

Annual Cumulated Index

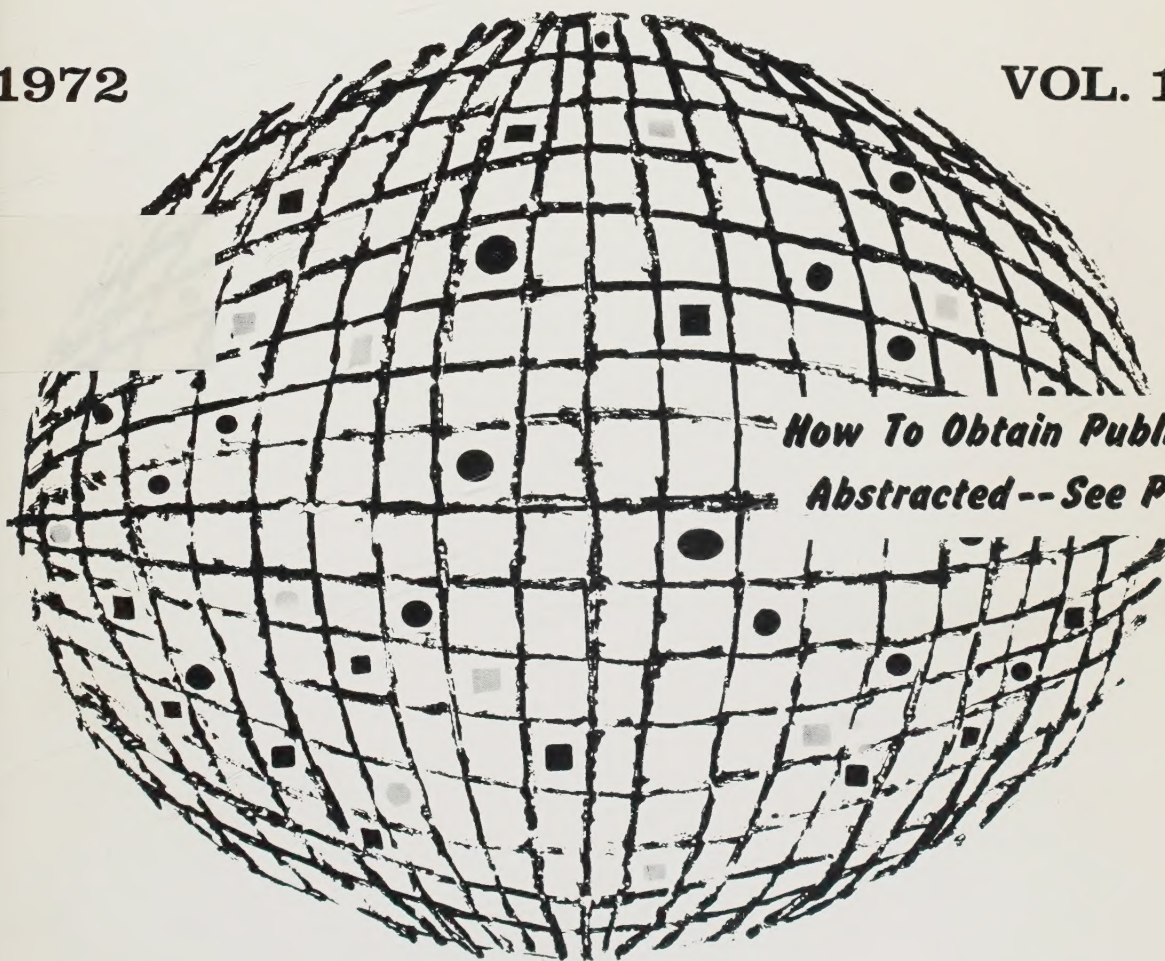
ACCESSION NOS. A72-10001 to A72-45794

INTERNATIONAL AEROSPACE ABSTRACTS

PART 1, PERIODICALS SCANNED, SUBJECT INDEX, A - L

1972

VOL. 12



*How To Obtain Publications
Abstracted--See Page IV*

PUBLISHED BY THE TECHNICAL INFORMATION SERVICE
AMERICAN INSTITUTE OF AERONAUTICS AND ASTRONAUTICS



Digitized by the Internet Archive
in 2023

500
I 57
U. 12
1972
pt. 1
A-L
N/C
Sci

INTERNATIONAL AEROSPACE ABSTRACTS

ANNUAL
CUMULATED
INDEX

PART 1

PERIODICALS SCANNED, SUBJECT INDEX, A - L

VOLUME 12

JANUARY - DECEMBER

1972

ACCESSION NUMBERS A72-10001 to A72-45794

INTERNATIONAL AEROSPACE ABSTRACTS is prepared and published semimonthly (except June and December, which have three issues) by the Technical Information Service, American Institute of Aeronautics and Astronautics, Inc., for the Institute and the National Aeronautics and Space Administration under Contract No. NASW-2422.

SUBSCRIPTION INFORMATION. Semimonthly issues: United States and Possessions, 1 year, \$110 postpaid; foreign countries, 1 year, \$125 postpaid. Cumulated index volumes: United States and Possessions, 1 year, \$75 postpaid; foreign countries, 1 year, \$90 postpaid.

EDITORIAL OFFICE: 750 Third Avenue, New York, N.Y. 10017. SUBSCRIPTION OFFICES: 750 Third Avenue, New York, N.Y. 10017; Third Avenue and Springtown Road, Alpha, N.J. 08865. Second-class postage paid at Phillipsburg, N.J. Copyright © 1972 by the American Institute of Aeronautics and Astronautics, Inc. (The indexes, however, may be reproduced for any bibliographic purpose.)

TELEPHONE: 212 TN 7-8300

TWX: 212 867-7265

March 1973

CONTENTS

PART 1

INTRODUCTION	iii
HOW TO OBTAIN PUBLICATIONS ABSTRACTED	iv
CROSS REFERENCES	iv
PERIODICALS SCANNED	v - xxv
SUBJECT INDEX, A - L	A1 - A1065A

PART 2

INTRODUCTION	iv
HOW TO OBTAIN PUBLICATIONS ABSTRACTED	v
CROSS REFERENCES	v
SUBJECT INDEX, M - Z	A1066 - A2171

PART 3

INTRODUCTION	iii
HOW TO OBTAIN PUBLICATIONS ABSTRACTED	iv
PERSONAL AUTHOR INDEX	B1 - B908
CONTRACT NUMBER INDEX	C1 - C33
MEETING PAPER & REPORT NUMBER INDEX	D1 - D14
ACCESSION NUMBER INDEX	E1 - E80

STAFF, AIAA

Administrator—Technical Information Programs, Robert R. Dexter

STAFF, TECHNICAL INFORMATION SERVICE

Director, John J. Glennon

Associate Director—Administrative, Thomas J. Meskel

Associate Director—Technical, Irene W. Bogolubsky

Abstracts Editor, Nanu Davis

Index Editor, Angelica Mihalakos

Chief Librarian, Patricia M. Marshall

INTRODUCTION

INTERNATIONAL AEROSPACE ABSTRACTS (IAA) is an abstracting and indexing service covering the world's published literature in the field of aeronautics and space science and technology. IAA is issued semimonthly, on the 1st and 15th of each month.

Coverage of Published Literature

The following types of publications are covered in IAA:

- Periodicals (including government-sponsored journals) and books.
- Meeting papers and conference proceedings issued by professional societies and academic organizations.
- Translations of journals and journal articles.

Coverage of Reports ("Unpublished" Literature)

Abstracts and indexes of report literature are issued in SCIENTIFIC AND TECHNICAL AEROSPACE REPORTS (STAR), which is published by the Scientific and Technical Information Office, National Aeronautics and Space Administration.

By special arrangement between NASA and the American Institute of Aeronautics and Astronautics, IAA is issued in coordination with the twice-monthly schedule of STAR, which appears on the 8th and 23rd of each month.

IAA and STAR both utilize identical subject categories and indexes, which are described below.

Thus the two services provide comprehensive access to the national and international unclassified report and published literature of current significance to aerospace science and technology.

Arrangement of the Semimonthly Issues

IAA is arranged in two major sections:

- (1) Abstracts Section. This section contains complete bibliographic citations with informative abstracts as required, arranged by appropriate subject categories to facilitate scanning. The subject categories are numbered from 01 to 34, and the scope of each category is outlined in the Table of Contents and again at the beginning of each category in the Abstracts Section. Each entry is prefixed by the IAA accession number.
- (2) Index Section. Five indexes are contained in this section: Subject, Personal Author, Contract Number, Meeting Paper and Report Number, and Accession Number. Each index is prefaced by explanatory notes.

Cumulated Indexes

The Semiannual Cumulated Index is issued promptly at the end of the first six months and the Annual Cumulated Index is issued promptly at the end of the twelve-month period.

Each cumulated index contains the following sections: A—Subject Index, B—Personal Author Index, C—Contract Number Index, D—Meeting Paper and Report Number Index, and E—Accession Number Index.

Indexing Vocabulary

The Preliminary Edition of the NASA THESAURUS (December 1967) (NASA SP-7030) is the authority for the indexing vocabulary that appears in the subject indexes to STAR and IAA. The NASA Thesaurus should be consulted for a total picture of the current indexing vocabulary and associated cross-reference structure. Copies of the NASA Thesaurus may be obtained from the National Technical Information Service or the U.S. Government Printing Office at a price of \$8.50 for the three-volume set. A one-volume NASA THESAURUS ALPHABETICAL UPDATE (September 1971) of 623 pages is available from the National Technical Information Service (NTIS), Springfield, Va. 22151, for \$6.00.

Information regarding SCIENTIFIC AND TECHNICAL AEROSPACE REPORTS and the availability of INTERNATIONAL AEROSPACE ABSTRACTS to organizations having contractual arrangements with NASA may be obtained from the following address:

National Aeronautics and Space Administration
Scientific and Technical Information Office
Attention: Code KSI
Washington, D. C. 20546

how to obtain publications abstracted

Documents announced are available from the AIAA Technical Information Service as follows:

- Paper copies of accessions announced in IAA and STAR and of other documents in the TIS library are available at \$5.00 per document up to a maximum of 20 pages. The charge for each additional page is \$0.25.
- Microfiche of documents announced in IAA are available at the rate of \$1.00 per microfiche on demand. Documents available in this manner are identified by the symbol # following the accession number in the Abstracts Section and in the Meeting Paper and Report Number and the Accession Number Indexes.
- Minimum air-mail postage to foreign countries is \$1.00.
- A number of publications, because of their special characteristics, are available only for reference in the library.

Address all inquiries and requests to:

Technical Information Service
American Institute of Aeronautics
and Astronautics, Inc.
750 Third Avenue, New York, N. Y. 10017

Telephone: 212 TN-7-8300
TWX: 212 867-7265

PLEASE REFER TO THE ACCESSION NUMBER WHEN REQUESTING PUBLICATIONS

CROSS REFERENCES

The subject index includes two types of cross references to aid the user of the index in locating the material being sought:

1. "USE" references (U) direct the user to alternate headings under which material on the subject will be found, for example

COLUMBIUM
U NIOBIUM

2. "NARROWER TERM" references (NT) refer the user to more specific headings in the same subject area, for example

LUMINESCENCE
NT ELECTROLUMINESCENCE

The periodicals listed in this section were scanned during the preparation of *International Aerospace Abstracts* for 1972. The periodicals were received regularly in all but a few instances. In the case of titles preceded by an asterisk, only the articles announced in *International Aerospace Abstracts* are available. All announced articles can be obtained from the AIAA Technical Information Service.

BM — Bimonthly
BW — Biweekly
Irreg. — Irregular
M — Monthly

Q — Quarterly
SA — Semiannual
SM — Semimonthly
W — Weekly

Abastumanskaia Astrofizicheskaia Observatoriia, Biulleten'. Akademiia Nauk Gruzinskoi SSR, Tbilisi. Irreg.

Académie des Sciences (Paris), Comptes Rendus, Série A — Sciences Mathématiques, Série B — Sciences Physiques. Académie des Sciences; Gauthier-Villars, Paris. W

Académie des Sciences (Paris), Comptes Rendus, Série C — Sciences Chimiques. Académie des Sciences; Gauthier-Villars, Paris. W

Académie Polonaise des Sciences, Bulletin, Série des Sciences Mathématiques, Astronomiques et Physiques. Académie Polonaise des Sciences; Państwowe Wydawnictwo Naukowe, Warsaw. M

Académie Polonaise des Sciences, Bulletin, Série des Sciences Techniques. Académie Polonaise des Sciences; Państwowe Wydawnictwo Naukowe, Warsaw. M

Académie Royale de Belgique, Classe des Sciences, Bulletin. Académie Royale de Belgique; Office International de Librairie, Brussels. M

Academy of Sciences, USSR, Izvestiya, Atmospheric and Oceanic Physics (Akademiia Nauk SSSR, Izvestiia, Fizika Atmosfery i Okeana). American Geophysical Union, Washington, D.C. M

Accademia Nazionale dei Lincei, Atti, Memorie — Classe di Scienze Fisiche, Matematiche e Naturali. Accademia Nazionale dei Lincei, Rome.

Accademia Nazionale dei Lincei, Atti, Rendiconti — Classe di Scienze Fisiche, Matematiche e Naturali. Accademia Nazionale dei Lincei, Rome. BM

ACM, Communications. Association for Computing Machinery, Baltimore, Md. M

Acoustical Society of America, Journal. Acoustical Society of America; American Institute of Physics, Inc., New York. M

Acta Astronomica. Polska Akademia Nauk; Państwowe Wydawnictwo Naukowe, Warsaw. Q

Acta Biologica et Medica Germanica. Akademie-Verlag GmbH, Berlin. M

Acta Cardiologica. Editions Acta Medica Belgica, Brussels. BM

Acta Cardiologica, Supplementum. Hôtel de Sociétés Scientifiques, Brussels.

Acta Científica. CITEFA, Buenos Aires. Q

Acta Electronica. Laboratoires d'Electronique et de Physique Appliquée, Limeil-Brévannes (Val de Marne), France. Q

Acta Geophysica Polonica. Polska Akademia Nauk; Państwowe Wydawnictwo Naukowe, Warsaw. Q

Acta Mathematica. Hungarian Academy of Sciences, Budapest. Irreg.

Acta Mechanica. Springer Verlag, Vienna. 8 issues per year

Acta Metallurgica. Pergamon Press, Inc., Elmsford, N.Y. M

**Acta Neuropathologica.* Springer Verlag, Berlin. Irreg.

**Acta Oto-Laryngologica.* Almqvist & Wiksell Periodical Co., Stockholm. M

Acta Physica. Akadémiai Kiadó, Budapest. BM

Acta Physica Austriaca. Österreichische Akademie der Wissenschaften; Springer Verlag, Vienna. Q

Acta Physica Polonica, Seria A. Polska Akademia Nauk, Instytut Fizyki and Polskie Towarzystwo Fizyczne, Warsaw.

Acta Physiologica Scandinavica. Scandinavian Physiological Society, Stockholm. 3 vols. per year

Acta Polytechnica Scandinavica, Civil Engineering and Building Construction Series. Scandinavian Council for Applied Research, Stockholm. Irreg.

Acta Polytechnica Scandinavica, Electrical Engineering Series. Scandinavian Council for Applied Research, Stockholm. Irreg.

Acta Polytechnica Scandinavica, Mathematics and Computing Machinery Series. Scandinavian Council for Applied Research, Stockholm. Irreg.

Acta Polytechnica Scandinavica, Mechanical Engineering Series. Scandinavian Council for Applied Research, Stockholm. Irreg.

Acta Psychologica. North-Holland Publishing Co., Amsterdam. M

Acta Technica. Akadémiai Kiadó, Budapest. 4 vols. per year

Acta Technica ČSAV. Československá Akademie Věd, Prague. BM

Acustica. S. Hirzel Verlag, KG, Stuttgart, West Germany. Irreg.

- Advances in Physics.* Taylor & Francis, Ltd., London. BM
- AEG-Telefunken, Technische Mitteilungen.* AEG-Telefunken, Berlin, West Germany. BM
- Aero Medical Society of India, Journal.* Institute of Aviation Medicine, Bangalore. Annual
- Aero-Revue.* Aero-Club der Schweiz and OSTIV; National-Zeitung AG, Basel. M
- Aeronautical Journal.* Royal Aeronautical Society, London. M
- Aeronautical Quarterly.* Royal Aeronautical Society, London. Q
- Aeronautical Society of India, Journal.* Aeronautical Society of India, New Delhi. Q
- L'Aéronautique et l'Astronautique.* Association Française des Ingénieurs et Techniciens de l'Aéronautique et de l'Espace and Société Française de l'Astronautique; Editions Air & Cosmos, Paris. M
- Aerospace Medicine.* Aerospace Medical Association, Washington, D.C. M
- L'Aerotecnica — Missili e Spazio.* Associazione Italiana di Aeronautica e Astronautica; Tamburini Editore S.p.A., Milan. BM
- AFEDS, Cahiers.* Association Française pour l'Etude et le Développement des Applications de l'Energie Solaire, Paris. Annual
- AIAA Journal.* American Institute of Aeronautics and Astronautics, Inc., New York. M
- AIAA Student Journal.* American Institute of Aeronautics and Astronautics, Inc., New York. Q
- AICHE Journal.* American Institute of Chemical Engineers, New York. BM
- Air University Review.* Aerospace Studies Institute, Maxwell Air Force Base, Ala. BM
- Aircraft Engineering.* Bunhill Publications, Ltd., London. M
- Airport Forum.* Bauverlag GmbH, Wiesbaden, West Germany. Q
- Akademia Athenon, Praktika.* Akademia Athenon, Athens.
- Akademiia Nauk Armianskoi SSR, Biurakanskaia Observatoriia, Soobshcheniia.* Akademiia Nauk Armianskoi SSR, Yerevan. Irreg.
- Akademiia Nauk Armianskoi SSR, Doklady.* Akademiia Nauk Armianskoi SSR, Yerevan. 10 issues per year
- Akademiia Nauk Armianskoi SSR, Izvestiia, Fizika.* Akademiia Nauk Armianskoi SSR, Yerevan. BM
- Akademiia Nauk Armianskoi SSR, Izvestiia, Mekhanika.* Akademiia Nauk Armianskoi SSR, Yerevan. BM
- Akademiia Nauk Armianskoi SSR, Izvestiia, Seriiia Tekhnicheskikh Nauk.* Akademiia Nauk Armianskoi SSR, Yerevan. BM
- Akademiia Nauk Azerbaidzhanskoi SSR, Doklady.* Akademiia Nauk Azerbaidzhanskoi SSR; Izdatel'stvo Elm, Baku. M
- Akademiia Nauk Azerbaidzhanskoi SSR, Izvestiia, Seriiia Fiziko-Tekhnicheskikh i Matematicheskikh Nauk.* Akademiia Nauk Azerbaidzhanskoi SSR; Izdatel'stvo Elm, Baku. BM
- Akademiia Nauk BSSR, Doklady.* Akademiia Nauk Belorusskoi SSR, Minsk. M
- Akademiia Nauk Gruzinskoi SSR, Soobshcheniia.* Akademiia Nauk Gruzinskoi SSR, Tiflis. M
- Akademiia Nauk Kazakhskoi SSR, Izvestiia, Seriiia Fiziko-Matematicheskaiia.* Akademiia Nauk Kazakhskoi SSR, Alma Ata. BM
- Akademiia Nauk Kazakhskoi SSR, Vestnik.* Akademiia Nauk Kazakhskoi SSR; Izdatel'stvo Nauka, Alma Ata. M
- Akademiia Nauk Latviiskoi SSR, Izvestiia, Seriiia Fizicheskikh i Tekhnicheskikh Nauk.* Akademiia Nauk Latviiskoi SSR, Riga. BM
- Akademiia Nauk SSSR, Doklady.* Akademiia Nauk SSSR; Izdatel'stvo Nauka, Moscow. 36 issues per year
- Akademiia Nauk SSSR, Izvestiia, Energetika i Transport.* Akademiia Nauk SSSR; Izdatel'stvo Nauka, Moscow. BM
- Akademiia Nauk SSSR, Izvestiia, Fizika Atmosfery i Okeana.* Akademiia Nauk SSSR; Izdatel'stvo Nauka, Moscow. M
- Akademiia Nauk SSSR, Izvestiia, Mekhanika Tverdogo Tela.* Akademiia Nauk SSSR; Izdatel'stvo Nauka, Moscow. BM
- Akademiia Nauk SSSR, Izvestiia, Mekhanika Zhidkosti i Gaza.* Akademiia Nauk SSSR; Izdatel'stvo Nauka, Moscow. BM
- Akademiia Nauk SSSR, Izvestiia, Metally.* Akademiia Nauk SSSR; Izdatel'stvo Nauka, Moscow. BM
- Akademiia Nauk SSSR, Izvestiia, Neorganicheskie Materialy.* Akademiia Nauk SSSR, Moscow. M
- Akademiia Nauk SSSR, Izvestiia, Seriiia Biologicheskaiia.* Akademiia Nauk SSSR; Izdatel'stvo Nauka, Moscow. BM
- Akademiia Nauk SSSR, Izvestiia, Seriiia Fizicheskaiia.* Akademiia Nauk SSSR; Izdatel'stvo Nauka, Moscow. M
- Akademiia Nauk SSSR, Izvestiia, Tekhnicheskaiia Kibernetika.* Akademiia Nauk SSSR; Izdatel'stvo Nauka, Moscow. BM
- Akademiia Nauk SSSR, Sibirskoe Otdelenie, Izvestiia, Seriiia Tekhnicheskikh Nauk.* Akademiia Nauk SSSR, Sibirskoe Otdelenie; Izdatel'stvo Nauka, Novosibirsk. 3 issues per year
- Akademiia Nauk SSSR, Vestnik.* Akademiia Nauk SSSR; Izdatel'stvo Nauka, Moscow. M
- Akademiia Nauk Tadzhikskoi SSR, Doklady.* Akademiia Nauk Tadzhikskoi SSR; Izdatel'stvo Donish, Dushanbe. M
- Akademiia Nauk Tadzhikskoi SSR, Institut Astrofiziki, Biulleten'.* Akademiia Nauk Tadzhikskoi SSR; Izdatel'stvo Donish, Dushanbe. Irreg.
- Akademiia Nauk Turkemenskoi SSR, Izvestiia, Seriiia Fiziko-Tekhnicheskikh, Khimicheskikh i Geologicheskikh Nauk.* Akademiia Nauk Turkemenskoi SSR; Izdatel'stvo Ylym, Ashkhabad. BM
- Akademiia Nauk Ukrains'koi RSR, Dopovidi, Seriiia A — Fiziko-Tekhnichni i Matematichni Nauki.* Akademiia Nauk Ukrains'koi RSR; Izdatel'stvo Naukova Dumka, Kiev. M
- Akademiia Nauk Ukrains'koi RSR, Dopovidi, Seriiia B — Geologii, Geofizika, Khimii i Biologiiia.* Akademiia Nauk Ukrains'koi RSR; Izdatel'stvo Naukova Dumka, Kiev. M

- Akademiia Nauk Ukrains'koi RSR, Visnik. Akademiia Nauk Ukrains'koi RSR; Izdatel'stvo Naukova Dumka, Kiev.*
- Akademiia Nauk Uzbekskoi SSR, Doklady. Akademiia Nauk Uzbekskoi SSR, Tashkent. M*
- Akademiia Nauk Uzbekskoi SSR, Izvestiia, Seriiia Fiziko-Matematicheskikh Nauk. Akademiia Nauk Uzbekskoi SSR, Tashkent. BM*
- Akademiia Nauk Uzbekskoi SSR, Izvestiia, Seriiia Tekhnicheskikh Nauk. Akademiia Nauk Uzbekskoi SSR, Tashkent. BM*
- Akademiia Navuk BSSR, Vestsi, Seryia Fizika-Tekhnichnykh Navuk. Akademiia Navuk Belaruskai SSR, Minsk. Q*
- Akusticheskii Zhurnal. Akademiia Nauk SSSR; Izdatel'stvo Nauka, Moscow. Q*
- Alata Internazionale. Etas Kompass, Milan. M*
- Alta Frequenza. Associazione Elettrotecnica ed Elettronica Italiana, Milan. M*
- Alta Frequenza (English Edition). Associazione Elettrotecnica ed Elettronica Italiana, Milan. M*
- Aluminium. Aluminium-Zentrale, e.V.; Aluminium-Verlag GmbH, Düsseldorf. M*
- American Ceramic Society Bulletin. American Ceramic Society, Inc., Columbus, Ohio. M*
- American Ceramic Society, Journal. American Ceramic Society, Inc., Columbus, Ohio. M*
- American Chemical Society, Journal. American Chemical Society, Washington, D.C. BW*
- American Heart Journal. C. V. Mosby Co., St. Louis, Mo. M*
- American Helicopter Society, Journal. American Helicopter Society, Inc., New York. Q*
- *American Journal of Botany. Botanical Society of America, Inc., City College, N.Y. 10 issues per year*
- American Journal of Cardiology. American College of Cardiology; Reuben H. Donnelley Corp., New York. M*
- American Journal of Ophthalmology. Ophthalmic Publishing Co., Chicago. M*
- American Journal of Physics. American Association of Physics Teachers; American Institute of Physics, Inc., New York. M*
- American Journal of Physiology. American Physiological Society, Bethesda, Md. M*
- American Journal of Psychology. University of Illinois Press, Urbana, Ill. Q*
- *American Journal of Science. Yale University, Kline Geology Laboratory, New Haven, Conn. M*
- *American Mathematical Society, Proceedings. American Mathematical Society, Providence, R. I. M*
- American Meteorological Society, Bulletin. American Meteorological Society, Boston. M*
- *American Mineralogist. Mineralogical Society of America, Washington, D.C. BM*
- American Society of Civil Engineers, Engineering Mechanics Division, Journal. American Society of Civil Engineers, New York. BM*
- American Society of Civil Engineers, Structural Division, Journal. American Society of Civil Engineers, New York. M*
- *Analytical Biochemistry. Academic Press, Inc., New York. M*
- *Analytical Chemistry. American Chemical Society, Washington, D.C. M*
- *Analytical Letters. Marcel Dekker, Inc., New York. M*
- *Anesthesiology. American Society of Anesthesiologists, Inc.; J. B. Lippincott Co., Philadelphia, Pa. M*
- Angewandte Informatik. Friedr. Vieweg & Sohn GmbH, Braunschweig. M*
- Annalen der Physik. Johann Ambrosius Barth Verlag, Leipzig, East Germany. Irreg.*
- Annales de Cardiologie et d'Angéiologie. L'Expansion Scientifique Française, Editeur, Paris. BM*
- Annales de Géophysique. Centre National de la Recherche Scientifique, Paris. Q*
- Annales de Physique. Centre National de la Recherche Scientifique; Masson & Cie., Paris. BM*
- Annales des Télécommunications. Centre National d'Etudes des Télécommunications, Issy-les-Moulineaux (Seine), France. BM*
- Annali di Geofisica. Istituto Nazionale de Geofisica, Rome. Q*
- *Annals of Mathematical Statistics. California State College at Hayward, Calif. BM*
- Annals of Physics. Academic Press, Inc., New York. M*
- *L'Antenna. II Rostro S.A.S., Rome. M*
- Antenny. Nauchno-Tekhnicheskoe Obshchestvo Radiotekhniki i Elektrosviazi imeni A. S. Popova; Izdatel'stvo Sviaz', Moscow. Irreg.*
- APL Technical Digest. Applied Physics Laboratory, Johns Hopkins University, Silver Spring, Md. BM*
- Aplikace Matematiky. Československá Akademie Věd, Matematický Ústav, Prague. BM*
- Applicable Analysis. Gordon & Breach Science Publishers, Ltd., London. Q*
- Applied Microbiology. American Society for Microbiology, Bethesda, Md. M*
- Applied Optics. Optical Society of America; American Institute of Physics, Inc., New York. M*
- Applied Physics Letters. American Institute of Physics, Inc., New York. SM*
- Applied Scientific Research. Martinus Nijhoff, The Hague. Irreg.*
- Applied Spectroscopy. Society for Applied Spectroscopy, Baltimore, Md. BM*
- Approach. Naval Safety Center; Division of Public Documents, Washington, D.C. M*
- Archiv für Elektronik und Übertragungstechnik. S. Hirzel Verlag, KG, Stuttgart, West Germany. Q*
- Archiv für Meteorologie, Geophysik und Bioklimatologie, Serie A — Meteorologie und Geophysik. Springer Verlag, Vienna. Irreg.*
- *Archiv für Mikrobiologie. Springer Verlag, Berlin. 4 vols. per year*
- Archiv für technisches Messen und industrielle Messtechnik (see Archiv für technisches Messen/-Messtechnische Praxis).*
- Archiv für technisches Messen/Messtechnische Praxis (formerly Archiv für technisches Messen und industrielle Messtechnik). Verlag R. Oldenbourg, Munich. M*
- Archive for Rational Mechanics and Analysis. Springer Verlag, Berlin. Irreg.*
- Archives des Sciences. Genève, Société de Physique et d'Histoire Naturelle; Librairie Payot S.A., Geneva. 3 issues per year*

- Archives of Environmental Health.* American Medical Association, Chicago. M
- Archiwum Automatyki i Telemechaniki.* Polska Akademia Nauk; Państwowe Wydawnictwo Naukowe, Warsaw. Q
- Archiwum Budowy Maszyn.* Polska Akademia Nauk, Komitet Budowy Maszyn; Państwowe Wydawnictwo Naukowe, Warsaw. Q
- Archiwum Elektrotechniki.* Polska Akademia Nauk; Państwowe Wydawnictwo Naukowe, Warsaw. Q
- Archiwum Mechaniki Stosowanej.* Polska Akademia Nauk, Instytut Podstawowych Problemów Techniki; Państwowe Wydawnictwo Naukowe, Warsaw. BM
- Archiwum Procesów Spalania.* Polska Akademia Nauk, Sekcja Spalania; Państwowe Wydawnictwo Naukowe, Warsaw. Q
- Arkiv för Geofysik.* Kungliga Svenska Vetenskapsakademien; Almqvist & Wiksells Boktryckeri AB, Stockholm. Irreg.
- Artificial Satellites.* Polish Academy of Sciences, Warsaw. Q
- ASCE, Transportation Engineering Journal.* American Society of Civil Engineers, New York. Q
- ASLE Transactions.* American Society of Lubrication Engineers; Academic Press, Inc., New York. M
- ASME, Transactions, Series B — Journal of Engineering for Industry.* American Society of Mechanical Engineers, New York. Q
- ASME, Transactions, Series C — Journal of Heat Transfer.* American Society of Mechanical Engineers, New York. Q
- ASME, Transactions, Series D — Journal of Basic Engineering.* American Society of Mechanical Engineers, New York. Q
- ASME, Transactions, Series E — Journal of Applied Mechanics.* American Society of Mechanical Engineers, New York. Q
- ASME, Transactions, Series F — Journal of Lubrication Technology.* American Society of Mechanical Engineers, New York. Q
- ASME, Transactions, Series G — Journal of Dynamic Systems, Measurement, and Control.* American Society of Mechanical Engineers, New York. Q
- Association for Computing Machinery, Journal.* Association for Computing Machinery, Inc., New York. Q
- Association Technique Maritime et Aéronautique, Bulletin.* Association Technique Maritime et Aéronautique, Paris. Annual
- Astrofizika.* Akademiia Nauk Armianskoi SSR, Yerevan. Q
- Astrometriia i Astrofizika.* Akademiia Nauk Ukrainskoi SSR; Izdatel'stvo Naukova Dumka, Kiev. Irreg.
- Astronautica Acta.* International Academy of Astronautics; Pergamon Press, Ltd., Oxford. BM
- Astronautical Society of the Republic of China, Transactions.* Astronautical Society of the Republic of China, Taiwan. Annual
- Astronautics and Aeronautics.* American Institute of Aeronautics and Astronautics, Inc., New York. M
- Astronautik.* Hermann Oberth-Gesellschaft, e.V., Hannover, West Germany. Q
- Astronautyka.* Polskie Towarzystwo Astronautyczne, Warsaw. Q
- Astronomical Institutes of Czechoslovakia, Bulletin.* Československá Akademie Věd, Prague. BM
- Astronomical Journal.* American Astronomical Society; American Institute of Physics, Inc., New York. 10 issues per year
- Astronomical Society of Australia, Proceedings.* Astronomical Society of Australia; Sydney University Press, Sydney. SA
- Astronomical Society of Japan, Publications.* Astronomical Society of Japan, c/o Tokyo Astronomical Observatory, Mitaka, Tokyo. Q
- Astronomical Society of the Pacific, Publications.* Astronomical Society of the Pacific, San Francisco. BM
- Astronomicheskii Vestnik.* Vsesoiuznoe Astronomo-Geodezicheskoe Obshchestvo; Izdatel'stvo Nauka, Moscow. Q
- Astronomicheskii Zhurnal.* Akademiia Nauk SSSR; Izdatel'stvo Nauka, Moscow. BM
- L'Astronomie.* Société Astronomique de France, Paris. BM
- Astronomie und Raumfahrt.* Deutsche Astronautische Gesellschaft, Berlin, East Germany. BM
- Astronomische Gesellschaft, Mitteilungen.* Astronomische Gesellschaft, Hamburg; G. Braun GmbH, Karlsruhe, West Germany. Irreg.
- Astronomische Nachrichten.* Akademie-Verlag GmbH, Berlin. Irreg.
- Astronomy and Astrophysics.* Springer Verlag, Berlin. M
- Astronomy and Astrophysics Supplement Series.* Leiden Observatory, Leiden. M
- Astronomy and Space.* David & Charles, Newton Abbot, Devon, England. M
- Astrophysical Journal.* American Astronomical Society; University of Chicago Press, Chicago. M
- Astrophysical Journal Supplement Series.* American Astronomical Society; University of Chicago Press, Chicago. M
- Astrophysical Letters.* Gordon & Breach Science Publishers, Ltd., London. M
- Astrophysics and Space Science.* D. Reidel Publishing Co., Dordrecht, Netherlands. M
- Atherosclerosis.* Elsevier Publishing Co., Amsterdam. BM
- Atmospheric Environment.* Pergamon Press, Ltd., Oxford. BM
- **Atomic Data.* Academic Press, Inc., New York. Q
- **Australian Journal of Chemistry.* Commonwealth Scientific and Industrial Research Organization, Melbourne. M
- Australian Journal of Physics.* Commonwealth Scientific and Industrial Research Organization, Melbourne. BM
- Australian Journal of Physics, Astrophysical Supplement.* Commonwealth Scientific and Industrial Research Organization, Melbourne. BM
- Australian Mathematical Society, Journal.* Australian Mathematical Society, Victoria; Wolters-Noordhoff NV, Groningen, Netherlands. 6 issues per year
- Australian Meteorological Magazine.* Commonwealth Bureau of Meteorology, Melbourne. Q

- Automatic Control Theory and Applications.* ACTA Press, Calgary, Canada. 3 issues per year
- Automatica.* Pergamon Press, Ltd., Oxford. BM
- Automation and Remote Control (Avtomatika i Telemekhanika).* Consultants Bureau, New York. M
- Automatizace.* Ministerstvo Průmyslu; Nakladatelství Technické Literatury, Prague. M
- Aviation Research Monographs.* University of Illinois, Urbana, Ill. Irreg.
- Aviation Review.* Smiths Industries, Ltd., Aviation Div., Wembley, Middx., England. Irreg.
- Aviation Week and Space Technology.* McGraw-Hill, Inc., New York. W
- Aviatsiia i Kosmonavtika.* Voenizdat, Moscow. M
- Aviatsionnaia Tekhnika.* Ministerstvo Vysshego i Srednego Spetsial'nogo Obrazovaniia SSSR; Izdanie Kazanskogo Aviatsionnogo Instituta, Kazan. Q
- Aviazione di Linea — Aeronautica e Spazio.* Publitelco International, Rome. M
- Aviazione di Linea, Difesa, e Spazio.* Rome. M
- Avtomatika.* Akademiia Nauk Ukrainskoi SSR; Izdatel'stvo Naukova Dumka, Kiev. BM
- Avtomatika i Telemekhanika.* Akademiia Nauk SSSR; Izdatel'stvo Nauka, Moscow. M
- Babeş-Bolyai, Universitas, Studia, Series Mathematica-Mechanica.* Babeş-Bolyai, Universitas, Cluj, Rumania. SA
- Babeş-Bolyai, Universitas, Studia, Series Physica.* Babeş-Bolyai, Universitas, Cluj, Rumania. SA
- Battelle Information* (Frankfurt). Battelle-Institut, e.V., Gemeinnützige Laboratorien für Vertragsforschung, Frankfurt am Main, West Germany.
- Battelle Research Outlook.* Battelle Memorial Institute, Columbus Laboratories, Columbus, Ohio. Q
- Beiträge aus der Plasmaphysik.* Akademie-Verlag GmbH, Berlin.
- Beiträge zur Physik der Atmosphäre.* Friedr. Vieweg & Sohn GmbH, Braunschweig. Q
- Bell System Technical Journal.* American Telephone & Telegraph Co., New York. 10 issues per year
- Bendix Technical Journal.* Bendix Corp., Southfield, Mich. 3 issues per year
- Bildmessung und Luftbildwesen.* Deutsche Gesellschaft für Photogrammetrie; Herbert Wichmann Verlag, Karlsruhe, West Germany. Q
- Biochemical and Biophysical Research Communications.* Academic Press, Inc., New York. SM
- **Biochemistry.* American Chemical Society, Washington, D.C. M
- **Biochimica et Biophysica Acta.* Elsevier Publishing Co., Amsterdam. W
- **Biometrics.* North Carolina State University, Institute of Statistics, Raleigh, N.C. Q
- Bionika.* Akademiia Nauk Ukrainskoi SSR; Izdatel'stvo Naukova Dumka, Kiev. Irreg.
- Biophysical Journal.* Biophysical Society; Rockefeller University Press, New York. M
- Biulleten' Eksperimental'noi Biologii i Meditsiny.* Akademiia Meditsinskikh Nauk SSSR; Izdatel'stvo Meditsina, Moscow. M
- B'lgarska Akademiia na Naukite, Fizicheski Institut s ANEB, Izvestiia.* B'lgarska Akademiia na Naukite, Otdelenie za Matematicheski i Fizicheski Nauki, Sofia. Irreg.
- B'lgarska Akademiia na Naukite, Institut po Elektronika, Izvestiia.* B'lgarska Akademiia na Naukite, Otdelenie za Matematicheski i Fizicheski Nauki, Sofia. Irreg.
- B'lgarska Akademiia na Naukite, Institut po Tekhnicheska Kibernetika, Izvestiia.* B'lgarska Akademiia na Naukite, Otdelenie za Tekhnicheski Nauki, Sofia. Irreg.
- B'lgarska Akademiia na Naukite, Institut po Tekhnicheska Mekhanika, Izvestiia.* B'lgarska Akademiia na Naukite, Otdelenie za Tekhnicheski Nauki, Sofia. Irreg.
- B'lgarska Akademiia na Naukite, Matematicheski Institut, Izvestiia.* B'lgarska Akademiia na Naukite, Sofia. Irreg.
- B'lgarska Akademiia na Naukite, Tsentralna Laboratoriia po Geodeziia, Izvestiia.* B'lgarska Akademiia na Naukite, Otdelenie za Matematicheski i Fizicheski Nauki, Sofia. Irreg.
- Bolgarskaia Akademiia Nauk, Doklady.* B'lgarska Akademiia na Naukite, Sofia. M
- Bosch Technische Berichte.* Robert Bosch GmbH, Stuttgart, West Germany. Irreg.
- Boundary-Layer Meteorology.* D. Reidel Publishing Co., Dordrecht, Netherlands. Q
- British Acoustical Society* (see *British Acoustical Society, Proceedings*).
- British Acoustical Society, Proceedings.* British Acoustical Society, London. M
- British Astronomical Association, Journal.* British Astronomical Association, Hounslow West, Middx., England. BM
- British Heart Journal.* British Medical Association, London. BM
- British Interplanetary Society, Journal.* British Interplanetary Society, London. M
- British Journal of Physiological Optics.* British Optical Association, London. Q
- Brüel and Kjaer Technical Review.* AS Brüel & Kjaer, Naerum, Denmark. Q
- Bucureşti, Institutul Politehnic Gheorghe Gheorghiu-Dej, Buletinul.* Institutul Politehnic Gheorghe Gheorghiu-Dej, Bucharest. BM
- Bucureşti, Universitatea, Analele, Matematică — Mecanică.* Redactia Analele Universitatii Bucureşti, Bucharest, Rumania. Irreg.
- Bulletin of the Atomic Scientists.* Educational Foundation for Nuclear Science, Chicago. M
- **Bulletins of American Paleontology.* Paleontological Research Institution, Ithaca, N.Y. 2 vols. per year
- California Management Review.* University of California, Graduate School of Business Administration, Berkeley. Q
- Cambridge Philosophical Society, Proceedings.* Cambridge University Press, London. BM
- Canada, National Research Council, Division of Mechanical Engineering and National Aeronautical Establishment, Quarterly Bulletin.* National Research Council of Canada, Ottawa. Q

- Canadian Aeronautics and Space Journal*. Canadian Aeronautics and Space Institute, Ottawa. M
- **Canadian Journal of Botany*. National Research Council of Canada, Ottawa. M
- **Canadian Journal of Microbiology*. National Research Council of Canada, Ottawa. M
- Canadian Journal of Physics*. National Research Council of Canada, Ottawa. SM
- Canadian Journal of Psychology*. Canadian Psychological Association; University of Toronto Press, Toronto. Q
- Canadian Society for Mechanical Engineering, Transactions*. Canadian Society for Mechanical Engineering, Montreal. Q
- Cardiology*. S. Karger AG, Basel. BM
- Cardiovascular Research*. British Cardiac Society; British Medical Association, London. Q
- CASI Transactions*. Canadian Aeronautics and Space Institute, Ottawa. SA
- CATCA Journal*. Canadian Air Traffic Control Association, Inc., Ottawa. SA
- Celestial Mechanics*. D. Reidel Publishing Co., Dordrecht, Netherlands. Q
- Československý Časopis pro Fysiku, Sekce A*. Československá Akademie Věd, Prague. BM
- Chartered Institute of Transport, Journal*. Chartered Institute of Transport, London. BM
- Chartered Mechanical Engineer*. Institution of Mechanical Engineers, London. M
- Chem Tech*. American Chemical Society, Washington, D.C. M
- Chemical Engineering Progress, Symposium Series*. American Institute of Chemical Engineers, New York. M
- Chemical Geology*. Elsevier Publishing Co., Amsterdam. 8 issues per year
- Chemical Physics Letters*. North-Holland Publishing Co., Amsterdam. BW
- **Chemie der Erde*. VEB Gustav Fischer Verlag, Jena, East Germany. Q
- Chemie-Ingenieur-Technik*. Gesellschaft Deutscher Chemiker; Verlag Chemie GmbH, Weinheim, West Germany. M
- Ciel et Terre*. Société Belge d'Astronomie, de Météorologie et de Physique du Globe, Brussels. BM
- Circulation*. American Heart Association, Inc., New York. M
- Circulation Research*. American Heart Association, Inc., New York. M
- **Clean Air*. Japan Air Cleaning Association, Tokyo. BM
- Cobalt*. Centre d'Information du Cobalt, Brussels. Q
- Combustion and Flame*. Combustion Institute; American Elsevier Publishing Co., Inc., New York. BM
- Combustion Science and Technology*. Gordon & Breach Science Publishers, Ltd., London. BM
- Comments on Modern Physics, Part C — Comments on Astrophysics and Space Physics*. Gordon & Breach Science Publishers, Ltd., London. BM
- Communications on Pure and Applied Mathematics*. New York University, Courant Institute of Mathematical Sciences; Interscience Publishers, New York. BM
- Component Technology*. Plessey Co., Ltd., Ilford, Essex, England.
- Composites*. Iliffe Science and Technology Publications, Ltd., Guildford, Surrey, England. Q
- Computer Journal*. British Computer Society, London. Q
- **Computers and Biomedical Research*. Academic Press, Inc., New York. Q
- Computers and Structures*. Pergamon Press, Ltd., Oxford. Q
- Computers in Biology and Medicine*. Pergamon Press, Inc., New York. Q
- Computing*. Springer Verlag, Vienna. Q
- COMSAT Technical Review*. Communications Satellite Corporation, Washington, D.C. SA
- Contamination Control/Biomedical Environments*. Blackwell Publishing Co., Inc., Los Angeles. BM
- Contemporary Physics*. Taylor & Francis, Ltd., London. BM
- **Contributions to Mineralogy and Petrology*. Springer Verlag, Berlin. 3 vols. per year
- Corrosion*. National Association of Corrosion Engineers, Inc., Houston, Tex. M
- Cosmic Electrodynamics*. D. Reidel Publishing Co., Dordrecht, Netherlands. Q
- Cosmic Research (Kosmicheskie Issledovaniia)*. Consultants Bureau, New York. BM
- COSPAR Information Bulletin*. COSPAR Secretariat, Paris. Irreg.
- Cryogenic Technology*. Cryogenic Society of America; Value Engineering Publications, Inc., Los Angeles. BM
- Cryogenics*. Iliffe Science & Technology Publications, Ltd., London. BM
- Current Science*. Current Science Association, Bangalore. SM
- Czechoslovak Journal of Physics, Section B*. Československá Akademie Věd, Prague. M
- Defence Science Journal*. Indian Ministry of Defence, New Delhi. Q
- Defense Management Journal*. Directorate for Management Improvement Programs, Office of the Assistant Secretary of Defense; Supt. of Documents, Washington, D.C. Q
- DEW-Technische Berichte*. Deutsche Edelstahlwerke Aktiengesellschaft, Krefeld, West Germany. Irreg.
- DFVLR-Nachrichten*. Deutsche Forschungs- und Versuchsanstalt für Luft- und Raumfahrt, e.V., Porz-Wahn, West Germany. Irreg.
- DGLR Mitteilungen*. Deutsche Gesellschaft für Luft- und Raumfahrt, e.V., Cologne. Q
- Differentsial'nye Uravneniia*. Izdatel'stvo Nauka i Tekhnika, Minsk. M
- Dinamika i Prochnost' Mashin*. Izdatel'stvo Khar'kovskogo Gosudarstvennogo Universiteta, Kharkov. Irreg.
- Dornier-Post (English Edition)*. Dornier AG, Munich. Q

- Earth and Extraterrestrial Sciences.* Gordon & Breach Science Publishers, Ltd., London. Irreg.
- Earth and Planetary Science Letters.* North-Holland Publishing Co., Amsterdam. M
- L'Echo des Recherches.* Centre National d'Etudes des Télécommunications, Issy-les-Moulineaux, France. Q
- Eesti NSV Teaduste Akadeemia, Toimetised, Füüsika-Matemaatika.* Izdatel'stvo Periodika, Tallin. Q
- Electrical Communication.* International Telephone and Telegraph Corp., New York. Q
- Electrical Communication Laboratory, Review.* Nippon Telegraph & Telephone Public Corp., Tokyo. BM
- Electro-Optical Systems Design.* Milton S. Kiver Publications, Inc., Madison, Wis. M
- Electrochemical Society, Journal.* Electrochemical Society, Inc., New York. M
- Electroencephalography and Clinical Neurophysiology.* International Federation of Societies for Electroencephalography and Clinical Neurophysiology; Elsevier Publishing Co., Amsterdam. M
- Electron Technology.* Polish Academy of Sciences, Institute of Electron Technology; Państwowe Wydawnictwo Naukowe, Warsaw. Irreg.
- Electronic Applications Bulletin.* N. V. Philips' Gloeilampenfabrieken; N. V. Uitgeversmaatschappij Centrex, Eindhoven. 4 issues per year
- Electronic Design.* Hayden Publishing Co., Inc., New York. BW
- Electronic Packaging and Production.* Milton S. Kiver Publications, Inc., Chicago. M
- Electronic Progress.* Raytheon Co., Lexington, Mass. Q
- Electronics.* McGraw-Hill, Inc., New York. BW
- Electronics and Communications in Japan (Denshi Tsushin Gakkai Ronbunshi).* Institute of Electronics and Communications Engineers of Japan; Institute of Electrical and Electronics Engineers, Inc., New York. M
- Electronics and Power.* Institution of Electrical Engineers, London. M
- Electronics Letters.* Institution of Electrical Engineers, London. BW
- Elektromekhanika.* Ministerstvo Vysshego i Srednego Spetsial'nogo Obrazovaniia SSSR, Novocherkassk. M
- Elektronik.* Franzis-Verlag, Munich. M
- Elektronika.* Wydawnictwa Czasopism Technicznych NOT, Warsaw. M
- *Elektrotechnische Zeitschrift, Ausgabe A.* Verband Deutscher Elektrotechniker; VDE-Verlag GmbH, Berlin, West Germany.
- Energomashinostroenie.* Ministerstvo Tiazhelogo, Energeticheskogo i Transportnogo Mashinostroeniia SSSR and Nauchno-Tekhnicheskoe Obshchestvo Mashinostroitel'noi Promyshlennosti; Izdatel'stvo Mashinostroenie, Leningrad. M
- Energy Conversion.* Pergamon Press, Ltd., Oxford. Q
- Engineering Fracture Mechanics.* Pergamon Press, Ltd., Oxford. Q
- Entropie.* Editions Barthélemy & Cie., Paris. BM
- *Environmental Biology and Medicine.* Gordon & Breach Science Publishers, Ltd., London.
- Environmental Research.* Academic Press, Inc., New York. BM
- *Environmental Science and Technology.* American Chemical Society; ACS Publications, Washington, D.C. M
- EOS.* American Geophysical Union, Washington, D.C. M
- *Erdöl und Kohle Erdgas Petrochemie vereinigt mit Brennstoff-Chemie.* German Society for Petroleum Science and Coal Chemistry; Industrieverlag von Hernhausen, KG, Hamburg, West Germany. M
- Ergonomics.* Ergonomics Research Society, Nederlandse Vereniging voor Ergonomie, International Ergonomics Association; Taylor & Francis, Ltd., London. Q
- ESRO/ELDO Bulletin.* European Space Research Organization and European Space Vehicle Launcher Development Organization, Neuilly-sur-Seine, France. Q
- Esso Air World.* ESSO International, Inc., New York. BM
- Eurocontrol.* Eurocontrol, Public Relations Div., Brussels. SA
- Experimental Brain Research.* Springer Verlag, Berlin. Irreg.
- *Experimental Cell Research.* International Society for Cell Biology; Academic Press, Inc., New York. M
- Experimental Mechanics.* Society for Experimental Stress Analysis, Westport, Conn. M
- *Experimental Medicine and Surgery.* Brooklyn Medical Press, Inc., Brooklyn, N.Y. Q
- Explosivstoffe.* Erwin Barth Verlag, KG, Mannheim, West Germany. M
- Facilities for Atmospheric Research.* National Center for Atmospheric Research, Boulder, Colo. Q
- *Faraday Society, Transactions.* Aberdeen University Press, Ltd., Aberdeen, Scotland. M
- *Federation Proceedings.* Federation of American Societies for Experimental Biology, Washington, D.C. Q
- Finommechanika.* Lapkiadó Vállalat, Budapest. M
- Fizika.* Ministerstvo Vysshego i Srednego Spetsial'nogo Obrazovaniia SSSR; Izdatel'stvo Tomskogo Universiteta, Tomsk. M
- Fizika Aerodispersnykh Sistem.* Izdatel'stvo Kievskogo Universiteta, Kiev. Irreg.
- Fizika Goreniia i Vzryva.* Akademiia Nauk SSSR, Sibirskoe Otdelenie; Izdatel'stvo Nauka, Novosibirsk. Q
- Fizika i Tekhnika Poluprovodnikov.* Akademiia Nauk SSSR; Izdatel'stvo Nauka, Leningrad. M
- Fizika Metallov i Metallovedenie.* Akademiia Nauk SSSR; Izdatel'stvo Nauka, Sverdlovsk. M
- Fizika Plazmy.* Ministerstvo Vysshego i Srednego Spetsial'nogo Obrazovaniia SSSR and Moskovskii Inzhenerno-Fizicheskii Institut; Atomizdat, Moscow. Irreg.
- Fiziko-Khimicheskaiia Mekhanika Materialov.* Akademiia Nauk Ukrainskoi SSR; Izdatel'stvo Naukova Dumka, Kiev. BM

- Fiziologicheskii Zhurnal SSSR*. Akademiia Nauk SSSR; Izdatel'stvo Nauka, Leningrad. M
- Fiziologichnii Zhurnal*. Akademiia Nauk Ukrainskoi SSR, Institut Fiziologii; Izdatel'stvo Naukova Dumka, Kiev. BM
- Flight International*. Royal Aero Club; IPC Business Press, Ltd., London. W
- Flug Revue/Flugwelt International*. Club der Luftfahrt von Deutschland, e.V., Bonn; Vereinigte Motor-Verlage GmbH, Stuttgart, West Germany. M
- Fluid — Apparecchiature Idrauliche e Pneumatiche*. Etas Kompass, Milan. BM
- Fluid Mechanics — Soviet Research*. Scripta Publishing Corp., Washington, D.C. BM
- Fluidics Quarterly*. Ann Arbor, Mich. Q
- FOA Reports*. Försvarets Forskningsanstalt, Stockholm. Irreg.
- **Folia Primatologica*. S. Karger AG, Basel. BM
- Forces Aériennes Françaises*. Comité d'Etudes Aéronautiques Militaires, Paris. M
- Forschung im Ingenieurwesen*. Verein Deutscher Ingenieure; VDI-Verlag GmbH, Düsseldorf. BM
- Forschungsinstitut für Anthropotechnik, Anthropotechnische Mitteilung*. Gesellschaft zur Förderung der astrophysikalischen Forschung, e.V., Meckenheim, West Germany. Irreg.
- Fortune*. Time, Inc., Chicago. M
- Franklin Institute, Journal*. Franklin Institute, Philadelphia, Pa.; Pergamon Press, Ltd., Oxford. M
- Frequenz*. Fachverlag Schiele & Schön, Berlin. M
- Fujitsu Scientific and Technical Journal*. Fujitsu, Ltd., Kanagawa, Japan. Q
- Funktsional'nyi Analiz i Teoriia Funktsii*. Izdatel'stvo Kazanskogo Universiteta, Kazan. Irreg.
- Fyzikálny Časopis*. Slovenská Akademia Vied, Bratislava. Q
- Geliotekhnika*. Akademiia Nauk Uzbekskoi SSR, Tashkent. BM
- Genève, Société de Physique et d'Histoire Naturelle, Compte Rendu des Séances*. Société de Physique et d'Histoire Naturelle de Genève, Geneva. 3 issues per year
- Geochimica et Cosmochimica Acta*. Geochemical Society and Meteoritical Society; Pergamon Press, Ltd., Oxford. M
- Geodesy and Aerophotography (Geodeziia i Aerofotos'emka)*. American Geophysical Union, Washington, D.C. BM
- Geodeziia, Kartografiia i Aerofotos'emka*. Izdatel'stvo L'vovskogo Universiteta, Lvov. Irreg.
- Geodeziia i Aerofotos'emka*. Ministerstvo Vysshogo i Srednego Spetsial'nogo Obrazovaniia SSSR; Izdatel'stvo Moskovskogo Instituta Inzhenerov Geodezii, Aerofotos'emki i Kartografii, Moscow. BM
- Geodeziia i Kartografiia*. Glavnoe Upravlenie Geodezii i Kartografii pri Sovete Ministrov SSSR; Izdatel'stvo Nedra, Moscow. M
- Geodezja i Kartografia*. Polska Akademia Nauk, Komitet Geodezji; Państwowe Wydawnictwo Naukowe, Warsaw. Q
- Geofisica e Meteorologia (see Rivista Italiana di Geofisica)*.
- Geofysikální Sborník*. Československá Akademie Věd, Geofysikální Ústav, Prague.
- Geofysiske Publikasjoner (Geophysics Norvegica)*. Norske Videnskaps-Akademi, Oslo. Irreg.
- Geological Society of America Bulletin*. Geological Society of America, Boulder, Colo. M
- Geomagnetism and Aeronomy (Geomagnetizm i Aeronomiia)*. American Geophysical Union, Washington, D.C. BM
- Geomagnetizm i Aeronomiia*. Akademiia Nauk SSSR; Izdatel'stvo Nauka, Moscow. BM
- Geophysical Fluid Dynamics*. Gordon & Breach Science Publishers, Ltd., London. M
- Geophysical Journal*. Royal Astronomical Society; Blackwell Scientific Publications, Ltd., Oxford. M
- Gerlands Beiträge zur Geophysik*. Akademische Verlagsgesellschaft Geest & Portig, KG, Leipzig, East Germany. BM
- Gidromekhanika*. Akademiia Nauk Ukrainskoi SSR; Izdatel'stvo Naukova Dumka, Kiev. Irreg.
- Göttingen, Akademie der Wissenschaften, Nachrichten, Mathematisch-physikalische Klasse*. Vandenhoeck & Ruprecht, Göttingen. Irreg.
- Groupe de Recherches de Géodésie Spatiale, Bulletin*. GRGS, Observatoire de Meudon, Meudon, France.
- Harvard Business Review*. Harvard University, Graduate School of Business Administration, Boston. BM
- **Health Physics*. American Health Physics Society; Pergamon Press, Ltd., Oxford. M
- Heat and Fluid Flow*. Institution of Mechanical Engineers, London. SA
- Heat Transfer — Japanese Research*. Scripta Publishing Corp., Washington, D.C. Q
- Heat Transfer — Soviet Research*. American Society of Mechanical Engineers, New York. BM
- High Temperature (Teplofizika Vysokikh Temperatur)*. Consultants Bureau, New York. BM
- **High Temperature Science*. Academic Press, Inc., New York. Q
- High Temperatures — High Pressures*. Pion, Ltd., London. BM
- Híradástechnika*. Lapkiadó Vállalat, Budapest. BM
- **Hortscience*. American Society for Horticultural Science, Joseph, Mich. Q
- Human Factors*. Human Factors Society, Inc., Santa Monica, Calif.; The Johns Hopkins Press, Baltimore, Md. M
- Hydraulics and Pneumatics*. Industrial Publishing Co., Cleveland, Ohio. M
- I & EC — Industrial and Engineering Chemistry, Product Research and Development*. American Chemical Society, Washington, D.C. Q
- Iași, Institutul Politehnic, Buletinul, Secția I — Matematică, Mecanică Teoretică, Fizică*. Iași, Institutul Politehnic, Iași, Rumania. SA

- Iași, *Institutul Politehnic, Buletinul, Secția III — Electrotehnică, Electronică, Automatizări*. Iași, Institutul Politehnic, Iași, Rumania. Irreg.
- Iași, *Institutul Politehnic, Buletinul, Secția IV — Mecanică Tehnică*. Iași, Institutul Politehnic, Iași, Rumania. SA
- IBM *Journal of Research and Development*. International Business Machines Corp., Armonk, N.Y. BM
- Icarus. Academic Press, Inc., New York. BM
- IEE *Reviews*. Institution of Electrical Engineers, London. Annual
- IEEE, *Proceedings*. Institute of Electrical and Electronics Engineers, Inc., New York. M
- IEEE *Journal of Quantum Electronics*. Institute of Electrical and Electronics Engineers, Inc., New York. M
- IEEE *Journal of Solid-State Circuits*. Institute of Electrical and Electronics Engineers, Inc., New York. BM
- IEEE *Spectrum*. Institute of Electrical and Electronics Engineers, Inc., New York. M
- IEEE *Transactions on Aerospace and Electronic Systems*. Institute of Electrical and Electronics Engineers, Inc., New York. BM
- IEEE *Transactions on Antennas and Propagation*. Institute of Electrical and Electronics Engineers, Inc., New York. BM
- IEEE *Transactions on Audio and Electroacoustics*. Institute of Electrical and Electronics Engineers, Inc., New York. Q
- IEEE *Transactions on Automatic Control*. Institute of Electrical and Electronics Engineers, Inc., New York. BM
- IEEE *Transactions on Biomedical Engineering*. Institute of Electrical and Electronics Engineers, Inc., New York. M
- IEEE *Transactions on Broadcasting*. Institute of Electrical and Electronics Engineers Inc., New York. Q
- IEEE *Transactions on Circuit Theory*. Institute of Electrical and Electronics Engineers, Inc., New York. Q
- IEEE *Transactions on Communication Technology* (see *IEEE Transactions on Communications*).
- IEEE *Transactions on Communications* (formerly *IEEE Transactions on Communication Technology*). Institute of Electrical and Electronics Engineers, Inc., New York. BM
- IEEE *Transactions on Computers*. Institute of Electrical and Electronics Engineers, Inc., New York. M
- IEEE *Transactions on Education*. Institute of Electrical and Electronics Engineers, Inc., New York. Q
- IEEE *Transactions on Electrical Insulation*. Institute of Electrical and Electronics Engineers, Inc., New York. Q
- IEEE *Transactions on Electromagnetic Compatibility*. Institute of Electrical and Electronics Engineers, Inc., New York. Q
- IEEE *Transactions on Electron Devices*. Institute of Electrical and Electronics Engineers, Inc., New York. M
- IEEE *Transactions on Engineering Management*. Institute of Electrical and Electronics Engineers, Inc., New York. Q
- IEEE *Transactions on Geoscience Electronics*. Institute of Electrical and Electronics Engineers, Inc., New York. Q
- IEEE *Transactions on Industrial Electronics and Control Instrumentation*. Institute of Electrical and Electronics Engineers, Inc., New York. Q
- IEEE *Transactions on Industry Applications*. Institute of Electrical and Electronics Engineers, Inc., New York. BM
- IEEE *Transactions on Information Theory*. Institute of Electrical and Electronics Engineers, Inc., New York. BM
- IEEE *Transactions on Instrumentation and Measurement*. Institute of Electrical and Electronics Engineers, Inc., New York. Q
- IEEE *Transactions on Magnetics*. Institute of Electrical and Electronics Engineers, Inc., New York. Q
- IEEE *Transactions on Manufacturing Technology*. Institute of Electrical and Electronics Engineers, Inc., New York. Q
- IEEE *Transactions on Microwave Theory and Techniques*. Institute of Electrical and Electronics Engineers, Inc., New York. M
- IEEE *Transactions on Nuclear Science*. Institute of Electrical and Electronics Engineers, Inc., New York. BM
- IEEE *Transactions on Parts, Hybrids, and Packaging*. Institute of Electrical and Electronics Engineers, Inc., New York. Q
- IEEE *Transactions on Reliability*. Institute of Electrical and Electronics Engineers, Inc., New York. Q
- IEEE *Transactions on Sonics and Ultrasonics*. Institute of Electrical and Electronics Engineers, Inc., New York. Q
- IEEE *Transactions on Systems, Man, and Cybernetics*. Institute of Electrical and Electronics Engineers, Inc., New York. Q
- Image Technology. Society of Photographic Scientists and Engineers; Acolyte Publications Corp., Los Angeles. BM
- *Immunochemistry. Pergamon Press, Ltd., Oxford. M
- Indian Academy of Sciences, *Proceedings, Section A*. Indian Academy of Sciences, Bangalore. M
- Indian Institute of Science, *Journal*. Indian Institute of Science, Bangalore. Q
- Indian Journal of Pure and Applied Mathematics. Indian National Science Academy, New Delhi. Q
- Indian Journal of Pure and Applied Physics. Council of Scientific and Industrial Research, New Delhi. M
- Indian Journal of Technology. Council of Scientific and Industrial Research, New Delhi. M
- Indian Rocket Society, *Journal*. Indian Rocket Society, Trivandrum, India. Q
- Indiana University Mathematics Journal. Indiana University, Dept. of Mathematics, Bloomington, Ind. M

- Industrial Laboratory (Zavodskaja Laboratorija).* Consultants Bureau, New York. M
- Industries Atomiques et Spatiales (formerly Sciences et Industries Spatiales).* Sertna, S.A., Geneva. BM
- INFOR — Canadian Journal of Operational Research and Information Processing.* INFOR Journal, Ottawa. Q
- Information and Control.* Academic Press, Inc., New York. M
- Information Display.* Society for Information Display; Information Display Publications, Inc., Los Angeles. BM
- Infrared Physics.* Pergamon Press, Ltd., Oxford. Q
- Ingegneria.* Editore Ulrico Hoepli, Milan. M
- Ingeniería Aeronáutica y Astronáutica.* Asociación de Ingenieros Aeronáuticos, Madrid. BM
- Ingenieur-Archiv.* Springer Verlag, Berlin. BM
- Institut Fourier, Annales.* Centre National de la Recherche Scientifique, Paris; Institut de Mathématiques Pures, Saint-Martin-d'Hères, France. Q
- Institut Henri Poincaré, Annales, Section A — Physique Théorique.* Gauthier-Villars, Paris. BM
- Institut Teoreticheskoi Astronomii, Biulleten'.* Akademiia Nauk SSSR, Institut Teoreticheskoi Astronomii; Izdatel'stvo Nauka, Leningrad. Irreg.
- Institute of Mathematics and Its Applications, Journal.* Academic Press, Inc. (London), Ltd., London. Q
- Institute of Navigation, Journal (see Journal of Navigation).*
- Institution of Electrical Engineers, Proceedings.* Institution of Electrical Engineers, London. M
- Institution of Engineers (India), Journal, Electronics and Telecommunication Engineering Division.* Institution of Engineers, Calcutta. 3 issues per year
- Institution of Engineers (India), Journal, Mechanical Engineering Division.* Institution of Engineers, Calcutta. BM
- Institution of Mechanical Engineers, Proceedings.* Institution of Mechanical Engineers, London. Irreg.
- *Institution of Radio and Electronics Engineers (Australia), Proceedings.* Institution of Radio and Electronics Engineers, Sydney. M
- Institution of Telecommunication Engineers, Journal.* Institution of Telecommunication Engineers, New Delhi. M
- Instruments and Control Systems.* Chilton Co., Philadelphia, Pa. M
- Instytut Lotnictwa, Prace.* Instytut Lotnictwa Wydziału Naukowo-Techniczne, Warsaw. Irreg.
- Instytut Maszyn Przepływowych, Prace.* Polska Akademia Nauk, Instytut Maszyn Przepływowych, Gdansk; Państwowe Wydawnictwo Naukowe, Warsaw. Irreg.
- Interavia.* Interavia S.A., Geneva. M
- International Chemical Engineering.* American Institute of Chemical Engineers, New York. Q
- International Journal for Numerical Methods in Engineering.* John Wiley & Sons, Ltd., Chichester, Sussex, England. Q
- International Journal of Applied Radiation and Isotopes.* Pergamon Press, Ltd., Oxford. M
- International Journal of Computer Mathematics, Section B.* Gordon & Breach Science Publishers, New York. Q
- International Journal of Control, First Series.* Taylor & Francis, Ltd., London. M
- International Journal of Electronics, First Series.* Taylor & Francis, Ltd., London. M
- International Journal of Engineering Science.* Pergamon Press, Ltd., Oxford. M
- International Journal of Fracture Mechanics.* Wolters-Noordhoff Publishing, Groningen, Netherlands. Q
- International Journal of Heat and Mass Transfer.* Pergamon Press, Ltd., Oxford. M
- International Journal of Man-Machine Studies.* Academic Press, Inc. (London), Ltd., London. Q
- International Journal of Mechanical Sciences.* Pergamon Press, Ltd., Oxford. M
- International Journal of Non-Linear Mechanics.* Pergamon Press, Ltd., Oxford. Q
- International Journal of Nondestructive Testing.* Gordon & Breach Science Publishers, London.
- International Journal of Powder Metallurgy.* American Powder Metallurgy Institute, New York. Q
- International Journal of Solids and Structures.* Pergamon Press, Ltd., Oxford. M
- *International Journal of Theoretical Physics.* Plenum Publishing Co., Ltd., London. Q
- International Metallurgical Reviews.* Institute of Metals, London; American Society for Metals, Metals Park, Ohio. Q
- Internationale Elektronische Rundschau.* Verlag für Radio-Foto-Kinotechnik GmbH, Berlin. M
- Internationale Zeitschrift für angewandte Physiologie einschließlich Arbeitsphysiologie.* Springer Verlag, Berlin. Q
- *Investigative Radiology.* J. B. Lippincott Co., Philadelphia. BM
- Inzhenerno-Fizicheskii Zhurnal.* Akademiia Nauk Belorusskoi SSR; Izdatel'stvo Nauka i Tekhnika, Minsk. M
- Irish Astronomical Journal.* Observatory, Armagh, Northern Ireland. Q
- ISA Transactions.* Instrument Society of America, Pittsburgh, Pa. Q
- Israel Journal of Technology.* Weizmann Science Press of Israel, Jerusalem. BM
- İstanbul Üniversitesi, Fen Fakültesi Mecmuası, Seri A — Sırf ve Tatbiki Matematik.* İstanbul Üniversitesi, İstanbul. Q
- ITA-Engenharia.* Instituto Tecnológico de Aeronáutica, Sao Jose dos Campos, Sao Paulo, Brazil. BM
- ITU Telecommunication Journal.* International Telecommunication Union, Geneva. M
- Japan Air Self Defence Force, Aeromedical Laboratory, Reports.* Aeromedical Laboratory, Tachikawa, Japan. Q
- Japan Institute of Light Metals, Journal.* Japan Institute of Light Metals, Tokyo. BM
- Japan Institute of Metals, Journal (Nippon Kinzoku Gakkai-shi).* Japan Institute of Metals, Sendai. M

- Japan Institute of Metals, Transactions.* Japan Institute of Metals, Sendai. BM
- Japan Society for Aeronautical and Space Sciences, Transactions.* Japan Society for Aeronautical and Space Sciences, Tokyo. Irreg.
- Japan Society of Materials Science, Journal.* Society of Materials Science, Kyoto. M
- Japanese Heart Journal.* Tokyo, University, Faculty of Medicine, Tokyo. BM
- Japanese Journal of Applied Physics.* Physical Society of Japan and Japan Society of Applied Physics, Tokyo. M
- Japanese Journal of Applied Physiology.* Physiological Society of Japan; University of Tokyo Press, Tokyo. Irreg.
- Japanese Journal of Physiology.* Physiological Society of Japan; University of Tokyo Press, Tokyo. BM
- Jemná Mechanika a Optika.* Ministerstvo Průmyslu; Státní Nakladatelství Technické Literatury, Prague. BM
- Jena Review.* VEB Verlag Technik, Berlin. BM
- JETP Letters (ZHETF Pis'ma v Redaktsiiu).* American Institute of Physics, Inc., New York. SM
- Journal de Mécanique.* Gauthier-Villars, Paris. Q
- Journal de Physiologie.* Masson & Cie., Paris. BM
- Journal de Physique.* Société Française de Physique, Paris. M
- Journal of Air Law and Commerce.* Southern Methodist University, School of Law, Dallas. Q
- Journal of Air Traffic Control.* Air Traffic Control Association, Inc., Washington, D.C. BM
- Journal of Aircraft.* American Institute of Aeronautics and Astronautics, Inc., New York. BM
- Journal of Applied Meteorology.* American Meteorological Society, Boston. BM
- Journal of Applied Physics.* American Institute of Physics, Inc., New York. 13 issues per year
- Journal of Applied Physiology.* American Physiological Society, Washington, D.C. M
- Journal of Applied Psychology.* American Psychological Association, Washington, D.C. BM
- Journal of Atmospheric and Terrestrial Physics.* Pergamon Press, Ltd., Oxford. M
- Journal of Bacteriology.* American Society for Microbiology, Bethesda, Md. M
- Journal of Biological Chemistry.* American Society of Biological Chemists, Inc., Baltimore, Md. M
- Journal of Biomechanics.* Pergamon Press, Ltd., Oxford. Q
- *Journal of Catalysis.* Academic Press, Inc., New York. BM
- Journal of Chemical Physics.* American Institute of Physics, Inc., New York. SM
- *Journal of Chromatographic Science.* Preston Technical Abstracts Co., Evanston, Ill. M
- *Journal of Chromatography.* Elsevier Publishing Co., Amsterdam. M
- Journal of Comparative and Physiological Psychology.* American Psychological Association, Inc., Washington, D.C. M
- Journal of Composite Materials.* Technomic Publishing Co., Inc., Stamford, Conn. BM
- Journal of Computational Physics.* Academic Press, Inc., New York. Q
- Journal of Computer and System Sciences.* Academic Press, Inc., New York. BM
- Journal of Differential Equations.* Academic Press, Inc., New York. BM
- Journal of Elasticity.* Wolters-Noordhoff Publishing, Groningen, Netherlands. Q
- Journal of Electrocardiology.* Research in Electrocardiology, Inc., Dayton, Ohio. Q
- Journal of Engineering Mathematics.* Wolters-Noordhoff Publishing, Groningen, Netherlands. Q
- Journal of Environmental Sciences.* Institute of Environmental Sciences, Mt. Prospect, Ill. BM
- Journal of Experimental Psychology.* American Psychological Association, Inc., Washington, D.C. M
- Journal of Fire and Flammability.* Technomic Publishing Co., Inc., Stamford, Conn. Q
- Journal of Fluid Mechanics.* Cambridge University Press, London. 20 issues per year
- Journal of General Physiology.* The Rockefeller University Press, New York. M
- Journal of Geomagnetism and Geoelectricity.* Society of Terrestrial Magnetism and Electricity, Kyoto, Japan. Q
- Journal of Geophysical Research.* American Geophysical Union, Washington, D.C. 36 issues per year
- *Journal of Heterocyclic Chemistry.* University Station, Provo, Utah. BM
- Journal of Hydronautics.* American Institute of Aeronautics and Astronautics, Inc., New York. Q
- Journal of Interdisciplinary Cycle Research.* International Institute for Interdisciplinary Cycle Research, Leiden; Swets & Zeitlinger N.V., Amsterdam. Q
- *Journal of Invertebrate Pathology.* Academic Press, Inc., New York. BM
- *Journal of Macromolecular Science, Part C — Reviews of Macromolecular Chemistry.* Marcel Dekker, Inc., New York. SA
- Journal of Materials.* American Society for Testing and Materials, Philadelphia, Pa. Q
- Journal of Materials Science.* Chapman & Hall, Ltd., London. M
- Journal of Mathematical Analysis and Applications.* Academic Press, Inc., New York. M
- Journal of Mathematical and Physical Sciences.* Indian Institute of Technology, Madras.
- Journal of Mathematical Physics.* American Institute of Physics, Inc., New York. M
- Journal of Mechanical Engineering Science.* Institution of Mechanical Engineers, London. Q
- Journal of Metals.* American Institute of Mining, Metallurgical and Petroleum Engineers, Inc., New York. M
- Journal of Microwave Power.* International Microwave Power Institute, Ltd., Edmonton, Alberta, Canada. Q
- Journal of Molecular Evolution.* Springer Verlag, Berlin, West Germany. 4 issues per volume
- *Journal of Molecular Spectroscopy.* Academic Press, Inc., New York. M
- Journal of Navigation (formerly Institute of Navigation, Journal).* Royal Institute of Navigation; John Murray (Publishers), Ltd., London. Q
- *Journal of Neuropathology and Experimental Neurology.* Ed. Abner Wolf, New York. Q

- Journal of Occupational Medicine.* Industrial Medical Association; Charles B. Slack, Inc., Thorofare, N.J. M
- Journal of Optimization Theory and Applications.* Plenum Publishing Corp., New York. M
- Journal of Physical Chemistry.* American Chemical Society, Washington, D.C. BW
- Journal of Physical Oceanography.* American Meteorological Society, Boston. Q
- Journal of Physics, Part A — General Physics.* Institute of Physics and The Physical Society, London. BM
- Journal of Physics, Part B — Atomic and Molecular Physics.* Institute of Physics and The Physical Society, London. M
- Journal of Physics, Part C — Solid State Physics.* Institute of Physics and The Physical Society, London. M
- Journal of Physics, Part D — Applied Physics.* Institute of Physics and The Physical Society, London. M
- Journal of Physics, Part E — Scientific Instruments.* Institute of Physics and The Physical Society, London. M
- Journal of Physics, Part F — Metal Physics.* Institute of Physics, London. BM
- **Journal of Physics and Chemistry of Solids.* Pergamon Press, Ltd., Oxford. M
- Journal of Plasma Physics.* Cambridge University Press, London. Q
- **Journal of Polymer Science, Part A2 — Polymer Physics.* Interscience Publishers, Inc., New York. M
- **Journal of Polymer Science, Part B — Polymer Letters.* Interscience Publishers, Inc., New York. M
- **Journal of Polymer Science, Part C — Polymer Symposia.* Interscience Publishers, Inc., New York. Irreg.
- **Journal of Psychiatric Research.* Pergamon Press, Ltd., Oxford. Q
- Journal of Quality Technology.* American Society for Quality Control, Inc., Milwaukee, Wis. Q
- Journal of Quantitative Spectroscopy and Radiative Transfer.* Pergamon Press, Ltd., Oxford. M
- Journal of Research, Section A — Physics and Chemistry.* National Bureau of Standards; Supt. of Documents, Washington, D.C. BM
- Journal of Research, Section B — Mathematical Sciences.* National Bureau of Standards; Supt. of Documents, Washington, D.C. BM
- Journal of Research, Section C — Engineering and Instrumentation.* National Bureau of Standards; Supt. of Documents, Washington, D.C. Q
- Journal of Science and Technology.* The General Electric and English Electric Companies Limited, London. Q
- Journal of Scientific and Industrial Research.* Council of Scientific and Industrial Research, New Delhi. M
- **Journal of Sedimentary Petrology.* Society of Economic Paleontologists and Mineralogists, Tulsa, Okla. Q
- Journal of Sound and Vibration.* British Acoustical Society; Academic Press, Inc., (London), Ltd., London. BM
- Journal of Spacecraft and Rockets.* American Institute of Aeronautics and Astronautics, Inc., New York. M
- **Journal of Statistical Physics.* Plenum Publishing Corp., New York.
- Journal of Strain Analysis.* Joint British Committee for Stress Analysis; Institute of Mechanical Engineers, London. Q
- Journal of the Astronautical Sciences.* American Astronautical Society, Inc., Washington, D.C. BM
- Journal of the Atmospheric Sciences.* American Meteorological Society, Boston. BM
- Journal of the Experimental Analysis of Behavior.* Society for the Experimental Analysis of Behavior, Inc., Indiana University, Bloomington, Ind. BM
- Journal of the Less-Common Metals.* Elsevier Sequoia S.A., Lausanne. M
- Journal of the Mechanics and Physics of Solids.* Pergamon Press, Ltd., Oxford. BM
- **Journal of Theoretical Biology.* Academic Press, Ltd., London. M
- Journal of Vacuum Science and Technology.* American Vacuum Society; American Institute of Physics, Inc., New York. BM
- **Journal of Virology.* American Society for Microbiology; Williams & Wilkins, Baltimore, Md. BM
- JSME, Bulletin.* Japan Society of Mechanical Engineers, Tokyo. BM
- Kakioka Magnetic Observatory, Memoirs.* Kakioka Magnetic Observatory, Kakioka, Japan.
- Karlsruhe, Universität, Institut für Strömungslehre und Strömungsmaschinen, Mitteilungen.* Verlag G. Braun, Karlsruhe, West Germany. Irreg.
- Kazanskii Aviatsionnyi Institut, Trudy, Seriya Aviatsionnaya Tekhnologiya i Organizatsiya Proizvodstva.* Kazanskii Aviatsionnyi Institut, Kazan. Irreg.
- Kazanskii Aviatsionnyi Institut, Trudy, Seriya Aviatsionnye Dvigateli.* Kazanskii Aviatsionnyi Institut, Kazan. Irreg.
- Kazanskii Aviatsionnyi Institut, Trudy, Seriya Optimal'nye Protsessy.* Kazanskii Aviatsionnyi Institut, Kazan. Irreg.
- Kazanskii Aviatsionnyi Institut, Trudy, Seriya Prikladnaya Mekhanika.* Kazanskii Aviatsionnyi Institut, Kazan. Irreg.
- Khimiya i Tekhnologiya Topliv i Masel.* Ministerstvo Neftpererabatyvayushchei i Neftekhimicheskoi Promyshlennosti SSSR, Akademiya Nauk SSSR, and Nauchno-Tekhnicheskoe Obshchestvo Nef-tianoi i Gazovoi Promyshlennosti; Izdatel'stvo Khimii, Moscow. M
- Kibernetika i Vychislitel'naya Tekhnika.* Akademiya Nauk Ukrainskoi SSR; Izdatel'stvo Naukova Dumka, Kiev. Irreg.
- Kleinheubacher Berichte.* Fernmeldetechnischer Zentralamt, Darmstadt, West Germany. Irreg.
- Koninklijke Nederlandse Akademie van Wetenschappen, Proceedings, Series B — Physical Sciences.* North-Holland Publishing Co., Amsterdam. 5 issues per year

- Kosmicheskaia Biologiia i Meditsina*. Ministerstvo Zdravookhraneniia SSSR; Izdatel'stvo Meditsina, Moscow. BM
- Kosmicheskie Issledovaniia*. Akademiia Nauk SSSR; Izdatel'stvo Nauka, Moscow. BM
- Kovové Materiály*. Slovenská Akademia Vied, Bratislava. BM
- Krymskaia Astrofizicheskaia Observatoriia, Izvestiia*. Akademiia Nauk SSSR; Izdatel'stvo Nauka, Moscow. BM
- Kvantovaia Elektronika* (Moscow). Akademiia Nauk Ukrainskoi SSR, Institut Poluprovodnikov; Izdatel'stvo Naukova Dumka, Kiev. Irreg.
- **Kybernetik*. Springer Verlag, Berlin. 2 vols. per year
- Kybernetika*. Československá Akademie Věd, Prague. BM
- Kyoto University, Faculty of Engineering, Memoirs*. Kyoto University, Kyoto. Q
- Kyushu University, Research Institute for Applied Mechanics, Reports*. Kyushu University, Fukuoka, Japan. Irreg.
- Laser*. Fachschriftenverlag Aargauer Tagblatt AG, Aarau, Switzerland. Q
- Leningradskii Universitet, Vestnik, Matematika, Mekhanika, Astronomiia*. Izdatel'stvo Leningradskogo Universiteta, Leningrad. Q
- Lietuvos Fizikos Rinkiny*. Akademiia Nauk Litovskoi SSR; Izdatel'stvo Mintis, Vilnius. Q
- Lietuvos Matematikos Rinkiny*. Akademiia Nauk Litovskoi SSR; Izdatel'stvo Mintis, Vilnius. Q
- Life Sciences, Part I — Physiology and Pharmacology*. Pergamon Press, Ltd., Oxford. SM
- Life Sciences, Part II — Biochemistry, General and Molecular Biology*. Pergamon Press, Ltd., Oxford. SM
- **Lithos*. Universitetsforlaget, Oslo. Q
- Logistics Spectrum*. Society of Logistics Engineers, Los Angeles. Q
- Lowell Observatory Bulletin*. Lowell Observatory, Flagstaff, Ariz. Irreg.
- Lubrication Engineering*. American Society of Lubrication Engineers, Park Ridge, Ill. M
- Machine Design*. Penton Publishing Co., Cleveland, Ohio. 31 issues per year
- **Macromolecules*. American Chemical Society, Washington, D.C. BM
- Magnitnaia Gidrodinamika*. Akademiia Nauk Latviiskoi SSR; Izdatel'stvo Zinatne, Riga. Q
- Manufacturing Engineering and Management*. Society of Manufacturing Engineers, Dearborn, Mich. M
- Marconi Review*. Marconi Co., Ltd., Chelmsford, Essex, England. Q
- Mashinostroenie*. Ministerstvo Vysshego i Srednego Spetsial'nogo Obrazovaniia SSSR; Izdanie Moskovskogo Tekhnicheskogo Uchilishcha imeni N. E. Baumana, Moscow. M
- Matematicheskaia Fizika*. Akademiia Nauk Ukrainskoi SSR; Izdatel'stvo Naukova Dumka, Kiev. Irreg.
- Matematichki Vesnik*. Društvo Matematičara, Fizičara i Astronoma SRS and Matematichki Institut, Belgrade. Q
- Matematicheskii Institut imeni V. A. Steklova, Trudy*. Akademiia Nauk SSSR, Moscow. Irreg.
- Materialprüfung*. VDI-Verlag GmbH, Düsseldorf. M
- Materials and Process Technology*. SAMPE Publications, Inc., Los Angeles. BM
- Materials Evaluation*. American Society for Non-destructive Testing, Inc., Evanston, Ill. M
- Materials Protection and Performance*. National Association of Corrosion Engineers, Houston, Tex. M
- Materials Research and Standards*. American Society for Testing and Materials, Philadelphia, Pa. M
- **Materials Research Bulletin*. Pergamon Press, Ltd., Oxford. M
- Materials Science and Engineering*. American Society for Metals, Metals Park, Ohio; Elsevier Sequoia S.A., Lausanne. BM
- **Mathematical Biosciences*. American Elsevier Publishing Co., Inc., New York. Q
- Mathematics of Computation*. American Mathematical Society, Providence, R.I. Q
- Mathematika*. University College, Dept. of Mathematics, London. SA
- Max-Planck-Institut für Aeronomie, Mitteilungen*. Springer Verlag, Berlin. Irreg.
- Meccanica*. Italian Association of Theoretical and Applied Mechanics; Tamburini Editore, Milan. Q
- Mechanika Teoretyczna i Stosowana*. Polskie Towarzystwo Mechaniki Teoretycznej i Stosowanej; Państwowe Wydawnictwo Naukowe, Warsaw. Q
- **Mechanisms of Ageing and Development*. Elsevier Sequoia S.A., Lausanne.
- Medical and Biological Engineering*. International Federation for Medical and Biological Engineering; Pergamon Press, Ltd., Oxford. BM
- Medical Research Engineering*. Medical-Research-Technology, Little Falls, N.J. BM
- Medicine and Science in Sports*. American College of Sports Medicine, Madison, Wis. Q
- Mekhanika Polimerov*. Akademiia Nauk Latviiskoi SSR; Izdatel'stvo Zinatne, Riga. BM
- Mekhanika Tverdogo Tela*. Akademiia Nauk SSSR; Izdatel'stvo Nauka, Moscow. Irreg.
- Mémoires Scientifiques de la Revue de Métallurgie*. Paris. M
- Mercury*. Astronomical Society of the Pacific, San Francisco. BM
- Mérés és Automatika*. Lapkiadó Vállalat, Budapest. M
- Messtechnik*. Friedr. Vieweg & Sohn GmbH, Braunschweig. M
- Metal Construction and British Welding Journal*. The Welding Institute, London. M
- Metal Progress*. American Society for Metals, Metals Park, Ohio. M
- Metal Science and Heat Treatment (Metallovedenie i Termicheskaia Obrabotka Metallov)*. Consultants Bureau, New York. BM
- Metal Science Journal*. Institute of Metals and Institution of Metallurgists, London. BM

- Metallofizika*. Akademiia Nauk Ukrainskoi SSR; Izdatel'stvo Naukova Dumka, Kiev. Irreg.
- Metallovedenie i Termicheskaiia Obrabotka*. Nauchno-Tekhnicheskoe Obshchestvo Mashinostroitel'noi Promyshlennosti; Izdatel'stvo Mashinostroenie, Moscow. Irreg.
- Metallovedenie i Termicheskaiia Obrabotka Metallov*. Ministerstvo Stankostroitel'noi i Instrumental'noi Promyshlennosti SSSR and Nauchno-Tekhnicheskoe Obshchestvo Mashinostroitel'noi Promyshlennosti; Izdatel'stvo Mashinostroenie, Moscow. M
- Metallurgia Italiana*. Associazione Italiana di Metallurgia, Milan. M
- Metallurgical Transactions*. Metallurgical Society of the American Institute of Mining, Metallurgical and Petroleum Engineers, Inc., New York; American Society for Metals, Metals Park, Ohio. M
- Metals Engineering Quarterly*. American Society for Metals, Metals Park, Ohio. Q
- Meteor-Forschungsergebnisse, Reihe B — Meteorologie und Aeronomie*. Gebrüder Borntraeger, Berlin, West Germany. Irreg.
- Meteoritics*. Meteoritical Society and Arizona State University Bureau of Publications, Tempe, Ariz. Q
- Meteorological Magazine*. Meteorological Office; Her Majesty's Stationery Office, London. M
- Meteorological Society of Japan, Journal*. Meteorological Society of Japan, c/o Japan Meteorological Agency, Tokyo. BM
- Meteorologiya i Gidrologiya*. Glavnoe Upravlenie Gidrometeorologicheskoi Sluzhby SSSR; Gidrometeoizdat, Moscow. M
- Meteorologische Rundschau*. Verband Deutscher Meteorologischer Gesellschaften; Springer Verlag, Berlin. BM
- Metricheskie Voprosy Teorii Funktsii i Otobrazhenii*. Akademiia Nauk Ukrainskoi SSR, Institut Prikladnoi Matematiki i Mekhaniki; Izdatel'stvo Naukova Dumka, Kiev. Irreg.
- Microelectronics and Reliability*. Pergamon Press, Ltd., Oxford. BM
- Microwave Journal*. Horizon House, Inc., Dedham, Mass. M
- MicroWaves*. Hayden Microwaves Corp., New York. M
- Middle East Technical University Journal of Pure and Applied Sciences*. Middle East Technical University, Ankara. 3 issues per year
- Mitsubishi Denki Laboratory Reports*. Mitsubishi Electric Corp., Central Research Laboratory, Amagasaki, Kyogo Prefecture, Japan. Irreg.
- Mitsubishi Technical Bulletin*. Mitsubishi Heavy Industries, Ltd., Tokyo. Irreg.
- **Modern Geology*. Gordon & Breach Science Publishers, Ltd., London. Q
- **Molecular Crystals and Liquid Crystals*. Gordon & Breach Science Publishers, Inc., New York. Q
- Monthly Weather Review*. U. S. Weather Bureau; Supt. of Documents, Washington, D.C. M
- The Moon*. D. Reidel Publishing Co., Dordrecht, Netherlands. Q
- Moskovskii Universitet, Vestnik, Serii I — Matematika, Mekhanika*. Izdatel'stvo Moskovskogo Universiteta, Moscow. BM
- Moskovskii Universitet, Vestnik, Serii III — Fizika, Astronomiia*. Izdatel'stvo Moskovskogo Universiteta, Moscow. BM
- Motortekhnische Zeitschrift*. Franckh'sche Verlags-handlung, Stuttgart, West Germany. M
- Mullard Technical Communications*. Mullard, Ltd., London. 4 issues per year
- Nachrichtentechnische Zeitschrift*. Nachrichtentechnische Gesellschaft; VDE-Verlag GmbH, Berlin. M
- Nagoya University, Faculty of Engineering, Memoirs*. Nagoya University, Nagoya. Irreg.
- Nagoya University, Research Institute of Atmospheric Sciences, Proceedings*. Research Institute of Atmospheric Sciences, Toyokawa-Shi, Aichi-Ken, Japan. Irreg.
- National Academy of Sciences, Proceedings*. National Academy of Sciences, Washington, D.C. M
- Nature*. Macmillan (Journals), Ltd., London. W
- Nature Physical Science*. Macmillan (Journals), Ltd., London. W
- Naturwissenschaftliche Rundschau*. Wissenschaftliche Verlagsgesellschaft mbH, Stuttgart, West Germany. M
- Naval Research Logistics Quarterly*. U.S. Navy, Office of Naval Research; Supt. of Documents, Washington, D.C. Q
- Naval Research Reviews*. U. S. Navy, Office of Naval Research; Supt. of Documents, Washington, D.C. M
- Navigation*. Institute of Navigation, Washington, D.C. Q
- Navigation (Paris)*. Institut Français de Navigation, Paris. Q
- Neirofiziologiia*. Akademiia Nauk SSSR; Akademiia Nauk Ukrainskoi SSR; Izdatel'stvo Naukova Dumka, Kiev. BM
- **Neuropsychologia*. Pergamon Press, Ltd., Oxford. Q
- New Scientist*. New Science Publications, London. W
- New York Academy of Sciences, Annals*. New York Academy of Sciences, New York. Irreg.
- New York Academy of Sciences, Transactions, Series 2*. New York Academy of Sciences, New York. 8 issues per year
- Nihon University, Research Institute of Science and Technology, Journal*. Nihon University, Tokyo. Irreg.
- Non-Destructive Testing*. IPC Science and Technology Press, Ltd., Guildford, Surrey, England. BM
- Note, Recensioni e Notizie*. Poste e Telecomunicazioni, Istituto Superiore, Rome. BM
- Nouvelle Revue d'Optique Appliquée*. Masson & Cie., Editeurs, Paris. BM
- Nuclear Engineering and Design*. North-Holland Publishing Co., Amsterdam. M
- Nuclear Fusion*. International Atomic Energy Agency, Vienna. Q
- **Nuclear Instruments and Methods*. North-Holland Publishing Co., Amsterdam. BW
- Nuclear Science and Engineering*. American Nuclear Society, Inc., Hinsdale, Ill. M

- Nuclear Technology.* American Nuclear Society, Inc., Hinsdale, Ill. M
- Numerische Mathematik.* Springer Verlag, Berlin. Irreg.
- Nuovo Cimento, Lettere.* Società Italiana di Fisica, Bologna. 36 issues per year.
- Nuovo Cimento, Rivista.* Società Italiana di Fisica; Editrice Compositori, Bologna. Q
- Nuovo Cimento, Rivista, Serie 2.* Società Italiana di Fisica; Editrice Compositori, Bologna.
- Nuovo Cimento, Sezione A.* Società Italiana di Fisica; Editrice Compositori, Bologna. 26 issues per year
- Nuovo Cimento, Sezione B.* Società Italiana di Fisica; Editrice Compositori, Bologna. 26 issues per year.
- The Observatory.* Royal Greenwich Observatory, Hailsham, Sussex, England. M
- Obzornik za Matematiko in Fiziko.* Izdaja Društvo Matematikov, Fizikov in Astronomov SR Slovenije, Ljubljana, Yugoslavia. Q
- L'Onde Electrique.* Société Française des Electroniciens et des Radioélectriciens; Editions Chiron S.A., Paris. M
- ONERA, TP.* Office National d'Etudes et de Recherches Aérospatiales, Chatillon-sous-Bagneux (Seine), France. Irreg.
- Operations Research.* Operations Research Society of America, Baltimore, Md. BM
- Ophthalmic Research.* S. Karger AG, Basel. BM
- Optica Acta.* Taylor & Francis, Ltd., London. M
- Optical Engineering* (formerly *SPIE Journal*). Society of Photo-Optical Instrumentation Engineers, Redondo Beach, Calif. BM
- Optical Sciences Center Newsletter.* University of Arizona, Optical Sciences Center, Tucson, Ariz. Irreg.
- Optical Society of America, Journal.* Optical Society of America, Inc., Washington, D.C.; American Institute of Physics, Inc., New York. M
- Optical Spectra.* Optical Publishing Co., Inc., Pittsfield, Mass. M
- Optics and Laser Technology.* Iliffe Science & Technology Publications, Ltd., Guildford, Surrey, England. Q
- Optics Communications.* North-Holland Publishing Co., Amsterdam. M
- **Optik.* Wissenschaftliche Verlagsgesellschaft mbH, Stuttgart, West Germany. M
- Optika i Spektroskopiia.* Akademiia Nauk SSSR; Izdatel'stvo Nauka, Leningrad. M
- **Organic Mass Spectrometry.* Heyden & Son, Ltd., London. BM
- **Organizational Behavior and Human Performance.* Academic Press, Inc., New York. BM
- Orion.* Schweizerische Astronomische Gesellschaft, Schaffhausen, Switzerland. BM
- Ortung und Navigation.* Deutsche Gesellschaft für Ortung und Navigation, e.V., Düsseldorf, West Germany. Q
- Osaka Prefecture, University, Bulletin, Series A — Engineering and Natural Sciences.* University of Osaka Prefecture, Osaka, Japan. Irreg.
- Osaka University, Technology Reports.* Osaka University, Osaka, Japan. SA
- Österreichische Akademie der Wissenschaften, Mathematisch-naturwissenschaftliche Klasse, Sitzungsberichte, Abteilung 2.* Österreichische Akademie der Wissenschaften; Springer Verlag, Vienna. Irreg.
- Otbor i Peredacha Informatsii.* Akademiia Nauk Ukrainskoi SSR; Izdatel'stvo Naukova Dumka, Kiev. Irreg.
- Oxidation and Combustion Reviews.* Elsevier Publishing Co., Amsterdam. SA
- Oxidation of Metals.* Plenum Publishing Corp., New York. Q
- Papers in Meteorology and Geophysics.* Meteorological Research Institute, Tokyo. Q
- Perception and Psychophysics.* Psychonomic Journals, Inc., Austin, Tex. M
- Perceptual and Motor Skills.* Missoula, Mont. BM
- Periodica Polytechnica, Electrical Engineering.* Budapest, Technical University, Budapest. Q
- Periodica Polytechnica, Mechanical Engineering.* Budapest, Technical University, Budapest. Q
- Pflügers Archiv.* Springer Verlag, Berlin.
- Philips Research Reports.* N. V. Philips' Gloeilampenfabrieken, Research Laboratories, Eindhoven. BM
- Philips Research Reports Supplements.* N. V. Philips' Gloeilampenfabrieken, Research Laboratories, Eindhoven. Irreg.
- Philips Serving Science and Industry.* N. V. Philips' Gloeilampenfabrieken, Scientific and Industrial Equipment Div., Eindhoven.
- Philips Technical Review.* N. V. Philips' Gloeilampenfabrieken, Research Laboratories, Eindhoven. M
- Philosophical Magazine, 8th Series.* Taylor & Francis, Ltd., London. M
- **Photochemistry and Photobiology.* Pergamon Press, Inc., Elmsford, N.Y. M
- Photogrammetria.* International Society of Photogrammetry; Elsevier Publishing Co., Amsterdam. BM
- Photogrammetric Engineering.* American Society of Photogrammetry, Falls Church, Va. M
- Photographic Applications in Science, Technology and Medicine.* Photographic Applications in Science and Technology, Inc., New York. BM
- Physica.* Physica Foundation; North-Holland Publishing Co., Amsterdam. Irreg.
- Physica Scripta.* Royal Swedish Academy of Sciences; Almqvist & Wiksell Periodical Co., Stockholm. M
- Physica Status Solidi (A) — Applied Research.* Akademie-Verlag GmbH, Berlin; Academic Press, Inc., New York. 3 issues per year
- Physical Review A — General Physics, 3rd Series.* American Physical Society; American Institute of Physics, Inc., New York. M
- Physical Review B — Solid State, 3rd Series.* American Physical Society; American Institute of Physics, Inc., New York. SM

- Physical Review C — Nuclear Physics, 3rd Series.* American Physical Society; American Institute of Physics, Inc., New York. M
- Physical Review D — Particles and Fields, 3rd Series.* American Physical Society; American Institute of Physics, Inc., New York. SM
- Physical Review Letters.* American Physical Society, Inc., New York. W
- Physical Society of Japan, Journal.* Physical Society of Japan, Tokyo. M
- Physics in Medicine and Biology.* Taylor & Francis, Ltd., London. Q
- Physics Letters.* North-Holland Publishing Co., Amsterdam. W
- Physics Letters, Section C — Physics Reports.* North-Holland Publishing Co., Amsterdam. 1 vol. per year
- Physics of Fluids.* American Institute of Physics, Inc., New York. M
- Physics of the Earth and Planetary Interiors.* North-Holland Publishing Co., Amsterdam. BM
- Physics Today.* American Institute of Physics, Inc., New York. M
- Physiological Society of Japan, Journal.* Physiological Society of Japan, Tokyo. M
- **Phytochemistry.* Pergamon Press, Ltd., Oxford. M
- Pisa, Scuola Normale Superiore, Annali, Scienze Fisiche e Matematiche.* Pisa, Scuola Normale Superiore, Pisa. Q
- Planetary and Space Science.* Pergamon Press, Ltd., Oxford. M
- Planseeberichte für Pulvermetallurgie/Powder Metallurgy Bulletin.* Metallwerk Plansee Aktiengesellschaft, Reutte, Austria. 3 issues per year
- Planseeberichte für Pulvermetallurgie vereinigt mit Powder Metallurgy (see Planseeberichte für Pulvermetallurgie/Powder Metallurgy Bulletin).*
- Plasma Physics.* Pergamon Press, Ltd., Oxford. M
- PMM — Journal of Applied Mathematics and Mechanics (Prikladnaia Matematika i Mekhanika).* Pergamon Press, Ltd., Oxford. BM
- PMTF — Zhurnal Prikladnoi Mekhaniki i Tekhnicheskoi Fiziki.* Akademiiia Nauk SSSR, Sibirskoe Otdelenie; Izdatel'stvo Nauka, Novosibirsk. BM
- Podstawy Sterowania.* Polska Akademia Nauk; Państwowe Wydawnictwo Naukowe, Warsaw. Q
- Point-to-Point Communication.* Marconi Communication Systems, Ltd., Chelmsford, England. 3 issues per year
- Polish Medical Journal (Polski Tygodnik Lekarski).* Państwowy Zakład Wydawnictw Lekarskich, Warsaw; National Technical Information Service, Springfield, Va. Irreg.
- Politechnika Częstochowska, Zeszyty Naukowe, Nauki Techniczne — Mechanika.* Wydawnictwa Politechniki Śląskiej, Gliwice, Poland. Irreg.
- Politechnika Śląska, Zeszyty Naukowe, Mechanika.* Wydawnictwa Politechniki Śląskiej, Gliwice, Poland. Irreg.
- Polska Akademia Nauk, Instytut Automatyki, Prace.* Polska Akademia Nauk, Warsaw. Irreg.
- Poluprovodniki i ikh Primenenie v Elektrotekhnike.* Akademiiia Nauk Latviiskoi SSR, Fiziko-Energeticheskii Institut; Izdatel'stvo Zinatne, Riga. Irreg.
- Poluprovodnikovye Pribory i ikh Primenenie.* Izdatel'stvo Sovetskoe Radio, Moscow. Irreg.
- Polymer Engineering and Science.* Society of Plastics Engineers, Inc., Greenwich, Conn. BM
- Pomiary, Automatyka, Kontrola.* Naczelna Organizacja Techniczna, Warsaw. M
- Pontificiae Academiae Scientiarum Scripta Varia.* Pontificia Academia Scientiarum; North-Holland Publishing Co., Amsterdam; American Elsevier Publishing Co., Inc., New York.
- Poroshkovaia Metallurgiiia.* Akamediiia Nauk Ukrainskoi SSR; Izdatel'stvo Naukova Dumka, Kiev. M
- Postępy Astronautyki.* Polskie Towarzystwo Astronautyczne, Lodz. Q
- Postępy Astronomii.* Polskie Towarzystwo Astronomiczne; Państwowe Wydawnictwo Naukowe, Warsaw. Q
- Postępy Fizyki.* Polskie Towarzystwo Fizyczne; Państwowe Wydawnictwo Naukowe, Warsaw. BM
- Priboroostroenie.* Ministerstvo Vysshego i Srednego Spetsial'nogo Obrazovaniia SSSR; Izdatel'stvo Leningradskogo Instituta Tochnoi Mekhaniki i Optiki, Leningrad. M
- Pribory i Sistemy Avtomatiki.* Izdatel'stvo Khar'kovskogo Gosudarstvennogo Universiteta, Kharkov. Irreg.
- Pribory i Tekhnika Eksperimenta.* Akademiiia Nauk SSSR; Izdatel'stvo Nauka, Moscow. BM
- Prikladnaia Matematika i Programmirovanie.* Akademiiia Nauk Moldavskoi SSR, Institut Matematiki s Vychislitel'nyim Tsentrom; Izdatel'stvo Shtiintsa, Kishinev. Irreg.
- Prikladnaia Matematika i Mekhanika.* Akademiiia Nauk SSSR, Izdatel'stvo Nauka, Moscow. BM
- Prikladnaia Mekhanika.* Akademiiia Nauk Ukrainskoi SSR, Otdelenie Matematiki, Mekhaniki i Kibernetiki; Izdatel'stvo Naukova Dumka, Kiev. M
- Priroda.* Akademiiia Nauk SSSR; Izdatel'stvo Nauka, Moscow. M
- Problemy Fiziki Atmosfery.* Izdatel'stvo Leningradskogo Universiteta, Leningrad. Irreg.
- Problemy Kosmicheskoi Fiziki.* Izdatel'stvo Kievskogo Universiteta, Kiev. Irreg.
- Problemy Prochnosti.* Akademiiia Nauk Ukrainskoi SSR, Institut Problem Prochnosti; Izdatel'stvo Naukova Dumka, Kiev. M
- Problemy Tekhnicheskoi Elektrodinamiki.* Akademiiia Nauk Ukrainskoi SSR; Izdatel'stvo Naukova Dumka, Kiev. Irreg.
- Proceedings of Vibration Problems.* Polska Akademia Nauk; Państwowe Wydawnictwo Naukowe, Warsaw. Q
- Prochnost' i Dinamika Aviatsonnykh Dvigatelei.* Izdatel'stvo Mashinostroenie, Moscow. Irreg.
- Progress of Theoretical Physics.* Research Institute for Fundamental Physics and The Physical Society of Japan; Kyoto University, Kyoto. M
- Progress of Theoretical Physics, Supplement.* Research Institute for Fundamental Physics and The Physical Society of Japan, Kyoto, Japan. Q
- Psychonomic Science.* Psychonomic Journals, Inc., Austin, Tex. SM
- Public Administration Review.* American Society for Public Administration, Washington, D.C. BM

- Pulkovo, Glavnaia Astronomicheskaiia Observatoriia, Izvestiia.* Izdanie Glavnoi Astronomicheskoi Observatorii, Leningrad. Irreg.
- Pure and Applied Chemistry.* International Union of Pure and Applied Chemistry; Butterworth & Co. (Publishers), Ltd., London. Irreg.
- Pure and Applied Geophysics.* Birkhäuser Verlag, Basel. BM
- Quality Progress.* American Society for Quality Control, Inc., Milwaukee, Wis. M
- Quarterly Journal of Mechanics and Applied Mathematics.* Oxford University Press, London. Q
- Quarterly of Applied Mathematics.* Brown University, Providence, R.I. Q
- **Quarterly Reviews of Biophysics.* International Union for Pure and Applied Biophysics; Cambridge University Press, London. Q
- **Radiation Botany.* Pergamon Press, Ltd., Oxford. BM
- **Radiation Research.* Academic Press, Inc., New York. 4 vols. per year
- Radio and Electronic Engineer.* Institution of Electronic and Radio Engineers, London. M
- Radio Engineering and Electronic Physics (Radio-tekhnika i Elektronika).* Scripta Publishing Corp., Washington, D.C. M
- Radio Research Laboratories, Journal.* Ministry of Posts and Telecommunications, Radio Research Laboratories, Tokyo. BM
- Radio Research Laboratories, Review.* Ministry of Posts and Telecommunications, Radio Research Laboratories, Tokyo. Q
- Radio Science.* American Geophysical Union, Washington, D.C. M
- Radiobiologia — Radiotherapia.* VEB Verlag Volk und Gesundheit, Berlin, East Germany. BM
- Radioelektronika.* Ministerstvo Vysshego i Srednego Spetsial'nogo Obrazovaniia SSSR; Izdatel'stvo Kievskogo Politekhnikheskogo Instituta, Kiev. M
- Radiofizika.* Ministerstvo Vysshego i Srednego Spetsial'nogo Obrazovaniia SSSR; Izdanie Gor'kovskogo Universiteta, Gorki. M
- Radiotekhnika.* Nauchno-Tekhnicheskoe Obshchestvo Radiotekhniki i Elektrosviazi; Izdatel'stvo Sviaz', Moscow. M
- Radiotekhnika (Kharkov).* Izdatel'stvo Khar'kovskogo Gosudarstvennogo Universiteta, Kharkov. Irreg.
- Radiotekhnika i Elektronika.* Akademiia Nauk SSSR; Izdatel'stvo Nauka, Moscow. M
- Raumfahrtforschung.* Deutsche Gesellschaft für Luft- und Raumfahrt, e.V., Stuttgart, West Germany. BM
- RCA Review.* RCA Research and Engineering, Princeton, N.J. Q
- La Recherche.* Société d'Editions Scientifiques, Paris. M
- La Recherche Aérospatiale.* Office National d'Etudes et de Recherches Aérospatiales, Chatillon-sous-Bagneux (Seine), France. BM
- La Recherche Spatiale.* Centre National d'Etudes Spatiales; Dunod Editeur, Paris. M
- Remote Sensing of Environment.* American Elsevier Publishing Co., Inc., New York. Q
- Report of Ionosphere and Space Research in Japan.* Science Council of Japan, Ionosphere Research Committee, Tokyo. Q
- Research/Development.* Technical Publishing Co., Thompson Div., Barrington, Ill. M
- Research Management.* Industrial Research Institute, Inc.; Interscience Publishers, New York. BM
- Respiration Physiology.* North-Holland Publishing Co., Amsterdam. BM
- Review of Scientific Instruments.* American Institute of Physics, Inc., New York. M
- Reviews of Geophysics and Space Physics.* American Geophysical Union, Washington, D.C. Q
- Reviews of Modern Physics.* American Physical Society; American Institute of Physics, Inc., New York. Q
- Reviews on High-Temperature Materials.* Freund Publishing House, Ltd., Scientific Publications Div., Tel Aviv. Q
- Revista de Aeronáutica y Astronáutica.* Ministerio del Aire, Madrid. M
- Revue de Médecine Aéronautique et Spatiale.* Société Française de Physiologie et de Médecine Aéronautique et Cosmonautique; Masson & Cie., Paris. Q
- Revue de Métallurgie.* Paris. M
- Revue de Physique Appliquée.* Société Française de Physique, Paris. M
- Revue des Corps de Santé des Armées.* Centre de Recherches du Service de Santé des Armées, Paris. BM
- Revue Française de Droit Aérien.* Société Française de Droit Aérien et Spatial, Paris. Q
- Revue Française de Mécanique.* Société Française des Mécaniciens, Paris. Q
- Revue Générale de l'Air et de l'Espace.* Editions Internationales, Paris. Q
- Revue Internationale des Hautes Températures et des Réfractaires.* Société Nationale Française des Hautes Températures et des Réfractaires; Masson & Cie., Paris. Q
- Revue Roumaine de Mathématiques Pures et Appliquées.* Académie de la République Socialiste Roumaine, Bucharest. 10 issues per year
- Revue Roumaine de Physique.* Académie de la République Socialiste Roumaine, Bucharest. BM
- Revue Roumaine des Sciences Techniques, Série de Mécanique Appliquée.* Académie de la République Socialiste Roumaine, Bucharest. BM
- Revue Scientifique et Technique CECLES/CERS.* Gauthier-Villars, Paris. Q
- Revue Technique Thomson — CSF.* Thomson — CSF, Service de Documentation Technique; Masson & Cie., Paris. Q
- Rivista Aeronautica.* Rome. M
- Rivista di Medicina Aeronautica e Spaziale.* Servizio Sanitario dell'Aeronautica, Rome. Q
- Rivista di Meteorologia Aeronautica.* Servizio Meteorologico dell'Aeronautica, Rome. Q
- Rivista Italiana di Geofisica (formerly Geofisica e Meteorologia).* Associazione Geofisica Italiana, Genoa. 3 issues per year

- **Rivista Marittima*. Amm. di Squadra Alberto Zamboni, Rome. M
- Royal Astronomical Society, Memoirs*. Royal Astronomical Society; Blackwell Scientific Publications, Oxford. 4 issues per year
- Royal Astronomical Society, Monthly Notices*. Royal Astronomical Society, London; Blackwell Scientific Publications, Oxford. M
- Royal Astronomical Society, Quarterly Journal*. Royal Astronomical Society, London; Blackwell Scientific Publications, Oxford. Q
- Royal Astronomical Society of Canada, Journal*. Royal Astronomical Society of Canada, Toronto. BM
- Royal Meteorological Society, Quarterly Journal*. Royal Meteorological Society, London. Q
- Royal Society (Edinburgh), Proceedings, Section A*. Royal Society of Edinburgh, Edinburgh. Irreg.
- Royal Society (London), Philosophical Transactions, Series A*. Royal Society, London. Irreg.
- Royal Society (London), Proceedings, Series A*. Royal Society, London. Irreg.
- Rozprawy Inżynierskie*. Polska Akademia Nauk, Instytut Podstawowych Problemów Techniki; Państwowe Wydawnictwo Naukowe, Warsaw. Q
- Ruimtevaart*. Nederlandse Vereniging voor Ruimtevaart, The Hague. Q
- SAE Aerospace Information Report*. Society of Automotive Engineers, Inc., New York. Irreg.
- SAE Aerospace Recommended Practice*. Society of Automotive Engineers, Inc., New York. Irreg.
- SAE Aerospace Standards*. Society of Automotive Engineers, Inc., New York. Irreg.
- SAFE Engineering*. Survival and Flight Equipment Association; Value Engineering Publications, Inc., Los Angeles. BM
- Samoletostroenie i Tekhnika Vozdushnogo Flota*. Izdanie Khar'kovskogo Gosudarstvennogo Universiteta, Kharkov. Irreg.
- SAMPE Quarterly*. Society of Aerospace Material and Process Engineers, Azusa, Calif. Q
- SAWE Journal*. Society of Aeronautical Weight Engineers, Inc., Los Angeles. BM
- Schweizer Archiv* (see *Schweizer Archiv für angewandte Wissenschaft und Technik*.)
- Schweizer Archiv für angewandte Wissenschaft und Technik*. Schweizer Verband für die Materialprüfungen und Schweizerische Gesellschaft für Vakuumphysik und Technik; Verlag Vogt-Schild AG, Solothurn, Switzerland. M
- Schweizerische Technische Zeitschrift*. Schweizer Technischer Verband, Zurich. M
- Science*. American Association for the Advancement of Science, Washington, D.C. W
- Science Progrès Découverte*. Société des Ingénieurs Civils de France; Dunod Editeur, Paris. M
- Science Progress*. Blackwell Scientific Publications, Ltd., Oxford. Q
- Sciences* (Paris). Hermann, Paris. BM
- Sciences et Industries Spatiales* (see *Industries Atomiques et Spatiales*).
- Sciences et Techniques de l'Armement*. Ministère d'Etat Chargé de la Défense Nationale, Paris. Q
- Scientific American*. Scientific American, Inc., New York. M
- Scripta Metallurgica*. Pergamon Press, Inc., New York. M
- Shell Aviation News*. Shell Oil Co., London. M
- Shemakhinskaia Astrofizicheskaia Observatoriia, Soobshchenie*. Akademiia Nauk Azerbaidzhanskoi SSR; Izdatel'stvo Elm, Baku. Irreg.
- SIAM Journal on Applied Mathematics*. Society for Industrial and Applied Mathematics, Philadelphia, Pa. 8 issues per year
- **SIAM Journal on Computing*. Society for Industrial and Applied Mathematics, Philadelphia, Pa. Q
- SIAM Journal on Control*. Society for Industrial and Applied Mathematics, Philadelphia, Pa. Q
- SIAM Journal on Mathematical Analysis*. Society for Industrial and Applied Mathematics, Philadelphia, Pa. 8 issues per year
- SIAM Journal on Numerical Analysis*. Society for Industrial and Applied Mathematics, Philadelphia, Pa. Q
- SIAM Review*. Society for Industrial and Applied Mathematics, Philadelphia, Pa. Q
- Siemens Forschungs- und Entwicklungsberichte*. Siemens Aktiengesellschaft; Springer Verlag, Berlin, West Germany. Q
- Siemens-Zeitschrift*. Siemens Aktiengesellschaft, Berlin, West Germany. M
- Signal*. Armed Forces Communications and Electronics Association, Washington, D.C. M
- Simulation*. Simulation Councils, Inc., La Jolla, Calif. M
- Sinteticheskie Almazы*. Gosudarstvennyi Planovyi Komitet Soveta Ministrov Ukrainskoi SSR; Ukrainskii Nauchno-Issledovatel'skii Konstruktor-sko-Tekhnologicheskii Institut Sinteticheskikh Sverkhtrverdykh Materialov i Instrumenta; Ukrainskii Nauchno-Issledovatel'skii Institut Nauchno-Tekhnicheskoi Informatsii i Tekhniko-Ekonomicheskikh Issledovani, Kiev. Irreg.
- Sky and Telescope*. Sky Publishing Corp., Cambridge, Mass. M
- Slaboproudý Obzor*. Státní Nakladatelství Technické Literatury, Prague. M
- Sloan Management Review*. Industrial Management Review Association; Massachusetts Institute of Technology, Cambridge, Mass. 3 issues per year
- SMPTE, Journal*. Society of Motion Picture and Television Engineers, Inc., New York. M
- Società Astronomica Italiana, Memorie*. Gia Società degli Spettroscopisti Italiani, Milan. Q
- Societas Scientiarum Torunensis, Studia, Sectio F — Astronomia*. Societas Scientiarum Torunensis, Torun; Państwowe Wydawnictwo Naukowe, Poznan. Irreg.
- Société Royale des Sciences de Liège, Bulletin*. Société Royale des Sciences de Liège; Université de Liège, Liege. Irreg.
- Society for Experimental Biology and Medicine, Proceedings*. Society for Experimental Biology and Medicine, New York. 11 issues per year
- Society for Information Display, Proceedings*. Society for Information Display; Western Periodicals Co., North Hollywood, Calif. Q
- Society of Environmental Engineers, Journal*. Society of Environmental Engineers, London. Q

- Society of Experimental Test Pilots, Technical Review.* Society of Experimental Test Pilots, Lancaster, Calif. SA
- Society of Instrument and Control Engineers, Transactions.* Society of Instrument and Control Engineers, Tokyo. M
- **Society of Rheology, Transactions.* Interscience Publishers, New York. SA
- **Soil Biology and Biochemistry.* Pergamon Press, Ltd., Oxford. Q
- Solar Energy.* International Solar Energy Society, Victoria, Australia; Pergamon Press, Ltd., Oxford. Q
- Solar Physics.* D. Reidel Publishing Co., Dordrecht, Netherlands. M
- Solar System Research (Astronomicheskii Vestnik).* Consultants Bureau, New York. Q
- Solid-State Electronics.* Pergamon Press, Ltd., Oxford. M
- Soprotivlenie Materialov i Teoriia Sooruzhenii.* Izdatel'stvo Budivel'nik, Kiev. Irreg.
- Sound and Vibration.* Acoustical Publications, Inc., Cleveland, Ohio. M
- Soviet Astronomy (Astronomicheskii Zhurnal).* American Institute of Physics, Inc., New York. BM
- Soviet Journal of Nondestructive Testing (Defektoskopiia).* Consultants Bureau, New York. BM
- Soviet Journal of Optical Technology (Optiko-Mekhanicheskaiia Promyshlennost').* Optical Society of America, Inc., Washington, D.C.; American Institute of Physics, Inc., New York. M
- Soviet Journal of Quantum Electronics (Kvantovaia Elektronika /Moscow/).* American Institute of Physics, Inc., New York. BM
- Soviet Physics — Acoustics (Akusticheskii Zhurnal).* American Institute of Physics, Inc., New York. Q
- Soviet Physics — Doklady (Akademiia Nauk SSSR, Doklady).* American Institute of Physics, Inc., New York. M
- Soviet Physics — JETP (Zhurnal Eksperimental'noi i Teoreticheskoi Fiziki).* American Institute of Physics, Inc., New York. M
- Soviet Physics — Technical Physics (Zhurnal Tekhnicheskoi Fiziki).* American Institute of Physics, Inc., New York. M
- Soviet Physics — Uspekhi (Uspekhi Fizicheskikh Nauk).* American Institute of Physics, Inc., New York. BM
- Soviet Science Review.* IPC Science and Technology Press, Ltd., Guildford, Surrey, England. BM
- Space Life Sciences.* D. Reidel Publishing Co., Dordrecht, Netherlands. Q
- Space Science Reviews.* D. Reidel Publishing Co., Dordrecht, Netherlands. 9 issues per year
- Spaceflight.* British Interplanetary Society, London. M
- Sperry Rand Engineering Review.* Sperry Rand Corp., New York. Q
- SPIE Journal (see Optical Engineering).*
- Sterne und Weltraum.* Verlag Bibliographisches Institut AG, Mannheim, West Germany. M
- STP Notes.* International Council of Scientific Unions, Inter-Commission on Solar-Terrestrial Physics, c/o National Academy of Sciences, Washington, D.C. Irreg.
- Strain.* British Society for Strain Measurement, London. Q
- Strength of Materials (Problemy Prochnosti).* Consultants Bureau, New York. Q
- Strömungsmechanik und Strömungsmaschinen (see Karlsruhe, Universität, Institut für Strömungslehre und Strömungsmaschinen, Mitteilungen).*
- Studia Scientiarum Mathematicarum Hungarica.* Akademiai Kiadó, Budapest. Irreg.
- Studia Geophysica et Geodaetica.* Československá Akademie Věd, Prague. Q
- Studies in Applied Mathematics.* MIT Press, Cambridge, Mass. Q
- Studii și Cercetări de Astronomie.* Academia Republicii Socialiste Romîne, Bucharest. SA
- Studii și Cercetări de Fizică.* Academia Republicii Socialiste Romîne, Bucharest. 10 issues per year
- Studii și Cercetări de Mecanică Aplicată.* Academia Republicii Socialiste Romîne, Bucharest. BM
- Studii și Cercetări Matematice.* Academia Republicii Socialiste Romîne, Bucharest. 10 issues per year
- Surface Science.* North-Holland Publishing Co., Amsterdam. M
- **Surveying and Mapping.* American Congress on Surveying and Mapping, Washington, D.C. Q
- **Synthetic Communications.* Marcel Dekker, Inc., New York. Q
- Systems, Computers, Controls (Denshi Tsushin Gakkai Ronbunshi).* Institute of Electronics and Communication Engineers of Japan; Scripta Publishing Corp., Washington, D.C. BM
- Tartuskaia Astrofizicheskaiia Observatoriia, Publikatsii.* Akademiia Nauk Estonskoi SSR, Tartu. Irreg.
- Tech Air.* Society of Licensed Aircraft Engineers and Technologists, Kingston-upon-Thames, England. M
- Technische Mitteilungen Krupp, Werksberichte.* Fried. Krupp GmbH, Essen, West Germany. Q
- Technika Lotnicza i Astronautyczna.* Stowarzyszenie Inżynierów i Techników Mechaników Polskich, Sekcja Lotnicza; Naczelna Organizacja Techniczna, Warsaw. M
- Technisch-ökonomische Informationen der zivilen Luftfahrt.* Hauptverwaltung der Zivilen Luftfahrt, Zentrallughafen Berlin-Schönefeld, East Germany. M
- Technological Forecasting and Social Change.* American Elsevier Publishing Co., Inc., New York. Q
- Technology Review.* Massachusetts Institute of Technology, Cambridge, Mass. 9 issues per year
- Tecnica Italiana.* Trieste. M
- Teknisk Tidskrift.* Svenska Teknologföreningen, Stockholm. W
- Telecommunications and Radio Engineering. Part I — Telecommunications, Part II — Radio Engineering (Elektrosviaz', Radiotekhnika).* Scripta Publishing Corp., Washington, D.C. M
- Teledyne Ryan Aeronautical Reporter.* Teledyne Ryan Aeronautical, San Diego, Calif. Q
- Telemetry Journal.* International Foundation for Telemetering; Value Engineering Publications, Inc., Los Angeles. BM

- Tellus*. Svenska Geofysiska Föreningen, Stockholm; Almqvist & Wiksells Boktryckeri AB, Uppsala. BM
- Teoreticheskaia i Matematicheskaia Fizika*. Akademiia Nauk SSSR; Izdatel'stvo Nauka, Moscow. M
- Teoriia Funktsii, Funktsional'nyi Analiz i ikh Prilozheniia*. Izdatel'stvo Khar'kovskogo Gosudarstvennogo Universiteta, Kharkov. Irreg.
- Teoriia Veroiatnostei i ee Primeneniia*. Akademiia Nauk SSSR; Izdatel'stvo Nauka, Moscow. Q
- Teoriia Veroiatnostei i Matematicheskaia Statistika*. Izdatel'stvo Kievskogo Universiteta, Kiev. Irreg.
- Teplofizika i Teplotekhnika*. Akademiia Nauk Ukrainkoi SSR; Izdatel'stvo Naukova Dumka, Kiev. Irreg.
- Teplofizika Vysokikh Temperatur*. Akademiia Nauk SSSR; Izdatel'stvo Nauka, Moscow. BM
- Teplovyie Napriazheniia v Elementakh Konstruktsii*. Akademiia Nauk Ukrainkoi SSR, Institut Mekhaniki; Izdatel'stvo Naukova Dumka, Kiev. Irreg.
- Thermochimica Acta*. Elsevier Publishing Co., Amsterdam. BM
- Thin Solid Films*. Elsevier Sequoia S. A., Lausanne. M
- Tohoku University, Institute of High Speed Mechanics, Reports*. Tohoku University, Sendai. Irreg.
- Tohoku University, Record of Electrical and Communication Engineering Conversazione*. Tohoku University, Sendai.
- Tohoku University, Research Institute for Strength and Fracture of Materials, Reports*. Tohoku University, Sendai. Irreg.
- Tokyo, University, Faculty of Engineering, Journal, Series B*. Tokyo, University, Faculty of Engineering, Tokyo. Irreg.
- Tokyo, University, Institute of Industrial Science, Reports*. Tokyo, University, Tokyo. Irreg. g.
- Tokyo, University, Institute of Space and Aeronautical Science, Bulletin*. Tokyo, University, Institute of Space and Aeronautical Science, Tokyo. Q
- Tokyo, University, Institute of Space and Aeronautical Science, Report*. Tokyo, University, Institute of Space and Aeronautical Science, Tokyo. Irreg.
- Tokyo, University, Tokyo Astronomical Observatory, Annals, Second Series*. Tokyo, University, Tokyo. Irreg.
- Tokyo Astronomical Observatory, Tokyo Astronomical Bulletin, Second Series*. Tokyo Astronomical Observatory, Tokyo. Q
- Tokyo Institute of Technology, Bulletin*. Tokyo Institute of Technology, Tokyo. Irreg.
- Torino, Accademia delle Scienze, Classe di Scienze Fisiche, Matematiche e Naturali, Atti*. Torino, Accademia delle Scienze, Turin. Irreg.
- Toshiba Review*. Tokyo Shibaura Electric Co., Ltd., Tokyo. BM
- **Toxicology and Applied Pharmacology*. Academic Press, Inc., New York. BM
- Transport Theory and Statistical Physics*. Marcel Dekker, Inc., New York. Q
- Transporturi Auto, Navale si Aeriene*. Ministerul Transporturilor and Consiliul National al Inginerilor si Technicienilor, Bucharest. M
- Trend in Engineering*. Office of Engineering Research, University of Washington, Seattle. Q
- Tsvetnaia Metallurgii*. Ministerstvo Vysshego i Srednego Spetsial'nogo Obrazovaniia SSSR; Izdanie Severokavkazskogo Gornometallurgicheskogo Instituta, Ordzhonikidze. BM
- Ukrains'kii Fizichnii Zhurnal*. Akademiia Nauk Ukrain'skoi RSR, Kiev. M
- Ukrainskii Matematicheskii Zhurnal*. Akademiia Nauk Ukrainkoi SSR; Izdatel'stvo Naukova Dumka, Kiev. BM
- Ultrasonics*. Iliffe Science & Technology Publications, Ltd., Guildford, Surrey, England. Q
- Unione Matematica Italiana, Bollettino*. Nicola Zanichelli Editore, Bologna. BM
- Universitas Comeniana, Acta Facultatis Rerum Naturalium — Mathematica*. Slovenské Pedagogické Nakladateľstvo, Bratislava. Irreg.
- Universitas Comeniana, Acta Facultatis Rerum Naturalium — Physica*. Slovenské Pedagogické Nakladateľstvo, Bratislava. Irreg.
- Urania (Madrid)*. Sociedad Astronómica de España y America, Barcelona; Union Nacional de Astronomia y Ciencias Afines, Madrid. SA
- Uspekhi Fizicheskikh Nauk*. Akademiia Nauk SSSR; Izdatel'stvo Nauka, Moscow. M
- Uspekhi Fiziologicheskikh Nauk*. Izdatel'stvo Nauka, Moscow. Q
- **VDI-Berichte*. Verein Deutscher Ingenieure; VDI-Verlag GmbH, Düsseldorf. BM
- VDI-Forschungsheft*. Verein Deutscher Ingenieure; VDI-Verlag GmbH, Düsseldorf. BM
- VDI-Z*. Verein Deutscher Ingenieure; VDI-Verlag GmbH, Düsseldorf. SM
- VDI-Z Fortschritt-Berichte, Reihe 1 — Konstruktionstechnik, Maschinenelemente*. Verein Deutscher Ingenieure; VDI-Verlag GmbH, Düsseldorf, West Germany. Irreg.
- VDI-Z Fortschritt-Berichte, Reihe 6 — Energietechnik, Wärmetechnik*. Verein Deutscher Ingenieure; VDI-Verlag GmbH, Düsseldorf. Irreg.
- VDI-Z Fortschritt-Berichte, Reihe 7 — Strömungstechnik*. Verein Deutscher Ingenieure; VDI-Verlag GmbH, Düsseldorf, West Germany. Irreg.
- VertiFlite*. American Helicopter Society, Inc., New York. M
- Le Vide*. Société Française des Ingénieurs et Techniciens du Vide, Paris. BM
- Vilnius, Astronomijos Observatorijos, Biuletenis*. Vilnius. Irreg.
- Vision Research*. Pergamon Press, Ltd., Oxford. M
- Voenno-Meditsinskii Zhurnal*. Tsentral'noe Voenno-Meditsinskoe Upravlenie Ministerstva Oborony SSSR; Izdatel'stvo Krasnaia Zvezda, Moscow. M
- Voprosy Dinamiki i Prochnosti*. Rizhskii Politehnicheskii Institut; Izdatel'stvo Zinatne, Riga. Irreg.
- Vychislitel'naia i Prikladnaia Matematika*. Izdatel'stvo Kievskogo Universiteta, Kiev. Irreg.

Vychislitel'naia Tekhnika i Voprosy Kibernetiki. Leningradskii Gosudarstvennyi Universitet, Vychislitel'nyi Tsentr; Izdatel'stvo Moskovskogo Universiteta, Moscow. Irreg.

Vychislitel'nye Metody i Programmirovaniye. Izdatel'stvo Moskovskogo Universiteta, Moscow. Irreg.

Wärme- und Stoffübertragung. Springer Verlag, Berlin. Q

Wear. Elsevier Sequoia S.A., Lausanne. M

Wehrmedizinische Monatsschrift. J. F. Lehmanns Verlag, Munich. M

**Wehrtechnik.* Wehr & Wissen Verlags Gesellschaft mbH, Darmstadt, West Germany. M

Welding Journal. American Welding Society, New York. M

Welding Production (Svarochnoe Proizvodstvo). Welding Institute, Cambridge. M

Weltraumfahrt Raketentechnik. Umschau Verlag, Frankfurt/Main. BM

**Western Pharmacology Society, Proceedings.* Frank McCaffrey, Publisher, Seattle. Annual.

Westinghouse Engineer. Westinghouse Electric Corp., Pittsburgh, Pa. BM

Wetter und Leben. Österreichische Gesellschaft für Meteorologie; Verlag Wetter & Leben, Vienna. BM

Wissenschaftliche Berichte AEG-Telefunken. AEG-Telefunken, Berlin. Q

Wissenschaftliche Zeitschrift. Dresden, Technische Universität, Dresden, East Germany. BM

WRC Bulletin. Welding Research Council, New York. 10 issues per year

Yamagata University, Bulletin (Engineering). Yamagata University, Yamagata, Japan.

Zagadnienia Drgan Nieliniowych. Polska Akademia Nauk, Instytut Podstawowych Problemów Techniki; Państwowe Wydawnictwo Naukowe, Warsaw. Irreg.

Zastosowania Matematyki. Polska Akademia Nauk, Instytut Matematyczny; Państwowe Wydawnictwo Naukowe, Warsaw. 3 issues per year

Zeitschrift für angewandte Mathematik und Mechanik. Akademie-Verlag GmbH, Berlin. M

Zeitschrift für angewandte Mathematik und Physik. Birkhäuser Verlag, Basel. BM

Zeitschrift für angewandte Physik. Deutsche Physikalische Gesellschaft, e.V., Springer Verlag, Berlin. M

Zeitschrift für elektrische Informations- und Energietechnik. Akademische Verlagsgesellschaft Geest & Portig, KG, Leipzig, East Germany.

Zeitschrift für experimentelle und angewandte Psychologie. Deutsche Gesellschaft für Psychologie; Verlag für Psychologie, Göttingen. Q

Zeitschrift für Flugwissenschaften. Deutsche Gesellschaft für Luft- und Raumfahrt, e.V., and Deutsche Forschungs- und Versuchsanstalt für Luft- und Raumfahrt, e.V.; Friedr. Vieweg & Sohn GmbH, Braunschweig. M

Zeitschrift für Geophysik. Deutsche geophysikalische Gesellschaft, Hamburg; Physica-Verlag, Würzburg, West Germany. BM

Zeitschrift für Luftrecht und Weltraumrechtsfragen. Köln, Universität, Institut für Luftrecht und Weltraumrechtsfragen; Carl Heymanns Verlag, KG, Cologne. Q

Zeitschrift für Metallkunde. Deutsche Gesellschaft für Metallkunde, e.V.; Riederer-Verlag GmbH, Stuttgart, West Germany. M

Zeitschrift für Meteorologie. Meteorologische Gesellschaft; Akademie-Verlag GmbH, Berlin. Irreg.

Zeitschrift für Naturforschung, Teil a. Verlag der Zeitschrift für Naturforschung, Tübingen. M

Zeitschrift für Physik. Deutsche physikalische Gesellschaft; Springer Verlag, Berlin. Irreg.

Zeitschrift für Vermessungswesen. Deutscher Verein für Vermessungswesen; Verlag Konrad Wittwer, Stuttgart, West Germany. M

**Zeitschrift für Werkstofftechnik.* Verlag Chemie GmbH, Weinheim, West Germany.

Zemlia i Vselennaia. Akademiia Nauk SSSR; Izdatel'stvo Nauka, Moscow. BM

Zentralblatt für Verkehrs-Medizin, Verkehrs-Psychologie, Luft- und Raumfahrt-Medizin. Deutsche Gesellschaft für Luft, und Raumfahrt-Medizin and Deutsche Gesellschaft für Verkehrs-Medizin; J. F. Lehmanns Verlag, Munich. Irreg.

Zhurnal Eksperimental'noi i Teoreticheskoi Fiziki. Akademiia Nauk SSSR; Izdatel'stvo Nauka, Moscow. M

Zhurnal Nauchnoi i Prikladnoi Fotografii i Kinematografii. Akademiia Nauk SSSR; Izdatel'stvo Nauka, Moscow. M

Zhurnal Prikladnoi Spektroskopii. Izdatel'stvo Nauka i Tekhnika, Minsk. M

Zhurnal Tekhnicheskoi Fiziki. Akademiia Nauk SSSR; Izdatel'stvo Nauka, Leningrad. M

Zhurnal Vychislitel'noi Matematiki i Matematicheskoi Fiziki. Akademiia Nauk SSSR; Izdatel'stvo Nauka, Moscow. BM

Zhurnal Vysshei Nervnoi Deiatel'nosti. Akademiia Nauk SSSR; Izdatel'stvo Nauka, Moscow. BM

Zpráva VZLÚ. Výzkumný a Zkušební Letecký Ústav, Prague. Irreg.

Zpravodaj VZLÚ. Výzkumný a Zkušební Letecký Ústav, Prague. BM

Either a Notation of Content or the actual title of the publication appears under each subject heading. They are listed under several subject headings which provide multiple access to the subject of each accession. The *IAA* accession number is located under and to the right of the NOC or the title. It is preceded by numbers identifying the issue and page of *International Aerospace Abstracts* where the accession is located.

To illustrate:

Issue Number	Page Number	Accession Number
14	p2146	A72-30920

A

A STARS

Magnetic field role in Ap stars abundance peculiarities model, discussing rotational circulation, convection, accretion and mass loss effects on surface

RR Lyrae stars absolute magnitude determination by statistical parallaxes method

Nuclear reactions in anomalous element abundances production for peculiar A stars, considering surface diffusion and surface and internal nuclear processes

Photoelectric measurements of Ca K line of southern/equatorial A stars, discussing abundance variation

Photoelectric photometry of Ca K-line for A stars of population I clusters

Observed light curve amplitude phase relations in Ap magnetic star UVB system, using oblique rotator model

Photoelectric UVB photometry for galactic cluster NGC 7039 region stars, discussing MK spectral classifications and peculiar A stars

Peculiar A stars in open cluster Tr 2 region from objective prism plate searches, showing membership by photometrical characteristics and proper motions

Spectrophotometry of nebulosity associated Ae and Be stars, discussing age, circumstellar dust shells geometry and red stellar objects

Ap stars with variable periods from magnetic and photometric data analysis

A model atmosphere analysis of the Ap star HR 465.

Pm existence evidence for HR 465 from analysis of Pm II spectral line data

Rotational velocities of Ap stars.

Spectrophotometric investigation of Ap stars. I - Two-dimensional quantitative spectral classification

Variation of the spectrophotometric temperature from the center of the disk to the limb of stars of the spectral classes B and A

Pulsating variables in the Pleiades cluster.

Magnetic-field variations in 78 Virginis, beta Coronae Borealis, and 73 Draconis.

Oxygen abundances of three population II horizontal-branch stars.

Transuranium elements in HD 25354.

Model atmosphere analysis of the A 31a-O supergiant HD 33579 in the Large Magellanic Cloud.

On circumstellar gas emission among pre-main-sequence stars in Ie Orionis and NGC 2264.

Investigation of type-A star condensations in the Perseus and Cassiopeia constellations

Spectral variabilities of magnetic peculiar A stars associated with atmospheric chemical composition anomalies, using inclined rotator model

Ultraviolet absorption lines in the spectrum of Vega.

A-3 AIRCRAFT

U.S. Navy cartography, describing RA-3B Skywarrior capabilities and photographic instrumentation

A-4 AIRCRAFT

A-4 Skyhawk horizontal stabilizer experimental graphite-epoxy composite construction, describing design, manufacturing and testing techniques [AIAA PAPER 72-358]

A-6 AIRCRAFT

Sound pressure levels and acoustic fatigue tests for 11,200 and 9,300 pound thrust J-52 engines comparison in A-6A aircraft

A-7 AIRCRAFT

A-7 D/E navigation/weapon delivery system flight testing, using photogrammetric technique

Flight test evaluation of A-7D/E emergency backup flight control system, describing hydraulic power control systems design and function

Catapult steam ingestion test of turbofan engines in A-7 aircraft, correlating compressor stall occurrences with temperature increase rate in distorted region

A-9 AIRCRAFT

Northrop A-9A attack aircraft production planning, discussing design features and management/engineering organizational changes in anticipation of USAF production contract

A-10 AIRCRAFT

A-10 prototype designed for production.

A-300 AIRCRAFT

European A300B airbus flying control hydraulic system and landing gear design for safety and reliability, fatigue life, weight and maintenance

European A300B airbus flap and slat systems and tailplane actuator for longitudinal pitch trim control

A-300B European Airbus cantilever wing design and manufacture, discussing skin forming, skin-stringer and torsion-box assembly, automatic riveting and root-end profile machining procedures

Airbus A-300 B design and characteristics for passenger transport on short and medium haul routes

ABBREVIATIONS

U SYMBOLS

ABDOMEN

Magnetometer and spirometer ventilation measurements from chest and abdomen movements during

carbon dioxide inhalation

ABEL FUNCTION

Statistical analysis of spectrographic plasma temperature measurements, obtaining numerical solution to Abel integral equation

ABERRATION

Spherical aberration effect on far field Fraunhofer diffraction for circular aperture illuminated by quasinomochromatic partially space coherent light

Aberration correction in collimator of Schmidt spectrograph camera by changing surface geometry and grating positioning

Charged particle motion equations for fifth order spherical aberration of quadrupole-octupole lens with arbitrary electrode and pole shapes

Aberration introduced by high satellite velocities, investigating application to laser telemetry

Three element einzel and asymmetric voltage lenses for electron optics, calculating focal lengths and spherical aberrations based on potential distribution inside equidiameter coaxial cylinders

Third order aberration coefficients of electron trajectories for two tube electrostatic lens

Dark field electron microscopy with small annular zone of objective lens to reduce chromatic aberration effects on resolution

Dispersive optical imaging systems for chromatic aberration correction, considering broadband holographic reconstruction and generation, optical information processing and diffraction pattern achromatization

Thermal defocusing of high intensity continuous Ar laser radiation in absorbing medium with allowance for spherical aberrations

Spectral image formation and aberration by spherical concave grating for point light source, using geometric optics method

Glass choice for two lens uncemented objectives, calculating surface and aberration coefficients

Analysis of multiple hologram optical elements with low dispersion and low aberrations.

Coma, astigmatism and spectral line curvature derivation for spherical mirror-concave grating assembly, calculating mounting resolution in terms of wavelength

Lateral chromatic aberration of a double-meniscus telescope in Chile

Experimental investigation of optical aberrations, due to temperature deformation and convective fluxes, by using a nonequal-arm interferometer with a coherent light source

Determination of the aberration constant and the coefficients of short-period nutation terms from observations by the Pulkovo polar tube during the period from 1953 to 1964

Computer aided analysis of hologram optical elements for aberration and dispersion reduction and recording on thick media

Effect of spherical spectacle lenses on the monochromatic aberration of the eye

Optical system parameters for electrophotographic print quality, discussing aberration effect on image optical density

Double star components light aberration dependence on relative velocity of source and observer, considering two reference systems

Optical system chromatic aberration correction relationship to focus plane position in white light based on Strehl and Hopkin criteria

24 p3425 A72-44772

ABILITIES

Instrument flying skills retention, discussing initial training, discrete procedural and tracking responses

01 p0018 A72-10564

Two explanations of temporal changes in ability-skill relationships - A literature review and theoretical analysis.

21 p3008 A72-41015

ABIOGENESIS

Preferential polymerization and adsorption of L-optical isomers of amino acids on kaolinite, indicating role in prebiotic protein origin

03 p0321 A72-13743

Martian atmospheric volatiles history, noting initial chemical conditions favorable to abiotic organic synthesis

04 p0569 A72-14503

Chemical evolution and life origin - Conference, Pont-a-Mousson, France, April 1970, Volume 1, Molecular evolution

04 p0467 A72-14751

Life origin in space from point of hydrocarbons, cyanides, abiogenic organic synthesis and protobionts evolution

04 p0467 A72-14752

Chemical box model of energy storage in covalent bonds and nonequilibrium distributions in prebiological synthesis leading to macromolecules

04 p0482 A72-14755

Biological self replicative description and function in chemical reaction networks in search of life origin from non-life-like matrix

04 p0482 A72-14756

Energetical conditions of primeval biosynthesis and transdehydration feasibility on simplified present day templates

04 p0468 A72-14757

Possible origin of dissymmetry of life, excluding synthesis under influence of optically active quartz

04 p0468 A72-14758

Shock wave contributions from micrometeorites, meteors, meteorites and thunder to organic compounds formation in primeval atmosphere

04 p0572 A72-14760

Pulse shock tube synthesis of amino acids in primitive environments, discussing thermodynamic relations and conversion efficiency

04 p0482 A72-14761

Aromatic and amino acid prebiotic syntheses under primitive earth, considering electric discharge and cyanide polymerizations

04 p0483 A72-14762

Lower aldehydes contribution to biochemically important compounds in abiogenic synthesis, considering amino acids formation

04 p0483 A72-14763

Laboratory simulation of Jovian atmospheric reactions, observing amino nitriles formation

04 p0572 A72-14764

Nucleotides condensation in aqueous system in prebiotic conditions, investigating effects of imidazole, cyanamide and polyornithine

04 p0483 A72-14766

Esters and amides participation in prebiotic polymers, discussing ribosome bonds and messenger RNA

04 p0468 A72-14767

Energy transfer conditions of transdehydration reactions on primeval earth leading to transphosphorylation, transacylation and peptide synthesis

04 p0468 A72-14768

Inorganic phosphates-nucleoside hypohydrous thermal reaction mechanism, discussing thermal polymerization of orthophosphates for phosphorylation and condensing agents in primordial synthesis

04 p0483 A72-14770

Atmospheric model for proteins abiogenesis, considering heteropolypeptides formation from hydrogen cyanide and water

04 p0468 A72-14772

Protobionts formation by random aggregation and reproduction from proteins and nucleic acids macromolecules

04 p0469 A72-14782

Coacervate drops oxidoreductases and stability in primitive prebiological systems, using polyphenol oxidase-carbohydrate-histone-quinones

04 p0469 A72-14784

Pigments participation in lipid systems formation, considering chlorophyll photochemical activity in surface active agents

04 p0469 A72-14785

Ion selective accumulation model of carbohydrates diffusing through artificial polymer membranes, relating prebiological systems to catalytic microsystems

04 p0469 A72-14788

Antibiotic polypeptide synthesis of gramicidin S and tyrocidine, using primitive model of sequential addition of amino acids on polynzymes

04 p0470 A72-14790

Genetic code numerical structure association with logarithmic optimization rule for hierarchy of structures from molecular biology experiments

04 p0470 A72-14794

Inorganic polyphosphates effect on phosphorus metabolism evolution in primary living organisms, noting polyphosphate glucokinase distribution in various microorganisms

04 p0470 A72-14797

Biological energy transformation origin and evolution, discussing inorganic pyrophosphates precursor to adenosine phosphates as energy carriers

04 p0470 A72-14798

Prebiological food origin in carbonaceous met eorites, considering extraterrestrial environments, organic synthesis and terrestrial analogs

04 p0471 A72-14803

Chemical evolution of carbonaceous chondrite organic compounds, discussing similarity to terrestrial abiogenic material

04 p0484 A72-14804

Extraterrestrial life on Mars and Venus and Jupiter atmospheres, discussing abiogenesis failures on life-supportable planets

04 p0471 A72-14805

Ionizing radiation as effective energy in primordial organic synthesis, discussing small molecule formation and subsequent condensation into polypeptides and polynucleotides

05 p0617 A72-16127

Catalytic action in organic catalyst predecessors of contemporary enzymes, discussing polymers of alpha-amino acids and hydrogen cyanide

05 p0624 A72-16128

Biological phosphate origin through atmosphere-hydrosphere interrelations, discussing concentrative processes, dehydration mechanics and evaporation

05 p0617 A72-16129

Exobiology research objectives, discussing planetary exploration data on origin, nature and distribution of life, spacecraft contamination, manned and unmanned missions and specific mission targets

05 p0714 A72-16133

Book on origin of life by natural causes covering physical geology, astronomy, biopoiesis and evolution of life stages, orogenetic cycle, fossils, and primeval atmosphere

07 p0917 A72-19185

Transcript of conference on origins of life covering cosmic evolution, abundance and distribution of biologically important elements, earth and Mars atmosphere evolution, etc

07 p1074 A72-19450

Origins of life - Conference, Princeton, New Jersey, May 1967

07 p1074 A72-19451

Organic origin of meteoritic hydrocarbons in early solar system related to Fischer-Tropsch reaction

07 p1076 A72-19590

Papers on exobiology covering abiogenesis, extraterrestrial life, primordial organic chemistry, biochemical evolution electronic factors, membranes origin, molecular chirality, protein and cellular evolution, etc

08 p1119 A72-22001

Extraterrestrial life origin and development possibilities from earth chemical and biological evolution description, noting external conditions requirements

08 p1119 A72-22002

Origin of life as chemical evolution product, tracing juvenile carbon history through planetary and geological phases

08 p1162 A72-22004

Chemical evolution in microenvironment reactions system due to dominant energy or mass parameter, discussing complex organic molecule synthesis

08 p1128 A72-22005

Electronic factors role in intermolecular interactions and biochemical evolution, applying quantum biochemistry

08 p1128 A72-22006

Statistical, physical and biotic theories on molecular chirality origin, considering catalytic processes and asymmetric processes with circularly polarized light

08 p1129 A72-22007

Structure, function and origin of biological membranes, considering related surface phenomena

08 p1119 A72-22008

Amino acid sequences of proteins from living organisms, considering evolutionary process

08 p1119 A72-22009

Genetic organization emergence, considering pretranslational evolution in nontranslational protein synthesis, nucleic acid evolution and gene origin

08 p1119 A72-22010

Terrestrial life origin understanding by investigating life possibilities in nonterrestrial environments

08 p1120 A72-22015

Life beyond solar system, discussing planetary formation and prebiological organic chemistry developments and interstellar communication

08 p1120 A72-22016

Abiogenic formation and fluorescence spectra of porphyrin, chlorin and bacteriochlorin during chemical evolution, using pyrrol-formaldehyde model

08 p1122 A72-22185

Extraterrestrial abiogenic organic hollow spheres of Orgueil meteorite evaluated according to intrinsic and extrinsic criteria

09 p1385 A72-22640

Review of NASA Ames Research Center 1971 conference on interstellar molecules and origin of life

09 p1265 A72-22645

Life origin and primordial organic chemistry, considering Darwinian evolution, spontaneous generation, primitive atmospheres, interstellar matter, energy sources, macromolecular synthesis, moon and Jupiter

12 p1760 A72-27529

Abiogenic formation of nucleic acid bases and nucleosides in photochemically synthesized self sustaining coacervates

12 p1761 A72-27657

Abiotic origin of organic compounds in carbonaceous chondrites, analysing Murchison and Murray meteorites by combined gas chromatography-mass spectroscopy technique

15 p2306 A72-31625

Prebiotic thymidine phosphorylation at 65 C by urea-phosphate mixtures in simulated desert conditions

15 p2185 A72-31629

Chemical evolution and the origin of life - Bibliography supplement 1970.

18 p2650 A72-36450

ABLATION

Carbon-oxygen reaction kinetic limitations on carbon ablation rate, discounting diffusional transport limits above 1650 K

03 p0457 A72-13955

Isotopic heat source unit multiple elliptical orbit reentry unperturbed by solar-lunar gravitational forces, deriving analytical model of grazing trajectories, aerodynamic heating and thermochemical ablation

03 p0457 A72-13959

Pulsed electric microthruster with solid fuel feed system, noting electrode geometry effects on performance and ablation patterns

[AIAA PAPER 72-210]

05 p0705 A72-16799

Hypersonic melting ablation waves simulation near stagnation region by frozen oil models

[AIAA PAPER 72-92]

05 p0750 A72-16977

Radar verification of sporadic E layer formation from meteoritic atoms and ions production by meteoritic ablation

08 p1154 A72-20728

Slip cast fused silica ablation in high temperature hydrogen-oxygen environment, comparing analytical results with measured data from rocket motor exhaust experiments

08 p1191 A72-21601

Statistical multiple regression equations for identification of artificial graphite properties effect on ablation performance

[AIAA PAPER 72-295]

11 p1669 A72-25233

Constituents, processing, fabrication and structure effects on artificial graphitic materials ablation performance in sublimation regime from high temperature tests

[AIAA PAPER 72-298]

11 p1742 A72-25235

Ablation phase duration during spacecraft decelerated hypersonic reentry flight, using theoretical model based on quasi-steady assumptions

11 p1745 A72-25815

Nose blunting, exposure time and initial temperature effects on axisymmetric bodies ablation surface cross hatching patterns, presenting test results on cones with various vertex angles

11 p1572 A72-26006

Parallel rail solid fuel pulsed electric microthruster performance, noting mathematical model for mass ablation and plasma acceleration mechanism

[AIAA PAPER 72-458]

11 p1708 A72-26194

Fabrication, and physical, mechanical and ablation properties of three dimensional carbon-carbon cylinder composite materials

12 p1834 A72-28086

Ablation rate growth phenomenon in meltable material with increasing thermal flux, discussing quartz glass characteristics

13 p2066 A72-30007

Artificial meteor ablation on iron oxides by arc heated air plasma stream for product and environment identification studies

14 p2150 A72-30319

Apollo heat shield silica reinforcement fiber and ablation char reactions in laboratory and actual reentry tests

14 p2172 A72-30922

Aerothermochemical analysis of thermosetting hydrocarbon plastic ablation rate under heat transfer at reentry vehicle hypersonic stagnation point, describing pyrolysis by chemical kinetic equation

15 p2335 A72-32149

Graphite ablation rate inhibition and surface temperature depression by chlorine gas in supersonic high temperature air environment 16 p2475 A72-32842

Analytical model for crosshatch ablation patterns geometric features and stability characteristics prediction based on viscoelastic melt layer interaction with gas boundary layer [AIAA PAPER 72-718] 16 p2480 A72-34030

Radar verification of sporadic E layer formation from meteoritic atoms and ions produced by meteoroid ablation 19 p2791 A72-38356

A parametric study of the transient ablation of Teflon. [ASME PAPER 72-HT-32] 20 p2986 A72-39671

Ablation rate growth phenomenon in fusible material with diminished thermal flux, discussing quartz glass characteristics 22 p3244 A72-42728

Spin response of symmetric ablating vehicle at zero angle of attack, noting spin-up by ablation-induced grooving and spin-down by crosshatching effects 24 p3362 A72-45339

Nonsimilar solution for laminar and turbulent boundary-layer flows over ablating surfaces. 24 p3364 A72-45782

ABLATIVE MATERIALS

Space shuttle low density ablative thermal protection systems, emphasizing low cost refurbishment techniques 01 p0091 A72-10766

Radiative heat transfer between gas flow and axisymmetric ablating body near stagnation point, considering ablation products effects under boundary layer chemical equilibrium conditions 02 p0300 A72-11577

Graphite surface temperature and ablation rate for various stagnation pressures, radiative heat fluxes, stagnation enthalpies, heat transfer coefficients and test gas compositions 02 p0249 A72-12021

Mechanical and thermochemical erosion during ablation of silicophenolic material 04 p0597 A72-15554

Ablation performance of dielectric heat shields for planetary entry, testing diffuse reflectance by convective and radiative heating 05 p0747 A72-16809

High speed boundary layer flow three dimensional disturbances interaction with thermal and ablative response in adjacent surface material, considering laminar and turbulent compressible flows [AIAA PAPER 72-93] 05 p0748 A72-16811

Graphite ablation in combined convective and radiative heating, considering mass and energy transfer effects [AIAA PAPER 72-88] 05 p0750 A72-16954

Compressible boundary layer flow past swept wavy wall with heat transfer and ablation, measuring pressure and temperature disturbances 07 p1101 A72-20247

Thermal boundary layer interaction with distortions in shape or material of adjacent surface for space shuttle design [AIAA PAPER 72-312] 11 p1614 A72-25246

Surface patterns from ablating, melting and flowing materials in supersonic flow of wind tunnel, rocket motor and flight test environments, comparing with theory [AIAA PAPER 72-313] 11 p1743 A72-25247

Carbon-phenolic composite ablation and expansion in thermal environment during reentry shielding, using flight and simulation tests [AIAA PAPER 72-363] 11 p1669 A72-25390

Mechanical behavior of three dimensional reinforced ablative composites, including carbon-phenolic, quartz-phenolic and quartz-carbon materials 11 p1670 A72-25459

Carbon-carbon composite ring structure tested for processing cycle, design properties and ablative performance in solid rocket nozzle environment 11 p1673 A72-25488

Space shuttle orbiter reentry heat shield materials, considering hot structures and hot radiative metallic, ceramic insulative and ablative heat shields 11 p1660 A72-26245

Elastomeric silicone ablator heat shields thermal characteristics from NASA Planetary Atmosphere Experiments Test vehicle earth atmosphere entry measurements [AIAA PAPER 72-326] 13 p2064 A72-28953

Boundary layer temperature profile for ablating asbestos-plastic composite samples measured under combined convection and radiant heat fluxes 14 p2172 A72-31003

Development of moldable carbonaceous materials for ablative rocket nozzles. 17 p2572 A72-35668

Mechanical tests of laminated plastics in solar installations 22 p3197 A72-43192

ABLATIVE NOSE CONES

Heat and mass transfer blowing correction correlations for graphite and charring ablator reentry nosetip and heat shield applications [AIAA PAPER 72-91] 05 p0748 A72-16810

Thermally expanding surface effects on aerodynamic roll torques on smoothly ablating spinning cones, comparing analytic study and hypersonic wind tunnel test results [AIAA PAPER 72-30] 05 p0608 A72-16923

Computer program for low temperature ablator nosetip shape change at angle of attack, comparing with supersonic wind tunnel tests on camphor models [AIAA PAPER 72-90] 07 p1098 A72-18952

Laminar near wake solutions for slender ablating cone under supersonic atmospheric entry conditions including boundary layer reactions [AIAA PAPER 72-116] 07 p0907 A72-18954

High modulus yarn carbon-carbon three dimensional orthogonal composite material ablative and thermomechanical performance in nose tip ground tests [AIAA PAPER 72-365] 13 p1983 A72-28956

Thermomechanical erosion prediction for ablative, composite material, reentry nosetip applications and model development for heating, pressure and shear forces [AIAA PAPER 72-299] 14 p2171 A72-30827

Low recession graphite nosetip design for ballistic reentry, considering blunt and sharp configurations in terms of thermally induced tensile strain survival [AIAA PAPER 72-705] 16 p2472 A72-34039

Ablative nose shape change effects on re-entry vehicle aerodynamic performance. [AIAA PAPER 72-974] 22 p3230 A72-42337

Ablative asymmetric conical nose bluntness changes effects on aerodynamic characteristics for moderate magnitude tilt angles 24 p3363 A72-45341

Roll dynamic behavior of a very slender reentry vehicle. 24 p3452 A72-45348

ABNORMALITIES

NT MAGNETIC ANOMALIES

NT NEUROSES

Neural effects on human visual resolution of horizontal and vertical gratings resulting from early abnormal visual inputs due to astigmatism 10 p1430 A72-24348

Mathematical model for Venus phase anomaly, noting upper limit of reflecting layer for refraction effect 20 p2972 A72-39874

ABORTED MISSIONS

Liquid propellant rocket abort fireball model, specifying heat flux as function of time 03 p0457 A72-13953

Missile destruct systems explosive transmission line manifolds, discussing designs for high reliability under severe environmental conditions 08 p1221 A72-20782

Booster launch vehicle guidance scheme for critical aborts from staging through burnout, minimizing aerodynamic phases for different landing sites 15 p2269 A72-32182

ABRASION

Glass sample mechanical strength testing, considering abrasion process, concentric ring stress calculation and laser light scattering techniques 12 p1832 A72-27007

Lunar rock abrasion and cataclastic rupture lifetimes for near earth micrometeoroid flux determination, using hypervelocity impact tests 15 p2309 A72-31956

ABRASION RESISTANCE

Steel coatings produced by plasma jets on experimental machine parts, determining friction wear resistance by successive tests 03 p0363 A72-13548

Titanium carbide based hard cermet alloys with Ni addition, testing wear resistance 03 p0372 A72-13549

Martensite and solid Cr-containing inclusion effects on wear resistance of cermet steel during dry friction with R18 steel 05 p0665 A72-16095

Impurity content, particle size and abrasion resistance role in abrasiveness of molybdenum disulfide 06 p0836 A72-18589

Polyurethane O ring seals for high pressure applications, discussing stress relaxation /creep/ behavior, resilience and tear and abrasion resistance 08 p1173 A72-21023

Wear resistance of steel and Ti alloys in free abrasive gas jet, noting surface microhardness increase effect 09 p1319 A72-23188

Carbon and low alloy steels resistance to abrasive wear as function of hardness, heat treatment and composition 12 p1829 A72-27455

Wear resistance of artificial and natural diamond grindstones in ruby cutting, noting tests for grain geometry and fabrication technique effects 12 p1814 A72-27765

Antiscratch properties of nitrided layers of creep-resisting steels at high temperatures 22 p3187 A72-41868

ABRASIVES

Ductile metal surface erosion by hard abrasive grains striking at grazing angles 03 p0373 A72-13650

Thermophysical aspects of abrasive belt grinding, determining maximum contact temperatures and heat balance 13 p1963 A72-28745

Facility for studying the failure of structural elements in a supersonic high-temperature flow containing a controlled number of abrasive particles 21 p3043 A72-41717

Wide-band abrasive grinding of complex surfaces with flexible contact wire elements 23 p3293 A72-43672

ABRIKOSOV THEORY

Abrikosov and Mendelsohn models of nonideal superconductors of second kind in transverse magnetic field, discussing Landau-Ginzburg parameters and critical current density 07 p1049 A72-20153

Abrikosov vortex lattice in superconductors, calculating resonance linewidth and vacancy formation energy 11 p1699 A72-25718

ABSOLUTE TEMPERATURE SCALES

U TEMPERATURE SCALES

ABSORBERS [MATERIALS]

NT NEUTRON ABSORBERS

NT SOLAR ENERGY ABSORBERS

Mossbauer spectra measurement of metallic iron, sodium nitroprusside, sodium ferrocyanide and ferrocyanide absorbers at 78-293 K, fitting temperature dependences and resonant velocity to models 01 p0114 A72-10324

Hollow rubber impact absorber stiffness and deformation characteristics derivation by classical elasticity theory, noting accuracy 06 p0895 A72-17797

Carbon dioxide laser IR radiation modulation by application of Stark effect in various molecular absorbers, showing absence of saturation 07 p1000 A72-19035

Real time hologram photosensitive materials, determining power requirements and resolution for diffraction gratings in saturable absorbers and absorbing liquids [CLEA PAPER 15.4] 07 p0984 A72-19397

Efficiency response of covered Si detectors to monoenergetic gamma rays, considering Lucite, Al, Cu and Pb absorbers 13 p1954 A72-28429

Fiberglass performance as duct liner in presence of spinning modes from free field measurements, noting ineffectiveness for plane wave attenuation 13 p2028 A72-29573

IR absorbent effects on evaporographic image contrast performance based on photometric study, presenting color photographs 15 p2188 A72-31615

Laser coupling through nonlinear gas filled absorber cell, discussing molecules mean free path 15 p2246 A72-31883

Rhodamine laser radiation effects on absorbing materials investigated by high speed cinematography and shock wave structure 16 p2404 A72-33991

Theory of spontaneous mode locking in lasers using a circuit model. 19 p2813 A72-38690

Fluctuation mechanism of ultrashort pulse generation by laser with saturable absorber. 23 p3297 A72-44184

ABSORPTANCE

Plant leaves light reflectance, transmittance and absorptance characteristics relationship to leaf mesophyll arrangement, considering interpretation of aircraft/spacecraft remotely sensed data 02 p0213 A72-11856

Cylindrical solar array absorptance as function of solar flux vector inclination, using Gier-Dunkle integrating sphere [AIAA PAPER 72-57] 05 p0616 A72-16909

Polymers ignition time measurement in cabinet with benzene flames and W filament lamps, noting black body radiation source absorptance and incident irradiance effects 17 p2636 A72-34719

ABSORPTION

Absorbed oxygen concentration variation with depth in Nb during oxidation 07 p1022 A72-20555

Hydrogen adsorption and absorption by niobium, investigating sticking probability and heat of solution 15 p2276 A72-31864

Helium absorption into nitrogen tetroxide (NTO) and aerazine-50 /A-50/. 22 p3215 A72-42869

Capillary circulation as a regulator of sodium reabsorption and excretion. 23 p3257 A72-43995

ABSORPTION BANDS

U ABSORPTION SPECTRA

ABSORPTION COEFFICIENT

U ABSORPTIVITY

ABSORPTION CROSS SECTIONS

Solar corona atomic states radiative and collisional transitions, inferring radiative recombination cross section from bound-free absorption coefficient

03 p0422 A72-13203

Solar UV radiation role in mesosphere, investigating absorption cross sections of ozone and molecular oxygen

03 p0411 A72-13385

Energetic electrons absorption cross sections in weakly ionized atomic oxygen gas, showing energy losses through excitation

05 p0655 A72-16071

Extreme UV absorption cross sections ratios for atomic oxygen in upper atmosphere, observing solar radiation attenuation with satellite instruments

09 p1297 A72-22578

Ion quadrupole effects in ion-molecule collisions, calculating capture cross sections and ion trajectories

09 p1354 A72-22658

Cross sections of Li nonresonant capture of Na ion charge, interpreting quasi-oscillatory structure

10 p1517 A72-25047

Ion dipole capture cross sections at low ion and rotational energies compared with reaction cross sections for ammonia and water parent-ion collisions

11 p1692 A72-26014

Absorption spectrum of molecular nitrogen in 730-980 Å band, investigating absorption cross sections and optical oscillator strengths

12 p1848 A72-27853

Wave equations and photon absorption cross section of relativistic electron in magnetic field, taking into account relativistic energies

13 p2002 A72-28647

Luminous molecular absorption cross sections in aeronomy, considering photodissociation, actinic solar radiation attenuation and UV to IR analysis

14 p2097 A72-30135

IR absorption coefficients of oxygen atom and molecule fields due to free-free electron transfers at specific elastic scattering cross sections

15 p2274 A72-31409

Born approximation for resonance bremsstrahlung emission and photon absorption cross sections at electron-ion scattering, solving multiparticle problem

15 p2279 A72-32697

Radar meteorology in the Soviet Union - 1970. IR emission of nitrogen layer heated by reflected shock wave, noting absorption cross sections under free-free electron transitions in neutral particle fields

19 p2835 A72-38776

Anomalous high concentration of lunar rock Xe-131 relation to Ba-130 nonthermal neutron-capture cross section in resonance energy region

20 p2967 A72-39180

Total absorption cross sections of several gases of aeronomic interest at 584 Å.

22 p3152 A72-42419

Photoionization and photoabsorption cross sections of CO₂ at 584 Å.

23 p3317 A72-44519

An experimental investigation of radiative properties of aluminum oxide particles.

24 p3461 A72-44809

ABSORPTION SPECTRA

NT FRAUNHOFER LINES

NT HERZBERG BANDS

NT TELLURIC LINES

Absorption cell heterodyne method for nondispersive IR detection of trace gases with molecular vibrational-rotational spectrum

[AIAA PAPER 71-1064]

01 p0023 A72-10532

Flare region curved absorption lines interpreted as photospheric and chromospheric mass motions

01 p0129 A72-10800

CH Cygni spectrum analysis in activity phase, discussing blue continuum, emission and UV absorption lines, radial velocity and stratification effects

01 p0131 A72-11008

Cosmic and X ray irradiated quartz particles as contributor to interstellar extinction, discussing grain radiation damage measurements and absorption spectra in wavelengths of approximately 1600 Å to 20 micrometers

01 p0134 A72-11163

Uranium and tungsten plasmas emission and absorption properties at shock tube generated pressures of 3-48 atm and temperatures of 7,000-12,000 K

01 p0112 A72-11339

Stratospheric and lower mesospheric temperature measurement by ground based passive microwave sensing, calculating oxygen absorption band lines brightness temperature emission spectra

02 p0213 A72-11861

High velocity interstellar Ca II near Vela pulsar 0833-45, discussing absorption line association with Vela X, Y, Z supernova remnant complex

02 p0279 A72-12191

Grating spectra of Jupiter North Equatorial Belt, noting absorption feature at 4.73 microns

02 p0280 A72-12206

Absorption spectrum of atomic Ca trapped in solid hydrocarbons, comparing with diffuse interstellar band at 4430 Å

02 p0284 A72-12632

Line spectrum of Of star zeta Puppis at 3150-8600 Å, comparing absorption spectrum to 9 Sgr

03 p0416 A72-13014

Absorption profiles of neutral helium lines lambda 4471 and lambda 4026 for BoV star tau Sco, observing flux near peak of forbidden component

03 p0417 A72-13022

Space observation of stars and interstellar medium, considering stellar energy distributions and line spectra, interstellar absorption lines, galactic nebulae and X ray sources

03 p0420 A72-13122

Absorption line formation in magnetic field for magnetograph interpretation of solar atmosphere

03 p0427 A72-13291

Relaxation and heating rate due to solar radiation absorption by 2.7 and 4.3 micron vibration-rotation bands of carbon dioxide

03 p0347 A72-13387

Absorption effects of dimers of water molecule in atmosphere, using spectroscopic and maser measurements

03 p0348 A72-13400

Jovian planets methane and ammonium absorption bands spectrophotometric investigation, noting Saturn spectral variations

03 p0436 A72-13819

Formaldehyde photoionization and absorption spectrum measurements in vacuum UV region, using single configuration self consistent field procedure for Rydberg states and model

03 p0321 A72-13856

Venus cloudy atmosphere IR absorption line spectra interpretation, suggesting HCl and HF formations dependence on condensation phases

03 p0439 A72-14149

Soviet book on long period variable stars covering spectral data photometric characteristics, spatial and kinematic properties, absorption effect and evolution

03 p0439 A72-14224

Abundance ratios in quasar PKS 0237-23 from absorption spectrum measurements and explosive nucleosynthesis calculations

04 p0570 A72-14526

Light wave electric field Franz-Keldysh effect on GaAs absorption edge, using electroabsorbance, electoreflectance and photoconductivity spectrum and internal photoeffect analysis

04 p0561 A72-14621

Early type supergiant far UV spectrum observations, showing broad absorption feature near 1720 Å

04 p0578 A72-15315

Missing solar UV opacity from band absorption coefficient comparison between photospheric diatomic molecules and metals and hydrogen

04 p0579 A72-15327

Uranus IR spectral albedo, discussing methane absorption

04 p0580 A72-15365

White dwarf Grw plus 70 deg 8247 circular polarization spectral structure with molecular absorption bands coincident with Minkowski bands

04 p0580 A72-15368

Distance estimation for supernova remnants and H II regions from H I absorption measurements

05 p0712 A72-15770

Radio absorption spectra sounding for planetary atmospheric impurities calculating water vapor content in Venus cloud level

05 p0715 A72-16169

Radiation transfer by resonant scattering in expanding nebula with applications to quasars having blueward absorption wings

05 p0716 A72-16374

Water molecules absorption lines in sunspots umbral near IR spectrum, noting improved spectrometric apparatus

05 p0719 A72-16515

Metastable He atoms concentration in plasma from absorption characteristics at temperatures 4-300 K and pressures 1-70 mm Hg

05 p0696 A72-16612

Radio quiet quasar PHL 957 absorption line spectra obtained at telescope with Cassegrain image tube and multichannel spectrometer and integrating TV camera

05 p0720 A72-16714

Quasar mass determination, attributing absorption line red shift to radially moving gas clouds

05 p0723 A72-17157

Interstellar Ca II, H and K optical absorption lines of bright O and early B stars in Orion region

05 p0723 A72-17200

Photoelectric spectrophotometric measurements of Jupiter atmosphere optical properties and structure, showing methane absorption band intensity latitudinal variations

06 p0881 A72-17928

Twilight atmospheric sounding in oxygen absorption bands to reduce noise level in secondary light scattering

06 p0807 A72-17943

Martian dust storm depth determination from carbon dioxide absorption and abundance observation on Mars by earth based spectroscopy

06 p0890 A72-18348

Balloon-borne radiometer-sonde measurement of stratospheric downward emission in absorption spectral region of water vapor rotational band

07 p0982 A72-19105

Classification-dispersion spectrograms of early decline of Nova Serpentis 1970, discussing diffuse enhanced absorption system behavior

07 p1071 A72-19338

Optically pumped gas lasers with electron transitions to molecular excited state and resonant absorption lines

07 p1006 A72-19634

Coupled coherent and incoherent excitons motion effect on optical absorption line shape, deriving diffusion equation from density matrix equation of motion

07 p1035 A72-19672

Carbon dioxide IR absorption lines broadening at 298 and 207 K by evacuated high-resolution Czerny-Turner spectrograph, comparing with values based on fixed collision cross section

07 p1038 A72-19834

Room temperature IR absorption spectra of B alloyed powdered synthetic diamonds

07 p1050 A72-20253

Local interstellar hydrogen survey from OAO-2 observations of Lyman alpha absorption at 1216 Å for B2 or earlier stars

08 p1235 A72-21392

UV absorption levels in different areas of Jupiter disk from spectrophotometric studies at 3300-4800 Å, noting temporal variations in reflectance

08 p1237 A72-21828

Absorption spectra and detection sensitivity enhancement by organic dye laser quenching with broadband cavity

09 p1323 A72-22601

Carbon monoxide in carbon dioxide atmosphere, determining IR absorption lines broadening at reduced temperatures

09 p1351 A72-22612

Pseudo-hemispherical properties applied to radiative transfer in absorbing-emitting medium involving specular directional surfaces

09 p1351 A72-22671

Ultrafast X ray absorption spectra features of inner atomic shell photoionization in molecules

09 p1356 A72-22827

Ultrafast X ray region photoionization absorption spectra features of inert gases, solids, rare earth elements and transition metals

09 p1357 A72-22845

Foreign gas collisional broadening of nitrous oxide absorption lines, obtaining optical collision cross sections

09 p1276 A72-23332

Rapid rotation effect on weak and intermediate strength early type stellar radiation spectral absorption lines

09 p1390 A72-23527

Seyfert galaxies emission, absorption, IR, and optical spectral characteristics, suggesting model with sharp forbidden and Balmer line outer region and broad wing core

10 p1532 A72-23885

Radio-emitting and radio-quiet quasar optical emission and absorption line spectra

10 p1534 A72-23897

Laser radar technique for invisible air pollutants remote sensing systems, comparing Raman backscattering resonance scattering and absorption schemes

10 p1489 A72-23952

Methane absorption line profile, intensity and width studied with magnetically tuned He-Ne laser

10 p1490 A72-24041

Atmospheric water vapor submillimeter absorption lines in high resolution radiation transmission measurements with Froome type plasma metal junction device

10 p1472 A72-24175

IR absorption spectrum of gaseous ozone, obtaining mechanical anharmonicity coefficients and zero order wave numbers

10 p1511 A72-24226

Absorption spectra and plasma of laser spark in hydrogen, studying electron and atoms temperature and concentrations time variations

10 p1491 A72-24359

Solar gravitational red shift measurement from solar and laboratory potassium absorption line comparison, using atomic beam resonance scattering technique

10 p1541 A72-24415

Interferometric photoelectric scans of interstellar Ca K lines in stellar spectra, noting interstellar Na lines presence

10 p1544 A72-24663

- Stellar absorption spectral line fineness indication for cold interstellar molecular clouds between observer and star
10 p1546 A72-24848
- IR spectrophotometric data for Jupiter, determining limb darkening nature and ammonia and methane absorption variations over belts, zones and Red spot
10 p1548 A72-24971
- Free convection-radiative heat transfer interaction of real gases in laminar boundary layer on vertical plate, using exponential wideband model for total band absorptance
[AIAA PAPER 72-278]
11 p1740 A72-25218
- Fine structure and IR transmission functions of carbon dioxide absorption bands at high pressure and temperature, calculating transition lines strength and position
11 p1620 A72-25275
- Stratospheric methane measurements over North America from solar absorption spectra observed from aircraft
11 p1622 A72-25911
- Fluorescence and absorption spectra from oxygen sulfur dichloride photodissociation in vacuum UV, discussing So formation
11 p1590 A72-26012
- Interstellar anomalous 6 centimeter formaldehyde absorption in diffuse dark nebulae, discussing quantum mechanics of collisional pumping process
11 p1720 A72-26112
- Venus spectrum carbon dioxide absorption lines model with double cloud system and adiabatic atmosphere
11 p1721 A72-26120
- Laser stimulated Raman scattering and IR absorption on crystal defects leading to atomic migration in solids
11 p1647 A72-26144
- Carbon dioxide laser cross relaxation effects on hole burning process in Doppler broadened gain or absorption line
11 p1647 A72-26146
- He-Ne laser with absorption cell, investigating high contrast power resonances due to Lamb dip at nonuniformly broadened absorption line center
11 p1649 A72-26340
- Solar X-rays absorption profiles and residual fluxes in D and E layers during 7 March 1970 eclipse from rocket measurements
12 p1863 A72-27146
- HD 4180 shell H lines width variations comparison with Be stars, noting thirty year period emission decrease followed by outer shell absorption
12 p1867 A72-27213
- Interstellar atomic hydrogen observations in radio nebula W 3 direction, noting 21-cm absorption line profile coincidence with Cn alpha recombination line in radial velocity
12 p1868 A72-27219
- Absorption spectrum of Cr cations in magnesium aluminate spinel crystals excited by strong optical pumping
12 p1854 A72-27596
- Surface pressure via satellite-borne measurements of atmospheric transmission near absorption band
12 p1802 A72-27710
- Absorption spectrum of molecular nitrogen in 730-980 A band, investigating absorption cross sections and optical oscillator strengths
12 p1848 A72-27853
- Atmospheric nitric acid vapor radiation absorption measurements at various partial pressures
12 p1805 A72-27993
- IR absorption bands in mechanically and chemically polished GaAs single crystals irradiated with varying neutron and electron doses
12 p1859 A72-28069
- Plasma spectral absorpton coefficients determination by organic dye laser with tunable radiation frequency
13 p2015 A72-29504
- Sulfur alloyed CdTe single crystals IR absorption spectrum, noting temperature effects
13 p2023 A72-29918
- Absorption effects on 10.6 micron laser beam in fluidized particulate crosswind, discussing calcium hydroxide performance
14 p2109 A72-30186
- Radio absorption spectra sounding for planetary atmospheric impurities calculating water vapor content in Venus cloud level
14 p2149 A72-30238
- Black holes due to gravitational collapses, including radiation emission/absorption, pulsars and binary stars
14 p2151 A72-30478
- Fe and Ti ion bands in lunar pyroxenes and olivines single crystals polarized absorption spectra
14 p2154 A72-30510
- Galactic supernova remnants radio frequency absorption line observations, deriving distances, radio luminosity function and distribution
14 p2158 A72-30726
- Nova Delphini evolution from metallic absorption lines observations before December 1967 maximum, obtaining dispersion variation with wavelength
14 p2159 A72-30741
- Fundamental and overlapping bands integrated intensities and nitrogen broadened half widths of rotational lines in nitrous oxide obtained from absorption measurements
14 p2135 A72-30895
- Cosmic background radiation temperature from interstellar CN band R branch absorption line in star zeta Ophiuchi spectrum
15 p2313 A72-32309
- K line of X ray absorption spectra for pure Ti and compounds, discussing effects of valence, microstructure and electron configuration
15 p2259 A72-32700
- C-13 and C-12 formaldehyde absorption near Sgr A and Sgr B2, noting optical depths and abundance ratio
15 p2315 A72-32712
- Solar Mg abundance and hyperfine structure from oscillator strengths measurement by comparing absorption lines at furnace temperatures
15 p2317 A72-32774
- Mercuric chloride, bromide and iodide gas phase UV absorption spectra, discussing correlation with intermolecular charge transfer transitions
16 p2360 A72-32926
- Upper atmospheric Na abundance from daytime spectroscopic absorption measurement compared with twilight glow observation
16 p2383 A72-32970
- N-type GaAs absorption spectra construction from transmission spectra, considering effects of irradiation by fast protons, electrons, neutrons and alpha particles
16 p2441 A72-33368
- Heavily doped ruby optical properties review, discussing N-lines, absorption and fluorescence spectra, interactions with phonon and photon fields and ionic reactions
16 p2441 A72-33522
- HD absorption spectrum measurements in vacuum UV region for Rydberg states and ionization energy determination
16 p2431 A72-33583
- Twilight atmospheric sounding in oxygen absorption bands to reduce noise level in secondary light scattering
16 p2386 A72-33784
- Titan spectrum absorption features, estimating hydrogen abundances
17 p2606 A72-34540
- Absorption spectra and plasma of laser spark in hydrogen, studying electron and atoms temperature and concentrations time variations
17 p2562 A72-34958
- Solar flares and prominences rotational motions from spectrographic observations of atomic Al absorption line periodic asymmetry
17 p2608 A72-35086
- Soft X-rays from Cygnus X-2 and from Cygnus X-1 /in eclipse/.
17 p2600 A72-35297
- Vibrational analysis of electronic absorption spectra of 3-methyldiazirine and 3-methyl-d3-diazirine in vapor phase
18 p2657 A72-36566
- Absorption of the 4- to 6-millimeter wavelength band in the atmosphere.
18 p2689 A72-36961
- Photoelectric spectrophotometric measurements of Jupiter atmosphere optical properties and structure, showing methane absorption band intensity latitudinal variations
18 p2730 A72-37153
- French monograph - Determination of the absolute value of the absorption in the bands of the Schumann-Runge system of molecular oxygen
19 p2836 A72-37476
- Comparison of theoretical and experimental limits of detection in atomic absorption spectrometry using air-acetylene and nitrous oxide-acetylene flames.
19 p2762 A72-37725
- Measurement of the equivalent widths of oxygen A-band absorption lines at different pressures
19 p2837 A72-37959
- Absorption line profile and equivalent line width derivation for planetary atmosphere with low and high optical thicknesses, assuming arbitrary scattering coefficients
19 p2863 A72-38071
- Theoretical determination of the absorption coefficient and the total band absorptance including a specific application to carbon monoxide.
19 p2881 A72-38395
- Investigation of the 0.63-micron line shift in an He-Ne/20/ laser with an absorbing cell
19 p2814 A72-38787
- Vibration spectra of the isomorphous proustite-pyrrargyrite series.
20 p2932 A72-39506
- Stellar emission and absorption line spectra formation in presence of magnetic field interpreted by radiative transfer equation solution, considering dwarf stars observation
20 p2956 A72-39753
- Emission and absorption line spectra of type I supernovae after luminosity maximum interpreted by heating and ionization mechanisms in shell and intensity computation
20 p2973 A72-39886
- Boundary conditions in the exciton absorption region.
21 p3096 A72-40139
- Influence of polarization of laser fields on nonlinear interference effects
21 p3062 A72-40405
- Two-step photodissociation of ammonia molecules excited by laser radiation.
21 p3013 A72-40724
- Absorption spectra in the far ultraviolet of Be, B, C, N, Mg, Al, and Si
21 p3013 A72-40818
- He-D3 spectroheliogram absorption features correlation with magnetic field regions and H alpha structures
21 p3108 A72-41279
- Photoelectrically observed diatomic carbon absorption lines in sunspot spectra for two energy bands
21 p3108 A72-41284
- Investigation of amplification spectra and triplet-triplet absorption in a laser with a rhodamine 6G solution
21 p3064 A72-41743
- Effect of a random magnetic field on the absorption line characteristics of stars
21 p3113 A72-41761
- Nonvelocity origin of excess red shift in companion galaxies from observation of H and K absorption lines of Ca II
22 p3220 A72-41962
- Millimeter absorption features corresponding with H alpha dark filaments on disk and emissive regions in solar prominences, discussing electron temperatures and densities
22 p3221 A72-42035
- Peculiar absorption and emission microstructures in the type IV solar radio outburst of March 2, 1970.
22 p3217 A72-42044
- Russian book - Radiation characteristics of gases at high temperatures.
22 p3243 A72-42075
- Comparative studies of various spectral lamp designs for atom-absorption analyses and use of double-discharge multielement lamps to account for non-selective interference
22 p3176 A72-42170
- Sensitivity enhancement of atom absorption measurements by the method of pulse vaporization from the microprobe into the flame
22 p3176 A72-42174
- Usability of a graphite dish for atom absorption analyses of laser collected samples
22 p3176 A72-42175
- Total absorption cross sections of several gases of aeromic interest at 584 A.
22 p3152 A72-42419
- Spectrophotometry /0.3 to 1.1 micron/ of visited and proposed Apollo lunar landing sites.
22 p3225 A72-42530
- Atmospheric nitric acid vapor radiation absorption measurements at various partial pressures
22 p3174 A72-43007
- Study of the variation of the intensity of vibration-rotation spectra of hydrogen halide molecules under the action of compressed foreign gases
22 p3209 A72-43047
- Type II supernova spectral intensity minima due to blueshifted absorption lines of hydrogen and Fe II based on observed and synthetic spectra wavelength comparison
23 p3334 A72-43257
- Gas absorption lines detection based on multiple light passage through absorbing medium during generation process, noting radiation spectra of neodymium glass laser
23 p3295 A72-43305
- Temperature and polarization dependence of arsenic sulfide single crystals and thin films intrinsic absorption edge, determining forbidden bandwidth and transitions types
23 p3324 A72-43688
- Ultraviolet absorption lines in the spectrum of Vega.
23 p3337 A72-43826
- Slab band absorptance for molecular gas radiation.
23 p3316 A72-44327
- Optically pumped gas lasers with electron transitions to molecular excited state and resonant absorption lines
24 p3408 A72-44566
- Microwave spectrum of compressed O2-foreign gas mixtures in the 48-81 GHz region.
24 p3378 A72-44871
- Some infrared diagnostic techniques in high temperature gasdynamics.
24 p3402 A72-45043

ABSORPTION SPECTROSCOPY

Resonance neutron transmission for nondestructive absorption spectroscopic evaluation of quantitative chemical or isotopic composition at depth in large samples

01 p0069 A72-10806

Primary cosmic ray electrons energy spectrum measurements, using balloon-borne absorption spectrometer

04 p0568 A72-15509

Spectroscopy model design using ruby laser highly monochromatic light pulses, electro-optical scanning and high speed photography to study atmospheric gases absorption spectra

09 p1322 A72-22205

Air pollution monitoring with tunable lasers employing Raman scattering, resonantly excited or hot gases emission and resonant absorption

09 p1322 A72-22313

Saturated absorption spectroscopy of ammonia, considering Stark effect on IR transition

10 p1491 A72-24122

Multiple reflection absorption cell for gaseous air pollutants IR radiation measurements over wide temperature, pressure and distance ranges

11 p1619 A72-25216

Dual resonant cavity absorption cell composed of Fabry-Perot interferometers excited by microwave sources, observing spectroscopic double resonance effects

12 p1806 A72-27264

Acousto-optical method and equipment for atmospheric gases absorption lines recording with ruby laser for radiation source

14 p2111 A72-30812

Tunable output dye and semiconductor lasers application to absorption spectroscopy and air pollution monitoring

17 p2564 A72-35381

Far UV radiating hot dense microplasma production by laser heating for measuring by resonant absorption small quantities of gaseous element

21 p3093 A72-41341

IR spectroscopy techniques based on Pfund triple-pass absorption cell, image slicer and achromatic doublet lenses, presenting graphs for prism dispersion design parameters

23 p3289 A72-43895

ABSORPTIVITY

U ABSORPTIVITY

ABSORPTIVITY

Optical excitation of divergent alkali atomic beam by radiation absorption, deriving absorption coefficient for line broadening and/or Doppler effect

03 p0393 A72-14062

Hydrogen plasma absorption coefficients at laser frequencies over 0.3371-10.6 microns

05 p0694 A72-15997

Giant M stars atmospheres absorption coefficient calculation from vibrational and pure rotational bands of H₂O, CO and OH

05 p0715 A72-16167

Spherical ice and graphite particles absorption, scattering and radiation pressure coefficients and albedo, noting application to interstellar extinction

06 p0875 A72-17296

Conductive and radiative energy transfer in absorbing, emitting and conducting medium bounded by two black plates, using Milne-Eddington type absorption coefficient

06 p0903 A72-18187

Spectral composition of emitted radiation, emissivity and absorptivity of Venus atmosphere at high temperatures

07 p1068 A72-18933

Jovian atmospheric absorption coefficient at 6-14 microns as function of frequency from hydrogen, methane and ammonia contributions

07 p1069 A72-19078

Light beam time stationary multifocal structure in medium with Kerr type nonlinearity, relating maximum energy density and absorption coefficients

07 p0944 A72-19635

Shock wave collision induced population inversion in electromagnetic shock tubes, measuring plasma absorption coefficient

07 p1044 A72-20074

Light absorptivity measurement in low loss liquid with interferometer based on refractivity dependence on temperature change due to absorption

09 p1309 A72-22602

Transition metals IR spectral absorptivity evaluation at room and liquid He temperatures from reflectivity measurement relative to vapor deposited Au mirror

09 p1309 A72-22604

Nongray treatment of nonisothermal IR radiative transfer problem in terms of mean absorption coefficient

09 p1354 A72-22668

Molecular gases absorption coefficients measurement in extreme UV, analyzing photoionization curves in energy range far beyond threshold

09 p1356 A72-22829

Negative reabsorption coefficient for induced emission of neutron moving in medium in magnetic field

09 p1364 A72-23357

Monochromatic absorption coefficients determination for Ar heated in wall-stabilized arc at high temperatures and pressures

10 p1517 A72-23836

Airborne IR radiometric measurements of upward vertical radiance from tropical sea surface at 10-12 microns, noting absorption coefficient dependence on water vapor

10 p1474 A72-24747

IR absorption coefficients in air at 6000-8500 K and 40-95 atm, interpreting absorption due to free-free electron transitions in neutral particle fields

13 p2006 A72-29676

Semiconducting glass filter time dependent transition, absorption coefficient and luminescent spectral dependences, using monopolised ruby laser

13 p1971 A72-29909

Hg vapor absorptivity dependence on wave number, atomic density and temperature in 2537 A resonance line region, discussing measurement by magnetic scanning or monochromator

14 p2131 A72-30853

Mean opacities and effective absorption coefficients measurement using wide bandwidths and path lengths

14 p2131 A72-30900

Absorption coefficient of H-He plasma measured in temperature and electron density range of inverse bremsstrahlung and photoionization absorption

15 p2284 A72-31522

Theoretical determination of the absorption coefficient and the total band absorptance including a specific application to carbon monoxide.

19 p2881 A72-38395

Atmospheric window at 10-12 micron wavelength, investigating absorption coefficient of clear atmosphere water vapor

21 p3048 A72-40398

Influence of the lowering of the ionization energy on the continuous radiation of an argon plasma

21 p3093 A72-41343

Mean coefficient of opacity in stellar atmosphere model calculations

21 p3110 A72-41443

Nonlinear molecular absorption cell for frequency stabilization of carbon dioxide laser radiation, discussing stability limit dependence on amplification, absorptivity and Q value

22 p3184 A72-42102

Absorption coefficient and gain of a GaAs injection laser

22 p3184 A72-42104

Semigray approximation to nongray radiative transfer, taking into account mean absorption coefficient variation with spatial position and photon propagation direction

23 p3314 A72-44328

Light beam time stationary multifocal structure in medium with Kerr type nonlinearity, relating maximum energy density and absorption coefficients

24 p3408 A72-44567

3.39 micron resonance line absorption in shocked methane.

24 p3410 A72-45044

GaAs semiconductor injection laser and amplifier-absorber emission and light pulse transmission characteristics determination, noting nonlinear absorptivity, bleaching threshold and pulse compression factor

24 p3412 A72-45619

Influence of a temperature dependent spectral absorption coefficient on radiative flux.

24 p3466 A72-45791

ABSTRACTS

1972 seminar supplement to bibliography and abstracts on electrical contacts, circuit breakers and arc phenomena.

18 p2664 A72-35986

1970-1971 Holm Seminar supplement to bibliography and abstracts on electrical contacts, circuit breakers and arc phenomena.

18 p2665 A72-36120

ABUNDANCE

Nighttime sodium layer observation by tuned laser beam resonance scattering technique, measuring seasonal variation in Na abundance and height distribution

01 p0063 A72-10915

Interstellar C12/C13 abundance ratio lower limit in direction of 20 Tau

02 p0280 A72-12192

Spectroscopic He abundance in population II stars from viewpoint of big-bang cosmology, taking into account neutrino emission according to photon-neutrino coupling theory

02 p0281 A72-12303

Li, Be and B abundances in Apollo 11, 12 and 14 and Lunik 16 missions fine and core samples

03 p0414 A72-12903

Isotopic composition of trapped helium, neon and argon in carbonaceous chondrites, observing covariance based on mass-dependent fractionation

03 p0414 A72-12904

Magnetic field role in Ap stars abundance peculiarities model, discussing rotational circulation, convection, accretion and mass loss effects on surface

03 p0416 A72-13010

Terrestrial planets internal constitution and thermal history model, emphasizing iron fractionation in structure

03 p0418 A72-13110

He abundances in universe, discussing stellar structure and evolution, He production, variable stars and globular clusters H-R diagrams shape

03 p0418 A72-13112

He abundance in population I and II stellar atmospheres

03 p0418 A72-13113

Helium abundance in stellar interiors, considering mass-luminosity relations of Hyades

03 p0419 A72-13114

He abundances in gaseous nebulae by optical and radio observation, discussing hydrogen and helium recombination spectra interpretation

03 p0419 A72-13115

Xe and Kr abundance and isotopic composition in silicate inclusions of iron meteorites

03 p0435 A72-13690

Nuclear astrophysics review, discussing chemical elements and isotopes abundance and cosmic nucleosynthesis

03 p0437 A72-13842

Nuclear reactions in anomalous element abundances production for peculiar A stars, considering surface diffusion and surface and internal nuclear processes

03 p0437 A72-13872

Mars atmosphere diatomic oxygen upper limit abundance, using high dispersion spectroscopic data from 1969 apparition

04 p0569 A72-14498

Abundance ratios in quasar PKS 0237-23 from absorption spectrum measurements and explosive nucleosynthesis calculations

04 p0570 A72-14526

Neutrino emission process effects on solar C-N-O cycle energy generation and C12/C13 abundance ratio

04 p0567 A72-14911

Galactic evolution and cosmology implications of primordial solar D/H ratio, discussing deuterium production mechanisms

04 p0574 A72-14980

Slowly rotating F, G and early K field stars data, computing Li abundance and isotope ratio

04 p0578 A72-15316

Photometric standard star 29 Piscium abundance analysis with flux constant hydrogen line blanketed model atmospheres

04 p0578 A72-15317

Solar silicon abundance from low excitation forbidden Si I lines

04 p0579 A72-15326

Photoelectric measurements of Ca K line of southern/equatorial A stars, discussing abundance variation

05 p0712 A72-15796

Major and trace element abundances in orogenic area volcanic rocks, considering geographic and stratigraphic relations and composition

05 p0658 A72-16721

Disk population F-type star photometric luminosities, motions and metal abundance indices, discussing ultrashort period cepheids

07 p1071 A72-19333

Oxygen isotopic abundances and equilibrium temperatures of meteoritic minerals, chondrules, meteorites and planets

07 p0985 A72-19589

Stellar structure calculation by real gas equation of state, considering He abundances and solar lines of ionizable metal atoms

07 p1078 A72-19925

Solar corona abundance and intensity measurements during 30 May 1965 eclipse

07 p1081 A72-20233

Chondrite normalized rare earth abundances in lunar solidand liquid-type materials from Mare Tranquillitatis and Oceanus Procellarum associated with evolution

08 p1233 A72-21218

Bulk and rare earth abundances in Luna 16 soil levels A and D by sequential instrumental neutron activation analysis

09 p1381 A72-22275

Astrophysical abundances analysis, discussing assumptions of local thermodynamic equilibrium and microturbulence in stellar atmospheres

09 p1386 A72-22659

Inelasticity fluctuations effect on cosmic ray showers development, proposing criteria for lateral electron distribution and relative abundance of hadrons and muons

10 p1529 A72-24213

Symmetric fission of superheavy nuclei, observing overabundance of rare earth elements

10 p1515 A72-24526

Spectrographic analysis of K-type supergiant epsilon Pegasi for effective temperature, surface gravity and heavy and light element abundances
10 p1543 A72-24621

Enhanced abundances of low energy heavy elements in solar cosmic rays due to preferential acceleration within flare region
10 p1530 A72-24673

Gas rich meteorites and lunar materials solar rare gases component observed and predicted relative abundance agreement indicating absence of fractionation in solar nebula formation
11 p1721 A72-26118

Abundance in cold stellar atmospheres, noting effect on atmospheric thermal stratification and energy transfer from molecular spectra
11 p1722 A72-26432

Cosmic and solar wind abundance analysis for D and He-3 in protosolar gas, noting chemical equilibrium reaction role in D enrichment
12 p1868 A72-27216

Handbook on elemental abundances in meteorites covering individual elements, emission and X ray spectrography, colorimetry, neutron activation and isotope dilution
12 p1876 A72-28204

Solar X-ray spectral lines at 1-60 A from coronal ion relative abundances obtained from Jordan ionization equilibrium calculations
13 p2034 A72-29940

Saturn thermal radio emission brightness temperature calculations for subcloud atmosphere ammonia abundance evaluation
14 p2152 A72-30490

Growth analysis curve of halo subdwarf Groombridge 1830 relative to sun, noting metal abundance
15 p2314 A72-32373

Solar Mg abundance and hyperfine structure from oscillator strengths measurement by comparing absorption lines at furnace temperatures
15 p2317 A72-32774

Solar corona Ca ion abundance from emission line measurements and electron density determination
15 p2318 A72-32785

Upper atmospheric Na abundance from daytime spectroscopic absorption measurement compared with twilight glow observation
16 p2383 A72-32970

Isotopic abundance analysis of primary cosmic radiation with nuclear emulsion technique, discussing mass measurements in Be, C, O, Ne, Mg and Fe tracks
16 p2447 A72-33731

Model for low energy galactic cosmic ray effects on young and F star Li abundance and H I region heating
16 p2448 A72-33740

The reddening, distance modulus, chemical composition and age of the galactic cluster NGC 752.
17 p2607 A72-34675

The solar abundance of gold.
17 p2607 A72-35077

Metallic abundances in the solar chromosphere.
17 p2613 A72-35498

Velocity and flux dependence of the solar-wind helium abundance.
17 p2602 A72-35607

The distribution of carbon in lunar samples from Apollo 11, 12 and 14.
17 p2615 A72-35685

The isotopic composition and elemental abundance of gallium in meteorites and in terrestrial samples.
18 p2723 A72-36061

Upper atmospheric sodium and stratospheric warnings.
18 p2687 A72-36643

Proton capture mean lifetimes in fast C-N cycle, presenting nitrogen/carbon abundance ratio variation with temperature
18 p2721 A72-36650

The helium abundance in thirty-three main sequence B stars.
18 p2726 A72-36726

A model atmosphere analysis of the Ap star HR 465.
18 p2727 A72-36736

Thermal release Xe analysis of neutron irradiated white inclusion samples from Allende carbonaceous meteorite, noting iodine and plutonium isotopes abundance
18 p2728 A72-36971

Molecular equilibrium abundances in interstellar H I gas clouds, noting formation dependence on gas density and degree of interstellar radiation extinction
19 p2854 A72-37230

Luminosities and motions of the F-type stars. II - Metal-deficient stars.
19 p2855 A72-37238

Elemental abundances in stone meteorites.
19 p2858 A72-37863

Saturn thermal radio emission brightness temperature calculations for subcloud atmosphere ammonia abundance evaluation
19 p2864 A72-38319

Coude spectra, abundance ratios and radial and rotational velocities of He rich stars, using microphotometer equivalent width tracings
19 p2866 A72-38502

He abundance relationship to solar wind bulk speed and temperature from Explorers 34 and 43 observations, noting dependence on sunspot number
19 p2853 A72-38749

Rocket observation of Ar XII-XVI, Ca XIV-XVIII, and Fe XIV, XV, XXIV in the extreme-ultraviolet spectrum of a solar flare.
20 p2963 A72-38913

Elemental abundance trends in the australite strewn field by non-destructive neutron activation.
20 p2900 A72-39839

Eu, La and Sm in sunspot spectra.
20 p2973 A72-39884

On the chemical composition of epsilon Pegasi.
20 p2974 A72-39901

The abundance of helium in the cosmos. I.
21 p3103 A72-40379

Oxygen abundances of three population II horizontal-branch stars.
21 p3109 A72-41330

Curve of growth analysis of F star beta Cas and 10 UMa atmospheres for Ca, Sc, Ti, Cr, Mn and Ni-to-Fe abundance ratios
21 p3110 A72-41444

Molecular abundances and gas-to-electron pressure ratios as function of temperatures and pressures in solar composition gaseous mixture of late type stellar atmospheres
21 p3110 A72-41446

Cosmic abundance of iron and nature of primitive material in meteorites.
22 p3220 A72-41963

The solar abundance of calcium and collision broadening of Ca I- and Ca II-Fraunhofer lines by hydrogen.
22 p3221 A72-42027

Solar silver abundance from spectral scans for Ag 3280.7 and 3382.9 A resonance lines, using spectral synthesis method, model atmosphere and limb darkening observations
22 p3221 A72-42028

Detection of molecular oxygen on Mars.
22 p3224 A72-42293

Sodium to calcium ion abundances ratio variation model in interstellar clouds, comparing with pulsar dispersion and LF radio absorption measurements
22 p3224 A72-42383

Studies of heavy-element synthesis in the galaxy. I - Separation of r- and s-process abundances.
22 p3228 A72-42563

Low abundance of solar photosphere iron from Fe I excitation and ionization computations, showing LTE departure effects on spectral lines
22 p3228 A72-42569

Giant stars iron abundance from narrow band spectrophotometric analysis and model atmospheres, isolating super metal rich stars below H-R diagram subgiant branch
23 p3334 A72-43256

Chondrite Al-Ir abundance association for L compositional class consistent with Lamer condensation mechanism
23 p3335 A72-43266

Production of light elements in the solar system.
23 p3335 A72-43487

The analysis of the small Magellanic Cloud supergiant HD 7583.
23 p3336 A72-43555

Rare earth and other abundances in the Murchison carbonaceous meteorite.
23 p3262 A72-44131

Upper limits on the atomic hydrogen abundance in 12 globular clusters.
23 p3340 A72-44246

Photoionization of N2, O2, NO, CO, and CO2 by soft X rays.
24 p3426 A72-45302

AC [CURRENT]

U ALTERNATING CURRENT

AC GENERATORS

Aircraft turbo-alternator speed control for constant frequency power supply, presenting theoretical relationships for electrohydraulic or mechanohydraulic control loops
04 p0466 A72-15462

Aircraft turboalternator governing theory for frequency error detection, comparing performance of mechanical- and electro-hydraulic governors
06 p0868 A72-18249

Aircraft cockpit electrical heating system, converting three phase ac energy from alternator with economy and safety
[SAE PAPER 720329]
11 p1577 A72-25591

Silicon carbide rotating rectifier alternator with solid lubricated bearings for high altitude environments, noting applicability to supersonic aircraft
17 p2498 A72-35565

ACCELERATED LIFE TESTS

Uniform low temperature compression effect on accelerated aging of Duralumin specimens, noting Plateau due to Guinier-Preston zones
02 p0245 A72-12539

Aerospace reliability methods, discussing distribution functions, sampling, accelerated life testing and

ACCELERATION [PHYSICS]

case histories of space electric rocket and microthruster power conditioner tests

Arrhenius model and graphical methods for temperature accelerated life tests in electrical insulation systems
04 p0526 A72-14441

Accelerated fatigue limits for Al and Mg alloys from transverse bend test data
06 p0827 A72-17398

Aerospace explosive components accelerated storage life and stability tests, basing method on Arrhenius reaction rate equation modification
08 p1220 A72-20762

Graphical analysis of accelerated life test data on insulating fluids, capacitors, bearings and electronic devices, using inverse power law model
08 p1176 A72-21587

Corrosion testing classification based on similarity between laboratory and operating conditions, emphasizing qualitative nature of accelerated tests
08 p1189 A72-22103

Accelerated full scale aircraft turbine engine corrosion tests in controlled environment, simulating salt, high temperature and humidity conditions
[NACE PAPER 76]
10 p1528 A72-24320

Adhesive bonded clad Al corrosion penetration rates from accelerated tests
[SAE PAPER 720344]
11 p1656 A72-25600

Grid translation accelerator system for Kaufman ion thrusters beam deflection, noting response time and accelerated life tests
[AIAA PAPER 72-485]
11 p1710 A72-26211

Rectifier tube cathode as colloid thruster electron gun type neutralizer, discussing efficiency and accelerated life tests
[AIAA PAPER 72-511]
11 p1711 A72-26228

Long life leak-proof hermetic compression seals for alkaline batteries, describing design, fabrication and accelerated thermal cycle test method
[ECS PAPER 72]
13 p1899 A72-28434

Accelerated reliability, life, fatigue and performance tests of automatic systems components, noting mathematical models for minimum time techniques
13 p1965 A72-29172

Propellant powders safe life prediction based on short-time tests, discussing aging effects on chemical stability after 7-11 years air conditioned storage
14 p2144 A72-30756

Double base solid propellants life determination from accelerated aging tests at elevated temperatures, discussing surface properties effect on weight loss and autocatalytic decomposition
14 p2144 A72-30757

Weibull life tests of Kemet solid tantalum chip capacitors at high accelerated voltages.
17 p2527 A72-34685

Evaluation of gold electrodeposits for use in dry circuit applications.
18 p2664 A72-35983

Evaluation of testing methods for gold plated or gold clad contacts.
18 p2664 A72-35984

Thermionic converters performance and life tests, discussing test equipment and diffusion effect on emitter stability
18 p2643 A72-36139

Endurance test results for microwave avalanche diode oscillators
18 p2671 A72-37146

Heat resistant alloys stress-rupture strength tests for operating temperatures based on equivalent high temperatures damageability
19 p2818 A72-38008

Prediction of deformability and fracture processes for polymer materials
20 p2943 A72-38943

Fabrication and accelerated life tests of self sustained electron emission cathode with Cr film vapor deposition on Cu disk base
21 p2997 A72-40790

A note on a comparison of confidence interval techniques in truncated life tests.
21 p3075 A72-40828

Influence of dispersion on the accuracy of estimating the fatigue life from the results of accelerated investigations by the prefracture method.
22 p2332 A72-41928

Accelerated life testing of thick film resistors.
24 p3384 A72-44668

Point and confidence interval estimates for acceleration and aging component probability distribution functions in accelerated life tests and reliability prediction
24 p3406 A72-44669

Lifetime estimation, optimal experimental design and stress level severity prediction in parametric and nonparametric accelerated life tests
24 p3406 A72-44671

ACCELERATION [PHYSICS]

NT ANGULAR ACCELERATION

NT DECELERATION

NT HIGH ACCELERATION

NT HIGH GRAVITY ENVIRONMENTS

NT IMPACT ACCELERATION

NT LUNAR GRAVITATIONAL EFFECTS
 NT PARTICLE ACCELERATION
 NT PHYSIOLOGICAL ACCELERATION
 NT PLASMA ACCELERATION
 NT SPIN REDUCTION
 NT TRANSVERSE ACCELERATION

Aluminized solid propellant transient burning rate augmentation as function of acceleration vector magnitude and orientation, applying centrifugal accelerations of zero to 140 g

01 p0114 A72-10378

Kinetic energy velocity and acceleration formulas of penny shaped crack propagation in brittle body under triaxial tensile stress

01 p0144 A72-11391

Absolute gravity acceleration determination using free-falling laser interferometer apparatus with rotation-insensitive mirror at different sites

02 p0207 A72-11597

Turbulent boundary layer fluid dynamic behavior under transpiration and acceleration effects, presenting mean velocity profile data, skin friction and mixing length model

[ASME PAPER 71-HT-F] 02 p0205 A72-12315

Self oscillations and drift motion of gyroscopic integrator of linear accelerations under hf vibrations, assuming ideal linear gimbal compensation

02 p0231 A72-12567

Particle motion in uniform acceleration field via Schwarzschild line element of general relativity, applying to clock paradox

03 p0388 A72-13227

Rocket acceleration effect on internal isotropic nozzle flow, giving formulas for thermodynamic variables

03 p0441 A72-13627

Relativistic flight of decreasing mass, increasing acceleration and constant thrust rocket description from earth and rocket observer viewpoints, noting light flash transmission and arrival times

03 p0441 A72-13836

Rigid body general motion dynamic effects due to acceleration of arbitrary order, using Samov-Mangeron recursive formulas

04 p0551 A72-15746

Dynamic manned vehicle cockpit simulator for visual and aural effects and acceleration changes, discussing STOL and VTOL characteristics

06 p0796 A72-18246

Orbit determination using Kalman-Bucy filter to estimate state and unmodeled acceleration approximated as first order stationary Gauss-Markov process

08 p1145 A72-20867

Heat transfer characteristics of transpired and accelerated turbulent boundary layer on porous plate, comparing with prediction techniques

[ASME PAPER 71-HT-BB] 08 p1251 A72-20880

Coherent radar pulse train clutter performance prediction for targets with range acceleration effects on Doppler response

08 p1133 A72-21405

Optical measurement of point velocity on surface of moving solid, applying to Mylar foil accelerated by plasma gun

09 p1310 A72-22773

Strong shock wave acceleration during passage through decreasing density region observed in experiments with explosions in Ar-H mixture

09 p1295 A72-22961

Nonlinear longitudinal aerodynamic characteristics effect on rigid aircraft response to normal acceleration due to atmospheric turbulence, using power spectral technique

09 p1263 A72-23461

Dimensional analysis proportionalities method parallel to formal similitude method for accelerative mechanics problems

10 p1503 A72-23919

Pneumatically assisted parachute deployment at high altitudes with low accelerations

10 p1421 A72-24273

Time optimal transfer trajectory in central Newtonian force field between two arbitrary points under jet acceleration

11 p1718 A72-25942

Breakup of accelerating liquid drops in gas dynamic flow, presenting unified theory for acceleration and aerodynamic effects

11 p1619 A72-26641

Reciprocating O ring seal sliding friction behavior prediction by elastohydrodynamic theory, noting dwell time, acceleration rate and previous deceleration effects

12 p1816 A72-28110

Positive acceleration force-produced displacements of helmet-attached reticle in front of left eye

12 p1777 A72-28330

Hypergravity effects on bats spatial orientation, noting resistance to head-pelvis and pelvis-head accelerations

13 p1907 A72-30015

German monograph on small variable-speed motors with high impulse performance, considering asynchronous cage type, dc shunt type and pneumatic motors

15 p2182 A72-31325

Skyнет I synchronous satellite orbit determinations and longitude acceleration due to tesseral harmonics of earth gravity, using tracking station range data

15 p2321 A72-31949

Human body or dummy mechanical impedance calculation by acceleration measurement at two point reference system with circular spring supporting mass

15 p2192 A72-32608

Potassium atomic beam aerodynamic acceleration by He-Ar free jet, determining beam intensity as function of nozzle-skimmer distance, carrier gas pressure and nozzle temperature

16 p2429 A72-33056

Explosive charge design to drive metal by detonation in terms of impulse, acceleration and final velocity, using Gurney model

16 p2398 A72-33355

Subcooling and acceleration effects on nucleate boiling heat flux, comparing heat transfer prediction models with experimental measurements

16 p2477 A72-33433

The gravitational acceleration perpendicular to the galactic plane

17 p2603 A72-34441

Flow in an accelerated rocket nozzle - Effect of variation of total mass. II

17 p2621 A72-34918

Flow near an accelerated porous flat plate

17 p2540 A72-35054

Strong shock wave acceleration during passage through decreasing density region observed in experiments with gas discharges and Ar-H mixture explosions

17 p2544 A72-35890

Mechanical component acceleration-induced stress and transient phenomena analysis by dynamic photoelastometry and interferometry, applying to elastic birefringent and other materials

18 p2734 A72-36373

On the prediction of acceleration response of air cushion vehicles to random seaways and the distortion effects of the cushion inherent in scale models

[AIAA PAPER 72-598] 18 p2642 A72-36538

Accelerated propagation of a shock wave in a shock tube

18 p2682 A72-36670

Two dimensional channel contraction induced flow acceleration effect on turbulence structure

18 p2683 A72-36995

Acceleration effects on burning velocity of aluminized condensed rocket propellant systems, calculating particle size and slag mass

19 p2847 A72-37360

The development of dynamic flight test techniques for the extraction of aircraft performance

[AIAA PAPER 72-785] 19 p2749 A72-38102

On the existence of an instantaneous rotation axis during the motion of a solid body with a constant point in Euclidian n-dimensional space

19 p2835 A72-38635

Ascent acceleration maximization of variable mass particle, calculating optimal parameters of multistage rocket

22 p3204 A72-42066

Fluid dynamic forces exerted by Newtonian fluid axisymmetric creeping flow on accelerating body of arbitrary shape, calculating pressure gradient via Navier-Stokes equation

23 p3347 A72-43726

Acceleration waves in orthotropic elastic materials

23 p3354 A72-44342

Dynamic model compensation algorithm accuracy for sequential estimation of time history of lunar satellite acceleration due to modeled surface mascons effects

24 p3440 A72-45139

ACCELERATION PROTECTION

Acceleration tolerance increase by static forearm muscular contraction exercise comparison to g-suit protection during human centrifuge tests

[AD-739063] 08 p1114 A72-20887

Dynamic deceleration anthropomorphic dummy tests of general aviation occupant lap belt/shoulder harness restraint systems

[SAE PAPER 720325] 11 p1583 A72-25588

Acceleration protection properties of modified partial pressure suit, determining tolerance limits by vision impairment criteria during centrifuge tests

12 p1776 A72-28319

Aircraft crash landing induced acceleration effects on seated occupants, discussing energy absorber system dynamic response characteristics for injury protective devices

15 p2191 A72-32603

Dilant suspensions impact energy absorbent properties, considering application to ejection seat cushions for occupant acceleration attenuation

15 p2191 A72-32604

Deceleration attenuation effectiveness of airbag restraint systems compared with seat belt-shoulder harness for aircraft occupants crash protection

15 p2191 A72-32605

Flight and centrifuge tested aircrew tilting supinating seats biomedical and technical adequacy as acceleration protective man machine system

19 p2761 A72-38707

Effect of psychotropic substances on human resistance to acceleration

21 p3006 A72-40443

ACCELERATION STRESSES (PHYSIOLOGY)
NT CENTRIFUGING STRESS

Human spine elastic deformation due to bending stresses, presenting statistical data on caudocephalad acceleration effects in vertebral column injuries

01 p0016 A72-10111

Human centrifuge tests for gravito-inertial force effect on ocular counterrolling in normal and deaf subjects

02 p0159 A72-11956

Parachuting and aerial towing physiological and force data FM telemetry for biomedical response assessment leading to human engineered equipment improvement and midair retrieval system development

02 p0168 A72-12138

Human centrifuge tests for semicircular canal gyroscopic stimulation during sensory deprivation, discussing angular acceleration detection thresholds

04 p0478 A72-14865

Acceleration force simulation for altered weight effect on animal tolerance to restraint, discussing body mass loss, reduced lymphocyte count and disorientation

04 p0472 A72-14866

Human vestibular stability under frontal and sagittal head tilts in rotating chairs, discussing motion sickness onset

05 p0622 A72-16640

High carbohydrate diet-induced hypoglycemia as potential cause of pilot unconsciousness during flight acceleration

[AD-736564] 06 p0767 A72-17878

Mathematical model for semicircular canal dynamic response to angular acceleration, emphasizing role of perilymph over endolymph in cupula displacement

07 p0917 A72-19491

Motion sickness experience correlations to vestibular tests in pilots and nonpilots

12 p1764 A72-28257

Vision influence on acute motion sickness elicitation in slow rotation room, comparing with vestibular factors

12 p1764 A72-28258

Supine human body mechanical impedance under combined stress of vibration and sustained acceleration

12 p1765 A72-28270

Modified Van der Pol wave motion oscillator model for prediction of aortic dynamic response to negative g impact accelerations

12 p1765 A72-28271

Ear oximeter design for human subject blood oxygen saturation estimation during increased g-loads

12 p1774 A72-28278

Acceleration stress effects on splanchnic blood flow due to organ displacement and neurogenic vasoconstriction in vascular beds

12 p1765 A72-28285

Tilt table test for gravitational stress effects on human pulmonary capillary blood flow

12 p1765 A72-28286

Human centrifuge studies of high positive acceleration effects on blood oxygenation and arterial oxygen and carbon dioxide tension

12 p1766 A72-28287

Pilot and back-seat man physiological responses during high-g aerial combat maneuvers in F-4E aircraft, discussing ECG, respiratory rate and minute volume

12 p1767 A72-28317

Pilot pursuit tracking performance under acceleration stress, simulating high performance aircraft dynamics via human centrifuge equipped with simulated head-up predictive gunsight

12 p1776 A72-28320

Human acceleration stress tolerance monitoring techniques for temporal, brachial and radial arterial blood flow and indirect systolic and diastolic blood pressure measurements

12 p1777 A72-28328

Thromboelastographic and coagulographic studies of gravitational effects on blood coagulation in cats under acceleration stress

13 p1904 A72-29309

Rat adrenal cortex morphology after 24 hour transverse acceleration stress, studying changes in lipid, ascorbic acid and RNA content and acid phosphatase activity

13 p1904 A72-29310

Dog thyroid gland structural changes under repeated radial acceleration, noting atrophic process and autonomous reactions roles

13 p1905 A72-29334

High gravity, cold and starvation space stress effects on oxidative metabolism of ethylmorphine, aniline and p-nitroanisole in male rat liver

15 p2185 A72-31700

Russian book - Intracranial blood circulation under conditions of accelerations and weightlessness

17 p2509 A72-35460

Synchronous and asynchronous BASH /body acceleration synchronous with heart beat/ effects on hemodynamics and ventilation in dogs and humans
18 p2648 A72-36033

Participation of cholinergic structures in the development of disturbances of the functional state of the cerebellum under the action of centripetal accelerations
19 p2757 A72-38033

Hematologic responses to hypobaric hyperoxia.
20 p2892 A72-39345

Vestibular labyrinth reactions and nystagmus thresholds in dogs during negative angular accelerations and simulated chronic galactic radiation from Co 60 gamma source
21 p2998 A72-40439

Study of hemodynamics during the action of decompression and accelerations
21 p3006 A72-40444

Hemodynamic reflexes during acceleration stresses, considering vessel walls, cardiac rhythm, blood distribution and sinus carotis receptors
22 p3141 A72-41983

Features of a speech signal during cumulative action of Coriolis accelerations
23 p3257 A72-44154

Relation between a pilot's sensory perception of linear accelerations and the aircraft motion.
24 p3377 A72-45654

Influence of vision on susceptibility to acute motion sickness studied under quantifiable stimulus-response conditions.
24 p3377 A72-45659

Human physiological responses to high magnitude short duration positive accelerations, considering peripheral vision loss as function of time
24 p3377 A72-45660

ACCELERATION TOLERANCE

Mice tolerance to long term accelerations or super-gravities, detailing physiological consequences
01 p0014 A72-10934

Navigators, pilots and airman trainees response to Coriolis accelerations, investigating nystagmus sensitivity coefficient relationship to motion sickness resistance
01 p0021 A72-11286

Aerospace vehicle acceleration effects on human performance, noting visual, motor and intellectual impairment levels relation to physiological tolerance limits
02 p0166 A72-11702

Sjoberg hypothesis for zero gravity produced inversion illusion mechanism in aircraft parabolic flight, noting otolithic membrane deflection result of force on maculae
02 p0167 A72-11710

Chin-sternum-heart syndrome from partial parachute failure, with close reference to atrial endocardial and myocardial lacerations
02 p0167 A72-11711

Leg cooling effect improving tolerance to positive headward acceleration in sitting position
04 p0479 A72-15210

Pathogenesis of in-flight illusory acceleration sensations, discussing amino acid level, protein metabolism rate and pyridoxin metabolism
05 p0619 A72-16642

Acceleration tolerance increase by static forearm muscular contraction exercise comparison to g-suit protection during human centrifuge tests
08 p1114 A72-20887

Positive acceleration effects on human cardiovascular system during centrifuge tests, studying ECG changes in terms of cardiac rhythm, heart rate and wave parameters
11 p1584 A72-26015

Centrifugation tolerance reduction after 14 days bed rest with moderate exercise, determining rehydration effects
12 p1766 A72-28295

Bed rest and positive radial acceleration effect on peripheral visual response time, considering blackout or grayout prediction possibilities
12 p1766 A72-28297

Valsalva and M-1 maneuvers acceleration tolerance protective effects during high-g centrifuging with and without anti-g suits
12 p1767 A72-28318

Acceleration protection properties of modified partial pressure suit, determining tolerance limits by vision impairment criteria during centrifuge tests
12 p1776 A72-28319

Miniature swine as human analog to investigate physiological response to high positive acceleration, comparing human and animal tolerances
12 p1768 A72-28329

Crash energy absorption for prevention of fatal injuries, considering human deceleration tolerance with respect to required energy absorber force-deflection relationship
15 p2192 A72-32630

Acceleration stress tolerance dependence on electron or ion transport across cell surface activation energy barrier, studying rat survival times
18 p2650 A72-36448

Human tolerance to high, sustained +Gz acceleration.
19 p2758 A72-38702

Problem of artificial gravitation in terms of experimental physiology
21 p3006 A72-40441

Acceleration tolerance of man after a lasting exposure to conditions of simulated weightlessness
21 p3006 A72-40442

Influence of high temperature on the onset of motion sickness
21 p3004 A72-41749

Influence of prolonged longitudinal accelerations on control habits
21 p3004 A72-41750

Hypothermia and resistance of mice to lethal exposures to high gravitational forces.
22 p3142 A72-42494

Relationship of sodium deprivation to +Gz acceleration tolerance.
24 p3377 A72-45653

ACCELEROMETERS

Passenger aircraft onboard automated inertial navigation devices, emphasizing accelerometer and gyroscope design and construction
01 p0096 A72-10070

Apollo 14 landing site gravity determination from accelerometer data
02 p0285 A72-12844

Upper atmospheric density measurements accuracy from triaxial accelerometer instrumented inflated falling sphere
04 p0519 A72-15156

Inertial navigation system accelerometer error autocompensation, using reversal by accelerometer forced rotation in stabilized platform plane
05 p0664 A72-17148

Microaccelerometer for satellite drag measurement and compensating thrust control
06 p0892 A72-18260

Gyro-pendulum accelerometers, calculating moving base oscillation effect on performance by random function representation through canonical expansions
06 p0819 A72-18723

Accelerometer sensitivity calibration by laser interferometer for vibration measurement, discussing frequency range, accuracy and advantage over spectral lamp
07 p0984 A72-19350

Time optimal self alignment of inertial platforms using gyros and accelerometers with Kalman-Bucy filter
07 p0989 A72-20279

Flight vehicle angular velocity measurement by accelerometers, deriving equations of motion
10 p1481 A72-24497

Vertical gravitational gradiometer capable of separating in space gravitational field elements and mechanical motion translational acceleration
11 p1635 A72-26463

Vibrating string accelerometer sea gravity meter with electronics for digital readout, discussing performance tests
11 p1635 A72-26499

Active notch filter circuits for extending accelerometers frequency response to near resonance, presenting error analysis of mismatching components
12 p1808 A72-27639

Neural atmospheric density profiles measurements in lower thermosphere by satellite-borne accelerometers, noting longitudinal variations at high latitudes
13 p1948 A72-28833

Ionospheric neutral density profile measurement by ultrasensitive triaxial electrostatic force rebalance accelerometer onboard Cannon Ball 2
15 p2227 A72-31962

Soft gyro and accelerometer failure detection for redundant gimbal inertial measurement units by skew sensors
15 p2270 A72-32187

Optimal algorithm for failure detection and identification in redundant gyro-accelerator sensor systems, including Monte Carlo simulation
15 p2270 A72-32188

Meridian direction determination with angular accelerometer, noting reduction in effects of component imperfections on accuracy
16 p2421 A72-33962

Improvements in the wide-band vertical quartz torsion accelerometer.
18 p2689 A72-36030

Three dimensional seismic monitoring system developed from inertial guidance gyroscopes and accelerometers, noting pole shift observation, tilting during earth tides and earthquakes forecasting
20 p2923 A72-39088

Linear and rotational quartz fiber accelerometers suitable for geophysical and inertial use.
20 p2923 A72-39103

High speed accelerometers to determine test platform tilt and translational motion displacements, discussing instrument configurations without gyroscopes
20 p2923 A72-39105

ACCOMMODATION

Acceleration measurement by reference mass displacement in spherical cavity, considering triaxial accelerometer with capacitive sensors and differential amplifier
22 p3175 A72-41929

Optimum damping for accelerometers.
22 p3175 A72-41930

Viscously damped miniature piezoresistive biaxial accelerometer for operation in single cavity to 250 F
22 p3179 A72-42701

Utilization of the CACTUS microaccelerometer as a detector of micrometeorite impacts
22 p3181 A72-43097

Electronically-damped pendulum acceleration measuring device with analog restoring mechanism. I
24 p3403 A72-45271

ACCEPTABILITY

Tolerance intervals in multiple type acceptance sampling plans with attribute-based inspection
11 p1749 A72-26790

Incentive contracts with price differential acceptance test plans to motivate producer to product improvement, defining admissible strategies in terms of risk limitation
13 p2066 A72-28354

Ultrasonic inspection effectiveness and equipment errors relationship to a priori acceptability of products
13 p1963 A72-28925

Acceptance testing of the MKL capacitor for space application
18 p2669 A72-37119

ACCEPTANCE

U ACCEPTABILITY

ACCEPTOR MATERIALS

Deep seated substitutional acceptor impurity levels in semiconductors
04 p0561 A72-15076

Acceptor level study of thermally diffused Be and Be-Li complexes in single crystal Si after quenching and annealing
13 p2022 A72-29628

Quasi-discrete acceptor states in zero gap n-type semiconductors, showing noncompensation at low temperatures
14 p2142 A72-30360

Theory of photon-induced hopping on acceptors in p-type germanium.
17 p2595 A72-34750

Thermally-stimulated current from the gold acceptor trapping level in silicon.
21 p3097 A72-40996

ACCESS TIME

Rescue operation capability for Skylab, discussing mission requirements, response time and vehicle configuration
24 p3449 A72-45132

ACCESSORIES

High strength Ti alloys for aircraft accessories structural materials, comparing room temperature physical properties of ultrahigh tensile steels and other alloys
03 p0373 A72-13617

Accessory reliability relation to on-time performance, discussing production route in terms of specification, design, development and manufacture
15 p2339 A72-32463

ACCIDENT INVESTIGATION

NT AIRCRAFT ACCIDENT INVESTIGATION

Oxygen hazards, mishaps and safety programs in NASA operations, considering material, design, cleaning and procedural deficiencies and failures
04 p0564 A72-14436

ACCIDENT PREVENTION

Cockpit information for pilot and flight crew as key to transport aircraft accident prevention, discussing cockpit layout and displays in terms of flight safety requirements
04 p0464 A72-14813

Pyrotechnic hazard classification for property and personnel protection in event of accidental explosion
08 p1220 A72-20768

Asbestos reinforced plastics safe handling and manipulation ensured by regulations provided precautions
11 p1583 A72-25549

Airport improvements needed for safety.
18 p2675 A72-36784

Toxicity of rocket fuels
24 p3433 A72-44781

ACCIDENTS

NT AIRCRAFT ACCIDENTS

ACCLIMATIZATION

NT ALTITUDE ACCLIMATIZATION

NT COLD ACCLIMATIZATION

Sweat depression during controlled hyperthermia in man - Effects on the sweat rate and sweat electrolytes
20 p2892 A72-39591

Heat acclimatization by exercise-induced elevation of body temperature.
22 p3151 A72-42741

ACCOMMODATION

NT VISUAL ACCOMMODATION

ACCOMMODATION COEFFICIENT

Trapping probability in gas-surface interactions from empirical accommodation coefficients, using simple model based on assumed attractive square well and impulsive-repulsive potential

05 p0624 A72-16394

Gas-solid surface interaction semicontinuous model, predicting accommodation coefficient as function of gas atoms initial energy on tungsten

07 p0970 A72-20081

Kinetic model for polyatomic gas heat transfer between parallel plates, considering boundary value problem with arbitrary accommodation coefficients

11 p1744 A72-25559

Burnett theory of thermal transpiration in capillary with wall accommodation for polyatomic gases, using Chapman-Enskog constitutive relations

11 p1746 A72-26010

Hot wire cell measurement of specific heat in low pressure gases, determining thermal conductivity and accommodation coefficient

11 p1634 A72-26367

Rarefied gas interaction with spacecraft surface, calculating aerodynamic forces and accommodation coefficient for Proton 2 satellite

14 p2162 A72-30474

Numerically computed momentum and energy accommodation coefficients and angular distributions of gas molecules reflected from solid crystalline surfaces applied to satellite drag calculation

16 p2430 A72-33065

ACCRETION

U DEPOSITION

ACCUMULATORS

NT DUST COLLECTORS

NT SOLAR COLLECTORS

NT SOLAR REFLECTORS

Accumulator type radar detector analysis by Markov chains method, discussing false alarm and detection probabilities

11 p1592 A72-25807

ACCURACY

Given motion realization in presence of constantly acting perturbations by pulsed correction, applying to signal transmission accuracy implementation

13 p2007 A72-30082

Operating conditions of photometers for optimum photomultiplier photon counting photometry, considering measurement precision dependence on experimental parameters

14 p2105 A72-30733

Doppler carrier frequency shift measurement accuracy, finding relationships in errors for coherent and incoherent pulse trains

15 p2195 A72-31657

Theoretical models for speed-accuracy tradeoff during difficult visual discrimination tasks under time pressure

18 p2655 A72-37220

ACETATES

NT TRIACETIN

ACETAZOLAMIDE

In vitro measurements of oxygen tension effect on teleost and amphibian retinal lactate dehydrogenase activity, discussing acetazolamide produced hypoxia effects

10 p1424 A72-23729

ACETONE

Dihydroxyacetone /DHA/ as nutrient in growing rats diet, showing unsuitability of regenerated DHA-containing formose mixtures for space crew diets

16 p2354 A72-33371

ACETYL COMPOUNDS

Cardiac membrane pain sensitivity in vagotomized cats under sensitizing acetylcholine influence during reduced cholinesterase activity

13 p1905 A72-29329

Aluminum oxide chromatography for ethanol-amine acetyl derivatives detection and separation in animal tissue extracts, using water-butanol solution as solvent

14 p2077 A72-30972

ACETYLACETONE

Electron paramagnetic resonance spectrum of vanadyl acetylacetonate dissolved in liquid crystal or isotropic solvent

21 p3013 A72-41177

ACETYLENE

Particle formation rates in thermal decomposition of acetylene in diffusion flame, noting activation energy

07 p1099 A72-19373

Alkyl substituent effects on gas phase acidities of toluene, p-xylene and acetylenes, using ion cyclotron resonance spectroscopy

07 p0936 A72-19494

Carburization kinetics of Nb in acetylene or methane at high temperatures and low pressure

09 p1319 A72-22985

Molecular process and pressure effects on hydrogen formation in methyl acetylene photolysis at 1236 Å

11 p1590 A72-26011

Carbon origin in comets associated with propyne photodissociation by solar 1216 Å Lyman alpha radiation

13 p2050 A72-29995

Measurement of the characteristic times of detonation-wave formation in a tube filled with an acetylene-air mixture

18 p2676 A72-35999

A modified acetylene method for the determination of cardiac output during muscular exercise.

20 p2898 A72-39807

ACHONDRITES

Pu-244 fission Xe isotopic composition parameters in achondrite meteorites, using lunar spallation systematics

01 p0124 A72-10058

Fission origin of cosmic ray fossil tracks in augite achondrite high-uranium-concentration meteorite Angra dos Reis

05 p0714 A72-16078

Johnstown achondrite meteorite composition, presenting published and unpublished data on minor and trace elements

05 p0722 A72-17154

Volatile and siderophile elements in achondrites and ocean ridge basalts from radiochemical neutron activation analysis

09 p1385 A72-22598

A re-examination of relationships among pyroxene-plagioclase achondrites.

20 p2900 A72-39840

Chondrite and achondrite Nb abundance from spark source mass spectroscopic analysis

21 p3104 A72-40492

ACID BASE EQUILIBRIUM

Acid base equilibrium effects on chlorophyll primary photosynthetic regulating mechanism, considering electron transfer to NADP and ATP formation

04 p0468 A72-14778

Acid-base balance shift during muscular exertion, determining pH and bicarbonate content variation by Astrup micromethod

06 p0765 A72-18062

Acid base balance in arterialized capillary blood in men after maximal short duration exercise

07 p0929 A72-19441

Aerobic work capacity indices of gas exchange pulse rate, pulmonary ventilation and acid base balance in runners, determining maximum oxygen utilization

09 p1268 A72-23596

Mathematical model of extracellular pH in brain tissue from blood and cerebrospinal fluid acid-base parameters for respiration central chemosensitive mechanism study

11 p1579 A72-26660

Extracellular acid-base changes in the dog myocardium during hypoxia and local ischemia, measured by means of glass micro-electrodes.

17 p2501 A72-34983

Interaction of chronic hypoxia and hypercapnia upon blood gases and acid base status.

17 p2504 A72-35166

Algorithms for selected blood acid-base and blood gas calculations.

17 p2510 A72-35973

Experimental studies on the alkali-acid equilibrium in the blood gases under the chronic action of low concentrations of lead.

24 p3374 A72-44824

ACIDITY

Gas phase basicities of aliphatic amines by ion cyclotron resonance spectroscopy

07 p0936 A72-19493

Alkyl substituent effects on gas phase acidities of toluene, p-xylene and acetylenes, using ion cyclotron resonance spectroscopy

07 p0936 A72-19494

ACIDS

NT AMINO ACIDS

NT ASCORBIC ACID

NT BUTYRIC ACID

NT CHROMIC ACID

NT DEOXYRIBONUCLEIC ACID

NT FATTY ACIDS

NT GLUTATHIONE

NT HYDROCHLORIC ACID

NT HYDROFLUORIC ACID

NT LACTIC ACID

NT LEUCINE

NT METHIONINE

NT NICOTINIC ACID

NT NITRIC ACID

NT NUCLEIC ACIDS

NT OLEIC ACID

NT OXIDASE

NT PEPTIDES

NT PERCHLORIC ACID

NT PHOSPHORIC ACID

NT PROTOPROTEINS

NT PYRUVATES

NT RIBONUCLEIC ACIDS

NT SULFURIC ACID

NT THYMIDINE

NT THYROXINE

NT TRYPTOPHAN

NT URIC ACID

Corrosion resistance of stainless steels in acid solutions, describing electrochemical cell for recording potential/current density and polarization curves

04 p0533 A72-15236

Burning rates dependence on pressure in mixtures of ammonium perchlorate with succinic, glutaric, adipic, azelaic, sebacic, fumaric and aminosuccinic acids

06 p0867 A72-18210

ACCLINAL VALLEYS

U VALLEYS

ACOUSTIC ATTENUATION

NT SHOCK WAVE ATTENUATION

Liquid-base foam sound absorbing properties for jet aircraft noise reduction

01 p0115 A72-10160

Sound propagation and absorption mechanism in liquid-base foams explored by bubble pulsation and coupling mathematical model and distributed parameter mechanical analog

01 p0115 A72-10161

Ultrasonic scatter effect on attenuation for macrostructure measurement, noting application to emulsions and metal grain boundaries

01 p0070 A72-11017

Noise reduction by acoustic interference, using sound generators operating in antiphase mode to noise input

02 p0262 A72-12897

Acoustic attenuation calculation for turbulent flow in rigid tubes, determining critical flow velocity dependence on wall roughness and sound wave frequency

03 p0340 A72-12954

Acoustic cavity resonators use for suppression of combustion instability modes, determining acoustic impedance and damping

03 p0457 A72-13954

Wall shear layers effect on sound attenuation spectra in acoustically lined rectangular ducts, noting dependence on Mach number

04 p0462 A72-14842

Sound attenuation in lined rectangular ducts with uniform steady flow, considering aircraft engine noise reduction

04 p0565 A72-15267

Longitudinal ultrasonic sound attenuation in superconducting Mo-Re alloys as function of temperature, magnetic field and frequency, using evaporated thin film CdS transducers

04 p0562 A72-15295

Sound velocity and attenuation variations with magnetic field from ultrasonic continuous wave spectrometry

07 p0984 A72-19321

Atmospheric acoustic attenuation measurement on sailplane, assessing turbulence backscattering cross section

07 p1031 A72-20597

Particle mass spatial distribution effect on particulate damping of combustion acoustic vibrations in solid rocket propellants

08 p1224 A72-21617

Sound field measurement in circular and rectangular air duct with sound-absorbing walls/mufflers/, deriving empirical formula for attenuation frequency characteristics

09 p1354 A72-23683

Sound transmission loss through double leaf walls, noting correction for LF calculations

11 p1687 A72-26038

Coupling between chemical kinetics and sound propagation, discussing conditions for amplification and attenuation of acoustic wave

13 p1912 A72-28547

Undesirable mechanical vibration control concepts for acoustic noise reduction, considering environment characteristics, attenuation degrees and passive and active control mechanisms

13 p2005 A72-29555

Building soundproofing codes for airport zoning ordinances, emphasizing wider latitude in land use options

13 p2067 A72-29561

Sound attenuation in lined air ducts, describing experimental determination of lining materials acoustical properties for central air heating systems

13 p2005 A72-29577

Tone burst pulse measurements of acoustic absorption coefficients in noisy environments for electronic simulation of wind tunnel noise

13 p2006 A72-29584

Ultrasound damping in Mg and Al alloys by structural grains and dislocation oscillations during work hardening, recrystallization and oversaturated solid solution decay

14 p2122 A72-30957

French book on industrial acoustics elements and metrology covering transmission, absorption, noise and complex sound measuring apparatus and preventive measures

15 p2275 A72-31524

Theoretical model for HF mechanical waves interaction with crystal lattices based on measurements

of high amplitude ultrasonic waves attenuation in metal crystals
15 p2292 A72-31835

Sound velocity and ultrasonic attenuation in anharmonic metal for collision dominated regime
15 p2277 A72-31889

Electron contribution to phonon damping in anharmonic metal for collision-free regime, evaluating relaxation times
15 p2277 A72-31890

Atmospheric sound absorption prediction based four-gases composition and energy transfer mechanisms, comparing results with experiments at different humidities
15 p2277 A72-32020

Microwave acoustic surface waves attenuation at solid and monatomic gas boundary, detailing frequency, molecular weight, pressure and temperature effects
15 p2278 A72-32505

Hypersonic sound attenuation and velocity dispersion in sulfur fluoride near critical point determined by light scattering measurement
16 p2422 A72-32946

Earplugs effectiveness for narrow band white noise real-ear attenuation and wearability
16 p2358 A72-33325

Acoustic attenuation and thrust loss incurred by shrouded multistage supersonic jet noise suppressor [AIAA PAPER 72-642]
16 p2381 A72-34090

Sound reduction by barriers on the ground.
17 p2580 A72-34235

Sound attenuation in acoustically lined circular ducts in the presence of uniform flow and shear flow.
17 p2582 A72-35411

Acoustic refraction and attenuation in cylindrical and annular ducts.
17 p2582 A72-35414

The utility of the Galerkin method for the acoustic transmission in an attenuating duct.
21 p3083 A72-40332

Optimization of acoustic linings in presence of wall shear layers.
21 p3083 A72-40334

A model of low-frequency sound propagation in a lined duct.
21 p3085 A72-41112

Ultrasonic evidence against multiple energy gaps in superconducting niobium.
22 p3190 A72-42476

Sound absorption in atmosphere at 20 C, predicting relaxation times and strengths in 100 Hz to 1 MHz as functions of relative humidity
23 p3285 A72-44112

Ultrasonic diffraction loss and phase change for broad-band pulses.
23 p3113 A72-44115

Ultrasonic attenuation and velocity in hot specimens by the momentary contact method with pressure coupling, and some results on steel to 1200 C.
23 p3294 A72-44116

ACOUSTIC COMBUSTION

U COMBUSTION STABILITY

ACOUSTIC DELAY LINES

Pulse compression of radar signals by ultrasonic liquid delay line, stressing wideband damped electroacoustic transducers construction
01 p0044 A72-11321

Wideband microwave acoustic delay line design featuring superior bandwidth, phase linearity, spurious echo and insertion loss characteristics
04 p0521 A72-14720

Optoacoustic processing of large time-bandwidth signals, calculating insertion loss vs delay time
12 p1810 A72-27935

Room temperature operation of microwave acoustic delay lines with magnesium aluminate spinel, discussing acoustic mode conversion and shear wave piezoelectric transducers
19 p2800 A72-37875

Variable-bandwidth frequency-modulation chirp pulse compression using a longitudinal acoustic-wave convolver at 1.3 GHz.
21 p3023 A72-41468

Magnesium alloys containing rare-earth metals as materials with special physical properties
22 p3192 A72-42817

ACOUSTIC DUCTS

Wall shear layers effect on sound attenuation spectra in acoustically lined rectangular ducts, noting dependence on Mach number
04 p0462 A72-14842

Sound propagation in acoustic ducts with shear flow and wall lining by Ritz-Galerkin technique
04 p0511 A72-14848

Aerodynamic noise interference generated by fluid flow in acoustically lined ducts
04 p0462 A72-15268

Acoustic mode propagation and interaction in hard walled cylindrical ducts, determining pressure and power spectral densities from pressure cross spectrum measurements
15 p2277 A72-32018

The utility of the Galerkin method for the acoustic transmission in an attenuating duct.
21 p3083 A72-40332

A model of low-frequency sound propagation in a lined duct.
21 p3085 A72-41112

The propagation of sound in a circular duct of continuously varying cross-sectional area.
22 p3207 A72-42911

Measurement, in a duct, of the space-structure of the discrete-frequency noise generated by an axial compressor.
22 p3216 A72-42913

ACOUSTIC EXCITATION

Motional feedback systems comparison for ultrasonic transducers operated as resonant emitters, describing circuitry for self excitation
01 p0070 A72-11019

Acoustical oscillations effect on free jet flow stability and boundary layer structure, using inviscid Orr-Sommerfeld equation for flow disturbances frequency, wavelength and velocity
03 p0340 A72-12913

Acoustic wave excitation in water droplet with giant pulse radiation from Q switched laser, noting diffraction effects on laser power density requirement
03 p0367 A72-13372

Endurance tests of D16AMO alloy sheets under high intensity acoustic, harmonic and electrodynamic vibrator loading
03 p0371 A72-13470

Transverse acoustoelectric surface wave domain in piezo-semiconducting body, obtaining gain coefficient and generation threshold criterion
05 p0702 A72-16283

Sound propagation within and radiated from annular duct flow, measuring acoustic distributions for single and multimode excitations
05 p0691 A72-16924

Acoustic emission systems application to materials nondestructive testing, discussing single and multiple piezoelectric transducer arrays with on-line computer analysis [SAE PAPER 720175]
06 p0819 A72-17323

Ion-acoustic collisionless shock generation by initial plasma density discontinuity in Q machine, correlating experimental results with numerical simulation
06 p0856 A72-17520

German monograph on vibration amplitudes interferometric measurement, discussing methods for resolution improvement and phase measurements, distortion and sonic field effects, etc
07 p0983 A72-19264

Periodically supported beams acoustically induced vibration response based on equivalent structural wavelength definition
07 p1089 A72-19330

Nonlinear modal response analysis of plate structures under random acoustic excitation, using finite element method and perturbation technique
08 p1245 A72-21607

Acoustically generated vibration stresses in rigidly clamped Al alloy circular plate, noting stress amplitude distribution dependence on loading frequency bandwidth
11 p1738 A72-26805

Silicone based elastomers acoustic excitation damping properties at 213-423 K, discussing testing technique and results at 200-1000 Hz
13 p1957 A72-29090

Ultrasonic wave excitation in potassium seeded flame, showing amplitude proportional to harmonic perturbation frequency imposed on plasma
14 p2170 A72-30417

Scattering of Langmuir waves produced by a beam with finite transverse dimensions.
19 p2839 A72-37337

Aircraft structures fatigue life expectancy under random acoustic excitation, describing testing methods and equipment
24 p3367 A72-44739

Endurance tests of D16AMO alloy sheets under high intensity acoustic, harmonic and electrodynamic vibrator loading
24 p3414 A72-44945

ACOUSTIC FATIGUE

Sound pressure levels and acoustic fatigue tests for 11,200 and 9,300 pound thrust J-52 engines comparison in A-6A aircraft
07 p0910 A72-18757

Acoustic loads effect on carrying capacity and vibration stability of longitudinally stiffened cylindrical metal panels, investigating fatigue strength and stress-strain state
07 p1091 A72-19760

Setup to determine sonic creep and acoustic fatigue in polymers under symmetrical and asymmetrical load cycles at sonic and ultrasonic oscillation frequencies
08 p1147 A72-21763

ACOUSTIC GENERATORS

U SOUND GENERATORS

ACOUSTIC IMPEDANCE

Acoustic impedance of body surface at thorax and at abdomen, showing dependence on frequency and body pressure and position
01 p0021 A72-11195

Acoustic cavity resonators use for suppression of combustion instability modes, determining acoustic impedance and damping
03 p0457 A72-13954

Analytical model for acoustic impedance of perforated plate liner with multiple frequency excitation, discussing effects of fluid motion, grazing flow and spectral excitation
04 p0548 A72-14699

Sound pressure in liquid layer bounded by oscillating plate under bending as function of boundary acoustic impedance
07 p1034 A72-18923

Interdigital acoustic surface wave transducer impedance characteristics calculation from equivalent circuit, demonstrating effectiveness on delay lines [AD-743552]
09 p1316 A72-23421

Sound radiation impedance of vibrating prolate spheroids as function of nearfield variation
11 p1688 A72-26064

Electromechanical coupling and acoustic impedance response in piezoelectric transducer with diffusion under fixed charge
11 p1636 A72-26590

Combustion surface acoustic admittance model of blended solid propellant with allowance for foam zone inertia and solid/gas interface reactions
12 p1889 A72-27980

Acoustic admittance measurement for burning surface of nitroglycerin gunpowders, using combustion product velocity and wave pressure ratio
16 p2391 A72-33257

IAD-3 amplitude-phase impedance defecoscope.
19 p2805 A72-38765

Scattering of acoustical waves by a prolate spheroidal obstacle.
23 p3313 A72-44118

ACOUSTIC INSTABILITY

Acoustic instability of plasma with current under equilibrium ionization and moderate neutral gas pressures
01 p0109 A72-10485

Unstable sound waves in uranium plasma, taking into account fission power density, radiation diffusion and ionization variations
01 p0112 A72-11336

Cross-field current driven ion acoustic instability in two plasma devices, causing neutral sheet phenomena, anomalous dispersion and ion heating [AD-740261]
06 p0858 A72-17541

Longitudinal ambipolar acoustic instability effect on duration of plasma particle motion to wall across magnetic field, using phase method
06 p0860 A72-17693

Collisionless thermalization of ion beam by interaction with plasma, noting acoustic instability growth
10 p1524 A72-24921

Nature of sound dispersion in a plasma
18 p2717 A72-37178

Nonlinear saturation of the ion-acoustic instability.
19 p2840 A72-37931

Nonlinear ion sound in a fully ionized current-carrying plasma
21 p3090 A72-40411

Ion acoustic instability in collisionless shocks.
23 p3320 A72-43522

ACOUSTIC MEASUREMENTS

Lf subaudible chest wall vibration recordings, discussing external, epicardial surface and intraventricular pressure precordial displacement tracings
01 p0017 A72-10120

Portable detector-recorder for automobile, blast furnace, railroad car, engine room and helicopter infrasonic noise measurements, discussing peak frequencies and subjective effects
01 p0101 A72-10157

Acoustic emission tests of nuclear pressure vessels and piping, detecting weld slag, porosity, fatigue microcracking and stress corrosion cracking
01 p0048 A72-10802

Acoustic emission characteristics from nuclear reactor irradiated steels during tensile and wedge opening load tests
01 p0068 A72-10803

Acoustic emission evaluation of damage of filament wound composite materials under tensile loading applied to spherical test shapes
01 p0069 A72-10804

Acoustic echo sounder as real time monitor of airport environmental meteorological parameters
01 p0103 A72-11137

Acoustic emission monitoring of boron epoxy composite, showing crack extension characterization by emission bursts
02 p0249 A72-11993

Aircraft engine noise effects in airport vicinities, discussing measurement scales, turbofan sources, noise reduction and future air traffic
02 p0154 A72-12022

Papers on noise and vibration control covering acoustics in free space, outdoors, small enclosures and rooms, measurement, analysis and design problems

02 p0258 A72-12100

Acoustic absorption materials weak shock wave reflection and attenuation determination by shadow-graph-schlieren photography and pressure transducers

02 p0259 A72-12177

Mechanical breakdown prediction of loaded fiberglass reinforced plastic by seismoacoustic technique, investigating load effects on seismoacoustic emission

02 p0250 A72-12679

Acoustic emission techniques in defect structure materials tests, discussing fracture strength, crack propagation, fatigue, plastic deformation and creep in metals, composites and rocks

03 p0362 A72-13225

French jet aircraft noise reduction research facilities, discussing in-flight and overfly noise measurements, various silencer configurations and Concorde engine tests

03 p0406 A72-13680

Tube wall temperature and acoustic noise spectra dependence on thermal flux density in bubble coalescence

03 p0458 A72-14162

Impulse noise reproduction for temporary threshold shift and impulse noise measurements, considering rise time, frequency response and limitations of tape recorders

04 p0521 A72-14847

Metrology and technology for sounds intense enough for physiological distress and mechanical structure damage, discussing accompanying high temperature and vibration

[ONERA, TP NO. 1009]

05 p0661 A72-16024

Intense noise measurement device for heat flow environments, discussing applications to jet engines, nozzle exits, turbine exhausts and volcanic craters

[ONERA, TP NO. 1010]

05 p0661 A72-16025

Combined radar-acoustic system for lower atmosphere temperature sounding, considering use in air pollution studies and short range weather forecasting

[AD-739790]

05 p0663 A72-16690

Jet engine silencing plug nozzle suppressor configurations acoustic and thrust performance measurements

[AIAA PAPER 72-160]

05 p0706 A72-16826

Aerodynamic noise measurement, discussing physical units, spectral analysis, conversion and correction formulas

05 p0614 A72-17195

JT8D engine exhaust noise field, considering internal noise sources contribution from exhaust duct sound pressure measurements

07 p1054 A72-19331

California airport noise standards instrumentation, discussing battery operated measurement of hourly and community noise equivalent levels

07 p0985 A72-19490

Jet noise intensity reduction by screen around nozzle exit, using acoustic and hot wire measurements

07 p0968 A72-19873

Noise level measurement scales, units datum points and mathematical formulas, suggesting method of quasi-peak level above masked threshold

07 p1035 A72-20164

Loudness scaling methods for transportation noises, discussing matching procedures, reference sources, etc

07 p0931 A72-20165

Standard procedures development for perceived noisiness or noise annoyance evaluation, taking into account spectral complexity, spectra weighting, time integration and onset duration

07 p0932 A72-20166

Noise rating methods for speech communication effectiveness evaluation, presenting charts and tables for intelligibility limits with various communication techniques and equipment

07 p0932 A72-20167

Small samples acoustic transmission loss measurement with constant energy flow in small duct

08 p1206 A72-21296

Mean sound pressure level measurements with mobile microphone carriers, noting difference from mean energy density measurement

08 p1165 A72-21297

Cross correlation analysis of turbulent jet flow noise with pressure fluctuation as acoustic source

[ASA PAPER H 12]

08 p1150 A72-21488

Structural Acoustic Monitor system for airframe structural proof testing, providing multichannel recording and aural monitoring of acoustic data derived from aircraft mounted accelerometers

10 p1459 A72-24146

Optimal distribution of resources in automatic systems for detection and measurement of random concentrated noises number in assigned frequency range

10 p1440 A72-24917

Acoustic measurement of solid-liquid interface motion and solidification during freezing of Hg and paraffins

10 p1563 A72-25044

Acoustic emission monitoring of postweld heat treatment cracking in Rene 41 weldments, correlating relative crack susceptibility of different microstructures

11 p1653 A72-25345

Acoustic emission analysis of deformation and fracture modes under straining of fiber glass-epoxy composite structures, including NOL rings and vessels

11 p1671 A72-25469

Subsonic jet noise directivity prediction from acoustic pressure measurements

11 p1706 A72-26041

IF amplifier automatic gain control /AGC/ for ultrasonic pulse echo measurements

11 p1633 A72-26055

Radiation resistance of baffled beam modes from far field acoustic power intensity

11 p1687 A72-26058

Atmospheric infrasound measurement techniques and instrumentation for long distance propagation, considering wind and temperature effects

11 p1635 A72-26509

Atmospheric pressure noise reducer for active microbarograph array, evaluating performance in field tests

11 p1613 A72-26510

Atmospheric turbulent coherent noise in pipe arrays design for infrasonic wave detection

11 p1689 A72-26511

Acoustic ray tracing of long range infrasonic signals from launch and reentry of Saturn 5 rockets

11 p1690 A72-26512

Infrasonic observations of acoustic auroras, using microbarographs and resonant detector recordings

11 p1627 A72-26517

Rolled polycrystalline metal samples principal anisotropy direction determination by acoustic measurements at ultrasonic frequencies

12 p1806 A72-27086

Measurement of spatially coherent and incoherent structure of axial compressor-generated noise modes propagating in duct

[ONERA, TP NO. 1045]

12 p1861 A72-28049

Composite materials evaluation methods, discussing high quality photographs, radiography, laser holographic interferometry, thermographic fluorescent phosphors, liquid crystals and acoustic techniques

12 p1815 A72-28101

Low flight altitude atmospheric parameters spatial and temporal variability effects on aircraft flyover noise measurement

13 p1991 A72-28841

Space-averaged sound pressure measurement by sequentially sampled microphone arrays, considering scanning rate and rms detector time constants effect

13 p1958 A72-29565

Acoustic measurements for STOL turboprop transport aircraft propeller configurations under static, taxi and flyover conditions, discussing quiet propeller noise signature

13 p1897 A72-29571

Fan engine compressor noise measurement by spinning mode synthesizer for use in duct liner optimization

13 p2028 A72-29574

Acoustic environmental prediction model for near, mid and far field rocket engine noise

13 p2028 A72-29582

Tone burst pulse measurements of acoustic absorption coefficients in noisy environments for electronic simulation of wind tunnel noise

13 p2006 A72-29584

Bibliography on noise control covering surface transportation, machinery and aircraft noise, industrial criteria, biodynamics, legislation and measurement

13 p2006 A72-29588

Sound transmission loss and diffraction measurements by combined correlation and Fourier techniques

13 p2006 A72-29768

Analytical models for potential flow through smooth edged orifice, comparing acoustical inittance predicted and experimental values

13 p2006 A72-29770

Tu-104 turboprop aircraft flight noise measurements and spectral changes at different distances from landing strip, evaluating public nuisance and resident reactions

14 p2072 A72-30446

Correlation measurements of LF current noise and frequency fluctuations in Gunn oscillators, emphasizing generation-recombination noise component

14 p2088 A72-30916

French book on industrial acoustics elements and metrology covering transmission, absorption, noise and complex sound measuring apparatus and preventive measures

15 p2275 A72-31524

Noise measurements during shock free and underexpanded operation modes of supersonic cold model jet at moderate exit Mach number

15 p2179 A72-32017

Acoustic mode propagation and interaction in hard walled cylindrical ducts, determining pressure and power spectral densities from pressure cross spectrum measurements

15 p2277 A72-32018

Message circuit noise evaluation in commercial telephone system, discussing noise measurements and weighting curves

15 p2202 A72-32575

Airport vicinity aircraft noise exposure contour calculated from measured data at Osaka Airport

16 p2372 A72-32885

Noise pollution measurements parameter selection based on human reactions and attitudes, discussing psychoacoustic experiments, ratings and acoustic instruments

16 p2390 A72-33165

Lateral inhibition in auditory perception proved by psychophysical study of nervous activity stimuli patterns, noting erroneous measurement of pure tone masked threshold

16 p2357 A72-33970

Turbulence induced sound pressure level measurement for noise generated by grill in air flow, using streamlined probe microphone

16 p2344 A72-34001

Direct correlation measurement of turbulent jet noise and flow by cross correlating narrow filtered input turbulence and output acoustic signals

[AIAA PAPER 72-640]

16 p2381 A72-34092

Externally blown flap impingement noise

[AIAA PAPER 72-664]

17 p2487 A72-35961

Acoustic emission technique as NDT method for quality control of brazed metal-ceramic bonding

18 p2695 A72-36458

Observations of Helmholtz waves in the lower atmosphere with an acoustic sounder

18 p2687 A72-36635

A device for recording acoustic signals of crack formation in brittle materials

19 p2802 A72-38018

Flyover noise testing of commercial jet airplanes.

[AIAA PAPER 72-786]

19 p2749 A72-38103

Noise generated by STOL core-jet thrust reversers.

[AIAA PAPER 72-791]

19 p2849 A72-38108

A time-frequency localization system applied to acoustic certification of aircraft.

[AIAA PAPER 72-836]

20 p2950 A72-39091

The broad range detection of incipient failure using the acoustic emission phenomena.

20 p2925 A72-39286

A new approach to the measurement of very low acoustic noise levels.

20 p2953 A72-39554

Tu-104 turboprop aircraft flight noise measurements and spectral changes at different distances from landing strip, evaluating annoyance factors and resident reactions

21 p3009 A72-41110

Book - Vibration and acoustic measurement handbook.

21 p3086 A72-41533

Design and development of the United Aircraft Research Laboratories acoustic research tunnel.

[AIAA PAPER 72-1005]

21 p3041 A72-41589

Correlator with orthogonal filters for acoustic diagnostics, noting Laguerre functions variations in signal pairs autocorrelation

22 p3176 A72-42133

Low flying aircraft wake vortices tracking, describing sensing techniques based on acoustic pulse deflection and velocity field measurements

22 p3179 A72-42709

Measurement, in a duct, of the space-structure of the discrete-frequency noise generated by an axial compressor.

22 p3216 A72-42913

Aeroacoustic, vibration and shock environments for the space shuttle orbiter.

24 p3448 A72-44679

Saturn systems holddown acoustic efficiency and normalized acoustic power spectrum.

24 p3433 A72-44681

Tone noise from rotor/stator interactions in high speed fans.

24 p3433 A72-44917

ACOUSTIC PROPAGATION

Schlieren photography for visualizing ultrasonic pulse propagation and reflection in solids and liquids, applying to crack detection in steel tubes

01 p0071 A72-11022

Acoustic pulse generation and transmission loss characteristics measurement by single pulse method with simple shape to facilitate Fourier analysis

03 p0388 A72-12955

Pressure field calculations for random vibrations in wide class of elastic shells containing acoustic medium, discussing turbulent boundary layer-caused pulsations

04 p0586 A72-15010

Non-Maxwellian plasma response to acoustic wave propagation in single ended Q device, investigating ion distribution function

06 p0855 A72-17509

Light intensity distribution from ultrasonic surface waves reflection to probe surface acoustic propagation characteristics [AD-739047] 06 p0848 A72-17851

Acoustic waves refraction, reflection and transmission from moving medium layer with space-dependent velocity, considering Poiseuille flow three sublayer approximation 06 p0848 A72-17852

Log-periodic interdigital transducer design to obtain wide bandwidth for acoustic surface waves 06 p0784 A72-18241

Nonlinear acoustic propagation in chemically reacting media, discussing quasi-frozen and quasi-equilibrium flow processes behind shock fronts 07 p0969 A72-19974

Sound wave propagation in plasma, attributing acoustic cavity resonance curve sharpening to collisional energy transfer from electrons to neutrals 08 p1213 A72-21256

Small samples acoustic transmission loss measurement with constant energy flow in small duct 08 p1206 A72-21296

Atmospheric stratification irregularities effects on sonic boom propagation, obtaining probability density functions 08 p1111 A72-21905

Acoustic approximation of pressure step discontinuity sound propagation in attenuating and dispersive ionosphere 08 p1162 A72-22139

Vibrating membrane generated acoustic pressure wave propagation in rarefied gas, applying to solid surface-gas interaction models 09 p1294 A72-22762

Strong magnetic fields and electric current densities effects on acoustic oscillations and instability in stationary inhomogeneous low temperature plasma flow in crossed fields 10 p1517 A72-23838

Delayed pulse echo and through-transmission ultrasonic techniques for nondestructive inspection and quality control of braze bonds in high current electric contact assemblies 10 p1487 A72-24173

Acoustic and elastic HF waves propagation in nonuniform cylindrical waveguides, deriving asymptotic approximate solutions 11 p1686 A72-25726

Bibliography on infrasonic sound wave generation, propagation and detection at ground level and ionospheric heights 11 p1690 A72-26520

Boundary reflection and transmission of N-shaped acoustic shock wave radiated from circular pipe into free air space 12 p1844 A72-27262

Maximum overpressures of supersonic aircraft maneuvering-produced sonic booms occurring at geometrical acoustic ray focus points/caustic cusps/ 13 p1898 A72-29586

Optical acoustic field recordings application to turbulent characteristics measurement for transparent media of fluid flows 15 p2232 A72-31267

French book on industrial acoustics elements and metrology covering transmission, absorption, noise and complex sound measuring apparatus and preventive measures 15 p2275 A72-31524

Nondispersive guidance structure for acoustic surface waves due to velocity reduction of thin conducting strip on piezoelectric substrate 15 p2278 A72-32506

Equations of motion for small vibrations superposed on time depending deformation of elastic body, discussing acoustic wave propagation 16 p2425 A72-33590

High-frequency ultrasonic devices. 17 p2526 A72-34564

The estimation of nonstationary spectra from moving acoustic source distributions. [AIAA PAPER 72-667] 17 p2583 A72-35486

Multipole expansion of sound radiation from moving rigid bodies. 18 p2710 A72-36404

Transient acoustic point source disturbance transmission in two dimensional idealized jet, noting velocity profile effects on noise radiated to far field 18 p2679 A72-36406

WKB approximation to suggest vertical phase velocity measurement at turning points of acoustic-gravity wave propagation in thermosphere 18 p2686 A72-36411

Spheroids with surface vibration at specified normal velocity distributions, calculating acoustic radiation by Green function approach 18 p2710 A72-36412

Ray geometry, travel time and spreading loss derivation for refracted/bottom-reflected ray propagation in channel with horizontal and vertical sound speed gradients 18 p2710 A72-36413

Acoustic ray deflection by aircraft wake vortices with viscous core, observing maximum deflection angles during large aircraft landing 18 p2641 A72-36417

Linear acoustic model to predict axial flow turbomachinery aerodynamic sound generation including flow effects on radiation 19 p2788 A72-38568

Propagation of internal acoustic-gravity waves around a spherical earth. 19 p2793 A72-38748

Observation and analysis of simulated ultrasonic acoustic emission waves in plates and complex structures. 20 p2925 A72-39284

Nonlinear acoustic propagation in chemically reacting media, discussing quasi-frozen and quasi-equilibrium flow processes behind shock fronts 20 p2955 A72-40031

Response of the average pressure acting on the surface of an emitting circular transducer due to different reflecting objects. 21 p3055 A72-40948

Closed form solution for the sonic boom in a polytropic atmosphere. 21 p2992 A72-41258

Measurement, in a duct, of the space-structure of the discrete-frequency noise generated by an axial compressor. 22 p3216 A72-42913

Forward scattering of laser coherent light by acoustic or turbulent wave pressure variations, noting phase fluctuation spectrum 23 p3313 A72-44113

Acceleration waves in orthotropic elastic materials. 23 p3354 A72-44342

Book - The effects of the turbulent atmosphere on wave propagation. 24 p3379 A72-44650

Acoustical holography with a scanned linear array. 24 p3401 A72-44705

ACOUSTIC PROPERTIES

NT ACOUSTIC IMPEDANCE

NT ACOUSTIC INSTABILITY

NT ACOUSTIC SCATTERING

NT ACOUSTIC VELOCITY

NT SOUND INTENSITY

Air flow and acoustic characteristics of speech sounds produced with turbulence noise at glottal constriction, using flow equations [AD-744389] 01 p0101 A72-10162

Acoustic absorption materials weak shock wave reflection and attenuation determination by shadow-graph-schlieren photography and pressure transducers 02 p0259 A72-12177

Jet flap type exhaust flows acoustic and fluid dynamic characteristics, measuring sound power output and noise spectra for various configurations [AIAA PAPER 72-130] 05 p0608 A72-16920

Environment acoustic resonant frequencies effect on flat steel plate vibration under direct and air flow vortex shedding excitations 06 p0894 A72-17768

Sound attenuation in lined air ducts, describing experimental determination of lining materials acoustical properties for central air heating systems 13 p2005 A72-29577

Acoustic tunnel effect in elastic waveguide, noting penetration coefficient and quantum mechanics potential barrier 16 p2364 A72-33588

Piezosemiconductor crystals acoustoelectric surface domain waveguide effect for classical and transverse surface waves 16 p2441 A72-33596

Jet noise reduction by screen placed across jet flow, investigating acoustic properties, velocity and pressure in mixing zone [AIAA PAPER 72-644] 16 p2381 A72-34088

Acoustic emission experiments design based on piezoelectric transducer, discussing signal detection and data acquisition methods 20 p2924 A72-39278

Factors affecting acoustic emission response from materials. 20 p2924 A72-39279

Acoustic efficiency of supersonic annular jets 21 p3045 A72-41098

Russian book - Dynamics and acoustics of machines. 22 p3182 A72-42126

Features of a speech signal during cumulative action of Coriolis accelerations 23 p3257 A72-44154

ACOUSTIC RADIATION

U SOUND WAVES

ACOUSTIC SCATTERING

Ultrasonic scatter effect on attenuation for macrostructure measurement, noting application to emulsions and metal grain boundaries 01 p0070 A72-11017

Closed form solution of wave equation for sound wave scattering by rotating cylinders and spheres 04 p0550 A72-15567

Wind profile measurements to 200 meters by acoustic echo sounder and Doppler shift, describing signal emission and data reduction 10 p1508 A72-25084

Fog, cloud, rain and snow detection by acoustic echo sounding, noting effects of energy scattered from atmospheric boundary layer velocity and temperature fluctuations 15 p2267 A72-32725

Acoustic radiation from multiple spheres. 17 p2579 A72-34226

Acoustic edge scattering of elastic surface waves. 17 p2579 A72-34227

Separation and analysis of the acoustic field scattered by a rigid sphere. 18 p2710 A72-36408

The acoustics of axial flow machines. 18 p2685 A72-37204

An integro-differential equation approach to acoustic scattering from fluid-immersed elastic bodies. 21 p3083 A72-40102

Multiple scattering of bending waves by random inhomogeneities. 22 p3235 A72-42460

Scattering of acoustical waves by a prolate spheroidal obstacle. 23 p3313 A72-44118

ACOUSTIC SIMULATION

Sonic boom simulation devices and techniques, including wind tunnels, ballistic ranges, spark discharges and shock tubes 08 p1147 A72-21906

Field and laboratory sonic boom simulators, noting required characteristics 09 p1292 A72-23323

Tone burst pulse measurements of acoustic absorption coefficients in noisy environments for electronic simulation of wind tunnel noise 13 p2006 A72-29584

Acoustically scaled simulation of sonic boom N-wave energy penetration into ocean for flat air-water interface 13 p1951 A72-29587

Canadian sonic boom simulation facilities. [ICAS PAPER 72-26] 21 p3040 A72-41151

ACOUSTIC STABILITY

U FREQUENCY STABILITY

ACOUSTIC VELOCITY

Sound wave propagation velocity in partially dissociated and ionized gas, discussing attenuation coefficient, chemical process relaxation time and high temperature oxygen and nitrogen calculations 01 p0051 A72-11212

Liquid n-octane, n-decane and n-undecane densities and adiabatic/isothermal compressibilities from sound velocity measurements at high pressures and 30-140 C 02 p0261 A72-12829

Sound velocity and attenuation variations with magnetic field from ultrasonic continuous wave spectrometry 07 p0984 A72-19321

Shock wave patterns near sonic line in accelerating or decelerating nonhomotropic flows, extending Busemann homentropic flow description 10 p1419 A72-24841

Acoustic wave diffraction at fixed plate boundary, determining velocity field by inverting Volterra-type integral equations 14 p2070 A72-31016

Sound velocity and ultrasonic attenuation in anharmonic metal for collision dominated regime 15 p2277 A72-31889

Hypersonic sound attenuation and velocity dispersion in sulfur fluoride near critical point determined by light scattering measurement 16 p2422 A72-32946

Measurements of ultrasonic velocities using a digital averaging technique. 18 p2691 A72-36401

Ray geometry, travel time and spreading loss derivation for refracted/bottom-reflected ray propagation in channel with horizontal and vertical sound speed gradients 18 p2710 A72-36413

Ultrasonic velocity measurement by small power He-Ne laser visualization of standing waves in Fresnel diffraction region 18 p2697 A72-36416

Intrinsically transonic /almost equal frozen and equilibrium sound velocities/ flows of chemically active gas mixture, developing nonlinear perturbation theory 19 p2745 A72-37390

Pressure propagation rate relation to local sound speed in unsteady anisentropic gas flow with particle-varying specific entropy 19 p2788 A72-38564

Position of the transition point through the sonic velocity behind the detonation front 21 p3045 A72-40987

Streamline and fieldline geometry with applications to MHD flow kinematic properties, discussing field and momentum relations decomposition in terms of sound velocity 23 p3322 A72-44270

ACOUSTIC VIBRATIONS

U SOUND WAVES

ACOUSTICS

NT HARMONIC GENERATIONS

NT MAGNETOACOUSTICS

NT MICROSONICS

NT PSYCHOACOUSTICS

NT UNDERWATER ACOUSTICS

Acoustical theory application to jet engine noise reduction, developing mathematical model for blade shock wave spacing in noise generation process

07 p1055 A72-20542

Infrasonic research - Conference, Pullman, Washington and Moscow, Idaho, November 1970

11 p1627 A72-26508

Signal mathematical model in optical and acoustic pattern recognition

12 p1786 A72-27571

Book on basic acoustics covering mathematical methods, diffraction phenomena, statistical theory of signal processing, wave acoustics, membrane sound radiation, music, source array theory, etc

16 p2427 A72-33973

A method of calculating acoustic resonance phenomena generated by the unsteadiness of singular pressure losses in the pipes

17 p2580 A72-34279

Acoustical holography imaging methods and applications, reviewing liquid levitation, sampling holography, dynamic surface deformation and scanned pulse-echo holography

19 p2797 A72-37604

Pulsed operation mode of acoustic system of damper-piezovibrator-layer load connected into electrical circuit of thyatron generator

19 p2805 A72-38764

Acoustic emission testing and microcracking processes

20 p2924 A72-39277

Dislocation motion as a source of acoustic emission

20 p2924 A72-39280

Correlation analysis techniques to characterize acoustic emission pulses from Mg alloys, obtaining time varying spectra

20 p2924 A72-39281

Acoustic emissions and energy transfer during crack propagation

20 p2981 A72-39957

The use of simple three-dimensional acoustic finite elements for determining the natural modes and frequencies of complex shaped enclosures

22 p3206 A72-42464

ACOUSTO-OPTICS

Acousto-optical extraction of energy stored in pulsed He-Ne laser cavity, using modulator with piezoelectric transducer at light-ultrasound interaction region

01 p0081 A72-11322

Acoustic /ultrasonic/ holography techniques for acoustic field recording and image reconstruction in coherent light, including applications

07 p0981 A72-18920

Mode conversion effects on Gaussian laser beam in acousto-optical modulation for optical communications

07 p1004 A72-19225

Far field diffraction of Gaussian light beam passing through ultrasonic cylindrical standing waves

11 p1687 A72-26052

Long wave radio and acoustic holograms recording by complex scanning for transmission over communication channels

11 p1636 A72-26714

Real time depth gated acoustic image holography, using scanning laser beam pulse echo technique

12 p1809 A72-27840

Optoacoustic processing of large time-bandwidth signals, calculating insertion loss vs delay time

12 p1810 A72-27935

Optimal parameters of electro-optical signal processor for phased array antennas, noting optical subsystem correspondence to optoacoustical spectrum analyzer

13 p1926 A72-28374

Acoustic /ultrasonic/ holography techniques for acoustic field recording and image reconstruction in coherent light, including applications

13 p1957 A72-29206

Acoustic holography Doppler effects due to sound source or receiver motion during recording process

13 p1958 A72-29615

Relaxation methods of magnetic and acoustic spectroscopy for studies of gravitational and inertial dipoles and quadrupoles in molecules and nuclei of solid bodies

14 p2143 A72-30963

Liquid optoacoustical modulator for laser radiation control operating on pulse amplitude modulated ultrasonic traveling waves with membrane partitions

16 p2400 A72-33081

Acousto-optic modulation with coupled Gunn oscillator-piezoelectric structure

20 p2960 A72-39702

Acoustic holography Doppler effects due to sound source or receiver motion during recording process

21 p3054 A72-40668

Electro-, magneto- and acousto-optical methods for laser Q-switching, discussing physical and operational principles

22 p3186 A72-42942

Optical considerations for an acoustooptic deflector

23 p3288 A72-43885

Time dependence of laser characteristics on external HF modulation of parameters by mirror oscillation and electrooptical and acoustooptical effects, noting laser mode locking

24 p3410 A72-45416

ACQUISITION

NT DATA ACQUISITION

NT TARGET ACQUISITION

Acquisition time for sideband modulated noiseless phase lock loops

03 p0325 A72-14191

ACROBATICS

Analysis of the fundamental parameters and flight properties of aerobatic aircraft in a statistical framework

23 p3252 A72-44336

ACRYLIC RESINS

Aircraft fuselage acrylic glazing design, covering passenger cabin window, cockpit windscreen and various surface coatings

12 p1753 A72-27008

Acrylics and polycarbonates properties in aircraft transparencies design, emphasizing cost and optical, mechanical, thermal and chemical properties

12 p1832 A72-27009

Vibration measurements of temperature dependent dynamic moduli of Al/resin/Al sandwich bars with cyanocrylate adhesives

21 p3118 A72-40720

Polyacrylonitrile based carbon fiber strengthening by fast neutron irradiation at high temperatures

22 p3196 A72-41965

ACRYLONITRILES

Resistivity, thermoelectric power and magnetoresistance of carbon fibers derived from heat treated polyacrylonitrile

07 p1024 A72-20550

Morphology and physicomechanical properties of carbonized polyacrylonitrile fibers by scanning electron microscopy, discussing macro and microdefects effects on strength characteristics

08 p1195 A72-21762

Carbonized and ion beam thinned polyacrylonitrile copolymer fibers examination by low angle electron scattering electromicroscopy technique

09 p1339 A72-23190

Glass styrene acrylonitrile bead filled composites tensile behavior, discussing relationship between yield stress, filler content, strain rate and temperature

11 p1673 A72-25487

Flexural strength of Pyco-bond polyacrylonitrile/PAN/ precursor carbon fiber substrates for carbon-carbon composite fabrication

12 p1835 A72-28092

ACTH

U ADRENOCORTICOTROPIN [ACTH]

ACTINIDE SERIES

NT ACTINIUM

NT PLUTONIUM ISOTOPES

NT THORIUM ISOTOPES

NT TRANSURANIUM ELEMENTS

NT URANIUM

NT URANIUM ISOTOPES

La superconductivity pressure dependence based on valency considerations, noting actinides metals and alloys localized magnetism explanation by simple model

09 p1368 A72-22557

ACTINIDE SERIES COMPOUNDS

NT THORIUM COMPOUNDS

NT THORIUM OXIDES

NT URANIUM CARBIDES

NT URANIUM COMPOUNDS

NT URANIUM FLUORIDES

NT URANIUM OXIDES

Phonon dispersion curves from inelastic neutron scattering for actinide and transition metals carbides, noting superconducting properties

09 p1369 A72-22564

ACTINIUM

State of development of an actinium fueled thermionic generator

18 p2644 A72-36169

ACTINOGRAPHS

U ACTINOMETERS

ACTINOMETERS

NT DICKE RADIOMETERS

NT INFRARED DETECTORS

NT INFRARED SCANNERS

NT INFRARED SPECTROMETERS

NT INFRARED SPECTROPHOTOMETERS

NT MICROWAVE RADIOMETERS

NT PYRANOMETERS

NT RADIOMETERS

NT SOLAR SPECTROMETERS

NT SPECTROHELIOGRAPHS

NT SPECTROPHOTOMETERS

NT SPECTRORADIOMETERS

NT ULTRAVIOLET SPECTROMETERS

NT ULTRAVIOLET SPECTROPHOTOMETERS

APZ-2 daytime actinometric radiosonde measuring long wave radiation balance in presence of short wave solar radiation

06 p0814 A72-17626

Cloud structure and cover determination from actinometric short wave solar radiation and IR cloud radiation measurements

23 p3311 A72-43627

ACTIVATION

Metal powders sintering activation mechanism, considering heterogeneous metals particles diffusion flow, mutual solubility and crystal lattices distortion

02 p0232 A72-11432

Chemical and physical activation mechanisms of sintering metal powder compacts

11 p1645 A72-26862

ACTIVATION [BIOLOGY]

Irreversible thermodynamics applications to physicochemical and biological stability, including allosteric activation model

04 p0482 A72-14754

Stellate ganglion stimulation and hypoxia effects on hemodynamics and coronary circulation in dogs, discussing myocardial oxygen consumption, sympathetic nerve vasoconstrictor effect and vasodilatory response

05 p0617 A72-16153

Stretch activation of myogenic oscillation of isolated contractile structures of heart muscle in ATP salt solution

07 p0923 A72-20427

ACTIVATION ANALYSIS

NT NEUTRON ACTIVATION ANALYSIS

Ultrapur metals microimpurities determination from crystal lattice and atomic properties, comparing spectral analysis activation, mass spectrometric, thermophysical, recrystallization and kinetic methods

07 p1049 A72-20149

Solar activity effects on biosphere processes, discussing radiation-induced molecular activation mechanisms in water and biological plasma calcium ion concentration changes

12 p1763 A72-28213

Comparison of infrared and activation analysis results in determining the oxygen and carbon content in silicon

17 p2511 A72-35330

Activation analysis in geochemistry and cosmochemistry; Proceedings of the Advanced Study Institute, Kjeller, Norway, September 7-12, 1970

20 p2898 A72-39826

Rocks and meteorites analysis techniques evaluation, using Apollo 11 fines results to evaluate activation analysis for geochemistry and cosmochemistry applications

20 p2899 A72-39827

In-situ geochemical analysis of Martian and lunar composition via alpha particle activation technique, discussing Surveyor instrument performance

20 p2899 A72-39828

Non-destructive activation analysis of some elements in stony meteorites by proton- and bremsstrahlung-irradiation

20 p2899 A72-39833

Numerical integration of gamma ray photopeak digital data from nondestructive activation analysis

20 p2899 A72-39834

ACTIVATION ENERGY

Germanium nitride thermolysis, discussing allotropic alpha and beta phases stability and activation energies

01 p0023 A72-10191

Empirical power law application to secondary creep, steady state hot working and high temperature tensile or compressive yielding, discussing activation parameters interrelations

02 p0247 A72-12814

Tungsten, molybdenum and tantalum disulfides oxidation rate determination by fluidized bed technique, calculating kinetic and diffusive processes activation energy

03 p0370 A72-13184

High temperature creep activation energies relationship to diffusion in TiC, ZrC and UC

03 p0371 A72-13461

Pure metals creep or self diffusion activation energy from hot-hardness data, noting temperature and elastic modulus effects

03 p0375 A72-13931

Impurity diffusion of Ag, Cd, In, Sn and Sb in magnesium single crystals, observing valence effect on activation energy

03 p0378 A72-14254

Ferritic steel nil-ductility transition temperature data analysis correlating irradiation results with activation fluences and temperature

04 p0547 A72-14430

Isothermal annealing measurements of zero-phonon line luminescence at 0.97 eV in electron irradiated Si, obtaining activation energy

04 p0560 A72-14546

Temperature and compression rate effects on metal powder packing density, obtaining activation energy from Boltzmann equation

05 p0665 A72-16089

Combustible materials ignition temperature, time lag and burning rate in oxygen enriched atmosphere, deriving activation energy for fire resistance estimates
05 p0681 A72-16773

Pure Al self diffusion at 130-200 C, determining activation energy from prismatic loop annealing rates
05 p0677 A72-17109

Analog simulation of normal thermal explosions and cool flames, observing oscillations limits, time dependence of parameters and effect of changes in activation energy or initial temperature
07 p1098 A72-19366

Electrons and ionized impurities interaction in thin quantizing layers, discussing donor activation energy and kinetic characteristics
07 p1048 A72-19640

Thermal decomposition kinetics of tetramethylene tetranitramine beta HMX from differential thermal analysis and activation energy calculation
08 p1219 A72-20755

Steady state creep model for high activation energy role in interstitial formation and migration in particle strengthened alloys
08 p1185 A72-20992

Alpha Ti plastic deformation behavior below 700 K, determining activation area and enthalpy as functions of stress and temperature
08 p1186 A72-21247

Asymptotic analysis of activation energy limit for radiant ignition of reactive solid with in-depth absorption
[AD-741533] 08 p1255 A72-22044

German monograph on lattice and solid metal surface transport processes, discussing atom migration, activation energies, impurity atom diffusion, Kossel-Stranski model, etc
08 p1212 A72-22173

Inhomogeneous sink distribution effect on vacancy annealing kinetics and activation energy in metals
10 p1499 A72-24983

Transition from metallic to activation conductivity in doped semiconductors, noting activation energy dependence on compensation degree
11 p1700 A72-25720

Thermal release patterns and activation energies of spallogenic He, Ne and Ar from Carbo iron meteorite
12 p1866 A72-27116

Energy metabolism and ATP balance characteristics during muscular activity as function of organism adaptation to activity
13 p1902 A72-28640

Activation energy of high temperature creep in Cr alloy with aluminum oxide, comparing with moving monovacancies in pure Cr
14 p2112 A72-30161

Zr oxidation kinetics at 440-850 C for 3 min maximum exposure time, observing type oxide change relationship to activation energy
14 p2113 A72-30247

Metal creep activation energy determination during plastic deformation process, using temperature differential method
14 p2115 A72-30412

Mo addition effect on high temperature creep resistance and diffusion activation energy of Nb alloys tested in torsion and tension at 1100-1500 C in vacuum
14 p2116 A72-30436

Volumetric analysis of Th, Zr and Li hydrides precipitation in Mg alloys, determining rate equation and activation energy
15 p2257 A72-32118

Metal melting heat relationship to diffusion activation energy with vacancy mechanism equal numerically to crystal internal energy maximum change
15 p2259 A72-32691

Strain release method for investigating thermally activated microflow mechanisms in solids, discussing technique for activation energy and relaxation strength measurements
16 p2372 A72-32822

C diffusion mobility and coefficients in W-Mo steels gamma and alpha phases, discussing ionization effect on activation energy increase
16 p2408 A72-33538

Temperature and stress dependence of steady state creep rate for dispersion strengthened Ag-gallium oxide alloys, noting grain size effect on activation energy
16 p2411 A72-34094

Combustible materials ignition temperature, time lag and burning rate in oxygen enriched atmosphere, deriving activation energy for fire resistance estimates
17 p2571 A72-35276

The role of Sm and Mn as activators in calcium sulphate and lithium tetraborate
18 p2718 A72-36347

Acceleration stress tolerance dependence on electron or ion transport across cell surface activation energy barrier, studying rat survival times
18 p2650 A72-36448

Alloying element effects on C free energy interaction coefficients in liquid Fe alloys at 1550 C by equilibrium distribution method
20 p2937 A72-39295

A possible problem in measuring hydrogen diffusivity at low temperatures by the Gorsky effect
22 p3190 A72-42443

Al alloy rupturing analysis in complex stress state, noting sublimation and self diffusion values of activation energy in torsional to tensile state transition
23 p3301 A72-43957

High temperature creep activation energies relationship to diffusion in TiC, ZrC and UC
24 p3413 A72-44936

Contribution to the study of the creep behavior of 18 per cent-nickel maraging steel
24 p3415 A72-45600

ACTIVE GLACIERS
U GLACIERS

ACTIVE SATELLITES
NT SYNCOM SATELLITES

ACTIVITY [BIOLOGY]
Central nervous system pharmacology, discussing somniferous, narcotic and neurotropic substances effects on brain activity
08 p1127 A72-21841

Solar activity effects on biospheric processes for biological and physicochemical systems in unsteady state, considering maximum effects on man at certain electromagnetic wave frequencies
12 p1773 A72-28211

Electrocorticograph monitoring of central nervous system state in dogs reanimated by artificial blood circulation after prolonged clinical death by drowning
12 p1764 A72-28215

Plant leaves biochemical activities study by light scattering techniques, discussing photometric, spectroscopic and bionics methods
13 p1955 A72-28518

Rat vena porta muscle cells spontaneous activity intensified by direct current depolarization and inhibited by hyperpolarization, noting effects of calcium and sodium ions
13 p1902 A72-28638

Adaptation period to inverted work-rest cycle observed with encephalograph, noting effect of brain bioelectric activity circadian rhythms stability
13 p1904 A72-29315

EEG diurnal rhythms during 72 hour insomnia, considering adaptation to altered work-rest cycle in subjects with stable and unstable brain activity rhythms
13 p1904 A72-29319

ECG heart rate recording of helicopter instructor pilots during flight training tasks, administrative work, automobile driving and eating
14 p2082 A72-31097

A note on the biological activity of the noble gas compound xenon trioxide
18 p2652 A72-36444

Computerized statistical simulation of automatism of spontaneously active smooth muscle strip, neglecting individual cell spontaneous activity
19 p2757 A72-37949

ACTIVITY CYCLES [BIOLOGY]
Twelve hour light-dark-dark cycle phase shift effects on monkey feeding behavior and serial task performance
02 p0157 A72-11703

Optimum duration of human circadian cycle with respect to energy cost during work hours, relating normal cycle change to prolonged space mission stresses
05 p0619 A72-16639

Circadian rhythms of activity-sleep time in free running birds and man in isolation
07 p0918 A72-19527

Circadian rhythms variations for sleep, EEG, temperature and activity in monkeys, indicating acrophase, amplitude and level regulation
07 p0918 A72-19528

Phase resetting behavior of circadian rhythm of pupal eclosion in fruitfly populations
07 p0918 A72-19529

Day/night workers sleep patterns in terms of intrasleep REM-NREM ultradian cycle, noting sleep temporal instability for night workers
10 p1428 A72-23730

Sleep-wakefulness cycle variations effect on reaction time and spontaneous tempo during time isolation experiment, showing tendency toward circadian rhythm
11 p1581 A72-26687

Nocturnal primate Aotus trivirgatus wakefulness-sleep cycles during dark/light periods expressed in REM/non-REM percentages
13 p1903 A72-29300

Pulse rate studies of human adaptation to 16 hour work-rest cycle, showing persistence of 24 hour cycle
13 p1904 A72-29316

Statistical periodic analysis of cyclic activity in human perceptual-motor performance
13 p1911 A72-29845

Relaxation phenomena in the biological carbon cycle under conditions of variable atmospheric CO2-content
17 p2500 A72-34897

International Interdisciplinary Cycle Research Symposium, 3rd, Noordwijk, Netherlands, August 22-28, 1971, Proceedings.
22 p3147 A72-42976

Mutual relations between different physiological functions in circadian rhythms in man.
22 p3147 A72-42979

ACTUATION
Accelerated aperiodic actuation of pendulous mass surface gyrocompass to meridian direction, using inertial moment from rotor start-up
10 p1481 A72-24496

ACTUATOR DISKS
Stator-rotor induced annular incompressible rotating flow, allowing for blade loading generated vorticity within actuator disk theory
[ASME PAPER 71-WA/FE-18] 05 p0599 A72-15929

Relaxation analysis of discontinuities in axisymmetric rotating actuator disk flow
11 p1569 A72-25622

Critique of general momentum theory of propeller actuator disk model, showing flow field determination from nonlinear elliptic differential equation solution
11 p1572 A72-25998

Nonlinear integral equations solution for heavily loaded actuator disk induced flow field, taking into account blade tip vortices and thrust coefficient effects
11 p1573 A72-26577

Application of cascade and actuator disc theories to computer aided design of fans.
24 p3363 A72-45359

ACTUATORS
Barium stypnate replacement for discontinued SR-4990 smokeless powder as propellant base charge in MK 24 actuator
08 p1222 A72-20784

Multiplex electrohydraulic system for aircraft fly by wire actuators with majority voting and pressure logic, discussing frequency response and environmental tests
08 p1113 A72-22152

Hydraulic actuator servomechanism performance dependence on asymmetrical spool valve lap and closed loop system stability
08 p1113 A72-22153

Bi-metallic actuator for spacecraft thermal control with design emphasis on external power source elimination, high reliability, frictionless operation, simplicity and low weight
09 p1305 A72-22249

Electromechanical redundant activating mechanism for F-4 aircraft dual tandem hydraulic power servo, noting application to fly by wire control
14 p2072 A72-30422

High pressure cryogenic hydraulically actuated valve for repeated sealing of liquid He-containing cell
15 p2183 A72-32436

Low-explosive actuated mechanical devices to actuate switches and valves, sever cables or bolts, dispensing fluids, inflating bags or starting engines
16 p2442 A72-33359

Jaguar powered flight controls, discussing wing spoilers, slab tailplane, rudder, autostabilization system and integrated packaging of actuators
16 p2353 A72-34144

ACUITY
NT VISUAL ACUITY

ACYCLATION
Energy transfer conditions of transdehydration reactions on primeval earth leading to transphosphorylation, transacylation and peptide synthesis
04 p0468 A72-14768

ADAPTATION
NT ACCLIMATIZATION
NT ALTITUDE ACCLIMATIZATION
NT COLD ACCLIMATIZATION
NT DARK ADAPTATION
NT DESERT ADAPTATION
NT LIGHT ADAPTATION
NT RETINAL ADAPTATION

Soyuz 9 flight crew physiological data, discussing mental and physical performance and adaptation and readaptation to space-earth environments
01 p0020 A72-10933

Eye-hand coordination modifiable parameters under optical distortion conditions, deriving quadratic equation for hand response adaptation
02 p0167 A72-11897

Concurrent and terminal display exposure effects on perceptual adaptation for localizing movements with displacing prism
03 p0319 A72-13878

Conditioned reflex as component of artificial conditioned-natural unconditioned reflex system controlling adaptive behavioral patterns, noting contribution to complex nervous activity understanding
04 p0476 A72-15582

Respiratory adaptation to pure oxygen excess pressure after cockpit depressurization from flight simulator tests with pressure-suited pilots, presenting ECG reactions
05 p0623 A72-16749

Adjustment to subjective horizontal, vertical and 45 deg tilt in dark as function of age in 3-20 year old subjects
08 p1124 A72-20989

Soviet papers on human higher nervous activity physiology covering conditioned reflexes and adaptive

behavior, neurotropic substance effects, mathematical and structural modeling, etc 08 p1118 A72-21834

Monaural perstimulatory loudness adaptation measurement by delayed and single simultaneous balance methods, discussing intensity, frequency and duration effects 08 p1127 A72-21897

Auditory adaptation tests confirmation of Small loudness model prediction of lower adaptation for test tone greater than adapting tone intensity 08 p1127 A72-21897

Skeletal bones ash content in man and primates, implying differences due to adaptive physiological function 10 p1424 A72-23736

Metabolic and hormonal response adaptation to prolonged hypodynamics in water immersion (head out), noting diurnal and nocturnal differences in circadian rhythms 12 p1765 A72-28267

Energy metabolism and ATP balance characteristics during muscular activity as function of organism adaptation to activity 13 p1902 A72-28640

Pulse rate studies of human adaptation to 16 hour work-rest cycle, showing persistence of 24 hour cycle 13 p1904 A72-29316

Heart rate diurnal rhythm adaptation to work-rest cycle change, using recumbent and sitting position data parameters 14 p2075 A72-30391

Human organism readaptation after prolonged hypokinesia and weightlessness, discussing coordination disturbances, vegetative and vascular system instabilities, reduced orthostatic stability and asthenia 14 p2076 A72-30745

Stress and adaptation responses to repeated acute acceleration 17 p2500 A72-34729

New experimental data on the morpho-physiological analysis of the adaptation phenomenon in the somatic reflex arch 17 p2504 A72-35023

Adaptability limits on protein-nuclein-water life under exobiological extremal conditions, considering macromolecules, extraterrestrial life search and origin 20 p2891 A72-38958

Cortical metabolism regulation and efferent systems of the adaptation process 21 p3000 A72-40760

Target distance and adaptation in distance perception in the constancy of visual direction 21 p3008 A72-41022

Role of the thyrotropic region of the hypothalamus in the adaptation activity of the organism 22 p3141 A72-42167

ADAPTERS

Automatic interplanetary station adapter to obtain reflected signals amplitude-altitude-frequency characteristics during ionospheric probes 05 p0657 A72-16271

ADAPTIVE CONTROL

NT LEARNING MACHINES

NT SELF ADAPTIVE CONTROL SYSTEMS

Soviet book on reliable logic units design covering adaptive redundant and nonredundant control systems, threshold functions, optimal adaptation algorithms, restoring circuits, etc 01 p0033 A72-10296

Adaptive statistical prediction algorithm for character recognition by computer simulation involving handprinted numerals 01 p0034 A72-10472

Three-failure-tolerant digital computer system design using adaptive majority voting in hardware and software for real time control application 02 p0185 A72-11488

Mathematical model for control process as adaptive memory tracker, discussing digital simulation 02 p0186 A72-11659

Online identification on human describing function by iterative differential analyzer, noting application to man-machine systems and online adaptive control systems 02 p0169 A72-12661

Self organizing adaptive aircraft control system with C criterion pitch axis performance and failure compensation 03 p0337 A72-12920

Differential and difference equations approximate solutions in finite state machine form, developing adaptive gain changer model in aircraft stability control system 03 p0338 A72-13164

Linear dynamic system sensitivity models simplification conditions application to adaptive nonsearching system synthesis algorithms 04 p0505 A72-14999

Adaptive control algorithm with disturbance prediction for solution of deterministic and stochastic optimization problems of linear equation of state and quadratic performance criteria 05 p0639 A72-15759

Quasi-steady continuous process adaptive optimal control, discussing algorithms and model for sensitivity matrix calculation and digital simulation for strategy 05 p0640 A72-16200

Model reference adaptive control system synthesis in presence of random perturbations, considering error signal derivative use to form parameter adjustment algorithm 05 p0640 A72-16208

Parameter adjustment algorithm for simplified sensitivity model in adaptive nonsearching control system of linear plant with polynomial transfer function 05 p0641 A72-16318

Airborne computer programmed adaptive optimal control for subsonic vehicle automatic landing with aerodynamic performance 05 p0685 A72-16430

Adaptive maximum likelihood receiver for direct ranging navigation, comparing with phase locked receivers 05 p0686 A72-16560

Adaptive model following control systems design by hyperstability approach for flight control and simulation [AIAA PAPER 72-95] 05 p0613 A72-16956

Adaptive control for linear discrete time stochastic systems with unknown gain parameters, considering open loop feedback optimal control using quadratic performance index [AD-739126] 06 p0791 A72-17305

Parameter adaptive self organizing control of linear discrete time systems, presenting stochastic approximation algorithms for feedback systems identification 06 p0791 A72-17306

Divergence prevention in decision directed adaptive recursive estimators in relation to error covariance 06 p0792 A72-17307

Dither adaptive control technique application to constant fuel rate problem, illustrating with analog computer solution 06 p0792 A72-17308

Optimum adaptive variable step size delta modulator-demodulator producing minimum error for Markov-Gaussian source 06 p0772 A72-17404

Adaptive sampling of continuous measurement signals, calculating mean sampling rate 06 p0773 A72-17572

Algorithmic procedure in compensator design for hyperstable discrete model reference adaptive systems/MRAS/ 07 p1027 A72-19294

Biological radar clutter control by adaptive systems techniques, developing computer simulation for angel tolerance from bird electromagnetic characteristics 07 p0942 A72-19305

Analog/hybrid simulation of noise effect on adaptive delta modulation system consisting of transmitter, receiver and error simulator 07 p0951 A72-20339

Adaptive statistical system with feedback loop for weather analysis and forecasting, examining learning process features 08 p1202 A72-22113

Adaptive algorithms for dynamic systems observation based on extremal data processing systems construction 09 p1283 A72-22219

Hyperstability conditions generalization for model reference adaptive systems, using positive definite kernels properties 09 p1290 A72-23098

Discrete and continuous dynamic adaptation algorithms construction for extremal quality functional trajectory equations of adaptive control system 09 p1283 A72-23435

Filtration and extrapolation of multivariable random processes described by linear differential equations system, examining adaptive filter synthesis 09 p1283 A72-23436

Algorithms for optimal adaptive control of steady motions of single channel discrete extremal systems with independent search, studying quality functional behavior 09 p1291 A72-23437

Adaptive neural nets of threshold logic units as models of perception and memory in biological systems 09 p1273 A72-23580

Decision and control including adaptive processes - IEEE Conference, Miami Beach, Florida, December 1971 10 p1454 A72-23776

Quadratic cost, nonlinear optimal adaptive stochastic control of linear plant and measurement models excited by white Gaussian noise and with unknown parameters 10 p1455 A72-23792

Adjustable structure model for parameter adaptive control, noting convexity of performance index function over evaluation interval 10 p1455 A72-23793

Digital adaptive sampling, stressing implementation problem 10 p1455 A72-23799

Adaptive optimal antenna array detection of unknown spatial location radar targets, noting tradeoff between array size and signal energy with respect to performance 10 p1434 A72-23809

Parameter adjustment algorithm for simplified sensitivity model in adaptive nonsearching control system of linear plant with polynomial transfer function 10 p1458 A72-25072

Stochastic control theory application to flight problem, discussing aircraft identification and adaptive control over wide environmental range 10 p1458 A72-25146

Control algorithm with variable structure for incomplete state information on third order system, using error and first derivative 12 p1794 A72-27674

Russian papers on adaptive control systems covering automata and game theory, learning models, Markov processes and probability theory 12 p1787 A72-27921

Frequency response data identification technique using adaptive hybrid computer to improve quality and acquisition time 13 p1935 A72-29103

Russian papers on large adaptive control systems covering pattern recognition, statistical analysis, simulation, reliability, etc 13 p1936 A72-29153

Two step adaptive control of multidimensional linear static system, using first and second step ratio and optimization equations 13 p1936 A72-29159

Early design phase reliability analysis of large adaptive systems in terms of domination and graph theories 13 p1965 A72-29171

Noise resistance techniques for calculating linear signal interpolation errors in adaptive quantizers 13 p1991 A72-29268

Adaptive radiometer dynamic properties and parameters optimization based on minimum mean square error criterion 14 p2088 A72-30373

Pilot trainer transfer function identification for man-machine and on-line adaptive control system using analog/hybrid computer 14 p2091 A72-30721

Adaptive reception of weak repetitive signals on background of intense fluctuating noise, synthesizing adaptive detection system for multipath propagation and small SNR 15 p2195 A72-31658

Adaptive radar tracking processes in presence of clutter, comparing efficiencies via mathematical models 15 p2196 A72-31747

Automatic control theory trends /1950-1970/, discussing nonlinear, discontinuous and adaptive systems, optimization problems, Liapunov stability theory, etc 15 p2212 A72-32576

High speed deterministic adaptive controller for linear and nonlinear plants, identifying control law from state and input data by linear regression procedure 15 p2212 A72-32794

Computer algorithms for adaptive optimal synthesis of complex electronic systems, using stochastic approximation and gradient search with data storage 16 p2367 A72-33265

Noise stability of frequency-time adaptive transmission systems for discrete information, using resolving feedback circuits 16 p2363 A72-33266

Adaptive reception in a channel with slow common fading 17 p2515 A72-34835

Adaptive compression of prediction of differential coding images 17 p2518 A72-35674

Design of model-reference adaptive control systems using Liapunov functions. 18 p2672 A72-36326

An adaptive processor for RF antenna arrays. 18 p2659 A72-36329

Digital controller for high pressure rocket engine. 18 p2721 A72-36335

Adaptive equalization of data transmission rate in telephonic systems, considering criteria and iterative algorithms 18 p2661 A72-36790

Optimally sensitive adaptive control techniques for systems with unknown time-varying parameters, suggesting applicability to ATC 19 p2776 A72-37289

Condition for the equivalence of two important adaptation algorithms and its relationship to effective estimates of probability-distribution parameters 19 p2825 A72-37439

Conditions for the effectiveness of adaptation algorithms based on an empirical Bayesian approach to statistics 19 p2825 A72-37440

Model reference adaptive control systems design based on optimal control, parametric optimization, stability and statistical estimation theory
19 p2778 A72-37722

Effects of incomplete adaptation and disturbance in adaptive control.
19 p2781 A72-38263

Lapunov functions for quadratic differential equations with applications to adaptive control.
19 p2826 A72-38264

Extended Kalman filter with fictitious noise input for adaptive tracking of time varying parameters applied to VTOL aircraft
19 p2781 A72-38265

Design techniques for model-reference adaptive control systems.
19 p2781 A72-38266

Adaptive control systems fundamental functions, principles, characteristics and applicability
19 p2782 A72-38312

Discrete and continuous dynamic adaptation algorithms construction for extremal quality functional trajectory equations of adaptive control system
19 p2770 A72-38518

Filtration and extrapolation of multidimensional random processes described by linear differential equations system, examining adaptive filter synthesis
19 p2770 A72-38519

Algorithms for optimal adaptive control of steady motions of single channel discrete extremal systems with independent search, studying quality functional behavior
19 p2782 A72-38520

Comparison of the quality of empirical and optimal adaptation algorithms in multiple-alternative choice problems
19 p2828 A72-38583

An adaptive technique for a redundant-sensor navigation system.
[AIAA PAPER 72-863]
20 p2952 A72-39134

An algorithm for linearly constrained adaptive array processing.
20 p2904 A72-39777

Effects of errors in the direction of incidence on the performance of an adaptive array.
20 p2904 A72-39786

Unknown plant self organizing time optimal controller with variable switching surface and adaptation logic net, noting effectiveness by computer simulation
21 p3037 A72-40639

A recursive least-squares approach to the on-line adaptive control problem.
21 p3037 A72-40640

Comparative analysis of frequency response determination methods for searchless adaptive systems
21 p3038 A72-40709

Effect of single-bit digitization in adaptive array control loops.
21 p3034 A72-41085

Prediction role in execution of manual control with display device to aid human operator adaptation
21 p3010 A72-41406

On a feedback communication system having iteration control in the forward channel.
21 p3039 A72-41826

Fluidic implementation of a perturbation extremum controller.
22 p3139 A72-42050

Optimally sensitive control for distributed parameter systems.
23 p3275 A72-43612

Synthesis of hyperstable discrete model reference adaptive systems.
23 p3276 A72-43867

Digital-computer simulation of the motion of a walking machine
23 p3278 A72-44002

A computational successive improvement scheme for adaptive optimal control processes.
23 p3268 A72-44549

Respiration control mechanism ensuring adaptation to power requirements and chemical environment maintenance in tissues, considering brain stem location
24 p3371 A72-44600

Robert Bruce's spider problem extended - Reliability of adaptive experimental systems.
24 p3406 A72-44666

ADAPTIVE CONTROL SYSTEMS
U ADAPTIVE CONTROL
ADAPTIVE FILTERS
Nonrecursive and recursive adaptive equalizers for digital communication, discussing computerized simulation of performance
04 p0493 A72-15520

Discrete-time adaptive Kalman filter based on learning process and parameter estimate updating in operational cycle, comparing with simple Kalman and Wiener filters
05 p0639 A72-15758

Stochastic differential equations for a posteriori probability distribution in problems of Markov process parameter estimation, adaptive filtering and signal detection
06 p0794 A72-18301

Dynamic system time varying parameters on-line estimation using adaptive extended Kalman filter based on predicted error covariance matrix alteration
08 p1144 A72-20847

Soviet book on determinate, stationary, nonstationary and industrial random processes prediction, covering adaptive filters and algorithms
08 p1146 A72-21675

Adaptive filter techniques application to maneuvering reentry vehicle tracking, using Wald sequential test, decision theory and stochastic approximation
10 p1509 A72-23779

Digital MTI detection filter using on-line adaptive procedure for adjustment
10 p1456 A72-23804

Modulated filter theory for AM signal analysis in linear resonant circuits, noting use for superheterodyne amplifier and phase discriminator design
13 p1930 A72-29046

Optimal algorithms for analysis, synthesis and correcting filter of self adaptive control systems
13 p1936 A72-29154

Linear and nonlinear continuous self adaptive frequency converter filters with minimum error under SNR change
13 p1936 A72-29156

Self organizing control system for optimal performance of navigation instruments, using adaptive algorithm for statistical error filtration
13 p1996 A72-29157

Stochastic differential equations for a posteriori probability distribution in problems of Markov process parameter estimation, adaptive filtering and signal detection
13 p1937 A72-29441

Controllable matched filter model for single circuit and twin circuit parametric converters
15 p2207 A72-31886

Probabilistic information model of adaptive predictor filters /APF/ with latent memory simulated on digital and analog computers
15 p2211 A72-31896

Maximum likelihood identification of time varying and random system parameters.
18 p2673 A72-36822

Real time estimation of trajectory for lifting reentry vehicle of shuttle orbiter type, discussing iterated nonlinear filter and adaptive filter
20 p2966 A72-39126

Adaptive filtering algorithms for Kalman filter optimal gain estimation, discussing Bayesian, maximum likelihood, correlation and covariance matching methods relationship
23 p3274 A72-43542

Asymptotic methods of calculating the effectiveness of one variant procedure of selecting operational subchannels in an adaptive multichannel communications system
23 p3266 A72-44207

ADDERS [CIRCUITS]
U ADDING CIRCUITS
ADDING CIRCUITS
Error correction in adders with systematic subcodes, preserving AN binary code error control properties
08 p1138 A72-21551

ADDITION RESINS
NT ACRYLIC RESINS
NT VINYL COPOLYMERS
ADDITIONS
NT ADMIXTURES
NT ANTIFREEZES
NT ANTIOXIDANTS
NT OIL ADDITIVES
NT PLASTICIZERS
NT PROPELLANT ADDITIVES
NT PROPELLANT BINDERS
Additives and reactive retardants flame inhibiting properties for polymers, discussing various testing techniques
01 p0090 A72-10286

Mass spectroscopic analysis of addition effects of Xe, hydrogen and oxygen on CO-H laser discharge
01 p0079 A72-10517

Supercritically doped transferred electron microwave amplifiers stabilization mechanisms, considering cathode contact, anode diffusion current and active region temperature gradient roles
01 p0036 A72-10636

Doping profile effects on reflection-type IMPATT diode microwave amplifiers, presenting power-gain vs frequency curves
01 p0037 A72-10643

Electrical properties of subsonic argon plasma stream seeded with uranium hexafluoride, using electrostatic probe
01 p0111 A72-11334

Polyethylene and polypropylene combustion, investigating additives and surrounding gaseous composition effects on flammability and volatile products during thermal degradation
02 p0248 A72-11767

Viscosity and additive effects on jet engine fuel antiwear properties improvement
02 p0270 A72-11968

VT-31 Ti alloy with Al, Mo, Cr and Fe additives, investigating ductile type fracture after heat treatment by electron microscopy and tensile tests
02 p0244 A72-12249

Au distribution parameters in Si semiconductor devices, using radioactive isotope diagnostic methods
03 p0400 A72-12970

Powdered chromium carbide-nickel alloys phosphorus addition effects on sintering temperature, shrinkage, density and hardness
03 p0372 A72-13546

Mo and C additives effects on austenite susceptibility to deformation martensite formation and steel resistance to hydroerosion
03 p0375 A72-13941

Ta and Nb addition effects on W solid solution strengthening, determining W-Nb-Ta alloys phase diagram and melting point
03 p0375 A72-13943

Li-diffused Si compared to conventionally doped materials under neutron irradiation, considering carrier removal
03 p0403 A72-14078

Alloy additions and heat treatment effects on mechanical properties and weldability of quenched and aged high strength Ni steels
03 p0378 A72-14173

Alloying elements and grain size effects on thermally induced surface reconstruction of Al film metallization on Si devices from thermal cycling tests
03 p0364 A72-14285

Sb 124 dopant redistribution in Ge semiconductor during diffusion alloying with In at 750-850 C
05 p0701 A72-15751

Additives effect on liquid hydrocarbon fuels ignition delay, testing peroxides, esters, polyethers and alcohols
05 p0703 A72-16958

Screened impurity scattering determination in heavily doped covalent semiconductors from Hall mobility and thermoelectric power measurements
05 p0702 A72-17073

Alloying elements effects upon iron mechanical properties, investigating lattice parameters, temperature dependence of yielding and plastic flow, solid solution strengthening and softening, etc
05 p0676 A72-17101

High strength Al-Zn-Mg-Cu alloys, testing heat treatment and Ag addition effects on tensile strength
05 p0677 A72-17112

Ag addition effects on high strength Al-Zn-Mg-Cu alloys tensile properties and resistance to stress corrosion cracking
05 p0677 A72-17113

Ni-Al alloy, investigating Y addition effect on vacancy agglomeration suppression during oxidation
06 p0829 A72-17787

Recombination coefficient, ionization rates and average lifetime of ions in rarefied carbon-arc flames, investigating pressure and additives effects
06 p0904 A72-18213

Molybdenum disulfides with varying purity level evaluated as solid lubricants and as lubricant additives in standard lubricating testing devices
06 p0836 A72-18588

Mn additions effects on austenitic stainless steels yield strength, work hardening characteristics, corrosion resistance and machinability
07 p1011 A72-19478

Se and Te additions effects on low carbon steels formability and machinability from metallurgical examination and workability tests
07 p0994 A72-19480

Al-Mg alloy with Ti, Zr, Mo and B additions under tensile and impact loads, investigating mechanical properties, strength and crack formation
07 p1014 A72-19839

Transition metals addition effect on Al-Cu alloys strength and aging characteristics, determining lattice constant increase by X ray microstructural analysis
07 p1014 A72-19841

Lubricating action of sulfur-containing additives and chlorine compounds in lubricants and cermet materials, noting effects of iron compounds formation in contact region
07 p0996 A72-19967

High neutron absorption doping material selection for enhancing explosive mixtures neutron radiographic image without interference with chemical reaction
08 p1220 A72-20769

Electron microscopic investigation of niobium-oxygen alloys with Zr and Hf additions, measuring oxygen solubility
08 p1187 A72-21787

German monograph on fracture formation and behavior in Ni maraging steel under repeated stress alternations, considering Al and Ti effects on steel strength
08 p1190 A72-22172

Ti, Zr, Mo, B and Mn additives effect on rupture characteristics of cast Al-Mg alloy under uniaxial tensile stress
09 p1328 A72-23033

Radiation induced extrinsic photoconductivity in Li doped Si, examining localized energy levels in forbidden gap 09 p1372 A72-23238

Ti alloys fracture strength in air and sea water obtained by bending tests of notched specimens, noting stress corrosion resistance enhancement by Mo addition 10 p1499 A72-24891

B-Al composite mechanical properties improvement through heat treatment and steel addition 11 p1653 A72-25478

Temperature dependence of Ni and Ni alloys and solid solutions microhardness, noting strengthening effect of Ti, Cr, Al and B additions 11 p1654 A72-25491

Co, Al and Mn additions effect on secondary hardening during aging in Fe-Mo-C martensite 11 p1655 A72-25511

Al addition effect on thermal and mechanical stability, forgeability, cold workability, aging and oxidation resistance of Ti-Mo beta alloys 11 p1656 A72-25516

Ti-Al-Mo alloys thermomechanical treatment, investigating alloying effects on hardening 11 p1660 A72-26132

Ductile type fracture after heat treatment of VT3-1 Ti alloy with Al, Mo, Cr and Fe additives investigated by electron microscopy and tensile tests 11 p1660 A72-26132

Semiconductor laser threshold current dependence on doping degree and temperature based on optical transition model and energy band theory 11 p1647 A72-26327

Transmittance and Faraday effect characteristics of Te doped InSb samples with free carriers measured at 10.6 microns 11 p1648 A72-26338

Ni additive effects on tungsten trioxide reduction with hydrogen and W powder sinterability 11 p1643 A72-26835

Mg addition effect on high temperature mechanical properties of nickel-alumina alloy, studying particle coarsening mechanism changes 11 p1664 A72-26856

Transition metals silicides additions effect on sintering and oxidation resistance at high temperatures of Ti and Zr diborides 11 p1665 A72-26874

Molybdenum disulfide addition effect on compounded model greases lubricating performance, determining oxidation stability, rust preventive behavior and consistency 12 p1832 A72-27047

Small signal theory of emitter current limited injection in negative mobility semiconductors at zero doping limit 12 p1788 A72-27165

P-n junction diodes fabricated by ion implantation doping, calculating I-V characteristics for comparison with measured breakdown voltages 12 p1789 A72-27312

Crystal growth, physical and spectroscopic properties and laser performance of Nd and Ho doped crystals with apatite structure 12 p1825 A72-27927

Electron irradiation effects on Li doped silicon solar cells, noting changes in donor concentration and defects formation 12 p1757 A72-28022

Li dopant radiation damage inhibiting effect on electron irradiated n-type silicon, discussing EPR and photoconductivity experimental results 12 p1856 A72-28023

Electron irradiation of Li doped Ge at low temperatures, measuring Hall effect and minority carriers diffusion length 12 p1857 A72-28055

Phonon scattering and induced energy levels in electron irradiated Sb doped Ge in n to p-type conversion region, measuring thermal conductivity and Hall effect 12 p1857 A72-28057

Radiation damage in carbon doped silicon irradiated at low temperatures by 2 MeV electrons, noting isotope shifts 12 p1857 A72-28059

Electron irradiation of n-type Si or Te doped GaAs, determining carrier removal rate, mobility changes and annealing characteristics 12 p1858 A72-28067

Impact fracture resistance of Cr-Mn-Si steel, investigating alloying effects on crack initiation and propagation 12 p1831 A72-28238

Rare earth metals addition effect on mechanical properties of electrolytically hydrogen-refined Cr, noting low temperature ductility 12 p1831 A72-28241

Semiconductor layers alloying by directional crystallization of compressed melts doped by contact with Al, Ge, Te, Al and Sb films 13 p2020 A72-28564

Plasticizers and modifiers effect on epoxy polymers structure from electron microscopy and IR spectroscopy, observing chemical reactions between aliphatic resin and hardening agent 13 p1983 A72-28689

Nonuniform concentration mechanism for observed drag reduction in flows with high molecular weight polymer additives, considering boundary layer with varying viscosity on sphere 13 p1942 A72-29113

Aviation fuels and additives effect on steel endurance limit at room temperature 13 p1980 A72-29487

Impurity concentration relationship to electrons and holes density and potential fluctuations in completely compensated crystalline semiconductors with randomly distributed donors and acceptors 13 p2024 A72-29993

Co, Mo, Ti and Al alloying effects on aging and hardening processes in Ni steel from hardness, thermal emf and electrical resistance measurements 14 p2115 A72-30408

Semiconductor gamma ray detectors development, using cadmium dichlorides, dibromides, diiodides and difluorides as doping agents in CdTe crystal growth 14 p2142 A72-30549

Work functions of dilute W alloys from vacuum emission vehicle and thermionic microscope measurements, noting additives effect 14 p2120 A72-30613

Modified geometrical model for sintering Ni-doped W, including surface tension effect at Ni-vapor interface 14 p2121 A72-30770

Electric arc plasma, predicting elements addition and electron density alteration effects on radial temperature distribution 14 p2139 A72-30778

High temperature oxidation resistance and mechanical properties of Fe-Al-Cr alloys with Ti and Mo additions 15 p2253 A72-31520

Transition metals additives effect on binary Mo alloys softening, noting influence of temperature and electron concentration change 15 p2258 A72-32135

Transition metal doped lithium niobate for holographic storage, measuring recording sensitivity, maximum diffraction efficiency and erase behavior 15 p2239 A72-32354

Antioxidant additives effect on chemical stability and rheological properties of silica gel lubricants with SU type mineral oil dispersion medium 16 p2413 A72-33173

Heavily doped ruby optical properties review, discussing N-lines, absorption and fluorescence spectra, interactions with phonon and photon fields and ionic reactions 16 p2441 A72-33522

Impurities and additives effects on electrode properties in Cs vapor thermionic converter, noting coadsorption model for Cs-W-O surface 17 p2496 A72-34598

Extractability of antioxidant additions from fuels by means of water and NaCl solutions 17 p2596 A72-35179

Thermionic converter I-V performance improvement via oxygen addition, examining feasibility of cesium oxide-cesium solution as source 18 p2647 A72-36204

Effects of small amounts of additional elements on stress corrosion cracking of Al-Zn-Mg alloys. VI. 19 p2821 A72-38555

Influence of cerium additions on the luminescence of europium and samarium ions in NaF single crystals 20 p2932 A72-39414

Mechanical properties improvement of Al alloys for machine construction applications, suggesting Ti, Zr and Be additions optimal rate 20 p2941 A72-39577

Enhancement of heat resistance in Kh14G14N3T steel by microadditions of boron 20 p2941 A72-39579

Recrystallization and polygonization conditions in high purity metals, noting critical temperature and additives effect 21 p3065 A72-40093

Effects of modification and additional elements on the solidification of Al-Si alloy - Studies on the solidification of Al-Si alloys in a shell mold. II. 21 p3067 A72-40937

The effect of alloying elements on creep rupture strength and microstructure of 12 percent chromium heat resisting steel. 21 p3069 A72-41014

Microalloying effect on creep and stress rupture characteristics of hot rolled and annealed Mo alloys 21 p3070 A72-41355

Deformable magnesium alloys with scandium and yttrium 22 p3192 A72-42820

Lasing properties of yttrium orthoaluminate doped with rare-earth metals 22 p3187 A72-42943

Constitution of the Ni-Cr-Fe system from 0 to 40 pct Fe including some effects of Ti, Al, Si, and Nb. 22 p3194 A72-43038

Free electrons and holes concentration calculated for quadratic dispersion law in doped semiconductors without degeneration, noting additive atoms effect 23 p3324 A72-43849

Application of a strongly doped semiconductor model to the study of thermodynamic and conductivity properties 24 p3432 A72-45068

ADDRESSING

Electroluminescent matrix display system with amorphous semiconductor threshold switches for isolation and memory, discussing performance and address waveforms 12 p1788 A72-27239

Machine oriented language for modular computer programming, discussing subprogram composition, conditional addresses and description table structure 19 p2769 A72-38089

Air traffic density effect on secondary surveillance radar operation in ATC for aircraft identification and position determination, proposing selective address system 21 p3080 A72-40289

ADENINES

NT RIBONUCLEIC ACIDS

Adenine, guanine, cytosine and other nitrogen compounds synthesis from carbon monoxide, hydrogen and ammonia mixtures by Fischer-Tropsch-like process 04 p0483 A72-14765

ADENOSINE DIPHOSPHATE [ADP]

Platelet electrophoretic mobility response to adenosine diphosphate (ADP) in patients with coronary artery disease 15 p2183 A72-31283

ADENOSINE TRIPHOSPHATE [ATP]

Preglycolytic energy metabolism in biochemical evolution, concerning anaerobic oxidation of pyruvate and acetaldehyde to acetate and ATP 04 p0471 A72-14799

ATP injection protection against Co 60 or Cs 137 gamma radiation in albino mice, guinea pigs and dogs 05 p0621 A72-16636

Thin layer chromatography technique for rapid quantification of bacterial cell adenosine triphosphate, using microscope ultraviolet photometer 06 p0763 A72-17872

Blood serum proteins thermal stability in patients with vegetative vascular and neuroendocrine syndromes, discussing ATP effects 09 p1266 A72-22877

Pressure sensitivity of Na-K-Mg ATPase activity from rat intestine, investigating inhibiting effects of oxygen, nitrogen and helium tension increases 10 p1424 A72-23731

Energy metabolism and ATP balance characteristics during muscular activity as function of organism adaptation to activity 13 p1902 A72-28640

Muscle cell ATP, creatine phosphate and lactate concentration changes relation to oxygen uptake during and after exercise 14 p2080 A72-30705

The influence of exogenous ATP on cardiac metabolism in acute hypoxia. 17 p2501 A72-34987

Muscle metabolism of ATP, CP, glycogen and lactates at rest and during submaximal and maximal exercise 21 p3005 A72-40421

Muscle metabolism during isometric exercise performed at constant force. 21 p3005 A72-40425

Visual acuity restoration improvement after flash blindness by monocular shielding and ingestion of vitamin complexes containing ATP with pyridoxal, considering twilight vision 21 p3012 A72-41748

Specific ATP action on metabolism of isolated heart - Influence of pH, divalent cation concentration and stability of complexes. 22 p3147 A72-42986

ADENOSINES

NT ADENOSINE DIPHOSPHATE [ADP]

NT ADENOSINE TRIPHOSPHATE [ATP]

Acid base equilibrium effects on chlorophyll primary photosynthetic regulating mechanism, considering electron transfer to NADP and ATP formation 04 p0468 A72-14778

Biological energy transformation origin and evolution, discussing inorganic pyrophosphates precursor to adenosine phosphates as energy carriers 04 p0470 A72-14798

Inhaled oxygen pressure variation effects on adenosines, glucose, lactate and pyruvate levels in rat brains, noting anoxic limit value relation to age 07 p0924 A72-20658

ADHEROMETERS

U ADHESION TESTS

ADHESION

Nonmetallic material properties effects on structural design for reliability, considering molecular chain folding, polymer crystallization, entropic molecular segregation, adhesion and intermolecular forces
01 p0092 A72-10986

Solid lubricant coatings adherence to porous materials, discussing porosity acquired by sulfuration treatment in melted salts bath on soft steel surface
06 p0823 A72-18590

Polymer films friction properties under high pressure, discussing Amonton law failure and adhesion theory application
06 p0837 A72-18597

Chopped fiber glass reinforced high density thermoplastic polyethylene composite, determining critical fiber length, interfacial adhesion and fracture toughness
08 p1193 A72-21684

Electrostatic adhesive devices for zero-g intra/extravehicular activities, noting applications to astronaut and cargo maneuvering, worksite restraint, tool and equipment tiedown, etc
10 p1431 A72-24650

Surface reaction mechanisms analysis in adhesion, friction, wear and lubrication, using electron diffraction, Auger spectroscopy and ellipsometry techniques
12 p1813 A72-27036

Temperature effects on crystalline solids adhesion, noting friction rise above seizure point
12 p1818 A72-28187

Apiezone lubricants physicochemical properties comparison, noting aromatic hydrocarbons effect on thermo-oxidation stability and polyisoprene rubber type polymer additive effect on adhesiveness
16 p2413 A72-33171

Adhesion effects on tensile and thermal expansion properties of aluminum oxide particles filled epoxy-urethane polymer at ambient and liquid nitrogen temperatures
16 p2415 A72-33415

High temperature oxide scale adherence on Fe-Cr-Al alloys with Y or Sc additions as promoting agents
16 p2410 A72-33817

Incore thermionic reactor cylindrical Mo emitter covered with two CVD W layers, discussing first layer adhesion and diffusion characteristics and work function stability
18 p2707 A72-36135

Adhesive wear theoretical model based on asperity interactions number, area and volume, considering implications for friction and surface temperature analysis
19 p2809 A72-38377

Application of statistical methods to studies of the surface properties of polymers
21 p3072 A72-40080

Reversible changes in polyethylene coating adhesion due to thermo-oxidative destruction of polyethylene
21 p3072 A72-40082

ADHESION TESTS

Sliding friction and normal force adhesion under ultrahigh vacuum environment, describing test apparatus for real time analysis via contact resistance measurement
08 p1176 A72-21436

Metal adhesive forces to clean Fe surface measured with LEED and Auger emission spectroscopy, noting binding energy correlation to oxygen
10 p1497 A72-24821

Clean metallic surfaces adhesion coefficients in vacuum at 77-293 K as function of load, loading time and contact cycles
12 p1818 A72-28193

Ice adhesive shear strength to steel bearing surfaces coated with bonded solid lubricants, describing low temperature test apparatus and results
[ASLE PREPRINT 72AM 4] 13 p1964 A72-28970

Detonation deposited coatings, determining adhesive strength as function of coating thickness and process technological parameters
14 p2107 A72-30432

Adhesion characteristics of alpha-aluminum oxide-nickel system from shear strength measurements, investigating effects of sintering parameters and Ti and Zr alloying components
20 p2940 A72-39445

Non-destructive testing of adhesive bonded metal-to-metal joints. II.
24 p3408 A72-45290

NDT techniques selection, economics and organization for aircraft industry, considering ultrasonic holographic and adhesion tests
24 p3408 A72-45292

ADHESIVE BONDING

Metal-skin honeycomb composite structure design and manufacture for Concorde rudder, noting structural adhesive bonding in aircraft construction
04 p0589 A72-15090

Adhesive bonded components in aircraft and aerospace structures, discussing manufacturing, metal surface preparation, inspection and environmental exposure
[SAE PAPER 720118] 06 p0835 A72-17325

Flexure analysis of isotropic Reissner flat plates bonded by adhesive layer, deriving stress distribution equations in general tensor form
[AIAA PAPER 71-148] 07 p1089 A72-19688

Tensile load elastostatic transfer from rectangular cross section web to two infinite parallel sheets, deriving Cauchy type integral equation for adhesive bond force density
07 p1095 A72-20241

Maximum allowable time between Ti metal surface preparation and agent application in adhesive bonding
07 p1024 A72-20254

Graphite fibers surface treatment and interfacial adhesive bonding, considering resin composites shear strength enhancement by sulfuric acid and sodium chlorate oxidation
08 p1194 A72-21697

Water effect at epoxy resin-steel interface on adhesive bond strength as function of vitrification temperature
08 p1196 A72-21863

Residual shrinkage and thermal stresses in adhesion bond models of metal coatings and cemented seams
08 p1248 A72-21865

Electrical measurement of moisture resistance and hydrophilicity of cast epoxy and organosilicon adhesives
12 p1833 A72-27449

Adhesive bonding of L-1011 body shell panels for improved fatigue strength and corrosion resistance
15 p2245 A72-32429

Fracture mechanics approach to adhesive joints.
17 p2633 A72-35282

Combined spot weld-adhesive bonding to join sheet metal parts with applications to propellant tanks and spacecraft and aircraft structures
[SME PAPER AD 72-710] 18 p2695 A72-36526

Stress distribution and displacements in adhesive bonded lap-jointed aerospace structures, presenting approximate solution
18 p2740 A72-37214

Strain distribution in and around strain gauges.
19 p2870 A72-37225

Stability analysis of internal pressure loaded crack in adhesive layer bonding elastic plate to rigid base using energy and critical load intensity criteria
19 p2870 A72-37245

Adhesive joints strength and polymeric film breakdown dependence on substrate molecular forces at base interface
19 p2806 A72-37533

Adhesion and transfer of PTFE to metals studied by Auger Emission Spectroscopy.
19 p2807 A72-37646

Holographic interference as a means for quality determination of adhesive bonded metal joints.
[ICAS PAPER 72-06] 21 p3060 A72-41131

Combined mode crack extension in adhesive joints.
23 p3305 A72-43493

The molecular-kinetic theory of polymer adhesion
23 p3307 A72-43930

Bonded joints - Squeeze-out /flash/ effect on fatigue strength.
23 p3353 A72-44248

Bonded honeycomb structures. II - Bonded joints and non-destructive testing.
24 p3407 A72-45288

Non-destructive testing of adhesive bonded metal-to-metal joints. I.
24 p3408 A72-45289

Non-destructive testing of adhesive bonded metal-to-metal joints. II.
24 p3408 A72-45290

ADHESIVES

NT GLUES

Aerospace adhesives applications, discussing thermal and mechanical properties, and cryogenic, epoxy, urethane silicone and fluorocarbon types
01 p0090 A72-10188

Adhesive materials based on room temperature vulcanizing silicone elastomers for space shuttle vehicle reusable surface insulation bonding
01 p0075 A72-10763

Adhesives and techniques for bonding plastics with plastics and nonplastic materials
02 p0236 A72-12610

Polymer adhesives chemistry and properties in 450 F air, discussing weight loss and strength values
03 p0381 A72-14233

Electrical contacts conduction principles, considering circuit voltage, current, variable resistance and resistive, mechanical, heating and adhesive properties
06 p0791 A72-18578

Adhesives use for assembly of mechanical, optical, nucleonic and electronic instruments including printed and integrated circuits
07 p0992 A72-20576

Adhesive bonded clad Al corrosion penetration rates from accelerated tests
[SAE PAPER 720344] 11 p1656 A72-25600

Tacky adhesive tearing between two flexible strips, solving Newtonian viscous fluid slow flow problem by iterative numerical scheme
12 p1798 A72-27831

Adhesives polymerization and rapid ambient temperature curing, using Co 60 gamma rays and electron beams
12 p1833 A72-28079

Tensile strength of fiber glass reinforced plastic elements joined by cover plates and nonlinearly elastic adhesives
13 p1962 A72-28737

Polymeric structural adhesives thermal stability evaluation, recommending thermodifferential analysis and calorimetry to supplement thermogravimetric method
16 p2415 A72-33510

Heat resistant adhesives properties and selection, discussing thermosetting-thermoplastic resins and ceramic materials for temperatures to 4400 F
16 p2415 A72-33597

A fracture mechanics analysis of adhesive failure in a single lap shear joint.
[SESA PAPER 1990A] 17 p2630 A72-34815

ADIABATIC CONDITIONS

Adiabatic charged particle orbits in magnetic null sheet with transverse electric and added normal magnetic fields
03 p0348 A72-13512

Local skin friction evaluation in compressible flow, using incompressible Clauser charts and sublayer methods for adiabatic and nonadiabatic situations
03 p0341 A72-13614

Solar wind protons adiabatic spatial cooling related to temperature anisotropy
05 p0709 A72-16067

Equilibrium temperature distribution on radiatively adiabatic smooth and rough planes uniformly irradiated by collimated solar flux
[AIAA PAPER 72-59] 05 p0749 A72-16876

Heat pipe operating conditions and evaporator, condenser and adiabatic parts, discussing fluid capillary transport for heat pipe calculation
05 p0750 A72-17047

Adiabatic-nuclei theory application to diatomic molecules excitation by electron impact, approximating fixed nuclei phase shifts dependence on inter-nuclear separation
06 p0852 A72-17826

Hadron era evolution, discussing equation of state, ultimate temperature, galactic formation and adiabatic exponent application to Friedman universes
06 p0886 A72-18096

Hydrogen and helium thermal dissociation and ionization at Jupiter and Saturn adiabatic atmospheric models conditions
08 p1211 A72-21127

Slow adiabatic motions of vibratory suspended bodies and determination of carrying body parameters and orientation from oscillations monitoring
08 p1206 A72-21229

Velocity space instability in hot electron plasma created by adiabatic compression in pulsed magnetic mirror, observing radiation bursts below electron cyclotron frequency during compression
[AD-740408] 08 p1213 A72-21257

MGD equations for ideal plasma steady plane adiabatic flow in magnetic field, considering analogy to Chaplygin equations
08 p1214 A72-21645

Self-similar adiabatic expansion of gas behind shock wave front sustained by radiation, describing gas pressure, density and velocity profiles
08 p1152 A72-22049

Adiabatic transition experimental implementation by molecular beam irradiating field frequency variation
10 p1491 A72-24210

Contact binary star systems model, considering superadiabatic energy transfer mechanism of convective envelope
10 p1550 A72-25199

Mass transfer effect on adiabatic wall enthalpy and recovery factors in laminar boundary layer flow at high injection rates, using self similar solutions
11 p1746 A72-26535

Cryogenic microwave equipment for solids study provided with adiabatic demagnetization cooling system, noting relaxation time measurement in magnetic fields
12 p1796 A72-27856

Adiabatic density perturbations damping by radiative viscosity and heat conductivity, taking into account plasma recombination in hot expanding Universe
14 p2148 A72-30202

Massive red supergiants radial pulsations from adiabatic theory application to convective envelope models based on mixing length theory and H-He ionization zones
14 p2159 A72-30743

Relict radio fluctuation observations, investigating adiabatic density perturbations related to formation of galaxies and galactic clusters
14 p2159 A72-30788

Adiabatic stellar shells stability in cases of rigid and compressible nucleus
15 p2304 A72-31334

- Adiabatic conditions influence on charge carriers dispersion determination of semiconductors based on Nernst-Ettingshausen effect
15 p2291 A72-31390
- Heat transfer to two dimensional laminar flow, calculating axial conduction and fluid preheating effects on adiabatic forced convection at low Peclet number
15 p2336 A72-32478
- Metal specimens yield point in adiabatic tension determined by thermoelectric method from temperature-stress and stress-strain diagrams
15 p2259 A72-32690
- Low energy cosmic ray deuteron and He 3 source spectra observation implications for adiabatic deceleration in solar cavity, discussing interstellar propagation
16 p2448 A72-33743
- New demonstration of the adiabatic theorem for conservative systems in wave mechanics
18 p2711 A72-36473
- Two chamber adiabatic test compression system design with controlled throttle for high temperature nitrogen and nitrous oxide-type gases with exothermal reactions
18 p2676 A72-37189
- Compressor exergetic efficiency calculation from gas energy losses caused by pressure drop and cooling, noting relations to isothermal, adiabatic and polytropic efficiencies
19 p2746 A72-37668
- On the adiabatic invariants of a quantified system perturbed by a coherent wave
19 p2834 A72-37789
- Rotationally symmetric temperature distribution in region between two coaxial circular cones for isothermal and adiabatic conditions, solving heat conduction equation
20 p2983 A72-39329
- The behavior of two-phase systems during adiabatic expansion
20 p2953 A72-39595
- A method of computing skin friction and adiabatic wall temperature in a laminar boundary-layer without pressure gradient.
21 p3046 A72-41202
- Liquid dielectrics specific heat determination by adiabatic calorimeter with monotonic heating
21 p3059 A72-41819
- Heat transfer, adiabatic enthalpy /temperature/ of the wall, and hydrodynamic resistance in the presence of turbulent and laminar flow of a compressible fluid in a round tube
22 p3164 A72-41883
- Accuracy of the conservation of the third adiabatic invariant of charged-particle motion in axisymmetric fields. II
22 p3217 A72-42209
- On the formation of plastic adiabatic bands in a thin tube subjected to a dynamic torsion
22 p3236 A72-42638
- Adiabatic density perturbations damping by radiative viscosity and heat conductivity, taking into account plasma recombination in hot expanding universe
23 p3333 A72-43231
- Self ignition behaviour of some liquid fuels in an adiabatic compression machine.
23 p3325 A72-44252
- Iterative solution for adiabatic radial pulsation in massive main sequence star, noting transition to non-linearity via Eddington stability integral extension
24 p3438 A72-44833
- Factors affecting phase-change paint heat-transfer data reduction with emphasis on wall temperatures approaching adiabatic conditions.
[AIAA PAPER 72-1030] 24 p3389 A72-45407
- ADIABATIC FLOW**
- Fluid dynamical study of accretion process with gravitating point source motion through adiabatic gas, applying to galaxies
01 p0126 A72-10289
- Pressure drop relation to entropy production in viscous low velocity adiabatic pipe flow, showing analogy with Oswatitsch theorem
01 p0051 A72-11255
- Ultralong wave baroclinic instability, obtaining linearized perturbation equations from layered geostrophic hydrostatic adiabatic model
04 p0541 A72-14451
- Pressure recovery calculation for subsonic adiabatic air flow through diffusers with tail pipes, assuming turbulent inlet boundary layer
10 p1415 A72-23855
- Adiabatic velocity profiles and pressure variations of developing laminar flow in circular tube, using finite difference computation in FORTRAN IV
10 p1463 A72-23863
- Possible regimes and solutions for adiabatic one dimensional compressible gas flow in convergent and divergent ducts with friction
12 p1797 A72-27348
- Small cross flow integral method for growth prediction of three dimensional compressible turbulent boundary layers on adiabatic walls
[AIAA PAPER 72-697] 16 p2345 A72-34046
- Stationary adiabatic plasma flow in the magnetosphere.
20 p2919 A72-39547
- ADIPOSE TISSUES**
- Pure oxygen atmosphere effects at 450 and 600 mm Hg on rats in vitro liver and adipose tissue lipid synthesis, measuring food intake and plasma components
10 p1424 A72-23739
- ADJOINTS**
- Galerkin method application to nonconservative nonself-adjoint aeroelasticity problems based on interpretation as mathematical formulation of virtual work principle
07 p1025 A72-18788
- Goodman-Lance method of adjoints extension for solving boundary value problems of nonlinear differential equation systems
08 p1197 A72-20786
- Multiple completeness characteristics of eigenvectors and adjoint vectors of polynomial operator packets in separable Hilbert space
08 p1198 A72-21096
- Variational principle of linear differential equations.
18 p2705 A72-36717
- ADMINISTRATION**
- U MANAGEMENT**
- ADMITTANCE**
- U ELECTRICAL IMPEDANCE**
- ADMIXTURES**
- Phase diagrams of Ru binary and ternary systems, noting admixtures interactions
14 p2123 A72-30992
- Stabilization of a superconducting modification of beryllium by an aluminum admixture
20 p2960 A72-39407
- ADRENAL GLAND**
- Adrenocortical steroids during acute exposure to environmental stresses, noting effects of injected cortisol removal, uptake and release
06 p0763 A72-17874
- Hypothalamus increased noradrenaline turnover after adrenal glands demedullation in rats given disulfiram inhibitor
07 p0924 A72-20621
- Rat adrenal cortex morphology after 24 hour transverse acceleration stress, studying changes in lipid, ascorbic acid and RNA content and acid phosphatase activity
13 p1904 A72-29310
- Serotonin precursor 5-oxytryptophan effects on hypothalamic-hypophyseal-adrenal complex under complete deafferentation of medial-basal hypothalamus
13 p1907 A72-30016
- Nervous-emotional stress as a problem of modern work physiology
22 p3148 A72-43170
- Adrenal morphology changes in rats subjected to hypokinesia
23 p3255 A72-43905
- ADRENAL METABOLISM**
- Hypertrophic effects of chronic exercise on plasma corticosterone and adrenal cortex in rat
04 p0473 A72-15219
- Phenamine and aminazine effects on subthreshold sound perception and adrenoreactive excitability of unstable subjects under emotional stress
04 p0476 A72-15586
- Circadian adrenal periodicity of plasma corticosteroid levels in man under random living schedule
09 p1265 A72-22643
- Adrenocortical response to prolonged high altitude hypoxia in hypothalamic deafferented rats, showing rapid neural stimulation with delayed humoral activation
12 p1763 A72-27829
- Hemodynamic thermoregulatory and sympathoadrenal responses to heat acclimatization in man during supine and upright position exercise
17 p2506 A72-35963
- Adrenaline and noradrenaline metabolic stages and production mechanism under various physiological and pathological conditions, noting application to flight emotional stress detection
21 p3002 A72-41196
- Exogenous modifications of circadian rhythms of adrenal hormones in man.
22 p3147 A72-42978
- Influence of elevated partial oxygen pressure on the sympathetic-adrenal and acetyl-choline systems
24 p3371 A72-44595
- Unconjugated urinary corticosterone excretion in laboratory rats exposed to high pressure helium-oxygen environments.
24 p3374 A72-45656
- ADRENALINE**
- U EPINEPHRINE**
- ADRENERGICS**
- Beta-adrenergic and vagal blockage altered autonomous control effects on left ventricular function in conscious dogs, noting heart rate, stroke volume and end-diastolic and end-systolic diameters
02 p0163 A72-12090
- Phenamine and aminazine effects on subthreshold sound perception and adrenoreactive excitability of unstable subjects under emotional stress
04 p0476 A72-15586
- Beta-adrenergic inhibitors effects on coronary blood flow and myocardial oxygen consumption of normal and coronary artery disease patients
08 p1118 A72-21549
- Propranolol as adrenergic beta receptor inhibiting agent for hyperthyroidism symptom amelioration
08 p1118 A72-21550
- Adrenergic innervation of internal carotid arteries in extra- and intracranial regions in dogs, using luminescence method
08 p1121 A72-22184
- Oxygen consumption and body temperature in anesthetized, paralyzed and artificially ventilated dogs cooled in water bath at 34 C, measuring hypercapnia and beta-adrenergic blockade effects
10 p1424 A72-23735
- Beta-adrenergic blocking effect on canine coronary and systemic hemodynamic adaptation during treadmill exercise
11 p1579 A72-25802
- Acute hypoxia effects on dog coronary blood flow and cardiac function from cardiac beta-adrenergic and hemodynamics study
12 p1760 A72-27482
- Pharmacological effects on the central adrenergic regulation mechanisms of blood circulation
17 p2504 A72-35019
- Nucleic acid contents in cholinergic and adrenergic spinal cord neurons and in their glial satellite-cells during hypoxic hypoxia and a post-hypoxia period
19 p2756 A72-37742
- ADRENOCORTICOTROPIN [ACTH]**
- Shock-induced fighting effect on pituitary adrenocorticotrophic hormone ACTH and adrenocortical steroids plasma concentration in rats, relating psychological stress to physiological function
05 p0617 A72-16080
- ADSORBENTS**
- Development of a desiccant CO2 adsorbent tailored for shuttle application.
[ASME PAPER 72-ENAV-11] 20 p2896 A72-39166
- ADSORPTION**
- NT CHEMISORPTION**
- Surface active materials adsorption on developing bubble surface, analyzing time dependence
03 p0458 A72-14155
- Ar, Kr, methane and nitrogen physisorption isotherms on stainless steel in low pressure cryogenic baths calculating mean adsorption energies
05 p0624 A72-16395
- Adsorption, corrosion and hydrogen embrittlement effects on crack formation in quenched carbon steels in active media, using tensile stress-rupture tests
08 p1190 A72-22183
- Adsorption role in planetary primordial rare gas origin based on adsorptivity pattern of pulverized Al-lende meteoritic samples at 113 K
09 p1385 A72-22597
- Electron reflection mechanism and gas adsorption effect at W /001/ surface in energy range 1-10 eV
09 p1370 A72-22804
- Nitrogen adsorption kinetics on bulk W targets investigated by ultrahigh vacuum, molecular beam, reflexion detector method
09 p1276 A72-22806
- Methane, hydrogen and oxygen adsorption and displacement on crystal surface of W investigated by thermal desorption and work function changes
09 p1276 A72-22807
- Carbon monoxide and hydrogen adsorption on graphite, measuring sticking probabilities
12 p1777 A72-27039
- Slag powdery material moisture content determination by absolute pyridine adsorption method of moisture extraction
12 p1813 A72-27450
- CdTe thin film solar cell room temperature prolonged operation instability, thermal degradation and performance improvement by gas adsorption removal
12 p1756 A72-28017
- Low energy electron diffraction structures due to CO and oxygen adsorption on clean Re surfaces produced by Ar ion bombardment at 20 to 920 C
13 p2020 A72-28522
- Statistical adsorption kinetics model with electron desorption of oxygen on polycrystalline W, noting sticking coefficients
13 p1912 A72-28523
- Na additions effects on Si growth velocity and morphology in Al-Si alloys, considering coupled zone adsorption mechanism
13 p1975 A72-28664
- High temperature contact creep tests in vacuum and in metal melts, noting adsorption effect on surfaces plastic deformation
13 p1963 A72-28768
- Effect on physical and mechanical properties of hard metals due to gas sorption by metallic films spray-coated on surfaces, describing vacuum apparatus
13 p1939 A72-29488

Surface phonon appearance criteria associated with crystal surface gas adsorption, discussing entropy variation and colliding particle-crystal energy exchange 15 p2280 A72-31858

Oxygen monolayer amounts adsorption on yttrium films and molybdenum foil investigated by Auger electron spectroscopy, observing growth of shifted peaks 15 p2292 A72-31860

Hydrogen adsorption and absorption by niobium, investigating sticking probability and heat of solution 15 p2276 A72-31864

Carbon monoxide adsorption on nickel surface, determining preferential orientation by extended Huckel calculations 15 p2276 A72-31867

Tight binding model for binding energy determination in transition atoms adsorption on same series transition metal substrate, using moments expansion technique 15 p2281 A72-32379

Molecular adsorption on semiconducting surfaces, discussing conditions for formation of local surface levels in forbidden gap 15 p2296 A72-32760

H I region molecular formation on interstellar dust grains, discussing nonequilibrium evaporation mechanism for adsorbed particles 16 p2452 A72-33128

Cs adsorption on W and Ti observed by combination of ellipsometry, Auger spectroscopy and surface potential difference measurements, noting sticking coefficient and coverage 16 p2442 A72-33833

Hydrocarbon electrochemical oxidation kinetics for fuel cells at low temperature, considering adsorption and bond cleavage 16 p2361 A72-33891

Oxygen adsorption effect in Cs-W thermionic converter system, comparing statistical-mechanical model analytical results with Alleau-Bacal experimental data 17 p2496 A72-34597

Impurities and additives effects on electrode properties in Cs vapor thermionic converter, noting coadsorption model for Cs-W-O surface 17 p2496 A72-34598

Ellipsometry for the study of equilibrium cesium adsorption. 17 p2552 A72-34599

W /100/ work function change during adsorption of oxygen, cesium, and oxygen-cesium co-adsorption 18 p2656 A72-36128

Work function, thermal stability, and atomic structure of electropositive films adsorbed on single crystals of metals 18 p2656 A72-36132

Possibility of an inhomogeneous charge distribution in an adsorbed layer 18 p2713 A72-36176

Quartz microbalance studies of an adsorbed helium film. 18 p2719 A72-36675

High vacuum technology applications in surface physics research, discussing atomic collisions and adsorption processes 18 p2712 A72-36827

Flash desorption spectrum and LEED studies of CO adsorption on W single crystal planes, measuring work function increase as function of coverage 18 p2657 A72-37040

Effect of surface heterogeneity on the adsorptive behavior of orbiting pressure gases. 19 p2869 A72-38752

Skylab regenerable carbon dioxide removal system. [ASME PAPER 72-ENAV-4] 20 p2896 A72-39173

Application of statistical methods to studies of the surface properties of polymers 21 p3072 A72-40080

Polymer adsorption as a cause of changes in contact interaction intensity between two solid surfaces 21 p3059 A72-40083

Relation between the work function and adsorption and catalytic properties of transition metal borides in the reaction of recombination of hydrogen and nitrogen atoms 22 p3187 A72-41926

Gas adsorption by refractory metal single crystals. 22 p3187 A72-41940

Manifestation of the effect of adsorptive reduction in strength under conditions of selective transport during boundary friction 22 p3183 A72-43138

Adsorbed oxygen inhibition of reactions of hydrogen with tungsten. 23 p3298 A72-43270

ADVANCING GLACIERS
U GLACIERS
ADVECTION
 Temperature advection mesostructure from wind measurements for precise short term forecasts 02 p0254 A72-12778

Thermal advection statistical relation to vertical motion, discussing conventional synoptic meteorological empirical facts utilization in numerical models for long term weather forecasting 02 p0254 A72-12779

Mountain barrier and convective area minimum size determination for numerical forecasting models, reducing primitive equations system to advection difference equation 04 p0544 A72-15459

Theoretical model of large scale topographical effects on wind generation through temperature advection, applying to Mars atmosphere general circulation. 10 p1531 A72-23707

Centered difference approximation for atmospheric model advection equation by two step Lax-Wendroff method, discussing computational instability due to lattice separation 11 p1680 A72-25768

Hybrid forecast model for hydrometeors short range prediction based on meteorological satellites cloud pattern observations and quasi-Lagrangian advection analog 13 p1993 A72-28858

AEOLOTROPISM
 Stresses induced by torsional vibration in twisted composite cylindrical shell of cylindrically aeolotropic materials for high and low frequencies 16 p2466 A72-33102

AERATION
 Combined centrifugal oil filter, pump and deaerator for gas turbine engine lubrication systems, noting heat transfer effectiveness increase 18 p2694 A72-36050

AERIAL EXPLOSIONS
 Tungusk meteorite explosion energy values for various altitudes from investigation of shock wave propagation in variable density atmosphere 14 p2152 A72-30492

Tungusk meteorite explosion energy values for various altitudes from investigation of shock wave propagation in variable density atmosphere 19 p2864 A72-38321

AERIAL IMAGERY
U AERIAL PHOTOGRAPHY
AERIAL PHOTOGRAPHY
 Aerial focal plane shuttered camera high velocity images mathematical model based on collinearity equations, incorporating translational and rotational camera motion during exposure for image motion compensation 01 p0066 A72-10461

Aerial triangulation for optimum photogrammetric project parameters, discussing flight altitude, bridging distance and control points for computerized optimization 01 p0066 A72-10462

Aerial multispectral scanners and ground data stations for water quality measurements and pollution abatement [AIAA PAPER 71-1096] 01 p0067 A72-10545

Earth resources information systems using satellite and aerial IR terrain photography and ground teams for international cooperation, emphasizing timber inventory 01 p0063 A72-10950

Airborne remote sensing of earth surface physical properties, using panchromatic and IR black and white, true color and IR false color photography 02 p0208 A72-11782

Silicate rocks mapping from aerial IR data, discussing method for discriminating emission from background radiation 02 p0208 A72-11787

Sedimentary rocks remote multispectral analysis by aerial data covering UV to microwave spectral regions 02 p0209 A72-11788

High altitude aircraft and Apollo 9 multispectral photography and simulated ERTS-A imagery evaluation, comparing with ground observations in Arizona 02 p0210 A72-11799

Environmental analysis of Lake Tahoe Basin from small scale multispectral aerial imagery, discussing color enhancement usefulness for interpretation and management of natural resources 02 p0210 A72-11800

Computer enhancement of multispectral satellite-and-air-photographs and imagery for earth resources 02 p0186 A72-11801

Aerial multispectral scanner data determination with filtering and smoothing along flight line over extended areas, deriving algorithm for cloud-shadowed area detection 02 p0212 A72-11817

Oil slicks aerial photographic and multispectral scanner investigation, discussing detection effectiveness of UV, blue, green and IR imagery 02 p0226 A72-11829

Small scale aerial photography use in regional agricultural survey, discussing equipment used, sampling techniques and data collection and interpretation 02 p0213 A72-11835

Computerized statistical identification of aerial photograph ground patterns, comparing elliptical boundary condition with minimum distance to mean classification models 02 p0187 A72-11842

Automated photometric wetland mapping using aerial color film microdensitometric analysis and computer techniques 02 p0215 A72-11886

Soviet aerial survey techniques for natural resources data, discussing photograph interpretation, fast aerospectrometers, data processing and multispectrum cameras 02 p0216 A72-11888

RADAM /Radar Amazon/ side-looking radar imagery and multiband aerial photography for mineral, vegetation, soil and water resources mapping in Brazil 02 p0216 A72-11890

Hyperaltitude photography evaluation for geological mapping, comparing Gemini 4 and aerial photographs 02 p0216 A72-11891

Urban geographic social-spatial pattern determination with aerial photographic interpretation 02 p0229 A72-12019

Frequency contrast characteristics derivation method with devices for determining transfer functions of objectives and film, using electron-optical bench 02 p0229 A72-12171

Quantitative reliability criteria for aerial photo decoding, noting dependence on observation time 02 p0229 A72-12172

Southeast Florida 13 year urban and agricultural development recorded by high altitude color and color-IR photographs, demonstrating capability for detail and macroscale patterns 02 p0230 A72-12199

Space and high altitude aerial photography agricultural ground data collection and processing for Arizona survey evaluation 02 p0220 A72-12200

Mesometeorological processes in tropic and subtropical zone based on cloud photographs obtained from aircraft and satellites 02 p0255 A72-12792

Cathode ray tube recorder for remote airborne photographic mission 03 p0360 A72-13711

Satellite photograph interpretations, discussing wind direction indication, cloud structure, automatic mapping and hydrographic exploration 03 p0351 A72-14306

Urban area aerial photography survey for large scale photomaps, discussing building feature examination and universal stereophotogrammetric instruments utilization 03 p0362 A72-14311

Book on aerial photoecology covering aerial survey images interpretation, processing and printing operations and economic considerations 04 p0514 A72-14572

Aerial photographic determination of sea state, using reflection at water surface of natural light diffuse component radiated by sky-sun combination 04 p0525 A72-15563

Side-looking airborne radar /SLAR/ images comparison with small-scale low-sun black and white aerial photographs 05 p0661 A72-16041

Buffalo photographic aircraft for oil slick remote sensing, using aerial cameras and thermal IR scanner 05 p0658 A72-16600

Film flatness in airborne cameras, reducing large area and short period photogrammetric deviations 06 p0815 A72-17758

Thermal IR imaging remote sensing device for aerial earth resource surveys, noting hydrogeology, volcanology, forest fire and geothermal region detection and ice sheet study applications 06 p0807 A72-17789

Remote sensing methods in geology, discussing air/satellite-borne black and white, color and multispectral photographic, TV, multispectral scanning, IR and radar techniques 06 p0809 A72-18228

Remote sensing possibilities by aerial photographic methods based on scanning, scatterometer, radiometer and vidicon systems, discussing ground resolution, data automation and satellite observation [DGLR PAPER 71-128] 06 p0818 A72-18234

Survey camera design for continuous film advancement and prismatic image displacement compensation 07 p0987 A72-19860

Unified time recording for aerial photographic surveys, using exact time synchronized control signal sequences in recording camera shutter release 07 p0988 A72-19893

Photogrammetric light beam refraction during aerial surveys, considering air pressure, temperature and humidity gradients in and out of camera carrier 08 p1165 A72-21161

Aerial photographs inclination angles determination from stereocomparator measurements and terrain angles interrelationship 08 p1165 A72-21162

Linear programming procedure for efficiency and cost optimization in aerial survey mission 08 p1165 A72-21164

U.S. Navy cartography, describing RA-3B Skywarrior capabilities and photographic instrumentation 08 p1169 A72-21699

Drobyshev stereograph corrector operation for aerial photographs processing with transformed beam of stereoprojector

09 p1308 A72-22483

Computer calculation of spectral brightness coefficients on aerial photographs, determining contrast features density gradients

09 p1308 A72-22484

Aerial stereopair photograph orientation for geodetic coordinate adjustment in terms of collinearity, coplanarity and scaling

09 p1308 A72-22486

Panoramic aerial cameras with revolving objective or mirror, presenting formulas for photoimage plots geometric characteristics

09 p1308 A72-22487

Correlation functions for angular vibrations of operating aerial camera during working cycle

09 p1310 A72-22947

Correction procedures for spherical surface transformation on plane for high altitude aerial photographs

09 p1310 A72-22948

Mean coordinate and distance errors in photogrammetric measurements of two neighboring models carried out by two image scales and four aerial cameras

09 p1311 A72-22969

Aerial photography interpretation for studies of natural environment and resources

09 p1312 A72-23277

Multifactor landscape synthesis of aerial imagery for regional surveys

09 p1301 A72-23278

Aerial photography for rural soil mapping, considering geographic, ecologic and agricultural production interpretation

09 p1301 A72-23279

Aerial photointerpretation for landscape analysis with respect to agricultural land use, considering geomorphologic, hydrographic, soil and microclimatic conditions

09 p1301 A72-23280

Urban geography of U.S. cities on vertical aerial photography, considering site, location, street orientation, expansion, business districts and transportation networks

09 p1301 A72-23281

False color aerial photographs interpretation for cultivated wooded area inventory

09 p1302 A72-23282

Multiband color aerial photography interpretation for forest appraisal in U.S.S.R.

09 p1302 A72-23285

Color aerial photographs interpretation for forest tree type composition determination, comparing to IR sensitive black and white films

09 p1302 A72-23286

Multiband aerial photography application to vegetal cover determination, evaluating film types, seasons and scales

09 p1302 A72-23287

Multiband photointerpretation of forested land units, using aerial black and white photographs and film-filter combinations

09 p1302 A72-23288

Color aerial photograph evaluation for forest damage demarkation, using film-filter combinations

09 p1302 A72-23289

False color aerial photographs for road quality classification in forests

09 p1302 A72-23290

Aerial photointerpretation in forest administration, discussing electronic data processing methods

09 p1302 A72-23291

Soil science and climatology use for archeological site detection on aerial photographs

09 p1303 A72-23296

Education and training of personnel for photointerpretation, discussing psychological, physiological and methodological aspects of aerial photointerpretation

09 p1272 A72-23298

Psychological aspects in aerial photointerpretation, discussing importance of perception of image contrast, contours and areal distribution

09 p1272 A72-23299

Internal and integral aerial photointerpretation, discussing enhancement of information quality, quantity and reliability through participation of experts in various specialized fields

09 p1303 A72-23300

Environmental applications of airborne IR imagery, discussing detection, mapping and monitoring of water bodies thermal patterns and anomalous heat manifestations on land

09 p1312 A72-23301

Terrain evaluation by aerial imagery, discussing various film types for conventional visible and IR black and white and color photography, thermal IR and/or radar

09 p1303 A72-23303

Black and white aerial photographs quantitative evaluation for differentiation and identification of land use patterns by microdensitometry, using statistical methods

09 p1313 A72-23306

Sea depth determination in coastal waters based on solar reflection aerial photographs interpretation, presenting formula as function of swell parameters

09 p1303 A72-23307

Automation of aerial photointerpretation based on application of photometric, microdensitometric and digital computer technology

09 p1313 A72-23308

Optical image filtering to simplify and facilitate automatic aerial photointerpretation processes

09 p1313 A72-23310

Zeiss aerial photographic lens systems imaging quality characteristics in visible and near IR spectral ranges

09 p1313 A72-23311

Aerial photography and photogrammetry objectives and requirements for natural resources surveys

09 p1304 A72-23312

Color interpretation of pedological factors from aerial photographs in relation to agricultural seasons and use of panchromatic and false color emulsions

09 p1304 A72-23313

Terrain evaluation for engineering purposes through aerial photointerpretation in terms of physiography, geology, soil and vegetation

09 p1304 A72-23314

Three stage retinal model for visual monitoring method applied to computerized photointerpretation of aerial photographs

09 p1284 A72-23624

Crop classification by airborne multispectral observations, suggesting sample regions selection method for spectral signatures identification based on statistical similarities

11 p1628 A72-26985

Film flatness in airborne cameras, reducing large area and short period photogrammetric deviations

12 p1809 A72-27818

Photogrammetric camera system imaging characteristics comparison with aerial reconnaissance, multispectral and return beam vidicon systems, noting economic benefits due to smaller scale imagery

12 p1805 A72-27819

Photomaps plotting from high altitude photographs, presenting expressions for segment areas selection

13 p1954 A72-28496

Computer program analysis of errors in mutual orientation elements on aerial photographs with different lengthwise overlaps, discussing error minimization

13 p1955 A72-28497

Jet aircraft photographic observation of solar corona polarization during March 1970 solar eclipse

13 p2043 A72-29545

Large scale mapping by photogrammetric method based on contour points of outdated small scale aerial survey photographs, noting root-mean-square errors

13 p1959 A72-29633

Photographic observation of satellites to sixth magnitude with K-24 aerial camera on Polaroid 3000 and 10,000 ASA film, recording time signals on magnetic tape

14 p2084 A72-30235

Aerial survey camera with automatic exposure control, discussing film emulsions sensitivity characteristics, object light intensity range and measuring methods

14 p2105 A72-30839

Computer controlled ground truth station for environmental agricultural aerial photographic remote sensors data processing, discussing system components, printout format and computer program

15 p2213 A72-31249

Airborne remote sensing missions and instrumentation to investigate Penobscot River water ecology for thermal, chemical and solid pollutants

15 p2221 A72-31252

Topographic mapping from airborne radar geodetic measurements, evaluating photogrammetric accuracy

15 p2224 A72-31603

Correction formulas for aerial photograph distortions due to internal refraction of light rays in separation of gas media by lateral surface of circular cylinder

15 p2277 A72-31214

Exposure calibration, orientation and point coordinate distortions in aerial photographs from one or two camera stations

15 p2240 A72-32378

Coastal environment remote sensing from satellite and aircraft imaging platforms for geological, oceanographic and ecological investigations

15 p2232 A72-32622

Balloon-nacelle for small scale photography and multispectral photometric ground measurements, describing automatic adjustment device for photographic lens diaphragm

16 p2349 A72-33633

Photogrammetric light beam refraction during aerial surveys, considering air pressure, temperature and humidity gradients in an out of camera carrier

17 p2552 A72-34452

Aerial photographs inclination angles determination from stereocomparator measurements and terrain angles interrelationship

17 p2552 A72-34453

Linear programming procedure for efficiency and cost optimization in aerial survey mission

17 p2521 A72-34455

Two dimensional images from remote sensors, discussing geometrical properties and imaging equations for aerial, IR and radar photographs

17 p2555 A72-35335

Screen equidensities in aerial photograph interpretation

17 p2555 A72-35337

Night photography at 10,000 feet.

17 p2557 A72-35556

Modulation measurement applied to the focusing of aerial cameras.

17 p2558 A72-35948

Landscape site and vegetation /timber/ predictions from color and IR aerial imagery compared with ground data

18 p2686 A72-36318

Multispectral photography in soil moisture determination and soil series differentiation.

18 p2686 A72-36320

Coherent optical terrain-relief determination using a matched filter.

18 p2691 A72-36491

Learning strategy-based pattern recognition system for automatic classification of terrain type from aerial photography

18 p2691 A72-36494

A new computer-assisted stereocomparator.

18 p2664 A72-36499

A digital portable line-drawing rectifier.

18 p2692 A72-36500

The accuracy of the intermittent photographic film advance in the camera of an airborne thermal scanner.

18 p2692 A72-36697

Psychophysical information content evaluation of aerial photographic images by human viewer for photointerpretation and search in reference library

20 p2894 A72-39042

Aerotriangulation by simultaneous adjustment of photogrammetric and geodetic observations /SAPGO/ incorporating geodetic distances, horizontal angles, Laplace azimuths, longitudes, latitudes and elevation differences

20 p2927 A72-39738

Photogrammetric refraction equation and integral interpretation for actual atmosphere, climate and weather conditions suitable for photographic flights

20 p2927 A72-39739

Solar altitude nomogram for estimating terrestrial ground objects heights from shadow length on aerial photographs

22 p3181 A72-43196

Waterways outfall detection from color and IR color aerial photography, describing photointerpretation technique

22 p3181 A72-43197

Investigations regarding the condition of normal equations in the case of block triangulation according to the bundle method. I

23 p3284 A72-43632

Balloon nacelle for terrain photography from very high altitudes

24 p3403 A72-45229

AERIAL RECONNAISSANCE

Remote airborne sensors for sea water oil pollution surveillance in near UV, thermal IR and microwave regions

01 p0057 A72-10535

NASA Earth Resources Survey program review, discussing satellite and aircraft observation application to agriculture, geology, hydrology, geography, oceanography and environment pollution

12 p1877 A72-27688

East African low level cross equatorial air current exploration, using light aircraft-borne Doppler radar wind finding equipment

12 p1840 A72-27703

Photogrammetric camera system imaging characteristics comparison with aerial reconnaissance, multispectral and return beam vidicon systems, noting economic benefits due to smaller scale imagery

12 p1805 A72-27819

Weather forecasting support of NASA programs involving earth oriented viewing and sensing experiments from aircraft and spacecraft

13 p1990 A72-28816

Aerial IR line scanner systems for forest fire detection, considering escalation from aircraft to space platform

15 p2221 A72-31250

Digital technique for automatic change detection in aerial reconnaissance side-looking radar imagery, discussing image correlators

17 p2557 A72-35554

Photomorphic units for regional analysis from hyperaltitude and spacecraft remote sensing data

18 p2690 A72-36321

AERIAL RUDDERS

Metal-skin honeycomb composite structure design and manufacture for Concorde rudder, noting structural adhesive bonding in aircraft construction

04 p0589 A72-15090

Solar rudder for spacecraft steering in form of right circular cone with ideally reflecting surface
11 p1727 A72-25943

Flight test of direct side force control by rudder deflection and asymmetrical drag on T-33 airplane, noting use in dive bombing
12 p1754 A72-27520

Jaguar powered flight controls, discussing wing spoilers, slab tailplane, rudder, autostabilization system and integrated packaging of actuators
16 p2353 A72-34144

AEROBES
Isolation of a polyvalent bacteriophage for *Escherichia coli*, *Klebsiella pneumoniae*, and *Aerobacter aerogenes*.
19 p2755 A72-37650

AERODONTALGIA
U TOOTH DISEASES

AERODYNAMIC AXIS
U AERODYNAMIC BALANCE

AERODYNAMIC BALANCE
Gas generator performance shifts involving military trim level variations by TF-30 engines in high relative humidity environment caused by condensation in inlet duct
07 p1052 A72-18759

Natural inertia moment effect of balance weight at wing tip on critical flutter rate
08 p1242 A72-21092

Aerodynamic center and center of pressure of slender small aspect ratio wing near solid or free surface, determining angle of attack effect
13 p1894 A72-29131

Experimental determination of asymmetry-induced trim angles of attack.
[AIAA PAPER 72-1032]
21 p2993 A72-41605

Effect on entry vehicle dynamic stability of aerodynamic and mass asymmetry coupling.
[AIAA PAPER 72-973]
22 p3231 A72-42338

AERODYNAMIC BRAKES
NT DRAG CHUTES
NT LEADING EDGE SLATS
NT SPLIT FLAPS
NT TRAILING-EDGE FLAPS
NT WING FLAPS

Parachute designs and applications to escape systems, paratrooping, supply dropping, aircraft braking, weapons systems stabilization, flight testing aids and sport
01 p0003 A72-10302

Static and dynamic load measurements for stress-strain behavior and load-time characteristics of aerodynamic decelerator canopy fabrics, using metal foil strain gages
02 p0287 A72-11507

F-111 aircraft landing gear and speedbrake hydraulic system control by single dual-function valve, describing design features and performance characteristics
08 p1111 A72-21024

Equipment for ground and sea recovery of sounding rocket payloads, discussing airbrakes, buoy and parachute assemblies
15 p2319 A72-31690

AERODYNAMIC BUZZ
U FLUTTER

AERODYNAMIC CENTER
U AERODYNAMIC BALANCE

AERODYNAMIC CHARACTERISTICS
NT AERODYNAMIC BALANCE
NT AERODYNAMIC DRAG
NT AERODYNAMIC STABILITY
NT INTERFERENCE DRAG
NT INTERFERENCE LIFT
NT JET LIFT
NT LIFT
NT ROTOR LIFT
NT STATIC AERODYNAMIC CHARACTERISTICS
NT SUPERSONIC DRAG
NT ZERO LIFT

Nonporous rigid parachute models three component measurements, using low speed wind tunnel for testing skirt length effects on aerodynamic characteristics
01 p0003 A72-10303

Aerodynamic behavior of thin jet-flapped airfoil, investigating integrodifferential equation solution
02 p0149 A72-11669

Turbulence degree effects on aerodynamic properties of planar decelerating cascades at Reynolds numbers 50,000-250,000, discussing blade boundary layer characteristics
[DGLR PAPER 71-096]
02 p0153 A72-12716

Aircraft spin characteristics due to superstall, comparing three stall types with respect to recovery, yaw damping and rate of rotation
[DGLR PAPER 71-057]
02 p0155 A72-12718

Unsolved aerodynamic problems in sub- and transonic civil and military aircraft design, considering flow problems during transonic flight, takeoff and landing
[DGLR PAPER 71-105]
02 p0153 A72-12745

Tip clearance effect on compressor blade aerodynamic characteristics, applying Boullay analysis to low aspect ratio rectangular wing
02 p0153 A72-12825

Acoustical oscillations effect on free jet flow stability and boundary layer structure, using inviscid Orr-Sommerfeld equation for flow disturbances frequency, wavelength and velocity
03 p0340 A72-12913

Circular jet discharging perpendicular to solid surface into transverse flow, discussing effects on infinitely thin circular wing aerodynamic characteristics
03 p0309 A72-13915

Geometrical and aerodynamic characteristics of circular cross section diffuser channels from turbulent boundary layer calculation at preparation flow stage
04 p0461 A72-14647

Upper atmospheric turbulence correlation to supersonic aircraft dynamics, noting Concorde contribution
04 p0542 A72-14681

Aerodynamic interference between parallel bodies for estimating aerodynamic characteristics of rocket engine with auxiliary boosters, obtaining flow field by slender body theory
05 p0600 A72-16005

Axial flow multistage compressor design, discussing high speed flow measurements and Reynolds number and blade airfoil shape effect on aerodynamic performance
05 p0601 A72-16483

Radial inflow gas turbine rotating blades aerodynamic characteristics, noting exducer shape effect on turbine performance
05 p0601 A72-16484

Stalled blade rows dynamic performance in terms of blade channel fluid inertia and surface boundary layer-caused time delay
05 p0602 A72-16487

Two dimensional cascade test of air-cooled turbine nozzle, describing aerodynamic characteristics and heat transfer properties
05 p0602 A72-16489

Slat-airfoil combinations aerodynamics modeled by single point vortex to represent leading edge slat, discussing on-line computer graphics program
[AIAA PAPER 72-221]
05 p0603 A72-16798

Sail rotors for hovering platform, calculating rotor performance based on ideal two-dimensional flexible airfoil section characteristics
[AIAA PAPER 72-66]
05 p0612 A72-16925

Two dimensional lift characteristics of multielement airfoils, using potential flow method based on surface source distribution and finite difference boundary layer method
[AIAA PAPER 72-3]
05 p0608 A72-16935

Nonsymmetrical aerodynamic damping moments on 10 deg cone at supersonic speeds and large angles of attack, comparing Newtonian theory prediction with wind tunnel test results
[AIAA PAPER 72-29]
05 p0609 A72-16947

Aerodynamic characteristics of STOL aircraft with externally blown jet augmented flaps, predicting interference between lifting surfaces and turbofan engines
[AIAA PAPER 72-63]
05 p0609 A72-16953

Aerodynamic and thermodynamic phenomena in Hartmann-Sprenger tube with converging walls and excited by subsonic or adapted supersonic jet
06 p0901 A72-17559

V-shaped wings supersonic characteristics at 0-15 deg angles of attack, investigating flow structure between wings by pitot tube rake
06 p0757 A72-18129

Nonuniform propeller streams effects on aerodynamic characteristics of high aspect ratio wing, using airfoil theory
[AD-745477]
07 p0908 A72-19092

Aerodynamic characteristics of hypersonic velocity meteor traveling in earth atmosphere and shock wave propagation generated by explosion in air and on ground
07 p1081 A72-20094

Aeromechanical analysis of flight conditions for conventional aircraft, including kinematics of curvilinear motions with constant speed
07 p0913 A72-20372

Book on dynamics of atmospheric flight covering unsteady motion, small disturbance theory, aerodynamic characteristics, aircraft stability and control, handling qualities, etc
08 p1109 A72-21491

Tube flight vehicle system thrust and power requirements prediction by aerodynamic analysis with division of near and far flow fields
08 p1107 A72-21608

Aerodynamic efficiency of plane slotted blade cascades of adjustable nozzle diaphragms in transport aircraft axial flow gas turbine engines
09 p1374 A72-23186

Nonlinear longitudinal aerodynamic characteristics effect on rigid aircraft response to normal acceleration due to atmospheric turbulence, using power spectral technique
09 p1263 A72-23461

Aerodynamic data acquisition with magnetic balance on wind tunnel model delta and AGARD G wing planforms and body of revolution
10 p1462 A72-24770

Spacecraft trajectories for reentry at hyperbolic velocity, examining aerodynamic control loads and characteristics in atmospheric skip
11 p1718 A72-25929

Russian book on An-12 turboprop transport aircraft structural and aerodynamic characteristics covering engine operation, piloting, stability, controllability, etc
12 p1755 A72-28343

Measurement techniques for separated gas flows mean and fluctuating aerodynamic properties, discussing improved optical geometry for laser Doppler anemometer
13 p1956 A72-28632

Inviscid incompressible flow past longitudinally curved small aspect ratio slender wing, investigating aerodynamic characteristics
13 p1893 A72-28729

Numerical solution of algebraic equation encountered in aerodynamics of hypersonic boundary layer interacting with external flow on thin solids of revolution
13 p1895 A72-29848

Arbitrary cascade profiles aerodynamic characteristics calculation via integral equation numerical solution for attached potential incompressible fluid problem
14 p2070 A72-31014

Transient flow induced by shock front impingement on Laval nozzles observed by schlieren method, noting time variations of temperature and pressure
15 p2179 A72-32144

Aerodynamic properties prediction procedure for thin jet-flapped airfoil in incompressible inviscid flow bounded by different types of boundaries
15 p2179 A72-32147

Aircraft instrumentation system accuracy relation to aerodynamic derivatives evaluated from flight data, proposing input and transient response measurement system
16 p2394 A72-33640

Aerodynamic stall characteristic prediction from static experimental data for airfoils, noting boundary layer effects
[AIAA PAPER 72-682]
16 p2346 A72-34060

Atmospheric properties effect on satellite aerodynamic characteristics, noting gas composition and upper atmospheric winds
[AIAA PAPER 72-659]
16 p2347 A72-34075

Leading edge serrations effect on rotor noise and aerodynamic characteristics, noting vortex and rotational noise reduction and overall efficiency decrease
[AIAA PAPER 72-655]
16 p2349 A72-34079

Experimental study of the aerodynamic characteristics of burning gas-air jets in the transient flow region of natural gas
17 p2637 A72-35169

Variable sweep wings aerodynamic characteristics in subsonic, transonic and supersonic flight, considering lift, drag, stability and control
18 p2643 A72-36976

Methodology for estimating STOL aircraft high lift systems characteristics.
[AIAA PAPER 72-779]
19 p2752 A72-38138

Burke-Shumman-Zeldovich model for aerodynamic characteristics of straight jet laminar diffusion flames, considering free, semibounded and slipstream types
19 p2882 A72-38460

Aerodynamics of a slender cone with asymmetric nose bluntness at Mach 14.
20 p2886 A72-39634

Aerodynamic structure analysis of steady flame of homogeneous gas mixtures, noting streamlines, isotherms, isobars and flame front curves
21 p3129 A72-40979

Application of the elementary-balance method to the calculation of the nonstationary temperature fields and aerodynamic characteristics of several versions of a surface-type heat exchanger
21 p3130 A72-41064

Aerodynamic interference between aircraft components - Illustration of the possibility for prediction.
[ICAS PAPER 72-49]
21 p2992 A72-41174

Aerodynamic characteristics of the slotted fin.
21 p2992 A72-41262

Numerical solution to the Navier-Stokes equations in the problem of a gas flow past a rectangle
22 p3166 A72-42252

Aerodynamic characteristics of bodies of revolution with large fineness ratios at Mach numbers ranging from 0.2 to 6.0
22 p3134 A72-42286

Flight mechanics of spin stabilized rotating disks for special ordnance delivery, considering aerodynamic parameters relation to dynamic stability and orientation
[AIAA PAPER 72-982]
22 p3134 A72-42332

Low-drag artillery projectile aerodynamic characteristics and dynamic flight behavior from wind tunnel, spark range and instrumented flight tests, describing mathematical trajectory simulation
[AIAA PAPER 72-979]
22 p3134 A72-42334

Free-flight projectiles aerodynamic characteristics and trajectories from yawsonde and radar track data, obtaining best fit coefficients by equations of motion numerical integration [AIAA PAPER 72-978] 22 p3134 A72-42335

Ablative nose shape change effects on re-entry vehicle aerodynamic performance. [AIAA PAPER 72-974] 22 p3230 A72-42337

The effects of protuberances and scaling parameters on the aerodynamic characteristics of an air-to-air cruciform missile. [AIAA PAPER 72-969] 22 p3231 A72-42342

Heat transfer effects on reentry vehicle surface boundary layer stability and aerodynamic characteristics, noting stall angle reduction and drag increase from wind tunnel tests [AIAA PAPER 72-960] 22 p3137 A72-42357

Steady state equations of motion, equilibrium shape and stability derivatives of elastic airplanes evaluated with finite element methods. 22 p3138 A72-42845

Main results of nonlinear rotor theory 23 p3247 A72-43419

An aerodynamics model applicable to the synthesis of conventional fixed-wing aircraft. [SAWE PAPER 908] 23 p3250 A72-43455

Conical caret wings supersonic characteristics, examining flow transition from weak to strong attached shock waves 24 p3361 A72-45114

Status of hotshot wind tunnels for hypersonic aerodynamic studies. 24 p3388 A72-45203

Flight test investigation of the aerodynamic behavior of various-sized stabilizers on a small helicopter. 24 p3362 A72-45328

Ablative asymmetric conical nose bluntness changes effects on aerodynamic characteristics for moderate magnitude tilt angles 24 p3363 A72-45341

Asymmetric nose bluntness effects on the aerodynamics of a slender cone at Mach 14. 24 p3363 A72-45342

Application of plane fixed equations of motion to reentry vehicle flight analysis. 24 p3452 A72-45345

The determination of a general relation between the aerodynamic properties of a single airfoil and those of the same airfoil arranged in an arbitrary cascade. 24 p3363 A72-45363

A method for estimation of axial turbomachinery stage characteristics on the basis of experimentally obtained data with a runner tested in a free blow-out aerodynamic scheme. 24 p3363 A72-45364

Aerodynamic characteristics of turbine blade cascades in unsteady incompressible and compressible fluid flow, considering axial flow turbine blades vibration 24 p3364 A72-45524

Aerodynamic characteristics of two-dimensional waverider configurations. 24 p3365 A72-45793

AERODYNAMIC CHORDS

U AIRFOIL PROFILES

U CHORDS [GEOMETRY]

AERODYNAMIC COEFFICIENTS

Sound radiation from axial flow fans running in turbulent flow, evaluating fluctuating lift on rotor blades due to incident gusts 01 p0002 A72-10220

Aircraft stability coefficient determination by numerical integration fitting to differential equations of motion 01 p0005 A72-11136

Motion of asymmetric body of revolution in rotating liquid, calculating drag on ellipsoid 02 p0204 A72-12175

Area rule for change in lift/drag ratio of hypersonic delta wing due to conical body addition on compression side 02 p0151 A72-12270

Power law bodies lift and drag coefficients interrelationship under Newtonian nonaffine similarity laws, presenting rules for equivalent transformations identification 02 p0151 A72-12273

Jet aircraft brake parachute loads under engine wake, evaluating velocity and drag coefficient influences 02 p0155 A72-12504

Wing-fuselage combination aerodynamic coefficients, comparing experimental data with subsonic linear and nonlinear theoretical results [DGLR PAPER 71-115] 02 p0153 A72-12723

Two dimensional airfoil pressure distribution measurements at high subsonic speeds, comparing normal force coefficients corrected for wind tunnel interference effects with theoretical calculations [DFVLR-SONDDR-168] 03 p0308 A72-13609

Dynamic damping coefficient extraction from reentry vehicle flight test telemetered lateral rate data 03 p0441 A72-13951

Gas-metal surface interactions effect on aerodynamic lift and drag coefficients in free molecular flow 03 p0342 A72-14059

Flat plate, sphere and circular cylinder drag and lift coefficients in free molecular flow 04 p0463 A72-15645

Multimoment solutions to convective heat transfer from sphere, discussing maximum drag coefficient and validity at all Knudsen numbers [ASME PAPER 71-WA/HT-1] 05 p0743 A72-15863

Heat transfer, drag and lift coefficients for free molecular flow over concave surfaces, describing Monte Carlo simulation technique [ASME PAPER 71-WA/HT-17] 05 p0744 A72-15876

Isothermal elastohydrodynamic theory for full range of pressure-viscosity coefficient, considering film thickness effect 06 p0821 A72-17805

Conical and spherical nose shapes effects on drag and static stability at Mach 10 07 p0908 A72-19695

Pressure distribution and force coefficients for cones at angles of incidence as function of Mach number, using extended method of equivalent axisymmetric bodies 10 p1417 A72-24028

Wind tunnel investigation of Reynolds number effects on boundary layer separation incidence and maximum lift coefficient of high-lift device equipped aircraft model 10 p1419 A72-24657

Lift and pressure fluctuations of cambered airfoil under periodic longitudinal and transverse gusts, applying to axial flow turbomachines [ASME PAPER 72-GT-30] 11 p1569 A72-25626

Hypersonic gun tunnel balance and pressure measurements on sharp leading edge delta wings, comparing experimental coefficients and shock angles with predicted values 11 p1571 A72-25735

Rotating airfoil experimental test program for verification of Himmelskamp and Dwyer-McCroskey theoretical analysis, presenting graphs of lift coefficient vs angle of attack 12 p1752 A72-28124

Supersonic aerodynamic influence coefficients matrices calculation for wings of arbitrary planform, constructing computer program 12 p1752 A72-28142

Satellite aerodynamics effect on atmospheric density determination, discussing drag coefficient dependence on altitude 13 p1990 A72-28821

Aerodynamic profiles lift coefficient determination by empirical formula based on potential flow lines obtained by conformal mapping 13 p1894 A72-29132

Roughened and smooth spherical wind sensors lift and drag, calculating aerodynamic coefficient spectra from velocity 13 p1894 A72-29620

Vortex-lattice method for subsonic aircraft aerodynamic coefficients calculation, verifying results with airbus lifting surface wind tunnel test data 15 p2178 A72-31401

Rarefied gas flow problems, discussing mean free path effects on sharp nosed conical and bluff bodies drag and heat transfer coefficients 15 p2218 A72-32314

Free molecular flow over rotating sphere satellite, deriving aerodynamic forces on differential surface to determine drag and lift coefficients 16 p2341 A72-32844

Atomic and molecular beams fluid dynamic applications in rarefied gas flows exemplified by satellite drag coefficient measurement 16 p2429 A72-33052

Aerodynamic coefficients determination from momentum and energy exchange between low velocity molecular jet and solid surfaces, describing time of flight measurement technique 16 p2390 A72-33069

Angle of attack increase of an airfoil in decelerating flow. 16 p2641 A72-36773

Prediction of the stalling of a wing section in incompressible flow [ONERA, TP NO. 1088] 19 p2746 A72-37760

V/STOL aircraft configurations with lifting counter-rotating disks, presenting aerodynamic coefficients from rotating water tank experiments 21 p2990 A72-41070

Lift on airfoils with separated boundary layers. 21 p2992 A72-41264

Measurement system decomposition for aerodynamic coefficient estimation. [AIAA PAPER 72-964] 22 p3177 A72-42345

Computation of the potential-theoretical flow around wing-fuselage combinations and a comparison with measurements 23 p3249 A72-44298

Effect of the ratio of the axial-flow velocities in front of and behind the cascade on the aerodynamic coefficients of a plane compressor cascade 24 p3360 A72-44995

Limitations in the acquisition of nonlinear aerodynamic coefficients from free-oscillation data by means of the Chapman-Kirk technique. 24 p3362 A72-45336

AERODYNAMIC CONFIGURATIONS

Equilibrium configuration of cable towed in circular path, presenting multivalued boundary value problem mathematical analysis [AD-737445] 01 p1012 A72-11132

Wing-fuselage combination aerodynamic coefficients, comparing experimental data with subsonic linear and nonlinear theoretical results [DGLR PAPER 71-115] 02 p0153 A72-12723

Supersonic wind tunnel investigation of drag characteristics of clustered booster configuration in longitudinal flow at Mach 1.5 to 4.0 [DGLR PAPER 71-120] 02 p0153 A72-12737

Subsonic three dimensional potential flow computational method lifting aerodynamic configurations analysis and design [AIAA PAPER 72-188] 07 p0907 A72-18958

Concorde aerodynamic configuration R and D, discussing wing layout in terms of drag, stability, control and weight distribution characteristics 07 p0911 A72-19057

Airfoil ram-wing air-water hybrid vehicle X-13 Am design and operational principles based on aerodynamic ground effect, discussing flight tested performance characteristics 09 p1262 A72-22971

Centrifugal turboengine diffuser with high enlargement area compared with logarithmic spiral types, discussing boundary layers, secondary flow, shapes and aerodynamic parameters 10 p1463 A72-23747

Optimal configuration of lifting bodies for hypersonic speeds, noting negligible effect of blunt leading edges 10 p1418 A72-24536

Transport aircraft aerodynamic design technology application to general aviation propeller driven twin engine aircraft, discussing wing loading and aspect ratio optimization [SAE PAPER 720337] 11 p1576 A72-25595

Far field sonic boom approach effects, describing Whitham theory extension for ultimate N wave deviations for body configurations with continuous or discontinuous tangent 16 p2347 A72-33010

Wind-tunnel Magnus testing of a canted fin or self-rotating configuration. 17 p2486 A72-35254

Three-dimensional structure and equivalence rule of transonic flows. 20 p2886 A72-39631

High subsonic transport aircraft design development based on supercritical aerodynamic configuration and advanced structural, flight control and propulsion system technologies [AIAA PAPER 72-756] 20 p2889 A72-40056

A stability analysis for tethered aerodynamically shaped balloons. 23 p3250 A72-43332

Effect of several wing tip modifications on a trailing vortex. 23 p3247 A72-43334

Effects of variations in lift and drag response to longitudinal control on the ease and quality of landing. 24 p3368 A72-45333

Gas dynamics problems of oblique shock waves around aerodynamic bodies, noting exact quasi-explicit and approximate explicit solutions 24 p3394 A72-45445

AERODYNAMIC DRAG

NT SUPERSONIC DRAG

Axial cords effects on parachute drag and stability characteristics and opening time, discussing wind tunnel and balloon drop tests results 01 p0004 A72-10306

Parachutes flow characteristics in low speed free descent, discussing glide angle effect on total drag and water channel flow pattern studies 01 p0004 A72-10309

Parachute opening shock and filling time calculation based on aerodynamic drag, air mass and effective porosity time functions, using momentum and continuity equations 01 p0004 A72-10310

Aerodynamic design of atmospheric reentry vehicles forebody, considering maximum drag for hypersonic bodies 02 p0149 A72-11726

Helicopter rotor tip drag relief estimate based on two dimensional drag divergence with Mach number, airfoil parameters and flight conditions 02 p0154 A72-12882

Small sphere hydrodynamic drag in ionized gas at local thermodynamic equilibrium, taking into account nonlinear transport properties variations with temperature [ASME PAPER 71-APM-CC] 04 p0558 A72-15176

Heat transfer and drag during air laminar flow in circular pipe with constant heat flux density at wall
07 p0966 A72-18938

Geostrophic drag coefficient for heterogeneous terrain as function of effective roughness length, considering surface friction effects in large scale atmospheric models
07 p1030 A72-19108

Body drag measurement in low density supersonic gas stream in various Knudsen number ranges
08 p1166 A72-21409

Spheres drag coefficient measurements in laminar flow as function of Reynolds number, using wind tunnel model magnetic suspension system
10 p1419 A72-24772

High intensity free stream turbulence effects on flow past circular cylinder at subcritical Reynolds numbers, measuring unsteady lift and drag
11 p1573 A72-26640

Momentum consideration aided air resistance calculations for cylinder, discussing position effects
13 p1893 A72-28705

Spacecraft optimal control after transfer from hyperbolic trajectory to planetary satellite orbit by atmospheric drag, minimizing engine thrust
14 p2129 A72-30470

Interplanetary spacecraft transfer maneuver for hyperbolic trajectory change into eccentric orbit, using aerodynamic drag to obtain nearly circular orbit
14 p2151 A72-30471

Aerodynamic drag at high latitudes observed from Molniya satellites orbit analysis, suggesting upper atmosphere density change
15 p2229 A72-31989

Optimum nonslender bodies of revolution minimum drag in free molecular flow under integral constraints
15 p2180 A72-32395

Lift and induced drag characteristics of jet flapped finite span wings in close proximity to ground, using method of matched asymptotic expansions
16 p2341 A72-32827

Free molecular flow over rotating sphere satellite, deriving aerodynamic forces on differential surface to determine drag and lift coefficients
16 p2341 A72-32844

Thrust recovery factor and base drag losses in annular jets as function of jet thickness to base diameter ratio, determining recirculation mass flow
18 p2683 A72-37045

Drag of a finite flat plate set parallel to a uniform flow.
18 p2683 A72-37045

An investigation of the flow around rectangular cylinders.
19 p2747 A72-38813

Sting-free measurements of sphere drag in laminar flow.
21 p2989 A72-40110

Long-term orbit prediction using two-variable asymptotic expansions and the automated manipulation capabilities of the FORMAC language.
[AIAA PAPER 72-938] 21 p3113 A72-41576

The design and operation of a large tube-vehicle aerodynamic testing facility.
[AIAA PAPER 72-1001] 21 p3041 A72-41586

Effect of gas slipping on drag in a system of parallel cylinders at low Reynolds numbers
22 p3133 A72-42268

Atmospheric density from spacecraft drag data by successive optimization of control laws, using quadratic programming
23 p3277 A72-44003

Drag spectra of simple structures in turbulence.
23 p3281 A72-44102

Determination of slender bodies of minimum total drag in hypersonic flow using Newton-Busemann pressure coefficient law.
23 p3249 A72-44267

On required guidance for transfer from hyperbolic trajectory to the planetary satellite orbit by aerodynamic drag in atmosphere.
24 p3450 A72-45176

Determination of aerodynamic drag from radar data.
24 p3362 A72-45337

Transonic wall interference effects on bodies of revolution
[AIAA PAPER 72-1008] 24 p3389 A72-45404

AERODYNAMIC FORCES

NT AERODYNAMIC DRAG

NT AERODYNAMIC LOADS

NT BLAST LOADS

NT GUST LOADS

NT HYPERSONIC FORCES

NT INTERFERENCE LIFT

NT JET LIFT

NT LIFT

NT ROTOR LIFT

NT SUPERSONIC DRAG

NT WING LOADING

NT ZERO LIFT

Resonant vibration and stresses of dynamically nonuniform annular cascade under aerodynamic interaction of alternating different blades
01 p0143 A72-11368

Stroboscopic measurement of elastic untwisting angles of axial compressor rotor vanes under centrifugal and aerodynamic forces
01 p0143 A72-11371

Aerodynamic forces and pressure distribution measurement on wing-body combination model, investigating boundary layer on wing upper surface
02 p0151 A72-12228

Unsteady supersonic aerodynamic forces on oscillating circular cylindrical shell calculated using linearized equation of potential flow
02 p0151 A72-12256

Rigid boundary effect on thin panel flutter speed, determining aerodynamic forces via linearized potential theory
03 p0443 A72-13402

Lifting surface linearized potential theory for unsteady aerodynamic forces on wing and horizontal tail surfaces, using computer program
03 p0308 A72-13541

Environmental forces effects on gravity oriented satellites attitude dynamics, considering earth atmosphere aerodynamic and solar radiation forces effects
07 p1085 A72-19060

Interference induced unsteady aerodynamic forces on tandem airfoils in subsonic flow, using two dimensional model
07 p0910 A72-20101

Laughing gull metabolism dependence on flight speed and angle during wind tunnel tests from oxygen consumption, carbon dioxide production and aerodynamic forces analyses
08 p1115 A72-21080

Aerodynamic and gravitational effects on relative motion of two orbiting point masses connected by flexible nonexpandable thread
08 p1240 A72-21143

Pressure sensor measurements of fluctuating aerodynamic forces on rotor blades related to compressor noise generation
[ASA PAPER H 6] 08 p1107 A72-21486

Flying machine using reaction forces on body moving in compressible fluids within piston device equivalent to air pressure pump
08 p1108 A72-21798

German monograph on shaft and wall effect in aerodynamic measurements with three orifice pressure probes in wind tunnels
09 p1259 A72-22320

Hovercraft internal and external aerodynamic forces, discussing control, suspension, yawing moments, directional and roll stability and random surfaces performances
09 p1260 A72-22824

Aerodynamic field around singular stagnation point of blunt body tip with detached shock, using Legendre functions
09 p1261 A72-22932

Pressure distribution and force coefficients for cones at angles of incidence as function of Mach number, using extended method of equivalent axisymmetric bodies
10 p1417 A72-24028

Aerodynamic forces calculation for constant vortex shear flows around airfoil fixed between rectilinear walls, noting resultant perpendicularity to Ox axis
10 p1465 A72-24115

Aerodynamic force and moment measurements on model in magnetic wind tunnel balance system, using field equations
10 p1461 A72-24765

Magnetic balance measurements of aerodynamic forces on spheres and slender cones in hypersonic low density wind tunnels, noting sting effect
10 p1462 A72-24771

Rectangular and D-shaped cylinders pressure distribution and aerodynamic force measurements in two dimensional flow as function of cross sectional height/width ratio
10 p1419 A72-24840

Plane irrotational motion of ideal incompressible fluid perturbed by profile movement and deformation, obtaining aerodynamic forces power
10 p1420 A72-24853

Subsonic unsteady aerodynamic pressures on blades of compressor wheel rotating freely in air stream
[ONERA, TP NO. 1077] 10 p1420 A72-24854

Computerization of panel flutter boundary calculations with aerodynamic forces derived from linear three dimensional unsteady potential flow theory
[AIAA PAPER 72-403] 11 p1731 A72-25424

Axial flow compressor and turbine loss coefficients, correlating blade rows geometric and aerodynamic variables effects
[ASME PAPER 72-GT-18] 11 p1703 A72-25617

Coupled librational motion of gravity oriented satellite in circular orbit under aerodynamic forces, discussing limiting stability and periodic solutions
11 p1726 A72-25914

Aerodynamic lag effects on wing bending dynamic response at supersonic speeds, noting application to stress estimation under gust loads
11 p1572 A72-25922

Unsteady aerodynamic forces on flat plate in locally perturbed incompressible potential flow, investigating angle of attack frequency response to periodic local perturbations
11 p1573 A72-26579

Breakup of accelerating liquid drops in gas dynamic flow, presenting unified theory for acceleration and aerodynamic effects
11 p1619 A72-26641

Asymptotic stability of mechanical system with two mathematical pendulums and rod subjected to axial follower, correcting aerodynamic and dissipative forces
12 p1847 A72-27979

Slender profile in nonuniform flow, deriving lift, normal force distribution and moment from vortex and source distribution induced flow field
13 p1894 A72-29005

Mathematical model for flow field inside raindrop under aerodynamic transient stresses before impingement at stagnation point of blunt body in supersonic flight
13 p1942 A72-29224

Integral equation for calculation of unsteady aerodynamic forces on helicopter lifting rotor blades, taking into account air compressibility
[ONERA, TP NO. 1081] 13 p1895 A72-29671

Rarefied gas interaction with spacecraft surface, calculating aerodynamic forces and accommodation coefficient for Proton 2 satellite
14 p2162 A72-30474

French monograph on hot-wire anemometry techniques covering support aerodynamic perturbations, crossed wire probes and turbulent flow free boundary
14 p2106 A72-30946

Hingeless elastic helicopter blades coupled flap-lag motion under quasi-steady aerodynamic loads, reducing equations of motion to coupled nonlinear differential equations
15 p2180 A72-31211

Aerodynamic effects on circular-orbiting cylindrical satellites coupled librational motion, analyzing equilibrium configurations stability by linearized and Liapunov direct method
15 p2320 A72-31818

Unsteady viscous flow effects on aerodynamic forces exerted on oscillating elliptic airfoil for various Reynolds numbers, angles of attack and frequencies
15 p2180 A72-32344

Supersonic flow aerodynamic window for high power laser beam extraction through nonabsorbing gas medium while supporting pressure difference between cavity and ambient atmosphere
[AIAA PAPER 72-710] 16 p2404 A72-34036

Nonlinear panel response from a turbulent boundary layer.
17 p2632 A72-35228

Optimal aerodynamic attitude stabilization of near-earth satellites.
17 p2622 A72-35488

Rotor and grid motions associated with holomorphic two dimensional fluid velocity, obtaining aerodynamic forces
19 p2746 A72-37787

Aerodynamic and gravitational effects on relative motion of two orbiting point masses connected by flexible nonexpandable thread
20 p2977 A72-39248

Russian book - Experimental studies of helicopter aerodynamics.
20 p2887 A72-39598

Unsteady aerodynamic and aeroelastic effects in turbomachine blade cascades supersonic flow, discussing trends in fan and compressor technology
21 p3118 A72-40969

Comparison of three oscillatory techniques for cones at incidence.
[AIAA PAPER 72-1015] 21 p3042 A72-41595

Nonstationary processes in the intervane apertures of turbomachines
22 p3133 A72-42247

Spin induced boundary layer distortion on rotating cone at supersonic speeds via spark shadowgraphs, correlating Magnus and normal force measurements with boundary layer configurations
[AIAA PAPER 72-967] 22 p3135 A72-42343

Recent progress regarding the measurement techniques in the hypersonic area
[ONERA, TP NO. 1055] 22 p3178 A72-42581

Aerodynamic solar semipassive hybrid system for continuous three dimensional attitude control of axisymmetric satellite in near-earth orbits, discussing operation, design and optimization
24 p3450 A72-45146

A study of dedicated control surfaces for direct sideforce control.
24 p3368 A72-45344

On certain aerodynamic processes for asteroids and comets.
24 p3445 A72-45463

Relation between a pilot's sensory perception of linear accelerations and the aircraft motion.
24 p3377 A72-45654

AERODYNAMIC HEAT TRANSFER

NT HYPERSONIC HEAT TRANSFER

NT SUPERSONIC HEAT TRANSFER

Factors affecting phase-change paint heat-transfer data reduction with emphasis on wall temperatures approaching adiabatic conditions.

[AIAA PAPER 72-1030] 24 p3389 A72-45407

AERODYNAMIC HEATING

NT SHOCK HEATING

Constant high tensile stress and rapid aerodynamic heating effect on maraging steels and Ti and Al alloys, evaluating test and simulation procedures for design data development

01 p0084 A72-10749
Isotopic heat source unit multiple elliptical orbit reentry unperturbed by solar-lunar gravitational forces, deriving analytical model of grazing trajectories, aerodynamic heating and thermochemical ablation

03 p0457 A72-13959
Equilibrium temperature formula derived for surface subjected to aerodynamic heating by gas from heat balance between convective and radiative heat flow

04 p0595 A72-14651
Stochastic aerodynamic heating of shallow shell in supersonic turbulent flow by Monte Carlo method

05 p0599 A72-15845
Linear two-temperature theory of thermoelasticity for investigating transient stresses arising from solid isotropic sphere aerodynamic heating

[ASME PAPER 71-WA/APM-14] 05 p0733 A72-15966
Vortex production of intense localized heating to leeward regions of bodies in hypersonic flows, proposing flow field models

[AIAA PAPER 72-77] 05 p0604 A72-16804
Plate surface temperature during aerodynamic heating in supersonic gas flow, using linearized Pohlhausen method

07 p0909 A72-19891
Rarefied flow fields and heating rates for space shuttle orbiter reentry at high angles of attack, using Monte Carlo simulation technique

[AIAA PAPER 72-314] 11 p1567 A72-25248
Color schlieren technique for simultaneous photographic recording of flow fields and heat transfer patterns in aerodynamic heating, noting application to shock-boundary layer interactions

11 p1629 A72-25257
Atmospheric model effects on space shuttle ascent and reentry trajectories and aerodynamic heating

13 p1990 A72-28813
Stochastic aerodynamic heating of shallow shell in supersonic turbulent flow by Monte Carlo method

15 p2178 A72-31264
Thermal simulation tests for kinetic heating of aerospace structures and materials, describing facilities for supersonic flight and atmospheric reentry

16 p2475 A72-32897
Inviscid surface streamlines and laminar, transitional and turbulent heating of blunt nose shuttle configurations in hypersonic flow

[AIAA PAPER 72-703] 16 p2345 A72-34041
Probability for spore sterilization by aerodynamic heating, considering straight line and decaying circular orbital Mars entry trajectories

16 p2461 A72-34165
Plate surface temperature during aerodynamic heating in supersonic gas flow, using linearized Pohlhausen method

17 p2485 A72-35139
Use of an infrared-imaging camera to obtain convective heating distributions.

20 p2926 A72-39640
Theoretical and experimental investigations on the problem of aerodynamic heating of re-entry vehicles.

[ICAS PAPER 72-39] 21 p3130 A72-41164
Correlations of peak heating in shock interference regions at hypersonic speeds.

21 p2992 A72-41309
Asbestos-textolite coating required thickness calculation with allowance for aerodynamic heating, discussing softening mechanisms

21 p3074 A72-41709
Telemetry acquisition of aerodynamic heat rates to conical, free-flight models at Mach 6 in an aeroballistic range.

22 p3155 A72-42703

AERODYNAMIC LIFT

U LIFT

AERODYNAMIC LOADS

NT BLAST LOADS

NT GUST LOADS

NT WING LOADING

Parachute inflation loads and times, presenting calculation method based on unsteady pressure distribution on decelerating inflating parabolic shell of revolution with unsteady starting vortex

01 p0004 A72-10311
Matrix method calculation for aerodynamic loads, transverse forces, bending moments, torques and twist of hinged main rotor blades in helicopter during forward flight

02 p0294 A72-12440
Steady and oscillatory subsonic aerodynamic loads prediction based on Doublet-Lattice method and

method of images, determining chord and spanwise loading on lifting surfaces

[AIAA PAPER 72-26] 05 p0607 A72-16917
Turbulent flow field velocity fluctuations errors by hot-wire anemometer filaments vibrations from fluctuating aerodynamic loads in Karman vortex street

05 p0664 A72-17013
Airloads and structural integrity flight testing / U.S. Air Force/, noting dynamic response, fatigue tests and temperature data acquisition

06 p0759 A72-18490
Downwash behind lifting surface related to loading in ideal incompressible gas by equations of motion linearization

07 p0908 A72-19110
Wing load distribution and induced drag control by warping, summarizing linear theory and wind tunnel test results

10 p1417 A72-24218
Hypersonic nonlinear aerodynamic loading effect on panel flutter, examining stability for various initial conditions

[AIAA PAPER 72-345] 11 p1728 A72-25374
Unsteady aerodynamic loadings of flexible aircraft with nonplanar wings and wing-tail surfaces in supersonic flow

[AIAA PAPER 72-378] 11 p1574 A72-25402
Axial flow turbines aerodynamic loading increase via control of velocity distribution and boundary layer evolution around airfoil profiles

[ASME PAPER 72-GT-78] 11 p1571 A72-25658
Nonlinear integral equations solution for heavily loaded actuator disk induced flow field, taking into account blade tip vortices and thrust coefficient effects

11 p1573 A72-26577
Low altitude gust load spectra above Czechoslovak territory interpreted in terms of equivalent velocity cumulative frequencies for light aircraft

14 p2071 A72-30282
Aeroelasticity, discussing gust and maneuver load alleviation, flutter suppression, aircraft stability, computerized aeroelastic analysis, aeroelastic optimization, composite structures, etc

15 p2322 A72-31202
Near flow field and aerodynamic loading in subsonic and supersonic flow over body-wing configuration, surveying numerical, kernel function and image methods

18 p2641 A72-36390
Evaluation of Reissner's correction for finite span aerodynamic effects.

18 p2736 A72-36774
Application of advanced methods to the determination of design loads of the Lockheed L-1011 TriStar.

[AIAA PAPER 72-775] 19 p2752 A72-38134
The application of non-planar lifting surface theory to the calculation of external-stress loads.

[AIAA PAPER 72-971] 22 p3135 A72-42340
Agricultural aircraft flight loads - Typical spectra and some observations on airworthiness.

24 p3366 A72-44734
An assessment of repeated loads on general aviation and transport aircraft.

24 p3366 A72-44736

AERODYNAMIC MOMENTS

U STABILITY DERIVATIVES

AERODYNAMIC NOISE

Acoustic, turbulent and thermal fluctuating motions interdependence in gas flow, considering application to aerodynamic noise theory

03 p0341 A72-13405
Aerodynamic noise interference generated by fluid flow in acoustically lined ducts

04 p0462 A72-15268
Noise generation from turbulent supersonic shear layers, including low supersonic and transonic ranges for jet noise applications

04 p0463 A72-15566
Multiple pure tone noise generation from turbofan blade to blade nonuniformities in rotor geometry, using two dimensional inviscid flow model

04 p0565 A72-15568
Pressure source model of sound radiated by sonic jet, deriving frequency spectra ratio and jet pressure

05 p0600 A72-16105
Leaning vanes for fan noise reduction, discussing rotor-stator plane fluctuating pressure amplitude decrease and radial distribution modification

[AIAA PAPER 72-126] 05 p0706 A72-16823
Cross flow effect on lifting fan noise at subsonic blade tip speeds, analyzing radiation pattern change due to inlet flow distortion

[AIAA PAPER 72-128] 05 p0608 A72-16921
Aerodynamic noise measurement, discussing physical units, spectral analysis, conversion and correction formulas

05 p0614 A72-17195
Diffraction theory relevance to aerodynamic noise theory, considering lf and hf behavior

06 p0847 A72-17767
Hovercraft noise and vibration source and reduction for improved crew and passenger comfort

07 p0912 A72-19648

Pressure sensor measurements of fluctuating aerodynamic forces on rotor blades related to compressor noise generation

[ASA PAPER H 6] 08 p1107 A72-21486
Cross correlation analysis of turbulent jet flow noise with pressure fluctuation as acoustic source

[ASA PAPER H 12] 08 p1150 A72-21488
Coherent and incoherent structures of aerodynamic noise, analyzing compressor near field and hot jet IR emission source

[ONERA, TPNO. 983] 09 p1294 A72-22816
Aerodynamic noise generation in turbulent fluid at low Mach number due to source near half plane by applying Kutta-Joukowski condition

10 p1415 A72-23724
Aerodynamic noise produced by gas jet flow around airfoil, discussing sound reduction

10 p1417 A72-24107
Aerodynamic noise generation mechanism of ideally expanded supersonic jet based on large scale flow instabilities, deriving mathematical model

10 p1418 A72-24331
IR measurement of hot jets turbulence intensity axial and transverse profiles, noting application to sound sources detection

10 p1563 A72-24656
Low pressure ratio Q-FAN propulsor noise reduction tests on wind tunnel model, discussing source components and design configurations

[ASME PAPER 72-GT-40] 11 p1569 A72-25634
Aircraft noise sources, showing noise intensity relationship to airfoil velocity and pressure ratio

13 p1897 A72-29568
Subsonic and supersonic heavily loaded axial flow rotors noise, discussing helicopter blade slap effect and compressor rotor-stator interaction

13 p1897 A72-29570
Fan engine compressor noise measurement by spinning mode synthesizer for use in duct liner optimization

13 p2028 A72-29574
Mathematical model for gas turbine engine inlet noise caused by shock wave impingement, noting dynamic wave system with overpressure and distortion

13 p2028 A72-29576
Acoustic dipole radiation by wall pressure fluctuations in turbulent boundary layer flow over rigid and plane surface at low Mach number

13 p1894 A72-29583
Tone burst pulse measurements of acoustic absorption coefficients in noisy environments for electronic simulation of wind tunnel noise

13 p2006 A72-29584
Aerodynamic noise and structural fatigue failure research and test facility, concerning supersonic jet and V/STOL aircraft

16 p2342 A72-32900
Turbulence induced sound pressure level measurement for noise generated by grill in air flow, using streamlined probe microphone

16 p2344 A72-34001
Aerodynamic normal shock noise measurements on nose cylinder bodies in transonic flow

[AIAA PAPER 72-669] 16 p2346 A72-34068
Airfoil vortex shedding noise in low-turbulence flow at helicopter blade Reynolds numbers, obtaining correlation coefficients for far field noise and surface pressure fluctuations

[AIAA PAPER 72-656] 16 p2347 A72-34078
Acoustic attenuation and thrust loss incurred by shrouded multistage supersonic jet noise suppressor

[AIAA PAPER 72-642] 16 p2381 A72-34090
American Helicopter Society Noise Subcommittee report on physical characteristics and major controlling parameters of rotor induced aerodynamic noise

[AHS PREPRINT 625] 17 p2483 A72-34476
Externally blown flap impingement noise.

[AIAA PAPER 72-664] 17 p2487 A72-35961
Internal noise reduction in hovercraft.

18 p2642 A72-36574
An expansion scheme for the noise from circular jets.

[DFVLR-SONDDR-217] 18 p2683 A72-36941
The intrinsic structure of turbulent jets.

18 p2684 A72-37201
Noise generated by STOL core-jet thrust reversers.

[AIAA PAPER 72-791] 19 p2849 A72-38108
Linear acoustic model to predict axial flow turbomachinery aerodynamic sound generation including flow effects on radiation

19 p2788 A72-38568
Noise radiation from V/STOL aircraft.

[ICAS PAPER 72-22] 21 p2995 A72-41147
Evaluation of transonic and supersonic wind-tunnel background noise and effects of surface pressure fluctuation measurements.

[AIAA PAPER 72-1004] 21 p3041 A72-41588
Design and development of the United Aircraft Research Laboratories acoustic research tunnel.

[AIAA PAPER 72-1005] 21 p3041 A72-41589

Jet noise generation theory /Lighthill-Ffowles Williams/ verification by model tests, discussing means of reducing or eliminating shock cells
[ICAS PAPER 72-55] 21 p3047 A72-41852

Basic directivity and spectra of jet noise with improved correction for refraction.
24 p3389 A72-44678

Aeroacoustic, vibration and shock environments for the space shuttle orbiter.
24 p3448 A72-44679

Investigation of propeller vortex noise including the effects of boundary layer control.
24 p3359 A72-44680

Radiation properties of the semi-infinite vortex sheet.
24 p3359 A72-44918

AERODYNAMIC STABILITY

Axial cords effects on parachute drag and stability characteristics and opening time, discussing wind tunnel and balloon drop tests results
01 p0004 A72-10306

Paratroop type parachutes breathing oscillations and stability characteristics, using high speed cinematography and kinetheodolites to track during steady state descent
01 p0004 A72-10307

Flutter problem wing-air flow energy exchange at instability limit, obtaining vibration mode shapes from homogeneous boundary value problem analog model
03 p0442 A72-13191

Communications and TV broadcasting antenna feeder cost-efficient designs, relating climatology, oscillation theory and structural aerodynamic stability
07 p0955 A72-19513

Ground effect wing vehicles stability in forward motion, deriving characteristic equations by linear analysis
10 p1421 A72-24844

Meteorological rising balloon systems accuracy limitation, noting response to wind field changes, aerodynamic self oscillations and radar tracking errors
13 p1990 A72-28817

Stability criteria for limiting oscillatory motion of coasting sounding rocket exiting atmosphere
13 p2051 A72-28886

Wind tunnel ventilation duct aerodynamic stability analysis for incompressible and slightly compressible flow
16 p2378 A72-33439

Longitudinal dynamic stability of hypersonic shuttle vehicle designed for operation to planetary atmosphere rim
16 p2462 A72-34019

Exploration of aeroelastic stability boundaries with a soft-in-plane hingeless-rotor model.
[AHS PREPRINT 610] 17 p2489 A72-34493

Parametric studies of instabilities associated with large, flexible rotor propellers.
[AHS PREPRINT 615] 17 p2490 A72-34496

Helicopter stability derivative extraction and data processing using Kalman filtering techniques.
[AHS PREPRINT 641] 17 p2490 A72-34501

Satellite orientation and stabilization systems aerodynamic compensation for circular orbit perturbations
17 p2621 A72-35034

Prediction of nose shape effects on nonlinear stability characteristics of slender cones.
20 p2886 A72-39628

Development of an inflatable fabric structure for the early stabilization of the B-1 crew escape capsule.
[AIAA PAPER 72-801] 20 p2888 A72-40053

Performance optimization of satellite semipassive aerodynamic attitude controller for near-earth orbits, considering damping time and pointing error
[AIAA PAPER 72-923] 21 p3082 A72-41567

Spin stabilization dispersive effect on marginally stable bodies due to precession rate, comparing analytical results with aeroballistic range measurements
24 p3362 A72-45340

AERODYNAMIC STALLING

Aircraft spin characteristics due to superstall, comparing three stall types with respect to recovery, yaw damping and rate of rotation
[DGLR PAPER 71-057] 02 p0155 A72-12718

Stalled blade rows dynamic performance in terms of blade channel fluid inertia and surface boundary layer-caused time delay
05 p0602 A72-16487

Flight initial spin testing, discussing aircraft autorotation due to stalled angle of attack and sideslip
06 p0759 A72-18492

Inlet duct and turbofan engine compatibility without stalling and surge conditions obtained by design optimization and wind tunnel testing
07 p1052 A72-18761

Incipient wing stall detection by unsteady pressure monitoring via flush-mounted microphones, discussing flow patterns on models
07 p0908 A72-19093

Dassault Falcon 10 turbofan powered executive aircraft, attributing safe stall characteristics to wing design optimization
08 p1108 A72-21274

Unsteady airfoil stall and stall flutter analysis, discussing application to space shuttle configuration
[AIAA PAPER 72-380] 11 p1730 A72-25404

Stall warning system for general aviation aircraft, using signal discriminator for rough or gusting air
[SAE PAPER 720331] 11 p1630 A72-25592

Finite difference method application to axial flow compressors rotating stall nonlinear analysis, taking into account blade row characteristics
[ASME PAPER 72-GT-3] 11 p1568 A72-25606

Leading edge boundary layer flow separation and reattachment processes in airfoil dynamic stall, considering effect of angle of attack rate of change
15 p2179 A72-32024

Aerodynamic stall characteristic prediction from static experimental data for airfoils, noting boundary layer effects
[AIAA PAPER 72-682] 16 p2364 A72-34060

Influence of airfoils on stall flutter boundaries of articulated helicopter rotors.
[AHS PREPRINT 621] 17 p2484 A72-34489

Determination of airfoil and rotor blade dynamic stall response.
[AHS PREPRINT 613] 17 p2490 A72-34495

Wind tunnel experiments on aerodynamic superstall, describing stability tests and models
17 p2492 A72-35374

F-111 stall inhibitor system with angle of attack limitation, describing interface with stability augmentation system
17 p2493 A72-35577

Prediction of the stalling of a wing section in incompressible flow
[ONERA, TP NO. 1088] 19 p2746 A72-37760

Status of U.S. Navy stall/post-stall/spin flight testing.
[AIAA PAPER 72-787] 19 p2749 A72-38104

Heat transfer effects on reentry vehicle surfaces boundary layer stability and aerodynamic characteristics, noting stall angle reduction and drag increase from wind tunnel tests
[AIAA PAPER 72-960] 22 p3137 A72-42357

Analytical method for combining the interaction of inlet distortion and turbulence.
23 p3247 A72-43330

Application of a time-dependent boundary-layer analysis to the problem of dynamic stall
23 p3249 A72-44058

Influence of tangential fluid injection on the performance of two-dimensional diffusers.
[ASME PAPER 72-FE-16] 23 p3280 A72-44064

AERODYNAMIC VEHICLES

U AIRCRAFT

AERODYNAMICS

NT AEROTHERMODYNAMICS

NT HYPERSONICS

NT ROTOR AERODYNAMICS

NT SUPERSONICS

Soviet book on rocket dynamics covering history, variable mass point aerodynamics and ballistics, numerical and computer methods and trajectory analysis
02 p0286 A72-12123

High subsonic velocity aerodynamics boundary problem, transforming compressible flow to incompressible
03 p0307 A72-13238

SLINGSHOT pilot aerodynamic test facility for very high acceleration, using encapsulated gas slug over fixed model
[AIAA PAPER 72-168] 05 p0645 A72-16962

Circular crown theorems with aerodynamics applications
06 p0756 A72-18109

Aerodynamics of vortex chambers with symmetrical air injection, discussing core and end boundary layer flows interaction and momentum loss from end surfaces friction
09 p1260 A72-22676

Data acquisition and reduction for model aerodynamics in superconducting magnetic suspension and balance of supersonic wind tunnel facility
10 p1461 A72-24766

German book on flow technology and fluid flow machines covering hydrodynamics, gas dynamics, aerodynamics, airfoils, wind tunnels, propellers, helicopters, turbomachines, blade cascades, etc
10 p1471 A72-25122

Turbine aerodynamics research trends, covering engine cooling, high work factor turbines, pneumatic variable geometry and computer analysis
11 p1572 A72-26036

Transparent materials study by interferometric methods, emphasizing holographic bench advantages for stress analysis and aerodynamic flows observation
[ONERA, TP NO. 1037] 12 p1812 A72-28048

Mechanics fundamentals in aerodynamical aircraft analysis, noting force concept and Newton theory
14 p2073 A72-30817

Internal aerodynamic problem solution by kinetic equation for Couette and Poiseuille flows and heat transfer between plane plates
16 p2343 A72-33153

Russian book on flight dynamics covering horizontal flight, takeoff, climb and landing characteristics,

meteorological conditions, helicopters, trajectory problems, stability and controllability analysis, etc
16 p2349 A72-33874

Generalization of basic equations of aerodynamics and electrodynamics.
17 p2539 A72-35043

Aerodynamic analysis of various flight conditions of conventional aircraft. III - Mechanical fundamentals /Dynamics of a point mass/
17 p2492 A72-35440

Hypersonic wake aerodynamics at high Reynolds numbers.
[AIAA PAPER 72-701] 17 p2486 A72-35484

Holography for aerodynamics.
19 p2799 A72-37682

Book - Combustion aerodynamics.
19 p2882 A72-38722

Russian book - Experimental studies of helicopter aerodynamics.
20 p2887 A72-39598

Aerodynamic test facility data on swept wings, peaky airfoils, aircraft flutter and transonic flow, discussing shock tubes and wind tunnels development
20 p2912 A72-39846

Research planning in steady compressible flow aerodynamics, discussing projects on annular wings, shockless transonic airfoils and Smith panel method for three dimensional flow problems
[ICAS PAPER 72-01] 21 p2990 A72-41126

AEROELASTICITY

NT AEROTHERMOELASTICITY

Aeroelastic stability of flat anisotropic sandwich plates in supersonic compressible fluid flow
02 p0297 A72-12614

Aeroelastic models construction for flutter analysis of aircraft design, noting error risk reduction
[DGLR PAPER 71-082] 02 p0299 A72-12722

Galerkin method application to nonconservative nonself-adjoint aeroelasticity problems based on interpretation as mathematical formulation of virtual work principle
07 p1025 A72-18788

Dynamically similar wind tunnel models for transonic aeroelastic studies of aircraft failures or structural damage and flutter margins
[ONERA, TP NO. 1082] 13 p1939 A72-29672

Aeroelasticity, discussing gust and maneuver load alleviation, flutter suppression, aircraft stability, computerized aeroelastic analysis, aeroelastic optimization, composite structures, etc
15 p2322 A72-31202

Slender rotating body aeroelastic behavior under inertial, gravitational, thrust, servocontrol, elastic and aerodynamic forces, presenting equilibrium equations in matrix form
15 p2319 A72-31210

Aeroelastic model response comparison to amplitudes of sectional and linear wind tunnel models, indicating incorrectness of direct scaling
16 p2342 A72-32904

The aeroelastic behaviour of hot-wire anemometer filaments in an air stream.
17 p2552 A72-34229

The controllable twist rotor performance and blade dynamics.
[AHS PREPRINT 614] 17 p2488 A72-34483

Exploration of aeroelastic stability boundaries with a soft-in-plane hingeless-rotor model.
[AHS PREPRINT 610] 17 p2489 A72-34493

Parametric studies of instabilities associated with large, flexible rotor propellers.
[AHS PREPRINT 615] 17 p2490 A72-34496

Analytical investigation of the effects of blade flexibility, unsteady aerodynamics, and variable inflow on helicopter rotor stall characteristics.
20 p2887 A72-38950

Unsteady aerodynamic and aeroelastic effects in turbomachine blade cascades supersonic flow, discussing trends in fan and compressor technology
21 p3118 A72-40969

A new method of calculating the natural vibrations of a free airplane.
[ICAS PAPER 72-05] 21 p3120 A72-41130

Theoretical and experimental features and methods of creep.
[ICAS PAPER 72-45] 21 p3069 A72-41170

Liapunov stability analysis of hybrid dynamical systems with multi-elastic domains.
21 p3086 A72-41519

Structural dynamics and aeroelasticity analysis of space shuttle, covering vibration modes, thermal protection system dynamics, ground winds, flutter, buffet and noise
22 p3237 A72-42761

Steady state equations of motion, equilibrium shape and stability derivatives of elastic airplanes evaluated with finite element methods.
22 p3138 A72-42845

Flutter analysis and unsteady pressure fields induced by pitching motions of wall mounted sweptback wing, verifying experimentally lifting surface theory in high subsonic range
22 p3241 A72-43094

Aeroelastic optimization of a panel in high Mach number supersonic flow. 23 p3343 A72-43327

Influence of wing deformations measured during flight tests upon the flight performance of a glider made of synthetic materials. I 23 p3252 A72-44452

AEROEMBOLISM

Computer assisted monitoring of ECG waveforms and heart sounds frequency spectra to detect bubble laden blood during decompression sickness 11 p1587 A72-26626

Interactions between gas bubbles and components of the blood - Implications in decompression sickness. 24 p3374 A72-45652

AEROLOGY

Gliding flight atmospheric energy utilization through aerology, discussing value of weather forecasts to glider pilots 04 p0542 A72-14684

AEROMAGNETISM

U GEOMAGNETISM

AEROMAGNETO FLUTTER

U FLUTTER

AERONAUTICAL ENGINEERING

Russian book - Calculation and analysis of flight-vehicle motion: Engineering handbook 17 p2492 A72-35451

AERONAUTICS

DGLR 1970 yearbook covering flight mechanics, relaxation in gas dynamics, space shuttle, flight simulation, reentry vehicles, turbulent boundary layer control, noise reduction, etc 02 p0206 A72-12895

Heat transfer research review, discussing gas turbines, aeronautics, astronautics, nuclear power, thermal pollution and controlled fusion challenges 09 p1412 A72-23684

Human and instrumental observations of aviation visibility, discussing measurements of extinction coefficient and light scatter and sensors testing 13 p1992 A72-28845

Aviation and astronautics - Conference, Tel Aviv-Haifa, March 1972 15 p2177 A72-31201

AERONOMY

Photochemical models of aeronomical formation and dissociation of hydrogen and ozone in mesosphere and stratosphere 03 p0346 A72-13377

AEROS aeronomy satellite solar cell array power supply system simulation tests under space conditions 04 p0466 A72-15650

Vlf propagation and D region aeronomy model for vlf phase behavior predictions and observations during two solar eclipses 05 p0630 A72-16618

Carbon dioxide atmospheric models for Mars and Venus, discussing aeronomy, Mariner probes, gas dissociation by solar radiation, and electron density inconsistency 09 p1386 A72-22685

Upper atmosphere atomic oxygen distribution calculated for D and E region aeronomy problems solution 13 p1947 A72-28604

Collisional relaxation and rotational intensity distributions in aeronomic spectra, including radiative losses effects from weak interaction model 13 p2008 A72-30057

Upper atmosphere research rockets missions, payloads and measurements, describing various international aeronomy research projects 13 p2052 A72-30081

Luminous molecular absorption cross sections in aeronomy, considering photodissociation, actinic solar radiation attenuation and UV to IR analysis 14 p2097 A72-30135

Report to COSPAR on West German space program covering meteorology, aeronomy, ionospheric physics, magnetosphere, solar wind and radiation, solar system and life sciences 15 p2338 A72-32014

Upper atmosphere atomic oxygen distribution calculated for D and E region aeronomy problems solution 24 p3398 A72-45104

Cross section parameters for electron impact excitation, noting mathematical models for aeronomical users 24 p3400 A72-45591

AEROPHYSICS

U ATMOSPHERIC PHYSICS

AEROS SATELLITE

Aeros satellite mass spectrometer, retarding potential analyzer and neutral gas thermograph onboard experiments, noting measurements and data transmission triggering by light direction sensor [DGLR PAPER 71-093] 02 p0284 A72-12727

Aeros satellite mass spectrometer design, discussing operation mode ion detection system, power supply, logarithmic electrometer and modulator 02 p0232 A72-12729

AEROS satellite active magnetic attitude control system, describing magnetometer system, sun and IR earth sensors, spin stabilization and axis and spin rate control torque generation 05 p0727 A72-16473

Spacecraft power system with Maximum Power Point Tracker, discussing German Aeros satellite and orbit simulation program 07 p0914 A72-19090

Engine ignition electronic system for triggering detonators in Aeros aeronomy satellite blastoff and release devices, discussing prototypes acceptance tests 11 p1610 A72-25803

Operational evaluation for sun stabilized attitude control system in Aeros satellite, describing laboratory equipment and component static and dynamic tests [DGLR PAPER 72-026] 13 p2052 A72-28967

AEROS research satellite control program, describing system objectives, operational testing, error analysis and command verification [DGLR PAPER 72-023] 13 p1918 A72-28968

German aeronomy research satellite Aeros mission objectives, discussing orbit layout, onboard equipment and operation 13 p2050 A72-30079

Aeros satellite magnetic properties, describing measurement procedures for component induced disturbance fields, dipole moments and eddy currents 13 p1940 A72-30080

German Aeros satellite mission and payload, noting mass spectrograph, EUV spectrometer for UV solar radiation and neutral particles temperature measuring instrument 20 p2974 A72-39935

Polar orbiting Aeros aeronomy satellite turnstile antenna system with nearly spherical radiation pattern, discussing design modifications for optimization 21 p3030 A72-40533

AEROSINUSITIS

Statistical survey of barosinusitis incidence in U.S. Navy flying personnel during altitude chamber training, discussing diagnostic methods and clinical management 12 p1765 A72-28274

AEROSOLS

Lidar measurements of atmospheric aerosol distributions over large areas including urban haze, scattering layers, trade wind inversion and Sahara dust stream in Caribbean [AIAA PAPER 71-1055] 01 p0057 A72-10526

Monostatic and bistatic lidar and solar radiometer sensing techniques for remote measuring of aerosol size distributions 01 p0066 A72-10528

Invariant imbedding theory of aerosols multiple scattering induced telephotometric errors, determining scattering coefficients relative to optical thickness by Monte Carlo method [AIAA PAPER 71-1062] 01 p0066 A72-10531

Particle mass monitor system based on piezoelectric microbalance combined with electrostatic precipitator collector, considering applications to air quality monitoring, laboratory aerosol research, process control, etc [AIAA PAPER 71-1100] 01 p0067 A72-10548

Atmospheric aerosol chemical composition analysis by nephelometer light scattering measurement of suspended particle mass concentration, visibility and size distribution and scattering-humidity relationship [AIAA PAPER 71-1101] 01 p0058 A72-10549

Analysis methods for microsize atmospheric aerosols and particulate contaminants from natural and industrial sources, discussing electron microscopy, electron probes, X ray diffraction, etc [AIAA PAPER 71-1104] 01 p0067 A72-10550

Aerosol and atmospheric scattering layers observability by satellite mounted optical detector at 3000-7000 Å, comparing wide angle receiver and limited view field steerable telescope [AIAA PAPER 71-1110] 01 p0058 A72-10554

Global satellite horizon-scanning monitoring technique permitting scattered solar radiation horizon profile conversion into aerosol vertical distribution [AIAA PAPER 71-1111] 01 p0058 A72-10555

Stratospheric aerosol boiling point measurement with photoelectric particle counter, observing sulfate radical as major constituent 01 p0059 A72-10833

Radiant heat attenuation of W seeded hydrogen aerosol at high pressure and temperature for gas core nuclear rocket propellant application 01 p0112 A72-11340

Atmospheric aerosols size/altitude distribution via sun aureole sky brightness and airborne particle counterpoint sampling measurements 02 p0213 A72-11860

Upper atmosphere ozone, aerosol and neutral constituent density profiles estimation by recursive filtering algorithm for satellite observation data 02 p0222 A72-12811

Atmospheric short wave radiation angular and vertical distribution relation to aerosol scattering parameters, using transport equation 05 p0658 A72-16291

Noncoagulating polydisperse aerosol deposition from two dimensional turbulent boundary layer and fully developed turbulent pipe flows [AIAA PAPER 72-81] 05 p0650 A72-16806

Charged aerosols for efficient power transduction in power conversion devices, deriving optimum particle radius to number of charges ratio for various operating conditions 06 p0760 A72-17422

Aerosol scattering coefficient in atmosphere, determining statistical characteristics of vertical and spectral structure 06 p0842 A72-18043

Powder concentration effects on corona particle charging efficiency of aerosols for electrostatic generators 06 p0760 A72-18335

Atmospheric aerosols optical thickness evaluation from solar radiation integral intensity 07 p1031 A72-19855

High energy UV solar radiation transfer by stratospheric aerosols to biosphere, considering radiation injury to human lung 09 p1298 A72-22662

Mathematical model of ion capture and annihilation by aerosol particles from ground level to 60 km 09 p1346 A72-23266

IR refractivity measurement for atmospheric aerosol substances and sea salts [AD-744397] 11 p1620 A72-25306

Residence time of water vapor and aerosols in troposphere and lower stratosphere, noting application to air pollution buildup by aircraft 13 p1991 A72-28836

Stratospheric aerosols physical properties and chemical composition, discussing various measuring techniques and results 13 p1991 A72-28839

Heatable chamber burners design to increase sensitivity of flame spectrophotometry, separating solvent from aerosols 13 p1958 A72-29525

Absorption effects on 10.6 micron laser beam in fluidized particulate crosswind, discussing calcium hydroxide performance 14 p2109 A72-30186

Turbulence effects on electron, ion, aerosol, water vapor and ozone concentration in atmospheric layers 15 p2222 A72-31395

Rocket-borne laser radar for aerosol observation in upper atmosphere, noting light scattering layer relation to noctilucent cloud appearance 15 p2231 A72-32331

Giant hygroscopic atmospheric dust particle concentration variations measured with light scattering monitor, noting frontal passage dependence on prefrontal concentration 16 p2386 A72-33604

Solar radiation absorption and scattering by particles in atmosphere, emphasizing absorption/backscatter ratio explanation 16 p2388 A72-34023

Effect of aerosol variation on radiance in the earth's atmosphere-ocean system. 17 p2547 A72-35194

Measurement of aerosol motion and wind velocity in the lower troposphere by Doppler optical radar. 18 p2706 A72-36638

Relation between impurity shear dispersion in the atmospheric ground layer and the turbulence characteristics 19 p2829 A72-38772

Approximate determination of the change in the aerosol distribution spectrum in a Venturi coagulator tube 20 p2928 A72-40039

Influence of hygroscopic substances on the transparency of aerosols from combustion products of condensed systems 20 p2987 A72-40043

A system of disc-stabilized dc arc and solution nebulization device for the investigation of multicomponent plasmas. 21 p3039 A72-40213

Optical properties and structure of the Jovian atmosphere. V - Probable structure of the ammonium aerosol layer 22 p3219 A72-41914

Laser radar/lidar/ for mapping aerosol structure. 23 p3298 A72-44542

Determination of the physical properties of atmospheric aerosol particles above the Atlantic 24 p3420 A72-44757

Rocket-borne GaAs laser radar system with scatter light detector and data processor for upper atmosphere aerosol and pollution measurements 24 p3409 A72-44778

AEROSPACE ENGINEERING

NT AERONAUTICAL ENGINEERING

Aerospace adhesives applications, discussing thermal and mechanical properties, and cryogenic, epoxy, urethane silicone and fluorocarbon types 01 p0090 A72-10188

Aerospace reliability methods, discussing distribution functions, sampling, accelerated life testing and

case histories of space electric rocket and microthruster power conditioner tests
04 p0526 A72-14441
Paris, May 1971

Marine and aerospace engineering - Conference,
04 p0463 A72-15551

Laser welding theory and applications to microelectronics, nuclear and aerospace fields
10 p1485 A72-23968

NASA program to develop heat resistant materials for aerospace applications, discussing refractory carbides, nitrides and borides temperature dependent behavior and properties
11 p1664 A72-26857

Space technology developments during 1970s and 1980s, discussing solar system exploration, space shuttle systems, cost effectiveness, international cooperation, nuclear propulsion systems, etc
13 p2051 A72-28453

Aerospace technology transfer to and utilization by industry for product development and improvement, discussing NASA structural analysis computer program [NASA/NASTRAN]
[ASME PAPER 72-DE-60] 14 p2175 A72-30875

Aerospace critical systems and future technologies, presenting illustrative diagram for functions combination and interrelations
14 p2175 A72-31140

Astronautical engineering - Conference, Mar del Plata, Argentina, October 1969
15 p2320 A72-31801

Acceptance testing of the MKL capacitor for space application
18 p2669 A72-37119

The potentialities of space technology in relation to oceanography and surface meteorology.
19 p2790 A72-37924

Successful engineering design teams characteristics in development of complex defense systems, discussing organization size, experience, documentation and procurement practices
21 p3132 A72-40972

National aerospace R and D facilities requirements, establishing priority order for V/STOL, aeropropulsion systems, high Reynolds number, large transonic and true-temperature hypersonic test facilities
[AIAA PAPER 72-1033] 21 p3043 A72-41608

Dynamic response of structures; Proceedings of the Symposium, Stanford University, Stanford, Calif., June 28, 29, 1971.
22 p3236 A72-42755

Some contributions to energetics by the Lewis Research Center and a review of their potential non-aerospace applications.
[ASME PAPER 72-AERO-12] 22 p3245 A72-43148

Detection of hazards associated with aerospace operations.
23 p3287 A72-43424

Aerospace vehicles preliminary design computer program to include cost, reliability, maintainability and safety parameters in addition to weight as performance determining factors
[SAWE PAPER 940] 23 p3342 A72-43480

Commercial space applications economics, discussing meteorological, navigational traffic control and communications satellites, nuclear waste disposal, space manufacturing, solar power generation, etc
24 p3441 A72-45216

AEROSPACE ENVIRONMENTS
NT CISLUNAR SPACE
NT DEEP SPACE
NT INTERPLANETARY SPACE
NT INTERSTELLAR SPACE
Soyuz 9 flight crew physiological data, discussing mental and physical performance and adaptation and readaptation to space-earth environments
01 p0020 A72-10933

Space environment weightlessness and radiation effects on leeches biorhythm, metabolism, reproduction and growth from rocket biological experiments
04 p0481 A72-15729

High energy particle and ionizing radiation effects on glasses in space environment
09 p1336 A72-22402

Cosmic radiation effects and damage on solar cells, discussing shielding, stability improvement, space environments, minority carrier lifetime and photosensitivity spectral distribution
10 p1422 A72-24312

Extravehicular life support systems for shuttle, space station, lunar base and Mars missions, considering thermal control, carbon dioxide control and oxygen supply subsystems
[AIAA PAPER 72-231] 10 p1430 A72-24441

Space environment and astronomical studies with sounding rockets, satellites and orbiting solar observations
10 p1548 A72-24974

Space and ground environments effect on cryogenic multilayer insulation materials, tabulating mechanical and thermophysical test data
[AIAA PAPER 72-286] 11 p1741 A72-25225

Electron beam machine for thin metal plates welding and cutting under space conditions, noting design features and performance
11 p1639 A72-25809

Outer space and earth surface galactic cosmic ray intensity data correlation analysis for studying interplanetary magnetic field structure
11 p1713 A72-25936

Space flight ecology and physiology, discussing atmospheric temperatures and radiation, biological effects of acceleration, deceleration and weightlessness and physiological stresses
11 p1584 A72-26018

High temperature materials powder metallurgy for space applications, discussing melting points
11 p1665 A72-26866

Geostationary satellites spacing dependence on quantifying factors, describing space environment experiments for satellite attitude stability and ground station antenna patterns and polarization effects
[AIAA PAPER 72-542] 12 p1780 A72-27365

ATS F Environmental Measurements Experiment package for synchronous altitude space environment and electromagnetic-ionospheric interactions studies
12 p1795 A72-27525

Solar cells array design and assembly techniques, discussing tests for Esro satellites aerospace environments
12 p1758 A72-28033

Noise and vibration control in industrial and aerospace environments, discussing materials and techniques for structural vibration damping
13 p2059 A72-29557

Environmental effects on aircraft structure operational reliability, discussing failure removal and protective coating lifetime
14 p2072 A72-30285

Environmental effects on spacecraft materials, structures and design, discussing sterilization, gravity, vacuum, micrometeoroids, radiation, etc
15 p2320 A72-31802

Cytological, genetic and physiological analyses of space flight factors effects on seeds and plants aboard Zond 5 probe
15 p2186 A72-31828

Space environment weightlessness induced perceptual deprivation, considering hand-eye coordination, visual judgments and motion and time perception
16 p2355 A72-33549

Biotelemetry and computer analysis techniques for steep states and wakefulness studies during aerospace flight
16 p2356 A72-33560

Space and upper atmosphere environmental effects on spacecraft and instrument surfaces, considering high energy particle radiation, interstellar and lunar dust effects, etc
18 p2712 A72-36832

Apparatus for programmed oral administration of drugs to large primates in altered environments.
18 p2654 A72-36921

Experimental investigation of an astronaut maneuvering scheme.
18 p2655 A72-37026

Strain rate, stress concentration and temperature effects on hydrogen environment embrittlement of metals
19 p2816 A72-37640

Solar activity effects on sun-earth space physical processes, considering galactic cosmic rays, comets, ionospheric disturbances, and nocturnal clouds
19 p2867 A72-38629

About the interaction between a satellite and its environmental ionospheric plasma.
21 p3090 A72-40454

Environmental characteristics and advantages of manufacturing in space, considering gravity, vacuum, temperature, pressure and radiation effects on materials and products processing
21 p3060 A72-40968

Effects of the space flight environment on man's immune system. I - Serum proteins and immunoglobulins.
22 p3150 A72-42493

Variable impedance transducer measuring instruments for in-flight aircraft performance tests under environmental thermal effects
22 p3180 A72-42711

AEROSPACE INDUSTRY
NT AIRCRAFT INDUSTRY
Industrial parachute R and D in UK, discussing management, technical staff requirements and government/industry liaison
01 p0004 A72-10304

Aerospace wire and cables testing methods standards for evaluating mechanical, electrical and chemical properties, coating thicknesses, continuity flaws, flammability, geometrical characteristics, etc
[SAE A1198] 01 p0006 A72-10384

Industrial challenge of European space R and D programs, discussing ELDO Europa 1 launcher vehicle and ESRO-HEOS satellite technological problems
01 p0146 A72-10948

Telemetry applications in aerospace industry - ISA Conference, Las Vegas, May 1971
02 p0179 A72-12402

Twisted shielded pair [TSP] time division multiplexed data bus with standard interfaces for use in aerospace applications
02 p0194 A72-12405

Refractory materials fabrication characteristics for aerospace technology, presenting listing of synergic agents for use with inhibitors
05 p0681 A72-16774

Space shuttle program evaluation, discussing national economic benefits relative to aerospace industry employment, domestic production, balance of trade, etc
06 p0893 A72-18612

Aerospace management systems effectiveness in design, development, test and engineering areas, discussing cost, scheduling and technical performance factors
[AIAA PAPER 72-243] 10 p1565 A72-25050

Inertia welded bimetallic fasteners for aerospace industrial applications, noting cost advantages
[ASM PAPER W 72-32.5] 12 p1817 A72-28166

Aerospace technology economic and social effects, relating U.S. space expenditures and gross national product
14 p2174 A72-30682

Weapon system program choice for development in aerospace industry, considering cost effectiveness and ranking illustrated on stand-off tactical interdiction missiles
16 p2482 A72-33598

Refractory materials fabrication characteristics for aerospace technology, presenting listing of synergic agents for use with halogenous inhibitors
17 p2571 A72-35277

French aerospace industry difficulties in procuring parts, suggesting purchasing centralization or setting up of parts stocks
17 p2639 A72-35951

Canadian industrial participation in domestic, U.S. and overseas space projects, emphasizing technology advancement as national objective
[AIAA PAPER 72-738] 18 p2742 A72-36544

Successful engineering design teams characteristics in development of complex defense systems, discussing organization size, experience, documentation and procurement practices
21 p3132 A72-40972

Industrial work study methods application to aerospace manufacturing for establishment of efficient work methods, facilities utilization and productivity controls
21 p3132 A72-41643

Employee motivation programs as a means of cost reduction in aerospace industries.
24 p3468 A72-45221

AEROSPACE MEDICINE
German Research and Test Institute for Aero- and Astronautics 1970 report covering flow mechanics, power conversion, aerospace medicine, atmospheric physics, etc
01 p0048 A72-11151

Case report on compensated hemolytic anemia associated with Gilbert syndrome, discussing implication in aviation
01 p0022 A72-11299

Case history of student aviator with psychosomatic Lymphogranuloma venereum related to vestibular apparatus
02 p0167 A72-11712

Medicopsychological surveillance of aircrew in fighter pilot school, stressing time factor in pilot training
04 p0467 A72-14569

Medical equipment advancements through NASA sponsored aerospace research program, describing prosthetic urethral valve, ear oximeter, radiation dosimeter and electromyographic muscle trainer
06 p0765 A72-18616

NASA sponsored medical R and D programs for space applications, stressing benefits to earthbound medical services
06 p0769 A72-18626

Functional diagnostics of teeth condition as pilot health factor in stomatological aviation medicine, discussing caries, parodontitis and odontalgia
07 p0922 A72-20374

Asthmatics evolution and treatments in armed forces aircrews, noting acetylcholine test
08 p1125 A72-21270

Hyperuricemia, gout and lithiasis among operating air crews, discussing diagnosis and relation to arteriosclerosis
08 p1125 A72-21271

Permanent flight unfitness attributable to air service, noting orthopedic traumatic sequelae, cardiovascular illnesses, psychological and ophthalmological causes
08 p1125 A72-21273

Space medical urological problems from experience with Biosatellite 3 monkey, discussing closed catheter

conduit system, urinary calcium changes in immobilized animals and urinary diuresis

10 p1424 A72-23728

Medical evaluation of manned space flight physiological effects, considering Mercury, Gemini and Apollo programs

11 p1585 A72-26100

Russian book on pathophysiological principles of air and space pharmacology covering stress and fatigue reduction and pilots and astronauts performance improvement

12 p1772 A72-27926

Aerospace medicine - Conference, Bal Harbour, Florida, May 1972

12 p1764 A72-28251

Low cost real time computerized C 14 radiorespirometry telemetering system for monitoring human metabolism data during space missions

12 p1774 A72-28277

Integrated medical and behavioral laboratory for detection and measurement of space flight stresses, specific etiologies and human tolerances and adaptivity

12 p1796 A72-28279

Review of aeromedical records for grounding USAF flying personnel during 1956-1970, noting increased age factor effect

12 p1776 A72-28316

Medication effects on pilot performance, covering tranquilizers, sedatives, antibiotics, stimulants, antihistamine and hypotension drugs

13 p1909 A72-28750

Flight psychiatry in NATO countries, discussing organization and facilities with respect to military and civil aviation

13 p1911 A72-29858

Low pressure chamber as aerospace medical diagnostics tool for flying personnel examinations regarding oxygen deficiency, low air pressure and air pressure fluctuations tolerance

14 p2080 A72-30819

Prophylactic otolaryngological investigation of vestibular analysis function in aviation medicine

15 p2186 A72-31769

Medical investigations during Salut space station flight, discussing weightlessness effects and efficiency evaluation of preventive measures for crewmembers high performance in space flight

15 p2189 A72-31918

Report to COSPAR on Polish space program covering artificial satellites tracking, aerospace medicine, meteorology and bioastronautics

15 p2337 A72-32004

Medical requirements for manned space flight, discussing physiological data monitoring and transmission, equipment miniaturization, telediagnosis, spacecraft environment protection, etc

16 p2358 A72-33562

Medical and technical aspects of rescue and survival of astronauts in high mountain and mountainous remote areas.

17 p2507 A72-34434

Russian book - Theory and practice of aviation medicine

19 p2760 A72-37447

USAF aerospace medical research on human capabilities as limiting factor in defense systems development, discussing environmental simulators and human test facilities

21 p3008 A72-40973

The use of cholesteric liquid crystals in the study of skin temperature and their applications in aviation medicine

21 p3009 A72-41192

An integrated medical system for long-duration space missions.

21 p3009 A72-41305

Airport medical design guide /with comment on certain operational matters/.

22 p3150 A72-42500

AEROSPACE SCIENCES

Laser sources for space research, considering He-Ne, carbon dioxide, Nd-YAG and argon lasers performance

02 p0237 A72-11695

Earth Resources Survey (ERS) program personnel training and education, discussing trainee selection, knowledge categories and training methods for remote sensing

02 p0304 A72-11855

Frequency allocation for space research, radio astronomy, time signal and earth resources exploration, reviewing allowable power flux density and emitter power

02 p0177 A72-12386

Space astronomy techniques - Conference, Munich, August 1970

03 p0352 A72-13026

Collaboration of World Health Organization and various international astronomical organizations for space technology applications to man-environment relationships and medical and communication sciences

07 p0933 A72-20300

Satellite, space probe and observatory data impact on space physics, considering solar wind, interplanetary magnetic field, Van Allen belt and Chapman-Ferraro theory

10 p1538 A72-24268

Space science advances and NASA Planetary Program, noting solar system evolution, life origin and Skylab and Space Shuttle programs

19 p2855 A72-37274

Space technological advance effects on human extraterrestrial, scientific, economic and sociological progresses

19 p2867 A72-38545

ESOC-Darmstadt - ESRO's European center of operations for space exploration

20 p2988 A72-39415

Book - Progress in aerospace sciences. Volume 12.

22 p3135 A72-42576

Life sciences and space research X; Proceedings of the Fourteenth Plenary Meeting, Seattle, Wash., June 21-July 2, 1971.

23 p3253 A72-43381

NASA space science, exploration and applications plans and policies in view of space shuttle capabilities, emphasizing cost reduction

24 p3440 A72-45162

AEROSPACE SYSTEMS

Electronics and aerospace systems - IEEE Conference, Washington, D.C., October 1971

02 p0177 A72-12376

P-channel MOS/silicon-on-sapphire transistor logic circuits for aerospace systems, investigating radiation hardness and performance potential

03 p0334 A72-14086

Systems analysis for equipment performance and data management in aerospace programs

03 p0460 A72-14199

Papers on aerospace structure by N. J. Hoff covering aircraft framework, stress analysis, structural stability, shell theories, bending, buckling, monocoque and sandwich structures, etc

04 p0591 A72-15238

Automatic control in space - Conference, Dubrovnik, Yugoslavia, September 1971

05 p0724 A72-16427

Nonlinear multivariable and linear systems optimal control in aerospace field, discussing use of performance indexes for fuel consumption, process evolution time or combination

05 p0725 A72-16453

Concatenated coded command system for low error probabilities at moderate SNR, emphasizing spaceborne portions implementation

07 p0949 A72-19299

Aerospace subsystem alternate designs and cost effectiveness evaluation and optimization, considering algorithm of three functions with minimal coupling

07 p1105 A72-19552

Aerospace systems radar target computer simulation model based on simple multiple reflector geometrical configuration

07 p0948 A72-20345

Aerospace explosive components accelerated storage life and stability tests, basing method on Arrhenius reaction rate equation modification

08 p1220 A72-20762

Aerospace type electroexplosive devices gross sensitivity to short damped rf energy burst

08 p1220 A72-20765

Space applications of camera tubes - Conference, Paris, November 1971

08 p1169 A72-21951

Robots/electromechanical systems with local computers and sensor controlling motors and effectors/space application categories and operating and decision making requirements

10 p1458 A72-23777

Dormant aerospace electronic system sedentary or nonoperating failure rate analysis by prediction technique

10 p1447 A72-24008

Work administration system for aerospace applications, considering contractual statements, corporate requirements, schedule accomplishment and cost effectiveness

[AIAA PAPER 72-244]

10 p1564 A72-24449

Aerospace vehicle high tensile strength fasteners stress corrosion cracking and hydrogen embrittlement

[AIAA PAPER 72-385]

11 p1653 A72-25407

Aerospace complex physical systems including human operator, discussing computerized design for behavior analysis by means of mathematical models

14 p2093 A72-30846

Aerospace critical systems and future technologies, presenting illustrative diagram for functions combination and interrelations

14 p2175 A72-31140

Astronautical digital computing hardware and software trends and implications, considering data rates, reliability, LSI, speed-storage tradeoff, etc

15 p2203 A72-31822

A comparison of voice communication techniques for aeronautical and marine applications.

17 p2512 A72-34267

Hybrid LSI logic modules for aerospace.

17 p2527 A72-34683

Techniques for control of long-term reliability of complex integrated circuits. I - Reliability assurance by test vehicle qualification.

17 p2528 A72-34686

Performance characteristics and design options for software controlled I/O processor for aerospace computer applications with high speed real time responses

17 p2521 A72-34702

International Aerospace Instrumentation Symposium, 18th, Miami, Fla., May 15-17, 1972, Proceedings.

22 p3178 A72-42676

Aerospace vehicle passive thermal protection systems heat shield and bulk insulation estimation by weight prediction in conceptual phases of design

[SAWE PAPER 934]

23 p3356 A72-43474

Space subsystems cost optimization technique for minimization of total spacecraft plus boost cost, studying orbital logistics spacecraft

[SAWE PAPER 941]

23 p3342 A72-43481

Rocketry and space age inauguration, considering technical, engineering, management and political problem areas

23 p3358 A72-44354

Space structures and materials technology utilization and transfer to world economic and social problems, considering thermal control, NDT, systems analysis and design

24 p3407 A72-45154

AEROSPACE VEHICLES

High performance aerospace vehicles transparent materials, discussing glasses, plastics and optical coatings, solar properties, refractive index, UV transmittance and radiation damage susceptibility

01 p0091 A72-10765

Rockets and spacecraft technology developments in U.S., U.S.S.R. and other nations, discussing satellite boosters, ballistic missiles, manned and unmanned spacecraft, lunar and interplanetary probes, etc

05 p0728 A72-16742

Electrofluid-dynamic wind tunnel velocity augmentation by enthalpy addition during expansion at constant static pressure and temperature for aerospace vehicles flight conditions simulation

[AIAA PAPER 72-166]

05 p0645 A72-16831

Aerospace structures harmonic vibration tests, discussing structures natural frequency spectrum, mode isolation, eigenmodes and inertial characteristics

06 p0896 A72-17948

Book on electricity and electronics for aerospace vehicles covering theoretical foundations, measuring instruments, batteries, generators, motors, radio receivers and transmitters, navigation equipment, autopilots, etc

15 p2182 A72-31511

Thermal simulation tests for kinetic heating of aerospace structures and materials, describing facilities for supersonic flight and atmospheric reentry

16 p2475 A72-32897

Aerospace vehicle explosive components initiation, separation and destruct systems

16 p2443 A72-33361

Integration of aerospace vehicle performance and design optimization.

[AIAA PAPER 72-948]

22 p3137 A72-42355

Balancing aerospace bodies on industrial balancing machines.

[SAWE PAPER 929]

23 p3293 A72-43469

Rotating aerospace vehicles dynamic balance error terms due to despin masses misalignment and aerodynamic effects

[SAWE PAPER 930]

23 p3342 A72-43470

AEROSTATS

U AIRSHIPS

AEROTHERMOCHEMISTRY

Aerothermochemical analysis of thermosetting hydrocarbon plastic ablation rate under heat transfer at reentry vehicle hypersonic stagnation point, describing pyrolysis by chemical kinetic equation

15 p2335 A72-32149

AEROTHERMODYNAMICS

A semiempirical method for the evaluation of aerothermodynamic properties in the intermediate hypersonic flow regimes.

[ICAS PAPER 72-03]

21 p2990 A72-41128

Electron-beam flow visualization - Applications in the definition of configuration aerothermal characteristics.

[AIAA PAPER 72-1016]

24 p3404 A72-45405

AEROTHERMOELASTICITY

Comparison of experimental and theoretical thermal fatigue lives for five nickel-base alloys.

19 p2815 A72-37639

AEROZINE

Helium absorption into nitrogen tetroxide (NTO) and aerazine-50 (A-50).

22 p3215 A72-42869

AFC [CONTROL]

U AUTOMATIC FREQUENCY CONTROL

AFCs [CONTROL SYSTEM]

U AUTOMATIC FLIGHT CONTROL

AFFERENT NERVOUS SYSTEMS

Pyramidal tract neuron reactions to antidromic and afferent stimuli in cats, determining somatosensor cortical neurons responses by intra- and extracellular potential outlets

02 p0159 A72-11768

Frog and rabbit sciatic nerve afferent impulse recordings during prolonged sinusoidal vibration of foot

04 p0474 A72-15235

Visceral afferentation role in vestibular system activity from experiments on rabbit stomach and rectum mechanoreceptor stimulation effects on vestibular-oculomotor reflexes

05 p0618 A72-16630

Cat respiratory center activity phase relation to arterial chemoreceptor afferent discharge oscillations effect on lung ventilation frequency

05 p0619 A72-16789

Nembutal barbiturate effects on afferent signals transmission and thalamocortical level of somatosensory system

08 p1116 A72-21195

Peripheral afferent input to monkey cortical efferent zones of distal forelimb muscle control, using single microelectrode for intracranial stimulation and cellular discharge recording

09 p1267 A72-23583

Russian book on visual sensory signal dynamics covering nerve signal transformation, light stimuli responses, afferent flow, bionics, neurocybernetics and communication theory

11 p1584 A72-26049

Amygdala projection to accessory olfactory bulb in rats, discussing main bulb, olfactory tubercle, pyriform cortex accessory bulb and amygdala relationships

11 p1581 A72-26770

High threshold afferents role in dorsal surface potential formation in cat spinal cord

13 p1905 A72-29327

Neuroinhibition in the regulation of emesis.

18 p2650 A72-36449

Synaptic patterns in the superficial layers of the superior colliculus of the monkey, *Macaca mulatta*.

19 p2758 A72-38647

Influence of a preceding afferent stimulation on the pyramidal activation of spinal motor neurons

21 p2999 A72-40588

Pyramidal control of the activity of interneurons related to various types of peripheral afferents

21 p2999 A72-40589

Cerebrum sections and related afferent processes as activator of automatic neuron mechanism control of motor activity, discussing segmentary spinal cord changes

21 p2999 A72-40593

Morpho-physiological structures thalamic afferent switching mechanisms of visceral analysers in motor, premotor, frontal and limbic cerebral sections

21 p3000 A72-40753

Polysynaptic sympatho-reticular and somatic afferent visceral links between internal organs and cerebrum in interoceptive reflex fields

21 p3000 A72-40755

Role of afferent and efferent connections in the formation and reproduction of trace processes in man

21 p3001 A72-40807

Analysis of the activity evoked in the cerebellar cortex by stimulation of the visual pathways.

21 p3003 A72-41460

Morphological and electrophysiological analysis of afferent receptor connections in cerebellar cortex, discussing fast conducting, diffuse reticular and inferior olive fiber paths

21 p3004 A72-41674

Electrophysiological analysis of defense reflex and unconditioned reaction and conditioned signal analyzers in nodal mechanisms of functional system /afferent synthesis, decision making, correction, etc/

21 p3004 A72-41675

Cerebral auditory system acoustic information processing, discussing ganglia and cochlea neurophysiological functions in response to afferent stimulations

22 p3146 A72-42786

Post-synaptic potentials of motor neurons of the facial nerve nucleus evoked by afferent and corticofugal pulse stimulation

23 p3257 A72-44091

The reflex and mechanical response of the inspiratory muscles to an increased airflow resistance.

24 p3372 A72-44958

AFFINITY

Phosphorus hydride electron affinity determination by electron photodetachment cross section measurement, using ion cyclotron resonance spectrometer

07 p0935 A72-19432

Photomultiplier negative electron affinity emitter materials photosensitivity performance, considering Cs-activated GaP and applications for low light level detection

15 p2291 A72-31531

AFRICA

Geomorphological and thermographic reconnaissance of Central Sahara, using orbital photographs

09 p1303 A72-23297

AFTERBODIES

Convergent-divergent nozzles thrust model measurement on supersonic aircraft afterbody [ONERA, TP NO. 978]

05 p0642 A72-15856

AFTERBURNERS

U AFTERBURNING

AFTERBURNING

Nonequilibrium chemistry effects on electrical properties of solid propellant rocket motors turbulent afterburning exhaust plumes, describing free electron sources

07 p0935 A72-19359

Boron ignition and combustion in air-augmented rocket afterburners.

17 p2636 A72-34902

Steady combustion limits in afterburner gas turbine engine chambers

20 p2987 A72-39922

Optimal synthesis of a two-parameter continuous controller for a jet engine with an afterburner

23 p3326 A72-44284

AFTERGLOWS

NT HELIUM AFTERGLOW

NT OXYGEN AFTERGLOW

Laboratory measurements of D region ion-molecule reactions using flowing afterglow system

03 p0347 A72-13388

Acoustic waves generation in afterglow of weakly ionized low pressure He plasma, using electrostatic probe

05 p0699 A72-17083

Electron-ion recombination rate measurements in flowing afterglow, using sampling mass spectrometer and floating double probe

06 p0851 A72-17318

Weakly ionized decaying afterglow plasma potential fluctuation and instability in magnetic field, using electrostatic probes

06 p0860 A72-17692

Vibrationally excited nitrogen photoionization spectrum obtained with quadrupole mass spectrometer in flowing nitrogen afterglow

07 p1037 A72-19434

Ambipolar diffusion in weakly ionized unstable plasma afterglow in presence of uniform axial magnetic field

07 p1047 A72-20558

An appraisal of the single Langmuir probe technique in the study of afterglow plasmas.

19 p2840 A72-37456

Diffusion cooling in neon, argon, and krypton afterglow plasmas.

19 p2841 A72-38378

A technique for recording Langmuir probe characteristics in afterglow plasmas.

21 p3051 A72-40212

Direct measurement of diffusion cooling in an afterglow plasma.

22 p3212 A72-42918

Measurement of the rate coefficient for the recombination of He⁺ with electrons.

23 p3315 A72-43869

Dissociative recombination at elevated temperatures. I - Experimental measurements in krypton afterglows.

23 p3316 A72-44346

AFTERIMAGES

Fragmentation and closure in afterimages of bright flash stimuli

03 p0317 A72-13938

Afterimage apparent motion preceding smooth eye movement association with target tracking, noting unequal impairment occurrence over entire visual field

07 p0927 A72-19034

Contrast enhancement for switch-on and off modes of bar patterns, noting spatial transients due to primary image interaction with negative afterimage

12 p1808 A72-27679

Frequency-specific color aftereffects as result of alternate exposure of subject to inspection gratings of different spatial frequencies

13 p1901 A72-28615

Foveal and nonfoveal afterimages effects on saccadic behavior of eye movement

13 p1907 A72-29971

Eye movement pattern monitoring to investigate retinal afterimage role in release of pursuit movements

17 p2508 A72-34886

Manipulation of projected afterimages by means of the physiological theory imposed on the observer.

18 p2654 A72-36920

Contour-contingent color aftereffects - Retinal area specificity.

19 p2755 A72-37273

Discontinuity of seen motion reduces the visual motion aftereffect.

19 p2760 A72-37600

Investigations concerning the problem of virtual contours in visual perception

19 p2759 A72-38719

The effect of size, retinal locus, and orientation on the visibility of a single afterimage.

21 p3003 A72-41253

Interactions between spatial and kinetic dimensions in movement aftereffect.

21 p3003 A72-41254

Complete assimilation of briefly presented lines.

23 p3261 A72-44150

The photopigment bleaching hypothesis of complementary after-images - A psychophysical test.

23 p3258 A72-44376

AGC [CONTROL]

U AUTOMATIC GAIN CONTROL

AGE DETERMINATION

U CHRONOLOGY

AGE FACTOR

Sphene U-Pb age resistance to thermal metamorphism, discussing zircon U-Pb and biotite and hornblende K-Ar ages within thermal aureole

01 p0052 A72-10069

Age and physique effects on human continuous work capacity, monitoring heart rates during task performance

01 p0018 A72-10568

Age related diminutions in ballistocardiographic and electrocardiographic amplitudes, observing relation to heart position lateralization and size reduction

03 p0314 A72-13144

Altitude hypoxia resistance and endurance in dogs of various ages, discussing homeostasis retention, altitude ceiling and survival time

04 p0474 A72-15234

Doppler ultrasonic probe phonocardiography for human cardiovascular velocity measurement, showing normal tracings and aging effects

05 p0617 A72-16154

Small lunar maria craters morphological maturity as function of age and dimensions

05 p0722 A72-17041

Electrocardiographic age trends in adult healthy populations, discussing diagnostic implications and overweight, exercise and latent coronary artery disease influence

06 p0761 A72-17425

Aging effect on visual acuity variations relation to refraction variations in flight deck personnel, noting eye functional value diminution

07 p0927 A72-19244

Adjustment to subjective horizontal, vertical and 45 deg tilt in dark as function of age in 3-20 year old subjects

08 p1124 A72-20989

Arterial hypoxemia development during hypoxic ontogenesis early stages related to age in dogs

09 p1266 A72-22879

Ventricular and supraventricular arrhythmias incidence during maximal treadmill exercise in normal man, noting age factor and cardiovascular disease presence effects

09 p1266 A72-23272

Human body efficiency in paced and unpaced performance as function of age

10 p1432 A72-24987

EEG measurement of sleep behavior patterns, discussing sleep stages, temporal patterns, circadian rhythm, intrasleep process stability and age factor

11 p1580 A72-26679

Hemodynamic criteria for physical fitness in airman, discussing age dependent variations in heart beat, arterial pressure and body temperature

11 p1590 A72-26987

Physiological index changes in parachutists of various ages, considering plasma recalcification, blood prothrombin, heparin time, fibrinolytic activity, pressure and heart beat

11 p1590 A72-26988

Triglyceridemia relation to age, relative weight and ischemic cardiopathy probability from ECG, anthropometry and lipid and glucid metabolism studies

12 p1759 A72-27238

Cosmic ray showers age parameter change with density of penetrating component, using Geiger counters and scintillator system

12 p1864 A72-27720

Galactic cluster lifetimes from observed age distribution comparison to evaporation times by numerical experiments with star cluster models

12 p1873 A72-27897

Review of aeromedical records for grounding USAF flying personnel during 1956-1970, noting increased age factor effect

12 p1776 A72-28316

New and old sunspot groups proper motions in large scale flow of solar photosphere investigated as function of age, noting angular momentum transport direction

13 p2036 A72-28834

Chlorella population age structure and cell requirements correlation with nutrient medium nitrogen and phosphorus absorption

13 p1909 A72-29311

Ar-39/Ar-38 cosmic ray exposure age calculation from Sikhote-Alin meteorite fall fragment content of Ar-39, Ar-38, Ne-21 and He-3

14 p2157 A72-30584

- Work capacity and physiological responses to maximum exercise in 54 year old men in relation to heart disease and cardiovascular hazard studies
17 p2505 A72-35822
- Developmental relationships between field independence and fixity-mobility.
18 p2651 A72-36906
- Assessment of life span age difference relations in visual perceptual tasks, taking into account maturational and generational differences
18 p2653 A72-36910
- Effect of set size, age, and mode of stimulus presentation on information-processing speed.
18 p2654 A72-36922
- Age dependence of changes in pupil diameter in the dark.
21 p3007 A72-40732
- Echocardiographic investigation of heart rate, sex and normal aging effects on mitral valve leaflet movement in healthy subjects
22 p3148 A72-43021
- Collagen in human myocardium as a function of age.
23 p3256 A72-43935
- The scoliosis of congenital heart disease.
24 p3370 A72-44560

AGE HARDENING

U PRECIPITATION HARDENING

AGENA ROCKET VEHICLES

- U.S. reconnaissance satellites development, discussing RAND project, Agena, Discoverer, Samos and Midas
12 p1876 A72-27109
- The Agena orbit transfer stage as an interim space tug.
24 p3451 A72-45195

AGGLOMERATION

- Euler and Lagrange methods of calculation for agglomeration of particles due to velocity drop disparities among particles in Laval nozzles
02 p0149 A72-11593
- Refractory metal powders spherical agglomerates growth and strength in rotating tumbler, noting particle size dependence on binder
11 p1643 A72-26829

AGGLUTINATION

- Light transmission measurements of blood flow to quantify red cell aggregation and dispersion
15 p2185 A72-31640

AGGREGATES

- Mathematical model of class of complex control systems composed of structures obtained from aggregates of ordered sets and random operators
19 p2777 A72-37380

AGING

- Electromagnetic cylindrical wave group aging properties, describing extragalactic red shift production mechanism
01 p0135 A72-11325
- VS type 2-W carbon resistor electrical aging operation, investigating optimal ambient temperature and duration
08 p1143 A72-22068

AGING [BIOLOGY]

- Hypophysectomy in rats, resulting in prolonged red blood cell survival due to oxygen consumption decrease and altered erythrocyte enzymatic processes
01 p0010 A72-10075
- Viruslike particles in salivary glands, muscles and nerves of normal and gamma irradiated *Drosophila melanogaster*, showing age dependent infection
08 p1116 A72-21198
- Blood circulation minute volume and peripheral resistance changes during human aging process, accounting for body weight
08 p1120 A72-22073
- Vascular-capillary study of age related angioarchitectonic features of human brain optic lobe
11 p1580 A72-26675
- Changes of the mitral echocardiogram with ageing and the influence of atherosclerotic risk factors.
18 p2652 A72-37031
- Age-induced long-term memory changes in animals
23 p3257 A72-44079
- Natural aging and radiation-induced life shortening in *Drosophila melanogaster*.
24 p3373 A72-45279

AGING [MATERIALS]

NT AGING [METALLURGY]

- High temperature strength degradation of graphite and boron reinforced epoxy composites after room temperature aging
01 p0090 A72-10728
- Integral operators functions approximation for elasticity and materials aging equations, noting transcendental functions in solutions
08 p1243 A72-21239
- Lithium diffusion into silicon by evaporation and homogenization technique, discussing dislocations and oxygen effects from aging in Ar at 150 C
12 p1757 A72-28025
- Paint coatings aging effect on D16T type alloy corrosion fatigue in NaCl solution, noting protective efficiency decrease
13 p1984 A72-29486

Explosives life limitation due to aging phenomena, discussing chemical and physical processes and environmental effects
14 p2143 A72-30752

Carboxy-terminated polybutadiene/ammonium perchlorate base solid propellants aging properties under long time storage conditions at 243-353 K, considering mechanical, dimensional and combustion properties
14 p2145 A72-30763

Pulsed solid state lasers with large area Si photodiode for output measurement in feedback control system to compensate flash lamp aging
15 p2247 A72-32027

Nitride precipitate platelets and dislocation loops formation in Nb-N alloys during aging at 535 C from electron microscope observations of structural changes
16 p2405 A72-32999

Point and confidence interval estimates for acceleration and aging component probability distribution functions in accelerated life tests and reliability prediction
24 p3406 A72-44669

AGING [METALLURGY]

Uniform low temperature compression effect on accelerated aging of Duralumin specimens, noting Plateau due to Guinier-Preston zones
02 p0245 A72-12539

Surface layers and aging influence on Bauschinger effect in profiled low carbon steel under low tension-compression load cycles
03 p0445 A72-13591

Mg-Zn alloys precipitation hardening mechanism at various aging stages, considering yield strength increase due to interface dislocations
03 p0374 A72-13717

Alloying elements effects on aging response of austenitic-ferritic alloys in Fe-Cr-Mn-Ni base, determining mechanical properties dependence on processing and heat treatment
03 p0377 A72-14170

Strain hardening for steel strength increase to 300 kg/sq mm by sequentially combined mechanical and thermal processing, involving plastic deformation, quenching and aging
04 p0527 A72-15454

Electron microscopic examination of molybdenum alloy thin plates aging at 700 C observing nucleation and precipitated phase
05 p0673 A72-16147

Aging effect on duraluminum electrical resistivity alteration at low temperature plastic deformation
05 p0679 A72-17181

Electron transmission microscope study of quenched Mo-N alloys supersaturated solid solution low temperature aging behavior, investigating recovery processes
06 p0830 A72-18056

Aging creep theory application to anisotropic strain hardenable metals
06 p0900 A72-18680

Aging kinetics in Co-Ni-Ti alloys, noting three dimensional periodically modulated structure development
06 p0834 A72-18742

Structural changes, mechanical properties, electrical resistance and lattice constant during aging of Al alloys containing Mg, Li and Mn
06 p0834 A72-18743

Increased microplastic deformation resistance, relaxation stability and aging of beryllium by cyclic heat treatment
07 p1013 A72-19740

Deformable thermally work hardenable Al-Mg-Li alloy, detailing phase composition changes during aging
07 p1014 A72-19838

Transition metals addition effect on Al-Cu alloys strength and aging characteristics, determining lattice constant increase by X ray microstructural analysis
07 p1014 A72-19841

Aging effect on brittleness and hardening of Fe-Ni-Mn alloy at various temperatures
07 p1016 A72-19939

Heat treatment of martensitically aging steels with Co, Ni and Mo, considering hardening effects and optimal conditions for high mechanical properties
07 p1020 A72-20414

High temperature nitriding of martensitically aging steels in ammonia-nitrogen mixtures, obtaining hard nonbrittle diffusion surface layers
07 p1020 A72-20418

Austeno-martensitic steel with 25 percent delta ferrite, examining microstructural changes due to aging at 550 C by thin slide electron microscopy
07 p1021 A72-20484

Stable austenite formation during maraging steel aging at 300-750 C determined by X ray diffraction
07 p1022 A72-20525

Precipitation effect on microstructure, coercive force, resistivity and cell formation changes in heterogeneous decomposition of supersaturated solid solutions and aging alloys
08 p1218 A72-21777

Fe-Ni alloys atom redistribution during aging before phase precipitation, discussing Mo and Co clusters in martensitic maraging steels
08 p1190 A72-22189

Microstructural transformations in preaged Ti alloys with unstable beta phase under external tensile stresses
09 p1328 A72-23032

Magnetic susceptibility of ternary Al-Mn alloys with Ti, Va, Cr, Fe, Co, Ni, Cu and Zn, describing microstructure and aging experiments
10 p1494 A72-23832

Sintering and aging effects on mechanical behavior of low carbon copper steel
10 p1488 A72-24696

Co, Al and Mn additions effect on secondary hardening during aging in Fe-Mo-C martensite
11 p1655 A72-25511

Al addition effect on thermal and mechanical stability, forgeability, cold workability, aging and oxidation resistance of Ti-Mo beta alloys
11 p1656 A72-25516

Cold working effect on Cu-Ni-Si-Mg and Cu-Ni-Si-Cr alloys age hardening behavior, presenting hardness and tensile strength vs aging time at 350 and 400 C
11 p1662 A72-26743

X ray diffraction patterns of aging nimonin alloys, noting effects of atomic volume difference between precipitation phase and matrix
13 p1976 A72-28766

Al-Zn alloy supersaturated solid solution decomposition during aging, studying single crystal lattice characteristics via X ray diffusive scattering techniques
13 p1976 A72-28902

Microhardness anisotropy of hardened and aged Be single crystal as function of purity
13 p1978 A72-29023

Maraging Fe-Ni-Co-Mo alloy ordered metastable omega phase formation during martensite aging from electron microscopic investigation, noting Co addition effects and precipitation
14 p2115 A72-30404

Co, Mo, Ti and Al alloying effects on aging and hardening processes in Ni steel from hardness, thermal emf and electrical resistance measurements
14 p2115 A72-30408

Al-Cu alloy structural changes after long term natural aging by X ray diffraction analysis
14 p2115 A72-30413

Uniformly distributed precipitates effect on hardness increase in aging of ferritic matrix Fe-Co-Ti and Fe-Co-Al alloys
14 p2119 A72-30605

Alloying effect on structural transformations and strain hardening during aging of two phase α -beta/Mg-Li-Zn alloys
14 p2124 A72-31031

Dispersion hardening of Nb-Zr-O and Nb-Hf-O alloys, discussing composition and heat treatment effects on aging, recrystallization temperature and grain growth
15 p2255 A72-31567

Dispersion hardening /aging/ effect on embrittlement of Ni base alloys in cold worked pipes during heat treatment
15 p2255 A72-31569

Plane strain fracture toughness tests of compact thick maraging steel specimens at various yield strength levels as function of aging
16 p2406 A72-33317

Discontinuous precipitation and site nucleation in quenched and aged Al based Zn alloys as function of temperature
16 p2410 A72-33812

Destabilization and aging mechanisms for ionic conductivity decrease in stabilized zirconia type electrolytes, discussing yttria stabilization
16 p2361 A72-33895

New observations of preprecipitation phenomena in Al-Mg and Al-Mg-Zn alloys
17 p2566 A72-34286

Interstitial and substitutional dynamic strain aging of Fe-Nb alloy and Al-Nb bearing steel at 295-950 K
18 p2699 A72-36342

The structure of the metastable precipitates formed during aging of an Al-Mg-Si alloy.
18 p2702 A72-36743

Some problems concerning microplastic deformation and isothermal transformation of Fe-Ni-C alloy. III - Effect of aging in the temperature range from 203 to 304 K on microplastic deformation at 77 K
19 p2814 A72-37419

Plane stress rupture criterion for age hardening materials during plastic deformation, calculating resistance to shear and torsion of solid and hollow round bars
19 p2818 A72-38009

Aging characteristics of Ti-Mo base beta alloys.
19 p2820 A72-38371

Quench-ageing behaviour of 40Co-38Ni-17Cr-5Ti alloy.
20 p2935 A72-39141

Formation of voids and dislocation loops in near-stoichiometric NiAl by aging at 700 to 900 C, and some effects on alloy properties. 20 p2937 A72-39288

X ray diffraction patterns of aging mimonic alloys, noting effects of atomic volume difference between precipitation phase and matrix 21 p3065 A72-40267

Dilatometric studies of volume compression effect during aging of mimonic alloy showing linear dependence of matrix lattice constant on gamma prime phase 21 p3068 A72-40957

Changes in the structure of nickel-beryllium alloys during deformation, recrystallization, and aging 21 p3068 A72-40959

Different forms of elimination of quenching lacunae in supersaturation in the case of aging of two alloys, Al-Cu and Al-Mg-Si 22 p3190 A72-42444

Carbide phases in nickel-based heat-resistant alloys 22 p3192 A72-43018

Investigation of the process of D16-alloy quenching in liquid nitrogen 23 p3294 A72-44095

Estimates of creep-fatigue interaction in irradiated and unirradiated austenitic stainless steels. 24 p3412 A72-44554

Contribution to the study of the creep behavior of 18 per cent-nickel maraging steel 24 p3415 A72-45600

AGITATION

NT ULTRASONIC AGITATION

Decay of isotropic turbulence generated by a mechanically agitated grid. 19 p2787 A72-38426

AGREEMENTS

Discrimination preference and effect on insurance of limit liability of international air carrier according to modified Montreal Interim Agreement 07 p1106 A72-20674

Book on world airlines economic regulation, analyzing multilateral international agreements, national aviation interests and competitive situation 11 p1748 A72-25923

Swiss franc revaluation effect on Warsaw Treaty liability limits, discussing legal problems 11 p1749 A72-26562

Warsaw Air Transport Convention second revision by Guatemala Protocol of 8 March 1971, discussing provisions for air carrier liability 14 p2174 A72-30821

AGRICULTURAL AIRCRAFT

U UTILITY AIRCRAFT

AGRICULTURE

Agricultural land use analysis by remote sensing, discussing side-looking airborne radar systems and image interpretation for local needs 01 p0056 A72-10456

Agriculture and natural vegetation remote sensing programs, discussing dichotomous keys for side-looking airborne radar imagery analysis 01 p0056 A72-10457

Forestry and agricultural applications of multiband photography, considering photointerpretation of black and white, color and IR photographs 01 p0057 A72-10459

Interpretation model for aircraft and spacecraft remote sensing of tropical agricultural systems 02 p0210 A72-11798

Small scale aerial photography use in regional agricultural survey, discussing equipment used, sampling techniques and data collection and interpretation 02 p0213 A72-11835

Sounding rockets in remote sensing programs for agricultural census and crop yield estimates in Argentina 02 p0228 A72-11854

Southeast Florida 13 year urban and agricultural development recorded by high altitude color and color-IR photographs, demonstrating capability for detail and macroscale patterns 02 p0230 A72-12199

Space and high altitude aerial photography agricultural ground data collection and processing for Arizona survey evaluation 02 p0220 A72-12200

Aerial photography for rural soil mapping, considering geographic, ecologic and agricultural production interpretation 09 p1301 A72-23279

Aerial photointerpretation for landscape analysis with respect to agricultural land use, considering geomorphologic, hydrographic, soil and microclimatic conditions 09 p1301 A72-23280

United Nations FAO interest in remote sensing techniques application to agricultural, forestry and fisheries resources survey and management 15 p2220 A72-31228

Computer controlled ground truth station for environmental agricultural aerial photographic remote sensors data processing, discussing system components, printout format and computer program 15 p2213 A72-31249

Lunar horticulture possible role as life support system of earth independent lunar colony 17 p2505 A72-35938

AILERONS

State sensitivity functions in aircraft parameter identification for lateral dynamics under aileron deflection from model response and in-flight test data 10 p1421 A72-23807

Aileron vibration pressure measurement in plane-parallel transonic flow, evaluating damping characteristics with allowance for shock motion caused nonlinear effects 14 p2071 A72-31026

AIR

NT ALVEOLAR AIR

NT COMPRESSED AIR

NT EXPIRED AIR

NT HIGH TEMPERATURE AIR

NT LIQUID AIR

Intracavity radiation induced air breakdown in TEA carbon dioxide laser for application in plasma heating. 02 p0238 A72-12205

Electron density and diffusion measurements in ionized air in front of strong shock wave with resonant microwave probe and electromagnetic induction technique 05 p0648 A72-16211

Cascade ionization of air by RF electric fields and intense laser pulses, solving Boltzmann equation for electron distribution 12 p1848 A72-27390

Air composition and thermodynamic properties at 12,000-25,000 K and 0.1-100 atm with allowance for Coulomb interaction effect on pressure and for ionization potential decrease 13 p2018 A72-29878

Combustion process in mixing gas jets of different density, using argon and nitrogen for internal flow and air for external jet 16 p2381 A72-34169

Numerical and shock tube experiments for variation of bound electron temperature and nonequilibrium chemical and radiative relaxation behind normal shock waves in air, using atom-molecule collision model 18 p2681 A72-36564

An experimental study of turbulent diffusion of helium jets issued upwards into the air at rest. 23 p3281 A72-44273

Effect of plasma mirror in the breakdown of air in a CO2 laser cavity. 24 p3412 A72-45775

AIR BEARINGS

U GAS BEARINGS

AIR BLASTS

U AERIAL EXPLOSIONS

AIR BREATHING ENGINES

NT GAS TURBINE ENGINES

NT JET ENGINES

NT PULSEJET ENGINES

NT RAMJET ENGINES

NT SUPERSONIC COMBUSTION RAMJET ENGINES

NT TURBOFAN ENGINES

NT TURBOJET ENGINES

NT TURBOPROP ENGINES

Air breathing propulsion systems for reducing engine noise level, discussing stoichiometric gas turbine engines, V/STOL propfans and variable-geometry supersonic inlet and exhaust nozzles 03 p0406 A72-13486

Aircraft air breathing propulsion technology, discussing two-place aircraft, turboprop power plants, helicopter engines and V/STOL, CTOL, subsonic transports and supersonic aircraft 04 p0565 A72-14825

German monograph on liquid air fractionation during flight of recoverable spacecraft carrier propelled by air breathing propulsion systems 09 p1374 A72-23160

Two-dimensional model for thermal compression. 22 p3136 A72-42868

AIR CARGO

U.S.S.R. high-subsonic freight transport jet aircraft IL-76 for arctic areas, Siberia and Far East, noting independence of large airports availability 03 p0310 A72-13471

American civil aviation future development, discussing passenger and freight markets growth, aircraft types and FAA role 04 p0464 A72-14811

Future civil air transport trends, considering passenger and cargo growth, travel frequency per capita income and STOL market 08 p1257 A72-22150

Air cargo growth potential, marketing and profitability, considering need for improvements in ground handling, rate structure, container standardization, documentation, etc 13 p1896 A72-28452

Air cargo intermodal and interline containers handling in warehouse storage, transportation and distribution, considering total pack and interlock requirements 16 p2372 A72-33174

AIR COOLING

Terminal handling environment and air cargo requirements for noncontainerized freight 16 p2372 A72-33175

Major civil airport passenger and cargo terminal complex design and layout planning, discussing various facilities and equipment requirements 16 p2373 A72-33329

Simulation of an air cargo handling system 17 p2372 A72-34472

Airborne towed cargo carrying bodies dynamic stability for single-point suspension system, using linearized small perturbation analysis [AIAA PAPER 72-986] 22 p3136 A72-42328

Boeing 747-F cargo aircraft, describing onboard and ground facilities for freight handling and loading 23 p3278 A72-43245

Air freight ground handling and distribution terminal facilities and methods, discussing future technical and organizational developments for efficient handling of increased traffic volume 23 p3358 A72-43246

Design of a military air cargo transportation system by use of a large scale mathematical programming model. 24 p3466 A72-44577

Statistical forecasting models for USAF CONUS outbound cargo airlift requirements by averaging and exponential smoothing models 24 p3466 A72-44578

AIR CONDITIONING

Sound attenuation in lined air ducts, describing experimental determination of lining materials acoustical properties for central air heating systems 13 p2005 A72-29577

AIR CONDITIONING EQUIPMENT

Soviet book on civil aircraft high altitude equipment covering air conditioning systems, oxygen equipment and cabin pressurization 02 p0156 A72-12295

Design and development program for air conditioning system of twin engine unpressurized Piper Navajo, noting flight test results [SAE PAPER 720328] 11 p1577 A72-25590

AIR COOLING

Forced air cooling of cylindrical body with distributed thermal input, calculating temperature distribution and optimum mechanical dimensions for temperature rise minimization 02 p0189 A72-11560

Heat transfer from gas to air-cooled turbine blade, obtaining solution by brute force technique 04 p0595 A72-14649

Two dimensional cascade test of air-cooled turbine nozzle, describing aerodynamic characteristics and heat transfer properties 05 p0602 A72-16489

Aircraft engines high pressure turbine guide vanes air cooling by internal insert, analyzing thermal stresses [AIAA PAPER 72-7] 05 p0707 A72-16864

Velocity and exit angle determination for flow behind turbine blade cascade with cooling air exhaust through blade trailing edges from continuity equations 05 p0707 A72-17063

Boundary conditions in heat conduction for nozzle blades with shrouds exposed to cooling air on one side 08 p1222 A72-20945

Steady heat conduction solution for intensified cooling of turbine rotor blade leading edge with holes and air channel 08 p1223 A72-20951

Profile thickness effect on air cooling of gas turbine disks in central and peripheral sections 08 p1223 A72-20952

Gas turbine nozzle guide vane trailing edge protection by air films cooling, measuring gas temperatures with chromel-alumel thermocouples 08 p1224 A72-21318

Heat transfer rates of impingement cooling in gas turbine airfoils, noting leading edge sharpness effects for slot and circular jet configurations [ASME PAPER 72-GT-7] 11 p1703 A72-25610

Local heat transfer coefficient distribution in multiple air jet cooled cavity, noting application to gas turbine blade leading edge cooling [ASME PAPER 72-GT-59] 11 p1745 A72-25650

Cooling efficiency and load endurance of aircraft turbine engine blades as function of ambient temperature and air flow rates 11 p1712 A72-26892

Gas side, coolant side and interstitial heat transfer in gas turbines transpiration air cooling 12 p1860 A72-27350

Air bleeding location to cool turbojet engine turbine of supersonic aircraft, presenting graphs 12 p1862 A72-28147

Simulation model test for effects of cooling air exhaust into gas flow area on turbine blading efficiency, obtaining dimensionless expression for experimental data generalization 12 p1862 A72-28148

Russian papers on cooled high temperature gas turbines covering engine theory and design, power plants development, heat transfer and air cooling systems 13 p2029 A72-29925

Computer aided thermal design of LSI module packs for forced convection air cooling, using modal conductance matrix method 16 p2368 A72-33195

Computer-aided thermal design of LSI packages. 17 p2527 A72-34681

Air film cooling in a nonadiabatic wall conical nozzle. 17 p2638 A72-35493

Air cooled CW 30 W carbon dioxide laser construction for technological applications, using radiation energy extraction through GeAs or GaAs plate 20 p2932 A72-39507

Influence of cooling-air exhaust into the air-gas flow area on the flow-rate characteristics of cooled profiles 20 p2963 A72-39923

Dimensionless pressure method to account for air density variations in gas turbine cooling system design 21 p3099 A72-41059

Influence of baffle geometry on heat transfer in the cooling channel of air-cooled blades 21 p3099 A72-41062

Pressure at the trailing edge and losses in turbine bladings with air injection into the blade wake 23 p3248 A72-43661

Gasdynamic investigation of a turbine with evaporative air cooling of the nozzle guide vanes 23 p3325 A72-43662

AIR CURRENTS

NT JET STREAMS [METEOROLOGY]

NT MERIDIONAL FLOW

NT VERTICAL AIR CURRENTS

Ionization movement of charged and neutral particles in F 2 region coupled to air movement by collision drag forces 11 p1621 A72-25839

East African low level cross equatorial air current exploration, using light aircraft-borne Doppler radar wind finding equipment 12 p1840 A72-27703

The aeroelastic behaviour of hot-wire anemometer filaments in an air stream. 17 p2552 A72-34229

Wind velocity components determination in Cartesian coordinates based on rectilinear uniform air particle motion, noting difference with respect to geostrophic approximation 23 p3310 A72-43532

AIR CUSHION VEHICLES

U GROUND EFFECT MACHINES

AIR DEFENSE

Optimal air defense strategy with budgetary constraints, considering artillery, airborne interceptor and mobile surface to air missile effectiveness against penetrating enemy 03 p0459 A72-14197

Book on man machine system experiments covering ATC, air defense, logistics organizations, space flight, battlefield operation, police dispatching, communications, etc 16 p2359 A72-33796

SAM-D control test vehicle trajectory planning and flight test analysis. 24 p3451 A72-45338

AIR DUCTS

Sound field measurement in circular and rectangular air duct with sound-absorbing walls /mufflers/, deriving empirical formula for attenuation frequency characteristics 09 p1354 A72-23683

Sound attenuation in lined air ducts, describing experimental determination of lining materials acoustical properties for central air heating systems 13 p2005 A72-29577

Wind tunnel ventilation duct aerodynamic stability analysis for incompressible and slightly compressible flow 16 p2378 A72-33439

AIR FILTERS

Dusty inlet air filtering in aircraft turbine engines, discussing engine operation, dust and filter characteristics 05 p0704 A72-16179

Gas turbine engine inlet solid particle separator designed as integral engine part, discussing semireverse flow superiority 07 p1052 A72-18755

Aircraft gas turbine engines smoke emission sampling by stained filter technique, comparing Navy specifications AS 1833 with SAE method ARP 1179 07 p1053 A72-18770

Air dust erosive damage to helicopter gas turbine engine parts, discussing inertial rotorless filtering systems 13 p2026 A72-28786

AIR FLOW

NT AIR CURRENTS

NT JET STREAMS [METEOROLOGY]

NT MERIDIONAL FLOW

NT VERTICAL AIR CURRENTS

Air flow and acoustic characteristics of speech sounds produced with turbulence noise at glottal constriction, using flow equations [AD-744389] 01 p0101 A72-10162

Gas turbine nozzles aerodynamic throat area air flow measurement, describing accuracy, standards, reference nozzles and mounting flanges [SAE ARP 1195] 01 p0065 A72-10390

Real gas effects in atmosphere to make sonic bang shock wave full dispersion and thickness wide variations 02 p0154 A72-11972

Lee waves characteristics relationship to air flow and temperature layers in troposphere based on satellite pictures 02 p0255 A72-12791

Flutter problem wing-air flow energy exchange at instability limit, obtaining vibration mode shapes from homogeneous boundary value problem analog model 03 p0442 A72-13191

Dynamic calibration by sound wave of hot wire operated by constant resistance method, using open resonance tube in homogeneous incompressible air flow 03 p0356 A72-13235

Supersonic diffusion flame in duct configuration to study mixing with combustion of two parallel methane and air flows 03 p0405 A72-13545

Hydrodynamic journal gas bearing with herringbone grooved portion for self generating air supply pump hydrostatic starting and stopping [ASME PAPER 71-WA/DE-7] 05 p0664 A72-15944

Air stream from air entry holes of aeronautical gas turbine combustor, investigating jets maximum penetration, flow path, and mixing 05 p0705 A72-16493

Homogeneous compressible turbulence field with large amplitude and density fluctuations generated in subsonic wind tunnel by rapid mixing of hot and cold air streams [AIAA PAPER 72-119] 05 p0652 A72-16980

Shock wave shape and strength alteration by radioisotope emissions from body surface in supersonic airstream 05 p0654 A72-17226

Ignition conditions for pyroxylin and polyvinyl-nitrate in air flow containing spherical aluminosilicate and aluminum oxide particles 06 p0903 A72-18211

Heat transfer and drag during air laminar flow in circular pipe with constant heat flux density at wall 07 p0966 A72-18938

Two phase flow model of water droplets velocity in air stream, using Fresnel biprism and laser differential scheme 07 p1000 A72-18940

Air flow turbulent behavior and dynamic characteristics dependence on underlying surface roughness variations 07 p1031 A72-20695

Atmospheric light scattering matrices from nighttime air flows, showing climatic variability and similarity between Crimean and Moscow measurements 07 p1031 A72-20700

Vaneless diffuser air flow calculation based on helical flow model with back currents in boundary layer 09 p1259 A72-22299

Parallel air and hydrogen flows confluence numerical examination to determine self ignition conditions in turbulent mixing layer, noting reaction zone [ONERA, TP NO. 981] 09 p1410 A72-22814

Pressure recovery calculation for subsonic adiabatic air flow through diffusers with tail pipes, assuming turbulent inlet boundary layer 10 p1415 A72-23855

Turbulent shear stress and kinetic energy characteristics of subsonic air flow in straight conical diffuser, using hot-wire anemometry measurements 10 p1416 A72-23862

Spanwise velocity distribution effect on drag measurement of short struts in two dimensional turbulent airstreams 10 p1417 A72-23881

Semiconductor air-air heat pumps with solar cell feed current, determining hot air flow temperature effects and energy conversion efficiency 10 p1423 A72-24319

Quasi-steady creeping flow in small airways of spherical, oblate and prolate ellipsoid and circular cylinder lung models, obtaining Stokes equations solutions 10 p1431 A72-24469

Shock layer emission associated with hypersonic air flow past spherical segment, solving flow equations by iteration technique 10 p1418 A72-24539

Subsonic unsteady aerodynamic pressures on blades of compressor wheel rotating freely in air stream [ONERA, TP NO. 1077] 10 p1420 A72-24854

Smoke generator for fluid flow visualization, presenting photographs of turbulent rotating air flow in cylindrical enclosure [AD-746416] 11 p1613 A72-26540

Single continuous algebraic correlation equation for convective heat transfer in cross flow for wide

Reynolds number range, considering applications to hot-wire anemometry 11 p1747 A72-26541

Perturbation velocity corrections for eccentric model position and different air flow ducting in rectangular wind tunnels [DFVLR-SONDDR-191] 11 p1573 A72-26581

Stability of free shear layer in wind tunnel two layered temperature differentiated air flow against small periodic disturbances, noting critical Richardson number 11 p1619 A72-26638

Rain droplets growth by collision and coalescence during fall through sheared air flow, discussing discrepancies between calculated and experimental collision efficiencies 11 p1619 A72-26642

Tornado model from atmospheric thermodynamics nonlinear equations, examining air flow from lower boundary layer and ground friction 11 p1682 A72-26880

Numerical shallow fluid model for air flow across orographic variable grid barrier, using idealized Andes Mountains range 12 p1838 A72-27023

Surface roughness effects on air flow in turbulent atmospheric boundary layer, using finite difference method 12 p1838 A72-27026

Gas turbine engine combustion chamber, investigating swirl vane air flow rate effects on circumferential nonuniformity of gas temperature field at outlet 12 p1861 A72-28132

Copper resistance thermoanemometer for channel unsteady air flow rate measurement, discussing design, operation principles and maximum error 12 p1812 A72-28146

Film cooling effectiveness for air-gas flow section of gas turbine engine under actual operating conditions 12 p1890 A72-28170

Heat transfer measurement during flat plate cooling by air film, using electrical calorimetric technique 12 p1890 A72-28176

Wind tunnel investigation of supersonic air flow behavior on rotatable right dihedral formed by two plane plates with sharp edges 13 p1894 A72-29636

Wind tunnel investigation of pressure perturbations on plane surface due to gas jet injected from surface into subsonic air drift flow 13 p1894 A72-29637

Heat transfer and hydraulic resistance for cooled air forced flows in narrow rectangular channels as function of pressure and Reynolds number 14 p2093 A72-30291

Air and carbon dioxide intensive injection effects on turbulent boundary layer of subsonic channel air flow 14 p2097 A72-31159

Wind tunnel measurement of intermittency in turbulent boundary layer on porous plate for alternating laminar and turbulent air flow 15 p2217 A72-31610

Fully developed turbulent air flow through concentric annuli, measuring inner wall shear stress distribution by zero-shear position location and sliding sleeve technique 16 p2375 A72-32875

Thermodynamic properties of axisymmetric and planar stagnation flows of air with gas injection, taking into account mass transfer effects on heat transfer rate 16 p2477 A72-33428

Turbulence induced sound pressure level measurement for noise generated by grill in air flow, using streamlined probe microphone 16 p2344 A72-34001

Flowing air glow discharge near IR emission spectrum as function of pressure, noting atomic lines 16 p2427 A72-34097

Calculation of airflow over an arbitrary ridge including diabatic heating and cooling. 18 p2706 A72-36629

Atmospheric flow turbulent behavior and dynamic characteristics dependence on underlying surface roughness variations 20 p2948 A72-39010

Atmospheric surface layer light scattering matrices from nighttime air flows, showing climatic variability and similarity between Crimean and Moscow measurements 20 p2948 A72-39014

Intensification of heat transfer in channels with turbulent gas flows 21 p3127 A72-40127

Influence of baffle geometry on heat transfer in the cooling channel of air-cooled blades 21 p3099 A72-41062

Perturbation analysis of aerodynamic test flow in Ludwig tubes, investigating nonsteady coupling effects on nozzle turbulent boundary layer [AIAA PAPER 72-994] 21 p2993 A72-41580

Electron beam visualization in hypersonic air flows. [AIAA PAPER 72-1017] 21 p3042 A72-41596

Nitrogen temperature determination in arc tunnel air flows. [AIAA PAPER 72-1022] 21 p3042 A72-41600

Throttle characteristics and mixing chamber geometry effects on low pressure gas ejector operation, noting air flow and pressure rates in air ejectors 22 p3133 A72-41859

Velocity distribution in turbulent air flow over perforated plates with gas injection in turbulent boundary layer 22 p3166 A72-42256

Interferometric investigation of natural convection in rectangular air cavities of different orientation 22 p3244 A72-42262

Experimental facility and diffusion technique for measuring turbulence characteristics during hydrocarbon fuels burning in air streams 23 p3287 A72-43658

Probability distribution of velocities and temperatures near a wall 23 p3279 A72-43696

Experimental study of the plane deformation of a homogeneous turbulence 23 p3280 A72-43822

An experimental study of flows in planar nozzles. [ASME PAPER 72-FLCS-2] 23 p3249 A72-44066

Effect of a line energy source at the boundary of a supersonic flow. 24 p3361 A72-45187

Investigation of the characteristics of turbulent air flow in a channel with elastic walls 24 p3393 A72-45257

AIR FREIGHT

U AIR CARGO

AIR INLETS

U AIR INTAKES

AIR INTAKES

NT ENGINE INLETS

NT HYPERSONIC INLETS

NT SUPERSONIC INLETS

Pressure and convective heat transfer distribution at air inlet central body surface, reducing Navier-Stokes equations to partial differential equations with similar solutions 04 p0596 A72-14971

Convective heat flow pressure and density measurements at surface of central body of air inlet with live point and axial symmetry 06 p0755 A72-17560

Gas turbine engine inlet solid particle separator designed as integral engine part, discussing semirverse flow superiority 07 p1052 A72-18755

Inlet duct and turbfan engine compatibility without stalling and surge conditions obtained by design optimization and wind tunnel testing 07 p1052 A72-18761

AIR JETS

Plane air jet ejection into dead ended rectangular and parabolic channels, discussing effects of geometry, length and pressure 03 p0309 A72-14156

Velocity profiles of turbulent three-dimensional incompressible air jet flow from rectangular orifice tangent to and along curved wall surface [ASME PAPER 71-WA/FE-2] 05 p0647 A72-15938

Pressure source model of sound radiated by sonic jet, deriving frequency spectra ratio and jet pressure 05 p0600 A72-16105

Axial structure of free air jet in rarefied atmosphere, measuring pressure and density 06 p0797 A72-17561

Air jet propelled flight vehicles optimal design parameters for constant altitude flight at given speed 07 p0911 A72-18991

Aerodynamic throttling effect due to air jet flow interaction in throat region of mainstream two dimensional nozzle flow 10 p1419 A72-24845

Ammonia-air opposed reacting jet /ORJ/ for flame stabilization, solving partial differential equations for flow field 10 p1564 A72-25141

Two phase axisymmetrical air jet turbulence intensity determination from heat distribution parameters in wake of wire heated by electric current 10 p1471 A72-25172

Two dimensional transverse subsonic hot-air jet interaction with freestream flow at various jet/freestream velocity ratios, measuring jet velocity and temperature distributions [AIAA PAPER 72-292] 11 p1567 A72-25230

Local heat transfer coefficient distribution in multiple air jet cooled cavity, noting application to gas turbine blade leading edge cooling [ASME PAPER 72-GT-59] 11 p1745 A72-25650

Turbulent intensity induced by wakes near secondary air jet inlet to gas turbine engine flame tube 12 p1861 A72-28131

Round air jet turbulent mixing with incompressible transverse flow, examining interaction behavior as function of relative momentum 13 p1943 A72-29641

Experimental study of the aerodynamic characteristics of burning gas-air jets in the transient flow region of natural gas 17 p2637 A72-35169

Topler schlieren study of diffusion flame structure of plane laminar hydrogen-air jets in rectangular channel with vortex generators 19 p2879 A72-37365

Space correlations of the fluctuating pressure in subsonic turbulent jets. 20 p2913 A72-39555

Effect of air injection on the torque produced by a trailing vortex. 23 p3247 A72-43333

Turbulent interaction of air jets issuing from perforated surfaces into free space, determining three dimensional flow field via Reichardt free turbulence theory 23 p3248 A72-43625

Basic directivity and spectra of jet noise with improved correction for refraction. 24 p3389 A72-44678

AIR MASSES

Tornado and funnel cloud comparison in seasonal and diurnal distributions, air mass instability, tropospheric vertical wind shear and geographical distribution 03 p0385 A72-14231

Air masses circulation in atmospheric upper layers during IQSY from meteor trail drifts observation by radar tracking method 08 p1161 A72-21882

Computer program for numerical analysis of atmospheric fronts in lower troposphere based on models for spatial distribution of hydrothermal characteristic in air mass 19 p2829 A72-38771

Direct observation of a complete unit of meridian circulation from the equatorial belt up to the polar front - Synthesis of concepts of the pseudofront, of the equatorial mesosystem, and of the subsidence well 21 p3078 A72-41344

AIR NAVIGATION

NT ALL-WEATHER AIR NAVIGATION

ATC separation minima and navigational errors on airways in general and long range oceanic environments 01 p0096 A72-10177

Avionics contribution to airspace decision making problems, considering navigation, surveillance radar, collision avoidance and ATC techniques 01 p0097 A72-10180

Stellar attitude reference and navigation associative processor with high computational speed for radar approach control in ATC 02 p0256 A72-12033

Optimal stochastic /Kalman/ filters application to integrated air and submarine navigation systems, discussing measurement errors modeling as bias and colored noise 02 p0256 A72-12050

L band in satellite system for aerial navigation aid, discussing position accuracy, data transmission and voice communication and modulation methods 02 p0257 A72-12642

Radio aids for air navigation and traffic control in Italy, discussing facilities development 02 p0257 A72-12748

Doppler system with navigation radar device, computer unit and data transmitter for continuous recording of aircraft position and speed 02 p0258 A72-12749

Maritime and aerial navigation radio aids, discussing recent technological advances 02 p0258 A72-12750

Communications and navigation trends in ATC, emphasizing use of improved existing systems 05 p0684 A72-15781

OMEGA system application to airborne long range navigation, describing aircraft position determination technique for extended flight over water without line-of-sight radio navigation aids 05 p0686 A72-16655

A-7 D/E navigation/weapon delivery system flight testing, using photogrammetric technique 05 p0663 A72-16656

Navy hovering vehicle versatile automatic control system for V/STOL flight test program, using airborne digital computer for navigation/guidance computations 05 p0687 A72-16661

Flight navigation technology current state and development trends, discussing transition from Doppler to inertial systems, use of computers and satellites, collision avoidance, etc 05 p0687 A72-16737

Flight safety and ATC planning in German Federal Republic and on international level, discussing regional control stations, radio frequencies, navigation systems, automation, etc 05 p0687 A72-16738

Acquisition probability equation for navigation systems terrain correlation devices, using two different correlation algorithms [AIAA PAPER 72-122] 05 p0688 A72-16974

Omega system in short range navigation supplementing VORTAC for coverage at low altitudes in mountain areas 06 p0844 A72-17334

Single satellite angle system and multiple satellite ranging and range difference systems in short haul air navigation, comparing with VORTAC 06 p0844 A72-17335

Noise, delay and interruption caused communication degradation effects on feedback control system performance, considering air navigation and computer aided command and control on battlefield 06 p0794 A72-18242

High accuracy north-seeking course-attitude inertial reference system for air navigation, using platform unit and automatic alignment for Schuler tuned operation 07 p0990 A72-20282

Head-up display flying under IMC and VMC flight conditions, considering takeoff, landing and navigation modes 08 p1204 A72-21004

Area navigation systems, discussing VOR/DME, Doppler and inertial systems, CRT displays, data links, etc 08 p1204 A72-21523

Cockpit instrumentation for jet transport aircraft flight path management, emphasizing dependability, safety and economy 08 p1168 A72-21524

Automation in planning and execution of flights, considering navigation, communication, flight instruments monitoring, control/stabilization and warning systems 09 p1269 A72-22780

Space flight experience application to human factors engineering problems in air and maritime navigation, considering use of small digital computers, display and sensing devices 09 p1348 A72-22785

Area navigation for Chicago-New York region, evaluating Decca Omnitrac 1A RNAV system installation in Boeing 727 aircraft 09 p1349 A72-23467

Flight testing of automated modular area navigation system for L-1011, describing computer, data storage and control-display units and electronic automatic chart system 10 p1509 A72-24271

Nonlinear filtering for random signals in statistically unknown noise, noting application to satellite orbit determination, aircraft navigation and missile tracking 11 p1611 A72-25986

Skyguide airborne computer navigation system for airline applications, discussing system components, flight crew monitoring and optimization 11 p1684 A72-26999

VOR and Doppler VOR ground station equipment based on reliable solid state radio transmitters and signal generating devices for aircraft navigation 12 p1779 A72-27104

Adaptive multibeam experiment for aeronautical and maritime services /AMEAMS/, discussing NASA ATSG satellite application to small mobile terminal communications system 12 p1842 A72-27383

Shoran systems with onboard computers for aircraft position and trajectory parameters, noting coordinate plotting for flight path recovery maneuvers 13 p1996 A72-28785

Information theory approaches to air navigation, discussing ATC, collision avoidance and computer applications 13 p1996 A72-29013

Critique of paper on error distributions in air navigation, noting inappropriateness of Gaussian distribution 13 p1996 A72-29015

Comment on paper on Gaussian logarithms use in air navigation 13 p1996 A72-29016

Navigation accuracy of corrected OMEGA close to transmitter, using aircraft flight test at 500 nm range 13 p1997 A72-29186

Aircraft applications of composite signal OMEGA configuration with phase data combined at separate carrier with weighting coefficients, discussing advantages over uncompensated navigation systems 13 p1998 A72-29192

Operational advantages of low cost VLF/OMEGA digital navigation system for various aircraft types 13 p1998 A72-29196

Aeronautical navigation/guidance standardization in conjunction with OMEGA, covering sensor and computer equipment life cycles 13 p1999 A72-29199

Small aircraft navigation over 10-400 mile course segments by raw OMEGA phase information dc presentation on conventional ID-249 course deviation indicator 13 p1999 A72-29201

OMEGA receiver integration into Navy P-3C airborne computerized navigation system, describing flight test, maintainability and laboratory simulation programs 13 p1999 A72-29202

Subtraction circuit design for impulse noise elimination at front end of aircraft oriented OMEGA navigation system receiver 13 p1999 A72-29204

Low-altitude flight imposed psychophysiological stresses due to air turbulence discomfort, instrument dial vibration and ground-based navigational objects recognition difficulty

14 p2080 A72-30747

Satellite communications and position finding for ships and aircraft compared with costs and reliability of ionospheric radio communication

15 p2193 A72-31300

Aircraft inertial navigation system, discussing mode selection unit, digital computer and control display for operator communication with system

15 p2267 A72-31596

Head-up display for aircraft three dimensional sky path observation during navigation and landing, discussing computer units, CRT and image generating subsystems

15 p2268 A72-32042

Navigation for general aviation and navigation training - Conference, Atlanta, February-March 1972

15 p2271 A72-32201

Area navigation requirements by general aviation, discussing random routing, ATC system and aircraft approach spacing

15 p2271 A72-32202

Great circle intermediate waypoint computation method for inertial navigation equipped aircraft

15 p2271 A72-32205

Computerized navigator training simulator for complete array of air navigation instruments, discussing design and human factors

15 p2214 A72-32208

Canadian Armed Forces air navigation training program, noting emphasis on training flights

15 p2272 A72-32209

USAF Academy air navigation training program, discussing systems development course and descriptive and applied astronomy

15 p2272 A72-32210

Fighter bomber Loran-inertial data processing with digital computer to combine navigation, guidance and weapon delivery into fully integrated system

16 p2420 A72-33246

Solid state modular ground based distance measuring equipment (DME) receiver for en route aircraft navigation and landing

16 p2420 A72-33521

Technical and operational aspects of L-band satellite system for air navigation, discussing verbal communication, direction finding and noise interference problems

16 p2421 A72-34138

Configuration and flight test of the only operational Air Force area navigation system

17 p2578 A72-35557

USAF development of electrostatic gyros for inertial air navigation, noting flight tests and associated airborne digital computer

17 p2578 A72-35558

The Omega navigation system - Its history, application and versatility

17 p2578 A72-35559

Book - Minimum operational characteristics for vertical guidance equipment used in airborne volumetric navigation systems

[DO-152] 17 p2578 A72-35800

Proportional navigation with a maneuvering target

19 p2830 A72-37290

OMEGA air and maritime navigation system development, test phase and application potential, discussing operational modes, propagation parameters, solar activity effects and signal loss

19 p2831 A72-37796

Inertial platform pursuant to ARINC-571 specifications, noting capability for integration into surface navigation system or autonomous operation

19 p2831 A72-37799

Development of STOLAND, a versatile navigation, guidance and control system

[AIAA PAPER 72-789] 19 p2831 A72-38106

Flight evaluation of three-dimensional area navigation for jet transport noise abatement

[AIAA PAPER 72-814] 19 p2750 A72-38116

Area navigation and its affect on aircraft operation and systems design

[AIAA PAPER 72-754] 19 p2831 A72-38125

Error analysis of hybrid aircraft inertial navigation systems

[AIAA PAPER 72-848] 20 p2950 A72-39081

Optimum aiding of inertial navigation systems using air data

[AIAA PAPER 72-847] 20 p2950 A72-39082

Updating inertial navigation systems with VOR/DME information

[AIAA PAPER 72-846] 20 p2950 A72-39083

Tactical aircraft weapon system development, describing navigation, target acquisition, release point guidance and delivery modes

[AIAA PAPER 72-896] 20 p2951 A72-39107

Reduction of air traffic congestion due to corridor effect of present airway route pattern through area navigation (R-NAV) based on VOR/DME inputs

20 p2952 A72-39750

NEWNAV Symposium, Frankfurt am Main, West Germany, October 5-7, 1971, Report. Volumes 1 & 2.

21 p3079 A72-40276

Modular navigation (MONA) dual channel automatic area navigation system, describing computer, flight data storage and control/display units

21 p3079 A72-40277

TCE-71A area navigation system based on modular design with provision for 20 waypoints parameter storage, describing computer, control display and automatic data entry units

21 p3079 A72-40278

Operational implementation of area navigation

21 p3079 A72-40279

Area navigation systems integration into existing ATC and man/machine relationship problems, considering cockpit workload coordination

21 p3079 A72-40280

An area navigation system for a long range airplane

21 p3079 A72-40281

Present status of self-contained navigation systems combining Doppler velocity sensors and attitude/heading references

21 p3079 A72-40282

Autonomous navigation systems, discussing Doppler navigation, inertial platforms and onboard computers

21 p3079 A72-40283

Geostationary satellite system for air navigation via voice and data communication, discussing ground facilities and avionics

21 p3080 A72-40284

An air traffic controller's view on area navigation and ATS requirements related thereto

21 p3081 A72-40299

Terminal airspace navigation and aircraft ground handling control, discussing air traffic controllers and pilots functions in context of workload and automation

21 p3081 A72-40546

Automated area navigation with real time track computation, discussing information processing by on-board computer for immediate pilot instruction

21 p3081 A72-40683

Collision avoidance system electromagnetic compatibility with radar altimeters designed for 1600 MHz aeronavigation band

21 p3018 A72-40881

Great circle navigation for inertial equipped aircraft, describing procedure for determining waypoint coordinates with reference to VORTAC stations

22 p3203 A72-42949

The effect of geometry on area navigation system errors

22 p3203 A72-43132

Possible impact of area navigation upon MLS requirements for azimuth angular coverage and range

24 p3422 A72-44643

AIR PIRACY

Papers on air piracy and international law based on McGill University Conference (October 1970), covering legal problem solving, hijacking, etc

01 p0146 A72-10321

Legal problems of aircraft hijacking, discussing jurisdiction, duty to prosecute, penalties, extradition, sanctions and international criminal tribunal

05 p0752 A72-15833

Aircraft hijacking control, examining international cooperation, extradition and treaties

05 p0752 A72-15834

International and domestic governmental interests in aircraft hijacking, discussing deterrents, enforcement and accepted action

05 p0752 A72-15835

Hague convention on aircraft hijacking, discussing international extradition, prosecution and punishment

05 p0752 A72-15836

International criminal court for aircraft hijacking, examining political and jurisdictional aspects

05 p0752 A72-15837

Hague convention of 16 December 1970 for repression of skyjacking, discussing definition, punishment, jurisdictional competence, arrest and preliminary inquiry, pursuit, extradition and prevention

05 p0753 A72-17165

Civil and military aircraft forced diversion, discussing legal counters and aircraft restoration

05 p0753 A72-17166

Clinical effects on atrio-ventricular pacing system of electromagnetic weapon detector systems used for air passenger screening at airports in air hijacking prevention efforts

10 p1428 A72-23740

Legal aspects in prevention of aircraft unlawful seizure in view of international cooperation, noting German Democratic Republic agreements

12 p1890 A72-27272

The onboard authority of the aircraft commanding officer as provided by the 1963 Tokyo Convention

17 p2639 A72-35763

AIR POLLUTION

Trace gas pollutant monitoring by microwave rotational absorption spectroscopy, discussing test results with Gunn diode cavity spectrometer

[AIAA PAPER 71-1048] 01 p0023 A72-10524

Gas filter correlation spectral analysis technique for measuring pollutant concentrations in presence of interfering gases, describing application to hydrochloric and hydrofluoric acids monitoring

[AIAA PAPER 71-1049] 01 p0066 A72-10525

Laser radar application to air pollution measurement, discussing techniques and instrumentation utilizing elastic, Raman and fluorescence scattering

[AIAA PAPER 71-1056] 01 p0028 A72-10527

Remote sensing of regional vertical air column pollutants, discussing sulfur dioxide and nitrogen dioxide measurements by correlation spectrometer

[AIAA PAPER 71-1060] 01 p0057 A72-10529

Gaseous pollutants remote detection by IR heterodyne radiometer with tunable lasers

[AIAA PAPER 71-1079] 01 p0080 A72-10538

FM/CW laser radar technique for smoke plume opacity remote measurement, discussing eye safety

[AIAA PAPER 71-1081] 01 p0080 A72-10539

Carbon dioxide laser IR heterodyne radiometer for remote sensing of atmospheric pollution

[AIAA PAPER 71-1083] 01 p0067 A72-10540

Raman scattering cross sections and depolarization ratios of atmospheric gaseous pollutants as function of incident photon energy

[AIAA PAPER 71-1086] 01 p0104 A72-10543

Smoke plume opacity or particulate content measurement by laser backscatter, using Q switched ruby and Nd lasers

[AIAA PAPER 71-1087] 01 p0058 A72-10544

Particle mass monitor system based on piezoelectric microbalance combined with electrostatic precipitator collector, considering applications to air quality monitoring, laboratory aerosol research, process control, etc

[AIAA PAPER 71-1100] 01 p0067 A72-10548

Atmospheric aerosol chemical composition analysis by nephelometer light scattering measurement of suspended particle mass concentration, visibility and size distribution and scattering-humidity relationship

[AIAA PAPER 71-1101] 01 p0058 A72-10549

Analysis methods for microsize atmospheric aerosols and particulate contaminants from natural and industrial sources, discussing electron microscopy, electron probes, X ray diffraction, etc

[AIAA PAPER 71-1104] 01 p0067 A72-10550

Air pollution circulation patterns remote sensing, describing multispectral stereo image pairs digital cross correlation

[AIAA PAPER 71-1106] 01 p0067 A72-10551

Remote sensing of atmospheric pollutants and trace contaminants, presenting high speed high resolution, Fourier interferometer breadboard model

[AIAA PAPER 71-1109] 01 p0068 A72-10553

Atmospheric carbon monoxide pollution sources, sink mechanism and remote sensing requirement

[AIAA PAPER 71-1120] 01 p0068 A72-10557

Mt. Agung volcanic eruption dust effects on monthly-mean lower stratospheric temperatures for tropical stations

01 p0096 A72-11284

Soyuz manned spacecraft meteorological observations, dealing cloud cover in various climatic zones, atmospheric turbidity and snow cover in mountain areas

02 p0253 A72-11731

World Weather Watch and Global Atmospheric Research Program remote sensing applications, considering weather prediction and modification, atmosphere pollution monitoring and global atmosphere mathematical modeling and simulation

02 p0208 A72-11784

Atmospheric pollutants time and spatial profiles monitoring by geosynchronous satellite remote sensors

02 p0211 A72-11806

Air pollution measurements by laser radar, using coherence properties to discriminate between backscatter due to molecular atmospheric constituents and pollutant particulates

02 p0212 A72-11816

Air transportation evolution and relation to atmospheric and noise pollution

03 p0459 A72-14151

Air pollutant detection by multiple slit correlation spectrometry and laser absorption technique, noting sensitivity enhancement by laser output increase

04 p0530 A72-14894

Remote air pollution detection by laser methods, comparing Raman backscattering, resonance backscattering and resonance absorption

04 p0531 A72-15300

Diffusion and fallout of polluting particulates emitted by aircraft engines, discussing effect of wing-tip vortices, plume visibility and monitoring, simulation and modeling

[ASME PAPER 71-WA/AV-2] 05 p0704 A72-15950

Combined radar-acoustic system for lower atmosphere temperature sounding, considering use in air pollution studies and short range weather forecasting

[AD-739790] 05 p0663 A72-16690

Air pollutant monitoring and remote analysis by Raman, fluorescence and resonance backscattering, Rayleigh scattering and absorption laser radar techniques

06 p0827 A72-18460

Army aircraft gas turbine engines pollution potential evaluation program, considering smoke emission, noise and invisible pollutants 07 p1053 A72-18772

Air pollution monitoring with tunable lasers employing Raman scattering, resonantly excited or hot gases emission and resonant absorption 09 p1322 A72-22313

Air pollutants lateral dispersion coefficient determination from turbulence intensity, presenting formula for wind direction frequency distribution function 09 p1344 A72-22436

Cloud and Aitken nuclei vertical distribution upwind and downwind of urban pollution sources from simultaneous airborne observations 09 p1345 A72-22443

Gaseous or solid particle Hg from fumaroles, suggesting natural and industrial sources of Hawaiian air pollution 09 p1305 A72-23648

Laser radar technique for invisible air pollutants remote sensing systems, comparing Raman backscattering resonance scattering and absorption schemes 10 p1489 A72-23952

Gaseous air pollutant detection and measurement by chemiluminescence method for continuous monitoring of given pollutant concentration 10 p1434 A72-24099

Air pollution monitoring by remote optical sensing techniques based on light scattering measurements, noting suitability of high power laser probes 10 p1480 A72-24100

Flame photometric detection of small concentrations of sulfur compounds in ambient air, describing spectrum scanning detector, rotating interference filter and correlation detector 10 p1480 A72-24101

Atmospheric electricity problems, considering air pollution effects on ion concentration and air conductivity and solar activity effects on ionosphere-earth potential difference 10 p1473 A72-24528

Clinical and laboratory examinations of workers exposed to trichlorofluoroethane vapor for long range health effects study 10 p1431 A72-24590

Spectrophotometric measurements of sky radiance distribution to determine atmospheric pollution, ozone content and radiation attenuation by clouds 10 p1476 A72-25085

Multiple reflection absorption cell for gaseous air pollutants IR radiation measurements over wide temperature, pressure and distance ranges [AIAA PAPER 72-276] 11 p1619 A72-25216

Combustion research for reducing jet aircraft pollutant emissions, discussing fuel atomization improvement, smoke reduction and combustor design techniques 11 p1705 A72-26037

Aitken condensation nuclei clouds microstructure and area contamination profiles, discussing small sources pollution and plumes polyfurfuration [AIAA PAPER 71-1125] 11 p1628 A72-26989

New York-New Jersey megalopolis offshore jetport feasibility, considering noise, air-water pollution, land conservation, cost, etc 13 p1938 A72-28792

Residence time of water vapor and aerosols in troposphere and lower stratosphere, noting application to air pollution buildup by aircraft 13 p1991 A72-28836

Estimated peak regional concentration of SST exhaust in stratosphere from expected flight operation levels 13 p1991 A72-28837

Stratospheric subsonic and supersonic aircraft emission estimation for water vapor and nitrogen oxides 13 p1991 A72-28838

SST water vapor and nitrogen oxides exhausts effect on stratospheric composition, developing nonequilibrium photochemical model 13 p1994 A72-28878

Future projections of commercial jet aircraft fuel demands, estimating engine exhaust effects on air quality 13 p1897 A72-28879

Stable air clouds localization from meteorological satellite photographs, noting atmospheric air pollution 15 p2265 A72-31236

Atmospheric air pollution study by space techniques via thermal radiation spectral measurements and laser sounding, considering spaceborne photography 15 p2220 A72-31237

Molecular absorption of microwaves by atmospheric impurity gases ozone, carbon monoxide and nitrous oxide up to 20 km 16 p2364 A72-33483

Climatic changes due to stratospheric perturbation by propulsion effluents of high altitude aircraft flights [AIAA PAPER 72-658] 16 p2388 A72-34076

Stratospheric pollution by SST exhaust gases, discussing water vapor and nitrogen oxides effects on ozone concentration 17 p2597 A72-35327

Tunable output dye and semiconductor lasers application to absorption spectroscopy and air pollution monitoring 17 p2564 A72-35381

Atmospheric composition to 40 km altitude from balloon-borne particle impacted electron microscope screens, discussing pollution effects from high flying aircraft exhaust gases 17 p2551 A72-35935

Radiation absorption and emission in atmosphere IR spectrum influenced by water droplets around atmosphere contamination particles 17 p2552 A72-35942

Air transport developments effects on economy and environment, discussing government power to control airport use and location and air pollution 17 p2639 A72-35952

Numerical prediction of the diffusion of exhaust products of supersonic aircraft in the stratosphere 19 p2748 A72-37824

A method for simulating wind conditions during atmospheric stagnation periods. 20 p2947 A72-38965

Hypersonic transports commercial applications, examining economic and noise and air pollution aspects [ICAS PAPER 72-32] 21 p2995 A72-41157

Electro-optical design and performance parameters of polluted air liquid droplet size distribution measurement by pulsed junction diode laser light external scattering 22 p3179 A72-42680

Theoretical model, laboratory experiments and in situ measurements by instrumented sailplane for investigating cloud and precipitation formation physics relationship to atmospheric pollutants cleansing 23 p3311 A72-44263

Laser radar /lidar/ for mapping aerosol structure. 23 p3298 A72-44542

Rocket-borne GaAs laser radar system with scatter light detector and data processor for upper atmosphere aerosol and pollution measurements 24 p3409 A72-44778

AIR PURIFICATION

Hot water ejector application to environmental control, considering noise suppression, air and gas purification and dust particles precipitation 10 p1460 A72-24491

Sealed cabin air regeneration by means of potassium superoxide, noting weight and space savings 11 p1586 A72-26594

AIR SAMPLING

Methane concentration of air sample from stratopause measured by gas chromatography, discussing sample integrity, analysis method and results 12 p1802 A72-27505

AIR SEA INTERACTIONS

U AIR WATER INTERACTIONS

AIR SICKNESS

U MOTION SICKNESS

AIR TO AIR MISSILES

Missile systems of U.S., U.S.S.R. and other nations, discussing ground-to-ground, ground-to-air, air-to-ground and air-to-air missiles 05 p0728 A72-16740

Design for air combat. [AIAA PAPER 72-749] 19 p2751 A72-38124

The effects of protuberances and scaling parameters on the aerodynamic characteristics of an air-to-air cruciform missile. [AIAA PAPER 72-969] 22 p3231 A72-42342

AIR TO AIR REFUELING

F-14 Tomcat test program for hydraulic systems, spinning, low speed performance, stalling, afterburning turbofan engines, in-flight refueling and automatic telemetry equipment 06 p0758 A72-17582

AIR TO AIR ROCKETS

U AIR TO AIR MISSILES

AIR TO SURFACE MISSILES

Missile systems of U.S., U.S.S.R. and other nations, discussing ground-to-ground, ground-to-air, air-to-ground and air-to-air missiles 05 p0728 A72-16740

Harpoon air-sea/sea-sea all-weather missile system, describing two phase guidance system based on inertial platform initial phase and radar terminal guidance 07 p1085 A72-20312

Pilot-fighter aircraft system mathematical model relating pilot performance to air to ground weapon delivery accuracy 17 p2493 A72-35564

Virtual target steering - A unique air-to-surface missile targeting and guidance technique. [AIAA PAPER 72-826] 20 p2951 A72-39100

Development and optimization of the SRAM guidance and control software. [AIAA PAPER 72-824] 20 p2951 A72-39102

AIR TRAFFIC

Future aircraft design trends for transcontinental and short haul operation, considering traffic forecasts, current transport aircraft and potential derivatives and technology [SAE PAPER 710749] 01 p0002 A72-10248

Pilot collision warning indicator performance in terminal area traffic, using computer fast-time simulation for traffic model 01 p0098 A72-11134

German Federal Republic territorial air traffic regulations covering general, VFR and IFR rules, equipment and personnel examination and certification, safety, takeoff and landing, accidents, etc 02 p0305 A72-12621

German book on air traffic law covering norms relative to vehicles and air space, international air law, organizations, etc 02 p0305 A72-12622

German commercial airports adaptation to traffic development, considering economic factors 05 p0643 A72-16187

Soviet air traffic service productivity increase and manpower saving by introduction of new airliner types 05 p0612 A72-16779

STOL transport passenger market demand model selection based on estimation of traffic patterns between two population centers and service frequency and fare considerations 06 p0905 A72-17586

Aircraft midair collision prevention in dense air traffic environments, suggesting problem solution based on proximity warning system 08 p1204 A72-21090

Thunderstorm detection and recording device with 200 km radius for weather prediction and air traffic information 09 p1312 A72-23269

Discusses geostationary satellites project for Atlantic and Pacific ocean air and ship traffic safety based on radar tracking and multiplex numerical data transmission 09 p1396 A72-23400

Optimal high capacity runway systems for major airports, discussing multiple systems in anticipation of future mass air traffic requirements 10 p1459 A72-24169

General aviation equipment standards in light of air traffic system safety needs, emphasizing Technical Standard Order system 11 p1748 A72-25571

Charter air traffic regulations under German air law, discussing legal safeguards relative to economic, personnel, technical and organizational aspects 11 p1748 A72-26559

Airport capacity and air traffic congestion effects on airport operations in terms of time and costs 15 p2339 A72-32454

Individual regions and nationwide air traffic demands forecasting for airport planning 16 p2481 A72-33311

Major civil airport planning, discussing information gathering and processing for aviation demand, aircraft movements revenue and cost forecasts and pricing policy evaluation 16 p2481 A72-33327

Major civil airport development plan, discussing traffic forecasts, runways, noise, airspace capacity, access systems, freight installations, maintenance facilities, navigation aids, buildings, etc 16 p2373 A72-33328

Airport planning requirements - An airline view. 17 p2535 A72-34224

Simulation models for airports performance evaluation through replication of traffic units actual movement 17 p2535 A72-34414

Functional equipment active and standby redundancy for flight safety and air traffic punctuality improvement, noting Boeing 747 aircraft redundant systems 17 p2492 A72-35476

Air transport developments effects on economy and environment, discussing government power to control airport use and location and air pollution 17 p2639 A72-35952

Air transport development between the UK and Europe - The next twenty years. 18 p2743 A72-37092

Reduction of air traffic congestion due to corridor effect of present airway route pattern through area navigation /R-NAV/ based on VOR/DME inputs 20 p2952 A72-39750

German monograph - Model-analytical investigation of short-haul air traffic with VTOL aircraft in the Federal Republic of Germany. 22 p3245 A72-43068

Independent parallel runway landing system to relieve air traffic congestion, investigating minimum spacing required to minimize collision risk 22 p3203 A72-43130

Critical assessment of air transport planning for German Federal Republic, advocating decentralized concept of major air terminals for intercontinental jumbo jet traffic 23 p3357 A72-43244

Airports planning for West Germany, discussing geographical air traffic patterns, economic and noise aspects [DGLR PAPER 72-034] 24 p3387 A72-44614

Airline operational problems from traffic volume increase, discussing flight safety, passenger comfort, schedule adherence and economy aspects [DGLR PAPER 72-037] 24 p3467 A72-44618

AIR TRAFFIC CONTROL

NT RADAR APPROACH CONTROL

ATC separation minima and navigational errors on airways in general and long range oceanic environments 01 p0096 A72-10177

Avionics contribution to airspace decision making problems, considering navigation, surveillance radar, collision avoidance and ATC techniques 01 p0097 A72-10180

Automated radar terminal system (ARTS) for monitoring and tracking all aircraft within radar range, displaying identification, altitude and ground speed information to air traffic controller 01 p0098 A72-10960

Phased scanning array for ATC radar beacon systems, airport or air route surveillance radars and ground landing systems 01 p0098 A72-10962

Inertial navigation role in automatic ATC systems, discussing path control accuracies, environmental conditions, noise and air pollution, etc 01 p0098 A72-11118

ATC system decision making problem and future technological and administrative improvements 02 p0255 A72-11718

Stellar attitude reference and navigation associative processor with high computational speed for radar approach control in ATC 02 p0256 A72-12033

Discrete address ATC radar beacon system operation and design 02 p0256 A72-12378

FAA air traffic control automation program, discussing en route stage, computer program, data processing and storage and terminal area navigation and display techniques 02 p0256 A72-12380

Uhf aeronautical satellite system, presenting ATC trends, international aspects, available flight levels, weather conditions and long haul conflicts 02 p0257 A72-12383

Computer-aided interactive graphic displays for ATC, discussing subsystems, data processing flow and operational capabilities 02 p0257 A72-12420

Tactical ATC display system for airport surveillance, precision approach and landing and operator/aircraft/machine operations by using terminal Area Surveillance Radar 02 p0230 A72-12421

Digital computer memory system for real time processing of air and naval traffic data, discussing logic design, time comparisons and optimum use 02 p0188 A72-12647

ATCAS air traffic control automation system emphasizing Italian situation 02 p0257 A72-12649

Radio aids for air navigation and traffic control in Italy, discussing facilities development 02 p0257 A72-12748

Flight planning by ATC, discussing problems due to runway feeding from several converging airways 03 p0386 A72-13415

ATC for North Atlantic air transportation, emphasizing collision risk model for safety standards assessment 04 p0544 A72-14484

ATC technology impact on flight operations and public value of aviation, discussing microwave landing system economic aspects 04 p0544 A72-14810

Terminal area air traffic guidance and control, discussing automation, all-weather precision approach and landing and failure detection 04 p0544 A72-14817

Air traffic control long range planning for airlines and general aviation, discussing use of IFR, RNAV and IPC equipment 04 p0545 A72-14818

Aircraft operations effects on community noise pollution, discussing ATC airline operational procedures modifications in terms of noise reduction 04 p0464 A72-14819

Air surveillance using satellite range-difference measurement from noninterrogated aircraft beacons for ATC 04 p0545 A72-14826

Airborne collision avoidance system equipment for general aviation aircraft, discussing logic functions, transmission modes, data handling tradeoffs and ATC procedure interactions 04 p0545 A72-14830

ATC radar beacon system developments, considering diversity transponders, interrogator environment control, electronic scan cylindrical array antenna design and discrete address mode 04 p0508 A72-14832

Computer technology projection in terms of cost and performance for future ATC system, determining data processing systems availability 04 p0496 A72-14834

Toulouse-Bretigny link involving ATC and flight simulators with Concorde cockpit replica 04 p0545 A72-15072

Mountain stations wind measurement usefulness for small aircraft traffic guidance 04 p0544 A72-15625

Communications and navigation trends in ATC, emphasizing use of improved existing systems 05 p0684 A72-15781

Flight safety and ATC planning in German Federal Republic and on international level, discussing regional control stations, radio frequencies, navigation systems, automation, etc 05 p0687 A72-16738

Automated scheduling algorithm for aircraft from terminal area to touchdown, discussing system features and STOL air traffic computerized simulation [AIAA PAPER 72-120] 05 p0688 A72-16905

Fast time simulation application to ATC systems, discussing control action exercise within strategic/tactical spectrum 05 p0645 A72-16994

Radio technical capabilities and limitations of ATC systems - Conference, Washington, D.C., November 1971 06 p0844 A72-17326

FAA air traffic control automation program, describing enroute and terminal ATC systems implementation 06 p0844 A72-17327

Development programs for ATC system improvement by digital computers and data displays applications 06 p0844 A72-17328

Airborne traffic display system using beacon and radar surveillance network and ground computer processing 06 p0844 A72-17329

Aircraft proximity control for ATC system using national secondary surveillance radar (SSR) for CAS-PWI functions 06 p0844 A72-17330

Airline pilot performance in automated ATC system involving use of surveillance data and instantaneous discrete communications 06 p0844 A72-17331

Pilot role in automated ATC system using onboard situation display with navigation and collision avoidance devices 06 p0844 A72-17332

Control concepts for future ATC system relative to airspace structure, management and geographic and jurisdictional boundaries 06 p0844 A72-17333

Supplementary Aviation Information Display for ATC, discussing remote sensing capability and cost savings 06 p0845 A72-17424

Terminal area ATC specialists and trainees job attitude and motivation from questionnaire on challenge, tasks, salary, work schedule, etc 06 p0766 A72-17865

Automated ATC guidance technique for aircraft curved flight trajectories, describing flight profiles synthesizing algorithms and computerized simulation technique [AIAA PAPER 72-121] 06 p0845 A72-17922

ATC study by computerized simulation, using successive approximation models 06 p0845 A72-17975

Nationwide real time automated ATC system interconnected by data transmission links, discussing radar signal acquisition/transfer and computer complex 06 p0845 A72-18283

ATC at single-runway airport analyzed by fast time simulation with high speed digital computers 07 p1032 A72-19064

FORTAN digital simulation of ATC radar beacon system making possible computer generated movie display 07 p0950 A72-19301

Boeing 707 cockpit simulator with computer generated displays, moving area navigation map and ATC information 07 p1033 A72-20336

V/STOL development for short haul air transportation, discussing requirements for quiet pollution-free operation, ATC systems, navigation and landing aids 08 p1108 A72-21010

Synchronous satellite surveillance system for transoceanic ATC, using suboptimal/modified Kalman/ filter for aircraft position and velocity computation 08 p1204 A72-21091

Aerosat program for ATC and communications via four geostationary satellites over Atlantic and Pacific Oceans, discussing technical and financial international provisions 08 p1256 A72-21203

ATC radar performance monitoring, considering advances in radar signal processing and digital display techniques 08 p1134 A72-21525

Ground based ATC information processing systems analysis, considering controllers work load 09 p1348 A72-22778

Anthropotechnical aspects of aircraft taxiing guidance in airfield runway areas, suggesting computerized operational system 09 p1269 A72-22779

ATC systems analysis by computerized real time environmental simulation, taking into account new aircraft types, navigation and supervision aids 09 p1348 A72-22782

Aircraft collision near misses under IFR and VFR conditions, discussing ATC coordination, equipment failure and personal and planning problems 09 p1349 A72-22972

ATC tasks work load assessment - Conference, Darmstadt University of Technology, June 1971 09 p1270 A72-23126

Human operator role in ATC systems analysis, evaluating tasks with respect to job demands and personal fulfillment 09 p1270 A72-23127

Air traffic control systems efficiency evaluation, discussing measures for criteria conflict solution 09 p1270 A72-23128

Operator mental processes during ATC task performance, discussing work load effect, mental representation and operator algorithm definition 09 p1270 A72-23129

Operator, task level and workload effects on operative strategy, showing controllers methods modification in ATC center 09 p1270 A72-23130

Landing sequence strategy variations for individual ATC operators, indicating dependence on flight progress data variation, existing maneuvering conditions and controller personality traits 09 p1271 A72-23131

Pilot and ATC radar controller workload variations relation, discussing distraction stress effects 09 p1271 A72-23132

Time analyses of ATC approach controller tasks, developing flow diagram for task component sequencing and quantifying 09 p1271 A72-23133

ATC operator stress factor evaluation from information theory analysis of radio telecommunication information content 09 p1271 A72-23134

ATC task analysis by subjective rating of work load, discussing information processing measures, scoring method and observer rating procedure 09 p1271 A72-23135

Time series analysis of physiological and work study data in ATC tasks, using heart rate as strain indicator 09 p1271 A72-23137

Frankfurt Airport air traffic controller opinion survey of attitudes toward work and working environment 09 p1271 A72-23138

Acceptable load standards in ATC tasks, defining moments of conscious brain control as mental load measure 09 p1271 A72-23139

ATC system analysis by fast time arithmetic simulation techniques, describing ground model development 09 p1272 A72-23141

Turbulence measurement, reporting and subsequent data handling by upgraded ATC system, suggesting R and D program to evaluate wake turbulence effects on airport capacity 09 p1346 A72-23466

Air traffic control messages syllabic and word prominence patterns, discussing impact on continuous speech recognition by machine 09 p1274 A72-23581

STARAN IV-X associative array processor for automation in ATC environment, considering air tracking, conflict prediction and resolution functions 10 p1442 A72-23818

Microwave equipment and technology application for instrument landing, terminal ATC, millimeter wave CAT detection and satellite communications 10 p1509 A72-24036

ICAO standardized taxiing guidance and airports surface traffic control procedures 10 p1459 A72-24171

Electronics and data processing technology effects on radar state of art, discussing automated air traffic control surveillance systems 10 p1435 A72-24490

Airborne VHF omnirange (VOR) systems minimum operational standards for navigation and communication in air traffic control 10 p1509 A72-24725

Operational aviation meteorological requirements, reviewing aircraft categories, ATC systems and avionics and navigational aids 10 p1508 A72-25078

STOL aircraft systems development coordination, considering vehicle design, airport facilities and related ground environment, transportation modes interface and airspace management

11 p1574 A72-25255
SECANT system of aircraft separation and control by nonsynchronous technique for midair collision avoidance

[SAE PAPER 720313] 11 p1683 A72-25577
Digital solid state altitude encoder for ATC transponder reporting, covering Gray and Gillham codes [SAE PAPER 720314] 11 p1630 A72-25578

ATC system, discussing flight data and radar processing functions and terminal automation program 11 p1683 A72-25875
Short sleep period and oxygen breathing effects on arousal level of air traffic controller during detection task performance

11 p1588 A72-26686
FAA automated ATC system, discussing subsystems related to operational and nonoperational computer program components, data entry and display, communication, personnel and environments 11 p1684 A72-27000
Trends in civil ATC discussing plans to increase terminal capacity, surveillance system and use of multiple synchronous satellites for ocean travel efficiency improvement

12 p1842 A72-27103
Continuous wave Doppler radar with microwave oscillator for ATC measurements and surveillance 12 p1789 A72-27403
STOL aircraft role in civil aviation, discussing short range operation, ATC, reduced noise and weather capability

12 p1754 A72-27518
Communication aspects of aeronautical satellite system, considering aircraft equipment, ground stations, ATC, type of access and frequency assignment 12 p1783 A72-27658
Aptitude screening test of ATC training applicants, using directional heading determination under aural distraction

12 p1773 A72-28252
Potential coronary heart disease susceptibility indicators in ATC population, using Framingham age/obesity parameters 12 p1764 A72-28265
Secondary surveillance radar systems design and planning for ATC application

13 p1917 A72-28698
Meteorological information requirements for V/STOL aircraft design, airport location, runway orientation, aircraft operations and ATC simulation 13 p1994 A72-28869
Information theory approaches to air navigation, discussing ATC, collision avoidance and computer applications

13 p1996 A72-29013
Statistical analysis for single airport ATC digital simulation using Poisson distribution law, calculating optimal number of channels 13 p1996 A72-29179
Aircraft antennas design for radio links to satellites for aeronautical communication and ATC, proposing use of beam steering system

13 p1932 A72-29347
Hypersonic commercial aircraft operational problems, considering passenger physiology limits flight profile, sonic pollution, traffic demands, route structure, etc 14 p2073 A72-30830
ATC operational systems, discussing global surveillance and voice and data communication between aircraft and earth station

14 p2129 A72-31141
ATC systems fast-time simulation, emphasizing importance of human operator performance realistic modeling 15 p2269 A72-32097
ATC procedures training by digital radar simulators, taking into account geographic terrain, radar, wind and aircraft characteristics and flight plans

15 p2214 A72-32098
Area navigation requirements by general aviation, discussing random routing, ATC system and aircraft approach spacing 15 p2271 A72-32202
ATC system organization in terms of optimal operating conditions for civil and military airspace users, discussing navigation systems, human factors, equipment reliability, etc

15 p2272 A72-32455
Aircraft on-time operation and air traffic problems, considering solution requirement formulation and funding suggestions 15 p2339 A72-32462
Book on man machine system experiments covering ATC, air defense, logistics organizations, space flight, battlefield operation, police dispatching, communications, etc

16 p2359 A72-33796
Integrated civil/military ATC system for upper airspace control /UAC/ center at Karlsruhe 16 p2421 A72-34108
Mediator plan for joint civil/military ATC organization at London center, discussing sectorization, control and radar facilities, flight plan processing and communications

16 p2421 A72-34109
Ranging signals for aeronautical satellite systems 17 p2516 A72-35220
Book - Minimum operational characteristics for vertical guidance equipment used in airborne volumetric navigation systems [DO-152] 17 p2578 A72-35800
ATC IC transponder used with secondary surveillance radar, discussing design features

18 p2662 A72-37048
Atmospheric turbulence and the ATC system. 18 p2663 A72-37049
Potential value of turn-rate telemetry in tracking of aircraft equipped with discrete address beacon system /DABS/ for ATC, discussing tracking algorithms design

19 p2830 A72-37282
The Gander automated air traffic system. 19 p2830 A72-37748
Study of the flow of air traffic and capacity of a control system 19 p2831 A72-37797
STOL-based short haul transportation feasibility for airport congestion alleviation from airline viewpoint, discussing system requirements, economic factors and safety

[AIAA PAPER 72-807] 19 p2750 A72-38120
4-D guidance system design with application to STOL air traffic control. 19 p2832 A72-38252
Air traffic flow control - Problems and approaches. 19 p2832 A72-38254
Application of optimization techniques to near terminal area sequencing and flow control.

19 p2832 A72-38255
An investigation of vehicle dependent aspects of terminal area ATC operation. 19 p2832 A72-38256
Operational implementation of area navigation. 21 p3079 A72-40279
Area navigation systems integration into existing ATC and man/machine relationship problems, considering cockpit workload coordination

21 p3079 A72-40280
Automatic position reporting, ATC communication, weather information and message identification via digital ground-air-ground data link, discussing operational and maintenance requirements 21 p3080 A72-40286
ATC services configuration with secondary surveillance radar and primary radar data acquisition system, discussing signal processing by automated decoder

21 p3080 A72-40288
Air traffic density effect on secondary surveillance radar operation in ATC for aircraft identification and position determination, proposing selective address system 21 p3080 A72-40289
Design, operation and performance of time-frequency midair collision avoidance system, noting air traffic controller backup for departure, enroute and arrival control

21 p3081 A72-40295
Midair collision prevention independent of ATC, discussing aircraft lighting, collision avoidance systems and proximity warning indicator 21 p3081 A72-40297
An air traffic controller's view on area navigation and ATS requirements related thereto.

21 p3081 A72-40299
Active transistorized directional dipole VHF receiving antennas for ATC and mobile applications and field intensity measurement 21 p3030 A72-40527
Radar double beam dielectric radiator antenna design for ATC in 1250-1350 MHz range

21 p3030 A72-40530
Terminal airspace navigation and aircraft ground handling control, discussing air traffic controllers and pilots functions in context of workload and automation 21 p3081 A72-40546
Shaped coverage patterns with satellite array antennas.

21 p3019 A72-40884
Future trends in air traffic control and landing. [ICAS PAPER 72-04] 21 p3082 A72-41129
Investigations on the use of a Kalman filtering method in tracking systems for air traffic control. [ICAS PAPER 72-43] 21 p3082 A72-41168
Discrete address beacon system /DABS/ development for surveillance and ground-air communications in support of ATC automation

22 p3204 A72-43151
Trends in the control of air-traffic flows in the air space 23 p3311 A72-43640
The optimal control of merging aircraft - Implementation of the hybrid air traffic controller. 23 p3277 A72-43868
Flight safety from general aviation viewpoint in West Germany, discussing ATC and flight rules relative to airspace use [DGLR PAPER 72-036] 24 p3467 A72-44615
Air traffic, collision risks, defense zones, airspace structure and central planning agency for flight safety problems reform [DGLR PAPER 72-038] 24 p3467 A72-44617

AIR TRANSPORTATION
Air transportation system design for safety and efficiency, discussing navigation facilities and surveillance systems employment for blunder prevention 01 p0098 A72-11117
STOL aircraft for solving noise reduction and land use problems in future transportation systems, discussing airport location and layout for growing air traffic 01 p0005 A72-11153
General and commercial aircraft service needs in air transportation, considering FAA and CAB roles and policies 02 p3034 A72-11716
Short haul air transport system need for future short takeoff and landing aircraft, considering airports, airways, economics and navigation and landing aids 02 p0154 A72-11719
Civil aviation air transportation contributing factors to American economy, considering disposable income, airline fares and time-trend variable 02 p3034 A72-11721
Short haul operating systems in air transportation environments, discussing terminal vs cruise configurations, costs and noise abatement 03 p0309 A72-13422
Air transport vs other travel, discussing time, costs, popularity and technology 03 p0459 A72-13485
Short-short haul STOL network economics for commuter ports in Detroit region, estimating service demand, aircraft number and maintenance costs 03 p0459 A72-13696
Soviet look on air transport economics covering efficiency and control improvement, maintenance, work and wages, tariffs, cost and revenues, etc 03 p0459 A72-14098
Air transportation evolution and relation to atmospheric and noise pollution 03 p0459 A72-14151
ATC for North Atlantic air transportation, emphasizing collision risk model for safety standards assessment 04 p0544 A72-14484
Air transportation and society - AIAA/FAA Conference, Key Biscayne, June 1971 04 p0544 A72-14809
American civil aviation future development, discussing passenger and freight markets growth, aircraft types and FAA role 04 p0464 A72-14811
Air transport maintenance regulation as part of National Aviation System program, discussing airworthiness, safety and reliability in relation to design requirements 04 p0526 A72-14814
Route charges system for Europe, stressing financial necessity 04 p0597 A72-15071
Canadian STOL design, development, production, airports and civil air transportation applications 05 p0751 A72-15775
Air transport planning in coordination with urban and country development in West Germany 05 p0644 A72-16697
Air transportation modal split analysis by computer simulation program for determining utilization of alternative travel modes between origins and destinations 06 p0905 A72-17973
Utah-Colorado-New Mexico-Arizona regional air transportation study, assessing scheduled air carrier service demand for 1971-1990 07 p1102 A72-19178
Eastbound and westbound transmeridian flights effect on body temperature and psychomotor and visual performance circadian rhythms, discussing readjustment times [AMRL-TR-71-89] 07 p0921 A72-20176
Computer simulation requirements for air and ground transportation system, emphasizing mathematical models capable of system performance relation to design parameters 07 p0952 A72-20362
Rhythmstasis as fundamental life characteristic analogous to homeostasis, discussing human circadian rhythm and cycle desynchrony during air travel 07 p0923 A72-20445
Discrimination preference and effect on insurance of limit liability of international air carrier according to modified Montreal Interim Agreement 07 p1106 A72-20674
V/STOL development for short haul air transportation, discussing requirements for quiet pollution-free operation, ATC systems, navigation and landing aids 08 p1108 A72-21010

Linear programming application to aircraft selection for tactical airlift fleet contingency planning [AD-736074] 08 p1256 A72-21468

Future civil air transport trends, considering passenger and cargo growth, travel frequency per capita income and STOL market 08 p1257 A72-22150

Book on IATA organization and functions, discussing international aviation history, conference machinery, enforcement of conference resolutions, air transportation economics, public corporations, etc 10 p1564 A72-23846

Future short haul aircraft transportation systems, discussing aircraft forms, noise reduction technology and runway requirements 12 p1754 A72-27660

STOL, VTOL and V/STOL air transportation systems development, characteristics and requirements, presenting economic forecast 12 p1754 A72-27661

Book on air transportation, covering history, government agencies roles in economic and safety regulation of air carriers, accounting, financial and legal aspects, etc 12 p1891 A72-28205

Air cushion aircraft landing systems advantages and suitability for arctic transportation applications 13 p1897 A72-28793

Multiscale numerical model for local weather development simulation, noting forecasting for long distance air travel 13 p1993 A72-28857

Warsaw Air Transport Convention second revision by Guatemala Protocol of 8 March 1971, discussing provisions for air carrier liability 14 p2174 A72-30821

Hierarchical system of helicopter service terminals, calculating passenger lots for single and multiloop arrangements under given stochastic input conditions 15 p2337 A72-31498

National airports system for UK civil air transportation, discussing economic, operational, accessibility and social aspects 15 p2214 A72-32321

Short haul airlines on-time operation, discussing ATC, weather, cargo and aircraft ground handling, cabin and flight services and aircraft reliability effects 15 p2339 A72-32452

Prediction models for dynamic environment experienced by cargo during air and rail transportation 15 p2339 A72-32610

Ultrashort haul common carrier air transportation system based on VTOL aircraft for suburban-to-city center trips, comparing with land based transport 16 p2480 A72-33113

VTOL short haul transportation applications discussing concept evolution and economic factors 16 p2480 A72-33181

Flexible wing applications to passenger and cargo transport, discussing gliding and soaring sport, emergency use, powered flight, rocket payload recovery, etc 16 p2347 A72-33182

Buoyancy systems and parawings application in short haul passenger transportation, discussing VTOL and STOL operations 16 p2348 A72-33183

Air cushion landing system application for civil air transportation, discussing operation, braking and parking 16 p2348 A72-33184

Air transportation - SAE/AIAA/ASME Conference, Washington, D.C., May-June 1972 16 p2481 A72-33306

Airport and air transportation benefits and costs to community and industry, considering institutional, environmental and economic issues 16 p2373 A72-33308

Airport economic and social impact on environs in terms of community development 16 p2373 A72-33309

Short haul air transportation system economic and political problems, noting community acceptance and passenger service standards 16 p2481 A72-33310

Individual regions and nationwide air traffic demands forecasting for airport planning 16 p2481 A72-33311

Commercial airport and air transport service economic impacts on business and industrial communities 16 p2481 A72-33312

Aero engines and propulsion systems development contribution to air transport economics and regularity, considering environmental factors 16 p2443 A72-33313

Commercial transport aircraft engine technology contribution to world air transportation, considering social and ecological compatibility with community 16 p2348 A72-33314

ICAO assistance to member states in various transport airports and navigation facilities economics including accounting and financial statistics 16 p2481 A72-33334

Planning model for German air transport. 17 p2638 A72-34244

The air bus as the aircraft of near future. II 17 p2492 A72-35439

Maintenance processes planning in air transportation, discussing aircraft availability, cost analysis and production management 17 p2560 A72-35441

Air transport developments effects on economy and environment, discussing government power to control airport use and location and air pollution 17 p2639 A72-35952

Airports: Key to the air transportation system; Proceedings of the Conference, Atlanta Ga., April 14-16, 1971. 18 p2675 A72-36776

Environmental considerations in airport development. 18 p2743 A72-36778

What's new in airport planning. 18 p2675 A72-36780

Boeing 747 aircraft impact on Chicago O'Hare airport design criteria, noting future terminal facilities planning 18 p2675 A72-36782

Air transport development between the UK and Europe - The next twenty years. 18 p2743 A72-37092

The future of general aviation in Europe. 18 p2743 A72-37093

Advanced subsonic transport technology. 19 p2748 A72-37677

STOL ride quality criteria - Passenger acceptance. [AIAA PAPER 72-790] 19 p2749 A72-38107

Helicopter search, rescue and transportation of wounded and ill persons in Denmark, discussing accidental hypothermia treatment 19 p2759 A72-38714

Short haul intercity air transportation systems requirements for successful competition with lower cost ground modes [ICAS PAPER 72-16] 21 p2995 A72-41141

Prototype interurban IFR STOL transportation system demonstration project, considering area navigation, scanning beam microwave landing systems and STOL port planning [ICAS PAPER 72-41] 21 p3040 A72-41166

Rigid form airship for transportation, discussing applications for special loads and scientific and service purposes, and design and construction problems 21 p2996 A72-41200

German monograph - Model-analytical investigation of short-haul air traffic with VTOL aircraft in the Federal Republic of Germany. 22 p3245 A72-43068

Critical assessment of air transport planning for German Federal Republic, advocating decentralized concept of major air terminals for intercontinental jumbo jet traffic 23 p3357 A72-43244

Minimum operational costs of passenger and cargo transport aircraft, considering effects of flight distance, wind conditions and optimum speed and altitude 23 p3252 A72-44338

Design of a military air cargo transportation system by use of a large scale mathematical programming model. 24 p3466 A72-44577

AIR WATER INTERACTIONS

Acoustically scaled simulation of sonic boom N-wave energy penetration into ocean for flat air-water interface 13 p1951 A72-29587

Upward and downward radiative transfer in atmosphere-ocean system model calculated by Monte Carlo method, noting turbidity effect on radiance 15 p2224 A72-31673

Barbados oceanographic meteorological experiment /BOMEX/ sea air interaction program in equatorial Atlantic, using real time synchronous satellite information 15 p2225 A72-31808

AIRBORNE EQUIPMENT

NT AIRBORNE/SPACEBORNE COMPUTERS

Agricultural land use analysis by remote sensing, discussing side-looking airborne radar systems and image interpretation for local needs 01 p0056 A72-10456

Remote airborne sensors for sea water oil pollution surveillance in near UV, thermal IR and microwave regions [AIAA PAPER 71-1073] 01 p0057 A72-10535

Rapid water pollution assessment by airborne chlorophyll measurement using differential, correlation and IR radiometers [AIAA PAPER 71-1097] 01 p0058 A72-10546

Microwave module circuit design for airborne phased array radar with distributed power generation, reception and phase shift functions, considering performance, reliability and cost 01 p0028 A72-10660

Pulse IMPATT diode Ka band microwave rf head mechanically steered antenna array for airborne monopulse tracker applications 01 p0039 A72-10661

Earth surface and atmosphere remote sensing by airborne microwave measurements, noting ocean surface emissance dependence on temperature, surface conditions and pollution 02 p0207 A72-11779

Object proportions estimation algorithms in single resolution element of airborne multispectral scanner 02 p0227 A72-11839

Airborne sensors terrain classification, considering sample points clustering approach and signature analysis 02 p0227 A72-11844

NASA/MSC earth observation aircraft program radar scatterometers, presenting system evaluation 02 p0172 A72-11849

Airborne high resolution multispectral TV camera system, describing special objective configuration for improved ground resolution 02 p0227 A72-11850

Multichannel multispectral airborne IR imaging system and video data processing for U.S. geological survey 02 p0227 A72-11851

Extended wavelength field spectroradiometry for multispectral scanner data interpretation in airborne observations 02 p0228 A72-11853

Side-looking airborne radar imagery for sea ice drift size, shape and surface characteristics determination [AD-733605] 02 p0215 A72-11882

Aerial Radiological Measuring System for environmental radiation detection and tracking, emphasizing snow mass prediction by terrain radiation attenuation measurement 02 p0215 A72-11884

Approximate signal-clutter ratio formulas for airborne pulse radar system, eliminating computer calculations 02 p0176 A72-12216

Army data analysis system for fixed and rotary wing aircraft flight testing, including airborne and computer controlled ground stations equipment 02 p0179 A72-12408

Electrically charged low mobility droplet production by water vapor condensation on to gaseous ions from aircraft static discharger 02 p0231 A72-12556

Passive airborne mapping of radiation sources, using fixed side-looking multilobed and scanning fan beam antenna pattern with coherent optical processing of film records 04 p0495 A72-14491

Airborne gamma ray spectrometer investigation circle, considering altitude, air density, source density and gamma ray attenuation coefficient effects 04 p0520 A72-14564

CAT detection by airborne laser Doppler radar and ground based ultrasensitive microwave Doppler radar methods 04 p0543 A72-14822

Airborne CAT detection by passive IR radiometry, reducing false alarms due to temperature anomalies 04 p0543 A72-14828

Airborne remote CAT detection equipment, examining pulsed Doppler laser and IR radiometry 04 p0521 A72-14831

Side-looking airborne radar (SLAR) images comparison with small-scale low-sun black and white aerial photographs 05 p0661 A72-16041

Airborne traffic display system using beacon and radar surveillance network and ground computer processing 06 p0844 A72-17329

Three component airborne magnetometer design, discussing direction reference system and stabilized platform 06 p0812 A72-17372

Aeromagnetic surveying with airborne fluxgate magnetometer, discussing field data compilation and interpretation 06 p0812 A72-17373

CNES airborne remote sensing of earth resources comparison with classical photodetection methods, discussing application to oceanography, geology, agriculture, hydrology and human activities 06 p0803 A72-17385

Trident aircraft air-system interrogator airborne first line test apparatus for electrical components malfunction diagnosis 06 p0796 A72-18154

Computerized Eros II airborne collision avoidance time frequency system design, considering radio transmission, synchronization and ground stations 06 p0845 A72-18247

Aircraft turboalternator governing theory for frequency error detection, comparing performance of mechanical- and electro-hydraulic governors 06 p0868 A72-18249

- Airborne ruby lidar application to cirrus and haze layers measurements, deriving optical parameters
06 p0777 A72-18448
- Solid state Ku-band local Gunn oscillator for airborne radar applications, discussing design and batch process fabrication
06 p0789 A72-18480
- IR spectral emittance measurement with airborne spectrometer for geological mapping over Pisgah Crater /California/
08 p1162 A72-22017
- Rock type discrimination from ratioed airborne thermal IR scanner images of Pisgah Crater /California/
08 p1162 A72-22018
- Small scale atmospheric turbulence measurement with airborne hot-wire anemometer, discussing optimal choice of experimental parameters
09 p1307 A72-22435
- Airborne gas chromatograph for real time diffusion analyses, describing flight test results with sulfur hexafluoride plumes
09 p1307 A72-22451
- Sea surface roughness mapping by airborne microwave radiometry with correction for viewing angle and atmospheric effects
09 p1297 A72-22525
- Development trends in airborne man machine flight control, discussing optimal division between human pilot and machine in relation to total system performance and economic factors
09 p1270 A72-22781
- Area navigation for Chicago-New York region, evaluating Decca Omnitrac 1A RNAV system installation in Boeing 727 aircraft
09 p1349 A72-23467
- Flight testing of automated modular area navigation system for L-1011, describing computer, data storage and control-display units and electronic automatic chart system
10 p1509 A72-24271
- Stochastic optimization of airborne laser seeker system design parameters to maximize target acquisition probability through regression analysis of data from computerized model
10 p1437 A72-24682
- Airborne VHF omnirange /VOR/ systems minimum operational standards for navigation and communication in air traffic control
10 p1509 A72-24725
- Single engine aircraft-borne weather radar with electronically scanned steerable phased array antenna [SAE PAPER 720315]
11 p1591 A72-25579
- Mechanical seal for airborne Stirling cycle cryogenic refrigerator, noting He cross leaks and sealing faces galling and blistering [ASLE PREPRINT 72AM 16]
13 p1964 A72-28973
- Design characteristics and in-flight performance tests of computerized airborne OMEGA receiver, noting time independent one mile accuracy
13 p1997 A72-29188
- Sky wave correction /Swanson/ model and computer program for real time propagation prediction for airborne OMEGA system
13 p1997 A72-29190
- Airborne thermal sensors time constants, giving temperature perturbation wavelength estimates
13 p1958 A72-29623
- Airplane-borne cylindrical field mill type instrument to record atmospheric electric field
13 p1961 A72-30085
- Aircraft or helicopter-borne IR radiometer for surface temperature of snow covers and glaciers and air-snow energy balance measurements
15 p2232 A72-31244
- Spaceborne and airborne remote sensing methods and applications for earth resources observation
15 p2221 A72-31245
- Airborne microwave hologram radar system, discussing along- and cross-track direction resolution realization by synthetic aperture technique and phased receiving array respectively
15 p2196 A72-31788
- Airborne ground mapping and meteorological radar with steerable phased array antenna without mechanical scanners
15 p2200 A72-32216
- Aircraft industry product support role in time delays minimization for aircraft operators, discussing malfunction report, minimum equipment decision and fault diagnosis
15 p2339 A72-32456
- Multi-environment reliability test program for airborne electronic systems under simulated temperature, humidity, vibration and shock conditions
15 p2215 A72-32616
- Computer simulation of airborne gamma ray spectrometer with prescribed photopeak windows from flight over surfaces with arbitrary-dimension radiation sources
16 p2392 A72-33617
- Airborne external instrumentation pod containing IR scanner and associated test equipment for land and water surveys
16 p2393 A72-33635
- Digital recording techniques for airborne data acquisition, emphasizing laser beam holographic recorders
16 p2394 A72-33642
- Airborne flight test data acquisition system modular design to provide digital readings from monitoring transducers analog signal
16 p2364 A72-33645
- An integrated system of airborne and ground-based instrumentation for flying qualities research with the X-22A airplane.
[AHS PREPRINT 654]
17 p2536 A72-34486
- A compact grating spectroheliograph for the MgII resonance lines.
17 p2554 A72-35079
- Airborne waveguide element reliable advanced solid state radar /RASSR/ phased array radiation patterns and design
17 p2531 A72-35571
- SHF airborne distributed phased array antenna system.
17 p2531 A72-35572
- Airborne equipment electric power supply standards to provide characteristics limits for compatibility with ground support systems [SAE AS 1212]
18 p2648 A72-36355
- Air/ground digital communications in airline operations.
18 p2660 A72-36561
- ATC IC transponder used with secondary surveillance radar, discussing design features
18 p2662 A72-37048
- Man-made electromagnetic noise in southern California and southern Nevada.
19 p2764 A72-37869
- Automated airborne recording system to obtain data on aircraft engines, subsystems and operational performance, considering cost and economic benefits [AIAA PAPER 72-752]
19 p2802 A72-38126
- Fast response solid state phase lock refractometer for airborne measurement of atmospheric refractive index
19 p2802 A72-38225
- Computer simulation aided airborne attack missile launch system design for safe separation from carrier aircraft, discussing ejection and control systems design
20 p2951 A72-39099
- Navigation satellite system based on triangular distance measurement between two satellites and aircraft, noting simplification of air- and satellite-borne equipment requirements
21 p3080 A72-40285
- ILS replacement by microwave landing system, considering landing phase range from acquisition to touchdown, terminal approach handling by airborne navigation system and economic advantages
21 p3081 A72-40294
- Propagation of horizontally polarized VLF waves - Systems implications.
21 p3021 A72-40905
- Digital processing for motion compensation in high resolution airborne synthetic aperture radar imagery in presence of simultaneous longitudinal, lateral and vertical maneuvers
21 p3022 A72-41076
- AIRBORNE TERRAIN ANALYSIS**
U TERRAIN ANALYSIS
AIRBORNE/SPACEBORNE COMPUTERS
- Scientific satellite with simple inertial system, deriving discrete feedback reentry guidance algorithms based on closed-form equations solvable by onboard computer
01 p0098 A72-10944
- STAR self testing and repairing fault tolerant digital computer for outerplanet exploration spacecraft, discussing architecture, reliability analysis, software and peripheral system automatic maintenance
02 p0184 A72-11482
- Distributed fault-tolerant aerospace digital computer design with duplicated central multiprocessor, triplicated memory and conventional redundancy local processors for error detection and correction
02 p0185 A72-11489
- Ferrite core memory for space flight devices, comparing 1 bit storage capacity power consumption with MOS cell
02 p0196 A72-12734
- Doppler system with navigation radar device, computer unit and data transmitter for continuous recording of aircraft position and speed
02 p0258 A72-12749
- Aircraft integrated data systems application to flight safety analysis, engine performance monitoring, crew proficiency, autoland evaluation, operations and logistics
04 p0495 A72-14726
- Airborne computer programmed adaptive optimal control for subsonic vehicle automatic landing with aerodynamic performance
05 p0685 A72-16430
- European reusable space tug, discussing computer controlled attitude stabilization and maneuvering system design for orbital rendezvous and docking
05 p0725 A72-16446
- Deep space probe MULTIPAC data system computer repairable during flight via command and telemetry links by reprogramming failed unit
05 p0633 A72-16573
- Navy hovering vehicle versatile automatic control system for V/STOL flight test program, using airborne digital computer for navigation/guidance computations
05 p0687 A72-16661
- Flight control systems development, discussing onboard computers use in subsystems functional integration, stabilization and landing systems, inertial navigation and flight simulation
05 p0687 A72-16736
- Flight navigation technology current state and development trends, discussing transition from Doppler to inertial systems, use of computers and satellites, collision avoidance, etc
05 p0687 A72-16737
- Programming systems for onboard unmanned deep space probe computers, describing Mariner and outer planet Grand Tour Programs
07 p0949 A72-19295
- On-line digital computer maximum likelihood estimate of Earth atmosphere profile ahead of flight vehicle using discrete measurements of density, temperature and pressure
08 p1156 A72-20853
- Strapdown inertial guidance and navigation systems state of art, discussing recent developments in computers, sensors and systems technology
08 p1204 A72-21089
- Space flight experience application to human factors engineering problems in air and maritime navigation, considering use of small digital computers, display and sensing devices
09 p1348 A72-22785
- European Special Space Tug electronic subsystem requirements, considering strapdown inertial measuring unit, remote sensors, computer and fail-safe backup system
09 p1396 A72-23258
- Sailplane computer displaying rate of climb simultaneously with airspeed for pilot determination of best strategy for local upcurrent-downcurrent conditions
09 p1316 A72-23550
- Robots /electromechanical systems with local computers and sensor controlling motors and effectors/ space application categories and operating and decision making requirements
10 p1458 A72-23777
- Fault tolerant redundancy for manned spacecraft computers considered as long term desirable solution from cost analysis
10 p1443 A72-23819
- Reliability program for SAAB 37 Viggen airborne computer, discussing prototype and components operating tests and failure rates
10 p1443 A72-23984
- Long time mission spacecraft computer reliability economics based on failure and step improvement costs evaluation
10 p1444 A72-24017
- Space shuttle flight crew/computer interface display and control functional requirements optimization by real time digital simulation
10 p1460 A72-24437
- Landing control algorithm using onboard digital computer for spacecraft hyperbolic velocity reentry, discussing simulation test results
11 p1684 A72-26898
- Skyguide airborne computer navigation system for airline applications, discussing system components, flight crew monitoring and optimization
11 p1684 A72-26999
- Aerospace guidance multiprocessor with memory units attached to time-multiplexed data bus, predicting performance in terms of queueing theory, Markov process and simulation
12 p1786 A72-27433
- Shoran systems with onboard computers for aircraft position and trajectory parameters, noting coordinate plotting for flight path recovery maneuvers
13 p1996 A72-28785
- Aeronautical navigation/guidance standardization in conjunction with OMEGA, covering sensor and computer equipment life cycles
13 p1999 A72-29199
- OMEGA receiver integration into Navy P-3C airborne computerized navigation system, describing flight test, maintainability and laboratory simulation programs
13 p1999 A72-29202
- Avionics equipment for signal processing onboard civil aircraft to improve flight safety, discussing uses of OMEGA navigation system and digital computers
15 p2193 A72-31178
- Astronautical digital computing hardware and software trends and implications, considering data rates, reliability, LSI, speed-storage tradeoff, etc
15 p2203 A72-31822
- Digital attitude and heading reference system computer for aircraft heading control, discussing design and performance features
16 p2367 A72-33244

- Univac 1832 multiprocessor avionics computer for airborne ASW, discussing input/output controllers and interfaces and IC design features 16 p2367 A72-33245
- Fighter bomber Loran-inertial data processing with digital computer to combine navigation, guidance and weapon delivery into fully integrated system 16 p2420 A72-33246
- S-3A Viking systems. 17 p2491 A72-34741
- Russian book - Mathematical methods of modeling in space studies 17 p2607 A72-35026
- A method of using a control computer in a system controlling onboard spacecraft equipment 17 p2522 A72-35027
- A method of realization of the functions of a program timer on a computer used in a spacecraft onboard equipment control system 17 p2522 A72-35028
- A probabilistic model of a control computer complex for estimating the efficiency of communication of a computer with data sources and receivers 17 p2522 A72-35029
- USAF development of electrostatic gyros for inertial air navigation, noting flight tests and associated airborne digital computer 17 p2578 A72-35558
- The SKC-2000 advanced aerospace computer. 17 p2523 A72-35578
- High performance 16-bit computer organization. 17 p2523 A72-35580
- Modular avionics computer design concept to permit tailoring for diverse applications via microprogramming 17 p2524 A72-35581
- Aerospace computer software validation and verification methods application to complex systems, discussing code execution and analysis tools, program diagnostics, cost and schedules 17 p2524 A72-35582
- Airline crew familiarization with DC-10 Computerized Flight Guidance System to calculate steering signal from raw data to follow flight path 19 p2831 A72-37899
- Development of coordinate signal transmission and data processing equipment for operation supervision in space travel 19 p2765 A72-38305
- A simplified analysis of the computational requirements for straddown attitude reference. [AIAA PAPER 72-827] 20 p2951 A72-39098
- Future trends of airborne computers. [AIAA PAPER 72-895] 20 p2905 A72-39109
- Modular navigation /MONA/ dual channel automatic area navigation system, describing computer, flight data storage and control/display units 21 p3079 A72-40277
- Autonomous navigation systems, discussing Doppler navigation, inertial platforms and onboard computers 21 p3079 A72-40283
- Spacecraft-borne computer and electronic systems interface for radio reception, transmission and TV imagery applications 21 p3014 A72-40309
- Automated area navigation with real time track computation, discussing information processing by on-board computer for immediate pilot instruction 21 p3081 A72-40683
- Microminiaturization, microprogramming, multiprocessing, and processing and memory module design technology of aerospace computers in different size ranges 21 p3025 A72-41113
- A new concept of flight displays compatible with digital airborne computers. 21 p3012 A72-41426
- Dynamic characteristics, stability and steady state accuracy for orbital gyroscope with digital control, noting bit density requirements of onboard computer 22 p3202 A72-42207
- The on-board computer of the Astronomical Netherlands Satellite /ANS/. 24 p3382 A72-45163
- Spacecraft rendezvous trajectories and targeting maneuvers onboard sequential computation, taking into account maneuver constraints and state vector update information 24 p3450 A72-45172
- Minicomputers application for long distance data transmission, noting multipurpose use of VT 1010/B computer in satellite operation program 24 p3382 A72-45391
- Automatic software diagnostic package for airborne computer, using testing computer for decision making based on received data 24 p3383 A72-45669

AIRCRAFT

- Aircraft and spacecraft conceptual definitions in national and international law 11 p1749 A72-26561

AIRCRAFT ACCIDENT INVESTIGATION

- Human ejection vertebral injury data in aircraft accidents by cross reference to final medical diagnosis, considering costs and prevention for seat systems 02 p0167 A72-11714
- Computerized error function method of wreckage trajectory analysis in aircraft accident investigation, using fundamental equations of motion 03 p0309 A72-13250
- Pilot in-flight incapacitation probability from airline reports, career termination studies and questionnaire responses 04 p0479 A72-14870
- Fatal aviation accident human factors investigation by roentgenography, noting flight environment factors, injury pattern relation to aircraft design and victim identification 06 p0768 A72-17880
- Uric acid to urea nitrogen ratio as assay test for identification of avian tissue in verifying bird ingestion or impact as aircraft accident cause [AD-737853] 07 p0922 A72-20184
- Forum choice in aircraft disaster litigation, discussing res ipsa loquitur, guest statute and vicarious liability 07 p1106 A72-20672
- Aviation insurance and claim servicing risks in aircraft accidents, discussing coverage, claims investigation, litigation and settlement 07 p1106 A72-20673
- General aviation aircraft structural safety studied with 1547 accident histories, noting IFR and turbulent weather conditions predominance [SAE PAPER 720308] 11 p1575 A72-25572
- Human, technical and environmental factors in accidents of naval F-104 squadron, considering temporal distribution of accidents and pilot physical condition 12 p1772 A72-27820
- Medical factors in air racing accidents, investigating drug, fatigue and gastrointestinal symptoms effects on pilot reaction to emergency 14 p2081 A72-31089
- General aircraft accident investigation approach, using subsequent psychosocial reconstruction of pilot lifestyle to explain accident-producing behavior 14 p2082 A72-31095
- Aircraft accident in the Faroe Islands in 1970 - Observations from a medical point of view, with special reference to spinal fractures. 17 p2508 A72-34556
- Grouping of the causative factors in investigation of aircraft accidents attributed to pilot errors. 17 p2508 A72-34557
- Jurisdictional problems in the autopsy of aircraft accident victims. 17 p2639 A72-34558
- Corporate aircraft pilot contribution to accident investigation in providing expertise, discussing various case histories 20 p2888 A72-39751
- AIRCRAFT ACCIDENTS**
- Cockpit information for pilot and flight crew as key to transport aircraft accident prevention, discussing cockpit layout and displays in terms of flight safety requirements 04 p0464 A72-14813
- Airborne collision avoidance system equipment for general aviation aircraft, discussing logic functions, transmission modes, data handling tradeoffs and ATC procedure interactions 04 p0545 A72-14830
- Atmospheric turbulence effects on aircraft flight and design, covering accidents and costs, turbulence generation, prediction, measurements and load alleviation devices [AIAA PAPER 72-219] 05 p0684 A72-16885
- Dazzle glare effects and acuity recuperation among aircrew, noting civil and military aircraft accidents during daytime and nighttime flights 08 p1125 A72-21272
- High performance aircraft takeoff and landing accidents, investigating survival rates 08 p1109 A72-21563
- Survival rates in USAF accidents during 1965-69, noting visual sighting as primary rescue factor 08 p1109 A72-21564
- Behavioral inaction under stress conditions similar to survivable aircraft accident, tabulating hesitation statistics 08 p1109 A72-21570
- Disorientation in naval aircraft accidents from psychophysiological and environmental factors, suggesting flight scheduling and training improvements 08 p1126 A72-21574
- Pilot survival probabilities under various conditions of high performance aircraft takeoff and landing accidents, suggesting emergency action guidelines for pilot training 10 p1428 A72-23732
- Book on general aviation safety covering statistical accident records, accident analysis, crashworthiness, preventive measures, etc 10 p1420 A72-23750

- Test facility design for aircraft crashworthiness: evaluation and improvement, considering survivable accident surrounding conditions, equipment and testing methods 11 p1576 A72-25586
- [SAE PAPER 720323] 11 p1576 A72-25586
- Safe aircraft fuels crashworthiness evaluation in terms of ignition susceptibility parameter, noting full scale crash environment simulation [ASME PAPER 72-GT-27] 11 p1702 A72-25623
- USAF aircraft accidents/incidents involving aircrewmembers with medical waiver on various visual, cardiopulmonary and other chronic pathological and psychiatric conditions 12 p1776 A72-28315
- Head-up omnidirectional two dimensional auditory display device for visual detection facilitation in aircraft collision avoidance systems 12 p1777 A72-28327
- General aviation crashworthy personnel restraint systems, discussing strap take-up devices, comfort, fit and ease of use 13 p1908 A72-28726
- Passenger behavioral inaction in survivable aircraft accidents, suggesting maladaptive behavior counteraction by leadership and/or training 13 p1908 A72-28727
- Aircraft accident statistical projections from human error review, analyzing situational circumstance limitations 14 p2081 A72-31086
- Atmospheric turbulence and the ATC system. 18 p2663 A72-37049
- Corporate business aviation performance record in light of aircraft accident statistics, noting high percentage of approach-landing accidents and means for improvement 20 p2888 A72-39743
- Aircraft accidents during nonprecision approaches under adverse weather conditions, discussing landing aids use for corporate jet aircraft 20 p2952 A72-39745
- Electrostatic charge on an aircraft and lightning striking the aircraft 21 p2994 A72-40171
- A survey of rotary-wing aircraft crashworthiness. 22 p3138 A72-42763
- An assessment of energy absorbing devices for prospective use in aircraft impact situations. 22 p3237 A72-42764
- Human tolerance limitations related to aircraft crashworthiness. 22 p3151 A72-42765
- Response of a seat-passenger system to impulsive loading. 22 p3151 A72-42766
- A study of USAF survival accidents 1 Jan. 1965-31 Dec. 1969. 23 p3259 A72-43425
- Intoxicating liquor and the general aviation pilot in 1971. 24 p3377 A72-45662
- AIRCRAFT ANTENNAS**
- Helicopter antenna placement, using scale models for three dimensional radiation pattern semiautomatic recording under free space conditions 01 p0024 A72-10149
- Computer controlled production test system for airborne phased array modules, describing various measurement capabilities 05 p0637 A72-16417
- Vertical dipole antenna design for CW Doppler radar midair collision avoidance system 05 p0629 A72-16571
- Received signal spectrum gravity center and effective antenna centers of airborne Doppler velocimeter in horizontal flight 11 p1606 A72-26730
- Test facility for aircraft and spacecraft antennas radiation patterns and optimal installation determination 12 p1795 A72-27412
- Preproduction OMEGA aircraft receivers and antennas development and flight testing, noting signal loss problems in high noise or precipitation static environments 13 p1998 A72-29198
- Test flights into weather at midlatitudes and tropical systems with airborne OMEGA navigation system, discussing E field and H field antennas 13 p1999 A72-29203
- Aircraft antennas design for radio links to satellites for aeronautical communication and ATC, proposing use of beam steering system 13 p1932 A72-29347
- Experimental investigation regarding Archimedean spiral antennas for the L-band, and radiator groups constructed from them whose radiation directions are controlled by a conduction matrix 21 p3028 A72-40510
- Determination of the radiation characteristics of aircraft antennas in flight 21 p3030 A72-40534
- Linear HF radar antenna array aperture synthesis for ionospherically propagated signal reception in air-

plane for achievement of ideal directivity without ionospheric compensation

21 p3022 A72-41080

AIRCRAFT APPROACH INSTRUMENTS

U APPROACH INDICATORS

AIRCRAFT APPROACH SPACING

ATC separation minima and navigational errors on airways in general and long range oceanic environments

01 p0096 A72-10177

Mathematical analysis of separation standards and aircraft navigational collision risk for parallel tracks in radar monitored systems

01 p0096 A72-10178

Statistical analysis of track keeping Strumble VOR data for lateral navigation separation standards and collision risk in continental environment

01 p0097 A72-10179

Terrain clearance during descent and approach of aircraft under radar control, discussing optimum profile, ATC, nav aids and rules

01 p0097 A72-10183

Area navigation requirements by general aviation, discussing random routing, ATC system and aircraft approach spacing

15 p2271 A72-32202

Operation principles, capabilities and tests of midair collision avoidance system with aircraft separation control by nonsynchronous techniques

21 p3081 A72-40296

AIRCRAFT BASES

U MILITARY AIR FACILITIES

AIRCRAFT BRAKES

NT LEADING EDGE SLATS

NT SPLIT FLAPS

NT TRAILING-EDGE FLAPS

NT WING FLAPS

Foot forces exerted at various aircraft brake-pedal angles, observing 20 degree zone with maximum effectiveness

[AD-73551]

01 p0018 A72-10567

Ti effects on aircraft equipment design, considering use of Ni plated brake cylinder, wheel, engine control rams, tie bolts and rings

03 p0373 A72-13618

Environmental tests on carbon fiber Vulcan air-brake flap, including thermal cycling, sustained loading, immersion, corrosion and lightning strike tests

05 p0681 A72-16998

Carbon-carbon composite material for high performance aircraft braking systems, noting weight savings and thermal characteristics improvements

12 p1835 A72-28093

AIRCRAFT BREATHING APPARATUS

U BREATHING APPARATUS

AIRCRAFT CABINS

U AIRCRAFT COMPARTMENTS

AIRCRAFT CARRIERS

Carrier system for controlled approach of Naval aircraft to provide pilot window to deck for tactical jet guidance for poor visibility landing

02 p0256 A72-12323

U.S. Navy automatic carrier landing system /ACLS/, discussing shore and ship based test techniques and problem areas

05 p0686 A72-16654

Carrier suitability testing for aircraft landing, considering landing gear and supporting structure under simulated shipboard conditions

06 p0759 A72-18497

Aircraft launch envelope investigation for minimum catapult end airspeed determination at carrier bow, discussing optimum test pilot launch technique

06 p0759 A72-18498

Night Carrier Landing Trainer flight and carrier environment simulator for A-7 aircraft pilot training, discussing performance predictions from computer data analysis

07 p0927 A72-19137

Carrier based attack aircraft allocation model formulation and solution for maximum inflicted target damage, using sequential unconstrained minimization technique with nonlinear programming

[AD-736073]

08 p1256 A72-21469

Pilot landing performance prediction criteria based on day and night carrier qualification trials and flight training

14 p2081 A72-31084

Simulator for physical forces experienced by carrier aircraft during catapult launches and arrested landings, considering external stores safe suspension

15 p2215 A72-32620

Direct lift control feasibility for integration into F-14A automatic carrier landing system /ACLS/, using moving-base six-degree-of-freedom simulation

[AIAA PAPER 72-873] 20 p2951 A72-39127

AIRCRAFT COMMUNICATION

Book on global communication law covering maritime transport, civil aviation, radio, space communication postal services, international cooperation, etc

02 p0305 A72-12575

Civil aviation communication systems, discussing short and long range communications, satellite chan-

nel capacities, digital data link systems, ATC, weather broadcasts, etc

03 p0322 A72-13416

Communications and navigation trends in ATC, emphasizing use of improved existing systems

05 p0684 A72-15781

Soviet book on aircraft radio equipment covering transmission and reception, velocity and coordinates measurements, siting and navigation, flying target interception, reconnaissance, landing systems, etc

05 p0637 A72-16530

Airline pilot performance in automated ATC system involving use of surveillance data and instantaneous discrete communications

06 p0844 A72-17331

Airline air/ground radio communications and data link service implementation for San Francisco-Hawaii center

06 p0770 A72-17337

Automation in planning and execution of flights, considering navigation, communication, flight instruments monitoring, control/stabilization and warning systems

09 p1269 A72-22780

Airborne VHF omnirange /VOR/ systems minimum operational standards for navigation and communication in air traffic control

10 p1509 A72-24725

Aircraft and water vehicles mobile communications via stationary satellite, discussing optimum multiple access and repeater configuration

12 p1781 A72-27376

Pacific Ocean meteorological data collection from military and civil aircraft in-flight reports, discussing computer processing for daily analysis and monthly and seasonal means

13 p1994 A72-28874

ATC operational systems, discussing global surveillance and voice and data communication between aircraft and earth station

14 p2129 A72-31141

Aeronautical communication satellite technical and economic survey, considering wave propagation, noise, aircraft antennas and VHF and UHF links

15 p2193 A72-31180

Economic analysis of aeronautical communication system via satellite, noting cost estimates and annual charge per user

21 p3081 A72-40298

Ground-based Doppler navigation waveguide slot antenna design for optimal directional multilobe reception from aircraft

21 p3028 A72-40509

AIRCRAFT COMPARTMENTS

Aircraft crash fire protection, using passenger compartment heat shield of fire-retardant polyisocyanurate foam and intumescent paint

03 p0310 A72-13484

Aircraft transparencies from civil operator viewpoint, considering replacement cost of flight deck and cabin windows

12 p1753 A72-27005

Concorde aircraft optical transparency components design characteristics and reliability tests, noting vision, pilot forward windshield, flight deck side windows and cabin windows

12 p1753 A72-27012

AIRCRAFT CONFIGURATIONS

Industry assisted state of art assessment of high lift turbofan configurations for USAF STOL tactical transport technology program

[SAE PAPER 710758]

01 p0003 A72-10255

Sonic boom generation, propagation and minimization, discussing atmospheric turbulence and temperature gradients and aircraft configuration effects

[AIAA PAPER 72-194]

05 p0612 A72-16849

VJ-101A and B V/STOL weapon system design, describing various propulsion system configurations

07 p0912 A72-19250

V/STOL weapon system VJ-101, describing He-231 design development from tailsitter concept to canard configuration with tilting wing-tip engines

07 p0912 A72-19251

Engine fan-compressor maximum noise reduction for given aircraft configuration by acoustic linings on nacelle inlet and exhaust walls

07 p1054 A72-19268

Iron rotational hysteresis effect in cold magnetic balance wind tunnel system for spinning aircraft configurations and subsonic flow regimes

10 p1462 A72-24776

Flutter analysis of propeller whirl flutter, twin boom aircraft, T tail configuration, servo tabs and all-moving tail, discussing structural variations effects on service life

[SAE PAPER 720309]

11 p1575 A72-25573

European passenger aircraft Airbus program, discussing various configurations performance, economic factors and technical support

12 p1753 A72-27108

Future short haul aircraft transportation systems, discussing aircraft forms, noise reduction technology and runway requirements

12 p1754 A72-27660

Relationship between static pressure error /position error/ and measurable flight parameters for different aircraft weights and configurations

16 p2393 A72-33637

B-1 aircraft design features, discussing aerodynamic configurational aspects, structural components and materials, engine inlets, fuel, hydraulic control and avionics systems

17 p2487 A72-34223

New VTOL transport aircraft designs by VFW Fokker. II

17 p2492 A72-35477

V/STOL developments in Hawker Siddeley Aviation Limited.

18 p2643 A72-37096

B-52 test vehicle flight demonstration program for control configured vehicles /CCV/ technology concepts validation, noting gross weight reduction

[AIAA PAPER 72-747]

19 p2751 A72-38123

Advanced technology transport /ATT/ aircraft configurations design parameters analysis, considering cruise speed, passenger capacities, ranges, noise level and economics

[AIAA PAPER 72-757]

19 p2751 A72-38127

V/STOL aircraft configurations with lifting counter-rotating disks, presenting aerodynamic coefficients from rotating water tank experiments

21 p2990 A72-41070

F-111A inlet nozzle dynamic distortion diagnostics for airframe-propulsion integration based on flight and transonic wind tunnel tests

[ICAS PAPER 72-18]

21 p2991 A72-41143

Analytic prediction of aircraft spin characteristics and analysis of spin recovery.

[AIAA PAPER 72-985]

22 p3136 A72-42329

An aerodynamics model applicable to the synthesis of conventional fixed-wing aircraft.

[SAWE PAPER 908]

23 p3250 A72-43455

Mission analysis and performance program as part of computerized aircraft configuration synthesis process, describing interfaces with other system modules

[SAWE PAPER 909]

23 p3250 A72-43456

Control requirements for control configured vehicles.

24 p3368 A72-45349

AIRCRAFT CONSTRUCTION

U AIRCRAFT STRUCTURES

AIRCRAFT CONTROL

NT HELICOPTER CONTROL

Aircraft pitching and yawing cross couplings compensation at high speed

01 p0005 A72-10506

European A300B airbus flap and slat systems and tailplane actuator for longitudinal pitch trim control

01 p0006 A72-10725

Handling qualities simulation program for augmentor wing jet STOL research aircraft considering control devices design

02 p0154 A72-11654

STOL aircraft roll moment control possibility for externally-blown jet flap due to engine failure

02 p0154 A72-11700

B-1 strategic supersonic bomber design, emphasizing variable sweep wing, landing gear, control and instrumentation

02 p0154 A72-12226

Soviet book on in-flight studies of aircraft stability and controllability covering dynamic characteristics, measurements, balancing curves, aerodynamic forces and limiting and special flight regimes

02 p0155 A72-12542

Self organizing adaptive aircraft control system with C criterion pitch axis performance and failure compensation

03 p0337 A72-12920

Aircraft power plant management, discussing integration of intake, engine and exhaust system from control standpoint

03 p0405 A72-13418

Pilots in aircraft systems management involving machine and air traffic environment

03 p0309 A72-13419

Control technique and flight quality for crew workload reduction to improve military and civil aircraft flight safety

03 p0310 A72-13640

Aircraft integrated data systems application to flight safety analysis, engine performance monitoring, crew proficiency, autoland evaluation, operations and logistics

04 p0495 A72-14726

Aircraft landing microwave guidance and control systems, considering general dynamic model for aircraft translational motion determination in earth fixed coordinate system

04 p0545 A72-14821

Airplane hydraulic control systems digital simulation, using method of characteristics for distributed parameter analysis of transmission line dynamics

[ASME PAPER 71-WA/FE-21]

05 p0615 A72-15928

Feedback gains for STOL aircraft display pilot interactive flight director design, using computerized ap-

proach-touchdown simulation and optimal control theory
[ASME PAPER 71-WA/AUT-9] 05 p0684 A72-15956

Aircraft steering dynamics model with translational and rotational equations, considering zero sideslip and acceleration and lift bank angle transfer functions
05 p0611 A72-16112

Dynamic stability, control and structural response of transonic jet transport to atmospheric turbulence
05 p0611 A72-16348

Optimization algorithms for jet transport aircraft in-ternally based flight trajectory control in turbulent atmosphere, comparing with ILS
05 p0685 A72-16472

Aircraft flight control system MTBF field operational and MIL-STD-781 testing, establishing data baseline for reliability predictions
05 p0638 A72-16662

Direct side force control by rudder deflection and asymmetrical drag utilization to cancel yawing moment, discussing variable stability T-33 flight tests
[AIAA PAPER 72-94] 05 p0613 A72-16946

Aircraft proximity control for ATC system using national secondary surveillance radar /SSR/ for CAS-PWI functions
06 p0844 A72-17330

Extremal field properties in optimal control problem applied to aircraft flight over assigned distance with minimum fuel consumption
06 p0758 A72-17727

Flight simulator for aircraft design, emphasizing compromise between performance and control requirements to avoid excess weight and drag
06 p0796 A72-18245

Multiplier method for discrete optimization problems with equality constraints, applying to time optimal control for V/STOL aircraft
06 p0794 A72-18387

Sensitivity functions for differential equations describing aircraft perturbed motion, noting dependence on time derivatives, system parameters and coordinates
07 p1032 A72-18977

Aircraft optimal control for case of continuous data flow on time variable flight conditions
07 p1032 A72-18979

Singular surfaces for time optimal control in zero sum differential games between two aircraft in three dimensional space, assuming spherical acceleration vectogram
07 p1027 A72-19279

Optimal thrust reversing in pursuit evasion games between two aircraft in horizontal plane, considering cost functions and termination criteria
07 p0912 A72-19282

Model-following control for nonlinear multivariable plants, considering implicit algorithm solution and application to variable stability aircraft control synthesis
07 p0961 A72-19708

Aircraft altitude two-loop feedback control system designed by compensation parameter variation technique, determining correlation between system sensitivity computations and observations
07 p0963 A72-20592

Book on dynamics of atmospheric flight covering unsteady motion, small disturbance theory, aerodynamic characteristics, aircraft stability and control, handling qualities, etc
08 p1109 A72-21491

Mystere business jet aircraft flight instruments, acceleration, control and stall characteristics
08 p1110 A72-21900

Soviet book on control system technology for flight vehicles covering production of mechanical, hydraulic, pneumatic, electric and electronic elements
08 p1179 A72-22024

Anthropotechnical aspects of V/STOL aircraft control, discussing instrument and control systems concepts based on development and flight tests of experimental Do-31 VTOL aircraft
09 p1270 A72-22784

DC 10 aircraft automatic flight guidance system, noting dual-dual fail-passive autoland
09 p1349 A72-23448

Individual style differences between operators of simulated aircraft control
09 p1273 A72-23579

Near optimal closed loop control laws for fixed time pursuit-evasion differential game between two aircraft in vertical plane, using dynamic modeling
10 p1421 A72-23805

State sensitivity functions in aircraft parameter identification for lateral dynamics under aileron deflection from model response and in-flight test data
10 p1421 A72-23807

Digital computers application as filters in launch vehicles and high performance aircraft attitude control systems, estimating number of computer operations
10 p1444 A72-24031

Stochastic control theory application to flight problem, discussing aircraft identification and adaptive control over wide environmental range
10 p1458 A72-25146

Extremal field properties in optimal control problem applied to aircraft flight over assigned distance with minimum fuel consumption
11 p1574 A72-25329

Flight airworthiness requirements development for supersonic transports, V/STOL and transport and general aviation aircraft, exploring critical control and stability parameters
[SAE PAPER 720306] 11 p1575 A72-25570

SECANT system of aircraft separation and control by nonsynchronous technique for midair collision avoidance
[SAE PAPER 720313] 11 p1683 A72-25577

Aft center of gravity travel effects on aircraft longitudinal control response characteristics
[SAE PAPER 720318] 11 p1575 A72-25581

Propulsion control systems design for military and commercial V/STOL aircraft, considering power management performance with minimum weight and maximum reliability and maintainability
[ASME PAPER 72-GT-79] 11 p1705 A72-25659

Flight tests of stability augmentation system for light airplane improving pilot control during IFR encounter
12 p1754 A72-27513

Flight test of direct side force control by rudder deflection and asymmetrical drag on T-33 airplane, noting use in dive bombing
12 p1754 A72-27520

Pilot-aircraft system model for relationship between weapons delivery accuracy and manual flight control system design, noting display, computation and control aids to pilot
12 p1773 A72-28121

FAA program for revision of aviation aircraft maximum allowable control forces specifications, taking into account female pilots capabilities
12 p1777 A72-28325

Low level vertical wind shear effect on aircraft control, considering runway selection with respect to surface wind conditions
13 p1993 A72-28862

Airplane attitude display motion relationship to external world as factor in pilot error due to visual frame of reference shift
14 p2083 A72-31151

Aircraft inertial navigation system, discussing mode selection unit, digital computer and control display for operator communication with system
15 p2267 A72-31596

L-1011 propulsion, fuel, flight control, navigation, avionics, communication, electrical, environmental control and auxiliary power systems, discussing structure and high lift devices
15 p2181 A72-32427

Aircraft electronic display for pilot precise control in complex tasks, discussing clarity, stability and readability of CRT images
15 p2181 A72-32632

Aircraft CRT electronic displays discussing operational flexibility versus control and monitor complexities, economics, reliability and human factors
15 p2182 A72-32636

Digital attitude and heading reference system computer for aircraft heading control, discussing design and performance features
16 p2367 A72-33244

Flight test instrumentation system for measurement of aircraft performance, stability and control characteristics during nonsteady flight
16 p2349 A72-33639

Russian book on flight dynamics covering horizontal flight, takeoff, climb and landing characteristics, meteorological conditions, helicopters, trajectory problems, stability and controllability analysis, etc
16 p2349 A72-33874

A pilot's opinion - VTOL control design requirements for the instrument approach task.
[AHS PREPRINT 644] 17 p2490 A72-34504

Russian book on aircraft design covering flight conditions, structure and control characteristics, production and stress analysis
17 p2492 A72-35448

Hybrid mechanical-electrical mechanizing techniques for aircraft flight control systems
17 p2493 A72-35576

Development of STOLAND, a versatile navigation, guidance and control system.
[AIAA PAPER 72-789] 19 p2831 A72-38106

STOL transport stability and control derivative prediction methods and accuracy requirements.
[AIAA PAPER 72-780] 19 p2752 A72-38139

Lift and control augmentation by spanwise blowing over trailing edge flaps and control surfaces.
[AIAA PAPER 72-781] 19 p2746 A72-38140

Optimal selection of stability augmentation parameters for excellent pilot acceptance.
19 p2752 A72-38227

An optimal model-following flight control system for manual control.
19 p2753 A72-38228

A generalized method for the identification of aircraft stability and control derivatives from flight test data.
19 p2753 A72-38260

Relationships among isometric forces measured in aircraft control locations.
19 p2761 A72-38706

A versatile Kalman technique for aircraft or missile state estimation and error analysis using radar tracking data.
[AIAA PAPER 72-838] 20 p2950 A72-39089

Advanced fighter controls flight simulator for all-systems compatibility testing.
[AIAA PAPER 72-837] 20 p2911 A72-39090

Synthesis and analysis of a fly-by-wire flight control system for an F-4 aircraft.
[AIAA PAPER 72-880] 20 p2887 A72-39119

Maneuver load control and relaxed static stability applied to a contemporary fighter aircraft.
[AIAA PAPER 72-870] 20 p2887 A72-39129

System analysis and synthesis for B-52 Control Configured Vehicle program, discussing flutter mode and maneuver load control and augmented stability configurations.
[AIAA PAPER 72-869] 20 p2887 A72-39130

Failsafe hydraulic actuator flight control for jet aircraft.
20 p2890 A72-39351

Test of direct lift control in the case of the experimental aircraft DFVLR-HFB 320
20 p2888 A72-39934

Flight-test experience in digital control of a remotely piloted vehicle.
[AIAA PAPER 72-883] 20 p2889 A72-40059

Instruments installation effect on soviet passenger aircraft pilot performance, discussing Tupolev aircraft control systems
21 p2994 A72-40173

Operation principles, capabilities and tests of midair collision avoidance system with aircraft separation control by nonsynchronous techniques
21 p3081 A72-40296

Concorde electrically signalled fly by wire control system with mechanical linkages for standby fail-safe redundancy
21 p2994 A72-41068

Improved qualitative flight data rating scales.
21 p2996 A72-41257

Lectures on theory of manual-vehicle control.
21 p3011 A72-41418

Results of the investigation of different extrapolation displays.
21 p3012 A72-41431

Evaluation of flight instrumentation for the identification of stability and control derivatives.
[AIAA PAPER 72-963] 22 p3136 A72-42346

An analysis of aircraft lateral-directional handling qualities using pilot models.
[AIAA PAPER 72-962] 22 p3137 A72-42347

The optimal control of merging aircraft - Implementation of the hybrid air traffic controller.
23 p3277 A72-43868

Liquid and solid precipitation on aircraft structure surfaces, discussing potential hazards to engine components and aircraft controls due to ice formation
23 p3252 A72-44339

Effects of variations in lift and drag response to longitudinal control on the ease and quality of landing.
24 p3368 A72-45333

Aircraft interception avoidance problem solved by differential game theory, discussing human operator decision making for random pursuit tracking
24 p3377 A72-45523

AIRCRAFT DESIGN

NT HELICOPTER DESIGN

Aircraft producibility considerations in preliminary design and production planning phases
[SAE PAPER 710746] 01 p0074 A72-10245

Aircraft design producibility to reduce production cost and enhance product profitability, using joint engineering and manufacturing team
[SAE PAPER 710748] 01 p0074 A72-10247

Future aircraft design trends for transcontinental and short haul operation, considering traffic forecasts, current transport aircraft and potential derivatives and technology
[SAE PAPER 710749] 01 p0002 A72-10248

TriStar commercial jet transport aircraft development, discussing design and flight tests for operating efficiency, reliability and safety
[SAE PAPER 710755] 01 p0003 A72-10252

Augmentor wing jet STOL research aircraft development progress report covering design, engine tests, performance prediction, control simulation and stability augmentation
[SAE PAPER 710757] 01 p0003 A72-10254

Propulsion system optimization for commercial transport aircraft design under Advanced Transport Technology study, considering impact on aircraft gross weight
[SAE PAPER 710760] 01 p0115 A72-10257

Propulsion system optimization in transonic transport aircraft design, considering nacelle integration, engine choice, noise attenuation and technology utilization
[SAE PAPER 710762] 01 p0115 A72-10259

Airline Propulsion Team approach to DC-10 aircraft power plant design for maximum operational effectiveness
[SAE PAPER 710778] 01 p0116 A72-10270

- Variable speed constant frequency power generation equipment influence weapon system effectiveness, considering weight and cost
01 p0008 A72-11067
- Human factors engineering of aircraft cockpit data entry keyboards on area navigation control and display units
01 p0021 A72-11318
- Alerting light and audio signals for aircraft pilots, considering implications for aircraft design
01 p0021 A72-11291
- Aircraft ride comfort problem in turbulent air, comparing free and fixed wing aircraft responses
02 p0154 A72-11720
- B-1 strategic supersonic bomber design, emphasizing variable sweep wing, landing gear, control and instrumentation
02 p0154 A72-12226
- Aircraft design interactive computer graphics technique, using human decision input response to computer output information
[DGLR PAPER 71-107] 02 p0300 A72-12733
- Unsolved aerodynamic problems in sub- and transonic civil and military aircraft design, considering flow problems during transonic flight, takeoff and landing
[DGLR PAPER 71-105] 02 p0153 A72-12745
- G-22Z aircraft design and operation, examining marketing problems
03 p0309 A72-13098
- Services and systems integration into total aircraft design, considering utilization and type effects
03 p0309 A72-13413
- Supersonic Tu 144 aircraft design, discussing engine and aerodynamic characteristics, stabilization and control, propulsion, wing structure, landing gear and operation
03 p0310 A72-13473
- Transonic air transport design, discussing wind tunnel tests, supercritical flow technology, sonic beam avoidance, cruising speed, operating costs and transport family development
03 p0310 A72-13487
- Ti effects on aircraft equipment design, considering use of Ni plated brake cylinder, wheel, engine control rams, tie bolts and rings
03 p0373 A72-13618
- VFW-614 short range twin jet passenger transport aircraft, analyzing service performance and economic efficiency requirements influence on design characteristics
03 p0310 A72-13643
- Metal-skin honeycomb composite structure design and manufacture for Concorde rudder, noting structural adhesive bonding in aircraft construction
04 p0589 A72-15090
- Canadian STOL design, development, production, airports and civil air transportation applications
05 p0751 A72-15775
- Wave drag reduction by antisymmetric wing and body arrangement, discussing application to transport aircraft at supersonic speeds
05 p0602 A72-16534
- Airbus A-300 B design and characteristics for passenger transport on short and medium haul routes
05 p0612 A72-16694
- VTOL transport aircraft use in densely populated urban areas, discussing travel time, airport requirements, noise and design problems
05 p0612 A72-16733
- Atmospheric turbulence effects on aircraft flight and design, covering accidents and costs, turbulence generation, prediction, measurements and load alleviation devices
[AIAA PAPER 72-219] 05 p0684 A72-16885
- Model following variable stability system for X-14B VTOL aircraft, discussing hardware design and flight evaluation
[AIAA PAPER 72-96] 05 p0613 A72-16978
- French civil aircraft displayed at 1971 Le Bourget Air Show, discussing design and performance characteristics of Airbus, Concorde, Caravelle, Corvette, Falcon, Frigate, STOL-A-904 and Mercure
05 p0614 A72-17193
- Flight simulator for aircraft design, emphasizing compromise between performance and control requirements to avoid excess weight and drag
06 p0796 A72-18245
- Tail first /canard/ and tandem wing configurations for natural STOL, discussing low cost aerial work aircraft
06 p0758 A72-18285
- Value engineering based cost data application to design of aircraft in production
06 p0906 A72-18435
- Procedures followed by test pilot on first flight of new aircraft design
06 p0758 A72-18488
- Crashproof rotorcraft STOL aircraft for rescue operation, discussing orthodox rigid and special rotary wings design, air tunnel experiment and flight tests
06 p0760 A72-18582
- Government role in widebody aircraft introduction to air carrier service, discussing aircraft maintenance, design and fail-safe structural configurations
07 p0911 A72-18831
- Air jet propelled flight vehicles optimal design parameters for constant altitude flight at given speed
07 p0911 A72-18991
- Aircraft performance parameters in terms of effect on lifting system service and fatigue life and on design
07 p0912 A72-19111
- VJ-101A and B V/STOL weapon system design, describing various propulsion system configurations
07 p0912 A72-19250
- V/STOL weapon system VJ-101, describing He-231 design development from tail-sitter concept to canard configuration with tilting wing-tip engines
07 p0912 A72-19251
- Aircraft design for acceptable vibration level, discussing flight vibration and runway response
07 p0928 A72-19269
- Mitsubishi T-2 two-place supersonic trainer, describing prototype airframe and propulsion system design and operational features
07 p0913 A72-20306
- French, British, Italian, U.S., German and Israeli military aircraft, presenting design and performance data
07 p0913 A72-20308
- Mercure short haul transport aircraft, emphasizing lightweight structural design with extensive use of integral machined components for fatigue safety
07 p0913 A72-20310
- Aircraft preliminary design procedure with integrated performance simulation, using time sharing computer facility
07 p0913 A72-20353
- Eight-place turboprop powered business jet aircraft design, discussing structure, fuel system, engines crew station and safety features
08 p1109 A72-21572
- Emergency Life Saving Instant Exit system in aircraft fuselage for use after crash landing, discussing design and ground testing
08 p1109 A72-21583
- Wing structural weight estimation for civil aircraft preliminary deriving generalized formula based on wing root bending moment for specified flight condition
09 p1262 A72-22909
- Fixed wing agricultural aircraft, comparing different designs in terms of performance, safety, handling and economic efficiency
09 p1262 A72-22940
- Airfoil ram-wing air-water hybrid vehicle X-113 Am design and operational principles based on aerodynamic ground effect, discussing flight tested performance characteristics
09 p1262 A72-22971
- DC-10 aircraft structural design, flight handling characteristics and fatigue tests
09 p1262 A72-23446
- Deterministic optimization of aircraft undercarriage suspension characteristics for taxiing induced vibration minimization, discussing damping and stiffness functions and hybrid computer solution
09 p1407 A72-23458
- Simply supported skew plates stability under combined loading, noting wing and tail design applications for high speed aircraft and missiles
10 p1555 A72-24196
- STOL and V/STOL transport aircraft design requirements consideration based on common propulsion and lift engine types use, noting fan lift solution superiority
10 p1421 A72-24865
- RCA SECANT aircraft collision avoidance system avionics design using nonsynchronous techniques
10 p1509 A72-24866
- Legal aspects of international cooperation on aircraft design and production, discussing work distribution, project management and liabilities sharing
10 p1565 A72-24881
- Mitsubishi XT-2 jet trainer aircraft, presenting design, structural and performance data
10 p1421 A72-25107
- STOL aircraft systems development coordination, considering vehicle design, airport facilities and related ground environment, transportation modes interface and airspace management
11 p1574 A72-25255
- Transport aircraft fuselage computerized design, determining optimal structural distribution for strength and displacement constraints
[AIAA PAPER 72-330] 11 p1727 A72-25366
- Automated optimization for preliminary design of supersonic aircraft wings, noting flutter, stresses and resonant frequency as dynamic constraints
[AIAA PAPER 72-333] 11 p1727 A72-25368
- Convective cooling system design for Mach 6 hyper-sonic transport Al alloy airframe, using water glycol loop network
[AIAA PAPER 72-334] 11 p1574 A72-25369
- Energy absorbing seat design for light aircraft, describing development and static and dynamic testing
[SAE PAPER 720322] 11 p1583 A72-25585
- Test facility design for aircraft crashworthiness evaluation and improvement, considering survivable accident surrounding conditions, equipment and testing methods
[SAE PAPER 720323] 11 p1576 A72-25586
- Transport aircraft aerodynamic design technology application to general aviation propeller driven twin engine aircraft, discussing wing loading and aspect ratio optimization
[SAE PAPER 720337] 11 p1576 A72-25595
- Propulsion system/airframe matching in hybrid V/STOL airplanes, stressing thrust vector management, lift engine bypass ratio and power plant packaging design
[ASME PAPER 72-GT-106] 11 p1576 A72-25671
- Super Guppy four engine aircraft characteristics, performance and loading device for bulky cargo air transportation
11 p1577 A72-25812
- LOX supply systems installation for civil transport aircraft crew and/or passenger breathing oxygen
[SAE AIR 1223] 11 p1584 A72-26030
- Structural design and optical problems of external vision and cockpit transparencies in military aircraft
12 p1753 A72-27002
- German VAK 191B V/STOL fighter aircraft design, development and flight tests, noting redundant control systems
12 p1753 A72-27166
- NDT application to aircraft design and reliability, discussing fatigue life analysis and in-service monitoring for structural elements, components and airframes
12 p1813 A72-27198
- Tu-154 aerodynamic design, discussing arrow wing and propulsion unit characteristics
12 p1753 A72-27268
- L-1011 flight test program, discussing aircraft design, flight station, controls, flying qualities, etc
12 p1754 A72-27519
- General Dynamics model 401 air superiority single engine fighter design stressing light weight structure and maneuverability at high speeds and angles of attack
13 p1896 A72-28575
- Computer calculation of second order curve segment discriminant in geometrical problem associated with aircraft lofting, assessing method accuracy
13 p1986 A72-28739
- Large amplitude flight simulator for fighter design refinement, noting extensive computer commitment
13 p1938 A72-28757
- Meteorological information requirements for V/STOL aircraft design, airport location, runway orientation, aircraft operations and ATC simulation
13 p1994 A72-28869
- Aircraft landing gear stress spectrum and design data during ground loading on airport runways, using linearized theory for model investigation
14 p2071 A72-30283
- Measuring technique importance for aircraft R and D, emphasizing quartz tensometer, digital control and signal processing
14 p2092 A72-30286
- Book of aircraft design illustrations covering three view and perspective form low drag airfoil, aspect ratio, plain split, slotted and multiple flaps
14 p2167 A72-30776
- Airbus design features, noting passenger number, operational range and propulsion engine number and location
14 p2072 A72-30813
- Suboptimal feedback control for aircraft gust alleviation design, using indirect perturbation information through normal acceleration factor measurement
15 p2181 A72-32025
- Book on airfoil section designs for light aircraft covering wind tunnel studies of lift drag ratio as function of angle of attack
15 p2179 A72-32250
- Aircraft design for operational reliability and maintainability, emphasizing working relations coordination between manufacturer and operator
15 p2181 A72-32459
- Concorde on-time operation as total management problem from design to airline operations, discussing techniques for in-flight failure diagnosis and onward reporting
15 p2181 A72-32460
- Fokker VTOL transport aircraft designs, considering payload, range, runway conditions, noise, military capabilities and operational costs
16 p2347 A72-33048
- V/STOL weapon system VJ-101 design, discussing one axis rocking device, suspension structure and hovering flight thrust control
16 p2347 A72-33049
- STOL aircraft for civil transport applications, considering optimum design concepts, noise reduction and terminal facility requirements
16 p2348 A72-33331
- B-1 aircraft design features, discussing aerodynamic configurational aspects, structural components and materials, engine inlets, fuel, hydraulic control and avionics systems
17 p2487 A72-34223
- V/STOL flight control - Trend and requirements
17 p2487 A72-34240
- The flight mechanics of STOL aircraft
17 p2488 A72-34241

Northrop A-9A attack aircraft production planning, discussing design features and management/engineering organizational changes in anticipation of USAF production contract

17 p2488 A72-34391

A-10 prototype designed for production.

17 p2488 A72-34392

The integration of composite structures into aircraft design.

17 p2492 A72-35281

Aerodynamic analysis of various flight conditions of conventional aircraft. III - Mechanical fundamentals /Dynamics of a point mass/

17 p2492 A72-35440

Russian book on aircraft design covering flight conditions, structure and control characteristics, production and stress analysis

17 p2492 A72-35448

Remote power control for aircraft generating and distribution systems.

18 p2648 A72-37034

V/STOL developments in Hawker Siddeley Aviation Limited.

18 p2643 A72-37096

V/STOL - Selection and problems of the new medium

18 p2643 A72-37215

Flow and circulation diagrams formed by events involved in optimum aircraft design configuration and structural weight selection, outlining calculation methods

19 p2748 A72-37452

Fast method for aircraft rebalance.

19 p2748 A72-37453

Active controls - Changing the rules of structural design.

19 p2748 A72-37681

Development of the Saab-Scania Viggen.

19 p2748 A72-37749

VJ-101 V/STOL aircraft design, development and flight testing, discussing takeoff and landing, hovering and transition flight and associated control problems

19 p2749 A72-38032

A computerized system for the preliminary design of commercial airplanes.

[AIAA PAPER 72-793]

19 p2749 A72-38110

A flutter optimization program for aircraft structural design.

[AIAA PAPER 72-795]

19 p2876 A72-38111

An integrated computer system for preliminary design of advanced aircraft.

[AIAA PAPER 72-796]

19 p2749 A72-38112

Design studies and model tests of the stowed tilt-rotor concept.

[AIAA PAPER 72-804]

19 p2750 A72-38113

Investigation of the commonality in development of military and commercial STOL transports.

[AIAA PAPER 72-808]

19 p2750 A72-38114

The DHC-7, first generation transport category STOL - Particular design challenges.

[AIAA PAPER 72-809]

19 p2750 A72-38115

Computer program for automated design of long haul transport aircraft, discussing cost effectiveness of composite materials for aircraft structure

[AIAA PAPER 72-794]

19 p2750 A72-38121

Aerodynamic design and development of the Lockheed S-3A Viking.

[AIAA PAPER 72-746]

19 p2751 A72-38122

B-52 test vehicle flight demonstration program for control configured vehicles /CCV/ technology concepts validation, noting gross weight reduction

[AIAA PAPER 72-747]

19 p2751 A72-38123

Design for air combat.

[AIAA PAPER 72-749]

19 p2751 A72-38124

Advanced technology transport /ATT/ aircraft configurations design parameters analysis, considering cruise speed, passenger capacities, ranges, noise level and economics

[AIAA PAPER 72-757]

19 p2751 A72-38127

Economic impact of applying advanced technologies to transport airplanes.

[AIAA PAPER 72-758]

19 p2751 A72-38128

Use of the flight simulator in the design of a STOL research aircraft.

[AIAA PAPER 72-762]

19 p2751 A72-38129

Designing aircraft structure for resistance and tolerance to battle damage.

[AIAA PAPER 72-773]

19 p2752 A72-38133

Application of advanced methods to the determination of design loads of the Lockheed L-1011 TriStar.

[AIAA PAPER 72-775]

19 p2752 A72-38134

Structural development of the L-1011 TriStar.

[AIAA PAPER 72-776]

19 p2876 A72-38135

System analysis and synthesis for B-52 Control Configured Vehicle program, discussing flutter mode and maneuver load control and augmented stability configurations

[AIAA PAPER 72-869]

20 p2887 A72-39130

Use of fixed and moving base flight simulators for the aerodynamic design and development of the S-3A airplane.

[AIAA PAPER 72-764]

20 p2888 A72-40052

Tilt-propotor VTOL aircraft design evaluation based on aerodynamic and aeroelastic model and full scale performance tests

[AIAA PAPER 72-803]

20 p2889 A72-40054

STOL performance criteria for military transport aircraft.

[AIAA PAPER 72-806]

20 p2889 A72-40055

High subsonic transport aircraft design development based on supercritical aerodynamic configuration and advanced structural, flight control and propulsion system technologies

[AIAA PAPER 72-756]

20 p2889 A72-40056

Airlines requirements for European airbus, discussing design of aircraft structure, control, pressurized cabin and propulsion system

21 p2994 A72-40174

Landing 'in the backyard' with quiet aircraft

21 p2994 A72-40376

Dutch monograph - Analysis of dynamic aircraft landing loads, and a proposal for rational design landing load requirements.

21 p2994 A72-40925

Noise radiation from V/STOL aircraft.

[ICAS PAPER 72-22]

21 p2995 A72-41147

Modern landing impact load calculations and old-fashioned requirements.

[ICAS PAPER 72-31]

21 p2995 A72-41156

VTOL aircraft noise reduction through design methods and flight path management in terminal area, evaluating acoustical annoyance to surrounding community

[ICAS PAPER 72-34]

21 p2995 A72-41159

Rigid form airship for transportation, discussing applications for special loads and scientific and service purposes, and design and construction problems

21 p2996 A72-41200

Human engineering requirements in aircraft system development.

21 p3011 A72-41423

Development of design criteria for predicting departure characteristics and spin susceptibility of fighter-type aircraft.

[AIAA PAPER 72-984]

22 p3136 A72-42330

The application of non-planar lifting surface theory to the calculation of external-store loads.

[AIAA PAPER 72-971]

22 p3135 A72-42340

Aircraft emergency evacuation systems, discussing door designs, inflatable escape slide and slide/lifeboat combination

22 p3138 A72-42520

Boeing aircraft altitude alerting systems development and design to meet FAR 91-51 requirements, discussing retrofit programs and altimeter encoding

22 p3179 A72-42689

Wing flutter prevention in SST structural design, using finite element model and lifting surface aerodynamic theory

22 p3237 A72-42760

A survey of rotary-wing aircraft crashworthiness.

22 p3138 A72-42763

An assessment of energy absorbing devices for prospective use in aircraft impact situations.

22 p3237 A72-42764

Dynamic aspects of Fokker F-28 aircraft design.

22 p3138 A72-42831

Aircraft synthesis analysis program /ASAP/ for computerized aircraft design, enabling large number of trade-off studies for design optimization

[SAWE PAPER 907]

23 p3250 A72-43454

An aerodynamics model applicable to the synthesis of conventional fixed-wing aircraft.

[SAWE PAPER 908]

23 p3250 A72-43455

Mission analysis and performance program as part of computerized aircraft configuration synthesis process, describing interfaces with other system modules

[SAWE PAPER 909]

23 p3250 A72-43456

Engine selection for specific aircraft design and mission, considering bypass and pressure ratios and turbine temperature effects on performance and weight

[SAWE PAPER 910]

23 p3250 A72-43457

The weight module - A keystone in the aircraft synthesis program.

[SAWE PAPER 912]

23 p3250 A72-43459

L-1011 computerized weight reporting system present and future capabilities.

[SAWE PAPER 932]

23 p3251 A72-43472

Aircraft design structural weight estimation based on post-design analysis of production aircraft, discussing weight factors application to new designs

[SAWE PAPER 936]

23 p3251 A72-43476

Analysis of the fundamental parameters and flight properties of aerobatic aircraft in a statistical framework

23 p3252 A72-44336

Harrier two seat aircraft design, performance, weapon systems, thrust vectoring and combat characteristics comparison with GR.1

23 p3252 A72-44391

Design and certification for executive type aircraft.

24 p3366 A72-44730

Fatigue design and test program for the American SST.

24 p3367 A72-44741

Observations on designing to combat fatigue and its effects on the economics of civil transport aircraft.

24 p3368 A72-44745

Aircraft/spacecraft design approach and performance data, considering space shuttle program

24 p3467 A72-45159

Lateral flight path control during aircraft landing in gusty cross-winds by lateral thrust deflection, discussing design optimization

24 p3368 A72-45330

Iterative methods for the aerodynamic calculation of thin wings in a subsonic flow

24 p3363 A72-45378

Control configured fighter and bomber aircraft based on flight control technology, discussing development programs

24 p3369 A72-45380

Military aircraft construction, design and economic requirements, discussing fighter payloads, armament efficiency and fire control systems

24 p3369 A72-45450

AIRCRAFT DETECTION

Air surveillance using satellite range-difference measurement from noninterrogated aircraft beacons for ATC

04 p0545 A72-14826

Automatic recognition of aircraft by Fourier harmonics of slope densities of silhouettes

07 p0949 A72-19053

The visibility range when observing an aircraft with and without field-glasses.

21 p3007 A72-40750

AIRCRAFT ENGINES

NT HELICOPTER ENGINES

Advanced technology air transports propulsion system requirements, considering design, engine performance and reliability, maintenance, airline problems, noise and pollution control

[SAE PAPER 710761]

01 p0115 A72-10258

Concorde engine performance, reviewing control, reheat and exhaust systems

[SAE PAPER 710775]

CF6 high bypass ratio turbofan engine design improvements for fuel consumption, thrust/weight ratio, starting, noise level, smoke emission, maintenance, monitoring and accessory replacement

[SAE PAPER 710779]

01 p0117 A72-10271

Aircraft hybrid electrical power systems, describing variable frequency generation and high voltage dc distribution

01 p0009 A72-11068

Thermal shock fatigue tests on aircraft gas turbine engine inlet nozzles, showing cracks as function of material

01 p0143 A72-11373

Thermal radial stresses in axial compressor disk-drum transition areas of operating AM-3 aircraft engine

01 p0143 A72-11374

Aircraft gas turbine rotating disks thermal and mechanical stresses under variable thermal conditions, describing test assembly

02 p0199 A72-11637

PT6 and JT15D gas turbine aircraft engines development and service experience

02 p0271 A72-11699

Q/STOL jet aircraft engines design for low noise levels, describing takeoff thrust, bypass ratio and turbine stages

02 p0271 A72-12501

Superalloys ductility and workability improvements without sacrificing elevated temperature strength for aircraft engine applications

02 p0246 A72-12566

Aircraft power plant management, discussing integration of intake, engine and exhaust system from control standpoint

03 p0405 A72-13418

Prop-fan engine for quiet STOL propulsion, discussing noise characteristics, weight advantage, response and reduced fuel consumption

03 p0406 A72-13697

Aircraft air breathing propulsion technology, discussing two-place aircraft, turbofan power plants, helicopter engines and V/STOL, CTOL, subsonic transports and supersonic aircraft

04 p0565 A72-14825

Soviet book on thermal and gas dynamic design of gas turbines in aircraft and liquid propellant rocket engines, covering three dimensional flows, temperature distribution, component cooling, etc

04 p0565 A72-15246

Aircraft gas turbine engine emission reduction, showing nitrogen oxide control with water injection

[ASME PAPER 71-WA/GT-9]

05 p0704 A72-15902

Aircraft engine exhaust geometry effects on smoke plume visibility, describing carbon particles light absorption characteristics by Beer-Lambert law

[ASME PAPER 71-WA/GT-10]

05 p0704 A72-15903

Jet engine test facilities for JT9D experimental and production models

[ASME PAPER 71-WA/GT-12]

05 p0642 A72-15904

Diffusion and fallout of polluting particulates emitted by aircraft engines, discussing effect of wing-

05 p0642 A72-15904

Diffusion and fallout of polluting particulates emitted by aircraft engines, discussing effect of wing-

05 p0642 A72-15904

Diffusion and fallout of polluting particulates emitted by aircraft engines, discussing effect of wing-

05 p0642 A72-15904

Diffusion and fallout of polluting particulates emitted by aircraft engines, discussing effect of wing-

05 p0642 A72-15904

Diffusion and fallout of polluting particulates emitted by aircraft engines, discussing effect of wing-

05 p0642 A72-15904

Diffusion and fallout of polluting particulates emitted by aircraft engines, discussing effect of wing-

05 p0642 A72-15904

Diffusion and fallout of polluting particulates emitted by aircraft engines, discussing effect of wing-

05 p0642 A72-15904

- tip vortices, plume visibility and monitoring, simulation and modeling
[ASME PAPER 71-WA/AV-2] 05 p0704 A72-15950
- Dusty inlet air filtering in aircraft turbine engines, discussing engine operation, dust and filter characteristics
05 p0704 A72-16179
- Aircraft gas turbine engine and components post-war development in Japan
05 p0705 A72-16499
- Aircraft and reusable spacecraft propulsion systems current status and future development, discussing noise and exhaust emission problems, V/STOL bypass and fan engines, ramjets, etc
05 p0705 A72-16735
- Aircraft engine anti-icing tests and evaluation describing ground and airborne techniques
[AIAA PAPER 72-162] 05 p0706 A72-16828
- Aircraft engines high pressure turbine guide vanes air cooling by internal insert, analyzing thermal stresses
[AIAA PAPER 72-7] 05 p0707 A72-16864
- Optimal reversion coefficient determination for passenger aircraft engine thrust reversal
05 p0614 A72-17060
- S-3A Viking land based antisubmarine warfare maritime and reconnaissance aircraft, describing flight controls, structural design, underslung poded engines and operational equipment
06 p0758 A72-17583
- Aircraft power plants sealing materials, emphasizing porous cermet seals heat resistance under thermal cyclic loads
06 p0797 A72-18658
- Aircraft gas turbine engine monitoring for failure prevention, evaluating condition through spectrum analysis and real time correlation techniques
07 p1053 A72-18766
- C-54 A/B aircraft engine air particle separator anti-seismic system design features, manufacturing techniques and testing
07 p1053 A72-18769
- Aircraft gas turbine engines smoke emission sampling by stained filter technique, comparing Navy specifications AS 1833 with SAE method ARP 1179
07 p1053 A72-18770
- Army aircraft gas turbine engines pollution potential evaluation program, considering smoke emission, noise and invisible pollutants
07 p1053 A72-18772
- National Environmental Policy Act /PL 91-190/ impact on Army aircraft turbine engine development in terms of performance, additional cost and time
07 p1053 A72-18773
- Manufacturer viewpoint on aircraft engine safe introduction into airline service, discussing JT9D engine design for 747 aircraft
07 p1053 A72-18830
- Aircraft engine test data processing by polynomial relations, assuming normal measurement error distribution
07 p0994 A72-18978
- Hot corrosion resistant Pt-Al coating for high temperature aircraft engine Ni alloy components, presenting cyclic sulfidation and thermal shock test results
07 p1012 A72-19573
- Aircraft electric power generation history, noting aircraft performance effect on electrical system design
07 p0914 A72-20201
- Commercially available aircraft turbofan engines specifications, describing design features and performance characteristics
07 p1055 A72-20625
- Onboard and ground based hydraulic starter systems design, construction and operation for aircraft turbine engines
08 p1224 A72-21484
- Variable pitch fans for STOL aircraft thrust/shaft engine, noting short field capability and quietness
09 p1374 A72-23447
- Accelerated full scale aircraft turbine engine corrosion tests in controlled environment, simulating salt, high temperature and humidity conditions
[NACE PAPER 76] 10 p1528 A72-24320
- NASA aerodynamic technology program, emphasizing airframe and engine development for next generation subsonic CTOL jet transport requirements
[SAE PAPER 720319] 11 p1575 A72-25582
- Two spool geared fan jet engine design and development for general aviation, discussing performance, reliability and ecological aspects
[SAE PAPER 720351] 11 p1703 A72-25602
- Air lubricated bearings for high performance aircraft gas turbines, studying design and performance in turboshaft engine
[ASME PAPER 72-GT-38] 11 p1638 A72-25632
- Variable pitch ultrahigh bypass ratio ducted fan engine design for STOL transport aircraft
[ASME PAPER 72-GT-61] 11 p1704 A72-25652
- Integral and remote powered lift fan engines design for large civilian VTOL transports
[ASME PAPER 72-GT-65] 11 p1704 A72-25654
- Aircraft gas turbine engines exhaust emission characteristics identification, considering ambient temperature and humidity effects
[ASME PAPER 72-GT-75] 11 p1705 A72-25657
- NASA quiet engine program, discussing noise reduction technology for subsonic civil transport aircraft propulsion system
[ASME PAPER 72-GT-96] 11 p1705 A72-25667
- Russian book on aircraft engine reliability covering defects, fractures and failure analysis, service life prediction, production deficiencies and operational conditions
11 p1706 A72-26068
- Countersink boring machines with programmed digital control systems for precision spacing multiple hole drilling in extended aircraft engine components
11 p1642 A72-26816
- Cooling efficiency and load endurance of aircraft turbine engine blades as function of ambient temperature and air flow rates
11 p1712 A72-26892
- Exhaust composition and smoke emission reduction from aircraft with gas turbine power plants
12 p1860 A72-27270
- Turbomeca Astafan geared fan engine with axial centrifugal compressor design, specifications and performance
12 p1861 A72-27748
- Air bleeding location to cool turbojet engine turbine of supersonic aircraft, presenting graphs
12 p1862 A72-28147
- Long range transport aircraft structures and composite materials technology for airframe and engine systems
[AIAA PAPER 72-362] 13 p1897 A72-28955
- Aircraft gas turbine engines synthetic lubricants thermal stability characteristics, describing coke deposition test apparatus and results
[ASLE PREPRINT 72AM 14] 13 p1983 A72-28971
- Time constant of aircraft gas turbine engines gas temperature regulating system, using two thermocouples with different rise times
13 p2028 A72-29138
- Aircraft engine components fatigue life assessment under small cycle temperature conditions, including temperature field and stress-strain determination in critical spot
14 p2145 A72-30279
- Optimum low noise engine selection for transport and combat aircraft relative to range or payload performance, considering CTOL, VTOL, SST and fighter aircraft
15 p2297 A72-32127
- Integrated data acquisition and processing system for inlet-aircraft engine matching, considering all-digital, analog and hybrid approach
15 p2298 A72-32319
- RB 211 three-shaft turbofan engine for L-1011 airliner, describing design for noise reduction
15 p2298 A72-32428
- Concorde engines design for maintainability and reliability to reduce turnaround time, discussing diagnostic facilities and on-wing maintenance features
15 p2298 A72-32457
- Aero engines and propulsion systems development contribution to air transport economics and regularity, considering environmental factors
16 p2443 A72-33313
- Commercial transport aircraft engine technology contribution to world air transportation, considering social and ecological compatibility with community
16 p2348 A72-33314
- Russian book on aircraft turbine and spacecraft rocket engine assembly covering process schedules, work organization, precision, joints and couplings, quality control, etc
16 p2399 A72-33373
- Russian book - Production of the principal elements and units of aircraft engines
17 p2560 A72-35456
- Internal engine generator application to commercial transport aircraft.
17 p2498 A72-35566
- Aircraft gas turbine engine fuel pump design, discussing sizing for given mass flow and pressure requirements with procedure for temperature rise calculations
18 p2694 A72-36049
- Performance of low pressure ratio ejectors for engine nacelle cooling.
[SAE AIR 1191] 18 p2721 A72-36530
- Procedure for the continuous sampling and measurement of gaseous emissions from aircraft turbine engines.
[SAE ARP 1256] 18 p2721 A72-36532
- NASA program for low cost turbojet and turbofan engine fabrication for missile and light aircraft propulsion
19 p2848 A72-37637
- Influence of the structural format on the range of critical rotational speeds of rotors in aircraft engines
20 p2963 A72-39801
- Aircraft engine lifetime and turbine blade reliability
20 p2963 A72-39916
- Russian book - The ASH-62IR engine /4th enlarged edition/.
21 p3098 A72-40463
- NASA's quiet engine programs.
22 p3217 A72-43152
- Engine selection for specific aircraft design and mission, considering bypass and pressure ratios and turbine temperature effects on performance and weight
[SAWE PAPER 910] 23 p3250 A72-43457
- IL-62 aircraft propulsion system design and installation details, operational surveillance system and maintenance operations
23 p3325 A72-43639
- Basic dimensionless geometrical relations for the combustion chambers of aircraft gas turbine engines
23 p3325 A72-43674
- Aircraft jet-engine control; Conference, Velestin, Czechoslovakia, June 12-16, 1972, Proceedings
23 p3326 A72-44276
- Aircraft gas turbine engine controllers and fuel pump testing under extreme fuel temperatures, noting cavitation characteristics
23 p3327 A72-44287
- Mathematical model for dynamics simulation of aircraft turboprop engines, using digital, analog and hybrid computers
23 p3327 A72-44288
- Aircraft gas turbine engines environmental effects, considering thermal radiation, acoustic emissions and exhaust gases in relation to propulsion system design parameters
23 p3328 A72-44296
- Test facilities for aeropropulsion systems, emphasizing utilization, cost and technical advantages, aircraft inlet-engine systems compatibility and test types
[AIAA PAPER 72-1034] 24 p3388 A72-45401
- AIRCRAFT EQUIPMENT**
- NT AIRCRAFT HYDRAULIC SYSTEMS
- NT AIRCRAFT LIGHTS
- NT AIRCRAFT TIRES
- NT BOMBING EQUIPMENT
- NT EJECTION SEATS
- Soviet book on civil aircraft high altitude equipment covering air conditioning systems, oxygen equipment and cabin pressurization
02 p0156 A72-12295
- Soviet book on electrical equipment and instrumentation of An-24 aircraft covering power sources, control, safety systems, engine, flight and navigation instruments and autopilot
05 p0615 A72-16400
- Soviet book on aircraft radio equipment covering transmission and reception, velocity and coordinates measurements, siting and navigation, flying target interception, reconnaissance, landing systems, etc
05 p0637 A72-16530
- Zener diode transient suppressors with electronic thermal switch for ground vehicle and aircraft applications
[AD-741529] 05 p0637 A72-16553
- DC 9 aircraft integrated data system simulator to facilitate interacting systems checking, input circuit integrity, performance degradation and calibration
06 p0796 A72-18284
- Concorde aircraft systems reliability and safety flight and simulator testing, discussing operational and environmental conditions and maintenance procedures
07 p0965 A72-20309
- Survival and flight equipment - Conference, Las Vegas, September 1971
08 p1109 A72-21560
- Altitude information warning devices and systems, discussing requirements and performance and qualification tests
[SAE ARP 1061] 11 p1632 A72-26032
- Onboard localization of aircraft electrical equipment failures, using list checkout, automatic indication and dynamic programming method
11 p1578 A72-26895
- Communication aspects of aeronautical satellite system, considering aircraft equipment, ground stations, ATC, type of access and frequency assignment
12 p1783 A72-27658
- Reliability requirements and optimization for complex systems, discussing method to improve component reliability of aircraft weapon system
13 p1961 A72-28353
- Aircraft electrical power systems design dependence on latitude, minimum weight requirement, reliability degree, environmental conditions and acceleration
13 p1899 A72-28693
- Cavitation failure of aircraft hydraulic plunger pump elements from microscopic and metallographic analysis
13 p1899 A72-28732
- Airborne OMEGA navigation system performance, discussing transmission facilities, three frequency receiver, flight tests and optimization of receiving antenna
13 p1998 A72-29191

High light transmission electrically conducting Hyviz and gold film laminates for aircraft windshields and window heating applications 13 p1898 A72-30038

Reduced voltage relay operation in aircraft high voltage ac power systems, describing RLC circuit theory, laboratory test arrangement and performance measurements 15 p2204 A72-31215

Collision avoidance techniques for midair collisions reduction, discussing airborne and ground based systems 15 p2272 A72-32213

Electromagnetic waves penetration through conducting gasket used to protect sensitive devices in aircraft, investigating field strength variation with distance from gasket 15 p2202 A72-32571

Sizing new generation aircraft wire and circuit breakers utilizing computer techniques 17 p2498 A72-35568

USSR electric impulse de-icing system design 18 p2648 A72-37033

Electronic primary flight control system requirements and equipment characteristics, discussing USAF and NASA fly by wire R and D programs [AIAA PAPER 72-882] 20 p2887 A72-39118

AIRCRAFT EXHAUST U EXHAUST GASES AIRCRAFT FUEL SYSTEMS

Lightweight low pressure plastic hose assemblies in aircraft and missile petroleum base fuel and synthetic lubricating oil systems at 395-710 R and up to 200 psi [SAE ARP 1180] 01 p0006 A72-10388

Aircraft fuel system gunfire vulnerability and fire and explosion protection techniques 08 p1112 A72-21579

Hydraulic starter systems for aircraft turbine engines, examining operation loads and fluid supply and pressure requirements 11 p1702 A72-25284

Utilization of wing and empennage volume for aircraft fuel tankage, presenting equations and charts for quick determination of available volume 11 p1576 A72-25811

Deterioration of shaft bearings of electromotor driving aircraft centrifugal fuel pump, determining lateral force acting on impeller 23 p3252 A72-43663

Reliability analysis of a jet engine fuel system with the aid of an analog computer using operational data 23 p3326 A72-44282

AIRCRAFT FUELS

Proposed gas turbine procurement standards for gaseous and liquid fuel specifications emphasizing fuel contaminants [ASME PAPER 71-WA/GT-3] 05 p0703 A72-15896

Fuels and lubricants development trends for subsonic and supersonic aircraft, discussing thermostable hydrocarbons, ramjet fuels, esters, oxidation inhibitors, metal deactivators, high pressure lubricant additives, etc 05 p0681 A72-16739

Purity requirements of aircraft gas turbine fuels, considering mechanical impurities, water, microorganisms, and surface active, corrosive, resinlike and paraffin substances 07 p1052 A72-20373

Fuel lubricity effects on aircraft engine fuel pump wear, discussing remedial use of corrosion inhibitors and change to noncorroding pump construction materials 08 p1222 A72-21450

Safe aircraft fuels crashworthiness evaluation in terms of ignition susceptibility parameter, noting full scale crash environment simulation [ASME PAPER 72-GT-27] 11 p1702 A72-25623

Crash safe turbine fuel to reduce fire probability and severity during aircraft ground crash, investigating physical and chemical properties [ASME PAPER 72-GT-28] 11 p1702 A72-25624

Physicochemical processes in metal surface layers subjected to contact friction with aircraft fuels presence, noting secondary compounds and thermal oxidation acceleration 12 p1817 A72-28183

Future projections of commercial jet aircraft fuel demands, estimating engine exhaust effects on air quality 13 p1897 A72-28879

Aviation fuels and additives effect on steel endurance limit at room temperature 13 p1980 A72-29487

Evaluation of film forming foams for the suppression of fuel fires in aircraft hangars. [WSCI PAPER 72-16] 20 p2982 A72-38974

Fuels, lubricating oils and hydraulic fluids for supersonic aircraft, discussing chemical properties, propellant combustion efficiency and production 20 p2945 A72-39930

AIRCRAFT GUIDANCE

Carrier system for controlled approach of Naval aircraft to provide pilot window to deck for tactical jet guidance for poor visibility landing 02 p0256 A72-12323

Terminal area air traffic guidance and control, discussing automation, all-weather precision approach and landing and failure detection 04 p0544 A72-14817

Aircraft landing microwave guidance and control systems, considering general dynamic model for aircraft translational motion determination in earth fixed coordinate system 04 p0545 A72-14821

Navy hovering vehicle versatile automatic control system for V/STOL flight test program, using airborne digital computer for navigation/guidance computations 05 p0687 A72-16661

Automated ATC guidance technique for aircraft curved flight trajectories, describing flight profiles synthesizing algorithms and computerized simulation technique [AIAA PAPER 72-121] 06 p0845 A72-17922

Ground based Doppler navigation system for wide range elevation and azimuth aircraft approach guidance, using linear directive antenna array for conical surface definition 06 p0845 A72-18183

Aircraft optimal terminal guidance nonlinear feedback control law, deriving maximum principle by digital computer program 07 p1033 A72-19287

Automatic laser tracking and ranging system for cooperative retroreflective aircraft targets, discussing design, performance, eyesafe distance and atmospheric attenuation [CLEA PAPER 9,3] 07 p0942 A72-19385

Control synthesis equations for aircraft motion on phase space surface 09 p1261 A72-22208

Civil aviation approach and landing guidance systems evolution, discussing ILS development, state of art and future requirements 13 p1996 A72-29014

Aeronautical navigation/guidance standardization in conjunction with OMEGA, covering sensor and computer equipment life cycles 13 p1999 A72-29199

Airport lighting for pilot guidance during approach and landing under category I-III visibility conditions, discussing runway layouts and power requirements 14 p2092 A72-30621

Fighter bomber Loran-inertial data processing with digital computer to combine navigation, guidance and weapon delivery into fully integrated system 16 p2420 A72-33246

Investigation of data rate requirements for low visibility approach with a scanning beam landing guidance system 17 p2578 A72-35562

Book - Minimum operational characteristics for vertical guidance equipment used in airborne volumetric navigation systems [DO-152] 17 p2578 A72-35800

Airline crew familiarization with DC-10 Computerized Flight Guidance System to calculate steering signal from raw data to follow flight path 19 p2831 A72-37899

Development of STOLAND, a versatile navigation, guidance and control system. [AIAA PAPER 72-789] 19 p2831 A72-38106

4-D guidance system design with application to STOL air traffic control. 19 p2832 A72-38252

Investigation of data rate requirements for low visibility approach with a scanning beam landing guidance system. 19 p2832 A72-38259

A landing approach guidance scheme for aircraft which are capable of executing steep approaches. 19 p2832 A72-38278

Tactical aircraft weapon system development, describing navigation, target acquisition, release point guidance and delivery modes [AIAA PAPER 72-896] 20 p2951 A72-39107

Microwave landing system effect on the flight guidance and control system. [AIAA PAPER 72-755] 20 p2952 A72-40057

Design and flight experience with a digital fly-by-wire control system using Apollo guidance system hardware on an F-8 aircraft. [AIAA PAPER 72-881] 20 p2889 A72-40060

Characteristics and prospects for a new landing guidance system. 21 p3080 A72-40293

Development and evaluation of an energy-oriented guidance logic for air combat models. [AIAA PAPER 72-949] 22 p3137 A72-42354

CW radar system for tactical aircraft real time command, control and positioning, using combination of frequency and time multiplexing for range measurement 22 p3203 A72-42946

AIRCRAFT HAZARDS

Boeing 707 rapid decompression at 25,000 feet, noting rivet hole fatigue damage 02 p0167 A72-11715

Statistical characteristics of range-guard intrusions and airspace collision conflicts in terminal area 05 p0611 A72-16110

Aircraft hydrocarbon fuel tank lightning protection in airframes, using adhesive bonding, high strength materials and high modulus fiber structures 07 p1086 A72-1876

Multiple swept stroke flash technique to test lightning effects on aircraft 07 p0964 A72-1876

Lightning simulation laboratory for aircraft strike testing, using high energy generators 07 p0964 A72-1877

Probability estimates for aircraft encounters with heavy rain 07 p1031 A72-2036

Aircraft hazard detection and warning system selection criteria 08 p1109 A72-2156

Hypoxia incidents in Strategic Air Command due to cabin pressurization malfunction 08 p1126 A72-2156

Probability estimates of aircraft encounters with hail, discussing variations with locality, hailstone size and height and supersonic transport experience 09 p1346 A72-2342

Turbulent jets effectiveness in protection of aircraft surfaces from rain, describing wind tunnel simulation of takeoff and landing 10 p1463 A72-2513

Hail damage to aircraft, predicting metal surface dent depth and deformation shape with computer program [AIAA PAPER 72-335] 11 p1574 A72-2537

Jet engine fuel fire hazard evaluation by controlled laboratory tests, analyzing ignition characteristics under simulated survivable aircraft crash accidents [SAE PAPER 720324] 11 p1702 A72-2558

Jet engine fuel modification to decrease fire hazard in survivable aircraft crashes [ASME PAPER 72-GT-25] 11 p1702 A72-2562

Aircraft windshield bird impact resistance, noting weight, speed, angle and window geometry effects 12 p1813 A72-2701

Legal aspects in prevention of aircraft unlawful seizure in view of international cooperation, noting German Democratic Republic agreements 12 p1890 A72-2727

Thunderstorm-associated aircraft mishaps relation to surrounding synoptic scale meteorological conditions, discussing storm interior condition contribution to flight stability upset 13 p1992 A72-2885

Thunderstorm penetration by F-100 aircraft to study turbulence hazard relation to updraft size and sheared period fluctuation-induced acceleration changes 13 p1992 A72-2885

Hailstone impact simulator for aircraft damage prediction in testing prospective structural designs 13 p1938 A72-2885

Mathematical criteria for probable and potential aircraft icing occurrence, using radiosonde and empirical climatological data 13 p1993 A72-2885

Lightning current tests of aircraft glass/carbon fiber reinforced plastics materials 13 p1898 A72-3004

Probabilistic analysis of aircraft crash-caused structural damage to nuclear power plant, using Monte Carlo method and yield line theory for perforation and collapse modes 16 p2421 A72-3360

Flight safety research, discussing NASA aviation hazards R and D programs involving fire, lightning and static, steep approaches, aircraft wakes, fog and visibility 20 p2888 A72-3974

Liquid and solid precipitation on aircraft structural surfaces, discussing potential hazards to engine components and aircraft controls due to ice formation 23 p3252 A72-4433

AIRCRAFT HYDRAULIC SYSTEMS

European A300B airbus flying control hydraulic system and landing gear design for safety and reliability, fatigue life, weight and maintenance 01 p0005 A72-1072

Concorde supersonic transport hydraulic control systems, describing design features with emphasis on reliability 03 p0312 A72-1396

Airplane hydraulic control systems digital simulation, using method of characteristics for distributed parameter analysis of transmission line dynamics [ASME PAPER 71-WA/FE-21] 05 p0615 A72-1592

F-14 Tomcat test program for hydraulic system spinning, low speed performance, stalling, afterburner turbofan engines, in-flight refueling and automatic telemetry equipment 06 p0758 A72-1758

Onboard and ground based hydraulic start systems design, construction and operation for aircraft turbine engines 08 p1224 A72-2144

Metric swaged pipe coupling design and development for aircraft hydraulic systems, presenting fatigue test results 08 p1179 A72-219

Hydraulic starter systems for aircraft turbine engines, examining operation loads and fluid supply and pressure requirements 11 p1702 A72-25284

Cessna 210 aircraft electrically driven hydraulic power pack for landing gear system, noting engine and flight tests [SAE PAPER 720327] 11 p1577 A72-25589

Freon 30 bidistillate as washing liquid for flight vehicle hydraulic systems, discussing industrial methylene chloride purification 11 p1675 A72-26818

L-1011 TriStar cartridge valves and manifolds, reservoirs and hydraulic service center design for speedy maintenance and servicing 14 p2073 A72-31050

Russian book - Assembly and testing of hydraulic and pneumatic systems of flight vehicles 19 p2753 A72-37300

Failsafe hydraulic actuator flight control for jet aircraft. 20 p2890 A72-39351

Aircraft hydraulic control systems modular design for maintainability, emphasizing component removal with minimum hydraulic fluid loss and air entrainment 22 p3140 A72-42294

Aircraft clamp-on flowmeter using IR heat source in thermistor bridge to monitor flow rate in hydraulic lines 22 p3180 A72-42715

Aircraft hydraulic secondary power system weight estimation, presenting components loads and weights breakdown in tables and charts [SAWE PAPER 935] 23 p3252 A72-43475

Error analysis of linear and nonlinear elements in hydraulic control circuits of flight vehicles, calculating accuracy of frequency response determination 23 p3252 A72-43671

AIRCRAFT INDUSTRY

Commercial transport market and technology forecasting, considering all-cargo, STOL, SST and CTOL aircraft [SAE PAPER 710750] 01 p0002 A72-10249

Le Bourget Exposition data for displayed civil transport aircraft 03 p0310 A72-13638

Common law liability of aviation manufacturers, discussing safety, airworthiness, maintenance, reporting, modifications and inspection requirements and evidence of negligence 07 p1106 A72-20671

Chemical compositions, properties and heat treatment of Ti, Al alloys and steels used in aircraft industry 11 p1652 A72-25286

Aircraft industry product support role in time delays minimization for aircraft operators, discussing malfunction report, minimum equipment decision and fault diagnosis 15 p2339 A72-32456

Financial methods employed in creating Brazilian aircraft industry via mixed public-private ownership 16 p2481 A72-33375

Polish aircraft industry production and fabrication techniques, discussing metal working, digital controlled machining and cost reduction 18 p2696 A72-37010

AIRCRAFT INSTRUMENTS

NT ALTIMETERS

NT ANEMOMETERS

NT APPROACH INDICATORS

NT ATTITUDE INDICATORS

NT AUTOMATIC PILOTS

NT FLIGHT RECORDERS

NT GYRO HORIZONS

NT GYROCOMPASSES

NT HOT-WIRE ANEMOMETERS

NT MAGNETIC COMPASSES

NT PLAN POSITION INDICATORS

NT POSITION INDICATORS

NT RADIO ALTIMETERS

NT RADIO DIRECTION FINDERS

NT RATE OF CLIMB INDICATORS

NT SPACECRAFT POSITION INDICATORS

NT SPEED INDICATORS

NT TACHOMETERS

Passenger aircraft onboard automated inertial navigation devices, emphasizing accelerometer and gyroscope design and construction 01 p0096 A72-10070

Polar navigation with transverse mercator technique for aircraft using secant geared ground position indicators 01 p0097 A72-10181

Pressure altimeter system minimum safe performance standards for subsonic aircraft operation, describing test procedures [SAE AS 942] 01 p0064 A72-10386

Airfield Vehicle Obstacle Indication Device short range high-definition radar system for aircraft navigation aid 02 p0173 A72-12042

Airborne pictorial navigation systems for visual indication of aircraft position in addition to digital readout 02 p0256 A72-12106

Soviet book on course-indicating systems and automatic navigation aids for civil aviation aircraft covering design, operation principles, error analysis and reliability 02 p0256 A72-12298

Aircraft in-flight monitoring instruments for meteorological service in U.S. 04 p0464 A72-14687

Cockpit information for pilot and flight crew as key to transport aircraft accident prevention, discussing cockpit layout and displays in terms of flight safety requirements 04 p0464 A72-14813

Time/frequency collision avoidance systems, discussing operating principle and economic aspects for airlines and general aviation 04 p0544 A72-14816

Soviet book on electrical equipment and instrumentation of An-24 aircraft covering power sources, control, safety systems, engine, flight and navigation instruments and autopilot 05 p0615 A72-16400

Aircraft and airports weather instrumentation for all-weather landing and takeoff, discussing application of laser technology and digital presentation 08 p1168 A72-21522

Cockpit instrumentation for jet transport aircraft flight path management, emphasizing dependability, safety and economy 08 p1168 A72-21524

U.S. Navy cartography, describing RA-3B Skywarrior capabilities and photographic instrumentation 08 p1169 A72-21699

Mystere business jet aircraft flight instruments, acceleration, control and stall characteristics 08 p1110 A72-21900

Anthropotechnical aspects of V/STOL aircraft control, discussing instrument and control systems concepts based on development and flight tests of experimental Do-31 VTOL aircraft 09 p1270 A72-22784

Automated navigation management in cockpit, considering modular navigation /MONA/ dual channel system of L-1011 TriStar 09 p1349 A72-23450

SECANT system of aircraft separation and control by nonsynchronous technique for midair collision avoidance [SAE PAPER 720313] 11 p1683 A72-25577

Pulse operated multichannel annunciator system for pilot warning of aircraft systems malfunctions, describing circuit design [SAE PAPER 720333] 11 p1630 A72-25593

Aircraft distance measuring equipment with VOR radio receivers and ground station transponder for pulse interrogation 12 p1842 A72-27105

Aircraft microminiature ILS with transmitter and localizer antenna to provide pilot with bearing and glide slope information for alignment with runway 12 p1842 A72-27106

Airborne gravimetry experiment yielding high resolution pressure and altitude measurements, describing equipment 13 p1994 A72-28877

Electronic head-up displays for aircraft instrument indication in symbolic form at pilot eye level 15 p2188 A72-31513

DAMIEN III digital magnetic tape recording system for aircraft flight test data acquisition, discussing components 16 p2393 A72-33629

Microwave /60 GHz/ radiometer for air temperature measurement outside aircraft during icing conditions 16 p2393 A72-33631

Aircraft instrumentation system accuracy relation to aerodynamic derivatives evaluated from flight data, proposing input and transient response measurement system 16 p2394 A72-33640

Error analysis of hybrid aircraft inertial navigation systems. [AIAA PAPER 72-848] 20 p2950 A72-39081

Altimeters development history from Wright brothers to Boeing 747, discussing altitude alert systems providing aural and visual warnings to pilot 20 p2952 A72-39747

Instruments installation effect on soviet passenger aircraft pilot performance, discussing Tupolev aircraft control systems 21 p2994 A72-40173

Aircraft instrument panel redesign to alleviate crew task, proposing integral displays and controls for flight information 21 p3080 A72-40291

Collision avoidance system electromagnetic compatibility with radar altimeters designed for 1600 MHz aeronavigation band 21 p3018 A72-40881

Application of the head-up display /HUD/ to a commercial jet transport. 21 p3060 A72-41256

The INAS device of Ferranti as integrated weapon system for the HS Harrier 21 p3083 A72-41846

An advanced strain level counter for monitoring aircraft fatigue. 22 p3179 A72-42688

Aircraft clamp-on flowmeter using IR heat source in thermistor bridge to monitor flow rate in hydraulic lines 22 p3180 A72-42715

AIRCRAFT LANDING

NT CRASH LANDING

Short haul air transport system need for future short takeoff and landing aircraft, considering airports, airways, economics and navigation and landing aids 02 p0154 A72-11719

Microwave aircraft landing system development, discussing contract definition, feasibility, prototype development, management planning and program costs 02 p0304 A72-12377

Aircraft ILS, covering history, adverse weather operations and replacement systems 02 p0257 A72-12645

STOL aircraft integrated landing approach flight control system with elevator and thrust control coupling to angle of attack, altitude and other state variables [DGLR PAPER 71-063] 02 p0155 A72-12705

TU-154 lift and drag augmenting devices for takeoff and landing characteristics improvement 03 p0310 A72-13472

ATC technology impact on flight operations and public value of aviation, discussing microwave landing system economic aspects 04 p0544 A72-14810

Terminal area air traffic guidance and control, discussing automation, all-weather precision approach and landing and failure detection 04 p0544 A72-14817

Aircraft landing microwave guidance and control systems, considering general dynamic model for aircraft translational motion determination in earth fixed coordinate system 04 p0545 A72-14821

Automated scheduling algorithm for aircraft from terminal area to touchdown, discussing system features and STOL air traffic computerized simulation [AIAA PAPER 72-120] 05 p0688 A72-16905

Step-scan landing system technique, using microwave fixed linear array for area coverage with pattern of narrow overlapping individually coded sequentially switched beams 06 p0846 A72-18397

Carrier suitability testing for aircraft landing, considering landing gear and supporting structure under simulated shipboard conditions 06 p0759 A72-18497

Crosswind landing under adverse runway conditions, illustrating technique with sketches 07 p0911 A72-18833

Night Carrier Landing Trainer flight and carrier environment simulator for A-7 aircraft pilot training, discussing performance predictions from computer data analysis 07 p0927 A72-19137

High performance aircraft takeoff and landing accidents, investigating survival rates 08 p1109 A72-21563

Buccaneer Mk 2 and F-4K Phantom takeoff and landing performance improvement due to boundary layer control by leading and trailing edge blowing 09 p1262 A72-22973

Turbulent jets effectiveness in protection of aircraft surfaces from rain, describing wind tunnel simulation of takeoff and landing 10 p1463 A72-25137

Helicopter landing on ships, discussing wind, visibility limitations and flight deck motions vs aircraft stability and handling characteristics 12 p1754 A72-27413

Pilot evaluation of C-5 automatic landing system in Category III weather environment 12 p1842 A72-27521

Workload modification effects on pilot neurological changes during Boeing 707 letdown, approach and landing 12 p1775 A72-28290

Slant range visibility measurements by lidar for aircraft landing operations under low clouds and fog at coastal region 13 p1992 A72-28847

Optimal angle selection of commercial aircraft glide path, taking into account vertical velocity, propulsion units operation and landing procedure 14 p2072 A72-30814

Aircraft copilot assistance to pilot in flight phases, emphasizing takeoff and landing and man machine system reliability 14 p2072 A72-30815

U.S.S.R. civil aviation regulations on takeoff and landing minimum conditions for cloud ceilings and visibility range for various aircraft characteristics and equipment

14 p2129 A72-30820

Pilot landing performance prediction criteria based on day and night carrier qualification trials and flight training

14 p2081 A72-31084

Tactical approach landing radar tests for low lift drag ratio aircraft in unpowered flight, using F-104D as test aircraft

15 p2267 A72-31694

Flight experiments to determine horizontal visual restriction effects on T-33 aircraft front cockpit during approaches and landings

15 p2180 A72-31697

Jet lift VTOL flight path optimization for minimum landing transition distance, evaluating deceleration as function of incidence and thrust vector angles

15 p2272 A72-32323

STRADA landing trajectory recording system for real time flight path restitution during approach and landing, using computer and lidar techniques

16 p2420 A72-32895

Aircraft flight characteristics for landing approach by spoiler-elevator deflection coupling, considering pitch, flight path angle and speed

16 p2343 A72-33423

Solid state modular ground based distance measuring equipment /DME/ receiver for en route aircraft navigation and landing

16 p2420 A72-33521

Computerized aircraft landing measurement system for civil airport, using optical, seismic and IR sensors

16 p2374 A72-33627

Helicopter/ship dynamic interface testing for launch and recovery capabilities under sea environment conditions, discussing visual landing aids, wind, visibility and ship motions

[AHS PREPRINT 650] Investigation of data rate requirements for low visibility approach with a scanning beam landing guidance system.

17 p2578 A72-35562

Computer control of aircraft landing.

17 p2578 A72-35950

Acoustic ray deflection by aircraft wake vortices with viscous core, observing maximum deflection angles during large aircraft landing

18 p2641 A72-36417

Application of electronic data processing airport analysis in airlines operations and for manufacturers.

19 p2747 A72-37277

Investigation of data rate requirements for low visibility approach with a scanning beam landing guidance system.

19 p2832 A72-38259

A landing approach guidance scheme for aircraft which are capable of executing steep approaches.

19 p2832 A72-38278

Dutch monograph - Analysis of dynamic aircraft landing loads, and a proposal for rational design landing load requirements.

21 p2994 A72-40925

Automatic landing and microwave guidance system potential.

21 p3040 A72-41072

An exploratory study of flying qualities of very large subsonic transport aircraft in landing approach.

[ICAS PAPER 72-07] Multiloop piloting aspects of longitudinal approach path control.

21 p2995 A72-41132

[ICAS PAPER 72-46] Allowable region of approach height and desirable approach path of aircraft for safe landing, presenting optimal control trajectories

23 p3252 A72-44497

Lateral flight path control during aircraft landing in gusty cross-winds by lateral thrust deflection, discussing design optimization

24 p3368 A72-45330

Effects of variations in lift and drag response to longitudinal control on the ease and quality of landing.

24 p3368 A72-45333

An investigation of parameters and factors governing manual control of STOL aircraft in landing approach.

[AIAA PAPER 72-987] Pilot workload assessment technique during transport aircraft approach and landing, correlating with aircraft serviceability, crew efficiency, navigation aids, meteorological conditions and control procedure factors

24 p3377 A72-45657

AIRCRAFT LANDING INSTRUMENTS

U LANDING INSTRUMENTS

AIRCRAFT LAUNCHING DEVICES

Aircraft launch envelope investigation for minimum catapult end airspeed determination at carrier bow, discussing optimum test pilot launch technique

06 p0759 A72-18498

AIRCRAFT LIGHTS

Midair collision prevention independent of ATC, discussing aircraft lighting, collision avoidance systems and proximity warning indicator

21 p3081 A72-40297

AIRCRAFT MAINTENANCE

Helicopter elastomeric bearing rotors, discussing downtime and cost reduction, maintenance, endurance and inspection

01 p0073 A72-10150

Advanced technology air transports propulsion system requirements, considering design, engine performance and reliability, maintenance, airline problems, noise and pollution control

[SAE PAPER 710761] Aircraft power plant design and installation influence on operational effectiveness, discussing manufacturers and operators cooperation for reliability and maintainability enhancement

[SAE PAPER 710777] DC-10 nondestructive testing manual, detailing section/subject format, methods, planned area accessibility and aircraft maintenance

01 p0115 A72-10258

Soviet look on air transport economics covering efficiency and control improvement, maintenance, work and wages, tariffs, cost and revenues, etc

03 p0459 A72-14098

Nondestructive testing for materials inspection and monitored aircraft maintenance programs

03 p0364 A72-14201

Air transport maintenance regulation as part of National Aviation System program, discussing airworthiness, safety and reliability in relation to design requirements

04 p0526 A72-14814

Turbojet aircraft engine overhauling planning and execution, discussing dismantling, washing, galvanic treatments, acceptance checks and quality controls

05 p0643 A72-16014

Military aircraft operations and logistics computerized simulation for support and maintenance cost estimates

06 p0758 A72-17974

MARS digital simulation model in GPSS for determining scheduled flight operations and maintenance resources effects on aircraft availability and usage rates

06 p0779 A72-17976

Trident aircraft air-system interrogator airborne first line test apparatus for electrical components malfunction diagnosis

06 p0796 A72-18154

Government role in widebody aircraft introduction to air carrier service, discussing aircraft maintenance, design and fail-safe structural configurations

07 p0911 A72-18831

X ray, ultrasonic and eddy current nondestructive testing of aircraft structure for maintenance and special problems

07 p0994 A72-18840

Common law liability of aviation manufacturers, discussing safety, airworthiness, maintenance, reporting, modifications and inspection requirements and evidence of negligence

07 p1106 A72-20671

Naval aircraft optimal repair and replacement policies determination for operation cost minimization by dynamic programming

08 p1256 A72-21470

Aircraft maintenance and reliability monitoring and control on scheduled airlines, considering component failure rate and mode analysis, sampling inspection and remedial action

09 p1261 A72-22901

C-5A Galaxy aircraft systems and components maintainability program

10 p1459 A72-23851

Corrosion resistant fabrication methods in jumbo jetliners components to reduce maintenance and repair downtime, discussing clad wing and fuselage skins

10 p1487 A72-24025

Aircraft scheduled maintenance, discussing turbine engine and component reliability protection, controlled overhaul, test and repair

10 p1565 A72-24867

Aircraft maintenance optimization, considering safety, reliability, punctuality and cost factors

10 p1422 A72-25108

Statistical diagnosis of aeronautical systems reliability and maintenance, using Benzer factorial analysis for data reduction

11 p1639 A72-25817

NDT application to aircraft design and reliability, discussing fatigue life analysis and in-service monitoring for structural elements, components and airframes

12 p1813 A72-27198

Bolkow 105C 5-place helicopter with twin turbine engine driven rigid glass-reinforced plastic rotor blades, emphasizing design philosophy of easy maintainability

13 p1898 A72-29871

Decision diagrams use in logic analysis for aircraft maintenance schedule testing relative to operational reliability control

13 p1967 A72-30041

Aircraft maintenance operations and personnel requirements planning for optimal economic effectiveness, formulating relations between work productivity, downtime and aircraft utilization

14 p2174 A72-30822

Electronic data processing in airline materiel supplies operations, discussing procedural efficiency improvement through reduction of stochastic effects inherent in aircraft maintenance operations

14 p2174 A72-30823

L-1011 TriStar cartridge valves and manifolds, reservoirs and hydraulic service center design for speedy maintenance and servicing

14 p2073 A72-31050

Airline maintenance program and facilities for Boeing 747 aircraft based on optimized service concept

15 p2181 A72-32430

Maintenance of the 747. II - BOAC. Maintenance processes planning in air transportation, discussing aircraft availability, cost analysis and production management

17 p2560 A72-35441

Technical experience in operating the equipment in the IL-62 aircraft

17 p2558 A72-35791

Private aircraft ownership and use for family travel and pleasure, discussing costs, maintenance and operational problems

[AIAA PAPER 72-812] A method of solving the operational planning problem for an engineering aircraft base

21 p3039 A72-40178

Russian book - The ASH-62IR engine /4th enlarged edition/. Detection of structural deterioration and associated airline maintenance problems.

[SAE PAPER 918] IL-62 aircraft propulsion system design and installation details, operational surveillance system and maintenance operations

23 p3293 A72-43465

Simulation procedure for mission and maintenance planning of an air force wing.

23 p3325 A72-43639

Naval helicopters applications to search and rescue, ASW, ground support and other roles, considering reliability and maintenance

24 p3365 A72-44663

Structural fatigue cost in aircraft maintenance and repair, considering inspections, defect rectification, preventive modifications, replacements and NDT

24 p3365 A72-44685

Wind tunnel stability tests of aerodynamic pitch damping of aircraft model oscillating in two degrees of freedom

24 p3367 A72-44744

AIRCRAFT MODELS

Low subsonic region unsteady interference effects on harmonically oscillating wing-tailplane model with variable sweep wing

[DGLR PAPER 71-081] Aeroelastic models construction for flutter analysis of aircraft design, noting error risk reduction

[DGLR PAPER 71-082] Wind tunnel stability tests of aerodynamic pitch damping of aircraft model oscillating in two degrees of freedom

02 p0152 A72-12709

State sensitivity functions in aircraft parameter identification for lateral dynamics under aileron deflection from model response and in-flight test data

10 p1421 A72-23807

Wind tunnel investigation of Reynolds number effects on boundary layer separation incidence and maximum lift coefficient of high-lift device equipped aircraft model

10 p1419 A72-24657

Magnetic simulation of gravity for wind tunnel investigations of aircraft jettison processes, considering Froude number and relationships between model and full scale aircraft

10 p1462 A72-24775

Fan-in-wing model noise due to cross flow generated in- and outflow distortions and steady rotor blade forces

[ASME PAPER 72-GT-92] Characteristics of an ejector-type engine simulator for STOL model testing.

[AIAA PAPER 72-1028] AIRCRAFT NOISE

NT JET AIRCRAFT NOISE

NT SONIC BOOMS

STOL aircraft for solving noise reduction and land use problems in future transportation systems, discussing airport location and layout for growing air traffic

01 p0005 A72-11153

Aircraft engine noise effects in airport vicinities, discussing measurement scales, turbofan sources, noise reduction and future air traffic

02 p0154 A72-12022

Rating scale judgments of aircraft noise based on surveys around airport 03 p0309 A72-12956

Prop-fan engine for quiet STOL propulsion, discussing noise characteristics, weight advantage, response and reduced fuel consumption 03 p0406 A72-13697

Air transportation evolution and relation to atmospheric and noise pollution 03 p0459 A72-14151

Aircraft operations effects on community noise pollution, discussing ATC airline operational procedures modifications in terms of noise reduction 04 p0464 A72-14819

Aircraft industry noise reduction efforts to meet FAA requirements for CTOL and STOL aircraft, emphasizing turbofan and compressor noise suppression and/or attenuation 04 p0565 A72-14820

Aircraft and other transient noise levels temporal characteristics effect on noise assessment 04 p0464 A72-14843

Sound attenuation in lined rectangular ducts with uniform steady flow, considering aircraft engine noise reduction 04 p0565 A72-15267

Civil aircraft technological constraints and requirements, discussing noise, congestion and performance characteristics of rotorcraft, STOL, VTOL, hypersonic and supersonic transports 05 p0611 A72-15774

Civil aviation R and D policy study, showing priorities for aircraft noise and congestion abatement and short haul systems 05 p0611 A72-15780

Aircraft noise measurement units and methods, discussing engine design for noise reduction 05 p0611 A72-16026

Aerospace vehicle noise induced structural vibration, presenting propellers, turbojet engine exhausts and sonic boom waves 05 p0739 A72-16597

VTOL transport aircraft use in densely populated urban areas, discussing travel time, airport requirements, noise and design problems 05 p0612 A72-16733

Airport surrounding communities survey on attitudes toward aircraft noise, noting daily activity disturbance, emotional reactions, economic effects, noise abatement awareness, etc 06 p0767 A72-17870

Airfield law in Schleswig-Holstein Appeals Court decision concerning property owner suit against operator for unnecessary noise 06 p0906 A72-18170

Rotorcraft based on VTOL concept for aircraft noise reduction in urban transportation 06 p0758 A72-18248

Army aircraft gas turbine engines pollution potential evaluation program, considering smoke emission, noise and invisible pollutants 07 p1053 A72-18772

Externally blown flap noise tests at various nozzle exhaust velocities for STOL aircraft noise reduction [AIAA PAPER 72-129] 07 p0908 A72-18962

California airport noise standards instrumentation, discussing battery operated measurement of hourly and community noise equivalent levels 07 p0985 A72-19490

Aircraft noise protective earplug design, employing perforated and slit modifications for additional protection without tympanic membrane pressure excess risk 07 p0933 A72-20187

Helicopter noise and vibration testing and cabin soundproofing for improved comfort 08 p1128 A72-22141

Commercial applications of quiet light aircraft technology, discussing cost and noise reduction [SAE PAPER 720339] 11 p1576 A72-25596

Turbofan engine trends for short haul conventional and STOL aircraft, considering variable pitch fans, reduction gears, thrust reversal and noise and environmental pollution [ASME PAPER 72-GT-86] 11 p1705 A72-25661

Fan-in-wing model noise due to cross flow generated in- and outflow distortions and steady rotor blade forces [ASME PAPER 72-GT-92] 11 p1571 A72-25666

Aircraft flyover house noise reduction data, noting application to indoors noise level estimation [SAE AIR 1081] 11 p1686 A72-26029

Infrasound observations of natural background and signals from Apollo 14 and aircraft, using thermistor flowmeter microphone array 11 p1690 A72-26515

Acoustic ray path method for computing atmospheric conditions effect on aircraft noise propagation, using digital computer 13 p1897 A72-28840

Low flight altitude atmospheric parameters spatial and temporal variability effects on aircraft flyover noise measurement 13 p1991 A72-28841

Aircraft noise sources, showing noise intensity relationship to airfoil velocity and pressure ratio 13 p1897 A72-29568

Aircraft fan and compressor noise generation mechanism, considering mass flow and lift forces fluctuations from rotor and stator airfoils 13 p2028 A72-29569

Acoustic measurements for STOL turboprop transport aircraft propeller configurations under static, taxi and flyover conditions, discussing quiet propeller noise signature 13 p1897 A72-29571

Bibliography on noise control covering surface transportation, machinery and aircraft noise, industrial criteria, biodynamics, legislation and measurement 13 p2006 A72-29588

Digital data processing techniques for aircraft engine noise data reduction, analyzing fan noise spectrum 13 p1925 A72-29840

Quiet RTOL /reduced takeoff and landing/ short haul aircraft cost comparison with Trident 3 aircraft up to design range stage length 15 p2180 A72-31320

Optimum low noise engine selection for transport and combat aircraft relative to range or payload performance, considering CTOL, VTOL, SST and fighter aircraft 15 p2297 A72-32127

Low noise aircraft-engine configuration feasibility, discussing turbofan engine noise reduction 15 p2181 A72-32322

High intensity sound effects on electronic equipment and components in aircraft noise environment, noting whisker diode and printed circuit board damage 15 p2209 A72-32621

Airport vicinity aircraft noise exposure contour calculated from measured data at Osaka Airport 16 p2372 A72-32885

Reduction of noise and acoustic-frequency vibrations in aircraft transmissions. [AHS PREPRINT 661] 17 p2491 A72-34508

Internal noise reduction in hovercraft. 18 p2642 A72-36574

Flyover noise testing of commercial jet airplanes. [AIAA PAPER 72-786] 19 p2749 A72-38103

Aircraft noise problem in piston engine to turbofan jumbo jet transports, discussing need for noise reduction research [AIAA PAPER 72-815] 19 p2750 A72-38117

A time-frequency localization system applied to acoustic certification of aircraft. [AIAA PAPER 72-836] 20 p2950 A72-39091

Acoustic pressure and sound intensity levels and noise annoyance international standards for civil aircraft noise reduction 20 p2888 A72-39803

Landing 'in the backyard' with quiet aircraft 21 p2994 A72-40376

Flying personnel auditory defects caused by environmental conditions, discussing aircraft noise, vibrations and atmospheric pressure effects 21 p3002 A72-40924

Noise radiation from V/STOL aircraft. [ICAS PAPER 72-22] 21 p2995 A72-41147

VTOL aircraft noise reduction through design methods and flight path management in terminal area, evaluating acoustical annoyance to surrounding community [ICAS PAPER 72-34] 21 p2995 A72-41159

Description and use of a method for characterizing noise sources in jets [ICAS PAPER 72-35] 21 p3046 A72-41160

Aircraft noise duration correction for effective perceived noise level /EPNL/ computation, eliminating mathematical anomaly incurred by present FAA and ICAO prescribed method 22 p3139 A72-42909

Statistical analysis of the sound level distribution of aircraft noise as a function of time 23 p3252 A72-44337

Airports planning for West Germany, discussing geographical air traffic patterns, economic and noise aspects [DGLR PAPER 72-034] 24 p3387 A72-44614

Multipoint real time all-day computerized noise monitoring system for diagnostic evaluation of airport, discussing design and applications 24 p3387 A72-44684

Tone noise from rotor/stator interactions in high speed fans. 24 p3433 A72-44917

AIRCRAFT PARTS

Integrity control procedures for machining, drilling and grinding of steel and Ti alloy aircraft parts, discussing nondestructive inspection method [SME PAPER IQ 71-238] 01 p0076 A72-10969

High strength Ti alloys for aircraft accessories structural materials, comparing room temperature physical properties of ultrahigh tensile steels and other alloys 03 p0373 A72-13617

AIRCRAFT PERFORMANCE

Ti effects on aircraft equipment design, considering use of Ni plated brake cylinder, wheel, engine control rams, tie bolts and rings 03 p0373 A72-13618

Relative cost comparisons of composite applications with conventional material components selected from F-111A supersonic fighter bomber 03 p0310 A72-14234

Fatigue behavior of notched or cracked aircraft structure parts, examining service life prediction problem 06 p0895 A72-17811

Cocuring technique optimization for primary aircraft components composite materials, discussing mechanical and dimensional properties test data, production cost analysis and cure time 12 p1815 A72-28077

Vibrational shot peening as a method of increasing the fatigue strength of critical aircraft elements 20 p2929 A72-39802

AIRCRAFT PERFORMANCE

NT HELICOPTER PERFORMANCE

TriStar commercial jet transport aircraft development, discussing design and flight tests for operating efficiency, reliability and safety [SAE PAPER 710755] 01 p0003 A72-10252

STOL and VTOL aircraft performance and efficiency, discussing landing and takeoff distances reduction 01 p0006 A72-11258

VFW-614 short range twin jet passenger transport aircraft, analyzing service performance and economic efficiency requirements influence on design characteristics 03 p0310 A72-13643

Air to air maneuverability of aircraft capable of in-flight thrust vectoring, indicating improved deceleration, normal acceleration g-force and turn rate 03 p0310 A72-13877

Civil aircraft technological constraints and requirements, discussing noise, congestion and performance characteristics of rotorcraft, STOL, VTOL, hypersonic and supersonic transports 05 p0611 A72-15774

Pilot evaluation of Boeing 747 handling, directional stability, stall, rudder feel forces, landing, inertial navigation and reliability 05 p0614 A72-16992

French civil aircraft displayed at 1971 Le Bourget Air Show, discussing design and performance characteristics of Airbus, Concorde, Caravelle, Corvette, Falcon, Fregate, STOL-A-904 and Mercure 05 p0614 A72-17193

Flight simulator for aircraft design, emphasizing compromise between performance and control requirements to avoid excess weight and drag 06 p0796 A72-18245

Federal Air Regulations procedures for civil transport aircraft flight testing under natural and/or simulated icing conditions 06 p0760 A72-18501

Aircraft performance and flight path optimization algorithms for minimum fuel-fixed range, using calculus of variations 07 p0912 A72-19091

Aircraft performance parameters in terms of effect on lifting system service and fatigue life and on design 07 p0912 A72-19111

Aircraft electric power generation history, noting aircraft performance effect on electrical system design 07 p0914 A72-20201

French, British, Italian, U.S., German and Israeli military aircraft, presenting design and performance data 07 p0913 A72-20308

Aeromechanical analysis of flight conditions for conventional aircraft, including kinematics of curvilinear motions with constant speed 07 p0913 A72-20372

DC-10 aircraft automatic landing performance and failure assessment monitor system 08 p1204 A72-21003

F-14 naval fighter aircraft flight test programs, discussing instrumentation and low-speed test results 08 p1108 A72-21005

Maneuvering aircraft sonic boom propagation and signatures prediction in stratified atmosphere by geometric acoustic method 08 p1110 A72-21904

Fixed wing agricultural aircraft, comparing different designs in terms of performance, safety, handling and economic efficiency 09 p1262 A72-22940

Airfoil ram-wing air-water hybrid vehicle X-113 Am design and operational principles based on aerodynamic ground effect, discussing flight tested performance characteristics 09 p1262 A72-22971

Flight tests of combination flight director displayed and attitude command control system effect on and attitude command control system effect on general aviation aircraft handling qualities during ILS approach [SAE PAPER 720316] 11 p1575 A72-25580

Super Guppy four engine aircraft characteristics, performance and loading device for bulky cargo air transportation

11 p1577 A72-25812

European passenger aircraft Airbus program, discussing various configurations performance, economic factors and technical support

12 p1753 A72-27108

STOL aircraft role in civil aviation, discussing short range operation, ATC, reduced noise and weather capability

12 p1754 A72-27518

L-1011 flight test program, discussing aircraft design, flight station, controls, flying qualities, etc

12 p1754 A72-27519

Airplane sideslip and yaw rate perturbations by continuous random vertical and side gusts, using low pass filtered white noise representation for mathematical modeling

12 p1755 A72-28125

Air cushion aircraft landing systems advantages and suitability for arctic transportation applications

13 p1897 A72-28793

European Airbus program, noting international cooperation juridical sources, content and organization, aircraft performance, financing, project chronology and Franco-German agreement

13 p2067 A72-28795

Aircraft flight conditions effect on low altitude critical air turbulence in terms of gust velocity components for CAT prediction

13 p1993 A72-28861

Stratospheric meteorological characteristics effects on Concorde supersonic flight performance, fuel consumption, dynamic behavior and passenger comfort

13 p1994 A72-28876

HR 200 training and acrobatic two seater low wing metal aircraft series production, dimensions and maximum takeoff weight performances

13 p1898 A72-30039

Hovercraft state of development and utilization potential, comparing performance to other transportation modes

14 p2073 A72-30818

Flight test instrumentation system for measurement of aircraft performance, stability and control characteristics during nonsteady flight

16 p2349 A72-33639

The use of airborne magnetic tape recorders for fatigue life monitoring.

17 p2553 A72-34812

The fly-by-wire systems approach to aircraft flying qualities.

17 p2493 A72-35575

Meteorological effects on SST performance, considering temperature, wind, turbulence, hydrometeors, ozone and radiation effects

17 p2577 A72-35790

Aircraft flight test facilities deficiencies and modernization impediments, recommending integrated facility research program establishment

19 p2783 A72-37676

Propulsion technology advance factors, stressing noise and exhaust emissions reduction, economic considerations and aircraft performance

19 p2848 A72-37679

The Dassault Mystere 20.

19 p2748 A72-37900

Flight test report on L-1011 aerodynamic characteristics, discussing high and low speed performance, stability and control, stall behavior, etc

19 p2748 A72-38030

The development of dynamic flight test techniques for the extraction of aircraft performance.

[AIAA PAPER 72-785]

19 p2749 A72-38102

Automated airborne recording system to obtain data on aircraft engines, subsystems and operational performance, considering cost and economic benefits

[AIAA PAPER 72-752]

19 p2802 A72-38126

Advanced technology transport (ATT) aircraft configurations design parameters analysis, considering cruise speed, passenger capacities, ranges, noise level and economics

[AIAA PAPER 72-757]

19 p2751 A72-38127

A-X Air Force flight evaluation.

[AIAA PAPER 72-770]

19 p2751 A72-38131

Maneuver load control and relaxed static stability applied to a contemporary fighter aircraft.

[AIAA PAPER 72-870]

20 p2887 A72-39129

Aerodynamic test facility data on swept wings, peaky airfoils, aircraft flutter and transonic flow, discussing shock tubes and wind tunnels development

20 p2912 A72-39846

STOL performance criteria for military transport aircraft.

[AIAA PAPER 72-806]

20 p2889 A72-40055

Defense systems development based on balance between theoretical studies and hardware prototyping for uncertainty reduction in performance and cost

21 p3132 A72-40971

High Reynolds number transonic wind tunnel facility (HIRT) for improved aerodynamic testing of modern combat and commercial aircraft performance, maneuverability and handling qualities

[AIAA PAPER 72-1035]

21 p3043 A72-41609

Flow distortion and performance measurements on a 12-inch fan-in-wing model for a range of forward speeds and angle of attack settings.

22 p3134 A72-42323

Flying experience with the SCI research aircraft and the P1127 prototype at the Royal Aircraft Establishment, Bedford, England.

22 p3136 A72-42324

Variable impedance transducer measuring instruments for in-flight aircraft performance tests under environmental thermal effects

22 p3180 A72-42711

Mission analysis and performance program as part of computerized aircraft configuration synthesis process, describing interfaces with other system modules

[SAWE PAPER 909]

23 p3250 A72-43456

Engine selection for specific aircraft design and mission, considering bypass and pressure ratios and turbine temperature effects on performance and weight

[SAWE PAPER 910]

23 p3250 A72-43457

Empty weight and cruise performance of very large subsonic jet transports.

[SAWE PAPER 919]

23 p3251 A72-43466

Analysis of the fundamental parameters and flight properties of aerobatic aircraft in a statistical framework

23 p3252 A72-44336

Aircraft/spacecraft design approach and performance data, considering space shuttle program

24 p3467 A72-45159

Control requirements for control configured vehicles.

24 p3368 A72-45349

AIRCRAFT PILOTS

NT TEST PILOTS

Disorientation and related experiences reported by pilots flying several aircraft types, comparing with previous reports

01 p0021 A72-11288

Alerting light and audio signals for aircraft pilots, considering implications for aircraft design

01 p0021 A72-11291

Automatic flight control systems value to aircraft pilot, stressing man machine interface

03 p0386 A72-13420

Saccadic eye movements significance for jet pilots, noting saccade rate diurnal fluctuations and alcohol and tranquilizer negative effects

05 p0616 A72-15800

Pilots oxygen uptake vs flight time and altitude as indicator of physical condition, noting large fluctuations and differences for individual pilots and different flights

05 p0623 A72-16748

Respiratory adaptation to pure oxygen excess pressure after cockpit depressurization from flight simulator tests with pressure-suited pilots, presenting ECG reactions

05 p0623 A72-16749

Aeromedical diagnostics for aircraft pilot hearing sense tests, considering cockpit environment and stress-produced impairments in central nervous system

05 p0623 A72-16781

Fighter pilots training by simulators, determining learning effectiveness by mathematical model based on renewal theory

[AIAA PAPER 72-161]

05 p0644 A72-16827

Aircraft pilot performance during instrument approach in low visibility conditions

07 p0925 A72-18832

Idiopathic subvalvular aortic stenosis characterized by muscular or membrane obstruction in left ventricular infundibulum, discussing diagnostic importance for pilots

07 p0933 A72-20189

Aircraft pilot seating protection from dynamic environment by active vibration isolation, discussing human frequency response characteristics

11 p1585 A72-26391

Life support equipment and pressure suit operational requirements from viewpoint of flight crews and test pilots

12 p1771 A72-27516

Multivariate algorithms of optimum content and form for cardiovascular risk assessment in pilots and air transport personnel

12 p1764 A72-28264

Pilots seating active and passive isolation from LF vibrations in helicopters and jet aircrafts, discussing human factors and dynamic environment

13 p1910 A72-29558

Aircraft copilot assistance to pilot in flight phases, emphasizing takeoff and landing and man machine system reliability

14 p2072 A72-30815

Aircraft pilot reaction capability for switch activation in response to voice countdown, tone initiation and termination, noting standard deviation

15 p2188 A72-31787

Human factors engineering techniques in pilot-aircraft-environment adaptation to ease workload and in performance efficiency improvement

17 p2493 A72-35792

Corporate aircraft pilot contribution to accident investigation in providing expertise, discussing various case histories

20 p2888 A72-39751

AIRCRAFT POWER SOURCES

U AIRCRAFT ENGINES

AIRCRAFT PRODUCTION

Aircraft producibility considerations in preliminary design and production planning phases

[SAE PAPER 710746]

A-300B European Airbus cantilever wing design and manufacture, discussing skin forming, skin-stringer and torsion-box assembly, automatic riveting and root-end profile machining procedures

03 p0365 A72-14301

Forging techniques and applications for YF-12A aircraft Ti alloy bulkhead production, considering diffusion bonding and die shimming

04 p0527 A72-14914

Value engineering based cost data application to design of aircraft in production

06 p0906 A72-18435

Legal aspects of international cooperation on aircraft design and production, discussing work distribution, project management and liabilities sharing

10 p1565 A72-24881

Shot peen contouring of Boeing 747 wing skins combined with incremental chip forming, noting principles and manufacturing process

[ASM PAPER W 72-31.4]

Computer method of link formation in multiple nomenclature aircraft production lines, minimizing idle time

13 p1966 A72-29464

HR 200 training and acrobatic two seater low wing metal aircraft series production, dimensions and maximum takeoff weight performances

13 p1898 A72-30039

B-1 production planning and engineering, discussing manpower, tooling, structural components tests, schedules and cost estimates

17 p2559 A72-34389

Northrop A-9A attack aircraft production planning, discussing design features and management/engineering organizational changes in anticipation of USAF production contract

17 p2488 A72-34391

Russian book on aircraft design covering flight conditions, structure and control characteristics, production and stress analysis

17 p2492 A72-35448

Russian book - Production of the principal elements and units of aircraft engines

17 p2560 A72-35456

Hi-Shear and Hi-Lok fastening systems for aircraft manufacture, comparing strength and weight with conventional rivets and bolts

[SAWE PAPER 901]

23 p3293 A72-43451

AIRCRAFT PROTRUBERANCES

U PROTRUBERANCES

AIRCRAFT RELIABILITY

Boeing 747B growth model FAA certification, discussing engine thrust, fuel capacity, taxi and flight weights and aircraft noise reduction

[SAE PAPER 710753]

01 p0003 A72-10251

Concorde airworthiness certification, discussing ground and flight test programs for performance, flying qualities and structures fatigue properties evaluation

[SAE PAPER 710756]

Aircraft power plant design and installation influence on operational effectiveness, discussing manufacturers and operators cooperation for reliability and maintainability enhancement

[SAE PAPER 710777]

Air transport maintenance regulation as part of National Aviation System program, discussing airworthiness, safety and reliability in relation to design requirements

04 p0526 A72-14814

Concorde aircraft systems reliability and safety flight and simulator testing, discussing operational and environmental conditions and maintenance procedures

07 p0965 A72-20309

Common law liability of aviation manufacturers, discussing safety, airworthiness, maintenance, reporting, modifications and inspection requirements and evidence of negligence

07 p1106 A72-20671

Aircraft maintenance and reliability monitoring and control on scheduled airlines, considering component failure rate and mode analysis, sampling inspection and remedial action

09 p1261 A72-22901

Commercial aircraft reliability program development from informal continuous product improvement to formalized methods based on reliability logic diagrams and probability calculations

10 p1421 A72-24019

Aircraft scheduled maintenance, discussing turbine engine and component reliability protection, controlled overhaul, test and repair

10 p1565 A72-24867

Aircraft maintenance optimization, considering safety, reliability, punctuality and cost factors
10 p1422 A72-25108

Flight airworthiness requirements development for supersonic transports, V/STOL and transport and general aviation aircraft, exploring critical control and stability parameters
[SAE PAPER 720306] 11 p1575 A72-25570

Inspectibility criteria for airframes with fatigue fail safe design requirements for small airplane certification
[SAE PAPER 720310] 11 p1575 A72-25574

Fatigue certification of general aviation aircraft in Australia, describing ground taxi load spectra and endurance and radiographic inspection of laminated spar caps
[SAE PAPER 720311] 11 p1734 A72-25575

Russian book on aircraft engine reliability covering defects, fractures and failure analysis, service life prediction, production deficiencies and operational conditions
11 p1706 A72-26068

NDT application to aircraft design and reliability, discussing fatigue life analysis and in-service monitoring for structural elements, components and airframes
12 p1813 A72-27198

Complete aircraft systems reliability and maintainability, discussing extraordinary variances causes, faulty data inferences and operational testing for equipment specifications validation
13 p1896 A72-28358

Strike aircraft reliability prediction in cost effectiveness analyses, showing failure probability distribution with time
13 p1896 A72-28360

Parametric approaches to statistical burn-in or debugging problems in aircraft reliability analysis
13 p1985 A72-28363

Environmental effects on aircraft structure operational reliability, discussing failure removal and protective coating lifetime
14 p2072 A72-30285

Computer algorithms and programs contribution to aircraft structure operational reliability and fatigue life calculation
14 p2164 A72-30288

Military systems cost reduction via civil avionics procurement techniques, discussing cost-reliability design criteria
15 p2338 A72-32215

Time parameter in military air operations, discussing weapon systems R and D, all-weather capability, communications, reliability and maintainability, manpower training, etc
15 p2339 A72-32453

Results of the reliability and maintainability demonstration of the OH-58A light observation helicopter.
[AHS PREPRINT 652] 17 p2491 A72-34507

Integrity of flight control system design.
18 p2643 A72-37032

Future aspects of business aviation, discussing pilot training and aircraft reliability and maintenance in context of flight safety
20 p2988 A72-39741

Unique features of the B-1 flight control systems.
[AIAA PAPER 72-872] 20 p2889 A72-40062

Modern landing impact load calculations and old-fashioned requirements.
[ICAS PAPER 72-31] 21 p2995 A72-41156

In-flight and flight-line monitor system to detect foreign object damage in jet engines.
22 p3179 A72-42690

ICAO structural airworthiness requirements relation to air transportation safety, considering maneuver and gust loads in terms of limit load concept
22 p3138 A72-42830

Reliability analysis in the estimation of transport-type aircraft fatigue performance.
22 p3241 A72-42971

Life estimation and prediction of fighter aircraft.
22 p3139 A72-42972

Statistical method of failure analysis for redundancy forms selection, noting aircraft safety and reliability
22 p3139 A72-42973

Testing procedures for the design and life estimation of fatigue-sensitive structures.
22 p3241 A72-42974

Optimal fleet reliability under fatigue and chance overload in service.
24 p3365 A72-44656

Naval helicopters applications to search and rescue, ASW, ground support and other roles, considering reliability and maintenance
24 p3365 A72-44685

Agricultural aircraft flight loads - Typical spectra and some observations on airworthiness.
24 p3366 A72-44734

AIRCRAFT SAFETY

Air transportation system design for safety and efficiency, discussing navigation facilities and surveillance systems employment for blunder prevention
01 p0098 A72-11117

Human ejection vertebral injury data in aircraft accidents by cross reference to final medical diagnosis, considering costs and prevention for seat systems
02 p0167 A72-11714

Aircraft crash fire protection, using passenger compartment heat shield of fire-retardant polyisocyanurate foam and intumescent paint
03 p0310 A72-13484

Safety factors of aircraft flight instruments, discussing altimeter and artificial horizon reading errors and modifications
03 p0319 A72-13698

ATC for North Atlantic air transportation, emphasizing collision risk model for safety standards assessment
04 p0544 A72-14484

Air transport maintenance regulation as part of National Aviation System program, discussing airworthiness, safety and reliability in relation to design requirements
04 p0526 A72-14814

Time/frequency collision avoidance systems, discussing operating principle and economic aspects for airlines and general aviation
04 p0544 A72-14816

Human factors relation to pressurized cabin development, discussing aircraft safety, high altitude tests, pressure loss predictions and cabin altitude selection
04 p0479 A72-14869

Aircraft collision avoidance system design and evaluation, developing closed form method for system alarm rate estimation
[AIAA PAPER 72-97] 05 p0688 A72-16945

Computerized Eros II airborne collision avoidance time frequency system design, considering radio transmission, synchronization and ground stations
06 p0845 A72-18247

Flight flutter boundary testing, describing steps to minimize risk
06 p0759 A72-18491

Crashproof rotorcraft STOL aircraft for rescue operation, discussing orthodox rigid and special rotary wings design, air tunnel experiment and flight tests
06 p0760 A72-18582

Bird hazards to aircraft, discussing protective measures
07 p0911 A72-18771

Air safety - Conference, Mexico City, October 1971
07 p0911 A72-18827

Aircraft safety factors, noting navigational and flight system in Concorde design
07 p0911 A72-18828

Government role in widebody aircraft introduction to air carrier service, discussing aircraft maintenance, design and fail-safe structural configurations
07 p0911 A72-18831

Antimisting kerosene fuels for aircraft crash fires reduction
07 p1050 A72-18837

Aircraft safety enhancement by computer controlled flight simulator training of air crews, discussing Boeing 747 program
07 p0926 A72-18839

Concorde aircraft systems reliability and safety flight and simulator testing, discussing operational and environmental conditions and maintenance procedures
07 p0965 A72-20309

Mercury short haul transport aircraft, emphasizing lightweight structural design with extensive use of integral machined components for fatigue safety
07 p0913 A72-20310

Common law liability of aviation manufacturers, discussing safety, airworthiness, maintenance, reporting, modifications and inspection requirements and evidence of negligence
07 p1106 A72-20671

Eight-place turboprop powered business jet aircraft design, discussing structure, fuel system, engines crew station and safety features
08 p1109 A72-21572

Dynamic response index /DRI/ minimization for personnel aircraft emergency catapult escape systems to reduce injury probability
08 p1112 A72-21576

Crashworthy upper torso restraint systems for general aviation, incorporating strap takeup devices
08 p1126 A72-21578

Collision avoidance systems requirements and criteria, evaluating Eros time frequency and Secant interrogation-and-reply systems
09 p1349 A72-22822

Runway fog dispersal system based on underground installed flight-discarded turbojet engines, discussing system efficiency and economics
09 p1292 A72-22910

Fixed wing agricultural aircraft, comparing different designs in terms of performance, safety, handling and economic efficiency
09 p1262 A72-22940

Aircraft collision near misses under IFR and VFR conditions, discussing ATC coordination, equipment failure and personal and planning problems
09 p1349 A72-22972

Dioscures geostationary satellites project for Atlantic and Pacific ocean air and ship traffic safety based on radar tracking and multiplex numerical data transmission
09 p1396 A72-23400

Book on general aviation safety covering statistical accident records, accident analysis, crashworthiness, preventive measures, etc
10 p1420 A72-23750

Aircraft maintenance optimization, considering safety, reliability, punctuality and cost factors
10 p1422 A72-25108

General aviation aircraft structural safety studied with 1547 accident histories, noting IFR and turbulent weather conditions predominance
[SAE PAPER 720308] 11 p1575 A72-25572

SECANT system of aircraft separation and control by nonsynchronous technique for midair collision avoidance
[SAE PAPER 720313] 11 p1683 A72-25577

Test facility design for aircraft crashworthiness evaluation and improvement, considering survivable accident surrounding conditions, equipment and testing methods
[SAE PAPER 720323] 11 p1576 A72-25586

Dynamic deceleration anthropomorphic dummy tests of general aviation occupant lap belt/shoulder harness restraint systems
[SAE PAPER 720325] 11 p1583 A72-25588

Flight crew training programs cost and quality, emphasizing safety and flight simulator application
11 p1590 A72-26998

Minimum safety flight altitudes for aircraft landing systems and lateral deviations for correction maneuver
12 p1842 A72-27269

OMEGA effect on oceanic airway safety, noting improvement over inertial navigation systems
13 p1998 A72-29197

Simulator for physical forces experienced by carrier aircraft during catapult launches and arrested landings, considering external stores safe suspension
15 p2215 A72-32620

SECANT collision avoidance system, describing operational principles and flight test results
16 p2421 A72-34137

The onboard authority of the aircraft commanding officer as provided by the 1963 Tokyo Convention
17 p2639 A72-35763

Airport improvements needed for safety.
18 p2675 A72-36784

FAA implemented airport certification legislation covering minimum safety standards, operation manual, emergency plan, fire and rescue service and pavement requirements
18 p2675 A72-36785

Integrity of flight control system design.
18 p2643 A72-37032

Survivable flight control system compatibility test program.
[AIAA PAPER 72-761] 19 p2752 A72-38143

Annual Corporate Aircraft Safety Seminar, 17th, Washington, D.C., April 17, 18, 1972, Proceedings.
20 p2887 A72-39740

Safety in commuter airline operation.
20 p2988 A72-39748

Aircraft emergency evacuation systems, discussing door designs, inflatable escape slide and slide/lifeboat combination
22 p3138 A72-42520

Aircraft structural safety criteria based on acceptable failure probability, determining critical load levels
22 p3138 A72-42829

ICAO structural airworthiness requirements relation to air transportation safety, considering maneuver and gust loads in terms of limit load concept
22 p3138 A72-42830

Statistical method of failure analysis for redundancy forms selection, noting aircraft safety and reliability
22 p3139 A72-42973

Allowable region of approach height and desirable approach path of aircraft for safe landing, presenting optimal control trajectories
23 p3252 A72-44497

AIRCRAFT SPECIFICATIONS

Le Bourget Exposition data for displayed civil transport aircraft
03 p0310 A72-13638

Aircraft electric power equipment transient voltage and EMC limits specifications
03 p0312 A72-14043

Trainer-combat turbojet or turboprop aircraft characteristics, comparing flight, weight, size, maintenance and development costs
05 p0611 A72-16178

Structural requirements for normal category plastic aircraft civil certification, noting compliance with Federal Aviation Regulations
[SAE PAPER 720304] 11 p1575 A72-25568

FAA program for revision of aviation aircraft maximum allowable control forces specifications, taking into account female pilots capabilities
12 p1777 A72-28325

- HR 200 training and acrobatic two seater low wing metal aircraft series production, dimensions and maximum takeoff weight performances 13 p1898 A72-30039
- Critical review of Mil-F-83300 V/STOL flying qualities specifications as applied to helicopter design and missions, suggesting inappropriateness for Navy helicopters [AHS PREPRINT 643] 17 p2490 A72-34503
- Investigation of the commonality in development of military and commercial STOL transports. [AIAA PAPER 72-808] 19 p2750 A72-38114
- ### AIRCRAFT STABILITY
- #### NT HOVERING STABILITY
- Aircraft stability coefficient determination by numerical integration fitting to differential equations of motion 01 p0005 A72-11136
- Aircraft ride comfort problem in turbulent air, comparing free and fixed wing aircraft responses 02 p0154 A72-11720
- Soviet book on in-flight studies of aircraft stability and controllability covering dynamic characteristics, measurements, balancing curves, aerodynamic forces and limiting and special flight regimes 02 p0155 A72-12542
- Aircraft spin characteristics due to superstall, comparing three stall types with respect to recovery, yaw damping and rate of rotation [DGLR PAPER 71-057] 02 p0155 A72-12718
- Aeroelastic models construction for flutter analysis of aircraft design, noting error risk reduction [DGLR PAPER 71-082] 02 p0299 A72-12722
- Flight vibration testing methods for ascertaining flutter stability of high speed aircraft [DGLR PAPER 71-083] 02 p0155 A72-12725
- Wind tunnel model instrumentation and captive trajectory facilities for aircraft stability, control and metric wing-pylon store tests for performance and structural predictions 03 p0339 A72-12921
- Differential and difference equations approximate solutions in finite state machine form, developing adaptive gain changer model in aircraft stability control system 03 p0338 A72-13164
- Dynamic stability, control and structural response of transonic jet transport to atmospheric turbulence 05 p0611 A72-16348
- NF-8D aircraft variable stability system ground/in-flight calibration for determination of flight control system dynamics effects on flying qualities 05 p0611 A72-16660
- Flight control systems development, discussing on-board computers use in subsystems functional integration, stabilization and landing systems, inertial navigation and flight simulation 05 p0687 A72-16736
- Direct side force control by rudder deflection and asymmetrical drag utilization to cancel yawing moment, discussing variable stability T-33 flight tests [AIAA PAPER 72-94] 05 p0613 A72-16946
- Model following variable stability system for X-14B VTOL aircraft, discussing hardware design and flight evaluation [AIAA PAPER 72-96] 05 p0613 A72-16978
- Motion dynamics of aircraft-autopilot closed loop system under influence of atmospheric turbulence and electric circuitry thermal noise 07 p0911 A72-18990
- Book on dynamics of atmospheric flight covering unsteady motion, small disturbance theory, aerodynamic characteristics, aircraft stability and control, handling qualities, etc 08 p1109 A72-21491
- Nonlinear longitudinal aerodynamic characteristics effect on rigid aircraft response to normal acceleration due to atmospheric turbulence, using power spectral technique 09 p1263 A72-23461
- Pitching moments effect on phugoid and height mode stability of aircraft in supersonic flight 09 p1263 A72-23622
- Flight airworthiness requirements development for supersonic transports, V/STOL and transport and general aviation aircraft, exploring critical control and stability parameters [SAE PAPER 720306] 11 p1575 A72-25570
- Runway motion stability of aircraft with three wheel landing gear, assuming elastic response to moment induced drift 12 p1753 A72-27235
- Hydrofluidic stability augmentation system (HYSAS) development for military helicopters, discussing test program and technical feasibility 12 p1754 A72-27407
- Flight tests of stability augmentation system for light airplane improving pilot control during IFR encounter 12 p1754 A72-27513
- Thunderstorm-associated aircraft mishaps relation to surrounding synoptic scale meteorological conditions, discussing storm interior condition contribution to flight stability upset 13 p1992 A72-28851

- Aeroelasticity, discussing gust and maneuver load alleviation, flutter suppression, aircraft stability, computerized aeroelastic analysis, aeroelastic optimization, composite structures, etc 15 p2322 A72-31202
- Hydrofluidic three-axis stability augmentation system to improve UH-1B helicopter damping and handling qualities during high speed gunfiring missions 16 p2350 A72-33650
- Russian book on flight dynamics covering horizontal flight, takeoff, climb and landing characteristics, meteorological conditions, helicopters, trajectory problems, stability and controllability analysis, etc 16 p2349 A72-33874
- An experimental investigation of STOL longitudinal flying qualities in the landing approach using the variable stability X-22A aircraft. [AHS PREPRINT 642] 17 p2490 A72-34502
- The world speed records of the SA 341 - Gazelle. [AHS PREPRINT 651] 17 p2491 A72-34506
- Hydrofluidic stability augmentation system for U.S. Army helicopters, emphasizing reliability, maintainability and reduced cost 17 p2492 A72-34928
- F-111 stall inhibitor system with angle of attack limitation, describing interface with stability augmentation system 17 p2493 A72-35577
- Special control of spiral flight curves with the neutral and maneuver points as ultimate positions of the indifference points 18 p2643 A72-36942
- STOL transport stability and control derivative prediction methods and accuracy requirements. [AIAA PAPER 72-780] 19 p2752 A72-38139
- Optimal selection of stability augmentation parameters for excellent pilot acceptance. 19 p2752 A72-38227
- A generalized method for the identification of aircraft stability and control derivatives from flight test data. 19 p2753 A72-38260
- Problems and solutions related to the design of a control augmentation system for a longitudinally unstable supersonic transport. [AIAA PAPER 72-871] 20 p2887 A72-39128
- Maneuver load control and relaxed static stability applied to a contemporary fighter aircraft. [AIAA PAPER 72-870] 20 p2887 A72-39129
- A new method of calculating the natural vibrations of a free airplane. [ICAS PAPER 72-05] 21 p3120 A72-41130
- Analytic prediction of aircraft spin characteristics and analysis of spin recovery. [AIAA PAPER 72-985] 22 p3136 A72-42329
- Development of design criteria for predicting departure characteristics and spin susceptibility of fighter-type aircraft. [AIAA PAPER 72-984] 22 p3136 A72-42330
- Evaluation of flight instrumentation for the identification of stability and control derivatives. [AIAA PAPER 72-963] 22 p3136 A72-42346
- Aircraft longitudinal stability under conditions of varying atmospheric density, thrust force and velocity, determining critical altitude for vanishing oscillations [AIAA PAPER 72-951] 22 p3138 A72-42358
- Steady state equations of motion, equilibrium shape and stability derivatives of elastic airplanes evaluated with finite element methods. 22 p3138 A72-42845
- Output-feedback control law for randomly distributed multivariable system. 23 p3275 A72-43608
- ### AIRCRAFT STRUCTURES
- #### NT AIRFRAMES
- #### NT FUSELAGES
- #### NT PLASTIC AIRCRAFT STRUCTURES
- Warpage control of large Al alloy forgings machining of jumbo jet components, using packing and storage methods [SAE PAPER 710801] 01 p0074 A72-10280
- Structural sandwich panel design, establishing simple stress and deflection formulas under transverse loading based on tests evaluating balsa as laminate core 01 p0138 A72-10723
- Aircraft interior materials selection relative to fire hazards and smoke emission properties [PI PAPER 18] 03 p0380 A72-13249
- High strength, stiffness and low density properties of boron/aluminum matrix composites in flight structures 04 p0585 A72-14745
- Papers on aerospace structure by N. J. Hoff covering aircraft framework, stress analysis, structural stability, shell theories, bending, buckling, monocoque and sandwich structures, etc 04 p0591 A72-15238
- Step-by-step perturbation method for calculating vibration modes of aerospace structure [ONERA, TP NO. 968] 04 p0592 A72-15552
- Hailstone impact simulator for prediction of hail damage to aircraft structures, presenting data on damage to flat metal sheets and spherical caps [AIAA PAPER 72-163] 05 p0645 A72-16957

- Unidirectional carbon fiber composites effects and use of stress envelopes in aircraft structure design 05 p0681 A72-16997
- Concorde airframe testing for thermal effects on structural strength and fatigue life, discussing facilities for flight conditions simulation 05 p0614 A72-17197
- Adhesive bonded components in aircraft and aerospace structures, discussing manufacturing, metal surface preparation, inspection and environmental exposure [SAE PAPER 720118] 06 p0835 A72-17325
- Fatigue behavior of notched or cracked aircraft structure parts, examining service life prediction problem 06 p0895 A72-17811
- Structural demonstration flight testing (U.S. Navy, of new aircraft, presenting maneuver checklist 06 p0759 A72-18489
- Airloads and structural integrity flight testing (U.S. Air Force), noting dynamic response, fatigue tests and temperature data acquisition 06 p0759 A72-18490
- Aircraft light alloy integral construction for stress concentration and fatigue failure avoidance, describing continuous casting process, stress relieving and ultrasonic flaw testing procedures 07 p0995 A72-19725
- Mercury short haul transport aircraft, emphasizing lightweight structural design with extensive use of integral machined components for fatigue safety 07 p0913 A72-20310
- Wilga 3 aircraft structure service life from structural fatigue theory and tests, emphasizing operational load distribution measurement 08 p1110 A72-21634
- Large automated tape placement machine tool design and construction for laying up aircraft structures from composite materials 08 p1177 A72-21690
- Heat treatment and machining for distortion control of large Al alloy forgings for DC 10 aircraft 09 p1317 A72-22476
- Automatic riveting machine for fuel tight aircraft structures, describing process technique and machine design details and features 09 p1319 A72-22906
- Corrosion resistant fabrication methods in jumbo jetliners components to reduce maintenance and repair downtime, discussing clad wing and fuselage skins 10 p1487 A72-24022
- Structural Acoustic Monitor system for airframe structural proof testing, providing multichannel recording and aural monitoring of acoustic data derived from aircraft mounted accelerometers 10 p1459 A72-24146
- Unsteady aerodynamic loadings of flexible aircraft with nonplanar wings and wing-tail surfaces in supersonic flow [AIAA PAPER 72-378] 11 p1574 A72-25402
- Aircraft wing structure fatigue life estimates based on flight load time histories from counter accelerometer [SAE PAPER 720305] 11 p1733 A72-25569
- Layered anisotropic fiber composite (Tetra-Core) for sandwich construction and aircraft applications, discussing design, fabrication and strength characteristics [SAE PAPER 720343] 11 p1638 A72-25599
- Crack initiation detecting and recording instrument with optical strain gages for double shear fatigue tests of aircraft fasteners 11 p1632 A72-25823
- Optical quality requirements for aircraft transparencies, considering resolution, haze, halation, light transmission, distortion, binocular deviation, double images, scratches and inclusions 12 p1832 A72-27003
- Optical qualities of aircraft windshields and direct vision windows, considering color, light transmission, faults, heating, distortion, inside reflections and double images 12 p1832 A72-27004
- Aircraft windscreen design, discussing high impact strength glass, electroconductive film, transparency service life and weight reduction 12 p1753 A72-27006
- Aircraft fuselage acrylic glazing design, covering passenger cabin window, cockpit windscreen and various surface coatings 12 p1753 A72-27008
- Acrylics and polycarbonates properties in aircraft transparencies design, emphasizing cost and optical, mechanical, thermal and chemical properties 12 p1832 A72-27009
- Polycarbonates applications in aircraft transparencies, discussing chemical, heat, impact and abrasion resistance, toughness and weathering 12 p1832 A72-27010
- Aircraft windscreen reliability, discussing delamination, interface shear stress effects and analogy to metal fatigue 12 p1812 A72-27011

Concorde aircraft optical transparency components design characteristics and reliability tests, noting visor, pilot forward windshield, flight deck side windows and cabin windows

12 p1753 A72-27012

Aircraft windshield bird impact resistance, noting weight, speed, angle and window geometry effects

12 p1813 A72-27014

Transparent aircraft polycarbonate glazing systems shielding properties for projectile and bird impacts

12 p1832 A72-27015

Chemically strengthened glass for eject-through frangible canopy design in aircraft emergency escape systems, noting protection against ejection injuries

12 p1813 A72-27016

Emergency escape from high performance military aircraft in flight and on ground, using explosive cord for transparent canopy material breakup

12 p1753 A72-27017

Metal matrix composites application to aircraft structures, describing design, analysis and fabrication of aircraft bulkhead with B-Al as main structural material

12 p1886 A72-28096

Graphite fiber-epoxy composite systems development for F-5 aircraft landing gear door, speed brake, leading and trailing edge flaps and horizontal stabilizer

12 p1835 A72-28097

Russian book on An-12 turboprop transport aircraft structural and aerodynamic characteristics covering engine operation, piloting, stability, controllability, etc

12 p1755 A72-28343

Boron and carbon fiber reinforced plastics applications in aircraft and engine structural components, discussing dynamic and impact damping properties compared to conventional materials

13 p1982 A72-28555

General Dynamics model 401 air superiority single engine fighter design stressing light weight structure and maneuverability at high speeds and angles of attack

13 p1896 A72-28575

Optimal design of thin walled minimum weight aircraft shell structures, using linear programming

13 p2058 A72-29143

Stress levels and fatigue in aircraft structures subjected to jet noise, noting stress calculation for skin panels and control surfaces

13 p1898 A72-29579

Dynamically similar wind tunnel models for transonic aeroelastic studies of aircraft failures or structural damage and flutter margins

13 p1939 A72-29672

Aircraft structures design and development with composite materials, considering materials characteristics relations to structural components dynamic response

13 p2060 A72-29691

Computer algorithms and programs contribution to aircraft structure operational reliability and fatigue life calculation

14 p2164 A72-30288

Ni-Cr-Ti steel aircraft structural element fatigue life calculation based on failure mechanism involving crack propagation

14 p2164 A72-30429

Mechanics fundamentals in aerodynamical aircraft analysis, noting force concept and Newton theory

14 p2073 A72-30817

Navy program for composites technology development in aircraft structures, discussing design, reliability and cost

14 p2073 A72-30860

L-1011 propulsion, fuel, flight control, navigation, avionics, communication, electrical, environmental control and auxiliary power systems, discussing structure and high lift devices

15 p2181 A72-32427

Adhesive bonding of L-1011 body shell panels for improved fatigue strength and corrosion resistance

15 p2245 A72-32429

Cost-saving techniques in helicopter structural test methods, suggesting system simulation, component replacement time calculation and computer techniques

16 p2373 A72-33221

Resonant vibration of thin walled rods and stiffened plates and cylindrical shells, noting aircraft and rocket structures

16 p2471 A72-33679

Application of boron/epoxy to the CH-54B Skyvane helicopter.

[ASME PREPRINT 670]

17 p2491 A72-34510

Full scale airframe fatigue testing of the CH-46.

[AHS PREPRINT 671]

17 p2491 A72-34511

Al alloys, high strength steels and Ti alloys in aircraft construction, reviewing premetal materials in heavier than air vehicles

17 p2568 A72-35375

Russian book on aircraft design covering flight conditions, structure and control characteristics, production and stress analysis

17 p2492 A72-35448

Boron- and graphite-epoxy and boron-aluminum composites forming, processing and costs for aircraft structural materials

17 p2560 A72-35663

Combined spot weld-adhesive bonding to join sheet metal parts with applications to propellant tanks and spacecraft and aircraft structures

[SME PAPER AD 72-710]

18 p2695 A72-36526

Analysis of a partially cracked panel.

18 p2735 A72-36771

Graphite-epoxy composites application to commercial transports for weight and cost reduction

19 p2873 A72-37680

A flutter optimization program for aircraft structural design.

[AIAA PAPER 72-795]

19 p2876 A72-38111

Structural development of the L-1011 Tri-Star.

[AIAA PAPER 72-776]

19 p2876 A72-38135

High subsonic transport aircraft design development based on supercritical aerodynamic configuration and advanced structural, flight control and propulsion system technologies

[AIAA PAPER 72-756]

20 p2889 A72-40056

Russian book - Handbook of aircraft materials.

21 p3072 A72-40459

Sheet metal economics in aircraft construction based on strength/weight and stiffness/weight comparison of Al alloys and Ti alloys in relation to cost and structural weight considerations

21 p3060 A72-41071

Aircraft structures weight reduction through fiber-matrix composite materials, discussing anisotropic elastic and failure behavior of composite light shell structures

[ICAS PAPER 72-38]

21 p3120 A72-41163

Russian book - Design principles in aircraft construction.

22 p3136 A72-42074

Digital data system with real time displays and multiprocessing capability for multistep of aircraft structure with operational manpower reduction, assessing performance

22 p3163 A72-42696

Book - Contributions to the theory of aircraft structures.

22 p3238 A72-42826

Transport aircraft wing compression panel failure in bending test due to stringer interruptions, analyzing structural deficiency via column and beam bending theories

22 p3183 A72-42827

Aircraft structural design loads definition by mission analysis criteria, taking into account gust loads via power spectral density method

22 p3138 A72-42828

Aircraft structural safety criteria based on acceptable failure probability, determining critical load levels

22 p3138 A72-42829

ICAO structural airworthiness requirements relation to air transportation safety, considering maneuver and gust loads in terms of limit load concept

22 p3138 A72-42830

Fatigue strength and fail-safe aspects of lug joint in aircraft structures, considering tension-compression load, fretting corrosion, prestress and residual stress

22 p3239 A72-42851

Vibration measurements of an airplane fuselage structure. I - Turbulent boundary layer excitation. II - Jet noise excitation.

22 p3139 A72-42912

Reliability analysis in the estimation of transport-type aircraft fatigue performance.

22 p3241 A72-42971

Hi-Shear and Hi-Lok fastening systems for aircraft manufacture, comparing strength and weight with conventional rivets and bolts

[SAWE PAPER 901]

23 p3293 A72-43451

Detection of structural deterioration and associated airline maintenance problems.

[SAWE PAPER 918]

23 p3293 A72-43465

Empty weight and cruise performance of very large subsonic jet transports.

[SAWE PAPER 919]

23 p3251 A72-43466

Moment sampling method as selfvalidating aircraft weight and balance accounting procedure

[SAWE PAPER 920]

23 p3251 A72-43467

Aircraft design structural weight estimation based on post-design analysis of production aircraft, discussing weight factors application to new designs

[SAWE PAPER 936]

23 p3251 A72-43476

The surface flaw in aircraft structures and related fracture mechanics analysis problems.

23 p3352 A72-44228

Liquid and solid precipitation on aircraft structure surfaces, discussing potential hazards to engine components and aircraft controls due to ice formation

23 p3252 A72-44339

Aircraft structures shock and blast loading characteristics from internal detonation, comparing computer program results with available data

24 p3365 A72-44610

Aircraft fatigue: Design, operational and economic aspects.

24 p3366 A72-44726

Optimum design of joints - The stress severity factor concept.

24 p3455 A72-44728

Fatigue testing of the F.28 Fellowship.

24 p3366 A72-44729

Design and certification for executive type aircraft.

24 p3366 A72-44730

Fan jet Falcon design and certification tests.

24 p3366 A72-44731

The application of Ti-6Al-4V titanium to helicopter fatigue loaded components.

24 p3366 A72-44732

Aircraft structures fatigue life expectancy under random acoustic excitation, describing testing methods and equipment

24 p3367 A72-44739

The importance of service inspection in aircraft fatigue.

24 p3367 A72-44740

Fatigue design and test program for the American SST.

24 p3367 A72-44741

Structural fatigue cost penalties in airline operations, considering inspection, maintenance and carrying capacity reduction

24 p3367 A72-44743

Structural fatigue cost in aircraft maintenance and repair, considering inspections, defect rectification, preventive modifications, replacements and NDT

24 p3367 A72-44744

Observations on designing to combat fatigue and its effects on the economics of civil transport aircraft.

24 p3368 A72-44745

Military aircraft construction, design and economic requirements, discussing fighter payloads, armament efficiency and fire control systems

24 p3369 A72-45450

AIRCRAFT TIRES

Aircraft landing gear wheel damage and antiskid mechanisms under operational conditions

08 p1109 A72-21485

Aircraft wheel mechanics, discussing freely turning and braked wheels, tire drift and antiskid braking systems for landing gear

11 p1574 A72-25287

Aircraft tires design and performance characteristics, considering VTOL and Concorde operating conditions

13 p1901 A72-30098

Ground and torque relation to swivel angle and lateral displacement of wheel rim plane, using string model for tire

21 p2996 A72-41260

AIRCRAFT WAKES

NT HELICOPTER WAKES

NT PROPELLER SLIPSTREAMS

NT SLIPSTREAMS

Jet aircraft brake parachute loads under engine wake, evaluating velocity and drag coefficient influences

02 p0155 A72-12504

Subsonic wind tunnel investigation of aircraft wake far field structure, measuring trailing vortex decay by yawhead pressure probe

[AIAA PAPER 72-40]

05 p0607 A72-16902

Turbulent boundary layer analogy mathematical model for turbulent mixing and buoyancy effects on aircraft trailing vortex wake motion and persistency

[AIAA PAPER 72-42]

05 p0607 A72-16903

Acoustic ray deflection by aircraft wake vortices with viscous core, observing maximum deflection angles during large aircraft landing

18 p2641 A72-36417

Effect of ground wind shear on aircraft trailing vortices.

20 p2886 A72-39630

Flight test studies of the formation of trailing vortices and a method to accelerate vortex dissipation.

[AIAA PAPER 72-988]

22 p3134 A72-42327

Unsteady wake effects on progressing/regressing forced rotor flapping modes.

[AIAA PAPER 72-957]

22 p3137 A72-42350

Low flying aircraft wake vortices tracking, describing sensing techniques based on acoustic pulse deflection and velocity field measurements

22 p3179 A72-42709

Effect of air injection on the torque produced by a trailing vortex.

23 p3247 A72-43333

Effect of several wing tip modifications on a trailing vortex.

23 p3247 A72-43334

Trailing vortex effects on wing pressure distribution from low speed wind tunnel tests, discussing effect of wing-vortex distance

24 p3362 A72-45331

Dynamic simulation of an aircraft under the effect of vortex wake turbulence.

24 p3368 A72-45346

AIRCRAFTS

U FLIGHT CREWS

AIRFIELD SURFACE MOVEMENTS

AIRFIELD SURFACE MOVEMENTS

Airfield surface radar detection equipment to control aircraft and ground vehicles under reduced visibility and darkness

02 p0173 A72-12105

Air/ground interface simulation in GPSS/360 for passenger transfer between airport terminal and aircraft

07 p1106 A72-20342

Anthropotechnical aspects of aircraft taxiing guidance in airfield runway areas, suggesting computerized operational system

09 p1269 A72-22779

ICAO standardized taxiing guidance and airports surface traffic control procedures

10 p1459 A72-24171

Runway motion stability of aircraft with three wheel landing gear, assuming elastic response to moment induced drift

12 p1753 A72-27235

AIRFOIL CHARACTERISTICS

U AIRFOILS

AIRFOIL PROFILES

NT WING PROFILES

NT WING SPAN

Two dimensional airfoil pressure distribution measurements at high subsonic speeds, comparing normal force coefficients corrected for wind tunnel interference effects with theoretical calculations

[DFVLR-SONDDR-168] 03 p0308 A72-13609

Two dimensional transonic airfoil section testing at ONERA S3MA wind tunnel, comparing results with helicopter rotor blades test data

[ONERA, TP NO. 1028] 03 p0308 A72-13642

Navier-Stokes equations solution for unsteady viscous flow around oscillating elliptic airfoil in turbomachinery flutter analysis, obtaining pressure and shear stress distributions

05 p0600 A72-16002

Finite pitch airfoil theory relations for turbomachine moving blade rows interference effect on cascade flutter

05 p0738 A72-16488

Computerized analytical model of two dimensional multicomponent airfoil in viscous subsonic flow

[AIAA PAPER 72-2] 05 p0606 A72-16861

Sail rotors for hovering platform, calculating rotor performance based on ideal two-dimensional flexible airfoil section characteristics

[AIAA PAPER 72-66] 05 p0612 A72-16925

Optimal airfoil profile for minimum drag in supersonic linearized gas flow with allowance for random fabrication errors and surface melting and sublimation at high temperatures

05 p0610 A72-17136

Laminar flow airfoils for gliders, optimizing profiles for favorable velocity and pressure distribution

05 p0610 A72-17194

Finite difference method for transonic airfoil design for wide range of angles of attack and Mach numbers

06 p0755 A72-17629

Hypersonic flow past final thickness delta wing, presenting conical flow equations with boundary value solution

06 p0757 A72-18128

Viscous flow through movable and immovable cascades of blades, determining velocity field by airfoil center line vortex distribution

06 p0757 A72-18131

Numerical analysis of computing velocity distribution in vortex row cascade profiles by method of singularities

07 p0965 A72-18787

Plane stationary flow of ideal incompressible fluid past large camber profiles of arbitrary shape and thickness, using computerized Fourier expansion

07 p0908 A72-18976

Irrational two dimensional transonic flow past symmetric profile with and without shock

07 p0909 A72-20068

Airfoil contour design as envelope of family of circles with centers lying on mean camber line

09 p1259 A72-22298

Axial flow turbines aerodynamic loading increase via control of velocity distribution and boundary layer evolution around airfoil profiles

[ASME PAPER 72-GT-78] 11 p1571 A72-25658

Rotating airfoil experimental test program for verification of Himmelskamp and Dwyer-McCroskey theoretical analysis, presenting graphs of lift coefficient vs angle of attack

12 p1752 A72-28124

Slender profile in nonuniform flow, deriving lift, normal force distribution and moment from vortex and source distribution induced flow field

13 p1894 A72-29005

Aerodynamic profiles lift coefficient determination by empirical formula based on potential flow lines obtained by conformal mapping

13 p1894 A72-29132

Arbitrary cascade profiles aerodynamic characteristics calculation via integral equation numerical solution for attached potential incompressible fluid problem

14 p2070 A72-31014

Local subsonic flow region in transonic free flow past airfoil profile, transforming flow differential equations into linear Beltrami equations system via Chaplygin transformation

15 p2178 A72-31473

Contracting or diverging stream flow mean velocity change effects on airfoil pressure distribution, circulation and lift, deriving vortex distribution expression

15 p2179 A72-32023

Book on airfoil section designs for light aircraft covering wind tunnel studies of lift drag ratio as function of angle of attack

15 p2179 A72-32250

Unsteady viscous flow effects on aerodynamic forces exerted on oscillating elliptic airfoil for various Reynolds numbers, angles of attack and frequencies

15 p2180 A72-32344

Collocation method for coupled bending-torsion vibrations of straight uniform cantilever beam with asymmetric airfoil cross section

16 p2464 A72-32908

Transonic airfoil section design to given surface pressure distribution, applying finite difference procedures to transonic small disturbance equations

[AIAA PAPER 72-679] 16 p2346 A72-34062

Influence of airfoils on stall flutter boundaries of articulated helicopter rotors.

[AHS PREPRINT 621] 17 p2484 A72-34489

Determination of airfoil and rotor blade dynamic stall response.

[AHS PREPRINT 613] 17 p2490 A72-34495

Comparison of two types of blade profile for axial-flow fans

18 p2720 A72-36000

Uniformly exact solution of the problem of the flow past a slender profile

20 p2886 A72-39904

Book - A theory of supercritical wing sections, with computer programs and examples.

21 p2993 A72-41534

Problem of uniform-jet flow around an airfoil

22 p3133 A72-42271

New results concerning the numerical calculation of the sonic flow around a given airfoil section

22 p3135 A72-42639

An improved solution of the two-dimensional jet-flapped airfoil problem.

23 p3247 A72-43329

Plane stationary flow of ideal incompressible fluid past large camber profiles of arbitrary shape and thickness, using computerized Fourier expansion

24 p3360 A72-45002

AIRFOIL SECTIONS

U AIRFOIL PROFILES

AIRFOIL THICKNESS

U AIRFOIL PROFILES

AIRFOILS

NT AERIAL RUDDERS

NT AILERONS

NT ARROW WINGS

NT CARET WINGS

NT CRUCIFORM WINGS

NT DELTA WINGS

NT ELEVATORS [CONTROL SURFACES]

NT FIXED WINGS

NT FLAPS [CONTROL SURFACES]

NT FLEXIBLE WINGS

NT HORIZONTAL TAIL SURFACES

NT JET FLAPS

NT LAMINAR FLOW AIRFOILS

NT LEADING EDGE SLATS

NT LIFTING ROTORS

NT LOW ASPECT RATIO WINGS

NT PARAWINGS

NT PROPELLER BLADES

NT RECTANGULAR WINGS

NT RIGID ROTORS

NT RING WINGS

NT ROTARY WINGS

NT SLENDER WINGS

NT SPLIT FLAPS

NT SPOILERS

NT SUPERCRITICAL WINGS

NT SUPERSONIC AIRFOILS

NT SWEPT WINGS

NT SWEPTBACK WINGS

NT THIN AIRFOILS

NT THIN WINGS

NT TILTING ROTORS

NT TIP DRIVEN ROTORS

NT TRAILING-EDGE FLAPS

NT TWISTED WINGS

NT UNSWEPT WINGS

NT VARIABLE SWEEP WINGS

NT WING FLAPS

NT WINGS

Unsteady flow about two dimensional airfoils, determining surface pressure fluctuations induced by turbulent boundary layers

01 p0001 A72-10217

Straight line computer solution of Chaplygin equation, with application to high subsonic gas flow incident on airfoil with local supersonic zone

02 p0149 A72-11581

Aerodynamic behavior of thin jet-flapped airfoil, investigating integrodifferential equation solution

02 p0149 A72-11669

Skin friction measurement in nonisobaric subsonic flow with pressure gradient over airfoil section by surface impact probes

02 p0151 A72-12275

Airfoil theory singular integrodifferential equation reduction to integral equations with quasi-regular and regular kernels, applying to jet flapped wing problem

03 p0381 A72-12987

Steady two dimensional cavity flow past infinite number of airfoils using linearized theory

04 p0461 A72-14460

Complex perturbation potential of constant vortex shear flows around airfoil activated by motion in presence of rectilinear wall

05 p0600 A72-16122

Slat-airfoil combinations aerodynamics modeled by single point vortex to represent leading edge slat, discussing on-line computer graphics program

[AIAA PAPER 72-221] 05 p0603 A72-16798

Turbulent boundary layer development for airfoil at high transonic speeds, discussing viscous-inviscid flow interaction

[AIAA PAPER 72-5] 05 p0606 A72-16863

Two dimensional airfoil unsteady stall in incompressible flow, comparing calculated loading during transient and sinusoidal pitching motions with measured values

[AIAA PAPER 72-37] 05 p0607 A72-16899

Two dimensional lift characteristics of multielement airfoils, using potential flow method based on surface source distribution and finite difference boundary layer method

[AIAA PAPER 72-3] 05 p0608 A72-16935

Transonic flow past wing airfoils, obtaining numerical solution by fitting mixed initial boundary conditions

07 p0909 A72-20079

Interference induced unsteady aerodynamic forces on tandem airfoils in subsonic flow, using two dimensional model

07 p0910 A72-20101

Jet-STOL augmentor wing consisting of moderately thick airfoil with full span leading edge slat and double surface trailing edge flap

08 p1110 A72-21899

Static pressure tube calibration for surface pressure measurements in flow over flat plate and airfoil

09 p1261 A72-22937

Airfoil ram-wing air-water hybrid vehicle X-113 Am design and operational principles based on aerodynamic ground effect, discussing flight tested performance characteristics

09 p1262 A72-22971

Aerodynamic noise produced by gas jet flow around airfoil, discussing sound reduction

10 p1417 A72-24107

Aerodynamic forces calculation for constant vortex shear flows around airfoil fixed between rectilinear walls, noting resultant perpendicularity to Ox axis

10 p1465 A72-24115

Unsteady airfoil stall and stall flutter analysis, discussing application to space shuttle configuration

[AIAA PAPER 72-380] 11 p1730 A72-25404

Unsteady lift on airfoils in moving cascades with inlet axial flow disturbances, estimating lift on reference blade between blade channels

[ASME PAPER 72-GT-5] 11 p1568 A72-25608

Heat transfer rates of impingement cooling in gas turbine airfoils, noting leading edge sharpness effects for slot and circular jet configurations

[ASME PAPER 72-GT-7] 11 p1703 A72-25610

Lift and pressure fluctuations of cambered airfoil under periodic longitudinal and transverse gusts, applying to axial flow turbomachines

[ASME PAPER 72-GT-30] 11 p1569 A72-25626

Airfoil vortex shedding noise in low-turbulence flow at helicopter blade Reynolds numbers, obtaining correlation coefficients for far field noise and surface pressure fluctuations

[AIAA PAPER 72-656] 16 p2347 A72-34078

Rotary wings lift and efficiency increase by circulation control via tangential blowing about bluff trailing edge airfoils

[AHS PREPRINT 603] 17 p2489 A72-34492

Study of circular arc airfoils with asymptotic critical Mach number. I

17 p2484 A72-34744

Study of circular arc airfoils with asymptotic critical Mach number. II

17 p2484 A72-34745

Transonic viscous flow around lifting two-dimensional airfoils.

[AIAA PAPER 72-678] 17 p2486 A72-35479

Angle of attack increase of an airfoil in decelerating flow.

18 p2641 A72-36773

Surface evaluation of airfoils via contouring.

19 p2806 A72-37605

Analysis of the interaction of jets and airfoils in two dimensions.

[AIAA PAPER 72-777] 19 p2746 A72-38136

Surface vorticity theory for axisymmetric potential flow past annular aerofoils and bodies of revolution with application to ducted propellers and cowls.
19 p2747 A72-38554

Aerodynamic test facility data on swept wings, peaky airfoils, aircraft flutter and transonic flow, discussing shock tubes and wind tunnels development.
20 p2912 A72-39846

Visualization study of flow near the trailing edge of an oscillating airfoil.
20 p2886 A72-40067

Periodic wave of oscillating and stationary two dimensional bodies immersed in uniform incompressible stream, investigating semiinfinite vortex trails relationship to oscillating airfoils
21 p2989 A72-40651

Some results from tests in the NAE high Reynolds number two-dimensional test facility on 'shockless' and other airfoils.
[ICAS PAPER 72-33] 21 p2991 A72-41158

Conformal mapping procedure for numerical generation of airfoils with local curvature singularities, presenting test problem results for zero trailing edge angle
21 p2992 A72-41259

Lift on airfoils with separated boundary layers.
21 p2992 A72-41264

Calculation of potential flow about aerofoils using approximation by splines.
22 p3135 A72-42849

The determination of a general relation between the aerodynamic properties of a single airfoil and those of the same airfoil arranged in an arbitrary cascade.
24 p3363 A72-45363

Computation of wall effects in ventilated transonic wind tunnels.
[AIAA PAPER 72-1007] 24 p3388 A72-45403

AIRFRAME MATERIALS

Ti alloys for airframe shell construction based on room temperature strength, stiffness and densities comparison with Al alloys, stainless steel and Be data
03 p0373 A72-13615

Ti alloys for aircraft structures, emphasizing weldability, tensile fatigue and residual strengths, shear-carrying qualities and fuselage shell design
03 p0373 A72-13616

Carbon fiber resin composite characteristics for airframe component design, comparing with metal materials
04 p0537 A72-14746

Aircraft hydrocarbon fuel tank lightning protection in airframes, using adhesive bonding, high strength materials and high modulus fiber structures
07 p1086 A72-18767

Thin wall airframe wire insulation relative thermal life and temperature rating evaluation procedure using Arrhenius plot
09 p1339 A72-23270

Compressive strength of Ti alloy airframe skin stringer panels reinforced with B-Al composite by brazing
[AIAA PAPER 72-359] 11 p1729 A72-25387

Fatigue strength characteristics of boron-epoxy reinforced Al stringers for helicopter airframe
[AIAA PAPER 72-392] 11 p1574 A72-25413

Boron/epoxy and graphite/epoxy composites application to aircraft structural design, discussing flight test and developmental programs
11 p1577 A72-26234

Long range transport aircraft structures and composite materials technology for airframe and engine systems
[AIAA PAPER 72-362] 13 p1897 A72-28955

Al alloys, high strength steels and Ti alloys in aircraft construction, reviewing premetal materials in heavier than air vehicles
17 p2568 A72-35375

Structural development of the L-1011 Tri-Star.
[AIAA PAPER 72-776] 19 p2876 A72-38135

Sheet metal economics in aircraft construction based on strength/weight and stiffness/weight comparison of Al alloys and Ti alloys in relation to cost and structural weight considerations
21 p3060 A72-41071

PRD-49, a new composite material - Its characteristics and its application to the BO-105 helicopter.
[SAWE PAPER 915] 23 p3305 A72-43462

The application of Ti-6Al-4V titanium to helicopter fatigue loaded components.
24 p3366 A72-44732

AIRFRAMES

Concorde airframe testing for thermal effects on structural strength and fatigue life, discussing facilities for flight conditions simulation
05 p0614 A72-17197

Statistical evaluation of welded airframe component fatigue damage increment during cyclic loading with constant force amplitude
10 p1559 A72-24922

Convective cooling system design for Mach 6 hypersonic transport Al alloy airframe, using water glycol loop network
[AIAA PAPER 72-334] 11 p1574 A72-25369

Inspectability criteria for airframes with fatigue fail safe design requirements for small airplane certification
[SAE PAPER 720310] 11 p1575 A72-25574

NASA aerodynamic technology program, emphasizing airframe and engine development for next generation subsonic CTOL jet transport requirements
[SAE PAPER 720319] 11 p1575 A72-25582

Airframe and wing fatigue life testing, discussing results recomputation for changed operating conditions
14 p2092 A72-30276

Welded steel airframe residual fatigue life tests by nonstationary random loading, applying to jet trainer aircraft landing gear
14 p2107 A72-30277

Computerized airframe manufacturing cost and weight analysis, using technique for detailed parts list generation from configuration concept as input
[SAWE PAPER 913] 23 p3293 A72-43460

Approaches to verification and solution of magnetic particle inspection problems.
24 p3407 A72-44903

Welding airframe structures in titanium using tensile loading to overcome distortion.
24 p3407 A72-45000

AIRGLOW

NT GEOCORONAL EMISSIONS
NT NIGHTGLOW
NT TWILIGHT GLOW
UV airglow in 1304 A line of oxygen from Cosmos 215 satellite
01 p0053 A72-10362

Lyman alpha, Lyman beta and Balmer alpha hydrogen airglow emission simultaneous measurements compared with solar radiation resonant scattering models
01 p0061 A72-10899

Computer program for atmospheric effects on IR radiation, calculating transmission and radiance spectra for various remotely sensed atmospheric, path and target conditions
02 p0187 A72-11862

Mountaintop high resolution spectral observations of diffuse isotropic submillimeter atmospheric and sky emission
02 p0274 A72-12194

Nitrogen dioxide producing chemiluminescent radiative and three-body recombination reaction at low pressures, determining airglow and oxygen atoms decay time by resonance fluorescence method
03 p0347 A72-13395

Bidirectional reflectance at several wavelengths from moonlit earth observations by airglow photometer on OGO-4 satellite
03 p0433 A72-13428

Quenching rate of vibrationally excited hydroxyl with molecular oxygen in fast flows for airglow studies in upper atmosphere
03 p0321 A72-13899

Van Rhijn height and intensity variations of 5577 A emission in night E layer airglow
04 p0518 A72-14960

Airglow considered as faint light emission during atomic and molecular dissociations in atmosphere, yielding clues to physical and chemical processes from spectrum
04 p0520 A72-15642

Bright O, C and carbon dioxide emissions in Martian airglow from temperature profile models based on Mariner UV spectrometry
06 p0803 A72-17446

Mariner 9 UV spectrometry observations of Mars airglow spectrum containing CO Cameron band and atomic oxygen and hydrogen lines
06 p0890 A72-18344

Ionospheric scintillations relationship to airglow emission spectrum at 6300 A
07 p0974 A72-18895

Airglow IR spectrum between 3 and 4 microns during morning and evening twilight, showing OH intensity drop
09 p1299 A72-22903

Airglow intensities and upper atmosphere physical processes relationship, discussing spectral features, emission brightness and excitation sources
10 p1474 A72-24714

Effective atmospheric emissivity for clear skies, showing dependence on surface vapor pressure
[AD-742882] 11 p1681 A72-26084

Luminous emissions of upper atmosphere, discussing relation to airglow and auroral phenomena
11 p1626 A72-26431

Airglow and auroral OI and NI allowed and spin forbidden transitions for above 9 eV excitation potential lines
14 p2098 A72-30145

Predawn airglow enhancement project, discussing magnetically conjugate photoelectron impact excitation observation and geophysical interpretation
14 p2098 A72-30147

Submillimeter isotropic background limits of stratosphere emission spectrum, using aircraft-borne Michelson interferometer and Rollin far IR detector
15 p2265 A72-31626

Near IR airglow observation by sound rocket to determine layer height diurnal variation and rocket axis zenith angle
15 p2231 A72-32328

Observation of the intensity ratio between /5,1/ and /9,4/ bands of OH emission in the night airglow.
17 p2546 A72-35059

Metastable atomic oxygen deactivation in upper atmosphere by inelastic collisions and by spontaneous irradiation, noting airglow intensity dependence on red lines irradiation
19 p2792 A72-38633

OH airglow IR observation from high altitude sites with bandpass filter, noting average spatial and diurnal fluctuations
19 p2794 A72-38861

Zodiacal light, airglow and lightning monitoring by wide field broad bandpass OSO-5 experiment, obtaining height profile, cell size and intensity variations of nightglow
21 p3054 A72-40619

Airglow observations with a Hadamard photometer.
22 p3169 A72-42023

Skylight intensity, polarization and airglow measurements during the total solar eclipse of 30 May 1965.
22 p3170 A72-42371

Theoretical calculations of the F-region tropical ultraviolet airglow intensity.
22 p3171 A72-42418

Observations of the airglow continuum.
22 p3174 A72-42888

Photochemistry of the airglow continuum.
22 p3153 A72-42889

Equatorial UV airglow azimuthal variations from spinning rocket measurements, attributing origin to electron collision excited atomic hydrogen Lyman alpha emission
23 p3282 A72-43263

Second positive system of nitrogen bands in the day airglow from Cosmos-224 data
23 p3282 A72-43356

AIRLINE OPERATIONS

Airport efficiency improvement measures, considering boarding gates, parking space, baggage handling, fire protection, monitoring and central control
02 p0200 A72-11717

Civil aviation air transportation contributing factors to American economy, considering disposable income, airline fares and time-trend variable
02 p0304 A72-11721

Air transport vs other travel, discussing time, costs, popularity and technology
03 p0459 A72-13485

Soviet look on air transport economics covering efficiency and control improvement, maintenance, work and wages, tariffs, cost and revenues, etc
03 p0459 A72-14098

Airline schedule keeping by Sud Lear all-weather landing system, discussing crew training
04 p0544 A72-14688

ATC technology impact on flight operations and public value of aviation, discussing microwave landing system economic aspects
04 p0544 A72-14810

Air traffic control long range planning for airlines and general aviation, discussing use of IFR, RNAV and IPC equipment
04 p0545 A72-14818

Aircraft operations effects on community noise pollution, discussing ATC airline operational procedures modifications in terms of noise reduction
04 p0464 A72-14819

Route charges system for Europe, stressing financial necessity
04 p0597 A72-15071

Toulouse-Bretigny link involving ATC and flight simulators with Concorde cockpit replica
04 p0545 A72-15072

United Air Lines computerized information retrieval system for message switching, flight planning and monitoring and aircraft parts inventory control
[IEEE PAPER 23,3] 04 p0598 A72-15713

Soviet air traffic service productivity increase and manpower saving by introduction of new airliner types
05 p0612 A72-16779

Air transportation modal split analysis by computer simulation program for determining utilization of alternative travel modes between origins and destinations
06 p0905 A72-17973

MARS digital simulation model in GPSS for determining scheduled flight operations and maintenance resources effects on aircraft availability and usage rates
06 p0779 A72-17976

Airfield law in Schleswig-Holstein Appeals Court decision concerning property owner suit against operator for unnecessary noise
06 p0906 A72-18170

Manufacturer viewpoint on aircraft engine safe introduction into airline service, discussing JT9D engine design for 747 aircraft

07 p1053 A72-18830

Utah-Colorado-New Mexico-Arizona regional air transportation study, assessing scheduled air carrier service demand for 1971-1990

07 p1102 A72-19178

Prediction of weather induced airline operating delays, discussing fog, snow, freezing rain, thunderstorms, crosswind, headwinds, CAT, wind shear, wet runways and tail winds

07 p1030 A72-19597

Federal regulation of airline mergers from viewpoint of history and current evaluating procedures in U.S.

07 p1106 A72-20675

Civil aviation physician duties for airline personnel and passenger benefit, discussing medical advice, health precautions, first aid training, etc

08 p1125 A72-21269

British regional airports development, discussing terminal facilities for scheduled and nonscheduled air carriers on domestic and international routes

10 p1459 A72-24170

Book on world airlines economic regulation, analyzing multilateral international agreements, national aviation interests and competitive situation

11 p1748 A72-25923

Skyguide airborne computer navigation system for airline applications, discussing system components, flight crew monitoring and optimization

11 p1684 A72-26999

Organizational changes due to electronic data processing /EDP/ introduction into INTERFLUG material-technical supply

12 p1890 A72-27273

Book on air transportation, covering history, government agencies roles in economic and safety regulation of air carriers, accounting, financial and legal aspects, etc

12 p1891 A72-28205

Complete aircraft systems reliability and maintainability, discussing extraordinary variances causes, faulty data inferences and operational testing for equipment specifications validation

13 p1896 A72-28358

Meteorological information requirements for V/STOL aircraft design, airport location, runway orientation, aircraft operations and ATC simulation

13 p1994 A72-28869

Electronic data processing in airline material supplies operations, discussing procedural efficiency improvement through reduction of stochastic effects inherent in aircraft maintenance operations

14 p2174 A72-30823

ATC operational systems, discussing global surveillance and voice and data communication between aircraft and earth station

14 p2129 A72-31141

Airline maintenance program and facilities for Boeing 747 aircraft based on optimized service concept

15 p2181 A72-32430

Total system approach to time scheduled aircraft operations - Conference, London, May 1972

15 p2339 A72-32451

Short haul airlines on-time operation, discussing ATC, weather, cargo and aircraft ground handling, cabin and flight services and aircraft reliability effects

15 p2339 A72-32452

Aircraft industry product support role in time delays minimization for aircraft operators, discussing malfunction report, minimum equipment decision and fault diagnosis

15 p2339 A72-32456

Concorde on-time operation as total management problem from design to airline operations, discussing techniques for in-flight failure diagnosis and onward reporting

15 p2181 A72-32460

Avionics effects on airline operations timekeeping, considering gains due to all-weather capability and engine monitoring vs possible losses due to equipment failures

15 p2208 A72-32461

Aircraft on-time operation and air traffic problems, considering solution requirement formulation and funding suggestions

15 p2339 A72-32462

Accessory reliability relation to on-time performance, discussing production route in terms of specification, design, development and manufacture

15 p2339 A72-32463

Jet aircraft gas turbine engine technology impact on safety, reliability, airline profitability and international trade

16 p2443 A72-33315

Developing countries civil aviation airlines evolution, considering government fund allocation, international money credibility, skilled manpower, equipment, fare and tourism expansion

16 p2481 A72-33332

Commercial airlines aircraft selection factors, considering size, range, economics, traffic, runway qual-

ity, maintenance and operating costs, reliability and cargo handling

16 p2348 A72-33333

Government regulations effects on local service airlines cost performance and growth strategies

16 p2481 A72-33374

Passenger transfer in airports with total separation between aircraft and permanent buildings for independent functioning, noting Dulles Airport mobile lounges

16 p2374 A72-34143

Airport planning requirements - An airline view

17 p2535 A72-34224

Maintenance of the 747. II - BOAC.

17 p2492 A72-34929

The legal position of civil air personnel

17 p2639 A72-35762

Air/ground digital communications in airline operations.

18 p2660 A72-36561

V/STOL - Selection and problems of the new medium

18 p2643 A72-37215

Application of electronic data processing airport analysis in airlines operations and for manufacturers.

19 p2747 A72-37277

Factors to be considered in airline scheduling.

19 p2883 A72-37745

How United trains DC-10 pilots.

19 p2760 A72-37898

Airline crew familiarization with DC-10 Computerized Flight Guidance System to calculate steering signal from raw data to follow flight path

19 p2831 A72-37899

Flight evaluation of three-dimensional area navigation for jet transport noise abatement.

[AIAA PAPER 72-814]

19 p2750 A72-38116

Day-to-day operational airplane-airport relationship, discussing runway grooving impact and friction coefficient measurement

[AIAA PAPER 72-813]

19 p2750 A72-38118

Application of optimization techniques to near terminal area sequencing and flow control.

19 p2832 A72-38255

Safety in commuter airline operation.

20 p2988 A72-39748

Visual simulation - A proven training method.

20 p2897 A72-39749

Airlines requirements for European airbus, discussing design of aircraft structure, control, pressurized cabin and propulsion system

21 p2994 A72-40174

A method of solving the operational planning problem for an engineering aircraft base

21 p3039 A72-40178

Operational implementation of area navigation.

21 p3079 A72-40279

System analysis for an airline operational environment through a computerized network simulation model.

21 p3025 A72-41077

Airport medical design guide /with comment on certain operational matters/.

22 p3150 A72-42500

Airline operational weighing and balancing of 747 aircraft, discussing accuracy and calibration procedures for electronic load cells, mobile platform scales and onboard aircraft weighing systems

[SAWE PAPER 917]

23 p3251 A72-43464

Detection of structural deterioration and associated airline maintenance problems.

[SAWE PAPER 918]

23 p3293 A72-43465

Minimum operational costs of passenger and cargo transport aircraft, considering effects of flight distance, wind conditions and optimum speed and altitude

23 p3252 A72-44338

Lockheed airline system simulation and aircraft scheduling models.

24 p3466 A72-44579

A systems analysis of subsonic versus supersonic jet travel.

24 p3466 A72-44580

Cost effective algorithm for optimal route aircraft scheduling for airlines by mixed integer multi-commodity flow technique and Dantzig-Wolfe decomposition

24 p3466 A72-44582

Applications of operational research in the airline industry.

24 p3466 A72-44583

Heuristic procedure solution for least cost commercial airline crew scheduling, emphasizing combinatorial space size reduction

24 p3466 A72-44584

Systems approach to airport passenger terminal planning.

24 p3387 A72-44585

International and regional scheduled air traffic terminals and general aviation airports characteristic objectives and operational aspects, discussing ATC, safety and noise problems

[DGLR PAPER 72-033]

24 p3387 A72-44616

Airline operational problems from traffic volume increase, discussing flight safety, passenger comfort, schedule adherence and economy aspects

[DGLR PAPER 72-037]

24 p3467 A72-44618

Structural fatigue cost penalties in airline operations, considering inspection, maintenance and carrying capacity reduction

24 p3367 A72-44743

Structural fatigue cost in aircraft maintenance and repair, considering inspections, defect rectification, preventive modifications, replacements and NDT

24 p3367 A72-44744

Observations on designing to combat fatigue and its effects on the economics of civil transport aircraft.

24 p3368 A72-44745

AIRLINERS

U COMMERCIAL AIRCRAFT

U PASSENGER AIRCRAFT

AIRPLANE PRODUCTION COSTS

Military systems cost reduction via civil avionics procurement techniques, discussing cost-reliability design criteria

15 p2338 A72-32215

Computerized airframe manufacturing cost and weight analysis, using technique for detailed parts list generation from configuration concept as input

[SAWE PAPER 913]

23 p3293 A72-43460

Economic and operational aspects of fatigue - Figures of a Swiss ground attack/fighter aircraft.

24 p3367 A72-44742

AIRPORT BEACONS

Discrete address beacon system /DABS/ development for surveillance and ground-air communications in support of ATC automation

22 p3204 A72-43151

AIRPORT LIGHTS

NT RUNWAY LIGHTS

Airport lights systems control with thyristors, discussing light intensity regulation, command board design and insulation test equipment

12 p1794 A72-27401

Airport lights system design for optical landing aids, discussing runway illumination conditions

12 p1795 A72-27402

Airport lighting for pilot guidance during approach and landing under category I-III visibility conditions, discussing runway layouts and power requirements

14 p2092 A72-30621

AIRPORT MOBILE LOUNGES

U MOBILE LOUNGES

STOL transport aircraft technology assessment, analyzing airports growth problems

[SAE PAPER 710751]

01 p0003 A72-10250

Acoustic echo sounder as real time monitor of airport environmental meteorological parameters

01 p0103 A72-11137

STOL aircraft for solving noise reduction and land use problems in future transportation systems, discussing airport location and layout for growing air traffic

01 p0005 A72-11153

Airport efficiency improvement measures, considering boarding gates, parking space, baggage handling, fire protection, monitoring and central control

02 p0200 A72-17177

Aircraft engine noise effects in airport vicinities, discussing measurement scales, turbofan sources, noise reduction and future air traffic

02 p0154 A72-12022

Airport terminal flow and interface transportation systems, discussing access, passenger traffic and cargo handling and government controls

03 p0339 A72-13414

Automated meteorological telemetry and interrogation response system with terminal extensions for Paris airport

04 p0508 A72-14695

German commercial airports adaptation to traffic development, considering economic factors

05 p0643 A72-16187

Spiralport design for maximum utilization of airport runways for landings and takeoffs

05 p0644 A72-16693

Water based offshore and floating island airports planning and construction, discussing economic, technical and social aspects

05 p0644 A72-16695

Newark airport program, discussing land preparation, public facilities, terminal area, building design, support systems, organization and scheduling

05 p0644 A72-16696

Air transport planning in coordination with urban and country development in West Germany

05 p0644 A72-16697

Airport financing, discussing funds, long term planning, commercial principles, private enterprise, loans and revenue

05 p0753 A72-16698

VTOL transport aircraft use in densely populated urban areas, discussing travel time, airport requirements, noise and design problems

05 p0612 A72-16733

Lounge planning model for airport terminal design simulation, taking into account scheduled arrivals and departures, aircraft types, passenger number, gate assignments, etc

06 p0780 A72-17979

ATC at single-runway airport analyzed by fast time simulation with high speed digital computers

07 p1032 A72-19064

Airfield surface system fast-time computer simulation model for airport planning systems analysis

07 p0965 A72-20341

Air/ground interface simulation in GPSS/360 for passenger transfer between airport terminal and aircraft

07 p1106 A72-20342

Wind shear, turbulence, precipitation, temperature, visibility and ceiling effects on airport capacity, suggesting weather data integration into ATC system for pilots information

08 p1147 A72-21521

Optimal high capacity runway systems for major airports, discussing multiple systems in anticipation of future mass air traffic requirements

10 p1459 A72-24169

British regional airports development, discussing terminal facilities for scheduled and nonscheduled air carriers on domestic and international routes

10 p1459 A72-24170

STOL aircraft systems development coordination, considering vehicle design, airport facilities and related ground environment, transportation modes interface and airspace management

11 p1574 A72-25255

New York-New Jersey megalopolis offshore jetport feasibility, considering noise, air-water pollution, land conservation, cost, etc

13 p1938 A72-28792

Slant Visual Range/Approach Light Contact Height Measurement System utilizing state of art technology for airport applications

13 p1938 A72-28848

Meteorological information requirements for V/STOL aircraft design, airport location, runway orientation, aircraft operations and ATC simulation

13 p1994 A72-28869

Building soundproofing codes for airport zoning ordinances, emphasizing wider latitude in land use options

13 p2067 A72-29561

Airport runway lighting systems development, noting lamp for night flights and control console

13 p1940 A72-30119

National airports system for UK civil air transportation, discussing economic, operational, accessibility and social aspects

15 p2214 A72-32321

Airport capacity and air traffic congestion effects on airport operations in terms of time and costs

15 p2359 A72-32454

Dallas/Fort Worth airport planning and construction economics impact on community economy and life style

16 p2373 A72-33307

Airport and air transportation benefits and costs to community and industry, considering institutional, environmental and economic issues

16 p2373 A72-33308

Airport economic and social impact on environs in terms of community development

16 p2373 A72-33309

Individual regions and nationwide air traffic demands forecasting for airport planning

16 p2481 A72-33311

Commercial airport and air transport service economic impacts on business and industrial communities

16 p2481 A72-33312

Major civil airport planning, discussing information gathering and processing for aviation demand, aircraft movements revenue and cost forecasts and pricing policy evaluation

16 p2481 A72-33327

Major civil airport development plan, discussing traffic forecasts, runways, noise, airspace capacity, access systems, freight installations, maintenance facilities, navigation aids, buildings, etc

16 p2373 A72-33328

Major civil airport passenger and cargo terminal complex design and layout planning, discussing various facilities and equipment requirements

16 p2373 A72-33329

FAA policy in issuing civil airport operating certificates and establishing minimum safety standards

16 p2373 A72-33330

ICAO assistance to member states in various transport airports and navigation facilities economics including accounting and financial statistics

16 p2481 A72-33334

Passenger transfer in airports with total separation between aircraft and permanent buildings for independent functioning, noting Dulles Airport mobile lounges

16 p2374 A72-34143

Airport planning requirements - An airline view.

17 p2535 A72-34224

Airport terminal design - The passenger's point of view.

17 p2535 A72-34225

STOL airports planning objectives, discussing ground and airspace congestion relief, terminal locations, flight safety and community acceptance

17 p2535 A72-34239

Kansas City International Airport facilities and features, discussing decentralized passenger processing system

17 p2535 A72-34242

Runway marking requirements for visibility under day and night conditions, considering night reflection value, color stability, durability, noninterference with flight operations, etc

17 p2535 A72-34243

Planning model for German air transport.

17 p2638 A72-34244

Simulation models for airports performance evaluation through replication of traffic units actual movement

17 p2535 A72-34414

Airports: Key to the air transportation system; Proceedings of the Conference, Atlanta Ga., April 14-16, 1971.

18 p2675 A72-36776

Federal legislation impact on airport and airway system planning, considering budget and schedule requirements

18 p2743 A72-36777

Environmental considerations in airport development.

18 p2743 A72-36778

Economics of a new regional airport.

18 p2743 A72-36779

What's new in airport planning.

18 p2675 A72-36780

Atlanta airport redesign and expansion program including runway reconfiguration taxiway relocation and passenger and cargo terminal system improvement to relieve congestion

18 p2675 A72-36781

Boeing 747 aircraft impact on Chicago O'Hare airport design criteria, noting future terminal facilities planning

18 p2675 A72-36782

Design of V/STOL ports.

18 p2675 A72-36783

Airport improvements needed for safety.

18 p2675 A72-36784

FAA implemented airport certification legislation covering minimum safety standards, operation manual, emergency plan, fire and rescue service and pavement requirements

18 p2675 A72-36785

Concrete airport pavement thickness determination methods comparison, noting design life dependence on safety factors

18 p2675 A72-36786

Airfield flexible pavement design - A state of the art paper.

18 p2675 A72-36787

Systems approach to integrated planning of airfield pavements design, construction, operation and maintenance, emphasizing need for mathematical models, constitutive parameters and limiting criteria

18 p2675 A72-36788

Airlines and aircraft manufacturers requirements for airport pavement evaluation/data system, discussing relationships between strength, landing gear design, aircraft weight, range, etc

18 p2675 A72-36789

Day-to-day operational airplane-airport relationship, discussing runway grooving impact and friction coefficient measurement [AIAA PAPER 72-813]

19 p2750 A72-38118

Airport medical design guide /with comment on certain operational matters/.

22 p3150 A72-42500

Independent parallel runway landing system to relieve air traffic congestion, investigating minimum spacing required to minimize collision risk

22 p3203 A72-43130

Critical assessment of air transport planning for German Federal Republic, advocating decentralized concept of major air terminals for intercontinental jumbo jet traffic

23 p3357 A72-43244

Dala /Sweden/ regional airport, describing planning and financing, approach lighting, ILS system and facilities for tourist traffic and industrial development

23 p3278 A72-43248

Systems approach to airport passenger terminal planning.

24 p3387 A72-44585

Airports planning for West Germany, discussing geographical air traffic patterns, economic and noise aspects [DGLR PAPER 72-034]

24 p3387 A72-44614

AIRPORT SURFACE DETECTION EQUIPMENT

Airfield surface radar detection equipment to control aircraft and ground vehicles under reduced visibility and darkness

02 p0173 A72-12105

Low cost vertical crossed beam radar systems for nonprecision approach in small airports, reducing track error

04 p0545 A72-14829

Surveillance radar for clutter rejection and signal loss reduction at airports, discussing system design features

18 p2662 A72-37046

AIRPORTS

NT HELIPORTS

Airport apron surface pavement strain measurements under field loading conditions, considering static and dynamic loads with finite element method

01 p0047 A72-10192

Terminal aerodrome forecasts usefulness and accuracy assessment

01 p0095 A72-10864

Lime, cement, fly ash and sand combination airport pavement design and testing, discussing material structural and chemical properties, compressive strength, costs, etc

02 p0200 A72-12023

Jet noise suppression near airports, discussing noise physical description, source relation to engine technology and ICAO certification standards

03 p0309 A72-13097

Economic evaluation of airport fog dispersal methods in the U.S., including crushed dry ice and liquid propane

04 p0542 A72-14677

California airport noise standards instrumentation, discussing battery operated measurement of hourly and community noise equivalent levels

07 p0985 A72-19490

Turbulence measurement, reporting and subsequent data handling by upgraded ATC system, suggesting R and D program to evaluate wake turbulence effects on airport capacity

09 p1346 A72-23466

Airport meteorological instrumentation, discussing ground wind, visibility, cloud height, air temperature and humidity detectors and radar equipment

10 p1484 A72-25093

Statistical analysis for single airport ATC digital simulation using Poisson distribution law, calculating optimal number of channels

13 p1996 A72-29179

Airport vicinity aircraft noise exposure contour calculated from measured data at Osaka Airport

16 p2372 A72-32885

Kansas City International Airport facilities and features, discussing decentralized passenger processing system

17 p2535 A72-34242

Application of electronic data processing airport analysis in airlines operations and for manufacturers.

19 p2747 A72-37277

Frankfurt/Main international airport central terminal facilities, describing efficiency oriented layout for large volume passenger and baggage handling and links to rail and road nets

23 p3278 A72-43247

Dala /Sweden/ regional airport, describing planning and financing, approach lighting, ILS system and facilities for tourist traffic and industrial development

23 p3278 A72-43248

International and regional scheduled air traffic terminals and general aviation airports characteristic objectives and operational aspects, discussing ATC, safety and noise problems [DGLR PAPER 72-033]

24 p3387 A72-44616

Airport power supply system to meet increased load terminal demands, describing main and emergency standby network layout and equipment

24 p3388 A72-45272

Low-altitude atmospheric turbulence around an airport.

24 p3421 A72-45334

AIRSHIPS

Unpredicted structural vibration in Comet and Electra aircraft, Graf Zeppelin dirigible, missile antennas, etc

02 p0292 A72-12002

Rigid form airship for transportation, discussing applications for special loads and scientific and service purposes, and design and construction problems

21 p2996 A72-41200

AIRSPACE

Control concepts for future ATC system relative to airspace structure, management and geographic and jurisdictional boundaries

06 p0844 A72-17333

ATC system organization in terms of optimal operating conditions for civil and military airspace users, discussing navigation systems, human factors, equipment reliability, etc

15 p2272 A72-32455

Study of the flow of air traffic and capacity of a control system

19 p2831 A72-37797

Terminal airspace navigation and aircraft ground handling control, discussing air traffic controllers and pilots functions in context of workload and automation

21 p3081 A72-40546

AIRSPEED

Linear airspeed and runway rate field displays, measuring initial response latencies, control reversals and root mean square tracking errors

06 p0845 A72-17717

Aircraft launch envelope investigation for minimum catapult end airspeed determination at carrier bow, discussing optimum test pilot launch technique

06 p0759 A72-18498

Air velocity calculation from hot-wire anemometer measurements in variable density flow, discussing correction factors checking method and application to internal combustion engine

09 p1315 A72-23390

Applications of a technique for estimating aircraft states from recorded flight test data.

[AIAA PAPER 72-965] 22 p3138 A72-42360

AIRWORTHINESS

U AIRCRAFT RELIABILITY

AIRWORTHINESS REQUIREMENTS

U AIRCRAFT RELIABILITY

ALADIN 2 AIRCRAFT

Aladin 2 noiseless STOL jet aircraft project, describing exhaust nozzle configuration, design and economics

02 p0155 A72-12503

ALARMS

U WARNING SYSTEMS

ALASKA

Regional geologic features of Alaska and Western Canada from Nimbus 4 satellite image dissection camera system (IDCS)/photographs

10 p1477 A72-25109

Wind patterns at meteor altitudes /75-105 kilometers/ above College, Alaska, associated with mid-winter stratospheric warmings.

18 p2689 A72-36962

ALBEDO

NT EARTH ALBEDO

Neutron albedo flux recording instrument with composite scintillation crystal and photomultiplier scanning to monitor near space

02 p0273 A72-11934

Uranus IR spectral albedo, discussing methane absorption

04 p0580 A72-15365

Mathematical model for radiative transfer properties of high albedo carbon dioxide and water cryodeposits on opaque substrate

[AIAA PAPER 72-58] 05 p0749 A72-16929

Transient lunar phenomena as changes in albedo due to dust movement or fluidization from lunar sample tests

06 p0877 A72-17650

Monte Carlo calculations of lunar photon albedo from galactic and solar proton bombardment for lunar soil composition information

07 p1070 A72-19139

Martian crater abundance correlation with surface albedo, discussing relative age of light and dark terrains

08 p1230 A72-20983

Martian violet clouds photometric studies, determining monochromatic albedo, optical thickness and Junge parameter

08 p1237 A72-21827

Venus, Mars, Jupiter and Saturn UV spectra from OAO-2 objective grating spectrophotometry, obtaining planetary albedos from G-type stars observations

09 p1382 A72-22288

Scattering computations of albedo reflectance for model media as function of incidence angle

09 p1299 A72-22808

Model for volcanic origin of Descartes Formation high albedo region, suggesting young age and endogenic nature of bright surface deposit

09 p1394 A72-23666

Monte Carlo random walk methods for directional emittance of one dimensional absorbing-scattering slab with reflecting boundaries, considering refractive index, optical thickness and albedo

[AIAA PAPER 72-309] 11 p1743 A72-25243

Neutron albedo flux recording instrument with composite scintillation crystal and photomultiplier scanning to monitor near space

13 p2030 A72-29246

Mars surface normal albedo distribution function from red light photometry data

14 p2152 A72-30489

Intensity and energy spectrum calculation of albedo electrons recorded in cosmic particle showers by gas discharge counters

14 p2105 A72-30629

Steady state thermal transfer during ablation and radiation of single scattering albedo with constant heat flux at boundary

14 p2171 A72-30892

Polarization observations of Saturnian satellite Iapetus leading and trailing hemispheres, showing albedo difference consistent with light curve amplitude

16 p2453 A72-33139

Solar radiation anisotropic nonconservative scattering in semiinfinite atmosphere, calculating plane and spherical albedo by exponential kernel approximation

16 p2446 A72-33463

German monograph - A method for the determination of the differential albedo for photons in the range from 1-17 MeV

19 p2836 A72-37484

Mars surface normal albedo distribution function from red light photometry data

19 p2864 A72-38318

Crop surface albedo measurements, taking into account cloudiness, zenith angle and day period effects

20 p2915 A72-38970

An albedo horizon sensor using hybrid circuitry.

21 p3050 A72-40122

Albedo and surface illuminance of a planet having a nonhomogeneous purely scattering atmosphere

21 p3050 A72-41796

Lunar albedo and temperature distribution from simultaneous photoelectric and far IR brightness temperature measurements of sunlit lunar surface

22 p3226 A72-42536

Venus high albedo, discussing compound reflecting layer and liquid Hg cloud models

24 p3436 A72-44692

ALCOHOLS

NT BISPHENOLS

NT ETHYL ALCOHOL

NT GLYCOLS

NT METHYL ALCOHOLS

NT PHENOLS

Alcohol ingestion effects on tracking performance during angular acceleration, observing nystagmic eye movements and eye-hand coordination

04 p0477 A72-14474

Pulsating flame spread on liquid alcohol surface over range of liquid temperatures, using shadow streak photography

07 p1099 A72-19375

Electron impact induced fragmentation of alkyl-N-/1-phenylethyl-/carbamates of primary, secondary and tertiary alcohols, using deuterium labeling and high resolution mass spectrometry

07 p0936 A72-19500

Alcohol ingestion effect on vestibular responses to angular acceleration and Coriolis stimulation, discussing nystagmus and subjective responses

14 p2082 A72-31090

ALDEHYDES

NT FORMALDEHYDE

Lower aldehydes contribution to biochemically important compounds in abiogenic synthesis, considering amino acids formation

04 p0483 A72-14763

ALDOSTERONE

Renin in differential diagnosis of hypertension.

19 p2757 A72-38144

The production and characterization of specific antibodies to aldosterone.

19 p2757 A72-38175

ALERTNESS

Book on sustained attention /vigilance/, discussing effects of signal frequency, magnitude and distribution, task complexity, noise, age, intelligence, etc

07 p0930 A72-19910

ALFVEN WAVES

U MAGNETOHYDRODYNAMIC WAVES

ALGAE

NT BLUE GREEN ALGAE

NT CHLORELLA

Holocene Bahamian oolites examination by scanning electron and light microscopy, observing aragonite crystals morphology, orientation and modification by boring activities of endolithic algae

05 p0654 A72-16037

Protein-rich food substitute from microalgae cultures for human nutrition, describing experimental production, protein value determination, special diets and food shortage relief

06 p0768 A72-18159

Molecular aspects of structural and functional circadian rhythms in chloroplasts of unicellular alga Acetabularia, emphasizing protein synthesis role

07 p0919 A72-19540

Bioengineering models of energy and mass exchange of algae under varying ambient conditions, noting mass cultivation possibility for oxygen regeneration in closed environments

20 p2893 A72-38959

ALGAL BLOOM

U ALGAE

ALGEBRA

NT ADJOINTS

NT BANACH SPACE

NT BINOMIAL THEOREM

NT CANONICAL FORMS

NT DETERMINANTS

NT DUFFING DIFFERENTIAL EQUATION

NT DYADICS

NT EIGENVALUES

NT EIGENVECTORS

NT GROUP THEORY

NT HERMITIAN POLYNOMIAL

NT HILBERT SPACE

NT HOMOMORPHISMS

NT JORDAN FORM

NT LIE GROUPS

NT LINEAR EQUATIONS

NT LINEAR TRANSFORMATIONS

NT MATRICES [MATHEMATICS]

NT NONLINEAR EQUATIONS

NT POLYNOMIALS

NT QUADRATIC EQUATIONS

NT SPINOR GROUPS

NT STATE VECTORS

NT STOKES THEOREM [VECTOR CALCULUS]

NT STRESS TENSORS

NT SUBGROUPS

NT TENSORS

NT VECTOR SPACES

NT VECTORS [MATHEMATICS]

NT VORTICITY

Algebraic structures of operator nodes with reduced elements

08 p1198 A72-21097

Sigma algebra and statistics system for optimal stopping of stochastic processes for continuous time case

09 p1340 A72-22424

Algebraic dimensional analysis developed algorithm to generate optimized dimensionless products set associated with physical phenomenon, using matrix methods

10 p1443 A72-23916

Numerical stability in linear algebraic equations, considering mapping from input data to desired output information

11 p1677 A72-25861

Operator identities unification and classification, presenting reformulation as algebraic closure properties of graphs

14 p2125 A72-30229

Motion concept formulation by linear algebra of n dimensional spaces, emphasizing tensor character of velocity and acceleration

21 p3084 A72-40816

A note on algebraic differential equations whose coefficients are entire functions of finite order.

22 p3198 A72-41948

ALGOL

Linear control systems optimal synthesis using ALGOL program for digital computers minimizing error square integral

15 p2210 A72-31687

Computer programming languages, discussing system dependent and problem-oriented languages, ALGOL, FORTRAN and applicability ranges

17 p2523 A72-35444

ALGOL ENGINE

Algol 3 solid propellant rocket motor design for Scout D and E launch vehicles first stage, considering high total impulse, payload/mass capability and propellant grains

[SAE PAPER 710765] 01 p0115 A72-10261

The Scout launch vehicle system.

24 p3450 A72-45165

ALGORITHMS

Optical radar target range estimation, determining suboptimum post detection signal processing algorithms in photon counting mode

01 p0024 A72-10047

Algorithms for mass and stiffness matrices synthesis from experimental vibration modes applied to cantilever beam

[SAE PAPER 710787] 01 p0137 A72-10278

Optimal control algorithm for spacecraft descent in atmosphere at speed near escape velocity, using game theory

01 p0135 A72-10298

Digital computer program high speed algorithm for high resolution images geometric correction, discussing application to ERTS return beam vidicon images

01 p0065 A72-10454

Adaptive statistical prediction algorithm for character recognition by computer simulation involving handprinted numerals

01 p0034 A72-10472

Algorithms for object apparent velocity calculation from linear acceleration and angular velocity integrators readings, estimating errors

01 p0135 A72-10507

Microwave oriented circuit analysis program /MODMAN/ to handle nonlinear, time-varying, lumped and distributed elements in time domain, using transmission line modeling algorithm

01 p0045 A72-10687

Scientific satellite with simple inertial system, deriving discrete feedback reentry guidance algorithms based on closed-form equations solvable by onboard computer

01 p0098 A72-10944

Step-by-step algorithmic numerical solution for nonlinear Volterra integro-differential equation, considering convergence

01 p0093 A72-11105

Signal flow graph theory based computer diagnosis using blocking gate approach, constructing algorithm for gates optimal locations determination for maximum faults distinguishability

02 p0184 A72-11479

- Random and algorithmic procedures employing three-valued logic system for sequential circuits fault detection test sequence generation 02 p0185 A72-11486
- Computer algorithm of initial functions for elastic thick finite hollow axisymmetric cylinders under static conditions 02 p0288 A72-11604
- Self adjustment for time optimal nonstationary system control, developing algorithm for flutter 02 p0196 A72-11675
- Aerial multispectral scanner data determination with filtering and smoothing along flight line over extended areas, deriving algorithm for cloud-shadowed area detection 02 p0212 A72-11817
- Object proportions estimation algorithms in single resolution element of airborne multispectral scanner 02 p0227 A72-11839
- ERTS-A satellite geometric and radiometric received image errors, presenting detection and correction with digital algorithms 02 p0171 A72-11847
- Computer simulation studies of hybrid pull-up bootstrap decoding algorithm, devising technique for efficient computational allocation and reliable identification of decoded data sections 02 p0187 A72-12154
- Estimation algorithm for arbitrary parameter of narrow band radio signal with unknown amplitude and phase during reception on additive normal noise background 02 p0176 A72-12218
- Isotropic incompressible turbulence numerical simulation, presenting algorithm for convolution sums calculation 02 p0205 A72-12367
- Algorithm design for objective high altitude fog prognosis, considering geostrophic vorticity, thermal advection, wind direction and dew point difference 02 p0254 A72-12782
- Upper atmosphere ozone, aerosol and neutral constituent density profiles estimation by recursive filtering algorithm for satellite observation data 02 p0222 A72-12811
- Optimal control algorithm synthesized from linear sampling theory for inertial platform alignment, requiring systematic error free optimal digital computer 02 p0258 A72-12899
- Remes algorithm modification for linear approximation problem solution, discussing geometric interpretation and convergence 03 p0381 A72-13619
- Optimization algorithms synthesis models, discussing conceptual-implementable transition 03 p0327 A72-13702
- Computerized design algorithm for ferrite core memory system, considering cross-temperature effect under worst driving conditions [IEEE PAPER 11,8] 03 p0327 A72-13766
- Linear radio receiver circuit synthesis for output signal structure and rotational choice, using reduction algorithm 03 p0323 A72-13894
- Multimass multiply branched multistage elastic systems natural frequencies and oscillation modes, presenting algorithm and iterative calculation procedure 03 p0449 A72-13913
- Finite memory uncertain stochastic controller, developing optimal and suboptimal algorithms 03 p0329 A72-14181
- Soviet book on linear automatic control systems with variable parameters covering pulse transfer function determination algorithms, signal transmission characteristics and systems stability 03 p0339 A72-14245
- Chain and branched type electrical and mechanical systems, establishing algorithms with linear flow graphs 04 p0504 A72-14516
- Sequential interpolating estimation algorithm derivation for distributed-parameter noisy dynamic systems described by nonlinear partial differential equations 04 p0538 A72-14669
- Computational efficiency of minimization algorithm for solving eigenvalue problem arising from dynamic structural analysis by finite element method 04 p0585 A72-14845
- Economically optimal operation of protection circuit for plant subject to stationary random process, determining failure rate of plant 04 p0496 A72-14995
- Linear dynamic system sensitivity models simplification conditions application to adaptive nonsearching system synthesis algorithms 04 p0505 A72-14999
- Modified quasi-linearization algorithm for solving nonlinear two-point boundary value problems based on performance index and cumulative error in differential equations 04 p0539 A72-15045
- Optimal control systems with terminal state constraints, presenting algorithm based on constraint-space conjugate gradient method for function minimization 04 p0506 A72-15111
- On-line digital spectrum analysis based on fast Fourier transform algorithm, exemplifying by plasma density fluctuations correlation 04 p0496 A72-15488
- Adaptive control algorithm with disturbance prediction for solution of deterministic and stochastic optimization problems of linear equation of state and quadratic performance criteria 05 p0639 A72-15759
- Optimization algorithm for simultaneous solutions to bivalent 0-1 Knapsack problems with linear target function and linear restrictions, using ALGOL 05 p0632 A72-15817
- Random phasing algorithms to reduce phase quantization lobes for radiation patterns of commutated phased array antennas 05 p0634 A72-15820
- Computational algorithm for optimal control problem with variable terminal point constrained on state space surface, using iteration technique for satisfying transversality condition [ASME PAPER 71-WA/AUT-6] 05 p0640 A72-15957
- Optimization algorithm in measurement conditions selection for satellite thermal sounding of atmosphere in 15 micron carbon dioxide band 05 p0655 A72-16174
- Quasi-steady continuous process adaptive optimal control, discussing algorithms and model for sensitivity matrix calculation and digital simulation for strategy 05 p0640 A72-16200
- Model reference adaptive control system synthesis in presence of random perturbations, considering error signal derivative use to form parameter adjustment algorithm 05 p0640 A72-16208
- Parameter adjustment algorithm for simplified sensitivity model in adaptive nonsearching control system of linear plant with polynomial transfer function 05 p0641 A72-16318
- Recurrent algorithms for optimal signal detection on background of random noise, using Markov processes 05 p0627 A72-16406
- Spacecraft reentry trajectory parameter selection and optimal control algorithm under random atmospheric density variation 05 p0685 A72-16429
- Roll control algorithm for parabolic velocity spacecraft reentry, using successive stepwise extrapolation of approach trajectory parameters 05 p0685 A72-16431
- Minimax solution of linear regulator problem, presenting algorithm for numerical computation 05 p0682 A72-16451
- Sensitivity algorithms for finite memory batch processing smoother /Kalman filter/, applying to ship inertial velocity error estimation 05 p0686 A72-16572
- Algorithms for optimal planning of trajectory measurement times during sampling several parameters 05 p0641 A72-16759
- Dynamic system observation accuracy in spacecraft trajectory measurement, deriving processing algorithm based on state-estimate error correlation matrix analysis with maximum likelihood procedure 05 p0721 A72-16760
- Satellite motion state vector accuracy estimate algorithm based on angular measurements of stellar positions relative to satellite sent probe 05 p0687 A72-16762
- Finite element algorithm derived for partial differential equation system governing laminar three dimensional boundary layer flow of multicomponent compressible fluid [AIAA PAPER 72-108] 05 p0604 A72-16817
- Automated scheduling algorithm for aircraft from terminal area to touchdown, discussing system features and STOL air traffic computerized simulation [AIAA PAPER 72-120] 05 p0688 A72-16905
- Time optimal trajectory graphical construction procedure from energy state approximation as basis of computational algorithm for real time onboard flight optimization [AIAA PAPER 72-123] 05 p0688 A72-16968
- Optimal control algorithm for nonlinear stochastic systems ensuring probability-wise stability and minimum error, using Liapunov theory and dynamic programming 05 p0691 A72-17141
- Suboptimal feedback control for nonlinear dynamic processes, presenting control algorithm based on linear plant optimal solution 06 p0792 A72-17314
- Facsimile bandwidth compression by picture elements reduction with contrast preservation, discussing analog processing algorithm and application to weather satellite photographs 06 p0772 A72-17406
- Backward differentiation formulas application to differential algebraic equations, obtaining efficient algorithm as compared to Gear-Nordsieck method 06 p0779 A72-17479
- Computer aided steady state response analysis for nonlinear electric circuits with periodic input, using Newton algorithm with rapid convergence 06 p0779 A72-17480
- Second variational algorithm for iterative solution of unconstrained optimal control problems, examining linearized feedback control 06 p0839 A72-17592
- Linear system digital simulation by matrix exponentiation with generalized hold order algorithm for accuracy improvement at less computer time 06 p0839 A72-17630
- Algorithm for gas turbine labyrinth seals design, presenting flow chart for seal leakage analysis [ASME PAPER 72-LUB-C] 06 p0821 A72-17803
- Algorithm for selective computation of large structural modifications effect on eigenmodes of linear structure 06 p0895 A72-17848
- Algorithm for bandwidth reduction of symmetric matrices for complex structural problems 06 p0897 A72-17968
- Nonsupervised learning algorithm steady state behavior for multicategory pattern classification by analysis and digital computer simulations 06 p0780 A72-18256
- Recognition algorithms of moving objects for patterns alone and in symbolic and motion context, indicating possible recognition mechanism degradation 06 p0780 A72-18257
- Waveguide integral equation numerical solution by moment method, suggesting algorithm for detecting and alleviating relative convergence behavior [AD-745595] 06 p0775 A72-18368
- Adaptive control system synthesis by steepest descent method, obtaining algorithms for parameters self adjustment loop construction 06 p0795 A72-18661
- Algorithm selection for optimization solutions by finite, ad hoc, conjugate, Newton and restricted step methods 07 p1025 A72-18783
- Numerical algorithm for Galerkin solutions of nonlinear ordinary differential equations in dynamic system applications 07 p1025 A72-18785
- Algorithm for constructing linear and nonlinear differential and algebraic equations of state variables of nonlinear electronic circuits 07 p0958 A72-18846
- Aircraft performance and flight path optimization algorithms for minimum fuel-fixed range, using calculus of variations 07 p0912 A72-19091
- Fast algorithm for space charge layer and semiconductor junction capacitance calculation, applying to impurity profile determination 07 p0954 A72-19120
- Feasible solutions to automatic control problems satisfying multiple state and control variable inequality constraints, discussing algorithmic numerical implementation 07 p0959 A72-19281
- Signal design for coherent M-ary communication systems by stochastic gradient algorithm for minimizing error rate 07 p0959 A72-19285
- Hyperstable algorithm for multinput and output systems identification through equation error method, representing scheme as equivalent time varying nonlinear feedback system 07 p1027 A72-19290
- Stochastic approximation algorithm with nonstationary regression function for signal parameter estimation, considering convergence, mean square error bound and applications 07 p1027 A72-19291
- Algorithmic procedure in compensator design for hyperstable discrete model reference adaptive systems /MRAS/ 07 p1027 A72-19294
- Digital differential analyzers number comparison in realization of direction cosine, Euler angle and quaternion attitude algorithms 07 p0949 A72-19296
- Range rate prediction algorithm for pulse Doppler ambiguity resolution by invariant imbedding method 07 p0941 A72-19303
- Asymptotically optimal rank algorithms for signal resolution at phase and amplitude detectors outputs 07 p0943 A72-19518
- Weak signal detection in additive mixture on non-Gaussian random-correlated noise, deriving algorithms for discrete- and continuous-time and coherent detection problems 07 p0943 A72-19521
- Suboptimum linear quadratic algorithm for optical radar signals postdetection processing and target range estimation 07 p0943 A72-19522

Aerospace subsystem alternate designs and cost effectiveness evaluation and optimization, considering algorithm of three functions with minimal coupling
07 p1105 A72-19552

Optimization algorithm for minimum margin efficiency of electronic circuits, applying to IC TTL gate and transistorized bistable multivibrator (flip-flop/
07 p0944 A72-19568

Artificial intelligence application to mass spectra interpretation, discussing heuristic Dendritic Algorithm based computer program to generate structural isomers
07 p0950 A72-19608

Smoothed randomized functionals and algorithms in adaptation and learning theory, accounting for constraints by generalized penalty function method
07 p0960 A72-19653

Model-following algorithm and equicontrollability in multivariable feedback control systems, considering application to decoupling problem
07 p0960 A72-19698

Algorithm for low order linear state variable models construction from measured data
07 p0950 A72-19701

Algebraic algorithm for reducing to state form multivariable control systems defined by linear constant differential operators
07 p0950 A72-19702

Model-following control for nonlinear multivariable plants, considering implicit algorithm solution and application to variable stability aircraft control synthesis
07 p0961 A72-19708

Two-variable second order system for multivariable systems predictive control, deriving algorithm for near time optimal control
07 p0961 A72-19709

Algorithm for iterative computation of time and fuel optimal control functions for linear systems, presenting flow chart
07 p0962 A72-19714

Toeplitz matrix in numerical solution of integral equation for cylindrical antenna and array, presenting rapid inversion algorithm by exploiting symmetry properties
[AD-743577] 07 p0957 A72-19795

Algorithm for solving boundary value problem of integrodifferential equations describing temperature field inside hollow thin walled rod within solar radiation field in vacuum
07 p1028 A72-20207

Algorithm for asynchronous multilevel sequential circuits design, stressing NOR networks
07 p0963 A72-20387

Real time recursive algorithms for estimating coefficients of fixed knot spline approximation to trajectory
08 p1197 A72-20849

Hybrid computer synthesis and simulation algorithm for optimal discrete nonlinear filters, giving timing, accuracy and equipment requirement estimates
08 p1137 A72-20851

Algorithm for asymptotic behavior approximation of semi-Markov processes with splitting set of states by Markov chain
08 p1198 A72-20997

Algorithm for asymptotic power series for Poisson process residence time function generation in band with delaying screen
08 p1198 A72-20998

Proton 2 and 4 and Cosmos 196 orientation by quick response algorithm from onboard three component magnetometer readings
08 p1240 A72-21138

Dynamic programming application to computer algorithm construction for elasticity theory two dimensional problems, solving boundary value problem for elliptic differential equation
08 p1243 A72-21235

Algorithm to compute inertial navigation system altitude and vertical velocity by closed feedback loop with accelerometer output mixed with pressure altitude reference
08 p1204 A72-21411

Green matrix computation algorithm extensible to spherical and toroidal closed shells of revolution for stress-strain state determination
08 p1246 A72-21672

Soviet book on determinate, stationary, nonstationary and industrial random processes prediction, covering adaptive filters and algorithms
08 p1146 A72-21675

Radio system operational reliability analysis by mathematical methods with use of digital computer, discussing statistical modeling algorithm
08 p1143 A72-22065

Prognosis algorithm to infer weather predictor by analogy as basis for statistical weather forecasting
08 p1203 A72-22126

Adaptive algorithms for dynamic systems observation based on extremal data processing systems construction
09 p1283 A72-22219

Paired Gill propeller anemometer response function in generalized wind vector sensor application, proposing algorithm for magnitude and direction errors reduction in output analyses
09 p1307 A72-22434

Computer algorithm for thermoplastic stress-strain state of thin shells of revolution based on plastic flow theory, taking into account loading history
09 p1401 A72-22724

Algorithm and formulas for lunar limb absolute heights determination in selenodetic reference points system from lunar photographs
09 p1388 A72-23057

Algorithm for transformation of generalized companion forms for multivariable linear systems into Jordan canonical form
09 p1341 A72-23071

Nonlinear systems controllers design based on Liapunov functions and time domain ratio criterion, presenting digital computer algorithm
09 p1290 A72-23090

Numerical algorithm for matrix case extension of transport problem in periodic media
09 p1342 A72-23368

Iterative algorithm for digital adaptive null steering of RF antenna arrays, demonstrating feasibility by computer simulation
09 p1289 A72-23416

Numerical algorithm for optimal coefficient equations in analytical design of complex control plants
09 p1291 A72-23426

Automatic classification algorithms using heuristic, partitioning and variational techniques
09 p1283 A72-23429

Discrete and continuous dynamic adaptation algorithms construction for extremal quality functional trajectory equations of adaptive control system
09 p1283 A72-23435

Algorithms for optimal adaptive control of steady motions of single channel discrete extremal systems with independent search, studying quality functional behavior
09 p1291 A72-23437

Algorithm for automatic construction of finite element approximation to Laplace equation, noting convergence
10 p1502 A72-23719

Revised algorithm for unconstrained optimization using quasi-Newton methods based on recurring factorization of approximation to Hessian matrix
10 p1502 A72-23723

Interplanetary spacecraft midcourse guidance stochastic control, deriving algorithm for computing optimum velocity correction and execution time with allowance for correction-dependent errors
10 p1508 A72-23778

Nonlinear programming and parameter optimization algorithms for constrained feedback control system design
10 p1441 A72-23790

Steepest descent variable step-size algorithm with dynamic programming for mean square error adaptive equalizer, noting convergence
10 p1455 A72-23794

Nonlinear programming solution of optimal control problems, using methods of centers and feasible directions
10 p1455 A72-23797

Probability density functions shape estimation by deterministic heuristic and entropy maximization algorithms
10 p1442 A72-23798

Stochastic projected gradient algorithm to maximize SNR subject under linear or nonlinear constraints, applying to detector antenna array processing
10 p1456 A72-23808

Algebraic dimensional analysis developed algorithm to generate optimized dimensionless products set associated with physical phenomenon, using matrix methods
10 p1443 A72-23916

Fifth order modified Runge-Kutta integration algorithm, presenting truncation error estimation method and computation procedure flow chart
10 p1505 A72-24091

Algorithms for spatially varying parameters estimation in nonlinear partial differential equations from noisy observations, noting diffusivity in heat equation
10 p1506 A72-24457

Asymptotically optimal detection/discrimination algorithms for weak signals on correlated noise background
10 p1436 A72-24508

Electronic circuits statistical optimization with Monte Carlo procedure, discussing methods and algorithms for accelerating evolutionary modeling
10 p1452 A72-24638

Agile beam electronically scanned multitarget phased array tracking radar, dwell allocation strategy and trajectory extrapolation algorithm effects on target handling capacity
10 p1437 A72-24685

Digital signal analyzer design based on fast Fourier transform algorithm shift register coupled with single flow-through arithmetic unit
10 p1446 A72-25062

Parameter adjustment algorithm for simplified sensitivity model in adaptive nonsearching control system of linear plant with polynomial transfer function
10 p1458 A72-25072

Algorithm for optimal binary search tree construction with minimum weighted and restricted maximum path lengths
11 p1676 A72-25354

Mean square error and functional state prediction algorithm for plants controlled by automatic system containing digital computer
11 p1600 A72-25439

Recurrent algorithms for inertialess Markov objects identification based on statistical solutions theory
11 p1609 A72-25443

Transfer functions algebraic determination for stationary object from random processes realizations, proposing algorithm
11 p1610 A72-25451

Pade table for formal power series with notation for extension to Laurent series, relating algebraic theory to bigradient determinants and numerical analysis algorithms
11 p1676 A72-25501

Stiffly stable implicit linear multistep algorithm for deriving stability properties from extended complex plane transformation
11 p1677 A72-25860

Spacecraft interplanetary guidance trajectory correction, deriving algorithm for optimal accuracy and minimum fuel expenditure
11 p1718 A72-25931

Algorithm for moving object hologram synthesis with digital computer
11 p1633 A72-26365

Random process quantization interval search algorithm based on signal approximation by n-th degree polynomial
11 p1602 A72-26439

Binary multiplication algorithms adaptable to IC functional elements for ultrahigh speed operations
11 p1602 A72-26547

Electronic filters realization by error function minimization, discussing parameter space algorithmic search and complex plane optimization methods
11 p1606 A72-26550

Nonlinear control system optimal bang-bang controls computation, noting algorithm obtained by parameter optimization
11 p1577 A72-26666

Position and minimum scattering algorithms for narrow band signal source received by spaced receivers forming antenna arrays with large separations
11 p1598 A72-26715

Space communications period forecasting algorithm for limited power ground based transmitters and spacecraft in earth orbit
11 p1598 A72-26735

Path connection algorithms for optimal IC layout on circuit board, using digital computer
11 p1607 A72-26784

Two step spacecraft reentry guidance involving skip trajectory at parabolic speeds, proposing algorithm for running coordinate and speed vector components values
11 p1684 A72-26896

Spacecraft roll stabilization during parabolic earth atmosphere reentry, developing single parameter multistep algorithm
11 p1684 A72-26897

Landing control algorithm using onboard digital computer for spacecraft hyperbolic velocity reentry, discussing simulation test results
11 p1684 A72-26898

Parabolic velocity atmospheric reentry navigation algorithm for spacecraft control, demonstrating guidance accuracy to landing point
11 p1684 A72-26899

Spacecraft motion control algorithm for reentry at escape velocity based on object motion model
11 p1684 A72-26900

Trajectory correction problem optimal measurement set, showing solution by linear programming simplex algorithm method
11 p1684 A72-26901

Inverse eigenvalue problem numerical solution for matrices and difference and differential equations, obtaining algorithms for parameters estimation
11 p1679 A72-26955

Recursive algorithm for numerical solution of Sturm-Liouville problem with periodic boundary conditions
11 p1679 A72-26958

Computer algorithms for scattering functions of condensed aluminum or magnesium oxides in combustion products for various temperatures and particle sizes
11 p1747 A72-26966

Finite difference method for bending stresses calculation in rotating disks subjected to irregularly distributed temperature, deriving digital computer program algorithm
11 p1712 A72-26976

Signal filtration algorithms and parameter estimation in additive non-Gaussian noise background by conditional Markov process theory

12 p1783 A72-27633

Control algorithm with variable structure for incomplete state information on third order system, using error and first derivative

12 p1794 A72-27674

Convergence rate of epsilon algorithm, using Pade table and analytic functions

12 p1837 A72-27717

Heuristic recognition algorithms with learning for homogeneous irreducible stationary Markov chain sequence of recognized objects

12 p1837 A72-27824

Fourth order polynomial method and computational algorithm for direct integration of n body systems, discussing two body encounters and binary systems

12 p1875 A72-27917

Algorithms for eigenvalue spectrum determination in Dirichlet and Neumann problems for Helmholtz equation in configuration domains

12 p1847 A72-27985

Atmospheric optics inverse problem solution, comparing orthogonal functions series expansion and regularization method algorithms

12 p1841 A72-27992

Algorithms for combinatorial problem optimal solution based on implicit enumeration method, applying to assembly line balancing

12 p1837 A72-28117

Hybrid computer Monte Carlo solution algorithm for parabolic partial differential equations with time varying boundary conditions, applying to ferromagnetic rod magnetization problem

12 p1787 A72-28119

Multivariate algorithms of optimum content and form for cardiovascular risk assessment in pilots and air transport personnel

12 p1764 A72-28264

Least squares method algorithm for estimating unsteady harmonic signal parameter in presence of normally distributed additive noise

13 p1915 A72-28435

Extremum search algorithm in multicomponent mixture optimization problem, using gradient method adaptation

13 p1924 A72-28460

Random retrieval algorithms in finite set of preset movement directions, considering quadratic function minimization

13 p1924 A72-28610

Numerical algorithm for Boltzmann equation solution with application to shock structure in one dimensional flow

13 p1985 A72-28617

Algorithmic method in ALGOL 60 for successive approximations of optimal control problems, discussing improved convergence

13 p1935 A72-28707

Numerical algorithm for guaranteed minimax /max-min/ estimates for multistep decision making processes, using ALGOL 60

13 p1924 A72-28708

Algorithm and computer program to calculate low run multiple nomenclature production process optimal parameters

13 p1962 A72-28741

Optimal cross section selection of rectangular beams in oblique bending by nonlinear programming and learning algorithm

13 p2056 A72-28914

Algorithm for meteor velocity calculation from radio observation data, noting symmetrical error distribution function of velocities

13 p1924 A72-29034

Computer programmed algorithm for conducting smooth piecewise polynomial third order approximation in spline function determination

13 p1986 A72-29065

Computer algorithms and programs for complex surface geometrical parameters calculation and discrete curve coordinates determination by interpolation

13 p1924 A72-29141

Computer algorithm for plates and shells internal forces and moments and stress-strain state determination from strain gage data

13 p2058 A72-29144

Optimal algorithms for analysis, synthesis and correcting filter of self adaptive control systems

13 p1936 A72-29154

Extremal correlation algorithm for automatic control of two image congruent superposition, using digital simulation and statistical trial techniques

13 p1924 A72-29161

Two phase algorithm for selecting optimal sets of characteristics for image recognition systems

13 p1925 A72-29164

Algorithm for optimal strategy in statistical plant control for machine parts production and assembly, discussing measuring equipment errors effects

13 p1965 A72-29168

Computer algorithm to calculate surfaces formed by equidistant conic sections, using successive approximation method

13 p1966 A72-29461

Kalman filter stability analysis by mathematical modeling, using floating point computer algorithm

13 p1934 A72-30000

Computer algorithms and programs contribution to aircraft structure operational reliability and fatigue life calculation

14 p2164 A72-30288

Flow equations for floating body flowmeters, discussing density and viscosity effect, instrument characteristics and computer algorithms

14 p2104 A72-30484

Linear stiff differential equations subdominant solutions, developing numerical integration algorithm

14 p2126 A72-30525

Stress-strain state of complex configured thin walled shell, deriving computer algorithm via tensor analysis and finite difference scheme

14 p2165 A72-30686

Complex systems optimization with respect to vector-valued cost function without prespecified constraints or criteria weighting, deriving algorithm for characteristic set of noninferior solutions

14 p2087 A72-30825

Russian book on averaging method in nonlinear mechanics covering algorithms and schemes based on variables change, asymptotic methods and applications

15 p2273 A72-31274

Critical examination of programming courses design and subject matter, emphasizing fundamental principles and algorithm construction

15 p2202 A72-31453

Nonlinear electronic /transistor/ system mapping-on by matrix dynamic transform algorithms, comparing with Newton-Raphson method

15 p2210 A72-31491

Parameter-dependent linear and nonlinear equation systems solution by approximation polynomials, developing numerical algorithms

15 p2261 A72-31496

Schedule analysis computer program algorithms for waterfall bar chart display and commodity flow processing and graphing through network

15 p2203 A72-31696

Algorithm to transpose large matrices in excess of direct access computer memory for external sequential storage

15 p2203 A72-31748

Computer program for symbolic network functions, using numerical algorithms for branches not represented by symbolic parameters

15 p2211 A72-31845

Mariner 9 TV experiment image data display, processing and production for real time analysis, noting computer algorithms

15 p2236 A72-31982

Relations between Haar and Walsh/Hadamard transforms to wield orthogonal transforms with common fast algorithm

15 p2264 A72-32081

Fuzzy algorithms and artificial intelligence for deep space navigation of vehicles from earth to space /planet/ location

15 p2270 A72-32185

Optimal algorithm for failure detection and identification in redundant gyro-accelerometer sensor systems, including Monte Carlo simulation

15 p2270 A72-32188

Steering algorithm for fail-safe guidance of continuously thrusting interplanetary spacecraft to maintain ballistic intercept target objective

15 p2271 A72-32195

Algorithmic calculation for composition changes due to nuclear reactions and convective mixing during stellar evolution

15 p2314 A72-32374

Algorithms for incorporating electromagnetic field into plasma numerical simulation to explain unwanted noise generation rates

15 p2288 A72-32421

Linear radio receiver circuit synthesis for output signal structure and rational selection, using reduction algorithm

15 p2202 A72-32705

Algorithms for photogrammetric model coordinates variance and covariance estimation, considering convergence properties

16 p2384 A72-33029

Algorithm for minimax parameter optimization by linear and quadratic programming with application to earth orbiting satellite orbital transfer

16 p2366 A72-33191

Computer algorithms for adaptive optimal synthesis of complex electronic systems, using stochastic approximation and gradient search with data storage

16 p2367 A72-33265

Joint maximum likelihood estimation of three parameters of Weibull distribution, obtaining modified quasi-linearization algorithm for nonlinear equations iterative solution

16 p2416 A72-33348

Semiimplicit time integration algorithm in atmospheric baroclinic models for short range weather forecasting in Canada

16 p2418 A72-33665

Algorithm for moving object hologram synthesis with digital computer

16 p2394 A72-33717

System models for R and D processes in terms of state variables and control vectors, deriving algorithm for optimization

16 p2482 A72-33864

Nonparametric probability density function modeling algorithms comparison for convergence rate and limit cycle stability relative to implementation ease

16 p2367 A72-33867

Structural information model for data compression algorithm synthesis, using piecewise signal approximation

16 p2395 A72-33954

Numerical construction of the Hill functions.

17 p2573 A72-34216

Rate of convergence of several conjugate gradient algorithms.

17 p2573 A72-34218

On behavior strategy solutions in two-person zero-sum finite extended games with imperfect information. I - A method for determination of minimally complex behavior strategy solutions.

17 p2574 A72-34343

Image enhancement by computer programs, discussing digital filtering, fast Fourier transform algorithm, data management and large matrix handling

17 p2520 A72-34404

Computer program algorithm for processing local landmark and cloud motion data recorded by satellite observation

17 p2520 A72-34410

A sequential algorithm for covariance matrix calculations.

17 p2574 A72-34416

Sizing an external-fueled in-core thermionic reactor.

17 p2495 A72-34588

Study of circular arc airfoils with asymptotic critical Mach number. II

17 p2484 A72-34745

An algorithm in arithmetic with a floating point to increase the accuracy of a sum

17 p2575 A72-34906

An algorithm for the automatic synthesis of nearly optimal 2-level-and-or combinational circuits.

17 p2533 A72-35058

An automated gradient projection algorithm for optimal control problems.

17 p2576 A72-35244

Algorithms for optimal planning of trajectory measurement times during sampling several parameters

17 p2533 A72-35262

Dynamic system observation accuracy in spacecraft trajectory measurement, deriving processing algorithm based on state-estimate error correlation matrix analysis with maximum likelihood procedure

17 p2610 A72-35263

Satellite motion state vector accuracy estimate algorithm based on angular measurements of stellar positions relative to satellite launched probe

17 p2578 A72-35265

Discrete-time demodulation of continuous-time signals.

17 p2516 A72-35332

Spectral factorization in periodically time-varying systems and application to navigation problems.

17 p2578 A72-35492

A suboptimal error reduction scheme for a long-term self-contained inertial navigation system.

17 p2578 A72-35560

Algorithms for selected blood acid-base and blood gas calculations.

17 p2510 A72-35973

Recursive bootstrap maximum likelihood estimators algorithms for identification of process modeled by stable linear difference equation under additive output measurement noise

18 p2672 A72-36056

Intraframe coding for picture transmission.

18 p2657 A72-36252

Computational algorithms compared for spatial frequency image filtering, considering tradeoffs between direct convolution and fast Fourier transform under equal point-spread functions assumption

18 p2658 A72-36263

Techniques for generating highly reliable redundant systems.

18 p2663 A72-36309

Extendible variable profile nozzle for various flow regimes operation, developing numerical design algorithm

18 p2641 A72-36661

Conical and cylindrical shell deformation with nonlinear one dimensional wave processes, describing algorithm for method of characteristics application

18 p2735 A72-36664

Adaptive equalization of data transmission rate in telephonic systems, considering criteria and iterative algorithms

18 p2661 A72-36790

Computation of optimal controls by a method combining quasilinearization and quadratic programming.

18 p2673 A72-36824

A-stable, accurate averaging of multistep methods for stiff differential equations.

18 p2705 A72-37019

Hopscotch algorithm for numerical integration of nonlinear hyperbolic partial differential equation systems based on finite difference method

18 p2705 A72-37020

Automatic computation of exponentials, logarithms, ratios and square roots.

18 p2705 A72-37021

Modifications and extensions of the sequential gradient-restoration algorithm for optimal control theory.

[AD-736265]

19 p2776 A72-37246

Linear electric circuits optimal synthesis as nonlinear programming of network parameters, discussing approximation algorithms

19 p2776 A72-37306

Extremal problems arising in the substantiation of heuristic procedures

19 p2824 A72-37381

Stochastic analogs of finite-converging learning algorithms for recognition systems

19 p2769 A72-37421

Condition for the equivalence of two important adaptation algorithms and its relationship to effective estimates of probability-distribution parameters

19 p2825 A72-37439

Conditions for the effectiveness of adaptation algorithms based on an empirical Bayesian approach to statistics

19 p2825 A72-37440

French monograph - Linear estimation of the parameters of multidimensional dynamic systems and statistical validation of the model - Applications to process identification

19 p2778 A72-37486

French monograph - Contribution to the study of extremal control systems

19 p2778 A72-37487

Some properties of iterative square-rooting methods using high-speed multiplication.

19 p2769 A72-37577

Computer solution of dynamic problems for bending of beams and thin plates beyond the elastic limit under alternating loads

19 p2877 A72-38194

Algorithm for linear multivariable systems synthesis via combined dynamic feedforward compensation and linear state variable feedback

19 p2779 A72-38232

Parameter identification of a class of multiple input/multiple output linear discrete-time systems.

19 p2826 A72-38269

On-line identification of multivariable stochastic feedback systems.

19 p2781 A72-38270

Recursive updating of smoothing and filtering algorithms for discretely observed continuous dynamic linear systems

19 p2826 A72-38274

Numerical solutions in the simplest problem of the calculus of variations.

19 p2827 A72-38382

Digital computer algorithm for electronic circuit calculations

19 p2774 A72-38422

Optimal recurrent and nonrecurrent algorithms for polynomial dividing functions of learning and recognition in form of adaptive threshold elements

19 p2769 A72-38465

Signal recognizing algorithms for class of large number of normal distributions with unknown probabilities, using statistical complex hypothesis verification

19 p2770 A72-38466

Discrete and continuous dynamic adaptation algorithms construction for extremal quality functional trajectory equations of adaptive control system

19 p2770 A72-38518

Algorithms for optimal adaptive control of steady motions of single channel discrete extremal systems with independent search, studying quality functional behavior

19 p2782 A72-38520

Simple algorithm for a search of the global extremum of a function of several variables and its application to the functional approximation problem

19 p2828 A72-38582

Comparison of the quality of empirical and optimal adaptation algorithms in multiple-alternative choice problems

19 p2828 A72-38583

Hybrid computer Monte Carlo solution algorithm for parabolic partial differential equations with time varying boundary conditions, applying to ferromagnetic rod magnetization problem

19 p2770 A72-38620

Certain algorithms for obtaining an approximate solution of incorrect problems on a set of monotonic functions

19 p2828 A72-38846

Proton 2 and 4 and Cosmos 196 orientation by high speed algorithm from onboard three component magnetometer readings

20 p2976 A72-39243

Memory requirements and computation times for implementing reduced consensus algorithms.

20 p2905 A72-39434

An algorithm for linearly constrained adaptive array processing.

20 p2904 A72-39777

The possibility of constructing an algorithmically universal hybrid computer

21 p3024 A72-40177

An algorithm for computer calculation of critical curves of longitudinal cryotrons

21 p3025 A72-40183

Variable metric algorithms - Necessary and sufficient conditions for identical behavior of nonquadratic functions.

21 p3074 A72-40227

Telemetric frame compression coefficient and shaping algorithm for spacecraft data processing systems for arbitrary number of active channels

21 p3014 A72-40326

The optimum design of small nonuniformly spaced arrays.

21 p3027 A72-40362

Russian book - Algorithms for calculation of navigation data on spacecraft position.

21 p3103 A72-40460

Transmission efficiency of gas chromatography algorithmic data compression and coding for spacecraft atmosphere studies

21 p3053 A72-40549

A computational technique for optimal control problems having singular arcs.

21 p3037 A72-40641

Frequency-sampling and transversal digital filter equalizers optimal design from specified unit impulse time response, using linear programming algorithm

21 p3033 A72-40900

An estimation algorithm with learning feature for an adaptive bit synchronizer.

21 p3021 A72-40908

Characterization and algorithm for optimal solution of stochastic linear programming to minimize cost

21 p3075 A72-41234

Computational solutions of matrix problems over an integral domain.

21 p3076 A72-41315

Gaussian elimination with floating point arithmetic, discussing algorithm for least squares scaling of matrices with less error than row and column norms equilibration

21 p3076 A72-41317

Algorithm for solving the schedule planning problem in mass production

[AD-742589]

21 p3132 A72-41790

An algorithm in the gradient method for synthesis of nonlinear control systems

21 p3039 A72-41804

Polak-Ribiere conjugate gradient algorithm modifications to eliminate minimization at each iteration for efficient implementation with convergence

22 p3198 A72-41931

Q-ary output data transmission channel with burst errors, discussing burst-b distance measure and binary block code decoding algorithm for error correction

22 p3153 A72-41979

Optimization algorithm for minimum margin efficiency of electronic circuits, applying to IC TTL gate and transistorized bistable multivibrator / flip-flop/

22 p3158 A72-42086

A minimization method of describing classes in pattern recognition

22 p3198 A72-42178

Readjustment algorithm for searchless self adaptive control system with reference standard by direct Liapunov method

22 p3205 A72-42186

Synthesis problems of optimum quick-response engine control systems

22 p3216 A72-42190

A control algorithm for the orbital reentry of a space vehicle

22 p3223 A72-42206

Characteristics of an optimal algorithm for detecting Gaussian signals against a pulse noise background for receivers with a logarithmic amplifier

22 p3154 A72-42238

Algorithm for identification of unsteady dynamic objects described by linear differential equation, noting quasi-optimal system operation

22 p3205 A72-42290

Clamped circular rigid-plastic plates subjected to central blast loading.

22 p3235 A72-42601

Application of computer mathematics procedures for prediction of phase diagrams

22 p3191 A72-42812

Atmospheric optics inverse problem solution, comparing orthogonal functions series expansion and statistical regularization method algorithms

22 p3202 A72-43006

Parallelized algorithms for computer solution of spanning tree, distance and path problems on cellular array of identical modules containing memory and combinational logic

22 p3157 A72-43023

A new approach to automatic scanning of contour maps.

22 p3174 A72-43024

German monograph - Iterative algorithms for ordinary differential equations and their suitability for parallel processing by means of symbol manipulation.

22 p3200 A72-43063

Book - Computer simulation of dynamic systems.

22 p3157 A72-43081

Minimization of finite automata

22 p3157 A72-43082

An algorithm for determining the absolutely minimum form of weakly determined functions

23 p3308 A72-43349

An adaptive replacement algorithm for paged-memory computer systems.

23 p3266 A72-43420

Random phasing algorithms to reduce phase quantization sidelobes for radiation patterns of commutated phased array antennas

23 p3268 A72-43428

Generalized numbers method for analysis and synthesis of linear circuits described by signal flow graph, noting algorithms for computer programming

23 p3269 A72-43443

Modeling a holographic process on a computer

23 p3287 A72-43531

A survey of methods of feasible directions for the solution of optimal control problems.

23 p3274 A72-43537

Adaptive filtering algorithms for Kalman filter optimal gain estimation, discussing Bayesian, maximum likelihood, correlation and covariance matching methods relationship

23 p3274 A72-43542

An improved general algorithm for arbitrary pole assignment.

23 p3275 A72-43546

Optimisation of contraction-mapping algorithm for calculating optimal controls.

23 p3275 A72-43607

Iterative method of computing the limiting solution of the matrix Riccati differential equation.

23 p3275 A72-43610

An algorithm to obtain the steady state response of nonlinear periodic systems.

23 p3267 A72-43852

Regulator vector selection algorithm for largest estimate of exponential absolute control stability region based on Popov frequency condition reformulation

23 p3276 A72-43853

Optimal minimax regulation of a dynamic system.

23 p3276 A72-43860

Efficient method to multiply successively functions of the companion matrix and applying the method to evaluate transient response.

23 p3309 A72-43862

Synthesis of hyperstable discrete model reference adaptive systems.

23 p3276 A72-43867

Optimal filtration algorithms of Markov parameters of discrete time signals in digital data transmission system with background noise, using Gaussian probability density approximation

23 p3264 A72-44005

Achievement of given motion by impulse correction under arbitrary disturbances /difference models/

23 p3313 A72-44044

A manifold imbedding algorithm for optimization problems.

23 p3268 A72-44197

Sequential analysis algorithm for data channel detection of received signal represented by Poisson sequence of quantum transitions under large SNR

23 p3266 A72-44206

Effectiveness of certain easily realized rank detection algorithms for noise-masked signals

23 p3266 A72-44216

The elastic analysis of the part-circular surface flaw problem by the alternating method.

23 p3353 A72-44232

Determination of the operational transfer functions of a gas turbine engine on a digital computer

23 p3327 A72-44292

Experimental design algorithm based on information quantity optimization, noting measuring instrumentation synthesis adaptable to operational conditions

23 p3292 A72-44463

A computational successive improvement scheme for adaptive optimal control processes.

23 p3268 A72-44549

A simple algorithmic method for the simulation of a spacecraft with flexible appendages.

23 p3343 A72-44552

Cost effective algorithm for optimal route aircraft scheduling for airlines by mixed integer multi-commodity flow technique and Dantzig-Wolfe decomposition

24 p3466 A72-44582

Optimum reception algorithms in communication systems with decision feedback in presence of noise in forward and return channel 24 p3379 A72-44747

Improvement of an algorithm for the rejection of points in the solution of a mutual orientation problem on a digital computer 24 p3401 A72-44861

Dynamic model compensation algorithm accuracy for sequential estimation of time history of lunar satellite acceleration due to modeled surface mascons effects 24 p3440 A72-45139

Linguistic message decoding algorithms for communication with extraterrestrial intelligences, considering unified procedure and key problems solutions 24 p3382 A72-45226

Application of advanced filtering methods to the determination of the interplanetary orbit of Mariner '71 24 p3443 A72-45427

Earth-based navigation capabilities for outer planet missions. [AIAA PAPER 72-906] 24 p3423 A72-45430

Algorithmic description of the generalized operational characteristic of a human operator 24 p3376 A72-45515

An iterative algorithm for solving the realization problem of a Boolean function by a single threshold element. 24 p3419 A72-45576

Computer algorithm for breakpoints and forcing functions determination for optimal curve fitting by piecewise differential approximation 24 p3419 A72-45632

The automatic computation of exponentials, logarithms, ratios, and square roots. 24 p3383 A72-45668

ALIGNMENT

NT SELF ALIGNMENT

Correlation filters alignment for optical character recognition, discussing kinematic mounting and in position techniques 02 p0225 A72-11750

Precision alignment device using He-Ne laser with small beam divergence 02 p0238 A72-12115

Optimal alignment and calibration of gyro stabilized platforms, using Kalman filter and minimal weighted squared errors 07 p0989 A72-20280

Inertial navigation system platform alignment and calibration by state space technique similar to Kalman filtering 16 p2420 A72-33697

German monograph - Development and testing of a laser autocollimator 19 p2810 A72-37480

All sky photography of auroral arcs alignment, noting oval distribution pattern 19 p2793 A72-38750

In-flight alignment and calibration of inertial measurement units. I - General formulation. II - Experimental results. 21 p3081 A72-41079

Automatic coaxial alignment system with photoelectric positioning sensors, discussing alignment errors as function of light source distance and components spacing 21 p3059 A72-41817

Optical alignment of planes and straight lines in space by reflecting prism systems and double ray bundles with mirror symmetry 24 p3424 A72-44768

ALIPHATIC COMPOUNDS

NT ACETONE

NT ACETYL COMPOUNDS

NT ACETYLACETONE

NT ACETYLENE

NT ACRYLONITRILES

NT ADENINES

NT ADENOSINE DIPHOSPHATE [ADP]

NT ADENOSINE TRIPHOSPHATE [ATP]

NT ADENOSINES

NT ALKYL COMPOUNDS

NT ALLYL COMPOUNDS

NT ANTHRACENE

NT BUTANES

NT BUTENES

NT CARBAMATES [TRADENAME]

NT CARBON TETRAFLUORIDE

NT CELLULOSE

NT CETANE

NT CHLORPROMAZINE

NT CYANAMIDES

NT CYANOGEN

NT CYCLIC HYDROCARBONS

NT CYCLOPROPANE

NT DIMETHYLHYDRAZINES

NT ETHYL ALCOHOL

NT ETHYLENE

NT GLUCOSE

NT GLUTAMATES

NT GLUTATHIONE

NT GLYCOKENS

NT GLYCOLS

NT GUANIDINES

NT HEPTANES

NT HYDRAZINES

NT ISOPROPYL COMPOUNDS

NT KETONES

NT LACTATES

NT LACTIC ACID

NT MALEATES

NT METHANE

NT METHYL ALCOHOLS

NT METHYL COMPOUNDS

NT METHYL NITRATE

NT NEMBUTAL [TRADEMARK]

NT NEOPENTANE

NT NITRATE ESTERS

NT NITROAMINES

NT NUCLEOSIDES

NT OCTANES

NT OLEIC ACID

NT PARAFFINS

NT PROPANE

NT PROPYLENE

NT STARCHES

NT SUCROSE

NT SUGARS

NT TRIMETHYL COMPOUNDS

NT URETHANES

Mass spectral analysis of aliphatic amino acid derivatives, obtaining diagnostic criteria for distinction of alpha, beta, gamma and N-methyl isomers 07 p0935 A72-18905

Gas phase basicities of aliphatic amines by ion cyclotron resonance spectroscopy 07 p0936 A72-19493

Polyethylene oxidative degradation study with gas chromatographic techniques, obtaining aliphatic and organic compounds at 75-200 C in varying oxygen concentrations 08 p1128 A72-21425

Aliphatic hydrocarbons in phytopathogenic fungi spores, discussing similarity to higher plant alkanes, functional roles and species distribution and occurrence 13 p1906 A72-29834

The steric analysis of aliphatic amines with two asymmetric centres by gas-liquid chromatography of diastereoisomeric amides. 17 p2510 A72-34337

ALKALI HALIDES

NT CESIUM IODIDES

NT SODIUM CHLORIDES

NT SODIUM FLUORIDES

NT SODIUM IODIDES

Alkali halide crystals optical dc dielectric strength determination, using carbon dioxide laser induced breakdown threshold data 03 p0368 A72-13607

[AD-737913]

Dynamics of flare formation by pulsed laser beam at surface of alkali halide crystals 07 p1007 A72-20124

Interatomic force model for elastic properties of alpha quartz and alkali halides generalized for specified structure under arbitrary pressure 07 p0980 A72-20519

Dynamics of the optical-pumping cycle of F centers in alkali halides - Theory and application to detection of electron-spin and electron-nuclear-double-spin resonance in the relaxed-excited state. 18 p2719 A72-36709

ALKALI METAL COMPOUNDS

Alkali antimonide photocathodes photoelectric yield /quantum efficiency/ relation to reversible variation of surface potential, noting critical current density temperature dependence 08 p1171 A72-21968

Investigation of radiation paramagnetic defects in alkaline-silicate glass subjected to the action of high quasi-hydrostatic pressures - Structure of hole defects 24 p3417 A72-45421

ALKALI METALS

NT CESIUM

NT CESIUM VAPOR

NT LIQUID POTASSIUM

NT LIQUID SODIUM

NT LITHIUM

NT LITHIUM ISOTOPES

NT POTASSIUM

NT POTASSIUM ISOTOPES

NT RUBIDIUM

NT RUBIDIUM ISOTOPES

NT SODIUM

NT SODIUM VAPOR

Japanese lava geochemical analysis, determining K, Rb, Sr, Ba and rare earth concentrations with mass spectrometric stable isotope dilution 01 p0051 A72-10059

Alkali ion scattering by NbTi alloy and SiC and components, comparing scattering coefficients 03 p0401 A72-13424

Optical excitation of divergent alkali atomic beam by radiation absorption, deriving absorption coefficient for line broadening and/or Doppler effect 03 p0393 A72-14062

Organic dye lasers radiation nonlinear interaction with alkali metals spark discharge plasma, showing angular and spectral broadening 04 p0532 A72-15573

Alkali liquid metal heat pipes, showing heat transport rate for boiling initiation [ASME PAPER 71-WA/HT-10] 05 p0743 A72-15870

Cylindrical alkali metal plasma column structure in single ended Q device under axial magnetic field 06 p0854 A72-17503

Hf fluctuations in density gradient of alkali plasma within Q device 06 p0858 A72-17536

Vibration viscometer measurement of viscosity of alkali metals Rb, Cs, Na and K near solidification temperature, studying oxygen effects on metal surface 11 p1746 A72-26236

Small amplitude plane wave speed variation with pressure for Na and K at absolute zero temperature, using crystal strain energy formulation 13 p2006 A72-29675

Current-voltage and specific power-energy relationships for high temperature electrochemical cells with alkali metal anodes and chalcogen or halogen cathodes 16 p2352 A72-33900

Work function, thermal stability, and atomic structure of electropositive films adsorbed on single crystals of metals 18 p2656 A72-36132

On strain energy and constitutive relations for alkali metals. 18 p2703 A72-37087

ALKALIES

NT POTASSIUM HYDROXIDES

Richardson and effective work functions measurements for thermionic emission from alkali and extended red-sensitive trialkali photocathodes, discussing error minimization 20 p2890 A72-39646

Repulsive potential determination for alkali cations, halide anions and anisotropic molecules from scattering experiments and bond energy data 21 p3087 A72-40555

Bond energy electrostatic potential calculation and equilibrium and rate constants prediction for alkali and halide ions association with neutrals 21 p3087 A72-40556

ALKALINE BATTERIES

Long life leak-proof hermetic compression seals for alkaline batteries, describing design, fabrication and accelerated thermal cycle test method [ECS PAPER 72] 13 p1899 A72-28434

Electrodes converting hydrogen, methanol or oxygen for use in fuel cells with alkaline electrolyte, using Ag-Pd, Ni, Si and C catalysts 16 p2351 A72-33885

Alkaline fuel cell development and trends, noting carbon dioxide removal technique and applications ranging from portable batteries to automobile power 16 p2351 A72-33887

ALKALINE EARTH METALS

NT BARIUM ISOTOPES

Japanese lava geochemical analysis, determining K, Rb, Sr, Ba and rare earth concentrations with mass spectrometric stable isotope dilution 01 p0051 A72-10059

Nonequilibrium ionization theories for high pressure discharge in inert gas-alkali metal vapor 10 p1515 A72-24414

ALKALINE EARTH OXIDES

NT BARIUM OXIDES

NT BERYLLIUM OXIDES

NT CALCIUM OXIDES

NT MAGNESIUM OXIDES

ALKALOIDS

NT MORPHINE

NT NICOTINE

NT RESERPINE

ALKALOSIS

Respiratory effects of hypochloremic alkalosis and potassium depletion in the dog. 21 p2997 A72-40418

Lack of effect of high altitude on hemoglobin oxygen affinity. 21 p3006 A72-40430

Physiologic effects of passive hyperventilation on oxygen delivery and consumption. 23 p3258 A72-44365

ALKANES

NT BUTANES

NT CETANE

NT HEPTANES

NT METHANE

NT NEOPENTANE

NT OCTANES

NT PARAFFINS

NT PROPANE

ALKENES

NT BUTENES

NT ETHYLENE

NT PROPYLENE

ALKYL COMPOUNDS

NT METHYL NITRATE

NT TRIMETHYL COMPOUNDS

Alkyl substituent effects on gas phase acidities of toluene, phylene and acetylenes, using ion cyclotron resonance spectroscopy

07 p0936 A72-19494

Electron impact induced fragmentation of alkyl-N-1-phenylethyl-carbamates of primary, secondary and tertiary alcohols, using deuterium labeling and high resolution mass spectrometry

07 p0936 A72-19500

Antiwear properties of mixed anhydrides of alkyl xanthogene and phosphorus containing acids for use as oil lubricant additives

09 p1336 A72-22499

Chromatographic analysis of reaction products of HCl-accelerated neopentane pyrolysis, showing tert-butyl chloride formation

10 p1434 A72-24235

Time estimate criterion of lasing breakdown in photodissociative iodine-alkyl lasers with iodine molecule buildup

12 p1819 A72-27053

Structure-property relationships in flame retardant systems - Relative effects of alkyl phosphates, phosphonates and phosphites on cellulose flammability.

20 p2987 A72-39698

Analytic criteria for laser quenching moment, generation power and stimulated emission energy for photodissociative iodine-alkyl lasers with iodine molecule buildup

24 p3412 A72-45706

ALKYNES

NT ACETYLENE

ALL SKY PHOTOGRAPHY

Pulsating auroras morphology in polar substorm, recording poleward expansion and eastward drifting patches with all sky cameras

08 p1157 A72-21117

Clear line-of-sight probabilities for atmosphere from whole sky photos, visual cloud cover, sunshine recorder traces, satellite and in-flight observations

13 p1989 A72-28809

Expanding auroral bulge front photographs during auroral substorm, noting violent curl motions and arcs formation

15 p2223 A72-31439

Observations of the auroral oval by the Alaskan meridian chain of stations.

17 p2548 A72-35594

All sky photography of auroral arcs alignment, noting oval distribution pattern

19 p2793 A72-38750

Photogrammetrically determined cloud-free lines-of-sight through the atmosphere.

20 p2947 A72-38963

Wide-angle photographs of the southern sky as a contribution to the planar photometry of the Galaxy

21 p3102 A72-40275

ALL-WEATHER AIR NAVIGATION

Airline schedule keeping by Sud Lear all-weather landing system, discussing crew training

04 p0544 A72-14688

All-weather landing aids for civil VTOL aircraft and helicopters, discussing Doppler and inertial navigations, instrument landing systems and ground visibility improvement

05 p0688 A72-16780

Aircraft and airports weather instrumentation for all-weather landing and takeoff, discussing application of laser technology and digital presentation

08 p1168 A72-21522

Pilot evaluation of C-5 automatic landing system in Category III weather environment

12 p1842 A72-27521

Time parameter in military air operations, discussing weapon systems R and D, all-weather capability, communications, reliability and maintainability, manpower training, etc

15 p2339 A72-32453

Avionics effects on airline operations timekeeping, considering gains due to all-weather capability and engine monitoring vs possible losses due to equipment failures

15 p2208 A72-32461

V/STOL flight control - Trend and requirements.

17 p2487 A72-34240

All weather landing for a STOL system.

19 p2831 A72-38105

ALLERGIC DISEASES

Human immunobiological status during prolonged maintenance in bioregenerative life support system, discussing possible allergic reaction to chlorella gaseous metabolites

13 p1910 A72-29312

ALLOCATIONS

NT RESOURCE ALLOCATION

ALLOTROPY

Allotropic transformations and recrystallization by precipitation hardening in pure Ti crystals, using field emission microscopy

02 p0242 A72-12007

Enthalpy measurements of allotropic transformation of Co alloys during hcp-fcc transition with additive elements

10 p1498 A72-24850

Grain boundary network of allotropic phase change for ductility enhancement in Fe-Ta alloys

11 p1668 A72-26941

Mutual solid solubilities of rare earth metals with Zr extended by splat quenching, noting metastable low temperature allotropic forms of solid solutions

14 p2119 A72-30609

Pure Co single crystals allotropic transformation effects on deformation behavior, noting flow stress and work hardening rate relationship to history

22 p3193 A72-43034

ALLOYS

NT ALUMINUM ALLOYS

NT ANTIMONY ALLOYS

NT AUSTENITIC STAINLESS STEELS

NT BAINITIC STEEL

NT BEARING ALLOYS

NT BERYLLIUM ALLOYS

NT BINARY ALLOYS

NT BISMUTH ALLOYS

NT BORON ALLOYS

NT BRASSES

NT BRONZES

NT CADMIUM ALLOYS

NT CARBON STEELS

NT CHROMIUM ALLOYS

NT CHROMIUM STEELS

NT COBALT ALLOYS

NT COPPER ALLOYS

NT ERBIUM ALLOYS

NT EUTECTIC ALLOYS

NT FERRITIC STAINLESS STEELS

NT GALLIUM ALLOYS

NT GERMANIUM ALLOYS

NT GOLD ALLOYS

NT HAFNIUM ALLOYS

NT HASTELLOY [TRADEMARK]

NT HEAT RESISTANT ALLOYS

NT HIGH STRENGTH ALLOYS

NT HIGH STRENGTH STEELS

NT INCONEL [TRADEMARK]

NT INDIUM ALLOYS

NT IRON ALLOYS

NT KOVAR [TRADEMARK]

NT LANTHANUM ALLOYS

NT LEAD ALLOYS

NT LIGHT ALLOYS

NT LIQUID ALLOYS

NT LITHIUM ALLOYS

NT MAGNESIUM ALLOYS

NT MANGANESE ALLOYS

NT MARAGING STEELS

NT MARTENSITIC STAINLESS STEELS

NT MERCURY ALLOYS

NT MOLYBDENUM ALLOYS

NT NEODYMIUM ALLOYS

NT NICHROME [TRADEMARK]

NT NICKEL ALLOYS

NT NICKEL STEELS

NT NIMONIC ALLOYS

NT NIOBIUM ALLOYS

NT PALLADIUM ALLOYS

NT PERMALLOYS [TRADEMARK]

NT PLATINUM ALLOYS

NT QUATERNARY ALLOYS

NT RARE EARTH ALLOYS

NT REFRACTORY METAL ALLOYS

NT RHENIUM ALLOYS

NT RHODIUM ALLOYS

NT RUTHENIUM ALLOYS

NT SILICON ALLOYS

NT SILVER ALLOYS

NT SODIUM ALLOYS

NT STAINLESS STEELS

NT STEELS

NT TANTALUM ALLOYS

NT TELLURIUM ALLOYS

NT TERNARY ALLOYS

NT THORIUM ALLOYS

NT TIN ALLOYS

NT TITANIUM ALLOYS

NT TUNGSTEN ALLOYS

NT UDIMET ALLOYS

NT URANIUM ALLOYS

NT VANADIUM ALLOYS

NT WASPALOY

NT WROUGHT ALLOYS

NT YTTRIUM ALLOYS

NT ZINC ALLOYS

NT ZIRCALOYS [TRADEMARK]

NT ZIRCONIUM ALLOYS

High transition temperature alloys, layered intermetallic and organic superconductors development and properties

01 p0113 A72-10163

High pressure gaseous hydrogen effect on space shuttle main engine components alloys under static loads, using surface flawed flat plate PTC samples

01 p0085 A72-10774

Statistical thermodynamics models for determining vacancy concentration and atoms and vacancies arrangement in metals and alloys under thermal equilibrium

03 p0378 A72-14255

Commercial alloy creep and rupture strength data correlation for predicting design creep properties [ASME PAPER 71-WA/MET-2] 05 p0671 A72-15907

Large length-to-diameter ratio two layer blank bimetallic hard alloy product manufacture by extrusion die method, noting mechanical properties

05 p0666 A72-16098

Steady state creep model for high activation energy role in interstitial formation and migration in particle strengthened alloys

08 p1185 A72-20992

Alloy composition, specimen stressing and surface conditions effects on stress corrosion cracking

08 p1189 A72-22106

Alloying addition effects on structural stability and particle-matrix cohesion in metal-alumina composites

11 p1665 A72-26864

Coherent phases transformations in alloys, investigating mechanical properties dependence on microstructural features

11 p1667 A72-26929

Creep rupture characteristics of alloy in uniaxial tension, considering transient, steady state and accelerated phases

13 p1981 A72-29890

Russian papers on phase diagrams of metallic systems covering thermodynamic, X ray and metallographic alloys analysis

14 p2122 A72-30976

Surface energy effect on alloy structure formation, analyzing crystal growth and formation from supersaturated solutions

15 p2253 A72-31221

Alloying effects on high temperature softening due to crystal lattice, stacking fault energy and decreased mobility interactions

15 p2254 A72-31564

Coherent potential approximation generalization for disordered alloy systems, showing different results for propagator and locator formalisms in multiple site approximation [ONERA, TP NO. 1126]

15 p2293 A72-32229

General analysis and synthesis of alloys and materials with inhomogeneous physical properties, noting thermal physicochemical methods for laminates and metal powders

16 p2405 A72-33095

Russian book on metal alloys structure and properties covering structural changes in solid bodies, metals atomic structure, diffusion, phase transformations and composite materials

17 p2568 A72-35446

Russian book - Plastic deformation of high-alloy steels and alloys

17 p2568 A72-35454

Russian book - Automation of the monitoring and study of metals

19 p2795 A72-37299

Precipitation rate characteristics in age hardenable quenched alloys explained by transient analysis of vacancy annealing kinetics

22 p3189 A72-42441

The limiting strength of worm metal surfaces.

22 p3194 A72-43039

Compound tellurides and their alloys for Peltier cooling - A review.

22 p3215 A72-43088

Effect of overheating on the creep resistance of metastable alloys

23 p3301 A72-43927

ALLYL COMPOUNDS

Allyl esters of phosphoric acid preparation and application as substitutes for heavy metal sulfides and silver compounds in single operation photographic process

16 p2392 A72-33363

ALMUCANTAR

U ELEVATION ANGLE

ALOUETTE SATELLITES

U.S.-Canadian Alouette/ISIS satellites case history, considering hardware, lunar sample analysis and satellite transmitted radio beacon signal reception and analysis

14 p2175 A72-31144

ALPHA PARTICLES

Excited state and electron densities in noble and atmospheric gas plasmas created by alpha particle induced ion irradiation, discussing plasma kinetic processes and superimposed electric field effects

01 p0112 A72-11335

Vanadium carbide diffraction spectrum reflection intensity under Mo and CuK-alpha irradiation, showing crystalline structure and interatomic ionic interaction

04 p0533 A72-14618

Solar wind model of electrons, protons and alpha particles velocity and temperature differences dependence on distance from sun

06 p0873 A72-18025

Magnetospherically trapped particles sources, losses and transport processes, presenting time averaged proton, electron and alpha particle distributions in trapping and pseudo-trapping regions

07 p1062 A72-20028

Nuclear transducer for atmospheric pressure measurements based on alpha radiation detection, discussing accuracy, linearity and possible error sources 07 p1033 A72-20307

Primary cosmic rays alpha particles and protons energy spectra similarity and intensity difference at .05 to 1.6 TeV, using Proton satellites data 07 p1064 A72-20631

Multiple-wire spark counter characteristics for alpha particle detection, discussing electrodes surface finish and gas filling 08 p1164 A72-20941

High resolution multiple particle spectrometer for measuring energetic protons, electrons and alpha particles during solar particle events 08 p1167 A72-21509

Surface contamination effect on alpha particle resolution of surface barrier detector/preamplifier combination for use in space environment 08 p1168 A72-21517

Solar wind model of electrons, protons and alpha particles velocity and temperature differences dependence on distance from sun 11 p1713 A72-25961

Alpha particles effect on carbon dioxide laser output power and emission spectra, using uranium acetate as radioactive source 11 p1651 A72-26552

Low radioactivity of surface exposed lunar rock from alpha spectrometry, indicating absence of radon outgassing 15 p2303 A72-31304

Alpha effect solar dynamo model magnetic field and velocity expansion in spherical harmonics, solving mean field induction equation 15 p2316 A72-32755

Magnetic field distribution measurement in axisymmetric plasma column inside Tokamak device by alpha particle beam from radioisotope 16 p2434 A72-32818

Geomagnetically trapped alpha particles. I - Off-equator particles in the outer zone. 17 p2548 A72-35595

The influence of molecular binding on the stopping power of alpha particles in hydrocarbons. 18 p2655 A72-37193

Average energy to form electron-hole pairs in GAP diodes with alpha particles. 20 p2908 A72-39564

In-situ geochemical analysis of Martian and lunar composition via alpha particle activation technique, discussing Surveyor instrument performance 20 p2899 A72-39828

Change of solar flare proton to alpha ratios during an energetic storm particle event. 21 p3101 A72-41297

Particle trajectory and time of flight measurement in search for anti-alpha particles in primary cosmic radiation, using magnetic spectrometer with spark chambers 22 p3219 A72-42568

ALPHA RADIATION
U ALPHA PARTICLES
ALPHANUMERIC CHARACTERS
NT BINARY DIGITS
NT DIGITS
Feature classifying filter for pattern recognition system simulated on computer for line printed numerals 01 p0034 A72-10473

Digital computers data output alphanumerical display by commercially available TV sets, describing system design 03 p0355 A72-13075

Alphanumeric data representation by TV receivers, describing coding device and gate system for video signal generation 05 p0634 A72-15813

High speed material transfer recording equipment for alphanumeric printers, toned image graphic and microimage computer printer applications 10 p1489 A72-23934

Logic character generator for CRT text display and DEC PDP 8/S graphics 11 p1601 A72-26290

Alphanumeric characters for small TV type raster displays, describing legibility experiment for character height optimization 13 p1911 A72-29821

Proximity and direction of arrangement in numeric displays. 21 p3008 A72-41017

ALSEP
U APOLLO LUNAR SURFACE EXPERIMENTS
PACKAGE
ALTERNATING CURRENT
Electropneumatic converter for pneumatic pulse transformation into dc or ac signal, using corona discharge current 03 p0311 A72-13556

NbN thin film stabilization by metal overlays with reduction in ac losses, discussing superconducting reversibility to normal transition 04 p0560 A72-14542

AC-DC energy conversion - Conference, Milan, Italy, November 1970 06 p0785 A72-18307

Ac and dc power regulation by switched capacitor, analyzing voltage spectrum for resistive load 07 p0958 A72-20389

Pulsed plasma flow interaction with spatially periodic magnetic field generated by coaxial coils with alternating currents, noting MHD stability 09 p1362 A72-23207

Self balancing ac bridge with double conversion of unbalance-signal and low capacitance sensor for displacement measurement 11 p1634 A72-26459

Alternating magnetic field effect on collisionless nonhomogeneous magnetoplasma ion acoustic oscillations stability, examining parametric excitation of Langmuir oscillations 13 p2016 A72-29604

HF follower currents effect on dc arc I-V characteristics, indicating use of HF follower arc for quasi-steady arc power control 13 p2017 A72-29645

Feedback ac compensating amplifier design for automatic AM signal envelope conversion, noting truncated equivalent transfer function expandability 13 p1933 A72-29972

Solid state ac square law function generator based on fixed elements and operating on electrical servo system principle 13 p1933 A72-29973

Polyphase ac power systems I-V characteristics determination via application of symmetrical sequence components principle, examining system protection and reliability aspects 15 p2204 A72-31216

Multispecies magnetoplasma ac electrical conductivity tensor collision factor from quantum mechanical convergent kinetic equation 15 p2287 A72-32411

Ion temperature diagnostic using a high power alternating current probe. 17 p2557 A72-35617

Conductance associated with interface states in MOS tunnel structures. 21 p3032 A72-40701

Effect of an alternating current on the steady characteristics of Josephson point contacts 22 p3208 A72-43109

ALTERNATING CURRENT GENERATORS
U AC GENERATORS
ALTERNATORS [GENERATORS]
U AC GENERATORS
ALTIMETERS
NT LASER ALTIMETERS
NT RADIO ALTIMETERS
Pressure altimeter system minimum safe performance standards for subsonic aircraft operation, describing test procedures 01 p0064 A72-10386

Safety factors of aircraft flight instruments, discussing altimeter and artificial horizon reading errors and modifications 03 p0319 A72-13698

Statistical analysis of cockpit simulator data on altimetry display for commercial aircraft 08 p1168 A72-21573

Skylab S-193 altimeter experimental mission objectives and spacecraft instrumentation, considering precision designs, oceanographic surface remote sensing and electromagnetic scattering measurement 09 p1306 A72-22317

Altitude information warning devices and systems, discussing requirements and performance and qualification tests 11 p1632 A72-26032

Altimeters development history from Wright brothers to Boeing 747, discussing altitude alert systems providing aural and visual warnings to pilot 20 p2952 A72-39747

Boeing aircraft altitude alerting systems development and design to meet FAR 91-51 requirements, discussing retrofit programs and altimeter encoding 22 p3179 A72-42689

ALTITUDE
NT FLIGHT ALTITUDE
NT HIGH ALTITUDE
NT LOW ALTITUDE
NT SIMULATED ALTITUDE
Lunar surface altitude measurements, considering difficulty due to reference level absence and accuracy improvement by photometric procedure 03 p0421 A72-13195

Gravity data free air and Bouguer correction /elevation correction/ by nomographic alignment chart 06 p0809 A72-18148

Electron attachment rate relation to altitude in radar observation of meteor trails 09 p1384 A72-22513

Terrestrial altitude differences effects on photogrammetric data accuracy in two step compensation with models 09 p1311 A72-22966

Digital solid state altitude encoder for ATC transponder reporting, covering Gray and Gillham codes 11 p1630 A72-25578

ALTITUDE ACCLIMATIZATION
Acute, short and long term and life long high altitude hypoxia exposure effects on pulmonary gas exchange control and efficiency during physical exercise 01 p0014 A72-10848

Sublethal X radiation effects on rat erythropoietic system during altitude hypoxia acclimatization 04 p0476 A72-15721

Plasma erythropoietin concentration in men and mice during altitude acclimatization 07 p0917 A72-19440

Corticosterone content in blood plasma, cerebral cortex and skeletal muscles during hypoxia adaptation in rats 08 p1121 A72-22083

Stepwise adaptation to high mountain conditions effect on brain and sural muscle oxidation processes in rats 08 p1121 A72-22085

Erythrocyte hemolysate cataphoresis studies of human hemoglobin changes during stepwise adaptation to high mountain conditions 09 p1266 A72-22880

High altitude acclimatization effects on human lung diffusing capacity for carbon monoxide at different oxygen tensions 10 p1425 A72-24476

Urine and plasma protein and creatinine measurements in acclimatized and unacclimatized men before, during and after high altitude ascent 10 p1426 A72-24482

Erythrocyte life span in mice under normal atmospheric pressure and various degrees of hypoxia acclimatization, using radioactive labeled diisopropyl phosphorofluoridate 11 p1579 A72-26608

Chronic hypoxia adapted rat myocardial tissue sensitivity to increased carbon dioxide tension 11 p1579 A72-26616

High altitude hypoxia preadaptation effects on left ventricle myocardium noradrenaline concentration in rats with experimental vitium cordis 12 p1761 A72-27648

Exercise role in ventilatory acclimatization to graded hypoxia in goats from carbon dioxide response curve measurements 12 p1762 A72-27727

Adrenocortical response to prolonged high altitude hypoxia in hypothalamic deafferented rats, showing rapid neural stimulation with delayed humoral activation 12 p1763 A72-27829

Pressure chamber training effects on rats chain motor reflexes hypoxia adaptation, noting sinocarotid receptors importance in compensatory-adaptive reactions 13 p1902 A72-28641

Concentrated and extended learning effects on formation rate and retention degree of conditioned reflex during mice adaptation to high altitude hypoxia 13 p1903 A72-28770

Stepwise altitude acclimatization and subsequent re-animation after blood loss caused clinical death effects on dog peripheral blood erythrocytes, reticulocytes, hemoglobin and hematocrit 14 p2076 A72-30671

Mountain inhabitants cardiocirculatory adaptation to chronic hypoxia, studying coronary flow and myocardial oxygen consumption and efficiency 15 p2187 A72-32498

Ventilatory peripheral chemoreflex response to hypoxia during physical exercise in native highlanders and altitude-acclimated lowlanders 17 p2499 A72-34345

Thyroidal influence on myocardial changes induced by simulated high altitude. 17 p2500 A72-34730

Myocardial metabolic changes in chronic hypoxia. 17 p2502 A72-34989

Role of the synthesis of nucleic acids and proteins in the adaptation of the organism to altitude hypoxia. 17 p2502 A72-34990

Cardiac performance and the coronary circulation of man in chronic hypoxia. 17 p2502 A72-34992

Pulmonary gas exchange in Andean natives at high altitude. 18 p2650 A72-36570

Hemopoiesis in the pig-tailed monkey Macaca nemestrina during chronic altitude exposure. 20 p2892 A72-39344

Regional lung function during early acclimatization to 3,100 m altitude. 21 p3005 A72-40424

Lack of effect of high altitude on hemoglobin oxygen affinity. 21 p3006 A72-40430

Hypoxic pulmonary steady-state diffusing capacity for CO and alveolar-arterial O2 pressure differences in growing rats after adaptation to a simulated altitude of 3500 m. 21 p3003 A72-41622

Cardiac output, arterial and mixed-venous O2 saturation, and blood O2 dissociation curve in growing rats adapted to a simulated altitude of 3500 m. 21 p3003 A72-41623

Cardiac hypertrophy, capillary and muscle fiber density, muscle fiber diameter, capillary radius and diffusion distance in the myocardium of growing rats adapted to a simulated altitude of 3500 m.
21 p3003 A72-41624

High altitude physiology: Cardiac and respiratory aspects; Proceedings of the Symposium, London, England, February 17, 18, 1971.
22 p3143 A72-42583

Adaptive processes responsible for natural acclimatization of human organism to low ambient pressures at high altitudes
22 p3143 A72-42584

Morphometric evaluation of changes in lung structure due to high altitude.
22 p3143 A72-42585

The carotid body in animals at high altitude.
22 p3143 A72-42589

Suprapontine influences on hypoxic ventilatory control.
22 p3143 A72-42590

Genetic aspects of the blunted chemoreflex ventilatory response to hypoxia in high altitude adaptation.
22 p3144 A72-42591

Succinic and lactic dehydrogenase activities in homogenates from myocardial tissues of guinea pigs, rabbits and dogs in high altitude environments
22 p3144 A72-42592

Coronary blood flow and myocardial metabolism in man at high altitude.
22 p3144 A72-42593

Anatomy of the coronary circulation at high altitude.
22 p3144 A72-42594

Resistance and capacitance vessels of the skin in permanent and temporary residents at high altitude.
22 p3144 A72-42595

Hypoxic acclimation effects on rats heart, liver and kidney mitochondria, measuring cytochrome oxidase and succinic dehydrogenase activities
22 p3144 A72-42673

Cardiocirculatory adaptation to chronic hypoxia. II - Comparative study of myocardial metabolism of glucose, lactate, pyruvate and free fatty acids between sea level and high altitude residents.
22 p3148 A72-43022

Mechanism of adaptation to hypoxic hypoxia
23 p3255 A72-43907

Altitude limit as function of acclimatization time length for investigation of enhanced resistance to acute hypoxia in rats
23 p3255 A72-43908

ALTITUDE CONTROL

Aircraft altitude two-loop feedback control system designed by compensation parameter variation technique, determining correlation between system sensitivity computations and observations
07 p0963 A72-20592

Algorithm to compute inertial navigation system altitude and vertical velocity by closed feedback loop with accelerometer output mixed with pressure altitude reference
08 p1204 A72-21411

Boeing aircraft altitude alerting systems development and design to meet FAR 91-51 requirements, discussing retrofit programs and altimeter encoding
22 p3179 A72-42689

ALTITUDE SICKNESS

Reproducibility of acute mountain sickness severity and duration in individuals under high altitude simulation, noting relationship to hypoxia
01 p0021 A72-11287

Mountain sickness relation to ventilation response to hypoxia, noting response intensity dependence on peripheral chemoreceptor sensitivity
12 p1771 A72-27481

Effects of simulated high altitude on renin-aldosterone and Na homeostasis in normal man.
21 p3005 A72-40422

Vascular headache of acute mountain sickness.
22 p3150 A72-42491

High altitude physiology: Cardiac and respiratory aspects; Proceedings of the Symposium, London, England, February 17, 18, 1971.
22 p3143 A72-42583

Chronic altitude sickness pathology based on anatomical and histological findings in abnormal mountain inhabitants autopsies, comparing with cardiovascular system morphology in normal people
22 p3143 A72-42586

Heart function and pulmonary circulation in humans suffering from chronic mountain sickness
22 p3143 A72-42587

Transarterial leakage - A possible mechanism of high altitude pulmonary oedema.
22 p3143 A72-42588

ALTITUDE SIMULATION

Hypothermia induced by hypoxia in rats, discussing colonic temperature during high altitude exposures and seasonal variations
01 p0011 A72-10214

Human factors relation to pressurized cabin development, discussing aircraft safety, high altitude tests, pressure loss predictions and cabin altitude selection
04 p0479 A72-14869

Diffuser for altitude simulation in rocket motor operation, featuring film cooling with water inflow by motor exhaust gas ejector action
05 p0704 A72-16004

Altitude chamber simulation of reentry bodies separation from ballistic missiles, examining body shape, nozzle dimensions, gas pressure and distance effects
05 p0645 A72-17198

Simulated testing of turbojet engine ingestion of missile exhaust, determining design criteria for aircraft engine inlets from altitude chamber test data
07 p1052 A72-18758

Hypoxia effect on aircraft pilot performance during altitude and flight simulation, testing instrument landing approaches
07 p0933 A72-20186

Physiological evaluation of modified jet transport passenger oxygen mask from altitude chamber experiments
08 p1126 A72-21571

Physiological and clinical effects of long distance flight in pressurized commercial planes with simulated altitudes over 1500 meters
12 p1771 A72-27486

Rocket engines simulated high altitude testing, using multiple stage ejector augmented supersonic diffuser system
13 p1938 A72-28692

ALTITUDE TESTS

NT HIGH ALTITUDE TESTS

Altitude-velocity dependence of turboprop engine equivalent horse power, propeller output and specific fuel consumption, discussing performance characteristics relation to ambient air temperature
05 p0708 A72-17100

Disposable emergency oxygen mask for air passengers based on continuous flow, phase dilution principle, describing altitude chamber tests with human subjects to study physiological responses
13 p1908 A72-28702

Ka-26 helicopter operational flight testing in high mountain environment, discussing takeoff, landing and climb performance as function of altitude dependent engine characteristics
23 p3251 A72-43638

ALTITUDE TOLERANCE

High altitude hypoxia effects on rat myocardium lactic dehydrogenase isozyme complement and anoxic tolerance
02 p0165 A72-12834

Hypoxia tolerance among pupil pilots during aeromedical instruction in decompression chamber, obtaining EEG and cardiac rhythm recordings
04 p0466 A72-14567

Altitude hypoxia resistance and endurance in dogs of various ages, discussing homeostasis retention, altitude ceiling and survival time
04 p0474 A72-15234

Student pilot syncope during altitude chamber training, discussing physiological mechanism from cardiovascular studies and psychiatric evaluation
06 p0767 A72-17879

Statistical survey of barosinusitis incidence in U.S. Navy flying personnel during altitude chamber training, discussing diagnostic methods and clinical management
12 p1765 A72-28274

ALTOCUMULUS CLOUDS

U CUMULUS CLOUDS

ALU [COMPUTER COMPONENTS]

U ARITHMETIC AND LOGIC UNITS

ALUMINA

U ALUMINUM OXIDES

ALUMINATES

Steel castings made in electric furnace with Al additive, observing magnesium and lime aluminates inclusions
03 p0371 A72-13199

Lasing properties of yttrium orthoaluminate doped with rare-earth metals
22 p3187 A72-42943

ALUMINIZING

U ALUMINUM COATINGS

ALUMINUM

NT ALUMINUM ISOTOPEs

NT POWDERED ALUMINUM

NT SINTERED ALUMINUM POWDER

Aluminum vacuum furnace fluxless brazing process, eliminating flux entrapment, postbrazing cleaning and water pollution
01 p0074 A72-10281

NDT program for detectability changes of tight defects in Al as function of applied load
01 p0085 A72-10756

Ductile tensile cracking macroscopic simulation with perforated pure Al specimens, determining fracture energy as function of hole size and pattern
01 p0086 A72-10987

Grain boundary migration measurements in bicrystalline Al under intense electric field, using optical microscope
01 p0089 A72-11182

Annealed pure Al polycrystals fatigue behavior data under elevated temperatures, using transmission electron microscopy
02 p0242 A72-15252

Low impulsive loading effect on strength creep resistance of polycrystalline Al at elevated temperatures
02 p0243 A72-12011

Secondary slip in impact loaded Al single crystal disks, interpreting face deformation bands
02 p0247 A72-12819

Mechanical response of Al and Cu under complex strain histories conditions, using endochronic theory of viscoplasticity without yield surface
03 p0444 A72-13504

Aluminum intergranular entropy estimation, neglecting coupling between atomic vibrations
03 p0376 A72-13969

Different pair potentials for simulating vacancy in Al, discussing program planning for relaxations calculation around vacancy to effect computing time reduction
03 p0378 A72-14253

Boundary segregate concentration during grain growth annealing of ultrapure Al as function of migration rate and distance
03 p0379 A72-14259

Alloying elements and grain size effects on thermally induced surface reconstruction of Al film metalization on Si devices from thermal cycling tests
03 p0364 A72-14285

High strength, stiffness and low density properties of boron/aluminum matrix composites in flight structures
04 p0585 A72-14745

Dip, torch, furnace and vacuum brazing of aluminum
04 p0526 A72-14836

Dislocation substructure in fatigued Al and Ni polycrystals surface layer and interior due to high and low stress cycling, discussing stacking fault energy influence
04 p0534 A72-15577

Anodic layer thickness effect on fatigue crack initiation and fracture mode in mono and polycrystalline aluminum
05 p0672 A72-16015

Al and steel plate penetration, perforation and fragmentation under hard steel sphere impact at and above ballistic velocities, investigating velocity and strain histories
05 p0672 A72-16115

Internal friction changes in aluminum single crystal after uniaxial plastic deformation and irradiation
05 p0673 A72-16148

Pure Al self diffusion at 130-200 C, determining activation energy from prismatic loop annealing rates
05 p0677 A72-17109

High purity polycrystalline Al hf low strain fatigue measurements by piezoelectrically driven expantile horn, estimating critical point defect concentration
06 p0893 A72-17420

Al sheet weld cracking, discussing hold-down, localized heating, welding speed and gap effects
06 p0820 A72-17702

Al content caused defect in gas tungsten arc welded Hastelloy, using electron microprobe analysis
06 p0820 A72-17708

Low temperature slip discontinuity and strength of pure Al crystals as function of strain rate
06 p0831 A72-18355

Two dimensional dynamic thermal stresses in Al plate, allowing for Newtonian surface heat transfer
06 p0899 A72-18642

Cavitation erosion of Al in liquid oxygen as function of static pressure and ultrasound frequency
07 p1034 A72-18921

Transient high speed deformations analysis of annealed Al under impact loads by three dimensional moire fringe techniques
07 p0983 A72-19131

Far UV Al line spectra from laser produced plasma in 35-50 A range
07 p1038 A72-19835

Three and four layer vacancy defects annealing in quenched Al for stacking fault removal
07 p1020 A72-20412

Al single crystals relationship between stress, strain and dislocation density ring elevated temperature creep by direct observation of etch pits
08 p1185 A72-20990

Plasma beam cutting of Al sheets, discussing heat effect on surface oxides and microstructure and plasmagenic gas influence
08 p1176 A72-21047

Gamma irradiation effects on temperature of reversible solid-to-liquid phase transformation in Al
08 p1185 A72-21075

X ray diffuse scattering from Al crystal at 100-500 V, considering phonon modes effects on anharmonicity and atomic deformation
08 p1186 A72-21591

Copper, zinc and aluminum mechanical properties comparison by cyclic and steady state compressive
08 p1186 A72-21591

- load tests, noting stress-strain curve relationship to strain rate 08 p1188 A72-21921
- Amorphous chromate and phosphate conversion coatings of Al, providing inert surface for painting 09 p1317 A72-22480
- Loading path effect on yield surfaces of pure Al at elevated temperatures under tension 09 p1328 A72-22993
- Diffusion coefficient and distribution of Ti atoms in thin Al film from electric current vs time curves for oxidation of solid solution 09 p1329 A72-23036
- Helically bound wire reinforced sprayed Al tubes and rings, investigating failure mechanism dependence on fracture modes from tensile and bending tests 09 p1330 A72-23174
- Hugoniot equation of state for impact shock wave propagation along fiber direction in Al epoxy matrix composites 09 p1407 A72-23235
- Metastable austenitic steel fiber to increase Al matrix strength to density ratio and fracture toughness 09 p1331 A72-23385
- Oxidation and substructural effects on low stress creep of Al near melting point 09 p1331 A72-23507
- Pulsed microplasma and intermediate current plasma welding of Al, comparing with tungsten arc and electron beam welding 09 p1320 A72-23628
- Dislocations distribution in Al single crystals observed by X ray topography, noting effects of critical work hardening with annealing and secondary recrystallization 10 p1495 A72-24068
- Surface defects absence after intergranular creep from Al bicrystals grain boundaries observation by transmission electron microscopy 10 p1495 A72-24084
- Autonomous combustion of Al sphere in controlled atmospheres oxygen-argon, nitrogen and air, identifying products 10 p1562 A72-24238
- Elastoplastic analysis of unidirectional filament reinforced boron/aluminum and boron/epoxy composites under longitudinal loading, using finite element techniques 10 p1555 A72-24254
- Photoionization cross sections for atoms and ions of Al, Si and Ar on basis of Hartree-Fock bound-electron and close coupling approximation free-electron wave functions 10 p1516 A72-24669
- Evaporation, superficial diffusion and oxidation role in grain junctions electromigration phenomenon in binary Al crystals traversed by high density continuous current 10 p1498 A72-24860
- B-Al metal matrix composites joining together and to Al and Ti, considering soldering, brazing, bonding and mechanical fastening [AIAA PAPER 72-360] 11 p1638 A72-25388
- Fatigue strength characteristics of boron-epoxy reinforced Al stringers for helicopter airframe [AIAA PAPER 72-392] 11 p1574 A72-25413
- Fracture toughness of anisotropic heterogeneous filamentary boron/aluminum composites, correlating test results with acoustic emissions from filament breakage 11 p1672 A72-25470
- Surface textures in rolled Al sheets, investigating friction and reduction 11 p1638 A72-25509
- Al addition effect on thermal and mechanical stability, forgeability, cold workability, aging and oxidation resistance of Ti-Mo beta alloys 11 p1656 A72-25516
- Hardcoat anodizing of Al surfaces, discussing preparation, racking, equipment and post treatments [SAE PAPER 720341] 11 p1638 A72-25598
- Adhesive bonded clad Al corrosion penetration rates from accelerated tests 11 p1656 A72-25600
- Tensile properties of continuously cast aluminum-carbon fiber composites, discussing fiber outgassing and metal coating for wetting promotion 11 p1659 A72-25859
- Dislocation velocity-stress relationship in plastically deformed Al at room temperature, noting entropy term in Gibbs free energy equation 11 p1661 A72-26652
- Microstructural properties of Ni-Al powder synthetic material from transmission and photoemission electron microscopy, discussing low and high temperature strength characteristics 11 p1645 A72-26855
- Filament reinforced boron-aluminum composites multiple fracture behavior dependence on cross section geometry from tensile test 11 p1668 A72-26944
- High purity Al single crystal orientation explained by Rowland transformation model, observing recrystallization grains 12 p1828 A72-27300
- Resin bonded B-Al composites, discussing fabrication techniques and mechanical properties 12 p1815 A72-28098
- Crystals deformation and orientation effects on Al polygonization process, noting dislocation densities dependence on stress axis orientation 13 p1972 A72-28464
- Brittle continuous and crazed anodic oxide coatings effect on Al filament stiffness, comparing with Dow analysis 13 p1974 A72-28663
- Al crystal block structure and size changes during creep evaluated by small-angle X ray scattering technique 13 p1977 A72-28909
- Cavitation erosion of Al in liquid oxygen as function of static pressure and ultrasound frequency 13 p1942 A72-29207
- Microscopic substructure in high temperature fatigued fcc austenitic steel and aluminum, studying cross slip lines and crack initiation 13 p1979 A72-29448
- High purity aluminum-aluminum oxide reversible oxidation, discussing mechanism based on electron charging due to beam 13 p1980 A72-29827
- Aluminum aircraft wheels ultrasonic inspection, noting reliability, simplicity and time economy as compared to eddy current or fluorescent penetrant methods 13 p1966 A72-30037
- HF transverse resonant vibrations of annular Al plates with polychlorovinyl and polyamide base coatings, noting damping and strain relationship to energy dissipation 14 p2164 A72-30427
- Refractory fiber metal reinforcement and matrix incorporation, considering SiC fiber reinforced Al 14 p2107 A72-30532
- Stress analysis of boron fiber-reinforced and isotropic Al panels under identical loading conditions 15 p2323 A72-31479
- Low energy electron spectroscopy measurement of thin oxide layer growth on Al surface, noting oxidation uniformity dependence on residual gas water content 15 p2276 A72-31859
- Positron annihilation lifetimes and trapping probabilities for vacancies and dislocations in Al single crystal 15 p2258 A72-32228
- Gallium arsenide-aluminum gallium arsenide double heterostructure wafer fabrication, describing reproducible liquid phase epitaxial growth 15 p2250 A72-32518
- Recovery-work hardening model of steady state creep for Al, assuming equal internal and applied stress 15 p2259 A72-32642
- Plastic flow, yield strength and fracture of unidirectional Al-B fiber composite sheet under biaxial tension 16 p2411 A72-33821
- Ti comparison with Al for effects on Fe alloy deformation and fracture, discussing intergranular failure suppression 16 p2411 A72-33823
- Al and Zr single thin strands burning rates at various total oxygen pressures, comparing photographic observation to computations 16 p2479 A72-34003
- Welded Al joints fatigue resistance from iterative nonlinear regression analysis with multiparameter endurance curves 16 p2412 A72-34141
- Temperature dependent aluminum-water reaction generation of free hydrogen and aluminum hydroxide 16 p2362 A72-34159
- Focusing properties and efficiency of EHF waveguide lens with Al honeycomb as guiding medium, noting design considerations and performance test results 17 p2525 A72-34368
- The dynamic stress-strain behavior in torsion of 1100-O aluminum subjected to a sharp increase in strain rate 17 p2629 A72-34808
- [ASME PAPER 72-APM-6] Plastic buckling theory, presenting yield surfaces in tension-torsion stress space for pure aluminum 17 p2632 A72-35245
- Fracture of boron filaments in an aluminum matrix 17 p2571 A72-35655
- Plastic anisotropy quantitative calculation formula verified on Cu, Ni and Al, discussing physical sense of coefficients 18 p2735 A72-36475
- Fatigue of boron-aluminum and carbon-aluminum fibre composites 18 p2701 A72-36625
- Study of point defects produced in aluminum by tempering and irradiation with electrons 18 p2702 A72-36705
- The forces for projectile penetration of aluminum 19 p2871 A72-37461
- Some results of an experimental study of stress distribution at monofilament tips 19 p2822 A72-37529
- Aluminum. II - A review of deformation properties of high purity aluminum and dilute aluminum alloys 19 p2818 A72-37832
- Plasma formation on Al target surface by ruby laser beam irradiation, discussing electron and ion velocities as functions of beam power density 19 p2811 A72-38197
- Some considerations on the residual stresses in orthogonal cut surface of aluminum 20 p2978 A72-38884
- Fine structure in quenched Fe-Al-C steels 20 p2938 A72-39300
- The transverse tensile properties of boron fiber reinforced aluminum matrix composites 20 p2938 A72-39302
- Stabilization of a superconducting modification of beryllium by an aluminum admixture 20 p2960 A72-39407
- Production and properties of carbon fiber-reinforced aluminum 20 p2940 A72-39442
- Mechanical properties of boron fiber reinforced aluminum matrix composite, describing experimental and control techniques 20 p2944 A72-39452
- Aluminum/plastic semifinished material - A new material for multiple applications 20 p2944 A72-39452
- Fatigue strength of welded aluminum-connections - Investigation with the aid of multiparameter life length lines 20 p2930 A72-39941
- Recrystallized Al monocrystals applications to optics and X ray spectroscopy, describing preparation methods 21 p3065 A72-40085
- Cyclic stress-strain induced buckling and fatigue failure in cold-rolled steel and tabulating and diagramming mechanical properties 21 p3065 A72-40233
- LF circularly polarized electromagnetic waves /helicons/ resonance crystal plates, deriving magnetoresistivity and Hall coefficient 21 p3066 A72-40624
- Observation on phenomena associated with a slowly varying surface barrier at niobium oxide and aluminum interface 21 p3097 A72-40702
- Plastic deformation in annealed aluminum bar containing circumferential semicircular notch 21 p3118 A72-40719
- Vibration measurements of temperature dependent dynamic moduli of Al/resin/Al sandwich bars with cyanacrylate adhesives 21 p3118 A72-40720
- The aluminum electrode in AlCl₃-alkali-halide melts 21 p3013 A72-40844
- Effects of environment on formation of finished surface in drilling aluminum and aluminum alloys 21 p3060 A72-40936
- Strain aging of pure aluminum annealed from pre-melting temperature 21 p3060 A72-40954
- Influence of dislocations in subgrains on the substructural hardening of aluminum 21 p3068 A72-40961
- High energy electrons monokinetic beam propagation in Cu and Al crystals, investigating critical voltage effect on contrast 21 p3069 A72-41342
- Fabricating aluminum matrix composites. I - A survey of aluminum matrix composites 22 p3182 A72-41996
- Alpha stabilizing Al and Sn suppression effect on beta-omega transformation during Ti alloy hardening 22 p3189 A72-42278
- Composite materials obtained by depositing boron layers under vacuum on aluminum sheets 22 p3190 A72-42646
- Analytical model of the flash produced in aluminum-aluminum hypervelocity impacts 22 p3207 A72-42867
- Deformation mechanism of aluminum and zinc single crystals during low-temperature cavitation 22 p3192 A72-43019
- Effect of grain size on the thermal diffusion of copper in aluminum 22 p3193 A72-43036
- Determination of mosaic-block disorientations in the creep of aluminum by the method of low-angle X-ray scattering 23 p3299 A72-43341
- Diffusion coefficients measurement in solid and liquid Al, discussing experimental techniques and temperature dependence 23 p3304 A72-44300
- Characteristics of pion and nucleon interaction with carbon and aluminum nuclei over the energy range from 30 to 300 GeV 23 p3331 A72-44435
- Electron-microscope study on the recrystallization in technically pure aluminum 24 p3412 A72-44719
- Boron-aluminum structural component for Shuttle 24 p3458 A72-44890

Low temperature slip discontinuity and strength of pure Al crystals as function of strain rate
24 p3416 A72-45742

ALUMINUM ALLOYS

Ni-Cr-Al alloys high temperature oxidation, detailing surface reactions and continuous oxide layer formation
[ECS PAPER 114] 01 p0082 A72-10172

Thermal conductivity, electrical resistivity, Lorentz ratio and thermopower of Ti, Al and Ni alloys for aerospace structures over 4-300 K range
01 p0113 A72-10173

Transmission electron microscopic investigation of heterogeneous nucleation of Al-Ag alloys metastable gamma prime phase, noting association with four dislocation types
01 p0083 A72-10209

Warpage control of large Al alloy forgings machining of jumbo jet components, using packing and storage methods
[SAE PAPER 710801] 01 p0074 A72-10280

Porosity and W inclusions effects on Al alloy weld strength, presenting radiographic and tensile test data
01 p0074 A72-10282

Nondestructive determination of temperature dependence of elastic moduli of Al alloy and Ni and stainless steels by resonant frequency method
01 p0084 A72-10518

Fiberglass overwrapped Al alloy for space shuttle cryogenic hydrogen and oxygen tanks, noting weight reduction and impeding effect on cyclic loading induced crack growth rate
01 p0139 A72-10738

Constant high tensile stress and rapid aerodynamic heating effect on maraging steels and Ti and Al alloys, evaluating test and simulation procedures for design data development
01 p0084 A72-10749

Torsional prestrain effects on 1100-F Al alloy thin walled tubes yield locus, calculating distortion degree by statistical characteristics
01 p0086 A72-11000

Coarse grained dispersion strengthened Al alloys, investigating solute solutions effects on steady state creep behavior
01 p0087 A72-11025

Hexagonal close packed Ti-Al alloys, determining stacking fault probability with X ray powder diffraction line profiles and Fourier analysis
01 p0087 A72-11029

Al-Mg alloy under reverse bending fatigue in aqueous sodium chloride with constant load and potentiostatic control, determining anodic polarization effects on fatigue life
01 p0087 A72-11033

Metallurgical defects in hot extruded aluminum alloys, describing investigation methods and remedies
01 p0077 A72-11041

Extruded anodized AlMgSi alloy matrix precipitate surface defects, noting wood grain effect, segregated bands, microstructural stains and heterogeneous zones
01 p0077 A72-11042

Extruded AlMgSi alloy manufacturing conditions effect on strength, surface finish and anodized appearance, discussing evenly distributed fine hardening precipitates, metal purity, etc
01 p0077 A72-11043

Precipitation hardened Al-Cu alloy microstructure relation to fatigue and tensile properties, emphasizing particle size and distribution, moving dislocations and grain boundary effects
01 p0088 A72-11044

Al-Mn system constitution, discussing metastable phase, high and room temperature modifications and transformation equilibrium
01 p0088 A72-11045

Mo and Zr additions induced mechanical strength increase of Ni-Al-Nb alloys in cast and deformed states at 20-1100 C
01 p0088 A72-11081

Al alloy powder metallurgy part production, discussing sintering procedures in nitrogen and dissociated ammonia in vacuum
02 p0233 A72-11440

Coextrusion of metal powder and ceramic dispersions clad alloyed Al as function of cartridge density and reactor core length
02 p0233 A72-11456

Residual buckling strength of Al alloy elastic column with fatigue crack
[SESA PAPER 1914A] 02 p0288 A72-11511

Directional solidification of off-eutectic Al-Be alloy, obtaining ultimate strength, elastic modulus and concentration perturbation caused by freezing rate changes
[AD-738212] 02 p0242 A72-11985

Al alloys compressed strips, determining anisotropy of toughness and crack sensitivity by tests
02 p0244 A72-12244

Fracture extension resistance features of aluminum alloys
02 p0245 A72-12510

Al-Mg-Si alloy fatigue, vibration creep and creep strength tests at room temperature, determining mean

stress effects on fatigue strength and cumulative damage
02 p0297 A72-12536

Uniform low temperature compression effect on accelerated aging of Duralumin specimens, noting Plateau due to Guinier-Preston zones
02 p0245 A72-12539

Passivation velocity apparatus for testing Al-Mg alloy sensitivity to corrosion under voltage
02 p0246 A72-12599

Dye penetrant surface defect indications on 2014-T6 Al gas metal arc weldments heat affected zone, considering minimization by arc stabilization and caustic etch time reduction
02 p0236 A72-12775

Fan shaped precipitate formation during supersaturated Al-Zr solid solution decomposition, discussing interpretation as grain boundary migration
02 p0247 A72-12820

Resistometric investigation of Ge addition effect on Al-Zn alloy clustering kinetics, determining Ge atom-vacancy binding energy
02 p0247 A72-12821

Tubular and rod extruded age hardenable Al alloys, determining mechanical anisotropic properties from yield loci and r values
03 p0369 A72-12957

Al-Mo alloys under high temperature, determining phase equilibria and intermetallic phases
03 p0370 A72-12961

Plane strain fracture toughness of notched high strength Al and Ti alloys at low temperatures
03 p0371 A72-13464

Scale factor and surface imbedded inserts effect on bending cyclic fatigue strength of nonhardened and roll hardened Al-Ti alloy
03 p0372 A72-13596

Silicide precipitation in Ti-Zr-Al-Si system, discussing microstructure correlation with mechanical properties
03 p0374 A72-13927

Fibrous structure of precipitates produced at bottom of trace due to friction in work hardened Al-Cu alloy solid solution
03 p0376 A72-13970

Temperature dependence of X ray interference lines for Al-V alloy obtained at high cooling rate, noting metastable solid solution thermal stability
03 p0377 A72-14022

Substructure of cast alloys based on Al-Mg system from electron diffraction microscopy
03 p0377 A72-14023

Creep rupture test program for Al alloys, circumventing parametric methods limitations by extrapolation procedure with graphical extension of isostress curves
03 p0378 A72-14174

Heat treatable Al alloys tensile and compressive moduli of elasticities data from USAF programs, comparing to long-accepted typical values
03 p0378 A72-14175

Portevin-Le Chatelier effect in Al-Mg single crystals during tensile tests, investigating strain rate influence on stress
03 p0378 A72-14257

Au-Al wire bond, discussing intermetallic phase formation under elevated temperature treatments and reliability design limitations
03 p0364 A72-14284

Shock precompression effect on dynamic fracture strength of steel and Al alloy, investigating crack initiation and growth
04 p0533 A72-14541

Heat input, interpass temperature and panel width effects on butt welds strength in Al alloy plate
04 p0526 A72-14838

Boron/aluminum composite sheet quality evaluation by radiography, ultrasonic C-scanning and micro-ohm resistance measurement, correlating with resistance weld strength
04 p0526 A72-14839

Creep surface in Al alloy under combined tension and torsion, obtaining strain rate vectors from probes
04 p0590 A72-15195

Foundry Al alloys elasticity limit estimation via regression formulas, discussing application to quality control
04 p0534 A72-15560

Anodizing effect on corrosion fatigue strength of sheet duralumin under low and high bending stress
04 p0535 A72-15662

Al-Zn-Mg alloy intergranular corrosion in unstressed condition, detecting anodic paths at grain boundaries by potentiostatic technique
04 p0535 A72-15731

Grain boundary region constituents corrosion behavior and solution chemistry within stress corrosion cracks in Al alloys observed from pH changes
04 p0535 A72-15733

Pitting potential and intergranular corrosion of anodically polarized Al and Al alloys in electrolytes
04 p0536 A72-15736

Fatigue crack propagation rates for aluminum alloy plates under mode I extensional loads and transverse mode II bending loads
[ASME PAPER 71-MET-J] 05 p0732 A72-15793

Forming of 7075-T6 Al in high pressure environments, predicting fracture occurrence via finite element stress analysis computer programs and pressure dependent model
[ASME PAPER 71-WA/PT-11] 05 p0671 A72-15912

Fe-Cr-Al and Fe-Cr-Si type ferritic steels, investigating additives effects on ductile-brittle transition temperature
05 p0672 A72-16012

Varying energy and gamma /quasi-steady/ models for point source blast waves from high speed solids impact, comparing 1100-0-aluminum shock decay data
05 p0736 A72-16101

Surface oxide film effects on hydrogen liberation rate from Al and alloys in high vacuum at 20-450 C
05 p0675 A72-16627

NMR behavior and magnetic susceptibility of intermetallic compound CeAl, noting exchange polarization of RKKY type between 4f electrons and conduction electrons
05 p0702 A72-16784

Laser pulse heating inability to quench in disorder in Fe-Al alloy
05 p0669 A72-16796

Fatigue test curves of notched Al alloys under bending with rotation
05 p0676 A72-17086

Al-AlCu intermetallic unidirectionally solidified eutectic composite structure and heat treatment effects on room temperature tensile properties
05 p0676 A72-17104

Age hardened Al-Cu single crystal anisotropy from stress-strain curves, using plane strain compression tests
[AD-743602] 05 p0677 A72-17106

High strength Al-Zn-Mg-Cu alloys, testing heat treatment and Ag addition effects on tensile strength
05 p0677 A72-17112

Ag addition effects on high strength Al-Zn-Mg-Cu alloys tensile properties and resistance to stress corrosion cracking
05 p0677 A72-17113

Directionally solidified Al-AlNi intermetallic eutectic composites creep tests, identifying time dependent fracture mechanism
05 p0678 A72-17114

Directionally solidified Al-AlNi intermetallic eutectic alloy microstructural characteristics and effects on creep fracture
05 p0678 A72-17115

Plastic flow stress around dislocations on Ni-Al intermetallic cube and octahedral cross slip systems
05 p0678 A72-17118

Impurities effect on microstructure alignment in unidirectionally solidified Al-AlNi eutectic intermetallic, noting fiberless region defects
05 p0679 A72-17123

Aging effect on duralumin electrical resistivity alteration at low temperature plastic deformation
05 p0679 A72-17181

Microwires and microstrips fabrication from high strength deformation resistant aluminum alloys
05 p0680 A72-17207

Accelerated fatigue limits for Al and Mg alloys from transverse bend test data
06 p0827 A72-17398

Ni-Al alloy, investigating Y addition effect on vacancy agglomeration suppression during oxidation
06 p0829 A72-17787

Preferred orientation effects on X ray stress measurement of Young modulus and Poisson ratio of Al alloy
06 p0829 A72-17793

Neutron irradiation effect on grain boundary relaxation in Al and Al-Li alloy by internal friction investigation
06 p0830 A72-18292

Al and Ti alloy fatigue after temperature reduction to 253, 77 and 4 K as function of surface purity after machining
06 p0831 A72-18356

V and Al addition effects on mechanical properties of oxygen rich Ti alloys
06 p0831 A72-18358

Anomalous temperature-strain rate dependence of Ni-Al intermetallic compound mechanical properties from plastic deformation mechanism
06 p0832 A72-18417

Hardening mechanisms of interaction between superlattice dislocations and point defects in Ni-Al intermetallic compound mechanical properties strain rate and temperature dependence
06 p0832 A72-18420

Refractory and structural steels and Al alloys, obtaining low cyclic plastic deformation and breaking stress curves
06 p0898 A72-18549

Plasticity of Al alloy thin walled tubular specimens under axial tension and internal pressure at 293, 173 and 93 K
06 p0833 A72-18561

Fractographic analysis of failure kinetics and crack formation in Al alloys, showing microfatigue intrusions and extrusions for various initial stress levels
06 p0834 A72-18653

Structural changes, mechanical properties, electrical resistance and lattice constant during aging of Al alloys containing Mg, Li and Mn
06 p0834 A72-18743

Al alloy plates and D-nosed specimens indentation and penetration under hail impact test
07 p1086 A72-18764

Monograph on diffusion couple technique for Ti-Al system interdiffusion phenomena, discussing layer growth, phase development, grain boundary diffusion mechanism, mass transport, etc.
07 p1011 A72-19267

Al alloy melts with Fe, Cr, Co and Ni, measuring kinematic viscosity by oscillatory-rotary method using logarithmic damping decrement
07 p1012 A72-19550

Y-Fe-Al alloys ternary system X ray structural analysis after arc furnace preparation, annealing and quench hardening
07 p1012 A72-19550

Formation kinetics, phase composition and structure of oxide films in binary and ternary iron-base chromium aluminum alloys, studying hydrogen penetration characteristics
07 p1048 A72-19681

Deformable thermally work hardenable Al-Mg-Li alloy, detailing phase composition changes during aging
07 p1013 A72-19771

Al-Mg alloy with Ti, Zr, Mo and B additions under tensile and impact loads, investigating mechanical properties, strength and crack formation
07 p1014 A72-19838

Recrystallized and unrecrystallized deformed semishinif wrought Al alloy under cyclic and static loads, investigating macrofracture kinetics
07 p1014 A72-19840

Transition metals addition effect on Al-Cu alloys strength and aging characteristics, determining lattice constant increase by X ray microstructural analysis
07 p1014 A72-19841

Cold working effects on plasticity of hardened Al at 20-400 C
07 p1015 A72-19902

Diffusion kinetics in Nb-Al system for varying time and temperatures
07 p1015 A72-19930

Environmental hydrogen embrittlement of Ti-Al alloy as function of test displacement rate and microstructure variation
07 p1016 A72-19933

Interfacial dislocations and failure in tension of directionally solidified Al-Cu-Mg eutectic
07 p1016 A72-19937

Gas quenching technique for vacuum brazing of Al, Ti and ferrous alloys, evaluating mechanical properties, surface contamination and He leak tightness
07 p0997 A72-19997

Al, Ti and ferrous alloys suitability for vacuum brazing-gas quenching processing for He leak-tight joints, using photomicrography
07 p0997 A72-19999

Filler metal compositions and procedures for Al alloys vacuum brazing, describing experimental vacuum furnace apparatus
07 p0997 A72-20000

Metallographic properties of vacuum brazed, heat treated and gas quenched Al alloys, low alloy steels and corrosion resistant steel alloys
07 p1017 A72-20001

Chemically etched notches effect on Al-Mg alloy mechanical properties
07 p1018 A72-20139

Precipitation hardening of quenched superconducting Nb-Al alloys, examining polycrystalline and single crystal samples and intermetallic phases
07 p1050 A72-20155

Al and Al-Si alloy thermal expansion at low temperatures, noting near-eutectic crystalline composition
07 p1019 A72-20156

Al wrought alloys dynamic elasticity modulus and Poisson ratio dependence on temperature, using ultrasonic measurement method
07 p1019 A72-20239

Rapidly and unidirectionally solidified Al alloys microstructure, discussing crystal dislocation origins and patterns
07 p1019 A72-20240

Stainless steel saturation with Al and Cr, investigating structure, microhardness, linear expansion and contact surface seizure reduction
07 p1020 A72-20419

Precipitation hardened Ni-Al alloy mechanical properties, relating ductility and strength to precipitate caused inhibition of microcrack initiation and propagation
07 p1021 A72-20438

Binary Al alloys with variable melting volume and liquid zone velocities, investigating crystallization during zone melting
07 p1022 A72-20572

Temperature dependence of electrical resistance and thermal conductivity in duralumin quenched at 77 K
07 p1022 A72-20663

Electrical resistance and thermal conductivity dependence on temperatures in duralumin quenched at 77 K
07 p1022 A72-20666

Al alloys welding with Pb sheathed linear ribbon RDX explosives by parallel plate process, achieving high weld strength
08 p1173 A72-20779

Optical properties changes of Al alloys containing impurities, noting band structure modification and tendency toward free electron response
08 p1186 A72-21593

German monograph on computerized statistical analysis of Al alloy fatigue test data, considering welded samples and thin plates
08 p1188 A72-21848

Guinier-Preston zone nucleation and growth as function of vacancies in Al-Cu alloy
08 p1190 A72-22166

Viscoplasticity techniques application to deforming portion strain and strain rate fields of axisymmetric Al alloy extrusion with various flow patterns
08 p1250 A72-22194

German monograph on deep drawing of pre-hardened and partially annealed Al and Al alloys, noting anisotropy effect of bottom zone of plate samples
09 p1317 A72-22329

Thermomechanical treatment effects on microstructure and mechanical properties of Al alloy
09 p1327 A72-22470

Heat treatment and machining for distortion control of large Al alloy forgings for DC 10 aircraft
09 p1317 A72-22476

ELDO launch vehicle cryogenic tanks fabrication, discussing Al alloy selection and mechanical properties at low temperatures, manufacturing processes and thermal insulation
09 p1318 A72-22690

Al alloys solid binary solution soft X ray emission spectra interpretation by rigid band and virtual bound state models
09 p1371 A72-22847

Soft X ray emission spectra from Al-Nb and Al-Pd alloys, deducing electron state density near Al ions
09 p1371 A72-22848

Al alloys degree of deformation dependence on pulse energy during extrusion by pulsed magnetic field, showing hardening effect
09 p1319 A72-22865

Ignition delay time and combustion mechanism of Al-Mg alloys single particles in combustion products of oxidizer-fuel mixture
09 p1373 A72-22885

Fracture toughness tests on Al-Cu alloy plate, noting insensitivity to strain rate
09 p1328 A72-22913

Fatigue striation formation and crack propagation mechanism in Al alloy films from electron microscope studies
09 p1328 A72-22917

Transmission electron microscope investigation of Al-Mg-Si alloy precipitation, showing Guinier-Preston zone visibility due to matrix elastic strain introduction
09 p1328 A72-22983

Ti, Zr, Mo, B and Mn additives effect on rupture characteristics of cast Al-Mg alloy under uniaxial tensile stress
09 p1328 A72-23033

Cumulative fatigue damage in Al-Zn-Mg alloy fillet welded joints, analyzing constant amplitude and programmed load fatigue test results
09 p1332 A72-23618

Data scatter reduction in Al-Zu-Mg welded specimens cumulative fatigue damage testing, noting fatigue life improvement by shot peening and static or dynamic prestressing
09 p1332 A72-23619

German monograph on transition elements Cr, Mn and Zr influence on Al-Zn-Mg alloys stress corrosion covering electron microscope studies and loop-bending tests
10 p1493 A72-23769

Electron microscopic study of cyclically deformed Al, Cu, Al-Mg-Zn alloy and carbon steel dislocation structure
10 p1494 A72-23830

Al and oxygen effects on commercially pure Ti microhardness and microstructure, noting interstitial and substitutional atom inclusions effects on hexagonal cell dimensions
10 p1494 A72-23831

Magnetic susceptibility of ternary Al-Mn alloys with Ti, Va, Cr, Fe, Co, Ni, Cu and Zn, describing microstructure and aging experiments
10 p1494 A72-23832

Micrographic observation of Al and Al-Cu intermetallics dendrites shape at birth in liquid of nearly eutectic composition
10 p1496 A72-24239

Transmission electron microscope examination of deformation microstructures adjacent to fatigue cracks in Al alloys
10 p1497 A72-24823

High strength steel strip reinforced aluminum, discussing fabrication techniques and mechanical properties
10 p1498 A72-24839

Mean stress effect on fatigue crack propagation rate in half inch thick Al alloy specimens of high and low fracture toughness
10 p1498 A72-24884

Al alloy notch-bend and compact-tension specimens thickness and crack length effects on plane-strain fracture toughness test results
10 p1498 A72-24886

Tensile, plane strain fracture toughness and fatigue tests of high strength Al alloy cylinders, discussing unstable crack growth conditions
10 p1498 A72-24887

Environmental sensitivity effect on crack propagation rates in steels and Al and Ti alloys, discussing corrosion fatigue
10 p1499 A72-24899

Lattice source interference method for detection of X ray diffraction in Al-Zn solid solutions, taking into account precipitation effects
10 p1499 A72-24981

Chemical compositions, properties and heat treatment of Ti, Al alloys and steels used in aircraft industry
11 p1652 A72-25286

Stress corrosion crack paths in Al-Zn-Mg alloys, showing normal coincidence with grain boundaries
11 p1652 A72-25289

Off axis and transverse tensile properties of boron reinforced Al alloys, correlating metallurgical structures with stress-strain curves and fractographic studies
11 p1654 A72-25479

Fatigue crack initiation and growth in filament reinforced Al alloys, noting interface crack tip stress distribution effects
11 p1654 A72-25480

Al microsegregation in Ti-Al and commercial Ti alloys, investigating effects of cooling rate from beta phase and of Al content
11 p1655 A72-25507

Neutron irradiation effects on GP zones and precipitates in ternary Al alloy, measuring X ray small angle scattering and electrical resistivity
11 p1655 A72-25514

Al alloys hand forgings fracture strength and stress corrosion characteristics from precracked specimens bending tests in air and sea water
11 p1658 A72-25833

Mn content effect on mechanical properties and corrosion fatigue and stress corrosion cracking resistance of Al-Mg casting alloys
11 p1658 A72-25850

Fracture toughness anisotropy and crack sensitivity of Al alloys extruded bars notched cylindrical samples
11 p1659 A72-26130

Microwires and microstrips fabrication from high strength deformation resistant Al alloys
11 p1660 A72-26142

Al alloy-graphite composites brazing and welding feasibility, tabulating spot welding parameters
11 p1641 A72-26491

Ga alloying effect on Al single crystals work hardening, noting Portevin-Chatelier effect at higher Ga contents
11 p1662 A72-26739

Statistical analysis of strain criteria and stochastic relations for Al alloy fatigue life and minimum creep rate at 175-250 C
11 p1663 A72-26800

Cyclic loads frequency and environmental effects on fatigue crack propagation rate, comparing theoretical results with Al alloy thin plates experimental data
11 p1663 A72-26802

Acoustically generated vibration stresses in rigidly clamped Al alloy circular plate, noting stress amplitude distribution dependence on loading frequency bandwidth
11 p1738 A72-26805

Multiphase Al alloys strengthening by dislocation substructures in repeated rolling and recovery cycles at elevated temperature
11 p1667 A72-26930

Anodic oxide film protective properties for Al and Al alloys, evaluating via film dissolution time observation in chromic and phosphoric acids mixture
12 p1829 A72-27457

Plastic deformation resistance nonuniformity in Al alloys, determining stresses
12 p1814 A72-27644

Flow rate limits increase and near homogeneous stress concentration in active hot extrusion of Al alloys
12 p1830 A72-27750

Al-Zn-Mg alloy tear resistance relationship to stress corrosion cracking from tear, tensile and corrosion tests

- Al alloy plate material microstructural variations and specimen orientation effects on tensile and fracture toughness properties 12 p1830 A72-28080
- Heat treated Al alloy forgings stress relief by cold deformation between quench and age, examining effect on tensile properties and residual stresses [ASM PAPER W 72-53,1] 12 p1817 A72-28165
- Electron structure of Al atoms in alloys with transition metals obtained from emission spectra 13 p1973 A72-28492
- Electron microprobe analysis of solute segregation near grain boundaries in Al-Zn-Mg alloy after quenching and aging heat treatment 13 p1973 A72-28652
- Na additions effects on Si growth velocity and morphology in Al-Si alloys, considering coupled zone adsorption mechanism 13 p1975 A72-28664
- Mo addition effect on Al and Ti diffusion from intermetallic compounds into Ni matrix, noting increased high temperature stress rupture life 13 p1975 A72-28670
- Al-Zn alloy supersaturated solid solution decomposition during aging, studying single crystal lattice characteristics via X ray diffusive scattering techniques 13 p1976 A72-28902
- Plastic strains and crack growth in Al alloy under static and repeated static loading 13 p1977 A72-28915
- Thermal effects on phase structure of welded joints of Al alloy with Cu addition 13 p1978 A72-29022
- Stress-service life relations for duralumin samples from impact and nonimpact tensile tests with cyclic axial loads, noting notch sensitivity 13 p1978 A72-29147
- Al and AlMg single crystals static recovery and stacking fault energy at 77-500 K in plastic deformation, noting cross slip onset at 500 K 13 p1978 A72-29222
- Iron content and stress level effect on flaking corrosion of Al alloy sheets, describing experimental technique 13 p1980 A72-29826
- Ti, B, Zr and Be trace additions effect on Al alloy grain refining from spectrochemical analysis 13 p1913 A72-29838
- Microstructure and mechanical properties of heat resistant Fe-Mn-Al alloys at 650-1150 C 13 p1981 A72-30093
- X ray analysis of Ti-Al alloys for cold rolled texture diagrams at low and high deformation levels 14 p2112 A72-30159
- Al inhibitive of Ti oxidation at 800-1000 C due to interatomic bonds, lower oxygen solubility and diffusion rates 14 p2113 A72-30166
- Literature survey of fatigue behavior of Al alloy welded joints, discussing testing and analysis methods 14 p2113 A72-30250
- Hot worked Al alloy machine elements mechanical properties scattering, discussing quality control procedures 14 p2114 A72-30275
- Al single crystals, investigating scale factor effects on stepwise deformation at 1.4 K 14 p2115 A72-30410
- Al-Cu alloy structural changes after long term natural aging by X ray diffraction analysis 14 p2115 A72-30413
- Welded Al alloys at temperatures above 100 C, discussing traditional and powder metallurgy and mechanical properties dependence on time, temperature and creep 14 p2116 A72-30528
- Chemical and mechanical properties relationship to stress corrosion in high strength Al-Cu and Al-Zn-Mg alloys, emphasizing grain boundaries cleavage energy 14 p2117 A72-30536
- Anodic salt-chromate stress corrosion resistance test of Al-Zn-Mg alloys, noting time reduction and correlation with natural environment exposures 14 p2117 A72-30541
- Microstructural changes relationship to corrosion susceptibility in ternary Al alloy obtained from stress corrosion cracking tests and electron metallography, noting precipitate-free region 14 p2118 A72-30542
- Quenching rate and alloying element content effects on precipitation extent and corrosion resistance of Al-Cu alloys, discussing microstructure, chemical composition and mechanical properties 14 p2119 A72-30604
- Uniformly distributed precipitates effect on hardness increase in aging of ferritic matrix Fe-Co-Ti and Fe-Co-Al alloys 14 p2119 A72-30605
- Metallurgical and superconducting properties of beta-tungsten structure niobium aluminide with high critical temperature 14 p2119 A72-30607
- Crystal lattice defects induced by cyclic straining in quenched Al-Zn alloy, noting fatigue effects on dislocations accumulation and grain boundary migration 14 p2120 A72-30610
- Modified Al-Si eutectic solidification behavior and microstructure, investigating LF mechanical vibration effects 14 p2120 A72-30617
- Ultrasound damping in Mg and Al alloys by structural grains and dislocation oscillations during work hardening, recrystallization and oversaturated solid solution decay 14 p2122 A72-30957
- Mo-Ni-Al system phase equilibria at 600 C from X ray and microstructural analysis, noting hardness dependence on composition 14 p2123 A72-30985
- Ni-Al-Nb-Mo system phase diagram from X ray and microstructural analysis, noting solid solubility and dependence of hardness and electrical resistivity on components 14 p2123 A72-30989
- Slip band blocking effect of disperse particles on crack suppression and creep rupture strength of intermetallic Al-Fe-Ni alloy 14 p2124 A72-31033
- Primary crystallization of intermetallic compounds in Al alloy as function of high melting metal concentration and casting temperature 14 p2124 A72-31034
- Cast Al alloys tendency to brittle failure in percussive bending tests estimated from force strain oscillograms 14 p2124 A72-31035
- Binary Al alloys intermetallic phases effects on microcracks nucleation and propagation at 300 C in uniaxial tension, considering alloying elements influence on mechanical properties 14 p2124 A72-31036
- Al-Mu-Li alloys phases mechanical and thermal properties under tensile and fatigue tests at room and elevated temperatures 14 p2124 A72-31037
- Mn, Zr and Cr alloying effects on grain size and solid solution decomposition of cast Al-Zn-Mg alloy bars 14 p2125 A72-31039
- High temperature oxidation resistance and mechanical properties of Fe-Al-Cr alloys with Ti and Mo additions 15 p2253 A72-31520
- Viscoelastic model for constitutive nonlinear creep law with combined strain and time hardening assumptions, evaluating material parameters for Al alloys 15 p2254 A72-31554
- Structural decomposition and hardening of supersaturated Al-Cu, Al-Cu-Ag, Al-Zn, Cu-Sn and Cu-Ni-Co solid solutions 15 p2255 A72-31565
- Al-Zn-Mg alloys hot cracking during solidification, discussing chemical composition, Al purity, temperature, aging, dissolved gases and grain refining additives effects 15 p2256 A72-31774
- Mechanical properties and residual stresses in and adjacent to interface of explosively welded Al-Zn-Mg alloy with steel, noting microcracks effect on weld strength 15 p2257 A72-32111
- Electron microscopic investigation of Al-Mn alloy precipitate structure and morphology after annealing induced decomposition 15 p2257 A72-32114
- Al-Zn-Mg-Cu forgings fracture toughness increase with Fe content reduction, discussing overload fracture following grain and stringers 16 p2405 A72-33000
- Al alloy welded seams corrosion fatigue strength increase by epoxy polymer coatings under cyclic tensile stresses 16 p2397 A72-33268
- Anodic oxide films separation from Al alloy surface using ethyl bromide at temperatures below 40 C 16 p2397 A72-33274
- Al-Mg solid solution creep at 570-800 K, discussing creep rate controlling mechanism due to Mg atoms interactions with dislocations 16 p2407 A72-33442
- Strain rate and temperature effects on supersaturated Al-Cu-Mg solid solution mechanical properties, considering ultimate tensile strength and hardening 16 p2407 A72-33443
- Al-Cu-Mg alloys room temperature age hardening, determining effects of tension load up to plastic deformation from measurements of mechanical properties and electrical resistance [DFVLR-SONDDR-188] 16 p2408 A72-33674
- Crack propagation in Al-Cu-Mg alloy sheet under vibratory bending loads, noting crack length to loading cycles number relationship 16 p2408 A72-33677
- Liquidus temperatures and isothermals in Al corner of Al-Ti-B alloy phase diagram, using differential thermal analysis 16 p2409 A72-33808
- Chill zone structures in Al-Cu alloys as function of heat sink, surface microprofile and liquid metal fluid flow 16 p2409 A72-33810
- Discontinuous precipitation and site nucleation in quenched and aged Al based Zn alloys as function of temperature 16 p2410 A72-33812
- High temperature oxide scale adherence on Fe-Cr-Al alloys with Y or Sc additions as promoting agents 16 p2410 A72-33817
- Error analysis of dynamic yield point measurements based on residual deformation from impact tests of Al alloy and steel specimens 16 p2472 A72-34016
- Permanent traction and torsion strains effect on ratio between pure compression and pure traction yield points of Al alloy 16 p2412 A72-34179
- Chemical diffusion in the titanium-aluminum system 17 p2510 A72-34275
- New observations of preprecipitation phenomena in Al-Mg and Al-Mg-Zn alloys 17 p2566 A72-34286
- Initial yield surface of a unidirectionally reinforced composite. [ASME PAPER 71-APMW-19] 17 p2623 A72-34301
- An experimental buckling study of skin-corrugated ring-stiffened curved panels. [SESA PAPER 1993A] 17 p2630 A72-34818
- Use of special gauges for determining crack growth rate in fatigue in the AU4G1 aluminum alloy 17 p2567 A72-34890
- Impact crater formation at intermediate velocities. [ASME PAPER 72-MAT-C] 17 p2631 A72-34967
- Separation of iron and annealing-out of lattice defects in rapidly-solidified aluminum-iron alloys. I - Microstructure and properties of quenched samples. II - Tempering behavior 17 p2567 A72-35174
- Aluminum alloys electron beam weldability, considering preheating, welding speed, voltage, pre- and post-weld heat treatments effects 17 p2561 A72-35799
- Complexonometrical analysis of molybdenum aluminides and Cu-Mo alloys without preliminary separation of components 18 p2655 A72-36097
- Metallurgical aspects in the development of AlMgSi alloys with a low sensitivity to quenching 18 p2699 A72-36224
- Precipitation caused surface defects on Al-Mg-Si alloy extrusions, considering segregation streaks, cooling induced microstructural stains and cold working-annealing produced heterogeneous zones 18 p2699 A72-36225
- Filler wire composition effects on solidification cracking resistance in weldable Al-Zn-Mg alloy 18 p2699 A72-36426
- Phase structure and solution kinetics of cast and wrought Al alloys after plastic deformation by rolling 18 p2700 A72-36585
- Ultrasonic velocity measurement of elastic constants of Al-Al3Ni unidirectionally solidified eutectic. 18 p2701 A72-36591
- Diffusion in the nickel-rich, Ni-Al solid solution at 1260 C. 18 p2701 A72-36593
- The structure of the metastable precipitates formed during ageing of an Al-Mg-Si alloy. 18 p2702 A72-36743
- Combustion propagation in cylindrical aluminum alloy specimens and some peculiarities of the aluminum combustion mechanism 19 p2847 A72-37362
- Zr and V alpha and beta stabilizing element effects on phase boundaries in arc fused Ti-Al alloy studied by diffusion layer method 19 p2817 A72-37754
- Aluminum. II - A review of deformation properties of high purity aluminum and dilute aluminum alloys. 19 p2818 A72-37832
- Microstructure and differential thermal analyses of ternary system Co-Mn-Al, presenting phase diagrams 19 p2818 A72-37852
- Investigation of the influence of surface treatment purity and procedure on the strength of the Kh18Ni10T and Kh16N6 steels and the AM6G alloy at normal and low temperatures 19 p2819 A72-38016
- Effect of additions of Cu and Zr on stress corrosion cracking of Al-Mg alloys. 19 p2820 A72-38370
- Optimization of thermo-mechanical deformation parameters for Ti-6Al-4V. 19 p2821 A72-38385
- Interpreting electron fractographs of stress corrosion in aluminum alloys. 19 p2821 A72-38387
- Effects of small amounts of additional elements on stress corrosion cracking of Al-Zn-Mg alloys. VI. 19 p2821 A72-38555
- Radiographic examination of rhenium-aluminum-boron and rhenium-silicon-boron ternary systems 19 p2822 A72-38679

- Book - Aluminum brazing handbook
19 p2810 A72-38720
Experimental creep buckling of circular cylindrical shell under uniform compression.
20 p2978 A72-38883
Distortion and residual stresses in welded aluminum structures.
20 p2928 A72-39204
Al-B and Al-Ti-B alloys fabrication, discussing quality control and grain refinement
20 p2936 A72-39207
The mechanism of oxidation of Ni-Cr-Al alloys.
20 p2937 A72-39214
The internal oxidation of Ni-Cr-Al alloys.
20 p2937 A72-39215
Formation of voids and dislocation loops in near-stoichiometric NiAl by aging at 700 to 900 C, and some effects on alloy properties.
20 p2937 A72-39288
X ray diffraction study of crystal structure of metastable phase in rapidly solidified Al-Zr alloys
20 p2939 A72-39307
Investigation of solid solution decay in cobalt-titanium, iron-cobalt-titanium-aluminum and iron-nickel-titanium-aluminum alloys
20 p2939 A72-39314
Mechanical properties improvement of Al alloys for machine construction applications, suggesting Ti, Zr and Be additions optimal rate
20 p2941 A72-39577
Interfacial characteristics of silicon carbide-coated boron-reinforced aluminum matrix composites.
20 p2941 A72-39791
Deformation and failure characteristics of joints in a Ni-Al system under the action of high thermal pulses
20 p2942 A72-39822
Effect of alloying on the decay of an aluminum-magnesium solid solution
20 p2942 A72-39823
Optimal planning of an experiment in a study of the properties of Ti-V-Al alloys
20 p2942 A72-39825
Fatigue-crack propagation characteristics of aluminum alloys in thick sections.
20 p2942 A72-39951
Burning of particles of an aluminum-magnesium alloy
20 p2987 A72-40041
Fatigue damage of aluminum alloy at high temperature.
21 p3066 A72-40716
Fatigue cumulative damage in cases of rotating-bending and torsional multistep loading.
21 p3118 A72-40933
Effects of environment on formation of finished surface in drilling aluminum and aluminum alloys.
21 p3060 A72-40936
Effects of modification and additional elements on the solidification of Al-Si alloy - Studies on the solidification of Al-Si alloys in a shell mold. II.
21 p3067 A72-40937
The nature of solid solutions of the titanium-vanadium-oxygen and titanium-vanadium-aluminum-oxygen systems
21 p3068 A72-40962
Ferromagnetic tau phase structure of Mn-Ac alloy with powder anisotropy related to platelet formation and twinning orientation
21 p3068 A72-40965
Fabrication studies of Nb3Al superconductors.
21 p3097 A72-41182
Mechanism of high temperature creep of aluminum-magnesium solid solution alloys.
21 p3069 A72-41299
Influence of the cycling frequency and directional anisotropy on the fatigue strength of AMg6BM aluminum-alloy sheet
21 p3070 A72-41356
Graphite content effect on vibration damping properties of Al-Sn and Al-Zn alloys
21 p3070 A72-41358
Resonant frequency, fatigue and energy dissipation relations for endurance limit determination in Al alloy specimens under vibrational loads
21 p3070 A72-41368
Plastic flow and strain hardening theories for short time tensile creep in high temperature metal formation, applying to Al alloys
21 p3125 A72-41510
Calculating the stability of centrally compressed thin-walled bars with various profiles
21 p3126 A72-41549
Metastable phases in very rapidly solidified aluminum-germanium alloys
21 p3070 A72-41644
Influence of stress raisers in the form of circular holes on the endurance in symmetric bending of AMg6BM aluminum-alloy sheet
21 p3071 A72-41704
Comparison of the resistance to fracture of the K1c of the AK4-IT1, V95T1, and D16T aluminum alloys and VT8 and VT9 titanium alloys under static and cyclic loading
21 p3071 A72-41705
Yielding and fracture of D16T alloy at low temperatures under conditions of complex stress-strain state
21 p3071 A72-41706
Stress-strain diagrams and fracture characteristics of fiber-reinforced aluminum alloys
22 p3189 A72-42300
Cyclic hardening of Al-Zn single crystals at constant plastic strain amplitude, observing similarity between fatigue hardening and work hardening
22 p3189 A72-42439
Thermoelastic martensite caused elastic vibration damping in Cu-Al-Ni alloy, observing shape memory effect
22 p3190 A72-42442
Different forms of elimination of quenching lacunae in supersaturation in the case of aging of two alloys, Al-Cu and Al-Mg-Si
22 p3190 A72-42444
Effect of rare earth metals on the structure and properties of aluminum and its alloys
22 p3192 A72-42818
Superconducting transition temperature increase in Nb-Al-Si alloys as function of composition under tetragonal lattice crystallization
22 p3192 A72-43020
Aluminized thoria dispersed NiCr and Ni-20Cr alloys with protective alumina scales from pack diffusion, observing oxidation resistance by isothermal and cyclic oxidation tests
22 p3193 A72-43030
Brittle striation formation role in corrosion fatigue crack propagation mechanism in Al-Zn-Mg alloy from test in NaCl solution under reversed anodic-cathodic current
22 p3193 A72-43033
Effect of cyclic stress wave form on corrosion fatigue crack propagation in Al-Zn-Mg alloys.
22 p3194 A72-43043
Studies on sizes and shapes of tensile test specimens for thin sheet materials of aluminum alloys.
22 p3195 A72-43125
Composite Al- and Ni-base alloys strengthened by B and W/Mo fibers respectively for reduced weight wing spars and high temperature applications
22 p3197 A72-43139
Flow-stress recovery of nickel-aluminum alloys.
23 p3299 A72-43563
Recovery of high temperature deformed Ni-Al alloys.
23 p3300 A72-43564
Tendency toward brittle failure of a simulated weld-seam region in Ti-Al-V system alloys
23 p3293 A72-43593
Stability of AlBMg2 particles against diffusive coagulation in aluminum-magnesium alloys
23 p3301 A72-43649
Al alloy sheet panel tests for cracks emanating from stress concentration areas at holes or cutout edge
23 p3347 A72-43713
Heat treatment effect on tensile and bending fatigue strength of Al alloy thin sheet
23 p3301 A72-43743
Experimental investigation of displacements and stresses in a rod during impact loading
23 p3348 A72-43795
Al alloy rupturing analysis in complex stress state, noting sublimation and self diffusion values of activation energy in torsional to tensile state transition
23 p3301 A72-43957
Fatigue fracture and crack propagation in aluminum alloys. II.
23 p3302 A72-43973
Shear-strain-rate effects in a high-strength aluminum alloy.
23 p3302 A72-43983
Peritectic solid phase transformations in cast homogenized Al-Cu-Li-Mn-Cd alloy, noting Li strengthening effect
23 p3303 A72-44093
Structure of the 01420 alloy with zirconium
23 p3303 A72-44094
Investigation of the process of D16-alloy quenching in liquid nitrogen
23 p3294 A72-44095
A study of cold-worked titanium-aluminum alloys by X-ray diffraction.
24 p3413 A72-44720
Fatigue crack closure at positive stresses.
24 p3457 A72-44819
Plane strain fracture toughness of notched high strength Al and Ti alloys at low temperatures
24 p3413 A72-44939
A study of the hardening of the subspinoidal alloy Fe-Ni-Al
24 p3415 A72-45395
The mechanism of void formation, void growth, and tensile fracture in an alloy consisting of two ductile phases.
24 p3415 A72-45481
The mutual solubilities of titanium and boron in pure aluminum.
24 p3415 A72-45482
Al and Ti alloy fatigue after temperature reduction to 253, 77 and 4 K as function of surface purity after machining
24 p3416 A72-45743
V and Al addition effects on mechanical properties of oxygen rich Ti alloys
24 p3416 A72-45745
Chemically etched notches effect on Al-Mg alloy mechanical properties
24 p3417 A72-45764
ALUMINUM ANTIMONIDES
Phase diagrams of AlSb-GaSb and InAs-GaAs systems, noting mixing energy for liquid and solid phases
19 p2845 A72-38207
ALUMINUM COATINGS
Lightning protective coatings for boron/epoxy composite materials, discussing high current damage mechanisms, simulation facility and test results on aluminum foils, meshes, etc
01 p0092 A72-10783
Anodized aluminum metallization for reducing electromigration induced failure modes in silicon wafers
03 p0365 A72-14286
Al and Al-Zr coating effects on heat resistant alloy turbine blades high temperature fatigue resistance under bending-torsion cyclic loads
05 p0671 A72-15990
Aluminized layer phase and chemical composition on heat resistant iron and nickel alloys
07 p1013 A72-19748
Aluminum plated pyrotechnics physical properties and performance for electroexplosive device applications, describing particle size distribution and loading pressure dependence of density
08 p1221 A72-20772
Cathodic processes in Al electrodeposition from ethyl pyridine bromide electrolyte, discussing phase equilibrium and electrical conductivity dependence on solution composition
09 p1318 A72-22529
Ellipsometric characterization of oxide films obtained by heat treatment of Al in air and vacuum, noting interface disruption due to gamma crystal penetration into coated metal
10 p1495 A72-24078
High temperature effects on stability, corrosion behavior, structure and protective effectiveness of Al coatings on Ni and Co alloys
11 p1664 A72-26852
Aluminizing process improvement by CaAl and ammonium chloride contents increase in powder
13 p1964 A72-29020
Phase composition, structure and strength properties of aluminizing coatings on Ni-Al alloys, noting plasticity increase due to Ta addition
13 p1980 A72-29485
Heat losses due to spacecraft installation discontinuities on aluminized Mylar multilayer insulation, predicting blanket performance
14 p2171 A72-30829
Tensile strength, toughness and corrosion resistance of dross aluminized carbon steel specimens under static, cyclic and impact loads
16 p2406 A72-33267
Stability and hot corrosion of aluminum coatings on the INCO 713C alloy and on cobalt alloys
18 p2701 A72-36595
Hot corrosion of experimental aluminum-coated cobalt-base alloys.
18 p2702 A72-36797
Profile and depth of microcraters formed in glass.
18 p2736 A72-36972
Acceleration effects on burning velocity of aluminized condensed rocket propellant systems, calculating particle size and slag mass
19 p2847 A72-37360
Formation of defects in reflecting coatings under the action of high temperatures
22 p3197 A72-43193
Al and Al-Zr coating effects on heat resistant alloy turbine blades high temperature fatigue resistance under bending-torsion cyclic loads
24 p3415 A72-45732
ALUMINUM COMPOUNDS
NT ALUMINATES
NT ALUMINUM ANTIMONIDES
NT ALUMINUM FLUORIDES
NT ALUMINUM NITRIDES
NT ALUMINUM OXIDES
NT ALUMINUM SILICATES
NT ANDESITE
NT FELDSPARS
NT KAOLINITE
NT PYROPHYLLITE
NT SAPPHIRE
Iron aluminides and borides diffusion layers morphology on alpha iron surface by metal surface/gas phase interaction, observing preferential orientation
03 p0376 A72-13971
Enhanced indirect optical absorption measurement in AlAs and GaP with energy denominator variation for direct band gap evaluation
13 p2022 A72-29627

Gallium aluminum arsenide light emitting diode thin structures grown on GaP substrates by liquid phase epitaxial method

15 p2290 A72-31381

Pd-Al intermetallic compound contact materials.

18 p2698 A72-35985

ALUMINUM FLUORIDES

Nuclear magnetic resonance of Al 27 in topaz /aluminum fluorosilicate/, determining nuclear quadrupolar coupling constant and asymmetry parameter

04 p0564 A72-15638

ALUMINUM ISOTOPES

Al 26 production rates from Al, Si, S, Mg and Ca in Bruderheim chondrite by weighted least squares analysis

03 p0435 A72-13691

ALUMINUM NITRIDES

Aluminum nitride amount and particle size measurement at austenitic grain coarsening temperatures in low carbon steels

11 p1656 A72-25755

Precipitation of aluminum nitride in low-alloy steel

21 p3068 A72-40956

ALUMINUM OXIDES

NT SAPPHIRE

GaAs, Si and alumina performance as substrates in integrated microwave circuits

01 p0046 A72-10700

Alumina dispersions structural stability in Fe and Ni based alloys metal matrices

02 p0241 A72-11445

Aluminum oxide dispersion hardened ferritic heat resisting Cr steel, describing liquid phase sintering effects on high temperature tensile strength

02 p0241 A72-11448

Metal-alumina-oxide-semiconductor capacitor flat band bias voltage measurement before and after thermal stressing, noting potential barrier in structure model

03 p0336 A72-14278

Corundum ceramics thermal stability, basing qualitative tests on thermal cycle number and quantitative tests on thermal gradient producing damage

05 p0680 A72-15755

Surface oxide film effects on hydrogen liberation rate from Al and alloys in high vacuum at 20-450 C

05 p0675 A72-16627

Soviet papers on anodic oxidation of metals covering aluminum and zirconium oxides, oxide films, anion sorption capacity, chemical composition, structure and physicochemical properties

05 p0667 A72-17050

Heating effect on potassium bichromate-saturated anodic aluminum oxide electrical characteristics, discussing surface conductivity and capacity and solution pH

05 p0667 A72-17052

Anion sorption mechanisms and product composition in anodic aluminum oxide filled with phosphate, chromate and sulfate solutions, discussing chemisorption compound formation and oxide dehydration

05 p0624 A72-17053

Electron microscopy for structure study of anodic aluminum oxides prepared by various methods, comparing electrograms of oxides after heating, boiling and filling with water

05 p0624 A72-17054

Sorption properties of anodic aluminum oxides prepared in orthophosphoric and chromic acid solutions, determining dependence on pH by isotopic labeling method

05 p0624 A72-17055

Current reversal effect on anodic aluminum oxide film prepared in phosphate electrolyte, using electron microscope and isotopic labeling

05 p0667 A72-17056

Thermal conductivity of aluminum, beryllium and magnesium oxides lattices at high temperatures

06 p0828 A72-17615

Aluminum oxide cloud formation for thermosphere temperature determinations, describing methane/oxygen payloads, spectrographs, photometers and atmospheric models

06 p0806 A72-17646

Moving heat source model of temperature profile and thermal stress propagation for laser drilled holes in alumina ceramic material

07 p0994 A72-19211

Bond dissociation energy of aluminum monoxide, tabulating flame compositions and temperatures

07 p1051 A72-19363

Photoelectric temperature measurements in contact zone during grinding of aluminum oxide ceramic materials by synthetic diamond disks

07 p0997 A72-20252

Dispersion strengthening of electrolytically deposited nickel-aluminum oxide alloys, comparing tensile tests to theoretical values

08 p1186 A72-21442

Quenched aluminum oxide rod residual stress profile from strain and heat transfer rate measurements and temperature distribution calculation

08 p1196 A72-21918

High strength solids compositional, heat treatment and chemical environmental effects on fracture strength, considering alumina as example

09 p1334 A72-22387

Alumina microstructure, grain size and impurities effects on ballistic performance, discussing results in terms of microplasticity

09 p1334 A72-22390

Thermomechanical and plastic deformation behavior of polycrystalline alumina at elevated temperatures

09 p1335 A72-22394

Nonbasal deformation modes activation in Czochralski sapphire and fine grained alumina polycrystals deformation, noting water weakening

09 p1335 A72-22395

Static fatigue of borosilicate glass, fused silica and polycrystalline alumina, presenting log stress vs log failure time plots

09 p1335 A72-22398

Cermet coating with enhanced microhardness by Ni electroplating with fine corundum particles, presenting optimum electrolytes

09 p1318 A72-22527

Protective aluminum oxide scale development on Ni-Cr-Al alloy, describing transient oxidation stage

09 p1332 A72-23584

Ellipsometric characterization of oxide films obtained by heat treatment of Al in air and vacuum, noting interface disruption due to gamma crystal penetration into coated metal

10 p1495 A72-24078

Nonstoichiometry of beta and beta-two aluminas in epitaxial coexistence from crystallographic investigation

10 p1433 A72-24082

Alpha corundum grains from Apollo 11 lunar dust sample, using X ray diffraction and electron microprobe analyses

10 p1536 A72-24152

High alumina ceramics metallization and hard soldering to metals for manufacturing vacuum jacket of transmitting thermionic tubes

10 p1488 A72-24642

Mullite as part of aluminum oxide-silicon dioxide system, discussing formation, structure, physical chemistry, additives effects and high alumina refractories

10 p1501 A72-24729

Fusion cast zirconia-alumina-silica refractories manufacturing process, phase diagrams, chemical and physical properties and industrial applications

10 p1502 A72-24734

Superconductive behavior of cold-worked sintered Nb wires, examining effects of aluminum oxide addition on residual resistivity, magnetization behavior and critical current density

11 p1662 A72-26742

Ball milling effects on alumina and tungsten carbide powder sinterability due to particle comminution and microstrains

11 p1642 A72-26827

Mg addition effect on high temperature mechanical properties of nickel-alumina alloy, studying particle coarsening mechanism changes

11 p1664 A72-26856

Alloying addition effects on structural stability and particle-matrix cohesion in metal-alumina composites

11 p1665 A72-26864

Computer algorithms for scattering functions of condensed aluminum or magnesium oxides in combustion products for various temperatures and particle sizes

11 p1747 A72-26966

Heat resistance of corundum based ceramics with multiphase additions under thermal cycling tests

13 p1983 A72-28568

Polycrystalline microstructure changes of corundum during high temperature creep tests, using optical microscopy

13 p1983 A72-28775

High purity aluminum-aluminum oxide reversible oxidation, discussing mechanism based on electron charging due to beam

13 p1980 A72-29827

Activation energy of high temperature creep in Cr alloy with aluminum oxide, comparing with moving monovacancies in pure Cr

14 p2112 A72-30161

Nonmetallized aluminum oxide ceramics brazing with metals under pressure using copper solder, noting optimum conditions for Kovar

15 p2243 A72-31225

High temperature steady creep of Nb and niobium-aluminum oxide alloys at 850-1400 C

15 p2254 A72-31561

Aluminum oxide reproducible layers plastic deformability or microhardness from molecular beam scattering distribution

16 p2430 A72-33064

Zinc oxide effect on alumina dispersion, energy of formation, nucleation and particle size reduction, calculating critical nucleus radii

16 p2476 A72-33255

Dynamic load tests for impact strength of ceramic composites with fiber reinforced alumina matrix, obtaining dynamic stress-strain curves

16 p2414 A72-33300

Adhesion effects on tensile and thermal expansion properties of aluminum oxide particles filled epoxy-urethane polymer at ambient and liquid nitrogen temperatures

16 p2415 A72-33415

Aluminum oxide high temperature equilibrium morphology in Ni matrix prepared via vapor deposition and internal oxidation methods

16 p2411 A72-33824

Dielectric breakdown in electrical insulators used in thermionic converters.

17 p2496 A72-34591

Carbon fibre composites with ceramic and glass matrices. II - Continuous fibres.

17 p2570 A72-34669

High strength alumina, boron, silicon carbide and graphite reinforcing fibers for composite materials

17 p2572 A72-35656

Effective separation technique for small diameter whiskers.

17 p2572 A72-35662

Effect of structural parameters and temperature on the effective thermal conductivity of plasma-sputtered aluminum oxide

18 p2696 A72-37188

Alpha aluminum oxide whiskers growth in presence of lead by vapor/liquid/solid phase mechanism in moist hydrogen at 1200-1400 C

19 p2823 A72-38279

Structural features of plasma and gas-flame deposited aluminum oxide coatings

19 p2810 A72-38680

Aluminum oxide and silicon carbide whiskers fabrication by homogeneous gas reaction process, discussing gas composition, temperature and substrate effects on production yield

20 p2940 A72-39440

Adhesion characteristics of alpha-aluminum oxide-nickel system from shear strength measurements, investigating effects of sintering parameters and Ti and Zr alloying components

20 p2940 A72-39445

Corundum polycrystalline microstructure changes during high temperature creep tests, using optical microscopy

21 p3072 A72-40269

Highly aluminous glasses in lunar soils and the nature of the lunar highlands.

21 p3104 A72-40490

Aluminized thoria dispersed NiCr and Ni-20Cr alloys with protective alumina scales from pack diffusion, observing oxidation resistance by isothermal and cyclic oxidation tests

22 p3193 A72-43030

Polycrystalline aluminum and magnesium oxide ceramics fracture strength, considering plastic deformation and twinning role in crack nucleation

23 p3305 A72-43505

Determination of the regions of action of various creep mechanisms in ceramic materials

23 p3307 A72-43932

Contribution to the study of phenomena of ordering of defects in single crystals of alumina- or zirconia-base refractory materials

23 p3302 A72-44000

Alpha aluminum whiskers growth in multie ceramic composition following vapor-liquid-solid phase

23 p3303 A72-44152

An experimental investigation of radiative properties of aluminum oxide particles.

24 p3461 A72-44809

Surface tension, density, and volume change on melting of Al₂O₃ systems, Cr₂O₃, and Sm₂O₃.

24 p3417 A72-44925

ALUMINUM SILICATES

NT ANDESITE

NT KAOLINITE

NT PYROPHYLLITE

Alumoborosilicate glass fibers vacuum tensile strength tests, noting fiber strength increase with vacuum and exposure time

07 p1023 A72-19778

Strength of titania and aluminum silicate under combined stresses.

19 p2822 A72-37271

Phase diagram, isomorphism and temperature dependence of hexagonal, monoclinic and triclinic modifications of Sr-Ba polycrystalline aluminosilicates

21 p3072 A72-40382

ALUMINUM 26

Early solar system nucleosynthesis of Al 26, discussing silicon and carbon burning and spallation

04 p0567 A72-14912

Lunar rheolite cosmogenic Al 26 and Na 22 distribution in Lunik 16 sample interpreted by lunar surface soil impact induced mixing

08 p1240 A72-22190

Aluminum 26 and manganese 53 produced by solar-flare particles in lunar rock and cosmic dust.

20 p2970 A72-39472

- Depth distributions of cosmic ray produced radionuclides in chondrites and achondrites, determining apheia from Al 26 activities 22 p3228 A72-42861
- ALUMINUM 27**
Nuclear magnetic resonance of Al 27 in topaz /aluminum fluorosilicate/, determining nuclear quadrupolar coupling constant and asymmetry parameter 04 p0564 A72-15638
- ALVEOLAR AIR**
Lung ventilation nonuniformity determination by single calm breath method, showing nitrogen concentration in alveolar phases 02 p0165 A72-12515
Single breath diffusing capacity and alveolar dead space measurements for carbon 18 monoxide using respiratory mass spectrometer 04 p0480 A72-15215
Single breath method for pulmonary diffusing capacity measurement with respect to total lung capacity and inspiration time 05 p0620 A72-17174
Compression cycles effects on alveolar volumes of sea lions and dogs excised lungs, noting decompression sickness prevention by airways cartilaginous reinforcement 08 p1116 A72-21186
Digital computer simulation of circulatory and respiratory systems interaction model for oxygen and carbon dioxide gas exchange between pulmonary blood and alveolar air 09 p1268 A72-22456
Four-parallel-compartment lung model for emptying pattern study, using expired nitrogen concentration data to calculate alveolar dilution ratio and emptying rate 14 p2079 A72-30703
Rebreathing studies of carbon dioxide pressure level effect on carbon dioxide content difference in arterial blood and alveolar gas during exercise and rest 17 p2499 A72-34346
Respiratory frequency and alveolar oxygen and carbon dioxide tension relationship to hypercapnia in man 17 p2506 A72-35965
Blood oxygenating ability of helium- and argon-oxygen environments relative to air, using alveolar gas equation to predict arterial oxygen pressure 18 p2649 A72-36438
A model of fluctuating alveolar gas exchange during the respiratory cycle. 18 p2650 A72-36571
- ALVEOLI**
Electron microscope examination of freeze-etched air-filled lung alveoli extracellular lining layer, discussing sample preparation techniques 05 p0623 A72-16787
Blood flow stratification effect on alveolar gas exchange in liquid filled lungs in dogs from Xe 133 concentration measurements 10 p1425 A72-24481
Sheet flow theory for pulmonary alveolar blood flow, discussing blood pressure effects, membrane tension, blood volume and transit time distribution 11 p1589 A72-26702
Alveolar carbon dioxide pressure-ventilation response curve measurement by Campbell rebreathing method in consecutive daily trials 13 p1906 A72-29846
Cell proliferation in lungs of mice exposed to elevated concentrations of oxygen. 17 p2499 A72-34548
- AMBIENT TEMPERATURE**
CW X-band Gunn oscillator in coaxial cavities, investigating frequency variation with ambient temperature 01 p0037 A72-10641
Aerodynamic compensation for ambient medium temperature effect on fluidic standard components and timing devices 04 p0466 A72-14993
Various work-rest cycles and environmental temperature effects on body temperature, determining external auditory canal and core temperature relationship 08 p1123 A72-20886
VS type 2-W carbon resistor electrical aging operation, investigating optimal ambient temperature and duration 08 p1143 A72-22068
CW X band Gunn microwave oscillators, measuring frequency variation relationship to ambient temperature 10 p1450 A72-24555
Environmental temperature effect on motion sickness sweating, discussing nausea and discomforting symptomology prediction 12 p1775 A72-28302
Sweating relation to body temperature after exhaustive exercise for various oxygen uptakes and ambient temperatures 14 p2079 A72-30702
Wall and ambient temperature distribution effects on free convection heat transfer from nonisothermal vertical flat plate in temperature stratified medium for Prandtl number range 16 p2477 A72-33434
- Thermal resistance of Gunn diodes - Analysis and measurement. 21 p3035 A72-41491
Frequency stability of Gunn oscillators with variation of ambient temperature. 24 p3385 A72-44980
- AMBIGUITY**
Radar detection and resolution, discussing computer analysis of interval modulated signal ambiguity properties and synthesis method 02 p0181 A72-12648
Man-machine systems communication ambiguities due to information misinterpretation involving sense organs, previous experience and expectational bias 04 p0478 A72-14850
Velocity measurement by Doppler light scattering due to particle finite residence time, estimating ambiguity and noise effects on turbulent spectra of frequency fluctuation 09 p1305 A72-22302
Information theory and ambiguity concept generalization for signal distinction by phase displacement in time and frequency 09 p1281 A72-23470
Cross-ambiguity function for a linear FM pulse compression radar. 19 p2764 A72-37868
- AMBIPOLAR DIFFUSION**
Electron-ion recombination and ambipolar diffusion disruption of electron density in cryogenic helium plasma, using cavity resonator measurements 03 p0399 A72-14067
Ambipolar diffusion influence on MHD generator electrical conductivity, discussing plasma radiation, electron escape generator geometry and efficiency and ignition temperature range 04 p0554 A72-14404
Plasma ambipolar diffusion coefficient and electron density determination from thermal density fluctuations cross spectrum based on Langmuir probe measurements 06 p0864 A72-18536
Ionization change induced striation instability of low temperature plasma with ambipolar diffusion in transverse magnetic field 07 p1043 A72-19878
Ambipolar diffusion in weakly ionized unstable plasma afterglow in presence of uniform axial magnetic field 07 p1047 A72-20558
Diurnal and seasonal variation of ambipolar diffusion coefficient in meteor trail zone within upper atmosphere 08 p1238 A72-21888
Positive plasma column theory for longitudinal cylindrical discharge problem in ambipolar conditions, stressing surface and bulk temperature effects 10 p1521 A72-24357
Ion and electron temperature ratios in hot plasma, discussing energy relaxation, heating and cooling effects and electrostatic confinement by ambipolar diffusion 10 p1524 A72-25032
Ionization change induced striation instability of low temperature plasma with ambipolar diffusion in transverse magnetic field 17 p2590 A72-35128
Determination of upper atmosphere parameters by measuring the ambipolar diffusion coefficient by the method of meteor trail radar observations 18 p2688 A72-36862
Diffusion cooling in neon, argon, and krypton afterglow plasmas. 19 p2841 A72-38378
Ambipolar diffusion noise in a semiconductor in the presence of a magnetic field. 19 p2846 A72-38599
The mass spectrographic measurement of gas separation with the aid of ambipolar effusion in neon-krypton mixtures 21 p3053 A72-40486
- AMBIT**
U FIELD THEORY (PHYSICS)
- AMBULANCES**
General aviation patient transportation, investigating military helicopter airlift performance 01 p0022 A72-11298
- AMIDES**
NT ACETAZOLAMIDE
NT CYANAMIDES
NT POLYIMIDES
NT SUCCINIMIDES
NT UREAS
Esters and amides participation in prebiotic polymers, discussing ribosome bonds and messenger RNA 04 p0468 A72-14767
The steric analysis of aliphatic amines with two asymmetric centres by gas-liquid chromatography of diastereoisomeric amides. 17 p2510 A72-34337
- AMINES**
NT ANILINE
NT CATECHOLAMINE
NT DIMETHYLHYDRAZINES
NT GUANIDINES
- NT NITROAMINES
NT SEROTONIN
NT TETRYL
NT TRYPTAMINES
Cyclohexylamine determination in aqueous solutions of sodium cyclamate by electron capture gas chromatography 07 p0935 A72-19488
Gas phase basicities of aliphatic amines by ion cyclotron resonance spectroscopy 07 p0936 A72-19493
Aluminum oxide chromatography for ethanol-amine acetyl derivatives detection and separation in animal tissue extracts, using water-butanol solution as solvent 14 p2077 A72-30972
Rhodamine 6G photodegradation resistance improvement in cooled solid matrices of polymethylmethacrylate, investigating time and temperature dependence of bleaching by linearly polarized lasers 16 p2401 A72-33386
The steric analysis of aliphatic amines with two asymmetric centres by gas-liquid chromatography of diastereoisomeric amides. 17 p2510 A72-34337
Model reactions between phthalic anhydride and o-phenylenediamine under polymerization-analogous conditions for polyimideazopyrrolone formation 19 p2762 A72-37647
Formation of hydrogen from amine oxidation and pyrolysis. 19 p2883 A72-38874
Burning rates of organic perchlorates of aliphatic, aromatic and heterocyclic amines and amidines with explosive compounds containing nitrogen dioxide group as oxidizer 22 p3153 A72-43181
- AMINO ACIDS**
NT GLUTATHIONE
NT LEUCINE
NT METHIONINE
NT PEPTIDES
NT PROTOPROTEINS
NT PYRUVATES
NT THYROXINE
NT TRYPTOPHAN
Hydrostatic pressure and temperature effects on growth of psychrophilic marine bacterium, emphasizing inhibited amino acid transport and respiration 01 p0011 A72-10322
Waterless amino acid synthesis in interstellar space, describing ammonia, methanol vapor, formic acid and formaldehyde reaction under UV radiation 01 p0023 A72-11157
Molecular evolutionary changes in amino acids of proteins due to mutant random fixation, comparing human and fish hemoglobin chains 02 p0158 A72-11761
Evolutionary rate of cistrons in vertebrates, discussing hemoglobin and cytochrome c changes involving amino acid mutant substitution 02 p0158 A72-11762
Cytochrome c X ray structure and molecular evolution rates, using amino acid sequence comparative data 02 p0158 A72-11763
Interstellar formaldehyde and ammonia molecules effects on prebiological amino acids evolution 02 p0165 A72-12846
Preferential polymerization and adsorption of L-optical isomers of amino acids on kaolinite, indicating role in prebiotic protein origin 03 p0321 A72-13743
Pulse shock tube synthesis of amino acids in primitive environments, discussing thermodynamic relations and conversion efficiency 04 p0482 A72-14761
Aromatic and amino acid prebiotic syntheses under primitive earth, considering electric discharge and cyanide polymerizations 04 p0483 A72-14762
Lower aldehydes contribution to biochemically important compounds in abiogenic synthesis, considering amino acids formation 04 p0483 A72-14763
Amino acid-phosphate anhydrides polymerization in presence of clay minerals, noting reactions superposition and monomer diffusion 04 p0483 A72-14774
Alpha amino acids proteinoids or thermal polymers enzyme activity, investigating hydrolytic activities and decarboxylation reactions 04 p0483 A72-14776
Protein evolution, discussing biological group amino and nucleic acid structure variations from phylogenetic tree of cytochrome c data 04 p0470 A72-14791
Distillation experiments showing volatility-caused amino acid contamination of commercially available aqueous hydrochloric acid 05 p0624 A72-16079
Catalytic action in organic catalyst predecessors of contemporary enzymes, discussing polymers of alpha amino acids and hydrogen cyanide 05 p0624 A72-16128

Pathogenesis of in-flight illusory acceleration sensations, discussing amino acid level, protein metabolism rate and pyridoxin metabolism

05 p0619 A72-16642

Rat tissue autolysis rate during hypokinesia, discussing relation to free amino acid background changes

05 p0619 A72-16648

Enzymically synthesized homopolynucleotide and lysine-rich proteinoid microparticles effect on aminocycl adenylate condensation as basis for genetic code origin

06 p0770 A72-17724

Mass spectral analysis of aliphatic amino acid derivatives, obtaining diagnostic criteria for distinction of alpha, beta, gamma and N-methyl isomers

07 p0935 A72-18905

Rapid eye movement sleep deprivation and hyperbaric oxygenation influence on gamma-aminobutyric acid levels in mice brains, suggesting protective mechanism against nerve cell oxygen intoxication

07 p0922 A72-20191

Amino acid sequences of proteins from living organisms, considering evolutionary process

08 p1119 A72-22009

Orgueil meteorite examination by mass spectroscopy and gas chromatography, identifying amino acids of extraterrestrial origin

09 p1393 A72-23549

Evolutionary significance of primary amino acid or nucleotide base sequences of DNAs within various phylogenetic groups

12 p1759 A72-27160

Nonprotein amino acids from spark discharges, comparing with Murchison meteorite amino acids

12 p1778 A72-27749

Nonprotein amino acids detection in presence of protein amino acids by amino acid analyzer, noting separation of chemically similar compounds

13 p1913 A72-29774

Biochemical analysis of cat brain regions for gamma-aminobutyric, aspartic and glutamic acids, glycogen and phosphatidopeptide concentrations during paradoxical sleep deprivation

16 p2356 A72-33559

The uptake, metabolism and release of C14-taurine by rat retina in vitro.

17 p2500 A72-34881

Dipeptidyl aminopeptidase. I - Application in sequencing of peptides.

17 p2511 A72-35167

Gas dynamics and chemistry of lightning-produced shock waves (thunder) in postulated primordial reducing atmosphere, noting amino acid production

18 p2650 A72-36443

Apollo and terrestrial geochemical samples examination for indigenous amino acids distribution and optical configuration, stressing close monitoring of contamination sources

19 p2762 A72-37648

Protein synthesis in the cell-free system of the human thyroid gland

19 p2757 A72-38212

Geochemistry of amino acid enantiomers - Gas chromatography of their diastereomeric derivatives.

19 p2762 A72-38224

Effects of free amino acid doses and of amino acid metabolism cofactors on the distribution of regional free amino acid resources in the brain and blood of animals

20 p2891 A72-39324

Amino acid substitution correlation with genetic code in human, bovine, ovine, porcine and salmon calcinons, suggesting mutation occurrence time during evolution

23 p3254 A72-43568

Recently published protein sequences. I.

23 p3254 A72-43570

AMMETERS

NT MICROMILLIAMMETERS

AMMONIA

NT LIQUID AMMONIA

Oscillation transient in molecular Q switched ammonia beam maser following Stark voltage pulse in resonant cavity

01 p0081 A72-11186

Ammonia beam maser with electret focuser providing semipermanent molecular separation under high vacuum for use in relaxation studies

01 p0081 A72-11187

Fluorine-ammonia as high energy liquid bipropellant for rocket engines, presenting ground test results regarding velocity and specific impulse characteristics as functions of mixture ratio

01 p0114 A72-11220

Interstellar formaldehyde and ammonia molecules effects on prebiological amino acids evolution

02 p0165 A72-12846

Jovian planets methane and ammonia absorption bands spectrophotometric investigation, noting Saturn spectral variations

03 p0436 A72-13819

Carbon dioxide laser modulation by molecular Stark effect in deuterated ammonia, observing pressure broadening coefficient

04 p0528 A72-14585

Saturated absorption spectroscopy of ammonia, considering Stark effect on IR transition

10 p1491 A72-24122

IR spectrophotometric data for Jupiter, determining limb darkening nature and ammonia and methane absorption variations over belts, zones and Red spot

10 p1548 A72-24971

Ammonia-air opposed reacting jet (ORJ) for flame stabilization, solving partial differential equations for flow field

10 p1564 A72-25141

Self priming high capacity spiral artery heat pipe with ammonia as working fluid for flight on OAO 3, discussing development models analysis, design and testing

[AIAA PAPER 72-258]

11 p1725 A72-25203

Ion dipole capture cross sections at low ion and rotational energies compared with reaction cross sections for ammonia and water parent-ion collisions

11 p1692 A72-26014

Heterogeneous-homogeneous catalytic effects on combustion rate of hydrocarbons, ammonia and hydrogen mixtures

13 p1912 A72-28777

Saturn thermal radio emission brightness temperature calculations for subcloud atmosphere ammonia abundance evaluation

14 p2152 A72-30490

Flat flame deflagration tube measurements of laminar flame velocities for propane-ammonia-air mixtures in fuel rich region

16 p2480 A72-34006

High temperature oxidation of ammonia.

17 p2511 A72-34904

Saturn thermal radio emission brightness temperature calculations for subcloud atmosphere ammonia abundance evaluation

19 p2864 A72-38319

Ammonia photolysis and the role of ammonia in chemical revolution.

20 p2898 A72-39375

Two-step photodissociation of ammonia molecules excited by laser radiation.

21 p3013 A72-40724

Shapes and widths of ammonia lines collision-broadened by hydrogen.

21 p3013 A72-40817

Optical properties and structure of the Jovian atmosphere. V - Probable structure of the ammonia aerosol layer

22 p3219 A72-41914

AMMONIUM CHLORIDES

Aluminizing process improvement by CaAl and ammonium chloride contents increase in powder

13 p1964 A72-29020

AMMONIUM COMPOUNDS

NT AMMONIUM CHLORIDES

NT AMMONIUM NITRATES

NT AMMONIUM PERCHLORATES

NT AMMONIUM PHOSPHATES

NT AMMONIUM SULFATES

Formation of urea and guanidine by irradiation of ammonium cyanide.

23 p3262 A72-43569

AMMONIUM NITRATES

Linear law and catalyst modification of ammonium nitrate combustion, using ammonium perchlorate-base propergols theory

02 p0270 A72-12165

Experimental hybrid rocket engine combustion chamber with solid oxidizer lining of ammonium nitrate and perchlorate eutectic mixture

05 p0708 A72-17249

AMMONIUM PERCHLORATES

Linear law and catalyst modification of ammonium nitrate combustion, using ammonium perchlorate-base propergols theory

02 p0270 A72-12165

Experimental hybrid rocket engine combustion chamber with solid oxidizer lining of ammonium nitrate and perchlorate eutectic mixture

05 p0708 A72-17249

Combustion of composite solid propellants with ammonium perchlorate base and pyrolyzable binder, investigating perchlorate grain size, binder concentration and catalyst effects

06 p0867 A72-17574

Burning rates dependence on pressure in mixtures of ammonium perchlorate with succinic, glutaric, adipic, azelaic, sebacic, fumaric and aminosuccinic acids

06 p0867 A72-18210

Solid propellant reaction kinetics at gaseous fuel and catalyst-containing ammonium perchlorate interface, studying ignition and deflagration

07 p1051 A72-19367

Quench combustion studies with two dimensional propellant sandwiches with ammonium perchlorate oxidizer and various binders, using high pressure com-

bustion vessel for deflagration characteristics determination

07 p1051 A72-19727

Pure and doped ammonium perchlorate deflagration rate sensitivity due to sample temperature and environmental pressure changes

07 p1051 A72-19729

Impact detonation mechanism in ammonium perchlorate mixtures with inflammable additions, determining critical detonation triggering stresses

09 p1373 A72-22890

Simple composite propellant modelled by ammonium perchlorate-wax mixtures, noting stoichiometric composition effects on explosive properties

09 p1373 A72-23141

Burning rate dependence on oxidizer particle size of ammonium or potassium perchlorate mixtures with organic fuels

09 p1373 A72-23146

Catalytic effects on ammonium perchlorate combustion pressure limits, noting distribution, concentration and particle size effects

13 p2025 A72-29303

Ammonium perchlorate burning rate temperature dependence as function of pressure and oxidizer particles size, noting low pressure deflagration limit [ONERA, TP NO. 1079]

13 p2025 A72-29669

IR internal reflection spectroscopy application to dynamic chemical changes study on ammonium perchlorate surface during thermal decomposition, observing crystal lattice transformation

15 p2296 A72-32313

Powdered Al additions effect on burning rates of three component mixture systems based on ammonium and potassium perchlorates

19 p2847 A72-37361

Ignition of a mixture of ammonium perchlorate and starch by incandescent wires

19 p2847 A72-37367

Iron-containing catalysts action mechanism during ammonium perchlorate-poly(methyl methacrylate) mixture burning in nitrogen atmosphere

19 p2847 A72-38456

Comment on 'The deflagration of single crystals of ammonium perchlorate.'

19 p2848 A72-38873

Ionization mechanism and condensed and gas phase kinetics of oxidizer burning during ammonium perchlorate combustion

22 p3215 A72-43140

Ionization zone formation and condensed and gaseous phase kinetics during ammonium perchlorate burning in nitrogen atmosphere

22 p3215 A72-43179

Microscopic and electron-microscopic investigation of the catalysis of ammonium perchlorate combustion

22 p3216 A72-43186

AMMONIUM PHOSPHATES

Polyphosphate and trimetaphosphate formation under potentially prebiotic conditions.

23 p3261 A72-43566

AMMONIUM SULFATES

Thermodynamic freezing theory of small solution droplets containing insoluble particles, considering ammonium sulfate concentration for ice formation in clouds

16 p2476 A72-33380

AMOEBA

Ultrasonically produced cavitation events correlation to amoeba cells number decrease under 1 MHz irradiation

04 p0475 A72-15299

Zn concentration in chromatoid bodies of ribosome crystals in Entamoeba invadens, using absorption spectroscopy, electron microprobe and dithione staining techniques

15 p2186 A72-31725

AMORPHOUS MATERIALS

High resolution electron microscope observation of voids in amorphous Ge films, noting density dependence on substrate temperature

04 p0562 A72-15152

Book on electronic processes in noncrystalline materials covering liquid metals, semimetals and semiconductors, Hall effect, phonons and polarons, thermoelectricity, photoconductivity, etc

06 p0866 A72-18516

Lunar dust grain fossil coatings of ultrathin metamictized amorphous layers resulting from solar wind ion implantation

08 p1230 A72-20982

Nonlinear viscoelastic body model for stress relaxation of amorphous linear polymers below vitrification temperature for various deformations, temperatures and deformation speeds

08 p1194 A72-21751

Fast neutron radiation damage to glass ceramics and amorphous semiconductors electrical properties

09 p1336 A72-22405

Amorphous chromate and phosphate conversion coatings of Al, providing inert surface for painting

09 p1317 A72-22480

Anisotropic electrical properties and void structure of amorphous Ge, discussing low- and high-field re-

- sistivity measurement in planar and transverse directions
09 p1371 A72-22873
- Graphitization kinetics of amorphous thin carbon films under light impulses, discussing crystallite sizes, optical and electrical properties and two-stage character
12 p1833 A72-27857
- Heat resistance of thermostable organic materials/amorphous glass and high polymers/, improving plastic stability by glass fibers addition, intermolecular arrangements modification and synthesis [ONERA, TP NO. 1107]
14 p2125 A72-30529
- Amorphous structure analysis of splat quenched Cu-Zr noncrystalline phase, using electron microscopy
16 p2410 A72-33814
- Successive graphitization of amorphous carbon
19 p2823 A72-38676
- Anisotropic electrical properties of amorphous germanium.
20 p2960 A72-39457
- Electron microscope investigation of the effect of fillers on the formation of supramolecular structures and on the type of breakdown in amorphous and crystalline polymers
21 p3072 A72-40084
- Amorphous materials; Proceedings of the Third International Conference on the Physics of Non-crystalline Solids, University of Sheffield, Sheffield, England, September 14-18, 1970.
22 p3196 A72-42790
- Glassy materials rheological behavior description in terms of stress function, discussing molecular processes transformation range thermodynamics
22 p3196 A72-42791
- The dynamic viscoelastic properties of some non-crystalline metals.
22 p3214 A72-42792
- Pair-correlation and angular distribution functions calculations for one and two dimensional amorphous structures
22 p3197 A72-42797
- Light scattering studies in amorphous media.
22 p3206 A72-42798
- Coherent/incoherent elastic/inelastic neutron scattering in amorphous solids, presenting neutron intensity and correlation functions
22 p3206 A72-42799
- AMORPHOUS SEMICONDUCTORS**
Thermal effects on reversible threshold switching in amorphous semiconductor thin films involving current controlled negative resistance
[AD-741462]
02 p0268 A72-12202
- Amorphous semiconductors dielectric properties based on randomly distributed local electron states in disordered solids, crystalline impurities and polymer aggregates
02 p0269 A72-12450
- Electron correlation effects on low temperature thermodynamics of amorphous semiconductors, predicting Curie law magnetic susceptibility and equilibrium electronic specific heat dependence on temperature
04 p0562 A72-15153
- Hydrostatic pressure effects on I-V characteristics of amorphous semiconductor germanium telluride sulfide arsenide
06 p0865 A72-17493
- Electron states in glassy amorphous semiconductors, constructing trial wave functions for valence band
06 p0866 A72-18180
- Effective current carrier electron and hole lifetime in amorphous photodiode semiconductor Se and As-Se films with randomly distributed capture levels
09 p1366 A72-22418
- Diamagnetic enhancement of magnetic susceptibility of amorphous semiconductors, considering mobility states and paramagnetic Van Vleck reduction
09 p1373 A72-23508
- Thin film tunnel triode using p-type amorphous semiconductors to achieve injected current amplification
10 p1451 A72-24624
- Hall-Weaire tight binding Hamiltonian solution in cycle free approximation for band structures and delta functions of amorphous semiconductors
11 p1700 A72-25725
- Electroluminescent matrix display system with amorphous semiconductor threshold switches for isolation and memory, discussing performance and address waveforms
12 p1788 A72-27239
- Reversible threshold switching in amorphous semiconductor alloys by carrier transport and recombinant electron injection
12 p1854 A72-27431
- Uniaxial elastic deformation pressure effects on electronic conduction in tetrahedrally bonded amorphous semiconducting thin films as function of temperature
13 p2021 A72-28574
- Optical weak absorption measurements in amorphous semiconductors AsS, GeAs and GeSbSe, showing dependence on band gap localized states
13 p2022 A72-29629
- Amorphous semiconductors theories, discussing electron states and transport properties in terms of Cohen, Mott and Gubanov models
15 p2293 A72-32234
- Conductance measurements for metal oxide-amorphous silicon junctions, showing temperature dependent tunneling
16 p2442 A72-33620
- An investigation of amorphous semiconductor memory devices utilizing thick film fabrication techniques.
17 p2527 A72-34682
- UHF and microwave dielectric properties of an amorphous semiconductor.
18 p2718 A72-36311
- Study of the mechanism of radiative recombination in vitreous and monocrystalline arsenic selenide.
19 p2844 A72-37684
- Photoconductivity and electroconductivity spectral distributions in glassy cadmium silicon germanium arsenide semiconductors at 300 K related to quantum mechanism
19 p2847 A72-38682
- Book - Amorphous semiconductors.
20 p2958 A72-38924
- Binary information storage with bipolar transistors, tunnel diodes, MIS and glass semiconductors, considering Gunn effect devices application
20 p2905 A72-39425
- Amorphous semiconductors for optical memory and other devices.
20 p2961 A72-39707
- As-Te-Ge amorphous semiconductor film optical memory effect due to crystallization and reversion during exposure to pulsed laser beam, noting writing and erasing characteristics
20 p2961 A72-39708
- Fast-neutron-compensated n-germanium as a model of amorphous semiconductors.
20 p2961 A72-39853
- Vitrification in ternary diamond-like semiconductors
21 p3096 A72-40380
- Theory of Poole-Frenkel conduction in low-mobility semiconductors.
22 p3214 A72-42317
- The switching behaviour of thin films of chalcogenide glass.
22 p3214 A72-42319
- Effect of substrate temperature on electrical properties of amorphous germanium films.
23 p3324 A72-44069
- Note on the experimental determination of photoconductive response characteristics of amorphous semiconductors.
24 p3431 A72-44716
- Preswitching electrical properties, 'forming,' and switching in amorphous chalcogenide alloy threshold and memory devices.
24 p3385 A72-44982
- An apparatus for measuring the Hall effect of high-resistivity materials in alternating electric and magnetic fields
24 p3405 A72-45698
- AMORPHOUSNESS**
U CRYSTALLINITY
AMPERAGE
U ELECTRIC CURRENT
AMPHIBIOUS AIRCRAFT
Comparative analysis of the operative costs of large amphibious hovercraft
18 p2643 A72-37212
- AMPHIBIOUS VEHICLES**
NT AMPHIBIOUS AIRCRAFT
AMPLIFICATION
NT POWER GAIN
NT SOUND AMPLIFICATION
NT WAVE AMPLIFICATION
Gain and bandwidth properties of microwave and optical devices with isotropic active medium, investigating transmission coefficient
02 p0189 A72-11566
- Two stage M-type amplifier with two electron beams and stepwise variation of cathode, calculating gain in linear approximation
02 p0189 A72-11569
- Wide range bias dependence of planar bipolar transistor dc and small signal current gain, comparing analytical findings with Si junction experiment
06 p0783 A72-17608
- Gain variations in channel electron multipliers, investigating total radiation exposure effect
[AD-741089]
07 p0984 A72-19324
- Dynamic programming method application to signal processing components selection for cascaded communication links to satisfy overall gain and noise figure
09 p1281 A72-23415
- Radial small-signal gain profile measurement in carbon dioxide laser discharge tube explained by axial gas temperature increase with discharge current
11 p1647 A72-26145
- Design analysis of emitter- and collector-base gain stabilized junction transistor amplifier at elevated temperatures using passive elements
11 p1606 A72-26569
- Earth station parabolic antenna gain-noise temperature ratio measurement using radio star and Applications Technology Satellite technique [AIAA PAPER 72-528]
12 p1779 A72-27354
- Whistler waves amplification in magnetosphere, obtaining particles pitch angle and energy diffusion coefficients and one dimensional Fokker-Planck equation
15 p2194 A72-31427
- Three-frequency parametric traveling wave amplifier gain and conversion factors calculation by numerical method with allowance for fast and slow space charge wave effects
15 p2206 A72-31661
- Image forming mechanism in photographic silver halide emulsions due to incident optical signals, considering latent image amplification process efficiency
19 p2800 A72-37857
- Diagram and gain measurements regarding antennas conducted with a helicopter for the range from 0.5 to 800 MHz
21 p3031 A72-40545
- Hydroxyl and water radio sources scale and geometry constraints placed by interstellar maser gain saturation relation to emission solid angle
21 p3062 A72-40565
- Optical communication channel optimization with binary signals preamplified in optical parametric amplifier, noting amplifier gain and SNR
21 p3016 A72-40783
- Drift of amplification factor and its effects in a tri-electrode electron gun.
21 p3033 A72-40995
- Independent cascaded multicomponent random variable system gain statistics relationship to individual component based on moment derivation, obtaining curves from variance equation
21 p3022 A72-41087
- Manual tracking control with continuously variable selective control gain in response to system state, noting intuitive optimization
21 p3011 A72-41425
- German monograph - Amplification measurements and investigation of 'super radiation' characteristics in the case of optically pumped rubies.
22 p3187 A72-43065
- AMPLIFICATION FACTOR**
U AMPLIFICATION
AMPLIFIER DESIGN
Transistorized pulse amplifier stage, showing gain as function of resistor parameters in collector circuit
01 p0035 A72-10200
- Supercritically doped transferred electron microwave amplifiers stabilization mechanisms, considering cathode contact, anode diffusion current and active region temperature gradient roles
01 p0036 A72-10636
- Wideband microwave parametric amplifier using balanced circuits to relax isolation requirements between signal, idler and pump circuits
01 p0038 A72-10655
- Computer program for design optimization of three-stage wideband low-noise integrated microwave amplifier
01 p0041 A72-10690
- Varactor diode microwave parametric amplifiers for radio astronomy interferometer, discussing system design features for gain and phase stabilities
02 p0192 A72-12043
- Dual-gate MOS transistor structure, operational principles and electrical characteristics, noting suitable properties for use in low noise microwave amplifier
03 p0330 A72-12969
- Dc, ac and transient models of IC operational amplifier for computer aided circuit design and analysis applications
03 p0329 A72-14180
- RC network synthesis technique using grounded gyator and summing amplifier, applying to thin film RC networks and IC operational amplifiers
04 p0504 A72-14570
- Computer aided design of single tuned parametric amplifiers, stressing voltage gain-bandwidth product
04 p0497 A72-14715
- Wideband tunnel diode amplifier design, discussing circulator off-band impedance characteristics improvement through voltage standing wave ratio suppression network
05 p0638 A72-16594
- Wideband tunnel diode microwave amplifier design with coaxial line, considering band-edge stability and impedance matching
06 p0785 A72-18310
- High power L-band microminiaturized hybrid type integrated transistor amplifier design and realization by computer
06 p0785 A72-18314

Broadband parametric amplifier design using computerized optimization procedure based on Gauss-Newton iteration technique

06 p0786 A72-18376

Transferred electron microwave oscillators design for various peak and average power levels, considering tradeoff between operating mode and device configuration

06 p0789 A72-18475

Amplifier amplitude characteristic nonlinearity effect on dynamic properties of autooscillatory temperature controller

07 p0981 A72-18926

Waveguide cavity Gunn microwave power amplifiers, predicting maximum small signal gain and FM and AM noise performance

07 p0958 A72-19921

Symmetrical amplitude-frequency characteristics of microwave reflection amplifiers with active resonators connected in series by nonhalf wave transmission line

08 p1138 A72-20791

Linear IC amplifier analysis by admittance parameters of equivalent two terminal pair network as function of frequency, temperature and supply voltage

09 p1285 A72-22342

Millimeter wave pumped X band balanced diode type parametric amplifier using GaAs Schottky barrier varactors for operation at room temperature

09 p1289 A72-23417

Permanent state operation optimization for fluid amplifier with jet interaction

10 p1422 A72-24125

Electric field profile in n-type GaAs layer biased above transferred electron threshold for small signal amplifier operation

10 p1450 A72-24554

Multistage broadband microwave amplifier design based on bipolar transistors cascade coupling, using scattering parameters

10 p1451 A72-24572

Nonlinear microwave power amplifiers with IMPATT diodes in stable and injection locked modes, predicting behavior for comparison with experiment

10 p1451 A72-24592

Book on logarithmic video amplifiers covering design, analysis, performance and applications

10 p1452 A72-24698

Stabilization bandwidth reduction in microwave parallel tuned tunnel diode amplifier circuits synthesis

10 p1453 A72-24910

Vortex fluid amplifier design with asymmetrical flow fields, discussing effects of geometrical parameters variations on performance characteristics

10 p1423 A72-25053

VHF and UHF radio transmitters with strip transmission lines, discussing transistor power amplifier design

10 p1441 A72-25116

Multiaxis radial circuits for transferred electron microwave oscillator performance optimization to obtain wideband CW amplification, discussing LSA tests

11 p1604 A72-25745

Feedback and feedforward circuits to double operational amplifier output voltage swing with increased slew rate

11 p1604 A72-25746

Two stage magnetic operational amplifier transfer function, time constants and control stability conditions, using difference equation approach

11 p1605 A72-26466

Design analysis of emitter- and collector-base gain stabilized junction transistor amplifier at elevated temperatures using passive elements

11 p1606 A72-26569

Tunnel diode amplifier for 8 GHz band, considering gain, bandwidth, noise factor and stability characteristics

12 p1790 A72-27533

Optimal design of broad passband in unilateral parametric balance amplifier

13 p1928 A72-28789

Method to obtain optimal efficiency gyroamplifier circuits with short waveguide selector by prior grouping of electronic oscillators

13 p1928 A72-28799

Selectivity evaluation for regenerative amplifiers of complex design

13 p1929 A72-28898

Bandpass amplifier design with differing two-circuit filters, discussing advantages and limitations

13 p1929 A72-28899

Single circuit amplifier design characterized by cascade connections of transistors to resonance network

13 p1929 A72-28900

Forward loop signal attenuation and phase shift diagrams for design of feedback amplifier and compensation network for dc flyback converter

13 p1899 A72-29110

Computerized synthesis of wideband series stabilized tunnel diode amplifier based on distributed constant elements

13 p1931 A72-29286

Large signal four-pole parameters and optimum conditions determination for RF high gain amplifiers with class C operated transistors

13 p1921 A72-29344

Feedback ac compensating amplifier design for automatic AM signal envelope conversion, noting truncated equivalent transfer function expandability

13 p1933 A72-29972

Cascade section parameters calculation for multisection amplifiers with composite transistors and correction elements

13 p1934 A72-29978

Narrow band retuned dc pumped amplifier-filter design based on diffron, considering electron beam interaction

14 p2088 A72-30798

Design and performance of microwave single stage relaxing avalanche diode reflection amplifier

14 p2088 A72-30918

Carrier wave propagation at semiconductor surface with electron drift, discussing solid state traveling wave amplifier design

15 p2290 A72-31288

Transistorized pulse amplifier stage, showing gain as function of resistor parameters in collector circuit

15 p2206 A72-31624

Nonlinear and phase delay distortion of FM modulation in tuned and detuned injection phase-locked oscillator-amplifiers

16 p2369 A72-33760

The fabrication and evaluation of a micropower transistor and hybrid RF amplifier.

17 p2528 A72-34688

Modular I-band solid-state microwave amplifier.

17 p2528 A72-34711

Design and analysis of transistorized, selective HF amplifiers with allowance for sensitivity properties

17 p2532 A72-35978

Optimal number of parallel transistor connections in feedback amplifier to improve SNR

18 p2665 A72-36108

Bilateral tunnel-diode amplifiers using ferrite transformers.

18 p2665 A72-36306

Spaceflight-qualified tunable C-band parametric amplifier system.

19 p2770 A72-37253

18 GHz paramps with both liquid helium and room temperature operations and with triple-tuned gain characteristics.

19 p2770 A72-37254

An X-band paramp with 0.85 dB noise figure /uncooled/ and 500 MHz bandwidth.

19 p2770 A72-37258

A C-band all ferrite integrated wideband high power GaAs avalanche diode amplifier.

19 p2771 A72-37264

Intermodulation characteristics of X-band IMPATT amplifiers.

19 p2771 A72-37265

Feedback influence coefficient on amplifier gain, using recurrent difference concept

19 p2777 A72-37314

German monograph - Multiple tuning of cooled parametric amplifiers

19 p2772 A72-37651

Microwave low noise amplifiers for use in radar systems.

20 p2907 A72-39220

Digital p-i-n diode microwave drive amplifier design guidelines, discussing sharp switching pulses and short circuit protection features

20 p2904 A72-39734

Low noise microwave parametric amplifier design for space communication receivers, using inverted diode balanced mixers

21 p3025 A72-40304

Calculation of two- and three-stage broadband amplifiers with parallel correction from the standpoint of a maximum quality factor with an optimally flat amplitude characteristic

21 p3027 A72-40477

Amplification cascade designs for harmonic and pulsed signals with a high frequency emitter correction

21 p3033 A72-40946

Determination of pulsed amplifier correction parameters with the aid of approximating polynomials

21 p3034 A72-41120

Fluidic flow-mode amplifiers physical dimensions and operating pressures restrictions, presenting design and performance evaluation theory and velocity profiles

22 p3139 A72-42048

Cross-modulation dynamic range of amplifiers used in the input stages of receiver equipment

23 p3271 A72-43839

AMPLIFIERS

NT BEAM PLASMA AMPLIFIERS

NT BROADBAND AMPLIFIERS

NT CROSSED FIELD AMPLIFIERS

NT CURRENT AMPLIFIERS

NT DIFFERENTIAL AMPLIFIERS

NT DISTRIBUTED AMPLIFIERS

NT FEEDBACK AMPLIFIERS

NT FLUID AMPLIFIERS

NT INTERMEDIATE FREQUENCY AMPLIFIERS

NT JET AMPLIFIERS

NT LIGHT AMPLIFIERS

NT LINEAR AMPLIFIERS

NT MAGNETIC AMPLIFIERS

NT MAGNETOSTATIC AMPLIFIERS

NT MICROWAVE AMPLIFIERS

NT PARAMETRIC AMPLIFIERS

NT PHOTOMULTIPLIER TUBES

NT POWER AMPLIFIERS

NT PREAMPLIFIERS

NT PUSH-PULL AMPLIFIERS

NT TRANSISTOR AMPLIFIERS

NT TRAVELING WAVE AMPLIFIERS

NT VOLTAGE AMPLIFIERS

Nonlinear equations for M-type amplifiers derived from Maxwell equations

02 p0189 A72-11567

Two stage M-type amplifier with two electron beams and stepwise variation of cathode, calculating gain in linear approximation

02 p0189 A72-11569

M-type amplifier operation with two electron beams and staggered dual section cathode

02 p0190 A72-11570

Stability criterion for system representing amplitude modulation amplifiers development, noting applicability to excitation functions

03 p0338 A72-13791

Tunnel diode amplifier stability under parameter variation due to fabrication tolerances, aging, heating, etc

05 p0638 A72-17189

Electron tube present and future applications as oscillators, high power and hf amplifiers and optoelectronic converters

06 p0784 A72-17775

Regulating amplifier with optoelectronic coupler for sonar sea bed layer measurements

09 p1284 A72-22239

Polynomial filter design with three layer RC distributed elements and operational amplifiers, investigating active elements effects on response

09 p1290 A72-23354

Phase shift methods for data transmission vestigial sideband signal generation, providing shaping functions by shift registers, weighing resistors, summing amplifiers and low pass filters

11 p1592 A72-25890

FM distortion in injection phase locked oscillator amplifiers from generalized Alder equation

12 p1793 A72-27965

Photodiode-operational amplifier circuit for pulsed laser systems energy variations monitoring, noting insensitivity to ambient light conditions

16 p2402 A72-33607

Synthesis of networks containing three-layer rectangular distributed RC elements and nonideal operational amplifiers

18 p2673 A72-36791

Tunnel diode amplifier stability under parameter variation due to fabrication tolerances, aging, heating, etc

19 p2775 A72-38625

Miniaturized piezoelectric transducer electronics versus charge amplifiers - A comparison of the two systems in vibration and pressure applications.

22 p3159 A72-42702

AMPLITRONS (TRADEMARK)

U PLANOTRONS

AMPLITUDE DISTRIBUTION ANALYSIS

Statistical synthesis of antenna arrays using phase amplitude distribution equivalent to reference array radiation pattern

02 p0196 A72-12758

Intracavity modulation of high-gain gas laser with traveling light waves nonuniform amplitude distribution, presenting results for lithium niobate crystal resonator equipped He-Ne laser

02 p0183 A72-12762

Holographic investigation of acoustical fields, describing shadowgraph recording apparatus for sound pressure amplitude distribution

03 p0352 A72-12918

Iterative synthesis of dipole antenna array for maximum directivity radiation pattern, considering amplitude-phase distributions

04 p0499 A72-15142

Amplitude characteristics of Q switched He-Xe laser at 3.5 microns, using rotating reflection prism and velocity equations

04 p0531 A72-15149

Amplitude fluctuations of laser beam with Gaussian amplitude distribution on short line-of-sight path propagation through artificial turbulent atmosphere

04 p0488 A72-15383

Diurnal phase and amplitude variations of long radio waves at great distances, explaining sunrise and sunset fades

04 p0492 A72-15443

Probability amplitude analysis of statistical behavior of fading signal envelope

04 p0493 A72-15457

Waveguide with slanted aperture, determining propagation mode and wave amplitude from radiation level at Brillouin angle

05 p0625 A72-15828

Nonlinear amplitude distribution of electromagnetic wave propagating in plasma near hybrid resonance frequencies

06 p0771 A72-17390

Nonlinear oscillation amplitude of ion beam due to phase bunching in interaction with plasma electrons

06 p0853 A72-17395

Statistical model of signal amplitude distribution and thermoelectron noise of photoelectron multiplier

06 p0816 A72-17837

Antenna radiation pattern synthesis, discussing current phase and amplitude distribution determination by iterative and quadratures solutions respectively

07 p0953 A72-19004

Geomagnetic Pc3 pulsations amplitude distribution patterns along meridional profile, determining source from maximum near 60 N

08 p1155 A72-20741

Symmetrical amplitude-frequency characteristics of microwave reflection amplifiers with active resonators connected in series by nonhalf wave transmission line

08 p1138 A72-20791

Sensitivity threshold of optical heterodyne receiver as function of laser radiation amplitude spectrum, using photodetector output noise

08 p1181 A72-20794

Aperture filtering effects on amplitude scintillation power spectra of paraboloid radio telescope over millimeter wave propagation path

08 p1136 A72-21982

LF noise generator with Rice variable amplitude probability distribution law, using shielded vacuum tube superregenerative amplifier

09 p1285 A72-22345

Radio emission from pulsar CP 1133, comparing amplitude and polarization characteristics of two subpulses

09 p1387 A72-22987

Phase and amplitude error effects on image reconstruction in conventional and weak signal enhancement holography

09 p1312 A72-23242

VLF atmospheric count comparability in broad- and narrow-band operation, presenting amplitude frequency response

09 p1301 A72-23268

MOS transistor current fluctuation relation to capture centers surface density, energy position and gate potential, determining spectral amplitude distribution

10 p1449 A72-24284

Synthesis of slot antenna on metallic wedge for amplitude radiation pattern, determining RMS approximation and fixed phase diagram

10 p1436 A72-24506

Regular and irregular classes of amplitude fluctuations within artificially stimulated VLF emissions by low power pulses from ground transmitter

10 p1440 A72-24950

Combined probability density of amplitude and phase difference distribution of signal and noise sum in moving target selection radar systems

11 p1596 A72-26307

Probability distribution density of amplitude difference of target signal and correlated noise sum for radar efficiency estimation

11 p1596 A72-26309

Narrow band process signal model for phase and amplitude difference distribution densities of alternating period compensation system output signal

11 p1596 A72-26310

Amplitude and phase local distribution analysis by filtering of spatial frequencies, examining holographic system by Hilbert and Fourier transformation

12 p1812 A72-27952

Mutual coupling in phased arrays of randomly spaced antennas, investigating probabilistic properties of main beam amplitude fluctuations

13 p1916 A72-28532

Periodic waveform expression in truncated Fourier series, determining polynomial coefficients relationship to amplitude density function

13 p1920 A72-29108

Amplitude probability distribution of radio waves reflected from traveling ionospheric disturbances superimposed on small scale irregularities

13 p1921 A72-29338

Avalanche photodiode optical detector noise amplitude distribution as function of operating conditions

13 p1971 A72-29924

Joint photon-count probability distribution measurement of electric field amplitude correlation function for random-Gaussian light fields produced by laser beam scattering

15 p2280 A72-31378

Three Josephson junction asymmetric feed quantum interferometer, discussing magnetic field sensitivity and amplitude variation increase

15 p2241 A72-32536

Two-magnon Raman scattering in antiferromagnets, obtaining amplitude-renormalization factor by extended Dyson-Maleev graphical approach to include corrections in transition operator M

15 p2295 A72-32548

Minimum values estimation of amplitude fluctuations dispersion and spectral line width for conventional and quartz crystal controlled oscillators

15 p2210 A72-32735

Digital data processing equipment for continuous ECG analysis, noting analog to digital converter and amplitude distribution analysis

17 p2522 A72-34914

Fundamental, harmonic and combination frequency components amplitude analysis via dual input describing function for nonlinear element response under two incommensurate frequency sinusoidal signals

18 p2671 A72-36051

The diurnal effect of the cosmic rays during the period 15 October 1965-30 June 1966. I - Method of analysis and statistical distribution.

18 p2722 A72-37159

Geomagnetic Pc 3 pulsations amplitude distribution patterns along meridional profile, determining source from maximum near 60 N

19 p2791 A72-38369

Nonlinear double T-shaped RC filter

19 p2774 A72-38417

Statistical synthesis of antenna arrays using phase amplitude distribution equivalent to reference array radiation pattern

20 p2907 A72-39064

Intracavity modulation of high-gain gas laser with traveling light waves nonuniform amplitude distribution, considering lithium niobate crystal resonator equipped He-Ne laser

20 p2931 A72-39068

Crack growth behavior correlation to acoustic emission signal amplitude distribution in high strength steel heat treated to different fracture toughness values

20 p2924 A72-39282

Machine elements vibration parameters from dynamic model of planetary gears, noting energy spectrum, correlation and amplitude distribution functions

22 p3182 A72-42132

A time-interval amplitude analyzer for turbulent flow processes and its application for the control of a chronophotographic measurement installation

22 p3177 A72-42393

Amplitude-time and polarization characteristics of the subpulses of the CP 1133 pulsar

22 p3230 A72-43136

Waveguide with slanted aperture, determining propagation mode and wave amplitude from radiation level at Brillouin angle

23 p3263 A72-43436

Influence of the phase-amplitude distribution of the field in the aperture of an antenna on its directional properties

23 p3270 A72-43773

Amplitude dependence of frequency in oscillators.

24 p3385 A72-44964

On the S/N-characteristics in PCM systems for a class of signals with representative amplitude distributions.

24 p3380 A72-45282

Frequency multiplication with a traveling-wave tube. I - Computation of the current harmonics in a traveling-wave tube by the large-signal theory.

24 p3386 A72-45284

Frequency multiplication with a traveling-wave tube. II - Numerical analysis of a traveling-wave frequency multiplier by the large-signal theory.

24 p3386 A72-45285

AMPLITUDE MODULATION

Information feedback application to AM laser communication system, predicting multiplicative error, background shot noise and photon arrival fluctuation effects on continuous parameter transmission

[AD-736731] 01 p0025 A72-10326

Parametric amplification of laser waves with amplitude and phase modulation under exponential signal growth applied to Raman scattering picosecond pulse field

01 p0079 A72-10346

AM and FM noise reduction of cavity and injection stabilized microwave Gunn and avalanche diode oscillators

01 p0037 A72-10644

Technical characteristics of vhf/AM receiving transmitter, noting MTBF improvement

02 p0182 A72-12651

Stability and perturbation of oscillator system with frequency fixed by all pass ring transmission function with delayed amplitude regulation

03 p0331 A72-13410

Spectrum of low modulation frequencies of He-Ne laser radiation produced by motion of external reflector of matched and unmatched three-mirror resonators

03 p0368 A72-13666

Stability criterion for system representing amplitude modulation amplifiers development, noting applicability to excitation functions

03 p0338 A72-13791

Computerized simulation for AM radio receiver waveform performance degradation under pulsed interference

03 p0324 A72-14035

Analog computer simulation for filtering, phasing, multiplication and addition in AM communication system

03 p0329 A72-14182

Gas lasers mode locking, describing use of amplitude and frequency modulation and moving mirrors

04 p0530 A72-14738

Quasi-monochromatic radio signal propagation for arbitrary amplitude and phase envelopes in nonlinear medium with nonlinearity caused by plasma heating

05 p0627 A72-16404

Unlimited phase locked loop analysis for AM signal by Fokker-Planck equation

05 p0637 A72-16554

Periodic quasi-noise spectrum and amplitude modulation of LF pulsed signals from earth in magnetosphere plasma

05 p0696 A72-16605

Broadband uhf power amplifier for AM signals output power of 100 W, using eight parallel transistors

06 p0774 A72-17750

AM/PM distortion intermodulation in FM/FDM radio systems during two-path propagation, using Fourier series method for noise power spectra calculation

06 p0775 A72-18239

Waveform distortion of strong field amplitude modulated plane electromagnetic wave propagating in anisotropic plasma

06 p0862 A72-18338

Binary single sideband phase modulation with simultaneous AM by signal and Hilbert transformation

06 p0776 A72-18395

Variance estimate of second order moment by nonlinear correlator in presence of additive amplitude and phase modulation and normal noise

07 p0939 A72-19021

Parametric converter mixers with FM and AM signal and pump oscillator, investigating SNR behavior

07 p0956 A72-19658

Hybrid computer and graphics terminals for real time dynamic man machine interaction, discussing AM communication system simulation

07 p0951 A72-20335

Rf excitation produced plasma instability, considering density fluctuation and drive frequency introduction by amplitude modulation

07 p1045 A72-20441

Quartz crystals ultrasonic vibrations produced by laser beam, noting light modulation depth dependence on effective cross section and amplitude

09 p1322 A72-22415

Microwave amplitude modulation during propagation through RF plasma under perpendicular low intensity time dependent magnetic field

10 p1520 A72-24345

Noise measurements of AM and FM microwave generators and amplifiers in nonlinear regime

10 p1452 A72-24643

Spectral distribution of signal power in AM, FM and PM PCM systems with time division multiplexing

10 p1439 A72-24909

Upper bound on probability of specified errors pattern occurrence for amplitude modulated digital communications systems subject to intersymbol interference and random noise

11 p1592 A72-25889

Single sideband AM microwave analog transmission systems using frequency division multiplex techniques

11 p1595 A72-26289

Statistical analysis of errors in altitude readings of phase comparison AM radio altimeters

11 p1633 A72-26303

Laser emission spectrum broadening due to saturable dye filter bleaching, discussing amplitude and phase modulation contributions

11 p1649 A72-26341

First order systems steady state frequency response to general harmonic amplitude modulated input, noting signal attenuation and absence of distortion

12 p1845 A72-27540

AM/PM conversion and transfer in nonlinear signal transmission systems, calculating coefficients as function of multicarrier powers for intelligible crosstalk

12 p1782 A72-27554

Optimal reception system synthesized for FM signal with phase fluctuation masked by narrow band AM and white noise

13 p1914 A72-28414

Spectrum analysis of PCM/AM-FM and PCM/FM-FM telemetry signals, using approximation technique to Fourier transform time signal to frequency domain

13 p1919 A72-29025

Modulated filter theory for AM signal analysis in linear resonant circuits, noting use for superheterodyne amplifier and phase discriminator design

13 p1930 A72-29046

Modulation oscillations in ferromagnetic core-based LF signal generators and frequency doublers, deriving

- differential equations for converter operation and formulas for static characteristics 13 p1930 A72-29049
- Parametric excitation of HF and LF plasma oscillations by AM SHF field, noting dependence on field strength at carrier frequency 13 p2015 A72-29436
- Natural instabilities development in laminar boundary layer of incompressible flow, considering AM spectrum and abscissa-ordinate development compared to Orr-Sommerfeld equation solution 13 p1943 A72-29784
- Feedback ac compensating amplifier design for automatic AM signal envelope conversion, noting truncated equivalent transfer function expandability 13 p1933 A72-29972
- Nonlinear AM and FM due to bonded nature of quasi-monochromatic whistler packets in magnetosphere 14 p2085 A72-30448
- Transmission lines with nonlinear capacitance semiconductor diodes, investigating electromagnetic traveling and standing waves instabilities and self amplitude modulation 14 p2086 A72-30795
- Optical communications photodetector sensitivity assessed from input power ratio of ideal and actual detector, noting amplitude modulated systems 15 p2235 A72-31621
- Signal spectrum sidebands asymmetry of LF waves in plasma with electric current and ion stream, suggesting amplitude and frequency modulation 15 p2284 A72-31650
- Whistler mode VLF signal transmission in ground transmitter and magnetically conjugate zones, observing spectrum broadening and AM in magnetosphere 15 p2197 A72-31919
- Time sharing radio communication system analysis with amplitude modulated carrier, noting power reduction, sideband content and multiplexing 15 p2201 A72-32566
- Interfering beams amplitude modulation, applying optical heterodyne techniques 15 p2202 A72-32676
- Magnetoelastic amplitude modulator of millimeter waves based on an antiferromagnetic/hemite/ 17 p2529 A72-34842
- Difference frequency signal from two sinusoidal voltages linear detection, estimating amplitude modulation envelope representation accuracy by Fourier series 17 p2518 A72-35781
- Spatial diversity technique based on predetector equal-gain combining for fast fading reduction of AM radio receiver, using phase shifter 18 p2661 A72-36845
- Synchronization and noise performance of mutually coupled oscillators. 18 p2668 A72-37036
- Wiener filter design for optimal processing of AM signals distorted during transmission through randomly dispersive medium 19 p2763 A72-37288
- Spectra of a frequency-shift-keyed signal amplitude-modulated by a sinusoidal wave. 20 p2904 A72-39771
- Controlled-carrier transmission of AM/VSB television from space. 21 p3016 A72-40770
- Optimal frequency-difference communications system with manipulated amplitudes 22 p3154 A72-42237
- Cross-modulation dynamic range of amplifiers used in the input stages of receiver equipment 23 p3271 A72-43839
- Analysis of a single-loop parametric amplifier by the phase plane method 24 p3384 A72-44893
- AMPLITUDE PROBABILITY ANALYSIS**
U AMPLITUDE DISTRIBUTION ANALYSIS
AMPLITUDES
 NT PULSE AMPLITUDE
 NT SCATTERING AMPLITUDE
 He-Ne laser amplitude fluctuations with hot and cold cathode discharge tube operation, determining emission spectral line width 05 p0669 A72-16613
- Electron plasma wave echoes experimental investigation, discussing amplitude decay under plasma and random noise influence 06 p0858 A72-17538
- Asymptotic approximation method for damping force as function of velocity from successive oscillations amplitudes measurement 07 p1096 A72-20474
- Steady state combination oscillations stability, examining geometrical properties of amplitude surfaces 14 p2133 A72-31128
- Amplitude-controlled harmonic oscillator transient response time reduction by sampling techniques in control loop without introducing distortion 16 p2369 A72-33763
- Complex amplitude four-pole network nonlinear conversion of sum of sinusoidal oscillations 22 p3158 A72-42083
- Use of rotated electrodes for amplitude weighting in interdigital surface-wave transducers. 22 p3178 A72-42619
- AN-24 AIRCRAFT**
 Soviet book on electrical equipment and instrumentation of An-24 aircraft covering power sources, control, safety systems, engine, flight and navigation instruments and autopilot 05 p0615 A72-16400
- ANACLINAL STREAMS**
U STREAMS
ANACLINAL VALLEYS
U VALLEYS
ANAEROBES
 Preglycolytic energy metabolism in biochemical evolution, concerning anaerobic oxidation of pyruvate and acetaldehyde to acetate and ATP 04 p0471 A72-14799
- ANALGESIA**
 Analgesic electrical stimulation in rat brainstem with other sensory modes unaffected 04 p0475 A72-15361
- ANALOG CIRCUITS**
 Analog fluidics systems status, exemplifying attitude reaction control for solar observation rocket and air gauging in textile industry 08 p1111 A72-20927
- Book on digital and analog monolithic IC systems, covering manufacturing methods, component design, MOS logic, arithmetic, error correction, codes, applications, etc 09 p1286 A72-23044
- Wide dynamic range analog multiplier with variable transconductance divider in operational transistor amplifier feedback path 11 p1603 A72-25742
- Integrated inductorless quadratic bandpass filters for constant bandwidth wide frequency range, using IC analog multipliers network 13 p1927 A72-28403
- A recognition method for technical diagnosis of analog electronic circuits 17 p2522 A72-34913
- Electromechanical measurement systems using analog transducers with ohmic resistance, electric and magnetic fields and digital/frequency and stochastic outputs 19 p2800 A72-37755
- Quadruple-redundancy management for fly-by-wire control system reliability, discussing analog circuit and digital computer voter/monitor techniques [ALAA PAPER 72-884] 20 p2910 A72-39117
- Assessment of the errors of a version of the hybrid quasi-analog system due to errors in quantization in time in the solution of systems of ordinary differential equations 21 p3024 A72-40158
- Analysis of the characteristics of an MOS transistor as a switching element 21 p3025 A72-40163
- Hybrid digital transmission systems based on optical fiber waveguides and analog repeaters, noting YAG laser light modulation by phase shift keyed sub-carrier 21 p3018 A72-40868
- Application of piezoelectric transducers for the measurement of static pressures 21 p3035 A72-41811
- Analog and digital automatic control systems for aerospace and process applications, discussing transfer function and state variable methods 22 p3162 A72-42714
- Circuit analysis and operation of analog multipliers with MOSFET, applying to industrial automatic control systems and measuring instruments 24 p3384 A72-44896
- ANALOG COMPUTERS**
 General purpose electronic modular units for human factors research bioinstrumentation, considering digital and analog computers, logic modules and interface and auxiliary equipment 01 p0048 A72-10569
- Synchros as electromechanical function generators and receivers for analog computers, examining errors in standard resolvers operation 03 p0328 A72-13841
- Analog computer simulation for filtering, phasing, multiplication and addition in AM communication system 03 p0329 A72-14182
- Simulation language for digital static checks for hybrid and analog computers 04 p0495 A72-14417
- Hsu-Howe iterative hybrid method for partial differential equations solution by time sharing analog components, using dynamic scaling and incremental formulations for reduced sensitivity 04 p0495 A72-14418
- Lf spectrum analysis instrumentation, describing stored data signals Fourier series parameters analog computation techniques 04 p0523 A72-15487
- Dynamic test facility for Symphony satellite attitude control, discussing sun and earth sensors and analog computer for motion simulator 05 p0643 A72-16432
- Digital differential analyzers number comparison in realization of direction cosine, Euler angle and quaternion attitude algorithms 07 p0949 A72-19296
- Cardiovascular analog computing circuits with outputs for left ventricular pressure maximum rise rate, cardiac stroke volume and atrioventricular conduction time 08 p1124 A72-20899
- Hybrid Monte Carlo techniques with digital and analog computers and minimal interface, simulating random walks for partial differential equations solution 08 p1138 A72-21602
- Analog and hybrid computers automated programming, setup and checking facilities for off and on-line program preparation and debugging 10 p1445 A72-24090
- Large scale integrated circuits for digital differential analyzers, giving operational specifications for shift registers, adders and integrators 10 p1448 A72-24276
- Analog computers application to resonance phenomena analysis in oscillating systems, describing programming of variable frequency harmonic oscillations 10 p1445 A72-24492
- Lower bound estimates of error distributions for analog computer solutions of linear algebraic equations 11 p1600 A72-25433
- Analog computer for practical evaluation of hologram interference fringes, analyzing errors 12 p1811 A72-27940
- Dynamic electrocardiography with analog computer program to detect, count and classify atypical ventricular depolarization complexes 12 p1775 A72-28281
- Analog and digital computers for automatic statistical analysis of unsteady random process recorded data, calculating correlation functions and expectancy 13 p1925 A72-29165
- Pilot trainer transfer function identification for man-machine and on-line adaptive control system using analog/hybrid computer 14 p2091 A72-30721
- Programmable digital differential analyzer for connection to digital computer, discussing dynamical problem solution and real time systems simulation capability 15 p2204 A72-32387
- Laser computer technology - Today and tomorrow. III** 17 p2523 A72-35186
- An analog computer technique for estimating sample times for digital simulation. 18 p2663 A72-36305
- A hybrid quasi-analog system for solving boundary value problems 21 p3024 A72-40159
- Computer simulations of transport processes. 21 p3024 A72-40247
- Stability criterion and imaginary axis displacement for real roots determination of algebraic equations on analog computers 21 p3025 A72-41806
- Real time analog computation at light speed and rapid access data storage in optical data processing systems, considering coherent electro-optical instrumentation 22 p3180 A72-42713
- Principles of modelling studies of fuel systems and hydraulic systems by electronic analog computers 22 p3157 A72-42922
- Constrained proportional controller dynamic equation solution on analog computer, determining limit cycle phase shift and nonlinearity effects on self oscillation parameters 24 p3403 A72-45322
- ANALOG DATA**
 Optimal inertialess transformation of output signals from several devices, noting method application to analog data processing systems 01 p0045 A72-10571
- Coding for analog and digital data transmission over channels with noiseless and noisy feedback links 02 p0197 A72-11680
- Format logic design for airborne memory controlled PCM telemetry multiplex digital and analog data system 02 p0187 A72-12130
- Multiprogrammed digital computer controlled acquisition and processing of quasi-static analog transducer data during spacecraft environmental simulation tests 02 p0200 A72-12478
- Interrogation frequency effects in random access analog multiplexers operating on flying capacitor at very high sampling frequencies 02 p0195 A72-12692
- Real time analog video magnetogram, describing differential photometer for electronic subtraction technique 03 p0357 A72-13286

Meteorological measurements representativeness and analog discrete filters synthesis with optimal data processing and weighting function averaging procedures

08 p1203 A72-22123

Wide bandwidth electron beam analog recorder and reproducer, using signal processing electronics and silver halide film

10 p1479 A72-23931

On-line analog display system for cardiovascular functions and beat-by-beat cardiac output derived from single aortic blood flow measurement

10 p1430 A72-24375

Surface acoustic wave technology in communication systems, discussing analog and digital matched filters and navigation, ATC and collision avoidance applications

10 p1483 A72-24940

Data transmission bandwidth requirements compression for band-limited functions, investigating feasibility through analog signal routing

11 p1592 A72-25887

Single sideband AM microwave analog transmission systems using frequency division multiplex techniques

11 p1595 A72-26289

SIDERAL program organization and computational method application to calculation of malfunction by drift of linear analog equipment

15 p2207 A72-31872

Registers and digital circuits with FETs and integrated operational amplifiers to permit analog measurements storage for display on CRT oscilloscope

15 p2204 A72-32499

Digital communication system for analog signal transmission by digital modulation techniques, presenting detection schemes

15 p2201 A72-32565

Discrete-time demodulation of continuous-time signals.

17 p2516 A72-35332

Electronically restored holographic data recording process for analog shape visualization with random access computer storage, discussing system design and capabilities

18 p2659 A72-36271

Video signals generation from binary data and mixing with analog information from cameras or tape recorders for simultaneous display on cathode ray tubes

19 p2769 A72-37936

Stable current-to-frequency converter with continuous integration of analog input signal providing digital output suitable for input to scalar

21 p2996 A72-40207

Analog and digital data recording systems, discussing accuracy, versatility and cost factor tradeoffs in selecting equipment for given applications

22 p3155 A72-42707

ANALOG SIMULATION

Analog computer simulation of automatic control systems containing time delay element in feedback loop, evaluating errors

01 p0044 A72-10152

Electronic analog models of human retina and visual system, discussing optical character recognition, signal processing, photoreceptor stimulation, visual cortex excitation and further model development

01 p0017 A72-10471

Spring fracture and vibration in injection pumps by analog model

02 p0236 A72-12437

Analog circuit method for slender profile flow field shock front boundary value problem for simple profile variation, using known mapping plane solutions

[DGLR PAPER 71-069] 02 p0153 A72-12743

Human arm arterial pressure and flow pulsations numerical analysis, constructing electrical analog circuit from mathematical model

03 p0317 A72-12951

Analog computer simulation for filtering, phasing, multiplication and addition in AM communication system

03 p0329 A72-14182

In vivo investigation of dogs natural mitral valve flow dynamics, developing cardiohemic system physical model for data analysis and electrical analog simulation

[ASME PAPER 71-WA/BHF-2] 05 p0621 A72-15949

German monograph on analog model of thermoregulation in human body at rest and at work, describing heat transfer

05 p0621 A72-16047

Vibration simulation of elastohysterical systems on analog computers using photoresistor-voltage relationship of polycrystalline photoresistors

06 p0900 A72-18674

Analog simulation of normal thermal explosions and cool flames, observing oscillations limits, time dependence of parameters and effect of changes in activation energy or initial temperature

07 p1098 A72-19366

Analog/hybrid simulation of noise effect on adaptive delta modulation system consisting of transmitter, receiver and error simulator

07 p0951 A72-20339

Analog simulation of dual-spin satellite dynamics and control, emphasizing Hughes gyrostat spacecraft

07 p1086 A72-20352

Geomagnetic phenomena associated with auroras and magnetic storms, investigating analog modeling experiment by stationary electrical discharges under laboratory conditions

07 p0980 A72-20457

Inflight validation of laboratory scaled-down simulation experiments on optimal hierarchy of colors for markers and signals

[AD-737901] 08 p1147 A72-21582

Conditioned reflex activity, discussing biological and nervous system, electric analog simulation and mathematical and structural modeling

08 p1127 A72-21842

Servomechanism with nonlinear static and Coulomb friction under autonomous operation, predicting stability boundaries by analog computer simulation

08 p1113 A72-22154

Cardiovascular system model for demonstration of biological system analog simulation and computation, describing components for heart pumping action and systemic circulation

09 p1268 A72-22454

Digital controller simulation by analog means with independent gain adjustment of proportional, derivative and integral modes

10 p1445 A72-24093

Analog simulation of hyperbolic differential equations with split boundary conditions, comparing to digital solutions to nonlinear flow

10 p1445 A72-24454

Dynamic processes of electric drive system with electromagnetic clutch modeled by analog computer element with logical input-output relation

10 p1423 A72-24755

Spacecraft structural dynamics, design and testing, using Fourier transform and analog vibration simulation

[AIAA PAPER 72-349] 11 p1728 A72-25378

Jet engine fuel fire hazard evaluation by controlled laboratory tests, analyzing ignition characteristics under simulated survivable aircraft crash accidents

[SAE PAPER 720324] 11 p1702 A72-25587

Circularly polarized ultrashort radio wave reflection from lunar and planetary surfaces, determining angular scattering spectrum

11 p1599 A72-26908

Equations of motion for torsional vibrations in system with nonlinear elastic term and variable moments of inertia, noting analog computer simulation

11 p1739 A72-26982

Transit time, retarded domain and suppressed domain mode simulation of Gunn oscillator, using LF analog

13 p1927 A72-28405

Analog simulation of Josephson superconducting junctions dc characteristics for two mixed microwave frequencies, discussing signal detection sensitivity improvement

13 p2021 A72-28648

Analog simulation of direct acting gas pressure regulators in terms of spring, flow and friction forces

13 p1956 A72-28703

Analog dynamic model of tracked air cushion vehicle for high speed ground transportation systems

13 p1896 A72-28704

Electrical analog simulation of internal combustion engines intake and exhaust systems nonstationary gas flow, considering cylinder, turbine and supercharger operation

13 p2027 A72-29136

Two compartment analog model of thermoregulation during rest and exercise, considering temperature, heat conductance, sweat rate and oxygen uptake

15 p2185 A72-31450

Solar flare and neutral sheet simulation by investigating behavior of plasma current through magnetic neutral point created by capacitor discharges

15 p2301 A72-32342

Voltage and current generalized immittance converter realization, using with current conveyor for simulation

16 p2367 A72-32856

Analog simulation method for highly redundant structure optimization based on reproducing structure mechanical behavior in stabilized stress states

16 p2463 A72-32899

Atmospheric boundary layer and diffusion over three dimensional mountainous terrain by laboratory simulation with meteorological wind tunnel and scale model

[AIAA PAPER 72-648] 16 p2419 A72-34085

Theory of the dynamic vibration neutralizer with motion-limiting stops.

[ASME PAPER 71-APMW-14] 17 p2625 A72-34317

The physically defined flame and its representation in the water model

18 p2656 A72-36242

Application of an analog computer to the calculation of partially plasticized rotating circular disks prepared from strain-hardenable materials

18 p2735 A72-36421

Microwave-analogy tests regarding light scattering at cosmic dust particles

19 p2804 A72-38507

Analog computer simulation for PCM-FM and four-phase DPSK digital radio receivers susceptibility to interference sources

20 p2905 A72-38985

Electrical modeling of the plane problem of elasticity theory in terms of stresses

21 p3116 A72-40164

Electronic simulator for calculating effective temperatures in the establishment of climatological procedures

21 p3077 A72-40166

Accuracy of alpha-analog simulation of linear algebraic equations in the case of a nonzero discrepancy vector

21 p3074 A72-40170

Analog model for two dimensional heat conduction equation, noting electrical networks for one dimensional difference equations solution

21 p3127 A72-40179

Simulation of physically nonlinear nonlinear beams

21 p3116 A72-40180

Electrical modeling of nonlinear problems of thermal engineering

21 p3128 A72-40182

The determination of active array impedance with multielement waveguide simulators.

21 p3026 A72-40357

Application of an agar-agar chamber for the study of electromagnetic waves in an inhomogeneous medium.

21 p3015 A72-40359

Susceptibility measurements on PCM-FM and four phase differential PSK digital receivers simulated on analog computer

21 p3016 A72-40852

Book - Computer simulation of dynamic systems.

22 p3157 A72-43081

Analysis by hydraulic analogy of rotating separation in compressors

22 p3167 A72-43091

Use of the simulation method for the solution of a dispersion problem for the propagation of symmetrical magnetic waves in a rectangular waveguide filled with a nonhomogeneous plasma

23 p3263 A72-43450

Computer simulation of fracture spreading in a visco-elastic solid.

23 p3267 A72-43702

Reliability analysis of a jet engine fuel system with the aid of an analog computer using operational data

23 p3326 A72-44282

Use of modeling and simulation methods in the design of gas turbine engine control systems

23 p3326 A72-44283

Dynamic and static characteristics of jet engine simulators

23 p3327 A72-44286

Analog model of gas turbine engine control systems, using statistical estimates and flow rate, heat conduction and dynamic equations

23 p3327 A72-44293

Examination of rocket control system by means of analog computer.

24 p3450 A72-45175

Constrained proportional controller dynamic equation solution on analog computer, determining limit cycle phase shift and nonlinearity effects on self oscillation parameters

24 p3403 A72-45322

Dynamic simulation of an aircraft under the effect of vortex wake turbulence.

24 p3368 A72-45346

ANALOG TO DIGITAL CONVERTERS

Land pattern mapping from monimager analysis, using coordinate digitizer system with planimetric computer input

02 p0187 A72-11874

Single scan TV-radiography system for providing A-D converter analog signal for digital data acquisition, obtaining transfer functions

04 p0522 A72-15226

Image processing of diagnostic echocardiogram by ultrahigh speed analog to digital converter interfacing digital computer

07 p0928 A72-19312

Charpy impact test computerized data acquisition and analysis system using analog to digital converter

07 p1090 A72-19735

Interference rejection method for high speed analog to digital converters, noting application to on-line computer systems

07 p0948 A72-20386

Flat electrically conducting screen with periodic filamentary structure as possible analog converter of electromagnetic field information

09 p1291 A72-23433

Analog to digital conversion system analysis and design with linear converter and nonlinear logarithmic amplifier, noting small signal resolution

09 p1284 A72-23678

Cybernetic equipment reliability and precision analysis from algorithmic, conversion and instrumental error

- rors, surveying digital, analog and hybrid computers and converters
11 p1608 A72-25427
- Image dissector system fabrication for two dimensional area scanning, applying to photograph digitization
11 p1631 A72-25688
- Amplitude-time quantization of radar pulse signals in analog-digital converter, improving noise threshold and ranging accuracy
11 p1595 A72-26294
- Quasi-equidistant binary-decimal codes for displacement digitizers, noting readout error probability reduction
11 p1602 A72-26448
- Semiautomatic analog to digital converter for pulse signals time dependent parameters, examining block diagrams and tunnel diode operation
11 p1605 A72-26456
- Arterial pressure data recording technique using magnetic tape recorder and automatic conversion to digital form
12 p1772 A72-27649
- Automatic digitizing and recording of analog information from oscilloscope photographs
13 p1959 A72-29755
- Analogue to digital converter for sinusoidal voltage amplitude pickup and subsequent digital coding with correction for conversion characteristic nonlinearity
13 p1934 A72-30020
- High accuracy relative attitude readout mechanization, discussing analog and digital design, closed loop analysis and simulation
15 p2270 A72-32191
- Airborne flight test data acquisition system modular design to provide digital readings from monitoring transducers analog signal
16 p2364 A72-33645
- A/D and D/A converter for color TV signal digital transmission over communication satellites, discussing system design features
17 p2524 A72-34262
- Contact-type level gauge with a transistorized decimal code converter
17 p2529 A72-34764
- Digital data processing equipment for continuous ECG analysis, noting analog to digital converter and amplitude distribution analysis
17 p2522 A72-34914
- A system for the mass examination of electrocardiograms.
19 p2760 A72-37853
- Electrically conducting plane screen with periodic filamentary structure as possible analog converter of electromagnetic field information
19 p2782 A72-38516
- Transformation of reactive ladders into digital circuits.
20 p2910 A72-39427
- Mean value of noisy signal quantized by analog/digital converter, noting input noise level relation to estimate accuracy
20 p2904 A72-39785
- Linear analog to pulsewidth converter insertion into control loop in dc/dc regulators for space applications to permit high sampling frequencies
21 p2997 A72-41081
- Increasing the linearity of the time scale of a time-amplitude-code converter
21 p3035 A72-41728
- Analysis of the basic metrological characteristics of Vernier time-pulse converters
21 p3035 A72-41729
- Elimination of an ambiguity in the reading of digital computational devices
21 p3035 A72-41810
- Integrating digital voltmeter - Operating principles and accuracy.
24 p3403 A72-45275
- ANALOGIES**
NT HYDRAULIC ANALOGIES
Pulmonary RC network and multiple breath nitrogen washout time constants mathematical relationship for breathing mechanics measurement, discussing lung compliance and resistance
04 p0478 A72-14862
- Submodel similarity relations in single indirect experiment design
08 p1257 A72-22176
- Thermal and electric flow analogy application to heat transfer determination on basis of three dimensional model
09 p1410 A72-22628
- Second order Cowley-Imai analogy application to transcribe gas dynamic perturbation solutions into magnetogasdynamic solutions for perfect gas axisymmetric super-Alfvénic flows
10 p1521 A72-24464
- Chaplygin gas flow equation for analogy between hydrodynamic and electrodynamic equations, noting special theory of relativity
23 p3312 A72-43404

ANALOGS

- Relativistic homogeneous anisotropic models
analogs construction in Newtonian cosmology
11 p1716 A72-25711
- Miniature swine as human analog to investigate physiological response to high positive acceleration, comparing human and animal tolerances
12 p1768 A72-28329
- ANALYSIS [MATHEMATICS]**
NT ABEL FUNCTION
NT ANALYTIC FUNCTIONS
NT APERIODIC FUNCTIONS
NT ASYMPTOTES
NT ASYMPTOTIC SERIES
NT BANACH SPACE
NT BESSEL FUNCTIONS
NT BETHE-SALPETER EQUATION
NT BIHARMONIC EQUATIONS
NT BLASIUSS EQUATION
NT BOREL SETS
NT BURGER EQUATION
NT CALCULUS
NT CALCULUS OF VARIATIONS
NT CAUCHY INTEGRAL FORMULA
NT CHANDRASEKHAR EQUATION
NT COLLINEARITY
NT COMBINATORIAL ANALYSIS
NT COMPLEX VARIABLES
NT CONFORMAL MAPPING
NT CONJUGATES
NT CONTINUITY [MATHEMATICS]
NT CONVOLUTION INTEGRALS
NT DELTA FUNCTION
NT DIFFERENTIAL CALCULUS
NT DIFFERENTIAL EQUATIONS
NT DUFFING DIFFERENTIAL EQUATION
NT EINSTEIN EQUATIONS
NT ELLIPTIC DIFFERENTIAL EQUATIONS
NT ELLIPTIC FUNCTIONS
NT ENTIRE FUNCTIONS
NT EXISTENCE THEOREMS
NT EXPONENTIAL FUNCTIONS
NT EXTREMUM VALUES
NT FALKNER-SKAN EQUATION
NT FOKKER-PLANCK EQUATION
NT FOURIER ANALYSIS
NT FOURIER SERIES
NT FOURIER TRANSFORMATION
NT FOURIER-BESSEL TRANSFORMATIONS
NT FREDHOLM EQUATIONS
NT FUNCTION SPACE
NT FUNCTIONAL ANALYSIS
NT FUNCTIONAL INTEGRATION
NT GAMMA FUNCTION
NT GAUSS EQUATION
NT GREEN FUNCTION
NT HALF PLANES
NT HALF SPACES
NT HANKEL FUNCTIONS
NT HARMONIC ANALYSIS
NT HARMONIC FUNCTIONS
NT HILBERT SPACE
NT HILBERT TRANSFORMATION
NT HILL DETERMINANT
NT HYPERBOLIC FUNCTIONS
NT HYPERGEOMETRIC FUNCTIONS
NT INTEGRAL CALCULUS
NT INTEGRAL EQUATIONS
NT INTEGRAL TRANSFORMATIONS
NT JACOBI INTEGRAL
NT JACOBI MATRIX METHOD
NT KERNEL FUNCTIONS
NT LAGUERRE FUNCTIONS
NT LAME WAVE EQUATIONS
NT LAPLACE TRANSFORMATION
NT LEBESGUE THEOREM
NT LEGENDRE FUNCTIONS
NT LIAPUNOV FUNCTIONS
NT LIMITS [MATHEMATICS]
NT LINEAR EQUATIONS
NT LIOUVILLE EQUATIONS
NT LIPSCHITZ CONDITION
NT LOGARITHMS
NT MATHIEU FUNCTION
NT MEASURE AND INTEGRATION
NT MEROMORPHIC FUNCTIONS
NT MINIMA
NT NEUMANN PROBLEM
NT NONHOLONOMIC EQUATIONS
NT NONLINEAR EQUATIONS
NT NUMERICAL ANALYSIS
NT NUMERICAL INTEGRATION
NT ORTHOGONAL FUNCTIONS
NT PADE APPROXIMATION
NT PARABOLIC DIFFERENTIAL EQUATIONS
NT PARTIAL DIFFERENTIAL EQUATIONS
NT PERIODIC FUNCTIONS
NT PHASE-SPACE INTEGRAL
NT POISSON EQUATION
NT POWER SERIES
NT QUADRATIC EQUATIONS
NT RATIONAL FUNCTIONS
NT RUNGE-KUTTA METHOD
NT SERIES [MATHEMATICS]
NT SINGULAR INTEGRAL EQUATIONS

- NT SINGULARITY [MATHEMATICS]
NT SPHERICAL HARMONICS
NT STURM-LIOUVILLE THEORY
NT TANGENTS
NT TAYLOR SERIES
NT TESSERAL HARMONICS
NT TRIGONOMETRIC FUNCTIONS
NT VECTOR ANALYSIS
NT VLASOV EQUATIONS
NT VOLTERRA EQUATIONS
NT VORTICITY
NT WEIERSTRASS FUNCTIONS
NT WEIGHTING FUNCTIONS
NT WHITTAKER FUNCTIONS
NT WIENER HOPF EQUATIONS
NT ZONAL HARMONICS
Geopotential induced secular perturbations, using second approximation to achieve analytic accuracy
15 p2309 A72-31934
- Direct methods of qualitative spectral analysis for the singular Sturm-Liouville equation with an unrestricted operator potential
23 p3308 A72-43578
- ANALYSIS OF VARIANCE**
Stellar and planetary atmosphere dynamics, deriving balance equations for variance analysis of angular momentum
16 p2453 A72-33247
- Smooth empirical Bayes estimation of observation error variances in linear systems.
17 p2576 A72-35248
- ANALYTIC FUNCTIONS**
NT ENTIRE FUNCTIONS
Multiple-input multiple-output linear time invariant feedback systems stability, investigating continuous-time case
04 p0507 A72-15694
- Elasticity theory three-dimensional axisymmetric problem reduction to two-dimensional analytic function boundary value problem
05 p0739 A72-16591
- Engineering curves and surfaces representation by spline functions, discussing computerized approximation methods for algebraic, transcendental and transfer functions
07 p1024 A72-18777
- Elastic equilibrium of infinite wedge with apical asymmetric notch, reducing to Hilbert problem for holomorphic vectors
07 p1093 A72-19976
- P-analytic functions application to strength analysis of zero moment shells of revolution with positive Gaussian curvature under concentrated loads
08 p1242 A72-20905
- Elasticity and potential theory axisymmetric problems solution for sphere and spherical cavity, constructing x-analytic functions for boundary surfaces
08 p1242 A72-20908
- Axisymmetric elasticity theory problems for stress-strain state of space with spherical incision, obtaining solutions with p-analytic functions
08 p1242 A72-20960
- Functional analysis techniques for existence of holonomic solutions to linear differential equation systems with singular points
09 p1342 A72-23254
- Differential geometry extremal problem of holomorphic embedding of complex curves in Kaehler manifold with constant holomorphic curvature, using Riemann surface moduli theory
10 p1506 A72-24862
- Convergence rate of epsilon algorithm, using Pade table and analytic functions
12 p1837 A72-27717
- Differentiation method for complex root calculation for system of nonlinear equations with analytic functions
13 p1985 A72-28710
- Series representations of p-analytic functions in Legendre functions of first and second kind, applying to axisymmetric problems solution in elasticity theory
13 p2057 A72-29079
- Criteria for nonlinear systems controllability in terms of state variable analytic function and derivatives, implying strong accessibility for manifolds including Euclidean spaces
18 p2673 A72-36616
- Elasticity theory three-dimensional axisymmetric problem reduction to two dimensional analytic function boundary value problem
19 p2872 A72-37563
- Methods of solving boundary value problems of linear conjugation for functions that are holomorphic in bicylindrical domains
21 p3074 A72-40254
- German monograph - Iterative algorithms for ordinary differential equations and their suitability for parallel processing by means of symbol manipulation.
22 p3200 A72-43063
- Reduction to diagonal form of some triangular-matrix classes in spaces of functions that are analytic in multicircular regions
23 p3308 A72-43581

Schauder bases in certain spaces of holomorphic functions
24 p3418 A72-44826

Analytic continuation of functions over infinite dimensional domains, covering Banach manifolds, hypoanalytical mappings, convexity and topology
24 p3418 A72-44827

Hyperbolic two body problem in celestial mechanics, discussing /E, r, alpha, beta/ summability procedure for analytic continuation
24 p3442 A72-45236

Approximation of analytic functions by trigonometric polynomials over an interval smaller than the period
24 p3419 A72-45550

ANALYTIC GEOMETRY

NT CONICS
NT ELLIPSES
NT EPICYCLOIDS
NT HYPERBOLAS
NT LOCI
NT MERCATOR PROJECTION
NT OBLATE SPHEROIDS
NT PROLATE SPHEROIDS
NT QUADRANTS
NT SPHEROIDS
NT TANGENTS
NT TORUSES

ANALYZERS

NT SIGNAL ANALYZERS
Electrostatic analyzer for very low energy particles, calculating trajectories
03 p0392 A72-14055

Cylindrical mirror electron energy analyzer, discussing theory, operation and design parameters [AD-745599]
07 p0984 A72-19322

Nonprotein amino acids detection in presence of protein amino acids by amino acid analyzer, noting separation of chemically similar compounds
13 p1913 A72-29774

The geometric factor of a cylindrical plate electrostatic analyzer.
17 p2553 A72-34639

ANASTIGMATISM

Anastigmatic optical systems with two high aperture ratio mirrors for UV image tubes
08 p1169 A72-21952

ANATASE

Xenolithic origin for silicate inclusions in anatase of Landes meteorite from West Virginia
13 p2036 A72-28753

ANATOMY

NT ADRENAL GLAND
NT AORTA
NT ARM [ANATOMY]
NT ARTERIES
NT BARORECEPTORS
NT BLADDER
NT BLOOD VESSELS
NT BONES
NT BRAIN
NT BRAIN STEM
NT BRONCHI
NT BRONCHIAL TUBE
NT CAPILLARIES [ANATOMY]
NT CARDIAC AURICLES
NT CARDIAC VENTRICLES
NT CARDIOVASCULAR SYSTEM
NT CEREBELLUM
NT CEREBRAL CORTEX
NT CEREBRUM
NT CHEMORECEPTORS
NT CHEST
NT CHIN
NT CHOROID MEMBRANES
NT CIRCULATORY SYSTEM
NT COCHLEA
NT COLLAGENS
NT CONNECTIVE TISSUE
NT CONSTRICTORS
NT CORNEA
NT CRANIUM
NT DIAPHRAGM [ANATOMY]
NT DIASTOLE
NT EAR
NT EARDRUMS
NT ENDOCRINE GLANDS
NT EPICARDIUM
NT ERYTHROCYTES
NT EYE [ANATOMY]
NT FEMUR
NT FINGERS
NT FOREARM
NT FOVEA
NT GLANDS [ANATOMY]
NT GLOMERULUS
NT GONADS
NT GRAVIRECEPTORS
NT HAND [ANATOMY]
NT HEAD [ANATOMY]
NT HEART
NT HEMATOPOIESIS
NT HEMATOPOIETIC SYSTEM
NT HIPPOCAMPUS
NT HUMAN BODY

NT INTRACRANIAL CAVITY
NT JOINTS [ANATOMY]
NT KIDNEYS
NT LABYRINTH
NT LEG [ANATOMY]
NT LEUKOCYTES
NT LIMBS [ANATOMY]
NT LIVER
NT LUNGS
NT LYMPHOCYTES
NT MIDDLE EAR
NT MUSCULOSKELETAL SYSTEM
NT MYOCARDIUM
NT NECK [ANATOMY]
NT NOSE [ANATOMY]
NT OCCIPITAL LOBES
NT OCULOMOTOR NERVES
NT ORGANS
NT OTOLITH ORGANS
NT PANCREAS
NT PARATHYROID GLAND
NT PELVIS
NT PHOTORECEPTORS
NT PITUITARY GLAND
NT PROPRIORECEPTORS
NT PUPILS
NT RESPIRATORY SYSTEM
NT RETICULOCYTES
NT RETINA
NT SCIATIC REGION
NT SEMICIRCULAR CANALS
NT SENSE ORGANS
NT SPLEEN
NT STERNUM
NT SYSTOLE
NT TESTES
NT THERMORECEPTORS
NT THROMBOPLASTIN
NT THYROID GLAND
NT TIBIA
NT ULNA
NT VASCULAR SYSTEM
NT VEINS
NT VERTEBRAL COLUMN
NT VESTIBULES

Anatomical-physiological, optical and behavioral-visual similarities of nonhuman and human primates
03 p0313 A72-13069

Thalamus functional and organizational anatomy studies from improved neurophysiological research methods, emphasizing cytoarchitectural differentiation functional significance
07 p0922 A72-20274

Human vocal apparatus anatomical and neural structure, considering linguistic sounds composition
22 p3147 A72-42789

ANDESITE

Eruptive center location and flow direction measurements for andesite and quartz latite lava flows in Mogollon Mountains
15 p2223 A72-31579

ANDROMEDA GALAXIES

X-ray emission from intergalactic gas in the neighbourhood of galaxies.
20 p2964 A72-39240

Estimate for the frequency of novae in the Andromeda Nebula and our Galaxy.
23 p3333 A72-43229

ANECHOIC CHAMBERS

Sidewall reflection induced boresight error in anechoic chamber used for missile test or simulation
08 p1141 A72-21421

RF simulator design for missile systems performance tests, discussing requirements, target array and anechoic chamber
[AIAA PAPER 72-861]
20 p2911 A72-39125

ANELASTICITY

Anelastic solid energy dissipation linear memory models based on viscoelasticity theory, applied to earth and metals experimental data and dynamic loading problems
02 p0294 A72-12447

Anelasticity effects due to defects and phase transformations in solids - Conference, Lausanne, Switzerland, June 1970
06 p0830 A72-18291

Nonlinear structural analysis of circular plates and shells of revolution with geometric and inelastic material nonlinearities, using direct stiffness method [AIAA PAPER 72-353]
11 p1729 A72-25382

Stress relaxation in anelastic materials, calculating spectra, complex modulus of elasticity and internal friction
12 p1883 A72-27541

Resonance type facility using dynamic hysteresis loop method to test metal fatigue and anelasticity in torsion at room and high temperatures
14 p2092 A72-30443

Anelastic damping of cold worked Nb sheet as function of vibration frequency, temperature, rolling rate and oxygen content
15 p2258 A72-32638

ANEMIAS

Case report on compensated hemolytic anemia associated with Gilbert syndrome, discussing implication in aviation
01 p0022 A72-11299

Physiological effects of transfusing 2,3-diphosphoglycerate (DPG) depleted red cells with high oxygen affinity in anemic hypoxic patients
04 p0473 A72-15211

ANEMOMETERS

NT HOT-FILM ANEMOMETERS
NT HOT-WIRE ANEMOMETERS
Laser optical anemometry system, describing fringe, Doppler and reference beam operation modes
01 p0081 A72-11168

Laser anemometer system for instantaneous velocity measurement in turbulent pipe flow, determining two point velocity correlation coefficients
01 p0071 A72-11169

Laser flow anemometer technology, discussing velocity and spatial resolution, chromatic and temporal coherence, signal processing, frequency discrimination, spectrum analyzer and tracking filter
02 p0224 A72-11743

Atmospheric turbulence detection sensors, reviewing microwave radar, acoustic, Doppler lidar, laser fringe anemometry and passive IR techniques
04 p0530 A72-14833

Paired Gill propeller anemometer response function in generalized wind vector sensor application, proposing algorithm for magnitude and direction errors reduction in output analyses
09 p1307 A72-22434

Anemometer probe with thermistors for low velocities of liquids derived from pulsed thermal conductivity gage
10 p1479 A72-24066

VHF remote control anemometer network with digital receiving station for wind measurement and gale warning system
10 p1463 A72-25013

Momentum anemometer for wind velocity and vorticity measurement, discussing design principle and performance advantages
10 p1484 A72-25089

Non-Newtonian pipe flow turbulence measurements by laser anemometer, describing optical system and signal processing instrumentation
[AD-742872]
11 p1646 A72-25554

Thermistor anemometers design and measurement of displacement or dispersion coefficients
11 p1636 A72-26699

Copper resistance thermoanemometer for channel unsteady air flow rate measurement, discussing design, operation principles and maximum error
12 p1812 A72-28146

Optical anemometers for mean and fluctuating velocities in premixed flame of town gas-air combustion system, noting velocity probability density distribution
13 p1955 A72-28546

Measurement techniques for separated gas flows mean and fluctuating aerodynamic properties, discussing improved optical geometry for laser Doppler anemometer
13 p1956 A72-28632

Velocimeter design for MHD boundary layer flow velocity measurement, using Doppler frequency shift of laser light scattered from added macroscopic particles
13 p1957 A72-29360

Satellite anemometry for ocean waves and weather forecasting, discussing Skylab microwave radiometer-scatterometer potential design
15 p2221 A72-31239

Operation and calibration of three blade rotating vane anemometer for rarefied gas flow velocity measurement
16 p2395 A72-33966

Laser Doppler anemometer for three dimensional liquid and gas flow velocity measurements in water tunnels
16 p2396 A72-34158

An automatic data processing system for laser anemometers.
19 p2795 A72-37287

Fluid mechanics anemometry based on laser light frequency modulation /Doppler effect/, describing measurement of extensions of vortices and oscillations in flow boundary layers
19 p2801 A72-37934

Cup anemometer response to fluctuating wind speeds.
20 p2920 A72-38966

Thermoanemometer measurements of turbulence degree in wake behind square mesh grids in water flow within low speed wind tunnel
20 p2912 A72-39364

Theoretical considerations of significance to the design of optical anemometers.
[ASME PAPER 72-HT-7]
20 p2926 A72-39678

Microstructure of turbulent flow in the stabilized flow region in a channel
21 p3045 A72-41054

ANEMOMETRY

Investigation of the operation of a vane anemometer in vacuum with the aid of an optical transducer for the rotational frequency

21 p3059 A72-41820

An improved pressure-sphere anemometer.

22 p3178 A72-42596

Fluid velocity measurement of oscillatory flow generated from vortex shedding by laser Doppler system, discussing frequency tracker design, continuous detection problem and application

22 p3178 A72-42677

ANEMOMETRY

U VELOCITY MEASUREMENT

ANESTHESIA

Effects of chloralose-urethan anesthesia on temperature regulation in dogs.

21 p2997 A72-40426

ANESTHESIOLOGY

Differential neurophysiological and psychological effects of subanesthetic concentrations of cyclopropane, diethyl ether, methoxyflurane and ethrane in conscious man

04 p0480 A72-15220

ANESTHETICS

NT CYCLOPROPANE

ANGELS

Biological radar clutter control by adaptive systems techniques, developing computer simulation for angel tolerance from bird electromagnetic characteristics

07 p0942 A72-19305

ANGIOGRAPHY

Correlation between ergometry, ballistocardiography and coronary angiography in 267 patients.

18 p2649 A72-36034

Continuous recording of His bundle electrogram during selective coronary cineangiography in man.

23 p3255 A72-43813

Effects of coronary arteriography on myocardial blood flow.

23 p3256 A72-43933

Clinicoarteriographic correlations in angina pectoris with and without myocardial infarction.

24 p3372 A72-45010

ANGLE OF ATTACK

NT ZERO ANGLE OF ATTACK

Circular cone in supersonic flow, obtaining self similar solution for effect of angle of attack on laminar boundary layer by finite difference method

02 p0150 A72-12095

Multivortex model of vortex sheet development on slender axisymmetric bodies at angle of attack

03 p0307 A72-12919

Finite difference integration based on theoretical model analysis of three dimensional turbulent boundary layer on sharp cone at angle of attack in supersonic flow

05 p0650 A72-16842

HP-115 slender wing research aircraft linear motion and undamped Dutch roll oscillations at high angles of attack

05 p0613 A72-16932

Nonsymmetrical aerodynamic damping moments on 10 deg cone at supersonic speeds and large angles of attack, comparing Newtonian theory prediction with wind tunnel test results

05 p0609 A72-16947

Finite difference method for transonic airfoil design for wide range of angles of attack and Mach numbers

06 p0755 A72-17629

V-shaped wings supersonic characteristics at 0-15 deg angles of attack, investigating flow structure between wings by pitot tube rake

06 p0757 A72-18129

Wake analysis of asymmetric hypersonic flow past two dimensional profiles at small angles of attack, using perturbation techniques

06 p0757 A72-18143

Vanes for sensing incidence angles of airstream with respect to aircraft, noting correlation coefficient

06 p0796 A72-18450

Flight initial spin testing, discussing aircraft autorotation due to stalled angle of attack and sideslip

06 p0759 A72-18492

Computer program for low temperature ablator nosetip shape change at angle of attack, comparing with supersonic wind tunnel tests on camphor models

07 p1098 A72-18952

Boundary layer transition on slender cone in hypersonic flow as function of nose bluntness, free stream Reynolds number and angle of attack

07 p0908 A72-18961

Pressure distribution and force coefficients for cones at angles of incidence as function of Mach number, using extended method of equivalent axisymmetric bodies

10 p1417 A72-24028

Similarity method solution of differential equations of motion for supersonic laminar boundary near symmetry plane of cone at angle of incidence

10 p1418 A72-24326

Supersonic flow around thin cruciform wing with antisymmetrical angle of attack distribution and horizontal plane with leading edge, considering flow separation at edges

10 p1420 A72-25118

Base pressure distribution measurement for free flying sharp cone at hypersonic speeds and high angles of attack

[AIAA PAPER 72-316]

11 p1567 A72-25250

Hypersonic base heating investigation on Mars atmosphere entry blunt bodies, taking into account gas composition and angle of attack effects

[AIAA PAPER 72-317]

11 p1568 A72-25251

Three dimensional laminar boundary layer on slender circular cone at angle of attack in supersonic flow, determining separated flow region via finite difference method

11 p1572 A72-25818

Nose bluntness effect on bodies of revolution pitching moment characteristics in incompressible flow at various angles of attack

11 p1573 A72-26576

Unsteady aerodynamic forces on flat plate in locally perturbed incompressible potential flow, investigating angle of attack frequency response to periodic local perturbations

11 p1573 A72-26579

Rotating airfoil experimental test program for verification of Himmelskamp and Dwyer-McCroskey theoretical analysis, presenting graphs of lift coefficient vs angle of attack

12 p1752 A72-28124

Skin friction response to angle and perturbation in flow past axisymmetric body with unsteady main stream

13 p1941 A72-28887

Aerodynamic center and center of pressure of slender small aspect ratio wing near solid or free surface, determining angle of attack effect

13 p1894 A72-29131

Numerical analysis of inviscid hypersonic flow characteristics in shock layer between bow shock and cone at angles of attack, taking into account laminar separated flow

14 p2069 A72-30328

Longitudinal and circumferential boundary layer characteristics for concave and convex axisymmetric bodies at small angles of attack, using Cooke equivalent radius concept

15 p2177 A72-31205

Leading edge boundary layer flow separation and reattachment processes in airfoil dynamic stall, considering effect of angle of attack rate of change

15 p2179 A72-32024

Book on airfoil section designs for light aircraft covering wind tunnel studies of lift drag ratio as function of angle of attack

15 p2179 A72-32250

Unsteady viscous flow effects on aerodynamic forces exerted on oscillating elliptic airfoil for various Reynolds numbers, angles of attack and frequencies

15 p2180 A72-32344

Singularity method treatment of vortex distribution induced velocity perturbations on flat plate at angle of attack, noting results similarity to lifting surface theory

15 p2180 A72-32466

Exact boundary layer calculations for heat and mass transfer on cones at angle of attack, considering Mach number, enthalpy ratio and cross flow effects

15 p2337 A72-32591

Influence of the angle of attack on the performance of high-deflection stator blades

17 p2484 A72-34889

F-111 stall inhibitor system with angle of attack limitation, describing interface with stability augmentation system

17 p2493 A72-35577

Viscous hypersonic flow over a flat plate at angle of attack with leeward boundary layer separation.

[AD-744593]

17 p2486 A72-35634

Angle of attack increase of an airfoil in decelerating flow.

18 p2641 A72-36773

Effect of angle of incidence on the response of cylindrical electrostatic probes at supersonic speeds.

20 p2926 A72-39602

The effect of angle of attack on boundary-layer transition on cones.

20 p2886 A72-39638

Lift on airfoils with separated boundary layers.

21 p2992 A72-41264

Comparison of three oscillatory techniques for cones at incidence.

[AIAA PAPER 72-1015]

21 p3042 A72-41595

Axisymmetric jet stretcher diffuser performance for ramjet engine inlet configurations, testing at angles of attack and supersonic flow velocities

[AIAA PAPER 72-1024]

21 p2993 A72-41602

Wall porosity and angle of attack effects on jet stretcher flow field for supersonic engine inlet testing, using three dimensional method of characteristics

[AIAA PAPER 72-1025]

21 p3042 A72-41603

Full-scale inlet/engine testing at high maneuvering angles at transonic velocities.

[AIAA PAPER 72-1026]

21 p3042 A72-41604

Experimental determination of asymmetry-induced trim angles of attack.

[AIAA PAPER 72-1032]

21 p2993 A72-41605

Finned missiles nonlinear rolling motion characteristics at large angles of attack, solving differential equation of motion by global nonlinear least squares method

[AIAA PAPER 72-980]

22 p3134 A72-42333

Supersonic flow past a suddenly set plate

22 p3136 A72-42906

Three dimensional supersonic flow past bodies with a smooth generatrix

23 p3248 A72-43651

Experiment of supersonic air intake buzz.

23 p3249 A72-44496

Occurrence and inhibition of large yawing moments during high-incidence flight of slender missile configurations.

[AIAA PAPER 72-968]

24 p3364 A72-45411

Lifting entry optimization equations for fixed angle of attack with path control for roll modulation of lift, considering space shuttle orbiter configuration

[AIAA PAPER 72-933]

24 p3443 A72-45435

ANGLES (GEOMETRY)

NT ANGLE OF ATTACK

NT BRAGG ANGLE

NT BREWSTER ANGLE

NT DIHEDRAL ANGLE

NT ELEVATION ANGLE

Long base radio interferometry at centimeter wavelength for angular measurement accuracy improvement in astronomy and geophysics

04 p0495 A72-15728

Photoelectric transducer with electric pulses as measure of rotating disk angle of turn, discussing design and measurement accuracy

05 p0662 A72-16124

Satellite angular coordinates determination by laser ranging from single station, using echo recording by Schmidt telescope

07 p0947 A72-20255

Aerial photographs inclination angles determination from stereocomparator measurements and terrain angles interrelationship

08 p1165 A72-21162

Formulas to evaluate differences in angles formed by coordinate systems of two star catalogs

09 p1388 A72-23053

Visual and haptic perception in angle reproduction matching task, noting performance differences relation to nature of form discrimination and task

10 p1433 A72-25126

Spacecraft orientation angle measurement by inertial sensors, analyzing equipment kinematic efficiency and limitations

11 p1684 A72-26913

Slope angle determination with respect to photograph surface from visible horizon line configuration

15 p2238 A72-32123

Angular measurement error for group and repetition techniques as function of observation time, deriving formulas for comparison in terms of economy and efficiency

16 p2389 A72-33030

Aerial photographs inclination angles determination from stereocomparator measurements and terrain angles interrelationship

17 p2552 A72-34453

ANGULAR ACCELERATION

Alcohol ingestion effects on tracking performance during angular acceleration, observing nystagmic eye movements and eye-hand coordination

04 p0477 A72-14474

Mathematical model for semicircular canal dynamic response to angular acceleration, emphasizing role of perilymph over endolymph in cupula displacement

07 p0917 A72-19491

Dog thyroid gland structural changes under repeated radial acceleration, noting atrophic process and autonomous reactions roles

13 p1905 A72-29334

Alcohol ingestion effect on vestibular responses to angular acceleration and Coriolis stimulation, discussing nystagmus and subjective responses

14 p2082 A72-31090

Airline pilot rotation perception during angular acceleration tests, noting power law description of subjective motion for three major body axes

16 p2358 A72-33649

Note on displacements in accelerating disks of variable thickness.

20 p2980 A72-39690

Flow analysis in the axial-flow compressor impeller with meridional stream acceleration.

24 p3394 A72-45371

ANGULAR CORRELATION

Action kinetics and radiation spectra of multiruby lasers, determining effect of crystal C axes angular orientation relative to ruby pairs geometrical axes

01 p0079 A72-10374

Correlation functions for angular vibrations of operating aerial camera during working cycle

09 p1310 A72-22947

Frequency and angular correlation function relationship for signal scattering cross section of extensive bodies

10 p1436 A72-24586

- Adiabatic effect of slow rotational molecular diffusion on perturbed angular correlations of gamma radiation for radioactive studies in viscous media 13 p2008 A72-29863
- Effect of voids on angular correlation of positron annihilation photons in molybdenum. 22 p3187 A72-41967
- Gamma-neutrino angular correlations in muon capture. 24 p3427 A72-45774
- ## ANGULAR DISTRIBUTION
- Solar X rays angular distribution during solar flares, considering anisotropy connection with short wave fadeouts correlation with H alpha flares and X ray bursts center-to-limb variation 01 p0118 A72-10420
- Limited scan microwave antenna design, discussing angular coverage, feed motion and focal field distribution 01 p0039 A72-10670
- Parallel electric field evidence near auroral ionosphere deduced from low energy particles, energy spectra and angular distribution 01 p0061 A72-10895
- Solid state laser emission angular divergence, considering active medium optical inhomogeneity and cavity parameters effects 01 p0081 A72-10976
- Solar wind electron density variations, discussing radio source interplanetary scintillation and angular distribution measurements at various distances from sun 02 p0277 A72-11902
- Angular straying of gravity center over cross section of diverging light beam in turbulent atmosphere 02 p0181 A72-12594
- Angular dependence of radiation emitted by earth-atmosphere system and reflected by space, noting application to radiation balance mean value computation 02 p0255 A72-12790
- Cosmic ray neutrons angular distribution and energy spectrum at 3200 m altitude, using ionization calorimeter and proportional counters 02 p0275 A72-12828
- Short wavelength continuous solar X-radiation polarization and angular distribution measurements, revealing physical processes in solar flares 03 p0409 A72-13126
- High energy cosmic ray track angular azimuthal distribution in lunar silicate rocks 04 p0577 A72-15154
- Gravitational radiation detector angular dependence, obtaining directivity pattern 05 p0656 A72-16184
- Atmospheric short wave radiation angular and vertical distribution relation to aerosol scattering parameters, using transport equation 05 p0658 A72-16291
- Anisotropic angular distribution of solar flare associated hard X-rays 05 p0709 A72-16519
- Scaling hypothesis testing by angular distributions from cosmic ray experiments 05 p0711 A72-17125
- Secondary cosmic ray shower charged particles angular distribution asymmetry in C-system and azimuthal plane related to single fireball formation 06 p0868 A72-17263
- High energy muon energy and angular distributions from electron-photon cascades, using emulsion chamber with X ray films 06 p0871 A72-17286
- Radiation intensity angular distribution from optically thick plane cloud layer reflection, relating photon survival probability and scattering functions 06 p0807 A72-17939
- Solar radiation angular field structure from upper atmospheric boundary scattering, taking into account underlying surface albedo fluctuations 06 p0807 A72-17942
- Interplanetary scintillation and angular dimensions of radio sources at 81.5 MHz, using diffraction theory 06 p0889 A72-18327
- Crystallographic texture of Mo sheet, analyzing angular dependence of Young modulus 06 p0832 A72-18366
- Cosmic ray muons integral energy spectrum and angular distribution at sea level represented by power law, using primary interaction model 07 p1063 A72-20475
- Computerized numerical calculation of muons production spectrum, angular distribution and Coulomb scattering in determining meteorological factors effects on cosmic rays 07 p1067 A72-20655
- High energy charged particles angular distribution measurements in equatorial region cosmic radiation above atmosphere by Proton 2 satellite 08 p1226 A72-20799
- Energy and angular distributions of electrons released during ion atom collisions from energy spectra studies, discussing autoionization transitions 08 p1210 A72-20836
- Angular distributions of proton polarization during elastic scattering by V, Cr, Ni and Co nuclei in high energy region 08 p1211 A72-21093
- Fourier transform and angular distribution of light diffusion by plasma with strong correlations 10 p1519 A72-24129
- Amplitude comparison direction finding systems, calculating error due to clutter from incident signal and noise angular distribution relationship to measured arrival angle 10 p1439 A72-24803
- Earth albedo neutrons energy and angular distributions, suggesting neutron source of inner radiation belt trapped protons 11 p1712 A72-25880
- Angular distribution of electrons at output of specimen observed by electron microscope, examining resolution problem for thin objects 11 p1635 A72-26483
- Circularly polarized ultrashort radio wave reflection from lunar and planetary surfaces, determining angular scattering spectrum 11 p1599 A72-26908
- Angular annihilation photon distribution curves from positron-electron annihilation method for metallic phase interaction with crystal lattice in synthetic diamonds 12 p1833 A72-27764
- Electron impact excitation spectrum of molecular oxygen, investigating angular behavior of differential scattering cross sections and energy dissipation 12 p1848 A72-27851
- Angular spectrum of second harmonic generation during two frequency interactions in KDP laser 13 p1969 A72-29524
- Directional dependence of sound wave emission by convective turbulence in solar atmosphere, considering cut-off frequency effects on transmitted acoustic spectrum 13 p2048 A72-29926
- Gas dynamics of steady rotating azimuthally dependent solar wind under magnetic field influence, calculating azimuthal distribution of radial velocity near earth orbit 13 p2034 A72-29960
- Angular distribution of first Stokes component for stimulated combinational scattering investigated under various excitation conditions 13 p1972 A72-29982
- Energetic particle flux observation at very low altitudes near geomagnetic equator, noting narrow distribution around 90-deg pitch angle 13 p2034 A72-30122
- Plasma radiation from collisionless MHD shock waves, discussing waves generation and angular distribution 14 p2138 A72-30555
- Energy and angular distribution of hydrogen and rare gas ions backscattered from polycrystalline metal surfaces 15 p2276 A72-31852
- Beam divergence prediction for multiple transverse laser modes, proposing tables and graphs to determine angular spread in far field 15 p2247 A72-32031
- Angular distribution and intensity of light scattered by carbon dioxide near critical point, noting temperature dependence of isothermal compressibility and long range correlation length 16 p2422 A72-32945
- Numerically computed momentum and energy accommodation coefficients and angular distributions of gas molecules reflected from solid crystalline surfaces applied to satellite drag calculation 16 p2430 A72-33065
- Radiation intensity angular distribution from optically thick plane cloud layer reflection, relating photon survival probability and scattering functions 16 p2426 A72-33780
- Solar radiation angular field structure from upper atmospheric boundary scattering, taking into account underlying surface albedo fluctuations 16 p2386 A72-33783
- Bidirectional optical scattering from dielectric materials of various pigmentation and surface roughnesses, obtaining cross section data to determine angular, spectral and polarization behavior 16 p2427 A72-33839
- Upper limit of the mean interaction path of cosmic protons generating extensive air showers 17 p2598 A72-34287
- Electrons angular distribution effect on photoionization branching ratio measurement by photoelectron spectroscopy 17 p2552 A72-34288
- Scintillation telescopes for muon angular distribution, designing test device for photomultiplier tubes selection 17 p2556 A72-35437
- Book - Angular scattering functions for spheroids 17 p2582 A72-35457
- Synchrotron radiation-like angular distribution of gravitational synchrotron radiation produced by ultrarelativistic geodesic particle orbits in Schwarzschild geometry 17 p2583 A72-35820
- A method of calculating the pitch angle distributions of particle fluxes based on rocket and satellite data. 17 p2558 A72-35840
- A spheric rate azimuth-profile of the 1955 Blackwell, Oklahoma, tornado. 18 p2706 A72-36639
- Vibrational excitation in N2 by electron impact in the 15-35-eV region. 19 p2837 A72-37546
- Observations of the solar wind with the European satellite Heos-1 19 p2850 A72-37785
- Determination of the angular divergence of laser radiation by a transforming system of prisms. 20 p2933 A72-39523
- Angular distribution of electrons elastically scattered from N2. 21 p3088 A72-40777
- Energy and angular distributions of secondary electrons resulting from ionizing collisions of electrons with helium and krypton. 21 p3088 A72-41493
- Effects of thermo-optical distortion on the radiation loss magnitude and spatial-angular radiation characteristics for a lamp-pumped rhodamine-6G laser 22 p3185 A72-42173
- Radiogoniometer error analysis for receiver internal noise and external interference sources, noting sources angular distribution effect on instrument error 22 p3158 A72-42233
- Pair-correlation and angular distribution functions calculations for one and two dimensional amorphous structures 22 p3197 A72-42797
- Angular distribution of interstellar atomic hydrogen. 23 p3315 A72-43834
- Galaxies and galactic cluster distance determination from Palomar chart angular diameters related to Holmberg-Vaucouleurs photometric systems 23 p3338 A72-44034
- Angular distribution of electrons autodetached from H- in slow collisions with He. 23 p3316 A72-44074
- Investigation of the angular distribution of particles on the basis of Cosmos-219 satellite data 23 p3343 A72-44174
- Angular distribution of extensive air showers in a range of large zenith angles 23 p3330 A72-44421
- Energy spectrum and angular distribution of cascades with an energy greater than 0.3 TeV, formed by cosmic muons 23 p3331 A72-44427
- Energy spectra and angular distributions of cosmic ray muons with an energy of 2 to 10 TeV 23 p3331 A72-44428
- Behavior of the spatial distribution function of shower particles near the axis of a cascade shower 23 p3331 A72-44432
- Angular distribution of high-energy cosmic-ray muons 23 p3331 A72-44434
- Study of the angular distribution of charged and neutral pions during inelastic interactions in the energy region above 1 TeV 23 p3291 A72-44443
- Angular and impulse characteristics of negative-pion interactions at an energy of 60 GeV in the emulsion 23 p3292 A72-44446
- Detection of earthward flow of keV protons in the geomagnetic tail at lunar distances. 23 p3333 A72-44532
- Crystallographic texture of sheet Mo alloys, analyzing angular dependence of Young modulus 24 p3416 A72-45752
- ## ANGULAR MOMENTUM
- Limited three body problem applied to planetary angular momentum increment due to accretion of particles in heliocentric orbits, discussing planet rotation laws 02 p0282 A72-12330
- Angular momentum conservation law compliance of generalized triple configuration model for spin-detonation nucleus, assuming transverse Chapman-Jouguet wave 03 p0342 A72-13734
- Global angular momentum balance, considering atmospheric frictional torques and fluxes, ocean wave mass exchanges and seasonal variations effects 03 p0384 A72-14142
- Cyg X-1 type X ray sources evolution, discussing white dwarf and supernovae stages, parent mass and angular momentum 04 p0568 A72-15508
- Angular momentum and Li diffusive transport induced by mild thermally driven turbulence associated with Goldreich-Schubert-Fricke instability, discussing solar rotation slowdown 05 p0720 A72-16718

ANGULAR MOTION

- Inelastic nuclear interactions between 200-GeV cosmic ray particles and polyethylene targets, correlating similarity property, angular momentum spectra and secondary particle pairs 06 p0868 A72-17258
- Fourth algebraic integral in Kovalevskaya solution of rotating body motion about fixed point regarding angular momentum components 08 p1208 A72-21357
- Gravitational field angular momentum transfer analogy with Einstein gravitational energy transfer in general relativity 10 p1511 A72-24246
- LF radiation effect on angular momentum distribution of interstellar grains with permanent dipole moments 10 p1541 A72-24473
- Post-Newtonian approximation for calculation of energy and angular momentum radiated in form of gravitational waves by two point particles system, noting masses in hyperbolic Kepler orbit 10 p1547 A72-24933
- Orbital eccentricity and angular momentum management scheme stability for satellite large attitude maneuver followed by trim maneuver sequence 11 p1719 A72-25978
- Internal gravity waves effects on energy budgets and vertical angular momentum transport over mountainous terrain in southwestern U.S. from handheld camera pictures on Apollo 9 11 p1682 A72-26472
- Jupiter, Saturn, Uranus, Neptune and Pluto state of knowledge, noting angular momentum fraction, red spot, albedos, densities, atmospheric compositions, natural satellites, etc 12 p1870 A72-27345
- Thin lubricant film angular inertia effect on externally pressurized MGD bearings load carrying capacity, solving nonlinear differential equation by Runge-Kutta method 13 p1963 A72-28747
- Limited three body problem applied to planetary angular momentum increment due to accretion of particles in heliocentric orbits, discussing planet rotation laws 13 p2039 A72-29214
- Latitude dependent time variations of solar differential rotation and global activity distribution asymmetry, assuming large scale convection due to angular momentum transport 13 p2046 A72-29730
- Stability analysis of gyrostal satellites possible equilibria under gravitational torques, considering inertia, equilibrium and angular momentum parameters 15 p2321 A72-32586
- Stellar and planetary atmosphere dynamics, deriving balance equations for variance analysis of angular momentum 16 p2453 A72-33247
- Spiral structure generation by outward angular momentum transfer, considering gravitational stress tensor, star-spiral wave momentum transfer and galactic secular evolution 16 p2457 A72-33683
- Model stability of globular star cluster with nonzero angular momentum, discussing gravitational effects 17 p2606 A72-34658
- The evolution of the solar inner rotation by the Eddington-Sweet type circulation under the influence of the solar wind torque 17 p2613 A72-35497
- Quantum fields interaction with classical sources on Schwarzschild background, noting mass, charge and angular momentum as sole measurable quantum numbers of black hole 18 p2726 A72-36716
- Einstein relativity principle incompatibility with conservation of angular momentum, discussing invariance of inertia reference systems and formulas for relative and absolute velocities 19 p2834 A72-37921
- Mathematical model of ideal incompressible gyroscopic fluid with internal angular momentum using kinematic equations 19 p2835 A72-37929
- Role of the swarm of satellite-particles on the origin of the earth's rotation 22 p3220 A72-41916
- Angular momentum conservation laws formulation for Einstein field equations solution in general relativity, applying to Kerr metric 24 p3425 A72-44787
- ANGULAR MOTION**
- U ANGULAR VELOCITY**
- ANGULAR RESOLUTION**
- Balloon-borne galactic X ray detection unit, obtaining high directivity with honeycomb collimator and angular resolution with solar sensor 03 p0353 A72-13043
- Angular coordinates and slope determination from monopulse radar measurements of two unresolved targets 05 p0629 A72-16578

- Radio sources and quasar structure angular resolution determination with distant radio telescope interferometry and microwave relay links 06 p0886 A72-18177
- Radio waves arrival angles distribution function in Fraunhofer diffraction zone upon plane wave normal incidence on inhomogeneous scattering layer 07 p0938 A72-19017
- Cer-Vit glass mirror replacement for AFCRL lunar laser observatory inverted Dall-Kirkham Cassegrain telescope, noting one arc sec resolution from wire and null optics tests 07 p0985 A72-19410
- Fluidic wind sensor measurements from low threshold to high velocities, noting wind angle resolution from output differential pressure signal 10 p1484 A72-25083
- Target angular position measurement by surveillance radar on background of correlated interference 11 p1595 A72-26296
- Solar radial brightness distribution, using mm observations during 7 March 1970 solar eclipse for improved angular resolution 13 p2042 A72-29531
- Roll angle detector for angular position measurement of two independent bodies, using optical-mechanical-electrical system 15 p2268 A72-32043
- Directivity pattern accuracy effects on angular coordinate determination by scanning active optical radars 16 p2362 A72-33188
- Three axis angular deviations measurement by flexible monitor system for spacecraft, using pulsed light sources, autocollimator and porro reflectors [AIAA PAPER 72-855] 20 p2951 A72-39106
- A variable spacing modulation collimator for X-ray astronomy 20 p2928 A72-39891
- Observations of sources of maser radio emission with an angular resolution of 0.0002 sec 21 p101 A72-41751
- Solar atmosphere fine structure observation limitations in terms of solar telescope angular resolution 24 p3404 A72-45529
- Orbiting telescopes improved angular resolution and access to UV spectra as advantages in determining stellar composition, mass, luminosity and distance 24 p3446 A72-45531
- ANGULAR VELOCITY**
- Fluidic device for measuring angular velocities based on pressure output proportional to shaft revolutions per unit time, discussing equivalent circuit 01 p0064 A72-10171
- Equilibrium rotating superdense baryons in general relativity theory, determining integral parameters /mass semiaxes quadrupole moment/ in angular velocity approximation 03 p0435 A72-13805
- Angular and linear velocities of plasmoid in coaxial accelerator under axisymmetric magnetic field 03 p0398 A72-14002
- Stratified fluid motion between two parallel infinite disks rotating with different angular velocities 04 p0511 A72-14857
- Display device for engine rotational speed nonuniformity parameters indication on oscilloscope without supplementary computation 05 p0662 A72-16125
- Planetary wave spectrum calculation by Galerkin method, discussing angular velocity of longest Rossby waves distortable by zonal flow 05 p0655 A72-16170
- Steady state angular motion stability of passive magnetically stabilized satellites, using Liapunov method 05 p0726 A72-16464
- Spacecraft banking control during reentry, deriving dynamic equations of angular motion 05 p0730 A72-17026
- Angular position of sun disoriented artificial earth satellites with angular velocities not exceeding 0.5 deg/sec, using harmonic analysis of magnetometric data 05 p0631 A72-17033
- Stationary stars rigid and differential rotation angular velocity limits, showing analogous conditions in general relativity 06 p0882 A72-18001
- Angular velocity vector active damping during spin-up of electrically supported gyro with mass-unbalance readout, using Euler equations of motion 07 p0986 A72-19691
- Rotating disk background and speed effects on perception of verticity motion in clockwise or counterclockwise direction 08 p1124 A72-20987
- Moment of forces on spacecraft with low angular velocities in variable magnetic field, using electrodynamics equations 08 p1240 A72-21140
- White dwarf's rotation parameters relation to angular velocity within general relativity compared to analogous calculations in Newtonian theory 08 p1234 A72-21284

- Kharlamov kinematic equations application to gyrostal motion problem, deriving angular velocity hodograph 08 p1207 A72-21350
- Solid body motion about fixed point, determining moving and fixed angular velocity hodographs 08 p1208 A72-21351
- Moving hodograph of angular velocity vector in solution to problem of body motion about fixed point 08 p1208 A72-21354
- Solid body motion with fixed point in central Newtonian force field, classifying angular velocity vector hodograph as function of dimensionless parameters 08 p1208 A72-21363
- Moving and inertial trihedron orientation determination from absolute angular velocity vector, solving Poisson equations system 08 p1205 A72-21802
- German monograph on optimal guidance of spin stabilized space bodies for combined attitude and angular velocity control and time optimal nutation damping 08 p1241 A72-21847
- Twin spool jet engine system, predicting shaft speed effects on whirling frequencies due to gyroscopic action with computer model 08 p1224 A72-22130
- Flight vehicle angular velocity measurement by accelerometers, deriving equations of motion 10 p1481 A72-24497
- Short period terms in earth rotation rate and polar motion, considering data truncation effects on periodograms 10 p1475 A72-24872
- Relativistic counterpart of Poincare condition for angular velocity of rigidly rotating star, discussing equilibrium disturbance effects 10 p1549 A72-25058
- Cosmic spherical rotating bodies angular velocity zonal distribution determination, noting application to Jupiter and Saturn 11 p1723 A72-26481
- Spacecraft motion stabilization about mass center and optimal angular velocity control using minimax technique 11 p1684 A72-26903
- Turboprop engines dynamic parameters experimental determination by rpm transient response to instantaneous fuel supply changes 13 p2027 A72-29137
- Solid state stepping motor drive controller to provide constant angular shaft velocity for scanner applications 13 p1933 A72-29767
- High resolution angular velocity measurement by high speed digital transducer feeding photosensor pick-up pulses into pulse shaping circuit 14 p2103 A72-30199
- Sub-Mercurial planet Vulcan observation data, calculating orbital elements, angular size and velocity radial distance and object diameter 14 p2149 A72-30234
- Permanent rotation of force-free gyroscope characterized by outer framework constant angular velocity, defining permanent axes of rotation 15 p2275 A72-31493
- Time dependent orthogonal coordinate system rotation by unit vector along effective axis, obtaining angular velocity and effective angle interpretation 15 p2275 A72-31590
- Turbulent diffusion limiting flux variation with angular rotation velocity of rough rotating disk 15 p2217 A72-31676
- Best fitting triaxial ellipsoid representation of seleno-equipotential surface at Apollo 12 landing site based on observed local gravity and moon angular velocity 15 p2308 A72-31922
- Moon radius from Lunar Orbiter 1 angular velocity data obtained from camera image motion compensator sensor /V/H sensor/ 17 p2603 A72-34207
- Simple Doppler radar using the CL8630 Gunn effect oscillator for the observation of small rotating objects 17 p2524 A72-34245
- On the dependence of the linear velocity of solar rotation on latitude and optical depth 17 p2607 A72-35076
- Saturn rotation period latitudinal difference, presenting graphic plots derived from various visual observations 17 p2619 A72-35958
- Using ring lasers as rate sensors 19 p2812 A72-38223
- High angular velocity device design problems, considering gyroscopes, ultracentrifuges, yarn-spinning textile machinery and dental drill 19 p2809 A72-38544
- Linear and rotational quartz fiber accelerometers suitable for geophysical and inertial use. [AIAA PAPER 72-822] 20 p2923 A72-39103
- Moment of forces on spacecraft with low angular velocities in variable magnetic field, using electrodynamics equations 20 p2976 A72-39245

Proportional control of space vehicles with the aid of auxiliary jet engines
20 p2977 A72-39593

Bi-planar wind tunnel free flight test and instrumentation for difference between nonplanar and planar dynamic stability of blunt and sharp half cones, providing angular documentation
[AIAA PAPER 72-983] 22 p3163 A72-42331

Generalized subharmonic response of a missile with slight configurational asymmetries.
[AIAA PAPER 72-972] 22 p3134 A72-42339

The bursting speed of a symmetrical conical disk with radial holes.
22 p3238 A72-42835

The role of eruptive centers of the atmosphere of Jupiter in the determination of the rotation velocity of the core
23 p3336 A72-43548

Influence of revolutions on efficiency and characteristics of the rotating axial cascade of blades.
24 p3363 A72-45361

ANHYDRIDES
NT PEROXIDES
Alcyclic dicarboxylic anhydride structure effects on cured epoxidized novalac resin physical and chemical properties
08 p1193 A72-21695

Antiwear properties of mixed anhydrides of alkyl xanthogene and phosphorus containing acids for use as oil lubricant additives
09 p1336 A72-22499

Model reactions between phthalic anhydride and o-phenylenediamine under polymerization-analogous conditions for polyimidazopyrrolone formation
19 p2762 A72-37647

ANILINE
Starvation effects on male rats, mice and guinea pigs hepatic drug metabolism, discussing ethylmorphine, p-nitroanisole and aniline
01 p0015 A72-11262

Reactions of aniline with isoamyl nitrite and phenyldiazonium borofluoride with caustic potash, investigating kinetics of chemical polarization of products nuclei
09 p1275 A72-22497

ANIMALS
NT AMOEBA
NT BATS
NT BIRDS
NT CATS
NT CHIMPANZEES
NT COLEOPTERA
NT DROSOPHILA
NT FISHES
NT FLAGELLATA
NT FROGS
NT GROUND SQUIRRELS
NT HOMEOTHERMS
NT HUMAN BEINGS
NT INSECTS
NT MAMMALS
NT MICE
NT MOLLUSKS
NT MONKEYS
NT PIGEONS
NT PRIMATES
NT PROTOZOA
NT PUPA
NT RABBITS
NT SNAKES
NT SPORES
NT SWINE
NT VERTEBRATES
NT WORMS

Telemetric instrumentation for remote physiological and behavioral observations of free roaming animals
07 p0930 A72-19912

Animal response to sonic booms, considering mink reactions in detail
08 p1119 A72-21909

Biological experiments on plants, animals and bacteria aboard Zond 5, 6 and 7 space probes, noting flight conditions effect on physiological functions and hereditary structures
11 p1579 A72-25941

ANIONS
Equilibrium concentrations of negative ions in nighttime D region, comparing computations to mass spectrometric measurements
01 p0063 A72-10917

D region positive and negative ion chemistry review, noting dominant roles of water ion clusters, NO cation and hydrates
02 p0219 A72-11979

Anion sorption mechanisms and product composition in anodic aluminum oxide filled with phosphate, chromate and sulfate solutions, discussing chemisorptive compound formation and oxide dehydration
05 p0624 A72-17053

Single collision beam experiments, swarms, Townsend current and capture processes in negative ions
05 p0693 A72-17219

Temperature effects on anodic polarization of Ti open surface and corrosion crevices, discussing critical potential relation to pitting
06 p0829 A72-17946

Tungsten and rhenium oxides negative ions source, presenting mass analysis table
07 p1037 A72-19323

D region negative ion reaction schemes, discussing reaction rates of nitrogen dioxide with hydrogen
09 p1275 A72-22592

Charged particles effect on plasma negative ions, examining Stark effect in energy level
11 p1693 A72-25714

Diatomic carbon negative ion search in HD 201626 and solar spectra, noting rotational lines coincidence with absorption features
13 p2038 A72-29010

Negative ions and collision frequency effects on circularly polarized ELF and VLF wave propagation in ionosphere
14 p2084 A72-30128

Energy curves of negative carbon dioxide ion as function of bending angle
14 p2134 A72-30749

Target anion effect on radioactive Sb and Te distribution formed by high energy proton irradiation of cesium salts containing oxygen
15 p2282 A72-32485

Recombination of protons and negative hydrogen ions in slow collisions.
18 p2713 A72-36953

Ion mobilities and ion-molecule reaction rates in oxygen.
19 p2836 A72-37457

Experimental technique for oxygen negative ions destruction by associative detachment reaction with hydrogen in oxygen-hydrogen mixtures, calculating transport and ionization coefficients
19 p2836 A72-37458

Electronic and nuclear magnetic resonances of the oxygen and hydrogen labile negative molecular ions.
20 p2956 A72-39189

Uranyl fluoride crystals luminescence spectrum study, calculating anion normal vibration frequencies
20 p2960 A72-39413

Electron attachment and compound formation in flames. V - Negative ion formation in flames containing chromium and potassium.
22 p3244 A72-42717

Crossover frequencies in multicomponent plasmas with negative ions.
23 p3323 A72-44525

Circularly polarized waves in magnetoplasmas containing negative ions.
23 p3323 A72-44533

ANISOLE
Starvation effects on male rats, mice and guinea pigs hepatic drug metabolism, discussing ethylmorphine, p-nitroanisole and aniline
01 p0015 A72-11262

ANISOTROPIC FLUIDS
Stratified anisotropic multifluid plasma wave propagation from transverse field equations, using Green function and Fourier transform method
06 p0773 A72-17597

Homogeneous turbulence with rotatory anisotropy, determining alternating tensor with moment equations
06 p0800 A72-17988

Anisotropic conducting fluid flow in presence of traveling magnetic field, determining Hall effect via solution to electromagnetic field distribution boundary value problem
08 p1214 A72-21648

Compressible anisotropic magnetoplasma filled cylindrical waveguide excitation by electric dipole, plotting electric field patterns as function of electron temperature and density
12 p1782 A72-27489

Homogeneous turbulence with rotatory anisotropy, determining alternating tensor with moment equations
14 p2093 A72-30214

ANISOTROPIC MEDIA
NT ANISOTROPIC FLUIDS
Plane and spherical geometry anisotropic plasma jet stability, considering uniform velocity streaming immersed in magnetic field surrounded by nonconducting medium
01 p0106 A72-10131

Oblique electromagnetic wave propagation modes in anisotropic ionized stratified medium, investigating electric field and polarization components
01 p0106 A72-10133

Hydroxyapatite isotropic and anisotropic elastic properties compared with experimentally observed anisotropic behavior of bone
01 p0018 A72-10625

Three dimensional problems in stability, elasticity and plasticity theory for isotropic, anisotropic and inhomogeneous bodies, noting applications to machine construction, civil engineering, geophysics, etc
02 p0288 A72-11602

Al alloys compressed strips, determining anisotropy of toughness and crack sensitivity by tests
02 p0244 A72-12244

Anisotropic and compressible work hardening materials three dimensional elastoplastic flow quasi-linear theory, deriving boundary integral equations
02 p0296 A72-12530

Nonstationary radiation transfer with one dimensional anisotropic scattering, deriving Bessel function expressions for quantum exit from semiinfinite medium
02 p0262 A72-12830

Plasma beam production with Penning type discharge, demonstrating anisotropic electron temperature
03 p0395 A72-13566

Fracture mechanics of interfacial cracks between two bonded dissimilar anisotropic elastic half spaces, presenting two dimensional analysis of stress fields
03 p0446 A72-13707

Electric field effects on electromagnetic wave packet motion in anisotropic nonlinear medium with electro-optical effect
03 p0322 A72-13737

Plastic torsion of prismatic and anisotropic rods, emphasizing inhomogeneity problems numerical solution
03 p0447 A72-13853

Immersion-type electroconductivity probe for anisotropic plasmas, calculating Hall coefficient
03 p0397 A72-13922

Anisotropic media elastoplastic behavior, developing plastic deformation theory from stress-strain relationships for linearly elastic media
03 p0454 A72-14216

Reciprocity relations for electromagnetic waves scattered by isolated, stratified and composite anisotropic obstacles
04 p0547 A72-14535

Cylindrical grid-like antenna in anisotropic compressible homogeneous plasma, obtaining magnetic field effects on wave dispersion by numerical solution
04 p0488 A72-15306

Plane harmonic electromagnetic wave diffraction by conducting parallel half planes in uniaxially anisotropic media
04 p0492 A72-15447

Distortional energy theory for predicting failure of orthotropic materials exposed to three dimensional stress state
05 p0732 A72-15942

Elastic stress field in hollow circular cylindrically anisotropic body under surface tractions expressed as Fourier series
[ASME PAPER 71-WA/APM-13] 05 p0734 A72-15967

Bimetallic rectangular plate with two interconnected layers of anisotropic and isotropic materials and large deflections in nonuniform pressure and temperature field
05 p0735 A72-16016

Anisotropic plasma rotational discontinuity theory, considering parallel and perpendicular components of plasma pressure and magnetic induction
05 p0695 A72-16074

Electromagnetic wave transmission and reflection by semiinfinite moving anisotropic plasma with parallel static magnetic field, considering incident H wave
05 p0696 A72-16623

Anisotropic plasma stability to magnetosonic wave near ion cyclotron frequency propagating almost perpendicular to magnetic field
05 p0698 A72-17017

Dispersion relations for frequencies near first two harmonics of perpendicular magnetosonic waves in relativistic anisotropic plasmas
05 p0698 A72-17020

Age hardened Al-Cu single crystal anisotropy from stress-strain curves, using plane strain compression tests
[AD-743502] 05 p0677 A72-17106

Conversion effectiveness of oscillations induced by electron beam in bounded anisotropic plasma into electromagnetic emission
06 p0860 A72-17700

Isotropic and anisotropic materials strength criteria and boundary surfaces in invariant stress tensor spaces
06 p0898 A72-18553

Aging creep theory application to anisotropic strain hardenable metals
06 p0900 A72-18680

Electrostatic wave instabilities at harmonics of electron cyclotron frequency in hot and cold anisotropic plasma with Maxwellian temperature distribution
07 p1039 A72-18824

Nonlinear monochromatic Alfvén wave propagation parallel to magnetic field in anisotropic plasma with long wavelength beam instability
07 p1039 A72-18915

Wave propagation in thin film optical waveguides with gyrotropic and anisotropic substrates, deriving TE and TM mode conversion conditions
[AD-739120] 07 p0940 A72-19230

Optical resonators using lossy anisotropic metal film linear polarizer for oscillation mode selection
[C.I.E.A PAPER 6,3] 07 p1004 A72-19382

Transverse electromagnetic instabilities in anisotropic plasmas, confirming by computer simulation energy constants derived from nonlinear Vlasov-Maxwell equations

07 p1041 A72-19509

Material anisotropy effect on stress-strain state and limiting load in plane plastic deformation

07 p1091 A72-19764

Anisotropic grounded dielectric or plasma layer motion effects on magnetic or electric current line source radiation patterns

07 p0946 A72-19802

Transverse anisotropy effect on collapse loads of plastic rotating disks and circular plates

07 p1093 A72-19946

Multiplication and mixing of electromagnetic waves in optically nonlinear anisotropic crystal media

07 p1007 A72-20119

Anisotropic equilibrium solution to Vlasov equation for high beta theta pinch plasma column

07 p1045 A72-20478

Refraction of electromagnetic wave with electric field perpendicular to applied magnetic field in anisotropic plasma cylinder cross section

07 p1046 A72-20507

Mellin transforms application to two dimensional elasticity problem for anisotropic wedge with continuous mechanical characteristics under concentrated force

08 p1243 A72-21238

Optimal design of anisotropic composite material annular plates by numerical method

08 p1246 A72-21673

Elastic stability of nonlinearly elastic anisotropic body analyzed via variational principles in three dimensional theory

08 p1246 A72-21707

Polarization corrections for normal electromagnetic waves passing from homogeneous to nonhomogeneous anisotropic medium

08 p1135 A72-21735

Anisotropy and nonuniformity of bonded glass mat thermoelectric properties, investigating thermal buckling origin

09 p1337 A72-22703

Dielectric tensor for electromagnetic waves in weakly inhomogeneous anisotropic media, taking into account permittivity and conductivity fluctuations

09 p1280 A72-23230

Nonlinear dispersive medium characteristics determination from higher harmonic oscillations and beats analysis based on traveling waves concept

09 p1353 A72-23486

Orthogonality conditions for VLF height gains in vertically inhomogeneous anisotropic earth ionosphere waveguide

09 p1282 A72-23517

Background medium anisotropy effect on electromagnetic waves scattering from ionospheric irregularities, calculating scattered power by Green function

09 p1282 A72-23519

Current-optical effects of anisotropic absorption of polarized and unpolarized light in rarefied cosmic media

10 p1525 A72-23763

Light polarization in anisotropic Zeeman laser under axial magnetic field

10 p1491 A72-24134

Quenched specimen anisotropic surface heating effect in liquid vaporization characteristics determination

10 p1561 A72-24207

Linear anisotropic composites with periodic spatial structure, determining elastic moduli and electrical conductivity variational bounds

10 p1556 A72-24346

Polarization characteristics and losses of anisotropic laser resonators composed of arbitrary number of mirrors

10 p1492 A72-24364

Photoelastic analysis of piezooptical and rheological properties of anisotropic composite glass plastics

10 p1557 A72-24626

Classical boundary value problems in theory of thermal stresses in piecewise continuous anisotropic elastic bodies under coupling conditions

10 p1563 A72-24994

Empirical multiaxial strength criteria for anisotropic composite materials

11 p1731 A72-25455

Fracture toughness of anisotropic heterogeneous filamentary boron/aluminum composites, correlating test results with acoustic emissions from filament breakage

11 p1672 A72-25470

Linear antenna in anisotropic plasma with ion depletion, calculating reactance change due to surrounding dielectric layer thickness

11 p1593 A72-25949

Fracture toughness anisotropy and crack sensitivity of Al alloys extruded bars notched cylindrical samples

11 p1659 A72-26130

Temperature anisotropy quasi-linear relaxation thermodynamics in collisionless plasma, analyzing system free energy

11 p1698 A72-26599

Plasma beam production with Penning type discharge, demonstrating anisotropic electron temperature

11 p1699 A72-26753

Radiation propagation in optically thin anisotropic noncrystalline media, obtaining explicit formulas for Stokes parameters of transmitted and scattered radiation

12 p1865 A72-27052

Three dimensional nonlinearly elastic anisotropic body with arbitrary elastic potential examined for large initial deformations, considering stress-strain state

12 p1877 A72-27077

Rolled polycrystalline metal samples principal anisotropy direction determination by acoustic measurements at ultrasonic frequencies

12 p1806 A72-27086

Perturbation theory for electromagnetic radiation in weakly anisotropic magnetoplasma, calculating Green function for delta function source oriented parallel to static magnetic field

12 p1783 A72-27668

Two dimensional reinforced plastic material anisotropic creep derivation from orthotropic plate time functions and stress tensor invariants

13 p2034 A72-28437

Strong field electromagnetic wave interactions with anisotropic plasmas, considering electron velocity distribution function

13 p2009 A72-28449

Anisotropic light scattering layer radiation intensity dependence on optical coordinate, obtaining integral equations for semiinfinite and finitely thick layers

13 p2001 A72-28502

Fiber glass reinforced plastic structure design based on anisotropy, calculating optimum angle between reinforcement and horizontal axis

13 p2058 A72-29463

Diffraction of plane waves scattered by impedance structures in anisotropic medium, noting wedge shaped region with cold plasma under external magnetic field

14 p2086 A72-30809

Wave propagation in inhomogeneous anisotropic time varying moving media, discussing generalized dispersion equation

15 p2196 A72-31688

Elastic properties of media with cracks, discussing elastic anisotropy and crack distribution

15 p2327 A72-31733

Ultrasonic wave propagation in single crystals, discussing linear elastic wave attenuation, anisotropic interactions, particle displacement polarization and energy flux deviation

15 p2292 A72-31834

Steepest descent path of integral describing transient plane wave propagation in anisotropic cold plasma, relating to evanescent wave arrival

15 p2285 A72-32109

Nonlinear anisotropic elastic constitutive equations for micromorphic and micropolar mixtures, investigating plane wave propagation via field equations with restricted coupling

15 p2278 A72-32446

Work hardening and anisotropy coefficients effects on deep drawing limit curves for extramild steel, noting rupture strain and deformation trajectories

16 p2396 A72-32873

Interaction forces between two dislocations in infinite weakly anisotropic media with bcc crystal lattice elastic properties

16 p2424 A72-33146

Forced vibrations of thick homogeneous anisotropic elastic sphere, studying dynamic response to uniformly distributed internal and external pressure

16 p2424 A72-33147

Iterative procedure for Maxwell equations exact solution for anisotropic birefringent medium, applying result to limiting polarization problem

16 p2425 A72-33490

Electromagnetic waves attenuation and phase velocity correction in polycrystals with anisotropic crystal distribution

16 p2365 A72-34013

Radiation from a magnetic line source covered with an anisotropic warm plasma slab

17 p2587 A72-34386

The plane solution for anisotropic elastic wedges under normal and shear loading.

[ASME PAPER 72-APM-13] 17 p2629 A72-34802

Strain history effect on isotropic and anisotropic plastic behavior.

[SESA PAPER 1940] 17 p2631 A72-34820

Polarization characteristics and losses of anisotropic laser resonators composed of arbitrary number of mirrors

17 p2563 A72-34963

Finite bending of a compressible anisotropic rectangular block into a hyperbolic shell.

17 p2634 A72-35438

Circular waveguides lined with artificial anisotropic dielectrics.

17 p2530 A72-35468

Local characteristics of ray propagation in an inhomogeneous anisotropic ionosphere.

18 p2686 A72-36229

Anisotropic circular cylinder stress analysis under uniaxial load, calculating elastic deformation

19 p2872 A72-37536

Use of generalized theory of optical diffraction for the study of second harmonic generation.

19 p2811 A72-37673

Energy propagation in a Cauchy elastic material.

19 p2878 A72-38718

Constitutive equations and optical yielding of anisotropic perfectly plastic dielectrics.

19 p2878 A72-38799

Constitutive equations and wave propagation of anisotropic perfectly plastic materials.

19 p2878 A72-38800

Scattering of electromagnetic pulse waves by conducting wedge in an uniaxially anisotropic medium.

20 p2903 A72-39269

Nonlinear monochromatic Alfvén wave propagation along magnetic field in anisotropic rarefied plasma with firehose instability

20 p2957 A72-39381

Anisotropic electrical properties of amorphous germanium.

20 p2960 A72-39457

On diffraction and focusing in anisotropic crystals.

20 p2961 A72-39779

Galaxy formation in generic dust filled anisotropic cosmology, analyzing density perturbations growth rate

20 p2972 A72-39872

On Maxwell's equations in three-dimensional anisotropic periodic media - Tensor formulation of the problem and the N-beam approximation.

20 p2962 A72-40019

Repulsive potential determination for alkali cations, halide anions and anisotropic molecules from scattering experiments and bond energy data

21 p3087 A72-40555

Connexions between the moduli for anisotropic elastic materials.

21 p3119 A72-41107

Filament wound pressure vessel isotenoid theory, considering composite material as macroscopically homogeneous anisotropic continuum

22 p3238 A72-42838

Circular waveguide in an anisotropic medium

23 p3264 A72-44156

Method for solving the problem of radiation in an anisotropic plasma

23 p3321 A72-44220

Generalized integral equations of radiative heat exchange.

23 p3357 A72-44536

Radiation from an electric dipole in anisotropic media.

24 p3424 A72-44706

Torsion analysis of prismatic bars of different cross sections based on dipolar stress theory, applying to anisotropic media

24 p3457 A72-44872

Idealized homogeneous and nonisotropic cosmological models with electromagnetic and massless scalar fields, noting Einstein equations

24 p3442 A72-45246

Two-dimensional problem of elasticity theory for an anisotropic inhomogeneous wedge

24 p3459 A72-45263

Methods for determining thermal properties of anisotropic systems.

24 p3465 A72-45633

Radiation propagation in optically thin anisotropic noncrystalline media, obtaining explicit formulas for Stokes parameters of transmitted and scattered radiation

24 p3425 A72-45705

ANISOTROPIC PLATES

Buckling of boron/aluminum and graphite/resin fiber composite anisotropic plates, giving load vs fiber orientation angle for various plate aspect ratios

01 p0139 A72-10739

Thermal conductivity and boundary conditions for unsteady thermal fields in thin anisotropic plates with heat emission

02 p0291 A72-11635

Aeroelastic stability of flat anisotropic sandwich plates in supersonic compressible fluid flow

02 p0297 A72-12614

Stress distribution for anisotropic elastic plate containing two or more arbitrary elliptical holes

02 p0298 A72-12674

Edge temperature effects on contact stress concentration in anisotropic plate with elliptic hole under mixed boundary conditions of thermoelasticity

03 p0450 A72-14109

Anisotropic plate with hole stiffened at edge by thin isotropic ring, calculating thermal stress distribution

03 p0450 A72-14113

Anisotropic elasticity effects on plane shock wave propagation for arbitrary loading directions in plate impact experiments 04 p0585 A72-14538

Interferometric holography application to photoelastic stress analysis of opaque anisotropic composite plates under static and dynamic transverse and in-plane loads 06 p0898 A72-18349

Generalized coupled thermoelasticity problem solution from wave equations for anisotropic plate in plane thermal stress state 07 p1094 A72-19987

Thermal stresses in anisotropic annular, circular and perforated plates with temperature dependent coefficients for lateral surfaces heat removal 08 p1245 A72-21505

Elasticity theory doubly periodic problem for unbounded anisotropic plate weakened by system of identical arbitrary holes with self balanced loads 08 p1246 A72-21807

German monograph on deep drawing of pre-hardened and partially annealed Al and Al alloys, noting anisotropy effect of bottom zone of plate samples 09 p1317 A72-22329

Anisotropic plate theory for perfectly plastic flow, expressing yield condition in terms of mixed stress-anisotropy tensors 09 p1403 A72-22765

Stress wave surfaces in graphite fiber-epoxy matrix anisotropic plates under transverse impact forces, using Mindlin approximation theory 10 p1555 A72-24255

Macroscopic elastic constants of three dimensional multilaminar composites with anisotropic layers, assuming stress and displacement continuity 10 p1555 A72-24256

Stress concentrations around circular openings and failure criteria for orthotropic and anisotropic composite laminated plates subjected to uniaxial, biaxial and shear loading 11 p1732 A72-25474

Linear contingency method for elasticity theory of anisotropic plane with elliptic hole, deriving boundary value problems solutions 11 p1733 A72-25543

Nonlinear first order differential equation for carrying capacity of anisotropic circular plates, curved elongate disks and shallow shells of revolution 13 p2054 A72-28457

Stress-strain concentrations near circular holes in fiberglass reinforced plastic plates under various types of load as function of hole diameter/plate width ratio, anisotropy and load 13 p1983 A72-28560

Anisotropic plate with doubly periodic system of elastic ring stiffened elliptic holes, calculating stresses at holes due to tensile forces applied at infinity 14 p2165 A72-30685

Optical anisotropy effects in birefringent materials by reflected shadow method and extension of theory for constrained zones around cracked plates under plane stress 14 p2167 A72-30903

Transverse shear deformations in laminated anisotropic plates from generalized treatment for isotropic and sandwich plates with homogeneous cores [AD-745613] 16 p2375 A72-32846

Anisotropic laminated plates theories reliability comparison, noting applications to thin and sandwich plates 17 p2625 A72-34326

On the analysis of unsymmetrical cross-ply rectangular plates. 17 p2626 A72-34328

Anisotropic rectangular plate free flexural vibration improved solution via Fourier analysis 18 p2734 A72-36419

Variational principle based three dimensional elasticity theory of micropolar anisotropic sandwich plates, considering transverse shear and strains and rotatory inertia 18 p2737 A72-37057

Contact interactions of smooth rigid punch impressing into thin laminar anisotropic reinforced plastic plate 19 p2872 A72-37541

German monograph - Computation of the stress condition in homogeneous anisotropic discs with the aid of an integral equation method 19 p2873 A72-37660

Cracks and screw dislocation arrays in anisotropic bimaterial plates. 20 p2937 A72-39291

Strongly coupled stress waves in heterogeneous plates. 20 p2980 A72-39616

Maximum deflection and bending moments of simply supported anisotropic rectangular plate under uniform transverse load, using double Fourier series 20 p2981 A72-39973

Structural stability of anisotropic plates and structures, developing method based on data for corresponding isotropic problem 22 p3239 A72-42847

Boundary value problems for concentrated forces acting inside semiinfinite anisotropic plate under plane stress, investigating failure modes of unidirectional composites 23 p3344 A72-43495

Influence of the imperfection of resonator elements on the characteristics of a triangular ring laser with a 90-degree Faraday rotator 24 p3408 A72-44622

Supersonic flutter of plane, rectangular, anisotropic, heterogeneous structures 24 p3459 A72-45440

ANISOTROPIC SHELLS

Highly elastic cylindrical layer reinforced with anisotropic shell, deriving stress-strain state and nonlinear elastic stability 02 p0299 A72-12687

Anisotropic shell supercritical deformation, deriving formula for lower critical load for shallow orthotropic spherical segment under external pressure 03 p0447 A72-13729

Curvilinear material anisotropy effects on temperature distributions of thin walled cylindrical shells of revolution 03 p0449 A72-13919

Stress distribution at hole in multilayer anisotropic shells of composite glass-plastic or cermet material 04 p0588 A72-15052

Laminated anisotropic imperfect circular cylindrical shells under axial compression, obtaining upper bound buckling load solution [AIAA PAPER 72-139] 05 p0740 A72-16893

Stress and displacement solutions to elastic deformation of homogeneous and composite anisotropic near cylindrical bodies, using Almansi algorithm 06 p0894 A72-17688

Elasticity theory method for nonlinear stress-strain relationships in thin anisotropic shells, discussing fiberglass reinforced cylindrical shell 08 p1247 A72-21810

Rotationally symmetric stress and strain distribution in anisotropic elastic shells of revolution [AD-745622] 09 p1405 A72-22944

Axially homogeneous stress and strain in anisotropic thin walled cylindrical shells, considering pure bending, stretching and twisting [ASME PAPER 71-APMW-4] 10 p1554 A72-24181

Elasticity theory for unsymmetric deformation of nonhomogeneous anisotropic cylindrical shells, using Donnell equations 10 p1555 A72-24252

Structural weight optimization with piecewise concave cost functionals defined on set in Euclidean space for anisotropic cylindrical shells 12 p1881 A72-27254

Proximate equations of two dimensional orthotropic shell theory obtained by asymptotic integration method, examining anisotropy effect 13 p2053 A72-28391

Stress-strain relations for inelastic deformation of anisotropic strain hardenable shells of revolution under arbitrary plasticity conditions 15 p2332 A72-32678

Cosserat surface uniqueness theorem for non-homogeneous anisotropic thermoelastic shells small motions and temperature variations superposed on large deformation 16 p2465 A72-32981

Determination of the natural frequencies of cylindrical shells of variable thickness 20 p2980 A72-39906

Aircraft structures weight reduction through fiber-matrix composite materials, discussing anisotropic elastic and failure behavior of composite light shell structures [ICAS PAPER 72-38] 21 p3120 A72-41163

Multilayer shell theories with allowance for transverse shear and transverse normal deformation of layers, noting viscoelastic material and anisotropic shallow shells 21 p3125 A72-41537

A linear asymptotic theory for anisotropic shells. 24 p3460 A72-45473

Mechanical behavior of fiber reinforced cylindrical shells. 24 p3461 A72-45783

ANISOTROPY

NT ELASTIC ANISOTROPY

NT PLASTIC ANISOTROPY

Tubular and rod extruded age hardenable Al alloys, determining mechanical anisotropic properties from yield loci and r values 03 p0369 A72-12957

Short wavelength continuous solar X-radiation polarization and angular distribution measurements, revealing physical processes in solar flares 03 p0409 A72-13126

Rolled metals and alloys with various lattice types and packing defect energies, showing elastic properties isotropy and Young modulus anisotropy 03 p0371 A72-13188

Nonparabolic n-InSb semiconductors, presenting microwave conductivity dc field induced anisotropy 04 p0560 A72-14543

Diurnal and seasonal variations of F region irregularities drift and anisotropy parameters during IQSY from aerial fading records, noting magnetic activity effect 04 p0517 A72-14955

High energy cosmic ray electrons anisotropy, considering diffusion from discrete source model 04 p0568 A72-15510

Anisotropic effects use in passive semiconductor magnetoplasma for submillimeter isolators and circulators development, describing transmission devices based on Faraday rotation 04 p0563 A72-15600

Magnetic stress anisotropy field in plated cylindrical Permalloy films, determining relationships to circumferential composition variation, geometry and easy-axis dispersion 04 p0564 A72-15717

Solar wind protons adiabatic spatial cooling related to temperature anisotropy 05 p0709 A72-16067

Atmospheric temperature effect on solar diurnal variation of muon component, considering asymptotic characteristics of cosmic ray anisotropy 05 p0709 A72-16257

Ferritic stainless steel roping /buckling/ morphology and texture explanation by anisotropic plastic flow 05 p0677 A72-17105

Dissipative effects in universe expansion, considering damping of anisotropy in homogeneous cosmological models [AD-745836] 06 p0880 A72-17885

Idealized model for anisotropy of metals inelastic characteristics due to plastic deformation, demonstrating applicability to polycrystalline materials 06 p0900 A72-18685

Three dimensional cosmic ray anisotropy and density distribution at earth orbit and in interplanetary space with allowance for primary particle and nucleon energy spectrum 07 p1065 A72-20645

Non spherical and nonadditive interactions contribution to third virial coefficient of polyatomic gas, discussing anisotropy, shape factor, and intermolecular forces 08 p1211 A72-21292

Heat transfer in shield-vacuum thermal insulation layers at various temperatures and pressures, noting conductivity anisotropy 08 p1253 A72-21451

Pulsed GaAs injection laser active region anisotropy and radiation polarization under spontaneous and coherent emission conditions 08 p1183 A72-21772

Metal single crystals use for corrosion tests, noting anisotropy, adsorption, oxidation and pitting 08 p1189 A72-22111

Mechanical properties anisotropy in heat resistant Ni alloys due to strengthening phase nonmetallic inclusions distribution, suggesting purification by vacuum melting 09 p1327 A72-22321

Anisotropic electrical properties and void structure of amorphous Ge, discussing low- and high-field resistivity measurement in planar and transverse directions 09 p1371 A72-22873

Space anisotropy responsible for solar semidiurnal variation of cosmic ray intensity studied with data from worldwide network of neutron monitor stations 09 p1377 A72-22929

Homogeneous anisotropic solutions of Einstein equations with cosmological term for universe with plane comoving frame filled with powder 09 p1352 A72-23361

Sobolev-Orlicz anisotropic spaces application to calculus of variations equations with strongly nonlinear coefficients 10 p1505 A72-24215

Boron fibers tensile and transverse strengths, relating severe anisotropy to residual stress pattern from preexistent flaws 11 p1672 A72-25484

Relativistic homogeneous anisotropic models analogs construction in Newtonian cosmology 11 p1716 A72-25711

Local and cosmological irreversibility and time anisotropy theories from thermodynamics, statistical mechanics, astrophysics and quantum-relativity viewpoints 11 p1716 A72-25775

Explorer 35 observations of solar wind electron density and temperature, noting anisotropy direction correlation with magnetic field vector alignment 11 p1713 A72-26392

Two dimensional Prandtl-Meyer flow anisotropy of ideal gas expanding into vacuum, using free path probe-molecule technique 12 p1799 A72-28178

Stress calculation in inflexible overlapping cemented joint of orthotropic layers, taking into account joining geometry and elastic properties anisotropy 13 p1962 A72-28396

- Solar wind distortion of stellar anisotropy of galactic cosmic rays, associating annual particle density variation with earth revolution about sun
13 p2029 A72-28590
- Polarimetric determination of angle between polarization planes of emission and external radiation field in three level gas laser, noting resonator anisotropy properties
13 p1970 A72-29687
- Transient North-South anisotropies in cosmic radiation intensity, noting occurrence during Forbush decreases
15 p2298 A72-31432
- Creep theory with anisotropic hardening compared to curves obtained from verification experiments with loading and unloading in steps
15 p2256 A72-31707
- Anisotropic and isotropic descriptions of physical process speeds in special relativity theory space-time metric
15 p2279 A72-32768
- Solar wind thermal anisotropy effects on least squares estimates of interplanetary shock parameters and associated normals from Rankine-Hugoniot equations
16 p2444 A72-32973
- Diffusion propagation and source distribution effects on cosmic ray charge composition and anisotropy in galactic disk, considering nuclear fragmentation
16 p2448 A72-33742
- Alfven wave firehose instability relaxation calculation to include nonlinear terms for explanation of solar wind temperature anisotropies by collisionless mechanism
16 p2449 A72-33933
- Electron diffraction patterns of previously deformed Ti-Nb alloy containing unequal populations of omega phase variants, noting anisotropy
17 p2566 A72-34673
- Galactic cosmic rays anisotropy prediction as function of energy for various assumed source distributions and magnetic field configurations
17 p2599 A72-34924
- Anisotropy and strong-coupling effects on the critical-magnetic-field curve of elemental superconductors.
18 p2719 A72-36710
- Solar cosmic ray anisotropy 27-day variations during IGY from global network stations neutron component data
18 p2722 A72-36876
- The north-south anisotropy and the cosmic-ray radial gradient in the vicinity of the earth.
18 p2722 A72-37164
- Persistent particle anisotropies and magnetospheric models.
20 p2916 A72-39233
- Anisotropy of Raman scattering by optical phonons in cubic zinc blende crystals, describing experimental arrangements
21 p3061 A72-40141
- Extension of Eliashberg's theory to type-II superconductors.
21 p3096 A72-40574
- Determination of conduction anisotropies in semiconductors.
21 p3097 A72-40697
- Three-dimensional cosmic ray anisotropy in interplanetary space. III, IV.
21 p3101 A72-41385
- Electroconductivity anisotropy effect on transverse Dember effect angular dependence and spectral distribution in p-type CdSb lattice
21 p3098 A72-41693
- Oxidation rate anisotropy investigation on coupon specimen of Ta-Mo alloy at 950 C
22 p3190 A72-42770
- Experimental study of the plane deformation of a homogeneous turbulence
23 p3280 A72-43822
- Diffusion processes of cosmic rays with energies between 2 and 20 GV during Forbush decreases - The diurnal effect.
24 p3434 A72-44785
- Reacting and nonreacting swirl recirculation bubble gasdynamic structure in fuel combustion systems, noting anisotropic turbulence from hot-wire anemometer measurements
24 p3461 A72-45024
- Solar wind distortion of stellar anisotropy of galactic cosmic rays, associating annual particle density variation with earth revolution about sun
24 p3435 A72-45090
- ANNEALING**
NT PULSE HEATING
Annealed pure Al polycrystals fatigue behavior data under elevated temperatures, using transmission electron microscopy
02 p0242 A72-11525
- Charge state effects on defect production mechanisms, configurations, mobility, annealing kinetics, interaction and dissociation in displacement damage in covalent semiconductors
03 p0403 A72-14077

- Boundary segregate concentration during grain growth annealing of ultrapure Al as function of migration rate and distance
03 p0379 A72-14259
- Annealing defects in n-type silicon, observing anomalous heat treatment temperatures of A and E centers
04 p0560 A72-14529
- Isothermal annealing measurements of zero-phonon line luminescence at 0.97 eV in electron irradiated Si, obtaining activation energy
04 p0560 A72-14546
- Annealing effects in plated-wire memory elements, investigating Cu and Permalloy interdiffusion at low temperatures by X ray diffraction and electron beam microprobe
04 p0503 A72-15715
- Annealing effects in plated-wire memory elements, discussing recrystallization in Permalloy films from grain size and magnetic dispersion observations
04 p0504 A72-15716
- Oxygen and/or nitrogen interstitial solute pick-up effects on yield stress during Nb annealing, discussing Hall-Petch plot parameter values
05 p0676 A72-16730
- Pure Al self diffusion at 130-200 C, determining activation energy from prismatic loop annealing rates
05 p0677 A72-17109
- Dynamic oversteering and annealing effects on fatigue life of convoluted metal bellows, using dynamic model and strain gage measurements
05 p0742 A72-17245
- Hydraulic sand blasting and annealing effects on Ti alloy sheet bending fatigue strength
06 p0831 A72-18357
- Microstructural changes and mechanical properties of deformed Nb alloy during annealing process, observing low temperature plasticity increase
06 p0835 A72-18747
- Phase diagrams of yttrium, erbium and ytterbium oxides at 1500-2400 C, using annealing and quenching method with differential thermal analysis
07 p1047 A72-18858
- Three and four layer vacancy defects annealing in quenched Al for stacking fault removal
07 p1020 A72-20412
- Phase diagrams, superconducting properties and annealing critical temperature of Nb-Al-Ge alloys, establishing four phase peritectic equilibria
08 p1218 A72-21778
- German monograph on deep drawing of pre-hardened and partially annealed Al and Al alloys, noting anisotropy effect of bottom zone of plate samples
09 p1317 A72-22329
- Electrical conductivity relationship to phase composition in thin CdTe films deposited on mica bases and annealed in Cd vapor
09 p1367 A72-22420
- Subgrain growth during annealing of rolled samples of Mo-Ti-C alloy and of single crystal Mo purified by electron beam zone melting
09 p1329 A72-23034
- Dislocations distribution in Al single crystals observed by X ray topography, noting effects of critical work hardening with annealing and secondary recrystallization
10 p1495 A72-24068
- Inhomogeneous sink distribution effect on vacancy annealing kinetics and activation energy in metals
10 p1499 A72-24983
- Mercury porosimetry for iron powders void and internal particle porosity change as function of compacting pressure, noting compressibility improvement by precompacting and annealing
11 p1639 A72-25828
- Bending stress in oxygen presaturated Nb during oxidation, cooling, dissolution and annealing, using thin film model
11 p1658 A72-25853
- Cold working effect on precipitation-recrystallization interaction in Cu-Ni-Zn alloy, discussing superposed strengthening mechanism during annealing
11 p1641 A72-26738
- Diffusion measurements during annealing of Pd-V, Pd-Ti and metal-ceramic systems by microprobe
11 p1664 A72-26853
- Transition temperature and other superconducting properties of annealed Nb-Al-Ge thin films
12 p1853 A72-27038
- Vapor annealing effect on vacuum evaporator CdSe thin films electroconductivity as function of pressure and temperature
12 p1854 A72-27249
- Low temperature irradiation and annealing effects in germanium, calculating charge states for donor and acceptor centers
12 p1857 A72-28054
- Recombination luminescence in irradiated Si, investigating thermal annealing and Li impurity effects
12 p1858 A72-28062
- Introduction rate and annealing of defects produced in Li-diffused float zone n-type Si by 30 MeV electrons and fission neutrons
12 p1858 A72-28064

- Annealing effects on gamma ray irradiated Li compensated p-type B doped Si semiconductor
12 p1858 A72-28065
- Annealing behavior of electrical properties and photoluminescence spectra in electron irradiated n-type GaAs semiconductors
12 p1859 A72-28068
- Ultrafine grained microstructures and mechanical properties of alloy steels developed by cold working followed by annealing
13 p1974 A72-28662
- Defect annealing in neutron irradiated Si by deep trap concentrations, using space charge limited current (SCLC)
13 p2022 A72-29630
- Temperature control and measurement in electric wire annealing for standard Pu/Pt-10 Rh thermocouples
13 p1960 A72-29766
- Electron shell structure in annealed and plastically deformed W-Re alloys from positron annihilation angular distributions
13 p1981 A72-29908
- Mo single crystal weakening after hot rolling and annealing, showing decreased dislocation density and hardness recovery by electron microscopy
14 p2112 A72-30160
- Primary recrystallization in TD-nickel bars on sublight optical level identified by transmission electron microscopy examination of deformation and annealing substructures
14 p2119 A72-30601
- Coarse grain transformation in TD-nickel bar subjected to deformation and annealing, noting abnormal growth caused by thermomechanical effects
14 p2119 A72-30602
- Vacancy annealing effect on beta phase transformation during tempering of Ti alloy with Mo, showing strain hardening and contraction increase
14 p2124 A72-31032
- Ti alloy initial H content effect on resistance to hot salt stress corrosion embrittlement and cracking, discussing annealing treatment influence
15 p2253 A72-31296
- Carbon distribution effect on cast Mo and alloys structure studied by electron microscopy, microdiffraction and X ray analysis, noting annealing from eutectic temperature
15 p2255 A72-31575
- Electron microscopic investigation of Al-Mn alloy precipitate structure and morphology after annealing induced decomposition
15 p2257 A72-32114
- Stainless steel surface alloy composition characterization as function of vacuum annealing temperature, using proton-induced X rays
15 p2258 A72-32527
- Prestrained and annealed elastic materials stress-strain relationship calculation in plastic range, compared with tensile and compression load tests results
16 p2472 A72-33948
- Separation of iron and annealing-out of lattice defects in rapidly-solidified aluminum-iron alloys. I - Microstructure and properties of quenched samples. II - Tempering behavior
17 p2567 A72-35174
- Room temperature ductility of different types of molybdenum after differing annealing
18 p2698 A72-36155
- Kinetics and annealing and mechanical properties of W chemical vapor deposition, discussing high temperature tests
18 p2656 A72-36398
- Changes of electrical and structural properties of Au thin films obtained by sputtering during the annealing process.
18 p2720 A72-36955
- Study of the structural stability and mechanical properties of molybdenum subjected to the prolonged action of temperature and stress
19 p2818 A72-38013
- The effects of composition and annealing conditions on the stability of columbium/niobium-treated low-carbon steels.
20 p2938 A72-39301
- Effect of twins produced by annealing on high-temperature failure of chromium-nickel-molybdenum steel
20 p2939 A72-39316
- Plastic deformation in annealed aluminum bar containing circumferential semicircular notch.
21 p3118 A72-40719
- Effect of cold work on the oxidation of nickel at high temperature.
21 p3067 A72-40846
- Strain aging of pure aluminum annealed from pre-melting temperature
21 p3060 A72-40954
- Precipitation rate characteristics in age hardenable quenched alloys explained by transient analysis of vacancy annealing kinetics
22 p3189 A72-42441

Surface layer grain boundary corrosion damage of Ti alloys during vacuum annealing, reducing rupture strength, vibration resistance and bending fatigue limit 23 p3293 A72-43589

Dislocation-substructure-strengthening and mechanical-thermal treatment of metals. 23 p3304 A72-44299

Temperature change direct measurement and annealing experiment via differential power analysis to determine stored energy release in metal plastic flow during compression 24 p3405 A72-44613

Relationship between the strength properties and the phase composition of annealed titanium alloys 24 p3414 A72-45383

The effect of annealing temperature on certain properties of molybdenum and tungsten fibers 24 p3415 A72-45396

Hydraulic sand blasting and annealing effects on Ti alloy sheet bending fatigue strength 24 p3416 A72-45744

ANNIHILATION REACTIONS

NT POSITRON ANNIHILATION

Antimatter existence on cosmological scale in universe, comparing calculated annihilation gamma ray spectrum with background observations 02 p0278 A72-11967

Particle motions in earth magnetospheric tail and core, estimating maximum rate of magnetic field annihilation and magnetic drift shell 07 p1062 A72-20027

Pulsed Si p-n junction mesoplasma dynamic I-V characteristics explained by mechanism based on hot carrier annihilation 12 p1853 A72-28113

Expanding universe models showing particle pairs annihilation at critical temperatures 18 p2725 A72-36525

Possibilities of determining complex form factors from experiments with polarized particles 21 p3086 A72-40100

Recombination and annihilation rates of interstitial atoms and vacancies in crystal lattices, taking account of diffusion 21 p3088 A72-41690

ANNOTATIONS

Data correlation and annotation of earth resources remote survey pictorial records 01 p0065 A72-10453

ANNUAL VARIATIONS

Hypoxemia induced by hypoxia in rats, discussing colonic temperature during high altitude exposures and seasonal variations 01 p0011 A72-10214

Diurnal and seasonal variations of scintillations in short wave radio signals of earth satellites and spacecraft 01 p0053 A72-10359

Daily, annual and long term ionoscat and sporadic E variations above Europe, using hf propagation measurements 01 p0055 A72-10432

Seasonal variation in lower thermosphere atomic oxygen concentration deduced from static diffusion models, using incoherent scatter and orbital decay temperature measurements 01 p0062 A72-10907

Nighttime sodium layer observation by tuned laser beam resonance scattering technique, measuring seasonal variation in Na abundance and height distribution 01 p0063 A72-10915

Annual movements of satellite signals scintillation boundary in subauroral ionosphere 01 p0031 A72-10920

ATS Faraday rotation measurement data on total electron content during geomagnetic storms, giving first midlatitude ionosphere average storm patterns and seasonal influence analysis 02 p0216 A72-11900

Diurnal and seasonal changes in occurrence frequency of rapid phase fluctuations in vlf received at Franz Josef Land correlated with geophysical observations 02 p0172 A72-11922

Atomic/molecular oxygen concentration ratio semi-annual variation at 130 km altitude from mass spectroscopic data analysis 02 p0218 A72-11947

Beacon satellite transmission determination of ionosphere total electron content, describing equivalent slab thickness and diurnal, seasonal and solar cycle behavior 02 p0221 A72-12460

Mesosphere meteorological sounding by acoustic grenade and pitot probe techniques, investigating seasonal and latitudinal variations 03 p0383 A72-13384

Computer calculation for atmospheric total mass and seasonal redistribution from pressure and temperature field data, discussing error sources 03 p0348 A72-13480

Stratospheric water vapor concentration annual variability from regression analysis of monthly measurements initiated as IQSY program 03 p0385 A72-14148

Time variations of zonal averages of albedo and absorbed solar radiation derived from brightness data of digitized satellite pictures 03 p0385 A72-14228

Tornado and funnel cloud comparison in seasonal and diurnal distributions, air mass instability, tropospheric vertical wind shear and geographical distribution 03 p0385 A72-14231

Two dimensional meridional ozone model for seasonal ozone concentration behavior at 15-45 km, taking into account advective and turbulent effects 03 p0351 A72-14360

Ionospheric electron content over New Delhi, observing seasonal and solar cycle variations of diurnal changes 04 p0515 A72-14930

Diurnal and seasonal variations of F region irregularities drift and anisotropy parameters during IQSY from aerial fading records, noting magnetic activity effect 04 p0517 A72-14955

Ionospheric absorption measurements at 2.2 MHz by vertical incidence pulse sounding method, observing diurnal and seasonal variations 04 p0518 A72-14965

Ionospheric radio absorption, observing diurnal and seasonal variations and sunspot numbers and solar flares effects 04 p0518 A72-14966

Southern Martian polar cap seasonal change, describing variation at vernal equinox and dry ice hypothesis 04 p0581 A72-15621

Power spectra of ionospheric electron content fluctuations from 6 year continuous records, noting gravity wave and seasonal daily variations 05 p0655 A72-16066

Seasonal variations of semidiurnal tidal winds at 90-110 km from harmonic analysis of ionospheric inhomogeneity drift data 05 p0658 A72-16290

Latitudinal, diurnal, seasonal and solar cycle variations in vhf-uhf scintillation producing irregularities in F layer electron density 05 p0630 A72-16617

F1 layer diurnal and seasonal model for medium to high latitudes, comparing calculated and observed electron density diurnal variations 06 p0804 A72-17458

Ionospheric disturbance in American zone during IGY-IGC, showing latitudinal, annual and diurnal solar variations effects and regional geomagnetic anomaly 06 p0806 A72-17641

Electron density distribution inhomogeneities from vhf Faraday rotation measurements, noting diurnal, seasonal, sunspot cycle and geomagnetic activity effects 06 p0806 A72-17642

Ozone observation and daily and seasonal variations at Cologne, noting longitudinal variations for monthly means 06 p0808 A72-18146

Meteorological satellites and Gemini and Apollo earth photographs, showing annual and diurnal oceanographic, hydrologic and geologic dynamic features 06 p0810 A72-18614

PE sub s harmonic components diurnal and seasonal variations and latitudinal dependence, investigating relationship to drift velocity in E region 06 p0811 A72-18749

Magnetic disturbance singularities searched for in horizontal intensity, showing field depressions around September 5 07 p0980 A72-20406

Annual variations of calibration factors of star pyranometers for copper-constantan and nichrome-constantan thermocouples 07 p0991 A72-20450

Interstellar gas role in cosmic ray yearly variations determined from solar short wave radiation induced gas ionization 07 p1065 A72-20640

Diurnal, sporadic and yearly variations in cosmic ray flux based on neutron component data, noting relation to solar activity cycles 07 p1066 A72-20647

F region ionization anomalous evening enhancement, discussing seasonal variations, solar activity and geomagnetic coordinates maximum in Yakutsk 08 p1153 A72-20707

Seasonal variation in ionospheric horizontal drift velocities under normal E and sporadic E conditions for middle latitudes 08 p1157 A72-21115

Semiannual latitude dependent mesospheric wind patterns from meteor trail observations, suggesting

heat inputs from solar radiation and magnetic storm related auroral heating 08 p1159 A72-21227

Tidal and seasonal wind variations from ionospheric drift If range measurements, comparing with radar-meteor data 08 p1160 A72-21528

Ionospheric drift patterns diurnal, seasonal and solar cycle variations from synoptic measurements over east Siberia by closely spaced receivers, using Briggs similar fades method 08 p1160 A72-21530

Seasonal and diurnal variations of earth albedo from turbidity measurements, showing lower atmosphere moisture effect 08 p1237 A72-21799

Diurnal and seasonal variation of ambipolar diffusion coefficient in meteor trail zone within upper atmosphere 08 p1238 A72-21888

North-south ionospheric movements at low latitude station, investigating diurnal and seasonal velocity variations from cross correlation and similar fades time delays measurements 08 p1136 A72-21981

Model calculation for seasonal effects on minor neutral constituents distribution in mesosphere and lower thermosphere, suggesting large scale meridional circulation role 09 p1274 A72-22354

D and E region electron density profile, investigating geographical, diurnal, seasonal and sunspot cycle variations 09 p1376 A72-22370

Synoptic measurement of midlatitude D region electron density diurnal and seasonal variations under quiet conditions, using differential absorption partial reflection experiment 09 p1376 A72-22372

Geomagnetic activity annual variations from daily international magnetic character figures analysis by time series numerical filter method, discussing sunspot cycle effect 09 p1298 A72-22584

Diurnal, seasonal and solar cycle variations in cosmic noise absorption during 1957-1966, showing various ionospheric layers contribution 09 p1385 A72-22586

Ionospheric potential and thunderstorm activity annual variations during 1959-70 solar cycle from radiosonde measurements in free atmosphere 09 p1301 A72-23265

Ecological study of damp wasteland according to seasons and with various photographic emulsions 09 p1303 A72-23293

Geomagnetic field short term variations as function of solar activity from solar radiation data harmonic analysis, relating large amplitude fluctuation to seasonal variations 09 p1304 A72-23503

Semiannual and annual modulation of geomagnetic field horizontal intensity, suggesting two component model of generating mechanism 10 p1476 A72-24960

Sporadic E layer variations monitoring in 50 MHz band, examining diurnal, seasonal, magnetic and meteoroid showers relationships of oblique incidence paths 10 p1441 A72-25152

Autumnal stratospheric temperature variations in northern and southern hemispheres from Nimbus 3 IR spectrometer 11 p1680 A72-25761

Joint ocean-atmosphere model response to solar zenith angle seasonal variation, noting snow cover and ocean surface effects on lower troposphere warming 11 p1620 A72-25766

Whistler dispersion and occurrence rate characteristics at low latitudes during solar cycle, noting annual variations and magnetospheric electron density 11 p1623 A72-26105

Computer calculation for atmospheric total mass and seasonal redistribution from pressure and temperature field data, discussing error sources 11 p1623 A72-26250

Geometric parameters variations of ionospheric N/h profiles and characteristics during magnetic storm, discussing prognosis procedures from solar activity, latitude and season 11 p1594 A72-26273

Noontime N/h profiles forecasts and annual variation in F region, relating solar activity levels to vertical distribution of electron concentration 11 p1594 A72-26277

Time and space characteristics of F scattering, investigating maximum appearance probability, intensity and seasonal and diurnal variations 11 p1595 A72-26280

F2 layer midlatitude local centers of anomalous noontime ionization during winter and summer solstices 11 p1623 A72-26283

Average plasma sheet configuration in geomagnetic tail at lunar orbit, presenting seasonal dependence and variations with geomagnetic activity

11 p1624 A72-26396

Atmospheric density annual and diurnal variations in lower ionosphere, from satellite radar tracking data, considering drag coefficient modeling and orbit determination techniques

11 p1625 A72-26410

Semiannual exospheric temperature and density variations from satellite observation and ionosonde measurements

11 p1626 A72-26420

Semiannual variation in ionospheric drifts, zonal winds and vertical shear at thermosphere base

11 p1626 A72-26475

Solar activity maximum annual variations effect on ionospheric parameters

12 p1868 A72-27306

Ionosphere electron content annual mean difference from semiannual amplitude as seasonal fluctuation indication for tropospheric circulation

12 p1803 A72-27774

F region mean electron density profile seasonal and solar cycle dependence, using Chapman function for nighttime F layer description

12 p1803 A72-27775

Seasonal atmospheric composition changes relation to midlatitude F 2 layer seasonal anomaly during high solar activity

12 p1803 A72-27776

Sporadic E layer structure and dynamics diurnal and seasonal variations from ionosondes frequency and drift measurements

12 p1804 A72-27781

Ionospheric absorption measurements during sunspot cycle at fixed frequencies, noting monthly and seasonal variations

12 p1804 A72-27782

Solar wind distortion of stellar anisotropy of galactic cosmic rays, associating annual particle density variation with earth revolution about sun

13 p2029 A72-28590

Latitudinal and diurnal development of seasonal anomaly in upper ionosphere from Alouette 1 data, discussing vertical electron density profiles

13 p1946 A72-28594

Diurnal and annual temperature variations at 30-60 km from statistical analysis of rocketsonde data, obtaining solar radiation errors magnitude

13 p1947 A72-28829

Mesosphere and stratosphere density and temperature variability with seasons and altitude

13 p1947 A72-28830

Diurnal and seasonal changes in occurrence frequency of rapid phase fluctuations in VLF received at Franz Josef Land correlated with geophysical observations

13 p1920 A72-29234

Atomic/molecular oxygen concentration ratio semiannual variation at 130 km altitude from mass spectroscopic data analysis

13 p1949 A72-29259

Meteorological-astronomical diurnal and seasonal environmental rhythm simulation for psychological stresses alleviation in long term space missions

13 p1910 A72-29322

Ionospheric absorption measurement by IF mode field strength recording with A3 circuit at 6 MHz, noting diurnal and seasonal variations

13 p1952 A72-29660

Jupiter, Saturn and earth atmospheric circulation seasonal variation data analogies, noting factors governing planetary atmospheric temperature

13 p2048 A72-29813

Range and frequency spread F diurnal and seasonal variations at magnetic equatorial station Thumba, noting geomagnetic activity effect

14 p2097 A72-30130

Seasonal changes in magnetospheric directional fluxes at synchronous altitudes due to solar wind induced field line knee effect and drift shell asymmetry

14 p2097 A72-30131

Seasonal features of nocturnal 6300 Å emission variation and decay coefficient in nightglow related to recombination coefficient for F layer ionization

14 p2097 A72-30132

Hydroxyl emission bands intensity, and vibrational and rotational temperatures sporadic and harmonic components in seasonal and diurnal variations

14 p2098 A72-30142

Semiannual equatorial wind oscillations in upper stratosphere and lower mesosphere dependence on temperature variations in high and middle latitudes

14 p2099 A72-30259

Thermospheric parameters seasonal and latitudinal variations calculation based on atmospheric model with components ionization and molecular oxygen dissociation as main heat sources

14 p2128 A72-30463

Lower ionospheric seasonal anomaly in electron density levels, noting diurnal and latitudinal characteristics at various heights

14 p2102 A72-30653

Ionospheric radio waves absorption and stratosphere temperature variations with respect to season and sunspot cycles, examining 1963-5 winter anomaly

15 p2195 A72-31555

Annual variations of singly charged positive He ion density distribution in solar wind from Vela 3 observations

15 p2299 A72-31944

Rocket and radar-meteor wind observations of zonal flow, noting annual and semiannual components for northern latitudes at 60-130 km

15 p2229 A72-31985

Thermospheric density annual and semiannual variations due to solar heat input into ozone layer and Joule heating, discussing decomposition into Fourier terms

15 p2229 A72-32255

Blanketing sporadic E layer latitude seasonal variations near geographic equator, noting spread F occurrence and solar cycle effects

15 p2231 A72-32265

Tropospheric meridional ozone profiles between Europe and South Africa from measurements aboard commercial airliners, noting seasonal variations

16 p2382 A72-32889

Seasonal rhythms of endocrine system in hibernating mammals, discussing central and peripheral biological clocks in relation to hypothalamus and pancreas/thyroid gland

16 p2353 A72-33100

Ionospheric electron content semiannual and seasonal variations as function of solar and geomagnetic activity from low and mid-northern latitude observations

16 p2385 A72-33378

On the winter anomaly of ionospheric absorption

17 p2546 A72-34695

Thermospheric molecular oxygen from solar extreme-ultraviolet occultation measurements

17 p2614 A72-35602

Geomagnetic activity annual variation investigation, showing 12-month wave existence

17 p2549 A72-35605

Observed seasonal change of the Martian polar cap

17 p2615 A72-35679

Signal reflection height seasonal variations effect on radio waves absorption estimation from vertical ionospheric sounding

18 p2662 A72-36881

Nocturnal and semiannual variations of the intensity of 5577 Å emission of atomic oxygen

19 p2789 A72-37511

F region ionization anomalous evening enhancement, discussing seasonal variations, solar activity effects and maximum value dependence on geomagnetic latitude and longitude

19 p2790 A72-38335

Secular and seasonal modifications of Mars surface, considering southern polar cap and 1971 dust storm

19 p2865 A72-38475

Regression-line studies of E-region seasonal anomaly

19 p2794 A72-38863

The variation of air density at 240 and 280 km from April to November 1967

20 p2916 A72-39235

Seasonal and latitudinal relation between Mars white clouds occurrence frequency and global water distribution, suggesting cloud composition as water vapor

20 p2968 A72-39241

On the diurnal and seasonal variations of the D- and E-regions above Kjeller

20 p2917 A72-39529

Intensity of turbulence within canopies with simple and complex roughness elements

20 p2948 A72-39798

Seasonal, nonseasonal and synoptic global variations in stratosphere temperature from satellite-measured radiances, discussing latitudinal warming-cooling relationships

21 p3048 A72-40253

Diurnal and seasonal behavior of discrete white clouds on Mars

21 p3110 A72-41454

Geomagnetic storm and seasonal effects on spread of monthly distribution and average behavior of midlatitude F region electron peak density and slab thickness

22 p3172 A72-42434

Falls of meteorites in Germany: Temporal distribution of the falls and deductions with regard to their origin - Hypotheses concerning the origin of the meteorites as well as further falls and findings in Germany

22 p3227 A72-42542

Time series analysis of meteoropathological disturbances of human regulation mechanisms, investigating annual variations of diurnal rhythms

22 p3147 A72-42977

Annual and solar-magnetic-cycle variations in the interplanetary magnetic field, 1926-1971

23 p3286 A72-44504

Annual variation of the interplanetary He⁺ velocity distribution at 1 AU

23 p3332 A72-44505

Solar wind distortion of stellar anisotropy of galactic cosmic rays, associating annual particle density variation with earth revolution about sun

24 p3435 A72-45090

Latitudinal and diurnal development of seasonal anomaly in upper ionosphere from Alouette 1 data, discussing vertical electron density profiles

24 p3398 A72-45094

Computer simulation of the F-region seasonal anomaly

24 p3400 A72-45586

ANNULAR FLOW

Electrically ionized striated plasma flow in annular channel, noting application to synchronous induction MHD generator

01 p0111 A72-11209

Turbulent flow development in concentric annuli from modified Reichart integral equation model for eddy diffusivity of momentum

02 p0203 A72-12103

Boundary layer suction intensity and slot location effects on performance of curvilinear annular diffuser for various Mach and Reynolds numbers

03 p0308 A72-13736

Annular MHD channel laminar flow generation at supercritical Reynolds numbers by strong magnetic fields

03 p0398 A72-14005

Critical thermal loads during external and internal heating of annular channels, discussing curvature effect on density level in thermal flux during forced fluid motion

03 p0458 A72-14157

Stator-rotor induced annular incompressible rotating flow, allowing for blade loading generated vorticity within actuator disk theory

[ASME PAPER 71-WA/FE-18] 05 p0599 A72-15929

Numerical solution to Navier-Stokes equations for viscous annular flow between rotating long eccentric cylinders

05 p0605 A72-16821

Sound propagation within and radiated from annular duct flow, measuring acoustic distributions for single and multimode excitations

[AIAA PAPER 72-197] 05 p0691 A72-16924

Transpiration cooling of laminar tangential Newtonian flow in annuli, obtaining temperature distribution

07 p1100 A72-19631

Flow stability of viscous fluid in annular space between rotating inner and axially oscillating coaxial outer cylinder, using perturbation method

07 p0971 A72-20089

Hydrodynamics of dispersed annular two phase flow in cylindrical channels characterized by concurrent motion of flow core and liquid film at wall

08 p1151 A72-21667

German monograph on experimental investigations of annular channels with axial flow of incompressible fluids covering graphical and computational determination of flow volume

09 p1293 A72-22332

Fully developed laminar flows in ducts with secondary motions, considering annuli with rotating core, pipe with swirl generator and straight rectangular duct

10 p1463 A72-23865

Intercomponent complex annular ducts design for gas turbine engines

10 p1416 A72-23872

Non-Newtonian Reiner-Rivlin fluid flow between two coaxial porous cylinders with longitudinal pulses applied to inner cylinder at finite time intervals

10 p1468 A72-24402

Convective motions in rotating laterally heated annulus with contacting rigid lid, determining radial temperature difference for transition to vortex regime

10 p1506 A72-24420

Helical turbulent flow through concentric annulus with rotating inner cylinder, examining axial and tangential velocity distribution and shear stresses

10 p1471 A72-25190

Hydromagnetic stability of rotating nondissipative inviscid incompressible conducting fluid annulus permeated by radially varying magnetic field, considering axisymmetric and nonaxisymmetric disturbances

11 p1619 A72-26639

Viscous flow stability between two rotating nonconcentric cylinders, obtaining approximate solution to eigenvalue problem by perturbation method

12 p1799 A72-27846

Optimization of heat pipe with wick and annulus liquid flow, investigating effect of pressure loss and recovery in vapor passage

[ASME PAPER 71-HT-V] 15 p2335 A72-31767

Steady laminar MHD flow of viscous incompressible electrically conducting fluid between long concentric rotating porous cylinders under radial magnetic field

15 p2287 A72-32397

Fully developed turbulent air flow through concentric annuli, measuring inner wall shear stress distribu-

- tion by zero-shear position location and sliding sleeve technique
16 p2375 A72-32875
- Stability of spiral flow and of the flow in a curved channel.
17 p2540 A72-35051
- Acoustic refraction and attenuation in cylindrical and annular ducts.
17 p2582 A72-35414
- An integral analysis of condensing annular-mist flow.
18 p2682 A72-36720
- Thrust recovery factor and base drag losses in annular jets as function of jet thickness to base diameter ratio, determining recirculation mass flow.
18 p2641 A72-36769
- Laminar flow in an annulus with porous outer wall.
18 p2683 A72-37054
- Numerical studies of flow between rotating coaxial disks.
19 p2784 A72-37374
- Flow between eccentric rotating cylinders.
[ASME PAPER 72-LUB-J] 19 p2786 A72-37699
- Heat transfer and resistance in a laminar gas flow with variable properties in an annular channel
19 p2786 A72-38040
- Theory of heat transfer in a two-dimensional porous cooled medium and application to an eccentric annular region.
[ASME PAPER 72-HT-47] 20 p2985 A72-39663
- Non-local effects in the stability of flow between eccentric rotating cylinders.
21 p3043 A72-40111
- Investigation of the critical heat flux density in heat transfer with and without turbulization of the flow at the inlet of an annular channel
21 p3129 A72-41057
- Acoustic efficiency of supersonic annular jets
21 p3045 A72-41098
- Discrete component of the noise spectrum of a supersonic annular jet
21 p3045 A72-41100
- Developing turbulent flow and heat transfer in concentric annuli.
[CSME PAPER 71-39] 24 p3465 A72-45253
- ANNULAR JETS**
U ANNULAR FLOW
U JET FLOW
- ANNULAR NOZZLES**
Curved-wall annular exhaust diffusers for hot engine parts IR shielding, evaluating performance tests for swirl flow and ejector secondary flow effects on pressure recovery
[ASME PAPER 71-WA/FE-35] 05 p0646 A72-15922
- Flow calculations for subsonic and transonic portions of ring nozzles and plane curvilinear channels
05 p0601 A72-16226
- Charged to neutral particle transformation capacity of wide aperture recharge target formed by supersonic gas jets in magnetic trap with annular nozzle
09 p1363 A72-23224
- Low speed performance and boundary layer growth in optimal annular diffuser with uniform center body diameter and conically diverging wall
10 p1415 A72-23856
- Turbulent boundary layer growth measurement on annular diffuser containing free vortex swirl
10 p1416 A72-23857
- Swirling flow effects on annular conical diffuser performance in axial flow turbomachines, showing stagnation region and inner body diameter dependence
14 p2069 A72-30580
- Method of characteristics for ideal gas flow in annular space of axisymmetric plug nozzle, noting flow visualization by schlieren photography
22 p3166 A72-42263
- Flow and energy loss distribution in annular stator nozzle cascades with cylindrical blade profiles of different twist, measuring flow exit angle along blade span
23 p3248 A72-43664
- ANNULAR PLATES**
Finite stretching of isotropic incompressible annular plate with inner edge rigid inclusion, noting edge zone thickness variation due to transverse normal strain
02 p0296 A72-12528
- Thickness function corresponding to constant velocity loading condition for orthotropic annular circular plate with uniform stress
04 p0591 A72-15279
- Deflection function for symmetrical bending of unloaded annular plate, constructing stiffness, mass and stability coefficient matrices by function manipulation
05 p0739 A72-16550
- Stability loss of circular annular plate under compression, determining critical loads with inner edge free and outer edge hinged or clamped
07 p1092 A72-19900
- Poisson equation boundary value problems summarized representation formulas for three layer annular sector with Dirichlet or Neumann conditions
08 p1205 A72-20963
- Thermal stresses in anisotropic annular, circular and perforated plates with temperature dependent coefficients for lateral surfaces heat removal
08 p1245 A72-21505
- Optimal design of anisotropic composite material annular plates by numerical method
08 p1246 A72-21673
- Annular plate with supporting edge beams and concentrated load, showing deflection decrease with stiffness
11 p1736 A72-25990
- Finite element method application to variable thickness circular and annular plates free transverse vibration
12 p1879 A72-27191
- HF transverse resonant vibrations of annular Al plates with polychlorovinyl and polyamide base coatings, noting damping and strain relationship to energy dissipation
14 p2164 A72-30427
- Large deflection calculation of circular and annular strain hardenable rigid plastic plates under axisymmetric load, using Kirchhoff-Love hypothesis and Tresca flow condition
14 p2165 A72-30440
- Finite element method application to thin plate bending problem to illustrate efficiency of sector elements for sectorial and annular plates
15 p2326 A72-31720
- Magnetic shielding effectiveness of metal cylinder tubes with periodically imbedded annular transverse Bloch walls of high permeability
16 p2369 A72-33669
- A comparison of flow and deformation theories in a radially stressed annular plate.
[ASME PAPER 72-APM-44] 17 p2627 A72-34781
- The carrying capacity of frames under the influence of concentrated forces
20 p2981 A72-39919
- Stresses and strains in the plastic range in an annular disk due to steady-state radial temperature variation.
21 p3121 A72-41210
- Equilibrium equations for given stress concentration in circular and annular plates under tensile loads with different yield points in tension and compression
21 p3126 A72-41545
- Symmetrical bending of circular plates using finite elements.
22 p3236 A72-42605
- On the use of a coordinate transformation for analysis of axisymmetric vibration of polar orthotropic annular plates.
24 p3457 A72-44883
- ANNULI**
Cascaded annular lens systems for focusing electromagnetic waves, noting advantages of axicon
03 p0388 A72-12967
- Dynamic radial vibrations and stresses in thick circular annulus of nonisotropic elastic material, using Hankel transform
08 p1246 A72-21793
- Thermal stresses in plane elasticity for doubly connected regions, considering temperature distribution, stress state problem formulation and nonconcentric annulus
15 p2329 A72-32287
- ANODES**
NT TUBE ANODES
Anode heat flux for cascade atmospheric Ar arc of Maecker type, checking anode heat transfer model validity
02 p0302 A72-12266
- Cathode and anode temperatures effect on effective heat of condensation of electrons at anode for particular current density and different cesium vapor pressures
02 p0156 A72-12858
- Magnetic fields effect on anode heat losses in MPD accelerator arcs, noting minimal charge current density
[AIAA PAPER 72-502] 11 p1711 A72-26225
- Anodic dissolution of metals during electrochemical precision processing, studying electrolyte composition and flow and mixing rates
11 p1640 A72-26255
- Electrochemical metal precision processing, discussing steels carbon content, surface purity, electrolyte anion composition and anode potential
11 p1640 A72-26256
- Stress corrosion crack initiation and propagation for Ti alloy in sodium chloride solutions, noting anodic dissolution
15 p2253 A72-31295
- Electron swarms in uniform electric fields, discussing anode current amplification/radial distribution and drift-diffusion equation
15 p2285 A72-32239
- ANODIC COATINGS**
Anodic layer thickness effect on fatigue crack initiation and fracture mode in mono and polycrystalline aluminum
05 p0672 A72-16015
- White thick layer anodic zirconium oxide water content determination by volumetric and thermogravimetric analysis of heated samples
05 p0667 A72-17051
- Heating effect on potassium bichromate-saturated anodic aluminum oxide electrical characteristics, discussing surface conductivity and capacity and solution pH
05 p0667 A72-17052
- Anion sorption mechanisms and product composition in anodic aluminum oxide filled with phosphate, chromate and sulfate solutions, discussing chemisorptive compound formation and oxide dehydration
05 p0624 A72-17053
- Electron microscopy for structure study of anodic aluminum oxides prepared by various methods, comparing electrograms of oxides after heating, boiling and filling with water
05 p0624 A72-17054
- Sorption properties of anodic aluminum oxides prepared in orthophosphoric and chromic acid solutions, determining dependence on pH by isotopic labeling method
05 p0624 A72-17055
- Current reversal effect on anodic aluminum oxide film prepared in phosphate electrolyte, using electron microscope and isotopic labeling
05 p0667 A72-17056
- Stress-strain characteristics of metal ductile filaments with elastic brittle coatings, noting strengthening effect on anodic oxide coated aluminum
09 p1330 A72-23379
- Hardcoat anodizing of Al surfaces, discussing preparation, racking, equipment and post treatments
[SAE PAPER 720341] 11 p1638 A72-25598
- Anodic oxide film protective properties for Al and Al alloys, evaluating via film dissolution time observation in chromic and phosphoric acids mixture
12 p1828 A72-27453
- Brittle continuous and crazed anodic oxide coatings effect on Al filament stiffness, comparing with Dow analysis
13 p1974 A72-28663
- Anodic oxide films separation from Al surface using ethyl bromide at temperatures below 40 C
16 p2397 A72-33274
- ANODIZING**
Extruded AlMgSi alloy manufacturing conditions effect on strength, surface finish and anodized appearance, discussing evenly distributed fine hardening precipitates, metal purity, etc
01 p0077 A72-11043
- Anodized aluminum metallization for reducing electromigration induced failure modes in silicon wafers
03 p0365 A72-14286
- Ti anodic behavior in anhydrous liquid ammonia, noting oxidation by halogen intermediary
04 p0484 A72-14976
- Anodizing effect on corrosion fatigue strength of sheet duralumin under low and high bending stress
04 p0535 A72-15662
- Pitting potential and intergranular corrosion of anodically polarized Al and Al alloys in electrolytes
04 p0536 A72-15736
- Soviet papers on anodic oxidation of metals covering aluminum and zirconium oxides, oxide films, anion sorption capacity, chemical composition, structure and physicochemical properties
05 p0667 A72-17050
- Thin film formation techniques including evaporation, sputtering, anodization, chemical vapor deposition, electrodeposition and sintering, discussing surface scattering, tunneling, Schottky emission and conduction mechanisms
06 p0790 A72-18571
- ANOMALIES**
U ABNORMALITIES
- ANORTHOSITE**
Electron microprobe analysis of plagioclase points and pyroxene grains of Apollo 15415 anorthositic genesis rock
02 p0282 A72-12411
- Crystallization age of Apollo 15 anorthosite rock 15415.9
06 p0888 A72-18270
- Mineralogic and petrologic study of lunar anorthosite slide 15415.18
06 p0888 A72-18271
- Texture, mineralogy and metamorphic history of lunar anorthosite 15415
06 p0889 A72-18272
- Lunar anorthosites and parent liquids chemical composition from trace element analysis
10 p1537 A72-24158
- Geological setting, petrography and history of Apollo 15 anorthosite sample, tracing fragmentation and thermal metamorphic events
11 p1722 A72-26239
- Radiogenic Ar 40/Ar 39 age and cosmic ray irradiation history of Apollo 15 anorthosite sample 15415, indicating Imbrian impact heating
12 p1862 A72-27111
- Highly aluminous glasses in lunar soils and the nature of the lunar highlands.
21 p3104 A72-40490

ANOXIA

- High altitude hypoxia effects on rat myocardium lactic dehydrogenase isozyme complement and anoxic tolerance 02 p0165 A72-12834
- Thyroidal influence on myocardial changes induced by simulated high altitude. 17 p2500 A72-34730
- Acute myocardial anoxia - Anatomical changes and their possible relation to immunological processes. 17 p2501 A72-34981
- Anoxic tolerance of the heart muscle in different types of chronic hypoxia. 17 p2502 A72-34991

ANTARCTIC REGIONS

- Solar cosmic ray flare recording in stratosphere in Murmansk and Antarctic regions during February-April 1969 07 p1066 A72-20649
- VLF signals Antarctic ice cap attenuation determined at Byrd station from relative phase and amplitude observations over short and long great circle paths 09 p1281 A72-23511
- Weather satellite data use to obtain forecasts for aircraft and ships in Southern Hemisphere and for Antarctic research stations 11 p1683 A72-26890
- Antarctica dry valley microbiology investigation for Martian life model 12 p1802 A72-27258
- Simultaneous determination of chord length and direction by artificial earth satellite geodetic observations in Arctic and Antarctic regions 13 p1945 A72-28493
- Midnight auroral electrojet time variations relationship to midday auroras latitudinal shift during South Pole magnetospheric substorms 13 p1950 A72-29382
- Upper atmosphere temperature and wind variations over Antarctic from meteorological rocket sounding, noting winter cyclonic vortex level 15 p2225 A72-31906
- Antarctic ice sheet complex permeability in VLF band from reduction of measurement data with buried dipole antenna under snow surface 15 p2200 A72-32104
- Antarctic D region reflection heights from relative phase measurements on VLF transmissions at several phase locked frequencies, interpreting results by waveguide mode theory 15 p2200 A72-32105
- Thermospheric composition variations in south polar regions during magnetically quiet periods fromOGO-6 observations, considering atmospheric heating by electron precipitation cyclic variations 16 p2383 A72-32964
- VLF hiss intensity, polarization, incidence angle and arriving direction observation at Antarctica station during magnetic disturbances 18 p2660 A72-36431
- VLF-ELF hiss polarization and right/left component ratios recording at antarctic station, using sweep polarimeter 18 p2660 A72-36432
- Structure and circulation of the upper atmosphere over East Antarctica in 1969 and 1970 20 p2949 A72-39949

ANTARCTICA

U ANTARCTIC REGIONS

ANTENNA ARRAYS

- NT ENDFIRE ARRAYS
- NT LINEAR ARRAYS
- NT STEERABLE ANTENNAS
- NT TURNSTILE ANTENNAS
- NT YAGI ANTENNAS
- Phased array antennas design and performance characteristics, examining feeding and electronic scanning problems with special attention to all-solid-state designs 01 p0038 A72-10659
- Far field patterns of hourglass reflector phased array for electronic despin of communications antenna on spin stabilized satellite 01 p0029 A72-10666
- Multifunction integrated microwave array antenna design emphasizing interlaced multifrequency bands into single aperture and mutual interaction effects reduction between elements 01 p0039 A72-10667
- Short backfire antenna gain increase, considering construction case, reflector arrangement and circular polarization 01 p0040 A72-10684
- Moderate gain superdirective antenna arrays design based on backfire principle, using parasitic elements 01 p0040 A72-10685
- Boundary value problem solution for multiple interleaved phased arrays of waveguide radiators operating at different frequencies, investigating transmission characteristics 01 p0042 A72-11234
- Mutual microwave coupling effects on element VSWR in linear dipole log periodic antenna array 01 p0043 A72-11242

- Propagating waves characteristics measurement on Yagi-Uda array, obtaining k-beta diagrams and phase velocities 01 p0043 A72-11244
- Automatically retrodirective performance from circular arrays and circularly continuous aperture antennas, applying method to cylindrical antennas 01 p0043 A72-11248
- Equivalent circuits and characteristics of multiwire and small active transistorized antennas including unipoles, loops, Franklin arrays and mast antennas 02 p0191 A72-11685
- Large reflector and phased array antennas, discussing synthesis and analysis, active impedance and blind spots, matching, beam steering and implementation 02 p0191 A72-11686
- Short backfire antenna directivity determination from plane conduction reflection coefficient 02 p0192 A72-12111
- Statistical synthesis of antenna arrays using phase amplitude distribution equivalent to reference array radiation pattern 02 p0196 A72-12758
- Time shared performance test monitor function, operation and self repair of corporate fed array radars with computer control for long time internal reliability 03 p0321 A72-13165
- Antenna arrays near-field radiation pattern prediction, using Harrington matrix methods 03 p0323 A72-14030
- Planar phased array antennas with uniform current amplitudes, calculating beam-pointing error dependence on array geometry, phase errors and scan angle. 03 p0325 A72-14179
- Phased antenna array blind spot detection and elimination, describing aperture match with inductive irises 04 p0486 A72-14493
- ATC radar beacon system developments, considering diversity transponders, interrogator environment control, electronic scan cylindrical array antenna design and discrete address mode 04 p0508 A72-14832
- Iterative synthesis of dipole antenna array for maximum directivity radiation pattern, considering amplitude-phase distributions 04 p0499 A72-15142
- Signal fluctuation effect on directional properties of multipole receiving antenna, calculating radiation pattern 04 p0499 A72-15143
- Dicke-type microwave radiometer for daily measurements of 2800 MHz solar flux, discussing antenna system and dynamic range 04 p0522 A72-15163
- Highly directional circular array antennas radiation characteristics calculation, showing sidelobe size dependence on aperture angle 04 p0499 A72-15240
- Antenna arrays performance optimization, emphasizing directivity and signal to noise power ratio 04 p0499 A72-15301
- Phase-amplitude current distribution calculation for plane array and curvilinear radiator based on given amplitude radiation pattern 04 p0500 A72-15405
- Random phasing algorithms to reduce phase quantization lobes for radiation patterns of commutated phased array antennas 05 p0634 A72-15820
- Radio pulse signal fixed source location estimate with nondirectional space diversity receivers in arbitrary configuration antenna array 05 p0625 A72-15822
- Radiative coupling of fed and unfed adjacent antennas in navigation systems rotating beam circular arrays, deriving equivalent circuit via quadrupole theory 05 p0635 A72-16300
- Reciprocal effects of rectangular guide-slot radiators with circular polarization, analyzing field ellipticity factor change for cross-cut slot under neighboring array slots influence 05 p0635 A72-16336
- Polarization and energy characteristics of two mutually orthogonal slots cut in rectangular guide, allowing for reciprocal effects of slot arms 05 p0635 A72-16337
- Radio direction finding techniques using amplitude-trigonometric interpolation between signals received at circular antenna array 05 p0628 A72-16555
- Computed performance of ILS glide slope transmitting arrays sited over flat ground planes of one dimensional perfectly conducting strips in free space 05 p0686 A72-16559
- Supersynthesis antenna array design by analytical approach involving isolation and separate optimization of parameters effects on spatial frequency component sampling 06 p0771 A72-17341
- Spherical reflector antenna phase aberration correction by planar array feeds, discussing synthesis procedure for mean square error minimization 06 p0781 A72-17344

- Multifrequency array antenna of interlaced open ended waveguide elements for L, S and C bands, reducing mutual interaction by cross polarization 06 p0782 A72-17360
- Small array technique for active impedance amplitude and phase measurement of large phased arrays 06 p0782 A72-17361
- Critique on condition for planar antennas physical reliability, concerning smoothness of aperture edges 06 p0782 A72-17362
- Electronically scanned steerable antenna array design with interelement coupling, considering maximum gain and radiation pattern control 06 p0773 A72-17497
- Optimum directional arrays design with linear programming simplex method generation of point elements excitation 06 p0774 A72-17855
- Toeplitz matrix in numerical solution of integral equation for cylindrical antenna and array, presenting rapid inversion algorithm by exploiting symmetry properties [AD-743577] 07 p0957 A72-19795
- Charged conductors in homogeneous collisionless magnetoactive plasma at hybrid frequencies, investigating antenna array quasi-electrostatic field one dimensional structure 08 p1138 A72-20746
- Random antenna radiation patterns probability distribution law and Dolph-Chebyshev array design, calculating minimum statistical sidelobe level 08 p1138 A72-20930
- Quasi-stationary three dimensional array excitation by large phase shift calculated for circular conducting elements 08 p1140 A72-21262
- Probabilistic characteristics of radiation pattern for multielement antenna with nonpolar phase front 09 p1285 A72-22575
- Iterative algorithm for digital adaptive null steering of RF antenna arrays, demonstrating feasibility by computer simulation 09 p1289 A72-23416
- FM/CW interferometric ionosonde used for interferometric direction finding, computing incident azimuth and elevation from baseline array phase differences 09 p1281 A72-23514
- Stochastic projected gradient algorithm to maximize SNR subject under linear or nonlinear constraints, applying to detector antenna array processing 10 p1456 A72-23808
- Adaptive optimal antenna array detection of unknown spatial location radar targets, noting tradeoff between array size and signal energy with respect to performance 10 p1434 A72-23809
- Synthesizing antenna arrays perpendicular to conducting screen by PSK signal theory, discussing optimal binary phasing and radiation patterns numerical data 10 p1450 A72-24507
- Receiving antennas polarization parameters selection in side-looking synthetic aperture radars 10 p1453 A72-24905
- Expected value of two dimensional Gaussian random array gain, assuming two dimensional isotropic noise field of single frequency 11 p1604 A72-26040
- Optimum synthesis of antenna array of slot radiators with passive elements, using nonlinear programming 11 p1597 A72-26708
- Aperture synthesis of ring antenna arrays radiation pattern using earth rotation 11 p1597 A72-26710
- Multipole synthesis compensating mutual coupling for orthonormalized radiation patterns in ring antenna array 11 p1598 A72-26711
- Radiation pattern forming circuit with compensated mutual coupling in phased antenna arrays, noting synthesis by matched multipoles 11 p1598 A72-26712
- Position and minimum scattering algorithms for narrow band signal source received by spaced receivers forming antenna arrays with large separations 11 p1598 A72-26715
- Communication and data relay satellites multibeam antennas characteristics, discussing multiple feed reflectors, bootlace lens configuration and phased arrays [ATA PAPER 72-530] 12 p1789 A72-27355
- Computerized antenna array design, using Automated Engineering and Scientific Optimization Program 12 p1792 A72-27735
- Iterative method for synthesis of reflector antenna array of dipole elements to provide given radiation pattern, obtaining impedance matching values 13 p1926 A72-28372
- Optimal parameters of electro-optical signal processor for phased array antennas, noting optical subsystem correspondence to optoelectrical spectrum analyzer 13 p1926 A72-28374

- Pulse excitation of traveling wave antenna array, describing spectral method of solving high resolution side-looking radar limitation 13 p1915 A72-28526
- Directivity characteristics of scannable planar antenna arrays, illustrating grating lobes presence effect 13 p1928 A72-28527
- Mutual coupling in phased arrays of randomly spaced antennas, investigating probabilistic properties of main beam amplitude fluctuations 13 p1916 A72-28532
- Rectangular slots linear array and feed network performance in reentry plasma environment, obtaining self and mutual impedances, gain and radiation pattern 13 p1916 A72-28537
- Wave channel type antenna design with modulated phase velocity and multiple use of antenna array 13 p1929 A72-28895
- Scattering matrix derivation for parallel plane waveguide array terminated in infinite plane, determining neighboring guides TEM modes mutual coupling 13 p1921 A72-29345
- Antenna array synthesis for radiation patterns prescribed by continuous function, proposing formulas for current determination 14 p2087 A72-30335
- Parabolic reflector fed by log-periodic dipole antenna array, predicting combined effects of feed phase center lateral and axial displacement on secondary performance 15 p2205 A72-31541
- Broadband arrays and multimode fed antenna excitation pattern mathematical synthesis in terms of optimization in Hilbert space 15 p2197 A72-31892
- Bandwidth log-periodic dipole array radiation pattern and impedance characteristics as function of design parameters 15 p2208 A72-32390
- Plane electromagnetic wave diffraction on periodic arbitrary profile array, presenting near and far field asymptotic characteristics 15 p2202 A72-32660
- Phase distribution randomization in switched antenna array, noting radiation pattern sidelobe compensation application 15 p2209 A72-32666
- Radio pulses from extensive air showers detected by antenna array with east-west oriented dipoles connected in parallel 16 p2444 A72-33036
- A synthesis of array antennas for high directivity and low sidelobes 17 p2525 A72-34354
- Phase optimization of antenna array gain with constrained amplitude excitation 17 p2513 A72-34355
- Pattern synthesis of hexagonal planar arrays 17 p2525 A72-34363
- Calculations showing the reduction in the frequency dependence of a two-element array antenna fed by microwave transistors 17 p2514 A72-34369
- A fast numerical method for determining the optimum SNR of an array subject to a Q factor constraint 17 p2514 A72-34372
- Frequency-scanned X-band waveguide array 17 p2525 A72-34374
- Radiation from a directive continuous spiral antenna array 17 p2526 A72-34376
- Design of an array of circular-loop antennas with optimum directivity 17 p2514 A72-34387
- Book - Theory and analysis of phased array antennas 17 p2515 A72-34621
- Solid state phased arrays for ECM applications 17 p2531 A72-35569
- SHF airborne distributed phased array antenna system 17 p2531 A72-35572
- Cylindrical phased arrays - Beam scanning and sidelobe control 17 p2531 A72-35573
- A wideband antenna array 17 p2531 A72-35766
- Antenna array analysis of arbitrarily-located, parallel center-fed dipoles with terminals in a common plane 18 p2666 A72-36328
- An adaptive processor for RF antenna arrays 18 p2659 A72-36329
- Optimal distributions for semi-circular arrays of isotropic radiators 18 p2666 A72-36330
- A new project of 8-cm radioheliograph 18 p2691 A72-36434
- A short-wave rotating antenna for 500-kW transmitter output 18 p2666 A72-36676
- Fourier series analysis of multielement circular loop antenna with arbitrary circumference for current distribution and self and mutual admittances 19 p2775 A72-38615
- Methods for monitoring the parameters of phased antenna arrays 19 p2767 A72-38622
- Plane wave diffraction in a plane waveguide array with protruding dielectric plates 19 p2768 A72-38655
- Statistical synthesis of antenna arrays using phase amplitude distribution equivalent to reference array radiation pattern 20 p2907 A72-39064
- Reliable advanced solid state radar (RASSR) array design featuring transmit-receive elements arranged in triangular grid and built-in test equipment 20 p2904 A72-39732
- An algorithm for linearly constrained adaptive array processing 20 p2904 A72-39777
- Effects of errors in the direction of incidence on the performance of an adaptive array 20 p2904 A72-39786
- Analysis and element pattern design of periodic arrays of circular apertures on conducting cylinders 21 p3026 A72-40351
- Analysis and design of TEM-line antennas 21 p3026 A72-40353
- The determination of active array impedance with multielement waveguide simulators 21 p3026 A72-40357
- The optimum design of small nonuniformly spaced arrays 21 p3027 A72-40362
- On the removal of blindness in phased antenna arrays by element positioning errors 21 p3027 A72-40363
- Gain of arrays of dipoles with a ground plane 21 p3027 A72-40364
- Radiation patterns of an antenna near a conducting strip 21 p3015 A72-40365
- Mutual coupling of infinite periodic phased arrays of arbitrarily oriented dipoles, investigating dipole length, orientation and phase effects on current distribution 21 p3027 A72-40368
- On the relationship between classical and matrix design methods for arrays of wire antennas 21 p3027 A72-40373
- Constrained optimization of the gain of an array of thin wire antennas 21 p3027 A72-40374
- A contribution to the theory of finite antenna groups, taking into consideration radiation coupling 21 p3028 A72-40503
- Statistically dilute antenna groups with enhanced minimum distance between elements 21 p3028 A72-40504
- Theoretical and experimental investigations, conducted with the aid of a plate containing holes, concerning the simulation of a statistically arranged antenna group 21 p3028 A72-40505
- Wave equation for infinitely long slotted screen in elliptic cylindric coordinates, noting radiation pattern for phased antenna array of metallized hyperbolic striplines 21 p3028 A72-40507
- Experimental investigation regarding Archimedean spiral antennas for the L-band, and radiator groups constructed from them whose radiation directions are controlled by a conduction matrix 21 p3028 A72-40510
- The effect of amplitude and phase tolerances on the phase characteristics of dipole arrays 21 p3028 A72-40512
- Shaped coverage patterns with satellite array antennas 21 p3019 A72-40884
- Effect of single-bit digitization in adaptive array control loops 21 p3034 A72-41085
- FM signal distortion during passage through two-element antenna array to determine usable bandwidth from transmission characteristics viewpoint 21 p3022 A72-41265
- Numerical integration of integral equation for phased array radiation modeled by impedance filaments in conductive plane, noting excitation by magnetic flux 22 p3159 A72-42663
- Random phasing algorithms to reduce phase quantization sidelobes for radiation patterns of commutated phased array antennas 23 p3268 A72-43428
- Radio pulse signal fixed source location estimate with nondirectional space diversity receivers in arbitrary configuration antenna array 23 p3263 A72-43430
- Design of radiating elements for large planar arrays - Accomplishments and remaining challenges 23 p3269 A72-43571
- Wideband limitations of waveguide arrays 23 p3270 A72-43573
- Antenna radiation patterns from statistical phase synthesis of antenna arrays, estimating directivity loss for in- and out-of-phase initial current distribution 23 p3265 A72-44203
- Discrete-antenna synthesis theory in the case of uniform approximation to a given radiation pattern 23 p3266 A72-44213
- Probabilistic characteristics of radiation pattern for multielement antenna with nonpolar phase front 24 p3384 A72-44754
- Coupled active parallel doublets network within external electromagnetic field at receiving station, investigating decoupling function between radiating elements 24 p3382 A72-45771
- ANTENNA COMPONENTS**
- NT ANTENNA COUPLERS
- NT ANTENNA FEEDS
- NT COUPLERS
- ANTENNA COUPLERS**
- NT COUPLING CIRCUITS
- Radiation pattern forming circuit with compensated mutual coupling in phased antenna arrays, noting synthesis by matched multipoles 11 p1598 A72-26712
- Mutual coupling in phased arrays of randomly spaced antennas, investigating probabilistic properties of main beam amplitude fluctuations 13 p1916 A72-28532
- Narrow strongly radiating slot voltage distribution, investigating cavity coupling with integral equation 15 p2209 A72-32659
- Spacecraft antenna feeder channel parameter control in flight 21 p3026 A72-40319
- ANTENNA DESIGN**
- Radio telescopes quality criteria, noting performance dependence on antennas dimensions and distribution 01 p0047 A72-10194
- Phased array antennas design and performance characteristics, examining feeding and electronic scanning problems with special attention to all-solid-state designs 01 p0038 A72-10659
- Low sidelobe pencil beam thinned phased arrays design involving element position selection 01 p0039 A72-10664
- Linear antenna array optimal power pattern synthesis by best approximation, using weighting function in man-machine iteration 01 p0029 A72-10665
- Multifunction integrated microwave array antenna design emphasizing interlacing multifrequency bands into single aperture and mutual interaction effects reduction between elements 01 p0039 A72-10667
- Tubular traveling wave antenna array for radar applications and microwave television transmitters, describing computer program for design 01 p0039 A72-10668
- Broadband beam scanned linear waveguide antenna array design with FMCW short range high resolution radar for airport navigational aid in fog 01 p0039 A72-10669
- Limited scan microwave antenna design, discussing angular coverage, feed motion and focal field distribution 01 p0039 A72-10670
- Broadband high gain large aperture Schwarzschild antenna systems design, considering compromises and tradeoffs in scan angle, F/D ratio and surface shapes 01 p0039 A72-10672
- Large aperture antenna feed design, calculating focused and unfocused amplitude and phase field distributions in front of circular aperture 01 p0029 A72-10674
- Dielectric cone feeds design for microwave antennas, presenting radiation patterns 01 p0029 A72-10675
- Corrugated horn antenna design, discussing difficulties associated with mode amplitude and phase control 01 p0040 A72-10679
- Radiation pattern of corrugated conical horn with wide flare angle, deriving horn feed design criteria 01 p0040 A72-10682
- Short backfire antenna gain increase, considering construction case, reflector arrangement and circular polarization 01 p0040 A72-10684
- Moderate gain superdirective antenna arrays design based on backfire principle, using parasitic elements 01 p0040 A72-10685
- Design, construction and testing of wideband circularly polarized dipole antenna suitable for ionospheric research 01 p0043 A72-11235
- Broadband dipole antenna design based on method of moments, noting VSWR and current distribution 01 p0043 A72-11241
- Nozzle shaped antenna for synchronous satellite, obtaining radiation patterns 01 p0043 A72-11245

Automatically retrodirective performance from circular arrays and circularly continuous aperture antennas, applying method to cylindrical antennas

01 p0043 A72-11248

Equivalent circuits and characteristics of multiwire and small active transistorized antennas including unipoles, loops, Franklin arrays and mast antennas

02 p0191 A72-11685

Narrow flare angle scalar antenna feed radiation pattern derivation, showing horn gain variation with respect to length

02 p0191 A72-11895

Dielectric loaded cavity or waveguide slot antennas for telemetry applications, describing design and fabrication

02 p0192 A72-12157

Limited scan antenna system for precision approach radar, detailing design for reflector, aperture gain and phased array

02 p0193 A72-12393

Linear aperture antennas approximate synthesis method, determining radiation pattern characteristics by solution of extremal problems in theory of linear integral operators

02 p0195 A72-12592

Optimal synthesis for radiator coordinates and complex amplitudes of linear antenna array for given radiation pattern

02 p0196 A72-12756

Statistical synthesis of antenna arrays using phase amplitude distribution equivalent to reference array radiation pattern

02 p0196 A72-12758

Isolated antenna system for shielded enclosure measurements at 20-200 MHz, discussing associated circuits design and performance tests

03 p0333 A72-14037

ATS F and G ground station mobile terminal, discussing system flexibility, utility and reliability features and parabolic antenna design

04 p0485 A72-14478

Wire antenna computer design to determine feed voltages for obtaining pattern synthesis and gain maximization, using matrix methods

04 p0495 A72-14492

Flange angle effects on sectional horn antenna E-plane radiation patterns and beam focusing and broadening

04 p0497 A72-14511

Book on metallic and dielectric antennas covering planar, cylindrical and plasma types for symmetrical, dipole and ring excitations

04 p0497 A72-14612

Arbitrarily located inclined resonant slot in waveguide antenna, obtaining condition for circularly polarized radiation from scattering parameters analysis

04 p0499 A72-15205

Geometric optics method accuracy in design of dual-mirror antenna illumination system, noting diffraction effects and near field influence

04 p0499 A72-15242

Antenna design and performance in random fields, using statistical description of fields

04 p0500 A72-15394

Antenna synthesis problems for given radiation pattern, discussing stable method of solution for amplitude or phase current distribution

04 p0500 A72-15404

Phase-amplitude current distribution calculation for plane array and curvilinear radiator based on given amplitude radiation pattern

04 p0500 A72-15405

Synthesis of currents along linear antennas, reducing to solution of integral equation

04 p0500 A72-15406

Conical logarithmic foil type spiral antenna, presenting model of wavelength lenses used in dielectric rod antennas

04 p0500 A72-15408

Broadband corrugated conical horn antennas with small flare angles, investigating radiation patterns and bandwidth

04 p0501 A72-15425

Small arbitrary shape antennas with inner transmission line loading, showing efficiency without external matching circuit

04 p0501 A72-15432

Time domain analysis of wire antennas including straight, vee and zigzag dipoles

04 p0502 A72-15448

Log periodic dipole antenna design with loop elements, discussing radiation patterns and resistance, efficiency, polarization and gain

04 p0503 A72-15673

Antenna synthesis problems approximate solution with reactive factor/supergain ratio, involving radiation pattern and aperture current expansion as orthogonal functions

05 p0634 A72-15819

French book on antenna application to radars and space techniques covering UHF techniques, mathematical theories and apparatus development

05 p0626 A72-16287

Microwave antennas, feed systems, strip transmission lines and test instrumentation, examining radiation patterns, design and polarization characteristics

05 p0635 A72-16330

Supersynthesis antenna array design by analytical approach involving isolation and separate optimization of parameters effects on spatial frequency component sampling

06 p0771 A72-17341

Radiation field from slot antennas on semiinfinite conducting cone surface, evaluating patterns for various cone angles, slot positions and azimuthal variations

06 p0781 A72-17342

Four uhf antennas buried beneath refractory concrete, discussing design, fabrication and power gain and azimuthal pattern measurements

06 p0771 A72-17345

E-plane dielectric slabs symmetrical loading effects on horn aperture efficiency enhancement from far field calculation

[AD-738714] 06 p0781 A72-17347

Optimal design of directive dielectric loaded circular waveguide antenna for parabolic reflectors and radar detection

06 p0782 A72-17356

Rectangular planar antenna array directivity from constituent linear arrays of dipoles or isotropic elements, using Forman method

06 p0782 A72-17358

Electronically scanned steerable antenna array design with interelement coupling, considering maximum gain and radiation pattern control

06 p0773 A72-17497

Pyramidal horn antenna with mesh conducting surface comparing response with geometrically similar horn with continuous walls

06 p0783 A72-17600

Single slotted waveguide linear arrays, discussing microwave antenna design and feeding and cross polarization suppression

06 p0784 A72-17740

Optimum directional arrays design with linear programming simplex method generation of point elements excitation

06 p0774 A72-17855

Hansen-Woodyard condition applicability in continuous linear array design for increased directivity with optimal excitation

06 p0775 A72-18238

Two-layer dielectric loaded cylindrical antenna with wall airgap, calculating radiation pattern by boundary value approach

06 p0775 A72-18240

Yagi antenna radiation pattern parameters optimization for maximum directional gain, minimum sidelobe and optimal slope curvature

07 p0952 A72-18852

Antenna radiation pattern synthesis, discussing current phase and amplitude distribution determination by iterative and quadratures solutions respectively

07 p0953 A72-19004

Statistical characteristics of antenna gain threshold as function of link trajectory during radiation pattern shift with respect to fixed orientation

07 p0953 A72-19006

Frequency-independent multimode equiangular/conical spiral antenna with thick wires, calculating current distribution and radiation pattern by numerical program

07 p0939 A72-19187

Wideband IR heterodyne receiver in spatially coherent array, discussing signal conversion efficiency, beam crossover control, mixer characteristics and microwave antenna comparison

07 p0940 A72-19237

Element position design of pencil beam thin phased arrays with low sidelobes

07 p0941 A72-19256

Lens antennas for amplitude and phase transformations, examining existence of solutions and bounds in terms of parameters

07 p0985 A72-19404

Communications and TV broadcasting antenna feeder cost-efficient designs, relating climatology, oscillation theory and structural aerodynamic stability

07 p0955 A72-19513

Corrugated surface wave antenna design with low sidelobe level radiation pattern, finding relief modulated impedance parameters

07 p0955 A72-19514

Linear antenna synthesis for minimum sidelobe level, eliminating superdirectivity effect

07 p0956 A72-19567

Corrugated conical horn antenna groove electromagnetic field analysis for design of scalar feed radiation pattern

07 p0945 A72-19661

Computer simulated phased arrays with randomly located elements, deriving peak sidelobe level for comparison with measurement

07 p0945 A72-19783

Conical reflector microwave antenna design including subreflector with horn feed, presenting ray and physical optics analysis for radiation patterns

07 p0957 A72-19786

Wideband dual mode dielectric loaded horn antenna, discussing structure and radiation patterns

07 p0957 A72-19793

Book on statistical antenna theory covering radiation patterns and other parameters for large multielement, mirror, and synthetic aperture antennas

07 p0957 A72-19862

Improved circuit theory for linear antenna array design, obtaining maximum directivity and corresponding current distributions and driving-point voltages and currents

07 p0958 A72-20193

Antenna optimal radiation patterns, discussing antenna synthesis based on desired far field characteristics

08 p1138 A72-20743

Parabolic antenna instantaneous phase center calculations, using radiation patterns from aperture field and current distribution methods

08 p1138 A72-20744

Optimum directive gain of circular Taylor patterns for planar aperture antenna design

08 p1143 A72-21987

Conjugate gradient method for computerized antenna radiation pattern synthesis using error functional minimization and iterative procedure

08 p1143 A72-21988

Hoghorn parabolic antenna design, presenting relations for dimensions, aperture field and radiation pattern calculation by computer

09 p1284 A72-22242

Horn antenna synthesis for determining impedance boundary conditions at walls for aperture field distribution

09 p1285 A72-22574

Phased array radar systems synthesis based on life cycle cost minimization, taking into account high-speed digital data processing

09 p1280 A72-23374

Log periodic dipole antenna design parameters effects on bidirectional radiation pattern

09 p1282 A72-23571

Adaptive optimal antenna array detection of unknown spatial location radar targets, noting tradeoff between array size and signal energy with respect to performance

10 p1434 A72-23809

Input impedance of plane antenna immersed in plasma within magnetic field and propagating sheath waves

10 p1520 A72-24132

Synthesis of linear antenna with integrated currents for specified ratio of antenna radiation to elementary radiator patterns

10 p1436 A72-24504

Optimal antennas statistical synthesis for minimum noise power for given signal gain

10 p1436 A72-24505

Synthesis of slot antenna on metallic wedge for amplitude radiation pattern, determining RMS approximation and fixed phase diagram

10 p1436 A72-24506

Synthesizing antenna arrays perpendicular to conducting screen by PSK signal theory, discussing optical binary phasing and radiation patterns numerical data

10 p1450 A72-24507

Current distribution approximation for toroidal antennas of small cross section under incident electromagnetic excitation

10 p1453 A72-25104

Gravitational wave antenna response to linear, mixed and randomly polarized sources, discussing Weber signals galactic nucleus source

11 p1717 A72-25882

Finite and infinite number element phased array antennas, deriving active impedance, element pattern and power gain

11 p1593 A72-26096

Optimum synthesis of antenna array of slot radiators with passive elements, using nonlinear programming

11 p1597 A72-26708

Minimum sidelobe radiation level of circular aperture antennas as function of gain and direction finding characteristics

11 p1597 A72-26709

Optimal sum-difference characteristics of nonsuperdirective convex slot spherical antennas for maximum directive gain and minimum spatial sidelobe radiation

11 p1598 A72-26713

Computerized antenna array design, using Automated Engineering and Scientific Optimization Program

12 p1792 A72-27735

Optimal directional gain and slope difference characteristics of cylindrical nonsuperdirective slot antennas, relating sidelobe-main lobe radiation

13 p1927 A72-28408

- Optimum aperture distributions for radiation pattern shaping for arbitrary superdirectivity ratio in antenna design 13 p1915 A72-28528
- Antenna synthesis and inverse problems solution by regularization methods, considering radiation patterns and random error effects 13 p1916 A72-28535
- Strip and line source antennas quality factor, examining relationship to superconductivity ratio 13 p1928 A72-28529
- Wave channel type antenna design with modulated phase velocity and multiple use of antenna array 13 p1916 A72-28535
- Design of parabolic reflector antenna with pyramidal horn radiator closed by quadratic waveguide, calculating radiation pattern 13 p1929 A72-28895
- Aircraft antennas design for radio links to satellites for aeronautical communication and ATC, proposing use of beam steering system 13 p1929 A72-29039
- Antenna array synthesis for radiation patterns prescribed by continuous function, proposing formulas for current determination 13 p1932 A72-29347
- Reflector networks analysis for optimal operation of electronic scanning antenna in illuminated grating 14 p2087 A72-30335
- Combination antenna unit with vertical monopole and two perpendicular slots in horizontal plane to yield steerable cardioid-shaped pattern for vertically polarized waves 15 p2195 A72-31670
- Broadband arrays and multimode fed antenna excitation pattern mathematical synthesis in terms of optimization in Hilbert space 15 p2206 A72-31776
- Bandwidth log-periodic dipole array radiation pattern and impedance characteristics as function of design parameters 15 p2197 A72-31892
- Monopole antenna height reduction by transistor amplifier incorporation in antenna structure 15 p2208 A72-32390
- Thin circular loop antenna input admittance and current distribution calculation comparison 15 p2208 A72-32391
- Time domain analysis of long thin bar antenna response to gravitational signals, estimating sensitivity limit via noise background analysis 15 p2209 A72-32673
- Numerical analysis of boundary value problem for finite cylindrical dipole antenna of arbitrary orientation in magnetized plasma approximated by uniaxial medium 16 p2423 A72-33013
- The analysis of deployable umbrella parabolic reflectors. 16 p2366 A72-34107
- Properties of a nonisosceles triangular grid planar phased array. 17 p2524 A72-34351
- A broad-band wide-angle scan matching technique for large environmentally restricted phased arrays. 17 p2524 A72-34352
- A synthesis of array antennas for high directivity and low sidelobes. 17 p2513 A72-34353
- Phase optimization of antenna array gain with constrained amplitude excitation. 17 p2525 A72-34354
- Cross coupling in a five horn monopulse tracking system. 17 p2513 A72-34355
- An electromagnetic analysis of a cylindrical homogeneous lens. 17 p2513 A72-34356
- Pattern synthesis of hexagonal planar arrays. 17 p2525 A72-34362
- On the behavior of thin-wire antennas and scatterers arbitrarily located within a parallel-plate region. 17 p2525 A72-34363
- Focusing properties and efficiency of EHF waveguide lens with Al honeycomb as guiding medium, noting design considerations and performance test results 17 p2513 A72-34365
- Shaped-beam synthesis of nonuniformly spaced linear arrays. 17 p2525 A72-34370
- A fast numerical method for determining the optimum SNR of an array subject to a Q factor constraint. 17 p2514 A72-34372
- Computer aided impedance matching of an interleaved waveguide phased array. 17 p2525 A72-34373
- Frequency-scanned X-band waveguide array. 17 p2525 A72-34374
- Radiation from a directive continuous spiral antenna array. 17 p2526 A72-34376
- A portable coaxial collinear antenna. 17 p2526 A72-34377
- Design of an array of circular-loop antennas with optimum directivity. 17 p2514 A72-34387
- Five-horn feed system design for improving large steerable antenna monopulse performance, discussing weight and cost reductions by focal length selection 17 p2526 A72-34467
- Book - Theory and analysis of phased array antennas 17 p2515 A72-34621
- Problem of antenna parameter optimization in the presence of random errors 17 p2529 A72-34831
- Relationship between antenna synthesis for a given radiation pattern and the synthesis of spatial signal processing systems 17 p2515 A72-34832
- Engineering approach to the design of tapered dielectric-rod and horn antennas. 17 p2530 A72-35362
- Surface waves in the corrugated conical horn. 17 p2517 A72-35387
- Steerable directional VHF antenna design for radio interferometric tracking and ranging of Symphonie satellite 17 p2536 A72-35432
- [DFVLR-SONDDR-222] Pattern synthesis of linear arrays using Fourier coefficient matching. 18 p2659 A72-36298
- Optimal distributions for semi-circular arrays of isotropic radiators. 18 p2666 A72-36330
- A short-wave rotating antenna for 500-kW transmitter output 18 p2666 A72-36676
- Low noise microwave receiving systems on a 64 m antenna. 19 p2763 A72-37255
- Log periodic dipole antenna systems for ILS localizers, noting reduced sensitivity to snow and ice 19 p2830 A72-37279
- Application of the Volterra series to the analysis and design of an angle track loop. 19 p2830 A72-37283
- Design of Cassegrain antennas employing dielectric cone feeds. 19 p2772 A72-37847
- Application of the computer to aerial design and development. 19 p2773 A72-37873
- Yagi-Uda helical antenna array with moderate gain and compact mechanical design, determining electrical characteristics 19 p2773 A72-37941
- Gain averages as criteria for antenna EMC-performance. 20 p2902 A72-39001
- Optimal synthesis for radiator coordinates and complex amplitudes of linear antenna array for given radiation pattern 20 p2907 A72-39062
- Statistical synthesis of antenna arrays using phase amplitude distribution equivalent to reference array radiation pattern 20 p2907 A72-39064
- Reflector profiles for the pencil-beam Cassegrain antenna. 20 p2903 A72-39221
- Reliable advanced solid state radar /RASSR/ array design featuring transmit-receive elements arranged in triangular grid and built-in test equipment 20 p2904 A72-39732
- Faraday rotation dual-mode ferrite reciprocal phaser with performance and cost advantages over toroidal type for microwave phased array applications 20 p2909 A72-39733
- Selection of an optimal design for a spacecraft antenna system 21 p3025 A72-40311
- Certain problems in designing highly directional spacecraft antennas 21 p3026 A72-40325
- Analysis and element pattern design of periodic arrays of circular apertures on conducting cylinders. 21 p3026 A72-40351
- Wave propagation on helical antennas. 21 p3015 A72-40352
- Analysis and design of TEM-line antennas. 21 p3026 A72-40353
- Performance of antennas in random fields. 21 p3026 A72-40355
- A flat-feed technique for phased arrays. 21 p3026 A72-40356
- A proposed approach for increasing the azimuthal resolution in HF radar. 21 p3015 A72-40360
- The optimum design of small nonuniformly spaced arrays. 21 p3027 A72-40362
- Gain of arrays of dipoles with a ground plane. 21 p3027 A72-40364
- On the radiation from an open-ended corrugated pipe carrying the HE sub 11 mode. 21 p3015 A72-40366
- The efficiency of near-field Cassegrainian antennas. 21 p3027 A72-40367
- On the efficiency and radiation patterns of mismatched shaped Cassegrainian antenna systems. 21 p3027 A72-40369
- Radiation efficiency of electrically small multiturn loop antennas. 21 p3027 A72-40370
- A metallized channel guide antenna for use over a cylindrical ground screen. 21 p3027 A72-40372
- On the relationship between classical and matrix design methods for arrays of wire antennas. 21 p3027 A72-40373
- Constrained optimization of the gain of an array of thin wire antennas. 21 p3027 A72-40374
- Antenna radiation patterns synthesis from individual elements amplitude and phase characteristics, using method based on steepest descent technique 21 p3028 A72-40506
- Design and investigations regarding a phase-controlled dipole group with radiation input 21 p3028 A72-40508
- Computerized design for cylindrical cage antenna, using polynomial approximation of current to reduce computer size and time requirements 21 p3028 A72-40511
- Two-hybrid mode feed design procedure and performance for small and large f/D ratio reflectors of microwave telescope 21 p3029 A72-40515
- Near-field Cassegrain antennas of high surface efficiency for satellite communication links 21 p3029 A72-40520
- A 3-meter Cassegrain antenna for the frequency range from 2.1 to 2.3 GHz 21 p3029 A72-40521
- A polydirectional antenna in polygon reflector design with cosecant-type elevation directional diagram for providing television in the 12-GHz frequency range 21 p3029 A72-40524
- Active transistorized directional dipole VHF receiving antennas for ATC and mobile applications and field intensity measurement 21 p3030 A72-40527
- Radiation patterns of dielectric antenna of size comparable to radiator wavelength in air, discussing narrow band and broadband configurations 21 p3030 A72-40528
- Radar double beam dielectric radiator antenna design for ATC in 1250-1350 MHz range 21 p3030 A72-40530
- Polar orbiting Aeros aeronomy satellite turnstile antenna system with nearly spherical radiation pattern, discussing design modifications for optimization 21 p3030 A72-40533
- Integral equation method for boundary value problem of logarithmic spiral antenna, noting suitability for digital computers 21 p3031 A72-40535
- Series-dipole antenna design based on Ehrenspeck short backfire antenna mirror method, noting small dimensions and cost reduction 21 p3031 A72-40539
- Reflector optimization of backfire antennas with the aid of the theory of the Fresnel zones 21 p3031 A72-40541
- Broad-band television transmitting antenna with polydirectional characteristics for the UHF-region 21 p3031 A72-40542
- Main-reflector-rim diffraction in back direction. 21 p3032 A72-40632
- Multiple beam fixed reflector antenna configuration selection for reliable satellite communication earth stations, considering tradeoffs between gain, transmitter power and receiver noise temperature 21 p3032 A72-40879
- Side and back lobe structures of directive antennas. 21 p3020 A72-40903
- A directional antenna represented by a system of two wires positioned on the generatrix of a relief impedance cylinder 21 p3033 A72-40942
- Electronically scannable plasma leaky wave antenna system. 21 p3022 A72-41325
- A dual frequency, dual polarized feed for radioastronomical applications. 21 p3034 A72-41400
- Null placing in radiation patterns by shaping antenna edges. 21 p3034 A72-41467
- Linear antenna synthesis for minimum sidelobe level, eliminating superdirectivity effect 22 p3158 A72-42085
- Diffraction by an infinite corner reflector transversely loaded by concentric dielectric slabs. 22 p3159 A72-42301
- Antenna synthesis problems approximate solution with reactive factor /supergain ratio/, involving radiation pattern and aperture current expansion as orthogonal functions 23 p3268 A72-43427
- Design of radiating elements for large planar arrays - Accomplishments and remaining challenges. 23 p3269 A72-43571

- Wideband limitations of waveguide arrays.
23 p3270 A72-43573
- Beam port coupled waveguide antenna radiation patterns for uniform and cosine plus pedestal radiating aperture distribution, using coupled mode theory
23 p3264 A72-43602
- A high-accuracy radio direction finder with a moving antenna
23 p3270 A72-43769
- Radiation patterns and structural design of two mirror millimeter wave Cassegrain antennas with horn radiator
23 p3271 A72-43778
- Thermal energy dissipation in artificial antennas of large broadcasting transmitters studying cooling systems
23 p3278 A72-44311
- Butler-matrix fed arrays, discussing phase differences, scan steps and sectors, sidelobe structure and attenuation
23 p3273 A72-44363
- Synthesis of horn antenna with impedance boundary conditions on walls and specified aperture field distribution
24 p3384 A72-44753
- ANTENNA FEEDS**
- Phased array antennas design and performance characteristics, examining feeding and electronic scanning problems with special attention to all-solid-state designs
01 p0038 A72-10659
- Limited scan microwave antenna design, discussing angular coverage, feed motion and focal field distribution
01 p0039 A72-10670
- High efficiency reflector antennas, discussing secondary subreflector for feed energy redistribution
01 p0039 A72-10671
- Large aperture antenna feed design, calculating focused and unfocused amplitude and phase field distributions in front of circular aperture
01 p0029 A72-10674
- Dielectric cone feeds design for microwave antennas, presenting radiation patterns
01 p0029 A72-10675
- Feed requirements and design of Effelsberg radio telescope with parabolic reflector operating down to 1 cm wavelengths
01 p0040 A72-10676
- Hybrid mode secondary focus feed realization for Effelsberg radio telescope, giving antenna radiation patterns
01 p0040 A72-10677
- Multimode feeds development for off-set Cassegrain tracking antennas
01 p0040 A72-10678
- Radiation pattern of corrugated conical horn with wide flare angle, deriving horn feed design criteria
01 p0040 A72-10682
- Self admittance and radiation conductance characteristics of stripline feed slots in waveguide walls
01 p0029 A72-10683
- Narrow flare angle scalar antenna feed radiation pattern derivation, showing horn gain variation with respect to length
02 p0191 A72-11895
- Prime focus paraboloid antenna performance with cylindrical hybrid mode feeds, detailing radiation patterns and distribution
02 p0173 A72-12110
- Center fed full wave dipole antenna with feed points displaced transverse to dipole axis, considering radiation patterns, electrical properties and power gain
02 p0177 A72-12325
- Wire antenna computer design to determine feed voltages for obtaining pattern synthesis and gain maximization, using matrix methods
04 p0495 A72-14492
- Two center-fed feed-point displaced dipole antennas, calculating mutual impedance for various combinations of displacements and heights
04 p0501 A72-15433
- Frequency response of passive dipole antennas fed by transistor circuit, investigating power gain, bandwidth and voltage SWR
04 p0503 A72-15670
- Electrical properties of unbalanced center-fed non-planar dipole antenna, discussing radiation patterns and resistance, power gain, aperture and efficiency
04 p0503 A72-15674
- Microwave antennas, feed systems, strip transmission lines and test instrumentation, examining radiation patterns, design and polarization characteristics
05 p0635 A72-16330
- Low cost automated digitized measurement for microwave antenna feed power gain and relative phase, using computer facilities
05 p0637 A72-16420
- Spherical reflector antenna phase aberration correction by planar array feeds, discussing synthesis procedure for mean square error minimization
06 p0781 A72-17344
- Corrugated conical horn antenna groove electromagnetic field analysis for design of scalar feed radiation pattern
07 p0945 A72-19661
- Conical reflector microwave antenna design including subreflector with horn feed, presenting ray and physical optics analysis for radiation patterns
07 p0957 A72-19786
- Balun-fed open sleeve dipole in front of metallic reflector for 225-400 MHz band operation, investigating radiation pattern and gain
07 p0957 A72-19794
- Circular and rectangular waveguide excited dielectric spheres as antenna feed, noting gain and polarization linearity
07 p0957 A72-19796
- Launching horn effect on radiation pattern of dielectric cone feeds, proposing wide angle sidelobe reduction via absorbent sheath
12 p1791 A72-27669
- Waveguides for primary and hybrid mode horns for secondary feeders of deep paraboloid reflector radio telescope in Effelsberg, West Germany
12 p1793 A72-27811
- Directional and mode characteristics of coaxial exciter for high area utilization and low halation paraboloid antennas
12 p1793 A72-27812
- Pulse excitation of traveling wave antenna array, describing spectral method of solving high resolution side-looking radar limitation
13 p1915 A72-28526
- Rectangular slots linear array and feed network performance in reentry plasma environment, obtaining self and mutual impedances, gain and radiation pattern
13 p1916 A72-28537
- Radiation patterns of linear equidistant fishbone-type dipole antenna array fed by long symmetrical transmission line
13 p1930 A72-29056
- Parabolic reflector fed by log-periodic dipole antenna array, predicting combined effects of feed phase center lateral and axial displacement on secondary performance
15 p2205 A72-31541
- Broadband arrays and multimode feed antenna excitation pattern mathematical synthesis in terms of optimization in Hilbert space
15 p2197 A72-31892
- Mathematical analysis of feed point displacement effects on linear dipole antennas, investigating radiation properties
16 p2362 A72-32852
- Quadratic phase feed for phased arrays as method of preventing degradation of sidelobe level of patterns due to quantization
17 p2526 A72-34384
- L band optimum monopulse high power feed using dominate and higher order waveguide modes to develop sum and difference patterns
17 p2526 A72-34421
- Five-horn feed system design for improving large steerable antenna monopulse performance, discussing weight and cost reductions by focal length selection
17 p2526 A72-34467
- Distribution of current in centre-fed cylindrical dipole antennas with arbitrarily displaced feed points.
17 p2526 A72-34517
- Solid state phased arrays for ECM applications.
17 p2531 A72-35569
- A multi-channel rotary joint for spacecraft applications.
19 p2770 A72-37260
- Design of Cassegrain antennas employing dielectric cone feeds.
19 p2772 A72-37847
- Application of the computer to aerial design and development.
19 p2773 A72-37873
- Radiation characteristics of dielectric cones.
20 p2904 A72-39773
- Microwave filters in antenna circuit feeder systems of space vehicles
21 p3026 A72-40318
- Spacecraft antenna feeder channel parameter control in flight
21 p3026 A72-40319
- A flat-feed technique for phased arrays.
21 p3026 A72-40356
- On the removal of blindness in phased antenna arrays by element positioning errors.
21 p3027 A72-40363
- On the efficiency and radiation patterns of mismatched shaped Cassegrain antenna systems.
21 p3027 A72-40369
- Design and investigations regarding a phase-controlled dipole group with radiation input
21 p3028 A72-40508
- Reflector antennas for satellite communication, discussing hybrid mode, dielectric and lens feeds, spherical and stepped reflectors, and high efficiency paraboloid antennas
21 p3028 A72-40513
- Coaxial exciter for parabolic antennas with high area efficiency and small halation
21 p3029 A72-40514
- Two-hybrid mode feed design procedure and performance for small and large f/D ratio reflectors of microwave telescope
21 p3029 A72-40515
- Spherical reflector as possible antenna for millimeter wave astronomy, discussing feed design for spherical aberration corrections
21 p3029 A72-40519
- A dual frequency, dual polarized feed for radioastronomical applications.
21 p3034 A72-41400
- Synthesis of horn antenna with impedance boundary conditions on walls and specified aperture field distribution
24 p3384 A72-44753
- Simple small primary feed for large opening angles and high aperture efficiency.
24 p3385 A72-44961
- ANTENNA FIELDS**
- U ANTENNA RADIATION PATTERNS**
- NT SIDELOBES**
- Helicopter antenna placement, using scale models for three dimensional radiation pattern semiautomatic recording under free space conditions
01 p0024 A72-10149
- X-band linear phased array tracking antenna with digital phase shifters and beam steering, evaluating beamwidth, gain and direction error
01 p0028 A72-10663
- Linear antenna array optimal power pattern synthesis by best approximation, using weighting function in man-machine iteration
01 p0029 A72-10665
- Far field patterns of hourglass reflector phased array for electronic despin of communications antenna on spin stabilized satellite
01 p0029 A72-10666
- Reflector antennas with very high front-to-back ratio - Theory and experiments on models.
01 p0029 A72-10673
- Dielectric cone feeds design for microwave antennas, presenting radiation patterns
01 p0029 A72-10675
- Hybrid mode secondary focus feed realization for Effelsberg radio telescope, giving antenna radiation patterns
01 p0040 A72-10677
- Corrugated conical horn antennas with arbitrary groove depth, considering far field radiation patterns
01 p0040 A72-10680
- Radiation patterns from rectangular guide horns with impedance walls, analyzing hybrid modes
01 p0040 A72-10681
- Radiation pattern of corrugated conical horn with wide flare angle, deriving horn feed design criteria
01 p0040 A72-10682
- Hertzian dipole radiation with impulsive currents in nondispersive dielectric half space
01 p0030 A72-10841
- Radiation patterns of symmetrical dipoles or small apertures on perfectly conducting sphere, using dyadic Green function analysis
01 p0030 A72-10844
- Radome enclosed Haystack parabolic antenna characteristics as radio astronomical instrument, discussing gain, polarization, interference susceptibility and noise temperature
01 p0032 A72-11233
- Boundary value problem solution for multiple interleaved phased arrays of waveguide radiators operating at different frequencies, investigating transmission characteristics
01 p0042 A72-11234
- Aperture and pattern space factors relationship for vector fields of rectangular and circular apertures, investigating characteristic functions
01 p0043 A72-11240
- Nozzle shaped antenna for synchronous satellite, obtaining radiation patterns
01 p0043 A72-11245
- Narrow flare angle scalar antenna feed radiation pattern derivation, showing horn gain variation with respect to length
02 p0191 A72-11895
- Prime focus paraboloid antenna performance with cylindrical hybrid mode feeds, detailing radiation patterns and distribution
02 p0173 A72-12110
- Equiphasic radiating apertures maximum directivity under nonaxial orientation conditions, discussing limitation dependence on illumination law for major and lateral lobes
02 p0194 A72-12570
- Linear aperture antennas approximate synthesis method, determining radiation pattern characteristics by solution of extremal problems in theory of linear integral operators
02 p0195 A72-12592
- Optimal synthesis for radiator coordinates and complex amplitudes of linear antenna array for given radiation pattern
02 p0196 A72-12756
- Scattering diagram for mutual cross coupling between antennas in Fresnel zone
02 p0196 A72-12757
- Statistical synthesis of antenna arrays using phase amplitude distribution equivalent to reference array radiation pattern
02 p0196 A72-12758

- Radiation pattern and reflected field analysis for incident plane wave on phased arrays of thick wall rectangular waveguides 03 p0330 A72-13168
- Antenna sidelobe radiation probability assessment for directional gain 03 p0333 A72-13832
- Digital computer solution for near field coupling between high and low gain antennas above conductive surface 03 p0323 A72-14029
- Antenna arrays near-field radiation pattern prediction, using Harrington matrix methods 03 p0323 A72-14030
- Planar phased array antennas with uniform current amplitudes, calculating beam-pointing error dependence on array geometry, phase errors and scan angle 03 p0325 A72-14179
- Rectangular slot antennas radiation through inhomogeneous plasma layer with dielectric window, obtaining input admittances by fields modal expansion 04 p0554 A72-14412
- Passive airborne mapping of radiation sources, using fixed side-looking multilobed and scanning fan beam antenna pattern with coherent optical processing of film records 04 p0495 A72-14491
- Phased antenna array blind spot detection and elimination, describing aperture match with inductive irises 04 p0486 A72-14493
- Flange angle effects on sectional horn antenna E-plane radiation patterns and beam focusing and broadening 04 p0497 A72-14511
- Iterative synthesis of dipole antenna array for maximum directivity radiation pattern, considering amplitude-phase distributions 04 p0499 A72-15142
- Signal fluctuation effect on directional properties of multipole receiving antenna, calculating radiation pattern 04 p0499 A72-15143
- Highly directional circular array antennas radiation characteristics calculation, showing sidelobe size dependence on aperture angle 04 p0499 A72-15240
- Geometric optics method accuracy in design of dual-mirror antenna illumination system, noting diffraction effects and near field influence 04 p0499 A72-15242
- Error distribution computation for combined Rayleigh-Gaussian statistics data, applying to antenna radiation beam-pointing example 04 p0500 A72-15303
- Antenna design and performance in random fields, using statistical description of fields 04 p0500 A72-15394
- Antenna synthesis problems for given radiation pattern, discussing stable method of solution for amplitude or phase current distribution 04 p0500 A72-15404
- Phase-amplitude current distribution calculation for plane array and curvilinear radiator based on given amplitude radiation pattern 04 p0500 A72-15405
- Spacecraft antenna radiation pattern numerical analysis using combined electric and magnetic integral equations 04 p0500 A72-15407
- Radiation pattern of radio astronomical paraboloidal reflector antenna in Dwingeloo, Netherlands, determining directivity and beam efficiency 04 p0501 A72-15423
- Broadband corrugated conical horn antennas with small flare angles, investigating radiation patterns and bandwidth 04 p0501 A72-15425
- Metrology and radio performance of steerable antenna paraboloidal reflector, considering profile measurements by optical range finder and laser methods 04 p0493 A72-15518
- Active loop-dipole antennas with height reduction properties at resonance, deriving input impedance power gain and radiation patterns 04 p0502 A72-15519
- Spherical antenna covered by lossy hot plasma layer, calculating radiation fields by transmission line theory 04 p0493 A72-15525
- Log periodic dipole antenna design with loop elements, discussing radiation patterns and resistance, efficiency, polarization and gain 04 p0503 A72-15673
- Electrical properties of unbalanced center-fed nonplanar dipole antenna, discussing radiation patterns and resistance, power gain, aperture and efficiency 04 p0503 A72-15674
- Antenna synthesis problems approximate solution with reactive factor/supergain ratio/, involving radiation pattern and aperture current expansion as orthogonal functions 05 p0634 A72-15819
- Random phasing algorithms to reduce phase quantization lobes for radiation patterns of commutated phased array antennas 05 p0634 A72-15820
- Antenna azimuthal radiation patterns and meteor radiant distribution effects on wind velocity measurement by radar observation of meteor trains 05 p0715 A72-16251
- Microwave antennas, feed systems, strip transmission lines and test instrumentation, examining radiation patterns, design and polarization characteristics 05 p0635 A72-16330
- Controlled polarization pattern of rectangular guide slots array as function of exciting wave parameters, presenting formulas for elliptical polarization distortion determination 05 p0635 A72-16331
- SNR effect on rms bearing error by amplitude comparison for nonscanning nontracking receiving system with two antenna lobes of arbitrary shape 05 p0629 A72-16577
- Electromagnetic and electroacoustic near zone fields of linear antenna in plasma measured by diagnostic probe 05 p0700 A72-17232
- Radiation field from slot antennas on semiinfinite conducting cone surface, evaluating patterns for various cone angles, slot positions and azimuthal variations 06 p0781 A72-17342
- Slot excited conical antenna, calculating first order diffraction coefficients by integral expressions for radiation field 06 p0781 A72-17343
- Four uhf antennas buried beneath refractory concrete, discussing design, fabrication and power gain and azimuthal pattern measurements 06 p0771 A72-17345
- E-plane dielectric slabs symmetrical loading effects on horn aperture efficiency enhancement from far field calculation [AD-738714] 06 p0781 A72-17347
- Half wavelength antenna radiation admittance into warm lossy two layer plasma half space, using effects of slot width and electron collision frequency 06 p0781 A72-17348
- Double parasitic loop counterpoise antenna radiation properties comparison to VOR systems, noting siting error reduction 06 p0782 A72-17357
- Antenna pattern sidelobe control for line sources and uniformly spaced linear arrays, using iterative sampling method 06 p0782 A72-17359
- Electronic scanning steerable phased array radar beam pointing capability improvement for moving target detection probability 06 p0772 A72-17423
- Microwave holography using transmitting and receiving antenna for generation of synthetic aperture in angular direction 06 p0814 A72-17486
- Electronically scanned steerable antenna array design with interelement coupling, considering maximum gain and radiation pattern control 06 p0773 A72-17497
- Noise parameters of space communication systems ground receiving antennas, considering noise effects on gain and radiation patterns 06 p0783 A72-17499
- Holographic methods of antenna radiation pattern measurement, noting applications to radio astronomy and radar 06 p0816 A72-17920
- Automatic measurements of wideband antenna radiation characteristics, using microwave generators linked with analyzers 06 p0775 A72-18194
- Hansen-Woodyard condition applicability in continuous linear array design for increased directivity with optimal excitation 06 p0775 A72-18238
- Two-layer dielectric loaded cylindrical antenna with wall airgap, calculating radiation pattern by boundary value approach 06 p0775 A72-18240
- Yagi antenna radiation pattern parameters optimization for maximum directional gain, minimum sidelobe and optimal slope curvature 07 p0952 A72-18852
- Antenna radiation pattern synthesis, discussing current phase and amplitude distribution determination by iterative and quadratures solutions respectively 07 p0953 A72-19004
- Linear array antenna radiation pattern synthesis for minimum sidelobe level outside of given intervals, calculating current distribution 07 p0953 A72-19005
- Statistical characteristics of antenna gain threshold as function of link trajectory during radiation pattern shift with respect to fixed orientation 07 p0953 A72-19006
- Two-channel direction finding with point source emission and spaced antennas reception, investigating cross correlation and background noise interference effects on accuracy 07 p0938 A72-19007
- Frequency-independent multimode equiangular/conical spiral antenna with thick wires, calculating current distribution and radiation pattern by numerical program 07 p0939 A72-19187
- Corrugated surface wave antenna design with low sidelobe level radiation pattern, finding relief modulated impedance parameters 07 p0955 A72-19514
- Corrugated conical horn antenna groove electromagnetic field analysis for design of scalar feed radiation pattern 07 p0945 A72-19661
- Circular semiinfinite dielectric rod antenna, determining near- and far-zone fields, gain and beamwidth under excitation by HE/sub 11/ hybrid mode 07 p0956 A72-19782
- Taylor type antenna radiation distribution for aperture edge behavior realization in E or H planes 07 p0945 A72-19785
- Conical reflector microwave antenna design including subreflector with horn feed, presenting ray and physical optics analysis for radiation patterns 07 p0957 A72-19786
- Interferometric measurement at 1415 MHz of radio telescope paraboloidal antenna radiation pattern, using cosmic radio sources with known flux density as signal source 07 p0945 A72-19789
- Wideband dual mode dielectric loaded horn antenna, discussing structure and radiation patterns 07 p0957 A72-19793
- Balun-fed open sleeve dipole in front of metallic reflector for 225-400 MHz band operation, investigating radiation pattern and gain 07 p0957 A72-19794
- Anisotropic grounded dielectric or plasma layer motion effects on magnetic or electric current line source radiation patterns 07 p0946 A72-19802
- Book on statistical antenna theory covering radiation patterns and other parameters for large multielement, mirror, and synthetic aperture antennas 07 p0957 A72-19862
- Moving isotropic plasma half space effect on magnetic or electric line source radiation patterns 07 p1044 A72-20192
- Antenna optimal radiation patterns, discussing antenna synthesis based on desired far field characteristics 08 p1138 A72-20743
- Parabolic antenna instantaneous phase center calculations, using radiation patterns from aperture field and current distribution methods 08 p1138 A72-20744
- Polarization distortion of partially polarized wave emission and reception by two channel horn antennas, noting radio astronomy, radar and optics applications 08 p1138 A72-20788
- Random antenna radiation patterns probability distribution law and Dolph-Chebyshev array design, calculating minimum statistical sidelobe level 08 p1138 A72-20930
- Impedance strip synthesis on symmetric cylindrical antenna excited by phased magnetic flux ring, determining radiation pattern for pure reactance conditions 08 p1131 A72-20932
- Homogeneous polarization diagrams synthesis for entire radiation pattern of single reflector pencil beam antenna, noting radiator aperture misalignment effect 08 p1138 A72-20933
- Gain function for planar phased array far field pattern, deriving calculation method for excitation pattern for prescribed radiated beam behavior 08 p1132 A72-21328
- Reciprocity theorem for antenna directivity pattern measurement of optical superheterodyne receiver for carbon dioxide laser radiation 08 p1140 A72-21376
- Two reflector Cassegrain antenna secondary reflector random fluctuations effects on drift in main lobe direction 08 p1143 A72-21846
- Antenna near field correction for backscatter gain in two-beam incoherent scatter radar measurements at Arecibo Observatory 08 p1137 A72-21983
- Optimum directive gain of circular Taylor patterns for planar aperture antenna design 08 p1143 A72-21987
- Conjugate gradient method for computerized antenna radiation pattern synthesis using error functional minimization and iterative procedure 08 p1143 A72-21988
- Electron temperature effects on radiation fields and resistance of short electric dipole antenna embedded in hot uniaxial plasma 08 p1215 A72-21991
- Probabilistic characteristics of radiation pattern for multielement antenna with nonpolar phase front 09 p1285 A72-22575

Monograph on slotted circular waveguide analysis covering boundary value problem solution by Wiener-Hopf and Galerkin procedures and application to far field determination
09 p1279 A72-22925

Power integral method for electric and magnetic dipole antennas vlf/elf radiation patterns in cold magnetoplasma, emphasizing focusing effects of refractive index surface
09 p1279 A72-23009

Radiation pattern of spacecraft dipole antenna mounted on conducting finite length cone calculated by superposition of radiated and diffracted waves
09 p1282 A72-23524

Log periodic dipole antenna design parameters effects on bidirectional radiation pattern
09 p1282 A72-23571

Synthesis of linear antenna with integrated currents for specified ratio of antenna radiation to elementary radiator patterns
10 p1436 A72-24504

Synthesis of slot antenna on metallic wedge for amplitude radiation pattern, determining RMS approximation and fixed phase diagram
10 p1436 A72-24506

Synthesizing antenna arrays perpendicular to conducting screen by PSK signal theory, discussing optimal binary phasing and radiation patterns numerical data
10 p1450 A72-24507

Fixed base two element interferometer for radio astronomy, obtaining beavertail radiation pattern by use of earth rotation
10 p1482 A72-24578

Dipole antenna near electric field, basing calculation method on integral equation for antenna surface charge distribution function
10 p1451 A72-24579

Wide rectangular low loss metal waveguide with dielectric layer on opposite walls, noting attenuation based on eigenwaves
10 p1451 A72-24585

Radiation pattern determination parabolic Cassegrain radio telescope reflector antennas from Fresnel zone emission source, using holographic technique
10 p1482 A72-24783

Radiation pattern of longitudinal magnetic dipole near circular cylinder parallel to flat screen
10 p1453 A72-24903

Microwave two reflector rectangular backfire antenna with dielectric surface wave structure as waveguide prolongation, obtaining far field radiation pattern
11 p1604 A72-25749

Minimum sidelobe radiation level of circular aperture antennas as function of gain and direction finding characteristics
11 p1597 A72-26709

Aperture synthesis of ring antenna arrays radiation pattern using earth rotation
11 p1597 A72-26710

Multipole synthesis compensating mutual coupling for orthonormalized radiation patterns in ring antenna array
11 p1598 A72-26711

Radiation pattern forming circuit with compensated mutual coupling in phased antenna arrays, noting synthesis by matched multipoles
11 p1598 A72-26712

Parasitic sidelobe suppression in radiation patterns of phase switching linear antenna array without gain loss
11 p1598 A72-26717

Microwave antenna radiation patterns from far field measurements by radio holograms with probe
11 p1598 A72-26718

Geostationary satellites spacing dependence on quantifying factors, describing space environment experiments for satellite attitude stability and ground station antenna patterns and polarization effects [AIAA PAPER 72-542]
12 p1780 A72-27365

Test facility for aircraft and spacecraft antennas radiation patterns and optimal installation determination
12 p1795 A72-27412

Radiation patterns of circular loop antenna in isotropic compressible plasma, discussing far fields for electromagnetic and electron plasma waves
12 p1790 A72-27491

Launching horn effect on radiation pattern of dielectric cone feeds, proposing wide angle sidelobe reduction via absorbent sheath
12 p1791 A72-27669

Numerical accuracy of electromagnetic field spherical wave expansions, considering horn antenna radiation pattern
12 p1791 A72-27670

HF backscatter pulse signal incidence elevation angle measurements based on amplitude ratio of two antennas with different vertical patterns
12 p1783 A72-27779

Directional and mode characteristics of coaxial exciter for high area utilization and low halation paraboloid antennas
12 p1793 A72-27812

Iterative method for synthesis of reflector antenna array of dipole elements to provide given radiation pattern, obtaining impedance matching values
13 p1926 A72-28372

Optimal directional gain and slope difference characteristics of cylindrical nonsuperdirective slot antennas, relating sidelobe-main lobe radiation
13 p1927 A72-28408

Optimum aperture distributions for radiation pattern shaping for arbitrary superdirectivity ratio in antenna design
13 p1915 A72-28528

Antenna synthesis and inverse problems solution by regularization methods, considering radiation patterns and random error effects
13 p1928 A72-28529

Optimization of monopulse antenna performance indices for specified sidelobe envelope function and/or specified pattern nulls
13 p1915 A72-28530

Dipole antenna radiation patterns in sinusoidally space-time periodic media
13 p1915 A72-28531

Numerical analysis of surface current density distribution and electromagnetic fields of conducting body, noting radiation patterns of radial dipole and quarter wavelength monopole
13 p1916 A72-28541

Diffraction antenna use in visual range to study troposphere modulated laser radiation propagation in turbulent atmosphere, presenting light intensity distribution
13 p1917 A72-28690

Aircraft measurements of radiation pattern of radar antenna system used for meteor height observation
13 p1919 A72-29027

Design of parabolic reflector antenna with pyramidal horn radiator closed by quadratic waveguide, calculating radiation pattern
13 p1929 A72-29039

Pyramidal horn primary element axial position effect on dual mirror Cassegrain microwave antenna main lobe pattern, obtaining optimal position
13 p1929 A72-29040

Radiation patterns of linear equidistant fishbone-type dipole antenna array fed by long symmetrical transmission line
13 p1930 A72-29056

Parabolic, Cassegrain, spherical and horn-parabolic axisymmetric mirror antennas, calculating primary radiating element orientation effects on radiation polarization characteristics
13 p1931 A72-29277

Narrow band linear filter output SNR relationship to orthogonal radiating elements system directional gain and radiation patterns
13 p1931 A72-29281

Rod antenna near field energy flow direction and intensity characterization by time independent and dependent components of Poynting vector
13 p1932 A72-29398

Radiation pattern reconstruction of radio telescope parabolic Cassegrain reflector antennas from Fresnel zone emission source, using holography and optical processing
14 p2103 A72-30221

Antenna array synthesis for radiation patterns prescribed by continuous function, proposing formulas for current determination
14 p2087 A72-30335

Wire antenna half-space problem analysis by Sommerfeld integral approach and plane wave reflection coefficient approximation
14 p2085 A72-30338

Combination antenna unit with vertical monopole and two perpendicular slots in horizontal plane to yield steerable cardioid-shaped pattern for vertically polarized waves
15 p2206 A72-31776

Bandwidth log-periodic dipole array radiation pattern and impedance characteristics as function of design parameters
15 p2208 A72-32390

Skewed wire antennas electric and magnetic near fields prediction from computer programs based on matrix inversion method
15 p2209 A72-32567

Optical modeling of antenna radiation patterns from radio hologram of Fresnel region field
15 p2209 A72-32664

Phase distribution randomization in switched antenna array, noting radiation pattern sidelobe compensation application
15 p2209 A72-32666

Microwave antenna near field apparent image and phase-amplitude distribution measurement with photocontrolled semiconductor panel
15 p2209 A72-32672

Rayleigh distribution of radio signals partially reflected from D region, noting amplitude fluctuations dependence on antenna radiation pattern
15 p2202 A72-32733

Mathematical analysis of feed point displacement effects on linear dipole antennas, investigating radiation properties
16 p2362 A72-32852

The analysis of deployable umbrella parabolic reflectors.
17 p2524 A72-34351

Phase optimization of antenna array gain with constrained amplitude excitation.
17 p2513 A72-34355

Analysis of antennas on finite circular cylinders with conical or disk end caps.
17 p2525 A72-34361

An electromagnetic analysis of a cylindrical homogeneous lens.
17 p2525 A72-34362

Pattern synthesis of hexagonal planar arrays.
17 p2525 A72-34363

A millimeter wave receiving antenna with an omnidirectional or directional scannable azimuth pattern and a directional vertical pattern.
17 p2525 A72-34364

Shaped-beam synthesis of nonuniformly spaced linear arrays.
17 p2525 A72-34370

Radiation from a directive continuous spiral antenna array.
17 p2526 A72-34376

A portable coaxial collinear antenna.
17 p2526 A72-34377

Quadratic phase feed for phased arrays as method of preventing degradation of sidelobe level of patterns due to quantization
17 p2526 A72-34384

Radiation from a magnetic line source covered with an anisotropic warm plasma slab.
17 p2587 A72-34386

Theoretical analyses on Apollo lunar surface electrical properties experiment transmitter antenna.
17 p2515 A72-34423

Automatic device for plotting antenna polar diagrams
17 p2529 A72-34766

Relationship between antenna synthesis for a given radiation pattern and the synthesis of spatial signal processing systems
17 p2515 A72-34832

Statistical estimate of the attainable sidelobe level in phase-switched antenna arrays with a nonlinear initial phase lead
17 p2529 A72-34833

Engineering approach to the design of tapered dielectric-rod and horn antennas.
17 p2530 A72-35362

Radiation pattern determination for an antenna receiving random signals
17 p2517 A72-35540

Airborne waveguide element reliable advanced solid state radar /RASSR/ phased array radiation patterns and design
17 p2531 A72-35571

Pattern synthesis of linear arrays using Fourier coefficient matching.
18 p2659 A72-36298

Antenna array analysis of arbitrarily-located, parallel center-fed dipoles with terminals in a common plane.
18 p2666 A72-36328

Optimal distributions for semi-circular arrays of isotropic radiators.
18 p2666 A72-36330

The transient radiated field of a coaxial aperture antenna.
18 p2660 A72-36331

Technique for compensating for reflector-antenna-surface errors with long correlation lengths.
18 p2667 A72-36691

An artificial dielectric lens suitable for high power applications.
18 p2671 A72-37148

Design of Cassegrain antennas employing dielectric cone feeds.
19 p2772 A72-37847

Cross-polarized radiation from convex spherical antennas with a phase-opposed field distribution
19 p2774 A72-38414

Analysis of the correlation functions of space-time wideband signals received by linear antennas
19 p2775 A72-38657

Dipole antenna radiation in homogeneous plasma layer magnetized by normal uniform magnetic field, calculating radiation pattern
19 p2768 A72-38661

Antenna pattern analysis for compatibility prediction.
20 p2902 A72-39000

Optimal synthesis for radiator coordinates and complex amplitudes of linear antenna array for given radiation pattern
20 p2907 A72-39062

Scattering diagram for mutual cross coupling between antennas in Fresnel zone 20 p2907 A72-39063

Statistical synthesis of antenna arrays using phase amplitude distribution equivalent to reference array radiation pattern 20 p2907 A72-39064

Reflector profiles for the pencil-beam Cassegrain antenna. 20 p2903 A72-39221

Phase shifter number reduction effects on phased radar array radiation pattern distortion and sidelobe reduction 20 p2907 A72-39268

Radiation characteristics of dielectric cones. 20 p2904 A72-39773

Circular-polarization antennas with controlled radiation patterns 21 p3026 A72-40314

Controlling the directive gain of weakly directional antennas during space-vehicle flight 21 p3026 A72-40324

Analysis and element pattern design of periodic arrays of circular apertures on conducting cylinders. 21 p3026 A72-40351

Wave propagation on helical antennas. 21 p3015 A72-40352

Analysis and design of TEM-line antennas. 21 p3026 A72-40353

A numerical solution for the near and far fields of an annular ring of magnetic current. 21 p3015 A72-40354

A flat-feed technique for phased arrays. 21 p3026 A72-40356

A rectangular beam waveguide resonator and antenna. 21 p3026 A72-40358

Application of an agar-agar chamber for the study of electromagnetic waves in an inhomogeneous medium. 21 p3015 A72-40359

On the removal of blindness in phased antenna arrays by element positioning errors. 21 p3027 A72-40363

Gain of arrays of dipoles with a ground plane. 21 p3027 A72-40364

Radiation patterns of an antenna near a conducting strip. 21 p3015 A72-40365

On the radiation from an open-ended corrugated pipe carrying the HE sub 11 mode. 21 p3015 A72-40366

On the efficiency and radiation patterns of mismatched shaped Cassegrain antenna systems. 21 p3027 A72-40369

Radiation efficiency of electrically small multirun loop antennas. 21 p3027 A72-40370

A metallized channel guide antenna for use over a cylindrical ground screen. 21 p3027 A72-40372

On the relationship between classical and matrix design methods for arrays of wire antennas. 21 p3027 A72-40373

A contribution to the theory of finite antenna groups, taking into consideration radiation coupling 21 p3028 A72-40503

Statistically dilute antenna groups with enhanced minimum distance between elements 21 p3028 A72-40504

Antenna radiation patterns synthesis from individual elements amplitude and phase characteristics, using method based on steepest descent technique 21 p3028 A72-40506

Wave equation for infinitely long slotted screen in elliptic cylindric coordinates, noting radiation pattern for phased antenna array of metallized hyperbolic striplines 21 p3028 A72-40507

The effect of amplitude and phase tolerances on the phase characteristics of dipole arrays 21 p3028 A72-40512

Correcting effects of corrugated boundaries on coaxial radiators asymmetry and sidelobes, investigating waveguide hybrid modes induced transverse fields 21 p3029 A72-40516

Combination of sum and difference diagrams of a dipole group in front of a parabolic reflector for a two-plane monopulse method 21 p3029 A72-40517

Integral equation and optics methods for far field radiation characteristics calculation of plane antennas with arbitrary reflector-source configurations 21 p3029 A72-40522

A polydirectional antenna in polygon reflector design with cosecant-type elevation directional diagram for providing television in the 12-GHz frequency range 21 p3029 A72-40524

Radiation patterns of dielectric antenna of size comparable to radiator wavelength in air, discussing narrow band and broadband configurations 21 p3030 A72-40528

Luneburg lens spherical antenna microwave radiation pattern, computing Maxwell equations via Tai method 21 p3030 A72-40529

Turnstile antennas polydirectional emission and polarization characteristics, discussing relationship formulation by Scott-Soo Hoo theorem 21 p3030 A72-40531

An antenna principle with universally polydirectional radiation for large spin-stabilized flight devices 21 p3030 A72-40532

Polar orbiting Aeros aeronomy satellite turnstile antenna system with nearly spherical radiation pattern, discussing design modifications for optimization 21 p3030 A72-40533

Determination of the radiation characteristics of aircraft antennas in flight 21 p3030 A72-40534

New combination of logarithmic-periodic dipole antennas for the short wave range 21 p3031 A72-40537

Radiation pattern and gain of reflector antenna with adjusting ring, discussing directivity and bandwidth 21 p3031 A72-40540

VHF-FM radio transmitting antenna for waves of circular, elliptical, and horizontally, vertically, or obliquely linear polarization 21 p3031 A72-40543

Diagram and gain measurements regarding antennas conducted with a helicopter for the range from 0.5 to 800 MHz 21 p3031 A72-40545

Eigenvalues associated with balanced hybrid modes expressed in closed form to derive conical scalar horn antenna far field radiation patterns 21 p3032 A72-40630

Bubnov-Galerkin solutions to wire-antenna problems. 21 p3032 A72-40631

Main-reflector-rim diffraction in back direction. 21 p3032 A72-40632

Radiation of EM waves with Walsh-function time variation - Preliminary results. 21 p3020 A72-40902

Plexiglas spheres and cubes effect on circular and rectangular waveguide aperture antennas directive radiation patterns and sidelobe reduction 21 p3021 A72-40904

A directional antenna represented by a system of two wires positioned on the generatrix of a relief impedance cylinder 21 p3033 A72-40942

Electronically scannable plasma leaky wave antenna system. 21 p3022 A72-41325

Null placing in radiation patterns by shaping antenna edges. 21 p3034 A72-41467

Computer-aided numerical solution for electric field structure of rod and plate, calculating field distortion by rod antennas and near lightning rod 21 p3086 A72-41671

Radiation patterns of wideband horn antenna loaded by dielectric belt, noting satellite and terrestrial radio relay applications 21 p3036 A72-41832

Linear antenna synthesis for minimum sidelobe level, eliminating superdirectivity effect 21 p3158 A72-42085

Radiation field of a plane aperture in an inhomogeneous stratified medium over a large-radius sphere 22 p3155 A72-42654

Theoretical study and wind tunnel simulation of the electrical phenomena of reentry 22 p3231 A72-43092

Antenna synthesis problems approximate solution with reactive factor /supergain ratio/, involving radiation pattern and aperture current expansion as orthogonal functions 23 p3268 A72-43427

Random phasing algorithms to reduce phase quantization sidelobes for radiation patterns of commutated phased array antennas 23 p3268 A72-43428

Design of radiating elements for large planar arrays - Accomplishments and remaining challenges. 23 p3269 A72-43571

Beam port coupled waveguide antenna radiation patterns for uniform and cosine plus pedestal radiating aperture distribution, using coupled mode theory 23 p3264 A72-43602

Optimisation of slope of difference-mode radiation pattern in sum-and-difference-comparison monopulse radar. 23 p3264 A72-43606

Influence of the phase-amplitude distribution of the field in the aperture of an antenna on its directional properties 23 p3270 A72-43773

Radiation patterns and structural design of two mirror millimeter wave Cassegrain antennas with horn radiator 23 p3271 A72-43778

Antenna radiation patterns from statistical phase synthesis of antenna arrays, estimating directivity loss for in- and out-of-phase initial current distribution 23 p3265 A72-44203

Discrete-antenna synthesis theory in the case of uniform approximation to a given radiation pattern 23 p3266 A72-44213

Butler-matrix fed arrays, discussing phase differences, scan steps and sectors, sidelobe structure and attenuation 23 p3273 A72-44363

Computer aided directivity measurements of large antennas in Fresnel zone 23 p3274 A72-44491

Field expressions for a circular loop antenna in terms of a new set of functions. 24 p3379 A72-44707

Probabilistic characteristics of radiation pattern for multielement antenna with nonpolar phase front 24 p3384 A72-44754

Simple small primary feed for large opening angles and high aperture efficiency. 24 p3385 A72-44961

Wideband antenna test facility. 24 p3389 A72-45554

Electromagnetic propagation from flanged waveguide, studying diffraction, radiation patterns and reflection/modal coefficients 24 p3381 A72-45642

Effects of pseudosonic and electroacoustic waves on the radiation of a plasma-coated spherical antenna. 24 p3386 A72-45645

ANTENNAS

NT AIRCRAFT ANTENNAS

NT CASSEGRAIN ANTENNAS

NT CYLINDRICAL ANTENNAS

NT DIPOLE ANTENNAS

NT DIRECTIONAL ANTENNAS

NT HELICAL ANTENNAS

NT HORN ANTENNAS

NT LENS ANTENNAS

NT LOG PERIODIC ANTENNAS

NT LOG SPIRAL ANTENNAS

NT LOOP ANTENNAS

NT MICROWAVE ANTENNAS

NT MISSILE ANTENNAS

NT MONOPOLE ANTENNAS

NT MONOPULSE ANTENNAS

NT OMNIDIRECTIONAL ANTENNAS

NT PARABOLIC ANTENNAS

NT RADAR ANTENNAS

NT RADIO ANTENNAS

NT SATELLITE ANTENNAS

NT SCHWARZSCHILD ANTENNAS

NT SLOT ANTENNAS

NT SPACECRAFT ANTENNAS

NT SPHERICAL ANTENNAS

NT SPIRAL ANTENNAS

NT STEERABLE ANTENNAS

NT TURNSTILE ANTENNAS

NT TWO REFLECTOR ANTENNAS

NT WAVEGUIDE ANTENNAS

NT YAGI ANTENNAS

Alternative derivation of Mei integral equation for numerical determination of current distribution along thin wire antennas 01 p0043 A72-11246

Traveling wave antenna for exciting ion cyclotron waves in cylindrical anisotropic magnetoplasma 02 p0188 A72-11468

Ferrite rod antennas calibration for radio frequency measurements up to 1 MHz 02 p0195 A72-12606

Isolation between two orthogonally polarized beams radiated by single paraboloidal reflector, discussing polarization coupling to earth receiving antenna [AIAA PAPER 72-531] 12 p1789 A72-27356

Atmospheric turbulence induced wave front distortion effects on fast-tracking laser antenna performance, considering infinite plane wave random complex phase modulation 14 p2110 A72-30550

Fourth order linear filter function suggested for pulse signal detection from gravitational antennas, noting parameters optimization 14 p2086 A72-30800

Antennas scattering coefficients measurement by ground and atmospheric radiation, permitting antenna noise temperature components determination 15 p2206 A72-31652

Antennas; Specialists' Meeting, Darmstadt, West Germany, February 22-24, 1972, Reports 21 p3027 A72-40502

Propagation of horizontally polarized VLF waves - Systems implications. 21 p3021 A72-40905

Electronic density and temperature deduced from the observation of the cone of resonance of an antenna in a magnetoplasma 22 p3212 A72-43049

Book - EMI prediction and analysis techniques. 22 p3156 A72-43198

A positive signature for the recognition of gravitational radiation. 23 p3337 A72-43943

ANTHRACENE

Fluorescence of anthracene single crystals whose surface is disturbed by an impurity

19 p2847 A72-38781

Quenching of fluorescence and the photoeffect in anthracene crystals

19 p2847 A72-38782

ANTHROPOMETRY

Anthropometric data utilization for military pilot/aircraft compatibility evaluation, discussing cockpit exclusion code development and implementation

12 p1777 A72-28324

Chamois leather mechanical response, comparing stress relaxation and frequency response characteristics to human skin for applications in anthropometric dummy construction

15 p2191 A72-32606

ANTIADRENERGICS

Beta-adrenergic blocking effect on canine coronary and systemic hemodynamic adaptation during treadmill exercise

11 p1579 A72-25802

Systemic haemodynamics in borderline arterial hypertension - Responses to static exercise before and under the influence of propranolol.

19 p2756 A72-37773

Effect of beta-adrenergic blockade on plasma volume in human subjects.

19 p2757 A72-38029

ANTIBIOTICS

NT PENICILLIN

Antibiotic polypeptide synthesis of gramicidin S and tyrocidine, using primitive model of sequential addition of amino acids on polyenzymes

04 p0470 A72-14790

Fourier transformation for natural abundance C 13 free induction decays of cyclic antibiotic valinomycin and K ion complex, noting chemical shift differences

13 p1913 A72-29862

Fourier transform C-13 nmr analysis of some free and potassium-ion complexed antibiotics.

20 p2898 A72-39399

ANTIBODIES

Normal and germ free rat antibody response to sheep erythrocyte inoculation in He-O atmosphere, analyzing microagglutinin and hemolysin titres [AD-736324]

04 p0471 A72-14861

The production and characterization of specific antibodies to aldosterone.

19 p2757 A72-38175

ANTICHOLINERGICS

Evoked cortical potentials changes from emotional visual word stimuli stress under amylin anticholinesterase drug influence

08 p1116 A72-21194

ANTICLINICAL MOUNTAINS

U MOUNTAINS

ANTICLINICAL VALLEYS

U VALLEYS

ANTICOAGULANTS

Human coagulating and anticoagulating blood system changes due to emotional stress during parachute jumps, noting plasma recalcification time increase

04 p0474 A72-15233

Ascorbic acid influence on blood coagulation and anticoagulation systems in dogs with acute hypoxia, discussing plasma recalcification time and heparin tolerance

12 p1764 A72-28217

ANTIURETICS

Renal clearance studies of left atrial distention effect in dog, indicating antiuretic hormone inhibition mechanism of diuresis

12 p1763 A72-27828

ANTIFERROMAGNETISM

Hydrostatic pressure effect on itinerant antiferromagnetic ordering in Cr-Fe alloys with Ru and Mn additions

12 p1828 A72-27432

Heisenberg antiferromagnet with noncollinear sublattices and linear dislocation, considering coupled spin wave states and density

13 p2023 A72-29910

Two-magnon Raman scattering in antiferromagnets, obtaining amplitude-renormalization factor by extended Dyson-Maleev graphical approach to include corrections in transition operator M

15 p2295 A72-32548

Magnetoelastic amplitude modulator of millimeter waves based on an antiferromagnetic/hematite/

17 p2529 A72-34842

Antiferromagnetic dispersion, absorption and light scattering in NiO and other face centred cubic crystals.

20 p2960 A72-39458

Resonance between spin waves and magneto-hydrodynamic waves in antiferromagnetic semiconductors and metals

21 p3096 A72-40415

Slow electromagnetic waves in antiferromagnetics near the point of transition to the ferromagnetic phase

21 p3098 A72-41685

Critical-point anomalies in the electron-paramagnetic-resonance linewidth and in the zero-field relaxation time of antiferromagnets.

24 p3432 A72-45674

ANTIFREEZES

Methyl alcohol-ethylene glycol self mixing antifreeze solution for precipitation gages

11 p1682 A72-26088

ANTIFRICTION BEARINGS

NT BALL BEARINGS

NT ROLLER BEARINGS

Tensometric damage detection in rolling contact bearings from bending stress spectrum, using Si strain and wire strain gages

01 p0078 A72-11379

Nonuniform magnetic field effects in MHD slider bearing, showing inertia terms contribution dependence on Hartmann number

[ASME PAPER 71-LUB-8]

02 p0235 A72-11533

Conical hydrostatic bearing optimization for minimum friction in laminar and turbulent flows, developing flow rate, load capacity and friction torque equations

[ASME PAPER 71-LUB-19]

02 p0235 A72-11539

Vertical shaft stability on elastic sliding bearings, considering passage through self oscillation zone

06 p0894 A72-17683

Filler particles orientation effects on plastic bearing materials friction and wear properties, discussing experimental testing methods

06 p0836 A72-18595

Sliding bearing structural features and materials effects on running and friction behavior at contact surface

07 p0998 A72-20524

Self lubricating materials for maintenance-free clocks antifriction bearings, discussing friction and wear behavior

09 p1319 A72-23562

Antifriction phase structure of friction formed thin surface layer of sulfurized iron-graphite metal-ceramic materials, using transmission microscopy

13 p1967 A72-30108

On the stability of rotor-and-bearing systems and on the calculation of sliding bearings.

18 p2696 A72-36708

Shaft support improvement by combining rolling and hydrodynamic journal bearings, noting wear and friction torque reduction

21 p3060 A72-40928

ANTIMATTER

NT ANTINUCLEONS

NT ANTIPARTICLES

NT ANTIPROTONS

NT POSITRONS

Antimatter existence on cosmological scale in universe, comparing calculated annihilation gamma ray spectrum with background observations

02 p0278 A72-11967

Hydrodynamics of matter-antimatter system embedded in thermal radiation, observing coalescence effect

03 p0416 A72-13013

X ray and gamma astronomy, discussing satellite-borne experiments for electromagnetic and nuclear reaction rates and antimatter existence in cosmic radiation

04 p0582 A72-15692

Antimatter search in primary cosmic rays by balloon-borne superconducting magnetic spectrometer capable of direct matter-antimatter separation

12 p1863 A72-27296

Universe evolution, discussing constituents, matter and antimatter, quasars and radio stars in various galaxies

14 p2157 A72-30623

Joining of two semiclosed worlds and a cosmological model of matter-antimatter asymmetry.

23 p3336 A72-43489

ANTIMONIDES

NT ALUMINUM ANTIMONIDES

NT CADMIUM ANTIMONIDES

NT GALLIUM ANTIMONIDES

NT GERMANIUM ANTIMONIDES

NT INDIUM ANTIMONIDES

Alkali antimonide photocathodes photoelectric yield /quantum efficiency/ relation to reversible variation of surface potential, noting critical current density temperature dependence

08 p1171 A72-21968

Physicochemical properties and composition diagrams of antimonides and arsenides of Zn, Cd, Al, In and Ga

15 p2290 A72-31194

Strain gage resistor with BiTeSb compound semiconductor film vacuum deposited on dielectric substrate, noting high sensitivity and operation without amplifiers

23 p3287 A72-43348

ANTIMONY

Target anion effect on radioactive Sb and Te distribution formed by high energy proton irradiation of cesium salts containing oxygen

15 p2282 A72-32485

Changes in the grain-boundary free energy and the segregation of tin and antimony at grain boundaries in CrV steels

24 p3415 A72-45394

ANTIMONY ALLOYS

Liquid quenched Sb-transition metal binary alloy constitution, finding metastable phases in quenched Cr-Sb and Mn-Sb alloys

13 p1975 A72-28672

Electroconductivity, thermal emf and Hall coefficient for single crystals of Bi-Sb alloys with Cd, In and Sn additions

19 p2847 A72-38683

Bi-Sb alloys for magneto-thermoelectric and thermomagnetic cooling.

22 p3215 A72-43089

ANTIMONY COMPOUNDS

NT ALUMINUM ANTIMONIDES

NT ANTIMONIDES

NT CADMIUM ANTIMONIDES

NT GALLIUM ANTIMONIDES

NT GERMANIUM ANTIMONIDES

NT INDIUM ANTIMONIDES

Wear behavior of molybdenum disulfide and antimony trioxide bonded solid film lubricant with air curing silicone resin, noting temperature and pretreatment effects

06 p0823 A72-18593

Antimony-halogen synergistic reactions in fire retardants, noting antimony oxychloride role

07 p0935 A72-19056

Antimony compounds single crystal whiskers permittivity determination at microwave frequencies from power reflection and transmission coefficients

09 p1366 A72-22417

Dielectric dispersion in SrSi filamentary single crystals as function of Curie temperature in lf and shf range

09 p1367 A72-22422

Comparative evaluation of zinc borate 2:3:5 with antimony oxide using various fire testing methods.

20 p2898 A72-39699

ANTIMONY ISOTOPES

Sb 124 dopant redistribution in Ge semiconductor during diffusion alloying with In at 750-850 C

05 p0701 A72-15751

ANTINUCLEONS

High energy hadrons time structure in extensive air showers, considering production of nucleon-antinucleon pairs in particle interactions

07 p1067 A72-20687

ANTIOXIDANTS

Antioxidation coatings of Ta and Ta alloys for high temperature long term operation, emphasizing sintered molybdenum disilicide

11 p1663 A72-26840

Antioxidative and antiwear action of S-containing and S-free phosphoric acid ester additives in lubricating oils

12 p1835 A72-28201

Antioxidant additives effect on chemical stability and rheological properties of silica gel lubricants with SU type mineral oil dispersion medium

16 p2413 A72-33173

Extractability of antioxidative additives from fuels by means of water and NaCl solutions

17 p2596 A72-35179

ANTIPARTICLES

NT ANTINUCLEONS

NT ANTIPROTONS

NT POSITRONS

Primary cosmic rays antinuclei content upper limit from emulsions investigations with balloons and satellites

14 p2148 A72-30885

Particle trajectory and time of flight measurement in search for anti-alpha particles in primary cosmic radiation, using magnetic spectrometer with spark chambers

22 p3219 A72-42568

ANTIPROTONS

Antiprotons abundance in primary cosmic radiation near geomagnetic equator from asymmetrical flux balloon measurements

03 p0407 A72-12992

Antiproton flux energy spectrum in Galactic interstellar space, discussing flux peak

03 p0408 A72-13005

Primary cosmic radiation antiproton flux, finding .005 ratio upper limit to proton flux with balloon-borne magnetic spectrometer

07 p1064 A72-20633

Antiproton energy spectrum in cosmic rays from primary proton-interstellar hydrogen collision in two fireball model

12 p1863 A72-27186

ANTIRADIATION DRUGS

ATP injection protection against Co 60 or Cs 137 gamma radiation in albino mice, guinea pigs and dogs

05 p0621 A72-16636

Radioprotectants /mexamine and cystamine/ effects on histo-hematic barrier permeability in rats under hypokinetic conditions

13 p1904 A72-29308

Ionizing radiation effects on mitosis and nucleic acid synthesis, noting protective chemical agents and hematological evaluation of radiation damage and marrow regeneration
22 p3141 A72-41986

ANTISERUMS
Immunohistochemical properties of human oxyhemoglobin comparison with complex of dog hemoglobin and human hemoglobin reactions in anti-hemoglobin serum
09 p1268 A72-23695

ANTISKID DEVICES
Aircraft landing gear wheel damage and antiskid mechanisms under operational conditions
08 p1109 A72-21485
Aircraft wheel mechanics, discussing freely turning and braked wheels, tire drift and antiskid braking systems for landing gear
11 p1574 A72-25287

ANTISUBMARINE WARFARE
Univac 1832 multiprocessor avionics computer for airborne ASW, discussing input/output controllers and interfaces and IC design features
16 p2367 A72-33245
S-3A Viking systems.
17 p2491 A72-34741

ANTISUBMARINE WARFARE AIRCRAFT
S-3A Viking land based antisubmarine warfare maritime and reconnaissance aircraft, describing flight controls, structural design, underslung podded engines and operational equipment
06 p0758 A72-17583
ASW aircraft magnetic anomaly detection (MAD)/system range limitation due to residual maneuver noise, discussing real time compensation for geomagnetic gradient interference
22 p3177 A72-42322
Naval helicopters applications to search and rescue, ASW, ground support and other roles, considering reliability and maintenance
24 p3365 A72-44685

ANTITANK MISSILES
French missile and rocket weapon systems based on solid propellants, describing various ground-to-ground, short and medium range, antitank and other missile types
03 p0441 A72-13644

ANTONOV AIRCRAFT
Russian book on An-12 turboprop transport aircraft structural and aerodynamic characteristics covering engine operation, piloting, stability, controllability, etc
12 p1755 A72-28343
Fiberglass reinforced plastic fuselage production for AN-2m aircraft, noting plastic-plastic and metal-plastic joints
13 p1897 A72-29462

ANXIETY
Anxiety relation to success or failure in naval flight training program
12 p1774 A72-28263
Effects of instructions on measures of state and trait anxiety in flight students.
17 p2507 A72-34464

AORTA
Idiopathic hypertrophic subaortic stenosis ballistocardiography, measuring ventricular function by angiography
03 p0314 A72-13142
Nonsurgical ultrasonic technique to measure wall displacement and pulsatile changes in thoracic aorta [AD-739809]
07 p0930 A72-19447
Idiopathic subvalvular aortic stenosis characterized by muscular or membrane obstruction in left ventricular infundibulum, discussing diagnostic importance for pilots
07 p0933 A72-20189
Aortic flow disturbances in vivo study by hot-film anemometer, considering peak flow velocity and pulse rate effects
07 p0934 A72-20537
Aortic constriction and release effects on kidney glomerulotubular balance in saline- and water-loaded dogs, studying sodium reabsorption changes
08 p1115 A72-21084
Arterial velocity profiles measurement in dogs thoracic aorta by hot-film probe, relating flow disturbances and turbulence to Reynolds number
10 p1431 A72-24468
Hemodynamic assessment of arterial blood flow from radiograph measurements of aorta branching points
11 p1582 A72-26774
Fluid mechanics of left ventricle model with mitral and aortic valves, showing ring vortex relation to diastole and closure
11 p1589 A72-26775
Single linear measure of systolic pressure gradient for calculation of aortic valve area in stenosis severity assessment
12 p1762 A72-27734
Modified Van der Pol wave motion oscillator model for prediction of aortic dynamic response to negative g impact accelerations
12 p1765 A72-28271

Temporal relation of the second heart sound to aortic flow in various conditions.
19 p2759 A72-38818
Aortic regurgitation variation with respiratory sinus arrhythmia and respiratory cycle in dogs during tachycardia and bradycardia
22 p3151 A72-42674

APATITES
U CALCIUM PHOSPHATES
U MINERALS

APERIODIC FUNCTIONS
Instability effect on aperiodic motion of nonlinear thermomechanical oscillator from periodic solutions
04 p0547 A72-14458

APERTURES
NT IRISES [MECHANICAL APERTURES]
Aperture and pattern space factors relationship for vector fields of rectangular and circular apertures, investigating characteristic functions
[AD-742948]
01 p0043 A72-11240
Linear aperture antennas approximate synthesis method, determining radiation pattern characteristics by solution of extremal problems in theory of linear integral operators
02 p0195 A72-12592
Highly directional circular array antennas radiation characteristics calculation, showing sidelobe size dependence on aperture angle
04 p0499 A72-15240
Critique on condition for planar antennas physical reliability, concerning smoothness of aperture edges
06 p0782 A72-17362
Resolution dependence on coherent properties of light source for aberration free annular aperture operating in partially coherent light, presenting composite intensity curves
07 p1008 A72-20545
Aperture filtering effects on amplitude scintillation power spectra of paraboloid radio telescope over millimeter wave propagation path
08 p1136 A72-21982
Aperture synthesis of ring antenna arrays radiation pattern using earth rotation
11 p1597 A72-26710
Photosensor aperture shape and line scan spacing effect in reducing facsimile camera aliasing
12 p1807 A72-27408
Transmitter aperture size and focus effects on scintillations of laser beam propagating through turbulent atmosphere
12 p1791 A72-27678
Optimum aperture distributions for radiation pattern shaping for arbitrary superdirectivity ratio in antenna design
13 p1915 A72-28528
Electromagnetic boundary value problem of two rectangular waveguides coupled by aperture radiating into free space, solving integral equation by moments method
15 p2205 A72-31357
Fourier transform /subtractive/ holographic imaging technique for microwave antenna apertures
16 p2368 A72-33072
Kirchhoff-Fresnel diffraction field fluctuation at plane screen aperture in turbulent atmosphere
16 p2425 A72-33487
Diffraction of electromagnetic waves by a two-dimensional aperture with arbitrary cross-sectional shape.
17 p2514 A72-34385
Multifunction microwave apertures - Concepts and potential.
17 p2531 A72-35574
Diffraction by an aperture between two wedges.
18 p2712 A72-36938
Use of amplitude filter to improve the partially space coherent diffraction of a defocused circular aperture.
19 p2833 A72-37402
Ultrasonic imaging system based on side-looking synthetic aperture radar principles, using B-scan technique
19 p2798 A72-37624
Experimental effects of finite transmitter-apertures on scintillations.
20 p2932 A72-39500
Coaxial exciter for parabolic antennas with high area efficiency and small halation
21 p3029 A72-40514
Beam port coupled waveguide antenna radiation patterns for uniform and cosine plus pedestal radiating aperture distribution, using coupled mode theory
23 p3264 A72-43602
Spectrophotometer linearity testing using the double-aperture method.
23 p3289 A72-43894
Light beam modulated by uniformly spaced circular apertures, calculating Fourier power spectrum for homogeneous and bivariate normal intensity distributions
23 p3289 A72-43900
Spaceborne astronomy by synthetic aperture optics for high resolution without cost and weight disadvantages of large telescopes, considering Michelson stellar interferometer
24 p3404 A72-45541

APEXES
Galactic spiral density waves instability effects, noting local centroid radial motion and apex deviation
09 p1384 A72-22519
Communication network vertex and mixed cutset definitions and computation from interchange graph of given finite connected undirected graph without loops and multiple edges
21 p3015 A72-40634

APHELIONS
Depth distributions of cosmic ray produced radionuclides in chondrites and achondrites, determining aphelia from Al 26 activities
22 p3228 A72-42861

APNEA
U RESPIRATION

APOGEES
Extremum of satellite orbit perigee or apogee height in Hohmann transfer
05 p0713 A72-16006

APOLLO FLIGHTS
Apollo 11 and 12 lunar soil samples, calculating mixing models by least squares and end member groups by Q mode factor analysis
01 p0124 A72-10057
Marsian surface nature from Surveyor and Apollo missions data on lunar particle size distribution
01 p0132 A72-11037
Apollo flight lunar spinels compositional variations, formulating modified Johnstone prism projections
01 p0134 A72-11162
Biochemical and physiological effects of Apollo flight diet, noting no significant variations in serum electrolytes, endocrine values, body fluids and hematologic parameters
02 p0167 A72-11707
Apollo 11 and 12 rock samples depth profiles for Al, Na, Mn, S, V, Ca, P, Co, Fe, Cu and Sc isotopic contents, estimating solar proton flux
02 p0282 A72-12327
Li, Be and B abundances in Apollo 11, 12 and 14 and Lunik 16 missions fine and core samples
03 p0414 A72-12903
Sedimentology of Apollo 11 and 12 soils, investigating grain size distribution
03 p0440 A72-14325
Lunar mare soil deformation and cracking from Surveyor and Apollo photographs
04 p0574 A72-14918
Flight laser altimeter for Apollo vehicle height measurements above lunar surface, using telescope relay and quartz crystal oscillator
05 p0660 A72-15786
Energy spectra of positive ion bursts on lunar night side from Apollo 12 and 14 Alsep suprathermal ion detectors data
06 p0872 A72-17462
Automated navigation aids interface with human operator, discussing Apollo flight experience and technology utilization in air and marine navigation
06 p0846 A72-18288
Apollo lunar fine samples total emittance as function of temperature, using spectral emittance measurement technique
09 p1388 A72-23028
Lunar orbiting rescue vehicle design for Apollo missions, discussing guidance, navigation and communications
09 p1396 A72-23156
Neutron capture effects on Gd isotopic composition and irradiation histories of lunar rocks from Apollo sites, using mass spectroscopic measurements
10 p1536 A72-24154
Stable remanent magnetization components of lunar rock samples from Apollo 11 and 12 missions, indicating liquid core origin
10 p1536 A72-24155
Neutron capture effect on isotopic composition variations of Sm in Apollo lunar samples, comparing with terrestrial abundance
10 p1537 A72-24156
Lunar basalt Eu abundance anomaly in Apollo 11 and 12 samples, considering partial melting with or without plagioclase
10 p1537 A72-24162
Zirconium rich metal oxides mineral group in Apollo 14 and 15 lunar rocks from feldspar-phryic basalt and pyroxene ferrobasalt, noting optical and chemical properties
11 p1717 A72-25868
Shock wave generation and propagation from Apollo rockets at orbital altitudes
11 p1690 A72-26513
Long range air coupled seismic wave recording from Apollo launchings, using microphones and seismographs arrays
11 p1690 A72-26514
Ground and flight crews coordinated effort in Apollo mission operations, noting experts on ground and spacecrew spot judgments capability
[AIAA PAPER 72-236]
11 p1586 A72-26557

U, Th, Pb and rare earth elements abundances and Pb 207/Pb 206 ages of Apollo lunar minerals by ion microprobe mass analysis

12 p1866 A72-27114

Apollo 11 and 12 lunar samples thermal properties, presenting diffusivity, conductivity and specific heat

12 p1869 A72-27334

Position information in lunar cartographic products evaluated by Apollo data, obtaining reliability factors

12 p1871 A72-27530

Apollo 15 and 16 TV, still and movie cameras, discussing astronomical activities of astronauts

12 p1807 A72-27546

Red cell mass plasma volume decrease in Apollo mission crews, indicating erythropoiesis inhibition

12 p1765 A72-28266

Significance of Apollo 11 and 12 lunar rock fragments of norite rich in K, rare earth elements and P/KREEP/ for lunar evolution assessment

13 p2037 A72-28990

Apollo 11 and 12 rock samples depth profiles for cosmogenic Al, Na, Mn, S, V, Ca, P, Co, Fe, Cu and Sc isotopic contents, estimating solar proton flux

13 p2039 A72-29211

Apollo centralized ground support and communication system, describing network support team, mission control center, instrumentation support team and manned space flight network

13 p1940 A72-29860

Magnetization and temperature interrelationship in high constant magnetic field for Apollo 11, 12 and 14 rocks, obtaining magnetic hysteresis curves

14 p2155 A72-30517

Astronauts physiological and psychological reliability, discussing Apollo flights and prolonged missions to other planets

14 p2079 A72-30677

U bearing phase zirkelite in Apollo 12 and 14 lunar rocks, using electron microprobe

15 p2303 A72-31303

Apollo lunar exploration program survey, reviewing information on lunar crust composition and thickness, lunar evolutionary processes and chronology and extraterrestrial particle fluxes

15 p2309 A72-31970

Lunar rock nature and properties from Apollo samples, discussing crust, Fra Mauro, interior, chronology, surface processes and earth-moon environment

15 p2314 A72-32376

Diopside and Cr-Zr-arnalcite occurrence on moon from Apollo 14166.6 fines, using petrographic and electron microprobe examination

16 p2461 A72-34163

Apollo and terrestrial geochemical samples examination for indigenous amino acids distribution and optical configuration, stressing close monitoring of contamination sources

19 p2762 A72-37648

Lunar landing sites selection approach for Apollo missions, examining mission design requirements, launch vehicle considerations and lunar composition

19 p2857 A72-37700

Spectral reflectance and emittance of Apollo 11 and 12 lunar material.

20 p2970 A72-39609

APOLLO LUNAR SURFACE EXPERIMENTS PACKAGE

Lunar remanent magnetism origin theory from Apollo and Explorer data, suggesting solar wind, earth magnetosphere and lunar dynamo sources

01 p0134 A72-11269

Photogrammetric techniques for Tranquility base experiment locations map based on surface and spacecraft photographs

02 p0280 A72-12198

ALSEP design and development, discussing reliability, power sources and astronaut interface constraints

04 p0577 A72-15092

ALSEP structural/thermal/ design, outlining package hardware configuration, passive thermal protection and materials selection procedures

04 p0508 A72-15093

ALSEP central station data subsystem, discussing power conditioning unit and electric power subsystem

04 p0508 A72-15094

ALSEP passive seismic experiment design, discussing instrument operation and performance parameters

04 p0508 A72-15095

ALSEP active seismic experiment design, investigating lunar subsurface geologic structure

04 p0508 A72-15096

Apollo 14 charged particle lunar environment experiment, describing ALSEP particle spectrometer

04 p0508 A72-15097

ALSEP lunar heat flow experiment, describing instrument for temperature and thermal conductivity measurements in lunar subsurface

04 p0577 A72-15098

ALSEP human engineering design criteria for crew interface, describing astronaut trainer

04 p0479 A72-15100

ALSEP data management, describing processing facility characteristics and support activities

04 p0509 A72-15101

Energy spectra of positive ion bursts on lunar night side from Apollo 12 and 14 Alsep suprathermal ion detectors data

06 p0872 A72-17462

ALSEP heat flow experiment design and calibration, presenting independent vertical temperature gradient and thermal conductivity measurements in regolith

12 p1869 A72-27331

ALSEP seismic records from Apollo 12 lunar module and Apollo 13 rocket stage impact, showing ringing phenomenon due to sphere curvature-caused energy dissipation

13 p2035 A72-28618

Apollo 16 lunar surface magnetometer cooling system variable conductance heat pipe/radiator design and thermal performance

14 p2171 A72-30828

[AIAA PAPER 72-271] Apollo lunar surface experiments package suprathermal ion detector measurements in lunar environment

15 p2309 A72-31957

Apollo 15 manned lunar landing, discussing geological data and surface experiment package and instruments

15 p2310 A72-31983

Suprathermal ion detector measurements on lunar surface by Apollo 12 and 14 astronauts to provide search for lunar exosphere phenomena

15 p2301 A72-32092

APOLLO PROJECT

Apollo mission profiles, discussing lunar landings, craters, evolution, samples and spacecraft instruments and hardware improvements

03 p0418 A72-13106

Apollo manned mission real time ground support computer simulation for NASA flight controller training to maximize flight crew safety

07 p0933 A72-20329

NASA space programs, discussing future Apollo, Skylab, orbiting space station, space shuttle and deep space projects

08 p1230 A72-21002

Apollo program management decisions based on reliability analysis, discussing incentive fees, testing optimization, engineering changes approval and flight readiness certification

10 p1486 A72-24007

Apollo, Luna and Zond lunar exploration contribution to solar system formation knowledge, discussing post-Apollo lunar and planetary exploration programs

11 p1715 A72-25252

Moonquakes and meteorite and manmade impacts as sources of seismic signals detected by Apollo lunar seismic stations

13 p2037 A72-28988

Bioastronautic results of Apollo space flight biomedical operations, discussing weightlessness, sleep impairment, motion sickness, preventive medicine, etc

15 p2189 A72-31827

Lunar interior structure and crust composition from artificial impact data recorded by Apollo seismometers

15 p2314 A72-32377

Spectrophotometry /0.3 to 1.1 micron/ of visited and proposed Apollo lunar landing sites.

22 p3225 A72-42530

Comments on the figure of the moon from Apollo landmark tracking.

22 p3226 A72-42534

Unique charts for space missions.

24 p3422 A72-44644

APOLLO SPACECRAFT

Apollo spacecraft guidance and control systems, reviewing navigation objectives, concepts and performances during cislunar, rendezvous and landing maneuver phases

01 p0097 A72-10943

Apollo heat shield silica reinforcement fiber and ablation char reactions in laboratory and actual reentry tests

14 p2172 A72-30922

Zero-gravity thermal performance of the Apollo cryogenic gas storage system.

19 p2869 A72-38830

The development of the Apollo entry thermal protection system.

21 p3115 A72-41124

Apollo/Saturn 5 spacecraft liquid propellants safety procedures in event of fire on explosion in operations building at Kennedy Space Center

23 p3343 A72-43552

APOLLO TELESCOPE MOUNT

Gimbale control moment gyro for Skylab telescope mount stringent pointing requirements, investigating normal and clamped operation modes and dynamic response of attitude control

01 p0097 A72-10382

APOLLO 11 FLIGHT

Book on Apollo 11 lunar rocks and minerals covering mineralogy, petrology, chemical and isotope analyses, bioscience, organic geochemistry, physical properties and measurements

01 p0122 A72-10001

Single domain grain distribution deduction method obtained from Neel theory, applying to Apollo 11 lunar dust iron grains

01 p0125 A72-10071

Critique of paper by Ringwood on petrogenesis of Apollo 11 lunar basalts composition and implications for lunar origin

02 p0275 A72-11600

Apollo 11 lunar fines behavior and gas evolution characteristics from high vacuum differential thermal analysis and mass spectroscopy

04 p0569 A72-14504

Apollo 11 lunar samples carbon compound geochemical analysis, using sequential scheme with minimum handling of solids and extracts

05 p0714 A72-16131

Critique of paper on heat capacity and thermal conductivity of Apollo 11 lunar rocks at liquid helium temperatures, noting constraints imposed by Mossbauer data

07 p1084 A72-20521

Carbon compound distribution on moon from Apollo 11 samples, comparing with earth data

08 p1120 A72-22013

Alpha corundum grains from Apollo 11 lunar dust sample, using X ray diffraction and electron microprobe analyses

10 p1536 A72-24152

Differentiated igneous textures of Apollo 11 lunar ferrobasalt samples, indicating fractional crystallization followed by crystal-liquid separation

10 p1537 A72-24157

Rb-Sr isotopic age determination on density and size fractions of Apollo 11 fine soil and basaltic materials

10 p1538 A72-24165

Vaporization and condensation effects on Apollo 11 glass spherules from microbreccia samples, suggesting concentration gradients as result of impact event

11 p1723 A72-26522

Crystallization experiments on Apollo 11 magmas of K and Rb-rich basalt, discussing plagioclase characteristics

11 p1723 A72-26523

Apollo 11 EASEP nickel resistance thermometer lunar surface data, presenting unshadowed equivalent brightness temperature and thermal parameters and emission directional dependence

12 p1869 A72-27330

Rates of solidification of Apollo 11 basalt and Hawaiian tholeiite.

20 p2967 A72-39181

Chemical and structural classification of Apollo 11 lunar rocks, showing lunar surface material temperature history and meteoritic component presence

20 p2900 A72-39842

APOLLO 12 FLIGHT

Apollo 12 lunar rock 12013, examining uranium distribution in apatite, whitlockite, zircon and beta phases

01 p0124 A72-10062

Apollo 12 lunar samples exoelectrons of thermally stimulated emission, noting concentration of traps for radiation history measurement

01 p0124 A72-10063

Apollo 12 lunar igneous rocks 12004, 12040, 12051 and 12053, obtaining Kr 78/Kr 83 and Xe 131/Xe 126 spallation component ratios correlation line

01 p0124 A72-10065

Apollo 14 lunar soil sample 14163 orthopyroxene composition, determining K, P and rare earth elements

01 p0125 A72-10066

Apollo 12 liquid oxygen cloud spectrum observations, describing spectrograph with off axis zone plate for transmission grating and sieve plate collimator

01 p0071 A72-11172

Apollo 12 lunar crystalline rock and fines magnetic properties measurement, noting magnetic minerals composition

02 p0278 A72-12026

Apollo 12 lunar soil samples solar wind noble gas analysis of KREEP fragments, estimating Surveyor Crater age

03 p0414 A72-12902

Apollo 12 retrieved Surveyor 3 TV camera mirror surface and camera-shroud organic contamination attributed to spacecraft outgassing and engine exhaust products

03 p0415 A72-12948

Lunar rock 12013 sawdust and fragment composition from neutron activation analysis, comparing to Java tektite J2

05 p0722 A72-17127

Diurnal temperature variations in lunar surface layer from Apollo 12 samples, comparing with Apollo 11 samples and IR measurements

07 p1068 A72-18874

Lunar seismograms for LM and S-4B impacts in Apollo 12 experiment, indicating modulation mirage effect on signal distortion 10 p1536 A72-24153

Crystallization sequence, petrology and mineralogy of Apollo 12 basalt sample 12009 10 p1537 A72-24160

Thermoluminescent and luminescent properties of Apollo 12 lunar fines, core tube samples and rock chips 10 p1537 A72-24163

Apollo 12 lunar rocks and fines sulfur concentrations and isotope ratios measurement 10 p1538 A72-24168

Apollo 12 material effect on tobacco tissue cultures, noting pigment increase 12 p1761 A72-27626

Lunar core-crust conductivity models compatibility with lunar surface field/interplanetary magnetic field transfer function from Apollo 12 magnetometer data 14 p2153 A72-30502

Apollo 12 fines thermal conductivity in vacuum at 200-400 K, using least squares technique for curve fit 14 p2154 A72-30509

Apollo 12 lunar fines spectral and thermal radiation properties as function of bulk density, presenting emittance as function of temperature and solar reflectance 14 p2154 A72-30513

Best fitting triaxial ellipsoid representation of seleno-equipotential surface at Apollo 12 landing site based on observed local gravity and moon angular velocity 15 p2308 A72-31922

Study by Mossbauer spectrometry of the iron distribution in mineralogical fractions separated from lunar rocks brought back by Apollo 12 17 p2607 A72-34917

Compositional characteristics of olivines from Apollo 12 samples. 18 p2723 A72-36063

Spectral emittance of Apollo-12 lunar fines. 20 p2970 A72-39486

Fragments of terra rock in the Apollo 12 soil samples and a structural model of the moon. 21 p3110 A72-41452

APOLLO 14 FLIGHT

Apollo 14 crystalline rocks and fragments Rb/Sr, Ar 40/Ar 39 or cosmic ray exposure ages from electron microprobe and petrographic microscope examination 01 p0123 A72-10051

Apollo 14 rocks, breccia fragments and soil samples ages from Ar 40/Ar 39 and cosmic ray dating, discussing basalt Ar release patterns 01 p0117 A72-10052

Apollo 14 Fra Mauro site basaltic rocks and breccia clast internal Rb-Sr isochrons, comparing to Tranquility Sea basalts 01 p0123 A72-10053

Glass compositions in Apollo 14 soil, discussing correspondence to Fra Mauro basalts, mare basalts and soils, and gabbroic anorthositic and potash granite 01 p0123 A72-10054

Dunite-norite olivine-rich microbreccia in Apollo 14 lunar fines sample 14002.8, discussing origin and chemical composition 01 p0126 A72-10106

Apollo 14 food system, describing new items, improvements in production methods, packaging and preparation with emphasis on rehydratable foods 02 p0166 A72-17066

Apollo 14 landing site gravity determination from accelerometer data 02 p0285 A72-12844

Apollo 14 basaltic evidence for selective volatilization on lunar surface, using electron probe analysis 03 p0439 A72-14273

Exploratory test of extrasensory perception to identify random order of symbols in space during Apollo 14 flight with four subjects on earth 04 p0565 A72-14888

Apollo 14 charged particle lunar environment experiment, describing ALSEP particle spectrometer 04 p0508 A72-15097

Lunar Imbrian Basin formation, discussing micrometeorite component composition of Apollo 14 soil samples 05 p0715 A72-16160

Apollo 14 lunar breccia samples, observing chondrules from meteoritic impact event 05 p0715 A72-16161

Lunar gravity measurements via Apollo 14 Doppler radio tracking over 100 kilometer band during low periapsis altitude orbits, relating to surface features 05 p0722 A72-17126

Chromian pleonaste and aluminous picotite in Apollo 14 fine grained microbreccias comparing with spinel composition in lunar basalts 06 p0878 A72-17672

Carbon chemistry of Apollo 14 size-fractionated fines, noting solar wind activity effect 07 p1082 A72-20290

Apollo 14 mission report covering crew training, launch, docking, lunar landing and surface activities 08 p1230 A72-21006

Low energy ions and negative particle fluxes simultaneous enhancements due to Apollo 14 lunar module impact, suggesting solar wind and gas cloud interaction as acceleration mechanism 09 p1388 A72-23018

Apollo 14 explosion seismic refraction data, showing lunar near surface regolith thickness and compressional wave velocity 09 p1390 A72-23495

Geochemistry of lunar opaque minerals in Apollo 14 crystalline rocks, including FeNi metal, ilmenite, spinels, schreibersite, baddeleyite, fayalite and tranquillityite 10 p1538 A72-24164

Surface orientation reconstruction of Apollo 14 lunar rocks from microstereoscopic studies of microcraters, soil covers and glass coatings, determining micrometeoroid erosion 11 p1719 A72-25975

Infrasound observations of natural background and signals from Apollo 14 and aircraft, using thermistor flowmeter microphone array 11 p1690 A72-26515

Apollo 14 basaltic rocks cooling deduced from divalent Mg and Fe ionic distribution in pyroxene, noting process interruption below 840 C 11 p1724 A72-26574

Shock deformation microstructures in Apollo 14 breccia and comparative terrestrial minerals, using transmission electron microscopy 11 p1724 A72-26951

Apollo 14 breccia sample inverted pigeonites /pyroxenes/ as evidence of lunar plutonic rocks, using optical, electron probe and X ray diffraction techniques 12 p1865 A72-27112

Electron microprobe analysis of chromian spinels from Apollo 14 rocks indicating crystallization from high aluminum low iron magma 12 p1865 A72-27113

Apollo 14 experiments to demonstrate flow patterns of convection and heat transfer in gases and liquids under weightlessness 13 p2035 A72-28614

U-Th-Pb ages in Apollo 14 basalts and initial radiogenic Pb in lunar rocks, comparing with Rb-Sr and K-Ar isotopic method 15 p2303 A72-31301

Lithology of Apollo 14 lunar clastic rocks from Fra Mauro region, noting different makeups of glassy matrix and particles, plagioclase, pyroxene and lithic clasts 16 p2457 A72-33675

Apollo 14 Rb-Sr isotope rock sample data, relating isochron age to igneous crystallization time 17 p2607 A72-35073

Analysis of vegetable seedlings grown in contact with Apollo 14 lunar surface fines. 17 p2505 A72-35925

Occurrence of chromian, hercynitic spinel /pleonaste/ in Apollo-14 samples and its petrologic implications. 22 p3153 A72-42862

Immiscible materials processing experiments in near weightlessness environments during Apollo 14 mission and on NASA short duration low gravity test facilities 24 p3407 A72-45155

Soil mechanical properties at the Apollo 14 site. 24 p3447 A72-45556

APOLLO 15 FLIGHT

Electron microprobe analysis of plagioclase points and pyroxene grains of Apollo 15415 anorthositic genesis rock 02 p0282 A72-12411

Apollo 15 mare basalts and breccias and premare igneous rocks, analyzing chemical composition and microstructure 06 p0888 A72-18262

Geologic setting of Apollo 15 breccias and basalt 06 p0888 A72-18263

Chemical, geochronological and petrogenetic analyses of Apollo 15 lunar mare basalt rock from Hadley Rille, comparing with Apollo 12 and 14 basalts 06 p0888 A72-18264

Apollo 15 rock 15555 age by argon-40-argon-39 dating 06 p0888 A72-18265

Largest Apollo 15 lunar rock mass spectrometry analyses of noble gases with gas retention age estimation and spallation Kr data 06 p0888 A72-18267

Trace element concentrations of Apollo 15 basalt and soil samples by atomic colorimetry and isotope dilution 06 p0888 A72-18269

Crystallization age of Apollo 15 anorthositic rock 15415.9 06 p0888 A72-18270

Apollo 15 geochemical X ray fluorescence experiment, noting differential lunar highland crust existence 06 p0889 A72-18273

Primordial radioelements and cosmogenic radionuclides in Apollo 15 basalt, breccia and soil samples 06 p0889 A72-18274

Apollo 15 mission report, discussing lunar module powered descent, surface exploration with LRV, scientific instrument module, extravehicular activity, etc 08 p1230 A72-21007

Apollo 15 lunar subsatellite particle experiment subsystem design for studying magnetosphere dynamics, plasmas-moon interaction and solar flare physics 08 p1168 A72-21519

Ionospheric disturbances due to shock front from Apollo 15 launching, using split signal observation in ion acoustic and normal mode 09 p1397 A72-23569

Lunar crust and mantle evolution from Rb-Sr ages of Apollo 15 mare basalt samples 10 p1537 A72-24161

Geological setting, petrography and history of Apollo 15 anorthositic sample, tracing fragmentation and thermal metamorphic events 11 p1722 A72-26239

Radiogenic Ar 40/Ar 39 age and cosmic ray irradiation history of Apollo 15 anorthositic sample 15415, indicating Imbrian impact heating 12 p1862 A72-27111

Apollo 15 lunar heat flow experiment, discussing temperature data from probes and long lived radioisotopes decay effects 12 p1869 A72-27332

Glazed rock fragments and glassy splatter origin in bottom of small lunar craters from Apollo 15 observation 15 p2306 A72-31577

Lunar orbital photography of astronomical and geophysical phenomena during Apollo 15 flight, noting solar corona and Milky Way 15 p2236 A72-31974

Apollo 15 manned lunar landing, discussing geological data and surface experiment package and instruments 15 p2310 A72-31983

Apollo 15 orbital science payload instruments for exploring lunar origin and evolution to relate to earth history 15 p2310 A72-31984

The Apollo 15 lunar heat-flow measurement. 18 p2724 A72-36285

Apollo 15 gravity analysis from the S-band transponder experiment. 18 p2724 A72-36286

Solid solution, subsolidus reduction and compositional characteristics of spinels in some Apollo 15 basalts. 23 p3262 A72-44135

Major element composition of glasses in three Apollo 15 soils. 23 p3339 A72-44137

Lunar ultramafic glasses, chondrules and rocks. 23 p3340 A72-44340

APOLLO 16 FLIGHT

Apollo 16 planned mission to moon surface near crater Descartes, describing objectives 10 p1547 A72-24942

Photogeologic evidence of differentiation and deposition of lunar highland volcanic rocks at Apollo 16 landing site 12 p1866 A72-27115

Lunar surface mapping for Mg, Al and Si along ground tracks swept out by orbiting Apollo 16 spacecraft, noting geochemical X ray fluorescent analysis 18 p2726 A72-36556

APOLLO 17 FLIGHT

Lunar surface profile, subsurface features and electrical properties measurement for Apollo 17 coherent radar and optical recording system 14 p2085 A72-30512

APPENDAGES

NT ARM [ANATOMY]

NT FOREARM

NT HAND [ANATOMY]

NT LEG [ANATOMY]

A simple algorithmic method for the simulation of a spacecraft with flexible appendages. 23 p3343 A72-44552

APPLICATIONS OF MATHEMATICS

Book on integral transforms for solving ordinary and partial differential equations in applied mathematics covering Laplace, Fourier and Hankel transforms 01 p0094 A72-11274

Book on applied functions of complex variable covering infinite series, Cauchy theorem, singularities, Laurent series, residue theorem, conformal mapping, Fourier and Laplace transforms, etc 13 p1985 A72-28433

Dual extremum principles in functional analysis, including applications in nonlinear programming, networks, optimization, control theory, fluid mechanics, etc 15 p2262 A72-31630

Mathematical problems in geophysical sciences - Conference, Rensselaer Polytechnic Institute, Troy, New York, July 1970 16 p2384 A72-33335

- Book on basic acoustics covering mathematical methods, diffraction phenomena, statistical theory of signal processing, wave acoustics, membrane sound radiation, music, source array theory, etc
16 p2427 A72-33973
- Book on mathematical methods for viscoelasticity problems covering shear stress, viscometric flow, stress analysis, Fourier and Laplace transforms, momentum, equilibrium and constitutive equations, etc
16 p2427 A72-33975
- Analytical foundations of experimental mechanics - Trends in analytical mechanics.
18 p2732 A72-36354
- Boundary minorizing of the solution of an equation connected with the Signorini problem
18 p2704 A72-36466
- Russian book - Mathematical theory of friction
19 p2806 A72-37350
- Russian book - Problems of applied mathematics and mechanics
19 p2784 A72-37376

APPLICATIONS PROGRAMS [COMPUTERS]

- Computer programming languages, discussing system dependent and problem-oriented languages, ALGOL, FORTRAN and applicability ranges
17 p2523 A72-35444

APPLICATIONS TECHNOLOGY SATELLITES

- ATS-F educational TV experiment in India, discussing domestic communication satellite development and nationwide coverage problems
02 p0278 A72-11960
- Real time programmable video data compression system for microwave transmission of ATS satellite pictures between acquisition station and central computer processing
02 p0173 A72-12128
- Organizational structure and functions of ESTEC /ESRO branch/ concerned with scientific research and application satellites development
[DGLR PAPER 71-048] 02 p0305 A72-12724
- ATS F and G ground station mobile terminal, discussing system flexibility, utility and reliability features and parabolic antenna design
04 p0485 A72-14478
- Synoptic and dynamic aspects of tornado-producing thunderstorms development from ATS 3 and aerological data, observing mesoscale convective disturbances
06 p0842 A72-18438
- NASA space applications program review, discussing potential of communication, navigation and earth observation satellites
06 p0893 A72-18610
- Spacecraft charging at synchronous orbit, constructing mathematical model of ATS 5
07 p1058 A72-19150
- Lf oscillations of magnetic field at ATS 1, presenting local time and frequency distributions
07 p0975 A72-19160
- ATS F and G satellites with 30 foot deployable antennas as three axis stabilized platforms in geostationary orbit with high pointing accuracy
07 p1085 A72-19275
- Earth-space path attenuation statistics and fade duration at 15.3 GHz, using ATS 5 satellite transmission and radiometric sun/sky techniques
07 p0948 A72-20496
- ATS specular thermal control louvre system performance in simulated solar vacuum environment as function of sun and blade angle, noting white paint effect
[AIAA PAPER 72-268] 11 p1740 A72-25209
- ATS observed ionospheric column electron content variation during March 1970 solar eclipse, discussing neutral winds effects
12 p1801 A72-27155
- Earth station parabolic antenna gain-noise temperature ratio measurement using radio star and Applications Technology Satellite technique
[AIAA PAPER 72-528] 12 p1779 A72-27354
- British defense and civil communications satellite program, discussing SkyNet, INTELSAT, ESRO and New Space Technology Program activities
[AIAA PAPER 72-548] 12 p1781 A72-27371
- Adaptive multibeam experiment for aeronautical and maritime services /AMEAMS/, discussing NASA ATS-G satellite application to small mobile terminal communications system
[AIAA PAPER 72-582] 12 p1842 A72-27383
- Space technology application to ATS F and G program, discussing high power requirements, parabolic antenna design, tracking accuracy and ground station simplification
12 p1870 A72-27523
- Reliability, quality and testing assurance in ATS F and G system, discussing computerized handling of spacecraft parts information
12 p1814 A72-27524
- ATS F Environmental Measurements Experiment package for synchronous altitude space environment and electromagnetic-ionospheric interactions studies
12 p1795 A72-27525
- ATS F/G radio beacon experiments for study of exosphere and ionosphere integrated electron content, spatial structure and time dependent behavior
12 p1782 A72-27526

ATS F/G spacecraft thermal control design verification by chamber thermal balance tests and performance prediction mathematical model of earth viewing module and orbital environment
12 p1877 A72-27527

Composite materials mechanical and thermal properties for ATS reflector supporting truss, noting graphite fiber reinforced epoxy plastic design, fabrication and tests
12 p1886 A72-28158

Experimental communications satellite system of ATS F and G geostationary satellites for specific application, discussing system performance measurement instruments
[AIAA PAPER 72-578] 13 p1918 A72-28986

NASA ATS F/G satellites for educational TV broadcasting in foreign countries, discussing technologies and case histories
15 p2196 A72-31829

Satellites use for position determination and data acquisition systems application to earth sciences and industry
17 p2603 A72-34398

SRET-1 'solar cells'
19 p2869 A72-37822

ATS F and G radio link with ground stations, discussing telemetry and command functions with redundancy for RF interference minimization
21 p3019 A72-40883

APPROACH

NT INSTRUMENT APPROACH

APPROACH CONTROL

- Stellar attitude reference and navigation associative processor with high computational speed for radar approach control in ATC
02 p0256 A72-12033
- Carrier system for controlled approach of Naval aircraft to provide pilot window to deck for tactical jet guidance for poor visibility landing
02 p0256 A72-12323
- STOL aircraft integrated landing approach flight control system with elevator and thrust control coupling to angle of attack, altitude and other state variables
[DGLR PAPER 71-063] 02 p0155 A72-12705
- Terminal area air traffic guidance and control, discussing automation, all-weather precision approach and landing and failure detection
04 p0544 A72-14817
- HH-53 rescue helicopter automatic approach and hover coupler for automatic transition from forward flight at constant deceleration and rate of descent
05 p0686 A72-16653
- Conventional open and closed loop servo analysis methods applied to Naval aircraft approach power compensator systems, using pilot model concepts
[AIAA PAPER 72-124] 05 p0612 A72-16922
- General aviation type light airplanes pilot workload during steep landing approach, comparing flight tested control response parameters with handling qualities criteria
[AIAA PAPER 72-125] 05 p0613 A72-16941
- Ground based Doppler navigation system for wide range elevation and azimuth aircraft approach guidance, using linear directive antenna array for conical surface definition
06 p0845 A72-18183
- Explicit analytic guidance technique for hyperbolic approach phases of lunar and interplanetary spacecraft trajectories from first order solution for perturbed planet centered trajectory
[AIAA PAPER 72-15] 07 p1032 A72-18944
- Landing sequence strategy variations for individual ATC operators, indicating dependence on flight progress data variation, existing maneuvering conditions and controller personality traits
09 p1271 A72-23131
- Time analyses of ATC approach controller tasks, developing flow diagram for task component sequencing and quantifying
09 p1271 A72-23133
- Unpowered shuttle orbiter piloted control during approach and landing, discussing energy management technique based on fixed base six degree of freedom simulation
[AIAA PAPER 72-227] 10 p1551 A72-24438
- Aircraft microminiature ILS with transmitter and localizer antenna to provide pilot with bearing and glide slope information for alignment with runway
12 p1842 A72-27106
- Helicopter automatic flight control approach/hover coupler systems, hands off stability and handling qualities
12 p1843 A72-27522
- Workload modification effects on pilot neurological changes during Boeing 707 letdown, approach and landing
12 p1775 A72-28290
- Target acquisition by systems with unlagged acceleration control or rate control with exponential time lag, discussing number of approach and control stick movements
13 p1911 A72-29819

Airport lighting for pilot guidance during approach and landing under category I-III visibility conditions, discussing runway layouts and power requirements
14 p2092 A72-30621

Tactical approach landing radar tests for low lift drag ratio aircraft in unpowered flight, using F-104D as test aircraft
15 p2267 A72-31694

Hybrid area navigation and microwave instrument landing system, discussing approach control and terminal guidance
15 p2271 A72-32206

An experimental investigation of STOL longitudinal flying qualities in the landing approach using the variable stability X-22A aircraft.
[AHS PREPRINT 642] 17 p2490 A72-34502

Investigation of data rate requirements for low visibility approach with a scanning beam landing guidance system.
17 p2578 A72-35562

Precision navigation for approach and landing operations.
19 p2832 A72-38253

Investigation of data rate requirements for low visibility approach with a scanning beam landing guidance system.
19 p2832 A72-38259

A landing approach guidance scheme for aircraft which are capable of executing steep approaches.
19 p2832 A72-38278

Aircraft accidents during nonprecision approaches under adverse weather conditions, discussing landing aids use for corporate jet aircraft
20 p2952 A72-39745

Design, operation and testing of integrated STOL flight control system, noting approach accuracy and passenger comfort improvement
21 p3080 A72-40292

ILS replacement by microwave landing system, considering landing phase range from acquisition to touchdown, terminal approach handling by airborne navigation system and economic advantages
21 p3081 A72-40294

Multiloop piloting aspects of longitudinal approach path control.
[ICAS PAPER 72-46] 21 p2995 A72-41171

Allowable region of approach height and desirable approach path of aircraft for safe landing, presenting optimal control trajectories
23 p3252 A72-44497

An investigation of parameters and factors governing manual control of STOL aircraft in landing approach.
[AIAA PAPER 72-987] 24 p3369 A72-45415

Viewing Phobos and Deimos for navigating Mariner 9.
[AIAA PAPER 72-927] 24 p3423 A72-45433

APPROACH INDICATORS

Slant Visual Range/Approach Light Contact Height Measurement System utilizing state of art technology for airport applications
13 p1938 A72-28848

Aircraft radar for weather data, ground mapping, avoidance modes and independent landing monitor function, presenting straight and slant approach simulation data
21 p3080 A72-40290

APPROXIMATION

- NT BORN APPROXIMATION
NT BORN-OPPENHEIMER APPROXIMATION
NT CHEBYSHEV APPROXIMATION
NT FINITE DIFFERENCE THEORY
NT FINITE ELEMENT METHOD
NT HARTREE APPROXIMATION
NT LEAST SQUARES METHOD
NT NEWTON-RAPHSON METHOD
NT OSEEN APPROXIMATION
NT PADE APPROXIMATION
NT PARTICLE IN CELL TECHNIQUE
NT POHLHAUSEN METHOD
NT RAYLEIGH-RITZ METHOD
NT RELAXATION METHOD [MATHEMATICS]
NT RITZ AVERAGING METHOD
NT SCHWARTZ METHOD
NT SOMMERFELD APPROXIMATION
- Imperfect nonlinear system elastic buckling critical load calculation by higher order approximation, using perturbation approach and discrete coordinate diagonalized system
01 p0136 A72-10035
- Optimal control of material point motion in thin spherical layer of central gravitational field, solving by approximation
01 p0127 A72-10355
- F 2 layer critical frequency variations relation to solar radio flux intensity, using mathematical approximations
01 p0059 A72-10613
- Linear antenna array optimal power pattern synthesis by best approximation, using weighting function in man-machine iteration
01 p0029 A72-10665

Reachable sets calculation for linear dynamical system control, suggesting iterative procedures for numerical approximations

01 p0034 A72-11124

Half range differential approximation for spherically symmetric radiative transfer in concentric spheres with and without internal heat sources

02 p0302 A72-12259

Markov chain successive approximation method for electromagnetic wave propagation in medium with random large discontinuities, using scalar parabolic equation

02 p0181 A72-12588

Remes algorithm modification for linear approximation problem solution, discussing geometric interpretation and convergence

03 p0381 A72-13619

Molecular collision model, comparing generalized phase shift approximation method with classical trajectory calculations for rotational inelasticity

03 p0391 A72-13857

Approximation method for determination of distributed parameter systems optimal control, considering state and control variable constraints

03 p0338 A72-13917

Approximation of functions with diophantine conditions by polynomials with integral coefficients

03 p0382 A72-13948

Nonlinear elliptical equations first boundary value problem, presenting approximation capacity and convergence of straight line procedure

04 p0538 A72-14625

Distributed parameter state regulator system, investigating order of spatial discretization error in finite difference approximation to optimal response, control and performance cost

[AD-738401]

05 p0639 A72-15805

Stationary nonlinear dynamic systems identification, using modified differential approximation technique

[ASME PAPER 71-WA/AUT-11]

05 p0682 A72-15955

Convergent finite difference schemes for Navier-Stokes equations initial boundary value problems, using Temam systems approximation method

06 p0840 A72-18132

Closure approximation for energy transfer mechanism of stationary locally isotropic turbulence in inertial and dissipation ranges

06 p0802 A72-18545

Engineering curves and surfaces representation by spline functions, discussing computerized approximation methods for algebraic, transcendental and transfer functions

07 p1024 A72-18777

Differential equations system with right side dependent on constant parameters, obtaining approximate numerical solution by maximum principle of control theory

07 p1026 A72-18967

Approximating trajectory solution to state constrained optimal control problems, discussing convergence

07 p0959 A72-19289

Parametric and adaptive non-parametric system identification procedures in boundary value problem of string on elastic foundation, considering various approximation methods

07 p1096 A72-20349

Conditional mean state estimate approximation for nonlinear systems by parallel computation to reduce computer time

08 p1145 A72-20868

Dynamic characteristics and nonlinear oscillations of liquid in spherical shell of revolution, modifying Lukovskii approximation method

08 p1148 A72-20962

Averaging method for systems with shocks, assessing exact and approximate solutions discrepancy over finite time intervals

08 p1206 A72-20967

Integral operators functions approximation for elasticity and materials aging equations, noting transcendental functions in solutions

08 p1243 A72-21239

Best approximation estimates for function of many variables by sums of two functions of smaller number of variables

08 p1199 A72-21299

Approximation method for gas ejection calculation, assuming zero mixer flow velocity and ejection coefficient and suction side optimum operation for uniform pressure distribution

08 p1107 A72-21320

Successive approximations method for stress concentration problem at hole in cylindrical shell

08 p1247 A72-21818

Weighted least squares stationary approximations to time varying linear systems, noting criterion for matrix choice

09 p1341 A72-23094

Stochastic approximation for identification of element with second order lag, noting convergence with optimum parameter

09 p1291 A72-23371

Linear theories of gravitational fields, discussing Lorentz invariant approximation use to obtain Einstein equations approximation

09 p1352 A72-23386

Taylor series truncation method for steady supersonic inviscid gas flow past nonaxisymmetric conical bodies

09 p1295 A72-23498

Increased accuracy cubic spline approximation to two-point boundary value problems for differential equation, noting truncation error

10 p1502 A72-23722

Revised algorithm for unconstrained optimization using quasi-Newton methods based on recurring factorization of approximation to Hessian matrix

10 p1502 A72-23723

Nonlinear diffraction of weak shock waves near rigid wall with sharp bend, obtaining approximate solution by matched asymptotic expansion method

10 p1468 A72-24432

Sensitivity loss from approximation to radar and sonar signal square law detectors in quadrature systems with postdetection integration

10 p1437 A72-24690

Electromagnetic theory of HF ripple ground wave backscattering from gently rippled sea surfaces, discussing approximations for separated transmitting and receiving antennas case

10 p1438 A72-24742

Approximate model to reduce differential equation order for linear system of series connected elementary aperiodic components with different time constants

10 p1457 A72-24753

Sufficient conditions for existence, uniqueness and finite-dimensional approximation of solution to first order infinite-dimensional vector differential equation

11 p1676 A72-25357

Suboptimal feedback control law synthesis for nonlinear systems, using second order approximation to optimal control

11 p1610 A72-25872

Russian book on approximate solutions of boundary value problems covering elliptic differential equations and Ritz, moment, straight lines and probability modeling methods

11 p1677 A72-26065

Error bounds for finite element methods and approximation with piecewise polynomials for elliptic differential equations solution

11 p1679 A72-26956

Error bounds relationship to norm in approximate numerical solutions of initial value problems for ordinary differential equations

11 p1679 A72-26957

Inverse contour problem of approximating functions for compacta of positive logarithmic capacity in complex plane

12 p1836 A72-27070

Two dimensional approximation for viscoelastic inhomogeneous material with hereditary properties varying in radial direction, deriving integrodifferential equations

12 p1878 A72-27088

Classical isoperimetric problem approximation via multipliers method, generating minimizing convergent sequence of arcs

12 p1836 A72-27510

Algorithmic method in ALGOL 60 for successive approximations of optimal control problems, discussing improved convergence

13 p1935 A72-28707

Computer programmed algorithm for conducting smooth piecewise polynomial third order approximation in spline function determination

13 p1986 A72-29065

Boundary value problems of Poisson equation for rectangle having side with mixed boundary conditions, discussing solution by summary representations and successive approximations methods

13 p1986 A72-29071

Nonlinear dispersive wave propagation problems singly and multiply periodic solutions, using perturbation and numerical approximation methods

14 p2130 A72-30227

Approximate analytical solution for spherical particle acceleration in uniform gas flow, examining nozzle geometry and particle size effects

14 p2095 A72-30924

Hollow elliptical waveguide numerical analysis by polygon approximation with computer program to obtain cutoff wavelength without Mathieu functions

14 p2087 A72-30943

Approximate periodic solution of satellite equation of motion based on Schwarzschild metric integration, noting relativistic effects

14 p2162 A72-31108

Approximate solution of nonlinear boundary value problems in high temperature conductive heat transfer

14 p2174 A72-31161

Lumped approximation to distributed RC notch networks for linear IC, deriving open circuit voltage transfer functions and root locus graphs

14 p2092 A72-31170

Parameter-dependent linear and nonlinear equation systems solution by approximation polynomials, developing numerical algorithms

15 p2261 A72-31496

Variable cross section rod free longitudinal and torsional vibration frequencies and mode shapes determined by slowly varying parameters approximation method

15 p2327 A72-31740

Optimal thrust direction for planetary escape at residual speed, using approximate explicit closed loop guidance scheme

15 p2268 A72-31821

Coherent potential approximation generalization for disordered alloy systems, showing different results for propagator and locator formalisms in multiple site approximation [ONERA, TP NO. 1126]

15 p2293 A72-32229

Asymptotic formula for approximation of mean cycle-slip time of phase locked loops with low SNR and steady state phase error

16 p2371 A72-33211

Approximation of mathematical models for continuous media with many degrees of freedom, local structure and interactions, discussing parameters similarity conditions

16 p2425 A72-33586

Linear normed space subsets approximation by sums based on Fourier-Laplace series

16 p2417 A72-34009

The approximate solution of parabolic initial boundary value problems by weighted least-squares methods.

17 p2573 A72-34217

Book - Approximation of elliptic boundary-value problems

17 p2574 A72-34622

On the first-exursion probability in stationary narrow-band random vibration. II.

[ASME PAPER 72-APM-16]

17 p2628 A72-34800

Sudden freeze approximation for fluid flow systems relaxation time at constant enthalpy and pressure

17 p2542 A72-35633

Approximations yielding closed equations for isotropic turbulence compared to laboratory and computer experiments, emphasizing Langevin type model equation for velocity

18 p2677 A72-36008

MHD inlet flow into channel, obtaining velocity profile numerical solution in Prandtl approximation with modified boundary conditions

18 p2714 A72-36121

Digital simulation of stiff linear dynamic systems.

18 p2663 A72-36315

Automatic computation of exponentials, logarithms, ratios and square roots.

18 p2705 A72-37021

Linear electric circuits optimal synthesis as nonlinear programming of network parameters, discussing approximation algorithms

19 p2776 A72-37306

Sufficient conditions for two stage stochastic optimal control difference approximation by finite dimensional extremum problem sequences

19 p2777 A72-37318

Certain properties of continuous stochastic approximation procedures

19 p2824 A72-37325

Structure of absolutely approximating and absolutely correct difference schemes

19 p2824 A72-37384

Large particle method differential approximations in difference equation schemes for gas dynamics problems, discussing viscous effects and solution stability

19 p2745 A72-37385

Approximation by fractional steps of control problems governed by parabolic equations and with boundary control

19 p2825 A72-37786

Convergence of a multipoint iteration method for solving nonlinear equations

19 p2826 A72-38215

Certain algorithms for obtaining an approximate solution of incorrect problems on a set of monotonic functions

19 p2828 A72-38846

The equivalence of several initial value methods for solving integral equations.

20 p2945 A72-39346

Approximation of partial sums of multiple conjugate Fourier series of functions whose measure of continuity is given in the mean by Poisson integrals

20 p2945 A72-39394

Solution of a boundary value problem for a class of nonlinear ordinary differential equations by the method of successive approximations

20 p2945 A72-39463

Book - Functional analysis and approximation theory in numerical analysis.

20 p2946 A72-39729

Quasi-homogeneous approximation for wing with curved subsonic leading edges at supersonic speeds [ICAS PAPER 72-54]

21 p2992 A72-41176

Nonlinear differential equation periodic solution approximation by pseudo-linear representation of nonlinear terms effects on single harmonic, using describing function matrix method

21 p3076 A72-41314

Radiation absorption calculation for nonisothermal gas containing combustion products, noting approximation for water vapor radiation

22 p3243 A72-41885

A collocation solution of the nonlinear equations for axisymmetric bending of shallow spherical shells.

22 p3232 A72-41938

Improved Curtis-Godson approximation in a non-homogeneous atmosphere.

22 p3201 A72-42511

Linear multistep methods for a class of functional differential equations.

22 p3199 A72-42774

An approximation to midcourse correction direction errors.

22 p3203 A72-42870

Approximate solutions of the relativistic gravitational field equations to describe clusters of galaxies.

22 p3229 A72-42993

Extension of the range of convergence of precise iterative methods

22 p3200 A72-43133

On the approximation of the thermal conductivity of rigid heat conductors as a Cauchy problem

23 p3356 A72-43721

Degenerate electron gas self energy approximation by dielectric function, calculating quasi-particle and plasmon properties

24 p3428 A72-44797

An approximate method for the calculation of the characteristics of axial-flow fans.

24 p3363 A72-45369

Approximation of continuous periodic functions by Faward sums

24 p3419 A72-45547

Spline functions application to approximation theory problem of determining diameters of subspaces and manifolds in Banach space

24 p3419 A72-45548

Evaluation of the norm of a function in terms of its Fourier coefficients, convenient in problems of approximation theory

24 p3419 A72-45549

Approximation of analytic functions by trigonometric polynomials over an interval smaller than the period

24 p3419 A72-45550

Approximation of a continuous function of two variables by particular sums of a Fourier-Laguerre series

24 p3419 A72-45647

APPROXIMATION METHODS

U APPROXIMATION

APSIDAL ANGLES

U ANGLES [GEOMETRY]

APSIDES

NT APHELIONS

NT APOGEES

NT PERIGEEES

NT PERIHELIONS

APTITUDE

Aptitude screening test of ATC training applicants, using directional heading determination under aural distraction

12 p1773 A72-28252

AQUEOUS SOLUTIONS

Aqueous solutions specular reflectance measurement, using organic dye laser spectrophotometer at 360-650 nm and reflectometer equipped spectrophotometer at 0.2-20 micron wavelengths

02 p0226 A72-11831

Cyanogen induced phosphorylation of sugars in aqueous solution, discussing system prebiotic plausibility

04 p0483 A72-14771

Distillation experiments showing volatility-caused amino acid contamination of commercially available aqueous hydrochloric acid

05 p0624 A72-16079

Anion sorption mechanisms and product composition in anodic aluminum oxide filled with phosphate, chromate and sulfate solutions, discussing chemisorptive compound formation and oxide dehydration

05 p0624 A72-17053

Cyclohexylamine determination in aqueous solutions of sodium cyclamate by electron capture gas chromatography

07 p0935 A72-19488

Polyglycol aqueous solutions selection as fire resistant hydraulic fluid from hydraulic bench tests performed with various type pumps

08 p1197 A72-22161

Microstructural effects on high strength Mg, Al and Ti alloys stress corrosion crack growth in aqueous environments, discussing correlations relative to composition and preferred orientation

11 p1668 A72-26946

Aqueous formaldehyde effects on *Bacillus subtilis* spores, showing sporostasis due to germination inhibition and sporocidic due to temperature dependent inactivation

16 p2357 A72-33772

Critical species in the transgranular stress corrosion cracking of titanium alloys in aqueous solutions.

17 p2567 A72-34733

Laser velocimeter measurement of Reynolds stress and turbulence in dilute polymer solutions.

17 p2541 A72-35252

Autoclaves for the study of the effects of deformation on the high temperature aqueous corrosion of metals.

21 p3039 A72-40216

Phase transition between solid hydrate and saturated solution of lithium chloride electrically detected on a lithium chloride heated hygrometer.

21 p3054 A72-40689

On the vortex street behind a circular cylinder in non-Newtonian flows.

21 p2992 A72-41227

Water-soluble insulin receptors from human lymphocytes.

24 p3373 A72-45375

ARAGONITE

Holocene Bahamian oolites examination by scanning electron and light microscopy, observing aragonite crystals morphology, orientation and modification by boring activities of endolithic algae

05 p0654 A72-16037

ARC CHAMBERS

Exploding wire restrike mechanisms, discussing shock generation for arc channels

02 p0260 A72-12362

Thermal flux model of lithium plasma source at various temperatures and pressures, using arc channel model with conducting cross section

02 p0268 A72-12859

ARC DISCHARGES

German monograph on toroidal electric arc plasma with allowance for induced flow, covering tube wall heat transfer, electric field, MHD vortex development, mathematical model, etc

02 p0263 A72-11650

Interelectrode gap position control of discharge in coaxial gas heater with arc rotated by magnetic field

02 p0201 A72-12865

Cross flow blown two dimensional stationary plasma arc deflection and temperature distribution as function of collisional drift velocity and electric field

03 p0397 A72-13921

Arc driven shock tubes performance prediction, presenting correlation equations for velocity calculation

[AD-738275] 04 p0510 A72-15499

Boundary conditions and equations of plasma arc discharge in cylindrical diode with azimuthal magnetic field

05 p0697 A72-16988

Low voltage arc discharge development in cesium vapor with glowing spherical plasma cluster formation in electrode gap

05 p0701 A72-17238

Initial development period of low voltage arc discharge in cesium vapor leading to quasi-neutral plasma formation

06 p0860 A72-17696

Pinched vortex tube high current arc discharges for continuous pumping of ion crystal YAG-Nd lasers

06 p0825 A72-17839

Multiple swept stroke flash technique to test lightning effects on aircraft

07 p0964 A72-18768

Approximate solution to Elenbass-Geller equation of arc electric and radiation characteristics as function of thermal conductivity by Galerkin method

07 p1043 A72-19879

German monograph on wall stabilized Ar arc column displacement by pulsed HF radiation heating covering power absorption determination based on theoretical model

09 p1358 A72-22341

Vacuum arc stationary cathode mechanism theoretical analysis, determining cathodic temperature and current density

10 p1524 A72-24930

Quasi-steady Ar MPD arc exhaust plume structure from spectroscopic and photographic investigation, noting dependence on arc current and mass flow rate [AIAA PAPER 72-499]

11 p1696 A72-26222

Boundary conditions and equations of plasma arc discharge in cylindrical diode with azimuthal magnetic field

12 p1850 A72-27132

Magnetic probe measurement of random fluctuations in transverse magnetic field caused by He plasma produced in arc discharge

15 p2287 A72-32408

Suppression of arc drop in thermionic converters.

17 p2497 A72-34612

Continuous arc generation in Ar via focused CW carbon dioxide TEA laser, inducing gas breakdown by focal volume preionization with single pulse

18 p2697 A72-36082

Arc discharge transition from diffusion to arc mode, presenting theory on I-V characteristics negative resistance section and on hysteresis causes

18 p2714 A72-36207

Excitation and ionization processes in a low-voltage arc discharge

18 p2714 A72-36213

The Maxwellization of electrons in Cs-plasma of a low-voltage arc discharge

18 p2715 A72-36215

On the discharge instability in thermionic converters with long electrodes

18 p2647 A72-36217

Model improvements for thermionic diode plasmas.

18 p2715 A72-36218

Polarization and interferometric investigations of discharge modes in thermionic energy converters

18 p2647 A72-36219

The influence of a nonequilibrium electron distribution function near the cathode and fractional coverage on the characteristics of a thermionic emission converter in the arc mode

18 p2647 A72-36220

Quantitative schlieren techniques applied to high current arc investigations.

19 p2797 A72-37588

Results of a computer simulation of an arc plasma in a curved discharge tube.

19 p2841 A72-38085

Study of tungsten and molybdenum coatings obtained by arc discharge in a vacuum

19 p2808 A72-38186

An apparatus to investigate plasmas at very high pressure.

21 p3056 A72-41004

Approximate calculation of a laminar arc discharge in a cylindrical channel

22 p3210 A72-42285

Spatial and temporal temperature distribution in plasma from a low-voltage aperiodic spark discharge in an atmosphere of argon

23 p3320 A72-43677

ARC GENERATORS

Lightning simulation laboratory for aircraft strike testing, using high energy generators

07 p0964 A72-18774

Investigation of electrical processes in high frequency condensed-spark generators

22 p3139 A72-42169

ARC HEATING

Ar jet simulation tests of thorium dispersed Ni and Co alloys for space shuttle Metallic Thermal Protection System, determining material degradation

01 p0086 A72-10978

Hot pressed baron nitride and composite oxidation tests in atmospheric arc jet, noting fabrication and composition effects on thermal shock and oxidation resistance

09 p1333 A72-22379

Arc furnace for thermal analysis of ultrarefractory materials

21 p3039 A72-40208

Nitrogen temperature determination in arc tunnel air flows.

[AIAA PAPER 72-1022] 21 p3042 A72-41600

Spectroscopic measurements for atmospheric nitrogen and helium arcs.

23 p3322 A72-44326

ARC JET ENGINES

Electron density and temperature fluctuations coupled through Ohm law for ionizable medium, applying to MHD generators and MPD arc thrusters [AIAA PAPER 72-101]

05 p0706 A72-16813

Electron density and temperature temporal and radial profiles in megawatt MPD-arc thruster exhaust, using Thomson scattering technique

[AIAA PAPER 72-209] 05 p0707 A72-16887

Near field megawatt single shot exhaust flow and propulsion characteristics of pulsed MPD arc thruster [AIAA PAPER 72-500]

11 p1711 A72-26223

Propulsive performance of a 30 kW arc-jet thruster stabilized by vortex and magnetic forces.

19 p2848 A72-37925

ARC LAMPS

CW Kr arc lamps for high power Nd-YAG laser pumping, testing operating life and electrical and spectral characteristics as function of design

09 p1324 A72-23080

High power CW Nd-YAG laser efficiency improvement by optical pump wavelength, power coupling and balance factors, noting krypton arc lamp contribution

15 p2247 A72-32029

Cs vapor photoionization by sequential method via thermally tunable Ga-As laser and arc-lamp monochromator radiation

17 p2585 A72-34614

Influence of gas pressure in arc lamps on the pumping efficiency of CW garnet lasers.

20 p2933 A72-39513

Control circuit for a power supply of a laser pump lamp.

20 p2933 A72-39524

ARC MELTING

Mechanical and microstructural properties of Be-base alloys consolidated by vacuum arc melting, reporting results of tensile tests, hardness measurements and microprobe analysis

05 p0674 A72-16389

Ti alloys evaluation technique of arc melting, processing and testing of miniature ingots, discussing alloying and microstructural effects and correlation with plate properties

05 p0674 A72-16390

Arc-air method application to groove planing, cutting and beveling, describing manual, semiautomatic and full-automatic units

07 p0994 A72-18932

Equilibrium diagram of Cr-Va alloy produced by arc melting under Ar atmosphere, using high temperature differential thermal analysis

07 p1019 A72-20160

Plasma arc and MIG/metal inert gas/welding combination with filler wire, obtaining high melting rates and penetration control

09 p1322 A72-23645

Refractory metals vacuum melting for ingot production and purification in arc and electron bombardment furnaces

14 p2107 A72-30531

Inhomogeneity of high melting temperature elements in titanium alloys.

18 p2701 A72-36693

Zr and V alpha and beta stabilizing element effects on phase boundaries in arc fused Ti-Al alloy studied by diffusion layer method

19 p2817 A72-37754

ARC SPRAYING

Plasma arc testing of space shuttle Nb and Co alloys thermal protection materials, using IR radiometric and photographic techniques

01 p0048 A72-10977

ARC WELDING

NT GAS TUNGSTEN ARC WELDING

NT PLASMA ARC WELDING

Heat input, interpass temperature and panel width effects on butt welds strength in Al alloy plate

04 p0526 A72-14838

Stress fields around moving weld arc on Al sheet from isotherm map, calculating compressive and tensile stresses from heat induced material expansion

06 p0820 A72-17705

Fine oxide particle inclusions in mild steel weld metal deposited by carbon dioxide shielded metal arc process, using electron micrography and diffraction pattern photography

06 p0820 A72-17706

Cast and wrought Ti alloys Ar arc weldments microstructural and mechanical properties after different heat treatment sequences

07 p1013 A72-19750

Cavity formation and drop transfer time correlation with welding current in powder covered/submerged/arc welding, using high speed X ray photography

07 p0998 A72-20396

Impurities effect on Mo plastic properties and toughness, suggesting lower vacuum arc welding rates and increased electron beam zone refining runs

09 p1326 A72-22228

Pulsed arc TIG welding with modulation of current from standard power source, comparing performance with steady dc method

09 p1320 A72-23632

Niobium and molybdenum carbide film deposition on steel substrates by open arc welding with partial carbon burnout

14 p2107 A72-30156

Servomechanism and reduction gear ratio selection for arc welding voltage regulator, taking into account welded joints properties

15 p2244 A72-31611

Gas shielded arc welding of Ni, discussing current density, energy, arc length and preheating temperature effects on welds porosity

18 p2695 A72-36427

Ways of reducing porosity in argon-arc welding of thin titanium sheets.

18 p2695 A72-36428

Investigation of the transport of electrode metal during welding in a carbon dioxide atmosphere

19 p2810 A72-38588

ARCHES

Interaction surfaces for structural members under combined axial, shear force and bending moment, investigating shear effect on yielding of arches

07 p1090 A72-19730

Free in-plane vibrations of hinged and fixed uniform circular arches, discussing natural frequencies and flexural and extensional vibration modes

10 p1560 A72-25186

Linear programming simplex method for static load limit of circular arch

11 p1739 A72-26921

Uniformly loaded parabolic arches lateral-torsional buckling, deriving governing linear differential equations from Clebsch-Kirchhoff equilibrium equations for thin curved bars

12 p1888 A72-28349

Dynamic response of thin circular arches to in-plane forced excitation under cyclic symmetric and unsymmetric support movement

14 p2169 A72-31175

A comparison of initial velocities for dynamic instability of a shallow arch.

18 p2738 A72-37080

Dynamic snap-buckling of shallow arches under inclined loads.

20 p2980 A72-39617

ARCTIC OCEAN

Autocorrelation functions of anomalous magnetic field and earth crust structure of central portion of Arctic Ocean, using sliding energy spectrum method

13 p1946 A72-28589

Autocorrelation functions of anomalous magnetic field and earth crust structure of central portion of Arctic Ocean, using sliding energy spectrum method

24 p3397 A72-45089

ARCTIC REGIONS

Arctic polar region geomagnetic perturbations during IQSY, noting diurnal variations

05 p0658 A72-16278

Simultaneous determination of chord length and direction by artificial earth satellite geodetic observations in Arctic and Antarctic regions

13 p1945 A72-28493

Lower Arctic thermosphere neutral composition changes due to disturbances, considering atomic hydrogen, nitric oxide, hydroxyl, water vapor, nitrogen and oxygen

15 p2225 A72-31912

Arctic environment surface effect vehicle design, considering structures, drag, lift, propulsive power and range

15 p2181 A72-32125

Structure and circulation of the upper atmosphere over East Antarctica in 1969 and 1970

20 p2949 A72-39949

On the classification of high-latitude auroras.

20 p2920 A72-39979

The occurrence of radio aurora at high latitudes - The IGY period, 1957-1959.

20 p2904 A72-39982

Application of differential OMEGA to remote environmental sensing.

24 p3421 A72-44639

ARGENTINA

Lunar magnetic variations at Trelew/Argentina/.

19 p2794 A72-38860

ARGON

NT ARGON ISOTOPES

Ionized argon recombination rate constant determination as function of temperature, using dual frequency laser interferometry measurement of corner expansion flow

01 p0050 A72-10851

Isotopic composition of trapped helium, neon and argon in carbonaceous chondrites, observing covariance based on mass-dependent fractionation

03 p0414 A72-12904

Hard sphere liquid Bernal model with cell method extension, determining liquid argon behavior near melting

03 p0388 A72-13151

Coronary blood flow measurement in various hemodynamic conditions by argon technique, determining oxygen consumption and coronary vascular resistance

03 p0315 A72-13183

Dimer formation effect on thermal diffusion factor at low temperatures for krypton-argon system

03 p0391 A72-13749

Effective cross sections of ion collisions with gaseous target and argon atoms collision with argon target by molecular beam intensity attenuation method

03 p0392 A72-14060

Two dimensional molecular dynamics digital simulation of Ar liquid-vapor interface at triple point, yielding strongly oscillatory density profile

03 p0393 A72-14263

Hanle effect mean-life measurements on aligned Ar fast ion beam particles, comparing results with beam-fol measurement

04 p0552 A72-15151

Ar, Kr, methane and nitrogen physisorption isotherms on stainless steel in low pressure cryogenic baths calculating mean adsorption energies

05 p0624 A72-16395

Vibrationally inelastic scattering of CO cations by Ar collision, measuring ion energy, mass and angular distribution with high resolution ion beam apparatus

05 p0693 A72-17169

Ar core polarizability effect on photoionization cross section calculation for ground state configuration

05 p0693 A72-17173

Metastable argon-carbon dioxide dissociation and electronic excitation of carbon monoxide or oxygen

07 p1037 A72-19496

Pressure broadened atomic line shapes calculation for Cs resonance line pressurized by Ar, using Lennard-Jones potentials

09 p1354 A72-22663

Magnetic field effect on threshold pressure reduction for He and Ar gas breakdown by carbon dioxide laser radiation, taking into account inhibition of radial electron diffusion

AD-741539 09 p1365 A72-23493

Photoionization cross sections for atoms and ions of Al, Si and Ar on basis of Hartree-Fock bound-electron and close coupling approximation free-electron wave functions

10 p1516 A72-24669

Isochoric heat capacity peaks of water and argon near boundary in two phase region at critical state

11 p1747 A72-26964

Argon and mercury ion engines operation, performance and control, evaluating safety and ease of handling from laboratory test data

13 p2026 A72-28931

Isoelectronic wavelength calculations for Ar line spectra, presenting table with identifications and interpolations

13 p2045 A72-29704

Thermoelectrical properties of ternary bismuth-antimony-tellurium alloy system obtained under Ar gas pressure in quartz and graphite crucibles

14 p2142 A72-30500

Ar and K electron cross section determination for momentum transfer, using dc conductivity measurement of high pressure plasma

14 p2134 A72-30803

Pressure effects of Ar and ⁴He mixtures on Cs atomic line shapes calculated assuming additivity of perturber interactions

14 p2134 A72-30838

Steady state electron mean energy variation between parallel plates in Ar and He calculated by Monte Carlo simulation for comparison

15 p2285 A72-32222

Differential collision cross sections for argon pairs with neon, methane and ethane at angular region of two crossed nozzle molecular beams

16 p2431 A72-33070

Nitrogen molecular beam rotational excitation by collision with argon beam, describing electron beam spectrographic experimental method and numerical simulation technique

16 p2431 A72-33071

Combustion process in mixing gas jets of different density, using argon and nitrogen for internal flow and air for external jet

16 p2381 A72-34169

Breakdown in argon and nitrogen under the influence of a 0.35-micron picosecond laser pulse.

17 p2564 A72-35508

Continuous arc generation in Ar via focused CW carbon dioxide TEA laser, inducing gas breakdown by focal volume preionization with single pulse

18 p2697 A72-36082

Ion-atom scattering and interatomic potentials for ions of noble metals and period II elements incident on neon and argon with energies in the range 8-25 keV.

19 p2387 A72-37883

Volume and enthalpy changes at critical point of condensed state, noting Ar enthalpy dependence on temperature

19 p2881 A72-38045

Shock tube boundary layers in ionized argon-helium mixtures.

20 p2914 A72-39639

Broadening and shift of magnesium lines by van der Waals interaction with argon atoms and by microfields.

22 p3208 A72-42388

Drift velocities, diffusion coefficients, and temperatures of photions in argon, nitrogen, and oxygen

22 p3209 A72-42926

Pulse discharge plasma in Ar with gas ionization level near unity, noting plasma cylinder parameters, electron temperature and I-V characteristics

22 p3212 A72-43103

Electronic detection of ionizing-particle tracks in liquid argon

23 p3291 A72-44442

Transport properties of a gas of diatomic molecules. VI - Classical trajectory calculations of the rotational relaxation time of the Ar-N₂ system.

24 p3427 A72-45308

Mass spectra stimulated by O+ and Ar+ interacting with a surface.

24 p3378 A72-45312

ARGON ISOTOPES

Apollo 14 rocks, breccia fragments and soil samples ages from Ar 40/Ar 39 and cosmic ray dating, discussing basalt Ar release patterns

01 p0117 A72-10052

L-chondrite Assam, determining He, Ne and Ar concentrations and isotopic compositions and galactic and solar flare irradiation track densities

01 p0124 A72-10060

Apollo 15 rock 15555 age by argon-40-argon-39 dating

06 p0888 A72-18265

Ar-39/Ar-38 cosmic ray exposure age calculation from Sikhote-Alin meteorite fall fragment content of Ar-39, Ar-38, Ne-21 and He-3

14 p2157 A72-30584

Argon 37/argon 39 activity ratios in meteorites and the spatial constancy of the cosmic radiation.
18 p2723 A72-36027

ARGON LASERS

Laser sources for space research, considering He-Ne, carbon dioxide, Nd-YAG and argon lasers performance
02 p0237 A72-11695

Soviet book on gas lasers covering operation, population inversion, helium-neon, argon and carbon dioxide lasers and atomic frequency standards
02 p0238 A72-12121

Dc excited argon laser anode oscillation noise, discussing relation to ballast resistance, suppression conditions and current fluctuation frequency response to laser fluctuation
02 p0239 A72-12826

Holographically produced zone plates for solar X ray imaging, using Ar laser produced interference figure
03 p0354 A72-13046

Traveling wave Ar laser with only fundamental TEM modes, examining mode self locking and composition and intensity as functions of frequency misalignment
03 p0366 A72-13366

Spectroscopic characteristics of continuous wave neutral argon laser using helium and chlorine for power enhancement
03 p0367 A72-13432

Pulsed Ar ion laser quantitative level population mechanism in gas discharges, discussing radiation trapping effects on 4s doublet based on spontaneous emission line data
04 p0529 A72-14602

Radiation intensity of CW argon ion laser with nonlinearly absorbing argon cell in cavity, showing pressure relation to amplification and absorption
04 p0530 A72-14658

Neutral atoms pressure distribution along capillary and pressure compensating channel during discharge in argon ion laser
05 p0670 A72-16990

Spectral characteristics of Ar ion laser emission for determination of stability region, mode sequence and beat signal levels
06 p0826 A72-18009

Magneto-optical effect on CW radiation intensity of Ar laser with cell in magnetic field for various gain conditions
07 p1009 A72-20615

Magnetic field effect on gain saturation in CW Ar laser associated with Zeeman splitting
08 p1184 A72-22036

High resolution Raman spectroscopy of low pressure gases, using single mode Ar laser
09 p1323 A72-22613

High power Ar laser frequency stabilization technique using multiple feedback loop with optical cavity discriminator stabilized against iodine vapor absorption line
09 p1325 A72-23337

High power Ar ion laser with plasma tube using current conducting graphite bore for stable long life operation
10 p1489 A72-23944

Raman spectra of azoanisole and anilindazine in liquid crystal states excited by Ar laser, revealing lattice vibrations attenuation near transition point
10 p1490 A72-24042

Vortex discharge in Ar as optical pumping source for ionic crystal CW lasers, comparing efficiency with YAG-Nd crystal pumping
11 p1648 A72-26331

Ar laser levels population inversion dependence on current density, discharge tube pressure and magnetic flux
11 p1649 A72-26350

Stable single frequency Ar laser radiation with coupled transitions emission
11 p1650 A72-26356

Neutral atoms pressure distribution along capillary and pressure compensating channel during discharge in argon ion laser
12 p1819 A72-27133

Organic dye desensitization of bleached AgBr phase holograms against printout darkening by Ar ion laser light
12 p1811 A72-27949

Thermal defocusing of high intensity continuous Ar laser radiation in absorbing medium with allowance for spherical aberrations
14 p2110 A72-30355

ADP or KDP crystal induced second harmonic emission from Ar laser resonator, noting crystal temperature effects on primary/secondary radiation phase synchronism
16 p2400 A72-33281

Ar laser levels population inversion dependence on current density, discharge tube pressure and magnetic flux
16 p2402 A72-33703

Stable single frequency Ar laser radiation with coupled transitions emission
16 p2403 A72-33709

CW argon ion laser characteristics at high steady discharge currents, discussing output limitation by low inversion utilization efficiency due to cavity mirrors optical degradation
16 p2404 A72-34035

Satellite measurement of ground-based CW Ar laser source scintillation, deriving log amplitude variance, probability distribution and power spectral density from telemetered data
17 p2513 A72-34289

Spectral characteristics of a single-frequency argon laser with an absorbing film.
20 p2932 A72-39509

Measurements of a mode-competition discriminant in a single-frequency argon ion ring laser.
21 p3062 A72-40240

Output power saturation with increasing discharge current in powerful argon CW lasers
21 p3062 A72-40404

Cross sections for the excitation of Ar II laser lines in electron-ion collisions.
21 p3063 A72-40725

Molecular-beam-stabilized argon laser.
23 p3296 A72-43817

ARGON PLASMA

Electrical properties of subsonic argon plasma stream seeded with uranium hexafluoride, using electrostatic probe
01 p0111 A72-11334

Argon-hydrogen plasma seeded with submicron tungsten particles, measuring composition, temperature, radiant heat output and opacity
01 p0112 A72-11343

Simulation of nuclear light bulb engine propellant radiative heating, using argon seeded with micronized carbon particles and 500 kw dc arc as radiant energy source
01 p0099 A72-11344

Wall stabilized Ar arc plasma, investigating Boltzmann equilibrium existence between spectral energy levels
02 p0264 A72-12025

Anode heat flux for cascade atmospheric Ar arc of Maecker type, checking anode heat transfer model validity
02 p0302 A72-12266

Argon plasma electromagnetic wave transformation and absorption measurements under various gas pressures
03 p0395 A72-13571

Power and gas consumption for inductive plasma formed in Ar atmosphere, measuring radial distribution of magnetic field axial component
03 p0395 A72-13652

Ar gas dc discharge plasma characteristics in crossed electric and magnetic fields, examining equivalent pressure concept
04 p0556 A72-14945

Argon and nitrogen plasma viscosity measurements, using pressure difference probe
04 p0558 A72-15344

Plasma satellite linewidth broadening due to density inhomogeneity, considering evidence based on light scattering from Ar plasma jet
04 p0559 A72-15355

Electron drift speed and multiplication rate in pulsed Ar positive column in axial electric field
04 p0553 A72-15669

Electric field strength, radiated power and radial temperature distribution measurements in high pressure Ar cascade arc
05 p0695 A72-16156

Radiation transport mechanism and transport coefficients in high pressure Ar cascade arc, measuring electric field strength, radiated power and radial temperature distribution
05 p0695 A72-16157

Continuously burning optical discharge in Ar and Xe at atmospheric pressures, evaluating laser beam energy absorption, electron density and plasma temperature
05 p0669 A72-16679

Argon plasma transient axial flow and heating characteristics in pinched column of linear z-pinch device with collapsing current sheets conversion to axial streaming velocity
05 p0696 A72-16886

Thermodynamic equilibrium relations in optically thin plasma models for hydrogen and argon systems
05 p0699 A72-17218

Nonequilibrium plasma production by induced electric field in helium and argon streams in magnetic field
05 p0700 A72-17229

Collisionless relaxation of ionpenetrating ion beams in Ar plasma, showing velocity spectrum broadening during Langmuir frequency periods
06 p0853 A72-17394

Quiescent large volume collisionless He and Ar plasma generation via hf electric fields, noting low cost
06 p0854 A72-17504

Magnetic multipole confinement of magnetic field-free He and Ar plasmas in vacuum chamber, observing decay
06 p0854 A72-17505

Boltzmann kinetic equation with electron-electron collision coefficients for isothermal weakly ionized cesium-argon plasma, using nodal point method
06 p0860 A72-17695

Ion heating caused by ion acoustic waves in ion streaming argon plasma
06 p0860 A72-17746

Argon ion spectra overlap with satellites to carbon and boron Lyman alpha lines, employing theta pinch
06 p0852 A72-17897

Cathode temperature measurement in erosion and heat transport reduction by cesium seeding of Ar plasma arc
06 p0862 A72-18334

Linear Z plasma pinch in Ar as spectroscopic source, investigating effects on shock-piston separation
06 p0865 A72-18544

Design equations for transpiration radiometer applicable to radiation measurement from confined Ar plasma
08 p1163 A72-20919

Plasma generator with Ar as ionizing medium for metal cutting and welding, discussing protection against secondary arc formation
08 p1176 A72-21048

Ar plasma in ion engine discharge chamber with primary and Maxwell electron bombardment, discussing ion production probabilities in perturbed and unperturbed cases
08 p1223 A72-21209

Electrostatic ion wave Landau damping in magnetic field of Ar plasma QP machine
08 p1213 A72-21250

Multimode cavity for simultaneous oxygen/argon plasma excitation and electron density measurements, noting gas pressure effect
08 p1213 A72-21323

Calorimetric gage for convective and radiative wall heat flux measurements in Ar arc plasma
08 p1254 A72-21628

Powder materials heating and melting temperatures calculation in free turbulent nitrogen and argon plasma jets
08 p1181 A72-22098

German monograph on wall stabilized Ar arc column displacement by pulsed HF radiation heating covering power absorption determination based on theoretical model
09 p1358 A72-22341

Transition probabilities of ionized Ar spectral lines for excitation temperature measurements
09 p1355 A72-22672

Turbulent mixing of high temperature Ar jet injected into ring slipstream of air in dc plasmatron with coaxial nozzle and fixed arc
09 p1410 A72-22677

Ionic and atomic temperature measurement in low pressure Ar plasma by X ray absorption spectroscopy
09 p1360 A72-22832

Radial temperature distribution in Ar plasma jet, assuming local thermodynamic equilibrium
09 p1364 A72-23387

Dense low temperature Ar and Hg plasmas, observing correlation between electrical conductivity and optical emission
10 p1517 A72-23835

Monochromatic absorption coefficients determination for Ar heated in wall-stabilized arc at high temperatures and pressures
10 p1517 A72-23836

Observation and ionization relaxation times of Ar plasma produced in shock tube at Mach 10-13, describing experimental arrangement
10 p1519 A72-24056

Microwave equipment for electron density profiles determination used in ionization relaxation start study of shock induced Ar plasma
10 p1519 A72-24067

Argon plasma jet mean flow velocity radial distribution measurement method
10 p1520 A72-24205

Ar/He plasma acoustic wave properties, expressing phase velocity and damping as function of ion-electron temperature ratio and relative species densities
10 p1520 A72-24300

Diaphragmless electrothermal shock tube for collision in preheated Ar, using RF plasma heater
10 p1459 A72-24410

Electron-neutral collisions effects on wavelength and damping of electrostatic waves propagation in Ar and He plasmas
10 p1525 A72-25143

Quasi-steady Ar MPD arc exhaust plume structure from spectroscopic and photographic investigation, noting dependence on arc current and mass flow rate
11 p1696 A72-26222

Shock-induced flow acceleration in Ar plasma, studying shock front behavior from high-speed photographs
11 p1696 A72-26374

Electromagnetic wave transformation and absorption in Ar plasma with nonmonotonic longitudinal density distribution
11 p1699 A72-26758

Velocity and temperature attenuation of argon and nitrogen jets expelled from plasma spray guns into physically identical ambient medium
13 p2011 A72-28920
Cs seeded nonequilibrium MHD Ar plasma stability in fully ionized seed regime
13 p2014 A72-29368
Thermal flux distribution in sectioned plasmatron channel with supersonic Ar plasma injection, discussing energy dissipation
13 p2017 A72-29634
He and Ar plasma transport by magnetic fields after expulsion from pulsed linear discharge
14 p2135 A72-30167
Pulsed Ar plasma temperature and charged particle concentration obtained as functions of elapsed discharge time by spectroscopic observation
14 p2139 A72-30780
Ar plasma spectral lines, calculating temperature functions of excitation to fourth ionization multiple at atmospheric pressure
14 p2139 A72-30782
Anomalous excitation of nitrogen positive bands in seeded Ar free plasma jet, measuring oscillator strengths of atoms
14 p2140 A72-30899
Solar cells insulating dielectrics breakdown tests in dilute Ar plasma at positive bias voltages to 20 kV
14 p2140 A72-30926
Ar plasma radiation dispersion by plane grating, measuring ionic spectral lines and continuous spectrum intensity time variation
15 p2286 A72-32340
Visible and UV stimulated emission in plasma of direct pinch discharge on Ar II and III ions, discussing application possibility to plasma diagnostics
16 p2400 A72-33297
Continuously burning optical discharge in Ar and Xe at atmospheric pressures, evaluating laser beam energy absorption, electron density and plasma temperature
16 p2402 A72-33691
Ionized gas-solid suspension thermal physical properties verification by micro-sized MgO dispersion in Ar plasma
[AIAA PAPER 72-688]
16 p2439 A72-34054
Positive and negative ions relative intensity measurement during nitrous oxide target molecules injection into sonic Ar plasma reaction channel, using quadrupole mass spectrometer
[AIAA PAPER 72-675]
16 p2440 A72-34064
Suppression of arc drop in thermionic converters.
17 p2497 A72-34612
The propagation of non-axisymmetric Alfvén waves in an argon plasma.
17 p2591 A72-35371
Collisional-rate coefficients for sodiumlike Ar VIII ions.
17 p2585 A72-35770
Electron density measurements in early stage of the high current pulsed discharge.
18 p2716 A72-36957
Effect of a cooling gas layer on the geometrical dimensions of an induction plasma
20 p2957 A72-39219
Effect of angle of incidence on the response of cylindrical electrostatic probes at supersonic speeds.
20 p2926 A72-39602
Influence of the lowering of the ionization energy on the continuous radiation of an argon plasma
21 p3093 A72-41343
Ar plasma diagnostics from stabilized arc emission spectra, noting thermodynamic equilibrium in central zone of arc channel
22 p3209 A72-41880
Anode heat transfer for a flowing argon plasma at elevated electron temperature.
22 p3210 A72-41952
Elastic electron-neutral interaction in argon in the vicinity of the Ramsauer minimum
22 p3211 A72-42642
A transpiration radiometer for measurement of total thermal radiation from a flowing plasma
22 p3179 A72-42691
Measurement of the electronic density in a hollow cathode discharge working with argon
22 p3181 A72-43098
Molecular gas presence effect on electron energy balance in atomic gases, noting inelastic collisions loss factor in heated Ar plasma containing nitrogen molecules
22 p3213 A72-43110
A study of the electronic and gasdynamic parameters of a hypersonic wake behind models moving in argon
22 p3168 A72-43111
Spatial and temporal temperature distribution in plasma from a low-voltage aperiodic spark discharge in an atmosphere of argon
23 p3320 A72-43677
Excitation mechanisms in the argon-ion spectrum at near laser conditions and temperatures and densities in a hollow cathode argon-arc discharge.
24 p3428 A72-44807

Velocity distribution function and balance parameters of electrons in a nonisothermal argon plasma at degrees of ionization from 0.000000001 to 0.01
24 p3428 A72-44968
ARGON 36
U ARGON ISOTOPES
ARGON 40
U ARGON ISOTOPES
ARGUMENTS [MATHEMATICS]
U INDEPENDENT VARIABLES
ARIEL 3 SATELLITE
Magnetically symmetric detection of the mid-latitude electron density trough by Ariel 3 satellite.
22 p3170 A72-42372
ARIP [IMPACT PREDICTION]
U COMPUTERIZED SIMULATION
U IMPACT PREDICTION
ARITHMETIC
NT DOUBLE PRECISION ARITHMETIC
NT FLOATING POINT ARITHMETIC
Moore-Penrose pseudoinverse matrix computation, using single and multiple modulus arithmetic method for reduced roundoff error
11 p1676 A72-25505
ARITHMETIC AND LOGIC UNITS
Programmable cellular cascades and arrays synthesis for realizing arbitrary Boolean functions or parallel arithmetic operations
04 p0498 A72-15107
Medium scale integration /MSI/ modules for arithmetic section in small, medium and process computers, emphasizing carry-lookahead procedure
13 p1926 A72-30053
Cellular-array arithmetic unit with multiplication and division.
17 p2519 A72-34297
ARM [ANATOMY]
NT FOREARM
Human arm arterial pressure and flow pulsations numerical analysis, constructing electrical analog circuit from mathematical model
03 p0317 A72-12951
Human body movements basic kinetics, measuring static force, angle and tangential acceleration of horizontal arm swings
04 p0478 A72-14707
Electromyographic determination of muscular compliance during arm movements, using on-line analog computer
04 p0478 A72-14708
Physical conditioning effect on central and peripheral circulatory responses to arm work, measuring cardiac output at 80 percent maximum aerobic power
04 p0473 A72-14900
Human arm muscle motor neuron reflex response to rectangular pulse excitation of ulnar nerve
04 p0476 A72-15587
Hand steadiness during unrestricted linear arm movements and eye-hand coordination tasks, showing tremor occurrence in up-down plane
10 p1432 A72-25113
Human hand-arm system vibration characteristics, describing mechanical impedance measurements for mathematical modeling
13 p1910 A72-29559
ARMED FORCES
NT ARMED FORCES [FOREIGN]
NT ARMED FORCES [UNITED STATES]
NT NAVY
Simulation procedure for mission and maintenance planning of an air force wing.
24 p3365 A72-44663
ARMED FORCES [FOREIGN]
Methods for measurement of the state of health
21 p3005 A72-40395
ARMED FORCES [UNITED STATES]
Decompression sickness treatment in USAF hyperbaric oxygen chambers
08 p1126 A72-21575
U.S. Navy cartography, describing RA-3B Skywarrior capabilities and photographic instrumentation
08 p1169 A72-21699
USAF Academy air navigation training program, discussing systems development course and descriptive and applied astronomy
15 p2272 A72-32210
AROMATIC COMPOUNDS
Jet fuels hydrocarbon composition effect on thermal stability, considering nonaromatic components influence on aromatic hydrocarbons oxidation products coagulation
02 p0271 A72-12800
Aromatic and amino acid prebiotic syntheses under primitive earth, considering electric discharge and cyanide polymerizations
04 p0483 A72-14762
Photoemission from tetracene organic semiconductors due to electron capture defect ionization by excitons
11 p1700 A72-25785
Aromatic polyimide binder for compression moldable high performance composites preparation with

thermal curing to obtain good thermal-oxidative stability and toughness
12 p1834 A72-28090
Aromatic hydrocarbons and fuels, investigating engine parameters effects on combustion and exhaust gases temperatures
13 p2025 A72-29074
Properties of pyrolytic oil hydrogenated aromatic fraction, noting suitability for jet fuels applications
14 p2145 A72-31075
Aromatic hydrocarbons - Methane ignition inhibitors
19 p2879 A72-37364
Investigation of certain complex compounds of triaryl phosphines /phosphites/ in optically sensilized photographic emulsions
21 p3052 A72-40390
Synthesis of polymers with conjugate bonds on the basis of dilithium-derivative aromatic hydrocarbons
23 p3262 A72-43929
AROUSAL
Human vestibulo-ocular responses to oscillatory rotational stimulation during various sleep and arousal stages, discussing Sugie-Jones reflex system mathematical model
04 p0474 A72-15249
Short sleep period and oxygen breathing effects on arousal level of air traffic controller during detection task performance
11 p1588 A72-26686
Circadian rhythm effects on introverts and extroverts biochemistry, physiology and performance, suggesting arousal mechanism differences
11 p1581 A72-26693
ARRAYS
NT ANTENNA ARRAYS
NT ENDFIRE ARRAYS
NT LARGE APERTURE SEISMIC ARRAY
NT LINEAR ARRAYS
NT PHASED ARRAYS
NT SOLAR ARRAYS
NT STEERABLE ANTENNAS
NT SYNTHETIC ARRAYS
NT TURNSTILE ANTENNAS
NT YAGI ANTENNAS
Mechanical constraints effects on loose spherical metal particles sintering rates, considering one, two and three dimensional arrays
02 p0232 A72-11433
Adaptive nonlinear optimization of the signal-to-noise ratio of an array subject to a constraint.
18 p2660 A72-36507
ARRHYTHMIA
Ventricular ectopic arrhythmias from treadmill exercise in patients observed during ECG monitoring
02 p0156 A72-11424
HIS bundle electrocardiography for arrhythmia studies, discussing conducting tissue potential recording, ventricular delay and block site determination and electrophysiological effects of drugs
02 p0157 A72-11473
Arrhythmias relation to coronary artery disease, discussing conduction defects, sudden death prodromata and prevention and digitalis as antiarrhythmic agent
02 p0157 A72-11476
Familial cardiomyopathy detection by electrocardiography noting arrhythmias, ventricular hypertrophy, abnormal Q waves and intraventricular conduction defects
04 p0466 A72-14443
Quotient of arrhythmia relation to physical work load, noting heart rate amplitude and frequency variations
04 p0472 A72-14899
Atheromatosis, chest angina and arrhythmia - Conference, Brussels, October 1970
08 p1117 A72-21541
Ventricular and supraventricular arrhythmias incidence during maximal treadmill exercise in normal man, noting age factor and cardiovascular disease presence effects
09 p1266 A72-23272
ECG, physical exercise and drug use in diagnosis and aeromedical evaluation of supraventricular arrhythmias, presenting case histories of pilots with wandering cardiac pacemakers
[AD-740987]
10 p1428 A72-23741
QRS wave detectors for arrhythmia and hemodynamic data analysis, using standardized FM magnetic tape containing various artifacts for evaluation
11 p1582 A72-25499
ECG diagnostics for arrhythmia assessment in flying personnel flight fitness examination
12 p1775 A72-28294
Induction of ventricular arrhythmias by elevation of arterial free fatty acids in experimental myocardial infarction.
17 p2502 A72-34997
Heart rate variability in a binary choice reaction task - An evaluation of some scoring methods.
22 p3143 A72-42550

Aortic regurgitation variation with respiratory sinus arrhythmia and respiratory cycle in dogs during tachycardia and bradycardia

22 p3151 A72-42674

Continuous ECG monitoring method /scattergram/ for arrhythmia pattern recognition in intensive care units

23 p3260 A72-43938

Analysis of intracavitary electrocardiograms through a saline bridge in the diagnosis of cardiac arrhythmias.

24 p3370 A72-44559

ARROW WINGS

Tu-154 aerodynamic design, discussing arrow wing and propulsion unit characteristics

12 p1753 A72-27268

ARSENIC

Zeeman patterns and energy level Lande g factors from spectrograms of As ion electrodeless discharge tubes in presence of 24,025 G magnetic field

07 p0987 A72-19832

Vapor pressure and composition in As-I system, investigating entropy and enthalpy changes and temperature dependence of equilibrium constant

09 p1373 A72-23481

ARSENIC COMPOUNDS

NT ARSENIDES
NT GALLIUM ARSENIDES
NT INDIUM ARSENIDES
NT PROUSTITE

Study of the mechanism of radiative recombination in vitreous and monocrytalline arsenic selenide.

19 p2844 A72-37684

Osarsite, a new osmium-ruthenium sulfarsenide from California.

22 p3172 A72-42450

Temperature and polarization dependence of arsenic sulfide single crystals and thin films intrinsic absorption edge, determining forbidden bandwidth and transitions types

23 p3324 A72-43688

ARSENIDES

NT GALLIUM ARSENIDES
NT INDIUM ARSENIDES
NT PROUSTITE

Preparation and electrical properties of thin cadmium antimonide and arsenide layers, comparing to single crystal films

02 p0268 A72-12281

Enhanced indirect optical absorption measurement in AlAs and GaP with energy denominator variation for direct band gap evaluation

13 p2022 A72-29627

Optical weak absorption measurements in amorphous semiconductors AsS, GeAs and GeSbSe, showing dependence on band gap localized states

13 p2022 A72-29629

Physicochemical properties and composition diagrams of antimonides and arsenides of Zn, Cd, Al, In and Ga

15 p2290 A72-31194

Peritectic interaction and phase diagrams of quaternary semiconductor CdAs-CdTe and CdP-CdSe systems

19 p2845 A72-38404

ARTERIES

NT AORTA

Rheological properties and architecture of arterial walls, using stress relaxation and stress-strain hysteresis tests on dog aorta, iliac and femoral strips

01 p0010 A72-10184

Arrhythmias relation to coronary artery disease, discussing conduction defects, sudden death prodromata and prevention and digitalis as antiarrhythmic agent

02 p0157 A72-11476

Antinatriuretic effect of acute thoracic and abdominal inferior vena cava constriction on arterial pressure, renal hemodynamics and electrolyte excretion

02 p0157 A72-11660

Femoral arterial blood pressure third order waves onset mechanism in narcotized dogs, noting changed blood and respiration dynamics

02 p0160 A72-12014

Human arm arterial pressure and flow pulsations numerical analysis, constructing electrical analog circuit from mathematical model

03 p0317 A72-12951

Xenon 133 myocardial clearance method accuracy and reliability in determining high and low left coronary artery blood flow under different hemodynamic conditions

03 p0319 A72-13181

Clinical assessment of degree of obstruction from coronary arteriograms of ischemic and rheumatic heart patients

03 p0316 A72-13847

Spinal mesenteric vascular reflexes of vasoconstriction effect of pressure drop in coeliac artery relation to Rein nutritional hepatic reflex

04 p0473 A72-15125

Blood viscosity and distributed external constraints and viscoelastic properties of vessels effects on wave

dispersion and dissipation in arteries and veins, using membrane model

04 p0481 A72-15466

Approximate numerical method for calculating flow profiles in arteries from local pressure measurements, taking into account Navier-Stokes equations nonlinear terms

[ASME PAPER 71-WA/BHF-3] 05 p0621 A72-15948

Human epicardial arterial circulation platelet aggregates role in sudden coronary death, discussing relation to atherosclerotic stenosis and acute thrombi

05 p0616 A72-16013

Functional condition of rabbits cerebrum precortical arteries during hypertension produced by intravenous noradrenaline infusion, discussing hypo and hyperkinesia

06 p0762 A72-17674

Dog mesentery terminal venous microvessel distensibility characteristics from response to arterial and venous pressure changes

06 p0765 A72-18196

Body thermal stress, local heating and arterial occlusion effects on sweat electrolyte content

07 p0929 A72-19437

Acid base balance in arterialized capillary blood in men after maximal short duration exercise

07 p0929 A72-19441

Clinical response to nitroglycerin therapy correlation with coronary angiography as diagnostic test for coronary artery disease in patients with chest pain

07 p0920 A72-19993

Coronary artery disease and vessel involvement severity predictions from electrocardiographic and vectorcardiographic patterns of anterior wall myocardial infarction

07 p0931 A72-19994

Nonlinear model for computer simulation of human arterial system, using finite difference technique for pressure and flow calculations

07 p0934 A72-20357

Intravascular pressure and extravascular structure effects on radial and longitudinal distensibility of arterial microvessels in dog mesentery

07 p0922 A72-20426

Arterial chemoreceptor deafferentation influence on rat respiratory response to hypoxic and hypercapnic gas mixture breathing

08 p1120 A72-22078

Adrenergic innervation of internal carotid arteries in extra- and intracranial regions in dogs, using luminescence method

08 p1121 A72-22184

Arterial hypoxemia development during hypoxic ontogenesis early stages related to age in dogs

09 p1266 A72-22879

Local and cardiac complications of selective percutaneous transluminal coronary arteriography, noting hemorrhages thromboses, embolisms, myocardial infarction, bradyarrhythmia and ventricular fibrillation

09 p1267 A72-23325

Arterial velocity profiles measurement in dogs thoracic aorta by hot-film probe, relating flow disturbances and turbulence to Reynolds number

10 p1431 A72-24468

Pulmonary capillary bed filling as function of arterial pressure in perfused frozen dog lungs

10 p1425 A72-24480

Hydraulic transmission line equations for computer simulation of arterial circulatory systems

10 p1431 A72-24811

Mathematical model for arterial system pressure, blood flow and dimensional changes, examining cardiac ejection dynamics and vasculature mechanical properties and viscoelasticity

10 p1432 A72-24812

Hemodynamic assessment of arterial blood flow from radiograph measurements of aorta branching points

11 p1582 A72-26774

Hemodynamic response to physical exercise stress in dogs with angiotensin-induced acute arterial hypertension

12 p1764 A72-28216

Arterial blood gas tensions, using sequential phased dilution for pilot oxygen delivery

12 p1764 A72-28255

Prolonged bed rest induced muscular activity restriction effect on arterial and venous tone in different body areas

14 p2074 A72-30385

Rebreathing studies of carbon dioxide pressure level effect on carbon dioxide content difference in arterial blood and alveolar gas during exercise and rest

17 p2499 A72-34346

Blood oxygenating ability of helium and argon-oxygen environments relative to air, using alveolar gas equation to predict arterial oxygen pressure

18 p2649 A72-36438

Digital computer simulation of human systemic arterial pulse wave transmission - A nonlinear model.

18 p2655 A72-37028

Systemic haemodynamics in borderline arterial hypertension - Responses to static exercise before and under the influence of propranolol.

19 p2756 A72-37773

Relationship of pulmonary artery to left ventricular diastolic pressures in acute myocardial infarction.

20 p2892 A72-39461

Reflexive cardiac rhythm changes and arterial tension during hypoxia, noting differences due to animals, controlled respiration and pharmacological effects

22 p3141 A72-41984

Anatomy of the coronary circulation at high altitude.

22 p3144 A72-42594

Carotid displacement pulse first time derivative recording as noninvasive technique for heart function assessment

24 p3370 A72-44561

Clinicoarteriographic correlations in angina pectoris with and without myocardial infarction.

24 p3372 A72-45010

ARTERIOSCLEROSIS

Early diagnostics of cerebral arteriosclerosis in flying personnel, investigating hypertension, neurocirculatory dystonia and myocarditic cardiosclerosis effects on flight performance

06 p0765 A72-18198

Hyperuricemia, gout and lithiasis among operating air crews, discussing diagnosis and relation to arteriosclerosis

08 p1125 A72-21271

Atheromatosis, chest angina and arrhythmia - Conference, Brussels, October 1970

08 p1117 A72-21541

Lipid metabolism abnormality relation to hypothyroidism leading to atherosclerosis, noting thyroid parenchyma atrophy from autoimmune thyroiditis

08 p1117 A72-21544

Blood lipid levels and dietary habits in atherosclerotic and healthy subjects, showing lipid and glucose metabolism disturbance increase in coronary cases

08 p1117 A72-21546

Dietary and pharmacological treatment of atherogenic hyperlipidemias from lipid-sugar balance and drug efficacy studies

08 p1117 A72-21547

Negative and positive emotional states influence on blood cholesterol and arterial pressure levels in dogs, suggesting common subcortical genesis of atherosclerosis and hypertension

09 p1264 A72-22498

Serum cholesterol, phospholipid and lipoprotein levels relation to atherosclerotic heart disease occurrence in USAF personnel

12 p1766 A72-28292

Clofibrate treatment for atherosclerotic cardiovascular disease prevention among Sabena flying personnel

12 p1766 A72-28293

Hypoxic theory for atherosclerosis formation, noting blood plasma protein concentration effects on oxygen diffusion

18 p2651 A72-37030

Changes of the mitral echocardiogram with ageing and the influence of atherosclerotic risk factors.

18 p2652 A72-37031

Hemodynamic indices in flight crew personnel during hypertonic sickness and atherosclerosis of coronary arteries

20 p2892 A72-39391

A special vitamin complex for prophylaxis of atherosclerosis in aviation personnel

23 p3261 A72-44153

Animal studies of effect of chronic exercise on the heart and atherosclerosis - A review.

24 p3370 A72-44563

Clinicoarteriographic correlations in angina pectoris with and without myocardial infarction.

24 p3372 A72-45010

H-V intervals in left bundle-branch block - Clinical and electrocardiographic correlations.

24 p3374 A72-45690

ARTHRITIS

Two stage description of middle germ layer chronic polyarthritis, noting heart muscle and vascular wall tissues necrosis

12 p1772 A72-27822

ARTHROPODS

NT COLEOPTERA
NT DROSOPHILA
NT INSECTS
NT MOLLUSKS
NT PUPA

ARTIFICIAL CLOUDS

Kr 85 clouds released by instantaneous point sources, measuring speed, height, short period concentrations, crosswind and downwind concentration integrations and dimensions

01 p0095 A72-10828

Plasma physical characteristics, considering experiments with Ba and Sr atom clouds introduced into ionosphere

03 p0394 A72-13196

Dynamic characteristics of buoyant low altitude clouds formed by solid rocket motor launches, determining initial temperature by motion pictures combined with conservation equations

[ASME PAPER 71-WA/FE-33] 05 p0724 A72-15923

- Artificial barium oxide clouds band spectrum analysis, calculating rotational and vibrational temperatures in total wavelength region 05 p0655 A72-16069
- Aluminum oxide cloud formation for thermosphere temperature determinations, describing methane/oxygen payloads, spectrographs, photometers and atmospheric models 06 p0806 A72-17646
- Winds velocity, direction and diffusion coefficients over Heiss Island from artificial luminous clouds observations 08 p1160 A72-21534
- Wind shear theory of midlatitude sporadic E formation, using wind profiles from artificial luminous cloud observations 08 p1161 A72-21540
- Geomagnetic field effects on initially spherically symmetric ion cloud diffusive motion in earth upper atmosphere 09 p1297 A72-22577
- Sunlight resonance scattering by spherically symmetric optically thick artificial Sr clouds, comparing photometric data with computed theoretical isophotes, line profiles and irradiances 09 p1297 A72-22579
- Tuned laser radar detection and ranging of high altitude Ba ion cloud by photon counting, discussing SNR requirement 10 p1440 A72-24963
- West German-United States Barium Ion Cloud Project meteorological support at Wallops Station, discussing magnetospheric magnetic and electric fields 13 p1947 A72-28802
- Artificial barium ion cloud spatial-temporal growth in ionosphere, solving ion diffusion equation by numerical methods 13 p1950 A72-29387
- Midlatitude sporadic E layer formation under wind shear action from artificial cloud data on lower thermosphere wind speed and direction 13 p1951 A72-29589
- Radiative transfer in freely expanding gaseous Ba clouds, deriving atomic states level populations ratio 15 p2223 A72-31428
- Rocket released artificial Cs plasma clouds in upper atmosphere, measuring electron density by HF radar observation 15 p2231 A72-32330
- Barium cloud striations deformation in ionosphere explained by equations of motion for plasma cloud thin bar model, discussing pinch effect 16 p2387 A72-33907
- Study of the motion of ionized artificial clouds in the upper atmosphere 18 p2688 A72-36864
- The anomaly of the neutral wind at a height of approximately 200 km at high latitudes. 20 p2918 A72-39536
- Electron-density increase in the E layer below an artificial barium cloud. 20 p2920 A72-39983
- The observation of chemical releases in the upper atmosphere. 22 p3152 A72-42022
- A possible connection between a barium cloud and electron intensity fluctuations observed on a rocket flight at Kiruna. 22 p3172 A72-42433
- ARTIFICIAL GRAVITY**
- Artificial gravity effects on space station crews performance, discussing unusual mechanical and perceptual phenomena 06 p0766 A72-17715
- Weightlessness effects on human organism, discussing physiological changes, artificial gravity by spacecraft rotation and exercise to counter adverse reactions 11 p1589 A72-26891
- Habitability factors in a rotating space station. 18 p2652 A72-36436
- Problem of artificial gravitation in terms of experimental physiology 21 p3006 A72-40441
- OFO A orbital flight recording of bullfrog vestibular gravity sensor nerve fiber pulses for assessing necessity of artificial gravity during prolonged weightlessness 23 p3254 A72-43391
- ARTIFICIAL HEART VALVES**
- Non-invasive assessment of prosthetic mitral paravalvular and intravalvular regurgitation. 17 p2498 A72-34221
- ARTIFICIAL INTELLIGENCE**
- Human touch deficiency in artificial pattern recognizers regarding handwriting, speech and pattern recognition involving nonevents 01 p0017 A72-10464
- Cellular electronic logic circuit planar array representing objects inertial motion, applying to traffic control, image processing and artificial intelligence 06 p0779 A72-17496
- Artificial intelligence applications for chemical inference, discussing modified heuristic DENDRAL computer program for cyclic structure and linear molecule identification 07 p0936 A72-19498
- Artificial intelligence application to mass spectra interpretation, discussing heuristic Dendritic Algorithm based computer program to generate structural isomers 07 p0950 A72-19608
- Air traffic control messages syllabic and word prominence patterns, discussing impact on continuous speech recognition by machine 09 p1274 A72-23581
- Language description of remotely sensed image data, noting application to artificial intelligence, linguistic analysis and retrieval 13 p1924 A72-28525
- Fuzzy algorithms and artificial intelligence for deep space navigation of vehicles from earth to space /planet/ location 15 p2270 A72-32185
- ARTIFICIAL RADIATION BELTS**
- Long term A3 absorption associated with nuclear explosion caused artificial radiation belts, discussing electron precipitation role in D region ionization 15 p2299 A72-31933
- ARTIFICIAL SATELLITES**
- NT AEROS SATELLITE
- NT ALOUETTE SATELLITES
- NT APPLICATIONS TECHNOLOGY SATELLITES
- NT BEACON SATELLITES
- NT COMMUNICATION SATELLITES
- NT COS-B SATELLITE
- NT COSMOS SATELLITES
- NT DISCOVERER SATELLITES
- NT EARTH RESOURCES TECHNOLOGY SATELLITES
- NT ELEKTRON SATELLITES
- NT ENVIRONMENTAL RESEARCH SATELLITES
- NT EOLE SATELLITES
- NT EOSS
- NT ESRO SATELLITES
- NT ESSA SATELLITES
- NT EXPLORER SATELLITES
- NT GEODETIC SATELLITES
- NT GEOPHYSICAL SATELLITES
- NT GRAVITY GRADIENT SATELLITES
- NT HEOS B SATELLITE
- NT HEOS SATELLITES
- NT INTELSAT SATELLITES
- NT INTERCOSMOS SATELLITES
- NT ISIS SATELLITES
- NT LUNAR ORBITER
- NT LUNAR SATELLITES
- NT METEOROLOGICAL SATELLITES
- NT MIDAS SATELLITES
- NT MOLNIYA SATELLITES
- NT NAVIGATION SATELLITES
- NT NAVSTAR SATELLITES
- NT NIMBUS SATELLITES
- NT OAO
- NT OGO
- NT OGO-A
- NT OGO-B
- NT OGO-D
- NT OGO-E
- NT ORBITAL SPACE STATIONS
- NT ORBITAL WORKSHOPS
- NT OSO
- NT OSO-E
- NT OSO-G
- NT OSO-H
- NT PAGEOS SATELLITE
- NT PAS
- NT PASSIVE SATELLITES
- NT PROTON SATELLITES
- NT RADIO ASTRONOMY EXPLORER SATELLITE
- NT RELAY SATELLITES
- NT SAN MARCO SATELLITE
- NT SAS-A
- NT SAS-D
- NT SIRIO SATELLITE
- NT SKYNET SATELLITES
- NT SYMPHONIE SATELLITES
- NT SYNCHRONOUS METEOROLOGICAL SATELLITE
- NT SYNCHRONOUS SATELLITES
- NT SYNCOM SATELLITES
- NT TIROS SATELLITES
- NT TRANSIT SATELLITES
- NT UHURU SATELLITE
- NT VENERA SATELLITES
- Criticism of artificial satellite theory for small eccentricities 01 p0123 A72-10016
- German book on gyroscope theory and applications, covering artificial satellites motion in gravitational field 03 p0360 A72-13675
- Jupiter-induced perturbations in orbital elements of Callisto artificial satellite, noting correction requirement due to Jupiter polar flattening 04 p0572 A72-14634
- Long period perturbations arising in orbits of artificial satellites with large surface to mass ratio under solar radiation pressure and earth oblateness effects 04 p0572 A72-14637
- Artificial earth satellites orbit plane determination accuracy in terms of local vertical sensor errors and gyroscope drift 05 p0717 A72-16441
- Earth satellite plane periodic oscillations damping with respect to center of mass in orbital plane during motion on elliptical Kepler orbit 05 p0730 A72-17030
- Angular position of sun disoriented artificial earth satellites with angular velocities not exceeding 0.5 deg/sec, using harmonic analysis of magnetometric data 05 p0631 A72-17033
- Artificial planetary satellites lifetime estimation from atmospheric drag, discussing critical height/atmospheric density relationship, satellite design and initial orbit height 05 p0722 A72-17042
- Research measurement error determination for two frequency Doppler measurement of artificial satellites 12 p1782 A72-27532
- Simultaneous determination of chord length and direction by artificial earth satellite geodetic observations in Arctic and Antarctic regions 13 p1945 A72-28493
- Geostationary artificial satellite orbital parameters calculation, taking into account lunar, solar and light pressure perturbations 14 p2150 A72-30451
- Nonoriented astronomical satellite attitude determination from onboard measurements of geomagnetic field and stellar luminosity 14 p2151 A72-30460
- Optimum elliptic orbit characteristics of planetary artificial satellite based on earth-planet-earth flight 14 p2151 A72-30472
- Computer calculation of artificial satellite ephemerides from Smithsonian mean orbital elements, comparing observed and computed topocentric equatorial coordinates 14 p2087 A72-30480
- Earth satellite orbit motion in terms of probability densities and distributions for large populations and single satellites 15 p2307 A72-31692
- Computational method for determining numerical values of relativity by two-way Doppler radio tracking and ranging data from planetary orbiting spacecraft 15 p2310 A72-31978
- Lift and drag on conical, cylindrical and spherical artificial satellites from spatial impulsive interaction model depending on gas temperature and surface conditions 16 p2347 A72-34167
- Prediction of upper atmosphere density over the lifetime of a satellite 17 p2547 A72-35215
- Influence of the Galilean Jovian satellites on the motion of an artificial satellite of Callisto 17 p2618 A72-35811
- On the effects of gravitational absorption on orbits of artificial earth satellites. 18 p2728 A72-36761
- Doppler effect characteristics and applications to artificial satellite tracking, considering computer program in orbit parameter calculations 19 p2765 A72-38172
- Influence of the terrestrial magnetic field on the motion of a satellite around its center of gravity 21 p3106 A72-41048
- Secular perturbations in the motion of artificial earth satellites 21 p3114 A72-41770
- On the tidal effects in the motion of artificial satellites. 24 p3441 A72-45233
- ARTILLERY**
- Prototype compact ruggedized crystal-controlled L-band artillery telemetry transmitter design and performance 02 p0192 A72-12156
- ARYL COMPOUNDS**
- U AROMATIC COMPOUNDS**
- ASBESTOS**
- Asbestos fiber reinforced plastics composites fabrication techniques, discussing possible applications 04 p0537 A72-15086
- Lungs fibrosis and cancer caused by asbestos fibers inhalation, noting environment control for protection against workers health hazards 11 p1583 A72-25548
- Asbestos reinforced plastics safe handling and manipulation ensured by regulations provided precautions 11 p1583 A72-25549
- Boundary layer temperature profile for ablating asbestos-plastic composite samples measured under combined convection and radiant heat fluxes 14 p2172 A72-31003
- Asbestos-textolite coating required thickness calculation with allowance for aerodynamic heating, discussing softening mechanisms 21 p3074 A72-41709
- ASCENT**
- NT CLIMBING FLIGHT**

- Ascent acceleration maximization of variable mass particle, calculating optimal parameters of multistage rocket 22 p3204 A72-42066
- ASCENT TRAJECTORIES**
- Superpressure balloons /tetroons/ performance characteristics, determining ascent rates and superpressure, stress and volume perturbations due to forced change in height 01 p0005 A72-10829
- Space shuttle optimal boost trajectories, showing payload increase by flying pitch profiles optimization [AAS PAPER 71-325] 02 p0286 A72-12423
- Shuttle ascent guidance and control, discussing self targeting, trajectory optimization problems and flight phases 06 p0892 A72-18178
- Atmospheric model effects on space shuttle ascent and reentry trajectories and aerodynamic heating 13 p1990 A72-28813
- Constrained payload-optimum extremal ascent trajectories for space shuttle vehicles. [AIAA PAPER 72-829] 20 p2966 A72-39097
- Space shuttle ascent trajectory optimization by Davidson/Broyden crude search technique for matrix updating [AIAA PAPER 72-907] 21 p3111 A72-41556
- Optimization of altitude and inclination change schedules during low thrust ascent to geosynchronous orbit. 24 p3440 A72-45150
- ASCORBIC ACID**
- Ascorbic acid influence on blood coagulation and anticoagulation systems in dogs with acute hypoxia, discussing plasma recalcification time and heparin tolerance 12 p1764 A72-28217
- ASCORBIC ACID METABOLISM**
- Enzyme activity and ascorbic acid concentration as index of rat thyroid gland tissue functional activity during hyperthermia 14 p2077 A72-31098
- ASDE**
- U AIRPORT SURFACE DETECTION EQUIPMENT
- ASHES**
- Skeletal bones ash content in man and primates, implying differences due to adaptive physiological function 10 p1424 A72-23736
- Regional stratigraphy and fabric distribution of volcanic ash flow sheets in northwestern Mogollon Plateau by flow direction technique 15 p2223 A72-31578
- Lunar ash flows - Isothermal approximation. 18 p2723 A72-36026
- Morphology and petrography of volcanic ashes. 18 p2685 A72-36222
- Complex index of refraction of airborne fly ash determined by laser radar and collection of particles at 13 km. 18 p2661 A72-36637
- ASPECT RATIO**
- NT HIGH ASPECT RATIO
- NT LOW ASPECT RATIO
- Continuum gas viscoseals performance, comparing two seal groove aspect ratio geometries 02 p0237 A72-12850
- Elliptic wing-vortex interaction for various aspect ratios 05 p0603 A72-16542
- Radar cross section computation and contours map for thin straight wire, noting resonant peak and interference null variations with frequency and aspect ratio 06 p0771 A72-17351
- Critical aspect ratio of W fiber in copper matrix for stress rupture applications 11 p1654 A72-25482
- Inviscid incompressible flow past longitudinally curved small aspect ratio slender wing, investigating aerodynamic characteristics 13 p1893 A72-28729
- Sound generation by finite rectangular plate vibrations, deriving radiated power as function of aspect ratio and vibration pattern 13 p2005 A72-29564
- Limit analysis for plates - A simple loading problem involving a complex exact solution. 19 p2872 A72-37599
- Downwash distribution at surface of rectangular planform wings with prescribed subsonic aerodynamic loading for various aspect ratios 19 p2747 A72-38809
- Fiberglass reinforced plastics tensile test specimens aspect ratio effect on tensile properties, considering deformation of orthotropic rectangular plate with uniform forced displacement 20 p2943 A72-38889
- ASPHALT**
- Ethylene-vinyl acetate-asphalt thermoplastic material properties, filler effects, application methods and commercial uses 12 p1835 A72-28094

- ASPHERICITY**
- Scatterplate, artificial hologram, moire and null lens methods for aspheric mirror testing for space astronomy and laser communication 20 p2922 A72-39033
- An immersion interferometer for monitoring the quality of second-order aspherical surfaces 21 p3058 A72-41808
- ASPHYXIA**
- Hypothermia, asphyxia and ionizing radiation effects on rat immunological defense mechanisms against particulate antigens 16 p2355 A72-33555
- ASPIRATION**
- U VACUUM
- ASSEMBLIES**
- Lightweight low pressure plastic hose assemblies in aircraft and missile petroleum base fuel and synthetic lubricating oil systems at 395-710 R and up to 200 psi [SAE ARP 1180] 01 p0006 A72-10388
- Automatic control for selective precision joint assembly of fuel pump equipment, reducing unfinished product volume 16 p2397 A72-33261
- ASSEMBLING**
- Circuit boards contact assembly by special type rivets, discussing technical and economic advantages for prototype or small series fabrication of printed circuit devices 06 p0784 A72-18192
- Adhesives use for assembly of mechanical, optical, nucleonic and electronic instruments including printed and integrated circuits 07 p0992 A72-20576
- Automatic assembly machines for IC batch production, involving terminal cutting and bending and RC element insertion 09 p1292 A72-23255
- Algorithms for combinatorial problem optimal solution based on implicit enumeration method, applying to assembly line balancing 12 p1837 A72-28117
- Equipment assembly design optimization by operational versions determination and criteria evaluation for optimal conditions, noting rotary wing design 23 p2394 A72-44024
- ASSESSMENTS**
- NT TECHNOLOGY ASSESSMENT
- Subjective probability distributions for random device-generated Bernoulli process unknowns, discussing distribution median and quartiles and hypothetical sample impact assessment techniques 05 p0616 A72-15812
- ASSIMILATION**
- Complete assimilation of briefly presented lines. 23 p3261 A72-44150
- ASSOCIATIONS**
- U ORGANIZATIONS
- ASSURANCE**
- Cost reduction by integration of assurance technologies from complex systems development risk management model [AIAA PAPER 72-245] 10 p1487 A72-24450
- ASTEROIDS**
- NT CERES ASTEROID
- NT ICARUS ASTEROID
- NT VESTA ASTEROID
- Minor planet Eros photographic observations by long-focus refracting telescopes and Ross cameras at various Yale observatories, tabulating ephemerides [AD-737017] 02 p0286 A72-12894
- Minor planets radar measurements contribution to astrometric corrections, obtaining solutions for conditional equations systems representative of Cerera observations 04 p0572 A72-14635
- Light phase curve model for nonatmospheric bodies covered with porous or dust-like surface layer 04 p0574 A72-14910
- Planetary mass errors effects on orbit determinations, discussing Ceres mass from influence on Pallas orbit 04 p0575 A72-15035
- Jupiter mass correction from minor planets /153/ Hilda, /279/ Thule and /334/ Chicago observations 04 p0576 A72-15036
- Asteroids origin, discussing Phaethon model, masses, distribution, fragmentation and disintegration 05 p0713 A72-15980
- Trajectory characteristics for multiple asteroid flyby missions to determine physical properties of minor planets [AIAA PAPER 72-52] 05 p0721 A72-16928
- Meridian circle planet and asteroid positions and deviations from ephemerides during 1950 to 1955 05 p0723 A72-17158
- Asteroid diameters and absolute magnitude distributions, noting characteristics, methods of calculation and hypotheses 06 p0875 A72-17494
- Numerical solution of equations for asteroidal mass distribution under collisional fragmentation 07 p1071 A72-19180

- Telescope observations of occultations of stars by outer planets, natural satellites and asteroids 09 p1387 A72-29277
- Pallada, Vesta, Irida and Harmony asteroids positions computed from observations with 400 mm photographic telescope 09 p1389 A72-23066
- Martian cratering by asteroid impact, discussing Palomar-Leiden asteroid statistics, Opik capture theory and evolutionary extrapolation limitations 10 p1531 A72-23705
- Photometric UVB and polarimetric observations of rotation period, polarization curves and phase coefficients of asteroid Flora, comparing with moon 10 p1531 A72-23709
- Asteroidal positions from plates from Zeiss astrograph at Turin Observatory, discussing reduction methods and error analysis 11 p1717 A72-25901
- Solar electric propulsion application to comet and asteroid rendezvous and docking CARD missions with sample return [AIAA PAPER 72-470] 11 p1722 A72-26201
- Minor planets orbital elements determination accuracy from planets coincident optical observations 13 p2035 A72-28439
- Asteroids and comets orbit perturbation equations for small eccentricity values 14 p2161 A72-31080
- Capture resonance of asteroid 1685 Toro by earth due to gravitational interaction at close encounters 15 p2307 A72-31721
- Relative orbit inclination dispersions of minor planets, fireballs and photographic and radio meteors, indicating common origin 16 p2456 A72-33515
- Parent-body models for the formation of iron meteorites. 17 p2615 A72-35687
- Some photometric parameters of the minor planet 2 Pallas. 18 p2723 A72-36086
- New method of calculating disturbed ephemeris of minor planets 21 p3102 A72-40095
- Flyby missions to comets, asteroids and meteors for obtaining solar system geological information, considering space dynamics feasibility 23 p3340 A72-44351
- Ephemerides and improved orbital elements of minor planets, noting general theory of relativity verification from astronomical observations of Icarus 24 p3437 A72-44758
- Correction of the orbits of 161 minor planets 24 p3437 A72-44763
- Observations of minor planets at the Crimean Astrophysical Observatory AN SSSR. XVIII 24 p3437 A72-44764
- Mission strategy for combined comet-asteroid flybys. [AIAA PAPER 72-939] 24 p3444 A72-45436
- Physical parameters of asteroids and interrelations with comets. 24 p3445 A72-45460
- Meteor streams orbital elements dispersion from photographic data, and asteroid stream percentage variation with concentration of orbits to ecliptic plane. 24 p3445 A72-45462
- On certain aerodynamic processes for asteroids and comets. 24 p3445 A72-45463
- On the existence of a resonance-captured 'quasi-satellite' of the earth. 24 p3446 A72-45471
- The possibility of a trans-Saturnian belt of particulate matter. 24 p3446 A72-45472
- Accuracy of the determination of the zero points of a fundamental catalog from observations of major and minor planets 24 p3447 A72-45676
- ASTHMA**
- Asthmatics evolution and treatments in armed forces aircrews, noting acetylcholine test 08 p1125 A72-21270
- ASTIGMATISM**
- First order imagery in neighborhood of base ray transversing arbitrary optical system, discussing relationships among anamorphic nature, astigmatism and image rotation 09 p1309 A72-22606
- Neural effects on human visual resolution of horizontal and vertical gratings resulting from early abnormal visual inputs due to astigmatism 10 p1430 A72-24348
- Coma, astigmatism and spectral line curvature derivation for spherical mirror-concave grating assembly, calculating mounting resolution in terms of wavelength 19 p2799 A72-37672
- German monograph - Contributions to the study of the astigmatic image. 22 p3207 A72-43067

- ASTRONICS**
 Power conditioning requirements and tradeoff considerations for space shuttle, warning against central power conversion use on orbiter and booster vehicles
 01 p0007 A72-11052
 Spacecraft electronic equipment requirements, discussing effects of planned missions
 [DGLR PAPER 71-104] 02 p0196 A72-12739
 Aerospace instrumentation - Conference, Cranfield Institute of Technology, England, March 1972
 16 p2393 A72-33626
 Development of electronic part failure rates for long-duration space missions.
 17 p2527 A72-34684
 Problems confronting the engineer in charge of procurement of components intended for electronic aerospace systems
 18 p2743 A72-37126
 European co-ordination activities with particular reference to the Space Components Co-ordination Committee.
 18 p2743 A72-37130
 Electronic packaging techniques in housing spaceborne computer, digital telemetry and other microelectronics for protection against severe aerospace environment
 20 p2909 A72-39767
- ASTROBIOLOGY**
 U EXOBIOLOGY
- ASTRODYNAMICS**
 Soviet book on celestial mechanics and astrodynamics covering classical and contemporary theory, many body problem, satellite perturbation, optimal and boundary value problems, etc
 07 p1078 A72-19952
 Book - Astrodynamics: Orbit correction, perturbation theory, integration
 19 p2868 A72-38723
 Transfer equations for stellar systems
 23 p3338 A72-44035
 Energy sources for extragalactic explosive phenomena in galactic nuclei and quasars, considering gravitation and double radio sources
 24 p3439 A72-45018
- ASTROGRAPHY**
 Apollo mapping camera system synchronized laser altimetry utilization in astro-photogrammetric triangulation
 12 p1872 A72-27816
 Exact positions of Mars as determined by the photographic method at Pulkovo in 1966 and 1967
 19 p2859 A72-37914
 Results of observations of the minor planet Icarus by the Maksutov meniscus astrograph in Chile
 19 p2859 A72-37916
 Comparison of IDS Catalog double stars having determined individual motions of their components
 19 p2859 A72-37917
 Orientation of astrographs in observations and measurements
 19 p2802 A72-37972
 Determination of the aberration constant and the coefficients of short-period nutation terms from observations by the Pulkovo polar tube during the period from 1953 to 1964
 19 p2861 A72-37976
 Attempt at determining the exact positions of Venus from photographic observations on the short-focus double astrograph and the 26-in. refractor of the Pulkovo observatory
 19 p2861 A72-37984
 Computer processed Mars photographic positional measurements with Pulkovo normal astrograph in 1965
 19 p2861 A72-37985
 Investigation of the UIM-21 coordinate-measuring machine
 19 p2802 A72-37988
 Jupiter surface maps for 1965-70 from drawings obtained with astrograph, noting high activity and eruptive changes after 1961-63 outburst
 22 p3220 A72-41920
- ASTROMETRY**
 Astrometric measurements of visual binaries by electronographic method, using Lallemand camera
 03 p0415 A72-13002
 Minor planets radar measurements contribution to astrometric corrections, obtaining solutions for conditional equations systems representative of Cerera observations
 04 p0572 A72-14635
 Disk diameter errors due to wire thickness in reduction of visual planetary observations
 09 p1311 A72-23062
 Computer processing of star meridian observations, concerning reduction to visible area, declinations, right ascensions and conversion
 09 p1283 A72-23063
 Mathematical model of block adjustment and star coordinate accuracy in photographic astrometry
 09 p1392 A72-23541
 Relative orientation of major axes of double radio sources, comparing with Brown ordering of galaxies on megaparsec scale
 10 p1541 A72-24472
- Occultation of beta Scorpii by Jupiter and Io to determine Jovian equatorial radius and oblateness
 10 p1548 A72-24970
 Long baseline radio interferometry with independent frequency standards for geodetic and astrometric applications
 15 p2199 A72-32074
 Quasars 3C273 and 3C279 superlight velocity and distances from interferometer pattern changes in 1970-1971
 16 p2450 A72-32865
 Comparison of several methods for determining the magnitude of turn for the screw of a positional contact micrometer in an astronomical universal instrument
 19 p2795 A72-37347
 Accuracy of the determination of the positions of stars and artificial satellites from an aircraft
 19 p2861 A72-37973
 Investigation of the screw turn magnitude of a contact micrometer attached to the Toepfer meridian circle on the basis of observed right ascensions of stars
 19 p2802 A72-37975
 Preliminary results of discussions of latitude observations by the prismatic astrolabe in Pulkovo /1963.2-1968.7/
 19 p2861 A72-37977
 Galaxies and galactic cluster distance determination from Palomar chart angular diameters related to Holmberg-Vaucouleurs photometric systems
 23 p3338 A72-44034
 Ground observation for outer planets natural satellites ephemeris, using astrometric telescopes, photographic and plate reduction techniques
 [AIAA PAPER 72-904] 24 p3443 A72-45426
- ASTRON THERMONUCLEAR REACTOR**
 Plasma layer growth and equilibrium magnetic fields for astron configurations, solving stream function by finite difference methods
 07 p1042 A72-19512
 Collective self fields generated from intense electron beams for high energy positive particle acceleration and Astron hot plasma confinement for fusion control
 10 p1523 A72-24788
- ASTRONAUT LOCOMOTION**
 Experimental investigation of an astronaut maneuvering scheme.
 18 p2655 A72-37026
- ASTRONAUT MANEUVERING EQUIPMENT**
 Medical and technical aspects of rescue and survival of astronauts in high mountain and mountainous remote areas.
 17 p2507 A72-34434
- ASTRONAUT PERFORMANCE**
 NT BLACKOUT PREVENTION
 Astronaut zero gravity adaptive responses in performance, locomotion, orientation, sleep and physiological and functional characteristics
 03 p0319 A72-13867
 Soviet book on astronaut activity psychological features covering space flight living conditions, space and time perception psychophysiological mechanism changes and weightlessness effects
 03 p0317 A72-14246
 Artificial gravity effects on space station crews performance, discussing unusual mechanical and perceptual phenomena
 06 p0766 A72-17715
 Medicobiological investigations of prolonged weightlessness effects on astronaut physiological system based on Soyuz flight program
 10 p1425 A72-24409
 Ground and flight crews coordinated effort in Apollo mission operations, noting experts on ground and spacecrew spot judgments capability
 [AIAA PAPER 72-236] 11 p1586 A72-26557
 Russian book on pathophysiological principles of air and space pharmacology covering stress and fatigue reduction and pilots and astronauts performance improvement
 12 p1772 A72-27926
 Zero gravity earth orbital cloud physics facility requirements and design concepts, noting experiments feasibility relative to astronaut performance
 13 p1990 A72-28815
 Astronauts physiological and psychological reliability, discussing Apollo flights and prolonged missions to other planets
 14 p2079 A72-30677
 Medical investigations during Salut space station flight, discussing weightlessness effects and efficiency evaluation of preventive measures for crewmembers high performance in space flight
 15 p2189 A72-31918
 Psychological and physiological parameters correlation for astronaut functional state relation to emotional tension level during ground and flight tests
 16 p2356 A72-33563
 Russian book - Space ergonomics.
 21 p3004 A72-40300
 Biological rhythms origin and mechanisms, discussing 24-hour cycle, subcellular biological clock and rhythm disruption effects in speologists, astronauts and pilots
 22 p3141 A72-41985
- Psychic adaptation of man to a long-duration stay in space
 22 p3149 A72-41988
 The prediction of the condition of man during a space flight
 22 p3149 A72-42067
 Motor activity capability of an astronaut in flight
 22 p3149 A72-42220
 Effects of weightlessness on astronauts - A summary.
 23 p3253 A72-43385
- ASTRONAUT TRAINING**
 ALSEP human engineering design criteria for crew interface, describing astronaut trainer
 04 p0479 A72-15100
 Apollo 14 mission report covering crew training, launch, docking, lunar landing and surface activities
 08 p1230 A72-21006
 Skylab launch and mission program, describing modular components, crew training, checkout, launch and docking procedures, flight plan and crew working schedules, rescue and reentry procedures, etc
 08 p1240 A72-21008
 Astronaut training obtained visually in lunar module simulator via film, spacecraft models and landing site relief models as sources for complex TV system
 08 p1147 A72-21335
 Soviet space crews selection and training based on professional and scientific background, emphasizing psychological qualities for working compatibility in space environment
 09 p1274 A72-23672
 Some aspects of survival and rescue of astronauts in polar regions.
 17 p2507 A72-34435
- ASTRONAUTICS**
 Astronautical research - IAF Conference, Konstanz, West Germany, October 1970
 01 p0130 A72-10926
 DGLR 1970 yearbook covering flight mechanics, relaxation in gas dynamics, space shuttle, flight simulation, reentry vehicles, turbulent boundary layer control, noise reduction, etc
 02 p0206 A72-12895
 Heat transfer research review, discussing gas turbines, aeronautics, astronautics, nuclear power, thermal pollution and controlled fusion challenges
 09 p1412 A72-23684
 Aviation and astronautics - Conference, Tel Aviv-Haifa, March 1972
 15 p2177 A72-31201
 Astronautical engineering - Conference, Mar del Plata, Argentina, October 1969
 15 p2320 A72-31801
- ASTRONAUTS**
 NT ORBITAL WORKERS
 Calcium metabolism perturbations in astronauts under weightlessness conditions and in immobilized test subjects, noting bone tissue renewal cycle modification, calciuria variations and bone calcification
 07 p0927 A72-19245
 Meteorological-astronomical diurnal and seasonal environmental rhythm simulation for psychological stresses alleviation in long term space missions
 13 p1910 A72-29322
 Zero-g showers for long duration space flight crews hygiene, describing flexible mummy bag and truncated conical shell design
 15 p2190 A72-32320
 Astronauts red cell mass changes associated with space flight due to space and earth environment differences
 16 p2356 A72-33564
- ASTRONAVIGATION**
 Russian book on flight navigation cybernetics covering Doppler, astro and radio inertial schemes and satellite systems
 12 p1843 A72-28344
 Requirements and techniques of interstellar navigation, discussing astronomical maps and observational phenomena at relativistic travel velocities
 15 p2267 A72-31291
 Spacecraft orientation according to reference celestial bodies direction determination, noting successive orientation permissible time intervals
 19 p2831 A72-38149
- ASTRONOMICAL CATALOGS**
 Radio sources structure in astronomical catalog, noting no difference between quasars and radio galaxies
 01 p0127 A72-10291
 Galactic superclusters and matter distribution in universe, considering systematic catalog errors and uncertainty of statistical tests
 03 p0421 A72-13172
 Astronomical catalog of 42 novae, presenting tables of exact positions
 03 p0433 A72-13489
 Statistical investigation of 1500 galaxies in MCG catalog with weak surface brightness, noting sculpture type spheroidal galaxies in Virgo cluster
 03 p0435 A72-13807
 Earth precession constant correction, considering Fricke catalogs
 04 p0576 A72-15039

Stellar radial velocities observation with photoelectric spectrometer, discussing catalog errors

04 p0577 A72-15280

Spectral and time variations at radio frequencies of QSO and radio galaxies from Parkes catalog

05 p0717 A72-16378

Lunar surface details absolute and relative heights, estimating accuracy by comparison of data from different catalogs

06 p0884 A72-18034

Observational parameters of 61 pulsars, tabulating names, right ascension and declination, galactic longitude and latitude and period and dispersion measures

08 p1233 A72-21179

Catalog of lunar craters central peaks and floor objects on visible hemisphere based on Kuiper photographic atlas

08 p1236 A72-21476

Space astronomy experiments with TV scanning, discussing data from Telescope catalog of UV observations and photometric and astrometric accuracy

08 p1170 A72-21957

Star catalogs comparison and stellar positional differences and motion studies using random field theory

09 p1388 A72-23052

Formulas to evaluate differences in angles formed by coordinate systems of two star catalogs

09 p1388 A72-23053

Lunar objects position accuracy assessment based on pairwise comparison of current selenodetic reference catalogs

09 p1388 A72-23054

Reference grid construction for lunar craters in system with scale and orientation independent of other systems, discussing preliminary catalog compilation from lunar photographs

09 p1388 A72-23055

Poltava latitude changes derived from Boss catalog stars observations with Bamberg zenith telescope, deducing declination system from 12 year observation cycle

09 p1300 A72-23069

Cassiopeia region galactic structure study via objective prism, cataloging stars radial velocities and distances

09 p1391 A72-23539

Data reduction for photographic catalog of AGK2-AGK3 stars in terms of random and systematic errors in plate constants

09 p1392 A72-23543

Large Magellanic Cloud star membership, comparing Sanduleak catalog based on objective-prism spectroscopy with Fehrenbach-Duflet catalog based on radial velocities

09 p1392 A72-23547

Precise optical positions of nine compact radio sources in AGK 3 catalog

10 p1536 A72-24140

Positions, flux densities and identifications for weak sources in Parkes catalog at 2700 MHz, including galaxies and quasars

10 p1545 A72-24792

Galaxies clusters classification on basis of relative contrast between brightest member and typical bright galaxy population of cluster

10 p1548 A72-24964

Fan beam surveys of radio sources with Cambridge telescope, presenting catalogs of galactic coordinates and flux density measurements

10 p1549 A72-25194

Lunar surface features absolute and relative heights, estimating accuracy by comparison of data from different catalogs

11 p1719 A72-25970

Intergalactic extinction relationship to large galactic clusters from statistical analysis of fourth and fifth Zwicky catalogs

12 p1872 A72-27759

Comparative study of lunar objects selenodetic coordinates catalogs based on continuous media deformation theory

13 p2037 A72-28987

Orbiter 4 photographs to update System of Lunar Craters /1966/, cataloging positions, diameters and morphological data

13 p2037 A72-28991

Solar eclipse timings by photoelectric, photographic and visual observation for comparison of Newcombe sun tables and improved lunar ephemeris reference systems

13 p2041 A72-29527

Star catalog zero-point improvement by Bessel method modification for lunar observation data reduction

14 p2149 A72-30210

Quasar color indices and redshift correlation, using catalog data on U, B and V colors

14 p2150 A72-30371

List of galaxies with UV continuum, noting emission lines, Seyferts, quasars and spectral energy distribution

15 p2304 A72-31326

Optical identification of two radio source samples from astronomical B2 catalog, providing finding charts and reference star positions for investigated fields

15 p2316 A72-32749

Observations of some small-diameter radio sources at 408 MHz.

17 p2603 A72-34440

Contribution of Danjon's astrolabe to the study of proper motions

18 p2726 A72-36727

Luminosities and motions of the F-type stars. II - Metal-deficient stars.

19 p2855 A72-37238

Spectrographic and photometric observations of supergiants and foreground stars, in the direction of the Large Magellanic Cloud.

19 p2858 A72-37855

Table for reduction of stellar radial velocities to the center of the sun

19 p2859 A72-37909

Corrections to the right ascensions of FK4 according to observations of fundamental star series with the meridian circle of the Cerro Calan Observatory /Chile/

19 p2859 A72-37911

Comparison of IDS Catalog double stars having determined individual motions of their components

19 p2859 A72-37917

Catalog of individual motions of stars in the open star cluster NGC 6866 and vicinity

19 p2860 A72-37918

Influence of the reference catalog system on the coordinates of determined stars in zonal meridional observations

19 p2861 A72-37974

Comparison of the declinations of Talcott pair centers, obtained from latitude observations by ZTF-135 in Pulkovo, with certain catalogs

19 p2861 A72-37978

Declinations of bright and weak stars determined separately from observations in the upper and lower culminations by the Struve-Ertel vertical circle during 1955-1961

19 p2861 A72-37981

Determination of mutual orientation in Euler angles for nine selenodetic catalogs

19 p2863 A72-38076

Accurate positions of radio sources at 408 MHz.

19 p2868 A72-38698

Observations at 408 MHz of radio sources from the 4C catalogue. IV - Declination range 20 to 0 deg.

19 p2869 A72-38825

Accurate flux densities at 5009 MHz of 1007 radio sources.

20 p2967 A72-39190

Flux densities, positions, and structures for a complete sample of intense radio sources at 1400 MHz.

21 p3105 A72-40575

A catalog of selenographic coordinates of points of the libration zones and the reverse side of the moon

21 p3114 A72-41767

Nebulae of the Southern Milky Way - An atlas.

21 p3114 A72-41847

Corrections to star catalogues from satellite observations.

22 p3220 A72-41997

Star catalog zero-point improvement by Bessel method modification for lunar observation data reduction

23 p3333 A72-43240

Spectrometric zonal standards - Selection of stars and methodology of their study

23 p3338 A72-44031

Observations of minor planets at the Crimean Astrophysical Observatory AN SSSR, XVIII

24 p3437 A72-44764

Compilation of azimuth tables for the North star /for the tropical zone/

24 p3438 A72-44866

Accuracy of the determination of the zero points of a fundamental catalog from observations of major and minor planets

24 p3447 A72-45676

Spectral classification of stars with respect to non-broadened low-dispersion spectra. III - Classification method and criteria

24 p3447 A72-45678

Spectral classification of stars with respect to non-broadened low-dispersion spectra. IV - Catalog of spectra of faint stars about the NGC 2129 cluster

24 p3447 A72-45679

Photographic observations of Mars at the Main Astronomical Observatory, AN USSR during 1963-1967

24 p3448 A72-45686

Proper motions of 122 eclipsing variables

24 p3448 A72-45688

ASTRONOMICAL COORDINATES

Astronomical method of satellite photograph reduction in geodesy using photogrammetric technique

02 p0231 A72-12602

Trapezium type star systems photographic observations, presenting rectangular coordinates and relative positions

02 p0286 A72-12878

Circumpolar region object position autonomous determination from arbitrarily zenith-oriented moving horizontal platform position coordinates

04 p0545 A72-15002

Astronomical coordinate system, examining equinox proper motion and precession corrections

04 p0575 A72-15029

Meridian circle planet and asteroid positions and deviations from ephemerides during 1950 to 1955

05 p0723 A72-17158

Transit instrument system year-to-year stability in astronomical time determination, considering seasonal wave causes and star coordinate errors

06 p0885 A72-18037

Selenographic coordinate system development, using lunar craters as reference point selection criteria

07 p1067 A72-18869

Comets heliographic coordinates and angles quadrants from orbital elements

08 p1229 A72-20832

Determination method for selenographic coordinates of points on lunar surface, discussing astronomical observations from moon

08 p1231 A72-21131

Disturbing parameters effect on spacecraft trajectory X coordinate values estimation, including planetary masses and coordinates, astronomical unit and light speed

08 p1232 A72-21151

Observational parameters of 61 pulsars, tabulating names, right ascension and declination, galactic longitude and latitude and period and dispersion measures

08 p1233 A72-21179

Stepwise adjustment of astronomo-geodetic grid, complying with exact solution

09 p1299 A72-22945

Soviet papers on astronomical studies covering coordinate systems motion and stellar and celestial body position determination in solar system

09 p1388 A72-23051

Formulas to evaluate differences in angles formed by coordinate systems of two star catalogs

09 p1388 A72-23053

Electromechanical system for wire drive along stellar right ascension of meridian circle of Odessa Astronomical Observatory

09 p1311 A72-23061

Star declinations from simultaneous observations at upper and lower culminations

09 p1388 A72-23064

Delphinus Nova positions determination from plates obtained with photographic telescope with/without diffraction gratings

09 p1389 A72-23067

Tago-Sato-Kosako comet positions determination from plates obtained with photographic telescope, tabulating averaged spherical coordinates

09 p1389 A72-23068

Mathematical model of block adjustment and star coordinate accuracy in photographic astrometry

09 p1392 A72-23541

Radio echo observation of Quadrantid meteor showers right ascension and declination, observing mean range and influx rate as function of universal time

10 p1545 A72-22408

Transit instrument system year-to-year stability in astronomical time determination, considering seasonal wave causes and star coordinate errors

11 p1719 A72-25973

Optical identification of two radio source samples from astronomical B2 catalog, providing finding charts and reference star positions for investigated fields

15 p2316 A72-32749

Coordinate system valid for Oppenheimer-Snyder spherical dust cloud collapse into black hole

16 p2452 A72-33046

Observations of some small-diameter radio sources at 408 MHz.

17 p2603 A72-34440

Ephemerides determination improvement of celestial bodies with nonperiodic trajectories, relating different observatories measurements

17 p2607 A72-35042

The Laplace plane and the masses of the planets

17 p2618 A72-35813

Corrections to the right ascensions of FK4 according to observations of fundamental star series with the meridian circle of the Cerro Calan Observatory /Chile/

19 p2859 A72-37911

Analysis of the division-line errors of the Pulkovo meridian circle by observations of stars

19 p2801 A72-37912

Influence of the reference catalog system on the coordinates of determined stars in zonal meridional observations

19 p2861 A72-37974

Declinations of bright and weak stars determined separately from observations in the upper and lower culminations by the Struve-Ertel vertical circle during 1955-1961

19 p2861 A72-37981

Right ascensions of the sun, Mercury, and Venus observed with the transit instrument at Nikolaev during 1966-1967

19 p2861 A72-37982

Attempt at determining the exact positions of Venus from photographic observations on the short-focus double astrograph and the 26-in. refractor of the Pul'kovo observatory

19 p2861 A72-37984

Determination of major planet coordinates by an expeditionary astrograph

19 p2861 A72-37986

Investigation of the UIM-21 coordinate-measuring machine

19 p2802 A72-37988

Coordinate system for use with high-latitude energetic-particle phenomena.

19 p2853 A72-38729

Astro-azimuth comparative studies with Wild T3, Wild T4, and Kern DKM3 theodolites.

[AIAA PAPER 72-842] 20 p2923 A72-39087

Disturbing parameters effect on spacecraft trajectory X coordinate values estimation, including planetary masses and coordinates, astronomical unit and light speed

20 p2969 A72-39256

A tabulation of pulsar observations.

20 p2969 A72-39390

Nonlogarithmic calculation of chronometer corrections in azimuthal methods of determining time /Struve's method, Struve-Pavlov method, Dellen's method, and other methods/

24 p3438 A72-44864

ASTRONOMICAL MAPS

Jupiter Red Spot 1968-1970 isodensity maps, deriving east-west and north-south photometric profiles for asymmetries

05 p0712 A72-15766

Double and multiple galaxies relative number and space distribution with respect to single galaxies number from sky survey map analysis

06 p0882 A72-18005

Maffei 2 galaxy radio maps and H line studies, discussing distances, intrinsic luminosity, flux density and apparent size

06 p0886 A72-18097

Stellar motion in asymmetric galaxies with three degrees of freedom, using four dimensional surface of section mapping and stochastic measurement

07 p1034 A72-19072

Faint planetary nebulae classification and measurement in northern Milky Way between Cygnus and Perseus from Schmidt camera survey

07 p1070 A72-19084

Image dissector, silicon photodiode and vidicon behavior comparison for medium resolution star mappers design for three axis stabilized vehicles

08 p1172 A72-21975

Polarization maps of extended extragalactic and galactic radio sources at 6 cm wavelength

10 p1545 A72-24793

Coma constellation hard X ray intensity sky map at 20-150 keV from balloon observations

10 p1530 A72-24948

Fan beam surveys of radio sources with Cambridge telescope, presenting catalogs of galactic coordinates and flux density measurements

10 p1549 A72-25194

Martian Sinus Meridiani and South Polar maps from mosaics of Mariner 6 and 7 wide angle photographs

12 p1871 A72-27664

Solar radio emission map at 1.2 mm wavelength obtained with He cooled Ge bolometer connected radio telescope

13 p2046 A72-29716

Requirements and techniques of interstellar navigation, discussing astronomical maps and observational phenomena at relativistic travel velocities

15 p2267 A72-31291

Mars observations in 1965, 1967 and 1969 by 150 mm and 400 mm refracting telescopes noting surface map and drawings

15 p2305 A72-31397

Solar instruments and methods for photosphere magnetic field measurement, noting spectroheliographic mapping in violet spectral region

15 p2306 A72-31647

Radio source concentration mapping near NGC 7331 and Stephan quintet group

16 p2455 A72-33469

Mars surface mapping from spectrophotometric studies of surface materials photometric function, composition and distribution, suggesting color due to limonite-stained soil particles

16 p2457 A72-33616

Radio maps of extragalactic sources at 2.7 and 5.0 GHz presented with physical data for various components

16 p2458 A72-33718

X ray astronomy observational procedures, discussing source location and models, X ray detectors, satellite-borne equipment, correlation maps and diffuse X ray background studies

17 p2612 A72-35377

The new Mariner 9 map of Mars.

18 p2729 A72-36988

The structure of the Crab Nebula at 2.7 and 5 GHz.

I.

19 p2855 A72-37340

Solution of the problem of cosmic triangulation by the generalized method of synchronous and quasi-synchronous straight lines

19 p2861 A72-37971

High resolution observations of 3C390.3 at 2.7 and 5 GHz.

21 p3111 A72-41471

Jupiter surface maps for 1965-70 from drawings obtained with astrograph, noting high activity and eruptive changes after 1961-63 outburst

22 p3220 A72-41920

The derivation of temperature gradient and electron density maps from EUV spectroheliograms.

22 p3222 A72-42036

ASTRONOMICAL MODELS

Iron meteorite formation model based on metal carbonyls low temperature thermal decomposition in comets

01 p0124 A72-10061

Radio source counts, cosmology and evolution in uniform model universes

01 p0127 A72-10323

Empirical model with near IR spectra from expanding circumstellar envelope, normal pulsating atmosphere, shock front and relaxation layers and expanding radiative cooling layer

01 p0128 A72-10791

Quiet solar wind kinetic model, comparing with exospheric, semikinetic and hydrodynamic models

01 p0119 A72-10878

Solar wind two component model with protons collisionless beyond ten solar radii, discussing effects of variable electron temperature

01 p0119 A72-10879

Similarity models of interstellar loop structures, investigating magnetic field and energy losses effects and cosmic ray emission

01 p0131 A72-11011

Cygnus X-6 soft X ray source location, presenting polycarbonate pulse-height spectrum and counter response to different model source energy spectra

01 p0121 A72-11096

Astronomical research, discussing Venus exploration, stellar evolution quasar structure, Maffei galaxies, black holes, dwarfs and neutron star model

01 p0133 A72-11099

Primeval fireball cosmic background radiation spectrum in homogeneous axisymmetric anisotropic world model including electron neutrino effects on expansion dynamics

01 p0121 A72-11139

Quasar model proposal as giant pulsar rejected discussing mass, radius, magnetic field strength, luminosity and gamma radiation

01 p0134 A72-11144

Neutrino flux from solar models differing in opacity, equations of state and nuclear cross section factors

01 p0122 A72-11146

Pulsar magnetosphere axisymmetric and vacuum oblique rotator models, emphasizing electromagnetic field properties

01 p0134 A72-11159

Spatially homogeneous rotating and expanding universe models, deriving Lagrangian function from Einstein field equations

01 p0103 A72-11260

Solar sector magnetism cross correlation, showing difference from classical Babcock model in boundary direction, rigid rotation and identical solar hemisphere polarities

01 p0134 A72-11267

Criticism of cyclonic reversal mechanism and dynamo theory for solar 22-year cycle, proposing penetrating magnetic and general field theory

02 p0276 A72-11641

Line splitting in emission near plasma frequency in drift pair solar radio bursts, considering causes by model involving electrons bunching through solar corona

02 p0276 A72-11646

Jet-like structure formation by close juxtaposition of 80 MHz sources observed in late phase of complex solar burst, presenting model for explanation

02 p0272 A72-11649

Planetary nebulae dynamic models, incorporating expanding shell thermal histories and thermal stability in terms of high temperature evolutionary phase

02 p0276 A72-11667

Eta Carinae model with IR spectrum details described by compact H II region photoionized by hot massive star radiation

02 p0277 A72-11668

Crab Nebula pulsar NP 0532 model for interaction and polarization of radio radiation with surrounding media

02 p0277 A72-11772

Compact extragalactic radio source spectrum analysis, discussing successive uncorrelated outburst models

02 p0277 A72-11775

Ultrahigh energy cosmic ray models indication of galactic origin and composition, based on energy spectrum flattening data

02 p0272 A72-11901

Extended Thomas-Fermi isolated atom model for pulsar outermost crust magnetic field effects, using pressure-density equations of state

02 p0277 A72-11903

Radio galaxy and quasar structure from 3.8 cm observations, fitting models to data

02 p0279 A72-12186

Quasar evolution models statistics suggesting relationship to radio galaxies, discussing continuity equation for density and luminosity changes

02 p0279 A72-12187

Interplanetary medium spherical solid component model from radio meteor orbit catalog, discussing density of interplanetary dust, meteor matter and cosmic fallout on sun

02 p0282 A72-12332

Photometric meteor mass determination, using models relating radiation intensity, meteor velocity, atmospheric density and instantaneous luminous flux

02 p0282 A72-12334

Variational solutions of nonlinear free boundary integrodifferential Euler equations for rotating star models

02 p0252 A72-12540

Oblique rotator model for time dependent light polarization of red long period variables, considering dust particle alignment in outer atmospheric layers near magnetic poles

02 p0283 A72-12630

Extinction curves for Mie scattering by interstellar grains, including refractive index differences in vacuum UV for methane, ammonia and water ice absorption

02 p0284 A72-12633

Astronomical model for solar cosmic ray bursts propagation including anisotropic particle diffusion along interplanetary magnetic field

03 p0407 A72-12944

Stellar secular stability during complex roots onset in model evolution, discussing radiative heat transport coefficient effects

03 p0416 A72-13004

Magnetic field role in Ap stars abundance peculiarities model, discussing rotational circulation, convection, accretion and mass loss effects on surface

03 p0416 A72-13010

Terrestrial planets internal constitution and thermal history model, emphasizing iron fractionation in structure

03 p0418 A72-13110

Giant planets internal constitution models, discussing Jupiter visual magnitude variability, Saturn ring system, cold matter equations of state and He abundances

03 p0418 A72-13111

Helium production in different cosmological models based on solar system, stars and nebulae observations and stellar evolution calculations

03 p0419 A72-13118

Lunar limb structure from occultation traces from point source stars, constructing model with levels and slopes

03 p0420 A72-13129

Lunar occultation light curve model for photoelectric data analysis, using least squares method

03 p0421 A72-13133

Hadrons in extensive air showers, predicting arrival time spectra from fireball and isobar-p ionization models for high energy interactions

03 p0409 A72-13147

Anisotropic universe model based on Einstein equations for metric with cosmological term

03 p0388 A72-13193

Nonoptical and optical observation derived coronal condensations models for active regions and flare associated events

03 p0423 A72-13211

Active and quiet solar atmosphere models from OSO satellite data, presenting emission lines and continua from abundant elements

03 p0423 A72-13215

Massive star evolution, discussing stellar structure theory uncertainties, young clusters, helium burning and evolutionary tracks

03 p0425 A72-13262

Magellanic Clouds and Galactic nucleosynthesis from chemical composition

03 p0426 A72-13263

Gaseous general relativistic kinetic theory, detailing matter model, thermodynamics, cosmology and Einstein field equation completion with Liouville or Boltzmann equation

03 p0388 A72-13266

Relativistic cosmological model, showing relation to fluid dynamics in Newtonian theory and space-time dependence on causality condition

03 p0426 A72-13267

Astrophysical cosmology, discussing universe expansion, Robertson-Walker models, radio sources, quasars, cosmic X ray background, intergalactic media, etc

03 p0426 A72-13268

Rotating relativistic stellar models, covering coordinate systems injection energy, convection, red shift, external gravitational waves and black holes
03 p0426 A72-13269

Galactic formation theories, discussing hot big bang and Friedmann models, primordial fireball and Hubble diagram
03 p0426 A72-13271

Cosmological density fluctuations in hadron state, examining relativistic free particle and high temperature hadron gas models
03 p0426 A72-13273

Sunspot and active region magnetic fields and thermodynamic structure from umbral and penumbral models, discussing magnetic fine structure
03 p0427 A72-13296

Solar magnetic field distribution in sunspots surface layers, considering photospheric three dimensional magnetohydrostatic model
03 p0431 A72-13337

Radio-astronomical evidence for magnetohydrodynamical pulsations in corona, considering solar radio burst model of pulsating structure due to synchrotron radiation
03 p0432 A72-13349

Solar cycle models physical mechanisms, discussing surface activities and nonaxisymmetric steady state solutions
03 p0433 A72-13357

Large scale solar magnetic field dynamo model in terms of force-free constituents series, deducing periodic solution by eigenvalue method
03 p0433 A72-13362

Lunar electrical conductivity model, determining vacuum transient response to time varying spatially uniform magnetic field
03 p0434 A72-13508

Inner solar system particle propagation model solved for radial gradient of galactic protons, comparing to Mariner 4 measurements
03 p0412 A72-13527

Cosmic ray energy changes in interplanetary space by model for solar X-ray bursts
03 p0413 A72-13534

Critique of quasar model of independent random pulse emitting sources conglomeration, noting brightness fluctuations incompatibility
03 p0435 A72-13802

X ray background model based on photons bremsstrahlung emission by subcosmic metagalactic electrons or protons
03 p0413 A72-13804

Electromagnetic pulsar models features and predictions, using rotating neutron stars with strong dipolar magnetic fields
03 p0437 A72-13873

Fe-S segregation role in early chemical and physical history, giving model of early lunar differentiation
03 p0439 A72-14274

Nucleosynthesis model for gamma ray astronomy, covering explosive events
03 p0413 A72-14275

Electromagnetic radiation in universe, discussing relic radio emission, energy density, hot model isotropic extragalactic component isolation, intergalactic gas, radio sources and quasars
03 p0414 A72-14317

Toroidal oscillations of spherical planetary models, presenting regular eigenfunction form near center
03 p0352 A72-14381

Outer planets satellites physics and chemistry, discussing steady state thermal models based on energy equilibrium between internal radioactive decay and surface radiation
04 p0568 A72-14495

Two-layer lunar model from variable viscosity media isostatic processes selenological investigation, suggesting hard top crust and deeper asthenosphere
04 p0569 A72-14505

Optical search for Ryle-Neville radio sources, discussing cosmological model constraints and quasar and radio galaxies optical and radio luminosity functions
04 p0570 A72-14549

One zone model formulation and mathematical behavior for evolution of galaxies, discussing stellar birth rate and end states
04 p0570 A72-14551

Coherent synchrotron radiation from model with charge distribution moving on ring, applying to pulsars
04 p0566 A72-14555

Solar model for capture rate in $Cl\ 37$ neutrino experiment, comparing different stellar evolution programs
04 p0566 A72-14562

Expanding source model for quasars and Seyfert galaxy nuclei radio outbursts from extension of radio galaxy evolution models
04 p0573 A72-14874

Pulsar model, discussing polar radiation diagram formation with source motion around neutron star
04 p0573 A72-14903

Blanketing effect of strong line spectra collisionally broadened wings, evaluating stellar atmospheric model computation
04 p0573 A72-14907

Light phase curve model for nonatmospheric bodies covered with porous or dust-like surface layer
04 p0574 A72-14910

Empirical dimensionless ratios between universal physical constants, supporting steady cosmological expanding universe model
04 p0574 A72-14983

Lunar sea surface model derivation from morphology data analysis, suggesting four-layer bottom relief of basaltoidal lava, rocks, breccia and surface regolith
04 p0576 A72-15069

F and early G dwarf stars atmospheric models and line data, deriving temperatures, abundances and gravities
04 p0577 A72-15282

Universe cluster expansion model, showing velocity dispersion increases from center to turnover radius
04 p0578 A72-15308

Interstellar sodium lines intensities and widths as discriminants for two component models of galactic H I cloud regions
04 p0578 A72-15310

Photometric standard star 29 Piscium abundance analysis with flux constant hydrogen line blanketed model atmospheres
04 p0578 A72-15317

Linear nonadiabatic pulsation constants for fundamental mode and first two harmonics of stellar models including Cepheids, observing mass scattering
04 p0579 A72-15319

NGC 5128 X ray spectrum from sounding rocket and balloon observations, presenting inverse Compton models
04 p0568 A72-15372

High energy cosmic ray electrons anisotropy, considering diffusion from discrete source model
04 p0568 A72-15510

Li, Be and B production rate in interstellar gas by galactic cosmic rays from diffusion model of fast particles, accounting for He component
05 p0708 A72-15760

Asteroids origin, discussing Phaethon model, masses, distribution, fragmentation and disintegration
05 p0713 A72-15980

Galactic cluster lifetimes compared with star cluster model evaporation times, discussing general galactic and interstellar clouds tidal fields effects
05 p0713 A72-16051

Encounterless one-dimensional constant density self gravitating system stability for symmetric disturbances, using analytic treatment and computer experiments
05 p0713 A72-16054

Lynden-Bell statistical mechanics predictions compared with most and least violently relaxed one dimensional self gravitating systems, using computer experiments
05 p0714 A72-16055

Vlasov equation phase space boundary integration for evolution of one dimensional self gravitating collisionless stellar systems with constant density
05 p0714 A72-16056

Collective relaxation of two phase space density collisionless one dimensional self gravitating stellar systems, following boundary curve motion
05 p0714 A72-16057

Cosmological models dynamics and structural evolution feedback from density inhomogeneities energy momentum tensor, using hf approximation
05 p0715 A72-16166

Large scale alternating solar magnetic field generation by outer shell convective flow, constructing oscillator hydromagnetic dynamo model
05 p0715 A72-16232

Cosmological evolution theories, discussing big bang theory, galactic evolution, quasars, pulsars, gravitational collapse, stellar evolution, supernovae, black holes, etc
05 p0716 A72-16311

Interstellar extinction curves for stellar far UV radiation, discussing required multicomponent interstellar dust model
05 p0720 A72-16717

Gamma ray absorption near Crab Nebula pulsar NP 0532 within beam model, discussing pair production in photon field
05 p0711 A72-17161

Neutron star and white dwarf strong magnetic field generation mechanism involving thermodynamic equilibrium states of electron gas
05 p0723 A72-17162

Periodic model of time evolving universe, examining stability of Einstein static solution to field equations
05 p0723 A72-17180

Perturbations in Godel universe, considering Einstein equations in relativistic cosmology
06 p0876 A72-17564

Radio emitting giant loops in the Galaxy, considering supernova radiation induced nebulae model to explain spectral and polarization properties
06 p0876 A72-17649

Galactic star clusters dynamic evolution, using King type equilibrium and stellar mass distribution models
06 p0879 A72-17860

Periodic comets orbital elements and nongravitational parameters, discussing mass loss rates, time effects and nuclear core-mantle model
06 p0880 A72-17863

Dissipative effects in universe expansion, considering damping of anisotropy in homogeneous cosmological models
06 p0880 A72-17885

Lunar gravitational field, relief and internal structure, suggesting two layer model and crust thickness change relation to field characteristics
06 p0881 A72-17926

Model computations for population I stars of 0.6, 0.8 and 1.2 solar masses, considering evolutionary sequences correspondence to planetary nebulae evolution
06 p0882 A72-17999

Interstellar gas motion model of nebulae formation by Wolf-Rayet stars
06 p0883 A72-18016

Star cluster stability in form of Einstein model of rotating spherically symmetrical mass system, using Newton approximation
06 p0883 A72-18018

Red shift and spectral line broadening model based on emitting and absorbing atom effects
06 p0883 A72-18023

Solar wind model of electrons, protons and alpha particles velocity and temperature differences dependence on distance from sun
06 p0873 A72-18025

Statistical mechanics of N-body self gravitating system one dimensional model, using canonical and microcanonical ensembles
06 p0885 A72-18075

Numerical experiments in collisionless stellar systems evolution by gravitational n-body calculations using computers
06 p0885 A72-18076

Isolated rotating disks of stars galactic evolution model for gravitational field studies, noting dynamic instabilities and final exponential mass distribution
06 p0885 A72-18077

Monte Carlo scheme for dynamic evolution of spherical stellar systems
06 p0885 A72-18080

Computer models for simulating self consistent collisionless stellar systems evolution under gravitational field
06 p0885 A72-18081

Galactic evolution model, tracing stellar and supernova nucleosynthesis influence on interstellar gas composition
06 p0886 A72-18082

Hadron era evolution, discussing equation of state, ultimate temperature, galactic formation and adiabatic exponent application to Friedman universes
06 p0886 A72-18096

Lunar surface temperature-independent and dependent plane homogeneous models for thermal properties study, discussing surface roughness and localized thermal anomalies
06 p0887 A72-18227

Astronomical model for Jovian decametric radio emission control by Io satellite based on two surface sources on planet and particle interaction with plasma
06 p0891 A72-18504

Microscopic calculations for nuclear forces, compressibility of neutron matter and maximum mass of neutron stars based on solid state model at high densities
06 p0891 A72-18507

Mass distribution gravitationally equivalent to L1 lunar potential model for finite torus shaped shell region sampled by Apollo spacecraft
07 p1067 A72-18871

Hubble diagram history, present status, extension and improvement, considering quasars, galactic red shifts and other extragalactic radio sources
07 p1068 A72-18999

Spiral galaxies hypothesis for higher mass-luminosity ratio of outer parts from undetected cold neutral hydrogen, using model of NGC 300
07 p1068 A72-19071

Galactic cepheid RS Puppis and surrounding ring-structured nebula luminous variations and evolution, using reflecting shell model
07 p1069 A72-19079

Model atmosphere and spectral analysis for two early B-type supergiant stars, deducing stellar mass and evolutionary phase
07 p1070 A72-19085

Solar modulated galactic cosmic rays radial gradient idealized model for comparable deceleration and convection effects
07 p1057 A72-19138

Metric tensor components of isotropic inhomogeneous cosmological model obtained from Einstein equations
07 p1072 A72-19340

Homogeneous isotropic Newtonian and Robertson-Walker cosmological models, discussing radiative transfer and optics
07 p1074 A72-19431

Dynamic model of galactic clusters in terms of cosmological turbulence, estimating velocity dispersion and rotation and chaotic velocity contributions to kinetic energy 07 p1076 A72-19805

Lunar gravitational anomalies and plumb deviations mapping, reflecting global structure of Lorell JPL-3 model 07 p0976 A72-19818

Earth and moon chemical composition differences based on model of lunar formation from circumterrestrial swarm of particles and larger objects 07 p1077 A72-19820

Pulsars suggested as rotating neutron stars based on collapsed star magnetic field strength, mass-radius relation and radio flux emission 07 p1080 A72-20055

Pulsar model based on neutron star rotation with skew magnetic field, considering radiated particle acceleration necessary for high energy activity in supernova remnants 07 p1080 A72-20057

Magnetosphere theory of pulsar electrodynamics, discussing unipolar inductor with iron sphere having uniform magnetization parallel to rotation axis 07 p1080 A72-20058

Solar model inconsistencies, considering He and Fe abundances and solar age approximation 07 p1083 A72-20464

Population I stars and open cluster age determination methods based on stellar evolution theory, discussing inherent uncertainties effects 07 p1083 A72-20467

Mars internal structure models with chondrite as potential core-forming material, discussing absence of internal origin magnetic field 07 p1084 A72-20518

Nonstationary and asymmetric cosmic ray modulation theory, discussing moving boundary problem and solar wind model with spherical singularity 07 p1065 A72-20643

Spectral characteristics of continuous radio emission of extragalactic binary objects, discussing model of binary radio source formation from dipole nucleus 08 p1231 A72-21118

Semitransparent particle model of Martian surface for reflective power at various incidence and reflection angles, discussing packing density and optical parameters 08 p1231 A72-21126

Zeta Puppis visual line spectrum discrepancy from non-LTE stellar atmospheres models, necessitating hydrostatic equilibrium deviations consideration for temperature derivation 08 p1232 A72-21178

Local deviation limits of universe from homogeneous isotropic model, considering velocity field perturbations and galaxy counts 08 p1234 A72-21381

Radio galaxy and quasar evolution models derived by formalism for number of sources in universe at any instant of cosmic time 08 p1234 A72-21382

Quasars and Seyfert galaxies radiation, discussing dust clouds, synchrotron and unstable plasma models 08 p1234 A72-21383

Tracking interferometer observations for compact radio source structure investigation with simple models constructed for several individual sources 08 p1235 A72-21384

Pulsar braking index and period-pulse width distribution calculations within proposed model leading to neutron star surface magnetic field strength estimates 08 p1235 A72-21389

Scorpius X-1 linear optical polarization, comparing intrinsic to interstellar theories 08 p1235 A72-21390

Models of galactic diffuse sources of soft cosmic X rays, estimating spectrum and intensity 08 p1228 A72-21650

Mixmaster world model with arbitrarily moving matter, using coordinate system with matrix of reference point components of three dimensional metric tensor 08 p1237 A72-21714

Brightness distribution and phase dependence measured for spheres with different colors and roughness for Mars surface optical parameters model validity 08 p1238 A72-21830

Cosmological model with negative and positive mass particles, discussing cosmological term, gravitation shielding, red shift and interacting Vorontsov Veliaminov galaxies 09 p1379 A72-22202

Quasi-stellar objects hydrogen L-alpha lines computation via cloud collapse and ionizing radiation flux model, comparing computed distribution with PHL 957 and 4C 05.34 observations 09 p1382 A72-22280

Nova outbursts hydrodynamic processes, studying mass loss mechanism based on direct shock wave ejection and pulsational instability 09 p1382 A72-22283

Redshifted L alpha flux upper limit restricting hot ionized gas models for gravitational binding of Coma galactic cluster 09 p1383 A72-22292

Model stability of globular star cluster with nonzero rotational moment, discussing gravitational effects 09 p1383 A72-22494

Spiral density waves in galactic model with differentially rotating interstellar gas and stars, deriving dispersion equation by frequency to wave numbers relation 09 p1384 A72-22517

Quasar rotation and pulsation periods within pulsar models, postulating supermassive stars /one million-one billion solar masses/ as energy sources 09 p1385 A72-22536

Astronomical models for gas kinematics near galactic center, discussing gas jets origin and kinetic energy 09 p1386 A72-22687

Cosmological implications of radioactive decays study by Rutherford, suggesting evolving nonstatic universe 09 p1386 A72-22688

Magnetic star theory, postulating stellar magnetic flux as slowly decaying relic of flux in prestar gas, considering dissipation processes and rotation 09 p1387 A72-22754

Quasar 3C279 flux density variation measurement as evidence for alternate model to explain apparent expansion rate of 10c 09 p1387 A72-22976

Markov processes in stellar dynamics, discussing relaxation and evaporation times and star velocity distribution for galactic cluster models 09 p1390 A72-23504

Spectrum of hot hydrogen plasma continuum radiation, discussing models for Scorpius X-1 source and inhomogeneous clouds 09 p1391 A72-23536

Eigenmodes growth rate in convectively unstable self gravitating gas sphere, using spherical harmonic series expansion and Laplace transforms 09 p1392 A72-23545

OH emission source and H II region bright knots coincidence in NGC 7538 nebula, suggesting physical model 09 p1392 A72-23548

Model for volcanic origin of Descartes Formation high albedo region, suggesting young age and endogenic nature of bright surface deposit 09 p1394 A72-23666

Seyfert galaxies emission, absorption, IR and optical spectral characteristics, suggesting model with sharp forbidden and Balmer line outer region and broad wing core 10 p1532 A72-23885

Radio source observational identification as radio and normal galaxies and quasars, examining models for compact and large double radio source features and mechanisms 10 p1533 A72-23886

Galactic center radio, IR, X ray, gamma ray and molecular spectral features, considering models for source component emission mechanisms and energy densities 10 p1533 A72-23887

Galactic nuclei evolution and stellar content models from nearby stars spectral synthesis 10 p1533 A72-23895

Quasar and radio galaxy emission intensity and polarization variation models, comparing with observations 10 p1534 A72-23901

Monodirectional jet mass ejection from black holes, developing hypothetical model based on squeezed toothpaste analogy 10 p1535 A72-23910

Variable radio structure model using relativistic electron cloud outbursts in stationary magnetic field tubes for faster than light velocities 10 p1536 A72-24139

Current lines of relativistic fluid investigated by Ehlers method, applying to MHD Godel type universes 10 p1520 A72-24220

Friedmann cosmological models in terms of conformally invariant gravitation theory, noting two physically connected universe halves 10 p1541 A72-24474

Cosmological models with astrophysical and geophysical properties by introducing particles mass field and dimensionless coupling constant in conformally invariant gravitational theory 10 p1541 A72-24475

Cepheid instability strip stellar models pulsation properties compared with delta Scuti stars and AI Velorum variables observation data for stellar evolution studies 10 p1542 A72-24611

OH emission characteristics of IR stars from model with asymmetrical expansion outward of circumstellar OH clouds 10 p1542 A72-24613

Binary stars convective zones reaction to periodic gravitational fluctuations due to stellar revolutions asynchronism, using incompressible fluid plane layer model 10 p1543 A72-24631

Rapid perturbation growth conditions for expanding universe, discussing background density decrease with time 10 p1543 A72-24661

Cepheid variables evolutionary and blue edge calculations reconciled with observation 10 p1544 A72-24665

Cen X-3 model with X ray emission from atmosphere heated by shock waves generated by surface pulsations of white dwarf 10 p1544 A72-24668

Pulsar radiation mechanism study from magnetosphere structure model, taking into account neutron star evaporated gas accumulation in gravitation-centrifugal force balance region 10 p1544 A72-24672

Zero-pressure universe model parameters from red shift and apparent magnitude data for clusters of galaxies 10 p1545 A72-24809

Red shift-absolute magnitude relation for uniform time-dependent universe expansion rate suggesting large scale clustering modifications based on light propagation model 10 p1545 A72-24810

Dynamo theory of magnetic stars, proposing symmetrical rotator as alternative to skew rotator 10 p1546 A72-24833

Optical and X ray pulsars, discussing Crab pulsar, emission behavior, pulse intensity, periodicity, polarization properties and antenna emission, plasma maser and Chiu models 10 p1547 A72-24919

Cygnus X-1 model with hard X rays from inverse Compton scattering of B star UV photons and IR synchrotron radiation from other component 10 p1530 A72-24944

High density models for ambient gas of eta Carinae star from X ray observations 10 p1530 A72-24947

Radio methods for cosmological model testing, discussing radio telescope requirements, source sampling procedures and counts as basic cosmological data 10 p1549 A72-25054

Field and geodetic line equations for light rays in open and closed isotropic radiative universe model 10 p1549 A72-25059

Close binary stars system model for totally eclipsing AW UMa light curves and line profiles, noting very low mass ratio 10 p1550 A72-25195

Contact binary star systems model, considering superadiabatic energy transfer mechanism of convective envelope 10 p1550 A72-25199

Cold static superdense model for white dwarf and neutron stars, using relativity theory and variational principles for stellar structure in hydrostatic equilibrium 11 p1715 A72-25528

V 1057 Cyg photometry and polarimetry, considering model with two circumstellar shells stellar flux absorption and reradiation 11 p1716 A72-25678

Stellar atmospheric structure physical parameters from model atmosphere calculations, applying method to G and K stars 11 p1717 A72-25904

Solar chromosphere-corona transition region theoretical and empirical models, studying acoustic flux generated above convective zone 11 p1717 A72-25906

Pulsar rotational models, considering white dwarves, neutron stars, oblique rotators, etc 11 p1718 A72-25907

Astronomical models of solar wind interaction with interstellar medium, determining magnetic field effects on shock wave 11 p1713 A72-25946

Interstellar gas motion model of nebulae formation by Wolf-Rayet stars 11 p1718 A72-25952

Star cluster stability in form of Einstein model of rotating spherically symmetrical mass system, using Newton approximation 11 p1718 A72-25954

Red shift and spectral line broadening model based on emitting and absorbing atom effects 11 p1718 A72-25959

Solar wind model of electrons, protons and alpha particles velocity and temperature differences dependence on distance from sun 11 p1713 A72-25961

Russian book on eclipsing binary stars covering limb darkening law, photometric eclipsing phases, computer applications and models 11 p1720 A72-26046

Perseus two armed spiral shock model based on O associations, young open clusters, H II regions, interstellar absorption lines and 21 cm hydrogen maps
11 p1720 A72-26110

Venus spectrum carbon dioxide absorption lines model with double cloud system and adiabatic atmosphere
11 p1721 A72-26120

Lunar occultations of IRC plus 10216 for IR radiation distribution, deducing model of late type carbon star surrounded by thermally reemitting dust shell
11 p1721 A72-26123

Interferometer investigations of Cassiopeia linear polarization at centimeter wavelengths, explaining results by source model incorporating Faraday depolarization
12 p1865 A72-27094

Fowler quasars and exploding galaxies model tested by hydrodynamic equations numerical solution for premain sequence contraction and relativistic collapse of nonrotating supermassive star
12 p1866 A72-27202

Elliptical radio galaxies and quasars intrinsic emitted radio power correlation to spectral indices interpreted as evolutionary track in terms of model
12 p1867 A72-27210

Radio observation of neutral hydrogen near galactic center, noting expanding and rotating ring of gas from kinematic model
12 p1867 A72-27211

UBV photometric properties and probability of discovery in blue light of detached close binaries models
12 p1867 A72-27214

Space-time model locally identical with Minkowski space in geometrical and causality features, implying non-Doppler red shift and cosmology
12 p1868 A72-27218

Lunar microwave emission, constructing thermophysical models for radio observations and brightness temperature variations
12 p1869 A72-27327

Lunar surface roughness thermal characteristics, comparing IR data with three realistic models
12 p1870 A72-27335

Lunar interior thermal history discussing mathematical models for radioactive heat source, initial conditions, temperature distribution and time dependent fractionation
12 p1870 A72-27336

Velocity dominated singularities generalized to solutions of Einstein equations with irrotational perfect fluid sources within hydrodynamic cosmological models
12 p1870 A72-27410

Grain heating model of H II region to explain 100 micron emission predominance in IR sources
12 p1871 A72-27693

Chandrasekhar statistical stellar dynamics assumption generality compared to Chandrasekhar diffusion process, discussing discontinuous model, relaxation time, escape probability and numerical results
12 p1872 A72-27893

Dynamical evolution of spherical star cluster under effect of internal encounters, using Monte Carlo models
12 p1873 A72-27896

Galactic cluster lifetimes from observed age distribution comparison to evaporation times by numerical experiments with star cluster models
12 p1873 A72-27897

Binary evolution in star cluster models from numerical methods of direct integration, noting domination by heavy binary and double star formation and disruption
12 p1873 A72-27899

Numerical experimentation in collisionless systems for Jeans instability, static self consistent models and spiral patterns
12 p1874 A72-27908

Noncovariant gravitation theory field equations based on preferred reference frame applied to homogeneous isotropic cosmological model, finding conservation law for total energy
12 p1875 A72-28154

Structural and integral parameters for rotating stellar configurations within Newton gravitation theory, giving equations for gravitational potential, outer surface geometry and multiple moments
13 p2035 A72-28677

Conformally flat linear axial symmetry chromometrically invariant cosmological models, discussing various types of spaces realized during model evolution
13 p2036 A72-28759

Expanding hot universe evolution from astrophysical cosmology point of view, emphasizing galaxy formation relation to state of matter and radiation in early universe
13 p2038 A72-29084

Interplanetary medium spherical solid component model from radio meteor orbit catalog, discussing density of interplanetary dust, meteor matter and cosmic fallout on sun
13 p2039 A72-29216

Photometric meteor mass determination, using models relating radiation intensity, meteor velocity, atmospheric density and instantaneous luminous flux
13 p2039 A72-29218

Avrett-Krook temperature correction procedure modified to improve, near surface convergence for blanketed model stellar atmospheres
13 p2040 A72-29406

Self consistent model for cosmic ray propagation from sources in Galaxy toward earth, using H and He isotope interstellar spectra
13 p2031 A72-29409

Lower solar chromosphere two dimensional models, noting effects of macroscopic velocity fields
13 p2045 A72-29709

Umbral model effect on Li abundance determination from sunspot spectra
13 p2045 A72-29711

Sunspot energy deficit relation to model depth, deriving facular model with two dimensional radiative transfer analysis
13 p2045 A72-29712

Observed continuous solar spectrum intensity comparison with photospheric models, noting bend-off due to veiled line haze
13 p2047 A72-29734

Sunspot magnetic field depth variations model, using configuration conditioned by Schluter-Temesvary similarity law
13 p2048 A72-29740

Model of solar wind expansion beyond heliosphere, taking into account effect of relative motion between cool interstellar atomic hydrogen and solar wind protons
13 p1033 A72-29801

Habing galactic model extension and confirmation from observations of high velocity neutral hydrogen clouds and outer spiral arm structure
13 p2048 A72-29817

Solar chromosphere model based on Lyman spectra observations, calculating temperature, gas and electron pressure and particle densities as function of height
13 p2049 A72-29932

Parker dynamo theory failure in explanation for galactic magnetic field origin and form, noting reasons
13 p2050 A72-29957

Electron temperature radial dependence in two fluid models of solar wind, noting unrealistic assumption of heat conduction dominated electron gas energy equation
13 p2034 A72-29961

Protoplanet cloud model of solar system as flat gas-dust disk, discussing density profile, gravitational stability and mass loss
14 p2148 A72-30206

Quasi-stationary spherical system structure model for stars of different masses with isotropic velocity distribution
14 p2149 A72-30212

Earth-moon system periodic orbits calculation by modified quasi-linearization combined with particular solutions method, using restricted three body model
14 p2149 A72-30232

Lunar core-crust conductivity models compatibility with lunar surface field/interplanetary magnetic field transfer function from Apollo 12 magnetometer data
14 p2153 A72-30502

Cylindrical model of interplanetary magnetic field-moon interaction, taking into account solar wind flow boundary condition asymmetries
14 p2154 A72-30514

Lunar interior thermal history and current state from theoretical temperature models, taking into account initial conditions, heat sources, differentiation and simulated convection
14 p2155 A72-30519

Expanding universe postulate vs tired light effect for cosmological red shift explanation, discussing possible tests
14 p2155 A72-30551

Crab Nebula X ray emission synchrotron model confirmation by sounding rocket polarimeter polarization detection data
14 p2156 A72-30565

Model for textural features and mineralogical composition of Ca and Al-rich inclusions in C3 chondrites during condensation in primitive solar nebula
14 p2157 A72-30585

OH and IR emission from NML Cygnus, discussing gas cloud model with flattening and gas expansion
14 p2157 A72-30681

Mass exchange and thermal time scales for shell source burning binary components with deep outer convective layers, interpreting numerical results from analytical model
14 p2159 A72-30739

Massive red supergiants radial pulsations from adiabatic theory application to convective envelope models based on mixing length theory and H-He ionization zones
14 p2159 A72-30743

Spiral structure density wave model of inner parts of Galaxy, calculating density, potential and velocity perturbation and dispersion in gas and stars
14 p2161 A72-30914

Galactic tidal interactions, computing mass loss for hyperbolic collisions and giant system formation from density distribution models
14 p2161 A72-31043

Quiet and active models for solar structure and processes in terms of elementary physical concepts
15 p2302 A72-31276

Model for hot stars mass outflow due to gas acceleration by radiation absorption in UV resonance lines
15 p2305 A72-31341

Particular and general exact solutions of Einstein equations for matter filled space under assumption of spherically symmetric distribution of perfect fluid
15 p2305 A72-31343

Flat homogeneous isotropic relativistic cosmological two fluid model, using Robertson-Walker metric
15 p2307 A72-31795

Two fluid cosmological model in conformal and conformally flat forms, deriving solutions in elementary functions
15 p2307 A72-31796

Callisto radio emission analysis by ice body model, noting brightness temperature calculation of ice surface
15 p2308 A72-31904

Nonhomologous expansion in modified Friedmann cosmological model, neglecting particle collisions
15 p2313 A72-32304

Lower zero age main sequence star models uncertainties, comparing nonmixing and mixing length theory for various composition atmospheres
15 p2314 A72-32367

Photoelectric photometry of binary VV Pup with 3-sec time resolution, suggesting qualitative model from eclipses identification
15 p2314 A72-32369

V/Vm insensitivity to red shift random shuffling based on luminosity function in Einstein-de Sitter cosmological model
15 p2314 A72-32375

Water bag model in cylindrical rotating two dimensional rod stellar system, showing kinetic energy minimum correspondence to collisionless Boltzmann equation
15 p2315 A72-32717

Coronal scattering effects on type 3 solar bursts, using radio sources scintillation model and Monte Carlo ray tracing technique
15 p2316 A72-32752

Alpha effect solar dynamo model magnetic field and velocity expansion in spherical harmonics, solving mean field induction equation
15 p2316 A72-32755

Vela pulsar speedup explanation by corequake release of elastic energy stored within solid neutron lattice
16 p2450 A72-32869

Temperature profile derivation for uppermost convection region of two solar convection zone models from finite amplitude convection theory
16 p2451 A72-33037

Quantitative evolution model for time variable flux densities and polarization characteristics of isolated moving type 4 events
16 p2444 A72-33041

Opacity corrections of main sequence stellar models of 2.25 solar masses in terms of Cox, Carson and Watson formulas
16 p2452 A72-33130

Fourier analysis of Pluto light curve in terms of geometrical model consisting of bright and dark areas
16 p2452 A72-33131

Diffuse X ray emission from galaxy interarm region, suggesting population of unresolvable low luminosity sources as emission model
16 p2445 A72-33138

Information propagation time direction of cosmological models in terms of conventional electrodynamic theory, contrasting with Wheeler-Feynman theory
16 p2424 A72-33286

Hellas-Hellepontus transition zone properties in origin model with impact and later isostatic subsidence
16 p2454 A72-33445

Negligible intergalactic matter model, deriving distance-red shift relation and comparing to acceleration parameter of homogeneous model
16 p2455 A72-33470

Magnitude redshift relation in flat Brans-Dicke cosmology, discussing gravitational constant effects on stellar evolution and galactic luminosity
16 p2455 A72-33471

Cen X-3 system X ray flux amplitude periodic variations, proposing model composed of source orbiting around massive body with ionized gas cloud in between
16 p2446 A72-33611

- Helium stars linear and nonlinear pulsation and evolutionary computations, establishing instability strip with two solar mass models 16 p2458 A72-33720
- Stellar magnetic oblique rotator internal motion field construction by perturbation technique estimating energy dissipation and turbulent viscosity 16 p2458 A72-33721
- Model for low energy galactic cosmic ray effects on young and F star Li abundance and H I region heating 16 p2448 A72-33740
- Solar wind velocity near Jupiter correlated to 10 geocentric phase during radio bursts, noting plasma-sphere models 16 p2459 A72-33904
- Stellar MHD, discussing strongly magnetic stars identification and slow rotation origin based on oblique rotator model 16 p2460 A72-33923
- Mathematical model for magnetosphere surrounding rotating neutron star, noting computer programs for Maxwell and plasma equations solution 16 p2460 A72-33927
- Fermi lectures by Dyson on neutron stars and pulsars origin and structure, using perfect gas and realistic models 16 p2460 A72-33974
- Stellar evolution and rotation data acquisition from photometric analysis of B-F main sequence stars, considering different models for rotating atmospheres 16 p2462 A72-34184
- NP 0532 precursor pulse as radiation scattered from main pulse beam by ring of material centered on pulsar 17 p2603 A72-34192
- Photoionizing models for the emission-line regions of quasi-stellar and related objects. 17 p2605 A72-34527
- Random gravitational encounters and the evolution of spherical systems. IV - Isolated systems of identical stars. 17 p2605 A72-34528
- The equilibria and oscillations of a family of uniformly rotating stellar disks. 17 p2605 A72-34529
- On galaxy formation from primeval universal turbulence. 17 p2606 A72-34574
- Model stability of globular star cluster with nonzero angular momentum, discussing gravitational effects 17 p2606 A72-34658
- A two-fluid solar wind model with anisotropic proton temperature. 17 p2599 A72-35097
- Disk-shaped diffusion model with inhomogeneous distribution of gas and heavy relativistic nuclei sources for galactic cosmic rays chemical composition 17 p2600 A72-35206
- Fundamental data for massive stars compared with theoretical models. 17 p2611 A72-35317
- Cosmological models interpretation of extragalactic radio source counts 17 p2612 A72-35350
- X ray astronomy observational procedures, discussing source location and models, X ray detectors, satellite-borne equipment, correlation maps and diffuse X ray background studies 17 p2612 A72-35377
- Quantum models for the lowest-order velocity-dominated solutions of irrotational dust cosmologies. 17 p2613 A72-35392
- Vibrational stability of supermassive stars stabilized dynamically by a uniform or differential rotation 17 p2613 A72-35461
- The tidal interaction of galaxies 17 p2613 A72-35473
- Faraday rotation in connection with Hoyle theory of intergalactic magnetic field existence in steady state cosmology, considering cosmological model with cosmic magnetic field 17 p2614 A72-35504
- Lunar local surface magnetic fields production mechanism, considering convection currents due to ionization of volcanic-ash-particle flow by electrodynamic model 17 p2614 A72-35586
- Astronomical model for primitive solar nebula showing planetary evolution in hot initial state under centrifugal forces 17 p2614 A72-35677
- Parent-body models for the formation of iron meteorites. 17 p2615 A72-35687
- A model for drift pair and hook burst emission from the solar corona. 17 p2617 A72-35712
- Vortex model of galactic clusters evolution, estimating velocity dispersion and rotation and chaotic velocity contributions to kinetic energy 17 p2617 A72-35729
- Lunar gravitational anomalies and plumb deviations mapping, reflecting global structure of Lorell JPL-3 model 17 p2618 A72-35743
- Earth and moon chemical composition differences based on model of lunar formation, from circumterrestrial swarm of particles and larger objects 17 p2618 A72-35745
- Fluid dynamics of convective stellar envelopes. 17 p2618 A72-35933
- Conformally flat linear axisymmetric chronometrically invariant cosmological models, discussing various types of spaces realized during model evolution 18 p2724 A72-36237
- Geochemically and geophysically consistent model of lunar accretion process to explain initial temperature distribution 18 p2725 A72-36291
- Velocity structure and properties of the lunar crust. 18 p2725 A72-36292
- Spiral galaxies self gravitating cold disk model, considering equilibrium state, instability, oscillation modes, bending motions, pressure effects and angular momentum distribution 18 p2725 A72-36386
- Expanding universe models showing particle pairs annihilation at critical temperatures 18 p2725 A72-36525
- Polarization and velocity field in the galaxy M 82. 18 p2727 A72-36729
- The metal-to-hydrogen ratio in F1-F5 stars, as determined by a model-atmosphere analysis of photoelectric observations of a group of weak metal lines. 18 p2727 A72-36737
- A working model for sunspot umbrae. 18 p2727 A72-36740
- Geometrical study of the shape and orientation of the tail of Comet Bennett /1969/ 18 p2728 A72-36764
- Binary, rotatory and oscillatory theories on pulsar existence, considering energy emission and Maxwell equations 18 p2728 A72-36765
- Radiative opacity and calculation of stellar models 18 p2728 A72-36766
- Underluminosity and magnetic fields in beta Lyrae. 18 p2729 A72-36982
- Lunar electrical conductivity. 18 p2729 A72-37000
- Lunar gravitational field, relief and internal structure, suggesting two layer model and crust thickness change relation to field characteristics 18 p2730 A72-37151
- On the ability of the luminosity-volume test to reveal the statistical evolution of the luminosity of quasi-stellar sources. 19 p2854 A72-37226
- The correlation of redshift with magnitude and morphology in the coma cluster. 19 p2854 A72-37228
- The structure of the Coma cluster of galaxies. 19 p2854 A72-37229
- Hydrostatic oxygen burning in stars. II. 19 p2854 A72-37236
- Linear pulsations and stability of differentially rotating stellar models. I - Newtonian analysis. II - General relativistic analysis. 19 p2855 A72-37247
- Computational models of gravitationally interacting galaxies. 19 p2855 A72-37344
- Russian book - Physics of the earth and planets: Figures and internal structure 19 p2856 A72-37474
- Double system HD 175514. III - Analysis of 1968 observations 19 p2858 A72-37810
- Pulsar properties correlation with radially oscillating coherent plasma of electron-positron pair production by strong electric field around central object 19 p2859 A72-37892
- Extent of information that can be obtained from the luminosity loss curves of eclipsing systems with extended atmospheres 19 p2860 A72-37953
- Single body and stellar cluster models of quasars and galactic nuclei stability, noting neutron and collapsing star lifetimes 19 p2862 A72-38052
- Direction of trailing in spiral galaxies 19 p2863 A72-38067
- Rotatory perturbations in anisotropic cosmology 19 p2864 A72-38078
- Secular stability. I - A Population I star near the main sequence. 19 p2864 A72-38099
- Pulsars as stellar population, considering physical models, pulse emission radiation mechanism and use in galaxy studies 19 p2865 A72-38476
- Neutron star matter properties and model calculations, investigating magnetic field decay 19 p2865 A72-38482
- Models concerning the kinematics of star clusters 19 p2866 A72-38489
- Hydrodynamic model calculations for dynamically unstable supermassive stars. 19 p2866 A72-38490
- A preliminary model for the shell ionisation of the nova RS Ophiuchi. 19 p2866 A72-38504
- Astronomical models for matter sources leading to galaxy formation, considering source nature and origin 19 p2867 A72-38505
- Chronology of first phases of formation of solar system solid objects, meteorites and primitive lunar rocks, describing models 19 p2867 A72-38548
- The influence of local conditions in the interstellar medium upon star formation. 19 p2868 A72-38699
- One fluid solar wind model prediction from corona base density and temperature for parameters at earth 19 p2863 A72-38733
- Electromagnetic background radiation in universe, discussing relic radio emission, energy density, hot model isotropic extragalactic component isolation, intergalactic gas, radio sources and quasars 19 p2854 A72-38815
- Differentially rotating magnetoid model for quasar and radio galaxies matter ejection and luminosity mechanisms in terms of magnetic field evolution and current sheet generation 20 p2965 A72-38903
- Observational evidence against supernovae being the source of the universal X-ray background. 20 p2965 A72-38906
- Hydrodynamic model of white dwarf envelope thermonuclear runaway evolution producing nova outburst, computed for various CNO nuclei initial abundances 20 p2966 A72-38908
- Interstellar medium hydroxyl radiation model, considering amplified spontaneous emission and hot spots 20 p2964 A72-38919
- The masses, densities and moments of inertia of Uranus and Neptune. 20 p2967 A72-39184
- An estimate of stellar wind mass loss during the red giant phase of evolution. 20 p2967 A72-39187
- Energy spectrum and composition of pulsar-accelerated cosmic rays. 20 p2964 A72-39343
- Moon model - An offset core. 20 p2969 A72-39374
- Statistical analysis for best fit of compact X ray object spectra to black body, bremsstrahlung and power law models 20 p2969 A72-39387
- Galaxy formation in generic dust filled anisotropic cosmology, analyzing density perturbations growth rate 20 p2972 A72-39872
- Examples of multiple solutions for equilibrium stars with helium cores. 20 p2973 A72-39878
- On the influence of the opacity values on static stellar models. I - Horizontal branch stars. 20 p2973 A72-39879
- Local Vogt-Russell theorem confirmation by linear approximation for stellar structure nonlinear differential equations, discussing equilibrium model local uniqueness and stellar stability 20 p2973 A72-39888
- Structure of spherically symmetrical clusters in the relaxation phase 20 p2974 A72-40022
- The Robertson-Walker cosmology and the Friedmann cosmology 20 p2975 A72-40071
- Model of a stationary star cluster of high binding energy 21 p3103 A72-40401
- Interaction between weak gravitational waves and a gas 21 p3084 A72-40402
- The origin and form of the galactic magnetic field. II. 21 p3104 A72-40479
- Solar wind models of energy transport mechanisms and nonthermal heating requirements, comparing predictions with spacecraft observation 21 p3100 A72-40484
- Spatially homogeneous general relativistic Bianchi cosmological models with diagonal metrics, noting field equations simplicity 21 p3104 A72-40569
- Weinberg model application to hot universe of weakly interacting particles at nonzero temperature, noting long range character 21 p3084 A72-40726
- Gravitational radiation interaction with background fluid of collisionless particles with zero rest mass in homogeneous isotropic Friedmann universe 21 p3105 A72-41028
- Numerical model of NGC 7662 consistent with line strengths and ratios, considering double shell structure and central star flux deviation from black body 21 p3105 A72-41033
- Statistical mechanics of light elements at high pressure. II - Hydrogen and helium alloys. 21 p3106 A72-41044

The chromospheric continuum observed at the total solar eclipse of 12 November 1966 and a model of the low chromosphere

21 p3109 A72-41328

Oxygen abundances of three population II horizontal-branch stars.

21 p3109 A72-41330

Finite radial oscillations of uniformly rotating gravitating magnetized fluid cylinder model of star formation dynamics

21 p3109 A72-41331

Least squares estimation of cosmological model parameters, comparing confidence limits with Solheim trial method

21 p3109 A72-41440

Cosmological model radiation pressure and density calculation by red shift-stellar magnitude ratios from galactic observations

21 p3109 A72-41441

Inhomogeneous cosmological models in terms of impulse energy tensor, discussing coupled Einstein equations, gauge invariance and Lorentz gauge

21 p3110 A72-41442

Fragments of terra rock in the Apollo 12 soil samples and a structural model of the moon.

21 p3110 A72-41452

Computer-aided numerical experiment of cluster mass increase by accretion in protostar evolution

21 p3113 A72-41754

Differential rotation of polytropic stellar models by structural equilibrium equations, disproving Porfiriev theory

21 p3114 A72-41775

The non-spherical nebulae of Nova Delphini 1967, Nova Vulpeculae 1968/II, and Nova Serpentis 1970.

22 p3221 A72-41999

The decay characteristics of models of solar hard X-ray bursts.

22 p3217 A72-42040

Sodium to calcium ion abundances ratio variation model in interstellar clouds, comparing with pulsar dispersion and LF radio absorption measurements

22 p3224 A72-42383

Double water-bag model stability for plane one dimensional stellar system, computing eigenfrequencies and eigenfunctions

22 p3224 A72-42384

Lunar thermal history model, considering nonuniform initial composition, radioactive element partitioning and melt cutoff value

22 p3225 A72-42529

The moon's thermal state and an interpretation of the lunar electrical conductivity distribution.

22 p3226 A72-42531

Cool supergiant stars atmospheric model for chemical composition change effects due to nuclear burning cycle

22 p3227 A72-42556

Internal dust effects on nebulae structure and spectrum, solving radiation transfer equation for spherical models with nonisotropic scattering

22 p3227 A72-42558

Effective temperatures of massive stars as a function of chemical composition and mass.

22 p3227 A72-42560

Nucleosynthesis theory for advanced thermonuclear evolution models of massive stars from helium burning through final hydrodynamic stages

22 p3227 A72-42561

Equation of state of neutron-star matter at sub-nuclear densities.

22 p3228 A72-42564

Neutron star model for magnetic field and superfluidity effects on cooling during pulsar stage

22 p3228 A72-42565

Extragalactic object categorization according to IR luminosities, considering radiation mechanism models and IR spectra relation to radio spectrum

22 p3228 A72-42571

Interstellar circular polarization - Data for six stars and the wavelength dependence.

22 p3228 A72-42572

Exact expressions for the properties of the zero-pressure Friedmann models.

22 p3229 A72-42890

21 cm observations of NGC45.

22 p3229 A72-42995

Protoplanet cloud model of solar system as flat gas-dust disk, discussing density profile, gravitational stability and mass loss

22 p3333 A72-43236

Quasi-stationary spherical system structure model for stars of different masses with isotropic velocity distribution

23 p3334 A72-43242

The emission-line spectrum of Cygnus A.

23 p3334 A72-43251

Sunlight scattering by double reflection on rough and absorbing surfaces, deriving fractional circular polarization from models for comparison with observation

23 p3334 A72-43254

Numerical models for He stars structural evolution, considering main sequence models of 1-8 solar masses and different carbon enrichments

23 p3334 A72-43258

Gamma radiation of Magellanic Clouds and metagalactic origin of cosmic rays.

23 p3328 A72-43264

Joining of two semiclosed worlds and a cosmological model of matter-antimatter asymmetry.

23 p3336 A72-43489

The cosmological evolution of radio sources of large angular extent.

23 p3336 A72-43554

Quasars as images of Seyfert nuclei.

23 p3336 A72-43559

Extended horizontal branch loci.

23 p3337 A72-43830

Galactic evolution - Program and initial results.

23 p3337 A72-43832

Quasar red shift relationship to cosmological distance, considering explanation in terms of gravitational and Doppler effects and unknown process

23 p3338 A72-43993

Calculation of stellar and diffuse radiation for a plane-parallel semiinfinite model of the Galaxy

23 p3338 A72-44027

Numerical models of elliptical galaxy based on rotational speed and integral equations for mass distribution

23 p3338 A72-44033

On irrotational Bianchi-type universes in the Brans-Dicke cosmology.

23 p3314 A72-44314

Interaction of the solar wind with the neutral component of the interstellar gas.

23 p3332 A72-44507

Venus high albedo, discussing compound reflecting layer and liquid Hg cloud models

24 p3436 A72-44692

The lunar conductivity profile and the nonuniqueness of electromagnetic data inversion.

24 p3436 A72-44693

Accretion disc models for compact X-ray sources.

24 p3435 A72-44828

Resonance effects on second order anharmonic pulsational amplitudes for polytropic main sequence evolutionary models, classifying Cepheid-type pulsators

24 p3437 A72-44832

Linear polarization survey for galactic background radiation at 1415 MHz in North Polar Spur, Cetus Arc and Loop III, noting continuous maxima shift

24 p3438 A72-44835

Luminosity variation in the one-zone Cepheid model.

24 p3438 A72-44837

On the physical nature of cosmic neutrino creation. I - Cosmological models with continuous creation. II - Cosmological models without continuous creation.

24 p3439 A72-44974

Lunar composition in terms of evolutionary mode based on inhomogeneous planetary accretion and high temperature condensation

24 p3439 A72-44977

Idealized homogeneous and nonisotropic cosmological models with electromagnetic and massless scalar fields, noting Einstein equations

24 p3442 A72-45246

Conditions in the early solar system, as inferred from meteorites.

24 p3445 A72-45458

Solar oblateness and neutrino flux measurement experiments, discussing agreement with solar interior and evolution models

24 p3446 A72-45527

ASTRONOMICAL OBSERVATORIES

NT HEAO

NT OAO

NT OSO

NT OSO-E

Abastumani Observatory 70 cm meniscus telescope, determining performance from primary focus field data

03 p0359 A72-13498

Laser satellite range measurement at Ondrejov astronomical observatory, describing radar system and experiment design

03 p0326 A72-14332

Spaceborne Uvicon/Celeste astronomical observatory for stellar UV TV pictures, discussing system design requirements

08 p1170 A72-21958

Radar equipment complex in Dushanbe for upper atmosphere wind measurements in meteor physics studies

09 p1308 A72-22506

Arecibo Observatory radio-radar telescope design and operation, discussing reflector wire mesh surface, computer control and data acquisition, ionosphere and pulsar studies and interferometry

10 p1459 A72-24310

Lick observatory image-dissector scanner for faint astronomical spectra, describing design and performance of system based on individual photon pulse counting and memory storage

11 p1631 A72-25691

Hale observatories computer system design for telescope control and data handling, using solid state techniques

11 p1601 A72-25696

Paris Observatory Danjon astrolabe observation of latitude variations, obtaining periodograms by Fourier analysis

12 p1868 A72-27217

Arecibo observatory research, discussing pulsars, radio source scintillation and ionospheric heating

12 p1795 A72-27427

K-2 astrophysical rocket observatory for far UV and X ray solar radiation recording, discussing trajectory, orientation and stabilization, electric and spectrographic instrumentation

14 p1263 A72-30970

Cerenkov counter for astronomical observatory high energy cosmic ray experiments, discussing UV-reflecting paint, radiator and photomultiplier positioning improvements

15 p2234 A72-31536

Astronomical observations from astrophysical observatory onboard orbital space station controlled by astronaut, discussing telescope orientation outside of spacecraft

15 p2242 A72-32740

Construction and optical equipment of astrophysical observatory Orion onboard Salyut space station, discussing mirror telescope, spectrograph and star tracker

15 p2242 A72-32741

Orion spaceborne astronomical observatory automatic control system for instrument orientation and star tracking, discussing servomechanism and pulse duration modulation

15 p2242 A72-32743

Spectrograph for Orion spaceborne astronomical observatory on Salyut space station calibrated with synchrotron radiation from particle accelerator

15 p2242 A72-32744

Photographic characteristics of high resolution film for Orion spaceborne astronomical observatory spectrograms, discussing aerospace environment effect on sensitivity and physicochemical properties

15 p2243 A72-32745

Book on Soviet astronomical reflecting telescopes, paraboloid mirrors, computer control, microphotometers and image converters

17 p2553 A72-34623

Corrections to the right ascensions of FK4 according to observations of fundamental star series with the meridian circle of the Cerro Calan Observatory /Chile/

19 p2859 A72-37911

Ground based optical astronomy developments, emphasizing faint objects positional observation, trigonometric parallaxes, data analysis and measuring techniques

19 p2865 A72-38477

A method of calculating the lag of the phase photoelectric installation of a time service

21 p3058 A72-41769

Figl astrophysical observatory design and instrumentation, describing solar radiation insulation, computerized data reduction, area scanning photoelectric photometer and Cassegrain spectrograph

22 p3178 A72-42541

Space astronomical observatory mission planning, analysis and operation and data utilization in terms of space and ground facility instruments and support subsystems

24 p3382 A72-45530

UV and IR observations of galactic and intergalactic matter from space stations, noting spatial resolution increase

24 p3446 A72-45532

Remotely controlled astronomical observatory telescope Cassegrain focus, evaluating computerized automated electronic system advantage over conventional instrument

24 p3405 A72-45543

Manned and unmanned space-based astronomical observatory systems pros and cons, discussing experiment management complexity and cost reduction

24 p3447 A72-45546

ASTRONOMICAL PHOTOGRAPHY

Southern radio sources optical identification by photography using fiber optics image tube

02 p0285 A72-12795

Trapezium type star systems photographic observations, presenting rectangular coordinates and relative positions

02 p0286 A72-12878

Minor planet Eros photographic observations by long-focus refracting telescopes and Ross cameras at various Yale observatories, tabulating ephemerides [AD-737017]

02 p0286 A72-12894

Astronomical photographic emulsions and phenidonehydroquinone developer relative detective quantum efficiency measurements

03 p0352 A72-13007

Coronal events in 5303 A wavelength, discussing loops and arches and slow and fast events from photographic recordings

03 p0422 A72-13209

Solar spectra photographic recording technique, using spectrographoheliography method with data reduction

03 p0429 A72-13313

Solar corona observations during total eclipse of 22 September 1968, presenting photographs, polarization measurements, photometric data, structure and isophotes

03 p0434 A72-13492

Solar limb flare observations on 4 November 1968, presenting photographs and intensive green coronal luminescence

03 p0434 A72-13493

Solar photospheric facula blue light limb photographs, determining spatial variation in contrast levels

03 p0434 A72-13494

Interference fringes production from binary stars focal images obtained with Lallemand electronic camera

03 p0435 A72-13798

Solar K corona intensity and electron density determination from photographs without eclipse

04 p0574 A72-14924

Electronographic photography of 3C 173 radio source and stars in same field

04 p0574 A72-14975

Large aperture ratio wide field VCN-UV camera exploration of night sky, presenting isophotes of zodiacal light and Milky Way

04 p0525 A72-15685

Planetary nebulae NGC 2392, 6210, 6826, 6720 and 6853 observations, presenting monochromatic photographs and isophotic contours

05 p0713 A72-16021

Mercury trajectory across solar disk plotted by telephoto lens cameras, for determining position angles, disk contact times and relative angular velocity

06 p0882 A72-17934

Solar magnetic field filamentary structure based on analysis of photospheric photographs and presunrise spectrograms obtained during Soviet stratospheric observatory flight

06 p0886 A72-18100

Jovian belts, zones, great red spot, white ovals and atmospheric rotation and circulation from methane photographs analysis, comparing to earth atmosphere

06 p0889 A72-18331

Solar eruptive prominence observations and photographs on 3 May 1971 at 0903-1029 UT with maximum height of 540,000 km

07 p1082 A72-20298

Tago-Sato-Kosaka comet isophote picture of 5 February 1970, noting tail composition, photographic magnitude and emission spectrum

08 p1229 A72-20831

Comets visual brightness determination by astronomical photographic photometry

08 p1229 A72-20834

Wolf-Rayet stars identification in spiral galaxy M33 /NGC 598/ from narrow band interference filter photographs, tabulating apparent magnitudes and emission indexes

09 p1382 A72-22281

Stellar magnitude equation for 400 mm photographic telescope, correcting star coordinates measurements

09 p1311 A72-23060

Delphinus Nova positions determination from plates obtained with photographic telescope with/without diffraction gratings

09 p1389 A72-23067

Tago-Sato-Kosaka comet positions determination from plates obtained with photographic telescope, tabulating averaged spherical coordinates

09 p1389 A72-23068

Photographic measurements of Saturn, observing atmospheric belt latitudes, ring dimensions and southern hemisphere bright spot rotation

10 p1531 A72-23711

Atmospheric vertical shear at visible cloud level in Jupiter equatorial zone from blue and red wavelength photographs

10 p1531 A72-23712

Photographic telescope Gautier used for photographs of moon together with stellar background, noting reduction method for lunar positions deduction

11 p1716 A72-25771

Asteroidal positions from plates from Zeiss astrograph at Turin Observatory, discussing reduction methods and error analysis

11 p1717 A72-25901

Compact galaxies morphology and related properties from blue and red prints of Palomar Sky Survey, correlating to color and apparent magnitude

11 p1717 A72-25902

Photographic observation of times of first and second contact and maximum phase for 15 February 1971 partial solar eclipse, discussing instruments and materials

11 p1717 A72-25903

Magnetically unaffected Fe I line profiles in sunspots from high resolution photographic spectra observation

12 p1867 A72-27205

Photographic position of comet Ikeya-Seki, presenting data reduction procedure

12 p1868 A72-27220

Martian storm of 1971, describing development, decline, structure and photographic data

12 p1870 A72-27425

Slit spectrogram and direct photograph observation of inner corona fine structure during 7 March 1970 solar eclipse, describing line and continuum intensities

13 p2042 A72-29533

White light and XUV coronas on 7 March 1970 from rocket photographs, comparing with X ray, Lyman alpha, Fe XIV and IR eclipse photographs

13 p2031 A72-29542

Polarization-color effect in K corona during 7 March 1970 eclipse observation, using Wollaston prism and filter combination

13 p2043 A72-29544

Jet aircraft photographic observation of solar corona polarization during March 1970 solar eclipse

13 p2043 A72-29545

Celestial pole region photographs obtained with TV equipment, emphasizing observations of faint meteoroids and gas trails

13 p2044 A72-29648

Photographic records of sunspot umbrae showing bright penumbral filament penetration

13 p2045 A72-29713

Spicular field morphology near solar limb from photographs taken with H alpha filter

15 p2305 A72-31512

Lunar orbital photography of astronomical and geophysical phenomena during Apollo 15 flight, noting solar corona and Milky Way

15 p2236 A72-31974

Mars violet haze and blue clearing for Syrtis Major-Arabia from photographic and photoelectric data

15 p2311 A72-32086

Alpha Lyra and beta Cen spectrograms by Orion observatory onboard Salyut space station, noting veiled and overexposed photographic films

15 p2316 A72-32742

Photographic characteristics of high resolution film for Orion spaceborne astronomical observatory spectrograms, discussing aerospace environment effect on sensitivity and physicochemical properties

15 p2243 A72-32745

Macroscopic velocity fields in solar prominence based on solar spectra and monochromatic photographs, proposing helical model

15 p2318 A72-32779

Photographic technique to obtain isophotic contours of solar corona polarized light during total eclipse

16 p2393 A72-33624

The solar spectrum - Wavelengths and identifications from 60 to 385 angstroms.

17 p2600 A72-35319

Earth based Mars photographic observations with direct image transmission via TV system, determining rotation period

17 p2619 A72-35956

Observations of six supernovae

18 p2728 A72-36762

Preliminary analysis of the solar image quality in the 'Amici' dome of the Arcetri Astrophysical Observatory

18 p2728 A72-36767

Mercury trajectory across solar disk plotted by telephoto lens cameras to determine position angles, disk contact times and relative angular velocity

18 p2730 A72-37158

Positions of the major planets and the moon observed at the 0.33 M photographic equatorial

19 p2858 A72-37856

Certain results of the statistical processing of a large series of large-scale television images of stars

19 p2860 A72-37957

Wide-angle photographs of the southern sky as a contribution to the planar photometry of the Galaxy

21 p3102 A72-40275

Image intensifier systems and their applications to astronomy.

22 p3181 A72-42989

Polarization of emission in the IC 4592 and IC 4601 nebulae

23 p3338 A72-44032

A meteor spectrum in the infrared region.

23 p3341 A72-44473

Coordinates of features on the Mariner 6 and 7 pictures of Mars.

24 p3436 A72-44695

Ground observation for outer planets natural satellites ephemeris, using astrometric telescopes, photographic and plate reduction techniques

[AIAA PAPER 72-904]

24 p3443 A72-45426

Photographic observations of variable stars in the proximity of NGC 6830

24 p3448 A72-45683

Photographic observations of Mars at the Main Astronomical Observatory, AN USSR during 1963-1967

24 p3448 A72-45686

ASTRONOMICAL PHOTOMETRY NT STELLAR SPECTROPHOTOMETRY

ASTRONOMICAL PHOTOMETRY

Icy halo influence on photometric continuum of comet Burnham within cometary head model

01 p0125 A72-10080

Cometary head model for photometric profiles of carbon molecular emission in comet Burnham assuming icy grain halo

01 p0125 A72-10081

Interplanetary and terrestrial dust detection, discussing zodiacal light photometric measurements by Helios space probe and light pressure, solar wind and Poynting-Robertson effect

01 p0126 A72-10201

Calibrations consistency of UVBY Beta and G and GNKMF photometries of binary stars with G or K giants and A or F main sequence components

01 p0132 A72-11014

Soviet monograph on variable stars observation covering photographic photometry, photoelectric observation, image processing devices and computer techniques

02 p0279 A72-12122

Photometric meteor mass determination, using models relating radiation intensity, meteor velocity, atmospheric density and instantaneous luminous flux

02 p0282 A72-12334

Photoelectric and visual timings of occultations for lunar motions, comparing accuracy and systematic instrument errors

03 p0420 A72-13127

Lunar surface altitude measurements, considering difficulty due to reference level absence and accuracy improvement by photometric procedure

03 p0421 A72-13195

Magellanic Clouds hot supergiants color-magnitude arrays from spectroscopic and photometric measurements

03 p0424 A72-13253

Single channel photometer measurement possibility in UVB magnitudes of variable stars

03 p0359 A72-13497

Soviet book on long period variable stars covering spectral data photometric characteristics, spatial and kinematic properties, absorption effect and evolution

03 p0439 A72-14224

Markarian galaxies photometric observations, presenting emission line intensities and UVB magnitudes

04 p0578 A72-15309

Photometric standard star 29 Piscium abundance analysis with flux constant hydrogen line blanketed model atmospheres

04 p0578 A72-15317

Faust project history, scientific objectives and present status, discussing stars, nebulae, quasars point sources and galactic photometry

04 p0583 A72-15691

Globular clusters NGC 1851 and 2808, reducing plate material with iris photometer

05 p0711 A72-15761

Jupiter Red Spot 1968-1970 isodensity maps, deriving east-west and north-south photometric profiles for asymmetries

05 p0712 A72-15766

Compact galaxies photometry, determining historical variability from photographic plates obtained by large aperture cameras

06 p0880 A72-17886

Structure, absolute photometry and polarization of corona from solar eclipse observation on 22 September 1968

06 p0883 A72-18026

Jovian atmosphere effect on photometric observations of beta Sco C occultation by Jupiter on 13 May 1971

06 p0886 A72-18153

Lunar photometric studies, discussing surface light scattering properties, data reduction and relative and systematic errors in brightness

06 p0817 A72-18224

Infrared telescopes /light collectors/, discussing diameter, photography, photometry and spectroscopy

06 p0818 A72-18298

High speed photometry of nova variables with white dwarf and late-type binary star flickering, using Cassegrain focus

06 p0889 A72-18332

Southern globular clusters /NGC 6362 and NGC 6752/ photometric standards, stellar photographic and color-magnitude diagrams

07 p1069 A72-19076

Isophote equidensity role in astronomical photometric investigation of solar corona, galactic nebulas, comets and extragalactic stellar systems

07 p1082 A72-20301

Comets visual brightness determination by astronomical photographic photometry

08 p1229 A72-20834

Quasars and Seyfert and N-galaxies compact nuclei radiation polarization from polarimetric and photometric observations

08 p1234 A72-21281

Martian violet clouds photometric studies, determining monochromatic albedo, optical thickness and Junge parameter

08 p1237 A72-21827

Photoelectric measurements of brightness of Galilean satellites of Jupiter as function of solar phase angle
08 p1238 A72-21831

Camera tube used in Faust program of spatial and astronomical UV photometry and spectrophotometry
08 p1169 A72-21953

UV/visible image converter for use with TV camera tubes for astronomical photometry and spectroscopy from satellites and sounding rockets
08 p1169 A72-21955

Electronic cameras to record and measure weak stars 1000-11000 Å, noting atmospheric turbulence suppression and night sky brightness reduction
08 p1170 A72-21962

Quasi-stellar radio sources spectroscopic and photometric observations, determining spatial distribution and bivariate radio and optical luminosity function
09 p1382 A72-22279

Photoelectric Fabry-Perot measurements of M8 and M42 nebulae H alpha and forbidden N II emission lines profiles, determining temperatures and turbulent motions
09 p1390 A72-23528

Photoelectric observation of eclipsing contact binary 44 i Bootis period changes
09 p1391 A72-23534

Eight color intermediate band photometric three dimensional star classification system, taking into account spectral classes, absolute magnitudes, Fe/H ratios and interstellar reddening
09 p1392 A72-23546

Mars south polar cap surface roughness and photometric function from Mariner 7 UV spectrometric experiment
10 p1531 A72-23708

Photometric UVB and polarimetric observations of rotation period, polarization curves and phase coefficients of asteroid Flora, comparing with moon
10 p1531 A72-23709

Negative search for post-eclipse brightening of Io and Europa satellites in 1970 based on single beam photometric observation
10 p1532 A72-23714

Optical properties of nuclei of normal, Seyfert and N-type galaxies and quasars from spectrographic and photometric observations
10 p1534 A72-23902

Peculiar A stars in open cluster Tr 2 region from objective prism plate searches, showing membership by photometrical characteristics and proper motions
10 p1545 A72-24828

Satellite photometric observation of diffuse celestial sources such as Milky Way, zodiacal light and gegenschein
10 p1546 A72-24863

Stellar physical parameters computed from multicolor photometric data on extra-atmospheric magnitudes by maximum likelihood method
11 p1715 A72-25296

Eclipse analyses confidence in eclipsing binary photometric solutions, discussing consistency with stellar interior model density distributions and interactions between member stars
11 p1716 A72-25677

III-V metal photocathodes for near IR and shorter wavelengths, noting performance improvements over conventional cathodes
11 p1630 A72-25683

Integrating silicon target vidicon photometer for two dimensional photometric images of planets and stars
11 p1631 A72-25686

Multichannel area stellar photometer using photosensitive cell array for individual photoelectron counting, applying to autoguidance
11 p1631 A72-25690

Rotating analyzer astronomical photopolarimeter automation by on-line computer control system
11 p1600 A72-25695

Structure, absolute photometry and polarization of corona from solar eclipse observation on 22 September 1968
11 p1719 A72-25962

Close binary stars photometric measurement with electronic camera, noting magnitude difference determination from recorded images
12 p1866 A72-27203

Milky Way spiral structure and star distribution, discussing photometric methods
12 p1875 A72-27967

Photometric meteor mass determination, using models relating radiation intensity, meteor velocity, atmospheric density and instantaneous luminous flux
13 p2039 A72-29218

Rocket-borne coronagraph photometry of solar corona during 7 March 1970 eclipse for streamer analysis
13 p2043 A72-29543

Satellite photometric observatory for solar corona intensity and polarization measurements during 7 March 1970 total eclipse
13 p2043 A72-29546

Relative brightnesses along solar radius from density photometry of corona at eclipses
13 p2046 A72-29715

Lunar eclipse of 25 September 1965, observing penumbra densities and isophotes in B and V spectral regions by photoelectric photometry
14 p2161 A72-30915

Photometric characteristics of two types of eruptive binary stars differing in hot spot brightness
15 p2305 A72-31340

Spherical mirror camera for southern galaxy planar photometry, discussing photographic calibration methods
15 p2306 A72-31597

Mars nonpolar region photometric and topographic characteristics from Mariner 6 and 7 UV spectrometer observations
15 p2311 A72-32084

Surface roughness effects on Mars photometric properties, allowing for scattering in terms of Minnaert law
15 p2311 A72-32085

Mars violet haze and blue clearing for Syrtis Major-Arabia from photographic and photoelectric data
15 p2311 A72-32086

Photometric search for Venus halo effect during 1970 inferior conjunction in relation to brightness maximum and ice in cloud tops
15 p2312 A72-32089

Mercury magnitude determination near superior conjunction with aid of coronagraph photography and photometric calibration
15 p2312 A72-32090

Mercury diameter measurement by photoelectric Hertzprung method during transit on 9 May 1970
15 p2312 A72-32091

IR photometry of IR-OH sources, showing IR colors correlation with velocity separation of OH emission peaks
15 p2315 A72-32711

Photometric, photographic and spectroscopic observations of Seyfert galaxies NGC 1068 and 1566, noting nuclear luminosity and surface brightness
15 p2315 A72-32713

Radio source Oj 287 photometric and polarimetric observations, noting optical intensity and plane polarization variability
16 p2452 A72-33134

Mars surface mapping from spectrophotometric studies of surface materials photometric function, composition and distribution, suggesting color due to limonite-stained soil particles
16 p2457 A72-33616

Radio sources reidentification in field of Coma Cluster of galaxies by Schmidt telescope
16 p2458 A72-33719

Local population II stars density upper limit in terms of mass-luminosity ratio based on U, B and V photometric observations
17 p2604 A72-34442

Photometric observations of Naro-Chavira IR stars, noting variable nature predominance
17 p2604 A72-34443

Photoelectric observation of H alpha, sodium deuteride and He solar umbra line profiles, using pressure scanning spectrometer
17 p2608 A72-35082

Some optical properties of the Venusian atmosphere and possible interpretations of photometric and polarization measurements
17 p2610 A72-35211

Photometric radii of Io and Europa.
17 p2619 A72-35946

Some photometric parameters of the minor planet 2 Pallas.
18 p2723 A72-36086

Physical observations of comets. XVII
18 p2726 A72-36722

Photometric behaviour of Saturn's rings as a function of the saturnocentric latitudes of the earth and the sun.
18 p2727 A72-36735

Observations of planetary nebulae at 1.65 to 3.4 microns.
19 p2854 A72-37233

Luminosities and motions of the F-type stars. II - Metal-deficient stars.
19 p2855 A72-37238

Correlation study of geodetic refraction effect on astronomical refraction anomalies for solar light source observation at large zenith distances
19 p2855 A72-37348

Russian book - Refraction of light rays in the atmosphere
19 p2834 A72-37448

Spectrophotometric study of eclipsing-variable system components. I
19 p2858 A72-37811

Multicolor photometry of the NGC 5194/5195 double system
19 p2858 A72-37812

Spectrographic and photometric observations of supergiants and foreground stars, in the direction of the Large Magellanic Cloud.
19 p2858 A72-37855

Occultation of beta Scorpii by Jupiter on May 13, 1971.
19 p2859 A72-37890

Certain results of the statistical processing of a large series of large-scale television images of stars
19 p2860 A72-37957

Photoelectric transit observations of Saturn and Mars, showing culmination in universal ephemerides time
19 p2862 A72-37987

Saturn ring thickness estimates according to observations in 1966
19 p2863 A72-38075

Photoelectric photometry of close visual binaries
19 p2866 A72-38499

Design and testing of a nine-channel photometer
19 p2804 A72-38500

Galactic structure at galactic longitudes from 230 to 355 deg on the basis of photoelectric UVB H beta photometry of 55 southern open star clusters
19 p2867 A72-38513

Absolute magnitudes of E and S0 galaxies in the Virgo and Coma clusters as a function of U-B color.
20 p2965 A72-38902

Emission lines and optical continuum of Seyfert radio galaxy 3C 120 from spectrophotometric scans
20 p2965 A72-38905

Photoelectric light curve of Nova Vulpeculae 1968 N. 1.
20 p2973 A72-39883

Far-infrared and uvby photometry of V 1057 Cygni.
20 p2973 A72-39887

Photometric study of the NGC 3587 planetary nebula /the Owl/ observed in H sub alpha light - Structure of hydrogen in the nebula
20 p2973 A72-39890

An Irtran-1 reflection filter for the 20-micron atmospheric window.
20 p2928 A72-39897

Photoelectric observations of the 1971-eclipse of 32 Cyg.
20 p2974 A72-39900

Wide-angle photographs of the southern sky as a contribution to the planar photometry of the Galaxy
21 p3102 A72-40275

Search for high frequency optical variability in X-ray sources.
21 p3100 A72-40685

Photometric analysis of X-ray photographs of sun obtained with rocket-borne zone plate camera in XUV region
21 p3108 A72-41289

High precision stellar electrophotometer design, using two channel single photoamplifier photometer and digital computer for statistical atmospheric noise damping
21 p3056 A72-41447

Comet integral brightness estimation by mathematical analysis of photometric characteristics
21 p3110 A72-41449

Photometric characteristics of Jupiter and Saturn at wavelengths between 0.48 to 0.33 micron
22 p3219 A72-41915

Spiral and halo structure of our galaxy on the basis of optical distance determinations.
22 p3222 A72-42136

Determination of the characteristics of scattering particles in the Venusian atmosphere on the basis of photometric measurements
22 p3223 A72-42215

A photoelectric study of Messier 81.
22 p3229 A72-42975

Galaxies and galactic cluster distance determination from Palomar chart angular diameters related to Holmberg-Vaucouleurs photometric systems
23 p3338 A72-44034

Spectrophotometry of the comet Tago-Sato-Kosaka 1969 IX
23 p3339 A72-44168

Signal-to-energy conversion function in the photometry of solar soft X-radiation with broad-band detectors.
23 p3329 A72-44238

Electronic imaging devices for astronomy from a space platform.
24 p3404 A72-45542

ASTRONOMICAL SPECTROSCOPY

Far UV astronomical studies with moderate spectral and spatial resolution instruments, discussing Lyman alpha line background
03 p0417 A72-13049

Magellanic Clouds hot supergiants color-magnitude arrays from spectroscopic and photometric measurements
03 p0424 A72-13253

Spectrographic observation of hot OB subdwarf HD 149382
03 p0435 A72-13799

Venusian polar tropopause and cloud layer from IR spectral recording in carbon dioxide band near inferior conjunction for crescent regions
03 p0436 A72-13814

Mars short wave line spectra from measurement with reflector, estimating nitrogen dioxide content in atmosphere
03 p0436 A72-13815

Meteor spectrum analysis, presenting tables for Soviet observations
03 p0438 A72-13979

- Radiation transfer by resonant scattering in expanding nebula with applications to quasars having blueward absorption wings 05 p0716 A72-16374
- Radio quiet quasar PHL 957 absorption line spectra obtained at telescope with Cassegrain image tube and multichannel spectrometer and integrating TV camera 05 p0720 A72-16714
- Martian dust storm depth determination from carbon dioxide absorption and abundance observation on Mars by earth based spectroscopy 06 p0890 A72-18348
- Astronomical IR spectroscopy of Alpha Ori, discussing OH line formation, LTE, rms turbulence velocity and abundance 07 p1072 A72-19345
- Spectroscopic observations and classification of luminous galactic nuclei with broad emission lines, discussing gas density, velocity and outflow and electron scattering 08 p1234 A72-21279
- Balloon observations of low energy Scorpius X-1 gamma ray spectrum 08 p1227 A72-21395
- SAS-D borne TV type UV sensitive detector with camera tubes for high resolution astronomical spectroscopy 08 p1169 A72-21954
- UV/visible image converter for use with TV camera tubes for astronomical photometry and spectroscopy from satellites and sounding rockets 08 p1169 A72-21955
- Quasi-stellar radio sources spectroscopic and photometric observations, determining spatial distribution and bivariate radio and optical luminosity function 09 p1382 A72-22279
- Spectroscopic evidence for spectral line structure of visible Venus cloud layers 09 p1386 A72-22670
- Large Magellanic Cloud star membership, comparing Sanduleak catalog based on objective-prism spectroscopy with Fehrenbach-Duflo catalog based on radial velocities 09 p1392 A72-23547
- Spectrophotometric observations of Venus, showing unreliability of evidence for dehydrated ferrous chloride in upper cloud layers 10 p1532 A72-23715
- Seyfert galaxies emission, absorption, IR and optical spectral characteristics, suggesting model with sharp forbidden and Balmer line outer region and broad wing core 10 p1532 A72-23885
- Galactic center radio, IR, X ray, gamma ray and molecular spectral features, considering models for source component emission mechanisms and energy densities 10 p1533 A72-23887
- Seyfert, N-type, compact and radio galaxies spectroscopic properties, noting two dwarf emission line galaxies as possible young galactic nuclei 10 p1534 A72-23896
- Radio-emitting and radio-quiet quasar optical emission and absorption line spectra 10 p1534 A72-23897
- Quasar and galactic nuclei emission line spectral data corrected for interstellar extinction 10 p1534 A72-23898
- Jupiter spectral observations, discussing presence of deuterated methane in atmosphere and comparison with solar spectra for telluric features identification 10 p1539 A72-24347
- Lick observatory image-dissector scanner for faint astronomical spectra, describing design and performance of system based on individual photon pulse counting and memory storage 11 p1631 A72-25691
- Computer controlled coude and Cassegrain scanner telescope spectrometers at McDonald Observatory, discussing design, instrument performance and computer program 11 p1632 A72-25698
- Cometary spectra analysis, noting resonance fluorescence mechanism of emissions 11 p1722 A72-26433
- Low noise receivers in radio astronomy, discussing accuracy requirements for line measurements and very long baseline interferometry 12 p1792 A72-27806
- Astronomical spectroscopy using ultraviolet resolution single Fabry-Perot interferometer in tandem with echelle Hilger monochromator 12 p1811 A72-27942
- Nova Delphini evolution from metallic absorption lines observations before December 1967 maximum, obtaining dispersion variation with wavelength 14 p2159 A72-30741
- Carbon dioxide abundance variations from Venus high resolution spectra, discussing HCl and hydrogen fluoride line formation 15 p2310 A72-31994
- Photometric, photographic and spectroscopic observations of Seyfert galaxies NGC 1068 and 1566, noting nuclear luminosity and surface brightness 15 p2315 A72-32713
- Spectroscopic analysis of condensations density and intensity variations in solar eruptive prominences, discussing hypothetical magnetic field effects 15 p2318 A72-32781
- Astronomical objects spectral lines red shift interpretation in terms of noncosmological origin and photon-photon interactions 16 p2450 A72-32863
- Quasars spectroscopic observations, noting red shift and line spectra errors and corrections 16 p2452 A72-33133
- Studies of extremely young clusters. VI - Spectroscopic observations of the ultraviolet-excess stars in the Orion Nebula cluster and NGC 2264. 17 p2605 A72-34530
- A comparison between the emission-line galaxies NGC 5253 and NGC 5408. 17 p2611 A72-35310
- Internal kinematics of two compact galaxies from spectroscopic observations, noting velocity dispersion, luminosity function and mass/light ratio 17 p2611 A72-35311
- The solar spectrum - Wavelengths and identifications from 60 to 385 angstroms. 17 p2600 A72-35319
- Least squares method for Y Cyg spectroscopic elements improvement based on radial velocity measurements, noting nonexistence of gamma velocity variability 19 p2858 A72-37809
- Spectrographic and photometric observations of supergiants and foreground stars, in the direction of the Large Magellanic Cloud. 19 p2858 A72-37855
- Measurement of the equivalent widths of oxygen A-band absorption lines at different pressures 19 p2837 A72-37959
- Expanding ring in Galactic center from analysis of microwave spectroscopic data, measuring expansion and rotation velocities 20 p2972 A72-39860
- Detection of molecular oxygen in the Martian atmosphere. 21 p3103 A72-40451
- Fabry-Perot spectrometer adjustment for the compensation of Doppler shift from rapidly rotating and rapidly flowing sources. 21 p3053 A72-40607
- The spectrum of N Del 67 and some remarks on chemical composition of the novae envelopes. 21 p3109 A72-41436
- Figl astrophysical observatory design and instrumentation, describing solar radiation insulation, computerized data reduction, area scanning photoelectric photometer and Cassegrain spectrograph 22 p3178 A72-42541
- Astrospectrography with a mirror telescope. II - One-prism spectrograph with 60 deg flint prism 22 p3178 A72-42545
- Spectral investigations of the comet Bennett 1970 II /1969 i/ 23 p3337 A72-43646
- Ionization structure and coarse and fine analyses in planetary nebulae spatial spectroscopic diagnostics based on line profile monochromatic intensity integral equation inversion 23 p3339 A72-44236
- Radial velocity periodic variability determination from shell star 88 Hercules hydrogen lines, obtaining hypothetical spectroscopic binary elements 23 p3340 A72-44237
- Orion nebula continuum spectrum energy distribution from spectrophotometric measurements, comparing color temperature with previously obtained data 24 p3438 A72-44839
- Fast Fourier transform algorithm for astronomical line spectra resolution enhancement, estimating central line intensity, line width parameter and line shape 24 p3438 A72-44841
- Emission and absorption spectral behavior observation by millimeter radio telescopes for molecules in interstellar space of Milky Way galaxy spiral arms 24 p3439 A72-44905
- Orbiting telescopes improved angular resolution and access to UV spectra as advantages in determining stellar composition, mass, luminosity and distance 24 p3446 A72-45531
- ASTRONOMICAL TELESCOPES**
- NT APOLO TELESCOPE MOUNT
- NT HELIOMETERS
- NT PYROHELIOMETERS
- NT SPECTROSCOPIC TELESCOPES
- NT STRATOSCOPE TELESCOPES
- NT X RAY TELESCOPES
- Stellar pair scale technique for determining multiplying factor of ocular micrometer drum in universal astronomical instrument 01 p0064 A72-10197
- Cassegrain type astronomical reflecting telescope design, describing auxiliary equipment 01 p0047 A72-10202
- Red interference filter design for high prominence telescope for H alpha line observation 01 p0064 A72-10203
- Anglo-Australian astronomical optical telescope construction, summarizing project organization, components and system design 02 p0199 A72-11640
- Low energy gamma ray telescope with active honeycomb collimator and anticoincidence detector, describing directivity techniques for galactic sources 03 p0408 A72-13030
- Optical multiplate spark chamber in balloon-borne gamma ray telescope, describing triggering signal from plastic scintillator directional Cerenkov counter and photographic recording system 03 p0353 A72-13035
- X ray astronomy techniques survey, covering image forming telescopes, detectors, nondispersive spectrometers and polarimeters 03 p0353 A72-13037
- Gimbaled telescope/UV spectrophotometer combination with star tracking facilities for use on ESRO TD-1 A satellite 03 p0355 A72-13061
- Solar prominence telescope design parameters and structural dimensions calculation using lens equation 03 p0356 A72-13197
- Abastumani Observatory 70 cm meniscus telescope, determining performance from primary focus field data 03 p0359 A72-13498
- Martian surface relief observation from earth distance, showing telescope resolution requirements above dense atmospheric layers 03 p0438 A72-13983
- OAQ space telescope of 120 inches aperture, discussing structural design, geometric configuration and stabilization and pointing control system [ALIA PAPER 72-201] 05 p0663 A72-16800
- Infrared telescopes /light collectors/, discussing diameter, photography, photometry and spectroscopy 06 p0818 A72-18298
- Cer-Vit glass mirror replacement for AFCRI lunar laser observatory inverted Dall-Kirkham Cassegrain telescope, noting one arc sec resolution from wire and null optics tests 07 p0985 A72-19410
- Small lunar based reflecting telescopes with Cassegrainian and catadioptric optical systems, discussing design and operation 08 p1164 A72-20976
- Telescopic requirements posed by Venus near sun, discussing sky brightness in image plane, atmospheric dust and Rayleigh scattering 08 p1230 A72-20993
- Binocular observation of astronomical objects, discussing binocular design of astronomical telescopes 08 p1165 A72-21087
- Telescope construction for solar prominences observation, discussing reflection prisms effect on light rays path and image displacement 08 p1165 A72-21088
- Stellar magnitude equation for 400 mm photographic telescope, correcting star coordinates measurements 09 p1311 A72-23060
- Integrating two dimensional silicon diode array vidicon astronomical photometer for telescope use 09 p1313 A72-23330
- Ground based IR astronomical telescope detectors, relating F number and optical requirements to near, far, and intermediate IR observation 10 p1481 A72-24249
- Large space telescope /I/ST/ project, discussing instrumentation, observation program and operational characteristics 11 p1630 A72-25681
- Hale observatories computer system design for telescope control and data handling, using solid state techniques 11 p1601 A72-25696
- Astronomical reflector telescope design, describing thermal effects on Al mirror and image intensification 12 p1807 A72-27428
- Astronomical pointing of radio telescopes using on-line computer 12 p1793 A72-27813
- Transistorized oscillators for variable-frequency generators designed to feed synchronous motor drives of equatorial telescopes 14 p2073 A72-30683
- Large astronomical telescopes construction, discussing aspherical surfaces control, grinding, polishing and optical testing procedures 15 p2234 A72-31612
- Astronomical observations from astrophysical observatory onboard orbital space station controlled by astronaut, discussing telescope orientation outside of spacecraft 15 p2242 A72-32740
- Construction and optical equipment of astrophysical observatory Orion onboard Salyut space station, discussing mirror telescope, spectrograph and star tracker 15 p2242 A72-32741
- Extra-atmospheric astronomical studies and instruments, discussing spaceborne, X ray and heavy orbit

ing telescopes and ground-space radio interferometer designs

16 p2462 A72-33516
Operational tests of the AFCRL 152-cm telescope.

17 p2555 A72-35198
Early data from the ultraviolet sky-scan telescope in the TD1 satellite.

19 p2857 A72-37524
Adaptation of the Schupmann medial telescope to a large scale astronomical optical system.

19 p2797 A72-37587
Radio astronomical observations in the 0.9 to 1.5 mm band using a 22-m radio telescope with an n-InSb receiver

19 p2858 A72-37803
Limiting magnitudes of stars in visual telescopic observations /Ground and extraatmospheric locations of instrument and observer/

19 p2859 A72-37907
Lateral chromatic aberration of a double-meniscus telescope in Chile

19 p2801 A72-37919
Experimental investigation of optical aberrations, due to temperature deformation and convective fluxes, by using a nonequal-arm interferometer with a coherent light source

19 p2801 A72-37920
Colorimetric and spectrophotometric gradient systems comparison for bright stars used in automatic telescope pointing control, discussing interstellar absorption

19 p2860 A72-37955
Experimental observations of the instability of stellar images from a bichromatic two-channel television system

19 p2860 A72-37956
Minimum perceivable stellar magnitudes in visual observations by naked eye and telescope, discussing image contrast and angular scale

19 p2860 A72-37961
Design of a system for automatic compensation of atmospheric dispersion

19 p2801 A72-37962
Reduction of the effect of mount deformation on the flexure of the telescope mirror

19 p2801 A72-37967
Method for determining thermal strains in astronomical mirrors

19 p2801 A72-37968
Investigation of the screw turn magnitude of a contact micrometer attached to the Toepfer meridian circle on the basis of observed right ascensions of stars

19 p2802 A72-37975
A program of wide scale pairs for determining the micrometer screw turn magnitude of the Pulkovo ZTL-180 wide-angle zenith telescope

19 p2802 A72-37979
Investigation of the Talcott levels of zenith telescopes and determination of their division value

19 p2802 A72-37980
Process control of the 100-meter telescope - Astronomical concept

19 p2803 A72-38485
Autocorrelation methods to obtain diffraction-limited resolution with large telescopes.

20 p2920 A72-38922
Fine guidance pointing stability of a 120-inch (3 meter) large space telescope /LST/.

[AIAA PAPER 72-853] 20 p2949 A72-39076
Astronomical telescope hybrid pointing control system with double gimbal control moment gyros and orthogonally mounted reaction wheels to achieve extreme accuracy and stability

[AIAA PAPER 72-854] 20 p2924 A72-39138
Gamma quanta recording efficiency and energy determination by gamma telescopes, calculating root-mean-square error of real gamma spectra

21 p3026 A72-40323
Multiple mirror astronomical telescope using laser source light collimated with central Cassegrain system, presenting expected diffraction patterns

21 p3052 A72-40378
A two-element telescope of high collecting efficiency for sub-millimetre astronomy.

21 p3055 A72-40825
Remote transmission of telescope coordinate readings by industrial television

21 p3056 A72-41448
Astrospectrography with a mirror telescope. II - One-prism spectrograph with 60 deg flint prism

22 p3178 A72-42545
OAO 3 satellite Copernicus onboard equipment, discussing UV reflecting and X ray telescopes, attitude sensor, star tracker, solar sensor and computer

22 p3231 A72-42985
A large multiple mirror telescope /MMT/ project.

22 p3180 A72-42988
New optical measurements of planetary diameters. II - Planet Venus.

24 p3436 A72-44694
Solar atmosphere fine structure observation limitations in terms of solar telescope angular resolution

24 p3404 A72-45529

Future orbital observatory modules for stellar and galactic astronomy.

24 p3453 A72-45533
Spaceborne astronomy by synthetic aperture optics for high resolution without cost and weight disadvantages of large telescopes, considering Michelson stellar interferometer

24 p3404 A72-45541
Future giant-aperture orbital space telescope design based on active optics and electro-optical techniques, discussing laser interferometry and precise servomechanisms roles

24 p3405 A72-45544

ASTRONOMY

NT INFRARED ASTRONOMY

NT RADAR ASTRONOMY

NT RADIO ASTRONOMY

NT SPACEBORNE ASTRONOMY

NT X RAY ASTRONOMY

Astronomical research, discussing Venus exploration, stellar evolution quasar structure, Maffei galaxies, black holes, dwarfs and neutron star model

01 p0133 A72-11099
Astronomy - Conference, University of Sydney, Australia, May 1971

02 p0276 A72-11639
Space astronomy techniques - Conference, Munich, August 1970

03 p0352 A72-13026
Astronomy - IAU Conference, Brighton, England, August 1970

03 p0417 A72-13101
Astronomical constants - IAU Conference, Heidelberg, August 1970

04 p0574 A72-15025
UV astronomy techniques and devices, discussing hot stars, stellar chemical composition and interstellar medium

04 p0582 A72-15686
Uniform time systems relevance to precise astronomical observations and accurate determination of irregularities in earth rotation, outlining proposals for time signals

07 p1032 A72-19068
Electronic imaging devices in astronomy, describing TV readout image tubes

07 p0985 A72-19580
Programming and operations of astronomer data acquisition system using NOVA computer

11 p1601 A72-25699
Book on astronomy covering optical and radio telescopes properties and atmospheres of inner and outer planets, stellar lifetimes and evolution, galaxies, cosmology, etc

15 p2306 A72-31516
Report to COSPAR on U.S. space program covering stellar astronomy, lunar and planetary research upper atmospheric physics, earth and life sciences, etc

15 p2337 A72-32006
Report to COSPAR on Indian space program covering organizations, ground station facilities, atmosphere and astronomy studies and international collaborations

15 p2338 A72-32012
Astronomy - Conference, University of Adelaide, Australia, December 1971

16 p2451 A72-33031
Book on stellar astronomy covering H-R diagram, solar system, nuclear energy sources, Milky Way Galaxy, quasars, cosmology, planetology, etc

16 p2453 A72-33275
Atmospheric refraction effects on ground based astronomical observations, using atmospheric model with concentric spherical shells having decreasing density with height

16 p2386 A72-33495
Measures of time in astronomy.

17 p2609 A72-35114
Origin of the planetary systems astronomical evidence in other stars.

24 p3444 A72-45453

ASTROPHYSICS

NT SOLAR PHYSICS

Astrophysical cosmology, discussing universe expansion, Robertson-Walker models, radio sources, quasars, cosmic X ray background, intergalactic media, etc

03 p0426 A72-13268
Nuclear astrophysics review, discussing chemical elements and isotopes abundance and cosmic nucleosynthesis

03 p0437 A72-13842
Black hole prediction in gravitational collapse of star and universe in terms of quantum principle, chemical mechanics and superspace dynamics

05 p0690 A72-16528
Cosmic plasma phenomena in astrophysics, discussing distribution, ionospheric disturbances, magnetospheric waves, solar wind, etc

05 p0723 A72-17217
Astrophysics and general relativity - Conference, Brandeis University, Waltham, Massachusetts, June-July 1968

07 p1073 A72-19426

Astrophysical study of cosmological evolution, discussing evidence from radio source counts and quasar spatial distribution

07 p1084 A72-20471
Shock tube spectroscopy role in laboratory astrophysics, stressing hook method effectiveness for quantitative analysis of shock heated gases in solar abundances determination

08 p1146 A72-21017
Hydrodynamic analogy for astrophysical effects of general relativity theory, analyzing Chaplygin gas motion in three dimensional curvilinear coordinate system

08 p1209 A72-21876
High energy astrophysics - Conference, Erice, Italy, May-June 1971

10 p1532 A72-23883
Local and cosmological irreversibility and time anisotropy theories from thermodynamics, statistical mechanics, astrophysics and quantum-relativity viewpoints

11 p1716 A72-25775
Constraint on astrophysical sources of gravitational waves, using microwave radiometers

11 p1721 A72-26124
Japanese cosmological studies covering evolutionary cosmology, astrophysics, relativity, nuclear physics and metagalactic phenomena

13 p2038 A72-29083
Expanding hot universe evolution from astrophysical cosmology point of view, emphasizing galaxy formation relation to state of matter and radiation in early universe

13 p2038 A72-29084
Astrophysical equipment for Cerenkov radiation measurement from atmospheric showers, discussing source of high energy gamma rays in galactic equator direction

14 p2146 A72-30201
Mars astrophysical observation from Mars 3, describing instruments and measurement results

15 p2308 A72-31901
Astronomical observations from astrophysical observatory onboard orbital space station controlled by astronaut, discussing telescope orientation outside of spacecraft

15 p2242 A72-32740
The equilibrium configuration of the gaseous component of the Galaxy.

17 p2611 A72-35312
Astrophysical theories of supernovae outbursts as stellar evolutionary nonstationary phase in terms of thermal instability of degenerated matter or stellar explosion

18 p2725 A72-36399
Collisional excitation and impact ionization coefficients of hydrogen

19 p2837 A72-37807
German book - Relativistic astrophysics

19 p2868 A72-38721
Lagrangian approach to kinematic-dynamo equations for astrophysical bodies, obtaining variational principle for eigenvalue computation

20 p2966 A72-38911
Figl astrophysical observatory design and instrumentation, describing solar radiation insulation, computerized data reduction, area scanning photoelectric photometer and Cassegrain spectrograph

22 p3178 A72-42541
Russian book - Problems of the physics of nebulae and unsteady stars.

23 p3338 A72-44026

ASYMMETRY
Motion of asymmetric body of revolution in rotating liquid, calculating drag on ellipsoid

02 p0204 A72-12175
Correcting effects of corrugated boundaries on coaxial radiators asymmetry and sidelobes, investigating waveguide hybrid modes induced transverse fields

21 p3029 A72-40516
Constant strength shells theory generalization from axially symmetric to nonsymmetric case, using Von Mises yield condition

21 p3117 A72-40680
Generalized subharmonic response of a missile with slight configurational asymmetries.

[AIAA PAPER 72-972] 22 p3134 A72-42339
Lyman alpha resonance line asymmetry calculation in dense hydrogen plasma, noting disagreement between theory and experiment

22 p3212 A72-42917
Asymmetric imperfections effect on spherical elastic shell buckling strength under uniform external pressure

23 p3351 A72-44104

ASYMPTOTES
Ordinary differential equations convergent solutions growth estimates, computing error function asymptotic growth rate

05 p0683 A72-17000
Book on asymptotic behavior and stability in ordinary differential equations covering linear and nonlinear systems, Liapunov and analytical-topological methods

07 p1026 A72-19184

Asymptotic motion stability for part of periodic and continuous systems variables, deriving solution uniqueness sufficient conditions

09 p1350 A72-22206

Asymptotic almost periodic differential equations solved by introducing semiseparated conditions concept

09 p1340 A72-22246

Difference equation inequalities in sampled data system stability analysis, discussing solution asymptotic behavior

09 p1342 A72-23252

Asymptotic behavior of unperturbed linear and nonlinear perturbed functional differential equations

11 p1677 A72-25524

Ergodic theorems for operators generated by Markov transients, examining asymptotic properties of stochastic learning model

12 p1787 A72-27924

Asymptotic stability of mechanical system with two mathematical pendulums and rod subjected to axial follower, correcting aerodynamic and dissipative forces

12 p1847 A72-27979

Delayed argument linear partial differential equations system integration, constructing asymptotic solution in nonresonant case

13 p1988 A72-30084

Navier-Stokes equation for unsteady asymptotic suction flow over flat plate, plotting velocity distribution profiles

15 p2178 A72-31406

Plane electromagnetic wave diffraction on periodic arbitrary profile array, presenting near and far field asymptotic characteristics

15 p2202 A72-32660

Structural analysis of gravitational field in asymptotic limit at spatial infinity, introducing three dimensional spacelike surface carrying initial data for spacetime

17 p2583 A72-35824

Diffraction by an aperture between two wedges

18 p2712 A72-36938

Asymptotic behavior of solutions of boundary value problems for systems of linear ordinary differential equations with a small parameter by the derivative

20 p2945 A72-39464

Improved criteria for hyperbolic-elliptic motion in the general three-body problem.

21 p3109 A72-41333

Asymptotic motion stability analysis with respect to part of variables, using Liapunov functions for solution boundedness conditions

22 p3204 A72-41901

Vertical asymptotes and bounds for certain solutions of a class of second order differential equations.

22 p3199 A72-42914

Asymptotic behavior of solutions of systems of conservative differential equations

23 p3308 A72-43693

ASYMPTOTIC METHODS

Edge loaded cylindrical shells of resolution nonlinear axisymmetric deformation determination from asymptotic solution of Reissner equations, using multiple scale perturbation technique

01 p0136 A72-10031

Rate-type viscoelastic materials, deriving weak shock structure by wave front, ray and singular surface theories and asymptotic expansions

01 p0101 A72-10033

Semi-Markov process sojourn time within reducible subset of states, examining asymptotic behavior with algorithm developed for linear operators disturbances

01 p0094 A72-11265

Time operator method in creep theory for orthotropic bodies, obtaining asymptotic solutions for laminar orthotropic rod and elastic plate vibration problems

02 p0289 A72-11617

Asymptotic methods application to differential equations in nonlinear solar convection theory at high Rayleigh number, noting discrepancy from numerical integration

02 p0276 A72-11644

Asymptotic method for investigating multiwave interaction processes in one dimensional weakly nonlinear distributed systems with slowly changing parameters

02 p0261 A72-12585

Hf wave scattering in inhomogeneous medium, examining asymptotic methods

03 p0390 A72-13973

Asymptotic methods for complex mixed problems of elasticity related to stress concentration in plates with cracks or inclusions

03 p0449 A72-14102

Asymptotic theory of heat transfer in two dimensional turbulent boundary layers of incompressible fluid at large Reynolds numbers

03 p0459 A72-14390

Weakly interacting waves Langevin equation in fluid, using characteristic functionals and time asymptotic methods

04 p0549 A72-15289

Asymptotically diagonal systems for variational expansions applied to elliptic partial differential equations, estimating convergence rate

04 p0540 A72-15374

Asymptotic theory of diffraction at waveguide open end, using generalization by ray and parabolic equation methods

04 p0489 A72-15385

Short wave asymptotic formulas for shadow zone of plane diffraction, discussing asymptotic solutions for field from point source

04 p0489 A72-15386

Open resonators stability analysis, describing integral equations eigenfunctions and eigenvalues short wave asymptotic expansions

04 p0502 A72-15435

Fabry-Perot open resonators, determining eigenvectors, resonant frequencies and diffraction losses by asymptotic perturbation method

04 p0502 A72-15436

Asymptotic integration method solution of heat transfer equation with constant wall temperature for low speed slip flow regime

[ASME PAPER 71-WA/HT-5] 05 p0599 A72-15866

Asymptotic two dimensional theory of shell structures, comparing with axiomatic formulation

05 p0738 A72-16349

Thin elastic shell postbuckling behavior from asymptotic integration solution for differential equations, permitting dynamic effect modeling

05 p0738 A72-16425

Static perturbation technique functional form for postbuckling equilibrium path analysis by asymptotic approximation, noting relationship to Koiter method

05 p0742 A72-17244

Validity proof of asymptotic methods in oscillation theory of one dimensional nonlinear dynamic systems described by hyperbolic and parabolic differential equations

06 p0839 A72-17681

Infinite homogeneous self gravitating compressed gas media nonlinear condensations, describing finite amplitude motion with asymptotic expansions

06 p0880 A72-17889

Asymptotic theory of turbulent boundary layer in incompressible liquid with positive pressure gradient and injection

06 p0799 A72-17910

Mixed boundary value problem of partial differential equations describing nonlinear viscoelastic vibration of clamped rods, examining asymptotic solution stability

06 p0901 A72-18716

Two point boundary value solution for N-body trajectories, comparing asymptotic with numerical integration solutions for several lunar and interplanetary trajectories

[AIAA PAPER 72-49] 07 p1068 A72-18945

Asymptotically optimal rank algorithms for signal resolution at phase and amplitude detectors outputs

07 p0943 A72-19518

Uniform asymptotic solution near wavefront of transient field propagation in inhomogeneous dispersive media

[AD-745077] 07 p0946 A72-19800

Elasticity theory axisymmetric problem for hollow cone, analyzing stress-strain state and boundary value problem by asymptotic methods

07 p1093 A72-19980

Asymptotic method applications to differential equations solution construction and stability analysis and to stochastic systems

07 p1028 A72-20206

Asymptotic approximation method for damping force as function of velocity from successive oscillations amplitudes measurement

07 p1096 A72-20474

Random vibration theory and Markov processes in nonlinear stochastic systems with probability and asymptotic methods application

08 p1205 A72-20965

Krylov-Bogoliubov asymptotic method for oscillation analysis in time lag systems under pulse inputs

08 p1206 A72-20970

Spectral density estimates for discrete time models of steady nonGaussian random processes, noting dispersion in asymptotic expression

08 p1198 A72-20996

Algorithm for asymptotic behavior approximation of semi-Markov processes with splitting set of states by Markov chain

08 p1198 A72-20997

Algorithm for asymptotic power series for Poisson process residence time function generation in band with delaying screen

08 p1198 A72-20998

Parametric oscillations of nonlinear systems prone to self excitation, using asymptotic method

08 p1206 A72-21243

Asymptotic method solution for boundary value problems for nonlinear differential equations describing transonic and slow supersonic flow past thin bodies

08 p1108 A72-21709

Asymptotic analysis of activation energy limit for radiant ignition of reactive solid with in-depth absorption

[AD-741533] 08 p1255 A72-22044

Grid plates of complex structure, determining stress-strain state by asymptotic solution of boundary value problem for sixth order differential equations

09 p1398 A72-22693

Hartman-Olech theorem to prove asymptotic stability of mechanical system with nonlinear elastic characteristic, analyzing differential equations of motion

09 p1343 A72-23612

Nonlinear diffraction of weak shock waves near rigid wall with sharp bend, obtaining approximate solution by matched asymptotic expansion method

10 p1468 A72-24432

Asymptotic dynamic response of infinite beam on elastic foundation to randomly moving load

11 p1727 A72-25292

Perturbation method for asymptotic solutions of initial value problems for hyperbolic wave equations with small nonlinearities

11 p1676 A72-25355

Nonstationary nonlinear multidegree-of-freedom systems resonant response analysis by asymptotic method, investigating gyroscopic system for combination differential resonances

11 p1629 A72-25422

First order asymptotic matching computational technique for calculation of perturbed moon-centered hyperbola parameters in earth-moon trajectory

11 p1720 A72-25996

Short wave oscillations point source problem near convex curve, deriving asymptotic expression for Green function

11 p1678 A72-26379

Linear multistep methods with variable matrix coefficients for asymptotic numerical integration of ordinary differential equations system

11 p1679 A72-26960

Multiple scale asymptotic method for nonlinear theory of dispersive periodic waves with slowly varying parameters, noting equations for irrotational motion of perfect relativistic fluid

12 p1843 A72-27170

Proximate equations of two dimensional orthotropic shell theory obtained by asymptotic integration method, examining anisotropy effect

13 p2053 A72-28391

Asymptotic approximation methods for boundary layers in singular perturbation theory for linear elliptic partial differential equations in two independent variables

13 p1940 A72-28425

Asymptotic and exact methods for light scattering problems in radiative transport theory, discussing finitely thick plane layer luminescence

13 p2001 A72-28503

Asymptotic expansion method for nonsinusoidal wave processes described by Lagrange-type partial differential equations, using averaged form of generalized Hamiltonian variational principle

13 p2003 A72-28718

Asymptotically bilateral solutions to partial differential equations, using fictitious regions and auxiliary unsteady problem methods

13 p1987 A72-29472

Asymptotic theory of turbulent flows established with bubbles, showing limiting relations existence at increasing liquid discharge rates

13 p1943 A72-29785

Asymptotic solution for velocity distribution in viscous liquid axisymmetric flow in conical diffusers

14 p2070 A72-31006

Russian book on averaging method in nonlinear mechanics covering algorithms and schemes based on variables change, asymptotic methods and applications

15 p2273 A72-31274

Rough surface elastic bodies stress calculation, using asymptotic method of boundary conditions

15 p2327 A72-31736

Transient torsional vibration of asymmetric rotor with limited power supply near critical speed calculated by asymptotic method

16 p2463 A72-32874

Asymptotic solution for inviscid conducting fluid flow past arbitrary wing profile in magnetic field

16 p2434 A72-32929

Asymptotic formula for approximation of mean cycle-slip time of phase locked loops with low SNR and steady state phase error

16 p2371 A72-33211

Supplement to the asymptotic theory of steady turbulent flows with bubbles

17 p2537 A72-34278

Guided elastic wave propagation near curved surfaces and in nonconstant thickness layers, discussing asymptotic solution and applications to Love, Rayleigh and Lamb waves

[ASME PAPER 72-APM-00] 17 p2580 A72-34306

Vibration perturbation of slender rotating beam with end masses, using method of matched asymptotic expansions

[ASME PAPER 72-APM-B] 17 p2625 A72-34318

Finite length inhomogeneous elastic rod free vibration, deriving asymptotic expressions for eigenvalues and eigenfunctions

17 p2625 A72-34320

Asymptotic solutions of inhomogeneous initial boundary value problems for weakly nonlinear partial differential equations.

17 p2574 A72-34342

Critical point regularity conditions and asymptotic solutions to the time stationary, linearized, inhomogeneous solar wind flow problem.

17 p2599 A72-35095

Asymptotically optimal procedures for certain types of moments of cutoff and terminal decisions in sequential estimation

17 p2576 A72-35419

An asymptotic solution for the large deflection of a circular plate with a central hole.

18 p2732 A72-36081

Fluid dynamics problems self similar solutions as descriptions of intermediate asymptotic behavior of solutions for initial, boundary and mixed problems

18 p2709 A72-36388

Asymptotic estimate of steady state solution to Euler equations for ideal incompressible fluid flow with free boundaries

18 p2682 A72-36805

Asymptotic solution of a second-order linear differential system

19 p2824 A72-37382

French monograph - An asymptotic theory of the Boltzmann equation and its application to the study of near continuum flows

19 p2785 A72-37489

Asymptotic method application to wave propagation in nonlinearly elastic rods, describing displacement field by perturbation series

19 p2875 A72-37885

Asymptotic series solution of optimal systems with small time-delay.

19 p2826 A72-38268

Riccati equation asymptotic theory, deriving a priori bound dependence on information and control energy rates and state dimensions

20 p2945 A72-39347

An asymptotic solution for steady flow above an infinite rotating disc with suction.

20 p2886 A72-40015

Elasticity theory axisymmetric problem for hollow cones analyzing stress-strain state and boundary value problem by asymptotic methods

20 p2982 A72-40036

An asymptotic method for the Vlasov equation. III - Transition from amplitude oscillation to linear Landau damping.

21 p3089 A72-40190

Asymptotic theory of an optically thick radiating gas flow past a smooth boundary at moderate radiation strength.

21 p2989 A72-40196

Asymptotic solution of the wave equation with variable velocity and boundary conditions.

21 p3075 A72-40838

The lift coefficient of a supercavitating jet-flapped foil in a free jet.

21 p2992 A72-41236

Numerical and asymptotic methods for solving the problem of complete boundary-layer stabilization

21 p3047 A72-41659

Asymptotic analysis of the behavior of an elastic rod under aperiodic intense loading

21 p3127 A72-41670

Asymptotic representation of the solution of a boundary value problem for a biharmonic equation degenerating into a fourth-order parabolic equation

22 p3198 A72-41899

Asymptotic expansion method for nonsinusoidal wave processes described by Lagrange-type partial differential equations, using averaged form of generalized Hamiltonian variational principle

22 p3204 A72-42095

Asymptotic method for nonlinear wave systems of periodic structure

22 p3155 A72-42657

Asymptotic behavior of solutions of nonlinear parabolic equations.

23 p3309 A72-43979

Velocity, enthalpy and turbulent energy distributions calculation for plane wake behind flat body by asymptotic solution based on turbulence theory

23 p3249 A72-44083

Asymptotic methods of calculating the effectiveness of one variant procedure of selecting operational subchannels in an adaptive multichannel communications system

23 p3266 A72-44207

Estimates of unknown parameter from quantized observations given as sequence of evenly distributed random values, noting optimal grouping equations for general distribution function

23 p3266 A72-44218

Asymptotic behavior of the solutions of the third external boundary value problem for a wave equation with two space variables

23 p3310 A72-44488

On exponential-asymptotic stability properties of Boltzmann's equation and a class of its modifications.

24 p3426 A72-44911

The large Reynolds number - Asymptotic theory of turbulent boundary layers.

24 p3392 A72-45248

A linear asymptotic theory for anisotropic shells.

24 p3460 A72-45473

ASYMPTOTIC SERIES

Matched asymptotic expansions method application to problems with two independent perturbation parameters, considering application to boundary layer and hypersonic flow theory

[ONFRA, TP NO. 1007] 07 p0970 A72-20076

Ordinary linear differential equation boundary value problem solution in form of asymptotic series in powers of small parameter

08 p1199 A72-21462

Fluid dynamics layer-type singular perturbation problems, constructing inner and outer asymptotic approximations with overlapping domains of validity

11 p1615 A72-25502

Numerical check on boundary layer equations asymptotic expansion solutions for Falkner-Skan reverse flow and unit Prandtl number compressible boundary layer with blowing

15 p2219 A72-32589

On the asymptotically spherical deformations of arbitrary membranes of revolution fixed along an edge and inflated by large pressures - A nonlinear boundary layer phenomenon.

21 p3118 A72-40840

Comparison of the classical and the global solutions of the ideal resonance problem.

21 p3085 A72-41047

ATAXIA

Tandem walking on floor with eyes closed as ataxia test for vestibular function assessment

12 p1770 A72-27476

ATELECTASIS

Pulmonary atelectasis and arterial-venous shunting and heart displacement prevention during centrifuging of dogs breathing oxygenated liquid fluorocarbon in water immersion respirator

11 p1579 A72-26609

ATHLETES

Atypical ECG of sportsmen, considering repolarization disorders due to ischemia, lesion, excitability and conduction signs

07 p0924 A72-20575

Longevity and cardiovascular mortality among former college athletes.

24 p3374 A72-45689

ATHODYDS

U RAMJET ENGINES

ATLANTIC OCEAN

Barbados oceanographic meteorological experiment /BOMEX/ sea air interaction program in equatorial Atlantic, using real time synchronous satellite information

15 p2225 A72-31808

Allowance for the ocean surface temperature in monthly weather forecasts for the Northern Atlantic Ocean

20 p2949 A72-39946

ATLAS CENTAUR LAUNCH VEHICLE

Real-time launch vehicle steering program selection. [AIAA PAPER 72-830]

20 p2977 A72-40058

ATLAS LAUNCH VEHICLES

NT ATLAS CENTAUR LAUNCH VEHICLE

ATMOSPHERES

Sound waves radiative damping in isothermal atmosphere, discussing relaxation influence on model response to body force and chromosphere dissipation effect on oscillation

10 p1543 A72-24622

ATMOSPHERIC ABSORPTION

U ATMOSPHERIC ATTENUATION

ATMOSPHERIC ATTENUATION

NT AURORAL ABSORPTION

Rain droplet size distribution effects on microwave attenuation at millimeter wavelengths, comparing calculation with measurement

01 p0027 A72-10406

Rain, snow and hail precipitation effects on radio link signal attenuation, scattering and fading along various transmission paths at millimeter and centimeter wavelengths

01 p0027 A72-10407

Spanish winter anomalous ionospheric short wave absorption observed by high precision ground based measurements

01 p0055 A72-10434

Ionospheric neutral gas wind and altitude effects on Spanish short wave absorption winter anomaly

01 p0055 A72-10435

Quantitative interpretation of correlation mask remote sensors UV, visible and IR spectral data, discussing beam transmittance attenuation by absorption, scattering and emission

01 p0066 A72-10530

Remote sensing of surface radiation temperature topographic variations by precision radiation ther-

mometer equipped aircraft, calibrating for atmospheric attenuation

02 p0210 A72-11803

Computer program for atmospheric effects on IR radiation, calculating transmission and radiance spectra for various remotely sensed atmospheric, path and target conditions

02 p0187 A72-11862

Thermal IR radiation attenuation by atmospheric particulates, comparing computer simulated brightness temperatures with airborne radiometer and Nimbus 3 observed data

02 p0213 A72-11863

Lower ionospheric nighttime absorption as ionization processes indicator, discussing relationship to geomagnetic activity

02 p0216 A72-11921

High resolution atmospheric transmission measurement of wavelength dependence of absorption losses in carbon dioxide of solid state Er laser radiation

02 p0238 A72-12201

Absorption effects of dimers of water molecule in atmosphere, using spectroscopic and maser measurements

03 p0348 A72-13400

Tropospheric forward electromagnetic scatter propagation path loss prediction by modified Yeh method with empirically derived correction function

03 p0323 A72-14031

Sonic boom generation, propagation and minimization, discussing atmospheric conditions and ground characteristics influence and means for boom signature reduction

04 p0464 A72-14815

Nighttime radio absorption from lower ionospheric ionization by Sco X-1 and Tau X-1 X rays, using full wave admittance method

04 p0519 A72-15161

Near sea level atmospheric effects on submillimeter radiation absorption in terms of dielectric coefficient theory

04 p0551 A72-15606

Atmospheric molecular and aerosol absorption effects on submillimeter radio wave propagation using laser, BWT and liquid He receiver-transmitter devices

04 p0551 A72-15607

Giant M stars atmospheres absorption coefficient calculation from vibrational and pure rotational bands of H₂O, CO and OH

05 p0715 A72-16167

Optical wave front transmission through turbulent atmosphere, predicting saturation phenomenon accompanying sea level turbulence

05 p0690 A72-16675

Terrestrial atmospheric effects on quasar red shift measurements, considering night sky emission lines and atmospheric window size limits

05 p0723 A72-17159

Atmospheric contrast degradation and turbulence effects on photography from space with computerized optimization of ground resolution

06 p0813 A72-17431

Oxygen telluric lines contours shape analysis, allowing for atmospheric nonisothermicity and inhomogeneity

06 p0852 A72-18050

Atmospheric effects on remotely sensed earth surface signature recognition, considering scattering, absorption and emission effects

06 p0809 A72-18233

Jovian atmospheric absorption coefficient at 6-14 microns as function of frequency from hydrogen, methane and ammonia contributions

07 p1069 A72-19078

Atmospheric attenuation due to rain based on links experiment and statistical study of equivalent precipitation for given path length and time percentage

07 p0939 A72-19188

Radio attenuation above 10 GHz based on theoretical model of equivalent precipitation on path using intensity spatial distribution function within rain cell

07 p0940 A72-19189

Automatic laser tracking and ranging system for cooperative retroreflective aircraft targets, discussing design, performance, eyesafe distance and atmospheric attenuation

07 p0942 A72-19385

Rain attenuation determination at 15 and 35 GHz under precipitation condition from emission measurement and correlation to regression line, using portable radiometric system

07 p0946 A72-19791

Turbojet and turbofan engines noise signatures and sonic boom effects, discussing frequency spectra, atmospheric attenuation and noise suppression systems

07 p0912 A72-20163

Atmospheric acoustic attenuation measurement on sailplane, assessing turbulence backscattering cross section

07 p1031 A72-20597

Long distance atmospheric propagation in earth-ionosphere waveguide, obtaining phase velocities and damping factors

08 p1131 A72-20802

Whistling atmospherics generation mechanism, showing ionic sound excitation by hydromagnetic wave propagation through magnetospheric rapid plasma concentration change regions
08 p1155 A72-20807

Radio absorption in lower ionosphere obtained from vertical distribution of electron density and production rates from solar protons energy spectrum
08 p1226 A72-20816

Terrestrial surface observation from space platform, considering atmospheric effects, surface spectral properties and information resolution and transmission
08 p1170 A72-21965

Spectroscope model design using ruby laser highly monochromatic light pulses, electro-optical scanning and high speed photography to study atmospheric gases absorption spectra
09 p1322 A72-22205

Transportable radio telescope for atmospheric attenuation and solar activity observations
09 p1316 A72-23509

Atmospheric water vapor submillimeter absorption lines in high resolution radiation transmission measurements with Froome type plasma metal junction device
10 p1472 A72-24175

Spectrophotometric measurements of sky radiance distribution to determine atmospheric pollution, ozone content and radiation attenuation by clouds
10 p1476 A72-25085

Nighttime E region electron density variation effects on MF and HF radio wave propagation, discussing ionospheric absorption detection experiments
11 p1593 A72-26070

Ionospheric radio wave absorption and intensity calculation, using vertical sounding data and riometric measurements
11 p1594 A72-26278

Nonlinear thermal effects of atmospheric absorption for high power carbon dioxide laser beams
11 p1651 A72-26747

Venus lower atmosphere enhanced microwave attenuation explained by water vapor and droplet layer, calculating mass density distributions
11 p1724 A72-26762

Line-of-sight radio link attenuation by atmospheric precipitation and phase interference fading during multipath propagation in 7-15 GHz range
12 p1785 A72-27802

Light beams propagation in clouds and fog, discussing scattering and attenuation coefficients
13 p1988 A72-28517

Four dimensional atmospheric model providing global moisture, temperature, pressure and density profiles as attenuation model inputs for earth resources satellite mission simulation
13 p1989 A72-28805

Ground terminals spatial diversity for earth satellite mm wave communication systems to avoid attenuations by rainfall
13 p1989 A72-28810

Lower ionospheric nighttime absorption as ionization processes indicator, discussing relationship to geomagnetic activity
13 p1948 A72-29233

Regional observation of atmospheric spectral transmittance by Bouguer and high/low star methods
13 p2044 A72-29650

IR absorption coefficients in air at 6000-8500 K and 40-95 atm, interpreting absorption due to free-free electron transitions in neutral particle fields
13 p2006 A72-29676

Ionospheric attenuation of 3-100 MHz radio waves, interpreting scatter mode propagation mechanism as total reflection from lower ionizational irregularities
14 p2086 A72-30658

Reflectivity-emissivity relationship for isothermal atmosphere with coherent scattering and continuous absorption, generalizing for noncoherent case with line opacity
14 p2131 A72-30890

High resolution atmospheric millimeter wave spectrum of attenuated solar radiation from sea level observations, using Fourier type IR techniques
15 p2224 A72-31671

Atmospheric sound absorption prediction based four-gases composition and energy transfer mechanisms, comparing results with experiments at different humidities
15 p2277 A72-32020

Azimuth display of attenuation instrument used with weather radar to measure rain induced attenuation over slant paths
15 p2207 A72-32101

Slant path radar attenuation events due to rain during summers at 10 GHz, obtaining statistics on frequency of occurrence, extent in azimuth and duration
15 p2200 A72-32103

Molecular absorption of microwaves by atmospheric impurity gases ozone, carbon monoxide and nitrous oxide up to 20 km
16 p2364 A72-33483

Atmospheric absorption height determination from orbital elements during solar radiation satellite observation
16 p2386 A72-33603

Solar radiation absorption and scattering by particles in atmosphere, emphasizing absorption/backscatter ratio explanation
16 p2388 A72-34023

Material injection RF blackout alleviation and plasma diagnostic measurement with electrostatic probes and S-band reflectometer during RAM C-III reentry flight
16 p2365 A72-34052

[AIAA PAPER 72-690]
On the winter anomaly of ionospheric absorption.
17 p2546 A72-34695

The absorption length for solar particles in the earth's atmosphere - Solar proton event November 18, 1968.
17 p2602 A72-35760

Laser IR radiation attenuation in natural and artificial fogs, noting dependence on particle size distribution
18 p2697 A72-36102

Laser optical and IR radiation attenuation in atmospheric precipitation, considering snow, rain and drizzle
18 p2697 A72-36103

Simplified method of calculating microwave diffraction loss over spherical earth.
18 p2660 A72-36517

Sea surface albedo for short wave solar radiation in terms of sun altitude and atmospheric transmittance, noting wind and surface roughness effects
18 p2687 A72-36642

Absorption of the 4- to 6-millimeter wavelength band in the atmosphere.
18 p2689 A72-36961

Investigation of the atmospheric boundary layer and clouds by the laser tracking method
18 p2698 A72-36969

Atmospheric pressure, density and scale height calculated from H Lyman-alpha absorption allowing for the variation in cross-section with wavelength.
19 p2793 A72-38859

Atmospheric transmittance measurements time and spatial representativeness optimization by allowing for fog element caused discontinuities
20 p2947 A72-38971

Atmospheric transmissivity in the 49- to 72-GHz band - Analysis and laboratory measurements.
21 p3021 A72-40906

Solar radiant energy reflection and absorption by cloud layers
21 p3049 A72-41795

Measurement of the vertical atmosphere transmittance in the IR spectral region with the aid of an artificial source
21 p3079 A72-41800

Ionospheric refractivity and attenuation surface deformation relationship to ion cyclotron whistlers near cross-over level between zero and critical coupling angles
22 p3168 A72-42006

Improved Curtis-Godson approximation in a non-homogeneous atmosphere.
22 p3201 A72-42511

Variation of tropospheric slant-path attenuation in the UK at 11.75 and 17 GHz.
22 p3155 A72-42751

Absorption profile of a planetary atmosphere - A proposal for a scattering independent determination.
23 p3289 A72-43889

Calculation of middle ultraviolet radiation detector response to solar radiation as a function of altitude.
23 p3289 A72-43897

Spectrometric zonal standards - Selection of stars and methodology of their study
23 p3338 A72-44031

Sound absorption in atmosphere at 20 C, predicting relaxation times and strengths in 100 Hz to 1 MHz as functions of relative humidity
23 p3285 A72-44112

Attenuation of ruby laser radiation in the boundary layer of the atmosphere during the temperature-dependent variations of the wavelength
24 p3411 A72-45424

ATMOSPHERIC BOUNDARY LAYER

Lidar measurements of atmospheric aerosol distributions over large areas including urban haze, scattering layers, trade wind inversion and Sahara dust stream in Caribbean
01 p0057 A72-10526

[AIAA PAPER 71-1055]
Momentum exchange coefficient for surface layer neutrally stable flow after surface roughness change, noting error possibility in flow estimates for heterogeneous terrain
01 p0094 A72-10827

Quasi-geotriptic wind field vertical motions in ground friction layer from continuity equation
02 p0254 A72-12780

Small scale turbulence time-space variability in atmospheric boundary layer in presence of unstable stratification from vertical air flow measurements
03 p0383 A72-13481

Image blurring effects due to atmospheric boundary layer refractivity turbulent fluctuations during remote optical radiation source observations
03 p0359 A72-13482

Obukhov contribution to turbulence in atmosphere with nonuniform temperature, discussing dynamic scale length and asymptotic states of boundary layer in unstable flows
03 p0385 A72-14333

Atmospheric static stability effect on turbulence layer thickness under nonuniform temperature, using correction factor dependent on Richardson number
03 p0386 A72-14334

Vertical wind velocity variances and spectra above atmospheric surface layer for flat and mountain terrains
03 p0386 A72-14335

Ekman boundary layer shear stress due to laminar and turbulent flow over hills
03 p0386 A72-14336

Finite difference schemes for surface and planetary boundary layer solutions using grid spacings proportional to mixing length and eddy viscosity
03 p0386 A72-14337

Electric or magnetic field tangential components at ground-air interface, discussing secondary electromagnetic sources
04 p0492 A72-15438

Planetary boundary layer mixing length flow hypothesis with dependence on Reynolds tangential stress permitting turbulent diffusion coefficient maximum values computation
04 p0519 A72-15458

Iterative method to solve planetary boundary layer differential equations, overcoming difficulties of previous approaches
04 p0519 A72-15460

Prandtl layer turbulence spectra parameterization from wind vector data, considering functional dependence on mean wind velocity, height and thermal stratification
04 p0544 A72-15623

Altitude dependent turbulence characteristics in atmospheric boundary layer over wavy ocean surface from wind pulsation measurements
06 p0841 A72-17624

Vertical two-point longitudinal velocity differences or wind shear in atmospheric boundary layer, obtaining standard deviation from turbulence measurements
06 p0841 A72-17666

Steady state geostrophic wind vector variation hodographs in planetary baroclinic boundary layer, considering thermal influence linear superposition on internal friction effects
06 p0841 A72-17667

Turbulent energy dissipation rate statistical characteristics above 1000 m from radar measurements, discussing atmospheric boundary layer quantities
06 p0841 A72-17940

Velocity and temperature pulsations as function of stratification parameter in atmospheric boundary layer
06 p0842 A72-18044

Surface layer humidity correlation to height of atmosphere emitting in IR spectral region, determining water vapor content by recording earth radiation angular distribution
06 p0808 A72-18046

Rain amount forecasting based on five level atmosphere model and hydrothermodynamics equations, calculating vertical currents under uniform atmospheric boundary layer stratification conditions
07 p1029 A72-18859

Numerical simulation of atmospheric turbulence in planetary boundary layer due to wind shear and/or unstable thermal stratification, noting buoyancy and planetary rotation effects
07 p1031 A72-20359

Atmospheric surface layer meteorological elements representative values determination as optimal filtration problem, examining data correlation with errors in initial statistical characteristics
08 p1203 A72-22121

Atmospheric boundary layer pressure field expansion into dual series of natural time dependent components to separate fluctuations within monthly period for weather forecasts
08 p1203 A72-22125

Earth location effect in Fresnel diffraction zone on comparator performance, measuring phase difference fluctuations in turbulent atmospheric boundary layer radio waves
09 p1284 A72-22232

Parametrization of turbulent flux of momentum, heat and moisture at ground in baroclinic planetary boundary layer
09 p1346 A72-22810

Rossby similarity for barotropic planetary boundary layer flows in terms of nondimensional Reynolds stress and eddy viscosity
09 p1346 A72-22811

Ground based radiometric measurements of vertical temperature profiles in planetary boundary layer, describing data reduction technique
11 p1681 A72-26083

Low cost radiation shield for thermistor deployment in atmospheric boundary layer, noting measurement accuracy relationship to data acquisition system

11 p1682 A72-26087

Small scale turbulence time-space variability in atmospheric boundary layer in presence of unstable stratification from vertical air flow measurements

11 p1682 A72-26251

Image blurring effects due to atmospheric boundary layer refractivity turbulent fluctuations during remote optical radiation source observations

11 p1633 A72-26252

Tornado model from atmospheric thermodynamics nonlinear equations, examining air flow from lower boundary layer and ground friction

11 p1682 A72-26880

Surface roughness effects on air flow in turbulent atmospheric boundary layer, using finite difference method

12 p1838 A72-27026

Atmospheric surface layer turbulent transfer mechanisms, studying direct measurements of momentum, heat and moisture turbulent fluxes

12 p1840 A72-27705

Earth atmosphere boundary layer nonstationary problems, considering diurnal changes of meteorological fields and nonperiodic evolution of elements from wind variations

12 p1841 A72-27988

Earth atmosphere general circulation model based on planetary boundary layer parameterization, considering surface stress and heat and moisture flux

13 p1988 A72-28442

Wind shear third and fourth moments and distribution function in atmospheric boundary layer, emphasizing longitudinal turbulent velocity vertical variations

13 p1993 A72-28860

Diurnal variability of atmospheric refraction index at UHF in boundary layer for various weather types during summer-fall season

13 p1995 A72-29590

Horizontal and vertical scales of atmospheric boundary layer turbulence for various temperature stratifications, noting space and time correlations for longitudinal wind velocity component

13 p1995 A72-29592

Convective clouds effect on air temperature gradient and turbulent heat fluxes in near-surface layers

13 p1995 A72-29593

Magnetosphere tail internal plasma boundary layer dynamics during substorms based on aurora data

14 p2103 A72-30663

Air injection as neutral atmospheric boundary layer thickening simulation, presenting mean velocity and turbulence intensity profiles

14 p2093 A72-30849

Turbulence effects on electron, ion, aerosol, water vapor and ozone concentration in atmospheric layers

15 p2222 A72-31395

Upper boundary layer conditions effects on atmospheric temperature profile reconstruction, by integro-differential equation substitution for Fredholm equation

15 p2265 A72-31399

Microscale static pressure fluctuation measurements in lower atmospheric boundary layer turbulent flow using Eulerian measurements

15 p2265 A72-31618

Mixing length theory derivation of barotropic planetary boundary layer profiles for geostrophic wind deviations, Reynolds stress, eddy viscosity and turbulent kinetic energy dissipation

15 p2224 A72-31675

Laser communication lines in atmospheric ground layer, comparing SNR for direct-reception and superheterodyne video systems

15 p2247 A72-31887

Three dimensional flow of steady neutral horizontally inhomogeneous planetary boundary layer, studying hodograph, velocity, vorticity, energetics and eddy coefficients

15 p2266 A72-32723

Fog, cloud, rain and snow detection by acoustic echo sounding, noting effects of energy scattered from atmospheric boundary layer velocity and temperature fluctuations

15 p2267 A72-32725

Turbulent energy dissipation rate statistical characteristics above 1000 m from radar measurements, discussing atmospheric boundary layer quantities

16 p2418 A72-33781

Atmospheric boundary layer and diffusion over three dimensional mountainous terrain by laboratory simulation with meteorological wind tunnel and scale model

[AIAA PAPER 72-648] 16 p2419 A72-34085

Atmospheric surface layer temperature, humidity and vertical wind velocity variances dependence on turbulent fluctuation inputs

16 p2419 A72-34148

Saltation threshold velocity simulation by dynamic model with terrestrial and Martian surface applica-

tions, using particle trajectory equations for near ground-atmosphere interface

17 p2614 A72-35637

On the boundary conditions in theoretical model calculations of the distributions of minor neutral constituents in the upper atmosphere.

18 p2659 A72-36294

Calculation of airflow over an arbitrary ridge including diabatic heating and cooling.

18 p2706 A72-36629

On the inflection point instability of a stratified Ekman boundary layer.

18 p2687 A72-36631

A theoretical study of the diurnal wind variations in the planetary boundary layer.

18 p2706 A72-36645

Investigation of the atmospheric boundary layer and clouds by the laser tracking method

18 p2698 A72-36969

Atmospheric boundary layer turbulence modeling, considering terrain roughness effects, vertical mixing, high frequency spectra, energy dissipation rate and vertical component variance

19 p2828 A72-38557

Similarity predictions for shear stress and heat flux cospectral behavior in atmospheric turbulent boundary layer

19 p2829 A72-38560

The indirect determination of stability, heat and momentum fluxes in the atmospheric boundary layer from simple scalar variables during dry unstable conditions.

20 p2947 A72-38964

Atmospheric surface layer light scattering matrices from nighttime air flows, showing climatic variability and similarity between Crimean and Moscow measurements

20 p2948 A72-39014

A wind-tunnel experiment concerning atmospheric vortex streets.

20 p2948 A72-39796

Instrumentation for measuring static pressure fluctuations within the atmospheric boundary layer.

20 p2927 A72-39799

An application of the shooting method to the stability problem for a stratified, rotating boundary layer.

21 p3043 A72-40106

Lower planetary boundary layer mesoscale flow patterns and transport climatology, using hourly averaged wind data from wind tower station network

21 p3077 A72-40252

An improved pressure-sphere anemometer.

22 p3178 A72-42596

Wind tunnel measurement for demonstrating similarity of atmospheric turbulent boundary layer mean velocity and shear stress at high Reynolds number

22 p3201 A72-42598

Atmospheric waves observed in the planetary boundary layer using an acoustic sounder and a microbarograph array.

22 p3202 A72-42599

Earth atmosphere boundary layer nonstationary problems, considering diurnal changes of meteorological fields and nonperiodic evolution of elements from wind variations

22 p3202 A72-43002

Relative movements of mid-latitude trough and scintillation boundary.

23 p3282 A72-43267

Pioneer 8 observation of diffuse magnetosphere-magnetopause boundary, noting proton flux intensity and flow angle

23 p3341 A72-44512

A method of calculating meteorological elements for mesoscale processes

24 p3420 A72-44633

Atmospheric boundary layer definition by height of maximum vertical kinetic energy flux, considering stable and unstable stratifications

24 p3421 A72-44954

Baroclinic effects on the resistance law for the planetary boundary layer of the atmosphere.

24 p3397 A72-44956

Attenuation of ruby laser radiation in the boundary layer of the atmosphere during the temperature-dependent variations of the wavelength

24 p3411 A72-45424

Incorporation of steep mountains into numerical forecasting models.

24 p3421 A72-45486

Measurement of the angular divergence and of the refraction of a laser beam in the ground layer of the atmosphere.

24 p3380 A72-45611

ATMOSPHERIC CHEMISTRY

Photochemical ion-molecule reactions in ionosphere by air exhaust device and RF mass spectrometer observation in geophysical rocket experiment

01 p0068 A72-10591

Venus atmospheric investigation by Venera 4, 5 and 6 probes, discussing satellite components and instrumentation, and atmospheric composition, depth, density, pressure, temperature and model

01 p0130 A72-10931

Oxygen and hydrogen atoms production in atmosphere by photodissociation, investigating terrestrial hydrogen escape efficiency

03 p0346 A72-13381

Laboratory measurements of D region ion-molecule reactions using flowing afterglow system

03 p0347 A72-13388

Quantum yield observations for photochemistry of ozone and singlet molecular oxygen in atmosphere

03 p0347 A72-13393

Venusian ionosphere thermal proton destruction, discussing helium and oxygen replacement candidates for principal ion components

03 p0434 A72-13537

Martian atmospheric volatiles history, noting initial chemical conditions favorable to abiotic organic synthesis

04 p0569 A72-14503

Laboratory simulation of Jovian atmospheric reactions, observing amino nitriles formation

04 p0572 A72-14764

Jupiter atmosphere chemical and photochemical analysis, using solar-composition adiabatic equilibrium model for coloration, electric discharge and UV irradiation studies

05 p0714 A72-16132

Night source ionized component profiles in chemistry and aeronomy of D and E regions, considering scattered L alpha and beta emissions and corpuscular fluxes

07 p0936 A72-20038

Neutral species chemical reactions in D and E regions, taking into account effects of photodissociation and transport by horizontal and vertical flow and molecular diffusion

07 p0936 A72-20039

D and E regions positive ion chemistry based on E and F regions ion-molecule reaction rate constants comparison with laboratory measurement

09 p1275 A72-22360

D and E region ion chemistry reaction rate measurements, noting hydration, charge exchange and ion-ion interchanges

09 p1275 A72-22366

Room temperature reactions involving ionospheric cluster ions, discussing rate constants measurement by stationary afterglow and drift tube facilities

09 p1275 A72-22367

Atmospheric metal ion chemistry, tabulating thermal energy binary and three body reaction rate data

10 p1434 A72-25160

D region chemistry based on earth albedo effects from airborne radio sounding experiments, suggesting visible light energy flux role

13 p1950 A72-29342

Ozone photochemical reactions measurements for quantum yield of UV photolysis in strong Hartley band with water vapor chain decomposition effects

14 p2083 A72-30134

Stratospheric particles analysis by X ray detector on scanning electron microscope, comparing results with data on volcanic particles and cosmic dust

15 p2227 A72-31958

Bibliography on SST upper atmospheric environment, listing references to stratospheric structure, composition and physical dynamics, chemical reactions with pollutants, transport properties, etc.

16 p2386 A72-33797

Oxygen molecule electron affinity role in ion chemistry of lower ionosphere, noting binding energy of ground state

17 p2585 A72-34260

Photochemistry of the lower troposphere.

17 p2511 A72-34635

High temperature turbulent jet facility for studying ionic species produced by high temperature air and ablation products interaction with cool ambient air

[AIAA PAPER 72-676] 17 p2536 A72-35480

Book - The earth's atmosphere

17 p2550 A72-35797

Gas dynamics and chemistry of lightning-produced shock waves /thunder/ in postulated primordial reducing atmosphere, noting amino acid production

18 p2650 A72-36443

Existence, structure and thermodynamic and kinetic stability of ClOO radical in Venus atmosphere, using quantum statistics methods for unimolecular decomposition rate

18 p2726 A72-36647

Stability of the Martian atmosphere.

22 p3224 A72-42292

Detection of molecular oxygen on Mars.

22 p3224 A72-42293

ATMOSPHERIC CIRCULATION

Venusian atmosphere heat transfer processes, calculating radiant fluxes and convective motion model

01 p0127 A72-10364

Neutral gas wind effect on Doppler shifts in frequency spectrum of atmospheric gravity waves in F region with resultant phase altitude dependence alteration

01 p0054 A72-10426

Air pollution circulation patterns remote sensing, describing multispectral stereo image pairs digital cross correlation

[AIAA PAPER 71-1106] 01 p0067 A72-10551

Ultrasonic rotameter for wind velocity circulation measurement, using cylindrical electroacoustic capacitor converter with solid dielectric for radiators and receivers
01 p0094 A72-10560

Tropospheric wind estimation from ATS 1 satellite cloud motions over equatorial Pacific
01 p0060 A72-10856

Topography and Coriolis effects on Martian atmospheric circulation, incorporating low radiative time constant and large variations in analytical model
01 p0135 A72-11279

Digital simulation of general atmospheric circulation via spatial finite difference dense grid, considering surface properties and pressure distribution maps
02 p0252 A72-11652

Tropospheric processes effects on Northern Hemisphere stratospheric meridional transformations in geopotential field and air circulation
02 p0253 A72-11732

Temperature advection mesostructure from wind measurements for precise short term forecasts
02 p0254 A72-12778

Atmospheric deviations of ageostrophic wind in jet stream domain, using dimensionless vector characteristics
02 p0255 A72-12787

Ageostrophic flow relations in tropospheric high wind fields, discussing Scheibe equation and vector calculation
02 p0255 A72-12788

Forced barotropic Rossby waves in homogeneous fluid in rotating cylindrical annulus with differentially rotating source-sink distribution
03 p0340 A72-12974

Dynamic modeling of stratospheric and mesospheric circulation and thermal structure
03 p0346 A72-13382

Disturbance evolution on zonal flow background in baroclinic atmosphere with given wind profile, determining average-time energy distribution
03 p0383 A72-13479

Global angular momentum balance, considering atmospheric frictional torques and fluxes, ocean water mass exchanges and seasonal variations effects
03 p0384 A72-14142

Tropical east-west atmospheric circulation geometrical, thermal and intensity characteristics during northern summer
03 p0384 A72-14143

Short period height and longer period kinetic energy oscillations in 10-level primitive equation model for circulation prediction in tropical region
03 p0385 A72-14232

Air exchange between stratosphere and troposphere from cosmic ray produced radionuclides and fallout comparison with weather development
03 p0351 A72-14359

Two dimensional meridional ozone model for seasonal ozone concentration behavior at 15-45 km, taking into account advective and turbulent effects
03 p0351 A72-14360

Stratospheric circulation and air temperature horizontal and vertical distribution, discussing CAT at supersonic transport heights
04 p0541 A72-14676

Gliding flight atmospheric energy utilization through aerology, discussing value of weather forecasts to glider pilots
04 p0542 A72-14684

Atmospheric tides wave dynamics in thermosphere, considering viscosity, thermal conduction, hydromagnetic forces and nonlinearity effects on transmission and excitation
04 p0514 A72-14722

Thermospheric neutral-air wind effects on ionospheric F 2 layer from atmospheric model
04 p0514 A72-14876

French monograph on atmospheric ozone utilization as tracer for troposphere-stratosphere exchanges covering investigations at various locations
05 p0654 A72-15799

Planetary wave spectrum calculation by Galerkin method, discussing angular velocity of longest Rossby waves distortable by zonal flow
05 p0655 A72-16170

Solar effects contradictory relationships with earth atmosphere, discussing geomagnetic disturbance, annual variations, stratospheric transport and high energy particles
05 p0656 A72-16233

Stratospheric rocket sounding on global scale for studies of atmospheric circulation in equatorial zone, polar regions and hemispheres
06 p0840 A72-17620

Solar radiative constant and stratospheric volcanic dust effects on circulation and climate anomalies
06 p0840 A72-17623

Meteor streams effect on atmospheric motions turbulence intensity based on radar observations
06 p0842 A72-18045

Jovian belts, zones, great red spot, white ovals and atmospheric rotation and circulation from methane photographs analysis, comparing to earth atmosphere
06 p0889 A72-18331

Tropical upper tropospheric motion field during Northern Hemisphere summer, computing energy exchange between zonal flow and eddies
06 p0842 A72-18437

Radar observed apparent land breeze front off Wallops Island, giving temperature and wind profiles
06 p0843 A72-18441

Solar photosphere active regions and large scale flow patterns from Greenwich sunspot statistics
07 p1068 A72-18886

Tropical disturbances effect on general atmospheric circulation, considering Hadley cell rising branch and cumulonimbus clouds heat release
07 p1029 A72-19096

Traveling ionospheric disturbance as diagnostic tool for thermospheric dynamics, monitoring wave polarization of ATS 3 signals
07 p0975 A72-19154

Solar magnetic field regularities analogy with terrestrial cyclones instead of convection cells in vertical heat transport
07 p1074 A72-19558

Horizontal transport in upper atmosphere by large scale circulation, presenting altitude variation of atmospheric constituents concentration for various eddy diffusion coefficient values
07 p0978 A72-20040

Venusian atmospheric circulation experiments with time dependent two layer primitive equations model, discussing hot house and Goody-Robinson radiation transfer implications
07 p1083 A72-20452

Circulation mechanics of gaseous atmospheres with zonal symmetry in motions and other properties, applying to Jupiter atmosphere
07 p1083 A72-20453

Magnetic field components of vertical currents at magnetosphere boundary and earth surface, using computerized Gaussian method
08 p1156 A72-20822

Linearized two level model for atmospheric motion equations systems, using Psi-balanced system for 24 hour forecast
08 p1156 A72-20995

Circulation motions in D and E regions, discussing planetary waves, tidal oscillations, gravity waves, turbulence and drift measurement
08 p1160 A72-21527

Energy transfer from radiative heat source near summer pole to radiative heat sink near winter pole, investigating large scale eddies and gravity waves
08 p1161 A72-21536

Wind measurements in lower thermosphere by meteor radar method, presenting models of prevailing circulation in meteor zone over Eurasia and Arctic
08 p1161 A72-21538

Air masses circulation in atmospheric upper layers during IQSY from meteor trail drifts observation by radar tracking method
08 p1161 A72-21882

Optimal variant of meteor wind patrol radar station for atmospheric circulation study
08 p1147 A72-21886

Energy and momentum removal from troposphere and lower atmosphere by mountain lee wave breaking, discussing effects on atmospheric circulation evolution and maintenance
08 p1203 A72-22167

Planetary scale circulation systems effects on photochemistry and transport processes of minor neutral constituents in mesosphere and lower thermosphere
09 p1274 A72-22353

Tropical storms generated midlatitude cloud bands relation to autumnal large scale circulation, analyzing heat and moisture injection effects
09 p1344 A72-22429

Wind vector field computation by forced dynamical adjustment to observed height field data, using Mintz-Arakawa two level atmospheric circulation model
09 p1344 A72-22433

Numerical integration of primitive equations for barotropic atmosphere, using spherical polar coordinates
09 p1346 A72-22809

Inferred perturbation effects of Arecibo large nighttime gravity wave on neutral atmosphere velocity and temperature
09 p1300 A72-23021

Wind velocity distribution structural laws in vertical and horizontal planes for large mesospheric and atmospheric processes
09 p1347 A72-23591

Microbaroms produced by ocean waves radiated in frasound, noting dependence on upper atmosphere temperature and winds
09 p1348 A72-23656

Theoretical model of large scale topographical effects on wind generation through temperature advection, applying to Mars atmosphere general circulation
10 p1531 A72-23707

Atmospheric vertical shear at visible cloud level in Jupiter equatorial zone from blue and red wavelength photographs
10 p1531 A72-23712

ESSA satellite observation of meridional circulation, noting roles of subsidence sinks, storm depressions and melting fronts
10 p1506 A72-24059

Noctilucent cloud wave structure, discussing motions in high atmosphere, ice crystal formation, energy sources and observations
10 p1474 A72-24707

Photochemical models to simulate composition and reactions of upper atmosphere, noting transport importance
10 p1474 A72-24713

Noctilucent cloud kinematics as indicators of mesospheric circulation and turbulence characteristics, discussing need for international scientific cooperation
10 p1476 A72-25006

Atmospheric wind velocity time variations at 80-100 km altitudes from ionospheric drift data, finding planetary oscillation periodicities relationship to solar activity cycle
11 p1620 A72-25273

Baroclinic wave field distributions and balances in rotating annulus with free surface in atmospheric circulation study, noting Ekman layer features
11 p1680 A72-25765

Asian subtropics western disturbances movement prediction by primitive equation barotropic model with east-west cyclic boundary conditions, presenting forecast charts and error statistics
11 p1681 A72-26077

Morning glory, showing squall formation by atmospheric hydraulic jump favored by slack pressure gradients, cloudless skies and low latitudes
11 p1681 A72-26080

Disturbance evolution on zonal flow background in baroclinic atmosphere with given wind profile, determining average-time energy distribution
11 p1682 A72-26249

Atmospheric vertical motions velocities prediction based on satellite cloud data
11 p1683 A72-26887

Time-spectral characteristics and geographic variations of large scale cloud activity in tropical Pacific
12 p1837 A72-27018

Kinematic estimate of large scale atmospheric vertical motion field patterns, using polynomial approximation of wind profiles
12 p1840 A72-27707

Ekman boundary layer in two level quasi-geostrophic general circulation numerical model, representing physical characteristics of boundary layer turbulence increase with height
12 p1840 A72-27708

Ionosphere electron content annual mean difference from semiannual amplitude as seasonal fluctuation indication for tropospheric circulation
12 p1803 A72-27774

Solar activity relation to geophysical phenomena, discussing atmospheric circulation and climatic variation cyclicity and sunspot corpuscular fluxes
12 p1842 A72-28207

Quasi-steady and sporadic corpuscular fluxes as basic solar activity effect on troposphere, showing magnetosphere interaction time relation to meridional atmospheric circulation changes
12 p1842 A72-28208

Earth atmosphere general circulation model based on planetary boundary layer parameterization, considering surface stress and heat and moisture flux
13 p1988 A72-28442

Global horizontal sounding technique balloon flights, determining Southern Hemisphere temperate latitude circulation climatology
13 p1988 A72-28443

Atmospheric motion equations numerical integration, presenting conservative finite difference approximation for quasi-uniform spherical grids derived from regular polyhedrons
13 p1985 A72-28445

Jupiter, Saturn and earth atmospheric circulation seasonal variation data analogies, noting factors governing planetary atmospheric temperature
13 p2048 A72-29813

Planetary wave spectrum calculation by Galerkin method, discussing discrete modes of longest Rossby waves distortable by zonal flow
14 p2099 A72-30239

Global atmospheric circulation barotropic spectral model application to satellite asymptotic data continuous processing
14 p2127 A72-30258

Semiannual equatorial wind oscillations in upper stratosphere and lower mesosphere dependence on temperature variations in high and middle latitudes
14 p2099 A72-30259

Aircraft atmospheric flow measurements of horizontal and vertical motions on mesoscales, using inertial reference system
14 p2127 A72-30300

Balloon flight tracking by Nimbus D satellite to sound tropical stratosphere air motions, noting northward drift maximum in Northern Hemisphere winter
14 p2128 A72-30350

Turbulent Ekman boundary layer characteristics in laboratory rotating apparatus compared with atmospheric field observation data and theories, noting similarity relation validity 14 p2094 A72-30418

Oceanic and atmospheric flow geostrophic adjustment by means of gravity-inertial wave propagation from initially imbalanced regions 15 p2222 A72-31278

Rocket and radar-meteor wind observations of zonal flow, noting annual and semiannual components for northern latitudes at 60-130 km 15 p2229 A72-31985

Radiative stellar envelopes circulation velocity calculation for various cylindrical rotation laws using perturbation method 15 p2314 A72-32371

Atmospheric motions prediction with numerical model based on discrete stratified fluid free oscillations 15 p2266 A72-32720

Nonrotating Hadley cells turbulence from steady one dimensional flow instabilities in thin nonrotating differentially heated atmosphere or ocean 15 p2219 A72-32722

Imposed southern boundary experimentation for large scale Northern Hemisphere midlatitude atmospheric flow numerical prediction, discussing factors contributing to model success 15 p2267 A72-32726

Vertical temperature profile retrieval from satellite radiance measurements for insertion into numerical atmospheric circulation model, discussing sensitivity test 15 p2267 A72-32728

Wind direction rotation with altitude and time dependent downward phase propagation observed by vapor trail experiments, suggesting upward propagation of atmospheric waves 16 p2383 A72-32969

Geophysical fluid dynamics approach to dynamical processes in ocean and atmospheric motions, discussing equations of motion, vorticity, geostrophism, Ekman layer, Rossby waves, etc 16 p2377 A72-33336

Planetary atmospheres and interiors in terms of dynamics, rotation, magnetic fields, Jupiter features, geomagnetism, earth baroclinic waves, global circulation and gravitation, etc 16 p2384 A72-33339

Climatic changes due to stratospheric perturbation by propulsion effluents of high altitude aircraft flights [AIAA PAPER 72-658] 16 p2388 A72-34076

Meridian circulation with rapid differential rotation in radiative stellar envelopes. 17 p2605 A72-34532

The evolution of the solar inner rotation by the Eddington-Sweet type circulation under the influence of the solar wind torque. 17 p2613 A72-35497

Shock tube investigation of low-density heated fluid element dynamic reaction to reflected shock wave passage, noting similarity to atmospheric thermals 17 p2542 A72-35615

Book - The earth's atmosphere 17 p2550 A72-35797

Terrestrial and solar atmospheres general circulations from laboratory experiments on rotating cylinders filled with differentially heated fluids, noting solar equatorial acceleration 17 p2551 A72-35941

Spatial variations in atmospheric predictability. 18 p2706 A72-36627

Equatorial tropospheric waves induced by diabatic heat sources. 18 p2687 A72-36628

Mathematical model for internal atmospheric gravity waves breaking process modification by momentum exchange between wave and mean flow 18 p2687 A72-36630

Observations of Helmholtz waves in the lower atmosphere with an acoustic sounder. 18 p2687 A72-36635

A note on the effects of pressure gradients on fluid flow with atmospheric applications. 18 p2706 A72-36644

Meteorological applications of the Nimbus 4 temperature-humidity infrared radiometer, 6.7 micron channel data. 18 p2707 A72-36718

Upward and downward motions of Venus atmosphere in terms of continuous cloud cover effects, considering solid cloud cover hypothesis 18 p2729 A72-36984

Features of zonal circulation in the stratosphere and lower mesosphere of the equatorial region during the period of increasing solar activity/1967-1968/ 19 p2790 A72-37999

Similarity theory of planetary atmosphere circulations applied to solar atmosphere in terms of radius and rotatory Mach number 19 p2863 A72-38066

Superrotation of the upper atmosphere. 20 p2916 A72-39336

The anomaly of the neutral wind at a height of approximately 200 km at high latitudes. 20 p2918 A72-39536

Stratospheric circulation variation in autumns preceding cold winters 20 p2949 A72-39947

Structure and circulation of the upper atmosphere over East Antarctica in 1969 and 1970 20 p2949 A72-39949

Effect of vertical flow structures on the cloud cover in the intratropical convergence zone 20 p2949 A72-39950

Response of the tropical atmosphere to local, steady forcing. 21 p3077 A72-40248

Temporal behavior of hemispherically averaged geostrophic zonal and meridional flow from dynamic climatology studies of Northern Hemisphere large scale circulation 21 p3077 A72-40251

Instability of rotational and gravitational modes of oscillation. 21 p3078 A72-40773

Direct observation of a complete unit of meridian circulation from the equatorial belt up to the polar front - Synthesis of concepts of the pseudofront, of the equatorial mesosystem, and of the subsidence well 21 p3078 A72-41344

Stratospheric general circulation patterns from geographical, vertical and annual distribution for Northern Hemisphere temperatures, geopotential heights and winds 21 p3078 A72-41611

Air motions in the tropical stratosphere deduced from satellite tracking of horizontally floating balloons. 21 p3078 A72-41612

Russian book - Long-term variations of atmospheric circulation and long-range hydrometeorological forecasts. 22 p3200 A72-42078

An updated theory for the quasi-biennial cycle of the tropical stratosphere. 22 p3201 A72-42503

Description of global-scale circulation cells in the tropics with a 40-50 day period. 22 p3201 A72-42506

A diagnostic study of the vorticity balance at 200 mb in the tropics during the Northern summer. 22 p3201 A72-42507

Nonlinear hydrothermodynamic model of steady atmospheric motion in equatorial latitudes with energy influx approximation 23 p3284 A72-43533

Synchronous observations of lower-ionospheric wind conditions in Dushanbe and at the equator 23 p3285 A72-44166

Scale analysis of atmospheric large-scale motions in low latitudes. 23 p3311 A72-44241

On the power law for the kinetic energy spectrum of large scale atmospheric flow. 24 p3398 A72-45483

ATMOSPHERIC COMPOSITION

NT ATMOSPHERIC MOISTURE

NT IONOSPHERIC COMPOSITION

Neutral H concentration in upper atmosphere during solar minimum, using ion thermal energies from rocket and satellite mass spectrometric, radio and proton whistler measurements 01 p0053 A72-10361

Atmospheric aerosol chemical composition analysis by nephelometer light scattering measurement of suspended particle mass concentration, visibility and size distribution and scattering-humidity relationship [AIAA PAPER 71-1101] 01 p0058 A72-10549

Remote sensing of atmospheric pollutants and trace contaminants, presenting high speed high resolution, Fourier interferometer breadboard model [AIAA PAPER 71-1109] 01 p0068 A72-10553

Airborne and spaceborne remote measurement and mapping of atmospheric nitric oxide, describing system configuration with mono or bistatic and pulsed or CW laser [AIAA PAPER 71-1112] 01 p0068 A72-10556

Atmospheric carbon monoxide pollution sources, sink mechanism and remote sensing requirement [AIAA PAPER 71-1120] 01 p0068 A72-10557

Stratospheric aerosol boiling point measurement with photoelectric particle counter, observing sulfate radical as major constituent 01 p0059 A72-10833

Seasonal variation in lower thermosphere atomic oxygen concentration deduced from static diffusion models, using incoherent scatter and orbital decay temperature measurements 01 p0062 A72-10907

Atmospheric aerosols size/altitude distribution via sun aureole sky brightness and airborne particle counterpoint sampling measurements 02 p0213 A72-11860

Atomic oxygen layer height and peak concentration in earth upper atmosphere, considering solar dissociation

radiation and turbulent diffusion for equinox conditions 02 p0217 A72-11924

Vertical concentration profile and diurnal variations of N and NO vs solar activity from satellite horizon airglow experiment 02 p0217 A72-11925

Atomic/molecular oxygen concentration ratio semi-annual variation at 130 km altitude from mass spectroscopic data analysis 02 p0218 A72-11947

Oxygen isotope ratios in iron meteorites magnetite crust and cosmic spherules as indicators for atmospheric oxygen development 02 p0279 A72-12117

Martian atmosphere and surface, covering atmospheric composition, optical thickness and pressure, violet and yellow clouds, surface relief and topography 02 p0282 A72-12326

Cosmos 65 global ozone contour data similarity with geomagnetic L shells configuration, discussing South Pacific region depletion area 02 p0221 A72-12466

Upper atmosphere ozone, aerosol and neutral constituent density profiles estimation by recursive filtering algorithm for satellite observation data 02 p0222 A72-12811

Jupiter atmospheric hydrogen-helium mixing ratio from binary star beta Sco occultation by planet in May 1971 03 p0416 A72-13009

Ozone photolysis in UV region, determining primary products from oxygen optical emission detection using time-resolved flow system 03 p0320 A72-13394

Magnetic storm effects on neutral atmospheric composition above 400 km, discussing energy deposition 03 p0349 A72-13518

Atmospheric model for mesosphere odd-nitrogen concentration relation to NO dissociation rate and downward flux through mesopause 03 p0350 A72-13526

Raman scattering cross section measurement for atmospheric nitrogen tetroxide, using Q switched ruby laser excitation source 03 p0367 A72-13601

Venus cloudy atmosphere IR absorption line spectra interpretation, suggesting HCl and HF formations dependence on condensation phases 03 p0439 A72-14149

Mars atmosphere diatomic oxygen upper limit abundance, using high dispersion spectroscopic data from 1969 apparition 04 p0569 A72-14498

Radio absorption spectra sounding for planetary atmospheric impurities calculating water vapor content in Venus cloud level 05 p0715 A72-16169

Vibrationally excited oxygen molecules formation and decomposition in upper atmosphere, calculating day and night equilibrium concentrations 05 p0657 A72-16252

Atmospheric neutron production by cosmic rays, calculating Cd-In ratio 05 p0662 A72-16258

Atmospheric composition and temperature effects on F1 region ion concentration structure from 140 to 220 km for low solar activity conditions 05 p0657 A72-16261

Venus cloud top chemical composition from spectroscopic data, discussing cloud refractive index and reflectivity 05 p0719 A72-16711

Venus daytime ionosphere at 100-500 km, discussing ion clustering processes below 100 km discussing UV haze layer and atmospheric composition 05 p0723 A72-17163

Upper atmosphere Na abundance compared to radio meteor rate after diurnal effects elimination 06 p0876 A72-17645

Molecular sieve adsorption sampler for stratospheric carbon 14 measurements from balloon collected carbon dioxide samples 06 p0807 A72-17824

Photoelectric spectrophotometric measurements of Jupiter atmosphere optical properties and structure, showing methane absorption band intensity latitudinal variations 06 p0881 A72-17928

Ozone observation and daily and seasonal variations at Cologne, noting longitudinal variations for monthly means 06 p0808 A72-18146

Mars, Venus and Jupiter atmosphere composition and structure from spectral analysis, discussing equilibrium temperature, radiative heat transfer, integrated density and adiabatic temperature gradient 07 p1073 A72-19353

Transcript of conference on origins of life covering cosmic evolution, abundance and distribution of biologically important elements, earth and Mars atmosphere evolution, etc 07 p1074 A72-19450

- Atmospheric ozone photochemistry, discussing pure oxygen and moist atmospheres, NO mechanism, tracer applications, stratospheric dynamics and Umkehr observations
07 p0979 A72-20228
- Upper atmosphere minor component distribution rearrangement, investigating transition time to diffusion equilibrium
08 p1155 A72-20803
- Sunlight irradiated atmosphere formaldehyde photolysis as hydrogen atom source, estimating photodecomposition rates from extinction rates and photochemical results
08 p1230 A72-20981
- Atmospheric Na, Li and K layers height, width, abundance and thickness from twilight glow measurements, using birefringent filter type photometers
08 p1159 A72-21224
- Venus atmosphere chemical composition, temperature and pressure, discussing model cloud layer, circulation and upper atmosphere structure
08 p1236 A72-21400
- Handbook on aviation meteorology covering atmospheric structure and composition, standard atmospheres, heat transfer, adiabatic processes, winds, cloud formations, precipitation, ice formation, fog, visibility, etc
08 p1200 A72-21479
- Venus upper clouds composition from Mariner 5 occultation data analysis concerning temperature and pressure profiles, abundances, polarization characteristics, reflection and emission spectra
08 p1236 A72-21496
- Planetary atmospheres composition diversity, discussing evolution of Mars, Venus, earth and Jupiter from primitive solar nebula
08 p1119 A72-22012
- Mesosphere ozone number densities from rocket photometric measurement of lunar UV radiation absorption
09 p1385 A72-22583
- Approximate expression for charge exchange spreading of proton beam precipitating into atmosphere, showing dependence on atmospheric structure, collision data and primary particle energy
09 p1377 A72-22591
- Layer-like atmosphere discontinuities effects on earth-space communications, noting electromagnetic waves alteration and reflection by grazing incidence
09 p1279 A72-22898
- Sounding rocket spectral measurements of low energy auroral ion composition during premidnight breakup
09 p1300 A72-23020
- Horizontal ozone distribution in middle stratospheric macrosynoptic situations, considering anticyclonal side and jet stream delta region
09 p1301 A72-23194
- Microorganisms effects on oxygen and compounds cycles, leading to changes in oxygen distribution in earth crust, hydrosphere, atmosphere and biomass
09 p1267 A72-23592
- Neutral atmosphere effects on lower ionosphere, considering D region atomic oxygen, nitric oxide and water vapor and electron density distributions
10 p1474 A72-24712
- Photochemical models to simulate composition and reactions of upper atmosphere, noting transport importance
10 p1474 A72-24713
- Magnetic storm effects in atmospheric neutral composition, noting thermospheric wind circulation role due to Joule heating within auroral zone
10 p1476 A72-24957
- Atmospheric constituents dimension, composition and dynamics from optical radar echo observation of laser light scattering
11 p1592 A72-25849
- Stratospheric methane measurements over North America from solar absorption spectra observed from aircraft
11 p1622 A72-25911
- Atmospheric carbon monoxide and nitrous oxide telluric line contours and line centers optical thickness, measuring solar radio emission transmissivity
11 p1628 A72-26881
- Ionospheric and neutral atmospheric temperature profile, composition and electron density and energy measurements by MR-12 rocket
11 p1628 A72-26905
- Atmospheric ozone inference from satellite IR horizon radiance measurements
12 p1799 A72-27030
- Atmospheric abundance ratios of gas inclusions in Muong Nong and Libyan Desert glass tektites by mass spectrometric analysis, indicating terrestrial origin
12 p1866 A72-27117
- Methane concentration of air sample from stratopause measured by gas chromatography, discussing sample integrity, analysis method and results
12 p1802 A72-27505
- Life on Mars, investigating ground based and probe observations of atmospheric composition and pressure, surface temperature and features and UV radiation
12 p1761 A72-27624
- Seasonal atmospheric composition changes relation to midlatitude F 2 layer seasonal anomaly during high solar activity
12 p1803 A72-27776
- Atmospheric nitric acid vapor radiation absorption measurements at various partial pressures
12 p1805 A72-27993
- Hypoxia effect on aircraft pilot performance, using Link GAT 1 trainer and controlled composition atmosphere under varied altitude conditions for simulated ILS landing approaches
12 p1776 A72-28310
- Upper atmosphere atomic oxygen distribution calculated for D and E region aeronomy problems solution
13 p1947 A72-28604
- SST water vapor and nitrogen oxides exhausts effect on stratospheric composition, developing nonequilibrium photochemical model
13 p1994 A72-28878
- Martian atmosphere and surface, covering atmospheric composition, optical thickness and pressure, violet and yellow clouds, surface relief and topography
13 p2039 A72-29210
- Atomic oxygen layer height and peak concentration in earth upper atmosphere, considering solar dissociative radiation and turbulent diffusion for equinox conditions
13 p1948 A72-29236
- Vertical concentration profile and diurnal variations of N and NO vs solar activity from satellite horizon airglow experiment
13 p1948 A72-29237
- Subauroral red arcs formation mechanism involving magnetosphere-ionosphere energy conduction and lower atmosphere neutral composition changes due to turbulent mixing
13 p1952 A72-29802
- Thermospheric atomic hydrogen concentration diurnal variations from time dependent continuity and diffusion equations, using Jacchia background atmosphere thermal and density structure formulas
13 p1953 A72-29806
- Radio absorption spectra sounding for planetary atmospheric impurities calculating water vapor content in Venus cloud level
14 p2149 A72-30238
- Jupiter and Saturn atmosphere composition, structure and radiative properties, presenting two zone stratosphere-troposphere model
14 p2161 A72-31072
- Light rays total, astronomical and photogrammetric refraction in planetary atmospheres with arbitrary composition
15 p2224 A72-31602
- Lower Arctic thermosphere neutral composition changes due to disturbances, considering atomic hydrogen, nitric oxide, hydroxyl, water vapor, nitrogen and oxygen
15 p2225 A72-31912
- Lower thermospheric neutral gas density and composition rocket-borne mass spectrometric measurements with liquid He cooled ion source
15 p2236 A72-31942
- Thermospheric composition global model for magnetically quiet conditions based onOGO-6 mass spectrometer measurements
15 p2227 A72-31954
- Satellite instrument to observe atmospheric composition by energy analysis of incoming gas stream, using velocity mass spectrometer for neutral particles measurement
15 p2236 A72-31966
- Mesospheric and lower thermospheric composition from neutral atmospheric particles measurement by rocket-borne instrument consisting of RF quadrupole mass spectrometer
15 p2228 A72-31967
- Aladdin experiment atmospheric composition, total neutral density, temperature and ion density vertical profiles
15 p2228 A72-31969
- Carbon dioxide abundance variations from Venus high resolution spectra, discussing HCl and hydrogen fluoride line formation
15 p2310 A72-31994
- Tropospheric meridional ozone profiles between Europe and South Africa from measurements aboard commercial airliners, noting seasonal variations
16 p2382 A72-32889
- Thermospheric composition variations in south polar regions during magnetically quiet periods fromOGO-6 observations, considering atmospheric heating by electron precipitation cyclic variations
16 p2383 A72-32964
- Lower thermosphere neutral composition from February 1969 rocket-borne mass spectrometer measurements over Fort Churchill, Canada
16 p2383 A72-32965
- Summer upper mesosphere and lower thermosphere positive ion composition at high latitudes from Nike Cajon rocket soundings
16 p2383 A72-32966
- Upper atmospheric trace constituents global mapping by laser radar probing from satellite, discussing feasibility and comparison with ground based system
16 p2365 A72-34074
- Atmospheric properties effect on satellite aerodynamic characteristics, noting gas composition and upper atmospheric winds
16 p2347 A72-34075
- [AIAA PAPER 72-659]
The bulk composition of Titan's atmosphere.
17 p2606 A72-34541
- Relaxation phenomena in the biological carbon cycle under conditions of variable atmospheric CO₂-content.
17 p2500 A72-34897
- Spectral observations of Venus in the frequency interval 18.5-24.0 GHz - 1964 and 1967-68.
17 p2610 A72-35120
- Remote measurements of the atmosphere using Raman scattering.
17 p2547 A72-35195
- Thermospheric molecular oxygen from solar extreme-ultraviolet occultation measurements.
17 p2614 A72-35602
- Atmospheric composition to 40 km altitude from balloon-borne particle impacted electron microscope screens, discussing pollution effects from high flying aircraft exhaust gases
17 p2551 A72-35935
- On the boundary conditions in theoretical model calculations of the distributions of minor neutral constituents in the upper atmosphere.
18 p2659 A72-36294
- Atmospheric ozone and the history of life.
18 p2686 A72-36626
- Water vapor flux periodic and spatial variations from airborne measurements, confirming height variation of maximum spectral density wavelength for crosswind runs
18 p2706 A72-36632
- Upper atmospheric sodium and stratospheric warnings.
18 p2687 A72-36643
- Existence, structure and thermodynamic and kinetic stability of ClOO radical in Venus atmosphere, using quantum statistics methods for unimolecular decomposition rate
18 p2726 A72-36647
- A model atmosphere analysis of the Ap star HR 465.
18 p2727 A72-36736
- Titan and its atmosphere.
18 p2729 A72-36989
- Photoelectric spectrophotometric measurements of Jupiter atmosphere optical properties and structure, showing methane absorption band intensity latitudinal variations
18 p2730 A72-37153
- Seasonal and latitudinal relation between Mars white clouds occurrence frequency and global water distribution, suggesting cloud composition as water vapor
20 p2968 A72-39241
- Jupiter atmosphere methane deuterium/hydrogen ratio estimate from exchange reaction and temperature studies
20 p2968 A72-39242
- Ammonia photolysis and the role of ammonia in chemical revolution.
20 p2898 A72-39375
- Atmospheric carbon monoxide and nitrous oxide telluric line contours and optical thickness in line centers, measuring solar radio emission transmissivity
20 p2919 A72-39568
- Equilibrium lunar atmospheric content of radon-222, noting earth based diffusion constants inapplicability in moon vacuum conditions
20 p2972 A72-39861
- Detection of molecular oxygen in the Martian atmosphere.
21 p3103 A72-40451
- Transmission efficiency of gas chromatography algorithmic data compression and coding for spacecraft atmosphere studies
21 p3053 A72-40549
- Jupiter atmospheric C12/C13 ratio for methane from equivalent width measurements in R[2] multiplet
21 p3107 A72-41273
- Venus atmosphere constituent abundances and temperature and pressure profiles from Venera probe data
21 p3110 A72-41451
- The composition of the Martian atmosphere - Minor constituents.
21 p3110 A72-41458
- Minor constituents in planetary atmospheres - Ultraviolet spectroscopy from the Orbiting Astronomical Observatory.
21 p3111 A72-41459
- Balloon optical experiments in IR, visible, UV and X ray regions, considering in situ measurements of atmospheric composition, electric field and cosmic dust
21 p3049 A72-41613

- Distribution of total ozone content in the atmosphere according to spacecraft observations
21 p3050 A72-41797
- Russian book - Aviation meteorology.
22 p3200 A72-42024
- Detection of molecular oxygen on Mars.
22 p3224 A72-42293
- Rocket radiometers measurement of oxygen IR atmospheric system altitude profile at night, noting auroral enhancement possibility
22 p3170 A72-42365
- Gaseous and particulate iodine in the marine atmosphere.
22 p3173 A72-42469
- Gaseous and particulate bromine in the marine atmosphere.
22 p3173 A72-42470
- Cool supergiant stars atmospheric model for chemical composition change effects due to nuclear burning cycle
22 p3227 A72-42556
- Low abundance of solar photosphere iron from Fe I excitation and ionization computations, showing LTE departure effects on spectral lines
22 p3228 A72-42569
- Inert gas effects on embryonic development.
22 p3145 A72-42744
- Atmospheric nitric acid vapor radiation absorption measurements at various partial pressures
22 p3174 A72-43007
- Physical and chemical properties and stratification of neutral matter in comet atmospheres, discussing neutral gas dynamics and surface brightness distribution in comet images
23 p3335 A72-43299
- A rocket measurement of the vertical distribution of atmospheric ozone.
23 p3285 A72-44242
- Stratospheric concentration of radioactive carbon from 1961-62 nuclear tests by balloon measurements over European U.S.S.R. territory during 1967-69
23 p3286 A72-44492
- Determination of the physical properties of atmospheric aerosol particles above the Atlantic
24 p3420 A72-44757
- Upper atmosphere atomic oxygen distribution calculated for D and E region aeronomy problems solution
24 p3398 A72-45104
- Distribution of hydrogen and helium in the upper atmosphere.
24 p3400 A72-45593
- ATMOSPHERIC CONDITIONS**
U METEOROLOGY
ATMOSPHERIC CONDUCTIVITY
NT IONOSPHERIC CONDUCTIVITY
- Balloon measurements of lower stratosphere ion conductivity, noting deviation from predicted values based on Thompson ion-ion recombination theory
06 p0808 A72-18094
- Ball lightning theory based on thin conducting ladder networks and three dimensional fine particle structures formation in electric fields
09 p1346 A72-22963
- Atmospheric electricity problems, considering air pollution effects on ion concentration and air conductivity and solar activity effects on ionosphere-earth potential difference
10 p1473 A72-24528
- Mathematical model of atmospheric electric clouds, calculating electric charges and fields from convection and conductivity data
13 p1996 A72-30086
- Magnetospheric and ionospheric potential electric fields, using variational process based on transverse/longitudinal conductivity ratios in plasma
14 p2100 A72-30633
- ATMOSPHERIC DENSITY**
- Lower thermosphere temperature, air density and pressure models, using auroral zone midlatitude neutral thermal and molecular diffusion coefficient measurements
01 p0053 A72-10187
- Average energy electron capture coefficient dependence on air density, temperature and altitude under gamma radiation
01 p0059 A72-10599
- Upper atmosphere neutral oxygen density diurnal variations from incoherent scatter and satellite drag data, noting deviations from Jacchia static diffusion model predictions
01 p0062 A72-10911
- Solar outer corona steamer density and temperature data from type 3 solar radio burst observation by space radio astronomy
03 p0424 A72-13223
- Upper atmospheric density measurements accuracy from triaxial accelerometer instrumented inflated falling sphere
04 p0519 A72-15156
- Rotating and nonuniform planetary exosphere model, examining density profiles
04 p0579 A72-15333
- Atmospheric density near 150 km altitude from Cosmos 316 orbital decay, noting density increases during geomagnetic storms
05 p0655 A72-16070
- Spacecraft reentry trajectory parameter selection and optimal control algorithm under random atmospheric density variation
05 p0685 A72-16429
- Upper atmosphere density fluctuations associated with solar activity and local time values, using Cosmos 14 satellite drag data
05 p0659 A72-17037
- Upper atmosphere density and heating near auroral zones, using satellite Molniya 1K data
06 p0805 A72-17637
- Upper atmosphere analytical model expressing density as function of exospheric temperature and altitude
06 p0806 A72-17658
- Low energy per pulse high repetition rate laser radar capabilities for atmospheric density measurement above 30 km
06 p0775 A72-18093
- Latitude dependent discrepancy between low latitude satellite drag deduced densities at high latitudes and Jacchia model
07 p0976 A72-19167
- Gas-surface interaction parameters and atmospheric density determination from satellite drag induced orbital decay measurements
07 p0910 A72-20116
- Atmospheric turbulence, wind velocity, temperature and density measurements at 90-250 km, using explosive contaminants release from Skylark rockets
07 p0979 A72-20265
- Laser radar observations of mesosphere and lower thermosphere optical scattering cross section variations due to tide-caused atmospheric density fluctuations
08 p1156 A72-21100
- Wind and density measurements by small sounding rockets, comparing results with ground observed radio wave absorption diurnal variations
08 p1160 A72-21531
- D region neutral gas winds, density changes and short wave radio absorption correlation, determining air mass flow rates from chaff fall rate measurements
08 p1160 A72-21532
- Satellite orbital inclination change due to rotating upper atmosphere with day-to-night density variation, deriving resonance conditions
08 p1241 A72-21640
- D region neutral gas winds, density variations and short wave absorption, determining correlation from ultralight chaff and absorption measurements at 2.83 MHz
09 p1277 A72-22374
- Frictioned force modification of lower thermosphere vertical neutral gas velocities with resulting atomic oxygen and molecular nitrogen density-height distribution deviation from barometric law
09 p1298 A72-22582
- Diurnal phase anomaly in upper atmospheric density and temperature inferred from satellite drag and incoherent scattering observations
09 p1298 A72-22590
- Vertical air density gradient in stratosphere as function of altitude
10 p1472 A72-24489
- Thermosphere and lower exosphere density and temperature variations from satellite decay
11 p1621 A72-25843
- Thermodynamic equilibrium theory for upper atmosphere /thermosphere/ temperature and density variations, noting Harris-Priester model
11 p1622 A72-25844
- Atmospheric neutral density measurement near 400 km during daytime by microphone density gage onOGO 6
11 p1625 A72-26407
- Atmospheric density annual and diurnal variations in lower ionosphere, from satellite radar tracking data, considering drag coefficient modeling and orbit determination techniques
11 p1625 A72-26410
- Semiannual exospheric temperature and density variations from satellite observation and ionosonde measurements
11 p1626 A72-26420
- Atmospheric density variations from meteorological rocket soundings, discussing data reduction methods and error sources for bead thermistor and inflatable falling sphere instruments
11 p1626 A72-26473
- Time dependent geopotential as function of position weighted atmospheric density from Poisson equation, noting satellite orbit perturbations due to mass shifts in planetary atmospheres
12 p1838 A72-27022
- Diving operations medical aspects significance for manned planetary surface exploration in high density atmospheres, considering protective clothing, breathing apparatus and gas mixtures, etc
12 p1769 A72-27415
- Upper atmosphere density measurement techniques used by Sputnik 3 and San Marco 1 and 2 satellites
12 p1802 A72-27683
- Self similar blast waves propagation, studying flow field in terms of shock front velocity and ambient atmospheric density variation ahead of front
12 p1889 A72-27832
- Solar cells calibration by high altitude aircraft, using extrapolation method to zero air density
12 p1758 A72-28041
- Atmospheric model for random density variations effects on space shuttle reentry parameters, using Monte Carlo trajectories for delta wing orbiter
13 p1990 A72-28814
- Rocket-borne inflatable sphere for radar signal backscatter calibrations at reentry altitudes and for simultaneous atmospheric density determination
13 p1918 A72-28819
- Satellite aerodynamics effect on atmospheric density determination, discussing drag coefficient dependence on altitude
13 p1990 A72-28821
- Ballistic density and wind determination from radiances observed by satellite IR spectrometer (SIRS) onboard Nimbus 3
13 p1991 A72-28825
- Mesosphere and stratosphere density and temperature variability with seasons and altitude
13 p1947 A72-28830
- Neutral atmospheric density profiles measurements in lower thermosphere by satellite-borne accelerometers, noting longitudinal variations at high latitudes
13 p1948 A72-28833
- Thermospheric density-temperature time lag, considering two dimensional time dependent model based on UV heat input dynamic excitation
13 p1951 A72-29388
- Atmospheric oxygen concentration latitudinal and diurnal variations from incoherent scatter and satellite drag data, noting compatibility with Jacchia model
13 p1951 A72-29389
- Satellite measurements of exospheric density variations during June 1968-December 1970 at 1070 and 900 km, discussing solar activity effect
13 p1952 A72-29803
- Tungusk meteorite explosion energy values for various altitudes from investigation of shock wave propagation in variable density atmosphere
14 p2152 A72-30492
- Ionospheric rotational temperature and density measurement, using fluorescence produced by rocket-borne electron beam gun
14 p2106 A72-30974
- Stochastic atmospheric density fluctuations effect on circular-orbiting satellite roll-yaw oscillations stability
15 p2319 A72-31457
- Temperature and density data deviation from stratosphere and mesosphere mean season model values at high latitudes
15 p2225 A72-31907
- Mesospheric air density and temperature measurements from rocket-borne resistance thermometers based on free molecular flow
15 p2225 A72-31911
- Lower Arctic thermosphere neutral composition changes due to disturbances, considering atomic hydrogen, nitric oxide, hydroxyl, water vapor, nitrogen and oxygen
15 p2225 A72-31912
- Nitric oxide gas release by rocket in auroral glow to determine atomic oxygen densities in ionosphere via observation of auroral light emission
15 p2226 A72-31936
- Lower thermospheric neutral gas density and composition rocket-borne mass spectrometric measurements with liquid He cooled ion source
15 p2236 A72-31942
- Ionospheric molecular oxygen density measurements during solar grazing ray absorption experiment on Ariel 3 satellite
15 p2226 A72-31950
- Atmospheric density and temperature measurements by rocket-borne spheres during 1972 winter, observing variability with altitude
15 p2227 A72-31959
- Ionospheric neutral density profile measurement by ultrasensitive triaxial electrostatic force rebalance accelerometer onboard Cannon Ball 2
15 p2227 A72-31962
- Upper atmosphere density from orbital drag on Cannon Ball II and Musket Ball satellites
15 p2227 A72-31963
- Aladdin experiment atmospheric composition, total neutral density, temperature and ion density vertical profiles
15 p2228 A72-31969
- Aerodynamic drag at high latitudes observed from Molniya satellites orbit analysis, suggesting upper atmosphere density change
15 p2229 A72-31989
- Polar/midlatitude model of atmospheric density variations from LOGACS low altitude satellite accelerometer experiment
15 p2229 A72-32000

Ion chemistry and heating of daytime ionosphere E and lower F regions, calculating neutral atmosphere densities, ion production rates and solar EUV radiation absorption

15 p2192 A72-32253

Ionospheric ion temperatures and velocities and electron and neutral densities from incoherent scatter observations during 11 February 1969 magnetic storm

15 p2229 A72-32254

Thermospheric density annual and semiannual variations due to solar heat input into ozone layer and Joule heating, discussing decomposition into Fourier terms

15 p2229 A72-32255

Exobase atomic hydrogen densities for zero ballistic net flux as function of temperature distribution, noting support of McAfee hypothesis by OGO-4 polar UV observations

16 p2384 A72-32979

On the possibility of a simultaneous measurement of wind speed, wind direction, air density and air temperatures at heights which correspond to the upper D-region /max. 95 km/ with chaff cloud sensors.

17 p2545 A72-34631

Measurements of molecular oxygen in the thermosphere.

17 p2546 A72-34694

Functional equations for optimal spacecraft or rocket interception by similar vehicle within limits of dense atmosphere

17 p2621 A72-35121

Prediction of upper atmosphere density over the lifetime of a satellite

17 p2547 A72-35215

Upward and downward motions of Venus atmosphere in terms of continuous cloud cover effects, considering solid cloud cover hypothesis

18 p2729 A72-36984

Tungusk meteorite explosion energy values for various altitudes from investigation of shock wave propagation in variable density atmosphere

19 p2864 A72-38321

The variation of air density at 240 and 280 km from April to November 1967.

20 p2916 A72-39235

The influence of vertical motions on the diurnal variations of temperature and density in the thermosphere.

20 p2916 A72-39236

Thermal oscillations in the high solar photosphere.

21 p3107 A72-41275

The total pulsation-frequency spectrum of a polytropic atmosphere

21 p3114 A72-41779

A calculated hydrogen distribution in the exosphere.

22 p3168 A72-42004

Atmospheric density from spacecraft drag data by successive optimization of control laws, using quadratic programming

23 p3277 A72-44003

Isothermal atmosphere inhomogeneities effects on electromagnetic cascade electrons integral energy spatial distribution

23 p3331 A72-44433

The estimation of accuracy of short-term atmosphere density prediction.

24 p3398 A72-45173

Minimum-time entry of space vehicles into a planetary atmosphere

24 p3452 A72-45442

Optimization of spacecraft reentry into a planetary atmosphere

24 p3453 A72-45597

ATMOSPHERIC DIFFUSION

Electronic computing wind vane for meteorological support during atmospheric diffusion studies

06 p0843 A72-18449

Mesosphere and lower thermosphere heating and associated solar UV radiation absorption calculation based on diurnally varying photochemical diffusive model

10 p1475 A72-24943

Upper atmosphere /thermosphere/ physical variations, discussing diffusive equilibrium, energy absorption and heat transfer

11 p1621 A72-25842

Non-Maxwellian collisionless transport properties of neutral gas constituents in planetary exospheres, discussing ballistic particle and heat transport and escape fluxes

11 p1716 A72-25846

Real time measurements of ground level and airborne particle concentrations and diffusion in 10-100 km range

11 p1681 A72-26081

Relative atmospheric dispersion in entropy/half squared vorticity/ - cascading inertial range of homogeneous two dimensional turbulence

12 p1839 A72-27031

Thermospheric atomic hydrogen concentration diurnal variations from time dependent continuity and diffusion equations, using Jacchia background atmosphere thermal and density structure formulas

13 p1953 A72-29806

SST contrails stratospheric dispersion by aircraft wake, atmospheric turbulence and exhaust gases temperature induced buoyancy

[AIAA PAPER 72-650] 16 p2388 A72-34084

Atmospheric boundary layer and diffusion over three dimensional mountainous terrain by laboratory simulation with meteorological wind tunnel and scale model

[AIAA PAPER 72-648] 16 p2419 A72-34085

Relation between impurity shear dispersion in the atmospheric ground layer and the turbulence characteristics

19 p2829 A72-38772

A method for simulating wind conditions during atmospheric stagnation periods.

20 p2947 A72-38965

Some features of instantaneous point source diffusion within a turbulent boundary layer.

21 p3078 A72-40467

Diffusion from a continuous source in relation to the Eulerian properties of turbulence.

21 p3046 A72-41248

ATMOSPHERIC ELECTRICITY

NT AURORAL ELECTROJET

NT ELECTROJET

NT EQUATORIAL ELECTROJET

NT IONOSPHERIC CURRENTS

Parallel electric field evidence near auroral ionosphere deduced from low energy particles, energy spectra and angular distribution

01 p0061 A72-10895

Magnetospheric wave and particle phenomena correlation to convection electric fields in nightside magnetosphere during isolated substorms

01 p0062 A72-10904

Vertical distribution of ionospheric and magnetospheric electric fields, estimating Joule heating

02 p0220 A72-12324

Air shower cores or relativistic monopoles as sources of straight lightning, considering thundercloud conditions over ocean and land areas

03 p0350 A72-14100

Magnetospheric current effects on geomagnetic field structure, noting electron and proton precipitation into auroral zone

05 p0657 A72-16275

Large drops coalescence, investigating approach rate dependence on electric field strength and distance

08 p1201 A72-21998

Potential gradient and air-earth current increases during period of increasing solar activity, discussing H alpha flare effects

09 p1378 A72-23264

Atmospheric electricity problems, considering air pollution effects on ion concentration and air conductivity and solar activity effects on ionosphere-earth potential difference

10 p1473 A72-24528

Atmospheric electricity measurements at Waldorf observatory during 7 March 1970 solar eclipse

12 p1799 A72-27139

Atmospheric electricity, turbulence and pseudosunrise effect during solar eclipse, analyzing space charge density and power spectra decay

12 p1800 A72-27140

Point discharge current and precipitation effect on atmospheric potential gradient vertical profile

12 p1839 A72-27501

Tropical thunderstorm precipitation current variations due to lightning produced atmospheric electric field changes, considering charged raindrops turbulent diffusion

12 p1839 A72-27502

Analytic models of large scale electric fields in atmosphere, considering geomagnetic Sq current in lower atmosphere and inner magnetosphere

12 p1804 A72-27790

Upper atmosphere electric fields derived from ionosphere-earth electric potential measurements following solar flare activity

12 p1804 A72-27805

Solar activity effects on atmospheric electricity during favorable weather conditions, discussing troposphere potential gradient and earth air current

13 p2029 A72-28622

Field mill measurement of atmospheric electric space charge density, discussing effects of snow melting and artificial charge sources

13 p1952 A72-29666

Airplane-borne cylindrical field mill type instrument to record atmospheric electric field

13 p1961 A72-30085

Mathematical model of atmospheric electric clouds, calculating electric charges and fields from convection and conductivity data

13 p1996 A72-30086

Solar event-related ionospheric horizontal electric fields derived from balloon measurement of mid-European and equatorial ionosphere potentials

15 p2223 A72-31556

Geomagnetic substorm magneto-ionospheric effect, discussing electric field transmission, magnetic field variations and currents flowing in dynamo region

15 p2230 A72-32259

A satellite survey of vector electric fields in the ionosphere at frequencies of 10 to 500 hertz. I - Isotropic, high-latitude electrostatic emissions.

19 p2768 A72-38742

A satellite survey of vector electric fields in the ionosphere at frequencies of 10 to 500 hertz. II - The electric component of ELF hiss.

19 p2768 A72-38743

A satellite survey of vector electric fields in the ionosphere at frequencies of 10 to 500 hertz. III - Low-frequency equatorial emissions and their relationship to ionospheric turbulence.

19 p2768 A72-38744

ATMOSPHERIC EMISSION

U AIRGLOW

ATMOSPHERIC ENTRY

NT HYPERBOLIC REENTRY

NT HYPERSONIC REENTRY

NT MANNED REENTRY

NT SPACECRAFT REENTRY

Orbital plane rotation and terminal impact ascending node and inclination of satellite during ballistic reentry

01 p0052 A72-10078

Temperature gradient induced in Lost City /Oklahoma/ olivine-bronzite chondrite by atmospheric friction from thermoluminescent emission measurements

01 p0126 A72-10109

Optimal control algorithm for spacecraft descent in atmosphere at speed near escape velocity, using game theory

01 p0135 A72-10298

Reentry glider approximate optimal atmospheric entry trajectories, maximizing function of terminal velocity, altitude, flight path and heading angles subject to three terminal nonlinear constraints

01 p0128 A72-10377

Crater 9 meteorite /Argentina/ entry trajectory and orbital calculations, determining masses and velocities from dynamic conditions at impact

02 p0275 A72-11599

Optimal closed loop control of stochastic nonlinear systems by expanded cost function applied to reduced terminal error atmospheric entry problem

05 p0685 A72-16462

Atmospheric reentry trajectory mechanics investigation method, considering flight path angle vs atmospheric density

05 p0728 A72-16704

Ablation performance of dielectric heat shields for planetary entry, testing diffuse reflectance by convective and radiative heating

05 p0747 A72-16809

Environmental analysis of gas particle/probe aeroshell interaction in rarefied flow of high altitude Jupiter entry

05 p0721 A72-16844

Spacecraft banking control during reentry, deriving dynamic equations of angular motion

05 p0730 A72-17026

Laminar near wake solutions for slender ablating cone under supersonic atmospheric entry conditions including boundary layer reactions

07 p0907 A72-18954

Atmospheric freestream pressure profiles determination from base pressure and flow phenomena of Mars, Venus or Jupiter entry probes

07 p0982 A72-18959

Transcendental series solution of Chini-Painleve nonlinear differential equations describing vehicle and meteorite oscillation during planetary atmospheric entry

07 p0964 A72-20594

Recursive and nonrecursive real time spline methods for nonlinear estimation of independent trajectory parameters for vehicle entering earth atmosphere

08 p1197 A72-20862

Perturbation solution of deceleration trajectory in ballistic reentry through rotating atmosphere with winds, assuming constant gravitational field and square law drag force

09 p1395 A72-22924

Mars and Venus probes entry into planetary atmospheres, discussing aerodynamics of trajectory control and soft landing

09 p1394 A72-23673

Mars atmospheric entry experiments for Viking 1975 mission, discussing onboard neutral gas mass spectrometer and retarding potential analyzer

10 p1540 A72-24381

Spacecraft trajectories for reentry at hyperbolic velocity, examining aerodynamic control loads and characteristics in atmospheric skip

11 p1718 A72-25929

Parabolic velocity atmospheric reentry navigation algorithm for spacecraft control, demonstrating guidance accuracy to landing point

11 p1684 A72-26899

Elastomeric silicone ablator heat shields thermal characteristics from NASA Planetary Atmosphere Experiments Test vehicle earth atmosphere entry measurements

13 p2064 A72-28953

Spacecraft optimal control after transfer from hyperbolic trajectory to planetary satellite orbit by atmospheric drag, minimizing engine thrust
14 p2129 A72-30470

Minimum weight phase change thermal control device for planetary descent probes, discussing test over various heat loads
[AIAA PAPER 72-287] 14 p2171 A72-30826

Hypersonic limit for equilibrium laminar constant pressure boundary layer equations of planetary entry, obtaining skin friction and heat transfer parameters
14 p2071 A72-31052

Blunt planetary entry vehicles thermal flux prediction, taking into account viscosity, conduction, dissociation, ionization, nongray radiation, surface emissivity and ablation effects
15 p2335 A72-31816

Electron density measurements in bow shock stagnation and conical afterbody regions during blunt body atmospheric reentry, using flush mounted electrostatic probes
[AIAA PAPER 72-694] 16 p2345 A72-34047

Blunt nose cone flow field characteristics microwave measurement at stagnation point during atmospheric reentry, using plasma diagnostic sensors with antennas and electrostatic probes
[AIAA PAPER 72-693] 16 p2345 A72-34049

Onboard radiometric measurement of bow shock generated UV radiation during atmospheric reentry of experimental sphere
[AIAA PAPER 72-692] 16 p2462 A72-34050

Probability for spore sterilization by aerodynamic heating, considering straight line and decaying circular orbital Mars entry trajectories
16 p2461 A72-34165

Synthesis of a nonlinear law for spacecraft motion control in the earth's atmosphere
17 p2621 A72-35201

Synthesis of a nonlinear law for the control of spacecraft motion in the atmosphere of the earth
17 p2621 A72-35202

Investigation of the range of landing area distances for earth atmosphere reentries at hypersonic velocities
17 p2622 A72-35204

Parameters influencing dynamic stability characteristics of Viking-type entry configurations at Mach 1.76.
17 p2622 A72-35494

Thermally controlled entry guidance for shuttle.
[AIAA PAPER 72-831] 20 p2951 A72-39096

Nuclear particle fluxes and radioactive isotopes production rate distribution from cosmic rays data along orbits, calculating iron meteorite dimensions prior to atmosphere entry
22 p3220 A72-41919

Development and performance analysis of a trajectory estimator for an entry through the Martian atmosphere.
[AIAA PAPER 72-953] 22 p3224 A72-42352

Taylor instability in the shock layer on a Jovian atmosphere entry probe.
22 p3136 A72-42873

Aerospace tug using atmospheric braking during return from geostationary orbit, discussing radiative thermal protection, mass, design and advantages
23 p3340 A72-44275

On required guidance for transfer from hyperbolic trajectory to the planetary satellite orbit by aerodynamic drag in atmosphere.
24 p3450 A72-45176

Radiation gasdynamics of planetary entry - Concepts and recent advances.
24 p3361 A72-45188

Space shuttle optimal entry trajectories for thermal protection system weight minimization, considering constant and variable angles of attack
[AIAA PAPER 72-977] 24 p3452 A72-45414

Minimum-time entry of space vehicles into a planetary atmosphere
24 p3452 A72-45442

ATMOSPHERIC ENTRY SIMULATION

Thin liquid surface water film cooling tests for mass loss under simulated reentry heating and shear conditions
10 p1563 A72-24648

Hypersonic base heating investigation on Mars atmosphere entry blunt bodies, taking into account gas composition and angle of attack effects
[AIAA PAPER 72-317] 11 p1568 A72-25251

Spacecraft reentry into random medium atmosphere, determining optimal control procedure for prescribed arrival region and time with simulation equation
11 p1686 A72-25930

Fusion silicide protective coatings performance for Ta alloys under simulated reentry conditions, noting oxidation rate, ductile brittle bend transition temperature and mechanical properties
[ASM PAPER W 72-13.6] 12 p1835 A72-28162

Thermal control techniques used in space simulation laboratory testing.
22 p3164 A72-42997

Theoretical study and wind tunnel simulation of the electrical phenomena of reentry
22 p3231 A72-43092

ATMOSPHERIC HEAT BUDGET

Quasi-biennial modulation of kinetic energy transfer in stratosphere, comparing with hemispheric energy, eddy transports and tropical zonal wind and temperature
06 p0841 A72-17632

Handbook on aviation meteorology covering atmospheric structure and composition, standard atmospheres, heat transfer, adiabatic processes, winds, cloud formations, precipitation, ice formation, fog, visibility, etc
08 p1200 A72-21479

Aircraft or helicopter-borne IR radiometer for surface temperature of snow covers and glaciers and air-snow energy balance measurements
15 p2232 A72-31244

Aircraft short wavelength measurements of cloud reflection and absorption properties for impact on earth radiation budgets
16 p2388 A72-34024

Book - The earth's atmosphere
17 p2550 A72-35797

Mass and heat budget estimations of the Atlantic SE trade wind flow at the equator.
24 p3420 A72-44756

ATMOSPHERIC HEATING

MHD wave modes nonlinear coupling by quantum field approach with Hamiltonian formulation, applying to solar coronal heating
01 p0129 A72-10797

Relaxation and heating rate due to solar radiation absorption by 2.7 and 4.3 micron vibration-rotation bands of carbon dioxide
03 p0347 A72-13387

Supercooled and warm fog dispersion technology, considering air heating, helicopter downwash and seeding methods
04 p0543 A72-14812

Vertical motions in stratified cloudy atmosphere as function of plane divergence distribution and heat influx
06 p0840 A72-17621

Upper atmosphere density and heating near auroral zones, using satellite Molniya 1K data
06 p0805 A72-17637

Ozone content and vertical distribution variations as causes of winter stratospheric warmings in Northern Hemisphere
07 p0973 A72-18861

Atmospheric heating and kinetic cooling nonlinear effects on IR carbon dioxide laser beam propagation, comparing digital simulation results with geometrical optics
[CLEA PAPER 2.6] 07 p0942 A72-19381

Storm available potential energy generation and boundary layer frictional dissipation estimation in heat transfer from ocean to atmosphere within east coast cyclone
07 p0980 A72-20451

Non-LTE effects on mechanical heating in gray atmosphere applied to nonradiative energy input estimates for solar chromosphere from negative hydrogen ion emission
08 p1235 A72-21391

Nimbus 4 satellite-borne selective chopper radiometer design characteristics, obtaining maps of stratospheric warmings in both hemispheres
08 p1173 A72-22168

Three parameter prognosis model for geopotential vertical profile in troposphere and stratosphere, describing vortex and heat influx in quasi-geostrophic and adiabatic approximations
09 p1297 A72-22549

Cen X-3 model with X ray emission from atmosphere heated by shock waves generated by surface pulsations of white dwarf
10 p1544 A72-24668

Mesosphere and lower thermosphere heating and associated solar UV radiation absorption calculation based on diurnally varying photochemical diffusive model
10 p1475 A72-24943

Magnetic storm effects in atmospheric neutral composition, noting thermospheric wind circulation role due to Joule heating within auroral zone
10 p1476 A72-24957

Coincidence effects of subionsospheric extraterrestrial radiation focusing on ionospheric changes and stratospheric warmings
12 p1804 A72-27804

Satellite radiance data for altitude and amplitude monitoring of stratospheric warming, comparing with rocketsonde and radiosonde observations
13 p1991 A72-28823

Time evolution of chromosphere layer heated by energetic particle stream during solar flare, noting cooling by Lyman continuum radiation transfer
13 p2032 A72-29721

Nonrotating Hadley cells turbulence from steady one dimensional flow instabilities in thin nonrotating differentially heated atmosphere or ocean
15 p2219 A72-32722

Thermospheric composition variations in south polar regions during magnetically quiet periods from

OGO-6 observations, considering atmospheric heating by electron precipitation cyclic variations
16 p2383 A72-32964

Venus comet-like interaction with solar wind explained via He outer atmosphere with preferential heating by wind
16 p2459 A72-33915

Calculation of airflow over an arbitrary ridge including diabatic heating and cooling.
18 p2706 A72-36629

Upper atmospheric sodium and stratospheric warmings.
18 p2687 A72-36643

Wind patterns at meteor altitudes /75-105 kilometers/ above College, Alaska, associated with mid-winter stratospheric warmings.
18 p2689 A72-36962

Ucra meteorite - Determination of differential atmospheric heating using its natural thermoluminescence.
19 p2858 A72-37859

Investigation of the mesoscale convective processes during the forthcoming GARP implementation.
20 p2948 A72-39800

Response of the tropical atmosphere to local, steady forcing.
21 p3077 A72-40248

Seasonal, nonseasonal and synoptic global variations in stratosphere temperature from satellite-measured radiances, discussing latitudinal warming-cooling relationships
21 p3048 A72-40253

Equatorial stratospheric waves induced by diabatic heat sources.
22 p3201 A72-42508

Influence of the heating of a turbulent atmosphere by a light beam on the fluctuations of the beam intensity.
24 p3425 A72-45601

ATMOSPHERIC IMPURITIES

U AIR POLLUTION

ATMOSPHERIC IONIZATION

NT AURORAL IONIZATION

Lower ionosphere ionization response to auroral particle fallout during 1968 substorms, using geomagnetic, VLF and balloon measurements
01 p0053 A72-10366

Midlatitude D layer observations during sunspot minimum, emphasizing atmospheric ionization and ozonospheric parameters
01 p0055 A72-10433

Short wave skip distance calculation as function of path inclination to ionospheric layer for linear and parabolic ionization distributions
01 p0028 A72-10612

Ionospheric ion formation and neutralization reaction rate coefficients determination by fitting measured electron concentration profiles with computer generated profiles
01 p0059 A72-10616

F region neutral thermosphere temperature perturbation and circulation pattern due to global wind with anomalies of ionization calculated from two dimensional dynamic model
01 p0096 A72-11283

Auroral current generation by ionization and space charge transport interaction between charged particles and atmospheres
02 p0273 A72-11928

Linear electron density distribution along faint meteor trail, discussing radio echo time-amplitude characteristics and ionization curve
02 p0282 A72-12335

Oxygen, hydrogen and nitrogen constituents in mesosphere, investigating ionization process in D region at midlatitudes
03 p0346 A72-13379

Associative attachment and gas-to-particle conversion mechanisms in positive and negative ion formation up to 50 km
03 p0347 A72-13390

Upper atmosphere He, Ne, Na and K atoms collisions with molecular oxygen, determining ejected electron energy during fast Na, K, Rb and Cs ionization for meteor phenomena modeling
03 p0438 A72-13980

X ray stars atmospheric ionization effects by vlf phase tracking relative to Omega navigation accuracy, diurnal shift variations and astrophysical data
04 p0486 A72-14877

Magnetic latitude effect on wave dispersion in drifts and random movements of ionization irregularities in E region, suggesting charged particle precipitation role
04 p0518 A72-14964

Nighttime radio absorption from lower ionospheric ionization by Sco X-1 and Tau X-1 X rays, using full wave admittance method
04 p0519 A72-15161

D region ionization by electron fluxes as explanation for latitudinal radio wave absorption
05 p0636 A72-16249

Daytime ionogram corrections for underlying ionization in absence of X-trace of sporadic E layer
05 p0657 A72-16265

Sporadic E ionization during 1955 partial solar eclipse, considering gravity waves effect due to fast moving shadow region cooling spot

06 p0805 A72-17466

Balloon measurements of lower stratosphere ion conductivity, noting deviation from predicted values based on Thompson ion-ion recombination theory

06 p0808 A72-18094

F 2 ionization distribution diurnal variations from airborne ionosonde measurements during June-July 1966 over Tamanrasset meridian, correlating magnetic activity with wind variations

06 p0810 A72-18731

F region ionization anomalous evening enhancement, discussing seasonal variations, solar activity and geomagnetic coordinates maximum in Yakutsk

08 p1153 A72-20707

Radar verification of sporadic E layer formation from meteoritic atoms and ions production by meteoritic ablation

08 p1154 A72-20728

F 2 region magnetic disturbances conjugacy mechanisms, considering vertical ionization profiles

08 p1155 A72-20801

D region extraionization and solar X-ray flux from vlf data, emphasizing solar spectral shape and use of continuity equation for ionization time history

08 p1227 A72-21116

Hydrogen and helium thermal dissociation and ionization at Jupiter and Saturn adiabatic atmospheric models conditions

08 p1211 A72-21127

Oxygen ionization and ion mobility measurements in air by open proportional counting chamber with electron counter and exoelectron emitter

09 p1305 A72-22203

Supersonic and subsonic measurements of mesospheric ionization at night, using Arcaas rocket parachute borne nose-tip and blunt probes

09 p1296 A72-22362

Effective electron loss rates in lower D region from ionization changes during solar X ray flares, noting water cluster ions destruction

09 p1376 A72-22369

Photometric parameters of Leonid meteor ionized trail and turbulent diffusion in M zone, determining electron attachment rate

09 p1384 A72-22510

Aspiration condenser spectrometry of small ion mobility as function of height and atmospheric conditions

09 p1346 A72-23267

Metal ion sheaths in midlatitude sporadic E layer caused by vertical redistribution of neutral ionization, discussing wind shear discontinuities

10 p1477 A72-25159

Ionization movement of charged and neutral particles in F 2 region coupled to air movement by collision drag forces

11 p1621 A72-25839

D region ionization by solar corpuscular streams, considering formation of charged particle concentration profiles

11 p1622 A72-25948

Anomalous F region ionization in darkened high latitudes during solar activity growth and abatement

11 p1623 A72-26270

F 2 layer midlatitude local centers of anomalous nighttime ionization during winter and summer solstices

11 p1623 A72-26283

Electron density and ionization changes in lower ionosphere during 7 March 1970 solar eclipse from 2.66 MHz absorption and Langmuir probe rocket measurements

12 p1800 A72-27148

Ionization and associated energy loss effects on particles acceleration in solar atmosphere, emphasizing Fermi mechanisms

12 p1863 A72-27303

Electron density profiles calculation from ionograms, obtaining equivalent delay caused by ionization below minimum plasma frequency

12 p1802 A72-27307

Upper atmosphere particle flux density determined from nocturnal electromagnetic absorption caused by geomagnetic storms, noting ionization process time lag in lower ionosphere

13 p1945 A72-28580

Variations of F 1 layer thickness and maximum ionization height for high and low solar activity periods obtained from vertical ionospheric sounding

13 p1946 A72-28595

Electric field nature required for DP current system development in disturbed high latitude ionosphere, discussing F 2 region ionization drift

13 p1946 A72-28596

Drift measurement of lower ionosphere ionizational inhomogeneities by space-diversity LF band broadcast reception

13 p1948 A72-29037

Linear electron density distribution along faint meteor trail, discussing radio echo time-amplitude characteristics and ionization curve

13 p2039 A72-29219

Auroral current generation by ionization and space charge transport interaction between charged particles and atmosphere

13 p2030 A72-29240

Thermospheric parameters seasonal and latitudinal variations calculation based on atmospheric model with components ionization and molecular oxygen dissociation as main heat sources

14 p2128 A72-30463

Photoelectron precipitation induced dissociation of atmospheric nitrogen molecules during moderate solar activity

14 p2102 A72-30659

Long term A3 absorption associated with nuclear explosion caused artificial radiation belts, discussing electron precipitation role in D region ionization

15 p2299 A72-31933

Ion chemistry and heating of daytime ionosphere E and lower F regions, calculating neutral atmosphere densities, ion production rates and solar EUV radiation absorption

15 p2192 A72-32253

Ionized and neutral atmospheres coupled ionospheric continuity and motion equations, discussing nonlinear force effects on F 2 height and electron density

15 p2230 A72-32257

Occurrence frequency of F 2 layer sporadic ionization in auroral zone, noting solar activity effect

17 p2551 A72-35867

Nonstationary electron-ion gas distribution in the ionosphere

18 p2689 A72-36878

F region ionization anomalous evening enhancement, discussing seasonal variations, solar activity effects and maximum value dependence on geomagnetic latitude and longitude

19 p2790 A72-38335

Radar verification of sporadic E layer formation from meteoritic atoms and ions produced by meteoroid ablation

19 p2791 A72-38356

Diurnally varying neutral wind effects on lower F region ionization distribution, noting Appleton anomaly disappearance time

19 p2794 A72-38865

Theoretical investigation of nitric oxide and its role in D-region ionization.

20 p2918 A72-39531

Mid-latitude D-region ionization associated with the 'slot' in radiation belt electrons.

20 p2964 A72-39533

Aspect-sensitive reflections from ionization irregularities in the F-region.

22 p3154 A72-42364

The solar X-ray spectrum deduced from a proportional counter experiment and the resultant production of ionization in the mesosphere.

22 p3170 A72-42368

Electron deposition in water vapor, with atmospheric applications.

22 p3171 A72-42420

The density dependent ionization balance of carbon, oxygen and neon in the solar atmosphere.

23 p3334 A72-43252

Isothermal ionization of the lower ionosphere under the action of radio waves

23 p3283 A72-43362

The effect of meteoric ion processes on radio studies of meteoroids.

23 p3336 A72-43558

Investigation of hadron interactions with atomic nuclei at energies greater than 100 GeV

23 p3329 A72-44404

Anomalous ionization in lower ionosphere recorded by riometers, considering ionospheric substorms caused by auroral absorption

24 p3396 A72-44849

Upper atmosphere particle flux density determined from nocturnal electromagnetic absorption caused by geomagnetic storms, noting ionization process time lag in lower ionosphere

24 p3397 A72-45080

Variations of F 1 layer thickness and maximum ionization height for high and low solar activity periods obtained from vertical ionospheric sounding

24 p3398 A72-45095

Electric field nature for DP current system development in disturbed high latitude ionosphere, discussing F 2 region ionization drift

24 p3398 A72-45096

ATMOSPHERIC MODELS

NT BREADBOARD MODELS

NT DYNAMIC MODELS

NT REFERENCE ATMOSPHERES

Lower thermosphere temperature, air density and pressure models, using auroral zone midlatitude neutral thermal and molecular diffusion coefficient measurements

01 p0053 A72-10187

VLF modulation/demodulation system performance prediction by atmospheric noise model, comparing results with measurements

01 p0025 A72-10327

Venusian atmosphere heat transfer processes, calculating radiant fluxes and convective motion model

01 p0127 A72-10364

Tropospheric transhorizon meter, decimeter and centimeter wave propagation mechanisms, suggesting model for scattering and partial reflection effects

01 p0054 A72-10402

Atmospheric wave propagation mode parameters frequency dependence analysis from duct model, calculating received signal time behavior by waveguide transfer function

01 p0027 A72-10408

Discrete ionospheric model of superionic two dimensional low density plasma flow past large bodies, using quasi-neutrality condition

01 p0001 A72-10588

Ion production rates during electron-flux-atmosphere interactions based on atmospheric models with different energy and angular distributions

01 p0059 A72-10597

Venus lower atmosphere from Venera 4, 5 and 6 and Mariner 5 data, evaluating greenhouse effect by microwave absorption and by nongray radiative model

01 p0129 A72-10795

Vertical ozone distribution model using four variable parameters for stratospheric studies, climatology, scattering or radiometric measurements from ground or satellite

01 p0059 A72-10834

Open magnetosphere mathematical models application to dayside auroras, investigating interplanetary magnetic field topology

01 p0060 A72-10885

Isolated magnetospheric substorms model, explaining electric field origin, cold plasma flow, magnetic field lines and particle phenomena

01 p0060 A72-10889

Lyman alpha, Lyman beta and Balmer alpha hydrogen airglow emission simultaneous measurements compared with solar radiation resonant scattering models

01 p0061 A72-10899

Upper atmosphere neutral oxygen density diurnal variations from incoherent scatter and satellite drag data, noting deviations from Jacchia static diffusion model predictions

01 p0062 A72-10911

Nimbus 3 and 4 satellite technological and meteorological performance, discussing atmospheric temperature humidity and ozone vertical sounding for numerical weather forecasting models

01 p0130 A72-10955

Approximate height formula for radio ray propagating through spherically stratified smoothly varying troposphere, evaluating exponential model atmosphere

01 p0032 A72-11253

Topography and Coriolis effects on Martian atmospheric circulation, incorporating low radiative time constant and large variations in analytical model

01 p0135 A72-11279

F region neutral thermosphere temperature perturbation and circulation pattern due to global wind with anomalies of ionization calculated from two dimensional dynamic model

01 p0096 A72-11283

Ionospheric spread-F mechanism as electromagnetic wave scattering on electron density inhomogeneities, calculating characteristic dependence of height interval on operational frequency

02 p0216 A72-11920

Magnetospheric substorm model for auroral activity sudden increase and ionospheric current development explanation by shock wave excitation in magnetospheric tail neutral layer

02 p0217 A72-11927

Magnetosphere deformation by solar wind, comparing accuracy of free molecular flow and double dipole models

02 p0218 A72-11948

Long period geomagnetic pulsation generation at boundary of magnetosphere and incoming solar wind, considering possibility from idealized model

02 p0218 A72-11950

Idealized model for small scale internal structure of magnetopause separating distorted geomagnetic field in magnetosphere from solar plasma flow in magnetosheath

02 p0218 A72-11977

Nighttime lower ionosphere electron density distribution models for vertically polarized radio wave propagation parameters

02 p0173 A72-12112

Venus cloud reflected radiation flux and polarization by Monte Carlo technique, using models with different particle size distributions

02 p0280 A72-12193

Magnetosphere model for low energy cosmic ray proton propagation mode to synchronous orbit satellite, calculating geomagnetic cutoffs and penetration regions

[AD-741079]

02 p0274 A72-12453

Solar proton entry observations over polar caps in relation to magnetosphere, magnetotail and magnetopause models

02 p0275 A72-12463

Thermal advection statistical relation to vertical motion, discussing conventional synoptic meteorological empirical facts utilization in numerical models for long term weather forecasting

02 p0254 A72-12779

Numerical weather prediction, discussing automatic forecasting, error sources, models and four-day validity in Northern Hemisphere

02 p0254 A72-12781

Nonducted vlf wave propagation near plasmapause during whistlers based on diffusive equilibrium and collisionless models for magnetospheric electron density distribution

02 p0222 A72-12873

Cyanide and carbon molecules and isotopes electronic systems opacity probability distribution functions for stellar equilibrium model atmospheres calculations

03 p0416 A72-13012

Extreme UV observations of solar chromosphere-corona transition region, evaluating various theoretical and empirical models

03 p0422 A72-13205

Active and quiet solar atmosphere models from OSO satellite data, presenting emission lines and continua from abundant elements

03 p0423 A72-13215

Solar chromosphere-corona transition region models based on UV resonance emission lines intensity, deriving temperature gradient from radio data

03 p0424 A72-13222

Mesospheric models - Conference, Frascati, Italy, July 1970

03 p0345 A72-13376

Photochemical models of aeronomic formation and dissociation of hydrogen and ozone in mesosphere and stratosphere

03 p0346 A72-13377

Meridional model of oxygen and hydrogen compounds reactions in mesosphere and lower thermosphere, determining diurnal variations and vertical profiles

03 p0346 A72-13378

Dynamic modeling of stratospheric and mesospheric circulation and thermal structure

03 p0346 A72-13382

Rocket measurement of highly collimated short duration bursts of auroral electrons, comparing with existing auroral models

03 p0349 A72-13515

Atmospheric model for mesosphere odd-nitrogen concentration relation to NO dissociation rate and downward flux through mesopause

03 p0350 A72-13526

Nonentraining axially symmetric steady state sloping model of severe storm, discussing validity and limitations

03 p0384 A72-14147

Short period height and longer period kinetic energy oscillations in 10-level primitive equation model for circulation prediction in tropical region

03 p0385 A72-14232

Two dimensional meridional ozone model for seasonal ozone concentration behavior at 15-45 km, taking into account advective and turbulent effects

03 p0351 A72-14360

Ultralong wave baroclinic instability, obtaining linearized perturbation equations from layered geostrophic hydrostatic adiabatic model

04 p0541 A72-14451

Linearized continuous baroclinic atmospheric model, discussing stability for planetary vorticity gradient

04 p0541 A72-14452

Various updating effects on meteorological data analysis accuracy, using balanced barotropic model

04 p0541 A72-14456

Energetic excitation of precursor compounds in gaseous phase for models of primordial atmospheres in thermodynamic equilibrium

04 p0552 A72-14759

Atmospheric model for proteins abiogenesis, considering heteropolypeptides formation from hydrogen cyanide and water

04 p0468 A72-14772

Thermospheric neutral-air wind effects on ionospheric F2 layer from atmospheric model

04 p0514 A72-14876

Optical angle of refraction through earth mean atmosphere determination by three models of refractivity and iterative methods

04 p0515 A72-14884

Blanketing effect of strong line spectra collisionally broadened wings, evaluating stellar atmospheric model computation

04 p0573 A72-14907

Ionospheric hydromagnetic and acoustic gravity wave interactions, examining stratified nonisothermal atmospheric model

04 p0516 A72-14934

Internal atmospheric gravity waves transient two-dimensional finite difference model, including nonlinear, viscosity and thermal conduction terms

04 p0544 A72-15119

F and early G dwarf stars atmospheric models and line data, deriving temperatures, abundances and gravities

04 p0577 A72-15282

Rotating and nonuniform planetary exosphere model, examining density profiles

04 p0579 A72-15333

Deactivation of A-state nitrogen molecules in auroras, reinterpreting rocket observations of nitrogen Vegard-Kaplan system in terms of atmospheric model based on mass spectrometer measurements

[AD-737434] 05 p0655 A72-16072

Jupiter atmosphere chemical and photochemical analysis, using solar-composition adiabatic equilibrium model for coloration, electric discharge and UV irradiation studies

05 p0714 A72-16132

F1 region ion structure during ionospheric magnetic disturbances by numerical simulation of quiet and disturbed conditions based on electron concentration profiles

05 p0656 A72-16247

Magnetospheric field model, assuming magnetostatic problem solution facilitated by equation linearity

05 p0657 A72-16274

Atmospheric optics and geophysics problems modeling arrangement reproducing radiation field within light scattering medium

05 p0658 A72-16293

Oxygen and hydrogen stable isotopes utilization for studying water vapor in precipitations, constructing meteorological model

05 p0684 A72-16793

Geomagnetic tail natural oscillations, applying model of plasma cylinder with free boundary immersed in interplanetary medium

05 p0659 A72-17044

Numerical two layer model of frontal motions development in atmosphere

06 p0840 A72-17384

F1 layer diurnal and seasonal model for medium to high latitudes, comparing calculated and observed electron density diurnal variations

06 p0804 A72-17458

Mathematical two dimensional model of vertical wind shear near convective cloud in free atmosphere

06 p0840 A72-17622

Stochastic dynamic equations for atmospheric prediction and numerical weather forecasting, using barotropic model

06 p0841 A72-17633

Upper atmosphere analytical model expressing density as function of exospheric temperature and altitude

06 p0806 A72-17658

He and heavy ions properties and behavior in solar wind from expanding solar corona theoretical models

06 p0874 A72-18065

Homogeneous isotropically scattering spherical media atmospheric model for radiative transfer problem, using combined operational method

06 p0842 A72-18083

Magnetospheric structure models during quiet solar periods

06 p0809 A72-18277

Pulse reflection of polarized plane electromagnetic wave from cold plasma ionosphere model with vertical magnetic field

06 p0777 A72-18729

Rain amount forecasting based on five level atmosphere model and hydrothermodynamics equations, calculating vertical currents under uniform atmospheric boundary layer stratification conditions

07 p1029 A72-18859

Diffusion model applicability to lateral transport in terrestrial and lunar exospheres, using kinetic theory

07 p1056 A72-18902

Magnetospheric field model from magnetosphere surface approximation by paraboloid of revolution

07 p0974 A72-18903

Fe I and Ti I excitation temperatures and ionization potentials of late G and K giant stellar atmospheres, comparing with model predictions

07 p1069 A72-19077

Model atmosphere and spectral analysis for two early B-type supergiant stars, deducing stellar mass and evolutionary phase

07 p1070 A72-19085

Wind, pressure and temperature diurnal and semidiurnal variations to 30 km altitude over tropical western Pacific, considering atmospheric model based on linearized equations of motion

07 p1029 A72-19099

Polar night jet idealized model with zero tropospheric and constant vertical stratospheric shear, considering instability due to small wave disturbances

07 p1030 A72-19103

Geostrophic drag coefficient for heterogeneous terrain as function of effective roughness length, considering surface friction effects in large scale atmospheric models

07 p1030 A72-19108

Radio attenuation above 10 GHz based on theoretical model of equivalent precipitation on path using intensity spatial distribution function within rain cell

07 p0940 A72-19189

Exact and approximate expressions derived for energy content of vertical air column extending from earth surface to stratosphere

07 p0977 A72-19856

Magnetospheric and polar substorms model for auroral particles acceleration and geomagnetic tail current diversion to auroral oval night side

07 p0977 A72-20029

Ionospheric F region storms model accounting for global electron density changes due to abundance ratio of atomic oxygen to molecular oxygen or nitrogen

07 p0979 A72-20047

Venusian atmospheric circulation experiments with time dependent two layer primitive equations model, discussing hot house and Goody-Robinson radiation transfer implications

07 p1083 A72-20452

Circulation mechanics of gaseous atmospheres with zonal symmetry in motions and other properties, applying to Jupiter atmosphere

07 p1083 A72-20453

IR radiation radiative transfer calculation for selected spectral intervals due to various model cloud droplet size distribution

07 p0980 A72-20456

Solar model inconsistencies, considering He and Fe abundances and solar age approximation

07 p1083 A72-20464

Synoptic velocity fluctuations from empirical structural functions of wind fields, proposing spectral kinetic energy distribution model for atmospheric turbulence

07 p1031 A72-20694

Atmospheric model for plasma motion along surface of geomagnetic tail under action of interplanetary, magnetic lines of forces

08 p1153 A72-20722

On-line digital computer maximum likelihood estimate of Earth atmosphere profile ahead of flight vehicle using discrete measurements of density, temperature and pressure

08 p1156 A72-20853

Venus clouds composition from spectral and polarization data, considering hydrochloric acid particles model

08 p1230 A72-20980

Linearized two level model for atmospheric motion equations systems, using Psi-balanced system for 24 hour forecast

08 p1156 A72-20995

Median true height atmospheric profile model synthesis from propagation parameters, using polynomial representations and alpha-Chapman layers

08 p1157 A72-21106

Mars atmosphere temperature profiles inference from outgoing radiation spectral characteristics, constructing atmospheric model

08 p1232 A72-21147

Zeta Puppis visual line spectrum discrepancy from non-LTE stellar atmospheres models, necessitating hydrostatic equilibrium deviations consideration for temperature derivation

08 p1232 A72-21178

Atmosphere hydrodynamic simulation model for cascade energy transfer in turbulent flow, using Euler gyro equations

08 p1158 A72-21190

Numerical modeling of Venus atmospheric circulation, taking into account short wave radiation absorption, boundary layer, mesoscale convection and horizontal friction

08 p1233 A72-21191

Radiative thermal flux model of Venus atmosphere, using Venera data and greenhouse effect

08 p1233 A72-21193

Jeans escape rate prediction validity for hydrogen atoms in upper atmosphere and error sources in physical models

08 p1159 A72-21401

Handbook on aviation meteorology covering atmospheric structure and composition, standard atmospheres, heat transfer, adiabatic processes, winds, cloud formations, precipitation, ice formation, fog, visibility, etc

08 p1200 A72-21479

Wind measurements in lower thermosphere by meteor radar method, presenting models of prevailing circulation in meteor zone over Eurasia and Arctic

08 p1161 A72-21538

Numerical forecasting model with precipitation as function of vertical velocity and humidity distribution, noting orographic influence and atmosphere static stability

08 p1200 A72-21796

Non-LTE atmospheric model calculations for H, He I and II spectra of O stars, discussing He abundances

08 p1239 A72-21949

Horizontally polarized impulsive plane electromagnetic wave reflection from perturbed linear ionosphere model, obtaining transient response as inverse Fourier transform

08 p1136 A72-21979

One dimensional atmospheric turbulent diffusion model and semiempirical equation, considering jumplike changes in particle velocity

08 p1201 A72-21999

Hydrodynamic models and computational schemes optimization in statistical weather forecasting

08 p1202 A72-22114

Model calculation for seasonal effects on minor neutral constituents distribution in mesosphere and lower thermosphere, suggesting large scale meridional circulation role

09 p1274 A72-22354

Model calculation for electron production rates due to photoionization and particle precipitation below 100 km at midlatitude during solar minimum and maximum years

09 p1375 A72-22357

Vertical macroturbulence diffusion coefficient and Na 22 and Be 7 flux from stratosphere to troposphere estimated using ground level measurements and two layer model

09 p1376 A72-22416

Steady state global climatic model for earth-atmosphere-ocean system, discussing perturbations effect on stability

09 p1343 A72-22426

Primitive equation multilayer model for winter precipitation prediction in U.S. northeast coastal region, noting correlation with observational data

09 p1344 A72-22428

Wind vector field computation by forced dynamical adjuement to observed height field data, using Mintz-Arakawa two level atmospheric circulation model

09 p1344 A72-22433

One dimensional model for climatological evaluation of ice phase seeding for isolated cumulus cloud modification

09 p1345 A72-22448

Three parameter prognosis model for geopotential vertical profile in troposphere and stratosphere, describing vortex and heat influx in quasi-geostrophic and adiabatic approximations

09 p1297 A72-22549

Atmospheric refraction effects on IR far field irradiance distribution based on model of nonlinear interaction including absorption, transverse flow and vibrational relaxation effects

09 p1350 A72-22607

Carbon dioxide atmospheric models for Mars and Venus, discussing aeronomy, Mariner probes, gas dissociation by solar radiation, and electron density inconsistency

09 p1386 A72-22685

OGO 4 satellite observed band limited ELF hiss characteristics explanation by model based on generation at large wave normal angle in equatorial region

09 p1279 A72-23008

EUV resonance radiation from He atoms and ions in geocorona, comparing model calculation based on solar radiation resonance scattering with rocket experiments

09 p1378 A72-23010

Thermospheric structure between 100 and 400 km from rocket soundings and ground observations, noting mass spectrometers chemical reactions influence on atmosphere model accuracy

09 p1300 A72-23015

Mathematical model of ion capture and annihilation by aerosol particles from ground level to 60 km

09 p1346 A72-23266

Frontogenesis models based on horizontal deformation field, noting uniform and nonuniform potential vorticity

09 p1347 A72-23652

Convective plumes model with heat flux, layer depth and surface turbulence intensity as parameters [AD-745511]

09 p1347 A72-23655

Steady state model for Venus atmosphere water vapor loss, noting hydrogen and oxygen escape due to dynamic outflow of constituents from upper region

09 p1393 A72-23657

Exospheric temperatures in hydrogen dominated planetary atmospheres for evaporative loss rates estimation, noting two component diffusive equilibrium model

09 p1393 A72-23661

Theoretical model of large scale topographical effects on wind generation through temperature advection, applying to Mars atmosphere general circulation

10 p1531 A72-23707

Van Allen proton belt model, considering ionosphere particle acceleration by stochastic interaction with hydromagnetic waves due to solar wind at magnetosphere shock front

10 p1529 A72-24245

Atmospheric models of vertical structure of semidiurnal atmospheric gravitational tides, taking into account Coriolis force and vertical acceleration components

10 p1473 A72-24530

Photochemical models to simulate composition and reactions of upper atmosphere, noting transport importance

10 p1474 A72-24713

Sporadic E layer structure model from radiosonde observation, noting peak plasma frequency variation and total reflection by blobs

10 p1441 A72-25153

Sporadic E layer altitude and density variations caused by lunar influences, using model for electrostatic field and wind shear effects

10 p1478 A72-25163

Model atmosphere with n homogeneous layers and ground surface for solar radiation flux calculation [AD-744410]

11 p1620 A72-25307

Joint ocean-atmosphere model response to solar zenith angle seasonal variation, noting snow cover and ocean surface effects on lower troposphere warming

11 p1620 A72-25766

Centered difference approximation for atmospheric model advection equation by two step Lax-Wendroff method, discussing computational instability due to lattice separation

11 p1680 A72-25768

Stellar atmospheric structure physical parameters from model atmosphere calculations, applying method to G and K stars

11 p1717 A72-25904

Solar chromosphere-corona transition region theoretical and empirical models, studying acoustic flux generated above convective zone

11 p1717 A72-25906

Plasma layer effect on natural oscillations of magnetosphere tail, using infinite plasma cylinder model immersed in interplanetary plasma

11 p1622 A72-25944

Magnetosphere neutral layer plasma conductivity determination from model of linear magnetic dipole in conducting fluid flow

11 p1622 A72-25945

Asian subtropical western disturbances movement prediction by primitive equation barotropic model with east-west cyclic boundary conditions, presenting forecast charts and error statistics

11 p1681 A72-26077

Wet and dry bent over plumes comparison, constructing plume paths for various atmospheric stability conditions

11 p1681 A72-26082

IR observation and theoretical considerations for Jupiter atmosphere inhomogeneous model with two cloud layers

11 p1721 A72-26119

Magnetosphere fast electron precipitation investigated by simulation experiments with model created by plasma stream interaction with dipole magnetic field

11 p1714 A72-26531

Geomagnetic tail model with plasma cylinder immersed into solar wind, obtaining dispersion equation for oscillations

11 p1627 A72-26532

Ionsospheric scattered wave propagation mode and weak echo delay explained by analysis-derived model

11 p1597 A72-26570

Analytic ray path solutions for HF radio wave transmission through plane stratified isotropic ionsospheric model

11 p1599 A72-26763

VLF phase changes due to particle precipitation into geomagnetic anomaly during solar proton events explained by exponential ionsospheric models with effective reflecting height

11 p1599 A72-26765

Tropical hurricane model describing initial whirlwind and self exciting wind velocity development and dependence on ocean surface temperature

11 p1682 A72-26879

Tornado model from atmospheric thermodynamics nonlinear equations, examining air flow from lower boundary layer and ground friction

11 p1682 A72-26880

Nonlinear medium range numerical weather forecasting method based on atmospheric spectral model

11 p1683 A72-26884

Baroclinic primitive equation prediction model for nontropical part of Northern Hemisphere with allowance for moisture exchange, radiative heat influx and cloud formation processes

11 p1683 A72-26886

Conditional instability of second kind /CISK/ model of surface cyclonic vorticity dependence on vertical distribution of latent heat release

12 p1838 A72-27019

Barotropic instability and vorticity equation of zonal flow with superposed Rossby waves limiting predictability of real atmosphere

12 p1838 A72-27021

Fourier phase angle models of intermittent atmospheric turbulence

12 p1838 A72-27025

Numerical model of global scale propagating waves in equatorial stratosphere generated by tropospheric heat sources for Kelvin and Rossby-gravity modes

12 p1839 A72-27029

Cosmogenic radionuclides pickup by cloud water and deposition in precipitation described by model

12 p1863 A72-27503

Atmospheric models for critical flux Richardson number prediction for turbulence maintenance in stratified flows

12 p1840 A72-27702

Ekman boundary layer in two level quasi-geostrophic general circulation numerical model, representing physical characteristics of boundary layer turbulence increase with height

12 p1840 A72-27708

Equivalent atmospheric turbulence models concept for structure function behavior of electromagnetic wave propagation, noting dependence on model characteristics

12 p1841 A72-27946

Baroclinic long wave dynamic instability in Kochin two layer frontal model, extending Richardson number range in absence of beta effect

12 p1841 A72-27987

Atmospheric thermal radiation flux calculation, showing carbon dioxide concentration effects on summer and winter models

12 p1805 A72-27991

Earth atmosphere general circulation model based on planetary boundary layer parameterization, considering surface stress and heat and moisture flux

13 p1988 A72-28442

Exponential functions model for D region vertical distribution of electron density profiles, taking into account solar X- and cosmic rays

13 p1945 A72-28581

Worldwide thunderstorm activity model selection from Schumann resonance observations, using ELF noise measurements in lowest earth-ionosphere cavity modes

13 p1988 A72-28600

Four dimensional atmospheric model providing global moisture, temperature, pressure and density profiles as attenuation model inputs for earth resources satellite mission simulation

13 p1989 A72-28805

Model determining system responses to nominal profiles of atmospheric parameters from orbital to 25 km altitudes

13 p1989 A72-28807

Precipitation exceedance rates charts for various risks, using statistical models

13 p1989 A72-28811

Atmospheric model effects on space shuttle ascent and reentry trajectories and aerodynamic heating

13 p1990 A72-28813

Atmospheric model for random density variations effects on space shuttle reentry parameters, using Monte Carlo trajectories for delta wing orbiter

13 p1990 A72-28814

Multiscale numerical model for local weather development simulation, noting forecasting for long distance air travel

13 p1993 A72-28857

Hybrid forecast model for hydrometeors short range prediction based on meteorological satellites cloud pattern observations and quasi-Lagrangian advection analog

13 p1993 A72-28858

Number density, particle, momentum and energy fluxes in model ion-exosphere with open magnetic field and asymmetric Maxwellian velocity distribution

13 p1948 A72-29115

Ionsospheric spread-F mechanism as electromagnetic wave scattering on electron density inhomogeneities, calculating characteristic dependence of height interval on operational frequency

13 p1948 A72-29232

Magnetospheric substorm model for auroral activity sudden increase and ionsospheric current development explanation by shock wave excitation in magnetospheric tail neutral layer

13 p1948 A72-29239

Magnetosphere deformation by solar wind, comparing accuracy of free molecular flow and double dipole models

13 p1949 A72-29260

Long period geomagnetic pulsation generation at boundary of magnetosphere and incoming solar wind, considering possibility from idealized model

13 p1949 A72-29262

Polar thermospheric wind calculation from convection electric field measurements in polar cap ionosphere, using simple ionsospheric model

13 p1950 A72-29385

Thermospheric density-temperature time lag, considering two dimensional time dependent model based on UV heat input dynamic excitation

13 p1951 A72-29388

Avrett-Krook temperature correction procedure modified to improve, near surface convergence for blanketed model stellar atmospheres

13 p2040 A72-29406

Model solar atmosphere from mm and cm wavelength high resolution observations of chromosphere by lunar limb antenna tracking during 7 March 1970 eclipse

13 p2042 A72-29532

Gravity wave propagation in realistic thermospheric model, considering temperature, wind, Coriolis force, viscosity, thermal conduction and ion drag effects

13 p1951 A72-29652

Solar pole-equator difference in effective temperature and mechanical heating, using atmospheric model 13 p2044 A72-29702

Lower solar chromosphere two dimensional models, noting effects of macroscopic velocity fields 13 p2045 A72-29709

Observed continuous solar spectrum intensity comparison with photospheric models, noting bend-off due to veiled line haze 13 p2047 A72-29734

Semiempirical line blanketing in solar model atmospheres, including limb darkening predictions 13 p2047 A72-29735

Dynamics and thermodynamic interactions connected with large, mesoscale and small scale stratiform clouds, describing mathematical models 13 p1995 A72-29849

Undisturbed and active solar photospheric turbulent velocity determination by comparing half widths of observed weak Fraunhofer line profiles with model calculation 13 p2049 A72-29929

Solar H alpha profile formation from non-LTE radiative transfer solutions through model atmosphere by integro-differential equation technique 13 p2049 A72-29931

Solar chromosphere model based on Lyman spectra observations, calculating temperature, gas and electron pressure and particle densities as function of height 13 p2049 A72-29932

Equatorial quiet solar atmosphere model for chromosphere-corona transition region based on cm radio observation and hydrodynamical conservation equations 13 p2049 A72-29933

Mathematical model of atmospheric electric clouds, calculating electric charges and fields from convection and conductivity data 13 p1996 A72-30086

Global atmospheric circulation barotropic spectral model application to satellite asymptotic data continuous processing 14 p2127 A72-30258

Radiative-dynamic model for static stability of rotating atmospheres, deriving mean equilibrium value of Richardson number in troposphere 14 p2127 A72-30341

Scale analysis of large scale tropical disturbances in conditionally unstable atmosphere, estimating geopotential height dependence on stream function via heat balance equation 14 p2128 A72-30345

Thermospheric parameters seasonal and latitudinal variations calculation based on atmospheric model with components ionization and molecular oxygen dissociation as main heat sources 14 p2128 A72-30463

Three layer atmospheric model for neutral gas motion-produced ionosphere and magnetosphere currents, electromagnetic field and charged particle concentration perturbations 14 p2100 A72-30632

Dipolar coordinate system for geomagnetic field dipole approximation in studies of diffusion and heat conduction in F region and outer ionosphere 14 p2102 A72-30652

Air injection as neutral atmospheric boundary layer thickening simulation, presenting mean velocity and turbulence intensity profiles 14 p2093 A72-30849

Jupiter and Saturn atmosphere composition, structure and radiative properties, presenting two zone stratosphere-troposphere model 14 p2161 A72-31072

Model Martian atmosphere, investigating effects of departures from electron density profile spherical symmetry on radio wave phase shift in bistatic radar occultation experiment 15 p2194 A72-31440

Upward and downward radiative transfer in atmosphere-ocean system model calculated by Monte Carlo method, noting turbidity effect on radiance 15 p2224 A72-31673

Book on dynamic meteorology covering synoptic disturbance model, numerical weather prediction and baroclinic waves origin 15 p2266 A72-31875

Temperature and density data deviation from stratosphere and mesosphere mean season model values at high latitudes 15 p2225 A72-31907

Photochemical model of N and NO distribution based on E region ion composition 15 p2226 A72-31916

Whistlers nose frequency and minimum group time delay determined from model magnetosphere and from measurement, noting precision effect on electric field calculation accuracy 15 p2198 A72-31947

Thermospheric composition global model for magnetically quiet conditions based onOGO-6 mass spectrometer measurements 15 p2227 A72-31954

Polar/midlatitude model of atmospheric density variations from LOGACS low altitude satellite accelerometer experiment 15 p2229 A72-32000

Atmospheric sound absorption prediction based four-gases composition and energy transfer mechanisms, comparing results with experiments at different humidities 15 p2277 A72-32020

Jupiter atmospheric greenhouse effect modeled by two layer emission, deriving temperatures from non-gray step function approximation of IR absorption 15 p2312 A72-32096

Microwave propagation delay due to atmosphere in satellite-to-earth communication based on spherical smoothly varying model and geometrical optics techniques 15 p2200 A72-32102

Ion pair production rate and electron number density in ionospheric D region from ground based and rocket measurements, discussing two ion model 15 p2229 A72-32252

Ionospheric models with constant electron density contours axially symmetrical to earth centered dipole magnetic field, discussing radio ray paths 15 p2230 A72-32263

Solar activity effects on integrated ion production rates at sunrise using atmospheric model 15 p2301 A72-32266

Lower zero age main sequence star models uncertainties, comparing nonmixing and mixing length theory for various composition atmospheres 15 p2314 A72-32367

Imposed southern boundary experimentation for large scale Northern Hemisphere midlatitude atmospheric flow numerical prediction, discussing factors contributing to model success 15 p2267 A72-32726

Vertical temperature profile retrieval from satellite radiance measurements for insertion into numerical atmospheric circulation model, discussing sensitivity test 15 p2267 A72-32728

Auroral electrojet polarization model, considering ionospheric Hall and Pedersen conductance maximum due to precipitation from electron plasma sheet inner edge [AD-745672] 16 p2444 A72-32961

Two layer model for diurnal temperature variations analysis for radiative heat transfer between lower atmosphere and underlying layer 16 p2417 A72-33293

Atmospheric refraction effects on ground based astronomical observations, using atmospheric model with concentric spherical shells having decreasing density with height 16 p2386 A72-33495

Atmospheric model for local mesometeorological deviations from large scale field distributions, taking into account synoptic scale influence 16 p2418 A72-33601

Planetary wave interaction in two level baroclinic atmosphere, using quasi-geostrophic equations 16 p2418 A72-33602

Semiimplicit time integration algorithm in atmospheric baroclinic models for short range weather forecasting in Canada 16 p2418 A72-33665

Model for magnetospheric substorm growth phase, noting dayside magnetopause convection onset, geomagnetic tail configurational changes and breakup with auroral electrojet development 16 p2387 A72-33903

Barium cloud striations deformation in ionosphere explained by equations of motion for plasma cloud thin bar model, discussing pinch effect 16 p2387 A72-33907

Digital equilibrium temperature model for diurnal surface thermal and energy transfer simulation based on Myrup analog solution 16 p2419 A72-33942

Band model and scaling approximation validity for computation of transmission profile in V4 band of methane in Jovian atmosphere 16 p2461 A72-34099

The bulk composition of Titan's atmosphere 17 p2606 A72-34541

Photochemistry of the lower troposphere 17 p2511 A72-34635

Consequences of an isotropic static plasma sheet in models of the geomagnetic tail 17 p2545 A72-34636

Measurements of molecular oxygen in the thermosphere 17 p2546 A72-34694

Solar chromosphere-corona transition region structure and energy balance calculation by static planar model compared with XUV resonance line observations 17 p2608 A72-35083

Effect of aerosol variation on radiance in the earth's atmosphere-ocean system 17 p2547 A72-35194

Flaring-tail model explanation for geomagnetic tail configuration changes during magnetospheric substorm growth phase 17 p2548 A72-35589

Stratospheric model for bremsstrahlung X ray relation emission to auroral electron flux, considering photon energy release in scintillation counters 17 p2551 A72-35872

Determination of the quenching of O(1D) by molecular nitrogen using the ionospheric modification experiment 18 p2685 A72-35991

Models for F region and topside ionospheric storms morphology, discussing electric current disturbance at polar region 18 p2685 A72-35994

UHF radio signals refraction angles and group delay times for biexponential model of ionospheric electron density profile 18 p2657 A72-36101

Local characteristics of ray propagation in an inhomogeneous anisotropic ionosphere 18 p2686 A72-36229

On the boundary conditions in theoretical model calculations of the distributions of minor neutral constituents in the upper atmosphere 18 p2659 A72-36294

Atmospheric model synthesis of observed electron temperatures and concentrations in tropical ionosphere during 8 March 1970 magnetic storm, noting F2 region features 18 p2686 A72-36296

On the reflection of whistler mode waves from model lower ionospheres 18 p2660 A72-36430

Spatial variations in atmospheric predictability 18 p2706 A72-36627

Mathematical model for internal atmospheric gravity waves breaking process modification by momentum exchange between wave and mean flow 18 p2687 A72-36630

Friction term formulation and convective instability in a shallow atmosphere 18 p2706 A72-36633

A model atmosphere analysis of the Ap star HR 465 18 p2727 A72-36736

The metal-to-hydrogen ratio in F1-F5 stars, as determined by a model-atmosphere analysis of photoelectric observations of a group of weak metal lines 18 p2727 A72-36737

Model ionosphere for D region at summer noon during sunspot maximum 18 p2689 A72-37207

Numerical methods of solving weather forecasting problems 19 p2828 A72-37386

A three dimensional, analytical magnetospheric model with defined magnetopause 19 p2789 A72-37410

Method of constructing a forecast chart of H sub 500 anomalies on the basis of several analyses 19 p2828 A72-38000

Atmospheric model for plasma motion along surface of geomagnetic tail under action of interplanetary magnetic lines of force 19 p2791 A72-38350

Critical frequencies and geometric parameters of parabolic ionosphere layer model in oblique backscatter sounding, using distance-frequency characteristics 19 p2791 A72-38360

Atmospheric boundary layer turbulence modeling, considering terrain roughness effects, vertical mixing, high frequency spectra, energy dissipation rate and vertical component variance 19 p2828 A72-38557

Non-Boussinesq effects and further development in a model of upper tropospheric frontogenesis 19 p2829 A72-38558

The possible use of Laguerre polynomials for representing the vertical structure of numerical models of the atmosphere 19 p2829 A72-38562

Computer program for numerical analysis of atmospheric fronts in lower troposphere based on models for spatial distribution of hydrothermal characteristic in air mass 19 p2829 A72-38771

A method for simulating wind conditions during atmospheric stagnation periods 20 p2947 A72-38965

Synoptic velocity fluctuations from empirical structural functions of wind fields, proposing spectral kinetic energy distribution model for atmospheric turbulence 20 p2948 A72-39009

Persistent particle anisotropies and magnetospheric models 20 p2916 A72-39233

Mars atmosphere temperature profiles inference from outgoing radiation spectral characteristics, constructing atmospheric model 20 p2968 A72-39252

Turbulence in dynamic models of the atmosphere 20 p2948 A72-39357

Plate convergence, transcurrent faults, and internal deformation adjacent to Southeast Asia and the Western Pacific. 20 p2917 A72-39479

Plasmapause nightside, dayside and bulge positive ion concentration measurements withOGO 5 mass spectrometer compared with magnetospheric convection model 20 p2919 A72-39544

Magnetic neutral sheet model in terms of self consistency between current and tail field in reversal region 20 p2919 A72-39548

A wind-tunnel experiment concerning atmospheric vortex streets. 20 p2948 A72-39796

On the chemical composition of epsilon Pegasi. 20 p2974 A72-39901

Computerized long term weather forecasting via mathematical modeling of atmospheric processes based on meteorological parameters worldwide observational data 20 p2948 A72-39939

Dynamic adjustment of initial model fields by using complete equations of hydrothermodynamics 20 p2949 A72-39943

Response of the tropical atmosphere to local, steady forcing. 21 p3077 A72-40248

Further study of the severe storm with a rotating updraft configuration. 21 p3077 A72-40466

Numerical experiment of radiative-convective equilibrium of the Martian atmosphere. 21 p3105 A72-40772

Instability of rotational and gravitational modes of oscillation. 21 p3078 A72-40773

Atmospheric model for numerical simulation of five minute oscillation field properties of solar granular convection-excited gravity waves 21 p3107 A72-41277

Mean coefficient of opacity in stellar atmosphere model calculations 21 p3110 A72-41443

Quasi-two dimensional turbulence model of energy spectra and potential entropy transfer in synoptic large scale quasi-horizontal atmospheric motions 21 p3049 A72-41793

Optical properties and structure of the Jovian atmosphere. V - Probable structure of the ammonium aerosol layer 22 p3219 A72-41914

Analytic expressions for electron energy transfer rates for nitrogen and oxygen vibrational excitation in ionosphere, applying to atmospheric and ionospheric computer modeling 22 p3168 A72-42001

Solar silver abundance from spectral scans for Ag 3280.7 and 3382.9 A resonance lines, using spectral synthesis method, model atmosphere and limb darkening observations 22 p3221 A72-42028

Stability of the Martian atmosphere. 22 p3224 A72-42292

Atmospheric effects on the surface cosmic ray meson intensity recorded in London. 22 p3218 A72-42369

Model atmosphere analysis of the A 31a-O supergiant HD 33579 in the Large Magellanic Cloud. 22 p3225 A72-42386

Daily variation of electron and proton geomagnetic cutoffs calculated for Fort Churchill, Canada. 22 p3170 A72-42401

Thermospheric atomic oxygen and molecular nitrogen densities fromOGO 6 neutral atmospheric composition experiment, comparing with prediction by Jacchia models 22 p3172 A72-42431

Prediction error growth computation by test-field model for inertial range atmospheric turbulent flows in three and two dimensions 22 p3167 A72-42501

Adjustment of the wind field to geopotential data in a primitive equations model. 22 p3200 A72-42502

Mars - The effects of topography on baroclinic instability. 22 p3225 A72-42504

Atmospheric frontal motion stability via two-layer homogeneous incompressible fluid model, solving eigenvalue problem by small perturbation method 22 p3201 A72-42505

Improved Curtis-Godson approximation in a non-homogeneous atmosphere. 22 p3201 A72-42511

Time dependent one dimensional numerical model of hail-bearing cumulus cloud, using microphysical process parameterization and exponential raindrop and hailstone size distributions 22 p3201 A72-42513

Hail formation model based on injection of finite embryo size classes into horizontally homogeneous steady nondivergent updraft, considering growth and accumulation zones 22 p3201 A72-42514

Cool supergiant stars atmospheric model for chemical composition change effects due to nuclear burning cycle 22 p3227 A72-42556

Baroclinic long wave dynamic instability in Kochin two layer frontal model, noting beta effect on wave disturbances 22 p3202 A72-43001

Atmospheric thermal IR radiation transmission function dependence on carbon dioxide concentration, calculating spectral and vertical distributions for standard, summer and winter model atmospheres 22 p3174 A72-43005

Allowance for the influence of orography in a dual-layer model of the atmosphere 23 p3310 A72-43343

Nonlinear hydrothermodynamic model of steady atmospheric motion in equatorial latitudes with energy influx approximation 23 p3284 A72-43533

Reproduction of the climatic distribution of meteorological elements on the basis of a nonadiabatic spectral model of the atmosphere 23 p3311 A72-43626

Theoretical estimate of the effective recombination coefficient in the D region. 23 p3284 A72-43818

Satellite-observed Southern Hemisphere cloud vortices in relation to conventional observations. 23 p3285 A72-44145

Modeling the rise and combustion of a cloud of light gas in the atmosphere 23 p3357 A72-44493

Model for the uneven illumination of polar caps by solar protons. 23 p3286 A72-44502

One-level fine-mesh limited-area grid numerical weather prediction atmospheric model, evaluating various finite difference schemes, boundary conditions and initialization methods 24 p3420 A72-44619

New optical measurements of planetary diameters. II - Planet Venus. 24 p3436 A72-44694

A method for balancing geopotential and wind fields 24 p3420 A72-44765

Boundary layer core flow model of concentrated columnar vortex interaction with plane solid nonrotating surface, applying to tornado interpretation 24 p3391 A72-45022

Exponential functions model for D region vertical distribution of electron density profiles, taking into account solar X- and cosmic rays 24 p3397 A72-45081

Worldwide thunderstorm activity model selection from Schumann resonance observations, using ELF noise measurements in lowest earth-ionosphere cavity modes 24 p3380 A72-45100

The estimation of accuracy of short-term atmosphere density prediction. 24 p3398 A72-45173

On the power law for the kinetic energy spectrum of large scale atmospheric flow. 24 p3398 A72-45483

On the instability of a three-layer atmosphere with an isentropic stratosphere. 24 p3399 A72-45484

Tropospheric wave motions with baroclinic basic flow in equatorial latitudes. 24 p3399 A72-45485

Incorporation of steep mountains into numerical forecasting models. 24 p3421 A72-45486

Conference on Theoretical Ionospheric Models, Pennsylvania State University, University Park, Pa., June 14-16, 1971, Proceedings. 24 p3399 A72-45579

Theoretical models of the D-region. 24 p3399 A72-45580

The relationship of theory and experiment in the D-region. 24 p3399 A72-45581

A numerical integration method useful for studying ionospheric phenomena. 24 p3399 A72-45582

Formulation of diurnal D-region models using a photochemical computer code and current reaction rates. 24 p3399 A72-45583

Mean dissociative and effective recombination coefficients of E region, discussing charged particle reactions effect on model formation 24 p3399 A72-45584

The development of a theoretical model of the atmosphere and the ionosphere. 24 p3399 A72-45585

Computer simulation of the F-region seasonal anomaly. 24 p3400 A72-45586

O/plus/ H/plus/ and He/plus/ ion distributions in a new polar wind model. 24 p3400 A72-45587

A theoretical model of the ionosphere dynamics with interhemispheric coupling. 24 p3400 A72-45588

Continuity equation for dynamic auroral ionospheric model relating electron density profiles to auroral arc brightness 24 p3400 A72-45589

A three-dimensional model of thermosphere dynamics. I - Heat input and eigenfunctions. II - Tidal waves. III - Planetary waves. 24 p3400 A72-45594

A thermospheric model from satellite orbital decay densities and incoherent scatter temperatures. 24 p3400 A72-45595

ATMOSPHERIC MOISTURE

Atmospheric water vapor role in waveguide effects above sea on millimeter and centimeter propagation along transhorizon and beyond horizon paths 01 p0026 A72-10403

Raman scattering from water vapor for Ar laser wavelengths in remote atmospheric humidity measurements [AIAA PAPER 71-1085] 01 p0104 A72-10542

Atmospheric water vapor vertical distribution from satellite IR spectrometer measurements, noting effects, absorption coefficients and temperature profiles errors 01 p0095 A72-10831

Nimbus 4 vertical atmospheric sounding techniques, obtaining temperature, water vapor and ozone profiles with Michelson IR interferometer 01 p0095 A72-10957

Visibility relationships to atmospheric liquid water content in fog derived from fog drop size distribution model 01 p0096 A72-11281

Atmospheric humid cover measurement with airborne/spaceborne microwave radiometric sounding, considering radiothermal radiation models 02 p0253 A72-11733

Microwave spectrometer remote sensing of atmospheric temperature and water vapor, discussing cloud, topography and sea state effects and multiple regression statistical method 02 p0228 A72-11859

Ocean winds velocity, temperature and humidity fluctuations second and third order structure functions, deriving Kolmogoroff constants 03 p0383 A72-13154

Wind velocity spatial derivative determination by radar observation of signal reflection from atmospheric water particles 03 p0383 A72-13483

Stratospheric water vapor concentration annual variability from regression analysis of monthly measurements initiated as IQSY program 03 p0385 A72-14148

Mars atmospheric water vapor observations, examining spectroscopic plates water line strengths at 8200 A 04 p0569 A72-14497

Ordinary and macroporous structured polycondensation oxidation-reduction polymers synthesis, discussing application to organic impurities removal from atmospheric moisture condensates 05 p0622 A72-16645

Airborne or satellite-mounted millimeter wave radiometer for atmospheric water vapor determination noting accuracy advantage over IR measurement 06 p0814 A72-17589

Satellite surface temperature measurements changes due to atmospheric specific humidity, noting increase in water vapor absorption coefficient with content 06 p0806 A72-17671

Specific moisture contents in stratosphere over European Soviet Union from balloon measurements 06 p0806 A72-17734

Indirect reduction of vertical atmospheric water vapor profile from measured outgoing thermal radiation by regularization method 06 p0842 A72-18039

Surface layer humidity correlation to height of atmosphere emitting in IR spectral region, determining water vapor content by recording earth radiation angular distribution 06 p0808 A72-18046

Total atmospheric water vapor content from solar radiation absorption observation at millimeter wavelengths 06 p0817 A72-18091

Broadbeam S band radar application to quantitative analysis of severe storms, calculating liquid water content 06 p0843 A72-18442

Gas generator performance shifts involving military trim level variations by TF-30 engines in high relative humidity environment caused by condensation in inlet duct 07 p1052 A72-18759

Meteorological elements vertical profiles under cloud cover condition by solving heat and humidity transfer equations based on satellite data 07 p1029 A72-18860

Atmospheric vapor pressure and temperature direct measurement, using copper-constantan thermocouples for wet-bulb temperature rapid fluctuations and thermistor for mean wet-bulb temperature 07 p0982 A72-19106

Atmospheric humidity forecasts from field evolution and transfer and specific humidity deficit description with equations system

07 p1031 A72-20699

Atmospheric vertical humidity profile from ground measurements of radio wave absorption at 1.35 cm water vapor line

08 p1158 A72-21192

Numerical forecasting model with precipitation as function of vertical velocity and humidity distribution, noting orographic influence and atmosphere static stability

08 p1200 A72-21796

Seasonal and diurnal variations of earth albedo from turbidity measurements, showing lower atmosphere moisture effect

08 p1237 A72-21799

Ground based Raman laser backscatter measurement of stratospheric water vapor content, noting 1 ppm accuracy

08 p1161 A72-21825

Droplet growth on passivated hygroscopic condensation nuclei in device with controllable relative humidity

08 p1172 A72-22000

Stress corrosion of uranium carbide ceramics in atmospheric environments containing water

09 p1335 A72-22399

Tropical storms generated midlatitudinal cloud bands relation to autumnal large scale circulation, analyzing heat and moisture injection effects

09 p1344 A72-22429

Radiometric method for atmospheric moisture data retrieval above radiosonde hygrometer cut-off or during malfunction, inferring average moisture decrease through radiative transfer equation

09 p1307 A72-22441

Continuous scan diffraction spectrometer for thermal sounding experiment on Meteor satellite, presenting vertical temperature and humidity profiles

09 p1347 A72-23588

Mesospheric clouds composed of molecular complexes of extraterrestrial origin, considering chemical reactions, hydroxyl luminescence, thermospheric water vapor and auroras

09 p1347 A72-23590

Atmospheric water vapor submillimeter absorption lines in high resolution radiation transmission measurements with Froome type plasma metal junction device

10 p1472 A72-24175

Martian atmosphere water vapor detection and mapping during Viking missions, discussing experimental approach and spectrometer choice

10 p1539 A72-24378

Hair hygrometer for FM radiosonde in-flight air humidity measurements, discussing design, operation and accuracy test in extreme weather conditions

10 p1483 A72-25005

Air hygrometer with heated electrolytic sensor for atmospheric humidity determination by automatic meteorological stations

10 p1483 A72-25016

Atmospheric humidity vertical profile determination by measuring microwave radiation from satellite

11 p1620 A72-25274

Atmospheric water vapor measurements by Raman backscatter from pulsed laser radar, comparing with meteorological tower data

11 p1680 A72-25347

Wet and dry bent over plumes comparison, constructing plume paths for various atmospheric stability conditions

11 p1681 A72-26082

Wind velocity spatial derivative determination by radar observation of signal reflection from atmospheric water particles

11 p1682 A72-26253

Statistical approach to atmospheric optics inverse problems solution, considering application to vertical temperature and humidity profiles determination

11 p1683 A72-26888

Two dimensional dynamic model numerical simulation for micro- and macrostructures of moist convective clouds, comparing to field observations

12 p1839 A72-27028

Ice formation on helicopter rotor blades, discussing atmospheric moisture and temperature conditions, blade surface temperature, centrifugal and aerodynamic forces and preventive measures

12 p1754 A72-27414

Atmospheric surface layer turbulent transfer mechanisms, studying direct measurements of momentum, heat and moisture turbulent fluxes

12 p1840 A72-27705

Total precipitable water in atmosphere vertical column relation to surface humidity from measurements at desert, coastal and maritime sites

13 p1989 A72-28812

Upper atmosphere water vapor sources and sinks, discussing Hadley cell circulation, convective storm, stratospheric-tropospheric interchange, methane oxidation and volcanic activity

13 p1948 A72-28835

Atmospheric desorbed water molecules and ions number density vertical distribution in lower ionosphere and thermosphere

15 p2225 A72-31913

Earth atmosphere water vapor mixing ratio profiles from relaxation method for full radiative transfer equation inverse solution

15 p2266 A72-32724

Barbados Oceanographic and Meteorological Experiment to compare synoptic scale-measured vertical vapor fluxes over tropical ocean

16 p2417 A72-33169

Fluctuations of water vapour content in the troposphere as derived from interferometric observations of celestial radio sources.

17 p2545 A72-34690

Water vapor flux periodic and spatial variations from airborne measurements, confirming height variation of maximum spectral density wavelength for crosswind runs

18 p2706 A72-36632

Investigation of moisture content in the atmosphere by the method of ground radar thermal measurements

20 p2949 A72-39945

Atmospheric window at 10-12 micron wavelength, investigating absorption coefficient of clear atmosphere water vapor

21 p3048 A72-40398

Sanitary-hygienic evaluation of the extraction method for water recycling in atmospheric moisture condensates

21 p3006 A72-40435

Diurnal variation in energy balance microclimate across coastal beach, noting surface moisture effect

21 p3078 A72-40468

Conceptual possibilities of studies of moisture content in the atmosphere from thermal radio emission in the submillimeter wavelength range

21 p3078 A72-41798

Sound absorption in atmosphere at 20 C, predicting relaxation times and strengths in 100 Hz to 1 MHz as functions of relative humidity

23 p3285 A72-44112

Determination of the physical properties of atmospheric aerosol particles above the Atlantic

24 p3420 A72-44757

MOS devices instability caused by water and hydroxyl molecules on silicon dioxide surface, noting optimal conditions for chemical stabilization

24 p3431 A72-44821

Electrical discharge-produced explosions aboard supertankers during cleaning operation and electrostatic charging of supersonic aircraft during passage through heavy rain, noting water drop disintegration

24 p3368 A72-44979

ATMOSPHERIC NEUTRON FLUX DENSITY

U ATMOSPHERIC RADIATION

U NEUTRON FLUX DENSITY

ATMOSPHERIC NOISE

U ATMOSPHERICS

ATMOSPHERIC OPTICS

Atmospheric refractive index structure parameter variation with height and measurement near ground [AD-739059]

02 p0253 A72-12546

Electrostatically induced stimulated Brillouin light scattering effect on atmospheric depolarization, obtaining solutions for steady state and transient conditions

[AD-736316]

03 p0367 A72-13429

Precipitation effects on optical transfer function of turbulent atmosphere at 1.2 km, comparing to clear, overcast and cloudy skies

05 p0656 A72-16176

Atmospheric optics and geophysics problems modeling arrangement reproducing radiation field within light scattering medium

05 p0658 A72-16293

Upper atmosphere twilight optical inhomogeneities relation to noctilucent clouds, using electrophotometry methods

06 p0807 A72-17933

Light field in cloud and fog plane layers from stationary collimated point source propagation

06 p0848 A72-17937

Angular transmittance model of visible light scattering through overcast cloud layer

07 p1030 A72-19411

Atmospheric aerosols optical thickness evaluation from solar radiation integral intensity

07 p1031 A72-19855

Correlation radius of intensity fluctuations of light beam focused in turbulent atmosphere

08 p1135 A72-21733

Methane contribution to thermal opacity in Uranus and Neptune atmospheres for atmospheric model synthesis

09 p1383 A72-22293

Radiative transfer equation for solar irradiance penetration of turbid atmosphere and plant canopy, using four point quadrature method

09 p1297 A72-22442

Atmospheric refractive index inhomogeneity statistics from interferometer measurements of distance-dependent phase fluctuations in near-ground

horizontal optical propagation paths under turbulence conditions

09 p1354 A72-23696

Optical path calculation in ionosphere and troposphere, determining term due to astronomical refraction with respect to frequency

10 p1475 A72-24859

Turbulence theory 2/3 law applicability to optical spherical wave propagation through turbulent atmosphere, comparing to von Karman model

11 p1686 A72-25772

Luminous emissions of upper atmosphere, discussing relation to airglow and auroral phenomena

11 p1626 A72-26431

Book on information theory of atmospheric visibility covering vision threshold conditions, eye as radiation detector and short waves field near ground

11 p1691 A72-26697

Statistical approach to atmospheric optics inverse problems solution, considering application to vertical temperature and humidity profiles determination

11 p1683 A72-26888

Angular variation and spot dancing of laser beam in atmospheric propagation, obtaining standard deviation

12 p1782 A72-27493

Intracavity gas cell for carbon monoxide laser oscillations restriction to lines coincident with atmosphere transmission bands, noting absorption by atmospheric water vapor

12 p1823 A72-27837

Atmospheric optics inverse problem solution, comparing orthogonal functions series expansion and regularization method algorithms

12 p1841 A72-27992

Optical measurement of crosswind from effects produced by atmospheric turbulence and wind velocity relationships

13 p1994 A72-28870

Parhelia phenomenon origin, proposing flat hexagonal ice platelets descending in relatively quiet atmosphere

13 p1954 A72-30087

Precipitation effects on optical transfer function of turbulent atmosphere at 1.2 km, comparing to clear, overcast and cloudy skies

14 p2099 A72-30245

Laser Doppler velocimeter designs for atmospheric applications, discussing illuminating techniques, SNR, performance comparison and system selection

15 p2237 A72-32051

Atmospheric transmittance calculation from 0.76-micron oxygen band fine structure parameters

16 p2417 A72-33289

Two beam optical recording instrument for atmospheric IR transmissivity, discussing spectrophotometers with changeable NaCl, KBr and LiF prisms

16 p2392 A72-33294

Light field in cloud and fog plane layers from stationary collimated point source propagation

16 p2426 A72-33778

Numerical evaluation of Chapman's grazing incidence integral χ/X , χ_i

17 p2549 A72-35609

Radiation transfer in planetary atmospheres with a three-term scattering indicatrix

17 p2618 A72-35810

A relative performance analysis of atmospheric laser Doppler velocimeter methods.

17 p2558 A72-35949

Preliminary analysis of the solar image quality in the 'Amici' dome of the Arcetri Astrophysical Observatory

18 p2728 A72-36767

Propagation of laser beams through the atmosphere. II

18 p2661 A72-36793

Auroral absorption and magnetospheric plasma dynamics pattern from arctic stations atmospheric opacity data

18 p2688 A72-36859

Facility and procedure for measuring the spectral transmittance of the atmosphere in the range from 0.48 to 12 microns with moderate resolution

18 p2692 A72-36965

Dependence of the optical transfer function of a turbulent atmosphere on the averaging time

18 p2707 A72-36968

Russian book - Refraction of light rays in the atmosphere

19 p2834 A72-37448

High energy gamma ray sources search by Cerenkov radiation recording from extensive air showers, noting atmospheric transparency effects

19 p2850 A72-37805

Design of a system for automatic compensation of atmospheric dispersion

19 p2801 A72-37962

An Irtan-1 reflection filter for the 20-micron atmospheric window.

20 p2928 A72-39897

Experiments on turbulence characteristics and multiwavelength scintillation phenomena.

21 p3048 A72-40140

- Simplified equation for amplitude scintillations in a turbulent atmosphere. 21 p3083 A72-40143
- Balloon measurements of tropospheric turbulence vertical profiles, obtaining temperature and refractive index structure coefficients 21 p3077 A72-40144
- Atmospheric window at 10-12 micron wavelength, investigating absorption coefficient of clear atmosphere water vapor 21 p3048 A72-40398
- Effect of environmental changes on the ghosting of distant objects in twin-glazed windows. 21 p3084 A72-40616
- Light pulse propagation through clouds - Models and experiments. 21 p3063 A72-40857
- Probability interpretation of radiative transfer to calculate magnetic field-originating spectral line formation dependence on solar atmosphere mean optical depth 21 p3107 A72-41276
- High precision stellar electrophotometer design, using two channel single photoamplifier photometer and digital computer for statistical atmospheric noise damping 21 p3056 A72-41447
- Balloon optical experiments in IR, visible, UV and X ray regions, considering in situ measurements of atmospheric composition, electric field and cosmic dust 21 p3049 A72-41613
- IR night vision instruments range calculation, taking into account atmospheric optics and electro-optical image converter characteristics 21 p3059 A72-41816
- Connection of the brightness indicatrices with the optical thickness of the atmosphere 22 p3200 A72-41874
- Optical properties and structure of the Jovian atmosphere. V - Probable structure of the ammonium aerosol layer 22 p3219 A72-41914
- Improved Curtis-Godson approximation in a non-homogeneous atmosphere. 22 p3201 A72-42511
- The effect of cloud scattering on the absorption of solar radiation by atmospheric dust. 22 p3201 A72-42512
- Determination of the refractive index of air by a dispersion method based on the use of radio waves 22 p3155 A72-42722
- Visibility variations at Schiphol-Airport, Amsterdam. 22 p3202 A72-42886
- Atmospheric thermal IR radiation transmission function dependence on carbon dioxide concentration, calculating spectral and vertical distributions for standard, summer and winter model atmospheres 22 p3174 A72-43005
- Atmospheric optics inverse problem solution, comparing orthogonal functions series expansion and statistical regularization method algorithms 22 p3202 A72-43006
- Absorption profile of a planetary atmosphere - A proposal for a scattering independent determination. 23 p3289 A72-43889
- The spectral albedo of water clouds in the 1- to 6-micron range 24 p3395 A72-44636
- Measurement of the angular divergence and of the refraction of a laser beam in the ground layer of the atmosphere. 24 p3380 A72-45611
- ### ATMOSPHERIC PHYSICS
- #### NT CLOUD PHYSICS
- Altitude dependent superrotation of earth upper atmosphere, using nonlinear continuity, momentum conservation and state equations of gas dynamics 01 p0052 A72-10076
- Small harmonic oscillations of isothermal atmosphere due to acoustic-gravity wave downward reflection caused by kinematic viscosity increase with altitude 01 p0102 A72-10229
- Radiative heat transfer equilibrium in Earth, Venus and Mars atmospheres, taking into account interaction with ground 01 p0058 A72-10561
- Venus atmospheric investigation by Venera 4, 5 and 6 probes, discussing satellite components and instrumentation, and atmospheric composition, depth, density, pressure, temperature and model 01 p0130 A72-10931
- German Research and Test Institute for Aero- and Astronautics 1970 report covering flow mechanics, power conversion, aerospace medicine, atmospheric physics, etc 01 p0048 A72-11151
- Steady state convection in solar atmosphere outer layers, plotting physical parameters as functions of geometrical depth 02 p0276 A72-11645
- Soyuz 6 multispectral aerogeophysical measurements of Usturt plateau and Caspian and Aral Seas, discussing remote sensing information yield on earth water/land and atmosphere properties 02 p0208 A72-11785
- Real gas effects in atmosphere to make sonic bang shock wave full dispersion and thickness wide variations 02 p0154 A72-11972
- Ionospheric effects related to production, maintenance and control of geomagnetically aligned Birke-land current system 02 p0219 A72-11978
- Micrometer particle formation by water vapor photolysis at 1500-1700 Å, noting particle production rate and implications to planetary atmosphere physics 02 p0220 A72-12207
- Algorithm design for objective high altitude fog prognosis, considering geostrophic vorticity, thermal advection, wind direction and dew point difference 02 p0254 A72-12782
- Wind velocity and direction vertical changes for weather dynamics, emphasizing jet streams 02 p0255 A72-12785
- Computer calculation for atmospheric total mass and seasonal redistribution from pressure and temperature field data, discussing error sources 03 p3348 A72-13480
- Ionosphere-magnetosphere interactions - Conference, New Delhi, February 1971 04 p0515 A72-14926
- Airglow considered as faint light emission during atomic and molecular dissociations in atmosphere, yielding clues to physical and chemical processes from spectrum 04 p0520 A72-15642
- European Space Research and Technology Center /ESTEC/ results in cosmic rays, ionospheric physics and surface physics 05 p0644 A72-16754
- Magnetospheric plasma sources, discussing wave-particle interactions and acceleration mechanisms 06 p0810 A72-18281
- Acoustic and gravity waves nonlinear propagation and structural deformation in isothermal and incompressible atmospheres with traveling wave induction 07 p0981 A72-20696
- Handbook on aviation meteorology covering atmospheric structure and composition, standard atmospheres, heat transfer, adiabatic processes, winds, cloud formations, precipitation, ice formation, fog, visibility, etc 08 p1200 A72-21479
- Discriminant analysis application to data on precipitation formation in convective cumulus clouds to relate process to surrounding atmosphere and cloud characteristics 08 p1201 A72-21993
- Book on stellar atmospheric physics covering gray and nongray atmospheres, radiation emission and absorption, transfer equation, Eddington approximation, spectral lines formation, etc 10 p1532 A72-23725
- Papers on thermospheric circulation covering atmospheric dynamics, ionosphere, gravity waves, noctilucent clouds, meteor trail winds, radar observations, etc 10 p1473 A72-24701
- Noctilucent clouds characteristics and interpretation, discussing height, observation latitudes, variations, drift, wave structure, auroral influence and particle size and density, etc 10 p1473 A72-24706
- Airglow intensities and upper atmosphere physical processes relationship, discussing spectral features, emission brightness and excitation sources 10 p1474 A72-24714
- Pulse radar radio altimeter for balloon atmospheric sounding 10 p1484 A72-25088
- Upper atmosphere physics - Conference, Erice, Italy, June 1970, Volume 2 11 p1621 A72-25834
- Ionospheric physics, attributing anomalies to plasma motions 11 p1621 A72-25835
- Computer calculation for atmospheric total mass and seasonal redistribution from pressure and temperature field data, discussing error sources 11 p1623 A72-26250
- Atmospheric infrasound measurement techniques and instrumentation for long distance propagation, considering wind and temperature effects 11 p1635 A72-26509
- Upper atmosphere neutral particle pressure, temperature and density profiles during 7 March 1970 solar eclipse from pitot tube soundings 12 p1800 A72-27144
- Transient planetary Rossby waves dynamics in winter stratosphere forced from below, using quasi-geostrophic midlatitude beta plane approximations 13 p1988 A72-28550
- Low flight altitude atmospheric parameters spatial and temporal variability effects on aircraft flyover noise measurement 13 p1991 A72-28841
- Acousto-optical method and equipment for atmospheric gases absorption lines recording with ruby laser for radiation source 14 p2111 A72-30812
- Atmospheric gravity waves effects in ionosphere, discussing F region traveling ionospheric disturbances, sporadic E layer and D region radar scattering 15 p2222 A72-31285
- Wind profiles, turbulence, and temperature and density distribution of neutral upper atmosphere obtained via sounding with Skylark rockets carrying chemical seeding payloads 15 p2223 A72-31435
- Atmospheric ion composition analysis by RF mass spectrometer during rocket ionosphere sounding, discussing meteor ionization layers 15 p2225 A72-31915
- Report to COSPAR on 1971 Soviet space programs, discussing moon, planets, cosmic radiation, interplanetary medium, magnetosphere, upper atmosphere, meteorological, orbital station and biomedical studies 15 p2337 A72-32002
- Report to COSPAR on French space program covering ionospheric and magnetospheric physics, meteorology, earth resources and exobiology 15 p2337 A72-32003
- Report to COSPAR on U.S. space program covering stellar astronomy, lunar and planetary research upper atmospheric physics, earth and life sciences, etc 15 p2337 A72-32006
- Stellar and planetary atmosphere dynamics, deriving balance equations for variance analysis of angular momentum 16 p2453 A72-33247
- Giant hygroscopic atmospheric dust particle concentration variations measured with light scattering monitor, noting frontal passage dependence on prefrontal concentration 16 p2386 A72-33604
- Mathematical model for atmospheric ions density fluctuation with time, noting absence of oscillating solutions 16 p2386 A72-33652
- Bibliography on SST upper atmospheric environment, listing references to stratospheric structure, composition and physical dynamics, chemical reactions with pollutants, transport properties, etc 16 p2386 A72-33797
- Atomic, molecular and ionic species detection in upper atmosphere by measurement of resonance fluorescence radiation excited by tunable laser radiation [AIAA PAPER 72-661] 16 p2388 A72-34073
- Atmospheric properties effect on satellite aerodynamic characteristics, noting gas composition and upper atmospheric winds [AIAA PAPER 72-659] 16 p2347 A72-34075
- Photogrammetric light beam refraction during aerial surveys, considering air pressure, temperature and humidity gradients in an out of camera carrier 17 p2552 A72-34452
- Russian book - Morphology and physics of the polar ionosphere 17 p2550 A72-35851
- Flow of a viscous liquid round a cylinder for Reynolds numbers 60 and 80. 18 p2679 A72-36233
- Free convection similarity and measurements in flows with and without shear. 18 p2706 A72-36634
- Singularities of nonstationary solutions to the equation of diffusion in a gravitational field. I, II 18 p2687 A72-36655
- Acoustic and gravity waves nonlinear propagation and structural deformation in isothermal and incompressible atmospheres with traveling wave induction 20 p2915 A72-39011
- Motion of a strong shock front in a nonuniform atmosphere 21 p3044 A72-40128
- Evanescence and internal gravity wave propagation effects on atmospheric dynamics, considering momentum transfer, energy dissipation and turbulence 22 p3168 A72-41964
- Theory of radiative heat transfer in polytropic atmospheres 22 p3229 A72-42962
- Latitudinal variation of temperature in the lower thermosphere /80 to 100 km/ 24 p3395 A72-44635
- Upper limits for an atmosphere on Io. 24 p3436 A72-44703
- Symposium on the Morphology and Physics of Magnetospheric Substorms, Moscow, USSR, August 3, 1971, Proceedings. 24 p3395 A72-44846
- A three-dimensional model of thermospheric dynamics. I - Heat input and eigenfunctions. II - Tidal waves III - Planetary waves. 24 p3400 A72-45594

ATMOSPHERIC PRESSURE

Lower thermosphere temperature, air density and pressure models, using auroral zone midlatitude neutral thermal and molecular diffusion coefficient measurements

01 p0053 A72-10187

Atmospheric temperature and pressure altitude effects on runway lengths and aircraft takeoff weights [ASCE PREPRINT 1242]

01 p0047 A72-10193

Pin electrode transversely excited atmospheric pressure carbon dioxide laser construction and pulse power outputs up to 60 kW [AD-738684]

01 p0079 A72-10516

Atmospheric ozone pressure variations in high altitude cyclones, anticyclones, troughs and crests at low pressure levels

02 p0207 A72-11734

Martian atmosphere and surface, covering atmospheric composition, optical thickness and pressure, violet and yellow clouds, surface relief and topography

02 p0282 A72-12326

Spherical planetary atmosphere tendency equation of pressure variation for horizontal stratification, using static and continuity equation in spherical harmonics

03 p0351 A72-14356

Uniform discharges in flowing carbon dioxide laser mixtures at atmospheric pressure, observing fluorescence intensity variation with discharge power density

03 p0369 A72-14400

Mode-locked transversely excited atmospheric pressure carbon dioxide laser pulse duration dependence on cavity modulation frequency and loss

04 p0529 A72-14588

Martian atmospheric pressure determination from carbon dioxide bands spectroscopic measurements

06 p0884 A72-18032

Atmospheric freestream pressure profiles determination from base pressure and flow phenomena of Mars, Venus or Jupiter entry probes [AIAA PAPER 72-202]

07 p0982 A72-18959

Wind, pressure and temperature diurnal and semidiurnal variations to 30 km altitude over tropical western Pacific, considering atmospheric model based on linearized equations of motion

07 p1029 A72-19099

Nuclear transducer for atmospheric pressure measurements based on alpha radiation detection, discussing accuracy, linearity and possible error sources

07 p1033 A72-20307

Venus atmosphere chemical composition, temperature and pressure, discussing model cloud layer, circulation and upper atmospheric structure

08 p1236 A72-21400

Atmospheric boundary layer pressure field expansion into dual series of natural time dependent components to separate fluctuations within monthly period for weather forecasts

08 p1203 A72-22125

Frictioned force modification of lower thermosphere vertical neutral gas velocities with resulting atomic oxygen and molecular nitrogen density-height distribution deviation from barometric law

09 p1298 A72-22582

Increased atmospheric pressure influence on blood coagulation in rabbits, showing post-decompression hypercoagulation followed by hypocoagulation

09 p1268 A72-23597

Martian atmospheric pressure determination from carbon dioxide bands spectroscopic measurements

11 p1719 A72-25968

Tropical depression analysis based on radar data, observing large divergence in maximum vorticity areas

11 p1681 A72-26079

Atmospheric pressure noise reducer for active microbarograph array, evaluating performance in field tests

11 p1613 A72-26510

Infrasound observations of acoustic auroras, using microbarographs and resonant detector recordings

11 p1627 A72-26517

Nonregular oceanic level fluctuations dependence on atmospheric pressure and tangential wind stress, deriving fluctuation spectrum from linear hydrodynamic model

11 p1682 A72-26882

Uniar surface neutral gas pressure measurement by Apollo 14 cold cathode ionization gage, determining day and night temperature effects on vacuum quality

12 p1805 A72-27041

Double discharge transversely excited atmospheric pressure TEA/ carbon dioxide laser construction, operation and output energy

12 p1819 A72-27266

Surface pressure via satellite-borne measurements of atmospheric transmission near absorption band

12 p1802 A72-27710

TEA pulsed carbon dioxide laser with continuous shaped electrodes, investigating hydrogen addition effects on power output and gain

12 p1827 A72-28224

Upper troposphere-lower stratosphere geostrophic wind deviation from rawinsonde and pressure-height data in El Paso-White Sands area, using finite difference method

13 p1988 A72-28447

Martian atmosphere and surface, covering atmospheric composition, optical thickness and pressure, violet and yellow clouds, surface relief and topography

13 p2039 A72-29210

Mars atmospheric temperature, pressure and electron density from radio occultation measurement with Mariner 6 and 7, noting frozen carbon dioxide in middle atmosphere

13 p2039 A72-29335

Hydrodynamic theory of atmospheric action center formation due to pressure migration for Northern troposphere two level meteorological forecasting

14 p2127 A72-30261

Air pressure and temperature changes during 7 March 1970 solar eclipse, showing primary wave structure with Fourier analysis

14 p2128 A72-30351

Long term atmospheric pressure fluctuations in relationship to solar activity over Northern Hemisphere, confirming 22 year cycle

14 p2101 A72-30648

Low pressure chamber as aerospace medical diagnostics tool for flying personnel examinations regarding oxygen deficiency, low air pressure and air pressure fluctuations tolerance

14 p2080 A72-30819

Apparent difference in Martian night and day side surfaces atmospheric pressure based on Mariner spacecraft occultations, noting effects of topography and electron layer

15 p2310 A72-31973

Air pressure effects on absorption dependence at IR wavelengths, using water vapor transmittance windows

15 p2202 A72-32657

Atmospheric energy spectra from two dimensional synoptic scales applicable to pressure or geopotential surface variables

15 p2266 A72-32721

Sea level wind and pressure data adjustment to governing dynamical equations by numerical variational analysis, using Sasaki matching technique

16 p2419 A72-33941

Russian book on atmosphere studies covering determination of periodic variations in meteorological elements to assess seasonal pressure, temperature and wind variations

17 p2546 A72-34975

Continuous natural background sources of microseismic motions due to atmospheric and ocean loading, wind, flowing water and local disturbances [AIAA PAPER 72-819]

20 p2915 A72-39104

Nonperiodic oceanic level fluctuations dependence on atmospheric pressure and tangential wind stress, deriving fluctuation spectrum from linear hydrodynamic model

20 p2948 A72-39569

Instrumentation for measuring static pressure fluctuations within the atmospheric boundary layer

20 p2927 A72-39799

Flying personnel auditory defects caused by environmental conditions, discussing aircraft noise, vibrations and atmospheric pressure effects

21 p3002 A72-40924

Venus atmosphere constituent abundances and temperature and pressure profiles from Venera probe data

21 p3110 A72-41451

Propagation of spherical and cylindrical shock waves in an inhomogeneous atmosphere with allowance for back pressure

21 p3047 A72-41662

Speech intelligibility during exercise at normal and increased atmospheric pressures

22 p3150 A72-42496

Sea level tropospheric pressure distribution persistence correlation to solar corpuscular radiation measured by planetary scale geomagnetic disturbance

22 p3219 A72-42517

Temperature of a free plasma filament in a high-frequency field at high pressures

23 p3322 A72-44464

ATMOSPHERIC RADIATION

NT AIRGLOW

NT AURORAL ARCS

NT AURORAS

NT DAWN CHORUS

NT DAYGLOW

NT GEOCORONAL EMISSIONS

NT IONOSPHERIC NOISE

NT NIGHTGLOW

NT RADIO AURORAS

NT RED ARCS

NT SKY RADIATION

NT STRATOSPHERE RADIATION

NT TWILIGHT GLOW

NT WHISTLERS

Planetary atmosphere IR radiative transfer model using matched asymptotic expansions method

01 p0125 A72-10099

Fabry-Perot interferometer application as filter with transmission windows at regular intervals in wave numbers to detect Raman scattered radiation from atmospheric gases

[AIAA PAPER 71-1078] 01 p0067 A72-10537

Nighttime ionosphere dynamical behavior, discussing motions effect on OI emission intensity

01 p0063 A72-10919

Atmospheric thermal sounding from meteorological satellites, reviewing measurement accuracy, equation kernel, spectral resolution, optimum measuring condition and interpretation techniques

01 p0070 A72-10959

Atmospheric primary and secondary cosmic ray propagation with close reference to two-fire-ball, H₂ quantum and excited baryon models of multiple meson production

01 p0121 A72-11122

Epithermal neutrons energy spectra in atmospheric equilibrium layers at 57 geomagnetic N, noting agreement with experimental error limits

02 p0273 A72-11918

Relief effects on atmospheric natural radioactivity vertical distribution

02 p0275 A72-12879

Bremsstrahlung emission by auroral electrons in upper atmosphere and penetration in lower atmosphere, comparing calculation with balloon measurement

04 p0566 A72-14879

Lower ionosphere 5577 and 5893 A and hydroxyl band emissions interrelationships, observing atomic O and vertical eddy transport effects

04 p0518 A72-14961

Atmospheric short wave radiation angular and vertical distribution relation to aerosol scattering parameters, using transport equation

05 p0658 A72-16291

Upper atmosphere atomic hydrogen H alpha emission, correlating intensity and hydroxyl vibration temperature

05 p0659 A72-17036

Azimuthal IR radiation distribution of atmospheric brightness cross sections at various zenith angles from balloon programmed-control radiometer data

06 p0808 A72-18042

Surface layer humidity correlation to height of atmosphere emitting in IR spectral region, determining water vapor content by recording earth radiation angular distribution

06 p0808 A72-18046

Narrow beam radiometer design and performance for atmospheric radiation studies including water vapor continuum absorption and high layer clouds emissivity

06 p0819 A72-18447

Night source ionized component profiles in chemistry and aeronomy of D and E regions, considering scattered L alpha and beta emissions and corpuscular fluxes

07 p0936 A72-20038

Epithermal neutron differential flux spectrum in equilibrium layers of atmosphere at 57 degrees north

07 p1066 A72-20652

Auroral X ray radiation measurements in midnight sector during solar storm of 8 March 1970

08 p1155 A72-20806

Excess radiation and primary cosmic ray intensity variations at 200-350 km during 1965-1969 solar cycle from Cosmos satellite data

08 p1227 A72-21156

Global radiation flux and energy sum calculation from turbidity factor and cloud cover parameters, comparing with measurements in tropics and polar region

08 p1201 A72-21797

Atmospheric vertical temperature profile inference from ground based measurement of microwave thermal emission spectrum from atmospheric oxygen

08 p1161 A72-21824

Planetary atmosphere diffuse radiation from limb side, applying to Mars atmospheric emission

08 p1238 A72-21832

Book on stellar atmospheric physics covering gray and nongray atmospheres, radiation emission and absorption, transfer equation, Eddington approximation, spectral lines formation, etc

10 p1532 A72-23725

Regular and irregular classes of amplitude fluctuations within artificially stimulated VLF emissions by low power pulses from ground transmitter

10 p1440 A72-24950

Overlap emissivity of atmospheric carbon dioxide and water vapor for computer simulated earth surface temperature calculations

11 p1628 A72-26986

Atmospheric thermal radiation flux calculation, showing carbon dioxide concentration effects on summer and winter models

12 p1805 A72-27991

Epithermal neutrons energy spectra in atmospheric equilibrium layers at 57 geomagnetic N, noting agreement with experimental error limits

13 p2030 A72-29230

Averaged atmospheric IR counter radiation values in cumulus clouds, using statistical characteristics 14 p2099 A72-30249

Vertical propagation of large scale disturbances in long wave radiation field into upper atmosphere, using linearized hydrothermodynamic equations 14 p2127 A72-30262

HCl and HF in carbon dioxide atmosphere, determining line intensities, halfwidths and shapes at room temperature 14 p2135 A72-30894

Jupiter and Saturn atmosphere composition, structure and radiative properties, presenting two zone stratosphere-troposphere model 14 p2161 A72-31072

Zeeman triplet with unsplit upper level formation in isothermic atmosphere under magnetic field, considering Doppler and Lorentz frequency profiles of transitions 15 p2304 A72-31332

Planetary cloudy atmosphere synthetic spectral line profile computation, using analytic scattering diagrams 15 p2192 A72-31649

Antennas scattering coefficients measurement by ground and atmospheric radiation, permitting antenna noise temperature components determination 15 p2206 A72-31652

Supernovae produced fluorescence pulses search in upper atmosphere by automatic coincident light receivers 15 p2313 A72-32233

Association between quasi-periodic VLF emission and micropulsation. 17 p2516 A72-35065

Radiation absorption and emission in atmosphere IR spectrum influenced by water droplets around atmosphere contamination particles 17 p2552 A72-35942

The influence of line shape and band structure on temperatures in planetary atmospheres. 18 p2726 A72-36640

Temperature sounding experiments for the Jovian planets. 18 p2726 A72-36641

Studies on radiation balance at a tropical station. 18 p2722 A72-36759

Preliminary results of observations of the pulsar CP 1133 with the aid of a device for recording Cerenkov flares of extensive atmospheric showers 19 p2850 A72-37806

Pion exchange and the cosmic-ray nucleon cascade. 19 p2851 A72-37923

Excess radiation and primary cosmic ray intensity variations at 200-350 km during 1965-1969 solar cycle from Cosmos satellite data 20 p2964 A72-39261

Radiative properties of upper and middle level clouds and of vertically developing clouds 20 p2949 A72-39948

Radiative transfer equations solution for stellar spherical atmosphere by Grant-Hunt method, approximating intensity derivative over angular variable with Legendre polynomials 21 p3109 A72-41433

Some results of measurements of short-wave and long-wave radiation fluxes from the Cosmos-320 satellite 22 p3168 A72-41875

Radiation, evaporation and the maintenance of turbulence under stable conditions in the lower atmosphere. 22 p3201 A72-42597

Variable strong atmospheric radio noise production under fair weather conditions without manmade signals, noting peaks before midnight and sunrise 22 p3173 A72-42885

Atmospheric thermal IR radiation transmission function dependence on carbon dioxide concentration, calculating spectral and vertical distributions for standard, summer and winter model atmospheres 22 p3174 A72-43005

Nuclear interactions in the atmosphere at energies greater than 100 TeV 23 p3330 A72-44411

Investigation of EAS characteristics at sea level with the aid of the classical method and by the method of recording radio emission 23 p3330 A72-44423

Low-energy nucleons in extensive air showers 23 p3331 A72-44424

Certain characteristics of the muon and electron components of extensive air showers at mountain level 23 p3331 A72-44425

Model for the uneven illumination of polar caps by solar protons. 23 p3286 A72-44502

Approximate formulas for the intensity of diffuse reflected emission from a semiinfinite atmosphere 24 p3448 A72-45685

ATMOSPHERIC REFRACTION
NT RADIO WAVE REFRACTION

Electromagnetic wave line-of-sight propagation based on geometrical optics for different refractivity profiles above sea, noting earth surface reflection role 01 p0026 A72-10404

Electromagnetic wave propagation anomalies over sea, comparing calculated and measured field strengths based on simultaneous refractivity vertical distribution measurement 01 p0026 A72-10405

Atmospheric radio refractive index computation errors derived from monthly averages of pressure, dry bulb temperature and vapor pressure 01 p0095 A72-10835

Radio signal fading analysis by ray tracing for transmission in spherically stratified atmosphere, assuming refractivity linear variation with height 02 p0179 A72-12414

Microwave propagation anomalies due to meteorological factors, discussing superrefractive atmospheric layers effects on radar data reliability and undesirable echoes appearance on display screen 02 p0182 A72-12746

Image blurring effects due to atmospheric boundary layer refractivity turbulent fluctuations during remote optical radiation source observations 03 p0359 A72-13482

Optical angle of refraction through earth mean atmosphere determination by three models of refractivity and iterative methods 04 p0515 A72-14884

Amplitude fluctuations of laser beam with Gaussian amplitude distribution on short line-of-sight path propagation through artificial turbulent atmosphere 04 p0488 A72-15383

High resolution measurement of microwave refraction including arrival and fire angles on short line-of-sight tropospheric paths 07 p0946 A72-19790

Photogrammetric light beam refraction during aerial surveys, considering air pressure, temperature and humidity gradients in and out of camera carrier 08 p1165 A72-21161

Meteorological radar measurements, noting missile tracking radio interferometer noise due to stochastic refractive ray bending and associated multipath conditions 08 p1136 A72-21978

Atmospheric refraction effects on IR far field irradiance distribution based on model of nonlinear interaction including absorption, transverse flow and vibrational relaxation effects 09 p1350 A72-22607

Two-laser optical distance measuring instrument with atmospheric refractivity correction, noting accuracy 11 p1646 A72-25305

IR refractivity measurement for atmospheric aerosol substances and sea salts [AD-744397] 11 p1620 A72-25306

Image blurring effects due to atmospheric boundary layer refractivity turbulent fluctuations during remote optical radiation source observations 11 p1633 A72-26252

Millimeter to meter waves propagation conditions prediction in horizontally inhomogeneous coastal foreground by meteorological parameters, considering wind effects on refractivity 12 p1784 A72-27798

Near horizon anomalies in astronomical refraction due to ground air layer effects on tropospheric processes 13 p1945 A72-28495

Diurnal variability of atmospheric refraction index at UHF in boundary layer for various weather types during summer-fall season 13 p1995 A72-29590

VLF long distance radio propagation in earth-ionosphere waveguide, considering earth magnetic field effects in mode conversion and refraction error calculation 13 p1922 A72-29655

Parhelia phenomenon origin, proposing flat hexagonal ice platelets descending in relatively quiet atmosphere 13 p1954 A72-30087

Venus atmospheric parameters below critical refraction and surface refractive index from signal amplitude measurement by radio holographic occultation techniques 14 p2151 A72-30467

Light rays total, astronomical and photogrammetric refraction in planetary atmospheres with arbitrary composition 15 p2224 A72-31602

Beam trajectory distortions due to turbulent air refractive index fluctuations in optical transmission line 15 p2197 A72-31885

Correction formulas for aerial photograph distortions due to internal refraction of light rays in separation of gas media by lateral surface of circular cylinder 15 p2277 A72-32124

Atmospheric refraction effects on ground based astronomical observations, using atmospheric model

with concentric spherical shells having decreasing density with height 16 p2386 A72-33495

Booker theorem generalization to cover wide range of ionospheric refractivity profiles containing variable electron density and collision frequency 16 p2386 A72-33662

Photogrammetric light beam refraction during aerial surveys, considering air pressure, temperature and humidity gradients in an out of camera carrier 17 p2552 A72-34452

Refraction correction of rocket tracking radar inputs in near real time. 18 p2661 A72-36636

Fourth moment of a wave propagating in a random medium. 18 p2712 A72-37025

Correlation study of geodetic refraction effect on astronomical refraction anomalies for solar light source observation at large zenith distances 19 p2855 A72-37348

High level atmospheric refraction of electromagnetic waves as function of elevation and meteorological element vertical stratification 19 p2764 A72-37349

Russian book - Refraction of light rays in the atmosphere 19 p2834 A72-37448

Indirect measurement of the atmospheric refraction index with the aid of radiosonde data 19 p2789 A72-37744

Thermistor temperature observation and correction for errors due to refraction anomalies in latitude measurements 19 p2801 A72-37913

Fast response solid state phase lock refractometer for airborne measurement of atmospheric refractive index 19 p2802 A72-38225

Propagation of internal acoustic-gravity waves around a spherical earth. 19 p2793 A72-38748

Photogrammetric refraction equation and integral interpretation for actual atmosphere, climate and weather conditions suitable for photographic flights 20 p2927 A72-39739

Mathematical model for Venus phase anomaly, noting upper limit of reflecting layer for refraction effect 20 p2972 A72-39874

Radiation field of a plane aperture in an inhomogeneous stratified medium over a large-radius sphere 22 p3155 A72-42654

Supersonic aircraft focused sonic boom suppression by slowing down during turning flight, obtaining conditions for focus cut-off at ground by atmospheric refraction 23 p3251 A72-44125

The influence of the atmosphere on the wavelength of the He-Ne laser and the solution of corrections of the laser interferometer. 24 p3409 A72-44771

Determination of refraction in the propagation of electromagnetic waves at the earth's surface 24 p3379 A72-44865

ATMOSPHERIC SCATTERING

NT TROPOSPHERIC SCATTERING

Atomic models of velocity uncorrelated radiation line scattering with frequency redistribution at large distance from atmosphere 01 p0104 A72-10094

Rain, snow and hail precipitation effects on radio link signal attenuation, scattering and fading along various transmission paths at millimeter and centimeter wavelengths 01 p0027 A72-10407

FM radio link superposed parabolic antenna systems adjustment for space diversity reception for scatter propagation and broadband multichannel transmission in 1.9 GHz range 01 p0027 A72-10410

Raman scattering from water vapor for Ar laser wavelengths in remote atmospheric humidity measurements [AIAA PAPER 71-1085] 01 p0104 A72-10542

Raman scattering cross sections and depolarization ratios of atmospheric gaseous pollutants as function of incident photon energy [AIAA PAPER 71-1086] 01 p0104 A72-10543

Aerosol and atmospheric scattering layers observability by satellite mounted optical detector at 3000-7000 Å, comparing wide angle receiver and limited view field steerable telescope [AIAA PAPER 71-1110] 01 p0058 A72-10554

Global satellite horizon-scanning monitoring technique permitting scattered solar radiation horizon profile conversion into aerosol vertical distribution [AIAA PAPER 71-1111] 01 p0058 A72-10555

Nonconservative radiative transfer in spherically symmetric system, calculating linearly polarized electron scattering atmosphere 01 p0102 A72-11127

Atmospheric scattering and absorption effects on target/background discrimination in environmental remote sensing at 0.4-3.0 microns spectral region

02 p0213 A72-11858

Ionospheric reflection height calculation according to oblique electromagnetic backscatter sounding data at two frequencies

02 p0172 A72-11943

Polarization and atmospheric inhomogeneity effects on solar radiative transfer in turbid atmospheres, using diffused reflection and transmission matrices

02 p0222 A72-12836

Radio wave scattering observation in turbulent lower ionosphere, determining vertical propagation velocity dispersion by statistical analysis

03 p0322 A72-13476

Multiple scattering polarization of sunlight reflected by terrestrial water clouds as function of particle shape and size, using doubling method

03 p0384 A72-14145

Singular integral equation in radiative transfer theory with polynomial scattering indicatrices

04 p0597 A72-15643

Ground and atmospheric scattered radiation discrimination by ground modulation based on chopper signal frequency analysis, considering feasibility from airborne tests results

06 p0814 A72-17587

Raman laser radar (LIDAR) for remote probing, discussing design, construction, testing, atmospheric scattering, and intensity and polarization measurements

06 p0824 A72-17588

Radiation intensity angular distribution from optically thick plane cloud layer reflection, relating photon survival probability and scattering functions

06 p0807 A72-17939

Solar radiation angular field structure from upper atmospheric boundary scattering, taking into account underlying surface albedo fluctuations

06 p0807 A72-17942

Twilight atmospheric sounding in oxygen absorption bands to reduce noise level in secondary light scattering

06 p0807 A72-17943

Brightness profiles of earth daytime horizon from Soyuz spacecraft photographic photometry, deriving atmospheric scattering coefficient relation to optical thickness vertical distribution

06 p0808 A72-18040

Aerosol scattering coefficient in atmosphere, determining statistical characteristics of vertical and spectral structure

06 p0842 A72-18043

Atmospheric directional scattering coefficients from vertical measurements of IR spectral sky brightness near solar almucantar and direct radiation

06 p0842 A72-18048

Photon radiative exit from scattering isothermal atmosphere containing atoms with two energy levels

06 p0848 A72-18051

Atmospheric light scattering matrices from nighttime air flows, showing climatic variability and similarity between Crimean and Moscow measurements

07 p1031 A72-20700

Geometric optics approximation for rf wave forward and backscatter characteristics by spherical overdense clouds for several electron density distributions

[AD-739797]

08 p1136 A72-21980

Backscattering by turbulent irregularities derived in context of single scattering corresponding to weak microwave reflections observed in atmospheric sounding

09 p1280 A72-23412

Atmospheric constituents dimension, composition and dynamics from optical radar echo observation of laser light scattering

11 p1592 A72-25849

Radio wave scattering observation in turbulent lower ionosphere, determining vertical propagation velocity dispersion by statistical analysis

11 p1593 A72-26246

Time and space characteristics of F scattering, investigating maximum appearance probability, intensity and seasonal and diurnal variations

11 p1595 A72-26280

Remote measurement of cloud ice and water content from Raman scattering of ground based laser signal

12 p1840 A72-27547

Ionospheric reflection height calculation according to oblique electromagnetic backscatter sounding data at two frequencies

13 p1920 A72-29255

Ionospheric attenuation of 3-100 MHz radio waves, interpreting scatter mode propagation mechanism as total reflection from lower ionizational irregularities

14 p2086 A72-30658

Reflectivity-emissivity relationship for isothermal atmosphere with coherent scattering and continuous absorption, generalizing for noncoherent case with line opacity

14 p2131 A72-30890

Steady state thermal transfer during ablation and radiation of single scattering albedo with constant heat flux at boundary

14 p2171 A72-30892

Aircraft laser radar measurements of atmospheric backscattering coefficients for cloud and underlying surface studies

15 p2266 A72-31908

Coronal scattering effects on type 3 solar bursts, using radio sources scintillation model and Monte Carlo ray tracing technique

15 p2316 A72-32752

Radiation intensity angular distribution from optically thick plane cloud layer reflection, relating photon survival probability and scattering functions

16 p2426 A72-33780

Solar radiation angular field structure from upper atmospheric boundary scattering, taking into account underlying surface albedo fluctuations

16 p2386 A72-33783

Twilight atmospheric sounding in oxygen absorption bands to reduce noise level in secondary light scattering

16 p2386 A72-33784

IR carbon dioxide laser radar with heterodyne detection, measuring SNR and atmospheric scattering coefficients for various weather conditions

17 p2516 A72-35192

On the choice of boundary conditions for integration of transfer equations.

17 p2577 A72-35695

Radiation transfer in planetary atmospheres with a three-term scattering indicatrix

17 p2618 A72-35810

Mie scattering models of zodiacal light based on spherical particles, commenting on inadequacy for nonspherical particles at elongations above 120 deg

19 p2792 A72-38506

Atmospheric surface layer light scattering matrices from nighttime air flows, showing climatic variability and similarity between Crimean and Moscow measurements

20 p2948 A72-39014

An application of atmospheric light scattering for contrast analysis in electro-optical detection systems.

20 p2923 A72-39056

Backscatter from gated fluctuating regions - A Bremmer series approach.

21 p3015 A72-40361

Albedo and surface illuminance of a planet having a nonhomogeneous purely scattering atmosphere

21 p3050 A72-41796

Determination of the characteristics of scattering particles in the Venusian atmosphere on the basis of photometric measurements

22 p3223 A72-42215

A comparison of the observed twilight with the vertical scatter distribution.

22 p3170 A72-42373

The effect of cloud scattering on the absorption of solar radiation by atmospheric dust.

22 p3201 A72-42512

Noctilucent clouds in daytime - Circumpolar particulate layers near the summer mesopause.

22 p3173 A72-42515

Backscattering of desorbed gas molecules from spacecraft

23 p3284 A72-43618

Absorption profile of a planetary atmosphere - A proposal for a scattering independent determination.

23 p3289 A72-43889

Density distribution of the radiation passing through a scattering medium from a bounded source

24 p3424 A72-44634

Approximate formulas for the intensity of diffuse reflected emission from a semiinfinite atmosphere

24 p3448 A72-45685

ATMOSPHERIC SHELLS

U ATMOSPHERIC STRATIFICATION

ATMOSPHERIC STRATIFICATION

Tropospheric layer structures effect on long range vhf radio communication, calculating wave modes attenuation rate and electric field patterns

01 p0032 A72-11238

Epithermal neutrons energy spectra in atmospheric equilibrium layers at 57 geomagnetic N, noting agreement with experimental error limits

02 p0273 A72-11918

Atomic oxygen layer height and peak concentration in earth upper atmosphere, considering solar dissociative radiation and turbulent diffusion for equinox conditions

02 p0217 A72-11924

Radio signal fading analysis by ray tracing for transmission in spherically stratified atmosphere, assuming refractivity linear variation with height

02 p0179 A72-12414

Small scale turbulence time-space variability in atmospheric boundary layer in presence of unstable stratification from vertical air flow measurements

03 p0383 A72-13481

Spherical planetary atmosphere tendency equation of pressure variation for horizontal stratification, using static and continuity equation in spherical harmonics

03 p0351 A72-14356

Northern Hemisphere mean zonal flow across arbitrary horizontal surfaces, evaluating vertical transports of kinetic energy

04 p0541 A72-14454

Vertical motions in stratified cloudy atmosphere as function of plane divergence distribution and heat influx

06 p0840 A72-17621

Velocity and temperature pulsations as function of stratification parameter in atmospheric boundary layer

06 p0842 A72-18044

Rain amount forecasting based on five level atmospheric model and hydrothermodynamics equations, calculating vertical currents under uniform atmospheric boundary layer stratification conditions

07 p1029 A72-18859

Ground focus line location of sonic bang propagating in stratified atmosphere with wind for transonically accelerating aircraft

07 p0912 A72-19645

Booms generated on ground by supersonic aircraft flying at high altitude through stratified atmosphere

08 p1149 A72-21019

Median true height atmospheric profile model synthesis from propagation parameters, using polynomial representations and alpha-Charman layers

08 p1157 A72-21106

Maneuvering aircraft sonic boom propagation and signatures prediction in stratified atmosphere by geometric acoustic method

08 p1110 A72-21904

Atmospheric stratification irregularities effects on sonic boom propagation, obtaining probability density functions

08 p1111 A72-21905

Thermal stratification of mesosphere and lower thermosphere at low latitudes with allowance for turbulent mixing, showing molecular oxygen and ozone radiative heating prevalence

09 p1347 A72-23589

Convective plumes model with heat flux, layer depth and surface turbulence intensity as parameters [AD-745511]

09 p1347 A72-23655

Spectral line formation in atmosphere with plane parallel layers and frequency independent source function, using matrix approach for transfer equation solution

10 p1535 A72-24058

Model atmosphere with n homogeneous layers and ground surface for solar radiation flux calculation [AD-744410]

11 p620 A72-25307

Hydromagnetic stability of isothermal stratified plasma atmosphere uniform flow over conducting liquid along magnetic field, discussing dispersion relation for static configuration

11 p1695 A72-26115

Small scale turbulence time-space variability in atmospheric turbulent layer in presence of unstable stratification from vertical air flow measurements

11 p1682 A72-26251

Abundance in cold stellar atmospheres, noting effect on atmospheric thermal stratification and energy transfer from molecular spectra

11 p1722 A72-26432

Analytic ray path solutions for HF radio wave transmission through plane stratified isotropic ionospheric model

11 p1599 A72-26763

Radio wave propagation control by superrefraction layers, investigating daily weather forecast technology improvement

12 p1784 A72-27797

Cloud tops height determination, considering IR radiation reflection by plane layer

12 p1841 A72-27990

Satellite radiance data to determine stratospheric layer thickness, comparing empirical regression equations to mean weighted temperatures

13 p1991 A72-28824

Aviation hazards due to stably stratified shear and turbulence zones, discussing meteorological analysis of 747 jumbo jet turbulence incident

13 p1994 A72-28865

Epithermal neutrons energy spectra in atmospheric equilibrium layers at 57 geomagnetic N, noting agreement with experimental error limits

13 p2030 A72-29230

Atomic oxygen layer height and peak concentration in earth upper atmosphere, considering solar dissociative radiation and turbulent diffusion for equinox conditions

13 p1948 A72-29236

Sonic boom magnitude and location in stratified atmosphere calculated from gas dynamical equations for lifting body of revolution

13 p1898 A72-29585

Midlatitude sporadic E layer formation under wind shear action from artificial cloud data on lower thermosphere wind speed and direction

13 p1951 A72-29589

Horizontal and vertical scales of atmospheric boundary layer turbulence for various temperature stratifications, noting space and time correlations for longitudinal wind velocity component

13 p1995 A72-29592

Oblique radio wave propagation through horizontally stratified ionosphere, considering electron collisions effects, reflection behavior and coupling levels
13 p1923 A72-29657

Interferometric investigation of temperature fields and heat transfer in air layers between vertical, inclined and horizontal parallel walls
14 p2170 A72-30251

Atmospheric stratification, wind profiles and vertical kinetic distribution of ions and neutral particles determined by rocket sounding
15 p2228 A72-31968

Computer calculations of horizontal linear antenna impedance for multilayer plane stratified medium, using induced emf method
16 p2368 A72-33492

Planetary wave interaction in two level baroclinic atmosphere, using quasi-geostrophic equations
16 p2418 A72-33602

Experimental evidences for a transient ion layer formation in connection with sudden ionospheric disturbances in the height range 20-50 km.
17 p2545 A72-34630

On the inflection point instability of a stratified Ekman boundary layer.
18 p2687 A72-36631

High level atmospheric refraction of electromagnetic waves as function of elevation and meteorological element vertical stratification
19 p2764 A72-37349

The motion of a vortex pair in a stratified atmosphere.
19 p2785 A72-37571

Internal wave instability in stratified jet streams
20 p2949 A72-39944

An application of the shooting method to the stability problem for a stratified, rotating boundary layer.
21 p3043 A72-40106

Wind profiles from velocity measurements at 20-160 meters, noting atmospheric stratification effect
21 p3078 A72-40766

Earth surface and background wind effects on mesoscale and large scale meteorological processes in free stably stratified atmosphere
21 p3078 A72-41794

Fine structure of temperature stratification in the troposphere and stratosphere
21 p3079 A72-41799

A comparison of the observed twilight with the vertical scatter distribution.
22 p3170 A72-42373

Atmospheric frontal motion stability via two-layer homogeneous incompressible fluid model, solving eigenvalue problem by small perturbation method
22 p3201 A72-42505

Noctilucent clouds in daytime - Circumpolar particulate layers near the summer mesopause.
22 p3173 A72-42515

Thermodynamic conditions for the development of convective clouds and a method of forecasting the quantity of rainfall
22 p3202 A72-42953

Cloud tops height determination, considering IR radiation reflection from plane layer
22 p3174 A72-43004

Allowance for the influence of orography in a dual-layer model of the atmosphere
23 p3310 A72-43443

Air temperature measurement errors due to instrument inertia under various meteorological conditions and atmospheric stratification
23 p3310 A72-43536

Atmospheric boundary layer definition by height of maximum vertical kinetic energy flux, considering stable and unstable stratifications
24 p3421 A72-44954

On the instability of a three-layer atmosphere with an isentropic stratosphere.
24 p3399 A72-45484

ATMOSPHERIC TEMPERATURE

NT AURORAL TEMPERATURE

NT IONOSPHERIC TEMPERATURE

Atmospheric temperature and pressure altitude effects on runway lengths and aircraft takeoff weights [ASCE PREPRINT 1242]
01 p0047 A72-10193

Average energy electron capture coefficient dependence on air density, temperature and altitude under gamma radiation
01 p0059 A72-10599

Nimbus 4 vertical atmospheric sounding techniques, obtaining temperature, water vapor and ozone profiles with Michelson IR interferometer
01 p0095 A72-10957

Atmospheric thermal sounding from meteorological satellites, reviewing measurement accuracy, equation kernel, spectral resolution, optimum measuring condition and interpretation techniques
01 p0070 A72-10959

Mt. Agung volcanic eruption dust effects on monthly-mean lower stratospheric temperatures for tropical stations
01 p0096 A72-11284

Microwave spectrometer remote sensing of atmospheric temperature and water vapor, discussing

cloud, topography and sea state effects and multiple regression statistical method
02 p0228 A72-11859

Stratospheric and lower mesospheric temperature measurement by ground based passive microwave sensing, calculating oxygen absorption band lines brightness temperature emission spectra
02 p0213 A72-11861

Temperature advection mesostructure from wind measurements for precise short term forecasts
02 p0254 A72-12778

Sunspot cycle 1958/70 effects on D region ionospheric absorption and stratospheric temperature measured by radiosonde
03 p0345 A72-12978

Ocean winds velocity, temperature and humidity fluctuations second and third order structure functions, deriving Kolmogoroff constants
03 p0383 A72-13154

Solar outer corona steamer density and temperature data from type 3 solar radio burst observation by space radio astronomy
03 p0424 A72-13223

Ground based atmospheric vertical temperature profiles measurement by Raman backscatter from molecular nitrogen
03 p0348 A72-13430

Meteorological elements, upper ionospheric data and solar radio emission intensities during winter stratomesospheric temperature rises
03 p0383 A72-13477

Earth limb radiance measurements inversion, yielding temperature distribution as function of altitude in real atmospheres
03 p0384 A72-14146

Temperature reduction produced by partial cloud cover effect on radiation received by Nimbus 3 IR radiometer
03 p0385 A72-14226

Obukhov contribution to turbulence in atmosphere with nonuniform temperature, discussing dynamic scale length and asymptotic states of boundary layer in unstable flows
03 p0385 A72-14333

Atmospheric static stability effect on turbulence layer thickness under nonuniform temperature, using correction factor dependent on Richardson number
03 p0386 A72-14334

Stratospheric circulation and air temperature horizontal and vertical distribution, discussing CAT at supersonic transport heights
04 p0541 A72-14676

Meteorological information assistance for Concorde aircraft test flights, discussing high tropospheric turbulence and lower stratospheric temperature predictions and instruments
04 p0542 A72-14680

Temperature variations in 30-100 km region of atmosphere, investigating solar radiation effects
04 p0516 A72-14935

Free atmosphere vertical temperature structure at mesoscale, using continuous recording sonde [AD-739147]
04 p0519 A72-15158

Electron energy derivation from contaminated Langmuir probe, explaining E region high temperature
05 p0654 A72-16007

Optimization algorithm in measurement conditions selection for satellite thermal sounding of atmosphere in 15 micron carbon dioxide band
05 p0655 A72-16174

Nighttime polar atmospheric structure and temperature variations due to gas kinetic and electron energy changes
05 p0656 A72-16240

Atmospheric temperature effect on solar diurnal variation of muon component, considering asymptotic characteristics of cosmic ray anisotropy
05 p0709 A72-16257

Atmospheric composition and temperature effects on F 1 region ion concentration structure from 140 to 220 km for low solar activity conditions
05 p0657 A72-16261

Diffusion equations of ion components of plane stratified plasma /ionosphere/, taking into account wind effect and vertical temperature distribution
05 p0658 A72-16402

Combined radar-acoustic system for lower atmosphere temperature sounding, considering use in air pollution studies and short range weather forecasting [AD-739790]
05 p0663 A72-16690

Pressure modulated carbon dioxide radiometer for remote temperature sounding in upper atmosphere
05 p0663 A72-16692

Sonic boom generation, propagation and minimization, discussing atmospheric turbulence and temperature gradients and aircraft configuration effects [AIAA PAPER 72-194]
05 p0612 A72-16849

Aluminum oxide cloud formation for thermosphere temperature determinations, describing methane/oxygen payloads, spectrographs, photometers and atmospheric models
06 p0806 A72-17646

Upper atmosphere analytical model expressing density as function of exospheric temperature and altitude
06 p0806 A72-17658

Venus 8.2 mm radio emission dependence on sunlight phase angle, considering implications regarding day/night atmospheric temperature variations
06 p0884 A72-18031

Nimbus 4 satellite selective chopper IR radiometer atmospheric temperature measurements from earth surface to 50 km altitude, describing instrument design, operation and performance
07 p1029 A72-19097

Wind, pressure and temperature diurnal and semidiurnal variations to 30 km altitude over tropical western Pacific, considering atmospheric model based on linearized equations of motion
07 p1029 A72-19099

Atmospheric vapor pressure and temperature direct measurement, using copper-constantan thermocouples for wet-bulb temperature rapid fluctuations and thermistor for mean wet-bulb temperature
07 p0982 A72-19106

Atmospheric turbulence, wind velocity, temperature and density measurements at 90-250 km, using explosive contaminants release from Skylark rockets
07 p0979 A72-20265

Atmospheric kinetic and temperature energy spectral balances in thermally stratified turbulent flow without shear
07 p0980 A72-20454

Upper atmosphere temperature measurement by homodyne detection of excited atoms and molecules radiation, using photodiode beat frequencies produced by spectral line emission
08 p1154 A72-20739

Mars atmosphere temperature profiles inference from outgoing radiation spectral characteristics, constructing atmospheric model
08 p1232 A72-21147

Venus atmosphere chemical composition, temperature and pressure, discussing model cloud layer, circulation and upper atmospheric structure
08 p1236 A72-21400

Mesospheric temperature and wind profiles during stratospheric warming from rocket grenade experiments
08 p1160 A72-21533

Auroral zone neutral wind velocity and atmospheric temperature correlations with geomagnetic activity, considering ion-neutral particle drag as accelerating mechanism during magnetic storms
08 p1161 A72-21535

Atmospheric vertical temperature profile inference from ground based measurement of microwave thermal emission spectrum from atmospheric oxygen
08 p1161 A72-21824

Upper atmospheric oxygen red line diurnal variations and midnight minimum, noting emission relation to kinetic temperature in magnetic storm
09 p1296 A72-22234

Weather analysis for mountainous terrain from potential temperature surface maps and vertical cross sections
09 p1344 A72-22431

Horizontal temperature variations relation to stratospheric CAT based on U-2 flight data
09 p1344 A72-22438

Atmospheric temperature vertical profiles by laser Raman backscatter measurements
09 p1307 A72-22439

Atmospheric temperature profiles real time retrieval from Nimbus 4 satellite IR spectrometric observation, describing method used in dynamical weather forecasting
09 p1345 A72-22440

Diurnal phase anomaly in upper atmospheric density and temperature inferred from satellite drag and incoherent scattering observations
09 p1298 A72-22590

Inferred perturbation effects of Arcibo large nighttime gravity wave on neutral atmosphere velocity and temperature
09 p1300 A72-23021

Clear air turbulence association with rapid temperature change over Bahrain, suggesting convectionally induced internal wave dissipation in inversion layer as turbulence mechanism
09 p1346 A72-23424

Continuous scan diffraction spectrometer for thermal sounding experiment on Meteor satellite, presenting vertical temperature and humidity profiles
09 p1347 A72-23588

Microbaroms produced by ocean waves radiated in infrasonic, noting dependence on upper atmosphere temperature and winds
09 p1348 A72-23656

Wind and temperature fields periodic updating, considering error reduction as function of time intervals between updates
09 p1348 A72-23659

Exospheric temperatures in hydrogen dominated planetary atmospheres for evaporative loss rates estimation, noting two component diffusive equilibrium model
09 p1393 A72-23661

Plane wave solutions to atmospheric gravity waves, including effects of nonlinearity, instability, molecular dissipation, temperature, wind and diurnal tides
10 p1473 A72-24705

Air, wet bulb and soil temperature indications from automatic telemetering meteorological stations, comparing with Hg thermometer readings

10 p1483 A72-25012

Satellite IR spectrometer sounding measurements reduction for atmospheric temperature profiles, obtaining coefficients by statistical regression and minimum information solutions

10 p1508 A72-25081

Successful operational satellite sounding probabilities with normal global cloud cover by vertical temperature profile radiometer

10 p1508 A72-25082

Atmospheric temperature measurement up to 2 km height, reviewing sounding equipment and techniques

10 p1508 A72-25091

Autumnal stratospheric temperature variations in northern and southern hemispheres from Nimbus 3 IR spectrometer

11 p1680 A72-25761

Lower atmosphere vertical temperature profiles determination from clear air ground based measurements of microwave thermal emission by oxygen

11 p1591 A72-25764

Thermosphere and lower exosphere density and temperature variations from satellite decay

11 p1621 A72-25843

Thermodynamic equilibrium theory for upper atmosphere /thermosphere/ temperature and density variations, noting Harris-Priester model

11 p1622 A72-25844

Heat conduction and radiative transfer equations of IR cooling by atomic O in thermosphere

11 p1622 A72-25848

Venus 8.2 mm radio emission dependence on sun-light phase angle, considering implications for day/night atmospheric temperature variations

11 p1719 A72-25967

Meteorological elements, upper ionospheric data and solar radio emission intensities during winter stratospheric temperature rises

11 p1682 A72-26247

Twilight and nighttime ionospheric temperatures from oxygen 6300 and 5577 A spectral line profiles obtained with Fabry-Perot interferometers

11 p1625 A72-26406

Atmospheric temperature measurement by neutral particle wake method, using satellite-borne mass spectrometer

11 p1634 A72-26408

Semiannual exospheric temperature and density variations from satellite observation and ionosonde measurements

11 p1626 A72-26420

Stratosphere geopotential height and temperature data observed at Northern Hemisphere radiosonde stations comparison with objectively analyzed data

11 p1682 A72-26474

Ionospheric and neutral atmospheric temperature profile, composition and electron density and energy measurements by MR-12 rocket

11 p1628 A72-26905

Carbon dioxide and dust effect on Martian atmospheric temperatures from time dependent calculations

12 p1865 A72-27033

Thermosphere temperature measurement by high velocity probe, admitting atmospheric sample via free molecular flow inlet

12 p1806 A72-27044

Ice formation on helicopter rotor blades, discussing atmospheric moisture and temperature conditions, blade surface temperature, centrifugal and aerodynamic forces and preventive measures

12 p1754 A72-27414

Temperature distribution and dissipation effects on compressible isothermal atmosphere Lamb waves vertical structure

12 p1839 A72-27504

Clear sky atmospheric thermal radiation from all-wave radiation and air temperature measurements, showing diurnal and desert condition induced deviations from empirical formula

12 p1840 A72-27706

Near-ground daytime temperature and humidity fine structure relation to heat flux, net radiation and temperature and wind gradients

12 p1841 A72-27711

Cloud top temperature measurement by satellite through comparison of visible and IR cloud images with concurrent airborne radar and lidar measurements

13 p1944 A72-28444

Corpuscular radiation intensity relationship to midlatitude mesosphere temperature from rocket and balloon sounding and ground measurements

13 p2029 A72-28603

Regression technique for determining temperature profiles in upper stratosphere from satellite measured radiances, noting accuracy

13 p1990 A72-28822

Satellite radiance data for altitude and amplitude monitoring of stratospheric warming, comparing with rocketsonde and radiosonde observations

13 p1991 A72-28823

Diurnal and annual temperature variations at 30-60 km from statistical analysis of rocketsonde data, obtaining solar radiation errors magnitude

13 p1947 A72-28829

Mesosphere and stratosphere density and temperature variability with seasons and altitude

13 p1947 A72-28830

Lower stratospheric turbulence and horizontal temperature gradients from RB-57F aircraft meteorological measurements

13 p1993 A72-28864

Mars atmospheric temperature, pressure and electron density from radio occultation measurement with Mariner 6 and 7, noting frozen carbon dioxide in middle atmosphere

13 p2039 A72-29335

Thermospheric density-temperature time lag, considering two dimensional time dependent model based on UV heat input dynamic excitation

13 p1951 A72-29388

Horizontal and vertical scales of atmospheric boundary layer turbulence for various temperature stratifications, noting space and time correlations for longitudinal wind velocity component

13 p1995 A72-29592

Convective clouds effect on air temperature gradient and turbulent heat fluxes in near-surface layers

13 p1995 A72-29593

Jupiter, Saturn and earth atmospheric circulation seasonal variation data analogies, noting factors governing planetary atmospheric temperature

13 p2048 A72-29813

Polar zone thermospheric temperature variations due to atmospheric cooling, H component variations and discrete perturbation

14 p2097 A72-30133

Outgoing 15 micron carbon dioxide band radiation measurement optimization for atmospheric thermal sounding by satellite

14 p2099 A72-30243

Air pressure and temperature changes during 7 March 1970 solar eclipse, showing primary wave structure with Fourier analysis

14 p2128 A72-30351

Thermosphere kinetic temperature diurnal variation from heat conduction equation periodic solution, determining heat sources from solar radiation atmospheric absorption

14 p2101 A72-30640

Wind tunnel tests for correction of temperature profile data in stratosphere and lower mesosphere obtained from SKUA rocket sounding

14 p2105 A72-30807

Upper boundary layer conditions effects on atmospheric temperature profile reconstruction, by integro-differential equation substitution for Fredholm equation

15 p2265 A72-31399

Ionospheric radio waves absorption and stratosphere temperature variations with respect to season and sunspot cycles, examining 1963-5 winter anomaly

15 p2195 A72-31555

Upper atmosphere temperature and wind variations over Antarctic from meteorological rocket sounding, noting winter cyclonic vortex level

15 p2225 A72-31906

Temperature and density data deviation from stratosphere and mesosphere mean season model values at high latitudes

15 p2225 A72-31907

Mesosphere and lower thermosphere temperature measurement by rocket-borne manometer, relating temperature variations to corpuscular flux intensity and sun generated geomagnetic excitations

15 p2225 A72-31910

Mesospheric air density and temperature measurements from rocket-borne resistance thermometers based on free molecular flow

15 p2225 A72-31911

Atmospheric density and temperature measurements by rocket-borne spheres during 1972 winter, observing variability with altitude

15 p2227 A72-31959

Aladdin experiment atmospheric composition, total neutral density, temperature and ion density vertical profiles

15 p2228 A72-31969

Selective chopper radiometer /SCR/ radiances comparison to rocketsonde data, showing vertical resolution of stratosphere and mesosphere temperature changes during midwinter disturbance

15 p2228 A72-31976

Monthly mean air temperature anomalies annual forecasts based on Fourier analysis of 1900-1970 statistical data

16 p2418 A72-33381

Microwave /60 GHz/ radiometer for air temperature measurement outside aircraft during icing conditions

16 p2393 A72-33631

Atmospheric surface layer temperature, humidity and vertical wind velocity variances dependence on turbulent fluctuation inputs

16 p2419 A72-34148

On the possibility of a simultaneous measurement of wind speed, wind direction, air density and air temperatures at heights which correspond to the upper D-region /max. 95 km/ with chaff cloud sensors.

17 p2545 A72-34631

Russian book on atmosphere studies covering determination of periodic variations in meteorological elements to assess seasonal pressure, temperature and wind variations

17 p2546 A72-34975

Water vapor, CO2 and particulate effects on the atmospheric temperature profile.

17 p2549 A72-35636

The influence of line shape and band structure on temperatures in planetary atmospheres.

18 p2726 A72-36640

Temperature sounding experiments for the Jovian planets.

18 p2726 A72-36641

Numerical integration of nonlinear convective flow equations for arbitrary atmospheric temperature and wind profiles, discussing cloud streets formation

19 p2828 A72-37998

Upper atmosphere temperature measurement by homodyne detection of excited atoms and molecules radiation, using photodiode beat frequencies produced by spectral line emission

19 p2791 A72-38367

Some results of a numerical experiment in the reconstruction of a temperature profile by a 'regularized' iteration method

19 p2829 A72-38769

The influence of vertical motions on the diurnal variations of temperature and density in the thermosphere.

20 p2916 A72-39236

Mars atmosphere temperature profiles inference from outgoing radiation spectral characteristics, constructing atmospheric model

20 p2968 A72-39252

Stratospheric winds and winter warmings in the Southern Hemisphere.

20 p2948 A72-39862

Regression technique for determining temperature profiles in the upper stratosphere from satellite-measured radiances.

21 p3052 A72-40249

Seasonal, nonseasonal and synoptic global variations in stratosphere temperature from satellite-measured radiances, discussing latitudinal warming-cooling relationships

21 p3048 A72-40253

Numerical experiment of radiative-convective equilibrium of the Martian atmosphere.

21 p3105 A72-40772

Temperature range estimation method for planetary atmospheric component generating spectral lines, applying to Venus observations at 7820 A carbon dioxide band

21 p3106 A72-41045

Thermal oscillations in the high solar photosphere.

21 p3107 A72-41275

Venus atmosphere constituent abundances and temperature and pressure profiles from Venera probe data

21 p3110 A72-41451

Ground and flight tests of the Ramzes rocket sonde.

21 p3115 A72-41499

Stratospheric general circulation patterns from geographical, vertical and annual distribution for Northern Hemisphere temperatures, geopotential heights and winds

21 p3078 A72-41611

Fine structure of temperature stratification in the troposphere and stratosphere

21 p3079 A72-41799

Theory of radiative heat transfer in polytropic atmospheres

22 p3229 A72-42962

Annual height and temperature distribution charts of polar and tropical tropopause over Northern Hemisphere

23 p3310 A72-43534

Air temperature measurement errors due to instrument inertia under various meteorological conditions and atmospheric stratification

23 p3310 A72-43536

Ground-based sensing of temperature profiles from angular and multi-spectral microwave emission measurements.

23 p3285 A72-44147

Radiation influences on a white-coated thermistor temperature sensor in a radiosonde.

24 p3401 A72-44620

Latitudinal variation of temperature in the lower thermosphere /80 to 100 km/

24 p3395 A72-44635

Corpuscular radiation intensity relationship to midlatitude mesosphere temperature from rocket and balloon soundings and ground measurements

24 p3435 A72-45103

A thermospheric model from satellite orbital decay densities and incoherent scatter temperatures.

24 p3400 A72-45595

ATMOSPHERIC TIDES

- Matrix calculation of forced atmospheric oscillations for Hall, Coriolis and Pedersen regions 01 p0053 A72-10090
- Thermally excited E layer tidal winds based on UV radiation as thermal source, using isothermal atmosphere model 01 p0055 A72-10429
- Internal gravity waves and tidal oscillations excitation mechanism in upper atmosphere 03 p0346 A72-13383
- Atmospheric tides wave dynamics in thermosphere, considering viscosity, thermal conduction, hydromagnetic forces and nonlinearity effects on transmission and excitation 04 p0514 A72-14722
- Seasonal variations of semidiurnal tidal winds at 90-110 km from harmonic analysis of ionospheric inhomogeneity drift data 05 p0658 A72-16290
- Laser radar observations of mesosphere and lower thermosphere optical scattering cross section variations due to tide-caused atmospheric density fluctuations 08 p1156 A72-21100
- Tidal and seasonal wind variations from ionospheric drift if range measurements, comparing with radar-meteor data 08 p1160 A72-21528
- Atmospheric models of vertical structure of semidiurnal atmospheric gravitational tides, taking into account Coriolis force and vertical acceleration components 10 p1473 A72-24530
- Plane wave solutions to atmospheric gravity waves, including effects of nonlinearity, instability, molecular dissipation, temperature, wind and diurnal tides 10 p1477 A72-24705
- Regular tidal winds and irregular gravity waves domination of E region transport processes 10 p1477 A72-25161
- Temporal variations of sporadic E layer blanketing frequency, virtual height and occurrence rate, calculating electron density profiles and tidal wind influence 10 p1441 A72-25162
- Midlatitude upper atmosphere wind, tide and turbulence measurements, using radar observations of meteor trails 14 p2099 A72-30248
- Mathematical model of atmospheric tides using Navier-Stokes equations for perfect gas in thermodynamic equilibrium 16 p2385 A72-33343
- Information-prediction value of the tidal solar-lunar rhythmicity of certain meteorological processes 17 p2577 A72-35779
- Height structure of tidal winds as inferred from incoherent scatter observations. 22 p3169 A72-42014
- The problem of the boundary conditions in thermosphere dynamics. 22 p3201 A72-42510
- Lunar and solar gravitational effects on earth atmosphere, describing latitudinal distribution of cyclone centers by momentum distribution of horizontal tide-generating forces 23 p3310 A72-43249

ATMOSPHERIC TURBULENCE

NT CLEAR AIR TURBULENCE

NT GUSTS

NT LOW LEVEL TURBULENCE

- Wind resonance in ionosphere under pressure fluctuations, noting turbulent friction factor above 110 km 01 p0058 A72-10589
- Sonic boom pressure signatures during F-104 overflights at Mach 1.3 and 30,000 ft, explaining variations by atmospheric turbulence 01 p0006 A72-11158
- Far field diffraction due to annular apertures of plane wave light rendered partially coherent by atmospheric turbulence 01 p0103 A72-11166
- Angular straying of gravity center over cross section of diverging light beam in turbulent atmosphere 02 p0181 A72-12594
- Wind altitude and maximal velocity computation for jet stream structure and turbulence 02 p0255 A72-12786
- Atmospheric deviations of ageostrophic wind in jet stream domain, using dimensionless vector characteristics 02 p0255 A72-12787
- Atmospheric turbulence induced laser beam spread estimation from spherical wave modulation transfer function 03 p0367 A72-13442
- Radio wave scattering observation in turbulent lower ionosphere, determining vertical propagation velocity dispersion by statistical analysis 03 p0322 A72-13476
- Small scale turbulence time-space variability in atmospheric boundary layer in presence of unstable stratification from vertical air flow measurements 03 p0383 A72-13481

Image blurring effects due to atmospheric boundary layer refractivity turbulent fluctuations during remote optical radiation source observations 03 p0359 A72-13482

Obukhov contribution to turbulence in atmosphere with nonuniform temperature, discussing dynamic scale length and asymptotic states of boundary layer in unstable flows 03 p0385 A72-14333

Atmospheric static stability effect on turbulence layer thickness under nonuniform temperature, using correction factor dependent on Richardson number 03 p0386 A72-14334

Curve of line width correlation application to alpha Orionis OH lines, determining atmospheric turbulence and thermal velocities 04 p0571 A72-14558

Meteorological information assistance for Concorde aircraft test flights, discussing high tropospheric turbulence and lower stratospheric temperature predictions and instruments 04 p0542 A72-14680

Upper atmospheric turbulence correlation to supersonic aircraft dynamics, noting Concorde contribution 04 p0542 A72-14681

Turbulent tropospheric temperature fluctuations effects on optical waves propagation with random scattering, considering amplitude, phase, angle-of-arrival and polarization 04 p0548 A72-14736

Atmospheric turbulence detection sensors, reviewing microwave radar, acoustic, Doppler lidar, laser fringe anemometry and passive IR techniques 04 p0530 A72-14833

Amplitude fluctuations of laser beam with Gaussian amplitude distribution on short line-of-sight path propagation through artificial turbulent atmosphere 04 p0488 A72-15383

Prandtl layer turbulence spectra parameterization from wind vector data, considering functional dependence on mean wind velocity, height and thermal stratification 04 p0544 A72-15623

Frequency-contrast characteristics of optical system producing image of distant object in turbulent boundary layer of atmosphere, determining refractive index fluctuation intensities 05 p0689 A72-16172

Precipitation effects on optical transfer function of turbulent atmosphere at 1.2 km, comparing to clear, overcast and cloudy skies 05 p0656 A72-16176

Dynamic stability, control and structural response of transonic jet transport to atmospheric turbulence 05 p0611 A72-16348

Optimization algorithms for jet transport aircraft internally based flight trajectory control in turbulent atmosphere, comparing with ILS 05 p0685 A72-16472

Goldberg-Unno method accuracy for solar photospheric microturbulent velocities, discussing correction for damping effect and LTE deviation 05 p0718 A72-16503

Optical wave front transmission through turbulent atmosphere, predicting saturation phenomenon accompanying sea level turbulence 05 p0690 A72-16675

Sonic boom generation, propagation and minimization, discussing atmospheric turbulence and temperature gradients and aircraft configuration effects [AIAA PAPER 72-194] 05 p0612 A72-16849

Atmospheric turbulence incompressible two dimensional model, comparing Navier-Stokes equations numerical integration results with finite difference simulation [AIAA PAPER 72-152] 05 p0651 A72-16871

Atmospheric turbulence effects on aircraft flight and design, covering accidents and costs, turbulence generation, prediction, measurements and load alleviation devices [AIAA PAPER 72-219] 05 p0684 A72-16885

Ionospheric turbulence induced scintillations of Intelsat geostationary satellite signals at 4 and 6 GHz [AIAA PAPER 72-179] 05 p0631 A72-16966

Rice exceedance statistics application to atmospheric turbulence, indicating strong nonGaussian second order distributions [AIAA PAPER 72-136] 05 p0684 A72-16969

Multifrequency plane, spherical and beam waves propagation, calculating temporal frequency spectra in turbulent atmosphere 06 p0771 A72-17339

Altitude dependent turbulence characteristics in atmospheric boundary layer over wavy ocean surface from wind pulsation measurements 06 p0841 A72-17624

Vertical two-point longitudinal velocity differences or wind shear in atmospheric boundary layer, obtaining standard deviation from turbulence measurements 06 p0841 A72-17666

Turbulent energy dissipation rate statistical characteristics above 1000 m from radar measurements, discussing atmospheric boundary layer quantities 06 p0841 A72-17940

Cumulus clouds vertical motion velocity spectra curves, turbulence dissipation rates and energy determination from aircraft measurements 06 p0842 A72-17941

Meteor streams effect on atmospheric motions turbulence intensity based on radar observations 06 p0842 A72-18045

Surface pressure fluctuations near axisymmetric stagnation point in flow over simple impinged body, showing fluid strain suppression of turbulence 06 p0757 A72-18133

Rising/falling spherical wind sensors responses to atmospheric wind perturbations on vertical wind profile, using Fourier transform techniques 06 p0843 A72-18445

Motion dynamics of aircraft-autopilot closed loop system under influence of atmospheric turbulence and electric circuitry thermal noise 07 p0911 A72-18990

Pattern recognition through atmospheric turbulence by reflected coherent light power spectrum recording technique, using Wiener-Khinchin theorem 07 p0982 A72-19054

Atmospheric turbulence measurements over sea from 30 m to 1 km, examining rms vertical velocity variations with altitude 07 p1030 A72-19104

Atmospheric eddy flux spatial variations in constant flux layer, noting heat and momentum flux variability of less than 10 percent 07 p1030 A72-19107

Atmospheric turbulence, wind velocity, temperature and density measurements at 90-250 km, using explosive contaminants release from Skylark rockets 07 p0979 A72-20265

Numerical simulation of atmospheric turbulence in planetary boundary layer due to wind shear and/or unstable thermal stratification, noting buoyancy and planetary rotation effects 07 p1031 A72-20359

Atmospheric acoustic attenuation measurement on sailplane, assessing turbulence backscattering cross section 07 p1031 A72-20597

Synoptic velocity fluctuations from empirical structural functions of wind fields, proposing spectral kinetic energy distribution model for atmospheric turbulence 07 p1031 A72-20694

Atmospheric free convection turbulence and diffusion, proposing statistical characteristics and formulas with horizontal thermal flux vertical and transverse velocity components 07 p1031 A72-20697

Optical signal heterodyne reception, discussing atmospheric distortion effects reduction 08 p1131 A72-20749

Atmosphere hydrodynamic simulation model for cascade energy transfer in turbulent flow, using Euler gyro equations 08 p1158 A72-21190

Lin parameter and eddy viscosity of atmospheric vortex streets, using TIROS and Gemini data 08 p1200 A72-21621

Correlation radius of intensity fluctuations of light beam focused in turbulent atmosphere 08 p1135 A72-21733

Displacement measurement of weight center of light beam transmitted through turbulent atmosphere 08 p1135 A72-21734

One dimensional atmospheric turbulent diffusion model and semiempirical equation, considering jumplike changes in particle velocity 08 p1201 A72-21999

Turbulent earth atmosphere optical inhomogeneities determination from solar limb image characteristics in motion pictures of solar disk edge 09 p1305 A72-22233

Small scale atmospheric turbulence measurement with airborne hot-wire anemometer, discussing optimal choice of experimental parameters 09 p1307 A72-22435

Air pollutants lateral dispersion coefficient determination from turbulence intensity, presenting formula for wind direction frequency distribution function 09 p1344 A72-22436

Parametrization of turbulent flux of momentum, heat and moisture at ground in baroclinic planetary boundary layer 09 p1346 A72-22810

Atmospheric turbulence inner scale measuring configuration consisting of light transmitter and two scintillation counter detectors 09 p1314 A72-23343

CW carbon dioxide laser Doppler radar for remote measurement of atmospheric wind velocity and turbulence, obtaining Doppler signal via homodyned radiation scattered by airborne particles 09 p1315 A72-23407

Backscattering by turbulent irregularities derived in context of single scattering corresponding to weak microwave reflections observed in atmospheric sounding 09 p1280 A72-23412

Nonlinear longitudinal aerodynamic characteristics effect on rigid aircraft response to normal acceleration due to atmospheric turbulence, using power spectral technique

09 p1263 A72-23461

Turbulence measurement, reporting and subsequent data handling by upgraded ATC system, suggesting R and D program to evaluate wake turbulence effects on airport capacity

09 p1346 A72-23466

Meteor trail photoobservations for atmospheric small scale turbulences vertical profile, determining eddy minima velocities and turbulent energy dissipation in M zone

09 p1393 A72-23650

Convective plumes model with heat flux, layer depth and surface turbulence intensity as parameters [AD-745511]

09 p1347 A72-23655

Atmospheric refractive index inhomogeneity statistics from interferometer measurements of distance-dependent phase fluctuations in near-ground horizontal optical propagation paths under turbulence conditions

09 p1354 A72-23696

Local and macroscopic thermal transport in turbulent air stream, discussing measurement from calorimeter instrumented sphere

10 p1417 A72-24148

Atmospheric isotropic turbulence kinetic energy dissipation and wind spectra estimation from Doppler spectra of precipitation particle velocities

10 p1507 A72-25001

Noctilucent cloud kinematics as indicators of mesospheric circulation and turbulence characteristics, discussing need for international scientific cooperation

10 p1476 A72-25006

Frequency distribution of ionospheric horizontal winds vertical shear, noting altitude independence, turbulence and viscous energy dissipation

10 p1477 A72-25157

Turbulence theory 2/3 law applicability to optical spherical wave propagation through turbulent atmosphere, comparing to von Karman model

11 p1686 A72-25772

Radio wave scattering observation in turbulent lower ionosphere, determining vertical propagation velocity dispersion by statistical analysis

11 p1593 A72-26246

Small scale turbulence time-space variability in atmospheric boundary layer in presence of unstable stratification from vertical air flow measurements

11 p1682 A72-26251

Image blurring effects due to atmospheric boundary layer refractivity turbulent fluctuations during remote optical radiation source observations

11 p1633 A72-26252

Atmospheric turbulent coherent noise in pipe arrays design for infrasonic wave detection

11 p1689 A72-26511

Correlation function of depolarized finite collimated Gaussian laser beam in atmospheric turbulent medium

11 p1599 A72-26748

Telescope performance reciprocity in laser transmitter or optical heterodyne receiver functionings, considering atmospheric turbulence effects

11 p1636 A72-26750

Fourier phase angle models of intermittent atmospheric turbulence

12 p1838 A72-27025

Atmospheric electricity, turbulence and pseudosunrise effect during solar eclipse, analyzing space charge density and power spectra decay

12 p1800 A72-27140

Ground surface shadow bands observations during 7 March 1970 solar eclipse by photoelectric detection, indicating atmospheric turbulence effect

12 p1800 A72-27142

Transmitter aperture size and focus effects on scintillations of laser beam propagating through turbulent atmosphere

12 p1791 A72-27678

Atmospheric surface layer turbulent transfer mechanisms, studying direct measurements of momentum, heat and moisture turbulent fluxes

12 p1840 A72-27705

Equivalent atmospheric turbulence models concept for structure function behavior of electromagnetic wave propagation, noting dependence on model characteristics

12 p1841 A72-27946

Diffraction antenna use in visual range to study troposphere modulated laser radiation propagation in turbulent atmosphere, presenting light intensity distribution

13 p1917 A72-28690

Small scale atmospheric turbulent motions sensing by FPS-16 Radar-Jimsphere meteorological balloon system, analyzing wind velocity data from dual radar measurements

13 p1990 A72-28818

Thunderstorm penetration by F-100 aircraft to study turbulence hazard relation to updraft size and short period fluctuation-induced acceleration changes

13 p1992 A72-28852

Laser Doppler-type remote sensor for wind velocity and atmospheric turbulence measurements

13 p1956 A72-28859

Lower stratospheric turbulence and horizontal temperature gradients from RB-57F aircraft meteorological measurements

13 p1993 A72-28864

Aviation hazards due to stably stratified shear and turbulence zones, discussing meteorological analysis of 747 jumbo jet turbulence incident

13 p1994 A72-28865

Optical measurement of crosswind from effects produced by atmospheric turbulence and wind velocity relationships

13 p1994 A72-28870

Atmospheric turbulence anisotropy from meteor trails radar observations statistics, presenting plots of velocity field transverse structure

13 p2038 A72-29036

Horizontal and vertical scales of atmospheric boundary layer turbulence for various temperature stratifications, noting space and time correlations for longitudinal wind velocity component

13 p1995 A72-29592

Subauroral red arcs formation mechanism involving magnetosphere-ionosphere energy conduction and lower atmosphere neutral composition changes due to turbulent mixing

13 p1952 A72-29802

Laser beam propagation in vacuum, imperfectly transparent medium and turbulent atmosphere

13 p1971 A72-29865

Directional dependence of sound wave emission by convective turbulence in solar atmosphere, considering cut-off frequency effects on transmitted acoustic spectrum

13 p2048 A72-29926

Undisturbed and active solar photospheric turbulent velocity determination by comparing half widths of observed weak Fraunhofer line profiles with model calculation

13 p2049 A72-29929

Nightglow small scale intensity fluctuations of 5777 A atomic oxygen emission due to turbulent transport of horizontal wind observed with photometers

14 p2098 A72-30143

Modulation transfer functions of optical system producing image of distant object in turbulent boundary layer of atmosphere, determining refractive index fluctuation intensities

14 p2130 A72-30241

Precipitation effects on optical transfer function of turbulent atmosphere at 1.2 km, comparing to clear, overcast and cloudy skies

14 p2099 A72-30245

Midlatitude upper atmosphere wind, tide and turbulence measurements, using radar observations of meteor trails

14 p2099 A72-30248

Atmospheric turbulent characteristics and velocity longitudinal component intensity profiles, applying to dynamic wind loads computation

14 p2127 A72-30264

Small transport aircraft horizontal tail surfaces flow characteristics determination for stress calculation during flight in turbulent atmosphere

14 p2071 A72-30284

Venera satellite parachute probe method for Doppler measurement of Venus atmosphere wind velocity and turbulence

14 p2151 A72-30466

Atmospheric turbulence induced wave front distortion effects on fast-tracking laser antenna performance, considering infinite plane wave random complex phase modulation

14 p2110 A72-30550

Random parameters effect on divergence of focused light beams in turbulent atmosphere, noting light patch dependence on illumination source diameter

14 p2131 A72-30810

Wind profiles, turbulence, and temperature and density distribution of neutral upper atmosphere obtained via sounding with Skylark rockets carrying chemical seeding payloads

15 p2223 A72-31435

Submillimeter plane monochromatic waves propagation in ground layer of turbulent atmosphere, deriving received signals levels fluctuations

15 p2195 A72-31653

Beam trajectory distortions due to turbulent air refractive index fluctuations in optical transmission line

15 p2197 A72-31885

Subcloud Venus atmospheric wind velocity and turbulence from Venera Doppler measurements

15 p2308 A72-31905

Optical pulse wave field longitudinal and transverse statistical correlations during propagation in turbulent atmosphere

15 p2198 A72-32061

Single degree of freedom system displacement response exceedance of given level under nonstationary random excitation, considering aircraft flight through turbulent region with variable intensity

15 p2279 A72-32592

Floating forces contribution to heat flux during turbulent mixing of upper atmosphere

16 p2417 A72-33292

Correlation function measurements of optical gravity center roaming of spatially limited light beams in turbulent atmosphere

16 p2364 A72-33486

Kirchhoff-Fresnel diffraction field fluctuation at plane screen aperture in turbulent atmosphere

16 p2425 A72-33487

Atmospheric turbulence from illuminance and intensity fluctuation measurements at focused light beam

16 p2364 A72-33488

Turbulent divergence of laser beams along oblique atmospheric path for vertical refractive index distribution, using Markov coherence model

16 p2364 A72-33489

Narrow light beam attenuation and scattering characteristics in turbid medium as function of distance from source from transport equation solution

16 p2426 A72-33779

Turbulent energy dissipation rate statistical characteristics above 1000 m from radar measurements, discussing atmospheric boundary layer quantities

16 p2418 A72-33782

Cumulus clouds vertical motion velocity spectra curves, turbulence dissipation rates and energy determination from aircraft measurements

16 p2418 A72-33782

Pasquill method adequacy for atmospheric stability conditions discrimination and prediction of horizontal and vertical turbulence intensities

16 p2419 A72-33943

Atmospheric turbulence statistical theory, discussing random flow field characterization by property expressed in ergodic theorem

17 p2537 A72-34273

Variable rate optical communication schemes over earth/space link neutralizing atmospheric turbulence effects

17 p2514 A72-34415

The effect of atmospheric turbulence on the error of an optoelectronic angle sensor

17 p2554 A72-34941

Structural mode vibration control system design for B-1 aircraft to improve ride during atmospheric turbulence and terrain following

17 p2493 A72-35563

On the size distribution of turbulent elements in the earth's atmosphere

17 p2549 A72-35717

Turbulent micro and macromotion velocities in solar photosphere from CN molecule vibrational band line contours

17 p2617 A72-35735

Focused irradiance fluctuations beyond a layer of turbulent atmosphere

17 p2518 A72-35754

Low order model and error rates for two dimensional turbulent motion prediction in atmosphere spectrum

18 p2677 A72-36009

Some observed properties of atmospheric turbulence

18 p2705 A72-36019

Statistical self-similarity and inertial subrange turbulence

18 p2678 A72-36021

Observations of the variability of dissipation rates of turbulent velocity and temperature fields

18 p2678 A72-36022

Friction term formulation and convective instability in a shallow atmosphere

18 p2706 A72-36633

Field fluctuations of a laser beam propagating in a turbulent atmosphere

18 p2661 A72-36656

Radar meteorology in the Soviet Union - 1970

18 p2707 A72-36719

Dependence of the optical transfer function of a turbulent atmosphere on the averaging time

18 p2707 A72-36968

Atmospheric turbulence and the ATC system

18 p2663 A72-37049

Astronomical observations supporting stellar atmosphere microturbulence concept, noting Cepheid variables high dispersion spectra, supergiants irregular changes and microturbulence hydrodynamic effect

19 p2857 A72-37525

Numerical study of the characteristic magnitudes of turbulence on the far sound field radiated by a subsonic jet

[ONERA, TP NO. 1058]

19 p2786 A72-37761

Atmospheric boundary layer turbulence modeling, considering terrain roughness effects, vertical mixing, high frequency spectra, energy dissipation rate and vertical component variance

19 p2828 A72-38557

Spectral characteristics of surface-layer turbulence

19 p2829 A72-38559

Similarity predictions for shear stress and heat flux cospectral behavior in atmospheric turbulent boundary layer

19 p2829 A72-38560

Aircraft measurements of dissipation of turbulent kinetic energy. 19 p2829 A72-38561

Relation between impurity shear dispersion in the atmospheric ground layer and the turbulence characteristics 19 p2829 A72-38772

The indirect determination of stability, heat and momentum fluxes in the atmospheric boundary layer from simple scalar variables during dry unstable conditions. 20 p2947 A72-38964

Synoptic velocity fluctuations from empirical structural functions of wind fields, proposing spectral kinetic energy distribution model for atmospheric turbulence 20 p2948 A72-39009

Atmospheric flow turbulent behavior and dynamic characteristics dependence on underlying surface roughness variations 20 p2948 A72-39010

Atmospheric free convection turbulence and diffusion, proposing statistical formulas for components of horizontal thermal flux, vertical and transverse velocity and free diffusion tensor 20 p2948 A72-39012

Atmospheric turbulence induced optical effects due to refractive index fluctuations, solving Maxwell equations for instantaneous intensity distribution function 20 p2948 A72-39055

Turbulence in dynamic models of the atmosphere. 20 p2948 A72-39357

The stability of a coupled wave-turbulence system in a parallel shear flow. 20 p2948 A72-39797

Intensity of turbulence within canopies with simple and complex roughness elements. 20 p2948 A72-39798

Propagation of weak shock waves through turbulence. 21 p3044 A72-40114

Experiments on turbulence characteristics and multiwavelength scintillation phenomena. 21 p3048 A72-40140

Balloon measurements of tropospheric turbulence vertical profiles, obtaining temperature and refractive index structure coefficients 21 p3077 A72-40144

Russian book - Large-scale motions in the convective zones of stars and large planets. 21 p3104 A72-40462

Diffusion from a continuous source in relation to the Eulerian properties of turbulence. 21 p3046 A72-41248

Rigid aircraft longitudinal dynamic response to random atmospheric turbulence, defining spectral gust alleviation factors in terms of mass scale and damping ratio parameters 21 p2996 A72-41641

Quasi-two dimensional turbulence model of energy spectra and potential enstrophy transfer in synoptic large scale quasi-horizontal atmospheric motions 21 p3049 A72-41793

Evanescence and internal gravity wave propagation effects on atmospheric dynamics, considering momentum transfer, energy dissipation and turbulence 22 p3168 A72-41964

Micro- and macroturbulent motions and the velocity spectrum of the solar photosphere. 22 p3221 A72-42030

Modulation transfer function for solar telescopes and atmospheric turbulence. 22 p3175 A72-42047

Prediction error growth computation by test-field model for inertial range atmospheric turbulent flows in three and two dimensions 22 p3167 A72-42501

Radiation, evaporation and the maintenance of turbulence under stable conditions in the lower atmosphere. 22 p3201 A72-42597

Study of target edge response viewed through atmospheric turbulence over water. 23 p3289 A72-43896

The intermittent small-scale structure of turbulence - Data-processing hazards. 23 p3282 A72-44305

Book - The effects of the turbulent atmosphere on wave propagation. 24 p3379 A72-44650

Low-altitude atmospheric turbulence around an airport. 24 p3421 A72-45334

On the instability of a three-layer atmosphere with an isentropic stratosphere. 24 p3399 A72-45484

Influence of the heating of a turbulent atmosphere by a light beam on the fluctuations of the beam intensity. 24 p3425 A72-45601

ATMOSPHERICS

NT DAWN CHORUS
NT HISS
NT IONOSPHERICS

NT SUDDEN ENHANCEMENT OF ATMOSPHERICS
NT WHISTLERS

Atmospheric waveforms in relation to source location, source vicinity electric field properties, VLF radio wave propagation, frequency spectra and lightning discharges 01 p0024 A72-10124

VLF modulation/demodulation system performance prediction by atmospheric noise model, comparing results with measurements 01 p0025 A72-10327

Bit error rate estimation for narrow band digital communication in presence of atmospheric radio noise bursts 01 p0025 A72-10334

Statistical analysis of atmospheric average arrival time distribution, using simultaneous data from Berlin and equatorial latitude positioned research ship Meteor 01 p0056 A72-10443

Atmospheric radio noise measurement by two methods for quasi-peak value, noting good correlation between techniques 01 p0031 A72-10923

Burst and quasi-continuous forms atmospheric radio noise short term time characteristics above different thresholds, considering pulse duration and spacing 01 p0031 A72-10998

Book on radio wave propagation covering ground, tropospheric and ionospheric waves, atmospheric and cosmic noise, reflection, attenuation, signal distortion, space communication, etc 04 p0487 A72-15269

Long distance atmospheric propagation in earth-ionosphere waveguide, obtaining phase velocities and damping factors 08 p1131 A72-20802

VLF atmospheric count comparability in broad- and narrow-band operation, presenting amplitude frequency response 09 p1301 A72-23268

Digital lightning goniometry for flash locations at great distances by atmospheric and whistlers analysis 09 p1304 A72-23471

ELF wideband noise receiver for atmospheric waveshape magnetic tape recording, computer processing and system simulation 12 p1791 A72-27637

Global ground stations for lower VLF atmospheric arrival directions and spectral parameters observation 12 p1804 A72-27792

Distant thunderstorm center location with VLF atmospheric, determining delay time difference of Fourier spectrum groups of 6 and 8 kHz 12 p1841 A72-27793

Sudden decreases of atmospheric due to solar flares effects on lower ionosphere, discussing noise propagation 15 p2230 A72-32256

First mode calculations for VLF atmospheric parameters of group delay time and spectral amplitude ratio based on Wait-Walters model 16 p2362 A72-32890

Low energy auroral electron precipitation associated ELF noise band observation by polar-orbiting satellite INJUN 5 17 p2517 A72-35593

Error investigation for the location of the sources of atmospheric by radio direction finding. 18 p2706 A72-36429

A spheric rate azimuth-profile of the 1955 Blackwell, Oklahoma, tornado. 18 p2706 A72-36639

Propagation of horizontally polarized VLF waves - Systems implications. 21 p3021 A72-40905

Variable strong atmospheric radio noise production under fair weather conditions without manmade signals, noting peaks before midnight and sunrise 22 p3173 A72-42885

ATOM CONCENTRATION

Plasma temperature and seed atom concentration in MHD generator ducts and combustion chambers by optical measurements, discussing boundary layer thickness, optical density, etc 01 p0072 A72-11218

Laser flare luminosity front displacements and atom density at surfaces of transparent dielectrics as function of pulse intensities 07 p1007 A72-20123

Quantum mechanical transport equation for radiation interactions with molecules subject to perturber atom collisions, describing macroscopic density matrix evolution [AD-739082] 07 p1039 A72-20683

Diffusion coefficient and distribution of Ti atoms in thin Al film from electric current vs time curves for oxidation of solid solution 09 p1329 A72-23036

Critical resolved shear stress and solute atom concentrations relationship in solid solution hardening of metal crystals 12 p1853 A72-27101

Hg vapor absorptivity dependence on wave number, atomic density and temperature in 2537 A resonance line region, discussing measurement by magnetic scanning or monochromator 14 p2131 A72-30853

Neutral atom concentration measurement in Cs ion beam, using high sensitivity detection gage to obtain emission indicatives 16 p2434 A72-32862

Exobase atomic hydrogen densities for zero ballistic net flux as function of temperature distribution, noting support of McAfee hypothesis by OGO-4 polar UV observations 16 p2384 A72-32979

Sensor design and principles for atomic oxygen concentration measurement in dissociated gases, using Ag thin film electrical resistance change during oxidation 16 p2390 A72-33162

Polarization and interferometric investigations of discharge modes in thermionic energy converters 18 p2647 A72-36219

Neutron-rich nuclei in a Fermi gas 19 p2837 A72-38060

Solid surface geometry, atomic composition and electronic structure observations, discussing Auger spectroscopy, field ion microscopy and electron diffraction and scattering techniques 19 p2803 A72-38389

Effect of evaporation of the volatile component on the electrical properties of Cdsb 19 p2845 A72-38402

Martian atmosphere atomic oxygen concentration estimation from Mariner 6 and 7 O 11304 and 1356 A data analysis 19 p2868 A72-38734

Alloying element effects on C free energy interaction coefficients in liquid Fe alloys at 1550 C by equilibrium distribution method 20 p2937 A72-39295

Investigation of the influence of cobalt on the redistribution of the atoms of the alloying elements in iron-base alloys by the NGR method 22 p3188 A72-42162

Relationship between the electrical resistivity and solute concentration in the solid solution of tantalum-hydrogen system. 24 p3412 A72-44718

ATOMIC BATTERIES

U RADIOISOTOPE BATTERIES

ATOMIC BEAMS

Neutral Cr beam excited states radiative lifetime measurement by beam foil method 03 p0390 A72-13016

Magnetic atomic beam absorption filter for high resolution solar field observations 03 p0357 A72-13290

Multiphotonic ionization of atomic cesium jet by Q switched ruby laser beam 03 p0392 A72-14061

Optical excitation of divergent alkali atomic beam by radiation absorption, deriving absorption coefficient for line broadening and/or Doppler effect 03 p0393 A72-14062

Target jet density variations effect on vacuum in neutral atom beam ionization region of fast neutral particle magnetic trap 09 p1363 A72-23223

Merging beams study of positive ion ionization by electron impact for atomic He, N and O 11 p1692 A72-26658

Hydrogen plasma ion density determination from atomic beam attenuation by resonant charge exchange with protons 15 p2284 A72-31582

Atomic and molecular beams fluid dynamic applications in rarefied gas flows exemplified by satellite drag coefficient measurement 16 p2429 A72-33052

Potassium atomic beam aerodynamic acceleration by He-Ar free jet, determining beam intensity as function of nozzle-skimmer distance, carrier gas pressure and nozzle temperature 16 p2429 A72-33056

Fast metastable hydrogen atom beam production by proton beam-Cs vapor charge exchanges 16 p2429 A72-33057

Time-of-flight measurements of molecular and atomic beams produced by cooled microwave discharge source, using hydrogen, helium, argon and nitrogen 16 p2430 A72-33061

An atomic oxygen beam system for the investigation of mass spectrometer response in the upper atmosphere. 19 p2795 A72-37515

ATOMIC CLOCKS

Soviet book on gas lasers covering operation, population inversion, helium-neon, argon and carbon dioxide lasers and atomic frequency standards 02 p0238 A72-12121

Precision timekeeping, discussing atomic standards and Cs and Rb controlled molecular oscillators stability, cost and size 04 p0521 A72-14835

Atomic clocks application to spacecraft position determination, discussing ground stations synchronization and accuracy improvement by lasers [ONERA, TP NO. 1020] 05 p0660 A72-15858

Toran O long range navigation system based on circular coordinates and rubidium vapor clocks for beat phase measurements, noting use of portable transmitters 06 p0846 A72-12827

Time metrology achievements review, discussing time unit development, atomic and molecular frequency standards, atomic clocks, time scales and time signal broadcasting 10 p1481 A72-24399

Microwave and optical quantum electronic sources for frequency standards, noting primary Cs reference and multimode laser-RF oscillator beat technique 12 p1824 A72-27867

Short term instability of frequency standard using AFC of quartz crystal oscillator by phase locking to optically pumped Rb 87 vapor clock 13 p1968 A72-29296

ATS-3 C band dual transponders for geographically distant clocks time synchronization, using Cs clocks for accuracy verification 15 p2200 A72-32080

Microwave and optical quantum electronic sources for frequency standards, noting primary Cs reference and multimode laser-RF oscillator beat technique 16 p2403 A72-33976

Around-the-world atomic clocks - Predicted relativistic time gains. 17 p2584 A72-35838

Around-the-world atomic clocks - Observed relativistic time gains. 17 p2584 A72-35839

ATOMIC COLLISIONS

Supersonic oxygen molecules nozzle beam reactive scattering on barium atoms, detailing exothermic reaction energy in barium oxide formation 02 p0170 A72-11912

Atomic oxygen coupled electron excitation and ionization by electron-atom and atom-atom collisions in nonequilibrium relaxation zone behind shock wave 02 p0207 A72-12896

Solar corona atomic states radiative and collisional transitions, inferring radiative recombination cross section from bound-free absorption coefficient 03 p0422 A72-13203

Collisional relaxation rate effects of atomic level polarization on spectral line formation in solar magnetic regions 03 p0427 A72-13294

Upper atmosphere He, Ne, Na and K atoms collisions with molecular oxygen, determining ejected electron energy during fast Na, K, Rb and Cs ionization for meteor phenomena modeling 03 p0438 A72-13980

Effective cross sections of ion collisions with gaseous target and argon atoms collision with argon target by molecular beam intensity attenuation method 03 p0392 A72-14060

Surface potential effects on splitting of p- and d-orbitals of atoms and ions approaching bcc and fcc substrates 03 p0393 A72-14340

Velocity dependence of ionization cross section of Ar, Kr and Xe during thermal energy metastable neon atoms impact, obtaining secondary electron ejection efficiency 04 p0553 A72-15640

Hydrogen 2p and 2s states formation during 1-25 keV atomic collisions with rare gases from Lyman alpha radiation cross section measurement 05 p0693 A72-17168

Molecular oxygen dissociation rate constant determination during interaction with He atoms in cylindrical shock tube 06 p0852 A72-17686

Solid thermal motion influence on atom colliding with solid surface linear semiinfinite atomic chain, presenting accommodation coefficient calculation method 06 p0853 A72-18140

Ionization mechanism for low voltage neon plasma arcs, determining non-Maxwellian energy distribution effects and excited atoms collisions role 06 p0862 A72-18333

Inelastic high energy multiple interactions between cosmic ray particles and atomic nucleus targets, using Wilson chamber and ionization calorimeter 07 p0988 A72-19864

Lyman alpha radiation emission cross sections due to H/2p and H/2s formation in protons and hydrogen atoms collisions with hydrogen molecules 07 p1038 A72-20678

Quantum mechanical transport equation for radiation interactions with molecules subject to perturber atom collisions, describing macroscopic density matrix evolution [AD-739082] 07 p1039 A72-20683

Repeatable hermetic seal quality determination by He bombardment technique based on measured leak rate decay with time 08 p1220 A72-20766

Hydrogen protons and atoms interaction with hydrogen and nitrogen molecules, showing electron transfers agreement with Franck-Condon principle 08 p1210 A72-20835

Energy and angular distributions of electrons released during ion atom collisions from energy spectra studies, discussing autoionization transitions 08 p1210 A72-20836

Exothermic capture processes with ionization during nonelastic ion atom collisions, discussing cross sections of He ion collisions with Ar, Kr and Xe atoms 08 p1210 A72-20837

Atomic variational scattering calculation by method of models, using modified Hamiltonian form to avoid difficulties due to inexact target wave functions 09 p1355 A72-22787

Polarization fraction calculation for Lyman alpha radiation from excited H atom collisions, using Glauber, Born and Vainshtein approximations 09 p1355 A72-22790

Semiquantal theory application to cross section calculation for excitation and ionization produced by impact between two H atoms 09 p1355 A72-22791

Attractive well potential effects on vibrational transition probability during atom-diatomic molecule collisional relaxation 10 p1514 A72-24335

Pressure dependence of gas laser intensity, taking into account velocity changing collisions with foreign gas atoms [AD-740403] 10 p1492 A72-24604

Collisional ionization cross sections measurement for gaseous metal atoms in hydrogen-oxygen flames at 2000-2800 K 11 p1591 A72-26659

Mercury vapor physicochemical processes kinematics in shock tube, determining electron gas energy balance equations and atom-atom collision cross sections 11 p1699 A72-26760

Many electron pseudopotential method for electron-atom scattering, calculating singlet s wave and p wave phase shifts 12 p1848 A72-27429

Na atoms D line radiation excited in collisions with molecular gases, noting transfer cross section dependence on kinetic energy for given quantum number change 13 p2009 A72-30063

Dissipative instability produced by colliding ions and atoms in weakly ionized plasma 14 p2136 A72-30303

Ar and K electron cross section determination for momentum transfer, using dc conductivity measurement of high pressure plasma 14 p2134 A72-30803

Atomic hydrogen 3s state destruction by impact on nitrogen, argon and hydrogen molecules, considering collisional ionization and electron capture mechanisms 14 p2134 A72-30883

Elastic and one-phonon inelastic scattering of monoenergetic He atoms from cleaved LiF crystal surface 15 p2281 A72-31862

Na-He atomic collisions induced D lines broadening, fine structure transitions cross sections and multipole polarization resonance levels relaxation 15 p2283 A72-32651

Sodium D lines broadening and shift parameters under atomic H and He collisions effect, calculating low lying states interatomic potentials 15 p2317 A72-32772

Molecular and atomic mechanisms for hydrogen-iodine exchange reaction dynamics, using classical trajectory analysis 16 p2360 A72-33581

Diatomic molecules dissociation investigation from effective cross section measurement of slow atomic negative ions formation by molecules collisions with fast ions and atoms 16 p2432 A72-34152

Redistribution of resonance radiation. I - The effect of collisions. 17 p2605 A72-34534

Shock-wave structure using nonlinear model Boltzmann equations. 17 p2542 A72-35614

High vacuum technology applications in surface physics research, discussing atomic collisions and adsorption processes 18 p2712 A72-36827

Absolute differential cross sections of electrons elastically scattered on neon atom. 18 p2713 A72-36952

Absolute detection and collisional destruction of 2.5-keV metastable hydrogen atoms produced by a charge-exchange process in cesium vapor. 19 p2837 A72-37547

Collisional excitation and impact ionization coefficients of hydrogen 19 p2837 A72-37807

The redistribution function of polarized light in the presence of collisions and of small magnetic fields -

Discussion of the polarization of the solar line Ca I 4227 A. 20 p2971 A72-39756

Electron loss in atom-molecule collisions. 21 p3087 A72-40473

Speed-dependent collisional width and shift parameters in spectral profiles. 21 p3088 A72-40820

The solar abundance of calcium and collision broadening of Ca I- and Ca II-Fraunhofer lines by hydrogen. 22 p3221 A72-42027

Larmor radius and collisional effects on the dynamic stability of a composite medium. 22 p3212 A72-42990

Dissipative instability produced by colliding ions and atoms in weakly ionized plasma 23 p3317 A72-43205

Charge state variation processes in hydrogen atom collisions with H2 molecules 23 p3315 A72-43304

Variation in the hyperfine state of a hydrogen atom during its collision with unsaturated hydrocarbons in the gaseous phase 23 p3317 A72-44477

Influence of atom-atom collisions on the collisional-radiative ionization and recombination coefficients of helium plasmas. 24 p3428 A72-44798

Classical calculations of H2O rotational excitation in energetic atom-molecule collisions. 24 p3427 A72-45309

ATOMIC ENERGY

U NUCLEAR ENERGY

ATOMIC ENERGY LEVELS

Solar corona atomic states radiative and collisional transitions, inferring radiative recombination cross section from bound-free absorption coefficient 03 p0422 A72-13203

Collisional relaxation rate effects of atomic level polarization on spectral line formation in solar magnetic regions 03 p0427 A72-13294

Orion and planetary gaseous nebula helium atoms metastable triplet states population calculations 04 p0578 A72-15314

Elemental nucleosynthesis, considering cosmological, stellar, galactic and solar system evolution and atomic nuclei energetic levels 07 p1083 A72-20466

Ultrasoft X ray absorption spectra features of inner atomic shell photoionization in molecules 09 p1356 A72-22827

Multiconfigurational interactions in atoms with incomplete electron shells, identifying K-alpha satellite emission lines 09 p1357 A72-22837

High atomic energy levels population at low temperature, density and thermal radiation fields conditions in interstellar medium 11 p1720 A72-26111

Atomic hydrogen 3s state destruction by impact on nitrogen, argon and hydrogen molecules, considering collisional ionization and electron capture mechanisms 14 p2134 A72-30883

Electromagnetic field-two level atoms coherent interactions, using semiclassical approximation 15 p2250 A72-32305

Rutile titanium dioxide molecular orbital energy level diagram deduction from X ray emission and absorption band spectra, noting Ti and O states roles 15 p2295 A72-32539

Energy level population and emission spectrum of C IV ion in planetary nebula with radiative excitation 16 p2458 A72-33688

Emission line polarization prediction for planetary nebula C IV ion emitted spectrum via theory for energy level population 16 p2458 A72-33689

UV laser parameters calculation for operation on Lyman transition between H atom resonant excited state and ground state 17 p2562 A72-34349

Spectral measurements of atomic level populations in a plasma 17 p2591 A72-35307

The exact evaluation of certain partial sums of the second order energies of atoms. I - The ground and the singly excited states. 17 p2586 A72-35829

Stellar multilevel spectral line formation solution by preconditioning procedure based on core frequency transfer determination by local saturation approximation 20 p2954 A72-39758

Transition probabilities and collision-induced transitions in excited levels of neon. 21 p3061 A72-40136

Populating excited states of incoherent atoms using coherent light. 21 p3088 A72-40778

Investigation of amplification spectra and triplet-triplet absorption in a laser with a rhodamine 6G solution 21 p3064 A72-41743

ATOMIC EXCITATIONS

Atomic oxygen coupled electron excitation and ionization by electron-atom and atom-atom collisions in nonequilibrium relaxation zone behind shock wave 02 p0207 A72-12896

Excited Hg atom and electron concentration measurement behind shock front in nonstationary plasma by continuous displacement recording of interference bands 03 p0357 A72-13374

Hydrogen 2p and 2s states formation during 1-25 keV atomic collisions with rare gases from Lyman alpha radiation cross section measurement 05 p0693 A72-17168

Ionization mechanism for low voltage neon plasma arcs, determining non-Maxwellian energy distribution effects and excited atoms collisions role 06 p0862 A72-18333

Intensity ratio and effective lifetime of excited oxygen atoms in pulsating aurora from auroral intensity and absorption observations, noting diurnal variations 07 p0974 A72-18897

Laser quantum theory for single mode steady state emission fluctuations and instability region with high density of excited atoms 07 p0999 A72-18910

Electron beam induced dissociative excitation of vacuum UV emission from atomic nitrogen multiplets, using normal incidence monochromator and pulse counting techniques [AD-736008] 07 p1036 A72-18925

Scattering cross section for excited oxygen atoms production by electron impact dissociation of molecular oxygen 07 p1037 A72-18964

Fe I and Ti I excitation temperatures and ionization potentials of late G and K giant stellar atmospheres, comparing with model predictions 07 p1069 A72-19077

Atomic selective two step photoionization and molecular photodissociation by tunable laser radiation, experimenting on Rb vapor and HCl respectively [CLEA PAPER 12,4] 07 p1005 A72-19395

Mg ion excitation by electron collision in solar chromosphere studies, calculating scattering cross sections 07 p1081 A72-20234

Semiquantal theory application to cross section calculation for excitation and ionization produced by impact between two H atoms 09 p1355 A72-22791

Ionic and atomic temperature measurement in low pressure Ar plasma by X ray absorption spectroscopy 09 p1360 A72-22832

Inner shell ionized atoms, discussing orbital electron rearrangement processes based on shakeoff events and radiative Auger transition 09 p1356 A72-22834

Excitation accompanying photoionization in atoms and molecules and relationship to electron correlation observed from rare gases inner and valence shell satellite lines measurements 09 p1356 A72-22835

Photoabsorption and simple and multiple excitations of rare gases internal atomic layers under X ray action, relating electron transition and relaxed core energies 09 p1357 A72-22836

Metal welded joints formation as diffusion intensification from atom jumps stimulation by phonons from atomic thermal vibrations or crystal defects generation 09 p1319 A72-22867

Magnetic mirror system to study Lorentz ionization of highly excited hydrogen atoms with quantum numbers 6-7 in strong magnetic fields 09 p1363 A72-23222

WR hot stars CIII, NIV and OV emission spectra structure associated with excitation of 2pn and pd ion configurations 10 p1549 A72-25169

Optical radiation from Hg bombardment ion thrusters downstream regions due to excited atoms radiative decay, examining exhaust interference with star tracker [AIAA PAPER 72-441] 11 p1707 A72-26182

Population inversion through metastable ion formation by atomic inner shell electrons photoionization, determining effectiveness relationship to emission source plasma composition 11 p1648 A72-26332

Stimulated laser emission in vacuum UV by liquid Xe excitation with electron beam, determining threshold current density, radiation divergence and line half width 12 p1820 A72-27582

Excitation cross section in dipole approximation of semiclassical impact parameter and Born approximation, using asymptotic expansion of hydrogen-like atoms oscillator strength 13 p2040 A72-29411

Solar corona IR Fe XIII lines during 12 November 1966 solar eclipse, discussing proton collisions as line-producing excitation mechanism 13 p2042 A72-29537

Auroral spectroscopic and excitation processes, discussing atomic oxygen production, emission ratios

and electron energy spectrum, UV and IR emissions, composition and temperature measurements 14 p2098 A72-30138

Infrasonic excitation of red oxygen emission at 6300 A during geomagnetic storms at middle latitudes 14 p2098 A72-30146

Ground state and metastable atoms and ions optical pumping, presenting critical survey on pumping and relaxation mechanisms, light propagation and spin exchange 14 p2109 A72-30325

Atomic hydrogen collisional and radiative transition rates, computing excitation and ionization cross sections 14 p2133 A72-30564

Ionospheric electrons and neutral particles temperature and concentration profiles explained by electron gas cooling due to atomic hydrogen excitation, calculating heat flow 14 p2101 A72-30641

Ar plasma spectral lines, calculating temperature functions of excitation to fourth ionization multiple at atmospheric pressure 14 p2139 A72-30782

First positive and first negative nitrogen emission excitation kinetic mechanisms, investigating shock tube measurements of nonequilibrium radiation 14 p2134 A72-30837

Anomalous excitation of nitrogen positive bands in seeded Ar free plasma jet, measuring oscillator strengths of atoms 14 p2140 A72-30899

Thermal expansion in simple solids and structural composites due to anharmonic vibrations, using atomic density model 15 p2322 A72-31257

Electron production cross section during He atom ionization by proton impact, noting peak existence for electrons near incident proton velocities 15 p2281 A72-32220

Eikonal distorted wave analysis of inelastic electron-atom collisions at intermediate energies application to electron impact induced atomic hydrogen 2s and 2p states excitation 15 p2282 A72-32646

Transverse modes competition in high power homogeneously broadened gas laser with confocal geometry, noting corresponding longitudinal mode in atomic excitation 16 p2403 A72-33941

Particle excitation processes in solar corona, ionosphere and astrophysics, discussing electron affinities, ion-molecule reactions, forbidden atomic transitions and Fe II problem 16 p2432 A72-34150

Excitation transfer and Penning ionization reactions between helium metastables and carbon monoxide. 18 p2713 A72-36563

The use of known helium line cross sections for investigation of unknown transition in neon. 18 p2713 A72-36954

Excited-state cesium photoionization cross sections. 19 p2837 A72-37838

Laser quantum theory for single mode emission fluctuations and instability region with high density of excited atoms, noting self consistent field effects 20 p2931 A72-39376

Transition probabilities and collision-induced transitions in excited levels of neon. 21 p3061 A72-40136

Cross sections for the excitation of Ar II laser lines in electron-ion collisions. 21 p3063 A72-40725

Populating excited states of incoherent atoms using coherent light. 21 p3088 A72-40778

Book - Excitation in heavy particle collisions. 21 p3088 A72-41525

Fundamental infrared lattice vibration spectrum and the laser-excited Raman spectrum of MoSe2. 22 p3185 A72-42321

Study of the Stark effect in the resonance lines of sodium by an atomic jet method 22 p3209 A72-43048

Book - Introduction to optical electronics. 23 p3295 A72-43650

Theory of dispersion in relation to light shifts. 24 p3409 A72-44921

ATOMIC EXPLOSIONS
U NUCLEAR EXPLOSIONS
ATOMIC GASES
U MONATOMIC GASES
ATOMIC MASS
U ATOMIC WEIGHTS
ATOMIC MOBILITIES
German monograph on lattice and solid metal surface transport processes, discussing atom migration, activation energies, impurity atom diffusion, Kossel-Stranski model, etc 08 p1212 A72-22173

Impurity atoms effects on grain boundary motion velocity, considering interactions with metal lattice vacancies 11 p1662 A72-26655

ATOMIC PHYSICS

Classical path theory of pressure broadening in radiating atomic system perturbed by other atoms 07 p1037 A72-19497

Atom interactions with rf field, using quantum mechanical interpretation in terms of photons 07 p1038 A72-20433

Physical properties of atoms, molecules and solid material in ultrastrong magnetic field, using quantum drift approximation 12 p1847 A72-27055

Magnetic dipole matrix elements for atomic transitions between Zeeman levels at microwave frequencies 17 p2585 A72-35769

Use of multiple basis sets in the Brueckner-Goldstone many-body perturbation theory for atomic problems. 17 p2586 A72-35772

A simple, radially correlated ground state wavefunction for two electron atoms. 17 p2586 A72-35828

Coupled multiconfigurational self-consistent-field method of atomic dipole polarizabilities. I - Theory and application to carbon. 21 p3087 A72-40776

Broadening and shift of magnesium lines by van der Waals interaction with argon atoms and by microfields. 22 p3208 A72-42388

Physical properties of atoms, molecules and solid material in ultrastrong magnetic field, using quantum drift approximation 24 p3427 A72-45708

ATOMIC RECOMBINATION
NT OXYGEN RECOMBINATION
Recombination of hydrogen atoms on the surfaces of solid bodies 19 p2838 A72-38199

Monte Carlo trajectory calculations of the three-body recombination and dissociation of diatomic molecules. 19 p2838 A72-38805

Emission and absorption RF recombination lines of interstellar neutral atomic H and He, discussing electron transition processes in nebula 20 p2975 A72-40070

Radiative recombination of atoms as a resonance scattering process. 21 p3087 A72-40560

Correlation between the work function of transition metal carbides and the surface recombination of hydrogen atoms in the region of homogeneity 21 p3070 A72-41372

Recombination and annihilation rates of interstitial atoms and vacancies in crystal lattices, taking account of diffusion 21 p3088 A72-41690

Relation between the work function and adsorption and catalytic properties of transition metal borides in the reaction of recombination of hydrogen and nitrogen atoms 22 p3187 A72-41926

ATOMIC SPECTRA
Pressure broadened atomic line shapes calculation for Cs resonance line pressurized by Ar, using Lennard-Jones potentials 09 p1354 A72-22663

Mossbauer lines diffusion broadening and weakening in crystals impurity atoms nuclear spectra 09 p1371 A72-23030

Comparison of theoretical and experimental limits of detection in atomic absorption spectrometry using air-acetylene and nitrous oxide-acetylene flames. 09 p1376 A72-23725

Quantitative spectroscopy of the aurora. I - The spectrum of bright aurora between 7000 and 9000 A at 7.5 A resolution. 21 p3049 A72-41724

ATOMIC STRUCTURE
Physical properties of monocarbides of Zr, Nb and alloys in homogeneity range, explaining electronic structure relationship to composition changes 02 p0241 A72-11453

Atomic structural mechanism of solid solution decomposition by nucleation and equilibrium phase particles in Fe-Co-Ti alloy, using X ray analysis and transmission microscopy 02 p0242 A72-12008

Ordered Cu-Au alloy atomic order parameters, using field ion microscopy 04 p0560 A72-14548

Transition metals and alloys electron structure and packing defect energy theory, discussing crystal atomic interactions and brittle breakdown 07 p1049 A72-20148

Effective photoionization sections of neutral atoms, discussing photon energy effects, subshell periodicity and continuum functions phase shift 09 p1356 A72-22828

X ray emission spectroscopy of electronic structure of transition metals and alloys, obtaining electron energy spectrum 09 p1370 A72-22841

Computer simulation of crack tip atomic structure in diamond, relating covalent bond structure to dislocation nucleation and propagation likelihood
09 p1338 A72-22923

X ray spectral analysis of Ti-Cu alloys electronic structure
09 p1329 A72-23043

Order-disorder transition in metastable splat cooled Ti rich Ti-Fe alloys from phase formation, constitution and crystal chemistry viewpoint
09 p1330 A72-23378

Neutron diffraction study of inorganic materials atomic structure, examining symmetry properties and group arrangements of hydrogen compounds
09 p1358 A72-23478

X ray diffraction study of molten Mg-Cd alloy atomic structure, demonstrating existence of Mg-Cd compounds
10 p1497 A72-24678

Atomic radius ratios and lattice constants in inter-metallic compounds Laves phases, presenting semistatistically calculated values for niobium difluoride based on rigid sphere model
10 p1527 A72-24978

Ordering degree effect on elementary excitation spectrum gaps in nonideally ordered solid systems, obtaining Green functions for valence and conduction electrons calculations
10 p1527 A72-24982

Russian book on transition metals and alloys electron structure and electronic properties covering paramagnetism, positron annihilation, magnetic transformations and electron heat capacity
11 p1659 A72-26069

Electronic structure of technological processes in powder metallurgy of high temperature materials
11 p1646 A72-26872

Electronic configuration effect on wetting characteristics of hard material mixed crystals, investigating transition metals carbides, nitrides and oxides
11 p1665 A72-26873

Micromechanics of deformed continua, discussing atomic structure effects on stress concentrations in composite materials, framed structures and grids
12 p1884 A72-27640

X ray spectral analysis of Ti-Mo system alloys, investigating K and L lines and electronic structure
13 p1972 A72-28491

Electron structure of Al atoms in alloys with transition metals obtained from emission spectra
13 p1973 A72-28492

Electron shell structure in annealed and plastically deformed W-Re alloys from positron annihilation angular distributions
13 p1981 A72-29908

Atomic spectroscopy role in modern physics, discussing 1913 genesis, golden age in 1930s and revival in 1960s
14 p2133 A72-30577

Electronic structure of binary phase diagrams of group III-VI transition metals, using valence separation and condensed state model
15 p2252 A72-31198

Heat capacity data analysis for solid solutions of superconducting Nb-Ti system, investigating electronic structure
15 p2296 A72-32692

K and L lines of X ray emission spectra of Ti in alloys with Nb, noting atomic structure change during alloy formation
15 p2259 A72-32701

Field-ion microscopy as experimental metallurgical technique for metal surface atomic structure studies, discussing image formation, ionization and field evaporation
16 p2392 A72-33444

Experimental evidence for stationary population inversions of atomic levels in an expanding hydrogen plasma
17 p2589 A72-34898

Russian book on metal alloys structure and properties covering structural changes in solid bodies, metals atomic structure, diffusion, phase transformations and composite materials
17 p2568 A72-35446

Study of certain features of the electronic structure of the ternary alloys Ni3/Mn, Fe/ and Ni3/Mn, Co/
17 p2568 A72-35518

Work function, thermal stability, and atomic structure of electropositive films adsorbed on single crystals of metals
18 p2656 A72-36132

Time spectrum and angular distribution for positron annihilation studies of electron structure and phase transformations of materials
19 p2845 A72-38401

X-ray spectra and electronic structure of titanium nitrides of limit composition and in the homogeneity range
19 p2821 A72-38406

Russian book on electron configuration model of condensed matter based on Hubbard model covering physicochemical properties of transition metals, alloys and compounds
21 p3066 A72-40348

Hydrostatic pressure effects on atomic configuration based on principle of equivalence related to Einstein gravitational equations
22 p3205 A72-42459

Physical properties and electronic structure of V1-x Crx/3Si ternary alloys
22 p3192 A72-43014

Influence of alloying elements on ordering in alloys of the nickel-molybdenum system
22 p3192 A72-43016

Angular distribution of electrons autodetached from H- in slow collisions with He.
23 p3316 A72-44074

Photoemission studies of wurtzite zinc oxide.
24 p3432 A72-45387

ATOMIC THEORY

NT HEISENBERG THEORY

Atomic models of velocity noncorrelated radiation line scattering with frequency redistribution at large distance from atmosphere
01 p0104 A72-10094

Materials science historical development from ancient theories of structure of matter to modern atomic and field theories leading to general theory of elastic continuum
02 p0297 A72-12611

Universal mathematical model of n-complete atomic theory, obtaining existence criterion for prehomogeneous relation in relation age
10 p1506 A72-24851

Atomic spectroscopy role in modern physics, discussing 1913 genesis, golden age in 1930s and revival in 1960s
14 p2133 A72-30577

ATOMIC WEIGHTS

Isotopic abundance analysis of primary cosmic radiation with nuclear emulsion technique, discussing mass measurements in Be, C, O, Ne, Mg and Fe tracks
16 p2447 A72-33731

ATOMIZATION

U ATOMIZING

ATOMIZERS

Cooling system based on vaporization of solar cell preheated solution drawn through chamber with atomizing injector
10 p1422 A72-24314

ATOMIZING

Melting atmosphere, atomizing media and consolidation techniques effects on Co base alloy powder products physical properties
02 p0240 A72-11436

Physical processes of fluids atomization in electric field, discussing droplet surface instability and boundary values of surface tension coefficient
05 p0667 A72-17185

High melting point alloy and metal powder production by vacuum atomization, using rotary vane and electron beam melting techniques
11 p1645 A72-26860

Optimization of high temperature supersonic gas jets for metal powders production by melts atomization, discussing excess air ratio effect on gas parameters
13 p2025 A72-29133

Cold flow tests of mixing and atomization characteristics of gas/liquid circular coaxial injector elements in pressurized facilities
14 p2146 A72-30920

Atomization of liquid droplets in a convective gas stream.
17 p2540 A72-35044

In-line holography of reacting liquid sprays.
19 p2798 A72-37619

Model for shock wave propagation through gas-liquid drop medium based on liquid phase atomization by boundary layer stripping
24 p3391 A72-45049

ATOMS

NT HELIUM ATOMS

NT HYDROGEN ATOMS

NT METASTABLE ATOMS

NT NITROGEN ATOMS

NT OXYGEN ATOMS

Free atoms and radicals elementary reactions, passing parent molecules through electrodeless rf or microwave discharge at various pressures and temperatures
03 p0320 A72-13392

ATP

U ADENOSINE TRIPHOSPHATE [ATP]

ATROPHY

Exercise and denervation effects on intrafusal muscle fibers morphology, noting 25-33 percent cross-sectional area atrophy in nuclear bag and chain fibers
04 p0472 A72-14895

ATS [SATELLITES]

U APPLICATIONS TECHNOLOGY SATELLITES

ATS 1

Geomagnetic storm field recovery near synchronous satellite ATS 1 in terms of ring current belt and plasma sheet variations
01 p0053 A72-10088

Tropospheric wind estimation from ATS 1 satellite cloud motions over equatorial Pacific
01 p0060 A72-10856

Magnetosphere model for low energy cosmic ray proton propagation mode to synchronous orbit satellite, calculating geomagnetic cutoffs and penetration regions
02 p0274 A72-12453

Hydrologic data collection via ATS 1 satellite for river and flood forecast of National Weather Service, planning geostationary operational environmental satellites /GOES/
09 p1296 A72-22315

ATS 3

Ionospheric total electron content measurement with geostationary ATS 3 satellite during solar eclipse of 7 March 1970, plotting Faraday rotation as function of time
01 p0059 A72-10838

Traveling ionospheric disturbances observations during March 1970 solar eclipse from ATS 3 total electron content measurements
12 p1801 A72-27156

Smoothed wind fields generated from ATS 3 cloud motions measurements observed on computer display system
13 p1991 A72-28827

ATS-3 C band dual transponders for geographically distant clocks time synchronization, using Cs clocks for accuracy verification
15 p2200 A72-32080

ATS 5

Unshocked solar wind detection by ATS 5 satellite during 8 March 1970 geomagnetic storm
15 p2299 A72-31960

ATS 6

ATS-F satellite short and long term data processing, detailing millimeter wave propagation experiment
02 p0177 A72-12384

ATS F ion thruster system for north-south station-keeping, discussing specific impulse, thrust vectoring, propellant system and power conditioning circuitry [AIAA PAPER 72-439]
11 p1707 A72-26180

The 20 and 30 GHz communications system for the ATS-F millimeter wave experiment.
21 p3019 A72-40882

ATTACHMENT

Associative attachment and gas-to-particle conversion mechanisms in positive and negative ion formation up to 50 km
03 p0347 A72-13390

ATTACHMENTS

U ACCESSORIES

ATTACK AIRCRAFT

NT BOMBER AIRCRAFT

NT BUCCANEER AIRCRAFT

NT FIGHTER AIRCRAFT

NT JAGUAR AIRCRAFT

Electronic displays for attack aircraft, discussing subsystems, simulation technique and pilot role [DFVLR-SONDDR-140]
02 p0225 A72-11756

Air to air maneuverability of aircraft capable of inflight thrust vectoring, indicating improved deceleration, normal acceleration g-force and turn rate
03 p0310 A72-13877

Combat aircraft lateral aiming performance optimization and evaluation based on criterion of bullet stream response to pilot roll commands
05 p0611 A72-16657

Fighter/attack aircraft turbojet and turbofan engines testing with/without afterburners
06 p0868 A72-18495

Attack helicopters engine failure problems, discussing flight test results in transition from powered high speed flight to autorotational flight
08 p1108 A72-21011

Test pilot role in attack aircraft avionics systems integration consisting of head-up display, projected map, digital computer, inertial platform, radar and Doppler systems, etc
08 p1165 A72-21012

Carrier based attack aircraft allocation model formulation and solution for maximum inflicted target damage, using sequential unconstrained minimization technique with nonlinear programming
08 p1256 A72-21469

Strike aircraft reliability prediction in cost effectiveness analyses, showing failure probability distribution with time
13 p1896 A72-28360

Electronic displays with weapon aiming sensors in aircraft navigator-attack systems
15 p2273 A72-32634

Development of the Saab-Scania Viggen.
19 p2748 A72-37749

A-X Air Force flight evaluation.
19 p2751 A72-38131

A study of dedicated control surfaces for direct sideforce control.
24 p3368 A72-45344

ATTENTION

Selective attention dichotic listening test as flying proficiency prediction criteria, discussing omission and intrusion errors
07 p0929 A72-19351

Book on sustained attention /vigilance/, discussing effects of signal frequency, magnitude and distribution, task complexity, noise, age, intelligence, etc
07 p0930 A72-19910

Character recognition experiments to determine attention control and temporal-spatial capacity limitation during visual information processing 12 p1768 A72-27074

Self estimated distractibility in subjects related to attention lapses during perceptual motor performance, indicating psychophysiological changes 12 p1776 A72-28307

Divided attention effect localization, using choice tracking task reaction times in sequential stage model for human information processing 13 p1911 A72-29852

Experimental tests of Voth-Mayman hypothesis of autokinesia mediation by attention distribution mechanism 18 p2653 A72-36904

Repression-sensitization and duration of visual attention. 18 p2654 A72-36917

ATTENUATION

NT ACOUSTIC ATTENUATION
NT ATMOSPHERIC ATTENUATION
NT AURORAL ABSORPTION
NT MICROWAVE ATTENUATION
NT RADAR ATTENUATION
NT RADIO ATTENUATION
NT SHOCK WAVE ATTENUATION
NT SIDELobe REDUCTION
NT WAVE ATTENUATION

ATTENUATION COEFFICIENTS

Water depth attenuation coefficients and bottom reflectance characteristics from large area multispectral scanner measurements for discharge and concentrations monitoring 02 p0211 A72-11812

Eigenfunctions, eigenvalues and microwave attenuation constants in square and rectangular waveguides with rounded corners 11 p1607 A72-26994

Theoretical and measured rainfall attenuation of millimeter waves, correlating attenuation coefficients, rain rate and drop size distributions 12 p1785 A72-27803

Light beams propagation in clouds and fog, discussing scattering and attenuation coefficients 13 p1988 A72-28517

Physical interpretation of electromagnetic waves attenuation function HF singularity during diffraction over spherical surface, applying to short wave diffraction in tropospheric model 15 p2195 A72-31651

Attenuation rate of electromagnetic waves for dominant ELF and VLF modes of earth crust waveguide 15 p2200 A72-32110

Electrons and photons interaction with relict radiation, establishing high energy gamma rays energy and intensity attenuation length 17 p2600 A72-35145

Light attenuation coefficient measurement in water of various turbidity with AR and Kr lasers, interpreting results by Mie scattering theory 20 p2931 A72-39270

Microwave filter of interdigital or comb construction, calculating attenuation coefficient relationship to impedance of slabline with cylindrical inner conductor 21 p3032 A72-40628

Electromagnetic-wave propagation along a horizontal wire above ground. 21 p3015 A72-40633

Propagation loss of centimeter and millimeter waves in rainfall. 21 p3023 A72-41833

The cosmic-ray spectral modulation above 2 GV. 1V - The influence on the attenuation coefficient of the nucleonic component. 24 p3434 A72-44783

ATTENUATORS

NT POTENTIOMETERS [RESISTORS]
NT PRINTED RESISTORS
NT RESISTORS
NT THERMISTORS

P-i-n variable attenuator with low phase shift. 19 p2773 A72-38294

Mathematical description and calculation of the steady-state regime of a microwave power stabilizer with a semiconductor attenuator 23 p3270 A72-43766

ATTITUDE [INCLINATION]

NT PITCH [INCLINATION]
NT ROLL
NT SATELLITE ORIENTATION
NT YAW

Recurrence relation derived for general normalized satellite inclination function with three parameters in series expansion for geogravitational potential 01 p0123 A72-10012

Spacecraft attitude determination with single-axis sensor and single natural radiation source with relative mutual motion, deriving error equations 01 p0032 A72-11224

Digital differential analyzers number comparison in realization of direction cosine, Euler angle and quaternion attitude algorithms 07 p0949 A72-19296

Nonoriented astronomical satellite attitude determination from onboard measurements of geomagnetic field and stellar luminosity 14 p2151 A72-30460

Receptive fields of units in the visual cortex of the cat in the presence and absence of bodily tilt. 19 p2758 A72-38646

High speed accelerometers to determine test platform tilt and translational motion displacements, discussing instrument configurations without gyroscopes [AIAA PAPER 72-818] 20 p2923 A72-39105

Interaction between attitude libration and orbital motion of a rigid body in a near Keplerian orbit of low eccentricity. 20 p2968 A72-39197

Tilt table tests for orthostatic tolerance, measuring heart rate, blood pressure and responses of fainers and nonfainters 21 p3008 A72-41020

Applications of a technique for estimating aircraft states from recorded flight test data. [AIAA PAPER 72-965] 22 p3138 A72-42360

Ablative asymmetric conical nose bluntness changes effects on aerodynamic characteristics for moderate magnitude tilt angles 24 p3363 A72-45341

ATTITUDE CONTROL

NT DIRECTIONAL CONTROL
NT LATERAL CONTROL
NT LONGITUDINAL CONTROL
NT SATELLITE ATTITUDE CONTROL
NT THRUST VECTOR CONTROL

Pintle-controlled rocket engine design with gimbaled supersonic splitline thrust vector control, featuring variable thrust, attitude controls and high propulsion efficiency [SAE PAPER 710763] 01 p0115 A72-10260

Gimbaled control moment gyro for Skylab telescope mount stringent pointing requirements, investigating normal and clamped operation modes and dynamic response of attitude control 01 p0097 A72-10382

Free flight simulation tests for V/STOL aircraft nonlinear attitude control system adaptation to helicopter pitch and roll control [DGLR PAPER 71-060] 02 p0155 A72-12714

Optimal control algorithm synthesized from linear sampling theory for inertial platform alignment, requiring systematic error free optimal digital computer 02 p0258 A72-12899

Spacecraft initial solar orientation techniques estimation and classification 05 p0685 A72-16444

European reusable space tug, discussing computer controlled attitude stabilization and maneuvering system design for orbital rendezvous and docking 05 p0725 A72-16446

Language for description of onboard control system location and attitude control operations during spacecraft maneuvering 05 p0726 A72-16456

Three dimensional global spacecraft attitude control system analytical design technique based on system stability considerations 05 p0726 A72-16457

Spacecraft precision off-on attitude control by pure jet torquing, using electronics based on control system idealized model 05 p0726 A72-16459

Large launch vehicle attitude control system absolute stability mathematical model, using quadratic Liapunov function for exponential property description 05 p0728 A72-16475

Spacecraft attitude control system reliability and performance improvement through nonorthogonal coordinates application, using matrix technique 05 p0728 A72-16477

Three-axis attitude control and stabilization system for sounding rocket payload, discussing performance from simulation and ground test results 05 p0728 A72-16478

Gas jet attitude control systems for spacecraft, discussing accuracy and time of active operation 05 p0728 A72-16479

High accuracy north-seeking course-attitude inertial reference system for air navigation, using platform unit and automatic alignment for Schuler tuned operation 07 p0990 A72-20282

Attitude reference platforms in ASTRID and DACHS control systems for high altitude research rockets 07 p0990 A72-20283

Analog fluidics systems status, exemplifying attitude reaction control for solar observation rocket and air gauging in textile industry 08 p1111 A72-20927

German monograph on optimal guidance of spin stabilized space bodies for combined attitude and angular velocity control and time optimal nutation damping 08 p1241 A72-21847

Dynamic and kinematic equations of attitude and translational motions of symmetric rigid body under body fixed force 09 p1351 A72-22991

Nighttime airglow layer effect application to autonomous navigation and orientation of piloted space vehicles 10 p1508 A72-23758

Digital computers application as filters in launch vehicles and high performance aircraft attitude control systems, estimating number of computer operations 10 p1444 A72-24031

Flight tests of combination flight director displayed and attitude command control system effect on and attitude command control system effect on general aviation aircraft handling qualities during ILS approach [SAE PAPER 720316] 11 p1575 A72-25580

Limiting stability cases of vehicle with linear attitude control and pointed at star by two power gyroscopes in conical suspensions 13 p2051 A72-28383

Oscillations of spacecraft with on-off attitude control under constant perturbation moment, calculating energy expenditures for desired orientation maintenance 14 p2162 A72-30459

Pulsed motion of gravity gradient vehicle in central gravity field, presenting expressions of optimized attitude control 14 p2162 A72-30473

Cassiopeia attitude control apparatus flight tests on Tactile rocket, describing aiming accuracy, target acquisition and gas consumption 15 p2321 A72-31824

High accuracy relative attitude readout mechanization, discussing analog and digital design, closed loop analysis and simulation 15 p2270 A72-32191

Flexible space vehicle multiple closed loop attitude control system design, discussing stability, structure interaction and performance by analog simulation 15 p2321 A72-32587

Digital attitude and heading reference system computer for aircraft heading control, discussing design and performance features 16 p2367 A72-33244

Spacecraft oscillatory motion as function of attitude control impulse and slave mechanism efficiency 17 p2622 A72-35205

Absolute stability analysis of attitude control systems for large boosters. 17 p2622 A72-35489

Multimode flight control for precision weapon delivery. 17 p2493 A72-35561

Development of a GH2/GO2 pulsejet engine with 6.7 kN thrust for the attitude control system of the space shuttle 19 p2848 A72-37495

A simplified analysis of the computational requirements for strapdown attitude reference. [AIAA PAPER 72-827] 20 p2951 A72-39098

Black Arrow satellite launch vehicle attitude control as part of inertial guidance system, describing four-gimbal gyroscopically stabilized platform and associated electronics 21 p3115 A72-40121

An attitude reference system with discrete correction capability. 22 p3203 A72-42864

The development of GH2/GO2-pulse mode rocket engines in the thrust range of 6,660-9,340 N /1,500-2,100 lbs/. 24 p3434 A72-45207

ATTITUDE GYROS

NT GYRO HORIZONS

ATTITUDE INDICATORS

NT GYRO HORIZONS

Autonomous star mapping attitude reference technique for providing three-axes attitude information on inertially stabilized or slowly spinning spacecraft 03 p0387 A72-13952

Airplane attitude display motion relationship to external world as factor in pilot error due to visual frame of reference shift 14 p2083 A72-31151

Vehicle orientation degrees of freedom remote measurement with mounted passive devices and polarization-modulated light, discussing data reduction and system accuracy 15 p2267 A72-31780

Optical sensors for spacecraft attitude determination, discussing operation principles based on solar radiation, albedo, IR contrast and stellar radiation detection 16 p2389 A72-32849

Attitude instruments, pitch and roll. I - Minimum performance standard for equipment. [SAE AS 1162] 18 p2692 A72-36534

Present status of self-contained navigation systems combining Doppler velocity sensors and attitude/heading references. 21 p3079 A72-40282

The wedge probe - A review.

24 p3404 A72-45355

ATTITUDE STABILITY

NT DIRECTIONAL STABILITY

NT GYROSCOPIC STABILITY

NT LATERAL STABILITY

NT LONGITUDINAL STABILITY

Attitude motion at equilibrium libration points of axisymmetric smallest body in restricted three body problem

01 p0123 A72-10011

Kalman linear filtering technique for spinning satellite attitude restitution, evaluating reliability by model for simulation of measurements by sensors [ONERA, TP NO. 953]

05 p0724 A72-16436

Long term spin and misalignment in orbit of Azur satellite with passive magnetic attitude control system

05 p0727 A72-16466

Liapunov direct method based approaches to hybrid dynamical systems stability, applying to attitude stability of flexible earth pointing satellite

[AIAA PAPER 72-18]

05 p0729 A72-16867

Spin-axis attitude stability in torque-free environment of dual spin spacecraft with energy losses in both bodies

[AIAA PAPER 72-16]

05 p0730 A72-16964

Environmental forces effects on gravity oriented satellites attitude dynamics, considering earth atmosphere aerodynamic and solar radiation forces effects

07 p0185 A72-19060

Orbital eccentricity and angular momentum management scene stability for satellite large attitude maneuver followed by trim maneuver sequence

11 p1719 A72-25978

Geostationary satellites spacing dependence on quantifying factors, describing space environment experiments for satellite attitude stability and ground station antenna patterns and polarization effects

[AIAA PAPER 72-542]

12 p1780 A72-27365

Operational evaluation for sun stabilized attitude control system in Aeros satellite, describing laboratory equipment and component static and dynamic tests

[DGLR PAPER 72-026]

13 p2052 A72-28967

Aerodynamic effects on circular-orbiting cylindrical satellites coupled librational motion, analyzing equilibrium configurations stability by linearized and Liapunov direct method

15 p2320 A72-31818

Flexible space vehicle multiple closed loop attitude control system design, discussing stability, structure interaction and performance by analog simulation

15 p2321 A72-32587

Small amplitude libration stability and damping system for gravitationally stabilized tethered orbiting radio interferometer satellite system

16 p2462 A72-34020

Geomagnetic attitude control of an axisymmetric spinning satellite.

17 p2619 A72-34201

Optimal aerodynamic attitude stabilization of near-earth satellites.

17 p2622 A72-35488

TD-1A - Europe's largest and most advanced satellite.

18 p2731 A72-37011

Attitude stability and performance of a dual-spin satellite with nutation damping.

19 p2862 A72-38022

Attitude stability of a dual-spin satellite with a large flexible solar array.

[AIAA PAPER 72-887]

20 p2975 A72-39114

Attitude dynamics of a three-axis stabilized satellite with a large flexible solar array.

[AIAA PAPER 72-857]

20 p2976 A72-39137

Astronomical telescope hybrid pointing control system with double gimbal control moment gyros and orthogonally mounted reaction wheels to achieve extreme accuracy and stability

[AIAA PAPER 72-854]

20 p2924 A72-39138

Periodic libration solutions in attitude control stability study of slowly spinning satellites under gravity gradient torques, using Floquet theory

20 p2968 A72-39195

Resonant attitude instabilities for a symmetric satellite in a circular orbit.

21 p3115 A72-41046

Effect of bearing flexibility on dual-spin satellite attitude stability.

21 p3115 A72-41303

Liapunov stability analysis of hybrid dynamical systems with multi-elastic domains.

21 p3086 A72-41519

Attitude perturbations of a spinning Jupiter Orbiter spacecraft.

[AIAA PAPER 72-920]

21 p3115 A72-41565

ATTRACTION

Psychological tests to judge maximum and minimum nonphysical subjective attraction forces between two parallel bars

18 p2654 A72-36919

Decomposition of the force function of two homogeneous spheroids with noncoinciding symmetry planes

21 p3114 A72-41771

ATTRITION [MATERIALS]

U COMMUNITION

AUDIO EQUIPMENT

NT MICROPHONES

AUDIO FREQUENCIES

Spectrometers for phase audible frequencies, discussing linearization theory and application to spectrum analyzer calculation

07 p0983 A72-19186

Perceived noise level correction for background noise effects based on frequency band SNR

07 p0932 A72-20170

Monaural perstimulatory loudness adaptation measurement by delayed and single simultaneous balance methods, discussing intensity, frequency and duration effects

08 p1127 A72-21896

Probe triggered audio frequency plasma oscillation period dependence on applied magnetic field and discharge current

13 p2010 A72-28544

AUDIO VISUAL EQUIPMENT

U TRAINING DEVICES

U VISUAL AIDS

AUDIOLOGY

Aeromedical diagnostics for aircraft pilot hearing sense tests, considering cockpit environment and stress-produced impairments in central nervous system

05 p0623 A72-16781

German book - Hearing, voice, balance /Physiology of the senses III/.

22 p3146 A72-42784

The physiology of hearing. I - The middle and the inner ear

22 p3146 A72-42785

AUDIOMETRY

Directional hearing perception threshold in normal and auditory-defective patients, studying frontal and median planes for rising and falling noise frequencies

02 p0158 A72-11740

Flight helmet optimal fitting technique, using automatic recording audiometer and noise source for acoustic leakage detection

04 p0479 A72-14873

Right ear prevalence in hearing process determined by dichotic speech audition

04 p0476 A72-15584

Hearing damage scaling methods, discussing audiometric frequencies effect and damage risk criteria

07 p0932 A72-20169

Monaural perstimulatory loudness adaptation measurement by delayed and single simultaneous balance methods, discussing intensity, frequency and duration effects

08 p1127 A72-21896

The physiology of hearing. I - The middle and the inner ear

22 p3146 A72-42785

AUDITORY DEFECTS

Directional hearing perception threshold in normal and auditory-defective patients, studying frontal and median planes for rising and falling noise frequencies

02 p0158 A72-11740

Hearing damage scaling methods, discussing audiometric frequencies effect and damage risk criteria

07 p0932 A72-20169

Design criteria for transportation system noise regulation, considering ambient noise, hearing damage, speech interference and subjective reactions

07 p0932 A72-20173

Stapedectomy postoperative complications as flying hazard, discussing pilot reaction to middle ear pressure changes

14 p2082 A72-31094

U.S. federal regulation on occupational noise exposure control for hearing loss prevention, discussing noise measurement, reduction and periodic tests

16 p2358 A72-33324

Flying personnel auditory defects caused by environmental conditions, discussing aircraft noise, vibrations and atmospheric pressure effects

21 p3002 A72-40924

AUDITORY PERCEPTION

Neurophysiological hearing mechanisms of inner ear in peripheral auditory pattern recognition

01 p0012 A72-10481

Neurophysiology of auditory pattern recognition of simple and complex sounds, using cats data on cochlear nerve neural mechanism

01 p0012 A72-10482

Auditory pathway neuron discharge response to complex sound stimuli and frequency discrimination of pattern recognition in cats

01 p0012 A72-10483

Intervening discrete elements effects on filled duration illusion in auditory, tactual and visual presentation

01 p0014 A72-10720

Body cooling effect on human vigilance in hot environments, testing reaction time to visual stimuli and auditory signal detection rate

01 p0021 A72-11290

Computer simulation of evoked cortical audio potentials in animals and humans, noting clinical application for hearing threshold measurements

01 p0016 A72-11324

Statistical long term speech spectrum analysis and perceptual evaluation, using digital bandpass filter technique

02 p0171 A72-11666

Inert gas narcosis under hyperbaric conditions relationship to mental performance and auditory and visual evoked responses in man

[AD-736736]

02 p0166 A72-11705

Cats cochlea and cochlear nucleus neural responses in auditory masking of low frequency tones, showing phase locked cells progressive desynchronization with intensity

04 p0475 A72-15251

High and low pass filtered clicks lateralization tests, suggesting lateral position discrimination dependence on If content and cochlear partition apical end

04 p0550 A72-15297

Formant-coded voiced speech parameters smoothing and quantizing effects subjective evaluation, obtaining average quantization threshold levels

04 p0487 A72-15298

Right ear prevalence in hearing process determined by dichotic speech audition

04 p0476 A72-15584

Phenamine and aminazine effects on subthreshold sound perception and adrenoreactive excitability of unstable subjects under emotional stress

04 p0476 A72-15586

Aeromedical diagnostics for aircraft pilot hearing sense tests, considering cockpit environment and stress-produced impairments in central nervous system

05 p0623 A72-16781

Bisensory performance in simultaneous auditory and visual verbal information recognition, demonstrating integrative action between hearing and vision

06 p0768 A72-17949

Dynamic manned vehicle cockpit simulator for visual and aural effects and acceleration changes, discussing STOL and VTOL characteristics

06 p0796 A72-18246

Standard procedures development for perceived noisiness or noise annoyance evaluation, taking into account spectral complexity, spectra weighting, time integration and onset duration

07 p0932 A72-20166

Perceived noise level correction for background noise effects based on frequency band SNR

07 p0932 A72-20170

Loudness and noisiness judgment contours, considering experimental subjective and objective conditions, subject age and sex and sound field characteristics

07 p0932 A72-20171

Mark VII ear performance calculation procedure for perceived loudness or noisiness levels relation to sound pressure, using experimental frequency weighting contours

08 p1127 A72-21895

Loudness function correlations to illusory spiral aftereffect persistence, motion sickness susceptibility and auditory reaction time in individuals

08 p1128 A72-22138

Vigilance performance prediction for difficulty-matched auditory and loosely and closely coupled visual intensity discrimination tasks

10 p1433 A72-25127

Auditory sensation overall loudness prediction for steady broad-band noise from summation of weighted intensities of power spectrum sub-bands

11 p1686 A72-25800

Audiometric determination of human temporary threshold shifts due to steady state and impulsive noise

11 p1583 A72-25873

Auditory flutter fusion frequency changes in humans during prolonged visual deprivation

12 p1769 A72-27418

Vestibular, auditory, acceleration and altitude decompression testing of pilot following endolymphatic shunt surgery for Menieres disease

12 p1771 A72-27485

Monograph on perceptual analysis of sound covering peripheral auditory system functions, subjective pitch perception, periodic pulse and white noise harmonic audibility, masking behavior, etc

15 p2188 A72-31514

Visual and acoustic image processing rates during letter sequencing tasks, suggesting implicit verbal control involvement

15 p2188 A72-32764

Auditory induction of fainter by louder sounds as perceptual phenomenon cancelling masking effects

16 p2354 A72-33170

Lateral inhibition in auditory perception proved by psychophysical study of nervous activity stimuli patterns, noting erroneous measurement of pure tone masked threshold

16 p2357 A72-33970

Calculating the perceived level of light and sound.

19 p2761 A72-38567

Myogenic and eardrum evoked auditory potentials and cortical responses to 0.2 millisecond voltage pulse acoustic stimuli 20 p2891 A72-38932

Determination of the functional state of the auditory analyzer through the action of short-term acoustic stimuli of increasing intensity 20 p2893 A72-38939

An aspect of the problem of pitch dependence on the duration of short sinusoidal signals. 20 p2897 A72-39217

Effect of electrical excitation of various auditory analyzer levels on a conditioned motor reflex 21 p3001 A72-40805

Display device design and human operator training based on visual and auditory sensation and perception principles, emphasizing fitting between man and information 21 p3010 A72-41407

1971 Rayleigh Gold Medal Address - Calculating the perceived level of light and sound. 22 p3205 A72-42462

Reactions of auditory cortex neurons to geniculocortical fiber stimulation 22 p3145 A72-42723

AUDITORY SENSATION AREAS

Postsynaptic electric potential responses to click of auditory cortex neurons in cats 02 p0158 A72-11757

Bats auditory cortex electrical responses to ultrasonic stimuli, determining maximum sensitivity frequency range 02 p0159 A72-11769

Electrophysiology for auditory temporal masking mechanism study of cat cochlear nucleus and inferior colliculus single neurons 05 p0620 A72-17175

Human cortical auditory evoked response to speech and sound effects, relating EEG interhemispheric wave amplitude asymmetry to stimulus meaningfulness 08 p1115 A72-20984

Cat auditory cortex neurons response to auditory and medial geniculate body electrical stimulation 12 p1761 A72-27651

Effect of electrical excitation of various auditory analyzer levels on a conditioned motor reflex 21 p3001 A72-40805

Evoked potentials of the primary auditory cortical zone produced by positive and inhibitive conditioned stimuli 21 p3001 A72-40806

Dependence of inhibitory areas of inferior colliculus neurons on the time characteristics of acoustic stimuli 22 p3145 A72-42724

AUDITORY SIGNALS

Alerting light and audio signals for aircraft pilots, considering implications for aircraft design 01 p0021 A72-11291

Vibrotactile warning device effectiveness under auditory and visual loadings, investigating reaction time and errors number 08 p1126 A72-21569

Head-up omnidirectional two dimensional auditory display device for visual detection facilitation in aircraft collision avoidance systems 12 p1777 A72-28327

Preferences for signaled over unsignaled noise from subjectively rated noise intensity experiments, discussing preparatory response vs information cognitive control interpretations 15 p2187 A72-32763

Response bias and sensitivity variations in psychophysical test of rats discrimination between standard and attenuated auditory signal intensities 16 p2356 A72-33648

Energy detection model for transient overshoot in tonal signals masked by narrow band auditory stimuli, discussing masking produced by gated sinusoid 16 p2359 A72-33972

Direct correlation measurement of turbulent jet noise and flow by cross correlating narrow filtered input turbulence and output acoustic signals [AIAA PAPER 72-640] 16 p2381 A72-34092

Effect of fringe on masking-level difference when gating from uncorrelated to correlated noise. 21 p2997 A72-40346

Reaction time to the second of two shortly spaced auditory signals both varying in intensity. 22 p3142 A72-42549

AUDITORY STIMULI

Bats auditory cortex electrical responses to ultrasonic stimuli, determining maximum sensitivity frequency range 02 p0159 A72-11769

Monotonous auditory stimulation frequency effects on human orienting reaction habituation and sleep onset 02 p0169 A72-12494

Human trace responses generation and storage under light stimulus reinforcement of sound conditioning from galvanic skin reactions observation 04 p0475 A72-15581

Human cortical auditory evoked response to speech and sound effects, relating EEG interhemispheric

wave amplitude asymmetry to stimulus meaningfulness 08 p1115 A72-20984

Hypothalamic single neuron unit discharge pattern response to acoustic, light and somatosensory stimulation in cats 08 p1116 A72-21471

Animal response to sonic booms, considering mink reactions in detail 08 p1119 A72-21909

Human reactions to sonic boom acoustic stimuli, noting startle reflex responses 09 p1267 A72-23320

Auditory sensation overall loudness prediction for steady broad-band noise from summation of weighted intensities of power spectrum sub-bands 11 p1686 A72-25800

Jet aircraft noise effect on sleeping EEG and subsequent waking performance, showing presence of carry-over effects 12 p1770 A72-27474

Cat auditory cortex neurons response to auditory and medial geniculate body electrical stimulation 12 p1761 A72-27651

Periodic, continuous and aperiodic white noise effects on human serial decoding performance, relating subjective and autonomic responses 12 p1775 A72-28289

Acoustic stimuli transients rise time and repetition rate effects on loudness, applying various steady state noise calculation methods to transients Fourier transforms 13 p2004 A72-29097

Vigilance effects for noise or vibration stimuli duration judgment task performed with or without simultaneous mental arithmetic task 14 p2080 A72-30964

Compensatory tracking task performance with continuous error information feedback via visual, auditory or electrocutaneous displays 14 p2083 A72-31152

Aircraft pilot reaction capability for switch activation in response to voice countdown, tone initiation and termination, noting standard deviation 15 p2188 A72-31787

Human cerebral hemodynamic changes during arousal and orienting reactions to auditory stimuli 16 p2353 A72-32993

Auditory display in dual-axis compensatory tracking task, discussing performance measures in terms of squared error integral and human operator describing functions 16 p2359 A72-33866

Lateral inhibition in auditory perception proved by psychophysical study of nervous activity stimuli patterns, noting erroneous measurement of pure tone masked threshold 16 p2357 A72-33970

Energy detection model for transient overshoot in tonal signals masked by narrow band auditory stimuli, discussing masking produced by gated sinusoid 16 p2359 A72-33972

Myogenic and eardrum evoked auditory potentials and cortical responses to 0.2 millisecond voltage pulse acoustic stimuli 20 p2891 A72-38932

Determination of the functional state of the auditory analyzer through the action of short-term acoustic stimuli of increasing intensity 20 p2893 A72-38939

An aspect of the problem of pitch dependence on the duration of short sinusoidal signals. 20 p2897 A72-39217

Psychometric test for auditory stimulus duration difference estimation, noting Weber fraction for temporal gaps marker condition 21 p3004 A72-40345

Evoked potentials of the primary auditory cortical zone produced by positive and inhibitive conditioned stimuli 21 p3001 A72-40806

Dependence of inhibitory areas of inferior colliculus neurons on the time characteristics of acoustic stimuli 22 p3145 A72-42724

Electrophysiological investigation of the excitation and inhibition processes in the auditory cortex 22 p3148 A72-43165

Nervous mechanisms of the acoustic stress reaction 22 p3148 A72-43169

Characteristics of conditioned reflexes to an ecologically adequate stimulus in hens 23 p3257 A72-44080

Electrophysiological analysis of limbic-reticular interaction during the orientating reflex 23 p3257 A72-44081

Neuronal and focal reactions of the parietal associative cortex to various peripheral stimuli 23 p3257 A72-44089

Responses of anterior suprasylvian gyrus neurons to peripheral stimuli of different modalities 23 p3257 A72-44090

Sonic boom startle - A field study in Meppen, West Germany. 24 p3374 A72-44916

AUDITORY TASKS

Selective attention dichotic listening test as flying proficiency prediction criteria, discussing omission and intrusion errors 07 p0929 A72-19351

Auditory adaptation tests confirmation of Small loudness model prediction of lower adaptation for test tone greater than adapting tone intensity 08 p1127 A72-21897

Vigilance performance prediction for difficulty-matched auditory and loosely and closely coupled visual intensity discrimination tasks 10 p1433 A72-25127

Cumulative partial sleep deprivation effects on human performance in auditory vigilance, routine addition and running digit span tests, observing circadian rhythms 11 p1581 A72-26683

Body orientation under vertical sinusoidal vibration. 21 p3008 A72-41019

Human operator dynamics for aural compensatory tracking. 22 p3149 A72-41950

Heart rate variability in a binary choice reaction task - An evaluation of some scoring methods 22 p3143 A72-42550

AUGER EFFECT

Equivalent circuit models in semiconductor transport for thermal, optical, Auger-impact and tunneling recombination-generation-trapping processes [AD-740495] 03 p0401 A72-13585

G-r noise in intrinsic photoconductors for Auger band-to-band radiative recombination 06 p0865 A72-17365

Inner shell ionized atoms, discussing orbital electrons rearrangement processes based on shakeoff events and radiative Auger transition 09 p1356 A72-22834

Carbon dioxide absorption kinetics on monocrySTALLINE Mo from Auger spectrometry and slow electrons diffraction 10 p1525 A72-24137

Metal adhesive forces to clean Fe surface measured with LEED and Auger emission spectroscopy, noting binding energy correlation to oxygen 10 p1497 A72-24821

Oxygen monolayer amounts adsorption on yttrium films and molybdenum foil investigated by Auger electron spectroscopy, observing growth of shifted peaks 15 p2292 A72-31860

Mo and stainless Ni-Cr steel surfaces chemical composition determination by Auger electron spectroscopy during heating in high vacuum 16 p2406 A72-33251

Cs adsorption on W and Ti observed by combination of ellipsometry, Auger spectroscopy and surface potential difference measurements, noting sticking coefficient and coverage 16 p2442 A72-33833

Single crystal disk substrate design with electron bombardment heating for LEED and Auger electron spectroscopy studies in ultrahigh vacuum 17 p2553 A72-34642

Adhesion and transfer of PTFE to metals studied by Auger Emission Spectroscopy. 19 p2807 A72-37646

Solid surface geometry, atomic composition and electronic structure observations, discussing Auger spectroscopy, field ion microscopy and electron diffraction and scattering techniques 19 p2803 A72-38389

L-S coupling interpretation of high-resolution LMM Auger spectra of Cu and Zn. 19 p2846 A72-38597

Crystalline solids surfaces with catalysis, electronics and corrosive reactions, discussing slow electron diffraction, ionic field microscopy and Auger spectroscopy techniques for surface cleanliness measurement 23 p3324 A72-44461

AUGMENTATION

Large scale high aspect ratio multielement suppressor nozzle arrays testing for augmentor wings and internally blown flaps 05 p0612 A72-16888

AURORAL ABSORPTION

Auroral absorption and DR currents development during magnetic storms, discussing corpuscular fluxes arrival from magnetospheric tail into lower ionosphere 01 p0059 A72-10619

Auroral absorption prediction during disturbed conditions in communications as function of frequencies and radio ranges at different geomagnetic time and coordinates 05 p0626 A72-16009

Intensity ratio and effective lifetime of excited oxygen atoms in pulsating aurora from auroral intensity and absorption observations, noting diurnal variations 07 p0974 A72-18897

Ionospheric disturbances and prediction dependence on solar and geophysical activities, discussing SID, pca, auroral absorption and F 2 region 11 p1623 A72-26267

Correlated particle flux, magnetic field, electron intensity and riometer absorption measurements during recovery phase of polar magnetic substorm on 6 March 1970

15 p2226 A72-31946

Magnetospheric geometry derivation from ISIS-1 observations of soft particles penetration into polar cap and auroral regions, discussing entry and energization mechanisms

15 p2227 A72-31953

Meridional motion of a corpuscular entry region from observations of riometric absorption

17 p2551 A72-35864

Height of the region of principal auroral radio-wave absorption in the presence of a sporadic E layer

17 p2519 A72-35869

Auroral absorption and magnetospheric plasma dynamics pattern from arctic stations atmospheric opacity data

18 p2688 A72-36859

Anomalous ionization in lower ionosphere recorded by riometers, considering ionospheric substorms caused by auroral absorption

24 p3396 A72-44849

AURORAL ACTIVITY

U AURORAS

AURORAL ARCS

NT RED ARCS

Rocket-borne measurement of particle fluxes and currents in auroral arc, determining pitch-angle distribution of electron and proton energies

01 p0120 A72-10897

Rocket-borne measurement of Birkeland ionospheric current density associated with auroral arc and electrojet

01 p0061 A72-10898

Quiet auroral arcs formation by ionospheric instability and field aligned current triggering

02 p0220 A72-12451

Electric field aligned sheet currents of low energy electrons and protons near auroral arc, obtaining magnetic signatures

03 p0349 A72-13516

Auroral substorms development phases, noting auroral arcs latitudinal shifting during genesis phase

05 p0657 A72-16273

Magnetic baylike disturbances and multiple midlatitude 6300-A auroral arcs during geomagnetic storm recovery phase and concurrent ionospheric current system

05 p0630 A72-16620

Geophysical data analysis for high latitude negative geomagnetic disturbances revealing geomagnetic pulsations during auroral arcs passage

08 p1155 A72-20809

Charged particles observations on 21 December 1968 by Explorer 40 and from ground, noting auroral light primary energy influx by precipitation band of electron intensities

[AD-740048]

09 p1299 A72-23005

Visual aurora and Explorer 40 satellite simultaneous observations of VLF radio noise, noting hiss associated with light emissions and associated charged particle flux

[AD-740047]

09 p1299 A72-23006

Auroral conjugate points relative motion during substorms, showing existence of equatorward and poleward auroral arc systems

11 p1625 A72-26404

Negative auroral arc infrasonic wave observations during substorm poleward expansions at Inuvik, Canada

11 p1627 A72-26516

Peak electron energy spectra during auroral substorm from high energy resolution balloon X ray measurements

12 p1804 A72-27787

Nocturnal low intensity auroral red arcs observations by meridian scanning photometer, comparing with green emission

14 p2097 A72-30136

Expanding auroral bulge front photographs during auroral substorm, noting violent curl motions and arcs formation

15 p2223 A72-31439

Photometric all sky observations of stable auroral red arcs on 8-9 March 1970, determining altitudes of 6300 A, 5577 A and 4278 A emissions

16 p2384 A72-32978

Auroral electron energy spectra at high latitudes from polar auroral arcs luminosity profile examination

17 p2550 A72-35853

All sky photography of auroral arcs alignment, noting oval distribution pattern

19 p2793 A72-38750

Formation of auroral patches in the midday sector during a substorm.

20 p2916 A72-39239

On the classification of high-latitude auroras.

20 p2920 A72-39979

The Harang discontinuity in auroral belt ionospheric currents.

20 p2920 A72-39980

O1 6300 and 5577 A, N1 5200 A and H beta 4861 A emission line measurement during 8-9 March 1970 auroral arc event

22 p3169 A72-42018

Continuity equation for dynamic auroral ionospheric model relating electron density profiles to auroral arc brightness

24 p3400 A72-45589

AURORAL ECHOES

Auroral backscatter echoes observations in ionospheric short wave propagation, using satellite oblique propagation ionograms and magnetograms

01 p0056 A72-10439

Optical aurora relationship to radio counterpart, showing backscattered signal peak amplitude close correlation to magnetic bay peaks

01 p0056 A72-10440

Auroral radio reflection regions spatial distribution from radar measurement, noting backscattering indicatrix independence on geographical latitudes

17 p2519 A72-35873

Results of simultaneous measurements of the spectrum of auroral radio echoes at two frequencies

17 p2519 A72-35874

Influence of ionospheric currents on the geometry of auroral radio echoes

17 p2519 A72-35875

Relationship between auroral radio echoes and other geophysical phenomena

17 p2519 A72-35876

Radar auroral echo VHF power spectrum analysis of ionospheric irregularities, using range-time-intensity film strips

22 p3171 A72-42415

Characteristics of nonuniform regions responsible for microwave signals auroral scattering, noting observations with two sidelobe radio interferometer

24 p3397 A72-45084

AURORAL ELECTROJETS

Rocket-borne measurement of Birkeland ionospheric current density associated with auroral arc and electrojet

01 p0061 A72-10898

Auroral current generation by ionization and space charge transport interaction between charged particles and atmospheres

02 p0273 A72-11928

Radio auroral electrojet aspect sensitivity and Farley two stream instability, discussing magnetic field distortion and orthogonal deviation as function of current strength and direction

07 p0976 A72-19163

Equatorial ring current relation to polar electrojet during magnetosphere geomagnetic storm, discussing magnetosphere-ionosphere current systems

09 p1298 A72-22580

Supersonic auroral motions relationship to infrasonic waves generation, showing acoustic pulse within electrojet arcs due to collisions with neutral gas of positive ions

11 p1624 A72-26403

Auroral current generation by ionization and space charge transport interaction between charged particles and atmosphere

13 p2030 A72-29240

Midnight auroral electrojet time variations relationship to midday auroras latitudinal shift during South Pole magnetospheric substorms

13 p1950 A72-29382

Ring current and polar electrojet effects on proton auroras oval during magnetic disturbances from H alpha line observation

13 p1952 A72-29659

Auroral electrojet polarization model, considering ionospheric Hall and Pedersen conductance maximum due to precipitation from electron plasma sheet inner edge

[AD-745672]

16 p2444 A72-32961

Model for magnetospheric substorm growth phase, noting dayside magnetopause convection onset, geomagnetic tail configurational changes and breakup with auroral electrojet development

16 p2387 A72-33903

Easterly and westerly polar electrojets intensity diurnal variations with respect to universal time and geo- and heliophysical phenomena

19 p2791 A72-38368

Parametric coupling of large amplitude pump wave to E layer plasma mode to explain auroral electrojet irregularities external production and control

19 p2793 A72-38746

Signatures for substorm development of the growth phase and expansion phase.

20 p2916 A72-39237

DP-2 mode daily magnetic variation in polar cap based on magnetic and auroral records, noting relationship to magnetospheric substorms

22 p3168 A72-42005

Longitudinal magnetospheric currents contribution to auroral electrojet from satellite observation data, noting magnetosphere electric field excitation of meridional Pedersen and Hall currents

22 p3169 A72-42225

AURORAL EMISSION

U AURORAS

U LIGHT EMISSION

AURORAL IONIZATION

Lower ionosphere ionization response to auroral particle fallout during 1968 substorms, using geomagnetic, VLF and balloon measurements

01 p0053 A72-10366

Metallic ion convergent flow role in sporadic E layer formation in auroral and equatorial ionosphere

06 p0810 A72-18730

Rocket sounding of auroral zone F region low energy electron precipitation and excitation and ionization processes

09 p1298 A72-22585

Magnetosheath electron precipitation effect on dayside auroral-oval plasma density and conductivity, relating precipitation heat flux to solar wind energy density

13 p1950 A72-29381

Auroral sporadic E layer diurnal distribution correlation to charged particle integral flux diurnal variations observed by satellite in winter, noting Kp index effect

14 p2102 A72-30655

N2 positive and N2+/+ band systems and the energy spectra of auroral electrons.

17 p2545 A72-34634

Auroral cosmic radio emission absorption mechanisms, considering ionization rate, recombination coefficient and collision frequency effects

17 p2602 A72-35865

AURORAL IRRADIATION

Synchrotron radiation from incoming auroral electrons based on Schwinger equation, accounting for hf backscatter sounder noise

01 p0060 A72-10839

Magnetospheric and polar substorms model for auroral particles acceleration and geomagnetic tail current diversion to auroral oval night side

07 p0977 A72-20029

Auroral X ray radiation measurements in midnight sector during solar storm of 8 March 1970

08 p1155 A72-20806

Auroral electron acceleration by longitudinal electric field due to protons defreezing above ionosphere

17 p2550 A72-35852

Auroral electron energy spectra at high latitudes from polar auroral arcs luminosity profile examination

17 p2550 A72-35853

Auroral proton energy time behavior estimation based on magnetic and ionospheric data from ground observations

17 p2550 A72-35855

AURORAL SPECTROSCOPY

Book on auroras, discussing primary particle-atmosphere interactions, H line emission, geometry, intensity, height and atmospheric temperature determination from auroral spectra

04 p0519 A72-15356

Sounding rocket spectral measurements of low energy auroral ion composition during premidnight breakup

09 p1300 A72-23020

Auroral spectrophotometric measurements in J/S-1 region and of O I line /5577/, discussing digital recording and computer averaging techniques

10 p1474 A72-24745

Auroral spectrum analysis in 1200-4000 A band, obtaining photon emission rates

11 p1624 A72-26402

Satellite-borne low energy electron and proton spectrometer for measuring auroral electron and proton spectra

13 p1960 A72-29841

Low energy particles spectrometer channels calibration for satellite auroral observation, discussing photomultiplier detector properties

13 p1960 A72-29843

Auroral emission spectrum intensity ratios for IBC 2 system observed via aircraft flown digital multichannel photometer

14 p2097 A72-30137

Auroral spectroscopic and excitation processes, discussing atomic oxygen production, emission ratios and electron energy spectrum, UV and IR emissions, composition and temperature measurements

14 p2098 A72-30138

Auroral spectra recorded at 2000-3000 A with fast Ebert Fastie scanning spectrometer aboard ESRO rockets

14 p2098 A72-30139

N2 positive and N2+/+ band systems and the energy spectra of auroral electrons.

17 p2545 A72-34634

Quantitative spectroscopy of the aurora. I - The spectrum of bright aurora between 7000 and 9000 A at 7.5 A resolution.

21 p3049 A72-41724

AURORAL TEMPERATURE

Auroral plasma particle discharge during motion in strong inhomogeneous magnetic field, magnetospheric instability due to temperature anisotropy

11 p1715 A72-26904

AURORAL ZONES

Auroral electron flux and energy spectrum observations by synchronous ATS 5 and polar OV-1-17 satellites 01 p0061 A72-10894

Parallel electric field evidence near auroral ionosphere deduced from low energy particles, energy spectra and angular distribution 01 p0061 A72-10895

Precipitated electron energy latitude and time variations from auroral-height measurement during IQSY, using meridian scanning photometers 01 p0120 A72-10896

Substorm electron drift relationship to cosmic noise absorption on auroral zone morning side, calculating electron energy loss 01 p0063 A72-10918

Auroral electron precipitation modulation dependence on energy explained by resonance at rebound frequency 02 p0222 A72-12598

Plasma sheet thinning in substorms correlated to auroral oval poleward expansion and associated phenomena in magnetotail 03 p0348 A72-13514

Rocket measurement of highly collimated short duration bursts of auroral electrons, comparing with existing auroral models 03 p0349 A72-13515

Midday oval, cusp region and polar cap auroral electron precipitation at low magnetic activity, presenting intensity vs altitude profiles for nitrogen ion line emissions 03 p0350 A72-13531

Magnetic perturbations in near polar region and morning-night sectors of auroral oval as function of current sources and modulation by universal time 05 p0657 A72-16276

Ionospheric scintillation fading observations by NASA satellite tracking and data acquisition networks, noting frequency dependence in auroral regions [AIAA PAPER 72-220] 05 p0631 A72-16858

Auroral zone vlf hiss and associated low energy electron precipitation in polar magnetosphere [AD-736327] 06 p0804 A72-17456

Sounding rocket observations of magnetic field aligned electron pitch angle distributions coincident with auroral precipitation band northern boundary 06 p0804 A72-17457

Energetic charged particles penetration into magnetosphere by auroral simulation experiments with artificial solar wind, observing magnetic field microfluctuations behind collisionless shock front 06 p0805 A72-17469

Upper atmosphere density and heating near auroral zones, using satellite Molniya 1K data 06 p0805 A72-17637

Magnetic flux determination in magnetosphere tail during substorm from auroral oval boundary and center location observation 06 p0807 A72-17985

Auroral zone electron precipitation events before and at negative magnetic bays onset, presenting balloon recordings of bremsstrahlung X-rays intensity 06 p0808 A72-18092

Auroral charged particle fluxes electrodynamic interaction with atmosphere, determining ion formation rate and electron concentration and conductivity 08 p1155 A72-20804

Polar orbiting satellite ESRO-1A 1-13 keV electron measurements compared to bottomside ionosonde measurements for auroral particle precipitation and F region electron density 08 p1226 A72-21099

High energy electron precipitation events in auroral zone X rays, showing exponential daytime and flat nighttime energy spectra 08 p1226 A72-21110

Auroral F region electron density enhancement relation to sporadic F2 and red oxygen emission 08 p1226 A72-21111

Propagation by direct backscatter on aligned irregularities in auroral F layer, noting horizontal ionization gradients role 08 p1158 A72-21220

Auroral zone neutral wind velocity and atmospheric temperature correlations with geomagnetic activity, considering ion-neutral particle drag as accelerating mechanism during magnetic storms 08 p1161 A72-21535

Midlatitude auroral zone positive ion mass spectrometer observations in E region, noting diurnal variation and sporadic E events 09 p1375 A72-22364

Rocket sounding of auroral zone F region low energy electron precipitation and excitation and ionization processes 09 p1298 A72-22585

Magnetic storm effects in atmospheric neutral composition, noting thermospheric wind circulation role due to Joule heating within auroral zone 10 p1476 A72-24957

Fast auroral hydromagnetic wave occurrence relation to substorm activity, suggesting role of enhanced particle population in magnetospheric region 10 p1476 A72-24962

Interplanetary magnetic field direction and high latitude ionospheric currents in dayside auroral regions, showing plasma drift induced magnetic disturbances 11 p1626 A72-26419

Auroral particle precipitation /keV electrons and protons/ morphology from ESRO 1A particle spectrometer measurement, discussing particle populations in day and night magnetospheres 12 p1864 A72-27786

Characteristics of nonuniform regions responsible for microwave signals auroral scattering, noting observations with two sidelobes radio interferometer 13 p1946 A72-28584

Subauroral zone F region disturbances latitudinal variations catalogs from vertical sounding data, taking into account ionospheric states 13 p1946 A72-28598

OMEGA phase shifts in auroral region due to solar phenomena, discussing methods eliminating PCA induced errors 13 p1997 A72-29185

Subauroral red arcs formation mechanism involving magnetosphere-ionosphere energy conduction and lower atmosphere neutral composition changes due to turbulent mixing 13 p1952 A72-29802

Data acquisition, reduction, quick-look data and standard and special programs for ESRO 1A and B auroral particle satellite experiment 13 p1925 A72-29868

Midlatitude VLF emissions intensity relationship to dayside auroral particle precipitation flux 15 p2194 A72-31437

Interplanetary magnetic field variations and auroral zone substorm activity observation, noting time delay between IMF southward turning and negative magnetic bay 16 p2451 A72-32974

Daytime irregular geomagnetic pulsation, P_{id}, and its relation to magnetospheric substorm. 17 p2546 A72-35062

Magnetospheric convection induced longitudinal or Fermi acceleration role in nighttime auroral particle flux production mechanism 17 p2601 A72-35592

Low energy auroral electron precipitation associated ELF noise band observation by polar-orbiting satellite INJUN 5 17 p2517 A72-35593

Observations of the auroral oval by the Alaskan meridian chain of stations. 17 p2548 A72-35594

Auroral zone splitting into various radiation intensity regions, discussing DR currents influence on particle motion in magnetosphere and structural relationship 17 p2550 A72-35856

Auroral motion analysis based on baylike disturbances against quiet field background during polar substorm 17 p2550 A72-35858

Electron profiles during negative magnetic bays in the auroral zone 17 p2551 A72-35860

Occurrence frequency of F 2 layer sporadic ionization in auroral zone, noting solar activity effect 17 p2551 A72-35867

Investigation of the characteristics of short wave propagation along the auroral radio path 17 p2519 A72-35877

Chatanika, Alaska, auroral-zone incoherent-scatter facility. 18 p2674 A72-36297

Local-time survey of plasma at low altitudes over the auroral zones. 19 p2792 A72-38739

Ionospheric and magnetospheric electric field strength measurements in auroral and polar cap regions by Ba ion cloud and double floating probe techniques 20 p2918 A72-39543

The Harang discontinuity in auroral belt ionospheric currents. 20 p2920 A72-39980

Magnetospheric propagation of auroral hiss with whistler mode dispersive properties, suggesting burst source locations and mechanisms 21 p3048 A72-40399

Rocket measurements of electron influx during a major magnetic storm with type A aurora. 23 p3332 A72-44515

Subauroral zone F region disturbances latitudinal variations catalogs from vertical sounding data, taking into account ionospheric states 24 p3398 A72-45098

AURORAS

NT AURORAL ARCS
NT RADIO AURORAS
NT RED ARCS

Meridional thermospheric wind effect on auroral atomic oxygen red line profile, noting inadequacy of diffusion hypothesis 01 p0052 A72-10079

Open magnetosphere mathematical models application to dayside auroras, investigating interplanetary magnetic field topology 01 p0060 A72-10885

Magnetospheric substorm model for auroral activity sudden increase and ionospheric current development explanation by shock wave excitation in magnetospheric tail neutral layer 02 p0217 A72-11927

Non-Boltzmann molecular nitrogen vibrational distribution in aurora during electron bombardment as function of altitude 02 p0221 A72-12456

Ionospheric propagation, reflection and absorption of vlf hiss in aurora from rocket observation during quiet and substorm conditions 02 p0221 A72-12458

Vibrational population of molecular nitrogen electronic states in normal auroras, examining electron impact and cascade contributions 03 p0349 A72-13524

Soviet book on calms and storms in upper atmosphere covering energy variations, auroras, geomagnetic storms, weather forecasting, etc 03 p0350 A72-13967

Low energy electrons anisotropic flux impulsive precipitations in structured aurora explained by potential difference along geomagnetic field lines of force 03 p0350 A72-14272

Forbidden O I and molecular nitrogen ions emission lines ratio variation with height in aurora 03 p0352 A72-14382

Bremsstrahlung emission by auroral electrons in upper atmosphere and penetration in lower atmosphere, comparing calculation with balloon measurement 04 p0566 A72-14879

Auroral behavior observation at midlatitude station, exhibiting correlation with solar activity as regards solar cycle recurrence and phase [AD-739061] 04 p0515 A72-14882

Book on auroras, discussing primary particle-atmosphere interactions, H line emission, geometry, intensity, height and atmospheric temperature determination from auroral spectra 04 p0519 A72-15356

Channel electron multiplier efficiency for protons of 0.2-10 keV from aurora rocket sounding 04 p0524 A72-15501

Deactivation of A-state nitrogen molecules in auroras, reinterpreting rocket observations of nitrogen Vegard-Kaplan system in terms of atmospheric model based on mass spectrometer measurements [AD-737434] 05 p0655 A72-16072

Charged particles injection effects on magnetic perturbations relation to integral auroral luminance intensity from whole sky photometry measurements 05 p0658 A72-16277

Equatorward motion of midday auroras during magnetospheric substorms, using all sky photographs 06 p0805 A72-17463

Vlf auroral hiss comparison with low energy electron precipitation, using Ogo 4 data 07 p1058 A72-19149

Systematic increase in auroral electrons mean energy with total precipitated energy 07 p1058 A72-19151

Simultaneous auroral X ray, bremsstrahlung and visible bursts observations from balloons. 07 p1058 A72-19166

Auroral forms dynamics dependence on solar wind and DP intensity in magnetosphere 07 p0977 A72-20030

Geomagnetic phenomena associated with auroras and magnetic storms, investigating analog modeling experiment by stationary electrical discharges under laboratory conditions 07 p0980 A72-20457

Auroral ionosphere radio self emission at supercritical frequencies from accelerated protons charge exchange effects, comprising radio bursts, storms and amplifications 08 p1153 A72-20713

Errors in ionospheric sounding of sporadic E layers with auroral presence, discussing continuous reflections duration distribution 08 p1155 A72-20817

Auroral emission rates for various transitions from cross section data and secondary electron spectra measurements 08 p1227 A72-21114

Pulsating auroras morphology in polar substorm, recording poleward expansion and eastward drifting patches with all sky cameras 08 p1157 A72-21117

Spectrophotographic recording of UV auroral emissions during rocket probe flight, noting excitation by electron impact on molecular nitrogen 08 p1159 A72-21225

Phase angle measurements of frequency-oxygen atom lifetime relationship in pulsating auroras

09 p1298 A72-22589

Pulsating polar auroral line emission spectra observation at 3914 and 5577 Å by rocket-borne photometers

09 p1301 A72-23262

Luminous emissions of upper atmosphere, discussing relation to airglow and auroral phenomena

11 p1626 A72-26431

Infrasound observations of acoustic auroras, using microbarographs and resonant detector recordings

11 p1627 A72-26517

Pc 5 type geomagnetic pulsations correlation with nighttime magnetosphere auroral magnetic disturbances from magnetograms obtained at Murmansk, College /Alaska/ and Tiksi

13 p1947 A72-28606

Magnetospheric substorm model for auroral activity sudden increase and ionospheric current development explanation by shock wave excitation in magnetospheric tail neutral layer

13 p1948 A72-29239

Midnight auroral electrojet time variations relationship to midday auroras latitudinal shift during South Pole magnetospheric substorms

13 p1950 A72-29382

Ring current and polar electrojet effects on proton auroras oval during magnetic disturbances from H alpha line observation

13 p1952 A72-29659

Electric field excited stable auroral red arc time dependent behavior, noting inconsistency with satellite and ground observation of 6300 Å emission for electron energy

13 p1953 A72-29812

Low energy particles spectrometer channels calibration for satellite auroral observation, discussing photomultiplier detector properties

13 p1960 A72-29843

Airglow and auroral OI and NI allowed and spin forbidden transitions for above 9 eV excitation potential lines

14 p2098 A72-30145

Auroral electron spectrum space-time dynamics during magnetospheric substorms, using X ray bremsstrahlung balloon data

14 p2101 A72-30637

Magnetosphere tail internal plasma boundary layer dynamics during substorms based on aurora data

14 p2103 A72-30663

Nitric oxide gas release by rocket in auroral glow to determine atomic oxygen densities in ionosphere via observation of auroral light emission

15 p2226 A72-31936

Electric and magnetic field effects on auroras formation, noting similarity with thermonuclear reactor plasma

16 p2456 A72-33518

Precipitation dynamics and energy spectrum of auroral electrons in the midnight sector during a magnetospheric substorm

17 p2550 A72-35854

Auroral substorm and proton auroras during moderate geomagnetic disturbances

17 p2550 A72-35857

Stratospheric model for bremsstrahlung X ray relation emission to auroral electron flux, considering photon energy release in scintillation counters

17 p2551 A72-35872

X-ray bremsstrahlung in the stratosphere and the auroral activity of January 21 and February 3, 1969

18 p2722 A72-36863

Earth magnetosphere pinch effect related to geomagnetic field pulsations and polar aurora luminosity fluctuations

18 p2688 A72-36867

Photometric observations from sounding rockets - Selection of horizontal sightings

19 p2789 A72-37784

Auroral ionosphere radio self emission at supercritical frequencies from accelerated protons charge exchange effects, comprising radio noise bursts, storms and amplifications

19 p2790 A72-38341

Airborne optical measurement comparison with satellite observation for auroral emissions and particle precipitation at noon, suggesting electron precipitation role

19 p2868 A72-38738

An evaluation of the intensity of Cerenkov radiation from auroral electrons with energies down to 100 eV

19 p2792 A72-38741

Aircraft and spacecraft high latitude optical measurements of magnetosphere-related emissions, discussing red arcs, IR auroras, X ray pulsations, conjugate effects, etc

20 p2918 A72-39539

Morphologic maps of pulsating aurora for late afternoon and evening geomagnetic sector near Tromsø during 1967-1969

20 p2918 A72-39540

High latitude particle precipitation and source regions in the magnetosphere

20 p2964 A72-39542

Auroral electron and proton distribution in magnetosphere and precipitation pattern from satellite, rocket and ground based observations

20 p2920 A72-39976

Auroral space-time regularities relationship to magnetospheric variations, precipitating electron fluxes, magnetic tail formation and substorms

20 p2920 A72-39977

Midday auroras and polar cap auroras

20 p2920 A72-39978

Auroral photometric observations at geomagnetically conjugate points

22 p3169 A72-42020

Type 3 solar burst distinction from auroral type high pass noise via spectrum analysis

22 p3222 A72-42043

Auroral EUV flux observation by Javelin sounding rocket photometers, comparing with visible and X ray emissions

22 p3171 A72-42417

Ray structures of polar auroras and their association with drift-current instability in a plasmoid

23 p3282 A72-43358

Nature of polar-aurora light intensity pulsations associated with P12-type geomagnetic pulsations

23 p3282 A72-43359

Quiet, growth, expansive and recovery phases of auroral morphology, noting interplanetary magnetic field turning relation to substorm

24 p3396 A72-44848

Pc 5 type geomagnetic pulsations correlation with nighttime magnetosphere auroral magnetic disturbances from magnetograms obtained at Murmansk, College /Alaska/ and Tiksi

24 p3398 A72-45106

AUSFORMING

Carbide precipitation effect on strength of ausrolled hardenable hypoeutectoid and hypereutectoid stainless steels

07 p1016 A72-19943

Work hardening after ausforming and heat treatment effects on mechanical properties of metastable austenitic Ni-Cr steel

08 p1190 A72-22165

Tempered hardness and tensile strength of ausforming Mn-Cr-B spring steels at low temperatures in austenite stable phase by electron microscopy

21 p3066 A72-40718

AUSTENITE

Mo and C additives effects on austenite susceptibility to deformation martensite formation and steel resistance to hydroerosion

03 p0375 A72-13941

Dissolved oxygen effect on structure and toughness of nonalloyed extruded steels, observing austenite recrystallization kinetics retardation after hot plastic deformation

05 p0672 A72-16143

Austenitizing conditions effects on hardness and microstructure of tempered steel, emphasizing martensite structure and grain size changes produced by controlled heat treatment

07 p0995 A72-19486

Tensile strength enhancement of dislocated martensites in Fe alloys by precipitate dispersion in austenite prior to transformation

07 p1016 A72-19936

Austenite stabilization in maraging steel by cumulative heat cycling, using dilatometric and X ray analysis techniques

07 p0998 A72-20483

Stable austenite formation during maraging steel aging at 300-750 °C determined by X ray diffraction

07 p1022 A72-20525

Quenched and tempered Ni carbon steel retained austenite transformation and crack observation by X ray diffraction under low cycle fatigue testing

09 p1329 A72-23149

Ni carbon steel microstructure changes in retained austenite phase and crack observation during low cycle fatigue testing

09 p1330 A72-23150

Aluminum nitride amount and particle size measurement at austenitic grain coarsening temperatures in low carbon steels

11 p1656 A72-25755

Austenite formation kinetics in Fe-C ferritic-pearlitic structure at 855 °C, comparing experimental data with theoretical calculations

11 p1662 A72-26744

Austenite grain growth characteristics of heat treated Ni maraging steel

13 p1976 A72-28673

Magnetic balance for magnetic saturation measurement and determination of retained austenite, Curie temperature, permeability and martensite content

16 p2391 A72-33237

The effect of plastic deformation on the martensite-to-austenite transition in an iron-nickel alloy

20 p2938 A72-39298

Martensite formation temperature decrease and grain size reduction caused by martensite crystals interaction with barriers in Fe alloy containing austenite beta phase particles

21 p3070 A72-41679

AUSTENITIC STAINLESS STEELS

Stress corrosion cracking of Cr-Ni austenitic stainless steel with Mo and Cu additions in boiling sulfuric medium

01 p0089 A72-11181

Austenitic steel under combined bending and torsion, showing fatigue strength dependence on temperature, load cycle asymmetry and stress concentration

03 p0371 A72-13469

Hydrogen charging of iron-chrome-nickel austenitic stainless alloys, investigating crack initiation in Inconel 600

03 p0373 A72-13600

Phosphorus-containing austenitic stainless steel, investigating quenching defects and precipitation from microstructure by transmission electron microscopy

03 p0379 A72-14260

Low temperatures and deformation rates effect on martensitic phase formation in Cr-Ni austenitic stainless steel under compression and tension

03 p0379 A72-14378

Metastable Fe-Cr-Ni austenitic stainless steels, demonstrating step phenomenon at elastic limit

05 p0672 A72-16011

Solidification, microsegregation and homogenization of austenitic stainless steels containing delta ferrite

05 p0672 A72-16142

Structural stabilization of austenitic steels with manganese, maintaining toughness and sensitivity to martensitic transformation by hammer hardening

05 p0673 A72-16145

Structural stabilization of austenitic steels with manganese, noting chemical purity and cleanliness conditions

05 p0673 A72-16146

Fatigue and fatigue-corrosion properties of high strength stainless maraging martensitic structural and stainless austenitic steels

05 p0680 A72-17206

Welding thermal energy effect on residual ferrite of austenitic chrome-nickel steel deposits

07 p1010 A72-18971

Micrographic evaluation of inclusions in austenitic stainless steel tubes ensuring surface quality control

07 p0994 A72-18972

Mn additions effects on austenitic stainless steels yield strength, work hardening characteristics, corrosion resistance and machinability

07 p1011 A72-19478

High pressure hydrogen effects on austenitic stainless steel embrittlement, determining yield, tensile and fracture strength

07 p1011 A72-19479

Austenitic stainless steel with improved corrosion resistance, yield strength and hot workability

07 p1011 A72-19487

Static and fatigue strength in tension of welded joints composed of low carbon and austenitic steel

07 p0996 A72-19767

Stress-strain state relationship to crack development morphology in elastic strain region of austenitic steel sample under cyclic bending

07 p1013 A72-19769

Adiabatic reversion of Ni martensitic steel to austenite under shear in orthogonal cutting

07 p0996 A72-19934

Test temperature effect on phase composition, mechanical properties and resistance to cavitation of unstable austenitic steels, describing test facility

07 p1018 A72-20140

Austeno-martensitic steel with 25 percent delta ferrite, examining microstructural changes due to aging at 550 °C by thin slide electron microscopy

07 p1021 A72-20484

Hydrogen embrittlement of stable austenitic Ni-Cu steel, observing intergranular decohesion in fractured specimens by microfractography, electron microscopy and X ray crystallography

07 p1021 A72-20485

Work hardening after ausforming and heat treatment effects on mechanical properties of metastable austenitic Ni-Cr steel

08 p1190 A72-22165

Crack propagation and substructure formation near fatigue crack in austenitic stainless steel observed by X ray diffraction and replica electron microscopy

09 p1329 A72-23148

Micrograin superplasticity in eutectoid steel, discussing effect of transformation to austenite

09 p1330 A72-23380

Metastable austenitic steel fiber to increase Al matrix strength to density ratio and fracture toughness

09 p1331 A72-23385

Electron beam welding focus effect on fusion zone penetration in thick austenitic stainless steel

09 p1321 A72-23643

Fe-Ni-C alloy mixed austeno-martensitic microstructure embrittlement, investigating mechanical properties after thermomechanical treatment

10 p1495 A72-40487

Fatigue crack propagation relation to plasticized zone formation at crack tip in ferritic carbon steels and in Cr-Ni austenitic stainless steels
10 p1558 A72-24855

Tensile ligament instability model for stress corrosion crack propagation velocity in austenitized steel tempered at 750 F
10 p1499 A72-24888

Fracture strength relation to austenite stability in steels with plastic deformation caused by strain induced austenite-martensite transformation
10 p1499 A72-24894

High temperature metallographic methods in microstructure study of austenitic heat resistant steel under plastic deformation and heat treatment
11 p1654 A72-25495

Iron emission spectrum in phase transformations and recrystallization study of austenitic and carbon steels under high temperature hardening
11 p1655 A72-25496

Austenitizing condition effect on lower bainite transformation in eutectoid carbon steel
11 p1656 A72-25515

Fatigue and fatigue-corrosion properties of high strength stainless maraging, martensitic structural and stainless austenitic steels
11 p1660 A72-26141

Creep tests for thermal pre cycling effect on time to failure and long term ductility of austenitic steel thin walled tubular samples
11 p1663 A72-26809

Austenizing temperature relationship to quenching rate in ultrahigh strength steels with high fracture toughness, recommending two step quench technique
12 p1829 A72-27695

Time-temperature-precipitation (TTP) diagrams and phase instabilities of high temperature exposed Mo containing austenitic stainless steels
13 p1974 A72-28658

Mechanical properties of nitrided austenitic steels at low temperatures, noting improved tensile strength
13 p1977 A72-29017

Austenite deformation effect on thermal stability and hardness of Ni steels at various C and Ni concentrations
13 p1977 A72-29019

Microscopic substructure in high temperature fatigued fcc austenitic steel and aluminum, studying cross slip lines and crack initiation
13 p1979 A72-29448

Temperature and strain rate dependence of austenitic stainless steel fracture by low cycle fatigue at high temperatures, studying striations with scanning electron microscopes
13 p1979 A72-29449

Creep rate dependence on high temperature oxidation in austenitic steel, noting preformed oxide layer and environment cycling effects
14 p2117 A72-30537

Stress relieving heat treatment for service failure prevention of stressed austenitic stainless steel components of high temperatures, noting cracking regulation by oxidation mechanism
14 p2117 A72-30538

Creep velocity and rupture strength calculated for tensile stress, noting high temperature tests of austenitic steel
14 p2121 A72-30697

Electron microscope study of precipitated fines of austenitic steel containing V and N, noting heat treatment effect on fcc crystal structure
15 p2254 A72-31523

Mo, W, Nb, Ti, V and N complex alloying to harden cast heat resistant austenitic steel, discussing phase composition and stress-rupture strength
15 p2254 A72-31563

Incoloy low cycle fatigue tests at high temperatures and different strain rates, discussing fatigue life at 10 and 60 min hold times
16 p2410 A72-33820

Low-temperature properties of nitrogen-alloyed austenitic chromium-nickel /molybdenum/ steels and chromium-manganese-nickel steels and their applicability as low-temperature ductile steels
17 p2566 A72-34395

Austenitic steel stress corrosion prevention at high temperatures and pressures, investigating inhibitor adsorption properties from capacitance measurements and polarization curves
17 p2568 A72-35474

Optimal composition equation with austenite retention index for high strength maraging stainless steel development for improved toughness
18 p2702 A72-36796

Contribution to the study of the stabilization of corrosion-resistant chromium-nickel austenitic steels
18 p2702 A72-37014

A study of the mechanical behaviors of austenitic stainless steels in the process of stress corrosion testing.
19 p2820 A72-38372

The role of metal dissolution in the process of stress corrosion cracking of austenitic stainless steel.
19 p2821 A72-38374

Microscopic substructure in face centered cubic metals fatigued at elevated temperatures.
20 p2935 A72-38880

Creep-fatigue interaction interpretation for austenitic stainless steels from crack growth viewpoint, investigating time and cycle dependent failure at elevated temperature
20 p2937 A72-39213

Enhancement of heat resistance in Kh14G14N3T steel by microadditions of boron
20 p2941 A72-39579

Dynamic recrystallization occurrence during deformation at elevated temperatures, examining subgrain structure role in austenitic stainless steels
20 p2942 A72-39990

The nitriding behaviour of austenitic stainless steels containing titanium.
21 p3066 A72-40686

Temperature and strain rate dependences of low cycle fatigue life at high temperatures of austenitic stainless steel, examining crack behavior and stress-strain relations
21 p3069 A72-41010

German monograph - Influence of programmed welding cycle temperatures on the microstructure formation and corrosion behavior of austenitic corrosion-resistant steels.
22 p3195 A72-43075

German monograph - The causes of hot crack formation in welded joints of austenitic steel with 16 percent chromium and 16 percent nickel.
22 p3195 A72-43079

Chemistry of grain boundaries and its relation to intergranular corrosion of austenitic stainless steel.
22 p3195 A72-43126

Estimates of creep-fatigue interaction in irradiated and unirradiated austenitic stainless steels.
24 p3412 A72-44554

Austenitic steel under combined bending and torsion, showing fatigue strength dependence on temperature, load cycle asymmetry and stress concentration
24 p3414 A72-44944

Measurement of stacking fault energy in CrMnNiN austenitic steel by the method of extended nodes
24 p3415 A72-45397

AUSTRALIA
Gosses Bluff impact structure in Central Australia, discussing geologic, seismic, gravity, and magnetic surveys and lunar crater analog
09 p1304 A72-23494

AUSTRALITES
Elemental abundance trends in the australite strewn field by non-destructive neutron activation.
20 p2900 A72-39839

AUTOCLAVES
Autoclaves for the study of the effects of deformation on the high temperature aqueous corrosion of metals.
21 p3039 A72-40216

AUTOCLAVING
Polyimide prepolymer formulation for glass and graphite reinforced composites autoclave processing via increased melt phase duration and temperature range
01 p0090 A72-10729

AUTOCOLLIMATORS
U COLLIMATORS

AUTOCORRELATION
Anomalous magnetic and gravitational fields energy spectra model, examining autocorrelation functions changes
02 p0217 A72-11932

Autocorrelation functions of topside incoherent scatter data, using computerized least square gradient search
02 p0220 A72-12454

Autocorrelation signal detection method application to spectrometry by modulation amplitude, investigating SNR
04 p0521 A72-14973

Hydrodynamic asymptotic characteristics of autocorrelation function for molecule velocity in classical liquid, obtaining Lagrangian diffusion coefficient
05 p0692 A72-16684

Logic circuit binary signal autocorrelation determination as function of 0 and 1 signals duration distribution considering AND and OR gates
05 p0632 A72-17094

Auto- and cross correlation functions for neuron reactions in vasomotorial center to adequate stimulation of cats vestibular apparatus
06 p0762 A72-17673

Factor analysis of frontal and occipital brain regions EEG indices interzonal variability, relating autocorrelation function parameters to neuron ensembles force level
06 p0764 A72-18057

Lightly damped nonlinear mechanical oscillators under random excitation, calculating stationary response frequency and autocorrelation by heuristic procedures
06 p0849 A72-18693

Scattered light coherence in optically thin vapors and ideal gases in energy level crossing experiment formulated in terms of autocorrelation function
08 p1206 A72-21294

Tropospheric scatter path characteristics as communication channel with random fluctuations, deriving signal autocorrelation function from mean power pulse response
08 p1132 A72-21329

Loose medium deformations and displacements fluctuations verification by statistical tests, noting inception information from autocorrelation and boundary conditions cross correlation functions
10 p1512 A72-24719

Auto and cross correlation functions of combined binary pseudorandom sequences in digital space communication systems
10 p1439 A72-24907

Uncertainty functions side maxima for phase manipulated signals with low sidelobe levels in autocorrelation functions, noting Doppler frequency shift effect
10 p1440 A72-24916

Multifilter detection system with phase autocorrelator, discussing design based on correction detection probability vs mismatch between signal and filter central frequencies
11 p1597 A72-26315

Switch detector output random process energy spectrum and autocorrelation function, noting distortion reduction by proper parameter choice
11 p1605 A72-26317

Autocorrelation functions of anomalous magnetic field and earth crust structure of central portion of Arctic Ocean, using sliding energy spectrum method
13 p1946 A72-28589

Anomalous magnetic and gravitational fields energy spectra model, examining autocorrelation functions changes
13 p1949 A72-29244

Randomized electromagnetic field propagation through uniform medium, deriving autocorrelation and intensity fluctuation spectrum expressions
13 p2007 A72-30124

Anomalous magnetic and gravitational field models autocorrelation function behavior dependence on circular cylindrical sources depth and spacing
14 p2101 A72-30647

Pulse and monochromatic short wave signals phase/amplitude autocorrelation functions and probability distributions during oblique incidence reflection from ionosphere
15 p2197 A72-31876

Landau-Placzek autocorrelation functions analysis method application to fluids transport coefficients LF characteristics
15 p2279 A72-32648

Spectral line width measurement accuracy based on digital autocorrelation of photon counting fluctuations, noting light field and photoelectric process limiting effects
16 p2357 A72-32949

Autocorrelation analysis of Mariner 2 data for solar wind velocity, noting 27 day recurrences
16 p2444 A72-32954

Time correlation functions for gases of linear molecules in a magnetic field.
17 p2589 A72-34894

Image autocorrelation function models and power spectra, obtaining probability distribution, variance and correlation coefficients of image orthogonal transformations
17 p2518 A72-35672

Recursive stochastic approximation of autocorrelation function for stationary random process based on mean-square error and maximum likelihood methods
19 p2824 A72-37285

Woodward ambiguity function extension to random signals, noting Gaussian signal in white noise with given autocorrelation function
19 p2766 A72-38418

Autocorrelation methods to obtain diffraction-limited resolution with large telescopes.
20 p2920 A72-38922

Fourier transformation relating autocorrelation to spectral density of power bounded and energy bounded functions, discussing unsteady stochastic processes
20 p2953 A72-39552

Time scales and correlations in a turbulent boundary layer.
21 p3047 A72-41626

Signal classification through quasi-singular detection with applications in mechanical fault diagnosis.
22 p3158 A72-41976

Correlator with orthogonal filters for acoustic diagnostics, noting Laguerre functions variations in signal pairs autocorrelation
22 p3176 A72-42133

Quantum impulse autocorrelation function of one dimensional harmonic crystal lattice, noting periodic time dependence at high and low temperatures
23 p3312 A72-43405

Power law behavior of autocorrelation and memory functions of statistical mechanics as t approaches infinity

23 p3309 A72-43870

Autocorrelation functions of anomalous magnetic field and earth crust structure of central portion of Arctic Ocean, using sliding energy spectrum method

24 p3397 A72-45089

Autocorrelation function of smooth steady random signal determination from consecutive derivative dispersions by MacLaurin, least squares and Taylor methods

24 p3380 A72-45317

AUTODYNES

Sensitivity of optical autodyne quantum receiver in presence of output noise, using photomultiplier signal model

07 p1000 A72-19022

Self oscillations of microwave autodyne oscillator loaded by two resonant cavities, noting radio spectroscopic applications

14 p2089 A72-31110

AUTOIONIZATION

Quantum mechanical calculations of autoionization structure in ionization of Ba positive ions by electron impact

03 p0391 A72-13746

Molecular oxygen photoelectron spectra at autoionization resonance frequencies, comparing with Franck-Condon calculations

04 p0552 A72-14892

Quasi-projection operators for calculating electron resonances in multitarget scattering tested on He ion autoionization system

12 p1847 A72-27385

Secondary autoionization reduction of recombination coefficient during dielectronic recombination process, considering importance in Fe ions

12 p1864 A72-27747

Hydrogen direct photoionization and photoexcited autoionization cross sections calculation for radiation in 600-800 Å region

16 p2431 A72-33579

Wave function and resonance parameters for autoionization and ground states of helium and hydrogen

17 p2586 A72-35774

Angular distribution of electrons autodetached from H- in slow collisions with He.

23 p3316 A72-44074

Multiphoton dissociation, predissociation, and autoionization of the hydrogen molecule.

24 p3427 A72-45476

AUTOKINESIS

Afterimage apparent motion preceding smooth eye movement association with target tracking, noting unequal impairment occurrence over entire visual field

07 p0927 A72-19034

Experimental tests of Voth-Mayman hypothesis of autokinesis mediation by attention distribution mechanism

18 p2653 A72-36904

AUTOMATA THEORY

Generalized cellular automata simulation by mathematical model network of identical automata with two states

05 p0641 A72-16317

Autonomous threshold elements diagnostic tests and verification control, noting cascade, pyramidal and branching schemes

06 p0785 A72-18303

Accuracy and reliability in engineering design of discrete automata without memory /logic circuits/, using Boolean algebra for mathematical models

11 p1600 A72-25434

Abstract family of multistorage tape acceptors and associated languages, discussing wedge operation and applications

12 p1787 A72-27675

Russian papers on adaptive control systems covering automata and game theory, learning models, Markov processes and probability theory

12 p1787 A72-27921

Multiple function stochastic automata performance in environment with random control processes, showing improved learning rate

12 p1787 A72-27922

Multiple input automata with optimal response to any input set, using maximum mean gain as criteria for response selection

12 p1787 A72-27923

Autonomous threshold elements diagnostic tests and verification control, noting cascade, pyramidal and branching schemes

13 p1934 A72-30071

Automata with behavior defined by input stimuli sequence and independent on initial state, considering neuron nets as example

15 p2203 A72-32173

Automata with specific properties of diagnostic, arranging and synchronizing word sets

16 p2366 A72-33086

Information lossless automata for unknown input sequences identification of arbitrary length, noting

solvability conditions and application to automata superposition

16 p2366 A72-33087

Automaton model with sequential description of control systems operations, discussing structure with states code recorded on shift register

16 p2366 A72-33088

Integral equations of a multiport network with a digital control automaton

21 p3036 A72-40154

A stochastic automata theoretical approach to dynamic programming.

22 p3199 A72-42633

Minimization of finite automata

22 p3157 A72-43082

Input delay influence on dynamic stability of potential finite automata in transition between two states, noting logic circuits synthesis based on Boolean algebra

23 p3274 A72-43350

Digital-computer simulation of the motion of a walking machine

23 p3278 A72-44002

Problems of complex object modeling based on heuristic self-organization

24 p3376 A72-45509

Finite Boolean function computation on sequential machine models, developing exchange inequalities between storage, time, et cetera, for relation of combinational and time complexities

24 p3383 A72-45650

Computer programming for minimization of time required for retranslation with compilers, discussing finite state machine modeling with circulating page loose system

24 p3383 A72-45670

AUTOMATIC CONTROL

NT ADAPTIVE CONTROL

NT AUTOMATIC FLIGHT CONTROL

NT AUTOMATIC FREQUENCY CONTROL

NT AUTOMATIC GAIN CONTROL

NT AUTOMATIC LANDING CONTROL

NT CASCADE CONTROL

NT DYNAMIC CONTROL

NT FEEDBACK CONTROL

NT FEEDFORWARD CONTROL

NT LEARNING MACHINES

NT NUMERICAL CONTROL

NT OFF-ON CONTROL

NT OPTIMAL CONTROL

NT PROPORTIONAL CONTROL

NT SELF ADAPTIVE CONTROL SYSTEMS

NT SELF ALIGNMENT

NT SEQUENTIAL CONTROL

NT TIME OPTIMAL CONTROL

Automatic control systems sensitivity, presenting literature survey

01 p0044 A72-10299

Aircraft high pressure oxygen cylinder system filler valve optimum standards, discussing automatic fill rate and pressure sensitive closing control, design, construction and performance

[SAE AS 1225] 01 p0006 A72-10385

Soviet papers on complex automatic control systems, covering elastic spacecraft stabilization, nonlinear dynamic systems controllability and random vibration spectra control

01 p0045 A72-10496

Ideally conducting plasma confined in vacuum by circularly polarized magnetic field, investigating MHD instabilities suppression by distributed automatic control system

01 p0109 A72-10503

Automatic device using tetragonal conducting film sheets to feed graphic information into computer

02 p0187 A72-12279

Radar digital control system, discussing cost effectiveness, block levels, flexibility, tradeoffs, data management, decision making and future applications

02 p0178 A72-12395

Computer controlled telemetry data acquisition station, noting cost effectiveness

02 p0179 A72-12407

Radio telescope variable profile antenna autocollimation adjustment for separating transmitted and received signals pulse-time characteristics

02 p0231 A72-12521

Nomogram determination of frequency characteristics of closed loop linear automatic control systems

02 p0197 A72-12563

ATCAS air traffic control automation system emphasizing Italian situation

02 p0257 A72-12649

Optimal control algorithm synthesized from linear sampling theory for inertial platform alignment, requiring systematic error free optimal digital computer

02 p0258 A72-12899

Time shared performance test monitor function, operation and self repair of corporate fed array radars with computer control for long time internal reliability

03 p0321 A72-13165

Soviet book on linear automatic control systems with variable parameters covering pulse transfer function determination algorithms, signal transmission characteristics and systems stability

03 p0339 A72-14245

Electronic system for electrodischarge machining, considering thyristor spark control and circuitry design for automatic feed down and short circuit clearance

04 p0502 A72-15530

Computer controlled automatic system for measuring electroconductivity and Hall effect in semiconductors, noting data acquisition instrumentation

04 p0496 A72-15534

Bang-bang automatic control of linear plant with discontinuous characteristics element, investigating periodic function oscillation

05 p0639 A72-15757

Ground based satellite control center data processing for Azur satellite, using automatic guidance

05 p0632 A72-16138

Direct and inverse problems of sensitivity theory, discussing solvability conditions, search optimization and applicability in automatic control

05 p0640 A72-16206

Automatic control in space - Conference, Dubrovnik, Yugoslavia, September 1971

05 p0724 A72-16427

Automatic craft for planet surface exploration, classifying propulsion gear

05 p0644 A72-16449

Automatic control of ESRO drag-free deep space probe for measuring Robertson matrix beta and gamma constants

05 p0727 A72-16468

Nonlinear control systems of vehicles angular orientation, investigating dynamic properties by method of harmonic linearization

05 p0727 A72-16474

Automatic control systems testing and evaluation - Conference, Saint Mary College of Maryland, August/September 1971

05 p0686 A72-16652

Large space vehicles automatic docking guidance and control system design, using single plane and six degrees of freedom analysis

05 p0729 A72-16874

Low wing loading STOL transport with ride smoothing automatic control system, noting thrust-weight ratio

05 p0613 A72-16942

Inertial navigation system accelerometer error autocorrelation, using reversal by accelerometer forced rotation in stabilized platform plane

05 p0664 A72-17148

Automatic optical tracking instrumentation at rocket launching station Tanegashima, describing automatic cinetheodolite

06 p0795 A72-17432

Nationwide real time automated ATC system interconnected by data transmission links, discussing radar signal acquisition/transfer and computer complex

06 p0845 A72-18283

Axiomatic determination of dynamic logic control systems based on Moore automaton elements and combined continuous and finite models

06 p0781 A72-18660

System properties of information patterns in complex hierarchical automatic control systems

07 p0949 A72-18927

Feasible solutions to automatic control problems satisfying multiple state and control variable inequality constraints, discussing algorithmic numerical implementation

07 p0959 A72-19281

Absolute stability region of linear portion of single loop automatic control system with one nonlinear element determined by frequency criteria

07 p0963 A72-19898

Automatic control of electroerosion machining by process computer, using pulse-voltage-metal removal relation

08 p1174 A72-21030

Transistorized static pulse generators for spark erosion machining, discussing operating principle, design, applications, automatic control system and maintenance procedures

08 p1146 A72-21038

Automatic systems efficiency determination, using characteristic equation roots sensitivity with respect to system parameters changes

08 p1146 A72-22063

Soviet papers on industrial plants automatic control systems organization, design and technological arrangement, covering information handling requirements and man machine interfaces

08 p1256 A72-22144

Automated administrative control systems design, discussing man machine interactions in industrial and economic enterprises management

08 p1256 A72-22145

- Data transmission system design in computerized administrative control system for industrial enterprise management 08 p1257 A72-22148
- Industrial enterprises preparation for computerized administrative control systems introduction 08 p1257 A72-22149
- Servomechanism with nonlinear static and Coulomb friction under autonomous operation, predicting stability boundaries by analog computer simulation 08 p1113 A72-22154
- Deviation accumulation conditions and maximum dynamic error of linear automatic control system under perturbation, including theorem for Bellman equation 08 p1146 A72-22177
- German monograph on models for automatic radar tracking methods covering error probabilities, reliability and false information reception 09 p1348 A72-22321
- Redundant polystable element designs with autonomous redundant state breakdown controls for reliability improvement in automatic control systems 09 p1290 A72-22547
- Liapunov direct method in synthesis of frequency-pulse system for automatic stabilization of spacecraft position 09 p1397 A72-23427
- Man machine automatic control system structural synthesis, treating system operation as nonlinear programming problem 09 p1291 A72-23438
- Automatic electron beam welding machine for small components, discussing design, performance and inspection methods 09 p1321 A72-23637
- Control system for stabilization of liquid propellant rockets Pogo oscillations, discussing structure, fuel tank and feed system, combustion chamber, control gain and accelerometer installations 10 p1551 A72-24027
- Informational reliability of automatic control system comparators, considering tolerance field contraction effect 10 p1456 A72-24081
- Spectral position of spontaneous self regulatory systems, comparing to classical wave spectra 10 p1511 A72-24221
- Automatic electromagnetic suspensions using tuned RLC saturable reactor control 10 p1460 A72-24761
- Optimal distribution of resources in automatic systems for detection and measurement of random concentrated noises number in assigned frequency range 10 p1440 A72-24917
- Automatic meteorological stations - Conference, Potsdam, East Germany, March 1970 10 p1507 A72-25007
- Automatic meteorological stations development in populated areas, foreseeing data gathering by sensors with satellite and radar efficiency taken into account 10 p1507 A72-25008
- Standardized automatic telemetering hydrometeorological station, discussing structure, operation, working principles and sensors 10 p1462 A72-25009
- Automatic remote transmitting meteorological station, discussing development, working principle, technological features and sensors 10 p1462 A72-25010
- Reliability, operational safety and system concept interrelationship in automatic meteorological stations 10 p1463 A72-25011
- Air, wet bulb and soil temperature indications from automatic telemetering meteorological stations, comparing with Hg thermometer readings 10 p1483 A72-25012
- Automatic telemetering meteorological stations and visual observation data processor control 10 p1507 A72-25020
- Classification of automatic meteorological ground stations networks in populated areas, discussing required equipment, data transmission, real time operation and costs 10 p1507 A72-25021
- Data acquisition and transfer efficiency and reliability in computerized automatic control systems for communications, listing probability and expectation criteria 11 p1600 A72-25436
- Error correlation technique to ensure reliability of discrete automatically controlled digital systems inputs, noting lower redundancy requirement 11 p1600 A72-25438
- Mean square error and functional state prediction algorithm for plants controlled by automatic system containing digital computer 11 p1600 A72-25439
- Absolute stability conditions of zero solution for PAM automatic control systems equations in terms of transfer function 11 p1609 A72-25446
- Automated echelle spectrograph data handling using computer control 11 p1716 A72-25693
- Rotating analyzer astronomical photopolarimeter automation by on-line computer control system 11 p1600 A72-25695
- Computer control data acquisition system for 46 meter radio telescope at Algonquin Observatory 11 p1631 A72-25697
- Automatic device using tetragonal conducting film sheets to feed graphic information into computer 11 p1601 A72-25704
- ATC system, discussing flight data and radar processing functions and terminal automation program 11 p1683 A72-25875
- Russian papers on automatic monitoring and electrical measurement methods covering optical systems, control devices, diagnostic test optimization, bionic applications, etc 11 p1611 A72-26435
- Discrete automatic monitoring and measuring systems with discrete random sequence and continuous process reconstructed output signals, deriving probability criteria for reading frequency determination 11 p1611 A72-26438
- Data display techniques in man operated automatic control system, assessing information volume versatility and operability 11 p1585 A72-26451
- Linear multiple section binary filters analysis and synthesis, discussing mesh functions spectra for signal measurement in automatic control systems 11 p1612 A72-26452
- Variational problems in automatic control theory, presenting existence theorems for solution of boundary value problems for nonlinear differential equations with deviating argument 12 p1837 A72-27995
- Russian book on random signal generation covering ultralow and audio frequency spectra, random number and pseudorandom signals simulation and automatic control 12 p1786 A72-28347
- Automatic control system synthesis by computer-aided version of grapho-analytical method 13 p1934 A72-28459
- Variable structure automatic control relay system design with reduced insensitivity zone and given transient process requirements 13 p1935 A72-28612
- Automatic electrostatic contour welding of IC microcircuit metallic casings, using contact and electrode voltage feedback signals 13 p1963 A72-28921
- Automatic statistical analyzer for radio meteor echo multiplicity recording in three coordinate /multivariable/ space, including instrument error allowance 13 p1929 A72-29032
- Extremal correlation algorithm for automatic control of two image congruent superposition, using digital simulation and statistical trial techniques 13 p1924 A72-29161
- Statistical homogeneity criteria for automatic equipment operation reliability, using Poisson flow model with random fluctuations 13 p1965 A72-29173
- Semiautomatic tracking device for satellites comprising laser telemetry equipment 13 p1939 A72-29674
- Feedback ac compensating amplifier design for automatic AM signal envelope conversion, noting truncated equivalent transfer function expandability 13 p1933 A72-29972
- Linear automatic control systems diagnostics and synthesis 13 p1937 A72-29998
- Absolute stability of nonlinear automatic control systems based on root locus trajectories and Popov line hodographs 13 p1937 A72-30094
- Single automatic potentiometer based maximum-minimum temperature control unit, noting elimination of dual temperature regulators 14 p2104 A72-30444
- Aerial survey camera with automatic exposure control, discussing film emulsions sensitivity characteristics, object light intensity range and measuring methods 14 p2105 A72-30839
- Nonlinear self excited oscillations with negative hysteresis in automatic control systems 14 p2091 A72-31127
- Automatically controlled plasma arc welding for uniform cross section weld seams production under fluctuating electric current conditions, describing electronic control system 15 p2244 A72-31773
- Automatic control theory trends /1950-1970/, discussing nonlinear, discontinuous and adaptive systems, optimization problems, Liapunov stability theory, etc 15 p2212 A72-32576
- Orion spaceborne astronomical observatory automatic control system for instrument orientation and star tracking, discussing servomechanism and pulse duration modulation 15 p2242 A72-32743
- Automaton model with sequential description of control systems operations, discussing structure with states code recorded on shift register 16 p2366 A72-33088
- Group perturbation method for accuracy analysis of nonlinear stochastic automatic control systems, noting computer time reduction 16 p2371 A72-33091
- Automatic control for selective precision joint assembly of fuel pump equipment, reducing unfinished product volume 16 p2397 A72-33261
- Monitor and regulator for automatic speed control and flow velocity measurement in wind tunnel 16 p2392 A72-33609
- Automatic remote mechanical system parameter control by electrical elements, introducing rigidity for mass sensitive measurement in dynamometry 16 p2370 A72-33956
- Time-optimality of a class of extremal systems with statistical signal processing 17 p2518 A72-35782
- Construction, analysis, and design of FM digital devices for controlling and measuring rapidly varying quantities 19 p2776 A72-37303
- Stability of nonlinear automatic systems with double pulse modulation, discussing systems with linear and nonlinear pulse elements 19 p2777 A72-37435
- Analysis of discrete automatic control systems with variable parameters by the method of orthogonal expansions. I, II 19 p2778 A72-37438
- Colorimetric and spectrophotometric gradient systems comparison for bright stars used in automatic telescope pointing control, discussing interstellar absorption 19 p2860 A72-37955
- A system for programmed control of the motion of the carriage of a microphotometer along two coordinates 19 p2801 A72-37966
- Automatic structural mode control system with aerodynamic vanes for B-1 strategic bomber turbulence excitation during low altitude terrain following missions [AIAA PAPER 72-772] 19 p2751 A72-38132
- Investigation of the structure of processes in discrete automatic control systems by the application of graph theory 19 p2779 A72-38180
- Structural-matrix methods for discrete automatic control system designs 19 p2779 A72-38185
- Joint Automatic Control Conference, 13th, Stanford University, Stanford, Calif., August 16-18, 1972, Preprints of Technical Papers. 19 p2779 A72-38226
- Automatically controlled delay in self-excited pulsating systems based on artificial muscles 19 p2761 A72-38464
- Process control of the 100-m telescope - Digital control 19 p2803 A72-38486
- Man machine automatic control system structural synthesis, treating system operation as nonlinear programming problem 19 p2782 A72-38521
- An automated instrument for monitoring the quality of recovered water. [ASME PAPER 72-ENAV-16] 20 p2895 A72-39161
- Reversible integrodifferentiator with automatic data input 21 p3024 A72-40162
- An air traffic controller's view on area navigation and ATS requirements related thereto. 21 p3081 A72-40299
- Failure diagnostics in mathematical models of automatic control systems 21 p3038 A72-40712
- Controlled-carrier transmission of AM/VSB television from space. 21 p3016 A72-40770
- Human consciousness and choice role in biological control process automation to define differences between manual and automatic control systems 21 p3009 A72-41405
- Entropy criterion in the estimation of the dynamic quality of automatic control systems 21 p3039 A72-41803
- Frequency stability criterion for variable-structure automatic control systems 22 p3162 A72-42185
- Analog and digital automatic control systems for aerospace and process applications, discussing transfer function and state variable methods 22 p3162 A72-42714

Closed loop pulsed automatic control system, determining discrete correcting element parameters from linear equalities

22 p3163 A72-43009

Polynomial operators for nonlinear systems analysis.

23 p3308 A72-43599

Trends in the control of air-traffic flows in the air space

23 p3311 A72-43640

Frequency stabilization of pure neon laser.

23 p3296 A72-43951

High-frequency fatigue testing facility, U-20P, with programmed control of the sample's vibration amplitude

23 p3278 A72-43970

Man in a control circuit during an information game synthesis

24 p3377 A72-45520

AUTOMATIC CONTROL VALVES

NT PRESSURE REGULATORS

AUTOMATIC DATA PROCESSING

U DATA PROCESSING

AUTOMATIC FLIGHT CONTROL

NT AUTOMATIC LANDING CONTROL

Passenger aircraft onboard automated inertial navigation devices, emphasizing accelerometer and gyroscope design and construction

01 p0096 A72-10070

Inertial navigation role in automatic ATC systems, discussing path control accuracies, environmental conditions, noise and air pollution, etc

01 p0098 A72-11118

Soviet book on course-indicating systems and automatic navigation aids for civil aviation aircraft covering design, operation principles, error analysis and reliability

02 p0256 A72-12298

FAA air traffic control automation program, discussing en route stage, computer program, data processing and storage and terminal area navigation and display techniques

02 p0256 A72-12380

STOL aircraft integrated landing approach flight control system with elevator and thrust control coupling to angle of attack, altitude and other state variables

02 p0155 A72-12705

Automatic flight control systems value to aircraft pilot, stressing man machine interface

03 p0386 A72-13420

Navy hovering vehicle versatile automatic control system for V/STOL flight test program, using airborne digital computer for navigation/guidance computations

05 p0687 A72-16661

BQM-34A and E/F target drone aircraft versatile automatic flight control system flight test program and results for basic and advanced flight modes

05 p0687 A72-16663

Automated ATC guidance technique for aircraft curved flight trajectories, describing flight profiles synthesizing algorithms and computerized simulation technique

06 p0845 A72-17922

Development trends in airborne man machine flight control, discussing optimal division between human pilot and machine in relation to total system performance and economic factors

09 p1270 A72-22781

Optimal solutions for apportionment between automatic and manual flight control, considering number and types of displays required

09 p1348 A72-22783

DC 10 aircraft automatic flight guidance system, noting dual-dual fail-passive autoland

09 p1349 A72-23448

Automated navigation management in cockpit, considering modular navigation /MONA/ dual channel system of L-1011 TriStar

09 p1349 A72-23450

Helicopter automatic flight control approach/hover coupler systems, hands off stability and handling qualities

12 p1843 A72-27522

Autoland system flight testing in Trident 3B and British Civil Aviation Authority approval for ICAO Cat 3a weather

16 p2420 A72-33539

Airline crew familiarization with DC-10 Computerized Flight Guidance System to calculate steering signal from raw data to follow flight path

19 p2831 A72-37899

Some effects of bias errors in redundant flight control systems.

19 p2779 A72-38237

Electronic primary flight control system requirements and equipment characteristics, discussing USAF and NASA fly by wire R and D programs

20 p2887 A72-39118

Microwave landing system effect on the flight guidance and control system.

20 p2952 A72-40057

Modular navigation /MONA/ dual channel automatic area navigation system, describing computer, flight data storage and control/display units

21 p3079 A72-40277

TCE-71A area navigation system based on modular design with provision for 20 waypoints parameter storage, describing computer, control display and automatic data entry units

21 p3079 A72-40278

Automated area navigation with real time track computation, discussing information processing by on-board computer for immediate pilot instruction

21 p3081 A72-40683

The use of minimum order state observers in digital flight-control systems.

24 p3382 A72-45343

AUTOMATIC FREQUENCY CONTROL

Time optimal phase locked AFC system synthesis based on Pontryagin maximum principle, comparing computerized and experimental transient response

01 p0024 A72-10049

AFC for suppressed-carrier SSB voice signal reception, using phase locking procedure or comparative zero-crossing-rate measurement

01 p0025 A72-10333

Telemetry receiver signal data quality in terms of RF, if AGC, AFC and AM rejection circuitry requirements

02 p0192 A72-12149

Transient characteristics of phase lock automatic frequency control system with integrating filter, using nonlinear phase-plane method

02 p0176 A72-12224

Submillimeter wavelength HCN laser stabilization, describing AFC and phase locking

04 p0532 A72-15596

Stability conditions and effective bandwidths of first and second degree pulsed phase locked AFC systems with proportionately integrating filter, using Z transform method

05 p0625 A72-15825

Microwave-range optical heterodyne system with magnetically tuned Zeeman effect laser emissions mixing and AFC

05 p0668 A72-16345

Automatic frequency adjustment of pair of He-Ne lasers with different oscillation frequency fluctuations under various heating conditions

06 p0825 A72-17840

Aircraft turboalternator governing theory for frequency error detection, comparing performance of mechanical- and electro-hydraulic governors

06 p0868 A72-18249

Phase locked AFC system, calculating phase detector response effects on dynamic properties

07 p0943 A72-19524

Stability regions of phase-locked AFC with nonlinear control circuit, describing system dynamics by differential equations

09 p1290 A72-23180

Error analysis of measurement-type servo systems with constant product /or quotient/ of dependent and independent variables applying to phase loop AFC operation

11 p1595 A72-26301

Dynamic range errors and noise bands for phase comparison radio range finders with mutual automatic frequency control in interrogator and transponder

11 p1596 A72-26302

Second order phase lock AFC system transient response duration calculation for rectangular and sawtooth characteristics of phase detector, using averaging method

13 p1921 A72-29284

Sinusoidal signal and stationary quasi-white Gaussian noise mixture effects on stochastic phase locked AFC system operation, noting phase error probability density function

13 p1921 A72-29285

Short term instability of frequency standard using AFC of quartz crystal oscillator by phase locking to optically pumped Rb 87 vapor clock

13 p1968 A72-29296

Vibration stability and interference transfer function of onboard transponder with phase lock AFC used in Doppler system for measuring spacecraft trajectory parameters

13 p1958 A72-29456

Nonlinear variable transformation method to determine locking band and transition processes in automatic phase and frequency control systems

14 p2087 A72-31132

Estimation-correlation principle application to harmonic signal receiver with unknown carrier frequency, using searching phase locked AFC circuit as estimation unit

15 p2202 A72-32667

Dispersion signal recording for klystron AFC radio spectrometer by low frequency magnetic field modulation

22 p3175 A72-41900

Investigation of the threshold properties of a phase-locked AFC detecting a sinusoidally frequency modulated signal against a noise background

22 p3154 A72-42231

Stability conditions and effective bandwidths of first and second degree pulsed phase locked AFC systems with proportionately integrating filter, using Z transform method

23 p3263 A72-43433

Application of an electronic computer to the calculation of the locking band in nonlinear phase-lock automatic frequency control systems

23 p3264 A72-43763

AUTOMATIC GAIN CONTROL

Double beam spectrophotometer with automatic gain controlled preamplifier to achieve insensitivity to signal strength change in noise at low cost

07 p0992 A72-20579

Transistorized microwave amplifier/limiter for upper part of decimeter wave range, suggesting limitation in automatic gain control transistors

10 p1451 A72-24588

IF amplifier automatic gain control /AGC/ for ultrasonic pulse echo measurements

11 p1633 A72-26055

Gain control of cat retina rapid light adaptation process to attenuate signals reaching retinal ganglion cells from photoreceptors

12 p1760 A72-27299

Gain control and contrast sensitivity in the vertebrate retina.

17 p2507 A72-34418

Phase locked loop model based on AGC circuitry, devising optimum control strategies

17 p2532 A72-34419

Certain features of the use of controllable-gain transistors

21 p3033 A72-40944

Noise resistance of optical communication lines with radio and optical AGC systems

23 p3264 A72-43770

AUTOMATIC LANDING CONTROL

Automated radar terminal system /ARTS/ for monitoring and tracking all aircraft within radar range, displaying identification, altitude and ground speed information to air traffic controller

01 p0098 A72-10960

Fail-operational automatic landing system for Boeing 747 aircraft, noting reduction in allowable minimum weather conditions in U.S. and UK

01 p0098 A72-10961

Terminal area air traffic guidance and control, discussing automation, all-weather precision approach and landing and failure detection

04 p0544 A72-14817

Airborne computer programmed adaptive optimal control for subsonic vehicle automatic landing with aerodynamic performance

05 p0685 A72-16430

U.S. Navy automatic carrier landing system /ACLS/, discussing shore and ship based test techniques and problem areas

05 p0686 A72-16654

Flight control systems development, discussing onboard computers use in subsystems functional integration, stabilization and landing systems, inertial navigation and flight simulation

05 p0687 A72-16736

DC-10 aircraft automatic landing performance and failure assessment monitor system

08 p1204 A72-21003

Landing control algorithm using onboard digital computer for spacecraft hyperbolic velocity reentry, discussing simulation test results

11 p1684 A72-26898

Pilot evaluation of C-5 automatic landing system in Category III weather environment

12 p1842 A72-27521

Statistical correlation techniques applied to jet aircraft autoland system dynamic ground tests with simulated engine and aerodynamic characteristics

16 p2420 A72-33641

Precision navigation for approach and landing operations.

19 p2832 A72-38253

Direct lift control feasibility for integration into F-14A automatic carrier landing system /ACLS/, using moving-base six-degree-of-freedom simulation

20 p2951 A72-39127

AUTOMATIC PATTERN RECOGNITION

U PATTERN RECOGNITION

AUTOMATIC PILOTS

Soviet book on electrical equipment and instrumentation of An-24 aircraft covering power sources, control, safety systems, engine, flight and navigation instruments and autopilot

05 p0615 A72-16400

Motion dynamics of aircraft-autopilot closed loop system under influence of atmospheric turbulence and electric circuitry thermal noise

07 p0911 A72-18990

Digital autopilot for SKYLAB orbital assembly attitude control during docking, discussing jet selection logic, inter-axis dependence and onboard computer

15 p2269 A72-32183

Airline crew familiarization with DC-10 Computerized Flight Guidance System to calculate steering signal from raw data to follow flight path

19 p2831 A72-37899

Virtual target steering - A unique air-to-surface missile targeting and guidance technique.
[AIAA PAPER 72-826] 20 p2951 A72-39100

AUTOMATIC ROCKET IMPACT PREDICTORS
U COMPUTERIZED SIMULATION
U IMPACT PREDICTION

AUTOMATIC TEST EQUIPMENT
Automatic ultrasonic testing equipment for NDT tests of helicopter rotor blades
01 p0071 A72-11021

Automatic device for thermal and thermomechanical fatigue tests of steel specimens, noting crack nucleation and growth by hardening due to lattice defects
02 p0200 A72-11996

Electrical and electronic measurement and test instrument - Conference, Ottawa, June 1971
02 p0200 A72-12476

Interim automatic scanning multichannel data acquisition system for environmental test laboratory, using programmable calculator
02 p0200 A72-12477

Multiprogrammed digital computer controlled acquisition and processing of quasi-static analog transducer data during spacecraft environmental simulation tests
02 p0200 A72-12478

Digital computer automated test equipment and procedures for remote sensors and electronics for scanning celestial sphere for X rays prior to spacecraft launch
02 p0200 A72-12479

Automatic recording of cyclic creep and strain curves for metals under low cycle static tension
03 p0444 A72-13468

Book on EMI test instrumentation and automatic measuring systems covering shielded enclosures, emission and susceptibility antennas and spectrum analyzers
04 p0486 A72-14611

Automated jet engine development facility, discussing assembly and test area and computer controlled operation
[ASME PAPER 71-WA/GT-6] 05 p0642 A72-15899

Bayesian analysis of onboard computer controlled aircraft avionics subsystem built-in test for failure detection
05 p0638 A72-16574

Automatic recording of crack length in slow fracture tests of flat high strength steel in water
05 p0741 A72-17087

Computerized modular automatic test equipment for commercial airliner avionics device performance, discussing data handling ability and cost effectiveness
06 p0796 A72-18250

Automatic testing machine for mechanical properties of metals under static loading
06 p0796 A72-18365

Automatic photoelectric device for measuring internal stresses and deformations of photographic films
07 p0988 A72-19861

Automated mechanical system for solid propellant sheet stretch tests in two directions as function of time
08 p1147 A72-21331

Automatic computer-controlled system with laser technology for quality inspection of mass produced automobile master brake cylinders
09 p1319 A72-22979

Thermogravimetric design, using electromagnetic microbalances and turbomolecular pump for automatic sorption isotherm measurements in surface area and pore size analyses
11 p1636 A72-26788

Two coordinate oscillograph recording device with automatic reversing for stress-strain tests under static and cyclic loads
11 p1637 A72-26814

Computer program to reduce automated multiaxial testing strain gage and applied loads data from tubular or flat specimens including fiber composites
12 p1787 A72-27999

Digital microwave power measuring device with automatic range selection
13 p1931 A72-29267

Structure-borne acoustic nondestructive testing for readiness assessment, fault isolation and automatic checkout of space vehicle mechanical devices
15 p2214 A72-31699

Computer controlled random environment test systems for large scale off-line data analysis and reduction, using Fourier analyzer
15 p2204 A72-32609

Method for calibration and verification of automatic liquidborne particle counter/light method/
[SAE ARP 1192] 18 p2692 A72-36533

Considerations in the design of an automatic visual field tester.
18 p2654 A72-37013

Program-controlled machine for the investigation of mechanical properties of materials under a complex stress.
19 p2795 A72-37575

Development of a digital control system for a spacecraft propulsion test facility.
19 p2783 A72-37641

Methods for monitoring the parameters of phased antenna arrays.
19 p2767 A72-38622

Selection of characteristics for automatic classification of welding defects in radiographic testing.
19 p2805 A72-38763

Reliable advanced solid state radar (RASSR)/ array design featuring transmit-receive elements arranged in triangular grid and built-in test equipment
20 p2904 A72-39732

Facility for measuring and recording the electrical resistance of metallic samples during mechanical tests
21 p3043 A72-41718

Facility for studying the thermophysical properties of materials by quasi-stationary methods
22 p3176 A72-42289

Digital computer technique and real time monitor software application to instrumentation data acquisition system, discussing design guidelines and gas turbine engine test example
22 p3156 A72-42681

Digital computer controlled testing equipment for separately driven coaxial gas turbine low and high pressure compressors, emphasizing reliability and flexibility in system design
22 p3157 A72-42682

Computer-operated data acquisition and control system for automatic diagnostic monitoring of propulsion research instrument
22 p3216 A72-42684

Development of a digital control system for a spacecraft propulsion test facility.
22 p3163 A72-42685

Nondestructive stability evaluation of large shell structures by direct computer controlled testing.
22 p3157 A72-42695

Digital data system with real time displays and multiprocessing capability for multitest of aircraft structure with operational manpower reduction, assessing performance
22 p3163 A72-42696

Cascade computer controlled system for LSI devices testing, considering interim buffer storage and programmable pattern generator
22 p3160 A72-42823

Machine with programmed load control for studying the fatigue and inelasticity of metals at room and elevated temperatures
23 p3278 A72-43969

Automatic recording of cyclic creep and strain curves for metals under low cycle static tension
24 p3458 A72-44943

Automatic software diagnostic package for airborne computer, using testng computer for decision making based on received data
24 p3383 A72-45669

Automatic testing machine for mechanical properties of metals under static loading
24 p3389 A72-45751

AUTOMATION
Automatized graphic information input into computer, using electric potential distribution introduced into conducting underlay sheet by current carrying drawing pen
03 p0326 A72-13093

FAA air traffic control automation program, describing enroute and terminal ATC systems implementation
06 p0844 A72-17327

Automated navigation aids interface with human operator, discussing Apollo flight experience and technology utilization in air and marine navigation
06 p0846 A72-18288

Automation in planning and execution of flights, considering navigation, communication, flight instruments monitoring, control/stabilization and warning systems
09 p1269 A72-22780

Automatic assembly machines for IC batch production, involving terminal cutting and bending and RC element insertion
09 p1292 A72-23255

Spatial filtering techniques and numerical classification methods for pattern recognition in automated photointerpretation
09 p1312 A72-23305

Automation of aerial photointerpretation based on application of photometric, microdensitometric and digital computer technology
09 p1313 A72-23308

Optical image filtering to simplify and facilitate automatic aerial photointerpretation processes
09 p1313 A72-23310

Automatic cloud cover mapping from satellite photographs, describing three step procedure of texture edge detection and cleaning, region coloring and map cleaning
10 p1478 A72-23782

Electronics and data processing technology effects on radar state of art, discussing automated air traffic control surveillance systems
10 p1435 A72-24490

Automatized graphic information input into computer, using electric potential distribution introduced

into conducting underlay sheet by current carrying drawing pen
11 p1601 A72-25705

Image-to-signal conversion by TV tube in automatic contactless measuring systems, producing mosaics of object by optical, X ray and ultrasonic techniques
11 p1634 A72-26460

FAA automated ATC system, discussing subsystems related to operational and nonoperational computer program components, data entry and display, communication, personnel and environments
11 p1684 A72-27000

Pattern recognition in mental process automation, noting character transformations, written symbols content analysis and syntactic description
12 p1786 A72-27576

Automatic ECG recording and analysis by electronic data processing equipment, discussing methods of data acquisition and transmission for routine diagnosis and prophylactic mass examinations
12 p1772 A72-27821

Automated problem solving in continuous stochastic processes, using nonergodic representation of Gaussian process with continuous spectral density
15 p2204 A72-32588

Russian book - Automation of the monitoring and study of metals
19 p2795 A72-37299

INTERKAMA 1971; International Congress with Exposition for Measurement Technology and Automation, 5th, Duesseldorf, West Germany, October 14-20, 1971, Reports
19 p2782 A72-38301

Automated data processing and display capabilities of radiation measuring systems for surveillance, protection and control in nuclear research, medicine and power production
19 p2802 A72-38306

Computers and automatic drafting machines as aids in artwork production for printed circuits
19 p2809 A72-38307

Automatic air targets recognition via digital radar data processing, discussing methods for noise signals suppression
21 p3081 A72-40547

Automatic transmission and application of sky wave corrections with differential OMEGA navigation, discussing test equipment, procedures and results
22 p3203 A72-42948

Book - Industrial robots - A survey: Details of construction, performance, prices, and applications /Enlarged edition/
22 p3183 A72-43099

Comparative merits of manned and unmanned /automated/ space exploration, considering lunar observatories, earth orbiting space stations and interplanetary missions
24 p3441 A72-45220

AUTOMOBILES
Air transport vs other travel, discussing time, costs, popularity and technology
03 p0459 A72-13485

Helicopters and turbotrains as space conserving alternatives for automobile urban transportation, emphasizing comfort and convenience
17 p2639 A72-35505

AUTONOMIC NERVOUS SYSTEM
NT SYMPATHETIC NERVOUS SYSTEM
Cardiac output and autonomic nervous system role in antidiuretic response to acute thoracic superior vena cava constriction
02 p0157 A72-11661

Beta-adrenergic and vagal blockade altered autonomic control effects on left ventricular function in conscious dogs, noting heart rate, stroke volume and end-diastolic and end-systolic diameters
02 p0163 A72-12090

Simulated sonic boom effect on tracking performance and autonomic response, noting heart rates, skin conductance and startle reflex
06 p0767 A72-17868

Autonomic blockade effects on reflex bradycardia due to phenylephrine induced arterial pressure in man during rest and supine exercise
07 p0925 A72-20688

Dynamic orthosympathetic control of cardiovascular system, studying efferent element link between autonomic vasomotor and cardiac centers and effector cells
08 p1118 A72-21548

Autonomic nervous system role in controlling coronary and cardiac responses to hypoxic hypoxia, measuring blood flow with Doppler ultrasonic flow transducer
12 p1767 A72-28313

Vagus nerve regeneration in humans after stomach cancer surgery
13 p1903 A72-28779

Respiratory and vasculomotor autonomic centers functional state relation to vestibular system from labyrinth electrical stimulation and shaking experiments
14 p2075 A72-30387

- Role of the autonomic nervous system in the hypoxic response of the pulmonary vascular bed.
18 p2650 A72-36572
- Hypothalamic control of the electrical activity of the spinal cord
21 p3000 A72-40598
- Cortical effects mechanisms in animal vegetative systems, noting biological oxidation and organic phosphorus compound studies
21 p3000 A72-40759
- Localization and structural-functional organization of the system of vagus nerve nuclei constituting the 'cardiac center' of the medulla oblongata
21 p3004 A72-41673
- Prediction of vegetative reactions in the case of stress and extreme effects upon the organism
22 p3149 A72-42069
- Respiration control mechanism ensuring adaptation to power requirements and chemical environment maintenance in tissues, considering brain stem location
24 p3371 A72-44600

AUTONOMY

- Autonomous Hamiltonian system with two degrees of freedom, investigating origin and periodic orbits stability with two time variable method
01 p0123 A72-10030
- Maximal contraction points of autonomous nonlinear system phase trajectories, using van der Pol differential equations
18 p2674 A72-37149
- Analytical assessment of the accuracy of autonomous space navigation from measurements of the flight altitude and zenithal distance of one reference star
22 p3202 A72-42222

AUTOPILOTS

U AUTOMATIC PILOTS

AUTOPSIES

- Jurisdictional problems in the autopsy of aircraft accident victims.
17 p2639 A72-34558

AUTOROTATION

- Flat plate wing autorotation experiments about spanwise axis in low speed wind tunnel
04 p0462 A72-15117
- Attack helicopters engine failure problems, discussing flight test results in transition from powered high speed flight to autorotational flight
08 p1108 A72-21011
- Coning motion, autorotation, and vortex systems of slender flight vehicles
22 p3231 A72-42904
- Flight test investigation of the aerodynamic behavior of various-sized stabilizers on a small helicopter.
24 p3362 A72-45328

AUXILIARY ELECTRIC POWER UNITS

U AUXILIARY POWER SOURCES

AUXILIARY EQUIPMENT [COMPUTERS]

NT PLOTTERS

NT PRINTERS [DATA PROCESSING]

AUXILIARY POWER SOURCES

NT NUCLEAR AUXILIARY POWER UNITS

NT SPACE POWER REACTORS

NT SPACE POWER UNIT REACTORS

- Aircraft turbo-alternator speed control for constant frequency power supply, presenting theoretical relationships for electrohydraulic or mecano-hydraulic control loops
04 p0466 A72-15462

- Mirage 3E liquid propellant auxiliary rocket engine, discussing intercept performance enhancement
05 p0705 A72-16708

- Ion engine performance optimization by power sharing with secondary batteries on synchronous equatorial satellites
[AIAA PAPER 72-206]
05 p0706 A72-16852

- Reduced voltage relay operation in aircraft high voltage ac power systems, describing RLC circuit theory, laboratory test arrangement and performance measurements
15 p2204 A72-31215

- Military transport helicopter optimum secondary power system, considering onboard auxiliary power unit, electric or hydraulic engine start system, environmental control, etc
[AHS PREPRINT 664]
17 p2494 A72-34480

- Auxiliary power and electric propulsion applications of thermionic reactor power systems in manned and unmanned space missions
18 p2644 A72-36168

AUXILIARY PROPULSION

- Specific impulse, mass and propellant efficiency characteristics of miniature motors using cryogenic fuels for auxiliary rocket thrusters
07 p0914 A72-18983

- Communication satellites auxiliary propulsion systems surveyed for attitude and stationkeeping systems selection
[AIAA PAPER 72-515]
13 p2052 A72-28978

AVAILABILITY

- Time ratio models of equipment availability for using and procuring agencies, considering per-

- formance effectiveness criterion and suboptimization risk
24 p3467 A72-44659

AVALANCHE DIODES

- RF intrinsic and up or down-converted modulation noise mutual relationship with application to IMPATT diode oscillators
01 p0035 A72-10114

- Doping profile effects on reflection-type IMPATT diode microwave amplifiers, presenting power-gain vs frequency curves
01 p0037 A72-10643

- AM and FM noise reduction of cavity and injection stabilized microwave Gunn and avalanche diode oscillators
01 p0037 A72-10644

- Phase locked IMPATT diode microwave oscillator transients for reflection amplifier or pulse modulated source applications
01 p0037 A72-10646

- Wideband modulation feedback technique for IMPATT diode oscillator AM-FM noise suppression
01 p0037 A72-10647

- CW power of single cavity multiple IMPATT diode oscillator at 9.1 GHz, comparing with moding of multiple device oscillators
01 p0038 A72-10649

- X band power, bandwidth, efficiency and temperature performance of one watt CW microwave integrated avalanche diode oscillator
01 p0038 A72-10650

- Resonant traveling wave IMPATT oscillators wave propagation and power output characteristics, taking into account metal conductor and semiconductor substrate losses
01 p0038 A72-10651

- Broadband high efficiency mode /HEM/ TRAPATT amplifiers for S band, discussing bandpass and input-output characteristics with Ichebycheff filter
01 p0038 A72-10652

- Voltage and current waveforms monitoring on sampling oscilloscope for TRAPATT microwave oscillator performance optimization
01 p0038 A72-10653

- Microwave TRAPATT oscillator efficiency, using avalanche diode in coaxial cavity, slug and tapered sleeve
01 p0038 A72-10654

- Pulse IMPATT diode Ka band microwave rf head mechanically steered antenna array for airborne monopulse tracker applications
01 p0039 A72-10661

- Hybrid IC at 30 GHz, considering IMPATT oscillators, circulators, frequency multipliers and filters configuration and performance
01 p0046 A72-10699

- Gunn and IMPATT diodes applications for microwave power oscillators and amplifiers in radio link equipment
01 p0042 A72-10711

- Solid state components for millimeter wave systems, including IMPATT diode power sources and amplifiers, P-I-N diode modulators and switches and Schottky barrier mixers
02 p0192 A72-12183

- Read avalanche diode noise theory, showing carrier current modulation and lf and hf noise coupling in nonlinear regime
03 p0333 A72-13848

- Narrow band medium power X, Ku and C band solid state amplifiers, demonstrating TWT replacement with GaAs and avalanche diodes
03 p0334 A72-14072

- CW avalanche diode microwave oscillator frequency modulation, using injected rf signal
03 p0334 A72-14075

- Zener diode surface and bulk breakdown mechanisms by scanning electron microscopy, discussing microplasma noise
03 p0336 A72-14289

- High power reflection-type pulsed microwave amplifier using high efficiency antiparallel avalanche diode pair connected at transmission line ends
04 p0497 A72-14714

- Heat flow resistance measurement in avalanche diodes, noting junction temperature effect
04 p0498 A72-15133

- Avalanche transit time diodes noise mechanisms and performance in microwave amplifier, oscillator and mixer applications
04 p0500 A72-15302

- CW 100 GHz Si IMPATT diodes with nearly abrupt junctions, discussing output power and dc and small signal analyses
04 p0502 A72-15594

- Large signal IMPATT diode microwave oscillator lumped model, considering steady state oscillation
04 p0503 A72-15672

- Microstrip configuration for microwave GaAs IMPATT diode oscillators and power amplifiers
05 p0633 A72-15782

- Distributed unidirectional microwave IMPATT diode amplifier and CW tests for X and C band circuits
05 p0633 A72-15783

- Zener diode transient suppressors with electronic thermal switch for ground vehicle and aircraft applications
[AD-741529]
05 p0637 A72-16553

- Noise spectra of double sided CW silicon TRAPATT oscillator comparable to silicon IMPATT oscillator
06 p0783 A72-17482

- Noise effect in IMPATT and Gunn diode oscillators on phase/frequency fluctuation using series/parallel connected multiple active devices
06 p0783 A72-17483

- Double heat sinking high power CW TRAPATT diode oscillators using integral metallic heat spreaders
06 p0784 A72-17788

- Low noise IMPATT diode design for arbitrary signal levels, using Read model
06 p0787 A72-18382

- IMPATT diode avalanche region microwave self oscillation mechanism explanation by cavity resonator and feedback theories
06 p0787 A72-18383

- GaAs IMPATT diode with plated heat sink for microstrip circuit applications, exemplifying X band oscillator experiment
06 p0787 A72-18385

- High efficiency microwave avalanche diode oscillators circuit design in TRAPATT mode
06 p0787 A72-18455

- System potential of microwave solid state generation and amplification, comparing IMPATT, TRAPATT, Gunn, LSA, transistor and transistor-multiplier devices
06 p0787 A72-18456

- Computer simulation data on pulsed IMPATT microwave oscillator performance improvement via double-drift diodes and second harmonic tuning
06 p0788 A72-18463

- IMPATT diode microwave oscillators and amplifiers calculating noise sideband correlation factor at randomly large signal frequencies
06 p0788 A72-18464

- GaAs IMPATT diodes technology and performance at C, X and K band frequencies
06 p0788 A72-18466

- Millimeter wave GaAs avalanche diode oscillator processing on plated Cu heat sinking block resulting in epitaxially grown p-n junctions
06 p0788 A72-18467

- Harmonic power extraction from series-stacked high efficiency avalanche diodes at superhigh frequencies on simple microstrip circuits
06 p0788 A72-18468

- IMPATT diode oscillator injection locking behavior from model, comparing results with experiment
06 p0788 A72-18469

- IMPATT driven pumps replacement of klystron for parametric amplifiers producing over 100 mW at 38-40 GHz with good stability and noise performance
06 p0788 A72-18470

- X band IMPATT and Gunn oscillator, calculating injection lock time, modulation bandwidth, noise and FM suppression and dynamic response
06 p0788 A72-18471

- GaAs IMPATT diodes performance improvement, describing fabrication methods to achieve 6.7 watts output at 15 percent efficiency
06 p0789 A72-18474

- Power generation and low noise amplification devices development during past decade, considering avalanche diodes, transferred electron and acoustoelectric devices and microwave transistors
07 p0952 A72-18825

- Gigahertz reflection amplifiers with low cost avalanche transit time diodes, measuring characteristics of amplification by synchronization at center frequency
07 p0955 A72-19191

- Abrupt junction Si IMPATT diodes large signal analysis, discussing subharmonic modes and second harmonics effects
07 p0956 A72-19591

- I-V characteristics of junction transistors with avalanche breakdown mechanism
07 p0958 A72-19895

- High power negative resistance amplifiers, calculating relationship among output, gain, gain compression and efficiency for comparison with GaAs avalanche diode amplifier experiment
07 p0958 A72-19920

- IMPATT diode thermal resistance measurement from heat diffusion effect on small signal impedance of p-n junction
07 p0958 A72-20684

- IMPATT diode microwave oscillator stabilized by two external resonant circuits, investigating self oscillation characteristics
08 p1138 A72-20745

- Optimal output power of avalanche transit time diode oscillator in millimeter band as function of electric field and diode geometry
08 p1141 A72-21378

- Optoelectronic elements for information system applications, discussing photomultipliers, photodiodes,

photoresistors, avalanche and photoparametric diodes response and bandwidth characteristics
08 p1169 A72-21844

Subharmonically injected phase locked microwave IMPATT oscillator
09 p1285 A72-22894

Au-Si n and Al-Si p diodes noise operating in avalanche with charges injected by radiation
09 p1287 A72-23113

Noise characteristics and mechanisms in avalanche diodes and transferred electron devices
09 p1287 A72-23115

Avalanche diode background noise in linear and nonlinear regimes, emphasizing source dependence on oscillation level
09 p1287 A72-23117

LF noise spectral density measurements in avalanche diodes as function of frequency, considering mean square voltage drift
09 p1287 A72-23118

Background noise in amplification and oscillation in Si and GaAs avalanche diodes
09 p1287 A72-23119

Background noise at 200 Hz-1 MHz of avalanche effect voltage regulating diodes
09 p1288 A72-23120

IMPATT diode junction temperature measurement with accuracy from breakdown voltage by pulse techniques
10 p1449 A72-24304

Coupled line microstrip circuit for high power and efficiency L and S band TRAPATT diode oscillators
10 p1450 A72-24307

GaAs abrupt junction IMPATT diode large signal operation analysis, noting oscillation efficiency HF fall-off characteristics
10 p1450 A72-24557

Nonlinear microwave power amplifiers with IMPATT diodes in stable and injection locked modes, predicting behavior for comparison with experiment
10 p1451 A72-24592

German book on HF semiconductor electronics covering planar and field effect transistors, varactors, n-p, p-i-n, avalanche and Schottky barrier diodes, Gunn devices, etc
10 p1452 A72-24699

Computer simulation for TRAPATT circuit response to periodic current impulse, noting avalanche diode microwave oscillation efficiency
10 p1458 A72-24935

Stacked TRAPATT diodes oscillator with microstripline circuit to obtain 1 kw peak power at 1 GHz
12 p1788 A72-27163

IMPATT diode and transferred electron Gunn devices for systems applications, comparing thermal noise and physical properties
12 p1788 A72-27295

K band Read avalanche diodes fabricated by epitaxial deposition and diffusion processes, measuring capacitance-voltage characteristics and oscillator power efficiency
12 p1790 A72-27441

Computer aided circuit design by TRAPATT diode model consisting of nonlinear capacitance shunted by voltage- and current-controlled switch
12 p1791 A72-27672

C and X band CW GaAs Schottky barrier IMPATT oscillators with nichrome as barrier metal, noting high power efficiency and low noise performance
12 p1793 A72-27966

Pulsed IMPATT diode oscillators, pulse power capabilities, considering microwave circuit, dc and pulse biasing, power limitation and circuit anomalies
13 p1931 A72-29109

Avalanche photodiode optical detector noise amplitude distribution as function of operating conditions
13 p1971 A72-29924

Design and performance of microwave single stage relaxing avalanche diode reflection amplifier
14 p2088 A72-30918

Amplitude and frequency characteristics of avalanche diode microwave oscillator loaded with resonant circuits, noting Q value effect on self oscillations
14 p2089 A72-31109

EHF double-drift IMPATT oscillator small and large signal behavior analysis with computer program, noting second harmonic tuning and single frequency operation possibilities
15 p2204 A72-31314

Equivalent circuit characterization of waveguide-mounted IMPATT diode oscillators and associated circuit parasitics at millimeter wave frequencies
15 p2205 A72-31315

Temperature and electric field profiles in two TRAPATT diode structures in nonoscillatory state under dc bias, comparing geometrical limitations on diamond heat sinks
15 p2205 A72-31316

IMPATT diode junction temperature effects on operation explained by small signal analysis
15 p2206 A72-31545

Lf white noise voltage theory of avalanche diode extended to small multiplication M values and unequal hole and electron avalanche ionization coefficients
15 p2206 A72-31642

Avalanche photodiodes for Nd and injection lasers radiation detection, reducing noise equivalent power
15 p2247 A72-32035

Avalanche photodiode with n-p-pi double diffused reach-through structure for visible and near-IR regions, noting high efficiency, low noise and gain stability
15 p2248 A72-32036

Pulsed IMPATT diode oscillators RF oscillations growth rate and frequency shift behavior during buildup period, comparing equivalent circuit derived electrical properties with measurements
15 p2208 A72-32472

Phase and gain response of wideband coaxial X band microwave avalanche diode amplifiers
16 p2368 A72-33073

High efficiency and power S-band pulsed oscillator using avalanche diode and microstrip circuit
16 p2369 A72-33759

Transient 10 MeV electron radiation effects on RF power and recovery time of GaAs Schottky barrier IMPATT diodes
16 p2370 A72-33766

Noise-to-carrier ratio and rms frequency deviation evaluation for X band Gunn and Si and GaAs avalanche diode oscillators
16 p2370 A72-34177

BARITT, IMPATT, TRAPATT and Gunn diodes, discussing power, noise and thermal dissipation problems
17 p2526 A72-34465

Pulsed Impatt diode oscillator circuit design and operation frequency prediction for high Q coaxial structures from equivalent circuit
17 p2526 A72-34466

Avalanche diode oscillators.
17 p2526 A72-34563

Novel and accurate methods for measuring small-signal and large-signal impedances of IMPATT diodes.
18 p2664 A72-35997

Influence of carrier diffusion on the intrinsic response time of semiconductor avalanches.
18 p2717 A72-36083

Installation of a production line for high-reliability silicon diodes - Results obtained: Application of the underlying principles to more complex components
18 p2670 A72-37121

Endurance test results for microwave avalanche diode oscillators
18 p2671 A72-37146

K-band high power single-tuned IMPATT oscillator stabilized by hybrid-coupled cavities.
19 p2771 A72-37263

A C-band all ferrite integrated wideband high power GaAs avalanche diode amplifier.
19 p2771 A72-37264

Intermodulation characteristics of X-band IMPATT amplifiers.
19 p2771 A72-37265

A 22 percent C.W. efficiency solid state microwave oscillator.
19 p2771 A72-37266

Millimeter-wave solid-state exciter-modulator-amplifier module for gigabit data-rate.
19 p2771 A72-37267

The effect of junction temperature on the output power of a silicon IMPATT diode.
19 p2773 A72-38145

A solid-state transponder source using high-efficiency silicon avalanche oscillators.
19 p2774 A72-38400

Electrical properties and fabrication details of integral diode matrices with controllable avalanche breakdown produced from zone melted silicon under temperature gradient
19 p2774 A72-38416

Harmonic oscillation characteristics of avalanche Si diode with nonlinear and negative resistance characteristics
20 p2908 A72-39705

High-power microwave amplifier using IMPATT diodes.
20 p2909 A72-39776

IMPATT diode circuits operation as microwave amplifiers, presenting data on intermodulation distortion, amplitude to pulse modulation conversion and reliability
20 p2910 A72-39851

Current and voltage waveform measurements with sampling oscilloscope and capacitive voltage-divide probe to verify TRAPATT diode oscillator theoretical model
21 p3032 A72-40635

Analysis of large-signal noise in Read oscillators.
21 p3032 A72-40698

Optical direct detection using avalanche devices.
21 p3018 A72-40867

Effects of tunneling on an IMPATT oscillator.
21 p3034 A72-41382

Linear theory of a microwave distributed amplifier based on an avalanche transit-time diode
23 p3271 A72-43776

Reciprocal synchronization of generators connected by a long line section
23 p3272 A72-44210

X-band silicon double-drift IMPATT diodes using multiple epitaxy.
23 p3273 A72-44334

Microwave phase shifting with gain using IMPATT diodes.
24 p3385 A72-44963

AVANCHES
NT ELECTRON AVALANCHE
NT TOWNSEND AVALANCHE
AVERAGE

Averaging techniques for nonlinear integral and integrodifferential equations, considering standard equations with and without rapid and slow variables, asymptotic series application to unsolved problems
07 p1027 A72-19609

Orbit prediction for artificial satellites via numerical averaging technique, presenting algorithm for planetary equations solution
[AIAA PAPER 72-934]
21 p3112 A72-41572

AVIATION
U AERONAUTICS
AVIATORS
U AIRCRAFT PILOTS
AVIONICS

Avionics contribution to airspace decision making problems, considering navigation, surveillance radar, collision avoidance and ATC techniques
01 p0097 A72-10180

Variable speed constant frequency power generation equipment influence weapon system effectiveness, considering weight and cost
01 p0088 A72-11067

Electronic displays for attack aircraft, discussing subsystems, simulation technique and pilot role [DFVLR-SONDDR-140]
02 p0225 A72-11756

Aircraft and spacecraft integrated avionics systems design with emphasis on telemetry, discussing space shuttle subsystems integration
02 p0179 A72-12403

Aircraft integrated data systems, discussing cost effectiveness, reliability and maintenance
03 p0327 A72-13417

Computer simulation techniques in aerospace ground equipment design for maintenance testing of avionic systems
03 p0329 A72-14196

Bayesian analysis of onboard computer controlled aircraft avionic subsystem built-in test for failure detection
05 p0638 A72-16574

Book on mechanization and error analysis of inertial navigation systems, stressing terrestrial applications
06 p0845 A72-17944

Computerized modular automatic test equipment for commercial airliner avionics device performance, discussing data handling ability and cost effectiveness
06 p0796 A72-18250

Minimum frequency separation between avionics receivers and transmitters for acceptable interference level
08 p1131 A72-20929

Test pilot role in attack aircraft avionics systems integration consisting of head-up display, projected map, digital computer, inertial platform, radar and Doppler systems, etc
08 p1165 A72-21012

Sailplane computer displaying rate of climb simultaneously with airspeed for pilot determination of best strategy for local upcurrent-downcurrent conditions
09 p1316 A72-23550

Reliable interconnections for U.S. Army avionics, determining best technique for terminating flat conductor cables with electrical connectors
10 p1447 A72-24012

Avionics systems electrical interface connection design information document creation and dissemination, using EMPRENT computer program
10 p1453 A72-24864

RCA SECANT aircraft collision avoidance system avionics design using nonsynchronous techniques
10 p1509 A72-24866

Bell lifting rotor systems, examining company contributions in electronics and avionics
10 p1421 A72-24877

Operational aviation meteorological requirements, reviewing aircraft categories, ATC systems and avionics and navigational aids
10 p1508 A72-25078

Integrated display system design with navigation update, weapon delivery, reconnaissance, bomb damage assessment, threat and terrain avoidance capabilities for multicrew military aircraft
11 p1684 A72-26292

Aircraft microminiature ILS with transmitter and localizer antenna to provide pilot with bearing and glide slope information for alignment with runway
12 p1842 A72-27106

Training cockpit TL-29 mean time of failure-free operation from measurement data during development tests and two year guarantee, calculating avionics devices reliability

14 p2092 A72-30281

Avionics equipment for signal processing onboard civil aircraft to improve flight safety, discussing uses of OMEGA navigation system and digital computers

15 p2193 A72-31178

Book on electricity and electronics for aerospace vehicles covering theoretical foundations, measuring instruments, batteries, generators, motors, radio receivers and transmitters, navigation equipment, autopilots, etc

15 p2182 A72-31511

Error analysis for digital avionics system involving Doppler navigation by intermittent scanning of single beam multimode radar, noting optimum statistical data processing

15 p2271 A72-32204

Military systems cost reduction via civil avionics procurement techniques, discussing cost-reliability design criteria

15 p2338 A72-32215

Avionics effects on airline operations timekeeping, considering gains due to all-weather capability and engine monitoring vs possible losses due to equipment failures

15 p2208 A72-32461

Aircraft electronic display for pilot precise control in complex tasks, discussing clarity, stability and readability of CRT images

15 p2181 A72-32632

Civil helicopter electronic display requirements contrasted with fixed wing aircraft

15 p2182 A72-32633

Electronic displays with weapon aiming sensors in aircraft navigator-attack systems

15 p2273 A72-32634

Electronic display in future avionics systems, emphasizing computer techniques and digital data exchange systems

15 p2242 A72-32635

Aircraft CRT electronic displays discussing operational flexibility versus control and monitor complexities, economics, reliability and human factors

15 p2182 A72-32636

Univac 1832 multiprocessor avionics computer for airborne ASW, discussing input/output controllers and interfaces and IC design features

16 p2367 A72-33245

Flight training simulator criteria and design considerations, noting avionics, model aircraft, control console and teaching aspects

16 p2374 A72-33501

Aerospace instrumentation - Conference, Cranfield Institute of Technology, England, March 1972

16 p2393 A72-33626

Integrated airborne-ground based instrumentation system for variable stability X-22A aircraft flying qualities research, discussing telemetry, mobile van, landing aids and airplane design

16 p2348 A72-33628

Hybrid LSI logic modules for aerospace

17 p2527 A72-34683

S-3A Viking systems.

17 p2491 A72-34741

NAECON '72; Proceedings of the National Aerospace Electronics Conference, Dayton, Ohio, May 15-17, 1972.

17 p2493 A72-35551

Configuration and flight test of the only operational Air Force area navigation system.

17 p2578 A72-35557

Multifunction microwave apertures - Concepts and potential.

17 p2531 A72-35574

Modular avionics computer design concept to permit tailoring for diverse applications via microprogramming

17 p2524 A72-35581

Technical experience in operating the equipment in the IL-62 aircraft

17 p2558 A72-35791

Aircraft FDM and TDM systems, considering signal processing, cable requirements and applications to aircraft weapon systems and telemetry [SAE AIR 1207]

18 p2692 A72-36529

Recent research applicable to the design of electronic displays.

18 p2653 A72-36902

Integrity of flight control system design.

18 p2643 A72-37032

ATC IC transponder used with secondary surveillance radar, discussing design features

18 p2662 A72-37048

Development and optimization of the SRAM guidance and control software.

[AIAA PAPER 72-824]

20 p2951 A72-39102

Electronic primary flight control system requirements and equipment characteristics, discussing USAF and NASA fly by wire R and D programs [AIAA PAPER 72-882]

20 p2887 A72-39118

Missile guidance electronic packaging and module design for circuit protection against X rays, gamma radiation and nuclear blast damages

20 p2909 A72-39766

Weight saving, vibration proofing and heat dissipating techniques in avionics packaging, considering B-1 bomber electronic multiplexing system example

20 p2909 A72-39768

Choice of optimal geometrical relationships in a transformer-type angle converter

21 p3058 A72-41805

AVOIDANCE

NT COLLISION AVOIDANCE

Heat exposure effect on Sidman avoidance performance in rats, discussing organism thermoregulatory capacity disruption and shock and body temperature regulation

02 p0169 A72-12525

Existence theorems for dynamical systems admissible controls for avoidance of given set of state spaces, considering control process governed by ordinary differential equations

[ASME PAPER 72-AUT-C]

19 p2778 A72-37723

Aircraft interception avoidance problem solved by differential game theory, discussing human operator decision making for random pursuit tracking

24 p3377 A72-45523

AXES [COORDINATES]

U COORDINATES

AXES [REFERENCE LINES]

NT AXES OF ROTATION

NT EARTH AXIS

Force system axial equilibrium conditions for reference coordinates to eliminate inadmissible axes, deriving theorem for applicability limits

02 p0260 A72-12439

AXES OF ROTATION

NT EARTH AXIS

Control axes misalignment effects on spinning satellite wobble damping and requirements for active momentum exchange controllers

02 p0286 A72-12267

Stability of plane rotating galaxies in magnetic field parallel to axis of rotation, showing linearized MHD equations self conjugate for radial disturbance case

03 p0435 A72-13806

Flat plate wing autorotation experiments about spanwise axis in low speed wind tunnel

04 p0462 A72-15117

Hodograph geometrical analysis of heavy gyrostal motion for center of mass and gyrostatic moment located on first and third principal axes of rotation

08 p1208 A72-21352

Descriptive geometric method for distribution of axes of uniform rotation of body containing ideal homogeneous incompressible fluid in uniform turbulent motion

08 p1209 A72-21364

Notched bend test crack opening displacement gage for continuous measurement of apparent rotation axis and true displacement location at crack tip

10 p1483 A72-24885

Moment of inertia of earth atmosphere relative to earth axis of rotation

11 p1622 A72-25974

Hove gyroscope on base uniformly rotating about axis perpendicular to drive axis, considering forced motion elimination possibility

13 p1961 A72-30023

Permanent rotation of force-free gyroscope characterized by outer framework constant angular velocity, defining permanent axes of rotation

15 p2275 A72-31493

Time dependent orthogonal coordinate system rotation by unit vector along effective axis, obtaining angular velocity and effective angle interpretation

15 p2275 A72-31590

Hydromagnetic flow between two rotating disks with noncoincident parallel axes of rotation.

19 p2841 A72-38436

On the existence of an instantaneous rotation axis during the motion of a solid body with a constant point in Euclidian n-dimensional space.

19 p2835 A72-38635

AXIAL COMPRESSION LOADS

Upset steel cylinders under axial compression loads, determining localized surface stress and strain critical values at fracture

01 p0141 A72-11032

Minimum weight web-core sandwich panels under axial compression loads, presenting numerical results for boron-epoxy and graphite-epoxy composites

01 p0142 A72-11131

Glass fiber surfaces of revolution under axisymmetric pressure loads combined with centrifugal forces

01 p0143 A72-11365

Thin circular cylindrical shells under uniform axial compression loads, examining axially symmetrical creep buckling

02 p0296 A72-12531

Random search method application to optimal design of closed circular cylindrical shells under axial compressive loading

04 p0587 A72-15020

Axially compressed semi-sandwich corrugated ring-stiffened cylindrical shell crippling local buckling and general instability prediction by finite difference energy method

[AIAA PAPER 72-138]

05 p0740 A72-16892

Laminated anisotropic imperfect circular cylindrical shells under axial compression, obtaining upper bound buckling load solution

[AIAA PAPER 72-139]

05 p0740 A72-16893

Small deflection theory for dynamic elastic buckling of stringer-stiffened cylindrical shells under axial impact, discussing optimum stiffener geometry

05 p0742 A72-17248

Nickel base alloy under axisymmetric tension compression tests, obtaining breaking load diagrams and fatigue and creep curves

06 p0833 A72-18638

Axially compressed cylindrical shells with axisymmetric imperfections, analyzing random buckling behavior and failure probability by statistical methods

07 p1089 A72-19689

Buckling under uniaxial compressive load of structural sections and stiffened flat plates reinforced with laminated composites

07 p1090 A72-19732

Freely supported three layer cylindrical panel stability and critical loads under combined uniform axial compression and transverse pressure

08 p1242 A72-20907

Polycarbonate yield dependence on temperature in uniaxial compression and tensile tests described by modification of Eyring theory of non-Newtonian viscosity

08 p1191 A72-21184

Stability and postbuckling equilibrium of nearly cylindrical shells of revolution under axial compression

08 p1244 A72-21291

Glass fiber reinforced plastics irreversible cumulative damage under axial cyclic tension compression loads with heat production

08 p1191 A72-21500

Elastic filler rigidity effect on cylindrical glass fiber reinforced plastic shells stability loss and critical load value under axial compression

08 p1245 A72-21503

Dynamic buckling of shallow circular cylindrical hinged panel under axial compression

08 p1249 A72-22087

Nonuniformly heated infinite elastic cylindrical shell stability under axial compression loads

09 p1402 A72-22734

Continuously supported railroad track under axial compression forces and moving load, noting critical velocity for high speed trains

09 p1409 A72-23558

Critical compressive buckling and stability of straight beams under axial and transverse loads calculated by three unknowns methods

10 p1560 A72-25121

Asymmetrically stiffened elastic cylindrical shells under axial compression, calculating critical loads for various end conditions

11 p1733 A72-25541

Finite element method for buckling coefficients of isotropic rectangular plate subject to linearly varying axial compression, using general linear geometric matrix

11 p1736 A72-25999

Computer calculation of minimum weight ribbed plates under axial compression by random search method and linear programming

12 p1878 A72-27083

Stability of transversely isotropic cylindrical shell with elastic filler under axial compression, deriving approximate equations for transverse shear stress effect

13 p2055 A72-28556

Combined axial compression and shear deformation effect on elastic columns buckling behavior, evaluating third order polynomials eigenvalues by computerized Newton-Raphson technique

14 p2168 A72-30934

Random temperature variations effect on life of Euler column with sandwich cross section under constant axial compressive load, using Norton nonlinear creep law

15 p2324 A72-31494

Axially compressed cylindrical shells buckling behavior, deriving formula based on equivalent axisymmetric imperfections concept in terms of shell radius/thickness ratio

15 p2331 A72-32553

Particulate composite model deformation and failure behavior under plane uniaxial compressive stress, using finite element method

15 p2258 A72-32556

Small nonaxisymmetric initial shape deviations effect on creep buckling and critical time of thin walled circular cylindrical shell in axial compression

16 p2474 A72-34134

Asymptotic singular perturbation solution to thick spherical shell with circular hole under axisymmetric external pressure

16 p2474 A72-34157

Geometric instabilities in isotropic plastic solids under increasing uniaxial compression.
[ASME PAPER 72-APM-28] 17 p2624 A72-34310

Dynamic buckling of shallow circular cylindrical hinged panel under axial compression
17 p2626 A72-34665

Buckling of a circular cylindrical shell in axial compression and SS4 boundary conditions.
17 p2632 A72-35236

Buckling of an elastic cylindrical shell during longitudinal impact against an obstacle
19 p2870 A72-37322

Synthesis of optimal cylindrical reinforced-plastic shells under external pressure and axial compression
19 p2872 A72-37534

Loading rig in which axially compressed thin cylindrical shells buckle near theoretical values.
19 p2783 A72-37730

Axissymmetric impact of compactible rods subjected to finite deformations.
21 p3117 A72-40455

Buckling of plates and cylindrical panels under the action of axial dynamic compression
22 p3232 A72-41923

Buckling of circular cylindrical shells under axial compression.
22 p3239 A72-42840

Axissymmetric-multilobe creep buckling transition in thin walled circular cylindrical shells under uniformly distributed axial compressive load
22 p3239 A72-42844

Buckling of integrally stiffened cylindrical shells - A review of experiment and theory.
22 p3239 A72-42846

Longitudinal rib reinforced cylindrical shell under axial compression loads, determining equilibrium stability with approximation of transcendental equations
23 p3347 A72-43748

Post-buckling of axially compressed plates.
24 p3455 A72-44632

AXIAL COMPRESSORS
U TURBOCOMPRESSORS
AXIAL FLOW

Sound radiation from axial flow fans running in turbulent flow, evaluating fluctuating lift on rotor blades due to incident gusts
01 p0002 A72-10220

He-Ne traversing laser velocimeter for instantaneous axial fluid velocity measurement, describing signal analyzing system, construction and calibration
02 p0224 A72-11744

Axial flow effect on vortex filaments stability by slender body analysis of force balance between Kutta-Joukowski lift and momentum flux inside filament
[AD-740965] 03 p0307 A72-13157

Underexpanded nitrogen jet from sonic orifice, investigating axial rotational temperature distribution
04 p0597 A72-15335

Axial flow multistage compressor design, discussing high speed flow measurements and Reynolds number and blade airfoil shape effect on aerodynamic performance
05 p0601 A72-16483

Argon plasma transient axial flow and heating characteristics in pinched column of linear z-pinch device with collapsing current sheets conversion to axial streaming velocity
[AIAA PAPER 72-208] 05 p0696 A72-16886

Blading, flow and characteristic line calculations for machine with axial turbulent flow, using plane cascade measurements
06 p0757 A72-18690

Axial flow turbomachines three dimensional flow theory, using orthogonal curved coordinate system
07 p0910 A72-20104

Bushing seal with pressure dependent clearance for reciprocating piston rod or rotating shaft, presenting laminar and turbulent axial flow theory
08 p1178 A72-21936

Free turbulent jet heat and mass exchange and axial flow characteristics
09 p1292 A72-22235

German monograph on experimental investigations of annular channels with axial flow of incompressible fluids covering graphical and computational determination of flow volume
09 p1293 A72-22332

Jet flaps for high turning compressor cascades in incompressible axial flow, calculating blade pressure and jet slope distributions
11 p1569 A72-25615

[ASME PAPER 72-GT-16]

Screw type axial flow pump impellers pressure losses generalization by dimensionless coefficient in Euler number form
12 p1752 A72-28139

Navier-Stokes equation for rotating liquid axial flow past porous plate, noting velocity distribution for suction and thinning effect for blowing
13 p1942 A72-29127

Ideal gas supersonic axial flow past circular cylinder, solving Navier-Stokes equations by Van Dyke matched asymptotic expansions method
15 p2178 A72-31463

Experimental and two-dimensional computational study of end losses from a theta pinch.
17 p2592 A72-35628

Three-dimensional non-free vortex flow in axial fans.
17 p2487 A72-35896

Comparison of two types of blade profile for axial-flow fans
18 p2720 A72-36000

The acoustics of axial flow machines.
18 p2685 A72-37204

Interaction effects between blade rows in turbomachines.
19 p2745 A72-37275

The motion of a vortex filament with axial flow.
19 p2786 A72-37598

Nonaxisymmetrical disturbances effect on stability of cylindrical fluid flow with exponential density variation in radial direction and axial and azimuthal velocities
21 p3045 A72-40682

Effect of the ratio of the axial-flow velocities in front of and behind the cascade on the aerodynamic coefficients of a plane compressor cascade
24 p3360 A72-44995

A study of loss of radial equilibrium solution in axial-flow blade row design calculations.
24 p3393 A72-45358

Influence of revolutions on efficiency and characteristics of the rotating axial cascade of blades.
24 p3363 A72-45361

A method for estimation of axial turbomachinery stage characteristics on the basis of experimentally obtained data with a runner tested in a free blow-out aerodynamical scheme.
24 p3363 A72-45364

Some experiences with the solution of potential flow in the plane cascade on the computer.
24 p3393 A72-45365

An approximate method for the calculation of the characteristics of axial-flow fans.
24 p3363 A72-45369

Experimental research on the wave resistance of a thin spindle with an annular shield in a supersonic axial flow
24 p3364 A72-45393

Aerodynamic characteristics of turbine blade cascades in unsteady incompressible and compressible fluid flow, considering axial flow turbine blades vibration
24 p3364 A72-45524

AXIAL FLOW COMPRESSORS
U TURBOCOMPRESSORS
AXIAL FLOW PUMPS
NT TURBINE PUMPS
AXIAL FLOW TURBINES

Estimation method for surface pressure distribution on cascade airfoil in retarded flow, applying to axial flow turbomachines design with suction performance and efficiency
01 p0001 A72-10396

Nonuniform flow along axial turbomachine blades, presenting pressure loss evaluation method under boundary layer effect on external walls
01 p0002 A72-11271

Vortex flow structure in axial gas turbines near inlet and outlet of blade row
03 p0307 A72-13538

Velocity field induced by blade row in axial flow turbine
06 p0755 A72-17844

Axial turbine three dimensional flow across blading compatible with velocity distribution, establishing mean surfaces of revolution equation
06 p0755 A72-17849

Temperature measurements of axial gas turbine rotor for start-up heating and cooling tests
08 p1223 A72-20953

Aerodynamic efficiency of plane slotted blade cascades of adjustable nozzle diaphragms in transport aircraft axial flow gas turbine engines
09 p1374 A72-23186

German monograph on flow calculation in axial thermal turbomachines covering boundary conditions and field computation for steady state inviscid flow
10 p1415 A72-23772

Hydraulic tank application to internal flow visualization in turbomachinery, describing test equipment and methods used for axial flow model
10 p1419 A72-24654

Equations of motion of steady viscous fluid flow in three dimensional boundary layer on walls of axial flow compressors and turbines, obtaining velocity field
10 p1420 A72-25120

Lift and pressure fluctuations of cambered airfoil under periodic longitudinal and transverse gusts, applying to axial flow turbomachines
[ASME PAPER 72-GT-30] 11 p1569 A72-25626

Gas-particle flow trajectories, velocities and pressure distribution in axial flow turbine stage, using cascade tunnel and high speed photographic techniques
[ASME PAPER 72-GT-57] 11 p1571 A72-25648

Axial flow turbines aerodynamic loading increase via control of velocity distribution and boundary layer evolution around airfoil profiles
[ASME PAPER 72-GT-78] 11 p1571 A72-25658

Computer program in ALGOL 60 language for calculation of long blades twist in axial flow turbines and compressors
13 p1893 A72-28782

Swirling flow effects on annular conical diffuser performance in axial flow turbomachines, showing stagnation region and inner body diameter dependence
14 p2069 A72-30580

Blade tip losses in bandaged axial turbines, noting effects of Mach number, initial flow turbulence and geometry
15 p2179 A72-31701

Linear acoustic model to predict axial flow turbomachinery aerodynamic sound generation including flow effects on radiation
19 p2788 A72-38568

Effect of the slope and curvature of meridional current lines on the long-blade twist in axial turbomachines
20 p2979 A72-39588

Determination of the statistical characteristics of a turbine stage and a group of turbine stages
23 p3328 A72-44295

Performance and flow properties change through a rocket turbine by presence of solid particles.
24 p3361 A72-45206

AXIAL LOADS
NT AXIAL COMPRESSION LOADS

Thin walled prismatic structural members under uneven axial moment distribution, formulating force deflection equations for torsional-flexural behavior
01 p0141 A72-11049

Static and dynamic buckling behavior of clamped shallow conical shells under axisymmetric loads
02 p0291 A72-11963

Stress concentration factors for fiber and matrix in axially loaded unidirectional composite with discontinuous fiber, using linearly elastic finite element analysis
02 p0292 A72-11987

Axissymmetric load influence on stability of eccentrically reinforced shells of revolution, determining critical loads and linear and nonlinear relations for moment-subcritical states
04 p0587 A72-15014

Semiinfinite elastic solid response to arbitrary axially directed line load, transforming simultaneous partial differential equations by Hankel transforms
[ASME PAPER 71-APMW-1] 04 p0589 A72-15180

Plates in uniaxial compression with various support conditions at unloaded boundaries, predicting behavior after buckling
04 p0591 A72-15288

Mechanical behavior of uniaxially loaded multilayered oriented fiber cylindrical composites, observing tensile transverse stresses
[ASME PAPER 71-MET-O] 05 p0732 A72-15792

Ring finite elements use in analysis of shells of revolution under axisymmetric loads
[ASME PAPER 71-WA/HT-22] 05 p0732 A72-15880

Elastic analysis of circular cylinders with stress singularities from boundary discontinuities, mixed displacement and axial load conditions
[ASME PAPER 71-WA/APM-18] 05 p0733 A72-15962

Column axial load carrying capacity optimization vs structural weight, using finite element displacement method for buckling load, mode shape and strain energy density
[AIAA PAPER 72-141] 05 p0740 A72-16894

Low frequency biaxial load effect on stress concentration factors for circular and elliptical holes in Plexiglas plates
06 p0898 A72-18350

Plasticity of Al alloy thin walled tubular specimens under axial tension and internal pressure at 293, 173 and 93 K
06 p0833 A72-18561

Deformability and strength of soft fiber reinforced plastics under biaxial tension, determining low temperature critical tensile stresses and elongation ratios
06 p0836 A72-18562

Fatigue testing machines for axial and torsional loadings at low temperatures in vacuum
06 p0797 A72-18667

Creep buckling of simply supported initially slightly curved column under variable axial load, describing deflection up to critical point
07 p1088 A72-19168

Axial impact of semiinfinite elastic cylindrical shell filled with inviscid compressible fluid, obtaining equations of motion
08 p1149 A72-21166

Stresses, strains and moments interrelationship in axisymmetrically loaded circular cylindrical shell under unsteady creep conditions
09 p1401 A72-22729

Fatigue fracture of polymethyl methacrylate at room temperature under uniaxial failure cyclic loading
09 p1339 A72-23244

Elastoplastic deformation of Zn single crystals under uniaxial tensile loads, noting critical stresses relationship to current pulses
10 p1553 A72-23766

Parametric dynamic stability equations and boundary conditions for thin walled open cross section beam under axial load, taking into account longitudinal deformation effect
[ASME PAPER 71-APM-LL] 10 p1554 A72-24184

Maximum dynamic to static deflection ratio for thermally induced vibrations of elastic beams and plates, considering damping and axial load effects
[ASME PAPER 71-APM-UU] 10 p1554 A72-24185

Transient strain in axially impacted hollow non-homogeneous cone with axially varying modulus of elasticity and density 10 p1555 A72-24195

Fiber reinforced materials mechanical properties calculation, taking into account various fiber orientations and multiaxial loads 10 p1501 A72-24493

Rigidity calculation of double row radial thrust angular ball bearing loaded by axial and radial force and torque 11 p1646 A72-26978

Elastic truncated thin conical shell response to dynamically applied axial force from numerical solution of nonlinear equations 12 p1881 A72-27244

Asymptotic stability of mechanical system with two mathematical pendulums and rod subjected to axial follower, correcting aerodynamic and dissipative forces 12 p1847 A72-27979

High modulus fiber composite circular tube specimens multiaxial load testing, noting gripping methods to reduce transitional strains 12 p1886 A72-28000

Thin walled tubular carbon steel specimen deformation pattern under biaxial tension and internal pressure at normal and low temperatures 12 p1830 A72-28227

Heated three layer plate with load-carrying layers of different materials, thicknesses and temperatures, calculating stability under uniaxial tension 13 p2055 A72-28736

Stress-service life relations for duralumin samples from impact and nonimpact tensile tests with cyclic axial loads, noting notch sensitivity 13 p1978 A72-29147

Axissymmetric geometry and load finite element structural analysis of isotropic elastic materials for parametric and optimization studies 13 p2062 A72-29875

Dynamic behavior of thin walled semiinfinite elastic cylindrical shell with liquid under axial impact loads 13 p1943 A72-30008

Large deflection calculation of circular and annular strain hardenable rigid plastic plates under axisymmetric load, using Kirchhoff-Love hypothesis and Tresca flow condition 14 p2165 A72-30440

Tubular materials plane stress-strain test facility for combined axial load and internal pressure effects, describing principal components 14 p2092 A72-30442

Average stress and strain across thickness of liquid filled cylindrical elastic thin walled shell with rigid bottom under axial impact loads 14 p2166 A72-30698

Time to failure under axial tension determined for gallium selenide single crystals at constant temperatures, noting tensile strength dependence 15 p2290 A72-31387

Elastoplastic stress concentration near elliptic hole in plate loaded in smallest axis direction 15 p2325 A72-31606

Variable rigidity effects of ball bearings on axial loading stability and failure of gyromotor supports 15 p2235 A72-31898

Stress concentrations in cylindrical shells with cut-outs under uniformly distributed axial tensile load, presenting exact solution of differential equation 15 p2328 A72-32138

Stress-strain diagrams for orthotropic glass fiber reinforced plastic plates with circular hole under uniaxial tensile load 16 p2471 A72-33681

Brittle creep rupture process in beam subjected to simultaneous loading with bending moment and axial force 16 p2474 A72-34128

Lateral deflection of axially loaded imperfect bar under creep, solving nonlinear integrodifferential equations by quasi-linearization technique 16 p2474 A72-34130

Static and tension fatigue and free edge delamination damage induced by uniaxial tensile loads in flat graphite/epoxy laminate coupons 17 p2571 A72-35291

Nonstationary parametric response of a nonlinear column. 18 p2738 A72-37079

Anisotropic circular cylinder stress analysis under uniaxial load, calculating elastic deformation 19 p2872 A72-37536

Stress redistribution caused by creep in a thick walled circular cylinder under axial and thermal loading. 19 p2874 A72-37716

Shells of revolution free of bending under uniform axial loading. 19 p2876 A72-37886

Finite element large deflection analysis of elastic-plastic shells of revolution subjected to axisymmetric loading. 20 p2982 A72-40064

Stability and non-stationary vibration of columns under periodic loads. 21 p3116 A72-40336

Influence of discontinuity stresses on main propellant tankage of a space shuttle orbiter. 21 p3121 A72-41211

Battened columns out-of-plane buckling under axial loads and/or moments, deriving relationship between applied loads and section characteristics 21 p3121 A72-41211

Simply supported column dynamic stability under axial periodic load, discussing external viscous damping effect 21 p3121 A72-41242

Dynamic behavior of thin walled semiinfinite elastic cylindrical shell with compressible liquid under axial impact loads 22 p3167 A72-42736

Longitudinal-torsional vibrations of a screw beam under axial excitation 22 p3240 A72-42954

Application of cylindrical samples to the determination of the resistance to crack propagation of materials 22 p3242 A72-43163

Limiting equilibrium of shallow conical shells of variable thickness 23 p3348 A72-43787

Strain-rupture criteria for simple and complex loads 23 p3349 A72-43954

Dynamic buckling of axially stiffened imperfect cylinders under axial impulse. 24 p3453 A72-44602

Nonlinear theory for static analysis of moderately thick circular cylindrical shells under axisymmetric loads applied to pyrolytic graphite 24 p3454 A72-44603

Bending evaluation of test section in tensile tests with axial loads and resistance strain gages, noting friction moment role 24 p3456 A72-44791

AXIAL STRAIN

Neo-Hookean material circular plate under finite axisymmetric stretching, showing approximately constant deformed thickness 04 p0590 A72-15196

Axissymmetric stress analysis in various weld configurations of stub end high pressure pipe connections, using finite element method 06 p0820 A72-17709

Elasticity and potential theory axisymmetric problems solution for sphere and spherical cavity, constructing x-analytic functions for boundary surfaces 08 p1242 A72-20908

Uniaxially stressed elastic /soft/ shells with fold formation during compressive strain, formulating equilibrium and boundary conditions for uniaxial region 08 p1247 A72-21812

Fiber thermoplastics matrix breakdown and mechanical properties enhancement, examining lateral and longitudinal strain during uniaxial tensile creep and recovery [PI PAPER 4] 09 p1337 A72-22541

Two dimensionally reinforced quartz-phenolic composite material dynamic fracture behavior under stress wave loading in uniaxial strain, noting spallation threshold time dependence 11 p1669 A72-25291

Room temperature uniaxial tension tests for elastic deformation of steel samples, showing quadratic stress-strain function 13 p1977 A72-29008

Elastic-plastic medium with doubly periodic square array of circular cylindrical voids, obtaining finite element solution for uniaxial deformation by variational principle [ASME PAPER 72-APM-36] 17 p2628 A72-34784

Axial-symmetric deformations of a rubber-like cylinder under initial stress. 18 p2738 A72-37081

Zero-moment reinforced axisymmetric shells 19 p2876 A72-38155

Method of sources for solving axisymmetrical problems in the theory of elasticity 19 p2877 A72-38202

Determination of stresses along the symmetry axis in the isometric problem on the basis of an elastooptical image of isochromes 21 p3122 A72-41347

AXIAL STRESS

Experimental development of homogeneous field of plane stresses gripped in biaxial traction, considering convex models under constraint 01 p0142 A72-11176

Finite element technique for stress analysis of rotating bodies under axially symmetric stresses 02 p0293 A72-12343

Nonlinear creep of glass fabric-plastic composite under loading in uniaxial stressed state 02 p0250 A72-12676

Stress concentration at circular, elliptical, square, rectangular and triangular holes in isotropic plates stiffened by discontinuous elements under uniaxial tension 03 p0452 A72-14133

Stress concentration at hypotrochoid hole in cylindrical shell under internal pressure and axial tensile stresses 03 p0453 A72-14138

Cyclic deformation and fatigue testing equipment and techniques for biaxial stress, stress concentration and pure bending 03 p0339 A72-14168

Plastic strain and rupture characteristics of thin walled tubular Ni samples under complex loading and biaxial tension 04 p0588 A72-15058

Dynamic theory of thin elastic beams under large deflection, taking into account shear deformation and axial stress resultants [ASME PAPER 71-APM-EE] 04 p0590 A72-15183

Uniaxial stress effect on monocrySTALLINE niobium stanide superconducting transition temperature, considering crystal structure 04 p0562 A72-15293

Stress-strain characteristics of nylon-polyurethane coated fabric under biaxial tension and shear forces 05 p0736 A72-16108

Principle stress errors in biaxial stress fields expressed in terms of transverse sensitivity, stress and Poisson ratios of material during strain gage calibration 06 p0895 A72-17798

Biaxial bending solution by tangent stiffness matrix method suitable for computer application 06 p0897 A72-17967

Cylindrical shell under internal pressure, detailing axial thermal stresses relaxation 06 p0900 A72-18669

Interaction surfaces for structural members under combined axial, shear force and bending moment, investigating shear effect on yielding of arches 07 p1090 A72-19730

Heat absorption and liberation by glass fabric laminates under uniaxial tension, determining thermal effects dependence on strain rate and test temperature by calorimetric measurements 08 p1195 A72-21853

Normal axial impact of thin liquid filled elastic cylindrical shell with rigid bottom on compressible fluid half space surface 09 p1350 A72-22207

Photoelastic measurement of stress concentration in three dimensional fiber reinforced brittle plastic matrix under uniaxial tension [PI PAPER 1] 09 p1398 A72-22538

Axial thermal stresses in beams, investigating error in elementary calculations 09 p1405 A72-22999

Ti, Zr, Mo, B and Mn additives effect on rupture characteristics of cast Al-Mg alloy under uniaxial tensile stress 09 p1328 A72-23033

Plastic deformation effect on structure and properties of steel sheet under biaxial tension at liquid nitrogen temperature 09 p1330 A72-23187

Transfer matrix method application to rocket vehicles structural dynamics, incorporating axial and aerodynamic lift forces in vibrational analysis 09 p1397 A72-23499

Dynamic response of pressurized thin walled circular cylindrical shell under initial biaxial stress and subjected to radial uniformly moving force, noting transient and steady state [ASME PAPER 71-APM-GGG] 10 p1554 A72-24186

Initially axially stressed Timoshenko beam equations of motion derived from three dimensional theories, discussing buckling loads and vibration frequencies 10 p1555 A72-24191

Metal creep under multiaxial stress states, proposing technique for numerical stress analysis data collection [SMRT PAPER 1.1/3] 10 p1556 A72-24395

Stability loss in thin convex shells of revolution under axisymmetric stress, obtaining integrals for equilibrium equations 10 p1557 A72-24630

Crystal grain size effect on fracture initiation in mild steel under triaxial stress, using notch tests at low temperatures 11 p1657 A72-25756

Velocity behavior of shear waves propagating in uniaxially prestressed isotropic elastic body 12 p1886 A72-27982

Recombination luminescence in irradiated Si, investigating uniaxial stress and temperature variations effects 12 p1858 A72-28061

- Uniaxial compressive stress apparatus for InSb investigation at low temperatures in large magnetic fields 13 p1959 A72-29753
- Plastic flow, yield strength and fracture of unidirectional Al-B fiber composite sheet under biaxial tension 16 p2411 A72-33821
- Buckling of shells with cutouts - Experiment and analysis. 17 p2634 A72-35405
- Creep fracture theory investigating ratio of ultimate creep rupture time to latent failure under multiaxial states of stress 19 p2874 A72-37704
- Experimental analysis of the stress distribution in the vicinity of a nonwelded rigid circular inclusion in the interior of a plate stressed in monoaxial tension 23 p3346 A72-43691
- Low cycle fatigue under biaxial strain controlled conditions. 23 p3354 A72-44259
- A comparison of the axial and reversed-torsional strain cycling low-cycle fatigue strength of several structural materials. 23 p3304 A72-44397
- Stress concentration of a cylindrical shell with one or two circular holes. 23 p3355 A72-44399
- AXIOMS**
- Axiomatic determination of dynamic logic control systems based on Moore automaton elements and combined continuous and finite models 06 p0781 A72-18660
- Axiomatic development of mechanics from geometrically formulated kinematics to statics of rigid bodies and systems, using virtual rate of work and reaction principles 13 p2000 A72-28477
- AXISYMMETRIC BODIES**
- Attitude motion at equilibrium libration points of axisymmetric smallest body in restricted three body problem 01 p0123 A72-10011
- Radiative heat transfer between gas flow and axisymmetric ablating body near stagnation point, considering ablation products effects under boundary layer chemical equilibrium conditions 02 p0300 A72-11577
- Computer algorithm of initial functions for elastic thick finite hollow axisymmetric cylinders under static conditions 02 p0288 A72-11604
- Multivortex model of vortex sheet development on slender axisymmetric bodies at angle of attack 03 p0307 A72-12919
- Unitary stress state and deformations in rotating axisymmetric disk, using function applicable to axisymmetric pipes 04 p0584 A72-14471
- Tangential blowing and wall cooling effects on axisymmetric models flow separation at Mach 6, comparing pressure distribution with Busemann formula 05 p0601 A72-16227
- Two dimensional and axisymmetric body viscous drag in incompressible flows, using implicit finite difference boundary layer method [AIAA PAPER 72-1] 05 p0606 A72-16860
- Axisymmetric bodies with discontinuous curvature in transonic flow, calculating surface pressure distribution [AIAA PAPER 72-137] 05 p0606 A72-16891
- Conirolis force effect on axially symmetric body oscillating slowly along axis in rotating viscous fluid 05 p0610 A72-17081
- Spin stabilized axisymmetric probe attitude deviation due to solar pressure in elliptic orbits 06 p0892 A72-17655
- Cornered axisymmetric blunt body sonic line in steady supersonic flow, showing incomparability with sonic shoulder of sphere 06 p0757 A72-18138
- Axisymmetric grid plate bending and torsion under normal forces and moment vectors loads, determining stress-strain state from finite difference equations 09 p1398 A72-22692
- Periodic axisymmetric waveguide with complex structure, obtaining slow wave dispersion equation solutions 10 p1439 A72-24901
- Direct numerical integration scheme for viscoelastoplastic response of isotropic axisymmetric shells under impulsive loads [AIAA PAPER 72-400] 11 p1731 A72-25421
- Nose blunting, exposure time and initial temperature effects on axisymmetric bodies ablation surface cross hatching patterns, presenting test results on cones with various vertex angles 11 p1572 A72-26006
- Finite difference method for free vibration of axisymmetric shells, using inertia force terms in shell bending theory equilibrium equations 11 p1737 A72-26429
- Mixed variational formulation and finite element method for axisymmetric cylindrical, conical, spherical and ellipsoidal shells 12 p1879 A72-27195
- Skin friction response to angle and perturbation in flow past axisymmetric body with unsteady main stream 13 p1941 A72-28887
- Axisymmetric geometry and load finite element structural analysis of isotropic elastic materials for parametric and optimization studies 13 p2062 A72-29875
- Hypersonic flow of nonequilibrium ionized monatomic inviscid radiating gas past axisymmetric blunt body with allowance for electron and ion temperatures difference 13 p1895 A72-29877
- Axisymmetric satellite rotation about center of mass in circular orbit under Newtonian gravitational field, considering precessional stability 13 p2052 A72-30002
- Axisymmetric celestial bodies equilibrium shapes in post-Newtonian approximation of general relativity using integrodifferential equation 14 p2161 A72-31077
- Shear stress distribution and local heat flux at surface of axisymmetric bodies for laminar and turbulent boundary layer flows 14 p2071 A72-31163
- Axisymmetric flight vehicles motion stability and transient behavior via Liapunov method, taking into account nonlinear characteristics 15 p2318 A72-31203
- Longitudinal and circumferential boundary layer characteristics for concave and convex axisymmetric bodies at small angles of attack, using Cooke equivalent radius concept 15 p2177 A72-31205
- Axisymmetric convergent cone profile synthesis to transform parallel flow at inlet to uniform sonic flow at outlet, examining solution convergence 15 p2177 A72-31206
- Collection efficiency of conical and blunted axisymmetric power law bodies in hypersonic flight through dust clouds and of impact angle and velocity 15 p2180 A72-32580
- Monte Carlo simulation method for flow field around two dimensional or axisymmetric body immersed in hypersonic rarefied gas flow 16 p2342 A72-32882
- Stress analysis of axisymmetric solids with asymmetric properties. 17 p2632 A72-35227
- Hydromagnetic boundary layer flow around an oscillating axisymmetric body. 18 p2683 A72-36932
- Incompressible potential flow solution for axisymmetric body-duct configurations. 18 p2683 A72-36940
- Classical plate theory for variable-thickness isotropic elastic axisymmetric circular plates in partial contact with each other and with rigid smooth surfaces of revolution 18 p2738 A72-37072
- Constant strength shells theory generalization from axially symmetric to nonsymmetric case, using Von Mises yield condition 21 p3117 A72-40680
- Base mounted cylinders effect on near wake of axisymmetric blunt base in supersonic flow [AIAA PAPER 72-1013] 21 p2993 A72-41594
- Numerical solution of boundary value problems in the statics of axisymmetric shells by the method of reducing to Cauchy problems 22 p3233 A72-42054
- Axisymmetric satellite rotation about center of mass in circular orbit under Newtonian gravitational field, considering precessional stability 22 p3231 A72-42730
- Hypersonic flow around plane and axisymmetric bodies of arbitrary shape with inviscid radiating gas. 24 p3360 A72-45110
- Occurrence and inhibition of large yawing moments during high-incidence flight of slender missile configurations. 24 p3364 A72-45411
- AXISYMMETRIC DEFORMATION**
- U AXIAL STRAIN**
- AXISYMMETRIC FLOW**
- NT ANNULAR FLOW**
- Sonic line neighborhood of uniform axisymmetric supersonic air jet impinging on perpendicular flat plate, measuring shock shapes and surface pressures 01 p0002 A72-11398
- Inertia effects in fully developed axisymmetric laminar flow between two parallel rotating walls, solving Navier-Stokes equation in nonlinear form [ASME PAPER 71-LUB-J] 02 p0234 A72-11529
- Steady sonic flow around three dimensional obstacles by pseudo-axisymmetrical flow approach, revealing singular perturbation of lift downstream at infinity 02 p0150 A72-12096
- Residence time of foreign gas introduced within wake recirculation region behind slender body in axisymmetric supersonic laminar/turbulent flow [AD-733525] 03 p0308 A72-13633
- Visual investigation of semibounded axisymmetric MHD flow of liquid eutectic K-Na alloy under strong magnetic field effect 03 p0399 A72-14014
- Premixed combustible system in laminar axisymmetric stagnation flow, considering steady state and transient response of state variables, blow off extinction, ignition and heat flux [AD-743387] 03 p0458 A72-14222
- Rotational symmetry solutions to differential equations of stationary barotropic or axisymmetric incompressible flow 03 p0344 A72-14345
- Finite difference scheme for collision of two axially symmetric liquid jets with free boundary in cylindrical coordinate system 03 p0344 A72-14370
- Generalized transformation of plane compressible and axisymmetric equation for self similar solutions of dissipative boundary layer for bodies with variable surface 04 p0510 A72-14468
- Orthotropicity orientation effect on supersonic flutter of infinite-length thin heterogeneous circular cylindrical structures in axisymmetric gas flow 04 p0584 A72-14520
- Boundary value problem for steady parallel axisymmetric irrotational flow of inviscid incompressible fluid past cylinder having common axis with tube 04 p0512 A72-15056
- Axisymmetric deflected turbulent jet flow, analyzing physical features and trajectories [ASME PAPER 71-APM-SS] 04 p0462 A72-15177
- Incompressible power law pseudo-plastic material plane flow in converging channel and axially symmetric converging flow in circular cone 04 p0513 A72-15287
- Hypersonic axially symmetric laminar boundary layer electrically conducting fluid flow in blunt body stagnation region in presence of radial magnetic field 05 p0600 A72-16063
- Composite three-dimensional axisymmetric turbulent jet system, discussing jet interaction relation to boundary layer contact and resulting turbulent mixing 05 p0649 A72-16229
- Transonic compressor design for minimum number of stages and hub/tip ratio and maximum inlet axial velocity, assuming axisymmetric flow 05 p0601 A72-16482
- Internal axisymmetrical steady inviscid rotational flow velocity profiles simulation by means of shaped wire gauze screens 05 p0650 A72-16830
- Turbulent shear stress, intensity and velocity field in coflowing axisymmetric jets, using eddy viscosity model [AIAA PAPER 72-47] 05 p0652 A72-16926
- Mach 2.65 axisymmetric mixed-compression inlet system diffuser and boundary layer bleed system performance estimates confirmed by tests [AIAA PAPER 72-45] 05 p0609 A72-16959
- Unsteady axisymmetric incompressible pipe flow stability near piston, using Navier-Stokes equations solution with finite difference forms 05 p0653 A72-17006
- Critical streamline length in axisymmetric and plane ideal gas flows past conical bodies as function of Mach number and form parameter 06 p0755 A72-17677
- Flow field quantities for nearly free axisymmetric steady molecular gas flow through circular orifice from high pressure region into vacuum 06 p0800 A72-18118
- Vorticity transport and definition of equations for axisymmetric incompressible viscous vortex ring, solving coupled system numerically [AIAA PAPER 72-151] 07 p0907 A72-18956
- Compressible axisymmetric coaxial jets turbulent mixing in constant area duct, considering axial and radial pressure distributions 07 p0967 A72-19094
- Axisymmetric flow of ideal incompressible liquid with free boundary and variable velocity, taking into account external mass forces effect 07 p0968 A72-19899
- Branching theory application to convection and axisymmetric flow formation in internally heated self gravitating liquid filled sphere 07 p0968 A72-19973
- Two dimensional and axisymmetric flow with heat addition, deriving flow field by inverse methods 07 p0909 A72-20062
- Rayleigh method convergence in ideal fluids axisymmetric flow stability with free boundaries and perturbations without mass forces 08 p1148 A72-20909
- Steady axisymmetrical twisted gas flow parameters in channels with geometries similar to turbojet engine units 08 p1149 A72-21310

Boundary condition for plane or axisymmetric stagnation point flow of micropolar fluid over flat plate, giving numerical solutions for turbulent characteristics 09 p1293 A72-22621

Wall law for axisymmetric turbulent boundary layers in zero pressure gradient fluid flow through circular cylinders, noting negative and positive wake regions [ASME PAPER 71-APM-VV] 10 p1465 A72-24177

Supersonic axisymmetric turbulent jet density fluctuations measurement by single beam schlieren system, using preheater to reduce jet static/ambient temperature difference 10 p1466 A72-24292

Axisymmetric turbulent jets local entrainment rate as function of axial distance from nozzle exit, using Ricou-Spalding porous wall technique 10 p1481 A72-24425

Axisymmetric plane transonic flow past convex corner point, obtaining characteristics by mapping into hodograph plane 10 p1468 A72-24435

Second order Cowley-Imai analogy application to transcribe gas dynamic perturbation solutions into magnetogasdynamics solutions for perfect gas axisymmetric super-Alfvénic flows 10 p1521 A72-24464

Axisymmetric three component flow of viscous incompressible fluid, finding exact solutions to second problem of dynamics 10 p1471 A72-25133

Navier-Stokes equations system integration for axisymmetric vortex flow of viscous incompressible three component fluid 10 p1471 A72-25134

Two phase axisymmetrical air jet turbulence intensity determination from heat distribution parameters in wake of wire heated by electric current 10 p1471 A72-25172

Relaxation analysis of discontinuities in axisymmetric rotating actuator disk flow [ASME PAPER 72-GT-26] 11 p1569 A72-25622

Supersonic axisymmetric turbulent boundary layer characteristics over circular cone, predicting blowing effect on separation 11 p1617 A72-25995

Wind velocities field in vortices leeward of islands derived from Navier-Stokes equation for isolated axisymmetric viscous vortex 12 p1839 A72-27032

Streamlines and fluid diffusion determination for axisymmetric irrotational and rotational flows in ducted propellers, noting conformal mapping of arbitrarily shaped domain onto rectangle 12 p1751 A72-27168

Steady barotropic inviscid flows of rarefied gas plasmas as free jet and within cylindrical channel in axisymmetric external magnetic field with Hall effect 13 p2018 A72-29823

Axisymmetric hypersonic motion around thin solid of revolution, taking into account boundary layer interaction with inviscid external flow 13 p1895 A72-29847

Unstable discharge regime of nonisothermal axisymmetric subsonic turbulent jet in acoustic field with local perturbations 13 p1943 A72-29883

Steady nonrotating axisymmetric viscous incompressible flows with zero and negative ring circulation flux, studying solutions in three dimensional phase space 14 p2094 A72-30708

Plane nonlinear wave propagation in transonic region of two dimensional and axisymmetric steady flows, considering disturbance at arbitrary point 14 p2095 A72-31000

Asymptotic solution for velocity distribution in viscous liquid axisymmetric flow in conical diffusers 14 p2070 A72-31006

Ideal gas axisymmetric flow created in supersonic flow interaction with blunt body with strong blowing at surface, obtaining boundary layer approximate solution 14 p2070 A72-31012

Finite difference solution to Navier-Stokes equations for axisymmetric flow of incompressible viscous fluid 15 p2216 A72-31446

Turbulent flow between rotating disk and turbine engine body calculated from equations of axisymmetric viscous incompressible fluid flow 15 p2217 A72-31702

Solution existence for singular boundary value problem involving swirling flow, corresponding to problem of axisymmetric flow above rotating disk 16 p2377 A72-33186

Axisymmetric jet impact on ground board for different nozzle configurations and heights in VTOL aircraft aerodynamic studies 16 p2377 A72-33404

Axisymmetric rotating flow past a circular disk 17 p2540 A72-35190

On the stability of axisymmetric systems to axisymmetric perturbations in general relativity. I - The equa-

tions governing nonstationary, stationary, and perturbed systems. 17 p2611 A72-35315

Flow problems solutions estimation by variational principles application, exemplifying by plane Couette and Poiseuille and axisymmetric pipe flow 18 p2679 A72-36391

Unsteady motion of a compressible viscous fluid in a spherical layer 18 p2682 A72-36882

On the steady flow between a rotating and a stationary disk with a uniform suction at the stationary disk. 18 p2683 A72-36994

Surface vorticity theory for axisymmetric potential flow past annular aerofoils and bodies of revolution with application to ducted propellers and cowls. 19 p2747 A72-38554

Unsteady axisymmetric flows of a liquid draining from a circular tank. 20 p2913 A72-39605

Branching theory application to convection and axisymmetric flow formation in internally heated self gravitating liquid filled sphere 20 p2915 A72-40030

Experimental study of heat transfer in a subsonic jet impinging normally on a plane baffle. 21 p3128 A72-40949

Optical method for measuring the concentrations of axisymmetric gas jets 21 p3055 A72-40990

An approximate method for solving problems involving separated flows past bodies 21 p2990 A72-41088

Heat transfer in separated regions in supersonic and hypersonic flows. [ICAS PAPER 72-14] 21 p2991 A72-41139

Calculation of heat shield with local mass injection in hypersonic flow. 21 p3131 A72-41235

Three-dimensional supersonic flows at large distances from a body of finite volume 21 p2994 A72-41661

Flow equations for axisymmetric compressible conical flow in Busemann nozzle, noting numerical method for integral lines construction for given Mach number 22 p3134 A72-42288

Fluid dynamic forces exerted by Newtonian fluid axisymmetric creeping flow on accelerating body of arbitrary shape, calculating pressure gradient via Navier-Stokes equation 23 p3347 A72-43726

Waves generated in the configuration of a magnetically confined and field-permeated axisymmetric jet. 23 p3322 A72-44307

Axisymmetric and two-dimensional flow with attached shock waves. 24 p3361 A72-45161

AXISYMMETRY U SYMMETRY

AXLES

U SHAFTS [MACHINE ELEMENTS]

AXONS

Functional organization and neurophysiological mechanisms of return corticothalamic system in anesthetized cats, showing axon terminal presynaptic depolarization 13 p1902 A72-28762

Visual cortex neuron reactions to antidromic stimulation of cat pyramidal tract, noting axon activation increased discrimination in analyzer 13 p1903 A72-28781

Neuronal fiber and synaptic axonal contact structure of cat spinal gray matter in corticospinal, rubrospinal and reticulospinal terminal zones by Golgi method 21 p2998 A72-40579

The ultrastructure of the lateral basilar region of the spinal cord. 21 p2998 A72-40581

Supraspinal effects in the activity of preganglionic sympathetic neurons delivering axons to the cervical sympathetic nerve 21 p3000 A72-40599

The effect of membrane parameters on the properties of the nerve impulse. 22 p3140 A72-41936

AZIDES [INORGANIC]

Electron spin resonance of divalent Mn ion doped in thallous azide single crystals, investigating temperature effects on spin Hamiltonian parameters 22 p3152 A72-42716

AZIMUTH

Electron and muon density fluctuations, trajectory distribution and azimuthal symmetry in cosmic ray air showers 06 p0870 A72-17279

Target azimuth and elevation estimation by four beam cluster, analyzing angle estimation accuracy as function of SNR by computerized Monte Carlo simulation 07 p0941 A72-19304

Loxodrome and geodetic line azimuths relationship on ellipsoid of revolution 08 p1158 A72-21159

Geodetic azimuth determination by multiple observations of bright stars near meridian 09 p1297 A72-22485

FM/CW interferometric ionosonde used for interferometric direction finding, computing incident azimuth and elevation from baseline array phase differences 09 p1281 A72-23514

Cross loop antenna for apparent azimuthal direction of incidence of VLF transmitter, showing night time bearing direction changes 12 p1784 A72-27794

Bearing azimuth measurement accuracy improvement by ATC beacon system/secondary surveillance radar using monopulse technique 18 p2662 A72-37047

A nomogram for look angles to geostationary satellites. 19 p2869 A72-37298

Astro-azimuth comparative studies with Wild T3, Wild T4, and Kern DKM3 theodolites. 20 p2923 A72-39087

Possible impact of area navigation upon M.L.S. requirements for azimuth angular coverage and range. 24 p3422 A72-44643

An approximate method of determining the azimuth from observations of the passage of the solar disk across the horizontal thread of the instrument's telescope 24 p3437 A72-44755

Nonlogarithmic calculation of chronometer corrections in azimuthal methods of determining time /Struve's method, Struve-Pavlov method, Dellen's method, and other methods/ 24 p3438 A72-44864

Compilation of azimuth tables for the North star /for the tropical zone/ 24 p3438 A72-44866

AZO COMPOUNDS

NT RDX

Ethyl radicals reactions in shock tube produced pyrolysis of azoethane, using time of flight mass spectrometer 07 p0935 A72-19433

Azomethane and azomethane-d6 IR and Raman spectra, discussing fundamental modes vibrational assignment based on band contours, isotopic shift ratios and group frequency correlations 16 p2360 A72-32923

AZOLES

NT ACETAZOLAMIDE

NT INDOLES

NT PYRROLES

NT TRYPTOPHAN

Nucleotides condensation in aqueous system in prebiotic conditions, investigating effects of imidazole, cyanamide and polymorphine 04 p0483 A72-14766

AZULENE

Ruby laser radiation nonlinear absorption by azulene solutions derived by taking into account two-photon transitions for comparison with measurement 03 p0366 A72-13367

AZUR SATELLITE

Azur satellite temperature control system for protection against internal heat dissipation and external thermal loads due to earth radiation and albedo 04 p0582 A72-15651

Satellite projects Azur, Dial and Heos - Conference, Bremen, West Germany, April 1971 05 p0714 A72-16134

Azur satellite for investigating polar regions, inner radiation belt and solar particle emission 05 p0715 A72-16135

Azur satellite project definition organizational structure and time schedule, noting management and implementation problems 05 p0752 A72-16136

Spurious commands at high altitudes due to hf disturbances in Azur satellites, discussing telecommand system 05 p0626 A72-16137

Ground based satellite control center data processing for Azur satellite, using automatic guidance 05 p0632 A72-16138

Azur satellite flight data evaluation of thermal behavior, measuring temperature with thermistors 05 p0746 A72-16139

Azur satellite ground station network with polar stations for telemetry reception 05 p0643 A72-16140

Azur project data processing, noting problems with computational equipment intended for industrial operation 05 p0752 A72-16141

Long term spin and misalignment in orbit of Azur satellite with passive magnetic attitude control system 05 p0727 A72-16466

Misalignment angle of Azur satellite orientation axis relative to geomagnetic field vector 06 p0892 A72-18145

Proton measurements with Azur satellite during solar particle events of March 1970, considering diffusion and convection transport theories
07 p1056 A72-18901

B

B STARS

B and Be type stars intrinsic polarization, considering UVB spectra and effects on observed polarization
02 p0283 A72-12628

Absorption profiles of neutral helium lines lambda 4471 and lambda 4026 for BoV star tau Sco, observing flux near peak of forbidden component
03 p0417 A72-13022

Spectrographic observation of hot OB subdwarf HD 149382
03 p0435 A72-13799

Interstellar Ca II, H and K optical absorption lines of bright O and early B stars in Orion region
05 p0723 A72-17200

Be stars emission line profile broadening due to surrounding gaseous ring in circular motion according to Kepler law
06 p0880 A72-17892

Model atmosphere and spectral analysis for two early B-type supergiant stars, deducing stellar mass and evolutionary phase
07 p1070 A72-19085

Gravity darkening effects on rapidly rotating B stars He I and Mg II spectral lines
09 p1391 A72-23530

OB star distribution in Puppis from UVB and H beta photometry, noting correlation with hydrogen concentration
10 p1542 A72-24615

Ca II K line profiles in front of distant OB stars, using pressure scanned Fabry-Perot interferometer and coude spectrograph
10 p1542 A72-24616

Spectrophotometry of nebulosity associated Ae and Be stars, discussing age, circumstellar dust shells geometry and red stellar objects
11 p1720 A72-26114

IR and optical observations of cluster surrounding Herbig Be type star BD plus 40.4124, noting extreme youth of group
11 p1721 A72-26122

HD 4180 shell H lines width variations comparison with Be stars, noting thirty year period emission decrease followed by outer shell absorption
12 p1867 A72-27213

B type main sequence star absolute energy flux envelope from ground based and OAO 2 observations, comparing with model atmosphere prediction
15 p2311 A72-31997

Early B stars with normal helium abundances and small rotational velocities, deducing gravity from H lines and ESW stark broadening
15 p2316 A72-32751

Discoveries on southern objective-prism plates. III. Three new hydrogen-deficient stars and a bright B-type subdwarf.
17 p2609 A72-35116

Limb darkening for B-type main sequence stars in the infrared.
17 p2612 A72-35383

The helium abundance in thirty-three main sequence B stars.
18 p2726 A72-36726

Changes in the spectrum of the star Be HD 217050
18 p2727 A72-36733

Variation of the spectrophotometric temperature from the center of the disk to the limb of stars of the spectral classes B and A
21 p3102 A72-40094

Pulsating variables in the Pleiades cluster.
21 p3105 A72-41032

The influence of ultraviolet line blanketing on the neutral helium triplet lines in B-type stars.
24 p3438 A72-44834

B-1 AIRCRAFT

B-1 aircraft design features, discussing aerodynamic configurational aspects, structural components and materials, engine inlets, fuel, hydraulic control and avionics systems
17 p2487 A72-34223

B-1 production planning and engineering, discussing manpower, tooling, structural components tests, schedules and cost estimates
17 p2559 A72-34389

Structural model vibration control system design for B-1 aircraft to improve ride during atmospheric turbulence and terrain following
17 p2493 A72-35563

Automatic structural model control system with aerodynamic vanes for B-1 strategic bomber turbulence excitation during low altitude terrain following missions
19 p2751 A72-38132

Development of an inflatable fabric structure for the early stabilization of the B-1 crew escape capsule.
20 p2888 A72-40053

Unique features of the B-1 flight control systems.
20 p2889 A72-40062

B-103 AIRCRAFT
U BUCCANEER AIRCRAFT

B-52 AIRCRAFT
System analysis and synthesis for B-52 Control Configured Vehicle program, discussing flutter mode and maneuver load control and augmented stability configurations
20 p2887 A72-39130

B-70 AIRCRAFT
Synoptic meteorological parameters vs CAT encountered in stratosphere by XB-70 airplane, presenting frequency distributions and probability tables
13 p1994 A72-28867

BABBITT METAL
U BEARING ALLOYS

BACILLUS
Dry heat resistance of bacillus spores on spacecraft metal surfaces for different pressures, atmospheres and materials
04 p0475 A72-15261

Aqueous formaldehyde effects on Bacillus subtilis spores, showing sporostasis due to germination inhibition and sporocide due to temperature dependent inactivation
16 p2357 A72-33772

The effects of various cure cycles upon the viability of Bacillus subtilis var. niger spores within solid propellant.
18 p2652 A72-36437

Lactate dehydrogenase from an extremely thermophilic bacillus.
23 p3259 A72-44450

BACK INJURIES

Aircraft accident in the Faroe Islands in 1970 - Observations from a medical point of view, with special reference to spinal fractures.
17 p2508 A72-34556

BACKFIRE

Short backfire antenna gain increase, considering construction case, reflector arrangement and circular polarization
01 p0040 A72-10684

Moderate gain superdirective antenna arrays design based on backfire principle, using parasitic elements
01 p0040 A72-10685

Series-dipole antenna design based on Ehrenspect short backfire antenna mirror method, noting small dimensions and cost reduction
21 p3031 A72-40539

BACKGROUND NOISE

Random background noise effect on nonlinear self oscillation envelope passage time moments, discussing relationship between amplitude and frequency stabilities
01 p0035 A72-10032

Information feedback application to AM laser communication system, predicting multiplicative error, background shot noise and photon arrival fluctuation effects on continuous parameter transmission
01 p0025 A72-10326

Twicks contribution to atmospheric radio noise background, discussing nighttime ionospheric source information
01 p0056 A72-10444

Estimation algorithm for arbitrary parameter of narrow band radio signal with unknown amplitude and phase during reception on additive normal noise background
02 p0176 A72-12218

Signal waveform ensuring maximum reception stability on correlated noise background with peak limiting
02 p0183 A72-12760

Optimal discrimination rule for dual frequency radar targets with inadequate echo signal and background noise level parameters
05 p0625 A72-15821

Nonparametric constant false alarm rate /CFAR/ radar extractor for target detection in background noise, using sign test
05 p0629 A72-16569

Two-channel direction finding with point source emission and spaced antennas reception, investigating cross correlation and background noise interference effects on accuracy
07 p0938 A72-19007

Optimal Bayesian system synthesis for simultaneous discrimination and parameter estimation of several signals in noise background
07 p0943 A72-19516

Signal detection in noise, investigating quantiles position optimization in nonparametric test statistics
07 p0943 A72-19519

Signal detection in stationary, Markov and other noise background, discussing functional method of statistical and probabilistic representation
07 p0943 A72-19520

Perceived noise level correction for background noise effects based on frequency band SNR
07 p0932 A72-20170

Estimation-correlation principle and optimal detector for incomplete a priori information signal reception on random and white noise background
08 p1131 A72-20790

Velocity measurement by Doppler light scattering due to particle finite residence time, estimating ambiguity and noise effects on turbulent spectra of frequency fluctuation
09 p1305 A72-22302

German monograph on frequency noise of microwave transistor power oscillators covering generation mechanism and spectral density determination
09 p1285 A72-22340

Optimal signal discrimination on arbitrary noise background, choosing functional from class of integral polynomials
09 p1277 A72-22475

Potential noise stability of wideband communications systems during discrete signal reception on combined background of quasi-white noise and spectrally lumped interference
09 p1277 A72-22569

Background noise in active semiconductor devices - Conference, Toulouse, France, September 1971
09 p1286 A72-23101

Band limited background noise variance measurements by analog and digital techniques
09 p1280 A72-23103

Microwave transistor noise factor measurement for various geometries and parameter values correlation with predictions
09 p1286 A72-23104

Two dimensional dynamic model for background noise generation in bipolar transistors, using equivalent circuit
09 p1286 A72-23105

Burst noise relationship to Si crystal dislocations and defects near emitter-base junction and surface zone in bipolar transistors
09 p1286 A72-23106

Transistor LF flicker background noise generation mechanism in terms of bulk effect due to temperature fluctuation or phonon electron interactions
09 p1286 A72-23107

MOS transistor low level background flicker noise equivalent voltage relationship to gate voltage and input capacitance and interface state density
09 p1286 A72-23108

P-channel MOS transistor LF background noise components analysis for different dependencies on gate bias and temperature
09 p1286 A72-23109

Background noise in FETs with junction gate, formulating hypothesis of warm carriers for transistor channel
09 p1287 A72-23110

Excess, shot and channel thermal noises performance-limiting effects on junction FETs in high input impedance applications, considering minimization method
09 p1287 A72-23111

LF excess flicker noise in metal semiconductor Schottky barrier diodes due to barrier height fluctuation
09 p1287 A72-23114

Avalanche diode background noise in linear and nonlinear regimes, emphasizing source dependence on oscillation level
09 p1287 A72-23117

Background noise in amplification and oscillation in Si and GaAs avalanche diodes
09 p1287 A72-23119

Background noise at 200 Hz-1 MHz of avalanche effect voltage regulating diodes
09 p1288 A72-23120

LF originated background noise in Gunn oscillators, developing evolution equation for oscillator weakly perturbed by noise
09 p1288 A72-23121

Current carrier flow parameter fluctuations associated with steady state transport noise in semiconductor devices, considering generation-recombination processes, drift, diffusion and dielectric relaxation
09 p1288 A72-23125

Double beam single detector wavelength modulation spectrometer for background elimination from observed spectra, noting application to semiconductors band structure determination
09 p1315 A72-23402

Dynamic programming method application to signal processing components selection for cascaded communication links to satisfy overall gain and noise figure
09 p1281 A72-23415

MOS transistor logic circuits pulse noise stability dependence on transient response, emphasizing supply voltage effect
10 p1449 A72-24290

Supercritical CW GaAs transferred electron broadband reflection amplifier power gain and noise figure at 34 GHz
10 p1449 A72-24301

Asymptotically optimal detection/discrimination algorithms for weak signals on correlated noise background

10 p1436 A72-24508

Modulating /multiplicative/ noise effects on output signal characteristics of receiver designed for optimal reception on background of Gaussian noise

10 p1439 A72-24906

Fluidic proportional and digital amplifiers environmental effects on sensitivity of gain, noise and null shift based on dependence on Reynolds number [ASME PAPER 72-GT-84]

11 p1577 A72-25660

Optimal synthesis and analysis of quasi-deterministic signal detection system with simultaneous parameter measurement on background noise

11 p1596 A72-26312

Weak signals detection at visible wavelengths with background noise, examining photoelectric recording and optimal detection characteristics of receiver

11 p1596 A72-26314

Holograms image formation characteristics with extended reference beam source, presenting reconstructed image and noise field calculations

11 p1633 A72-26352

Infrasound observations of natural background and signals from Apollo 14 and aircraft, using thermistor flowmeter microphone array

11 p1690 A72-26515

Cryogenic Josephson junction magnetometer in magnetocardiography, discussing high ambient noise levels in unshielded environment

12 p1769 A72-27288

Schottky barrier gate FET design, device packaging and low noise characteristics

12 p1788 A72-27294

Signal filtration algorithms and parameter estimation in additive non-Gaussian noise background by conditional Markov process theory

12 p1783 A72-27633

Binary logic circuits with interconnected repeaters and inverters, discussing signal level selection to ensure maximum noise stability

12 p1786 A72-28120

Least squares method algorithm for estimating unsteady harmonic signal parameter in presence of normally distributed additive noise

13 p1915 A72-28435

Optimal optical measurement for two dimensional object position on plane in Gaussian background noise, calculating mean square error for false identification probability determination

13 p1920 A72-29280

Compressor directivity determination at discrete frequencies by tone power separation from noise background, using Fourier analysis of sound pressure autocorrelation

13 p2028 A72-29572

Quantization background noise during hologram approximation by step function, discussing effect on diffraction field forming reconstructed image

13 p1959 A72-29684

Correlation between internal noise sources of microwave transistors at low collector currents

14 p2088 A72-30917

Adaptive reception of weak repetitive signals on background of intense fluctuating noise, synthesizing adaptive detection system for multipath propagation and small SNR

15 p2195 A72-31658

Probability functional formulas for quasi-determine signal on unsteady normal noise background for use in false alarm and correct detection

15 p2195 A72-31664

Signal parameter estimation accuracy in nonoptimal reception on noise background with random uniformly distributed initial phase

15 p2195 A72-31665

Optimum processing structure /likelihood functional/ determination for signal sequence detection given noisy common background image sets

15 p2196 A72-31783

Time domain analysis of long thin bar antenna response to gravitational signals, estimating sensitivity limit via noise background analysis

16 p2423 A72-33013

Holograms image formation characteristics with extended reference beam source, presenting reconstructed image and noise field calculations

16 p2394 A72-33705

Search radar constant false alarm rate receiver circuit for background noise and clutter compensation, using matched dispersive delay lines flanking hard limiter

16 p2365 A72-33762

BARITT, IMPATT, TRAPATT and Gunn diodes, discussing power, noise and thermal dissipation problems

17 p2526 A72-34465

Detection of a two-frequency signal against a noise background of unknown intensity

17 p2516 A72-34849

Measures of effectiveness for special signal detectors of simple structure

17 p2516 A72-35222

Frequency-modulation sensitivity and frequency-pushing factor of a Pd-n-p/+ punchthrough microwave diode.

18 p2667 A72-36686

Correlation between the reliability of silicon bipolar transistors and their excess background noise

18 p2669 A72-37110

Binary logic circuits with interconnected repeaters and inverters, discussing signal level selection to ensure maximum noise stability

19 p2767 A72-38621

Signal waveform ensuring maximum reception stability on correlated noise background with peak limiting

20 p2903 A72-39066

External background and internal noise effects on automatic tracking systems accuracy, noting optimal operating point on transducer response curve

21 p3014 A72-40320

Photographic material characteristics for adequate diffraction efficiency and contrast and noise levels and acceptable nonlinear distortions of holograms, noting optical transfer function optimization

21 p3052 A72-40389

Image quality of binary and multigradation microwave holograms, noting HF components and background noise

21 p3055 A72-40794

Evaluation of transonic and supersonic wind-tunnel background noise and effects of surface pressure fluctuations measurements.

[AIAA PAPER 72-1004]

21 p3041 A72-41588

Optimum spatial filter for an anisotropic background-noise.

21 p3036 A72-41839

Pulse time positioning under background noise in radar and radio navigation range finders, noting root-mean-square errors and transient response

22 p3153 A72-42117

Investigation of the threshold properties of a phase-lock AFC detecting a sinusoidally frequency modulated signal against a noise background

22 p3154 A72-42231

Radiogoniometer error analysis for receiver internal noise and external interference sources, noting sources angular distribution effect on instrument error

22 p3158 A72-42233

Characteristics of an optimal algorithm for detecting Gaussian signals against a pulse noise background for receivers with a logarithmic amplifier

22 p3154 A72-42238

Interactions of signal and background variables in visual processing.

22 p3152 A72-42931

Optimal discrimination rule for dual frequency radar targets with inadequate echo signal and background noise level parameters

23 p3263 A72-43429

Analysis of optimal space-time signal discrimination

23 p3266 A72-44217

Potential noise stability of wideband communications systems during discrete signal reception on combined background of quasi-white noise and spectrally lumped interference

24 p3379 A72-44748

BACKGROUND RADIATION

Primeval fireball cosmic background radiation spectrum in homogeneous axisymmetric anisotropic world model including electron neutrino effects on expansion dynamics

01 p0121 A72-11139

Silicate rocks mapping from aerial IR data, discussing method for discriminating emission from background radiation

02 p0208 A72-11877

Atmospheric scattering and absorption effects on target/background discrimination in environmental remote sensing at 0.4-3.0 microns spectral region

02 p0213 A72-11858

Mountaintop high resolution spectral observations of diffuse isotropic submillimeter atmospheric and sky emission

02 p0274 A72-12194

Gamma ray astronomy, discussing energy spectrum, diffuse background flux, extragalactic origin and Crab Nebula emission

03 p0408 A72-13027

Major sources of background counts for collimation gamma ray detector, measuring radiation direction and energy spectrum from balloon altitudes

03 p0352 A72-13032

Far UV astronomical studies with moderate spectral and spatial resolution instruments, discussing Lyman alpha line background

03 p0417 A72-13049

Diffuse gravitational background radiation in universe, assuming gravitational field fluctuations macroscopic nature and Einstein equations applicability

03 p0417 A72-13095

Diffuse cosmic background radiation measurements, emphasizing microwave and X ray spectra and excitation mechanism

03 p0409 A72-13138

X ray background model based on photons bremsstrahlung emission by subcosmic metagalactic electrons or protons

03 p0413 A72-13804

Universal steady X ray background theory, examining superposition of radiation from pulsars in various galaxies

04 p0566 A72-14909

Radio signal parameters with unknown envelope approximated by orthonormal function series during white noise background reception

05 p0625 A72-15823

Background phonon X ray and gamma quanta intensities dependence on solar activity from Geiger counter recordings in deep space

05 p0711 A72-17046

Proton bombarded CsI crystal spallation-caused radioactive decay products contribution to background rate in satellite X ray telescope detector

06 p0853 A72-18084

Cosmological red shift and galactic evolution effects on line features in X ray background due to young pulsars in supernova remnants

06 p0891 A72-18509

Dark adaptation with logarithmically time decreasing background luminance, noting threshold time lag variation with rate of background change

07 p0930 A72-19827

Achromatic and chromatic thresholds during dark adaptation against varying background luminances, noting trend change at transition from cone to rod function

07 p0930 A72-19828

Hypotheses for excess background radiation at 200-500 km, suggesting single high energy electrons or electron clusters

07 p1064 A72-20638

Incoherently light radiating object and background light focusing on photosensitive mosaic, observing linear restoration by comparison of mean square error with Wiener filter theory

09 p1350 A72-22611

Nonthermal emission and ejection of matter from galactic nuclei, discussing radio, optical and IR synchrotron sources and background radiation

10 p1535 A72-23906

X ray background radiation from discrete sources, considering inverse Compton mechanism in galaxies and intergalactic space and soft component origin

10 p1529 A72-23913

Spectrum studies of extragalactic diffuse background radiation fields consisting of X ray and thermal or microwave background

10 p1529 A72-23914

Radial temperature distribution determination in nitrogen plasma jet from continuous spectral background intensity measurement

10 p1519 A72-24131

Diffuse gravitational background radiation in universe, assuming gravitational field fluctuations macroscopic nature and Einstein equations applicability

11 p1716 A72-25703

Cosmic X ray background intensity and spectrum interpretation in terms of metagalactic origin within evolutionary cosmology framework

13 p2030 A72-29087

Brightenings and surgelike spikes associated with low amplitude soft solar X-ray background flux in H alpha above limb, assessing energy budget

13 p2032 A72-29718

Solar cyclic intensity variation of excessive radiation with respect to galactic radiation background at low altitudes from satellite data analysis

14 p2146 A72-30475

Electromagnetic emission in universe, discussing background radiation spectrum, extragalactic source brightness, intergalactic gas and energy density

14 p2152 A72-30479

White dwarf background radiation and optical emission variations due to thermal bremsstrahlung from stellar coronae

14 p2147 A72-30554

Earth velocity through microwave background, discussing absolute and relative motion, inertial frame and distant matter distribution and Mach principle

14 p2157 A72-30624

Composition of radiation excess over primary cosmic ray background recorded by Cosmos satellites below midlatitude belt region

14 p2147 A72-30626

Submillimeter isotropic background limits of stratosphere emission spectrum, using aircraft-borne Michelson interferometer and Rollin far IR detector

15 p2265 A72-31626

Extraterrestrial He I 584 A background radiation suggested from rocket and satellite observations, noting interstellar medium temperature determination from isophotes

15 p2309 A72-31945

Background spallation source errors in satellite measurements of diffuse cosmic X ray spectrum with crystal scintillators

15 p2300 A72-31986

Cosmic background radiation temperature from interstellar CN band R branch absorption line in star zeta Ophiuchi spectrum

15 p2313 A72-32309

Galactic background continuous radiation observation at 15 GHz, determining brightness temperature and thermal radiation component

15 p2313 A72-32348

Cosmic microwave background radiation origin by energy dissipation associated with primordial chaotic universe

16 p2459 A72-33770

Effect of target-background luminance contrast on binocular depth discrimination at photopic levels of illumination.

17 p2508 A72-34879

Galactic and metagalactic background radiation

18 p2722 A72-36723

X ray observation inadequacy in detection of background radiation surface brightness fluctuations due to irregular distribution within galactic cluster sources

18 p2729 A72-37006

Electromagnetic background radiation in universe, discussing relic radio emission, energy density, hot model isotropic extragalactic component isolation, intergalactic gas, radio sources and quasars

19 p2854 A72-38815

Observational evidence against supernovae being the source of the universal X-ray background.

20 p2965 A72-38906

On the physical nature of cosmic electromagnetic absorption. V - The Einstein-de Sitter cosmology with plasma coupled to radiation at non-relativistic temperature.

20 p2967 A72-39185

On the physical nature of cosmic electromagnetic absorption. VI - The Einstein-de Sitter cosmology with plasma coupled to radiation at relativistic temperature.

20 p2967 A72-39186

Radiation models and explanations for absence of ground level gamma ray background periodic fluctuations

20 p2964 A72-39386

On a galactic origin for the soft X-ray background.

21 p3100 A72-41029

Radio signal parameters with unknown envelope approximated by orthonormal function series during white noise background reception

23 p3263 A72-43431

Galactic submillimeter background radiation energy density limit, taking into account recalibrated gamma ray flux measurements agreement with cosmic ray-interstellar matter interactions

23 p3329 A72-43942

Linear polarization survey for galactic background radiation at 1415 MHz in North Polar Spur, Cetus Arc and Loop III, noting continuous maxima shift

24 p3438 A72-44835

Increase in the ratio of the energy of ultrashort laser pulses to the energy of the background radiation.

24 p3411 A72-45613

BACKLOBES

Side and back lobe structures of directive antennas.

21 p3020 A72-40903

BACKSCATTERING

Auroral backscatter echoes observations in ionospheric short wave propagation, using satellite oblique propagation ionograms and magnetograms

01 p0056 A72-10439

Optical aurora relationship to radio counterpart, showing backscattered signal peak amplitude close correlation to magnetic bay peaks

01 p0056 A72-10440

Smoke plume opacity or particulate content measurement by laser backscatter, using Q switched ruby and Nd lidars

01 p0058 A72-10544

Backscatter hf radar signature analysis in relation to medium scale traveling ionospheric disturbances, using computer ray tracing technique

01 p0030 A72-10837

Radar backscatter time response waveforms for cube from lf data and diffraction analysis

01 p0030 A72-10843

Modified Born approximation for electromagnetic backscattering cross section from turbulent plasmas, noting attenuation leading to saturation and cross-polarization

01 p0031 A72-10846

Radar target thin rectangular plate model backscattering from incident and reflected waves, noting front and trailing edge phenomena with emphasis on side edge contribution

01 p0032 A72-11250

Total ozone estimation by interpolation from Nimbus 4 satellite data on backscattered UV earth radiance attenuation

01 p0096 A72-11285

Ionospheric reflection height calculation according to oblique electromagnetic backscatter sounding data at two frequencies

02 p0172 A72-11943

Spatial-temporal correlation functions of field due to electromagnetic waves backscattering from random inhomogeneities in extended layer

02 p0180 A72-12580

Ground based atmospheric vertical temperature profiles measurement by Raman backscatter from molecular nitrogen

03 p0348 A72-13430

Hf backscattering of plane electromagnetic wave at oblique incidence on conducting circular metallic disk, noting polarization dependence on angle

04 p0493 A72-15524

Short narrow light pulse reflection from thick turbid medium with strong anisotropic scattering, obtaining backscattering signal power from unsteady transport equation solution

05 p0690 A72-16292

High frequency electric field backscattering by plane electromagnetic wave incident on perfectly conducting sphere with radially inhomogeneous dielectric coating

05 p0630 A72-16621

Solar flare X-ray emission Compton backscattering from Fe lines examination

05 p0710 A72-16720

Mf/hf/vhf scattering from sea, deriving received power and spectral energy density dependence on grazing angle, frequency, range and surface impedance

06 p0770 A72-17338

Air pollutant monitoring and remote analysis by Raman, fluorescence and resonance backscattering, Rayleigh scattering and absorption laser radar techniques

06 p0827 A72-18460

Atmospheric lee waves three dimensional structures through high sensitivity Doppler radar measurements based on backscatter from refractive index inhomogeneities

07 p1029 A72-19100

Atmospheric acoustic attenuation measurement on sailplane, assessing turbulence backscattering cross section

07 p1031 A72-20597

Critical frequencies and geometrical parameters of parabolic model in oblique backscatter ionospheric sounding, using distance-frequency characteristics

08 p1154 A72-20732

Scattered signal power approximation during ionospheric oblique backscatter sounding, using geometrical optics method

08 p1130 A72-20733

Optimum pulse duration for ionospheric oblique backscatter sounding, determining receiver signal power input dependence on pulse duration

08 p1131 A72-20820

Propagation by direct backscatter on aligned irregularities in auroral F layer, noting horizontal ionization gradients role

08 p1158 A72-21220

Sky wave backscattering with narrow beam antenna coupled with signal modulations and Doppler shift as means of sea state observation and environmental monitoring

08 p1134 A72-21493

Ground based Raman laser backscatter measurement of stratospheric water vapor content, noting 1 ppm accuracy

08 p1161 A72-21825

Geometric optics approximation for rf wave forward and backscatter characteristics by spherical overdense clouds for several electron density distributions

08 p1136 A72-21980

Antenna near field correction for backscatter gain in two-beam incoherent scatter radar measurements at Arecibo Observatory

08 p1137 A72-21983

Airborne radar measurement of 2.25 cm backscatter from sea surface, obtaining wind speed by computerized clustering data analysis techniques

09 p1296 A72-22312

Atmospheric temperature vertical profiles by laser Raman backscatter measurements

09 p1307 A72-22439

Electromagnetic scattering by ungrounded conducting sphere above ground plane, calculating lf ground wave backscatter

09 p1279 A72-22905

Backscattering by turbulent irregularities derived in context of single scattering corresponding to weak microwave reflections observed in atmospheric sounding

09 p1280 A72-23412

Backscattering properties of ground observed with HF high resolution oblique sounding equipment

09 p1281 A72-23512

HF radio wave backscatter from sea surface to obtain gravity wave structure information

10 p1438 A72-24739

Electromagnetic theory of HF radio ground wave backscattering from gently rippled sea surfaces, discussing approximations for separated transmitting and receiving antennas case

10 p1438 A72-24742

Superhigh frequency electromagnetic waves diffraction by conducting screen circular aperture with phase change by dielectric disk and multiple internal reflections, noting patterns and backscattering apparatus

11 p1597 A72-26371

Radar backscattering cross section and power of conducting cylindrical spacecraft in compressible electron-ion plasma environment

12 p1779 A72-27173

HF backscatter pulse signal incidence elevation angle measurements based on amplitude ratio of two antennas with different vertical patterns

12 p1783 A72-27779

Satellite altimetry based on ocean backscattering, analyzing received signal model and altitude errors

13 p1955 A72-28533

Radar range reduction by snowfall, considering path attenuation and clutter power backscattered from near target precipitation

13 p1917 A72-28699

Rocket-borne inflatable sphere for radar signal backscatter calibrations at reentry altitudes and for simultaneous atmospheric density determination

13 p1918 A72-28819

Internal rarefied gas flow, taking into account molecular backscattering due to wall surface roughness

13 p1942 A72-29117

Ionospheric reflection height calculation according to oblique electromagnetic backscatter sounding data at two frequencies

13 p1920 A72-29255

Moon and Venus relief from backscattering diagrams based on radar echoes, calculating root-mean-square angles of surface inclination

14 p2151 A72-30468

Signal level fluctuations line spectra energy characteristics comparison for oblique and oblique-backscatter sounding, noting changes in harmonics intensity and period

14 p2085 A72-30638

Electromagnetic waves backscattering in magnetoactive plasma containing random inhomogeneities of electron density, calculating field spatial-time and cross correlation functions

14 p2086 A72-30789

Meter and decimeter wave reflected signals distribution and surface backscattering patterns effective beamwidth investigation by method based on Doppler effect

14 p2086 A72-30792

Photon correlation spectrometer for laboratory wind tunnel measurement of laser Doppler signals backscattered from dust particles

14 p2111 A72-30854

Energy and angular distribution of hydrogen and rare gas ions backscattered from polycrystalline metal surfaces

15 p2276 A72-31852

Aircraft laser radar measurements of atmospheric backscattering coefficients for cloud and underlying surface studies

15 p2266 A72-31908

First and second order backscattering, beam divergence, angular field of view, field size and receiver distance of water clouds illuminated by continuous lidar beam

15 p2200 A72-32154

Singly scattered radiation in weakly inhomogeneous turbulent plasma for incidence angles greater than critical angle, calculating backscattered wave depolarization from radiative transport equation

15 p2288 A72-32425

D region electron concentration and collision frequency with neutral molecules from radio waves backscattered by inhomogeneities in propagation medium

16 p2385 A72-33484

Solar radiation absorption and scattering by particles in atmosphere, emphasizing absorption/backscatter ratio explanation

16 p2388 A72-34023

Backscatter of solar resonance radiation. I.

17 p2598 A72-34626

The solar wind H and He⁺/+ content.

17 p2598 A72-34627

Auroral radio reflection regions spatial distribution from radar measurement, noting backscattering indicatrix independence on geographical latitudes

17 p2519 A72-35873

A dynamical theory for the contrast of perfect and imperfect crystals in the scanning electron microscope using backscattered electrons.

18 p2692 A72-36749

Experimental indications of plasma instabilities induced by laser heating.

19 p2840 A72-37549

Critical frequencies and geometric parameters of parabolic ionosphere layer model in oblique backscatter sounding, using distance-frequency characteristics

19 p2791 A72-38360

Scattered signal power approximation during ionospheric oblique backscatter sounding, using geometrical optics method 19 p2766 A72-38361

I unar radar backscattering measurement of 0.86 cm circularly polarized radiation, noting echo polarization ratio and depolarization variations with incidence angle 19 p2868 A72-38735

A multiple-scattering model of the diffuse component of lunar radar echoes. 20 p2903 A72-39473

Stimulated thermal and Mandelstam-Brillouin scattering of light in liquid nitrogen and oxygen. 20 p2933 A72-39520

Backscatter from gated fluctuating regions - A Bremmer series approach. 21 p3015 A72-40361

Aspect-sensitive reflections from ionization irregularities in the F-region. 22 p3154 A72-42364

Direct and cross polarized backscatter power from a turbulent plasma. 23 p3320 A72-43521

Backscattering of desorbed gas molecules from spacecraft 23 p3284 A72-43618

The effect of the subsurface on the depolarization of rough-surface backscatter. 24 p3380 A72-45635

A practical evaluation of earth-backscatter simulation and an estimate of the HF ground-scatter coefficient. 24 p3380 A72-45636

Approximate temperature distribution for a diffuse, highly reflecting material. 24 p3465 A72-45790

BACKWARD WAVE TUBES

Electrostatic focusing field inhomogeneity /gradients/ effects on high frequency electron-wave interaction processes in linear beam backward wave oscillator tube 07 p0952 A72-18845

Buildup of oscillations in crossed-field backward-wave oscillators. 24 p3385 A72-44973

BACKWARD WAVES

One dimensional periodic slow wave structure interaction with charged particles beam, considering system operation as TWT and backward wave tube 13 p1931 A72-29288

Resonator polarization parameters effect on backwave attenuation in three and four mirror TW ring laser, noting colliding waves intensity dependence on polarization angle 24 p3411 A72-45505

BACTERIA

NT BACILLUS

NT CLOSTRIDIUM BOTULINUM

NT ESCHERICHIA

NT HYDROGENOMONAS

NT PSEUDOMONAS

Hydrostatic pressure and temperature effects on growth of psychrophilic marine bacterium, emphasizing inhibited amino acid transport and respiration 01 p0011 A72-10322

Space flight biological effects on lysogenic bacteria and human cells in culture 01 p0011 A72-10365

Pigment system and primary photosynthesis evolution, using comparative analysis of bacteriochlorophyll, bacterioviridin and chlorophyll 04 p0469 A72-14780

Bacterial respiration through oxidative phosphorylation origin hypotheses, discussing photosynthesis and sulfate respiration in anoxygenic atmosphere and thioacillus and aerobic evolution in oxygen atmosphere 04 p0470 A72-14795

Thin layer chromatography technique for rapid quantification of bacterial cell adenosine triphosphate, using microscope ultraviolet photometer 06 p0763 A72-17872

Effect of salt on activity, stability and allosteric properties of catabolic threonine deaminase from extremely halophilic bacteria 09 p1275 A72-22535

Thermolabile triose phosphate isomerase in psychrophilic Clostridium at moderate temperatures 10 p1426 A72-24750

Biological experiments on plants, animals and bacteria aboard Zond 5, 6 and 7 space probes, noting flight conditions effect on physiological functions and hereditary structures 11 p1579 A72-25941

Ionic and hydrophobic interactions effects on Micrococcus lysodeikticus membrane stabilization process 14 p2075 A72-30595

Spacecraft bacteria population resistance to simulated Jovian trapped radiation belt electrons and solar wind protons, noting dependence on isolate, dose and electron energy 15 p2186 A72-31993

Isolation of extremely halophilic carbohydrate-utilizing bacteria, using acid formation from various sugars as carbohydrate metabolism index 15 p2187 A72-32729

Studies of the electron transport chain of extremely halophilic bacteria. VII - Solubilization properties of menadiene reductase. 19 p2755 A72-37649

Survival of common terrestrial microorganisms under simulated Jovian conditions. 19 p2755 A72-37721

Cytoplasmic heredity theory linking mitochondria origin to bacteria 19 p2758 A72-38549

Mathematical model of two-component alga-bacteria biocenosis 21 p2997 A72-40431

Functional reliability of the biological component of a life support system 21 p2998 A72-40448

Effects of simulated space vacuum on bacterial cells. 23 p3254 A72-43395

BACTERIOLOGY

Lipid composition of growing and starving cells of Arthrobacter crystallopoietes. 17 p2505 A72-35835

A re-evaluation of material effects on microbial release from solids. 23 p3253 A72-43383

BACTERIOPHAGES

Bacteriophage synergistic inactivation by heat and ionizing radiation from kinetic model describing dose rate and temperature dependences 06 p0768 A72-18185

Isolation of a polyvalent bacteriophage for Escherichia coli, Klebsiella pneumoniae, and Aerobacter aerogenes. 19 p2755 A72-37650

BAFFLES

Sound reflection by dense doubly periodic grating parallel to rigid baffle, describing asymptotic characteristics by double lattice virtual mass including mirror image 03 p0387 A72-12914

Electron bombardment ion thruster performance characteristics with variable magnetic baffle and hollow cathode 11 p1710 A72-26214

Variable magnetic baffle as control device for Kaufman electron bombardment ion thrusters with hollow cathode 13 p2027 A72-28949

Experimental study of heat transfer in a subsonic jet impinging normally on a plane baffle. 21 p3128 A72-40949

Influence of baffle geometry on heat transfer in the cooling channel of air-cooled blades 21 p3099 A72-41062

BAGS

NT GAS BAGS

BAINITE

Tempered Fe-Cr-C-Co steels microstructural and mechanical properties, investigating martensite and bainite 03 p0375 A72-13929

Austenitizing condition effect on lower bainite transformation in eutectoid carbon steel 11 p1656 A72-25515

BAINITIC STEEL

Heat treatment effects on martensitic bainitic steel hardness, tensile strength and impact endurance, examining carbide and alpha phases 11 p1666 A72-26922

Creep tests on 2-1/4 per cent chromium 1 per cent molybdenum steel in bainitic condition. 19 p2817 A72-37713

BAKEOUT

U DEGASSING

BALANCED AMPLIFIERS

U PUSH-PULL AMPLIFIERS

BALANCING

Wheel balancing by static and dynamic trial method, using Churchill Mark 3 apparatus 15 p2213 A72-31635

Balancing procedure for statically determinate turbine rotors with multiple supports 16 p2443 A72-33241

Vibration technology: Balancing flexible rotors; Conference, Technische Universitaet Berlin, Berlin, West Germany, March 23, 24, 1970, Summaries 18 p2731 A72-36064

Survey regarding present views, directives and standards, and the customary approaches for balancing flexible rotors 18 p2731 A72-36065

Orthogonal functions application to flexible rotors balance, expressing deflections vs angular velocity as sum of eigenvectors 18 p2731 A72-36066

Comparison of the balancing of a flexible rotor following the methods Federn-Kellenberger and Moore. 18 p2731 A72-36067

Flexible rotors balancing theory based on Fredholm integral equations, considering two- and three-bearing supported shafts with arbitrary mass distribution 18 p2731 A72-36068

Flexible rotor balancing over operational rotational speeds, deriving matrix equation for general conditions based on distributed and concentrated unbalance concept 18 p2732 A72-36071

Balancing of a flexible rotor by means of mode separation. 18 p2732 A72-36072

Statistical analysis of influence coefficients and unbalance forces measurement errors in balancing of rotors 21 p2996 A72-41229

Airline operational weighing and balancing of 747 aircraft, discussing accuracy and calibration procedures for electronic load cells, mobile platform scales and onboard aircraft weighing systems [SAWE PAPER 917] 23 p3251 A72-43464

Balancing aerospace bodies on industrial balancing machines. [SAWE PAPER 929] 23 p3293 A72-43469

BALL BEARINGS

High speed radial thrust multipoint ball bearing design, discussing contact resistance, ball motion, ring deflection and centrifugal force effect on performance and service life 01 p0078 A72-11378

Series hybrid fluid film-rolling element bearing analytical and test evaluation for high speed thrust load turbine applications [ASME PAPER 71-LUB-15] 02 p0235 A72-11537

Elastic strain effects in ball bearing supports on motion of gyroscope Cardan suspension 02 p0231 A72-12565

Ball bearings rolling and spinning friction coefficients determination as function of stress at contact point, race and ball diameter 03 p0363 A72-13561

Vibration measurements of gyromotors with aerodynamic spherical and ball bearings 09 p1263 A72-22347

Ball bearing rolling contact lubricating oil film thickness theoretical prediction compared with experiment 09 p1318 A72-22850

Rigidity calculation of double row radial thrust annular ball bearing loaded by axial and radial force and torque 11 p1646 A72-26978

Ball bearings lubricated with oils and fire-resistant fluids, testing fatigue life relationship to steel quality, fluid film thickness and viscosity 12 p1816 A72-28108

Deep groove ball bearing endurance tests to determine running conditions and lubricant film thickness/surface roughness ratio effects on fatigue life 12 p1816 A72-28112

Radial bearing placed on journal of Cardan suspension, investigating ball dimension errors effect on gyro drift rate 13 p1962 A72-28385

Rolling-element bearings life estimation based on ASME engineering design guide, taking into account materials properties and processing, misalignment, speed and lubrication characteristics [ASME PAPER 72-DE-29] 14 p2108 A72-30870

Variable rigidity effects of ball bearings on axial loading stability and failure of gyromotor supports 15 p2235 A72-31898

Steady flow of conducting fluid in MHD ball bearing clearance between two eccentric spheres, deriving load, friction moment and optimum operation mode 18 p2696 A72-36818

A stand for quality control of the vibrational characteristics of 'ultraquiet' radial ball bearings 19 p2807 A72-37663

Testing of plastic lubricants in ball bearings with rocking motion on the TsKB 16-T test stand 23 p3307 A72-43975

BALLISTIC CAMERAS

Accuracy of the determination of the positions of stars and artificial satellites from an aircraft 19 p2861 A72-37973

BALLISTIC MISSILES

NT INTERCONTINENTAL BALLISTIC MISSILES

NT INTERMEDIATE RANGE BALLISTIC MISSILES

NT MINUTEMAN ICBM

NT POLARIS MISSILES

NT POSEIDON MISSILES

Altitude chamber simulation of reentry bodies separation from ballistic missiles, examining body shape, nozzle dimensions, gas pressure and distance effects [ONERA, TP NO. 1029] 05 p0645 A72-17198

Hypersonic missile trail conductivity measurement on ballistic test stand, calculating electron concentration decrease 14 p2069 A72-30312

Sonar techniques application to radar, stressing utilization of preformed channels in rapid and distant detection of satellites and ballistic missiles
15 p2197 A72-31874

Low recession graphite nosetip design for ballistic reentry, considering blunt and sharp configurations in terms of thermally induced tensile strain survival
[AIAA PAPER 72-705] 16 p2472 A72-34039

Minimum ballistic factor missile shapes.
19 p2746 A72-37522

Hypersonic missile trail conductivity measurement on ballistic test stand, calculating electron concentration decrease
23 p3247 A72-43214

Spin stabilized ballistic air-to-ground or ground-to-ground rocket, discussing dynamic stability-impact error relationship
[SAWE PAPER 928] 23 p3342 A72-43468

Parallel processing of ballistic missile defense radar data with PEPE.
24 p3383 A72-45667

BALLISTIC RANGES

Sonic boom simulation devices and techniques, including wind tunnels, ballistic ranges, spark discharges and shock tubes
08 p1147 A72-21906

The design and operation of the Air Force Flight Dynamics Laboratory Ballistic Impact Test Facility.
[AIAA PAPER 72-998] 21 p3041 A72-41584

A large viewfield laser photographic system for inflight model contour measurements in an aeroballistic range.
22 p3179 A72-42679

Telemetry acquisition of aerodynamic heat rates to conical, free-flight models at Mach 6 in an aeroballistic range.
22 p3155 A72-42703

BALLISTIC TRAJECTORIES

Orbital plane rotation and terminal impact ascending node and inclination of satellite during ballistic reentry
01 p0052 A72-10078

Perturbation solution of deceleration trajectory in ballistic reentry through rotating atmosphere with winds, assuming constant gravitational field and square law drag force
09 p1395 A72-22924

Ballistic density and wind determination from radiances observed by satellite IR spectrometer /SIRS/ onboard Nimbus 3
13 p1991 A72-28825

Exobase atomic hydrogen densities for zero ballistic net flux as function of temperature distribution, noting support of McAfee hypothesis byOGO-4 polar UV observations
16 p2384 A72-32979

Range correction computations for weapons dropped from aircraft.
19 p2747 A72-37286

Equations for the general motion of a rocket in a resistant medium
24 p3452 A72-45448

BALLISTICS

NT INTERIOR BALLISTICS

NT TERMINAL BALLISTICS

Soviet book on rocket dynamics covering history, variable mass point aerodynamics and ballistics, numerical and computer methods and trajectory analysis
02 p0286 A72-12123

A study of the electronic and gasdynamic parameters of a hypersonic wake behind models moving in argon
22 p3168 A72-43111

BALLISTOCARDIOGRAPHY

Ballistocardiography and clinical studies - Conference, Atlantic City, 2 May 1970
03 p0314 A72-13141

Idiopathic hypertrophic subaortic stenosis ballistocardiography, measuring ventricular function by angiography
03 p0314 A72-13142

Regular sinus rhythm bundle branch block effect on ballistocardiogram dynamics
03 p0314 A72-13143

Age related diminutions in ballistocardiographic and electrocardiographic amplitudes, observing relation to heart position lateralization and size reduction
03 p0314 A72-13144

Ballistocardiographic measurement of net cranial blood inflow during cardiac ejection
03 p0314 A72-13145

Hf ballistocardiography in erect position, noting tracing quality in Starr table
03 p0318 A72-13146

Ballistocardiographic and angiographic correlations of ventricular function in patients with idiopathic hypertrophic subaortic stenosis
04 p0466 A72-14442

Circulatory assist and ballistocardiographic studies; Proceedings of the Fifteenth Annual Meeting, Atlantic City, N.J., May 1, 1971.
18 p2648 A72-36032

Correlation between ergometry, ballistocardiography and coronary angiography in 267 patients.
18 p2649 A72-36034

Mathematical models for flow ejection and aorta pressures based on displacement ballistocardiography and time dependent incompressible flow theories respectively
18 p2649 A72-36035

Some preliminary observations on the correlation of the high frequency /acceleration/ direct-body ballistocardiogram with the apex cardiogram, carotid pulse and their derivatives.
18 p2649 A72-36036

Computerized simulation of ballistocardiograph subjective evaluation and objective manual measurements, correlating heart beat with ideal pattern
18 p2652 A72-36037

Digital computer technique for ballistocardiography simulation, using distributed parameters for vessel segments in circulatory system model
18 p2652 A72-36038

Two-mass system as human body dynamic model in ballistocardiography, outlining transfer function parameter computation procedure
18 p2652 A72-36039

A large-scale model of the human cardiovascular system and its application to ballistocardiography.
[ASME PAPER 72-AUT-Q] 23 p3259 A72-43635

BALLOON FLIGHT

Superpressure balloons /tetroons/ performance characteristics, determining ascent rates and superpressure, stress and volume perturbations due to forced change in height
01 p0005 A72-10829

Behavior of spherical balloons in wind shear layers.
18 p2643 A72-36963

Balloon-borne UV spectrophotometer observation of Mg II resonance doublet at 2795 and 2802 A in stellar spectra, comparing to Ca II line widths
20 p2965 A72-38907

Composition of cosmic-ray nuclei at high energies.
20 p2965 A72-39716

Balloon-borne telescope search for solar neutrons and gamma rays during enhanced solar activity periods
21 p3101 A72-41298

Air motions in the tropical stratosphere deduced from satellite tracking of horizontally floating balloons.
21 p3078 A72-41612

BALLOON SOUNDING

Balloon measurements for differential energy spectra of cosmic ray protons and He over half solar cycle 1965-1969, using Geiger tube hodoscope.
[AD-745870] 01 p0119 A72-10876

Cost effective ship-based research balloon fleet for scientific experiments meeting stringent space research budget requirements
01 p0048 A72-10954

Extraterrestrial gamma ray flux contribution to total 0.7-4.5 MeV radiation at various latitudes by balloon sounding
01 p0120 A72-11007

Pulsar NP 0532 pulsed hard X ray energy spectrum measurement, using balloon sounding data
01 p0134 A72-11160

Antiprotons abundance in primary cosmic radiation near geomagnetic equator from asymmetrical flux balloon measurements
03 p0407 A72-12992

Optical multiplate spark chamber in balloon-borne gamma ray telescope, describing triggering signal from plastic scintillator directional Cerenkov counter and photographic recording system
03 p0353 A72-13035

Balloon-borne galactic X ray detection unit, obtaining high directivity with honeycomb collimator and angular resolution with solar sensor
03 p0353 A72-13043

Solar observation survey, considering sounding rockets, OSO, balloons, orbiting observatories, spectral resolution, spectral features and solar flare
03 p0409 A72-13050

Solar UV flux measurements by balloon-borne grating monochromator, using FM-FM analog and PCM telemetry systems for computerized data analysis
03 p0409 A72-13051

High spectral resolution balloon-borne spectrograph for near UV solar Mg II resonance lines
03 p0354 A72-13053

Scientific balloon data management system, discussing airborne and ground station equipment for telemetry, command and flight control
03 p0327 A72-13725

Bremsstrahlung emission by auroral electrons in upper atmosphere and penetration in lower atmosphere, comparing calculation with balloon measurement
04 p0566 A72-14879

Jimsonde high resolution temperature 'nsor for FPS-16 Radar/Jimisphere wind system, analyzing rms errors
04 p0522 A72-15157

Primary cosmic ray electrons energy spectrum measurements, using balloon-borne absorption spectrometer
04 p0568 A72-15509

Remote sensing with sounding rockets and balloons, discussing cost, mineralogical surveys, land use and hydrological assessments
05 p0654 A72-15756

Upper atmosphere supplementary electron flux data relationship to geomagnetic disturbance obtained from high altitude balloon experiments
05 p0709 A72-16236

X ray detection on Jupiter with actively collimated balloonborne scintillation counter, noting decametric emission due to electron precipitation
06 p0872 A72-17445

Specific moisture contents in stratosphere over European Soviet Union from balloon measurements
06 p0806 A72-17734

High energy gamma rays from Cygnus region, using balloon flight measurements with spark chamber telescope
06 p0873 A72-17891

Azimuthal IR radiation distribution of atmospheric brightness cross sections at various zenith angles from balloon programmed-control radiometer data
06 p0808 A72-18042

Balloon measurements of lower stratosphere ion conductivity, noting deviation from predicted values based on Thompson ion-ion recombination theory
06 p0808 A72-18094

Sounding rocket programs and balloon implemented upper atmosphere research in Australia
07 p1070 A72-19088

X ray pulsar observed near Crab Nebula by balloonborne telescope, discussing identification with NP 0527 or NP 0532
07 p1070 A72-19122

Simultaneous auroral X ray, bremsstrahlung and visible bursts observations from balloons.
07 p1058 A72-19166

Low energy gamma radiation spectrum from galactic center region, using balloon altitude observation
07 p1059 A72-19420

Balloon measurement of low energy cosmic gamma ray flux, obtaining energy spectrum
07 p1059 A72-19585

Extragalactic origin of diffuse low energy cosmic gamma rays, using balloon-borne detector system
07 p1063 A72-20392

Primary cosmic radiation antiproton flux, finding .005 ratio upper limit to proton flux with balloon-borne magnetic spectrometer
07 p1064 A72-20633

High energy electrons and gamma quantum flux in upper atmospheric layers from high altitude balloon measurements
07 p1065 A72-20639

High energy gamma radiation intensity from galactic plane in Cygnus-Cassiopeia region, using balloon-borne telescope
08 p1227 A72-21215

Balloon observations of low energy Scorpius X-1 gamma ray spectrum
08 p1227 A72-21395

Electronography in space astronomy, discussing use of Lallemand electronic camera as photon receptor onboard balloons or rockets
08 p1170 A72-21963

Hard X radiation source in Vela X supernova remnant direction detected during balloon flight on 25 November 1970
09 p1383 A72-22290

Energetic solar X-ray burst of 11 February 1970 observed by balloon-borne NaI scintillation detector launched from Antarctica, comparing to OSO 5 data
09 p1377 A72-22930

Balloon sounding observations of lower stratosphere secondary cosmic radiation bursts due to solar activity
10 p1529 A72-24069

Coma constellation hard X ray intensity sky map at 20-150 keV from balloon observations
10 p1530 A72-24948

Magnetometers for balloon-borne X ray astronomy payload azimuth determination, noting misorientation, earth and spurious magnetic fields effects on measurement effectiveness
10 p1530 A72-24954

Calibration technique for meteorological superpressure balloon hygrometers designed for horizontal sounding of troposphere and stratosphere
10 p1484 A72-25087

Pulse radar radio altimeter for balloon atmospheric sounding
10 p1484 A72-25088

French-U.S. Fole meteorological satellite project to map Southern Hemisphere winds, describing system based on pressurized balloons for data acquisition
11 p1680 A72-25813

Cosmic ray proton and He nuclei differential energy spectra measurements by balloon-borne ionization spectrometer
11 p1712 A72-25881

Global horizontal sounding technique balloon flights, determining Southern Hemisphere temperature latitude circulation climatology
13 p1988 A72-28443

- French tetrahedral and spherical meteorological balloons, discussing projects Eole and Essov to sound Southern Hemisphere and stratosphere respectively
13 p1897 A72-28828
- X ray flux associated with gravitational radiation pulses, determining upper limit with balloon-borne apparatus
13 p2007 A72-30121
- Balloon flight tracking by Nimbus D satellite to sound tropical stratosphere air motions, noting northward drift maximum in Northern Hemisphere winter
14 p2128 A72-30350
- Primary cosmic rays antinuclei content upper limit from emulsions investigations with balloons and satellites
14 p2148 A72-30885
- Diffuse cosmic gamma ray flux density and energy spectrum observation at equatorial balloon altitude, discussing photon count, flux and spectra
15 p2299 A72-31924
- Planetary divergence field estimation via Lagrangian tracers and Eole experimental balloons data, developing spatial analysis method
15 p2266 A72-31952
- Japanese report to COSPAR on space research by sounding rockets, balloons and SHINSEI scientific satellite
15 p2338 A72-32011
- Balloon flight observation of charge composition fine details and gross features of isotopic abundance in near relativistic cosmic rays
16 p2447 A72-33729
- A search for high energy gamma-rays from solar active regions.
17 p2599 A72-35092
- Atmospheric composition to 40 km altitude from balloon-borne particle impacted electron microscope screens, discussing pollution effects from high flying aircraft exhaust gases
17 p2551 A72-35935
- Some space instruments for the study of micrometeoroids.
17 p2558 A72-35940
- High energy gamma radiation from the galactic centre region.
18 p2722 A72-36998
- Anomalous increase in the total X-ray background at balloon altitude.
19 p2853 A72-38755
- A balloon search for extraterrestrial high energy gamma-rays in the northern hemisphere.
20 p2965 A72-39876
- Balloon measurements of tropospheric turbulence vertical profiles, obtaining temperature and refractive index structure coefficients
21 p3077 A72-40144
- Sounding balloon services for extraterrestrial, atmospheric and terrestrial studies, emphasizing NCAR Balloon Flight Station facilities at Palestine, Texas
21 p2996 A72-41610
- Balloon optical experiments in IR, visible, UV and X ray regions, considering in situ measurements of atmospheric composition, electric field and cosmic dust
21 p3049 A72-41613
- Conjugate features of magnetospheric electron dynamics observed at balloon altitudes.
21 p3049 A72-41614
- Balloon techniques in X ray astronomy, considering emission mechanisms of discrete cosmic sources
21 p2996 A72-41616
- Particle, plasma and field detectors for rocket investigations in and above atmosphere, considering PCM telemetry system and balloon-borne X ray telescope system
21 p3057 A72-41617
- Magnetospheric substorm onset examined via simultaneous balloon X ray and electric field measurements, discussing ATS 5 observations
22 p3170 A72-42409
- Balloon nacelle for terrain photography from very high altitudes
24 p3403 A72-45229
- BALLOONS**
NT HIGH ALTITUDE BALLOONS
NT METEOROLOGICAL BALLOONS
NT TETHERED BALLOONS
Pageos balloon satellite orbital perturbations due to erratic solar radiation pressure induced accelerations, comparing modified Smith perturbation model calculations with photometric observations
15 p2228 A72-31975
- Solar radiation pressure effects on balloon satellite behavior, noting orbital eccentricity variations
16 p2463 A72-34182
- Spherelike deformations of a balloon.
19 p2878 A72-38716
- BALMER SERIES**
Lyman alpha, Lyman beta and Balmer alpha hydrogen airglow emission simultaneous measurements compared with solar radiation resonant scattering models
01 p0061 A72-10899
- Dust continuous spectrum and Balmer line intensity ratio in Orion Nebula from slit spectroscopy observations
[AD-745076] 02 p0284 A72-12631
- Flare spectra of AD Leo during strong burst, comparing Balmer discontinuity and line widths with UV Cet stars
06 p0883 A72-18020
- Doppler broadening elimination in red Balmer line of atomic hydrogen at 6563 A by high resolution saturation spectroscopy
07 p1037 A72-19132
- Unstable binary RW Aur spectrophotometric study with stellar evolution and outer atmosphere implications, relating Balmer continuum to UV excess
08 p1233 A72-21277
- H Balmer lines H alpha/H beta ratios as electron temperature indicators in nonequilibrium plasmas
09 p1359 A72-22666
- Flare spectra of AD Leonis during strong burst, comparing Balmer discontinuity and line widths with UV Cet stars
11 p1718 A72-25956
- Spectrophotometry of inner corona and quiescent prominence during 7 March 1970 solar eclipse, discussing Balmer line analysis
13 p2042 A72-29536
- Early star absolute magnitude from equivalent H gamma and delta line widths and Balmer hydrogen series line
19 p2859 A72-37908
- The chromospheric continuum observed at the total solar eclipse of 12 November 1966 and a model of the low chromosphere.
21 p3109 A72-41328
- Simultaneous measurements of H alpha and H beta Balmer lines and He D3 line in faint prominences, showing emission intensity ratios dependence on layer total optical thickness
22 p3221 A72-42034
- On circumstellar gas emission among pre-main-sequence stars in Ie Orionis and NGC 2264.
22 p3227 A72-42555
- BALSA**
Structural sandwich panel design, establishing simple stress and deflection formulas under transverse loading based on tests evaluating balsa as laminate core
01 p0138 A72-10723
- BANACH SPACE**
Necessary conditions for inequality-type mixed constraint optimal control, using abstract multiplier rule for Banach space of continuous and bounded measurable functions
04 p0506 A72-15201
- Functional analytical formulation of steady creep processes, using error estimations in solution of equations with monotonic potential operators in Banach spaces
09 p1409 A72-23567
- Measurable multiapplications and convex integrals properties in complete probability and Banach spaces
11 p1678 A72-26476
- Successive approximation for solving parabolic equation with abstract function, using Chaplygin method for Cauchy boundary value problem in Banach space
13 p1987 A72-29646
- Iteration methods to compute inverse for nonsingular linear operator on Banach space
15 p2261 A72-31495
- Nonlinear equations systems iterative solution methods convergence, generalizing Varga matrix splitting technique to nonlinear mappings in Banach space
15 p2264 A72-32465
- Banach space order and compactness properties extension to general case of arbitrary regular space, discussing system topologies
18 p2704 A72-36461
- Interpolation theorems for nonlinear operators acting on locally convex spaces constituting projective and inductive limits of Banach spaces
18 p2704 A72-36513
- Nonzero solutions of boundary value problems for second order ordinary and delay-differential equations.
18 p2705 A72-36617
- Analytic continuation of functions over infinite dimensional domains, covering Banach manifolds, hypoanalytical mappings, convexity and topology
24 p3418 A72-44827
- Spline functions application to approximation theory problem of determining diameters of subspaces and manifolds in Banach space
24 p3419 A72-45548
- BAND STRUCTURE OF SOLIDS**
Mixed zincblende ternary and quaternary alloys, comparing empirical pseudopotential and dielectric model methods for energy gap calculation
03 p0404 A72-14262
- Second harmonic generation, coherence lengths and second order susceptibilities near band edge in InSb as function of magnetic field
03 p0404 A72-14269
- Metal-alumina-oxide-semiconductor capacitor flat band bias voltage measurement before and after thermal stressing, noting potential barrier in structure model
03 p0336 A72-14278
- N- and p-type semiconductors energy band structure bending near interface
05 p0702 A72-16197
- Electron theories of chemisorption and catalysis on semiconductor surfaces, considering band theory applicability range
07 p1048 A72-19561
- Optical properties changes of Al alloys containing impurities, noting band structure modification and tendency toward free electron response
08 p1186 A72-21593
- Pressure effects on transition temperature and electronic structure of narrow band superconductors
09 p1368 A72-22562
- Fluorescent X ray spectroscopy for K and L emission band structures of Mg, Al and V and metal compounds
09 p1370 A72-22839
- Ta and W X ray spectra fine structure measurement, providing electron states density in unoccupied regions of energy bands of solids
09 p1370 A72-22842
- Electron spectroscopy for chemical analysis /ESCA/ application to band structure measurements in transition metals, discussing photoexcitation, energy loss and escape depth
09 p1371 A72-22843
- Double beam single detector wavelength modulation spectrometer for background elimination from observed spectra, noting application to semiconductors band structure determination
09 p1315 A72-23402
- Book on semiconductors covering electrical properties, energy band structure, impurities, epitaxial growth, silicon dioxide, surface properties, p-n junctions and measurement techniques
10 p1528 A72-25123
- Hall-Weaire tight binding Hamiltonian solution in cycle free approximation for band structures and delta functions of amorphous semiconductors
11 p1700 A72-25725
- Semiconductor laser threshold current dependence on doping degree and temperature based on optical transition model and energy band theory
11 p1647 A72-26327
- Metallic chromium band structure determination by Green functions method, explaining transition metals X ray emission lines by single electron approach
13 p1972 A72-28489
- Vanadium emission spectra studies of energy band structure in vanadium silicides, showing p-subzone splitting
13 p1980 A72-29798
- Graphite band structure investigated by secondary electron emission, observing electron transitions to higher excited states
15 p2260 A72-31856
- Electronic energy band structures for alpha and gamma phase Ce, using exchange potential and plane wave method
15 p2293 A72-32227
- Metal-insulator-metal tunnel junctions, investigating effect of nonparabolic band structure energy-momentum relation on I-V characteristics
16 p2370 A72-34101
- Electric contact between metal and n-type semiconductor, investigating contact pressure effects on electron tunneling and phonon conductance to provide band structure
18 p2718 A72-36488
- Electronic and optical phenomena in semiconductors.
19 p2844 A72-37445
- Book - Amorphous semiconductors.
20 p2958 A72-38924
- Structure of the energy bands of titanium, hafnium, and tantalum monocarbides
20 p2939 A72-39311
- Quantum limit studies in single crystal and pyrolytic graphite.
21 p3097 A72-41186
- Light emitting diodes /LED/ materials characteristics, heterojunction band structures and optical spectral ranges, considering application to information processing
21 p3035 A72-41649
- Two band superconductor state density vs energy, noting energy spectrum extremal points
21 p3098 A72-41697
- Thermal conductivity in the two-band model of superconducting transition metals containing nonmagnetic impurities.
23 p3323 A72-43274
- Theory of microwave amplification with electron transfer
23 p3269 A72-43550
- The pressure dependence of the E2 reflectivity peak and of the dielectric constant in III-V semiconductors.
23 p3324 A72-44321

- Interpretation of X-ray emission bands of AIII-BV compounds 24 p3432 A72-44914
- Thermal conductivity in dirty transition-metal superconductors near the upper critical field. 24 p3432 A72-45675
- ## BANDPASS FILTERS
- ### NT CRYSTAL FILTERS
- ### NT TRACKING FILTERS
- Incoherent optical communications fixed receiver passband, determining SNR for pulse time and code modulation with discrete time 01 p0024 A72-10198
- RF interference in angle-modulated system with predetection linear bandpass filter, calculating output power spectral density in baseband 01 p0045 A72-10332
- Broadband high efficiency mode (HEM/ TRAPATT) amplifiers for S band, discussing bandpass and input-output characteristics with Ichebycheff filter 01 p0038 A72-10652
- Waveguide channel microwave bandpass filters for radio relay systems, discussing methods of improving group delay in passband and attenuation at harmonic frequencies 01 p0041 A72-10694
- Optimum power allocation in design of phase-coherent receiver having bandpass limiter, extending technique from single channel to two channel system 02 p0174 A72-12136
- Interference polarization filter by modulation and phase detection for passband narrowing and secondary maxima attenuation, discussing application to photoelectric recording system 03 p0356 A72-13096
- Active all-pass circuits transfer function and synthesis, including delay lines, phase correctors and wide-band phase shifter applications 03 p0338 A72-13169
- Low sensitivity distributed-active bandpass network with effective use of capacitance to save space and weight 04 p0506 A72-15307
- Computer search for optimum narrow band FM and PM systems bandpass filters, noting low index angle modulated signals 06 p0783 A72-17484
- Steepened microwave bandpass filters with bypass and flattened reflection coefficient and delay, discussing design and implementation 07 p0954 A72-19175
- Low and high pass, bandpass and bandstop active filters, tabulating cut-off frequencies, thermal stability, impedance, power dissipation and voltage specifications 07 p0955 A72-19248
- Orthogonal mode waveguide cavities bandpass filters for communication satellite transponders, comparing with Chebyshev design 07 p0958 A72-20489
- Orthogonal functions representation of received signals in ideal signal sequences transmission in linear systems with matched filters and frequency band limitation 08 p1132 A72-21326
- Transmission and passband properties of polyethylene echelette gratings and combined filters for long wave IR spectrum 08 p1210 A72-22038
- German monograph on optimal design of HF bandpass filters with lumped elements, covering LC coupled two- and four-circuit systems 09 p1284 A72-22328
- Total ozone measurements by selective transmission filter ozonometer comparable to Dobson spectrophotometer 09 p1307 A72-22453
- Tunable dye laser system with narrow band filter for Raman spectroscopy of gases 09 p1326 A72-23351
- Thermal and electric fields interaction in LF integrated circuits design, applying thermal feedback loops to bandpass filter, delay circuit and Schmidt-trigger oscillator 10 p1448 A72-24280
- Narrow bandpass waveguide filters synthesis, using orthogonal mode cavities to realize negative coupling elements 10 p1451 A72-24591
- Optimal filter for narrow band stochastic signal processing, using Wiener theory 10 p1441 A72-25103
- Interference polarization filter by modulation and phase detection for passband narrowing and secondary maxima attenuation, discussing application to photoelectric recording system 11 p1632 A72-25708
- Bandpass filter harmonic signal phase shift distortion effect on transient response in PSK of multichannel transmission 12 p1783 A72-27630
- Integrated inductorless quadratic bandpass filters for constant bandwidth wide frequency range, using IC analog multipliers network 13 p1927 A72-28403
- Bandpass amplifier design with differing two-circuit filters, discussing advantages and limitations 13 p1929 A72-28899
- Pulse signal transmission through bandpass error free wideband PCM communications systems 13 p1919 A72-29055
- Transfer matrices determination for two terminal pair network derived from four terminal pair network, considering bandpass filters 13 p1931 A72-29060
- Forced oscillations in RC amplifier with negative feedback through nonlinear bandpass filter with varicaps 13 p1931 A72-29266
- Narrow band retuned dc pumped amplifier-filter design based on diffron, considering electron beam interaction 14 p2088 A72-30798
- Minimum amplitude and phase distortion selective bandpass filters/ equalizers for satellite communications, noting realizability in UHF and microwave bands 14 p2089 A72-31048
- Rietz-Kantorovich method reduction of scalar problem for wave propagation along direction surface to boundary value problem, discussing parametric resonance and periodic waveguides 14 p2132 A72-31118
- Incoherent optical communications fixed receiver passband, determining SNR for pulse time and code modulation with discrete time 15 p2195 A72-31622
- Equivalent baseband and passband delay line and transversal equalizers derivation for linear modulation systems, obtaining relationship between tap coefficients 15 p2211 A72-31844
- Lossless low pass ladder network synthesis in terms of reflection coefficient poles and zeros with application to bandpass matching problem 15 p2212 A72-32248
- Low pass sampling bandwidth selection for digital mechanization of matched filter bit-synchronizer combination, discussing data rate vs SNR performance 16 p2363 A72-33217
- Bandpass-filtered geophysical and meteorological time series data statistical evaluation by comparison with filtered test series with same variance and autocorrelation function 16 p2363 A72-33383
- Bandpass filters set synthesis in crab eye configuration, noting design principles and telephone techniques 17 p2524 A72-34295
- Output signal-to-noise ratio of a nonlinear device and bandpass filter. 18 p2666 A72-36334
- Technique for varying the conversion loss against frequency of a surface-wave transducer without apodization. 18 p2667 A72-36692
- Synthesis of networks containing three-layer rectangular distributed RC elements and nonideal operational amplifiers 18 p2673 A72-36791
- Representation of real narrowband signals through nonuniformly displaced basal functions with positive coefficients 19 p2768 A72-38668
- Properties of metal interference filters for 1200-3000 Å, of dielectric mirrors for 1700-3000 Å and of multielectric narrow passband interference filters for 2000-3000 Å 20 p2923 A72-39051
- A frequency transformation chart for RC-active band-pass filters. 20 p2907 A72-39432
- Design equations for comb type bandpass filter formed by cascade connection of symmetrical networks containing coupled waveguides and coaxial lines 22 p3158 A72-42125
- Electronic analyzer of structural vibration frequency characteristics and mutual spectra, considering bandpass filter and automatic frequency spectra recorder 22 p3176 A72-42134
- An approach for generation of second order RC-active filters. 23 p2376 A72-43863
- On the performance of digital communication systems with bandpass limiters. I - One-link system. II - Two-link system. 23 p2365 A72-44181
- Monolithic quartz and ceramic bandpass filters for narrow band analog data transmission systems 23 p2373 A72-44347
- Theory of magnetically tunable band-pass filters 23 p3273 A72-44360
- ## BANDS
- Stability loss condition for long rectangular cross section band from nonlinear elastic material with internal constraints, discussing critical loads and deformations 16 p2467 A72-33120
- ## BANDWIDTH
- ### NT BROADBAND
- ### NT SPECTRAL LINE WIDTH
- Gain and bandwidth properties of microwave and optical devices with isotropic active medium, investigating transmission coefficient 02 p0189 A72-11566
- I-V characteristics and bandwidth properties of distributed emission amplifier within magnetic field, analyzing averaged electron trajectories and hf potential distribution 02 p0189 A72-11568
- Wireless electronic time distributing system, investigating integrable digital receiver circuit and frequency bandwidths 02 p0197 A72-12696
- Wideband microwave acoustic delay line design featuring superior bandwidth, phase linearity, spurious echo and insertion loss characteristics 04 p0521 A72-14720
- Bandwidth widening of waveguide H-plane Y-circulator with cylindrical ferrite post coated by dielectric sleeve 04 p0499 A72-15244
- Broadband corrugated conical horn antennas with small flare angles, investigating radiation patterns and bandwidth 04 p0501 A72-15425
- Stability conditions and effective bandwidths of first and second degree pulsed phase locked AFC systems with proportionately integrating filter, using Z transform method 05 p0625 A72-15825
- Reflection and transmission characteristics of circularly polarized horn antenna, discussing bandwidth properties, phase differences, polarization characteristics and voltage SWR 05 p0635 A72-16334
- Bandwidth properties and design of shielded asymmetrical striplines filled by dielectric 05 p0636 A72-16340
- Monopole antenna with lumped mutual coupling between driven and folded sections, noting staggered resonant frequencies and bandwidth broadening from input impedance analysis 06 p0782 A72-17355
- Facsimile bandwidth compression by picture elements reduction with contrast preservation, discussing analog processing algorithm and application to weather satellite photographs 06 p0772 A72-17406
- Log-periodic interdigital transducer design to obtain wide bandwidth for acoustic surface waves 06 p0784 A72-18241
- Comb type slow wave structures properties outside passband, obtaining dispersion and field distribution expressions by electrodynamic analysis 08 p1135 A72-21738
- Small signal microwave transistors design with arsenic and phosphorus diffused emitters, comparing performance in terms of power gain-bandwidth product, maximum frequency and noise figure 08 p1142 A72-21743
- Weak signal turnaround transponder design for pseudonoise coded ranging systems, discussing bandwidth optimization and performance comparison between various receiver configurations 10 p1452 A72-24688
- Stabilization bandwidth reduction in microwave parallel tuned tunnel diode amplifier circuits synthesis 10 p1453 A72-24910
- Data transmission bandwidth requirements compression for band-limited functions, investigating feasibility through analog signal routing 11 p1592 A72-25887
- Moving sound sources spectral analysis techniques, discussing computer controlled one-third octave band and narrowband analysis 13 p2005 A72-29566
- Mean opacities and effective absorption coefficients measurement using wide bandwidths and path lengths 14 p2131 A72-30900
- Multiple port waveguide circulators bandwidth performance calculation to include higher order cylindrical and evanescent modes 15 p2205 A72-31356
- Generalized locking equation for microwave oscillator bandwidth prediction for arbitrary cavity configurations and waveforms, considering strong harmonics presence 15 p2205 A72-31358
- High speed and resolution laser scanning by optomechanical methods, discussing theoretical bandwidth, resolution limits, position error correction measures and performance optimization 15 p2248 A72-32037
- Low pass sampling bandwidth selection for digital mechanization of matched filter bit-synchronizer combination, discussing data rate vs SNR performance 16 p2363 A72-33217
- The fabrication and evaluation of a micropower transistor and hybrid RF amplifier. 17 p2528 A72-34688

Design of band-limited signal with no intersymbol interference f An extension of sampling function.

19 p2767 A72-38606

Representation of real narrowband signals through nonuniformly displaced basal functions with positive coefficients

19 p2768 A72-38668

Bandwidth and threshold calculations for angle-tuned parametric oscillators.

19 p2813 A72-38689

Sensor selection for electromagnetic instrumentation system with sufficient sensitivity and bandwidth to demonstrate electroexplosive device compliance with MIL-E-6051D specified safety margin

20 p2962 A72-38979

Radiation pattern and gain of reflector antenna with adjusting ring, discussing directivity and bandwidth

21 p3031 A72-40540

Extending the range of attenuation measurements.

21 p3022 A72-40999

FM signal distortion during passage through two-element antenna array to determine usable bandwidth from transmission characteristics viewpoint

21 p3022 A72-41265

Variable-bandwidth frequency-modulation chirp pulse compression using a longitudinal acoustic-wave convolver at 1.3 GHz.

21 p3023 A72-41468

Instrumentation systems design for extended bandwidth data acquisition, discussing problem areas in transducers, amplifiers and signal conditioning, data recording and playback

22 p3157 A72-42712

Stability conditions and effective bandwidths of first and second degree pulsed phase locked AFC systems with proportionately integrating filter, using Z transform method

23 p3263 A72-43433

Reflectivity dependence of triple polarization grid on elements spacing and wires orientation, noting bandwidth of ray guide matching transformer

23 p3269 A72-43446

Wideband limitations of waveguide arrays.

23 p3270 A72-43573

Monolithic quartz and ceramic bandpass filters for narrow band analog data transmission systems

23 p3273 A72-44347

Effects of bandlimiting on the coherent detection of PSK, ASK and FSK signals.

24 p3380 A72-44900

BANG-BANG CONTROL

U OFF-ON CONTROL

BANKING FLIGHT

U TURNING FLIGHT

BARANY CHAIR

Vestibular and optical stimuli interaction in human orientation, testing via Barany chair on rotating platform surrounded by optokinetic drum

21 p3007 A72-40751

*RDEEN APPROXIMATION

U BARRIER LAYERS

U ELECTRICAL PROPERTIES

U SURFACE PROPERTIES

BARDEEN-COOPER-SCHRIEFFER THEORY

U BCS THEORY

BARIUM

NT BARIUM ISOTOPES

Optical emission spectrum of Ba and CuO combustion products during nozzle expansion into vacuum

01 p0146 A72-11312

Supersonic oxygen molecules nozzle beam reactive scattering on barium atoms, detailing exothermic reaction energy in barium oxide formation

02 p0170 A72-11912

Excess Xe 131 in lunar Ba feldspar rocks, discussing results of reactor irradiation experiments with fast and epithermal neutrons

03 p0414 A72-12901

Quantum mechanical calculations of autoionization structure in ionization of Ba positive ions by electron impact

03 p0391 A72-13746

Tuned laser radar detection and ranging of high altitude Ba ion cloud by photon counting, discussing SNR requirement

10 p1440 A72-24963

Artificial barium ion cloud spatial-temporal growth in ionosphere, solving ion diffusion equation by numerical methods

13 p1950 A72-29387

Radiative transfer in freely expanding gaseous Ba clouds, deriving atomic states level populations ratio

15 p2223 A72-31428

Thermionic energy conversion with a Ba-Cs-diode.

17 p2496 A72-34603

Investigation of physical processes and optimization of thermionic converters with a Cs-Ba filling

18 p2647 A72-36203

Electron-density increase in the E layer below an artificial barium cloud.

20 p2920 A72-39983

Electron impact effects on Ba I, Ba II and Sr I selected spectral line Doppler widths calculated for

laser-generated plasmas for chemical release simulation

21 p3092 A72-40821

BARIUM COMPOUNDS

NT BARIUM FLUORIDES

NT BARIUM OXIDES

NT BARIUM TITANATES

Barium perchlorate thermal decomposition mechanism, presenting pressure-time and weight-loss curves

07 p1051 A72-19360

Barium styphnate replacement for discontinued SR-4990 smokeless powder as propellant base charge in MK 24 actuator

08 p1222 A72-20784

Phase diagram, isomorphism and temperature dependence of hexagonal, monoclinic and triclinic modifications of Sr-Ba polycrystalline aluminosilicates

21 p3072 A72-40382

BARIUM FLUORIDES

Heat resistance of magnesium, barium and calcium fluorides as solid lubricants in air, hydrogen and water vapor at 100-1100 C

06 p0836 A72-18433

Cooperative and sequential sensitization effect on He emissive states population in polycrystalline barium and yttrium fluorides with trivalent Yb

10 p1525 A72-24044

BARIUM ISOTOPES

Anomalous high concentration of lunar rock Xe-131 relation to Ba-130 nonthermal neutron-capture cross section in resonance energy region

20 p2967 A72-39180

BARIUM OXIDES

Artificial barium oxide clouds band spectrum analysis, calculating rotational and vibrational temperatures in total wavelength region

05 p0655 A72-16069

BARIUM TITANATES

Temperature compensated high dielectric constant material, discussing low loss at microwave frequencies, reproducibility and mechanical properties

01 p0044 A72-11308

Surface moisture effect on dielectric properties of ultrafine barium titanate particulates of varying particle size

[ACS PAPER 7-E-69F]

02 p0269 A72-12416

Dielectric properties of high purity polycrystalline barium titanate, observing temperature effects as function of heat treatment

[AD-737022]

02 p0269 A72-12417

Polarization characteristics of ferroelectric barium strontium titanates in solid solution at 4-100 K

10 p1527 A72-24984

Ceramic dielectrics capacitors, considering perovskites and barium titanate physicochemical properties

11 p1702 A72-26545

Photovoltaic effects in CdS films evaporated onto barium titanate single crystal and ceramic ferroelectric substrates

12 p1856 A72-28014

Ferroelectric nature of superficial layer on barium titanate crystals from scanning electron microscope and optical observations

15 p2291 A72-31681

Phase transitions effect on dc electrical resistance of barium titanate investigated for yttrium-doped polycrystals and for reduced single crystals

15 p2294 A72-32483

Controlled self heating effect in semiconducting barium titanate positive temperature coefficient resistor substrate heater for planar Si devices

17 p2527 A72-34680

Formation of fluorine-containing solid solutions based on barium titanate

19 p2845 A72-38407

Electrical properties of thick-film barium titanate dielectrics produced by flame spraying.

19 p2846 A72-38616

Dielectric dispersion of irradiated BaTiO₃ near the phase transition.

22 p3215 A72-42934

Physical and electrical properties of thin-film barium titanate prepared by RF sputtering on silicon substrates.

22 p3215 A72-42999

BARKHAUSEN EFFECT

Supermagnetic magnetization and ac core loss temperature dependence under slow temperature cycling in vacuum, noting anomalous Barkhausen effect

04 p0564 A72-15718

BAROCLINIC WAVES

Stratospheric CAT relationships to baroclinic zones and Richardson number examined from aircraft observed cross sections data

01 p0096 A72-11282

Disturbance evolution on zonal flow background in baroclinic atmosphere with given wind profile, determining average-time energy distribution

03 p0383 A72-13479

Ultralong wave baroclinic instability, obtaining linearized perturbation equations from layered geostrophic hydrostatic adiabatic model

04 p0541 A72-14451

Steady state geostrophic wind vector variation hodographs in planetary baroclinic boundary layer, considering thermal influence linear superposition on internal friction effects

06 p0841 A72-17667

Parametrization of turbulent flux of momentum, heat and moisture at ground in baroclinic planetary boundary layer

09 p1346 A72-22810

Long period pulsations of finite amplitude baroclinic wave, noting stable limit cycle for small friction effect

09 p1347 A72-23653

Post bifurcation finite amplitude baroclinic instability, emphasizing wave vectors configuration with quadratic nonlinear interactions

09 p1347 A72-23654

Baroclinic wave field distributions and balances in rotating annulus with free surface in atmospheric circulation study, noting Ekman layer features

11 p1680 A72-25765

Disturbance evolution on zonal flow background in baroclinic atmosphere with given wind profile, determining average-time energy distribution

11 p1682 A72-26249

Streak topography for three dimensional structure of thermal convection in rotating fluid under horizontal temperature gradient, noting time variations of baroclinic waves

12 p1809 A72-27701

Baroclinic long wave dynamic instability in Kochin two layer frontal model, extending Richardson number range in absence of beta effect

12 p1841 A72-27987

Baroclinic instability formulation as initial value problem compared to normal mode studies, considering cyclone development in atmosphere

13 p1945 A72-28446

Second order nongeostrophic effects on exponential amplification of two layer baroclinic wave system in uniform zonal current

14 p2127 A72-30342

Book on dynamic meteorology covering synoptic disturbance model, numerical weather prediction and baroclinic waves origin

15 p2266 A72-31875

Planetary atmospheres and interiors in terms of dynamics, rotation, magnetic fields, Jupiter features, geomagnetism, earth baroclinic waves, global circulation and gravitation, etc

16 p2384 A72-33339

Planetary wave interaction in two level baroclinic atmosphere, using quasi-geostrophic equations

16 p2418 A72-33602

Mars - The effects of topography on baroclinic instability.

22 p3225 A72-42504

Baroclinic long wave dynamic instability in Kochin two layer frontal model, noting beta effect on wave disturbances

22 p3202 A72-43001

Tropospheric wave motions with baroclinic basic flow in equatorial latitudes.

24 p3399 A72-45485

BAROCLINITY

Linearized continuous baroclinic atmospheric model, discussing stability for planetary vorticity gradient

04 p0541 A72-14452

Baroclinic primitive equation prediction model for nonpolar part of Northern Hemisphere with allowance for moisture exchange, radiative heat influx and cloud formation processes

11 p1683 A72-26886

Semiimplicit time integration algorithm in atmospheric baroclinic models for short range weather forecasting in Canada

16 p2418 A72-33665

Baroclinic effects on the resistance law for the planetary boundary layer of the atmosphere.

24 p3397 A72-44956

BAROMETRIC PRESSURE

U ATMOSPHERIC PRESSURE

BARORECEPTORS

Cat mean renal nerve activity modification by hypothalamus stimulation and baroreceptor reflex interactions, discussing mean aortic pressure variation effects

04 p0477 A72-15722

Carotid sinus counterpressure as baroreceptor stimulus in intact dog, recording arterial pressure response in closed loop gain

[AD-739805]

07 p0917 A72-19439

Control parameters of the blood-pressure regulatory system. I - Heart rate sensitivity.

22 p3145 A72-42771

BAROTRAUMA

Statistical survey of barosinusitis incidence in U.S. Navy flying personnel during altitude chamber training, discussing diagnostic methods and clinical management

12 p1765 A72-28274

Case report on dive decompression induced maxillary sinus barotrauma due to sinus pressure buildup caused by ostium blockage

22 p3150 A72-42497

Paranasal sinus barotrauma in military flying personnel, discussing radiographic diagnostic methods and hypobaric test procedures for flight status restoration time determination

24 p3378 A72-45664

BAROTROPIC FLOW

Forced barotropic Rossby waves in homogeneous fluid in rotating cylindrical annulus with differentially rotating source-sink distribution

03 p0340 A72-12974

Rotational symmetry solutions to differential equations of stationary barotropic or axisymmetric incompressible flow

03 p0344 A72-14345

Barotropic stability of stratified shear flow to non-geostrophic disturbances by linear analysis

04 p0541 A72-14453

Numerical integration of primitive equations for barotropic atmosphere, using spherical polar coordinates

09 p1346 A72-22809

Rossby similarity for barotropic planetary boundary layer flows in terms of nondimensional Reynolds stress and eddy viscosity

09 p1346 A72-22811

Asian subtropics western disturbances movement prediction by primitive equation barotropic model with east-west cyclic boundary conditions, presenting forecast charts and error statistics

11 p1681 A72-26077

Barotropic instability and vorticity equation of zonal flow with superposed Rossby waves limiting predictability of real atmosphere

12 p1838 A72-27021

Steady barotropic inviscid flows of rarefied gas plasmas as free jet and within cylindrical channel in axisymmetric external magnetic field with Hall effect

13 p2018 A72-29823

Global atmospheric circulation barotropic spectral model application to satellite asymptotic data continuous processing

14 p2127 A72-30258

Planetary wave description by linear difference equation for vorticity transport on hemisphere, considering Laplace operator error

14 p2099 A72-30260

Scale analysis of atmospheric large-scale motions in low latitudes.

23 p3311 A72-44241

BAROTROPISM

Various updating effects on meteorological data analysis accuracy, using balanced barotropic model

04 p0541 A72-14456

Mixing length theory derivation of barotropic planetary boundary layer profiles for geostrophic wind deviations, Reynolds stress, eddy viscosity and turbulent kinetic energy dissipation

15 p2224 A72-31675

BARRICADES

U BARRIERS

BARRIER ISLANDS

U ISLANDS

BARRIER LAKES

U LAKES

BARRIER LAYERS

Barrier capacitance effect on transient characteristics of light diodes, obtaining time dependence of p-n junction volume charge voltage and recombination emission intensity

09 p1284 A72-22211

Josephson dc and ac effects in plane junctions with thin semiconducting film barrier of evaporated material between two superconductors

09 p1370 A72-22800

Microbarrier mechanisms of 1/f noise for resistive materials and semiconductor devices

09 p1280 A72-23102

Cadmium sulfide solar cells stress analysis in relation to degradation caused by fabrication technology, discussing barrier layer formation process

12 p1757 A72-28020

Fretting corrosion fatigue prevention by barrier approach, discussing test program and application to helicopter part fatigue life increase

[AHS PREPRINT 672] 17 p2626 A72-34512

Schottky diode frequency converter characteristics, considering series resistance, housing reactance, barrier layer capacitance, noise sources and noise temperature

19 p2773 A72-37937

Observation on phenomena associated with a slowly varying surface barrier at niobium oxide and aluminum interface.

21 p3097 A72-40702

BARRIERS

Externally pressurized automatic barrier seals for high pressure applications in chemical industry, nuclear power plants and deep-submergence vessels, discussing theory, design and test results

[AHS PREPRINT 72AM 17] 13 p1964 A72-28974

BARS

NT ELASTIC BARS

NT PRISMATIC BARS

Lateral vibration of thin conical bar with clamped base and free tip, calculating characteristic modes and frequencies

01 p0138 A72-10509

Torsion and bending by transverse load for homogeneous orthotropic slightly curved bars

03 p0444 A72-13499

Natural vibration frequencies calculation of straight bars with stepwise variable cross sections by iterative technique based on method of three unknowns

04 p0584 A72-14522

Approximate maximum shock stress analysis for curved bar bending vibration due to longitudinal impact by disregarding elements inertia with regard to axial motion

05 p0737 A72-16285

Split Hopkinson pressure bar for studying material plastic behavior under impact, discussing principles, equipment and test results

06 p0814 A72-17742

X ray and resistance strain gage techniques for bar and metal plate simultaneous residual stress determination

07 p0993 A72-20606

Longitudinal elastic wave propagation along composite bar with conical sections and interface discontinuities in material properties, solving multiple reflection by finite difference method

08 p1245 A72-21606

German monograph on multielement linear mechanical oscillator analysis covering behavior of harmonically excited bar chains of arbitrary structure

09 p1350 A72-22337

Resonant frequency and vibration modes of variable cross section bar in elastic medium under transversal force, noting dynamic programming combined with optimization principle

12 p1845 A72-27538

Creep stability of bars and thin plates and shells for given loading force, considering instability criteria

13 p2054 A72-28481

Partial differential equations for longitudinal, torsional and transverse vibrations of bars with variable composition

13 p2006 A72-29885

Lateral deflection of axially loaded imperfect bar under creep, solving nonlinear integrodifferential equations by quasi-linearization technique

16 p2474 A72-34130

Transverse vibrations of bars with concentrated additional masses

17 p2627 A72-34772

An analysis of the split Hopkinson bar technique for strain-rate-dependent material behavior.

[ASME PAPER 72-APM-26] 17 p2628 A72-34792

Three dynamic conical bar theories, solving transient axisymmetrical motion via method of characteristics

[ASME PAPER 72-APM-20] 17 p2581 A72-34797

Contactless parameter measurements of a vibrating bar.

17 p2554 A72-35148

Longitudinal-torsional vibrations of a screw beam under axial excitation

22 p3240 A72-42954

The use of bar buckling eigenfunctions in the stability analysis of clamped skew plates.

23 p3355 A72-44456

BARYCENTER

U CENTER OF GRAVITY

BARYONS

Equilibrium rotating superdense baryons in general relativity theory, determining integral parameters /mass semiaxes quadrupole moment/ in angular velocity approximation

03 p0435 A72-13805

Equation of state for matter at 10-500 trillion g/cc, applying to baryon matter and neutron stars

04 p0571 A72-14557

CP-noninvariance model of baryon interaction and charge asymmetry of universe, postulating kappa particle /neutral massive fermion/

06 p0875 A72-17275

Transcendence of baryon number conservation law, discussing static black hole properties as final massive star collapse state

07 p1076 A72-19667

Baryon number nonmeasurability of Schwarzschild black hole by strong interactions, extending results to Kerr-Newman holes

09 p1387 A72-22875

Baryon number nonexistence for static black holes and resulting baryonic conservation law transcendence and noninteraction with outside universe

12 p1848 A72-28152

Static black hole noninteraction with exterior world by meson fields, noting baryon number conservation in general relativity

17 p2612 A72-35388

Nuclear energy sources in overdense celestial bodies

19 p2862 A72-38061

BASALT

Apollo 14 Fra Mauro site basaltic rocks and breccia clast internal Rb-Sr isochrons, comparing to Tranquility Sea basalts

01 p0123 A72-10053

Lunar basalts 10044 and 12021 Fe oxidation state in plagioclase and distribution in crystal structure, using Mossbauer spectroscopy

01 p0124 A72-10064

Critique of paper by Ringwood on petrogenesis of Apollo 11 lunar basalts composition and implications for lunar origin

02 p0275 A72-11600

Apollo 14 basaltic evidence for selective volatilization on lunar surface, using electron probe analysis

03 p0439 A72-14273

Northeast Bank, Southern California Borderland volcanic petrology and geologic history, investigating basaltic rocks, hyaloclastites and fossil fragments

04 p0520 A72-15589

Southern Great Basin upper Cenozoic high Sr87/Sr86 and Sr/Rb ratio basalt initial composition, showing mantle material derivation

05 p0655 A72-16043

Volcanic basalt geochemistry in Afar Triple Junction, suggesting relation to crustal thinning and melting zone shallowing under rift

05 p0658 A72-16722

Chromian pleonaste and aluminous picotite in Apollo 14 fine grained microbreccias comparing with spinel composition in lunar basalts

06 p0878 A72-17672

Apollo 15 mare basalts and breccias and premare igneous rocks, analyzing chemical composition and microstructure

06 p0888 A72-18262

Geologic setting of Apollo 15 breccias and basalt

06 p0888 A72-18263

Chemical, geochronological and petrogenetic analyses of Apollo 15 lunar mare basalt rock from Hadley Rille, comparing with Apollo 12 and 14 basalts

06 p0888 A72-18264

Lunar mare basalt 15555 age by Rb-Sr and K-Ar techniques

06 p0888 A72-18266

Trace element concentrations of Apollo 15 basalt and soil samples by atomic spectrophotometry, colorimetry and isotope dilution

06 p0888 A72-18269

Primordial radioelements and cosmogenic radionuclides in Apollo 15 basalt, breccia and soil samples

06 p0889 A72-18274

Fractional crystallization and crustal contamination roles in origin of quaternary basaltic magmas from Black Rock Desert Region in Utah

06 p0810 A72-18515

Geomorphic evidence for basalt lava tubes and channels in Lunar Marius Hills, comparing with terrestrial analogs

07 p1067 A72-18870

Lava tube formation in pahoehoe basalt and flow activity in vent near Alae Crater, Hawaii

07 p0980 A72-20462

Basalt plates craters produced by steel balls, noting profiles at normal and oblique impacts

08 p1232 A72-21153

Lunik 16 landing site geologic similarity to Apollo 11 and 12 sites on basaltic mare fill, noting impact bombardment developed regolith presence

09 p1379 A72-22251

Electron microprobe analysis of Lunik 16 basalt fragments, noting similarity to Apollo 11 and 12 igneous rocks

09 p1379 A72-22252

Optical petrographic, electron microprobe and single crystal X ray diffraction analysis of basaltic and monomineralic soil fragments of Lunik 16 core sample from Sea of Fertility

09 p1379 A72-22257

Lunik 16 microbasalt sample containing skeletal olivine, plagioclase, ilmenite and interstitial pyroxene, comparing to ferromagnesian rich Apollo 11 and 12 basalts

09 p1379 A72-22258

Electron microprobe analyses of Lunik 16 mare basalt fragment G37 with high Al and low Mg content, discussing fragments G46 and G51

09 p1380 A72-22260

Luna 16 rock sample B-1 petrology, mineralogy and chemistry, noting fine grained ophitic basalt nature

09 p1380 A72-22262

Rb-Sr internal isochron determination of Luna 16 maria basalt age, discussing major lunar magmatic activity time interval

09 p1380 A72-22263

Gas retention and cosmic ray exposure ages of Luna 16 basalt fragment from Mare Fecunditatis

09 p1380 A72-22264

Volatile and siderophile elements in achondrites and ocean ridge basalts from radiochemical neutron activation analysis

09 p1385 A72-22598

Thermal conductivity, diffusivity and specific heat of lunar soil and basalt analogs, using Luna 16 samples 10 p1532 A72-23753

Chemical composition features of basalts from British Tertiary Volcanic Province, discussing possible evolution 10 p1472 A72-23915

Differentiated igneous textures of Apollo 11 lunar ferrobalt samples, indicating fractional crystallization followed by crystal-liquid separation 10 p1537 A72-24157

Crystallization sequence, petrology and mineralogy of Apollo 12 basalt sample 12009 10 p1537 A72-24160

Lunar crust and mantle evolution from Rb-Sr ages of Apollo 15 mare basalt samples 10 p1537 A72-24161

Lunar basalt Eu abundance anomaly in Apollo 11 and 12 samples, considering partial melting with or without plagioclase 10 p1537 A72-24162

Rb-Sr isotopic age determination on density and size fractions of Apollo 11 fine soil and basaltic materials 10 p1538 A72-24165

Zirconium rich metal oxides mineral group in Apollo 14 and 15 lunar rocks from feldspar-phyrlic basalt and pyroxene ferrobalt, noting optical and chemical properties 11 p1717 A72-25868

Crystallization experiments on Apollo 11 magmas of K and Rb-rich basalt, discussing plagioclase characteristics 11 p1723 A72-26523

Apollo 14 basaltic rocks cooling deduced from divalent Mg and Fe ionic distribution in pyroxene, noting process interruption below 840 C 11 p1724 A72-26574

U-Th-Pb ages in Apollo 14 basalts and initial radiogenic Pb in lunar rocks, comparing with Rb-Sr and K-Ar isotopic method 15 p2303 A72-31301

Compositional characteristics of olivines from Apollo 12 samples. 18 p2723 A72-36063

Apollo 11 and 12 mare basalts and gabbros - Classification, compositional variations, and possible petrogenetic relations. 19 p2864 A72-38295

Lava tubes of the Cave Basalt, Mount St. Helens, Washington. 19 p2790 A72-38296

Rates of solidification of Apollo 11 basalt and Hawaiian tholeiite. 20 p2967 A72-39181

Basalt plates craters produced by high velocity impact of steel spheres, noting profiles at normal and oblique angles 20 p2978 A72-39258

Instrumental neutron activation analysis of igneous rock abundances in petrogenic and stratigraphic problems, applying to Colombia River basalts and Apollo 11 rock samples 20 p2899 A72-39829

Phenocryst fabric in lunar basalt sample 12052 from the Ocean of Storms. 21 p3106 A72-41115

Uranium distribution in basalt fragments of five lunar samples. 23 p3261 A72-43399

Solid solution, subsolidus reduction and compositional characteristics of spinels in some Apollo 15 basalts. 23 p3262 A72-44135

BASE FLOW

Atmospheric freestream pressure profiles determination from base pressure and flow phenomena of Mars, Venus or Jupiter entry probes [AIAA PAPER 72-202] 07 p0982 A72-18959

The structure of blunt base wakes in swirling flow. 24 p3391 A72-45023

Flow model for the determination of the heat transfer on the base of vehicles with clustered H2-O2 rocket engines. 24 p3434 A72-45201

BASE HEATING

Hypersonic base heating investigation on Mars at atmosphere entry blunt bodies, taking into account gas composition and angle of attack effects [AIAA PAPER 72-317] 11 p1568 A72-25251

Turbulent base heating on a slender re-entry vehicle. 21 p2992 A72-41308

Flow model for the determination of the heat transfer on the base of vehicles with clustered H2-O2 rocket engines. 24 p3434 A72-45201

BASE PRESSURE

Base pressure determination for subsonic isothermal central and peripheral jets of incompressible fluid discharging into subsonic slipstream 03 p0342 A72-13912

Wake outflow concept application to flow separation phenomena, enabling determination of base pressure for drag calculations [DFVLR-SONDDR-176] 05 p0603 A72-16702

Atmospheric freestream pressure profiles determination from base pressure and flow phenomena of Mars, Venus or Jupiter entry probes [AIAA PAPER 72-202] 07 p0982 A72-18959

Solar five minute oscillations in isothermal atmosphere by base pressure fluctuations 09 p1382 A72-22287

Base pressure drag reduction on rectangular wings with blunt trailing edges from low speed wind tunnel measurements [DFVLR-SONDDR-219] 10 p1419 A72-24842

Base pressure distribution measurement for free flying sharp cone at hypersonic speeds and high angles of attack [AIAA PAPER 72-316] 11 p1567 A72-25250

Inert and reactive gas injection in near wake behind blunt bodies in supersonic flow, considering influence on base pressure and temperature 17 p2487 A72-35930

Thrust recovery factor and base drag losses in annular jets as function of jet thickness to base diameter ratio, determining recirculation mass flow 18 p2641 A72-36769

An investigation of the flow around rectangular cylinders. 19 p2747 A72-38813

BASES [CHEMICAL]

Gas phase basicities of aliphatic amines by ion cyclotron resonance spectroscopy 07 p0936 A72-19493

BASES [FOUNDATIONS]

U FOUNDATIONS

BATCH PROCESSING

Sensitivity algorithms for finite memory batch processing smoother [Kalman filter], applying to ship inertial velocity error estimation 05 p0686 A72-16572

Test conditions, specimen batch and method effects on accuracy of rapid fatigue limit tests with increasing stress amplitude 05 p0741 A72-17085

Partial differential equation language [PDEL] for batch and interactive digital simulation of PDE models 07 p0951 A72-20327

Solution of the problem of a fast Fourier transform in a homogeneous associative parallel processor 19 p2779 A72-37993

BATHING

Zero-g showers for long duration space flight crews hygiene, describing flexible mummy bag and truncated conical shell design 15 p2190 A72-32320

BATHS

NT SALT BATHS

BATS

Hypergravity effects on bats spatial orientation, noting resistance to head-pelvis and pelvis-head accelerations 13 p1907 A72-30015

BATTERIES

U ELECTRIC BATTERIES

BATTERY CHARGERS

Charging methods for Ni-Cd batteries used in satellites, noting life increase and weight reduction 01 p0007 A72-11054

BATTERY SEPARATORS

U SEPARATORS

BAUSCHINGER EFFECT

Analytic yield surface in work hardening including stress in transition range after load change [Bauschinger effect] 01 p0144 A72-11388

Surface layers and aging influence on Bauschinger effect in profiled low carbon steel under low tension-compression load cycles 03 p0445 A72-13591

Sign-variable nonisothermal plastic deformation and creep behavior of polycrystalline construction materials, taking into account Bauschinger effect 09 p1401 A72-22726

Bauschinger effect analysis based on yield theory, noting effects of stress relaxation and isotropic hardening 16 p2471 A72-33786

BAYARD-ALPERT IONIZATION GAGES

Ultrahigh vacuum measurement by Bayard-Alpert hot cathode ionization gages, showing ion current component influence on lower pressure limit 07 p0914 A72-19907

BAYES THEOREM

Dynamic model for estimating Bayesian recursive images by linear Kalman filtering 01 p0046 A72-10866

Spectral texture effects on remotely sensed high altitude automatic IR image interpretation, using Bayesian probability techniques [AD-734261] 02 p0228 A72-11873

Bayesian analysis of onboard computer controlled aircraft avionics subsystem built-in test for failure detection 05 p0638 A72-16574

Bayes theorem based iterative method for image restoration by treating degraded images as probability-

frequency functions, noting adaptability to computer processing 05 p0690 A72-16671

Coupled detection-estimation of Gauss-Markov processes in white Gaussian noise, deriving Bayes optimal recursive rules 06 p0775 A72-18388

Bayesian estimate of signal parameters in random noise background under mutually exclusive hypotheses about statistical properties 07 p0943 A72-19515

Optimal Bayesian system synthesis for simultaneous discrimination and parameter estimation of several signals in noise background 07 p0943 A72-19516

R and D management policies choices with respect to Bayesian decision-theoretic model in simulated environments 07 p1105 A72-19553

Bayes estimators for Poisson distribution random parameters and reliability function, using Monte Carlo method and maximum likelihood estimation 08 p1200 A72-21590

Bayesian analysis application to reliability and life parameter estimation for Weibull failure model, using Monte Carlo simulation 10 p1503 A72-23978

Bayes analysis application to Weibull distribution parameters estimation, using entropy concept for figure of merit to assess reliability analysis 10 p1444 A72-23987

Decision theory and cost-benefit modeling application to large government funded systems development programs, discussing Bayesian techniques 10 p1564 A72-23993

Optimal random search noise recognition systems with Bayes teaching technique 13 p1924 A72-29162

Bayesian estimation for nonlinear filtration of nonstationary non-Gaussian radio signals, deriving second central moments and parameter estimate errors 15 p2195 A72-31656

Statistical inferences on two parameter Weibull reliability function from classical, Bayesian and structural probability viewpoint 15 p2264 A72-31800

Random scale parameter of Weibull distribution with known shape parameter obtained via empirical Bayes estimation 16 p2398 A72-33346

Bayesian recursive linear Kalman filtering technique for image estimation with noise background elimination, proposing time invariant dynamic model to provide stationary statistics 17 p2520 A72-34403

Smooth empirical Bayes estimation of observation error variances in linear systems. 17 p2576 A72-35248

Bayesian recursive estimation by Kalman filtering for enhancement of image corrupted by additive random noise 17 p2557 A72-35539

Two dimensional recursive filter for Bayesian estimate of pictorial data represented by dynamic model of random field with exponential autocorrelation 18 p2658 A72-36261

Conditions for the effectiveness of adaptation algorithms based on an empirical Bayesian approach to statistics 19 p2825 A72-37440

Book - Fundamentals of pattern recognition. 20 p2905 A72-39575

Book - Bayesian statistics: A review. 20 p2946 A72-39728

Bayes theorem for radio signals parameter estimation on random noise background, using rectangular function of losses 21 p3016 A72-40797

Bayesian decision analysis of the hazard rate for a two-parameter Weibull process. 22 p3198 A72-41981

Determining optimum burn-in and replacement times using Bayesian decision theory. 22 p3182 A72-41982

Machine vibration diagnostics and damping, emphasizing filter lattice foundation structures, probability analysis and Bayes formula application 22 p3182 A72-42127

Bayesian statistical decision theory and reliability-based design. 22 p3240 A72-42967

BAYESIAN STATISTICS

U BAYES THEOREM

BBGKY HIERARCHY

Two dimensional plasma under dc magnetic field, investigating thermal equilibrium with Liouville equation and BBGKY hierarchy 01 p0107 A72-10145

Book on unmagnetized plasma theory covering Vlasov and Klimontovich models, electrostatic solutions, plasma oscillations, nonlinear phenomena, statistical descriptions, BBGKY correlations, etc 07 p1041 A72-19449

Correlations analysis method for homogeneous and inhomogeneous systems under external field based on BBGKY hierarchy and decomposition of reduced distribution functions

11 p1689 A72-26480
Kramer and Couette flows using the Bhatnagar-Gross-Krook model.

20 p2913 A72-39418
Lowest order two particle correlation function solution to BBGKY hierarchy obtained via Green function with Fourier transform satisfying analyticity requirements for causality

20 p2956 A72-39725
Balescu-Guernsey-Lenard kinetic equation for homogeneous dilute electron gas extended to higher densities, specifying conditions for BBGKY hierarchy correlation functions solution

20 p2958 A72-39815

BCC LATTICES

U BODY CENTERED CUBIC LATTICES

BCC THEORY

BCS theory for transition metals and alloys superconductivity, discussing electron phonon coupling, transition temperatures and Cooper pair fluctuations

09 p1368 A72-22556

BEACON SATELLITES

Beacon satellite transmission determination of ionosphere total electron content, describing equivalent slab thickness and diurnal, seasonal and solar cycle behavior

02 p0221 A72-12460

Ionospheric inhomogeneity studies from angle of arrival recordings of satellite beacon transmissions, using phase radiometer interferometry

09 p1305 A72-23576

Satellite beacons observations from 1964 to 1970.

17 p2547 A72-35125

Characteristics of the abrupt scintillation boundary.

22 p3170 A72-42363

BEACONS

NT AIRPORT BEACONS

NT RADAR BEACONS

NT RADIO BEACONS

NT RADIO DIRECTION FINDERS

Onboard orbital navigation system analysis on space shuttle radio range and range rate measurement data relative to ground beacon, using Kalman filter

08 p1203 A72-20856

BEADS

Electrode vertex angle effect on fused weld bead geometry related to plate thickness in tungsten inert gas (TIG) welding

09 p1320 A72-23634

Glass styrene acrylonitrile bead filled composites tensile behavior, discussing relationship between yield stress, filler content, strain rate and temperature

11 p1673 A72-25487

BEAM COLUMNS

U BEAMS [SUPPORTS]

U COLUMNS [SUPPORTS]

BEAM CURRENTS

High current relativistic electron beam properties, noting application in thermonuclear synthesis and accelerators

12 p1788 A72-27250

Fast electron gun with subnanosecond switching times and 100 mA peak beam current for delayed coincidence studies of atomic decays

13 p1933 A72-29761

BEAM PLASMA AMPLIFIERS

Two stream instabilities of low density beam-plasma interaction in finite and zero magnetic fields

02 p0267 A72-12839

Higher harmonics intensities dependence on fundamental of electron oscillation in beam generated plasma

10 p1524 A72-24920

Suppression of instabilities in a beam-plasma system by a modulation of the electron beam.

21 p3089 A72-40199

Linear and Alfvén waves propagation in incompressible beam-plasma systems, deriving dispersion law

21 p3092 A72-40994

BEAM SPLITTERS

Goos-Hanchen nonpolarized light effect for laser beam separation into rectilinearly polarized beams during reflection

01 p0101 A72-10042

Double passed Michelson interferometer with polarizing beam splitter, quarter wave plates and cube corner reflectors to obtain immunity to mirror misalignment

11 p1635 A72-26500

Laser interference fringe jitter due to wavelength instability, suggesting pulse shape blurring intensity variation control by flat or large-angle wedge beam splitter

15 p2249 A72-32166

Design of an inexpensive, 30 cm diameter, long path difference interferometer.

17 p2553 A72-34640

Laser mode suppression arrangements consisting of Michelson interferometers with polarization prism as beam splitting element

18 p2697 A72-36112

Gain and visualization of the modes of a thermally stabilized HCN laser.

19 p2810 A72-37455

A laser beam divider with continuous adjustment of the intensity ratio

23 p3294 A72-43225

BEAM SWITCHING

Step-scan landing system technique, using microwave fixed linear array for area coverage with pattern of narrow overlapping individually coded sequentially switched beams

06 p0846 A72-18397

In-line eight stage digital light deflector with prisms and polarization switch, using Pockels effect with transverse field

07 p1003 A72-19222

Holographic memory devices for bulk information recording, discussing use of image converter for brightness amplification and lithium niobate electro-optical deflector for beam switching

12 p1807 A72-27588

Optimal energy response conditions for single pulse emission by noninstantaneous switching of ruby and Nd glass lasers

13 p1969 A72-29612

Fast electron gun with subnanosecond switching times and 100 mA peak beam current for delayed coincidence studies of atomic decays

13 p1933 A72-29761

Optimal energy response conditions for single pulse emission by noninstantaneous switching of ruby and Nd glass lasers

21 p3063 A72-40665

BEAM WAVEGUIDES

Beam guides for optical and millimeter wave communication, discussing optical pipelines and iris, lens and reflector waveguides

02 p0191 A72-11684

Lens type beam waveguide for optical trunk communication, discussing transmission medium, terrain layout, bandwidth, terminal equipment, misalignment and multibeam application

04 p0497 A72-14483

Long wave propagation in curved ducts and pipes, considering plane wave transition and distortion

04 p0548 A72-14698

Optical data transmission system with dielectric single-mode glass fiber waveguide, PCM semiconductor laser diode transmitter and avalanche photodiode receiver

06 p0774 A72-17770

Wave propagation in single node clad glass fiber light waveguide, discussing fiber core minimum diameter and various loss mechanisms

06 p0825 A72-17773

Data transmitting dielectric light waveguide production problems, noting light scattering and absorption losses due to glass material impurities

06 p0825 A72-17774

Stimulated Raman emission in glass fiber optical waveguides with low threshold broadband gain, permitting construction of wideband amplifiers and oscillators

07 p0953 A72-18876

Thin film optical waveguide with crystal quartz as substrate, observing reversible TE to TM mode conversion due to anisotropy

07 p0953 A72-18878

Integrated miniature guided wave optical transmission systems using crystals adapted to thin film nonlinear interaction and photolithographic technique

07 p1004 A72-19228

Metal clad dielectric slab waveguide for integrated optics, obtaining dispersion equation solution and propagation modes from simplified model

07 p0940 A72-19229

Linear and circular birefringence of low loss single mode glass fiber dielectric optical waveguide as function of length

07 p0940 A72-19232

Element position design of pencil beam thin phased arrays with low sidelobes

07 p0941 A72-19256

Round-the-world short wave signals propagation and waveguides effective volume and attenuation characteristics, relating ionospheric effects and nonlinear beam defocusing

08 p1130 A72-20704

Material dispersion contribution to signal envelope delay distortion in weakly guiding dielectric optical fiber waveguides

09 p1314 A72-23340

Intense relativistic electron beam-plasma interactions in finite cavities, calculating neutral gas charge production and gas breakdown times

10 p1518 A72-23960

Hollow dielectric waveguide used for carbon dioxide laser gas discharge, noting increased gain, volumetric output and saturation parameters

15 p2245 A72-31386

Multimode optical fiber waveguide theoretical model to predict pulse propagation dispersion for comparison with measurements

15 p2194 A72-31546

Quasi-optical transmission line stability improvement, investigating pulsating light beam concept

15 p2202 A72-32663

Carbon dioxide waveguide gas laser performance characteristics, noting mode pattern stability and insensitivity to resonator disturbances

16 p2402 A72-33396

Analysis of an optical beam waveguide consisting of a tapered lens-like medium and its applications.

17 p2580 A72-34382

Wave-guiding properties of stripe-geometry double heterostructure injection lasers.

18 p2698 A72-36981

Circumterrestrial short wave signals propagation and waveguides effective volume and attenuation characteristics, relating ionospheric effects and nonlinear beam defocusing

19 p2765 A72-38332

Optical communications in Japan.

19 p2766 A72-38602

Reduction of temperature difference in shielding pipes for light-beam transmission.

20 p2903 A72-39267

A rectangular beam waveguide resonator and antenna.

21 p3026 A72-40358

Self focusing effect on wave beam propagation in optical lens waveguides, discussing system nonlinearity

22 p3186 A72-42656

Reflectivity dependence of triple polarization grid on elements spacing and wires orientation, noting bandwidth of ray guide matching transformer

23 p3269 A72-43446

BEAMS

Stress intensity factors for circular crack near surface of semfinite solid, considering pure beam bending and approximate thickness effect for plate deep surface flaw

01 p0140 A72-10991

BEAMS [RADIATION]

NT ATOMIC BEAMS

NT ELECTRON BEAMS

NT GAMMA RAY BEAMS

NT ION BEAMS

NT LIGHT BEAMS

NT MICROBEAMS

NT MOLECULAR BEAMS

NT NEUTRAL BEAMS

NT NEUTRON BEAMS

NT PARTICLE BEAMS

NT PHONON BEAMS

NT PHOTON BEAMS

NT PION BEAMS

NT PROTON BEAMS

NT RADAR BEAMS

Low sidelobe pencil beam thinned phased arrays design involving element position selection

01 p0039 A72-10664

Pulse widths formed by relativistic beaming pulsars effect on emission spectra

01 p0133 A72-11130

Gaussian electromagnetic wave beam diffraction and scattering problems solutions by optics formula application to beam transformation through optical systems

02 p0261 A72-12603

Weakly divergent beam propagation of electromagnetic waves in statistically inhomogeneous nonlinear medium with dielectric constant dependence, using small perturbation method

05 p0625 A72-15818

Multifrequency plane, spherical and beam waves propagation, calculating temporal frequency spectra in turbulent atmosphere

06 p0771 A72-17339

Radio wave beam trajectories in laminar isotropic plasma layer, using dynamic systems theory

06 p0774 A72-17731

Radio wave beam trajectories in laminar isotropic plasma layer, using dynamic systems theory

11 p1591 A72-25335

Low cost microwave scanning beam landing systems for interim instrument landing system replacement in civil aviation

15 p2272 A72-32217

Gaussian electromagnetic radiation beam propagation in turbulent medium, calculating broadening dependence on outer scale by modified Karman spectrum characterization

17 p2580 A72-34291

Weakly divergent beam propagation of electromagnetic waves in statistically inhomogeneous nonlinear medium with dielectric constant dependence, using small perturbation method

23 p3263 A72-43426

Numerical simulation of the relaxation of a beam of charged particles in a strong electric field

23 p3315 A72-43530

BEAMS [SUPPORTS]

NT BOX BEAMS

NT CANTILEVER BEAMS
 NT CURVED BEAMS
 NT I BEAMS
 NT RECTANGULAR BEAMS

Saint Venant problem solutions of cylindrical beam in linear theory of micropolar elasticity in terms of three functions

01 p0137 A72-10318

Maximum logarithmic decrement vs frequency of damped oscillation of elastic thin beam including internal and viscous resistance

01 p0144 A72-11384

Local buckling and collapse of thin walled lipped channel beams under critical end moments

01 p0144 A72-11396

Moment sensors for strain gaged beam systems analysis, noting application to bending moments determination

02 p0287 A72-11510

Beams and plates resting on elastic base with loads moving along line or strip, calculating wave processes based on half space dynamic model

02 p0290 A72-11629

Minimum weight beams and frames calculation for random loads taking into account material carrying capacity

02 p0291 A72-11727

Newtonian quasi-static crack propagation theory application to nonlinear structures, considering slender beams, plates and circular cylindrical shells

02 p0292 A72-12029

Beam theory application to cylindrical and conical shells bending, deriving flexibility functions from membrane equations

02 p0296 A72-12529

Straight beams and rectangular frames stress-strain calculation under pulsed loading, taking into account shock waves finite propagation velocity and internal damping

02 p0300 A72-12855

Elastic-plastic stress-strain analysis of beams with uniform cross section under combined loadings by finite element method

03 p0449 A72-13975

Infinite elastic-plastic beam impact by semiinfinite elastic rod, computing strain-time profiles

04 p0583 A72-14447

Torsion of hollow beam consisting of two homogeneous isotropic rods with different elastic properties and simply connected cross sections, solving by conformal mapping

04 p0586 A72-14992

Dynamic theory of thin elastic beams under large deflection, taking into account shear deformation and axial stress resultants

[ASME PAPER 71-APM-EE] 04 p0590 A72-15183

Sandwich beam design, deriving linear programming formulation suitable for computer treatment

04 p0590 A72-15191

Statically indeterminate and determinate elastic beams optimal design for maximum-minimum deflection under distributed load

04 p0590 A72-15192

Shock response of simply supported sandwich beam with viscoelastic core, using four element model for dynamic shear properties

04 p0591 A72-15274

Integral equation for lowest natural frequency of vibrating beams, using eigenfunction theory

04 p0593 A72-15565

Minimum weight design of perfectly plastic continuous sandwich beams with two equal spans for movable loads

04 p0593 A72-15647

Saint Venant problem for orthotropic almost cylindrical beams, investigating elongation, bending due to couple and transversal loads and torsion due to torque

04 p0594 A72-15747

Infinitely long Euler-Bernoulli damped periodic aluminum beam with elastic springs, determining distance for steady state sinusoidal response to spatial decay

05 p0736 A72-16111

Optimal design of statically determinate sandwich beams for given deflection at specified cross section

05 p0737 A72-16119

Large deflection microstructure continuum model for composite beam flexural wave propagation and free vibration, deriving equations of motion

[AIAA PAPER 72-140] 05 p0741 A72-16937

Scaling laws for vibrating beams and plates, stressing shear and rotary inertia effects

06 p0894 A72-17769

Bending tests of beam with different creep characteristics in tension and compression

06 p0899 A72-18639

Beams and square plates nonlinear vibration response to random concentrated driving force solved numerically on digital computer

06 p0901 A72-18718

Finite element solutions for buckling of columns and beams, investigating restraints and cross section partial plasticity effects

07 p1088 A72-19117

Optimality criterion for beams and frames with segmentwise constant cross sections and alternative loading exceeding plastic load carrying capacity

07 p1088 A72-19119

Periodically supported beams acoustically induced vibration response based on equivalent structural wavelength definition

[ASA PAPER E 14] 07 p1089 A72-19330

Minimum weight design of elastic sandwich beam with segmentwise constant stiffness under displacement and stress constraints, using iterative solution and finite element analysis

[AD-745488] 07 p1092 A72-19825

Bounds for impulsively loaded plastic structures, considering fixed end beam with uniform velocity distribution

07 p1093 A72-19947

Nonlinear theory of thin walled open elastic beams with deformations by large cross sectional rotation, using potential energy principle

07 p1096 A72-20430

Perturbation solution to nonlinear nonuniform torsion of thin walled open elastic beams with strain hardening dependent on torque-rotation behavior

07 p1096 A72-20431

Pinned-free beam response to transient support excitation, using pinned-pinned beam modal parameters

07 p1096 A72-20526

Circular elastoplastic beam under combined torsion and tension via Mindlin elastic model for materials with microstructure, taking into account work hardening

07 p1097 A72-20534

Nonlinear large amplitude vibration of beams for various support conditions, using finite element matrix displacement method

08 p1245 A72-21626

Thin viscoelastic beam free oscillations and material properties description by Volterra type nonlinear integral equation

08 p1249 A72-21869

Nonlinear beam and plate analysis, obtaining smooth elastic-plastic transition through modified Richard moment-rotation equation application

08 p1249 A72-21923

Nonlinear programming analysis of free vibration of simply supported beam

08 p1249 A72-22136

German monograph on ring shaped continuous beams calculation, deriving optimum support under torsional stress

09 p1397 A72-22335

Tensionless contact area between beam and elastic half space determined by approximate technique

09 p1398 A72-22623

Axial thermal stresses in beams, investigating error in elementary calculations

09 p1405 A72-22999

Slip contact joint frictional damping of vibration of beam on elastic support

09 p1408 A72-23464

Vibration frequencies of slender beams and circular plates with boundary stiffness and damping

[ASA PAPER E 5] 09 p1408 A72-23525

Parametric dynamic stability equations and boundary conditions for thin walled open cross section beam under axial load, taking into account longitudinal deformation effect

[ASME PAPER 71-APM-LL] 10 p1554 A72-24184

Maximum dynamic to static deflection ratio for thermally induced vibrations of elastic beams and plates, considering damping and axial load effects

[ASME PAPER 71-APM-UU] 10 p1554 A72-24185

Initially axially stressed Timoshenko beam equations of motion derived from three dimensional theories, discussing buckling loads and vibration frequencies

10 p1555 A72-24191

Steady two dimensional flow of monatomic rarefied gas past semiinfinite beam

10 p1418 A72-24543

Critical compressive buckling and stability of straight beams under axial and transverse loads calculated by three unknowns methods

10 p1560 A72-25121

Asymptotic dynamic response of infinite beam on elastic foundation to randomly moving load

11 p1727 A72-25292

Dynamic deflections and bending moments of simply supported Bernoulli-Euler beam under traveling mass loads

[AIAA PAPER 72-338] 11 p1728 A72-25371

Plastic behavior of laterally loaded beams and rectangular plates, formulating upper and lower bound theorems

[AIAA PAPER 72-343] 11 p1728 A72-25372

Stress analysis of short beam bending of graphite fiber reinforced epoxy composites

11 p1671 A72-25464

Asymmetric three layer beam design for elastic impact, proposing functional equation integration by computer method

11 p1732 A72-25531

Static loading and monoharmonic excitation influence on transverse vibrations of eccentrically prestressed metallic beam

11 p1732 A72-25535

Bending deflection calculation for laminated beams with layers of different rigidity

11 p1733 A72-25546

Matrix displacement method for nonuniform beam vibration problems, using internal nodes concept

11 p1735 A72-25740

Radiation resistance of baffled beam modes from far field acoustic power intensity

11 p1687 A72-26058

Anisotropic cylindrical beam bending by transverse load in elastic plane, reducing to Almansi problem

11 p1736 A72-26091

Energy method for boundary conditions of beam vibrations under linear viscoelastic stress-strain law, deriving uniqueness, boundedness and stability theorems

12 p1885 A72-27848

Minimum weight reliable beams and frames calculation for random loads, using one degree of freedom system to obtain closed form solution

14 p2164 A72-30237

Sandwich beams structural optimization for given deflection by iterative finite element procedure

14 p2168 A72-30927

Natural frequencies of beams with stepwise variable cross sections, approximating deflection shape by sectionwise representation of inertia load

15 p2323 A72-31454

First mode ultraharmonics in nonlinear beam vibration with various boundary conditions and structural properties

16 p2463 A72-32845

Thermoelastic stress bounds in fiber reinforced composite beams of arbitrary cross section, examining conditions for applicability of elementary beam theory

16 p2464 A72-32915

Brittle creep rupture process in beam subjected to simultaneous loading with bending moment and axial force

16 p2474 A72-34128

Stability analysis of a pinned-end beam undergoing non-linear free vibration

17 p2623 A72-34236

Vibration perturbation of slender rotating beam with end masses, using method of matched asymptotic expansions

[ASME PAPER 72-APM-B] 17 p2625 A72-34318

Nonlinear vibrations of a hinged beam including nonlinear inertia effects

[ASME PAPER 72-APM-51] 17 p2627 A72-34779

Transverse vibration of a viscoelastic beam carrying an arbitrary number of mass bodies

17 p2631 A72-35053

Flexure of micropolar elastic beams

17 p2631 A72-35056

On the finite deflections of thin beams

17 p2634 A72-35404

Monograph - The elastic flexural-torsional buckling of beam-columns by discrete element techniques

17 p2634 A72-35548

Steady state response of nonlinear beam under periodic loading, using finite element techniques for nonlinear differential equation

18 p2732 A72-36078

Flat beam linear vibration analysis from mode measurement and moire technique, applying to prototype turbine compressor blade

18 p2734 A72-36375

Thickness-punch size ratio effects on stress state response of elastic plates and beams in flat contact under symmetric loads due to rigid punches

18 p2734 A72-36378

Resonant mode sound field radiated by nonuniform slender circular cross section free-free beams, using dipole array modeling

18 p2710 A72-36410

On the dynamic response of an infinite Bernoulli-Euler beam

18 p2735 A72-36758

Infinite plate with a supported reinforced circular hole

18 p2738 A72-37071

Timoshenko finite element beam theory application to flexural vibration problems, considering shear deformation and rotary inertia effects

18 p2740 A72-37206

Experimental determination of viscoelastic characteristics

18 p2740 A72-37211

Theory for transverse vibrations of beams during elastoplastic deformations

19 p2877 A72-38179

Computer solution of dynamic problems for bending of beams and thin plates beyond the elastic limit under alternating loads

19 p2877 A72-38194

Transverse isotropy effects on beams static behavior, considering Green functions, deflection under distributed loads and beam-column deflection

20 p2980 A72-39613

Beams on bilinear elastic foundations.
20 p2980 A72-39692

Simulation of physically nonlinear elastoplastic beams
21 p3116 A72-40180

Forced motion of isotropic and transversely isotropic viscoelastic Timoshenko beams using measured material.
21 p3116 A72-40331

The effects of discrete masses and elastic supports on continuous beam natural frequencies.
21 p3116 A72-40335

A consistent approach for treating distributed loading in the matrix force method.
21 p3122 A72-41261

Numerical solution of a boundary value problem arising in the deflection of beams and shells.
21 p3122 A72-41311

Inhomogeneous beam torsional vibration modes and frequencies calculation by initial parameters method, replacing beam by series connected oscillators
22 p2332 A72-41865

Three dimensional thermoelastodynamic theory for elastic beams, deriving nonlinear motion equations by combined expansion and variational methods
22 p2335 A72-42523

Differential equation for maximum beam deflections in transverse bending based on trapezoidal rule
22 p3240 A72-42958

Variational analysis of sandwich beams under static loads, presenting shear deformation and normal stress distributions
[ASME PAPER 72-APM-R] 23 p3350 A72-44055

Stability and vibration of transversely isotropic beams under initial stress.
23 p3350 A72-44057

Equivalent linear solution for transient free vibration of beams with strain dependent, frequency independent stress-strain hysteresis loop with sharp corners
23 p3352 A72-44120

Bounds to bending frequencies of a rotating beam.
23 p3354 A72-44249

Forced vibration analysis of sandwich beams with viscoelastic core.
23 p3354 A72-44253

Non-linear free vibration of a beam with time-dependent material properties.
23 p3355 A72-44374

Technique for measuring damping properties of thin viscoelastic layers.
24 p3402 A72-44885

Pure antiplane stress and equilibrium of isotropic elastic beams, considering suspended cylinders
24 p3459 A72-44989

BEAMSHAPING
U COLLIMATION
BEARING [DIRECTION]
SNR effect on rms bearing error by amplitude comparison for nonscanning nontracking receiving system with two antenna lobes of arbitrary shape
05 p0629 A72-16577

Bearing estimation performance of monopulse tracking with passive linear arrays, using computer simulation for various integration times and input S/N ratios
06 p0774 A72-17809

Azimuth-bearing error dispersion in surveillance radar measurements, using Markov chains
11 p1595 A72-26297

Cross loop antenna for apparent azimuthal direction of incidence of VLF transmitter, showing night time bearing direction changes
12 p1784 A72-27794

Error investigation for the location of the sources of atmospheric by radio direction finding.
18 p2706 A72-36429

Bearing azimuth measurement accuracy improvement by ATC beacon system/secondary surveillance radar using monopulse technique
18 p2662 A72-37047

Present status of self-contained navigation systems combining Doppler velocity sensors and attitude/heading references.
21 p3079 A72-40282

BEARING ALLOYS
Fatigue cracks nucleation in steel bearings subjected to cyclic contact stresses
03 p0377 A72-14020

BEARINGS
NT ANTIFRICTION BEARINGS
NT BALL BEARINGS
NT FOIL BEARINGS
NT GAS BEARINGS
NT JOURNAL BEARINGS
NT LIQUID BEARINGS
NT ROLLER BEARINGS
NT THRUST BEARINGS
Helicopter elastomeric bearing rotors, discussing downtime and cost reduction, maintenance, endurance and inspection
01 p0073 A72-10150

Carbon fiber reinforced thermoplastics tested for gears and bearings applications, including wear, static,

dynamic, surface tension, stereoscan and microscopy effects
04 p0537 A72-14748

Bearing operating characteristics within transition range between laminar and fully developed turbulent flow, accounting for film thickness variation and pressure gradients
04 p0528 A72-15701

Dynamic analysis of vertical rotor rotating in elastic sliding bearings, analyzing precession stability and self oscillation zone
04 p0594 A72-15748

Friction and wear characteristics at high temperature of plain bearing embedded with pellets of graphite, sodium fluoride and tungsten disulfide lubricating mixture
06 p0823 A72-18584

Modified PV criterion for self lubricated dry bearings, observing bearing length and diameter effect on steady state temperature
06 p0823 A72-18594

Random vibrations and antitorque moments of rigid shaft with precision bearings, considering effects of geometrical fabrication defects and nonuniform film thickness
06 p0824 A72-18722

Mathematical model for multiple bearing supported isotropic undamped rotors with arbitrary stiffness and mass distribution, taking into account horizontal/vertical motion coupling
07 p1096 A72-20529

Vibrational characteristics dependence on structural flexibility in gimbal bearings and supporting structure of two axis free gyroscopes and single axis rate gyroscopes
08 p1173 A72-22129

Vibration of reciprocating engine crankshafts and steam turbine, alternator and gas turbine rotor shafts supported on hydrodynamic sleeve bearings
08 p1225 A72-22133

Dynamics of rigid rotor supported on squeeze oil film bearings
08 p1225 A72-22134

Complete and simplified equations of motion for rate gyro installed in flight vehicle, taking into account bearing torques
[DFVLR-SONDDR-190] 11 p1635 A72-26580

Rigid body model for nonholonomic kinematic linkages of tangentially sliding nonrolling bearings, noting virtual displacements and mechanical work
12 p1845 A72-27539

Ice adhesive shear strength to steel bearing surfaces coated with bonded solid lubricants, describing low temperature test apparatus and results
[ASLE PREPRINT 72AM 4] 13 p1964 A72-28970

Monograph on rotor-bearing stability and sliding bearing calculation covering rigid and flexible supports, gyroscopic effects, cavitation, load capacity, etc
15 p2243 A72-31349

Application of boundary layer concepts to turbulent lubrication theory of bearings and seals
18 p2696 A72-37052

Properties of internally lubricated glass-fortified thermoplastics for gears and bearings.
19 p2822 A72-37896

Calculation of the tightness of threshold joints of gas turbine engine rotor bearings
20 p2979 A72-39589

Effect of bearing flexibility on dual-spin satellite attitude stability.
21 p3115 A72-41303

Experimental investigation of the elastic characteristics of composite bearings in turbine machinery for the purpose of increasing their efficiency and reliability during nonlinear vibrations of the rotor
22 p3181 A72-41860

Technological utilization of Weissenberg viscoelastic effect for sliding bearings centripetal pressure lubrication, noting analogy with human and animal skeletal joints lubrication
22 p3183 A72-42875

Deterioration of shaft bearings of electromotor driving aircraft centrifugal fuel pump, determining lateral force acting on impeller
23 p3252 A72-43663

Bearing supports elasticity effect on pendulum vibration of rigid rotating shaft with disk, noting vibrational frequencies relation to resonant frequencies
23 p3293 A72-43668

Disk fillets stressed state, determining concentration coefficient and bearing capacity effect
23 p3347 A72-43747

BEAT
U SYNCHRONISM
BEAT FREQUENCIES

Natural fluctuations effect on beat frequency dependence of opposed waves in ring laser on rotation velocity
05 p0668 A72-16405

Spectral characteristics of Ar ion laser emission for determination of stability region, mode sequence and beat signal levels
06 p0826 A72-18009

Toran O long range navigation system based on circular coordinates and rubidium vapor clocks for beat phase measurements, noting use of portable transmitters
06 p0846 A72-18287

Nonlinear dispersive medium characteristics determination from higher harmonic oscillations and beats analysis based on traveling waves concept
09 p1353 A72-23486

Coherent and noncoherent modes of optical beating in laser Doppler velocity measurement using light scattered from single and multiple particles
10 p1481 A72-24412

IR radiation generation by Raman scattering and difference frequency mixing with Q switched Nd-YAG laser, noting peak power and photon conversion efficiency
11 p1647 A72-26149

Solenoid-produced local axial magnetic field influence on beat signal frequency characteristics in ring laser with nearly linearly polarized emission
11 p1650 A72-26357

Quantum beats in transitions from levels subject to optical cascades
12 p1847 A72-27184

Microwave and optical quantum electronic sources for frequency standards, noting primary Cs reference and multimode laser-RF oscillator beat technique
12 p1824 A72-27867

Solenoid-produced local axial magnetic field influence on beat signal frequency characteristics in ring laser with nearly linearly polarized emission
16 p2403 A72-33710

Microwave and optical quantum electronic sources for frequency standards, noting primary Cs reference and multimode laser-RF oscillator beat technique
16 p2403 A72-33976

A method of phase detection of the beat signal in FM-CW radar.
17 p2514 A72-34383

Plasma heating by nonlinear damping of resonantly excited longitudinal oscillations produced by two parallel laser beams with difference frequency equal to plasma frequency
21 p3090 A72-40342

The phase difference between coupled laser oscillations
22 p3184 A72-42109

Nonlinearity and inhomogeneity effects on plasma wave excitation by beating two laser beams, taking into account Lorentz force modulation by large amplitude plasma wave
22 p3185 A72-42475

Moire screens coded with pseudo-random sequences.
23 p3289 A72-43892

BED REST
Long term bed rest effect on humans and primates, detailing cardiovascular metabolic and musculoskeletal physiological systems
[AD-737557] 01 p0014 A72-10932

Bed rest and centrifuging effects on human plasma thyroid hormone level, discussing total protein, albumin and thyroxin binding globulin concentrations
12 p1770 A72-27477

Centrifugation tolerance reduction after 14 days bed rest with moderate exercise, determining rehydration effects
12 p1766 A72-28295

Plasma protein concentration, volume and hematocrit changes during exercise, bed rest and high forward acceleration
12 p1766 A72-28296

Bed rest and positive radial acceleration effect on peripheral visual response time, considering blackout or grayout prediction possibilities
12 p1766 A72-28297

Thermoregulation changes during simulated weightlessness of prolonged bed rest, noting lower sweating threshold and decreased vasodilation/autonomic dysfunction/
12 p1767 A72-28301

Six day bed rest effect on external respiration and subcutaneous tissue oxygen metabolism, noting oxygen consumption decline
13 p1905 A72-29324

Prolonged bed rest induced muscular activity restriction effect on arterial and venous tone in different body areas
14 p2074 A72-30385

Disproportional changes in hematocrit, plasma volume, and proteins during exercise and bed rest.
17 p2506 A72-35966

Calcium metabolism under stress and in repose.
23 p3254 A72-43389

Health condition changes in test subjects during strict bed rest in hypokinetic recumbent and antiothostatic position subject to lower body negative pressure
23 p3259 A72-43913

Rheographic investigation of cerebral, pulmonary and peripheral circulation during bed rest in antiothostatic position
23 p3255 A72-43914

Cardiac output, hemodynamic and gas exchange variations as function of basal metabolism during bed rest in hypokinetic recumbent or antiorthostatic position

23 p2355 A72-43915

Ophthalmoscopic, photocalibrometric and ophthalmodynamometric examinations of test subjects visual acuity during bed rest in hypokinetic antiorthostatic position

23 p2355 A72-43916

Otorhinolaryngological organ response during hypokinetic antiorthostatic bed rest for control, exercising and muscular electric-stimulated groups

23 p2356 A72-43917

Physical training as a prophylactic measure against the hypodynamic syndrome

23 p3260 A72-43920

Metabolic changes in healthy humans caused by prolonged bed rest in horizontal position, noting prevention by physical exercises and electric muscle stimulation

23 p3260 A72-43921

Cerebral blood filling reduction and blood vessel tone deterioration during 120 day clinostatic hypokinesia of healthy male subjects

23 p3256 A72-43922

Induction of hemodynamic deterioration by the hypogravic state - An evaluation of mechanisms and prevention.

24 p3373 A72-45199

BEDIASITES

Geological verification in search for origin of vagabond tektites, commenting on Caribbean label bediasite find

15 p2303 A72-31307

BEDS [PROCESS ENGINEERING]

High-speed carburizing with natural gas in a fluidized bed

20 p2929 A72-39582

BEHAVIOR

NT DECONDITIONING

NT HUMAN BEHAVIOR

Behavior concept formulation for visceral systems, considering digestive system data and extension from motor function concepts

24 p3370 A72-44586

BELL AIRCRAFT

Bell lifting rotor systems, examining company contributions in electronics and avionics

10 p1421 A72-24877

BELL MILITARY AIRCRAFT

U MILITARY AIRCRAFT

BELLMAN THEORY

High order optimality conditions of singular controls, considering Pontryagin maximum principle, Bellman dynamic programming and functional analysis

01 p0044 A72-10297

Regularization theorems for epsilon solutions to Bellman functions in optimal quick response problems

06 p0847 A72-17728

Optimal strategies conditions for game problems in conflictly controlled system, discussing minimax technique and Bellman equation solution

07 p1028 A72-19971

Self similar invariant group solutions to Bellman nonlinear partial differential equation for optimal correction problems of control systems motion with random disturbances

07 p0963 A72-20322

Deviation accumulation conditions and maximum dynamic error of linear automatic control system under perturbation, including theorem for Bellman equation

08 p1146 A72-22177

Regularization theorems for epsilon solutions to Bellman functions in optimal quick response problems

11 p1608 A72-25330

Optimal strategies conditions for game problems in conflict controlled system, discussing minimax technique and Bellman equation solution

20 p2947 A72-40028

BELLOWS

Unitized bellow radioisotope thermoelectric generator concept for long term stability, using standardized design, fabrication and qualification [ASME PAPER 71-WA/ENER-1]

05 p0615 A72-15940

Dynamic overstressing and annealing effects on fatigue life of convoluted metal bellows, using dynamic model and strain gage measurements

05 p0742 A72-17245

BELTRAMI FLOW

Local subsonic flow region in transonic free flow past airfoil profile, transforming flow differential equations into linear Beltrami equations system via Chaplygin transformation

15 p2178 A72-31473

BELTS

Nonlinear oscillations amplitude, frequency and instability regions of moving belt as function of longitudinal velocity

13 p1964 A72-29150

BENARD CELLS

Physical and numerical experiments on layered convection in a density-stratified fluid.

17 p2543 A72-35764

Friction term formulation and convective instability in a shallow atmosphere.

18 p2706 A72-36633

BENCHES

U SEATS

BENDING

NT ELASTIC BENDING

Nb alloys bend ductility at various temperatures, showing silicide coatings and electron beam and gas tungsten arc welding effects on mechanical properties

01 p0083 A72-10284

Bare and coated Nb alloy in high temperature vacuum conditions, discussing tensile and bend tests and mechanical properties

01 p0084 A72-10747

Solid rectangular beams under bending tests, obtaining tension-compression stress-strain curves

01 p0141 A72-11002

Ti-Nd and Ti-Nd-Al alloys heat treatment effects on tensile and bending strengths

02 p0244 A72-12245

Cylindrical shafts with deep circumferential grooves, determining effective stress concentration under axial tension or bending

03 p0451 A72-14125

Cyclic deformation and fatigue testing equipment and techniques for biaxial stress, stress concentration and pure bending

03 p0339 A72-14168

Bend tests for minimum radius/thickness ratio of Ti and Be alloy sheets in pressurized fluid [ASME PAPER 71-WA/PT-8]

05 p0671 A72-15913

Stress state of variable thickness long elastic shallow shell in bending and torsion, applying equations to large turbine blades

05 p0735 A72-15986

Bending tests of beam with different creep characteristics in tension and compression

06 p0899 A72-18639

Glass ceramics mechanical properties as function of temperature during bending, taking into account scale factor

09 p1337 A72-22742

Axially homogeneous stress and strain in anisotropic thin walled cylindrical shells, considering pure bending, stretching and twisting [ASME PAPER 71-APMW-4]

10 p1554 A72-24181

Bending of rectangular cross section cantilever beam with cylinder reinforced circular opening, calculating interface stress distribution as function of thickness and elasticity moduli ratio

11 p1733 A72-25545

High strength steel flat plates brake formability from bend tests on sheared edges specimens, noting Hutchinson method sensitivity for different crack propagation propensities materials

11 p1657 A72-25819

Al alloys hand forgings fracture strength and stress corrosion characteristics from precracked specimens bending tests in air and sea water

11 p1658 A72-25833

Ti-Nb and Ti-Nb-Al alloys heat treatment effects on tensile and bending strengths

11 p1659 A72-26131

Glass textolites and high strength oriented plastics fracture mechanism in tension and bending, noting equalizing effect through proper cohesion characteristics between layers

11 p1674 A72-26804

Normal and tangential force factors in casing shaping by bend roll method

11 p1642 A72-26817

Finite difference method for bending stresses calculation in rotating disks subjected to irregularly distributed temperature, deriving digital computer program algorithm

11 p1712 A72-26976

Nonlinear fracture toughness determination via three point bending test simulation by elastic-plastic finite element computer program

12 p1830 A72-27731

Surface piezoelectric effects of mechanical bending of noncentrosymmetric CdS semiconductor wafers

13 p2020 A72-28524

Microcuts as equivalent mechanical stress concentrators for breakdown energy estimation in flat polymethyl methacrylate glass specimens under impact bending loads

13 p1983 A72-28563

Optimal cross section selection of rectangular beams in oblique bending by nonlinear programming and learning algorithm

13 p2056 A72-28914

Infinite plane plates sound radiation due to bending waves interactions with density and stiffness fluctuations in material

13 p2004 A72-29094

Bending of clamped skew plate under uniform loading, using Gaydon-Shephard eigenfunction expansion method

16 p2463 A72-32836

Bending of skew plates of variable rigidity.

17 p2626 A72-34329

Elastoplastic bending of rectangular plates with large deflection.

[ASME PAPER 72-APM-34] 17 p2628 A72-34785

Estimation of the accuracy of the method of measuring the bending of strips in order to determine residual stresses.

19 p2806 A72-37574

Transport aircraft wing compression panel failure in bending test due to stringer interruptions, analyzing structural deficiency via column and beam bending theories

22 p3183 A72-42827

Solid powder metallurgy tungsten alloys, determining scale factor effect on bending strength and fatigue limit

23 p3301 A72-43751

Stress state of variable thickness long elastic shallow shell in bending and torsion, applying equations to large turbine blades

24 p3460 A72-45728

BENDING DIAGRAMS

Optical mirror method for bending strains study in welding cycles with applications to sheet metal thermal stress strain rates

09 p1318 A72-22738

BENDING FATIGUE

Al-Mg alloy under reverse bending fatigue in aqueous sodium chloride with constant load and potentiostatic control, determining anodic polarization effects on fatigue life

01 p0087 A72-11033

Fatigue test machine for alternating cantilever bend and torsion testings at 50 Hz and 1.5-300 K

01 p0049 A72-11381

Combined bending/torque fatigue test machines design, operation, calibration and results, developing probabilistic S-N diagram from cycles-to-failure data statistical analysis

02 p0199 A72-11514

Resonance type rotating bending fatigue testing machine using specimens with attached inertial mass, presenting test results with carbon steel specimens

02 p0201 A72-12823

Temperature dependence of low temperature endurance of Cr-Ni steels in bending fatigue tests

03 p0371 A72-13463

Fatigue breakdown and energy dissipation dependence on stress during bending of cylindrical steel and iron specimens

03 p0372 A72-13589

Crack propagation rates during bending fatigue tests on flat hardened steel as function of stress intensity and plasticity area

03 p0445 A72-13593

Fatigue crack onset and propagation from bending behavior of revolving flat specimens

03 p0445 A72-13594

Scale factor and surface imbedded inserts effect on bending cyclic fatigue strength of nonhardened and roll hardened Al-Ti alloy

03 p0372 A72-13596

Anodizing effect on corrosion fatigue strength of sheet duralumin under low and high bending stress

04 p0535 A72-15662

Fatigue test curves of notched Al alloys under bending with rotation

05 p0676 A72-17086

Accelerated fatigue limits for Al and Mg alloys from transverse bend test data

06 p0827 A72-17398

Hydraulic sand blasting and annealing effects on Ti alloy sheet bending fatigue strength

06 p0831 A72-18357

Resolved shear stress formula for shafts under simultaneous tangential bending and torsion acting at dangerous points of cross section

06 p0899 A72-18643

Sheet metal fatigue test method for transverse 100-1000 Hz bending at normal and high temperatures, applying to 1.5 mm Ti alloy sheet

06 p0900 A72-18671

Stress variation effect on strength values obtained by low cycle fatigue tests involving bending with rotation

07 p1014 A72-19847

Cr-Ti-V-B alloys rod specimens grain size and brittleness-viscosity transition temperature after heat treatment, cooling and bending tests

07 p1023 A72-20668

Notched bend test crack opening displacement gage for continuous measurement of apparent rotation axis and true displacement location at crack tip

10 p1483 A72-24885

Stress analysis of short beam bending of graphite fiber reinforced epoxy composites

11 p1671 A72-25464

Locati and Prot methods for metal fatigue limits evaluated by axial and rotating bending tests on steel specimens

11 p1657 A72-25824

Rotating bending fatigue limit correlation with non-propagating crack for steel specimens with hole

15 p2329 A72-32140

Equipment for low cycle fatigue bending, torsion and tension-compression tests, considering design and performance

16 p2394 A72-33846

Fatigue of boron-aluminum and carbon-aluminum fibre composites.

18 p2701 A72-36625

Resistance to brittle fracture of high-strength steels in various structural states

19 p2819 A72-38014

On a method of analysis of the strain energy changes taking place during the rotatory bending fatigue test of carbon steels and an effect of the pearlite patches to these changes.

20 p2935 A72-38881

Possibility of determining the fracture toughness of materials on the basis of the form of static bend test fracture samples.

20 p2941 A72-39714

Fatigue cumulative damage in cases of rotating-bending and torsional multistep loading.

21 p3118 A72-40933

Non-stationary random vibration of non-linear structures.

21 p3125 A72-41517

Influence of stress raisers in the form of circular holes on the endurance in symmetric bending of AM6BM aluminum-alloy sheet

21 p3071 A72-41704

Heat treatment effectiveness criteria for thermomechanically strengthened steels, using creep rupture, fatigue, bending and tensile tests

23 p3300 A72-43643

Heat treatment effect on tensile and bending fatigue strength of Al alloy thin sheet

23 p3301 A72-43743

The stress-strain relation in the low-cycle fatigue of metallic materials under rotating-beam bending.

24 p3454 A72-44626

Temperature dependence of low temperature endurance of Cr-Ni steels in bending fatigue tests

24 p3413 A72-44938

Hydraulic sand blasting and annealing effects on Ti alloy sheet bending fatigue strength

24 p3416 A72-45744

Method for applying a fatigue crack to impact test specimens made from tough materials.

24 p3417 A72-45765

BENDING MOMENTS

Human spine elastic deformation due to bending stresses, presenting statistical data on caudocephalad acceleration effects in vertebral column injuries

01 p0016 A72-10111

Stress intensity factors for circular crack near surface of semiinfinite solid, considering pure beam bending and approximate thickness effect for plate deep surface flaw

01 p0140 A72-10991

Moment sensors for strain gaged beam systems analysis, noting application to bending moments determination

02 p0287 A72-11510

Matrix method calculation for aerodynamic loads, transverse forces, bending moments, torques and twist of hinged main rotor blades in helicopter during forward flight

02 p0294 A72-12440

Bending stress analysis of rectangular plate with variable stiffness applied to marine propeller blade

02 p0298 A72-12673

Bending moments in transversely isotropic rectangular cantilever plate of low shear rigidity

02 p0299 A72-12684

Plane discrete elastic lattice plates buckling, presenting plane and bending state of force equations

03 p0444 A72-13502

Stress-strain state of transverse isotropic plate with hole under bending and torsional moments

03 p0452 A72-14136

Fiber flexural stiffness determination from bending moment and deflection relation, using bend test

03 p0365 A72-14300

Variable thickness plate under cylindrical bending, considering stress concentration around circular hole

04 p0586 A72-14991

Cyclic bending stress distribution in fir tree turbine blade root for arbitrary loading phase

06 p0899 A72-18629

Interaction surfaces for structural members under combined axial, shear force and bending moment, investigating shear effect on yielding of arches

07 p1090 A72-19730

Membrane and bending moment stresses distribution at elliptical hole in circular cylindrical shell, solving boundary value problems

08 p1243 A72-21234

Stress concentration and elastohydrodynamic values at curvilinear hole in fiberglass reinforced plastic plate under bending moment

08 p1243 A72-21237

Transverse shear effect during bending of cantilever plates with low shear rigidity

08 p1248 A72-21864

Secondary normal stresses in fixed flange zone of thin walled nonlinearly elastic pipe under bending moment and torsion

08 p1249 A72-22096

Nonlinear plane bending of thin elastic rectilinear bar guide elements under concentrated force and torque

09 p1397 A72-22350

Optimum thickness variation in annular strip/curved beam/ under bending moment at constant stress based on Mises-Hencky yield criterion

10 p1558 A72-24847

Dynamic deflections and bending moments of simply supported Bernoulli-Euler beam under traveling mass loads

[AIAA PAPER 72-338]

11 p1728 A72-25371

Aerodynamic lag effects on wing bending dynamic response at supersonic speeds, noting application to stress estimation under gust loads

11 p1572 A72-25922

Free and forced vibrations of two dimensional grids with simple and bridge-type boundary conditions, presenting closed form solutions for nodal deflections and moments

15 p2332 A72-32561

Membrane and bending stress analysis for thin circular cylindrical shells with elliptic hole

16 p2464 A72-32918

Creep deformation upper bounds for smooth pipe bends under constant external bending moments, using energy method analysis

16 p2473 A72-34123

Brittle creep rupture process in beam subjected to simultaneous loading with bending moment and axial force

16 p2474 A72-34128

Nonuniformly thick combined cylindrical shell vibrations, studying radial displacement, bending moment and shearing force

18 p2735 A72-36695

Thermal stability of skewed plates

19 p2871 A72-37430

The unit stress state in a cylindrical tank with a flat bottom and a partly cantilevered shell

20 p2979 A72-39594

Maximum deflection and bending moments of simply supported anisotropic rectangular plate under uniform transverse load, using double Fourier series

20 p2981 A72-39973

Experimental investigation of the carrying capacity in bending of steel box-section beams

22 p2322 A72-41870

Differential equation for maximum beam deflections in transverse bending based on trapezoidal rule

22 p3240 A72-42958

BENDING THEORY

Flexible viscoelastic orthotropic plates and shells obeying linear heredity relations, solving stability and bending problems by Laplace transform

02 p0290 A72-11625

Unidirectional and bidirectional composite laminates subjected to cylindrical bending under uniformly distributed and concentrated loads

02 p0292 A72-11989

Prismatic shells membrane and bending fields induced by concentrated forces, applying Fourier analysis to semiinfinite plates geometry

02 p0296 A72-12527

Beam theory application to cylindrical and conical shells bending, deriving flexibility functions from membrane equations

02 p0296 A72-12529

Bending stresses in composite shell at conical interface between metal and fiberglass reinforced plastic portions under internal pressure

02 p0298 A72-12683

Crack notched three point loaded bend specimens plain strain fracture toughness determination, showing relation between elastic work and stress intensity factor

03 p0442 A72-12960

Torsion and bending by transverse load for homogeneous orthotropic slightly curved bars

03 p0444 A72-13499

Two dimensional boundary value problems for rectangular plates in bending with rigidity variation, using Kantorovich, trigonometric and Horvay functions

03 p0449 A72-13907

Transversely isotropic plates with elastic circular insert, calculating stress concentration at holes under bending

03 p0451 A72-14123

Dynamic stress concentration at circular hole generated by plane bending wave propagation in thin plate, analyzing dependence on vibration frequency

03 p0453 A72-14139

Circumferential undulations of flanges from theory of nonsymmetrical bending of circular plates

04 p0584 A72-14472

Yield point elongated and strain hardened rectangular plates, calculating plastic coefficients in geometrically nonlinear bending problem

04 p0588 A72-15057

Uniform circular plates axisymmetric elastic deformation under various static loadings and boundary conditions, solving flexural equilibrium equations

04 p0590 A72-15184

Shell bending and Timoshenko-type theory to solve stresses of semiinfinite elastic circular cylindrical shells produced by radial pressure pulses

[ASME PAPER 71-WA/APM-16]

05 p0733 A72-15964

Thin cylindrical shell bending deformation from axisymmetric temperature distribution generated by narrow heating element

05 p0736 A72-16113

Plastic zone formation and fatigue crack propagation rate during high cyclic bending of metals

05 p0674 A72-16326

Triangular/KLI/ and quadrilateral/KQT/ thin shallow shell elements with 20 degrees of freedom, basing bending behavior on discrete Kirchhoff formulation

05 p0739 A72-16549

Deflection function for symmetrical bending of unloaded annular plate, constructing stiffness, mass and stability coefficient matrices by function manipulation

05 p0739 A72-16550

Biaxial bending solution by tangent stiffness matrix method suitable for computer application

06 p0897 A72-17967

Soviet book on nonmetallic material strength during nonuniform heating covering, load endurance, bending phenomena and thermal stability of fiberglass, pyroceramics and reinforced plastics

06 p0796 A72-18521

Temperature induced bending of thin freely supported rectangular plate, obtaining stress-strain state

06 p0899 A72-18564

Collocation least square solutions of boundary value problems, applying to prismatic bar torsion and plate bending

07 p1025 A72-18790

Stress-strain state relationship to crack development morphology in elastic strain region of austenitic steel sample under cyclic bending

07 p1013 A72-19769

Symmetrical bending of variable thickness circular plate solved by classical method and Reissner and Vekua equations

07 p1092 A72-19852

Bending and torsion of thin isotropic rod with identical principal rigidities in bending, writing elastic curve equation in cylindrical coordinate system

08 p1209 A72-21367

Friction and bending effect on unidirectional glass fiber reinforced plastic ring deformation distribution

08 p1191 A72-21504

Elastic shell geometry and rigidity effects on critical load in pure bending within structurally orthotropic theory, taking into account reinforcing rib eccentricity

08 p1247 A72-21816

Bending under concentrated load of laminated cantilever plate with low interlaminar rigidity, taking into account low shear resistance effects

08 p1248 A72-21860

German monograph on bending theory extension for stress analysis of disks and cylindrical shells

09 p1397 A72-22333

Axisymmetric grid plate bending and torsion under normal forces and moment vectors loads, determining stress-strain state from finite difference equations

09 p1398 A72-22692

Bending theory of homogeneous isotropic micropolar cantilever beam loaded by moments at edges

09 p1399 A72-22700

Existence and uniqueness theorem for weak solution of clamped elastic plate equilibrium problem, using micropolar flat plate bending theory

10 p1555 A72-24202

Freely supported rectangular plate flexure under arbitrarily distributed load, obtaining differential equations solution in trigonometric polynomials

10 p1559 A72-24996

Nonlinear bending and buckling of axisymmetric sandwich shells based on finite element approach

[AIAA PAPER 72-356]

11 p1729 A72-25385

Bending deflection calculation for laminated beams with layers of different rigidity

11 p1733 A72-25546

Bending stress in oxygen presaturated Nb during oxidation, cooling, dissolution and annealing, using thin film model

11 p1658 A72-25853

Bending of simply supported thin square plate clamped around central circular hole and under uniformly distributed transverse load

11 p1736 A72-25985

Finite difference method for free vibration of axisymmetric shells, using inertia force terms in shell bending theory equilibrium equations

11 p1737 A72-26429

Transverse bending theory for sandwich plates, considering core and face equilibrium and compatibility equations

11 p1737 A72-26587

Longitudinal bending stability of hard polymer rods under compression load and creep

11 p1675 A72-26824

Electrical and thermal conductivity, elastic properties and resistance to bending of porous tungsten in porosities region

11 p1665 A72-26868

Bending of unbounded plate coupled to elastic isotropic half space with vertical and horizontal springs, calculating contact stresses by double Fourier transforms

12 p1878 A72-27082

Bending problem for circular three layer plate with rigid circular insert, studying deflection under bending moment

12 p1879 A72-27090

Stress-strain state in pure bending for infinite elastic strip with circular central hole, using integral Fourier transforms

13 p2053 A72-28390

Limiting load calculation for thin walled I-beam in oblique bending and torsion beyond elastic limit

13 p2055 A72-28734

Bending of rectangular plates clamped at three edges, establishing sufficient conditions for application of simple iterations to linear algebraic equations solution

13 p2057 A72-29077

Rigidity of developable surfaces with cylindrical connections and without plane domains, subjected to infinitesimally small bendings

13 p2061 A72-29793

Infinitesimally small slip bendings of sign-variable curved surface of revolution with parabolic boundary parallels

13 p2061 A72-29794

Rigid smooth body pressing into elastic plate surface subjected to cylindrical bending, discussing contact problem and transverse shear strain

13 p2062 A72-29950

Boundary values for bending of plates with weak orthotropy from Vekua plate theory

13 p2062 A72-29951

Thin wedge shaped shell bending under normal loads, discussing boundary value problems

13 p2062 A72-30066

Bending deflections of rectangular plates with laminated orthotropic layers analysis by finite element displacement, comparing with carbon fiber reinforced plastic structures

14 p2167 A72-30905

Thin elastic plates finite displacement flexure behavior, using piecewise linear finite element incremental stiffness technique

14 p2168 A72-30933

Cosserat strip bending by singular shear stresses, normal stress dipoles and spin moments, confirming Saint Venant principle

15 p2324 A72-31484

Finite element analysis of circular and elliptical plates with curved boundaries, discussing high precision triangular plate bending element modification for accuracy improvement

15 p2326 A72-31715

Mixed triangular finite element model for plate bending problems including shear deformation effects, discussing error analysis and convergence

15 p2326 A72-31716

Finite element method application to thin plate bending problem to illustrate efficiency of sector elements for sectorial and annular plates

15 p2326 A72-31720

Bending of uniformly loaded circular plate with mixed boundary conditions, calculating deflection and bending moments

15 p2332 A72-32579

Plane stress solution for thin walled cantilever beam with end load extended for beam width effects in composite orthotropic beam bending

16 p2463 A72-32841

Linear theory for spirally sinusoidal stress distributions in elastic helicoidal shells applied to pure bending problem

16 p2465 A72-33003

Instantaneous and time dependent solutions for thin rectangular plates nonlinear creep bending within framework of Karman theory

16 p2473 A72-34126

Natural bending frequency comparable to rotational frequency in rotating cantilever beam.

17 p2625 A72-34324

Governing equation derivation for coupled extension, flexure and torsion in pretwisted curved beams of thin walled open section, using three dimensional elasticity

[ASME PAPER 72-APM-5] 17 p2630 A72-34809

Effect of end attachment on the strength of fiber reinforced composite cylinders.

[SESA PAPER 1994A] 17 p2630 A72-34817

Stresses in a welded diaphragm due to boundary contraction and normal uniform pressure.

[SESA PAPER 181 I] 17 p2631 A72-34821

The evaluation of the stress intensity factors for cracks subjected to tension, torsion, and flexure by an efficient numerical technique.

[ASME PAPER 72-MAT-B] 17 p2631 A72-34966

Shear deformation in heterogeneous anisotropic plates.

17 p2633 A72-35294

Finite bending of a compressible anisotropic rectangular block into a hyperbolic shell.

17 p2634 A72-35438

Monograph - The finite-element method in plate bending analysis

17 p2634 A72-35547

Computerized numerical integration for nonlinear bending of tapered slender cantilever beams under concentrated tip loads

17 p2635 A72-35975

Bending and vibration of multilayered sandwich plates, presenting static and dynamic analysis method

17 p2635 A72-35976

Bending of rectangular plates of linearly varying thickness

18 p2736 A72-36991

A rational approach to creep design.

19 p2874 A72-37706

Fatigue limits of cylindrical test pieces in rotative bending and in tension-compression, investigating strain gradient effect

19 p2875 A72-37788

Shells of revolution free of bending under uniform axial loading.

19 p2876 A72-37886

Bubnov-Vlasov variational method for thin parallelogram plates bending under complex loads, calculating edge skew and side length effects

19 p2877 A72-38160

Plane bending problems in the theory of elasticity for nonhomogeneous solids

19 p2877 A72-38162

Pure bending of a rectangular plate made of heteromodulus material

20 p2978 A72-39020

Plate bending analysis with hybrid triangular and rectangular finite elements, deriving stiffness matrix via optimized stress functions

20 p2979 A72-39556

An equivalent grid framework for skew plates in flexure.

20 p2980 A72-39689

Plane strain bending of laminated fibre-reinforced plates.

20 p2982 A72-40021

The influence of end plate and bulkhead on the shell of variable rectangular profile subjected to simultaneous torsion and bending at middle planes.

20 p2982 A72-40065

Bent plates and shells equations and rupture modes, characterizing cracks and stress intensity

21 p3122 A72-41338

Mixed finite element analysis of elasto-plastic plates in bending.

21 p3124 A72-41502

A collocation solution of the nonlinear equations for axisymmetric bending of shallow spherical shells.

22 p3232 A72-41938

Bending of a rectangular plate with a clamped edge and an internal symmetric cut

22 p3234 A72-42291

Stress analysis in two dimensional bending process using the photo-rheological stress analysis.

22 p3183 A72-42483

Symmetrical bending of circular plates using finite elements.

22 p3236 A72-42605

Numerical solution of bending stresses in elastic cantilever plates under surface and edge loads, noting boundary layer, load concentration and sweep back effects

22 p3236 A72-42609

Numerical solution of a boundary-value bending problem for rectangular plates with free and freely supported opposite edges

23 p3345 A72-43645

A nonlinear problem of pure bending of a three-layer plate with a corrugated sheet filler

23 p3346 A72-43655

Stress intensity factors for embedded elliptical crack in semiinfinite solid and for semicircular surface crack in plate under tension and/or bending

23 p3353 A72-44231

Bending evaluation of test section in tensile tests with axial loads and resistance strain gages, noting friction moment role

24 p3456 A72-44791

Theory of thin elastic shells applied to pipe bends subjected to bending and internal pressure.

24 p3456 A72-44795

Fracture of WC-Co from a continuum viewpoint.

24 p3413 A72-44815

BENDING VIBRATION

Flexural vibrations of arbitrary ring with axial symmetric cross section, noting validity for natural frequencies prediction

01 p0138 A72-10395

Natural bending-torsional vibrations of turbine blades connected by ring junctions, using dynamic pliability principle

01 p0143 A72-11370

Chordwise bending vibrations and flutter of thin isotropic rectangular plates, considering static and dynamic responses

03 p0443 A72-13404

Conforming rectangular and triangular finite elements for plate free vibrations analysis in bending

04 p0585 A72-14846

Approximate maximum shock stress analysis for curved bar bending vibration due to longitudinal impact by disregarding elements inertia with regard to axial motion

05 p0737 A72-16285

Dynamic properties of turbine wheels under bending vibrations, classifying resonant frequencies on basis of vibration modes

06 p0899 A72-18644

Flexural, longitudinal and torsional vibration damping of various size rods, taking into account surface layer energy loss

06 p0900 A72-18675

Shallow axially symmetrical spherical shell flexural vibrations, obtaining equations iterative solution

06 p0901 A72-18705

Beams and square plates nonlinear vibration response to random concentrated driving force solved numerically on digital computer

06 p0901 A72-18718

Sound pressure in liquid layer bounded by oscillating plate under bending as function of boundary acoustic impedance

07 p1034 A72-18923

Composite elastic beams equations under initial stress, investigating flexural wave propagation and structural stability

07 p1090 A72-19733

Torsional bending vibrations mode shapes of space frame with variable elastic and mass characteristics, determining eigenvalue error limits

08 p1205 A72-20957

Coupled motions of rotating free solid body and elastic rod torsional bending vibrations with precession and forced vibrations from energy exchange

08 p1205 A72-20959

Ritz-Galerkin process applied to coupled differential equations of motion of pretwisted tapered cantilever turbine blade vibrating in flexure

08 p1244 A72-21483

Dynamic buckling and plate to shell transition of thick spherical caps under large amplitude axisymmetric flexural vibrations

08 p1249 A72-22135

Quadrilateral four node nonconforming plate bending finite elements for structural vibration and stability analysis

08 p1250 A72-22142

Variable rigidity circular isotropic plate vibration and bending, determining flexure surface and natural frequencies in terms of Fourier-Bessel series

09 p1399 A72-22699

Perturbation analysis of nonlinear free flexural vibrations of circular cylindrical shell, using Donnell equations

09 p1405 A72-22998

Damping coefficient increase in welded bodies under uniform stress and compression, torsion and bending vibration

09 p1406 A72-23076

Nonlinear mode coupling in equations of motion for thin panel vibration as function of membrane stretching-bending energy ratio

09 p1408 A72-23465

Circular plates free flexural vibrations with and without damping, calculating resonant frequencies from corresponding Bessel functions

10 p1555 A72-24194

Free flexural vibration of truncated conical shells, using Galerkin method and Donnell type basic equation

10 p1559 A72-25024

Free in-plane vibrations of hinged and fixed uniform circular arches, discussing natural frequencies and flexural and extensional vibration modes

10 p1560 A72-25186

Aerodynamic damping of turbomachine blade vibrations under varied conditions of stagger angle, pressure ratio and relative velocity, using pure bending mode excitation

[ASME PAPER 72-GT-8] 11 p1568 A72-25611

Helicopter rotor blades bending vibrations, examining scale effects, dynamic similarity and natural frequencies via series of Legendre polynomials

[AD-745569] 11 p1734 A72-25733

Flexural vibrating free edge plate transducer with stepped thickness for high directional ultrasonic radiation generation in fluids

11 p1687 A72-26060

Convergence of plate bending eigenvalue solutions from conforming displacement finite elements based on thick plate free vibration conversion to isoperimetric variational problem

12 p1879 A72-27194

Flexural vibrations of nonrotating turbopump rotor due to kinematic excitation of casing, deriving integral equation yielding stress-strain state and fatigue strength 12 p1886 A72-28150

Coupled flexural longitudinal vibrations of circular arc girder with symmetrical cross section, discussing optimal design 15 p2324 A72-31487

Flexural vibrations of ring with arbitrary cross section, proposing theory for natural frequencies prediction by Ritz method 15 p2329 A72-32141

Rotating shaft bending vibrations under harmonically varying transverse load and periodic parametrically exciting axial force, using linearized theory of small displacements 16 p2463 A72-32877

Collocation method for coupled bending-bending torsion vibrations of straight uniform cantilever beam with asymmetric airfoil cross section 16 p2464 A72-32908

Nonlinear flexural vibrations of a clamped circular plate. [ASME PAPER 72-APM-18] 17 p2628 A72-34798

Anisotropic rectangular plate free flexural vibration improved solution via Fourier analysis 18 p2734 A72-36419

Bending waves diffraction and scattering by mass impedance loadings of infinite plane plate, considering point load and semiinfinite rib arrays 18 p2739 A72-37203

Timoshenko finite element beam theory application to flexural vibration problems, considering shear deformation and rotary inertia effects 18 p2740 A72-37206

Experimental investigation of flexural vibration damping in supported square plates with coatings 19 p2876 A72-38004

Propagation of bending-torsional waves in a thin curved rod with allowance for the shear effect 19 p2877 A72-38189

Computer solution of dynamic problems for bending of beams and thin plates beyond the elastic limit under alternating loads 19 p2877 A72-38194

Bending vibrations of finite length prismatic bar moved in longitudinal direction through tubelike supports, using variational technique 20 p2979 A72-39332

Determination of flexural-vibration deflections of structural elements with allowance for internal friction damping 20 p2981 A72-39921

Dispersion of flexural waves in circular cylindrical shells. 20 p2982 A72-39975

Simulation of flexural vibrations of rods without concentrated masses 21 p3116 A72-40168

Bending vibration test of glass-textolites, noting temperature effect on vibration damping properties 21 p3073 A72-41357

Application of a method using slowly changing parameters for the approximate calculation of transverse vibrations of rods 21 p3126 A72-41550

Rheological properties of molybdenum and platinum of bamboo structure under bending loads 21 p3071 A72-41712

Numerical analysis of wave processes in a three-layer strip with rigid filler 22 p3232 A72-41872

Bending waves propagation through flat plate forming rigid sound bridge between two parallel plates, calculating energy transfer at LF oscillations 22 p3234 A72-42128

Unsteady rotor aerodynamics at low inflow and its effect on flutter. [AIAA PAPER 72-959] 22 p3135 A72-42349

On eigenvalue boundary problems of transversely vibrating sandwich beams. 22 p3240 A72-42910

Nonaxisymmetric vibrations of arbitrarily thick circular cylindrical shells 23 p3345 A72-43624

Experimental investigation of displacements and stresses in a rod during impact loading 23 p3348 A72-43795

Free flexural vibrations of an elliptical plate with simply supported edge. 23 p3352 A72-44121

Bounds to bending frequencies of a rotating beam. 23 p3354 A72-44249

BENDS [PHYSIOLOGY]

U DECOMPRESSION SICKNESS

BENZENE

Catalytic action of metal oxides on isopropylbenzene hydroperoxide decomposition in liquid phase 08 p1129 A72-22094

Energy and time characteristics of Raman scattering by benzene in laser cavity as function of medium thickness and cavity length 13 p1969 A72-29523

Benzene isochoric specific heat curves along saturation line in biphasic and single phase states, noting variations near critical point 15 p2334 A72-31393

BERNOULLI EQUATION

U BERNOULLI THEOREM

BERNOULLI THEOREM

Subjective probability distributions for random device-generated Bernoulli process unknowns, discussing distribution median and quartiles and hypothetical sample impact assessment techniques 05 p0616 A72-15812

Near ground pressure differentials caused by large transport aircraft induced wake vortices, comparing measured data with Bernoulli formula theoretical values 12 p1752 A72-28122

Simplified conservation laws for finite-difference computations. 20 p2946 A72-39637

Isometric motion in relativistic magnetohydrodynamics. 21 p3091 A72-40567

BERNSTEIN ENERGY PRINCIPLE

Growth rate estimation of negative energy Bernstein and ion acoustic waves explosive interaction, noting collisionless shock turbulence 08 p1212 A72-21248

Nonlinear instability of Bernstein modes pumped by an electromagnetic wave. 24 p3430 A72-45571

BERYLLIUM

NT BERYLLIUM ISOTOPES

Beryllium microstructure and hexagonal close packed polycrystal material residual thermal stresses, calculating thermal expansion coefficients 01 p0087 A72-11028

Substructure variations and crystal lattice periods dependence on compression stress in beryllium single crystals during plastic deformation due to base slip 03 p0376 A72-14018

Li, Be and B production rate in interstellar gas by galactic cosmic rays from diffusion model of fast particles, accounting for He component 05 p0708 A72-15760

Beryllium joining by resistance welding, electron beam welding, dip brazing and braze welding 06 p0820 A72-17701

Increased microplastic deformation resistance, relaxation stability and aging of beryllium by cyclic heat treatment 07 p1013 A72-19740

Basal and prismatic crystal dislocations in Be, measuring critical resolved shear stress dependence on temperature at 300-500 K 08 p1185 A72-20991

Beryllium sheet and foil application to lightweight space structures, discussing mechanical properties [AIAA PAPER 72-404] 11 p1726 A72-25425

Be elastic constants at 25-300 C, using ultrasonic pulse technique 11 p1657 A72-25774

Hot isostatic pressing techniques for thin wall Be tubes manufacture 11 p1643 A72-26831

Zone refined prism slip oriented Be single crystals deformation substructure analysis by synergistic method combining transmission electron microscopy, X ray topography and X ray diffraction profile analysis 11 p1666 A72-26928

Be foil electrical resistance change during and after pulsed laser irradiation and annealing 12 p1853 A72-27067

Oxide content and sheet microstructure directionality effects on Be powder and ingot sheets notch strength, noting thickness dependence [ASM PAPER W 72-12,6] 12 p1830 A72-28164

Mechanical properties of thick Be plate produced by diffusion bonding of thin sheets from ingot material 13 p1973 A72-28655

Microhardness anisotropy of hardened and aged Be single crystal as function of purity 13 p1978 A72-29023

Acceptor level study of thermally diffused Be and Be-Li complexes in single crystal Si after quenching and annealing 13 p2022 A72-29628

Quasi-longitudinal and quasi-transverse plane wave propagation in anisotropic elastic-plastic solids, approximating Be single crystal behavior 14 p2163 A72-30176

German book on welding of special metals covering Ti, Zr, Mo, Ta, W, Va, Nb and Be welding techniques 16 p2398 A72-33372

Be doped p-type Si piezoresistance and hole transport properties dependence on temperature, crystal orientation and doping concentration 16 p2442 A72-33834

The temperature dependence of the friction stress for basal dislocations in beryllium in the range 300-500 K. 20 p2935 A72-39191

Stabilization of a superconducting modification of beryllium by an aluminum admixture 20 p2960 A72-39407

Mechanical properties improvement of Al alloys for machine construction applications, suggesting Ti, Zr and Be additions optimal rate 20 p2941 A72-39577

Be foil electrical resistance change during and after pulsed laser irradiation and annealing 24 p3432 A72-45720

BERYLLIUM ALLOYS

Directional solidification of off-eutectic Al-Be alloy, obtaining ultimate strength, elastic modulus and concentration perturbation caused by freezing rate changes [AD-738212] 02 p0242 A72-11985

Phase composition and structure of Be alloys containing Ru, Os, Rh or Ir, noting isomorphous beryllides existence 03 p0375 A72-13942

Bend tests for minimum radius/thickness ratio of Ti and Be alloy sheets in pressurized fluid [ASME PAPER 71-WA/PT-8] 05 p0671 A72-15913

Mechanical and microstructural properties of Be-base alloys consolidated by vacuum arc melting, reporting results of tensile tests, hardness measurements and microprobe analysis 05 p0674 A72-16389

Kinetic data analysis of internal oxidation in dilute Ni-Be alloys, deriving activation energy and diffusivity of oxygen in Ni 07 p1021 A72-20435

Quenched beryllium bronze alloy plastic deformation effects on anomalous and ordinary stress relaxation processes 12 p1828 A72-27292

Changes in the structure of nickel-beryllium alloys during deformation, recrystallization, and aging 21 p3068 A72-40959

BERYLLIUM COMPOUNDS

NT BERYLLIUM OXIDES

Solid phase reaction kinetics in zirconium beryllide alloys with Ta and Nb at 900-1400 C, noting Be diffusion effect 16 p2408 A72-33535

BERYLLIUM ISOTOPES

Cosmic Li, Be and B nuclei charge and isotopic composition measured by particle telescopes, finding L/M ratio 01 p0121 A72-11120

Be isotopic ratio in galactic cosmic rays, noting mean interstellar hydrogen density and rays age 16 p2448 A72-33738

BERYLLIUM OXIDES

Thermal conductivity of aluminum, beryllium and magnesium oxides lattices at high temperatures 06 p0828 A72-17615

Refractory steels heat resistance improvement by surface saturation with Be and subsequent oxidation in air at 900-1000 C, comparing with aluminized steels 15 p2255 A72-31574

Dielectric breakdown in electrical insulators used in thermionic converters. 17 p2496 A72-34593

Physical-mechanical properties of beryllium oxide and investigation of its electrical resistance under irradiation in a reactor 18 p2703 A72-36147

BERYLLIUM POISONING

Ultrastructural and morphometric studies of beryllium oxide-contaminated environment effect on monkey and dog lung tissue 07 p0925 A72-20686

BERYLLIUM 7

Vertical macroturbulence diffusion coefficient and Na 22 and Be 7 flux from stratosphere to troposphere estimated using ground level measurements and two layer model 09 p1376 A72-22416

Be 7 destruction via nuclear decay instigated by atomic electron capture in interstellar medium, considering Ar 37, Ca 41, Ti 44, V 49, Cr 51, Mn 53 and Fe 54 16 p2447 A72-33736

BERYLLIUM 9

Pionic X ray fields and transitions in Li 6, Be 9, C 12 and O 16, obtaining 2p level absorption broadening 10 p1515 A72-24418

BESSEL FUNCTIONS

NT HANKEL FUNCTIONS

WKB type solution for electromagnetic wave propagation in circularly cylindrical coordinate system with rho-dependent refractivity, using Bessel function 04 p0491 A72-15384

Air-filled elliptical waveguide with nonmagnetic metal wall, determining dominant TE mode attenuation by perturbation method with Bessel function 04 p0491 A72-15426

Particular solutions to inhomogeneous Bessel and Legendre equations in resonance case 08 p1198 A72-20973

Electromagnetic impulse wave impingement on semiinfinite isotropic plasma slabs with arbitrary in-

cidence angle and polarization, calculating signal reflection in terms of Bessel functions

08 p1137 A72-21990

Circular plates free flexural vibrations with and without damping, calculating resonant frequencies from corresponding Bessel functions

10 p1555 A72-24194

Probability density function of hologram exposure irradiation in terms of Bessel function, adding uniform beam coherently to random speckle pattern

11 p1636 A72-26749

Determinant with first and second kind Bessel functions elements, presenting zeros estimates

12 p1836 A72-27072

Fourier-Bessel superposition and Laplace transformation methods for surface displacement produced by time dependent dipole in elastic half space, noting buried dipole case

19 p2876 A72-37887

Bessel series solution to electromagnetic field and pulse function of cylindrical conducting screen located in monochromatic plane wave

22 p3155 A72-42667

BETA PARTICLES

Boron concentrations in Mo-Hf alloy samples from neutron activation analysis, measuring Li 8 beta radiation with plastic scintillation detector

16 p2391 A72-33238

Some aspects of the use of small needle-shaped semiconductor detectors in the determination of regional distribution and transport of labelled compounds.

18 p2655 A72-37195

Bremsstrahlung from cylindrical beta sources.

21 p3088 A72-41383

BETATONS

Energy-phase time transformations of damped Liapunov system applied to nonlinear spring pendulum and betatron transient oscillations

01 p0103 A72-11387

BETHE-SALPETER EQUATION

First and second moment of an optical wave propagating in a random medium - Equivalence of the solution of the Dyson and Bethe-Salpeter equation to that obtained by the Huygens-Fresnel principle.

17 p2580 A72-34290

BEVATRON

Bevatron nuclear fragmentation of N 14 nuclei, discussing isotopic fragments identification

03 p0391 A72-13692

Depth ionization properties and biological effects of bevatron produced heavy ion beams, discussing utilization in tumor therapy, space biology and radiobiology

03 p0316 A72-13693

Inclusive isotope spectra of secondary nuclei produced by Bevatron heavy ion fragmentation in carbon and polyethylene targets, noting partial differential cross sections

10 p1517 A72-25144

BIAS

NT RESPONSE BIAS

Bias and variance prediction efficiency in two stage sampling designs

03 p0383 A72-14368

Wide range bias dependence of planar bipolar transistor dc and small signal current gain, comparing analytical findings with Si junction experiment

06 p0783 A72-17608

P-channel MOS transistor LF background noise components analysis for different dependencies on gate bias and temperature

09 p1286 A72-23109

Fixed-bias floating double-probe technique with simple Langmuir-probe characteristics.

19 p2804 A72-38592

BIBLIOGRAPHIES

Automatic control systems sensitivity, presenting literature survey

01 p0044 A72-10299

Soviet progress and bibliography on fault tolerant digital computers design, emphasizing redundancy application to achieve high reliability

02 p0184 A72-11484

Survey and bibliography of extrapolation processes in numerical analysis based on polynomial or rational functions

02 p0252 A72-11546

Bibliography on linear-quadratic-Gaussian problems covering quadratic criteria, state estimation, stochastic control, computations and applications

02 p0198 A72-12813

Literature review of structural safety, treating load, strength, dynamic structural and structural reliability analyses and design aspects

10 p1560 A72-25174

Bibliography on infrasonic sound wave generation, propagation and detection at ground level and ionospheric heights

11 p1690 A72-26520

Nd-YAG laser bibliography covering oscillation, dynamics, engineering, materials and harmonic generation

12 p1826 A72-27957

Bibliography on noise control covering surface transportation, machinery and aircraft noise, industrial criteria, biodynamics, legislation and measurement

13 p2006 A72-29588

Lunar research bibliography covering earth-moon system, moon motion, gravitational field, structure, thermal history, composition, photometry, spacecraft exploration, etc

14 p2155 A72-30521

Bibliography on SST upper atmospheric environment, listing references to stratospheric structure, composition and physical dynamics, chemical reactions with pollutants, transport properties, etc

16 p2386 A72-33797

1972 seminar supplement to bibliography and abstracts on electrical contacts, circuit breakers and arc phenomena.

18 p2664 A72-35986

1970-1971 Holm Seminar supplement to bibliography and abstracts on electrical contacts, circuit breakers and arc phenomena.

18 p2665 A72-36120

Digital image enhancement heuristic, superresolution and positive restoration techniques, providing bibliography

18 p2658 A72-36264

Chemical evolution and the origin of life - Bibliography supplement 1970.

18 p2650 A72-36450

A table of solutions of the one-dimensional Burgers equation.

19 p2828 A72-38717

Book - Law and politics in outer space: A bibliography.

21 p3132 A72-41535

A bibliographical survey of acoustic emission.

24 p3408 A72-45293

BICARBONATES

U CARBONATES

BICRYSTALS

Grain boundary migration measurements in bicrystalline Al under intense electric field, using optical microscope

01 p0089 A72-11182

Surface defects absence after intergranular creep from Al bicrystals grain boundaries observation by transmission electron microscopy

10 p1495 A72-24084

BIHARMONIC EQUATIONS

Bi-harmonic stress and displacement potentials for two dimensional boundary problems in elasticity theory, using Galerkin method

03 p0453 A72-14207

Cauchy problem for nonlinear biharmonic equation in Euclidean n-space, deriving a priori inequality estimate by logarithmic convexity of functional F

04 p0539 A72-15044

Bi-harmonic boundary value problems solution by summary representations method and conformal mapping for plane with two circular holes

08 p1242 A72-20906

Rectangular domain boundary value problem biharmonic equation and Cauchy system equivalence, noting semigroup properties analysis in terms of nonclassical imbedding variables

11 p1737 A72-26663

Inverse transformations in mathematical models of elasticity and plasticity problems reducible to biharmonic equation

16 p2468 A72-33163

Block five diagonal matrices and the fast numerical solution of the biharmonic equation.

17 p2574 A72-34446

Chebyshev acceleration application to Jacobi, Gauss-Seidel and related iterative methods for solution of coupled harmonic equations, comparing to block SOR method

17 p2574 A72-34447

Solutions to certain elliptic equations, which are positive in the vicinity of an isolated singular point

20 p2947 A72-39867

Asymptotic representation of the solution of a boundary value problem for a biharmonic equation degenerating into a fourth-order parabolic equation

22 p3198 A72-41899

BILLETS

Optimal selection of flawless nose cones from graphite billets, obtaining mathematical model based on ultrasonic reflection test data

07 p1086 A72-20350

Chemical composition, physical properties, microstructure and production of 1300 kg powder metallurgy forged billets

11 p1644 A72-26845

Kinetic forming of conical Al component from solid cylindrical billet, analyzing forming and inertia stresses, impact velocity and displacement-time history

15 p2244 A72-31708

BILLOW CLOUDS

U CLOUDS [METEOROLOGY]

BIMETALS

Two component flow and optimal strength ratios between core and shell materials during extrusion of composite bimetallic specimens into circular tubes

01 p0077 A72-11078

Bimetallic rectangular plate with two interconnected layers of anisotropic and isotropic materials and large deflections in nonuniform pressure and temperature field

05 p0735 A72-16016

Large length-to-diameter ratio two layer blank bimetallic hard alloy product manufacture by extrusion die method, noting mechanical properties

05 p0666 A72-16098

Bimetallic actuator for spacecraft thermal control with design emphasis on external power source elimination, high reliability, frictionless operation, simplicity and low weight

09 p1305 A72-22249

Numerical solution of integral equations for dislocation densities and stress singularities associated with cracks and pile ups in bimetallic media

09 p1398 A72-22622

Phase transformations and recrystallization study of Ti-steel bimetal with emission microscope, observing high temperature formation of titanium and vanadium carbides

11 p1654 A72-25493

Inertia welded bimetallic fasteners for aerospace industrial applications, noting cost advantages [ASM PAPER W 72-32,5]

12 p1817 A72-28166

Electron probe microanalysis of Mo-Pd system diffusion at 1000-1600 C, measuring chemical diffusion coefficient as function of temperature, concentration and activation energy

13 p1978 A72-29221

Laminar composite materials with special physical properties

20 p2940 A72-39451

Theoretical interpretation of emf generation between noncompressed parts of bimetallic junction traversed by shock wave, taking into account radiation pressure of phonon gas

22 p3207 A72-43050

High strength bimetallic rivets produced by inertia welding Al-Ti alloy shank with pure Ti tail, noting weight and cost reduction for aerospace vehicle production [SAE PAPER 902]

23 p3293 A72-43452

Tensile strength of tungsten reinforced nickel, determining temperature effect on fibers deformation after vacuum rolling simultaneously with plastic matrix

24 p3416 A72-45749

BINARY ALLOYS

Binary alloys ground state energy and superstructures, examining bcc and fcc Ising model systems with first and second neighbor interactions

01 p0083 A72-10210

Al-Mn system constitution, discussing metastable phase, high and room temperature modifications and transformation equilibrium

01 p0088 A72-11045

Binary and ternary alloys of Cr and Fe with Ni, determining interaction coefficient and molar enthalpy for Cr at 1600 C by mass spectrometry

05 p0676 A72-17103

Vacancy effects on residual electrical resistance of binary ordering fcc lattice alloys as function of composition and annealing temperature

06 p0832 A72-18422

Monograph on diffusion couple technique for Ti-Al system interdiffusion phenomena, discussing layer growth, phase development, grain boundary diffusion mechanism, mass transport, etc.

07 p1011 A72-19267

Structure, hardness, density and electrical resistance of binary alloys V-Ti, V-Cr, V-Al and V-Sn

07 p1013 A72-19741

Quantum mechanical electron motion problem in binary alloy crystal lattice, discussing Bloch approximation, energy spectra, and third element admixture conductivity effects

07 p1049 A72-20150

Binary alloys concentration distribution determination in migrating liquid-solid plane phase interfaces range during crystallization

07 p1022 A72-20571

Binary Al alloys with variable melting volume and liquid zone velocities, investigating crystallization during zone melting

07 p1022 A72-20572

X ray K absorption edges in binary solid solutions of Co, Fe and Ni with localized hole increases

09 p1371 A72-22846

Al alloys solid binary solution soft X ray emission spectra interpretation by rigid band and virtual bound state models

09 p1371 A72-22847

Diffusion measurements during annealing of Pd-V, Pd-Ti and metal-ceramic systems by microprobe

11 p1664 A72-26853

Phase structure of Cr rich Cr-Ni, Cr-Fe, Cr-Co and Cr-Ni-Fe alloy particles produced by evaporation in Ar using X ray diffraction

13 p1974 A72-28660

Liquid quenched Sb-transition metal binary alloy constitution, finding metastable phases in quenched Cr-Sb and Mn-Sb alloys

13 p1975 A72-28672

Temperature dependent electron density of state and dc resistivity of disordered binary alloys, using single band thermal disorder model

13 p2022 A72-29626

Binary ordering alloys with fcc lattice, studying volume effects on solubility of impurity atoms in interstices

13 p2023 A72-29907

Phase diagram of cast and annealed Cr-Sc alloys by differential thermal, X ray, metallographic and microhardness analyses

13 p1981 A72-29953

Sintering of binary systems Co-Ni Co-Fe and Fe-Ni with infinite mutual solubility at different temperatures

13 p1966 A72-29954

X ray and metallographic analyses of Ni-Mo, Ni-Ta, Ni-Nb, Ni-Zr and Ni-Ti alloys crystallized at high cooling rates, observing metastable phases

14 p2115 A72-30405

Phase diagrams of Ru binary and ternary systems, noting admixtures interactions

14 p2123 A72-30992

Binary systems phase diagrams qualitative and quantitative analysis based on free atoms electron state energy ratios, formulating solid solubility criterion

14 p2123 A72-30994

Composition dependence of ultrasonic velocity in binary Mg base alloys measured by pulse method

14 p2143 A72-31030

Binary Al alloys intermetallic phases effects on microcracks nucleation and propagation at 300 C in uniaxial tension, considering alloying elements influence on mechanical properties

14 p2124 A72-31036

Li addition effects on Mg mechanical properties temperature dependence and notch sensitivity of binary Mg-Li alloys

14 p2125 A72-31041

Sm and Eu binary alloys, investigating physicochemical interactions and phase diagrams

15 p2289 A72-31187

Concentration dependence of interdiffusion coefficient in binary metallic systems with continuous and bounded solid solutions

15 p2243 A72-31572

Transition metals additives effect on binary Mo alloys softening, noting influence of temperature and electron concentration change

15 p2258 A72-32135

Geometric/chemical model of lattice dimensions of Laves phases of binary alloy bcc and fcc structures

16 p2409 A72-33801

Gravimetric and polarographic determination of W in binary W-Mo alloys, noting methods accuracy

18 p2655 A72-36098

The effect of Mo, Al, and C on phase transformations in Ni alloys

19 p2814 A72-37417

Solid-state phase transformations

19 p2815 A72-37442

Hall and resistance measurements on single crystal HgTe-InTe alloy systems for high pressure phases in terms of conduction state, band structure and impurity effects

19 p2844 A72-37464

German monograph - The effect of alloying elements on the dry high temperature oxidation of cobalt in the temperature range from 800 C to 1000 C in air and pure oxygen

19 p2816 A72-37656

Shrinkage concentration behavior of two phase systems /Co-Ni, Co-Fe, Fe-Ni, Fe-Cu/ in sintering correlated with diffusion parameters

19 p2808 A72-38280

Young and shear moduli of binary Fe base alloys as functions of composition and temperature by ultrasonic pulse echo technique

20 p2937 A72-39287

Unidirectionally oriented pseudobinary eutectic solidification in ternary systems, investigating crystallographic and mechanical characteristics of ZrCuSi fibers embedded in Cu matrix

20 p2940 A72-39441

Phase diagram study of Cr-Ga alloys, investigating intermetallic compounds presence and polymorphic transformation and temperature effects

20 p2942 A72-39987

Absolute thermoelectric power of chromium-ruthenium alloys.

20 p2942 A72-39988

Matthiessen rule on binary alloy electrical resistivity temperature derivative, discussing data deviations in substitutional alloys after quenching, radiation damage and plastic deformation

22 p3189 A72-42298

Binary and multicomponent Re alloys with W, Mo, Ni, Co and Cr, noting elastic and strength properties for torsional suspension structures

22 p3191 A72-42805

German monograph - Determination of the diffusion coefficient of hydrogen in the binary iron-nickel system at 25 and 58 C.

22 p3194 A72-43057

X ray and differential thermal analysis for phase diagrams of binary alloys of samarium oxides and gadolinium oxides with calcium oxides, noting solid solutions formation

23 p3304 A72-43250

X ray, microstructural and differential thermal analysis for binary Zr alloys, noting formation of ternary phases and solid solutions

23 p3300 A72-43588

BINARY CODES

Convolutional coding, Viterbi decoding and binary phase shift keyed modulation for reliable communication on power limited satellite and space channels

01 p0026 A72-10342

Orthogonal convolutional coding with on-off signaling and Viterbi decoding for synchronous multiple access communication with bound bit error rate

01 p0026 A72-10343

Walsh functions, sequence and Gray codes computations on finite binary n-tuple domain

03 p0326 A72-14248

Rate 1/n binary convolutional code free distance upper bound derivation and largest input sequence determination for equal weight

06 p0776 A72-18392

Range sidelobe suppression technique for Barker type phase reversal codes in digital processor for pulse compression

08 p1133 A72-21404

Error correction in adders with systematic sub-codes, preserving AN binary code error control properties

08 p1138 A72-21551

Algorithm for optimal binary search tree construction with minimum weighted and restricted maximum path lengths

11 p1676 A72-25354

Phase noise and transient times for binary quantized digital phase locked loops in white Gaussian noise

11 p1592 A72-25886

Average time between successive false target indications in surveillance binary signal detector with variable storage capacity

11 p1595 A72-26295

Mutually coupled continuous time orthogonal binary random processes, illustrating transition from discrete to exponential interval distribution

11 p1611 A72-26298

Spectral correlation and transition probabilities of mutually dependent orthogonal binary random signals

11 p1595 A72-26299

Quasi-equidistant binary-decimal codes for displacement digitizers, noting readout error probability reduction

11 p1602 A72-26448

Phase metering information converters with digital analog computation, discussing analysis of prototype semiconductor model with ten-digit binary codes

11 p1602 A72-26449

Statistical analysis of random mismatched tapped delay line filters effect on binary phase shift keying pulse compression codes peak-to-sidelobe and SNR

15 p2196 A72-31792

Adjacent channel discrimination enhancement in Gray-scale binary coded two dimensional array, using checkerboard filter for pattern noise suppression

15 p2238 A72-32162

Converter of the Gray code to a conventional binary code

17 p2515 A72-34762

Effectiveness of error-correcting codes during reception on the whole in the presence of additive normal white noise

21 p3014 A72-40310

Q-ary output data transmission channel with burst errors, discussing burst-b distance measure and binary block code decoding algorithm for error correction

22 p3153 A72-41979

Code correcting asymmetric-error bursts during information exchange between computers

22 p3156 A72-42189

Communication systems with binary convolutional signal encoding and threshold decoding, discussing orthogonal checkout sums distribution for correct and erroneous synchronization

22 p3154 A72-42235

Computer-aided binary code sequence selection for data acquisition system in PCM-TDMA satellite communication, evaluating performance and reliability

24 p3379 A72-44779

BINARY DATA

EROS program thematic mapping system for binary graphic overlays of open water, snow and ice, reflective IR vegetation and human works

01 p0066 A72-10460

Pattern recognition by computerized local processing of binary matrix representations

01 p0018 A72-10476

Coherent demodulation of continuous phase binary FSK signals in additive white noise, determining error probability

02 p0174 A72-12135

Near optimum limiting and blanking levels /error probability/ selection for binary signal matched filter reception in Gaussian and impulse noise, discussing performance simulation

04 p0486 A72-14485

Edge-coding operators for two dimensional binary picture black-white boundary pattern recognition suitable for use in parallel processing systems

04 p0496 A72-15203

Logical synthesis of hybrid off-on control systems with proportional and binary variables, presenting example of fluid power, electronic and fluidic implementation [ASME PAPER 71-WA/FLCS-1]

05 p0640 A72-15919

Logic circuit binary signal autocorrelation determination as function of 0 and 1 signals duration distribution considering AND and OR gates

05 p0632 A72-17094

Binary differentially coherent phase shift keyed system, evaluating error probability performance in presence of thermal noise and intersymbol interference

06 p0772 A72-17408

Binary single sideband phase modulation with simultaneous AM by signal and Hilbert transformation

06 p0776 A72-18395

Binary detector with dual gating function between first and second quantization processes, estimating false alarm and rejection probabilities

07 p0937 A72-18851

Input binary sequence transformation in chain of series connected on-off neuron models, applying to n-stage linear filter analysis

08 p1138 A72-20870

Huffman sequence synthesis by z transform zero pattern selection to obtain high energy for given peak amplitude, noting signal ambiguity functions

10 p1437 A72-24679

Auto and cross correlation functions of combined binary pseudorandom sequences in digital space communication systems

10 p1439 A72-24907

Optimum decision rule for sync word location in binary data frame, noting sum maximization of correlation and energy correction terms

11 p1592 A72-25888

Optical correlation technique, converting input data into area charts with binary valued density

12 p1820 A72-27495

Computer technique to synthesize binary holograms for wave beams analysis in quasi-optical communication channels

15 p2242 A72-32674

Video signals generation from binary data and mixing with analog information from cameras or tape recorders for simultaneous display on cathode ray tubes

19 p2769 A72-37936

Binary information storage with bipolar transistors, tunnel diodes, MIS and glass semiconductors, considering Gunn effect devices application

20 p2905 A72-39425

Small-size phase holograms for binary data storage

21 p3058 A72-41744

Flawless operation probability for information transmission reliability of electronic logic circuits with binary data inputs

23 p3271 A72-43784

Forward-error correction with decision feedback.

23 p3268 A72-44175

BINARY DIGITS

Binary multiplication algorithms adaptable to IC functional elements for ultrahigh speed operations

11 p1602 A72-26547

BINARY MIXTURES

NT EUTECTIC ALLOYS

NT EUTECTICS

Monatomic He-Ar binary gas mixtures heat transfer to cylinders in low Reynolds number flow, considering internal energy effects

02 p0303 A72-12358

Steady normal shock wave analysis in binary inert monatomic gas mixtures using kinetic theory moment method

04 p0513 A72-15340

Slush, boiling methane and methane mixture characteristics, noting advantages as potential rocket, aircraft and motor vehicle fuels

04 p0564 A72-15542

Flow parameters behind shock waves propagating in carbon dioxide-nitrogen mixtures at Mach numbers from 5 to 10

07 p0966 A72-18936

Thermal conductivities of gaseous binary mixtures of methyl nitrate with helium, neon, argon and nitrogen

07 p1051 A72-19365

Statistical-hydrodynamic description of nonequilibrium gas dynamics of single component and binary mixtures and systems with chemical reactions

07 p0968 A72-19886

- Hot-wire measurement of binary gaseous mixtures in unsteady concentration fields, investigating heat loss
07 p0993 A72-20587
- Binary gas mixtures calculation for Schmidt, Prandtl and Lewis number dependence on pressure, temperature and chemical composition
07 p1101 A72-20600
- Third harmonic radiation generation in phase matched mixture of Rb vapor and Xe, observing non-linear susceptibility
[AD-739764] 08 p1211 A72-21197
- Curvature and thickness corrective terms in Rankine-Hugoniot relation for shock wave propagation of ideal gases binary mixture
10 p1417 A72-24117
- Thermal conductivity of two- and three phase solid mixtures of silicone rubber and Al, Pb, Ni and Bi powders, using line source method
11 p1744 A72-25264
- Binary gas mixture slipping rate determination from joined solution of Hamel kinetic model linearized equations, and Navier-Stokes and Boltzmann equations
14 p2096 A72-31013
- Stationary heat conduction between stagnant binary gas mixture and two constant temperature plane parallel walls for arbitrary Knudsen numbers
15 p2334 A72-31462
- Velocity independent fast response hot-wire probe for binary gas mixtures composition measurement, describing design and operational principle based on dimensional analysis
16 p2389 A72-32829
- Binary gas mixture density correlation functions from initial value problem based on linearized Boltzmann equation for analysis of Rayleigh-Brillouin scattering
16 p2428 A72-32942
- Pohlhausen type integral method for dissociative binary mixture nonequilibrium laminar boundary layer on flat plate, using Crocco relationship between enthalpy and velocity profile
16 p2378 A72-33436
- Viscosity and thermal conductivity of moderately dense gas mixtures.
17 p2636 A72-34737
- Statistical-hydrodynamic description of nonequilibrium gas dynamics of single component and binary mixtures and systems with chemical reactions
17 p2540 A72-35134
- Theory of sound propagation in mixtures of monatomic gases.
17 p2583 A72-35613
- Investigation of physical processes and optimization of thermionic converters with a Cs-Ba filling
18 p2647 A72-36203
- Heterogeneously combusting binary gas mixture ignition time as function of initial state and thermokinetic properties, noting heat conduction equations for fuel and oxidizer
19 p2879 A72-37358
- Effect of concentration gradient on composition of sampled gas. II - Experimental verification.
19 p2805 A72-38870
- Experimental investigation of the detonation properties of hydrogen-oxygen and hydrogen-nitric oxide mixtures at initial pressures up to 40 atmospheres.
19 p2883 A72-38875
- Analytical and low-speed experimental diffusion-thermo effects in turbulent binary boundary layers.
[ASME PAPER 72-HT-56] 20 p2985 A72-39660
- Holographic technique for investigation of critical phenomena in aniline-cyclohexane and triethylamine-water binary critical mixtures, noting phase transition visualization
21 p3056 A72-41219
- Transport properties of a gas of diatomic molecules. VI - Classical trajectory calculations of the rotational relaxation time of the Ar-N₂ system.
24 p3427 A72-45308
- BINARY STARS**
NT COMPANION STARS
NT ECLIPSING BINARY STARS
- Calibrations consistency of UVBY beta and G₁KMF photometries of binary stars with G or K giants and A or F main sequence components
01 p0132 A72-11014
- Astrometric measurements of visual binaries by electronic method, using Lallemand camera
03 p0415 A72-13002
- Occultation curves for optical and radio lunar occultation analysis of radio sources, considering detection and measurement of binary systems
03 p0420 A72-13130
- Interference fringes production from binary stars focal images obtained with Lallemand electronic camera
03 p0435 A72-13798
- Binary systems formation probability during triple encounters, observing dependence on system/potential energy ratio
03 p0435 A72-13809
- Stellar evolution in close binary systems, discussing post main sequence stage, hydrodynamical processes and dwarf binaries
03 p0437 A72-13868
- Lunar limb slope from photoelectric measurements of occultations, noting relation to double star astronomy
06 p0879 A72-17861
- Close binary system average gravity and effective temperature at Roche limit for 90 deg phase and both conjunctions, taking into account mass ratios and orbital inclination
06 p0882 A72-18002
- VV Pup binary light variations correlation with primary component variable disk dimensions, considering nova-like processes
06 p0882 A72-18003
- High speed photometry of nova variables with white dwarf and late-type binary star flickering, using Cassegrain focus
06 p0889 A72-18332
- Orbital elements from radial velocity measurements for single line K giant binary star 4 Ursae Minoris
07 p1071 A72-19337
- Zeta Orionis spectra at 922-1453 Å from rocket spectroscopy, matching lines with stellar atmosphere models
07 p1072 A72-19346
- Soviet book on compact binary stellar systems with globular components covering disk darkening, eclipsing, absolute dimensions and masses, etc
08 p1229 A72-20910
- Unstable binary RW Aur spectrophotometric study with stellar evolution and outer atmosphere implications, relating Balmer continuum to UV excess
08 p1233 A72-21277
- Spectral types and magnitudes of O and WC stars of binary gamma Velorum system
09 p1382 A72-22282
- Periodic intensity and period variations of X ray pulsating source Cen X-3 caused by occulting binary system from Uhuru satellite observation
09 p1382 A72-22289
- Visual binary star investigations, considering parallaxes, masses, absolute magnitudes and orbit computation
09 p1390 A72-23502
- Binary stars convective zones reaction to periodic gravitational fluctuations due to stellar revolutions asynchronism, using incompressible fluid plane layer model
10 p1543 A72-24631
- Cygnus X-1 model with hard X rays from inverse Compton scattering of B star UV photons and IR synchrotron radiation from other component
10 p1530 A72-24944
- Contact binary star systems model, considering superadiabatic energy transfer mechanism of convective envelope
10 p1550 A72-25199
- Close binary stars photometric measurement with electronic camera, noting magnitude difference determination from recorded images
12 p1866 A72-27203
- Binary evolution in star cluster models from numerical methods of direct integration, noting domination by heavy binary and double star formation and disruption
12 p1873 A72-27899
- Black holes due to gravitational collapses, including radiation emission/absorption, pulsars and binary stars
14 p2151 A72-30478
- Low mass neutron star source of pulsed X radiation in binary Centaurus X-3 ejected during low energy supernova explosion
14 p2156 A72-30570
- Spectroscopic binary orbital elements calculated by FORTRAN IV computer programs, considering period, radial velocity Fourier coefficients and element improvement by least squares method
14 p2159 A72-30736
- Mass exchange and thermal time scales for shell source burning binary components with deep outer convective layers, interpreting numerical results from analytical model
14 p2159 A72-30739
- Dynamic behavior of three masses moving under mutual gravitational attraction examined by numerical experiments for binary star formation via third star hyperbolic escape
14 p2160 A72-30877
- Photometric characteristics of two types of eruptive binary stars differing in hot spot brightness
15 p2305 A72-31340
- Uhuru observed galactic X ray sources related to binary systems or supernova remnants, noting galaxy clusters
16 p2454 A72-33362
- Binary nature of the B supergiant in the error box of the Vela X-ray source.
17 p2604 A72-34521
- The rotation of close binaries
18 p2725 A72-36474
- Evolution of close binary systems with intermediate initial mass ratios.
18 p2728 A72-36741
- Underluminosity and magnetic fields in beta Lyrae.
18 p2729 A72-36982
- Collapsed objects absence in eccentric binary star systems and nonevidence of black holes formation effect on multiple line binaries
18 p2729 A72-36983
- Double system HD 175514. III - Analysis of 1968 observations
19 p2858 A72-37810
- Comparison of IDS Catalog double stars having determined individual motions of their components
19 p2859 A72-37917
- Orientation of astrophotographs in observations and measurements
19 p2802 A72-37972
- Comparison of the declinations of Talcott pair centers, obtained from latitude observations by ZTF-135 in Pulkovo, with certain catalogs
19 p2861 A72-37978
- Photoelectric photometry of close visual binaries
19 p2866 A72-38499
- Tidal perturbation of the non-radial oscillations of a star.
20 p2974 A72-39895
- Physical properties of interstellar matter surrounding binary stars from astronomical spectroscopy, discussing eruptions and photometric changes
20 p2975 A72-40069
- A spectral study of the nebula NGC 7635 and the star BD +60.2522 deg
21 p3113 A72-41755
- Orbit of the visual double star ADS 7896 equals JDS 2052 equals A 2768
21 p3114 A72-41848
- The non-spherical nebulae of Nova Delphini 1967, Nova Vulpeculae 1968/II, and Nova Serpentis 1970.
22 p3221 A72-41999
- Double star components light aberration dependence on relative velocity of source and observer, considering two reference systems
22 p3225 A72-42458
- Radial velocity periodic variability determination from shell star 88 Herculis hydrogen lines, obtaining hypothetical spectroscopic binary elements
23 p3340 A72-44237
- Centaurus X-3 - Possible reactivation of an old neutron star by mass exchange in a close binary.
24 p3439 A72-44976
- BINARY SUMMATORS**
U ADDING CIRCUITS
BINARY SYSTEMS [DIGITAL]
U DIGITAL SYSTEMS
BINARY SYSTEMS [MATERIALS]
NT BINARY ALLOYS
NT BINARY MIXTURES
NT EUTECTIC ALLOYS
NT EUTECTICS
- Hydrogen partial molar volume in metal-hydrogen two component systems under externally applied uniform hydrostatic stress field, using thermodynamic analysis
01 p0083 A72-10205
- Reactive diffusion in binary systems, explaining diffusive saturation process from phenomenological viewpoint
05 p0701 A72-15753
- Nb-Ga system equilibrium phase diagram determination by differential thermal, tempering microstructural and X ray analysis techniques, discussing various compounds formation temperatures and characteristics
07 p1050 A72-20161
- Silicon-silicon dioxide system, investigating effect of heating in dry and moist He on capture-center and recombination parameters by thermal and pyrolytic techniques
08 p1216 A72-21068
- Binary system molar energy diagram plotting, covering superheated, saturation and liquid phase regions
08 p1255 A72-22170
- Mullite as part of aluminum oxide-silicon dioxide system, discussing formation, structure, physical chemistry, additives effects and high alumina refractories
10 p1501 A72-24729
- Elastic fields of dislocation loop in two phase material consisting of isotropic elastic half spaces
12 p1884 A72-27567
- Pumping current pulse duration effect on lasing threshold of injection lasers with diffusion junctions and heterojunctions in GaAs-AlAs system
12 p1824 A72-27877
- Internal parameters of injection lasers based on diffusion and epitaxial p-n junctions and heterojunctions in GaAs-AlAs system at 300 K
12 p1825 A72-27878
- Hf binary systems phase diagrams, noting components effect on melting point, polymorphous transformations and mutual solubility
14 p2122 A72-30979

- Chalcogenide semiconductor compounds of b-subgroup transition elements, discussing binary system diagrams, stoichiometric composition and electrical properties
15 p2290 A72-31193
- Electronic structure of binary phase diagrams of group III-VI transition metals, using valence separation and condensed state model
15 p2252 A72-31198
- Russian papers on physical chemistry of surface effects in melts covering binary and multicomponent alloys, silicates, oxides and salts at high temperatures
15 p2253 A72-31220
- Elastic dilatational field association with twist disclination loop interaction with free surface of two phase system interface
15 p2331 A72-32504
- Internal parameters of injection lasers based on diffusion and epitaxial p-n junctions and heterojunctions in GaAs-AlAs system at 300 K
16 p2404 A72-33987
- Measurement of the electron work function in binary and ternary transition metal-nonmetal systems.
17 p2595 A72-34602
- High temperature cesium vapor sources based on a cesium-graphite system for thermionic converters
18 p2646 A72-36201
- Adhesion characteristics of alpha-aluminum oxide-nickel system from shear strength measurements, investigating effects of sintering parameters and Ti and Zr alloying components
20 p2940 A72-39445
- Conditions and mechanism of formation of suboxide phases in the niobium-oxygen system
21 p3066 A72-40381
- Phase diagrams, microhardness and composition of sintered binary B compounds with Zr, Hf, Ta, Cr, Mo, W, Re, Fe, Ni, and Si
21 p3070 A72-41371
- Application of computer mathematics procedures for prediction of phase diagrams
22 p3191 A72-42812
- Charge, direction and temperature dependence of semiconductor electrotransmission in dc field, considering metals diffused in Ge, Se, Te, Si, BiTe, GaAs and InAs
23 p3324 A72-43642
- Contribution to the study of some HfO₂-MO systems
23 p3302 A72-43999
- Interpretation of X-ray emission bands of AIII-BV compounds
24 p3432 A72-44914
- BINARY TO DECIMAL CONVERTERS**
Quasi-equidistant binary-decimal codes for displacement digitizers, noting readout error probability reduction
11 p1602 A72-26448
- BINAURAL HEARING**
Cross correlation model for interpreting empirical results on binaural noise masking level differences in sinusoidal signal detection, comparing with equalization-cancellation model
04 p0550 A72-15296
- Right ear prevalence in hearing process determined by dichotic speech audition
04 p0476 A72-15584
- Selective attention dichotic listening test as flying proficiency prediction criteria, discussing omission and intrusion errors
07 p0929 A72-19351
- Binaural frequency discrimination in masking level difference /MLD/ noise under homophasic and antiphase conditions
13 p2006 A72-29771
- Effect of fringe on masking-level difference when gating from uncorrelated to correlated noise.
21 p2997 A72-40346
- BINDERS [ADHESIVES]**
U ADHESIVES
- BINDERS [MATERIALS]**
NT PROPELLANT BINDERS
Refractory metal powders spherical agglomerates growth and strength in rotating tumbler, noting particle size dependence on binder
11 p1643 A72-26829
- Continuous woven fabric or roving filament reinforced thermoplastics production, discussing polymer binder systems, coupling agents, impregnation technique, processing parameters and equipment
12 p1815 A72-28083
- Aromatic polyimide binder for compression moldable high performance composites preparation with thermal curing to obtain good thermal-oxidative stability and toughness
12 p1834 A72-28090
- Development of moldable carbonaceous materials for ablative rocket nozzles.
17 p2572 A72-35668
- Epoxy-thiocol binder viscoelastic deformation under short and long term loads, noting stress-strain linearity limit
21 p3073 A72-41360
- BINOCULAR VISION**
Functional organization of visual cortex in monkeys, discussing monocular and binocular responses, trigger and stimulus abstraction
01 p0011 A72-10467
- Sensorimotor preconditions of single image impression in human binocular vision
01 p0018 A72-10477
- Neuronal mechanisms of binocular vision and space perception from tests on cats and men, discussing neurophysiological models of stereopsis
01 p0012 A72-10479
- Stereopsis spring coupled magnetic dipole model of binocular stereoscopic depth perception in man
01 p0012 A72-10480
- Binocular depth perception based on two retinal images spatial frequency content
02 p0164 A72-12486
- Human binocular visual system fusional information processing, evaluating compensatory eye movements role in overcoming retinal image disparity
07 p0929 A72-19314
- Objects visual detection probability distribution as function of angular size, contrast and search time, comparing binocular and monocular searches effectiveness
07 p0931 A72-19919
- Binocular observation of astronomical objects, discussing binocular design of astronomical telescopes
08 p1165 A72-21087
- Response latencies and correlation in single units and visual evoked potentials in cat striate cortex following monocular and binocular stimulations
11 p1582 A72-26771
- Voluntary eye movement and convergence effects on relation between binocularly perceived and physical distance ratios
16 p2358 A72-33647
- Visual depth perception response functions for sine and square wave modulated binocular parallax
17 p2498 A72-34293
- Effect of target-background luminance contrast on binocular depth discrimination at photopic levels of illumination.
17 p2508 A72-34879
- REM period functional maintenance of coordinated eye movement facilitation and binocular depth perception accuracy following sleep
17 p2509 A72-35462
- The tracking of targets located outside of Panum's area.
17 p2505 A72-35916
- Quantitative decision criteria for identification of visual evoked responses obtained during binocular rivalry.
18 p2652 A72-36312
- Vergence eye movements to pairs of disparity stimuli with shape selection cues.
18 p2651 A72-36612
- The neurophysiology of binocular vision.
19 p2755 A72-37250
- Hering's law of equal innervation and the position of the binoculus.
19 p2756 A72-37828
- Monocular and biocular magnifiers for night vision equipment.
20 p2921 A72-39030
- Viewing stereoscopically through binocular optical systems.
21 p3054 A72-40728
- Liminal stimuli binoptic detection variation with ratio of left eye to right eye detection probabilities
21 p3007 A72-40734
- Apparent movement and change in perceived location of a stimulus produced by a change in accommodative vergence.
21 p3002 A72-41024
- Visual experience as a determinant of the response characteristics of cortical receptive fields in cats.
21 p3003 A72-41461
- BINOCULARS**
Gyroscopic device for compensating displacement of sextants or binoculars optical axis due to spontaneous hand movements
07 p0988 A72-19894
- BINOMIAL COEFFICIENTS**
Time and frequency domain properties of orthogonal nonrecursive binomial sequences, discussing digital filters synthesis
03 p0381 A72-13408
- BINOMIAL THEOREM**
Planetary disturbing function expansion, using classical binomial or Laplace series methods on large scale digital computer with Poisson program
06 p0878 A72-17665
- BIOASSAY**
Microbiological examination of space hardware, discussing viable organisms neutralization buried inside solid materials, sampling procedures and culture media
01 p0019 A72-10820
- Nonsterile space flight hardware effects on planetary quarantine, evaluating contamination sources, design and mission parameters, cleanliness conditions and bioload
01 p0020 A72-10824
- Free radicals participation in cell membrane biopotential generation mechanism, comparing properties of protein molecules with semiconductors
02 p0169 A72-12348
- Human male gonadotropin secretion relation to sleep stages, using electrophysiologic recordings and radioimmunoassay techniques
05 p0620 A72-17128
- Uric acid to urea nitrogen ratio as assay test for identification of avian tissue in verifying bird ingestion or impact as aircraft accident cause
07 p0922 A72-20184
- [AD-737855]
A note on the biological activity of the noble gas compound xenon trioxide.
18 p2652 A72-36444
- A simple combination mass spectrometer inlet and oxygen electrode chamber for sampling gases dissolved in liquids.
19 p2762 A72-38146
- Quantitation of serum proteins on whole blood-electroimmunodiffusion technique applicable to capillary blood.
22 p3150 A72-42495
- The presence of P700 in chloroplast fragments prepared by short time incubation with Triton X-100.
23 p3258 A72-44325
- Acrylamide polymerization - New method for determining the oxygen content in blood.
24 p3376 A72-45376
- BIOASTRONAUTICS**
Soyuz 9 flight crew physiological data, discussing mental and physical performance and adaptation and readaptation to space-earth environments
01 p0020 A72-10933
- Space flight ecology and physiology, discussing atmospheric temperatures and radiation, biological effects of acceleration, deceleration and weightlessness and physiological stresses
11 p1584 A72-26018
- Extraterrestrial life search, noting radio contact with civilizations, bioastronautics, Martian conditions and physicochemical experiments
14 p2076 A72-30694
- Bioastronautic results of Apollo space flight biomedical operations, discussing weightlessness, sleep impairment, motion sickness, preventive medicine, etc
15 p2189 A72-31827
- Medical requirements for manned space flight, discussing physiological data monitoring and transmission, equipment miniaturization, telediagnosis, spacecraft environment protection, etc
16 p2358 A72-33562
- Life sciences and space research X: Proceedings of the Fourteenth Plenary Meeting, Seattle, Wash., June 21-July 2, 1971.
23 p3253 A72-43381
- Effects of weightlessness on astronauts - A summary.
23 p3253 A72-43385
- BIOCHEMISTRY**
NT BACTERIOLOGY
NT BIOGEOCHEMISTRY
NT ENZYMOLOGY
Biochemical and physiological effects of Apollo flight diet, noting no significant variations in serum electrolytes, endocrine values, body fluids and hematologic parameters
02 p0167 A72-11707
- Physical interpretations of physiological control, covering history, biochemical oscillator viewpoint of life and conferences
02 p0160 A72-12039
- Respiratory system frequency response analysis for chemical regulation of breathing, using time domain method and step functions
02 p0168 A72-12040
- Noceptive chemical action in rat skin vessels, showing fiber types for impulse transmission
02 p0164 A72-12511
- Soviet book on gravitation receptor covering evolution of structural, cytochemical and functional organization in invertebrates /statocyst/ and vertebrates /vestibular apparatus/
03 p0316 A72-13850
- Chemical evolution and life origin - Conference, Pont-a-Mousson, France, April 1970, Volume 1, Molecular evolution
04 p0467 A72-14751
- Chemical box model of energy storage in covalent bonds and nonequilibrium distributions in prebiological synthesis leading to macromolecules
04 p0482 A72-14755
- Biological self replicative description and function in chemical reaction networks in search of life origin from non-life-like matrix
04 p0482 A72-14756
- Lower aldehydes contribution to biochemically important compounds in abiogenic synthesis, considering amino acids formation
04 p0483 A72-14763

Biochemical functions of organisms in evolution of biosphere, discussing redox reactions, elementary compositions and metal compounds role in photosynthesis

04 p0470 A72-14796

Mathematical model physical structure, effectiveness and limitations for circadian rhythms, discussing Princeton and modified biochemical models

07 p0930 A72-19530

Cerebral vascular disorder biochemical analysis, noting retinal vascular change relation to coronary arteriosclerosis and anoxia and flight stress effect on serum lipid and cholesterol

07 p0923 A72-20448

Extraterrestrial life origin and development possibilities from earth chemical and biological evolution description, noting external conditions requirements

08 p1119 A72-22002

Electronic factors role in intermolecular interactions and biochemical evolution, applying quantum biochemistry

08 p1128 A72-22006

Review of biology and biochemistry of memory, suggesting molecular level mechanism of cerebral information processing

10 p1424 A72-23925

Human body biochemical energy conversion processes during muscular activity, discussing nutrition, circulation and respiration roles

11 p1585 A72-26075

Physiological and biochemical responses of *Paramecium caudatum* to hypo- and hyperbaric stresses, discussing protoplasmic inactivation by high oxygen pressure

12 p1766 A72-28299

Physiological effects on anesthetized and conscious dogs during exposure at 80,000 ft for different decompression rates, discussing cardiovascular, biochemical and pathological effects

12 p1768 A72-28322

Plant leaves biochemical activities study by light scattering techniques, discussing photometric, spectroscopic and bionics methods

13 p1955 A72-28518

Five-component cyclic model of retinal photopigment kinetics for photochemical changes corresponding to rod adaptation in rat and man in dark

13 p1906 A72-29966

Low molecular active hormones isolation from cat blood, obtaining eluates with phosphate buffer by chromatography

14 p2077 A72-30971

Biochemical analysis of cat brain regions for gamma-aminobutyric, aspartic and glutamic acids, glycogen and phosphatidopeptide concentrations during paradoxical sleep deprivation

16 p2356 A72-33559

The uptake, metabolism and release of C/14-taurine by rat retina in vitro.

17 p2500 A72-34881

Chemical evolution and the origin of life - Bibliography supplement 1970.

18 p2650 A72-36450

Significance of the nature of an increase in physical strain as it affects the adaptation of an organism to intense muscular activity

20 p2891 A72-38933

Effect of copper, cobalt and manganese salts on certain morphological-biochemical components of the blood in young sheep of the Hissar breed

20 p2893 A72-40075

Physical and chemical identification methods for biochemical reactions and energy balance of muscular contraction and shaking

21 p3003 A72-41469

Succinic and lactic dehydrogenases activities in homogenates from myocardial tissues of guinea pigs, rabbits and dogs in high altitude environments

22 p3144 A72-42592

Determination of copper, iron, cobalt, nickel, and manganese in biological samples of vegetable origin

23 p3260 A72-43924

BIOCLIMATOLOGY

Russian book - Climatic conditions and the thermal state of man.

21 p3006 A72-40458

Time series analysis of meteoropathological disturbances of human regulation mechanisms, investigating annual variations of diurnal rhythms

22 p3147 A72-42977

BIOCONTROL SYSTEMS

Book on hibernation and hypothalamus covering central nervous system regulating mechanisms, biologic rhythmicity, migration, thermoregulation, torpor, human implications, etc

01 p0010 A72-10169

Pattern recognition in biological and technical systems - Conference, Berlin, April 1970

01 p0017 A72-10463

Receptor activity control from clinical physiological and electrophysiological observation data analysis, noting central nervous system role and feedback and self adaptation capabilities

02 p0157 A72-11543

Human short term thermoregulation feedback-feed-forward control mechanism, using hypothalamic temperature as set point

02 p0168 A72-12036

Physical interpretations of physiological control, covering history, biochemical oscillator viewpoint of life and conferences

02 p0160 A72-12039

Mathematical models for man-machine control behavior in biodynamic environments including manual control performance and interface elements

03 p0318 A72-13162

Human postural control system dynamic model, discussing stick man pitch axis dynamics digital simulation and difficulties in linearizing equations of motion

03 p0318 A72-13163

Eye movement control device for electronystagmography, describing construction, line drawing and basic circuits

03 p0319 A72-13724

Human neuromuscular coordination control optimization, discussing preprogrammed open-loop control with feedback monitoring loop

04 p0477 A72-14705

Human and animal controlled self rotating maneuvers during free fall, comparing theoretical motion analysis with photographs of falling cats

04 p0478 A72-14709

Coincidence model tests of photoperiodic time measurement relation to circadian system in moth *Pectinophora gossypiella*, using induction by skeleton photoperiods and light cycles

07 p0919 A72-19533

Ecdysone hormonal control of *Drosophila* circadian rhythms and synchronizing mechanisms, discussing light stimulation and neurohormone secretion

07 p0919 A72-19537

Control system model integrating human left ventricle and circulatory system mechanics and regulation by central nervous system

07 p0934 A72-20356

Digital simulation of human cardiovascular system, noting blood pressure control by physiological reflexes

08 p1125 A72-21475

Conditioned reflex mechanisms responsible for regulation of emotions in higher order animal and human neurophysiology

08 p1118 A72-21837

Respiration control during hyperoxia, discussing chemoreceptor significance in minute volume respiration rate reduction mechanism from Pamir mountain aborigines oxygen breathing reaction studies

08 p1120 A72-22076

Human left ventricle measurements, modeling, control and simulation for heart monitoring purposes, describing muscle performance mathematical model and stress effect prediction control system

10 p1429 A72-23924

Myocardium biopulse-controlled cardiosynchronizer as key component of biocontrol systems for cardiological studies

11 p1585 A72-26455

Thermoregulation changes during simulated weightlessness of prolonged bed rest, noting lower sweating threshold and decreased vasodilation/autonomic dysfunction/

12 p1767 A72-28301

Supercellular regulators of triggering mechanism of regenerative reaction in sternum erythropoietic bone marrow tissue

13 p1901 A72-28636

Coronary system autoregulation patterns and mechanisms from coronary flow shift measurements during circumflex artery perfusion experiments in dogs

13 p1901 A72-28637

Neuronal mechanisms of muscular motor activity control, analyzing cerebrum-motoneuron connections, spinal potentials, monosynaptic responses and depolarization

13 p1907 A72-29981

Parameter estimation in dynamic biological control systems based on multicompartmental input-output behavior

15 p2192 A72-32766

Hippocampus morphology and physiology in relationship to emotion and memory mechanisms, time links, visceral activity and motivations and endocrine control

16 p2353 A72-33099

Water immersion tests to study body fluid balance disturbances during weightlessness, observing diuretic reflex control of blood volume

16 p2355 A72-33551

Russian book - Mechanisms regulating physiological functions

17 p2503 A72-35014

Pharmacological effects on the central adrenergic regulation mechanisms of blood circulation

17 p2504 A72-35019

Biomembrane hydration mechanism of Na-K ion pump of living cell based on fractionation at air-sea interface

18 p2649 A72-36441

Neuroinhibition in the regulation of emesis.

18 p2650 A72-36449

Servo action in human voluntary movement.

18 p2654 A72-36999

A human left ventricular control system model for cardiac diagnosis.

18 p2655 A72-37029

Vertical posture control mechanisms in man

19 p2757 A72-37992

Frequency response studies of human and avian respiratory regulation.

19 p2761 A72-38229

Biological systems activity in controlling extremal problems of nervous and muscular systems, noting external stimulation minimization

19 p2761 A72-38577

Russian book - Problems of the stability of biological system.

20 p2891 A72-38957

Adaptability limits on protein-nuclein-water life under exobiological extremal conditions, considering macromolecules, extraterrestrial life search and origin

20 p2891 A72-38958

Thermodynamic properties and mathematical modeling of complex biological systems, considering energy and mass exchange in photosynthesizing organisms for exobiological life support

20 p2891 A72-38960

The silent period in man during muscle lengthening produced by loading

20 p2892 A72-39590

Russian book - Mechanisms of descending control of spinal cord activities.

21 p2998 A72-40577

A possible anatomical basis for descending control of impulse transmission through the dorsal horn.

21 p2998 A72-40578

Synaptic suprasegmental control mechanisms of spinal cord motor neurons

21 p2999 A72-40584

Pyramidal control of the activity of interneurons related to various types of peripheral afferents

21 p2999 A72-40589

Systems analysis approach to the study of spinal mechanisms.

21 p2999 A72-40590

Cerebrum sections and related afferent processes as activator of automatic neuron mechanism control of motor activity, discussing segmentary spinal cord changes

21 p2999 A72-40593

Participation of supraspinal structures in the formation and control of a system of arbitrary cyclic motions of man

21 p2999 A72-40594

Role of efferent influences of temporo-rhinencephalic cerebral structures in pre-adjustment alterations of spinal motor neuron excitability

21 p2999 A72-40596

Vasomotor reflexes and the principle of descending control

21 p2999 A72-40597

Hypothalamic control of the electrical activity of the spinal cord

21 p3000 A72-40598

Man movements directed at reaching a preset goal

21 p3006 A72-40710

Nervous and humoral stimulation and hypoxia effects on erythropoiesis control, studying human blood serum additions to bone marrow cultures

21 p3001 A72-40762

Unsteady state description of living corneal mass transport modes, elucidating cornea thickness control mechanism

21 p3001 A72-40912

A mathematical model of the chemoreflex control of ventilation.

21 p3008 A72-40917

Parametric adjustment to a shifting target alternating with saccades to a stationary reference point.

21 p3009 A72-41250

Human consciousness and choice role in biological control process automation to define differences between manual and automatic control systems

21 p3009 A72-41405

A model for analysing the coordination of manual movements.

21 p3010 A72-41413

The functional organisation of object directed human intended-movement and the forming of a mathematical model.

21 p3011 A72-41422

Localization and structural-functional organization of the system of vagus nerve nuclei constituting the 'cardiac center' of the medulla oblongata

21 p3004 A72-41673

Hemodynamic reflexes during acceleration stresses, considering vessel walls, cardiac rhythm, blood distribution and sinus carotis receptors

22 p3141 A72-41983

- Intermittent movement control theory for prediction of visual correction applied to target aiming during illumination loss 22 p3142 A72-42546
- Carotid rete role in brain protection against extreme elevations of systemic blood pressure, presenting goat cerebral blood flow measurement procedure 22 p3144 A72-42671
- Control parameters of the blood-pressure regulatory system. I - Heart rate sensitivity. 22 p3145 A72-42771
- Control parameters of the blood-pressure regulatory system. II - Open-loop gain, reference pressure and basal heart rate. 22 p3145 A72-42772
- Biological system transfer-function extraction using swept-frequency and correlation techniques. 22 p3151 A72-42773
- Hypothalamic control of the systemic and lung circulation and functional significance of this control 22 p3148 A72-43168
- Respiratory control system benchmark simulation on a hybrid computer for Cheyne-Stokes breathing, emphasizing equations for arterial and venous carbon dioxide and oxygen stores 23 p3268 A72-44551
- Respiration control mechanism ensuring adaptation to power requirements and chemical environment maintenance in tissues, considering brain stem location 24 p3371 A72-44600
- Control, by the visual cortex, of the posterior lateral thalamic group in the cat 24 p3372 A72-45009
- BIODYNAMICS**
- Mathematical models for man-machine control behavior in biodynamic environments including manual control performance and interface elements 03 p0318 A72-13162
- Biomechanics - Conference, Eindhoven, Netherlands, August 1969 04 p0477 A72-14703
- External biodynamic models for human mechanical response to various environmental forces, emphasizing injury mechanisms 04 p0481 A72-15266
- Aircraft ejection simulation by human thoraco-lumbar spine flexion dynamic model, using strength of materials theory and shear effects for curved elastic beam [ASME PAPER 71-WA/BHF-7] 05 p0620 A72-15947
- Book on applied mechanics covering hydromechanics, biomechanics, transonic and hypersonic shock structures, random vibrations, plasticity, viscoplasticity, etc 06 p0896 A72-17958
- Dynamic response and functional state of human operator subjected to harmonic and random vibrational excitations, discussing biodynamic nonlinear oscillatory system model construction 06 p0770 A72-18728
- Mathematical model for semicircular canal dynamic response to angular acceleration, emphasizing role of perilymph over endolymph in cupula displacement 07 p0917 A72-19491
- Human biodynamic and behavioral response to whole body vibration, discussing subjective judgment of vibration intensity and effects on performance 10 p1431 A72-24797
- Optimum performance typewriter keyboard design, discussing biomechanical improvements in finger positioning facilitation, operator postural muscular strain reduction, etc [AD-740259] 10 p1433 A72-25114
- Bibliography on noise control covering surface transportation, machinery and aircraft noise, industrial criteria, biodynamics, legislation and measurement. 13 p2006 A72-29588
- Crash helmet performance prediction through maximum strain criteria, using brain injury biodynamic model 15 p2192 A72-32607
- Baboon heart endocardial structure dynamic behavior, comparing left ventricle septum and epicardium contractile force and intramyocardial pressure changes 15 p2187 A72-32748
- Biological structures study, proposing generalized thermodynamics for dissipative structures role in living beings functions 16 p2354 A72-33519
- Differential equations system solution satisfying dual integral equations, noting biomechanics applications 16 p2417 A72-33828
- Two-mass system as human body dynamic model in ballistocardiography, outlining transfer function parameter computation procedure 18 p2652 A72-36039
- Experimental investigation of an astronaut maneuvering scheme. 18 p2655 A72-37026
- The measurement of three-dimensional body movements by the use of photogrammetry. 20 p2898 A72-39806
- Man movements directed at reaching a preset goal 21 p3006 A72-40710
- BIOELECTRIC POTENTIAL**
- Multichannel topography of human scalp alpha EEG potential fields 01 p0016 A72-10072
- Computer simulation of evoked cortical audio potentials in animals and humans, noting clinical application for hearing threshold measurements 01 p0016 A72-11324
- Postsynaptic electric potential responses to click of auditory cortex neurons in cats 02 p0158 A72-11757
- Free radicals participation in cell membrane biopotential generation mechanism, comparing properties of protein molecules with semiconductors 02 p0169 A72-12348
- Vestibular nuclei bulbar complex evoked potentials under visceral and somatic nerves electric stimulation in anesthetized cats 02 p0164 A72-12512
- Human muscular electrical activity in various body positions, noting potentials during natural and unaccustomed postures 03 p0317 A72-13990
- Phylo-ontogenetic maturation of corticopetal projections of visual cortex, using evoked potential measurements in rabbits 06 p0763 A72-17736
- Phase shifts of circadian rhythm of optic nerve potentials from isolated eye of sea hare in darkness 07 p0919 A72-19534
- Field and intracellular potentials in cat trochlear nucleus following vestibular nerve and nuclei stimulation for synaptic organization study of vestibulo-ocular reflex 07 p0923 A72-20501
- Neuronal systems short-latency paired interactions detection method, obtaining histogram for action potentials 07 p0934 A72-20624
- Evoked cortical potentials changes from emotional visual word stimuli stress under amylid anticholinesterase drug influence 08 p1116 A72-21194
- Cortical synthesis and information handling properties of evoked potential in human normal and pathological behavior 08 p1119 A72-21840
- Neurophysiological mechanisms of sleep, studying sleep and wakefulness state evoked potentials relation to cortex and subcortical activity levels 09 p1264 A72-22224
- Photostimulated potentials of human visual cortex, determining retinal macular area involvement 10 p1426 A72-24786
- Average evoked potentials correlates of two flash perceptual discrimination in cats, discussing parallel changes as function of interflash intervals and peripheral level 10 p1427 A72-25178
- Lenticular conditioning-shock stimulation effect on cat visual cortex response to light stimuli, noting lateral gyrus photically evoked potential amplitude increase 11 p1578 A72-25801
- Transistorized amplifier input elements design for biopotentials recording, providing minimum noise at high input impedance 11 p1585 A72-26468
- Response latencies and correlation in single units and visual evoked potentials in cat striate cortex following monocular and binocular stimulations 11 p1582 A72-26771
- Cat auditory cortex neurons response to auditory and medial geniculate body electrical stimulation 12 p1761 A72-27651
- Neuron networks dynamic behavior in terms of linear differential equations for membrane potential changes and neuron threshold 12 p1772 A72-27925
- ECG P-wave-like deflections caused by strong diaphragmatic action potentials in obese woman with fever and erysipelas 13 p1908 A72-28569
- Deep brain structure biopotential correlations during man sleep development, using electrosuabortograms 13 p1901 A72-28634
- Monovalent K and Na and bivalent Ca and Mg plasma ion ratio effect on thrombocyte electrokinetic potential 13 p1901 A72-28635
- Digital evoked brain potential detector using multichannel amplitude analyzers 13 p1908 A72-28645
- High threshold afferents role in dorsal surface potential formation in cat spinal cord 13 p1905 A72-29327
- Selective chromatic adaptation in cone photoreceptors of cynomolgus macaque monkeys, using late receptor potential as response index 13 p1907 A72-29967
- Myelinated nerve fiber mathematical model for action potential transmission mechanism analysis during relative refractory phases 14 p2079 A72-30597
- Electroretinographic illumination potentials dependence on extracellular chloride ion concentration in isolated frog retina 15 p2186 A72-32491
- Conditioned slow negative potential of human brain cortex dependence on motivation, emphasizing punishment avoidance conditions 16 p2353 A72-33097
- Isolated retina receptor potential amplitude relation to visual pigment bleaching kinetics, indicating excitation-inhibition receptor response generation mechanism 19 p2756 A72-37830
- Myogenic and eardrum evoked auditory potentials and cortical responses to 0.2 millisecond voltage pulse acoustic stimuli 20 p2891 A72-38932
- Propriospinal ducts of the lateral funiculus and their possible role in transmission of pyramidal stimuli 21 p2999 A72-40583
- Study of the conductivity of the motor neuron membrane during supraspinal stimulation 21 p2999 A72-40585
- Synaptic potentials of sensor and motor neurons of trigeminal nuclei during corticofugal stimulation 21 p2999 A72-40587
- Role of pyramidal and extrapyramidal components of cortically-induced efferent stimuli in the mechanism of cortical motor activity coordination 21 p2999 A72-40591
- Hypothalamic control of the electrical activity of the spinal cord 21 p3000 A72-40598
- Supraspinal effects in the activity of preganglionic sympathetic neurons delivering axons to the cervical sympathetic nerve 21 p3000 A72-40599
- Evoked potentials of the primary auditory cortical zone produced by positive and inhibitive conditioned stimuli 21 p3001 A72-40806
- Some structural and functional characteristics of a retina projection onto the visual cortex of cats 21 p3001 A72-40808
- Analysis of the activity evoked in the cerebellar cortex by stimulation of the visual pathways. 21 p3003 A72-41460
- Effect of selenium on the formation of the electrical potential in the retina 22 p3148 A72-41898
- Computation of the shape and velocity of a nerve pulse 22 p3149 A72-42156
- Electromyographic investigation of diaphragm cross contraction following spinal cord section in cats, noting diaphragm motoneurons excitation by breathing center pulses 22 p3142 A72-42281
- Reactions of auditory cortex neurons to geniculocortical fiber stimulation 22 p3145 A72-42723
- Temperature transmission from biopotential radiotelemetry transmitters. 22 p3151 A72-42745
- Factors limiting the increase in stroke volume obtainable by positive inotropism - Investigations regarding the sufficient heart in the case of continued postextrasystolic potentiation 22 p3145 A72-42748
- Electrophysiological investigation of the excitation and inhibition processes in the auditory cortex 22 p3148 A72-43165
- A rapid assay of dipolar and extradiipolar content in the human electrocardiogram. 23 p3259 A72-43811
- Excitation contraction correlates in true ischemia. 23 p3255 A72-43814
- Synaptic events during specific and nonspecific inhibition of visual cortex neurons 23 p3257 A72-44088
- Neuronal and focal reactions of the parietal associative cortex to various peripheral stimuli 23 p3257 A72-44089
- Post-synaptic potentials of motor neurons of the facial nerve nucleus evoked by afferent and corticofugal pulse stimulation 23 p3257 A72-44091
- Photopic and scotopic contributions to the human visually evoked cortical potential. 23 p3261 A72-44380
- Component analysis of electroretinogram in dark and light adapted sheep eye, noting rod and cone receptor potentials and transient and dc responses 23 p3261 A72-44382
- Sensitivity of the human ERG and VEP to sinusoidally modulated light. 23 p3258 A72-44383
- Techniques for analysing differences in VEPs: Colored and patterned stimuli. 23 p3258 A72-44387

- Ensemble characteristics of the human visual evoked response - Periodic and random stimulation. 24 p3374 A72-44575
- Influence of the sympathetic nervous system on the presynaptic inhibition of the dorsal surface potential of the spinal cord 24 p3370 A72-44589
- BIOELECTRICITY**
- Auditory pathway neuron discharge response to complex sound stimuli and frequency discrimination of pattern recognition in cats 01 p0012 A72-10483
- Fish electroreceptor system morphology, physiology and evolution, considering electric current action, peripheral coding activity and central subsystems 02 p0157 A72-11545
- Synaptic mechanisms of vestibulospinal and reticulospinal effect on transmission to lumbar motoneurons in monkeys 02 p0158 A72-11760
- Nociceptive chemical action in cat skin vessels, showing fiber types for impulse transmission 02 p0164 A72-12511
- Hippocampus electric activity and cardiac rhythms variations responses to various intensity electric stimulation of central gray matter 02 p0165 A72-12881
- Conduction velocity groups in cat optic nerve from antidromic responses recorded in peripheral retina and area centralis 03 p0315 A72-13621
- Optic nerve axon diameters in central and peripheral cat retina related to conduction velocity groups 03 p0315 A72-13622
- Multichannel IC spike height discriminator for separating electrical activity of neural units recorded with microelectrode 04 p0481 A72-15223
- Bioelectric activity study of cat and dog cerebral intercentral relations during various motor activities and poses 04 p0474 A72-15231
- Cerebral neurons population electric stimulation effect on deep sleep duration in Parkinsonism patients 04 p0476 A72-15585
- Cat respiratory center activity phase relation to arterial chemoreceptor afferent discharge oscillations effect on lung ventilation frequency 05 p0619 A72-16789
- Sudden death in myocardial infarction, discussing heart electrical stability, neural control, arrhythmias and cardiac conduction disturbances 06 p0761 A72-17381
- Marine gastropod mollusk synaptic transmission mechanism, discussing various chemical transmitters, two phase potential, receivers, electrical interaction and electrophysiological conditioning 06 p0764 A72-17996
- Sensor systems terminals location in cats colliculus anterior through electrical response measurement to light and sound signals and skin stimulation 07 p0915 A72-18865
- Electrical cardiac activity computer simulation model including biophysically faithful conduction system and electrocardiograms for high fidelity production 07 p0929 A72-19313
- Stimulation transmission tracts, synaptic mechanisms and tonic activity of cat sympathetic ganglia 07 p0924 A72-20617
- Motoneuron pool fraction determination in human monosynaptic response of healthy and neuropathological subjects, comparing diagnostic methods 07 p0924 A72-20619
- Comparative EEG characteristics of frontal and occipital human brain cortex, relating psychophysiological and neurophysiological factors 08 p1116 A72-21196
- Hypothalamic single neuron unit discharge pattern response to acoustic, light and somatosensory stimulation in cats 08 p1116 A72-21471
- Bulbar respiratory neuron discharge pattern response to nasal and tracheal receptor stimulation in cats, relating changes in neuronal activity and intratracheal pressure 08 p1117 A72-21473
- Cat retina ganglion cell threshold and latent responses to separate stimulation of receptive field center and periphery 08 p1117 A72-21474
- Physiology of sleep phases and dreams, discussing data on highly organized and interacting neurohumoral mechanisms exhibiting alternating forms of brain bioelectric activity 08 p1118 A72-21838
- Protein biosynthesis inhibitors retardation of noradrenaline and serotonin induced hyperpolarization of neuron membranes in cortical sensorimotor region of rabbits 08 p1122 A72-22192
- German monograph on Ranvier node steady state I-V characteristics transition range and control by al-

- tered external solutions and morphological effects on nerve fiber 09 p1264 A72-22336
- Photically induced and spontaneously discharged neuron impulse propagation through direct pathways from superior colliculus to dorsal and ventral lateral geniculate nuclei in cats 09 p1265 A72-22863
- Laryngeal motoneuron activity during Hering-Breuer reflexes, noting inspiratory fibers firing inhibition and activation during lung inflation 09 p1266 A72-22975
- Mitogenic and IR radiation and plant bioelectricity in photogrammetry, using metabolic energy-photoemulsion relation 09 p1312 A72-23283
- Efferent vestibular activity in response to horizontal plane rotary stimulation in frog, showing efferent relations between both ears 10 p1426 A72-25099
- Single lateral geniculate neuron recording during receptive field-centered flashing spot variations for intensity response function comparison with optic neurons in cats 10 p1427 A72-25177
- Intraelectroretinographic analysis of light signal spatial summation at different retinal nerve levels in frogs 11 p1585 A72-26454
- Cortico-subcortical connections transection effect on cat lateral geniculate body and visual cortex neurons spontaneous activity 12 p1761 A72-27652
- Neuronal spike activity changes in rabbit visual and sensorimotor neocortex and hippocampus during EEG activation 13 p1902 A72-28643
- Illumination code efficiency in impulse activity of neurons of outer geniculate body of cat visual system, emphasizing pulse per group technique 13 p1903 A72-28780
- Visual cortex neuron reactions to antidromic stimulation of cat pyramidal tract, noting axon activation increased discrimination in analyzer 13 p1903 A72-28781
- Adaptation period to inverted work-rest cycle observed with encephalograph, noting effect of brain bioelectric activity circadian rhythms stability 13 p1904 A72-29315
- Dynamic bioelectric impedance level of tissue area between active electromyograph electrodes related to human skeletal muscle fatigue 13 p1905 A72-29332
- Myelinated nerve fiber mathematical model for action potential transmission mechanism analysis during relative refractory phases 14 p2079 A72-30597
- Cerebral cortex electric shock stimulation effects on phrenic nerve discharges in bivagotomized and curarized cats 14 p2077 A72-30842
- Cat bulbar respiratory neuron discharge modification by single electric shock stimulation of cerebral cortex 14 p2077 A72-30843
- Linear systems theory for mathematical model of retinal image and ganglion cell excitation, calculating receptor layer luminance distributions for several stimulus patterns 15 p2184 A72-31367
- Monkey retinal ganglion and lateral geniculate nucleus cell maintained discharge rate indication of receptive field organization for various light stimulus intensities 15 p2184 A72-31370
- Bioelectric activity of the medulla oblongata during hypothermia and bloodletting 17 p2504 A72-35024
- Synaptic patterns in the superficial layers of the superior colliculus of the monkey, *Macaca mulatta*. 19 p2758 A72-38647
- Influence of cooling of the sensorimotor region of the cerebral cortex on the neurons of the mesencephalic reticular formation 20 p2890 A72-38926
- Changes in the overall electrical activity of the mesencephalic reticular formation, the hippocampus, and the cerebral cortex under the influence of hydrocortisone and DOCA 20 p2890 A72-38929
- Operative memory mechanism as visual system neuron chain storage of stimuli from image recognition time measurements 20 p2891 A72-38936
- Device for eliminating the artifact of electrical stimulation when recording evoked pulse activity of neurons 20 p2893 A72-38938
- Morphological changes in spinal cord neurons of animals due to the decreased intensity of supraspinal stimulation 21 p2998 A72-40580
- Neuronal organization of descending systems of the spinal cord 21 p2998 A72-40582

- Intracellular study of rubrospinal neurons and of their synaptic activation during the stimulation of the sensorimotor cortical region 21 p2999 A72-40586
- Pyramidal control of the activity of interneurons related to various types of peripheral afferents 21 p2999 A72-40589
- Possible role of supraspinal formations in the fixation of trace alterations at the segmental apparatus level of the spinal cord 21 p2999 A72-40592
- Synchronization in the work of motor neurons during arbitrary motor activity of various types 21 p2999 A72-40595
- Role of afferent and efferent connections in the formation and reproduction of trace processes in man 21 p3001 A72-40807
- Patterns of spontaneous and reflexly-induced activity in phrenic and intercostal motoneurons. 21 p3003 A72-41462
- Morphological and electrophysiological analysis of afferent receptor connections in cerebellar cortex, discussing fast conducting, diffuse reticular and inferior olive fiber paths 21 p3004 A72-41674
- The effect of membrane parameters on the properties of the nerve impulse. 22 p3140 A72-41936
- New modifications of manipulators for investigations using microelectrodes 22 p3149 A72-42073
- Dependence of inhibitory areas of inferior colliculus neurons on the time characteristics of acoustic stimuli 22 p3145 A72-42724
- Effect of a polarizing current on the activity of neurons of the respiratory center 22 p3145 A72-42725
- Dynamics of the electrical activity of various regions of the neocortex during the sleep-wakefulness cycle 22 p3147 A72-42955
- The effect of electrical stimulation of the olfactory bulbs on the behaviour of cats and on the electrical activity of the neo- and archepaleocortex 22 p3147 A72-42960
- The electrical activity of the isolated frog retina in buffered chloride-deficient Ringer's solution 22 p3147 A72-42987
- Nervous mechanisms of the acoustic stress reaction 22 p3148 A72-43169
- Changes in the impulse activity of cortical neurons during selective reinforcement of a chosen range of their interpulse intervals 23 p3257 A72-44087
- Classification of neurons in the lumbosacral section of the spinal cord according to their discharge during evoked locomotion 23 p3257 A72-44092
- Preprocessing of nerve pulse sequences for analysis by digital computer 23 p3261 A72-44349
- Elaboration of steady changes in the firing rate of cortical neuron populations 24 p3370 A72-44587
- Cat hypothalamus regions neurons background activity characterized by single nonrhythmic spikes with large interspike intervals, noting frequency of discharge bursts 24 p3370 A72-44588
- Pulse activity of neurons in the thermal regulation center of the anterior hypothalamus during chill shivering 24 p3371 A72-44594
- Functional organization of the periphery effect in retinal ganglion cells. 24 p3371 A72-44908
- First-breath response of medullary inspiratory neurons to the mechanical loading of inspiration. 24 p3372 A72-44959
- Control, by the visual cortex, of the posterior lateral thalamic group in the cat 24 p3372 A72-45009
- Temperature-sensitive neurons in the brain stem - Their responses to brain temperature at different ambient temperatures. 24 p3373 A72-45232
- BIOENGINEERING**
- NT ANTHROPOMETRY
- NT BALLISTOCARDIOGRAPHY
- NT BIOMINSTRUMENTATION
- NT BIOMETRICS
- NT BIOTELEMETRY
- NT BODY MEASUREMENT [BIOLOGY]
- NT CARDIOGRAPHY
- NT ELECTROCARDIOGRAPHY
- NT ELECTROENCEPHALOGRAPHY
- NT ELECTROMYOGRAPHY
- NT ELECTRORETINOGRAPHY
- NT PLETHYSMOGRAPHY
- Medical equipment advancements through NASA sponsored aerospace research program, describing prosthetic urethral valve, ear oximeter, radiation dosimeter and electromyographic muscle trainer 06 p0765 A72-18616

- Moving visual stimuli apparatus with independent control over size, shape, background intensity, orientation and velocity of motion, describing cat neuronal sensitivity studies
07 p0926 A72-19032
- Hybrid computer simulation of cardiovascular system in biomedical engineering education
09 p1268 A72-22455
- Electrode system for ventricular defibrillation, noting current density role and rounded edge effectiveness
11 p1588 A72-26628
- Lumped parameter nonlinear RC circuit lung model for positive pressure respirator design
11 p1588 A72-26631
- Electrode design and implantation method for chronic experiments, discussing information loss factor elimination
14 p2078 A72-30393
- Apparatus for programmed oral administration of drugs to large primates in altered environments.
18 p2654 A72-36921
- Device for eliminating the artifact of electrical stimulation when recording evoked pulse activity of neurons
20 p2893 A72-38938
- Quantitative determination of fluorescence within the eye without disrupting the integrity of the eyeball
20 p2893 A72-38941
- Bioengineering models of energy and mass exchange of algae under varying ambient conditions, noting mass cultivation possibility for oxygen regeneration in closed environments
20 p2893 A72-38959
- Techniques and procedure for differential ballistocardiography of extremities.
20 p2897 A72-39325
- Functional reliability of the biological component of a life support system
21 p2998 A72-40448
- BIOGENESIS**
U BIOLOGICAL EVOLUTION
- BIOGENY**
Ecogenesis of volcanic island of Surtsey after 1967 lava eruption, discussing terrestrial and marine littoral and sublittoral biomes
04 p0473 A72-14916
- BIOGEOCHEMISTRY**
Molecular paleontology of fossil organic remnants in Molluscan shell proteins
04 p0467 A72-14753
- Phosphate solubilization and activation on primitive earth, using apatite solubility as function of pH
04 p0483 A72-14769
- Precambrian paleobiological history from fossil records, discussing heterotrophic living systems and eucaryote emergence in evolutionary organization development
08 p1162 A72-22003
- Carbon isotopic studies of organic matter in Precambrian rocks
09 p1304 A72-23496
- Prokaryotic algae associated with Australian proterozoic stromatolites.
22 p3174 A72-42981
- BIOINSTRUMENTATION**
NT BIOTELEMETRY
Chlorella algae size distribution curves by combining device for counting electrical conductivity pulses with discriminator for gamma scintillation spectrometry
01 p0017 A72-10400
- General purpose electronic modular units for human factors research bioinstrumentation, considering digital and analog computers, logic modules and interface and auxiliary equipment
01 p0048 A72-10569
- Parachuting and aerial towing physiological and force data FM telemetry for biomedical response assessment leading to human engineered equipment improvement and midair retrieval system development
02 p0168 A72-12138
- Electrical thermometer mounted on breathing mask for electropneumograms, measuring temperature change in respiration air flow
02 p0169 A72-12518
- Multichannel IC spike height discriminator for separating electrical activity of neural units recorded with microelectrode
04 p0481 A72-15223
- Nonsurgical ultrasonic technique to measure wall displacement and pulsatile changes in thoracic aorta [AD-73989]
07 p0930 A72-19447
- Biomedical transducers for NASA space program, discussing spray-on electrodes and telemetering for ECG respiration and body temperature
07 p0931 A72-19917
- Battery powered dc integrated circuit for temperature regulation in small experimental animals, using thermistor probes and heating pads
08 p1114 A72-20895
- Mathematical, physical and engineering aspects of electro- and magnetocardiography, noting heart field nondipolar properties and heart vector determination difficulties
09 p1273 A72-23414
- Semiautomatic measurement of human oxygen uptake, discussing apparatus and accuracy
10 p1432 A72-24991
- Electronic and hematocrit devices to investigate cardiovascular system functions including blood coagulation process, pressure and flow
11 p1585 A72-26464
- Pneumatic thermistor transducer to measure steep ejection time interval between cardiac volume pulse upstroke start and maximum rise rate occurrence
11 p1588 A72-26633
- Nose installed thermistor device for in-flight monitoring of pilot respiration and pulse rate
12 p1769 A72-27417
- Considerations in the design of an automatic visual field tester.
18 p2654 A72-37013
- Hand tremor measurement methods, discussing pickup system selection for given tasks
21 p3012 A72-41521
- New modifications of manipulators for investigations using microelectrodes
22 p3149 A72-42073
- Biological instrumentation for the Viking 1975 mission to Mars.
23 p3259 A72-43396
- An integrated multi-purpose biology instrument utilizing a single detector, the mass spectrometer.
23 p3287 A72-43397
- A critical assessment of an open circuit technique for measuring oxygen consumption.
23 p3260 A72-43937
- Analysis of a nuclear magnetic resonance blood flowmeter for pulsatile flow.
24 p3401 A72-44574
- BIOLOGICAL ACTIVITY**
U ACTIVITY [BIOLOGY]
BIOLOGICAL ANALYSIS
U BIOASSAY
BIOLOGICAL CELLS
U CELLS [BIOLOGY]
BIOLOGICAL CLOCKS
U RHYTHM [BIOLOGY]
BIOLOGICAL EFFECTS
NT RELATIVE BIOLOGICAL EFFECTIVENESS [RBE]
Space flight biological effects on lysogenic bacteria and human cells in culture
01 p0011 A72-10365
- Biological efficiency of secondary radiations from 70 GeV protons interaction with target, discussing dose dependences and restoration process relative rates
02 p0161 A72-12057
- Radiobiological effects of nonuniform body irradiation, discussing regeneration process stimulation by partially shielded bone marrow
02 p0161 A72-12060
- Nonuniform high energy proton irradiation of dogs, evaluating and predicting tissue biological effects
02 p0161 A72-12061
- Primary cosmic ray interaction with tissues, emphasizing biological effects and nuclear reactions induced radioactivity in astronaut body
03 p0313 A72-12911
- Depth ionization properties and biological effects of bevatron produced heavy ion beams, discussing utilization in tumor therapy, space biology and radiobiology
03 p0316 A72-13693
- Semiconductor devices potential interference and biological exposure hazards in microwave leakage field, considering shielding and filtering methods for reducing susceptibility
03 p0320 A72-14032
- Biological effects of unfocused laser radiation on DNA and RNA synthesis and cell activities in thymine dependent E. coli strain
04 p0477 A72-14610
- Space environment weightlessness and radiation effects on leeches biorhythm, metabolism, reproduction and growth from rocket biological experiments
04 p0481 A72-15729
- Biological damage inflicted to rats by protons, X rays and gamma rays
06 p0762 A72-17675
- Biological hazards of high intensity light sources, considering physiological factors involved in threshold eye damage values determination
08 p1125 A72-21333
- Thromboelastographic study of renin and angiotensin effect on blood clotting system of anesthetized and unanesthetized dogs
08 p1121 A72-22095
- Embryogenesis of fertile chicken eggs in pure oxygen at reduced pressure
09 p1265 A72-22642
- UV radiation intensity altitude dependence and absorption by ozone, considering diurnal and annual variations and biological effects
09 p1268 A72-23625
- Lungs fibrosis and cancer caused by asbestos fibers inhalation, noting environment control for protection against workers health hazards
11 p1583 A72-25548
- Industrial safety rules recommendations for lasers based on radiation biological effects and eye optical and physiological properties
12 p1771 A72-27615
- Geomagnetic field perturbation biological effects, studying geomagnetic storm field energy levels and magnetic flux variables relation to human sensitivity thresholds
12 p1773 A72-28210
- Solar activity effects on biospheric processes for biological and physicochemical systems in unsteady state, considering maximum effects on man at certain electromagnetic wave frequencies
12 p1773 A72-28211
- Solar activity effects on biosphere processes, discussing radiation-induced molecular activation mechanisms in water and biological plasma calcium ion concentration changes
12 p1763 A72-28213
- Biomedical effects on air crews of chemical fire suppression agent Halon 1301 /bromotrifluoromethane/ during simulated aircraft cabin fires
12 p1776 A72-28308
- Three year varied dose and acute exposure gamma irradiation of dogs, noting radiobiological effects from hematological, cytological and physiological examinations
13 p1903 A72-29307
- Proton irradiation effects on monkey central nervous system, showing inflammatory reaction and neurological astrocyte gliofibrin accumulation
13 p1906 A72-29833
- Serotonin precursor 5-oxytryptophan effects on hypothalamic-hypophyseal-adrenal complex under complete deafferentation of medial-basal hypothalamus
13 p1907 A72-30016
- Electromagnetic pulsed radiation fields effects on monkeys and dogs behavior and blood chemistry, noting biological hazard absence
14 p2078 A72-30423
- Luna 16 fine lunar soil fraction biological effect on mice
14 p2079 A72-30469
- Cytological, genetic and physiological analyses of space flight factors effects on seeds and plants aboard Zond 5 probe
15 p2186 A72-31828
- Biological structures study, proposing generalized thermodynamics for dissipative structures role in living beings functions
16 p2354 A72-33519
- Nonionizing electromagnetic radiation effects in biological systems, discussing microwave penetration, therapeutic warming, light scattering in tissues and medical instrument applications
16 p2359 A72-33754
- LF whole body vibration effects on rat escape conditioning in terms of frequency, amplitude and controls for noise and activation
16 p2357 A72-33868
- Visible and invisible nonionizing radiation produced human injuries, considering visual and retinal effects and induced thermal stresses
17 p2499 A72-34300
- Magnetic field effects in enzymes, tissue respiration and some metabolism characteristics of an intact organism
17 p2503 A72-35003
- Effects of magnetic fields on microorganisms
17 p2503 A72-35004
- Mechanism of the biological action of a constant magnetic field
17 p2503 A72-35005
- Influence of a magnetic field on radiation-induced chromosome aberrations in plants
17 p2503 A72-35007
- Pathologic-anatomic characterization of changes induced by magnetic fields in experimental animals
17 p2503 A72-35008
- Clinical hygienic and experimental data on magnetic field effects under working conditions
17 p2503 A72-35012
- Methodical and methodological characteristics of a magneto-biological experiment
17 p2503 A72-35013
- Effect of lunar ground on radiation damage in mice
17 p2504 A72-35214
- Space flight effects on chlorella cell survival and mutability in Zond automatic stations
17 p2504 A72-35278
- Soyuz 5 satellite vehicle space flight factors effect on chlorella cells, investigating survival rates and mutability
17 p2505 A72-35279
- Chromosome aberrations and germination speedup in Soyuz 5 carried barley seeds, noting stimulating effect by preflight ethylenimine treatment
17 p2505 A72-35280

- Analysis of vegetable seedlings grown in contact with Apollo 14 lunar surface fines. 17 p2505 A72-35925
- The influence of clinostat rotation on the fertilized amphibian egg. 18 p2649 A72-36435
- Roentgenologic studies of the effects of rapid decompression and hypoxia on the gall bladder in cats. 19 p2758 A72-38705
- The resonance mechanism of the biological action of vibration 20 p2897 A72-39409
- Changes in the wear resistance of polymer surface layers in aggressive and biologically active media 21 p3072 A72-40081
- Biological rhythms origin and mechanisms, discussing 24-hour cycle, subcellular biological clock and rhythm disruption effects in speleologists, astronauts and pilots 22 p3141 A72-41985
- Inert gas effects on embryonic development. 22 p3145 A72-42744
- Effects of simulated space vacuum on bacterial cells. 23 p3254 A72-43395

BIOLOGICAL EVOLUTION

- NT ABIOTIC GENESIS
- Molecular evolutionary changes in amino acids of proteins due to mutant random fixation, comparing human and fish hemoglobin chains 02 p0158 A72-11761
- Evolutionary rate of cistrons in vertebrates, discussing hemoglobin and cytochrome c changes involving amino acid mutant substitution 02 p0158 A72-11762
- Cytochrome c X ray structure and molecular evolution rates, using amino acid sequence comparative data 02 p0158 A72-11763
- Retinomotor light/darkness responses phylogenetic variations, discussing retinal elements structural and functional development in fishes and amphibians 02 p0164 A72-12484
- Interstellar formaldehyde and ammonia molecules effects on prebiological amino acids evolution 02 p0165 A72-12846
- Life origin in space from point of hydrocarbons, cyanides, abiogenic organic synthesis and protoions evolution 04 p0467 A72-14752
- Biological self replicative description and function in chemical reaction networks in search of life origin from non-life-like matrix 04 p0482 A72-14756
- Nucleic acid, protein and cell primordial sequence, ribosomes and genetic code for life origin, discussing experiments on homopolyamine acids reaction with mononucleotides 04 p0468 A72-14775
- Pigment system and primary photosynthesis evolution, using comparative analysis of bacteriochlorophyll, bacterioviridin and chlorophyll 04 p0469 A72-14780
- Molecular evolution of biological membrane from lipid film to lipoprotein particle assembly, using bacterial biochemistry 04 p0469 A72-14786
- Protein evolution, discussing biological group amino and nucleic acid structure variations from phylogenetic tree of cytochrome c data 04 p0470 A72-14791
- DNA primary structure variability relation to origin and evolution, discussing taxon scale in existing animal, plant and microorganism systems 04 p0470 A72-14792
- Ribosomes origin and rRNA evolution, considering biogenesis from coacervate to protocell and protein biosynthesis 04 p0470 A72-14793
- Bacterial respiration through oxidative phosphorylation origin hypotheses, discussing photosynthesis and sulfate respiration in anoxygenic atmosphere and thiobacillus and aerobic evolution in oxygen atmosphere 04 p0470 A72-14795
- Biochemical functions of organisms in evolution of biosphere, discussing redox reactions, elementary compositions and metal compounds role in photosynthesis 04 p0470 A72-14796
- Preglycolitic energy metabolism in biochemical evolution, concerning anaerobic oxidation of pyruvate and acetaldehyde to acetate and ATP 04 p0471 A72-14799
- Hereditary endosymbiotic model of microbial evolution of Precambrian prokaryotic and eukaryotic cells 04 p0471 A72-14800
- Prebiological food origin in carbonaceous met conites, considering extraterrestrial environments, organic synthesis and terrestrial analogs 04 p0471 A72-14803
- Extraterrestrial life origin and evolution, estimating possibilities on Mars, Venus and Jupiter 04 p0471 A72-14806

- Astrogenic and planetogenic environments characteristics examination for stellar spectral classes effect on intelligent life evolutionary pace and existence probability 04 p0573 A72-14887
- Soviet book on gravitational effects on animal evolution covering land and aqueous conditions adaptation and weightlessness in space 06 p0763 A72-17818
- Human biology, including evolution, organism structure, organizations of people, degeneracy, interactions with environment and philosophical concepts 06 p0765 A72-18315
- Extraterrestrial life origin and development possibilities from earth chemical and biological evolution description, noting external conditions requirements 08 p1119 A72-22002
- Precambrian paleobiological history from fossil records, discussing heterotrophic living systems and eucaryote emergence in evolutionary organization development 08 p1162 A72-22003
- Genetic organization emergence, considering pretranslational evolution in nontranslational protein synthesis, nucleic acid evolution and gene origin 08 p1119 A72-22010
- Cellular evolution investigation using molecular biology, microbial physiology and ecology 08 p1119 A72-22011
- Respiratory function control and physiological adaptation mechanisms evolution during changing earth atmosphere oxygen content, noting hypoxia sensitivity development 08 p1121 A72-22080
- Energetic motor activity rule hypothesis for physiological mechanisms of certain ontogenesis patterns, suggesting motor activity as excess anabolism induction factor 09 p1264 A72-22225
- Biological experiments of Viking Mars lander 1975 mission regarding Oparin-Haldane evolution hypothesis 10 p1430 A72-24384
- Evolutionary significance of primary amino acid or nucleotide base sequences of DNAs within various phylogenetic groups 12 p1759 A72-27160
- Liver and muscle type isozymes of DPN-linked glycerol-3-P dehydrogenase in chickens in terms of tissue distribution, ontogeny and avian evolution 12 p1759 A72-27161
- Coherent brain model for evolution mechanisms of biological resonance in neuron network signal flow 13 p1908 A72-28455
- Phylogenetic origin of cytoplasmids from Cyanophyceae algae involved in endosymbiosis with colorless Cryptophyte 13 p1907 A72-29996
- Atmospheric ozone and the history of life. 18 p2686 A72-36626
- Evolutionary clock - Nonconstancy of rate in different species. 19 p2758 A72-38551
- Comparative studies of the respiratory functions of mammalian blood. 21 p3002 A72-40919
- Prokaryotic algae associated with Australian proterozoic stromatolites. 22 p3174 A72-42981
- Empirical support for a stochastic model of evolution. 23 p3254 A72-43565
- Amino acid substitution correlation with genetic code in human, bovine, ovine, porcine and salmon catonins, suggesting mutation occurrence time during evolution 23 p3254 A72-43568

BIOLOGICAL MODELS

U BIONICS

BIOLOGICAL RHYTHM

U RHYTHM [BIOLOGY]

BIOLOGY

- Physical and biological sciences approaches to attainment of knowledge, noting indeterminateness in organic realm 07 p0934 A72-20394
- Biologist view of behavioristic approach to psychoacoustics, criticizing mechanical concept of living organism as inadequate for understanding human sensory system 11 p1583 A72-25732

BIO LUMINESCENCE

- Adrenergic innervation of internal carotid arteries in extra- and intracranial regions in dogs, using luminescence method 08 p1121 A72-22184
- Temperature effects on blood electrobioluminescence, relating luminescence peaks to protein and lipid molecular structure changes 09 p1268 A72-23694

BIOMECHANICS

U BIODYNAMICS

BIOMEDICAL DATA

- Computer controlled scintiscanning for pulmonary blood flow distribution, discussing real time data monitoring, contour plots and three dimensional and wall reflection maps 01 p0020 A72-11038
- Thermovisors /recording IR detectors/ development, discussing application to biomedical investigations and disease diagnosis 01 p0022 A72-11293
- MORL and Orbital Biomedical Laboratory projects, reviewing crew accommodation, spacecraft and booster requirements and biomedical measurements 05 p0724 A72-16177
- Computers in biomedicine - Conference, University of Hawaii, January 1972 07 p0928 A72-19306
- Biotelemetry applications in medicine, animal experiments and ecology, including ergonomics, internal bleeding detection, fetal monitoring, animal brain implantations, animal movement tracking, etc 07 p0931 A72-19916
- Bioelectric ECG and EEG signal analysis using hybrid computer techniques and parameter optimization for autocorrelation function modeling 07 p0933 A72-20333
- Diurnal and beat-to-beat variation factors in vectorcardiograms, noting respiratory movements, electrode location shift, skin-electrode impedance and heart electrical center mobility 08 p1127 A72-21849
- Hybrid computer simulation of cardiovascular system in biomedical engineering education 09 p1268 A72-22455
- Multichannel oscillograph for real time biomedical studies of LF physiological processes 09 p1270 A72-22881
- Multichannel automatic data acquisition and processing in ergonomic measurements of radar controller work from ECG, EOG, EMG and respiration 09 p1271 A72-23136
- On-line analog display system for cardiovascular functions and beat-by-beat cardiac output derived from single aortic blood flow measurement 10 p1430 A72-24375
- Computerized image analysis, establishing desirable scene characteristics for biomedical display in automated system 11 p1602 A72-26388
- Digital computer technique for computation of pulmonary mechanics parameters, using phasor method and Fourier series analysis of respiratory flow signals 11 p1587 A72-26620
- Left ventricular volume time course from computer processing of video angiocardigraphic data based on X ray densitometry measurements 11 p1587 A72-26627
- Random sample comparison of computer program for ECG diagnoses and physicians readings 11 p1590 A72-26975
- Arterial pressure data recording technique using magnetic tape recorder and automatic conversion to digital form 12 p1772 A72-27649
- Bioastronautic results of Apollo space flight biomedical operations, discussing weightlessness, sleep impairment, motion sickness, preventive medicine, etc 15 p2189 A72-31827
- Left ventricle intracavity volume measurements based on biplane angiographic data 15 p2190 A72-32497
- Medical requirements for manned space flight, discussing physiological data monitoring and transmission, equipment miniaturization, telediagnosis, spacecraft environment protection, etc 16 p2358 A72-33562
- A system for the mass examination of electrocardiograms. 19 p2760 A72-37853
- Probability threshold of data element similarity as separation criterion for automatic multiparameter biomedical data classification 20 p2893 A72-38937
- Application of sample quantiles to the compression of telemetric transmission and statistical processing of medical information 22 p3150 A72-42221

BIOMETEOROLOGY

U BIOCLIMATOLOGY

BIOMETRICS

- NT ANTHROPOMETRY
- NT BALLISTOCARDIOGRAPHY
- NT BODY MEASUREMENT [BIOLOGY]
- NT CARDIOGRAPHY
- NT ELECTROCARDIOGRAPHY
- NT ELECTROENCEPHALOGRAPHY
- NT ELECTROMYOGRAPHY
- NT ELECTRORETINOGRAPHY
- NT MAGNETOCARDIOGRAPHY
- NT PHONOCARDIOGRAPHY
- NT PLETHYSMOGRAPHY

Spatio-temporal scalp mapping localization of human visual evoked responses to full field light adapted stimulation, comparing to half-field situation
01 p0015 A72-11185

Magnetometer and spirometer ventilation measurements from chest and abdomen movements during carbon dioxide inhalation
05 p0619 A72-16790

Biological cell sorting by differential fluorescence generated electric signals via laser beam illuminated liquid stream
09 p1273 A72-23403

Ultrasonic Doppler flowmeter for instantaneous measurement of blood vessel flow velocity by averaging frequency shift over received signal power density spectrum
10 p1430 A72-24373

Human body calorimetry with water cooled garment for dynamic and continuous recording of heat dissipation from surface over extended time
10 p1431 A72-24485

TV microscopic system for on-line measurement of cat omentum microvessels diameter relative to heart action
11 p1587 A72-26621

Electrolyte hydrostatic pressure measurement in limited volume biological compartments by fluid filled glass micropipette used in microtransducer capacity
11 p1587 A72-26623

Arterial pressure data recording technique using magnetic tape recorder and automatic conversion to digital form
12 p1772 A72-27649

Piezoelectric transducer for indirect on-wrist blood pressure measurements for clinical environment
12 p1772 A72-27961

Human acceleration stress tolerance monitoring techniques for temporal, brachial and radial arterial blood flow and indirect systolic and diastolic blood pressure measurements
12 p1777 A72-28328

Noninvasive polygraphic technique to assess cardiovascular responses to intravenous glucagon injection
13 p1901 A72-28570

Left ventricle intracavity volume measurements based on biplane angiographic data
15 p2190 A72-32497

Automated constant cuff-pressure system to measure average systolic and diastolic blood pressure in man.
17 p2507 A72-34298

Reproducibility of indirect /CO₂/ Fick method for calculation of cardiac output.
17 p2506 A72-35971

Quantitative decision criteria for identification of visual evoked responses obtained during binocular rivalry.
18 p2652 A72-36312

An automatic measuring and recording system for clinical electro-oculography.
19 p2759 A72-37400

Optimal vascular pressure measurements with transducers located outside body with rigid and elastic tube couplings
19 p2760 A72-37757

A method for spiropgraphic display of functional residual capacity and other lung volumes.
21 p3005 A72-40427

Electrically sensed changes in chest and abdomen diameter for tidal volume, respiratory frequency and minute ventilation measurements
21 p3006 A72-40428

Determination of corneal configuration by the measurement of its derivatives.
21 p3055 A72-40745

Biological system transfer-function extraction using swept-frequency and correlation techniques.
22 p3151 A72-42773

BIONICS

Human body dynamics, discussing configuration, modeling techniques, kinematics, equations of motions and various limb motions examples
01 p0016 A72-10110

Bone tissue elastic behavior based on Voigt model of two phase composite material, using ultrasonically determined hydroxyapatite elastic moduli
01 p0136 A72-10112

Electronic analog models of human retina and visual system, discussing optical character recognition, signal processing, photoreceptor stimulation, visual cortex excitation and further model development
01 p0017 A72-10471

Neuronal mechanisms of binocular vision and space perception from tests on cats and men, discussing neurophysiological models of stereopsis
01 p0012 A72-10479

Stereopsis spring coupled magnetic dipole model of binocular stereoscopic depth perception in man
01 p0012 A72-10480

Site binding model of nucleic acid-protein interactions for chemical evolution and genetic code studies
02 p0159 A72-11765

Chlorella growth rate model, presenting specific photosynthetic and urea and carbon dioxide utilization rates
02 p0160 A72-12038

Radiation induced disease development related to dose, dose rate and radiation quality, discussing different models
02 p0161 A72-12053

Mathematical models for man-machine control behavior in biodynamic environments including manual control performance and interface elements
03 p0318 A72-13162

Primitive earth model of ion selective enzymatic asymmetric synthetic membrane for accelerated nutrients and metabolites transfer studies
04 p0469 A72-14787

Ion selective accumulation model of carbohydrates diffusing through artificial polymer membranes, relating prebiological systems to catalytic microsystems
04 p0469 A72-14788

Steady state heat transfer problem solutions in living tissue modeled as cylindrical shells, discussing blood flow and temperature distributions in extremities
05 p0745 A72-15885

[ASME PAPER 71-WA/HT-34] Aircraft ejection simulation by human thoraco-lumbar spine flexion dynamic model, using strength of materials theory and shear effects for curved elastic beam
05 p0620 A72-15947

[ASME PAPER 71-WA/BHF-7] Hydrodynamic model of human systemic arterial circulation to test artificial heart pumps
05 p0621 A72-15954

German monograph on analog model of thermoregulation in human body at rest and at work, describing heat transfer
05 p0621 A72-16047

Mathematical model for blood leucocyte population changes after radiation exposure within Blair model leucocytes hemopoietic to cardiovascular systems transport
05 p0618 A72-16635

Bacteriophage synergistic inactivation by heat and ionizing radiation from kinetic model describing dose rate and temperature dependences
06 p0768 A72-18185

EEG discharges virtual dipolar sources computation, using mathematical model with homogeneous spherical conductive medium to simulate human head
06 p0769 A72-18201

Human breathing metabolic simulation device for evaluating respiratory diagnostic, monitoring, support and resuscitation equipment
06 p0769 A72-18618

Computer graphics system simulation of saccadic eye movement made for time optimal control behavior study, incorporating eye muscle characteristics
07 p0928 A72-19309

Mathematical model physical structure, effectiveness and limitations for circadian rhythms, discussing Princeton and modified biochemical models
07 p0930 A72-19530

Bioelectric ECG and EEG signal analysis using hybrid computer techniques and parameter optimization for autocorrelation function modeling
07 p0933 A72-20333

Control system model integrating human left ventricle and circulatory system mechanics and regulation by central nervous system
07 p0934 A72-20356

Nonlinear model for computer simulation of human arterial system, using finite difference technique for pressure and flow calculations
07 p0934 A72-20357

Human behavior analysis based on nine component functional brain model, discussing information transmission mechanism via nerve path channels
07 p0923 A72-20460

Kalman filter estimator for nonlinear human pilot model parameters including time delay
08 p1145 A72-20861

Convective heat transfer from human form, using cylindrical model and aluminum statue physical replica in oven and wind tunnel air flow studies
08 p1123 A72-20892

Conditioned reflex activity, discussing biological and nervous system, electric analog simulation and mathematical and structural modeling
08 p1127 A72-21842

Auditory adaptation tests confirmation of Small loudness model prediction of lower adaptation for test tone greater than adapting tone intensity
08 p1127 A72-21897

Cardiovascular system model for demonstration of biological system analog simulation and computation, describing components for heart pumping action and systemic circulation
09 p1268 A72-22454

Digital computer simulation of circulatory and respiratory systems interaction model for oxygen and carbon dioxide gas exchange between pulmonary blood and alveolar air
09 p1268 A72-22456

Mathematical model of skin contact cooling tube device for human body thermoneutrality maintenance in various environments
09 p1270 A72-22821

Adaptive neural nets of threshold logic units as models of perception and memory in biological systems
09 p1273 A72-23580

Three stage retinal model for visual monitoring method applied to computerized photointerpretation of aerial photographs
09 p1284 A72-23624

Stochastic model for eye movements during fixation on stationary target
10 p1429 A72-23795

Human left ventricle measurements, modeling, control and simulation for heart monitoring purposes, describing muscle performance mathematical model and stress effect prediction control system
10 p1429 A72-23924

Operator independence test for human performance reliability modelling based on symptom detection and fault location of sonar system failure
10 p1429 A72-24002

Hot thermistor and hot-wire anemometer principles for phonocardiographic transducer design, using theory of hydraulic amplification with high SNR
10 p1430 A72-24374

Quasi-steady creeping flow in small airways of spherical, oblate and prolate ellipsoid and circular cylinder lung models, obtaining Stokes equations solutions
10 p1431 A72-24469

Elastic lung shaped model for distribution analysis of weight induced stresses, strains and surface pressures in lung
10 p1425 A72-24479

Artificial heart-lungs model with contractile polymer membrane as synthetic muscles to react with gases and liquids, discussing design features
10 p1431 A72-24640

Open capillaries control mechanism of pulmonary diffusion capacity, presenting mathematical interpretation of humoral and hydraulic blood pressure control
10 p1426 A72-24787

Hydraulic transmission line equations for computer simulation of arterial circulatory systems
10 p1431 A72-24811

Mathematical model for arterial system pressure, blood flow and dimensional changes, examining cardiac ejection dynamics and vasculature mechanical properties and viscoelasticity
10 p1432 A72-24812

Russian book on visual sensor signal dynamics covering nerve signal transformation, light stimuli responses, afferent flow, bionics, neurocybernetics and communication theory
11 p1584 A72-26049

Olfactory receptor models sensitivity, discussing threshold dependence on adsorbed odoriferous agent amount and exposure time
11 p1585 A72-26453

Lumped parameter nonlinear RC circuit lung model for positive pressure respirator design
11 p1588 A72-26631

Fluid mechanics of left ventricle model with mitral and aortic valves, showing ring vortex relation to diastole and closure
11 p1589 A72-26775

Impact tests on anthropomorphic dummies for protection effectiveness evaluation of lap belt, Air Force shoulder harness-lap belt and airbag-lap belt restraints [AD-741530]
12 p1769 A72-27471

Receptor membrane pulse generation electronic model with tunnel diode negative resistance circuit
12 p1771 A72-27578

Coherent brain model for evolution mechanisms of biological resonance in neuron network signal flow
13 p1908 A72-28455

Plant leaves biochemical activities study by light scattering techniques, discussing photometric, spectroscopic and bionics methods
13 p1955 A72-28518

Human torso surface mathematical model to determine equivalent heart dipole and quadrupole locations for ECG measurements
13 p1908 A72-28571

Qualitative microscopic model for biologic postsynaptic membrane with tunneling chemical bonds, noting selective ionic conductivity as function of electric field
13 p1909 A72-28769

Pulmonary oxygen transport dynamic model representing lung gas-side airway and alveolar regions and blood-side capillary bed
13 p1909 A72-28996

Statistical activity analysis procedure for random nerve network model, determining representative point trajectory in phase space via similarity matrix
13 p1909 A72-29176

Quantitative model to describe vestibular detection of body sway motion in postural response mode
13 p1905 A72-29374

Five-component cyclic model of retinal photopigment kinetics for photochemical changes corresponding to rod adaptation in rat and man in dark

13 p1906 A72-29966

Myelinated nerve fiber mathematical model for action potential transmission mechanism analysis during relative refractory phases

14 p2079 A72-30597

Four-parallel-compartment lung model for emptying pattern study, using expired nitrogen concentration data to calculate alveolar dilution ratio and emptying rate

14 p2079 A72-30703

Environmental chamber simulation to show terrestrial microorganisms survival under Jovian atmospheric conditions

15 p2183 A72-31293

Two compartment analog model of thermoregulation during rest and exercise, considering temperature, heat conductance, sweat rate and oxygen uptake

15 p2185 A72-31450

Hill model for myocardium activity, taking into account contractile state variations and characteristic force-velocity curve

15 p2187 A72-32492

Chamois leather mechanical response, comparing stress relaxation and frequency response characteristics to human skin for applications in anthropometric dummy construction

15 p2191 A72-32606

Crash helmet performance prediction through maximum strain criteria, using brain injury biodynamic model

15 p2192 A72-32607

Parameter estimation in dynamic biological control systems based on multicompartmental input-output behavior

15 p2192 A72-32766

Nonlinear theory of pulmonary ventilation distribution in two compartment model of human lungs

16 p2358 A72-33025

Computerized angiographic heart geometry analysis for three dimensional ventricle models of man and dog, using Ta markers

16 p2354 A72-33424

Simulation of the human cardiovascular system - A model with normal responses to change of posture, blood loss, transfusion, and autonomic blockade.

17 p2507 A72-34445

A new model for estimating space proton dose to body organs.

17 p2508 A72-35354

Mathematical model for flow limitation in collapsible tube in relation to pressure in pulmonary and circulatory system

17 p2510 A72-35972

Digital computer technique for ballistocardiography simulation, using distributed parameters for vessel segments in circulatory system model

18 p2652 A72-36038

Two-mass system as human body dynamic model in ballistocardiography, outlining transfer function parameter computation procedure

18 p2652 A72-36039

A stochastic bioburden model for spacecraft sterilization.

18 p2652 A72-36442

A model of fluctuating alveolar gas exchange during the respiratory cycle.

18 p2650 A72-36571

Model to account for visual responses to light flashes of dark adapted eye, discussing perceived brightness variation with intensity

18 p2651 A72-36611

Digital computer simulation of human systemic arterial pulse wave transmission - A nonlinear model.

18 p2655 A72-37028

A human left ventricular control system model for cardiac diagnosis.

18 p2655 A72-37029

Object code storage in the static portion of a short-time memory

19 p2759 A72-37423

Models of neurons reacting to input signal alternation in space and time

19 p2759 A72-37424

Neuron mathematical model synthesis from algorithms to construct neural networks and single threshold element in network form

19 p2759 A72-37425

Computerized statistical simulation of automatism of spontaneously active smooth muscle strip, neglecting individual cell spontaneous activity

19 p2757 A72-37949

Automatically controlled delay in self-excited pulsating systems based on artificial muscles

19 p2761 A72-38464

Russian book - Problems of the stability of biological system.

20 p2891 A72-38957

Thermodynamic properties and mathematical modeling of complex biological systems, considering energy and mass exchange in photosynthesizing organisms for exobiological life support

20 p2891 A72-38960

An electronic model of visual receptive fields.

20 p2897 A72-39271

Man movements directed at reaching a preset goal

21 p3006 A72-40710

Threshold detection model for foveal viewing by human observers using naked eye

21 p3007 A72-40733

Crystalline lens optical structure in human eye, representing on and off axis imaging characteristics by mathematical model

21 p3007 A72-40737

Unsteady state description of living corneal mass transport modes, elucidating cornea thickness control mechanism

21 p3001 A72-40912

A mathematical model of the chemoreflex control of ventilation.

21 p3008 A72-40917

A model for analysing the coordination of manual movements.

21 p3010 A72-41413

The design of a nonlinear multi-parameter model for the human operator.

21 p3011 A72-41421

The functional organisation of object directed human intended-movement and the forming of a mathematical model.

21 p3011 A72-41422

The effect of membrane parameters on the properties of the nerve impulse.

22 p3140 A72-41936

Control parameters of the blood-pressure regulatory system. II - Open-loop gain, reference pressure and basal heart rate.

22 p3145 A72-42772

Mutual relations between different physiological functions in circadian rhythms in man.

22 p3147 A72-42979

A large-scale model of the human cardiovascular system and its application to ballistocardiography. [ASME PAPER 72-AUT-Q]

23 p3259 A72-43635

A rapid assay of dipolar and extradiapolar content in the human electrocardiogram.

23 p3259 A72-43811

Information aspects in visual perimetry, obtaining memory requirement for control computer in automated perimetry

23 p3261 A72-44378

Respiratory control system benchmark simulation on hybrid computer for Cheyne-Stokes breathing, emphasizing equations for arterial and venous carbon dioxide and oxygen stores

23 p3268 A72-44551

Relative position of the rib within the chest and its determination on living subjects with the aid of a computer program.

24 p3372 A72-44957

BIOPHYSICS

NT HEALTH PHYSICS

Conformal electron interactions in biopolymer and hypermolecular biological systems, discussing calcium ions effects, enzyme activity, muscle contractions and information theory

07 p0915 A72-18803

Microwave radiation - Biophysical considerations and standards criteria.

17 p2507 A72-34299

Russian book - Effect of magnetic fields on biological objects

17 p2502 A72-35001

Physical phenomena occurring in living objects under the action of constant magnetic fields

17 p2502 A72-35002

Methodical and methodological characteristics of a magneto-biological experiment

17 p2503 A72-35013

Comparison of physical, biophysical and physiological methods of evaluating the thermal stress associated with wearing protective clothing.

20 p2898 A72-39808

Biology and molecular biophysics progress review, discussing synthetic semibiological systems, molecular pathology, free radicals and longevity

22 p3142 A72-42474

BIOREGENERATION

U REGENERATION (PHYSIOLOGY)

BIOREGENERATIVE LIFE SUPPORT SYSTEMS

U CLOSED ECOLOGICAL SYSTEMS

BIOSATELLITE 3

Space medical urological problems from experience with Biosatellite 3 monkey, discussing closed catheter conduit system, urinary calcium changes in immobilized animals and urinary diuresis

10 p1424 A72-23728

BIOSENSORS

U BIOINSTRUMENTATION

BIO SIMULATION

U BIONICS

BIO SPHERE

U EARTH HYDROSPHERE

U LOWER ATMOSPHERE

BIO SYNTHESIS

Waterless amino acid synthesis in interstellar space, describing ammonia, methanol vapor, formic acid and formaldehyde reaction under UV radiation

01 p0023 A72-11157

Chemical box model of energy storage in covalent bonds and nonequilibrium distributions in prebiological synthesis leading to macromolecules

04 p0482 A72-14755

Energetical conditions of primeval biosynthesis and transdehydration feasibility on simplified present day templates

04 p0468 A72-14757

Possible origin of dissymmetry of life, excluding synthesis under influence of optically active quartz

04 p0468 A72-14758

Energetic excitation of precursor compounds in gaseous phase for models of primordial atmospheres in thermodynamic equilibrium

04 p0552 A72-14759

Pulse shock tube synthesis of amino acids in primitive environments, discussing thermodynamic relations and conversion efficiency

04 p0482 A72-14761

Aromatic and amino acid prebiotic syntheses under primitive earth, considering electric discharge and cyanide polymerizations

04 p0483 A72-14762

Antibiotic polypeptide synthesis of gramicidin S and tyrocidine, using primitive model of sequential addition of amino acids on polyezymes

04 p0470 A72-14790

Ribosomes origin and rRNA evolution, considering biogenesis from coacervate to protocell and protein biosynthesis

04 p0470 A72-14793

Prebiological food origin in carbonaceous meteorites, considering extraterrestrial environments, organic synthesis and terrestrial analogs

04 p0471 A72-14803

Ionizing radiation as effective energy in primordial organic synthesis, discussing small molecule formation and subsequent condensation into polypeptides and polynucleotides

05 p0617 A72-16127

Biological phosphate origin through atmosphere-hydrosphere interrelations, discussing concentrative processes, dehydration mechanics and evaporation

05 p0617 A72-16129

Porphyrin exobiology, discussing organic and random biosynthesis and extraterrestrial existence based on interstellar spectral evidence

05 p0617 A72-16130

Enzymically synthesized homopolynucleotide and lysine-rich proteinoid microparticles effect on aminoacyl adenylate condensation as basis for genetic code origin

06 p0770 A72-17724

Book on origin of life by natural causes covering physical geology, astronomy, biopoiesis and evolution of life stages, orogenetic cycle, fossils, and primeval atmosphere

07 p0917 A72-19185

Transcript of conference on origins of life covering cosmic evolution, abundance and distribution of biologically important elements, earth and Mars atmosphere evolution, etc

07 p1074 A72-19450

Chemical evolution in microenvironment reactions system due to dominant energy or mass parameter, discussing complex organic molecule synthesis

08 p1128 A72-22005

Electronic factors role in intermolecular interactions and biochemical evolution, applying quantum biochemistry

08 p1128 A72-22006

Cosmic sources of organic compounds from chemical evolution viewpoint, discussing comets, interstellar space, prestellar nebulae and cool stellar atmospheres

08 p1120 A72-22014

Protein biosynthesis R and D, discussing rate control, structure and medical and nutritional applications

14 p2076 A72-30600

Pancreas insular apparatus biosynthesis of neurohumoral mechanism compounds stimulating coronary ectasia hormones discharge from brain into blood in cats with alloxan diabetes

14 p2077 A72-30973

The effects of acute hypoxia on lipid synthesis in the rat heart.

17 p2501 A72-34979

Myocardial protein synthesis in acute myocardial hypoxia and ischemia.

17 p2501 A72-34980

Role of the synthesis of nucleic acids and proteins in the adaptation of the organism to altitude hypoxia.

17 p2502 A72-34990

Dietary regulation of fatty acid synthesis in rat liver and hepatic autotransplants.

19 p2757 A72-38147

BIOT METHOD

Biot variational principle for phase change problem with constant heat flux boundary condition and without melt removal, noting linear temperature profile choice

08 p1254 A72-21611

On the two-dimensional deformation of a semi-infinite porous elastic medium.

18 p2736 A72-36929

BIOTECHNOLOGY

Cryobiology phenomena and applications, considering mode of action of various substances for freezing injury protection

19 p2762 A72-38828

BIOTELEMETRY

Miniaturized micropower biomultiplexer telemetry system utilizing hybrid techniques

02 p0192 A72-12133

Parachuting and aerial towing physiological and force data FM telemetry for biomedical response assessment leading to human engineered equipment improvement and midair retrieval system development

02 p0168 A72-12138

ECG telemetry systems parameters, discussing manufacturers specifications and standardized laboratory performance test data

02 p0169 A72-12139

Implanted telemetry development for cardiovascular research, discussing blood pressure, flow and hydraulic impedance relationships

02 p0169 A72-12140

Human pulse wave propagation velocity measurement, using biotelemetry system of photoresistance sensors and endoscopic bulbs connected to electrocardiograph

02 p0169 A72-12159

Electrocardiography telemetry system for intense radiation environment, describing electrode and transmitter implantation in monkey and heart signal transmission and reception

05 p0623 A72-16678

Cerebro-spinal fluid pressure remote monitoring by intracranially implanted radio pressure transducers, describing receiver-detector-recorder system

07 p0930 A72-19911

Telemetric instrumentation for remote physiological and behavioral observations of free roaming animals

07 p0930 A72-19912

Satellite system for telemetering environmental and physiological data from winter den of hibernating black bear, discussing instrumentation and equipment performance

07 p0931 A72-19913

Electrochemical energy cells for biological telemetry equipment, noting mercury cell use in implanted heart pacemakers

07 p0914 A72-19914

Biomedical telemetry instrumentation for radio sensing and transmitting biological information from animals and man, including location by satellite-borne receivers

07 p0931 A72-19915

Biotelemetry applications in medicine, animal experiments and ecology, including ergonometics, internal bleeding detection, fetal monitoring, animal brain implantations, animal movement tracking, etc

07 p0931 A72-19916

Biomedical transducers for NASA space program, discussing spray-on electrodes and telemetering for ECG respiration and body temperature

07 p0931 A72-19917

Respiration rate transmitter with miniature pressure transducer for measuring pneumograph variations in animals over FM-FM telemetry system

08 p1124 A72-20898

Common collector micropower monolithic transmitter for single or multichannel biomedical telemetry

11 p1586 A72-26563

Monolithic micropower command receiver to extend lifetime of implanted biotelemetry system

11 p1586 A72-26564

Cotton wick probe-transducer assembly for pneumograph recording of rabbit respiratory rate

11 p1587 A72-26619

Biotelemetry system for EEG monitoring of free swimming diver at 15 meter depth, discussing power requirements, antenna design and signal attenuation

12 p1770 A72-27478

Biotelemetry and computer analysis techniques for steep states and wakefulness studies during aerospace flight

16 p2356 A72-33560

Medical requirements for manned space flight, discussing physiological data monitoring and transmission, equipment miniaturization, telediagnosis, spacecraft environment protection, etc

16 p2358 A72-33562

Implantable blood pressure telemetry system

19 p2762 A72-38824

Radiorespirometry in the case of work and sports activities

22 p3149 A72-42071

Application of sample quantiles to the compression of telemetric transmission and statistical processing of medical information

22 p3150 A72-42221

Temperature transmission from biopotential radiotelemetry transmitters.

22 p3151 A72-42745

OFO A orbital flight recording of bullfrog vestibular gravity sensor nerve fiber pulses for assessing necessity of artificial gravity during prolonged weightlessness

23 p3254 A72-43391

Use of implantable telemetry systems for study of cardiovascular phenomena.

23 p3260 A72-43996

BIOTITE

Sphene U-Pb age resistance to thermal metamorphism, discussing zircon U-Pb and biotite and hornblende K-Ar ages within thermal aureole

01 p0052 A72-10069

BIPROPELLANTS

U LIQUID ROCKET PROPELLANTS

BIRDS

NT HOMEOTHERMS

NT PIGEONS

Bird hazards to aircraft, discussing protective measures

07 p0911 A72-18771

Biological radar clutter control by adaptive systems techniques, developing computer simulation for angel tolerance from bird electromagnetic characteristics

07 p0942 A72-19305

Uric acid to urea nitrogen ratio as assay test for identification of avian tissue in verifying bird ingestion or impact as aircraft accident cause

07 p0922 A72-20184

Laughing gull metabolism dependence on flight speed and angle during wind tunnel tests from oxygen consumption, carbon dioxide production and aerodynamic forces analyses

08 p1115 A72-21080

Concord aircraft windshield panels bird impact resistance, noting effects of edge clamping width, ply thickness, composition and temperature

12 p1812 A72-27013

Aircraft windshield bird impact resistance, noting weight, speed, angle and window geometry effects

12 p1813 A72-27014

BIREFRINGENCE

Nonmammalian vertebrate retinal receptor rods and cones birefringence as function of fixation, temperature and immersing medium

01 p0014 A72-10862

Second order electro-optic effect in diamond, discussing birefringence due to dispersion and random residual strains

02 p0260 A72-12545

Birefringent filter theory and optical properties, discussing transmission profile and error sources

03 p0352 A72-12947

Solc-type tunable birefringent filter for near UV spectrum, discussing optical design and transmission characteristics

03 p0355 A72-13058

Optics and electronics of digitized birefringent filter solar magnetograph to isolate magnetic sensitive lines

03 p0357 A72-13287

Solar magnetic field observations with birefringent filter for 5324 A Fe I line, showing H alpha fine structure

03 p0430 A72-13316

Low birefringent orthoferrites for optical devices, considering improvement in Faraday rotation detection of magnetic domains in single crystal platelets

03 p0360 A72-13760

Optical birefringent networks synthesis, describing use of building blocks of polarizers, birefringent crystals and optical compensators

04 p0548 A72-14737

Magnetoionic mode reciprocity for oblique incident electromagnetic wave propagation through birefringent stratified media

04 p0492 A72-15445

CdTe condensed films hexagonal modification and twinning boundaries birefringence reflection, using electron microscope and diffraction analysis

07 p1047 A72-18856

Linear and circular birefringence of low loss single mode glass fiber dielectric optical waveguide as function of length

07 p0940 A72-19232

Refractivity measurement of pure hexagonal structure 2H SiC over visible range, determining birefringence from curve fitting of data to Cauchy dispersion equation

09 p1309 A72-22603

Optical simulation of plastic strain distribution with models prepared from organic glass, investigating birefringence effect

09 p1406 A72-23182

Gamma irradiation effects on epoxy-diane resin creep and stress relaxation properties indicated by loaded specimens birefringence patterns

13 p1984 A72-29481

Tunable wide field birefringent element /filter magnetograph/ to separate polarized magnetic signal from selected spectral line width

13 p2045 A72-29706

Optical anisotropy effects in birefringent materials by reflected shadow method and extension of theory for constrained zones around cracked plates under plane stress

14 p2167 A72-30903

German monograph on optical transmission measurement interferometer with plane-parallel birefrin-

gent crystal plates covering plate combination selection based on interference pattern mathematics

15 p2233 A72-31525

Iterative procedure for Maxwell equations exact solution for anisotropic birefringent medium, applying result to limiting polarization problem

16 p2425 A72-33490

Orientational Kerr effect direct observation via birefringence relaxation time measurement in self focusing region of mode locked Q switched laser picosecond pulses

17 p2561 A72-34190

Experiments using the birefringence of fluids in motion

18 p2679 A72-36367

Mechanical component acceleration-induced stress and transient phenomena analysis by dynamic photoelastometry and interferometry, applying to elastic birefringent and other materials

18 p2734 A72-36373

Distribution of illumination in a point image in the presence of birefringence in the optical system /case of axial symmetry/

19 p2836 A72-38789

Optically induced variation of birefringence in ferroelectric materials.

20 p2959 A72-39045

Transparent film thickness, refractivity and birefringence measurements by white light interferometric gage, noting performance insensitivity to chemical composition, film temperature and haze level

21 p3053 A72-40601

A laser beam divider with continuous adjustment of the intensity ratio

23 p3294 A72-43225

Stress induced birefringence in an isolated and a shortcircuited KH2PO4 crystal.

23 p3324 A72-44322

BISMUTH

Photoemissive properties of bismuth-cesium films

17 p2595 A72-34754

BISMUTH ALLOYS

MnBi thin films as potential storage media within holographic optical memory system having write-in reference beam for readout

07 p0950 A72-19399

Structural and orientation study of sequentially evaporated MnBi thin films on glass substrates using electron diffraction and transmission microscopy

16 p2441 A72-33207

Electroconductivity, thermal emf and Hall coefficient for single crystals of Bi-Sb alloys with Cd, In and Sn additions

19 p2847 A72-38683

Bi-Sb alloys for magneto-thermoelectric and thermomagnetic cooling.

22 p3215 A72-43089

BISMUTH COMPOUNDS

NT BISMUTH OXIDES

NT BISMUTH TELLURIDES

Solar activity effects on bismuth chloride hydrolysis tests from statistical results following solar flares

12 p1773 A72-28212

Mutual interactions of thorium, lanthanides, and bismuth in Th-Ln-Bi solutions - Evidence for the formation of ThLnBi₃/y compounds.

20 p2942 A72-39986

BISMUTH OXIDES

Pyrochlore and perovskite preparation and structure in bismuth rhodium oxide system, discussing variable position parameter, occupancy factor and structure stability

13 p2022 A72-29375

BISMUTH TELLURIDES

BiTe crystal critical growth rate calculation based on theory for diffusional supercooling of melt with excess Te

08 p1217 A72-21338

Spectral analysis for Cu, Cl, Br and I impurity distribution in doped bismuth telluride crystals prepared by Bridgeman method

13 p2023 A72-29979

Concentration dependences and equilibrium values of the impurity distribution coefficients in bismuth telluride

19 p2845 A72-38177

Strain gage resistor with BiTeSb compound semiconductor film vacuum deposited on dielectric substrate, noting high sensitivity and operation without amplifiers

23 p3287 A72-43348

BISPENOLS

Zinc dithiophosphate and bisphenol effects on surface activation of additive compositions with succinimide base in lubricant applications

07 p1023 A72-19903

BISTABLE AMPLIFIERS

U FLIP-FLOPS

BISTABLE CIRCUITS

Electroluminescent image converter with positive optical feedback, investigating steady state bistable operation mode stability

02 p0193 A72-12341

- Bistable fluidic amplifiers switching dynamics, developing analytic performance prediction method from flow visualization studies
[ASME PAPER 71-WA/FLCS-8] 05 p0615 A72-15916
- Electroluminescent image converter with positive optical feedback, investigating steady state bistable operation mode stability 08 p1143 A72-21947
- FM mode locked Nd-YAG pulsed laser controlled bistable phase position operation, using modulator cut as Brewster angle prism 09 p1325 A72-23089 [AD-741511]
- Flow control circuits design based on unvented bistable fluid amplifiers 10 p1422 A72-23970
- Chalcogenide semiconductor monostable threshold and bistable memory switching devices, discussing fabrication and performance 13 p1934 A72-30090
- Fluidic digital logic devices vs electromechanical-electronic equivalents, describing Coanda effect application to bistable jet amplifiers /flip-flops/ as switching or memory devices 15 p2182 A72-31218
- The L14-120GJ, a new bistable image storage tube 18 p2667 A72-36677
- A CW Gunn diode bistable switching element. 22 p3159 A72-42610
- Bistable trigger stages composed of digital multiplexer with IC logic modulus replacing NAND or NOR circuits 23 p3267 A72-43990
- BISTATIC REFLECTIVITY**
- Bistatic radar scatter communication effective coverage analysis, considering dependence on equipment and target locations and properties 03 p0321 A72-13092
- Clear air atmospheric target detection, comparing bistatic and monostatic radar techniques
[AIAA PAPER 72-175] 05 p0630 A72-16835
- BIT SYNCHRONIZATION**
- Time division multiple access systems for satellite transmission, discussing burst transmission control problem associated with transmitting end synchronization 01 p0033 A72-11303
- Time division multiple access systems transmitting and receiving end synchronization control criteria derivation, discussing code pattern selection for reliable detection 01 p0033 A72-11304
- Frame synchronization performance tests for PCM telemetry system, considering code selection, frame length and data recovery 02 p0175 A72-12147
- Pulse amplitude modulated tester with shift register generated sequence and conventional data /PCM/ bit synchronizer and detector 02 p0192 A72-12148
- Digital data transition tracking loop as practical implementation of optimum self bit synchronizer in Mariner spacecraft telemetry demodulators 10 p1437 A72-24687
- Meteor trail radar operated under digital controller synchronization and programmed for alternate and simultaneous two orthogonal directions search 10 p1438 A72-24715
- Clock synchronization of multichannel radio communications systems using orthogonal signals with overlapping transmission spectra 11 p1598 A72-26727
- Message distortions analysis in PCM communications systems due to phase fluctuations of synchronization signal 11 p1598 A72-26728
- Lunar radar measurement for remotely located clock time synchronization, discussing applications to deep space tracking, computer technique for time delay correction and accuracy 15 p2199 A72-32069
- NASA global tracking network clock time synchronization to microseconds accuracy via GEOS-11 satellite 15 p2199 A72-32079
- Carrier synchronization and polyphase signal detection in digital communication network for high speed data transmission, deriving reconstructed noisy signal error probability 16 p2363 A72-33218
- Telemetric frame synchronization with the aid of distributed and concentrated frame periods 21 p3024 A72-40329
- Decision directed phase locked loops acquisition properties improvement technique for PCM bit synchronizer of random nonreturn to zero data 21 p3038 A72-40872
- An estimation algorithm with learning feature for an adaptive bit synchronizer. 21 p3021 A72-40908
- Communication systems with binary convolutional signal encoding and threshold decoding, discussing orthogonal checkout sums distribution for correct and erroneous synchronization 22 p3154 A72-42235

- Symbol synchronization advances impact on PCM bit synchronizers design, discussing symbol detection and timing extraction circuits 22 p3155 A72-42706
- Frame synchronization in time-multiplexed PCM telemetry with variable frame length. 23 p3265 A72-44182
- Alkali metal vapor Q switches for synchronizing mode-locked laser pulse trains with external events. 23 p3297 A72-44189
- BITS**
- Bias and spread in extreme value theory performance tests of communications systems, comparing with bit error rate tests 02 p0173 A72-12129
- BIVARIATE ANALYSIS**
- Dynamic optimization procedure for bivalent knapsack problem solution involving large number of variables 15 p2203 A72-31750
- BLACK AND WHITE PHOTOGRAPHY**
- Side-looking airborne radar /SLAR/ images comparison with small-scale low-sun black and white aerial photographs 05 p0661 A72-16041
- Black and white vs color photography application to photogeological interpretation of West Greenland Precambrian terrain 09 p1303 A72-23294
- Black and white aerial photographs quantitative evaluation for differentiation and identification of land use patterns by microdensitometry, using statistical methods 09 p1313 A72-23306
- Color enhanced black and white IR satellite images for oceanographic applications 11 p1620 A72-25346
- BLACK ARROW LAUNCH VEHICLE**
- U BLACK KNIGHT ROCKET VEHICLE**
- BLACK BODY RADIATION**
- Photometric calibration of long wavelength vacuum UV standards by synchrotron and plasma black body radiation 01 p0073 A72-11399
- Materials spectral emission properties measurement, comparing with absolute black body model 04 p0596 A72-14652
- Black radiation kinetics of photon thermalization in body cavity in static thermodynamic equilibrium 06 p0847 A72-17732
- High temperature black body model based on induction heating of graphite crucible, noting application to stellar energy spectral distribution determination 07 p0991 A72-20404
- Nonideal black body temperature measurement with IR radiometer, discussing error dependence on object temperature and emissivity and background temperature 07 p0993 A72-20692
- Black body X ray sources creation due to neutron stars rotational energy dissipation by strain hysteresis in crust 09 p1382 A72-22284
- Book on heat transfer by thermal radiation, covering black body radiation, electromagnetic theory, energy exchange, Monte Carlo solution, and absorbing and emitting media 09 p1411 A72-23046
- Nonisothermal hydrogen plasma channel flow and radiative heat transfer combined with convective and conductive transfer between isothermal black parallel boundaries 11 p1692 A72-25219
- Black radiation kinetics of photon thermalization in body cavity in static thermodynamic equilibrium 11 p1685 A72-25336
- Relativistic statistical mechanics invariant formula for coherence degree of plane blackbody radiation beam in arbitrary Lorentz frame, noting transformation law of temperature 12 p1846 A72-27741
- Blackness degree calculation for semitransparent film on nontransparent substrate with layer temperature gradients, allowing for polarization emission and multiple reflections 14 p2130 A72-30296
- Energy release mechanism during early universe expansion leading to distortion of relic black body spectrum, noting Comptonization effects 16 p2461 A72-34151
- Experimental achievement of optical pumping of a carbon dioxide molecular laser 19 p2814 A72-38790
- Experimental setup for the investigation of the spectral radiative capability of metals 22 p3175 A72-41893
- BLACK HOLES [ASTRONOMY]**
- Astronomical research, discussing Venus exploration, stellar evolution quasar structure, Maffei galaxies, black holes, dwarfs and neutron star model 01 p0133 A72-11099
- Gravitational lens effect in black holes detection, computing light curves 03 p0416 A72-13011

- Rotating relativistic stellar models, covering coordinate systems injection energy, convection, red shift, external gravitational waves and black holes 03 p0426 A72-13269
- Halos around black holes, showing luminosities caused by synchrotron radiation of magnetized plasma 03 p0435 A72-13803
- Gravitational waves proposed origin, considering black holes, star collapse, white dwarf and neutron star formation and galaxy center neutron star clustering 04 p0576 A72-15074
- Black hole prediction in gravitational collapse of star and universe in terms of quantum principle, chemical mechanics and superspace dynamics 05 p0690 A72-16528
- Transcendence of baryon number conservation law, discussing static black hole properties as final massive star collapse state 07 p1076 A72-19667
- Spectral distribution of electromagnetic radiation emitted by charge moving in gravitational field of spherically symmetric black holes 07 p1081 A72-20226
- Black hole vibrations explained as gravitational waves in spiral orbits 09 p1383 A72-22291
- Baryon number nonmeasurability of Schwarzschild black hole by strong interactions, extending results to Kerr-Newman holes 09 p1387 A72-22875
- Gravitational radiation spectrum and energy computation from point test particle falling radially into Schwarzschild black hole 09 p1393 A72-23646
- Long wave trains of gravitational waves from vibrating black hole, stressing hole dynamical entity 09 p1394 A72-23697
- General relativistic gravitational waves analogy with electromagnetic radiation, examining relation to collapsed astronomical objects from black hole properties 10 p1533 A72-23893
- Bright black holes from quasars condensation toward Schwarzschild radius, investigating primeval galaxies angular momentum increase and core concentration due to frictional effects 10 p1535 A72-23909
- Monodirectional jet mass ejection from black holes, developing hypothetical model based on squeezed toothpaste analogy 10 p1535 A72-23910
- Gravitational collapse /black holes/ search in universe, noting application of optical astronomy and radiation detectors on satellites and rockets 10 p1541 A72-24407
- Secondary component of eclipsing binary beta Lyræ as massive main sequence star in rapid nonuniform motion, refuting black hole suggestion 11 p1717 A72-25869
- Gravitational wave observation interpretations, discussing Weber theory of galactic nucleus isotropic radiation and synchrotron radiation sources in terms of black hole existence 11 p1717 A72-25883
- Black hole concept in general relativity and gravitational collapse, considering deviations from spherical symmetry and gravitational wave emanation from Galactic center 12 p1871 A72-27690
- Stellar gravitational collapse to neutron stars and black holes, discussing gravitational wave emission from Galactic center 12 p1875 A72-27958
- Baryon number nonexistence for static black holes and resulting baryonic conservation law transcendence and noninteraction with outside universe 12 p1848 A72-28152
- Luminosity variation of star in circular orbit around extreme Kerr black hole due to Doppler effects and gravitational field light focusing 13 p2041 A72-29416
- Relativistic analysis for synchrotron gravitational radiation emitted by particle in circular orbit around Schwarzschild black hole, noting astrophysical implications 13 p2007 A72-30123
- Black holes due to gravitational collapses, including radiation emission/absorption, pulsars and binary stars 14 p2151 A72-30478
- Relativistic theory gravitational analogue to electromagnetic radiation, suggesting black hole collision as galactic center flux mechanism 15 p2273 A72-31286
- Coordinate system valid for Oppenheimer-Snyder spherical dust cloud collapse into black hole 16 p2452 A72-33046
- Time evolution of a rotating black hole immersed in a static scalar field. 17 p2605 A72-34536
- Static black hole noninteraction with exterior world by meson fields, noting baryon number conservation in general relativity 17 p2612 A72-35388

Weak electromagnetic fields around a rotating black hole. 17 p2612 A72-35391

Russian book - Theory of gravitation and the evolution of stars 17 p2613 A72-35452

Pulses of gravitational radiation of a particle falling radially into a Schwarzschild black hole. 18 p2711 A72-36714

Quantum fields interaction with classical sources on Schwarzschild background, noting mass, charge and angular momentum as sole measurable quantum numbers of black hole 18 p2726 A72-36716

Collapsed objects absence in eccentric binary star systems and nonevidence of black holes formation effect on multiple line binaries 18 p2729 A72-36983

Black hole rotational energy extraction by super-radiant scattering with impinging wave amplification and by floating particle orbits with zero net radiation reaction 19 p2857 A72-37720

Gravitational spin interaction. 19 p2835 A72-38425

Polarization characteristics of Schwarzschild black hole gravitational synchrotron radiation in terms of Stokes parameters 21 p3107 A72-41215

Black hole physics compatibility with thermodynamics second law formulation based on black hole area as entropy measure 21 p3085 A72-41216

Gravitational radiation from charged black holes. 23 p3336 A72-43499

Accretion disc models for compact X-ray sources. 24 p3435 A72-44828

Rotating black holes - Separable wave equations for gravitational and electromagnetic perturbations. 24 p3439 A72-45014

Radiation pressure supported stars, degenerate dwarfs, neutron stars and black holes high energy observations from space platforms 24 p3446 A72-45536

BLACK KNIGHT ROCKET VEHICLE

Waxwing solid propellant rocket motor design for third stage propulsion of Black Arrow satellite launcher 13 p2026 A72-28932

Black Arrow satellite launch vehicle attitude control as part of inertial guidance system, describing four-gimbal gyroscopically stabilized platform and associated electronics 21 p3115 A72-40121

BLACKBURN B-103 AIRCRAFT

U BUCCANEER AIRCRAFT

BLACKOUT [PHYSIOLOGY]

NT BLACKOUT PREVENTION

Aerospace vehicle acceleration effects on human performance, noting visual, motor and intellectual impairment levels relation to physiological tolerance limits 02 p0166 A72-11702

High carbohydrate diet-induced hypoglycemia as potential cause of pilot unconsciousness during flight acceleration [AD-736564] 06 p0767 A72-17878

BLACKOUT [PROPAGATION]

NT ATMOSPHERICS

NT COSMIC NOISE

NT DAWN CHORUS

NT ELECTROMAGNETIC NOISE

NT HISS

NT IONOSPHERIC CROSS MODULATION

NT IONOSPHERIC NOISE

NT IONOSPHERICS

NT SHOT NOISE

NT SUDDEN ENHANCEMENT OF ATMOSPHERICS

NT THERMAL NOISE

NT WHISTLERS

Pulse position modulation system for minimizing rf blackout during 2 kW S band reentry telemetry transmission 02 p0175 A72-12158

Spacecraft reentry communications, discussing plasma sheaths, blackout alleviation and flight experiments 05 p0628 A72-16562

BLACKOUT PREVENTION

Fainting prevention in flying personnel, discussing constitutional susceptibility, health irregularities, alcohol, heavy smoking, lack of sleep, emotions and medical histories 03 p0316 A72-13722

Bed rest and positive radial acceleration effect on peripheral visual response time, considering blackout or grayout prediction possibilities 12 p1766 A72-28297

BLADDER

Röntgenologic studies of the effects of rapid decompression and hypoxia on the gall bladder in cats. 19 p2758 A72-38705

BLADDER MECHANICS

U DIAPHRAGMS

BLADDERS

NT EXPULSION BLADDERS

BLADDERS [MECHANICS]

U DIAPHRAGMS [MECHANICS]

BLADE TIPS

Helicopter rotor tip drag relief estimate based on two dimensional drag divergence with Mach number, airfoil parameters and flight conditions 02 p0154 A72-12882

Constraining U-shaped frames for blade edges protection during hydrojet shot blasting of compressor blades for gas turbine engines 11 p1642 A72-26819

French monograph on flow near rotor blade tips, discussing three dimensional circulation and boundary layer effects, energy losses, velocity and pressure distributions, etc 14 p2069 A72-30950

Blade tip losses in banded axial turbines, noting effects of Mach number, initial flow turbulence and geometry 15 p2179 A72-31701

Linear air mass flow injection at helicopter rotor blade tips, considering effects on trailing vortex circulation strength [AHS PREPRINT 624] 17 p2484 A72-34498

Complex vortex core fine structure around propeller tip observed via smoke and stroboscopic lighting, presenting photographs 19 p2786 A72-37747

The dissipation of tip vortices by mass injection with application to rotor systems. 24 p3362 A72-45329

The use of complex coordinates in the study of rotor dynamics. [AIAA PAPER 72-954] 24 p3369 A72-45413

BLADES [CUTTERS]

Force distribution in refractory Ti alloy cutting with circular self turning blades, noting effects of feeding speed, cut area and cutter angle 13 p1966 A72-29467

BLANKS

Deformation limits in thin and thick walled metal blanks axisymmetric drawing process, determining stress-strain state based on prescribed velocity field 13 p1963 A72-28743

BLASIUS EQUATION

The linearized solutions as applied to the half-jet mixing. 18 p2683 A72-36928

BLASIUS FLOW

Rotation effects on three dimensional infinitesimal wave stability in Blasius boundary layer 02 p0205 A72-12354

Velocity distribution in mixing layer between fluid at rest and in uniform stream by solving Blasius equation with boundary points 05 p0653 A72-17078

BLAST DEFLECTORS

Scale model tests of high thrust engine blast deflection fence combinations for protection of adjacent roadway traffic 16 p2374 A72-33698

BLAST LOADS

Blast wave techniques for exothermic processes in relation to propulsion systems, using shock or detonation tubes, point explosions, reflected shocks and implosion vessels [AD-737415] 01 p0117 A72-10939

Cylindrically symmetric blast wave generated by infinitely long line explosion in cold and homogeneous gas rotating rigidly within self gravitational field 07 p1070 A72-19134

One dimensional blast wave theory for trajectory analysis of shocks driven by solid explosives in linear shock tubes 14 p2093 A72-30179

Diatomic gas flow behind blast wave, discussing vibrational nonequilibrium effects and solution of governing equations via characteristics method 16 p2378 A72-33440

Clamped circular rigid-plastic plates subjected to central blast loading. 22 p3235 A72-42601

Dynamic blast loads on preheated and prestressed thin plates. 24 p3454 A72-44607

Aircraft structures shock and blast loading characteristics from internal detonation, comparing computer program results with available data 24 p3365 A72-44610

Effect of a line energy source at the boundary of a supersonic flow. 24 p3361 A72-45187

BLASTOFF

U ROCKET LAUNCHING

BLEACHING

Amplitude holograms diffraction effectiveness increase by conversion to phase holograms through photoemulsion bleaching, evaluating various bleaching agents effectiveness 05 p0663 A72-16614

BLOOD

High efficiency low noise volume /Lippmann-Bragg/ holograms recorded on photographic plate, using bleaching-darkening procedure 11 p1629 A72-25316

Holograms with high diffraction efficiency, describing bleaching experiments and SNR measurements in reconstructed image 12 p1810 A72-27887

Consensual photopupil responses to light flashes recorded in full dark adaptation, noting bleaching and backgrounds effects 13 p1907 A72-29969

Dark adaptation studies of bleach-induced visual threshold rise and subsequent return to rhodopsin level 15 p2184 A72-31365

Rhodamine 6G photodegradation resistance improvement in cooled solid matrices of polymethylmethacrylate, investigating time and temperature dependence of bleaching by linearly polarized lasers 16 p2401 A72-33386

Holograms with high diffraction efficiency, describing bleaching experiments and SNR measurements in reconstructed image 16 p2395 A72-33996

Isolated retina receptor potential amplitude relation to visual pigment bleaching kinetics, indicating excitation-inhibition receptor response generation mechanism 19 p2756 A72-37830

The photopigment bleaching hypothesis of complementary after-images - A psychophysical test. 23 p3258 A72-44376

GaAs semiconductor injection laser and amplifier-absorber emission and light pulse transmission characteristics determination, noting nonlinear absorptivity, bleaching threshold and pulse compression factor 24 p3412 A72-45619

BLEED-OFF

U PRESSURE REDUCTION

BLEEDING

Air bleeding location to cool turbojet engine turbine of supersonic aircraft, presenting graphs 12 p1862 A72-28147

Suppression effects of hyperoxic breathing gases on red blood cell and erythropoietin hormone production following blood loss 12 p1766 A72-28298

Effects of long periods of clinical death from drowning or lethal blood loss on higher nervous activity in reanimated dogs 13 p1902 A72-28642

Bioelectric activity of the medulla oblongata during hypothermia and bloodletting 17 p2504 A72-35024

BLENDS

U MIXTURES

BLIND LANDING

Carrier system for controlled approach of Naval aircraft to provide pilot window to deck for tactical jet guidance for poor visibility landing 02 p0256 A72-12323

Head-up display flying under IMC and VMC flight conditions, considering takeoff, landing and navigation modes 08 p1204 A72-21004

BLINDNESS

NT FLASH BLINDNESS

Neural substrates of sensory tactile vision substitution for information mediation in blind subjects, using TV camera 01 p0011 A72-10470

BLISTERS [PROTUBERANCES]

U PROTUBERANCES

BLOCH BAND

Bloch walls and Landau domain configurations in iron whiskers from DC to 200 kHz by direct magnetization measurements 11 p1659 A72-25912

Orbiting electron magnetic susceptibility derivation from many band Hamiltonian using Bloch representation to avoid decoupling transformation ambiguity 15 p2282 A72-32547

BLOCKING

Mass blocking of subsonic isentropic swirling flow through convergent axisymmetric nozzle, considering radial velocity component effect on vorticity 03 p0342 A72-13957

Pyrometric obturation devices effect on sample temperature level during high temperature tests with radiant heating 13 p1960 A72-29903

Steady two dimensional motion during horizontal motion of body at high Richardson number in stratified fluid, considering blocking mechanism 21 p2990 A72-40653

BLOOD

NT ERYTHROCYTES

NT LEUKOCYTES

NT LYMPHOCYTES

NT RETICULOCYTES

NT THROMBOPLASTIN

NT WHITE BLOOD CELLS

CO hemoglobin concentration measurement in blood of smokers, nonsmokers and deceased crewmembers of crashed aircraft

01 p0010 A72-10211

Chronic microwave irradiation effects on experimental animal blood forming systems, examining peripheral blood count changes and nuclei and mitosis abnormalities in erythroblastic and lymphoid cells

02 p0158 A72-11708

Biological dosimetry in acute human irradiation from cytogenic study of peripheral blood and bone marrow

04 p0467 A72-14606

Organism blood volume and losses determination by measuring human body electrical resistance, noting unsatisfactory results

06 p0768 A72-17994

Temperature effects on blood electrobioluminescence, relating luminescence peaks to protein and lipid molecular structure changes

09 p1268 A72-23694

Continuous and intermittent maximal exercise effects on human muscle intracellular and capillary blood pH

10 p1425 A72-24477

Human oxygen intake and blood lactic acid removal kinetics during recovery from mild steady work on bicycle ergometer

10 p1426 A72-24989

Light absorption and scattering factors in whole blood related to hemoglobin concentration, discussing oxygen saturation, cardiac output and pathological conditions

11 p1588 A72-26630

Human centrifuge studies of high positive acceleration effects on blood oxygenation and arterial oxygen and carbon dioxide tension

12 p1766 A72-28287

Serum cholesterol, phospholipid and lipoprotein levels relation to atherosclerotic heart disease occurrence in USAF personnel

12 p1766 A72-28292

Radioprotectants /mexamine and cystamine/ effects on histo-hematic barrier permeability in rats under hypokinetic conditions

13 p1904 A72-29308

Hemoglobin determination in whole blood with Specol-Zeiss spectrophotometer, comparing accuracy to cyanmethemoglobin measurements

14 p2080 A72-30787

Low molecular active hormones isolation from cat blood, obtaining eluates with phosphate buffer by chromatography

14 p2077 A72-30971

Hyperbaric environment decompression effects on human blood and urine chemistry and hemostatic system, showing physiological parameter alteration in presence and absence of bends symptoms

14 p2081 A72-31087

Rebreathing studies of carbon dioxide pressure level effect on carbon dioxide content difference in arterial blood and alveolar gas during exercise and rest

17 p2499 A72-34346

Interaction of chronic hypoxia and hypercapnia upon blood gases and acid base status.

17 p2504 A72-35166

Effects of free amino acid doses and of amino acid metabolism cofactors on the distribution of regional free amino acid resources in the brain and blood of animals

20 p2891 A72-39324

Effect of copper, cobalt and manganese salts on certain morphological-biochemical components of the blood in young sheep of the Hissar breed

20 p2893 A72-40075

Comparative studies of the respiratory functions of mammalian blood.

21 p3002 A72-40919

Cardiac output, arterial and mixed-venous O₂ saturation, and blood O₂ dissociation curve in growing rats adapted to a simulated altitude of 3500 m.

21 p3003 A72-41623

Dependence of muscle efficiency on oxygen concentration in the venous blood

22 p3141 A72-42157

Experimental studies on the alkali-acid equilibrium in the blood gases under the chronic action of low concentrations of lead.

24 p3374 A72-44824

Acrylamide polymerization - New method for determining the oxygen content in blood.

24 p3376 A72-45376

Interactions between gas bubbles and components of the blood - Implications in decompression sickness.

24 p3374 A72-45652

Human left ventricular volume determined by peripheral venous scintillation angiocardigraph isotope method, comparing with X ray method

02 p0157 A72-11475

Blood viscosity and distributed external constraints and viscoelastic properties of vessels effects on wave dispersion and dissipation in arteries and veins, using membrane model

04 p0481 A72-15466

Viscosity and constraints effects on wave dispersion and dissipation in blood vessels, comparing theory with experiments on dogs

04 p0481 A72-15467

Hydrodynamic model of human systemic arterial circulation to test artificial heart pumps [ASME PAPER 71-WA/AUT-13]

05 p0621 A72-15954

Blood self purification enteral mechanism in dogs, determining leukocyte population changes before and after feeding and intravenous interferon injections

07 p0915 A72-18867

Fluid mechanics of blood pulsatile flow in microcirculation, considering plasma layer nature and trans-capillary mass transfer

07 p0931 A72-20087

Nonlinear model for computer simulation of human arterial system, using finite difference technique for pressure and flow calculations

07 p0934 A72-20357

Blood circulation minute volume and peripheral resistance changes during human aging process, accounting for body weight

08 p1120 A72-22073

Cardiovascular system model for demonstration of biological system analog simulation and computation, describing components for heart pumping action and systemic circulation

09 p1268 A72-22454

Hydraulic transmission line equations for computer simulation of arterial circulatory systems

10 p1431 A72-24811

Electrocorticograph monitoring of central nervous system state in dogs reanimated by artificial blood circulation after prolonged clinical death by drowning

12 p1764 A72-28215

Water immersion tests to study body fluid balance disturbances during weightlessness, observing diuretic reflex control of blood volume

16 p2355 A72-33551

Simulation of the human cardiovascular system - A model with normal responses to change of posture, blood loss, transfusion, and autonomic blockade.

17 p2507 A72-34445

Pharmacological effects on the central adrenergic regulation mechanisms of blood circulation

17 p2504 A72-35019

Russian book - Intracranial blood circulation under conditions of accelerations and weightlessness

17 p2509 A72-35460

Vasopressin /antidiuretic hormone/ role in central vascular volume and fluid balance maintenance during continuous positive pressure breathing in dogs

17 p2505 A72-35917

Circulatory assist and ballistocardiographic studies; Proceedings of the Fifteenth Annual Meeting, Atlantic City, N.J., May 1, 1971.

18 p2648 A72-36032

Control of the circulating blood mass in the case of a functional detachment of various amounts of pulmonary tissue

21 p3012 A72-41825

Analysis of femoral venous blood during maximum muscular exercise.

22 p3145 A72-42742

Hypothalamic control of the systemic and lung circulation and functional significance of this control

22 p3148 A72-43168

BLOOD COAGULATION

Human coagulating and anticoagulating blood system changes due to emotional stress during parachute jumps, noting plasma recalcification time increase

04 p0474 A72-15233

Microcirculation study of intravascular erythrocyte aggregation /blood sludge/ in rats

07 p0920 A72-19686

Dietary lipid effect on platelet adhesion and aggregation, blood coagulation and fibrinolysis and relation to atherosclerosis and thrombosis

08 p1117 A72-21543

Thromboelastographic study of renin and angiotensin effect on blood clotting system of anesthetized and unanesthetized dogs

08 p1121 A72-22095

Increased atmospheric pressure influence on blood coagulation in rabbits, showing post-decompression hypercoagulation followed by hypocoagulation

09 p1268 A72-23597

Ascorbic acid influence on blood coagulation and anticoagulation systems in dogs with acute hypoxia, discussing plasma recalcification time and heparin tolerance

12 p1764 A72-28217

Thromboelastographic and coagulographic studies of gravitational effects on blood coagulation in cats under acceleration stress

13 p1904 A72-29309

Blood coagulation changes at high altitude predisposing to pulmonary hypertension.

17 p2498 A72-34222

Hypocapnic hypoxia effects on blood coagulation and fibrinolysis

19 p2756 A72-37880

Blood coagulation behavior in rats under fall induced intense trauma, attributing phenomenon to increase in extrinsic thromboplastin from damaged tissue

21 p3002 A72-41194

BLOOD FLOW

Computer controlled scintiscanning for pulmonary blood flow distribution, discussing real time data monitoring, contour plots and three dimensional and wall reflection maps

01 p0020 A72-11038

Computer aided biplane roentgen videometry system for dynamic circulatory structure studies including blood flow and heart volume determination

01 p0020 A72-11040

Oxygen distribution in human brain under counter-current capillary blood flow conditions, presenting mathematical simulation for transport in Krogh system

02 p0168 A72-12037

Implanted telemetry development for cardiovascular research, discussing blood pressure, flow and hydraulic impedance relationships

02 p0169 A72-12140

Epinephrine and norepinephrine effects on cerebral blood circulation volume and oxygen tension in tissues

02 p0165 A72-12517

Human arm arterial pressure and flow pulsations numerical analysis, constructing electrical analog circuit from mathematical model

03 p0317 A72-12951

Ballistocardiographic measurement of net cranial blood inflow during cardiac ejection

03 p0314 A72-13145

Xenon 133 myocardial clearance method accuracy and reliability in determining high and low left coronary artery blood flow under different hemodynamic conditions

03 p0319 A72-13181

Myocardial blood flow measurement by Xe 133 clearance method after direct application of isotope into subendocardial and subepicardial layers of left ventricle

03 p0315 A72-13182

Holographic measurement of red blood cell rotation in orifice flow, transforming orientation into form distribution data

04 p0479 A72-15140

Steady state heat transfer problem solutions in living tissue modeled as cylindrical shells, discussing blood flow and temperature distributions in extremities

[ASME PAPER 71-WA/HT-34]

Analytical model for living biological tissue transient heat transfer, taking into account conduction, storage, generation, convection and blood flow effects

[ASME PAPER 71-WA/HT-36]

Approximate numerical method for calculating flow profiles in arteries from local pressure measurements, taking into account Navier-Stokes equations nonlinear terms

[ASME PAPER 71-WA/BHF-3]

In vivo investigation of dogs natural mitral valve flow dynamics, developing cardiohemodynamic system physical model for data analysis and electrical analog simulation

[ASME PAPER 71-WA/BHF-2]

Light scattering time dependence, erythrocyte aggregation rates and hydrodynamic characteristics in ox, pig and horse blood stream

05 p0621 A72-16230

Cardiac murmur level dependence on blood stream Reynolds number, tracing cardiac noise origin to blood turbulence

06 p0762 A72-17676

Blood flow mathematical formulation, considering tissues constitutive equations, geometrical configurations, arterial wave propagation, etc

06 p0768 A72-17959

Hyperoxia effect on kidney blood flow erythropoietic properties in rabbits, noting inhibiting effect on erythroblast cells mitotic activity in bone marrow culture

06 p0765 A72-18061

Reciprocal temperature changes in dogs during constant thermomodulation for coronary sinus blood flow measurement

06 p0769 A72-18197

Microcirculation study of intravascular erythrocyte aggregation /blood sludge/ in rats

07 p0920 A72-19686

BLOOD CIRCULATION

- NT BRAIN CIRCULATION
- NT CARBOXYHEMOGLOBIN
- NT CORONARY CIRCULATION
- NT INTRACRANIAL CIRCULATION
- NT INTRAVASCULAR SYSTEM
- NT ISCHEMIA
- NT PULMONARY CIRCULATION

- Fluid mechanics of blood pulsatile flow in microcirculation, considering plasma layer nature and transcapillary mass transfer
07 p0931 A72-20087
- Aortic flow disturbances in vivo study by hot-film anemometer, considering peak flow velocity and pulse rate effects
07 p0934 A72-20537
- Muscle blood flow relation to oxygen consumption from measurements during bicycle ergometer exercises, using Xe 133 clearance method
08 p1123 A72-20888
- Splanchnic vascular bed role in human blood pressure regulation from lower body negative pressure tests, measuring blood flow from hepatic dye removal rates
08 p1123 A72-20889
- Beta-adrenergic inhibitors effects on coronary blood flow and myocardial oxygen consumption of normal and coronary artery disease patients
08 p1118 A72-21549
- Electromagnetic velocity and flow measurements techniques application to cardiovascular patients, discussing utilization problems
09 p1272 A72-23275
- Alternative heating local heat clearance probes for human muscle blood flow measurement
09 p1273 A72-23442
- Ultrasonic Doppler flowmeter for instantaneous measurement of blood vessel flow velocity by averaging frequency shift over received signal power density spectrum
10 p1430 A72-24373
- On-line analog display system for cardiovascular functions and beat-by-beat cardiac output derived from single aortic blood flow measurement
10 p1430 A72-24375
- Arterial velocity profiles measurement in dogs thoracic aorta by hot-film probe, relating flow disturbances and turbulence to Reynolds number
10 p1431 A72-24468
- Mathematical model for arterial system pressure, blood flow and dimensional changes, examining cardiac ejection dynamics and vasculature mechanical properties and viscoelasticity
10 p1432 A72-24812
- Assessment of regional myocardial temperature changes effect on blood flow measurements by heated cross-thermocouples in dogs
10 p1432 A72-25071
- Electronic and hematocrit devices to investigate cardiovascular system functions including blood coagulation process, pressure and flow
11 p1585 A72-26464
- Forearm skin and muscle blood flow change measurements during whole body heating, using plethysmography, isotopic labeling and blood sampling techniques
11 p1587 A72-26617
- Hemodynamic variables relation to coronary blood flow and myocardial oxygen consumption during upright bicycle exercise
11 p1587 A72-26618
- Water filled volume and strain gage phthysmography for forearm blood flow measurement during isometric exercise
11 p1587 A72-26622
- Vascular-capillary study of age related angioarchitectonic features of human brain optic lobe
11 p1580 A72-26675
- Sheet flow theory for pulmonary alveolar blood flow, discussing blood pressure effects, membrane tension, blood volume and transit time distribution
11 p1589 A72-26702
- Left ventricular dynamic function in terms of internal diameter, pressure and flow in dogs at rest and during isoproterenol and metaraminol infusions
11 p1582 A72-26773
- Hemodynamic assessment of arterial blood flow from radiograph measurements of aorta branching points
11 p1582 A72-26774
- Fluid mechanics of left ventricle model with mitral and aortic valves, showing ring vortex relation to diastole and closure
11 p1589 A72-26775
- Instantaneous and continuous blood flow velocity measurement by Doppler ultrasonic flowmeter using transcutaneous and implanted probes
11 p1589 A72-26778
- Isotopic labeled microspheres for cat uveal and retinal blood flow and oxygen consumption determination, studying increased intraocular pressure and carbon dioxide tension effects
12 p1763 A72-27841
- Acceleration stress effects on splanchnic blood flow due to organ displacement and neurogenic vasoconstriction in vascular beds
12 p1765 A72-28285
- Tilt table test for gravitational stress effects on human pulmonary capillary blood flow
12 p1765 A72-28286
- Autonomic nervous system role in controlling coronary and cardiac responses to hypoxic hypoxia, measuring blood flow with Doppler ultrasonic flow transducer
12 p1767 A72-28313
- Human acceleration stress tolerance monitoring techniques for temporal, brachial and radial arterial blood flow and indirect systolic and diastolic blood pressure measurements
12 p1777 A72-28328
- Coronary system autoregulation patterns and mechanisms from coronary flow shift measurements during circumflex artery perfusion experiments in dogs
13 p1901 A72-28637
- Whole blood flow dependence on optical density from light transmission measurement, showing photometric effects of red cell aggregation, deformation and orientation
15 p2185 A72-31639
- Light transmission measurements of blood flow to quantify red cell aggregation and dispersion
15 p2185 A72-31640
- Increase in skeletal muscle performance during emotional stress in man.
17 p2500 A72-34942
- Mathematical models for flow ejection and aorta pressures based on displacement ballistocardiography and time dependent incompressible flow theories respectively
18 p2649 A72-36035
- Coronary flow determination in experimental conditions with the use of radioactive xenon.
19 p2755 A72-37475
- Coronary collateral circulation and myocardial blood flow reserve.
19 p2755 A72-37500
- Temporal relation of the second heart sound to aortic flow in various conditions.
19 p2759 A72-38818
- motion.
20 p2891 A72-38935
- A modified acetylene method for the determination of cardiac output during muscular exercise.
20 p2898 A72-39807
- Influence of intracellular convection on the oxygen release by human erythrocytes.
21 p3003 A72-41625
- Blood flow, oxygen uptake, and capillary filtration in resting skeletal muscle.
22 p3150 A72-42668
- The effect of hypoxia on the coronary blood flow in reserpinized dogs.
24 p3370 A72-44562
- Analysis of a nuclear magnetic resonance blood flowmeter for pulsatile flow.
24 p3401 A72-44574
- BLOOD PLASMA**
- Stabilized human plasma protein solution analysis, noting albumin presence
03 p0316 A72-13855
- Plasma renin activity during supine physical exercise as function of salt loading
04 p0480 A72-15214
- Hemodynamic and blood oxygen parameter changes comparison in dogs during hypoxia at rest and muscle activity in various oxygen concentrations
04 p0474 A72-15232
- Conversion of angiotensin to angiotensin 2 in dog pulmonary circulation, studying peptide synthesis, radioimmunoassay and in vivo and plasma in vitro metabolism
04 p0475 A72-15465
- Plasma erythropoietin concentration in men and mice during altitude acclimatization
07 p0917 A72-19440
- Acid base balance in arterialized capillary blood in men after maximal short duration exercise
07 p0929 A72-19441
- Thermal stability variations in blood serum protein after electrical stimulation of rabbit hypothalamic structures
07 p0920 A72-19649
- Wien intravascular effect on plasma carbon dioxide gradients near pulmonary capillary wall, discussing free energy requirements
08 p1114 A72-20890
- Light-dark cycles and physiological stress stimuli effects on circadian rhythm in rat blood serum serotonin levels
08 p1115 A72-21081
- Dose dependent hyperglycemia and hypopolemia response to pentobarbital sodium injection in rats from plasma glucose and fatty acid analysis
08 p1116 A72-21187
- Lipid metabolism abnormality relation to hypothyroidism leading to atherosclerosis, noting thyroid parenchyma atrophy from autoimmune thyroiditis
08 p1117 A72-21544
- Blood lipid levels and dietary habits in atherosclerotic and healthy subjects, showing lipid and glucose metabolism disturbance increase in coronary cases
08 p1117 A72-21546
- Corticosterone content in blood plasma, cerebral cortex and skeletal muscles during hypoxia adaptation in rats
08 p1121 A72-22083
- Inhibitive effect of immobilization on urinary catecholamine excretion and blood plasma thyroxine level in rats
09 p1265 A72-22648
- Blood serum proteins thermal stability in patients with vegetative vascular and neuroendocrine syndromes, discussing ATP effects
09 p1266 A72-22877
- Human blood serum 11-oxy corticosteroid content after maximum stress exercise, noting heart rate and blood pressure changes
09 p1266 A72-22878
- Prolonged water immersion effects on renal function and plasma volume in trained and untrained subjects, noting deleterious effect on orthostatic tolerance and work capacity
10 p1428 A72-23738
- Urine and plasma protein and creatinine measurements in acclimatized and unacclimatized men before, during and after high altitude ascent
10 p1426 A72-24482
- Serum peptidase activity determination as enzymatic diagnostic test for myocardial infarction
11 p1579 A72-25851
- Myocardial infarction stress effect on serum cortisol, plasma free fatty acid and urinary catecholamine levels
11 p1582 A72-26787
- Bed rest and centrifuging effects on human plasma thyroid hormone level, discussing total protein, albumin and thyroxine binding globulin concentrations
12 p1770 A72-27477
- Multihour immersion effects on blood plasma protein and electrolyte concentration in trained and untrained subjects
12 p1770 A72-27480
- Red cell mass plasma volume decrease in Apollo mission crews, indicating erythropoiesis inhibition
12 p1765 A72-28266
- Plasma protein concentration, volume and hematocrit changes during exercise, bed rest and high forward acceleration
12 p1766 A72-28296
- Monovalent K and Na and bivalent Ca and Mg plasma ion ratio effect on thrombocyte electrokinetic potential
13 p1901 A72-28635
- Mechanical vibration induced physiological changes in rats, determining plasma Ca, Mg and inorganic phosphate concentration and xanthine oxidase activity response to frequency and g-levels
13 p1910 A72-29560
- Hypokinesia effect on fluid and electrolyte metabolism change patterns in rabbits from blood plasma studies
14 p2075 A72-30389
- Effects of in vivo inhalation of 100% oxygen at reduced pressure on serum and red cell lipids.
[AD-746090] 17 p2508 A72-34553
- Disproportional changes in hematocrit, plasma volume, and proteins during exercise and bed rest.
17 p2506 A72-35966
- Algorithms for selected blood acid-base and blood gas calculations.
17 p2510 A72-35973
- Fluid transfer between blood and tissues during exercise.
18 p2650 A72-36560
- Hypoxic theory for atherosclerosis formation, noting blood plasma protein concentration effects on oxygen diffusion
18 p2651 A72-37030
- The effect of chronic erythrocytic polycythemia and high altitude upon plasma and blood volumes.
19 p2757 A72-38028
- Effect of beta-adrenergic blockade on plasma volume in human subjects.
19 p2757 A72-38029
- Variation of the acetylcholine content and of the cholinesterase activity in the blood under muscular strain
20 p2891 A72-38934
- Hemopoiesis in the pig-tailed monkey *Macaca nemestrina* during chronic altitude exposure.
20 p2892 A72-39344
- Nervous and humoral stimulation and hypoxia effects on erythropoiesis control, studying human blood serum additions to bone marrow cultures
21 p3001 A72-40762
- Blood serum enzymes activity changes in polytraumatized humans injured in automobile accidents
21 p3002 A72-41188
- Human plasma free fatty acids relation to lactic acid concentration and maximum aerobic power, noting carbohydrate availability as exercise capacity limiter
21 p3003 A72-41520
- Effect of hypoxia and physical activity on plasma enzyme levels in man.
21 p3003 A72-41522

- Changes in blood serum proteins under the effect of hyperoxia in intact rats with thyroid gland dysfunction 22 p3142 A72-42283
- Effects of the space flight environment on man's immune system. I - Serum proteins and immunoglobulins. 22 p3150 A72-42493
- Quantitation of serum proteins on whole blood-electroimmunodiffusion technique applicable to capillary blood. 22 p3150 A72-42495
- Human prolactin - 24-hour pattern with increased release during sleep. 23 p3316 A72-43977
- Metabolism of angiotensin II in sodium depletion and hypertension in humans. 23 p3257 A72-43998
- Human blood monocytes - Stimulators of granulocyte and mononuclear colony formation in vitro. 24 p3373 A72-45374
- BLOOD PRESSURE**
- NT HYPERTENSION**
- NT SYSTOLIC PRESSURE**
- Right heart ventricle intracardiac phonocardiograms, recording pulmonary early diastolic click simultaneous with artery pressure curve diastolic wave 01 p0010 A72-10121
- Femoral arterial blood pressure third order waves onset mechanism in narcotized dogs, noting changed blood and respiration dynamics 02 p0160 A72-12014
- Implanted telemetry development for cardiovascular research, discussing blood pressure, flow and hydraulic impedance relationships 02 p0169 A72-12140
- Human arm arterial pressure and flow pulsations numerical analysis, constructing electrical analog circuit from mathematical model 03 p0317 A72-12951
- Spinal mesenteric vascular reflexes of vasoconstriction effect of pressure drop in coeliac artery relation to Rein nutritional hepatic reflex 04 p0473 A72-15125
- Splanchnic vasoconstriction in hyperthermic man independent of falling blood pressure 04 p0480 A72-15217
- Cat mean renal nerve activity modification by hypothalamus stimulation and baroreceptor reflex interactions, discussing mean aortic pressure variation effects 04 p0477 A72-15722
- Dog mesentery terminal venous microvessel distensibility characteristics from response to arterial and venous pressure changes 06 p0765 A72-18196
- Carotid sinus counterpressure as baroreceptor stimulus in intact dog, recording arterial pressure response in closed loop gain 07 p0917 A72-19439 [AD-739805]
- Intravascular pressure and extravascular structure effects on radial and longitudinal distensibility of arterial microvessels in dog mesentery 07 p0922 A72-20426
- Improperly controlled learning processes relationship to hypertonic blood pressure irregularities pathogenesis in rats, investigating negative emotional reactions effects 07 p0925 A72-20659
- Sex differences of chronic effect of environmental stress on blood pressure and information processing in rats, observing neurotic hypertonic blood pressure irregularity 07 p0925 A72-20660
- Autonomic blockade effects on reflex bradycardia due to phenylephrine induced arterial pressure in man during rest and supine exercise 07 p0925 A72-20688
- Splanchnic vascular bed role in human blood pressure regulation from lower body negative pressure tests, measuring blood flow from hepatic dye removal rates 08 p1123 A72-20889
- Cardiovascular analog computing circuits with outputs for left ventricular pressure maximum rise rate, cardiac stroke volume and atrioventricular conduction time 08 p1124 A72-20899
- Pulsatile blood pressure and ECG in squirrel monkeys, considering catheter electromanometer system and implanted arterial cannulas long stability 08 p1124 A72-20900
- Digital simulation of human cardiovascular system, noting blood pressure control by physiological reflexes 08 p1125 A72-21475
- Pulmonary capillary bed filling as function of arterial pressure in perfused frozen dog lungs 10 p1425 A72-24480
- Open capillaries control mechanism of pulmonary diffusion capacity, presenting mathematical interpretation of humoral and hydraulic blood pressure control 10 p1426 A72-24787
- Mathematical model for arterial system pressure, blood flow and dimensional changes, examining cardiac ejection dynamics and vasculature mechanical properties and viscoelasticity 10 p1432 A72-24812
- Electronic and hematocrit devices to investigate cardiovascular system functions including blood coagulation process, pressure and flow 11 p1585 A72-26464
- Sheet flow theory for pulmonary alveolar blood flow, discussing blood pressure effects, membrane tension, blood volume and transit time distribution 11 p1589 A72-26702
- Left ventricular dynamic function in terms of internal diameter, pressure and flow in dogs at rest and during isoproterenol and metaraminol infusions 11 p1582 A72-26773
- Arterial pressure data recording technique using magnetic tape recorder and automatic conversion to digital form 12 p1772 A72-27649
- Single linear measure of systolic pressure gradient for calculation of aortic valve area in stenosis severity assessment 12 p1762 A72-27734
- Piezoelectric transducer for indirect on-wrist blood pressure measurements for clinical environment 12 p1772 A72-27961
- Arterial blood gas tensions, using sequential phased dilution for pilot oxygen delivery 12 p1764 A72-28255
- Human acceleration stress tolerance monitoring techniques for temporal, brachial and radial arterial blood flow and indirect systolic and diastolic blood pressure measurements 12 p1777 A72-28328
- Prevention of weightlessness effects on blood hydrostatic pressure, musculoskeletal system and sensorimotor performance, discussing space flight training and space environment simulation tests 13 p1909 A72-28787
- Automated constant cuff-pressure system to measure average systolic and diastolic blood pressure in man. 17 p2507 A72-34298
- Hemodynamic changes in man during immersion with the head above water. 17 p2507 A72-34543
- Mathematical models for flow ejection and aorta pressures based on displacement ballistocardiography and time dependent incompressible flow theories respectively 18 p2649 A72-36035
- Effects of vagotomy and increased blood pressure on the incidence of decompression-induced pulmonary hemorrhage. 18 p2650 A72-36446
- Systemic haemodynamics in borderline arterial hypertension - Responses to static exercise before and under the influence of propranolol. 19 p2756 A72-37773
- Determination of systolic time intervals using the apex cardiogram and its first derivative. 19 p2759 A72-38817
- Implantable blood pressure telemetry system. 19 p2762 A72-38824
- Relationship of pulmonary artery to left ventricular diastolic pressures in acute myocardial infarction. 20 p2892 A72-39461
- An indirect method for evaluation of left ventricular function in acute myocardial infarction. 20 p2892 A72-39462
- Separation of central effects of CO₂ and nicotine on ventilation and blood pressure. 21 p3001 A72-40918
- Tilt table tests for orthostatic tolerance, measuring heart rate, blood pressure and responses of fainthearts and nonfainters 21 p3008 A72-41020
- Effect of fasting on tolerance to moderate hypoxia. 22 p3150 A72-42487
- Carotid rete role in brain protection against extreme elevations of systemic blood pressure, presenting goat cerebral blood flow measurement procedure 22 p3144 A72-42671
- Spinal cord heating and cooling effects on body temperature, respiratory and heart rates and arterial blood pressure, investigating feeding and drinking behaviors 22 p3150 A72-42672
- Control parameters of the blood-pressure regulatory system. I - Heart rate sensitivity. 22 p3145 A72-42771
- Control parameters of the blood-pressure regulatory system. II - Open-loop gain, reference pressure and basal heart rate. 22 p3145 A72-42772
- Lower-body negative pressure as a method of preventing shifts associated with changes in the hydrostatic pressure of blood 23 p3256 A72-43919
- Evaluation of the pulse-contour method of determining stroke volume in man. 23 p3256 A72-43934
- Use of implantable telemetry systems for study of cardiovascular phenomena. 23 p3260 A72-43996
- Increased fluid turnover and the activity of the renin-angiotensin system under various experimental conditions. 23 p3257 A72-43997
- Carotid displacement pulse first time derivative recording as noninvasive technique for heart function assessment 24 p3370 A72-44561
- General index for the assessment of cardiac function. 24 p3372 A72-45011
- BLOOD VESSELS**
- NT AORTA**
- NT ARTERIES**
- NT CAPILLARIES (ANATOMY)**
- NT GLOMERULUS**
- NT VEINS**
- Distensibility and stress relaxation characteristics of capacitance and resistance vessels of isolated rabbit ear as function of basal tone 04 p0473 A72-15124
- Viscosity and constraints effects on wave dispersion and dissipation in blood vessels, comparing theory with experiments on dogs 04 p0481 A72-15467
- Teflon diffusion membrane for in vivo blood and intramycardial tissue gas tension measurement by mass spectroscopy without chemically bonded heparin surface 08 p1124 A72-20901
- Ultrasonic Doppler flowmeter for instantaneous measurement of blood vessel flow velocity by averaging frequency shift over received signal power density spectrum 10 p1430 A72-24373
- TV microscopic system for on-line measurement of cat omentum microvessels diameter relative to heart action 11 p1587 A72-26621
- Irreversibility mechanism in postpartum ductus arteriosus closure in guinea pigs, studying vessel cellular changes and smooth muscle response to oxygen pressure 12 p1762 A72-27826
- Platelet aggregates role in intramycardial vessel circulation impedance in patients dying suddenly of coronary artery disease 15 p2186 A72-31770
- Mathematical model for flow limitation in collapsible tube in relation to pressure in pulmonary and circulatory system 17 p2510 A72-35972
- Coronary collateral circulation and myocardial blood flow reserve. 19 p2755 A72-37500
- Blood vessel reactions to natural defense and conditioned reflexes from plethysmography and blood pressure measurements, discussing cortical effects mechanisms 21 p3000 A72-40758
- Unresponsiveness of pial precapillary vessels to catecholamines and sympathetic nerve stimulation. 22 p3140 A72-41934
- Effect of vibration on the permeability of the blood-brain barrier 22 p3149 A72-42070
- Resistance and capacitance vessels of the skin in permanent and temporary residents at high altitude. 22 p3144 A72-42595
- Photoelastic analysis of cardiovascular-magnitude stress pattern produced by flow through gelatin-agar walled channels for analysis of mechanical stresses on blood vessel walls 23 p3260 A72-43936
- BLOWDOWN WIND TUNNELS**
- Blowdown wind tunnel internal and external noise fields prediction by empirical method, considering valves, burners, turbulent boundary layers and exhaust jets as sources [AIAA PAPER 72-668] 16 p2374 A72-34070
- Generating high Reynolds-number flows. 19 p2787 A72-38222
- Flow quality improvements in a blowdown wind tunnel using a multiple shock entrance diffuser. [AIAA PAPER 72-1002] 21 p3041 A72-41587
- Computer control of the General Dynamics High Speed Wind Tunnel. 22 p3157 A72-42697
- An initial two-dimensional wall interference investigation in a transonic wind tunnel with variable porosity test section walls. [AIAA PAPER 72-1011] 24 p3389 A72-45409
- BLOWERS**
- Influence of revolutions on efficiency and characteristics of the rotating axial cascade of blades. 24 p3363 A72-45361
- BLOWING**
- Navier-Stokes equations asymptotic solution for compressible weightless conducting fluid flow in plane channel with intense blowing from walls 05 p0648 A72-16219

Tangential blowing and wall cooling effects on axisymmetric models flow separation at Mach 6, comparing pressure distribution with Busemann formula 05 p0601 A72-16227

Forebody blowing induced dynamic instability effect on slender cones at hypersonic speeds, presenting theory based on unsteady imbedded Newtonian flow concepts [AIAA PAPER 72-31] 05 p0607 A72-16919

Jet peak velocity decay in single and multielement nozzles for STOL aircraft externally blown flaps, noting noise reduction due to flow mixing [AIAA PAPER 72-48] 05 p0608 A72-16927

Wall blowing discontinuity effect on two dimensional incompressible turbulent boundary layers, discussing flow relaxation length separation by penetration point trajectory 07 p0966 A72-18841

Initial dynamic length effects on heat transfer in turbulent boundary layer with blowing demonstrated by subsonic wind tunnel tests 08 p1151 A72-21665

Buccaneer Mk 2 and F-4K Phantom takeoff and landing performance improvement due to boundary layer control by leading and trailing edge blowing 09 p1262 A72-22973

Uniform flow past semiinfinite flat plate for large Reynolds numbers and strong blowing, noting injected fluid region separation from free stream by shear boundary layer 10 p1467 A72-24369

Supersonic axisymmetric turbulent boundary layer characteristics over circular cone, predicting blowing effect on separation 11 p1617 A72-25995

Flow characteristics in air injection through porous surface of blunt bodies, noting blowing parameter effect on boundary layer flow 12 p1752 A72-28143

Calculation procedure for reaction thrust of semibounded turbulent jet in boundary layer blowing and blow type anticing systems 13 p1897 A72-28728

Navier-Stokes equation for rotating liquid axial flow past porous plate, noting velocity distribution for suction and thinning effect for blowing 13 p1942 A72-29127

Blowing and suction effects on free convection boundary layer on semiinfinite vertical flat plate, taking into account temperature difference between plate and fluid 16 p2477 A72-33429

Blowing and suction effects on heat transfer and friction coefficients of transpired turbulent boundary layer, presenting theoretical models and experimental results 16 p2378 A72-33431

Rotary wings lift and efficiency increase by circulation control using tangential blowing about bluff trailing edge airfoils [AHS PREPRINT 603] 17 p2489 A72-34492

Influence of blowing on the resistance of a sphere in laminar viscous fluid flow 21 p3047 A72-41665

BLOWOUTS

A method for estimation of axial turbomachinery stage characteristics on the basis of experimentally obtained data with a runner tested in a free blow-out aerodynamical scheme. 24 p3363 A72-45364

BLUE GREEN ALGAE

Green and blue-green algae reflectance and transmittance characteristics, selecting spectral bands for multispectrum scanning of algal suspensions in water bodies 02 p0213 A72-11857

Artificial microfossil permineralization of blue green algae in silica, simulating Precambrian geochemical preservation 04 p0514 A72-14415

Blue green algae *Anacystis nidulans* photorecovery after Co 60 gamma radiation exposures, using white and red light 04 p0475 A72-15516

Phylogenetic origin of cytoplasmids from Cyanophyceae alga involved in endosymbiosis with colorless Cryptophyte 13 p1907 A72-29996

Blue green algae *Anacystis nidulans* UV light-sensitive mutants photorecovery capacity following irradiation 16 p2356 A72-33673

Ultrastructure and geologic relations of some two-aeon old Nostocacean algae from northeastern Minnesota. 17 p2544 A72-34336

Prokaryotic algae associated with Australian proterozoic stromatolites. 22 p3174 A72-42981

BLUFF BODIES

Convergent power series solution in powers of time for unsteady viscous flow near stagnation after impulsive motion of bluff body from vorticity distribution viewpoint 06 p0757 A72-18135

Incompressible laminar subcritical flow with separated wake past symmetric two dimensional bluff body, calculating upstream pressure distribution and separation point 12 p1751 A72-27172

Rarefied gas flow problems, discussing mean free path effects on sharp nosed conical and bluff bodies drag and heat transfer coefficients 15 p2218 A72-32314

Attachment length as stability criterion for bluff-body stabilized electrodeless arc, showing linear dependence on flow velocity ratio to power density 15 p2336 A72-32406

Crococo-Lee theory extension to flow behavior prediction for two dimensional supersonic turbulent near wake behind bluff body during recompression 16 p2343 A72-33402

Grid-generated turbulence distortion approaching two dimensional bluff body stagnation region 16 p2344 A72-33569

Periodic vortex formation and shedding in flows past bluff bodies, considering cylinder forced and self excited vibrations and interaction with wake 18 p2679 A72-36389

An experimental investigation of the formation of vortices behind the isosceles triangular cross-sectional obstacles protruding from the plane wall. 21 p2992 A72-41246

Length of the separation region behind a bluff body in a bounded flow 23 p3248 A72-43685

BLUFFS (LANDFORMS)

U CLIFFS

BLUNT BODIES

Plane shock wave and blunt body interaction in supersonic gas flow in two-diaphragm shock tube 04 p0461 A72-14639

Hypersonic axially symmetric laminar boundary layer electrically conducting fluid flow in blunt body stagnation region in presence of radial magnetic field 05 p0600 A72-16063

Inviscid variable density core flow in thin compressible boundary layer near stagnation point of smooth blunt body 05 p0601 A72-16216

Blunt bodies-shock wave interaction in shock tubes, using interferometer with laser light source and high speed streak camera 05 p0601 A72-16225

Newtonian theory for maximum lift drag ratio of blunt-cone cylinder bodies, optimizing rocket reentry nose shape 05 p0602 A72-16535

Numerical solution of supersonic flow past blunt bodies with large mass injection, deriving finite difference equations 06 p0756 A72-18114

Ideal gas flow past blunt body in supersonic stream, discussing sonic lines, characteristics and Mach number 06 p0756 A72-18119

Lax finite difference scheme application to transonic two dimensional Laval nozzle and supersonic blunt body flow with detached shock wave, considering inviscid thermally nonconducting 06 p0756 A72-18126

Cornered axisymmetric blunt body sonic line in steady supersonic flow, showing incomparability with sonic shoulder of sphere 06 p0757 A72-18138

Supersonic near wake flow around blunt and sharp cones with trailing edge turbulent boundary layer 06 p0757 A72-18141

Transitional and turbulent heat transfer measurements on yawed blunt cone nosetip in supersonic air flow at various angles of attack [AIAA PAPER 72-212] 07 p0964 A72-18960

Monatomic ionized radiating gas nonequilibrium flow in blunt body stagnation region behind shock wave during hypersonic atmospheric reentry 07 p0909 A72-20083

Flow structure between bow shock wave and blunted cone surface, studying interior shock waves by numerical solution via finite difference methods 07 p0910 A72-20108

Boundary layer transition effect on three dimensional shock interactions due to blunt protuberances and axial compression corner 08 p1150 A72-21629

Aerodynamic field around singular stagnation point of blunt body tip with detached shock, using Legendre functions 09 p1261 A72-22932

Vorticity effect on shock wave-boundary layer interactions on blunt edged compression surfaces of hypersonic inlets 10 p1419 A72-24649

Hypersonic base heating investigation on Mars atmosphere entry blunt bodies, taking into account gas composition and angle of attack effects [AIAA PAPER 72-317] 11 p1568 A72-25251

Nonequilibrium partially ionized viscous shock layer on blunt body, determining electron temperature and electron-ion density profiles 11 p1744 A72-25560

BLUNT BODIES

Nose blunting, exposure time and initial temperature effects on axisymmetric bodies ablation surface cross hatching patterns, presenting test results on cones with various vertex angles 11 p1572 A72-26006

Nose bluntness effect on bodies of revolution pitching moment characteristics in incompressible flow at various angles of attack 11 p1573 A72-26576

Flow characteristics in air injection through porous surface of blunt bodies, noting blowing parameter effect on boundary layer flow 12 p1752 A72-28143

Mathematical model for flow field inside raindrop under aerodynamic transient stresses before impingement at stagnation point of blunt body in supersonic flight 13 p1942 A72-29224

Friction drag and heat transfer on long blunt-nosed cylinder in supersonic flow, determining location of transition zone as function of Mach number 13 p1895 A72-29642

Hypersonic flow of nonequilibrium ionized monatomic inviscid radiating gas past axisymmetric blunt body with allowance for electron and ion temperatures difference 13 p1895 A72-29877

Ideal gas axisymmetric flow created in supersonic flow interaction with blunted body with strong blowing at surface, obtaining boundary layer approximate solution 14 p2070 A72-31012

Mass entrainment products effect on radiative and convective heat transfer during decomposition of graphite blunt body in steady hypersonic flow of radiating air 14 p2174 A72-31158

Blunt planetary entry vehicles thermal flux prediction, taking into account viscosity, conduction, dissociation, ionization, nongray radiation, surface emissivity and ablation effects 15 p2335 A72-31816

Collection efficiency of conical and blunted axisymmetric power law bodies in hypersonic flight through dust clouds and of impact angle and velocity 15 p2180 A72-32580

Thermal radiation effects on semiinfinite planar blunt leading edged body hypersonic flow field, using Lax and Rusanov artificial viscosity methods 15 p2337 A72-32593

Fast numerical solution for supersonic flow past flat-faced blunt body by integration from stagnation point, noting computing time on CDC 6600 16 p2341 A72-32840

German monograph on supersonic flow past blunt sharp edged cones, comparing Van Dyke and method of characteristics results with schlieren photos and shadowgraphs 16 p2343 A72-33505

Flat plate leading edge blunting and wall cooling effects on supersonic laminar flow ramp-induced separation [AIAA PAPER 72-716] 16 p2344 A72-34032

Inviscid surface streamlines and laminar, transitional and turbulent heating of blunt nose shuttle configurations in hypersonic flow [AIAA PAPER 72-703] 16 p2345 A72-34041

Electron density measurements in bow shock stagnation and conical afterbody regions during blunt body atmospheric reentry, using flush mounted electrostatic probes [AIAA PAPER 72-694] 16 p2345 A72-34047

Blunt nose cone flow field characteristics microwave measurement at stagnation point during atmospheric reentry, using plasma diagnostic sensors with antennas and electrostatic probes [AIAA PAPER 72-693] 16 p2345 A72-34049

Viscous shock layer analysis application to blunt nosed reentry vehicle plasma layer nonequilibrium flow species distribution, considering electron density [AIAA PAPER 72-689] 16 p2346 A72-34053

Sonic boom induced flow field at supersonic/hypersonic speeds, using shock expansion method and hypersonic equivalence principle for sharp and blunt nosed bodies [AIAA PAPER 72-652] 16 p2349 A72-34082

Inert and reactive gas injection in near wake behind blunt bodies in supersonic flow, considering influence on base pressure and temperature 17 p2487 A72-35930

Calculation of spatial ideal gas flows without a symmetry plane 18 p2642 A72-36901

Experimental investigation of the flow past a cylinder with a flat nose 19 p2745 A72-37397

Aerodynamics of a slender cone with asymmetric nose bluntness at Mach 14. 20 p2886 A72-39634

Instability of hypersonic viscous shock layer with finite rate chemistry. 20 p2886 A72-39635

Formation of a shock wave around a blunt conical body placed in a rarefied hypersonic flow 21 p2993 A72-41340

- Viking configuration pitch damping derivatives as influenced by support interference and test technique at transonic and supersonic speeds.
[AIAA PAPER 72-1012] 21 p3041 A72-41593
- Base mounted cylinders effect on near wake of axisymmetric blunt base in supersonic flow
[AIAA PAPER 72-1013] 21 p2993 A72-41594
- Total enthalpy measurement from blunt body gas cap emission in arc-heated wind tunnels - Results and application.
[AIAA PAPER 72-1021] 21 p2993 A72-41599
- Laminar boundary layer at critical point of blunt body in molecular oxygen flow, noting wall influence on condensation
22 p3243 A72-42257
- Behavior of the lines of flow in the proximity of the stagnation points of blunt bodies
22 p3136 A72-42905
- The structure of blunt base wakes in swirling flow.
24 p3391 A72-45023
- Periodicity in exothermic hypersonic flows about blunt projectiles.
24 p3463 A72-45035
- Ablative asymmetric conical nose bluntiness changes effects on aerodynamic characteristics for moderate magnitude tilt angles
24 p3363 A72-45341
- Asymmetric nose bluntiness effects on the aerodynamics of a slender cone at Mach 14.
24 p3363 A72-45342
- Aerodynamic characteristics of two-dimensional waverider configurations.
24 p3365 A72-45793

BLUNTNESS

U ELLIPTICITY

BLURRING

- Focused image holographic interferometer for reduced blur in deep object image reconstruction with white light source
02 p0224 A72-11747
- Image blurring effects due to atmospheric boundary layer refractivity turbulent fluctuations during remote optical radiation source observations
03 p0359 A72-13482
- Camera shake under stress of tracking moving targets viewed briefly in poor light, considering blur in horizontal and vertical dimension
10 p1483 A72-24986
- Image blurring effects due to atmospheric boundary layer refractivity turbulent fluctuations during remote optical radiation source observations
11 p1633 A72-26252
- Laser interference fringe jitter due to wavelength instability, suggesting pulse shape blurring intensity variation control by flat or large-angle wedge beam splitter
15 p2249 A72-32166
- Space-variant image motion degradation and restoration.
18 p2658 A72-36258

BODIES OF REVOLUTION

- NT CELESTIAL SPHERE
- NT CONICAL BODIES
- NT CYLINDRICAL BODIES
- NT PARABOLIC BODIES
- NT POINCARÉ SPHERES
- NT ROTATING CYLINDERS
- NT ROTATING SPHERES
- NT SLENDER CONES
- NT SPHERES
- NT TORUSES
- Edge loaded cylindrical shells of revolution nonlinear axisymmetric deformation determination from asymptotic solution of Reissner equations, using multiple scale perturbation technique
01 p0136 A72-10031
- Glass fiber surfaces of revolution under axisymmetric pressure loads combined with centrifugal forces
01 p0143 A72-11365
- Tube and hollow sphere revolving in thermal flux under surface pressure load, obtaining stress-strain state and random temperature dependences of creep
02 p0289 A72-11618
- Motion of asymmetric body of revolution in rotating liquid, calculating drag on ellipsoid
02 p0204 A72-12175
- Acoustical field from streamlined body of revolution moving in homogeneous gaseous medium past semiinfinite rigid screen, using Wiener-Hopf method for diffraction radiation
03 p0340 A72-12916
- Curvilinear material anisotropy effects on temperature distributions of thin walled cylindrical shells of revolution
03 p0449 A72-13919
- MHD boundary layer on rotating disk and on body of revolution in longitudinal flow at large Stewart numbers
03 p0399 A72-14013
- Convex figures in mathematical geodesy, applying function h for ellipse and ellipsoid of revolution
03 p0351 A72-14328
- Axisymmetric load influence on stability of eccentrically reinforced shells of revolution, determining

critical loads and linear and nonlinear relations for moment-subcritical states
04 p0587 A72-15014

Ring finite elements use in analysis of shells of revolution under axisymmetric loads
[ASME PAPER 71-WA/HT-22] 05 p0732 A72-15880

Variable thickness shallow spherical shells of revolution axisymmetric loads carrying capacity, determining limit equilibrium through application of Tresca yield point concept
05 p0734 A72-15983

Navier-Stokes equations numerical solution for laminar incompressible flow past paraboloid of revolution at zero angle of attack
[AIAA PAPER 72-1101] 05 p0604 A72-16818

Laminar incompressible flow over yawed spinning bodies of revolution by Navier-Stokes solutions, discussing flow fields and corresponding force coefficients
[AIAA PAPER 72-112] 05 p0605 A72-16820

Three dimensional hypersonic turbulent boundary layer under normal and longitudinal pressure gradients and cross flow along windward symmetry plane of body of revolution
[AIAA PAPER 72-186] 05 p0605 A72-16841

Spectral properties of differential displacement equations system describing natural vibrations of shell of revolution with m waves along parallel
06 p0897 A72-17990

Photoelastic analysis of cylindrical shells of revolution with one hemispheric closed end and reinforcing flanges at opposite end rim, examining boundary conditions effects
06 p0899 A72-18640

Load bearing capacity of shells of revolution, applying viscoplastic strain hardenable material model
06 p0899 A72-18656

Magnetospheric field model from magnetosphere surface approximation by paraboloid of revolution
07 p0974 A72-18903

Laminar-turbulent incompressible boundary layer transition prevention by suction slots on bodies of revolution, determining optimal suction power/slot distance conditions by variational methods
07 p0968 A72-19737

Stress-strain state of homogeneous isotropic medium bounded by noncanonical surfaces of revolution, using perturbation method
07 p1091 A72-19755

Contact discontinuity motion past slender body of revolution in shock tube, solving unsteady supersonic flow problem by method of integral transformation
07 p0909 A72-20072

P-analytical functions application to strength analysis of zero moment shells of revolution with positive Gaussian curvature under concentrated loads
08 p1242 A72-20905

Dynamic characteristics and nonlinear oscillations of liquid in spherical shell of revolution, modifying Lukovskii approximation method
08 p1148 A72-20962

Stability and postbuckling equilibrium of nearly cylindrical shells of revolution under axial compression
08 p1244 A72-21291

Hodograph geometrical analysis of heavy gyrostat motion for center of mass and gyrostatic moment located on first and third principal axes of rotation
08 p1208 A72-21352

Green matrix computation algorithm extensible to spherical and toroidal closed shells of revolution for stress-strain state determination
08 p1246 A72-21672

Optimal temperature gradients determination over thickness of shell of revolution under axisymmetric heating, formulating variational problem for conditional extremum of elastic energy functional
09 p1399 A72-22706

Heat conduction, stress-strain state and thermoelasticity of massive bodies of revolution under nonuniform heating
09 p1400 A72-22709

Thermoelastic problem of open orthotropic multilayer shell of revolution, obtaining one dimensional boundary value problem solutions by numerical orthogonalization method
09 p1400 A72-22712

Thermal insulations in form of thin shells of revolution with rigid external and elastic internal layers resting on rigid core
09 p1400 A72-22713

Stress-strain state of shallow shells of revolution for large displacements, reducing determination to system of nonlinear differential equations
09 p1400 A72-22714

Computer algorithm for thermoplastic stress-strain state of thin shells of revolution based on plastic flow theory, taking into account loading history
09 p1401 A72-22724

Finite difference analysis of dynamic deformation of thin elastoplastic shells of revolution under intense heating
09 p1401 A72-22728

Rotationally symmetric stress and strain distribution in anisotropic elastic shells of revolution
[AD-745622] 09 p1405 A72-22944

Natural axisymmetric vibration of thin elastic shell of revolution, deriving eigenvalues convergence to spectrum lower bound by asymptotic method
10 p1557 A72-24429

Kinematic impact theory for inertial motion of rigid bodies of revolution and energy flow through wire grid
10 p1512 A72-24520

Stability loss in thin convex shells of revolution under axisymmetric stress, obtaining integrals for equilibrium equations
10 p1557 A72-24630

Aerodynamic data acquisition with magnetic balance on wind tunnel model delta and AGARD G wing planforms and body of revolution
10 p1462 A72-24770

Violation effect of moment equilibrium about normal in shell of revolution and helical shell theory, discussing distribution
10 p1560 A72-25171

Nonlinear structural analysis of circular plates and shells of revolution with geometric and inelastic material nonlinearities, using direct stiffness method
[AIAA PAPER 72-353] 11 p1729 A72-25382

Nose bluntiness effect on bodies of revolution pitching moment characteristics in incompressible flow at various angles of attack
11 p1573 A72-26576

Body of revolution /saucer/ with nongeodesic internal stresses under gravitational field in terms of general relativity theory
12 p1843 A72-27048

Structural effects of meridian imperfections in symmetrically loaded elastic thin shell of revolution
12 p1881 A72-27255

Optimal weight and load capacity of ellipsoidal cylindrical shell of revolution of constant thickness with central circular hole under uniform internal pressure
12 p1885 A72-27977

Energy method based approximate calculation for natural frequencies of single layer compound shells of revolution
12 p1886 A72-28144

Axisymmetric stability of spherical cap rigidly clamped at contour of shells of revolution, using variational difference method for uniformly distributed external pressure
13 p2053 A72-28393

Nonlinear first order differential equation for carrying capacity of anisotropic circular plates, curved elongate disks and shallow shells of revolution
13 p2054 A72-28457

Electromagnetic wave diffraction on ideally conducting homogeneous bodies of revolution with arbitrary complex permittivity and permeability, using variables separation method
13 p1920 A72-29279

Green function solution for electric field intensity in space due to electric dipole at another point under boundary conditions on surface of revolution
13 p1921 A72-29341

Monge surface shells reduced to bodies of revolution by small parameter method for solution of momentless theory equations
13 p2058 A72-29489

Sonic boom magnitude and location in stratified atmosphere calculated from gas dynamical equations for lifting body of revolution
13 p1898 A72-29585

Infinitesimally small slip bendings of sign-variable curved surface of revolution with parabolic boundary parallels
13 p2061 A72-29794

Static deformation of laminar orthotropic shells of revolution with variable rigidity, using integral correlation method
13 p2061 A72-29795

Axisymmetric hypersonic motion around thin solid of revolution, taking into account boundary layer interaction with inviscid external flow
13 p1895 A72-29847

Numerical solution of algebraic equation encountered in aerodynamics of hypersonic boundary layer interacting with external flow on thin solids of revolution
13 p1895 A72-29848

Three dimensional axisymmetric problem for stressed state of elastic homogeneous cylindrical orthotropic bodies of revolution, using method based on small parameters
13 p2062 A72-29948

Spectral properties of differential displacement equations system describing natural vibrations of shell of revolution with m waves along parallel
14 p2163 A72-30217

Minimum drag bodies of revolution in supersonic flow obtained by combining steepest descent method with integral flow model
14 p2069 A72-30231

Carrying capacity of rigidly hinged shell of revolution with concentric reinforcing rib, applying to shallow spherical shell under uniform external pressure 14 p2166 A72-30687

Unsteady laminar boundary layer on body of revolution with axial and torsional oscillations, calculating velocity distribution and shear stress variation 15 p2178 A72-31402

Numerical calculation of stresses and displacements in variable radius bodies of revolution under axially symmetric torsional load, using Fredholm type integral equation 15 p2324 A72-31480

Viscoplastic flow of inhomogeneous shells of revolution obeying Tresca condition, noting plastic deformation velocity relation to stresses 15 p2325 A72-31605

Body of revolution motion in fixed center Newtonian field, investigating plane trajectories of center of inertia 15 p2307 A72-31677

Torsion problem of bodies of revolution bounded by two intersecting spherical surfaces, obtaining solution by Mehler-Fock transform 15 p2330 A72-32294

Optimum nonslender bodies of revolution minimum drag in free molecular flow under integral constraints 15 p2180 A72-32395

Ideally conducting and dielectric coaxial solids of revolution, investigating joint excitation by TM wave 15 p2209 A72-32658

Stress-strain relations for inelastic deformation of anisotropic strain hardenable shells of revolution under arbitrary plasticity conditions 15 p2332 A72-32678

Vibrational frequency density analysis of thin spherical and cylindrical shells of revolution, using asymptotic integration method 16 p2464 A72-32935

Natural vibration frequency spectra of circular cylindrical and spherical shells of revolution, using Bessel function 16 p2465 A72-32936

Incompressible flow drag caused by slot suction provided in bodies of revolution for preventing laminar boundary layer transition into turbulent state 16 p2344 A72-33678

Study of the stability of certain relative equilibria of a symmetrical satellite 17 p2620 A72-34282

Flows between stationary surfaces of revolution, having similarity solutions. [ASME PAPER 72-APM-4] 17 p2537 A72-34304

Buckling and vibration analysis for stiffened orthotropic shells of revolution. 17 p2632 A72-35242

A hypersonic flow about a body of revolution with fanned jet injection 17 p2487 A72-35805

Shell of revolution natural vibration spectrum, investigating moment and momentless type systems of differential equations 18 p2735 A72-36665

Electromagnetic radiation and scattering from loaded bodies of revolution of arbitrary shape, calculating plane wave scattering from apertures in cylinders and hemispheres 18 p2662 A72-36927

Incompressible potential flow solution for axisymmetric body-duct configurations. 18 p2683 A72-36940

Shells of revolution free of bending under uniform axial loading. 19 p2876 A72-37886

Oscillations, statics and transfer matrices of composite shells of revolution contacting elastic bases, using initial parameters method 19 p2876 A72-38156

Surface vorticity theory for axisymmetric potential flow past annular aerofoils and bodies of revolution with application to ducted propellers and cowlings. 19 p2747 A72-38554

Experimental results regarding drag in supersonic flow without lift in the case of flight bodies with three in front pointed bodies [DFVLR-SONDDR-215] 19 p2747 A72-38686

Pressure pulsation measurements at nose of well-streamlined body of revolution at high Reynolds numbers, noting turbulent pressure field intensity growth and decay 20 p2912 A72-39362

Finite element large deflection analysis of elastic-plastic shells of revolution subjected to axisymmetric loading. 20 p2982 A72-40064

On the asymptotically spherical deformations of arbitrary membranes of revolution fixed along an edge and inflated by large pressures - A nonlinear boundary layer phenomenon. 21 p3118 A72-40840

Calculation of sandwich shells of revolution at large elastic-plastic deflections. 21 p3125 A72-41512

Solution for shallow shells of revolution with allowance for large deflections by the method of integral relations 22 p2322 A72-41869

An inverse problem in the momentless theory of shells of revolution situated in a temperature field 22 p2322 A72-41895

Steady-state creep of shells of revolution in the case of the Tresca criterion 22 p2323 A72-42051

Aerodynamic characteristics of bodies of revolution with large fineness ratios at Mach numbers ranging from 0.2 to 6.0 22 p3134 A72-42286

Effects of rifling and N-vanes on the Magnus characteristics of bodies of revolution. [AIAA PAPER 72-970] 22 p3135 A72-42341

Finite element method optimization of orthotropic layered shells of revolution under mechanical and thermal loadings, considering stress-strain relationships [SAWE PAPER 939] 23 p3344 A72-43479

Stress state of arbitrary contour body of revolution under torsion using finite difference method 23 p3347 A72-43744

Boundary layer on bodies of revolution in longitudinal flows 24 p3390 A72-44723

Vortex control on an inclined body of revolution. 24 p3362 A72-45335

Transonic wall interference effects on bodies of revolution. [AIAA PAPER 72-1008] 24 p3389 A72-45404

Radar cross sections of conducting bodies of revolution, noting electric/magnetic polarizability tensors in LF Rayleigh scattering 24 p3381 A72-45639

Body of revolution /saucer/ with nonequidistant internal stresses under gravitational field in terms of general relativity theory 24 p3425 A72-45701

Variable thickness shallow spherical shells of revolution axisymmetric loads carrying capacity, determining limit equilibrium through application of Tresca yield point concept 24 p3460 A72-45725

Average circumferential pressure on inclined bodies of revolution at hypersonic speed. 24 p3365 A72-45788

BODY CENTERED CUBIC LATTICES

Ti alloys omega phase transformations by cryogenic cooling of bcc beta phase, interpreting electron diffraction pattern change in terms of displacement type reactions 01 p0082 A72-10204

Carbon atoms thermodynamic properties in bcc and fcc Fe-Si-C solid solutions from equilibrium measurements with hydrogen-methane gas mixtures as function of temperature and carburizing gas composition 01 p0083 A72-10207

Binary alloys ground state energy and superstructures, examining bcc and fcc Ising model systems with first and second neighbor interactions 01 p0083 A72-10210

Cobalt and lanthanum with face and body centered lattices, studying plastic deformation during allotropic transformations under sliding friction and gripping 01 p0074 A72-10579

Critique of theoretical and experimental findings on slip geometry in bcc metals, especially Fe-Si alloy single crystals 01 p0089 A72-11300

Yield stress of solid solution iron and Fe-Ge alloys with bcc structure, obtaining interaction energy between solute atoms and screw dislocation 03 p0402 A72-13974

Bcc Mo and Nb after cold working observing internal friction relaxation peaks as function of stress, strain, temperature and strain rate 06 p0831 A72-18296

Cu, Al and Pb bcc metals, investigating dislocation structure and creep characteristics change mechanism at transition from low to high temperature 07 p1014 A72-19822

Hardening mechanisms during plastic deformation of pure bcc metals, discussing stresses relation to fine structure and crystal dislocation paths 07 p1018 A72-20142

Cold brittleness of transition metal alloys with bcc lattices, discussing elastic characteristics, packing defects energy, plastic deformation and rhenium admixture 07 p1018 A72-20143

Bcc solid solutions formation in Cr-W binary alloys, investigating interface reaction and two phase grain boundary diffusion by X ray diffraction and microscopy 08 p1185 A72-21246

Phonon dispersion curves of bcc transition metals for normal lattice vibration modes 09 p1369 A72-22680

Ti, Zr and Hf hcp-bcc phase transformation isochromat spectroscopic investigation, noting fine structures to confirm electron state density 09 p1371 A72-22849

Recrystallization of dispersion strengthened alloys with bcc lattice, deriving equations for grain size changes 09 p1328 A72-23031

Radiation damage in bcc metal Mo and W foils under energetic Au ion irradiation, noting vacancy dislocation loops 09 p1331 A72-23506

Elastic constants of dilute Mo-Re alloys with bcc structure, determining randomly distributed point defects low concentration effects with T-matrix method 11 p1656 A72-25724

Deformation drawing textures of bcc metals, including W 11 p1644 A72-26838

Compression creep in ordered binary and ternary ordered bcc Ni alloys investigated by transmission electron microscopy 11 p1667 A72-26937

Interdiffusion studies in bcc phase of Zr-Ti alloy, using geoscan electron microprobe 13 p1973 A72-28653

Plastic deformation in bcc metal single crystals, discussing glide and work hardening, dislocations, core structure and atomic calculations 13 p2061 A72-29874

Equiatomic ordered, bcc TiFe and TiNi electron density in outer energy band from X ray K emission spectra 13 p1981 A72-30006

Low and medium strain rates and temperature effects on bcc structure polycrystalline Nd and Mo, determining mechanical properties of yield and flow 14 p2114 A72-30367

Interaction forces between two dislocations in infinite weakly anisotropic media with bcc crystal lattice elastic properties 16 p2424 A72-33146

Fcc in thin films and bcc in thick vacuum condensates deposited from Nb molecular beams obtained by evaporation and condensation in mass spectrometer 16 p2407 A72-33528

Crystal lattice disarrangement by melting In-Tl alloy, noting fcc and bcc metastable phases formation during rapid crystallization 16 p2441 A72-33536

Quenching produced martensitic transformations from equilibrium beta phase region for Ti alloys with Ta 16 p2408 A72-33618

Geometric/chemical model of lattice dimensions of Laves phases of binary alloy bcc and fcc structures 16 p2409 A72-33801

Thermodynamic interaction parameters of solid solution bcc V-Ti-Cr alloys by Knudsen effusion method combined with mass spectrometer 16 p2409 A72-33803

Bcc lattice sum calculation method in Langevin function terms, noting validity at low temperatures 16 p2442 A72-34175

Radiation damage to refractory metals as related to thermionic applications. 17 p2566 A72-34595

Impurity controlled deformation mechanism for softening control of interstitial bcc alloys, discussing low temperature and composition effects 18 p2699 A72-36341

Substitutional-interstitial interactions in bcc alloys. 18 p2699 A72-36396

Nucleation and growth of deformation twins in Mo-35 at. % Re alloy. 18 p2702 A72-36748

Beta to omega phase transformation and structure in Zr and Ti alloys bcc solid solutions by dark field electron microscopy, diffraction and ultrasonic technique 21 p3065 A72-40092

Deformation microstructure of fine grained and plate-like structure two phase Ti alloys, noting plasticity decrease in beta phase presence 21 p3068 A72-40963

On the growth kinetics of Laves phase precipitates in Fe-Ti alloys at elevated temperatures. 21 p3069 A72-41011

Ti based beta alloy strain hardening and failure characteristics, emphasizing initial deformation phase and microdefect onset and development 21 p3071 A72-41716

Equiatomic ordered bcc TiFe and TiNi electron density in outer energy band from X ray K emission spectra 22 p3190 A72-42733

The effect of pre-strain on the yield behavior of vanadium. 24 p3413 A72-44721

BODY COMPOSITION [BIOLOGY]

Annual clinical and physiological evaluation of test pilots physical performance over ten year period from body composition, pulmonary function and work capacity measurements 14 p2082 A72-31093

BODY FLUIDS

NT BLOOD
NT CEREBROSPINAL FLUID
NT ENDOLYMPH
NT ERYTHROCYTES
NT LEUKOCYTES

NT LYMPH
NT LYMPHOCYTES
NT RETICULOCYTES
NT SALIVA
NT SWEAT
NT THROMBOPLASTIN
NT URINE
NT WHITE BLOOD CELLS
Prolonged jet flight effect on passenger interstitial and intracellular fluid volumes from plasma, extracellular and total body water measurements, noting dehydration and foot swelling 06 p0767 A72-17866
Urea determination in urine and water wastes for recycling process, using N-dimethylaminobenzaldehyde colorimetric method 13 p1910 A72-29325
Hypokinesia effect on fluid and electrolyte metabolism change patterns in rabbits from blood plasma studies 14 p2075 A72-30389
Water immersion tests to study body fluid balance disturbances during weightlessness, observing diuretic reflex control of blood volume 16 p2355 A72-33551
Vasopressin/antidiuretic hormone/role in central vascular volume and fluid balance maintenance during continuous positive pressure breathing in dogs 17 p2505 A72-35917
Algorithms for selected blood acid-base and blood gas calculations. 17 p2510 A72-35973
Fluid transfer between blood and tissues during exercise. 18 p2650 A72-36560
Cardiovascular system venous part responsiveness to central nervous and humoral influences 22 p3148 A72-43167
Increased fluid turnover and the activity of the renin-angiotensin system under various experimental conditions. 23 p3257 A72-43997

BODY KINEMATICS
Human body dynamics, discussing configuration, modeling techniques, kinematics, equations of motions and various limb motions examples 01 p0016 A72-10110
Fluid immersed body velocity fluctuations due to irregular molecular impacts 01 p0001 A72-10234
Variable volume spherical cavity motion in ideal liquid near plane surface 02 p0202 A72-11586
Motion of asymmetric body of revolution in rotating liquid, calculating drag on ellipsoid 02 p0204 A72-12175
Three dimensional laminar boundary layer about finite body nonuniformly moving along rectilinear trajectory 02 p0206 A72-12618
Human body movements basic kinetics, measuring static force, angle and tangential acceleration of horizontal arm swings 04 p0478 A72-14707
Human and animal controlled self rotating maneuvers during free fall, comparing theoretical motion analysis with photographs of falling cats 04 p0478 A72-14709
Human body kinematics numerical analysis, obtaining space-time resolution by photogrammetric restitution and electronic data processing of photographic recordings 04 p0478 A72-14710
Invariant manifolds in rigid body motion about fixed point, considering Euler-Poincaré, Lagrange-Poisson and Kovalevskaya cases 04 p0549 A72-15197
Hydrodynamic resistance reduction for bodies moving under water, analyzing dynamic equations of viscous incompressible fluid 04 p0514 A72-15703
Dynamic analysis of straight shaft with constant noncircular section and internal friction forces, delineating trajectories for shaft center of symmetry 04 p0593 A72-15707
Rigid body general motion dynamic effects due to acceleration of arbitrary order, using Samov-Mangeron recursive formulas 04 p0551 A72-15746
Magnetometer and spirometer ventilation measurements from chest and abdomen movements during carbon dioxide inhalation 05 p0619 A72-16790
Wake behind body moving in plasma parallel to magnetic field, observing coupling with parallel ion acoustic waves and with perpendicular Bernstein modes 06 p0875 A72-17525
Relative motion of two mass points linked by flexible weightless tether in orbit around planet 06 p0891 A72-18695
Free solid body kinetic moment vector effects on long period motion in resonant state during transition from rotational to somersaulting mode 06 p0849 A72-18699

Nonlinear resonance oscillations of flexible rod and elastic cylindrical shell under potential and nonpotential forces, investigating motion instability 06 p0900 A72-18704
Nonlinear solid body system rotating and oscillating parts effect on spatial vibration stability, deriving excitation-natural frequencies relationship 06 p0850 A72-18711
Elastic body dynamics partial differential equations transformation into boundary value problem for Monge-Ampère equation 07 p1095 A72-20218
Sphere unsteady motion in viscoelastic liquids, noting falling-ball technique use for elastic parameters determination 07 p0973 A72-20549
Motion of two symmetrical rigid bodies connected by frictionless spherical hinge positioned at dynamic symmetry axes intersection 08 p1206 A72-21168
Slow adiabatic motions of vibratory suspended bodies and determination of carrying body parameters and orientation from oscillations monitoring 08 p1206 A72-21229
Motion equations order reduction for solid body with fixed point 08 p1207 A72-21340
Transformation of integrodifferential equation of motion of heavy solid body about fixed point 08 p1207 A72-21341
Polynomial solutions to integrodifferential equation of motion of solid body with fixed point for Lagrange conditions 08 p1207 A72-21342
Motion of body similar to Lagrange gyroscope, using Kolmogoroff theorem 08 p1207 A72-21343
Algebraic invariant relation of integrodifferential equation of motion of solid body about fixed point for Hess conditions, proving uniqueness 08 p1207 A72-21344
Motion of heavy solid body about fixed point for Hess conditions, analyzing Euler-Poisson equations solution properties 08 p1207 A72-21345
Solutions existence for algebraic invariant relation to integrodifferential equation of motion of solid body about fixed point in trigonometric and exponential polynomials class 08 p1207 A72-21346
Solutions existence for nonlinear invariant relation to integrodifferential equations of motion of solid body about fixed point 08 p1207 A72-21347
Solutions existence conditions for integrodifferential equation of motion of solid body about fixed point 08 p1207 A72-21349
Solid body motion about fixed point, determining moving and fixed angular velocity hodographs 08 p1208 A72-21351
Integrodifferential equation exponential solutions for body motion about fixed point 08 p1208 A72-21353
Moving hodograph of angular velocity vector in solution to problem of body motion about fixed point 08 p1208 A72-21354
Goriachev-Chaplygin solution to gyroscopic motion of body around fixed point for periodic motion 08 p1208 A72-21355
Sretenskii-Chaplygin integral in polynomial form for solution to gyrostat motion problem 08 p1208 A72-21356
Asymptotically uniform motions of heavy solid body with fixed point, assuming moving hodograph intersections with Staude cone 08 p1208 A72-21358
Solutions existence and uniqueness for linear invariant relation to gyrostat motion under nonholonomic constraint 08 p1208 A72-21362
Solid body motion with fixed point in central Newtonian force field, classifying angular velocity vector hodograph as function of dimensionless parameters 08 p1208 A72-21363
Helical line deformation in solid body motion about fixed point 08 p1209 A72-21366
Unsteady incompressible laminar boundary layer theory on two dimensional body motion through fluid at rest at infinity, considering skin friction 08 p1151 A72-21794
Dynamic and kinematic equations of attitude and translational motions of symmetric rigid body under body fixed force 09 p1351 A72-22991
Perturbed motion of rotating solid body with viscous fluid filled cavity, linearizing motion and Navier-Stokes equations 09 p1295 A72-23487
Bent lever equilibrium and relativistic mass for point body in motion, introducing von Laue energy flow inertia into d'Alembert principle 10 p1505 A72-24074

Kinematic impact theory for inertial motion of rigid bodies of revolution and energy flow through wire grid 10 p1512 A72-24520
Hydrodynamic field generated by sphere motion along viscous fluid filled cylinder axis beyond Stokes regime 10 p1470 A72-24852
Hand steadiness during unrestricted linear arm movements and eye-hand coordination tasks, showing tremor occurrence in up-down plane 10 p1432 A72-25113
Algorithm for moving object hologram synthesis with digital computer 11 p1633 A72-26365
Slow drop of heavy rigid spheres through vertical tube filled with viscous liquid, noting minimization of errors due to temperature and trajectory path 11 p1617 A72-26501
Rigid body model for nonholonomic kinematic linkages of tangentially sliding nonrolling bearings, noting virtual displacements and mechanical work 12 p1845 A72-27539
Algorithm for meteor velocity calculation from radio observation data, noting symmetrical error distribution function of velocities 13 p1924 A72-29034
Radar observation of meteor geocentric velocity dependence on radiant elongation angle 13 p2038 A72-29035
Human leg muscle reflex excitability changes during angular acceleration, suggesting vestibular apparatus as coordination means in quasi-static and dynamic movement control 14 p2075 A72-30388
Body of revolution motion in fixed center Newtonian inertia, investigating plane trajectories of center of inertia 15 p2307 A72-31677
Spherical, cylindrical or plane piston motion in nonuniform medium with radiative energy transfer, obtaining approximate analytic solutions and temperature profile behind shock front 15 p2336 A72-32394
Heavy body mass distribution gravitational effects in nonlocal linear theory, noting refractive index, rosette motion and perihelion advance 15 p2278 A72-32484
Unsteady boundary layer flow equations for arbitrarily smooth bodies moving relatively slowly through rotating liquid [DFVLR-SONDDR-211] 16 p2376 A72-33007
Lagrange equations of second kind for rigid systems, using balances of linear and angular momentum for mass point or rigid body 16 p2466 A72-33021
Algorithm for moving object hologram synthesis with digital computer 16 p2394 A72-33717
Three dynamic conical bar theories, solving transient axisymmetrical motion via method of characteristics [ASME PAPER 72-APM-20] 17 p2581 A72-34797
Two-mass system as human body dynamic model in ballistocardiography, outlining transfer function parameter computation procedure 18 p2652 A72-36039
Servo action in human voluntary movement. 18 p2654 A72-36999
Experimental investigation of an astronaut maneuvering scheme. 18 p2655 A72-37026
On the existence of an instantaneous rotation axis during the motion of a solid body with a constant point in Euclidean n-dimensional space. 19 p2835 A72-38635
The measurement of three-dimensional body movements by the use of photogrammetry. 20 p2898 A72-39806
Participation of supraspinal structures in the formation and control of a system of arbitrary cyclic motions of man 21 p2999 A72-40594
Steady two dimensional motion during horizontal motion of body at high Richardson number in stratified fluid, considering blocking mechanism 21 p2990 A72-40653
Man movements directed at reaching a preset goal 21 p3006 A72-40710
Control simulation models of three dimensional joint angle motions, including circle, ellipse and straight line trajectories and orientations in space 22 p3162 A72-42187
Inverse problems of the dynamics of a ponderous solid with one fixed point 23 p3312 A72-43219
Flight mechanics analysis of various flight conditions for conventional aircraft. V - Mechanical foundations/dynamics of rigid bodies/ 23 p3251 A72-43641
Motion of a solid with a nonholonomic constraint around a fixed point in a conservative force field 23 p3313 A72-43800
Free-transverse vibrations of an axially moving mass. 23 p3355 A72-44457

BODY MEASUREMENT [BIOLOGY]
NT ANTHROPOMETRY

Computer aided biplane roentgen videometry system for dynamic circulatory structure studies including blood flow and heart volume determination 01 p0020 A72-11040

Acoustic impedance of body surface at thorax and at abdomen, showing dependence on frequency and body pressure and position 01 p0021 A72-11195

Organism blood volume and losses determination by measuring human body electrical resistance, noting unsatisfactory results 06 p0768 A72-17994

Cardiovascular changes produced by whole body vibration of dogs and pigs, obtaining resonant frequencies of organ systems 10 p1426 A72-24484

Biological similarity theory for numerical relationships of morphometric and physiometric organization in mammals, using allometric growth equations and body weight correlations 10 p1432 A72-25098

Single linear measure of systolic pressure gradient for calculation of aortic valve area in stenosis severity assessment 12 p1762 A72-27734

Human torso surface mathematical model to determine equivalent heart dipole and quadrupole locations for ECG measurements 13 p1908 A72-28571

Echocardiographic determination of left ventricular dimensions, volumes and performance. 19 p2762 A72-38819

Electrically sensed changes in chest and abdomen diameter for tidal volume, respiratory frequency and minute ventilation measurements 21 p3006 A72-40428

Relative position of the rib within the chest and its determination on living subjects with the aid of a computer program. 24 p3372 A72-44957

BODY SIZE [BIOLOGY]

Dimensional analysis and similarity theories application to biological organisms relationships between body size and metabolism 11 p1585 A72-26074

BODY SWAY TEST

Quantitative model to describe vestibular detection of body sway motion in postural response mode 13 p1905 A72-29374

Effects of visual cues on the standing body sway of males and females. 18 p2654 A72-36918

Vertical posture control mechanisms in man 19 p2757 A72-37992

BODY TEMPERATURE

Body cooling effect on human vigilance in hot environments, testing reaction time to visual stimuli and auditory signal detection rate 01 p0021 A72-11290

Optimum muscle work conditions experiments with rabbits, correlating total work performance and power output with muscle temperature variations 02 p0160 A72-12013

Skin and hypothalamic temperature effects on human thermoregulatory responses, developing control mechanism for peripheral effects on skin sensors. 02 p0160 A72-12041

Chronic centrifugation effects on rat deep body temperature by implant biotelemetry, comparing with body mass and food consumption changes 02 p0163 A72-12089

Heat exposure effect on Sidman avoidance performance in rats, discussing organism thermoregulatory capacity disruption and shock and body temperature regulation 02 p0169 A72-12525

Thermoregulatory hypothalamic and body sites for behavioral temperature regulation in squirrel monkey 03 p0314 A72-13072

Biological tissue heat transport dimensionless parameters for steady state and transient analysis of homeotherm thermoregulation 04 p0472 A72-14864

Heat acclimatization, work habituation and exercise effects on body thermoregulation, measuring tympanic temperature, sweat rate and oxygen intake 04 p0472 A72-14896

Peripheral modifications to exercise induced central drive for sweating, determining rates as functions of internal temperature 04 p0479 A72-15212

Potassium cyanide effect on phospholipid exchange in rat brain and liver during histotoxic hypoxia as function of body temperature 05 p0618 A72-16357

Heat production increase by muscular contractions due to noradrenaline in cold adapted rats 05 p0620 A72-17215

Body thermal stress, local heating and arterial occlusion effects on sweat electrolyte content 07 p0929 A72-19437

Circadian rhythms variations for sleep, EEG, temperature and activity in monkeys, indicating acrophase, amplitude and level regulation 07 p0918 A72-19528

Weak If electric field influence on circadian rhythms of human rectal temperature and activity 07 p0918 A72-19531

Spectral photosensitivities for phase shifting of circadian body temperature rhythms in pocket mice 07 p0919 A72-19535

Biomedical transducers for NASA space program, discussing spray-on electrodes and telemetering for ECG respiration and body temperature 07 p0931 A72-19917

Eastbound and westbound transmeridian flights effect on body temperature and psychomotor and visual performance circadian rhythms, discussing readjustment times 07 p0921 A72-20176

Human temperature regulation during upright and supine exercise, showing nonlinear relationships between perspiration and skin and core temperatures 07 p0922 A72-20275

Various work-rest cycles and environmental temperature effects on body temperature, determining external auditory canal and core temperature relationship 08 p1123 A72-20886

Convective heat transfer from human form, using cylindrical model and aluminum statue physical replica in oven and wind tunnel air flow studies 08 p1123 A72-20892

Peripheral thermoregulation in arctic canines, showing subzero bath-immersed foot temperature maintenance above tissue freezing point 08 p1120 A72-22019

Mathematical model of skin contact cooling tube device for human body thermoneutrality maintenance in various environments 09 p1270 A72-22821

Calorimetric measurements of human body temperature and of hot saline solution drinking effects on sweating rate 09 p1267 A72-23440

Oxygen consumption and body temperature in anesthetized, paralyzed and artificially ventilated dogs cooled in water bath at 34 C, measuring hypercapnia and beta-adrenergic blockade effects 10 p1424 A72-23735

Human body calorimetry with water cooled garment for dynamic and continuous recording of heat dissipation from surface over extended time 10 p1431 A72-24485

Assessment of regional myocardial temperature changes effect on blood flow measurements by heated cross-thermocouples in dogs 10 p1432 A72-25071

German papers on human body energy balance and temperature control covering energy conversion processes, chemical secretions, muscle activity, etc 11 p1584 A72-26071

Human body thermoregulatory processes under varying environmental conditions and metabolic rates, discussing role of blood circulation, sweating, nervous stimuli, hormones, etc 11 p1584 A72-26073

Thermodynamic analysis of heat of evaporation of sweat, considering ambient temperature and humidity effects, body heat storage and presence of solutes 11 p1586 A72-26610

Forearm skin and muscle blood flow change measurements during whole body heating, using plethysmography, isotopic labeling and blood sampling techniques 11 p1587 A72-26617

Cumulative sleep deficit, preceding sleep or wakefulness period duration and body temperature effects on reaction time in multiple choice visual task 11 p1581 A72-26690

Biothermal response of increased core temperature in rhesus monkey to mechanical vibration, noting implications for pilot performance during prolonged buffeting 12 p1774 A72-28268

Ear site body temperature measurement relation to radiant heating of scalp and upper face 12 p1768 A72-28333

Cardiovascular system functional state elevation during controlled cooling, studying hemodynamic changes 14 p2075 A72-30386

Sweating relation to body temperature after exhaustive exercise for various oxygen uptakes and ambient temperatures 14 p2079 A72-30702

Water cooled suits efficiency and effectiveness for heat removal, noting importance of head area 14 p2081 A72-31085

Cardiac output and body temperature response to prolonged intermittent exercise 15 p2185 A72-31448

Heat, noise and vibration stress combined effects on skin and rectal temperature, heart rate, weight loss and biochemical urinalysis 17 p2508 A72-34551

Thermal neutral temperature of rats in helium-oxygen, argon-oxygen, and air. 17 p2500 A72-34728

Clinical IR thermography with Thermovision camera for body temperature discontinuity detection, discussing image resolution 18 p2655 A72-37196

Circadian rhythms in physiological and psychological functions related to jet travel, studying body temperature variations and psychomotor performance during isolation and varying light-dark cycle conditions 20 p2897 A72-39723

Human tryptophan and tyrosine metabolism - Effects of acute exposure to cold stress. 21 p2997 A72-40417

Russian book - Climatic conditions and the thermal state of man. 21 p3006 A72-40458

Oxygen consumption in liquid breathing mice. 22 p3142 A72-42488

Heat acclimatization by exercise-induced elevation of body temperature. 22 p3151 A72-42741

Temperature transmission from biopotential radiotelemetry transmitters. 22 p3151 A72-42745

Thermal balance in man during 24 hours in a controlled environment 22 p3145 A72-42747

Evidence for a metabolic limitation of survival in hypothermic hamsters. 23 p3258 A72-44364

Role of the dorso-medial area of the posterior hypothalamus in thermal regulation and its functional relationships with the anterior hypothalamus 24 p3371 A72-44592

Analysis of changes in thermal regulation after destruction of the medial preoptic area of the hypothalamus 24 p3371 A72-44593

Pulse activity of neurons in the thermal regulation center of the anterior hypothalamus during chill shivering 24 p3371 A72-44594

Temperature-sensitive neurons in the brain stem - Their responses to brain temperature at different ambient temperatures. 24 p3373 A72-45232

BODY TEMPERATURE REGULATION
U THERMOREGULATION

BODY VOLUME [BIOLOGY]

Combined photoelectric-photographic and plethysmographic technique for continuous measurement of rabbit ear vein diameter and tissue volume changes 09 p1273 A72-23443

Left ventricle intracavity volume measurements based on biplane angiographic data 15 p2190 A72-32497

BODY WEIGHT

Chronic centrifugation effects on rat deep body temperature by implant biotelemetry, comparing with body mass and food consumption changes 02 p0163 A72-12089

Posthypoxic thirst and relative dehydration of rats after return from hypoxia to normoxia, measuring body weight and water intake 02 p0165 A72-12835

Acceleration force simulation for altered weight effect on animal tolerance to restraint, discussing body mass loss, reduced lymphocyte count and disorientation 04 p0472 A72-14866

Blood circulation minute volume and peripheral resistance changes during human aging process, accounting for body weight 08 p1120 A72-22073

Biological similarity theory for numerical relationships of morphometric and physiometric organization in mammals, using allometric growth equations and body weight correlations 10 p1432 A72-25098

Weight loss due to respiratory tract evaporative water loss during exercise, from humidity change, ventilatory exchange and oxygen uptake data 11 p1586 A72-26613

Triglyceridemia relation to age, relative weight and ischemic cardiopathy probability from ECG, anthropometry and lipid and glucid metabolism studies 12 p1759 A72-27238

Physiological effects on prolonged weightlessness in dogs aboard Cosmos 110 biosatellite, emphasizing body weight loss and enzyme activity and bone tissue mineral concentration changes 16 p2354 A72-33547

Heat, noise and vibration stress combined effects on skin and rectal temperature, heart rate, weight loss and biochemical urinalysis 17 p2508 A72-34551

Body weight decreases in some primate exposed primates. 18 p2650 A72-36447

Effect of hyperoxic media on the stability of rats during acute carbon monoxide exposure 21 p2998 A72-40437

BODY-WING AND TAIL CONFIGURATIONS

- Aerodynamic forces and pressure distribution measurement on wing-body combination model, investigating boundary layer on wing upper surface
02 p0151 A72-12228
- Force and pressure distribution measurements on delta wing-body combination in compressible flow, investigating Reynolds number effect
[DGLR PAPER 71-118] 02 p0152 A72-12707
- Unsteady pressure distribution on harmonically oscillating circular cylindrical fuselage body with conical nose and delta wing with straight, cubic or sinusoidal leading edges
[DGLR PAPER 71-080] 02 p0153 A72-12730
- Subsonic doublet-lattice lifting surface method non-planar aspects refinement, using wing-tail configurations
05 p0600 A72-16109
- Simply supported skew plates stability under combined loading, noting wing and tail design applications for high speed aircraft and missiles
10 p1555 A72-24196
- Finite difference method computation of multi-isocked three dimensional wing-body supersonic flow fields with real gas effects, applying to delta winged space shuttle
[AIAA PAPER 72-702] 16 p2345 A72-34042
- Aerodynamic interference between aircraft components - Illustration of the possibility for prediction.
[ICAS PAPER 72-49] 21 p2992 A72-41174
- Configuration analysis as applied to aerospace vehicle design synthesis.
[SAWE PAPER 911] 23 p3342 A72-43458
- BODY-WING CONFIGURATIONS**
- Initial dihedral wing-body interaction for supersonic leading edges, determining expansion of velocity potential on root chord
14 p2069 A72-30365
- Unified area rule for hypersonic and supersonic wing-bodies.
17 p2485 A72-35251
- Near flow field and aerodynamic loading in subsonic and supersonic flow over body-wing configuration, surveying numerical, kernel function and image methods
18 p2641 A72-36390
- Experimental results regarding drag in supersonic flow without lift in the case of flight bodies with three in front pointed bodies
[DFVLR-SONDDR-215] 19 p2747 A72-38686
- Experimental investigations of separated flows on wing-body combinations with very slender wings at free-stream Mach numbers from 0.5 to 2.2.
[ICAS PAPER 72-25] 21 p2991 A72-41150
- Computation of the potential-theoretical flow around wing-fuselage combinations and a comparison with measurements
23 p3249 A72-44298
- BOEING AIRCRAFT**
- Boeing 347 helicopter program, discussing simulation, wind tunnel, whirl tower, bench testing, flight test development and demonstration
05 p0614 A72-16993
- Boeing aircraft altitude alerting systems development and design to meet FAR 91-51 requirements, discussing retrofit programs and altimeter encoding
22 p3179 A72-42689
- PRD-49, a new composite material - Its characteristics and its application to the BO-105 helicopter.
[SAWE PAPER 915] 23 p3305 A72-43462
- BOEING MILITARY AIRCRAFT**
- U MILITARY AIRCRAFT**
- BOEING 707 AIRCRAFT**
- Boeing 707 rapid decompression at 25,000 feet, noting rivet hole fatigue damage
02 p0167 A72-11715
- Boeing 707 cockpit simulator with computer generated displays, moving area navigation map and ATC information
07 p1033 A72-20336
- Operating cost comparisons between Concorde and Boeing 707 and 747 aircraft, considering profitability
20 p2888 A72-39818
- BOEING 747 AIRCRAFT**
- Boeing 747B growth model FAA certification, discussing engine thrust, fuel capacity, taxi and flight weights and aircraft noise reduction
[SAE PAPER 710753] 01 p0003 A72-10251
- Fail-operational automatic landing system for Boeing 747 aircraft, noting reduction in allowable minimum weather conditions in U.S. and UK
01 p0098 A72-10961
- Pilot evaluation of Boeing 747 handling, directional stability, stall, rudder feel forces, landing, inertial navigation and reliability
05 p0614 A72-16992
- Manufacturer viewpoint on aircraft engine safe introduction into airline service, discussing JT9D engine design for 747 aircraft
07 p1053 A72-18830
- Shot peen contouring of Boeing 747 wing skins combined with incremental chip forming, noting principles and manufacturing process
[ASM PAPER W 72-31,4] 12 p1817 A72-28160

Airline maintenance program and facilities for Boeing 747 aircraft based on optimized service concept
15 p2181 A72-32430

Meteorological data analysis for CAT encounter of Boeing 747 flight over Nantucket Island on 4 November 1970
16 p2418 A72-33525

Maintenance of the 747. II - BOAC.

- 17 p2492 A72-34929
- Functional equipment active and standby redundancy for flight safety and air traffic punctuality improvement, noting Boeing 747 aircraft redundancy systems
17 p2492 A72-35476
- Boeing 747 aircraft impact on Chicago O'Hare airport design criteria, noting future terminal facilities planning
18 p2675 A72-36782
- Operating cost comparisons between Concorde and Boeing 707 and 747 aircraft, considering profitability
20 p2888 A72-39818
- Boeing 747-F cargo aircraft, describing onboard and ground facilities for freight handling and loading
23 p3278 A72-43245
- Airline operational weighing and balancing of 747 aircraft, discussing accuracy and calibration procedures for electronic load cells, mobile platform scales and onboard aircraft weighing systems
[SAWE PAPER 917] 23 p3251 A72-43464

BOEING 7207 AIRCRAFT

- Fatigue design and test program for the American SST.
24 p3367 A72-44741

BOGOLIUBOV THEORY

- Bogoliubov-Mitropolski-Hale integral manifold theorem for perturbed nonlinear differential equations, using generalized variation of parameters formula
03 p0381 A72-12907
- Averaged Bogoliubov-derived chains of kinetic theory gas dynamics equations with strong statistical correlation for macroprocess description
08 p1149 A72-21175
- Beecham-Kryloff-Bogoliubov approximation method application to a degree of freedom nonlinear systems, using averaged kinetic energy and virtual work terms in Lagrange equation
09 p1342 A72-23454
- Quantum condensation in finite volume boson gas, using Bogoliubov quasi-expectation value method
10 p1563 A72-24676
- Relativistic plasma particle correlation function based on transverse electromagnetic field energy density treatment by enlarged Bogoliubov hypothesis
14 p2140 A72-30881
- Weak homogeneous turbulence analysis by Bogoliubov statistical mechanics theory, deriving kinetic equations for nonlinear wave interaction
15 p2278 A72-32383
- Long wave fluctuations in nonequilibrium gas with pair collisions, using Bogoliubov equations for simultaneous correlation functions
15 p2282 A72-32450

BOILERS

- Mathematical model of combustion region of steam boilers or gas turbines based on turbulent flow and transport equations
11 p1747 A72-26592

BOILING

- NT FILM BOILING
NT LEIDENFROST PHENOMENON
NT NUCLEATE BOILING
- Stratospheric aerosol boiling point measurement with photoelectric particle counter, observing sulfate radical as major constituent
01 p0059 A72-10833
- Alkali liquid metal heat pipes, showing heat transport rate for boiling initiation
[ASME PAPER 71-WA/HT-10] 05 p0743 A72-15870
- Minimum weight passive insulation requirements for hypersonic cruise vehicles.
17 p2638 A72-35256
- Combined buoyancy and flow direction effects on saturated boiling critical heat flux in liquid nitrogen.
21 p3130 A72-41184
- German monograph - Heat transfer at a vapor bubble growing on a heated wall during boiling.
22 p3244 A72-43059

BOLKOW AIRCRAFT

- Bolkow 105C 3-place helicopter with twin turbine engine driven rigid glass-reinforced plastic rotor blades, emphasizing design philosophy of easy maintainability
13 p1898 A72-29871

BOLOGRAMS**U BOLOGRAMS****BOLOGRAMS**

- Gallium-doped Ge bolometers and triglycine sulfate pyroelectric far IR detector, testing performance as functions of frequency and temperature
04 p0525 A72-15601
- Low temperature Ga doped Ge bolometer for IR detection, improving sensitivity by load resistance noise elimination
05 p0662 A72-16195

Solar radio emission map at 1.2 mm wavelength obtained with He cooled Ge bolometer connected radio telescope
13 p2046 A72-29716

A horizon sensor with a bolometer and electrooptical modulators
17 p2556 A72-35385

Pure and compensated Ge and Si far IR spectral properties at liquid He temperatures for bolometer detector application
21 p3013 A72-40822

BOLTS

- Bolted joint thermal conductance, considering interfacial pressure distribution and surface roughness effects
[AIAA PAPER 72-282] 11 p1741 A72-25222
- Bolted connections strength in graphite fiber-epoxy resin composites reinforced by colaminated boron film
11 p1672 A72-25476

BOLTZMANN DISTRIBUTION

- Wall stabilized Ar arc plasma, investigating Boltzmann equilibrium existence between spectral energy levels
02 p0264 A72-12025
- Boltzmann distribution of nitrogen ions according to rotational energy levels in nitrogen ionization by slow electrons impact
12 p1847 A72-27050
- Cascade ionization of air by RF electric fields and intense laser pulses, solving Boltzmann equation for electron distribution
12 p1848 A72-27390
- Theory of sound propagation in mixtures of monatomic gases.
17 p2583 A72-35613
- Boltzmann distribution of nitrogen ions according to rotational energy levels in nitrogen ionization by slow electrons impact
24 p3427 A72-45703

BOLTZMANN TRANSPORT EQUATION

- Brownian motion kinetic equation from Boltzmann equation for two component neutral gas by simultaneous expansion in density and mass ratios
01 p0050 A72-10233
- Nonsteady molecular beam approximation for strong shock structure problem, considering Boltzmann equation
03 p0399 A72-14053
- One dimensional Boltzmann equation with linearized small perturbation, determining secondary conditions
03 p0399 A72-14347
- Random method to solve basic rarefied gas /Boltzmann/ equation, applying to elastic collisions
04 p0551 A72-14518
- Random method solution of Boltzmann equation for pseudoshock /relaxation mixing/, applying to random collisions of molecular beams
04 p0551 A72-14519
- Rarefied gas heat transfer problem between two parallel plates of different temperatures, evaluating nonlinear Boltzmann equation with Monte Carlo techniques
04 p0595 A72-14599
- Electron heating by oscillating electric field in presence of steady magnetic field, solving Boltzmann transport equation for electron velocity distribution in plasma
04 p0556 A72-14947
- Boltzmann equation collision integral statistical models, solving shock structure in monatomic gas
04 p0513 A72-15339
- Monograph on nonequilibrium relativistic kinetic theory covering heuristic approach, Boltzmann equation, H theorem, equilibrium distributions, relativistic thermodynamics, phenomenological transport theory, heat conduction coefficients, etc
05 p0689 A72-16289

Chapman-Enskog method modification for gas flow Prandtl boundary layer zero approximation distribution function construction, applying Mises transform to Boltzmann equation
05 p0653 A72-17209

Boltzmann kinetic equation with electron-electron collision coefficients for isothermal weakly ionized cesium-argon plasma, using nodal point method
06 p0860 A72-17695

Transport processes theory in mixtures of chemically active gases using Boltzmann equation and Sonin polynomials expansion
06 p0852 A72-17989

Boltzmann equation solution analysis for Maxwell-Lorentz gas in electric field, discussing conditions for electron velocity distribution isotropic part evolution towards Maxwellian distribution
06 p0861 A72-18162

Uniqueness theorems for linearized Boltzmann equation with Maxwell boundary conditions, using Gauss theorem and Schwartz inequality
08 p1149 A72-21252

Boltzmann neutron transport equation solution for homogeneous slabs and spheres, noting dominant critical eigenfunction existence and total flux boundedness, continuity and positivity
09 p1358 A72-23072

- Collision operator behavior in linear Boltzmann equation model of molecular gas in Hilbert space
10 p1510 A72-24102
- LTE solutions of relativistic Boltzmann equation in presence of external electromagnetic field
10 p1513 A72-24856
- Chapman-Enskog method modification for gas flow
Prandtl boundary layer zero approximation distribution function construction, applying Mises transform to Boltzmann equation
11 p1614 A72-25332
- Existence and uniqueness of general solutions of initial value problem for nonlinear Maxwell-Boltzmann equation with finite time interval
12 p1836 A72-27122
- Transient current density in plasma subjected to pulsed electric field derived from Boltzmann transfer equation
12 p1850 A72-27278
- Russian papers on light scattering covering electromagnetic propagation in turbid media, transport equation solution methods, unsteady scattering, spectral line radiation and nonlinear phenomena
13 p2001 A72-28501
- Shock waves internal structure in gas of elastic spheres, solving nonlinear Boltzmann equation
13 p1944 A72-30029
- Transport processes theory in chemically active gases mixtures using Boltzmann equation and Sonin polynomials expansion
14 p2133 A72-30216
- Two dimensional numerical solution of semiconductor steady state transport equations, applying to MOS and bipolar transistors
14 p2142 A72-30847
- Binary gas mixture slipping rate determination from joined solution of Hamel kinetic model linearized equations, and Navier-Stokes and Boltzmann equations
14 p2096 A72-31013
- Nonlinear Boltzmann equation prediction of time correlation functions with long asymptotic time tails
15 p2278 A72-32307
- Microscopic theory of weakly ionized plasma conductivity, showing particle diffusion function or transition probability description by linear Boltzmann equation
15 p2287 A72-32412
- Fluctuation renormalized transport coefficients in corrected nonlinear transport equations derivation from generalized Fokker-Planck equation
15 p2337 A72-32653
- Water bag model in cylindrical rotating two dimensional rod stellar system, showing kinetic energy minimum correspondence to collisionless Boltzmann equation
15 p2315 A72-32717
- Thermal molecular jets mixing produced by Knudsen effusion from porous wall, obtaining Boltzmann equation approximate solution by moment method via assumed distribution function
16 p2429 A72-33055
- Thermionic Cs arc theory applicability evaluation, considering collision dominated transport equations for plasma
17 p2587 A72-34616
- Solution of the Boltzmann equation for a fully ionized plasma in an oscillatory electric field and a steady magnetic field. V - Explicit solution for a homogeneous plasma in a high-frequency electric field.
17 p2589 A72-35057
- Quantum Boltzmann equation for a laser.
17 p2563 A72-35160
- Eigenvalues and eigenvectors for solutions to the radiative transport equation.
17 p2576 A72-35259
- Solution to a relaxation problem by the discrete velocity method with the aid of the Boltzmann equation
17 p2586 A72-35809
- The Cauchy problem for the nonlinear Boltzmann equation in general relativity
18 p2710 A72-36471
- Electron-relaxation effects in transferred-electron devices revealed by new simulation method.
18 p2667 A72-36689
- Combined finite element-weighted residuals method for linearized BGK Boltzmann kinetic theory equation, considering cylindrical Couette flow
18 p2684 A72-37168
- French monograph - An asymptotic theory of the Boltzmann equation and its application to the study of near continuum flows
19 p2785 A72-37489
- Relaxation of a reacting gas described by the Boltzmann kinetic equation
19 p2838 A72-38856
- The relativistic Boltzmann equation.
20 p2955 A72-40012
- Limiting properties of solutions of the Boltzmann equation.
21 p3086 A72-40264
- Boltzmann kinetic equation for nonideal plasma with allowance for polarization effects, noting collision integral convergence
21 p3090 A72-40412
- Predvoditelev critical revision of hydrodynamic and heat transfer theory based on Navier-Stokes and Boltzmann equations, developing statistical system of molecular interactions
22 p3165 A72-41951
- Particle collisions integral in Boltzmann equation for arbitrary distribution function, with particular attention to two dimensional flows
22 p3205 A72-42266
- The internal boundary value problem for the Boltzmann equation in the steady state and weakly nonlinear
23 p3280 A72-43820
- Calculation of transport coefficients of a non-Lorentzian plasma
23 p3321 A72-43821
- On exponential-asymptotic stability properties of Boltzmann's equation and a class of its modifications.
24 p3426 A72-44911
- BOLTZMANN-VLASOV EQUATION**
Boltzmann equation solution in terms of irreducible spherical tensors and Talmi coefficients, calculating stress tensor for fully ionized plasma in strong magnetic field
09 p1341 A72-22681
- Galactic disk systems relaxation time due to particle encounters, discussing validity of Boltzmann-Vlasov equation
12 p1872 A72-27894
- Numerical algorithm for Boltzmann equation solution with application to shock structure in one dimensional flow
13 p1985 A72-28617
- BOLZA PROBLEMS**
Second order optimality conditions for variable end time terminal control problems.
[AIAA PAPER 72-932]
21 p3039 A72-41571
- BOMBER AIRCRAFT**
B-1 strategic supersonic bomber design, emphasizing variable sweep wing, landing gear, control and instrumentation
02 p0154 A72-12226
- Titanium-boron-epoxy composite materials selection and fracture mechanics criteria for B-1 bomber structural design
09 p1317 A72-22477
- Passive detection radar system for bombers, calculating target distance during horizontal flight
11 p1597 A72-26316
- Interdiction bombing mission effectiveness model for bad and good weather aircraft type selection depending on weather conditions at target site
13 p1896 A72-28400
- Control configured fighter and bomber aircraft based on flight control technology, discussing development programs
24 p3369 A72-45386
- BOMBING EQUIPMENT**
The application of non-planar lifting surface theory to the calculation of external-store loads.
[AIAA PAPER 72-971]
22 p3135 A72-42340
- BOMBS (PRESSURE GAGES)**
U PRESSURE GAGES
- BOMBS [SAMPLERS]**
U SAMPLERS
- BONDING**
NT ADHESIVE BONDING
NT CERAMIC BONDING
NT EXPLOSIVE WELDING
NT METAL BONDING
NT METAL-METAL BONDING
NT RESIN BONDING
Adhesive materials based on room temperature vulcanizing silicone elastomers for space shuttle vehicle reusable surface insulation bonding
01 p0075 A72-10763
- Clad-to-core bond testing in radioisotope irradiation strips by pulsed laser ultrasonic schlieren system
01 p0080 A72-10811
- Plane strain analysis of two bonded semiinfinite elastic media with different thermomechanical properties and cracks, calculating stress factors and maximum stress angles
01 p0140 A72-10990
- Adhesives and techniques for bonding plastics with plastics and nonplastic materials
02 p0236 A72-12610
- Elastic shaft bonded to dissimilar elastic disk, considering torsion problem
04 p0583 A72-14449
- Thin sintered fluoride films bonding with monoaluminum phosphate, investigating friction and wear behavior
06 p0821 A72-17804
- Plane elastostatic problem of stress concentration near flat interface inclusion in bonded dissimilar materials
09 p1405 A72-22997
- Delayed pulse echo and through-transmission ultrasonic techniques for nondestructive inspection and quality control of braze bonds in high current electric contact assemblies
10 p1487 A72-24173
- Elastic constants and bond stress distribution for discontinuous fiber-reinforced three dimensional composite subjected to uniaxial tension
[AIAA PAPER 72-397]
11 p1731 A72-25418
- Debonded laminar composite torsional stress intensification analysis near circular shaped imperfection based on Hankel transform and dual integral equations solution
15 p2261 A72-32247
- Plastic packages for complex microcircuits.
17 p2528 A72-34717
- Report on Flip Chip and Beam Lead bonding for electronic circuits.
[SAE AIR 1141]
18 p2666 A72-36528
- Coating of fibers and the fabrication of fiber-reinforced composite materials
20 p2929 A72-39443
- BONE MARROW**
Chronic microwave irradiation effects on experimental animal blood forming systems, examining peripheral blood count changes and nuclei and mitosis abnormalities in erythroblastic and lymphoid cells
02 p0158 A72-11708
- Radiobiological effects of nonuniform body irradiation, discussing regeneration process stimulation by partially shielded bone marrow
02 p0161 A72-12060
- Biological dosimetry in acute human irradiation from cytogenic study of peripheral blood and bone marrow
04 p0467 A72-14606
- Proliferative blood forming tissue activity under chronic gamma ray irradiation in guinea pigs by quantitative methods, showing myeloid and reticular disturbances of bone marrow
04 p0467 A72-14607
- Hypoxia effect on diurnal mitotic activity rhythm of marrow erythropoiesis system of guinea pigs in pressure chamber
05 p0618 A72-16631
- Supercellular regulators of triggering mechanism of regenerative reaction in sternum erythropoietic bone marrow tissue
13 p1901 A72-28636
- Nervous and humoral stimulation and hypoxia effects on erythropoiesis control, studying human blood serum additions to bone marrow cultures
21 p3001 A72-40762
- Pyrogenal injection test for hematopoietic tissue function in dogs, describing response as transient leukopenia followed by pronounced leukocytosis due to bone marrow granulocyte ejection
23 p3255 A72-43911
- BONES**
NT CEREBRUM
NT CRANIUM
NT FEMUR
NT INTRACRANIAL CAVITY
NT PELVIS
NT SCIATIC REGION
NT STERNUM
NT TIBIA
NT ULNA
Bone tissue elastic behavior based on Voigt model of two phase composite material, using ultrasonically determined hydroxyapatite elastic moduli
01 p0136 A72-10112
- Hydroxyapatite isotropic and anisotropic elastic properties compared with experimentally observed anisotropic behavior of bone
01 p0018 A72-10625
- Aseptic bone necrosis pathology from radiographic studies in dogs with decompression sickness noting articular cartilage erosion and joint dysplasia and exostosis
06 p0764 A72-17876
- Calcium metabolism perturbations in astronauts under weightlessness conditions and in immobilized test subjects, noting bone tissue renewal cycle modification, calciuria variations and bone calcification
07 p0927 A72-19245
- Skeletal bones ash content in man and primates, implying differences due to adaptive physiological function
10 p1424 A72-23736
- Calcium and phosphorus excretion relation to bone density changes in immobilized Macaca nemestrina monkeys
12 p1760 A72-27473
- Comparative study of two direct methods of bone mineral measurement.
17 p2508 A72-34552
- BOOLEAN ALGEBRA**
NT BOOLEAN FUNCTIONS
Logically stable failures of discrete combination devices by practical behavior in response to given input vectors, using alpha state Boolean algebras
04 p0496 A72-14994
- Probabilistic logic method, concepts and elementary operations in combining Boolean algebra and probability theory
08 p1197 A72-20869

Accuracy and reliability in engineering design of discrete automata without memory /logic circuits/, using Boolean algebra for mathematical models
11 p1600 A72-25434

Input delay influence on dynamic stability of potential finite automata in transition between two states, noting logic circuits synthesis based on Boolean algebra
23 p3274 A72-43350

BOOLEAN FUNCTIONS

Minimum length fault tests design for irredundant combinational logic circuits containing single faults based on Boolean difference function
02 p0185 A72-11485

Logic functions for magnetic bubble devices based on interaction of circular magnetic domains in rare earth iron oxides, considering gates for dynamic memory
[IEEE PAPER 2,3] 03 p0327 A72-13753

Programmable cellular cascades and arrays synthesis for realizing arbitrary Boolean functions or parallel arithmetic operations
04 p0498 A72-15107

Sign behavior of switching function defined for plane fuel-optimal flight on elliptical coast trajectories
05 p0728 A72-16705

Sequential machine realization with trigger or flip-flop elements and Boolean function feedback
10 p1445 A72-24401

Polish monograph on minimal representations and identification of Boolean function symmetry in combinational logic network synthesis, using two dimensional topological model
12 p1793 A72-27224

Multivalued logical function synthesis with multistage logical network through hypercomplex representation and linear transformation
12 p1794 A72-27497

Circuit synthesis for random numbers probabilistic digital transducers reduced to synthesis of random binary signal converters, noting method description with Boolean functions
16 p2372 A72-34012

Computer adapted for Boolean functions analysis and synthesis, describing structure and method of design
18 p2664 A72-36792

Linear programming application to the solution of some optimum problems of reliability theory
19 p2825 A72-37995

Memory requirements and computation times for implementing reduced consensus algorithms.
20 p2905 A72-39434

Network algebra simplification through computerized minimization of Boolean functions, describing FORTRAN IV program
21 p3038 A72-41001

A minimization method of describing classes in pattern recognition
22 p3198 A72-42178

An algorithm for determining the absolutely minimum form of weakly determined functions
23 p3308 A72-43349

An iterative technique for determining the minimal number of variables for a totally symmetric function with repeated variables.
23 p3308 A72-43421

An iterative algorithm for solving the realization problem of a Boolean function by a single threshold element.
24 p3419 A72-45576

Finite Boolean function computation on sequential machine models, developing exchange inequalities between storage, time, et cetera, for relation of combinational and time complexities
24 p3383 A72-45650

BOOMS [EQUIPMENT]

Spin stabilized satellites attitude dynamics during rigid booms extension, deriving equations of motion approximate solution
11 p1726 A72-25915

Frequency shift and mode shapes for equatorial vibrations of flexible boom on spin stabilized satellite, applying to thermal flutter resonance and nutational stability
15 p2320 A72-31803

Spacecraft boom deployment dynamics environmental simulation and testing for preflight system reliability evaluation
15 p2321 A72-32627

Predictions of solar induced response of thin-walled open-section booms for design.
18 p2733 A72-36364

BOOST

U ACCELERATION [PHYSICS]

BOOSTER RECOVERY

Booster launch vehicle guidance scheme for critical aborts from staging through burnout, minimizing aerodynamic phases for different landing sites
15 p2269 A72-32182

BOOSTER ROCKET ENGINES

NT ALGOL ENGINE

Europa 3 candidate propulsion modules system analysis, considering payload, mission flexibility, or-

bital injection precision, synchronous satellite design influence, satellite-booster interfaces and costs
02 p0287 A72-12731

Supersonic wind tunnel investigation of drag characteristics of clustered booster configuration in longitudinal flow at Mach 1.5 to 4.0
[DGLR PAPER 71-120] 02 p0153 A72-12737

Control system design computerized optimization technique based on high speed repetitive simulations and gradient minimization, considering application to reusable and expendable boost vehicles
[AIAA PAPER 72-98] 05 p0729 A72-16812

Laminar and turbulent convective heating distributions on delta wing space shuttle boosters with interference effects
[AIAA PAPER 72-315] 11 p1567 A72-25249

Boron-epoxy reinforced Ti tubular truss for application to space shuttle booster thrust structure, evaluating performance
[AIAA PAPER 72-393] 11 p1730 A72-25414

Design features of Soyuz life support and launch escape systems and Vostok rocket booster stage
23 p3343 A72-44335

BOOSTER ROCKETS

Boron-epoxy tubular struts for one third scale space shuttle booster thrust truss structure, discussing design, analysis, fabrication, weight, test and quality control
01 p0138 A72-10735

Composite space shuttle booster and orbiter engine support structures design and analysis, stressing weight savings
01 p0139 A72-10740

Test program to evaluate metallic materials candidates for space shuttle booster thermal protection system
01 p0085 A72-10755

Europa 3 booster rocket development for future European space programs, discussing performance characteristics, project management and international cooperation aspects
05 p0724 A72-16310

Longitudinal vibrations stability of launching rocket body, allowing for propellant sloshing, body dynamic deformation and motor dynamics
05 p0731 A72-17186

Transverse vibrations stability of launching rocket body, allowing for propellant sloshing and body elastic deformation
05 p0731 A72-17187

Hot versus shielded aerodynamic surfaces trade study for space shuttle booster wings and fins design, considering materials, structural weight and cost estimates
[AIAA PAPER 72-390] 11 p1726 A72-25411

Space shuttle booster and orbiter thermal protection systems, examining heat sink, metallic reradiative, reusable surface insulation and surface cooled designs
[AIAA PAPER 72-391] 11 p1726 A72-25412

Dynamic behavior of M-4S rocket devices for strap-on booster separation and nose cone and flare deployment
22 p3232 A72-43143

BOOSTERS

Aerodynamic interference between parallel bodies for estimating aerodynamic characteristics of rocket engine with auxiliary boosters, obtaining flow field by slender body theory
05 p0600 A72-16005

High pressure injector optimum design and performance for gas jet boosters, using one dimensional theory with friction allowance
12 p1861 A72-27535

BOOSTERS [EXPLOSIVES]

Leads and booster explosives replacements for tetryl, discussing military specifications and safety criteria of various newly developed compounds and mixtures
08 p1220 A72-20770

BORANES

Book on liquid rocket propellants development, history and ignition problem covering nitrogen tetroxide, hydrogen peroxide, fluorine compounds, boranes and monopropellants
19 p2884 A72-38675

BORATES

NT LITHIUM BORATES

Borated steels strength under static bending, cyclic flexure and torsion and impact loads, correlating fatigue strength, residual stresses and core properties
13 p1979 A72-29477

Comparative evaluation of zinc borate 2:3:3.5 with antimony oxide using various fire testing methods.
20 p2898 A72-39699

Structons /close-neighbor arrangements/ stability and characteristics in anhydrous borate crystals and glasses containing bridging and nonbridging or tribonded oxygens
22 p3197 A72-42795

BOREL SETS

Minimal dynamic systems invariant Borel probabilistic measure with metric space and topological entropy equality
08 p1210 A72-22187

Markovian characteristics of time dependent excursions and independent incursions processes provided with limits to left and continuous to right, noting Poisson punctual process and Borel sets
10 p1505 A72-24114

BORES

U CAVITIES

BORESIGHTS

Sidewall reflection induced boresight error in anechoic chamber used for missile test or simulation
08 p1441 A72-21421

X band radar target cross section representation by discrete point reflector models, deriving boresight error mean and variance in presence of n-target sources
15 p2201 A72-32474

BORIDES

NT CHROMIUM BORIDES

NT TITANIUM BORIDES

Zirconium diboride-silicon carbon-graphite composition for lifting entry vehicle hot leading edges, investigating mechanical behavior by tension and flexural tests
01 p0091 A72-10767

Iron aluminides and borides diffusion layers morphology on alpha iron surface by metal surface/gas phase interaction, observing preferential orientation
03 p0376 A72-13971

Phase composition and electrical and mechanical properties of compacted zirconium diboride/tungsten alloys after sintering in argon, carbonaceous medium and vacuum
06 p0832 A72-18428

Phase diagram of Ta-B system by thermal, X ray and microstructural analyses
06 p0833 A72-18434

Transition metal borides chemical bonding mechanism from Nb and Cr boride phases thermal emf and expansion, resistivity, Hall coefficient and carrier mobility
07 p1017 A72-19992

Oxide scale formation on zirconium diboride materials, observing microstructural features as function of temperature and reaction time
[AD-737020] 09 p1333 A72-22380

Mo-Zr solid solutions internal boriding, discussing diffusion controlled process and hardness dependence on Zr
10 p1494 A72-23833

Electrical discharge machining of zirconium diboride, considering operations and tooling requirements
[AIAA PAPER 72-329] 11 p1637 A72-25365

Isolation and sintering techniques and thermoemission properties of lanthanum, yttrium and gadolinium borides
11 p1645 A72-26858

X ray diffraction discovery of borides with yttrium chromium boride type orthorhombic structure
13 p1984 A72-29799

Optimum dispersion time and size particle determination for zirconium diboride powder grinding in vibrating mill, using gas flow ratio method
13 p1967 A72-30101

Equilibrium states difference of ternary metal-boron-nitrogen systems, taking into account chemical bond type and crystal structure of boride and nitride atoms
14 p2112 A72-30154

Zirconium diboride oxidation processes at temperatures above 520 C, noting zirconium oxide formation
14 p2121 A72-30850

Dynamic elastic moduli of diffusion saturated high melting point nitrides, carbides and borides of Ti, Zr, Nb, W, Mo and Ta
15 p2252 A72-31199

Chemical phase analysis for determining phase composition of products formed in borides, carbides and borocarbides mixtures
18 p2656 A72-36100

NASA research on refractory carbides, nitrides and borides, discussing electronic and defect structures, hot extrusion, uranium nitride, cermet for bearings and composite evaluation
18 p2701 A72-36594

Phase equilibria in the hafnium-niobium-boron and tantalum-chromium-boron systems
19 p2819 A72-38285

HfB2 and ZrN alloys

Electrolytic and nonelectrolytic diffusion methods for protective coatings production from gas, liquid or solid phase, discussing wear resistance enhancement in boridized steels
20 p2929 A72-39449

Certain physical properties of the borides of cobalt and nickel
21 p3068 A72-40953

Relation between the work function and adsorption and catalytic properties of transition metal borides in the reaction of recombination of hydrogen and nitrogen atoms
22 p3187 A72-41926

BORING MACHINES

Countersink boring machines with programmed digital control systems for precision spacing multiple hole drilling in extended aircraft engine components 11 p1642 A72-26816

BORN APPROXIMATION

Modified Born approximation for electromagnetic backscattering cross section from turbulent plasmas, noting attenuation leading to saturation and cross-polarization 01 p0031 A72-10846

Preresonance Raman scattering tensor in Born-Oppenheimer approximation of molecular wave functions 10 p1491 A72-24110

Electromagnetic wave scattering on inhomogeneities by Born approximation, estimating maximum error for small correlation radius 10 p1436 A72-24503

Space-time correlation of field amplitude and phase in plane waveguide with statistically irregular boundary, using Born approximation and perturbation theory method 13 p1928 A72-28471

Excitation cross section in dipole approximation of semiclassical impact parameter and Born approximation, using asymptotic expansion of hydrogen-like atoms oscillator strength 13 p2040 A72-29411

Ionization energy loss of relativistic heavy nuclei for close collisions as function of charge, computing Born approximation corrections via Mott exact cross section 15 p2282 A72-32647

Born approximation for resonance bremsstrahlung emission and photon absorption cross sections at electron-ion scattering, solving multiparticle problem 15 p2279 A72-32697

Calculation procedure involving wave function for vibrational correction to electron scattering cross section of hydrogen molecule in Born approximation 17 p2585 A72-34261

Collisional-rate coefficients for sodiumlike Ar VIII ions. 17 p2585 A72-35770

Direct and cross polarized backscatter power from a turbulent plasma. 23 p3320 A72-43521

Propagation of the mutual coherence of optical waves in a random medium. 24 p3424 A72-44711

Electron scattering by molecules with and without vibrational excitation. V - Elastic scattering and non-resonant vibrational excitation of N₂ at 30-83 eV. 24 p3427 A72-45305

BORN-MAYER EQUATION

U BORN APPROXIMATION

BORN-OPPENHEIMER APPROXIMATION

Semiempirical method for determining electron wave-function parameters in solids 20 p2959 A72-38955

BORON

NT BORON ISOTOPES

Continuous casting of metallic tubular structural elements reinforced with boron filaments, stressing application to space shuttle structures 01 p0074 A72-10731

Acoustic emission monitoring of boron epoxy composite, showing crack extension characterization by emission bursts 02 p0249 A72-11993

Boron-containing polymer heterogeneous combustion determination using hybrid regression rate with thermal degradation and surface temperature data 02 p0270 A72-12260

High strength, stiffness and low density properties of boron/aluminum matrix composites in flight structures 04 p0585 A72-14745

Boron/aluminum composite sheet quality evaluation by radiography, ultrasonic C-scanning and micro-ohm resistance measurement, correlating with resistance weld strength 04 p0526 A72-14839

Li, Be and B production rate in interstellar gas by galactic cosmic rays from diffusion model of fast particles, accounting for He component 05 p0708 A72-15760

Boron ignition and combustion mechanisms based on high speed photographs of laser ignited boron particles [AIAA PAPER 72-72] 05 p0703 A72-16801

Boron containing solid propellant combustion efficiency and fuel-air ratio determination from particle laden plume nonequilibrium effects in ducted subsonic flow [AIAA PAPER 72-36] 05 p0750 A72-16972

Neutral B I vacuum UV spectra from hollow cathode light source, remeasuring electron transitions to higher accuracy 06 p0852 A72-17896

Nb-Mo alloys behavior in aggressive boron containing medium at high temperatures, relating boride phases growth rate to component percentages 07 p1012 A72-19680

Boron addition effects on scaling resistance of Ni-Cr steel at high temperatures 07 p1012 A72-19738

Room temperature IR absorption spectra of B alloyed powdered synthetic diamonds 07 p1050 A72-20253

Thermal and mechanical properties of randomly reinforced fiber/resin composites including boron/epoxy, Thorne/epoxy and S glass/epoxy materials 08 p1192 A72-21682

Composite filament wound boron-epoxy rocket motor combustion chamber design, fabrication and hydrostatic tests 08 p1177 A72-21692

Boron and carbon fiber reinforced plastics anisotropic stress-strain properties, considering fiber misalignments curvature and low shear resistance effects 08 p1196 A72-21857

Titanium-boron-epoxy composite materials selection and fracture mechanics criteria for B-1 bomber structural design 09 p1317 A72-22477

Elastoplastic analysis of unidirectional filament reinforced boron/aluminum and boron/epoxy composites under longitudinal loading, using finite element techniques 10 p1555 A72-24254

B-Al metal matrix composites joining together and to Al and Ti, considering soldering, brazing, bonding and mechanical fastening [AIAA PAPER 72-360] 11 p1638 A72-25388

Colaminated boron-polyimide film effect on strength of graphite fiber-epoxy resin composite double lap bolted joints [AIAA PAPER 72-382] 11 p1730 A72-25405

Fatigue strength characteristics of boron-epoxy reinforced Al stringers for helicopter airframe [AIAA PAPER 72-392] 11 p1574 A72-25413

Boron-epoxy reinforced Ti tubular truss for application to space shuttle booster thrust structure, evaluating performance [AIAA PAPER 72-393] 11 p1730 A72-25414

Boron-epoxy reinforced composite metal shear web design for space shuttle orbiter main engine thrust beam structure [AIAA PAPER 72-395] 11 p1726 A72-25416

Selective reinforcement with high strength boron filament to achieve cost effectiveness and weight savings for composite structures [AIAA PAPER 72-396] 11 p1731 A72-25417

Boron-epoxy composite design for aircraft structures, discussing materials variations, strength prediction inadequacies and full scale tests 11 p1670 A72-25454

Failure modes effect on compressive strength of boron-epoxy composites tested on coupons, honeycomb sandwich columns and beams 11 p1671 A72-25466

Embedded strain gage technique for subsurface tensile testing of boron-epoxy composites 11 p1671 A72-25467

Fracture toughness of anisotropic heterogeneous filamentary boron/aluminum composites, correlating test results with acoustic emissions from filament breakage 11 p1672 A72-25470

Bolted connections strength in graphite fiber-epoxy resin composites reinforced by colaminated boron film 11 p1672 A72-25476

Off axis and transverse tensile properties of boron reinforced Al alloys, correlating metallurgical structures with stress-strain curves and fractographic studies 11 p1654 A72-25479

Boron fibers tensile and transverse strengths, relating severe anisotropy to residual stress pattern from preexistent flaws 11 p1672 A72-25484

Fracture surface energy and acoustic emission of boron fiber-epoxy resin composite, using linear elastic fracture mechanics and compliance variation methods 11 p1674 A72-25858

High performance continuous filament reinforcements for nonmetallic matrix composites, emphasizing boron and graphite fibers 11 p1674 A72-26229

Filament reinforced boron-aluminum composites multiple fracture behavior dependence on cross section geometry from tensile test 11 p1668 A72-26944

Dynamic properties of thermosetting plastic composites unidirectionally reinforced by high elastic moduli boron and carbon fiber for aircraft structural applications 12 p1882 A72-27343

Chemical vapor deposition of boron on carbon monofilament substrate to eliminate fracture and boron damage and achieve good strength 12 p1834 A72-28085

Resin bonded B-Al composites, discussing fabrication techniques and mechanical properties 12 p1815 A72-28098

Boron and carbon reinforced fiberglass plastics tensile strength characteristics, presenting static fatigue curves vs Poisson coefficient and elastic modulus for various fiber contents 13 p1982 A72-28552

Relaxation and internal friction characteristics of beta-rhombohedral B at 80-1000 K, using LF vacuum oscillator with inverted torsion pendulum 14 p2122 A72-30958

Boron reaction characteristics in ducted rockets under varying primary chamber conditions detailing various gaseous propellants effects 15 p2296 A72-32311

Laser ignition and combustion of boron particles, developing oxide coating and droplet burning models for low and high temperature stages respectively 15 p2296 A72-32582

Alpha to beta transformation of rhombohedral B, investigating lattice structure on heating stage in electron microscope 16 p2405 A72-33204

Boron concentrations in Mo-Hf alloy samples from neutron activation analysis, measuring Li 8 beta radiation with plastic scintillation detector 16 p2391 A72-33238

Plastic flow, yield strength and fracture of unidirectional Al-B fiber composite sheet under biaxial tension 16 p2411 A72-33821

Application of boron/epoxy to the CH-54B Skycrane helicopter. [AHS PREPRINT 670] 17 p2491 A72-34510

Boron ignition and combustion in air-augmented rocket afterburners. 17 p2636 A72-34902

Fracture of boron filaments in an aluminum matrix. 17 p2571 A72-35655

High strength alumina, boron, silicon carbide and graphite reinforcing fibers for composite materials 17 p2572 A72-35656

High strength-high modulus boron vapor deposited on a carbon monofilament substrate. 17 p2572 A72-35657

Boron- and graphite-epoxy and boron-aluminum composites forming, processing and costs for aircraft structural materials 17 p2560 A72-35663

Photocolorimetric determination of boron in nickel and titanium borides via Magnezone I in alkaline medium, determining solution pH, reaction time, light absorption, etc 18 p2655 A72-36099

Fatigue of boron-aluminum and carbon-aluminum fibre composites. 18 p2701 A72-36625

Machining boron-epoxy composites. 19 p2809 A72-38386

Variation of the coordination number of boron during heat treatment of aluminoborosilicate fiberglass 19 p2823 A72-38681

RF shielding and electrical properties of boron and carbon fiber reinforced composites. 20 p2944 A72-38987

The transverse tensile properties of boron fiber reinforced aluminum matrix composites. 20 p2938 A72-39302

Influence of boron on the structure and certain properties of electron-beam melted molybdenum 20 p2939 A72-39313

Boron and carbon fibers fabrication and properties for composite materials reinforcing elements, noting strength and stiffness dependence on stress orientation 20 p2944 A72-39437

Mechanical properties of boron fiber reinforced aluminum matrix composite, describing experimental and control techniques 20 p2940 A72-39447

Boron p-type region impurity concentration calculation technique to establish anomalous base profile in p-n bipolar transistors 20 p2908 A72-39567

Enhancement of heat resistance in Kh14G14N3T steel by microadditions of boron 20 p2941 A72-39579

Interfacial characteristics of silicon carbide-coated boron-reinforced aluminum matrix composites. 20 p2941 A72-39791

Boron polyimide composite development. 21 p3072 A72-40553

Boron fiber reinforced composites technology assessment and utilization, stressing cost reduction [ICAS PAPER 72-30] 21 p2995 A72-41155

Composite materials obtained by depositing boron layers under vacuum on aluminum sheets 22 p3190 A72-42646

High strength boron and borsic fiber reinforced aluminum composites. 23 p3299 A72-43491

Thermal diffusion annealing improved Ni-B composite electrolytic coatings with uniform B distribution over bulk matrix 23 p3303 A72-44012

- Boron-aluminum structural component for Shuttle.
24 p3458 A72-44890
- Influence of boron on the structure and properties of electron-beam melted molybdenum
24 p3414 A72-45380
- BORON ALLOYS**
- Fe-Ra-B ternary alloy, investigating phase equilibria and isothermal cross sections with X ray analysis
03 p0374 A72-13739
- Hf-B system alloys phase diagram and impurities effect, discussing synthesis and heat treatment regime
07 p1010 A72-18857
- Deposition of Ni-B coatings with specified electrical resistance onto fiberglass cloth reinforced plastics
09 p1318 A72-22528
- Mo corner of Mo-B phase diagram constructed from microstructural analysis and microhardness, melting point and lattice constant measurements
12 p1828 A72-27291
- Liquidus temperatures and isothermals in Al corner of Al-Ti-B alloy phase diagram, using differential thermal analysis
16 p2409 A72-33808
- Phase composition and isothermal cross section diagrams of Cr-Ni-B system at 800 C, using X ray and microstructural analyses
19 p2822 A72-38678
- Radiographic examination of rhenium-aluminum-boron and rhenium-silicon-boron ternary systems
19 p2822 A72-38679
- Al-B and Al-Ti-B alloys fabrication, discussing quality control and grain refinement
20 p2936 A72-39207
- Thermal fatigue resistance of KhN70VMluT boronized alloy
20 p2941 A72-39585
- Some results of an investigation of the tungsten-nickel-boron ternary system
21 p3066 A72-40393
- Boron and carbon contents effect on elastic properties strength and ductility of electron beam melted Mo-B alloys
24 p3414 A72-45381
- The mutual solubilities of titanium and boron in pure aluminum.
24 p3415 A72-45482
- BORON CARBIDES**
- Steels gas-powder facing with boron carbide, testing microhardness and wear resistance
03 p0363 A72-13547
- Oxidizability of boron-carbon compounds at high temperatures, determining chemical composition effect on oxidation resistance
18 p2703 A72-36095
- Enthalpy and heat capacity of boron carbide at temperatures ranging from 273 to 2600 K
18 p2704 A72-37191
- BORON COMPOUNDS**
- NT BORANES
NT BORATES
NT BORIDES
NT BORON CARBIDES
NT BORON FLUORIDES
NT BORON HYDRIDES
NT BORON NITRIDES
NT BORON OXIDES
NT CHROMIUM BORIDES
NT LITHIUM BORATES
NT TITANIUM BORIDES
- Boron/potassium nitrate parachute mortar design for aircraft and spacecraft applications, comparing with high-low propellant
08 p1221 A72-20783
- Fractography of high boron ceramics under ballistic impact, suggesting macroscopic and microscopic textures relationship to stress states and microstructure
09 p1334 A72-22391
- Phase diagrams, microhardness and composition of sintered binary B compounds with Zr, Hf, Ta, Cr, Mo, W, Re, Fe, Ni, and Si
21 p3070 A72-41371
- BORON FLUORIDES**
- IR mass spectrometric study of OBF in Ne and Ar matrices, discussing molecular structure
16 p2360 A72-33223
- BORON HYDRIDES**
- NT BORANES
- Ni plating by chemical reduction method in boron hydride solution, deducing stabilizing effect of sulfur compounds and Pb salts from catalyst poisoning theory
11 p1641 A72-26265
- BORON ISOTOPES**
- Cosmic Li, Be and B nuclei charge and isotopic composition measured by particle telescopes, finding I/M ratio
01 p0121 A72-11120
- BORON NITRIDES**
- Cold pressed powdered boron nitride, Mo, W, Nb disulfides and diselenides, investigating thermal dissociation in He by X ray analysis
03 p0380 A72-13551
- Composite plasma sprayed coatings of Cu, Ni and boron nitride, noting antifriction and wear characteristics
06 p0822 A72-18429

- Hot pressed boron nitride and composite oxidation tests in atmospheric arc jet, noting fabrication and composition effects on thermal shock and oxidation resistance
09 p1333 A72-22379
- UV radiation effects on pyrolytic boron nitride lattice imperfections, using space environment simulator
09 p1336 A72-22404
- Boron nitride coated boron fibers for metal matrix composite reinforcement, discussing surface nitriding process by heating
12 p1815 A72-28088
- Hexagonal and cubic boron nitride surface wetting by liquid metals as function of contact interaction and chemical affinity
15 p2253 A72-31224
- Thermal conductivity of compact samples of cubic BN
19 p2823 A72-38408
- BORON OXIDES**
- Gaseous boron dioxide and oxyfluoride heat of formation determination by mass spectroscopy and molecular effusion technique
[AD-740421] 07 p0936 A72-19682
- BORON TRIFLUORIDE**
- U BORON FLUORIDES**
- BOROSILICATE GLASS**
- Static fatigue of borosilicate glass, fused silica and polycrystalline alumina, presenting log stress vs log failure time plots
09 p1335 A72-22398
- Variation of the coordination number of boron during heat treatment of alumoborosilicate fiberglass
19 p2823 A72-38681
- Phototropic borosilicate glass optical density variation by exposure to UV or blue light, considering utilization for digital data storage and/or cathode ray tubes
22 p3180 A72-42941
- BOSE-EINSTEIN STATISTICS**
- U QUANTUM STATISTICS**
- BOSONS**
- NT ALPHA PARTICLES
NT LIGHT BEAMS
NT MESONS
NT PHOTONS
NT PIONS
- Quantum condensation in finite volume boson gas, using Bogoliubov quasi-expectation value method
10 p1563 A72-24676
- Resonant and semiweak process production cross sections for massive Lee-Wick spin-zero and spin-one bosons at high energies
15 p2280 A72-31290
- BOUGUER LAW**
- Quasi-specular and Lambert reflection of short radio waves from lunar surface dependent on central portion of near side
05 p0631 A72-17039
- Gravity data free air and Bouguer correction/elevation correction/ by nomographic alignment chart
06 p0809 A72-18148
- Error corrections for UV photometric measurements with light filters involving Bouguer formula
15 p2233 A72-31400
- BOUNDARIES**
- NT FLUID BOUNDARIES
NT FREE BOUNDARIES
NT GAS-SOLID INTERFACES
NT GRAIN BOUNDARIES
NT JET BOUNDARIES
NT LIQUID-LIQUID INTERFACES
NT LIQUID-SOLID INTERFACES
NT LIQUID-VAPOR INTERFACES
- BOUNDARY LAYER COMBUSTION**
- Numerical methods for inverse solution to turbulent swirling boundary layer combustion flow problem
13 p2063 A72-28420
- Energy supply calculation for two dimensional steady laminar compressible boundary layer flows with hypersonic hydrogen-air combustion
15 p2334 A72-31465
- Counterflow diffusion flame gas dynamic structure analysis in porous cylinder forward stagnation region, using surface and boundary layer approximations
15 p2336 A72-32310
- Supersonic and hypersonic combustion processes three dimensional characteristics, comparing wind tunnel test data with boundary layer equations numerical integration results
[ICAS PAPER 72-21] 21 p3130 A72-41146
- Propagation of the front of an exothermic reaction in condensed mixtures whose components interact through a high-melting layer
22 p3245 A72-43177
- BOUNDARY LAYER CONTROL**
- NT POROUS BOUNDARY LAYER CONTROL
- Laminar free convection from vertical nonisothermal right circular cone with boundary layer control by injection or suction, investigating heat transfer by perturbation method
02 p0204 A72-12232
- Wall blowing discontinuity effect on two dimensional incompressible turbulent boundary layers,

- discussing flow relaxation length separation by penetration point trajectory
07 p0966 A72-18841
- Spatial boundary layer variations in low speed wind tunnel working section due to settling chamber screens, discussing mesh variations effects on Preston tube measured pressure coefficient distributions
07 p0966 A72-19061
- Laminar-turbulent incompressible boundary layer transition prevention by suction slots on bodies of revolution, determining optimal suction power/slot distance conditions by variational methods
07 p0968 A72-19737
- Buccaneer Mk 2 and F-4K Phantom takeoff and landing performance improvement due to boundary layer control by leading and trailing edge blowing
09 p1262 A72-22973
- Calculation procedure for reaction thrust of semibounded turbulent jet in boundary layer blowing and blow type anticing systems
13 p1897 A72-28728
- Incompressible flow drag caused by slot suction provided in bodies of revolution for preventing laminar boundary layer transition into turbulent state
16 p2344 A72-33678
- Free jet reenergization efficiency, mixing distance and similarity analysis for boundary layer control at sharp trailing edges and cusps
[AIAA PAPER 72-700] 16 p2345 A72-34043
- Approximation by fractional steps of control problems governed by parabolic equations and with boundary control
19 p2825 A72-37786
- Heat flux and friction force minimization problems equivalence in optimal control of incompressible boundary layer on isothermal plate
20 p2914 A72-39918
- The boundary layer of higher order at the stagnation line of a yawed cylinder in the case of strong suction or injection
23 p3249 A72-44297
- Vortex control on an inclined body of revolution.
24 p3362 A72-45335
- BOUNDARY LAYER FLOW**
- NT BOUNDARY LAYER SEPARATION
NT REATTACHED FLOW
NT SECONDARY FLOW
NT SEPARATED FLOW
- Two dimensional unsteady incompressible boundary layer near forward stagnation point of infinite plane wall with uniform suction or injection, obtaining iterative solution
01 p0050 A72-11106
- Three dimensional boundary layer gas flow in large pressure gradient region, using two dimensional boundary layer equations
02 p0201 A72-11580
- Incompressible boundary layer theory development to include second order curvature effects, determining suction velocity to maintain constant displacement thickness on sphere
02 p0204 A72-12104
- Compressible boundary layer flow problems, using weighted residuals method with exponentials in velocity and enthalpy approximations
02 p0204 A72-12258
- Rotation effects on three dimensional infinitesimal wave stability in Blasius boundary layer
02 p0205 A72-12354
- Unsteady boundary layer flow of viscous incompressible fluid between two rotating coaxial parallel disks
02 p0205 A72-12538
- Turbulence degree effects on aerodynamic properties of planar decelerating cascades at Reynolds numbers 50,000-250,000, discussing blade boundary layer characteristics
[DGLR PAPER 71-096] 02 p0153 A72-12716
- Nozzle boundary layer effects on resistojets performance, presenting conical design model in heater stagnation conditions
03 p0405 A72-12973
- Elastico-viscous incompressible fluid laminar boundary layer flow past infinite plane porous wall, deriving velocity and temperature distributions by two-sided Laplace transform technique
03 p0340 A72-13024
- Wall jet flow displacement on curved surface, deriving two dimensional solution for second-order boundary layer equations
03 p0307 A72-13159
- Boundary layer suction intensity and slot location effects on performance of curvilinear annular diffuser for various Mach and Reynolds numbers
03 p0308 A72-13736
- Plane mixing boundary layer flow of high temperature turbulent gas jet in longitudinal magnetic field
03 p0397 A72-13998
- Intermittency factor of diffuser flow boundary layer with positive pressure gradient, using hot wire anemometers and multichannel analyzer
04 p0461 A72-14411
- Velocity and shear stress in laminar boundary layer flow on flat plate with narrow suction slot
04 p0461 A72-14461

- Generalized transformation of plane compressible and axisymmetric equation for self similar solutions of dissipative boundary layer for bodies with variable surface 04 p0510 A72-14468
- German monograph on two dimensional unsteady boundary layer calculation with unstable effects, using Navier-Stokes equations 04 p0512 A72-15245
- Planetary boundary layer mixing length flow hypothesis with dependence on Reynolds tangential stress permitting turbulent diffusion coefficient maximum values computation 04 p0519 A72-15458
- Low Reynolds number nonequilibrium stagnation heat transfer with helium, argon and hydrogen injection into air boundary and thin viscous shock layers [ASME PAPER 71-WA/HT-19] 05 p0744 A72-15878
- Longitudinal curvature effects on laminar and turbulent boundary layer flows predicted from Navier-Stokes equations, noting mixing length assumption validity [ASME PAPER 71-WA/FE-37] 05 p0645 A72-15920
- Theoretical model for turbulent mixing of confined jet, including wall boundary layer [ASME PAPER 71-WA/FE-31] 05 p0646 A72-15925
- High velocity unsteady flow calculations in metal pipes by numerical methods for boundary conditions, including turbomachinery, column separation and gas accumulator [ASME PAPER 71-WA/FE-13] 05 p0646 A72-15931
- Hypersonic axially symmetric laminar boundary layer electrically conducting fluid flow in blunt body stagnation region in presence of radial magnetic field 05 p0600 A72-16063
- Knudsen boundary layer role in physicochemical hydrodynamics of heterogeneous reactions and flows with surface reactions, using Boltzmann equation 05 p0746 A72-16209
- Book on heat and mass transfer, covering research results over 1953-1969 on supersonic aircraft and missiles cooling problems, rarefied gas dynamics boundary layer flow, etc 05 p0747 A72-16399
- Noncoagulating polydisperse aerosol deposition from two dimensional turbulent boundary layer and fully developed turbulent pipe flows [AIAA PAPER 72-81] 05 p0650 A72-16806
- Boundary layer of gas-particle flows with pressure gradient, numerically integrating momentum equation for cascade particulate flow [AIAA PAPER 72-87] 05 p0604 A72-16808
- High speed boundary layer flow three dimensional disturbances interaction with thermal and ablative response in adjacent surface material, considering laminar and turbulent compressible flows [AIAA PAPER 72-93] 05 p0748 A72-16811
- Finite element algorithm derived for partial differential equation system governing laminar three dimensional boundary layer flow of multicomponent compressible fluid [AIAA PAPER 72-108] 05 p0604 A72-16817
- Mach 2.65 axisymmetric mixed-compression inlet system diffuser and boundary layer bleed system performance estimates confirmed by tests [AIAA PAPER 72-45] 05 p0609 A72-16959
- Chapman-Enskog method modification for gas flow Prandtl boundary layer zero approximation distribution function construction, applying Mises transform to Boltzmann equation 05 p0653 A72-17209
- Low turbulence wind tunnel with closed circuit design and pressure gradient adjustment capability for turbulent boundary layer studies 06 p0795 A72-17713
- Turbulence model for near-wall boundary layer flows, solving differential equations for kinetic energy and length scale 06 p0802 A72-18527
- Monograph on boundary layer generation, presenting two dimensional singular perturbation method 07 p0967 A72-19265
- Second order effects in incompressible boundary layer flow with heat transfer, deriving numerical solutions for skin friction 07 p0968 A72-19625
- Matched asymptotic expansions method application to problems with two independent perturbation parameters, considering application to boundary layer and hypersonic flow theory [ONERA, TP NO. 1007] 07 p0970 A72-20076
- Compressible boundary layer flow past swept wavy wall with heat transfer and ablation, measuring pressure and temperature disturbances 07 p1101 A72-20247
- Laminar and turbulent wall boundary layer and shock attenuation effects on flow uniformity in shock tubes 08 p1149 A72-21018
- Rectangular channel mixed boundary layer flow patterns dependence on inlet edge configurations, channel geometry and hydrodynamic flow core parameters 08 p1150 A72-21317
- Plane potential flow problem for laminar boundary layer on rotating infinite cylindrical blade, using conformal coordinate transformation 08 p1108 A72-21614
- Near wall collateral layer with velocity vector magnitude changes existence in three dimensional turbulent boundary layer flow 08 p1150 A72-21615
- Accuracy tests of Wang method for calculating three dimensional laminar compressible boundary layer flow equations 08 p1150 A72-21625
- Unsteady incompressible laminar boundary layer theory on two dimensional body motion through fluid at rest at infinity, considering skin friction 08 p1151 A72-21794
- Aerodynamics of vortex chambers with symmetrical air injection, discussing core and end boundary layer flows interaction and momentum loss from end surfaces friction 09 p1260 A72-22676
- Rossby similarity for barotropic planetary boundary layer flows in terms of nondimensional Reynolds stress and eddy viscosity 09 p1346 A72-22811
- Galerkin method for numerical simulation of incompressible boundary flows in box geometries with periodic and free slip conditions, noting Taylor-Green vortex decay 09 p1294 A72-22941
- Low speed performance and boundary layer growth in optimal annular diffuser with uniform center body diameter and conically diverging wall 10 p1415 A72-23856
- Turbulent shear stress calculation from mean velocity data for complex flows with inappropriate boundary layer approximations, using method of characteristics 10 p1463 A72-23866
- Turbulent shear layer flow in reattachment region downstream of backward facing step and non-monotonic return to ordinary boundary layer state, noting eddy length scale decrease 10 p1468 A72-24467
- Transverse shear flow stability analysis based on disturbance energy balance determination, applying to ducted and jet stream boundary layer flows 10 p1469 A72-24531
- Laminar and turbulent boundary layer flow stability with forward separation areas 10 p1418 A72-24535
- Diffuser performance and idling characteristics in shock tube at Mach 8, discussing pressure recovery factor laminar and transition flows in boundary layer 10 p1419 A72-24545
- Perturbation analysis for forced flow past semi-infinite flat plate parallel to uniform mainstream, calculating two dimensional laminar film condensation by boundary layer theory 10 p1469 A72-24563
- Parabolic boundary layer finite difference model for predicting film cooling and heat transfer near flush injection slots in gas turbine combustors [AIAA PAPER 72-291] 11 p1614 A72-25229
- Heat transfer and laminarization prediction by two equation turbulence model for accelerated boundary layer flows at low Reynolds number 11 p1743 A72-25260
- Chapman-Enskog method modification for gas flow Prandtl boundary layer zero approximation distribution function construction, applying Mises transform to Boltzmann equation 11 p1614 A72-25332
- Viscous liquid impulsive flow past semi-infinite plate, showing leading edge effects and boundary layer singularity existence 11 p1614 A72-25351
- Two dimensional flow losses of turbine blade cascade with incompressible boundary layer injection [ASME PAPER 72-GT-46] 11 p1570 A72-25638
- Mass transfer effect on adiabatic wall enthalpy and recovery factors in laminar boundary layer flow at high injection rates, using self similar solutions 11 p1746 A72-26535
- Modified gas dynamic functions of total momentum of plane boundary layer for arbitrarily oriented control surfaces and for stratified flows with potential layer 11 p1574 A72-26973
- Turbulence model based on transport equations for Reynolds stress tensor and energy dissipation rate, deriving simplified version for boundary layer flows 12 p1798 A72-27830
- Convective heat transfer for fluid flow on plate with internal heat sources in boundary layer, solving laminar-turbulent transition equations by difference method 12 p1889 A72-28138
- Flow characteristics in air injection through porous surface of blunt bodies, noting blowing parameter effect on boundary layer flow 12 p1752 A72-28143
- Velocimeter design for MHD boundary layer flow velocity measurement, using Doppler frequency shift of laser light scattered from added macroscopic particles 13 p1957 A72-29360
- Acoustic dipole radiation by wall pressure fluctuations in turbulent boundary layer flow over rigid and plane surface at low Mach number 13 p1894 A72-29583
- Longitudinal vortices development in time-increasing boundary layers at concave walls, showing dependence on Reynolds number and boundary layer thickness 13 p1942 A72-29597
- Incompressible boundary layer velocity profile on swept wings, comparing critical Reynolds number to straight wing value 13 p1894 A72-29639
- Hypersonic turbulent boundary layer flow parameters and heat exchange during blowing of coolant air and He through slot 13 p1895 A72-29901
- Numerical integration of boundary layer equations through region of reverse flow past parallel flat plate with negative surface velocity 13 p1944 A72-30033
- Cylindrical model of interplanetary magnetic field-moon interaction, taking into account solar wind flow boundary condition asymmetries 14 p2154 A72-30514
- Ideal gas axisymmetric flow created in supersonic flow interaction with blunted body with strong blowing at surface, obtaining boundary layer approximate solution 14 p2070 A72-31012
- Shear stress distribution and local heat flux at surface of axisymmetric bodies for laminar and turbulent boundary layer flows 14 p2071 A72-31163
- Microelectronic devices liquid cooling by free and forced convection, investigating component size effects on heat transfer by boundary layer analysis and experiment 14 p2091 A72-31172
- Longitudinal and circumferential boundary layer characteristics for concave and convex axisymmetric bodies at small angles of attack, using Cooke equivalent radius concept 15 p2177 A72-31205
- Numerical check on boundary layer equations asymptotic expansion solutions for Falkner-Skan reverse flow and unit Prandtl number compressible boundary layer with blowing 15 p2219 A72-32589
- Three dimensional flow of steady neutral horizontally inhomogeneous planetary boundary layer, studying hodograph, velocity, vorticity, energetics and eddy coefficients 15 p2266 A72-32723
- Boundary layer ionization on flat plate and cylindrical plasma probes in high speed flow, considering ionized continuum flow and collisionless plasma 16 p2374 A72-32831
- Unsteady boundary layer flow equations for arbitrarily smooth bodies moving relatively slowly through rotating liquid [DFVLR-SOONDDR-211] 16 p2376 A72-33007
- Flow equations for corner boundary layer with favorable pressure gradients, indicating separation type main velocity profile 16 p2378 A72-33406
- Blowing and suction effects on free convection boundary layer on semi-infinite vertical flat plate, taking into account temperature difference between plate and fluid 16 p2477 A72-33429
- Steam-condensate mixture boundary layer flow along curved body surface with arbitrary pressure gradient at low Mach number and constant physical properties 16 p2378 A72-33437
- Drag reducing polymers influence on velocity gradients at wall for turbulent pipe flow, observing viscous sublayer thickening 16 p2379 A72-33574
- Supersonic vortex boundary layer flow velocity profiles behind flat plate indentation for Mach numbers 1.7-3.0 and Reynolds numbers to 40,000,000 16 p2380 A72-33857
- Three dimensional small perturbation effects on laminar and turbulent low and high speed boundary layer flows [AIAA PAPER 72-713] 16 p2344 A72-34034
- Transformations of the compressible boundary layer equations. 17 p2538 A72-34341
- Boundary layer velocity profiles on a helicopter rotor blade in hovering and forward flight [AHS PREPRINT 622] 17 p2484 A72-34482
- The effect of axial boundary motion on pressure surge generation [ASME PAPER 71-WA/FE-15] 17 p2539 A72-34969
- Flow over infinite wedge with mass transfer by boundary suction or injection, solving nonlinear boundary layer equations by parametric differentiation method 17 p2485 A72-35230

- Contribution to the study of flows with surface chemical reactions in the boundary layer
17 p2541 A72-35455
- Effects of vorticity, displacement speed and curvature on heat transfer with dissipation.
17 p2638 A72-35747
- Iterative calculation of a three-dimensional boundary layer and comparison with experiment
17 p2638 A72-35748
- On the extension of particular solutions of the energy equation of compressible turbulent boundary layers.
17 p2544 A72-35954
- The bounding theory of turbulence and its physical significance in the case of turbulent Couette flow.
18 p2677 A72-36006
- Behavior of boundary layers on rough compressor blades
18 p2641 A72-36420
- Boundary layer and inviscid main stream interaction in asymmetric supersonic steady gas flow incident on circular cone at high Reynolds numbers
18 p2641 A72-36662
- Response of heat transfer from a moving flat plate in a parabolic flow.
18 p2741 A72-36798
- The unsteady boundary layer flow in a convergent channel.
18 p2683 A72-36930
- Hydromagnetic boundary layer flow around an oscillating axisymmetric body.
18 p2683 A72-36932
- The forces on a flat plate in a Couette flow.
18 p2683 A72-36996
- Application of boundary layer concepts to turbulent lubrication theory of bearings and seals.
18 p2696 A72-37052
- Laminar flow in an annulus with porous outer wall.
18 p2683 A72-37054
- Alternate singular perturbation theory of high Reynolds number flow over flat plate to eliminate asymptotic matching and composite solution for accuracy improvement
18 p2684 A72-37083
- Prandtl equations solution nonuniqueness for outside boundary layer flow tangential velocity inversely proportional to power of abscissa measured distance
19 p2784 A72-37394
- Flow equations for flat plate turbulent boundary layer with Reynolds, continuity and energy components, deriving semiempirical differential equation for turbulence scale
19 p2785 A72-37471
- Inversion of a laminar boundary layer during the injection of CO₂ through a vertical porous surface under natural convection conditions
19 p2881 A72-38191
- Hydromagnetic flow between two rotating disks with noncoincident parallel axes of rotation.
19 p2841 A72-38436
- Motion of particles injected from the surface into stagnation-point flow.
20 p2913 A72-39611
- Compressible boundary-layer equations solved by the method of parametric differentiation.
20 p2914 A72-39614
- The prediction of compressible turbulent boundary-layer flows with mass addition.
[ASME PAPER 72-HT-58] 20 p2914 A72-39658
- A two-equation model of turbulence applied to the prediction of heat and mass transfer in wall boundary layers.
[ASME PAPER 72-HT-15] 20 p2986 A72-39685
- An inverse problem in boundary-layer flows - Numerical determination of pressure gradient for a given wall shear.
21 p3043 A72-40108
- A method for determining the motion in a laminar boundary layer.
21 p3045 A72-40813
- Calculation of heat shield with local mass injection in hypersonic flow.
21 p3131 A72-41235
- The motion of a viscous fluid past an impulsively started semi-infinite flat plate.
21 p3046 A72-41316
- Multicomponent diffusion and heat transfer in flows of a chemically balanced ionized gas past bodies
21 p3047 A72-41658
- Stewartson transformation correlating three dimensional compressible boundary layer growth on impulsively moving body, assuming small cross flow
21 p3047 A72-41782
- Transverse magnetic field effect on unsteady incompressible laminar MHD boundary layer flow, noting cylindrical body oscillations in fluid
21 p3095 A72-41786
- Time-periodic solutions of boundary layer equation systems
22 p3164 A72-41908
- Symmetrical plane-parallel boundary layer at a sudden onset of motion
22 p3164 A72-41909
- Diffusion toward a particle in the case of shear flow of a viscous liquid - Approximation of the diffusion boundary layer
22 p3165 A72-41910
- Differential equations for heat transfer in turbulent boundary layer flow of incompressible fluid with constant thermophysical characteristics
22 p3166 A72-42253
- Effect of external turbulence on the boundary layer of a flow
22 p3166 A72-42258
- Theory of a boundary layer with abruptly varying boundary conditions
22 p3166 A72-42259
- German monograph - Three-dimensional boundary layers at curved walls.
22 p3167 A72-43051
- Boundary layer flow on a circular cylinder moving in a fluid at rest.
23 p3248 A72-43715
- The effects of magnetic field oscillations on the boundary layer flow past a magnetized plate.
23 p3321 A72-43725
- A simple theory for the two-dimensional compressible turbulent boundary layer.
[ASME PAPER 72-FE-15] 23 p3280 A72-44062
- Second order boundary layer solutions on a curved surface.
[ASME PAPER 72-FE-21] 23 p3280 A72-44063
- A note on the laminar mixing of two uniform parallel semi-infinite streams.
23 p3281 A72-44301
- Pressure fluctuations resulting from the interaction between a shock wave and a turbulent boundary layer.
23 p3359 A72-44682
- Boundary layer on bodies of revolution in longitudinal flows
24 p3390 A72-44723
- Use of characteristics for boundaries in time dependent finite difference analysis of multidimensional gas dynamics.
24 p3359 A72-44879
- Water tunnel study of turbulent boundary layers structure in incompressible fluid with longitudinal pressure gradient at inlet section of converging and diverging nozzles
24 p3390 A72-45006
- Boundary layer core flow model of concentrated columnar vortex interaction with plane solid nonrotating surface, applying to tornado interpretation
24 p3391 A72-45022
- Developing laminar and turbulent duct flow with chemical reaction.
24 p3378 A72-45061
- The large Reynolds number - Asymptotic theory of turbulent boundary layers.
24 p3392 A72-45248
- Stability of the laminar flow of a 'power-law' non-Newtonian fluid in the boundary layer on a flat plate
24 p3393 A72-45255
- Study of a viscous flow in rotating centrifugal impellers.
24 p3363 A72-45368
- Similarity problems of a non-isothermal boundary layer of an incompressible non-linear viscous medium with regard for dissipation.
24 p3395 A72-45634
- Nonsimilar solution for laminar and turbulent boundary-layer flows over ablating surfaces.
24 p3364 A72-45782
- A finite-difference method for boundary layers with reverse flow.
24 p3395 A72-45789
- BOUNDARY LAYER NOISE**
U AERODYNAMIC NOISE
U BOUNDARY LAYERS
- BOUNDARY LAYER SEPARATION**
Chapman-Korst model for prediction of flow characteristics within plume induced boundary layer separation in rocket propelled vehicles during power-on maneuvers
01 p0050 A72-10376
- Critique of self similar solutions for physical property models of laminar boundary layer separation due to adverse pressure gradients, noting viscosity-enthalpy relation
02 p0204 A72-12265
- Two dimensional wedge shaped body base heat transfer to separated nonreattaching flow region in subsonic wind tunnel
[ASME PAPER 71-HT-DJ] 02 p0152 A72-12314
- Closed boundary layer separation regions in super- and hypersonic flow, deriving mathematical model for neutral stability curves calculation
[DGLR PAPER 71-065] 02 p0153 A72-12715
- Blade cascades pressure distribution for plane incompressible flow with boundary layer separation near trailing edges, replacing blade profiles by vortex fields
[DGLR PAPER 71-097] 02 p0153 A72-12728
- Geometrical and aerodynamic characteristics of circular cross section diffuser channels from turbulent boundary layer calculation at pre separation flow stage
04 p0461 A72-14647
- Stalled blade rows dynamic performance in terms of blade channel fluid inertia and surface boundary layer-caused time delay
05 p0602 A72-16487
- Jet interaction induced supersonic turbulent boundary layer separation, obtaining flat plate pressure measurements and jet plume shadowgraphs
05 p0602 A72-16537
- Two dimensional turbulent boundary layer before rectangular step, investigating heat exchange in separation regions
05 p0751 A72-17048
- Flow analysis and dimensioning data for parallel walled radial diffusers, stating flow separation criterion
09 p1260 A72-22629
- Book on steady laminar supersonic and hypersonic wakes covering near and far region solutions, boundary layer separation, etc
09 p1261 A72-23029
- Wind tunnel investigation of Reynolds number effects on boundary layer separation incidence and maximum lift coefficient of high-lift device equipped aircraft model
10 p1419 A72-24657
- Reversed flow solutions of Falkner-Skan equation in boundary layer theory
11 p1676 A72-25361
- Supersonic turbine stator and rotor blading design corrected for boundary layer displacement thickness, discussing limitations due to normal shock wave at flow separation
[ASME PAPER 72-GT-63] 11 p1571 A72-25653
- Three dimensional laminar boundary layer on slender circular cone at angle of attack in supersonic flow, determining separated flow region via finite difference method
11 p1572 A72-25818
- Supersonic axisymmetric turbulent boundary layer characteristics over circular cone, predicting blowing effect on separation
11 p1617 A72-25995
- Turbulent separating and reattaching supersonic boundary layer flows in two dimensional compression corner, noting Reynolds number effect on separated shear layer length
11 p1618 A72-26634
- Flow separation effects on critical lift of helicopter rotor, using blade angle of attack criterion
11 p1573 A72-26893
- Turbulent boundary layer separation zone subsonic flow before two dimensional rectangular step, examining flow pattern and static pressure distribution
14 p0296 A72-31020
- Leading edge boundary layer flow separation and reattachment processes in airfoil dynamic stall, considering effect of angle of attack rate of change
15 p2179 A72-32024
- Laminar boundary layer separation point in steady two dimensional constant density flow past solid surface, deriving pressure-vorticity gradient relationship
15 p2218 A72-32467
- Three dimensional boundary layer separation on slender bodies, delta wings and propulsion intake systems, reviewing computing techniques for interfering inviscid flow fields
16 p2341 A72-32826
- Mass flow rate and mean density measurements in separated laminar boundary layers with large transverse density gradients, analyzing density difference effects on instability
16 p2379 A72-33571
- Lateral pressure gradient and suction effects on laminar incompressible boundary layer separation on curved surfaces predicted by generalized tow-layer flow model
[AIAA PAPER 72-698] 16 p2380 A72-34045
- Viscous hypersonic flow over a flat plate at angle of attack with leeside boundary layer separation.
[AD-744593] 17 p2486 A72-35634
- Incident thermal flux parameters and wall temperature effects on flow characteristics in pre separation zone of laminar boundary layer and separation point location
17 p2487 A72-35927
- Swirling flows vortex breakdown in nozzles, diffusers and combustion chambers, considering analogy to boundary layer separation
18 p2641 A72-36385
- Rotational theory of laminar boundary layer separation of incompressible fluid from smooth surface under pressure gradients
18 p2682 A72-36887
- Calculation of axisymmetric swirling and non-swirling turbulent jets
18 p2682 A72-36890
- Determination of the separation parameter of an incompressible magnetohydrodynamic boundary layer by applying the dimensionality theory
18 p2717 A72-37181
- Numerical tests of resolution of detached flows on thick bodies
18 p2684 A72-37198

Integral and correlation methods for separation and reattachment phenomena in aerodynamics, applying to turbulent boundary layer [ONERA, TP NO. 1072] 19 p2786 A72-37762
Re-developing turbulent boundary layers behind yawed separation bubbles. 19 p2747 A72-38812
Flow separation at the edges of some types of tail sections used in supersonic aircraft and in rocket technology 20 p2885 A72-39597
Cooled supersonic turbulent boundary layer separated by a forward facing step. 20 p2886 A72-39632
Lift on airfoils with separated boundary layers. 21 p2992 A72-41264
Fundamental studies of turbulent boundary layers with injection or suction through porous wall. III - Investigations on the separation of turbulent boundary layers in strong adverse pressure gradients with injection through porous flat plate. 22 p3165 A72-41945
Calculation of separation points in incompressible turbulent flows. 23 p3279 A72-43328
Reduction of end losses in cascades of cambered blades 23 p3248 A72-44025
Application of a time-dependent boundary-layer analysis to the problem of dynamic stall. 23 p3249 A72-44058
Interferograms of turbulent boundary layer separation in critical blowing of gas through porous plate, noting velocity and concentration profiles of blowing parameters 23 p3281 A72-44082
A numerical experiment on two-dimensional turbulent separation. 24 p3389 A72-44687
Turbulent supersonic boundary layer flow in the neighborhood of a 90 deg corner. 24 p3361 A72-45204

BOUNDARY LAYER STABILITY
Closed boundary layer separation regions in super- and hypersonic flow, deriving mathematical model for neutral stability curves calculation [DGLR PAPER 71-065] 02 p0153 A72-12715
Acoustical oscillations effect on free jet flow stability and boundary layer structure, using inviscid Orr-Sommerfeld equation for flow disturbances frequency, wavelength and velocity 03 p0340 A72-12913
Boundary layers nonlinear resonant instability, investigating Tollmien-Schlichting wave triads interactions with energy transfer from primary shear flow to disturbance 03 p0340 A72-13160
Boundary layer stability and turbulence observation by flow visualization using dense Al flake suspension 09 p1292 A72-22304
Permeable porous plate surface properties effect on boundary layer stability 09 p1293 A72-22408
Compressible boundary layer stability at subsonic speeds, using orthogonalization calculation method 09 p1293 A72-22409
Laminar Ekman boundary layer instability for incompressible fluid over rigid boundary with fixed vertical temperature gradient, investigating internal gravity waves generation 14 p2100 A72-30347
Three dimensional boundary layer instability, obtaining linearized perturbation equation on basis of Navier-Stokes equation 15 p2216 A72-31471
Numerical solution to stabilization temperatures of supersonic boundary layer under intense surface cooling without constraints on disturbance wave number and Reynolds number 16 p2343 A72-33155
Mass flow rate and mean density measurements in separated laminar boundary layers with large transverse density gradients, analyzing density difference effects on instability 16 p2379 A72-33571
Spreading of a turbulent disturbance. 17 p2541 A72-35249
Stability of laminar boundary layers on concave walls in presence of magnetic field. 20 p2958 A72-40066
An application of the shooting method to the stability problem for a stratified, rotating boundary layer. 21 p3043 A72-40106
Numerical and asymptotic methods for solving the problem of complete boundary-layer stabilization 21 p3047 A72-41659
Symmetrical plane-parallel boundary layer at a sudden onset of motion 22 p3164 A72-41909
Three-dimensional disturbances in the boundary layer along a concave wall 22 p3165 A72-42111
Heat transfer effects on reentry vehicle surfaces boundary layer stability and aerodynamic characteristics, noting stall angle reduction and drag increase from wind tunnel tests [AIAA PAPER 72-960] 22 p3137 A72-42357
Hydrodynamic weak-turbulence facility, equipment, and procedure for studying the stability of laminar boundary layers 24 p3388 A72-45258
Thermal diffusion and convective stability. II - An analysis of the convected fluxes. 24 p3465 A72-45561

BOUNDARY LAYER TRANSITION

Laminar free jets characteristics, investigating transition to turbulence 02 p0150 A72-11730
Free stream and shock layer disturbances effect on hypersonic boundary layer transition in wind tunnels from hot wire measurements 02 p0230 A72-12274
Hypersonic boundary layer transition in presence of wind tunnel noise, indicating rms sound pressure relationship to transition Reynolds number 02 p0151 A72-12278
Ekman boundary layer shear stress due to laminar and turbulent flow over hills 03 p0386 A72-14336
Heat flux calculation in laminar turbulent boundary layer transition zone using Schlichting model of turbulent spot formation 05 p0649 A72-16222
Wind tunnel disturbances effects on hypersonic boundary layer transition on sharp cones, comparing hot-wire anemometer and surface pressure measurements [AIAA PAPER 72-181] 05 p0605 A72-16825
Rotating homogeneous incompressible fluid flow field over step with interior geostrophic regions, horizontal surfaces Ekman layers and vertical shear layers 05 p0653 A72-17008
Transitional and turbulent heat transfer measurements on yawed blunt cone nosetip in supersonic air flow at various angles of attack [AIAA PAPER 72-212] 07 p0964 A72-18960
Boundary layer transition on slender cone in hypersonic flow as function of nose bluntness, free stream Reynolds number and angle of attack [AIAA PAPER 72-216] 07 p0908 A72-18961
Laminar-turbulent incompressible boundary layer transition prevention by suction slots on bodies of revolution, determining optimal suction power/slot distance conditions by variational methods 07 p0968 A72-19737
Flat plate boundary layer transition equations for supersonic wind tunnels, taking into account free stream turbulence 08 p1150 A72-21616
Boundary layer transition effect on three dimensional shock interactions due to blunt protuberances and axial compression corner [AD-743741] 08 p1150 A72-21629
Laminar/turbulent boundary layer transition on parabolic wing profile in supersonic wind tunnel, noting critical Reynolds number increase with leading edge thickness 09 p1259 A72-22407
Baroclinic wave field distributions and balances in rotating annulus with free surface in atmospheric circulation study, noting Ekman layer features 11 p1680 A72-25765
Ekman boundary layer in two level quasi-geostrophic general circulation numerical model, representing physical characteristics of boundary layer turbulence increase with height 12 p1840 A72-27708
Uniform vertical magnetic field effect on Ekman layer over horizontal plate at rest relative to rotating conducting liquid 13 p2011 A72-29006
Free stream turbulence and pressure gradient effects on boundary layer transition, correlating theoretical prediction methods and experimental results 14 p2093 A72-30253
Equilibrium diabatic Ekman layer geostrophic drag, heat and mass transfer coefficients, presenting velocity and temperature profiles 14 p2100 A72-30346
Laminar Ekman boundary layer instability for incompressible fluid over rigid boundary with fixed vertical temperature gradient, investigating internal gravity waves generation 14 p2100 A72-30347
Turbulent Ekman boundary layer characteristics in laboratory rotating apparatus compared with atmospheric field observation data and theories, noting similarity relation validity 14 p2094 A72-30418
Laminar to turbulent boundary layer transition in supersonic flow over flat plate investigated in supersonic wind tunnels, noting unit Reynolds number effect 14 p2069 A72-31004

Hypersonic transition boundary layers, obtaining disturbance convection velocities as function of fluctuation scale and wall distance 15 p2219 A72-32581
Hypersonic boundary layer profiles upstream of transition point on cone surface from pitot surveys, heat transfer and wall pressure measurements and spark schlieren photographs 16 p2341 A72-32837
Incompressible flow drag caused by slot suction provided in bodies of revolution for preventing laminar boundary layer transition into turbulent state 16 p2344 A72-33678
Spreading of a turbulent disturbance. 17 p2541 A72-35249
Mechanism by which a two-dimensional roughness element induces boundary-layer transition. 17 p2542 A72-35611
On the inflection point instability of a stratified Ekman boundary layer. 18 p2687 A72-36631
Drag of a flat plate with transition in the absence of pressure gradient. 18 p2641 A72-36775
Transition to a turbulent flow mode in the boundary layer of a plane plate with various turbulence scales in the incident flow 18 p2682 A72-36889
Solution of the equations of the compressible boundary layer/laminar, transition, turbulent/ by an implicit finite difference technique. 19 p2785 A72-37521
The effect of angle of attack on boundary-layer transition on cones. 20 p2886 A72-39638
Transition in compressible free shear layers. 21 p2993 A72-41310
Three-dimensional disturbances in the boundary layer along a concave wall 22 p3165 A72-42111
Calculation of laminar boundary layers by means of a differential-difference method. 22 p3167 A72-42578
The structure of blunt base wakes in swirling flow. 24 p3391 A72-45023
A comparison of disturbance levels measured in hypersonic tunnels using a hot-wire anemometer and a pitot pressure probe. [AIAA PAPER 72-1003] 24 p3388 A72-45402

BOUNDARY LAYERS
NT ATMOSPHERIC BOUNDARY LAYER
NT COMPRESSIBLE BOUNDARY LAYER
NT HYPERSONIC BOUNDARY LAYER
NT LAMINAR BOUNDARY LAYER
NT SUPERSONIC BOUNDARY LAYERS
NT THERMAL BOUNDARY LAYER
NT THREE DIMENSIONAL BOUNDARY LAYER
NT TURBULENT BOUNDARY LAYER
Electron work function and electrode physicochemical properties and surface temperature on boundary layer formation and thickness at electrodes in MHD channel 01 p0009 A72-11206
Nonuniform flow along axial turbomachine blades, presenting pressure loss evaluation method under boundary layer effect on external walls 01 p0002 A72-11271
MHD boundary layer calculation for conducting fluid along semiinfinite flat plate with transverse magnetic field, deriving momentum and kinetic energy integral equations 01 p0113 A72-11383
Oil pumping ability of tapered roller bearing, using boundary layer theory [ASME PAPER 71-LUB-21] 02 p0236 A72-11541
Nozzle boundary layers effect on reattachment position of two dimensional jet to adjacent flat plate, noting Reynolds number influence 02 p0150 A72-11729
Aerodynamic forces and pressure distribution measurement on wing-body combination model, investigating boundary layer on wing upper surface 02 p0151 A72-12228
Electron temperature profile across nonequilibrium stagnation point boundary layer in partially ionized gas, investigating charged particles interaction with body in ionosphere 02 p0262 A72-12268
MHD flow due to impulsive rotation of infinite disk, observing magnetic field strength effects on velocity components and boundary layer displacement thickness 02 p0267 A72-12772
Rigid boundary effect on thin panel flutter speed, determining aerodynamic forces via linearized potential theory 03 p0443 A72-13402
MHD boundary layer on rotating disk and on body of revolution in longitudinal flow at large Stewart numbers 03 p0399 A72-14013

Buoyancy effect on shear stress and heat transfer in horizontal boundary layer, considering Boussinesq approximation

03 p0343 A72-14320

Nonsteady high-rate heat transfer control in boundary layer by conjugate problem treatment and reduction to Volterra equation, considering limiting-regime and stability

04 p0596 A72-14666

Time dependent hydromagnetic oscillations in contained rotating conducting fluid under magnetic field, using interior boundary layer expansion

04 p0549 A72-15115

Initial boundary layer effect on turbulent free shear layer velocity profiles, deriving procedure applicable at any streamwise station

05 p0645 A72-15795

Hypersonic air inlet of revolution with mixed supersonic compression, analyzing shock-boundary layer interaction process

[ONERA, TP NO. 977]

05 p0599 A72-15857

Boundary layer growth measurements in optimum annular diffusers, discussing pressure recovery and mean total pressure loss

[AIAA PAPER 72-86]

05 p0604 A72-16807

Helicopter rotor boundary layer, comparing analytical shear stress and velocity distributions obtained by momentum integral techniques with hot wire probe experimental data

[AIAA PAPER 72-38]

05 p0607 A72-16900

Combined viscous-inviscid analytical procedure for predicting boundary layer effects on supersonic inlet flow field

[AIAA PAPER 72-44]

05 p0609 A72-16975

Unsteady boundary layer on hemisphere embedded on infinite plane during normal liquid impingement, using inner and outer expansions method to study separation time

05 p0653 A72-17003

Shock wave deceleration and boundary layer mass loss effects on electron density and ionization levels of air in shock tube

05 p0700 A72-17225

Radar observed apparent land breeze front off Wallops Island, giving temperature and wind profiles

06 p0843 A72-18441

Compensation of shock wave attenuation due to boundary layer by varying shock tube driver chamber area, using central body of suitable length and profile

06 p0797 A72-18546

Sensitivity predictions of boundary layer pressure fluctuations for round, square and rectangular transducers

07 p0986 A72-19596

Storm available potential energy generation and boundary layer frictional dissipation estimation in heat transfer from ocean to atmosphere within east coast cyclone

07 p0980 A72-20451

Parabolic differential equation system for boundary layer behavior of steady plane gas flow

08 p1107 A72-20911

Vaneless diffuser air flow calculation based on helical flow model with back currents in boundary layer

09 p1259 A72-22299

Viscous boundary layer equations for MHD flow near rear stagnation point at small Reynolds number

09 p1296 A72-23674

Heat and mass transfer analogy based on coefficients ratio and boundary layer theory

09 p1412 A72-23686

Centrifugal turboengine diffuser with high enlargement area compared with logarithmic spiral types, discussing boundary layers, secondary flow, shapes and aerodynamic parameters

10 p1463 A72-23747

Dielectric and semiconductor crystals surface defects, considering electric polarization structures

10 p1525 A72-23761

Confined three dimensional boundary layers prediction, describing finite difference methods for flow equations solution

10 p1464 A72-23871

Reynolds number and mainstream turbulence effects on laminar separation bubbles behavior in boundary layers on turbine blades in cascade

10 p1416 A72-23873

Inverse boundary value problem of optically inhomogeneous layer nonuniform profile construction from optical field distribution

10 p1510 A72-24050

Thermal radiation effects on natural convection boundary layer adjacent to vertical flat surface with uniform heat flux input

10 p1562 A72-24466

Heat transfer process in boundary layer of transparent gas flowing past plane emitting plate with prescribed surface heat flux

10 p1418 A72-24540

Fluid dynamics layer-type singular perturbation problems, constructing inner and outer asymptotic approximations with overlapping domains of validity

11 p1615 A72-25502

Boundary value problems in boundary layer theory, discussing Falkner-Skan equation similar solutions existence theorems

11 p1677 A72-25525

Turbocompressor deceleration cascades blades surface roughness effects on boundary layer, noting pressure and velocity distributions

[ASME PAPER 72-GT-48]

11 p1570 A72-25640

Hub and shroud boundary layer growth in centrifugal compressor vaneless diffusers, comparing predicted and measured performance at high pressure ratio per stage

[ASME PAPER 72-GT-54]

11 p1570 A72-25645

Axial flow turbines aerodynamic loading increase via control of velocity distribution and boundary layer evolution around airfoil profiles

[ASME PAPER 72-GT-78]

11 p1571 A72-25658

Diffraction coefficients of scalar field for higher order edges and vertices, noting far field behavior of boundary layer expansion

11 p1617 A72-26158

Boundary layer turbulence development by gas flow interaction with arc plasma in supersonic nozzle, causing light emission fluctuations

[AIAA PAPER 72-415]

11 p1617 A72-26165

Magnetospheric midday boundary width dependence on geomagnetic dipole axis orientation, discussing different positions for magnetosphere boundary

11 p1628 A72-26914

Boundary layer analysis of wide capillary tube, deriving approximate error estimates

12 p1798 A72-27714

Iterative solution existence for elastic equilibrium problem of thin plates and shells near boundary layers

12 p1886 A72-27997

Asymptotic approximation methods for boundary layers in singular perturbation theory for linear elliptic partial differential equations in two independent variables

13 p1940 A72-28425

Boundary layer theory for convective heat transfer of two dimensional film cooling systems in turbulent regime, noting momentum, enthalpy and concentration equations

13 p2063 A72-28630

Boundary layer approach to local potential solution of diffusion equations, applying to transpiration cooled half space and heat conduction in melting solid

13 p2064 A72-28885

Liquid droplets behavior in high velocity gas jets, deriving fluid flow model solutions near symmetry axis and for liquid-gas boundary layer

[DFVLR-SONDDR-200]

13 p1941 A72-29003

Nonuniform concentration mechanism for observed drag reduction in flows with high molecular weight polymer additives, considering boundary layer with varying viscosity on sphere

13 p1942 A72-29113

Electrode boundary layer electrical breakdown mechanism with allowance for steep temperature gradients at surface, considering Joule heating or electrostatic field effect as causes

13 p2013 A72-29361

Heat transfer dynamics during cooling of thin vertical plates, observing boundary layer formation and motion

13 p2065 A72-29454

Unsteady laminar natural and forced convection at transparent medium boundary layer radiating surface, noting turbulence effects on heat exchange

13 p2066 A72-29902

Computation method for rotating and nonrotating viscous flows boundary vorticity iteration parameters for use with time centered or alternating direction implicit time differencing approximation

14 p2093 A72-30228

Boundary layer temperature profile for ablating asbestos-plastic composite samples measured under combined convection and radiant heat fluxes

14 p2172 A72-31003

Many-term formulas for parabolic differential equations solution in boundary layer theory, using linearized second order ordinary differential equations

15 p2216 A72-31467

Kinematic eddy viscosity for incompressible two dimensional turbulent flow, obtaining Navier-Stokes equations and conditions for equilibrium and nonequilibrium boundary layers

15 p2216 A72-31470

Deflection and energy dissipation of thin cascade profiles in transonic flow for given pressure distribution, noting boundary layers and separated flow

15 p2178 A72-31501

Heat transfer and longitudinal temperature distribution at Hartmann-Sprenger tube inlet calculated approximately on basis of boundary layer data in steady compressible flow

15 p2217 A72-31685

Electric and magnetic fields fluctuations in region between shock wave front and magnetosphere boundary, noting resulting energy dissipation

15 p2225 A72-31902

Exact boundary layer calculations for heat and mass transfer on cones at angle of attack, considering Mach number, enthalpy ratio and cross flow effects

15 p2337 A72-32591

Power law fluids impulsively started flow over plate, presenting analytical expressions for velocity distribution, shear stress and boundary layer thickness

16 p2375 A72-32833

Convective and radiative heat transfer in compressible gas boundary layer

16 p2343 A72-32995

Viscous boundary layer generated weak shock wave effects on gas dynamic laser medium density homogeneity

[AIAA PAPER 72-709]

16 p2380 A72-34037

Aerodynamic stall characteristic prediction from static experimental data for airfoils, noting boundary layer effects

[AIAA PAPER 72-682]

16 p2346 A72-34060

A method of solving partial differential equations for boundary layers

17 p2537 A72-34195

On the extension of an infinite elastic plate containing an axisymmetric hole.

[ASME PAPER 72-APM-G]

17 p2624 A72-34313

Heat transfer by free convection from a longitudinally vibrating vertical plate.

17 p2637 A72-35045

Symmetries of the boundary-layer equations under groups of linear transformations.

17 p2541 A72-35241

Rotation of a cylinder about an eccentric parallel axis in a viscous fluid.

18 p2680 A72-36479

A new method of analysis in laminar flow theory.

18 p2681 A72-36551

Drag of a finite flat plate set parallel to a uniform flow.

18 p2683 A72-37045

Solution of the general heat transfer problem by the integral Tolubinskii method for a longitudinal flow past cylindrical bodies

18 p2742 A72-37182

Coriolis force influence on convective stability in viscoelastic fluid layer heated from below, contrasting with rotation effects on ordinary viscous fluid

20 p2982 A72-39326

Boundary-layer effects on pressure variations in Ludwig tubes.

20 p2914 A72-39620

Shock tube boundary layers in ionized argon-helium mixtures.

20 p2914 A72-39639

Sweet's mechanism for the destruction of magnetic flux.

20 p2955 A72-40017

The solution of sharp-cone boundary-layer equations in the plane of symmetry.

21 p2989 A72-40650

On the asymptotically spherical deformations of arbitrary membranes of revolution fixed along an edge and inflated by large pressures - A nonlinear boundary layer phenomenon.

21 p3118 A72-40840

Some results from tests in the NAE high Reynolds number two-dimensional test facility on 'shockless' and other airfoils.

[ICAS PAPER 72-33]

21 p2991 A72-41158

Convection instability in viscous incompressible fluid layer with free boundaries under modulated external force field

22 p3243 A72-42099

A new concept for correcting the attenuation effects in a shock tube.

24 p3388 A72-44985

Model for shock wave propagation through gas-liquid drop medium based on liquid phase atomization by boundary layer stripping

24 p3391 A72-45049

BOUNDARY LUBRICATION

Soviet book on temperature resistance of lubrication boundary layers and solid lubrication coatings during friction of metals and alloys

08 p1179 A72-22023

Al alloy and brass deformation compression tests inadequacy for friction determination and boundary agents, EP additives and hydrodynamic and solid lubricants evaluation

08 p1181 A72-22195

Application of boundary layer concepts to turbulent lubrication theory of bearings and seals.

18 p2696 A72-37052

Manifestation of the effect of adsorptive reduction in strength under conditions of selective transport during boundary friction

22 p3183 A72-43138

BOUNDARY VALUE PROBLEMS

NT NEUMANN PROBLEM

Book on uniqueness theorems in linear elasticity covering three and two dimensional elastostatics, whole and half spaces, mixed boundary value problems, elastodynamics, etc

01 p0136 A72-10003

Overdetermined collocation method change into Ritz-Galerkin method for applications to boundary value problems with eigenvalues 01 p0093 A72-10122

Mixed boundary value problem of Laplace equation solution by dual trigonometric series equations approach, applying to microstrip transmission line capacitance determination 01 p0093 A72-10508

Correspondence principle application to numerical solution for plane boundary value problem of linear viscoelasticity theory based on Kelvin point force solution to field equations 01 p0138 A72-10512

Linear heat transfer boundary value problem series solution in Cartesian and cylindrical coordinate systems 01 p0145 A72-10575

Difference analog of nonlinear hydrodynamic boundary value problem from Navier-Stokes steady state theory 01 p0050 A72-10576

Invariant imbedding technique application to linear partial differential equations boundary value problems conversion to Cauchy problem via generalized Riccati transformations 01 p0093 A72-11116

Equilibrium configuration of cable towed in circular path, presenting multivalued boundary value problem mathematical analysis [AD-737445] 01 p0102 A72-11132

Boundary conditions for monatomic gas flow in constant cross section channel with heat supply and ionization 01 p0111 A72-11211

Boundary value problem solution for multiple interleaved phased arrays of waveguide radiators operating at different frequencies, investigating transmission characteristics 01 p0042 A72-11234

Direct method for dual and triple integral equations involving inverse Mellin transforms in potential mixed boundary value problems 01 p0094 A72-11390

Nonclassical shell theory development from three dimensional boundary value problems solution in elasticity theory 02 p0288 A72-11606

Affine similarity in static problems with mixed boundary conditions for inhomogeneous anisotropic linearly and nonlinearly elastic and viscoelastic and elastoplastic bodies 02 p0288 A72-11607

Three dimensional elasticity mixed boundary value problems associated with Laplace equation in half space, including slotted regions and stamp contact solutions 02 p0289 A72-11610

Nonlinear boundary value problem of creep for isotropic bodies with random mechanical properties under random loads, calculating structural component reliability and service life 02 p0289 A72-11619

Flow passage geometry optimization in compressor rotor design treated as boundary value problem with variational calculus solution 02 p0151 A72-12179

Lower bound deformation theorem for rigid plastic continua under impulsive loads, emphasizing kinematically admissible velocity field 02 p0259 A72-12237

Gas slip flow and transverse oscillations boundary value problems solution, using Wiener Hopf integral equation 02 p0205 A72-12355

Isothermal analogy for thermal stress in cylindrical shells, presenting orthogonal coordinate boundary condition equations [ASME PAPER 71-PVP-18] 02 p0294 A72-12471

Analog circuit method for slender profile flow field shock front boundary value problem for simple profile variation, using known mapping plane solutions [DGLR PAPER 71-069] 02 p0153 A72-12743

Static isotropic elastic body first and second boundary value problems solutions for inside and outside m dimensional sphere 02 p0300 A72-12876

Principal boundary value problems solution for Helmholtz equation in half space with spherical cavities, reducing problems to infinite systems of algebraic equations 03 p0387 A72-12915

Uniform progressing wave expansion solution to wave equation for transition region boundary value problems 03 p0388 A72-12988

Plane electromagnetic wave reflection and transmission at moving boundary between two dielectric media 03 p0321 A72-13091

High subsonic velocity aerodynamics boundary problem, transforming compressible flow to incompressible 03 p0307 A72-13238

Elastic bodies deformations theory, formulating boundary value problems 03 p0443 A72-13451

Ritz approximation to two dimensional strain elasticity and heat flow boundary value problems, considering piecewise linear and cubic functions for complete triangulation 03 p0381 A72-13620

Linear viscoelastic solid defined by constitutive equations replacing bounded domain in time interval on real axis, deriving theorem regarding solution of second problem of limits 03 p0447 A72-13787

Two dimensional boundary value problems for rectangular plates in bending with rigidity variation, using Kantorovich, trigonometric and Horvay functions 03 p0449 A72-13907

Two dimensional boundary value problem in elasticity for rectangular prism vibrations, considering dynamic stress and frequency characteristics 03 p0449 A72-13908

Heat transfer coefficients to both sides of finite one dimensional slab subject to phase-change coating technique boundary conditions, deriving thin wing correction factors 03 p0457 A72-13956

Edge temperature effects on contact stress concentration in anisotropic plate with elliptic hole under mixed boundary conditions of thermoelasticity 03 p0450 A72-14109

Two dimensional elasticity theory, discussing first, second and mixed boundary value problems solution in contour integral form 03 p0451 A72-14116

Biharmonic stress and displacement potentials for two dimensional boundary problems in elasticity theory, using Galerkin method 03 p0453 A72-14207

Rotationally symmetric force free magnetic field boundary value problem, using linear elliptic differential equation 03 p0400 A72-14352

Rotationally symmetric static incompressible infinite conducting plasma elliptic differential equation reduction to boundary value problem 03 p0400 A72-14353

Linear elastic Cosserat continuum mixed boundary-initial value problem uniqueness theorem, using Kirchhoff proof in classical elastostatics 03 p0382 A72-14363

Green vector function smoothness in elliptic boundary value problem with pseudodifferential conditions 03 p0383 A72-14372

Maxwell boundary conditions method application in kinetic theory of gases, investigating linearized plane Couette flow 04 p0510 A72-14594

Nonlinear elliptical equations first boundary value problem, presenting approximation capacity and convergence of straight line procedure 04 p0538 A72-14625

Steady heat conduction boundary value problem solution by generalized Kantorovich method of reduction to ordinary differential equations 04 p0595 A72-14642

Linear distributed parameter system optimal boundary control by direct method using linear combination of finite number of orthonormal functions 04 p0505 A72-14670

Canonical form for boundary conditions of thin elastic shells with oscillating loads applied on edges 04 p0587 A72-15013

Shooting method and contraction mapping application to existence-uniqueness theorem derivation for numerical solution of second order delay differential equations boundary value problems 04 p0539 A72-15042

Shooting and imbedding methods for theoretical analysis and approximate numerical solution of two-point boundary value problems involving n-vector-valued functions [AD-743615] 04 p0539 A72-15043

Modified quasi-linearization algorithm for solving nonlinear two-point boundary value problems based on performance index and cumulative error in differential equations 04 p0539 A72-15045

Boundary value problem for steady parallel axisymmetric irrotational flow of inviscid incompressible fluid past cylinder having common axis with tube 04 p0512 A72-15056

Nonlinear hereditary elasticity theory boundary value problem solution using complex potentials in successive approximation algorithm for stress concentration and nonlinear creep analysis 04 p0588 A72-15059

Uniform circular plates axisymmetric elastic deformation under various static loadings and boundary conditions, solving flexural equilibrium equations 04 p0590 A72-15184

Dynamic boundary value problem for elastic half space with rotational concentrated moment of variable magnitude, using Fourier and Laplace transforms 04 p0591 A72-15198

Fundamental frequency calculation method for bars and plates with arbitrary fixity of rotations, discussing buckling and vibration with realistic boundary conditions 04 p0591 A72-15275

Buckling of radially constrained imperfect circular ring loaded within perfect rigid circular boundary, obtaining numerical solution by discrete treatment 04 p0591 A72-15286

R-function theory application for solution of boundary value problems in electrodynamics, considering field behavior at infinity 04 p0488 A72-15377

Plane wave diffraction by infinite strip grating, providing closed form solution by boundary value problem reduction to singular integral equation 04 p0490 A72-15411

Electromagnetic wave propagation in plane and spherical waveguide channels with conducting lower wall, investigating transverse wave spectrum dependence on curvature and boundary conditions 04 p0492 A72-15441

Quasi-linear parabolic equations loaded system first boundary value problem for heat and mass transfer equations inverse problems 04 p0540 A72-15545

Dirichlet problem reduction to boundary value problem via invariant imbedding techniques and Fredholm integral equation method 04 p0540 A72-15632

Master equation for vibrational relaxation of diatomic dilute gases, discussing restrictions on experimental initial conditions and scattering cross sections 04 p0553 A72-15634

Piecewise linear approximation of inverse nonstationary conductive heat transfer through unbounded plate with arbitrary temperature distribution and asymmetric boundary conditions 05 p0742 A72-15847

Continuous media stationary motion stability using initial boundary value problem of partial differential equations in perturbations [ASME PAPER 71-WA/APM-17] 05 p0647 A72-15963

Elastic boundary value problems static and geometric field parameters pointwise upper and lower bounds, determining solution coefficients by error energy minimization 05 p0735 A72-16062

Hybrid representation for structural component by vibration modes with free or fixed connection points and boundary conditions selection to optimize accuracy 05 p0736 A72-16084

Laplace equation under Robin boundary conditions over unit square, discussing numerical solution by difference approximation and iterative procedure 05 p0682 A72-16100

Elastically supported cantilever stability with continuous lateral restraint under uniform distributed axial load, developing boundary conditions 05 p0737 A72-16118

Nonstationary plane shock wave propagation in inelastic medium with soil properties, discussing boundary problem solution and numerical analysis 05 p0689 A72-16284

One dimensional nonhomogeneous wave equations solution for linear and hyperbolic moving boundary conditions applied to resonator fields 05 p0627 A72-16407

Optimal control problem formulation as nonlinear two point boundary value problems, comparing linear systems and Riccati equations for solution 05 p0726 A72-16455

Transfer equation system solution for nonscattering medium with stationary homogeneous magnetic field, considering boundary value problem in Fraunhofer line theory 05 p0690 A72-16513

Vortical flow of incompressible fluid in finite region bounded by potential flow and with Bernoulli constant jump at boundary 05 p0649 A72-16581

Homogeneous viscoelastic boundary value problem, demonstrating Volterra principle validity 05 p0739 A72-16590

Elasticity theory three-dimensional axisymmetric problem reduction to two-dimensional analytic function boundary value problem 05 p0739 A72-16591

Boundary conditions and equations of plasma arc discharge in cylindrical diode with azimuthal magnetic field 05 p0697 A72-16988

Mixed boundary value problem of infinite elastic plate with parabolic crack, obtaining solution by complex variable method 05 p0741 A72-17004

MHD shock waves stability, showing Hall term effect on number of shock boundary conditions 05 p0699 A72-17025

Velocity distribution in mixing layer between fluid at rest and in uniform stream by solving Blasius equation with boundary points 05 p0653 A72-17078

- Optimal control of system described by parabolic partial differential equations with constraints on change rate of boundary conditions 05 p0683 A72-17137
- Physical processes of fluids atomization in electric field, discussing droplet surface instability and boundary values of surface tension coefficient 05 p0602 A72-17185
- Integro-differential initial value problem solution, differentiating for time variable and integrating for space variable 06 p0838 A72-17383
- Ordinary differential equations with highest derivatives multiplied by small parameters, discussing initial value problems and use of implicit function theorem methods 06 p0839 A72-17628
- Steady heat conduction boundary value problems from complementary variational principles 06 p0902 A72-17780
- Ordinary differential equation eigenvalues, presenting method based on interior zeros of one parameter solutions to second order equation with one endpoint boundary condition 06 p0839 A72-17883
- Numerical integration solution of nonlinear equations and two point boundary value problems, using quasi-linearization and imbedding methods 06 p0839 A72-17957
- Macroscopic boundary conditions of gas-solid interface interaction as function of gas temperature and transport coefficients variation in shock reflection problems 06 p0902 A72-18107
- Convergent finite difference schemes for Navier-Stokes equations initial boundary value problems, using Temam systems approximation method 06 p0840 A72-18132
- Collisionless plasma oscillations in external uniform magnetic field, described by initial value problem for nonrelativistic linearized Vlasov-Maxwell equations 06 p0862 A72-18251
- Single species one dimensional Vlasov plasma linearized analysis as initial value problem with periodic boundary conditions, using Hamilton variational principle 06 p0864 A72-18537
- Approximate trigonometric solution to thermoelastic boundary value problem of plate with doubly periodic system of holes under unsteady temperature and thermal stress fields 06 p0899 A72-18563
- Photoelastic analysis of cylindrical shells of revolution with one hemispheric closed end and reinforcing flanges at opposite end rim, examining boundary conditions effects 06 p0899 A72-18640
- Thin walled elastic isotropic shallow shell with thermal boundary conditions, obtaining thermoelastic solution in series form 06 p0899 A72-18657
- Shallow elastic shell under periodic distributed torque loading, investigating static stability enhancement through nonlinear boundary value problem periodic solutions 06 p0900 A72-18697
- Nonlinear elastic systems with distributed parameters, obtaining single frequency mode random oscillations solution of boundary value problem by asymptotic method and Markov process 06 p0850 A72-18700
- Nonlinear oscillations of liquids in complex geometrically shaped moving vessels, using approximation methods for boundary value problem solution in Cartesian coordinate system 06 p0802 A72-18712
- Single frequency oscillations in nonlinear mechanical systems described by one dimensional mixed boundary value problems, using asymptotic methods 06 p0850 A72-18715
- Mixed boundary value problem of partial differential equations describing nonlinear viscoelastic vibration of clamped rods, examining asymptotic solution stability 06 p0901 A72-18716
- Collocation least square solutions of boundary value problems, applying to prismatic bar torsion and plate bending 07 p1025 A72-18790
- Convergence conditions for Galerkin method, applying to boundary value problems of structural stability and critical buckling loads 07 p1025 A72-18798
- Singular integral equations numerical solution from Gauss-Chebyshev formulas for mixed boundary value problems 07 p1026 A72-18808
- Weakly damped harmonic oscillator, using perturbation methods for approximate solution to boundary value problem differential equation 07 p1034 A72-18816
- Two point boundary value solution for N-body trajectories, comparing asymptotic with numerical integration solutions for several lunar and interplanetary trajectories [AIAA PAPER 72-49] 07 p1068 A72-18945
- Differential equation initial value problem solution error bounds construction by interval arithmetic to guarantee exact solution inclusion 07 p1026 A72-18968
- Laplace equation internal Dirichlet and Neumann boundary value problems solution procedure for thermal potential of steady temperature field 07 p1098 A72-18988
- German book on nonlinear free boundary value problems of two dimensional hydrodynamics covering gravity, capillary and irrotational waves, liquid flow in channel, etc 07 p0967 A72-19183
- First passage time boundary value problem for first order phase locked loop systems, determining probability density function of time to cycle-slip 07 p0959 A72-19273
- Bounds estimation for thermal explosion critical parameters for exothermic reaction, using geometric transformation 07 p1098 A72-19364
- Linear multivariable discrete time cyclic system sensitivity model yielding sensitivity functions with respect to any system parameters and initial conditions 07 p0961 A72-19706
- Free vibration determination method for thin rectangular plate with arbitrary boundary conditions and thickness variations 07 p1092 A72-19857
- Axisymmetric single phase Stefan problem with boundary condition of second kind, obtaining temperature distribution along solidifying zone 07 p1101 A72-19892
- Soviet book on celestial mechanics and astrodynamics covering classical and contemporary theory, many body problem, satellite perturbation, optimal and boundary value problems, etc 07 p1078 A72-19952
- Electrodynamics and magnetoelasticity nonlinear Emden-Fowler equation solutions, considering heavy current carrying filaments equilibrium and boundary value problems 07 p1035 A72-19975
- Elasticity theory axisymmetric problem for hollow cone, analyzing stress-strain state and boundary value problem by asymptotic methods 07 p1093 A72-19980
- Multiple point boundary value problem with linear integrodifferential equation simplification 07 p1028 A72-19983
- Boundary value problems in supporting surfaces vibrations theory, constructing Green function from part of differential operator 07 p1093 A72-19984
- Navier-Stokes equation numerical solution methods, expressing boundary conditions by separate equations for vorticity and stream function 07 p0970 A72-20077
- Transonic flow past wing airfoils, obtaining numerical solution by fitting mixed initial boundary conditions 07 p0909 A72-20079
- Perfect fluid two dimensional steady flow equation solution for viscous flow with specified boundary conditions, considering vortex flow 07 p0971 A72-20099
- Boundary conditions for unsteady flow fields bounded by incompressible elastic thick plane wall fixed to rigid surface 07 p0972 A72-20113
- Algorithm for solving boundary value problem of integrodifferential equations describing temperature field inside hollow thin walled rod within solar radiation field in vacuum 07 p1028 A72-20207
- Nonlinear oscillations of liquid in movable conical containers, presenting approximate procedures for solving weight boundary value problem of eigenvalues 07 p0972 A72-20211
- Three dimensional stressed state of isotropic plate with elliptical holes under tension, solving boundary value problems 07 p1095 A72-20216
- Elastic body dynamics partial differential equations transformation into boundary value problem for Monge-Ampere equation 07 p1095 A72-20218
- Boundary value problem related to iteration equation of generalized axisymmetric potential theory, obtaining exact solution via Jacobi polynomials and difference scheme 07 p1036 A72-20219
- Computer interactive graphics for digital simulation of engineering fields modeled by partial differential equations boundary value problems 07 p0951 A72-20337
- Parametric and adaptive non-parametric system identification procedures in boundary value problem of string on elastic foundation, considering various approximation methods 07 p1096 A72-20349
- Nonstationary and asymmetric cosmic ray modulation theory, discussing moving boundary problem and solar wind model with spherical singularity 07 p1065 A72-20643
- Goodman-Lance method of adjoints extension for solving boundary value problems of nonlinear differential equation systems 08 p1197 A72-20786
- First boundary value problem solution of nonlinear Poisson equation in rectangular region by finite difference equations approximation 08 p1198 A72-20902
- Biharmonic boundary value problems solution by summary representations method and conformal mapping for plane with two circular holes 08 p1242 A72-20906
- Boundary conditions in steady and unsteady heat conduction for gas turbine rotors, using blade-disk temperature relation 08 p1222 A72-20944
- Boundary conditions in heat conduction for nozzle blades with shrouds exposed to cooling air on one side 08 p1222 A72-20945
- Axisymmetric potential theory boundary value problems for iterative elliptic differential equation in rectangle and half strip 08 p1198 A72-20961
- Poisson equation boundary value problems summary representation formulas for three layer annular sector with Dirichlet or Neumann conditions 08 p1205 A72-20963
- Librational transverse oscillations boundary value problems of heavy thread on orbiting satellite, determining equilibrium and eigenfunctions 08 p1240 A72-21142
- Boundary points regularity for second order elliptic equation with continuous coefficients 08 p1198 A72-21165
- Membrane and bending moment stresses distribution at elliptical hole in circular cylindrical shell, solving boundary value problems 08 p1243 A72-21234
- Dynamic programming application to computer algorithm construction for elasticity theory two dimensional problems, solving boundary value problem for elliptic differential equation 08 p1243 A72-21235
- Uniqueness theorems for linearized Boltzmann equation with Maxwell boundary conditions, using Gauss theorem and Schwartz inequality 08 p1149 A72-21252
- Convergence and stability criteria of monotonic difference schemes for linear parabolic differential equations with interface boundary conditions 08 p1199 A72-21286
- Nonlocal elliptical boundary value problem solvability in terms of smooth functions, deriving Green formula and homeomorphism theorems 08 p1199 A72-21300
- Thermal conductivity and thermal diffusion coefficients determination for plane plate heated unilaterally from above under fourth kind boundary conditions 08 p1252 A72-21313
- Matsevityi nonlinear resistances method for contact heat exchange boundary value problems of fourth kind 08 p1252 A72-21319
- Green functions in heat conduction solutions for hollow cylinder with mixed boundary conditions 08 p1253 A72-21448
- Poisson heat transfer equation for complex boundary three dimensional region, solving by constant sign functions with aid of R conjunctions 08 p1253 A72-21456
- Heat exchange extremum boundary value problems for flow direction reversal, considering thermal treatment of porous materials 08 p1253 A72-21457
- Ordinary linear differential equation boundary value problem solution in form of asymptotic series in powers of small parameter 08 p1199 A72-21462
- Operator approach solution to boundary value problems with infinite defect for differential equations with deviating argument, considering Fredholm alternative validity and compressed mappings application 08 p1199 A72-21465
- Linear time optimal problem with analytical perturbations of initial conditions, determining optimal control switching points from convergent series representation 08 p1145 A72-21466
- Towed cable flight vehicle system motion in uniform flow field, calculating equilibrium configuration during coordinated turn from two point boundary value problem numerical solution 08 p1110 A72-21604
- Spherically symmetric Stefan problem with boundary condition of second kind, obtaining temperature distribution 08 p1255 A72-21671
- Coordinate sequences construction method for complex regions and various boundary conditions, deriving closed form solution to elliptical equation 08 p1200 A72-21702
- R function and variational methods solution for mixed boundary value problem of Laplace equation applied to stationary heat conduction and electrodynamic problems 08 p1209 A72-21704

- Asymptotic method solution for boundary value problems for nonlinear differential equations describing transonic and slow supersonic flow past thin bodies 08 p1108 A72-21709
- Perforated flexible polymer plates stressed state problem with boundary conditions and viscoelastic and creep properties effects 08 p1248 A72-21861
- Resonant frequencies of rectangular plate with two sides subject to mixed boundary conditions, expressing vibration modes in terms of Fourier series 08 p1249 A72-21946
- Boundary value solutions and computer programs for one dimensional laminar flame propagation equations 08 p1129 A72-22040
- Probability density and distribution functions of first arrival time at boundary by steady normal random process 09 p1289 A72-22217
- Laplace operator eigenvalue computation for simply connected region with homogeneous Dirichlet and Neumann boundary conditions and finite difference problem 09 p1340 A72-22296
- Ordinary differential operators eigenvalues calculation, noting numerical integration scheme for initial value problem 09 p1340 A72-22461
- Two point boundary value problems solved by finite difference method using optimal sequence of nodes 09 p1341 A72-22464
- Coordinate mapping for solutions of Einstein initial value problem for vacuum gravitational fields 09 p1350 A72-22471
- Nonlinear initial boundary value problem for time dependent convection-diffusion equation with ionization and recombination reactions 09 p1341 A72-22472
- Boundary value problem solution for first order elliptic system on plane 09 p1341 A72-22488
- Mixed boundary value problem for infinite parallel cracks row solved by reduction to Fredholm integral equation 09 p1398 A72-22534
- Cylindrically guided hybrid TE and TM electromagnetic wave reflection and transmission from Maxwell equations and boundary value problems solution 09 p1278 A72-22605
- Boundary condition for plane or axisymmetric stagnation point flow of micropolar fluid over flat plate, giving numerical solutions for turbulent characteristics 09 p1293 A72-22621
- Grid plates of complex structure, determining stress-strain state by asymptotic solution of boundary value problem for sixth order differential equations 09 p1398 A72-22693
- Thermoelastic problem of open orthotropic multilayer shell of revolution, obtaining one dimensional boundary value problem solutions by numerical orthogonalization method 09 p1400 A72-22712
- Boundary value problems in micropolar theory of elasticity, obtaining displacement and rotation vectors from singular integral equations 09 p1402 A72-22745
- Monograph on slotted circular waveguide analysis covering boundary value problem solution by Wiener-Hopf and Galerkin procedures and application to far field determination 09 p1279 A72-22925
- Boundary value problem for degenerate quasi-linear parabolic differential equation, showing solution existence and smoothness dependence on region width 09 p1342 A72-23485
- Vibration frequencies of slender beams and circular plates with boundary stiffness and damping [ASA PAPER E 5] 09 p1408 A72-23525
- Ritz-Galerkin procedure used for nonlinear boundary value problems solution, noting convergence of perturbed Galerkin method 09 p1343 A72-23561
- Increased accuracy cubic spline approximation to two-point boundary value problems for differential equation, noting truncation error 10 p1502 A72-23722
- Mixed boundary elasticity solutions for plane with cuts on real axis, using hyperelliptic Riemann surface 10 p1553 A72-23768
- German monograph on flow calculation in axial thermal turbomachines covering boundary conditions and field computation for steady state inviscid flow 10 p1415 A72-23772
- Steady compressible fluid flow and plane shock wave propagation in pipe bends, discussing parameter effects and boundary conditions 10 p1464 A72-23878
- Inverse boundary value problem of optically inhomogeneous layer nonuniform profile construction from optical field distribution 10 p1510 A72-24050
- Boundary value problems for buckling and initial postbuckling of clamped shallow spherical and conical thin walled sandwich shells under uniformly distributed hydrostatic pressure [ASME PAPER 71-APM-YY] 10 p1554 A72-24182
- Parametric dynamic stability equations and boundary conditions for thin walled open cross section beam under axial load, taking into account longitudinal deformation effect [ASME PAPER 71-APM-LL] 10 p1554 A72-24184
- Linear initial value problem of partially mixed cylindrical wake in uniformly stratified fluid, obtaining exact solutions for density and velocity distributions 10 p1466 A72-24299
- Plane transonic gas flows through Laval nozzle and symmetrical wedge-shaped profile, solving boundary value problem by reduction to singular integral equation 10 p1418 A72-24433
- Analog simulation of hyperbolic differential equations with split boundary conditions, comparing to digital solutions to nonlinear flow 10 p1445 A72-24454
- Modified sweep variation method for optimal control programs, solving two point boundary value problem by linear perturbation technique 10 p1551 A72-24455
- Minimum fuel continuous low thrust orbit transfer problem of optimal control, solving boundary value problem with Multiple Substitution Polynomials and Marquardt method 10 p1552 A72-24486
- Plane and antipane elasticity boundary value problems reduced to integral equations by dislocation layers, noting closed form solutions for half and whole space 10 p1557 A72-24561
- Laboratory electromagnetic scale modelling for studying geophysical and propagation boundary value problems 10 p1512 A72-24741
- Boundary value problems for overdetermined elliptical systems of differential equations with arbitrary sized rectangular matrix 10 p1506 A72-24777
- Classical boundary value problems in theory of thermal stresses in piecewise continuous anisotropic elastic bodies under coupling conditions 10 p1563 A72-24994
- Linear continuous time systems optimal dual control problem solution by reduction to partial differential equation in finite domain with suitable boundary conditions 10 p1458 A72-25170
- Finite element method for boundary value radiative and convective heat transfer problems [AIAA PAPER 72-274] 11 p1740 A72-25214
- Perturbation method for asymptotic solutions of initial value problems for hyperbolic wave equations with small nonlinearities 11 p1676 A72-25355
- Hypersonic nonlinear aerodynamic loading effect on panel flutter, examining stability for various initial conditions [AIAA PAPER 72-345] 11 p1728 A72-25374
- Geometric interpretation of solution existence for nonlinear ordinary differential equations with linear and nonlinear boundary conditions, analyzing funnel of solutions 11 p1676 A72-25503
- Boundary value problems in boundary layer theory, discussing Falkner-Skan equation similar solutions existence theorems 11 p1677 A72-25525
- Linear contingency method for elasticity theory of anisotropic plane with elliptic hole, deriving boundary value problems solutions 11 p1733 A72-25543
- Kinetic model for polyatomic gas heat transfer between parallel plates, considering boundary value problem with arbitrary accommodation coefficients 11 p1744 A72-25559
- Boundary value problems to initial value problems transformation method extended by physical parameters invariant properties, noting fluid mechanics nonlinear equations 11 p1616 A72-25878
- Equilibrium stability of hyperelastic bodies under finite strain, deriving differential equations and boundary conditions of critical equilibrium states 11 p1686 A72-25916
- Russian book on approximate solutions of boundary value problems covering elliptic differential equations and Ritz, moment, straight lines and probability modeling methods 11 p1677 A72-26065
- Inhomogeneous strings oscillations determination in nonstationary inverse boundary value problems with integral equations 11 p1689 A72-26381
- Heat equation for insulated uniform body, examining definition and continuity of mapping from linear manifold of assumed boundary values 11 p1747 A72-26555
- Rectangular domain boundary value problem biharmonic equation and Cauchy system equivalence, noting semigroup properties analysis in terms of nonclassical imbedding variables 11 p1737 A72-26663
- Integral equation numerical solution applications to rectangular solid capacitance calculation and mixed boundary value problems 11 p1679 A72-26954
- Error bounds relationship to norm in approximate numerical solutions of initial value problems for ordinary differential equations 11 p1679 A72-26957
- Recursive algorithm for numerical solution of Sturm-Liouville problem with periodic boundary conditions 11 p1679 A72-26958
- Lowest natural vibration frequencies of conical shell for various boundary conditions, using finite difference scheme 12 p1878 A72-27081
- Finite difference equations for plate and shell calculations with various boundary conditions 12 p1878 A72-27089
- Existence and uniqueness of general solutions of initial value problem for nonlinear Maxwell-Boltzmann equation with finite time interval 12 p1836 A72-27122
- Boundary conditions and equations of plasma arc discharge in cylindrical diode with azimuthal magnetic field 12 p1850 A72-27132
- Elastic inhomogeneous continuum stability dependence on internal stress tensors field and boundary conditions, noting application to composite materials 12 p1843 A72-27171
- Ergodic boundary in initial conditions space for turbulent two dimensional flow, explaining phenomenon in terms of negative temperatures for point vortex model 12 p1797 A72-27183
- Book on finite element method application to boundary value problems, nonlinear continuum thermodynamics and thermoviscoelasticity 12 p1882 A72-27325
- Hybrid cylindrical shell finite element, determining natural frequencies from equilibrium equations, stress functions stress-strain relationships and boundary force transfer matrices 12 p1882 A72-27339
- Harmonically oscillating rectangular wing in unsteady transonic flow, obtaining two part boundary value problem for linear potential equation 12 p1751 A72-27545
- Helmholtz equation numerical solution for potential field problems with arbitrary boundary conditions of wave propagation, diffusion and thermal conduction in mathematical physics 12 p1846 A72-27553
- Stress boundary value problems for infinite wedges in linear elasticity theory solved by Mellin transforms 12 p1883 A72-27561
- Volume averages of stress and strain changes induced by Poisson ratio variation in boundary value problems of three dimensional classical elastostatics 12 p1884 A72-27566
- Energy method for boundary conditions of beam vibrations under linear viscoelastic stress-strain law, deriving uniqueness, boundedness and stability theorems 12 p1885 A72-27848
- Uniqueness theorem for solution to boundary value problem in anisotropic viscoelasticity, considering stress-strain relation in nonlinear Volterra equation form 12 p1886 A72-27983
- Russian papers on functional analysis covering approximate solution of linear integral equations, averaging principle for partial differential equations and boundary value problems 12 p1837 A72-27994
- Variational problems in automatic control theory, presenting existence theorems for solution of boundary value problems for nonlinear differential equations with deviating argument 12 p1837 A72-27995
- Generalized Fourier transformation method for mixed boundary value problems of second order parabolic differential equation in unbounded region, noting singular differential operator 12 p1837 A72-27998
- Hybrid computer Monte Carlo solution algorithm for parabolic partial differential equations with time varying boundary conditions, applying to ferromagnetic rod magnetization problem 12 p1787 A72-28119
- Laplace equation iterative solution for boundary value problems in structural hardening and heat resistance formulation, noting convergence 12 p1887 A72-28226
- Thin circular plate free vibrations with mixed boundary conditions from differential equations for vibration modes of circular isotropic plate in dimensionless polar coordinates 13 p2053 A72-28395

Baroclinic instability formulation as initial value problem compared to normal mode studies, considering cyclone development in atmosphere

13 p1945 A72-28446

Numerical methods to solve boundary value problems of monochromatic transport equations in light scattering media optics

13 p2001 A72-28504

Heat transfer to surfaces in turbulent compressible gas flows with various boundary conditions

13 p2063 A72-28627

Iterative solution of coupled nonlinear differential equations under boundary conditions for flow and heat transfer of Rivlin-Ericksen fluid between rotating parallel disks

13 p1986 A72-28881

Inverse variants of Galerkin-Krylov method, discussing convergence patterns of approximate solutions to boundary value problems

13 p1986 A72-29063

Boundary value problems of Poisson equation for rectangle having side with mixed boundary conditions, discussing solution by summary representations and successive approximations methods

13 p1986 A72-29071

Green function solution for electric field intensity in space due to electric dipole at another point under boundary conditions on surface of revolution

13 p1921 A72-29341

Harmonic functions skew derivative problem reduction to study of integrodifferential equation by constraints imposition on boundary condition coefficients

13 p1987 A72-29469

Variational principles for linearized dynamic and static problems of elastic incompressible bodies for highly elastic initial deformations

13 p2059 A72-29499

Eigenstate field parameter bounds in elastomechanics natural vibration problems

13 p2059 A72-29598

Successive approximation for solving parabolic equation with abstract function, using Chaplygin method for Cauchy boundary value problem in Banach space

13 p1987 A72-29646

Neumann problem for eigenvalues with homogeneous boundary conditions, using R-functions for complex-type regions

13 p1987 A72-29792

Boundary values for bending of plates with weak orthotropy from Vekua plate theory

13 p2062 A72-29951

Two dimensional boundary value problems of elasticity for simply connected noncanonical domains, using small parameter method

13 p2062 A72-29952

Thin wedge shaped shell bending under normal loads, discussing boundary value problems

13 p2062 A72-30066

Asymptotic solutions to dynamic problems of thermoelasticity estimation under homogeneous boundary conditions

13 p2062 A72-30067

Inviscid plane Couette flow infinitesimal instability as initial value problem, using distribution-theoretic approach

14 p2126 A72-30230

Boundary value problems in dynamics of Cosserat infinite elastic medium with finite crack, noting couple stresses effect on dynamic stress concentration

14 p2164 A72-30299

Composite two-material circular sector two dimensional stationary temperature field determined for certain thermal conduction coefficient ratios

14 p2170 A72-30573

Critical force instability analysis for rectangular plates with mixed boundary conditions, using deflection forms in Fourier series

14 p2165 A72-30575

Coordinate functions in Kantorovich variational method, noting application to stationary heat conduction boundary value problems

14 p2170 A72-30592

Gas surface interactions models, computing scattering kernels by reduction to boundary value problem

14 p2134 A72-30880

Initial value method for Ambarzumian integral equation by transformation to Cauchy system

14 p2126 A72-30889

Acoustic wave diffraction at fixed plate boundary, determining velocity field by inverting Volterra-type integral equations

14 p2070 A72-31016

Orthogonal projection method for nonstationary heat conduction boundary value problem with thermal conductivity and specific heat as prescribed functions of position

14 p2126 A72-31049

Rietz-Kantorovich method reduction of scalar problem for wave propagation along direction surface to boundary value problem, discussing parametric resonance and periodic waveguides

14 p2132 A72-31118

Approximate solution of nonlinear boundary value problems in high temperature conductive heat transfer

14 p2174 A72-31161

Piecewise linear approximation of inverse nonstationary conductive heat transfer through unbounded plate with arbitrary temperature distribution and asymmetric boundary conditions

15 p2334 A72-31266

Electromagnetic boundary value problem of two rectangular waveguides coupled by aperture radiating into free space, solving integral equation by moments method

15 p2205 A72-31357

Constitutive equations for multipolar solid with memory, deriving boundary conditions and free energy equation from first and second thermodynamics laws respectively

15 p2273 A72-31363

Three dimensional elasticity boundary value problems solution via multidimensional Fourier transforms, applying to semiinfinite solid and hollow cones

15 p2324 A72-31481

Eigenvalue equation, orthogonality theorem and wear eigenfunction expansion for boundary value coupling of second order Sturm-Liouville systems

15 p2262 A72-31588

Optimal segment boundaries with composite error function in piecewise approximation chosen by dynamic program in scalar state variable, noting uniqueness properties

15 p2262 A72-31634

Boundary conditions for resonant frequencies calculation of turbine blades with Z-shaped and combined coupling sections

15 p2326 A72-31704

Nonlinear creep, viscoelasticity and elastoplasticity boundary value problems, discussing matrix constitutive differential equation formulation and higher order numerical methods

15 p2326 A72-31712

Finite element analysis of circular and elliptical plates with curved boundaries, discussing high precision triangular plate bending element modification for accuracy improvement

15 p2326 A72-31715

Rough surface elastic bodies stress calculation, using asymptotic method of boundary conditions

15 p2327 A72-31736

Boundary value problem solution uniqueness relation to existence for nonlinear differential equations of arbitrary order satisfying solution compactness condition

15 p2263 A72-31753

Boundary value problems for discrete spectrum of nonlinear ordinary differential operators on unbounded intervals

15 p2263 A72-31760

Iterative solution of boundary value problem in multiple burn rocket trajectory optimization

15 p2308 A72-31820

First boundary value problem solution for circle in static elasticity theory using Fredholm equation and source-sink method

15 p2328 A72-31849

Thin wire parallel to interface between two homogeneous half spaces, deriving transmission current wave propagation constant from boundary value problem solution

15 p2200 A72-32108

Aerodynamic properties prediction procedure for thin jet-flapped airfoil in incompressible inviscid flow bounded by different types of boundaries

15 p2179 A72-32147

Saturating nonlinear feedback systems stability under bounded input excitation, discussing error signals magnitude and duration

15 p2212 A72-32246

Dynamic boundary value problems for elastic materials with microstructure reduction to tensor equations of motion subject to initial and boundary conditions

15 p2329 A72-32283

Uniqueness, existence and smoothness theorems for elliptic dynamic boundary problems in elasticity theory

15 p2329 A72-32286

Mechanical models in thermoelasticity associated with boundary problems of classical physical fields with postulated laws of variation and periodicity

15 p2330 A72-32288

Nonlinear elastic material approximation by piecewise linear material with linear boundary value problems, discussing isotropic case based on singular surfaces theory

15 p2330 A72-32295

Reduced density matrix dependence on nonzero boundary conditions, considering Salzburg-Kirkwood integral equations

15 p2282 A72-32448

Special boundary value problems solution method for Mathieu differential equation, transforming Mathieu equation to Hill differential equation via Fourier series expansion

15 p2264 A72-32468

Nonlinear stability theory for plane Poiseuille flow under finite amplitude perturbations, solving Orr-Sommerfeld boundary value problem via finite difference method

15 p2218 A72-32469

Elastic wave scattering by moving slab, calculating reflection and transmission coefficients for various incidence angles, frequencies and motion velocities

15 p2219 A72-32476

Bending of uniformly loaded circular plate with mixed boundary conditions, calculating deflection and bending moments

15 p2332 A72-32579

Infinite integral evaluation with integrand formed by product of H function and double contour integral, with application to boundary value problems solution

15 p2265 A72-32600

Equilibrium equations for boundary value problems in Vekua theory with moments allowance for plate with circular hole under bending and torsion

15 p2333 A72-32682

Weight minimization for simple structures with single natural frequency constraint, solving nonlinear two point boundary value problem by variational and numerical methods

16 p2463 A72-32834

First mode ultraharmonics in nonlinear beam vibration with various boundary conditions and structural properties

16 p2463 A72-32845

Linearized supersonic flow past harmonically vibrating cylindrical body, solving boundary value problem by cylindrical integral transformation

16 p2342 A72-32878

Regge calculus representation existence for solutions of initial value problem for spaces with axial symmetry

16 p2422 A72-32879

Variational principle for boundary value problem of elastic-plastic torsion of circular bars under quasi-static finite deformation

16 p2464 A72-32914

Static boundary value problem of axisymmetric elasticity for elastic isotropic media with small energy contribution to potential due to moment effects

16 p2464 A72-32934

Binary gas mixture density correlation functions from initial value problem based on linearized Boltzmann equation for analysis of Rayleigh-Brillouin scattering

16 p2428 A72-32942

Difference scheme for initial value problem of one dimensional Vlasov equation for collisionless electron plasma with homogeneous ion background

16 p2434 A72-33006

Equilibrium equations and boundary conditions for elastic buckling of open cylindrical sandwich shell under compressive forces applied to freely supported edges

16 p2467 A72-33116

Elastic bending of rectangular continuous orthotropic plate with variable rigidities and elastic foundation coefficients for discontinuous boundary conditions along one edge

16 p2467 A72-33118

Solution existence for singular boundary value problem involving swirling flow, corresponding to problem of axisymmetric flow above rotating disk

16 p2377 A72-33186

Initial value problem for compressible viscous heat-conducting fluid flows with basic rotation and density stratification in gravitational field

16 p2377 A72-33337

Differential boundary value problem solution by FORTRAN program using finite difference method

16 p2416 A72-33524

Triple and quadruple integral equations solution in analogy to Fourier-Bessel series with mixed boundary values, using Erdelyi, Kober, Sneddon and Srivastava operators

16 p2416 A72-33663

Stress concentration in elastic layer with circular slot analyzed by reducing mixed boundary value problem to initial condition problem via invariant imbedding

16 p2471 A72-33827

Spacecraft free fall trajectory calculation, using numerical optimization procedure based on Hamilton principle for two point boundary value problems

16 p2460 A72-34021

Numerical analysis of boundary value problem for finite cylindrical dipole antenna of arbitrary orientation in magnetized plasma approximated by uniaxial medium

16 p2366 A72-34107

Perturbation method for two point boundary value problem for fluid flow applied to optimal reentry control problem

16 p2462 A72-34166

The approximate solution of parabolic initial boundary value problems by weighted least-squares methods.

17 p2573 A72-34217

Book - The method of weighted residuals and variational principles: With application in fluid mechanics, heat and mass transfer

17 p2573 A72-34250

A first initial boundary value problem for a semilinear heat equation.

17 p2573 A72-34339

Asymptotic solutions of inhomogeneous initial boundary value problems for weakly nonlinear partial differential equations. 17 p2574 A72-34342

Block five diagonal matrices and the fast numerical solution of the biharmonic equation. 17 p2574 A72-34446

Distribution of current in centre-fed cylindrical dipole antennas with arbitrarily displaced feed points. 17 p2526 A72-34517

Book - Theory and analysis of phased array antennas 17 p2515 A72-34621

Book - Approximation of elliptic boundary-value problems 17 p2574 A72-34622

Self-adjusting hybrid schemes for shock computations. 17 p2575 A72-34648

Study of circular arc airfoils with asymptotic critical Mach number. II 17 p2484 A72-34745

Stresses in a welded diaphragm due to boundary contraction and normal uniform pressure. [SESA PAPER 1811] 17 p2631 A72-34821

Existence of multiple solutions for nonlinear elliptic boundary value problems. 17 p2575 A72-34936

Theory of nonlinear viscoelasticity and its applications 17 p2631 A72-35109

Book - Nonlinear partial differential equations in engineering, Volume 2 17 p2576 A72-35449

Initial-boundary-value problem of the formation of an electrical discharge in a flow. 17 p2592 A72-35627

On the choice of boundary conditions for integration of transfer equations. 17 p2577 A72-35695

Solution to a boundary value problem in the theory of diffraction of electromagnetic waves at a circular hole in a plane screen between two media 17 p2518 A72-35724

General theory of spherically symmetric boundary-value problems of the linear transport theory. 17 p2583 A72-35825

Solvability of the first boundary value problem of higher-order elliptic quasi-linear equations with discontinuous and rapidly increasing Orlicz-class coefficients 17 p2577 A72-35842

The first Cauchy-Goursat problem of a hyperbolic-type equation degenerating at the boundary and having singular coefficients at the degeneration line 17 p2577 A72-35844

MHD inlet flow into channel, obtaining velocity profile numerical solution in Prandtl approximation with modified boundary conditions 18 p2714 A72-36121

Flat plate withdrawal at high speed from quiescent liquid baths, calculating velocity profile via boundary condition transformation and eigenfunction expansion method 18 p2678 A72-36122

Fluid dynamics problems self similar solutions as descriptions of intermediate asymptotic behavior of solutions for initial, boundary and mixed problems 18 p2709 A72-36388

Scattering of elastic waves by moving objects. 18 p2709 A72-36403

Transmission of sound in ducts with thin shear layers - Convergence to the uniform flow case. 18 p2710 A72-36405

Separation and analysis of the acoustic field scattered by a rigid sphere. 18 p2710 A72-36408

Solution of heat transfer problems with the aid of Laplace transforms. I - Development of analytical solutions for two specific boundary value problems 18 p2740 A72-36422

The stability of Poiseuille flow in a pipe of circular cross-section. 18 p2681 A72-36480

Compact self adjoint differential operators in family of Hilbert interpolation spaces, applying perturbation theorem to boundary value problems 18 p2704 A72-36511

Cluster variation method for boundary free energy solution in lattice model applied to Ising phase and gas-liquid interface and longer range interaction 18 p2711 A72-36565

The numerical solution of Fredholm integral equations of the second kind with singular kernels. 18 p2705 A72-36603

Error bounds for the Galerkin method applied to singular and nonsingular boundary value problems. 18 p2705 A72-36604

A singular multi-parameter eigenvalue problem in second order ordinary differential equations. 18 p2705 A72-36615

Nonzero solutions of boundary value problems for second order ordinary and delay-differential equations. 18 p2705 A72-36617

Boundary value problems for second order, ordinary differential equations involving a parameter. 18 p2705 A72-36619

Stability of difference schemes for elliptic equations in terms of the Dirichlet boundary conditions 18 p2705 A72-36801

Solution of some mixed boundary value problems of conducting medium thermodynamics by the method of variable separation 18 p2715 A72-36802

Optimality conditions in a problem of heat transfer process control 18 p2741 A72-36809

Diffraction and potentials of multilayers 18 p2736 A72-37003

Axial-symmetric deformations of a rubber-like cylinder under initial stress. 18 p2738 A72-37081

On the accuracy and application of the point matching method for shallow shells. 18 p2739 A72-37090

Integral equation method for solution of boundary value problems of structural mechanics. I - Ordinary differential equations. II - Elliptic partial differential equations. 18 p2739 A72-37169

A numerical method for coupled differential equations. 18 p2705 A72-37174

Boundary value problem for degenerate equations with discrete coefficients 19 p2824 A72-37317

Boundary conditions in the presence of Hall current or finite ion Larmor radius effects. 19 p2839 A72-37338

Boundary value problem approximate solution for Stokes flow of unbounded viscous Newtonian fluid past single body, applying algorithm to spheroidal shapes 19 p2784 A72-37369

The stress boundary value problem for plane strain deformations of an ideal fibre-reinforced material. 19 p2870 A72-37371

Computer method for plasticity theory boundary value problem for medium with unknown equations of state, using complex load simulating device 19 p2870 A72-37387

Complex systems dynamics and stability problems, deriving equations of motion and boundary conditions from principle of least action 19 p2784 A72-37388

An initial value method for dual integral equations. 19 p2824 A72-37413

Formal extension of the possibilities of the method of integral transforms in the study of linear distributed systems with constant parameters 19 p2834 A72-37432

Convergence of Rothe's method in the construction of bounded almost periodic and periodic solutions to a parabolic boundary value problem 19 p2824 A72-37433

Instabilities in semiconductors with negative differential mobility. 19 p2844 A72-37465

French monograph - An asymptotic theory of the Boltzmann equation and its application to the study of near continuum flows 19 p2785 A72-37489

Vortical flow of incompressible fluid in finite region bounded by potential flow and with Bernoulli constant jump at boundary 19 p2785 A72-37552

Homogeneous viscoelastic boundary value problem, demonstrating Volterra principle validity 19 p2872 A72-37562

Elasticity theory three-dimensional axisymmetric problem reduction to two dimensional analytic function boundary value problem 19 p2872 A72-37563

Approximation by fractional steps of control problems governed by parabolic equations and with boundary control 19 p2825 A72-37786

Homogeneous linear partial differential equation for optimal control with boundary condition formed by terminal component, noting weighting functions for linear plant 19 p2778 A72-37989

Dynamic meteorological problems solution by four dimensional analysis, discussing information deficiency effect on boundary value problems analysis in numerical weather forecasting 19 p2828 A72-37997

Solution of boundary value problems in heat conduction by the method of the successive averaging of a desired function 19 p2881 A72-38042

Mixed boundary value problem in the theory of elasticity for a half-space with circular lines of separation between boundary conditions 19 p2876 A72-38152

An eigenfunction method for solving the second boundary-value problem in the theory of elasticity 19 p2877 A72-38182

A characteristic problem for a hyperbolic-type equation degenerating at the boundary 19 p2825 A72-38187

A technique for numerical solution of boundary value problems in the plane theory of elasticity by the finite-difference method 19 p2878 A72-38204

Identification of parameters in nonlinear boundary conditions of distributed systems with linear fields. 19 p2780 A72-38245

Modified Ritz method to find optimum boundaries to elliptic systems governed by Laplace or Poisson equation 19 p2826 A72-38246

Control theory stability criteria applied to discrete time feedback systems, investigating numerical integration methods for initial value problems solution 19 p2826 A72-38250

Nonlinear interaction of a small cold beam and a plasma. II. 19 p2841 A72-38444

Investigation of a mixed boundary value problem for one class of second-order hyperbolic equations with a nonlinear operator-type right-hand side 19 p2827 A72-38447

Investigation of generalized and classical solutions of a mixed boundary value problem in a finite domain for one class of nonlinear second-order parabolic equations 19 p2827 A72-38448

Scattering resonances of electromagnetic wave by an infinite plane grating with reflector. 19 p2767 A72-38612

Hybrid computer Monte Carlo solution algorithm for parabolic partial differential equations with time varying boundary conditions, applying to ferromagnetic rod magnetization problem 19 p2770 A72-38620

A boundary value problem for a mixed-type equation with two perpendicular parabolic-degeneration lines 19 p2828 A72-38630

The Helmholtz equation in a waveguide /Factorization of the boundary condition from infinity/ 19 p2768 A72-38848

An intermediate matching technique for solving two point boundary value problems using the perturbation method. 20 p2910 A72-39198

Librational transverse oscillations boundary value problems of heavy thread on orbiting satellite, determining equilibrium and eigenfunctions 20 p2977 A72-39247

Proof of existence theorems for the principal dynamic problems of thermoelasticity 20 p2978 A72-39317

Fractional steps method of difference schemes for approximate numerical solution of parabolic and elliptic initial boundary value problems 20 p2945 A72-39327

The equivalence of several initial value methods for solving integral equations. 20 p2945 A72-39346

Solution of a problem with a skew derivative in a half-space for certain elliptical equations 20 p2945 A72-39393

Solution of some boundary value problems in the theory of potential gas flows and weak shock wave propagation 20 p2913 A72-39404

Solution of a boundary value problem for a class of nonlinear ordinary differential equations by the method of successive approximations 20 p2945 A72-39463

Asymptotic behavior of solutions of boundary value problems for systems of linear ordinary differential equations with a small parameter by the derivative 20 p2945 A72-39464

Certain properties of differential operators with variable coefficients dependent on the domain format 20 p2946 A72-39465

Expansion of a theory of elasticity operator in a series of eigenfunctions 20 p2979 A72-39467

Solution of mixed boundary value problems in heterogeneous media for multiply connected regions of complex shape by a structural method 20 p2946 A72-39469

Polymoment homogeneous solution characteristics in the theory of elasticity for design calculations 20 p2979 A72-39587

Compressible boundary-layer equations solved by the method of parametric differentiation. 20 p2914 A72-39614

A modified gradient technique for solving boundary and initial value problems. 20 p2946 A72-39618

Book - Functional analysis and approximation theory in numerical analysis. 20 p2946 A72-39729

A thermal boundary layer on a nonisothermal plate 20 p2987 A72-39917

Electrodynamics and magnetoelasticity nonlinear Emden-Fowler equation solutions, considering cur-

- rent carrying heavy filaments equilibrium and boundary value problems 20 p2955 A72-40032
- Elasticity theory axisymmetric problem for hollow cones analyzing stress-strain state and boundary value problem by asymptotic methods 20 p2982 A72-40036
- Finite difference boundary value method for solving one-dimensional eigenvalue equations. 21 p3074 A72-40107
- Boundary conditions in the exciton absorption region. 21 p3096 A72-40139
- A hybrid quasi-analog system for solving boundary value problems 21 p3024 A72-40159
- Methods of solving boundary value problems of linear conjugation for functions that are holomorphic in bicylindrical domains 21 p3074 A72-40254
- Classes of uniqueness of solutions to a boundary value problem in an infinite layer for systems of linear difference-differential equations 21 p3074 A72-40257
- Limiting equation for solving a boundary value problem in a multilayer domain 21 p3074 A72-40258
- Integral equation method for boundary value problem of logarithmic spiral antenna, noting suitability for digital computers 21 p3031 A72-40535
- Initial-value methods in the theory of Fredholm integral equations. II. 21 p3075 A72-40550
- Electromagnetic-wave propagation along a horizontal wire above ground. 21 p3015 A72-40633
- Necessary conditions for optimality in a general class of non-linear mixed boundary value control problems. 21 p3037 A72-40644
- Asymptotic solution of the wave equation with variable velocity and boundary conditions. 21 p3075 A72-40838
- Buckling of elastic bars with varying stiffness and nonideal boundary conditions. 21 p3118 A72-40932
- Synthesis of Tolubinskii's integral method and the perturbation method in nonstationary transport problems with nonlinear boundary conditions 21 p3129 A72-41053
- Application of Tolubinskii's integral method to the solution of boundary value problems of nonstationary convective diffusion 21 p3129 A72-41056
- Another boundary value problem of the linear theory of elasticity in regions with a fractionally-grained boundary 21 p3119 A72-41091
- Numerical solution of a boundary value problem arising in the deflection of beams and shells. 21 p3122 A72-41311
- Constitutive equations and boundary value problems in discrete theory of elasticity, noting linear systems of prismatic rods and lattice type shells 21 p3123 A72-41390
- Boundary value problems of lattice plates statics for transversally loaded homogeneous strip, noting elastically supported continuous plates 21 p3123 A72-41394
- Book on nonhomogeneous boundary value problems covering Hilbert theory for trace and interpolation spaces, elliptic operators and variational equations 21 p3076 A72-41526
- Book on nonhomogeneous boundary value problems for different classes of linear evolution parabolic operators, with applications to optimal control problems 21 p3076 A72-41527
- Numerical and asymptotic methods for solving the problem of complete boundary-layer stabilization 21 p3047 A72-41659
- Steady state or periodic solution to initial boundary value problems for heat conduction equation with nonlinear terms and boundary conditions 21 p3131 A72-41667
- Asymptotic representation of the solution of a boundary value problem for a biharmonic equation degenerating into a fourth-order parabolic equation 22 p3198 A72-41899
- Solution method for some boundary problems of nonlinear hyperbolic-type equations and propagation of weak shock waves 22 p3164 A72-41904
- Time evaluation of discontinuity occurrence in solutions of boundary problems for second-order hyperbolic quasi-linear systems 22 p3198 A72-41912
- A calculated hydrogen distribution in the exosphere. 22 p3168 A72-42004
- Alpha force-free magnetic field representation for solution of boundary value problem for chromosphere and lower corona magnetic fields 22 p3222 A72-42037
- Numerical solution of boundary value problems in the statics of axisymmetric shells by the method of reducing to Cauchy problems 22 p3233 A72-42054
- Analogies between linearized and linear problems in elasticity theory in the case of uniform initial states 22 p3233 A72-42061
- Quasi-regularity of infinite systems in problems of two-dimensional elasticity theory for doubly connected domains 22 p3233 A72-42063
- Finite difference theory for Lamé equations of elastic waves propagation in two dimensional body under mixed boundary conditions 22 p3234 A72-42144
- Pontryagin equations for Markov process limits probability, solving problem of one dimensional steady random process limits for given initial probability density function 22 p3205 A72-42227
- The problem of the boundary conditions in thermosphere dynamics. 22 p3201 A72-42510
- Calculation of laminar boundary layers by means of a differential-difference method. 22 p3167 A72-42578
- On the effect of the form of the strain energy function on the solution of a boundary-value problem in finite elasticity. 22 p3236 A72-42606
- Variable-step truncation error estimates for Runge-Kutta methods of order 4 or less. 22 p3199 A72-42746
- Square edged semiinfinite circular cylindrical shell, deriving boundary value problem closed form solution based on Novozhilov complex form cylinder equations 22 p3238 A72-42839
- Variational solution of a nonlinear boundary value problem for unsteady flow of gas. 22 p3199 A72-42854
- On eigenvalue boundary problems of transversely vibrating sandwich beams. 22 p3240 A72-42910
- Vertical asymptotes and bounds for certain solutions of a class of second order differential equations. 22 p3199 A72-42914
- Second order differential equations with general boundary conditions. 22 p3199 A72-42915
- German monograph - Heat stresses in circular plates subject to finite deflections. 22 p3241 A72-43058
- Plasma-electromagnetic interaction with surface wave propagation along boundary, obtaining boundary conditions for longitudinal and transverse wave amplitudes with allowance for particles interaction 22 p3213 A72-43117
- Method of solving boundary-value problems for a Langmuir probe in a dense plasma 22 p3213 A72-43119
- Boundary value problems of viscous fluid dynamic system generated by Navier-Stokes equations, using Hopf theory 22 p3208 A72-43137
- Book - The method of fractional steps: The solution of problems of mathematical physics in several variables 22 p3208 A72-43200
- Boundary value problems for concentrated forces acting inside semiinfinite anisotropic plate under plane stress, investigating failure modes of unidirectional composites 23 p3344 A72-43495
- Approximate optimal control solution to boundary value problem for one dimensional heat conduction equation, using Fredholm linear integral and degenerate kernels 23 p3274 A72-43526
- Some numerical results using Kalaba's new approach to optimal control and filtering. 23 p3274 A72-43543
- Boundary value problems for a mixed-composite type of equation in an unbounded domain 23 p3308 A72-43628
- Construction of the solution of a two-dimensional mixed boundary value problem for an arbitrary doubly connected region 23 p3345 A72-43629
- Numerical solution of a boundary-value bending problem for rectangular plates with free and freely supported opposite edges 23 p3345 A72-43645
- Nonlinear thin elastic plate deformation differential relations and static boundary conditions along contour, verifying theory by bending experiment on rectangular plate 23 p3348 A72-43791
- Approximation for boundary value problem of homogeneous stationary combustion in laminar gas flow through cylindrical tube 23 p3356 A72-43798
- The internal boundary value problem for the Boltzmann equation in the steady state and weakly nonlinear 23 p3280 A72-43820
- Asymptotic behavior of solutions of nonlinear parabolic equations. 23 p3309 A72-43979
- A priori bounds and upper and lower solutions for nonlinear second-order boundary-value problems. 23 p3309 A72-43980
- Dirichlet series in eigenvalues of boundary value problems for an arbitrary second-degree elliptic differential operator 23 p3309 A72-44043
- Application of the 'vanishing viscosity' method to improve stability conditions for higher-accuracy difference schemes used with the heat-conduction equation 23 p3356 A72-44046
- Series solution of the three-dimensional elasticity problem of a layer. 23 p3350 A72-44049
- Reflection of pulses at the interface between an elastic rod and an elastic half-space. 23 p3314 A72-44119
- Free flexural vibrations of an elliptical plate with simply supported edge. 23 p3352 A72-44121
- A manifold imbedding algorithm for optimization problems. 23 p3268 A72-44197
- Problem of error estimation during solution of internal boundary value problems in microwave electrodynamics 23 p3265 A72-44201
- Incompressible continuous media three dimensional boundary problems solution by pure shear state analysis, discussing application to plasticity theory 23 p3314 A72-44222
- Numerical evaluation of elastic stress intensity factors by the boundary-integral equation method. 23 p3353 A72-44233
- Integration scheme for two-dimensional impulsive waves in a linear acoustic medium. 23 p3314 A72-44250
- Multistage rocket optimal control, deriving conditions for existence of minimum of performance index function of mass, position and velocity initial and final values 23 p3343 A72-44264
- One dimensional steady conducting gas flow in nonaccelerating coordinate system under magnetic field, calculating pressure, density and temperature variations with boundary shock wave 23 p3281 A72-44265
- Stress distribution in a homogeneous elastic sphere containing a penny shaped crack of prescribed shape. 23 p3354 A72-44268
- Boundary value problems for multidimensional hyperbolic equations with degeneration 23 p3310 A72-44487
- Asymptotic behavior of the solutions of the third external boundary value problem for a wave equation with two space variables 23 p3310 A72-44488
- Scattering of obliquely incident waves by inhomogeneous fibers. 24 p3379 A72-44710
- Periodic solutions of a nonlinear mixed problem for the Navier-Stokes equations 24 p3418 A72-44780
- Free vibrations of thick, layered cylinders having finite length with various boundary conditions. 24 p3425 A72-44884
- Elastic bodies deformations theory, formulating boundary value problems 24 p3458 A72-44926
- The effect of shear on a penny-shaped crack at the interface of an elastic half-space and a rigid foundation. 24 p3459 A72-45250
- Riemann boundary value problem with a shift in multiply connected regions for quasi-linear elliptic systems of equations 24 p3419 A72-45260
- Computation of wall effects in ventilated transonic wind tunnels. 24 p3388 A72-45403
- [AIAA PAPER 72-1007] Dual extremum variational principles relevant to nonlinear heat transfer, applying to temperature distribution on thin walled spherical spacecraft surface 24 p3465 A72-45474
- Solution of a boundary-value thermoelasticity problem for a turbine blade by the polymoment method 24 p3460 A72-45623
- The first initial-boundary value problem for a nonuniform parabolic equation. 24 p3419 A72-45631
- A priori estimates at the boundary for solving second-order elliptic integrodifferential equations 24 p3420 A72-45648
- Comparison of linear and Riccati equations used to solve optimal control problems. 24 p3420 A72-45776
- Best finite elements distribution around a singularity. 24 p3420 A72-45786

BOURDON TUBES

Thin walled Bourdon tube manometric spring deformation analysis by Ritz method in second approximation

09 p1397 A72-22349

Differential error of fused quartz Bourdon tube precision pressure gages as function of absolute pressure level tested for nitrogen

13 p1959 A72-29764

BOUSSINESQ APPROXIMATION

Linear spin-down of stratified rotating Boussinesq fluid in circular cylinder as function of Prandtl number, noting solar interior problem

01 p0051 A72-11231

Buoyancy effect on shear stress and heat transfer in horizontal boundary layer, considering Boussinesq approximation

03 p0343 A72-14320

Finite element solution for Boussinesq approximation of two dimensional viscous fluid dynamic problems, using variational principle

07 p0965 A72-18794

Boussinesq solution for elastic surface deflection due to continuous pressure with polynomial distribution over triangular area

12 p1884 A72-27568

Boussinesq problem for homogeneous viscoelastic half space governed by deformation law of typical body under concentrated or sinusoidal loads

13 p2062 A72-30092

Magnetic field effect on finite amplitude convection in fluids complying with Boussinesq approximation, discussing maximum Nusselt number shift

16 p2452 A72-33039

Non-Boussinesq effects and further development in a model of upper tropospheric frontogenesis.

19 p2829 A72-38558

A temperature adjustment process in a Boussinesq fluid via a buoyancy-induced meridional circulation.

21 p3044 A72-40112

BOW SHOCK WAVES

U BOW WAVES

U SHOCK WAVES

BOW WAVES

Pioneer 8 plasma wave measurements at distant bow shock crossings, considering solar wind-magnetosheath interaction

01 p0062 A72-10903

Anomalous earth bow shock locations during 1969 from plasma and magnetic observations aboard European satellite Heos-1

02 p0274 A72-12461

Solar wind plasma flow through earth bow shock, deriving specific heats ratio based on one-fluid theory and conservation equations

03 p0412 A72-13509

Nonstationary behavior of collisionless shock waves in plasma wind tunnel, suggesting interpretation of magnetosphere magnetic field structure near earth bow shock

04 p0559 A72-15468

Earth bow shock magnetic field data correlation with Ogo 5 flux gate magnetometer, using Tidman-Northrop theory

07 p0975 A72-19145

MHD shock normals calculation by magnetic coplanarity formula, applying to bow shock crossing of Pioneer 6

07 p1040 A72-19157

Flow structure between bow shock wave and blunted cone surface, studying interior shock waves by numerical solution via finite difference methods

07 p0910 A72-20108

Mariner 4 trajectory relation to proposed location of bow wave caused by solar wind interaction with Mars ionosphere, noting planet orbit aberration effects

09 p1385 A72-22581

Earth bow shock laminar profile at low Mach number by crossing satellites on 12 February 1969, determining mean velocity along normal

09 p1387 A72-23004

Electron plasma oscillations distribution upstream from earth bow shock, evaluating OGO-E plasma wave detector data

09 p1300 A72-23019

Earth bow shock nonuniform structure observation correlation with interplanetary field orientation, using Explorer 33 and 35 data

11 p1722 A72-26395

Magnetosheath pressure, magnetic field, temperature, particle density and stream velocity computed for earth bow shock in oblique interplanetary field with solar wind

11 p1723 A72-26526

Earth-solar wind bow shock structure from OGO-5 observations during passage from interplanetary medium into magnetosheath

13 p1950 A72-29379

Comet-like interaction of Venus atmosphere with solar wind from Venus probe data, noting absence of bow shock wave and ionospheric tail

13 p2050 A72-29956

Numerical analysis of inviscid hypersonic flow characteristics in shock layer between bow shock and

cone at angles of attack, taking into account laminar separated flow

14 p2069 A72-30328

Unipolar steady electromagnetic bow shock interaction of Mercury with solar wind, calculating planetary surface temperature

15 p2303 A72-31305

Earth bow shock wave structure model based on development of strong density gradient in magnetic field-free cosmic plasma

16 p2387 A72-33935

Electron density measurements in bow shock stagnation and conical afterbody regions during blunt body atmospheric reentry, using flush mounted electrostatic probes

[ALAA PAPER 72-694]

16 p2345 A72-34047

Onboard radiometric measurement of bow shock generated UV radiation during atmospheric reentry of experimental sphere

[ALAA PAPER 72-692]

16 p2462 A72-34050

Magnetohydrodynamic theory for the interaction of an interplanetary double-shock ensemble with the earth's bow shock.

22 p3170 A72-42404

Earth collisionless plasma bow shock oblique structure assessment by pulsation index Ip devised from empirical results

23 p3341 A72-44511

Weak electrostatic turbulence observation in earth bow shock magnetic field gradient, suggesting cyclotron drift instability role

23 p3342 A72-44523

Pressure and magnetic field probe measurements in transverse shock waves in ionizing hydromagnetic regimes, investigating bow shock effects on accuracy

24 p3390 A72-44708

Radiation gasdynamics of planetary entry - Concepts and recent advances.

24 p3361 A72-45188

Effects of upstream unsteadiness on hypersonic flow past a wedge.

24 p3364 A72-45565

BOX BEAMS

Thin walled box beam optimal design, noting cross section areas and dimensions with permissible walls and flanges safety and stability

08 p1243 A72-21240

Transverse strain coefficient for steel box-section beam under tension, presenting test values for deformations before and beyond elastic limit

14 p2166 A72-30692

Experimental investigation of the carrying capacity in bending of steel box-section beams

22 p3232 A72-41870

BRADYCARDIA

Autonomic blockade effects on reflex bradycardia due to phenylephrine induced arterial pressure in man during rest and supine exercise

07 p0925 A72-20688

Case report of pilot near-syncope episode with bradycardia due to hyperactive right carotid sinus reflex

12 p1771 A72-27487

Bradycardia diving reflex to apneic face immersion related to physical exercise

17 p2506 A72-35964

Aortic regurgitation variation with respiratory sinus arrhythmia and respiratory cycle in dogs during tachycardia and bradycardia

22 p3151 A72-42674

Continuous recording of His bundle electrogram during selective coronary cineangiography in man.

23 p3255 A72-43813

BRAGG ANGLE

Bragg crystal spectrometer for Sco X-1 spectrum scanning, using Aerobee 170 rocket

[AD-736552]

03 p0353 A72-13039

He-like lines in solar X-ray spectrum observed by Bragg crystal spectrometer, noting absolute wavelengths determination with shaft encoder for angle readout

11 p1714 A72-26572

X ray Brillouin scattering investigation of phonon phenomena for small momentum transfers with Bragg condition nearly satisfied

15 p2250 A72-32308

BRAIDED STREAMS

U STREAMS

BRAIN

NT BRAIN STEM

NT CEREBELLUM

NT CEREBRAL CORTEX

NT CEREBRUM

NT HIPPOCAMPUS

Intracellular pH prime regulation in rat brain during acute and sustained hypercapnia, discussing cellular bicarbonate accumulation

01 p0012 A72-10623

Hypoxia, hyperoxia and hypercapnia short period effect on rat brain oxygen supply, measuring blood gas values, tissue oxygen partial pressure time variations, etc

02 p0159 A72-11957

Nervous respiratory disorder in patients with diencephalic and vegetative vascular syndromes, discussing arterial hypoxemia development and resulting oxygen insufficiency

02 p0160 A72-12012

Insulin injection or carbohydrate consumption effects on serotonin and tryptophan concentrations in rat brains

02 p0165 A72-12845

Acute and chronic hypercapnia effect on lactate, pyruvate, alpha-ketoglutarate, glutamate and phosphocreatine contents of rat brain

03 p0316 A72-13677

Electrophysiology for auditory temporal masking mechanism study of cat cochlear nucleus and inferior colliculus single neurons

05 p0620 A72-17175

Rat brain acetylated and unacetylated coenzyme A aberration in marginally hyperoxic space capsule environments

06 p0763 A72-17875

Hologram data treatment comparison to human brain function, discussing recognition signals, Pavlovian qualities and intelligence function

06 p0768 A72-17997

Factor analysis of frontal and occipital brain regions EEG indices interzonal variability, relating autocorrelation function parameters to neuron ensembles force level

06 p0764 A72-18057

RNA content changes in ground squirrel brain during active and hibernation states

06 p0764 A72-18058

Retina, tectum opticum and Rostral brain structures role in analysis and processing of visual sensory stimuli in toad distinguishing between prey and enemies

07 p0915 A72-18775

Sensor systems terminals location in cats colliculus anterior through electrical response measurement to light and sound signals and skin stimulation

07 p0915 A72-18865

Human behavior analysis based on nine component functional brain model, discussing information transmission mechanism via nerve path channels

07 p0923 A72-20460

Inhaled oxygen pressure variation effects on adenosines, glucose, lactate and pyruvate levels in rat brains, noting anoxic limit value relation to age

07 p0924 A72-20658

Brain structures role in fixation of temporal relationships in information memory function of central nervous system

08 p1118 A72-21836

Physiology of sleep phases and dreams, discussing data on highly organized and interacting neurohumoral mechanisms exhibiting alternating forms of brain bioelectric activity

08 p1118 A72-21838

Breathing regulation characteristics showing reflex control of respiratory functions in normal environment and brain tissue receptor control under hypoxia

08 p1121 A72-22079

Stepwise adaptation to high mountain conditions effect on brain and sural muscle oxidation processes in rats

08 p1121 A72-22085

Soviet book on psychic phenomena and brain, covering cybernetics, dialectical materialist implications, consciousness, psychophysiology and cerebral neurodynamic structures

08 p1121 A72-22164

Photically induced and spontaneously discharged neuron impulse propagation through direct pathways from superior colliculus to dorsal and ventral lateral geniculate nuclei in cats

09 p1265 A72-22863

Review of biology and biochemistry of memory, suggesting molecular level mechanism of cerebral information processing

10 p1424 A72-23925

Mathematical model of extracellular pH in brain tissue from blood and cerebrospinal fluid acid-base parameters for respiration central chemosensitive mechanism study

11 p1579 A72-26660

Kespiration control by extracellular pH in medullary tissue, studying chemoreceptor response to hydrogen ion concentration in cat cerebrospinal fluid

11 p1579 A72-26661

Vascular-capillary study of age related angioarchitectonic features of human brain optic lobe

11 p1580 A72-26675

Thyroid and adrenocortical hormonal state effect on cell number and functional maturation of brain, discussing neurogenesis in infants

12 p1760 A72-27298

Thermoregulation in deeply hibernating rodents during separate chilling and steady hibernation temperature maintenance of skin and brain

12 p1762 A72-27827

Coherent brain model for evolution mechanisms of biological resonance in neuron network signal flow

13 p1908 A72-28455

Digital evoked brain potential detector using multichannel amplitude analyzers 13 p1908 A72-28645

Adaptation period to inverted work-rest cycle observed with encephalograph, noting effect of brain bioelectric activity circadian rhythms stability 13 p1904 A72-29315

Electric stimulation of rabbit brain limbic formations [claustrum, amygdala, hippocampus], showing effect on emotional response motor and vegetative components 14 p2076 A72-30668

Human brain sensorimotor region EEG dependence on proprioceptive influence, instruction for active movement and preparation passive movement of hand 16 p2353 A72-32992

Biochemical analysis of cat brain regions for gamma-aminobutyric, aspartic and glutamic acids, glycogen and phosphatide concentrations during paradoxical sleep deprivation 16 p2356 A72-33559

Bioelectric activity of the medulla oblongata during hypothermia and bloodletting 17 p2504 A72-35024

Sperry neuronal specificity hypothesis for nerve cell connections formation between eye and brain during embryonic development, proposing systems matching theory 17 p2504 A72-35070

Russian book - Intracranial blood circulation under conditions of accelerations and weightlessness 17 p2509 A72-35460

Language and speech capacity of the right hemisphere. 19 p2757 A72-38150

Synaptic patterns in the superficial layers of the superior colliculus of the monkey, Macaca mulatta. 19 p2758 A72-38647

Proteinase activity in different regions of the brain during development and inhibition of a conditioned passive-avoidance reflex 20 p2890 A72-38927

Effects of free amino acid doses and of amino acid metabolism cofactors on the distribution of regional free amino acid resources in the brain and blood of animals 20 p2891 A72-39324

Negative /painful/ stimulus cessation relation to emotionally positive zone activation in rat brain during self stimulation experiments 20 p2892 A72-39410

Localization and structural-functional organization of the system of vagus nerve nuclei constituting the 'cardiac center' of the medulla oblongata 21 p3004 A72-41673

New modifications of manipulators for investigations using microelectrodes 22 p3149 A72-42073

Modulating effect of limbic brain formations on the blood system 22 p3142 A72-42282

Suprapontine influences on hypoxic ventilatory control. 22 p3143 A72-42590

Dependence of inhibitory areas of inferior colliculus neurons on the time characteristics of acoustic stimuli 22 p3145 A72-42724

Mechanism of adaptation to hypoxic hypoxia 23 p3255 A72-43907

Influence of elevated partial oxygen pressure on the sympathetic-adrenal and acetyl-choline systems 24 p3371 A72-44595

BRAIN CIRCULATION

Oxygen distribution in human brain under counter-current capillary blood flow conditions, presenting mathematical simulation for transport in Krogh system 02 p0168 A72-12037

Epinephrine and norepinephrine effects on cerebral blood circulation volume and oxygen tension in tissues 02 p0165 A72-12517

Ballistocardiographic measurement of net cranial blood inflow during cardiac ejection 03 p0314 A72-13145

Book on experimental brain hypoxia covering changes in hemodynamics, energy metabolisms, electrolyte and water movement and cerebral and peripheral venous blood serum proteins 09 p1264 A72-22238

Objective evaluation of main rheoencephalogram parameter for disturbed brain blood circulation 12 p1773 A72-28218

Human brain stem vascular-capillary network density and dimensional characteristics 13 p1901 A72-28462

High altitude natives cerebral arterial-venous oxygen difference measurement during ambient air and oxygen breathing, showing chronic hypoxia effect on cerebral blood flow 14 p2079 A72-30704

Human cerebral hemodynamic changes during arousal and orienting reactions to auditory stimuli 16 p2353 A72-32993

Cerebral blood flow and metabolic changes during wakefulness, sleep, coma and epileptic seizures in terms of homeostatic mechanisms 16 p2356 A72-33558

Studies of the influence of theophylline on the vasodilating action of different medications on the cerebral and coronary circulation of man 18 p2651 A72-36799

Unresponsiveness of pial precapillary vessels to catecholamines and sympathetic nerve stimulation. 22 p3140 A72-41934

Effect of vibration on the permeability of the blood-brain barrier 22 p3149 A72-42070

Carotid rete role in brain protection against extreme elevations of systemic blood pressure, presenting goat cerebral blood flow measurement procedure 22 p3144 A72-42671

Rheographic investigation of cerebral, pulmonary and peripheral circulation during bed rest in antithrostatic position 23 p3255 A72-43914

Cerebral blood filling reduction and blood vessel tone deterioration during 120 day clinostatic hypokinesia of healthy male subjects 23 p3256 A72-43922

Comparative study of regional hemodynamics during tilt test and lower body negative pressure exposure. 24 p3373 A72-45131

BRAIN DAMAGE

High energy proton irradiation late pathological effects on rabbit brains, discussing brain lesions and radiation dosages [CERN-71-16] 02 p0161 A72-12056

Frontal lobe damage effect on conditional motor reflexes, communication capability and emotional behavior in baboon apes 04 p0476 A72-15583

Human craniocerebral trauma dependence on impact conditions, giving case histories 05 p0619 A72-16643

Cerebral vascular disorder biochemical analysis, noting retinal vascular change relation to coronary arteriosclerosis and anoxia and flight stress effect on serum lipid and cholesterol 07 p0923 A72-20448

Book on experimental brain hypoxia covering changes in hemodynamics, energy metabolisms, electrolyte and water movement and cerebral and peripheral venous blood serum proteins 09 p1264 A72-22238

Tentorium cerebelli microstructure and leaflets strength in study of chronic and acute hypoxia injury to fetus during pregnancy and labor 09 p1266 A72-23193

Hydrogen peroxide formation relationship to lipid peroxidation and seizures in brain during high pressure oxygen exposure 12 p1766 A72-28300

Destructive changes in rabbit brain and eyes under pulsed laser beam irradiation 13 p1910 A72-29333

Human and animal central nervous system repair processes for brain damage caused motor function disturbances 14 p2078 A72-31100

Crash helmet performance prediction through maximum strain criteria, using brain injury biodynamic model 15 p2192 A72-32607

Brain tumors in irradiated monkeys. 17 p2505 A72-35647

Reflex and conditional movement observation of central nervous system function restitution in Macaca mulatta monkeys with cortical lesions, studying pathological forced grasping 18 p2651 A72-36977

Language and speech capacity of the right hemisphere. 19 p2757 A72-38150

Supplementary cues and delayed-alternation performance of frontal monkeys. 20 p2892 A72-39372

Higher nervous activity of monkeys two years after the extirpation of the dorsolateral frontal cortex 21 p3001 A72-40803

Role of the reticular formation of the mid-brain in the storage and recreation of a system of conditioned reflexes 21 p3001 A72-40809

BRAIN STEM

Human brain stem vascular-capillary network density and dimensional characteristics 13 p1901 A72-28462

Role of the reticular formation of the mid-brain in the storage and recreation of a system of conditioned reflexes 21 p3001 A72-40809

Eye movements evoked by collicular stimulation in the alert monkey. 24 p3371 A72-44906

First-breath response of medullary inspiratory neurones to the mechanical loading of inspiration. 24 p3372 A72-44959

Temperature-sensitive neurons in the brain stem - Their responses to brain temperature at different ambient temperatures. 24 p3373 A72-45232

BRAKES [FOR ARRESTING MOTION]

NT AERODYNAMIC BRAKES
NT AIRCRAFT BRAKES
NT DRAG CHUTES
NT LEADING EDGE SLATS
NT SPLIT FLAPS
NT TRAILING-EDGE FLAPS
NT WHEEL BRAKES
NT WING FLAPS

BRAKES [FORMING OR BENDING]

High strength steel flat plates brake formability from bend tests on sheared edges specimens, noting Hutchinson method sensitivity for different crack propagation propensities materials 11 p1657 A72-25819

BRAKING

Transfer from high elliptical to circular orbit, using successive spacecraft braking maneuvers in planetary atmosphere with incomplete information 01 p0130 A72-10927

Aerospace tug using atmospheric braking during return from geostationary orbit, discussing radiative thermal protection, mass, design and advantages 23 p3340 A72-44275

BRANCHING [MATHEMATICS]

Multiplication operator unidimensional perturbation by independent variable, considering spectral function density poles and branch points 03 p0382 A72-13728

Approximations and bifurcations in flight dynamic system, investigating singular point motion over trajectory during partition process 05 p0611 A72-16582

Existence and bifurcation conditions of singular point consisting of spliced focus spliced out of ordinary trajectories, investigating stability 05 p0690 A72-16593

Multiple elastic postbuckling path generation at coincident branching points for system with many degrees of freedom 07 p1087 A72-19113

Branching theory application to convection and axisymmetric flow formation in internally heated self gravitating liquid filled sphere 07 p0968 A72-19973

Existence and branching of analytical solutions to equations describing oscillatory-rotatory motions of system of two pendulums with different masses 07 p1036 A72-20217

Periodic two-parameter solution families of dynamic systems having first integral, showing stability and bifurcation existence criteria relationships to dimensionality and Hamiltonian systems 15 p2261 A72-31309

Approximations and bifurcations in flight dynamic system, investigating singular point motion over trajectory during partition process 19 p2748 A72-37553

Existence and bifurcation conditions of singular point consisting of focus fused from ordinary trajectories, investigating dynamic system stability 19 p2834 A72-37565

Branching theory application to convection and axisymmetric flow formation in internally heated self gravitating liquid filled sphere 20 p2915 A72-40030

The branch and boundary method as a regular method of solving irregular problems of mathematical programming. I 22 p3198 A72-42188

Continuum and finite element branching studies of the circular plate. 22 p3235 A72-42603

BRANCHING [PHYSICS]

Product of net branching factor and induction period in hydrocarbon oxidation at low temperatures, tabulating results 07 p1051 A72-19374

Perfect and imperfect plastic column buckling, describing bifurcation and stability theory for elastic-plastic and rigid-plastic bodies 13 p2054 A72-28480

Transients analysis for nonlinear branched dynamic systems by integral manifold and small parameter method 13 p2007 A72-29997

Perturbation scheme for branching analysis of post-buckling behavior in elastic spherical shells 16 p2465 A72-33001

Electrons angular distribution effect on photoionization branching ratio measurement by photoelectron spectroscopy 17 p2552 A72-34288

Complex stress-intensity factors at bifurcated cracks. 21 p3117 A72-40675

BRASSES

Grain orientation effect on fatigue crack propagation in notched test specimens cut from cold rolled prestressed annealed brass plate 03 p0375 A72-13934

- Electrolyte temperature, pH and mixing rate effects on anodic dissolution of steels and brass in electrochemical precision processing, using thermokinetic data processing 11 p1640 A72-26257
- The influence of grain and twin boundaries in fatigue cracking. 21 p3069 A72-41350
- Experimental investigation of electromagnetic cascades at an energy greater than 20 GeV 23 p3291 A72-44444
- BRAVAIS CRYSTALS**
- X ray diffraction analysis of dilute Nb-C alloys epsilon phase, discussing Bravais lattice and unit cell dimensions 03 p0375 A72-13932
- BRAYTON CYCLE**
- Nuclear Brayton space power systems, discussing efficiency, isotope decay and reactor design 04 p0546 A72-14423
- BRAZING**
- Book on vacuum brazing covering dissimilar metals joining, stress cracking, corrosion resistance, joint design, heat treatment and production engineering problems 01 p0073 A72-10165
- Aluminum vacuum furnace fluxless brazing process, eliminating flux entrapment, postbrazing cleaning and water pollution 01 p0074 A72-10281
- Brazed joints shear strength and ductility tests, discussing deformation, hardness, corrosion, irradiation, structure and microanalysis 01 p0074 A72-10285
- Refractory alloy weldability and brazing, discussing manual and automatic tungsten arc and electron beam processes and fillers 01 p0075 A72-10752
- Dip, torch, furnace and vacuum brazing of aluminum 04 p0526 A72-14836
- High temperature brazing of heat resistant alloys, determining tensile strengths 05 p0666 A72-16189
- Beryllium joining by resistance welding, electron beam welding, dip brazing and braze welding 06 p0820 A72-17701
- Ti-Ni-Cu and Ti-Zr-Be alloys for brazing Ti heat exchangers, discussing flow characteristics and corrosion resistance 06 p0820 A72-17703
- Gas quenching technique for vacuum brazing of Al, Ti and ferrous alloys, evaluating mechanical properties, surface contamination and He leak tightness 07 p0997 A72-19997
- Al, Ti and ferrous alloys suitability for vacuum brazing-gas quenching processing for He leak-tight joints, using photomicrography 07 p0997 A72-19999
- Filler metal compositions and procedures for Al alloys vacuum brazing, describing experimental vacuum furnace apparatus 07 p0997 A72-20000
- Metallographic properties of vacuum brazed, heat treated and gas quenched Al alloys, low alloy steels and corrosion resistant steel alloys 07 p1017 A72-20001
- Ti honeycomb brazing, discussing filler metals, furnace temperature and atmosphere control and use of protected graphite as furnace material 07 p0998 A72-20288
- Ti alloy sheets diffusion brazing, describing chemical cleaning, auxiliary metal cladding, heating and pressure augmented fusion processes involved in high quality joints production 10 p1497 A72-24658
- Filler metal paste application effect on Hastelloy sheet brazing quality, describing results in terms of mechanical properties and microstructural characteristics 11 p1637 A72-25342
- Compressive strength of Ti alloy airframe skin stringer panels reinforced with B-Al composite by brazing [AIAA PAPER 72-359] 11 p1729 A72-25387
- B-Al metal matrix composites joining together and to Al and Ti, considering soldering, brazing, bonding and mechanical fastening [AIAA PAPER 72-360] 11 p1638 A72-25388
- Space shuttle heat shield metallic refractory, superalloy and composite materials joining, discussing vacuum furnace brazing of Al/B matrix structures [AIAA PAPER 72-387] 11 p1638 A72-25408
- Al alloy-graphite composites brazing and welding feasibility, tabulating spot welding parameters 11 p1641 A72-26491
- Nonmetalized aluminum oxide ceramics brazing with metals under pressure using copper solder, noting optimum conditions for Kovar 15 p2243 A72-31225
- Developments in vacuum braze coating of aero-engine nozzle guide vanes. 17 p2559 A72-34937
- Compatibility of brazed joints with potassium and vacuum. 17 p2567 A72-34938
- Brazed-welded lightweight high pressure aerospace tube-fittings. 17 p2560 A72-34939
- Study of vacuum furnace atmospheres for brazing titanium honeycomb panels. 17 p2560 A72-34940
- Nondestructive ultrasonic inspection of braze bonds in high current electrical contact assemblies. 18 p2695 A72-36116
- Book - Aluminum brazing handbook 19 p2810 A72-38720
- Brazing furnaces and heat treatment under vacuum 22 p3163 A72-42635
- BREADBOARD MODELS**
- Reliability data collection methods, considering equipment initial design, breadboard models, prototype, production, acceptance, qualification, field installation and operation 10 p1443 A72-23975
- Solar electric propulsion subsystem performance tested on breadboard model, noting electrical power conversion, command, thrust vector control and propellant supply [AIAA PAPER 72-507] 11 p1711 A72-26227
- Surface wave devices signal processing for space communication, developing fast lock up spread spectrum communication link breadboard 13 p1920 A72-29106
- BREAKAWAY**
- U BOUNDARY LAYER SEPARATION
- BREAKERS [ELECTRIC]**
- U CIRCUIT BREAKERS
- BREATHING**
- NT HIGH ALTITUDE BREATHING
- NT OXYGEN BREATHING
- Respiratory system frequency response analysis for chemical regulation of breathing, using time domain method and step functions 02 p0168 A72-12040
- Human reaction to inhalation of gas mixtures with 3-9 percent carbon dioxide, measuring respiration rates, minute breathing volume, heart rates, arterial pressures, etc 05 p0618 A72-16632
- Bulbar respiratory neuron discharge pattern response to nasal and tracheal receptor stimulation in cats, relating changes in neuronal activity and intratracheal pressure 08 p1117 A72-21473
- Respiratory control system benchmark simulation on hybrid computer for Cheyne-Stokes breathing, emphasizing equations for arterial and venous carbon dioxide and oxygen stores 23 p3268 A72-44551
- BREATHING APPARATUS**
- NT OXYGEN MASKS
- NASA technology transfer from information dissemination and service to product development, noting firemen breathing system 17 p2639 A72-35506
- BREATHING MODE**
- U BREATHING VIBRATION
- BREATHING VIBRATION**
- Paratroop type parachutes breathing oscillations and stability characteristics, using high speed cinematography and kinetheodolites to track during steady state descent 01 p0004 A72-10307
- BRECCIA**
- Apollo 14 rocks, breccia fragments and soil samples ages from Ar 40/Ar 39 and cosmic ray dating, discussing basalt Ar release patterns 01 p0117 A72-10052
- Apollo 14 Fra Mauro site basaltic rocks and breccia clast internal Rb-Sr isochrons, comparing to Tranquility Sea basalts 01 p0123 A72-10053
- Hibonite/Ca-Al-Ti rich xenoliths/ from Leoville and Allende polymict brecciated HL group chondritic meteorites 01 p0125 A72-10067
- Dunite-norite olivine-rich microbreccia in Apollo 14 lunar fines sample 14002.8, discussing origin and chemical composition 01 p0126 A72-10106
- Lunar sea surface model derivation from morphology data analysis, suggesting four-layer bottom relief of basaltoid lava, rocks, breccia and surface regolith 04 p0576 A72-15069
- Impact breccias in carbonate rocks of Sierra Madera /Texas/, investigating microstructure, chemical composition, petrography and mineralogy 05 p0654 A72-16038
- Apollo 14 lunar breccia samples, observing chondrules from meteoritic impact event 05 p0715 A72-16161
- Chromian pleonaste and aluminous picotite in Apollo 14 fine grained microbreccias comparing with spinel composition in lunar basalts 06 p0878 A72-17672
- Apollo 15 mare basalts and breccias and premare igneous rocks, analyzing chemical composition and microstructure 06 p0888 A72-18262
- Geologic setting of Apollo 15 breccias and basalt 06 p0888 A72-18263
- Primordial radioelements and cosmogenic radionuclides in Apollo 15 basalt, breccia and soil samples 06 p0889 A72-18274
- Apollo 12 and 14 lunar soils K, Rb and Sr isotopic composition evaluation, noting microbreccia as major nonbasaltic constituent 11 p1723 A72-26497
- Vaporization and condensation effects on Apollo 11 glass spherules from microbreccia samples, suggesting concentration gradients as result of impact event 11 p1723 A72-26522
- Shock deformation microstructures in Apollo 14 breccia and comparative terrestrial minerals, using transmission electron microscopy 11 p1724 A72-26951
- Apollo 14 breccia sample inverted pigeonites /pyroxenes/ as evidence of lunar plutonic rocks, using optical, electron probe and X ray diffraction techniques 12 p1865 A72-27112
- Lunar breccia and crystalline rocks thermomagnetic magnetization characteristics, presenting alternating field and thermal demagnetization curves 14 p2154 A72-30507
- Pu 244/U 238 fission track retention age of whitlockite crystal in lunar breccia 14321 from Fra Mauro formation 15 p2307 A72-31722
- Lunar surface breccias origin, using exploration data to reappraise ballistic theory of giant craters and maria formation in favor of volcanic concepts 16 p2461 A72-34180
- Lunar pentlandite and sulfidization reactions in microbreccia 14315.9. 18 p2729 A72-36973
- Xenon isotope fission component due to extinct Pu-244 in lunar breccia, noting storage details in terms of crustal material dating 20 p2967 A72-39182
- On the applicability of lunar breccias for paleomagnetic interpretations. 22 p3226 A72-42532
- Occurrence of chromian, hercynitic spinel /pleonaste/ in Apollo-14 samples and its petrologic implications. 22 p3153 A72-42862
- Uranium distribution in basalt fragments of five lunar samples. 23 p3261 A72-43399
- BREECHES**
- U CLOSURES
- BREEDER REACTORS**
- Mathematical model and inelastic stress analysis for metal creep-fatigue interaction and progressive deformation in breeder reactors operation 09 p1407 A72-23200
- Deformation substructures in stainless steels under low cycle high strain fatigue tests evaluation for application as fuel cladding for fast breeder reactors 16 p2411 A72-33825
- BREGUET AIRCRAFT**
- Wind tunnel testing of Dassault-Breguet-Dornier Alpha Jet twin engine trainer, emphasizing tests for wing-empenage flutter and jet induced interference effects 13 p1940 A72-30077
- BREMSSTRAHLUNG**
- Bremsstrahlung X rays from electron precipitation associated with discrete vlf emissions, recording wave-particle experiment near plasmopause with balloon-borne counters in Antarctica 03 p0413 A72-13536
- X ray background model based on photons bremsstrahlung emission by subcosmic metagalactic electrons or protons 03 p0413 A72-13804
- Bremsstrahlung emission by auroral electrons in upper atmosphere and penetration in lower atmosphere, comparing calculation with balloon measurement 04 p0566 A72-14879
- Metagalactic gamma rays from relativistic electron bremsstrahlung interactions under assumption of single power law source 05 p0710 A72-16712
- Hard X ray emission by thermal plasma, applying relativistic corrections to photon bremsstrahlung Maxwell distribution and cross section 06 p0873 A72-18004
- Auroral zone electron precipitation events before and at negative magnetic bays onset, presenting balloon recordings of bremsstrahlung X-rays intensity 06 p0808 A72-18092
- Simultaneous auroral X ray, bremsstrahlung and visible bursts observations from balloons. 07 p1058 A72-19166

Magnetic bremsstrahlung energy straggling and radiation reaction, calculating particle and emitted photon distribution
07 p1037 A72-19668

Solar radio bursts classification, discussing normal and magnetic bremsstrahlung and plasma waves conversion
07 p1079 A72-20012

Absorption by Nd laser generated ionized Al plasma of extreme UV radiation due to inverse bremsstrahlung and photoionization
09 p1360 A72-22831

X ray observation inconsistency with matter creation in steady state universe due to inner bremsstrahlung from neutron decay
11 p1713 A72-26125

Electron energy, mobility and bremsstrahlung in weakly ionized nonisothermal plasmas, using Kogan approximation
11 p1698 A72-26647

High X ray luminosity associated with richest galaxy clusters, noting inverse Compton effect by relativistic electrons and bremsstrahlung from hot gas
13 p2040 A72-29412

Spectral radio observations of 7 March 1970 solar eclipse, noting McMath plages intense activity source flux characteristics and weaker source bremsstrahlung emission
13 p2044 A72-29551

High energy electron heating of solar flare plasma with X-ray emission due to thermal and nonthermal bremsstrahlung
13 p1033 A72-29745

White dwarf background radiation and optical emission variations due to thermal bremsstrahlung from stellar coronae
14 p2147 A72-30554

Absorption coefficient of H-He plasma measured in temperature and electron density range of inverse bremsstrahlung and photoionization absorption
15 p2284 A72-31522

Nonionizing component of underground high energy cosmic radiation investigated with anticoincidence screen and counters, noting bremsstrahlung as photons source
15 p2301 A72-32232

Bremsstrahlung photon emission rate from Maxwellian plasma, determining soft X ray diagnostic techniques applicability for laser produced plasmas
15 p2285 A72-32271

Born approximation for resonance bremsstrahlung emission and photon absorption cross sections at electron-ion scattering, solving multiparticle problem
15 p2279 A72-32697

Runaway electrons in toroidal plasma investigation by thick target bremsstrahlung measurement, noting energy distribution and runaway rate estimates
17 p2591 A72-35370

Stratospheric model for bremsstrahlung X ray relation emission to auroral electron flux, considering photon energy release in scintillation counters
17 p2551 A72-35872

Ion-ion correlation effects on electron-nucleus neutrino bremsstrahlung
18 p2723 A72-36089

X-ray bremsstrahlung in the stratosphere and the auroral activity of January 21 and February 3, 1969
18 p2722 A72-36863

Bremsstrahlung as a possible source of UHF emissions from lightning
19 p2828 A72-37894

Plasma electron velocity distributions determined from the polarization of free-free bremsstrahlung
19 p2841 A72-38439

Inverse bremsstrahlung caused fast cascade of electrons with Boltzmann energy distribution to explain laser induced gas breakdown via plasma heating
20 p2934 A72-39645

Non-destructive activation analysis of some elements in stony meteorites by proton- and bremsstrahlung-irradiation
20 p2899 A72-39833

Non-thermal bremsstrahlung of fast electrons and flare of stars
20 p2974 A72-39894

The effect of target absorption on the attenuation characteristics of bremsstrahlung generated at constant medium potentials
21 p3087 A72-40474

Bremsstrahlung from cylindrical beta sources
21 p3088 A72-41383

The interaction of Sco X-1 with its environment
22 p3218 A72-42387

Electron bremsstrahlung from hot plasma in the presence of strong magnetic field
24 p3431 A72-45627

BREWSTER ANGLE

Effects of thermal lensing in glass lasers
19 p2810 A72-37512

BRIDGES (STRUCTURES)

Structural analysis of cable stayed bridge scale model with fractional and full loading, showing system linear behavior with small displacements and real nonlinearities, respectively
[SESA PAPER 1896]
02 p0199 A72-11515

Thin airfoil and bridge deck flutter derivative from transient oscillatory states in test procedure
02 p0298 A72-12665

BRIGHTNESS

Quadrantid meteoritic shower upper atmosphere contamination effects on twilight and night sky brightness
02 p0283 A72-12467

Solar corona shape, structure and brightness changes during 11 year cycle from monochromatic and total eclipse white light observations
03 p0423 A72-13210

Magnetograph scans of solar disk center supergranulation, showing downdrafts relation to magnetic field strength and chromosphere and photosphere brightness
03 p0429 A72-13307

Critique of quasar model of independent random pulse emitting sources conglomeration, noting brightness fluctuations incompatibility
03 p0435 A72-13802

Statistical investigation of 1500 galaxies in MCG catalog with weak surface brightness, noting sculpture type spheroidal galaxies in Virgo cluster
03 p0435 A72-13807

Statistical processing of phase dependence of Martian integral brightness at 0.3-1.1 microns, noting abrupt reflectivity decrease
03 p0436 A72-13816

Simultaneous brightness contrast under scotopic conditions, investigating fovea rod and cone systems interaction in subjects with normal color vision
03 p0317 A72-13937

Extragalactic radio sources luminosity function and luminosity density function from radio index surface brightness, discussing evolution and agreement with models
05 p0722 A72-17156

Lunar photometric studies, discussing surface light scattering properties, data reduction and relative and systematic errors in brightness
06 p0817 A72-18224

Light polarization in Honda comet head, discussing brightness distribution
08 p1229 A72-20833

Comets visual brightness determination by astronomical photographic photometry
08 p1229 A72-20834

Comet brightness variations correlation with geomagnetic field and solar corpuscular flux variations in interplanetary space
08 p1231 A72-21132

Brightness distribution and phase dependence measured for spheres with different colors and roughness for Mars surface optical parameters model validity
08 p1238 A72-21830

Photoelectric measurements of brightness of Galilean satellites of Jupiter as function of solar phase angle
08 p1238 A72-21831

Computer calculation of spectral brightness coefficients on aerial photographs, determining contrast features density gradients
09 p1308 A72-22484

Negative search for post eclipse brightening of Io and Europa satellites in 1970 based on single beam photometric observation
10 p1532 A72-23714

Airglow intensities and upper atmosphere physical processes relationship, discussing spectral features, emission brightness and excitation sources
10 p1474 A72-24714

Lunar crater region ray systems origin and brightness variation mechanism from surface vitreous spherules examination
11 p1715 A72-25300

Relative brightnesses along solar radius from density photometry of corona at eclipses
13 p2046 A72-29715

Radio bursts and X ray emissions associated with 15-16 November 1970 solar chromosphere flares, noting brightness maximum differences
14 p2146 A72-30483

Monochromatic brightness coefficient measurements for Jupiter and Saturn disk centers and Uranus
14 p2152 A72-30491

Zodiacal light brightness and polarization measurement from OSO-5 with photometers at 4180 and 6820 A
16 p2385 A72-33467

Radial velocities and brightness distribution in active and quiet solar atmosphere from magnetograph measurements, discussing motion directions in photosphere and chromosphere
19 p2858 A72-37818

Monochromatic brightness coefficient measurements for Jupiter and Saturn disk centers and Uranus
19 p2864 A72-38320

Brightness matrix of a flat powdered layer with opaque particles in the single-scattering approximation
19 p2836 A72-38783

New observations of solar magnetic and brightness fields
20 p2971 A72-39763

The minimum brightness gain required in viewers using image intensifiers
21 p3055 A72-40744

Comet integral brightness estimation by mathematical analysis of photometric characteristics
21 p3110 A72-41449

Eclipsed binary brightness curve determination by least squares method, using weighted gravity center point observations
21 p3113 A72-41760

1971 Rayleigh Gold Medal Address - Calculating the perceived level of light and sound
22 p3205 A72-42462

Quasars as images of Seyfert nuclei
23 p3336 A72-43559

Master oscillator/power amplifier laser systems output beam divergence and far field brightness, comparing to Gaussian plane waves
23 p3296 A72-43901

BRIGHTNESS DISCRIMINATION

Head mounted monkey eye orientation measuring system for performance of brightness discrimination tasks
03 p0318 A72-13073

Contrast vision enhancement in Hermann grid with variable figure-ground ratio, using Baumgartner receptive field hypothesis
03 p0315 A72-13624

Comet Bennett tail and coma surface brightness distribution, estimating solar wind velocity
05 p0717 A72-16426

Meteor trails radar ranging system with circular vernier scanning and brightness indication with high accuracy
09 p1308 A72-22507

Model to account for visual responses to light flashes of dark adapted eye, discussing perceived brightness variation with intensity
18 p2651 A72-36611

Photometric behaviour of Saturn's rings as a function of the saturnocentric latitudes of the earth and the sun
18 p2727 A72-36735

Mach band measurement by psychological compensation technique, causing band disappearance by changes in stimulus pattern luminance and brightness distribution relations
19 p2760 A72-37827

Investigations concerning the problem of virtual contours in visual perception
19 p2759 A72-38719

The effects of simultaneous and successive contrast on perceived brightness
24 p3372 A72-44910

BRIGHTNESS TEMPERATURE

Quiet solar corona thermal emission flux at 169 MHz, showing constant brightness and electron temperatures during cycle
01 p0123 A72-10045

Optical/electrical apparatus for measuring high brightness temperatures in 6,000-100,000 K range
01 p0068 A72-10620

Atmospheric humid cover measurement with airborne/spaceborne microwave radiometric sounding, considering radiothermal radiation models
02 p0253 A72-11733

Natural and artificial snowpacks microwave brightness temperature variations with snow depth, free water content and underlying material characteristics
02 p0212 A72-11832

Remote passive microwave sensing of ocean surface wind fields, discussing sea microwave brightness temperature dependence on wind speed
02 p0214 A72-11864

Martian radio emission at 8.57 mm during 1971 approach, comparing brightness temperature to Jupiter
02 p0280 A72-12196

Saturn radio emission and brightness temperature measurements, determining rings optical thickness upper limit
03 p0438 A72-13977

Radio astronomical observation of two local sources associated with unipolar sunspot group 275 and bipolar group 282, investigating emission directivity and brightness temperature
04 p0572 A72-14636

Brightness temperatures and directionality of IR emission from rough lunar surface of crater field
05 p0714 A72-16104

Brightness temperatures over Mars south polar cap from Mariner 9 IR radiometry, comparing to Mariner 6 and 7
06 p0890 A72-18343

Interstellar heterocyclic carbon ring molecules furan and imidazole search from upper limits in galactic sources brightness temperature
06 p0891 A72-18502

Radiation temperature of carbon monoxide molecules in solar atmosphere from vibratory-rotatory spectral measurements
07 p1077 A72-19811

- Solar radio emission, considering sources of slowly varying waves, brightness temperature distribution, frequency spectra and fluctuations
08 p1228 A72-20827
- Microwave absorption in high pressure hydrogen based on radio astronomical measurements of Uranus brightness temperature
08 p1239 A72-22088
- Cosmos 243 microwave radiation analysis over cultivated terrain, showing radio brightness temperature dependence on soil temperature and humidity effect on emissivity
09 p1297 A72-22495
- Saturn radio emission detection and measurement at 49.5 cm, determining equivalent disk brightness temperature
10 p1531 A72-23710
- Lunar microwave emission, constructing thermophysical models for radio observations and brightness temperature variations
12 p1869 A72-27327
- Solar radial brightness distribution, using mm observations during 7 March 1970 solar eclipse for improved angular resolution
13 p2042 A72-29531
- Saturn thermal radio emission brightness temperature calculations for subcloud atmosphere ammonia abundance evaluation
14 p2152 A72-30490
- Nighttime lunar surface thermal properties from differential IR flux scans with earth based Cassegrain telescope, noting difference in brightness temperature gradients between highlands and maria
14 p2153 A72-30503
- Flux densities, electron energies and brightness temperature determination from radio telescope observations of galactic sources and nonthermal radiation
14 p2155 A72-30553
- Saturn rings gas-dust atmosphere, thickness and motion, considering planetary radio emission and brightness temperature
14 p2161 A72-31073
- Callisto radio emission analysis by ice body model, finding brightness temperature calculation of ice surface
15 p2308 A72-31904
- Venus brightness temperature and phase dependence at 2.7 cm wavelength during 1968-1970
15 p2311 A72-32088
- Cosmic background radiation temperature from interstellar CN band R branch absorption line in star zeta Ophiuchi spectrum
15 p2313 A72-32309
- Galactic background continuous radiation observation at 15 GHz, determining brightness temperature and thermal radiation component
15 p2313 A72-32348
- Solar vacuum UV flux measurement by photon ion chambers aboard WRESAT I satellite, obtaining 4600 K brightness temperature
16 p2452 A72-33040
- Microwave absorption in high pressure hydrogen based on radio astronomical measurements of Uranus brightness temperature
17 p2606 A72-34651
- Measurements of the limb darkening in the forbidden MgI line at 4571.1 Å.
17 p2608 A72-35078
- ESRO 2 satellite observation of solar X-ray emission from active limb prominence, obtaining temperatures and emission measures as function of time
17 p2608 A72-35085
- Solar thermal radio burst temperature and emission measure determination from flux spectrum, noting consistency with radio observation
17 p2608 A72-35090
- A revision of Jupiter brightness temperatures in the frequency interval 18.5-24.0 GHz /1968/.
17 p2610 A72-35119
- Spectral observations of Venus in the frequency interval 18.5-24.0 GHz - 1964 and 1967-68.
17 p2610 A72-35120
- Russian book on pyrometry principles covering high temperature measurement, error analysis, heat transfer and brightness temperature
17 p2556 A72-35447
- Radiation temperature of carbon monoxide molecules in solar atmosphere from vibratory-rotatory spectral measurements
17 p2618 A72-35736
- A photoelectric method for measuring the temperature pulsations of solids
19 p2799 A72-37664
- Measurement of Jovian radio emission at a wavelength of 2.94 m
19 p2864 A72-38080
- Saturn thermal radio emission brightness temperature calculations for subcloud atmosphere ammonia abundance evaluation
19 p2864 A72-38319
- Absolute measurement of the solar brightness in the spectral region between 100 and 500 microns.
22 p3225 A72-42389
- The Cygnus X-region. VII - Radio continuum search for a ring of filaments around the area.
22 p3225 A72-42390
- Brightness temperature of the terrestrial sky at 2.66 GHz.
22 p3173 A72-42516
- Lunar albedo and temperature distribution from simultaneous photoelectric and far IR brightness temperature measurements of sunlit lunar surface
22 p3226 A72-42536
- Directional far IR emission from sunlit lunar surface, determining brightness temperature as function of observer and sun elevation angles and surface parameters
22 p3226 A72-42537
- Identification and removal of phase errors in interferometry.
23 p3287 A72-43259
- Vacuum ultraviolet absorption measurements on ionized species.
23 p3316 A72-44330
- Individual reddening laws of O-type stars. I - Computation method, first results
24 p3437 A72-44829
- Orion nebula continuum spectrum energy distribution from spectrophotometric measurements, comparing color temperature with previously obtained data
24 p3438 A72-44839
- The quiet sun brightness distributions at millimeter wavelengths and chromospheric inhomogeneities.
24 p3438 A72-44840
- BRILLOUIN EFFECT**
Electrostrictively induced stimulated Brillouin light scattering effect on atmospheric depolarization, obtaining solutions for steady state and transient conditions
[AD-736316] 03 p0367 A72-13429
- Waveguide with slanted aperture, determining propagation mode and wave amplitude from radiation level at Brillouin angle
05 p0625 A72-15828
- Laser emission intensity enhancement based on stimulated Brillouin scattering effect by raising pumping level, energy density and pulse duration
12 p1821 A72-27587
- X ray Brillouin scattering investigation of phonon phenomena for small momentum transfers with Bragg condition nearly satisfied
15 p2250 A72-32308
- Rayleigh-Brillouin light scattering in He-Xe gas mixtures, noting thermal fluctuations effect
16 p2422 A72-32943
- Stimulated thermal and Mandelstam-Brillouin scattering of light in liquid nitrogen and oxygen.
20 p2933 A72-39520
- Fabry-Perot interferometer measurements of Brillouin scattering from He-Ne laser excited low temperature condensed gases
21 p3051 A72-40151
- Waveguide with slanted aperture, determining propagation mode and wave amplitude from radiation level at Brillouin angle
23 p3263 A72-43436
- Stimulated entropy /temperature/ scattering and its influence on stimulated Mandelstam-Brillouin scattering
23 p3297 A72-44478
- Gain and line width in stimulated Brillouin scattering in gases.
24 p3412 A72-45616
- BRITTLE MATERIALS**
Kinetic energy velocity and acceleration formulas of penny shaped crack propagation in brittle body under triaxial tensile stress
01 p0144 A72-11391
- Strength and strain theory statistical analysis for perfectly brittle and plastic materials, assuming ultimate or elastic limit strain as governing factor
07 p1097 A72-20536
- Single and multiple fractures in brittle matrix fibrous composites, discussing fracture energetics, stress-strain curves and hysteresis effects
09 p1338 A72-23164
- Stress intensity factor for circular crack embedded in finite thickness solid under uniform tension, noting semielliptical surface flaw in brittle material
[ASME PAPER 71-APMW-6] 10 p1554 A72-24183
- Statistical estimation method for brittle metals fracture strength, taking into account stress nonuniformities due to dislocation defects
11 p1738 A72-26803
- Thermal shock produced edge effect, analyzing brittle material heat resistance and failure, using thermoelastic heated cylinder
14 p2165 A72-30437
- Stress analysis for brittle body with thermoinsulated crack under mechanical load and temperature field, noting limiting equilibrium equation
16 p2469 A72-33272
- Cumulative damage probability in dynamic or static fatigue failure of brittle graphite materials as function of stress
16 p2414 A72-33321
- Brittle creep rupture process in beam subjected to simultaneous loading with bending moment and axial force
16 p2474 A72-34128
- Note on dynamic fracture toughness measurement.
17 p2566 A72-34257
- Point-loaded discs and blocks applicable to tensile testing of brittle materials.
19 p2870 A72-37223
- A device for recording acoustic signals of crack formation in brittle materials
19 p2802 A72-38018
- Thermal boundary equilibria in brittle bodies with heat conducting cracks under combined loads and temperature fields
19 p2877 A72-38198
- The fiber and filament reinforcement of plastic and brittle matrix materials
20 p2944 A72-39438
- Tendency toward brittle failure of a simulated weld-seam region in Ti-Al-V system alloys
23 p3293 A72-43593
- Brittle ceramic materials strength, showing porosity effect dependence on Weibull homogeneity parameter value
23 p3306 A72-43750
- Statistical strength and plasticity criterion for materials in a complex stress-strain state
23 p3349 A72-43953
- Investigation of the strength of construction materials for various principal-stress relations
23 p3349 A72-43955
- Test equipment for heat resistance determination of brittle refractory material, noting data processing procedure and formulas for temperature distribution and thermal stress
23 p3278 A72-43962
- Fiber and filament reinforcement of plastic and brittle matrix materials
24 p3414 A72-45276
- BRITTLENESS**
Interstitial impurities and grain size effects on cold brittleness in W melts in deformed and recrystallized states
01 p0088 A72-11082
- Alloy steels temper brittleness analysis, using internal friction characteristics as functions of time and temperature
02 p0247 A72-12816
- High alloy chromium and manganese steels brittle fracture susceptibility, showing notch effects
03 p0371 A72-13466
- Testing temperature effect on intergranular fracture propagation in steel sensitive to tempering brittleness
03 p0372 A72-13599
- Breakdown of three dimensional brittle medium weakened by concentric systems of interconnected circular cracks, using Fredholm integral equations
03 p0447 A72-13732
- Stress concentration around circular hole in infinite semibrittle plate under omnidirectional tension at infinity or pressure at hole contour
03 p0452 A72-14127
- Tensile ductile-brittle transition temperature and slip mechanism of thoriated Cr, comparing with unalloyed Cr
05 p0678 A72-17117
- Cyclic loading effects on resistance to brittle fracture of low carbon structural steels, using crack with criterion
06 p0831 A72-18353
- Plasticity onset and brittle fracture of annealed steel as function of preceding strains
06 p0831 A72-18354
- Tempering temperature effect on hydrogen penetration level and brittleness of hardened carbon steel
07 p1014 A72-19773
- Aging effect on brittleness and hardening of Fe-Ni-Mn alloy at various temperatures
07 p1016 A72-19939
- Reversible hydrogen brittleness development conditions in metals, deriving equations for hydrogen content effect on plasticity dip
07 p1018 A72-20132
- Cold brittleness of transition metal alloys with bcc lattices, discussing elastic characteristics, packing defects energy, plastic deformation and rhenium admixture
07 p1018 A72-20143
- Impurities and crystal lattice role in metal brittleness, discussing stress concentration and relaxation, crack initiation and plastic deformation
07 p1018 A72-20145
- Rare earth metals effects on chromium brittle transition temperature, showing maximum plasticity with lanthanum addition
07 p1019 A72-20151
- Cr-Ti-V-B alloys rod specimens grain size and brittleness-viscosity transition temperature after heat treatment, cooling and bending tests
07 p1023 A72-20668
- Tensile strength estimation for two dimensional composite with brittle matrix and randomly orientated discontinuous elastic fibrous reinforcement
08 p1244 A72-21324

C and Re effects on brittleness threshold temperature and plasticity of Mo-Re alloy

09 p1326 A72-22227

Brittle fracture dynamics, deriving motion equations and stability conditions of surface cracks under stress waves from energy balance and angular momentum conservation law

09 p1404 A72-22916

Stress-strain characteristics of metal ductile filaments with elastic brittle coatings, noting strengthening effect on anodic oxide coated aluminum

09 p1330 A72-23379

Stress corrosion cracking mechanism of low carbon steels to explain transcrystalline brittle mechanical cracks development along grain boundaries

11 p1666 A72-26923

Pure biocarbons for skeletal fixation of limb prosthetic devices, noting load bearing applications dependence on brittle characteristics

12 p1773 A72-28095

Cast Al alloys tendency to brittle failure in percussive bending tests estimated from force strain oscillograms

14 p2124 A72-31035

Neutron irradiation effects on structural materials brittle fracture initiation and propagation mechanisms, discussing residual elements influence on radiation defect stabilization

15 p2258 A72-32486

Surface energy and cleavage plane observation of brittle fracture for W single crystal in tension as function of orientation and temperature

18 p2702 A72-36750

German monograph - Significance of the manganese-carbon ratio in the brittle-fracture behavior and weldability of high-strength fine-grained structural steels

19 p2816 A72-37661

Evaluation of the tendency to brittle fracture of turbine rotors made from steels of medium strength

19 p2876 A72-38001

Resistance to brittle fracture of high-strength steels in various structural states

19 p2819 A72-38014

Brittle lacquer of air-drying type, investigating coating ingredients and plasticizers effect on strain sensitivity for various temperature and humidity levels

20 p2920 A72-38890

Quasi-static impact of hard hemisphere against brittle half space, investigating fracture mechanics

20 p2981 A72-39952

The stress gradient as a cause for the manifestation of the scale effect in brittle fracture of materials

21 p3123 A72-41364

Brittle fracture under dynamic loading conditions

22 p3239 A72-42848

Probabilistic model for tensile strength of brittle fibers, discussing clamping effects at various gauge lengths and Weibull flaw structure

23 p3305 A72-43490

Inelastic transverse strain coefficient and Poisson ratio dependences on plastic and brittle properties

23 p3348 A72-43752

Cold shortness of 14Kh2NZMA steel

23 p3303 A72-44023

Dynamic fracture criteria for ductile and brittle metals

23 p3354 A72-44260

High alloy chromium and manganese steels brittle fracture susceptibility, showing notch effects

24 p3414 A72-44941

Cyclic loading effects on resistance to brittle fracture of low carbon structural steels, using crack width criterion

24 p3416 A72-45740

Plasticity onset and brittle fracture of annealed steel as function of preceding strains

24 p3416 A72-45741

Reversible hydrogen brittleness development conditions in metals, deriving equations for hydrogen content effect on plasticity dip

24 p3416 A72-45758

BROADBAND

Broadband beam scanned linear waveguide antenna array design with FMCW short range high resolution radar for airport navigational aid in fog

01 p0039 A72-10669

Broadband high gain large aperture Schwarzschild antenna systems design, considering compromises and tradeoffs in scan angle, F/D ratio and surface shapes

01 p0039 A72-10672

Low loss wideband characteristics of groove and H guides for efficient signal transmission

02 p0190 A72-11679

Si p-n-p punchthrough X band oscillator, discussing wideband tuning and low noise properties and applications

07 p0955 A72-19252

Broadband cylindrical monopole antenna with adjustable quasi-distributed capacitive loading, comparing theoretical and experimental admittances

11 p1604 A72-25744

Broadband diode phase shifter design, discussing switched and loaded line, reflection and lumped element high pass and low pass circuits

11 p1607 A72-26992

Input match conditions for broadband mixer conversion loss minimization, comparing optimization procedures

15 p2208 A72-32392

A broad-band wide-angle scan matching technique for large environmentally restricted phased arrays.

17 p2513 A72-34353

Analysis of the correlation functions of space-time wideband signals received by linear antennas

19 p2775 A72-38657

An ultra-broadband probe for RF radiation measurements.

20 p2921 A72-38993

Broad-band transistorized receiving antennas in the frequency range between 10 kHz and 10 MHz

21 p3030 A72-40526

Broad-band television transmitting antenna with polydirectional characteristics for the UHF-region

21 p3031 A72-40542

Application of logarithmic characteristics to calculate wideband load matching of an oscillator

23 p3271 A72-43836

Ultrasonic diffraction loss and phase change for broad-band pulses.

23 p3313 A72-44115

BROADBAND AMPLIFIERS

Broadband high efficiency mode/HEM/ TRAPATT amplifiers for S band, discussing bandpass and input-output characteristics with Ichebycheff filter

01 p0038 A72-10652

Wideband microwave parametric amplifier using balanced circuits to relax isolation requirements between signal, idler and pump circuits

01 p0038 A72-10655

Gain vs bandwidth characteristics of broadband microwave parametric amplifiers

01 p0038 A72-10656

Computer program for design optimization of three-stage wideband low-noise integrated microwave amplifier

01 p0041 A72-10690

Directional couplers design for broadband microwave integrated circuits

01 p0046 A72-10702

Broadband uhf power amplifier for AM signals output power of 100 W, using eight parallel transistors

06 p0774 A72-17750

Wideband tunnel diode microwave amplifier design with coaxial line, considering band-edge stability and impedance matching

06 p0785 A72-18310

Microwave thin film microstrip IC tunnel diode amplifiers for broadband high performance receivers, discussing design, construction and performance

06 p0786 A72-18374

Broadband parametric amplifier design using computerized optimization procedure based on Gauss-Newton iteration technique

06 p0786 A72-18376

Miniature modular wideband parametric amplifier for centimeter range, using IC optimal coupled circuit with passband dependent on diode time constant

07 p0956 A72-19570

Hf and shf power transistor gain, efficiency and electrical characteristics for wideband linear amplifiers

08 p1139 A72-21051

Operational and equivalent circuit characteristics of low noise hf and shf transistors in wideband amplifiers

08 p1139 A72-21052

Supercritical CW GaAs transferred electron broadband reflection amplifier power gain and noise figure at 34 GHz

10 p1449 A72-24301

Multistage broadband microwave amplifier design based on bipolar transistors cascade coupling, using scattering parameters

10 p1451 A72-24572

Multiaxis radial circuits for transferred electron microwave oscillator performance optimization to obtain wideband CW amplification, discussing LSA tests

11 p1604 A72-25745

High quality GaAs varactor diodes for double diode low noise wideband parametric amplifiers at idler frequencies up to 43 GHz without refrigeration

12 p1788 A72-27174

Wideband push-pull transistorized power amplifier free of nonlinear distortions due to scattering inductance of load transformer

13 p1926 A72-28378

Compensation of nonlinear selectivity distortions in radio receivers with broadband preamplification stages, noting circuit diagrams for preselector correctors

13 p1927 A72-28412

Optimal design of broad passband in unilateral parametric balance amplifier

13 p1928 A72-28789

Computerized synthesis of wideband series stabilized tunnel diode amplifier based on distributed constant elements

13 p1931 A72-29286

Broadband high power L-band phased array amplifier chain.

17 p2528 A72-34710

Bilateral tunnel-diode amplifiers using ferrite transformers.

18 p2665 A72-36306

A C-band all ferrite integrated wideband high power GaAs avalanche diode amplifier.

19 p2771 A72-37264

Electron bunching and output gap interaction in broad-band klystrons.

19 p2772 A72-37566

German monograph - Multiple tuning of cooled parametric amplifiers

19 p2772 A72-37651

Calculation of two- and three-stage broadband amplifiers with parallel correction from the standpoint of a maximum quality factor with an optimally flat amplitude characteristic

21 p3027 A72-40477

Determination of pulsed amplifier correction parameters with the aid of approximating polynomials

21 p3034 A72-41120

Optimization of planar transistor operation modes in cascades with inductive correction

21 p3034 A72-41121

Miniature modular wideband parametric amplifier for centimeter range, using Q optimal coupled circuit with passband dependent on diode time constant

22 p3158 A72-42088

Ultrasonic response of a CW dye laser to selective extinction.

23 p3297 A72-44186

A wide-band Gunn-effect CW waveguide amplifier.

23 p3272 A72-44193

BROADCASTING

Long distance monitoring method for short wavelength radio transmission to remote countries

02 p0182 A72-12671

Communication satellites for European radio and TV broadcasts, discussing use of American, CETS-C and Symphonie satellites

04 p0494 A72-15677

TV programs direct broadcasting by satellites, discussing frequency range, amplitude vs frequency modulation, satellite stabilization and economic aspects

04 p0494 A72-15678

Satellite broadcasting juridical aspects, discussing control over frequency spectrum, geostationary orbits appropriation, copyrights, broadcast contents and advertising

04 p0494 A72-15679

Symphonie communication satellite applications in radio and TV broadcasting, discussing Retelsat network, Socrate and Memini projects, educational TV, etc

04 p0494 A72-15680

Satellite broadcasting for direct individual and community reception as mass communication means, discussing UN role and international juridical problems

07 p1104 A72-19472

Anik communications satellite for Canadian domestic television and radio broadcasting networks

07 p0944 A72-19655

Direct broadcasting communication satellites, discussing frequency allocation, modulation and data processing systems

07 p0948 A72-20266

UHF band satellite TV broadcasting system with FM, calculating required field strength and transmitter power

10 p1435 A72-24033

Combined educational and TV network satellite distribution system for public broadcasting service, discussing cost reduction techniques

10 p1435 A72-24035

Fixed and broadcast communication satellites for educational information dissemination in U.S., discussing commercial, multipurpose domestic and hybrid systems

12 p1779 A72-27352

Satellite technology for TV broadcasting service to Canadian remote areas, considering new frequency band allocation

12 p1781 A72-27373

Time data dissemination techniques, discussing astronomical and atomic time scales, frequency standards, broadcasting and TV, navigation and satellite systems

14 p2085 A72-30364

Frequency sharing between broadcast satellites and tropospheric scatter systems.

20 p2901 A72-38978

Controlled-carrier transmission of AM/VSB television from space.

21 p3016 A72-40770

Planning of a broadcast-satellite service.

21 p3016 A72-40771

Utilization of frequency bands allocated to satellite broadcasting for regional or domestic systems.

21 p3018 A72-40875

Geostationary satellite direct TV broadcasting system extension to 12 GHz band, considering receiving installations, antennas, performance and costs

21 p3018 A72-40876

- Orbital and frequency sharing between the broadcasting-satellite service and the fixed-satellite service.
21 p3018 A72-40877
- BROKEN CLOUDS**
U CLOUDS [METEOROLOGY]
- BROMIDES**
NT SILVER BROMIDES
- BROMINATION**
Studies on flame-resistant epoxy resin - Pyrolysis of tetra-brominated epoxy resin and flame-resistant mechanism.
18 p2704 A72-36519
- BROMINE**
Chlorine, bromine and iodine first spectral lines observation in IR region with liquid nitrogen cooled lead sulfide detector
09 p1276 A72-22614
Bromine additions effect on normal laminar flame propagation velocity of methane-air mixture at high pressures
09 p1411 A72-22889
Gaseous and particulate bromine in the marine atmosphere.
22 p3173 A72-42470
- BROMINE COMPOUNDS**
NT SILVER BROMIDES
Fire retardant capabilities of bromine and chlorine compounds in polymers
[PI PAPER 13]
03 p0380 A72-13247
Biomedical effects on air crews of chemical fire suppression agent Halon 1301 /bromotrifluoromethane/ during simulated aircraft cabin fires
12 p1776 A72-28308
Tetrafluorodibromomethane - A new fire extinguishing agent in civil aviation
17 p2512 A72-35793
Semiconductor properties of iodine and bromine molecular complexes of /1-phenyl-3-isindolyl-/ /1-phenyl-3-pseudoisindolenylidene-/ phenylmethane and /1-p-tolyl-3-isindolyl-/ /1-p-tolyl-3-pseudoisindolenylidene-/ phenylmethane.
19 p2847 A72-38641
- BRONCHI**
Quasi-steady creeping flow in small airways of spherical, oblate and prolate ellipsoid and circular cylinder lung models, obtaining Stokes equations solutions
10 p1431 A72-24469
Breathing rate response to oral instructions in relationship to nervous system, bronchial muscle tonus and gas metabolism rate reflex-type changes
21 p3001 A72-40761
- BRONCHIAL TUBE**
Mathematical model for flow limitation in collapsible tube in relation to pressure in pulmonary and circulatory system
17 p2510 A72-35972
- BRONZES**
Wear mechanism of lead-bronze dry sliding in air on hardened steel ring
11 p1638 A72-25510
Powder metallurgy sintering process variables for dimensional control of bronze parts, discussing strength and porosity level specifications
11 p1640 A72-26243
Quenched beryllium bronze alloy plastic deformation effects on anomalous and ordinary stress relaxation processes
12 p1828 A72-27292
Steady state creep measurements of lead-phosphor bronze discontinuous fiber composites under nonuniform deformation, comparing to fiber and matrix alone
15 p2261 A72-32299
Cubic sodium tungsten bronze electrocatalytic activity increase for oxygen reduction by traces of Pt
16 p2361 A72-33883
- BROWNIAN MOVEMENTS**
Brownian motion kinetic equation from Boltzmann equation for two component neutral gas by simultaneous expansion in density and mass ratios
01 p0050 A72-10233
Statistical description of Brownian particle motion in turbulent flow, using theory of canonical correlations
05 p0648 A72-16171
Brownian particle sedimentation rate and diffusion coefficient determination by holographic double exposure interferometry
06 p0816 A72-17982
Centered Gaussian process oscillations [Brownian motion], obtaining divergence rate in sequence of finite partitions
10 p1504 A72-24054
Probabilistic derivation of quantum mechanics wave equations for Brownian motion and spatial-temporal diffusion
10 p1505 A72-24071
Random number method for particle motion in homogeneous turbulence field, using Brownian motion Markov process for turbulence approximation
13 p1940 A72-28421
- Statistical description of Brownian particle velocity in turbulent flow, using theory of canonical correlations
14 p2093 A72-30240
Spatial diffusion dynamics, spin, and the Pauli equation
17 p2573 A72-34193
Inertial effects in motion driven by hydrodynamic fluctuations.
24 p3430 A72-45560
- BRUDERHEIM METEORITE**
Al 26 production rates from Al, Si, S, Mg and Ca in Bruderheim chondrite by weighted least squares analysis
03 p0435 A72-13691
- BRUSHES**
Friction, wear and noise of slip ring and brush contacts for synchronous satellite use.
18 p2693 A72-35982
The testing of contact materials for slip rings and brushes for space application.
18 p2698 A72-36117
- BUBBLE CHAMBERS**
Bubble chamber high energy particle tracks semiautomatic measuring device, using small on-line computer for data processing
06 p0813 A72-17438
- BUBBLES**
Sound propagation and absorption mechanism in liquid-base foams explored by bubble pulsation and coupling mathematical model and distributed parameter mechanical analog
01 p0115 A72-10161
Gas bubble damage centers in organic glass produced by quasi-steady ruby laser pulse induced high temperature heating, using high speed photography
01 p0079 A72-10373
Vapor bubble growth on heated surface with random temperature distribution and liquid microfilm for water and boiling potassium
02 p3033 A72-12862
Motion picture technique for studying vapor bubbles formation, determining temperature fluctuations on heated surface below active region
03 p0457 A72-14153
Surface active materials adsorption on developing bubble surface, analyzing time dependence
03 p0458 A72-14155
Tube wall temperature and acoustic noise spectra dependence on thermal flux density in bubble coalescence
03 p0458 A72-14162
Fluid motion model with gas bubbles, noting energy dependence on temperature and density
05 p0649 A72-16224
Ultrasonic transducer monitoring of decompression-caused gas bubbles in rat thigh muscle tissue for decompression sickness time course development studies
07 p0921 A72-20183
Numerical solution of disintegration and surface stability of gas bubbles under nonspherical free oscillation
08 p1149 A72-21295
Reynolds number and mainstream turbulence effects on laminar separation bubbles behavior in boundary layers on turbine blades in cascade
10 p1416 A72-23873
Experimentally produced vortex ring structure and stability, using dye and hydrogen bubble techniques for flow field, ring velocity and growth rate observations
10 p1466 A72-24327
Shock wave propagation and damping in system of constant density gas bubble suspension in liquid flow with uniform velocity
13 p1940 A72-28436
Asymptotic theory of turbulent flows established with bubbles, showing limiting relations existence at increasing liquid discharge rates
13 p1943 A72-29785
High Jakob numbers effect on bubble growth rates during nucleate boiling, taking into account liquid inertia
14 p2172 A72-31053
Thermal flux transmitted from hot surface to boiling fluid near nucleation site measured simultaneously with bubble growth rate
14 p2172 A72-31056
German monograph on heat transfer and stability limits for boiling and nonboiling falling films covering surface and bubble boiling conditions
15 p2334 A72-31503
Coriolis forces effect on bubbles trajectories in rotating containers, determining critical Reynolds number
17 p2537 A72-34209
Supplement to the asymptotic theory of steady turbulent flows with bubbles
17 p2537 A72-34278
Motion of a fluid and gas bubbles with allowance for their relative displacement
18 p2682 A72-36891
- Dynamics of dissolution of gas bubbles or pockets in tissues.
18 p2655 A72-37027
Precordial monitoring for pulmonary gas embolism and decompression bubbles.
19 p2762 A72-38710
Conjugate-flow theory for heterogeneous compressible fluids, with application to non-uniform suspensions of gas bubbles in liquids.
21 p3044 A72-40120
German monograph - Heat transfer at a vapor bubble growing on a heated wall during boiling.
22 p3244 A72-43059
Analysis and correlation of data on pressure fluctuations in separated flow.
23 p3247 A72-43331
Reacting and nonreacting swirl recirculation bubble gasdynamic structure in fuel combustion systems, noting anisotropic turbulence from hot-wire anemometer measurements
24 p3461 A72-45024
- BUCCANEER AIRCRAFT**
Buccaneer Mk 2 and F-4K Phantom takeoff and landing performance improvement due to boundary layer control by leading and trailing edge blowing
09 p1262 A72-22973
- BUCKLING**
NT CREEP BUCKLING
NT ELASTIC BUCKLING
NT EULER BUCKLING
NT THERMAL BUCKLING
Buckling of boron/aluminum and graphite/resin fiber composite anisotropic plates, giving load vs fiber orientation angle for various plate aspect ratios
01 p0139 A72-10739
Local buckling and collapse of thin walled lipped channel beams under critical end moments
01 p0144 A72-11396
Plate buckling elastoplastic process derivation allowing for secondary plastic deformation onset, examining stress discontinuity at overloading and unloading zones boundary
02 p0289 A72-11614
Static and dynamic buckling behavior of clamped shallow conical shells under axisymmetric loads
02 p0291 A72-11963
Vibration and buckling analysis of doubly curved composite monocoque plates and shells of positive and negative Gaussian curvature, examining stacking sequence effect
02 p0292 A72-11990
Postshear buckling, diagonal tension behavior of rectangular laminated boron-epoxy plates clamped on each side, observing stacking sequence effect
02 p0249 A72-11995
Circular cylindrical shells buckling under edge compression at various boundary conditions, obtaining critical loads and wave number from Donnell equations
02 p0292 A72-12107
Computer program for thermal stress and buckling analysis of nonuniformly heated segmented ring-stiffened cylindrical and conical shells
02 p0293 A72-12252
Truncated conical shell buckling under combined torsion and internal pressure load, discussing prebuckling stress conditions
02 p0298 A72-12666
Free vibration and buckling of orthotropic skew plates with different edge conditions, using Ritz variational method
04 p0584 A72-14508
Skew plates buckling with different edge support conditions, presenting Rayleigh-Ritz method results for various combinations of side ratio, skew angle and loadings
04 p0584 A72-14509
Fundamental frequency calculation method for bars and plates with arbitrary fixity of rotations, discussing buckling and vibration with realistic boundary conditions
04 p0591 A72-15275
Postbuckling behavior of cantilever columns with variable flexural rigidity, basing solution method on buckling mode assumption and principle of minimum total potential
04 p0591 A72-15278
Buckling of radially constrained imperfect circular ring loaded within perfect rigid circular boundary, obtaining numerical solution by discrete treatment
04 p0591 A72-15286
Plates in uniaxial compression with various support conditions at unloaded boundaries, predicting behavior after buckling
04 p0591 A72-15288
Load or compression eccentricity effect on buckling and postbuckling behavior of flat plates, presenting stress distribution curves
05 p0737 A72-16116
Thin elastic shell postbuckling behavior from asymptotic integration solution for differential equations, permitting dynamic effect modeling
05 p0738 A72-16425

Slot length effect on buckling load of cylindrical shell with circular holes

05 p0739 A72-16543

Meridional curvature effect on thin walled cylindrical shell buckling under external constant directional lateral pressure

05 p0739 A72-16546

Axially compressed semi-sandwich corrugated ring-stiffened cylindrical shell crippling local buckling and general instability prediction by finite difference energy method

[AIAA PAPER 72-138]

05 p0740 A72-16892

Laminated anisotropic imperfect circular cylindrical shells under axial compression, obtaining upper bound buckling load solution

[AIAA PAPER 72-139]

05 p0740 A72-16893

Ferritic stainless steel roping/buckling/ morphology and texture explanation by anisotropic plastic flow

05 p0677 A72-17105

Postbuckling collapse, end shortening, stiffness and ultimate load for geometrically imperfect simply supported plates with stress free edges

06 p0896 A72-17964

Convergence conditions for Galerkin method, applying to boundary value problems of structural stability and critical buckling loads

07 p1025 A72-18798

Finite element solutions for buckling of columns and beams, investigating restraints and cross section partial plasticity effects

07 p1088 A72-19117

Axially compressed cylindrical shells with axisymmetric imperfections, analyzing random buckling behavior and failure probability by statistical methods

07 p1089 A72-19689

Buckling under uniaxial compressive load of structural sections and stiffened flat plates reinforced with laminated composites

07 p1090 A72-19732

Buckling of arbitrary open cylindrical shells, investigating noncircularity effect

07 p1093 A72-19949

Monte Carlo digital simulation of probabilistic buckling behavior of indeterminate structure under initial stresses due to random geometric lack-of-fit

07 p1095 A72-20348

Gravitational field simulation by centrifugal force for structural stability and self weight buckling studies

07 p1096 A72-20428

Stability and postbuckling equilibrium of nearly cylindrical shells of revolution under axial compression

08 p1244 A72-21291

Composite viscous polymer cylindrical shells buckling modes under prolonged loading, taking into account initial imperfections

08 p1248 A72-21859

Tapered I-beams elastic twisting and flexural-torsional buckling, considering critical loads as function of taper ratio

08 p1249 A72-21924

Dynamic buckling of shallow circular cylindrical hinged panel under axial compression

08 p1249 A72-22087

Boundary value problems for buckling and initial postbuckling of clamped shallow spherical and conical thin walled sandwich shells under uniformly distributed hydrostatic pressure

[ASME PAPER 71-APM-YY]

10 p1554 A72-24182

Initially axially stressed Timoshenko beam equations of motion derived from three dimensional theories, discussing buckling loads and vibration frequencies

10 p1555 A72-24191

Stiffened panels initial buckling under longitudinal compression, presenting results obtained by numerical methods

10 p1558 A72-24843

Flugge equations for circular cylindrical shells buckling under compression, considering Donnell theory limits, stress determination and boundary conditions

10 p1560 A72-25025

Critical compressive buckling and stability of straight beams under axial and transverse loads calculated by three unknowns methods

10 p1560 A72-25121

Computer analysis of shells bifurcation buckling, presenting graphical results

[AIAA PAPER 72-352]

11 p1729 A72-25381

Nonlinear bending and buckling of axisymmetric sandwich shells based on finite element approach

[AIAA PAPER 72-356]

11 p1729 A72-25385

Computerized analysis of prismatic rectangular plate assemblies natural frequencies and initial buckling stresses

11 p1734 A72-25731

Computer program for bifurcation buckling analysis of shells under collapse load, using strain energy methods and two dimensional finite difference grid

11 p1736 A72-25980

Finite element method for buckling coefficients of isotropic rectangular plate subject to linearly varying axial compression, using general linear geometric matrix

11 p1736 A72-25999

Boundary surfaces during plastic buckling of hollow cylindrical shell under combined loading by external pressure and axial force

12 p1880 A72-27231

Axial compression stability critical load and buckling of cylindrical shells resting on Winklerian elastic base, using dynamic programming

12 p1885 A72-27972

Uniformly loaded parabolic arches lateral-torsional buckling, deriving governing linear differential equations from Clebsch-Kirchhoff equilibrium equations for thin curved bars

12 p1888 A72-28349

Perfect and imperfect plastic column buckling, describing bifurcation and stability theory for elastic-plastic and rigid-plastic bodies

13 p2054 A72-28480

Pressure law for flow between two parallel plates describing medium action on plates, noting plate flutter analogy to buckling

13 p2056 A72-29002

Axisymmetric ductile rotating shaft failure modes, considering fatigue, buckling and impact stress factors

[ASME PAPER 72-DE-40]

14 p2167 A72-30873

Spherical cap dynamic buckling under impulsive loading, comparing prediction by energy criterion with experiment using spray deposited explosive

15 p2323 A72-31405

Stability analysis of thin walled circular cylindrical shell under shearing force action to one end, calculating buckling modes

15 p2324 A72-31483

Local buckling analysis for triangular-corrugated core sandwich panels in compression, noting buckling mode nodal line features

15 p2326 A72-31709

Modified Rayleigh-Ritz method to obtain lower bounds of eigenvalues, applying to uniform cantilever column buckling

15 p2275 A72-31710

Filler influence on critical load and buckling zone size in circular elastic three layer ring under uniformly distributed vertical load in rigid cavity

15 p2328 A72-31745

Axially compressed cylindrical shells buckling behavior, deriving formula based on equivalent axisymmetric imperfections concept in terms of shell radius/thickness ratio

15 p2331 A72-32553

Buckling behavior of simply supported elastic folded plate structures without and with transverse stiffeners under symmetrical and asymmetrical uniform vertical loads

15 p2332 A72-32562

Buckling strain effects on critical stresses in design of longitudinally corrugated shells for axial compression

15 p2333 A72-32680

Sandwich structures buckling calculation by transfer matrices with allowance for cross section shearing

16 p2471 A72-33680

Geometric instabilities in isotropic plastic solids under increasing uniaxial compression.

[ASME PAPER 72-APM-28]

17 p2624 A72-34310

Improved bounds for buckling loads of tapered inelastic columns.

17 p2626 A72-34330

An experimental buckling study of skin-corrugated ring-stiffened curved panels.

[SESA PAPER 1993A]

17 p2630 A72-34818

Buckling of a circular cylindrical shell in axial compression and SS4 boundary conditions.

17 p2632 A72-35236

Buckling and vibration analysis for stiffened orthotropic shells of revolution.

17 p2632 A72-35242

Plastic buckling theory, presenting yield surfaces in tension-torsion stress space for pure aluminum

17 p2632 A72-35245

Shear buckling of an elastically supported fiber.

17 p2633 A72-35290

Buckling of shells with cutouts - Experiment and analysis.

17 p2634 A72-35405

A method for selection of significant terms in the assumed solution in a Rayleigh-Ritz analysis.

17 p2634 A72-35408

Buckling of orthotropic, curved, sandwich panels subjected to edge shear loads.

18 p2735 A72-36770

Loading rig in which axially compressed thin cylindrical shells buckle near theoretical values.

19 p2783 A72-37730

Buckling of circular cylindrical shells under compression. III - Solutions based on the Donnell type equations considering prebuckling edge rotations.

19 p2878 A72-38299

Dynamic snap-buckling of shallow arches under inclined loads.

20 p2980 A72-39617

Cyclic stress-strain induced buckling and fatigue failure in cold-rolled steel and tabulating and diagramming mechanical properties

21 p3065 A72-40233

An iterative procedure to obtain exact buckling criteria for columns under combined action of variable continuous load and concentrated forces.

21 p3118 A72-40927

Buckling of elastic bars with varying stiffness and nonideal boundary conditions.

21 p3118 A72-40932

Battened columns out-of-plane buckling under axial loads and/or moments, deriving relationship between applied loads and section characteristics

21 p3121 A72-41211

Buckling of inelastic cylindrical shells under axial impact.

21 p3124 A72-41507

Buckling of plates and cylindrical panels under the action of axial dynamic compression

22 p3332 A72-41923

Stress-strain state at holes in plates in the case of asymmetric buckling modes

22 p3333 A72-42059

Nonlinear buckling of cylindrical shells.

22 p3336 A72-42607

Buckling of circular cylindrical shells under axial compression.

22 p3339 A72-42840

The influence of production imperfections on design of optimum structures.

22 p3339 A72-42841

Buckling of integrally stiffened cylindrical shells - A review of experiment and theory.

22 p3339 A72-42846

A note on buckling of spherical caps with initial asymmetric imperfections.

23 p3351 A72-44060

Stability of orthotropic stiffened composite plates.

23 p3352 A72-44109

The use of bar buckling eigenfunctions in the stability analysis of clamped skew plates.

23 p3355 A72-44456

Dynamic buckling of axially stiffened imperfect cylinders under axial impulse.

24 p3453 A72-44602

Mapping of large dynamic deflections of structures.

24 p3454 A72-44606

Post-buckling of axially compressed plates.

24 p3455 A72-44632

Free vibration frequencies and critical buckling loads for thin walled shells of revolution constructed out of layered or heterogeneous anisotropic materials.

24 p3455 A72-44676

Buckling and lateral vibration of rectangular plates subject to inplane loads - A Ritz approach.

24 p3458 A72-44887

BUDGETING

Federal legislation impact on airport and airway system planning, considering budget and schedule requirements

18 p2743 A72-36777

BUFFER STORAGE

Time resolution buffer for multichannel scaler, applying to digital signal averaging

11 p1632 A72-25701

Cascade computer controlled system for LSI devices testing, considering interim buffer storage and programmable pattern generator

22 p3160 A72-42823

BUFFERS [CHEMISTRY]

Gaseous buffering for oxygen fugacity control in high temperature gas systems at one atmosphere

12 p1778 A72-28104

BUFFETING

Biothermal response of increased core temperature in rhesus monkey to mechanical vibration, noting implications for pilot performance during prolonged buffeting

12 p1774 A72-28268

BUILDING MATERIALS

U CONSTRUCTION MATERIALS

BUILDING STRUCTURES

U BUILDINGS

BUILDINGS

Urban area aerial photography survey for large scale photomaps, discussing building feature examination and universal stereophotogrammetric instruments utilization

03 p0362 A72-14311

Building soundproofing codes for airport zoning ordinances, emphasizing wider latitude in land use options

13 p2067 A72-29561

BULK MODULUS

High pressure bulk modulus test rig for composite material specimen nondestructive test, discussing measurement method and errors

09 p1315 A72-23391

Pure metals bulk modulus pressure dependence from detonation generated shock wave data, using empirical relations between propagation velocity and material flow rate

11 p1662 A72-26741

BULKHEADS

Forging techniques and applications for YF-12A aircraft Ti alloy bulkhead production, considering diffusion bonding and die shimming

04 p0527 A72-14914

Ring assembly with hinged cross section and uniform radial and transverse loads, determining deflection dependence on bulkheads and rigidity of supports
[AIAA PAPER 72-355] 11 p1729 A72-25384

Superposed forced oscillations of liquid and of elastically mounted bulkhead with translational harmonic displacements of cavity, noting damping increase 13 p1942 A72-29498

BUMPERS

Shock heating caused material phase transformation effects on bumper shield performance, studying thin metal sheets response to like-material spheres impact 14 p2168 A72-30921

BUNCHING

NT ELECTRON BUNCHING

BUOYANCY

Open cycle gas core nuclear rocket engine, determining scaling laws for buoyancy force effect on fuel containment at various flow parameters 01 p0099 A72-11348

Buoyancy effect on shear stress and heat transfer in horizontal boundary layer, considering Boussinesq approximation 03 p0343 A72-14320

Dynamic characteristics of buoyant low altitude clouds formed by solid rocket motor launches, determining initial temperature by motion pictures combined with conservation equations [ASME PAPER 71-WA/FE-33] 05 p0724 A72-15923

Turbulent boundary layer analogy mathematical model for turbulent mixing and buoyancy effects on aircraft trailing vortex wake motion and persistency [AIAA PAPER 72-42] 05 p0607 A72-16903

Numerical simulation of atmospheric turbulence in planetary boundary layer due to wind shear and/or unstable thermal stratification, noting buoyancy and planetary rotation effects 07 p1031 A72-20359

Cavity flow driven by buoyancy and shear, obtaining flow and temperature fields from Navier-Stokes equation numerical solution 10 p1467 A72-24366

Numerical simulation of three dimensional shape-preserving convective elements from buoyancy release in incompressible fluid, using Navier-Stokes equations 12 p1839 A72-27027

Buoyancy systems and parawings application in short haul passenger transportation, discussing VTOL and STOL operations 16 p2348 A72-33183

A temperature adjustment process in a Boussinesq fluid via a buoyancy-induced meridional circulation. 21 p3044 A72-40112

Combined buoyancy and flow direction effects on saturated boiling critical heat flux in liquid nitrogen. 21 p3130 A72-41184

Buoyancy effects on laminar heat transfer in the thermal entrance region of horizontal rectangular channels with uniform wall heat flux for large Prandtl number fluid. 22 p3243 A72-41956

BUOYS

Equipment for ground and sea recovery of sounding rocket payloads, discussing airbrakes, buoy and parachute assemblies 15 p2319 A72-31690

Eole program for tracking and gathering information from drifting buoys at sea 17 p2617 A72-35720

BURGER EQUATION

Wiener-Hermite random variable expansion technique with time dependent base for turbulence applied to Burger equation 07 p0967 A72-19502

Predictor-corrector multiple iteration technique for three dimensional viscous flow problems applied to hypersonic leading edges and Burger equation [PIBAL-72-19] 13 p1893 A72-28422

Burgers binary and Shkarofsky multiple collision theory numerical application to electrical conductivity in partially ionized solar magnetoplasma 13 p2018 A72-29714

General closed form solutions to Burger equation with forcing terms in Navier-Stokes equation for turbulence studies 18 p2677 A72-36004

Cameron-Martin-Wiener /C-M-W/ representations of nonlinear random process tested on Burger turbulence for real fluid problem 18 p2677 A72-36010

Burgers model equation for shear flow turbulence with complex physical processes and nonlinearities in governing equations 21 p3047 A72-41637

BURNERS

Burner design for solid propellants burning properties dynamic testing, using broadband tuned Helmholtz resonator for instability onset delay 04 p0509 A72-15497

Flame structure studies of stabilizing region of near stoichiometric laminar burner methane-air flame 09 p1411 A72-23147

Heatable chamber burners design to increase sensitivity of flame spectrophotometry, separating solvent from aerosols 13 p1958 A72-29525

BURNING

U COMBUSTION

BURNING PROCESS

U COMBUSTION

BURNING RATE

Aluminized solid propellant transient burning rate augmentation as function of acceleration vector magnitude and orientation, applying centrifugal accelerations of zero to 140 g 01 p0114 A72-10378

Active ingredient oxidizing potential and pressure effects on burning rate of explosive substances 02 p0302 A72-12292

Heat transfer to liquid fuel burning from sandfilled pan burner, measuring burning rate, wick temperature distribution and flame radiation heat flux distribution as function of time 03 p0458 A72-14221

Heat transfer in kinetic burning in turbulent boundary layer on porous surface for carbon dioxide blown in air stream with dissociated oxygen 05 p0746 A72-16223

Combustible materials ignition temperature, time lag and burning rate in oxygen enriched atmosphere, deriving activation energy for fire resistance estimates 05 p0681 A72-16773

Solid propellant flame spectral and temporal details during unstable and stable combustion, using middle infrared spectrometer 05 p0703 A72-16896

Combusting polymers gasification effective heat values determination from correlation of surface regression rate and oxygen impingement rate data [AIAA PAPER 72-34] 05 p0749 A72-16898

Wall thermal radiation influence on solid propellants burning rate in electrically heated tube furnace, noting correlation with laminar flame theory [AIAA PAPER 72-35] 05 p0703 A72-16938

Burning gunpowder surface reactions relative to temperature, chemical enthalpy and acoustic waves of pressure, velocity and density 05 p0751 A72-17211

Composite propellant powder combustion velocities as function of pressure, discussing powder sensitivity, limiting kinetic stage changes and surface monovariant equilibrium 06 p0867 A72-17568

Powder combustion rate dependence on light irradiation intensity 06 p0902 A72-17908

Operational stability of rocket engine with combustion chamber having charge of two propellant types with different burning rate dependences on pressure 06 p0867 A72-18206

Plane two dimensional flow in channel of rocket engine with solid propellant combustion, obtaining burning rates 06 p0867 A72-18207

Burning rates dependence on pressure in mixtures of ammonium perchlorate with succinic, glutaric, adipic, azelanic, sebacinic, fumaric and aminosuccinic acids 06 p0867 A72-18210

Photorecorder for burning rate measurements, consisting of electric motor driven film carrying rotating drum in slitted housing and flame front imaging optical system 06 p0817 A72-18215

Solid charge design for hybrid rocket engine with constant liquid propellant component consumption, deriving differential equation for perforated grain burning rate 07 p1053 A72-18994

Flame temperatures, composition profiles and burning rates in liquid n-heptane droplet and sphere combustion 07 p1051 A72-19362

Pure and doped ammonium perchlorate deflagration rate sensitivity due to sample temperature and environmental pressure changes 07 p1051 A72-19729

Necessary conditions for burning rate stepwise variation with time of condensed systems 08 p1254 A72-21657

Burning velocity inhibitors effect on hydrocarbon-oxygen-nitrogen mixtures ignition by hot wires [AD-744624] 08 p1129 A72-22039

Burning velocity measurement techniques for methane-air mixtures 08 p1255 A72-22047

Flame autostabilization mechanism during gaseous oxygen-liquid ammonia mixture combustion in liquid fuel rocket engine chamber, measuring mean burnout time 08 p1224 A72-22091

Pressure effect on combustion rate of Mg particles in water vapors 09 p1411 A72-22887

Burning rate of composite solid propellant charges, noting application in solid propellant pressure accumulators 09 p1411 A72-22893

Burning rate dependence on oxidizer particle size of ammonium or potassium perchlorate mixtures with organic fuels 09 p1373 A72-23146

Active ingredient oxidizing potential and pressure effects on burning rate of explosive substances 10 p1561 A72-23767

Burning gunpowder surface reactions relative to temperature, chemical enthalpy and acoustic waves of pressure, velocity and density 11 p1744 A72-25337

Wall effects on deflagration, combustion rate, and self and hot-point ignition temperature and delay 11 p1747 A72-26789

Inert gas-oxygen mixtures fire retardant properties under atmospheric and hypobaric pressures, measuring effectiveness by standard fabric burning rate 12 p1890 A72-28309

Quasi-steady state combustion theories compared with observations of hydrocarbon fuel droplet and flame zone diameters, noting underestimation of burning rate 13 p2063 A72-28545

Heterogeneous-homogeneous catalytic effects on combustion rate of hydrocarbons, ammonia and hydrogen mixtures 13 p1912 A72-28777

Solid rocket propellant combustion instability research, discussing data acquisition and reduction, motor instrumentation, motors and burning rate measurements 13 p2024 A72-28929

Metallized solid propellants burning rate augmentation by internal ballistics effect of spinning rocket motor, deriving relationship between burning rate, pressure level and acceleration 13 p2025 A72-29302

Solid propellants burning rate dynamic response to rapid pressure changes, discussing equations applicability to combustion extinction prediction as function of pressure decay rate 13 p2065 A72-29304

Ammonium perchlorate burning rate temperature dependence as function of pressure and oxidizer particles size, noting low pressure deflagration limit [ONERA, TP NO. 1079] 13 p2025 A72-29669

Solid combustibles flame spread rates in compressed atmospheres, noting dependence on oxygen concentration 14 p2170 A72-30340

High efficiency hybrid rocket motor based on polyester fuel and RFNA oxidizer, determining correlation between burning rate, oxidizer and total flow rates 15 p2297 A72-31207

Acoustic admittance measurement for burning surface of nitroglycerin gunpowders, using combustion product velocity and wave pressure ratio 16 p2391 A72-33257

Al and Zr single thin strands burning rates at various total oxygen pressures, comparing photographic observation to computations 16 p2479 A72-34003

Mixed-mode propulsion - Optimum burn profile for two-mode systems. 17 p2596 A72-34212

Flame autostabilization mechanism during gaseous oxygen-liquid ammonia mixture combustion in liquid fuel rocket engine chamber, measuring mean burnout time 17 p2597 A72-34662

Combustible materials ignition temperature, time lag and burning rate in oxygen enriched atmosphere, deriving activation energy for fire resistance estimates 17 p2571 A72-35276

Acceleration of burning by a shock wave interacting with the flame 18 p2740 A72-36240

Solid rocket propellant erosion burning in turbulent gas flow, discussing burning velocity dependence on Pobedonostsev criterion 19 p2878 A72-37351

Erosion combustion effect on unsteady solid rocket propellant burning stability during engine nozzle opening, noting combustion velocity and surface temperature 19 p2879 A72-37353

Steady combustion thermal stability of condensed explosives for burning rate limitation by condensed phase chemical reactions, noting surface temperature effects 19 p2879 A72-37356

Acceleration effects on burning velocity of aluminized condensed rocket propellant systems, calculating particle size and slag mass 19 p2847 A72-37360

Powdered Al additions effect on burning rates of three component mixture systems based on ammonium and potassium perchlorates 19 p2847 A72-37361

Characteristics of the development of steady burning rates during the ignition of gasless compositions by a hot surface

19 p2882 A72-38452

Ignition, unsteady burning and flame collapse of a unitary fuel particle

19 p2882 A72-38453

Effect of chemical reaction reversibility on the temperature and pressure dependence of burning rates

19 p2882 A72-38455

Influence of water vapor on the normal flame velocity of a methane-air mixture at high pressures

19 p2882 A72-38459

Detonation and burning characteristics of liquid oxygen-liquid methane mixtures.

19 p2848 A72-38834

Measurements of burning velocity in a flat flame front.

19 p2883 A72-38872

Comment on 'The deflagration of single crystals of ammonium perchlorate.'

19 p2848 A72-38873

Burning of particles of an aluminum-magnesium alloy

20 p2987 A72-40041

Reagent concentration and temperature fluctuation effects on turbulent burning rate, noting temperature pulsations influence on energy balance

21 p3128 A72-40976

Physical model of the onset of turbulent burning of compacted systems in a half-closed volume

21 p3131 A72-41699

Ionization mechanism and condensed and gas phase kinetics of oxidizer burning during ammonium perchlorate combustion

22 p3215 A72-43140

Ionization zone formation and condensed and gaseous phase kinetics during ammonium perchlorate burning in nitrogen atmosphere

22 p3215 A72-43179

Burn-out rate of a solid-propellant slab in contact with a solid-oxidizer layer

22 p3245 A72-43180

Burning rates of organic perchlorates of aliphatic, aromatic and heterocyclic amines and amidines with explosive compounds containing nitrogen dioxide group as oxidizer

22 p3153 A72-43181

Flow direction and velocity effects on metal burning rates of low carbon and Ni-Cr steels in pure oxygen, using diffusion model

22 p3245 A72-43185

BURNING TIME

Optimal design criteria for multigrain solid propellant rockets, considering powder weight, burning time and combustion chamber length

05 p0704 A72-16351

Start reaction effect on burning time sequence of hydrogen combustion in air

08 p1129 A72-22171

German monograph on flight performance optimization of solid propellant rockets covering thrust values, burning time, rocket design and orbits within earth atmosphere

10 p1550 A72-23770

Oscillatory gas combustion mechanism and stability boundary characteristics, determining burning time from flame height and flow rate

11 p1745 A72-25753

Overall characteristics of optimal quasi-steady plasma thruster system, discussing mass, burning time and thrust variations as function of power supply and pulse duration

[ALAA PAPER 72-456] 11 p1708 A72-26192

Device for measuring the kinetic characteristics of particle combustion

20 p2928 A72-40050

Flame structure and flame reaction kinetics. VI - Structure, mechanism and properties of rich hydrogen + nitrogen + oxygen flames.

24 p3461 A72-44919

BURNOUT

Dry areas occurrence on heating surface in pool boiling near burnout heat flux, discussing nucleate and film boiling stability and hysteresis

07 p1099 A72-19621

Effect of the temperature on the burn-out of hydrogen diffusion flames in a supersonic flow in a closed channel

21 p3129 A72-40983

BURNS [INJURIES]

Heat transfer through fabrics by convection, conduction, radiation and vaporization related to skin temperature and thermal injury

03 p0319 A72-13700

Epithelial follicle and mast cell role in peroxidase activity of thyroid gland during experimental burn development

13 p1905 A72-29330

BURSTS

NT RADIO BURSTS

NT SOLAR RADIO BURSTS

Data transmission systems with decision feedback in presence of burst noise, calculating statistical rela-

tions among received sequences as function of duration and spacing

16 p2372 A72-33795

BUSHINGS

Bushing seal with pressure dependent clearance for reciprocating piston rod or rotating shaft, presenting laminar and turbulent axial flow theory

08 p1178 A72-21936

Stability characteristics of floating bush bearings. [ASME PAPER 71-LUB-9]

19 p2807 A72-37698

Influence of the cycling frequency on the fatigue and corrosion fatigue of steel samples with bushings

22 p3242 A72-43155

X-ray inspection of the AWACS radome attachment locations.

24 p3406 A72-44902

BUTANES

Induction period, light emission, pressure change and cool flame explosion limits in butane oxidation, studying reaction products in negative temperature coefficient region

07 p1099 A72-19368

BUTENES

Thickening properties of butoxyacrosil products of butyl alcohol vapor and silicon dioxide surface reactions for use as oil lubricant additives

09 p1336 A72-22500

BUTT JOINTS

Heat input, interpass temperature and panel width effects on butt welds strength in Al alloy plate

04 p0526 A72-14838

Electron beam welding with filler metal, describing spot and butt welding applications

06 p0819 A72-17498

German monograph - Improvement of the ductility characteristics of flash butt welding joints involving carbon steels by pulse normal annealing and hot heading in the welding machine

19 p2807 A72-37659

BUTYLENE

U BUTENES

BUTYRIC ACID

Rapid eye movement sleep deprivation and hyperbaric oxygenation influence on gamma-aminobutyric acid levels in mice brains, suggesting protective mechanism against nerve cell oxygen intoxication

07 p0922 A72-20191

BYPASSES

Thermodynamic cycle parameter effects on bypass turbofan jet engine fuel consumption and performance under various flight conditions and engine ratings

23 p3326 A72-44281

C

C BAND

GaAs IMPATT diodes technology and performance at C, X and K band frequencies

06 p0788 A72-18466

Medium power high gain, CW transferred electron microwave amplifiers at C band, describing bandwidth, saturation, intermodulation distortion and dynamic range characteristics

06 p0789 A72-18483

ATS-3 C band dual transponders for geographically distant clocks time synchronization, using Cs clocks for accuracy verification

15 p2200 A72-32080

Spaceflight-qualified tunable C-band parametric amplifier system.

19 p2770 A72-37253

C-5 AIRCRAFT

C-5A Galaxy aircraft systems and components maintainability program

10 p1459 A72-23851

Pilot evaluation of C-5 automatic landing system in Category III weather environment

12 p1842 A72-27521

C-54 AIRCRAFT

C-54 A/B aircraft engine air particle separator anti-ice system design features, manufacturing techniques and testing

07 p1053 A72-18769

C-130 AIRCRAFT

Multichannel multispectral scanner system for NASA C-130 earth resources aircraft, describing electronic equipment and calibration sources

01 p0048 A72-10946

CABIN ATMOSPHERES

NT SPACECRAFT CABIN ATMOSPHERES

CO contamination of cabin and hazard to pilots, discussing concentrations, avoidance, control and analysis

07 p0933 A72-20267

Sealed cabin air regeneration by means of potassium superoxide, noting weight and space savings

11 p1586 A72-26594

Insecticide dichlorvos vapor toxicity in aircraft cabin atmosphere at 8000 ft, studying plasma cholinesterase activity, erythrocytes, dark adaptation and bronchial resistance

14 p2081 A72-31082

Environmental, medical and acoustic investigations with underwater laboratory, discussing cabin atmosphere control, depressurization, health conditions and sonar operation

20 p2898 A72-39938

CABINS

Internal noise reduction in hovercraft.

18 p2642 A72-36574

CABLES

Aerospace wire and cables testing methods standards for evaluating mechanical, electrical and chemical properties, coating thicknesses, continuity flaws, flammability, geometrical characteristics, etc

[SAE AS 1198] 01 p0006 A72-10384

Equilibrium configuration of cable towed in circular path, presenting multivalued boundary value problem mathematical analysis

[AD-737445] 01 p0102 A72-11132

Explosive welding of heat exchanger tubes and detonation produced compressive joining of cables as applications of explosive metalworking procedures

07 p0994 A72-18931

CABLES [ROPES]

Librational transverse oscillations boundary value problems of heavy thread on orbiting satellite, determining equilibrium and eigenfunctions

08 p1240 A72-21142

Towed cable flight vehicle system motion in uniform flow field, calculating equilibrium configuration during coordinated turn from two point boundary value problem numerical solution

08 p1110 A72-21604

Nonlinear dynamic response of single elastic cables with low initial tension, examining free and forced vibrations with incremental deformations theory

10 p1560 A72-25185

Flexible cable in uniform flow field, calculating coupling between longitudinal and transverse modes to obtain centripetal acceleration effects on tension

18 p2734 A72-36418

Librational transverse oscillations boundary value problems of heavy thread on orbiting satellite, determining equilibrium and eigenfunctions

20 p2977 A72-39247

CADMIUM

Hydrogen generation mechanism during cadmium plating of steel, describing porosity testing technique

04 p0527 A72-15548

Atmospheric neutron production by cosmic rays, calculating Cd-In ratio

05 p0662 A72-16258

Phonon limited mean free path in Cd by limiting point method, proposing model with elastic anisotropy

08 p1217 A72-21592

Superconducting energy gaps and transition temperatures of disordered cadmium and zinc films.

19 p2844 A72-37690

He-Cd lasers using recirculation geometry.

21 p3061 A72-40239

CADMIUM ALLOYS

X ray diffraction study of molten Mg-Cd alloy atomic structure, demonstrating existence of Mg-Cd compounds

10 p1497 A72-24678

Cd effect on alpha-beta transformation temperature and phase equilibrium in Ti rich end of Ti-Cd phase diagram, using metallographic and X ray techniques

16 p2409 A72-33806

CADMIUM ANTIMONIDES

Preparation and electrical properties of thin cadmium antimonide and arsenide layers, comparing to single crystal films

02 p0268 A72-12281

Electrical conductivity and thermal emf as function of temperature in CdSb, discussing energy spectrum and crystallization

09 p1372 A72-23479

Temperature dependence of Ge solubility in CdSb single crystals from microstructural observations and measurements of microhardness and electrical properties

09 p1372 A72-23480

Double doping effect on electrical properties of Te and Hg doped and Te and In doped CdSb single crystals

13 p2020 A72-28565

Effect of evaporation of the volatile component on the electrical properties of CdSb

19 p2845 A72-38402

Electrical conductivity of pressed cadmium antimonide

20 p2959 A72-39218

Electroconductivity anisotropy effect on transverse Demer effect angular dependence and spectral distribution in p-type CdSb lattice

21 p3098 A72-41693

CADMIUM COMPOUNDS

NT CADMIUM ANTIMONIDES

NT CADMIUM SELENIDES

NT CADMIUM SULFIDES

NT CADMIUM TELLURIDES

CADMIUM NICKEL BATTERIES

U NICKEL CADMIUM BATTERIES

CADMIUM SELENIDES

Vapor annealing effect on vacuum evaporator CdSe thin films electroconductivity as function of pressure and temperature

12 p1854 A72-27249

Memory and photoconductivity in CdSe polycrystals at 77 and 300 K, plotting photocurrent vs illumination levels

13 p2024 A72-30012

Negative photoconductivity in CdSe single crystals due to free carrier mobility decrease after surface treatment in gas discharge, noting neutron traps role

13 p2024 A72-30046

Free carrier mobility dependence on excitation light intensity in CdSe single crystals with negative photoconductivity

14 p2141 A72-30169

Solid-gas phase equilibria and thermodynamic properties of cadmium selenide.

17 p2511 A72-35329

Undamped photocurrent fluctuations in CdSe single crystals

18 p2718 A72-36348

Peritectic interaction and phase diagrams of quasi-binary semiconductor CdAs-CdTe and CdP-CdSe systems

19 p2845 A72-38404

Cd Se polycrystal memory and photoconductivity at 77 and 300 K, plotting photocurrent vs illumination levels

22 p3214 A72-42734

CADMIUM SILVER BATTERIES

U SILVER CADMIUM BATTERIES

CADMIUM SULFIDES

CdS single crystal field emission spectral characteristics at room and cryogenic temperatures, discussing intrinsic and impurity levels

02 p0269 A72-12888

Surface energy states of CdS basal plane based on photovoltage inversion effect model

03 p0400 A72-12991

Copper sulfide-cadmium sulfide single crystal photovoltaic heterojunctions, showing optically induced and thermal effects on short circuit current degradation

03 p0389 A72-13603

Self focusing effect of Q switched single mode ruby laser emission in CdS crystal, noting 60 kw minimum threshold power

03 p0369 A72-14064

Internal Q switching in CdS laser activated by exciton recombination, observing lag in emission onset after input pulses delivery

04 p0528 A72-14575

Photoluminescence of Er cations in CdS, observing group I co-dopants sensitizing behavior and broad-band emission spectra

04 p0563 A72-15472

Ultrasonic delay lines design and construction for 100-2000 MHz using evaporated CdS on sapphire and quartz and sputtered ZnO transducers

05 p0626 A72-16010

Spontaneous oscillations generation on transverse surface wave, discussing experimental realization with semiconducting CdS single crystals

05 p0626 A72-16282

Electronic characteristics of real CdS surfaces in room atmosphere and ultrahigh vacuum

07 p1050 A72-20458

Photometers with CdS cells, discussing calibration difficulties

07 p0992 A72-20584

Sintered cadmium sulfide films microstructure analyzed by X rays, discussing structural changes effects on dark resistance and photosensitivity

09 p1366 A72-22414

Chemisorbed oxygen effect on electrical properties of monocrystalline cadmium sulfide thin plates with high resistivity

10 p1525 A72-24211

Oxygen chemisorption surface states effects on electrical conductivity of CdS single crystals and evaporated films

11 p1701 A72-25855

Many element GaAs and CdS semiconductor laser achieving high power output by electron beam pumping

12 p1822 A72-27616

Electronic fringe counter with CdS cell photosensors, dc bridge and strip recorder for interferometric applications

12 p1792 A72-27762

Photovoltaic effect and energy band model of solar cell cadmium-sulfide-copper-disulfide heterojunctions

12 p1855 A72-28007

Thin film Cu-CdS solar cell electrochemical plating potential and solution composition effects on copper sulfide surface layer formation and cell efficiency

12 p1855 A72-28008

Low photon IR photovoltaic response of CdS-metal junction, noting energy conversion efficiency

12 p1855 A72-28009

Postdip heat treatment effects on thin film copper sulfide-cadmium sulfide junction solar cells spectral response, diode parameters and resistance

12 p1855 A72-28010

CdS thin film conductivity reactions to grain boundary and stacking faults, correlating grain size to mobility

12 p1856 A72-28012

Photovoltaic effects in CdS films evaporated onto barium titanate single crystal and ceramic ferroelectric substrates

12 p1856 A72-28014

Improved efficiency of cadmium sulfide-copper sulfide thin film solar cells, noting optimization of layer formation, gridding and encapsulation

12 p1756 A72-28016

Heat treatment and electron irradiation tests for spatial reliability of CdS and CdTe thin film solar cells, noting photovoltaic properties

12 p1756 A72-28019

Cadmium sulfide solar cells stress analysis in relation to degradation caused by fabrication technology, discussing barrier layer formation process

12 p1757 A72-28020

Surface piezoelectric effects of mechanical bending of noncentrosymmetric CdS semiconductor wafers

13 p2020 A72-28524

CdS crystals lasing in air at atmospheric pressure and room temperature by low voltage electron beam pumping through Ni film

15 p2245 A72-31319

Photon loss coefficients and gain measurement in CdS electron beam pumped lasers, noting absorption mechanism and efficiency

15 p2246 A72-31668

Trapped charge effect on photovoltaic properties of copper sulfide-cadmium sulfide single crystal heterojunction in terms of tunneling by photocapacitance technique

15 p2294 A72-32520

Dosimetric characteristics of CdS semiconductor detector and photoresistors for gamma rays recording

16 p2390 A72-33076

Preparation and properties of nonheat-treated single crystal Cu₂S-CdS heterojunctions.

17 p2595 A72-35331

Experimental determination of the coefficients of radiantly stimulated diffusion of sulphur in cadmium sulfide

20 p2959 A72-38954

Temperature dependence of electroconductivity and photosensitivity in CdS films

20 p2959 A72-39223

Relaxation oscillations induced in semi-insulating CdS with helium neon laser irradiation.

20 p2934 A72-39817

Mode-coupling effects in thin platelet semiconductor lasers.

21 p3064 A72-41381

Photovoltaic properties of single-crystal CdS-Cu₂S cells.

22 p3214 A72-42457

Cadmium sulfide single crystals suitable for electron-beam-pumped lasers.

24 p3432 A72-45607

CADMIUM TELLURIDES

Lf noise measurements of mercury telluride and Cd-Hg-Te semiconducting thin films using vacuum tube preamplifier and step-up transformer

02 p0268 A72-11523

Electric and photoelectric properties of CdTe films, describing solar cells preparation

04 p0465 A72-14593

CdTe condensed films hexagonal modification and twinning boundaries birefringence reflection, using electron microscope and diffraction analysis

07 p1047 A72-18856

Performance characteristics of electro-optical material cadmium telluride for intracavity modulator of carbon dioxide lasers

07 p1003 A72-19223

Cadmium mercury telluride photovoltaic cell features, noting gigahertz range frequency response, heterodyne sensitivity, operating temperature and nonstoichiometric p-n junction preparation

07 p1003 A72-19224

Light modulation by exciton electric absorption in thin high impedance recrystallized CdTe films within strong electric fields, showing spectral distribution curves

09 p1366 A72-22419

Electrical conductivity relationship to phase composition in thin CdTe films deposited on mica bases and annealed in Cd vapor

09 p1367 A72-22420

CdTe thin film solar cell room temperature prolonged operation instability, thermal degradation and performance improvement by gas adsorption removal

12 p1756 A72-28017

Photoelectric properties of cadmium telluride thin film solar cells, discussing energy gap temperature dependence, work function and current variations anomalies

12 p1756 A72-28018

Heat treatment and electron irradiation tests for spatial reliability of CdS and CdTe thin film solar cells, noting photovoltaic properties

12 p1756 A72-28019

Electron radiation damage and edge emission of cadmium telluride, presenting cathodoluminescence spectra

12 p1859 A72-28071

Carrier concentration Hall mobility and photoconductivity in n- and p-type CdTe after neutron and electron bombardment

12 p1859 A72-28072

Sulfur alloyed CdTe single crystals IR absorption spectrum, noting temperature effects

13 p2023 A72-29918

Semiconductor gamma ray detectors development, using cadmium dichlorides, dibromides, diiodides and difluorides as doping agents in CdTe crystal growth

14 p2142 A72-30549

CdTe single crystals photoplastic characteristics, detailing illumination effect on yield stress and resistivity

15 p2294 A72-32501

Investigation of resistance strain gauges based on zinc telluride and cadmium telluride semiconductor films

19 p2845 A72-38206

Photoluminescence and photoconductivity of hole-type cadmium telluride single crystal films

19 p2845 A72-38403

Peritectic interaction and phase diagrams of quasi-binary semiconductor CdAs-CdTe and CdP-CdSe systems

19 p2845 A72-38404

Influence of impurities on the high-temperature electrical conductivity of CdTe crystals

19 p2847 A72-38677

Mercury-cadmium telluride photoconductive detectors array for S-192 multispectral scanner for Skylab earth scanning experiments

23 p3288 A72-43879

Mercury-cadmium telluride multispectral photoconductive detectors, discussing fabrication techniques and performance characteristics

23 p3288 A72-43880

Mercury-cadmium telluride photodiode detectors for near IR laser receivers, discussing time response and I-V characteristics as function of temperature

23 p3296 A72-43881

CALCIFICATION

Calcium metabolism perturbations in astronauts under weightlessness conditions and in immobilized test subjects, noting bone tissue renewal cycle modification, calciuria variations and bone calcification

07 p0927 A72-19245

Calcium metabolism conditions in calcified tissues of rats during a lasting hypodynamia and thyrocalcitonin administration

21 p2997 A72-40432

CALCITE

Fluid inclusions in quartz crystals from calcite in Precambrian metasedimentary rocks in South-West Africa

07 p0975 A72-18907

Quartz and calcite spectral emission polarization calculation from Fresnel equation, comparing results with field measurements with broadband IR radiometer

21 p3097 A72-40603

CALCIUM

NT CALCIUM ISOTOPES

High velocity interstellar Ca II near Vela pulsar 0833-45, discussing absorption line association with Vela X, Y, Z supernova remnant complex

02 p0279 A72-12191

Interferometric photoelectric scans of interstellar Ca I 4226 line for stars with interstellar Ca II K-lines, discussing deduced electron densities

02 p0280 A72-12197

Absorption spectrum of atomic Ca trapped in solid hydrocarbons, comparing with diffuse interstellar band at 4430 A

02 p0284 A72-12632

Zeeman spectroheliograms of photospheric magnetic fields in Ca I 6102.7 A line

03 p0430 A72-13317

Photoelectric measurements of Ca K line of southern/equatorial A stars, discussing abundance variation

05 p0712 A72-15796

Photoelectric photometry of Ca K-line for A stars of population I clusters

05 p0712 A72-15797

Interstellar Ca II, H and K optical absorption lines of bright O and early B stars in Orion region

05 p0723 A72-17200

Conformal electron interactions in biopolymer and hypermolecular biological systems, discussing calcium ions effects, enzyme activity, muscle contractions and information theory

07 p0915 A72-18803

Coronal condensation of 10 September 1970, observing iron and calcium emission lines

07 p1082 A72-20297

- Ca II K line profiles in front of distant OB stars, using pressure scanned Fabry-Perot interferometer and coude spectrograph 10 p1542 A72-24616
- Microprobe analysis of Murchison and Vigarano meteorites, noting fractionation processes for Ca distribution in olivines 13 p2036 A72-28752
- Ca and Na ionization equilibrium ratio in dust filled interstellar clouds, considering cosmic ray and charge transfer influence 13 p2040 A72-29405
- Photospheric network, magnetic fields, Ca emission and continuum faculae from multichannel magnetograph observations 13 p2045 A72-29705
- Mg filterheliogram comparison with Ca spectroheliogram, noting correlation coefficient between location and intensity of bright features on sun 13 p2045 A72-29708
- Singly ionized Ca and Mg electron impact broadened resonance lines from rapid scanning Fabry-Perot spectrometer measurements in shock tube generated high temperature plasma 15 p2282 A72-32643
- Quiescent solar prominences internal motions from fine structure wavelength shift observations in Ca II K line spectra 15 p2318 A72-32780
- Solar corona Ca ion abundance from emission line measurements and electron density determination 15 p2318 A72-32785
- Complex Ca lubricants strength, colloidal and mechanical stability and thermal hardening relationship to dispersion medium viscosity 16 p2413 A72-33172
- Characteristics of the Ca II K-line profiles in the quiet sun. 21 p3108 A72-41280
- Nonvelocity origin of excess red shift in companion galaxies from observation of H and K absorption lines of Ca II 22 p3220 A72-41962
- The solar abundance of calcium and collision broadening of Ca I- and Ca II-Fraunhofer lines by hydrogen. 22 p3221 A72-42027
- High resolution spectroscopy of the disk chromosphere. II - Time sequence observations of Ca I H and K emissions. 22 p3221 A72-42032
- CALCIUM CARBONATES**
- NT ARAGONITE
- NT CALCITE
- CALCIUM COMPOUNDS**
- NT ARAGONITE
- NT CALCITE
- NT CALCIUM FLUORIDES
- NT CALCIUM OXIDES
- NT CALCIUM PHOSPHATES
- NT FLUORITE
- NT PEROVSKITES
- NT SCHEELITE
- Aluminizing process improvement by CaAl and ammonium chloride contents increase in powder 13 p1964 A72-29020
- The role of Sm and Mn as activators in calcium sulphate and lithium tetraborate. 18 p2718 A72-36347
- CALCIUM FLUORIDES**
- Heat resistance of magnesium, barium and calcium fluorides as solid lubricants in air, hydrogen and water vapor at 100-1100 C 06 p0836 A72-18433
- Green luminescence intensity dependence on lasing power during two-photon excitation of Er and Ho ions in calcium difluoride by neodymium laser 15 p2246 A72-31422
- CALCIUM ISOTOPES**
- Temperature fluctuations and fine structures in solar atmosphere from Ca II IR lines 03 p0414 A72-12926
- CALCIUM METABOLISM**
- Immobilization hypercalcaemia, discussing treatment by diet-induced extracellular volume depletion and possible pathophysiologic mechanism of intercompartmental fluid and electrolyte shift 04 p0479 A72-14871
- Calcium metabolism perturbations in astronauts under weightlessness conditions and in immobilized test subjects, noting bone tissue renewal cycle modification, calciuria variations and bone calcification 07 p0927 A72-19245
- Isolation stress effect on excretory products in unrestrained chimpanzee, suggesting Ca to P excretion ratio as physiological stress indicator [AD-739467] 07 p0921 A72-20179
- Calcium and phosphorus excretion relation to bone density changes in immobilized Macaca nemestrina monkeys 12 p1760 A72-27473
- Physiological evaluation of diastole mechanism in rat hypertrophied myocardium as function of heart rate, Ca ion concentrations and temperature 13 p1901 A72-28521

- Temperature and extracellular Ca level effects on mammalian ventricular myocardium force-frequency relationships, determining contractile tension, velocity and phase duration 13 p1907 A72-30045
- Weightlessness effects on calcium and electrolyte metabolism from measurements during Gemini 7 flight, using dietary control and excreta collection techniques 16 p2355 A72-33552
- Comparative study of two direct methods of bone mineral measurement. 17 p2508 A72-34552
- Calcium metabolism conditions in calcified tissues of rats during a lasting hypodynamia and thyrocalcin administration 21 p2997 A72-40432
- Calcium metabolism under stress and in repose. 23 p3254 A72-43389
- CALCIUM OXIDES**
- X ray and differential thermal analysis for phase diagrams of binary alloys of samarium oxides and gadolinium oxides with calcium oxides, noting solid solutions formation 23 p3304 A72-43250
- CALCIUM PHOSPHATES**
- Phosphate solubilization and activation on primitive earth, using apatite solubility as function of pH 04 p0483 A72-14769
- Lunar rock 14310 whitlockite richness in rare earth elements relative to associated apatite 16 p2454 A72-33446
- CALCIUM 45**
- U CALCIUM ISOTOPES**
- CALCULATION**
- U COMPUTATION**
- CALCULUS**
- NT ASYMPTOTIC SERIES
- NT COLLINEARITY
- NT CONTINUITY [MATHEMATICS]
- NT DIFFERENTIAL CALCULUS
- NT FOURIER SERIES
- NT FOURIER-BESSEL TRANSFORMATIONS
- NT INTEGRAL CALCULUS
- NT LIMITS [MATHEMATICS]
- NT PADE APPROXIMATION
- NT POWER SERIES
- NT SERIES [MATHEMATICS]
- NT TAYLOR SERIES
- NT VECTOR ANALYSIS
- NT VORTICITY
- Regge calculus representation existence for solutions of initial value problem for spaces with axial symmetry 16 p2422 A72-32879
- CALCULUS OF VARIATIONS**
- Flow passage geometry optimization in compressor rotor design treated as boundary value problem with variational calculus solution 02 p0151 A72-12179
- Variational perturbation problem solution in power series form for elliptic functional description of elastic continuous medium state by Euler-Lagrange equations 02 p0259 A72-12233
- Variational solutions of nonlinear free boundary integrodifferential Euler equations for rotating star models 02 p0252 A72-12540
- Variational problem of conducting fluid flow in MHD channel at large magnetic Reynolds numbers at induction saturation 03 p0397 A72-13999
- Elastoplastic bodies with crack at tip, determining limiting loads and crack propagation from variational relations 03 p0451 A72-14117
- Nonconservative stability problems, obtaining eigenvalues with adjoint variational methods [AD-742170] 04 p0583 A72-14446
- Spacecraft trajectories optimization by gradient method combination with Euler equations in calculus of variations 04 p0571 A72-14631
- Asymptotically diagonal systems for variational expansions applied to elliptic partial differential equations, estimating convergence rate 04 p0540 A72-15374
- Free oscillations of liquid masses contained in tanks, analyzing variational and Ritz methods 04 p0513 A72-15557
- Correlation energy calculation for system of fermions by means of variational method 05 p0702 A72-16785
- Elasticity theory equations for orthotropic plate bending, derived from combination variational and difference-differential procedures 05 p0741 A72-17144
- Second variational algorithm for iterative solution of unconstrained optimal control problems, examining linearized feedback control 06 p0839 A72-17592
- Kalman-Bucy colored noise filtering discrete time results and continuous time linear minimum variance estimation by calculus of variations 06 p0793 A72-17955

- Variational solutions to linear integral equations and extremal functions in physical gas dynamics problems, using stepwise constant trial functions 08 p1150 A72-21620
- R function and variational methods solution for mixed boundary value problem of Laplace equation applied to stationary heat conduction and electrodynamic problems 08 p1209 A72-21704
- Thermoelasticity theory for transversely isotropic shells, obtaining variational formulation of noncoupled quasi-static problem 08 p1247 A72-21811
- Optimal temperature gradients determination over thickness of shell of revolution under axisymmetric heating, formulating variational problem for conditional extremum of elastic energy functional 09 p1399 A72-22706
- Plastic compression of short cylinders prepared from incompressible rigid-plastic material with variable vertical yield point distribution, deriving variational equation of plastic flow 09 p1406 A72-23183
- Positive to quasi-stochastic matrix reduction by similar variation method, determining largest characteristic number and eigenvector 09 p1343 A72-23490
- Sobolev-Orlicz anisotropic spaces application to calculus of variations equations with strongly nonlinear coefficients 10 p1505 A72-24215
- Modified sweep variation method for optimal control programs, solving two point boundary value problem by linear perturbation technique 10 p1551 A72-24455
- Electromagnetic wave diffraction by dielectric steps in waveguides, calculating microwave scattered field by modified residue calculus technique 10 p1451 A72-24593
- Variational methods for approximate solutions to Fredholm integral equations describing stress intensity factors and plastic regions of Dugdale cracks [AD-744365] 10 p1558 A72-24892
- Variational equations of motion for three layered laminated sandwich beam vibrations, assuming small elastic deformations and axial and bending motion [AIAA PAPER 72-399] 11 p1731 A72-25420
- Inferential structure of variational statements for equations of motion and constitutive relations, noting function space choice 11 p1690 A72-26554
- Nonlocal variational mechanics problems approach by Balakrishnan epsilon technique, deriving methods for Lagrange function construction and Lagrange multipliers introduction 11 p1691 A72-26722
- Distribution theory application to fixed end point problem in variational calculus for extremal containing corners, obtaining Euler equation 12 p1885 A72-27849
- Variational problems in automatic control theory, presenting existence theorems for solution of boundary value problems for nonlinear differential equations with deviating argument 12 p1837 A72-27995
- Variational solution to axisymmetric problem of rigid stamp quasi-static impression into elastoplastic half space 13 p2053 A72-28387
- Axisymmetric stability of spherical cap rigidly clamped at contour of shells of revolution, using variational difference method for uniformly distributed external pressure 13 p2053 A72-28393
- Galerkin boundary method as variational approach to low Peclet number heat transfer in laminar flow 13 p2063 A72-28418
- Lagrange multiplier method derivation of variational functional for finite element method and applications to plate and shell problems 13 p2055 A72-28623
- Gravitational theory strong discontinuity conditions, using basis variational equation for field and media model construction in general relativity theory 13 p2002 A72-28711
- Variational form to determine equations and boundary conditions for elastic isotropic homogeneous nonferromagnetic body subjected to external load, temperature and electromagnetic field actions 13 p2061 A72-29797
- Generalized solution regularity of arbitrary order quasi-linear elliptic equations, indicating continuity conditions of variational problems 13 p1987 A72-30001
- Variational problem solution for solid strained body with nonlinear stress-strain relation, applying finite element method 14 p2130 A72-30189
- Differential equations for shallow orthotropic shells with variable thickness obtained by Bubnov-Galerkin variational method, presenting error assessment 14 p2163 A72-30195

Coordinate functions in Kantorovich variational method, noting application to stationary heat conduction boundary value problems

14 p2170 A72-30592

Magnetospheric and ionospheric potential electric fields, using variational process based on transverse/longitudinal conductivity ratios in plasma

14 p2100 A72-30633

Nonlinear equilibrium, stability and vibration equations of shallow sandwich shells with isotropic outer layer and rigid compressible filler obtained by variational method

14 p2166 A72-30700

Epitaxial film system parameters determination based on variational technique of computing electromagnetic waves reflectance and transmissivity in semiconductor structures

14 p2142 A72-30811

Variational calculus methods for periodic solutions of autonomously perturbed Hamiltonian systems of differential equations

15 p2263 A72-31759

Quantum mechanics variational methods reformulation for turbulent diffusion of marked particles

16 p2379 A72-33570

Control function improvement method for flight dynamics variational problems solution, discussing dynamic programming, trajectories with uncontrolled elements and coordinate transformation

17 p2607 A72-35036

Flight vehicle, control system and perturbations models synthesis from variational problem solution via control functions improvement

17 p2621 A72-35037

Variational and probabilistic methods for multiphase media, noting applications in electrodynamics, nonlinear plasticity and mechanics

17 p2632 A72-35110

Invariant imbedding and optimum beam design with displacement constraints.

17 p2634 A72-35406

Local potential concept based variational method for eigenvalue problems of disturbance damping or amplification in stability analysis

17 p2583 A72-35641

Calculus of variations and finite difference method for combined free and forced convective heat transfer through vertical noncircular ducts, calculating Nusselt number

18 p2741 A72-36926

Application of conformal transformation to the variational method - Buckling loads of polygonal plates.

18 p2738 A72-37074

Variational method in the control system invariance problem

19 p2778 A72-37990

Numerical integration method with recurrent power series for motion and variational equations of elliptic restricted three body problem

19 p2862 A72-38019

Bubnov-Vlasov variational method for thin parallelogram plates bending under complex loads, calculating edge skew and side length effects

19 p2877 A72-38160

Numerical solutions in the simplest problem of the calculus of variations.

19 p2827 A72-38382

Book - Some aspects of the optimal control of distributed parameter systems.

20 p2946 A72-39731

Bounds for heat transport in a porous layer.

21 p3127 A72-40119

Application of variational methods to the solution of some thermal shock problems

21 p3128 A72-40978

Variational theorems for harmonic waves in elastic composites with periodic structures, considering wave propagation in layered and in fiber reinforced composites

21 p3119 A72-41101

A method of numerical integration for trajectories with variational equations.

21 p3111 A72-41557

Variational formulation and computer solution for thermal boundary layer flow over flat plate in entrance region, assuming temperature dependent thermal conductivity and viscosity

22 p3156 A72-41959

Gravitational theory strong discontinuity conditions, using fundamental variational equation for field and media model construction in general relativity theory

22 p3204 A72-42089

Modified Newton-Kantorovich variational method for calculating flows in subsonic and transonic portions of circular nozzles, noting savings in computer time

23 p3248 A72-43659

Variational analysis of sandwich beams under static loads, presenting shear deformation and normal stress distributions

23 p3350 A72-44055

Modified Hellinger-Reissner variational method applicable to harmonic waves moving normal to fiber reinforced layered elastic composite, tabulating eigenfrequencies

23 p3351 A72-44061

Heat conduction with allowance for the temperature dependence of the coefficient of thermal conductivity. II - Correctness of the variational formalism

23 p3357 A72-44085

Duality in problems of the calculus of variations and optimal control

24 p3419 A72-45390

Minimum-time entry of space vehicles into a planetary atmosphere

24 p3452 A72-45442

CALDERAS

Height-depth ratios of lunar craters and terrestrial calderas from topographic measurements

02 p0278 A72-11908

CALIBRATING

NT WIND TUNNEL CALIBRATION

Flight test procedures for subsonic transport aircraft pitot static pressure system, recommending trailing cone calibration method

01 p0064 A72-10389

Computer image processing for photoreconnaissance, enhancement and calibration applications

01 p0070 A72-10870

Calibrations consistency of UBVY beta and GNMK photometries of binary stars with G or K giants and A or F main sequence components

01 p0132 A72-11014

Linearization errors and calibration functions for hot-wire anemometry taking into account higher order velocity fluctuations

01 p0071 A72-11170

Photometric calibration of long wavelength vacuum UV standards by synchrotron and plasma black body radiation

01 p0073 A72-11399

ERTS return beam vidicon system geometric calibration for high resolution photoimage maps cartographic referencing and register, discussing optical and electronic distortion sources

02 p0225 A72-11818

Steerable receiving antennas L/S band solar calibration error statistical analysis, obtaining 0.5 db uncertainty by monitoring antenna gain-to-noise temperature ratio

02 p0192 A72-12159

Steerable vhf/uhf receiving antennas stellar calibration error analysis, obtaining worst-case uncertainty of 0.4 db by monitoring antenna gain-to-noise temperature ratio

02 p0175 A72-12161

Electronic equipment and calibration procedures for 86 MHz radio interferometer providing synchronized astronomical observations

02 p0194 A72-12576

Ferrite rod antennas calibration for radio frequency measurements up to 1 MHz

02 p0195 A72-12606

Absolute UV calibration of rocket photometers used to update OAO calibration for determining energy distribution of reference stars

03 p0355 A72-13065

Rocket-borne spectrometers calibration for observing absolute intensity and center-to-limb variations of sun in vacuum UV region

03 p0355 A72-13066

Dynamic calibration by sound wave of hot wire operated by constant resistance method, using open resonance tube in homogeneous incompressible air flow

03 p0356 A72-13235

Calibration of polarimetric measurements in terms of magnetic fields, using Stokes parameters without line formation dependence

03 p0427 A72-13280

Calibration technique for low energy IR radiometers, calculating detector field of view energy content or photons number from mirror reflectivity and temperature

03 p0359 A72-13441

Portable electronic wattmeter for nonsinusoidal waveform low power factor circuit measurement, discussing design, calibration and applications

03 p0332 A72-13757

Thermal flux sensors high temperature calibration, using vacuum chamber technique

03 p0362 A72-14163

High temperature fatigue crack growth studies by compliance calibration test method, evaluating temperature and cycle rates effects

03 p0339 A72-14169

Pressure measuring method with piston manometers for absolute vacuum gage calibration

04 p0507 A72-14440

Linearized constant temperature hot-wire anemometer calibration for shock tube unsteady flow velocity measurements with low strength wave propagation

04 p0521 A72-14920

Al finished and Au plated triple calibration sphere as multispectral optical sensor for testing Cook hypothesis concerning satellite drag dependence on surface material

04 p0500 A72-15305

Laboratory spectrophotometer calibration for specular light over 0.5-2.5 micron range by means of stacked glass plates, noting accuracy

04 p0524 A72-15535

Acoustic radiation pressure of small radius spherical obstacle in high level harmonic plane field for application to microphone calibration

[ONERA, TP NO. 1008]

05 p0661 A72-16023

Numerical method for cylindrical microwave cavities calibration for plasma diagnostics, noting computer programs applicability for arbitrary electron density radial distributions

05 p0662 A72-16418

NF-8D aircraft variable stability system ground/in-flight calibration for determination of flight control system dynamics effects on flying qualities

05 p0611 A72-16660

Computer controlled vacuum optical calibration bench for astronomical satellites, describing pumping system

05 p0644 A72-16755

Spark calorimeter calibration by particle accelerator induced high energy pions, noting neutral and charged particles track detectors high geometric resolution

06 p0811 A72-17292

Self calibration of surveying cameras for three dimensional object photography without control points, using homologous ray method

06 p0815 A72-17754

Double frequency stroboscopic method for absolute calibration of vibration transducers, analyzing errors

06 p0815 A72-17766

Principle stress errors in biaxial stress fields expressed in terms of transverse sensitivity, stress and Poisson ratios of material during strain gage calibration

06 p0895 A72-17798

Light generator aided autonomous calibration of Cerenkov spectrometer for continuous primary cosmic nuclear flux measurements

06 p0815 A72-17832

Absolute gravity meter based on gradiometer system with additional mass, discussing working principle and calibration procedure

06 p0817 A72-18149

Short and long term spectral modulation of primary cosmic rays above 2 GV during solar cycle 19 descending phase, presenting neutron monitors calibration procedure

06 p0874 A72-18160

Sensitivity calibration of dual beam vertically pointing FM-CW radar, presenting antenna main lobe radiation patterns

06 p0776 A72-18443

Complex systems calibration based on computer derived transfer function, discussing theory, Fortran calibration program, error analysis and applications

07 p0949 A72-18818

Precision frequency calibrator for Raman spectrometers, using Fabry-Perot etalon

07 p0983 A72-19318

Small gage thermocouples calibration procedure, noting data correlation with thermoelectric theory

07 p0984 A72-19326

Accelerometer sensitivity calibration by laser interferometer for vibration measurement, discussing frequency range, accuracy and advantage over spectral lamp

07 p0984 A72-19350

Temperature effects on hot-wire anemometer calibrations, plotting Nusselt number variation with Reynolds number

07 p0990 A72-20369

Annual variations of calibration factors of star pyranometers for copper-constantan and nichrome-constantan thermocouples

07 p0991 A72-20450

Muon telescopes calibration for cosmic rays rigid component variations by data comparison with variable aperture telescope

08 p1162 A72-20720

Overheat resistance calibration of constant temperature hot-wire anemometers at low velocities in water with variable temperature

[ASME PAPER 71-HT-9]

08 p1163 A72-20873

Miniature three-position pressure valve for on-board calibration of pressure transducers in wind tunnel models, noting time lag reduction

08 p1164 A72-20923

Interlaboratory comparison of piston-cylinder pressure calibration based on albite breakdown to jadeite and quartz under pressure

08 p1165 A72-21298

Calibration technique for conductive thermal flux sensors operating at low temperatures

08 p1166 A72-21315

Yaw calibrations of Preston tubes for wall shear stress measurements in two and three dimensional turbulent boundary layers

08 p1254 A72-21627

Reflected signal and receiver noise interference error in antenna temperature and calibration measurements by artificial moon method in centimeter and decimeter bands

08 p1142 A72-21726

Multihole flow probe measurement data evaluation by multidimensional approximation of calibration curves and surfaces

09 p1260 A72-22631

Calibrator for millimeter wave horn radiometers, using radiation from load immersed in liquid nitrogen

09 p1310 A72-22652

Capacitive electret pressure sensors calibration for interior measurements in turbine engines, jets and exhaust nozzles

[ONERA, TP NO. 982] 09 p1310 A72-22815

Static pressure tube calibration for surface pressure measurements in flow over flat plate and airfoil

09 p1261 A72-22937

Temperature effects on low pressure calibration in vacuum gage metrology

09 p1312 A72-23249

System methodology application to filter design for inertial reference unit calibration in digital test station for FB-111 aircraft navigation system

10 p1456 A72-23820

Reference transfer method for in situ calibration of ionization gages, determining pressure ratio of molecular gas flow through fixed orifices

10 p1480 A72-24147

Carbon dioxide concentration effect on calibration of linearized hot-wire anemometer in operation at constant temperature

10 p1480 A72-24217

Calibration procedure for crack length determination based on in test crack opening displacement monitoring

10 p1559 A72-24900

Calibration technique for meteorological superpressure balloon hygrometers designed for horizontal sounding of troposphere and stratosphere

10 p1484 A72-25087

Calibration model for UV stellar photometer using secondary electron conduction/SEC vidicon

11 p1631 A72-25684

High tension exciter output voltage measurement based on cathode ray oscilloscope and high voltage probe, stressing calibration procedure

[SAE AIR 1092] 11 p1604 A72-26028

Ion thruster performance calibration investigating double ion content, back ingestion, beam spreading and propellant flow rate

[AIAA PAPER 72-475] 11 p1709 A72-26206

Dynamic calibration of inclined and crossed hot-wire flowmeters for absolute turbulence intensity measurements, using known sinusoidal oscillations in steady flow

11 p1636 A72-26637

Thermistor vacuum gage with interchangeable sensing heads, providing improved pressure response and direct interchanging without recalibration

11 p1636 A72-26776

Calorimeter calibration for laser energy and power measurements in terms of electrical energy based on voltage, resistance and frequency standards

11 p1652 A72-26781

Vacuum gage calibration standardization by piston manometer method of pressure determination from direct force-area measurement

12 p1805 A72-27037

Four-phase radio continuum receiver with digital demodulation and signal integration for transfer into on-line computer, discussing calibration

12 p1793 A72-27808

Silicon solar cell calibrations for space applications, discussing equivalent diagram, I-V characteristics and stratospheric balloon measurement

12 p1758 A72-28040

Solar cells calibration by high altitude aircraft, using extrapolation method to zero air density

12 p1758 A72-28041

Solar cell calibration in uncollimated sunlight, obtaining standards for solar simulator intensity

12 p1759 A72-28042

Secondary standard solar cells calibration method based on solar spectral response comparison with primary standard, discussing error correction method

12 p1759 A72-28043

Low energy particles spectrometer channels calibration for satellite auroral observation, discussing photomultiplier detector properties

13 p1960 A72-29843

Heated thin film gages calibration for skin friction measurements in laminar and turbulent flows, discussing wall temperature distribution and turbulence effects

15 p2241 A72-32577

Spectrograph for Orion spaceborne astronomical observatory on Salyut space station calibrated with synchrotron radiation from particle accelerator

15 p2242 A72-32744

Laser interferometric calibration for vibration measurement, discussing operation principle and detector error

16 p2391 A72-33248

Spectrophotometers and photometers calibration and standardization, emphasizing necessity for periodic control of instrument parameters

16 p2394 A72-33872

Calibration and application techniques for platinum resistance thermometers. [ASME PAPER 71-WA/TEMP-2]

17 p2554 A72-34965

A recalibration of the absolute magnitudes of supergiants.

17 p2609 A72-35115

The absolute calibration of periodic microwave phase shifters without a standard phase shifter.

17 p2531 A72-35470

Calibration of the flux density of Cassiopeia A and Cygnus A in the range 300-9375 MHz.

17 p2617 A72-35728

Dynamic characteristics of electrical measuring instruments and transducers, discussing static calibration curve, dynamic tests and parameters determination

17 p2557 A72-35757

Signal generator designed for calibration and control of interferometric radar station to observe and study radio echoes induced by meteor trails

17 p2519 A72-35959

Performance of a modified Askania iris photometer.

18 p2692 A72-36768

Procedure for the calibration of photoelectric components in the IR spectral range

18 p2693 A72-37005

A program of wide scale pairs for determining the micrometer screw turn magnitude of the Pulkovo ZTL-180 wide-angle zenith telescope

19 p2802 A72-37979

Muon telescopes calibration for cosmic rays hard component variations by data comparison with variable aperture standard telescope

19 p2803 A72-38348

Design of a reduced-state suboptimal filter for self-calibration of a terrestrial inertial navigation system. [AIAA PAPER 72-849]

20 p2949 A72-39080

Stable microprecision test platforms construction and microseismic effects on motion sensing instrument calibration including gyroscopes and inertial navigation and guidance systems

[AIAA PAPER 72-893] 20 p2911 A72-39110

Hot wire data corrections in low and in high turbulence intensity flows.

21 p3051 A72-40220

Some results of calibrating CG-2 gravimeters /Sharpe/ by the tilt method.

21 p3053 A72-40499

Diagram and gain measurements regarding antennas conducted with a helicopter for the range from 0.5 to 800 MHz

21 p3031 A72-40545

In-flight alignment and calibration of inertial measurement units. I - General formulation. II - Experimental results.

21 p3081 A72-41079

Calibration procedure to correct for the effects of dielectric containers in microwave plasma density measurements.

21 p3056 A72-41377

Hot wire anemometer calibration for measurements of small gas velocities.

22 p3175 A72-41953

Objective-prism plates photometric computerized calibration method based on continuum energy distribution of standard stars within photographic plate field

22 p3177 A72-42376

Analysis of the structure of the flow downstream of a sudden widening

22 p3167 A72-42643

Integration sphere facility with water cooled long arc xenon sources for pyranometer calibration, discussing operation theory and system design

22 p3163 A72-42692

Use of a linear air bearing sled for dynamic calibration of velocity transducers.

22 p3179 A72-42693

Compliance calibrations of a contoured and face grooved double cantilever beam specimen.

24 p3413 A72-44817

CALIFORNIA

Northeast Bank, Southern California Borderland volcanic petrology and geologic history, investigating basaltic rocks, hyaloclastites and fossil fragments

04 p0520 A72-15589

CALORIC REQUIREMENTS

Evaluation of cardiopulmonary function and work performance in man during caloric restriction.

21 p3005 A72-40423

CALORIC STIMULI

Vestibular system tests using optokinetic, caloric, positional and rotational stimuli

01 p0022 A72-11292

Influence of thermal, osmotic, and chemical stimulations on food and water intake

17 p2504 A72-35016

CALORIMETERS

Calorimeter for measuring energy pulses and wavelengths from frequency doubled neodymium to carbon dioxide lasers

02 p0224 A72-11748

Spectrophotometer and tristimulus mask calorimeter using double grating mirror dispersion system

03 p0358 A72-13427

Pulsed Nd laser beam polarization components energy measurement by double reflecting plate calorimeter, checking accuracy against NBS liquid cell calorimeter

04 p0531 A72-15479

Multilayer X ray chamber for gamma quanta energy spectrum determination by primary photon impact and absorber calorimetric methods

06 p0869 A72-17266

Spark calorimeter calibration by particle accelerator induced high energy pions, noting neutral and charged particles track detectors high geometric resolution

06 p0811 A72-17292

Transient effects due to electromagnetic cascades in Pb during Cu wall passage in ionization calorimeter

07 p0988 A72-19871

Calorimetric gage for convective and radiative wall heat flux measurements in Ar arc plasma

08 p1254 A72-21628

Hollow sphere calorimeter for high power pulsed laser energy measurements in broad spectral range, comparing with liquid calorimeter

09 p1323 A72-22656

Local and macroscopic thermal transport in turbulent air stream, discussing measurement from calorimeter instrumented sphere

10 p1417 A72-24148

Levitron calorimetry for solid and liquid Mo enthalpy measurement, calculating specific heat and heat of fusion

10 p1496 A72-24243

Self balanced microwave static calorimeter with substantial delay time, discussing system instability conditions

11 p1634 A72-26450

Calorimeter calibration for laser energy and power measurements in terms of electrical energy based on voltage, resistance and frequency standards

11 p1652 A72-26781

Portable X ray calorimeter for simultaneous fluence and front surface dose measurement in Ta from pulsed electron accelerations

15 p2241 A72-32440

Polymeric structural adhesives thermal stability evaluation, recommending thermogravimetric analysis and calorimetry to supplement thermogravimetric method

16 p2415 A72-33510

Russian monograph on heat measurement covering methods and instruments for heat flux determination, radiometers, thermal conductivity gages and electrical calorimeters

17 p2556 A72-35495

A graphite calorimeter

18 p2693 A72-37192

Liquid dielectrics specific heat determination by adiabatic calorimeter with monotonic heating

21 p3059 A72-41819

Nonstationary method for measuring the heat conductivity of liquids and gases under high pressures

22 p3243 A72-41886

CALORIMETRY

U HEAT MEASUREMENT

CALUTRONS

U CYCLOTRONS

CAMBER

NT WING CAMBER

Circular arc blades two dimensional cascade performance test data for various cambers comparison with potential theory data

05 p0602 A72-16485

Hydrodynamic characteristics of a cambered hydrofoil with a jet flap.

[ASME PAPER 71-APMW-17] 17 p2537 A72-34303

Plane stationary flow of ideal incompressible fluid past large camber profiles of arbitrary shape and thickness, using computerized Fourier expansion

24 p3360 A72-45002

CAMERA SHUTTERS

Meteor passage time determination by optical shutter with wedge-shaped blades for light flux periodic intersection and production of two discontinuous lines for identification

06 p0816 A72-17930

High speed photography ultrafast shutter based on polymethylene cyanide dyes saturability for measuring mode locked ruby laser pulse duration

15 p2241 A72-32535

Meteor passage time determination by optical shutter with wedge-shaped blades for light flux periodic intersection and production of two discontinuous lines for identification

18 p2693 A72-37155

Central band-type wide angle camera shutter design, noting stress examination in machine parts by optical method

21 p3052 A72-40306

CAMERA TUBES

- NT IMAGE DISSECTOR TUBES
 NT IMAGE ORTHICONS
 NT ORTHICONS
 NT RETURN BEAM VIDICONS
 NT VIDICONS
- Low light television camera tubes application to navigation safety in congested areas, reconnaissance and other watchkeeping system
 07 p1032 A72-19070
- Space applications of camera tubes - Conference, Paris, November 1971
 08 p1169 A72-1951
- Camera tube used in Faust program of spatial and astronomical UV photometry and spectrophotometry
 08 p1169 A72-1953
- SAS-D borne TV type UV sensitive detector with camera tubes for high resolution astronomical spectroscopy
 08 p1169 A72-1954
- UV/visible image converter for use with TV camera tubes for astronomical photometry and spectroscopy from satellites and sounding rockets
 08 p1169 A72-1955
- TD-1 satellite mounted slow analysis camera with supervidicon image tube to observe cosmic ray tracks in spark chamber
 08 p1170 A72-1961
- Electronic cameras to record and measure weak stars 1000-11000 A, noting atmospheric turbulence suppression and night sky brightness reduction
 08 p1170 A72-1962
- Image tube, film and mechanical scan camera imaging systems comparison for spacecraft-borne planetary photography based on maximum data return at acceptable cost
 08 p1170 A72-1964
- Low light level small intensifier/vidicon camera tube using bombardment induced conductivity target, and planar photocathode, detailing design and performance
 08 p1171 A72-1969
- Design and operation of digital image recorder based on single stage intensifier and silicon target intensifier television camera tube coupled to large memory
 11 p1631 A72-25685
- Image-to-signal conversion by TV tube in automatic contactless measuring systems, producing mosaics of object by optical, X ray and ultrasonic techniques
 11 p1634 A72-26460
- Intensified electron bombarded Si camera tube performance in low light level TV systems, predicting sensor resolution vs irradiance characteristics
 12 p1810 A72-27934
- A transmitting television tube for collecting information from streamer spark chambers
 23 p3290 A72-44160
- CAMERAS**
- NT BALLISTIC CAMERAS
 NT FRAMING CAMERAS
 NT HIGH SPEED CAMERAS
 NT LALLEMAND CAMERAS
 NT PANORAMIC CAMERAS
 NT SCHMIDT CAMERAS
 NT TELEVISION CAMERAS
- Aerial focal plane shuttered camera high velocity images mathematical model based on collinearity equations, incorporating translational and rotational camera motion during exposure for image motion compensation
 01 p0066 A72-10461
- Camera slit lamp apparatus design for anterior eye diagnosis in two dimensional and stereoscopic photography and ophthalmic application
 04 p0478 A72-14725
- Self calibration of surveying cameras for three dimensional object photography without control points, using homologous ray method
 06 p0815 A72-17754
- Return beam vidicon multispectral camera system for ERTS A and B, describing camera system design and performance characteristics in terms of ERTS mission purpose
 07 p0986 A72-19601
- Survey camera design for continuous film advancement and prismatic image displacement compensation
 07 p0987 A72-19860
- Design and operation of hand control of automatic camera for astrogodesy used for measuring artificial earth satellites orbits
 08 p1165 A72-21021
- Correlation functions for angular vibrations of operating aerial camera during working cycle
 09 p1310 A72-22947
- Camera shake under stress of tracking moving targets viewed briefly in poor light, considering blur in horizontal and vertical dimension
 10 p1483 A72-24986
- X and gamma ray astronomy with multiple pinhole cameras and a posteriori image synthesis, obtaining SNR gain
 11 p1629 A72-25313
- Apollo 15 and 16 TV, still and movie cameras, discussing astronomical activities of astronauts
 12 p1807 A72-27546

- Image deformation sources correction in space photography, discussing stationary and moving cameras and panoramic and complex sensing systems
 12 p1809 A72-27817
- Solid state array camera based on diffused junction phototransistors, discussing sensor technology and fabrication
 12 p1810 A72-27931
- Photographic observation of satellites to sixth magnitude with K-24 aerial camera on Polaroid 3000 and 10,000 ASA film, recording time signals on magnetic tape
 14 p2084 A72-30235
- Aerial survey camera with automatic exposure control, discussing film emulsions sensitivity characteristics, object light intensity range and measuring methods
 14 p2105 A72-30839
- Radioisotope camera based on electron avalanche in liquid Xe, noting spatial and energy resolution advantages over existing gamma ray cameras
 15 p2234 A72-31537
- Exposure calibration, orientation and point coordinate distortions in aerial photographs from one or two camera stations
 15 p2240 A72-32378
- Apollo-borne modified Hasselblad 500 EL Data moon camera and lenses, discussing design features and photographic applications
 16 p2388 A72-32825
- Apollo 9, Skylab and Earth Resources Technology Satellite-borne multiband cameras performance requirements and tolerances comparison, considering geometric and spectroradiometric properties
 16 p2395 A72-34103
- Stellar oriented Apollo metric mapping camera system for photo geodesy, discussing planned coverage triangulation methods, control network and gravity model improvements
 16 p2396 A72-34105
- Determination of the parameters of a satellite camera
 17 p2556 A72-35360
- Night photography at 10,000 feet.
 17 p2557 A72-35556
- Modulation measurement applied to the focusing of aerial cameras.
 17 p2558 A72-35948
- The accuracy of the intermittent photographic film advance in the camera of an airborne thermal scanner.
 18 p2692 A72-36697
- Clinical IR thermography with Thermovision camera for body temperature discontinuity detection, discussing image resolution
 18 p2655 A72-37196
- Optical design and production of low cost oscilloscope camera incorporating reliable setting for correct exposure and focus
 20 p2921 A72-39031
- Optimum diopter value for a view-finder of photographic camera.
 21 p3054 A72-40729
- CAMOUFLAGE**
- Determining the detectability range of camouflaged targets.
 17 p2510 A72-35690
- CANADA**
- Regional geologic features of Alaska and Western Canada from Nimbus 4 satellite image dissection camera system /IDCS/ photographs
 10 p1477 A72-25109
- CANARD CONFIGURATIONS**
- Tail first /canard/ and tandem wing configurations for natural STOL, discussing low cost aerial work aircraft
 06 p0758 A72-18285
- V/STOL weapon system VJ-101, describing He-231 design development from tailsitter concept to canard configuration with tilting wing-tip engines
 07 p0912 A72-19251
- Fighter aircraft maneuverability, range and armament requirements, discussing canard vs delta configurations
 11 p1577 A72-26657
- Vortex sheet simulation method for slender wing-canard surface nonlinear interaction investigation
 16 p2458 A72-33695
- CANCER**
- NT LEUKEMIAS
- Hazard rate of recurrence in patients with malignant melanoma, investigating survival
 02 p0167 A72-11713
- Lungs fibrosis and cancer caused by asbestos fibers inhalation, noting environment control for protection against workers health hazards
 11 p1583 A72-25548
- Hazard rate of recurrence in germinal cell tumors of the testis.
 22 p3150 A72-42498
- New cancer therapy treatment techniques using space dosimetric concepts.
 24 p3374 A72-45112
- Hodgkins disease post-surgery recurrence hazard rate in flying personnel, developing statistical base for decision regarding return to military flying duty
 24 p3377 A72-45661

CANNULAE

- Pulsatile blood pressure and ECG in squirrel monkeys, considering catheter electromanometer system and implanted arterial cannulas long stability
 08 p1124 A72-20900

CANONICAL FORMS

- Solution stability of linear differential equations systems with harmonic coefficients, using Jordan canonical forms and perturbation method
 03 p0382 A72-13918
- Canonical form for boundary conditions of thin elastic shells with oscillating loads applied on edges
 04 p0587 A72-15013
- Computer aided Foldy-Wouthuysen canonical transformation on Dirac Hamiltonian with electromagnetic potentials included
 04 p0496 A72-15627
- Stability-instability criterion of time varying linear systems, using canonical form of differential equations
 [ASME PAPER 71-WA/AUT-20]
- German monograph on Poincare orbit stability in restricted three body problem, using canonical mappings of annulus and perturbation method
 05 p0689 A72-16044
- Gyrostal translational rotational motion equations in canonical form without trigonometric expressions in Hamiltonian
 05 p0724 A72-16164
- Statistical description of Brownian particle motion in turbulent flow, using theory of canonical correlations
 05 p0648 A72-16171
- Optimal final value control systems in phase-variable canonical form, discussing feedback gain singularity structure for single and multiple input systems
 06 p0793 A72-17954
- Statistical mechanics of N-body self gravitating system one dimensional model, using canonical and microcanonical ensembles
 06 p0885 A72-18075
- Algorithm for transformation of generalized companion forms for multivariable linear systems into Jordan canonical form
 09 p1341 A72-23071
- Dimensional analysis pi-theorem local generalization by Lie transformation group investigation, constructing local canonical coordinate systems to obtain factoring properties of certain functions
 10 p1503 A72-23921
- Lie transformations for perturbed canonical system of differential equations solution, proposing parameter square root series development for resonance problems of celestial mechanics
 10 p1536 A72-24119
- Asymmetric Einstein equations with impulse-energy tensor in canonical form derived from variational principle, defining space-time continuum as pseudo-Riemann manifold
 10 p1510 A72-24120
- Digital computer simulation of random processes specified by canonical expansion, discussing quantization steps for storage requirements reduction
 11 p1600 A72-25432
- Canonical equations for frequency demodulator using feedback, calculating harmonic distortion for sinusoidal modulating signal
 11 p1593 A72-25891
- Statistical mechanics of one dimensional model for many body self gravitating system with canonical and microcanonical ensembles, noting isothermal solution of Vlasov equation
 12 p1846 A72-27907
- Statistical description of Brownian particle velocity in turbulent flow, using theory of canonical correlations
 14 p2093 A72-30240
- Optimal regulator inverse problem analysis for multiinput systems with integral type performance indices, using state variable canonical form
 17 p2534 A72-35527
- Direct and inverse transformations between phase variable and canonical forms.
 19 p2826 A72-38230
- Canonic model representations for communication receiver to analyze and simulate input-output behavior as nonlinear signal processing black box
 21 p3019 A72-40889
- Satellite vibration-rotation motions studied via canonical transformations.
 [AIAA PAPER 72-919]
- A method for calculating canonical realizations for linear, unsteady, discrete systems
 23 p3277 A72-43989
- CANOPIES**
- Static and dynamic load measurements for stress-strain behavior and load-time characteristics of aerodynamic decelerator canopy fabrics, using metal foil strain gages
 02 p0287 A72-11507
- Chemically strengthened glass for eject-through frangible canopy design in aircraft emergency escape systems, noting protection against ejection injuries
 12 p1813 A72-27016

Emergency escape from high performance military aircraft in flight and on ground, using explosive cord for transparent canopy material breakup

12 p1753 A72-27017

Intensity of turbulence within canopies with simple and complex roughness elements.

20 p2948 A72-39798

CANTILEVER BEAMS

Algorithms for mass and stiffness matrices synthesis from experimental vibration modes applied to cantilever beam

[SAE PAPER 710787] 01 p0137 A72-10278

Pretwisted tapered cantilever beam torsional vibration natural frequencies determination by Galerkin method for solution of differential equation of motion

02 p0297 A72-12533

Time delay effect on stability of viscoelastic cantilever column under retarded follower load

04 p0590 A72-15186

Postbuckling behavior of cantilever columns with variable flexural rigidity, basing solution method on buckling mode assumption and principle of minimum total potential

04 p0591 A72-15278

Unstable propagation and brittle fracture arrest in steels from double cantilever beam test under compression

05 p0677 A72-17107

Semiempirical stress analysis of cantilevered thin walled cylinder, obtaining local stresses via strain gages

[SAE PAPER 720285] 06 p0893 A72-17324

Critical loads for elastic buckling of monosymmetric beams and cantilevers

06 p0897 A72-17969

Forced transverse vibration damping of end loaded elastic cantilever beam, determining hysteresis loop contour from resonance curves

06 p0900 A72-18673

External pressure effects on cantilever rotating shaft vibration, determining critical whirling speed as function of pressure and area distribution by energy method

07 p1096 A72-20528

Bending theory of homogeneous isotropic micropolar cantilever beam loaded by moments at edges

09 p1399 A72-22700

Linear mechanical elastic systems divergence with infinitely large frequency onset, noting discrete cantilever beam under nonconservative forces

[ASME PAPER 71-APM-DDD] 10 p1555 A72-24189

External load effects on natural frequencies of free end and centrally loaded cantilever beams and supported or clamped circular plates

10 p1558 A72-24814

Pontryagin maximum principle application to minimum deflection of cantilever beam under own weight

10 p1558 A72-24880

Bending of rectangular cross section cantilever beam with cylinder reinforced circular opening, calculating interface stress distribution as function of thickness and elasticity moduli ratio

11 p1733 A72-25545

Cantilever beam transverse vibrations induced by time varying linear displacements of clamped end under external loads, taking into account internal energy dissipation

11 p1738 A72-26797

Simultaneous nonhomogeneous internal and external friction effects on nonconservative force systems motion stability, considering cantilever beam compression

12 p1845 A72-27321

Collapse loads of symmetrically tapered cantilever beams under uniformly distributed end shear, considering optimum tapering angle for minimum weight

13 p2059 A72-29596

Minimum weight hinged and unhinged cantilever truss design as variational problem, using dynamic programming method

14 p2166 A72-30690

Modified Rayleigh-Ritz method to obtain lower bounds of eigenvalues, applying to uniform cantilever column buckling

15 p2275 A72-31710

Cantilever beam tapered linearly in horizontal and vertical planes, obtaining computer solution for free transverse vibration fundamental frequency and harmonics

15 p2328 A72-32022

Plane stress solution for thin walled cantilever beam with end load extended for beam width effects in composite orthotropic beam bending

16 p2463 A72-32841

Collocation method for coupled bending-bending torsion vibrations of straight uniform cantilever beam with asymmetric airfoil cross section

16 p2464 A72-32908

Magnetoelastic buckling of beams and thin plates of magnetically soft material.

[ASME PAPER 72-APM-35] 17 p2624 A72-34311

Natural bending frequency comparable to rotational frequency in rotating cantilever beam.

17 p2625 A72-34324

Stability of a beam on an elastic foundation subjected to a follower force.

17 p2626 A72-34331

Computerized numerical integration for nonlinear bending of tapered slender cantilever beams under concentrated tip loads

17 p2635 A72-35975

Identification of parameters in nonlinear boundary conditions of distributed systems with linear fields.

19 p2780 A72-38245

Stresses in a perforated, continuously loaded cantilever beam.

21 p3117 A72-40453

On the destabilizing effect in a non-conservative system with slight internal and external damping.

21 p3124 A72-41483

Investigation of the stability and vibrations of beams of variable rigidity by the method of bilateral estimates

22 p3234 A72-42147

On eigenvalue boundary problems of transversely vibrating sandwich beams.

22 p3240 A72-42910

Crack propagation speed measurements with wedge loaded double cantilever beam of PMMA, calculating stress intensity, strain energy release rate and kinetic energy

23 p3346 A72-43709

Plastic design of regular orthotropic grids with two adjacent edges fixed, free, or hinged.

24 p3456 A72-44794

Compliance calibrations of a contoured and face grooved double cantilever beam specimen.

24 p3413 A72-44817

CANTILEVER MEMBERS

NT CANTILEVER BEAMS

NT CANTILEVER PLATES

Fatigue test machine for alternating cantilever bend and torsion testings at 50 Hz and 1.5-300 K

01 p0049 A72-11381

Concentrated inertias effects on cantilever beams and shafts free vibrations by Laplace transform technique

04 p0591 A72-15276

Double cantilevered specimen crack growth, computing fracture surface energies from dynamical cleavage analysis

05 p0735 A72-16019

Elastically supported cantilever stability with continuous lateral restraint under uniform distributed axial load, developing boundary conditions

05 p0737 A72-16118

Autoparametric excitation in relation to divergence and flutter of autonomous mechanical cantilever systems under nonpotential circulatory forces

06 p0851 A72-18726

Ritz-Galerkin process applied to coupled differential equations of motion of pretwisted tapered cantilever turbine blade vibrating in flexure

08 p1244 A72-21483

Matrix progression method analysis of free vibration problem for cantilever thin circular cylindrical elastic shells, using Flugge equations

16 p2475 A72-34173

CANTILEVER PLATES

Bending moments in transversely isotropic rectangular cantilever plate of low shear rigidity

02 p0299 A72-12684

Bending under concentrated load of laminated cantilever plate with low interlaminar rigidity, taking into account low shear resistance effects

08 p1248 A72-21860

Transverse shear effect during bending of cantilever plates with low shear rigidity

08 p1248 A72-21864

Vibration of trapezoidal cantilever plates with partial root chord support.

21 p3121 A72-41225

Numerical solution of bending stresses in elastic cantilever plates under surface and edge loads, noting boundary layer, load concentration and sweep back effects

22 p3236 A72-42609

CANTILEVER WINGS

U WINGS

CAPACITANCE

Mixed boundary value problem of Laplace equation solution by dual trigonometric series equations approach, applying to microstrip transmission line capacitance determination

01 p0093 A72-10508

Stainless steel electrodes resistive and capacitive properties in contact with saline solutions of various concentrations and over extensive frequency range and current densities

03 p0318 A72-12953

Densibility and stress relaxation characteristics of capacitance and resistance vessels of isolated rabbit ear as function of basal tone

04 p0473 A72-15124

Low sensitivity distributed-active bandpass network with effective use of capacitance to save space and weight

04 p0506 A72-15307

Semiconductor device physical behavior, discussing energy levels, impurity conduction, p-n junction capacitance and bipolar and unipolar transistor I-V characteristics

06 p0790 A72-18575

Multilayer thin film microcircuits and printed circuits partial capacitance and potential coefficient approximate calculation by matrix method

07 p0953 A72-19016

Fast algorithm for space charge layer and semiconductor junction capacitance calculation, applying to impurity profile determination

07 p0954 A72-19120

Flow graph analysis of optimal operation of frequency multipliers with idler circuits using nonlinear n-p junction capacitance

08 p1140 A72-21061

Junction FET drain source capacitance theory based on two-region physical model, taking into account carrier drift velocity saturation effect

08 p1142 A72-21745

Barrier capacitance effect on transient characteristics of light diodes, obtaining time dependence of p-n junction volume charge voltage and recombination emission intensity

09 p1284 A72-22211

Alternative TEM and waveguide type equivalent circuits for rectangular resonator loaded by lumped capacitance

09 p1289 A72-23365

Capacitance depth gage for thin liquid films thickness measurement, noting application to interface waves amplitude and frequency measurements

09 p1316 A72-23410

Capacitance gap sensor with logarithmic output response and adjustment for minimum error

10 p1482 A72-24641

Bipolar insulated gate FET IC buffer driver, discussing input and output interface capacitance and impedance characteristics and application to transistor-transistor logic

11 p1603 A72-25269

Self balancing ac bridge with double conversion of unbalance-signal and low capacitance sensor for displacement measurement

11 p1634 A72-26459

Integral equation numerical solution applications to rectangular solid capacitance calculation and mixed boundary value problems

11 p1679 A72-26954

Fall time calculation and junction capacitance effect in diodes with nonuniform base doping switched off by voltage and current generators

11 p1607 A72-26963

K band Read avalanche diodes fabricated by epitaxial deposition and diffusion processes, measuring capacitance-voltage characteristics and oscillator power efficiency

12 p1790 A72-27441

Varactor broken voltage-capacitance curve due to uncompensated impurities concentration change at p-n junction

13 p1926 A72-28379

Energy distribution in plasma jet as function of capacitance and energy of storage elements and storage circuit inductance

13 p2015 A72-29452

Active RC circuit synthesis by state model method, minimizing capacitances of admittance matrix for microelectronic circuit technology

15 p2210 A72-31595

Rotor displacement measurement of electrostatic gyroscope by capacitive sensor using spherical electrode

15 p2236 A72-31899

Parametric resonance in an oscillatory circuit with a nonlinear p-n junction capacitance

17 p2533 A72-34757

Measurements of the plasma sheath capacitance using a simple tunnel diode oscillator.

17 p2558 A72-35847

The capacitances of anisotropic heterojunctions with continuously varying energy band gap and electron affinity in the transition region.

18 p2719 A72-36944

High-stability capacitance strain gauge for use at extreme temperatures.

18 p2693 A72-37210

Effect of a junction capacitance nonlinearity on the spectral characteristics of a tunnel diode current

20 p2906 A72-38897

Phenomena and interpretation of the transients caused by temperature change on capacitance of metal-oxide-metal systems.

21 p3097 A72-40690

Carrier transport and storage effects in Au ion implanted SiO₂ structures.

21 p3097 A72-40699

A theoretical investigation on the generation current in silicon p-n junctions under reverse bias.

21 p3097 A72-40703

Low capacitance high speed lead tin telluride photodiodes via liquid phase epitaxial growth, discussing frequency response to Nd-YAG and carbon dioxide lasers

22 p3159 A72-42620

Frequency dependent deep level trap admittance and field effect transcapacitance of p-n junctions calculated by truncated space charge approximation

22 p3161 A72-43086

Capacitance voltage characteristics instability of metal-aluminum oxide-silicon dioxide-silicon (MAOS) structures, suggesting polarization effect in layer formed during deposition and annealing

23 p3324 A72-44070

Effect of capacitance on gain in a transversely pulsed CO₂ discharge.

23 p3298 A72-44534

Standardization of resistance and capacitance elements nonlinearity measurement procedure, proposing constant amplitude supply voltage

24 p3386 A72-45392

CAPACITANCE SWITCHES

Ultrasonic flaw detector pulse transducers operation using electrodynamic and capacitance receivers

03 p0361 A72-13987

A fast, high repetition rate avalanche transistors pulser for capacitive loads.

20 p2907 A72-39435

CAPACITORS

Metal-alumina-oxide-semiconductor capacitor film band bias voltage measurement before and after thermal stressing, noting potential barrier in structure model

03 p0336 A72-14278

Active RC circuit with grounded capacitors capable of functioning as differentiator, bridge, inductance simulator, bandpass filter and oscillator

03 p0337 A72-14354

Lumped capacitors, inductors, resistors and gyrators for use at microwave frequencies, discussing design and applications up to X band

04 p0497 A72-14717

Dielectrophoresis force measurements and wedge shaped capacitor separation properties in satellite zero gravity conditions

04 p0549 A72-14988

Capacitor-fed parallel chopper as phase sensitive demodulator, discussing design, stability, linearity and wide dynamic frequency range

04 p0507 A72-15522

Thin film resistors and capacitors design, considering stability, power, size, film thickness, parasitic inductance capacitance and resistance and dielectric loss properties

06 p0790 A72-18573

Thin film conductors, distributed film resistors and capacitors design and associated IC layout to form functional arrays

06 p0790 A72-18574

Monolithic Si IC design and fabrication including resistors, capacitors, diodes, n-p-n, p-n-p, and field effect transistors and inductors

06 p0791 A72-18576

Rectangular capacitor overheating calculation with allowance for heat transfer from all surfaces, discussing chassis heat removing action computation during natural cooling

07 p0953 A72-18930

Ac and dc power regulation by switched capacitor, analyzing voltage spectrum for resistive load

07 p0958 A72-20389

Computer storage array of isolated electrodes imbedded between capacitor parallel plates, discussing read-write cycle time, expected performance and experimental techniques

10 p1443 A72-23933

Ion implantation for varicaps and p-n-p bipolar transistors fabrication, examining implanted impurities profiles

10 p1449 A72-24285

Condenser charging by dc-dc converter consisting of SCR series inverter, transformer and rectifier-filter circuit, considering power consumption

11 p1577 A72-25278

Ceramic dielectrics capacitors, considering perovskites and barium titanate physicochemical properties

11 p1702 A72-26545

Russian book on penetrating radiation effect on radio components covering resistors and capacitors electrophysical characteristics and parameters changes under gamma and neutron radiation

12 p1793 A72-28342

Reliability tests on miniature ceramic capacitors encapsulated by epoxy-novolac block polymer compounds

13 p1919 A72-29061

Destabilizing factors effect on parameters of transistorized single circuit phase modulator with varicap control

13 p1932 A72-29455

Electroexplosive devices firing energy parameters determination by capacitor discharge system providing exponential pulses terminated at adjustable width

14 p2143 A72-30200

Electrohydraulic and electromagnetic metal forming, using capacitor stored energy conversion into hydraulic shock waves or magnetic pressure to deform sheet metal components, pipes, etc

15 p2243 A72-31323

Weibull life tests of Kemet solid tantalum chip capacitors at high accelerated voltages.

17 p2527 A72-34685

Two fluid MHD model to study cylindrical plasma condenser resonance properties in crossed axial magnetic and alternating electric fields

17 p2593 A72-35881

Two fluid MHD model for flat plasma condenser in crossed magnetic and alternating electric fields, calculating impedance and disturbed plasma parameters

17 p2593 A72-35882

Current and capacitance transient responses of MOS capacitor. I - General theory and applications to initially depleted surface without surface states.

18 p2718 A72-36346

Amplitude limits to the theory of resonant absorption in cold plasmas.

18 p2716 A72-36960

Use of the third-harmonic method for the selection of metal-bonded polycarbonate capacitors which are stable in time

18 p2669 A72-37115

Acceptance testing of the MKL capacitor for space application

18 p2669 A72-37119

A large-signal theory for current-driven frequency multipliers.

19 p2775 A72-38609

Dynamic error of storing voltages at capacitors in the storage channel of an integrator of variable structure

21 p3024 A72-40165

On the determination of minority carrier lifetime and surface recombination velocity from the transient response of MOS capacitors.

23 p3324 A72-44071

CAPE KENNEDY LAUNCH COMPLEX

Kennedy Space Center area afternoon convective thunderstorm activity and associated weather phenomena prediction via multivariate regression analysis

13 p1989 A72-28803

CAPILLARIES

A capillary-fed annular colloid thruster.

17 p2598 A72-35491

Quantitation of serum proteins on whole blood-electroimmunodiffusion technique applicable to capillary blood.

22 p3150 A72-42495

CAPILLARIES [ANATOMY]

Wien intravascular effect on plasma carbon dioxide gradients near pulmonary capillary wall, discussing free energy requirements

08 p1114 A72-20890

Radial diffusion and convection capillary model for analysis of tissue protein concentration and colloidal osmotic pressure changes during transcappillary fluid movement

08 p1114 A72-20896

Continuous and intermittent maximal exercise effects on human muscle intracellular and capillary blood pH

10 p1425 A72-24477

Pulmonary capillary bed filling as function of arterial pressure in perfused frozen dog lungs

10 p1425 A72-24480

Vascular-capillary study of age related angiarchitectonic features of human brain optic lobe

11 p1580 A72-26675

Albino rats spinal cord capillaries ultrastructure upon hypothermy, noting endothelial cells sinking to lower levels from microscopic observation

12 p1760 A72-27304

Human brain stem vascular-capillary network density and dimensional characteristics

13 p1901 A72-28462

Cardiac hypertrophy, capillary and muscle fiber density, muscle fiber diameter, capillary radius and diffusion distance in the myocardium of growing rats adapted to a simulated altitude of 3500 m.

21 p3003 A72-41624

Blood flow, oxygen uptake, and capillary filtration in resting skeletal muscle.

22 p3150 A72-42668

CAPILLARY CIRCULATION

U CAPILLARY FLOW

CAPILLARY FLOW

Kinetic energy correction in capillary viscometry, observing pressure drops and mass flow rates

02 p0202 A72-11724

Oxygen distribution in human brain under counter-current capillary blood flow conditions, presenting mathematical simulation for transport in Krogh system

02 p0168 A72-12037

Heat pipe operating conditions and evaporator, condenser and adiabatic parts, discussing fluid capillary transport for heat pipe calculation

05 p0750 A72-17047

Viscoelastic effect on cylindrical liquid jets capillary breakup after ejection into inviscid atmosphere

05 p0654 A72-17246

Capillary forces effects on free surface liquid behavior in partial or total weightlessness, reviewing sloshing problem mathematical treatments

06 p0802 A72-18717

Viscosity measurement error estimates for Newtonian incompressible fluid flow through deformed capillary tube

07 p0991 A72-20535

Surface tension determination at immiscible liquids or liquid-gas phase interfaces by capillary rise measurement of droplet

09 p1294 A72-22678

Quasi-steady creeping flow in small airways of spherical, oblate and prolate ellipsoid and circular cylinder lung models, obtaining Stokes equations solutions

10 p1431 A72-24469

Temperature dependence of gas flow coefficients at low pressures, determining isothermal permeability and heats of transport of He, Ne and Ar capillary flow

10 p1469 A72-24600

Open capillaries control mechanism of pulmonary diffusion capacity, presenting mathematical interpretation of humoral and hydraulic blood pressure control

10 p1426 A72-24787

Burnett theory of thermal transpiration in capillary with wall accommodation for polyatomic gases, using Chapman-Enskog constitutive relations

11 p1746 A72-26010

Tilt table test for gravitational stress effects on human pulmonary capillary blood flow

12 p1765 A72-28286

Capillary heat convective diffusion model of liquid layer sandwiched between two planes for calculating slag and metal movement rates

16 p2476 A72-33157

Effects of diffusion impairment on O₂ and CO₂ courses in pulmonary capillaries.

17 p2506 A72-35967

Mathematical model for surface tension induced thermocapillary fluid flow influence on conductive heat transfer through condensate film broken by non-wetting strips

20 p2985 A72-39654

Brazing furnaces and heat treatment under vacuum

22 p3163 A72-42635

Capillary circulation as a regulator of sodium reabsorption and excretion.

23 p3257 A72-43995

CAPILLARY TUBES

Heat conduction in vacuum insulated capillaries to prevent failure of level indicators and controllers based on condensation in evaporating cryogenic liquid

03 p0456 A72-13883

Plasma discharge instability in air in polyethylene and organic glass capillaries with evaporating walls, using time lapse filming

05 p0693 A72-15840

Heat pipe evaporation zone length based on desiccation length calculations for various capillary cross sections and thermal loads

05 p0743 A72-15853

Creep characteristics of unidirectional plastics reinforced by hollow glass fibers with insignificant capillary effect

08 p1196 A72-21868

Capillary evaporation cooling system with water as working medium, measuring effectiveness in terms of heat flux density vs water consumption

10 p1561 A72-24023

Boundary layer analysis of wide capillary tube, deriving approximate error estimates

12 p1798 A72-27714

Variometer system for sailplanes sinking or climbing rates direct readout, describing pressure difference measuring concept based on reservoir-capillary system

21 p3051 A72-40225

Variometer system for sailplanes sinking or climbing rates direct readout, describing pressure difference measuring concept based on reservoir-capillary system

23 p3292 A72-44451

CAPILLARY WAVES

NT BAROCLINIC WAVES

NT GRAVITY WAVES

Nonlinear development of capillary waves in a fluid jet

18 p2682 A72-36885

Steady capillary-gravitational waves of finite amplitude generated by pressure periodically distributed along the flow surface of a fluid of finite depth.

21 p3044 A72-40261

CAPSULES

Water radiolysis within sealed Al capsules in nuclear reactor, calculating pressure rise due to water decomposition via predictive models derived by multiple regression analysis

04 p0546 A72-14429

CAPTIVE TESTS

NT STATIC TESTS

Wind tunnel model instrumentation and captive trajectory facilities for aircraft stability, control and metric wing-pylon store tests for performance and structural predictions

03 p0339 A72-12921

CAPTURE CROSS SECTIONS U ABSORPTION CROSS SECTIONS CAPTURE EFFECT

Jupiter outer satellite origin, considering capture orbit dimensions based on three body elliptical problem

02 p0275 A72-11594

Spatial distribution of gaseous nitrogen molecules scattered from metal surface, estimating beam capture coefficient

03 p0392 A72-14056

Solar model for capture rate in C13 neutrino experiment, comparing different stellar evolution programs

04 p0566 A72-14562

Neutron energy spectrum of radiative pion captured by carbon 12, using gamma and neutron counters

05 p0692 A72-16688

Single collision beam experiments, swarms, Townsend current and capture processes in negative ions

05 p0693 A72-17219

Statistical and probabilistic analyses of comet groups existence with similar orbital elements, considering gravitational capture by trans-Neptunian planets

07 p1075 A72-19559

Exothermic capture processes with ionization during nonelastic ion atom collisions, discussing cross sections of He ion collisions with Ar, Kr and Xe atoms

08 p1210 A72-20837

Multiphonon capture of charge carriers by deep impurity centers in homopolymers semiconductors from generalized Lucovsky model

08 p1216 A72-21094

Numerical analysis of capture area ratio effect on shock wave propagation from free stream into moving flowing duct

08 p1150 A72-21619

Gd and Sm isotopic composition measurement in Luna 16 soil with largest low energy neutron fluence

09 p1380 A72-22265

Mathematical model of ion capture and annihilation by aerosol particles from ground level to 60 km

09 p1346 A72-23266

Neutron capture effects on Gd isotopic composition and irradiation histories of lunar rocks from Apollo sites, using mass spectroscopic measurements

10 p1536 A72-24154

Neutron capture effect on isotopic composition variations of Sm in Apollo lunar samples, comparing with terrestrial abundance

10 p1537 A72-24156

MOS transistor current fluctuation relation to capture centers surface density, energy position and gate potential, determining spectral amplitude distribution

10 p1449 A72-24284

Capture range and acquisition time analysis of phase locked loop with active filter

10 p1458 A72-24934

Ion dipole capture cross sections at low ion and rotational energies compared with reaction cross sections for ammonia and water parent-ion collisions

11 p1692 A72-26014

Nonadiabatic and atmosphere induced energy losses as causes of proton capture in geomagnetic field

11 p1715 A72-26915

Three body problem study of satellite capture by planets in elliptical orbits, deriving orbital elements in terms of mass ratio and planetary orbit eccentricity

12 p1865 A72-27096

Capture within restricted three body problem for close single encounters between massless particles and binary system lesser component

12 p1872 A72-27758

N region capture centers effects on small signal impedance in p-n diode structure during passage of strong dc current

13 p1933 A72-29977

Earth capture of dust particles moving in ecliptic plane heliocentric orbits, using three gravitational bodies analysis

14 p2153 A72-30494

Capture resonance of asteroid 1685 Toro by earth due to gravitational interaction at close encounters

15 p2307 A72-31721

Capture zone in noninteracting particles rarefied flow around magnetic dipole with transfer into finite orbits under small perturbations

17 p2593 A72-35906

A possible mechanism for the capture of micrometeoritic particles by the earth and other planets of the solar system

17 p2619 A72-35939

Proton capture mean lifetimes in fast C-N cycle, presenting nitrogen/carbon abundance ratio variation with temperature

18 p2721 A72-36650

Yields of gamma rays emitted following capture of negative muons by Si28 and Mg24

19 p2837 A72-38026

Earth capture of dust particles moving in ecliptic plane heliocentric orbits, using three gravitational bodies analysis

19 p2864 A72-38323

Capture of a signal with a linearly varying frequency in an astatic phase autotuning system

19 p2766 A72-38420

External noise effect on capture conditions in ring laser, noting capture bandwidth narrowing with noise spectral density increase

24 p3410 A72-45423

Gamma-neutrino angular correlations in muon capture

24 p3427 A72-45774

CARBAMATES [TRADENAME] NT URETHANES

Electron impact induced fragmentation of alkyl-N-1-phenylethyl-carbamates of primary, secondary and tertiary alcohols, using deuterium labeling and high resolution mass spectrometry

07 p0936 A72-19500

CARBIDES

NT BORON CARBIDES

NT CEMENTITE

NT CHROMIUM CARBIDES

NT HAFNIUM CARBIDES

NT MOLYBDENUM CARBIDES

NT NIOBIUM CARBIDES

NT SILICON CARBIDES

NT TANTALUM CARBIDES

NT TITANIUM CARBIDES

NT TUNGSTEN CARBIDES

NT URANIUM CARBIDES

NT VANADIUM CARBIDES

NT ZIRCONIUM CARBIDES

High temperature carbide dispersion strengthened Nb alloys, using heat and thermomechanical treatments

01 p0085 A72-10863

Oxygen content and stoichiometry effects on metal carbides grain growth in liquid phase sintering, discussing carbide-metal interface solution reaction as rate controlling mechanism

02 p0240 A72-11434

Physical properties of transition metal nitrides, carbonitrides and nitride-based cemented hard alloys, discussing carbides stability in presence of high pressure nitrogen

02 p0241 A72-11450

Oxygen determination in cemented carbides, metal powders and presintered and finished sintered products by vacuum fusion method, comparing with neutron activation method

02 p0245 A72-12548

Mixed cubic carbide diffusion layer formation on carbon steel surface, using chemical transport reaction analysis

06 p0828 A72-17570

Rhenium carbide synthesis at high pressure and temperature, searching for superconducting properties

06 p0828 A72-17617

Co and carbide containing alloys, investigating milling and sintering temperature effects on technological and physical properties

06 p0829 A72-17831

Phase equilibria of Mo-Mn-C and W-Mn-C systems by X ray analysis, showing eutectoid decomposition involving rhombic modification

06 p0833 A72-18432

Surface and interfacial energies measurement by multiphase equilibrium method for refractory metal monocarbides with liquid cobalt

07 p1010 A72-19136

Carbide precipitation effect on strength of ausrolled hardenable hypoeutectoid and hypereutectoid stainless steels

07 p1016 A72-19943

Temperature and alloy composition effects on coarsening rate of metal carbide particles in dissimilar metallic matrix

07 p1021 A72-20436

Cast Nb alloys plasticity enhancement by heat treatment, discussing solid solution decay kinetics and carbides composition of Nb-Mo-Zr-C system

09 p1327 A72-22229

Intermetallics and carbide forming additions of Cr, Ti, Ce, V and Nb for hardening of cold worked Mn rich steel from crystal dislocations growth

09 p1327 A72-22230

Thermal shock resistant composite materials with carbide or oxide matrices based on concept of crack propagation prevention, noting superiority from thermal simulation tests

09 p1334 A72-22384

Phonon dispersion curves from inelastic neutron scattering for actinide and transition metals carbides, noting superconducting properties

09 p1369 A72-22564

Electron microscopic, area diffraction and spectral analyses of carbide precipitates in Cr-Mo steels with different heat treatments and microstructures

10 p1494 A72-23828

Phase transformations and recrystallization study of Ti-steel bimetal with emission microscope, observing

high temperature formation of titanium and vanadium carbides

11 p1654 A72-25493

Metallographic examination of stainless steel specimens exposed to long term creep rupture tests, noting carbides precipitation and stress induced grain boundary migration

11 p1658 A72-25832

Electronic configuration effect on wetting characteristics of hard material mixed crystals, investigating transition metals carbides, nitrides and oxides

11 p1665 A72-26873

Carbide precipitation effect on structure and high temperature strength of Co based alloys

11 p1667 A72-26932

Electron microscope study of commercial Ni superalloys, discussing intermetallic compound and carbide precipitation hardening

12 p1827 A72-27137

Two phase and three phase composition of ternary alloys Nb-C-Re at 2000 C from X ray, metallographic and chemical analysis

13 p1973 A72-28567

Two phase structure solidification of monovariant eutectic Co-Cr-C alloys near pseudobinary cut

13 p1976 A72-28674

Precipitated carbide role in Cr-Ni stainless steels high temperature properties and creep rupture strength

13 p1979 A72-29447

Diffusion kinetics and thermodynamic characteristics of solid phase interactions in systems cobalt-transition metal carbides

13 p1981 A72-30104

Conditions for obtaining high porosity materials of complex carbides by combined reduction-carbization of metal oxides with soot in vacuum

13 p1967 A72-30114

Iron carbide single crystal growth texture due to anisotropy of interatomic interactions associated with oriented covalent Fe-C bonds

14 p1212 A72-30774

Phase diagrams of Ni-C and Co-C systems with metastable equilibrium lines, investigating microstructure and microhardness of carbide eutectic

14 p1213 A72-30990

Interstitial phases, crystal structure and chemical bonds of titanium, vanadium and niobium carbides, comparing with transition metal carbides

15 p2252 A72-31195

Dynamic elastic moduli of diffusion saturated high melting point nitrides, carbides and borides of Ti, Zr, Nb, W, Mo and Ta

15 p2252 A72-31199

Vacuum vaporization of niobium, tantalum, zirconium and hafnium carbide phases, using Langmuir method

15 p2253 A72-31200

Chemical phase analysis for determining phase composition of products formed in borides, carbides and borocarbides mixtures

18 p2656 A72-36100

NASA research on refractory carbides, nitrides and borides, discussing electronic and defect structures, hot extrusion, uranium nitride, cermets for bearings and composite evaluation

18 p2701 A72-36594

Stainless steels high temperature creep rupture strength relationship to carbide precipitation morphology

21 p3069 A72-41013

Correlation between the work function of transition metal carbides and the surface recombination of hydrogen atoms in the region of homogeneity

21 p3070 A72-41372

Dependence of the properties of monocarbides of group IV-V transition metals on carbon content

22 p3189 A72-42198

Carbide phases in nickel-based heat-resistant alloys

22 p3192 A72-43018

Contact interaction between high-melting compounds and liquid metals. I - Interaction between subgroup IVA metals and metals of the iron family

23 p3299 A72-43287

Physicomaterial properties of titanium-tungsten solid alloys with deficiency of carbon in the carbide solid solution lattice

24 p3415 A72-45385

CARBOHYDRATE METABOLISM NT HYPERGLYCEMIA NT HYPOGLYCEMIA

Insulin injection or carbohydrate consumption effects on serotonin and tryptophan concentrations in rat brains

02 p0165 A72-12845

Carbohydrate metabolism, glycolytic ferment activities and leukocyte size under ionizing radiation, showing compensatory bone marrow cell formation with leukopenia

04 p0467 A72-14609

Coacervate drops oxidoreductases and stability in primitive prebiological systems, using polyphenol oxidase-carbohydrate-histone-quinones

04 p0469 A72-14784

- Daily prolonged exercises effects on human muscle glycogen utilization, noting reduced lactate accumulation and increased free fatty acid levels
04 p0480 A72-15213
- Hypertension and blood sugar and lipid level increase as ischemic heart disease risk factors
08 p1117 A72-21542
- Isolation of extremely halophilic carbohydrate-utilizing bacteria, using acid formation from various sugars as carbohydrate metabolism index
15 p2187 A72-32729
- Myocardial lipid and carbohydrate metabolism in fasting men during prolonged exercise.
17 p2499 A72-34347
- Substrate utilization and glycolysis in the heart.
17 p2501 A72-34977
- Effect of nicotinic acid on myocardial metabolism in man at rest and during exercise.
17 p2506 A72-35968
- Cortico-visceral studies of spinal cord reticular formation stimulation and destruction effects on electroencephalogram, cardiac activity and interoceptive glycemic reflexes
21 p3000 A72-40757
- Cardiocirculatory adaptation to chronic hypoxia. II. Comparative study of myocardial metabolism of glucose, lactate, pyruvate and free fatty acids between sea level and high altitude residents.
22 p3148 A72-43022
- Evidence for a metabolic limitation of survival in hypothermic hamsters.
23 p3258 A72-44364
- Localization and dynamic changes of glycogen in frog retina adapted to darkness or light, I, II.
23 p3258 A72-44377
- CARBOHYDRATES**
NT ADENINES
NT ADENOSINE DIPHOSPHATE [ADP]
NT ADENOSINE TRIPHOSPHATE [ATP]
NT ADENOSINES
NT CELLULOSE
NT GLUCOSE
NT GLYCOGENS
NT NUCLEOSIDES
NT STARCHES
NT SUCROSE
NT SUGARS
- Ion selective accumulation model of carbohydrates diffusing through artificial polymer membranes, relating prebiological systems to catalytic microsystems
04 p0469 A72-14788
- Carbohydrate based gelling agent for gas turbine fuel, describing development and chemical and physical properties
[ASME PAPER 72-GT-9] 11 p1702 A72-25612
- Synthetic carbohydrates toxicity effects on rat liver lysosomes application to astronaut potential food sources
14 p2074 A72-30381
- Human plasma free fatty acids relation to lactic acid concentration and maximum aerobic power, noting carbohydrate availability as exercise capacity limiter
21 p3003 A72-41520
- CARBON**
NT CARBON ISOTOPES
- Cometary head model for photometric profiles of carbon molecular emission in comet Burnham assuming icy grain halo
01 p0125 A72-10081
- Carbon atoms thermodynamic properties in bcc and fcc Fe-Si solid solutions from equilibrium measurements with hydrogen-methane gas mixtures as function of temperature and carburizing gas composition
01 p0083 A72-10207
- Simulation of nuclear light bulb engine propellant radiative heating, using argon seeded with micronized carbon particles and 500 kw dc arc as radiant energy source
01 p0099 A72-11344
- Soviet book on cool carbon stars covering spectral features, atmospheric composition and temperatures
02 p0281 A72-12296
- Carbon-oxygen reaction kinetic limitations on carbon ablation rate, discounting diffusional transport limits above 1650 K
03 p0457 A72-13955
- Ni-C solid solution, determining room temperature neutron irradiation effects on C distribution during decomposition
03 p0378 A72-14251
- Carbon chemistry of moon based on lunar samples analysis
04 p0573 A72-14807
- Early solar system nucleosynthesis of Al 26, discussing silicon and carbon burning and spallation
04 p0567 A72-14912
- Emission line of neutral carbon in solar spectrum at 1993.6 Å from balloon-borne spectrography
06 p0876 A72-17566
- Diffusive mobility of C in Mo single crystals and Mo-Re alloy, using autoradiography and electron microscopy
06 p0829 A72-17733
- Internal friction in annealed and deformed tungsten at room temperature to 950 C, examining carbon contents, dislocations and temperature effects on carbon Snoek peak
06 p0830 A72-18295
- Carbon effects on strength, ductility, brittle transition and plastic strains of tungsten at high temperatures
06 p0833 A72-18634
- Cast electron-beam remelted Mo, investigating carbon and zirconium carbide additions effects on cold shortness and low temperature plasticity
06 p0833 A72-18645
- Self diffusion coefficients of carbon and oxygen in dolomite
07 p0937 A72-20520
- Nonconducting samples preparation for scanning electron microscope, using carbon as coating material
07 p0992 A72-20578
- Carbon determination in Cr-Ni steels and Ni alloys by layerwise spectral analysis, using electrode gap with He
07 p0993 A72-20609
- Cast Nb-C alloys carbon solubilities of 1.4 and 0.25 percent at 2100 and 1200 C, showing molten microstructure and measuring procedures
07 p1023 A72-20669
- Thermal stress measurement and thermoelastic behavior of carbon-carbon-materials for reentry nose cones, describing gage mounting, temperature compensation and data recording
08 p1164 A72-20921
- Type R Corona Borealis variable stars luminosity variations attributed to formation of carbon layer from He nuclear transformation process at stellar core-envelope boundary
08 p1231 A72-21086
- Temperature distribution and zone melting in carbon thin films heated by electron beam, using Sn crystal indicators
08 p1253 A72-21446
- Origin of life as chemical evolution product, tracing juvenile carbon history through planetary and geological phases
08 p1162 A72-22004
- Carbon compound distribution on moon from Apollo 11 samples, comparing with earth data
08 p1120 A72-22013
- Routine method for ultrathin carbon support film production for electron microscopy, noting mechanical stability and strength
08 p1172 A72-22020
- VS type 2-W carbon resistor electrical aging operation, investigating optimal ambient temperature and duration
08 p1143 A72-22068
- C and Re effects on brittleness threshold temperature and plasticity of Mo-Re alloy
09 p1326 A72-22227
- Radiative transition probabilities and recombination coefficients of ion C IV
09 p1354 A72-22664
- Main sequence star evolution relation to pulsar formation, discussing stellar core density at carbon ignition with respect to critical density limit
09 p1394 A72-23698
- Carbon effects on internal friction of low temperature Fe-Ni alloy during martensitic transformation
10 p1495 A72-24083
- Vaporization characteristics of carbon heat shields under radiative heating, presenting estimates of vaporization heat from energy balance
[AIAA PAPER 72-296] 11 p1741 A72-25234
- Diffusive mobility of C in Mo single crystals and Mo-Re alloy, using autoradiography and electron microscopy
11 p1652 A72-25340
- Carbon-carbon composite ring structure tested for processing cycle, design properties and ablative performance in solid rocket nozzle environment
11 p1673 A72-25488
- Grain size and carbon content effects on recrystallized Mo wire ductility at room and low temperatures
11 p1657 A72-25758
- Carbon solubility in Nb at 1500-2150 C, determining saturation concentrations from electrical resistivity vs reaction time curves
11 p1662 A72-26740
- Carbon-graphite fracture mechanics dependence on graphite crystallite structure, discussing crystal size effects on strength
11 p1674 A72-26812
- Carbon and other inclusions effects on cast W strength at elevated temperatures from microscopic observation
11 p1666 A72-26877
- Carbon and oxygen distribution and content effects on Mo mechanical properties and embrittlement
11 p1666 A72-26878
- Electron microscope observed dislocation splitting in bent thin tantalum carbide sheet, analyzing results in terms of strain rate law and carbon diffusion model
11 p1669 A72-26948
- Graphitization kinetics of amorphous thin carbon films under light impulses, discussing crystallite sizes, optical and electrical properties and two-stage character
12 p1833 A72-27857
- Carbon-carbon composite material for high performance aircraft braking systems, noting weight savings and thermal characteristics improvements
12 p1835 A72-28093
- Pure biocarbons for skeletal fixation of limb prosthetic devices, noting load bearing applications dependence on brittle characteristics
12 p1773 A72-28095
- Thin surface film lamination in antifriction carbon-graphite materials under critical specific pressure, discussing crystalline phase in wear products
12 p1818 A72-28192
- Re single crystal LEED diffraction pattern, showing surface carbon structure
13 p2021 A72-28800
- Diatom carbon negative ion search in HD 201626 and solar spectra, noting rotational lines coincidence with absorption features
13 p2038 A72-29010
- Carbon origin in comets associated with propyne photodissociation by solar 1216 Å Lyman alpha radiation
13 p2050 A72-29995
- Tungsten and carbon combined solubility in solid niobium at 2000, 1700 and 1100 C
14 p2113 A72-30165
- Low carbon and nitrogen concentrations in chromium ferritic stainless steel obtained with gas rinsing at reduced pressure, noting weldability and corrosion resistance
14 p2119 A72-30606
- Carbon distribution effect on cast Mo and alloys structure studied by electron microscopy, microdiffraction and X ray analysis, noting annealing from eutectic temperature
15 p2255 A72-31575
- Carbon resistance thermometers time response and thermal diffusivity measurements in liquid helium temperature range
15 p2234 A72-31581
- Decarburization kinetics of Nb wires with dissolved carbon in high temperature oxygen flow, monitoring electrical resistivity and CO partial pressure
15 p2244 A72-32113
- Co-Cr-C system carbon activity and solubility at 950-1200 C, deriving equation for temperature dependence and solid solution-carbide precipitation zone boundaries
16 p2407 A72-33441
- C diffusion mobility and coefficients in W-Mo steels gamma and alpha phases, discussing ionization effect on activation energy increase
16 p2408 A72-33538
- Energy level population and emission spectrum of C IV ion in planetary nebula with radiative excitation
16 p2458 A72-33688
- Emission line polarization prediction for planetary nebula C IV ion emitted spectrum via theory for energy level population
16 p2458 A72-33689
- The distribution of carbon in lunar samples from Apollo 11, 12 and 14.
17 p2615 A72-35685
- Contact contamination - Formation of carbonaceous deposits on electrical contacts.
18 p2665 A72-36119
- Proton capture mean lifetimes in fast C-N cycle, presenting nitrogen/carbon abundance ratio variation with temperature
18 p2721 A72-36650
- Carbon and graphite sublimation in inert gas flow at 2800-3000 K, determining rate dependence on temperature under kinetic and diffusive conditions
18 p2704 A72-37186
- Burning of carbon particles in a supersonic chemically active gas flow
19 p2882 A72-38454
- Successive graphitization of amorphous carbon
19 p2823 A72-38676
- Alloying element effects on C free energy interaction coefficients in liquid Fe alloys at 1550 C by equilibrium distribution method
20 p2937 A72-39295
- Coupled multiconfigurational self-consistent-field method of atomic dipole polarizabilities. I - Theory and application to carbon.
21 p3087 A72-40776
- The reduction of chlorine on carbon in AlCl₃-KCl-NaCl melts.
21 p3013 A72-40843
- Photoelectrically observed diatomic carbon absorption lines in sunspot spectra for two energy bands
21 p3108 A72-41284
- Diatom carbon lines search in sunspot umbras spectrum from solar telescope observations
21 p3108 A72-41285
- Inelasticity of cosmic neutron interactions in carbon
21 p3102 A72-41840

Rapid determination of total carbon content in titanium carbide 22 p3176 A72-42200

Approximation of energy generation and nucleosynthesis during hydrostatic carbon burning in massive stars, noting neutrino-dominated evolution effects 22 p3228 A72-42562

A study of the rates of carbon-carbon dioxide reaction in the temperature range 839 to 1050 C. 22 p3153 A72-43037

Numerical models for He stars structural evolution, considering main sequence models of 1-8 solar masses and different carbon enrichments 23 p3334 A72-43258

Thin film deposition of carbon on polypropylene, noting morphological templates role in enhancement of polymer nucleation during recrystallization 23 p3305 A72-43269

Titanium carbonitrides alloying with Ni in nitrogen atmosphere, noting N concentration effect on cermets wear resistance 23 p3298 A72-43281

The carbon chemistry of the moon. 23 p3339 A72-44149

Characteristics of pion and nucleon interaction with carbon and aluminum nuclei over the energy range from 30 to 300 GeV 23 p3331 A72-44435

Structural and strength characteristics of carbon materials, considering composites preparation and applications 24 p3418 A72-45748

CARBON COMPOUNDS

NT ARAGONITE

NT BORON CARBIDES

NT CALCITE

NT CARBIDES

NT CARBONATES

NT CEMENTITE

NT CHROMIUM CARBIDES

NT DOLOMITE [MINERAL]

NT HAFNIUM CARBIDES

NT MOLYBDENUM CARBIDES

NT NIOBIUM CARBIDES

NT POLYCARBONATES

NT SILICON CARBIDES

NT TANTALUM CARBIDES

NT TITANIUM CARBIDES

NT TUNGSTEN CARBIDES

NT URANIUM CARBIDES

NT VANADIUM CARBIDES

NT ZIRCONIUM CARBIDES

Apollo 11 lunar samples carbon compound geochemical analysis, using sequential scheme with minimum handling of solids and extracts 05 p0714 A72-16131

IR emission of oxygen reaction with carbon oxysulfide, investigating molecular vibrational transitions 10 p1510 A72-24133

Carboids effects on pyrolytic coke structure and graphite product properties 13 p1984 A72-29072

Physical, mechanical and thermal characteristics of reimpregnated pyrolyzed carbon-carbon and graphite-graphite composites [ICAS PAPER 72-29] 21 p3073 A72-41154

CARBON DIOXIDE

Electric quadrupole to magnetic dipole f-values for CO fourth positive and nitrogen Lyman-Birge-Hopfield systems, using curve of growth method 01 p0103 A72-10092

Collision excited carbon dioxide molecule vibrational relaxation rate constant based on statistical model 01 p0104 A72-10493

High resolution atmospheric transmission measurement of wavelength dependence of absorption losses in carbon dioxide of solid state Er laser radiation 02 p0238 A72-12201

Relaxation and heating rate due to solar radiation absorption by 2.7 and 4.3 micron vibration-rotation bands of carbon dioxide 03 p0347 A72-13387

Nitrogen to carbon dioxide vibrational energy transfer time measurement in gas dynamic laser 04 p0531 A72-15352

Southern Martian polar cap seasonal change, describing variation at vernal equinox and dry ice hypothesis 04 p0581 A72-15621

Carbon dioxide-carbon monoxide vibrational energy transfer rate at 730-2325 K from measurements following heating in shock tube 04 p0553 A72-15641

Reduced collision integrals for components of Venus and Mars type carbon dioxide atmospheres at 1000-11,000 K, using intermolecular interaction potentials 05 p0712 A72-15851

Human reaction to inhalation of gas mixtures with 3-9 percent carbon dioxide, measuring respiration rates, minute breathing volume, heart rates, arterial pressures, etc 05 p0618 A72-16632

Pressure modulated carbon dioxide radiometer for remote temperature sounding in upper atmosphere 05 p0663 A72-16692

Mathematical model for radiative transfer properties of high albedo carbon dioxide and water cryodeposits on opaque substrate [AIAA PAPER 72-58] 05 p0749 A72-16929

Carbon dioxide frost identification on Martian polar caps by Fourier spectroscopy 06 p0881 A72-17900

Population inversion of carbon dioxide molecules in gas flow expanding from nozzle 06 p0852 A72-17904

Small distance range anisotropic intermolecular interaction potentials for carbon dioxide and nitrogen oxide from beams elastic scattering data 06 p0852 A72-17983

Martian atmospheric pressure determination from carbon dioxide bands spectroscopic measurements 06 p0884 A72-18032

Martian dust storm depth determination from carbon dioxide absorption and abundance observation on Mars by earth based spectroscopy 06 p0890 A72-18348

Metastable argon-carbon dioxide dissociation and electronic excitation of carbon monoxide or oxygen 07 p1037 A72-19496

Carbon dioxide IR absorption lines broadening at 298 and 207 K by evacuated high-resolution Czerny-Turner spectrograph, comparing with values based on fixed collision cross section 07 p1038 A72-19834

Cometary carbon dioxide molecules annihilation by recharging and dissociative charge exchange with solar protons 08 p1229 A72-20830

Martian height gradients from 1.6 micron carbon dioxide band intensity, using telescopes with prismatic quartz spectrometer 08 p1231 A72-21125

Diatom oxygen and carbon dioxide density profiles effects on photoionization rates in D region [AD-741091] 09 p1274 A72-22356

Carbon monoxide in carbon dioxide atmosphere, determining IR absorption lines broadening at reduced temperatures 09 p1351 A72-22612

Spectroscopic measurements of light emission from carbon dioxide positive ions and carbon monoxide in metastable He interaction with carbon dioxide 09 p1354 A72-22667

Carbon dioxide atmospheric models for Mars and Venus, discussing aeronomy, Mariner probes, gas dissociation by solar radiation, and electron density inconsistency 09 p1386 A72-22685

Pressure, temperature and nozzle size effects on molecular cluster formation in expanding supersonic jets of rare gases, nitrogen and carbon dioxide 09 p1294 A72-22853

Carbon dioxide absorption kinetics on monocrytalline Mo from Auger spectrometry and slow electrons diffraction 10 p1525 A72-24137

Carbon dioxide concentration effect on calibration of linearized hot-wire anemometer in operation at constant temperature 10 p1480 A72-24217

Laser source spectroscopic determination of pure and nitrogen perturbed carbon dioxide transition lines half-widths 10 p1491 A72-24227

Fast iodine ions charge exchange in dense carbon dioxide supersonic jet, determining electron capture cross sections by least squares method 10 p1516 A72-25036

Thermal radiation shielding of porous surface on heated plate by absorbing gas transpiration, suggesting carbon dioxide, metal vapors and particulate mixture [AIAA PAPER 72-277] 11 p1740 A72-25217

Fine structure and IR transmission functions of carbon dioxide absorption bands at high pressure and temperature, calculating transition lines strength and position 11 p1620 A72-25275

Martian atmospheric pressure determination from carbon dioxide bands spectroscopic measurements 11 p1719 A72-25968

Cameron bands phosphorescent yield of carbon monoxide from carbon dioxide photodissociation in helium buffer 11 p1590 A72-26013

Venus spectrum carbon dioxide absorption lines model with double cloud system and adiabatic atmosphere 11 p1721 A72-26120

Carbon monoxide quantum yield measurements of carbon dioxide photolysis by radiation at 1470 and 1500-1670 A 11 p1590 A72-26423

Overlap emissivity of atmospheric carbon dioxide and water vapor for computer simulated earth surface temperature calculations 11 p1628 A72-26986

Carbon dioxide and dust effect on Martian atmospheric temperatures from time dependent calculations 12 p1865 A72-27033

Sulfur dioxide and carbon dioxide interaction with clean silver surface at ultrahigh vacuum, using Auger electron spectroscopy and work function measurement 13 p1912 A72-28684

Venus atmosphere IR synthetic spectra of carbon dioxide band and water line formation for isotropic scattering, comparing with terrestrial clouds 13 p2040 A72-29410

Vibrational relaxation mechanism in supersonic flows of chemically reacting carbon dioxide-nitrogen mixture, using numerical integration 13 p1913 A72-29502

Carbon dioxide arc plasma emissivity in visible range at atmospheric pressure and 6500-9500 K, discussing diatomic carbon concentration 13 p2016 A72-29520

Carbon dioxide turbulent flow heat exchange in single phase near critical region under forced and free convection 13 p2066 A72-29900

Outgoing 15 micron carbon dioxide band radiation measurement optimization for atmospheric thermal sounding by satellite 14 p2099 A72-30243

Energy curves of negative carbon dioxide ion as function of bending angle 14 p2134 A72-30749

HCl and HF in carbon dioxide atmosphere, determining line intensities, halfwidths and shapes at room temperature 14 p2135 A72-30894

Radiative transfer in Mars and above-cloud Venus carbon dioxide atmospheres, studying diurnal variations in temperature profile 14 p2160 A72-30897

Air and carbon dioxide intensive injection effects on turbulent boundary layer of subsonic channel air flow 14 p2097 A72-31159

Reduced collision integrals for components of Venus and Mars type carbon dioxide atmospheres at 1000-11,000 K, using intermolecular interaction potentials 15 p2302 A72-31270

Simultaneous vibration-translation and vibration-vibration exchanges between colliding carbon dioxide and nitrous oxide excited molecules 15 p2280 A72-31686

Carbon dioxide abundance variations from Venus high resolution spectra, discussing HCl and hydrogen fluoride line formation 15 p2310 A72-31994

Angular distribution and intensity of light scattered by carbon dioxide near critical point, noting temperature dependence of isothermal compressibility and long range correlation length 16 p2422 A72-32945

Power spectrum of light scattered from surface waves thermally excited on carbon dioxide liquid-vapor interface near critical point 16 p2423 A72-32948

Lifetime and quenching of metastable CO produced by dissociative recombination of positive carbon dioxide ions in He afterglow 16 p2432 A72-33771

Dissociative excitation of vacuum ultraviolet emission features by electron impact on molecular gases. III - CO₂. 17 p2585 A72-34734

Water vapor, CO₂ and particulate effects on the atmospheric temperature profile. 17 p2549 A72-35636

Experimental study of conditions for heat transfer deterioration in a turbulent carbon dioxide flow under supercritical pressure 18 p2742 A72-37185

Development of a desiccant CO₂ adsorbent tailored for shuttle application. [ASME PAPER 72-ENAV-11] 20 p2896 A72-39166

Separation of central effects of CO₂ and nicotine on ventilation and blood pressure. 21 p3001 A72-40918

Temperature range estimation method for planetary atmospheric component generating spectral lines, applying to Venus observations at 7820 A carbon dioxide band 21 p3106 A72-41045

Detection of crystals in CO₂ jet plumes. 21 p3046 A72-41306

Questions in the theory of monomolecular decay of a one-component gas and the dissociation constant of CO₂ at high temperatures 21 p3088 A72-41657

Martian topography according to ground-based radar measurements and the CO₂ absorption observed from the earth and from the Mariner 6 and 7 spacecraft 21 p3114 A72-41766

Calculation of the radiation of two plane isothermal layers of carbon dioxide and/or water vapor 22 p3242 A72-41884

- Energy degradation calculation for electron interaction with carbon dioxide molecules, discussing relationship with Mariner UV data 22 p3171 A72-42421
- A study of the rates of carbon-carbon dioxide reaction in the temperature range 839 to 1050 C. 22 p3153 A72-43037
- Photoionization and photoabsorption cross sections of CO₂ at 584 Å. 23 p3317 A72-44519
- Flame structure and flame reaction kinetics. VII - Reactions of traces of heavy water, deuterium and carbon dioxide added to rich hydrogen+ nitrogen+ oxygen flames. 24 p3378 A72-44920
- High speed mixing of nitrogen vibrationally excited with carbon dioxide 24 p3464 A72-45065
- Regeneration of oxygen from carbon dioxide and water. 24 p3375 A72-45183
- Dissociative attachment in carbon dioxide. 24 p3427 A72-45303
- CARBON DIOXIDE CONCENTRATION**
- Ventilatory and metabolic responses of unanesthetized dogs exposed to various carbon dioxide concentrations at 2 and 18 C, discussing oxygen uptake relation to cold 02 p0159 A72-11954
- Acute hypercapnia neurotropic effect in rabbits, describing carbon dioxide inhalation period, preanoxic and narcotic stages and recovery phase 02 p0160 A72-12015
- Mars carbon dioxide distribution map determination of surface topography from spectrophotometric observations of equatorial region 04 p0569 A72-14499
- Magnetometer and spirometer ventilation measurements from chest and abdomen movements during carbon dioxide inhalation 05 p0619 A72-16790
- Carbon dioxide-air-helium molecular systems population excitation rates with current, gas composition and partial pressures dependence 08 p1183 A72-22028
- Hypoxic and normoxic gas mixture breathing during intense muscular activity, relating oxygen consumption and carbon dioxide elimination magnitudes and motor performance 08 p1121 A72-22081
- Human external respiration characteristics changes during increasing hypercapnia, relating carbon dioxide concentration rate to compensatory mechanisms and endurance 08 p1121 A72-22084
- Added elastic load tests for thoracic elastance change effects on human response to carbon dioxide inhalation, using rebreathing technique 12 p1762 A72-27726
- Exercise role in ventilatory acclimatization to graded hypoxia in goats from carbon dioxide response curve measurements 12 p1762 A72-27727
- Native highlander and lowlander chemoreflex ventilatory response to transient carbon dioxide inhalation at low and high altitudes 12 p1762 A72-27728
- Atmospheric thermal radiation flux calculation, showing carbon dioxide concentration effects on summer and winter models 12 p1805 A72-27991
- Regression analysis for steady state N₂ inequality in O₂ consumption calculations. 17 p2507 A72-34542
- Relaxation phenomena in the biological carbon cycle under conditions of variable atmospheric CO₂ content. 17 p2500 A72-34897
- Interaction of chronic hypoxia and hypercapnia upon blood gases and acid base status. 17 p2504 A72-35166
- The effect of changing CO₂ concentration on radiative heating rates - Further comments. 20 p2947 A72-38969
- Integrated water vapor electrolysis oxygen generator and hydrogen depolarized carbon dioxide concentrator development. 20 p2896 A72-39170 [ASME PAPER 72-ENAV-7]
- Atmospheric thermal IR radiation transmission function dependence on carbon dioxide concentration, calculating spectral and vertical distributions for standard, summer and winter model atmospheres 22 p3174 A72-43005
- CARBON DIOXIDE LASERS**
- Carbon dioxide laser electrical plasma properties from probe and techniques, discussing effects of electron energy distributions, dissociation and N, He and Xe additions 01 p0079 A72-10514
- Molecular Stark effect modulation of IR carbon dioxide laser radiation, using density matrix technique 01 p0079 A72-10515
- Pin electrode transversely excited atmospheric pressure carbon dioxide laser construction and pulse power outputs up to 60 kW [AD-738684] 01 p0079 A72-10516
- Carbon dioxide laser IR heterodyne radiometer for remote sensing of atmospheric pollution [AIAA PAPER 71-1083] 01 p0067 A72-10540
- Single mode carbon dioxide laser action from quasi-optical mirror emission channels 01 p0080 A72-10578
- Nuclear pumped laser, noting electrically excited carbon dioxide laser experiment and high temperature multiple ionized plasma concepts 01 p0082 A72-11329
- Nuclear radiation enhancement of carbon dioxide laser performance, discussing low pressure CW and high pressure pulsed discharges 01 p0082 A72-11330
- Carbon dioxide laser pumping with nuclear reactions, indicating improved laser performance due to additional ionization by energetic charged particles 01 p0082 A72-11331
- Laser sources for space research, considering He-Ne, carbon dioxide, Nd-YAG and argon lasers performance 02 p0237 A72-11695
- Calorimeter for measuring energy pulses and wavelengths from frequency doubled neodymium to carbon dioxide lasers 02 p0224 A72-11748
- Soviet book on gas lasers covering operation, population inversion, helium-neon, argon and carbon dioxide lasers and atomic frequency standards 02 p0238 A72-12121
- Intracavity radiation induced air breakdown in TEA carbon dioxide laser for application in plasma heating 02 p0238 A72-12205
- Rabbit and monkey corneal damage following CW carbon dioxide laser irradiation, discussing hazard level derivation [FPRC/1314] 02 p0163 A72-12413
- Carbon dioxide IR laser construction, laboratory implementation and experimental results 02 p0239 A72-12693
- Cross-excited carbon-dioxide-nitrogen laser with pulse sharpening effect due to self-Q-switching, finding optimal nitrogen mixing ratio for peak power 02 p0239 A72-12827
- Saturation effect on power gain-bandwidth product of carbon dioxide regenerative ring laser amplifiers operating below threshold 03 p0366 A72-12964
- Sequential dielectric breakdown of air by focused radiation from mode locked pulsed carbon dioxide TEA laser 03 p0366 A72-12966
- Excited IR fluorescence in gas compounds with negligible absorption, using CW carbon dioxide laser 03 p0367 A72-13554
- Alkali halide crystals optical dc dielectric strength determination, using carbon dioxide laser induced breakdown threshold data [AD-737913] 03 p0368 A72-13607
- Small signal gain and radiant power of carbon dioxide gas dynamic laser, presenting temperature distribution and population inversion 03 p0368 A72-13920
- Uniform discharges in flowing carbon dioxide laser mixtures at atmospheric pressure, observing fluorescence intensity variation with discharge power density 03 p0369 A72-14400
- Tactical optical ground communication systems, discussing use of GaAs and carbon dioxide lasers and ultrawideband data links 04 p0485 A72-14482
- Electron energy distribution in carbon dioxide laser mixtures under lasing and nonlasing conditions 04 p0528 A72-14540
- Carbon dioxide laser modulation by molecular Stark effect in deuterated ammonia, observing pressure broadening coefficient 04 p0528 A72-14585
- Atmospheric pressure pulsed carbon dioxide laser using preionization by injected high energy electrons from surrounding glow discharge, obtaining highest output from gas mixture [AD-746376] 04 p0529 A72-14586
- Mode-locked transversely excited atmospheric pressure carbon dioxide laser pulse duration dependence on cavity modulation frequency and loss 04 p0529 A72-14588
- Self mode locked dual polarization carbon dioxide laser, obtaining simultaneous active stabilization and frequency modulation 04 p0529 A72-14604
- Relaxation processes in Michelson interferometer as integral part of carbon dioxide laser cavity in phase Q switching regime 04 p0530 A72-14990
- Carbon dioxide gas dynamic laser mixture at high pressure, investigating gain and vibrational kinetics 04 p0531 A72-15336
- He plasma generation by transversely excited carbon dioxide laser, determining density and temperature profiles of luminous fireball 04 p0558 A72-15345
- Visual display IR spectrometer for pulsed transversely excited carbon dioxide laser, tabulating observed wavelengths [AD-740011] 04 p0524 A72-15540
- Tunable coherent IR signal generation and propagation by mixing carbon dioxide laser and millimeter wave klystron output in GaAs loaded waveguide 04 p0532 A72-15614
- Output coupling apertures effect on carbon dioxide laser spatial coherence, considering resonator mode structure 05 p0667 A72-16001
- Ultrasonic diffraction grating for noninterference sampling of high power carbon dioxide laser beam, discussing diffraction profiles obtained from lasers operating in Gaussian and donut modes 05 p0669 A72-16608
- Carbon dioxide laser Q switching by molecular gases intracavity Stark modulation with sine or square wave electric field, using methyl chloride and difluoroethane 05 p0669 A72-16609
- HF and/or HF-carbon dioxide transfer laser potential power output and design criteria, considering deuterium and fluorine combustion, reaction product expansion and mixing rate [AIAA PAPER 72-147] 05 p0670 A72-16970
- Carbon dioxide laser single mode operation dynamics measured by scanning Fabry-Perot interferometer and conventional reference oscillator [AD-739101] 05 p0670 A72-17191
- Quasi-stationary carbon dioxide laser with pulse excitation, noting high population inversion values 06 p0826 A72-17916
- Carbon dioxide laser pumping at atmospheric pressure by electron beam controlled electrical discharge, discussing measured electrical and laser properties 07 p0999 A72-18875
- Carbon dioxide laser IR radiation modulation by application of Stark effect in various molecular absorbers, showing absence of saturation 07 p1000 A72-19035
- Gas kinetic cooling by absorption of carbon dioxide laser radiation, explaining by vibrational energy transfer and relaxation rates 07 p1000 A72-19046
- Gases for carbon dioxide laser lines modulation by molecular Stark effect, presenting data for fluoromethane, monomethylamine, methyl mercaptan, vapors methanol and trichloroethylene 07 p1001 A72-19193
- Kinetic model for gas dynamic laser energy extraction from carbon dioxide-nitrogen-helium mixture, predicting gain, saturation and pulse length 07 p1001 A72-19195
- High voltage axially pulsed carbon dioxide laser performance test, determining output energy dependence on tube parameters 07 p1001 A72-19197
- FM-CW radar range measurement by carbon dioxide laser, considering laser output nonlinear variation due to frequency pulling/pushing and refractivity changes 07 p0940 A72-19205
- High power carbon dioxide laser beam applications to deep penetration metal welding, including cutting tests 07 p0994 A72-19214
- Single mode high power pulsed nitrogen/carbon dioxide laser with unstable resonator coupling and diffraction limited focusing 07 p1002 A72-19215
- High power nitrogen-carbon dioxide cross beam electric discharge convection laser amplifier with rectangular channel 07 p1003 A72-19216
- Atmospheric pressure carbon dioxide-nitrogen-helium lasers with high output energy densities, using auxiliary discharge for volumetric excitation 07 p1003 A72-19217
- Pulsed combustion heated gas dynamic carbon dioxide laser, comparing with continuous version 07 p1003 A72-19219
- Transversely excited atmospheric /TEA/ carbon dioxide laser in single pulse and high repetition rate operation 07 p1003 A72-19220
- Performance characteristics of electro-optical material cadmium telluride for intracavity modulator of carbon dioxide lasers 07 p1003 A72-19223
- Wideband laser communication for space applications, comparing carbon dioxide and Nd-YAG systems on basis of SNR 07 p0941 A72-19239
- Atmospheric heating and kinetic cooling nonlinear effects on IR carbon dioxide laser beam propagation, comparing digital simulation results with geometrical optics [CLEA PAPER 2.6] 07 p0942 A72-19381

- Carbon dioxide lasers and GaAs electro-optical crystals 110iMHz bandwidth with coupling modulation technique 07 p1005 A72-19413
- Pulsed IR carbon dioxide TEA laser for two dimensional interferometry of theta pinch plasma during discharge 07 p1005 A72-19416
- Plastics cutting and drilling with carbon dioxide IR laser beam, discussing economics and commercially available equipment 07 p0999 A72-20554
- Transient plasma diagnostics using carbon dioxide laser interferometry and absorption for electron density and temperature determination 07 p1008 A72-20557
- Na deactivation effect on carbon dioxide-nitrogen gas dynamic laser gain 07 p1008 A72-20564
- Plasma diagnostics using carbon dioxide laser absorption and interferometry, comparing electron densities with shock data 07 p1008 A72-20565
- Gain saturation measurements in carbon dioxide TEA pulsed amplifiers at 330 torr 07 p1009 A72-20569
- Noble and molecular gases addition in reactions induced in ethylene by carbon dioxide-nitrogen-helium laser 07 p1009 A72-20693
- Pulsed carbon dioxide laser welding of miniature explosive detonators 08 p1221 A72-20778
- Nonlinear vibrational relaxation equations for expanding carbon dioxide-helium-nitrogen laser gas mixture, obtaining mode temperatures and gain coefficients by Runge-Kutta technique 08 p1149 A72-21261
- Amplitude-phase distortions of optical beam during nonlinear amplification in carbon dioxide laser with periodic correction 08 p1182 A72-21264
- Reciprocity theorem for antenna directivity pattern measurement of optical superheterodyne receiver for carbon dioxide laser radiation 08 p1140 A72-21376
- TEA atmospheric pressure carbon dioxide laser driven by 200 kV Marx generator pulse 08 p1183 A72-21800
- Self mode locking operation of transversely excited atmospheric pressure carbon dioxide pulsed laser with helical pumping 08 p1184 A72-22075
- Carbon dioxide laser radiation interaction with solids, applying to fused quartz drilling 09 p1323 A72-22904
- Pulsed carbon dioxide laser operation, measuring pulse energy variation with gas pressure, expansion nozzle shape and output mirror transmission 09 p1323 A72-22980
- Pulsed carbon dioxide laser heating of theta pinch plasma by inverse bremsstrahlung and induced Compton processes 09 p1364 A72-23233
- Plasma production from hydrogen solid targets by pulsed carbon dioxide TEA laser, noting diagnostic methods 09 p1325 A72-23237
- Pulsed carbon dioxide laser output monitor with Ge cylinder using photon drag effect to measure radiation pulse profile 09 p1326 A72-23389
- CW carbon dioxide laser Doppler radar for remote measurement of atmospheric wind velocity and turbulence, obtaining Doppler signal via homodyned radiation scattered by airborne particles 09 p1315 A72-23407
- Magnetic field effect on threshold pressure reduction for He and Ar gas breakdown by carbon dioxide laser radiation, taking into account inhibition of radial electron diffusion [AD-741539] 09 p1365 A72-23493
- Excitation and relaxation of upper laser state in carbon dioxide discharge from Q spoiled pulse-produced fluorescence measurements 09 p1326 A72-23577
- Oxygen jet-carbon dioxide laser beam cutting in mild and stainless steels, noting speed and material thickness limitations 09 p1321 A72-23639
- Electric discharge carbon dioxide laser performance in terms of optical beam quality, electrical efficiency and gas utilization 10 p1489 A72-23943
- Materials processing with carbon dioxide lasers, noting cutting, welding and hole drilling applications 10 p1485 A72-23969
- Mass spectrometric analysis of positive ions in carbon dioxide laser systems with nitrogen-helium mixture 10 p1492 A72-24411
- Modular carbon dioxide laser design and operational features, reporting measured data on plasma tube current, pressure and gas mixture flow rate effects on power output 10 p1492 A72-24565
- IR carbon dioxide laser amplifier with fundamental mode output power in excess of 500 W, describing multistage mirror section design and test results 10 p1492 A72-24581
- Carbon dioxide laser output power enhancement methods, discussing gas transport, atmospheric pressure and gas dynamic lasers 10 p1492 A72-24849
- Low voltage transversely excited gas transport CW carbon dioxide laser, discussing construction and power output, gain and efficiency 11 p1646 A72-25304
- Carbon dioxide-helium-nitrogen laser with nonlinearly absorbing cell, presenting emission pulse duration and rate 11 p1646 A72-25712
- Radial small-signal gain profile measurement in carbon dioxide laser discharge tube explained by axial gas temperature increase with discharge current 11 p1647 A72-26145
- Carbon dioxide laser cross relaxation effects on hole burning process in Doppler broadened gain or absorption line 11 p1647 A72-26146
- Electrically excited carbon dioxide-nitrogen laser using high repetition rate discharge pulses from pin electrode array transverse to supersonic flow 11 p1647 A72-26147
- Ternary chalcopyrite semiconductors refractivity measurement over range of wavelengths and optical nonlinear coefficient for second harmonic generation from carbon dioxide laser 11 p1701 A72-26148
- Transversely excited pulsed carbon dioxide laser, measuring spatial resolution of gain 11 p1647 A72-26323
- Molecular energy levels population inversions calculated from vibrational temperatures in carbon dioxide laser discharge plasma 11 p1649 A72-26339
- Passive Q factor modulation in carbon dioxide laser by resonance absorption saturation in osmium tetroxide vapors, noting vapor pressure effects 11 p1650 A72-26355
- Discharge current effect on refractive index in carbon dioxide laser 11 p1650 A72-26361
- Alpha particles effect on carbon dioxide laser output power and emission spectra, using uranium acetate as radioactive source 11 p1651 A72-26552
- Nonlinear thermal effects of atmospheric absorption for high power carbon dioxide laser beams 11 p1651 A72-26747
- High pressure electroionization carbon dioxide and nitrogen filled carbon dioxide lasers 11 p1652 A72-26793
- Thin Se film for recording mode structure of 10.6 micron carbon dioxide laser emission, describing optical equipment 11 p1652 A72-26795
- Double discharge transversely excited atmospheric pressure /TEA/ carbon dioxide laser construction, operation and output energy 12 p1819 A72-27266
- Kinetics and cavity intensity models for output characteristics of pulsed electric discharge carbon dioxide lasers 12 p1820 A72-27287
- Time delayed amplification effects in TEA carbon dioxide lasers, measuring gain decay times for various gas mixtures 12 p1823 A72-27753
- Theta pinch plasma heating by carbon dioxide laser transverse pulses, substantiating theoretical considerations by experimental observations 12 p1852 A72-27880
- Pressure effects on resonance fluorescence lifetimes in sulfur hexafluoride-air mixtures exposed to carbon dioxide laser radiation 12 p1826 A72-27929
- TEA pulsed carbon dioxide laser with continuous shaped electrodes, investigating hydrogen addition effects on power output and gain 12 p1827 A72-28224
- Spatially resolved gain measurements in carbon dioxide laser amplifier, considering gas mixture, flow rate, temperature, pressure and current effects 13 p1967 A72-28448
- Fabry-Perot interferometer for line structure of helical TEA-carbon dioxide laser, noting variable frequency single mode emission 13 p1968 A72-28687
- Q switched carbon dioxide laser based on PM by rotating mirror in one arm of Michelson interferometer, establishing phase relationships 13 p1968 A72-29287
- Deep penetration welding and cutting with high power CW carbon dioxide lasers, describing experimental setup 13 p1965 A72-29422
- Carbon dioxide laser vibrational-rotational band small signal gain factor dependence on time clapping after breakdown of equilibrium distribution 13 p2008 A72-29503
- Stable single frequency operation of molecular laser using carbon dioxide-helium mixture, ensuring vibrational-rotational transition by special selection of active element parameters 13 p1970 A72-29682
- Carbon dioxide laser light scattering measurements of turbulence in high beta collisionless plasma shock wave 13 p2018 A72-29853
- Carbon dioxide power laser effects on IR spectra of HCl-ethylene and sulfur dioxide-ethylene mixtures, focusing with Ge lens 13 p1971 A72-29870
- TEA carbon dioxide laser time dependent gain and cavity losses analysis, using lasing onset delay with current pulse 14 p2109 A72-30184
- Inversion population distribution during nonexcited carbon dioxide and excited nitrogen molecules plane jets interaction in diffusion carbon dioxide laser 14 p2109 A72-30314
- Proton beam effect on carbon dioxide laser discharge I-V characteristics and emission power 14 p2109 A72-30352
- Plasma emission spectrum of circulating and sealed carbon dioxide molecular laser, discussing concentration dependencies 14 p2110 A72-30786
- High power carbon dioxide laser construction, specifications and operation for applications to laboratory and industrial processing of glass, ceramics and metals 14 p2111 A72-30857
- Difference-frequency mixing of pulsed carbon dioxide lasers with non-phase-matched GaAs for submillimeter wave generation 15 p2290 A72-31384
- Hollow dielectric waveguide used for carbon dioxide laser gas discharge, noting increased gain, volumetric output and saturation parameters 15 p2245 A72-31386
- Rotatory gas temperature determination in carbon dioxide laser discharge plasma, plotting dependence on discharge current 15 p2245 A72-31419
- Carbon dioxide TEA high output pulsed laser, testing wide range of carbon dioxide-nitrogen-helium mixtures at various pressures 15 p2246 A72-31638
- Computer simulation for performance of carbon dioxide laser heterodyne communication system with photoconductive n-type mercury-cadmium telluride detector/mixer 15 p2198 A72-32062
- Transversely excited pulsed carbon dioxide-nitrogen-helium laser with electrical discharge determined optimum partial pressure 15 p2249 A72-32236
- High temperature lattice and radiative thermal conductivity measurements utilizing carbon dioxide laser and IR detector for diffusivity and mean extinction coefficient phase data 15 p2250 A72-32507
- Numerical results of carbon dioxide-nitrogen-water gas dynamic laser comparison with arc-driven supersonic laser in gas dynamic mode 15 p2250 A72-32517
- Transversely excited pulsed carbon dioxide laser with and without hydrogen addition, observing gain spatial and temporal dependence 15 p2251 A72-32529
- Dense helium theta pinch plasma heating by TEA carbon dioxide laser, studying temperature and density with high speed photography and spectrography 15 p2251 A72-32530
- Sealed room temperature gas laser output oscillating on 5-micron carbon monoxide or 10-micron carbon dioxide lines 15 p2251 A72-32533
- Transverse electric discharge pulsed carbon dioxide laser, measuring refractivity time history by interferometry for comparison with prediction 15 p2251 A72-32537
- High power carbon dioxide lasers review covering CW, Q switched and pulsed atmospheric pressure lasers and various excitation techniques 16 p2399 A72-32848
- Pulsed discharge development mechanism relationship to carbon dioxide laser lasing process, considering positive space charge ion role 16 p2401 A72-33369
- Holograms on bismuth and paraffin thin films with pulsed high power TEA carbon dioxide IR laser, discussing photosensitivity and capability for interferometric measurement 16 p2392 A72-33390
- Intense emission from high pressure pulsed carbon dioxide chemical transfer laser by flash photolysis initiated deuterium-fluorine exothermic chain reactions 16 p2401 A72-33392

Carbon dioxide waveguide gas laser performance characteristics, noting mode pattern stability and insensitivity to resonator disturbances 16 p2402 A72-33396

Single frequency and mode carbon dioxide laser frequency and power stabilization by phase control with electronic servosystem 16 p2402 A72-33621

Passive Q factor modulation in carbon dioxide laser by resonance absorption saturation in osmium tetroxide vapors, noting vapor pressure effects 16 p2402 A72-33708

Refractive index in carbon dioxide laser effect on discharge current 16 p2403 A72-33714

Transversely excited high pressure carbon dioxide laser cavity dumping with reproducible time delay between current excitation and gain-switched laser pulses 16 p2403 A72-33844

Theta pinch plasma heating by carbon dioxide laser transverse pulses, substantiating theoretical considerations by experimental observations 16 p2439 A72-33989

Discharge stabilization in closed cycle carbon dioxide electric discharge convection lasers by aerodynamic, RF power and tandem techniques [AIAA PAPER 72-723] 16 p2404 A72-34026

Study of transient phenomena by a TEA CO2 laser associated with a liquid-crystal detector 17 p2562 A72-34285

Flow conditioning in electric discharge convection lasers. 17 p2562 A72-34638

Competition effects on spatial coherence in a CO2 laser. 17 p2562 A72-34725

Possible mechanism for CO2-discharge current variation under the influence of laser radiation 17 p2562 A72-34840

IR carbon dioxide laser radar with heterodyne detection, measuring SNR and atmospheric scattering coefficients for various weather conditions 17 p2516 A72-35192

Hybrid injection locking of higher power CO2 lasers. 17 p2564 A72-35343

Passive Q switching extension of carbon dioxide laser output frequency range using dichloro-difluoro methane as saturable absorber 17 p2564 A72-35347

Carbon dioxide laser light scattering from cyclotron harmonic waves in steady state rarefied collisionless plasma, noting associated electron density fluctuations 17 p2591 A72-35378

Monochromatic carbon dioxide TEA laser 17 p2564 A72-35424

Electrothermal cutting processes using a CO2 laser. [IEEE PAPER TOD-71-118] 17 p2560 A72-35644

Excitation of a long-pulse CO2 laser with a short-pulse longitudinal electron beam. 17 p2565 A72-35815

Atmospheric pressure carbon dioxide pulsed IR laser to obtain 80 w peak power by optical pumping with TEA HBr laser and filter 17 p2565 A72-35816

RF augmentation in CO2 closed-cycle dc electric-discharge convection lasers. 17 p2565 A72-35818

Continuous arc generation in Ar via focused CW carbon dioxide TEA laser, inducing gas breakdown by focal volume preionization with single pulse 18 p2697 A72-36082

Experimental analysis of the vibrational-rotational line content of a Q-switched CO2 laser. 18 p2697 A72-36501

Vibrational relaxation of the bending mode of shock-heated CO2 by laser-absorption measurements. 18 p2697 A72-36562

Simple inexpensive laboratory-quality Rogowski TEA laser. 19 p2810 A72-37514

Momentum transfer and plasma formation above a surface with a high-power CO2 laser. 19 p2811 A72-37864

CW gasdynamic thermally excited and selectively pumped CO2-N2 mixing laser. 19 p2811 A72-38097

Doppler Q switching in a single-mode CO2 laser by a rotating mirror. 19 p2812 A72-38594

Influence of plasma kinetic processes on electrically excited CO2 laser performance. 19 p2812 A72-38598

Calculations of gain and power output for a gasdynamic laser. 19 p2813 A72-38693

Radio-frequency preionization in a supersonic transverse electrical discharge laser. 19 p2813 A72-38694

A simple self-mode-locked atmospheric pressure CO2 laser. 19 p2813 A72-38695

Experimental achievement of optical pumping of a carbon dioxide molecular laser 19 p2814 A72-38790

Air cooled CW 30 W carbon dioxide laser construction for technological applications, using radiation energy extraction through GeAs or GaAs plate 20 p2932 A72-39507

Gas breakdown in the laser as the limitation of pulsed high-pressure CO2 lasers. 20 p2934 A72-39565

Interferometric study of a TEA-CO2 laser produced plasma. 20 p2958 A72-39816

Laser output power increase with plasma dynamic carbon dioxide laser configuration, noting steady population inversion in pure hydrogen atoms 20 p2934 A72-39932

Mode locked carbon dioxide with transverse pulse pumping, using Ge ultrasonic diffraction cell as active loss modulator 20 p2934 A72-39965

Single longitudinal mode operation of a transversely excited CO2 laser. 21 p3062 A72-40243

A new method of exciting uniform discharges for high pressure lasers. 21 p3062 A72-40568

Transverse CO2 laser action at several atmospheres. 21 p3062 A72-40572

Carbon dioxide laser excitation by injection of plasma jets produced by capillary plasmatrons 21 p3063 A72-40835

Q-switched CO2 lasers with variable pulse delay. 21 p3064 A72-41006

Single transverse mode operation of a pulsed volume excited atmospheric pressure CO2 laser using an unstable resonator. 21 p3064 A72-41197

Nonlinear molecular absorption cell for frequency stabilization of carbon dioxide laser radiation, discussing stability limit dependence on amplification, absorptivity and Q value 22 p3184 A72-42102

Pulse energy and temporal/spatial distribution of carbon dioxide laser pumped by energy transfer from vibrationally excited DF produced by deuterium-fluorine chain reaction 22 p3185 A72-42617

Pulsed atmospheric-pressure carbon-dioxide laser initiated by a cold-cathode glow-discharge electron gun. 22 p3186 A72-42753

Inversion population distribution during nonexcited carbon dioxide and excited nitrogen molecules plane jets interaction in diffusion carbon dioxide laser 23 p3294 A72-43217

Steady-state lasing spectrum of a CO2 laser at reduced working-mixture pressures 23 p3295 A72-43681

Gain measurements of matrix-type TEA CO2 laser. 23 p3296 A72-44072

Effect of capacitance on gain in a transversely pulsed CO2 discharge. 23 p3298 A72-44534

Laser-source spectroscopy. II - Experimental study of line broadening for the 00-1/10-0, 02-0/ transition of CO2 disturbed by N2: Application of the theory of Anderson, Tsao, and Curmutte to the calculation of pure and N2-disturbed CO2 linewidths 23 p3298 A72-44535

Focusing characteristics of CO2 laser beam. 24 p3409 A72-44776

Pulsed carbon dioxide laser medium composition, pressure and electrical parameters effects on output power, energy and efficiency from mathematical model solution of kinetic equations 24 p3409 A72-44966

Pulsating conditions in the evaporation of optical materials under the influence of CO2 laser radiation. 24 p3411 A72-45610

Effect of plasma mirror in the breakdown of air in a CO2 laser cavity. 24 p3412 A72-45775

CARBON DIOXIDE REMOVAL

Electrochemical carbon dioxide concentrator materials compatibility to space shuttle life support environment, comparing with LiOH method 01 p0018 A72-10768

Extravehicular life support systems for shuttle, space station, lunar base and Mars missions, considering thermal control, carbon dioxide control and oxygen supply subsystems [AIAA PAPER 72-231] 10 p1430 A72-24441

Alkaline fuel cell development and trends, noting carbon dioxide removal technique and applications ranging from portable batteries to automobile power 16 p2351 A72-33887

Bioengineering models of energy and mass exchange of algae under varying ambient conditions, noting mass cultivation possibility for oxygen regeneration in closed environments 20 p2893 A72-38959

Bosch CO2 reduction unit research and development. [ASME PAPER 72-ENAV-10] 20 p2896 A72-39167

Bosch carbon dioxide reduction process for manned spacecraft oxygen recovery, analyzing carbon and water forming reactions with iron as catalyst [ASME PAPER 72-ENAV-9] 20 p2896 A72-39168

Skylab regenerable carbon dioxide removal system. [ASME PAPER 72-ENAV-4] 20 p2896 A72-39173

Determination of oxygen consumption by use of the paramagnetic oxygen analyzer. 21 p3006 A72-40429

CARBON DIOXIDE TENSION

NT HYPERCAPNIA

NT HYPOCAPNIA

Breathing control during speech, noting carbon dioxide response, hyperventilation and apnea 04 p0480 A72-15218

Rebreathing technique to estimate human mixed venous oxygen and carbon dioxide tension changes at start of exercise under respiratory stress and natural conditions 08 p1122 A72-20883

Wien intravascular effect on plasma carbon dioxide gradients near pulmonary capillary wall, discussing free energy requirements 08 p1114 A72-20890

Direct single electrode measurement of carbon dioxide partial pressure in liquids and gases, using pH changes due to gas diffusion 09 p1317 A72-23671

Isotopic labeled microspheres for cat uveal and retinal blood flow and oxygen consumption determination, studying increased intraocular pressure and carbon dioxide tension effects 12 p1763 A72-27841

Human centrifuge studies of high positive acceleration effects on blood oxygenation and arterial oxygen and carbon dioxide tension 12 p1766 A72-28287

Physiological and subjective responses of physically fit young men to combined exercise-carbon dioxide stress tests 12 p1767 A72-28311

Alveolar carbon dioxide pressure-ventilation response curve measurement by Campbell rebreathing method in consecutive daily trials 13 p1906 A72-29846

Rebreathing studies of carbon dioxide pressure level effect on carbon dioxide content difference in arterial blood and alveolar gas during exercise and rest 17 p2499 A72-34346

Respiratory frequency and alveolar oxygen and carbon dioxide tension relationship to hypercapnia in man 17 p2506 A72-35965

Effects of diffusion impairment on O2 and CO2 time courses in pulmonary capillaries. 17 p2506 A72-35967

Reproducibility of indirect /CO2/ Fick method for calculation of cardiac output. 17 p2506 A72-35971

Experimental studies on the alkali-acid equilibrium in the blood gases under the chronic action of low concentrations of lead. 24 p3374 A72-44824

CARBON DISULFIDE

Nonlinear wave propagation of laser beams in absorbing fluid media, comparing computer model calculation results with experiment on liquid carbon disulfide cell 07 p1006 A72-19837

Chemistry and performance characteristics of flash photolysis and microwave discharge initiated CW carbon disulfide/oxygen lasers 09 p1325 A72-23236

Bond dissociation energy calculation for carbon disulfide in vacuum UV from fluorescence threshold energy of incident photons, measuring absorption coefficient at 1200-1400 A 13 p1914 A72-30060

CARBON FIBERS

Graphite fiber composite fan blade design for subsonic turbofan engines, discussing weight and fatigue sensitivity reductions and performance test results [SAE PAPER 710771] 01 p0116 A72-10265

Radiographic detection of small flaws in bulk graphite and carbon/carbon composites, improving image quality and sensitivity by contrasting liquid impregnation 01 p0069 A72-10808

Graphite filament reinforced plastics strength, performance properties, fabrication processes and tooling concepts [SME PAPER EM 71-205] 01 p0076 A72-10968

Unidirectional glass/graphite fiber-epoxy resin composite, discussing fabrication and performance tests for mechanical properties [SME PAPER EM 71-192] 01 p0092 A72-10971

Price/demand/cost economic aspects of carbon fiber reinforced plastics composites in aero-engine applications 04 p0536 A72-14743

Carbon fiber reinforced composites properties and design limitations relative to elastic anisotropy in pump and fan applications 04 p0536 A72-14744

Carbon fiber resin composite characteristics for air-frame component design, comparing with metal materials

04 p0537 A72-14746

Sliding friction and wear behavior of carbon fiber reinforced composites with thermosetting resins, thermoplastic polymers and metal base materials

04 p0537 A72-14747

Carbon fiber reinforced thermoplastics tested for gears and bearings applications, including wear, static, dynamic, surface tension, stereoscan and microscopy effects

04 p0537 A72-14748

Carbon fiber reinforced material porosity source, applying equilibrium configurations of liquid films on parallel uniform cylindrical rod hexagonal and cubic arrays

04 p0537 A72-15087

Carbon fiber-resin laminates ballistic impact resistance, discussing damage and interlaminar shear strength

04 p0537 A72-15089

IR spectroscopy analysis of oxidation treatment, chemical and structural changes during carbon fiber formation from acrylic precursors

05 p0680 A72-16076

Unidirectional carbon fiber composites effects and use of stress envelopes in aircraft structure design

05 p0681 A72-16997

Environmental tests on carbon fiber Vulcan air-brake flap, including thermal cycling, sustained loading, immersion, corrosion and lightning strike tests

05 p0681 A72-16998

Carbon fiber laminates for helicopter components weight reduction

05 p0681 A72-16999

Heat resistant reinforced plastics from glass and pyrolytic carbon fibers by silicoorganic polymer treatment

06 p0835 A72-17735

Composite propeller blades with carbon fiber reinforced plastics spar for hovercraft, presenting mechanical properties test data for different composite configurations

07 p0912 A72-19062

Resistivity, thermoelectric power and magnetoresistance of carbon fibers derived from heat treated polyacrylonitrile

07 p1024 A72-20550

Carbon fibers elastic modulus inference from electrical conductivity inverse correlation with sound propagation rates

08 p1191 A72-21498

Carbon/epoxy composite reinforced plastic materials feasibility for application to aircraft landing gear wheel fabrication

08 p1193 A72-21686

Graphite fiber reinforcement of glass composite structure for increased cost effectiveness as compared to laminates and sandwich structures

08 p1193 A72-21694

Graphite fibers surface treatment and interfacial adhesive bonding, considering resin composites shear strength enhancement by sulfuric acid and sodium chlorate oxidation

08 p1194 A72-21697

Boron and carbon fiber reinforced plastics anisotropic stress-strain properties, considering fiber misalignments curvature and low shear resistance effects

08 p1196 A72-21857

Carbon fiber reinforced epoxy resin composites, testing fracture behavior in flexural and shear modes under static, fatigue and creep loading

09 p1334 A72-22389

Fiber orientation effects on physical properties of carbon fiber-epoxy resin composites

[PI PAPER 3] 09 p1337 A72-22540

Unidirectional and orthogonally cross-ply carbon fiber reinforced plastics laminates, determining interlaminar shear strength and fatigue life

[PI PAPER 8] 09 p1337 A72-22543

Carbon fiber reinforced epoxy resin composites fracture toughness dependence on fiber strength, diameter, volume fraction, modulus, fiber/matrix interface strength and temperature

[PI PAPER 9] 09 p1337 A72-22544

Pultrusion process for carbon fiber reinforced plastic, compared with wet lay up technique, noting mechanical properties

[PI PAPER 10] 09 p1318 A72-22545

Tensile microstrain and cyclic loading behavior of carbon fiber reinforced plastic composites at elevated temperature

09 p1338 A72-23169

Carbon fiber reinforced plastic toughness from strain concentration and plastic flow observation near crack tip by moiré technique

09 p1339 A72-23170

Temperature effects on kinetics of methane decomposition on carbon fiber at high temperatures, showing characteristics relationship to carbon gasification reactions

10 p1433 A72-24086

Molded carbon technique-produced carbon fiber/carbon composites, discussing flexural strength, toughness, crack resistance and rocket nozzle application

10 p1500 A72-24200

Tensile strength of notched carbon and glass fiber reinforced epoxy resin composites as function of crack size

10 p1500 A72-24253

Stress wave surfaces in graphite fiber-epoxy matrix anisotropic plates under transverse impact forces, using Mindlin approximation theory

10 p1555 A72-24255

Carbon-phenolic composite ablation and expansion in thermal environment during reentry shielding, using flight and simulation tests

[AIAA PAPER 72-363] 11 p1669 A72-25390

Uniaxial, biaxial and shear loading tests on filament wound carbon-carbon composite tubes and rings

11 p1670 A72-25458

Mechanical behavior of three dimensional reinforced ablative composites, including carbon-phenolic, quartz-phenolic and quartz-carbon materials

11 p1670 A72-25459

Thermal expansion measurements on graphite reinforced plastics, using Leitz dilatometer

11 p1670 A72-25460

Stress analysis of short beam bending of graphite fiber reinforced epoxy composites

11 p1671 A72-25464

Vacuum mold preparation and flexural testing of miniature carbon fiber reinforced composite specimens

11 p1671 A72-25468

Tensile properties of continuously cast aluminum-carbon fiber composites, discussing fiber outgassing and metal coating for wetting promotion

11 p1659 A72-25859

Book on carbon fibers in composite materials covering fiber testing and mechanical properties

11 p1674 A72-25924

High performance continuous filament reinforcements for nonmetallic matrix composites, emphasizing boron and graphite fibers

11 p1674 A72-26229

Rapid laser heating induced stress generation in carbon fiber-polyethyl methacrylate composite

12 p1833 A72-27286

Dynamic properties of thermosetting plastic composites unidirectionally reinforced by high elastic moduli boron and carbon fiber for aircraft structural applications

12 p1882 A72-27343

Graphite fiber with high tensile strength and modulus and good elongation at low cost for aerospace applications

12 p1834 A72-28084

Chemical vapor deposition of boron on carbon monofilament substrate to eliminate fracture and boron damage and achieve good strength

12 p1834 A72-28085

Fabrication, and physical, mechanical and ablation properties of three dimensional carbon-carbon cylinder composite materials

12 p1834 A72-28086

Fiber reinforced Mod 3 carbon-carbon composites mechanical and thermal properties comparison with polycrystalline bulk graphite

12 p1834 A72-28087

Flexural strength of Pyco-bond polyacrylonitrile /PAN/ precursor carbon fiber substrates for carbon-carbon composite fabrication

12 p1835 A72-28092

Graphite fiber-epoxy composite systems development for F-5 aircraft landing gear door, speed brake, leading and trailing edge flaps and horizontal stabilizer

12 p1835 A72-28097

Boron and carbon reinforced fiberglass plastics tensile strength characteristics, presenting static fatigue curves vs Poisson coefficient and elastic modulus for various fiber contents

13 p1982 A72-28552

High modulus yarn carbon-carbon three dimensional orthogonal composite material ablative and thermomechanical performance in nose tip ground tests

[AIAA PAPER 72-365] 13 p1983 A72-28956

Glass and carbon fiber reinforced plastic beam specimens dynamic moduli and loss factors determination from vibration frequency and decay rate measurements

13 p1984 A72-29095

High strength carbon fiber reinforced plastics, discussing fabrication techniques, fiber structural, physical and mechanical properties and potential technological applications

13 p1984 A72-30075

Carbon fiber reinforced plastics nondestructive testing by ultrasonic compressional and shear wave resonance

14 p2107 A72-30856

Thermal expansion of carbon-carbon composites as function of temperature and fiber orientation by dilatometric measurements

15 p2260 A72-31256

Carbon and graphite fiber reinforced composites elastic constants derived from ultrasonic immersion technique

15 p2261 A72-32503

Acoustic emission from carbon fiber-epoxy composite during continuous tensile stress cycling

16 p2413 A72-32868

Griffith equation applicability to graphite fiber fracture strength by measurement of work to break and critical flaw

16 p2413 A72-32871

Friction and wear properties of carbon fiber reinforced polymers sliding against metals in pure and sea water and aqueous solutions

16 p2396 A72-33123

Carbon fibers reinforced polymer wear rate decrease in organic fluids associated with films development on steel counterface, noting application in lubricated systems

16 p2397 A72-33124

Carbon fibers for composite materials reinforcement, discussing mechanical properties and economic factors

17 p2569 A72-34188

Impurity effects in carbon fibres.

17 p2569 A72-34667

Carbon fibre composites with ceramic and glass matrices. I - Discontinuous fibres.

17 p2570 A72-34668

Carbon fibre composites with ceramic and glass matrices. II - Continuous fibres.

17 p2570 A72-34669

Study of the surface reactivity of carbon fibers by gas chromatography

17 p2570 A72-34891

Failure mechanism for carbon fibers in epoxy novolac matrices under tensile loads

17 p2633 A72-35286

Observations of failure modes in carbon composite materials.

17 p2571 A72-35288

Data generation for engineering design with advanced composites.

17 p2571 A72-35653

High strength alumina, boron, silicon carbide and graphite reinforcing fibers for composite materials

17 p2572 A72-35656

High strength-high modulus boron vapor deposited on a carbon monofilament substrate.

17 p2572 A72-35657

High performance graphite ribbon - An advanced reinforcement material.

17 p2572 A72-35659

Carbon fiber structure at graphitization temperatures to 3100 C in terms of surface energy and internal stress accounting for low shear strength

17 p2572 A72-35660

Boron- and graphite-epoxy and boron-aluminum composites forming, processing and costs for aircraft structural materials

17 p2560 A72-35663

Carbon-carbon composite process and fabrication techniques, discussing heat treatment effects and physical properties correlation to material structure

17 p2561 A72-35666

Carbon-carbon composites for space shuttle reentry thermal protection.

17 p2572 A72-35667

Development of moldable carbonaceous materials for ablative rocket nozzles.

17 p2572 A72-35668

Mechanical properties of carbon filament wound carbon matrix composite from tensile tests, noting reinforcement efficiency

17 p2573 A72-35669

The development of high strength three dimensionally reinforced graphite composites.

17 p2573 A72-35670

Fatigue of boron-aluminum and carbon-aluminum fibre composites.

18 p2701 A72-36625

RF shielding and electrical properties of boron and carbon fiber reinforced composites.

20 p2944 A72-38987

Boron and carbon fibers fabrication and properties for composite materials reinforcing elements, noting strength and stiffness dependence on stress orientation

20 p2944 A72-39437

Production and properties of carbon fiber-reinforced aluminum

20 p2940 A72-39442

Transverse tensile properties of an unbonded model composite.

20 p2941 A72-39790

An interpretation of radiation effects on mechanical properties of carbon fibres based on a 'sheath' and 'core' model of fibre structure.

20 p2944 A72-39794

Processing of carbon/carbon composites - An overview.

21 p3072 A72-40552

Two-dimensional lattice orientation and three-dimensional crystallinity in carbon fibres.

21 p3073 A72-40687

Non-destructive examination of fibre reinforced polymers with special reference to continuous carbon fibre reinforcement.
[ICAS PAPER 72-44] 21 p3073 A72-41169

Polycrylonitrile based carbon fiber strengthening by fast neutron irradiation at high temperatures 22 p3196 A72-41965

Field emission from carbon fibres - A new electron source. 22 p3208 A72-41966

Fabrication and properties of graphite fiber reinforced magnesium. 22 p3193 A72-43035

The use of a torsion machine to measure the shear strength and modulus of unidirectional carbon fiber reinforced plastic composites. 23 p3306 A72-43562

CARBON ISOTOPES

Interstellar C12/C13 abundance ratio lower limit in direction of 20 Tau 02 p0280 A72-12192

Cyanide and carbon molecules and isotopes electronic systems opacity probability distribution functions for stellar equilibrium model atmospheres calculations 03 p0416 A72-13012

Single breath diffusing capacity and alveolar dead space measurements for carbon 18 monoxide using respiratory mass spectrometer 04 p0480 A72-15215

Carbon isotopic studies of organic matter in Precambrian rocks 09 p1304 A72-23496

C-13 and C-12 formaldehyde absorption near Sgr A and Sgr B2, noting optical depths and abundance ratio 15 p2315 A72-32712

Jupiter atmospheric C12/C13 ratio for methane from equivalent width measurements in R(2) multiplet 21 p3107 A72-41273

CARBON MONOXIDE

Self broadened rotational half widths for Lorentzian line shape and slit function in CO fundamental, using line center transmission measurements 01 p0104 A72-10095

CO hemoglobin concentration measurement in blood of smokers, nonsmokers and deceased crewmembers of crashed aircraft 01 p0010 A72-10211

Atmospheric carbon monoxide pollution sources, sink mechanism and remote sensing requirement [AIAA PAPER 71-1120] 01 p0068 A72-10557

Pulmonary functional inhomogeneities effects on steady state oxygen and CO diffusing capacity estimates in gas transfer resistances terms 01 p0014 A72-10847

Pulsed laser emission in carbon monoxide, calculating molecular excited state populations 02 p0237 A72-11471

Effective cross sections for charged and excited particles formation from He, Ne and Ar ion collisions with CO molecules, using mass spectrometry 03 p0393 A72-14065

Combustion reactions of water catalyzed gas-phase oxidation of carbon monoxide in premixed stagnation flow at atmospheric pressure [AD-743563] 03 p0459 A72-14223

Reaction kinetics of NO and CO formation in lean premixed hydrocarbon-air flames 04 p0594 A72-14409

Carbon monoxide oxidation by hydroxyl radicals at high and low temperatures from transition state theory, confirming flame and shock tube results [WSCI PAPER 71-36] 04 p0482 A72-14584

Human blood carboxyhemoglobin saturation relation to inspired air oxygen and CO concentrations from small closed rebreathing system tests [AD-740929] 04 p0472 A72-14863

Single breath diffusing capacity and alveolar dead space measurements for carbon 18 monoxide using respiratory mass spectrometer 04 p0480 A72-15215

Carbon dioxide-carbon monoxide vibrational energy transfer rate at 730-2325 K from measurements following heating in shock tube 04 p0553 A72-15641

Diatomic molecules forbidden transitions moments, Franck-Condon factors and lifetimes, calculating CO Cameron system intensity by perturbation theory 05 p0692 A72-16750

Vibrationally inelastic scattering of CO cations by Ar collision, measuring ion energy, mass and angular distribution with high resolution ion beam apparatus 05 p0693 A72-17169

Dissociative excitation of CO and metastable fragments by electron impact on carbon dioxide, investigating cross sections 06 p0803 A72-17447

Temperature dependence of carbon monoxide reaction rate with hydroxyl, noting activation energy 07 p0935 A72-19376

Carbon monoxide induced hypoxia inhibition of reflex vasoconstriction in man in presence of normal arterial oxygen tension 07 p0929 A72-19438

Radiation temperature of carbon monoxide molecules in solar atmosphere from vibratory-rotatory spectral measurements 07 p1077 A72-19811

CO hypoxia effect on oxygen transport during exercise, discussing changes in cardiac and respiratory functions and work capacity 08 p1114 A72-20893

Carbon monoxide in carbon dioxide atmosphere, determining IR absorption lines broadening at reduced temperatures 09 p1351 A72-22612

Spectroscopic measurements of light emission from carbon dioxide positive ions and carbon monoxide in metastable He interaction with carbon dioxide 09 p1354 A72-22667

Einstein A coefficients, band oscillator strengths and absolute band strengths calculation for comet tail band system of CO cations 09 p1355 A72-22789

High pressure CO and N plasmas production by uncoupling electron temperature from number density, measuring electron-ion recombination rates 10 p1518 A72-23962

CO Cameron system band intensity from measurements of equivalent widths of resolved rotational lines, using Doppler growth curve for line strength conversion 10 p1514 A72-24095

High altitude acclimatization effects on human lung diffusing capacity for carbon monoxide at different oxygen tensions 10 p1425 A72-24476

Cameron bands phosphorescent yield of carbon monoxide from carbon dioxide photodissociation in helium buffer 11 p1590 A72-26013

Carbon monoxide quantum yield measurements of carbon dioxide photolysis by radiation at 1470 and 1500-1670 Å 11 p1590 A72-26423

Atmospheric carbon monoxide and nitrous oxide telluric line contours and line centers optical thickness, measuring solar radio emission transmissivity 11 p1628 A72-26881

Carbon monoxide and hydrogen adsorption on graphite, measuring sticking probabilities 12 p1777 A72-27039

Carbon monoxide dynamics in chlorella reactor closed environment and in man-chlorella system at relatively constant level 14 p2078 A72-30377

Phase diagrams of Ni-C and Co-C systems with metastable equilibrium lines, investigating microstructure and microhardness of carbide eutectic 14 p2123 A72-30990

Carbon monoxide adsorption on nickel surface, determining preferential orientation by extended Huckel calculations 15 p2276 A72-31867

Decarburization kinetics of Nb wires with dissolved carbon in high temperature oxygen flow, monitoring electrical resistivity and CO partial pressure 15 p2244 A72-32113

CO overtone band and vibrational transitions in CW carbon disulfide-oxygen chemical laser, discussing pressure effects 15 p2250 A72-32525

Carbon monoxide oxidation reactions temperature dependence, correlating high to low temperature results via transition state theory 16 p2360 A72-33511

Lifetime and quenching of metastable CO produced by dissociative recombination of positive carbon dioxide ions in He afterglow 16 p2432 A72-33771

Decay rate coefficients at 250-370 K for three-body recombination kinetics of O and CO, considering CO, carbon dioxide and nitrogen as third body 17 p2511 A72-34736

Radiation temperature of carbon monoxide molecules in solar atmosphere from vibratory-rotatory spectral measurements 17 p2618 A72-35736

Emission spectra of comet tail carbon monoxide molecular ion indicating constant or slowly varying electron transition moment 17 p2618 A72-35826

Excitation transfer and Penning ionization reactions between helium metastables and carbon monoxide. 18 p2713 A72-36563

Flash desorption spectrum and LEED studies of CO adsorption on W single crystal planes, measuring work function increase as function of coverage 18 p2657 A72-37040

Theoretical determination of the absorption coefficient and the total band absorbance including a specific application to carbon monoxide. 19 p2881 A72-38395

Atmospheric carbon monoxide and nitrous oxide telluric line contours and optical thickness in line centers, measuring solar radio emission transmissivity 20 p2919 A72-39568

Calculation of solar CO vibration-rotation line profiles and equivalent widths. 20 p2973 A72-39889

Hypoxic pulmonary steady-state diffusing capacity for CO and alveolar-arterial O2 pressure differences in growing rats after adaptation to a simulated altitude of 3500 m. 21 p3003 A72-41622

Behavior of carbon monoxide in the upper photosphere 21 p3114 A72-41777

Chemisorption of CO on tungsten /100/- Combined flash desorption and electron stimulated desorption study. I. 22 p3152 A72-42297

Electron impact excitation cross sections and energy degradation in CO. 22 p3172 A72-42422

Collisional excitation of carbon monoxide in interstellar clouds. 22 p3227 A72-42553

Influence of a preliminary exposure to carbon monoxide on the development of hypokinetic disturbances in albino rats 23 p3255 A72-43909

Electron scattering by molecules with and without vibrational excitation. IV - Elastic scattering and excitation of the first vibrational level for N2 and CO at 20 eV. 24 p3427 A72-45304

Excitation of vacuum ultraviolet radiation by electron impact on carbon monoxide - Some unresolved questions near threshold. 24 p3379 A72-45313

Dissociation of carbon monoxide in the discharge of a continuous-flow CO laser 24 p3411 A72-45499

CARBON MONOXIDE LASERS

Mass spectroscopic analysis of addition effects of Xe, hydrogen and oxygen on CO-He laser discharge 01 p0079 A72-10517

Completely sealed off room temperature CO laser system, discussing performance and continuous wave power 01 p0080 A72-10852

CW longitudinal flow carbon monoxide chemical laser system analysis, discussing vibrational levels, population densities, excitation and relaxation processes and dynamic model 03 p0368 A72-13858

CW CO laser by discharging premixed carbon disulfide-oxygen flame, suggesting chemical pumping mechanism and flame laser possibility 04 p0529 A72-14589

Electron energy distribution in carbon monoxide lasers, considering excitation effects on exchange processes, power transfer to vibration levels and vibrationally excited molecules influence 07 p0999 A72-18883

Laser action in carbon monoxide vibrational-rotational bands produced by electrical excitation of carbon monoxide-nitrogen-oxygen-helium mixtures following expansion in supersonic nozzle 07 p1001 A72-19047

Spectral characteristics and small signal gains of carbon monoxide laser, using optimum gas compositions 07 p1003 A72-19218

Carbon monoxide laser output power variation as function of oxygen tension 12 p1823 A72-27755

Intracavity gas cell for carbon monoxide laser oscillations restriction to lines coincident with atmosphere transmission bands, noting absorption by atmospheric water vapor 12 p1823 A72-27837

CO-He laser vibrational population distribution and small signal gain measurements, comparing with prediction based on V-V anharmonic exchange relaxation 12 p1827 A72-28222

Transverse flow transverse pulsed chemical CO laser, describing Q switching, pulse duration power efficiency and chemical deactivation processes 14 p2109 A72-30187

CW tunable semiconductor laser measurement of CO laser amplifier gain line shape for several vibration-rotation lines 15 p2245 A72-31382

Sealed room temperature gas laser output oscillating on 5-micron carbon monoxide or 10-micron carbon dioxide lines 15 p2251 A72-32533

Electrical CO mixing gas dynamic laser. [AIAA PAPER 72-725] 17 p2564 A72-35483

Forced-convective-flow carbon monoxide laser. 22 p3184 A72-41968

Transient oscillator analysis of a high-pressure electrically excited CO laser. 22 p3184 A72-41970

Energy exchange processes in a low temperature N2-CO transfer laser. 22 p3184 A72-41993

- IR CW laser emission from arc generated flowing CO active medium, describing thermal dissociation of oxygen followed by carbon disulfide injection
22 p3185 A72-42611
- Molecular vibration levels inversion ratios increase by vibrationally cold CO addition to CW CO chemical laser, observing R-branch emission lines
22 p3185 A72-42615
- A new method of measuring temperature, inversion ratio, and pressure-broadened linewidth in a CW molecular laser.
23 p3297 A72-44188
- Dissociation of carbon monoxide in the discharge of a continuous-flow CO laser
24 p3411 A72-45499
- Electrical characteristics of a CO laser discharge plasma
24 p3411 A72-45500
- CARBON MONOXIDE POISONING**
- CO contamination of cabin and hazard to pilots, discussing concentrations, avoidance, control and analysis
07 p0933 A72-20267
- Effect of hyperoxic media on the stability of rats during acute carbon monoxide exposure
21 p2998 A72-40437
- Expired air as a source of spacecraft environment carbon monoxide contamination
24 p3375 A72-45120
- CARBON STEELS**
- Mixed cubic carbide diffusion layer formation on carbon steel surface, using chemical transport reaction analysis
06 p0828 A72-17570
- Se and Te additions effects on low carbon steels formability and machinability from metallurgical examination and workability tests
07 p0994 A72-19480
- Tempering temperature effect on hydrogen penetration level and brittleness of hardened carbon steel
07 p1014 A72-19773
- Plasma spraying process effects on carbon steel coatings structure and bonding, considering optimal parameters, properties control and phase transformations
07 p0996 A72-19966
- Niobium carbide coatings for carbon steels and cermets, comparing with titanium carbide coatings
08 p1186 A72-21724
- Soviet book on corrosion cracking of carbon steels covering chemical composition, structure, mechanical properties, anode and cathode processes role and adsorption losses
08 p1190 A72-22163
- Adsorption, corrosion and hydrogen embrittlement effects on crack formation in quenched carbon steels in active media, using tensile stress-rupture tests
08 p1190 A72-22183
- Quenched and tempered Ni carbon steel retained austenite transformation and crack observation by X ray diffraction under low cycle fatigue testing
09 p1329 A72-23149
- Ni carbon steel microstructure changes in retained austenite phase and crack observation during low cycle fatigue testing
09 p1330 A72-23150
- Electron microscopic study of cyclically deformed Al, Cu, Al-Mg-Zn alloy and carbon steel dislocation structure
10 p1494 A72-23830
- Fatigue crack propagation relation to plasticized zone formation at crack tip in ferritic carbon steels and in Cr-Ni austenitic stainless steels
10 p1558 A72-24855
- Carbon steel fatigue crack propagation rate dependence on strength and stress history, discussing conditions for crack nonpropagation
10 p1499 A72-24889
- Iron emission spectrum in phase transformations and recrystallization study of austenitic and carbon steels under high temperature hardening
11 p1655 A72-25496
- Austenitizing condition effect on lower bainite transformation in eutectoid carbon steel
11 p1656 A72-25515
- Liquid environments effect on mild steel fatigue strength, discussing effects of viscosity, compressibility and entry rate into cracks
11 p1656 A72-25738
- Aluminum nitride amount and particle size measurement at austenitic grain coarsening temperatures in low carbon steels
11 p1656 A72-25755
- Electrochemical metal precision processing, discussing steels carbon content, surface purity, electrolyte anion composition and anode potential
11 p1640 A72-26256
- Safe welding procedures for carbon manganese steels, noting hydrogen cracking association with hardening of heat affected zone
11 p1641 A72-26490
- Underbead hardness determination in carbon and low alloy steels, noting weld tests/theory correlation
11 p1641 A72-26493

- Austenite formation kinetics in Fe-C ferritic-pearlitic structure at 855 C, comparing experimental data with theoretical calculations
11 p1662 A72-26744
- Stress corrosion cracking mechanism of low carbon steels to explain transcrystalline brittle mechanical cracks development along grain boundaries
11 p1666 A72-26923
- Fractographic study of stress corrosion fractures of low carbon steels with electron microscope
11 p1666 A72-26924
- High strength hypereutectoid steel with low carbon needle-like martensite matrix obtained by conventional heat treatment
12 p1827 A72-27100
- Carbon and low alloy steels resistance to abrasive wear as function of hardness, heat treatment and composition
12 p1829 A72-27455
- Fatigue failure tests of low carbon Mn steel, analyzing structural damage under cyclic loads in relation to temperature curve
12 p1829 A72-27458
- Thin walled tubular carbon steel specimen deformation pattern under biaxial tension and internal pressure at normal and low temperatures
12 p1830 A72-28227
- Stepwise compression loading effect on yield stress of carbon and alloy steels in cylindrical samples with end plane cylindrical notches filled with solid lubricant
12 p1831 A72-28237
- High stress state mechanical properties of steels with different carbon contents and heat treatments
13 p1979 A72-29478
- Tensile strength, toughness and corrosion resistance of dross aluminized carbon steel specimens under static, cyclic and impact loads
16 p2406 A72-33267
- Understressing and coxing effects effect on deeply notched carbon steel fatigue behavior, emphasizing crack initiation and breakdown
16 p2472 A72-33947
- Niobium carbide coatings for carbon steels and cermets, comparing with titanium carbide coatings
17 p2567 A72-35124
- The application of a dislocation model to the strain and temperature dependence of the strain hardening exponent n in the Ludwik-Hollomon relation between stress and strain in mild steels.
18 p2701 A72-36589
- Fe-Ni-C alloys internal damping, martensitic structure and mechanical properties after quenching and tempering, discussing Mo and Cr additions
19 p2806 A72-37418
- German monograph - Improvement of the ductility characteristics of flash butt welding joints involving carbon steels by pulse normal annealing and hot heading in the welding machine
19 p2807 A72-37659
- German monograph - Significance of the manganese-carbon ratio in the brittle-fracture behavior and weldability of high-strength fine-grained structural steels
19 p2816 A72-37661
- The comparison of torsion and tension creep data for a 0.18 per cent carbon steel.
19 p2816 A72-37709
- Creep delay in low-carbon steel at room temperature
19 p2818 A72-38011
- On a method of analysis of the strain energy changes taking place during the rotatory bending fatigue test of carbon steels and an effect of the pearlite patches to these changes.
20 p2935 A72-38881
- Acoustic emission testing and microcracking processes.
20 p2924 A72-39277
- Fine structure in quenched Fe-Al-C steels.
20 p2938 A72-39300
- The effects of composition and annealing conditions on the stability of columbium/nibium-treated low-carbon steels.
20 p2938 A72-39301
- Chromizing of steel sheet by diffusion
20 p2929 A72-39581
- High-speed carburizing with natural gas in a fluidized bed
20 p2929 A72-39582
- Internal oxidation in carburized layers of alloyed steels
20 p2929 A72-39584
- Effect of the structure of carbon steels on their dynamic properties during dynamic loading
21 p3067 A72-40923
- Precipitation of aluminum nitride in low-alloy steel
21 p3068 A72-40956
- Low carbon steel S-N diagram for stresses ranging to fatigue limit, noting cyclic creep, macroplastic cyclic stress and fatigue failure
21 p3122 A72-41353
- Decarburization kinetics of low alloy ferritic steels in sodium.
22 p3194 A72-43042

- Inelastic effects during metal fatigue
22 p3195 A72-43156
- Exponential type equation for carbon steel stretched sample necking profile curve
23 p3348 A72-43753
- The cyclic plastic strain and cumulative fatigue damage - Fatigue damage caused by the stress below the fatigue limit.
24 p3454 A72-44628
- CARBON TETRACHLORIDE POISONING**
- Morphological changes in the lungs and kidneys during prolonged intoxication of the organism by carbon tetrachloride
19 p2760 A72-38035
- CARBON TETRAFLUORIDE**
- An experimental study in the application of the Raman scattering technique as a remote sensor of gas temperature and number density in hypersonic CF₄ flow.
[AIAA PAPER 72-1018]
21 p3057 A72-41597
- CARBON 12**
- Neutrino emission process effects on solar C-N-O cycle energy generation and C 12/C 13 abundance ratio
04 p0567 A72-14911
- Neutron energy spectrum of radiative pion captured by carbon 12, using gamma and neutron counters
05 p0692 A72-16688
- Pionic X ray fields and transitions in Li 6, Be 9, C 12 and O 16, obtaining 2p level absorption broadening
10 p1515 A72-24418
- Carbon 12/13 isotope ratio measurement for interstellar ionized CH molecules toward stars with strong interstellar lines
17 p2604 A72-34524
- CARBON 13**
- Neutrino emission process effects on solar C-N-O cycle energy generation and C 12/C 13 abundance ratio
04 p0567 A72-14911
- High C 13 content in carbonaceous phases of carbonaceous chondrites accounted for by Rayleigh distillation with oxidized and reduced forms of carbon
10 p1547 A72-24951
- Fourier transformation for natural abundance C 13 free induction decays of cyclic antibiotic valinomycin and K ion complex, noting chemical shift differences
13 p1913 A72-29862
- Beam maser spectrometric measurements of normal, C-13 and O-18 formaldehyde transitions, determining coupling constants for all rotational transitions hyperfine structure
16 p2431 A72-33132
- Carbon 12/13 isotope ratio measurement for interstellar ionized CH molecules toward stars with strong interstellar lines
17 p2604 A72-34524
- CARBON 14**
- C 14 diffusion coefficients in W and W-Re alloys single crystals at 1500-1800 C, discussing trace activation energy and frequency factor
05 p0676 A72-16731
- Cosmic ray exposure age of australites and far-east tektites, using C14 content as indication of terrestrial age
06 p0878 A72-17761
- Molecular sieve adsorption sampler for stratospheric carbon 14 measurements from balloon collected carbon dioxide samples
06 p0807 A72-17824
- Terrestrial stony meteorites age determination from C 14 content
09 p1386 A72-22661
- Viking Lander carbon 14 assimilation experiment for life detection in Martian soils
10 p1540 A72-24385
- Interstellar nitrogen-15 and U169.3 - Possibly a new methanol line.
21 p3107 A72-41272
- Stratospheric concentration of radioactive carbon from 1961-62 nuclear tests by balloon measurements over European U.S.S.R. territory during 1967-69
23 p3286 A72-44492
- CARBONACEOUS METEORITES**
- NT ORGUEIL METEORITE**
- Isotopic composition of trapped helium, neon and argon in carbonaceous chondrites, observing covariation based on mass-dependent fractionation
03 p0414 A72-12904
- Comet collisions in planetary nebulae as source of organic compounds in universe in preplanetary era, noting nucleic acid bases in carbonaceous meteorites
04 p0471 A72-14802
- Prebiological food origin in carbonaceous meteorites, considering extraterrestrial environments, organic synthesis and terrestrial analogs
04 p0471 A72-14803
- Chemical evolution of carbonaceous chondrite organic compounds, discussing similarity to terrestrial abiogenic material
04 p0484 A72-14804
- Uranium content and radiogenic ages by fission track analysis in hypersthene, bronzite, amphoterite and carbonaceous chondrites
06 p0878 A72-17791

- High C 13 content in carbonaceous phases of carbonaceous chondrites accounted for by Rayleigh distillation with oxidized and reduced forms of carbon 10 p1547 A72-24951
- Allende carbonaceous chondrite composition analysis, suggesting formaldehyde presence and significance about possible origins 10 p1549 A72-25022
- X ray fluorescence spectrometric analysis of carbonaceous chondrites for chemical subgroups 11 p1723 A72-26525
- Abiotic origin of organic compounds in carbonaceous chondrites, analysing Murchison and Murray meteorites by combined gas chromatography-mass spectroscopy technique 15 p2306 A72-31625
- Thermal release Xe analysis of neutron irradiated white inclusion samples from Allende carbonaceous meteorite, noting iodine and plutonium isotopes abundance 18 p2728 A72-36971
- Cosmic abundance of iron and nature of primitive material in meteorites. 22 p3220 A72-41963
- Cosmogenic radionuclides in the Allende and Murchison carbonaceous chondrites. 22 p3225 A72-42466
- Isotopic compositions of rare gases in the carbonaceous chondrites Mokoia and Allende. 22 p3229 A72-42899
- Rare earth and other abundances in the Murchison carbonaceous meteorite. 23 p3262 A72-44131
- CARBONACEOUS ROCKS**
- Impact breccias in carbonate rocks of Sierra Madera [Texas], investigating microstructure, chemical composition, petrography and mineralogy 05 p0654 A72-16038
- Carbon isotopic studies of organic matter in Precambrian rocks 09 p1304 A72-23496
- Elemental abundances in stone meteorites. 19 p2858 A72-37863
- Prokaryotic algae associated with Australian proterozoic stromatolites. 22 p3174 A72-42981
- CARBONATES**
- NT ARAGONITE
- NT CALCITE
- NT DOLOMITE [MINERAL]
- NT POLYCARBONATES
- Acid-base balance shift during muscular exertion, determining pH and bicarbonate content variation by Astrup micromethod 06 p0765 A72-18062
- Composition of initial mixtures for production of the gaseous C-H-O fuel for fuel cells with molten alkaline carbonates. 19 p2754 A72-37778
- CARBONIZATION**
- Carbonized and ion beam thinned polyacrylonitrile copolymer fibers examination by low angle electron scattering electromicroscopy technique 09 p1339 A72-23190
- Aircraft gas turbine engines synthetic lubricants thermal stability characteristics, describing coke deposition test apparatus and results [ASLE PREPRINT 72AM 14] 13 p1983 A72-28971
- High-speed carburizing with natural gas in a fluidized bed 20 p2929 A72-39582
- CARBONYL COMPOUNDS**
- Iron meteorite formation model based on metal carbonyls low temperature thermal decomposition in comets 01 p0124 A72-10061
- Trimethylphosphite interaction with acetyl- and benzoyl-p-quinone in dry nitrogen atmosphere, noting phosphate formation through intermediate bipolar ion 06 p0770 A72-17986
- Iron-nickel-molybdenum carbonyl powders 23 p3298 A72-43276
- Nucleic acid hybridization with RNA immobilized on filter paper. 24 p3379 A72-45773
- CARBOXYHEMOGLOBIN**
- Volumetric analysis of blood oxygen and CO, showing combination with hemoglobin without significant molecular volume increase 05 p0619 A72-16786
- CARBOXYHEMOGLOBIN TEST**
- Human blood carboxyhemoglobin saturation relation to inspired air oxygen and CO concentrations from small closed rebreathing system tests [AD-740929] 04 p0472 A72-14863
- CARBOXYL GROUP**
- Radical concentrations in gamma irradiated poly(ethylene 2,6-naphthalene dicarboxylate) by ESR spectrum analysis 10 p1433 A72-23847
- CARBOXYLIC ACIDS**
- NT LACTIC ACID
- NT NICOTINIC ACID
- NT OLEIC ACID
- NT TRYPTOPHAN
- CARBURETORS**
- Flow characteristics of pin type nozzles in constant pressure carburetors of Otto cycle engines 02 p0206 A72-12853
- CARBURIZING**
- Carburization of various irons in methane-hydrogen atmosphere at 750 C, comparing activity coefficients and solubility limits 04 p0533 A72-14978
- Carburization kinetics of Nb in acetylene or methane at high temperatures and low pressure 09 p1319 A72-22985
- Thermionic characteristics of carburized tungsten-rhenium alloys. 18 p2656 A72-36131
- Carbide hardening of chromium-molybdenum-vanadium steel 20 p2941 A72-39578
- Internal oxidation in carburized layers of alloyed steels 20 p2929 A72-39584
- Chromium carbides synthesis by carburizing chromium hydroxide or oxalate in hydrogen-methane gas mixture at temperatures below 1000 C 22 p3188 A72-41974
- CARCINOMA**
- U CANCER**
- CARDIAC AURICLES**
- Physical exercise effect on ECG atrial recovery wave duration and magnitude in humans with A-V blocks 02 p0166 A72-12891
- Computerized oesocardiogram for left auricle mechanical activity examination, comparing with catheterization technique 07 p0934 A72-20608
- CARDIAC VENTRICLES**
- Right heart ventricle intracardiac phonocardiograms, recording pulmonary early diastolic click simultaneous with artery pressure curve dirotic wave 01 p0010 A72-10121
- Extrasystolic potentiation of ventricular contraction effect on dog mitral valve function, using roentgen videodensitometry 01 p0015 A72-11036
- Paroxysmal supraventricular tachycardia initiated by sinus beats in patient, observing A-V nodal conduction delay by ECG and electrophysiological methods 02 p0156 A72-11423
- Ventricular ectopic arrhythmias from treadmill exercise in patients observed during ECG monitoring 02 p0156 A72-11424
- HIS bundle electrocardiography for arrhythmia studies, discussing conducting tissue potential recording, ventricular delay and block site determination and electrophysiological effects of drugs 02 p0157 A72-11473
- Canine and human ventricular myocardium microelectrophysiologic studies of postextrasystolic T wave change relation to cellular repolarization and contractile potentiation magnitude 02 p0157 A72-11474
- Human left ventricular volume determined by peripheral venous scintillation angiocardigraph isotope method, comparing with X ray method 02 p0157 A72-11475
- Beta-adrenergic and vagal blockage altered autonomous control effects on left ventricular function in conscious dogs, noting heart rate, stroke volume and end-diastolic and end-systolic diameters 02 p0163 A72-12090
- Idiopathic hypertrophic subaortic stenosis ballistocardiography, measuring ventricular function by angiography 03 p0314 A72-13142
- Exercise ECG correlation to morphological patterns of selective cinecoronary arteriography and ventriculography, revealing significant information on occlusion and stenosis 03 p0314 A72-13178
- Ballistocardiographic and angiographic correlations of ventricular function in patients with idiopathic hypertrophic subaortic stenosis 04 p0466 A72-14442
- Familial cardiomyopathy detection by electrocardiography noting arrhythmias, ventricular hypertrophy, abnormal Q waves and intraventricular conduction defects 04 p0466 A72-14443
- Doppler cardiometry determination of human cardiovascular velocities in patients with heart diseases, discussing impaired left ventricular function detection 05 p0617 A72-16155
- Asymmetrical hypertrophic cardiomyopathy symptoms simulating mitral stenosis, suggesting electrocardiography, chest X ray and hemodynamic studies as diagnostic procedures 06 p0761 A72-17380
- Ventricular function determination by computer graphic techniques for increasing speed, accuracy, reliability and scope of angiocardigraphic analyses determining human heart dimensions 07 p0928 A72-19308
- Idiopathic subvalvular aortic stenosis characterized by muscular or membrane obstruction in left ventricular infundibulum, discussing diagnostic importance for pilots 07 p0933 A72-20189
- Continuous transducer measurement of left ventricular wall thickness in open chest dogs, adapting mutual inductance coil technique 08 p1124 A72-20897
- Vectorcardiographic and ECG diagnosis of left anterior hemiblock combined with complete right bundle branch block, discussing coexisting myocardial infarction influence 08 p1127 A72-21850
- Ventricular myocardium contractile function disorder diagnosis by phase coordinate method with intracardial hemodynamics application 08 p1122 A72-22186
- Ventricular and supraventricular arrhythmias incidence during maximal treadmill exercise in normal man, noting age factor and cardiovascular disease presence effects 09 p1266 A72-23272
- Intraventricular conduction defects incidence and mortality in acute myocardial infarction, noting left anterior hemiblock dominance 09 p1266 A72-23273
- Clinical effects on atrio-ventricular pacing system of electromagnetic weapon detector systems used for air passenger screening at airports in air hijacking prevention efforts 10 p1428 A72-23740
- Human left ventricle measurements, modeling, control and simulation for heart monitoring purposes, describing muscle performance mathematical model and stress effect prediction control system 10 p1429 A72-23924
- Left ventricular volume time course from computer processing of video angiocardigraphic data based on X ray densitometry measurements 11 p1587 A72-26627
- Electrode system for ventricular defibrillation, noting current density role and rounded edge effectiveness 11 p1588 A72-26628
- Left ventricular dynamic function in terms of internal diameter, pressure and flow in dogs at rest and during isoproterenol and metaraminol infusions 11 p1582 A72-26773
- Fluid mechanics of left ventricle model with mitral and aortic valves, showing ring vortex relation to diastole and closure 11 p1589 A72-26775
- High altitude hypoxia preadaptation effects on left ventricle myocardium noradrenaline concentration in rats with experimental vitium cordis 12 p1761 A72-27648
- Dynamic electrocardiography with analog computer program to detect, count and classify atypical ventricular depolarization complexes 12 p1775 A72-28281
- Heart enzyme activity under experimental myocardial ischemia in rabbits determined for blood, left and right ventricles and atrium 13 p1901 A72-28463
- Piloting aptitude evaluation from ECG during hypoxia, considering right intraventricular conduction and ventricular repolarization anomalies 13 p1906 A72-29857
- Contractile responses of guinea pig, rat and human isolated ventricular myocardium to increased stimulation frequency 13 p1907 A72-30044
- Temperature and extracellular Ca level effects on mammalian ventricular myocardium force-frequency relationships, determining contractile tension, velocity and phase duration 13 p1907 A72-30045
- Quantitative angiocardiology of abnormal left ventricular function and contractile spectrum in ischemic heart disease patients 14 p2077 A72-30968
- Radiocardiography method for ventricular volume measurements, recording subclavian vein-injected radioisotope passage through cardiac cavities 15 p2190 A72-32495
- Indicator dilution methods for ventricular volume measurements from washout curves, discussing intraventricular blood mixing uniformity 15 p2190 A72-32496
- Left ventricle intracavity volume measurements based on biplane angiographic data 15 p2190 A72-32497
- Baboon heart endocardial structure dynamic behavior, comparing left ventricle septum and epicardium contractile force and intramycocardial pressure changes 15 p2187 A72-32748
- Computerized angiographic heart geometry analysis for three dimensional ventricle models of man and dog, using Ta markers 16 p2354 A72-33424
- Influence of hyperosmolality on left ventricular stiffness. 17 p2499 A72-34727

- Induction of ventricular arrhythmias by elevation of arterial free fatty acids in experimental myocardial infarction. 17 p2502 A72-34997
- Acquired complete right bundle branch block without overt cardiac disease - Clinical and hemodynamic study of 37 patients. 17 p2505 A72-35821
- A human left ventricular control system model for cardiac diagnosis. 18 p2655 A72-37029
- Left ventricular dynamics during handgrip. 19 p2755 A72-37243
- Analysis of left ventricular wall motion by reflected ultrasound - Application to assessment of myocardial function. 19 p2755 A72-37497
- Evaluation of left ventricular function by echocardiography. 19 p2755 A72-37498
- Determination of systolic time intervals using the apex cardiogram and its first derivative. 19 p2759 A72-38817
- Echocardiographic determination of left ventricular dimensions, volumes and performance. 19 p2762 A72-38819
- Determination of the elastic modulus of the left-ventricle myocardium with the aid of X-ray kymography. 20 p2893 A72-38940
- The mitral apparatus - Functional anatomy of mitral regurgitation. 20 p2892 A72-39460
- Relationship of pulmonary artery to left ventricular diastolic pressures in acute myocardial infarction. 20 p2892 A72-39461
- An indirect method for evaluation of left ventricular function in acute myocardial infarction. 20 p2892 A72-39462
- Cardiac hypertrophy, capillary and muscle fiber density, muscle fiber diameter, capillary radius and diffusion distance in the myocardium of growing rats adapted to a simulated altitude of 3500 m. 21 p3003 A72-41624
- The standard 12-lead scalar electrocardiogram - An assessment of left ventricular performance. 23 p3255 A72-43812
- Comparison of the vectors of the ventricular depolarization and repolarization of man during immersion in a standing position. 24 p3372 A72-44924
- H-V intervals in left bundle-branch block - Clinical and electrocardiographic correlations. 24 p3374 A72-45690
- Clinical and anatomic implications of intraventricular conduction blocks in acute myocardial infarction. 24 p3374 A72-45691
- CARDIOGRAMS**
- Image processing of diagnostic echocardiogram by ultrahigh speed analog to digital converter interfacing digital computer. 07 p0928 A72-19312
- Computerized oesocardiogram for left auricle mechanical activity examination, comparing with catheterization technique. 07 p0934 A72-20608
- A rapid assay of dipolar and extradiapolar content in the human electrocardiogram. 23 p3259 A72-43811
- The standard 12-lead scalar electrocardiogram - An assessment of left ventricular performance. 23 p3255 A72-43812
- CARDIOGRAPHY**
- NT BALLISTOCARDIOGRAPHY
- NT ELECTROCARDIOGRAPHY
- NT MAGNETOCARDIOGRAPHY
- NT PHONOCARDIOGRAPHY
- Human left ventricular volume determined by peripheral venous scintillation angiocardigraph isotope method, comparing with X ray method. 02 p0157 A72-11475
- Radiotelemetric cardiorespiratory determinations during submaximal dynamic exercise. 02 p0168 A72-12134
- Computerized polycardiographic data processing covering 23 cardiac and respiratory characteristics, using rabbits data. 07 p0926 A72-18868
- Electrophysiological responses to maximum exercise in healthy humans from polarcardiographic display of heart vector changes. 07 p0916 A72-18891
- Ventricular function determination by computer graphic techniques for increasing speed, accuracy, reliability and scope of angiocardigraphic analyses determining human heart dimensions. 07 p0928 A72-19308
- Cardiographic interpretation of computerized apexo-carotid diagram, using heart-motor pump comparison. 07 p0934 A72-20607
- Local and cardiac complications of selective percutaneous transfemoral coronary arteriography, noting hemorrhages thromboses, embolisms, myocardial infarction, bradyarrhythmia and ventricular fibrillation. 09 p1267 A72-23325

- Human left ventricle measurements, modeling, control and simulation for heart monitoring purposes, describing muscle performance mathematical model and stress effect prediction control system. 10 p1429 A72-23924
- Ear densitograph for noninvasive cardiac performance measurements during physical activities, exercise tests, flight conditions and for critical patients long-term monitoring. 11 p1582 A72-25500
- Left ventricular volume time course from computer processing of video angiocardigraphic data based on X ray densitometry measurements. 11 p1587 A72-26627
- Human cardiovascular function change as indication of hypoxic circulatory stress, using noninvasive cardiographic measurements of cardiac electromechanical time intervals. 12 p1769 A72-27470
- Medical monitoring system for enclosed men, using ultrasonic Doppler-cardiography for heart rate determination. 14 p2078 A72-30384
- Quantitative angiocardiology of abnormal left ventricular function and contractile spectrum in ischemic heart disease patients. 14 p2077 A72-30968
- Calibrated LF acceleration vibrocardiography to examine hemodynamics indices relation to main wave amplitudes. 15 p2188 A72-31313
- Apexocardiograms and carotid pulse measurements as indicators of cardiac function and myocardial contractility. 15 p2190 A72-32494
- Radiocardiography method for ventricular volume measurements, recording subclavian vein-injected radioisotope passage through cardiac cavities. 15 p2190 A72-32495
- Computerized angiographic heart geometry analysis for three dimensional ventricle models of man and dog, using Ta markers. 16 p2354 A72-33424
- Non-invasive assessment of prosthetic mitral paravalvular and intravalvular regurgitation. 17 p2498 A72-34221
- Changes of the mitral echocardiogram with ageing and the influence of atherosclerotic risk factors. 18 p2652 A72-37031
- Analysis of left ventricular wall motion by reflected ultrasound - Application to assessment of myocardial function. 19 p2755 A72-37497
- Evaluation of left ventricular function by echocardiography. 19 p2755 A72-37498
- Echocardiography in the diagnosis of congenital mitral stenosis and in evaluation of the results of mitral valvotomy. 19 p2755 A72-37499
- Determination of systolic time intervals using the apex cardiogram and its first derivative. 19 p2759 A72-38817
- Echocardiographic determination of left ventricular dimensions, volumes and performance. 19 p2762 A72-38819
- Echocardiographic investigation of heart rate, sex and normal aging effects on mitral valve leaflet movement in healthy subjects. 22 p3148 A72-43021
- Effects of coronary arteriography on myocardial blood flow. 23 p3256 A72-43933
- Clinicoarteriographic correlations in angina pectoris with and without myocardial infarction. 24 p3372 A72-45010
- General index for the assessment of cardiac function. 24 p3372 A72-45011
- CARDIOLOGY**
- Respiration effects on human heart rate deceleration and biphasic cardiac response in aversive shock conditioning situation. 01 p0010 A72-10195
- Photo-optical techniques in biomedical data acquisition, discussing cineangiography and X ray tomography applications in cardiological research work. 06 p0766 A72-17437
- Cardiac catheterization practice review, discussing pediatric and adult cardiology, risk reduction, diagnostic aids, relationship to radiology and laboratory equipment complexity. 07 p0923 A72-20553
- Abnormal ECG in healthy man due to former disease, subclinical disease, congenital anomalies, hereditary disease or functional aberrations. 07 p0924 A72-20574
- Atypical ECG of sportsmen, considering repolarization disorders due to ischemia, lesion, excitability and conduction signs. 07 p0924 A72-20575
- Computerized oesocardiogram for left auricle mechanical activity examination, comparing with catheterization technique. 07 p0934 A72-20608

- Ventricular myocardium contractile function disorder diagnosis by phase coordinate method with intracardial hemodynamics application. 08 p1122 A72-22186
- Cardiac cycle intervals measurement with multibeam cathode oscilloscope synchronized with multichannel polycardiographic automatic recording machine. 09 p1272 A72-23192
- Clinical reliability and normal variations of Frank ECG computer analysis by Smith-Hyde program for healthy and cardiac patients. 09 p1272 A72-23274
- Myocardium biopulse-controlled cardio-synchronizer as key component of biocontrol systems for cardiological studies. 11 p1585 A72-26455
- Cardiac membrane pain sensitivity in vagotomized cats under sensitizing acetylcholine influence during reduced cholinesterase activity. 13 p1905 A72-29329
- Exchangeable potassium in heart disease - Long-term effects of potassium supplements and amiloride. 17 p2500 A72-34932
- Acquired complete right bundle branch block without overt cardiac disease - Clinical and hemodynamic study of 37 patients. 17 p2505 A72-35821
- Work capacity and physiological responses to maximum exercise in 54 year old men in relation to heart disease and cardiovascular hazard studies. 17 p2505 A72-35822
- Reproducibility of indirect /CO₂/ Fick method for calculation of cardiac output. 17 p2506 A72-35971
- A human left ventricular control system model for cardiac diagnosis. 18 p2655 A72-37029
- Myocardium automatism, excitability, conductivity and contractility under cooling, noting complete inhibition at 9-3 deg C. 22 p3141 A72-42072
- Evaluation of the pulse-contour method of determining stroke volume in man. 23 p3256 A72-43934
- CARDIOTACHOMETERS**
- ECG amplifier and cardiotaohometer for exercise studies, using digital algorithm for heart rate computation and ECG signal preprocessing for R wave detection. 14 p2080 A72-30707
- Exercise cardiotaohometer with heart rate display on beat to beat basis, R wave recognition circuit and noise linear filtering efficiency. 14 p2082 A72-31092
- CARDIOVASCULAR SYSTEM**
- NT AORTA
- NT ARTERIES
- NT BLOOD VESSELS
- NT CAPILLARIES [ANATOMY]
- NT CARDIAC AURICLES
- NT CARDIAC VENTRICLES
- NT DIASTOLE
- NT EPICARDIUM
- NT ERYTHROCYTES
- NT GLOMERULUS
- NT HEART
- NT HEMATOPOIESIS
- NT HEMATOPOIETIC SYSTEM
- NT LEUKOCYTES
- NT LYMPHOCYTES
- NT MYOCARDIUM
- NT RETICULOCYTES
- NT SYSTOLE
- NT THROMBOPLASTIN
- NT VEINS
- Long term bed rest effect on humans and primates, detailing cardiovascular metabolic and musculoskeletal physiological systems. 01 p0014 A72-10932
- Implanted telemetry development for cardiovascular research, discussing blood pressure, flow and hydraulic impedance relationships. 02 p0169 A72-12140
- In vivo investigation of dogs natural mitral valve flow dynamics, developing cardiohemic system physical model for data analysis and electrical analog simulation. [ASME PAPER 71-WA/BHF-2] 05 p0621 A72-15949
- Hydrodynamic model of human systemic arterial circulation to test artificial heart pumps. [ASME PAPER 71-WA/AUT-13] 05 p0621 A72-15954
- Doppler ultrasonic probe phonocardiography for human cardiovascular velocity measurement, showing normal tracings and aging effects. 05 p0617 A72-16154
- Doppler cardiometry determination of human cardiovascular velocities in patients with heart diseases, discussing impaired left ventricular function detection. 05 p0617 A72-16155
- Mathematical model for blood leucocyte population changes after radiation exposure within Blair model.

leucocytes hemopoietic to cardiovascular systems transport 05 p0618 A72-16635

Cardiac acceleration by voluntary muscle contractions of minimal duration in men due to vagal tone inhibition 07 p0929 A72-19442

Cardiovascular and respiratory responses to intraarterial injection of K and Na ions in dogs for peripheral receptor site determination 07 p0921 A72-20177

Hyperbaric oxygen exposure effect on cardiovascular system in rats, discussing pulmonary edema relation to hypertensive left ventricular failure 07 p0921 A72-20182

Control system model integrating human left ventricle and circulatory system mechanics and regulation by central nervous system 07 p0934 A72-20356

Cardiographic interpretation of computerized apexo-carotid diagram, using heart-motor pump comparison 07 p0934 A72-20607

Cardiovascular analog computing circuits with outputs for left ventricular pressure maximum rise rate, cardiac stroke volume and atriocentric conduction time 08 p1124 A72-20899

Digital simulation of human cardiovascular system, noting blood pressure control by physiological reflexes 08 p1125 A72-21475

Dynamic orthosympathetic control of cardiovascular system, studying efferent element link between autonomic vasomotor and cardiac centers and effector cells 08 p1118 A72-21548

Cardiovascular system model for demonstration of biological system analog simulation and computation, describing components for heart pumping action and systemic circulation 09 p1268 A72-22454

Hybrid computer simulation of cardiovascular system in biomedical engineering education 09 p1268 A72-22455

Electromagnetic velocity and flow measurements techniques application to cardiovascular patients, discussing utilization problems 09 p1272 A72-23275

On-line analog display system for cardiovascular functions and beat-by-beat cardiac output derived from single aortic blood flow measurement 10 p1430 A72-24375

Cardiovascular changes produced by whole body vibration of dogs and pigs, obtaining resonant frequencies of organ systems 10 p1426 A72-24484

Positive acceleration effects on human cardiovascular system during centrifuge tests, studying ECG changes in terms of cardiac rhythm, heart rate and wave parameters 11 p1584 A72-26015

Cardiovascular responses to positive pressure oxygen breathing from blood pressure and heart and respiratory rate measurements 11 p1584 A72-26017

Human cardiovascular function change as indication of hypoxic circulatory stress, using noninvasive cardiographic measurements of cardiac electromechanical time intervals 12 p1769 A72-27470

Cat and rat cardiac and cardiovascular reflexes response to electric pulse stimulation of sensorimotor cerebral cortex 12 p1761 A72-27647

Multivariate algorithms of optimum content and form for cardiovascular risk assessment in pilots and air transport personnel 12 p1764 A72-28264

Clofibrate treatment for atherosclerotic cardiovascular disease prevention among Sabena flying personnel 12 p1766 A72-28293

Physiological effects on anesthetized and conscious dogs during exposure at 80,000 ft for different decompression rates, discussing cardiovascular, biochemical and pathological effects 12 p1768 A72-28322

Noninvasive polygraphic technique to assess cardiovascular responses to intravenous glucagon injection 13 p1901 A72-28570

Cardiovascular and respiratory changes in dogs exposed to acute overheating, relating ECG changes to adrenergic and hypoxia effects 14 p2074 A72-30382

Cardiovascular system functional state elevation during controlled cooling, studying hemodynamic changes 14 p2075 A72-30386

Simulation of the human cardiovascular system - A model with normal responses to change of posture, blood loss, transfusion, and autonomic blockade. 17 p2507 A72-34445

Pathology of the cardiovascular system in terms of the theory of cortico-visceral interrelations 21 p3000 A72-40756

Hemodynamic reflexes during acceleration stresses, considering vessel walls, cardiac rhythm, blood distribution and sinus carotis receptors 22 p3141 A72-41983

The function of external respiration in mental activity 22 p3150 A72-42284

New mechanical device for producing traumatic shock in dogs - Circulatory and respiratory responses. 22 p3142 A72-42490

High altitude physiology: Cardiac and respiratory aspects; Proceedings of the Symposium, London, England, February 17, 18, 1971. 22 p3143 A72-42583

Chronic altitude sickness pathology based on anatomical and histological findings in abnormal mountain inhabitants autopsies, comparing with cardiovascular system morphology in normal people 22 p3143 A72-42586

Limbico-neocortical, cardiovascular and hormonal system vegetative shifts associated with emotional behavior response, presenting neurogenic stress model for animals 22 p3148 A72-43166

Cardiovascular system venous part responsiveness to central nervous and humoral influences 22 p3148 A72-43167

Nervous-emotional stress as a problem of modern work physiology 22 p3148 A72-43170

Studies on weightlessness in a primate in the Biosatellite 3 experiment. 23 p3253 A72-43388

A large-scale model of the human cardiovascular system and its application to ballistocardiography. [ASME PAPER 72-AUT-Q] 23 p3259 A72-43635

Photoelastic analysis of cardiovascular-magnitude stress pattern produced by flow through gelatin-agar walled channels for analysis of mechanical stresses on blood vessel walls 23 p3260 A72-43936

Use of implantable telemetry systems for study of cardiovascular phenomena. 23 p3260 A72-43996

A special vitamin complex for prophylaxis of atherosclerosis in aviation personnel 23 p3261 A72-44153

Experimental development of a method for long-term implantation of plastic catheters in different sections of the cardiovascular system 24 p3375 A72-45118

Longevity and cardiovascular mortality among former college athletes. 24 p3374 A72-45689

CARDS
 Plaque program for logic network wiring on IC box cards 03 p0327 A72-13167

CARET WINGS
 Thin shock layer theory of lifting properties of reentry caret and flat delta wings and waveriders at high incidence angles and Mach number 02 p0152 A72-12345

V-shaped wings supersonic characteristics at 0-15 deg angles of attack, investigating flow structure between wings by pitot tube rake 06 p0757 A72-18129

Conical caret wings supersonic characteristics, examining flow transition from weak to strong attached shock waves 24 p3361 A72-45114

CARGO
NT AIR CARGO
 Prediction models for dynamic environment experienced by cargo during air and rail transportation 15 p2339 A72-32610

CARGO AIRCRAFT
 Super Guppy four engine aircraft characteristics, performance and loading device for bulky cargo air transportation 11 p1577 A72-25812

Dynamic input to cargo in turbojet aircraft studied during C141 and CSA flights, discussing instrumentation, test procedures, data reduction processes and results 15 p2181 A72-32625

Boeing 747-F cargo aircraft, describing onboard and ground facilities for freight handling and loading 23 p3278 A72-43245

Minimum operational costs of passenger and cargo transport aircraft, considering effects of flight distance, wind conditions and optimum speed and altitude 23 p3252 A72-44338

CARGO SHIPS
NT TANKER SHIPS
CARGO SPACECRAFT
 Space shuttle vehicle configurations with reusable booster and orbiter modules, discussing cargo capacity, maneuvering capability, mission duration, engine characteristics and acceleration constraints 07 p1085 A72-19058

CARNOT CYCLE
 Relativistic thermodynamics development based on invariant entropy concept, considering frictionless heat conduction and Carnot cycles 19 p2835 A72-37928

CAROTID SINUS REFLEX
 Carotid sinus counterpressure as baroreceptor stimulus in intact dog, recording arterial pressure response in closed loop gain 07 p0917 A72-19439

Case report of pilot near-syncope episode with bradycardia due to hyperactive right carotid sinus reflex 12 p1771 A72-27487

Pressure chamber training effects on rats chain motor reflexes hypoxia adaptation, noting sinocarotid receptors importance in compensatory-adaptive reactions 13 p1902 A72-28641

Venous responses to stimulation of carotid chemoreceptors by hypoxia and hypercapnia. 18 p2648 A72-36025

Hemodynamic reflexes during acceleration stresses, considering vessel walls, cardiac rhythm, blood distribution and sinus carotis receptors 22 p3141 A72-41983

Carotid rete role in brain protection against extreme elevations of systemic blood pressure, presenting goat cerebral blood flow measurement procedure 22 p3144 A72-42671

CARRIER FREQUENCIES
NT HARMONIC GENERATIONS
 Phase locking loop synchronized quartz oscillator for integral frequency multiplication in wideband carrier frequency systems 07 p0954 A72-19174

Optimal continuous recording of amplitude-phase distributions on spatial carrier frequency for light wave modulation and optical antenna simulation 08 p1132 A72-21263

Maximum likelihood estimate of carrier frequency and arrival direction of radio signals in background noise for large aperture antennas 08 p1133 A72-21373

Error probability and reception stability in synchronous detection of phase manipulated signals with additive Gaussian noise at multiplied carrier frequency 10 p1436 A72-24587

Statistical characteristics of IR receivers with parametric carrier frequency conversion, describing noise index minimization technique 12 p1846 A72-27889

Doppler carrier frequency shift measurement accuracy, finding relationships in errors for coherent and noncoherent pulse trains 15 p2195 A72-31657

Estimation-correlation principle application to harmonic signal receiver with unknown carrier frequency, using searching phase locked AFC circuit as estimation unit 15 p2202 A72-32667

Statistical characteristics of IR receivers with parametric carrier frequency conversion, describing noise index minimization technique 16 p2427 A72-33998

Shaping circuit for complex RF pulse consisting of simultaneous equallength square pulses with different frequencies, discussing carrier frequencies selection 21 p3022 A72-41118

Transient response of threshold lowering circuit with frequency converter for single contour IF amplifier with resonant frequency equal to carrier frequency 22 p3153 A72-42121

CARRIER INJECTION
 Punch-through transit time negative resistance semiconductor device utilizing injection from Schottky barrier, deriving small signal theory for microwave impedance 01 p0042 A72-10787

IMPATT diode oscillator injection locking behavior from model, comparing results with experiment 06 p0788 A72-18469

Strong electric field recombinational domains in semiconductors with mobile holes and electrons during band-band illumination or double injection 07 p1048 A72-19638

Magnetodiode model of intrinsic semiconductor slab under Lorentz force and double injection inducing ambipolar drift and carrier redistribution 08 p1142 A72-21746

Numerical solution of theta pinch in electron-hole plasma of Ge semiconductor under surface recombination as contactless method of current carrier injection 08 p1218 A72-22178

HF thermal noise in single and double injection space charge limited solid state diodes 09 p1288 A72-23124

Small signal theory of emitter current limited injection in negative mobility semiconductors at zero doping limit 12 p1788 A72-27165

- Te-doped GaAs injection laser, investigating crystal growth dislocations effects on output radiation-injection current characteristics 12 p1822 A72-27617
- P-n-p-n junction thyristor turnoff process under reverse anode voltage at high injection level, examining current voltage curve and switching time constant 13 p1932 A72-29293
- N region capture centers effects on small signal impedance in p-n-n diode structure during passage of strong dc current 13 p1933 A72-29977
- MOS transistor injection level dependent theory, calculating drain region saturation conductance by iterative procedure 15 p2205 A72-31318
- Stability of the dynamic parameters of a transistor in a small signal mode superimposed on a static injection mode 17 p2596 A72-35801
- Thermal noise in double injection diodes operating in the insulator regime 18 p2667 A72-36979
- Behavior of epitaxial bipolar transistors in the strong injection regime 18 p2668 A72-37103
- Charge injection into the gate dielectric of MOS transistors during junction avalanche 18 p2668 A72-37104
- The static current-voltage characteristic of four-layer structures in two-collector operation at a low injection level 19 p2846 A72-38573
- Effect of the filling of the capture levels with increasing current on the formation of negative resistance under double injection conditions 19 p2846 A72-38574
- Interpretation of the preswitching behaviour of chalcogenide-glass switches in terms of a space-charge-injection mechanism 21 p3034 A72-41466
- General transport theory of noise in pn junction-like devices. II - Carrier correlations and fluctuations for high injection 22 p3160 A72-43084
- Static and dynamic characteristics of double-injection currents in p'-n-n' diode structures with deep impurities and nonideally injecting junctions 23 p3268 A72-43346
- Strong electric field recombinational domains in semiconductors with mobile holes and electrons during band-band illumination or double injection 24 p3431 A72-44570
- Noise properties of the injection-limited Gunn diode 24 p3385 A72-44962
- CARRIER MOBILITY**
- NT ELECTRON MOBILITY**
- NT HOLE MOBILITY**
- Hall effect mobility dependence on dispersion law in degenerate electron gas on semiconductor surface 02 p0270 A72-12890
- Two dimensional analysis of carrier circulation in MOS transistors for arbitrary polarization, including surface effects 03 p0330 A72-13166
- Carrier mobility measurement in inhomogeneous semiconductors based on bulk photovoltaic and photomagnetolectric effects 03 p0402 A72-13862
- Carrier transport effects in semiconductors for carrier recombination time approaching relaxation time 03 p0333 A72-13863
- Charge state effects on defect production mechanisms, configurations, mobility, annealing kinetics, interaction and dissociation in displacement damage in covalent semiconductors 03 p0403 A72-14077
- Li-diffused Si compared to conventionally doped materials under neutron irradiation, considering carrier removal 03 p0403 A72-14078
- Minority carrier diffusion effect on current gain in miniature bipolar transistors 04 p0498 A72-15132
- Carrier mobility field dependence effects on validity of gradual channel approximation in insulated-gate field effect transistors, discussing velocity field relationship 04 p0498 A72-15135
- MOS inversion layer mobility theory and surface charge scattering mechanism 07 p0954 A72-19121
- Physical parameters of transistor, discussing carrier transfer, space charge and potential drop as function of current and voltage changes 08 p1139 A72-21058
- One dimensional model for drift transistor at low injection level with minority carrier mobility dependence on impurity concentration 08 p1140 A72-21063
- Sn additions influence on Te structural characteristics relation to microhardness and current carrier mobility variations 09 p1322 A72-22204

- Franck-Condon phonon displacement effects on mobility edge and energy gap in disordered materials 09 p1357 A72-22986
- Small signal theory of emitter current limited injection in negative mobility semiconductors at zero doping limit 12 p1788 A72-27165
- Electron irradiation of Li doped Ge at low temperatures, measuring Hall effect and minority carriers diffusion length 12 p1857 A72-28055
- Semiconductor devices with extended slow wave-carrier interaction region for vacuum traveling wave tube replacement 13 p1927 A72-28401
- Mobility-field characteristics of GaAs below Gunn threshold with magnetoresistance technique, relating to device performance and other material parameters 13 p2021 A72-28573
- Negative photoconductivity in CdSe single crystals due to free carrier mobility decrease after surface treatment in gas discharge, noting neutron traps role 13 p2024 A72-30046
- Free carrier mobility dependence on excitation light intensity in CdSe single crystals with negative photoconductivity 14 p2141 A72-30169
- Localized electronic states near mobility edge in semiconductor, considering eigenfunction behavior in random lattice problem 14 p2143 A72-30878
- Gunn effect - Bulk instabilities 17 p2594 A72-34562
- Influence of carrier diffusion on the intrinsic response time of semiconductor avalanches 18 p2717 A72-36083
- Transient behaviour of laser generated carrier mobility in n-Ge 18 p2697 A72-36351
- Electrical characteristics of bulk n-InP oscillators 18 p2666 A72-36456
- Measurement of Hall mobility of current carriers in inhomogeneous semiconductor samples 18 p2720 A72-36964
- Measurements of the field-effect and effective mobilities in MOS transistors 20 p2907 A72-39272
- Theory of Poole-Frenkel conduction in low-mobility semiconductors 22 p3214 A72-42317
- Dependence of MOS transistor parameters on carrier mobility 23 p3272 A72-44139
- CARRIER MODULATION**
- U MODULATION**
- CARRIER ROCKETS**
- U LAUNCH VEHICLES**
- CARRIER WAVES**
- FM communication systems with Gaussian and clipped noise carriers, calculating SNR 01 p0024 A72-10129
- Notch noise loading tests on predetection tape recording of FM carriers, showing noise power ratio dependence on record level and bias levels and output equalization 02 p0175 A72-12146
- Carrier wave growth during propagation through negative differential mobility n-type GaAs under nonuniform dc bias conditions 07 p1047 A72-19044
- Hybrid carrier and modulation tracking loops exploiting sideband coherency for phase coherent tracking, telemetry and command system performance improvements 07 p0939 A72-19066
- Pulse overlapping effects on phase jittering in carrier regeneration with quaternary phase shift keying 07 p0945 A72-19662
- Aircraft applications of composite signal OMEGA configuration with phase data combined at separate carrier with weighting coefficients, discussing advantages over uncompensated navigation systems 13 p1998 A72-29192
- Carrier wave behavior in n-type GaAs slab under crossed dc electric and magnetic fields, investigating traveling space charge amplifier magnetic control 14 p2143 A72-30941
- Carrier wave propagation at semiconductor surface with electron drift, discussing solid state traveling wave amplifier design 15 p2290 A72-31288
- Carrier synchronization and polyphase signal detection in digital communication network for high speed data transmission, deriving reconstructed noisy signal error probability 16 p2363 A72-33218
- Propagation of pulsed-carrier signals in random media 17 p2514 A72-34380
- Controlled-carrier transmission of AM/VSB television from space 21 p3016 A72-40770
- Digital command system second-order subcarrier tracking loop performance 21 p3038 A72-40870

- Spontaneous emission of plasma waves in the presence of a finite amplitude wave 21 p3093 A72-41494

CARTESIAN COORDINATES

- Geocentric coordinates transformation from system related to mean pole and mean equator into instantaneous pole and instantaneous equator system, noting Cartesian coordinates 17 p2548 A72-35359

- Wind velocity components determination in Cartesian coordinates based on rectilinear uniform air particle motion, noting difference with respect to geostrophic approximation 23 p3310 A72-43532

CARTIDGE ACTUATED DEVICES

- U ACTUATORS**
- U EXPLOSIVE DEVICES**
- CASCADE CONTROL**

- Network synthesis of cascaded threshold logic elements to separate binary patterns into two classes by iterative computation of parameters 01 p0034 A72-10474

- Analytical inversion of quasi-orthogonal matrix for Simpson method of state feedback gains calculation in multiloop linear mode control systems 05 p0639 A72-15807

- German book on time variable multiparameter control systems covering reduction, canonical forms, decoupling, feedback stabilization, observers, inversion and multiloop synthesis 06 p0794 A72-18517

- Complex sampling with cascaded triple input majority logic redundant systems, deriving failure probability 07 p0949 A72-19173

- Multistage broadband microwave amplifier design based on bipolar transistors cascade coupling, using scattering parameters 10 p1451 A72-24572

- On structures for nonrecursive digital filters 17 p2516 A72-35221

- Certain features of the use of controllable-gain transistors 21 p3033 A72-40944

- Amplification cascade designs for harmonic and pulsed signals with a high frequency emitter correction 21 p3033 A72-40946

- Optimization of planar transistor operation modes in cascades with inductive correction 21 p3034 A72-41121

CASCADE FLOW

- Estimation method for surface pressure distribution on cascade airfoil in retarded flow, applying to axial flow turbomachines design with suction performance and efficiency 01 p0001 A72-10396

- One dimensional unsteady flow in turbine engines rotating and static vane cascades, discussing vibrations propagation 02 p0202 A72-11584

- Turbulence degree effects on aerodynamic properties of planar decelerating cascades at Reynolds numbers 50,000-250,000, discussing blade boundary layer characteristics 02 p0153 A72-12716

- Blade cascades pressure distribution for plane incompressible flow with boundary layer separation near trailing edges, replacing blade profiles by vortex fields [DGLR PAPER 71-096] 02 p0153 A72-12728

- Circular arc blades two dimensional cascade performance test data for various cambers comparison with potential theory data 05 p0602 A72-16485

- Two dimensional cascade performance data correction for rotating blade row stream surface inclination in axial flow turbines 05 p0602 A72-16486

- Finite pitch airfoil theory relations for turbomachine moving blade rows interference effect on cascade flutter 05 p0738 A72-16488

- Two dimensional cascade test of air-cooled turbine nozzle, describing aerodynamic characteristics and heat transfer properties 05 p0602 A72-16489

- Cascade nozzle gas particle flow properties, discussing flow pressure experiments and theory at different streamlines 05 p0602 A72-16490

- Turbine blade local heat transfer coefficient calculation with digital computer program and naphthalene blade mass transfer in cascade flow 05 p0747 A72-16498

- Boundary layer of gas-particle flows with pressure gradient, numerically integrating momentum equation for cascade particulate flow [AIAA PAPER 72-87] 05 p0604 A72-16808

- Velocity and exit angle determination for flow behind turbine blade cascade with cooling air exhaust through blade trailing edges from continuity equations 05 p0707 A72-17063

- Flow visualization in supersonic axial compressor by short exposure schlieren photography of shock

- wave patterns in rotating annular cascade of compressor blades
[ONERA, TP NO. 1026] 05 p0708 A72-17192
- Viscous flow through movable and immovable cascades of blades, determining velocity field by airfoil center line vortex distribution
06 p0757 A72-18131
- Cascading turbomachine blades vibration measurement in subsonic and sonic high temperature gas flows, describing test facility
06 p0797 A72-18689
- Numerical analysis of computing velocity distribution in vortex row cascade profiles by method of singularities
07 p0965 A72-18787
- Two dimensional subsonic flow behind symmetrical blade cascade, taking into account initial flow turbulence
07 p0909 A72-20078
- Gas flow analysis of heat transfer coefficient in turbine blade cascades of active and reactive profiles
08 p1222 A72-20946
- Potential equations and singularities methods comparison for two dimensional flow field cascades and stress distribution elasticity theories
09 p1260 A72-22627
- Supersonic flow through stationary and rotating cascades, using method of characteristics
09 p1260 A72-22630
- Secondary flow types and measurement in axial flow compressor cascades, discussing energy losses
09 p1260 A72-22633
- Aerodynamic efficiency of plane slotted blade cascades of adjustable nozzle diaphragms in transport aircraft axial flow gas turbine engines
09 p1374 A72-23186
- Reynolds number and mainstream turbulence effects on laminar separation bubbles behavior in boundary layers on turbine blades in cascade
10 p1416 A72-23873
- Nonuniform vortex flow of compressible gas past cascade of plates, noting monochromatic pressure waves at harmonics of plate vibration frequency
10 p1418 A72-24538
- Linearized method of characteristics application to supersonic flow past oscillating flat plate cascades with supersonic leading edge locus
[AIAA PAPER 72-377] 11 p1730 A72-25401
- Unsteady lift on airfoils in moving cascades with inlet axial flow disturbances, estimating lift on reference blade between blade channels
[ASME PAPER 72-GT-5] 11 p1568 A72-25608
- Jet flaps for high turning compressor cascades in incompressible axial flow, calculating blade pressure and jet slope distributions
[ASME PAPER 72-GT-16] 11 p1569 A72-25615
- Shocked flow and pressure loss computation for axial flow compressor cascades, using time dependent finite difference technique
[ASME PAPER 72-GT-31] 11 p1569 A72-25627
- Cascade technology for centrifugal compressor vaned diffuser design, comparing performance results with conventional diffuser data
[ASME PAPER 72-GT-39] 11 p1569 A72-25633
- Two dimensional transonic turbine blade cascade downstream flow losses determination
[ASME PAPER 72-GT-43] 11 p1570 A72-25637
- Two dimensional flow losses of turbine blade cascade with incompressible boundary layer injection
[ASME PAPER 72-GT-46] 11 p1570 A72-25638
- Supersonic turbine cascade flow properties and pressure distributions on blades, comparing calculated results with experimental data
[ASME PAPER 72-GT-47] 11 p1570 A72-25639
- Two dimensional cascades supersonic exit flow field, using Oswatitsch method of characteristics and conservation laws
[ASME PAPER 72-GT-49] 11 p1570 A72-25641
- Flow data reduction validity for supersonic axial compressors, presenting experimental results for rotating supersonic cascade
[ASME PAPER 72-GT-100] 11 p1571 A72-25669
- Computer program for gas turbine characteristics and influence coefficients calculation, allowing for cascade loss distribution during flow choking
12 p1862 A72-28151
- Arbitrary cascade profiles aerodynamic characteristics calculation via integral equation numerical solution for attached potential incompressible fluid problem
14 p2070 A72-31014
- Isoenergetic and irrotational planar supersonic cascade ideal gas flow computation by analytic method of characteristics
15 p2178 A72-31466
- Velocity profiles for three dimensional turbulent boundary layer on end wall of axial flow compressor cascade passage under adverse pressure gradients
16 p2342 A72-32901
- Calculation of two-dimensional cascades in isentropic flow
17 p2484 A72-34893
- Calculation of the plane potential flow past rotating radial blade cascades
19 p2746 A72-38547
- Unsteady aerodynamic and aeroelastic effects in turbomachine blade cascades supersonic flow, discussing trends in fan and compressor technology
21 p3118 A72-40969
- Two-dimensional subsonic linearized theory of the unsteady flow through a blade-row with small steady pitch and camber angle.
[ICAS PAPER 72-12] 21 p2990 A72-41137
- Flow and energy loss distribution in annular stator nozzle cascades with cylindrical blade profiles of different twist, measuring flow exit angle along blade span
23 p3248 A72-43664
- Flow parameters and geometric factors effect on wake structure behind nozzle cascades with cooling air ejection through blade trailing edges, evaluating energy losses due to flow mixing process
23 p3248 A72-43665
- Reduction of end losses in cascades of cambered blades
23 p3248 A72-44025
- Double hierarchy in repeated cascade theory of turbulence.
24 p3390 A72-44997
- Extension of the Prandtl-Glauert similarity rule to loss including cascade flow.
24 p3363 A72-45352
- Determination of pressure losses in turbomachines.
24 p3393 A72-45353
- Study of a turbine type flowmeter with helical blades.
24 p3404 A72-45354
- Application of cascade and actuator disc theories to computer aided design of fans.
24 p3363 A72-45359
- Influence of revolutions on efficiency and characteristics of the rotating axial cascade of blades.
24 p3363 A72-45361
- The determination of a general relation between the aerodynamic properties of a single airfoil and those of the same airfoil arranged in an arbitrary cascade.
24 p3363 A72-45363
- Some experiences with the solution of potential flow in the plane cascade on the computer.
24 p3393 A72-45365
- Suction side velocity distribution parameter characteristic relationship to profile geometrical parameters in turbine blade cascade system
24 p3394 A72-45366
- An approximate method for the calculation of the characteristics of axial-flow fans.
24 p3363 A72-45369
- Frictionless core flow and friction layers at turbomachine walls and blades for real two dimensional cascade flow modeling
24 p3394 A72-45370
- Aerodynamic characteristics of turbine blade cascades in unsteady incompressible and compressible fluid flow, considering axial flow turbine blades vibration
24 p3364 A72-45524
- CASCADE WIND TUNNELS**
Cascade wind tunnel and water table determination for trajectories and velocities of suspended particles in fluid flow through axial compressor stage
07 p0907 A72-18756
- Researches on the two-dimensional retarded cascade. I, II.
22 p3133 A72-41944
- CASCADES**
Monte Carlo simulation on high energy cosmic ray propagation and multiplication in high altitude emulsion chamber observations, examining two-fire-ball and H-quantum models
01 p0121 A72-11123
- Resonant vibration and stresses of dynamically nonuniform annular cascade under aerodynamic interaction of alternating different blades
01 p0143 A72-11368
- Cascaded annular lens systems for focusing electromagnetic waves, noting advantages of axicon
03 p0388 A72-12967
- Blading, flow and characteristic line calculations for machine with axial turbulent flow, using plane cascade measurements
06 p0757 A72-18690
- Turbojet engine compressor efficiency relationship to cascade characteristics diagram, using influence coefficients
07 p1054 A72-18995
- Transient effects due to electromagnetic cascades in Pb during Cu wall passage in ionization calorimeter
07 p0988 A72-19871
- Turbulence velocity field analysis by repeated cascade theory via partial Fourier transform, predicting Kolmogoroff law in line with experimental results
07 p0972 A72-20112
- Nucleonic cascade model analysis of underground vertical muon curve for primary cosmic ray nucleon spectrum below 40 TeV
10 p1529 A72-24417
- Interaction between generating lines in coupled channels with arbitrary line broadening, studying radiation generation regimes in cascade circuit
13 p1970 A72-29680
- German monograph - Computational and experimental investigations regarding the operational characteristics of a three-stage axial-flow compressor with high performance per stage
19 p2745 A72-37490
- CASCADES (FLUID DYNAMICS)**
U FLUID DYNAMICS
- CASCADE MOSFET**
U FIELD EFFECT TRANSISTORS
- CASE BONDED PROPELLANTS**
Case bonded solid rocket propellants mechanical strength characteristics determination by photoelastic stress measurements or viscoelastic calculation
14 p2145 A72-30765
- CASE HISTORIES**
Case report on compensated hemolytic anemia associated with Gilbert syndrome, discussing implication in aviation
01 p0022 A72-11299
- Case history of student aviator with psychosomatic Lymphogranuloma venereum related to vestibular apparatus
02 p0167 A72-11712
- Fainting prevention in flying personnel, discussing constitutional susceptibility, health irregularities, alcohol, heavy smoking, lack of sleep, emotions and medical histories
03 p0316 A72-13722
- ECG, physical exercise and drug use in diagnosis and aeromedical evaluation of supraventricular arrhythmias, presenting case histories of pilots with wandering cardiac pacemakers
[AD-740987] 10 p1428 A72-23741
- Case report of fighter pilot disorientation episode during night flying exercise, suggesting psychological stress factor
11 p1584 A72-26019
- Case report of pilot near-syncope episode with bradycardia due to hyperactive right carotid sinus reflex
12 p1771 A72-27487
- U.S.-Canadian Alouette/ISIS satellites case history, considering hardware, lunar sample analysis and satellite transmitted radio beacon signal reception and analysis
14 p2175 A72-31144
- Private aircraft ownership and use for family travel and pleasure, discussing costs, maintenance and operational problems
[AIAA PAPER 72-812] 19 p2750 A72-38119
- Corporate aircraft pilot contribution to accident investigation in providing expertise, discussing various case histories
20 p2888 A72-39751
- Case report on dive decompression induced maxillary sinus barotrauma due to sinus pressure buildup caused by ostium blockage
22 p3150 A72-42497
- CASES (CONTAINERS)**
NT ROCKET ENGINE CASES
- CASING**
Turbine casing components stresses in presence of creep, demonstrating calculation method validity for thick-walled structures by elastoplastic analogy
05 p0734 A72-15985
- Free convective heat transfer measurement from solid copper inner cylinder to cylindrical casing
09 p1410 A72-22351
- Bending roller adjustment parameters for casing shaping in machining process
11 p1642 A72-26815
- Normal and tangential force factors in casing shaping by bend roll method
11 p1642 A72-26817
- Heat transfer to casing in axial clearance space between nozzle diaphragm and turbine wheel
12 p1861 A72-28134
- Dimensional chains calculation in differential method of manufacturing complex precision elements of casings
13 p1962 A72-28740
- Turbine casing components stresses in presence of creep, demonstrating calculation method validity for thick-walled structures by elastoplastic analogy
24 p3460 A72-45727
- CASPIAN SEA**
Soyuz 6 multispectral aerogeophysical measurements of Usturt plateau and Caspian and Aral Seas, discussing remote sensing information yield on earth water/land and atmosphere properties
02 p2028 A72-11785
- CASSEGRAIN ANTENNAS**
Multimode feeds development for offset Cassegrain tracking antennas
01 p0040 A72-10678
- Rayleigh distance for reflection from curved surfaces in Cassegrain subreflector geometrical optics design
04 p0499 A72-15207
- Phase errors and main lobe orientation changes during beam scanning of two reflector Cassegrain antennas
08 p1139 A72-20934

Two reflector Cassegrain antenna secondary reflector random fluctuations effects on drift in main lobe direction

08 p1143 A72-21846

Radiation pattern determination parabolic Cassegrain radio telescope reflector antennas from Fresnel zone emission source, using holographic technique

10 p1482 A72-24783

Pyramidal-horn primary element axial position effect on dual mirror Cassegrain microwave antenna main lobe pattern, obtaining optimal position

13 p1929 A72-29040

Parabolic, Cassegrain, spherical and horn-parabolic axisymmetric mirror antennas, calculating primary radiating element orientation effects on radiation polarization characteristics

13 p1931 A72-29277

Radiation pattern reconstruction of radio telescope parabolic Cassegrain reflector antennas from Fresnel zone emission source, using holography and optical processing

14 p2103 A72-30221

Near sidelobes in Cassegrain antenna systems

18 p2668 A72-37039

Low noise microwave receiving systems on a 64 m antenna

19 p2763 A72-37255

Design of Cassegrain antennas employing dielectric cone feeds

19 p2772 A72-37847

Reflector profiles for the pencil-beam Cassegrain antenna

20 p2903 A72-39221

The efficiency of near-field Cassegrainian antennas

21 p3027 A72-40367

On the efficiency and radiation patterns of mismatched shaped Cassegrainian antenna systems

21 p3027 A72-40369

Near-field Cassegrain antennas of high surface efficiency for satellite communication links

21 p3029 A72-40520

A 3-meter Cassegrain antenna for the frequency range from 2.1 to 2.3 GHz

21 p3029 A72-40521

Radiation patterns and structural design of two mirror millimeter wave Cassegrain antennas with horn radiator

23 p3271 A72-43778

CASSEGRAIN OPTICS

Cassegrain type astronomical reflecting telescope design, describing auxiliary equipment

01 p0047 A72-10202

High resolution UV stellar spectroscopy in star stabilized Skylark rocket vehicle, using Cassegrain echelle optics and image intensification

03 p0354 A72-13056

Rayleigh distance for reflection from curved surfaces in Cassegrain subreflector geometrical optics design

04 p0499 A72-15207

High speed photometry of nova variables with white dwarf and late-type binary star flickering, using Cassegrain focus

06 p0889 A72-18332

Cer-Vit glass mirror replacement for AFCRL lunar laser observatory inverted Dall-Kirkham Cassegrain telescope, noting one arc sec resolution from wire and null optics tests

07 p0985 A72-19410

Small lunar based reflecting telescopes with Cassegrainian and catadioptric optical systems, discussing design and operation

08 p1164 A72-20976

Rocket-borne Cassegrain optic stellar electrophotometer for early star observations in 1300-2000 A region

19 p2796 A72-37585

Adaptation of the Schupmann medial telescope to a large scale astronomical optical system

19 p2797 A72-37587

Multiple mirror astronomical telescope using laser source light collimated with central Cassegrain system, presenting expected diffraction patterns

21 p3052 A72-40378

A large multiple mirror telescope (MMT) project

22 p3180 A72-42988

Remotely controlled astronomical observatory telescope Cassegrain focus, evaluating computerized automated electronic system advantage over conventional instrument

24 p3405 A72-45543

CASSIOPEIA A

Cas A, Tau A, Cyg A and Orion Nebula absolute flux density measurements at centimeter wavelengths

04 p0578 A72-15313

Cassiopeia A secular flux density decrease relative to Cygnus A and Taurus A at 1.4 and 3 GHz, discussing application to antennas and radio telescopes calibration

09 p1390 A72-23529

Interferometer investigations of Cassiopeia linear polarization at centimeter wavelengths, explaining

results by source model incorporating Faraday depolarization

12 p1865 A72-27094

Calibration of the flux density of Cassiopeia A and Cygnus A in the range 300-9375 MHz

17 p2617 A72-35728

CASSIOPEIA CONSTELLATION

Cassiopeia region galactic structure study via objective prism, cataloging stars radial velocities and distances

09 p1391 A72-23539

Investigation of type-A star condensations in the Perseus and Cassiopeia constellations

22 p3229 A72-42951

Investigation of several nebulae in Cassiopeia with a Fabry-Perot interferometer

23 p3333 A72-43233

High energy gamma ray point sources in Cassiopeia and Cygnus regions, using extensive air shower Cerenkov flashes detection technique

23 p3329 A72-43941

CASTIGLIANO VARIATIONAL THEOREM

Castigliano theorem in energy method, considering global static constraints and restriction for generalized force variables reduction through integration

05 p0732 A72-15803

Castigliano variational theorem for algebraic equation solution of thermal stresses determination in elastic parallelepiped, using Maxwell stress functions as cosine binomial series

24 p3459 A72-45267

CASTING

NT INVESTMENT CASTING

NT SLIP CASTING

Continuous casting of metallic tubular structural elements reinforced with boron filaments, stressing application to space shuttle structures

01 p0074 A72-10731

Substructure of cast alloys based on Al-Mg system from electron diffraction microscopy

03 p0377 A72-14023

Low cost metal matrix composition fabrication techniques, considering plasma spraying and continuous casting

03 p0364 A72-14236

Carbon impurity effects on molybdenum ingot formation, detailing crystal growth, size reduction and length

04 p0533 A72-14987

Economical methods for cast maraging steel production, describing composition, heat treatment and mechanical properties

07 p1010 A72-18970

Aircraft light alloy integral construction for stress concentration and fatigue failure avoidance, describing continuous casting process, stress relieving and ultrasonic flaw testing procedures

07 p0995 A72-19725

Physical properties, combustion characteristics and applications of pyrotechnic castable composition for smoke generation

08 p1222 A72-20785

X ray diffraction and chemical phase analysis of Nb alloys in cast and heat treated state, considering hardening mechanism

09 p1327 A72-22636

Fusion cast zirconia-alumina-silica refractories manufacturing process, phase diagrams, chemical and physical properties and industrial applications

10 p1502 A72-24734

Metal forming techniques for gas turbine engines, considering isothermal, radial and powder metallurgy preform forgings, contoured cross and form rolling, and squeeze casting

11 p1638 A72-25649

Thermoplastic materials casting procedures to mold high melting point metal compound powders

11 p1645 A72-26861

Powder metallurgy versus melting and casting of high temperature alloys, tool steels and specialty alloys

11 p1646 A72-26869

Commercial and laboratory Mg alloys for die and sand casting, high strength and extruding applications

14 p2113 A72-30269

Squeeze casting for precision shaping mechanical properties, surface finish and cost reduction in metal working

14 p2108 A72-30862

Cast Al alloys tendency to brittle failure in percussive bending tests estimated from force strain oscillograms

14 p2124 A72-31035

Die-casting machine design trends, considering uses of elbow lever and hydraulic systems and programmed control

16 p2399 A72-34142

Metals and alloys solidification concepts, applying to casting techniques development

20 p2936 A72-39211

Fabricating aluminum matrix composites. I - A survey of aluminum matrix composites

22 p3182 A72-41996

Fabrication of shaping cermet elements of die-casting molds for plastics by the hydrostatic pressing method

22 p3182 A72-42199

Heat resistant ZrSi₂ alloy precision and ground cast specimens, determining short and long term strength and fatigue

23 p3301 A72-43761

Some technological factors influencing the ductility of thermoplastic dross and the properties of niobium-carbide-based finished products

23 p3293 A72-44009

CASTING SOLVENTS

U PLASTICIZERS

CASTINGS

Nondestructive radioactive gas penetrant tests for porosity and fatigue damage in jet engine castings

01 p0069 A72-10813

Plastic deformation, heat treatment and grinding of set blank W casts for strip and foil production

01 p0088 A72-11085

Titanium melting, casting and molding techniques, discussing shapes, sizes and physical properties

03 p0370 A72-13100

Steel castings made in electric furnace with Al additive, observing magnesium and lime aluminate inclusions

03 p0371 A72-13199

Diffusion welding of cast and wrought Udimet 700 superalloy gas turbine engine components, discussing interfacial grain boundary migration and microstructural homogeneity effects on weld joint quality

07 p0997 A72-19998

Ultrasonic oscillations effects on alloy castings grain size and heat resistance, suggesting waveguide direction for oriented solidification

11 p1642 A72-26822

Carbon and other inclusions effects on cast W strength at elevated temperatures from microscopic observation

11 p1666 A72-26877

Ordered crystallization casting of Ni superalloys for turbine blades, using power down and high rate solidification processes

11 p1646 A72-26894

Primary crystallization of intermetallic compounds in Al alloy as function of high melting metal concentration and casting temperature

14 p2124 A72-31034

CATABOLISM

Effect of salt on activity, stability and allosteric properties of catabolic threonine deaminase from extremely halophilic bacteria

09 p1275 A72-22535

CATALASE

Erythrocytes catalase activity and number content relationship in human and albino rats blood, discussing compensatory effects

06 p0764 A72-18060

CATALOGS (PUBLICATIONS)

NT ASTRONOMICAL CATALOGS

CATALYSIS

Catalytic action in organic catalyst predecessors of contemporary enzymes, discussing polymers of alpha-amino acids and hydrogen cyanide

05 p0624 A72-16128

Electron theories of chemisorption and catalysis on semiconductor surfaces, considering band theory applicability range

07 p1048 A72-19561

Ni plating by chemical reduction method in boron hydride solution, deducing stabilizing effect of sulfur compounds and Pb salts from catalyst poisoning theory

11 p1641 A72-26265

Heterogeneous-homogeneous catalytic effects on combustion rate of hydrocarbons, ammonia and hydrogen mixtures

13 p1912 A72-28777

Nitriles, nitrogen bases and porphyrin-like pigments catalytic synthesis products analysis by mass spectroscopy gas and other chromatographies

14 p2157 A72-30583

Thermocatalytic pyrolysis for hydrogen generation from liquid hydrocarbon fuels with absolute cracking reaction efficiency

16 p2361 A72-33890

Microscopic and electron-microscopic investigation of the catalysis of ammonium perchlorate combustion

22 p3216 A72-43186

CATALYSTS

NT ELECTROCATALYSTS

Catalytic effects on ammonium perchlorate combustion pressure limits, noting distribution, concentration and particle size effects

13 p2025 A72-29303

Steam-hydrogen treatment tests for high temperature stability of noble metal catalysts in hydrogen-oxygen reaction initiation

15 p2192 A72-32225

Rising temperature reactor technique to evaluate catalysts for initiating hydrogen-oxygen reaction in gas mixtures at 78 K

15 p2193 A72-32550

- Raney Pd-Ag catalysts for methanol oxidation in alkaline electrolyte in fuel cells 16 p2361 A72-33879
- Bosch carbon dioxide reduction process for manned spacecraft oxygen recovery, analyzing carbon and water forming reactions with iron as catalyst [ASME PAPER 72-ENAV-9] 20 p2896 A72-39168
- Catalytic efficiencies of H₂O, D₂O, NO, and HCl in the vibrational relaxation of HF and DF. 24 p3378 A72-45306
- ### CATALYTIC ACTIVITY
- Hydrodynamic convective stability in catalytic chemical reaction with thermal and concentration coupling dependent on Lewis number 02 p3031 A72-12092
- Heat transfer from burning gas mixture flow to receiver wall, taking into account exothermal reactions due to catalytic effects 03 p0458 A72-14166
- Molecular oxygen evolution Mn catalyst photoactivation as two-quantum process, discussing kinetic model computer simulation 04 p0484 A72-15740
- Manganese catalyst photoactivation process for oxygen photosynthetic evolution investigated in Mn-deficient *Anacystis nidulans* cells 05 p0624 A72-15811
- Catalytic oxidation of gaseous products formed during thermal treatment of human wastes, considering hopcalite, Cu-Cr, Cu-Co, Pt and Pd 05 p0622 A72-16646
- Surface catalytic properties effect on multicomponent gas hypersonic boundary layer with simultaneous vibrational-dissociative relaxation, considering plate and blunt body laminar boundary layer 06 p0757 A72-18130
- Catalytic action of metal oxides on isopropylbenzene hydroperoxide decomposition in liquid phase 08 p1129 A72-22094
- Cation polymerization of beta-propiolactone without initial kinetics dependence on monomers concentration, relating acyl ion bonding and electron donor groups 09 p1275 A72-22496
- Continuous cotalimetric and thermocatalytic titration processes theory, deriving titration curves equations 12 p1755 A72-27444
- Alloying component effect on Pt catalytic activity in anodic oxidation of methanol for fuel cells 16 p2361 A72-33881
- Cubic sodium tungsten bronze electrocatalytic activity increase for oxygen reduction by traces of Pt 16 p2361 A72-33883
- Catalytic dissociation, hydrogen embrittlement, and stress corrosion cracking. 17 p2566 A72-34256
- Graph-analytical method of determining cetane numbers of light catalytic gas oil grades 17 p2571 A72-35178
- Iron-containing catalysts action mechanism during ammonium perchlorate-poly(methyl methacrylate) mixture burning in nitrogen atmosphere 19 p2847 A72-38456
- Relation between the work function and adsorption and catalytic properties of transition metal borides in the reaction of recombination of hydrogen and nitrogen atoms 22 p3187 A72-41926
- Adsorbed oxygen inhibition of reactions of hydrogen with tungsten. 23 p3298 A72-43270
- Catalytic efficiencies of H₂O, D₂O, NO, and HCl in the vibrational relaxation of HF and DF. 24 p3378 A72-45306
- ### CATHODE RAY TUBES
- #### NT PICTURE TUBES
- Flight display systems current state and future developments, discussing dual attitude indicators and automatic chart systems CRTs, engine displays and malfunction warning systems 03 p0357 A72-13423
- Cathode ray tube recorder for remote airborne photographic mission 03 p0360 A72-13711
- High resolution CRT application to UV film recording and radar and X ray scanning 03 p0360 A72-13712
- Three color optical pyrometer with microsecond resolution time based on three-wavelength double ratio method, displaying temperature/time relationship on cathode ray oscilloscope 04 p0522 A72-15476
- Hybrid computer aided design of thick electrostatic electron lenses by Laplace equation solution in terms of cylindrical harmonics, applying to CRT 06 p0779 A72-17481
- Frequency characteristics of traveling wave deflection system for wideband CRT deflector, improving sensitivity by low beam accelerating voltage 10 p1446 A72-23939
- Semiconductor lasers with high energy electron pencil beam excitation for high capacity computer storage application 10 p1492 A72-24513
- High tension exciter output voltage measurement based on cathode ray oscilloscope and high voltage probe, stressing calibration procedure 11 p1604 A72-26028
- Logic character generator for CRT text display and DEC PDP 8/S graphics 11 p1601 A72-26290
- Interactive computer graphics with three dimensional real time CRT display of air combat maneuvers for fighter pilot training 11 p1613 A72-26291
- #### NT CELL CATHODES
- COLD CATHODE TUBES
- COLD CATHODES
- HOLLOW CATHODES
- HOT CATHODES
- PHOTOCATHODES
- PHOTOMULTIPLIER TUBES
- THERMIONIC CATHODES
- NT TUBE CATHODES
- Directly heated cathode effect on He-Ne laser power output and relaxation oscillations in discharge gap 02 p0239 A72-12763
- Cathode and anode temperatures effect on effective heat of condensation of electrons at anode for particular current density and different cesium vapor pressures 02 p0156 A72-12858
- Differential pressure effects of gas-liquid configuration on porous electrode activity in oxygen cathodes 03 p0311 A72-12923
- Low pressure glow cathode triodes gas discharges, determining electron energy distribution function in double layer by probe measurements 03 p0400 A72-14349
- Kaufman thruster ion sources, discussing refractory metal, oxide coated, liquid mercury and hollow cathodes design, performance and durability 04 p0564 A72-14433
- Microwave signals detection with virtual cathode in klystron repeller by electrons screening at velocity modulated electron beam 08 p1136 A72-21766
- Cathodic processes in Al electrodeposition from ethyl pyridine bromide electrolyte, discussing phase equilibrium and electrical conductivity dependence on solution composition 09 p1318 A72-22529
- Vacuum arc stationary cathode mechanism theoretical analysis, determining cathodic temperature and current density 10 p1524 A72-24930
- Helium-neon laser with Hg cathode in gas discharge tube, providing 250 mW output at 6328 Å 13 p1969 A72-29518
- Optical field emission effects on photoelectron emission nonlinearity from metal cathode using ultrashort mode locked laser pulses 15 p2250 A72-32303
- Electrochemical development of high energy batteries using organic solvents, organic cathode depolarizers and fused salts 16 p2351 A72-33888
- Directly heated cathode effect on He-Ne laser power output and relaxation oscillations in discharge gap 20 p2931 A72-39069
- Signal-to-noise ratio of a photodetector with a virtual cathode 21 p3055 A72-40802
- ### CATIONS
- #### NT FERRIC IONS
- #### NT MANGANESE IONS
- #### NT METAL IONS

Cation distribution observation over nonequivalent lattice sites in shocked orthopyroxene, noting Mg and Fe order-disorder

01 p0053 A72-10293

High latitude magnetotail highly directed nearly monoenergetic positive ions population observation during geomagnetic storms, using Vela satellites electrostatic analyzers

01 p0060 A72-10887

D region positive and negative ion chemistry review, noting dominant roles of water ion clusters, NO cation and hydrates

02 p0219 A72-11979

Plasma sheet positive ions flux enhancement detection at lunar distance during lunar eclipse and geomagnetic storm

02 p0283 A72-12452

Positive ion composition in equatorial D region, investigating reaction kinetics

03 p0412 A72-13522

Yb and Er cations dominant sites examination in zinc selenide from fluorescence emission spectra

03 p0404 A72-14265

Photoluminescence of Er cations in CdS, observing group I co-dopants sensitizing behavior and broad-band emission spectra

04 p0563 A72-15472

Vibrationally inelastic scattering of CO cations by Ar collision, measuring ion energy, mass and angular distribution with high resolution ion beam apparatus

05 p0693 A72-17169

Photodissociation cross sections of methyl chloride and nitrous oxide cations, using ion cyclotron resonance technique

07 p0936 A72-19492

D and E regions positive ion chemistry based on E and F regions ion-molecule reaction rate constants comparison with laboratory measurement

09 p1275 A72-22360

Oxygen, nitric oxide and water cluster positive ion composition from mass spectrometer experiments in lower ionosphere, noting ion production and low temperature effects

09 p1375 A72-22363

Midlatitude auroral zone positive ion mass spectrometer observations in E region, noting diurnal variation and sporadic E events

09 p1375 A72-22364

Cation polymerization of beta-propiolactone without initial kinetics dependence on monomers concentration, relating acyl ion bonding and electron donor groups

09 p1275 A72-22496

Einstein A coefficients, band oscillator strengths and absolute band strengths calculation for comet tail band system of CO cations

09 p1355 A72-22789

Ferrites electrical conductivity variations with time caused by cations distribution modification after cooling

10 p1525 A72-24121

Mass spectrometric analysis of positive ions in carbon dioxide laser systems with nitrogen-helium mixture

10 p1492 A72-24411

Merging beams study of positive ion ionization by electron impact for atomic He, N and O

11 p1692 A72-26658

Absorption spectrum of Cr cations in magnesium aluminate spinel crystals excited by strong optical pumping

12 p1854 A72-27596

Cation self diffusion coefficients in potassium oxide-strontium oxide-silicon dioxide glass, using radioactive tracers and sequential etching technique

13 p1912 A72-28625

Lateral diffusion measurement for mass identified positive ions in oxygen, noting spiralling, charge exchange and collisions effects on ion-molecule system

15 p2281 A72-32224

Exchange diffusion process contribution to human red blood cell transmembrane cation movement from sodium tracer influx studies

15 p2187 A72-32746

Energy difference measurement between 2S and 2P levels of multiply charged O 16 positive ion, using Stark quenching technique

16 p2432 A72-33768

Hydrogen and hydrocarbon diatomic molecules and cations rotational state upper limits determination, noting potential energy functions

16 p2432 A72-34098

Diurnal variation of the H⁺ flux between the ionosphere and the plasmasphere.

19 p2793 A72-38759

Diffusive spreading of weak plasma discontinuities in the presence of two kinds of positive ion

23 p3283 A72-43363

Measurement of the rate coefficient for the recombination of He⁺ with electrons.

23 p3315 A72-43869

CATS

Gain control of cat retina rapid light adaptation process to attenuate signals reaching retinal ganglion cells from photoreceptors

12 p1760 A72-27299

CAUCHY INTEGRAL FORMULA

Power series method with Cauchy formula for non-linear partial differential equations solution in unsteady periodic temperature oscillations

06 p0905 A72-18727

Initial value method for Ambartzumian integral equation by transformation to Cauchy system

14 p2126 A72-30889

Calculation of coefficients and error estimation for the interpolation quadrature formulas of simplest Cauchy-type integrals and singular open-contour integrals

18 p2705 A72-36808

CAUCHY PROBLEM

Invariant imbedding technique application to linear partial differential equations boundary value problems conversion to Cauchy problem via generalized Riccati transformations

01 p0093 A72-11116

Velocity field of sonic flow about aircraft wing profile, solving mixed Cauchy problem

01 p0001 A72-11178

Quasi-linear parabolic equations, investigating conditions for Cauchy-Dirichlet problem solution

03 p0383 A72-14380

Second order parabolic equations C Cauchy problem solution with dissipation level, using maximum principle

04 p0538 A72-14626

Nonlinear heat conduction equation explicit solution in combustion theory with allowance for gas dynamics model equation and resulting Cauchy problem solution

04 p0595 A72-14643

Cauchy-Poisson problem of infinitely deep fluid wave motion resulting from initial particle velocities and horizontal equilibrium surface change

04 p0511 A72-14648

Cauchy problem for nonlinear biharmonic equation in Euclidean n-space, deriving a priori inequality estimate by logarithmic convexity of functional F

04 p0539 A72-15044

Metal powder materials at high loading rates, obtaining stress state diagram from Cauchy problem solution with inertia components in equilibrium equations

05 p0672 A72-16088

Relativistic hydrodynamics, considering Cauchy problem in fluid evolution, ideal isentropic fluids, electromagnetic field effect and viscous/heat conducting thermodynamic flow models

06 p0846 A72-17252

Wave diffusion related to phenomena governed by linear hyperbolic partial differential equations of second order, presenting Cauchy problem solution

07 p1035 A72-20090

Theorems for averaging of first order linear hyperbolic system with time lag, proving existence and uniqueness of solution to Cauchy problem

07 p1028 A72-20214

Iterative solution of Cauchy problem of partial differential equations nonlinear system with time lag, formulating uniqueness theorem

08 p1198 A72-20904

Iterative solution to gas dynamics equations for hypersonic flow past slender three dimensional body, applying to Cauchy problem

08 p1107 A72-20971

Finite difference method explicit solution of Cauchy problem for system of heat conduction differential equations

08 p1254 A72-21464

Soviet book on Riemann-Hilbert problem method in electromagnetic waves theory, covering wave diffraction, scattering and propagation, waveguides and open resonators

08 p1137 A72-22021

Total variation of parabolic equations solutions, noting upper bound and explicit results for Cauchy and mixed problems

09 p1343 A72-23587

Converging or diverging high intensity charged particle beams arbitrary profile shaping, obtaining solution via Laplace equation through reduction to Cauchy problem

10 p1521 A72-24362

Rectangular domain boundary value problem biharmonic equation and Cauchy system equivalence, noting semigroup properties analysis in terms of nonclassical imbedding variables

11 p1737 A72-26663

Successive approximation for solving parabolic equation with abstract function, using Chaplygin method for Cauchy boundary value problem in Banach space

13 p1987 A72-29646

Polynomial spline function for approximate solution of Cauchy problem for nonlinear differential equations of order n

14 p2126 A72-30716

Poisson ratio changes effect on equilibrium problems solutions in thin plate theory via invariant imbedding technique, using Cauchy system formulation

15 p2330 A72-32444

Existence and uniqueness theorems for Cauchy problem solution for linear singular integrodifferential operator equation

16 p2417 A72-34010

Conditions for the uniqueness of the solution to the Cauchy problem for special systems of equations with variable coefficients

17 p2575 A72-34775

Converging or diverging high intensity charged particle beams arbitrary profile shaping, obtaining solution via Laplace equation through reduction to Cauchy problem

17 p2589 A72-34961

The first Cauchy-Goursat problem of a hyperbolic-type equation degenerating at the boundary and having singular coefficients at the degeneration line

17 p2577 A72-35844

The Cauchy problem for the nonlinear Boltzmann equation in general relativity

18 p2710 A72-36471

Rotatory motions of a body with a liquid-containing cavity

19 p2787 A72-38151

The equivalence of several initial value methods for solving integral equations.

20 p2945 A72-39346

Temperature distribution control in n-dimensional space via quasi-inversion method with Fourier transformation for Cauchy problem solution of heat conductivity equation

20 p2983 A72-39466

Classes of uniqueness of solutions to the Cauchy problem

21 p3074 A72-40255

A method for determining the motion in a laminar boundary layer.

21 p3045 A72-40813

A method for solving Cauchy problems for systems of differential equations with rational coefficients

21 p3075 A72-41093

Convergence of the successive approximation method in the problem of flows past bodies with strong injection

21 p2990 A72-41096

Electrodynamical mathematical model for electroconductivity of nonuniform plasma with Hall effect, calculating current distribution from Riemann problem solution

22 p3210 A72-41888

Solution method for some boundary problems of nonlinear hyperbolic-type equations and propagation of weak shock waves

22 p3164 A72-41904

Numerical solution of boundary value problems in the statics of axisymmetric shells by the method of reducing to Cauchy problems

22 p3233 A72-42054

Book - The method of fractional steps: The solution of problems of mathematical physics in several variables

22 p3208 A72-43200

Representation of the solution of a nonlinear differential equation in the form of a path integral

23 p3308 A72-43580

On the approximation of the thermal conductivity of rigid heat conductors as a Cauchy problem.

23 p3356 A72-43721

Cauchy problem for abstract Love equations

23 p3309 A72-44042

Hypersonic flow around plane and axisymmetric bodies of arbitrary shape with inviscid radiating gas.

24 p3360 A72-45110

Riemann boundary value problem with a shift in multiply connected regions for quasi-linear elliptic systems of equations

24 p3419 A72-45260

CAUSTICS

U ALKALIES

CAVITATION

U CAVITATION FLOW

CAVITATION CORROSION

Ultrasonic cavitation effects on martensitic specimens, observing plastic deformation, softening, phase transformations and decay

03 p0370 A72-13187

Cavitation erosion of Al in liquid oxygen as function of static pressure and ultrasound frequency

07 p1034 A72-18921

Cavitation phenomena role in liquid drop impact erosion of steam turbine blades leading edges

07 p0967 A72-19262

Test temperature effect on phase composition, mechanical properties and resistance to cavitation of unstable austenitic steels, describing test facility

07 p1018 A72-20140

Cavitation failure of aircraft hydraulic plunger pump elements from microscopic and metallographic analysis

13 p1899 A72-28732

- Cavitation erosion of Al in liquid oxygen as function of static pressure and ultrasound frequency
13 p1942 A72-29207
- Cryogenic liquids cavitation erosion of plastic and cold-short metals at 77 K, determining vapor pressure effect
13 p1979 A72-29479
- Deformation mechanism of aluminum and zinc single crystals during low-temperature cavitation
22 p3192 A72-43019

CAVITATION FLOW

- Plane cavity flow past symmetric ogival obstacles, applying variational principle to fixed point theorem
02 p0206 A72-12625
- Steady two dimensional cavity flow past infinite number of airfoils using linearized theory
04 p0461 A72-14460
- Ultrasonically produced cavitation events correlation to amoeba cells number decrease under 1 MHz irradiation
04 p0475 A72-15299
- Zhukovskii potentials for ideal fluid motion in spherical or cylindrical cavity with arbitrary radial partitions
05 p0648 A72-16218
- Cumulative jet formation in elliptical cavity, investigating effect on liquid explosives ignition
06 p0799 A72-17909
- Cavitation flow around plate in transverse gravitational field, investigating boundary condition approximation on free boundary
06 p0799 A72-17913
- Anticavitation properties improvement of volute centrifugal pumps during low flow rate operation by reducing back currents with truncated cone
07 p0914 A72-18984
- Bistable hydraulic servomechanisms limit cycle stable oscillations from bang-bang control and cavitation effects, discussing valve driving gear hysteresis and time lag
08 p1113 A72-22155
- Liquid flow cavitation impact on rotating disk surfaces, showing pitting characteristics dependence on physicochemical properties of specimens
09 p1327 A72-22297
- Cavity flow driven by buoyancy and shear, obtaining flow and temperature fields from Navier-Stokes equation numerical solution
10 p1467 A72-24366
- Loaded hydraulic cylinder response to step inputs in on-off servos with three position valves, considering cavitation effect on system natural frequency [ASME PAPER 72-AUT-A]
10 p1423 A72-25052
- Single spiral vortex cavity termination model for second order solution of flat plate hydrofoil cavitation flow
11 p1616 A72-25879
- Relaxation hypothesis of cavitation erosion based on small perturbations, eliminating theory-experiment contradictions
13 p1941 A72-28776
- Surface phase transformation during cavitation erosion in Co and Fe alloys, suggesting stacking fault energy effect on erosion resistance
14 p2119 A72-30603
- Rocket body longitudinal autooscillation modes, taking into account pipeline fluid discontinuous cavitation oscillations
17 p2620 A72-34469
- Cavitation zone structure behind circular cylinder model in plane flow investigated by high speed motion picture photography and with short exposure time flash
17 p2544 A72-35897
- Cavitation study of pump with semiopen impeller, obtaining hydraulic performance, flow photographs and noise level
17 p2561 A72-35899
- Mechanism for relaxation of cavitation erosion based on small perturbations, eliminating theory-experiment contradictions
21 p3044 A72-40271
- Conformal mapping for interaction of two dimensional flow of ideal fluid and injected counterflow with jet formation, calculating cavitation void dimensions
22 p3165 A72-42065
- Interferometric investigation of natural convection in rectangular air cavities of different orientation
22 p3244 A72-42262
- Perturbation of the shape of the cavity during motion in a ponderable liquid
23 p3280 A72-43797

CAVITIES

- Thermal stresses, temperature distribution and displacement fields in elastic solid with spherical cavity and external crack
01 p0144 A72-11385
- Current lines and temperature fields in square cavity with one movable wall and viscous flow and heat transfer, solving equations numerically
03 p0456 A72-13629
- Black radiation kinetics of photon thermalization in body cavity in static thermodynamic equilibrium
06 p0847 A72-17732

- Cavity formation and drop transfer time correlation with welding current in powder covered /submerged/ arc welding, using high speed X ray photography
07 p0998 A72-20396
- Nonlinear system of differential equations for gravity perturbation on geometrical form of thin axisymmetric cavity in heavy fluid
08 p1151 A72-21705
- Spherical wave functions in analysis of infinite systems of algebraic equations describing elastic wave diffraction in sequence of spherical cavities
08 p1246 A72-21706
- Black radiation kinetics of photon thermalization in body cavity in static thermodynamic equilibrium
11 p1685 A72-25336
- Cavitation by creep of Mg alloys, using density measurements and metallurgical examinations
11 p1661 A72-26650
- Axisymmetric stress field in infinite homogeneous isotropic elastic solid with crack surrounding cylindrical cavity, solving elastic equilibrium equations
11 p1738 A72-26720
- Fourier transform approximate inversion solution for transient pulse propagation from spherical cavity with surface under impulsive pressure in viscoelastic medium
12 p1844 A72-27196
- Series solution for coaxial spherical cavity effect on torsional stress of finite length elastic circular cylinder
13 p2059 A72-29491
- Thermal emissivity and directivity for V groove and rectangular cavities, optimizing geometry and surface properties for maximum focusing of emitted energy [ASME PAPER 72-HT-L]
20 p2984 A72-39651
- Heat transfer by laminar natural convection in low aspect ratio cavities. [ASME PAPER 72-HT-52]
20 p2985 A72-39661
- Asymptotic behavior of the flow created by a shock wave incident on a wedge-shaped cavity
21 p3047 A72-41668
- Simple analyses for the non-symmetric dynamic expansion of cylindrical cavities.
22 p3240 A72-42893

CAVITY RESONATORS

- Supersonic wind tunnel study of flow induced pressure oscillations in shallow rectangular cavity, investigating resonant frequencies and pressure mode shapes
01 p0049 A72-10221
- CW X-band Gunn oscillator in coaxial cavities, investigating frequency variation with ambient temperature
01 p0037 A72-10641
- Acousto-optical extraction of energy stored in pulsed He-Ne laser cavity, using modulator with piezoelectric transducer at light-ultrasound interaction region
01 p0081 A72-11322
- Spatially periodic coupled cavity slow wave structures for multibeam microwave tube stabilization without absorber
02 p0190 A72-11575
- Pulsed ruby laser with complex mirror resonator including optical delay line, observing mode locking effects in emission dynamics
02 p0238 A72-12290
- Closed rectangular cavity resonator with conducting walls, calculating differences of electromagnetic zero point fluctuation radiation pressure
02 p0260 A72-12434
- He-Ne laser active medium excitation and resonator geometry effects on TEM wave field
02 p0239 A72-12520
- Cavity resonator thermal stabilization, using gas pressure controlled membrane
02 p0196 A72-12698
- Laser with convex-plane resonator and cross sectional variable mirror transmission, showing effective transverse mode selection and diffraction divergence
02 p0239 A72-12767
- Abnormal rf hysteresis and bias voltage effect in resonant cavity Gunn devices
03 p0331 A72-13646
- Quantum mechanical analysis of detuning in cascaded cavity molecular beam masers
03 p0368 A72-13747
- Acoustic cavity resonators use for suppression of combustion instability modes, determining acoustic impedance and damping
03 p0457 A72-13954
- Ionizing radiation effects in cavities of microwave Gunn oscillators, noting large dose rate effects on circuit performance
03 p0335 A72-14094
- High power CW gas dynamic laser mode-control experiment with unstable resonator at high Fresnel number, obtaining near and far field intensity distribution
04 p0529 A72-14605
- Radiation intensity of CW argon ion laser with non-linearly absorbing argon cell in cavity, showing pressure relation to amplification and absorption
04 p0530 A72-14658

- Nonlinear nonlaminar 3D electron motion calculation through output cavity of klystron amplifier by Green function
04 p0497 A72-14697
- Superregenerative linear mode amplification in Q switched He-Xe laser as function of resonator phase, length and signal angle
04 p0531 A72-15147
- Open resonators stability analysis, describing integral equations eigenfunctions and eigenvalues short wave asymptotic expansions
04 p0502 A72-15435
- Fabry-Perot open resonators, determining eigenvectors, resonant frequencies and diffraction losses by asymptotic perturbation method
04 p0502 A72-15436
- Resonance degeneration removal in earth-ionosphere spherical cavity resonator, calculating eigenfrequencies by perturbation method
04 p0492 A72-15444
- Electron tube with Fabry-Perot cavity resonator with grooved and smooth mirrors for millimeter and submillimeter wave generation
04 p0503 A72-15598
- Conical cavity resonator design for submillimeter wave electron beam devices, investigating mode and resonant frequency dependence on cavity size
05 p0636 A72-16364
- Carbon dioxide laser Q switching by molecular gases intracavity Stark modulation with sine or square wave electric field, using methyl chloride and difluoroethane
05 p0669 A72-16609
- IMPATT diode avalanche region microwave self oscillation mechanism explanation by cavity resonator and feedback theories
06 p0787 A72-18383
- LSA oscillators performance and control optimization, discussing multiaxis radial microwave cavity effectiveness in oscillation starting and coupling to coaxial transmission line
06 p0789 A72-18481
- Single mode high power pulsed nitrogen/carbon dioxide laser with unstable resonator coupling and diffraction limited focusing
07 p1002 A72-19215
- Direct coupled waveguide cavity resonator equalizer networks, determining reflection coefficient, phase, amplitude and time delay characteristics by scattering matrix theory
07 p0955 A72-19327
- Kinetic equations for laser active medium disturbances and electromagnetic field modes in cavities with losses
07 p1006 A72-20117
- Output characteristics of Q switched liquid laser as function of pumping pulse, cavity mirror reflectivity and cavity length
07 p1008 A72-20544
- Microwave temperature sensor for radiation environment use, discussing cavity resonator design and operation, thermal cycling tests and comparative radiometer technique
07 p0993 A72-20677
- Symmetrical amplitude-frequency characteristics of microwave reflection amplifiers with active resonators connected in series by nonhalf wave transmission line
08 p1138 A72-20791
- Emission dynamics of pulsed laser with optical delay line in resonator
08 p1181 A72-20797
- End holes effects on dielectric constant measurement of long glass tubes by cylindrical microwave resonant cavity
08 p1164 A72-20940
- He-Ne laser resonator misalignment effect on output power, determining mirror arrangement precision tolerance for set fluctuation levels
08 p1181 A72-21163
- Sound wave propagation in plasma, attributing acoustic cavity resonance curve sharpening to collisional energy transfer from electrons to neutrals
08 p1213 A72-21256
- Multimode cavity for simultaneous oxygen/argon plasma excitation and electron density measurements, noting gas pressure effect
08 p1213 A72-21323
- Diffraction losses and corrections for lower order transverse modes and resonance conditions in optical resonators with cylindrical mirrors
08 p1133 A72-21371
- Digital frequency shift keying modulation of Gunn microwave oscillator by cavity placed between output and transmission line
08 p1141 A72-21432
- Elimination of spherical cavity resonators natural frequencies degeneration through symmetry disrupting disturbance, using group theory for fields and frequencies calculations
08 p1209 A72-21737
- Group and symmetry theory application to degenerate mode splitting in magnetron cavity systems with electromagnetic fields disturbances
08 p1142 A72-21740

Nd-glass laser time characteristics and radiation ordering from cavity lengthening 08 p1183 A72-21771

Ruby laser power output losses at 80 K with spectral line suppression dependence on surface reflection coefficient of plane parallel plate in resonator 08 p1183 A72-22026

Multidimensional function extremum for sectioned resonator type gyroamplifier efficiency optimization 08 p1172 A72-22050

Transition metal superconducting thin films and rf cavity surface protective coverings, investigating properties by low energy electron diffraction and Auger spectroscopy 09 p1368 A72-22560

Cavity resonator frequency detuning effects on FM and AM noise in cavity stabilized Gunn microwave oscillator 09 p1285 A72-22651

Q factor over temperature range of microwave resonator coupled with drifting indium antimonide plasma 09 p1285 A72-22895

High power Ar laser frequency stabilization technique using multiple feedback loop with optical cavity discriminator stabilized against iodine vapor absorption line 09 p1325 A72-23337

Alternative TEM and waveguide type equivalent circuits for rectangular resonator loaded by lumped capacitance 09 p1289 A72-23365

Pulsed ruby laser with complex mirror resonator with optical delay line, observing mode locking effects in emission dynamics 10 p1488 A72-23764

Cochlea enclosed two dimensional cavity potential flow model for fluid mechanical theory of hearing 10 p1430 A72-24295

Short and long term frequency stability improvement in X band klystron oscillator stabilized by high Q superconducting cavity 10 p1449 A72-24303

Polarization characteristics and losses of anisotropic laser resonators composed of arbitrary number of mirrors 10 p1492 A72-24364

Narrow bandpass waveguide filters synthesis, using orthogonal mode cavities to realize negative coupling elements 10 p1451 A72-24591

Classical laser theory, investigating anharmonic oscillators interaction with electromagnetic field in resonant cavity [AD-740404] 10 p1492 A72-24603

Focal spherical laser resonator deformation analysis based on perturbation method, investigating forced oscillation 10 p1493 A72-25150

Spherical specularly reflecting nonresonant cavities for use as absorption cells in far IR spectroscopy, predicting performance 11 p1629 A72-25301

Mode locked ruby laser having triangular ring cavity with four prisms to obtain reliable single-transverse-mode Q switched and normal operation 11 p1647 A72-26150

Mode properties and energy losses for unstable laser resonator with curved and sharp edged mirrors 11 p1648 A72-26336

Microwave resonators excited in coupled and E sub zero modes, determining equivalent circuit and Sommerfeld resonator Q factor and guide wavelength 11 p1605 A72-26369

Mode chart and unloaded quality factor of elliptic microstrip resonator operating in inverse or radial TM modes 11 p1607 A72-26996

Dual resonant cavity absorption cell composed of Fabry-Perot interferometers excited by microwave sources, observing spectroscopic double resonance effects 12 p1806 A72-27264

Kinetics and cavity intensity models for output characteristics of pulsed electric discharge carbon dioxide lasers 12 p1820 A72-27287

Power resonance and frequency stabilization of gas laser with nonlinear absorption cell, considering He-Ne laser with Fabry-Perot resonator 12 p1820 A72-27584

Gas laser with strong absorption saturation to obtain high peak power and frequency self stabilization by generation of quasi-traveling wave in resonator 12 p1820 A72-27585

Injection semiconductor laser mode selection and output enhancement by introducing external spectrally selective elements into resonator 12 p1821 A72-27589

Laser with unstable telescopic resonator and large radiation loss, calculating energy characteristics and power efficiency 12 p1821 A72-27590

Fast response thermal compensation system for gas laser resonator length and frequency stabilization, discussing fabrication and design calculation 12 p1822 A72-27607

Solid state laser resonator inhomogeneous dielectric and mirror elements matching effects on Q factor and output power 12 p1822 A72-27609

Laser resonator transverse and longitudinal mode selection techniques, considering single frequency stabilization, gain saturation theory and applications 12 p1826 A72-27964

Nb superconducting resonant cavities application to linear accelerator and RF particle separator structures in GHz region for wall energy loss reduction 13 p1922 A72-29348

Noise control by Helmholtz resonators, considering equivalent circuits via feedback schemes 13 p2005 A72-29567

Kinetic equations derived for electromagnetic field inside cavity with resonance medium and external source, determining sensitivity thresholds, gain factors and spectral compositions 13 p1969 A72-29677

Approximate analytical method for diffraction losses and corrections to lower transverse modes and resonance condition in symmetrical stable cavities with round spherical mirrors 13 p1970 A72-29679

Kinetics of monopulse development in cavity with nonlinear element converting generated radiation into second harmonic, considering energy and time characteristics 13 p1970 A72-29683

Discharge tube geometry effects on sensitivity of plasma electron density measurement by cylindrical cavity resonators 13 p2018 A72-29822

Conversion efficiency and polarization behavior of Gunn diodes in resonant cavities, using I-V characteristics 13 p1937 A72-29866

TEA carbon dioxide laser time dependent gain and cavity losses analysis, using lasing onset delay with current pulse 14 p2109 A72-30184

Liquid and two phase liquid-gaseous hydrogen density determination via dielectric constant measurement by open-ended microwave cavity 14 p2103 A72-30197

Kinetic instability bursts during heating of electron plasma in cylindrical resonator with standing electromagnetic waves 14 p2136 A72-30308

Kinetic instabilities during electron plasma heating in HF field of cylindrical resonator, discussing electron energy distribution function effect 14 p2137 A72-30309

Self oscillations of microwave autodyne oscillator loaded by two resonant cavities, noting radio spectroscopic applications 14 p2089 A72-31110

Two cavity self exciting SHF microwave oscillator with resistance coupling through low Q-factor resonant diaphragm, noting frequency stability 14 p2090 A72-31121

Generalized locking equation for microwave oscillator bandwidth prediction for arbitrary cavity configurations and waveforms, considering strong harmonics presence 15 p2205 A72-31358

Open terminations of cylindrical waveguide periodically loaded by metallic irises, investigating cavity resonator size effects on resonant frequency, mode and quality factor 15 p2194 A72-31547

Wave packet theory application to multimode laser cavity electromagnetic/optical/field analysis 15 p2251 A72-32649

Millimeter band open cavity resonator using trihedral reflector diffraction grating and inclination control for mode selection 16 p2364 A72-33491

Transversely excited high pressure carbon dioxide laser cavity dumping with reproducible time delay between current excitation and gain-switched laser pulses 16 p2403 A72-33844

Supersonic flow aerodynamic window for high power laser beam extraction through nonabsorbing gas medium while supporting pressure difference between cavity and ambient atmosphere [AIAA PAPER 72-710] 16 p2404 A72-34036

Natural frequencies of a cylindrical microwave cavity containing a coaxial cylindrical dielectric sample 17 p2513 A72-34334

He-Ne laser resonator misalignment effect on output power, determining mirror arrangement precision tolerance for set fluctuation levels 17 p2562 A72-34454

Pulsed Impatt diode oscillator circuit design and operation frequency prediction for high Q coaxial structures from equivalent circuit 17 p2526 A72-34466

Variable output coupling device for far infrared laser. 17 p2562 A72-34643

Polarization characteristics and losses of anisotropic laser resonators composed of arbitrary number of mirrors 17 p2563 A72-34963

Superconducting-cavity-stabilised oscillator of high stability. 17 p2530 A72-35386

Numerical calculation of energy storage, wave dispersion and propagation in waveguides of periodic resonator chains at high frequencies 18 p2657 A72-36105

Excitation of a confocal spherical laser resonator. 19 p2810 A72-37403

Using ring lasers as rate sensors. 19 p2812 A72-38223

Theoretical study and demonstration of the coupling of modes of a resonant cavity by an electron beam 19 p2774 A72-38543

Transverse mode selection in injection lasers with widely spaced heterojunctions. 19 p2812 A72-38595

Theory of spontaneous mode locking in lasers using a circuit model. 19 p2813 A72-38690

Laser with convex-plane resonator and cross sectional variable mirror transmission, showing effective transverse mode selection and diffraction divergence 20 p2931 A72-39073

Unstable resonator theory with geometrical optics and diffraction approximation, applying to laser mode selection and beam divergence reduction 20 p2932 A72-39501

Rectangular aperture diaphragm dimension determination for ring laser resonator principal transverse mode selection and higher modes suppression 20 p2933 A72-39510

A rectangular beam waveguide resonator and antenna. 21 p3026 A72-40358

Single transverse mode operation of a pulsed volume excited atmospheric pressure CO2 laser using an unstable resonator. 21 p3064 A72-41197

Automatic measurement of microwave-cavity parameters using stable sampled control loops. 21 p3034 A72-41465

Optical elements of a laser-pumped dye laser 21 p3064 A72-41737

The effect of an interferometer selector on the spectrum of the characteristic frequencies of a dispersion resonator 22 p3176 A72-42245

Approximate theory of the CW gasdynamic laser with an unstable resonator. 22 p3186 A72-42631

Pressure dependent microwave cavity breakdown field relationship to steady state plasma luminosity interpretation as evidence of RF confinement of low density plasma 22 p3212 A72-42897

Plasma diagnostics by means of microwave cavity resonators 22 p3212 A72-42950

Possibility of determining the three-dimensional distribution of a plasma with the aid of an SHF resonator 22 p3214 A72-43122

Kinetic instability bursts during heating of electron plasma in cylindrical resonator with standing electromagnetic waves 23 p3317 A72-43210

Kinetic instabilities during electron plasma heating in HF field of cylindrical resonator, discussing electron energy distribution function effect 23 p3317 A72-43211

Approximate calculation of a cavity resonator for n given initial natural frequencies 23 p3269 A72-43449

Junction circulator shunt conductance and susceptance-slope parameter calculation by constituent resonator input admittance formation, describing quarter wave mode operation 23 p3270 A72-43604

Laser radiation geometric divergence and variation of transmitted intensity with mirror transmissivity at centerline for unstable cavity viewed as oscillator-amplifier 23 p3296 A72-43902

Properties of a superconducting point contact contained in a resonator 23 p3324 A72-44221

Improved calculation of resonant frequencies of Helmholtz resonators. 23 p3315 A72-44372

Influence of the imperfection of resonator elements on the characteristics of a triangular ring laser with a 90-degree Faraday rotator 24 p3408 A72-44622

A new method of optical coupling of two laser cavities which permits stable generation of ultrashort optical pulses 24 p3410 A72-45075

Resonator polarization parameters effect on backwave attenuation in three and four mirror TW ring laser, noting colliding waves intensity dependence on polarization angle

24 p3411 A72-45505

Effect of plasma mirror in the breakdown of air in a CO2 laser cavity.

24 p3412 A72-45775

Cavity Vapor Generators

Minicavity reactor rocket engine combining high specific impulse of central gaseous fueled cavity and low weight NERVA type fuel elements in driver region external to moderator-reflector zone

01 p0100 A72-11358

Ceilings [Meteorology]

Remote meteorological elements sensing in terminal area, discussing radar, ceilings, thunderstorm warning, slant range visibility, low level winds and wind shear

04 p0543 A72-14692

U.S.S.R. civil aviation regulations on takeoff and landing minimum conditions for cloud ceilings and visibility range for various aircraft characteristics and equipment

14 p2129 A72-30820

Ceilometers

U Cloud Height Indicators

Celescopes

Space astronomy experiments with TV scanning, discussing data from Telescope catalog of UV observations and photometric and astrometric accuracy

08 p1170 A72-21957

Spaceborne Univicon/Telescope astronomical observatory for stellar UV TV pictures, discussing system design requirements

08 p1170 A72-21958

Celestial Bodies

NT A STARS
NT ACHONDrites
NT ANDROMEDA GALAXIES
NT ASTEROIDS
NT AUSTRALITES
NT B STARS
NT BEDIASITES
NT BINARY STARS
NT BRUDERHEIM METEORITE
NT CARBONACEOUS METEORITES
NT CASSIOPEIA A
NT CEPHEID VARIABLES
NT CERES ASTEROID
NT CHONDRITES
NT COMET TAILS
NT COMETS
NT CRAB NEBULA
NT DEIMOS
NT DRACONID METEOROIDS
NT DWARF STARS
NT EARLY STARS
NT EARTH [PLANET]
NT ECLIPSING BINARY STARS
NT EUROPA
NT EXTARS
NT EXTRASOLAR PLANETS
NT GALAXIES
NT GEMINID METEOROIDS
NT GIANT STARS
NT GLOBAL CLUSTERS
NT HOT STARS
NT IAPETUS
NT ICARUS ASTEROID
NT INFRARED STARS
NT IO
NT IRON METEORITES
NT JUPITER [PLANET]
NT LEONID METEOROIDS
NT MAGNETIC STARS
NT MAIN SEQUENCE STARS
NT MARS [PLANET]
NT MERCURY [PLANET]
NT METEORITES
NT METEOROID DUST CLOUDS
NT METEOROID SHOWERS
NT METEOROIDS
NT MICROMETEOROIDS
NT MILKY WAY GALAXY
NT MOON
NT MRKOS COMET
NT NATURAL SATELLITES
NT NEBULAE
NT NEPTUNE [PLANET]
NT NEUTRON STARS
NT NOVAE
NT O STARS
NT ORGUEIL METEORITE
NT ORIONID METEOROIDS
NT PERSEID METEOROIDS
NT PHOBOS
NT PLANETARY NEBULAE
NT PLANETS
NT PLUTO [PLANET]
NT PROTOSTARS
NT PULSARS
NT QUADRANTID METEOROIDS
NT QUASARS
NT RADIO GALAXIES

NT RADIO METEORS
NT RADIO SOURCES [ASTRONOMY]
NT RADIO STARS
NT REFERENCE STARS
NT SATURN [PLANET]
NT SIKHOTE-LIN METEORITE
NT SOLAR SYSTEM
NT SPIRAL GALAXIES
NT SPORADIC METEOROIDS
NT STAR CLUSTERS
NT STARS
NT STONY METEORITES
NT SUBDWARF STARS
NT SUN
NT SUPERGIANT STARS
NT SUPERNOVAE
NT T TAURI STARS
NT TEKTITES
NT TITAN
NT TUNGUSK METEORITE
NT URANUS [PLANET]
NT VARIABLE STARS
NT VENUS [PLANET]
NT VESTA ASTEROID
NT VIRGO STAR CLUSTER
NT WHITE DWARF STARS

Space law existence, contents and legal sources, discussing international decisions on outer space and celestial bodies use

01 p0147 A72-11108

United Nations proposals concerning legal principles for use of natural resources of celestial bodies and ocean floor

07 p1103 A72-19464

Rotating gas and dust clouds as basis of ring and disk structures in celestial bodies

10 p1539 A72-24311

Russian book on satellite-borne electro-optical IR radiometers design for celestial bodies spectral radiance and energy distribution measurement

11 p1634 A72-26376

Cosmological origin of red shift in spectral lines of astronomic bodies, suggesting interpretation based on inelastic interactions between photons of essentially nonzero mass

11 p1723 A72-26507

Encounter trajectory design for solar electric propulsion rendezvous with low mass celestial bodies, noting target characteristics

[AIAA PAPER 72-424]

13 p2036 A72-28939

Cosmic objects and phenomena frequency distribution functions monotone decrease with respect to importance, considering star clusters, binaries, lunar craters, solar activity, etc

14 p2160 A72-30912

Axisymmetric celestial bodies equilibrium shapes in post-Newtonian approximation of general relativity using integrodifferential equation

14 p2161 A72-31077

Ephemerides determination improvement of celestial bodies with nonperiodic trajectories, relating different observatory measurements

17 p2607 A72-35042

Problem of n bodies with a variable gravitational constant, and some dynamic characteristics of large-scale cosmic systems

19 p2863 A72-38077

Accretion processes leading to formation of meteorite parent bodies.

24 p3444 A72-45454

Celestial Geodesy

Molodenski integral equation for gravitational field calculation at point M on earth surface as function of neighboring region astronomical geodetic measurements

09 p1299 A72-22675

Terrestrial and lunar orbital and rotational motion behavior, discussing kinematic theory and ground and space vehicle based observation techniques

19 p2865 A72-38479

Error analysis of astronomical-geodetic network compensation methods, noting distortions minimization in polygon nodes by large blocs compensation with computers aid

22 p3173 A72-42721

Celestial Mechanics

Book on celestial mechanics covering Hamiltonian systems and equations of motion for three body problem

02 p0285 A72-12857

Magellanic Clouds kinematics, composition and other properties, discussing radio sources, atomic abundances, stellar luminosity limits, regional magnetic fields and polarization

03 p0424 A72-13252

Precession from proper motions of stars with respect to galaxies, discussing correction for systematic errors

04 p0575 A72-15027

Isolated fixed points existence in area preserving mappings considered with normal form for periodic Hamiltonians in celestial mechanics

04 p0576 A72-15041

Book on orbit determination, space navigation and celestial mechanics covering two body problem in-

tegration, units and constants, perturbation theory, orbit correction, etc

05 p0712 A72-15862

Soviet book on qualitative methods in celestial mechanics covering differential equations of motion averaging schemes, Newton type convergence method, three body problems, etc

06 p0879 A72-17821

Two body problem trajectory equation method simplification, reducing entire solution to two integral evaluations

06 p0881 A72-17931

Soviet book on celestial mechanics and astrodynamics covering classical and contemporary theory, many body problem, satellite perturbation, optimal and boundary value problems, etc

07 p1078 A72-19952

Soviet monograph on universal gravitation covering prerelativistic theories, inverse square law, relativistic effects, celestial mechanics, stellar structures and evolution, etc

08 p1231 A72-21025

Gravitational system dynamics, discussing massive-light star mixtures with collisions and systems with equal mass objects

08 p1231 A72-21121

Saturn ring motion stability factors for atomized material resistance to gravitational field, discussing ring thickness, density and other parameters

08 p1231 A72-21128

Celestial mechanics considerations for many body problem with finite and infinite macroobjects motions correlation and conservation principles elucidation

08 p1236 A72-21641

Book on perturbation theory in celestial mechanics, covering disturbing function, Lagrange method and Delaunay theory

09 p1389 A72-23246

Book on perturbation theory in celestial mechanics, covering absolute perturbation, Hill lunar theory and application to Jupiter satellites

09 p1389 A72-23247

Lie transformations for perturbed canonical system of differential equations solution, proposing parameter square root series development for resonance problems of celestial mechanics

10 p1536 A72-24119

Lunar motion as plane restricted three body problem in celestial mechanics

11 p1722 A72-26478

Vertex deviation of stellar samples in terms of reflection and galactic potential perturbation

12 p1867 A72-27212

Small perturbations in collisionless stellar dynamics, discussing linear modes for flat axisymmetric galaxy and effects introduced by nonlinear theory of spiral structure

12 p1874 A72-27904

Relativistic and Newtonian theory compared for orbiting satellite matter release criteria and subreleasing change effects during gravitational collapse of central dense core

13 p2040 A72-29407

Two body model for three body problem of uniformly distributed and isotropically expanding gravitational matter of Einstein-Sitter universe, noting metagalaxy cooling rate

14 p2149 A72-30211

Invariant mechanics principles for two body system dynamic properties, analyzing mass center motion, system energy and gravitational theory role

14 p2152 A72-30481

Book on astronomy covering optical and radio telescopes properties and atmospheres of inner and outer planets, stellar lifetimes and evolution, galaxies, cosmology, etc

15 p2306 A72-31516

The tidal interaction of galaxies

17 p2613 A72-35473

Two body problem trajectory equation method simplification, reducing entire solution to two integral evaluations

18 p2730 A72-37156

Third integral of equations of motion in axisymmetric potential field, noting Jeans theorem for phase density in star system

19 p2863 A72-38068

Regularized first order algorithm for ideal resonance problem in solar system, considering solution in terms of elliptic functions

20 p2968 A72-39199

Near parabolic orbit and short periodic comets motion, discussing circumsolar cloud and nongravitational disturbances

20 p2974 A72-40068

Recent developments in the theory of the motion of the moon.

21 p3102 A72-40124

Comparison of the classical and the global solutions of the ideal resonance problem.

21 p3085 A72-41047

Stationary motions of a triaxial body and their stabilities.

21 p3109 A72-41334

- Interactions between stars and local dust formations
21 p3113 A72-41758
- Celestial mechanics principles application to geostationary satellites in equatorial plane and in earth-moon system libration points, considering Jupiter and Saturn stationary satellites
22 p3222 A72-42141
- The dependence on inclination of the planetary perturbations of the orbits of long-period comets.
22 p3224 A72-42378
- Book on moons and planets covering celestial mechanics, solar system origin, stellar formation, comets, asteroids, meteorites, planetary interiors, surfaces, atmospheres, etc
22 p3228 A72-42750
- Two body model for three body problem of uniformly distributed and isotropically expanding gravitational matter of Einstein-Sitter universe, noting metagalaxy cooling rate
23 p3334 A72-43241
- Poorly founded systems of equations in astronomical practice and methods for their solution
24 p3437 A72-44760
- Celestial mechanics ideal resonance problem global solution via Bohlin-von Zeipel perturbation technique, modifying Hamiltonian expansion point and separatrix and libration region singularities suppression method
24 p3440 A72-45138
- Hyperbolic two body problem in celestial mechanics, discussing E , r , α , β , summability procedure for analytic continuation
24 p3442 A72-45236
- Dynamic behavior of three point mass system with variable body mass ratios and constant total system mass, applying results to stellar systems
24 p3442 A72-45240
- Precompiler to simplify programming of celestial mechanics problems in TRIGMAN formula manipulation system, introducing data tube SERIES into FORTRAN program
24 p3442 A72-45242
- A gasdynamical view on the motion, heating and accretion of solid bodies in the solar system.
24 p3444 A72-45456
- CELESTIAL NAVIGATION**
NT ASTRONAVIGATION
- Space vehicles guidance with UV optical systems, describing photometric celestial images with various receptors and different wavelength bandwidth selection
03 p0354 A72-13054
- Polar region performance of OMEGA navigation system, noting addition of selectable grid reference, multiple parallel DR system, manual celestial computation and bearing resolver
13 p1999 A72-29200
- Statistical data processing method for accuracy evaluation of satellite orbits parameters obtained from onboard measurements of two stars angular positions
14 p2151 A72-30454
- Measurement data processing in celestial navigation based on least squares method, calculating errors correlation matrix
15 p2267 A72-31731
- Satellite motion state vector accuracy estimate algorithm based on angular measurements of stellar positions relative to satellite launched probe
17 p2578 A72-35265
- CELESTIAL OBSERVATION**
U ASTRONOMY
- CELESTIAL REFERENCE SYSTEMS**
- Solar eclipse timings by photoelectric, photographic and visual observation for comparison of Newcombe sun tables and improved lunar ephemeris reference systems
13 p2041 A72-29527
- The Laplace plane and the masses of the planets
17 p2618 A72-35813
- Influence of the reference catalog system on the coordinates of determined stars in zonal meridional observations
19 p2861 A72-37974
- Investigation of the screw turn magnitude of a contact micrometer attached to the Toepfer meridian circle on the basis of observed right ascensions of stars
19 p2802 A72-37975
- Spacecraft orientation according to reference celestial bodies direction determination, noting successive orientation permissible time intervals
19 p2831 A72-38149
- A determination of the motion of the ecliptic.
23 p3337 A72-43833
- Lorentz-covariant reference-tetrad theories of gravitation
24 p3425 A72-44913
- CELESTIAL SPHERE**
- Electromechanical system for wire drive along stellar right ascension of meridian circle of Odessa Astronomical Observatory
09 p1311 A72-23061
- CELL CATHODES**
- Quinones as reversible redox couples for rechargeable cathodes, noting air regeneration capacity in organic electrolytes
16 p2352 A72-33898

CELL DIVISION

Euglena cell division timing control by endogenous circadian rhythm, showing direct entrainment by low frequency dark-light cycles
07 p0919 A72-19539

Cell proliferation in lungs of mice exposed to elevated concentrations of oxygen.
17 p2499 A72-34548

CELLS [BIOLOGY]

NT AXONS
NT CARBOXYHEMOGLOBIN
NT CHROMOSOMES
NT COLLAGENS
NT ERYTHROCYTES
NT HEMATOPOIESIS
NT HEMOGLOBIN
NT LEUKOCYTES
NT LYMPHOCYTES
NT MITOCHONDRIA
NT NEURONS
NT OXYHEMOGLOBIN
NT RETICULOCYTES

Space flight biological effects on lysogenic bacteria and human cells in culture
01 p0011 A72-10365

Three dimensional organization of spherical colonies formed by L5178Y cells grown in soft agar cultures from light and scanning electron microscopy
01 p0015 A72-11039

Neurosecretory cell functional activity of supraoptic and paraventricular hypothalamic nuclei in rats after electrical stimulation of midbrain reticular formation
02 p0158 A72-11759

Foresight, forecast and prognosis concepts in physiology, discussing intuition role and relation between molecular and cellular processes and organism activity
02 p0163 A72-12346

Free radicals participation in cell membrane biopotential generation mechanism, comparing properties of protein molecules with semiconductors
02 p0169 A72-12348

Nucleic acid, protein and cell primordial sequence, ribosomes and genetic code for life origin, discussing experiments on homopolymers amino acids reaction with mononucleotides
04 p0468 A72-14775

Hereditary endosymbiotic model of microbial evolution of Precambrian prokaryotic and eukaryotic cells
04 p0471 A72-14800

Ultrasonically produced cavitation events correlation to amoeba cells number decrease under 1 MHz irradiation
04 p0475 A72-15299

Origin and development of plasma membrane derived invaginations in *Vinca rosea*, observing endocytosis in plant cells
05 p0616 A72-15810

Soyuz 5 satellite vehicle space flight factors effect on chlorella cells, investigating survival rates and mutability
05 p0623 A72-16776

Synaptic contacts in vertebrate retinas, reviewing bipolar terminals, ganglion cells and amacrine responses from electron microscopy
06 p0762 A72-17719

Retinal ganglion cell spikes timing in mammalian retina, using electroretinography and computer analysis
06 p0762 A72-17721

Thalamus functional and organizational anatomy studies from improved neurophysiological research methods, emphasizing cytoarchitectural differentiation functional significance
07 p0922 A72-20274

Cellular evolution investigation using molecular biology, microbial physiology and ecology
08 p1119 A72-22011

Biological cell sorting by differential fluorescence generated electric signals via laser beam illuminated liquid stream
09 p1273 A72-23403

Continuous and intermittent maximal exercise effects on human muscle intracellular and capillary blood pH
10 p1425 A72-24477

Thyroid and adrenocortical hormonal state effect on cell number and functional maturation of brain, discussing neurogenesis in infants
12 p1760 A72-27298

Albino rats spinal cord capillaries ultrastructure upon hypothermy, noting endothelial cells sinking to lower levels from microscopic observation
12 p1760 A72-27304

Irreversibility mechanism in postpartum ductus arteriosus closure in guinea pigs, studying vessel cellular changes and smooth muscle response to oxygen pressure
12 p1762 A72-27826

Rat vena porta muscle cells spontaneous activity intensified by direct current depolarization and inhibited by hyperpolarization, noting effects of calcium and sodium ions
13 p1902 A72-28638

Epithelial follicle and mast cell role in peroxidase activity of thyroid gland during experimental burn development
13 p1905 A72-29330

Interval scanning photomicrography for recording growth of microbial cell populations during incubation
13 p1911 A72-29749

Synthetic carbohydrates toxicity effects on rat liver lysosomes application to astronaut potential food sources
14 p2074 A72-30381

Organ cell lysosomes polymorphic properties and formation by Golgi complex, discussing role in neurocyte structure restitution following gamma irradiation
14 p2075 A72-30594

Potassium, sodium and calcium ion distribution in skeletal muscle subcellular organelles, discussing lipid, protein and nucleic acid binding
14 p2076 A72-30670

Gravity effects on plant organ orientation with respect to force direction from *Chara rhizoid* cell statoliths
15 p2189 A72-31932

Dynamics of secondary vacuole movement within cytoplasm of *Tradescantia virginiana* hair cells
15 p2186 A72-32350

Soyuz 5 satellite vehicle space flight factors effect on chlorella cells, investigating survival rates and mutability
17 p2505 A72-35279

Lipid composition of growing and starving cells of *Arthrobacter crystallopoietes*.
17 p2505 A72-35835

Biomembrane hydration mechanism of Na-K ion pump of living cell based on fractionation at air-sea interface
18 p2649 A72-36441

Acceleration stress tolerance dependence on electron or ion transport across cell surface activation energy barrier, studying rat survival times
18 p2650 A72-36448

Freeze etching techniques in electron microscopic investigations of biological cells molecular structure
18 p2653 A72-36829

Computerized statistical simulation of automatism of spontaneously active smooth muscle strip, neglecting individual cell spontaneous activity
19 p2757 A72-37949

Receptive fields of units in the visual cortex of the cat in the presence and absence of bodily tilt.
19 p2758 A72-38646

Adaptability limits on protein-nuclein-water life under exobiological extremal conditions, considering macromolecules, extraterrestrial life search and origin
20 p2891 A72-38958

Book - Energy metabolism of human muscle.
20 p2893 A72-39700

Biological rhythms origin and mechanisms, discussing 24-hour cycle, subcellular biological clock and rhythm disruption effects in speleologists, astronauts and pilots
22 p3141 A72-41985

Effects of simulated space vacuum on bacterial cells.
23 p3254 A72-43395

Intracellular potassium in cells of the distal tubule.
24 p3373 A72-45231

Human blood monocytes - Stimulators of granulocyte and mononuclear colony formation in vitro.
24 p3373 A72-45374

CELLULOSE

Double base propellant nitroglycerin interactions with inhibition materials cellulose acetate and ethyl cellulose, noting time and temperature effects
14 p2145 A72-30767

Structure-property relationships in flame retardant systems - Relative effects of alkyl phosphates, phosphonates and phosphites on cellulose flammability.
20 p2987 A72-39698

CELLULOSE NITRATE

Ignition conditions for pyroxylin and polyvinyl-nitrate in air flow containing spherical aluminosilicate and aluminum oxide particles
06 p0903 A72-18211

Thermochemical methods for plasticized/stabilized cellulose nitrate kinetic constants determination for lifetime estimation, presenting isothermal decomposition curves
14 p2144 A72-30753

Effective stabilizer content measurement in smokeless powder propellants, discussing nitrogen dioxide generation by cellulose nitrate and glycerin trinitrate decomposition
14 p2144 A72-30755

Plastic deformation at a stably growing crack tip.
17 p2569 A72-34252

CELSIUS TEMPERATURE SCALE
U TEMPERATURE SCALES
CEMENTATION

Mechanical and microstructural properties of steels for effective surface cementation, suggesting Mo and Cr optimal contents
20 p2941 A72-39576

Study of the hot pressing kinetics for niobium-cemented tungsten and titanium carbide alloys
22 p3182 A72-42191

CEMENTITE
X ray analysis of cementite and titanium carbide precipitates in Cr-Mn-Mo-Ti steels weld zones
07 p1019 A72-20159
Magnetic domains in cobalt and cementite observed by electron microscopy, investigating thin film thickness effect on temperature
10 p1496 A72-24088

CENSORED DATA [MATHEMATICS]
Maximum likelihood estimation for Weibull distribution parameters from multicensored samples by Monte Carlo simulation
08 p1200 A72-21589
Best linear invariant estimation of Weibull parameters - Samples censored by time and truncated distributions.
22 p3199 A72-42969
Statistical techniques for severely censored random samples with known and unknown probability distribution functions
24 p3418 A72-44665

CENTAUR LAUNCH VEHICLE
NT ATLAS CENTAUR LAUNCH VEHICLE
CENTAURUS CONSTELLATION
Centaurus A NGC 5128 nucleus IR radiation measurement, suggesting small nonstellar core superposed on extended reddened stellar component
01 p0132 A72-11091
Centaurus region hard X ray flux temporal variations from OSO-3 X ray telescope observations
16 p2446 A72-33458

CENTER OF GRAVITY
Axial and radial displacements determination in rotor center of gravity for gyroscope with elastic suspension
03 p0360 A72-13560
Controlled motion dynamics of spacecraft performing maneuvers, applying point transformation to third-order nonlinear system moving about center of mass in lateral motion
05 p0730 A72-17029
Earth satellite plane periodic oscillations damping with respect to center of mass in orbital plane during motion on elliptical Kepler orbit
05 p0730 A72-17030
Center of mass motion of spacecraft in central gravitational field, analyzing programming of size and position of elements in mass geometry leading to arbitrarily large displacements
05 p0731 A72-17032
Lunar center of mass position with respect to visible hemisphere physical surface calculated from photogrammetric analysis and Lunar Orbiter 1 data
08 p1232 A72-21158
Hodograph geometrical analysis of heavy gyrostator motion for center of mass and gyrostatic moment located on first and third principal axes of rotation
08 p1208 A72-21352
Gyrostator inertial motion under nonholonomic constraint of mass center coincidence with fixed point
08 p1208 A72-21360
Body center of mass position for stable fall in viscous fluid, determining terminal velocity as function of body geometry
10 p1470 A72-25067
Aft center of gravity travel effects on aircraft longitudinal control response characteristics
[SAE PAPER 720318] 11 p1575 A72-25581
Received signal spectrum gravity center and effective antenna centers of airborne Doppler velocimeter in horizontal flight
11 p1606 A72-26730
Simulated gravity environment tests of vertical jump features, recording work performed, body center of gravity upward velocity, potential and kinetic energy changes
12 p1770 A72-27479
Axisymmetric satellite rotation about center of mass in circular orbit under Newtonian gravitational field, considering precessional stability
13 p2052 A72-30002
Invariant mechanics principles for two body system dynamic properties, analyzing mass center motion, system energy and gravitational theory role
14 p2152 A72-30481
Lunar center of mass position with respect to visible hemisphere physical surface calculated from photogrammetric analysis and Lunar Orbiter 1 data
20 p2969 A72-39263
Influence of the terrestrial magnetic field on the motion of a satellite around its center of gravity
21 p3106 A72-41048
Axisymmetric satellite rotation about center of mass in circular orbit under Newtonian gravitational field, considering precessional stability
22 p3231 A72-42730

CENTER OF PRESSURE
Aerodynamic center and center of pressure of slender small aspect ratio wing near solid or free surface, determining angle of attack effect
13 p1894 A72-29131

CENTERS

Centers and foci composition of united trajectories of two autonomous scalar second order differential equations
15 p2262 A72-31551

CENTIGRADE TEMPERATURE SCALE
U TEMPERATURE SCALES

CENTRAL NERVOUS SYSTEM
NT BRAIN
NT BRAIN STEM
NT CEREBELLUM
NT CEREBRAL CORTEX
NT CEREBRUM
NT HIPPOCAMPUS
NT SPINAL CORD
NT SPINE
NT THALAMUS
Book on hibernation and hypothalamus covering central nervous system regulating mechanisms, biologic rhythmicity, migration, thermoregulation, torpor, human implications, etc
01 p0010 A72-10169
Receptor activity control from clinical physiological and electrophysiological observation data analysis, noting central nervous system role and feedback and self adaptation capabilities
02 p0157 A72-11543
Rat central nervous system oxygen toxicity seizure susceptibility relation to circadian rhythms
04 p0472 A72-14867
Short and long term mental and physical work effects on central nervous system and motor apparatus in young people
04 p0474 A72-15230
Conditioned reflex as component of artificial conditioned-natural unconditioned reflex system controlling adaptive behavioral patterns, noting contribution to complex nervous activity understanding
04 p0476 A72-15582
Cat mean renal nerve activity modification by hypothalamus stimulation and baroreceptor reflex interactions, discussing mean aortic pressure variation effects
04 p0477 A72-15722
Aeromedical diagnostics for aircraft pilot hearing sense tests, considering cockpit environment and stress-produced impairments in central nervous system
05 p0623 A72-16781
Control system model integrating human left ventricle and circulatory system mechanics and regulation by central nervous system
07 p0934 A72-20356
Entropy effect in two dimensional conditional reflex decision situations upon rats central nervous analysis-synthesis processes
07 p0925 A72-20661
Central nervous plasticity and stereotypy intercorrelation in conditional reflex two dimensional decision situations
07 p0925 A72-20662
Brain structures role in fixation of temporal relationships in information memory function of central nervous system
08 p1118 A72-21836
Central nervous system pharmacology, discussing somniferous, narcotic and neurotropic substances effects on brain activity
08 p1127 A72-21841
Electrocorticograph monitoring of central nervous system state in dogs reanimated by artificial blood circulation after prolonged clinical death by drowning
12 p1764 A72-28215
Central nervous system symptoms and simple bends in gas decompression sickness cases during USAF operational flying
12 p1775 A72-28283
Proton irradiation effects on monkey central nervous system, showing inflammatory reaction and neuroglial astrocyte glycogen accumulation
13 p1906 A72-29833
Human and animal central nervous system repair processes for brain damage caused motor function disturbances
14 p2078 A72-31100
Effect of a magnetic field on the nervous system
17 p2503 A72-35010
Neuropathological evaluation of monkeys exposed to body-alone X-radiation.
18 p2649 A72-36439
Manipulation of projected afterimages by means of the physiological theory imposed on the observer.
18 p2654 A72-36920
Reflex and conditional movement observation of central nervous system function restitution in Macaca mulatta monkeys with cortical lesions, studying pathological forced grasping
18 p2651 A72-36977
Possible role of supraspinal formations in the fixation of trace alterations at the segmental apparatus level of the spinal cord
21 p2999 A72-40592

Participation of supraspinal structures in the formation and control of a system of arbitrary cyclic motions of man
21 p2999 A72-40594
Breathing rate response to oral instructions in relationship to nervous system, bronchial muscle tonus and gas metabolism rate reflex-type changes
21 p3001 A72-40761
The functional organization of object directed human intended-movement and the forming of a mathematical model.
21 p3011 A72-41422
Electrophysiological analysis of defense reflex and unconditioned reaction and conditioned signal analyzers in nodal mechanisms of functional system /afferent synthesis, decision making, correction, etc/
21 p3004 A72-41675
Effect of vibration on the permeability of the blood-brain barrier
22 p3149 A72-42070
Cardiovascular system venous part responsiveness to central nervous and humoral influences
22 p3148 A72-43167
Studies on weightlessness in a primate in the Biosatellite 3 experiment.
23 p3253 A72-43388

CENTRAL NERVOUS SYSTEM STIMULANTS
The simultaneous action of stimulants and tranquilizers on the efficiency of a human operator
23 p3260 A72-43923

CENTRAL PROCESSING UNITS
NT ARITHMETIC AND LOGIC UNITS
Optimal operation assignment and data array storage allocation in data system consisting of central processing unit and peripheral computer controlling data flow
09 p1283 A72-23439
Process computer technology, discussing data recognition, on-line open loop operation and system characteristics
13 p1926 A72-30051
Medium scale integration /MSI/ modules for arithmetic section in small, medium and process computers, emphasizing carry-lookahead procedure
13 p1926 A72-30053
Control center relation to process control computers in production engineering, discussing information flow and communication in man machine systems
19 p2761 A72-38310

CENTRIFUGAL COMPRESSORS
Centrifugal compressor diagonal type impeller profiling through ruled surfaces delineated by rectilinear generatrices, calculating velocity field of rotating cascade
05 p0603 A72-16626
Centrifugal impeller slip factor prediction from three dimensional flow influences, discussing fluid passage guidance, flow separation, eddy and viscous effects
05 p0610 A72-17247
Compressible flow measurement and loss prediction in radial vaneless diffuser in centrifugal compressor, using hot-wire anemometers
10 p1416 A72-23861
Cascade technology for centrifugal compressor vaneless diffuser design, comparing performance results with conventional diffuser data
[ASME PAPER 72-GT-39] 11 p1569 A72-25633
Radial inflow compressor feasibility, discussing blade loadings for various pressure ratios and efficiency of rotor and diffuser
[ASME PAPER 72-GT-52] 11 p1570 A72-25644
Hub and shroud boundary layer growth in centrifugal compressor vaneless diffusers, comparing predicted and measured performance at high pressure ratio per stage
[ASME PAPER 72-GT-54] 11 p1570 A72-25645
Design considerations in selecting geometries for high pressure ratio single stage centrifugal compressors
[ASME PAPER 72-GT-91] 11 p1571 A72-25665
Discharge coefficients of centrifugal screw-type swirl injector with helical channel, calculating drag and surface geometry effects
11 p1712 A72-26970
Pressurized air assisted gas turbine fuel system, describing single stage centrifugal turbocompressor and rotary-lobe compressor designs and performance characteristics
18 p2694 A72-36043

CENTRIFUGAL FORCE
Aluminized solid propellant transient burning rate augmentation as function of acceleration vector magnitude and orientation, applying centrifugal accelerations of zero to 140 g
01 p0114 A72-10378
Glass fiber surfaces of revolution under axisymmetric pressure loads combined with centrifugal forces
01 p0143 A72-11365
Stroboscopic measurement of elastic untwisting angles of axial compressor rotor vanes under centrifugal and aerodynamic forces
01 p0143 A72-11371

- Displacement equations for rotating cylinder of revolution with stress on boundary corresponding to centrifugal force
03 p0445 A72-13625
- Gravitational field simulation by centrifugal force for structural stability and self weight buckling studies
07 p1096 A72-20428
- Ideal incompressible fluid sloshing under centrifugal force in partially filled conical cavity rotating at constant angular velocity
08 p1149 A72-21244
- Rotational, centrifugal and Coriolis force effects on turbulent boundary layer development, discussing changes in structure and shear stress distribution
10 p1464 A72-23870
- Nonlinear analysis of helicopter rotor blade free transverse vibration under air and centrifugal loadings during forward flight, using matrix method
15 p3233 A72-31407
- Astronomical model for primitive solar nebula showing planetary evolution in hot initial state under centrifugal forces
17 p2614 A72-35677
- CENTRIFUGAL PUMPS**
- Anticavitation properties improvement of volute centrifugal pumps during low flow rate operation by reducing back currents with truncated cone
07 p0914 A72-18984
- Military jet engines centrifugal fuel pumps power requirements for throttled operation, noting pressure stability improvement at low flow rates
18 p2694 A72-36041
- Centrifugal pumps performance instability, considering mass flow rate/pressure curve characteristics as function of impeller slip, fluid prerotation and hydraulic losses
18 p2694 A72-36042
- Inlet throttle centrifugal fuel pumps for jet engine augmentation, discussing design features, performance, noise, life and reliability characteristics
18 p2694 A72-36044
- Combined centrifugal oil filter, pump and deaerator for gas turbine engine lubrication systems, noting heat transfer effectiveness increase
18 p2694 A72-36050
- Comparison of the experimental characteristics of disk-type and rotodynamic centrifugal pumps
20 p2930 A72-39924
- Deterioration of shaft bearings of electromotor driving aircraft centrifugal fuel pump, determining lateral force acting on impeller
23 p3252 A72-43663
- Amplitude-phase-frequency characteristics of a high-rpm centrifugal pump
23 p3294 A72-44021
- CENTRIFUGES**
- NT HUMAN CENTRIFUGES**
- High angular velocity device design problems, considering gyroscopes, ultracentrifuges, yarn-spinning textile machinery and dental drill
19 p2809 A72-38544
- CENTRIFUGING**
- Valsalva and M-1 maneuvers acceleration tolerance protective effects during high-g centrifuging with and without anti-g suits
12 p1767 A72-28318
- CENTRIFUGING STRESS**
- Aircraft gas turbine rotating disks thermal and mechanical stresses under variable thermal conditions, describing test assembly
02 p0199 A72-11637
- Chronic centrifugation effects on rat deep body temperature by implant biotelemetry, comparing with body mass and food consumption changes
02 p0163 A72-12089
- Histological examination of transverse acceleration stress effect on inner ear development of gestating rat embryos
07 p0923 A72-20446
- High gravity environment exposure effects on gravity preference in chronically centrifuged rats, showing dependence on reference level
08 p1122 A72-20787
- Positive acceleration effects on human cardiovascular system during centrifuge tests, studying ECG changes in terms of cardiac rhythm, heart rate and wave parameters
11 p1584 A72-26015
- Pulmonary atelectasis and arterial-venous shunting and heart displacement prevention during centrifuging of dogs breathing oxygenated liquid fluorocarbon in water immersion respirator
11 p1579 A72-26609
- Bed rest and centrifuging effects on human plasma thyroid hormone level, discussing total protein, albumin and thyroxine binding globulin concentrations
12 p1770 A72-27477
- Centrifugation tolerance reduction after 14 days bed rest with moderate exercise, determining rehydration effects
12 p1766 A72-28295
- Neck proprioception effects and otolith organ activity in perceived visual target elevation under centrifuging stress
12 p1776 A72-28305

- Organism response to extreme overload factors, discussing centrifuging and vibration stress effects on mean swimming time and post-irradiation survival time in mice
16 p2355 A72-33554
- Effects of combined O-G simulation and hypergravity on eggs of the nematode, *Ascaris suum*. (DFVLR-SONDDR-225)
17 p2499 A72-34547
- Stress and adaptation responses to repeated acute acceleration.
17 p2500 A72-34729
- Hypothermia and resistance of mice to lethal exposures to high gravitational forces.
22 p3142 A72-42494
- CENTRIPETAL FORCE**
- Flexible cable in uniform flow field, calculating coupling between longitudinal and transverse modes to obtain centripetal acceleration effects on tension
18 p2734 A72-36418
- Participation of cholinergic structures in the development of disturbances of the functional state of the cerebellum under the action of centripetal accelerations
19 p2757 A72-38033
- Optimal modes of operation of a centripetal-compressor wheel with preswirling of the flow
24 p3364 A72-45622
- CENTROIDS**
- Centroid shift of diffraction line due to X ray diffractometer geometry in stress measurement
04 p0547 A72-14527
- Galactic spiral density waves instability effects, noting local centripetal radial motion and apex deviation
09 p1384 A72-22519
- CEPHALAGIA**
- U HEADACHE**
- CEPHEID VARIABLES**
- Cepheid variables mass discrepancy from evolution and pulsation theories, emphasizing opacity changes, luminosity values and effective temperature
01 p0133 A72-11128
- RR Lyrae variables intermediate band photometry, tabulating magnitudes and color of 125 stars
01 p0133 A72-11129
- DT Cyg and T Vul cepheid variables light curves and periodic variations from photoelectric observations
03 p0416 A72-13018
- RR Lyrae stars absolute magnitude determination by statistical parallaxes method
03 p0421 A72-13139
- Absolute magnitudes and mass-radius relationship of RR Lyrae stars for stellar evolution calculations
03 p0421 A72-13140
- Cepheid variables compared for Milky Way and Small and Large Magellanic Clouds, discussing amplitudes, period-luminosity relations and light curves
03 p0425 A72-13255
- Small Magellanic Cloud NGC 371 region photometric studies for cepheids period-luminosity relations, noting domination by young supergiant stars
03 p0425 A72-13258
- Magellanic Clouds cepheid variables compared to Milky Way cepheids, discussing evolution tracks
03 p0425 A72-13261
- Lunisolar precession and equinox motion from Cepheids proper motion, using recently determined distance values
04 p0576 A72-15038
- Linear nonadiabatic pulsation constants for fundamental mode and first two harmonics of stellar models including Cepheids, observing mass scattering
04 p0579 A72-15319
- Beta Cephei type variable stars, determining KP Persei times of maximum light, mean UVB magnitudes and light ranges
06 p0882 A72-18006
- Galactic cepheid RS Puppis and surrounding ring-structured nebula luminous variations and evolution, using reflecting shell model
07 p1069 A72-19079
- Disk population F-type star photometric luminosities, motions and metal abundance indices, discussing ultrashort period cepheids
07 p1071 A72-19333
- Ultrashort period cepheids presence in blue stragglers of old disk population
07 p1071 A72-19334
- Shock wave properties in RR Lyra type star atmospheres, discussing high temperature region structure behind wave front and emission line profiles
08 p1229 A72-20841
- RR Lyrae variables period-luminosity relations explained by linearized pulsation calculations for quenching of first harmonic
08 p1235 A72-21388
- Long period Cepheids in galactic spherical component, confirming two groups according to spectral characteristics
09 p1384 A72-22514
- Periodic variations of 12 Cepheids from 4 to 45 days
09 p1384 A72-22515
- Cepheid instability strip stellar models pulsation properties compared with delta Scuti stars and AI

- Velorum variables observation data for stellar evolution studies
10 p1542 A72-24611
- Cepheid variables evolutionary and blue edge calculations reconciled with observation
10 p1544 A72-24665
- Short period RR Lyrae variables, presenting light curves in UB system
10 p1550 A72-25198
- Color photoelectric light pulsations curve of RU Cam variable star during October 1969-August 1970, noting constant mean luminosity and color
14 p2158 A72-30729
- Sequential three color photometry of dwarf cepheid DY Pegasi, noting smooth color variation with phase
15 p2314 A72-32370
- Astronomical observations supporting stellar atmosphere microturbulence concept, noting Cepheid variables high dispersion spectra, supergiants irregular changes and microturbulence hydrodynamic effect
19 p2857 A72-37525
- Photometry of RR Lyrae variables in the globular cluster NGC 6981.
21 p3111 A72-41475
- A more accurate determination of the structural features of the instability strip of classical Cepheids from Gascoigne's photoelectric data in the Small Magellanic Cloud
21 p3113 A72-41757
- A survey for RR Lyrae stars at high galactic latitude.
22 p3222 A72-42137
- Resonance effects on second order anharmonic pulsational amplitudes for polytropic main sequence evolutionary models, classifying Cepheid-type pulsators
24 p3437 A72-44832
- Luminosity variation in the one-zone Cepheid model.
24 p3438 A72-44837
- CERAMAL PROTECTIVE COATINGS**
- U CERMETS**
- U PROTECTIVE COATINGS**
- CERAMALS**
- U CERMETS**
- CERAMIC BONDING**
- Temperature effect on bonding strength between ceramic whiskers or fibers and metal matrices attributed to thermal expansion coefficients disparity
16 p2413 A72-33206
- Acoustic emission technique as NDT method for quality control of brazed metal-ceramic bonding
18 p2695 A72-36458
- CERAMIC COATINGS**
- Space shuttle orbiter reentry heat shield materials, considering hot structures and hot radiative metallic, ceramic insulative and ablative heat shields
11 p1660 A72-26245
- Structural design characteristics of low density fiber ceramic materials coated with refractory ceramics for space shuttle reusable surface insulation thermal protection systems
13 p2056 A72-28957
- [AIAA PAPER 72-372]
Ceramic-to-metal seal development for thermionic fuel elements.
18 p2695 A72-36156
- Ceramic coatings measure the complex stresses in gas-turbine blades.
19 p2875 A72-37732
- Structural features of plasma and gas-flame deposited aluminum oxide coatings
19 p2810 A72-38680
- Chemical composition, refractivity and temperature dependence of blackness levels of aluminum oxide-chromium oxide-phosphorus oxide ceramic coatings flame sprayed on steel
21 p3072 A72-40384
- CERAMIC NUCLEAR FUELS**
- Stress corrosion of uranium carbide ceramics in atmospheric environments containing water
09 p1335 A72-22399
- CERAMICS**
- NT CERAMIC NUCLEAR FUELS**
- NT PYROCERAM (TRADEMARK)**
- Coextrusion of metal powder and ceramic dispersions clad alloyed Al as function of cartridge density and reactor core length
02 p0233 A72-11456
- Corundum ceramics thermal stability, basing qualitative tests on thermal cycle number and quantitative tests on thermal gradient producing damage
05 p0680 A72-15755
- Sprayed single component ceramic coating thermal stability enhancement techniques, noting limitations
05 p0680 A72-16093
- Finite element micromechanical analysis of porous and filled ceramic composites for internal stresses and deformations
05 p0738 A72-16423
- Rare earth tungstate refractory ceramics, determining mechanical properties, crystalline structure and electrical/chemical parameters
05 p0675 A72-16700

Metals, insulators, semiconductors and ceramics thermophysical parameters measurement during monotonic heating or cooling at 123-3273 K
06 p0904 A72-18514

Soviet book on superduty refractory porous ceramics covering preparation, structure and properties as thermal insulators, high temperature filters and catalyst carriers
06 p0836 A72-18520

Soviet book on nonmetallic material strength during nonuniform heating covering, load endurance, bending phenomena and thermal stability of fiberglass, pyroceramics and reinforced plastics
06 p0796 A72-18521

Rhodamine 6G dye laser tuning by variable birefringence filter using lead lanthanum zirconate titanate electrooptic ceramics for wavelength selection
07 p1002 A72-19203

Moving heat source model of temperature profile and thermal stress propagation for laser drilled holes in alumina ceramic material
07 p0994 A72-19211

Strain biased transparent ferroelectric electro-optic ceramics for coherent transducers /page composers/ for holographic memories and optical data processing [CLEA PAPER 18,6]
07 p0950 A72-19401

Photoelectric temperature measurements in contact zone during grinding of aluminum oxide ceramic materials by synthetic diamond disks
07 p0997 A72-20252

Thermal shock transient test burner to test gas turbine ceramics under simulated operational environment conditions
08 p1147 A72-21434

Press forged ceramic crystals deformation, recrystallization, strength and fracture properties, comparing sapphires, rubies and spinels
08 p1196 A72-21917

Ceramics in severe environments - Conference, North Carolina State University, Raleigh, December 1970
09 p1333 A72-22376

Thermodynamics of ceramic oxide corrosion by sulphur and oxygen bearing atmospheres, considering formation products and furnace refractory materials choice
09 p1333 A72-22377

High temperature radiographic techniques for measurements of molten ceramics density, melting point, phase transitions, surface tension and viscosity up to 3000 C
09 p1333 A72-22378

Fracture mechanical analysis for stability criteria and propagation behavior of thermal stress cracks in brittle ceramics in severe thermal environments
09 p1333 A72-22382

Zirconia ceramics for high performance storage heaters, discussing operating conditions, optimal properties for heater design, engineering evaluation tests and in-service performance
[AD-737021] 09 p1333 A72-22383

Silicon nitride ceramics resistance to thermal shock and stress in severe environments
09 p1334 A72-22386

Crystalline ceramics compressive fracture strength and microhardness tests at room temperature, suggesting microplasticity role in failure mechanisms
09 p1334 A72-22388

Fractography of high boron ceramics under ballistic impact, suggesting macroscopic and microscopic textures relationship to stress states and microstructure
09 p1334 A72-22391

Ceramic materials stress-strain behavior dependence on microstructural factors, discussing point defects, pore size and grain boundaries
09 p1334 A72-22392

Compression creep mechanisms in ceramic materials at elevated temperatures by lattice dislocations, grain boundary sliding and stress directed diffusion
09 p1334 A72-22393

Ceramic fiber reinforced Ni base alloy for gas turbine blades, improving creep resistance at high temperatures
09 p1335 A72-22396

Performance characteristics and limitations of electrode and insulation materials for open and closed cycle MHD generators, noting ceramic compositions for channel
[AD-737019] 09 p1335 A72-22401

Ceramic laser materials failure due to optically induced damage, estimating stresses and changes in refractive indices under thermal effects
09 p1336 A72-22403

Fast neutron radiation damage to glass ceramics and amorphous semiconductors electrical properties
09 p1336 A72-22405

Glass ceramics mechanical properties as function of temperature during bending, taking into account scale factor
09 p1337 A72-22742

Strength and fracture energies and toughness in fibre reinforced ceramics
09 p1339 A72-23171

Recording holographic networks in polycrystalline transparent ferroelectric ceramics of lead and lanthanum titanate-zirconate system
10 p1480 A72-24111

Sintered prepolarized perovskite type ferroelectric ceramics adiabatic depolarization and energy conversion under shock wave action
10 p1422 A72-24128

Physicochemical principles of inorganic materials production, considering heat resistant alloys, oxygen free and oxide cermets, glasses, glass ceramics and protective coatings
10 p1501 A72-24408

High alumina ceramics metallization and hard soldering to metals for manufacturing vacuum jacket of transmitting thermionic tubes
10 p1488 A72-24642

Papers on high temperature oxides covering refractory glasses, glass-ceramics, mullite, oxide spinels, glass networks theory and physical chemistry principles application
10 p1501 A72-24726

Refractory glass-ceramics forming systems characteristics and production, discussing crystallization factors
10 p1501 A72-24728

Slip casting process for ceramics, cermets and metal powders, discussing slurry preparation, deflocculating agents, binders and molding process
10 p1502 A72-24733

High temperature metal fiber reinforced ceramic matrix composites for turbine vanes, showing strength toughness and crack depths dependence on interfacial bond
[ASME PAPER 72-GT-51] 11 p1704 A72-25643

Dense silicon nitride and carbide ceramics for gas turbines, discussing critical properties for thermal stress calculation
[ASME PAPER 72-GT-56] 11 p1674 A72-25647

Ceramic dielectrics capacitors, considering perovskites and barium titanate physicochemical properties
11 p1702 A72-26545

Continuous hot pressing of high density reactive ceramic and metal powder materials in alumina die
11 p1643 A72-26832

Diffusion measurements during annealing of Pd-V, Pd-Ti and metal-ceramic systems by microprobe
11 p1664 A72-26853

Mica glass ceramics mechanical properties and thermal shock behavior in terms of microstructural variables, discussing fracture propagation and secondary cracks formation
11 p1675 A72-26949

Photovoltaic effects in CdS films evaporated onto barium titanate single crystal and ceramic ferroelectric substrates
12 p1856 A72-28014

Sliding dry friction of hard refractory metals and ceramics, discussing surface changes as function of load, sliding speed, temperature and mechanical properties
12 p1817 A72-28184

Electronic heating test arrangement for high temperature testing of metals and electrically conducting ceramics in vacuum, describing temperature control systems
12 p1796 A72-28249

Heat resistance of corundum based ceramics with multiphase additions under thermal cycling tests
13 p1983 A72-28568

Reliability tests on miniature ceramic capacitors encapsulated by epoxy-novolac block polymer compounds
13 p1919 A72-29061

Antifriction phase structure of friction formed thin surface layer of sulfurized iron-graphite metal-ceramic materials, using transmission microscopy
13 p1967 A72-30108

Deep diffused layer sintering of metal-ceramic cutting alloys with variable Co content for increased wear resistance and tensile strength
13 p1982 A72-30112

Coating materials for metal surface wear inhibition by adhesive and abrasive interactions minimization, discussing laminar solids, plastics, ceramics and soft metals
[ASME PAPER 72-DE-48] 14 p2108 A72-30874

Nonmetallized aluminum oxide ceramics brazing with metals under pressure using copper solder, noting optimum conditions for Kovar
15 p2243 A72-31225

Ceramic envelope electron multiplier design with hemispherically shaped dynodes, discussing electron optics, photosensitivity and applications
15 p2234 A72-31533

Friction and adhesive and abrasive wear of ceramics, discussing effect of environmental water and hydrocarbons
15 p2260 A72-32129

Time-temperature correlated phase transformations in zirconia nucleated magnesium-aluminum-silicon oxide glass ceramics for isothermal heat treatment
16 p2413 A72-33205

Dynamic load tests for impact strength of ceramic composites with fiber reinforced alumina matrix, obtaining dynamic stress-strain curves
16 p2414 A72-33300

Heat resistant adhesives properties and selection, discussing thermosetting-thermoplastic resins and ceramic materials for temperatures to 4400 F
16 p2415 A72-33597

Effect of fast-neutron irradiation on ceramics and ceramic-metal seals.
17 p2559 A72-34591

Implications of ceramic-insulator irradiation results for thermionic reactor design.
17 p2496 A72-34592

Ceramic waveguide microwave integrated circuits.
17 p2534 A72-35570

Composites technology, costs and performance review covering metal matrix composites, ceramic reinforced plastics and whisker composites
17 p2571 A72-35652

Effect of neutron spectra on the swelling of ceramic insulators and implications for thermionic reactor design.
18 p2703 A72-36146

HfB2 and ZrN alloys
19 p2845 A72-38409

The relationship between the thick film conductor and substrate and its influence on conductor properties.
20 p2908 A72-39494

Weibull distribution government of dispersion of destructive temperature gradients characteristic of fireproof ceramic materials heat resistance
21 p3074 A72-41713

Prediction of thermal-shock resistance during heating at very high rates.
22 p3241 A72-43000

Microscopic aspects of fracture in ceramics.
23 p3305 A72-43504

Polycrystalline aluminum and magnesium oxide ceramics fracture strength, considering plastic deformation and twinning role in crack nucleation
23 p3305 A72-43505

Brittle ceramic materials strength, showing porosity effect dependence on Weibull homogeneity parameter value
23 p3306 A72-43750

Determination of the regions of action of various creep mechanisms in ceramic materials
23 p3307 A72-43932

Alpha aluminum whiskers growth in multilayer ceramic composition following vapor-liquid-solid phase
23 p3303 A72-44152

Monolithic quartz and ceramic bandpass filters for narrow band analog data transmission systems
23 p3273 A72-44347

Laser spin melting experiments for glass production in space from high melting metal and rare earth oxide ceramics
24 p3417 A72-45156

CEREBELLUM

Human craniocerebral trauma dependence on impact conditions, giving case histories
05 p0619 A72-16643

Tentorium cerebelli microstructure and leaflets strength in study of chronic and acute hypoxia injury to fetus during pregnancy and labor
09 p1266 A72-23193

Amygdala projection to accessory olfactory bulb in rats, discussing main bulb, olfactory tubercle, pyriform cortex accessory bulb and amygdala relationships
11 p1581 A72-26770

Cat cerebellum cortex evoked response impulses interaction during stimulation of hypothalamus and peripheral nerves
14 p2076 A72-30669

Participation of cholinergic structures in the development of disturbances of the functional state of the cerebellum under the action of centripetal accelerations
19 p2757 A72-38033

Influence of a preceding afferent stimulation on the pyramidal activation of spinal motor neurons
21 p2999 A72-40588

Analysis of the activity evoked in the cerebellar cortex by stimulation of the visual pathways.
21 p3003 A72-41460

Morphological and electrophysiological analysis of afferent receptor connections in cerebellar cortex, discussing fast conducting, diffuse reticular and inferior olive fiber paths
21 p3004 A72-41674

CEREBRAL CORTEX

Neuron responses in cat visual system /retina, geniculate body, primary, secondary and tertiary visual cortex/ to simple visual stimulus pattern
01 p0011 A72-10466

Functional organization of visual cortex in monkeys, discussing monocular and binocular responses, trigger and stimulus abstraction
01 p0011 A72-10467

Computer simulation of evoked cortical audio potentials in animals and humans, noting clinical application for hearing threshold measurements

01 p0016 A72-11324

Postsynaptic electric potential responses to click of auditory cortex neurons in cats

02 p0158 A72-11757

Pyramidal tract neuron reactions to antidromic and afferent stimuli in cats, determining somatosensor cortical neurons responses by intra- and extracellular potential outlets

02 p0159 A72-11768

Bats auditory cortex electrical responses to ultrasonic stimuli, determining maximum sensitivity frequency range

02 p0159 A72-11769

Visual response to monocularly and dichoptically presented flashed patterns, discussing physiological mechanism based on cortical visual field concept

02 p0164 A72-12485

Cortical responses to visually displayed word and nonsense syllable stimuli, using EEG and computer techniques

04 p0474 A72-15248

Cerebral neurons population electric stimulation effect on deep sleep duration in Parkinsonism patients

04 p0476 A72-15585

Human visual system selective adaptability to speed, size and orientation, suggesting motion analysis by visual cortex neural subsystems

06 p0761 A72-17603

Cerebral cortex striate area relation to visual field in various animals

06 p0763 A72-17722

Phylo-ontogenetic maturation of corticopetal projections of visual cortex, using evoked potential measurements in rabbits

06 p0763 A72-17736

Short-time memory and electrographic effective and trace processes relationship from visual and Rolandian cortical regions activity and Tarkhanov galvanocutaneous reaction

06 p0764 A72-17993

EEG study of cortical aftereffects to peripheral stimulation in cats

07 p0915 A72-18866

Hypothalamic stimulation conditioned negative fear reflex in cats before/after neocortex isolation

07 p0920 A72-19859

Human cortical auditory evoked response to speech and sound effects, relating EEG interhemispheric wave amplitude asymmetry to stimulus meaningfulness

08 p1115 A72-20984

Evoked cortical potentials changes from emotional visual word stimuli stress under amylol anticholinesterase drug influence

08 p1116 A72-21194

Nembutal barbiturate effects on afferent signals transmission and thalamocortical level of somatosensory system

08 p1116 A72-21195

Comparative EEG characteristics of frontal and occipital human brain cortex, relating psychophysiological and neurophysiological factors

08 p1116 A72-21196

Cortical synthesis and information handling properties of evoked potential in human normal and pathological behavior

08 p1119 A72-21840

Corticosterone content in blood plasma, cerebral cortex and skeletal muscles during hypoxia adaptation in rats

08 p1121 A72-22083

Protein biosynthesis inhibitors retardation of noradrenaline and serotonin induced hyperpolarization of neuron membranes in cortical sensorimotor region of rabbits

08 p1122 A72-22192

Neurophysiological mechanisms of sleep, studying sleep and wakefulness state evoked potentials relation to cortex and subcortical activity levels

09 p1264 A72-22224

Negative and positive emotional states influence on blood cholesterol and arterial pressure levels in dogs, suggesting common subcortical genesis of atherosclerosis and hypertension

09 p1264 A72-22498

Functional organization of monkey cortical efferent zones in distal forelimb muscle control from intracortical microstimulation studies, showing stimulation thresholds distribution

09 p1267 A72-23582

Peripheral afferent input to monkey cortical efferent zones of distal forelimb muscle control, using single microelectrode for intracranial stimulation and cellular discharge recording

09 p1267 A72-23583

Visual evoked cortical responses in objective refraction related to retinal image clarity for clinical applications

11 p1582 A72-25349

Lenticular conditioning-shock stimulation effect on cat visual cortex response to light stimuli, noting

lateral gyrus photically evoked potential amplitude increase

11 p1578 A72-25801

Response latencies and correlation in single units and visual evoked potentials in cat striate cortex following monocular and binocular stimulations

11 p1582 A72-26771

Extrageniculate vision in monkey, discussing circle vs triangle and red vs green discrimination

11 p1582 A72-26772

Interhemispheric effects on choice reaction times to single and multiple letter displays, analyzing cerebral dominance and visual information transmission compared with verbal response

12 p1768 A72-27075

Visual cortex neuronal background activity in unanesthetized rabbits under stimulation and depression of lateral geniculate body and mesencephalic reticular formation, considering synaptic organization

12 p1761 A72-27646

Cat and rat cardiac and cardiovascular reflexes response to electric pulse stimulation of sensorimotor cerebral cortex

12 p1761 A72-27647

Cat auditory cortex neurons response to auditory and medial geniculate body electrical stimulation

12 p1761 A72-27651

Cortico-subcortical connections transaction effect on cat lateral geniculate body and visual cortex neurons spontaneous activity

12 p1761 A72-27652

Deep brain structure biopotential correlations during man sleep development, using electrosuicortico-grams

13 p1901 A72-28634

Neuronal spike activity changes in rabbit visual and sensorimotor neocortex and hippocampus during EEG activation

13 p1902 A72-28643

Functional organization and neurophysiological mechanisms of return corticothalamic system in anesthetized cats, showing axon terminal presynaptic depolarization

13 p1902 A72-28762

Visual cortex neuron reactions to antidromic stimulation of cat pyramidal tract, noting axon activation increased discrimination in analyzer

13 p1903 A72-28781

Cat visual cortex receptive field responses to light bands of variable widths and intervals

14 p2074 A72-30256

Visual cortex repetitive stimulation effect on primary response habituation in young normal rabbits and adults with septum pellucidum lesion

14 p2076 A72-30596

Cat cerebellum cortex evoked response impulses interaction during stimulation of hypothalamus and peripheral nerves

14 p2076 A72-30669

Cerebral cortex electric shock stimulation effects on phrenic nerve discharges in bivagotomized and curarized cats

14 p2077 A72-30842

Cat bulbar respiratory neuron discharge modification by single electric shock stimulation of cerebral cortex

14 p2077 A72-30843

Conditioned slow negative potential of human brain cortex dependence on motivation, emphasizing punishment avoidance conditions

16 p2353 A72-33097

The neurophysiology of binocular vision.

19 p2755 A72-37250

Changes of the catecholamine content in the brain of albino rats under overstrain caused by running in a rotating drum

19 p2757 A72-38034

Receptive fields of units in the visual cortex of the cat in the presence and absence of bodily tilt.

19 p2758 A72-38646

Influence of cooling of the sensorimotor region of the cerebral cortex on the neurons of the mesencephalic reticular formation

20 p2890 A72-38926

RNA content in the cortex neurons in connection with the change in its function during the emergence of an animal from hypothermia

20 p2890 A72-38928

Changes in the overall electrical activity of the mesencephalic reticular formation, the hippocampus, and the cerebral cortex under the influence of hydrocortisone and DOCA

20 p2890 A72-38929

Myogenic and eardrum evoked auditory potentials and cortical responses to 0.2 millisecond voltage pulse acoustic stimuli

20 p2891 A72-38932

Determination of the functional state of the auditory analyzer through the action of short-term acoustic stimuli of increasing intensity

20 p2893 A72-38939

Study of bilateral cortical nerve connections between the prearcuate gyrus and various cortical regions

20 p2891 A72-39323

Supplementary cues and delayed-alternation performance of frontal monkeys.

20 p2892 A72-39372

Intracellular study of rubrospinal neurons and of their synaptic activation during the stimulation of the sensorimotor cortical region

21 p2999 A72-40586

Synaptic potentials of sensor and motor neurons of trigeminal nuclei during corticofugal stimulation

21 p2999 A72-40587

Pyramidal control of the activity of interneurons related to various types of peripheral afferents

21 p2999 A72-40589

Role of pyramidal and extrapyramidal components of cortically-induced efferent stimuli in the mechanism of cortical motor activity coordination

21 p2999 A72-40591

Role of efferent influences of temporo-rhinencephalic cerebral structures in pre-adjustment alterations of spinal motor neuron excitability

21 p2999 A72-40596

Russian book - Cortico-visceral interrelations in physiology, biology and medicine.

21 p3000 A72-40752

Morpho-physiological structures thalamic afferent switching mechanisms of visceral analysers in motor, premotor, frontal and limbic cerebral sections

21 p3000 A72-40753

Polysynaptic sympatho-reticular and somatic afferent visceral links between internal organs and cerebrum in interoceptive reflex fields

21 p3000 A72-40755

Pathology of the cardiovascular system in terms of the theory of cortico-visceral interrelations

21 p3000 A72-40756

Blood vessel reactions to natural defense and conditioned reflexes from plethysmography and blood pressure measurements, discussing cortical effects mechanisms

21 p3000 A72-40758

Cortical effects mechanisms in animal vegetative systems, noting biological oxidation and organic phosphorus compound studies

21 p3000 A72-40759

Cortical metabolism regulation and effector systems of the adaptation process

21 p3000 A72-40760

Higher nervous activity of monkeys two years after the extirpation of the dorsolateral frontal cortex

21 p3001 A72-40803

Characteristics of certain parameters of memory for visual signals in lower monkeys

21 p3001 A72-40804

Effect of electrical excitation of various auditory analyzer levels on a conditioned motor reflex

21 p3001 A72-40805

Evoked potentials of the primary auditory cortical zone produced by positive and inhibitive conditioned stimuli

21 p3001 A72-40806

Some structural and functional characteristics of a retina projection onto the visual cortex of cats

21 p3001 A72-40808

Visual experience as a determinant of the response characteristics of cortical receptive fields in cats.

21 p3003 A72-41461

Morphological and electrophysiological analysis of afferent receptor connections in cerebellar cortex, discussing fast conducting, diffuse reticular and inferior olive fiber paths

21 p3004 A72-41674

Reactions of auditory cortex neurons to geniculocortical fiber stimulation

22 p3145 A72-42723

Cerebral auditory system acoustic information processing, discussing ganglia and cochlea neurophysiological functions in response to afferent stimulations

22 p3146 A72-42786

Dynamics of the electrical activity of various regions of the neocortex during the sleep-wakefulness cycle

22 p3147 A72-42955

The effect of electrical stimulation of the olfactory bulbs on the behaviour of cats and on the electrical activity of the neo- and archipaleocortex

22 p3147 A72-42960

Electrophysiological investigation of the excitation and inhibition processes in the auditory cortex

22 p3148 A72-43165

Limbico-neocortical, cardiovascular and hormonal system vegetative shifts associated with emotional behavior response, presenting neurogenic stress model for animals

22 p3148 A72-43166

Changes in the impulse activity of cortical neurons during selective reinforcement of a chosen range of their interpulse intervals

23 p3257 A72-44087

Synaptic events during specific and nonspecific inhibition of visual cortex neurons

23 p3257 A72-44088

Neuronal and focal reactions of the parietal associative cortex to various peripheral stimuli

23 p3257 A72-44089

Techniques for analysing differences in VERs:
Colored and patterned stimuli.

23 p3258 A72-44387

Elaboration of steady changes in the firing rate of cortical neuron populations

24 p3370 A72-44587

Control, by the visual cortex, of the posterior lateral thalamic group in the cat

24 p3372 A72-45009

CEREBRAL VASCULAR ACCIDENTS

Cerebral vascular disorder biochemical analysis, noting retinal vascular change relation to coronary arteriosclerosis and anoxia and flight stress effect on serum lipid and cholesterol

07 p0923 A72-20448

CEREBROSPINAL FLUID

Cerebro-spinal fluid pressure remote monitoring by intracranially implanted radio pressure transducers, describing receiver-detector-recorder system

07 p0930 A72-19911

Respiration control by extracellular pH in medullary tissue, studying chemoreceptor response to hydrogen ion concentration in cat cerebrospinal fluid

11 p1579 A72-26661

Cerebrospinal fluid pH change effects on cat respiratory response before and after vagotomy, showing vagal activity relation to central chemical control of respiration

12 p1762 A72-27825

CEREBRUM

Split human cerebrum physiology, discussing corpus callosum as interhemispheric nervous process transfer, and right and left hemispheres functional differentiation and asymmetry

02 p0157 A72-11544

Bioelectric activity study of cat and dog cerebral intercentral relations during various motor activities and poses

04 p0474 A72-15231

Functional condition of rabbits cerebrum precortical arteries during hypertension produced by intravenous noradrenaline infusion, discussing hypo and hyperkinesia

06 p0762 A72-17674

Early diagnostics of cerebral arteriosclerosis in flying personnel, investigating hypertonia, neurocirculatory dystonia and myocardial cardiosclerosis effects on flight performance

06 p0765 A72-18198

Behavioral properties of somatosensory-motor interhemispheric transfer.

17 p2505 A72-35463

Frontal cerebrum region and elementary mental activity

18 p2649 A72-36400

Cerebrum sections and related afferent processes as activator of automatic neuron mechanism control of motor activity, discussing segmentary spinal cord changes

21 p2999 A72-40593

Responses of anterior suprasylvian gyrus neurons to peripheral stimuli of different modalities

23 p3257 A72-44090

CERENKOV COUNTERS

Optical multplate spark chamber in balloon-borne gamma ray telescope, describing triggering signal from plastic scintillator directional Cerenkov counter and photographic recording system

03 p0353 A72-13035

Light generator aided autonomous calibration of Cerenkov spectrometer for continuous primary cosmic nuclear flux measurements

06 p0815 A72-17832

Cerenkov counter for astronomical observatory high energy cosmic ray experiments, discussing UV-reflecting paint, radiator and photomultiplier positioning improvements

15 p2234 A72-31536

CERENKOV EFFECT

U CERENKOV RADIATION

CERENKOV RADIATION

Cerenkov radiation detection by human eye, discussing relativistic muons passage through vitreous humor and retina

02 p0272 A72-11754

High energy gamma ray telescope based on absorption induced Cerenkov radiation in low density gas, using parabolic mirror for focusing on photomultiplier tubes

03 p0352 A72-13033

Gas-Cerenkov detector for 10-100 MeV gamma rays based on conversion and Compton scattering in plastic scintillator

03 p0352 A72-13034

Tachyon generation of gravitational radiation analogous to Cerenkov emission of electromagnetic radiation

05 p0711 A72-17160

High energy gamma quanta point sources from extensive air showers Cerenkov flares records, finding flux limits of radio galaxy and pulsars

07 p1064 A72-20635

Astrophysical equipment for Cerenkov radiation measurement from atmospheric showers, discussing

source of high energy gamma rays in galactic equator direction

14 p2146 A72-30201

Extensive air showers at zenith, measuring associated UHF radio pulses with optical Cerenkov emission receiver as trigger source

14 p2147 A72-30858

Radiation source motion at superluminal speed in vacuum, defining conditions for Vavilov-Cerenkov and Doppler effects

15 p2279 A72-32767

Temporal distribution of Cerenkov light from extensive air showers, discussing experimental setup and pulse shape

17 p2599 A72-35140

Analysis of geometry effects in the detection of Cerenkov light from extensive air showers.

17 p2599 A72-35141

Monte Carlo calculation of radial and time dependence of isophote diagrams for Cerenkov light in 0.1 to 1 TeV extensive air shower

17 p2599 A72-35142

A model for drift pair and hook burst emission from the solar corona.

17 p2617 A72-35712

Detection of high-energy gamma rays from the Crab Nebula.

19 p2850 A72-37503

High energy gamma ray sources search by Cerenkov radiation recording from extensive air showers, noting atmospheric transparency effects

19 p2850 A72-37805

Preliminary results of observations of the pulsar CP 1133 with the aid of a device for recording Cerenkov flares of extensive atmospheric showers

19 p2850 A72-37806

An evaluation of the intensity of Cerenkov radiation from auroral electrons with energies down to 100 ev.

19 p2792 A72-38741

Charged particle uniform motion in sinusoidally space-time periodic medium, determining Cerenkov and transition radiation field spectrum from Brillouin diagram

21 p3088 A72-41378

Spontaneous emission of plasma waves in the presence of a finite amplitude wave.

21 p3093 A72-41494

Wave excitation during inclined charged-particle flight through a waveguide

21 p3089 A72-41841

Astrophysical equipment for Cerenkov radiation measurement from atmospheric showers, discussing source of high energy gamma rays in galactic equator direction

23 p3328 A72-43226

The EAS power spectrum at sea level for $N = 10$ million to 1 billion particles

23 p3330 A72-44418

EAS Cerenkov glow and the relation of shower strength to the primary-particle energy

23 p3330 A72-44419

Experiment for studying the pulse shape of Cerenkov emission at large distances from an extensive air shower

23 p3330 A72-44420

Generation of plasma oscillation by beam-plasma interaction.

24 p3430 A72-45574

CERES ASTEROID

Planetary mass errors effects on orbit determinations, discussing Ceres mass from influence on Pallas orbit

04 p0575 A72-15035

CERIUM

NMR behavior and magnetic susceptibility of inter-metallic compound CeAl, noting exchange polarization of RKKY type between 4f electrons and conduction electrons

05 p0702 A72-16784

Ti-Ce-S alloys phase equilibria with isothermal cross section, discussing eutectic alloys anomalous structure and cerium monosulfide preparation method

08 p1187 A72-21784

Ce-N alloys phase diagram from durometric, X ray, metallographic and differential thermal analyses

14 p2123 A72-30991

Phase diagrams of Hf-Ce and Hf-Er alloys, plotting hardness and electroconductivity curves

15 p2289 A72-31188

Electronic energy band structures for alpha and gamma phase Ce, using exchange potential and plane wave method

15 p2293 A72-32227

Influence of cerium additions on the luminescence of europium and samarium ions in NaF single crystals

20 p2932 A72-39414

CERIUM COMPOUNDS

NT CERIUM OXIDES

CERIUM OXIDES

Lattice and photon components of thermal conductivity of cerium dioxide at high temperatures

07 p1044 A72-19881

Some results of studies of cathode luminescence in cerium-activated glass

19 p2845 A72-38190

CERMETS

Thermomechanical conditions of plasticity-to-brittleness transition temperature for optimal rolling of cermet W strips

01 p0078 A72-11088

Molybdenum-zirconium oxide cermets oxidation behavior, noting change of Mo oxidation characteristic from linear to parabolic time law above molybdenum oxide melting point

02 p0246 A72-12550

Titanium carbide based hard cermet alloys with Ni addition, testing wear resistance

03 p0372 A72-13549

Molybdenum-uranium dioxide cermet fuel pins fission heating at 1145 K in forced convection He cooled reactor, measuring dimensional changes and U 235 burnup

04 p0546 A72-14424

Ceramic whisker and fiber reinforcement of metals, discussing manufacturing and testing problems

04 p0533 A72-15088

Martensite and solid Cr-containing inclusion effects on wear resistance of cermet steel during dry friction with R18 steel

05 p0665 A72-16095

Hot pressing /extrusion/ of rods from metal-ceramic Ti, using pure and cermet powders with tungsten carbide

06 p0822 A72-18426

Aircraft power plants sealing materials, emphasizing porous cermet seals heat resistance under thermal cyclic loads

06 p0797 A72-18658

Corrosion resistance decrease and embrittlement in Ni-Mo cermet alloys after heat treatment from electrical resistance measurement

07 p1017 A72-19965

Lubricating action of sulfur-containing additives and chlorine compounds in lubricants and cermet materials, noting effects of iron compounds formation in contact region

07 p0996 A72-19967

Niobium carbide coatings for carbon steels and cermets, comparing with titanium carbide coatings

08 p1186 A72-21724

Cermet coating with enhanced microhardness by Ni electroplating with fine corundum particles, presenting optimum electrolytes

09 p1318 A72-22527

Explosive strain hardening of hard metal-ceramic alloy, presenting photographs of carbide and cobalt phases structural changes after impact loading

09 p1337 A72-22892

Physicochemical principles of inorganic materials production, considering heat resistant alloys, oxygen free and oxide cermets, glasses, glass ceramics and protective coatings

10 p1501 A72-24408

Slip casting process for ceramics, cermets and metal powders, discussing slurry preparation, deflocculating agents, binders and molding process

10 p1502 A72-24733

Temperature, oxygen pressure and exposure time effects on oxidation characteristics of molybdenum-zirconium oxide cermets

11 p1665 A72-26865

Cermets technology applications, discussing powder metallurgy role and sintering mechanism

11 p1665 A72-26871

Microstructure and mechanical properties of molecular cermets produced from slip-cast fused silica of different porosity by alumothermal reduction method

13 p1967 A72-30115

Chemical composition, powder particle size, porosity and heat treatment effects on sulfurized iron-graphite cermets durability

13 p1984 A72-30118

Electron microscopic investigation of slip processes during plastic deformation of WC-Co based cermets, observing WC grain boundary sliding and Co phase crystal lattice transformations

15 p2257 A72-32117

Effect of fast-neutron irradiation on ceramics and ceramic-metal seals.

17 p2559 A72-34591

Niobium carbide coatings for carbon steels and cermets, comparing with titanium carbide coatings

17 p2567 A72-35124

Thermionic converters fuel tests by uranium dioxide-Mo cermets irradiation, noting fission gas retention and metallic matrix deformation

18 p2708 A72-36141

Behavior of tungsten-clad Mo-UO₂ fuel under neutron irradiation at high temperature.

18 p2708 A72-36143

Local thermionic emission from bare and covered surfaces of cermetelectrodes.

18 p2646 A72-36193

NASA research on refractory carbides, nitrides and borides, discussing electronic and defect structures, hot extrusion, uranium nitride, cermets for bearings and composite evaluation

18 p2701 A72-36594

- Influence of heat treatment on the properties of Cr-SiO cermet thin films 19 p2844 A72-37948
- Strength and plasticity of molybdenum during short-term tests 19 p2819 A72-38218
- Dispersion hardening fabrication of hollow cooled blades of thin cermet layer and embedded plastic metal core, using aluminum oxynitrate in water-alcohol solution 19 p2809 A72-38282
- Effect of molybdenum on the properties of TiC-Ni cermet hard alloys 19 p2819 A72-38283
- Emissivity and electrical resistivity of tungsten-yttrium oxide cermets as function of composition at 1200-3200 K 19 p2819 A72-38286
- Constitution and property relations regarding cermets and other multiphase materials 20 p2940 A72-39453
- Transverse tensile properties of an unbonded model composite 20 p2941 A72-39790
- Prospects of using carbonitrides as the hard component of cermet hard alloys 22 p3188 A72-42195
- Gas permeability of high-porosity nickel cermet 22 p3188 A72-42196
- Fabrication of shaping cermet elements of die-casting molds for plastics by the hydrostatic pressing method 22 p3182 A72-42199
- Niobium and molybdenum alloys containing borides and carbides of the IV-a group metals 22 p3191 A72-42814
- Analysis of the mechanisms of yield-stress variation during compacting of metal-ceramic materials by rolling 23 p3298 A72-43278
- Titanium carbonitrides alloying with Ni in nitrogen atmosphere, noting N concentration effect on cermets wear resistance 23 p3298 A72-43281
- Thermal stability of sulphides of some metals in iron-base cermets 23 p3298 A72-43285
- Influence of the protective medium during sintering on the properties of iron-base cermets 23 p3299 A72-43289
- Growth rate of refractory oxide particles in nickel cermets 23 p3299 A72-43290
- Thermophysical properties of highly porous thermochemically treated metal-ceramic iron 23 p3299 A72-43295
- Microstructural aspects of the fracture of two-phase alloys 23 p3299 A72-43510
- Metalceramic alloy of the B2Zr type 23 p3302 A72-44010
- Some strength characteristics of graphite/zirconium carbide composites 23 p3307 A72-44013
- Influence of the cooling rate after sintering on the structure and properties of the ZrGr1.5D2.5 cermet 23 p3303 A72-44014
- Influence of the sintering medium on the quality of metalceramic hard alloys containing zirconium and hafnium carbides 23 p3303 A72-44017
- Compressive strength of Cu-W fiber metal matrix composite as function of temperature, comparing to cermets 24 p3416 A72-45750

CERTIFICATION

- Boeing 747B growth model FAA certification, discussing engine thrust, fuel capacity, taxi and flight weights and aircraft noise reduction [SAE PAPER 710753] 01 p0003 A72-10251
- Concorde airworthiness certification, discussing ground and flight test programs for performance, flying qualities and structures fatigue properties evaluation [SAE PAPER 710756] 01 p0003 A72-10253
- NERVA fuel quality control, discussing planning, nondestructive tests, computer data acquisition and certification systems 02 p0258 A72-11552
- Structural requirements for normal category plastic aircraft civil certification, noting compliance with Federal Aviation Regulations [SAE PAPER 720304] 11 p1575 A72-25568
- Inspectability criteria for airframes with fatigue fail safe design requirements for small airplane certification [SAE PAPER 720310] 11 p1575 A72-25574
- Fatigue certification of general aviation aircraft in Australia, describing ground taxi load spectra and endurance and radiographic inspection of laminated spar caps [SAE PAPER 720311] 11 p1734 A72-25575
- FAA policy in issuing civil airport operating certificates and establishing minimum safety standards 16 p2373 A72-33330

Autoland system flight testing in Trident 3B and British Civil Aviation Authority approval for ICAO Cat 3a weather 16 p2420 A72-33539

FAA implemented airport certification legislation covering minimum safety standards, operation manual, emergency plan, fire and rescue service and pavement requirements 18 p2675 A72-36785

A time-frequency localization system applied to acoustic certification of aircraft. [AIAA PAPER 72-836] 20 p2950 A72-39091

Design and certification for executive type aircraft. 24 p3366 A72-44730

Fan jet Falcon design and certification tests. 24 p3366 A72-44731

The fatigue and fail-safe program for the certification of the Lockheed Model 286 rigid rotor helicopter. 24 p3366 A72-44733

CESIUM

NT CESIUM VAPOR
Multiphotonic ionization of atomic cesium jet by Q switched ruby laser beam 03 p0392 A72-14061

Cathode temperature measurement in erosion and heat transport reduction by cesium seeding of Ar plasma arc 06 p0862 A72-18334

Pressure broadened atomic line shapes calculation for Cs resonance line pressurized by Ar, using Lennard-Jones potentials 09 p1354 A72-22663

Emitter conduction bands with negative electron affinity energy from surface barrier lowering of Cs p-type semiconductors 10 p1526 A72-24351

Liquid Rb and Cs density and thermal expansion measurements near fusion point, discussing temperature dependence and gamma ray irradiation method 11 p1746 A72-26237

Thermal-to-electric power conversion efficiency of nonequilibrium MHD generator with Cs seeded noble gases, considering electrode configuration and gas dynamic effects 13 p1900 A72-29356

Pressure effects of Ar and He mixtures on Cs atomic line shapes calculated assuming additivity of perturber interactions 14 p2134 A72-30838

Target anion effect on radioactive Sb and Te distribution formed by high energy proton irradiation of cesium salts containing oxygen 15 p2282 A72-32485

Lattice dynamical model for Cs vibration frequency distribution, specific heat and electrical and thermal resistivity calculations 16 p2441 A72-33584

Oscillator strength and ground state photoionization cross sections computation for Na, K, Rb and Cs atoms, including core polarization correction to dipole moment 16 p2431 A72-33724

Ellipsometry for the study of equilibrium cesium adsorption. 17 p2552 A72-34599

Thermionic energy conversion with a Ba-Cs diode. 17 p2496 A72-34603

Photoemissive properties of bismuth-cesium films 17 p2595 A72-34754

Emitter conduction bands with negative electron affinity energy from surface barrier lowering of Cs p-type semiconductors 17 p2595 A72-34952

W/100/ work function change during adsorption of oxygen, cesium, and oxygen-cesium co-adsorption 18 p2656 A72-36128

Optical constants of cesium in the wavelength range from 0.3 to 2.5 microns and their dependence on temperature and state of matter 24 p3426 A72-44800

Optical properties of thin cesium films over the wavelength range from 0.3 to 0.9 microns and their electrical resistance 24 p3426 A72-44801

CESIUM COMPOUNDS

NT CESIUM IODIDES

NT CESIUM OXIDES

CESIUM DIODES

Thermionic converter electrode performance of electron emission current density in terms of Cs arrival rate and surface temperature 07 p0915 A72-20568

Diffused electron and ion currents through grid anode of cesium thermionic diode, determining electron temperature and potential distribution in electrode gap 08 p1113 A72-21747

Cs diode discharge current oscillations in Knudsen plasma containing electron and positive ion fluxes from thermionic emission and surface Cs ionization 09 p1361 A72-22960

Thermionic converter model analysis for performance stability and inhomogeneities in Cs diode, considering emission current dependence on temperature 11 p1578 A72-26759

Oxygen adsorption effect in Cs-W thermionic converter system, comparing statistical-mechanics model analytical results with Alleau-Bacal experimental data 17 p2496 A72-34597

Cs diode discharge current oscillations in collisionless Knudsen plasma containing electron and positive ion fluxes from thermionic emission and surface Cs ionization 17 p2593 A72-35889

Thermionic effect-based cesium plasma converter operation as caloelectric converter and cesium diode 18 p2645 A72-36190

Vapor pressure influence of Ba-Cs thermionic converter diodes on I-V characteristics and work functions in terms of anomalous Schottky effect 18 p2646 A72-36194

I-V-characteristics of a plane parallel cesium diode with tantalum and tungsten emitter. 18 p2646 A72-36196

The ignited mode of cesium thermionic diode. II - The charge influence on the volt-ampere characteristics. 18 p2647 A72-36211

Short cesium plasma discharge diode as physical model for thermionic converter, studying ionization, recombination and microwave radiation 18 p2714 A72-36212

Determination of the emission potential of cesium-coated surfaces at high temperatures with a plane-parallel cesium diode. I - Technology. II - Physical foundations and measurement results 19 p2754 A72-37779

CESIUM HALIDES

NT CESIUM IODIDES

CESIUM IODIDES

Vacuum chamber sputtering techniques for CsI/Tl/ and NaI/Tl/ thin films for soft proton scintillation detector 06 p0816 A72-17834

Proton bombarded CsI crystal spallation-caused radioactive decay products contribution to background rate in satellite X ray telescope detector 06 p0853 A72-18084

CESIUM ION

Cesium contact ion thruster, investigating carburized thoriated tungsten filaments electron emission under ion bombardment [AIAA PAPER 72-440] 11 p1707 A72-26181

Cs contact ion microthrusters, neutral fraction measurements, analytical methods and testing procedures [AIAA PAPER 72-495] 11 p1711 A72-26218

Low energy Cs ion beam energy loss during traverse through near-thermal equilibrium Cs plasma as function of plasma density, comparing measurements with theoretical predictions 13 p2011 A72-29000

Energy spectra of Cs+ ions scattered by the surface of a tungsten single crystal 24 p3429 A72-45501

CESIUM OXIDES

Cesium oxide system stable phases as sources of Cs and oxygen vapors in thermionic energy converters, increasing power and reservoir operating temperature 09 p1263 A72-22959

Cesium oxide system stable phases as sources of Cs and oxygen vapors in thermionic energy converters, increasing power and reservoir operating temperature 17 p2498 A72-35888

Thermionic converter I-V performance improvement via oxygen addition, examining feasibility of cesium oxide-cesium solution as source 18 p2647 A72-36204

CESIUM PLASMA

Photoresonance cesium plasma development and decay, determining density spatial-temporal behavior and recombination and polar diffusion coefficients by probe measurements 03 p0396 A72-13664

Circularly polarized microwave damping at electron cyclotron frequency in low density magneto cesium plasma, investigating power absorption coefficient and refractive index 04 p0555 A72-14853

German monograph on spectroscopic investigation of Cs plasma electron density and temperature and excited atom density in various operational states of thermionic converter 04 p0560 A72-15699

Bound states and Coulomb interaction effects on thermodynamic properties of cesium plasma calculated on computer for different pressures and temperatures 05 p0693 A72-15838

Wave induced Q machine cesium plasma loss produced by current-driven collisional drift instability 06 p0857 A72-17527

Resonance charge exchange cross section measurements for Cs at 2 eV within Q machine, discussing ion energy resolution improvement 06 p0859 A72-17552

Boltzmann kinetic equation with electron-electron collision coefficients for isothermal weakly ionized cesium-argon plasma, using nodal point method 06 p0860 A72-17695

- Cesium plasma thermionic converters, discussing performance and efficiency improvement by governing electron transport in interelectrode space and cation generation
06 p0760 A72-18308
- Spectrographic measurement of electron temperature and ion density profiles in cesium plasma thermionic converter
06 p0862 A72-18309
- Low voltage arc plasma in low pressure Cs vapors, determining charged particle concentration and potential distribution in interelectrode gap
06 p0863 A72-18413
- Vibration modes and stability of nonequilibrium low density He-Cs plasma in magnetic field
07 p1043 A72-19876
- Pulsed radiography of X ray absorption by plasma behind incident shock wave in Cs vapors, noting mirror behind shock front and wave reflection
07 p1044 A72-19887
- Microwave radiation intensity and spectral frequencies of Knudsen discharge in cesium plasma
07 p1046 A72-20515
- Electrical conductivity measurement of dense nonideal Cs plasma at high pressure and temperatures
12 p1849 A72-27057
- Low energy Cs ion beam energy loss during traverse through near-thermal equilibrium Cs plasma as function of plasma density, comparing measurements with theoretical predictions
13 p2011 A72-29000
- Cs seeded nonequilibrium MHD Ar plasma stability in fully ionized seed regime
13 p2014 A72-29368
- Resonant irradiation effect on cesium discharge plasma, charge density, electron temperature and electric field strength
13 p2017 A72-29610
- Electron energy distribution, ions mass spectral composition and spatial charge concentration of currentless photoresonant Ce plasma obtained by associative ionization
14 p2136 A72-30175
- Electronic density measurement in ionized Cs vapor by observation of fundamental series lines mixture, comparing to Stark widening theory based profiles
14 p2134 A72-30852
- Bound states and Coulomb interaction of continuum particles effects on thermodynamic properties of cesium plasma calculated on computer for different pressures and temperatures
15 p2283 A72-31259
- Cs plasma electron density radial distributions from resonance absorption in discharge tube
15 p2286 A72-32302
- Rocket released artificial Cs plasma clouds in upper atmosphere, measuring electron density by HF radar observation
15 p2231 A72-32330
- Neutral atom concentration measurement in Cs ion beam, using high sensitivity detection gage to obtain emission indicatrices
16 p2434 A72-32862
- The influence of the electron temperature and other parameters on the electron density of a cesium plasma in a thermionic converter.
17 p2497 A72-34611
- Thermionic Cs arc theory applicability evaluation, considering collision dominated transport equations for plasma
17 p2587 A72-34616
- Low voltage arc plasma in low pressure Cs vapors, determining charged particle concentration and potential distribution in interelectrode gap
17 p2588 A72-34861
- Pulsed radiography of X ray absorption by plasma behind incident shock wave in Cs vapors, noting mirror behind shock front and wave reflection
17 p2590 A72-35135
- Work function theory for Cs-/W/ and Cs-O-/W/.
18 p2656 A72-36133
- Thermionic effect-based cesium plasma converter operation as caloelectric converter and cesium diode.
18 p2645 A72-36190
- Analytical description of thermionic converter phenomena, assuming position linearity of interelectrode electron energy distribution and local thermodynamic equilibrium in cesium plasma near collector
18 p2646 A72-36200
- Probe measurements of a cesium plasma in a simulated thermionic energy converter.
18 p2647 A72-36206
- Nonequilibrium relaxation phenomena in the near-emitter region of the thermionic converter.
18 p2647 A72-36209
- Excitation and ionization processes in a low-voltage arc discharge
18 p2714 A72-36213
- The Maxwellization of electrons in Cs-plasma of a low-voltage arc discharge
18 p2715 A72-36215
- Model improvements for thermionic diode plasmas.
18 p2715 A72-36218
- Forbidden line intensities in cesium plasmas.
19 p2840 A72-37776
- Excited-state cesium photoionization cross sections.
19 p2837 A72-37838
- Resonant irradiation effect on Cs discharge plasma charge density, electron temperature and electric field strength
21 p3091 A72-40664
- Impedance of a partially ionized cesium plasma.
21 p3091 A72-40694
- Amplitude and phase space potential oscillations measurements with hot electron probe in collisional Cs plasma compared with linear drift wave theory
21 p3093 A72-41376
- Measurement of ionic parameters of a cesium plasma with the help of a grid probe with a cooled collector
22 p3211 A72-42645
- Caloric state equation for isentropes and temperature calculation of nonideal Cs plasma produced in high density vapors by shock wave compression
23 p3318 A72-43320
- Special features of photoresonance perturbation relaxation in a low-temperature discharge plasma
23 p3319 A72-43409
- Low frequency oscillations of cesium and mercury vapor plasmas, noting intensity distribution, radiation pattern and polarization characteristics of microwave emission
23 p3319 A72-43411
- Electrical conductivity measurement of dense nonideal Cs plasma at high pressure and temperatures
24 p3431 A72-45710
- CESIUM VAPOR**
- Molecular Cs role in multiphoton ionization process during interaction with low intensity Q switched Nd-glass laser radiation
05 p0670 A72-17082
- Low voltage arc discharge development in cesium vapor with glowing spherical plasma cluster formation in electrode gap
05 p0701 A72-17238
- Initial development period of low voltage arc discharge in cesium vapor leading to quasi-neutral plasma formation
06 p0860 A72-17696
- Low voltage arc plasma in low pressure Cs vapors, determining charged particle concentration and potential distribution in interelectrode gap
06 p0863 A72-18413
- Cs and Hg vapors compressibility factor in supercritical range as function of density, considering charged particles and atoms polarization interactions in ionized metal vapors
07 p1040 A72-18943
- Transients determined for Cs vapor discharge phases, observing current fluctuations between steady states in negative resistance zone above 0.2 torr
07 p1046 A72-20517
- Cesium oxide system stable phases as sources of Cs and oxygen vapors in thermionic energy converters, increasing power and reservoir operating temperature.
09 p1263 A72-22959
- Sound radiation by shock wave front in cesium vapors, describing experimental shock tube
13 p2017 A72-29608
- Cs vapors thermal conductivity at various temperatures and pressures, using low emissivity Ni cylinders.
13 p2065 A72-29896
- Electronic density measurement in ionized Cs vapor by observation of fundamental series lines mixture, comparing to Stark widening theory based profiles
14 p2134 A72-30852
- Giant pulse radiation in Q factor modulated Nd glass laser frequency stabilization by molecular Cs vapor
15 p2245 A72-31411
- Fast metastable hydrogen atom beam production by proton beam-Cs vapor charge exchanges
16 p2429 A72-33057
- Cs adsorption on W and Ti observed by combination of ellipsometry, Auger spectroscopy and surface potential difference measurements, noting sticking coefficient and coverage
16 p2442 A72-33833
- Impurities and additives effects on electrode properties in Cs vapor thermionic converter, noting coadsorption model for Cs-W-O surface
17 p2496 A72-34598
- Cs vapor photoionization by sequential method via thermally tunable Ga-As laser and arc-lamp monochromator radiation
17 p2585 A72-34614
- Low voltage arc plasma in low pressure Cs vapors, determining charged particle concentration and potential distribution in interelectrode gap
17 p2588 A72-34861
- Cesium oxide system stable phases as sources of Cs and oxygen vapors in thermionic energy converters, increasing power and reservoir operating temperature.
17 p2498 A72-35888
- Plasma immersion probe measurements of electron work function.
18 p2690 A72-36127
- Switch properties of thermionic diodes with cesium vapor.
18 p2645 A72-36178
- Cylindrical Cs thermionic converter with unique emitter and five collectors, measuring I-V characteristics to determine emitter work function, ignition voltage and electric power
18 p2646 A72-36191
- High temperature cesium vapor sources based on a cesium-graphite system for thermionic converters
18 p2646 A72-36201
- Investigation of physical processes and optimization of thermionic converters with a Cs-Ba filling
18 p2647 A72-36203
- Thermionic converter I-V performance improvement via oxygen addition, examining feasibility of cesium oxide-cesium solution as source
18 p2647 A72-36204
- Ionization of mercury vapor and cesium vapor in a nuclear reactor.
18 p2713 A72-36208
- Thermodynamic properties of Cs-vapors.
18 p2713 A72-36210
- Arc mode thermionic converter at low cesium vapor pressures
18 p2647 A72-36216
- Polarization and interferometric investigations of discharge modes in thermionic energy converters
18 p2647 A72-36219
- Study of cesium vapor pressure by the boiling point method
18 p2713 A72-37179
- Absolute detection and collisional destruction of 2.5-keV metastable hydrogen atoms produced by a charge-exchange process in cesium vapor.
19 p2837 A72-37547
- Thermionic performance of fluoride CVD tungsten-niobium converter.
19 p2754 A72-37781
- Sound radiation generation by shock wave front in Cs vapors, describing experimental shock tube
21 p3091 A72-40662
- Alkali metal vapor Q switches for synchronizing mode-locked laser pulse trains with external events.
23 p3297 A72-44189
- The ionization of caesium vapour by the method of space charge amplification.
23 p3316 A72-44344
- CESIUM 137**
- ATP injection protection against Co 60 or Cs 137 gamma radiation in albino mice, guinea pigs and dogs.
05 p0621 A72-16636
- CESNA MILITARY AIRCRAFT**
- U MILITARY AIRCRAFT
- CESNA 210 AIRCRAFT
- Cesna 210 aircraft electrically driven hydraulic power pack for landing gear system, noting engine and flight tests
11 p1577 A72-25589
- CETANE**
- Graph-analytical method of determining cetane numbers of light catalytic gas oil grades
17 p2571 A72-31578
- CH-46 HELICOPTER**
- Full scale airframe fatigue testing of the CH-46.
17 p2491 A72-34511
- CH-54 HELICOPTER**
- S-64 Skycrane helicopter current and anticipated applications in commerce and industry, considering logging operations in ecologically sensitive or rugged areas, bridge construction, etc
16 p2348 A72-33185
- Application of boron/epoxy to the CH-54B Skycrane helicopter.
17 p2491 A72-34510
- CHAFF**
- Experimental determination of fall rate of 'N5' chaff on the heights 50-90 km.
21 p3049 A72-41498
- CHAIRS**
- U SEATS
- CHALCOGENIDES**
- NT ALUMINUM OXIDES
- NT ANATASE
- NT BARIUM OXIDES
- NT BERYLLIUM OXIDES
- NT BISMUTH OXIDES
- NT BISMUTH TELLURIDES
- NT BORON OXIDES
- NT CADMIUM SELENIDES
- NT CADMIUM SULFIDES
- NT CADMIUM TELLURIDES
- NT CALCIUM OXIDES
- NT CARBON DIOXIDE
- NT CARBON DISULFIDE
- NT CARBON MONOXIDE
- NT CESIUM OXIDES
- NT CHROMITES
- NT CHROMIUM OXIDES
- NT COBALT OXIDES
- NT COESITE
- NT COPPER OXIDES
- NT COPPER SULFIDES
- NT DISULFIDES
- NT ENSTATITE

NT GALLIUM SELENIDES
 NT HAFNIUM OXIDES
 NT HEAVY WATER
 NT HEMATITE
 NT HYDROGEN PEROXIDE
 NT HYDROGEN SULFIDE
 NT ILMENITE
 NT INDIUM TELLURIDES
 NT IRON OXIDES
 NT LEAD SULFIDES
 NT LEAD TELLURIDES
 NT MAGNESIUM OXIDES
 NT MAGNETITE
 NT MERCURY TELLURIDES
 NT METAL OXIDES
 NT MOLYBDENUM DISULFIDES
 NT MOLYBDENUM OXIDES
 NT NICKEL OXIDES
 NT NIOBIUM OXIDES
 NT NITRIC OXIDE
 NT NITROGEN DIOXIDE
 NT NITROGEN OXIDES
 NT NITROGEN TETROXIDE
 NT NITROUS OXIDES
 NT OXIDES
 NT PEROXIDES
 NT POLYSULFIDES
 NT POTASSIUM OXIDES
 NT PYROXENES
 NT QUARTZ
 NT RUTILE
 NT SAPPHIRE
 NT SCHEELITE
 NT SELENIDES
 NT SILICON DIOXIDE
 NT SILICON OXIDES
 NT SULFIDES
 NT SULFUR OXIDES
 NT TANTALUM OXIDES
 NT TELLURIDES
 NT THORIUM OXIDES
 NT TIN TELLURIDES
 NT TITANIUM OXIDES
 NT TROLITE
 NT TUNGSTEN OXIDES
 NT URANIUM OXIDES
 NT VANADIUM OXIDES
 NT WURTZITE
 NT YTTRIUM OXIDES
 NT ZINC OXIDES
 NT ZINC SELENIDES
 NT ZINC SULFIDES
 NT ZINC TELLURIDES
 NT ZINCBLLENDE
 NT ZIRCONIUM OXIDES

Electron microscopy and diffraction analysis of lattice imperfections of layered superconducting transition metal dichalcogenide intercalation complexes
 01 p0113 A72-10019

Frequency response and I-V characteristics of metal/chalcogenide glass/metal diode structures
 04 p0498 A72-15079

Lattice expansion of metal chalcogenide superconducting organometallic structures with aromatic or aliphatic Lewis bases sandwiched into van der Waal gap
 08 p1216 A72-21214

Frequency response of spectral noise amplitude in chalcogenide glass switches
 09 p1366 A72-22215

Electron energy threshold measurements in irradiated II-VI compounds interpreted in terms of damage on metal and chalcogenide sublattices
 12 p1859 A72-28070

Friction characteristics of high melting point metal chalcogenides as function of load and temperature, noting friction coefficient variations
 12 p1817 A72-28185

Chalcogenide semiconductor monostable threshold and bistable memory switching devices, discussing fabrication and performance
 13 p1934 A72-30090

Chalcogenide semiconductor compounds of b-subgroup transition elements, discussing binary system diagrams, stoichiometric composition and electrical properties
 15 p2290 A72-31193

High electric field effects on I-V characteristics of Te-As-Ge-Si type chalcogenide thin film, noting Poole-Frenkel emission and electron tunneling roles
 15 p2291 A72-31641

Laser irradiation induced refractive index change in evaporated chalcogenide glass films of As-S-Ge system
 16 p2401 A72-33395

Structure, electrical conductivity and electron transport mechanisms in chalcogenide glasses
 17 p2596 A72-35750

Interdependence of the commutation and memorization effects and the thermal behavior in a series of chalcogenide glasses
 18 p2718 A72-36344

Electrical changes in the surface region of chalcogenide glasses.
 19 p2822 A72-37454

Interpretation of the preswitching behaviour of chalcogenide-glass switches in terms of a space-charge-injection mechanism.
 21 p3034 A72-41466

The switching behaviour of thin films of chalcogenide glass.
 22 p3214 A72-42319

Preswitching electrical properties, 'forming,' and switching in amorphous chalcogenide alloy threshold and memory devices.
 24 p3385 A72-44982

CHANCE-VOUGHT MILITARY AIRCRAFT U MILITARY AIRCRAFT CHANDRASEKHAR EQUATION

Chandrasekhar statistical stellar dynamics assumption generality compared to Chandrasekhar diffusion process, discussing discontinuous model, relaxation time, escape probability and numerical results
 12 p1872 A72-27893

On a resolution of the equations governing the second order correlation functions for an isotropic hydromagnetic turbulence.
 22 p3212 A72-43100

Characteristics and constants of motion method for collisional kinetic equations.
 24 p3426 A72-44984

CHANNEL CAPACITY

Time division multiple access system with 100/50 M bit/s channel capacity for Symphonie and Intelsat satellite speech channels
 01 p0033 A72-11302

Coding for data communication over discrete time channels without feedback under various fidelity criteria, discussing channel capacity
 02 p0171 A72-11681

Reconstruction errors, quantization noise and channel bandwidth in high order digital to analog conversion
 06 p0779 A72-17783

Technical standards for educational and community TV by satellite, considering picture quality requirement, modulations, SNR, threshold and fade margin, and channel width
 10 p1435 A72-24034

Communication satellite technology trends, discussing channel capacity, attitude stabilization, antenna pointing accuracy, energy conversion and storage, frequency reuse and onboard switching
 11 p1725 A72-25254

Intelsat V satellite system with large telephone channels capacity and full earth station network connectivity, discussing system concepts and technology [AIAA PAPER 72-536]
 12 p1780 A72-27359

Satellite supplement to domestic communication systems, discussing network management, system reliability, broadband capacity, earth station flexibility and market proposals [AIAA PAPER 72-554]
 12 p1781 A72-27374

Optical PCM communication system with megabits/sec information rate based on dye laser with combined frequency-time division multiplexing
 15 p2198 A72-32060

Random multiple access data transmission systems with feedback for message confirmation and retransmission in event of errors, evaluating channel capacity
 16 p2372 A72-33794

Comparison of circuit call capacity of demand-assignment and preassignment operation.
 17 p2512 A72-34270

Texture measurements in earth resources data management system by automatic photointerpretation with analog and digital techniques, discussing data processing rate requirements
 17 p2520 A72-34409

Video data transmission minimum channel capacity requirement calculation from rate distortion function of source with known probability distribution
 18 p2637 A72-36253

An optical communication system using envelope modulation.
 19 p2766 A72-38604

High speed, high density digital recording.
 22 p3175 A72-41933

CHANNEL FLOW

X-type pseudoshock at high Mach number compared with lambda-type pseudoshock, discussing loss at duct center by leading shock wave
 01 p0050 A72-10397

Electrically ionized striated plasma flow in annular channel, noting application to synchronous induction MHD generator
 01 p0111 A72-11209

Boundary conditions for monatomic gas flow in constant cross section channel with heat supply and ionization
 01 p0111 A72-11211

Ion oscillation theory for electrodynamic channel Poiseuille and Hagen-Poiseuille type flows, using transport and dispersion equations in various ionized media
 01 p0111 A72-11214

Differential equations solution for turbulent two dimensional jet flows bounded by parallel planes
 02 p0156 A72-12000

Electrohydrodynamic ideal incompressible fluid flow in flat and circular channels, determining electric potential and field distribution
 02 p0266 A72-12431

MHD flow development in parallel plate channel entrance region, obtaining numerical solution for velocity distribution, pressure drop and length at different Hartmann numbers
 02 p0266 A72-12493

Two dimensional MHD channel flow of inviscid fluid in circular nonuniform magnetic field
 02 p0267 A72-12771

Elliptic equations solutions for electromagnetic effect in MHD rectangular channels using relationship to Laplace equations
 03 p0397 A72-13995

Variational problem of conducting fluid flow in MHD channel at large magnetic Reynolds numbers at induction saturation
 03 p0397 A72-13999

Magnetic field and current density distributions in cylindrical conduction MHD channel with arbitrary number of pole-electrode pairs
 03 p0398 A72-14000

Annular MHD channel laminar flow generation at supercritical Reynolds numbers by strong magnetic fields
 03 p0398 A72-14005

Electric field intensity and pulsation spectra variation along rectangular channel in transverse magnetic field, noting current density changes
 03 p0398 A72-14006

Steady laminar viscous conducting fluid flow in infinite rectangular channel in crossed electric and magnetic fields, deriving flow rate and potential distribution
 03 p0398 A72-14008

Steady flow of viscous incompressible conducting fluid in rectangular channel with sectional walls under longitudinal external magnetic field, deriving velocity distribution
 03 p0398 A72-14009

Magnetic field distribution in linear MHD channel for large Reynolds numbers, determining current density and longitudinal field component
 03 p0398 A72-14010

Heat transfer in rectangular annular channel during external heating under supercritical pressure, discussing thermal flux, mass flow rates and enthalpy
 03 p0457 A72-14152

Plane air jet ejection into dead ended rectangular and parabolic channels, discussing effects of geometry, length and pressure
 03 p0309 A72-14156

Critical thermal loads during external and internal heating of annular channels, discussing curvature effect on density level in thermal flux during forced fluid motion
 03 p0458 A72-14157

Numerical solutions of integral equation for transition and turbulent flows through pipes and channels, discussing computer simulations
 04 p0510 A72-14469

Forced convective heat transfer of laminar flow in curved channel with square cross section at constant wall heat flux
 04 p0510 A72-14595

Heat transfer from nitrogen plasma jet mixed with cold gas to cooled reactor channel walls at various channel expansion degree values
 04 p0555 A72-14645

MHD approximation to solve natural convection problem in vertical channel under external inhomogeneous magnetic field, noting fluid flow rate
 04 p0555 A72-14646

Geometrical and aerodynamic characteristics of circular cross section diffuser channels from turbulent boundary layer calculation at preseparation flow stage
 04 p0461 A72-14647

Stratified fluid motion between two parallel infinite disks rotating with different angular velocities
 04 p0511 A72-14857

Laser light beam attenuation, considering turbulent pulsation effects in closed channel fluid flow axial region
 04 p0530 A72-14989

Boundary value problem for steady parallel axisymmetric irrotational flow of inviscid incompressible fluid past cylinder having common axis with tube
 04 p0512 A72-15056

Disk pump driven fluid layer device for density stratified water channel flow measurements, using hydrogen bubble technique
 04 p0509 A72-15118

Incompressible power law pseudo-plastic material plane flow in converging channel and axially symmetric converging flow in circular cone
 04 p0513 A72-15287

Magnetic field effect on heat transfer in steady plane laminar conducting incompressible viscoelastic fluid flow in channel with nonconducting walls
 04 p0560 A72-15580

- Navier-Stokes equations numerical solution by computerized simulation for viscous channel flow with diaphragm orifice reducing cross section
04 p0513 A72-15644
- Radial pressure distribution in laminar flow of compressible fluid between two coaxial disks from analog computer study
04 p0514 A72-15702
- Rectangular channel flow of two immiscible viscoelastic Maxwell fluids with transient pressure gradient, deriving interface velocity, flow rate and wall resistance components
04 p0514 A72-15705
- Confined laminar jet mixing of two uniform streams flowing in parallel plate channel, obtaining velocity field from linearized governing equation
[ASME PAPER 71-WA/APM-2] 05 p0647 A72-15973
- Navier-Stokes equations asymptotic solution for compressible weightless conducting fluid flow in plane channel with intense blowing from walls
05 p0648 A72-16219
- Flow calculations for subsonic and transonic portions of ring nozzles and plane curvilinear channels
05 p0601 A72-16226
- MHD flow of viscous fluid between two oscillating flat plates, observing velocity damping by magnetic field
05 p0699 A72-17179
- Equilibrium turbulent flow of incompressible fluid in plane diffusers, taking into account channel cross section including viscous sublayer
06 p0801 A72-18144
- Plane two dimensional flow in channel of rocket engine with solid propellant combustion, obtaining burning rates
06 p0867 A72-18207
- German book on nonlinear free boundary value problems of two dimensional hydrodynamics covering gravity, capillary and irrotational waves, liquid flow in channel, etc
07 p0967 A72-19183
- Heat transfer in thermal entrance region with turbulent flow between parallel plates, solving energy equation by difference methods
07 p1099 A72-19622
- Wall stabilized dc arc channel for plasma viscosity and flow characteristics studies, using pressure probe
07 p1043 A72-19877
- Hot gas heat transfer measurements in separation, reattachment and redevelopment regions downstream of abrupt circular channel expansion
[ASME PAPER 71-HT-DD] 08 p1251 A72-20881
- Heat transfer in laminar and turbulent Newtonian fluid flow in narrow channels with allowance for temperature dependence of viscosity and energy dissipation
08 p1148 A72-20955
- Heat transfer effect on Poiseuille flow in channel, using modified Orr-Sommerfeld equation with additional viscosity gradient terms
08 p1252 A72-21253
- Electrostatic ion wave stability in electrogasdynamic channel flow from approximate numerical solution of dispersion equations
08 p1211 A72-21305
- Steady axisymmetrical twisted gas flow parameters in channels with geometries similar to turbojet engine units
08 p1149 A72-21310
- Conjugate solution for Poisson equation of heat transfer in laminar flow with developed velocity profile in flat channel with internal constant heat sources
08 p1252 A72-21314
- Air injection from wall slot into turbulent boundary layer of high temperature gas channel flow, calculating film cooling effectiveness in flat plate
08 p1252 A72-21316
- Rectangular channel mixed boundary layer flow patterns dependence on inlet edge configurations, channel geometry and hydrodynamic flow core parameters
08 p1150 A72-21317
- Turbulent friction coefficients and velocity distribution in channel and pipe flow, using eddy viscosity model
08 p1150 A72-21623
- Supersonic plasma flow in narrow rectangular channel and free incompressible inviscid conducting liquid jet motion within pulsating transverse magnetic field
08 p1214 A72-21652
- Electric eddy currents formation during thermal acceleration of inviscid quasi-linear plasma in profiled channel
08 p1215 A72-21654
- Hydrodynamics of dispersed annular two phase flow in cylindrical channels characterized by concurrent motion of flow core and liquid film at wall
08 p1151 A72-21667
- German monograph on experimental investigations of annular channels with axial flow of incompressible fluids covering graphical and computational determination of flow volume
09 p1293 A72-22332
- Asymmetric flow in plane channel characterized by diffusional transport of turbulent shear stress and kinetic energy from rough to smooth wall regions
10 p1467 A72-24368
- Laminar flow dispersion coefficient for curved tubes and channels determined by mathematical model, permitting concentration distribution computation
10 p1468 A72-24371
- Interacting viscous conducting media flow in inclined channel in presence of transverse magnetic field, using Moiseev asymptotic method for steady flows with wavy interface
10 p1522 A72-24546
- Interaction solutions of steady crossed field MHD channel flows for perfect, singly ionizing monatomic and thermodynamically unspecified gases
10 p1523 A72-24789
- Hydrodynamic forces in sinusoidal vibrations of disk in water channel with toroidal vorticity wake pattern, applying results to flapping wing mechanics
10 p1471 A72-25129
- Nonisothermal hydrogen plasma channel flow and radiative heat transfer combined with convective and conductive transfer between isothermal black parallel boundaries
[AIAA PAPER 72-279] 11 p1692 A72-25219
- Noncoincidence of maximum velocity and zero shear stress due to asymmetric turbulent velocity profiles, considering effect on momentum, heat and mass transfer in noncircular channels
11 p1618 A72-26534
- Heat and momentum transfer of binary gas mixture flow in parallel plate channel with mass injection from porous wall, calculating velocity, pressure and temperature distributions
11 p1746 A72-26538
- Perturbation analysis of perfect gas unsteady transonic irrotational inviscid flow in two dimensional channel, presenting numerical computation of flow structure temporal change
11 p1618 A72-26635
- Computerized numerical model of mixed subsonic and supersonic gas flow with sonic transition in turbine curvilinear channel
11 p1574 A72-26967
- Discharge and pressure recovery coefficients of blocked gas flow in curvilinear channel with guide vanes, minimizing losses and separation at convex wall
11 p1574 A72-26971
- Viscous incompressible gas turbulent flow in axisymmetric channel under preliminary twist conditions at inlet, using computer numerical solution
12 p1752 A72-28126
- Copper resistance thermoanemometer for channel unsteady air flow rate measurement, discussing design, operation principles and maximum error
12 p1812 A72-28146
- Nonuniform inlet velocity profile effect on laminar flow development between parallel plates, solving equations by finite difference method
13 p1941 A72-28706
- Laminar channel flow stability loss dependence on Reynolds number and wave number, discussing conditions for separated flow self oscillations
13 p1941 A72-28765
- Uniform suction effect at stationary plate on longitudinal and transverse velocities of plane Couette flow between parallel plates
13 p1941 A72-28884
- Pressure law for flow between two parallel plates describing medium action on plates, noting plate flutter analogy to buckling
13 p2056 A72-29002
- Slow viscous incompressible conducting fluid MHD flow between two nonparallel walls, obtaining velocity profile solution in power series for small Reynolds numbers
13 p2020 A72-30047
- Heat transfer and hydraulic resistance for cooled air forced flows in narrow rectangular channels as function of pressure and Reynolds number
14 p2093 A72-30291
- Velocity perturbation functions in linear theory for bounded stream flow past slender profile
14 p2070 A72-31018
- Turbulent friction relation to averaged velocity profile of liquid flow in pipes and channels
14 p2096 A72-31019
- Forced convection and thermal boundary condition in parallel and tapered passages, discussing Nusselt numbers for exponentially decreasing wall heat fluxes
14 p2173 A72-31062
- Air and carbon dioxide intensive injection effects on turbulent boundary layer of subsonic channel air flow
14 p2097 A72-31159
- Hydromagnetic channel flow stability computation via energy method, solving eigenvalue problem by direct forward numerical integration
15 p2283 A72-31212
- Convective heat transfer in fully developed MHD channel flow between two parallel electrically conducting plates
15 p2335 A72-31636
- Converging plane-walled channels, calculating laminar flow development and heat transfer by finite difference method
15 p2336 A72-32481
- Variable amplitude and phase velocity electromagnetic traveling wave field distribution in diverging MHD induction machine channel with liquid metal flow
16 p2435 A72-33282
- Faraday ring currents induction by radial magnetic field in low pressure plasma supersonic ring channel flow driven by inductive hydrodynamic shock tube
16 p2437 A72-33749
- Electromagnetic characteristics of MHD channels with nonconducting walls at finite magnetic Reynolds numbers
17 p2587 A72-34456
- Flow of a real gas in annular channels with curvilinear walls at large MHD-interaction parameters
17 p2587 A72-34457
- Transverse edge effect in a rectangular MHD channel with a sectional side wall
17 p2587 A72-34458
- Shear-layer flow regimes and wave instabilities and reattachment lengths downstream of an abrupt circular channel expansion
[ASME PAPER 72-APM-2] 17 p2538 A72-34811
- Micromorphic description of turbulent channel flow
17 p2538 A72-34868
- Wall stabilized dc arc channel for plasma viscosity and flow characteristics studies, using pressure probe
17 p2590 A72-35127
- Unsteady temperature distribution for laminar flow in a porous straight channel
17 p2541 A72-35434
- Effect of a distributed sand roughness on the spectrum of wall pressure pulsations in a turbulent flow in a tube
17 p2541 A72-35542
- Laminar gas flow in narrow channels of constant and variable cross sections in the presence of heat transfer
17 p2543 A72-35807
- MHD inlet flow into channel, obtaining velocity profile numerical solution in Prandtl approximation with modified boundary conditions
18 p2714 A72-36121
- One-dimensional theory of flows with combustion
18 p2740 A72-36246
- Turbulence characteristics of flows with large velocity gradients in rectangular MHD channel with copper walls
18 p2715 A72-36813
- The unsteady boundary layer flow in a convergent channel
18 p2683 A72-36930
- Two dimensional channel contraction induced flow acceleration effect on turbulence structure
18 p2683 A72-36995
- Slow motion in a two-dimensional semi-infinite channel with moving walls
18 p2683 A72-37044
- Oscillatory flow of a viscous fluid in a flexible walled two dimensional channel
18 p2684 A72-37064
- Estimation of the conductance of channels for rarefied gas flow by means of an optical analogue
19 p2795 A72-37466
- Study of flow in a passage in the presence of transverse alternating pressure gradients
19 p2785 A72-37467
- Investigation of heat exchange during film boiling of underheated liquid under conditions of forced flow in channels
19 p2881 A72-38036
- Heat transfer and resistance in a laminar gas flow with variable properties in an annular channel
19 p2786 A72-38040
- Magnetohydrodynamic channel flow with an arbitrary inlet velocity profile
19 p2842 A72-38446
- The mechanics of an organized wave in turbulent shear flow. II - Experimental results
19 p2789 A72-38793
- Heat transfer in a channel with a porous wall for turbine cooling application
[ASME PAPER 72-HT-39] 20 p2986 A72-39667
- Intensification of heat transfer in channels with turbulent gas flows
21 p3127 A72-40127
- Stability loss in Poiseuille flow within two dimensional channel during Reynolds number passage through critical value
21 p3044 A72-40265
- Mixing of slipstreams in a channel of constant cross section in the presence of a recirculation zone
21 p3129 A72-40982
- Microstructure of turbulent flow in the stabilized flow region in a channel
21 p3045 A72-41054
- Investigation of the critical heat flux density in heat transfer with and without turbulization of the flow at the inlet of an annular channel
21 p3129 A72-41057

- Influence of baffle geometry on heat transfer in the cooling channel of air-cooled blades
21 p3099 A72-41062
- Investigation of the influence of nonuniform conditions at the inlet and of secondary flows on the flow parameters in arbitrarily twisted channels
21 p3045 A72-41067
- Investigation of the interaction between a plasma flow and an axisymmetric magnetic field
21 p3094 A72-41655
- Buoyancy effects on laminar heat transfer in the thermal entrance region of horizontal rectangular channels with uniform wall heat flux for large Prandtl number fluid.
22 p3243 A72-41956
- Convective instability of a fluid in hydrodynamically connected vertical channels
22 p3166 A72-42260
- Interferometric investigation of natural convection in rectangular air cavities of different orientation
22 p3244 A72-42262
- Approximate calculation of a laminar arc discharge in a cylindrical channel
22 p3210 A72-42285
- Pressure effect at arbitrary Knudsen numbers.
23 p3279 A72-43216
- Length of the separation region behind a bluff body in a bounded flow
23 p3248 A72-43685
- Photoelastic analysis of cardiovascular-magnitude stress pattern produced by flow through gelatin-agar walled channels for analysis of mechanical stresses on blood vessel walls
23 p3260 A72-43936
- Magnetohydrodynamic flow between parallel rotating disks. I - Influence of finite wall-conductance.
23 p3322 A72-44400
- Instabilities in the reaction zones of detonation waves.
24 p3462 A72-45029
- Investigation of the characteristics of turbulent air flow in a channel with elastic walls
24 p3393 A72-45257
- Linearized analysis of magnetohydrodynamic channel entrance flow.
24 p3430 A72-45573
- CHANNELS**
Optimal answer-back communications systems using feedback channel for error checking
09 p1277 A72-22568
- Ray geometry, travel time and spreading loss derivation for refracted/bottom-reflected ray propagation in channel with horizontal and vertical sound speed gradients
18 p2710 A72-36413
- A simple formula for the maximum stress in a twisted angle or channel.
22 p3240 A72-42894
- CHANNELS (DATA TRANSMISSION)**
Linear stochastic-parameter output channel, examining signal quadrature components statistical characteristics
01 p0024 A72-10199
- Convolutional coding and decoding techniques in communication systems, discussing distance properties, optimal decoder in memoryless channel, error probabilities and bit synchronization
01 p0025 A72-10336
- Optimal burst correcting codes for bursty channels, comparing with automatic repeat-request
01 p0025 A72-10337
- Forward error correction code performance on hf troposcatter and satellite channels, considering adaptive and nonadaptive convolutional and cyclic coding
01 p0026 A72-10338
- Nonsystematic quick-look-in convolutional codes for sequential decoding in deep space channels
01 p0026 A72-10339
- Optimal metric programmable high speed sequential decoder for convolutional code deep space channels
01 p0026 A72-10340
- High speed decision sequential decoder design and tests for digital errors, white noise and real channels
01 p0026 A72-10341
- Coding for analog and digital data transmission over channels with noiseless and noisy feedback links
02 p0197 A72-11680
- Coding for data communication over discrete time channels without feedback under various fidelity criteria, discussing channel capacity
02 p0171 A72-11681
- Low loss wideband circular wave guide bend characteristics and branching filters for millimeter wave large capacity digital transmission
02 p0190 A72-11682
- Telemetry receiver signal data quality in terms of RF, if AGC, AFC and AM rejection circuitry requirements
02 p0192 A72-12149
- Optimization methods in digital data transmission systems, discussing equalization circuits for base band channel using metallic lines
02 p0182 A72-12691
- Soviet book on statistical theory of digital data transmission through parallel channels covering optimal and suboptimal reception systems under signal fading and interference
03 p0323 A72-13968
- Two channel radio interferometry, determining limiting accuracy characteristics under arbitrary phase error
05 p0660 A72-15829
- Block orthogonal M-ary communication over fading dispersive channel with intermittent on-off noiseless feedback, calculating upper and lower bounds on error probability
06 p0776 A72-18389
- Channel coding/decoding schemes compatibility with TV data compressor for planetary missions in real time transmission
07 p0941 A72-19274
- Optimal control of linear multivariable plants with one or more quality criteria, considering control channels and game theory
07 p0962 A72-19720
- Adjacent channel interference effects in multicarrier telephony FM communications system
07 p0948 A72-20493
- Single-channel-per-voice-carrier transmission system application to data communication and small earth station operation, discussing modular design and performance
07 p0948 A72-20494
- On-line equalization of digital communication channels, discussing extended discrete Kalman filter use as adaptive equalizer
08 p1131 A72-20855
- Tropospheric scatter path characteristics as communication channel with random fluctuations, deriving signal autocorrelation function from mean power pulse response
08 p1132 A72-21329
- Gating duration influence in reception channel on singular signal detection in normal noise
09 p1278 A72-22571
- Multichannel automatic data acquisition and processing in ergonomic measurements of radar controller work from ECG, EOG, EMG and respiration
09 p1271 A72-23136
- Radio receiver-transmitter system for synchronous heterodyne signal detection of 6 GHz band electromagnetic channel pulsed response, discussing operational principles and accuracy
09 p1280 A72-23353
- CAMAC modular digital data handling system for communication with computer, discussing compatibility and data acquisition in astronomy application
11 p1600 A72-25692
- Time resolution buffer for multichannel scaler, applying to digital signal averaging
11 p1632 A72-25701
- Multichannel clock with dekatrons using multiple crossbar connector for program commutation and command pulse splitting
13 p1933 A72-29919
- Linear stochastic-parameter output channel, examining signal quadrature components statistical characteristics
15 p2195 A72-31623
- Adjacent channel discrimination enhancement in Gray-scale binary coded two dimensional array, using checkerboard filter for pattern noise suppression
15 p2238 A72-32162
- Computer technique to synthesize binary holograms for wave beams analysis in quasi-optical communication channels
15 p2242 A72-32674
- Adaptive reception in a channel with slow common fading
17 p2515 A72-34835
- Optimal predistortion efficiency for multiplicative disturbances in radio signal transmitting channel, noting Rayleigh distribution of signal fluctuations
17 p2518 A72-35778
- Telemetric frame compression coefficient and shaping algorithm for spacecraft data processing systems for arbitrary number of active channels
21 p3014 A72-40326
- Error correcting codes applied to satellite channels.
21 p3018 A72-40874
- Satellite adjacent-channel interference due to multicarrier transponder operation.
21 p3020 A72-40892
- Convolution noise and distortion in FDM/FM systems.
21 p3020 A72-40893
- Impulse noise in FM receivers in the presence of adjacent channel interference and thermal noise.
21 p3020 A72-40894
- Binary symmetric channel error effects on PCM color image transmission.
22 p3153 A72-41977
- Q-ary output data transmission channel with burst errors, discussing burst-b distance measure and binary block code decoding algorithm for error correction
22 p3153 A72-41979
- Code correcting asymmetric-error bursts during information exchange between computers
22 p3156 A72-42189
- Two channel radio interferometry, determining limiting accuracy characteristics under arbitrary phase error
23 p3287 A72-43437
- Forward-error correction with decision feedback.
23 p3268 A72-44175
- Optimal equalization of discrete signals passed through a random channel.
23 p3265 A72-44178
- On the performance of digital communication systems with bandpass limiters. I - One-link system. II - Two-link system.
23 p3265 A72-44181
- Frame synchronization in time-multiplexed PCM telemetry with variable frame length.
23 p3265 A72-44182
- Sequential analysis algorithm for data channel detection of received signal represented by Poisson sequence of quantum transitions under large SNR
23 p3266 A72-44206
- Gating duration influence in reception channel on singular signal detection in normal noise
24 p3379 A72-44750
- Semaphore channel signaling reliability, presenting error protection and correction system
24 p3381 A72-45770
- CHAOTIC CLOUD PATTERNS**
U CLOUDS [METEOROLOGY]
CHAPLYGIN EQUATION
Straight line computer solution of Chaplygin equation, with application to high subsonic gas flow incident on airfoil with local supersonic zone
02 p0149 A72-11581
- Chaplygin compressibility law in calculation of flow characteristics around compressor blading of axial turbomachines
03 p0308 A72-13544
- Nth order linear differential inequalities reduction to first order, permitting Chaplygin theorem infinite applicability limit and solution by quadratures
03 p0382 A72-14313
- Trigonometric series solution of Tricomi problem for Chaplygin-type equation in half plane
04 p0461 A72-14628
- Hydrodynamic analogy for astrophysical effects of general relativity theory, analyzing Chaplygin gas motion in three dimensional curvilinear coordinate system
08 p1209 A72-21876
- Successive approximation for solving parabolic equation with abstract function, using Chaplygin method for Cauchy boundary value problem in Banach space
13 p1987 A72-29646
- Chaplygin gas flow equation for analogy between hydrodynamic and electrodynamic equations, noting special theory of relativity
23 p3312 A72-43404
- CHAPMAN SHEAR LAYER**
U SHEAR LAYERS
CHAPMAN-ENSKOG THEORY
Chapman-Enskog method modification for gas flow Prandtl boundary layer zero approximation distribution function construction, applying Mises transform to Boltzmann equation
05 p0653 A72-17209
- Transport coefficients calculation in gas kinetic theory by relativistic generalization of Enskog-Chapman method
10 p1510 A72-24106
- Chapman-Enskog method modification for gas flow Prandtl boundary layer zero approximation distribution function construction, applying Mises transform to Boltzmann equation
11 p1614 A72-25332
- Third order constitutive equations for transport coefficients in rarefied gases, using Chapman-Enskog theory
11 p1617 A72-26009
- Viscosity and thermal conductivity of moderately dense gas mixtures.
17 p2636 A72-34737
- Numerical evaluation of Chapman's grazing incidence integral $\chi(X, \chi_i)$.
17 p2549 A72-35609
- Analysis of the transport coefficients for simple dense fluids - Application of the modified Enskog theory.
21 p3084 A72-40723
- Kinetic theory of turbulent flow.
24 p3394 A72-45563
- Kinetic equations for a chemically reacting plasma.
24 p3430 A72-45566
- CHAPMAN-FERRARO PROBLEM**
Satellite, space probe and observatory data impact on space physics, considering solar wind, interplanetary magnetic field, Van Allen belt and Chapman-Ferraro theory
10 p1538 A72-24268
- CHAPMAN-VOUGET FLAME**
U CHEMICAL EQUILIBRIUM
U DETONATION

U FLAME PROPAGATION
CHARACTER RECOGNITION

Human touch deficiency in artificial pattern recognizers regarding handwriting, speech and pattern recognition involving nonevents

01 p0017 A72-10464

Electronic analog models of human retina and visual system, discussing optical character recognition, signal processing, photoreceptor stimulation, visual cortex excitation and further model development

01 p0017 A72-10471

Adaptive statistical prediction algorithm for character recognition by computer simulation involving handprinted numerals

01 p0034 A72-10472

Correlation filters alignment for optical character recognition, discussing kinematic mounting and in position techniques

02 p0225 A72-11750

Truth table classification and numerical identification of character patterns of elements in groups and clusters

09 p1265 A72-22644

Visual search model from perceptual theory, animal studies and search data, discussing selection, inspection and naming single cued letters in visual array

09 p1274 A72-23647

Character recognition experiments to determine attention control and temporal-spatial capacity limitation during visual information processing

12 p1768 A72-27074

Phi-spatial filter method for straight or curved line geometric feature extraction of characters, using coherent optical system

12 p1820 A72-27494

Holographic method of character recognition, describing transformation from real space Cartesian coordinates to characteristic space

12 p1846 A72-27955

Alphanumeric characters for small TV type raster displays, describing legibility experiment for character height optimization

13 p1911 A72-29821

Visual and acoustic image processing rates during letter sequencing tasks, suggesting implicit verbal control involvement

15 p2188 A72-32764

Visual half-field differences in the recognition of bilaterally presented single letters and vertically spelled words.

18 p2653 A72-36908

Novelty, recency and frequency effects on visual recognition and pseudo-recognition thresholds.

18 p2653 A72-36909

Proximity and direction of arrangement in numeric displays.

21 p3008 A72-41017

Interactions of signal and background variables in visual processing.

22 p3152 A72-42931

CHARACTERISTIC EQUATIONS

U EIGENVALUES

U EIGENVECTORS

CHARACTERISTIC FUNCTIONS

U EIGENVALUES

U EIGENVECTORS

CHARACTERISTIC METHOD

U METHOD OF CHARACTERISTICS

CHARACTERS

U SYMBOLS

CHARGE CARRIERS

NT FREE ELECTRONS

NT HOLES [ELECTRON DEFICIENCIES]

NT MAJORITY CARRIERS

NT MINORITY CARRIERS

Read avalanche diode noise theory, showing carrier current modulation and If and hf noise coupling in nonlinear regime

03 p0333 A72-13848

Carrier mobility measurement in inhomogeneous semiconductors based on bulk photovoltaic and photomagnetolectric effects

03 p0402 A72-13862

Charge state effects on defect production mechanisms, configurations, mobility, annealing kinetics, interaction and dissociation in displacement damage in covalent semiconductors

03 p0403 A72-14077

Piezoelectric interaction between Lamb waves and charge carriers in piezoelectric plate inserted into semiconductor

06 p0865 A72-17388

Third harmonic generation in Ge induced by conduction nonlinearly during bulk heating of charge carriers by microwave fields

07 p1047 A72-19023

Semiconductors theory for multivalley energy spectrum and multivalued equilibrium distribution of carriers during electron phonon interactions

07 p1048 A72-19641

Multiphonon capture of charge carriers by deep impurity centers in homopolary semiconductors from generalized Lucovsky model

08 p1216 A72-21094

GaAs semiconductor injection lasers, discussing time characteristics of current carriers, population inversion and resonator Q factor modulation

08 p1184 A72-22032

Sn additions influence on Te structural characteristics relation to microhardness and current carrier mobility variations

09 p1322 A72-22204

Effective current carrier electron and hole lifetime in amorphous photodielectric semiconducting Se and As-Se films with randomly distributed capture levels

09 p1366 A72-22418

Avalanche carrier multiplication influence on semiconductor device p-n junction quality, discussing current distribution and I-V characteristics during avalanche breakdown

10 p1446 A72-23849

Width of space charge layer of reverse-biased p-n junction in p-n-p-n structure effect on current density, mobile charge carriers and constituent transistors gain coefficients

10 p1526 A72-24584

Quasi-continuous charge carrier traps in molecular single crystals associated with polarization energy dissipation

11 p1700 A72-25782

Space charge limited current theory of thin film organic semiconductor systems, investigating energy spectrum of traps and free carrier capture kinetics

11 p1700 A72-25783

Charge carrier photoproduction and energy structure of trans-bis-indonylene (TBB) semiconductor thin films

11 p1700 A72-25784

Charge carrier density, neutral gas density, electric potential and electron temperature profiles in cylindrical diffusion column, considering electron pressure

11 p1698 A72-26646

Reversible threshold switching in amorphous semiconductor alloys by carrier transport and recombinative electron injection

12 p1854 A72-27431

Theory of magnetotail elongation based on magnetosphere neutral layer drift notion due to electric current from trapped charge carriers inside surrounding plasma sheath

12 p1802 A72-27770

Electron bombardment effects on transport properties and carrier lifetime degradation of Li doped Si solar cells

12 p1856 A72-28024

Nonequilibrium carrier distribution in drift junction transistor, considering base region hindering field effect on transit time, current gain cut-off and frequency response

13 p1926 A72-28371

Electron distribution near semiconductor-metal contact, discussing current carriers quantum properties effects

13 p2021 A72-28679

Temperature and charge carrier density dependence of conduction electron optical effective mass in semiconductor compounds

13 p2021 A72-28788

Epitaxial GaAs carrier concentration profile, deep traps detection and properties determination, using Schottky barrier on semiconductors

13 p2024 A72-30035

Adiabatic conditions influence on charge carriers dispersion determination of semiconductors based on Nemst-Ettingshausen effect

15 p2291 A72-31390

MOS junction transistor turn-off behavior calculation based on model with carrier source and drain for channel formation

15 p2207 A72-31891

Superconductivity, temperature and tunneling effects in low carrier density semiconductor systems /tin, germanium and indium tellurides, lanthanum triselenide and strontium titanium oxide/

15 p2293 A72-32325

Charge carrier motion in semiconductor with electron interactions, considering heating in presence of negligible electric field

16 p2441 A72-33278

Studies of the free path of the current carriers in molybdenum

17 p2568 A72-35517

Charge carriers interaction with metal ions studied from electrical transport of Fe and Co in Fe-Cr alloy

17 p2569 A72-35521

Measurement of carrier lifetime in the base of silicon diodes - Application to the control of manufacturing techniques.

18 p2669 A72-37108

Drude theory of electromagnetic waves in an inclined magnetic field. I - One-band model of charge carriers.

19 p2840 A72-37510

Low-temperature photoluminescence of GaAs under conditions of strong interaction of the nonequilibrium carriers.

19 p2847 A72-38821

Carrier transport and storage effects in Au ion implanted SiO₂ structures.

21 p3097 A72-40699

The field strength conditions for measuring the carrier lifetime in semiconductor crystals by the light flash method

21 p3098 A72-41487

Semiconductors theory for multivalley energy spectrum and multivalued equilibrium distribution of carriers during electron phonon interactions

24 p3431 A72-44572

CHARGE DISTRIBUTION

Potential and ion charge distribution in proximity to conducting sphere moving in low density collisionless ion-electron plasma

01 p0109 A72-10371

Bipolar transistor model for device and circuit performance prediction, determining parameter from charge distribution by regional approximation technique

01 p0042 A72-10786

Charged particle motion in pulsar electromagnetic fields, discussing coherent synchrotron radiation and charge bunching

03 p0438 A72-13874

Zincblende ternary and quaternary alloy systems, calculating charge distribution in space by pseudopotential approach

03 p0404 A72-14261

Coherent synchrotron radiation from model with charge distribution moving on ring, applying to pulsars

04 p0566 A72-14555

Transit time and LSA oscillations at millimeter and submillimeter wavelengths in n-type GaAs

04 p0563 A72-15593

Semiconductor-dielectric system for controlling space charge and valley population redistribution by external field

05 p0702 A72-16201

Semiconductors theory for multivalley energy spectrum and multivalued equilibrium distribution of carriers during electron phonon interactions

07 p1048 A72-19641

Self consistent problem solution for planar magnetron diode with low cathode field and charge density not exceeding density of Brillouin zone

08 p1142 A72-21703

High temperature and pressure detonation gas expansion as shock wave from cylindrical volume, calculating flow velocity, pressure and density

10 p1561 A72-23759

Dipole antenna near electric field, basing calculation method on integral equation for antenna surface charge distribution function

10 p1451 A72-24579

Magnetic fields effect on anode heat losses in MPD accelerator arcs, noting minimal charge current density

11 p1711 A72-26225

Surface charge density in thermoplastic recording, showing potential-relief modulation dependence on frequency, scanning rate and electron beam properties

13 p1954 A72-28402

Field mill measurement of atmospheric electric space charge density, discussing effects of snow melting and artificial charge sources

13 p1952 A72-29666

Electron energy distribution, ions mass spectral composition and spatial charge concentration of currentless photoresonant Ce plasma obtained by associative ionization

14 p2136 A72-30175

Time invariance violation in charge asymmetry experiment, showing K-meson decay rate difference reversal from world to antiworld with particle unchanged

14 p2130 A72-30265

Electric field and volume charge density distribution in bipolar conductivity semiconductor with recombination instability

15 p2291 A72-31392

Charge and mass densities relation for stationary charged dust distribution in general relativity, investigating Einstein-Maxwell equations for stationary gravitational field

15 p2275 A72-31591

Cosmic ray nuclei charge and isotope composition measurement, discussing data for Li, Be, B and 15-30Z nuclei

16 p2447 A72-33727

Balloon flight observation of charge composition fine details and gross features of isotopic abundance in near relativistic cosmic rays

16 p2447 A72-33729

Diffusion propagation and source distribution effects on cosmic ray charge composition and anisotropy in galactic disk, considering nuclear fragmentation

16 p2448 A72-33742

An improved measurement of the charge ratio of cosmic ray muons in the range 10-300 GeV/c.

17 p2599 A72-34920

Calculation of the dependence of the charge density on the distribution of the potential in crossed symmetric electric and magnetic fields

17 p2593 A72-35903

A comparison of measurements of the charge spectrum of solar cosmic rays from nuclear emulsions and the Explorer 35 solid-state detector.

18 p2721 A72-35988

Possibility of an inhomogeneous charge distribution in an adsorbed layer

18 p2713 A72-36176

Composition of cosmic-ray nuclei at high energies.

20 p2965 A72-39716

Semiconductors theory for multivalency energy spectrum and multivalued equilibrium distribution of carriers during electron phonon interactions

24 p3431 A72-44572

CHARGE EXCHANGE

NT RESONANCE CHARGE EXCHANGE

Negative hydrogen ion production during charge exchange between protons in thick Li, Na, K and Mg vapor jets

06 p0863 A72-18410

Auroral ionosphere radio self emission at supercritical frequencies from accelerated protons charge exchange effects, comprising radio bursts, storms and amplifications

08 p1153 A72-20713

Cometary carbon dioxide molecules annihilation by recharging and dissociative charge exchange with solar protons

08 p1229 A72-20830

D and E region ion chemistry reaction rate measurements, noting hydration, charge exchange and ion-atom interchanges

09 p1275 A72-22366

Approximate expression for charge exchange spreading of proton beam precipitating into atmosphere, showing dependence on atmospheric structure, collision data and primary particle energy

09 p1377 A72-22591

Fast iodine ions charge exchange in dense carbon dioxide supersonic jet, determining electron capture cross sections by least squares method

10 p1516 A72-25036

Radial profiles of ionized He flux and protons in magnetosphere, taking into account charge exchange processes and fluctuating electrostatic fields

11 p1624 A72-26397

Toroidal plasmas heating by neutral injection, discussing ion acceleration, charge exchange and fast ion trajectories

11 p1697 A72-26582

Ionospheric oxygen ions loss rate in charge exchange reactions with hydrogen, molecular nitrogen and oxygen and atomic oxygen photoionization rate

13 p1953 A72-29811

Hydrogen plasma ion density determination from atomic beam attenuation by resonant charge exchange with protons

15 p2284 A72-31582

Lateral diffusion measurement for mass identified positive ions in oxygen, noting spiraling, charge exchange and collisions effects on ion-molecule system

15 p2281 A72-32224

Fast metastable hydrogen atom beam production by proton beam-Cs vapor charge exchanges

16 p2429 A72-33057

Hamiltonian for first order wave function in charge exchange perturbation theory

17 p2584 A72-34259

Absolute detection and collisional destruction of 2.5-keV metastable hydrogen atoms produced by a charge-exchange process in cesium vapor.

19 p2837 A72-37547

Auroral ionosphere radio self emission at supercritical frequencies from accelerated protons charge exchange effects, comprising radio noise bursts, storms and amplifications

19 p2790 A72-38341

Dissociation of molecular ions formed by charge exchange in an in-line tandem mass spectrometer.

19 p2763 A72-38801

Chemical reaction rates for dissociation and exchange in nonisothermal plasma from molecular energy level occupation investigation

20 p2957 A72-39018

CHARGE SEPARATION

U POLARIZATION [CHARGE SEPARATION]

CHARGE TRANSFER

Charged transfer devices and IGFET bucket brigade structures, discussing design measures and fabrication procedures for increased reliability

03 p0336 A72-14280

Current transport and I-V characteristics of metal-semiconductor-metal structures with back-to-back contact interfaces

04 p0562 A72-15128

Measuring apparatus for differential cross sections of charge transfer and elastic scattering of atomic projectiles by gas targets

04 p0553 A72-15539

Spectral distribution of electromagnetic radiation emitted by charge moving in gravitational field of spherically symmetric black holes

07 p1081 A72-20226

Physical parameters of transistor, discussing carrier transfer, space charge and potential drop as function of current and voltage changes

08 p1139 A72-21058

Emission characteristics of relativistic charge in rectilinear motion within gravitational wave field

08 p1206 A72-21072

Propagation time of charge diffusion across magnetic field in bounded plasma

08 p1215 A72-21879

Thermal energy reaction rates determination for partial charge transfer chemical reactions, comparing with electron transfer efficiencies

10 p1514 A72-24336

Cross sections of Li nonresonant capture of Na ion charge, interpreting quasi-oscillatory structure

10 p1517 A72-25047

Fermi level and scattering phase function nomograms for semiconductors with parabolic and isotropic energy bands, noting charge transfer effects

11 p1700 A72-25781

Organic semiconductors for photovoltaic cell applications, discussing structural characteristics, improved charge transfer and crystallographic conductivity mechanisms

12 p1856 A72-28015

Model potential method for calculating positively charged diatomic sodium molecular ions potential energy curves and resonance charge transfer cross sections

12 p1848 A72-28350

Vertical distribution of atomic nitrogen ions in F region produced by dissociative photoionization and charge transfer, suggesting undiscovered source at 300 km altitude

13 p1954 A72-29815

Ferric ion traces evidenced in lunar and meteoritic titanagites by charge transfer bands observations during heating, interpreting origin as caused by cosmic radiation

14 p2154 A72-30515

Mercuric chloride, bromide and iodide gas phase UV absorption spectra, discussing correlation with intermolecular charge transfer transitions

16 p2360 A72-32926

CW laser transitions in singly ionized Te vapor spectrum at 4843-9378 Å, indicating charge transfer as dominant excitation mechanism

16 p2401 A72-33394

Reaction rate coefficient evaluation for charge transfer from doubly positive carbon ion to helium at 100-100,000 K, discussing effect on interstellar medium

16 p2360 A72-33455

Charge, direction and temperature dependence of semiconductor electrotransmission in dc field, considering metals diffused in Ge, Se, Te, Si, BiTe, GaAs and InAs

23 p3324 A72-43642

CHARGED PARTICLES

NT ALPHA PARTICLES

NT ANIONS

NT ANTIPROTONS

NT ARGON PLASMA

NT ARTIFICIAL RADIATION BELTS

NT BETA PARTICLES

NT CATIONS

NT CESIUM PLASMA

NT COLD PLASMAS

NT COLLISIONLESS PLASMAS

NT CONDUCTION ELECTRONS

NT COSMIC PLASMA

NT DEUTERIUM PLASMA

NT DEUTERONS

NT ELECTRON PLASMA

NT ELECTRONS

NT FERRIC IONS

NT FREE ELECTRONS

NT HELIUM PLASMA

NT HIGH ENERGY ELECTRONS

NT HIGH TEMPERATURE PLASMAS

NT HOT ELECTRONS

NT HYDROGEN PLASMA

NT INNER RADIATION BELT

NT MAGNETICALLY TRAPPED PARTICLES

NT MANGANESE IONS

NT METAL IONS

NT METALLIC PLASMAS

NT NONEQUILIBRIUM PLASMAS

NT NONUNIFORM PLASMAS

NT NUCLEI [NUCLEAR PHYSICS]

NT OUTER RADIATION BELT

NT PHOTOELECTRONS

NT PLASMA CLOUDS

NT PLASMA LAYERS

NT PLASMA SHEATHS

NT PLASMA SLABS

NT PLASMAS [PHYSICS]

NT POSITRONS

NT PROTON BELTS

NT PROTONS

NT RADIATION BELTS

NT RAREFIED PLASMAS

NT RECOIL PROTONS

NT RELATIVISTIC PLASMAS

NT ROTATING PLASMAS

NT SOLAR PROTONS

NT SOLAR WIND

NT STELLAR WINDS

NT THERMAL PLASMAS

NT TOROIDAL PLASMAS

Collisionless motion of solar wind ions in helical magnetic field, giving transfer function of charged particles

01 p0118 A72-10360

Charged particles magnetic scattering on cyclotron instability waves of radiation belt plasma, estimating proton relaxation time

01 p0119 A72-10608

Carbon dioxide laser pumping with nuclear reactions, indicating improved laser performance due to additional ionization by energetic charged particles

01 p0082 A72-11331

Auroral current generation by ionization and space charge transport interaction between charged particles and atmospheres

02 p0273 A72-1928

Charged particle motion in strong magnetic field, considering magnetic moment and longitudinal adiabatic invariants

02 p0268 A72-12843

Adiabatic charged particle orbits in magnetic null sheet with transverse electric and added normal magnetic fields

03 p0348 A72-13512

Plasmoid transport in quadrupole and octupole magnetic fields, measuring plasma amounts in axial region charged particle densities and flux densities at vacuum chamber wall

03 p0395 A72-13568

Charged particle motion in pulsar electromagnetic fields, discussing coherent synchrotron radiation and charge bunching

03 p0438 A72-13874

Effective cross sections for charged and excited particles formation from He, Ne and Ar ion collisions with CO molecules, using mass spectrometry

03 p0393 A72-14065

Nuclear radiation interference and damage effects in galactic and solar cosmic ray measurements during charged particle experiments by deep space missions

03 p0438 A72-14085

Relativistic equations of motion of charged particle interacting with plane electromagnetic wave propagating at arbitrary angle to uniform magnetic field for magnetosphere model

04 p0554 A72-14406

Gamma ray and neutron emissions from sun, considering acceleration of charged particles in solar atmosphere

04 p0566 A72-14724

Nonrelativistic charged particle resonating with circularly polarized transverse electromagnetic wave in nonuniform magnetic field, showing Fresnel diffraction pattern-like motion

04 p0557 A72-14951

Apollo 14 charged particle lunar environment experiment, describing ALSEP particle spectrometer

04 p0508 A72-15097

Nuclear charge composition and energy spectra measurement for hydrogen, helium and medium nuclei in 12 April 1969 solar particle event

04 p0567 A72-15325

Second virial coefficient, temperature derivatives and additive components for $1/12$ -7 potential of charged particle interaction in gas

05 p0692 A72-15841

Charged particle acceleration by nonstationary sinusoidal electric fields in earth magnetosphere based on mathematical model

05 p0709 A72-16256

Charged particles injection effects on magnetic perturbations relation to integral auroral luminance intensity from whole sky photometry measurements

05 p0658 A72-16277

Charged particle motion equations for fifth order spherical aberration of quadrupole-octupole lens with arbitrary electrode and pole shapes

05 p0638 A72-16989

Fast charged particles measurement in inner radiation belt by Cerenkov counter mounted on Cosmos 137 satellite indicating presence of high energy electrons

05 p0711 A72-17035

Ion charge composition in plasma-electron beam system in strong longitudinal magnetic field, noting multiply charged ions production under high temperature conditions

05 p0701 A72-17235

Plasma heating and compression with nonadiabatic charged particle motion in uniform magnetic field

05 p0701 A72-17239

Secondary cosmic ray shower charged particles angular distribution asymmetry in C-system and azimuthal plane related to single fireball formation

06 p0868 A72-17263

- Heavy nonrelativistic single charge particle recording in cosmic rays at sea level, using scintillation and anticoincidence Cerenkov counters
06 p0870 A72-17276
- Charged aerosols for efficient power transduction in power conversion devices, deriving optimum particle radius to number of charges ratio for various operating conditions
06 p0760 A72-17422
- Energetic charged particles penetration into magnetosphere by auroral simulation experiments with artificial solar wind, observing magnetic field microfluctuations behind collisionless shock front
06 p0805 A72-17469
- Computerized simulation of high intensity beam charged particle trajectories in electromagnetic fields with rotational symmetry, applying to ion extraction
06 p0852 A72-17491
- Low voltage arc plasma in low pressure Cs vapors, determining charged particle concentration and potential distribution in interelectrode gap
06 p0863 A72-18413
- Cosmic rays generation by charged particles acceleration in electromagnetic constant crossed fields during magnetic stars contraction to neutron star dimensions
07 p1056 A72-19042
- Wide gap spark chamber feeding technique for compensation of charged particle track drift due to avalanches
07 p0988 A72-19956
- High energy charged particles angular distribution measurements in equatorial region cosmic radiation above atmosphere by Proton 2 satellite
08 p1226 A72-20799
- Auroral charged particle fluxes electrodynamic interaction with atmosphere, determining ion formation rate and electron concentration and conductivity
08 p1155 A72-20804
- Measuring equipment for charged particles spatial distribution in cosmic ray showers, considering multiaxial and secondary young showers
08 p1226 A72-21077
- Fokker-Planck equations for charged particle dynamics rederived for random fields, finding pitch angle scattering
08 p1227 A72-21385
- Mesosphere region positively and negatively charged particles concentration and mobility measurements by sounding rocket experiments
09 p1375 A72-22361
- Plasma emitter shape determination in accelerating electric field for charged particle flux production
09 p1358 A72-22490
- Charged particles observations on 21 December 1968 by Explorer 40 and from ground, noting auroral light primary energy influx by precipitation band of electron intensities
09 p1299 A72-23005
- Visual aurora and Explorer 40 satellite simultaneous observations of VLF radio noise, noting hiss associated with light emissions and associated charged particle flux
09 p1299 A72-23006
- Charged to neutral particle transformation capacity of wide aperture recharge target formed by supersonic gas jets in magnetic trap with annular nozzle
09 p1363 A72-23224
- Picoampere charged particle beam symmetry and magnitude monitor consisting of four transmission ion chambers
09 p1315 A72-23405
- Charged and neutral particles radial distribution across positive isothermal plasma column in high current discharges
10 p1521 A72-24355
- Converging or diverging high intensity charged particle beams arbitrary profile shaping, obtaining solution via Laplace equation through reduction to Cauchy problem
10 p1521 A72-24362
- Incompressible fluid jet propagation beyond charged particle source exit section, investigating electrohydrodynamic interaction parameter
10 p1522 A72-24549
- Multiply charged ion plasmas production in heavy ion accelerator by laser beam interaction with vaporized target material
10 p1516 A72-25033
- Charged particles effect on plasma negative ions, examining Stark effect in energy level
11 p1693 A72-25714
- Charged particle thermodynamics in ionosphere, considering energy exchange due to collisions or thermal conductivity
11 p1621 A72-25837
- Ionization movement of charged and neutral particles in F 2 region coupled to air movement by collision drag forces
11 p1621 A72-25839
- Fast charged particle flux measurement in inner radiation belt by Cosmos 137 satellite in January-February 1967
11 p1713 A72-25947
- D region ionization by solar corpuscular streams, considering formation of charged particle concentration profiles
11 p1622 A72-25948
- Nonrelativistic quantum concept of electromagnetic field interaction with charged microparticles
11 p1692 A72-26093
- Sunspots contact region charged particles acceleration by plasma flow induced electric field, noting Fermi type mechanism
11 p1695 A72-26107
- Plasmod transport in quadrupole and octupole magnetic fields, measuring axial charged particle and flux densities at vacuum chamber wall
11 p1699 A72-26755
- Radiative properties of charged particles moving in attractive Coulomb fields related to repulsive fields by symmetry relationships
12 p1848 A72-28155
- Russian book on electrodynamic plasma acceleration covering charged particles motion in electromagnetic field and pulsed, MHD, steady and Hall accelerators
12 p1853 A72-28341
- Russian book on geomagnetic field cosmic rays covering charged particle motion theory, extratroposphere currents, magnetosphere tail and solar wind effects, etc
12 p1864 A72-28345
- Charged particles propagation in magnetic field and scattering medium with constant and variable transport paths, applying to proton propagation for solar flares
13 p2029 A72-28576
- Book on theory of fully ionized plasmas covering Coulomb systems equilibrium and nonequilibrium states, charged particle radiation and interactions with EM fields
13 p2011 A72-29098
- Auroral current generation by ionization and space charge transport interaction between charged particles and atmosphere
13 p2030 A72-29240
- One dimensional periodic slow wave structure interaction with charged particles beam, considering system operation as TWT and backward wave tube
13 p1931 A72-29288
- Charged particle beams focusing in combined dual spiral system with homogeneous magnetic field along axis
13 p1932 A72-29292
- Homogeneous plasma column generation by HF generator, probing for electron temperature and charged particle concentration
13 p2015 A72-29507
- Magnetospheric ring current relation to polar magnetic substorm from charged particle measurements by satellites and magnetic field measurements at ground
13 p1952 A72-29658
- Positively and negatively charged plasma components thermodynamic density fluctuations effect on ionospheric and magnetospheric slowly varying electric fields measurement
13 p1953 A72-29810
- Cylindrical electrostatic analyzers in rocket and satellite instruments for space low energy charged particles measurements
13 p1960 A72-29842
- Data acquisition, reduction, quick-look data and standard and special programs for ESR0 1A and B auroral particle satellite experiment
13 p1925 A72-29868
- Charged particle inertial-electrostatic containment in spherical diode gas discharge gap, measuring flux radial and energy distributions
13 p1933 A72-29915
- Millimeter and submillimeter radiation produced by diffraction phenomena during charged particle passage near periodic structures, discussing physical properties and oscillator development
14 p2088 A72-30598
- Auroral sporadic E layer diurnal distribution correlation to charged particle integral flux diurnal variations observed by satellite in winter, noting Kp index effect
14 p2102 A72-30655
- Second virial coefficient, temperature derivatives and additive components for $1/2-7/$ potential of charged particle interaction in gas
15 p2280 A72-31260
- Charge and mass densities relation for stationary charged dust distribution in general relativity, investigating Einstein-Maxwell equations for stationary gravitational field
15 p2275 A72-31591
- Quasar electromagnetic radiation emission in terms of general relativistic coupling between gravitational field and charged particle radiation field
15 p2306 A72-31592
- Magnetospheric geometry derivation from ISIS-1 observations of soft particles penetration into polar cap and auroral regions, discussing entry and energization mechanisms
15 p2227 A72-31953
- Satellite charged particle observations and polar cap rimeter absorption measurements during solar cosmic ray events, noting electrons and protons contributions
15 p2300 A72-31965
- Ionization energy loss of relativistic heavy nuclei for close collisions as function of charge, computing Born approximation corrections via Mott exact cross section
15 p2282 A72-32647
- Relativistic charged particles produced transition radiation as diffuse cosmic X rays source, discussing validity based on interstellar space energy density consideration
15 p2301 A72-32716
- Charged particle energy dissipation in cold collisional plasma, discussing collisions effect on power spectrum
16 p2436 A72-33651
- Plasma emitter shape determination in accelerating electric field for charged particle flux production
17 p2588 A72-34653
- Low voltage arc plasma in low pressure Cs vapors, determining charged particle concentration and potential distribution in interelectrode gap
17 p2588 A72-34861
- Charged and neutral particles radial distribution across positive isothermal plasma column in high current discharges
17 p2589 A72-34955
- Converging or diverging high intensity charged particle beams arbitrary profile shaping, obtaining solution via Laplace equation through reduction to Cauchy problem
17 p2589 A72-34961
- Charged particle stream neutralization and stabilization in solar corona, noting plasma wave and relation to type 3 radio bursts
17 p2608 A72-35093
- Kinetic equations with radiation effects
17 p2590 A72-35155
- Investigation of energetic charged particles and VLF emissions on the 'Interkosmos-3' satellite
17 p2600 A72-35209
- A method of calculating the pitch angle distributions of particle fluxes based on rocket and satellite data
17 p2558 A72-35840
- Two dimensional turbulence model for charge fluctuations statistical mechanics of nonlinear guiding center plasma
18 p2714 A72-36014
- On the acceleration of charged particles to cosmic ray energies
19 p2852 A72-38483
- Radiation of charged particle moving uniformly in a nonstationary magnetoactive plasma
19 p2843 A72-38570
- Radiation from a particle in static electric and magnetic fields
20 p2956 A72-39459
- Particle charging behind shock waves in suspensions
20 p2914 A72-39627
- Exact solutions of the Einstein-Maxwell equations for an accelerated charge
20 p2955 A72-40008
- Lunar shadowing of charged particles with arbitrary gyroradii and steady drift transverse to magnetic field applied to detector in low lunar orbit
21 p3104 A72-40482
- Short distance behaviour of the pair correlation function for classical plasmas
21 p3091 A72-40570
- A charged particle in the field of a transverse electromagnetic plane wave - A group-theoretical analysis
21 p3084 A72-40722
- Formation of intense charged particle beams in a current-carrying plasma
21 p3092 A72-40834
- Spatial spark jitter measurements of highly charged nuclei for optical spark chambers
21 p3055 A72-41003
- Charged particle uniform motion in sinusoidally space-time periodic medium, determining Cerenkov and transition radiation field spectrum from Brillouin diagram
21 p3088 A72-41378
- Hamiltonian analysis of charged particle motion in the pulsar rotating magnetic field
21 p3111 A72-41472
- Wave excitation during inclined charged-particle flight through a waveguide
21 p3089 A72-41841
- Radiation of an oscillating charge in a three-dimensional periodically inhomogeneous medium
21 p3023 A72-41844
- Accuracy of the conservation of the third adiabatic invariant of charged-particle motion in axisymmetric fields. II
22 p3217 A72-42209
- Determination of the duration of the diffusional motion of charges in a plasma with allowance for bulk ionization
22 p3213 A72-43116

- Numerical simulation of the relaxation of a beam of charged particles in a strong electric field
23 p3315 A72-43530
- Study of the angular distribution of charged and neutral pions during inelastic interactions in the energy region above 1 TeV
23 p3291 A72-44443
- Relationship between the energies of charged and neutral particles generated in the energy region above 100 GeV
23 p3332 A72-44447
- Association between interplanetary shock waves and delayed solar particle events.
23 p3332 A72-44503
- Charged particles propagation in magnetic field and scattering medium with constant and variable transport mean free path, applying to proton propagation for solar flares
24 p3435 A72-45076
- Steady-state distribution of the charged and neutral particle concentration in a bounded high-temperature turbulent plasma
24 p3429 A72-45493
- Transformation of trapped charged particles to transit particles under the influence of a high-frequency electric field
24 p3429 A72-45494
- Charged and neutral cosmic rays radioactive isotope and momentum distribution measuring techniques in high energy particle astronomy observatories/HEAO/
24 p3404 A72-45540
- Mean dissociative and effective recombination coefficients of E region, discussing charged particle reactions on model formation
24 p3399 A72-45584
- CHARGING**
Spacecraft charging at synchronous orbit, constructing mathematical model of ATS 5
07 p1058 A72-19150
- Quinones as reversible redox couples for rechargeable cathodes, noting air regeneration capacity in organic electrolytes
16 p2352 A72-33898
- CHARPY IMPACT TEST**
Charpy impact test computerized data acquisition and analysis system using analog to digital converter
07 p1090 A72-19735
- Charpy impact strength data for unidirectional graphite, boron and glass-resin composites tested in fiber direction, noting tensile stress-strain characteristics importance
11 p1672 A72-25471
- Precracked Charpy specimens for fracture toughness impact and slow bend tests of Ti alloys, using energy values
13 p1974 A72-28656
- Charpy impact tests of neutron irradiated nuclear reactor component steels to determine ductile/brittle transition temperature, describing setup and gas heating and cooling procedures
16 p2373 A72-33222
- The use of pre-cracked Charpy specimens to determine dynamic fracture toughness.
20 p2981 A72-39964
- CHARRING**
Apollo heat shield silica reinforcement fiber and ablation char reactions in laboratory and actual reentry tests
14 p2172 A72-30922
- CHARTS**
NT FLOW CHARTS
NT GRAPHS [CHARTS]
NT METEOROLOGICAL CHARTS
NT PATTERSON MAP
Ishihara charts readings in artificial daylight at low color temperatures, low light intensity and limited exposure time by normal and color defective subjects
03 p0317 A72-13939
- Recently published protein sequences. I.
23 p3254 A72-43570
- CHASSIS**
Calculation of the temperature field of a heated zone of complex form consisting of a chassis and built-in components
18 p2742 A72-37187
- CHEBYSHEV APPROXIMATION**
Chebyshev polynomials best approximation with respect to linear space spanned by odd degree polynomials, obtaining extreme point sets
04 p0539 A72-14729
- Chebyshev approximation by nonlinear families on general compact space with local Haar condition
04 p0539 A72-14730
- Plane Poiseuille flow stability from Orr-Sommerfeld equation solution by Chebyshev polynomials expansion and QR matrix eigenvalue algorithm
05 p0653 A72-17009
- Unified design charts for communication systems filter networks with inverse Chebyshev and elliptic function responses
06 p0787 A72-18400
- Chebyshev phase and time delay approximations existence and characterization
12 p1836 A72-27572

- Alternant theorems for characterization of minimum solutions in multidimensional Chebyshev approximation of functions connected with Markov systems
15 p2261 A72-31497
- Chebyshev acceleration application to Jacobi, Gauss-Seidel and related iterative methods for solution of coupled harmonic equations, comparing to block SOR method
17 p2574 A72-34447
- Computerized design of electric filters with given frequency response, discussing attenuation characteristic approximation by Chebyshev method
19 p2776 A72-37307
- Minimax method of optimizing electric circuits in the absence of constraints on the variable parameters
19 p2777 A72-37309
- An improved method for the solution of the heat equation in Chebyshev series.
19 p2879 A72-37370
- CHECKOUT**
Simulation language for digital static checks for hybrid and analog computers
04 p0495 A72-14417
- Turbojet aircraft engine overhauling planning and execution, discussing dismantling, washing, galvanic treatments, acceptance checks and quality controls
05 p0643 A72-16014
- GERT simulation program as stochastic network analysis technique for modeling policies and processes in performance tests and checkout
06 p0780 A72-17977
- Radome checkout ensuring reproducibility by insertion phase delay measurement
06 p0822 A72-18195
- Parametric approaches to statistical burn-in or debugging problems in aircraft reliability analysis
13 p1985 A72-28363
- CHECKOUT EQUIPMENT**
U TEST EQUIPMENT
- CHEMICAL ANALYSIS**
NT ELECTROPHOTOMETRY
NT GAS ANALYSIS
NT GAS SPECTROSCOPY
NT KARL FISCHER REAGENT
NT MICROANALYSIS
NT NEUTRON ACTIVATION ANALYSIS
NT OZONOMETRY
NT POTENTIOMETRIC ANALYSIS
NT QUALITATIVE ANALYSIS
NT QUANTITATIVE ANALYSIS
NT SPECTROSCOPIC ANALYSIS
NT URINALYSIS
NT VOLUMETRIC ANALYSIS
- Chemical analysis of iron meteorites, tabulating Ni, Co, P and C content
01 p0126 A72-10108
- Toxicological control and chemical analysis of out-gassing products from nonmetals in high temperature oxygen atmosphere, investigating use within LM crew compartment
01 p0019 A72-10771
- Stabilized human plasma protein solution analysis, noting albumin presence
03 p0316 A72-13855
- Erlchmanite /natural osmium disulfide/ chemical analysis and X ray data, noting osmium abundance
03 p0351 A72-14369
- Apollo 11 lunar samples carbon compound geochemical analysis, using sequential scheme with minimum handling of solids and extracts
05 p0714 A72-16131
- Chemical, geochronological and petrogenetic analyses of Apollo 15 lunar mare basalt rock from Hadley Rille, comparing with Apollo 12 and 14 basalts
06 p0888 A72-18264
- Classification of mass spectra on computers /COM-SOC/ for compound characterization of complex mixtures with geochemical and environmental applications
07 p0980 A72-20393
- Luna 16 rock sample B-1 petrology, mineralogy and chemistry, noting fine grained ophitic basalt nature
09 p1380 A72-22262
- X ray diffraction and chemical phase analysis of Nb alloys in cast and heat treated state, considering hardening mechanism
09 p1327 A72-22636
- Viking Lander mass spectroscopic analysis of organic compounds, water and volatile constituents of Martian atmosphere and surface
10 p1540 A72-24383
- Titanium oxide, carbide and nitride fractional determination in Ni-Ti alloy, noting optimum extraction conditions
11 p1655 A72-25513
- High pressure cannular combustor with continuous analytical and sampling system for simulated gas turbine engines emission measurements
[ASME PAPER 72-GT-88] 11 p1705 A72-25663
- Chemical ionizing mass spectrometry with electron bombardment of reactant gas, discussing plasma chromatography
11 p1590 A72-26389

- Heat resistant alloys conjugate phases extraction, separation and chemical analysis, discussing control of minor phases as precipitation products
13 p1978 A72-29443
- Nonprotein amino acids detection in presence of protein amino acids by amino acid analyzer, noting separation of chemically similar compounds
13 p1913 A72-29774
- Ti, B, Zr and Be trace additions effect on Al alloy grain refining from spectrochemical analysis
13 p1913 A72-29838
- Orthogonality condition application to continuum mechanics systems with zero free energy, viscoelastic materials and chemical problems
14 p2130 A72-30419
- Solid surface inspection by X ray diffraction, electron microscopy and chemical techniques
14 p2131 A72-30693
- The effect of firing temperature on properties of natural steatite and pyrophyllite.
17 p2569 A72-34666
- Book - Chemical properties and analysis of refractory compounds
18 p2655 A72-36094
- Complexonometrical analysis of molybdenum aluminides and Cu-Mo alloys without preliminary separation of components
18 p2655 A72-36097
- Chemical phase analysis for determining phase composition of products formed in borides, carbides and borocarbides mixtures
18 p2656 A72-36100
- Apollo and terrestrial geochemical samples examination for indigenous amino acids distribution and optical configuration, stressing close monitoring of contamination sources
19 p2762 A72-37648
- Mineralogy, bulk chemistry and sample shape and mass of Seoni /India/ chondrite, observing extensive recrystallization
19 p2858 A72-37860
- Activation analysis in geochemistry and cosmochemistry; Proceedings of the Advanced Study Institute, Kjeller, Norway, September 7-12, 1970.
20 p2898 A72-39826
- Rocks and meteorites analysis techniques evaluation, using Apollo 11 fines results to evaluate activation analysis for geochemistry and cosmochemistry applications
20 p2899 A72-39827
- In-situ geochemical analysis of Martian and lunar composition via alpha particle activation technique, discussing Surveyor instrument performance
20 p2899 A72-39828
- Trace element geochemistry of Apollo 16 soil 68501.
23 p3337 A72-43939
- The carbon chemistry of the moon.
23 p3339 A72-44149
- Phase extraction and analysis in superalloys - Summary of investigations by ASTM Committee E-4 Task Group I.
23 p3304 A72-44257
- The chemical classification of iron meteorites. VI - A reinvestigation of irons with Ge concentrations lower than 1 ppm.
24 p3436 A72-44697
- CHEMICAL ATTACK**
NT INTERGRANULAR CORROSION
Resin selection for manufacture of chemically resistant glass fiber reinforced polyesters, considering structural factors of chain for susceptibility to alkaline hydrolysis
16 p2414 A72-33304
- Changes in the wear resistance of polymer surface layers in aggressive and biologically active media
21 p3072 A72-40081
- CHEMICAL BONDS**
NT COVALENT BONDS
Bond dissociation energy of aluminum monoxide, tabulating flame compositions and temperatures
07 p1051 A72-19363
- Transition metal borides chemical bonding mechanism from Nb and Cr boride phases thermal emf and expansion, resistivity, Hall coefficient and carrier mobility
07 p1017 A72-19992
- Metals and alloys breakdown toughness and mechanical properties predictions under various loading conditions, discussing interatomic bonds and plastic deformation zone size
07 p1019 A72-20146
- Ferroelectrics with strong hydrogen bonds, deriving self consistent optical phonon frequency and coupled proton-phonon vibration spectrum
09 p1366 A72-22221
- Chemical bond effect on K emission spectrum of oxygen and fluorine
09 p1275 A72-22522
- Electron paramagnetic resonance investigation of III-V compound semiconductor crystals, observing large magnetic moments, heteropolar chemical bonding and impurities
13 p2021 A72-28572

Qualitative microscopic model for biologic postsynaptic membrane with tunneling chemical bonds, noting selective ionic conductivity as function of electric field

13 p1909 A72-28769

Chemical bond in Cu-Ti intermetallic phases, from X ray K absorption edges studies

13 p1981 A72-29914

Bond dissociation energy calculation for carbon disulfide in vacuum UV from fluorescence threshold energy of incident photons, measuring absorption coefficient at 1200-1400 Å

13 p1914 A72-30060

Iron carbide single crystal growth texture due to anisotropy of interatomic interactions associated with oriented covalent Fe-C bonds

14 p2121 A72-30774

Interstitial phases, crystal structure and chemical bonds of titanium, vanadium and niobium carbides, comparing with transition metal carbides

15 p2252 A72-31195

Stoichiometric composition, crystal structure and chemical bond variations in Ta-O system

15 p2290 A72-31197

Intermolecular hydrogen bond study of hydroxyl group in caranol and caranol-o compounds, listing IR absorption bands for valence oscillations

15 p2192 A72-32100

Hydrocarbon electrochemical oxidation kinetics for fuel cells at low temperature, considering adsorption and bond cleavage

16 p2361 A72-33891

Use of X-ray photoelectron spectroscopy to study bonding in Cr, Mn, Fe, and Co compounds.

18 p2657 A72-36568

The influence of molecular binding on the stopping power of alpha particles in hydrocarbons.

18 p2655 A72-37193

Book - Amorphous semiconductors.

20 p2958 A72-38924

Bond energy electrostatic potential calculation and equilibrium and rate constants prediction for alkali and halide ions association with neutrals

21 p3087 A72-40556

Filler quantity and type effects on mechanical energy losses in polymers, discussing molecular interaction and chemical bond influences

23 p3306 A72-43731

Synthesis of polymers with conjugate bonds on the basis of dilithium-derivative aromatic hydrocarbons

23 p3262 A72-43929

Supramolecular structure artificial defects and bond strength influence on mechanical strength of pyrographite

24 p3418 A72-45761

HEMICAL CLEANING

Hydrogen evolution and ferric ion corrosion inhibition by synergistic action of substituted thioureas and thioamides to minimize metal corrosion during acid cleaning

13 p1980 A72-29624

HEMICAL COMPOSITION

NT CARBON DIOXIDE CONCENTRATION

Dunite-norite olivine-rich microbreccia in Apollo 14 lunar fines sample 14002.8, discussing origin and chemical composition

01 p0126 A72-10106

Lunik 16 core-tube soil sample petrology and chemical composition

01 p0126 A72-10107

Deformable stainless steels empirical diagram for structural state estimation from chemical composition, considering various austenite, martensite and ferrite combinations

02 p0243 A72-12241

Ti-Al-Mo alloys thermomechanical treatment, investigating alloy composition effects on hardening

02 p0244 A72-12246

Chemical composition and morphology of silicate spherules, comparing to lunar rocks, meteorites and tektites

02 p0280 A72-12283

High strength low alloy type ferrite pearlite steel microstructural and compositional variations effect on work hardening, ductility and impact toughness

02 p0246 A72-12558

Magellanic Clouds and Galactic nucleosynthesis from chemical composition

03 p0426 A72-13263

Rocket fuel combustion products composition and combustion chamber temperature determination

03 p0405 A72-13474

Meteorite structure and chemical composition, describing investigation methods, origin and evolution

03 p0438 A72-13976

Lunar craters and maria origin from rock and sample chemical composition and magnetic differentiation

03 p0439 A72-14302

Semiconductor film compound decomposition, chemical composition and metastable modifications presence during condensation in vacuum, discussing defect formation in crystal structure

05 p0701 A72-15752

Bulk type variable resistors with properties controlled by composition during fabrication, evaluating inorganic binders with optimal properties

05 p0701 A72-15754

Impact breccias in carbonate rocks of Sierra Madera /Texas/, investigating microstructure, chemical composition, petrography and mineralogy

05 p0654 A72-16038

Quasar primordial He content prediction from primordial temperature fluctuations necessary for galaxy formation

05 p0717 A72-16384

Pb and Sr isotopic composition measurements on eclogites from South Africa

05 p0658 A72-16551

Venus cloud top chemical composition from spectroscopic data, discussing cloud refractive index and reflectivity

05 p0719 A72-16711

Lunar rock 12013 sawdust and fragment composition from neutron activation analysis, comparing to Java tektite J2

05 p0722 A72-17127

Ni corrosion by hydrogen sulfide, determining nickel sulfide scale chemical composition and crystallographic orientation by electron and X ray diffraction

06 p0828 A72-17606

Bond zones morphology and composition in Invar-based explosive welds, using metallographic and electron microprobe techniques

06 p0820 A72-17707

Lunar surface rocks, soil and breccia chemical composition, discussing element concentration, radiation effects on surface chemistry and volcanism

06 p0887 A72-18226

Economical methods for cast maraging steel production, describing composition, heat treatment and mechanical properties

07 p1010 A72-18970

Thermodynamic models of gas-solid equilibria in cosmochemical systems containing H, O, Si, Mg, S, C, Cl and F

07 p1075 A72-19587

Aluminized layer phase and chemical composition on heat resistant iron and nickel alloys

07 p1013 A72-19748

Earth and moon chemical composition differences based on model of lunar formation from circumterrestrial swarm of particles and larger objects

07 p1077 A72-19820

Filler metal compositions and procedures for Al alloys vacuum brazing, describing experimental vacuum furnace apparatus

07 p0997 A72-20000

Chemical composition, thermal properties and shock propagation in solar wind plasma

07 p1061 A72-20018

Temperature and alloy composition effects on coarsening rate of metal carbide particles in dissimilar metallic matrix

07 p1021 A72-20436

Microscopic, chemical and morphological studies of ultralarge meteoric spherules in Yakut ASSR, noting composition

08 p1229 A72-20838

Venus atmosphere chemical composition, temperature and pressure, discussing model cloud layer, circulation and upper atmospheric structure

08 p1236 A72-21400

Soviet book on corrosion cracking of carbon steels covering chemical composition, structure, mechanical properties, anode and cathode processes role and adsorption losses

08 p1190 A72-22163

Lunik 16 lunar soil samples petrogenesis and chemical composition, comparing to Apollo regoliths

09 p1381 A72-22271

Lunik 16 soil sample chemical composition indicating similarity of Sea of Fertility to Sea of Tranquility sites geochemical characteristics

09 p1381 A72-22273

Mg alloys compositions, melting points, mechanical properties and applications

09 p1327 A72-22479

Analytic determination of Nb low content in highly alloyed Ni base alloys

09 p1276 A72-22637

Chemical composition features of basalts from British Tertiary Volcanic Province, discussing possible evolution

10 p1472 A72-23915

Lunar anorthosites and parent liquids chemical composition from trace element analysis

10 p1537 A72-24158

Deformable wrought stainless steels phase diagram for structural state estimation from chemical composition, considering various austenite, martensite and ferrite combinations

11 p1659 A72-26127

X ray fluorescence spectrometric analysis of carbonaceous chondrites for chemical subgroups

11 p1723 A72-26525

Chemical composition, physical properties, microstructure and production of 1300 kg powder metallurgy forged billets

11 p1644 A72-26845

W-Ni-Mo alloys obtained by powdered metals sintering, investigating mechanical properties, phase distribution and composition

11 p1666 A72-26876

Low cycle fatigue deformation of lamellar eutectic and cast Ni-Sr alloys, noting microstructure and chemical composition effects on fracture energy

11 p1668 A72-26939

Chemical and ionizational equilibrium equations of heterogeneous gas mixture composition with allowance for condensed phase ionization

11 p1747 A72-26965

High energy solar and galactic cosmic ray chemical composition, considering electron component abundances and beryllium-boron ratio

12 p1863 A72-27426

Zn,-Ge and P based semiconductor alloy specimens chemical composition determination via ac polarograms

12 p1854 A72-27443

Heat resistant blade alloy test temperature effects on fatigue life, tensile strength, hardness and chemical composition

12 p1831 A72-28230

Microprobe analysis of Timmersoi hypersthene chondrite from Niger Republic, noting equilibrium between olivine and orthopyroxene at 850 °C

13 p2035 A72-28751

Stratospheric aerosols physical properties and chemical composition, discussing various measuring techniques and results

13 p1991 A72-28839

Jet fuel hydrocarbon group chemical composition effects on antiwear characteristics in sliding friction and rolling simulation experiments

13 p2024 A72-29073

Quenching rate and alloying element content effects on precipitation extent and corrosion resistance of Al-Cu alloys, discussing microstructure, chemical composition and mechanical properties

14 p2119 A72-30604

Composition, strength and plasticity of ultralight Mn-Li alloys with two-phase alpha-beta base

14 p2125 A72-31040

Composition diagrams and properties of intermetallic compounds of magnesium in binary and ternary systems

15 p2252 A72-31196

Stoichiometric composition, crystal structure and chemical bond variations in Ta-O system

15 p2290 A72-31197

Diffusion effects on stellar surface chemical composition, emphasizing solar atmosphere conditions

15 p2305 A72-31342

Alloying characteristics of heat resistant Ni base Ni-Cr-Al-Ti-Nb-Mo disk alloy

15 p2255 A72-31566

Chemical inhomogeneity of high melting metals and alloys of Ti, Zr, Nb and Cr from radio isotopic and nuclear emission studies

15 p2255 A72-31576

Cosmic ray chemical composition from particle sampling by rockets and satellites, comparing galactic rays, solar rays and sun

15 p2299 A72-31648

Lateral distribution, radiation spectra and pulse shapes calculated from mathematical models of cosmic ray showers radio emission, noting chemical composition of primary particle

15 p2230 A72-32262

Stainless steel surface alloy composition characterization as function of vacuum annealing temperature, using proton-induced X rays

15 p2258 A72-32527

Mo and stainless Ni-Cr steel surfaces chemical composition determination by Auger electron spectroscopy during heating in high vacuum

16 p2406 A72-33251

Isotopic composition of primary cosmic radiation - Conference, Lyngby, Denmark, March 1971

16 p2446 A72-33726

Supernova explosion mechanism and quantitative game for galactic chemical evolution, discussing relationship to cosmic rays

16 p2459 A72-33744

Composition effect on strain-transformation and precipitation hardening of beta Ti alloys at 800-1100 °F

16 p2410 A72-33813

The reddening, distance modulus, chemical composition and age of the galactic cluster NGC 752.

17 p2607 A72-34675

Disk-shaped diffusion model with inhomogeneous distribution of gas and heavy relativistic nuclei sources for galactic cosmic rays chemical composition

17 p2600 A72-35206

Earth and moon chemical composition differences based on model of lunar formation, from circumterrestrial swarm of particles and larger objects

17 p2618 A72-35745

- Compositional characteristics of olivines from Apollo 12 samples. 18 p2723 A72-36063
- Oxidizability of boron-carbon compounds at high temperatures, determining chemical composition effect on oxidation resistance 18 p2703 A72-36095
- Morphology and petrography of volcanic ashes. 18 p2685 A72-36222
- Effects of nuclear reactions on the stability of degenerate stars. 19 p2864 A72-38100
- Apollo 11 and 12 mare basalts and gabbros - Classification, compositional variations, and possible petrogenetic relations. 19 p2864 A72-38295
- Activity-composition relations in the fayalite-forsterite solid solution between 900 and 1300 C at low pressures. 20 p2915 A72-39178
- The effects of composition and annealing conditions on the stability of columbium /niobium/-treated low-carbon steels. 20 p2938 A72-39301
- On the chemical composition of epsilon Pegasi. 20 p2974 A72-39901
- Chemical composition, refractivity and temperature dependence of blackness levels of aluminum oxide-chromium oxide-phosphorus oxide ceramic coatings flame sprayed on steel 21 p3072 A72-40384
- Thermodynamic parameters and reacting multicomponent mixture composition, using state equations and energy conservation equations for reaction kinetics 21 p3013 A72-40989
- The spectrum of N Del 67 and some remarks on chemical composition of the novae envelopes. 21 p3109 A72-41436
- Czech book - Moldavites and tektites. 21 p3111 A72-41536
- A survey for RR Lyræ stars at high galactic latitude. 22 p3222 A72-42137
- Universe evolution study from contemporary chemical composition of cosmic matter, noting concentration changes of protons, neutrons and He 4 22 p3222 A72-42140
- Study of the composition of inclusions in synthetic diamond crystals by the local analysis method 22 p3196 A72-42155
- Rapid determination of total carbon content in titanium carbide 22 p3176 A72-42200
- Lunar interior composition constraints from chemical composition of igneous rocks on surface 22 p3226 A72-42533
- Effective temperatures of massive stars as a function of chemical composition and mass. 22 p3227 A72-42560
- Giant stars iron abundance from narrow band spectrophotometric analysis and model atmospheres, isolating super metal rich stars below H-R diagram subgiant branch 23 p3334 A72-43256
- Infrared spectroscopy for chemical composition of inorganic and organic products formed on friction surfaces of gas turbine parts immersed in hydrocarbon fuels 23 p3325 A72-43974
- Influence of the chemical composition of Kh25N16G7AR steel on its heat resistance 23 p3303 A72-44098
- Mineralogy, petrology and chemistry of lunar rock 12039. 23 p3339 A72-44127
- Mundrabilla meteorites geographical location, external appearance, microstructure and chemical composition, suggesting shower occurrence 23 p3339 A72-44130
- Rare earth and other abundances in the Murchison carbonaceous meteorite. 23 p3262 A72-44131
- Evidence for vapor fractionation in the origin of chondrules. 23 p3339 A72-44134
- Solid solution, subsolidus reduction and compositional characteristics of spinels in some Apollo 15 basalts. 23 p3262 A72-44135
- Major element composition of glasses in three Apollo 15 soils. 23 p3339 A72-44137
- Chemical composition of Luna 16 and Luna 20 rock samples from Sea of Fertility and Apollonius Crater 24 p3440 A72-45109

CHEMICAL COMPOUNDS

- Lower aldehydes contribution to biochemically important compounds in abiogenic synthesis, considering amino acids formation 04 p0483 A72-14763
- Nonstoichiometric compounds thermodynamic properties in terms of indistinguishability of ions /atoms/ in different valence states 07 p1048 A72-19544

- Application of computer mathematics procedures for prediction of phase diagrams 22 p3191 A72-42812
- CHEMICAL EFFECTS
- Heat treated carbonized, cyanided, nitrided and boronized steel fatigue strength dependence on static strength, residual stress, brittleness and stress concentration from test data 02 p0244 A72-12242
- Active ingredient oxidizing potential and pressure effects on burning rate of explosive substances 02 p0302 A72-12292
- High strength solids compositional, heat treatment and chemical environmental effects on fracture strength, considering alumina as example 09 p1334 A72-22387
- Active ingredient oxidizing potential and pressure effects on burning rate of explosive substances 10 p1561 A72-23767
- Chemical surface treatment effects on mechanically gripped fiberglass rods tensile strength 11 p1674 A72-25827
- Heat treated carbonized, cyanided, nitrided and boronized steels fatigue limit dependence on static strength, residual stress, brittleness and stress concentration 11 p1659 A72-26128
- Glass fiber reinforced thermoplastic resins chemical and hydrolytic resistance, noting composites and polymers long term performance prediction in aggressive environments 12 p1833 A72-27405
- Tribochemical effects during friction of non-lubricated amorphous and crystalline polymer surfaces under mild and hard contacting conditions 12 p1835 A72-28200
- Chemical interaction effects on single crystal sapphire filament strength in Ni and Ni alloy matrices during heat treatment in inert atmosphere 13 p1974 A72-28661
- Reactional diffusion in metal surface layers due to chemically active external media involving solid reaction products formation 15 p2255 A72-31570
- Chemical effects in plasma condensation. 24 p3429 A72-45457

CHEMICAL ELEMENTS

- NT ACTINIDE SERIES
- NT ACTINIUM
- NT ALKALI METALS
- NT ALKALINE EARTH METALS
- NT ALUMINUM
- NT ALUMINUM ISOTOPES
- NT ANTIMONY
- NT ARGON
- NT ARGON ISOTOPES
- NT ARSENIC
- NT BARIUM
- NT BARIUM ISOTOPES
- NT BERYLLIUM
- NT BERYLLIUM ISOTOPES
- NT BISMUTH
- NT BORON
- NT BORON ISOTOPES
- NT BROMINE
- NT CADMIUM
- NT CALCIUM
- NT CALCIUM ISOTOPES
- NT CARBON
- NT CARBON ISOTOPES
- NT CERIUM
- NT CESIUM
- NT CESIUM VAPOR
- NT CHLORINE
- NT CHROMIUM
- NT COBALT
- NT COPPER
- NT DEUTERIUM
- NT DEUTERIUM PLASMA
- NT DYSPROSIUM
- NT ERBIUM
- NT EUROPIUM
- NT FLUORINE
- NT GADOLINIUM
- NT GALLIUM
- NT GALLIUM ISOTOPES
- NT GERMANIUM
- NT GOLD
- NT HAFNIUM
- NT HALOGENS
- NT HELIUM
- NT HELIUM ATOMS
- NT HELIUM FILM
- NT HELIUM ISOTOPES
- NT HOLMIUM
- NT HYDROGEN
- NT HYDROGEN ATOMS
- NT HYDROGEN IONS
- NT HYDROGEN ISOTOPES
- NT HYDROGEN PLASMA
- NT INDIUM
- NT IODINE
- NT IODINE ISOTOPES
- NT ITRIDIUM
- NT IRON

- NT ISOTOPES
- NT KRYPTON ISOTOPES
- NT LANTHANUM
- NT LEAD [METAL]
- NT LEAD ISOTOPES
- NT LIGHT ELEMENTS
- NT LIQUID HELIUM
- NT LIQUID HYDROGEN
- NT LIQUID NITROGEN
- NT LIQUID POTASSIUM
- NT LIQUID SODIUM
- NT LITHIUM
- NT LITHIUM ISOTOPES
- NT LUTETIUM
- NT MAGNESIUM
- NT MAGNESIUM ISOTOPES
- NT MANGANESE
- NT MANGANESE ISOTOPES
- NT MERCURY [METAL]
- NT MERCURY VAPOR
- NT METALLIC HYDROGEN
- NT MOLYBDENUM
- NT NEODYMIUM
- NT NEON
- NT NEON ISOTOPES
- NT NICKEL
- NT NIOBIUM
- NT NITROGEN
- NT NITROGEN ATOMS
- NT NITROGEN IONS
- NT NITROGEN ISOTOPES
- NT NUCLIDES
- NT OXYGEN ISOTOPES
- NT OXYGEN PLASMA
- NT PALLADIUM
- NT PLATINUM
- NT PLUTONIUM ISOTOPES
- NT POTASSIUM
- NT POTASSIUM ISOTOPES
- NT POWDERED ALUMINUM
- NT PRASEODYMIUM
- NT PROMETHIUM
- NT RADIOACTIVE ISOTOPES
- NT RADON
- NT RADON ISOTOPES
- NT RARE EARTH ELEMENTS
- NT RARE GASES
- NT REFRACTORY METALS
- NT RHODIUM
- NT RUBIDIUM
- NT RUBIDIUM ISOTOPES
- NT SAMARIUM
- NT SAMARIUM ISOTOPES
- NT SCANDIUM
- NT SELENIUM
- NT SILICON
- NT SILVER
- NT SINTERED ALUMINUM POWDER
- NT SODIUM
- NT SODIUM VAPOR
- NT SOLID NITROGEN
- NT STRONTIUM
- NT STRONTIUM ISOTOPES
- NT SULFUR
- NT SULFUR ISOTOPES
- NT TANTALUM
- NT TELLURIUM
- NT TERBIUM
- NT THALLIUM
- NT THORIUM ISOTOPES
- NT TIN
- NT TIN ISOTOPES
- NT TITANIUM
- NT TITANIUM ISOTOPES
- NT TRACE ELEMENTS
- NT TRANSURANIUM ELEMENTS
- NT TRITIUM
- NT TUNGSTEN
- NT URANIUM
- NT URANIUM ISOTOPES
- NT VANADIUM
- NT XENON
- NT XENON ISOTOPES
- NT YTTERBIUM
- NT YTTRIUM
- NT ZINC
- NT ZIRCONIUM
- Nondestructive identification of alloy elements by nondispersive X ray fluorescence spectroscopy using Si/Li detectors and radioisotope sources for mobile applications 01 p0069 A72-10805
- Nuclear astrophysics review, discussing chemical elements and isotopes abundance and cosmic nucleosynthesis 03 p0437 A72-13842
- Handbook on elemental abundances in meteorites covering individual elements, emission and X ray spectrography, colorimetry, neutron activation and isotope dilution 12 p1876 A72-28204
- Critique on experiment to measure gravitational constant differences between two elements, discussing errors in statistical analysis 16 p2426 A72-33769

CHEMICAL ENERGY

NT ENERGY OF FORMATION

Chemical box model of energy storage in covalent bonds and nonequilibrium distributions in prebiological synthesis leading to macromolecules

04 p0482 A72-14755

Biological energy transformation origin and evolution, discussing inorganic pyrophosphates precursor to adenosine phosphates as energy carriers

04 p0470 A72-14798

Reversible thermodynamic cycle of chemical to electric energy conversion with electron gas as working body, discussing Gibbs-Helmholtz equations

16 p2350 A72-32994

Physical and chemical identification methods for biochemical reactions and energy balance of muscular contraction and shaking

21 p3003 A72-41469

Chemical energy transformation to mechanical energy and heat in muscles during exercise, considering energy sources for contraction, oxidations, glycolysis and lactic anaerobic mechanism

21 p3003 A72-41470

CHEMICAL EQUILIBRIUM

NT ACID BASE EQUILIBRIUM

Angular momentum conservation law compliance of generalized triple configuration model for spin-detonation nucleus, assuming transverse Chapman-Jouguet wave

03 p0342 A72-13734

Three dimensional transverse wave structure effect on detonation wave and Chapman-Jouguet gross properties, using planar model

04 p0510 A72-14410

Vapor pressure and composition in As-I system, investigating entropy and enthalpy changes and temperature dependence of equilibrium constant

09 p1373 A72-23481

One dimensional pulsating detonations calculation with induction zone kinetics, obtaining Chapman-Jouguet steady solution profiles

11 p1745 A72-25983

Dimensionless heat transfer equations of reacting media in chemical equilibrium, using Lewis-Semenov criterion

12 p1889 A72-28140

Equilibrium states difference of ternary metal-boron-nitrogen systems, taking into account chemical bond type and crystal structure of boride and nitride atoms

14 p2112 A72-30154

Chemical equilibrium models of low temperature condensation from solar nebula relating to planetary composition

15 p2311 A72-32083

Equilibrium distribution of chemical species in a reacting gas mixture

17 p2512 A72-35808

Multicomponent diffusion and heat transfer in flows of a chemically balanced ionized gas past bodies

21 p3047 A72-41658

CHEMICAL EXPLOSIONS

NT GAS EXPLOSIONS

Analog simulation of normal thermal explosions and cool flames, observing oscillations limits, time dependence of parameters and effect of changes in activation energy or initial temperature

07 p1098 A72-19366

Steady combustion thermal stability of condensed explosives for burning rate limitation by condensed phase chemical reactions, noting surface temperature effects

19 p2879 A72-37356

Method of measuring the fine structure of detonation fronts in solid explosives.

24 p3463 A72-45039

Chemical explosion energy distribution between gases and propelled mass, discussing momentum and kinetic energy transfer

24 p3463 A72-45040

CHEMICAL EXTINGUISHERS

U FIRE EXTINGUISHERS

CHEMICAL FUELS

NT AEROSINE

NT AIRCRAFT FUELS

NT GASOLINE

NT HYDROCARBON FUELS

NT HYDROGEN FUELS

NT JET ENGINE FUELS

High energy chemical propellant combustion under adiabatic and nonadiabatic conditions, calculating product equilibrium state as functions of temperature and pressure with computer program

06 p0903 A72-18212

The impact of aerospace technology on energy conversion in the 70's.

[ASME PAPER 72-AERO-11] 22 p3140 A72-43147

CHEMICAL INDICATORS

Indicator dilution methods for ventricular volume measurements from washout curves, discussing intraventricular blood mixing uniformity

15 p2190 A72-32496

CHEMICAL KINETICS

U REACTION KINETICS

CHEMICAL LASERS

CW longitudinal flow carbon monoxide chemical laser system analysis, discussing vibrational levels, population densities, excitation and relaxation processes and dynamic model

03 p0368 A72-13858

CW CO laser by discharging premixed carbon disulfide-oxygen flame, suggesting chemical pumping mechanism and flame laser possibility

04 p0529 A72-14589

Pulsed chemical laser started by transverse electrical discharge, observing output energy dependence on fluorine compound used

04 p0530 A72-14974

Flash photolysis HF chemical laser pulse delay measurements, showing pressure, flash lamp intensity and optical cavity loss dependence

05 p0668 A72-16606

HF and/or HF-carbon dioxide transfer laser potential power output and design criteria, considering deuterium and fluorine combustion, reaction product expansion and mixing rate

05 p0670 A72-16970

Handbook on lasers and optical technology covering gas, dye, liquid, injection and insulating crystal lasers, materials, sources, transmission, hazards and holographic recording

06 p0826 A72-17945

Chemical lasers technology, considering population inversion, excited state molecules production, potential energy surfaces calculation and computer simulation

06 p0826 A72-18457

Self pulsed electrically initiated HF and DF chemical laser with high pulse repetition frequency gain switched operation

06 p0826 A72-18458

Atmospheric pressure pulsed chemical laser based on reaction between fluorine and hydrogen or deuterium

07 p0999 A72-18877

Laser action in pulsed transverse discharge initiated chemical reactions forming hydrogen and deuterium halides, noting production of previously unobserved transitions

07 p0999 A72-18879

CW diffusion type chemical HF laser and two-vibrational level HF molecular models, analyzing laser performance

07 p1000 A72-18955

HF diffusion type chemical laser fluid dynamic and optical properties, discussing computerized numerical analysis

07 p1001 A72-19063

Continuous chemical laser optimum optic axis position for maximum multimode power operation and intensity distribution

08 p1182 A72-21557

Time dependent progress of vibrational-rotational transitions in hydrogen-fluorine chemical laser investigated by oscillography with IKM-1 monochromator

08 p1183 A72-21715

Chemistry and performance characteristics of flash photolysis and microwave discharge initiated CW carbon disulfide/oxygen lasers

09 p1325 A72-23236

Lasing length, power and efficiency of cw HF chemical laser with nitrogen or He diluent

09 p1325 A72-23241

Chemical lasers diatomic and multiautomic molecules dissociation in nonequilibrium conditions, discussing vibrational energy exceeding gas temperature

11 p1646 A72-25713

Chemical laser with deuterium and nitrogen fluorides mixture, examining excited molecules emission spectra

11 p1649 A72-26351

Time estimate criterion of lasing breakdown in photodissociative iodine-alkyl lasers with iodine molecule buildup

12 p1819 A72-27053

Chemical laser dynamics review, discussing population inversion, molecular vibrational relaxation and reactions initiation methods

12 p1822 A72-27605

Spectral output of pulsed discharge initiated hydrogen fluoride chemical laser as function of pressure and gas composition

12 p1823 A72-27839

Quasi-stationary supersonic plasma flame generation by lamp-pumped rhodamine laser, studying shock wave structure by high speed cinematography

12 p1825 A72-27882

Computer simulation of pulsed hydrofluoric acid laser pumped by chain reaction, investigating cavity and chemical parameters effects on laser pulse

12 p1826 A72-27938

Population inversion in exothermal decomposition reactions of multiautomic molecules for chemical and collision laser systems

13 p1912 A72-28778

Energy and time characteristics of Raman scattering by benzene in laser cavity as function of medium thickness and cavity length

13 p1969 A72-29523

Pulsed chemical high pressure laser efficiency and output energy increase due to carbon dioxide introduction into deuterium-fluorine mixture

13 p1970 A72-29698

Transverse flow transverse pulsed chemical CO laser, describing Q switching, pulse duration power efficiency and chemical deactivation processes

14 p2109 A72-30187

Molecular iodine photolysis in photodissociative laser due to selective pumping, noting recombination-like storage mechanism

14 p2110 A72-30354

CO overtone band and vibrational transitions in CW carbon disulfide-oxygen chemical laser, discussing pressure effects

15 p2250 A72-32525

Intense emission from high pressure pulsed carbon dioxide chemical transfer laser by flash photolysis initiated deuterium-fluorine exothermic chain reactions

16 p2401 A72-33392

Chemical laser with deuterium and nitrogen fluorides mixture, examining excited molecules emission spectra

16 p2402 A72-33704

Rhodamine laser radiation effects on absorbing materials investigated by high speed cinematography and shock wave structure

16 p2404 A72-33991

Spectroscopy of pulsed HF chemical lasers using an infrared vidicon camera tube.

17 p2562 A72-34641

HF vibrational relaxation measurements using the combined shock tube-laser-induced fluorescence technique.

17 p2511 A72-34735

Gain and relaxation studies in transversely excited HF lasers.

17 p2564 A72-35344

HF chemical lasers pumped by atomic fluorine with molecular hydrogen, calculating intensity and efficiency by reaction kinetics analysis for comparison with computer solutions

21 p3062 A72-40617

Experimental CW chemical laser studies.

[AIAA PAPER 72-712] 21 p3063 A72-40920

Pulse energy and temporal/spatial distribution of carbon dioxide laser pumped by energy transfer from vibrationally excited DF produced by deuterium-fluorine chain reaction

22 p3185 A72-42617

The photochemical iodine laser - A high-power laser

22 p3186 A72-42940

Application of gasdynamic flows in laser technology

22 p3187 A72-43176

Generation spectrum kinetics of a photodissociative iodine laser

23 p3297 A72-44480

Analytic criteria for laser quenching moment, generation power and stimulated emission energy for photodissociative iodine-alkyl lasers with iodine molecule buildup

24 p3412 A72-45706

CHEMICAL MACHINING

NT ELECTROCHEMICAL MACHINING

Ni plating by chemical reduction method in boron hydride solution, deducing stabilizing effect of sulfur compounds and Pb salts from catalyst poisoning theory

11 p1641 A72-26265

Ti fabrication advances in forging, diffusion bonding, hot forming, chemical milling and laser cutting

21 p3061 A72-41335

Chemically etched notches effect on Al-Mg alloy mechanical properties

24 p3417 A72-45764

CHEMICAL MILLING

U CHEMICAL MACHINING

CHEMICAL PROPERTIES

NT ACIDITY

NT HEAT OF COMBUSTION

NT HEAT OF FORMATION

NT HEAT OF SOLUTION

NT HEAT OF VAPORIZATION

NT SALINITY

NT THERMOCHEMICAL PROPERTIES

Fe, Ni and Co based high temperature thin gauge sheet alloys, discussing chemical and mechanical properties, fabrication and availability

01 p0084 A72-10742

Lime, cement, fly ash and sand combination airport pavement design and testing, discussing material structural and chemical properties, compressive strength, costs, etc

02 p0200 A72-12023

Extruded superalloy powder structural shapes preparation by filled billet technique for improved chemical and mechanical properties

07 p0994 A72-19483

Chlorendic acid based Hetron 92C fire retardant chemical resistant polyester for fiberglass reinforced structure applications

08 p1192 A72-21677

Alicyclic dicarboxylic anhydride structure effects on cured epoxidized novolac resin physical and chemical properties

08 p1193 A72-21695

Synthetic fire resistant hydraulic fluids, comparing chlorinated hydrocarbons and phosphate esters chemical properties with water based products

08 p1197 A72-22160

Carbohydrate based gelling agent for gas turbine fuel, describing development and chemical and physical properties

[ASME PAPER 72-GT-9] 11 p1702 A72-25612

Crash safe turbine fuel to reduce fire probability and severity during aircraft ground crash, investigating physical and chemical properties

[ASME PAPER 72-GT-28] 11 p1702 A72-25624

Russian book on Nb in ferrous metallurgy covering physicochemical properties, steels, slags, ore reduction and smelting for Nb alloys production

11 p1659 A72-26048

Impact glass-like objects as evidence of meteoritic origin of Lonar Crater (India), discussing physical, chemical and optical properties

11 p1723 A72-26521

Superalloys properties and utilization at high temperatures, discussing chemical resistance, diffusion treatment, B and Zr action and grain size

14 p2116 A72-30527

Chemical and mechanical properties relationship to stress corrosion in high strength Al-Cu and Al-Zn-Mg alloys, emphasizing grain boundaries cleavage energy

14 p2117 A72-30536

Explosives life limitation due to aging phenomena, discussing chemical and physical processes and environmental effects

14 p2143 A72-30752

Physicochemical properties and composition diagrams of antimonides and arsenides of Zn, Cd, Al, In and Ga

15 p2290 A72-31194

Antioxidant additives effect on chemical stability and rheological properties of silica gel lubricants with SU type mineral oil dispersion medium

16 p2413 A72-33173

Design criteria for fiber reinforced thermoplastic resins performance optimization, discussing temperature, humidity and chemicals effects

16 p2415 A72-33417

Book - Chemical properties and analysis of refractory compounds

18 p2655 A72-36094

Ordinary chondrite chemical and mineralogical properties establishment during solar system formation, noting fractionation events

20 p2969 A72-39334

Fuels, lubricating oils and hydraulic fluids for supersonic aircraft, discussing chemical properties, propellant combustion efficiency and production

20 p2945 A72-39930

Russian book on electron configuration model of condensed matter based on Hubbard model covering physicochemical properties of transition metals, alloys and compounds

21 p3066 A72-40348

Russian book - Handbook of aircraft materials.

21 p3072 A72-40459

Physicochemical properties of rare earth metals for alloying Al, Mg, Cu and Ti, noting getter and permanent magnet materials

22 p3191 A72-42806

Effect of rare earth metals on the structure and properties of aluminum and its alloys

22 p3192 A72-42818

Physical and chemical properties and stratification of neutral matter in comet atmospheres, discussing neutral gas dynamics and surface brightness distribution in comet images

23 p3335 A72-43299

Influence of hydraulic extrusion on the composition and properties of the Nb3Sn compound

23 p3323 A72-43597

CHEMICAL PROPULSION

NT HYBRID PROPULSION

Current and future rocket and spacecraft propulsion systems based on chemical propellants, nuclear thermoelectric, electrostatic and electromagnetic power generators

05 p0705 A72-16743

Nuclear rocket for space tug, comparing performance and operational costs with chemical propulsion

13 p2000 A72-28926

Electrostatic ion thruster and hydrazine monopropellant systems for communication satellites, noting weight savings

17 p2596 A72-34265

CHEMICAL REACTIONS

NT ACYLATION

NT ATOMIC RECOMBINATION

NT BROMINATION

NT CARBONIZATION

NT COPOLYMERIZATION

NT DECARBONYLATION

NT DECARBOXYLATION

NT DEIONIZATION

NT DEOXIDIZING

NT DESULFURIZING

NT ELECTROCHEMICAL OXIDATION

NT EXOTHERMIC REACTIONS

NT FERMENTATION

NT GLYCOLYSIS

NT HALOGENATION

NT HYDROGENATION

NT HYDROLYSIS

NT ION RECOMBINATION

NT METAL-WATER REACTIONS

NT NITRIDING

NT OXIDATION

NT OXYGEN RECOMBINATION

NT OXYGENATION

NT PHOSPHORYLATION

NT PHOTOCHEMICAL REACTIONS

NT PHOTOCROMISM

NT PHOTODECOMPOSITION

NT PHOTOLYSIS

NT PHOTOOXIDATION

NT PHOTOSYNTHESIS

NT PYROLYSIS

NT RADIOLYSIS

NT REDUCTION [CHEMISTRY]

NT SULFATION

NT THERMAL DISSOCIATION

NT TITRATION

Temperature, concentration and heat conductivity profiles of chemically reacting gas mixtures with thermal gradient, using classical transfer equations

01 p0023 A72-10489

Mathematical analogy between nonequilibrium and viscous inert transonic flows for reacting mixtures with relaxation and freezing

02 p0150 A72-11736

Hydrodynamic convective stability in catalytic chemical reaction with thermal and concentration coupling dependent on Lewis number

02 p0301 A72-12092

Dichlorodifluoromethane-fluorine flame structure, taking samples by molecular beam sampling system for analysis by mass spectrometry

02 p0303 A72-12483

Interstellar molecules formation by radiative association and chemical reactions

03 p0320 A72-13121

Meridional model of oxygen and hydrogen compounds reactions in mesosphere and lower thermosphere, determining diurnal variations and vertical profiles

03 p0346 A72-13378

Thermal simulator of flows with chemical wall reaction, plotting surface temperature variations with distance

03 p0456 A72-13793

Computer program for construction and integration of chemical reaction rate equations, applying to nitric oxide formation and decomposition

[WSCIPAPER 71-27] 04 p0482 A72-14583

Macroscopic integrodifferential transport equations for gas mixture with internal degrees of freedom and chemical reactions from model kinetic equation

04 p0552 A72-14633

Adenine, guanine, cytosine and other nitrogen compounds synthesis from carbon monoxide, hydrogen and ammonia mixtures by Fischer-Tropsch-like process

04 p0483 A72-14765

Amino acid-phosphate anhydrides polymerization in presence of clay minerals, noting reactions superposition and monomer diffusion

04 p0483 A72-14774

X ray spectral analysis of microchemical changes in surface films of titanium alloys during diffusive interaction with silicon carbide abrasive

04 p0534 A72-15654

Stress corrosion crack tip electrochemical reactions simulation on Ti and alloy surfaces, using modified rotating disk apparatus with pH measurement

04 p0536 A72-15739

Thermal nozzle combustion effects on supersonic flow of chemically reacting gas in thermodynamic equilibrium

05 p0599 A72-15846

Knudsen boundary layer role in physicochemical hydrodynamics of heterogeneous reactions and flows with surface reactions, using Boltzmann equation

05 p0746 A72-16209

Velocity field time history of interacting shear waves in infinite homogeneous chemically reacting fluid for turbulent combustion studies

05 p0747 A72-16367

Laser induced gas breakdown in chemical reactions and explosions during plasma creation, using time resolved spectroscopy and titanium oxide probes

05 p0624 A72-16666

Additive and natural ionization in combustion reactions, discussing flame chemistry, ionic species and measurements

05 p0751 A72-17224

IR chemiluminescence study of chlorine reaction with hydrogen iodide at enhanced collision energies, investigating energy conversion efficiency and forward scattering

06 p0770 A72-17300

Transport processes theory in mixtures of chemically active gases using Boltzmann equation and Sonin polynomials expansion

06 p0852 A72-17989

Large diatomic and polyatomic molecules formation from big radicals in interstellar medium, noting association reaction role

06 p0891 A72-18506

Chemical reaction delayed effect on triple shock front confluence point trajectory in detonations, developing qualitative detonation cell model

06 p0904 A72-18530

Antimony-halogen synergistic reactions in fire retardants, noting antimony oxychloride role

07 p0935 A72-19056

Steady two dimensional laminar compressible boundary layer of reacting gas mixture with surface vaporization and fuel injection, using integral method

07 p0967 A72-19129

Temperature dependence of carbon monoxide reaction rate with hydroxyl, noting activation energy

07 p0935 A72-19376

Ethyl radicals reactions in shock tube produced pyrolysis of azoethane, using time of flight mass spectrometer

07 p0935 A72-19433

Statistical-hydrodynamic description of nonequilibrium gas dynamics of single component and binary mixtures and systems with chemical reactions

07 p0968 A72-19886

Nonlinear acoustic propagation in chemically reacting media, discussing quasi-frozen and quasi-equilibrium flow processes behind shock fronts

07 p0969 A72-19974

Neutral species chemical reactions in D and E regions, taking into account effects of photodissociation and transport by horizontal and vertical flow and molecular diffusion

07 p0936 A72-20039

Kinetic theory and nonequilibrium distribution functions of reacting gases with simultaneous reactions

07 p1035 A72-20114

Noble and molecular gases addition in reactions induced in ethylene by carbon dioxide-nitrogen-helium laser

07 p1009 A72-20693

Hot wire ignitor modeling including measured H value and heat generation by explosive chemical reaction

08 p1219 A72-20754

Differential thermal and X ray analyses of ignition and preignition solid-solid reactions in Zr-Mo trioxide delay system over 440-475 C

08 p1219 A72-20756

Chemical reactions in shock waves, discussing diatomic molecules dissociation and combustion processes

08 p1148 A72-21016

Origin of life as chemical evolution product, tracing juvenile carbon history through planetary and geological phases

08 p1162 A72-22004

Chemical evolution in microenvironment reactions system due to dominant energy or mass parameter, discussing complex organic molecule synthesis

08 p1128 A72-22005

Asymptotic analysis of activation energy limit for radiant ignition of reactive solid with in-depth absorption

[AD-741533] 08 p1255 A72-22044

Chemionization in oxyhydrogen plasma detonation waves

08 p1129 A72-22045

German monograph on heat transfer in chemically reacting gases covering laminar and turbulent tube flows for dissociated diminitrogen tetroxide

09 p1274 A72-22339

Reactions of aniline with isoamyl nitrite and phenyldiazonium borofluoride with caustic potash, investigating kinetics of chemical polarization of products nuclei

09 p1275 A72-22497

Parallel air and hydrogen flows confluence numerical examination to determine self ignition conditions in turbulent mixing layer, noting reaction zone

[ONERA, TP NO. 981] 09 p1410 A72-22814

Thermospheric structure between 100 and 400 km from rocket soundings and ground observations, noting mass spectrometers chemical reactions influence on atmosphere model accuracy

09 p1300 A72-23015

Mesospheric clouds composed of molecular complexes of extraterrestrial origin, considering chemical reactions, hydroxyl luminescence, thermospheric water vapor and auroras

09 p1347 A72-23590

Kinetic equations derivation for rarefied chemically reacting monatomic or stable molecular gases

10 p1514 A72-23845

- Laser induced chemical decomposition of copper maleate and fumarate and fragment reaction with low hydrocarbons, comparing with thermal heating
10 p1433 A72-23951
- Thermal energy reaction rates determination for partial charge transfer chemical reactions, comparing with electron transfer efficiencies
10 p1514 A72-24336
- Trajectory dynamics for fluorine atoms reaction with H molecules, predicting total available energy from energy release on potential energy surface
10 p1434 A72-24343
- Atmospheric metal ion chemistry, tabulating thermal energy binary and three body reaction rate data
10 p1434 A72-25160
- High voltage electron microscope applications to materials reactions in gaseous environments, exemplifying by stress corrosion morphology in stainless steel, Al-Zn-Mg and Ti-Al
11 p1668 A72-26945
- Cosmic and solar wind abundance analysis for D and He-3 in protosolar gas, noting chemical equilibrium reaction role in D enrichment
12 p1868 A72-27216
- Chemical laser dynamics review, discussing population inversion, molecular vibrational relaxation and reactions initiation methods
12 p1822 A72-27605
- Molecular-mechanical theory of external friction, taking into account surface roughness, time and temperature dependent mechanical properties and chemical processes
12 p1818 A72-28195
- Competition criteria for chemical reactions selection in nonequilibrium computer calculations on combustion systems properties, noting seeded flames and rocket exhausts
13 p1912 A72-28548
- Hydrocarbon-air mixtures reaction in incident shock waves of pressure greater than 25 atmospheres, correlating with shock tube results
13 p2063 A72-28549
- Plasticizers and modifiers effect on epoxy polymers structure from electron microscopy and IR spectroscopy, observing chemical reactions between aliphatic resin and hardening agent
13 p1983 A72-28689
- Chemical reactions between solids during boundary friction, presenting literature review on mechanochemical or tribo-chemical reactions between solid lubricants and metal surfaces
[ASLE PREPRINT 72AM 1] 13 p1964 A72-28969
- Vibrational relaxation mechanism in supersonic flows of chemically reacting carbon dioxide-nitrogen mixture, using numerical integration
13 p1913 A72-29502
- Concentration profile derivation for fluid flow near rotating disk with chemical reactions, considering concentration gradient and barodiffusion effects
13 p1944 A72-30049
- Transport processes theory in chemically active gases mixtures using Boltzmann equation and Sonin polynomials expansion
14 p2133 A72-30216
- Fe light emission for simulated meteor conditions, measuring ionization and spectral emission cross sections for Fe reactions with nitrogen and oxygen for 350-2000 eV
14 p2156 A72-30562
- Double base propellant nitroglycerin interactions with inhibition materials cellulose acetate and ethyl cellulose, noting time and temperature effects
14 p2145 A72-30767
- Sm and Eu binary alloys, investigating physicochemical interactions and phase diagrams
15 p2289 A72-31187
- Thermal nozzle combustion effects on supersonic flow of chemically reacting gas in thermodynamic equilibrium
15 p2334 A72-31265
- Epoxide resins for application in composite materials, discussing crosslinking reactions, temperature effects on cure, and electrical and physical properties
15 p2260 A72-31441
- Chemical interaction within crystals for generation of stacking fault vacancies and phenomena associated with solid solution microheterogeneity dislocations, discussing heat resistance
15 p2254 A72-31558
- Diffusion layer formation on metallic surfaces, discussing saturation, crystallization, phase structure, chemical reactions, thermal and contact conditions
15 p2253 A72-31571
- Steam-hydrogen treatment tests for high temperature stability of noble metal catalysts in hydrogen-oxygen reaction initiation
15 p2192 A72-32225
- IR internal reflection spectroscopy application to dynamic chemical changes study on ammonium perchlorate surface during thermal decomposition, observing crystal lattice transformation
15 p2296 A72-32313
- Red blood cell metabolite 1,3 diphosphoglycerate determination method by rapid deproteinization, concentration by precipitation and enzymatic reaction
15 p2190 A72-32488
- Rising temperature reactor technique to evaluate catalysts for initiating hydrogen-oxygen reaction in gas mixtures at 78 K
15 p2193 A72-32550
- Doubly ionized Mg, Ca and Ba atoms termolecular association rate constants with various molecular neutrals, comparing doubly charged with singly charged ions cluster reaction rates
16 p2360 A72-32924
- Nonequilibrium steady quasi-one dimensional expanding nozzle flow of chemically reacting gas mixture, using time dependent finite difference technique [AIAA PAPER 72-684]
16 p2480 A72-34058
- Entropy and chemical change. I - Characterization of product /and reactant/ energy distributions in reactive molecular collisions: Information and entropy deficiency.
17 p2511 A72-34738
- Statistical-hydrodynamic description of nonequilibrium gas dynamics of single component and binary mixtures and systems with chemical reactions
17 p2540 A72-35134
- Contribution to the study of flows with surface chemical reactions in the boundary layer
17 p2541 A72-35455
- The reaction of hydrogen peroxide with nitrogen dioxide and nitric oxide.
17 p2511 A72-35466
- Chemical reactions in inhomogeneous mixtures - The effect of the scale of turbulent mixing.
17 p2543 A72-35640
- Equilibrium distribution of chemical species in a reacting gas mixture
17 p2512 A72-35808
- Polymerization characteristics of 4-ferrocenyl-1, 3-pentadiene monomer, discussing synthesis on molar scale
17 p2512 A72-35934
- Olivine-garnet reaction in peridotites from Tanzania.
17 p2551 A72-35937
- Chemical reactions effects on gas dynamics, considering relaxation phenomena in fluid flow
18 p2679 A72-36384
- Statistical model of chemical reactions in nonisothermal low pressure plasma.
18 p2715 A72-36567
- Energetic and topological effects in surface chemical reactions, considering intermolecular dispersion and dipole forces and chemisorption
18 p2657 A72-36828
- Nonequilibrium transport equations for chemically reacting inhomogeneous gas mixtures, using Hermitian tensor polynomials of molecular velocities
18 p2713 A72-36895
- Critical conditions of thermal explosion in the presence of chemical and mechanical heat sources
19 p2879 A72-37357
- Intrinsically transonic /almost equal frozen and equilibrium sound velocities/ flows of chemically active gas mixture, developing nonlinear perturbation theory
19 p2745 A72-37390
- Model reactions between phthalic anhydride and o-phenylenediamine under polymerization-analogous conditions for polyimideazopyrrolone formation
19 p2762 A72-37647
- Effect of chemical reaction reversibility on the temperature and pressure dependence of burning rates
19 p2882 A72-38455
- Nitrous oxide production from ozone photolysis reaction with molecular nitrogen
19 p2762 A72-38753
- Chemical reaction rates for dissociation and exchange in nonisothermal plasma from molecular energy level occupation investigation
20 p2957 A72-39018
- Activity-composition relations in the fayalite-forsterite solid solution between 900 and 1300 C at low pressures.
20 p2915 A72-39178
- Aluminum oxide and silicon carbide whiskers fabrication by homogeneous gas reaction process, discussing gas composition, temperature and substrate effects on production yield
20 p2940 A72-39440
- Nonlinear acoustic propagation in chemically reacting media, discussing quasi-frozen and quasi-equilibrium flow processes behind shock fronts
20 p2955 A72-40031
- Velocity distribution in turbulent mixing of compressible reacting gases, noting flame length measurement of submerged H jet
21 p3129 A72-40981
- Internal energy and conductive and frictional dissipation, mass, momentum and energy production as functions of density, entropy and geometric state variables
21 p3130 A72-41228
- Equation of state of a mixture of nonideal chemically reacting gases
22 p3152 A72-41881
- Solid-state reactions during the production of TZM molybdenum alloy by powder metallurgical methods
22 p3187 A72-41972
- Self-propagating high-temperature synthesis of refractory inorganic compounds
22 p3188 A72-42165
- Kinetic equations of chemically reacting gas mixtures
22 p3152 A72-42267
- A study of the rates of carbon-carbon dioxide reaction in the temperature range 839 to 1050 C.
22 p3153 A72-43037
- German monograph - Solution of the boundary layer equations for chemically reacting gases by a collocation method.
22 p3167 A72-43071
- Polyphosphate and trimetaphosphate formation under potentially prebiotic conditions.
23 p3261 A72-43566
- Studies in prebiotic synthesis. VII - Solid-state synthesis of purine nucleosides.
23 p3262 A72-43567
- The kinetics of the reaction between oxygen and sulfur on a Ni(111) surface.
24 p3378 A72-44951
- Laminar high speed mixing of nonequilibrium dissociating gases.
24 p3392 A72-45056
- Developing laminar and turbulent duct flow with chemical reaction.
24 p3378 A72-45061
- Nucleic acid hybridization with RNA immobilized on filter paper.
24 p3379 A72-45773
- CHEMICAL REACTORS**
Jacketed tubular chemical reactor optimal startup control, presenting distributed maximum principle for diffusional parameter system
02 p0301 A72-12093
- Heat transfer from nitrogen plasma jet mixed with cold gas to cooled reactor channel walls at various channel expansion degree values
04 p0555 A72-14645
- Regeneration of oxygen from carbon dioxide and water.
24 p3375 A72-45183
- CHEMICAL RELAXATION**
U MOLECULAR RELAXATION
CHEMICAL SHIFT
U CHEMICAL EQUILIBRIUM
CHEMICAL STERILIZATION
Space flight hardware sterilization, considering dry heat and chemical destruction
01 p0019 A72-10822
- CHEMICAL TESTS**
NT CHEMICAL ANALYSIS
NT ELECTROPHOTOMETRY
NT GAS ANALYSIS
NT GAS SPECTROSCOPY
NT KARL FISCHER REAGENT
NT MICROANALYSIS
NT NEUTRON ACTIVATION ANALYSIS
NT OZONOMETRY
NT POTENTIOMETRIC ANALYSIS
NT QUALITATIVE ANALYSIS
NT QUANTITATIVE ANALYSIS
NT SALT SPRAY TESTS
NT SPECTROSCOPIC ANALYSIS
NT URINALYSIS
NT VOLUMETRIC ANALYSIS
Solar activity effects on bismuth chloride hydrolysis tests from statistical results following solar flares
12 p1773 A72-28212
- Study of titanium and titanium oxide structures corresponding to different kinetics of oxidation obtained at 850 C
20 p2936 A72-39206
- CHEMICAL WARFARE**
Comparison of physical, biophysical and physiological methods of evaluating the thermal stress associated with wearing protective clothing.
20 p2898 A72-39808
- CHEMILUMINESCENCE**
Nitrogen dioxide producing chemiluminescent radiative and three-body recombination reaction at low pressures, determining airglow and oxygen atoms decay time by resonance fluorescence method
03 p0347 A72-13395
- IR chemiluminescence study of chlorine reaction with hydrogen iodide at enhanced collision energies, investigating energy conversion efficiency and forward scattering
06 p0770 A72-17300
- Gaseous air pollutant detection and measurement by chemiluminescence method for continuous monitoring of given pollutant concentration
10 p1434 A72-24099
- IR emission of oxygen reaction with carbon oxysulfide, investigating molecular vibrational transitions
10 p1510 A72-24133
- Microphotometric chemiluminescence measurement for analysis of turbulent flame fine structure for homogeneous air-fuel mixtures at high Reynolds numbers
16 p2479 A72-34005

- IR chemiluminescence technique /method of arrested relaxation/ to measure spectral energy distribution among Cl and H1 and D1 reaction products
19 p2763 A72-38802
- CHEMISORPTION**
Electron theories of chemisorption and catalysis on semiconductor surfaces, considering band theory applicability range
07 p1048 A72-19561
- Chemisorbed oxygen effect on electrical properties of monocrystalline cadmium sulfide thin plates with high resistivity
10 p1525 A72-24211
- Oxygen adsorption effects on Mo orientation contrasts and emission image under electron microscope
10 p1513 A72-24875
- Oxygen chemisorption surface states effects on electrical conductivity of CdS single crystals and evaporated films
11 p1701 A72-25855
- Oxygen chemisorption effect on rare gas beams reflection from refractory metals polycrystalline surfaces, interpreting experimental results by simple correlation model
16 p2431 A72-33068
- Contact contamination - Formation of carbonaceous deposits on electrical contacts.
18 p2665 A72-36119
- Energetic and topological effects in surface chemical reactions, considering intermolecular dispersion and dipole forces and chemisorption
18 p2657 A72-36828
- A LEED investigation of the chemisorption of nitrous oxide on a tungsten /100/ surface.
20 p2898 A72-39188
- Chemisorption of CO on tungsten /100/- Combined flash desorption and electron stimulated desorption study. I.
22 p3152 A72-42297
- CHEMONUCLEAR PROPULSION**
U CHEMICAL PROPULSION
U NUCLEAR PROPULSION
CHEMORECEPTORS
Cat respiratory center activity phase relation to arterial chemoreceptor afferent discharge oscillations effect on lung ventilation frequency
05 p0619 A72-16789
- Respiration control during hyperoxia, discussing chemoreceptor significance in minute volume respiration rate reduction mechanism from Pamir mountain aborigines oxygen breathing reaction studies
08 p1120 A72-22076
- Arterial chemoreceptor deafferentation influence on rat respiratory response to hypoxic and hypercapnic gas mixture breathing
08 p1120 A72-22078
- Breathing regulation characteristics showing reflex control of respiratory functions in normal environment and brain tissue receptor control under hypoxia
08 p1121 A72-22079
- Olfactory receptor models sensitivity, discussing threshold dependence on adsorbed odoriferous agent amount and exposure time
11 p1585 A72-26453
- Mathematical model of extracellular pH in brain tissue from blood and cerebrospinal fluid acid-base parameters for respiration central chemosensitive mechanism study
11 p1579 A72-26660
- Respiration control by extracellular pH in medullary tissue, studying chemoreceptor response to hydrogen ion concentration in cat cerebrospinal fluid
11 p1579 A72-26661
- Mountain sickness relation to ventilation response to hypoxia, noting response intensity dependence on peripheral chemoreceptor sensitivity
12 p1771 A72-27481
- Acute hypoxia effects on dog coronary blood flow and cardiac function from cardiac beta-adrenergic and hemodynamics study
12 p1760 A72-27482
- Native highlander and lowlander chemoreflex ventilatory response to transient carbon dioxide inhalation at low and high altitudes
12 p1762 A72-27728
- Cerebrospinal fluid pH change effects on cat respiratory response before and after vagotomy, showing vagal activity relation to central chemical control of respiration
12 p1762 A72-27825
- Ventilatory peripheral chemoreflex response to hypoxia during physical exercise in native highlanders and altitude-acclimated lowlanders
17 p2499 A72-34345
- Venous responses to stimulation of carotid chemoreceptors by hypoxia and hypercapnia.
18 p2648 A72-36025
- A mathematical model of the chemoreflex control of ventilation.
21 p3008 A72-40917
- The carotid body in animals at high altitude.
22 p3143 A72-42589
- Genetic aspects of the blunted chemoreflex ventilatory response to hypoxia in high altitude adaptation.
22 p3144 A72-42591

- Comparison of three methods for quantitating respiratory response to hypoxia in man.
24 p3372 A72-44960
- Water-soluble insulin receptors from human lymphocytes.
24 p3373 A72-45375
- CHEMOSPHERE**
Molecular oxygen photodissociation in Schumann-Runge bands, discussing determination of solar radiation penetration depth into chemosphere
03 p0412 A72-13386
- CHEMOTHERAPY**
Time zone shift and p-chlorophenylalanine desynchronizing effects on sleep alteration and circadian rhythms in monkeys
03 p0318 A72-13071
- Isoniazid tuberculosis chemoprophylaxis safety in aviation personnel, discussing renal function, serum transaminase activity, hematology, electrocardiograms and neurological examinations
04 p0479 A72-14872
- Myorelaxant 3,5-dimethyl-4-bromopyrazole injection effect on rabbit and dog heart during direct extracardiac nerve stimulation
05 p0618 A72-16358
- Civil aeronautics environment relation to psychiatrists and medical psychologists treatment of air navigation personnel, discussing chemotherapeutic and psychotherapeutic treatment administration problems
07 p0927 A72-19243
- Clinical response to nitroglycerin therapy correlation with coronary angiography as diagnostic test for coronary artery disease in patients with chest pain
07 p0920 A72-19993
- Hypnotic drug use effect on pilot performance and flight safety, using glutethimide, flurazepam and placebo in double blind study
07 p0933 A72-20188
- Myocardial infarction effects on drug tolerance and hemodynamic changes due to digitalis doses, discussing toxic arrhythmias
08 p1115 A72-21082
- Hyperlipidemia progressive increase among flying personnel, showing Clofibrate treatment effect on lowering rate
08 p1117 A72-21545
- Dietary and pharmacological treatment of atherogenic hyperlipidemias from lipid-sugar balance and drug efficacy studies
08 p1117 A72-21547
- Propranolol as adrenergic beta receptor inhibiting agent for hyperthyroidism symptom amelioration
08 p1118 A72-21550
- ECG, physical exercise and drug use in diagnosis and aeromedical evaluation of supraventricular arrhythmias, presenting case histories of pilots with wandering cardiac pacemakers
10 p1428 A72-23741
- Left ventricular dynamic function in terms of internal diameter, pressure and flow in dogs at rest and during isoproterenol and metaraminol infusions
11 p1582 A72-26773
- Clofibrate treatment for atherosclerotic cardiovascular disease prevention among Sabena flying personnel
12 p1766 A72-28293
- Amitravite /biological protectant/ effect on natural immunity state of dogs exposed to chronic gamma irradiation simulating space flight environment
14 p2074 A72-30380
- Succinate and glutathione as protective agents against chronic effects of hyperbaric oxygen toxicity in rats
14 p2082 A72-31091
- Exchangeable potassium in heart disease - Long-term effects of potassium supplements and amiloride.
17 p2500 A72-34932
- Increased tolerance of leukemic mice to arabinosyl cytosine with schedule adjusted to circadian system.
17 p2505 A72-35397
- Studies of the influence of theophylline on the vasodilating action of different medications on the cerebral and coronary circulation of man
18 p2651 A72-36799
- Apparatus for programmed oral administration of drugs to large primates in altered environments.
18 p2654 A72-36921
- Effect of beta-adrenergic blockade on plasma volume in human subjects.
19 p2757 A72-38029
- Calcium metabolism conditions in calcified tissues of rats during a lasting hypodynamia and thyrocalcin administration
21 p2997 A72-40432
- Ocular and induced visual effects of systemic and topical drugs in terms of eye neuroanatomy and pharmacology, stressing glaucoma therapy
22 p3150 A72-42499
- The simultaneous action of stimulants and tranquilizers on the efficiency of a human operator
23 p3260 A72-43923

CHEST

- Lf subaudible chest wall vibration recordings, discussing external, epicardial surface and intraventricular pressure precordial displacement tracings
01 p0017 A72-10120
- Magnetometer and spirometer ventilation measurements from chest and abdomen movements during carbon dioxide inhalation
05 p0619 A72-16790

CHILLING**U COOLING****CHIMES****U AUDITORY SIGNALS****CHIMPANZEES****NT MONKEYS**

- Isolation stress effect on excretory products in unrestrained chimpanzee, suggesting Ca to P excretion ratio as physiological stress indicator
[AD-739467] 07 p0921 A72-20179
- Isolation stress effect on micturition circadian rhythm and diuresis occurrence in unrestrained chimpanzee under entrained and free running conditions
[AD-739468] 07 p0921 A72-20180
- Isolation stress effect on circadian rhythmic patterns of EEG activity during sleep-wake and sleep cycles in unrestrained chimpanzee
[AD-739469] 07 p0921 A72-20181

CHIN

- Chin-sternum-heart syndrome from partial parachute failure, with close reference to atrial endocardial and myocardial lacerations
02 p0167 A72-11711

CHIPS

- LSI/MOS logic circuits radiation effects prediction from modeling studies of individual devices on test chip
03 p0334 A72-14087

- Report on Flip Chip and Beam Lead bonding for electronic circuits.
[SAE AIR 1141] 18 p2666 A72-36528

CHIRP**NT CHIRP SIGNALS****CHIRP SIGNALS**

- Acoustic surface wave chirp filters application in pulse compression radar system, considering various piezoelectric substrate materials characteristics
14 p2089 A72-31045
- Variable-bandwidth frequency-modulation chirp pulse compression using a longitudinal acoustic-wave convolver at 1.3 GHz.
21 p3023 A72-41468

CHLORATES

- Chlorate based oxygen generator assembly, discussing tests, advantages and applications
04 p0482 A72-14568
- Potassium chlorate/red phosphorus mixtures sensitivity tests for initiation by electrostatic discharge, heating and impact
08 p1221 A72-20776
- Contaminant analysis in gaseous oxygen generated by chlorate candle combustion, using Draeger tubes
12 p1779 A72-28254

CHLORELLA

- Chlorella algae size distribution curves by combining device for counting electrical conductivity pulses with discriminator for gamma scintillation spectrometry
01 p0017 A72-10400
- Chlorella growth rate model, presenting specific photosynthetic and urea and carbon dioxide utilization rates
02 p0160 A72-12038
- Gibberellic acid effects on Chlorella algae growth rates, using algal suspension optical density as measuring technique
03 p0313 A72-12975
- Space flight effects on chlorella cell survival and mutability in Zond automatic stations
05 p0623 A72-16775
- Soyuz 5 satellite vehicle space flight factors effect on chlorella cells, investigating survival rates and mutability
05 p0623 A72-16776
- Chlorella population age structure and cell requirements correlation with nutrient medium nitrogen and phosphorus absorption
13 p1909 A72-29311
- Human immunobiological status during prolonged maintenance in bioregenerative life support system, discussing possible allergic reaction to chlorella gaseous metabolites
13 p1910 A72-29312
- Carbon monoxide dynamics in chlorella reactor closed environment and in man-chlorella system at relatively constant level
14 p2078 A72-30377
- Man, chlorella and wheat plant in life-supporting biological system, showing compatibility relative to gas and water exchange
15 p2189 A72-31826
- Space flight effects on chlorella cell survival and mutability in Zond automatic stations
17 p2504 A72-35278

- Soyuz 5 satellite vehicle space flight factors effect on chlorella cells, investigating survival rates and mutability 17 p2505 A72-35279
- Mathematical model of two-component alga-bacteria biocenosis 21 p2997 A72-40431
- CHLORIDES**
- NT AMMONIUM CHLORIDES
- NT DICHLORIDES
- NT HYDROCHLORIC ACID
- NT HYDROGEN CHLORIDES
- NT IRON CHLORIDES
- NT LITHIUM CHLORIDES
- NT POTASSIUM CHLORIDES
- NT SODIUM CHLORIDES
- NT SULFUR CHLORIDES
- Electrochemical crevice corrosion process of Ti in hot concentrated chloride solution, discussing temperature, set potential and surface treatment 03 p0374 A72-13714
- Chloride ion concentration effect on polarization behavior of Fe-Ni alloy, noting cathodic curve parallel shift in noble potential direction 11 p1652 A72-25290
- Scintillation TiCl₄/I₂Be/ crystal response to 8 GeV ionizing negative pions, noting pulse shape and resolution characteristics 15 p2291 A72-31535
- Electroretinographic illumination potentials dependence on extracellular chloride ion concentration in isolated frog retina 15 p2186 A72-32491
- Respiratory effects of hypochloremic alkalosis and potassium depletion in the dog. 21 p2997 A72-40418
- Effect of chloride on the anodic dissolution of titanium in methanolic solutions. 21 p3013 A72-40842
- CHLORINE**
- Energy levels and mean life measurements of Cl ions at 500-2800 Å using beam-foil spectra technique 02 p0170 A72-12547
- Spectroscopic characteristics of continuous wave neutral argon laser using helium and chlorine for power enhancement 03 p0367 A72-13432
- Electron impact Stark broadening of ionized chlorine lines in pulsed arc plasma using laser interferometric and spectroscopic measurements 03 p0396 A72-13748
- Mass spectroscopic rate constants for reactions of negative ions of rhenium and tungsten oxides with chlorine and nitrogen dioxide 04 p0484 A72-15639
- IR chemiluminescence study of chlorine reaction with hydrogen iodide at enhanced collision energies, investigating energy conversion efficiency and forward scattering 06 p0770 A72-17300
- Chlorine, bromine and iodine first spectral lines observation in IR region with liquid nitrogen cooled lead sulfide detector 09 p1276 A72-22614
- Raman band rotational structure computer simulation, noting application to gaseous chlorine spectrum analysis 09 p1358 A72-23050
- Graphite ablation rate inhibition and surface temperature depression by chlorine gas in supersonic high temperature air environment 16 p2475 A72-32842
- The reduction of chlorine on carbon in AlCl₃-KCl-NaCl melts. 21 p3013 A72-40843
- CHLORINE COMPOUNDS**
- NT AMMONIUM CHLORIDES
- NT AMMONIUM PERCHLORATES
- NT CHLORATES
- NT CHLORIDES
- NT CHLORINE FLUORIDES
- NT CHLOROSILANES
- NT DICHLORIDES
- NT HYDROCHLORIC ACID
- NT IRON CHLORIDES
- NT LITHIUM CHLORIDES
- NT PERCHLORATES
- NT POTASSIUM CHLORIDES
- NT POTASSIUM PERCHLORATES
- NT SODIUM CHLORIDES
- NT SULFUR CHLORIDES
- Fire retardant capabilities of bromine and chlorine compounds in polymers 03 p0380 A72-13247
- Plasticized PVC compounds, investigating chlorine based fire retardants role in increasing flame resistance [PAPER 14] 03 p0380 A72-13248
- Lubricating action of sulfur-containing additives and chlorine compounds in lubricants and cermet materials, noting effects of iron compounds formation in contact region 07 p0996 A72-19967
- Existence, structure and thermodynamic and kinetic stability of ClOO radical in Venus atmosphere, using quantum statistics methods for unimolecular decomposition rate 18 p2726 A72-36647
- CHLORINE FLUORIDES**
- High temperature ClF reaction kinetics in thermal decomposition shock tube study, using chlorine atom two-body emission 04 p0484 A72-15463
- CHLOROPHYLLS**
- Rapid water pollution assessment by airborne chlorophyll measurement using differential, correlation and IR radiometers [ALAA PAPER 71-1097] 01 p0058 A72-10546
- Plant leaves light reflectance, transmittance and absorbance characteristics relationship to leaf mesophyll arrangement, considering interpretation of aircraft/spacecraft remotely sensed data 02 p0213 A72-11856
- Acid base equilibrium effects on chlorophyll primary photosynthetic regulating mechanism, considering electron transfer to NADP and ATP formation 04 p0468 A72-14778
- Structural lipids role in accumulating light energy during prebiological evolution, using conductance studies in lipid-chlorophyll-water system 04 p0468 A72-14779
- Pigment system and primary photosynthesis evolution, using comparative analysis of bacteriochlorophyll, bacterioviridin and chlorophyll 04 p0469 A72-14780
- Pigments participation in lipid systems formation, considering chlorophyll photochemical activity in surface active agents 04 p0469 A72-14785
- CHLOROPLASTS**
- Molecular aspects of structural and functional circadian rhythms in chloroplasts of unicellular alga Acetabularia, emphasizing protein synthesis role 07 p0919 A72-19540
- Photon trapping in photosystem II of photosynthesis - The fluorescence rise curve in the presence of 3-[3,4-dichlorophenyl]-1,1-dimethylurea. 17 p2505 A72-35761
- The presence of P700 in chloroplast fragments prepared by short time incubation with Triton X-100. 23 p3258 A72-44325
- CHLOROSILANES**
- Trimethylchlorosilane film boiling for silicon carbide deposit on vertical heated tungsten filaments, investigating mass transport rate 04 p0595 A72-14600
- CHLORPROMAZINE**
- Chlorpromazine tranquilizer influence on squirrel monkeys in electric shock tests, shifting postevent aggressivity to pre event anticipation 07 p0916 A72-18975
- CHOLESTEROL**
- Cholesterol esters polymorphic and mesomorphic behavior, using differential scanning calorimetry, X ray powder diffractometry and positron annihilation techniques 04 p0484 A72-15262
- Negative and positive emotional states influence on blood cholesterol and arterial pressure levels in dogs, suggesting common subcortical genesis of atherosclerosis and hypertension 09 p1264 A72-22498
- Some optical properties of liquid crystals 20 p2961 A72-39850
- The use of cholesteric liquid crystals in the study of skin temperature and their applications in aviation medicine 21 p3009 A72-41192
- CHOLINERGIC BLOCKING AGENTS**
- U ANTICHOLINERGICS**
- CHOLINERGICS**
- NT ANTICHOLINERGICS
- Antimotion sickness drugs effectiveness based on acetylcholine or norepinephrine induced changes of balance between vestibular and reticular neurons 10 p1427 A72-23726
- Nuclein acid contents in cholinergic and adrenergic spinal cord neurons and in their glial satellite-cells during hypoxic hypoxia and a post-hypoxia period 19 p2756 A72-37742
- Participation of cholinergic structures in the development of disturbances of the functional state of the cerebellum under the action of centripetal accelerations 19 p2757 A72-38033
- CHOLINESTERASE**
- Cardiac membrane pain sensitivity in vagotomized cats under sensitizing acetylcholine influence during reduced cholinesterase activity 13 p1905 A72-29329
- Variation of the acetylcholine content and of the cholinesterase activity in the blood under muscular strain 20 p2891 A72-38934
- CHONDRITES**
- NT BRUDERHEIM METEORITE
- NT CARBONACEOUS METEORITES
- NT ORGUEIL METEORITE
- L-chondrite Assam, determining He, Ne and Ar concentrations and isotopic compositions and galactic and solar flare irradiation track densities 01 p0124 A72-10060
- Hibonite /Ca-Al-Ti rich xenoliths/ from Leoville and Allende polymict brecciated HL group chondritic meteorites 01 p0125 A72-10067
- Temperature gradient induced in Lost City /Oklahoma/ olivine-bronzite chondrite by atmospheric friction from thermoluminescent emission measurements 01 p0126 A72-10109
- Martian internal structure, investigating oxidation rate of chondritic material 02 p0277 A72-11752
- Siderophilic element content relation to oxidation state of ordinary chondrites, using Ir/Ni concentrations from neutron activation analysis 02 p0277 A72-11896
- Mineralogical and chemical compositions of Markovka chondrite 02 p0280 A72-12284
- Whole rock Rb-Sr measurements of hypersthene /including black/ chondrites for shock and reheating effects, noting data conformance to 4.5-4.6 gigayear isochron 04 p0571 A72-14566
- Shock transformed chondrite texture observed in thin plates by UV fluorescence 05 p0722 A72-17151
- Alfianello meteorite inspection by optical microscopy for petrological features of shock metamorphism in chondrites 05 p0722 A72-17152
- Oxygen isotopic temperatures and mineral compositions of equilibrated ordinary chondrites 07 p1076 A72-19588
- Xe and Kr mass fractionation and isotopic anomalies in ordinary chondrites, analyzing meteorite samples by mass spectrometry 07 p1084 A72-20497
- Mars internal structure models with chondrite as potential core-forming material, discussing absence of internal origin magnetic field 07 p1084 A72-20518
- Chondrite normalized rare earth abundances in lunar solidand liquid-type materials from Mare Tranquillitatis and Oceanus Procellarum associated with evolution 08 p1233 A72-21218
- Microprobe analysis of Timmersoi hypersthene chondrite from Niger Republic, noting equilibrium between olivine and orthopyroxene at 850 C 13 p2035 A72-28751
- Model for textural features and mineralogical composition of Ca and Al-rich inclusions in C3 chondrites during condensation in primitive solar nebula 14 p2157 A72-30585
- Chondrite Pawel microspectral analysis with laser beam vaporization of sample from microzone 16 p2450 A72-32850
- Enstatite chondrite Abee isotopic ratios of Gd, Sm and Eu comparison with terrestrial samples 16 p2457 A72-33566
- Platinum and gold in chondritic meteorites. 17 p2610 A72-35149
- Mineralogy, bulk chemistry and sample shape and mass of Seoni /India/ chondrite, observing extensive recrystallization 19 p2858 A72-37860
- Mineralogical and chemical researches on L-chondrites - Gргenti. 19 p2858 A72-37862
- Metal/silicate fractionation in the solar system. 20 p2967 A72-39177
- Ordinary chondrite chemical and mineralogical properties establishment during solar system formation, noting fractionation events 20 p2969 A72-39334
- Iron transport in chondrites - Evidence from the Warrenton meteorite. 21 p3104 A72-40491
- Chondrite and achondrite Nb abundance from spark source mass spectroscopic analysis 21 p3104 A72-40492
- Solar wind noble gases and solar flare emitted Fe group nuclei energetic tracks in chondrite Weston, considering galactic cosmic ray generated tracks 22 p3228 A72-42863
- Chondrite Al-Ir abundance association for L compositional class consistent with Larimer condensation mechanism 23 p3335 A72-43266
- Spectrographic, photometric and chemical identification of Giacobinid /Draconid/ meteoroids, noting compositional similarity to carbonaceous and olivine-bronzite chondrites 23 p3336 A72-43600
- Irradiation history of grain aggregates in ordinary chondrites - Possible clues to the advanced stages of accretion. 24 p3444 A72-45455
- Conditions in the early solar system, as inferred from meteorites. 24 p3445 A72-45458

CHONDRULE

- Chondrules occurrence in iron meteorite, investigating bulk chemical composition and mineral properties
01 p0127 A72-10294
- Apollo 14 lunar breccia samples, observing chondrules from meteoritic impact event
05 p0715 A72-16161
- Oxygen isotopic abundances and equilibrium temperatures of meteoritic minerals, chondrules, meteorites and planets
07 p0985 A72-19589
- Igneous and microbreccia lithic fragments, glasses and chondrules from Luna 16 fines, confirming lunar surface melting and igneous differentiation
09 p1379 A72-22253
- Chondrule like spherules from supercooled molten oxide and silicate droplets by carbon dioxide laser heating compared with meteoritic chondrules
15 p2303 A72-31306
- Iron transport in chondrites - Evidence from the Warrenton meteorite.
21 p3104 A72-40491
- Evidence for vapor fractionation in the origin of chondrules.
23 p3339 A72-44134
- Lunar ultramafic glasses, chondrules and rocks.
23 p3340 A72-44340

CHOPPERS (ELECTRIC)

U ELECTRIC CHOPPERS

CHORDS (GEOMETRY)

- Earth chord length determinations, using synchronous photographic satellite observations with simultaneous topocentric distance data from laser measurement
14 p2103 A72-31076

CHOROID MEMBRANES

- Intravascular injection and histology studies of human embryonic and fetal choroidal vasculature development
19 p2755 A72-37398

CHORUS (DAWN PHENOMENON)

U DAWN CHORUS

CHORUS PHENOMENON

U DAWN CHORUS

CHROMATES

NT POTASSIUM CHROMATES

- Amorphous chromate and phosphate conversion coatings of Al, providing inert surface for painting
09 p1317 A72-22480
- Thick phase holograms in dichromated gelatin, discussing physical properties requirements and reliable processing procedures
15 p2239 A72-32355

CHROMATOGRAPHY

- Aluminum oxide chromatography for ethanol-amine acetyl derivatives detection and separation in animal tissue extracts, using water-butanol solution as solvent
14 p2077 A72-30972

CHROME

U CHROMIUM

CHROMIC ACID

- Sorption properties of anodic aluminum oxides prepared in orthophosphoric and chromic acid solutions, determining dependence on pH by isotopic labeling method
05 p0624 A72-17055

CHROMITES

- Mossbauer and X ray structural analysis of nickel ferrite-chromite magnetic moments, comparing with theoretical data
14 p2141 A72-30171

CHROMIUM

- Neutral Cr beam excited states radiative lifetime measurement by beam foil method
03 p0390 A72-13016
- Fe XI to XV emission lines from transitions and isoelectronic spectra in manganese, chromium and vanadium
03 p0391 A72-13750
- Sigma phase formation in chromous ferrite, investigating vacuum diffusion, hot and cold working, welding and additives effects
03 p0375 A72-13940
- Si p-n-p and Cr-n-p junction transit time diode oscillators microwave and dc characteristics comparison, noting similarity
04 p0499 A72-15206
- Wear, bending and corrosion resistance of stainless steels with Cr thermal vacuum diffused coating
04 p0535 A72-15661
- Quantum yield of ruby crystals luminescence for excitation in UV region, noting Cr concentration effect
10 p1490 A72-24043
- Powder metallurgy Ni-Cr thoria cleaning by reduction with atmosphere of hydrogen plus HCl or HBr
10 p1488 A72-24697
- Absorption spectrum of Cr cations in magnesium aluminate spinel crystals excited by strong optical pumping
12 p1854 A72-27596
- Rare earth metals addition effect on mechanical properties of electrolytic hydrogen-refined Cr, noting low temperature ductility
12 p1831 A72-28241

Metallic chromium band structure determination by Green functions method, explaining transition metals X ray emission lines by single electron approach
13 p1972 A72-28489

Temporal, energetic and spectral properties of stimulated emission from Cr doped ruby laser irradiated by Co 60 gamma rays
13 p1969 A72-29613

K beta emission spectrum of metallic Cr, discussing structural X ray analysis revealed cubic structure
14 p2116 A72-30414

Y and La action on oxidation rates of Cr and Mo at high temperature in air
15 p2252 A72-31191

Debye-Waller factors measurement for Mo and Cr surfaces near normal incidence based on LEED
15 p2292 A72-31857

Circularly polarized photon echo decay measurement as function of Cr concentration in ruby, noting relationships to temperature, pulse separation and external magnetic field
15 p2295 A72-32545

Properties of high-purity chromium

The grain-size-dependences of the failure mode and ductility transition temperatures of melted chromium and tungsten.
20 p2935 A72-39139

An investigation of a possible correlation between the laser output of a ruby rod and the chromous ion concentration.
20 p2934 A72-39643

Spin wave theory and sublattice magnetization of Cr obtaining wave velocity
21 p3097 A72-40626

Temporal, energy and spectral properties of Cr laser output, considering ruby absorption before/after Co 60 gamma irradiation and radiation density distribution during pumping flashes
21 p3063 A72-40666

Fabrication and accelerated life tests of self sustained electron emission cathode with Cr film vapor deposition on Cu disk base
21 p2997 A72-40790

Electron attachment and compound formation in flames. V - Negative ion formation in flames containing chromium and potassium.
22 p3244 A72-42717

High-temperature creep of polycrystalline chromium.
23 p3304 A72-44449

CHROMIUM ALLOYS

NT CHROMIUM STEELS

Ni-Cr-Al alloys high temperature oxidation, detailing surface reactions and continuous oxide layer formation
[ECS PAPER 114]
01 p0082 A72-10172

Dispersion strengthened Ni-Cr alloys processing technique and mill products development, noting increased strength at elevated temperatures
01 p0075 A72-10744

Thoriated Ni-Cr alloys oxidation kinetics at high temperatures, discussing oxide formations as function of Cr content
01 p0089 A72-11164

Ti-Cr alloys omega phase formation by measurements of hardness, Young modulus and internal friction
02 p0246 A72-12672

Pressure induced d band deformation effect on magnetic susceptibility of Ti-V and V-Cr alloys
03 p0370 A72-13087

Structural features of heat resistant Ni-Cr alloy from electron diffraction microscopy, observing coherent lattice bond and plastic deformation
03 p0376 A72-14015

Low temperature heat capacity of chromium silicide, observing superconducting transition and magnetic susceptibility
03 p0377 A72-14024

Grain size and precipitate parameters effect on creep properties of Ni-Cr alloys
03 p0379 A72-14339

Quenched and tempered Ni-Cr-Nb-Co alloy, describing cellular precipitation mechanism
04 p0533 A72-14977

Fe-Cr-Al and Fe-Cr-Si type ferritic steels, investigating additives effects on ductile-brittle transition temperature
05 p0672 A72-16012

Quaternary Mo-Zr-Cr-C system, investigating fcc phase liquidation from phase diagram by chemical, metallographic and X ray analyses
05 p0666 A72-16099

Zr and Zr-Cr alloys corrosion behavior in steam, noting parabolic rate law breakaway point to linear rate
05 p0676 A72-16797

Binary and ternary alloys of Cr and Fe with Ni, determining interaction coefficient and molar enthalpy for Cr at 1600 C by mass spectrometry
05 p0676 A72-17103

Tensile ductile-brittle transition temperature and slip mechanism of thoriated Cr, comparing with unalloyed Cr
05 p0678 A72-17117

Critical cleavage stresses dependence on ordering degree in Ni-Cr alloy
06 p0835 A72-18745

Formation kinetics, phase composition and structure of oxide films in binary and ternary iron-base chromium aluminum alloys, studying hydrogen penetration characteristics
07 p1013 A72-19771

Microstructure and high temperature mechanical properties of unidirectionally solidified pseudobinary Fe-Cr-Nb eutectic alloy
07 p1016 A72-19938

Jerky flow /serrated yielding/ in Co-Ni-Cr-C fcc alloys during tensile testing, noting no correlation to dislocation-precipitate interactions
07 p1016 A72-19940

Rare earth metals effects on chromium brittle transition temperature, showing maximum plasticity with lanthanum addition
07 p1019 A72-20151

Equilibrium diagram of Cr-Va alloy produced by arc melting under Ar atmosphere, using high temperature differential thermal analysis
07 p1019 A72-20160

Fe addition effects on structural and mechanical properties of heat resistant Ni-Cr alloys
07 p1020 A72-20416

Stainless steel saturation with Al and Cr, investigating structure, microhardness, linear expansion and contact surface seizure reduction
07 p1020 A72-20419

Diffusion creep influence on grain boundary-adjacent precipitate free zone formation in Ni-Cr alloys subjected to high temperature tensile and creep tests
07 p1021 A72-20437

Internal oxidation behavior of Cu-Cr-Si ternary alloys microstructure comparison with Ni-Cr binary alloys, discussing oxide-matrix interface nucleation
07 p1021 A72-20439

Cr-Ti-V-B alloys rod specimens grain size and brittleness-viscosity transition temperature after heat treatment, cooling and bending tests
07 p1023 A72-20668

Bcc solid solutions formation in Cr-W binary alloys, investigating interface reaction and two phase grain boundary diffusion by X ray diffraction and microscopy
08 p1185 A72-21246

Cr-Tb alloys monotectic, eutectic and eutectoidal phase transformations study with differential thermal, metallographic, X ray structural and durometric analysis
08 p1187 A72-21781

Plastic deformation characteristics of Fe-Cr-Ni alloy single crystals at low temperatures
08 p1188 A72-21790

Samaria distribution effect on Ni-Cr alloy oxidation rate for various oxygen pressures, discussing behavior of electroplated and bulk specimens
09 p1332 A72-23585

Manufacturing process for dispersion strengthened nickel-chromium-thorium dioxide alloys for space shuttle thermal protection system panels, discussing joining optimization and mechanical properties
11 p1659 A72-26035

Temperature and strain rate effects on superplasticity of Ni-Cr eutectic alloy
11 p1659 A72-26129

Dispersion strengthened nickel-chromium-thoria alloy production methods, noting halogen gas phase diffusion process
11 p1645 A72-26850

Low cycle fatigue deformation of lamellar eutectic and cast Ni-Sr alloys, noting microstructure and chemical composition effects on fracture energy
11 p1668 A72-26939

Relative valence effect of transition metal additions on alpha-gamma phase equilibrium in Fe-Cr-Mn system
12 p1827 A72-27099

Hydrostatic pressure effect on itinerant antiferromagnetic ordering in Cr-Fe alloys with Ru and Mn additions
12 p1828 A72-27432

Nitride phase microstructure in ferrocromium nitrided in liquid state, comparing electrolytic etching and film coloration methods
12 p1829 A72-27454

Quenched powder metallurgy of high strength-high conductivity wrought Cu-Zr and Cu-Zr-Cr alloys, using nitrogen atomization
13 p1974 A72-28659

Phase structure of Cr rich Cr-Ni, Cr-Fe, Cr-Co and Cr-Ni-Fe alloy particles produced by evaporation in Ar using X ray diffraction
13 p1974 A72-28660

Two phase structure solidification of monovariant eutectic Co-Cr-C alloys near pseudobinary cut
13 p1976 A72-28674

- Phase diagram of cast and annealed Cr-Sc alloys by differential thermal, X ray, metallographic and microhardness analyses 13 p1981 A72-29953
- Metal particle decomposition products composition in slags from smelted Cr, Ti, Ni and Zr alloys, using X ray microanalysis 14 p2112 A72-30157
- Activation energy of high temperature creep in Cr alloy with aluminum oxide, comparing with moving monovacancies in pure Cr 14 p2112 A72-30161
- Optimal mechanical properties of Ti alloys with Cr, Mo, V, Nb and Ta additions, considering tensile strength, impact toughness, elongation and flattening 14 p2113 A72-30164
- Sn alloying effect on heat resistant Ni-Cr alloys plastic strain resistance and strength at room and high temperatures 14 p2114 A72-30274
- Nickel ion charge sign and magnitude estimation in Ni-Cr alloy by electron transfer method 14 p2116 A72-30415
- Co-Cr alloy high temperature oxidation kinetics reduction by Y addition, presenting metallographic study 14 p2118 A72-30543
- Co-Cr alloy oxidation as function of temperature and oxygen partial pressure, discussing solid state diffusion 14 p2118 A72-30544
- Ni additions effect on Fe-Cr alloys oxidation behavior at high temperatures during varied exposure time periods, noting dichromium trioxide scale formation 14 p2118 A72-30545
- Cr-containing Fe-alloy and Ni steels, investigating thermal cycling effects on thermal resistance by factorial program 14 p2118 A72-30546
- Accelerated intergranular corrosion and grain boundary precipitation mechanisms in stainless steel Fe-Ni-Cr alloy, using Huey, acid and Strauss tests 14 p2118 A72-30548
- Cr-N alloy phase diagram from thermal and X ray analysis, metallographic observation and hardness tests, noting melts crystallization 14 p2123 A72-30987
- High temperature oxidation resistance and mechanical properties of Fe-Al-Cr alloys with Ti and Mo additions 15 p2253 A72-31520
- Hyperfine magnetic field reduction produced in Fe-Cr alloy single crystal by Cr atoms observed by Mossbauer method, proposing spin disturbance mechanism 15 p2293 A72-32230
- Forming techniques and heat treatment effects on recrystallization characteristics of heat resistant Cr alloy, noting high temperature influence on crystal structure 16 p2407 A72-33531
- Mo and W simultaneous addition effects on Fe-Ni-Nb alloy properties, noting heat resistance increase and Nb solid solubility decrease 16 p2408 A72-33534
- Internal nitridation zones and growth kinetics for Cr and Cr-Ti alloys at 10000-1400 C, using Maak analysis 16 p2409 A72-33807
- High temperature oxide scale adherence on Fe-Cr-Al alloys with Y or Sc additions as promoting agents 16 p2410 A72-33817
- Susceptibility of the NiCr 15 Fe chromium-nickel alloy /Remanit 1675 SEW and Thermax 1675/ to intercrystalline corrosion 17 p2566 A72-34396
- Charge carriers interaction with metal ions studied from electrical transport of Fe and Co in Fe-Cr alloy 17 p2569 A72-35521
- Phase stability and mechanical properties of carbide and boride strengthened chromium-base alloys 18 p2700 A72-36579
- Grain-boundary relaxations in an Fe-Ni-Cr alloy 18 p2700 A72-36588
- Chromium-based powdered alloys used in highly alloyed steel welding 19 p2809 A72-38289
- Phase diagram of the chromium-holmium system 19 p2821 A72-38474
- X-ray analysis of iron-chrome solid solutions 19 p2821 A72-38572
- Phase composition and isothermal cross section diagrams of Cr-Ni-B system at 800 C, using X ray and microstructural analyses 19 p2822 A72-38678
- A review of the science, technology, and applications of dispersion strengthened Ni-Cr- and Co-Cr-base alloys. 20 p2936 A72-39209
- The mechanism of oxidation of Ni-Cr-Al alloys. 20 p2937 A72-39214
- The internal oxidation of Ni-Cr-Al alloys. 20 p2937 A72-39215
- Exploratory investigation of Y, La, and Hf coatings for nitridation protection of chromium alloys. 20 p2944 A72-39290
- Chromizing of steel sheet by diffusion 20 p2929 A72-39581
- Phase diagram study of Cr-Ga alloys, investigating intermetallic compounds presence and polymorphic transformation and temperature effects 20 p2942 A72-39987
- Absolute thermoelectric power of chromium-ruthenium alloys. 20 p2942 A72-39988
- Effects of scale porosity, second-phase oxides, and doping in the high-temperature oxidation of cobalt and dilute cobalt-chromium alloys. 21 p3067 A72-40845
- Calorimetric investigation of atom ordering effects in a Ni2Cr alloy 21 p3068 A72-40958
- Crystallization and structure of hypereutectic iron-carbon-chromium alloys 21 p3071 A72-41788
- Study of the properties of porous materials of nickel-molybdenum and nickel-chromium-molybdenum alloys 22 p3188 A72-42193
- Physical properties and electronic structure of V1-x Crx/3Si ternary alloys 22 p3192 A72-43014
- Grain size and temperature effects on Cr and Al diffusion coefficients and mobility in Ni-20Cr and thoriated dispersed NiCr alloys from measurement at 1038-1200 C 22 p3193 A72-43028
- Mechanical properties of heat and corrosion resistant nonmagnetic Ni-Cr-Nb spring alloys with W addition tested in aggressive and nitric acid base media 23 p3300 A72-43595
- Metalceramic alloy of the B2Zr type 23 p3302 A72-44010
- Phase transformations in chromium-titanium compounds. 24 p3413 A72-44922
- Three-phase equilibria of cast and annealed V-Zr-Cr alloy by X ray, metallographic and melting point analyses 24 p3414 A72-45384
- Growth kinetics of dispersed thorium in Ni and Ni-Cr alloys. 24 p3415 A72-45480
- CHROMIUM BORIDES**
- X ray diffraction discovery of borides with yttrium chromium boride type orthorhombic structure 13 p1984 A72-29799
- CHROMIUM CARBIDES**
- Powdered chromium carbide-nickel alloys phosphorus addition effects on sintering temperature, shrinkage, density and hardness 03 p0372 A72-13546
- Porous materials fabrication from chromium carbide powders, considering compaction procedures involving sinusoidal and pulsating vibrations 07 p1017 A72-19968
- Chromium carbides synthesis by carburizing chromium hydroxide or oxalate in hydrogen-methane gas mixture at temperatures below 1000 C 22 p3188 A72-41974
- High-temperature thermodynamic properties of the chromium carbides determined using the torsion-effusion technique. 22 p3193 A72-43029
- CHROMIUM COMPOUNDS**
- NT CHROMATES
- NT CHROMIC ACID
- NT CHROMITES
- NT CHROMIUM BORIDES
- NT CHROMIUM CARBIDES
- NT CHROMIUM OXIDES
- NT POTASSIUM CHROMATES
- Some data on interatomic interaction in solid high-melting compounds of titanium, vanadium, and chromium with light metals 17 p2569 A72-35520
- Isobar-isothermal potentials, entropy and formation heat of chromium silicides from thermoelectromotive force measurements of high temperature galvanic elements 23 p3298 A72-43286
- CHROMIUM OXIDES**
- NT CHROMITES
- Hot corrosion of thorium dispersed nickel and thorium dispersed Ni-Cr alloy in high velocity gas stream of jet fuel combustion products 07 p1010 A72-18753
- Ni additions effect on Fe-Cr alloys oxidation behavior at high temperatures during varied exposure time periods, noting dichromium trioxide scale formation 14 p2118 A72-30545
- Production and properties of materials of the Si3N4-Cr2O3 system 23 p3298 A72-43283
- Surface tension, density, and volume change on melting of Al2O3 systems, Cr2O3, and Sm2O3. 24 p3417 A72-44925
- CHROMIUM STEELS**
- High chromium ferritic stainless steels weldability and mechanical properties, showing C, N, Ti and residuals effects on recrystallization, toughness, tensile behavior and corrosion resistance 01 p0083 A72-10283
- Stress corrosion cracking of Cr-Ni austenitic stainless steel with Mo and Cu additions in boiling sulfuric medium 01 p0089 A72-11181
- Aluminum oxide dispersion hardened ferritic heat resisting Cr steel, describing liquid phase sintering effects on high temperature tensile strength 02 p0241 A72-11448
- Temperature-time dependent torsional strength and fracture failure of Cr-Ni steel microalloyed with La and Ce as function of grain boundaries 02 p0243 A72-12010
- Temperature dependence of low temperature endurance of Cr-Ni steels in bending fatigue tests 03 p0371 A72-13463
- High alloy chromium and manganese steels brittle fracture susceptibility, showing notch effects 03 p0371 A72-13466
- Stepwise thermomechanical treatment effect on improved cyclic fatigue strength of Ni-Cr sheet steel with tension and rolling deformations 03 p0372 A72-13598
- Hydrogen charging of iron-chrome-nickel austenitic stainless alloys, investigating crack initiation in Inconel 600 03 p0373 A72-13600
- Titanium sulfide initiation of pitting corrosion of Ti stabilized corrosion resistant Cr-Ni-Ti steels 03 p0379 A72-14367
- Potential change under pitting corrosion and repassivation on Cr-Ni steels alloyed with V, Si, Mo and Re 04 p0535 A72-15730
- Martensite and solid Cr-containing inclusion effects on wear resistance of cermet steel during dry friction with R18 steel 05 p0665 A72-16095
- High temperature low cycle fatigue of Cr-Mo-V steel, observing crack growth rate correlation with crack tip stress 05 p0673 A72-16321
- Cr and U contents effect on high strength Cr-Mo-Va alloy steel sheet hot cracking susceptibility, using Huxley test method 06 p0820 A72-17704
- Hardened and tempered Ni-Cr-Mo steel, testing rest periods caused fatigue life increase in terms of cycles to failure 06 p0895 A72-17802
- Hardenability and pearlite stage isothermal transformation properties of direct-quenching low Cr case-hardening steels, discussing Mn, Mo and Ni alloying effects on machinability 07 p0995 A72-19571
- High Cr ferritic steels intergranular and stress corrosion properties and resistance to sea water, organic and inorganic acids and acid mixtures 07 p0995 A72-19572
- Spot and seam welding of Cr ferritic stainless steel thin sheets, discussing electric current loading in relation to sheet thickness and contact pressure 07 p0995 A72-19575
- Boron addition effects on scaling resistance of Ni-Cr steel at high temperatures 07 p1012 A72-19738
- Long-time isothermal temper embrittlement in Ni-Cr-Mo-V steels, noting tensile ductility decrease and intergranular fracture 07 p1015 A72-19932
- X ray analysis of cementite and titanium carbide precipitates in Cr-Mn-Mo-Ti steels weld zones 07 p1019 A72-20159
- Internal friction measurements of tempered martensitic Cr steel quenched from 1100 C, connecting friction peaks with precipitation phenomena 07 p1021 A72-20486
- Carbon determination in Cr-Ni steels and Ni alloys by layerwise spectral analysis, using electrode gap with He 07 p0993 A72-20609
- Explosive loading effect on Cr-Ni stainless steel structure with electron microscope study of gamma, alpha and epsilon phases 08 p1187 A72-21780
- Ar-H microplasma welding of thin Cr steel sheets with narrow seams for aircraft engines and precision equipment casings 09 p1318 A72-22548
- Electron microscopic, area diffraction and spectral analyses of carbide precipitates in Cr-Mo steels with different heat treatments and microstructures 10 p1494 A72-23828
- Transitional ferrite phase formation in Fe-Cr-Ni alloy evidenced on electron micrographs and diffraction patterns 11 p1657 A72-25760
- Wear micromechanism in hard and brittle chromium steels under cyclic slide friction loads 12 p1818 A72-28194
- Impact fracture resistance of Cr-Mn-Si steel, investigating alloying effects on crack initiation and propagation 12 p1831 A72-28238

Tempered or recrystallized chromium steels tensile behavior at 0 to 700 C, showing strength dependence on martensite transformation induced dislocation structure

13 p1975 A72-28667

Precipitated carbide role in Cr-Ni stainless steels high temperature properties and creep rupture strength

13 p1979 A72-29447

Chromium stainless steel fatigue life reduction due to embrittlement in gaseous hydrogen atmosphere at room temperature, noting alleviating effect of atmosphere contaminants

13 p1979 A72-29484

Ni-Cr-Mo stainless maraging steel, investigating yield strength, toughness, corrosion resistance and weldability

14 p2113 A72-30270

Ni, Si and Mn alloying effect on structural transformations, phase composition and mechanical properties of cast Cr-Ni steels

14 p2114 A72-30273

Low carbon and nitrogen concentrations in chromium ferritic stainless steel obtained with gas rinsing at reduced pressure, noting weldability and corrosion resistance

14 p2119 A72-30606

Incoloy low cycle fatigue tests at high temperatures and different strain rates, discussing fatigue life at 10 and 60 min hold times

16 p2410 A72-33820

Graph-analytic technique to plot Cr steel stress relaxation curve from primary and isochronous creep diagrams

16 p2472 A72-33848

Creep tests on Cr martensite stainless steel, showing inapplicability of Garofalo equation for stress dependence of secondary creep rate during variable stress experiment

16 p2412 A72-34112

Low-temperature properties of nitrogen-alloyed austenitic chromium-nickel/molybdenum/steels and chromium-manganese-nickel steels and their applicability as low-temperature ductile steels

17 p2566 A72-34395

Contribution to the study of the stabilization of corrosion-resistant chromium-nickel austenitic steels

18 p2702 A72-37014

A comparison between the tensile and compressive creep behaviour of an 11 per cent chromium steel

19 p2814 A72-37222

Temperature effects on the strainrange partitioning approach for creep-fatigue analysis

19 p2815 A72-37638

German monograph - Effect of molybdenum and degree of age hardening on the corrosion properties of maraging chromium steels

19 p2816 A72-37654

Creep tests on 2-1/4 per cent chromium 1 per cent molybdenum steel in bainitic condition

19 p2817 A72-37713

A new morphological element on the viscous breakdown microsurface of hypoeutectoid steels

19 p2817 A72-37737

Chromium-based powdered alloys used in highly alloyed steel welding

19 p2809 A72-38289

Stress corrosion cracking of 18% Cr ferritic stainless steels

19 p2820 A72-38300

Effect of twins produced by annealing on high-temperature failure of chromium-nickel-molybdenum steel

20 p2939 A72-39316

Mechanical and microstructural properties of steels for effective surface cementation, suggesting Mo and Cr optimal contents

20 p2941 A72-39576

Carbide hardening of chromium-molybdenum-vanadium steel

20 p2941 A72-39578

Tempered hardness and tensile strength of austempering Mn-Cr-B spring steels at low temperatures in austenite stable phase by electron microscopy

21 p3066 A72-40718

Fracture toughness of the heat-affected zone in 14CrMoV69 steel and 18Ni maraging steel

21 p3067 A72-40850

The properties and structures of a heat resistant 1Cr-Mo-V steel and alloy A-286 after long time exposures at elev. temps.

21 p3069 A72-41012

The effect of alloying elements on creep rupture strength and microstructure of 12 percent chromium heat resisting steel

21 p3069 A72-41014

Free energy changes and boundary segregation of tin and antimony in CrV steels

21 p3070 A72-41648

German monograph - The causes of hot crack formation in welded joints of austenitic steel with 16 percent chromium and 16 percent nickel

22 p3195 A72-43079

Strain hardening effect of Ni, Mn and Mo in Cr steel after high temperature annealing

23 p3301 A72-43742

Investigation of the thermal fatigue of Kh18N10T steel under complex stress-strain state conditions

23 p3301 A72-43956

Influence of the chemical composition of Kh25N16G7AR steel on its heat resistance

23 p3303 A72-44098

Corrosion and electrochemical properties of Kh15N5D2T and Kh15N4AM3 oxidized steels

23 p3303 A72-44099

Estimation of creep and fatigue behaviour under cyclic loading

24 p3456 A72-44793

Temperature dependence of low temperature endurance of Cr-Ni steels in bending fatigue tests

24 p3413 A72-44938

High alloy chromium and manganese steels brittle fracture susceptibility, showing notch effects

24 p3414 A72-44941

Changes in the grain-boundary free energy and the segregation of tin and antimony at grain boundaries in CrV steels

24 p3415 A72-45394

Measurement of stacking fault energy in CrMnNi austenitic steel by the method of extended nodes

24 p3415 A72-45397

CHROMOSOMES

Inhaled ozone effect on chromosome aberrations break frequencies in circulating blood lymphocytes of irradiated Chinese hamsters

01 p0015 A72-11149

Chromosome aberrations and germination speedup in Soyuz 5 carried oat seeds, noting stimulating effect by preflight ethylenimine treatment

05 p0623 A72-16777

Pulsed and continuous rf irradiation effects on mitotic activity and chromosomal aberrations in regenerating rat liver tissue

07 p0917 A72-19443

Influence of a magnetic field on radiation-induced chromosome aberrations in plants

17 p2503 A72-35007

Chromosome aberrations and germination speedup in Soyuz 5 carried barley seeds, noting stimulating effect by preflight ethylenimine treatment

17 p2505 A72-35280

CHROMOSPHERE

Feautrier numerical solutions to transfer equation of polarized continuum radiation from sunspot in chromosphere

01 p0101 A72-10096

H alpha spectra and combined filtergram observations of chromospheric fine structure, using Becker model

03 p0414 A72-12929

Solar chromosphere fine structure at limb, measuring spicules and bright mottles lifetime

03 p0415 A72-12930

L alpha limb flux during total solar eclipse of 12 November 1966 from rocket measurements, comparing with chromosphere model

[AD-739763]

03 p0415 A72-12931

Topological features of force free magnetic field near bipolar sunspots, considering chromospheric fibrils and filaments in H alpha lines

03 p0415 A72-12932

Solar UV and X radiation, considering chromospheric temperature and density profiles and coronal electron densities

03 p0409 A72-13123

Extreme UV observations of solar chromosphere-corona transition region, evaluating various theoretical and empirical models

03 p0422 A72-13205

Flare associated waves suggested by optically observed phenomena, using time lapse photography of solar chromosphere

03 p0423 A72-13212

Areas index relationship to different phenomena in chromosphere, corona and interplanetary space, investigating coronal radio diameter during solar cycle and cosmic rays

03 p0423 A72-13214

Solar far UV spectrum observations for chromospheric coronal structure determination, reviewing ionization balance, relative abundances and limb/disk ratios

03 p0423 A72-13216

Solar chromosphere-corona transition region models based on UV resonance emission lines intensity, deriving temperature gradient from radio data

03 p0424 A72-13222

Solar magnetic field structure determination in active regions from H alpha morphology obtained with chromospheric magnetograph, discussing emerging flux region role

03 p0428 A72-13304

Magnetograph scans of solar disk center supergranulation, showing downdrafts relation to magnetic field strength and chromosphere and photosphere brightness

03 p0429 A72-13307

Five-minute plasma oscillations in solar photospheric and low chromospheric magnetic fields, discussing evidence, properties and production mechanism

[AD-743346]

03 p0430 A72-13319

Small scale magnetic field theories, concerning solar prominence structure, chromospheric and coronal heating and particle production in flares

03 p0430 A72-13333

Solar active region properties at millimeter wavelengths, suggesting chromospheric magnetic field measurement possibility from polarization

03 p0432 A72-13348

OSO-G satellite spectroheliograms of chromospheric, transition zone and coronal lines, indicating magnetic field spread with height

03 p0432 A72-13351

Solar chromospheric flare spectrophotometric data on 8 July 1966, presenting line spectra, ground state and populations in excited energy levels

03 p0413 A72-14242

Solar flares, presenting line width changes curves, chromospheric observation by spectrohelioscope and solar flux measurements

04 p0567 A72-14923

Solar radiation effects on earth atmosphere with MR-12 and M-100 meteorological rockets launched at onset of chromospheric flare, noting atmospheric parameters measurements

04 p0580 A72-15453

Horizontally averaged nonthermal velocities determination in lower solar chromosphere, observing Doppler widths of weak rare earth emission lines in H and K wings

05 p0718 A72-16504

Intensity variations of CN photospheric and K line chromospheric network with time

05 p0718 A72-16505

Fine H alpha fibrils in middle chromosphere, discussing optical thickness and absorption features

05 p0718 A72-16506

H alpha fine structure, investigating chromospheric magnetic field distribution

05 p0718 A72-16507

Solar chromospheric fine structure at active region, magnetic polarity boundaries from high resolution H-alpha filtergrams

05 p0718 A72-16508

UV spectrophotometry of late-type giant star /Arcurus/ from Aerobee rocket, identifying Mg II doublet resonance line for stellar chromosphere

06 p0881 A72-17893

Interplanetary shock wave inclination to ecliptic plane dependence on chromospheric flare and earth projection heliolatitude differences

06 p0884 A72-18027

Fine structure elements of chromosphere, discussing spicules, fibrils and thermal effects

07 p1077 A72-19808

Initial/premaximal/ phase model of chromospheric flare in terms of explosion theory, determining temperature, shock front and plasma velocities

07 p1077 A72-19809

Mg ion excitation by electron collision in solar chromosphere studies, calculating scattering cross sections

07 p1081 A72-20234

Solar corona structure during 22 September 1968 total eclipse noting N-S asymmetry and correspondence of large details to formations in photosphere and chromosphere

08 p1228 A72-20825

Transverse magnetic field measurement over sunspot in chromosphere, noting fan-shaped field line divergence

08 p1232 A72-21135

Non-LTE effects on mechanical heating in gray atmosphere applied to nonradiative energy input estimates for solar chromosphere from negative hydrogen ion emission

08 p1235 A72-21391

Coronal nonthermal radio emissions occurrence in absence of visible flares due to chromospheric perturbation

10 p1529 A72-24525

Sound waves radiative damping in isothermal atmosphere, discussing relaxation influence on model response to body force and chromosphere dissipation effect on oscillation

10 p1543 A72-24622

Solar chromosphere double limb effect attributed to instrument, discussing application to height measurement

11 p1717 A72-25905

Solar chromosphere-corona transition region theoretical and empirical models, studying acoustic flux generated above convective zone

11 p1717 A72-25906

Interplanetary shock wave inclination to ecliptic plane dependence on chromospheric flare and earth projection heliolatitude differences

11 p1719 A72-25963

Active chromosphere coupling to magnetic field determined by subphotospheric motions, discussing active regions rotation period

11 p1720 A72-26117

Spectral line variations in transition region from photosphere to chromosphere during March 1970 solar eclipse

13 p2041 A72-29530

Model solar atmosphere from mm and cm wavelength high resolution observations of chromosphere by lunar limb antenna tracking during 7 March 1970 eclipse

13 p2042 A72-29532

Spectrographic observation of flash spectrum during 7 March 1970 solar eclipse, showing significant coronal line emission origin in chromosphere inter-spicular regions

13 p2042 A72-29534

Aerobee rocket far UV flash spectrum observations of chromosphere and corona during 7 March 1970 solar eclipse

13 p2042 A72-29539

Lower solar chromosphere two dimensional models, noting effects of macroscopic velocity fields

13 p2045 A72-29709

Short lived chromospheric absorbing features in H alpha wings, noting development into active center

13 p2046 A72-29717

Flare related impulsive EUV solar emission lines enhancement in chromosphere-corona transition region

13 p2032 A72-29720

Time evolution of chromosphere layer heated by energetic particle stream during solar flare, noting cooling by Lyman continuum radiation transfer

13 p2032 A72-29721

Solar magnetic field fine structure from chromospheric morphology, using high resolution H alpha filtergram and magnetogram

13 p2046 A72-29731

Comparative spectroheliograms of He 10830 A and H alpha lines in chromosphere

13 p2047 A72-29733

Solar chromosphere model based on Lyman spectra observations, calculating temperature, gas and electron pressure and particle densities as function of height

13 p2049 A72-29932

Equatorial quiet solar atmosphere model for chromosphere-corona transition region based on cm radio observation and hydrodynamical conservation equations

13 p2049 A72-29933

Energy storage in chromospheric magnetic flux ropes in solar flares, discussing kink perturbation instability suppression

13 p2049 A72-29936

Radio bursts and X ray emissions associated with 15-16 November 1970 solar chromosphere flares, noting brightness maximum differences

14 p2146 A72-30483

Geomagnetic storms caused by quasi-stationary directed corpuscular streams resulting from solar chromosphere flares

14 p2147 A72-30487

Solar photosphere and low chromosphere spectral lines non-LTE empirical analysis, relating coefficients of departure from LTE to elemental state temperatures

15 p2317 A72-32771

Sunspot area east-west asymmetry dependence on location in chromospheric facula or plage, considering solar atmosphere optical and geometric depth changes

15 p2318 A72-32787

K2 III star Arcturus far UV chromospheric emission line spectrum observation with rocket-borne spectrometer, identifying hydrogen L alpha and O I

16 p2453 A72-33136

Solar chromosphere bright mottles and spicules lifetime relationship from H alpha photograph isophotometry of limb

16 p2456 A72-33509

Solar chromosphere-corona transition region structure and energy balance calculation by static planar model compared with XUV resonance line observations

17 p2608 A72-35083

Soft X-ray and microwave observations of hot regions in solar flares.

17 p2608 A72-35089

Plasma turbulence in solar atmosphere upper layers related to chromospheric flares and radio bursts

17 p2612 A72-35349

Metallic abundances in the solar chromosphere.

17 p2613 A72-35498

Chromospheric structure, magnetic field configuration, radiative transfer and energy balance relationship to solar prominences formation from corona

17 p2616 A72-35693

Some new Dy II identifications in the solar spectrum.

17 p2616 A72-35696

The chromosphere in continuum emission observed at the total solar eclipse on 7 March 1970.

17 p2616 A72-35698

Solar mottles characteristics as seen on large scale H alpha filtergrams

17 p2616 A72-35700

Photographic magnetograms comparison with H alpha filtergrams, investigating chromospheric features relationship to photospheric magnetic fields

17 p2616 A72-35702

EUV observations of solar quiet region with OSO 6 spectroheliometer, noting chromospheric network structure

17 p2616 A72-35703

Spectral analysis of highly inhomogeneous chromospheric flares.

17 p2617 A72-35709

Fine structure elements of chromosphere, discussing spicules, fibrils and thermal effects

17 p2617 A72-35733

Initial /premaximal/ phase model of chromospheric flare in terms of explosion theory, determining temperature, shock front and plasma velocities

17 p2602 A72-35734

Solar flares and radio bursts significance for chromosphere and corona studies, considering radiation frequency-source location relations

17 p2603 A72-35957

Geomagnetic storms correlation with chromospheric flare series and with central meridian passages of recurrent positive phases

18 p2723 A72-36087

Solar chromospheric flare details motion differences from spectrum analysis and H alpha line frame photography, noting radial velocities difference

19 p2851 A72-37816

Relation between chromosphere flare motion and ejections and the magnetic field

19 p2851 A72-37817

Radial velocities and brightness distribution in active and quiet solar atmosphere from magnetograph measurements, discussing motion directions in photosphere and chromosphere

19 p2858 A72-37818

Spectral line contours in the solar chromosphere, hydrogen line. IV - Contours in the chromosphere on the disk

19 p2859 A72-37905

Spectral line profiles of the solar chromosphere. III - Relationship between the line profiles and their intensity gradients

19 p2860 A72-37950

Geomagnetic storms caused by quasi-stationary directional corpuscular streams resulting from solar chromosphere flares

19 p2851 A72-38316

New observations of solar magnetic and brightness fields.

20 p2971 A72-39763

Characteristics of the Ca II K-line profiles in the quiet sun.

21 p3108 A72-41280

He II line emission in cold regions of solar prominences and chromosphere, noting hydrogen, metal and He I emissions

21 p3108 A72-41281

The chromospheric continuum observed at the total solar eclipse of 12 November 1966 and a model of the low chromosphere.

21 p3109 A72-41328

Intensity ratios of He I and H lines in a prominence and the chromosphere.

21 p3109 A72-41329

Study of the chromosphere in the D3He line during the eclipse of September 22, 1968

21 p3114 A72-41764

Observation procedures in high resolution spectrophotometry of solar chromospheric spectral fine structures

22 p3221 A72-42031

High resolution spectroscopy of the disk chromosphere. II - Time sequence observations of Ca II H and K emissions.

22 p3221 A72-42032

Alpha force-free magnetic field representation for solution of boundary value problem for chromosphere and lower corona magnetic fields

22 p3222 A72-42037

Magnetic field change rate related to chromospheric activity in McMath Regions 8863, 10385 and 11415, discussing flare associated effects and total flux

22 p3217 A72-42039

Mathematical models from UV, IR and radio observations of chromosphere and transition region to corona, noting temperature effects of shock wave dissipation

22 p3229 A72-42903

Photometric elements of corpuscular unstable AH Vir eclipsing binary at 4400 and 5600 A, comparing stellar gas stream and solar chromosphere densities

23 p3338 A72-44028

The quiet sun brightness distributions at millimeter wavelengths and chromospheric inhomogeneities.

24 p3438 A72-44840

Physical conditions in the solar corona from spectral observations of the eclipse of March 7, 1970

24 p3448 A72-45684

CHROMOTOGRAPHY

NT THIN LAYER CHROMATOGRAPHY

CHRONAXY

DNA-RNA molecular hybridization testing of chronon theory of circadian timekeeping in protozoa cells

07 p0920 A72-19542

CHRONIC CONDITIONS

Hypertrophic effects of chronic exercise on plasma corticosterone and adrenal cortex in rat

04 p0473 A72-15219

Two stage description of middle germ layer chronic polyarthritis, noting heart muscle and vascular wall tissues necrosis

12 p1772 A72-27822

Electrode design and implantation method for chronic experiments, discussing information loss factor elimination

14 p2078 A72-30393

High altitude natives cerebral arterial-venous oxygen difference measurement during ambient air and oxygen breathing, showing chronic hypoxia effect on cerebral blood flow

14 p2079 A72-30704

Succinate and glutathione as protective agents against chronic effects of hyperbaric oxygen toxicity in rats

14 p2082 A72-31091

Myocardial ultrastructure in acute and chronic hypoxia.

17 p2502 A72-34988

Myocardial metabolic changes in chronic hypoxia.

17 p2502 A72-34989

Anoxic tolerance of the heart muscle in different types of chronic hypoxia.

17 p2502 A72-34991

Cardiac performance and the coronary circulation of man in chronic hypoxia.

17 p2502 A72-34992

The effect of chronic erythrocytic polycythemia and high altitude upon plasma and blood volumes.

19 p2757 A72-38028

Hemopoiesis in the pig-tailed monkey *Macaca nemestrina* during chronic altitude exposure.

20 p2892 A72-39344

Chronic altitude sickness pathology based on anatomical and histological findings in abnormal mountain inhabitants autopsies, comparing with cardiovascular system morphology in normal people

22 p3143 A72-42586

Heart function and pulmonary circulation in humans suffering from chronic mountain sickness

22 p3143 A72-42587

Cardiocirculatory adaptation to chronic hypoxia. II - Comparative study of myocardial metabolism of glucose, lactate, pyruvate and free fatty acids between sea level and high altitude residents.

22 p3148 A72-43022

Physiological and hematological effects of chronic irradiation.

23 p3254 A72-43392

Animal studies of effect of chronic exercise on the heart and atherosclerosis - A review.

24 p3370 A72-44563

Experimental studies on the alkali-acid equilibrium in the blood gases under the chronic action of low concentrations of lead.

24 p3374 A72-44824

CHRONOGRAPHS

U CHRONOMETERS

CHRONOLOGY

NT GEOCHRONOLOGY

Age determination of Raco meteorite /Argentina/ by K-Ar method, noting olivine and rhombic pyroxene composition

01 p0126 A72-10104

Nucleic acid, protein and cell primordial sequence, ribosomes and genetic code for life origin, discussing experiments on homopolyamine acids reaction with mononucleotides

04 p0468 A72-14775

Crystallization age of Apollo 15 anorthositic rock 15415,9

06 p0888 A72-18270

Chronology of universe - Conference, Padua, Italy, November 1970

07 p1083 A72-20463

Population I stars and open cluster age determination methods based on stellar evolution theory, discussing inherent uncertainties effects

07 p1083 A72-20467

Big bang theory for age determination of galaxies, considering formation through gravitational instability and primeval gas velocity distribution fluctuations

07 p1084 A72-20470

CHRONOMETERS

Geophysical and gravimetric measurement time recording techniques, describing satellite tracking photochronograph and electronic printing chronographs

04 p0525 A72-15571

Electronic chronometer design problems, describing quartz clock components and temperature and voltage variation effect on accuracy

04 p0525 A72-15572

Method and equipment for checking chronometers by one-second timing radio signals under field conditions

19 p2795 A72-37346

Nonlogarithmic calculation of chronometer corrections in azimuthal methods of determining time

/Struve's method, Struve-Pavlov method, Dellen's method, and other methods/

24 p3438 A72-44864

CHRONOPHOTOGRAPHY

Flare associated waves suggested by optically observed phenomena, using time lapse photography of solar chromosphere

03 p0423 A72-13212

A time-interval amplitude analyzer for turbulent flow processes and its application for the control of a chronophotographic measurement installation

22 p3177 A72-42393

CHRONOTRONS

U PULSE RATE

U TIME LAG

CHUGGING

U COMBUSTION STABILITY

CHUTES

Aircraft emergency evacuation systems, discussing door designs, inflatable escape slide and slide/lifeboat combination

22 p3138 A72-42520

CINEFLUOROGRAPHY

U MOTION PICTURES

U RADIOGRAPHY

CINEMATOGRAPHY

Schlieren cinematographic and holographic diagnostic of giant pulse ruby laser produced plasma in Xe [CLEA PAPER 12,2]

07 p1040 A72-19393

Q switched laser system emitting light pulses for high speed cinematography synchronized illumination

11 p1649 A72-26343

Apollo 15 and 16 TV, still and movie cameras, discussing astronomical activities of astronauts

12 p1807 A72-27546

Scatter plate and lens methods of holographic cinematography

21 p3054 A72-40615

CINERADIOGRAPHY

U MOTION PICTURES

U RADIOGRAPHY

CINETHEODOLITES

Automatic optical tracking instrumentation at rocket launching station Tanegashima, describing automatic cinetheodolite

06 p0795 A72-17432

CIRCADIAN RHYTHMS

Time zone shift and p-chlorophenylalanine desynchronizing effects on sleep alteration and circadian rhythms in monkeys

03 p0318 A72-13071

Rat central nervous system oxygen toxicity seizure susceptibility relation to circadian rhythms

04 p0472 A72-14867

Hypoxia effect on diurnal mitotic activity rhythm of marrow erythropoiesis system of guinea pigs in pressure chamber

05 p0618 A72-16631

Optimum duration of human circadian cycle with respect to energy cost during work hours, relating normal cycle change to prolonged space mission stresses

05 p0619 A72-16639

Transmeridian flight psychological effects on aircrews, discussing anxiety, stress, circadian rhythm disruption and sleep loss effects on performance deterioration

06 p0766 A72-17816

Circadian rhythms of activity-sleep time in free running birds and man in isolation

07 p0918 A72-19527

Circadian rhythms variations for sleep, EEG, temperature and activity in monkeys, indicating acrophase, amplitude and level regulation

07 p0918 A72-19528

Phase resetting behavior of circadian rhythm of pupal eclosion in fruitfly populations

07 p0918 A72-19529

Mathematical model physical structure, effectiveness and limitations for circadian rhythms, discussing Princeton and modified biochemical models

07 p0930 A72-19530

Weak if electric field influence on circadian rhythms of human rectal temperature and activity

07 p0918 A72-19531

Circadian periodicity of resistance to ionizing radiation in pocket mouse at high and low metabolic rate

07 p0918 A72-19532

Coincidence model tests of photoperiodic time measurement relation to circadian system in moth *Pectinophora gossypiella*, using induction by skeleton photoperiods and light cycles

07 p0919 A72-19533

Phase shifts of circadian rhythm of optic nerve potentials from isolated eye of sea hare in darkness

07 p0919 A72-19534

Spectral photosensitivities for phase shifting of circadian body temperature rhythms in pocket mice

07 p0919 A72-19535

Phase shifting effect of light on circadian rhythm and photoreceptive pigment location in *Drosophila* in postpubertal stages

07 p0919 A72-19536

Ecdysone hormonal control of *Drosophila* circadian rhythms and synchronizing mechanisms, discussing light stimulation and neurohormone secretion

07 p0919 A72-19537

Metabolic control of temperature compensation in circadian rhythm of *Euglena gracilis* strain

07 p0919 A72-19538

Euglena cell division timing control by endogenous circadian rhythm, showing direct entrainment by low frequency dark-light cycles

07 p0919 A72-19539

Molecular aspects of structural and functional circadian rhythms in chloroplasts of unicellular alga *Acetabularia*, emphasizing protein synthesis role

07 p0919 A72-19540

DNA-RNA molecular hybridization testing of chronon theory of circadian timekeeping in protozoa cells

07 p0920 A72-19542

Eastbound and westbound transmeridian flights effect on body temperature and psychomotor and visual performance circadian rhythms, discussing readjustment times

[AMRL-TR-71-89] 07 p0921 A72-20176

Isolation stress effect on micturition circadian rhythm and diuresis occurrence in unrestrained chimpanzee under entrained and free running conditions

[AD-739468] 07 p0921 A72-20180

Isolation stress effect on circadian rhythmic patterns of EEG activity during sleep-wake and sleep cycles in unrestrained chimpanzee

[AD-739469] 07 p0921 A72-20181

Rhythmogenesis as fundamental life characteristic analogous to homeostasis, discussing human circadian rhythm and cycle desynchrony during air travel

07 p0923 A72-20445

Mitosis duration and mitotic activity diurnal rhythms in esophageal epithelium of rats given thyroxine

07 p0924 A72-20623

Light-dark cycles and physiological stress stimuli effects on circadian rhythm in rat blood serum serotonin levels

08 p1115 A72-21081

Circadian adrenal periodicity of plasma corticosterone levels in man under random living schedule

09 p1265 A72-22643

Day/night workers sleep patterns in terms of intrasleep REM-NREM ultradian cycle, noting sleep temporal instability for night workers

10 p1428 A72-23730

Diurnal rhythm and loss of sleep effects on human efficiency - Conference, Strasbourg, July 1970

11 p1580 A72-26676

Human performance dependence on time of day, discussing circadian and physiological rhythms relation and environmental change effects

11 p1580 A72-26677

Sleep deprivation effects relation to work duration, time of day, circadian rhythm, memory function, task performance, environmental factors, drug use and age

11 p1580 A72-26678

EEG measurement of sleep behavior patterns, discussing sleep stages, temporal patterns, circadian rhythm, intrasleep process stability and age factor

11 p1580 A72-26679

Time displacement effects on human physiological and psychological functions, discussing circadian rhythm phase shift and performance deficits

11 p1580 A72-26681

Cumulative partial sleep deprivation effects on human performance in auditory vigilance, routine addition and running digit span tests, observing circadian rhythms

11 p1581 A72-26683

Sleep, lack of sleep and circadian rhythm effects on psychometric test performance

11 p1581 A72-26684

Sleep interruption, sleep deprivation and continuous darkness effects on circadian rhythms in human performance

11 p1581 A72-26685

Sleep-wakefulness cycle variations effect on reaction time and spontaneous tempo during time isolation experiment, showing tendency toward circadian rhythm

11 p1581 A72-26687

Human functional level performance characteristics, noting relationship between spontaneous rhythm diurnal variations in psychic and physical performance

11 p1589 A72-26691

Sleep deprivation effect on circadian rhythms in human performance, psychological fatigue ratings, catecholamine excretion and urine flow

11 p1581 A72-26692

Circadian rhythm effects on introverts and extroverts biochemistry, physiology and performance, suggesting arousal mechanism differences

11 p1581 A72-26693

Transzonal air travel as cause of psychological and physiological rhythm change effects on pilot performance

11 p1589 A72-26694

Project Pegasus vigilance tasks for mental performance aspects of time zone change effects on human circadian rhythms

11 p1589 A72-26695

Time zone transition induced circadian rhythm disturbance effect on military personnel mental and physiological performance

11 p1589 A72-26696

Metabolic and hormonal response adaptation to prolonged hypodynamics in water immersion /head out/, noting diurnal and nocturnal differences in circadian rhythms

12 p1765 A72-28267

Circadian rhythms of visual accommodation responses and physiological correlations during target tracking, recording monocular focus state by IR optometer

12 p1767 A72-28306

Latent desynchronization caused by disturbances in circadian rhythms, noting rapid eye movement state

13 p1904 A72-29314

Adaptation period to inverted work-rest cycle observed with encephalograph, noting effect of brain bioelectric activity circadian rhythms stability

13 p1904 A72-29315

Pulse rate studies of human adaptation to 16 hour work-rest cycle, showing persistence of 24 hour cycle

13 p1904 A72-29316

Heart rate change regularities during inverted work-rest cycle of isolated man, noting relation to circadian rhythm

13 p1904 A72-29317

Diurnal changes in gas exchange and metabolic rate under normal and inverted day-night schedule conditions, studying human adaptation to shifted schedule

13 p1904 A72-29318

EEG diurnal rhythms during 72 hour insomnia, considering adaptation to altered work-rest cycle in subjects with stable and unstable brain activity rhythms

13 p1904 A72-29319

Sleep deprivation effects on diurnal urine potassium excretion, showing individual circadian rhythm variations

13 p1904 A72-29320

Illumination intensity effects on circadian periodicity and behavioral thresholds in Rhesus monkey, demonstrating exception to Aschoff rule

13 p1906 A72-29844

Work capacity evaluation from fatigue, biological rhythm, tissue respiration and oxygen consumption studies, discussing pharmacological stimulation effects

14 p2078 A72-30376

Human respiratory rate diurnal rhythm adjustments during inverted work-rest cycles in isolation chamber with controlled comfortable atmospheres

14 p2075 A72-30390

Heart rate diurnal rhythm adaptation to work-rest cycle change, using recumbent and sitting position data parameters

14 p2075 A72-30391

Noise and vibration stress combined effects on human mental performance as function of time of day, taking into account circadian rhythm factor

14 p2081 A72-31083

Increased tolerance of leukemic mice to arabinosyl cytosine with schedule adjusted to circadian system

17 p2505 A72-35397

EEG investigation of circadian variations in qualitative and quantitative RNA content in human leukocytes, noting changes during sleep

18 p2651 A72-36624

Circadian rhythms in physiological and psychological functions related to jet travel, studying body temperature variations and psychomotor performance during isolation and varying light-dark cycle conditions

20 p2897 A72-39723

Human tryptophan and tyrosine metabolism - Effects of acute exposure to cold stress

21 p2997 A72-40417

Biological rhythms origin and mechanisms, discussing 24-hour cycle, subcellular biological clock and rhythm disruption effects in speleologists, astronauts and pilots

22 p3141 A72-41985

Thermal balance in man during 24 hours in a controlled environment

22 p3145 A72-42747

Time series analysis of meteoropathological disturbances of human regulation mechanisms, investigating annual variations of diurnal rhythms

22 p3147 A72-42977

Exogenous modifications of circadian rhythms of adrenal hormones in man

22 p3147 A72-42978

Mutual relations between different physiological functions in circadian rhythms in man

22 p3147 A72-42979

Studies on weightlessness in a primate in the Biosatellite 3 experiment

23 p3253 A72-43388

Human prolactin - 24-hour pattern with increased release during sleep

23 p3316 A72-43977

Use of implantable telemetry systems for study of cardiovascular phenomena.

23 p3260 A72-43996

CIRCLES [GEOMETRY]

NT GREAT CIRCLES

Circle moving under fluid dynamic and gravitational forces in viscous incompressible flow, describing dynamic interaction by numerical method [AIAA PAPER 72-111]

05 p0604 A72-16819

Graphical design technique based on Nyquist plane construction using circle criterion for nonlinear systems controller synthesis

14 p2091 A72-30375

Composite two-material circular sector two dimensional stationary temperature field determined for certain thermal conduction coefficient ratios

14 p2170 A72-30573

CIRCUIT BOARDS

Ultrasonic bonding tip design for densely wired electronic circuit boards, analyzing standing wave phenomena and resonant frequency

[SAE PAPER 710789] 01 p0074 A72-10279

Analog matrix, input data and procedure for Al frame and Cu-clad printed circuit board module thermal resistance analysis using ECAP program

01 p0035 A72-10380

Circuit boards contact assembly by special type rivets, discussing technical and economic advantages for prototype or small series fabrication of printed circuit devices

06 p0784 A72-18192

Printed circuit boards and RC elements soldered connections reliability under high temperature and excessive current conditions, discussing test procedure and evaluation criteria

07 p0994 A72-19247

Path connection algorithms for optimal IC layout on circuit board, using digital computer

11 p1607 A72-26784

Screen printed large thick film multilayer interconnection board assemblies for electronic packaging, discussing fabrication and feasibility

16 p2368 A72-33194

Regeneration metering methods and equipment for acidic and alkaline etching of normal plated circuit boards.

20 p2929 A72-39491

Automation of high reliability multilayer printed circuit board fabrication.

22 p3184 A72-43173

CIRCUIT BREAKERS

Sizing new generation aircraft wire and circuit breakers utilizing computer techniques.

17 p2498 A72-35568

1970-1971 Holm Seminar supplement to bibliography and abstracts on electrical contacts, circuit breakers and arc phenomena.

18 p2665 A72-36120

CIRCUIT DIAGRAMS

Lunar Roving Vehicle navigation subsystem power converter design, discussing circuits, performance and voltage regulators and preregulators

01 p0009 A72-11069

Plasma diagnostics facilities design, circuit diagrams and operation based on Q switched ruby laser and optical recording system

02 p0237 A72-11407

Bulk effect diodes combination with YIG elements to provide oscillator operation up to 18 GHz, discussing design, circuit diagrams and performance

10 p1448 A72-24037

Voltage-frequency converter network design and operation, presenting circuit diagram

10 p1453 A72-24817

SCR trigger circuits design generating short control pulses for converters based on SCR elements, presenting circuit diagrams

11 p1603 A72-25280

Digital correlator systems design for nonstationary signals, presenting circuit diagrams for multichannel centering system and memory operation

11 p1602 A72-26445

Semiautomatic analog to digital converter for pulse signals time dependent parameters, examining block diagrams and tunnel diode operation

11 p1605 A72-26456

Circuitry and operational characteristics of variable output voltage regulator with low temperature coefficient, noting suitability for monolithic integration

12 p1792 A72-27740

Ionospheric radio adsorption measuring device with readout data convenient for visual and computer processing, discussing block and circuit diagrams

13 p1955 A72-28602

Eddy current sensor for mechanical vibration measurements, describing circuit design for stable and reliable operation at 30 MHz

13 p1930 A72-29051

Pressure measurement between compressor impeller blades during steady and transient operation, discussing system circuit diagram

13 p1957 A72-29139

Standard and bilinear z transformation techniques for digital sampling filters block diagrams derivation

16 p2369 A72-33671

Symbol generators for the representation of switching circuits by data display devices according to the television principle

19 p2769 A72-37935

Multivibrator with p-n-p and n-p-n transistors, noting circuit diagram, operation and power dissipation

20 p2906 A72-38898

Modified Dobson ozone spectrophotometer with revised electronic design circuitry, considering high voltage power supply, photomultiplier tube circuit, amplifier and electromechanical phase sensitive rectifier

20 p2921 A72-38968

Ionospheric radio absorption measuring device with readout data convenient for visual and computer processing, discussing block and circuit diagrams

24 p3402 A72-45102

CIRCUIT PROTECTION

Pulse width modulated transistor series inverter with inductor transformer in low power applications, noting short circuit and no-load protection

01 p0007 A72-11060

Sequential faults examination on three-phase distribution transformer, suggesting protection scheme modifications

03 p0313 A72-14186

Fast acting nonmechanical self healing mercury fuse for high current circuit protection

03 p0335 A72-14203

Economically optimal operation of protection circuit for plant subject to stationary random process, determining failure rate of plant

04 p0496 A72-14995

Transistor damage by electrostatic discharges, noting charge stored by humans and protection techniques

08 p1140 A72-21064

MOSFET for input impedance measuring amplifier, discussing input stage temperature drift and protection from overvoltage

10 p1482 A72-24599

Polyphase ac power systems I-V characteristics determination via application of symmetrical sequence components principle, examining system protection and reliability aspects

15 p2204 A72-31216

Solid state dc power controller design functional requirements, considering system overcurrent protection, power control by low voltage signals, power output to load status, etc

15 p2182 A72-31219

Electronic equipment shielding against electromagnetic radiation and circuit protection against unwanted electrical signals

15 p2209 A72-32570

The use of semiconductor diodes to protect a radar receiver

18 p2663 A72-37217

Effect of electrical generator parameters on transient suppressors.

19 p2753 A72-37291

The lightning arrester-connector - A new concept in system electrical protection.

20 p2889 A72-38989

Digital p-i-n diode microwave drive amplifier design guidelines, discussing sharp switching pulses and short circuit protection features

20 p2904 A72-39734

Missile guidance electronic packaging and module design for circuit protection against X rays, gamma radiation and nuclear blast damages

20 p2909 A72-39766

Saturation protection of a maser amplifier by the pulse-modulated pumping method

21 p3063 A72-40785

CIRCUIT RELIABILITY

Efficiency/reliability design requirements of driven transistor synchronous rectifiers in low output voltage applications

01 p0042 A72-11053

Fail-safe sequential machines realization using k-out-of-n code for state assignment and onset and off-set methods for excitation circuit construction

02 p0184 A72-11477

Fault-tolerant digital computer logic design for dynamic and interactive recovery with data integrity after error, discussing hardware and software functions requirements

02 p0184 A72-11480

Mathematical reliability modeling for fault tolerant digital computers, summarizing error masking and standby sparing reliability equations

02 p0184 A72-11481

STAR self testing and repairing fault tolerant digital computer for outerplanet exploration spacecraft, discussing architecture, reliability analysis, software and peripheral system automatic maintenance

02 p0184 A72-11482

Soviet progress and bibliography on fault tolerant digital computers design, emphasizing redundancy application to achieve high reliability

02 p0184 A72-11484

Minimum length fault tests design for irredundant combinational logic circuits containing single faults based on Boolean difference function

02 p0185 A72-11485

Three-failure-tolerant digital computer system design using adaptive majority voting in hardware and software for real time control application

02 p0185 A72-11488

Reliable combinational logic networks, deriving conditions for fault locatability from directed graph formal model

02 p0185 A72-11491

Failure modes of IC containing MOS devices, considering threshold voltage variations, oxide and silicon defects and leakage

02 p0194 A72-12443

Redundancy configuration effect on electronic system reliability, discussing MTBF and cost analysis

02 p0194 A72-12445

Avalanche injected current relationship to emitter-base junction breakdown damage in planar n-p-n gated transistors

03 p0336 A72-14279

Charged transfer devices and IGFET bucket brigade structures, discussing design measures and fabrication procedures for increased reliability

03 p0336 A72-14280

MIS semiconductors radiation-hardening mechanisms and radiation effects on electrical properties and degradation

03 p0405 A72-14281

MOS Si-gate arrays for static, dynamic and programmable read-only memories, investigating information storage reliability

03 p0336 A72-14282

Defective IC device glass surface passivation effects on scanning electron microscope analysis

03 p0365 A72-14287

Semiconductor-thermoplastic-dielectric hybrid ICs reliability, discussing interelement adhesive bonding properties and thermally induced strains effects

03 p0337 A72-14294

Low temperature liquid bath tests for IC environmental reliability, monitoring wire bonding, metallization, surface contamination, sealing and die bonding

03 p0337 A72-14296

Logically stable failures of discrete combination devices by practical behavior in response to given input vectors, using alpha state Boolean algebras

04 p0496 A72-14994

Economically optimal operation of protection circuit for plant subject to stationary random process, determining failure rate of plant

04 p0496 A72-14995

Variable conductance heat pipe technology for overcoming thermal resistance barrier in electronic package design

04 p0596 A72-15227

German monograph on thermionic power supply equipment converter network reliability covering I-V characteristics and failure probability calculation

04 p0466 A72-15696

Plastic encapsulated transistors and IC moisture resistance tests for reliability under laboratory and field conditions

06 p0782 A72-17363

Printed circuit boards and RC elements soldered connections reliability under high temperature and excessive current conditions, discussing test procedure and evaluation criteria

07 p0994 A72-19247

MOS IC reliability based on p-channel enhancement mode transistors, discussing failure modes and mechanisms

08 p1142 A72-21588

Inexpensive solid state microwave sources development and applications considering spectrum allocations, health hazards and reliability problems

09 p1285 A72-22595

N fail-safe logics for circuit fault restoration, comparing with failure probability of majority voting scheme and quadded logic

09 p1283 A72-23420

Random access memory with single error correction circuitry, predicting failure, card and module removal rates by computer simulation

10 p1443 A72-23980

Global NASA communications network /NASCOM/ reliability, discussing design and performance goals

10 p1435 A72-23992

Pulse width modulated regulating dc-to-dc converter with small number of transistors to improve circuit reliability

10 p1452 A72-24680

IC plastic encapsulation reliability problems related to die stability, wire bond and package moisture integrity

11 p1606 A72-26546

Eddy current sensor for mechanical vibration measurements, describing circuit design for stable and reliable operation at 30 MHz

13 p1930 A72-29051

Mathematical model for computation of electronic circuit drift reliability and circuit production yields, discussing operational parameter allowance

14 p2091 A72-31165

IC reliability assessment based on defects and failure mechanisms analysis instead of MTBF estimations

14 p2091 A72-31166

Low power TTL IC in plastic and hermetic packages tested for reliability via critical dc parameters measurement in initial and post-stress states

14 p2091 A72-31168

Polyphase ac power systems I-V characteristics determination via application of symmetrical sequence components principle, examining system protection and reliability aspects

15 p2204 A72-31216

Relay circuits malfunction due to interactions between coil induced currents and diode coil shunts, discussing circuit design and operating conditions

15 p2204 A72-31217

Electronic circuit reliability prediction model with statistical dependence for detailed failure modes

16 p2371 A72-33345

Computerized calculation of electronic circuit and equipment reliability and quality control, presenting task examples and printout form

16 p2368 A72-33347

Techniques for control of long-term reliability of complex integrated circuits. I - Reliability assurance by test vehicle qualification.

17 p2528 A72-34686

Techniques for control of long-term reliability of complex integrated circuits. II - A technique for the prediction of failure rates for MSI and LSI devices.

17 p2528 A72-34687

Report on Flip Chip and Beam Lead bonding for electronic circuits.

18 p2666 A72-36528

[SAE AIR 1141] Microwave power junction transistor design factors effects on long and short term reliability and MTBF

18 p2666 A72-36552

Microwave junction transistor geometric design factors effect on reliability and performance, comparing overlay, interdigitated, mesh and inverse overlay structures

18 p2666 A72-36553

Au alloys metallization system as alternative to aluminumizing for junction transistor reliability improvement, considering metal migration, microcracking and current leakage

18 p2666 A72-36554

Analysis of sensitization mechanisms of low consumption integrated circuits

18 p2668 A72-37107

Reliability of integrated circuits with plastic encapsulation

18 p2669 A72-37114

Reliability of nichrome film resistors deposited in vacuum by sublimation on a glass substrate

18 p2669 A72-37117

Organization of fabrication to obtain high-reliability hybrid circuits

18 p2669 A72-37118

Quality and reliability evaluation method for integrated circuits using MOS transistors - Option: Circuits on request

18 p2671 A72-37141

Test structures - Powerful technique for quality evaluation and reliability assessment of MSI and LSI /medium and large scale integrated circuits/.

18 p2671 A72-37143

Electronic control systems for industrial applications, discussing electrical and mechanical properties, circuit reliability and mechanical design features

19 p2782 A72-38314

Probability density - A new approach to system electromagnetic compatibility testing of digital circuits.

20 p2906 A72-38980

Heat transfer coefficient measurement and thermal network analysis computer program for improving performance and reliability of microelectronic package/board and chip/substrate systems

20 p2908 A72-39497

Microelectronic component system temperature distribution measurement by IR microscope and electrical technique to determine beam-lead IC thermal performance

20 p2908 A72-39498

Reliable advanced solid state radar /RASSR/ array design featuring transmit-receive elements arranged in triangular grid and built-in test equipment

20 p2904 A72-39732

Electronic packaging techniques in housing spaceborne computer, digital telemetry and other microelectronics for protection against severe aerospace environment

20 p2909 A72-39767

Electronic packaging and LSI techniques cost efficient use in meeting weight, volume, reliability, circuit speed and thermal protection requirements

20 p2909 A72-39769

Burn-in technique cost effectiveness in semiconductor and IC reliability enhancement, noting failure rate relationship to operating time

20 p2909 A72-39770

Effect of feedback and protective circuits on the reliability of electronic equipment

22 p3158 A72-42118

Automation of high reliability multilayer printed circuit board fabrication.

22 p3184 A72-43173

Allowance for correlation in the prediction of reliability parameters for radio equipment

23 p3270 A72-43767

Flawless operation probability for information transmission reliability of electronic logic circuits with binary data inputs

23 p3271 A72-43784

Ranking the reliability of two designs by Monte Carlo techniques.

24 p3383 A72-44655

CIRCUITS

NT ADDING CIRCUITS

NT ANALOG CIRCUITS

NT AUTODYNES

NT BISTABLE CIRCUITS

NT CIRCULATORS (PHASE SHIFT CIRCUITS)

NT COINCIDENCE CIRCUITS

NT COUNTING CIRCUITS

NT COUPLING CIRCUITS

NT DELAY CIRCUITS

NT DIGITAL INTEGRATORS

NT DISCRIMINATORS

NT ECHO SUPPRESSORS

NT ELECTRIC BRIDGES

NT EQUIVALENT CIRCUITS

NT FEEDBACK CIRCUITS

NT FLIP-FLOPS

NT FLUID SWITCHING ELEMENTS

NT FLUIDIC CIRCUITS

NT GATES [CIRCUITS]

NT INTEGRATED CIRCUITS

NT ITERATIVE NETWORKS

NT LC CIRCUITS

NT LIMITER CIRCUITS

NT LINEAR CIRCUITS

NT LOGIC CIRCUITS

NT MAGNETIC CIRCUITS

NT MATRICES [CIRCUITS]

NT MEDIUM SCALE INTEGRATION

NT MICROWAVE CIRCUITS

NT MIXING CIRCUITS

NT MULTIVIBRATORS

NT NEGATIVE RESISTANCE CIRCUITS

NT OHMS LAW

NT PHANTASTONS

NT PHASE DETECTORS

NT PHASE SHIFT CIRCUITS

NT PNEUMATIC CIRCUITS

NT POWER SUPPLY CIRCUITS

NT PRINTED CIRCUITS

NT RC CIRCUITS

NT RL CIRCUITS

NT RLC CIRCUITS

NT SCALERS

NT SWEEP CIRCUITS

NT SWITCHING CIRCUITS

NT SYNCHROSCOPES

NT THRESHOLD GATES

NT TRANSISTOR CIRCUITS

NT TRIGGER CIRCUITS

NT VARACTOR DIODE CIRCUITS

Circuit theory optimization techniques in computer aided electric circuits and devices design, discussing algorithms, sequential methods, convergence speed, topologies, system responses, etc

02 p0197 A72-11688

Hybrid circuit production, considering face down assembly of flip chip and beam lead semiconductor devices

02 p0195 A72-12608

Mean wind direction determining circuit for meteorological data collecting system

10 p1484 A72-25018

Circuit theory - IEEE Conference, North Hollywood, April 1972

15 p2211 A72-31843

Electric circuits design by combined network synthesis and optimization methods, noting approximation by nonlinear programming

19 p2776 A72-37308

Russian book - Mathematical modeling and electrical circuit theory, Number 8.

21 p3023 A72-40153

Russian book - Mathematical modeling and electrical circuit theory.

21 p3036 A72-40176

CIRCULAR CONES

Circular cone in supersonic flow, obtaining self similar solution for effect of angle of attack on laminar boundary layer by finite difference method

02 p0150 A72-12095

Laminar free convection from vertical nonisothermal right circular cone with boundary layer control by

injection or suction, investigating heat transfer by perturbation method

02 p0204 A72-12232

Incompressible power law pseudo-plastic material plane flow in converging channel and axially symmetric converging flow in circular cone

04 p0513 A72-15287

Surface pressure approximation formula for inclined circular cone in supersonic flow

05 p0603 A72-16547

Solar rudder for spacecraft steering in form of right circular cone with ideally reflecting surface

11 p1727 A72-25943

Supersonic axisymmetric turbulent boundary layer characteristics over circular cone, predicting blowing effect on separation

11 p1617 A72-25995

Flow distribution for inviscid nonconducting uniform supersonic stream past unyawed semiinfinite circular cone with attached shock wave

17 p2483 A72-34325

Closed form solution to conical inviscid hypersonic flow over circular cone at zero angle of attack

17 p2486 A72-35433

Rotationally symmetric temperature distribution in region between two coaxial circular cones for isothermal and adiabatic conditions, solving heat conduction equation

20 p2983 A72-39329

CIRCULAR CYLINDERS

Linear spin-down of stratified rotating Boussinesq fluid in circular cylinder as function of Prandtl number, noting solar interior problem

01 p0051 A72-11231

Natural vibrations of closed crosswise reinforced orthotropic circular cylindrical shells, using digital computer solution

01 p0142 A72-11363

Split-film anemometer probe determination of convective heat transfer coefficient azimuthal dependence in low Reynolds number flow over cylinders, discussing axial heat losses

02 p0224 A72-11725

Liquid motion in circular cylinder with elastic bottom under longitudinal excitation, representing dynamic and kinematic free surface conditions as nonlinear equations

02 p0204 A72-12254

Unsteady supersonic aerodynamic forces on oscillating circular cylindrical shell calculated using linearized equation of potential flow

02 p0151 A72-12256

Vertical thin circular cylindrical shells partially or completely filled with stationary liquid, determining free vibration characteristics with finite element theory

02 p0293 A72-12371

Plastic collapse limit analysis for combined edge and pressure loading on circular cylindrical shells for Tresca yield condition

02 p0295 A72-12474

Thin circular cylindrical shells under uniform axial compression loads, examining axially symmetrical creep buckling

02 p0296 A72-12531

Circular cylindrical sandwich panel and rectangular sandwich plates dynamic stability under periodic external loads derived from mathematical model

02 p0298 A72-12664

Time dependent unsteady flows visualization around circular cylinders and flat plates decelerated from steady speed

02 p0206 A72-12773

Orthotropicity orientation effect on supersonic flutter of infinite-length thin heterogeneous circular cylindrical structures in axisymmetric gas flow

04 p0584 A72-14520

Thermoviscoelastic stress analysis for hollow circular cylinder with reinforcing interlayer under pressure, axial tension and nonstationary temperature field

04 p0587 A72-15016

Random search method application to optimal design of closed circular cylindrical shells under axial compressive loading

04 p0587 A72-15020

Stress concentration around elliptic hole in infinitely long circular cylindrical shell under torsional loads

04 p0589 A72-15122

Axially symmetric torsional waves in elastic circular composite cylinders, plotting dispersion diagrams

04 p0590 A72-15185

Radiated pressure field in unbounded acoustic medium produced by pulsed elastic cylindrical circular shell

04 p0590 A72-15188

Temperature fluctuation structure in turbulent wake behind heated circular cylinder, investigating thermal convection, production and diffusion

04 p0596 A72-15330

WKB type solution for electromagnetic wave propagation in circular cylindrical coordinate system with rho-dependent refractivity, using Bessel function

04 p0488 A72-15384

- Numerical solution for diffraction on conducting finite and infinite lattice of cylinders with circumferential cross section
04 p0491 A72-15416
- Flat plate, sphere and circular cylinder drag and lift coefficients in free molecular flow
04 p0463 A72-15645
- Elastic analysis of circular cylinders with stress singularities from boundary discontinuities, mixed displacement and axial load conditions
[ASME PAPER 71-WA/APM-18]
05 p0733 A72-15962
- Elastic stress field in hollow circular cylindrically anisotropic body under surface tractions expressed as Fourier series
[ASME PAPER 71-WA/APM-13]
05 p0734 A72-15967
- Torsional vibration induced by periodic circumferential shear force on composite circular cylinder with varying rigidity and density, obtaining solutions for various boundary conditions
05 p0740 A72-16727
- Laminated anisotropic imperfect circular cylindrical shells under axial compression, obtaining upper bound buckling load solution
[AIAA PAPER 72-139]
05 p0740 A72-16893
- Flutter of thin elastic circular cylindrical fluid filled shells, presenting potential flow theory for coupled hydrodynamic forces
06 p0894 A72-17763
- Viscous incompressible flow past circular cylinder at Reynolds numbers 20-100 by finite difference methods, taking into account wake region behind body
06 p0756 A72-18125
- Nonstationary thermal interaction between thermally inert circular disk in bounded cylinder with controlled temperature, describing control process by third order differential equation
07 p1098 A72-19263
- Two and three dimensional quasi-static coupled thermal diffusivity problem for deformable body, determining physicochemical state of solid circular cylinder under cyclic loads
07 p1090 A72-19752
- Liquid sloshing in circular cylindrical cavity with ribs mounted radially to walls, calculating oscillation frequencies and virtual masses
08 p1148 A72-20968
- Three dimensional nonstationary heat conduction of hollow circular cylinder in medium with different temperature
08 p1251 A72-20972
- Viscous incompressible flow past circular cylinder at Reynolds numbers 100-1000, obtaining oscillatory drag, lift and torque by governing equations numerical solution
08 p1107 A72-21251
- Tube flight vehicle system thrust and power requirements prediction by aerodynamic analysis with division of near and far flow fields
08 p1107 A72-21608
- Axisymmetric thermoelastic state of isotropic infinitely long circular cylinder with external annular cut, determining cut plane normal thermal stresses
08 p1245 A72-21668
- Orthotropic circular cylindrical elastic shell vibration mode shape analysis by Vlasov equations, using asymptotic method
08 p1247 A72-21813
- Dynamic buckling of shallow circular cylindrical hinged panel under axial compression
08 p1249 A72-22087
- Fundamental vibrations of long circular cylinder made of bipolar elastic solid, discussing dispersion equations
09 p1398 A72-22620
- Stresses, strains and moments interrelationship in axisymmetrically loaded circular cylindrical shell under unsteady creep conditions
09 p1401 A72-22729
- Temperature and internal pressure effects on circular cylindrical shell stability under tension and compression, deriving critical temperature and loads
09 p1402 A72-22736
- Imperfection influence on nonlinear stability of long circular cylindrical shells subject to critical hydrostatic pressure
09 p1403 A72-22763
- Perturbation analysis of nonlinear free flexural vibrations of circular cylindrical shell, using Donnell equations
09 p1405 A72-22998
- Pressure distribution around circular cylinder with shrouds of various geometry for suppressing flow induced vibrations at subcritical and transition Reynolds number
09 p1261 A72-23315
- Electromagnetic wave scattering by arbitrarily oriented circular ice cylinders, deriving far field intensities for linearly polarized incident waves
09 p1280 A72-23341
- Nonlinear vibrations of thin circular cylindrical shells under arbitrary boundary and loading conditions
09 p1407 A72-23456
- Torsion of embedded infinite elastic circular cylindrical fiber with penny shaped crack, investigating breaking behavior from Fredholm integral equation iterative solution
10 p1553 A72-24094
- Wall law for axisymmetric turbulent boundary layers in zero pressure gradient fluid flow through circular cylinders, noting negative and positive wake regions
[ASME PAPER 71-APM-VV]
10 p1465 A72-24177
- Dynamic response of pressurized thin walled circular cylindrical shell under initial biaxial stress and subjected to radial uniformly moving force, noting transient and steady state
[ASME PAPER 71-APM-GGG]
10 p1554 A72-24186
- Partial differential equation for thin walled circular cylindrical shells, deriving solutions for displacement and stresses in terms of surface coordinates low degree polynomials
10 p1557 A72-24560
- Radiation pattern of longitudinal magnetic dipole near circular cylinder parallel to flat screen
10 p1553 A72-24903
- Bending of rectangular cross section cantilever beam with cylinder reinforced circular opening, calculating interface stress distribution as function of thickness and elasticity moduli ratio
11 p1733 A72-25545
- Linear impulsive spin down from rigid body rotational equilibrium of radiation penetrated opaque compressible fluid in circular cylinder
11 p1680 A72-25555
- Von Mises yield criterion extended to thin walled circular cylinder plastic torsional straining, noting variations of anisotropic parameters and yield stresses with shear strain
[ASME PAPER 71-MET-Y]
11 p1735 A72-25877
- Experimental data on twin vortices formed behind impulsively started or uniformly accelerated circular cylinders
11 p1572 A72-26375
- High intensity free stream turbulence effects on flow past circular cylinder at subcritical Reynolds numbers, measuring unsteady lift and drag
11 p1573 A72-26640
- Plastic percentage reduction of area and elongation for circular cylindrical sample in tensile deformation, proposing stress analysis method for metallic sleeves under low cycle loads
11 p1738 A72-26810
- Dynamics snap-through instability existence conditions in nonlinear plane deformation of shallow circular cylindrical elastic shell under impulsive loading
12 p1880 A72-27241
- Steady three dimensional viscous vortex within circular cylinder with tangential fluid influx from jets on outer surface and efflux through sink on bottom
[AD-741352]
12 p1798 A72-27716
- Stress distribution in circular cylindrical shell weakened by two identical holes on common generatrix
12 p1886 A72-27984
- Closed thin circular cylindrical shells external pressure pulse and structural parameters effects on stability under dynamic loading
12 p1886 A72-28129
- Circular cylindrical shell under distributed edge load along circular hole contour, calculating stress concentration by trigonometric series solution for shallow shell equation
12 p1886 A72-28130
- Analytical solution to difference stability equations, evaluating adequacy of difference scheme for circular cylindrical shell and rectangular hinged plate under compression
13 p2053 A72-28389
- Harmonic functions system for resonant vibrations of liquid in elastic circular cylindrical tank, calculating shells surface pressure from equations of motion
13 p1940 A72-28394
- Viscous incompressible flow between two coaxial rotating circular cylinders with small uniform injection at inner cylinder, obtaining solution of Navier-Stokes equations
13 p1941 A72-28883
- Series solution for coaxial spherical cavity effect on torsional stress of finite length elastic circular cylinder
13 p2059 A72-29491
- Rheological stress-strain relations in nonlinear viscoelasticity theory, calculating relaxation parameters for isotropic viscoelastic circular cylinder
13 p2059 A72-29493
- Nonequilibrium dissociating inviscid nitrogen flow pattern over spheres and circular cylinders, obtaining temperature, pressure and density fields
13 p1895 A72-30032
- Gravitational wave diffraction by liquid on surface of vertical circular cylindrical shells, determining velocity potentials
14 p2093 A72-30192
- Stress analysis of thick walled hollow viscoelastic circular cylinder enclosed in elastic shell and subjected to nonlinear creep conditions, noting temperature effects
14 p2165 A72-30439
- Ideal liquid theory application for unsteady separated flow calculation around arbitrary shape bodies, noting numerical solution for plane flow around circular cylinder
14 p2070 A72-31010
- Free stream turbulence effect on mass transfer from circular cylinder in cross flow as function of Schmidt and Reynolds numbers, using electrochemical measurement method
14 p2096 A72-31061
- Steady asymptotic suction profiles in free convection laminar boundary layer flows on heated vertical circular cylinder
14 p2096 A72-31070
- Ideal gas supersonic axial flow past circular cylinder, solving Navier-Stokes equations by Van Dyke matched asymptotic expansions method
15 p2178 A72-31463
- Stability analysis of thin walled circular cylindrical shell under shearing force action to one end, calculating buckling modes
15 p2324 A72-31483
- Three dimensional structure of transverse uniform flow around motionless circular cylinder for Reynolds number 45,000, investigating correlations of velocities on parallels to generatrices
15 p2179 A72-31684
- Complex conjugate fourth order partial differential equations for circular cylindrical shells deformation, comparing accuracy with Flugge, Morley and Novozhilov equations
15 p2331 A72-32559
- Differential equations for stress-strain state of circular cylindrical shell with circular holes resting on elastic base under external pressure
15 p2333 A72-32686
- Natural vibration frequency spectra of circular cylindrical and spherical shells of revolution, using Bessel function
16 p2465 A72-32936
- Hydrodynamic equations for low speed steady external rarefied gas flows past circular cylinder, noting drag and heat transfer coefficients
16 p2344 A72-33568
- Magnetothermoelastic temperature distribution effects due to linear heat source in infinite circular cylinder acted upon by magnetic field
16 p2425 A72-33595
- Spanwise correlation measurement of vortex shedding behind circular cylinder in subcritical Reynolds number region
16 p2379 A72-33658
- Transient elastic wave propagation in circular cylinder during sudden torsional shear stress application to end surface, noting surface particle velocity and stress
16 p2426 A72-33660
- Imperfect circular cylindrical shells creep and elastic buckling under nonuniform external loads, solving ordinary differential equations via finite difference technique
16 p2474 A72-34133
- Dynamic buckling of shallow circular cylindrical hinged panel under axial compression
17 p2626 A72-34665
- Elastic-plastic medium with doubly periodic square array of circular cylindrical voids, obtaining finite element solution for uniaxial deformation by variational principle
[ASME PAPER 72-APM-36]
17 p2628 A72-34784
- Buckling of a circular cylindrical shell in axial compression and SS4 boundary conditions.
17 p2632 A72-35236
- Cavitation zone structure behind circular cylinder model in plane flow investigated by high speed motion picture photography and with short exposure time flash
17 p2544 A72-35897
- Flow of a viscous liquid round a cylinder for Reynolds numbers 60 and 80.
18 p2679 A72-36233
- Propagation and attenuation of harmonic waves in a viscoelastic circular cylinder.
18 p2738 A72-37070
- A proof of the accuracy of a set of simplified buckling equations for circular cylindrical elastic shells.
18 p2739 A72-37091
- Thermal displacements and stresses in cylindrical shells due to instantaneous line heat sources.
19 p2870 A72-37272
- Numerical solution of the problem of the motion of a circular cylinder in a viscous fluid flow
19 p2784 A72-37395
- Experimental investigation of the flow past a cylinder with a flat nose
19 p2745 A72-37397
- German monograph - A contribution to the clarification of the carrying characteristics of closed isotropic circular cylindrical shells
19 p2871 A72-37478
- Anisotropic circular cylinder stress analysis under uniaxial load, calculating elastic deformation
19 p2872 A72-37536

- Stress redistribution caused by creep in a thick walled circular cylinder under axial and thermal loading. 19 p2874 A72-37716
- Buckling of circular cylindrical shells under compression. III - Solutions based on the Donnell type equations considering prebuckling edge rotations. 19 p2878 A72-38299
- Experimental creep buckling of circular cylindrical shell under uniform compression. 20 p2978 A72-38883
- Dispersion of flexural waves in circular cylindrical shells. 20 p2982 A72-39975
- Stresses in a circular cylindrical shell having two circular cutouts. 20 p2982 A72-40063
- Ultrasonic sound beam measurement of flow circulation variations in circular cylinder wake, evaluating probability distribution of beam phase fluctuations. 21 p2990 A72-40947
- Time dependent deformation of isotropic viscoelastic materials, discussing rectilinear shear, circular cylinder torsion, spiral shear of layer and conical layer torsion. 21 p3119 A72-41075
- Non-Hertzian contact stresses in a smoothly cradled heavy cylinder. 21 p3119 A72-41108
- On the vortex street behind a circular cylinder in non-Newtonian flows. 21 p2992 A72-41227
- Effect of gas slipping on drag in a system of parallel cylinders at low Reynolds numbers. 22 p3133 A72-42268
- Stresses in a circular cylindrical shell with arbitrary holes. 22 p3238 A72-42837
- Square edged semiinfinite circular cylindrical shell, deriving boundary value problem closed form solution based on Novozhilov complex form cylinder equations. 22 p3238 A72-42839
- Buckling of circular cylindrical shells under axial compression. 22 p3239 A72-42840
- Axisymmetric-multilobe creep buckling transition in thin walled circular cylindrical shells under uniformly distributed axial compressive load. 22 p3239 A72-42844
- Effects of non-homogeneity on the stresses in a rotating cylinder. 22 p3240 A72-42877
- German monograph - Cooling of geometrically simple bodies (flat plate, cylinder, sphere) by convection and radiation. 22 p3244 A72-43062
- Stresses around an axial crack in a pressurized cylindrical shell. 23 p3346 A72-43705
- Boundary layer flow on a circular cylinder moving in a fluid at rest. 23 p3248 A72-43715
- Longitudinal rib reinforced cylindrical shell under axial compression loads, determining equilibrium stability with approximation of transcendental equations. 23 p3347 A72-43748
- Laplace equation for homogeneous magnetic field perturbation by superconducting elliptical cylinder and by two parallel circular cylinders. 23 p3313 A72-43779
- Numerical determination of the stress concentration around a hole in a circular cylindrical shell. 23 p3348 A72-43799
- Improved method for determining shear stresses and checking the strength of circular cylinders in transverse bending. 23 p3349 A72-43968
- The torsion of a circular cylinder containing a symmetric array of edge cracks. 23 p3350 A72-44048
- Second order boundary layer solutions on a curved surface. [ASME PAPER 72-FE-21] 23 p3280 A72-44063
- Longitudinal curvature and displacement speed effects on incompressible laminar boundary layers. 24 p3393 A72-45249
- CIRCULAR ORBITS**
- NT STATIONARY ORBITS**
- Optimal control for thrusting rocket guidance with controllable steering angle rate during insertion into circular orbit, using flat earth approximation. 01 p0097 A72-10383
- Transfer from high elliptical to circular orbit, using successive spacecraft braking maneuvers in planetary atmosphere with incomplete information. 01 p0130 A72-10927
- Motion stability of sphere and homogeneous semi-infinite rotating cylinder in circular orbits and monoenergetic streams, integrating by trajectories. 02 p0285 A72-12832
- Analytic solution for optimal control circular orbit escape with constant thrust rocket, using Euler-Lagrange equations and perturbation technique. 03 p0437 A72-13839
- Satellite attitude control in circular orbit by actively varying inertia via angular rate sensing and use of fluid transfer logic. 05 p0725 A72-16440
- Regional communications coverage by controlled satellite constellations with low altitude circular orbits, developing analog or digital simulation method for mission planning. 07 p0945 A72-19690
- Stationary motions, stability of satellite with rotary gyroscope and gimbals in circular orbit and central Newtonian force field. 08 p1241 A72-21801
- Stationary motions stability of four rotor vertical gyroscopic system on satellite in circular orbit in Newtonian central force field. 08 p1205 A72-21804
- Liapunov stability of circular equatorial motions of light bodies in Kerr gravitational field of massive rotating body, using geodesic lines equations. 08 p1210 A72-22071
- German monograph on optimal attitude control of satellites with rotors and simultaneous spin reduction, covering motion equations for stable equilibrium and circular orbit. 09 p1394 A72-22330
- Coupled librational motion of gravity oriented satellite in circular orbit under aerodynamic forces, discussing limiting stability and periodic solutions. 11 p1726 A72-25914
- Energy optimal single impulse transfer from hyperbolic trajectory to circular orbit. 11 p1718 A72-25926
- Satellite circular orbit trajectory plane time optimal relocation, examining turn angle angular position and modulus of maximum lateral acceleration. 11 p1718 A72-25928
- Two and three impulse trajectories for fixed time and angle rendezvous between vacant circular coplanar orbits, defining optimality domain. 11 p1719 A72-25977
- Planar restricted three body problem periodic solutions with bridges connecting direct and retrograde circular orbits. 11 p1721 A72-26153
- Near circular orbit elements determination as functions of satellite initial speed and coordinates deviation by mathematical expectation procedure. 11 p1724 A72-26912
- Orbital and rotational motion stability of solid body containing elastic rods and fluid-filled cavity. 13 p2002 A72-28715
- Axisymmetric satellite rotation about center of mass in circular orbit under Newtonian gravitational field, considering precessional stability. 13 p2052 A72-30002
- Relativistic analysis for synchrotron gravitational radiation emitted by particle in circular orbit around Schwarzschild black hole, noting astrophysical implications. 13 p2007 A72-30123
- Interplanetary spacecraft transfer maneuver for hyperbolic trajectory change into eccentric orbit, using aerodynamic drag to obtain nearly circular orbit. 14 p2151 A72-30471
- Dynamic system motion stability estimation with Liapunov function in quadratic form, applying to circular satellite orbit stability in axisymmetric gravitational field. 14 p2161 A72-31079
- Aerodynamic effects on circular-orbiting cylindrical satellites coupled librational motion, analyzing equilibrium configurations stability by linearized and Liapunov direct method. 15 p2320 A72-31818
- Electromagnetic radiation frequency spectrum and mean power from accelerated magnetic dipoles in circular and Keplerian orbits, noting implications for pulsars. 16 p2453 A72-33285
- Long-term prediction of artificial satellite motion along almost circular orbits allowing for a random number of zonal harmonics. 16 p2607 A72-35033
- Satellite orientation and stabilization systems aerodynamic compensation for circular orbit perturbations. 17 p2621 A72-35034
- Existence proof and boundary regions for multiple solutions in minor planets circular orbits determination. 18 p2723 A72-36085
- French monograph - Optimal impulse corrections for near-circular orbits - Comparison of various thruster configurations. 19 p2856 A72-37491
- Compact expressions for maximum and minimum eclipse durations of spacecraft circular orbit, presenting numerical data as aid to spacecraft design. 19 p2862 A72-38021
- Resonant attitude instabilities for a symmetric satellite in a circular orbit. 21 p3115 A72-41046
- A two-parameter survey of periodic orbits in the restricted problem of three bodies. 21 p3106 A72-41049

First approximation for spacecraft observations of noctilucent clouds from circular orbits with optimal optical axis orientations. 21 p3049 A72-41438

Orbital and rotational motion stability of rigid body containing elastic rods and fluid-filled cavity. 22 p3204 A72-42092

Axisymmetric satellite rotation about center of mass in circular orbit under Newtonian gravitational field, considering precessional stability. 22 p3231 A72-42730

Analysis of the possibility of planetary escape by means of the solar sail. 22 p3230 A72-43072

Relativistic test particle escape from circular orbit around central mass due to mass loss, considering orbiting body corrections due to general relativity. 23 p3335 A72-43265

CIRCULAR PLATES

Carrying capacity solutions for perforated circular plates of rigid plastic material by kinematic method. 01 p0143 A72-11366

Edge effect equations for stability, vibration and deflection of asymmetric three layer circular plate and cylindrical shell with filler. 02 p0288 A72-11605

Static solution for circular plates of cylindrically monoclinic materials. 02 p0293 A72-12277

Nonlinear deflections and radial surface stresses in thin elastic circular glass plates with coaxial rings. 02 p0249 A72-12418

Rigid plastic circular plate dynamic model with yield time delay, discussing residual deflection as function of load duration. 02 p0293 A72-12426

Circularly symmetrical disks with circular hole and loaded by pressure at edges, calculating linear and power-law strain hardening. 02 p0297 A72-12535

Time harmonic electromagnetic wave diffraction by thin conducting circular disk at different media plane interface, calculating induced surface current density and scattering cross section. 03 p0322 A72-13237

Stress concentration of isotropic rotating multiply connected circular and elliptic plates weakened by two circular holes. 03 p0450 A72-14114

Circular disk with external radial cracks, obtaining limiting equilibrium stress-strain state through singular integral equation solution. 03 p0451 A72-14115

Elastoplastic circular plates optimum shakedown design under cyclic loading. 04 p0585 A72-14613

Uniform circular plates axisymmetric elastic deformation under various static loadings and boundary conditions, solving flexural equilibrium equations. 04 p0590 A72-15184

Neo-Hookean material circular plate under finite axisymmetric stretching, showing approximately constant deformed thickness. 04 p0590 A72-15196

Thickness function corresponding to constant velocity loading condition for orthotropic annular circular plate with uniform stress. 04 p0591 A72-15279

Circular disks, rings and perforated plates steady state field components, evolving forced and free vibration natural frequency equations. 04 p0592 A72-15505

Hf backscattering of plane electromagnetic wave at oblique incidence on conducting circular metallic disk, noting polarization dependence on angle. 04 p0493 A72-15524

Stability control of rotating circular plates with edge slots and membrane stresses by finite element method. [ASME PAPER 71-WA/AUT-2] 05 p0733 A72-15951

Thin circular flat plate simply supported at three points on circumference, obtaining vibration mode shapes and eigenvalues. 05 p0738 A72-16532

Thermoelasticity equations for thermal shock effect on freely supported circular plate, describing deformation and temperature field interactions. 05 p0741 A72-17147

Elastic constants measurement using vibrating wire strain gages on diametrically loaded circular disk and ring specimens. 06 p0818 A72-18325

Elastic stability of laminated circular plate with rectangular anisotropy under in-plane compression forces along edge. 07 p1090 A72-19693

Symmetrical bending of variable thickness circular plate solved by classical method and Reissner and Vekua equations. 07 p1092 A72-19852

Stability loss of circular annular plate under compression, determining critical loads with inner edge free and outer edge hinged or clamped. 07 p1092 A72-19900

Transverse anisotropy effect on collapse loads of plastic rotating disks and circular plates. 07 p1093 A72-19946

Steady viscous incompressible fluid flow in circular disk with prescribed velocity components at low Reynolds numbers, considering computer tested numerical method

07 p0972 A72-20102

Thermal stresses in anisotropic annular, circular and perforated plates with temperature dependent coefficients for lateral surfaces heat removal

08 p1245 A72-21505

Heavy falling body elastic impact against circular plate center analyzed by Timoshenko type wave equation

08 p1247 A72-21814

Stress-strain state of circular three layer laminar plates freely supported at circumference and loaded at edge

09 p1399 A72-22694

Variable rigidity circular isotropic plate vibration and bending, determining flexure surface and natural frequencies in terms of Fourier-Bessel series

09 p1399 A72-22699

Stressed state of circular elastic plate with press-fitted equiaxial disk

09 p1406 A72-23181

Vibration frequencies of slender beams and circular plates with boundary stiffness and damping [ASA PAPER E 5]

09 p1408 A72-23525

Circular plates free flexural vibrations with and without damping, calculating resonant frequencies from corresponding Bessel functions

10 p1555 A72-24194

Green function for stress components in circumferentially loaded circular disk, noting conformal mapping for arbitrary shape

10 p1557 A72-24717

Thin circular plate quasi-static thermal stresses induced by transient temperature distribution on upper face, obtaining series form solution in terms of Bessel functions

10 p1558 A72-24720

External load effects on natural frequencies of free end and centrally loaded cantilever beams and supported or clamped circular plates

10 p1558 A72-24814

Nonlinear structural analysis of circular plates and shells of revolution with geometric and inelastic material nonlinearities, using direct stiffness method [AIAA PAPER 72-353]

11 p1729 A72-25382

Elastic-plastic analysis of large deflection of axisymmetrically loaded circular plates, using incremental theory

11 p1737 A72-26426

Acoustically generated vibration stresses in rigidly clamped Al alloy circular plate, noting stress amplitude distribution dependence on loading frequency bandwidth

11 p1738 A72-26805

Bending problem for circular three layer plate with rigid circular insert, studying deflection under bending moment

12 p1879 A72-27090

Finite element method application to variable thickness circular and annular plates free transverse vibration

12 p1879 A72-27191

Variable shear modulus circular isotropic plate torsion by rigid circular stamp, obtaining stresses and displacements by Fourier analysis

12 p1881 A72-27319

Thin circular plate free vibrations with mixed boundary conditions from differential equations for vibration modes of circular isotropic plate in dimensionless polar coordinates

13 p2053 A72-28395

Nonlinear first order differential equation for carrying capacity of anisotropic circular plates, curved elongate disks and shallow shells of revolution

13 p2054 A72-28457

Free and forced vibrations of circular plates with associated rigidities and masses, obtaining orthogonality condition for natural vibration modes

13 p2059 A72-29501

Large deflection calculation of circular and annular strain hardenable rigid plastic plates under axisymmetric load, using Kirchhoff-Love hypothesis and Tresca flow condition

14 p2165 A72-30440

Large deflection vibrations of free circular plate of lenticular section with constant temperature gradient through thickness, noting thermal stresses effect

15 p2325 A72-31552

Finite element analysis of circular and elliptical plates with curved boundaries, discussing high precision triangular plate bending element modification for accuracy improvement

15 p2326 A72-31715

Large amplitude deflections and induced stresses in uniformly pressure loaded circular plate on elastic foundation, using von Karman coupled nonlinear partial differential equations

15 p2331 A72-32558

Dynamic response and buckling mode of elastically supported circular plates with initial tension under arbitrary surface load

15 p2332 A72-32578

Bending of uniformly loaded circular plate with mixed boundary conditions, calculating deflection and bending moments

15 p2332 A72-32579

Kinematic equations of motion for elastic shaft with circular plate under external forces and moments, noting transverse and torsional vibrations

16 p2469 A72-33250

Stress analysis for circular disk with diametral crack under symmetric and antisymmetric loads, solving integral equations via factorization

16 p2469 A72-33273

Stress analysis in circular disk loaded along circumference, noting results identity for stress presentation by Fourier series, Poisson integral and Green function

16 p2470 A72-33593

Quasi-static thermal stresses in circular disk due to rotating point heat source on surface

16 p2470 A72-33594

Large amplitude vibration of a circular plate with concentric rigid mass.

[ASME PAPER 71-APMW-11] 17 p2625 A72-34319

Nonlinear flexural vibrations of a clamped circular plate.

[ASME PAPER 72-APM-18] 17 p2628 A72-34798

An asymptotic solution for the large deflection of a circular plate with a central hole.

18 p2732 A72-36081

Sonic boom duration effects on thin circular elastic plate transient axisymmetric vibration via Hankel and Laplace transforms

18 p2734 A72-36409

Classical plate theory for variable-thickness isotropic elastic axisymmetric circular plates in partial contact with each other and with rigid smooth surfaces of revolution

18 p2738 A72-37072

Mathematical analogies in a theory of shallow spherical shells and plates allowing for transverse shear

19 p2872 A72-37540

Load capacity of tension-bent and compression-bent circular plates

19 p2877 A72-38161

Short-wave asymptotic representation of the solution to the problem of diffraction by a circular disk

19 p2769 A72-38849

Elastoplastic axisymmetric bending of a clamped circular plate under the action of a conically-distributed variable load

20 p2978 A72-39022

Uniformly loaded thin elastic isotropic circular plate with partly clamped and simply supported edges, determining deflection via solution of biharmonic differential equation

20 p2979 A72-39331

The influence of finite-deformations upon the creep behavior of circular plates.

20 p2980 A72-39693

Thermoelastic problems for multiply-connected plates with heat dissipation at both plane surfaces.

21 p3121 A72-41237

Determination of the limits of applicability of a continuous model when calculating a discrete polar lattice disk

21 p3122 A72-41346

Stress-strain state of thin circular perforated Cu plate under uniform tensile load, showing applicability of small elastoplastic finite deformation theory

21 p3122 A72-41351

Regime factor and stress concentration parameter for sudden heating of solid cylinders and disks, noting thermal stability criterion with allowance for statistical strength

21 p3123 A72-41361

Minimum weight design of circular plates with limited thickness.

21 p3125 A72-41515

Book - Analysis of plates.

21 p3125 A72-41530

Equilibrium equations for given stress concentration in circular and annular plates under tensile loads with different yield points in tension and compression

21 p3126 A72-41545

Hydrodynamic forces acting on rigid disk and circular membrane vibrating in ideal incompressible fluid, noting dependence on phase shift between vibration modes

21 p3126 A72-41552

Weight minimization for elastic circular plates of variable thickness under uniformly distributed load with given stress function conditions

22 p2322 A72-41896

Clamped circular rigid-plastic plates subjected to central blast loading.

22 p2325 A72-42601

Continuum and finite element branching studies of the circular plate.

22 p2325 A72-42603

Symmetrical bending of circular plates using finite elements.

22 p2326 A72-42605

Optimum design of circular sandwich plates.

22 p2329 A72-42843

Extensional vibration of a certain type of composite circular plate with a central hole.

22 p3240 A72-42879

Vibrations of circular plates of variable thickness under an inplane force.

22 p3240 A72-42908

German monograph - Heat stresses in circular plates subject to finite deflections.

22 p3241 A72-43058

Limiting equilibrium of shells of revolution and circular plates with allowance for shear stresses

23 p3348 A72-43789

Dynamic response of circular plates to pulse loads.

23 p3354 A72-44254

A method of determining the eigenfrequencies of closed circular conical plates in the Vlasov-Mustari hypothesis

24 p3459 A72-45441

CIRCULAR POLARIZATION

Design, construction and testing of wideband circularly polarized dipole antenna suitable for ionospheric research

01 p0043 A72-11235

Circularly polarized electromagnetic wave propagation through afterglow helium slab plasma near electron cyclotron frequency

02 p0266 A72-12653

Right handed circularly polarized electromagnetic wave propagation in hot inhomogeneous plasma, deriving local dispersion equation by WKB methods

03 p0393 A72-12949

Strong circularly polarized electromagnetic wave scattering by plasma electron as function of amplitude and magnetic field with radiation reaction

03 p0321 A72-13077

Sacramento Peak magnetograph, discussing modified Doppler-Zeeman analyzer for separate measurements of circularly polarized line displacement

03 p0356 A72-13284

Circular polarization parasitical signal reduction in variable profile antennas by curved wire grating, noting application to solar magnetic field studies by radio methods

03 p0331 A72-13289

Jupiter and Venus cloudy atmosphere reflected sunlight circular polarization measurement, noting sense variations with phase angle and location on disk

03 p0439 A72-14150

Absorption effects on circular polarization in synchrotron radiation, discussing frequency and magnetic field dependence

04 p0570 A72-14550

Circularly polarized microwave damping at electron cyclotron frequency in low density magneto cesium plasma, investigating power absorption coefficient and refractive index

04 p0555 A72-14853

Nonrelativistic charged particle resonating with circularly polarized transverse electromagnetic wave in nonuniform magnetic field, showing Fresnel diffraction pattern-like motion

04 p0557 A72-14951

Hf circularity polarized field strength and plasma density self consistent stationary distribution in weakly inhomogeneous constant magnetic field

04 p0558 A72-15175

Arbitrarily located inclined resonant slot in waveguide antenna, obtaining condition for circularly polarized radiation from scattering parameters analysis

04 p0499 A72-15205

Circular polarization change with wavelength in white dwarf Grw plus 70 deg 8247

04 p0580 A72-15367

White dwarf Grw plus 70 deg 8247 circular polarization spectral structure with molecular absorption bands coincident with Minkowski bands

04 p0580 A72-15368

Semiconductor slab electroconductivity measurement based on circularly polarized microwave propagation in circular waveguide

04 p0502 A72-15533

Reflection and transmission characteristics of circularly polarized horn antenna, discussing bandwidth properties, phase differences, polarization characteristics and voltage SWR

05 p0635 A72-16334

Polarization changes with distance from microwave antenna in near and intermediate zones for circularly and elliptically polarized fields in square and rectangular apertures

05 p0635 A72-16335

Reciprocal effects of rectangular guide-slot radiators with circular polarization, analyzing field ellipticity factor change for cross-cut slot under neighboring array slots influence

05 p0635 A72-16336

Magneto-optical effects on circular polarization in sunspots within Fe I 6302.5 A line

05 p0719 A72-16514

Nonlinear propagation effects of monochromatic circularly polarized vlf waves (whistlers, heli cons/ along field lines in magnetosphere

05 p0658 A72-16603

Circularly polarized hydromagnetic wave propagation upstream in solar wind, noting Doppler shifted whistler and slow electron cyclotron modes

06 p0872 A72-17449

Variable circular polarization in optical emission of X ray source Sco X-1, noting oscillations amplitude

06 p0878 A72-17785

Magnetic field decay in solar microwave burst region evaluated from circular polarization degree time profile

06 p0891 A72-18505

Circular polarization measurements of extragalactic radio sources at 1.4 and 5 GHz

09 p1393 A72-23568

Circular polarization measurements of Crab Nebula pulsar NP 0532, including main pulse leading and trailing edge components

[AD-736711]

09 p1394 A72-23675

Intensity dependent propagation characteristics of circularly polarized high power laser radiation in dense electron plasma, calculating energy losses

10 p1522 A72-24607

Nonlinear interaction between circular coherent light and modulating electromagnetic waves in presence of quadratic electrooptical effect, noting frequency shift

10 p1493 A72-24912

Reflected light beam transverse shift calculated by energy flux conservation argument, noting circular polarization and quasi-limit total reflection

10 p1513 A72-24932

Circularly polarized ultrashort radio wave reflection from lunar and planetary surfaces, determining angular scattering spectrum

11 p1599 A72-26908

Communication satellites microwave circular array antenna for wideband circularly polarized isotropic radiation

[ALAA PAPER 72-529]

12 p1789 A72-27419

Linearly and circularly polarized electromagnetic field effective scattering areas relationships, considering radar reflection in reverse direction

12 p1783 A72-27629

Reflectometer based on quasi-optical transmission line using conversion of incident and reflected waves into opposed circularly polarized components

13 p1954 A72-28375

Circular polarization disputed for Seyfert galaxy NGC 1068, quasar 3C 273 and X ray source Sco X-1

13 p2041 A72-29414

Strong circularly polarized electromagnetic wave scattering by plasma electron with radiation reaction, determining cross section as function of amplitude and magnetic field strength

13 p2015 A72-29427

Negative ions and collision frequency effects on circularly polarized ELF and VLF wave propagation in ionosphere

14 p2084 A72-30128

Anisotropic homogeneous plasmas, deriving computer model to predict effects of circularly polarized parallel plasma waves in external uniform magnetic field direction on instabilities

14 p2140 A72-30938

Variable circular polarization of X ray star SCO X-1 optical radiation due to Thomson scattering in magnetooactive plasma shell

15 p2304 A72-31328

Circularly polarized photon echo decay measurement as function of Cr concentration in ruby, noting relationships to temperature, pulse separation and external magnetic field

15 p2295 A72-32545

Hydroxyl emission sources classification from observed main line polarization and satellite lines

15 p2315 A72-32710

Optical circular polarization search in quasars, Seyfert galaxies nuclei, BL Lac and OJ 287

16 p2456 A72-33472

New measurements of circular polarization and an ephemeris for the variable white dwarf G195-19.

17 p2611 A72-35298

Polarization of solar active regions at 9.5 mm wavelength.

17 p2617 A72-35707

Polarization observations of solar radio emission at the 3.15-cm wavelength

19 p2858 A72-37801

Lunar radar backscattering measurement of 0.86 cm circularly polarized radiation, noting echo polarization ratio and depolarization variations with incidence angle

19 p2868 A72-38735

Linear and circular polarization of synchro-Compton radiation scattered by optically thin power law distribution of gyrating ultrarelativistic electrons

20 p2965 A72-39893

Circular polarisation measurements of the zodiacal light.

20 p2920 A72-39899

Circular-polarization antennas with controlled radiation patterns

21 p3026 A72-40314

Nonlinear theory of the monochromatic circularly polarized VLF and ULF waves in the magnetosphere.

21 p3015 A72-40480

Higher harmonics and transport coefficients of plasmas in circularly polarized magnetic fields and additional electromagnetic fields.

21 p3091 A72-40489

LF circularly polarized electromagnetic waves /helicons/ resonance crystal plates, deriving magnetoresistivity and Hall coefficient

21 p3066 A72-40624

Interstellar circular polarization - Data for six stars and the wavelength dependence.

22 p3228 A72-42572

Sunlight scattering by double reflection on rough and absorbing surfaces, deriving fractional circular polarization from models for comparison with observation

23 p3334 A72-43254

Interstellar circular polarization.

23 p3336 A72-43556

Discovery of interstellar circular polarization in the direction of the Crab Nebula.

23 p3336 A72-43557

Radiation from a free electron interacting with a circularly polarized laser pulse.

23 p3296 A72-43875

Circularly polarized waves in magnetoplasmas containing negative ions.

23 p3323 A72-44533

CIRCULAR SHELLS

Circular cylindrical shells buckling under edge compression at various boundary conditions, obtaining critical loads and wave number from Donnell equations

02 p0292 A72-12107

Elastic equilibrium in circular conical orthotropic shells of linearly variable thickness, investigating stresses under arbitrary loads

02 p0297 A72-12615

Buckling of radially constrained imperfect circular ring loaded within perfect rigid circular boundary, obtaining numerical solution by discrete treatment

04 p0591 A72-15286

Elastic equilibrium of circular conical orthotropic shells with linearly varying thickness, determining real and complex roots of stress state characteristic equation

04 p0594 A72-15710

Circular conical orthotropic shells of linearly variable thickness loaded by distributed and concentrated forces and moments, analyzing stress-strain state by numerical methods

04 p0594 A72-15749

Stress and deflection distribution for circular and elliptical toroidal shells under internal pressure from first order differential equations solutions

07 p1088 A72-19118

Stress-strain state of circular conical shell of linearly variable thickness within small elastoplastic deformation theory, assuming specific convective heat transfer at surface

09 p1401 A72-22722

Moment stress-strain state of two layer circular cylindrical shells under creep conditions

11 p1733 A72-25542

Two dimensional static solutions for cylindrical shells with nonhomogeneous boundary conditions, discussing numerical results for circular shell

12 p1880 A72-27230

Finite circular cylindrical shell under uniform pressure on outer rim, comparing stresses and displacements

13 p2055 A72-28624

Dynamic response of thin circular arches to in-plane forced excitation under cyclic symmetric and unsymmetric support movement

14 p2169 A72-31175

Shells of revolution free of bending under uniform axial loading.

19 p2876 A72-37886

Nonlinear theory for static analysis of moderately thick circular cylindrical shells under axisymmetric loads applied to pyrolytic graphite

24 p3454 A72-44603

CIRCULAR TUBES

Two component flow and optimal strength ratios between core and shell materials during extrusion of composite bimetallic specimens into circular tubes

01 p0077 A72-11078

Start-up flow of viscous incompressible fluid under constant head in entrance region of circular tube

03 p0344 A72-14343

Stainless steel circular tubes size and fittings effects on pneumatic pulse wave distortion and attenuation in fluidic pulse generation system

08 p1111 A72-20928

Monograph on slotted circular waveguide analysis covering boundary value problem solution by Wiener-Hopf and Galerkin procedures and application to far field determination

09 p1279 A72-22925

Adiabatic velocity profiles and pressure variations of developing laminar flow in circular tube, using finite difference computation in FORTRAN IV

10 p1463 A72-23863

IR radiative energy transfer to laminar flow of non-gray absorbing emitting gases through circular tube

10 p1563 A72-25038

Tubular specimens for testing mechanical properties of fiber reinforced composites under axial loading, discussing design, fabrication and end attachment problems

11 p1670 A72-25456

Eddy current extensometer for monitoring long term creep in diameter of pressurized tubular stainless steel specimens

11 p1613 A72-25821

Creep tests for thermal pre cycling effect on time to failure and long term ductility of austenitic steel thin walled tubular samples

11 p1663 A72-26809

High modulus fiber composite circular tube specimens multiaxial load testing, noting gripping methods to reduce transitional strains

12 p1886 A72-28000

Thermal load effect on convective heat transfer in turbulent flow of viscous incompressible liquid in circular tube

15 p2334 A72-31262

Maxwell equations solution for electromagnetic field in circular cylindrical tubes, deriving recursion formulas for computer processing

16 p2364 A72-33668

Magnetic shielding effectiveness of metal cylinder tubes with periodically imbedded annular transverse Bloch walls of high permeability

16 p2369 A72-33669

Spatial and temporal load pulse parameters for circular cylindrical shells /tubes/ dynamic plastic deformation

[ASME PAPER 72-APM-29]

17 p2628 A72-34790

Heat and mass transfer in initial section of circular pipe under stabilized laminar flow, using modified Leveque method

17 p2637 A72-35131

Sound attenuation in acoustically lined circular ducts in the presence of uniform flow and shear flow.

17 p2582 A72-35411

Propagation of an impurity in a laminar flow in a circular tube

18 p2682 A72-36892

Contribution to the theoretical calculation of sandwich structures with tube core

18 p2736 A72-36939

Turbulent mixing of fluids of different density moving in a tube

21 p3044 A72-40129

Unsteady laminar flow in a tube with arbitrary variation of the flow rate in time

22 p3164 A72-41892

Experimental investigation of finite-amplitude acoustic oscillations in a closed tube.

23 p3314 A72-44124

Determination of the radial heat conductivity of multilayer tubes for thermionic converters

24 p3461 A72-44875

CIRCULATION

NT ATMOSPHERIC CIRCULATION

NT BLOOD CIRCULATION

NT BRAIN CIRCULATION

NT CARBOXYHEMOGLOBIN

NT CORONARY CIRCULATION

NT INTERCRANIAL CIRCULATION

NT INTRAVASCULAR SYSTEM

NT ISCHEMIA

NT PERIPHERAL CIRCULATION

NT PULMONARY CIRCULATION

CIRCULATORS [PHASE SHIFT CIRCUITS]

Nonreciprocal microwave ferrite device design, outlining loss-free, cyclic symmetrical, multiport junction circulator theory

01 p0041 A72-10695

Ferrite-loaded waveguide Y-junction field mode identification by eigenvalue phase-frequency characteristics measurement, applying to millimeter wave circulator synthesis

01 p0041 A72-10697

Self consistent junction circulator theory, considering lossless ferrite loaded symmetric n-port junction and numerical design procedures

03 p0330 A72-13232

Bandwidth widening of waveguide H-plane Y-circulator with cylindrical ferrite post coated by dielectric sleeve

04 p0499 A72-15244

Wideband tunnel diode amplifier design, discussing circulator off-band impedance characteristics improvement through voltage standing wave ratio suppression network

05 p0638 A72-16594

L- and X-band Y junction waveguide circulators for medium and peak high powers in radar applications, discussing operation principle and design

06 p0785 A72-18311

Dissipative magnetic parameters measurement in ferrite and insertion loss measurement in waveguide Y-circulators below microwave resonance
06 p0786 A72-18367

Ferrite loaded X band waveguide Y junctions eigenvalue frequency dependence measurement to identify modal resonance and arrange displacement for circulator operation
12 p1790 A72-27508

Ferrite microwave limiter-filters and circulators using resonant rotation of polarization plane
13 p1927 A72-28409

Quasi-one dimensional spectral analysis of input signal by delay line circulator, discussing ring frequency characteristic influence on harmonic signal buildup efficiency
13 p1930 A72-29043

Multiple port waveguide circulators bandwidth performance calculation to include higher order cylindrical and evanescent modes
15 p2205 A72-31356

Three resonant mode waveguide circulator adjustment with eigenvalues associated to resonant field patterns
15 p2208 A72-32388

Series stabilization reflection type tunnel diode microwave amplifier synthesis with allowance for real circulator reactance
18 p2665 A72-36107

Slotted-line measurement of insertion loss in three-port ferrite junction circulator.
19 p2775 A72-38636

Junction circulator shunt conductance and susceptance-slope parameter calculation by constituent resonator input admittance formation, describing quarter wave mode operation
23 p3270 A72-43604

CIRCULATORY SYSTEM

NT AORTA

NT ARTERIES

NT BLOOD VESSELS

NT CAPILLARIES [ANATOMY]

NT GLOMERULUS

NT VASCULAR SYSTEM

NT VEINS

Physical conditioning effect on central and peripheral circulatory responses to arm work, measuring cardiac output at 80 percent maximum aerobic power
04 p0473 A72-14900

Control system model integrating human left ventricle and circulatory system mechanics and regulation by central nervous system
07 p0934 A72-20356

Oxygen intake and cardiac output measurements during various treadmill and bicycle ergometer exercises, relating exercise type to heart rate and arteriovenous oxygen differences
08 p1123 A72-20885

Hydraulic transmission line equations for computer simulation of arterial circulatory systems
10 p1431 A72-24811

Heart and circulatory system functional diagnostics, discussing ECG, blood pressure, X ray, phonocardiographical and pulmonary examinations
12 p1760 A72-27271

Human cardiovascular function change as indication of hypoxic circulatory stress, using noninvasive cardiographic measurements of cardiac electromechanical time intervals
12 p1769 A72-27470

Gas mask-caused air flow resistance effects on respiratory and circulatory response to exercise, assessing maximal oxygen uptake
13 p1906 A72-29818

Physiological and psychological effects of noise noting vulnerability of circulatory apparatus, neurovegetative system and stomach
14 p2079 A72-30696

Digital computer technique for ballistocardiography simulation, using distributed parameters for vessel segments in circulatory system model
18 p2652 A72-36038

Fluid transfer between blood and tissues during exercise.
18 p2650 A72-36560

CIRRUS CLOUDS

Airborne ruby lidar application to cirrus and haze layers measurements, deriving optical parameters
06 p0777 A72-18448

CISLUNAR SPACE

Explorer 35 and OGO 3 data on picogram size dust particle distribution in cislunar and selenocentric space, showing fluctuations during meteor shower periods
15 p2309 A72-31937

CITIES

Urban geography of U.S. cities on vertical aerial photography, considering site, location, street orientation, expansion, business districts and transportation networks
09 p1301 A72-23281

CIVIL AVIATION

General and commercial aircraft service needs in air transportation, considering FAA and CAB roles and policies
02 p0304 A72-11716

Civil aviation air transportation contributing factors to American economy, considering disposable income, airline fares and time-trend variable
02 p0304 A72-11721

Soviet book on civil aircraft high altitude equipment covering air conditioning systems, oxygen equipment and cabin pressurization
02 p0156 A72-12295

Soviet book on course-indicating systems and automatic navigation aids for civil aviation aircraft covering design, operation principles, error analysis and reliability
02 p0256 A72-12298

Civil aviation communication systems, discussing short and long range communications, satellite channel capacities, digital data link systems, ATC, weather broadcasts, etc
03 p0322 A72-13416

American civil aviation future development, discussing passenger and freight markets growth, aircraft types and FAA role
04 p0464 A72-14811

Civil aircraft technological constraints and requirements, discussing noise, congestion and performance characteristics of rotorcraft, STOL, VTOL, hypersonic and supersonic transports
05 p0611 A72-15774

Canadian STOL design, development, production, airports and civil air transportation applications
05 p0751 A72-15775

Civil aviation R and D policy study, showing priorities for aircraft noise and congestion abatement and short haul systems
05 p0611 A72-15780

Rotary wing aircraft design features and performance, discussing military and civilian helicopters and future developments
05 p0612 A72-16734

Civil and military aircraft forced diversion, discussing legal counters and aircraft restoration
05 p0753 A72-17166

French civil aircraft displayed at 1971 Le Bourget Air Show, discussing design and performance characteristics of Airbus, Concorde, Caravelle, Corvette, Falcon, Fregate, STOL-A-904 and Mercure
05 p0614 A72-17193

Federal Air Regulations procedures for civil transport aircraft flight testing under natural and/or simulated icing conditions
06 p0760 A72-18501

Aviation insurance and claim servicing risks in aircraft accidents, discussing coverage, claims investigation, litigation and settlement
07 p1106 A72-20673

Future civil air transport trends, considering passenger and cargo growth, travel frequency per capita income and STOL market
08 p1257 A72-22150

LOX supply systems installation for civil transport aircraft crew and/or passenger breathing oxygen [SAE AIR 1223]
11 p1584 A72-26030

Charter air traffic regulations under German air law, discussing legal safeguards relative to economic, personnel, technical and organizational aspects
11 p1748 A72-26559

Trends in civil ATC discussing plans to increase terminal capacity, surveillance system and use of multiple synchronous satellites for ocean travel efficiency improvement
12 p1842 A72-27103

Instrument landing systems specifications for civil and military aviation, suggesting replacement type development based on existing configurations
12 p1842 A72-27110

STOL aircraft role in civil aviation, discussing short range operation, ATC, reduced noise and weather capability
12 p1754 A72-27518

Civil aviation approach and landing guidance systems evolution, discussing ILS development, state of art and future requirements
13 p1996 A72-29014

Flight psychiatry in NATO contrics, discussing organization and facilities with respect to military and civil aviation
13 p1911 A72-29858

V/STOL aircraft potential for short haul civil air traffic, discussing present technology and investment costs in comparison with advanced ground transportation systems
13 p1898 A72-30076

Psychological criteria for flying personnel selection in civil aviation, noting performance prediction based on maximum likelihood estimates
14 p2080 A72-30816

U.S.S.R. civil aviation regulations on takeoff and landing minimum conditions for cloud ceilings and visibility range for various aircraft characteristics and equipment
14 p2129 A72-30820

Avionics equipment for signal processing onboard civil aircraft to improve flight safety, discussing uses of OMEGA navigation system and digital computers
15 p2193 A72-31178

Low cost microwave scanning beam landing systems for interim instrument landing system replacement in civil aviation
15 p2272 A72-32217

National airports system for UK civil air transportation, discussing economic, operational, accessibility and social aspects
15 p2214 A72-32321

ATC system organization in terms of optimal operating conditions for civil and military airspace users, discussing navigation systems, human factors, equipment reliability, etc
15 p2272 A72-32455

Management information system role in cost effective civil and military aircraft operations, discussing hardware modification and human resources and communication system adaptation
15 p2339 A72-32548

Air cushion landing system application for civil air transportation, discussing operation, braking and parking
16 p2348 A72-33184

Commercial airport and air transport service economic impacts on business and industrial communities
16 p2481 A72-33312

Civil aviation safety - Conference, Beirut, Lebanon, November-December 1971
16 p2481 A72-33326

Major civil airport planning, discussing information gathering and processing for aviation demand, aircraft movements revenue and cost forecasts and pricing policy evaluation
16 p2481 A72-33327

Major civil airport passenger and cargo terminal complex design and layout planning, discussing various facilities and equipment requirements
16 p2373 A72-33329

FAA policy in issuing civil airport operating certificates and establishing minimum safety standards
16 p2373 A72-33330

STOL aircraft for civil transport applications, considering optimum design concepts, noise reduction and terminal facility requirements
16 p2348 A72-33331

Developing countries civil aviation airlines evolution, considering government fund allocation, international money credibility, skilled manpower, equipment, fare and tourism expansion
16 p2481 A72-33332

Commercial airlines aircraft selection factors, considering size, range, economics, traffic, runway quality, maintenance and operating costs, reliability and cargo handling
16 p2348 A72-33333

ICAO assistance to member states in various transport airports and navigation facilities economics including accounting and financial statistics
16 p2481 A72-33334

The role of the International Civil Aviation Organization [ICAO] in organizing Search and Rescue Services [SAR].
17 p2638 A72-34430

The legal position of civil air personnel
17 p2639 A72-35762

Environmental considerations in airport development.
18 p2743 A72-36778

USSR electric impulse de-icing system design.
18 p2648 A72-37033

The future of general aviation in Europe.
18 p2743 A72-37093

Supercritical aerodynamics technology, noting lifting surface cross sectional profile and structural weight reduction
19 p2746 A72-37678

Inertial platform pursuant to ARINC-571 specifications, noting capability for integration into surface navigation system or autonomous operation
19 p2831 A72-37799

Future aspects of business aviation, discussing pilot training and aircraft reliability and maintenance in context of flight safety
20 p2988 A72-39741

Corporate business aviation performance record in light of aircraft accident statistics, noting high percentage of approach-landing accidents and means for improvement
20 p2888 A72-39743

Acoustic pressure and sound intensity levels and noise annoyance international standards for civil aircraft noise reduction
20 p2888 A72-39803

Airlines requirements for European airbus, discussing design of aircraft structure, control, pressurized cabin and propulsion system
21 p2994 A72-40174

A method of solving the operational planning problem for an engineering aircraft base
21 p3039 A72-40178

An air traffic controller's view on area navigation and ATS requirements related thereto.

21 p3081 A72-40299

Application of the head-up display /HUD/ to a commercial jet transport.

21 p3060 A72-41256

Economic and social aspects of commercial aviation at supersonic speeds.

[ICAS PAPER 72-51]

Russian book - Aviation meteorology.

22 p3200 A72-42024

CLADDING

Bond zone wave formation in explosion cladding, predicting critical collision velocity and angle with fluid flow model

01 p0077 A72-11031

Coextrusion of metal powder and ceramic dispersions clad alloyed Al as function of cartridge density and reactor core length

02 p0233 A72-11456

Heat treatment effect on elastic properties of steel clad material for devices in sulfuric acid, discussing structural changes and optimal conditions

07 p1020 A72-20415

Thin oxidation resistant alloy claddings for superalloys, comparing performance with aluminide coatings by cyclic furnace and high velocity burner rig tests

14 p2113 A72-30271

Gas shielded strip electrode welding and cladding, discussing electric arc behavior, weld bead penetration depth, drop transfer speed, weld microstructure, etc

15 p2243 A72-31324

Slurry explosives for metal cladding, discussing applications to pipe joints, bearing sleeves, recoil rods, gun barrels and cylinder liners

16 p2398 A72-33357

Deformation substructures in stainless steels under low cycle high strain fatigue tests evaluation for application as fuel cladding for fast breeder reactors

16 p2411 A72-33825

Thermionic fuel cladding development, compatibility, stability and performance for uranium carbide-tungsten and uranium oxide-tungsten systems at high temperatures under irradiation

18 p2709 A72-36164

CLAMPS

Static deflections determination of thin rectangular plates with point clamped restraints, using Ritz method with Lagrange multipliers

10 p1555 A72-24193

Probabilistic model for tensile strength of brittle fibers, discussing clamping effects at various gage lengths and Weibull flaw structure

23 p3305 A72-43490

Vibration frequencies and modes determination for clamped rectangular plates of orthotropic material, using weighted residual technique and polynomial approximation

24 p3455 A72-44683

CLARK Y AIRFOIL

U AIRFOIL PROFILES

CLASSICAL MECHANICS

NT ASTRODYNAMICS

NT CELESTIAL MECHANICS

NT KEPLER LAWS

NT ORBITAL MECHANICS

Inertial-gravitational mass ratio in classical and quantum case, proving equivalence principle non-validity for Brans-Dicke gravitation theory compared to Einstein theory

01 p0102 A72-10861

Perturbed motion differential equations for stability and integration problems in mechanics

08 p1205 A72-20964

Applied nonlinear mechanics problems solutions by linearization of differential equations

09 p1343 A72-23602

Atomic hydrogen viscosity and thermal conductivity coefficients for 1-100,000 K, using quantum theory for low temperatures and classical mechanics for high temperatures

13 p2065 A72-29299

Quasi-classical mechanical approximation in molecular scattering, using Monte Carlo methods for Jacobian determinant evaluation

14 p2134 A72-30836

Diatomic molecules partition functions derivation by classical and quantum mechanical theories for simple harmonic oscillator and square-well potential

15 p2280 A72-31693

CLASSICAL MECHANICS

NT DICHOTOMIES

NT HIERARCHIES

NT INDEXES [DOCUMENTATION]

Automatic classification over extended remote sensing test sites, examining causes of variation in multispectral scanner data response

02 p0228 A72-11875

Red, blue and color anomalous ratio carbon stars properties determination from comparative analysis of R-N and C classifications

03 p0433 A72-13490

Classification of mass spectra on computers /COM-SOC/ for compound characterization of complex mixtures with geochemical and environmental applications

07 p0980 A72-20393

Truth table classification and numerical identification of character patterns of elements in groups and clusters

09 p1265 A72-22644

Automatic classification algorithms using heuristic, partitioning and variational techniques

09 p1283 A72-23429

Eight color intermediate band photometric three dimensional star classification system, taking into account spectral classes, absolute magnitudes, Fe/H ratios and interstellar reddening

09 p1392 A72-23546

Galaxies clusters classification on basis of relative contrast between brightest member and typical bright galaxy population of cluster

10 p1548 A72-24964

Stellar photometric classification by comparing color indices to indices of standard stars with UPX-YZVS system, outlining computer method

11 p1715 A72-25294

Solar proton event classification system with index of three digits representing proton flux, absorption and sea level neutron monitor response measurements

11 p1714 A72-26425

Planetary nebula classification based on forbidden line ratios and morphology, discussing galactic plane distribution, radial velocities and evolution

12 p1867 A72-27209

Electrochemical oxidation and classification of fuel cells according to electrolyte, electrode, fuel, catalyst and temperature

16 p2351 A72-33877

Classification of the magnetohydrodynamic motions of a rotating fluid

19 p2839 A72-37392

Probability threshold of data element similarity as separation criterion for automatic multiparameter biomedical data classification

20 p2893 A72-38937

CLASSIFYING

Biological cell sorting by differential fluorescence generated electric signals via laser beam illuminated liquid stream

09 p1273 A72-23403

Theorem proved for pattern classification system effectiveness for system reliability prediction

10 p1504 A72-23996

Ti alloy metastable phases classification, including alpha-prime, secondary alpha, omega, beta and alpha phases

12 p1828 A72-27290

Rectangular, elliptical and parabolic waveguides TM and TE modes relation and cutoff wavelength analysis by finite element method, suggesting mode classifying system

15 p2205 A72-31354

CLAYS

NT KAOLINITE

Amino acid-phosphate anhydrides polymerization in presence of clay minerals, noting reactions superposition and monomer diffusion

04 p0483 A72-14774

Urease-active colloidal organo-complex extraction from Dublin clay loam soil, describing filtration procedure

13 p1913 A72-29399

CLEAN ROOMS

Planetary quarantine microbial contamination control, considering clean room concept and microbiologic barrier techniques

01 p0019 A72-10821

CLEANERS

NT AIR FILTERS

CLEANING

Powder metallurgy Ni-Cr thoria cleaning by reduction with atmosphere of hydrogen plus HCl or HBr

10 p1488 A72-24697

High and ultrahigh vacuum equipment and components selection, discussing gas-surface interactions, contamination and cleaning problems

19 p2835 A72-38391

CLEANLINESS

Nonsterile space flight hardware effects on planetary quarantine, evaluating contamination sources, design and mission parameters, cleanliness conditions and bioload

01 p0020 A72-10824

Steel cleanliness conditions for formation and decantation of inclusions due to deoxidation during production up to solidification

03 p0371 A72-13198

Forecasting technique for accumulated particulate contamination on spacecraft assemblies, discussing cleanliness optimization and test procedures

07 p0915 A72-18763

Electric contact phenomena in ultraclean and specifically contaminated metallic systems, noting resistance relationship to load curves and surface conditions

10 p1448 A72-24172

High level cleanliness maintenance and contamination control for instrument unit ring guidance system in Saturn 5 launch vehicle

24 p3388 A72-45297

CLEAR AIR TURBULENCE

Stratospheric CAT relationships to baroclinic zones and Richardson number examined from aircraft observed cross sections data

01 p0096 A72-11282

Clear air turbulence radiometric detection by IR vertical scan technique, associating atmospheric lapse rate anomalies with CAT related temperature inversions

02 p0225 A72-11820

Stratospheric circulation and air temperature horizontal and vertical distribution, discussing CAT at supersonic transport heights

04 p0541 A72-14676

CAT, cloud cover and icing forecasting for aviation in terms of numerical model and real atmosphere

04 p0542 A72-14689

CAT inducing atmospheric conditions effects on SST flight, discussing turbulence in convective clouds and kinetic energy spectra of atmospheric motions

04 p0543 A72-14693

CAT detection by airborne laser Doppler radar and ground based ultrasensitive microwave Doppler radar methods

04 p0543 A72-14822

Airborne CAT detection by passive IR radiometry, reducing false alarms due to temperature anomalies

04 p0543 A72-14828

Airborne remote CAT detection equipment, examining pulsed Doppler laser and IR radiometry

04 p0521 A72-14831

Clear air atmospheric target detection, comparing bistatic and monostatic radar techniques

05 p0630 A72-16835

Clear air intermittent turbulence energy budget from aircraft data, obtaining turbulence parameters along aircraft path through application of electronic filters

09 p1344 A72-22437

Horizontal temperature variations relation to stratospheric CAT based on U-2 flight data

09 p1344 A72-22438

Clear air turbulence association with rapid temperature change over Bahrain, suggesting convectionally induced internal wave dissipation in inversion layer as turbulence mechanism

09 p1346 A72-23424

Microwave equipment and technology application for instrument landing, terminal ATC, millimeter wave CAT detection and satellite communications

10 p1509 A72-24036

GMD-1 tracking system for mesoscale wind data, minimizing elevation angle errors in jet stream CAT program by upwind release of rawinsonde

10 p1508 A72-25080

High level Canberra flight for three dimensional picture of wind and temperature fields, showing CAT, gravity waves and smooth flight characteristics

12 p1841 A72-27709

Aircraft flight conditions effect on low altitude critical air turbulence in terms of gust velocity components for CAT prediction

13 p1993 A72-28861

CAT forecasting based on fluid mechanics experimental studies of stratified shear flows stability and meteorological analyses of aircraft CAT encounters

13 p1994 A72-28866

Synoptic meteorological parameters vs CAT encountered in stratosphere by XB-70 airplane, presenting frequency distributions and probability tables

13 p1994 A72-28867

Persistent intense CAT in upper level frontal zone, discussing synoptic features, vertical wind shears, radar echoes and turbulence intensity

13 p1995 A72-29622

Clear air turbulence nonlinear generation mechanism based on finite amplitude periodic waves in stratified shear flow critical layers, considering buoyancy, viscosity and heat conduction effects

14 p2127 A72-30226

Meteorological data analysis for CAT encounter of Boeing 747 flight over Nantucket Island on 4 November 1970

16 p2418 A72-33525

Atmospheric turbulence and the ATC system.

18 p2663 A72-37049

Simplified equation for amplitude scintillations in a turbulent atmosphere.

21 p3083 A72-40143

CAT probabilities relationship to temperature radiance gradients determined by IR spectrometers onboard Nimbus satellites

23 p3310 A72-43614

Clear air turbulence detection possibility by optical laser radar and turbulent fluctuation correlations

23 p3264 A72-43898

Measurements of air motion in regions of clear air turbulence using high-power Doppler radar.

24 p3421 A72-44978

CLEARANCES

- Bushing seal with pressure dependent clearance for reciprocating piston rod or rotating shaft, presenting laminar and turbulent axial flow theory
08 p1178 A72-21936
- Brazing furnaces and heat treatment under vacuum
22 p3163 A72-42635

CLEAVAGE

- Double cantilevered specimen crack growth, computing fracture surface energies from dynamical cleavage analysis
05 p0735 A72-16019
- Critical cleavage stresses dependence on ordering degree in Ni-Cr alloy
06 p0835 A72-18745
- Chemical and mechanical properties relationship to stress corrosion in high strength Al-Cu and Al-Zn-Mg alloys, emphasizing grain boundaries cleavage energy
14 p2117 A72-30536
- Tectonic dewatering and strain in the Michigamme Slate, Michigan.
18 p2686 A72-36223
- Surface energy and cleavage plane observation of brittle fracture for W single crystal in tension as function of orientation and temperature
18 p2702 A72-36750
- Estimation of the cleavage strength of polycrystalline metals from the internal energy
19 p2818 A72-38010
- Hydrogen gas effects on cleavage cracking in Ti-Al-Mo-V samples under static and cyclic loading
20 p2939 A72-39308

CLIFFS

- Radar observations of Martian craters and scarp during 1971 opposition
04 p0579 A72-15359

CLIMATE

- Solar radiative constant and stratospheric volcanic dust effects on circulation and climate anomalies
06 p0840 A72-17623
- Bicycle ergometer measurements of thermoregulation input and output under wide range of work load and climatic conditions, deriving correlation equation
11 p1579 A72-25874

CLIMATOLOGY

NT BIOCLIMATOLOGY

NT MICROCLIMATOLOGY

- Earth radiation climatology, noting qualitative agreement between calculated and satellite measured outgoing radiation data with allowance for inaccuracies due to albedo levels overrating
01 p0095 A72-10958
- Meteorological tests for mathematical models in study of climate changes
06 p0843 A72-18451
- Communications and TV broadcasting antenna feeder cost-efficient designs, relating climatology, oscillation theory and structural aerodynamic stability
07 p0955 A72-19513
- Atmospheric light scattering matrices from nighttime air flows, showing climatic variability and similarity between Crimean and Moscow measurements
07 p1031 A72-20700
- Steady state global climatic model for earth-atmosphere-ocean system, discussing perturbations effect on stability
09 p1343 A72-22426
- Soil science and climatology use for archeological site detection on aerial photographs
09 p1303 A72-23296
- Worldwide inventory and monitoring of ice and snow aggregations via satellite photography, discussing climatological aspects
09 p1303 A72-23302
- Solar activity relation to geophysical phenomena, discussing atmospheric circulation and climatic variation cyclicity and sunspot corpuscular fluxes
12 p1842 A72-28207
- Global horizontal sounding technique balloon flights, determining Southern Hemisphere temperate latitude circulation climatology
13 p1988 A72-28443
- Thunderstorm encounter probability at SST altitudes for selected cross country routes, using radar observation data
13 p1992 A72-28853
- Mathematical criteria for probable and potential aircraft icing occurrence, using radiosonde and empirical climatological data
13 p1993 A72-28856
- Local climatic forecasts via influence equations based on past meteorological data as initial conditions, obtaining solution by operational analysis methods
16 p2418 A72-33379
- Climatic changes due to stratospheric perturbation by propulsion effluents of high altitude aircraft flights [AIAA PAPER 72-658]
16 p2388 A72-34076
- A climatology of the potential vertical extent of giant cumulonimbus in some selected areas.
18 p2707 A72-36700
- A square equal-area map of the world.
20 p2915 A72-38961

Numerical climatic-change experiments - The effect of man's production of thermal energy.
20 p2947 A72-38962

Atmospheric surface layer light scattering matrices from nighttime air flows, showing climatic variability and similarity between Crimean and Moscow measurements
20 p2948 A72-39014

Electronic simulator for calculating effective temperatures in the establishment of climatological procedures
21 p3077 A72-40166

Temporal behavior of hemispherically averaged geostrophic zonal and meridional flow from dynamic climatology studies of Northern Hemisphere large scale circulation
21 p3077 A72-40251

Lower planetary boundary layer mesoscale flow patterns and transport climatology, using hourly averaged wind data from wind tower station network
21 p3077 A72-40252

Russian book - Calculated wind velocities at heights of the lower atmospheric layer.
22 p3200 A72-42077

Climatology of the occurrences of thundery weather over Gauhati Airport.
22 p3202 A72-42887

Reproduction of the climatic distribution of meteorological elements on the basis of a nonadiabatic spectral model of the atmosphere
23 p3311 A72-43626

CLIMBING FLIGHT

- USAF V-51R noise protector earplugs modification to allow for pressure equalization during aircraft climb and descent
12 p1774 A72-28276
- STOL aircraft minimum noise takeoff trajectories determination, taking into account engine thrust and listeners distance from noise source [AIAA PAPER 72-665]
16 p2349 A72-34072
- The dynamics of the ascending flight of sounding rockets [ONERA, TP NO. 1056]
22 p3231 A72-42582
- Maximum principle and penalty function technique for flight optimization, noting optimal control for climbing flight
24 p3369 A72-45444

CLINICAL MEDICINE

- Clinical electrocardiography diagnostic capability, discussing phase plane cardiogram sensitivity to aberrations in QRS contours
01 p0017 A72-10148
- Ballistocardiography and clinical studies - Conference, Atlantic City, 2 May 1970
03 p0314 A72-13141
- Coronary angiography findings in 263 patients of different age groups compared with history of angina pectoris, risk factors and ECG at rest
03 p0314 A72-13177
- Clinical response to nitroglycerin therapy correlation with coronary angiography as diagnostic test for coronary artery disease in patients with chest pain
07 p0920 A72-19993
- Idiopathic subvalvular aortic stenosis characterized by muscular or membrane obstruction in left ventricular infundibulum, discussing diagnostic importance for pilots
07 p0933 A72-20189
- Flight personnel statistical survey of clinical, physical and psychic causes of temporary and permanent flight service unfitness
07 p0923 A72-20447
- Reliability of electroencephalography as diagnostic method from specialists interpretation of curve morphological features, discussing normal and pathological record evaluation
08 p1124 A72-21000
- Dietary and pharmacological treatment of atherogenic hyperlipidemias from lipid-sugar balance and drug efficacy studies
08 p1117 A72-21547
- Clinical death period and reanimation concepts, noting erroneous interpretations of irreversible histological alterations, revival attempt period and organism self reanimation potential
09 p1266 A72-22876
- Physiological and clinical effects of long distance flight in pressurized commercial planes with simulated altitudes over 1500 meters
12 p1771 A72-27486
- Clinical diagnosis of ST/T depression in resting ECG, noting coronary heart disease and left ventricular hypertrophy
12 p1772 A72-27733
- NASA reliability and quality assurance methodology to improve hospital biomedical equipment, using space electric rocket test example
12 p1814 A72-27960
- Frontal sinus hematoma incidence in flying personnel and scuba divers, discussing diagnosis and clinical treatment
12 p1765 A72-28275
- Annual clinical and physiological evaluation of test pilots physical performance over ten year period from

CLOSED ECOLOGICAL SYSTEMS

- body composition, pulmonary function and work capacity measurements
14 p2082 A72-31093
- Coronary heart disease discriminatory factors from comparison with healthy controls, noting diastolic hypertension significance
15 p2183 A72-31282
- Diagnostic errors in draft age patients, noting doctor, examination methods, disease type and patient factors and psychosomatic disturbance detection
16 p2359 A72-34149
- Clinical observations as a research method in physiology
17 p2504 A72-35017
- Clinical IR thermography with Thermovision camera for body temperature discontinuity detection, discussing image resolution
18 p2655 A72-37196
- A system for the mass examination of electrocardiograms.
19 p2760 A72-37853
- A model corporate pilot physical program.
20 p2897 A72-39746
- The Macruz index and its clinical evaluation in electrocardiography with regard to the selection and control of air crews
21 p3009 A72-41193
- CLOCK PARADOX**
Particle motion in uniform acceleration field via Schwarzschild line element of general relativity, applying to clock paradox
03 p0388 A72-13227
- Lorentz transformation between fixed and inertial reference frame in uniform gravitational field, discussing application to clock paradox problem
03 p0388 A72-13228
- Earth rotational direction and speed effects on terrestrial circumnavigation relativistic time, suggesting clock paradox empirical proof
06 p0849 A72-18381
- Around-the-world atomic clocks - Observed relativistic time gains.
17 p2584 A72-35839
- CLOCKS**
NT ATOMIC CLOCKS
NT CHRONOMETERS
Propagation delays for clock synchronization from synchronous satellite tracking by range measurements
05 p0628 A72-16563
- Self lubricating materials for maintenance-free clocks antifriction bearings, discussing friction and wear behavior
09 p1319 A72-23562
- Multichannel clock with dekatrons using multiple crossbar connector for program commutation and command pulse splitting
13 p1933 A72-29919
- Time/frequency technology application to reliable aircraft collision avoidance system, discussing precision time-ordered techniques, frequency control and synchronization and flying clocks
15 p2268 A72-32072
- NASA global tracking network clock time synchronization to microseconds accuracy via GEOS-11 satellite
15 p2199 A72-32079
- CLOSE PACKED LATTICES**
Beryllium microstructure and hexagonal close packed polycrystalline material residual thermal stresses, calculating thermal expansion coefficients
01 p0087 A72-11028
- Hexagonal close packed Ti-Al alloys, determining stacking fault probability with X ray powder diffraction line profiles and Fourier analysis
01 p0087 A72-11029
- Ti, Zr and Hf hcp-bcc phase transformation isochromat spectroscopic investigation, noting fine structures to confirm electron state density
09 p1371 A72-22849
- Quenching produced martensitic transformations from equilibrium beta phase region for Ti alloys with Ta
16 p2408 A72-33618
- Electron microscope double contrast images to identify Burgers vectors of close packed metal crystal dislocations
19 p2846 A72-38590
- Phonon dispersion relations and Debye characteristic temperature for Ti, Hf and Y hcp lattices
24 p3415 A72-45629
- CLOSED CIRCUIT TELEVISION**
Remote transmission of telescope coordinate readings by industrial television
21 p3056 A72-41448
- CLOSED CYCLES**
NASA closed cycle MHD facility for power generation, discussing system components, design and operation [AIAA PAPER 72-103]
05 p0616 A72-16936
- CLOSED ECOLOGICAL SYSTEMS**
Miniaturized magnetic mass spectrometer for trace contaminants continuous monitoring and control, discussing applications to closed atmospheric systems in spacecraft and undersea environments [AIAA PAPER 71-1122]
01 p0068 A72-10558

Human blood carboxyhemoglobin saturation relation to inspired air oxygen and CO concentrations from small closed rebreathing system tests
[AD-740929] 04 p0472 A72-14863

Closed loop life support systems, discussing manned ninety day test in space station simulator, Soviet experiments and water and oxygen regeneration
10 p1432 A72-24973

Human immunobiological status during prolonged maintenance in bioregenerative life support system, discussing possible allergic reaction to chlorella gaseous metabolites
13 p1910 A72-29312

Vapor-liquid equilibrium analysis of water soluble volatile organic compounds in closed airtight systems by gas chromatography
13 p1910 A72-29326

Carbon monoxide dynamics in chlorella reactor closed environment and in man-chlorella system at relatively constant level
14 p2078 A72-30377

Man, chlorella and wheat plant in life-supporting biological system, showing compatibility relative to gas and water exchange
15 p2189 A72-31826

Thermodynamic properties and mathematical modeling of complex biological systems, considering energy and mass exchange in photosynthesizing organisms for exobiological life support
20 p2891 A72-38960

Space station atmospheric revitalization system design, covering temperature, humidity, carbon dioxide, contaminant and oxygen generation and composition control and vehicle configuration
[ASME PAPER 72-ENAV-24] 20 p2894 A72-39153

Functional reliability of the biological component of a life support system
21 p2998 A72-40448

Expired air as a source of spacecraft environment carbon monoxide contamination
24 p3375 A72-45120

The problem of decontaminating and preserving drinking water in spacecraft water supply systems
24 p3375 A72-45121

Regeneration of oxygen from carbon dioxide and water
24 p3375 A72-45183

Spacecraft food synthesis, using carbon dioxide and water from chemically regenerated human metabolic and waste products
24 p3376 A72-45277

CLOSED FAULTS

U GEOLOGICAL FAULTS

CLOSED LOOP SYSTEMS

U FEEDBACK CONTROL

CLOSTRIDIUM BOTULINUM

Thermolabile triose phosphate isomerase in psychrophilic Clostridium at moderate temperatures
10 p1426 A72-24750

CLOSURE LAW

Closure problem in statistical theory of isotropic turbulent velocity field
03 p0342 A72-13900

Closure schemes and retention of third moments in stochastic dynamic equations for numerical weather prediction, discussing imperfect forcing effects and kinetic energy relations
03 p0385 A72-14230

Closure approximation in hierarchy stochastic differential operator equations in statistical mechanics
04 p0540 A72-15257

Closure approximation for energy transfer mechanism of stationary locally isotropic turbulence in inertial and dissipation ranges
06 p0802 A72-18545

CLOSURES

Fragmentation and closure in afterimages of bright flash stimuli
03 p0317 A72-13938

CLOTH

U FABRICS

CLOTHING

NT FLIGHT CLOTHING

NT HELMETS

NT PRESSURE SUITS

NT PROTECTIVE CLOTHING

NT SPACE SUITS

NT SUITS

Russian book - Climatic conditions and the thermal state of man.
21 p3006 A72-40458

CLOUD CHAMBERS

Particle multiplicity and momentum spectra for high energy inelastic nuclear interactions in Wilson chamber with polyethylene target
06 p0868 A72-17261

Muon track curvatures in Wilson chamber magnetic field for calibrating ionization levels of logarithmic increase
06 p0811 A72-17293

Semiautomatic stereophotographic processing of cosmic ray shower particle interaction data from Wilson chamber
07 p0988 A72-19865

Study of high energy /25-10,000 GeV/ interactions with a multiplate cloud chamber using Monte Carlo simulations for energy calibration.
17 p2585 A72-34922

CLOUD COVER

Venus subcloud layer, investigating radiant heat transfer in convective lower atmosphere
01 p0128 A72-10370

Lake effect cloud examination by TIROS and ESSA photography, noting parallel bands with larger dimensions than cloud streets
01 p0095 A72-11280

Soyuz manned spacecraft meteorological observations, dealing cloud cover in various climatic zones, atmospheric turbidity and snow cover in mountain areas
02 p0253 A72-11731

Space TV images use in hydrospherical temperature discontinuity front location, examining cloud cover distributions over Sea of Japan
02 p0214 A72-11872

Meteorological precipitation and earth surface under cloud characteristics from airborne microwave radiation measurements using millimeter and centimeter waves
02 p0216 A72-11889

Ageostrophic vertical wind field determination from satellite cloudiness data, including geopotential pressure equations
02 p0253 A72-12537

Venusian polar tropopause and cloud layer from IR spectral recording in carbon dioxide band near inferior conjunction for crescent regions
03 p0436 A72-13814

Temperature reduction produced by partial cloud cover effect on radiation received by Nimbus 3 IR radiometer
03 p0385 A72-14226

Cloud interference-free sea surface temperatures, using techniques to reduce noise effect in Nimbus IR radiometer data
03 p0385 A72-14227

CAT, cloud cover and icing forecasting for aviation in terms of numerical model and real atmosphere
04 p0542 A72-14689

Daytime cloud cover space-time patterns from satellite sensed brightness values during 1967-1971
04 p0542 A72-14690

Venus cloud top chemical composition from spectroscopic data, discussing cloud refractive index and reflectivity
05 p0719 A72-16711

Noctilucous cloud studies prehistory, reviewing Jesse contributions in 1885-1901
05 p0659 A72-16723

Vertical motions in stratified cloudy atmosphere as function of plane divergence distribution and heat influx
06 p0840 A72-17621

Meteorological elements vertical profiles under cloud cover condition by solving heat and humidity transfer equations based on satellite data
07 p1029 A72-18860

Angular transmittance model of visible light scattering through overcast cloud layer
07 p1030 A72-19411

Venus clouds composition from spectral and polarization data, considering hydrochloric acid particles model
08 p1230 A72-20980

Meteosat geostationary satellite international program for earth cloud cover observation and meteorological data relays between ground stations as part of Global Atmospheric Research Program
08 p1241 A72-21204

Venus upper clouds composition from Mariner 5 occultation data analysis concerning temperature and pressure profiles, abundances, polarization characteristics, reflection and emission spectra
08 p1236 A72-21496

Global radiation flux and energy sum calculation from turbidity factor and cloud cover parameters, comparing with measurements in tropics and polar region
08 p1201 A72-21797

Martian violet clouds photometric studies, determining monochromatic albedo, optical thickness and Junge parameter
08 p1237 A72-21827

Sensor spatial resolution effects on satellite estimation of earth cloud cover, simulating cloud distribution and size
09 p1345 A72-22450

Spectral line formation in cloudy planetary atmospheres, applying to Venus
09 p1386 A72-22669

Spectroscopic evidence for spectral line structure of visible Venus cloud layers
09 p1386 A72-22670

Spectrophotometric observations of Venus, showing unreliability of evidence for dihydrated ferrous chloride in upper cloud layers
10 p1532 A72-23715

Automatic cloud cover mapping from satellite photographs, describing three step procedure of texture edge detection and cleaning, region coloring and map cleaning
10 p1478 A72-23782

Noctilucous clouds characteristics and interpretation, discussing height, observation latitudes, variations, drift, wave structure, auroral influence and particle size and density, etc
10 p1478 A72-24706

Successful operational satellite sounding probabilities with normal global cloud cover by vertical temperature profile radiometer
10 p1508 A72-25082

IR observation and theoretical considerations for Jupiter atmosphere inhomogeneous model with two cloud layers
[AD-742156] 11 p1721 A72-26119

Venus spectrum carbon dioxide absorption lines model with double cloud system and adiabatic atmosphere
11 p1721 A72-26120

Meteorological satellite information and communication aspects, stressing METEOSAT European project for permanent cloud cover observation in visible and IR bands
[AIAA PAPER 72-547] 12 p1839 A72-27370

Laboratory simulation of diffuse reflectivity from plane parallel cloudy planetary atmosphere, comparing to theory
12 p1796 A72-27947

Cloud top temperature measurement by satellite through comparison of visible and IR cloud images with concurrent airborne radar and lidar measurements
13 p1944 A72-28444

Mars surface particulate matter eroded by atmospheric winds, noting erosive and settling velocities and yellow clouds distribution
13 p2036 A72-28794

Clear line-of-sight probabilities for atmosphere from whole sky photos, visual cloud cover, sunshine recorder traces, satellite and in-flight observations
13 p1989 A72-28809

Slant range visibility measurements by lidar for aircraft landing operations under low clouds and fog at coastal region
13 p1992 A72-28847

Single layer overcast clouds visible light angular transmittance profiles, noting correlation with hemispheric and narrow-angle pyrheliometric transmittances
13 p1995 A72-29621

Radiative transfer in Mars and above-cloud Venus carbon dioxide atmospheres, studying diurnal variations in temperature profile
14 p2160 A72-30897

Planetary cloudy atmosphere synthetic spectral line profile computation, using analytic scattering diagrams
15 p2192 A72-31649

Photometric search for Venus halo effect during 1970 inferior conjunction in relation to brightness maximum and ice in cloud tops
15 p2312 A72-32089

Relative vorticity and balanced height distributions from cloud velocities associated with cloud structure of extratropical cyclone over continental U.S.
16 p2419 A72-33945

Aircraft short wavelength measurements of cloud reflection and absorption properties for impact on earth radiation budgets
16 p2388 A72-34024

Upward and downward motions of Venus atmosphere in terms of continuous cloud cover effects, considering solid cloud cover hypothesis
18 p2729 A72-36984

Crop surface albedo measurements, taking into account cloudiness, zenith angle and day period effects
20 p2915 A72-38970

Effect of vertical flow structures on the cloud cover in the intratropical convergence zone
20 p2949 A72-39950

Diurnal and seasonal behavior of discrete white clouds on Mars.
21 p3110 A72-41454

Solar radiant energy reflection and absorption by cloud layers
21 p3049 A72-41795

Jupiter surface maps from synoptic observations with refracting telescope, considering white cloud formations and atmosphere motions
22 p3220 A72-41921

Venus high albedo, discussing compound reflecting layer and liquid Hg cloud models
24 p3436 A72-44692

CLOUD GLACIATION

Ice particles and frozen droplets formation on nuclei in supercooled cloud by shock waves under laboratory conditions
06 p0843 A72-18452

Cumulus and stratocumulus ice crystal and nuclei concentrations, drop size distributions, glaciation differences and enhancement mechanisms
07 p1030 A72-19101

Cumulus cloud microstructure measurement by single particle optical spectrometer, inferring transition from water to ice phase regions from droplet size and number distributions 09 p1307 A72-22444

Noctilucent cloud wave structure, discussing motions in high atmosphere, ice crystal formation, energy sources and observations 10 p1474 A72-24707

Thermodynamic freezing theory of small solution droplets containing insoluble particles, considering ammonium sulfate concentration for ice formation in clouds 16 p2476 A72-33380

Mathematical formulation of ice crystal formation and propagation mechanism in seeded supercooled convective clouds 23 p3311 A72-43722

CLOUD HEIGHT INDICATORS

Upper cloud boundary height determination using Cosmos 320 satellite combined reflected solar and intrinsic radiation measurements 02 p0253 A72-12213

Cloud base altitude measurement by optical telemetry using TNN 1000 apparatus, noting reduced maintenance 04 p0521 A72-14691

Airport meteorological instrumentation, discussing ground wind, visibility, cloud height, air temperature and humidity detectors and radar equipment 10 p1484 A72-25093

Cloud height measurements and instrumentation, discussing rotating and fixed beam triangulation and French lidar and ruby laser ranging ceilometers 10 p1484 A72-25094

Cloud tops height determination, considering IR radiation reflection by plane layer 12 p1841 A72-27990

Cloud height measurement with rotating beam ceilometers, discussing precision and representativeness 13 p1992 A72-28849

Automatic ceilometer systems for sky state reporting, discussing computerized cloud simulation model, instrumentation and data sampling 13 p1992 A72-28850

Relative vorticity and balanced height distributions from cloud velocities associated with cloud structure of extratropical cyclone over continental U.S. 16 p2419 A72-33945

Cloud tops height determination, considering IR radiation reflection from plane layer 22 p3174 A72-43004

CLOUD PHOTOGRAPHS

Mesometeorological processes in tropic and subtropical zone based on cloud photographs obtained from aircraft and satellites 02 p0255 A72-12792

Mass and energy exchange in tropical convective cloud systems from ATS cloud photographs 09 p1344 A72-22430

Numerical wind profiles calculation over Mediterranean based on satellite photograph sequences of clouds 15 p2220 A72-31235

Stable air clouds localization from meteorological satellite photographs, noting atmospheric air pollution 15 p2265 A72-31236

Satellite-observed Southern Hemisphere cloud vortices in relation to conventional observations. 23 p3285 A72-44145

CLOUD PHOTOGRAPHY

Computer programs for global disk and landmarks registration of cloud motions from satellite data for ocean weather monitoring applications 01 p0070 A72-10871

WINDCO interactive man-computer system for automated cloud motion tracking using precisely aligned digital ATS satellite pictures 01 p0070 A72-10872

Lake effect cloud examination by TIROS and ESSA photography, noting parallel bands with larger dimensions than cloud streets 01 p0095 A72-11280

Aerial multispectral scanner data determination with filtering and smoothing along flight line over extended areas, deriving algorithm for cloud-shadowed area detection 02 p0212 A72-11817

Satellite photograph interpretations, discussing wind direction indication, cloud structure, automatic mapping and hydrographic exploration 03 p0351 A72-14306

Meteorological satellites TV, visual and IR cloud imaging and atmospheric sounding techniques for short and long range weather forecasting 06 p0892 A72-18066

Nimbus satellite image dissector camera system for continuous meteorological scanning, noting special suitability for cloud and ice features discrimination from brightness changes 08 p1171 A72-21967

Cloud top temperature measurement by satellite through comparison of visible and IR cloud images

with concurrent airborne radar and lidar measurements 13 p1944 A72-28444

Computer program algorithm for processing local landmark and cloud motion data recorded by satellite observation 17 p2520 A72-34410

Automated cloud tracking using precisely aligned digital ATS pictures. 17 p2521 A72-34411

Photogrammetrically determined cloud-free lines-of-sight through the atmosphere. 20 p2947 A72-38963

Weather satellites - Their role in the application of environmental services to the marine industries. 24 p3420 A72-44648

CLOUD PHYSICS

Cloud energy dissipation coefficient determination by ruby laser device, applying to water content and liquid particle concentration, vapor cloud and aerosol concentration 01 p0094 A72-10562

Kr 85 clouds released by instantaneous point sources, measuring speed, height, short period concentrations, crosswind and downwind concentration integrations and dimensions 01 p0095 A72-10828

Cloud temperature determination from satellite IR images, presenting error corrections for various U.S.S.R. locations 01 p0095 A72-10956

Venus cloud reflected radiation flux and polarization by Monte Carlo technique, using models with different particle size distributions 02 p0280 A72-12193

Size determination for stationary space charge clouds in streaming media from theoretical model of tanks filled with electrostatically chargeable inflammable fluids 02 p0261 A72-12554

Dust particle dynamical behavior during cloud collisions, discussing grain distribution in resultant cloud 02 p0284 A72-12638

Multiple scattering polarization of sunlight reflected by terrestrial water clouds as function of particle shape and size, using doubling method 03 p0384 A72-14145

Cloud streeting in earth atmosphere, discussing satellite observations and theoretical formation mechanisms 04 p0541 A72-14457

CAT inducing atmospheric conditions effects on SST flight, discussing turbulence in convective clouds and kinetic energy spectra of atmospheric motions 04 p0543 A72-14693

Stepped-leader theory in cloud-to-ground electrical discharges, estimating step-length for different electric fields by equivalence to electron avalanche transition 04 p0543 A72-14880

Jovian atmosphere and clouds explained by physico-chemical and meteorological data, discussing cloud motions, colors and Great Red Spot 04 p0580 A72-15363

Gas cloud motions in Seyfert galaxy NGC 7469 center from image tube spectra, discussing size, mass and radial velocities 04 p0580 A72-15370

Mathematical two dimensional model of vertical wind shear near convective cloud in free atmosphere 06 p0840 A72-17622

Positive corona streamers interactions with cloud droplets atomized from water and glycerin solution, discussing atmospheric significance 06 p0841 A72-17823

Droplets coalescence in clouds, considering microturbulence effects due to laminar shear flow 07 p1030 A72-19102

IR radiation radiative transfer calculation for selected spectral intervals due to various model cloud droplet size distribution 07 p0980 A72-20456

Cloud and precipitation dynamic processes effects on reflected radar signal statistical characteristics 08 p1137 A72-21996

Cloud and precipitation elementary processes effects on reflected radar signal fluctuation spectrum during hydrometeor formation 08 p1201 A72-21997

Large drops coalescence, investigating approach rate dependence on electric field strength and distance 08 p1201 A72-21998

Cloud and Aitken nuclei vertical distribution upwind and downwind of urban pollution sources from simultaneous airborne observations 09 p1345 A72-22443

Supercooled cloud water droplets in free fall shattered by shock waves measuring ice crystal formation probability 09 p1345 A72-22446

Noctilucent cloud kinematics as indicators of mesospheric circulation and turbulence characteristics, discussing need for international scientific cooperation 10 p1476 A72-25006

Gas and dust cloud evolution with allowance for dimensional finiteness and stellar evolution into red supergiant after hydrogen depletion 11 p1715 A72-25297

Fog and cloud microstructure and density distributions from directional light scattering coefficient /halo indicatrix/ 11 p1683 A72-26883

Aitken condensation nuclei clouds microstructure and area contamination profiles, discussing small sources pollution and plumes polyfurfurcation [AIAA PAPER 71-1125] 11 p1628 A72-26989

Time-spectral characteristics and geographic variations of large scale cloud activity in tropical Pacific 12 p1837 A72-27018

Two dimensional dynamic model numerical simulation for micro- and macrostructures of moist convective clouds, comparing to field observations 12 p1839 A72-27028

Developing cumulus clouds annihilation, considering ascending and descending spontaneous convective streams initiated by explosions 12 p1841 A72-27989

Cloud statistics stratification by climatological regime, month and time of day, extending simulation to drop size distributions and liquid water content 13 p1989 A72-28808

Zero gravity earth orbital cloud physics facility requirements and design concepts, noting experiments feasibility relative to astronaut performance 13 p1990 A72-28815

Two phase flow model of cloud and star formation by galactic shocks in quasi-steady interstellar gas flow in spiral gravitational field 13 p2040 A72-29404

Venus atmosphere IR synthetic spectra of carbon dioxide band and water line formation for isotropic scattering, comparing with terrestrial clouds 13 p2040 A72-29410

Dynamics and thermodynamic interactions connected with large, mesoscale and small scale stratiform clouds, describing mathematical models 13 p1995 A72-29849

Mathematical model of atmospheric electric clouds, calculating electric charges and fields from convection and conductivity data 13 p1996 A72-30086

Light intensity and linear polarization for single scattering by ice clouds in visible and IR, approximating crystals with long circular cylinders 14 p2128 A72-30349

Jupiter cloud models, observational characteristics and temperature error at 5 micron wavelength 15 p2312 A72-32095

Noctilucent cloud research, discussing morphology, rocket studies and ice particle theory 16 p2386 A72-33605

Numerical calculation for axisymmetric gas cloud rotation effects on collapse, noting implications for star formation and fragmentation 16 p2458 A72-33722

Relative vorticity and balanced height distributions from cloud velocities associated with cloud structure of extratropical cyclone over continental U.S. 16 p2419 A72-33945

Convective clouds fluid dynamic numerical modeling, considering plumes, thermals and vortex rings formation [AIAA PAPER 72-651] 16 p2419 A72-34083

Slipping stream instability of a self-gravitating hydromagnetic gas cloud. 17 p2613 A72-35501

Verification of theory for plasma of finite-size particles. 17 p2592 A72-35618

On depolarization of visible light from water clouds for a monostatic lidar. 18 p2706 A72-36646

Numerical integration of nonlinear convective flow equations for arbitrary atmospheric temperature and wind profiles, discussing cloud streets formation 19 p2828 A72-37998

Studies of vertical motions in cloud systems by using a coherent pulse radar in the decimeter wavelength range 19 p2829 A72-38773

Fog and cloud microstructure and particle size distributions from directional light scattering coefficient /halo indicatrix/ 20 p2948 A72-39570

Radiative properties of upper and middle level clouds and of vertically developing clouds 20 p2949 A72-39948

Cloud liquid water content measurement via digital radar system, presenting two dimensional display of storm system characteristics 21 p3077 A72-40250

Light pulse propagation through clouds - Models and experiments. 21 p3063 A72-40857

The observation of chemical releases in the upper atmosphere. 22 p3152 A72-42022

Time dependent one dimensional numerical model of hail-bearing cumulus cloud, using microphysical

process parameterization and exponential raindrop and hailstone size distributions

22 p3201 A72-42513

Hail formation model based on injection of finite embryo size classes into horizontally homogeneous steady nondivergent updraft, considering growth and accumulation zones

22 p3201 A72-42514

Thermodynamic conditions for the development of convective clouds and a method of forecasting the quantity of rainfall

22 p3202 A72-42953

Developing cumulus clouds annihilation, considering ascending and descending spontaneous convective streams initiated by explosions

22 p3202 A72-43003

Theoretical model, laboratory experiments and in situ measurements by instrumented sailplane for investigating cloud and precipitation formation physics relationship to atmospheric pollutants cleansing

23 p3311 A72-44263

Modeling the rise and combustion of a cloud of light gas in the atmosphere

23 p3357 A72-44493

The spectral albedo of water clouds in the 1- to 6-micron range

24 p3395 A72-44636

CLOUD SEEDING

Warm fog dissipation by helicopter downwash mixing, heat, hygroscopic particle and polyelectrolytes seeding

04 p0543 A72-14694

Supercooled and warm fog dispersion technology, considering air heating, helicopter downwash and seeding methods

04 p0543 A72-14812

Soviet papers on cloud seeding effects and meteorological radar studies covering precipitation formation, atmospheric model and reflected signal statistical characteristics

08 p1201 A72-21992

Intense precipitation contour zone distinguishing methods error estimation in seeding experiments on frontal clouds

08 p1201 A72-21994

One dimensional model for climatological evaluation of ice phase seeding for isolated cumulus cloud modification

09 p1345 A72-22448

Mathematical model for numerical simulation of warm fog modification by seeding hygroscopic particles, taking into account turbulent diffusion and horizontal wind advection

13 p1992 A72-28844

Airport runway fog dispersal in UK, discussing cost projection for chemical seeding system combined with lidar remote sensing

16 p2418 A72-33500

Mathematical formulation of ice crystal formation and propagation mechanism in seeded supercooled convective clouds

23 p3311 A72-43722

CLOUD STREETS

U CLOUDS [METEOROLOGY]

CLOUDS

NT ARTIFICIAL CLOUDS

NT CIRRUS CLOUDS

NT CLOUDS [METEOROLOGY]

NT CONVECTION CLOUDS

NT CUMULONIMBUS CLOUDS

NT CUMULUS CLOUDS

NT ELECTRON CLOUDS

NT HYDROGEN CLOUDS

NT MAGELLANIC CLOUDS

NT NOCTILUCENT CLOUDS

NT PLASMA CLOUDS

NT STRATOCUMULUS CLOUDS

Seasonal and latitudinal relation between Mars white clouds occurrence frequency and global water distribution, suggesting cloud composition as water vapor

20 p2968 A72-39241

CLOUDS [METEOROLOGY]

NT ARTIFICIAL CLOUDS

NT CIRRUS CLOUDS

NT CONVECTION CLOUDS

NT CUMULONIMBUS CLOUDS

NT CUMULUS CLOUDS

NT NOCTILUCENT CLOUDS

NT STRATOCUMULUS CLOUDS

Channel clearing through clouds by laser beam, considering cross section expansion dynamics, channel growth rate, cloud motion and blurring

01 p0078 A72-10155

Sky light polarization, cloudiness and view angle effects on oil remote detection over water surface, describing passive radiometric techniques

01 p0057 A72-10536

Tropospheric wind estimation from ATS 1 satellite cloud motions over equatorial Pacific

01 p0060 A72-10856

Quantitative cloud information from satellite IR thermal imagery and vertical temperature profile data

02 p0211 A72-11808

Remote sensing applications to operational weather forecasting including ground optical measurement of cloud base height and radar observation of precipitation

02 p0253 A72-11825

Venus cloudy atmosphere IR absorption line spectra interpretation, suggesting HCl and HF formations dependence on condensation phases

03 p0439 A72-14149

Jupiter and Venus cloudy atmosphere reflected sunlight circular polarization measurement, noting sense variations with phase angle and location on disk

03 p0439 A72-14150

Light field in cloud and fog plane layers from stationary collimated point source propagation

06 p0848 A72-17937

Radiation intensity angular distribution from optically thick plane cloud layer reflection, relating photon survival probability and scattering functions

06 p0807 A72-17939

Water and ice clouds spectral brightness coefficients in IR region of spectra from aircraft measurements

06 p0842 A72-18049

Geometric optics approximation for rf wave forward and backscatter characteristics by spherical overdense clouds for several electron density distributions

08 p1136 A72-21980

Tropical storms generated midlatitude cloud bands relation to autumnal large scale circulation, analyzing heat and moisture injection effects

09 p1344 A72-22429

Radiational cooling and heating rates for ice and water clouds based on radiative divergence measurements with allowance for latent load

09 p1348 A72-23660

Atmospheric vertical motions velocities prediction based on satellite cloud data

11 p1683 A72-26887

Cosmogenic radionuclides pickup by cloud water and deposition in precipitation described by model

12 p1863 A72-27503

Remote measurement of cloud ice and water content from Raman scattering of ground based laser signal

12 p1840 A72-27547

Light beams propagation in clouds and fog, discussing scattering and attenuation coefficients

13 p1988 A72-28517

Smoothed wind fields generated from ATS 3 cloud motions measurements observed on computer display system

13 p1991 A72-28827

Convective clouds effect on air temperature gradient and turbulent heat fluxes in near-surface layers

13 p1995 A72-29593

Calibrated thermal emission spectra under extreme temperature, surface strahlstrahlung and cloud conditions from Nimbus 4 IR spectroscopy

15 p2223 A72-31510

Aircraft laser radar measurements of atmospheric backscattering coefficients for cloud and underlying surface studies

15 p2266 A72-31908

First and second order backscattering, beam divergence, angular field of view, field size and receiver distance of water clouds illuminated by continuous lidar beam

15 p2290 A72-32154

Fog, cloud, rain and snow detection by acoustic echo sounding, noting effects of energy scattered from atmospheric boundary layer velocity and temperature fluctuations

15 p2267 A72-32725

Airborne electrostatic probe for cloud droplet size measurement, calculating flow distribution and particle trajectories

16 p2390 A72-33150

Spectroscopic sounding of clouds and snow and ice covers from below /earth surface/ and above /space or plane/

16 p2417 A72-33288

Light field in cloud and fog plane layers from stationary collimated point source propagation

16 p2426 A72-33778

Radiation intensity angular distribution from optically thick plane cloud layer reflection, relating photon survival probability and scattering functions

16 p2426 A72-33780

Investigation of the atmospheric boundary layer and clouds by the laser tracking method

18 p2698 A72-36969

Photogrammetrically determined cloud-free lines-of-sight through the atmosphere.

20 p2947 A72-38963

The effect of cloud scattering on the absorption of solar radiation by atmospheric dust.

22 p3201 A72-42512

Cloud structure and cover determination from actinometric short wave solar radiation and IR cloud radiation measurements

23 p3311 A72-43627

CLUMPS

Particle interactions in real and numerically simulated plasmas, considering effects of macroparticles formation via idealized clustering

17 p2590 A72-35143

CLUSTERS

U CLUMPS

CLUTCHES

Oscillations excitation, proposing models for percussive rotational action machines operation and dog tooth clutches processes

13 p1954 A72-28386

CLUTTER

Clutter suppression by amplitude weighted pulse trains in coherent radar, obtaining optimum weights and signal-to-clutter gain as function of Doppler frequency

01 p0030 A72-10789

Approximate signal-clutter ratio formulas for airborne pulse radar system, eliminating computer calculations

02 p0176 A72-12216

MTI radar system design philosophy for target detection in land clutter environment

02 p0178 A72-12390

Radar measurement accuracy in log-normal clutter of fluctuating targets in random noise or intentional interference

02 p0178 A72-12401

Range resolution effect on distributed radar target detection in white noise and clutter, using square law envelope detector with linear integrator

05 p0628 A72-16567

Pulsed coherent radar with pulse position random modulation, discussing subclutter visibility, target attenuation and blind speeds cancellation and radial speed measurement without range ambiguities

06 p0775 A72-18184

Coherent radar pulse train clutter performance prediction for targets with range acceleration effects on Doppler response

08 p1133 A72-21405

Clutter correlated lognormal random variables generation from statistically independent Gaussian random variables for radar simulations

08 p1134 A72-21423

Noncoherent detection of sinusoidal signal imbedded in clutter and Gaussian noise, obtaining probability density as function of SNR and clutter-to-noise ratio

10 p1437 A72-24691

Amplitude comparison direction finding systems, calculating error due to clutter from incident signal and noise angular distribution relationship to measured arrival angle

10 p1439 A72-24803

Pulse-pulse frequency agility influence on radar detection in sea and rain clutter with decorrelation, eliminating multiple-time-around echoes

13 p1917 A72-28695

Frequency agile radar techniques for improving detection and range resolution and reducing interference and sea and ground clutter

13 p1917 A72-28696

Radar clutter models and comparison with measurements, discussing parameters for description and main functions for suppression

13 p1922 A72-29396

Adaptive radar tracking processes in presence of clutter, comparing efficiencies via mathematical models

15 p2196 A72-31747

Sea clutter measurement at low grazing angles by high resolution radar, noting non-Rayleigh probability density and variation with frequency, pulsewidth and polarization

15 p2196 A72-31786

Search radar constant false alarm rate receiver circuit for background noise and clutter compensation, using matched dispersive delay lines flanking hard limiter

16 p2365 A72-33762

Time-compressed displays for target detection.

17 p2510 A72-35945

Tracking radar system rain clutter reduction by backscatter polarization technique for signal phase and magnitude adjustment

18 p2659 A72-36310

Determination of the reflecting power of a hilly terrain, knowing the reflective power of a flat terrain of the same nature

24 p3381 A72-45769

COAGULATION

NT BLOOD COAGULATION

Jet fuels hydrocarbon composition effect on thermal stability, considering nonaromatic components influence on aromatic hydrocarbons oxidation products coagulation

02 p0271 A72-12800

Protoplanetary bodies mass distribution by coagulation theory, using inverse power law

06 p0884 A72-18030

Protoplanetary bodies mass distribution by coagulation theory, using inverse power law

11 p1719 A72-25966

- Electronic and hematocrit devices to investigate cardiovascular system functions including blood coagulation process, pressure and flow
11 p1585 A72-26464
- Investigation of the coagulation and breaking of droplets of comparable dimensions in an electric field
20 p2956 A72-40038
- Approximate determination of the change in the aerosol distribution spectrum in a Venturi coagulator tube
20 p2928 A72-40039
- Stability of Al₃Mg₂ particles against diffusive coagulation in aluminum-magnesium alloys
23 p3301 A72-43649

COALESCENCE

U COALESCING

COALESCING

- Tube wall temperature and acoustic noise spectra dependence on thermal flux density in bubble coalescence
03 p0458 A72-14162
- Droplets coalescence in clouds, considering microturbulence effects due to laminar shear flow
07 p1030 A72-19102
- Large drops coalescence, investigating approach rate dependence on electric field strength and distance
08 p1201 A72-21998
- Rain droplets growth by collision and coalescence during fall through sheared air flow, discussing discrepancies between calculated and experimental collision efficiencies
11 p1619 A72-26642
- Continuous NDT of coalescers /jet fuel filters/ by liquid crystals, detecting split seams, cap leaks, cracks, material imperfections and epoxy filled voids [ASME PAPER 72-DE-25]
14 p2108 A72-30867
- # COANDA EFFECT
- Modular fluidic elements in pneumatic logic system based on Coanda effect
02 p0156 A72-11999
- Two dimensional flow attachment to flat plates, investigating Coanda effect
06 p0798 A72-17776
- Pneumatic fluidic logic elements design based on Coanda effect to realize conjunction, equivalence, nonequivalence, alternative and implication functions
10 p1423 A72-25112

COARSENESS

- Temperature and alloy composition effects on coarsening rate of metal carbide particles in dissimilar metallic matrix
07 p1021 A72-20436

COASTAL ECOLOGY

- Coastal environment remote sensing from satellite and aircraft imaging platforms for geological, oceanographic and ecological investigations
15 p2232 A72-32622

COASTING FLIGHT

- Rocket motion in general central force field, obtaining primer vector integration for optimal coasting arc during orbital transfer
06 p0890 A72-18386
- Stability criteria for limiting oscillatory motion of coasting sounding rocket exiting atmosphere
13 p2051 A72-28886

COASTS

- Statistical characteristics of rough sea compared with variable magnetic fields near Crimean coast in Black Sea
02 p0218 A72-11951
- Coastline effect on electric field strength of geomagnetic micropulsations
03 p0344 A72-12977
- Millimeter to meter waves propagation conditions prediction in horizontally inhomogeneous coastal foreground by meteorological parameters, considering wind effects on refractivity
12 p1784 A72-27798
- Statistical characteristics of rough sea compared with variable magnetic fields near Crimean coast in Black Sea
13 p1949 A72-29263

COATING

- NT ANODIZING
- NT ELECTROPLATING
- NT ENCAPSULATING
- NT METALLIZING
- # COATINGS
- NT ALUMINUM COATINGS
- NT ANODIC COATINGS
- NT CERAMIC COATINGS
- NT ELECTROPLATING
- NT ENCAPSULATING
- NT GLASS COATINGS
- NT GLAZES
- NT GOLD COATINGS
- NT INORGANIC COATINGS
- NT LACQUERS
- NT MAGNETIC FILMS
- NT METAL COATINGS
- NT METALLIZING
- NT NICKEL COATINGS
- NT PAINTS
- NT PLASTIC COATINGS
- NT PRIMERS [COATINGS]
- NT PROTECTIVE COATINGS

NT SPRAYED COATINGS

NT THERMAL CONTROL COATINGS

NT ZINC COATINGS

- Nonconducting samples preparation for scanning electron microscope, using carbon as coating material
07 p0992 A72-20578
- Niobium carbide coatings for carbon steels and cermets, comparing with titanium carbide coatings
08 p1186 A72-21724
- Soviet book on temperature resistance of lubrication boundary layers and solid lubrication coatings during friction of metals and alloys
08 p1179 A72-22023
- Selective surfaces and coatings for solar energy conversion systems, discussing semiconductor photoconverters, white-black surfaces, cooling systems and optimal optical properties
10 p1422 A72-24315
- Multilayer dielectric reflective coatings performance in solid state laser pumping systems
11 p1649 A72-26345
- Silicon solar cells antireflection coatings for performance loss minimization, obtaining improvement with titanium dioxide compared to silicon monoxide coatings
12 p1757 A72-28027
- Titanium dioxide thin film antireflection coating to minimize reflection losses in Si solar cells, discussing fabrication and optical and electrical characteristics
12 p1757 A72-28028
- Detonation deposited coatings, determining adhesive strength as function of coating thickness and process technological parameters
14 p2107 A72-30432
- Dc and RF sputter deposition in ionized inert gas of thin film coatings solid state microelectronics, solid lubricants and corrosion resistance applications [ASME PAPER 72-DE-37]
14 p2108 A72-30871
- Minimum ion source temperatures for glow discharge ion flux deposition of films and coatings on metallic and nonmetallic substrates
15 p2244 A72-31573
- Coating of fibers and the fabrication of fiber-reinforced composite materials
20 p2929 A72-39443
- # COAXIAL CABLES
- Coaxial connector standard interfaces for optimum microwave performance, discussing single connector reflection coefficient measurement equipment and procedures
01 p0041 A72-10693
- Low loss high power hf coaxial, twin wire and surface waveguides for long distance transmission
02 p0190 A72-11677
- Microwave precision coaxial connectors in terms of dimensional specifications, material properties, surface characteristics and other parameters for transmission standards effects
03 p0330 A72-13230
- Admittance calculation for vertical monopole antenna driven by coaxial line, approximating current distribution by polynomial with complex coefficients
04 p0501 A72-15429
- Coaxial and stripline wideband microwave hybrid ring junctions equivalent to magic Tees with improved electrical properties
05 p0636 A72-16344
- Wideband tunnel diode microwave amplifier design with coaxial line, considering band-edge stability and impedance matching
06 p0785 A72-18310
- A portable coaxial collinear antenna
17 p2526 A72-34377
- The transient radiated field of a coaxial aperture antenna
18 p2660 A72-36331
- Investigation of stepped irregularities in coaxial lines with allowance for higher-order modes
23 p3263 A72-43447
- # COAXIAL FLOW
- Velocity and temperature effects on momentum and temperature equalization in coaxial turbulent jet mixing in pipe inlet section [DFVLR-SONDDR-183]
01 p0051 A72-11257
- Coaxial flow gaseous core nuclear reactor system dynamic analysis, developing mathematical model and equations solution by computer program
01 p0100 A72-11352
- Compressible axisymmetric coaxial jets turbulent mixing in constant area duct, considering axial and radial pressure distributions
07 p0967 A72-19094
- Non-Newtonian Reiner-Rivlin fluid flow between two coaxial porous cylinders with longitudinal pulses applied to inner cylinder at finite time intervals
10 p1468 A72-24402
- Circulating toroidal vortex pattern in initial region of turbulent coaxial jet stream mixing obtained with hot-wire anemometer, static pressure probes and shadowgraphy [ASME PAPER 72-APM-30]
17 p2538 A72-34789
- Flow pattern of two impinging circular jets
17 p2540 A72-35233

COAXIAL PLASMA ACCELERATORS

- Self magnetic coaxial plasma accelerator integral output data, presenting mass velocities and thrust measurement [DGLR PAPER 71-103]
02 p0266 A72-12736
- Filamentary magnetic structure production on plasma current sheath of coaxial deuterium operated accelerator for laboratory observations of solar flare processes
03 p0411 A72-13338
- Coaxial plasma source energetic characteristics, establishing plasmoid energy linear dependence on battery stored energy
03 p0395 A72-13567
- Angular and linear velocities of plasmoid in coaxial accelerator under axisymmetric magnetic field
03 p0398 A72-14002
- Magnetic and electric field intensities measurement with charged particle beams in coaxial high temperature plasma sources
06 p0863 A72-18415
- Turbulent mixing of high temperature Ar jet injected into ring slipstream of air in dc plasmatron with coaxial nozzle and fixed arc
09 p1410 A72-22677
- Microwave, X ray and corpuscular emission by gas discharges in coaxial plasma gun, measuring pressure and current distribution
09 p1362 A72-23212
- Coaxial plasma source energetic characteristics, establishing plasmoid energy linear dependence on battery stored energy
11 p1699 A72-26754
- Current distribution over coaxial plasma gun outer electrode, attributing current concentration at electrode edge to accelerator cavity conductivity anisotropy
13 p2012 A72-29140
- Coaxial source accelerating circuit resistance, capacitance and inductance effect on velocity imparted to plasma jet
13 p2015 A72-29453
- Magnetic and electric field intensities measurement with charged particle beams in coaxial high temperature plasma sources
17 p2588 A72-34864
- Potential drops near electrodes in a pulsed plasma accelerator
22 p3213 A72-43108

COAXIAL TRANSMISSION

U COAXIAL CABLES

COBALT

- Cobalt and lanthanum with face and body centered lattices, studying plastic deformation during allotropic transformations under sliding friction and gripping
01 p0074 A72-10579
- Surface and interfacial energies measurement by multiphase equilibrium method for refractory metal monocarbides with liquid cobalt
07 p1010 A72-19136
- Maximum internal friction onset temperature and magnitude in Co as function of thermomechanical treatment and crystal lattice defects
09 p1329 A72-23035
- Magnetic domains in cobalt and cementite observed by electron microscopy, investigating thin film thickness effect on temperature
10 p1496 A72-24088
- Interference between recrystallization and allotropic transformation of cold rolled and annealed Co investigated by internal damping measurements
11 p1661 A72-26649
- Diffusion kinetics and thermodynamic characteristics of solid phase interactions in systems cobalt-transition metal carbides
13 p1981 A72-30104
- Tensile deformation of Co single crystal in high temperature fcc phase, noting dislocations effect on work hardening
16 p2410 A72-33819
- Thermodynamic properties of liquid Co and Pd metals by levitation calorimetry, including specific heat, heats of fusion and surface emissivities
16 p2480 A72-34025
- Charge carriers interaction with metal ions studied from electrical transport of Fe and Co in Fe-Cr alloy
17 p2569 A72-35521
- Study of the diffusion of iron and cobalt along the grain boundaries of tungsten
17 p2569 A72-35522
- The dry wear behaviour of porous cobalt
18 p2696 A72-36795
- German monograph - Studies of high-temperature corrosion of cobalt and cobalt alloys with radioactive isotopes
19 p2816 A72-37657
- Self-diffusion of cobalt in coarse grained polycrystalline Ni-Co alloys at low temperature
20 p2935 A72-39016
- The effect of mixed milling on the sintering of WC-Co hardmetals
22 p3188 A72-41975
- Martensitic transformation in filamentary cobalt crystals
22 p3192 A72-43017

- Pure Co single crystals allotropic transformation effects on deformation behavior, noting flow stress and work hardening rate relationship to history
22 p3193 A72-43034
- Simultaneous neutron-activation analyses of scandium, cobalt, iron, and zinc in biological objects with the aid of a total-absorption gamma spectrometer
23 p3259 A72-43347
- Fracture of WC-Co from a continuum viewpoint.
24 p3413 A72-44815

COBALT ALLOYS

- Magnetic transformation effect on creep behavior of fcc nickel-cobalt alloy compared with self diffusion data in Curie temperature vicinity
01 p0083 A72-10391
- Arc jet simulation tests of thorium dispersed Ni and Co alloys for space shuttle Metallic Thermal Protection System, determining material degradation
01 p0086 A72-10978
- Melting atmosphere, atomizing media and consolidation techniques effects on Co base alloy powder products physical properties
02 p0240 A72-11436
- Atomic structural mechanism of solid solution decomposition by nucleation and equilibrium phase particles in Fe-Co-Ti alloy, using X ray analysis and transmission microscopy
02 p0242 A72-12008
- Ta-Co system phase diagram from differential thermal, X ray, and microstructural analyses, determining composition, temperature, structural type and lattice constant
03 p0374 A72-13740
- Heat treated single-phase Pr-Co powder compacts, measuring coercivity as function of annealing or sintering temperature
[IEEE PAPER 7,3] 03 p0402 A72-13756
- Cobalt-rare earth single particles hysteresis loops interpretation, considering coercive force relationship to particle size
[IEEE PAPER 22,1] 03 p0402 A72-13781
- Vapor pressure and partial thermodynamic functions of Co-Ni alloys, observing negative deviations from Raoult law
03 p0374 A72-13928
- Nb-Co-Sn and Nb-Ni-Sn ternary systems, investigating intermetallic compounds existence by X ray analysis
03 p0375 A72-13944
- Quenched and tempered Ni-Cr-Nb-Co alloy, describing cellular precipitation mechanism
04 p0533 A72-14977
- Dispersion strengthened Co alloys structural stability, tensile and creep rupture strengths and hot corrosion properties
06 p0829 A72-17829
- Fe-Co alloy athermal transformation to bcc martensite at industrial cooling rates, investigating effects on mechanical properties
06 p0829 A72-17830
- Co and carbide containing alloys, investigating milling and sintering temperature effects on technological and physical properties
06 p0829 A72-17831
- Aging kinetics in Co-Ni-Ti alloys, noting three dimensional periodically modulated structure development
06 p0834 A72-18742
- Jerky flow /serrated yielding/ in Co-Ni-Cr-C fcc alloys during tensile testing, noting no correlation to dislocation-precipitate interactions
07 p1016 A72-19940
- Heat treatment of martensitically aging steels with Co, Ni and Mo, considering hardening effects and optimal conditions for high mechanical properties
07 p1020 A72-20414
- Monograph on Co alloy permanent magnets covering principles, magnetization and testing, alnicos, magnet steel and miscellaneous alloy technology, fine particle magnets and applications
08 p1217 A72-21481
- Ti-Co intermediate phase transformations discussing lattice formation, intermetallics melting points and stoichiometric composition
08 p1187 A72-21783
- High temperature Co-base alloy for nuclear, chemical and reentry vehicle applications
09 p1327 A72-22478
- X ray K absorption edges in binary solid solutions of Co, Fe and Ni with localized hole increases
09 p1371 A72-22846
- Enthalpy measurements of allotropic transformation of Co alloys during hcp-fcc transition with additive elements
10 p1498 A72-24850
- Young modulus of Ti-Co and Ti-C-Ni hard composites as function of volumetric fraction, using bending tests
11 p1660 A72-26487
- Microstructure and mechanical properties of dispersion strengthened Co alloys, investigating heat treatment effects
11 p1664 A72-26851

- High temperature effects on stability, corrosion behavior, structure and protective effectiveness of Al coatings on Ni and Co alloys
11 p1664 A72-26852
- Carbide precipitation effect on structure and high temperature strength of Co based alloys
11 p1667 A72-26932
- Dislocation bands in electrolytically hydrogen charged fcc Ni-Co alloy, describing band structure in terms of band axis and planes and Burgers vector
11 p1669 A72-26947
- W addition effect on Co-Nb alloys, noting phase structure transformation from cubic to hexagonal due to mean electron density increase
12 p1829 A72-27642
- Russian book on hard alloys strength covering WC-Co and WC-TiC-Co alloys microstructure, thermal stresses and fracture mechanism
12 p1831 A72-28348
- Annealed and quenched Fe-Mo-Co system, defining phase relationships in Fe-rich corner at 2200, 2000 and 1800 F
13 p1973 A72-28650
- Two phase structure solidification of monovariant eutectic Co-Cr-C alloys near pseudobinary cut
13 p1976 A72-28674
- Co-Cu alloy phase formation and separation morphology changes with temperature and anomalous diffusive X ray scattering in solid solutions
13 p1976 A72-28905
- Ni-Co alloys Nerst-Ettingshausen and Hall effects anomalous constants relationship determination from emf and electrical conductivity measurements
13 p1977 A72-28910
- Cu surface contamination effect on hot crack susceptibility and weldability of Co based superalloys
13 p1965 A72-29419
- Combined thermal, vibrational and dimensional treatments effect on WC-Co alloy physical and mechanical properties, noting tensile and impact strength increase
13 p1979 A72-29480
- Sintering of binary systems Co-Ni Co-Fe and Fe-Ni with infinite mutual solubility at different temperatures
13 p1966 A72-29954
- Deep diffused layer sintering of metal-ceramic cutting alloys with variable Co content for increased wear resistance and tensile strength
13 p1982 A72-30112
- Cobalt-base superalloys powder-metallurgical fabrication techniques and related effects on physical and mechanical properties
13 p1982 A72-30126
- Co-Cr alloy high temperature oxidation kinetics reduction by Y addition, presenting metallographic study
14 p2118 A72-30543
- Co-Cr alloy oxidation as function of temperature and oxygen partial pressure, discussing solid state diffusion
14 p2118 A72-30544
- Surface phase transformation during cavitation erosion in Co and Fe alloys, suggesting stacking fault energy effect on erosion resistance
14 p2119 A72-30603
- Uniformly distributed precipitates effect on hardness increase in aging of ferritic matrix Fe-Co-Ti and Fe-Co-Al alloys
14 p2119 A72-30605
- Superlattice structure and electron correlation of Co-Sn system, using X ray and metallographic analyses
15 p2257 A72-32115
- Co-Cr-C system carbon activity and solubility at 950-1200 C, deriving equation for temperature dependence and solid solution-carbide precipitation zone boundaries
16 p2407 A72-33441
- C concentration and temperature dependence of graphite wetting by liquid Ni and Co and melts of Ni-C and Co-C alloys, noting nonequilibrium effect
16 p2415 A72-33537
- Si stabilization of laves and intermediate phases in Nb-Fe-Si and Nb-Co-Si systems
16 p2409 A72-33805
- High-temperature resistant cobalt alloys
17 p2567 A72-35173
- Composition dependence of density in NiTi and CoTi.
18 p2701 A72-36592
- Stability and hot corrosion of aluminum coatings on the INCO 713C alloy and on cobalt alloys
18 p2701 A72-36595
- Behavior of Fe-21.6 Ni, Fe-18.4 Ni-15.0 Co, Fe-16.8 Ni-5.0 Mo subjected to cumulative thermal cycling at 300 C/hr
18 p2701 A72-36701
- Hot corrosion of experimental aluminium-coated cobalt-base alloys.
18 p2702 A72-36797
- Self-diffusion of cobalt in the ternary system Co-Ni-Fe
19 p2814 A72-37416

German monograph - The effect of alloying elements on the dry high temperature oxidation of cobalt in the temperature range from 800 C to 1000 C in air and pure oxygen
19 p2816 A72-37656

German monograph - Studies of high-temperature corrosion of cobalt and cobalt alloys with radioactive isotopes
19 p2816 A72-37657

Microstructure and differential thermal analyses of ternary system Co-Mn-Al, presenting phase diagrams
19 p2818 A72-37852

Self-diffusion of cobalt in coarse grained polycrystalline Ni-Co alloys at low temperature.
20 p2935 A72-39016

Quench-ageing behaviour of 40Co-38Ni-17Cr-5Ti alloy.
20 p2935 A72-39141

Mercury embrittlement of age-hardened Cu-1.9 wt pct cobalt and Cu-3.6 wt pct titanium.
20 p2938 A72-39296

Stress dependent cyclic creep rupture tests of Ti and Co-base alloys and stainless steel at 1300 F
20 p2938 A72-39305

Decomposition, solubility and coherent phase stability of modulated structure Co-Ni-Ti system at high nucleation temperatures
20 p2939 A72-39312

Investigation of solid solution decay in cobalt-titanium, iron-cobalt-titanium-aluminum and iron-nickel-titanium-aluminum alloys
20 p2939 A72-39314

Powder-metallurgical production of dispersion-hardened nickel and cobalt alloys
20 p2929 A72-39454

Method of investigating the wear of hard tungsten carbide cobalt alloys in a liquid nitrogen medium.
20 p2941 A72-39715

Effects of scale porosity, second-phase oxides, and doping in the high-temperature oxidation of cobalt and dilute cobalt-chromium alloys.
21 p3067 A72-40845

Diffusion of cobalt in Ni-Co alloys at temperatures up to 1000 C
21 p3070 A72-41645

Structural and reaction kinetic characteristics of /W, Ti and Ta/C-Co systems, considering solubility, surface energy, diffusion, segregation and grain growth
21 p3071 A72-41849

Temperature dependence of the thermal electromotive force and of the Nerst-Ettingshausen effect in nickel-cobalt alloys
22 p3187 A72-41855

Investigation of the influence of cobalt on the redistribution of the atoms of the alloying elements in iron-base alloys by the NGR method
22 p3188 A72-42162

Fine grained WC phase structure, physicochemical and cutting properties of Ti-Co alloy, using W powder prepared by tungsten oxide reduction in single stage muffle furnace
22 p3188 A72-42192

Influence of temperature on the mechanical properties of metallic compounds
22 p3191 A72-42804

Magnetic properties of the powders of highly dispersed iron-cobalt-nickel alloys
23 p3299 A72-43288

Investigation of the structural state of the InNDK40T7 high-coercivity alloy
23 p3300 A72-43594

Desulfurization of cobalt, nickel, and their eutectic carbon alloys during noncrucible zone melting in vacuum
23 p3300 A72-43647

The creep of dispersion-strengthened Ni-Co alloys.
24 p3413 A72-44923

Co-V solid solution decomposition by equilibrium phase precipitation at aging temperatures, using electron microscopic and X ray analysis
24 p3414 A72-45382

COBALT COMPOUNDS

- NT COBALT OXIDES
- Crystal structure of iron-zirconium disulfide and cobalt-zirconium disulfide systems
10 p1496 A72-24089
- X ray and Mossbauer spectral analyses of thermomagnetically treated nickel ferrite samples containing Co, investigating ordering mechanism
13 p2020 A72-28490
- Effect of copper, cobalt and manganese salts on certain morphological-biochemical components of the blood in young sheep of the Hissar breed
20 p2893 A72-40075
- Certain physical properties of the borides of cobalt and nickel
21 p3068 A72-40953
- Complex compounds of cobalt and nickel with hydrazine
23 p3262 A72-44165

COBALT OXIDES

CoO single crystal creep rate at different temperatures, stresses and oxygen pressures, noting slip occurrence

03 p0373 A72-13647

COBALT 60

Blue green algae *Anacystis nidulans* photorecovery after Co 60 gamma radiation exposures, using white and red light

04 p0475 A72-15516

ATP injection protection against Co 60 or Cs 137 gamma radiation in albino mice, guinea pigs and dogs

05 p0621 A72-16636

Resonance occurrence in generation-recombination noise spectrum of Co 60 gamma irradiated Ge single crystals, investigating Hall effect

09 p1372 A72-23112

Temporal, energetic and spectral properties of stimulated emission from Cr doped ruby laser irradiated by Co 60 gamma rays

13 p1969 A72-29613

Co 60 gamma radiation effect on stimulated ruby laser emission delay time, pulse duration, energy curve and intensity

13 p1972 A72-30005

Properties of stimulated neodymium laser emission under the action of Co 60 gamma emission

19 p2812 A72-38214

Temporal, energy and spectral properties of Cr laser output, considering ruby absorption before/after Co 60 gamma irradiation and radiation density distribution during pumping flashes

21 p3063 A72-40666

Instrumental neutron-activation determination of cobalt and certain other elements in plant materials

22 p3183 A72-42471

Co 60 gamma radiation effect on stimulated ruby laser emission delay time, pulse duration, energy curve and intensity

22 p3186 A72-42731

COCHLEA

Neurophysiological hearing mechanisms of inner ear in peripheral auditory pattern recognition

01 p0012 A72-10481

Neurophysiology of auditory pattern recognition of simple and complex sounds, using cats data on cochlear nerve neural mechanism

01 p0012 A72-10482

Cats cochlea and cochlear nucleus neural responses in auditory masking of low frequency tones, showing phase locked cells progressive desynchronization with intensity

04 p0475 A72-15251

High and low pass filtered clicks lateralization tests, suggesting lateral position discrimination dependence on lf content and cochlear partition apical end

04 p0550 A72-15297

Electrophysiology for auditory temporal masking mechanism study of cat cochlear nucleus and inferior colliculus single neurons

05 p0620 A72-17175

Field and intracellular potentials in cat trochlear nucleus following vestibular nerve and nuclei stimulation for synaptic organization study of vestibulo-ocular reflex

07 p0923 A72-20501

Cochlea enclosed two dimensional cavity potential flow model for fluid mechanical theory of hearing

10 p1430 A72-24295

Hybrid computer simulation of cochlea mathematical model, noting nonlinear damping

16 p2359 A72-33971

Cerebral auditory system acoustic information processing, discussing ganglia and cochlea neurophysiological functions in response to afferent stimulations

22 p3146 A72-42786

COCKPIT SIMULATORS

Respiratory adaptation to pure oxygen excess pressure after cockpit depressurization from flight simulator tests with pressure-suited pilots, presenting ECG reactions

05 p0623 A72-16749

Dynamic manned vehicle cockpit simulator for visual and aural effects and acceleration changes, discussing STOL and VTOL characteristics

06 p0796 A72-18246

Boeing 707 cockpit simulator with computer generated displays, moving area navigation map and ATC information

07 p1033 A72-20336

Statistical analysis of cockpit simulator data on altimetry display for commercial aircraft

08 p1168 A72-21573

Naval air test center participation in development of air-to-air combat simulation.

19 p2783 A72-38130

COCKPITS

Human factors engineering of aircraft cockpit data entry keyboards on area navigation control and display units

01 p0020 A72-11138

Aircraft cockpit electrical heating system, converting three phase ac energy from alternator with economy and safety

[SAE PAPER 720329] 11 p1577 A72-25591

Anthropometric data utilization for military pilot/aircraft compatibility evaluation, discussing cockpit exclusion code development and implementation

12 p1777 A72-28324

Training cockpit TL-29 mean time of failure-free operation from measurement data during development tests and two year guarantee, calculating avionic devices reliability

14 p2092 A72-30281

Flight experiments to determine horizontal visual restriction effects on T-33 aircraft front cockpit during approaches and landings

15 p2180 A72-31697

CODERS

One-way error correcting system with 1/3 rate interleaved block code, testing coder performance over 1300 km vhf ionosscatter path and 1500 km hf path

02 p0175 A72-12153

Satellite time-of-day code generator for data recording time identification, using ICs mounted on thick film multilayer printed ceramic substrates

07 p0944 A72-19605

Digital solid state altitude encoder for ATC transponder reporting, covering Gray and Gillham codes [SAE PAPER 720314]

11 p1630 A72-25578

Data processing in isolated crab biological strain receptor formed by muscle, transducer and encoder, noting pulse frequency modulation in encoding process

12 p1771 A72-27577

Binary PSK signals optimized on minimax and quadratic criteria, noting design of coders and decoders on shift registers with external logic

13 p1914 A72-28415

Ultrasonic flaw detector data analysis, discussing digital computer interface and encoders

16 p2397 A72-33202

Stochastic coder electronic circuit for random numbers conversion into electrical voltages and vice versa, noting compactness and low cost

23 p3273 A72-44460

CODES

Code performance evaluation over real digital channels, characterizing channel error process by multigap statistics

03 p0325 A72-14183

Dexter - A one-dimensional code for calculating thermionic performance of long converters.

17 p2521 A72-34587

Time-optimal mathematical models operating with low-frequency pulse-frequency-modulated input information converted to an intermediate digital code

17 p2524 A72-35786

CODING

NT DECODING

NT REDUNDANCY ENCODING

NT SIGNAL ENCODING

Reliable data transmission block coding techniques including burst error, fire, Reed-Solomon and product codes and majority decoding algorithm

01 p0025 A72-10335

Convolutional coding and decoding techniques in communication systems, discussing distance properties, optimal decoder in memoryless channel, error probabilities and bit synchronization

01 p0025 A72-10336

Skill acquisition in performance of three phase code transformation task

01 p0021 A72-11193

Time sharing three phase code transformation multitask effects on sustained performance

01 p0021 A72-11194

Coding for analog and digital data transmission over channels with noiseless and noisy feedback links

02 p0197 A72-11680

Coding for data communication over discrete time channels without feedback under various fidelity criteria, discussing channel capacity

02 p0171 A72-11681

Natural formations optical spectral reflectance optimal coding with speedy digital computer processing advantage for remote sensing of earth surface

02 p0187 A72-11811

High density digital tape recorder with combined phase encoded digital electronics and helical scan video transport

02 p0229 A72-12152

Edge-coding operators for two dimensional binary picture black-white boundary pattern recognition suitable for use in parallel processing systems

04 p0496 A72-15203

Alphanumeric data representation by TV receivers, describing coding device and gate system for video signal generation

05 p0634 A72-15813

Surface wave parametric signal processing, obtaining cross correlation of digitally coded input signals

05 p0631 A72-17074

Adaptive variable length coding for efficient compression of spacecraft TV data of Grand Tour missions

06 p0771 A72-17401

Image data coding by adaptive block classification and quantization of source output symbols, evaluating performance

06 p0772 A72-17402

Spatial digital transform coding of color images using three primary color data planes

06 p0772 A72-17403

Channel coding/decoding schemes compatibility with TV data compressor for planetary missions in real time transmission

07 p0941 A72-19274

Illumination code efficiency in impulse activity of neurons of outer geniculate body of cat visual system, emphasizing pulse per group technique

13 p1903 A72-28780

Meaningful shape coding for aircraft switch knobs.

17 p2510 A72-35944

Error search reading tasks to investigate practical applicability of blinking display coding techniques, noting reading speed reduction compared to steady display

21 p3008 A72-41018

Dual mode - An efficient encoding method of nonsynchronous data signals on PCM.

21 p3023 A72-41827

COEFFICIENT OF FRICTION

Ball bearings rolling and spinning friction coefficients determination as function of stress at contact point, race and ball diameter

03 p0363 A72-13561

Hydrodynamic lubricating films with viscosity variations perpendicular to direction of motion, evaluating friction coefficient changes for constant film thickness and load carrying capacity [ASME PAPER 72-LUB-E]

06 p0821 A72-17806

Polymer films friction properties under high pressure, discussing Amonton law failure and adhesion theory application

06 p0837 A72-18597

Graphite fluoride as solid lubricant, investigating friction coefficient and wear resistance

06 p0837 A72-18598

Sputtered molybdenum disulfide lubrication on polished metal surfaces with low friction coefficient, strong adherence, high density and small particle size

06 p0824 A72-18607

Friction coefficient, standard wear and surface layer temperature of seal for dry friction pairs in jet engines, investigating crystal lattice parameters

07 p0996 A72-19768

Surface friction coefficient dependence on Mach number and velocity gradients in adiabatic compressible laminar gas flow

08 p1107 A72-21311

Turbulent friction coefficients and velocity distribution in channel and pipe flow, using eddy viscosity model

08 p1150 A72-21623

Wear resistance and friction coefficients in physiologic solution of thermoplastic materials for prosthetic application in hip joints

08 p1194 A72-21760

Metal rolling speed effect on force and friction reduction by ultrasonic vibrations imposed on rollers, noting coefficient of friction dependence on deformation

12 p1814 A72-27645

Friction characteristics of high melting point metal chalcogenides as function of load and temperature, noting friction coefficient variations

12 p1817 A72-28185

Optimal efficiency of satellite passive nutation damper, noting system moment of inertia and flywheel axis relationship and viscous friction coefficient

14 p2162 A72-30458

PTFE thin films interspersal with lumps and streaks from transfer to smooth surface during low speed sliding, discussing friction coefficient under various conditions

16 p2396 A72-32870

Fillers effect on polytetrafluoroethylene friction properties, electroconductivity and thermal conductivity, noting friction coefficient reduction by laminar filler structures

16 p2413 A72-33269

Blowing and suction effects on heat transfer and friction coefficients of transpired turbulent boundary layer, presenting theoretical models and experimental results

16 p2378 A72-33431

Heat transfer and friction coefficients for turbulent flow in rough tubes as function of Reynolds and Prandtl number, using von Karman method

16 p2478 A72-33513

Friction of rubber on ice.

17 p2560 A72-35225

Friction and wear of electroplated hard gold deposits for connectors

18 p2693 A72-35981

Electric contact phenomena in ultra clean and specifically contaminated systems. 18 p2717 A72-36115

Antifiction and electrical properties of WSe₂-NbSe₂ quasi-binary alloys 23 p3299 A72-43292

COEFFICIENTS

NT ACCOMMODATION COEFFICIENT
NT AERODYNAMIC COEFFICIENTS
NT ATTENUATION COEFFICIENTS
NT BINOMIAL COEFFICIENTS
NT COEFFICIENT OF FRICTION
NT COHERENCE COEFFICIENT
NT CORRELATION COEFFICIENTS
NT COUPLING COEFFICIENTS
NT DIFFUSION COEFFICIENT
NT DISCHARGE COEFFICIENT
NT FLOW COEFFICIENTS
NT HEAT TRANSFER COEFFICIENTS
NT INFLUENCE COEFFICIENT
NT IONIZATION COEFFICIENTS
NT NOZZLE THRUST COEFFICIENTS
NT ONSAGER PHENOMENOLOGICAL COEFFICIENT
NT RECOMBINATION COEFFICIENT
NT SCATTERING COEFFICIENTS
NT STRUCTURAL INFLUENCE COEFFICIENTS
NT WIGNER COEFFICIENT

Conversion coefficients of optical heterodyne receiver mixer for various amplitude-phase distributions of interfering signal 07 p1000 A72-19012

COENZYMES

NT CYTOCHROMES
NT GLUTATHIONE
Rat brain acetylated and unacetylated coenzyme A aberration in marginally hyperoxic space capsule environments 06 p0763 A72-17875

COERCIVITY

Heat treated single-phase Pr-Co powder compacts, measuring coercivity as function of annealing or sintering temperature [IEEE PAPER 7.3] 03 p0402 A72-13756

Cobalt-rare earth single particles hysteresis loops interpretation, considering coercive force relationship to particle size [IEEE PAPER 22.1] 03 p0402 A72-13781

Precipitation effect on microstructure, coercive force, resistivity and cell formation changes in heterogeneous decomposition of supersaturated solid solutions and aging alloys 08 p1218 A72-21777

COESITE

Metastable coesite crystal growth in highly strained quartz under 5-20 kb pressures and 450-900 C 14 p2099 A72-30322

COGNITION

Some effects of cognitive similarity on proactive and retroactive interference in short-term memory. 22 p3142 A72-42548

COHERENCE

Coherence function and phase shift dependence of free ocean surface on angular energy distribution in two dimensional wind induced wave spectrum 06 p0841 A72-17625

Microdensitometer system analysis by partial coherence theory, determining optical transfer function for linear operation 07 p0987 A72-19830

Q switched ruby laser radiation spatial coherence, considering modes relationship to permittivity inhomogeneities and changes due to holes burning in population inversion 12 p1821 A72-27591

Visual aid-to-eye direct coupling, evaluating partial coherence effects on imagery optical performance by computer program 20 p2931 A72-39050

COHERENCE COEFFICIENT

Second harmonic generation, coherence lengths and second order susceptibilities near band edge in InSb as function of magnetic field 03 p0404 A72-14269

Output coupling apertures effect on carbon dioxide laser spatial coherence, considering resonator mode structure 05 p0667 A72-16001

Propagation of the mutual coherence of optical waves in a random medium. 24 p3424 A72-44711

COHERENT ACOUSTIC RADIATION

Coherent and incoherent structures of aerodynamic noise, analyzing compressor near field and hot jet IR emission source [ONERA, TP NO. 983] 09 p1294 A72-22816

COHERENT ELECTROMAGNETIC RADIATION

NT COHERENT LIGHT

Ionospheric integral electron concentration data from measurements of Elektron 1 and 3 satellites coherent radio wave emission 08 p1155 A72-20800

Emission of coherent microwave radiation from a relativistic electron beam propagating in a spatially modulated field. 17 p2589 A72-34874

Applicability bounds for the equation describing the mean field in a discrete scattering medium with allowance for the correlation of the scatterers 22 p3155 A72-42660

COHERENT LIGHT

Far field diffraction due to annular apertures of plane wave light rendered partially coherent by atmospheric turbulence 01 p0103 A72-11166

Multiple scattering of incident coherent light wave propagating in turbulent medium, considering irradiance intensity fluctuations and spectral and correlation characteristics 01 p0103 A72-11167

Spherical aberration effect on far field Fraunhofer diffraction for circular aperture illuminated by quasi-monochromatic partially space coherent light 01 p0103 A72-11188

Objects optical granularity in diffuse coherent light, noting similarity to image formation in diffuse incoherent light 01 p0073 A72-11313

Air pollution measurements by laser radar, using coherence properties to discriminate between backscatter due to molecular atmospheric constituents and pollutant particulates 02 p0212 A72-11816

Impending metal fatigue failure holographic detection by optical correlation of coherent light reflection from deformed surface structure as function of time 02 p0294 A72-12442

Distribution moments mathematical method for partially coherent light beam propagation through random phase screens in linear and nonlinear media 02 p0181 A72-12589

Fourier transform lens design in coherent optical filtering systems 03 p0358 A72-13439

Coherence of excitations produced in crystal by Raman effect via two beam method 03 p0368 A72-13796

Passive airborne mapping of radiation sources, using fixed side-looking multilobed and scanning fan beam antenna pattern with coherent optical processing of film records 04 p0495 A72-14491

Laser coherent monochromatic light for cybernetics research in pattern classification, discussing fingerprints and letters 04 p0531 A72-15137

Book on lasers and applications covering theories of light, polarization, coherence, resonators, mirrors, modes, electro-optical effect, communication, holography, etc 06 p0827 A72-18524

Acoustic /ultrasonic/ holography techniques for acoustic field recording and image reconstruction in coherent light, including applications 07 p0981 A72-18920

Pattern recognition through atmospheric turbulence by reflected coherent light power spectrum recording technique, using Wiener-Khinchin theorem 07 p0982 A72-19054

Wideband IR heterodyne receiver in spatially coherent array, discussing signal conversion efficiency, beam crossover control, mixer characteristics and microwave antenna comparison 07 p0940 A72-19237

Angle scintillation in laser radar return from retroreflector, comparing measurement with theoretical derivation in terms of phase fluctuation parameter [CLEA PAPER 2.1] 07 p0942 A72-19377

Laser beam diffraction effects on self induced thermal distortion in crosswind, noting dependence on Fresnel number [CLEA PAPER 2.4] 07 p0942 A72-19379

Resolution dependence on coherent properties of light source for aberration free annular aperture operating in partially coherent light, presenting composite intensity curves 07 p1008 A72-20545

Scattered light coherence in optically thin vapors and ideal gases in energy level crossing experiment formulated in terms of autocorrelation function 08 p1206 A72-21294

Pulsed GaAs injection laser active region anisotropy and radiation polarization under spontaneous and coherent emission conditions 08 p1183 A72-21772

Learning systems mathematical scheme to identify classes invariant with respect to transformation groups, realizing functionals with coherent and incoherent optics 09 p1282 A72-22218

Partially coherent imaging in microdensitometer, investigating conditions for linear operation from difference between high and low contrast edge images 09 p1309 A72-22608

Simulated superposed coherent and chaotic /thermal/ radiation of arbitrary spectral shape, using laser beam modulation and photocount statistics 09 p1352 A72-23240

Coherent and noncoherent modes of optical beating in laser Doppler velocity measurement using light scattered from single and multiple particles 10 p1481 A72-24412

Nonlinear interaction between circular coherent light and modulating electromagnetic waves in presence of quadratic electrooptical effect, noting frequency shift 10 p1493 A72-24912

Four-photon parametric frequency selection within broad stimulated emission lines during coherent light interaction, considering dye solution laser pumping 11 p1648 A72-26335

Probability density function of hologram exposure irradiation in terms of Bessel function, adding uniform beam coherently to random speckle pattern 11 p1636 A72-26749

Spatial and temporal coherence effects on image formation by in-line Fraunhofer holography 12 p1806 A72-27121

Ruby laser coherent light scattering by cylindrical electron beam under longitudinal magnetic field 12 p1820 A72-27586

Mode selection in high coherence ruby laser using KDP Q switch 12 p1823 A72-27618

Resonant interaction and self transparency effect of coherent ultrashort light pulse passing through semiconductor 12 p1824 A72-27868

Frequency modulation and transient effects in resonant propagation of coherent light pulses 12 p1826 A72-27939

Acoustic /ultrasonic/ holography techniques for acoustic field recording and image reconstruction in coherent light, including applications 13 p1957 A72-29206

Spatial coherence measurement of ruby laser light by interference method, calculating diffraction pattern contrast curves 13 p1968 A72-29510

Coherent laser light propagation in resonance media with level splitting, determining Lorentz and broadened resonance lines 13 p1969 A72-29515

TV speckle pattern recording for coherent laser light measurement of mechanical vibrations in micrometer range 13 p1961 A72-30026

Human eye relative luminous efficiency for near IR and UV coherent light, using ruby laser pumped tunable dye laser primary and second harmonic outputs 15 p2184 A72-31380

Book on coherent optical computers covering lens design, power sources, computation mathematics, modulation, detection, digital techniques and applications 15 p2203 A72-31499

Sine, square and triangular wave targets for optical transfer function measurements, comparing modulations in partial coherent light under different illumination conditions 15 p2246 A72-31613

Spacecraft onboard compact low-power coherent optical data processing system, using GaAs laser and paraboloid mirror segments 15 p2248 A72-32052

Extended Huygens-Fresnel principle for mutual coherence /cross correlation/ function of finite optical beam propagation in turbulent medium 15 p2249 A72-32161

Variable area modulation dual signal recording onto single input device for coherent optical correlators 15 p2249 A72-32165

Coherent light signal optoelectronic processing techniques application to engineering components displacement measurement and vibration amplitude real time imaging 15 p2238 A72-32168

Coherence narrowing during multiple scattering of resonance radiation in atomic vapor, treating polarization transfer in terms of classical tensors 15 p2281 A72-32221

Microwave modulated incoherent light for large volume scenes holography, noting object image reconstruction by coherent light transillumination of hologram 15 p2242 A72-32675

Coherent emission lines in visible spectrum from triply ionized Er in barium yttrium fluoride, discussing energy level transitions associated with various lines 16 p2401 A72-33387

Resonant interaction and self transparency effect of coherent ultrashort light pulse passing through semiconductor 16 p2403 A72-33977

Three dimensional model images information content increasing in coherent light interference shadow marking, noting automatic systems for distant objects recognition 17 p2529 A72-34844

- Holographic image reconstruction using He-Ne laser as coherent light source and black-white and color photographic emulsions 17 p2554 A72-34930
- Laser and mercury lamp outputs spatial coherence measurement by speckle patterns produced with ground glass as random inhomogeneous medium 17 p2565 A72-35752
- Coherent optical terrain-relief determination using a matched filter. 18 p2691 A72-36491
- Nonholographic coherent optical correlation for automatic stereoperception. 18 p2691 A72-36493
- Use of amplitude filter to improve the partially space coherent diffraction of a defocused circular aperture. 19 p2833 A72-37402
- Real time holographic contouring and coherent light interferometry of gear tooth surfaces. 19 p2797 A72-37606
- Coherent radiation emission by indium antimonide in a transverse magnetic field 19 p2845 A72-38176
- Coherent optical signal superregenerative amplification in Q switched gas laser, calculating sensitivity of He-Ne laser light amplifier 19 p2813 A72-38663
- Macroscopic photon echo polarization and radiation intensity in Cr ion doped ruby laser stimulated by coherent light pulses 19 p2814 A72-38780
- Optical information processing analysis for coherent optics and holography, discussing characteristic spectral bands, sampling and signal averaging 20 p2922 A72-39035
- Partially coherent light for image formation of objects with amplitude, phase and complex variations, discussing system concepts, coherence control, apodization and techniques 20 p2931 A72-39048
- Significance of OTF methods in assessing lenses to be used with partially coherent illumination. 20 p2931 A72-39049
- The effect of pump coherence on frequency conversion and parametric amplification. 21 p3014 A72-40238
- Russian book - Principles of holography and coherent optics. 21 p3052 A72-40388
- Populating excited states of incoherent atoms using coherent light. 21 p3088 A72-40778
- Interferometric investigation of the phase fluctuations of coherent optical emission in the atmosphere 22 p3186 A72-42661
- Real time analog computation at light speed and rapid access data storage in optical data processing systems, considering coherent electro-optical instrumentation 22 p3180 A72-42713
- Comparison of theoretical and experimental results concerning spatial filtering in coherent optics 23 p3288 A72-43724
- Conditions for space invariance in optical data processors used with coherent or noncoherent light. 23 p3288 A72-43887
- Forward scattering of laser coherent light by acoustic or turbulent wave pressure variations, noting phase fluctuation spectrum 23 p3313 A72-44113
- Approximate formulae for mixed modulated coherent and partially polarized chaotic light. 24 p3425 A72-44769
- Wideband parametric up-conversion of infrared waves into visible region using tunable dye laser pumping. 24 p3410 A72-45286
- Wave and polarization equations for short coherent light pulses transmission in linear amplifying and absorbing media, noting single pulse formation in lasers 24 p3410 A72-45420
- Laser frequency measurement by comparison with stable molecular oscillator Doppler shift produced by reflection of UHF modulated coherent optical signal 24 p3411 A72-45425
- COHERENT RADAR**
- Clutter suppression by amplitude weighted pulse trains in coherent radar, obtaining optimum weights and signal-to-clutter gain as function of Doppler frequency 01 p0030 A72-10789
- Radar signal digital processing for replacing analog circuitry, discussing rf signal representation, sidelobe reduction, coherent processors and filter design 02 p0178 A72-12396
- Pulsed coherent radar with pulse position random modulation, discussing subclutter visibility, target attenuation and blind speeds cancellation and radial speed measurement without range ambiguities 06 p0775 A72-18184
- Coherent radar pulse train clutter performance prediction for targets with range acceleration effects on Doppler response 08 p1133 A72-21405
- Lunar surface profile, subsurface features and electrical properties measurement for Apollo 17 coherent radar and optical recording system 14 p2085 A72-30512
- Studies of vertical motions in cloud systems by using a coherent pulse radar in the decimeter wavelength range 19 p2829 A72-38773
- COHERENT RADIATION**
- NT COHERENT ACOUSTIC RADIATION
- NT COHERENT ELECTROMAGNETIC RADIATION
- NT COHERENT LIGHT
- Two dimensional scanning electron beam pumped laser, describing production of coherent emission 01 p0079 A72-10522
- Laser power transmission, examining heat transformation into coherent radiation by closed cycle gas dynamic laser system 01 p0080 A72-10925
- Coherence properties of polarized radiation in weak magnetic fields, considering scattering redistribution for normal Zeeman triplet 03 p0427 A72-13292
- Charged particle motion in pulsar electromagnetic fields, discussing coherent synchrotron radiation and charge bunching 03 p0438 A72-13874
- Coherent synchrotron radiation from model with charge distribution moving on ring, applying to pulsars 04 p0566 A72-14555
- Quantum coherent spin wave interactions in ferromagnetics, showing retained emission field 07 p1007 A72-20125
- Relation for detector-aperture size for spatially coherent detection with dependent scattering applied to realistic laser radar signal signatures 09 p1278 A72-22618
- Flexural vibrating free edge plate transducer with stepped thickness for high directional ultrasonic radiation generation in fluids 11 p1687 A72-26060
- Relativistic statistical mechanics invariant formula for coherence degree of plane blackbody radiation beam in arbitrary Lorentz frame, noting transformation law of temperature 12 p1846 A72-27741
- Microwave horn and lens antennas radiation spatial coherence characteristics, noting effect on picture contrast 13 p1928 A72-28475
- Radiation coherence enhancement in pulsed semiconductor injection laser by voltage controlled barium zirconite piezoceramic element 15 p2245 A72-31416
- Coherent CW radiation by tunable GaAs injection laser in external dispersive cavity at 77 K, discussing monochromatic output spectral analysis by Fabry-Perot interferometer 16 p2401 A72-33393
- Competition effects on spatial coherence in a CO₂ laser. 17 p2562 A72-34725
- Rhesus monkey retinas ultrastructural alteration and damage in rods and cones produced by Q switched ruby laser coherent radiation 17 p2509 A72-35396
- Radiation coherence in a monopulse single-mode semiconductor injection laser 19 p2811 A72-37736
- Experimental evidence of an X-ray laser/Coherent radiation/copper/II/ gel target/ neodmium-glass pump/. 19 p2811 A72-37774
- On the adiabatic invariants of a quantified system perturbed by a coherent wave 19 p2834 A72-37789
- Influence of an optically nonhomogeneous medium on the coherence of laser radiation and the possibility of obtaining a holographic image 19 p2812 A72-38536
- Group theory for spontaneous coherent radiation of multilevel sources, noting angular distribution of photon echo effects 23 p3295 A72-43306
- Coherent cross section effects on primary particle energy in inelastic proton interaction with carbon nuclei at 20-60 GeV 23 p3332 A72-44439
- The efficient generation of coherent radiation continuously tunable from 2500 A to 3250 A. 24 p3409 A72-44803
- COHERENT SCATTERING**
- D region echo amplitude distribution, observing coherent scattering contribution 03 p0349 A72-13523
- Reflectivity-emissivity relationship for isothermal atmosphere with coherent scattering and continuous absorption, generalizing for noncoherent case with line opacity 14 p2131 A72-30890
- Applicability bounds for the equation describing the mean field in a discrete scattering medium with allowance for the correlation of the scatterers 22 p3155 A72-42660
- Coherent/incoherent elastic/inelastic neutron scattering in amorphous solids, presenting neutron intensity and correlation functions 22 p3206 A72-42799
- Light scattering in a sphere in the presence of an arbitrary source distribution 22 p3207 A72-42965
- General characteristics of proton-nucleon and coherent interactions at an energy of 67 GeV 23 p3317 A72-44415
- On the validity of a generalized Kirchhoff's Law for a nonisothermal scattering and absorptive medium. 24 p3424 A72-44698
- COHERENT SOUND**
- U COHERENT ACOUSTIC RADIATION
- U SOUND WAVES
- COHERENT SOURCES**
- U COHERENT RADIATION
- U RADIATION SOURCES
- COHERENT TRANSMISSION**
- U COHERENT RADIATION
- COHESION**
- Metals mechanical behavior, considering plastic deformability, strain hardening, cohesion and engineering performance prediction 01 p0086 A72-10985
- Alloying addition effects on structural stability and particle-matrix cohesion in metal-alumina composites 11 p1665 A72-26864
- COHOMOLOGY**
- U HOMOMOLOGY
- COINCIDENCE CIRCUITS**
- Gamma ray detection system using scintillation counter and active anticoincidence shield 03 p0352 A72-13028
- Coincidence counting applied to the activation analysis of meteorites and rocks. 20 p2900 A72-39841
- COINING**
- Mg-Al powder mixtures sintering and coining, describing fabrication procedure, microstructure and mechanical properties 21 p3067 A72-40832
- COKE**
- Aircraft gas turbine engines synthetic lubricants thermal stability characteristics, describing coke deposition test apparatus and results [ASLE PREPRINT 72AM 14] 13 p1983 A72-28971
- Carboids effects on pyrolytic coke structure and graphite product properties 13 p1984 A72-29072
- I-V characteristics of electric noise generated by flame between double probe electrodes during coke particle burning in air flow 19 p2882 A72-38458
- COLD ACCLIMATIZATION**
- Heat production increase by muscular contractions due to noradrenaline in cold adapted rats 05 p0620 A72-17215
- Heat and cold acclimatization in hamsters, relating thermoregulatory response to helium-cold hypothermia induction 08 p1115 A72-21085
- Cold adaptation effects on rat skeletal muscle tissue Vant-Hoff coefficient, considering phosphorylation and oxidation rate, P/O and mitochondrial ATP-ase activity 13 p1902 A72-28639
- Modifications of the rate of renewal of norepinephrine in various peripheral organs of the rat during exposure and acclimatization to cold 23 p3258 A72-44244
- COLD CATHODE TUBES**
- NT PHOTOMULTIPLIER TUBES
- He-Ne laser amplitude fluctuations with hot and cold cathode discharge tube operation, determining emission spectral line width 05 p0669 A72-16613
- Pulsed atmospheric-pressure carbon-dioxide laser initiated by a cold-cathode glow-discharge electron gun. 22 p3186 A72-42753
- COLD CATHODES**
- Legibility of cold cathode, side illumination and straight projection electronic digital displays under varying ambient light and viewing positions 01 p0016 A72-10118
- Triplasmatron using crossed field hydrogen discharge between cold cathode and disk anode, noting pulse modulation applications 13 p1927 A72-28380
- Relaxation oscillations in He gas discharge tubes with cold Mo cathode as function of pressure and discharge length 15 p2245 A72-31408
- COLD DRAWING**
- Crystal-morphology role in refraction of cold drawn polyethylene samples of varying lamellar thickness and density, relating elastic restoring force to crystal deformation 12 p1832 A72-27283
- COLD FLOW TESTS**
- Cold flow tests of mixing and atomization characteristics of gas/liquid circular coaxial injector elements in pressurized facilities [AIAA PAPER 71-672] 14 p2146 A72-30920

COLD FORMING
U COLD WORKING
COLD GAS

Heat transfer from nitrogen plasma jet mixed with cold gas to cooled reactor channel walls at various channel expansion degree values

04 p0555 A72-14645

Molecular diffusion laser gain determination from interaction kinetics between diatomic and cold working gases, examining annihilation processes

10 p1491 A72-24360

Molecular diffusion laser gain determination from interaction kinetics between diatomic and cold working gases, examining annihilation processes

17 p2563 A72-34959

Stability of a plasma conductor with axial current, surrounded by cold gas with a pressure gradient

19 p2842 A72-38533

COLD PLASMAS

Electron thermal boundary layer effects on Langmuir probe measurements in subsonic cold plasma flow

01 p0071 A72-11191

Electrical conductivities dependence on assumed values of elastic collision cross sections of electrons with neutral and charged particles in low temperature plasma

01 p0110 A72-11205

Magnetosonic perturbations caused by ideally conducting sphere expansion in cold plasma, determining electric field and magnetic induction time dependences

02 p0217 A72-11939

Low temperature plasma electron density measurements using ruby laser light scattering method

02 p0264 A72-12210

Cold plasma flow rate determination from emission inhomogeneities, using time of flight method and high speed streak photography for instantaneous velocity measurements

03 p0396 A72-13663

Electron-ion recombination and ambipolar diffusion disruption of electron density in cryogenic helium plasma, using cavity resonator measurements

03 p0399 A72-14067

Quasi-linear relaxation of fast ion beam in cold plasma moving transverse to magnetic field

04 p0554 A72-14403

Electromagnetic absorption heating in cold randomly inhomogeneous plasma, discussing consequences of thermal particle motion neglect

04 p0489 A72-15393

Nonlinear MHD wave trains in cold collisionless plasma investigated by numerical and analytical methods

05 p0698 A72-17018

Nonlinear scattering of microwave signals incident on unmagnetized cold plasma column

06 p0859 A72-17547

Pulsating point charge potential in cold homogeneous boundless magnetoplasma with complex permittivity tensor coefficients for quadrupole probes theory

06 p0859 A72-17638

Pulse reflection of polarized plane electromagnetic wave from cold plasma ionosphere model with vertical magnetic field

06 p0777 A72-18729

Elf/vlf radiation resistance of finite electric dipole oriented at arbitrary angle in cold uniform magnetoplasma, deriving general integral expression

07 p1039 A72-18823

Ionization change induced striation instability of low temperature plasma with ambipolar diffusion in transverse magnetic field

07 p1043 A72-19878

Electrical conductivity of nonideal low temperature plasma as function of metallization densities, applying to semiconductors and mercury vapor systems

07 p1043 A72-19880

Methane pyrolysis in glow discharges /cold plasmas/, discussing chemical reactions initiated by high energy electrons inelastic collisions with gas molecules

07 p0937 A72-20286

Far field radiation pattern from magnetic line source covered with moving uniaxial or isotropic nondispersive dielectric or cold plasma sheaths

08 p1137 A72-21985

Power integral method for electric and magnetic dipole antennas vlf/elf radiation patterns in cold magnetoplasma, emphasizing focusing effects of refractive index surface

09 p1279 A72-23009

Dense low temperature Ar and Hg plasmas, observing correlation between electrical conductivity and optical emission

10 p1517 A72-23835

Strong magnetic fields and electric current densities effects on acoustic oscillations and instability in stationary inhomogeneous low temperature plasma flow in crossed fields

10 p1517 A72-23838

Microwaves propagation through circular waveguide partially filled with lossless cold electron

plasma dielectric, presenting computed dispersion curves for waveguide and plasmaguide modes

10 p1522 A72-24677

Low temperature plasma electron density measurements using ruby laser light scattering method

11 p1693 A72-25706

Zero temperature relativistic plasma ground state energy calculation using Fermi momentum and Green function

11 p1694 A72-25715

Electromagnetic wave field effects on cold magnetoactive plasma potential oscillations, solving dispersion equation for sub-ion gyroscopic frequencies

12 p1849 A72-27066

VLF and LF electromagnetic ground wave propagation between points on smooth curved lunar surface surrounded by free space or cold isotropic plasma

12 p1783 A72-27635

Quasi-static and full wave calculation of VLF/ELF input impedance of arbitrarily oriented loop antenna in cold collisionless multicomponent magnetoplasma

13 p2009 A72-28542

Magnetosonic perturbations caused by ideally conducting sphere expansion in cold plasma, determining electric field and magnetic induction time dependences

13 p1949 A72-29251

Dispersion of polyhelical nonrelativistic electron flow interacting with slow waves of magnetized cold plasma, observing instability in presence of Doppler effects

14 p2136 A72-30304

Electromagnetic waves propagation in inhomogeneous moving cold electron plasma without external magnetic field and collisions, investigating dynamo-optical effects

14 p2086 A72-30790

Diffraction of plane waves scattered by impedance structures in anisotropic medium, noting wedge shaped region with cold plasma under external magnetic field

14 p2086 A72-30809

Nonlinear coupling of wave modes in cold magnetized plasma, applying to electrostatic wave transformation in connection with solar type 3 radiation

15 p2283 A72-31431

Mathematical model for modified ordinary electromagnetic wave propagation in presence of two cold counterstreaming plasma electron beams, noting instability regions and growth rate

15 p2286 A72-32274

Analytical solution of dispersion equation for ionization instability threshold in unbounded low temperature plasma, noting independence of relaxation rates

15 p2286 A72-32277

Small-amplitude near-steady oblique shock waves in cold collisionless plasma, considering magnetoacoustic and Alfvén waves

15 p2287 A72-32414

Turbulent heating and resistivity in cool electron theta pinches due to IF long wavelength modified two stream and drift instabilities

15 p2288 A72-32426

Heat conductivity effect on structure and critical Mach number of shock wave propagation across magnetic field in cold rarefied plasma

16 p2435 A72-33152

Charged particle energy dissipation in cold collisional plasma, discussing collisions effect on power spectrum

16 p2436 A72-33651

Conducting fluid flow near neutral sheet in magnetic field, assuming cold polar wind plasma geomagnetic tail

16 p2438 A72-33930

Coupled mode equations derivation for wave interactions in plasmas, considering oscillations production and cold magnetized plasma

17 p2589 A72-34923

Ionization change induced striation instability of low temperature plasma with ambipolar diffusion in transverse magnetic field

17 p2590 A72-35128

Electrical conductivity of nonideal low temperature plasma as function of metallization densities, applying to semiconductors and mercury vapor systems

17 p2590 A72-35129

Theory of magnetically conjugate transport of cold plasma in the outer low-latitude ionosphere

17 p2548 A72-35218

VLF wave propagation and its interaction with the magnetoplasma.

17 p2516 A72-35357

On the stability of obliquely propagating whistlers.

17 p2517 A72-35600

Whistler side-band growth due to nonlinear wave-particle interaction.

17 p2517 A72-35601

A photon rest mass and the dispersion of longitudinal electric waves in interstellar space.

18 p2728 A72-36923

Amplitude limits to the theory of resonant absorption in cold plasmas.

18 p2716 A72-36960

Unsteady weakly nonlinear waves in a multicomponent plasma with allowance for weak dissipation

19 p2842 A72-38528

Uniform low temperature gas discharge plasma diagnostics in shielded volume, noting application of stable plasma generation effect for isotope analysis

22 p3210 A72-42152

Noncoherent excitation of plasma vibrations by an almost monoenergetic relativistic beam

22 p3213 A72-43114

Electron-energy distribution in a low-temperature plasma

22 p3213 A72-43118

Dispersion of polyhelical nonrelativistic electron flow interacting with slow waves of magnetized cold plasma, observing instability in presence of Doppler effects

23 p3317 A72-43206

Kinetics of impact-radiative ionization and recombination

23 p3318 A72-43296

Excitation of potential oscillations in a plasma by a flow of phased oscillators

23 p3319 A72-43401

Special features of photoresonance perturbation relaxation in a low-temperature discharge plasma

23 p3319 A72-43409

Ray tracing in ionosphere and magnetoionic theory application to coupling in cold plasma waves, considering linear waves, electrodes, particles and echoes as exciters

23 p3319 A72-43516

Wave attenuation during plasma propagation, discussing particle collisions, absorption effect on geometric optics and linear mode coupling in cold magnetized plasma

23 p3320 A72-43519

Methods of solving one-dimensional problems of radiative gasdynamics

23 p3320 A72-43528

Electromagnetic wave field effects on cold magnetoactive plasma potential oscillations, solving dispersion equation for sub-ion gyroscopic frequencies

24 p3431 A72-45719

COLD PLATES

U COLD SURFACES

COLD ROLLING

Cold rolled Zircaloy 2 sheet microstructure, microstrains and hardness by X ray diffraction and electron microscopy

11 p1657 A72-25757

Plane plastic deformation during single pass rolling of corrugated metal sheet, determining stress-strain fields for first and second phases

13 p1964 A72-29148

X ray analysis of Ti-Al alloys for cold rolled texture diagrams at low and high deformation levels

14 p2112 A72-30159

Dislocation substructures effect on relaxation and internal friction peak in cold rolled Mo single crystals after annealing

14 p2122 A72-30956

Polycrystalline Mo-Re alloy under cold longitudinal, transverse, cross and pack rolling, noting twin and dislocation microstructures

15 p2256 A72-31669

Anelastic damping of cold worked Nb sheet as function of vibration frequency, temperature, rolling rate and oxygen content

15 p2258 A72-32638

The structure and properties of thermomechanically treated beta-III titanium.

18 p2700 A72-36586

Analysis of the mechanisms of yield-stress variation during compacting of metal-ceramic materials by rolling

23 p3298 A72-43278

Effects of hydrostatic stress on the yielding of cold rolled metals and fiber-reinforced composites.

23 p3299 A72-43496

COLD STRENGTH

Cast electron-beam remelted Mo, investigating carbon and zirconium carbide additions effects on cold shortness and low temperature plasticity

06 p0833 A72-18645

Cold shortness of W and related refractory metals, noting oxide phases and impurities effects on mechanical properties temperature dependence

09 p1326 A72-22226

Mo alloy under impact tests, investigating notch sharpness effects on cold shortness threshold and strength

23 p3301 A72-43756

COLD SURFACES

Experimental cold plates provided with heat pipes for thermal control of electronic equipment [AIAA PAPER 72-269]

11 p1740 A72-25210

Three-phase heat transfer - Transient condensing and freezing from a pure vapor onto a cold horizontal plate - Analysis and experiment.

22 p3243 A72-41957

COLD TOLERANCE

Helium-cold hypothermia induction and maintenance effect on hamster myocardia, with ventricle analysis of hypoxic damage, glycogen and catecholamines 04 p0476 A72-15720

Peripheral thermoregulation in arctic canines, showing subzero bath-immersed foot temperature maintenance above tissue freezing point 08 p1120 A72-22019

Aircrews tolerance to cold water and life raft exposure, discussing prediction model based on thermal insulation effectiveness, assumed metabolism and body surface area and mass [AD-740276] 10 p1428 A72-23734

Thermally protective life rafts and clothing evaluation for cold sea survival potential assessment and tolerance limit determination 14 p2081 A72-31088

High gravity, cold and starvation space stress effects on oxidative metabolism of ethylmorphine, aniline and p-nitroanisole in male rat liver 15 p2185 A72-31700

Myocardium automatism, excitability, conductivity and contractility under cooling, noting complete inhibition at 9-3 deg C 22 p3141 A72-42072

COLD WALLS
U COLD SURFACES
U WALLS

COLD WATER
Thermally protective life rafts and clothing evaluation for cold sea survival potential assessment and tolerance limit determination 14 p2081 A72-31088

COLD WEATHER
Temperature indetermination and large scale weather patterns in winter from 70 year temperature records 10 p1507 A72-25003

Stratosphere circulation variation in autumns preceding cold winters 20 p2949 A72-39947

COLD WEATHER TESTS
Engine lubrication under cold weather conditions, discussing polymer thickened and synthetic oils, automotive and industrial gear oils, hydraulic oils and lubricating greases 03 p0363 A72-13450

Human tryptophan and tyrosine metabolism - Effects of acute exposure to cold stress. 21 p2997 A72-40417

COLD WORKING
NT COLD ROLLING
NT ELECTROHYDRAULIC FORMING
NT EXPLOSIVE FORMING

Cryogenically formed prestressed stainless steel glass fiber reinforced vessels, demonstrating structural performance for space shuttle life support oxygen/nitrogen high pressure gas tanks 01 p0139 A72-10770

Bcc Mo and Nb after cold working observing internal friction relaxation peaks as function of stress, strain, temperature and strain rate 06 p0831 A72-18296

Cold working effects on plasticity of hardened Al at 20-400 C 07 p1015 A72-19902

Metals cold working mechanics about stress state and yield points, proposing theoretical model for mechanism and applications in extrusion molding, drawing and hollow forging 07 p0999 A72-20599

Metal cold working mechanics, discussing model based on equality of internal and external forces needed for plastic deformation 08 p1176 A72-21439

Critical supercurrents in heat treated and cold worked Nb-Ti wires, proposing pinning model based on enhancement of Ginzburg-Landau parameter in cell walls 08 p1186 A72-21594

Cold working effect on precipitation-recrystallization interaction in Cu-Ni-Zn alloy, discussing superposed strengthening mechanism during annealing 11 p1641 A72-26738

Superconductive behavior of cold-worked sintered Nb wires, examining effects of aluminum oxide addition on residual resistivity, magnetization behavior and critical current density 11 p1662 A72-26742

Cold working effect on Cu-Ni-Si-Mg and Cu-Ni-Si-Cr alloys age hardening behavior, presenting hardness and tensile strength vs aging time at 350 and 400 C 11 p1662 A72-26743

Heat treated Al alloy forgings stress relief by cold deformation between quench and age, examining effect on tensile properties and residual stresses [ASM PAPER W72-53,1] 12 p1817 A72-28165

Ultrafine grained microstructures and mechanical properties of alloy steels developed by cold working followed by annealing 13 p1974 A72-28662

Surface cold-working as a means of increasing the short-term fatigue endurance of machine elements 19 p2808 A72-38015

Nucleation of new grains in recrystallization of cold-worked metals. 20 p2930 A72-39995

Effect of cold work on the oxidation of nickel at high temperature. 21 p3067 A72-40846

Hydrogen cold work peak measurements in Nb, showing hydrogen atoms-dislocations binding energy extent and temperature effects on internal friction 22 p3189 A72-42440

Martensitic transformation during deformation in titanium alloys with a metastable beta phase 23 p3300 A72-43591

Fatigue-crack growth in 20% cold-worked Type 316 stainless steel at elevated temperatures. 24 p3435 A72-44555

A study of cold-worked titanium-aluminum alloys by X-ray diffraction. 24 p3413 A72-44720

COLEOPTERA
Coleoptera flight muscle system anatomy, presenting instantaneous lift forces measurement systems 06 p0755 A72-17563

COLLAGENS
Confinement, physical deconditioning and hypercapnia effects on human musculoskeletal protein by chromatographic method for quantifying urinary peptides and free amino acids 06 p0767 A72-17869

Pathological significance of high oxygen tension exposure effects on acid soluble collagen extracted from mouse skin 12 p1760 A72-27483

Collagen in human myocardium as a function of age. 23 p3256 A72-43935

COLLAPSE
Postbuckling collapse, end shortening, stiffness and ultimate load for geometrically imperfect simply supported plates with stress free edges 06 p0896 A72-17964

COLLECTORS
U ACCUMULATORS

COLLIMATION
Radio telescope variable profile antenna autocollimation adjustment for separating transmitted and received signals pulse-time characteristics 02 p0231 A72-12521

Neutral density glass collimating absorption lens for ideally uniform laser beams production 09 p1315 A72-23347

Low energy elastic scattering cross section measurements for helium-nitrogen system, using two collimated aerodynamically intensified crossed molecular beams 10 p1515 A72-24338

Beam divergence prediction for multiple transverse laser modes, proposing tables and graphs to determine angular spread in far field 15 p2247 A72-32031

COLLIMATORS
Apollo 12 liquid oxygen cloud spectrum observations, describing spectrograph with off axis zone plate for transmission grating and sieve plate collimator 01 p0071 A72-11172

Low energy gamma ray telescope with active honeycomb collimator and anticoincidence detector, describing directivity techniques for galactic sources 03 p0408 A72-13030

NASA spacecraft instrumentation for high energy phenomena measurements, discussing collimated proportional counters, wire grid digitized spark chambers and modulation and slit collimators 03 p0353 A72-13038

Balloon-borne galactic X ray detection unit, obtaining high directivity with honeycomb collimator and angular resolution with solar sensor 03 p0353 A72-13043

Aberration correction in collimator of Schmidt spectrograph camera by changing surface geometry and grating positioning 03 p0362 A72-14358

German monograph - Development and testing of a laser autocollimator 19 p2810 A72-37480

Three axis angular deviations measurement by flexure monitor system for spacecraft, using pulsed light sources, autocollimator and porro reflectors [AIAA PAPER 72-855] 20 p2951 A72-39106

A variable spacing modulation collimator for X-ray astronomy. 20 p2928 A72-39891

COLLINEARITY
Aerial focal plane shuttered camera high velocity images mathematical model based on collinearity equations, incorporating translational and rotational camera motion during exposure for image motion compensation 01 p0066 A72-10461

COLLISION AVOIDANCE
Mathematical analysis of separation standards and aircraft navigational collision risk for parallel tracks in radar monitored systems 01 p0096 A72-10178

Statistical analysis of track keeping Strumble VOR data for lateral navigation separation standards and collision risk in continental environment 01 p0097 A72-10179

Avionics contribution to airspace decision making problems, considering navigation, surveillance radar, collision avoidance and ATC techniques 01 p0097 A72-10180

Pilot collision warning indicator performance in terminal area traffic, using computer fast-time simulation for traffic model 01 p0098 A72-11134

FAA activity in collision avoidance system and pilot warning instrument areas 02 p0256 A72-12379

ATC for North Atlantic air transportation, emphasizing collision risk model for safety standards assessment 04 p0544 A72-14484

Time/frequency collision avoidance systems, discussing operating principle and economic aspects for airlines and general aviation 04 p0544 A72-14816

Collision avoidance systems and pilot warning instruments, minimizing cost by pilot detection, evaluation and avoidance execution 04 p0545 A72-14823

National Aviation System technology, discussing wide body jets, smokeless turbopans, all-weather operational capability, collision avoidance and noise reduction 04 p0597 A72-14824

Airborne collision avoidance system equipment for general aviation aircraft, discussing logic functions, transmission modes, data handling tradeoffs and ATC procedure interactions 04 p0545 A72-14830

Statistical characteristics of range-guard intrusions and airspace collision conflicts in terminal area 05 p0611 A72-16110

Vertical dipole antenna design for CW Doppler radar midair collision avoidance system 05 p0629 A72-16571

Aircraft collision avoidance system design and evaluation, developing closed form method for system alarm rate estimation [AIAA PAPER 72-97] 05 p0688 A72-16945

Computerized Eros II airborne collision avoidance time frequency system design, considering radio transmission, synchronization and ground stations 06 p0845 A72-18247

Collisional avoidance system operation evaluation, noting protected airspace volume requirement 07 p1032 A72-18835

Aircraft midair collision prevention in dense air traffic environments, suggesting problem solution based on proximity warning system 08 p1204 A72-21090

UFO sighting case history and analysis, discussing bright light approaching on collision course during night instrument flight rules 09 p1269 A72-22646

Collision avoidance systems requirements and criteria, evaluating Eros time frequency and Secant interrogation-and-reply systems 09 p1349 A72-22822

Eros and ATA /Air Transport Association/ time-frequency collision avoidance systems, discussing synchronization methods, back-up mode operation, threat computation and displays 09 p1349 A72-22823

C-band pulse beacon ranging system for collision avoidance, detailing interrogation, response and system test modes 09 p1349 A72-22908

Aircraft collision near misses under IFR and VFR conditions, discussing ATC coordination, equipment failure and personal and planning problems 09 p1349 A72-22972

RCA SECANT aircraft collision avoidance system avionics design using nonsynchronous techniques 10 p1509 A72-24866

Pilot warning systems for visual midair collision avoidance, noting reaction to imminent threats, scanning patterns and display sector size effects [SAE PAPER 720312] 11 p1583 A72-25576

SECANT system of aircraft separation and control by nonsynchronous technique for midair collision avoidance [SAE PAPER 720313] 11 p1683 A72-25577

Physiological effects of intense anticollision flash light backscatter pulses on instrument rated pilots 12 p1775 A72-28303

Detection range, color, brightness and flash subjective response tests to evaluate light signals for nighttime sea navigation and visual collision avoidance 12 p1777 A72-28326

Head-up omnidirectional two dimensional auditory display device for visual detection facilitation in aircraft collision avoidance systems 12 p1777 A72-28327

Information theory approaches to air navigation, discussing ATC, collision avoidance and computer applications 13 p1996 A72-29013

Time/frequency technology application to reliable aircraft collision avoidance system, discussing precision time-ordered techniques, frequency control and synchronization and flying clocks

15 p2268 A72-32072

Collision avoidance techniques for midair collisions reduction, discussing airborne and ground based systems

15 p2272 A72-32213

SECANT collision avoidance system, describing operational principles and flight test results

16 p2421 A72-34137

A time-frequency high performance collision avoidance system.

19 p2830 A72-37764

[ONERA, TP NO. 1091]
Midair collision causes and prevention, considering pilot responsibilities, anticollision devices and procedures

19 p2831 A72-37800

Aircraft radar for weather data, ground mapping, avoidance modes and independent landing monitor function, presenting straight and slant approach simulation data

21 p3080 A72-40290

Design, operation and performance of time-frequency midair collision avoidance system, noting air traffic controller backup for departure, enroute and arrival control

21 p3081 A72-40295

Operation principles, capabilities and tests of midair collision avoidance system with aircraft separation control by nonsynchronous techniques

21 p3081 A72-40296

Midair collision prevention independent of ATC, discussing aircraft lighting, collision avoidance systems and proximity warning indicator

21 p3081 A72-40297

Collision avoidance system electromagnetic compatibility with radar altimeters designed for 1600 MHz aeronavigation band

21 p3018 A72-40881

Independent parallel runway landing system to relieve air traffic congestion, investigating minimum spacing required to minimize collision risk

22 p3203 A72-43130

Midair collision prevention for Army aircraft.

24 p3422 A72-44645

SECANT midair collision avoidance system based on nonsynchronous microsec pulse transmission and receiving via randomly selected frequency, describing modular components and operating principles

24 p3422 A72-44647

Safety design of space station against collision hazards with artificial orbiting bodies.

24 p3449 A72-45143

COLLISION PARAMETERS

NT COLLISION RATES

Bond zone wave formation in explosion cladding, predicting critical collision velocity and angle with fluid flow model

01 p0077 A72-11031

Detonation waves collision in variable gas medium with plane, cylindrical or spherical obstruction, determining gas parameters behind reflected shock wave

02 p0201 A72-11579

Plasma ion temperature and neutral collision frequency determination by Langmuir probes

[AD-739452] 02 p0264 A72-12262

Fm of gas laser emission during sinusoidal modulation of relative excitation, evaluating collision parameters determination method

02 p0180 A72-12581

Collision integral for classical electron plasma, concerning Born-Bogoliubov-Green-Kirkwood-Yvon equations for long range interaction potential and motions of multiple particles

03 p0399 A72-14069

Reduced collision integrals for components of Venus and Mars type carbon dioxide atmospheres at 1000-11,000 K, using intermolecular interaction potentials

05 p0712 A72-15851

Collisional radiative model of population densities of metastable electron levels of orthohelium in low pressure rf helium plasma

05 p0694 A72-15998

Potential parameters determination from collision integrals in thermodynamic properties calculation for combustion products at moderate and low temperatures

05 p0751 A72-17067

Coupled equations for collision amplitudes in three body system involving particle redistribution

06 p0851 A72-17391

Boltzmann kinetic equation with electron-electron collision coefficients for isothermal weakly ionized cesium-argon plasma, using nodal point method

06 p0860 A72-17695

Magnetic effects on Lorentz plasma collision processes, calculating electron distribution function in presence of strong arbitrarily oriented magnetic and weak electric fields

06 p0864 A72-18535

Numerical solution of equations for asteroidal mass distribution under collisional fragmentation

07 p1071 A72-19180

Approximate expression for charge exchange spreading of proton beam precipitating into atmosphere, showing dependence on atmospheric structure, collision data and primary particle energy

09 p1377 A72-22591

Reduced mass and asymmetry differences effects on elastic collision integrals and thermal diffusion factors for isotopic hydrogen molecules

10 p1515 A72-24340

Rain droplets growth by collision and coalescence during fall through sheared air flow, discussing discrepancies between calculated and experimental collision efficiencies

11 p1619 A72-26642

Ion-molecule collision frequencies in gases by phase coherent pulsed ion cyclotron resonance spectrometry [ONERA, TP NO. 1071]

14 p2133 A72-30524

Reduced collision integrals for components of Venus and Mars type carbon dioxide atmospheres at 1000-11,000 K, using intermolecular interaction potentials

15 p2302 A72-31270

Differential collision cross sections for argon pairs with neon, methane and ethane at angular region of two crossed nozzle molecular beams

16 p2431 A72-33070

The collision singularity in a perturbed n-body problem.

17 p2609 A72-35107

On the collision of a cold elastic plate with a hot elasto-plastic plate.

21 p3124 A72-41482

Parameters influencing the theoretical calculation of the thermal conductivity of a nitrogen plasma

23 p3321 A72-43692

Calculation of transport coefficients of a non-Lorentzian plasma

23 p3321 A72-43821

Kinetic equations for a chemically reacting plasma.

24 p3430 A72-45566

COLLISION RATES

MHD equations for plasma of arbitrary collision frequency in weakly inhomogeneous magnetic field, considering collisional and resonant particle effects

01 p0108 A72-10241

Differential phase shift and absorption measurements of partially reflected radio waves, providing electron density and collision frequency data from 70-90 km

01 p0030 A72-10836

Collision frequencies definition in kinetic theory of gases, expressing ionospheric electron conductivity

03 p0345 A72-12979

Global morphology of integrated product with respect to D and E regions electron concentration height and collision frequency

03 p0345 A72-12981

Electronic collision frequency relationship with radio frequency in F region, investigating height, diurnal and seasonal variations

04 p0516 A72-14933

Dispersion relation for MHD wave propagation through partially ionized magnetoplasma, discussing collision frequencies effects

04 p0556 A72-14943

Rate constant for quenching of B⁺/super 2Sigma⁺ plus state of CN radical as function of quenching collision relative velocity and total pressure in fluorescence cell

04 p0553 A72-15635

Electron concentration and collisions number fluctuations effect on D region profiles based on radio waves partial reflection data

05 p0656 A72-16244

Gas discharge plasma detection characteristics, examining electron and ion densities and collision rates dependence on electromagnetic field frequency and amplitude

09 p1361 A72-22956

Collisional cyclotron instability nature in ionized gases in presence of Ramsauer effect

10 p1520 A72-24224

Quasi-linear approximation equations for relativistic charged particles beam dissipative instability in collisional plasma, noting electrons heating at high collision frequencies

12 p1852 A72-27860

Martian ionosphere electromagnetic wave propagation characteristics for E, F1 and F2 models, calculating refractive index for zero and nonzero collision frequencies

13 p1922 A72-29474

Negative ions and collision frequency effects on circularly polarized ELF and VLF wave propagation in ionosphere

14 p2084 A72-30128

D region electron concentration and collision frequency with neutral molecules from radio waves backscattered by inhomogeneities in propagation medium

16 p2385 A72-33484

Booker theorem generalization to cover wide range of ionospheric refractivity profiles containing variable electron density and collision frequency

16 p2386 A72-33662

Excitation of molecular vibration on collision - Simultaneous vibrational and rotational transitions in hydrogen + argon at high collision velocities.

17 p2585 A72-35467

Collisional-rate coefficients for sodiump-like Ar VIII ions.

17 p2585 A72-35770

Gas discharge plasma detection characteristics, examining electron and ion densities and collision rates dependence on electromagnetic field frequency and amplitude

17 p2593 A72-35885

Determination of the quenching of O(1D) by molecular nitrogen using the ionospheric modification experiment.

18 p2685 A72-35991

Model ionosphere for D region at summer noon during sunspot maximum.

18 p2689 A72-37207

D-region electron densities and collision frequencies from Faraday rotation and differential absorption measurements.

19 p2793 A72-38858

Measurements of enhanced absorption of electromagnetic waves and effective collision frequency due to parametric decay instability.

21 p3092 A72-40829

D-region measurements with the differential-absorption, differential-phase partial-reflection experiments.

22 p3172 A72-42423

Elastic electron-neutral interaction in argon in the vicinity of the Ramsauer minimum

22 p3211 A72-42642

Variation with electron velocity powers of electron collision frequency and energy transport coefficients in weakly ionized plasmas - Earth's lower ionosphere.

23 p3285 A72-43994

COLLISION WARNING DEVICES

U COLLISION AVOIDANCE

U WARNING SYSTEMS

COLLISIONLESS PLASMAS

Two dimensional collisionless plasmas instability with neutral points, discussing sheet pinch with periodic structure

01 p0105 A72-10022

Higher order cyclotron harmonic resonance of electrons with electromagnetic wave propagation through collisionless magnetoplasma, deriving energy oscillation time period

01 p0105 A72-10023

Scattering cross section of electromagnetic wave by collisionless plasma perpendicular to applied magnetic field

01 p0105 A72-10025

Similarity theory for electrostatic and magnetic collisionless shocks at zero ion temperature, using numerical simulation results

01 p0106 A72-10029

Electrostatic wave-particle interactions in inhomogeneous collisionless plasma, calculating resonant distribution function, charge densities and trapping periods

01 p0107 A72-10136

Nonlinear hydromagnetic waves in finite beta collisionless plasma, calculating space-time evolution with nonlinear integrodifferential equation

01 p0107 A72-10143

Collisionless plasma shock wave measurements in magnetic field, determining plasma temperature and free electron densities

01 p0108 A72-10236

Nonlocal theory of electrostatic trapped particle instability in collisionless toroidal plasma, estimating particle mode nonlinear diffusion coefficient

01 p0108 A72-10239

Nonlocal behavior of ion sound instability in collisionless nonuniform confined plasma shock wave

01 p0108 A72-10240

Potential and ion charge distribution in proximity to conducting sphere moving in low density collisionless ion-electron plasma

01 p0109 A72-10371

Solar wind two component model with protons collisionless beyond ten solar radii, discussing effects of variable electron temperature

01 p0119 A72-10879

Higher moment Vlasov equations of collisionless fully ionized plasma for studying solar wind proton thermal anisotropy, heat flux and distribution function

01 p0119 A72-10880

High speed streak cameras applicability to low density theta pinch studies, describing image converters design, operation and block diagrams

02 p0263 A72-11410

Decay interactions among plasma wave and two opposed electromagnetic waves in homogeneous layer of isotropic collisionless plasma, observing stimulated Raman scattering

02 p0180 A72-12579

Transverse shock waves fine structure and saturation of ion-acoustic turbulence in collisionless plasma, using magnetic field probe and MHD equations

03 p0399 A72-14068

- Ion-wave current instabilities theory, showing inhomogeneities generated by field aligned currents in collisionless plasma 04 p0559 A72-15350
- One dimensional collisionless plasma instability driven by cold electron beam, determining limits from beam trapping 04 p0559 A72-15353
- Electromagnetic wave propagation and stability in inhomogeneous collisionless plasma under static magnetic field 04 p0490 A72-15401
- Collision resonance effects on transverse wave propagation direction in collisionless plasma for upper ionospheric sounding 04 p0490 A72-15403
- Nonstationary behavior of collisionless shock waves in plasma wind tunnel, suggesting interpretation of magnetosphere magnetic field structure near earth bow shock 04 p0559 A72-15468
- Collisionless shock wave interaction with particle stream in upper solar corona from decameter radio observation 05 p0708 A72-15764
- Cylindrical positive probe behavior in high speed collisionless mesothermal plasma flow [ONERA, TP NO. 1000] 05 p0660 A72-15860
- Vlasov equation stability properties of collisionless plasma and stellar gas, removing energy variation difficulties with multiple water bag model 05 p0694 A72-16060
- Self action penetration of electromagnetic wave through dense collisionless plasma layer in high vacuum, using antenna microwave probes 05 p0695 A72-16601
- Electron heating in weakly ionized collisionless beam plasma discharge as function of neutral gas pressure and plasma column length 05 p0697 A72-16986
- Electron heating model in perpendicular collisionless plasma shock waves based on electron trapping by turbulent electric field 05 p0697 A72-17014
- Existence conditions for steady MHD shock waves propagating in collisionless plasma along magnetic field, observing dependence on pressure anisotropy 05 p0698 A72-17016
- Nonlinear MHD wave trains in cold collisionless plasma investigated by numerical and analytical methods 05 p0698 A72-17018
- Longitudinal electrostatic waves in perpendicular collisionless plasma shock, investigating stability 05 p0698 A72-17021
- Relativistic electron pitch-angle diffusion driven by oblique lf whistler-mode turbulence in collisionless plasma immersed in static magnetic field 05 p0699 A72-17024
- Laminar leading edge of collisionless plasma perpendicular shock structure and distribution functions, considering instability calculations 05 p0654 A72-17227
- Electron temperature gradient instability in collisionless shocks propagating across magnetic field 05 p0700 A72-17228
- Collisionless relaxation of interpenetrating ion beams in Ar plasma, showing velocity spectrum broadening during Langmuir frequency periods 06 p0853 A72-17394
- Collisionless solar wind in spiral interplanetary magnetic field, using two fluid model with hydrodynamically treated electrons 06 p0872 A72-17441
- Quiescent large volume collisionless He and Ar plasma generation via hf electric fields, noting low cost 06 p0854 A72-17504
- Perturbed density and ion velocity distribution functions of grid-excited ion acoustic waves in collisionless plasma in single ended Q device 06 p0855 A72-17511
- Ion-acoustic collisionless shock generation by initial plasma density discontinuity in Q machine, correlating experimental results with numerical simulation 06 p0856 A72-17520
- Electrostatic wave propagation and damping in thermally ionized collisionless alkali plasma, determining electron and ion densities, electron temperature and ion distribution function 06 p0856 A72-17521
- Electrons spatial and temporal response in collisionless plasma to externally applied voltage pulse 06 p0856 A72-17522
- Spontaneous collisionless drift waves due to pressure gradient in hydrogen plasma column, studying magnetic field and reflecting conditions effects 06 p0857 A72-17534
- Collisionless drift waves in thermally ionized Li plasma column under variable shear magnetic field 06 p0857 A72-17535
- Plasma wave growth from large diameter electron beam interaction with quiet collisionless unmagnetized discharge plasma, measuring linear dispersion properties 06 p0858 A72-17539
- Electron beam interaction with collisionless plasma, obtaining beam spatial distribution function from velocity diffusion coefficient measurement 06 p0858 A72-17540
- Electrostatic hf wave propagation in one dimensional collisionless plasma, describing electron trapping and oscillations and resonance-produced sidebands 06 p0858 A72-17544
- Trapped ion instability in collisionless plasma ion acoustic waves, discussing sideband waves frequency spectrum and growth rate 06 p0859 A72-17545
- Collisionless plasma oscillations in external uniform magnetic field, described by initial value problem for nonrelativistic linearized Vlasov-Maxwell equations 06 p0862 A72-18251
- Ion-acoustic solitary waves formation and interaction in collisionless warm plasma, using Vlasov equation for ions and Boltzmann distribution for electrons 07 p1041 A72-19507
- Collisionless plasma electronic shock waves /stationary heat discontinuity/ observation, proving stationary shock wave existence 07 p1043 A72-19874
- Solar wind and geomagnetic tail interaction with moon, discussing lunar Mach cone evidence for anisotropic wave propagation in magnetized collisionless warm plasma 07 p1061 A72-20025
- Collisionless ion beam plasma simulation of ionospheric plasma with Langmuir interpretation of density and frequency agreement 07 p1044 A72-20367
- Reverse deflection and contraction of collisionless plasma beam during motion along curved magnetic field lines 07 p0979 A72-20378
- Quasi-linear theory validity for turbulent collisionless plasmas, considering bump-in-tail and weak symmetric two-stream instabilities 07 p1045 A72-20481
- Charged conductors in homogeneous collisionless magnetoactive plasma at hybrid frequencies, investigating antenna array quasi-electrostatic field one dimensional structure 08 p1138 A72-20746
- Growth rate estimation of negative energy Bernstein and ion acoustic waves explosive interaction, noting collisionless shock turbulence 08 p1212 A72-21248
- Stability of steady large amplitude whistler wave supported by weak electrostatic waves in collisionless magnetoplasma, constructing distribution function via Vlasov equation solution 08 p1213 A72-21258
- Electron beam interaction with bounded homogeneous plasma layer natural oscillations, using collisionless kinetic equation 08 p1215 A72-21720
- Collisionless plasmas numerical simulation with weighted particles and periodically reconstructed distribution function, estimating diffusion rates 09 p1358 A72-22462
- Electrostatic longitudinal waves propagation and detection in isotropic collisionless hot electron plasma, calculating Landau dispersion curve and damping 09 p1359 A72-22794
- Self consistent collisionless theory of turbulent low Mach number ion-acoustic shocks, noting resistive heating 09 p1360 A72-22872
- Stable large amplitude high Mach number ion acoustic shocks in collisionless plasma, obtaining electron density as function of time 09 p1364 A72-23445
- Collisionless plasma spherical probe RF sheath model based on quasi-static approximation and electrostatic theory 09 p1365 A72-23520
- Quadrupole probe theory for hot collisionless isotropic plasma, noting impedance dependence on electron temperature at resonance and optimum dimension relationship to Debye length 10 p1523 A72-24798
- Collisionless thermalization of ion beam by interaction with plasma, noting acoustic instability growth 10 p1524 A72-24921
- Temperature anisotropy quasi-linear relaxation thermodynamics in collisionless plasma, analyzing system free energy 11 p1698 A72-26599
- Electron heating in weakly ionized collisionless beam plasma discharge as function of neutral gas pressure and plasma column length 12 p1850 A72-27130
- Plasma ion temperature determination by measuring transient current to cylindrical Langmuir probe under collision free conditions [AD-739815] 12 p1851 A72-27399
- Stability properties for collisionless plasma and encounterless self gravitational stellar gas described by Vlasov equations 12 p1875 A72-27916
- Quasi-static and full wave calculation of VLF/ELF input impedance of arbitrarily oriented loop antenna in cold collisionless multicomponent magnetoplasma 13 p2009 A72-28542
- Book on nonlinear coherent and turbulent collisionless plasma theory covering collective /wave-particle and wave-wave/ interactions and mathematical methods 13 p2011 A72-29099
- Weak ion-acoustic quasi-shock wave propagation in collisionless plasma, determining long time behavior of precursor ion stream reflected by electrostatic potential 13 p2012 A72-29125
- Computerized simulation of single large amplitude whistler wave propagation in plasma, noting collisionless damping, oscillations and equilibrium 13 p2012 A72-29128
- Alternating magnetic field effect on collisionless nonhomogeneous magnetoplasma ion acoustic oscillations stability, examining parametric excitation of Langmuir oscillations 13 p2016 A72-29604
- Carbon dioxide laser light scattering measurements of turbulence in high beta collisionless plasma shock wave 13 p2018 A72-29853
- Helicon/whistler/ turbulence spectra in collisionless plasma due to ion scattering, considering self trapping and stability along magnetic field with Landau absorption decay 14 p2137 A72-30357
- Non-Maxwellian inhomogeneous collisionless plasma equilibrium and stability, proposing statistical thermodynamic model 14 p2137 A72-30394
- Plasma radiation from collisionless MHD shock waves, discussing waves generation and angular distribution 14 p2138 A72-30555
- Electromagnetic waves propagation in inhomogeneous moving cold electron plasma without external magnetic field and collisions, investigating dynamical optical effects 14 p2086 A72-30790
- Waves and particles interaction in weakly turbulent collision-free Vlasov plasma under pure Coulomb interaction and zero magnetic field 14 p2140 A72-30937
- Lagrangian complex amplitude derivation for monochromatic electrostatic wave in unmagnetized collisionless plasma, investigating nonlinear Landau damping effects on instability 14 p2140 A72-30939
- Numerical analysis of steady one dimensional quasi-shock waves in collisionless plasma within longitudinal uniform magnetic field, noting oscillations behind wave front 15 p2284 A72-31584
- Nanosecond response magnetic probes to measure fast disturbances in oblique shock waves within collisionless plasma, describing experimental technique 15 p2235 A72-31646
- Solar wind model dividing interplanetary space in one fluid and two fluid collisionless regions, discussing proton thermal anisotropy 15 p2300 A72-31996
- Small-amplitude near-steady oblique shock waves in cold collisionless plasma, considering magnetoacoustic and Alfvén waves 15 p2287 A72-32414
- End effect in current response of highly negative cylindrical Langmuir probe in collisionless plasma flow, discussing use for ion temperature determination 15 p2288 A72-32418
- Contaminated Langmuir probes LF admittance measurements in mercury vapor plasma, considering dielectric relaxation in insulating layers 15 p2241 A72-32516
- Boundary layer ionization on flat plate and cylindrical plasma probes in high speed flow, considering ionized continuum flow and collisionless plasma 16 p2374 A72-32831
- Difference scheme for initial value problem of one dimensional Vlasov equation for collisionless electron plasma with homogeneous ion background 16 p2434 A72-33006
- Alfvén wave firehose instability relaxation calculation to include nonlinear terms for explanation of solar wind temperature anisotropies by collisionless mechanism 16 p2449 A72-33933
- Investigation of two types of collisionless linear dampings of electromagnetic waves in a non-homogeneous magnetized plasma 17 p2588 A72-34870
- Carbon dioxide laser light scattering from cyclotron-harmonic waves in steady state rarefied collisionless plasma, noting associated electron density fluctuations 17 p2591 A72-35378

Water bag model application to one dimensional inhomogeneous two-stream collisionless electron plasma stability computation, noting electrostatic modes

17 p2592 A72-35619

Electron cyclotron drift instability linear theory application to controlled fusion and collisionless shocks, proving anomalous resistance to current flow normal to magnetic field

17 p2592 A72-35624

Beam-generated collisionless ion-acoustic shocks.

17 p2592 A72-35626

Quiescent large-volume collisionless HF discharge plasma generator with zero magnetic field, noting low noise level due to self-stabilizing feature

17 p2592 A72-35814

Influence of reflected ions on the magnetic structure of a collisionless shock front.

17 p2592 A72-35819

Cs diode discharge current oscillations in collisionless Knudsen plasma containing electron and positive ion fluxes from thermionic emission and surface Cs ionization

17 p2593 A72-35889

Turbulent heating of electrons and ions in a collisionless shock wave.

18 p2715 A72-36599

Quasi-linear theory of plasmas situated in a weak UHF electric field and a constant magnetic field

18 p2715 A72-36654

Determination of the plasma density in a collisionless plasma.

18 p2717 A72-37041

Discontinuities in a collisionless plasma flow having a strong magnetic field.

18 p2717 A72-37042

Longitudinal waves in a perpendicular collisionless plasma shock. IV - Gradient B.

19 p2838 A72-37329

Mathematical model for perfectly absorbing spherical Langmuir probe in collisionless plasma, obtaining plasma density and ion temperature

19 p2842 A72-38524

Drift instabilities in an inhomogeneous collisionless plasma

20 p2957 A72-39355

Reductive perturbation method application to Vlasov equation governing one dimensional motion of collisionless plasmas, investigating nonlinear modulation of plasma waves

21 p3089 A72-40188

Collisionless momentum transfer interactions in laser produced plasma on solid target, refuting Wright model

21 p3090 A72-40339

Alternating magnetic field effect on ionoacoustic oscillations stability of collisionless nonhomogeneous magnetoplasma, examining parametric excitation of Langmuir oscillations

21 p3091 A72-40658

Low frequency electrostatic waves in a turbulent plasma.

21 p3092 A72-41221

Sideband waves excitation by large amplitude ion-acoustic waves in collisionless plasma, noting frequency spectrum and growth rate agreement with trapped particles theory

21 p3094 A72-41629

Resonances in the collisionless heating of a plasma by transit time magnetic pumping.

21 p3094 A72-41631

Investigation of the heating of the plasma ion component by a collisionless shock wave

23 p3318 A72-43310

Stationary solitary, snoidal and sinusoidal ion acoustic waves.

23 p3320 A72-43520

Damping of finite-amplitude electron plasma waves in a collisionless plasma.

23 p3321 A72-44075

Earth collisionless plasma bow shock oblique structure assessment by pulsation index I_p devised from empirical results

23 p3341 A72-44511

COLLISIONS

NT ATOMIC COLLISIONS
NT COULOMB COLLISIONS
NT INELASTIC COLLISIONS
NT IONIC COLLISIONS
NT METEORITE COLLISIONS
NT MIDAIR COLLISIONS
NT MOLECULAR COLLISIONS
NT PARTICLE COLLISIONS

Fluid jets formation in collisions between metal plates for large angles at subsonic velocities

13 p1963 A72-28771

Fluid jets formation region in subsonic collisions between metal plates at large angles

21 p3059 A72-40262

The topology of the regularized integral surfaces of the 3-body problem.

23 p3309 A72-43982

COLLOCATION

Overdetermined collocation method change into Ritz-Galerkin method for applications to boundary value problems with eigenvalues

01 p0093 A72-10122

Collocation method for coupled bending-bending torsion vibrations of straight uniform cantilever beam with asymmetric airfoil cross section

16 p2464 A72-32908

Comparison of two methods of astrogeodetic geoid determination based on least squares prediction and collocation.

21 p3048 A72-40469

Solution of the Stefan problem by the collocation method

21 p3130 A72-41089

A collocation solution of the nonlinear equations for axisymmetric bending of shallow spherical shells.

22 p3232 A72-41938

COLLOIDAL GENERATORS

Fission and fusion propulsion for deep space missions, discussing gas and colloid core reactors, controlled fusion, MHD and laser plasma systems

24 p3423 A72-45168

COLLOIDAL PROPELLANTS

One millipound colloid thruster power conditioning and control system design, presenting circuit diagrams, fault protection efficiency and high voltage transformer

01 p0009 A72-11070

Flow characteristics of colloid core reactor rocket engine, studying two component vortex flows with solid to gas mass density ratios over 100

[AD-735527] 01 p0100 A72-11359

Electrical measurements on capillary-fed colloid thruster with Zener diode-like I-V characteristic and constant propellant mass flow rate

04 p0565 A72-15204

Duration test and performance of annular colloid thruster, noting specific impulse increase and electrostatic vectoring

[AIAA PAPER 72-483] 11 p1710 A72-26209

Capillary fed annular colloid thruster operating characteristics, considering I-V relationship, thrust and exhaust velocities and propulsive efficiency

[AIAA PAPER 72-490] 11 p1710 A72-26215

Electric propulsion systems assessment for military spacecraft, discussing ion, colloid, pulsed and quasi-steady plasma thrusters

[AIAA PAPER 72-493] 11 p1711 A72-26217

Rectifier tube cathode as colloid thruster electron gun type neutralizer, discussing efficiency and accelerated life tests

[AIAA PAPER 72-511] 11 p1711 A72-26228

A capillary-fed annular colloid thruster.

17 p2598 A72-35491

COLLOIDING

Living organisms defense and preservation via refrigeration and vacuum combined use in lyophilization technique

12 p1769 A72-27293

COLLOIDS

NT AEROSOLS
NT COLLOIDAL PROPELLANTS
NT FOG

Solid state colloidal plasma physics, discussing statistical ionization mechanics, electron emission and recombination, rocket exhausts, MHD generation, metal vapors electrostatic precipitation, etc

02 p0267 A72-12842

Abiogenic formation of nucleic acid bases and nucleosides in photochemically synthesized self sustaining coacervates

12 p1761 A72-27657

COLONIES

Three dimensional organization of spherical colonies formed by L5178Y cells grown in soft agar cultures from light and scanning electron microscopy

01 p0015 A72-11039

COLOR

RR Lyrae variables intermediate band photometry, tabulating magnitudes and color of 125 stars

01 p0133 A72-11129

Photoelectric lunar occultation measurements of multiple star systems, determining separate colors from simultaneous multichannel observations

06 p0880 A72-17862

Inorganic photochromic and cathodochromic recording materials in single crystal and powder forms, considering color change properties during light or electron beam exposures

06 p0866 A72-17950

Computed and observed color indices of intermediate band UPXYZVS and wideband UVB photometric systems, evaluating response curve validity for parameter determination

11 p1715 A72-25295

Graphic color display adapted to traffic control for direct operator-computer dialogue, noting instruction repertoire, switching device and input devices

16 p2420 A72-32894

Extraversion, neuroticism, and color preferences.

18 p2653 A72-36903

Optical system chromatic aberration correction relationship to focus plane position in white light based on Strehl and Hopkin criteria

24 p3425 A72-44772

COLOR BLINDNESS

U COLOR VISION

COLOR CENTERS

Impurity-related color centers and electron-hole traps in quartz by electron spin resonance and thermoluminescence observations

02 p0207 A72-11598

Dynamics of the optical-pumping cycle of F centers in alkali halides - Theory and application to detection of electron-spin and electron-nuclear-double-spin resonance in the relaxed-excited state.

18 p2719 A72-36709

COLOR PERCEPTION

U COLOR VISION

COLOR PHOTOGRAPHY

Environmental analysis of Lake Tahoe Basin from small scale multispectral aerial imagery, discussing color enhancement usefulness for interpretation and management of natural resources

02 p0210 A72-11800

Digital computer mapping of terrain by clustering techniques, using color IR film emulsion layers as three band spectrometer

02 p0215 A72-11879

Southeast Florida 13 year urban and agricultural development recorded by high altitude color and color-IR photographs, demonstrating capability for detail and macroscale patterns

02 p0230 A72-12199

Holographic multicolor moving map display using photoresist recording and He-Cd laser

05 p0660 A72-15787

False color aerial photographs interpretation for cultivated wooded area inventory

09 p1302 A72-23282

Multiband color aerial photography interpretation for forest appraisal in U.S.S.R.

09 p1302 A72-23285

Color aerial photographs interpretation for forest tree type composition determination, comparing to IR sensitive black and white films

09 p1302 A72-23286

Color aerial photograph evaluation for forest damage demarcation, using film-filter combinations

09 p1302 A72-23289

False color aerial photographs for road quality classification in forests

09 p1302 A72-23290

Black and white vs color photography application to photozoological interpretation of West Greenland Precambrian terrain

09 p1303 A72-23294

Multispectral remote sensing techniques, equipment and applications, discussing color and IR camera, line scanning and radar systems and automated interpretation devices

09 p1312 A72-23304

Color interpretation of pedological factors from aerial photographs in relation to agricultural seasons and use of panchromatic and false color emulsions

09 p1304 A72-23313

Color schlieren technique for simultaneous photographic recording of flow fields and heat transfer patterns in aerodynamic heating, noting application to shock-boundary layer interactions

11 p1629 A72-25257

Three dimensional medium recording of multicolor holographic interferometry, comparing scale factor, spatial frequency and optical distortions with two dimensional medium

15 p2233 A72-31412

IR absorbent effects on evaporographic image contrast performance based on photometric study, presenting color photographs

15 p2188 A72-31615

Color band selection for Mars lander multispectral imaging system for surface constituent discrimination

15 p2307 A72-31809

Computer processed image enhancement applications to spacecraft returned photoreconnaissance, discussing data transmission and resolution vs recognition and color quality

17 p2520 A72-34408

A two-dimensional color schlieren technique.

17 p2554 A72-34933

Encoding and decoding of color information using two-dimensional spatial filtering.

17 p2556 A72-35537

Landscape site and vegetation /timber/ predictions from color and IR aerial imagery compared with ground data

18 p2686 A72-36318

Multicolor photometry of the NGC 5194/5195 double system

19 p2858 A72-37812

Binary symmetric channel error effects on PCM color image transmission.

22 p3153 A72-41977

- Waterways outfall detection from color and IR color aerial photography, describing photointerpretation technique 22 p3181 A72-43197
- COLOR TELEVISION**
- Remote sensor data analysis using color TV display system and interactive graphics equipment on-line to IBM 360/44 computer 02 p0226 A72-11838
- Spatial digital transform coding of color images using three primary color data planes 06 p0772 A72-17403
- Review of 1971 Picture Coding Symposium at Purdue University, discussing intraframe, interframe and color TV signal coding 09 p1279 A72-22899
- A/D and D/A converter for color TV signal digital transmission over communication satellites, discussing system design features 17 p2524 A72-34262
- Encoding and decoding of color information using two-dimensional spatial filtering. 17 p2556 A72-35537
- Color TV tube design without difference current generator, describing scanning unit saddle coils fabrication technique 18 p2667 A72-36678
- Experimental observations of the instability of stellar images from a bichromatic two-channel television system 19 p2860 A72-37956
- Binary symmetric channel error effects on PCM color image transmission. 22 p3153 A72-41977
- COLOR VISION**
- Temporal characteristics of wavelength and luminance modulated light perception, discussing visual system dynamics of color discrimination 02 p0164 A72-12487
- Photopic spectral curves of relative luminous efficiency for congenital deficiencies of color vision, using optical bench, interference filters and Bachstein flicker photometer 03 p0316 A72-13935
- Simultaneous brightness contrast under scotopic conditions, investigating fovea rod and cone systems interaction in subjects with normal color vision 03 p0317 A72-13937
- Ishihara charts readings in artificial daylight at low color temperatures, low light intensity and limited exposure time by normal and color defective subjects 03 p0317 A72-13939
- Human visual system frequency specific color adaptation, considering neural channels sensitivity to color and frequency input 06 p0761 A72-17412
- Color defective vision performance predictions during day and night tests of aviation color signal light discrimination 06 p0767 A72-17871
- Human vision light adaptation effects on dichromatic color matches for bipartite centrally fixated circular matching field 07 p0927 A72-19033
- Achromatic and chromatic thresholds during dark adaptation against varying background luminances, noting trend change at transition from cone to rod function 07 p0930 A72-19288
- Spectral response and vision thresholds of human eye for light detection and color sensation 08 p1125 A72-21332
- Inflight validation of laboratory scaled-down simulation experiments on optimal hierarchy of colors for markers and signals 08 p1147 A72-21582
- Three color response of human vision, noting relationships to color matching function and brightness 09 p1269 A72-22617
- Proposed cone sensitivities relation to Wright color discrimination lines, tabulating optimum weighting factors and longest to shortest chromaticity steps ratios 09 p1269 A72-22619
- Isolated specific color dependent waveforms of visual evoked response to strong colored lights relating luminance and wave amplitude changes 09 p1267 A72-23500
- Spatial frequency specificity of edge contour color aftereffects 10 p1427 A72-25182
- Extrageniculate vision in monkey, discussing circle vs triangle and red vs green discrimination 11 p1582 A72-26772
- One stage approximation to color conversion model, predicting gain setting control dependence on achromatic contrast 12 p1809 A72-27681
- Automated scanning spectroradiometer for color vision test stimuli and luminescence measurements, applying computer analysis of spectral data 12 p1811 A72-27944
- Frequency-specific color aftereffects as result of alternate exposure of subject to inspection gratings of different spatial frequencies 13 p1901 A72-28615
- Color discrimination threshold determination for spectral sensitivity in subjects with congenital color vision disorders 13 p1903 A72-28763
- Selective chromatic adaptation in cone photoreceptors of cynomolgus macaque monkeys, using late receptor potential as response index 13 p1907 A72-29967
- Matched luminance chromatic stimuli wavelength effects on human visual latency 14 p2074 A72-30267
- Opponent color responses of monkey optic tract fibers to monochromatic lights, using chromatic adaptation and microelectrode recording 15 p2184 A72-31369
- Detection and recognition of colored signal lights. 17 p2510 A72-35691
- The effect of chlordiazepoxide on visual field, extraocular muscle balance, colour matching ability and hand-eye co-ordination in man. 17 p2505 A72-35915
- Image processing by digital computer. 18 p2663 A72-36247
- An analytical description of the line element in the zone-fluctuation model of colour vision. I, II. 18 p2651 A72-36606
- Fly colour vision. 18 p2651 A72-36609
- Hue shifts accompany phase induced modulation enhancement of sinusoidally flickering lights. 18 p2651 A72-36613
- Contour-contingent color aftereffects - Retinal area specificity. 19 p2755 A72-37273
- Psychophysical procedures to investigate selective visual adaptation to light of different wavelengths from test gratings with various orientations and spatial frequencies 19 p2756 A72-37829
- Spectral sensitivity after prolonged intense spectral light exposure of rhesus monkey corneas, demonstrating long term loss of cone photopigment response 21 p3000 A72-40739
- The photopigment bleaching hypothesis of complementary after-images - A psychophysical test. 23 p3258 A72-44376
- Visual sensitivity measurement in retinal areas with stepwise change from one monochromatic light to another, discussing eye movements effects and perception thresholds 23 p3258 A72-44385
- Techniques for analysing differences in VERS: Colored and patterned stimuli. 23 p3258 A72-44387
- Small field tritanopia of central fovea in terms of dichromatic area color response mechanism and adaptation speed 23 p3259 A72-44390
- COLORATION**
- U COLOR**
- COLORIMETRY**
- Proposed cone sensitivities relation to Wright color discrimination lines, tabulating optimum weighting factors and longest to shortest chromaticity steps ratios 09 p1269 A72-22619
- Urea determination in urine and water wastes for recycling process, using N-dimethylaminobenzaldehyde colorimetric method 13 p1910 A72-29325
- Photocolorimetric determination of boron in nickel and titanium borides via Magnezon I in alkaline medium, determining solution pH, reaction time, light absorption, etc 18 p2655 A72-36099
- Colorimetric and spectrophotometric gradient systems comparison for bright stars used in automatic telescope pointing control, discussing interstellar absorption 19 p2860 A72-37955
- The effect exerted on pictorial-analytical measurements at the television microscope by subjective contrast enhancement with color filters 21 p3055 A72-40749
- COLUMBIUM**
- U NIOBIUM**
- COLUMBUS**
- Creep buckling of slender or thin-walled structures, taking into account strain rate dependent time-hardening and elastic deformation effects 19 p2875 A72-37884
- COLUMNS [SUPPORTS]**
- NT TAPERED COLUMNS**
- Initial crack effect on slender column compression load carrying capacity, deflection and stress intensity factor 01 p0140 A72-10989
- Optimal shape calculation for partially elastic and elastoplastic column under conservative load based on static stability criterion 03 p0447 A72-13851
- Column axial load carrying capacity optimization vs structural weight, using finite element displacement method for buckling load, mode shape and strain energy density [AIAA PAPER 72-141] 05 p0740 A72-16894
- Residual stresses and geometrical imperfections effects on compressive strength of thin walled welded box columns 07 p1088 A72-19114
- Finite element solutions for buckling of columns and beams, investigating restraints and cross section partial plasticity effects 07 p1088 A72-19117
- Creep buckling of simply supported initially slightly curved column under variable axial load, describing deflection up to critical point 07 p1088 A72-19168
- Perfect and imperfect plastic column buckling, describing bifurcation and stability theory for elastic-plastic and rigid-plastic bodies 13 p2054 A72-28480
- Finite plane elastic buckling deformations of incompressible composite columns reinforced by straight parallel fibers 13 p2059 A72-29599
- Combined axial compression and shear deformation effect on elastic columns buckling behavior, evaluating third order polynomials eigenvalues by computerized Newton-Raphson technique 14 p2168 A72-30934
- Random temperature variations effect on life of Euler column with sandwich cross section under constant axial compressive load, using Norton nonlinear creep law 15 p2324 A72-31494
- Unsymmetrical coupled columns stability under nonconservative lateral and end loading, using finite element method 15 p2331 A72-32557
- Preloaded thin walled open section elastic column dynamic stability under free longitudinal vibrations, deriving criterion for flexural and torsional vibrations nonlinear coupling 15 p2332 A72-32560
- Low speed wind tunnel investigation of vortex formation effect on angle section columns galloping response, varying stiffness and damping characteristics 15 p2332 A72-32594
- Thin walled elastic structures optimization by overall and local buckling coincidence, discussing compression column design 16 p2468 A72-33200
- Compressed initially bent Shanley column analyzed for geometric imperfection coupling and material behavior effects on critical time to creep collapse 16 p2474 A72-34131
- Exact differential equation derived for optimal design of straight nonprismatic column subject to creep buckling 16 p2474 A72-34132
- Monograph - The elastic flexural-torsional buckling of beam-columns by discrete element techniques 17 p2634 A72-35548
- Nonstationary parametric response of a nonlinear column. 18 p2738 A72-37079
- Stability and non-stationary vibration of columns under periodic loads. 21 p3116 A72-40336
- An iterative procedure to obtain exact buckling criteria for columns under combined action of variable continuous load and concentrated forces. 21 p3118 A72-40927
- Battened columns out-of-plane buckling under axial loads and/or moments, deriving relationship between applied loads and section characteristics 21 p3121 A72-41211
- Simply supported column dynamic stability under axial periodic load, discussing external viscous damping effect 21 p3121 A72-41242
- Column buckling under random initial deformations influence, determining mean square nonstationary deflection by Green function technique 23 p3351 A72-44106
- Liapunov method extension to dynamically loaded elastically end-restrained columns stability and frames forced vibration boundedness problems [ASCE PREPRINT 1639] 23 p3352 A72-44110
- COMA**
- Cerebral blood flow and metabolic changes during wakefulness, sleep, coma and epileptic seizures in terms of homeostatic mechanisms 16 p2356 A72-33558
- COMBAT**
- Sleep loss and work-rest cycle effects on combat efficiency, considering psychomotor reactivity, vigilance and decision making capacity 11 p1588 A72-26688
- Man computer weapons effectiveness and system test environment /WESTE/ instrumentation system with Decca navigation for simulated combat environmental flight tests 12 p1754 A72-27515
- Pilot and back-seat man physiological responses during high-aerial combat maneuvers in F-4E aircraft, discussing ECG, respiratory rate and minute volume 12 p1767 A72-28317

Multimode flight control for precision weapon delivery. 17 p2493 A72-35561

Design for air combat. 19 p2751 A72-38124
[AIAA PAPER 72-749]
Naval air test center participation in development of air-to-air combat simulation. 19 p2783 A72-38130
[AIAA PAPER 72-765]
Designing aircraft structure for resistance and tolerance to battle damage. 19 p2752 A72-38133
[AIAA PAPER 72-773]
Development and evaluation of an energy-oriented guidance logic for air combat models. 22 p3137 A72-42354
[AIAA PAPER 72-949]
Game theoretical modeling of fighter aircraft turning tactics competition in pursuit combat, using minimax technique 22 p3138 A72-42359
[AIAA PAPER 72-950]

COMBINATIONS [MATHEMATICS]

Probability model of statistical independence relationships among two events and environmental event, examining all combinations of definition statements for reliability analysis 10 p1504 A72-24015

COMBINATORIAL ANALYSIS

NT BINOMIAL COEFFICIENTS
NT COMBINATIONS [MATHEMATICS]
NT PARTITIONS [MATHEMATICS]
NT PERMUTATIONS
Irredundant multiple output combinational logic network fault detection and diagnosis theorems derivation from structural models in labeled direct graph form 02 p0184 A72-11478

Minimum length fault tests design for irredundant combinational logic circuits containing single faults based on Boolean difference function 02 p0185 A72-11485

Reliable combinational logic networks, deriving conditions for fault locatability from directed graph formal model 02 p0185 A72-11491

Generating function procedure of combinatorial identities for sums of composition coefficients applied to graph theory 03 p0383 A72-14374

Logically stable failures of discrete combination devices by practical behavior in response to given input vectors, using alpha state Boolean algebras 04 p0496 A72-14994

Combinational tree networks of AND and OR gates without internal fan-out, proposing test generation strategy for maximizing detected multifault sets size 05 p0640 A72-16163

Algorithms for combinatorial problem optimal solution based on implicit enumeration method, applying to assembly line balancing 12 p1837 A72-28117

Data file optimal arrangement by programmed procedures formulated as combinatorial problem, using branch-and-bound method for solution 12 p1787 A72-28118

Data file optimal arrangement for retrieval by programmed procedures formulated as combinatorial problem, using branch-and-bound method for solution 19 p2770 A72-38619

Heuristic procedure solution for least cost commercial airline crew scheduling, emphasizing combinatorial space size reduction 24 p3466 A72-44584

COMBINED STRESS

Plastic collapse limit analysis for combined edge and pressure loading on circular cylindrical shells for Tresca yield condition 02 p0295 A72-12474
[ASME PAPER 71-PVP-22]
Orthotropic glass fabric laminate creep under combined torsion and tension, describing test facility 02 p0250 A72-12677

Austenitic steel under combined bending and torsion, showing fatigue strength dependence on temperature, load cycle asymmetry and stress concentration 03 p0371 A72-13469

Plastic stability of cylindrical shells under combined internal pressure and axial compression loads 03 p0448 A72-13904

Mathematical plasticity theory of stress-strain relations under complex loading, including broken line trajectories 03 p0453 A72-14211

Ductility and fracture of metallic thin walled tubular samples under complex stress of internal pressure and axial tension 03 p0454 A72-14215

Rectangular plates nonlinear vibrations under combined static and vibrational loads, using Bubnov-Galerkin method on Karman type nonlinear differential equations 04 p0588 A72-15061

Creep surface in Al alloy under combined tension and torsion, obtaining strain rate vectors from probes 04 p0590 A72-15195

Combined stress wave propagation in thin walled prestressed tube under longitudinal and torsional impact loading 06 p0898 A72-18321

Resolved shear stress formula for shafts under simultaneous tangential bending and torsion acting at dangerous points of cross section 06 p0899 A72-18643

Low temperature test facility for cryogenic and rocket materials under combined tension and torsion 06 p0797 A72-18648

Biaxial tension and combined tension-torsion induced initial yield surfaces and plastic deformation onset, using localized strain theory 08 p1195 A72-21852

Design information for machinery to incorporate welding positions and joints, fatigue mechanisms, loads, combined stresses and plate and cast materials properties 09 p1409 A72-23621

Equivalent stress and plastic strain rates, based on shear stress hypothesis for theory of anisotropic plasticity of plastic materials under combined stress 10 p1553 A72-23745

Simply supported skew plates stability under combined loading, noting wing and tail design applications for high speed aircraft and missiles 10 p1555 A72-24196

Constrained zones and stress intensity factors in cracked thin elastic plates under combined tensile and shear loads 11 p1735 A72-25893

Incremental growth of beams under combined direct load and cyclically varying curvature 11 p1735 A72-25897

Nonuniform heating effect on stability of eccentrically stiffened smooth cylindrical shells under combined loading 12 p1885 A72-27973

Steady state combination oscillations stability, examining geometrical properties of amplitude surfaces 14 p2133 A72-31128

Safe stress range for metal fatigue deformation preceding fracture under combined cyclic and steady push-pull loads 16 p2468 A72-33228

An approach to the analysis of the nonlinear deformation and fatigue response of components subjected to complex service load histories. 18 p2733 A72-36355

Strength of titania and aluminum silicate under combined stresses. 19 p2822 A72-37271

Combined stress creep of non-linear viscoelastic material. 19 p2822 A72-37714

Stress criterion for creep rupture in tubes under combined axial load and internal pressure, deriving stress concentration from high temperature tests 19 p2874 A72-37715

Thermal boundary equilibria in brittle bodies with heat conducting cracks under combined loads and temperature fields 19 p2877 A72-38198

An experimental investigation of yield surfaces at elevated temperatures. 21 p3117 A72-40678

An iterative procedure to obtain exact buckling criteria for columns under combined action of variable continuous load and concentrated forces. 21 p3118 A72-40927

Combined tension-torsion elastic-plastic waves as propagating singular surfaces. 21 p3121 A72-41244

Longitudinal-torsional vibrations of a screw beam under axial excitation 22 p3240 A72-42954

Photoelastic analysis with Stokes vector and new methods for the determination of characteristic parameters in three dimensional photoelasticity. 23 p3354 A72-44255

Austenitic steel under combined bending and torsion, showing fatigue strength dependence on temperature, load cycle asymmetry and stress concentration 24 p3414 A72-44944

COMBUSTIBILITY

U FLAMMABILITY

COMBUSTIBLE FLOW

HF tracer gas detection in inert and combustive flows, using IR absorption technique for gaseous flow visualization 05 p0651 A72-16904

Numerical methods for inverse solution to turbulent swirling boundary layer combustion flow problem 13 p2063 A72-28420

Mechanism and characteristics of condensed system ignition by a dispersed flow 19 p2882 A72-38451

Mixing of slipstreams in a channel of constant cross section in the presence of a recirculation zone 21 p3129 A72-40982

Flow direction and velocity effects on metal burning rates of low carbon and Ni-Cr steels in pure oxygen, using diffusion model 22 p3245 A72-43185

Approximation for boundary value problem of homogeneous stationary combustion in laminar gas flow through cylindrical tube 23 p3356 A72-43798

Propagation of blast waves in a combustible gas. 24 p3462 A72-45034

One dimensional theory of electric discharge detonation effects in flame propagation within square duct with combustible gas mixture, applying to electrochemical pulse jet engine 24 p3464 A72-45064

COMBUSTION

NT AFTERBURNING
NT BOUNDARY LAYER COMBUSTION
NT DEFLAGRATION
NT FUEL COMBUSTION
NT HYDROCARBON COMBUSTION
NT HYPERSONIC COMBUSTION
NT METAL COMBUSTION
NT PROPELLANT COMBUSTION
NT SOLID PROPELLANT IGNITION
NT SPONTANEOUS COMBUSTION
NT SUPERSONIC COMBUSTION

Combustible fuel-air mixture laminar and turbulent flame propagation mathematical model, with reference to detonation and prevention 03 p0456 A72-13876

Rotating flow introduction effects on jet noise levels, combustion and turbulent mixing processes and flame stability 16 p2480 A72-34087

COMBUSTION CHAMBERS

Combustion chamber and nozzle materials for fluorine and/or metal combustors high energy propellant rocket engines, considering cooled and uncooled nozzles and spoiler plates 01 p0117 A72-10941

Plasma temperature and seed atom concentration in MHD generator ducts and combustion chambers by optical measurements, discussing boundary layer thickness, optical density, etc 01 p0072 A72-11218

Polyethylene-FLOX hybrid stage optimum combustion chamber pressure, representing pressure dependent factors by simple analytical models 01 p0117 A72-11221

Optical visualization and probe measurements on combustion characteristics of liquid fuel in compression-ignition engine swirl chamber 02 p0271 A72-12436

Rocket fuel combustion products composition and combustion chamber temperature determination 03 p0405 A72-13474

Air-augmented shrouded and ducted rocket secondary combustor performance parameter analysis based on one dimensional conservation equations 03 p0405 A72-13834

Gas turbine combustors performance model, using reaction rate equation from elementary mass balance equation 05 p0704 A72-15898

[ASME PAPER 71-WA/GT-5] Hydrogen fueled supersonic burning combustor testing, determining wall static pressure, hydrogen radial distribution, Pitot pressure and Mach number at combustor exit 05 p0704 A72-16107

Optimal design criteria for multigrain solid propellant rockets, considering powder weight, burning time and combustion chamber length 05 p0704 A72-16351

Soot oxidation rate from diffusion flame measurements extrapolated for gas turbine combustion chambers 05 p0747 A72-16368

High intensity combustion chamber design for gas turbine of jet engine, considering primary, secondary and dilution zones 05 p0705 A72-16491

Air stream from air entry holes of aeronautical gas turbine combustor, investigating jets maximum penetration, flow path, and mixing 05 p0705 A72-16493

Heat and corrosion resisting alloys development for gas turbine combustion liner, presenting microstructure of specimens after thermal shock test 05 p0675 A72-16494

Thermodynamic function error influence on rocket engine combustion product characteristics including combustion chamber temperature and specific pressure pulse 05 p0751 A72-17069

Stable molecules spatial concentration profiles in high intensity combustion chamber, using quartz sampling probe and gas chromatograph 05 p0751 A72-17088

Operational stability of rocket engine with combustion chamber having charge of two propellant types with different burning rate dependences on pressure 06 p0867 A72-18206

Self regenerating molten seed electrodes for open cycle MHD power generators longevity, regulating combustion chamber and gas flow seeding 06 p0862 A72-18336

Equations derived for powder burning in semiclosed chamber from phenomenological theory of unsteady burning, solving equations for variations in critical nozzle diameter 08 p1254 A72-21658

Gas temperature variation effects on powder burning stability in rocket combustion chamber from unsteady powder burning theory 08 p1255 A72-21659

Composite filament wound boron-epoxy rocket motor combustion chamber design, fabrication and hydrostatic tests 08 p1177 A72-21692

Recirculation criteria for confined jet flames in cylindrical combustion chamber, using Thring-Newby number 09 p1411 A72-23144

Optical method based on spectral line center intensity recording to measure plasma temperature in MHD generators channels and combustion chambers 10 p1525 A72-25111

Gas turbine engines emission data correlation based on combustor theoretical model, proposing correction factors for data reduction to standard test conditions [ASME PAPER 72-GT-60] 11 p1704 A72-25651

High pressure annular combustor with continuous analytical and sampling system for simulated gas turbine engines emission measurements [ASME PAPER 72-GT-88] 11 p1705 A72-25663

Mixing parameter design of high loading spray type combustor for lift jet engine, using primary zone [ASME PAPER 72-GT-99] 11 p1705 A72-25668

Nitrogen oxide emission characteristics of experimental compact combustors with kerosene type fuel, showing dependence on primary zone temperature and air-fuel ratio [ASME PAPER 72-GT-108] 11 p1705 A72-25672

Oscillatory relaxation combustion in annular chamber, applying kinematic theory to combustion frequencies and regions calculation 11 p1745 A72-25752

Mathematical model of combustion region of steam boilers or gas turbines based on turbulent flow and transport equations 11 p1747 A72-26592

Gas turbine engine combustion chamber, investigating swirl vane air flow rate effects on circumferential nonuniformity of gas temperature field at outlet 12 p1861 A72-28132

Russian book on combustion and turbulent mixing processes in jet engines covering temperature and velocity profiles, combustion chamber design and fuel injection characteristics 12 p1862 A72-28340

Russian book on theory of ramjet and rocket ramjet engines covering supersonic diffuser operational principles and design, nozzle, combustion chamber and ejector 12 p1862 A72-28346

Fuel injection, mixing and combustion processes investigation in model cylindrical swirl chamber, describing flow visualization method for turbulence observation 15 p2297 A72-32297

Boron reaction characteristics in ducted rocket engines under varying primary chamber conditions detailing various gaseous propellants effects 15 p2296 A72-32311

Russian book on solid propellant rocket engines covering combustion chamber and nozzle layouts, working cycle and thrust control 16 p2443 A72-33350

Lifetime nomogram for evaporating drop at vapor combustion, applying thermomechanical and aerodynamic decay to jet engine combustion chamber [DFVLR-SONDDR-203] 16 p2477 A72-33422

Computer program for the calculation of the thrust and of the firing data of internal cylindrical rocket burners with different profiles 17 p2523 A72-35417

Swirling flows vortex breakdown in nozzles, diffusers and combustion chambers, considering analogy to boundary layer separation 18 p2641 A72-36385

Supplemental internal gaseous film cooling combined with external cooling of combustion chamber walls, analyzing effectiveness via nonadiabatic model [AICHE PREPRINT 3] 18 p2741 A72-36550

Effect of fuel on gas corrosion in jet engine combustion chambers 19 p2849 A72-38091

A Monte Carlo model of turbulent mixing for the prediction of NO production in steady-flow combustors. [WSCI PAPER 72-8] 20 p2982 A72-38973

The film vaporization combustor and its physical principles. I - The vaporizer section of the combustor. II - The reaction chamber and the combustion [DFVLR-SONDDR-194] 20 p2963 A72-39074

Steady combustion limits in afterburner gas turbine engine chambers 20 p2987 A72-39922

Optimum design of MHD generator combustion chamber, noting effects of heating temperature, oxygen enrichment degree and flow velocities 21 p2997 A72-41065

Basic dimensionless geometrical relations for the combustion chambers of aircraft gas turbine engines 23 p3325 A72-43674

Jets breakup, liquid propellant evaporation and cross sectional area variation in rocket motor combustion chambers 24 p3433 A72-44998

COMBUSTION CONTROL

Plasticized PVC compounds, investigating chlorine based fire retardants role in increasing flame resistance [PI PAPER 14] 03 p0380 A72-13248

Directionality and far field structure of combustion generated noise, using premixed turbulent flame models [AIAA PAPER 72-198] 05 p0748 A72-16875

Nitrogen oxide emission control in gas turbine combustion by lowering flame temperature [ASME PAPER 72-GT-22] 11 p1744 A72-25620

Combustion research for reducing jet aircraft pollutant emissions, discussing fuel atomization improvement, smoke reduction and combustor design techniques 11 p1705 A72-26037

Experiments on methods for improved fuel ignition in scramjet combustion systems. [ICAS PAPER 72-15] 21 p3099 A72-41140

Response of convectively controlled burning to nonlinear disturbances. 24 p3464 A72-45055

COMBUSTION EFFICIENCY

Flame spread rate over combustible polymer fuel specimens as function of surface, sample, composition, pressure and oxygen mole fraction 02 p0301 A72-11965

Chemical efficiency improvement of aluminum combustion with nitric acid in organic solid fuel 03 p0405 A72-13540

Boron containing solid propellant combustion efficiency and fuel-air ratio determination from particle laden plume nonequilibrium effects in ducted subsonic flow [AIAA PAPER 72-36] 05 p0750 A72-16972

Composite propellant powder combustion velocities as function of pressure, discussing powder sensitivity, limiting kinetic stage changes and surface monovariant equilibrium 06 p0867 A72-17568

Controllable high energy hydrogen-oxygen rocket propulsion systems performance and combustion characteristics, considering mixture ratio, pressure, chamber geometric characteristics, injection area and velocity ratios 11 p1703 A72-25298

Heterogeneous-homogeneous catalytic effects on combustion rate of hydrocarbons, ammonia and hydrogen mixtures 13 p1912 A72-28777

High efficiency hybrid rocket motor based on polyester fuel and RFNA oxidizer, determining correlation between burning rate, oxidizer and total flow rates 15 p2297 A72-31207

Powdered Al additions effects on burning rates of three component mixture systems based on ammonium and potassium perchlorates 19 p2847 A72-37361

Influence of pressure on the combustion process of aluminum powders 19 p2847 A72-37368

Fuels, lubricating oils and hydraulic fluids for supersonic aircraft, discussing chemical properties, propellant combustion efficiency and production 20 p2945 A72-39930

Experimental performance of coaxial injectors in thrust-variable LO2/GH2-rocket engines. 24 p3434 A72-45181

COMBUSTION HEAT

U HEAT OF COMBUSTION

COMBUSTION INSTABILITY

U COMBUSTION STABILITY

COMBUSTION PHYSICS

Combustion fronts in relativistic hydrodynamics, considering theorem of detonation and deflagration velocity distribution 01 p0145 A72-11179

Pure solid and composite propellants combustion theory based on laminarized solutions to energy and flow conservation equations 02 p0270 A72-11766

Linear law and catalyst modification of ammonium nitrate combustion, using ammonium perchlorate-base propergols theory 02 p0270 A72-12165

Boron-containing polymer heterogeneous combustion determination using hybrid regression rate with thermal degradation and surface temperature data 02 p0270 A72-12260

Optical visualization and probe measurements on combustion characteristics of liquid fuel in compression-ignition engine swirl chamber 02 p0271 A72-12436

Dichlorodifluoromethane-fluorine flame structure, taking samples by molecular beam sampling system for analysis by mass spectrometry 02 p0303 A72-12483

Flame retardant mechanism in hydrocarbon polymer combustion, discussing halogen adverse effect on thermal stability [PI PAPER 10] 03 p0380 A72-13244

Combustion reactions of water catalyzed gas-phase oxidation of carbon monoxide in premixed stagnation flow at atmospheric pressure [AD-743563] 03 p0459 A72-14223

Nonlinear heat conduction equation explicit solution in combustion theory with allowance for gas dynamics model equation and resulting Cauchy problem solution 04 p0595 A72-14643

Bipropellant fuel droplets combustion in oxidizing atmospheres from spherico-symmetrical nonconvective quasi-steady state model, discussing supercritical pressures and forced convection probability 04 p0596 A72-15273

Emitting-absorbing flames diagnostics, measuring spectrally resolved radiant energy with fiber optic probe data [ASME PAPER 71-WA/FU-1] 05 p0661 A72-15915

Velocity field time history of interacting shear waves in infinite homogeneous chemically reacting fluid for turbulent combustion studies 05 p0747 A72-16367

Combustible materials ignition temperature, time lag and burning rate in oxygen enriched atmosphere, deriving activation energy for fire resistance estimates 05 p0681 A72-16773

Boron ignition and combustion mechanisms based on high speed photographs of laser ignited boron particles [AIAA PAPER 72-72] 05 p0703 A72-16801

Additive and natural ionization in combustion reactions, discussing flame chemistry, ionic species and measurements 05 p0751 A72-17224

Magneto-viscous interactions in combustion plasma, measuring velocity distributions for ordinary hydrodynamic and MHD flow with transverse magnetic field 06 p0859 A72-17618

Nonsteady powder combustion under harmonically varying pressure 06 p0902 A72-17907

Powder combustion rate dependence on light irradiation intensity 06 p0902 A72-17908

Reactive solid or fuel combustion, deriving equations for movement and deformation of reaction front during oxidant diffusion through ash mantle 06 p0902 A72-18155

Time characteristics preceding self-ignition of solid particle system suspended in gas, discussing quasi-steady state duration 06 p0903 A72-18202

Erosion burning in cylindrical ballistite powder N specimens under 50-80 kg/sq cm in simulated constant pressure combustion chamber with supersonic and subsonic nozzles 06 p0903 A72-18208

Induction period, light emission, pressure change and cool flame explosion limits in butane oxidation, studying reaction products in negative temperature coefficient region 07 p1099 A72-19368

Ionic winds with restricted entrainment and gauze electrode, considering diffusion flame aeration in combustion systems 07 p1037 A72-19372

Physical properties, combustion characteristics and applications of pyrotechnic castable composition for smoke generation 08 p1222 A72-20785

Evaporation and combustion of liquids injected into high temperature supersonic flow, considering interrelation with pressure variations 08 p1253 A72-21454

Necessary conditions for burning rate stepwise variation with time of condensed systems 08 p1254 A72-21657

Equations derived for powder burning in semiclosed chamber from phenomenological theory of unsteady burning, solving equations for variations in critical nozzle diameter 08 p1254 A72-21658

Start reaction effect on burning time sequence of hydrogen combustion in air 08 p1129 A72-22171

Dinitroxydiethyl nitramine burning, describing experimental facilities used to determine temperature profile of combustion front 09 p1411 A72-22884

Numerical prediction of inert and reacting steady internal two dimensional recirculating flows by finite difference method, including turbulence and combustion models 10 p1561 A72-23868

Radial temperature and water vapor concentration profiles of radiating combustion source from optical method, using IR band model 12 p1811 A72-27945

Combustion surface acoustic admittance model of blended solid propellant with allowance for foam zone inertia and solid/gas interface reactions

12 p1889 A72-27980

Quasi-steady state combustion theories compared with observations of hydrocarbon fuel droplet and flame zone diameters, noting underestimation of burning rate

13 p2063 A72-28545

Optical anemometers for mean and fluctuating velocities in premixed flame of town gas-air combustion system, noting velocity probability density distribution

13 p1955 A72-28546

Competition criteria for chemical reactions selection in nonequilibrium computer calculations on combustion systems properties, noting seeded flames and rocket exhausts

13 p1912 A72-28548

Catalytic effects on ammonium perchlorate combustion pressure limits, noting distribution, concentration and particle size effects

13 p2025 A72-29303

Powder combustion on metal plate at constant pressure based on two-phase model of condensed system thermal decomposition

13 p2065 A72-29879

Shock waves amplification by interaction with burning gas-liquid mixture, noting triangular profile of pressure variations behind wave front

13 p2065 A72-29888

Solid combustibles flame spread rates in compressed atmospheres, noting dependence on oxygen concentration

14 p2170 A72-30340

Entropy waves effect on gas pressure oscillations during powder combustion in semiclosed volume, noting resonant frequencies equation

16 p2475 A72-33096

Aerogel combustion kinetics and continuous flame formation on coal, Mg, Al and Al alloy powders, using track method

16 p2476 A72-33252

Combustion process in mixing gas jets of different density, using argon and nitrogen for internal flow and air for external jet

16 p2381 A72-34169

Smoke development of plastics under various fire parameters.

17 p2570 A72-34718

Boron ignition and combustion in air-augmented rocket afterburners.

17 p2636 A72-34902

Combustion fronts velocity comparison with light speed in relativistic hydrodynamics and MHD

17 p2589 A72-34911

Combustion driven resonance tubes.

17 p2597 A72-34974

Combustible materials ignition temperature, time lag and burning rate in oxygen enriched atmosphere, deriving activation energy for fire resistance estimates

17 p2571 A72-35276

The physically defined flame and its representation in the water model

18 p2656 A72-36242

The track method and its application in studies of atomized-fuel combustion kinetics

18 p2720 A72-36243

One-dimensional theory of flows with combustion

18 p2740 A72-36246

Solid rocket propellant erosion burning in turbulent gas flow, discussing burning velocity dependence on Pobodonostsev criterion

19 p2878 A72-37351

Pressure rise during combustion in semiclosed volume with reduced gas flow cross section in condensed system channel

19 p2879 A72-37354

Heterogeneously combusting binary gas mixture ignition time as function of initial state and thermokinetic properties, noting heat conduction equations for fuel and oxidizer

19 p2879 A72-37358

Combustion propagation in cylindrical aluminum alloy specimens and some peculiarities of the aluminum combustion mechanism

19 p2847 A72-37362

Error of the statistical method for determining the dependence of the combustion characteristics of particles upon particle size

19 p2879 A72-37363

Chain interaction during the inhibited burning of hydrogen

19 p2880 A72-37741

Mechanism and characteristics of condensed system ignition by a dispersed flow

19 p2882 A72-38451

Characteristics of the development of steady burning rates during the ignition of gasless compositions by a hot surface

19 p2882 A72-38452

Ignition, unsteady burning and flame collapse of a unitary fuel particle

19 p2882 A72-38453

Burning of carbon particles in a supersonic chemically active gas flow

19 p2882 A72-38454

Iron-containing catalysts action mechanism during ammonium perchlorate-polyethyl methacrylate mixture burning in nitrogen atmosphere

19 p2847 A72-38456

I-V characteristics of electric noise generated by flame between double probe electrodes during coke particle burning in air flow

19 p2882 A72-38458

Book - Combustion aerodynamics.

19 p2882 A72-38722

Measurements of burning velocity in a flat flame front.

19 p2883 A72-38872

Comparison of homogeneous gas-phase reaction kinetics for complete segregation and complete micromixing.

20 p2982 A72-38972

The film vaporization combustor and its physical principles. I - The vaporizer section of the combustor. II - The reaction chamber and the combustion

[DFVLR-SONDDR-194]

20 p2963 A72-39074

Turbulent combustion induced noise, discussing scaling rules for sound power and directional characteristics of radiated sound

20 p2984 A72-39557

Experimental investigation of the combustion process of two-component heterogeneous condensed systems at low pressures

20 p2987 A72-40042

Characteristics of models of detonation spinning in various combustible media

20 p2987 A72-40045

Device for measuring the kinetic characteristics of particle combustion

20 p2928 A72-40050

Unsteady burning of reacting mixture of air and condensed-phase combustion products in closed variable volume, noting mathematical model for parameters calculation

21 p3128 A72-40977

Physical model of the onset of turbulent burning of compacted systems in a half-closed volume

21 p3131 A72-41699

Experimental investigation of the effect of an electric field on a laminar flame

22 p3243 A72-41889

Popping phenomena with the hydrazine nitrogen-tetroxide propellant system.

22 p3215 A72-42866

Modeling the rise and combustion of a cloud of light gas in the atmosphere

23 p3357 A72-44493

Flame structure and flame reaction kinetics. VI - Structure, mechanism and properties of rich hydrogen+ nitrogen+ oxygen flames.

24 p3461 A72-44919

International Colloquium on Gasdynamics of Explosions and Reactive Systems, 3rd, Marseille, France, September 12-17, 1971, Proceedings.

24 p3461 A72-45016

A theoretical model for the combustion of droplets in super-critical conditions and gas pockets.

24 p3463 A72-45050

Low speed steady one dimensional flow models for monodisperse spray deflagration, considering homogeneous, heterogeneous and premixed combustion

24 p3464 A72-45054

The shock-combustion /expansion-combustion/polar with allowance for variation of the specific heat ratio of a gas passing through a flame front

24 p3465 A72-45446

COMBUSTION PRODUCTS

Thermodynamic properties of gases at high temperatures, tabulating composition, enthalpy, entropy and thermal conductivity of combustion products with ion seeding

01 p0145 A72-11202

Optical emission spectrum of Ba and CuO combustion products during nozzle expansion into vacuum

01 p0146 A72-11312

Jet fuels hydrocarbon composition effect on thermal stability, considering nonaromatic components influence on aromatic hydrocarbons oxidation products coagulation

02 p0271 A72-12800

Materials stability testing in high temperature propane-butane combustion product flow, selecting compact silicon carbide for structural use in redox medium

02 p0251 A72-12866

Flammability smoke hazards and combustion product toxicity tests of plastics

[PI PAPER 2]

03 p0379 A72-13243

Rocket fuel combustion products composition and combustion chamber temperature determination

03 p0405 A72-13474

Kinetic-analytical models for nitric oxide formation in combustion processes, evaluating heterogeneous effects

[WSCIPAPER 71-28]

04 p0482 A72-14581

Potential parameters determination from collision integrals in thermodynamic properties calculation for combustion products at moderate and low temperatures

05 p0751 A72-17067

Thermodynamic function error influence on rocket engine combustion product characteristics including combustion chamber temperature and specific pressure pulse

05 p0751 A72-17069

High energy chemical propellant combustion under adiabatic and nonadiabatic conditions, calculating product equilibrium state as functions of temperature and pressure with computer program

06 p0903 A72-18212

Hot corrosion of thoria dispersed nickel and thoria dispersed Ni-Cr alloy in high velocity gas stream of jet fuel combustion products

07 p0101 A72-18753

Nitric oxide formation rate in combustion products of propane-air and hydrogen-air diluent flames

07 p0935 A72-19361

Combustion product plasma electrical conductivity dependence on neutral component density fluctuation

07 p0144 A72-19888

Turbulized combustion product plasma electrical conductivity, noting temperature dependent variation

08 p2124 A72-21649

Ignition delay time and combustion mechanism of Al-Mg alloys single particles in combustion products of oxidizer-fuel mixture

09 p1373 A72-22885

Emissivity calculation for radiant heat flux from isothermal gas mixture of hydrocarbon fuel combustion products

10 p1561 A72-23839

Autonomous combustion of Al sphere in controlled atmospheres oxygen-argon, nitrogen and air, identifying products

10 p1562 A72-24238

Computer algorithms for scattering functions of condensed aluminum or magnesium oxides in combustion products for various temperatures and particle sizes

11 p1747 A72-26966

Russian book on combustion products thermodynamic and thermophysical properties covering fuels and propellants characteristics, equilibrium fuel compositions, gas phase transfer and expansion processes, etc

12 p1890 A72-28336

Future projections of commercial jet aircraft fuel demands, estimating engine exhaust effects on air quality

13 p1897 A72-28879

Nonequilibrium ionization phenomena effects on electric conductivity of combustion gas-particle plasma generated by aluminized fuel seeded with potassium nitrate

13 p2013 A72-29363

Combustion products thermodynamic parameters for natural gas burning in oxygen atmosphere, plotting gas temperature and flow rates against pressure and excess oxidant ratio

13 p2065 A72-29451

Destructive effect of combustion and pyrolysis products in intake air on fire extinguishers foam production

14 p2084 A72-30339

Combustion product plasma electrical conductivity dependence on neutral component density fluctuation

17 p2590 A72-35136

Review of jet engine emissions.

19 p2848 A72-37645

Formation of hydrogen from amine oxidation and pyrolysis.

19 p2883 A72-38874

Influence of hygroscopic substances on the transparency of aerosols from combustion products of condensed systems

20 p2987 A72-40043

Unsteady burning of reacting mixture of air and condensed-phase combustion products in closed variable volume, noting mathematical model for parameters calculation

21 p3128 A72-40977

The simulation of high pressure hydrogen/oxygen rocket engines.

[AIAA PAPER 72-1027]

21 p3042 A72-41606

Radiation absorption calculation for nonisothermal gas containing combustion products, noting approximation for water vapor radiation

22 p3243 A72-41885

Infrared spectroscopy for chemical composition of inorganic and organic products formed on friction surfaces of gas turbine parts immersed in hydrocarbon fuels

23 p3325 A72-43974

Combustion product gas dynamic motion effects on detonation front propagation, discussing reacting blast wave and finite kinetic rate models and asymptotic results

24 p3391 A72-45027

Pressure, temperature, current density, and potential difference fluctuations in subsonic flow of combustion products plasma, noting steadiness, ergodicity and distribution functions 24 p3429 A72-45502

COMBUSTION STABILITY

NT FLAME STABILITY

Diamant B launcher first stage Valois rocket motor combustion if, acoustic mode and if instabilities [ONERA, TP NO. 1027] 03 p0406 A72-13641
Acoustic cavity resonators use for suppression of combustion instability modes, determining acoustic impedance and damping 03 p0457 A72-13954

Burner design for solid propellants burning properties dynamic testing, using broadband tuned Helmholtz resonator for instability onset delay 04 p0509 A72-15497

Solid propellant flame spectral and temporal details during unstable and stable combustion, using middle infrared spectrometer [AIAA PAPER 72-32] 05 p0703 A72-16896

L instability in rocket motors with heterogeneous propellants, investigating sideways sandwich model [AIAA PAPER 72-33] 05 p0703 A72-16897
Two dimensional stability of condensed systems combustion, evaluating effects of heat transfer from combustion region 06 p0902 A72-17906

Gunpowder burning stability in semiclosed volume from automatic control theory methods application to temperature and pressure dynamics 06 p0903 A72-18205

Homogeneous laminar combustion in semiclosed cylindrical tube, relating stability to hydrodynamic and thermodynamic flow parameters longitudinal high frequency disturbances 07 p1101 A72-19988

Small perturbation stability of discontinuous solution of equations of motion for solid fuel combustion processes 08 p1253 A72-21463

Gas temperature variation effects on powder burning stability in rocket combustion chamber from unsteady powder burning theory 08 p1255 A72-21659

LF self oscillation processes associated with burning powders, showing origin in thermal relaxation instability in heated condensed phase layer 09 p1411 A72-22883

Supersonic combustion of liquid fuels, hydrogen and propane, discussing initiation and stabilization in supersonic flow 12 p1889 A72-27686

Solid rocket propellant combustion instability research, discussing data acquisition and reduction, motor instrumentation, motors and burning rate measurements 13 p2024 A72-28929

Liquid propellant rocket performance, stability and compatibility prediction techniques, noting effect on design time and cost 14 p2146 A72-30919

Acoustic admittance measurement for burning surface of nitroglycerin gunpowders, using combustion product velocity and wave pressure ratio 16 p2391 A72-33257

Combustion instability oscillations damping in rocket motors by short nozzles, calculating acoustic losses 17 p2635 A72-34233

Erosion combustion effect on unsteady solid rocket propellant burning stability during engine nozzle opening, noting combustion velocity and surface temperature 19 p2879 A72-37353

Steady combustion thermal stability of condensed explosives for burning rate limitation by condensed phase chemical reactions, noting surface temperature effects 19 p2879 A72-37356

Steady combustion limits in afterburner gas turbine engine chambers 20 p2987 A72-39922

Critical description of combustion stability in a turbulent flow of a homogeneous mixture 21 p3129 A72-40980

A nonacoustic wave instability of processes in a solid-fuel engine 22 p3217 A72-43182

Shock wave velocity, combustion front and pressure measurements of unstable detonations in propane-oxygen-nitrogen mixtures, comparing with double discontinuity theory 24 p3462 A72-45030

Diffusion flame in homologous turbulent shear flows. 24 p3395 A72-45564

COMBUSTION TEMPERATURE

Aromatic hydrocarbons and fuels, investigating engine parameters effects on combustion and exhaust gases temperatures 13 p2025 A72-29074

COMBUSTION VIBRATION

Flames vibratory propagation appearance conditions at constant volume, considering expansion and compression waves amplitude 03 p0456 A72-13794

Particle mass spatial distribution effect on particulate damping of combustion acoustic vibrations in solid rocket propellants 08 p1224 A72-21617

Liquid rocket LF unsteady transient behavior calculation from droplet evaporation and combustion parameters 10 p1528 A72-24644

Soviet papers on vibrational combustion systems covering flames relaxation in annular combustion chambers 11 p1745 A72-25751

Oscillatory relaxation combustion in annular chamber, applying kinematic theory to combustion frequencies and regions calculation 11 p1745 A72-25752

Oscillatory gas combustion mechanism and stability boundary characteristics, determining burning time from flame height and flow rate 11 p1745 A72-25753

Oscillatory relaxation combustion regions determination in high pressure gas injection tubes, noting flame propagation rate relationship with mixing concentration 11 p1745 A72-25754

Solid propellants oscillatory burning with gas phase time lag, solving nonsteady governing differential equations by numerical integration 13 p2065 A72-29301

Combustion instability oscillations damping in rocket motors by short nozzles, calculating acoustic losses 17 p2635 A72-34233

Investigation of the resonant combustion of a rocket charge with longitudinal slots 18 p2720 A72-36241

Combustion noise generation by burning fuel-air mixtures induced pressure fluctuations as result of time variable heat release rate due to turbulence 18 p2741 A72-36505

COMBUSTION WAVES

U FLAME PROPAGATION

COMBUSTION WIND TUNNELS

Supersonic and hypersonic combustion processes three dimensional characteristics, comparing wind tunnel test data with boundary layer equations numerical integration results [ICAS PAPER 72-21] 21 p3130 A72-41146

COMBUSTORS

U COMBUSTION CHAMBERS

COMET TAILS

Tago-Sato-Kosaka and Bennett comets plasma tails interaction with interplanetary magnetic field, demonstrating cometary events correlatability with solar wind data 01 p0128 A72-10419

Emission spectra of comet tail carbon monoxide molecular ion indicating constant or slowly varying electron transition moment 17 p2618 A72-35826

Geometrical study of the shape and orientation of the tail of Comet Bennett /1969i/ 18 p2728 A72-36764

Natural oscillations of type-I comet tails 19 p2864 A72-38081

Comet tail wave motion explanation via consideration as plasma cylinder with free boundary tangential discontinuity surface immersed in interplanetary plasma 22 p3221 A72-42011

COMET 4 AIRCRAFT

Unpredicted structural vibration in Comet and Electra aircraft, Graf Zeppelin dirigible, missile antennas, etc 02 p0292 A72-12002

COMETS

NT COMET TAILS

NT MRKOS COMET

Iron meteorite formation model based on metal carbonyls low temperature thermal decomposition in comets 01 p0124 A72-10061

Icy halo influence on photometric continuum of comet Burnham within cometary head model 01 p0125 A72-10080

Cometary head model for photometric profiles of carbon molecular emission in comet Burnham assuming icy grain halo 01 p0125 A72-10081

Monte Carlo method application to meteor stream formation by meteor material ejection from comet nucleus, determining age of Draconids 02 p0282 A72-12333

Numerical integration of element T /transit time through perihelion/ in perturbations of near parabolic comet orbits 03 p0436 A72-13829

Comet hypotheses, examining orbit axes and perihelions spatial distribution as possible interstellar origin 03 p0438 A72-13978

Orbit distributions of hypothetical comets from Jovian surface eruptions, calculating orbital elements with computer 03 p0439 A72-14240

Comet orbits with perihelion distances and inclinations from Jupiter, calculating osculating orbital elements and distributions 03 p0439 A72-14241

Comet collisions in planetary nebulae as source of organic compounds in universe in preplanetary era, noting nucleic acid bases in carbonaceous meteorites 04 p0471 A72-14802

French Lyman alpha photometer experiment onOGO 5 satellite, describing geocoronal observations, extraterrestrial emission and Bennett and Encke comets hydrogen envelopes 04 p0582 A72-15684

Meteor observation and counting, discussing meteor stream formation along comet orbit 05 p0712 A72-15975

Comet Bennett tail and coma surface brightness distribution, estimating solar wind velocity 05 p0717 A72-16426

Periodic comets orbital elements and nongravitational parameters, discussing mass loss rates, time effects and nuclear core-mantle model 06 p0880 A72-17863

Statistical analysis of eccentricity changes in nearly parabolic comets, showing data samples relation to Bernoulli random variable with two different unknown parameters 07 p1072 A72-19339

Statistical and probabilistic analyses of comet groups existence with similar orbital elements, considering gravitational capture by trans-Neptunian planets 07 p1075 A72-19559

Short period comets orbital evolution and major planets gravitational effects, discussing cometary cloud formation, diffusion, motion and discovery 07 p1078 A72-19981

Stellar perturbations of eccentric orbits of long period comets 07 p1081 A72-20232

Planetary perturbation of orbits of long period comets with large perihelion distances 07 p1081 A72-20236

Comet characteristics as indicators of cosmic space conditions, including relation to solar activity 07 p1081 A72-20272

Isophote equidensity role in astronomical photometric investigation of solar corona, galactic nebulas, comets and extragalactic stellar systems 07 p1082 A72-20301

Cometary carbon dioxide molecules annihilation by recharging and dissociative charge exchange with solar protons 08 p1229 A72-20830

Tago-Sato-Kosaka comet isophote picture of 5 February 1970, noting tail composition, photographic magnitude and emission spectrum 08 p1229 A72-20831

Comets heliographic coordinates and angles quadrants from orbital elements 08 p1229 A72-20832

Light polarization in Honda comet head, discussing brightness distribution 08 p1229 A72-20833

Comets visual brightness determination by astronomical photographic photometry 08 p1229 A72-20834

Comet brightness variations correlation with geomagnetic field and solar corpuscular flux variations in interplanetary space 08 p1231 A72-21132

Cosmic sources of organic compounds from chemical evolution viewpoint, discussing comets, interstellar space, prestellar nebulae and cool stellar atmospheres 08 p1120 A72-22014

Comet gas production and interaction with solar wind, discussing visible plasma tail within flow pattern 09 p1387 A72-22755

Einstein A coefficients, band oscillator strengths and absolute band strengths calculation for comet tail band system of CO cations 09 p1355 A72-22789

Tago-Sato-Kosaka comet positions determination from plates obtained with photographic telescope, tabulating averaged spherical coordinates 09 p1389 A72-23068

Short period comets origin and orbital evolution, discussing Jupiter perturbations and statistical study 10 p1536 A72-24143

Comet rendezvous and outer planet exploration mission operations by unmanned nuclear electric propulsion /NEP/ system with incore thermionic reactors for electric power generation [AIAA PAPER 72-428] 11 p1722 A72-26173

Solar electric propulsion application to comet and asteroid rendezvous and docking CARD missions with sample return
[AIAA PAPER 72-470] 11 p1722 A72-26201
Cometary spectra analysis, noting resonance fluorescence mechanism of emissions
11 p1722 A72-26433
Photographic position of comet Ikeya-Seki, presenting data reduction procedure
12 p1868 A72-27220
Trans-Plutonian planet effect on Halley comet, considering perihelion errors and comet residuals
13 p2038 A72-29012
Monte Carlo method application to meteor stream formation by meteor material ejection from comet nucleus, determining age of Draconids
13 p2039 A72-29217
Carbon origin in comets associated with propyne photodissociation by solar 1216 A Lyman alpha radiation
13 p2050 A72-29995
Comet core ice particle dust cover failure conditions, noting critical dust matrix thickness relation to sun proximity
14 p2160 A72-30831
Asteroids and comets orbit perturbation equations for small eccentricity values
14 p2161 A72-31080
Comets formation from Jupiter satellite Io surface eruption using particle trajectory analysis and comet orbital elements calculation
15 p2305 A72-31391
Solar wind and planetary atmosphere interaction observation by simulation of ionization mechanism in comet, using gun produced plasma stream and gas cloud
15 p2301 A72-32341
Comet Tago-Sato-Kosaka /1969g/ L alpha emission image recorded by f/2 objective-grating spectrograph aboard Aerobee rocket, discussing ice sublimation in nucleus
16 p2455 A72-33466
Comets Tago-Sato-Kosaka and Bennet UV observational data interpretation for origin, constitution and interaction with solar wind, emphasizing total gas production
16 p2459 A72-33914
Direct infrared measurements of thermal radiation from the nucleus of comet Bennett.
17 p2604 A72-34525
A possible mechanism for the capture of micrometeoritic particles by the earth and other planets of the solar system.
17 p2619 A72-35939
Physical observations of comets. XVII
18 p2726 A72-36722
Dust particle sizes in cometary atmospheres and the heliocentric distance
20 p2970 A72-39726
Near parabolic orbit and short periodic comets motion, discussing circumsolar cloud and nongravitational disturbances
20 p2974 A72-40068
Comet integral brightness estimation by mathematical analysis of photometric characteristics
21 p3110 A72-41449
Cometary parent bodies transfer to short period orbits by Jupiter caused gravitational disturbances, noting qualitative analysis of orbits evolution
22 p3219 A72-41913
Terminal orbit of comet 1937 V /Finsler/
22 p3220 A72-41917
The dependence on inclination of the planetary perturbations of the orbits of long-period comets.
22 p3224 A72-42378
Physical and chemical properties and stratification of neutral matter in comet atmospheres, discussing neutral gas dynamics and surface brightness distribution in comet images
23 p3335 A72-43299
Spectral investigations of the comet Bennett 1970 II /1969 i/
23 p3337 A72-43646
Spectrophotometry of the comet Tago-Sato-Kosaka 1969 IX
23 p3339 A72-44168
Flyby missions to comets, asteroids and meteors for obtaining solar system geological information, considering space dynamics feasibility
23 p3340 A72-44351
Two early missions to comets in 1977-1980 as precursors to more ambitious missions in 1984-1986, discussing exploration objectives and spacecraft configurations
23 p3340 A72-44352
Search for trans-Plutonian planets with the aid of periodic comets
24 p3437 A72-44759
Application of the restricted hyperbolic three-body problem to a star-sun-comet system.
24 p3442 A72-45234
Mission strategy for combined comet-asteroid flybys.
[AIAA PAPER 72-939] 24 p3444 A72-45436

Particle fragmentation, mass distribution and chemical composition of cometary meteoroids in earth orbit, noting collisional erosion and similarity to stony meteorites
24 p3445 A72-45459
Physical parameters of asteroids and interrelations with comets.
24 p3445 A72-45460
On certain aerodynamic processes for asteroids and comets.
24 p3445 A72-45463
The structure and formation of comets.
24 p3445 A72-45464
Impacting polar plasma thermalization during comet close approach to sun, considering solar wind-comet interaction role
24 p3445 A72-45470
Statistical analysis of comet observations, calculating relationships between comet head angular diameter and heliocentric and geocentric distances and apparent brightness
24 p3448 A72-45687

COMFORT

Aircraft ride comfort problem in turbulent air, comparing free and fixed wing aircraft responses
02 p0154 A72-11720
A time-sharing computer program for defining human thermal comfort conditions in any atmosphere.
[ASME PAPER 72-ENAV-33] 20 p2905 A72-39142
Design, operation and testing of integrated STOL flight control system, noting approach accuracy and passenger comfort improvement
21 p3080 A72-40292
Design of vibration absorbers minimizing human discomfort.
21 p3009 A72-41231
Applied research into the effects of vibration upon displays.
21 p3011 A72-41424

COMMAND AND CONTROL

Scientific balloon data management system, discussing airborne and ground station equipment for telemetry, command and flight control
03 p0327 A72-13725
Unified single rf channel tracking, telemetry and command control systems for guidance of unmanned vehicles, including pilotless aircraft and satellites
05 p0685 A72-16556
Noise, delay and interruption caused communication degradation effects on feedback control system performance, considering air navigation and computer aided command and control on battlefield
06 p0794 A72-18242
Real time computer simulation of command and control in transportation systems, detailing models, and programming technique and ATC controller effectiveness evaluation
07 p0952 A72-20363
Solar electric propulsion subsystem performance tested on breadboard model, noting electrical power conversion, command, thrust vector control and propellant supply
[AIAA PAPER 72-507] 11 p1711 A72-26227
ATS F and G radio link with ground stations, discussing telemetry and command functions with redundancy for RF interference minimization
21 p3019 A72-40883

COMMAND GUIDANCE

Fully redundant relay and data command system for SAS-A satellite, discussing operation and reliability tests
03 p0442 A72-14397
Spurious commands at high altitudes due to hf disturbances in Azur satellites, discussing telecommand system
05 p0626 A72-16137
Helios solar probe project command station design, discussing equipment details and command transmission operation sequence
[DGLR PAPER 72-018] 13 p1939 A72-28963
Virtual target steering - A unique air-to-surface missile targeting and guidance technique.
[AIAA PAPER 72-826] 20 p2951 A72-39100
CW radar system for tactical aircraft real time command, control and positioning, using combination of frequency and time multiplexing for range measurement
22 p3203 A72-42946

COMMAND SERVICE MODULES

Apollo 15 gravity analysis from the S-band transponder experiment.
18 p2724 A72-36286

COMMAND SYSTEMS

U COMMAND GUIDANCE

COMMAND-CONTROL

U COMMAND AND CONTROL

COMMERCIAL AIRCRAFT

NT ELECTRA AIRCRAFT

NT EUROPEAN AIRBUS

NT SUPERSONIC COMMERCIAL AIR TRANSPORT

Commercial transport market and technology forecasting, considering all-cargo, STOL, SST and CTOL aircraft
[SAE PAPER 710750] 01 p0002 A72-10249

Propulsion system optimization for commercial transport aircraft design under Advanced Transport Technology study, considering impact on aircraft gross weight
[SAE PAPER 710760] 01 p0115 A72-10257
Jet noise reduction technology, hardware and tests for NASA Quiet Engine Program to develop low noise subsonic civil transport aircraft propulsion system
[SAE PAPER 710774] 01 p0116 A72-10266
General and commercial aircraft service needs in air transportation, considering FAA and CAB roles and policies
02 p0304 A72-11716

Deterministic model for new product innovation adoption rate in commercial aircraft jet engine market.
07 p1105 A72-20269

Statistical analysis of cockpit simulator data on altimetry display for commercial aircraft
08 p1168 A72-21573

Marchetti SV-20-A twin engine winged commercial utility helicopter, describing design details, on-board systems and payload accommodations
09 p1262 A72-22907

Wing structural weight estimation for civil aircraft preliminary deriving generalized formula based on wing root bending moment for specified flight condition
09 p1262 A72-22909

Reliability design for airborne ecological system for jumbo jets, discussing toilet flushing and multiple server queueing model
10 p1429 A72-23999

Commercial aircraft reliability program development from informal continuous product improvement to formalized methods based on reliability logic diagrams and probability calculations
10 p1421 A72-24019

Commercial applications of quiet light aircraft technology, discussing cost and noise reduction
[SAE PAPER 720339] 11 p1576 A72-25596

Propulsion control systems design for military and commercial V/STOL aircraft, considering power management performance with minimum weight and maximum reliability and maintainability
[ASME PAPER 72-GT-79] 11 p1705 A72-25659

Charter air traffic regulations under German air law, discussing legal safeguards relative to economic, personnel, technical and organizational aspects
11 p1748 A72-26559

High cruise altitude operational advantages for commercial transport aircraft utilizing technological innovations in structures, propulsion, controls, avionics and aerodynamics
13 p1996 A72-28875

Future projections of commercial jet aircraft fuel demands, estimating engine exhaust effects on air quality
13 p1897 A72-28879

Optimal angle selection of commercial aircraft glide path, taking into account vertical velocity, propulsion units operation and landing procedure
14 p2072 A72-30814

Hypersonic commercial aircraft operational problems, considering passenger physiology limits flight profile, sonic pollution, traffic demands, route structure, etc
14 p2073 A72-30830

Commercial airlines aircraft selection factors, considering size, range, economics, traffic, runway quality, maintenance and operating costs, reliability and cargo handling
16 p2348 A72-33333

Internal engine generator application to commercial transport aircraft.
17 p2498 A72-35566

Graphite-epoxy composites application to commercial transports for weight and cost reduction
19 p2873 A72-37680

Active controls - Changing the rules of structural design.
19 p2748 A72-37681

Flyover noise testing of commercial jet airplanes.
[AIAA PAPER 72-786] 19 p2749 A72-38103

A computerized system for the preliminary design of commercial airplanes.
[AIAA PAPER 72-793] 19 p2749 A72-38110

Investigation of the commonality in development of military and commercial STOL transports.
[AIAA PAPER 72-808] 19 p2750 A72-38114

Economic and social aspects of commercial aviation at supersonic speeds.
[ICAS PAPER 72-51] 21 p2996 A72-41851

COMMERCIAL AVIATION

U CIVIL AVIATION

U COMMERCIAL AIRCRAFT

COMMUNITION

NT GRINDING [COMMUNITION]

Ball milling effects on alumina and tungsten carbide powder sinterability due to particle comminution and microstrains
11 p1642 A72-26827

COMMUNICATING

NT AIRCRAFT COMMUNICATION

NT ELECTROCATANEUS COMMUNICATION

COMMUNICATION SYSTEMS

U TELECOMMUNICATION

COMMUNICATION THEORY

NT SYLLABLES

NT WORDS [LANGUAGE]

Convolutional coding and decoding techniques in communication systems, discussing distance properties, optimal decoder in memoryless channel, error probabilities and bit synchronization

01 p0025 A72-10336

Error correction techniques of convolutional coding with Viterbi maximum likelihood decoding for communications systems design, using computer simulation

01 p0026 A72-10344

Statistical model for communication probability estimate based on signal-to-interference and SNR criteria

01 p0031 A72-10997

Coding for data communication over discrete time channels without feedback under various fidelity criteria, discussing channel capacity

02 p0171 A72-11681

Bias and spread in extreme value theory performance tests of communications systems, comparing with bit error rate tests

02 p0173 A72-12129

Electromagnetic noise and effects on communication systems, considering statistical parameters definition and measurements

03 p0324 A72-14036

Code performance evaluation over real digital channels, characterizing channel error process by multiplex statistics

03 p0325 A72-14183

Block orthogonal M-ary communication over fading dispersive channel with intermittent on-off noiseless feedback, calculating upper and lower bounds on error probability

06 p0776 A72-18389

Soviet book on laser communication statistical theory covering coherent and noncoherent optical signal detection and discrimination, SNR optimal reception, beam scanning, etc

06 p0777 A72-18518

Signal design for coherent M-ary communication systems by stochastic gradient algorithm for minimizing error rate

07 p0959 A72-19285

Bayesian estimate of signal parameters in random noise background under mutually exclusive hypotheses about statistical properties

07 p0943 A72-19515

Russian book on visual sensor signal dynamics covering nerve signal transformation, light stimuli responses, afferent flow, bionics, neurocybernetics and communication theory

11 p1584 A72-26049

Institute of Electrical and Electronics Engineers, Southwestern Annual Conference and Exhibition, 24th, Dallas, Tex., April 19-21, 1972, Record.

17 p2514 A72-34413

COMMUNITIES

NT MOUNTAIN INHABITANTS

COMMUTATION

Multichannel clock with dekatrons using multiple crossbar connector for program commutation and command pulse splitting

13 p1933 A72-29919

Interdependence of the commutation and memorization effects and the thermal behavior in a series of chalcogenide glasses

18 p2718 A72-36344

COMMUTATORS

NT DECOMMUTATORS

Multichannel integral commutators with MOSFET as switching elements, calculating transmission errors

10 p1449 A72-24288

High voltage single nanosecond pulse generator for variable load using commutator with shaping line charging circuit

16 p2368 A72-33077

German monograph - Investigations concerning a new frequency changer with 'forced' commutation for supplying power to one- or multiple phase consumers

19 p2753 A72-37482

Ferrite component for waveguide commutator used as microwave switching element and modulator, noting application in navigation instruments and avionics

23 p3270 A72-43768

Commutation switch based on an injection semiconductor laser.

24 p3412 A72-45620

COMPACTING

High energy rate compacting methods in powder metallurgy, considering use of high explosives in water or air and impulse pressing of metal powders

02 p0233 A72-11438

Material characteristics effect on compaction behavior of metal powders, stressing density and pressure measurements

02 p0242 A72-11460

Presintering effects on dimensional change of iron powder compacts, using dilatometric, thermogravimetric, differential thermal analyses and resistivity measurements

02 p0233 A72-11461

Porous materials fabrication from chromium carbide powders, considering compaction procedures involving sinusoidal and pulsating vibrations

07 p1017 A72-19968

Mercury porosimetry for iron powders void and internal particle porosity change as function of compacting pressure, noting compressibility improvement by precompacting and annealing

11 p1639 A72-25828

Conventional and explosive compacting effect on density distribution in green briquettes, investigating normal and shear stresses

11 p1643 A72-26830

Explosive compaction of metal powders by direct method with emphasis on W

11 p1643 A72-26833

Device for comparing powders friability to ascertain quality of compacts fabricated on automatic sintering presses, noting applications in ceramic, chemical and pharmaceutical industry

12 p1795 A72-27468

Compacting kinetics of fiber reinforced sandwich composites during hot pressing controlled by plastic matrix sliding velocity

13 p1967 A72-30103

Thermal conductivity of compact samples of cubic BN

19 p2823 A72-38408

Effect of inertial loading on the compression of powdered materials by a vibration process

21 p3061 A72-41369

Al powder bonding during compaction by explosively driven plates, measuring shock wave amplitudes, pressure drop, layer separation and critical pressures in spill plane

22 p3184 A72-43183

Electron diffusion across a shock wavefront in metals

22 p3208 A72-43184

Calculation of radial pressures in metal-fiber-reinforced materials during compacting

23 p3298 A72-43277

Study of the process of powder knurling to articles

23 p3292 A72-43279

Influence of the oxidation of finely dispersed graphite powders on their compactibility

23 p3307 A72-44018

COMPACTNESS

U VOID RATIO

COMPARISON STARS

Secondary component of eclipsing binary beta Lyrae as massive main sequence star in rapid nonuniform motion, refuting black hole suggestion

11 p1717 A72-25869

Accretion disc models for compact X-ray sources.

24 p3435 A72-44828

Centaurus X-3 - Possible reactivation of an old neutron star by mass exchange in a close binary.

24 p3439 A72-44976

COMPARATORS

Earth location effect in Fresnel diffraction zone on comparator performance, measuring phase difference fluctuations in turbulent atmospheric boundary layer radio waves

09 p1284 A72-22232

Informational reliability of automatic control system comparators, considering tolerance field contraction effect

10 p1456 A72-24081

Radar echo maximum intensity display by digital comparator with shift register video signals storage in National Severe Storms Laboratory

11 p1591 A72-25762

A new computer-assisted stereocomparator.

18 p2664 A72-36499

COMPARTMENTS

NT AIRCRAFT COMPARTMENTS

NT ANECHOIC CHAMBERS

NT PRESSURE CHAMBERS

NT PRESSURIZED CABINS

NT SPACECRAFT CABINS

NT TEST CHAMBERS

NT VACUUM CHAMBERS

COMPASSES

NT GYROCOMPASSES

NT MAGNETIC COMPASSES

COMPATIBILITY

Anthropometric data utilization for military pilot/aircraft compatibility evaluation, discussing cockpit exclusion code development and implementation

12 p1777 A72-28324

Discrete and continuous systems spurious solutions avoidance through Hamilton principle reciprocal form derivation of geometric compatibility conditions

[ASME PAPER 72-APM-54]

17 p2627 A72-34777

Airborne equipment electric power supply standards to provide characteristics limits for compatibility with ground support systems

18 p2648 A72-36535

COMPENSATION

Hammerstein form nonlinear systems class invertibility and reproducibility criteria derivation, noting decoupling possibility by dynamic precompensation and nonlinear state feedback

10 p1502 A72-23781

Alternating period compensation system velocity characteristics shaping problems, determining pulse repetition periods parameters by graph-analytical method

11 p1596 A72-26311

Noninteractive compensation of linear multivariable control systems based on matrix block diagram technique

15 p2213 A72-32799

Prolonged weightlessness effects on cardiovascular, digestive, musculoskeletal and nervous systems, blood and metabolism, noting compensatory reactions

16 p2354 A72-33546

Linearizing compensation for nonlinear control system transformation into linear system without approximation, discussing differential operator matrix definition and random noise effects

23 p3277 A72-43945

COMPENSATORS

Minimal order precompensator with state feedback for decoupling linear time-invariant multivariable control system, discussing design parameters determination from linear equations

04 p0506 A72-15109

Algorithmic procedure in compensator design for hyperstable discrete model reference adaptive systems [MRAS]

07 p1027 A72-19294

Compensator improvement for relative stability and frequency response of large space vehicle, using nonlinear programming

10 p1442 A72-23791

Feedback ac compensating amplifier design for automatic AM signal envelope conversion, noting truncated equivalent transfer function expandability

13 p1933 A72-29972

Stability bounds for nonlinear systems designed via frequency domain stability criteria.

[ASME PAPER 72-AUT-L]

23 p3275 A72-43636

Digital filter design using observers.

23 p3276 A72-43864

COMPENSATORY TRACKING

Laser station coordinate and Geos B satellite position compensation with simultaneous optical and laser observations

02 p0219 A72-12045

Radar systems of effectiveness for moving target selection with alternating period compensation devices, allowing for signals and noise statistical properties

11 p1596 A72-26306

Compensatory tracking task performance with continuous error information feedback via visual, auditory or electrocutaneous displays

14 p2083 A72-31152

Auditory display in dual-axis compensatory tracking task, discussing performance measures in terms of squared error integral and human operator describing functions

16 p2359 A72-33866

Congruent and spurious motion in the learning and performance of a compensatory tracking task.

17 p2510 A72-35692

Digital tracking with phased arrays.

19 p2765 A72-38261

Human operator dynamics for aural compensatory tracking.

22 p3149 A72-41950

COMPETITION

Medical factors in air racing accidents, investigating drug, fatigue and gastrointestinal symptoms effects on pilot reaction to emergency

14 p2081 A72-31089

COMPILATION [COMPUTERS]

U COMPILERS

COMPILER PROGRAMS

U COMPILERS

COMPILERS

Time shared electronically patched hybrid computer for design automation, discussing remote terminal graphics capabilities and simulation language compiler

06 p0778 A72-17476

Precompiler to simplify programming of celestial mechanics problems in TRIGMAN formula manipulation system, introducing data tube SERIES into FORTRAN program

24 p3442 A72-45242

Computer programming for minimization of time required for retranslation with compilers, discussing finite state machine modeling with circulating game loose system

24 p3383 A72-45670

COMPLETENESS

Shape functions for finite element analysis in n-dimensional space, examining completeness of polynomial interpolation and computational efficiency

15 p2326 A72-31713

Completeness proof for linear elasticity theory set of three harmonic functions based on theory of linear differential equations with constant coefficients
16 p2466 A72-33018

COMPLEX NUMBERS

Stellar secular stability during complex roots onset in model evolution, discussing radiative heat transport coefficient effects
03 p0416 A72-13004

Differentiation method for complex root calculation for system of nonlinear equations with analytic functions
13 p1985 A72-28710

Complex eigenvalues of frequency for Laplace tidal equation with negative equivalent depth, noting unstable modes role in solar differential rotation
14 p2100 A72-30344

Discrete system feedback design based on complex number plane mapping, determining gain
15 p2213 A72-32800

A constructive method of solving the Liapounov equation for complex matrices.
22 p3199 A72-42775

The use of complex coordinates in the study of rotor dynamics.
[AIAA PAPER 72-954] 24 p3369 A72-45413

COMPLEX SYSTEMS

Reliability behavior of complex systems with stand-by redundancy under different failure and repair echelons
02 p0194 A72-12446

Simulation of complex systems - Conference, Tokyo, September 1971
02 p0188 A72-12654

Hybrid computer for solving complex problems in distributed parameter systems in terms of parabolic differential equations
02 p0188 A72-12655

Complex structures mass and stiffness matrices reduction by automatic condensation, calculating lowest eigenfrequencies and eigenmodes of substitute systems
[DGLR PAPER 71-108] 02 p0299 A72-12721

Complex systems stochastic survivability estimates dependence on delay depth and initial conditions of interaction
05 p0640 A72-16204

Book on discrete event computer simulation for complex systems synthesis and analysis covering random numbers use, languages, and interactive man machine applications
06 p0779 A72-17812

GERTS II simulation program for graphically modeling and analyzing complex stochastic systems, discussing applications to assembly line, project management, conveyor and inventory systems
06 p0780 A72-17978

Complex bodies time dependent temperature distribution from temperature measurements at arbitrary points, using Duhamel integral
06 p0904 A72-18512

Complex systems calibration based on computer derived transfer function, discussing theory, Fortran calibration program, error analysis and applications
07 p0949 A72-18818

System properties of information patterns in complex hierarchical automatic control systems
07 p0949 A72-18927

Two-variable second order system for multivariable systems predictive control, deriving algorithm for near time optimal control
07 p0961 A72-19709

Multivariable linear systems control structure via optimal control theory with quadratic criterion, permitting compensation for nonzero mean value and slowly varying perturbations
07 p0961 A72-19711

Consistent finite element method to analyze random response of complex structures based on standard modal approach
08 p1248 A72-21823

Reliability of complex systems performing function with time dependent quantity
08 p1180 A72-22061

Economic factors influence on reliability optimization of complex radio systems and elements
08 p1143 A72-22066

Numerical algorithm for optimal coefficient equations in analytical design of complex control plants
09 p1291 A72-23426

Hierarchical control structures aggregation and construction for class of complex systems
09 p1292 A72-23489

Compensator improvement for relative stability and frequency response of large space vehicle, using nonlinear programming
10 p1442 A72-23791

Multistage systems maintainability, presenting equations for optimum allocation of demonstration tests to repairable elements
10 p1443 A72-23982

Complex system mission worth optimization by redundancies discussing MISDGRAD computer program to evaluate cost-reliability for mission without maintenance
10 p1550 A72-23994

Design review as management tool for complex systems quality and reliability assurance, discussing Skylab program
10 p1486 A72-24005

Complex system represented by fault-free with independent components, calculating confidence interval for failure probability by moment method
10 p1444 A72-24018

Cost reduction by integration of assurance technologies from complex systems development risk management model
[AIAA PAPER 72-245] 10 p1487 A72-24450

Mathematical statistics application to complex systems modeling, considering group method of data handling, simulation and regression methods
10 p1457 A72-24634

Parameter identification method for mathematical extremal control model of complex structure for static plants based on regression analysis
10 p1458 A72-25192

Time to failure determination in complex service systems, examining Markov processes
11 p1609 A72-25435

Book on sensitivity theory covering continuous and sampled data systems, linear, nonlinear and self exciting dynamic systems, optimal systems, large systems, controllability, etc
11 p1611 A72-26021

Rank correlation coefficient method for complex control plants parameters selection, applying to aircraft power system monitoring
11 p1612 A72-26442

Complex bipolar IC logic circuits realization by economical high speed techniques using metal bonding or cells available in library
11 p1606 A72-26548

Criterion selection and minimum margin search for optimization of complex electronic circuit parameters described by mathematical models
11 p1612 A72-26736

Reliability requirements and optimization for complex systems, discussing method to improve component reliability of aircraft weapon system
13 p1961 A72-28353

Statistical principles of reliability assessment and sequential testing of complex systems, considering confidence level, probability of acceptance and cost factors
13 p1984 A72-28361

Mathematical models for complex system debugging in initial life period, noting maximum likelihood estimates for failure rate functions
13 p1962 A72-28365

Dimensional chains calculation in differential method of manufacturing complex precision elements of casings
13 p1962 A72-28740

Optimal viability of complex system with ambient medium interaction, using stochastic game theory
13 p1936 A72-29174

Signal system design with digital displays for deviation control in complex multiparameter technological processes, using algorithm to estimate efficiency
13 p1936 A72-29177

Complex elastic systems natural frequencies computation from measured dynamic response to harmonic excitation, applying to helicopter and transport aircraft
14 p2164 A72-30326

Complex systems optimization with respect to vector-valued cost function without prespecified constraints or criteria weighting, deriving algorithm for characteristic set of noninferior solutions
14 p2087 A72-30825

Aerospace complex physical systems including human operator, discussing computerized design for behavior analysis by means of mathematical models
14 p2093 A72-30846

Nonlinear differential equations of motion of complex configuration, developing stable solution method
15 p2261 A72-31489

Complex structures dynamic analysis by component mode technique, treating modal characteristics as random variables
15 p2331 A72-32555

Computer algorithms for adaptive optimal synthesis of complex electronic systems, using stochastic approximation and gradient search with data storage
16 p2367 A72-33265

Uniqueness principle application to construction of gravitational field generated by complex of elastic bodies for mass tensor
16 p2424 A72-33366

Freedoms retention determination eigenvalue analysis of complex structures large dynamic matrices deriving transformation vectors based on maximum swept volume deformation modes
17 p2576 A72-35253

Stability and transient behavior of composite nonlinear systems.
17 p2534 A72-35530

Mathematical model of class of complex control systems composed of structures obtained from aggregates of ordered sets and random operators
19 p2777 A72-37380

Complex systems dynamics and stability problems, deriving equations of motion and boundary conditions from principle of least action
19 p2784 A72-37388

Integrated systems design procedures as exemplified by Europa 1, 2 and 3 rockets and Symphonie communication satellite development
19 p2869 A72-38302

Signal recognizing algorithms for class of large number of normal distributions with unknown probabilities, using statistical complex hypothesis verification
19 p2770 A72-38466

Application of matricial formalisms to the specification of light polarization changing systems.
20 p2928 A72-40025

Optimal control of complex time lag systems with series connected lumped and distributed parameters described by linear differential equations
22 p3162 A72-42241

Asymptotic reliability estimates of monotonically structured complex logic systems with low and high component failure rates equivalent with exponential or Weibull distributions
23 p3267 A72-44004

A survey and comparison of methods for determining confidence bounds on system reliability from subsystem data.
24 p3406 A72-44652

Automatic complex control systems with digital computer application for optimal control of production systems, selecting optimality criterion from hierarchically distributed local criteria
24 p3387 A72-45513

COMPLEX VARIABLES

NT ANALYTIC FUNCTIONS
NT BESSEL FUNCTIONS
NT CAUCHY INTEGRAL FORMULA
NT CONFORMAL MAPPING
NT CONJUGATES
NT ELLIPTIC FUNCTIONS
NT ENTIRE FUNCTIONS
NT EXPONENTIAL FUNCTIONS
NT GAMMA FUNCTION
NT HANKEL FUNCTIONS
NT HARMONIC FUNCTIONS
NT HYPERBOLIC FUNCTIONS
NT HYPERGEOMETRIC FUNCTIONS
NT LAGUERRE FUNCTIONS
NT LEGENDRE FUNCTIONS
NT LOGARITHMS
NT MATHIEU FUNCTION
NT MEROMORPHIC FUNCTIONS
NT NONHOLONOMIC EQUATIONS
NT ORTHOGONAL FUNCTIONS
NT RATIONAL FUNCTIONS
NT SINGULARITY [MATHEMATICS]
NT SPHERICAL HARMONICS

Accuracy of spacecraft trajectory determination by complex expressions in multidimensional geometric representation
01 p0127 A72-10353

Stressed state of reinforced flexibility nonlinear rods under torsion, using theory of functions of complex variables
03 p0447 A72-13731

Mixed boundary value problem of infinite elastic plate with parabolic crack, obtaining solution by complex variable method
05 p0741 A72-17004

Amplitude and phase modulated radar pulse train representation by complex number sequences, discussing generation, processing, and Z transform application to combination codes
06 p0773 A72-17495

Coordinate sequences construction method for complex regions and various boundary conditions, deriving closed form solution to elliptical equation
08 p1200 A72-21702

Angle tracking radar receiver signal analysis simplification by use of complex variables
10 p1437 A72-24684

Stiffly stable implicit linear multistep algorithm for deriving stability properties from extended complex plane transformation
11 p1677 A72-25860

Complex square stochastic matrix spectral inverse, examining nonzero eigenvalues on unit circle
11 p1677 A72-26152

Electronic filters realization by error function minimization, discussing parameter space algorithmic search and complex plane optimization methods
11 p1606 A72-26550

Inverse contour problem of approximating functions for compacta of positive logarithmic capacity in complex plane
12 p1836 A72-27070

Book on applied functions of complex variable covering infinite series, Cauchy theorem, singularity

ties, Laurent series, residue theorem, conformal mapping, Fourier and Laplace transforms, etc
13 p1985 A72-28433

Linear functional equations with constant coefficients for generalized partial derivative operators introduced in certain spaces of functions of many complex variables
13 p1987 A72-30083

Complex conjugate fourth order partial differential equations for circular cylindrical shells deformation, comparing accuracy with Fluegge, Morley and Novozhilov equations
15 p2331 A72-32559

Investigation of the convergence region boundary in a power series of functions of two complex variables
21 p3075 A72-41090

Versatile stretching of a disc shaped as a plane with elliptic aperture.
22 p3236 A72-42627

Square edged semiinfinite circular cylindrical shell, deriving boundary value problem closed form solution based on Novozhilov complex form cylinder equations
22 p3238 A72-42839

Identification and removal of phase errors in interferometry.
23 p3287 A72-43259

COMPLEXITY
NT TASK COMPLEXITY
Stimulus complexity and the EEG - Differential effects of the number and the variety of display elements.
17 p2507 A72-34248

COMPLIANCE (ELASTICITY)
U MODULUS OF ELASTICITY

COMPLICATION
U COMPLEXITY

COMPONENT RELIABILITY
Uhf varactors reliability, establishing rejection criterion by statistical analysis
02 p0194 A72-12444

Reliability behavior of complex systems with standby redundancy under different failure and repair echelons
02 p0194 A72-12446

Optimal smoothing application to testing of inertial navigation systems, gyros and component failure detection during mission
02 p0258 A72-12810

Regenerative system reliability, examining oscillation mode selector
03 p0333 A72-13833

Circuit application consideration in selecting design, materials, processes and packaging for IC component reliability
03 p0337 A72-14295

Oxygen hazards, mishaps and safety programs in NASA operations, considering material, design, cleaning and procedural deficiencies and failures
04 p0564 A72-14436

Metallurgical treatment control reliability in machine part mechanical properties quality evaluation
05 p0671 A72-15993

Reliability analysis of redundant and nonredundant systems with different component failures, using probability theory
08 p1180 A72-22053

Economic factors influence on reliability optimization of complex radio systems and elements
08 p1143 A72-22066

Aircraft maintenance and reliability monitoring and control on scheduled airlines, considering component failure rate and mode analysis, sampling inspection and remedial action
09 p1261 A72-22901

C-5A Galaxy aircraft systems and components maintainability program
10 p1459 A72-23851

Complete reliability program major activity areas identification, discussing various components interrelations
10 p1485 A72-23973

Reliability program for SAAB 37 Viggen airborne computer, discussing prototype and components operating tests and failure rates
10 p1443 A72-23984

Maximum likelihood method of combining system and component data for reliability estimates
10 p1444 A72-24016

Aircraft scheduled maintenance, discussing turbine engine and component reliability protection, controlled overhaul, test and repair
10 p1565 A72-24867

Silicon solar cell interconnectors design for 5-10 years mission life, considering launch induced vibration stresses and thermal cycling stresses during mission
12 p1758 A72-28037

Reliability requirements and optimization for complex systems, discussing method to improve component reliability of aircraft weapon system
13 p1961 A72-28353

Reliability prediction of system with components having independent and constant rate failures
13 p1961 A72-28357

Telecommunication satellites microwave components, emphasizing reliability requirements in multiplex systems
13 p1933 A72-29835

Welded machine component service history effects on residual fatigue life from statistical evaluation of factor experiment
14 p2107 A72-30278

High reliability long life heat pipe thermal control system for space station application [AIAA PAPER 72-261]
14 p2171 A72-30835

French quality assurance of electronic components, discussing organizational links with international bodies
14 p2174 A72-30848

Thin film resistor manufacture and evaluation for stability and long-life characteristics
14 p2091 A72-31171

Achieving fail safe design in rotors.
[AHS PREPRINT 673]
17 p2491 A72-34513

Ballistic-damage-tolerant composite flight control components.
[AHS PREPRINT 674]
17 p2626 A72-34514

Development of electronic part failure rates for long-duration space missions.
17 p2527 A72-34684

Techniques for generating highly reliable redundant systems.
18 p2663 A72-36309

High reliability electronic components; International Conference, Toulouse, France, March 6-10, 1972, Proceedings
18 p2668 A72-37101

Survey of current component reliability problems and methods for prevention.
18 p2668 A72-37102

Analysis of sensitization mechanisms of low consumption integrated circuits
18 p2668 A72-37107

Correlation between the reliability of silicon bipolar transistors and their excess background noise
18 p2669 A72-37110

The detection of unreliable contacts by noise measurements.
18 p2720 A72-37111

Acceptance testing of the MKL capacitor for space application
18 p2669 A72-37119

Microwave varactors for communications satellites
18 p2670 A72-37122

Industrial production of high-quality active semiconductor components
18 p2670 A72-37123

Reliable component procurement for Symphonie satellite, discussing parts list, specifications and subcontract monitoring and inspection
18 p2670 A72-37124

Problems confronting the engineer in charge of procurement of components intended for electronic aerospace systems
18 p2743 A72-37126

Reliability assurance of space equipment components, discussing drift and failure modes, computerized simulation and thermal maps
18 p2743 A72-37127

Standardization and reliability assurance on the national and European levels
18 p2743 A72-37128

Standardization and quality assurance of electronic devices on the national and European levels
18 p2743 A72-37129

European co-ordination activities with particular reference to the Space Components Co-ordination Committee.
18 p2743 A72-37130

Department of Defense Reliability Analysis Center.
18 p2676 A72-37131

Components analysis laboratory with curve tracers, third harmonic index equipment, noise meters, TV X ray system and metallographic microscopes
18 p2676 A72-37132

Production and test facilities availability effect on costs involved in obtaining item at required quality level, examining component rejects and defectives
18 p2670 A72-37133

Qualification procedure for high reliability electronic part requirements for noncontinuous production
18 p2744 A72-37134

CNET Reliability Center and its activities in the field of aerospace devices
18 p2676 A72-37135

Development and production of French high-reliability components: The Concerto Program - The CNES-Concerto certificate
18 p2744 A72-37136

Microwave and optoelectronic devices performance and component reliability, considering varactors, p-i-n, avalanche and Gunn diodes, ICs, FETs, light emitters and liquid crystals
18 p2720 A72-37137

Reliability of semiconductor optoelectronic components - Analysis of the long-term behavior
18 p2670 A72-37138

Test structures - Powerful technique for quality evaluation and reliability assessment of MSI and LSI /medium and large scale integrated circuits/.
18 p2671 A72-37143

Endurance test results for microwave avalanche diode oscillators
18 p2671 A72-37146

TOP 1369 traveling wave amplifier tube
18 p2671 A72-37147

Essential factors in reliability prediction and stress analysis of structural component with wide load and temperature variations
19 p2874 A72-37710

Relation between the reliability and allowable stress amplitude in fatigue design.
20 p2977 A72-38879

Variation analysis and design of experiments as an aid to design quality assurance.
20 p2930 A72-39856

Microelectronic component reliability prediction technique with near Weibull method accuracy in absence of detailed sampling life test results
20 p2930 A72-39857

Functional reliability of the biological component of a life support system
21 p2998 A72-40448

Probability model and causal approach to failure mechanisms and reliability of control systems applied to IC
21 p3024 A72-40711

Characteristic properties and estimation of reliability functions for redundant systems
21 p3038 A72-40713

Information criterion for optimal planning of reliability acceptance tests maximizing average effect
21 p3038 A72-40714

Single and double sample Dodge-Romig lot tolerance percent defective /LTPD/ rectifying inspection plans, using standard tables
21 p3059 A72-40827

Allowance for correlation in the prediction of reliability parameters for radio equipment
23 p3270 A72-43767

Evaluation of the reliability of diversity reception by antennas of different polarizations
23 p3271 A72-43777

Effects of projectile damage on critical helicopter components.
24 p3454 A72-44609

A concept of service life for estimating the reliability of machines and devices
24 p3405 A72-44623

Reliability, safety, maintainability and system effectiveness disciplines acquisition, processing, dissemination and exchange via Government-Industry Data Exchange Program and Failure Rate Data Program
24 p3467 A72-44660

Accelerated life testing of thick film resistors.
24 p3384 A72-44668

Point and confidence interval estimates for acceleration and aging component probability distribution functions in accelerated life tests and reliability prediction
24 p3406 A72-44669

Reliability of modular computer systems with varying configuration and load requirements.
24 p3383 A72-45673

Metallurgical treatment control reliability in machine part mechanical properties quality evaluation
24 p3416 A72-45735

COMPONENTS
Automatic electron beam welding machine for small components, discussing design, performance and inspection methods
09 p1321 A72-23637

COMPOSITE MATERIALS
NT CERMETS
NT COMPOSITE PROPELLANTS
NT LAMINATES
NT METAL MATRIX COMPOSITES
NT REINFORCED PLASTICS
NT THREE DIMENSIONAL COMPOSITES
NT WHISKER COMPOSITES

Bone tissue elastic behavior based on Voigt model of two phase composite material, using ultrasonically determined hydroxyapatite elastic moduli
01 p0136 A72-10112

Composite materials application for space shuttle structures, relating structural weight to payloads
01 p0090 A72-10727

Composite space shuttle booster and orbiter engine support structures design and analysis, stressing weight savings
01 p0139 A72-10740

Fiber reinforced filament wound composites for pressure vessel applications, investigating mechanical properties
01 p0090 A72-10741

Zirconium diboride-silicon carbon-graphite composition for lifting entry vehicle hot leading edges, investigating mechanical behavior by tension and flexural tests
01 p0091 A72-10767

Characterization of graphite/polyimide composites for space shuttle applications

01 p0092 A72-10784

Acoustic emission evaluation of damage of filament wound composite materials under tensile loading applied to spherical test shapes

01 p0069 A72-10804

Radiographic detection of small flaws in bulk graphite and carbon/carbon composites, improving image quality and sensitivity by contrasting liquid impregnation

01 p0069 A72-10808

High modulus high strength graphite composites for aerospace structures, noting materials, machining properties and applications

[SME PAPER EM 71-191] 01 p0092 A72-10965

Unidirectional fiber array reinforced composites with improved longitudinal tensile strength and stiffness compared with structural metals

[SME PAPER EM 71-283] 01 p0092 A72-10966

Fiber reinforced composite rotating disks stress-strain state calculation, discussing steady state closed solutions and approximate methods

01 p0142 A72-11175

Viscoelastic parameters calculation for orthotropic composite materials reinforced by unidirectional fibers, giving time dependence of relaxation functions

01 p0142 A72-11177

Strain gage tests on three dimensional composites for reentry vehicle structural design evaluation

02 p0287 A72-11506

Three dimensional heat conduction behavior in laminated composites calculated from continuum model using asymptotic developments

02 p0300 A72-11547

Hugoniot analysis of shock disturbance propagation with steady velocity through composite material, deriving conservation equations

02 p0248 A72-11982

Macroscopic fracture mechanics of composite laminates, discussing flawed specimen static strength prediction

02 p0249 A72-11983

Stress waves propagation in woven-fabric composites, obtaining dynamic moduli and vibration damping coefficients by resonance technique [AD-736006] 02 p0291 A72-11984

Composites response to shock loading via Hugoniot synthesis based on theory of mixtures, expressing mass, momentum and energy balance

02 p0291 A72-11986

Stress concentration factors for fiber and matrix in axially loaded unidirectional composite with discontinuous fiber, using linearly elastic finite element analysis

02 p0292 A72-11987

Unidirectional and bidirectional composite laminates subjected to cylindrical bending under uniformly distributed and concentrated loads

02 p0292 A72-11989

Vibration and buckling analysis of doubly curved composite monocoque plates and shells of positive and negative Gaussian curvature, examining stacking sequence effect

02 p0292 A72-11990

Stress analysis for transverse deformation of fiber reinforced composites

02 p0249 A72-11991

Ultrasonic measurement of orthotropic laminated composites elastic moduli, describing stress-strain response [AD-736007] 02 p0249 A72-11994

Postshear buckling, diagonal tension behavior of rectangular laminated boron-epoxy plates clamped on each side, observing stacking sequence effect

02 p0249 A72-11995

Epoxy- and polyimide-graphite composites electrical dissipation factor and capacitance measurements as guide to molding quality, describing equipment

02 p0250 A72-12609

Glass fabric reinforced composite materials stress distribution under longitudinal loading, using finite element method with two dimensional model

03 p0381 A72-13720

Thermography capabilities and limitations for design analysis and quality control in nondestructive testing of material test vehicle carbon-carbon composite cones

03 p0364 A72-14026

Relative cost comparisons of composite applications with conventional material components selected from F-111A supersonic fighter bomber

03 p0310 A72-14234

Static load transfer to discontinuous elastic filament in fiber reinforced composite, determining fiber force longitudinal distribution by approximation to Fredholm integral equation

03 p0455 A72-14384

Stress channelling in transversely isotropic elastic composites, comparing classical theory with ideal fiber reinforced composite plane deformation theory

03 p0455 A72-14385

Designing with composite materials - Conference, London, October 1971

04 p0536 A72-14742

Carbon fiber reinforced material porosity source, applying equilibrium configurations of liquid films on parallel uniform cylindrical rod hexagonal and cubic arrays

04 p0537 A72-15087

Composite materials testing with four point loading method, studying environmental and creep effects in flexure

04 p0537 A72-15091

Fiber reinforced composites with transversely isotropic constituents, discussing various mathematical models for elastic constants calculation

04 p0590 A72-15189

S-glass fiber bundles and composites under quasi-static loads, investigating strength characteristics and failure mechanism

04 p0592 A72-15474

Mechanical behavior of uniaxially loaded multilayered oriented fiber cylindrical composites, observing tensile transverse stresses

[ASME PAPER 71-MET-O] 05 p0732 A72-15792

Polyfluoroethylene-based composite materials mechanical properties, discussing strengthening mechanism of filler additions

05 p0682 A72-15989

Composite materials durability and strength estimations, using reliability theory for failure rate characteristic

05 p0680 A72-15991

Finite element micromechanical analysis of porous and filled ceramic composites for internal stresses and deformations

05 p0738 A72-16423

Large deflection microstructure continuum model for composite beam flexural wave propagation and free vibration, deriving equations of motion

[AIAA PAPER 72-140] 05 p0741 A72-16937

Photothermoelastic analysis of shrinkage stresses near discontinuity in fiber composite material, relating matrix cracking to fiber packing

06 p0835 A72-17800

Microscopic-macroscopic transition in heterogeneous metal polycrystals and multiphase composites at finite strain

06 p0897 A72-18068

Fiber pull-out from elastic matrix, calculating shear stress and load distribution dependence on elastic properties and fiber length

06 p0897 A72-18152

Fiber reinforced materials mechanical properties, showing strength dependence on stress-strain behavior of fibers and binders and fiber volumetric proportions

06 p0835 A72-18252

Structural and strength characteristics of carbon graphite materials, considering composites preparation and applications

06 p0836 A72-18361

Fibrous composite materials experimental failure studies at high temperatures and cyclic loading

06 p0838 A72-18654

Compression strength theory for monodirectional reinforced homogeneous anisotropic and piecewise homogeneous composite materials, using microvolume stability loss failure mechanism

06 p0838 A72-18655

Temperature distribution in composite media with internal heat generation, solving diffusion equation via Vodka type orthogonality relationship

07 p1100 A72-19626

Real time computer aided mechanical testing and data analysis system for composites, confirming computer analysis by motion pictures of thin walled graphite/epoxy composite fracture

07 p0965 A72-19734

Mechanical strength and microstructural characterization of sapphire ribbons and continuous filaments for composite materials

07 p1023 A72-19929

Limit analysis of ductile fiber reinforced structures, obtaining critical load of composite sandwich ring

07 p1093 A72-19950

Tensile strength estimation for two dimensional composite with brittle matrix and randomly orientated discontinuous elastic fibrous reinforcement

08 p1244 A72-21324

Material design for filament wound graphite-graphite fiber/matrix composite heat shields for improved performance during reentry

08 p1245 A72-21597

Optimal design of anisotropic composite material annular plates by numerical method

08 p1246 A72-21673

Prestressed glass reinforced composites mechanical behavior, taking into account manufacture induced residual stress concentrations

08 p1192 A72-21674

Random filament misalignment effects on rigidity and tensile strength of unidirectional graphite composites under shear loading

08 p1192 A72-21681

Stress rupture data from S glass composite matrix effectiveness tests, noting skewed lifetime distribution in statistical patterns

08 p1192 A72-21683

Carbon/epoxy composite reinforced plastic materials feasibility for application to aircraft landing gear wheel fabrication

08 p1193 A72-21686

Graphite reinforced epoxy stiffeners for variable geometry fuel tank to meet light weight requirement, discussing billet fabrication, assembly and installation

08 p1176 A72-21688

Graphite fiber reinforced composites with high mechanical strength and modulus at low weights, fatigue resistance, vibration damping and tailorable thermal expansion coefficient

08 p1193 A72-21689

Large automated tape placement machine tool design and construction for laying up aircraft structures from composite materials

08 p1177 A72-21690

Graphite fibers surface treatment and interfacial adhesive bonding, considering resin composites shear strength enhancement by sulfuric acid and sodium chlorate oxidation

08 p1194 A72-21697

Reinforcing fiber frame incurvation influence on elasticity and thermal expansion coefficients of composite material

08 p1194 A72-21754

Composite viscous polymer cylindrical shells buckling modes under prolonged loading, taking into account initial imperfections

08 p1248 A72-21859

Hot pressed boron nitride and composite oxidation tests in atmospheric arc jet, noting fabrication and composition effects on thermal shock and oxidation resistance

09 p1333 A72-22379

High temperature tests of graphite composites in air, determining material loss time dependence and correlation with observed strength data after oxidation

09 p1333 A72-22381

Thermal shock resistant composite materials with carbide or oxide matrices based on concept of crack propagation prevention, noting superiority from thermal simulation tests

09 p1334 A72-22384

Yttria stabilized hafnia based graphite and tungsten composites, investigating factors affecting thermal shock resistance

09 p1327 A72-22385

Titanium-boron-epoxy composite materials selection and fracture mechanics criteria for B-1 bomber structural design

09 p1317 A72-22477

Penny shaped interface crack between elastic layer and half space, calculating stress intensity factors and strain energy release rate for aluminum-epoxy combination

09 p1398 A72-22530

Interlaminar shear testing of composite materials, discussing short beam, scissor and torsional methods [PI PAPER 7] 09 p1337 A72-22542

Fiber composites mechanical properties - Conference, Teddington, England, November 1971

09 p1338 A72-23162

Aligned fibrous composites microstructural parameters, showing fiber thickness effect on fracture, fabrication, matrix cracking, creep resistance and fatigue

09 p1338 A72-23163

Single and multiple fractures in brittle matrix fibrous composites, discussing fracture energetics, stress-strain curves and hysteresis effects

09 p1338 A72-23164

Core and tube duplex fiber reinforced composites with fracture toughness capable of high stress level operation

09 p1338 A72-23166

Discontinuous rigid or creeping fiber reinforced composite materials, predicting steady state creep behavior

09 p1338 A72-23167

Two dimensional creeping flow in fiber reinforced composite under uniform tension, discussing matrix shear stress and fiber direct stress distributions

09 p1338 A72-23168

Stress concentration in elastic composite reinforced by two dimensional continuous parallel fiber array with one broken fiber

09 p1339 A72-23172

Tractions at interface between fiber and matrix in fiber reinforced composites, considering axially symmetric deformations and stress fields

09 p1339 A72-23173

High pressure bulk modulus test rig for composite material specimen nondestructive test, discussing measurement method and errors

09 p1315 A72-23391

Torsion of embedded infinite elastic circular cylindrical fiber with penny shaped crack, investigating breaking behavior from Fredholm integral equation iterative solution

10 p1553 A72-24094

Molded carbon technique-produced carbon fiber/carbon composites, discussing flexural strength, toughness, crack resistance and rocket nozzle application

10 p1500 A72-24200

Shock response of two constituent composites /Elkonites/, predicting Hugoniot states with allowance for thermal energy transfer 10 p1556 A72-24259

Dynamic shear modulus and damping of polystyrene composites filled with glass, salt and foam, including skin effect correction 10 p1500 A72-24260

Linear equations relating elastic compliance coefficients of anisotropic two-phase fiber reinforced composites 10 p1556 A72-24262

Linear anisotropic composites with periodic spatial structure, determining elastic moduli and electrical conductivity variational bounds 10 p1556 A72-24346

Fiber reinforced materials mechanical properties calculation, taking into account various fiber orientations and multiaxial loads 10 p1501 A72-24493

Statistical bounding approach to fracture analysis of fiber reinforced composite materials tensile strength 10 p1502 A72-24483

Low thermal flux glass fiber composite over-wrapped tubing with metallic liners for leak free cryogenic propulsion plumbing systems 11 p1637 A72-25364 [AIAA PAPER 72-328]

Initially sharp cylindrical pressure pulse propagation and stress wave attenuation in linear elastic fiber reinforced composites 11 p1730 A72-25415 [AIAA PAPER 72-394]

Elastic constants and bond stress distribution for discontinuous fiber-reinforced three dimensional composite subjected to uniaxial tension 11 p1731 A72-25418 [AIAA PAPER 72-397]

Composite materials testing and design - ASTM Conference, Anaheim, California, April 1971 11 p1670 A72-25452

Empirical multiaxial strength criteria for anisotropic composite materials 11 p1731 A72-25455

Fatigue failure modes of composite materials, considering fiber breakage, delamination, matrix cracking, interface debonding and void growth 11 p1670 A72-25461

Fiber toughening mechanisms in continuous filament unidirectionally reinforced composites with elastoplastic matrices, discussing tensile energy storage in debonded region 11 p1671 A72-25463

Micromechanical and impact test investigation of unidirectional fiber composites impact resistance properties, considering longitudinal, transverse and shear modes 11 p1672 A72-25472

Anisotropic graphite composite laminates cutouts stress analysis by finite element method, predicting structural reinforcement behavior 11 p1672 A72-25475

Elastic glass and Thorneil fiber/epoxy matrix composite material creep tests, determining creep rate dependence on specimen geometry and stress state 11 p1672 A72-25481

Random filament misalignment effect on reinforced composite strength, discussing bundle, tensile and shear strengths 11 p1673 A72-25486

Glass styrene acrylonitrile bead filled composites tensile behavior, discussing relationship between yield stress, filler content, strain rate and temperature 11 p1673 A72-25487

Carbon-carbon composite ring structure tested for processing cycle, design properties and ablative performance in solid rocket nozzle environment 11 p1673 A72-25488

Experimental weave pattern for three dimensional continuously woven fiber glass reinforced composite fabric impregnated with epoxy resin 11 p1673 A72-25597 [SAE PAPER 720340]

Layered anisotropic fiber composite (Tetra-Core) for sandwich construction and aircraft applications, discussing design, fabrication and strength characteristics 11 p1638 A72-25599 [SAE PAPER 720343]

Book on carbon fibers in composite materials covering fiber testing and mechanical properties 11 p1674 A72-25924

High performance continuous filament reinforcements for nonmetallic matrix composites, emphasizing boron and graphite fibers 11 p1674 A72-26229

Fiber-matrix composites overall strength optimization, emphasizing matrix and interface effects 11 p1674 A72-26231

Production manufacturing processes improvements for composite materials 11 p1674 A72-26232

Boron/epoxy and graphite/epoxy composites application to aircraft structural design, discussing flight test and developmental programs 11 p1577 A72-26234

Thermal stresses in homogeneous isotropic and composite curved beams for temperature distribution in polynomial form with coefficients representing functions of two remaining coordinates 11 p1737 A72-26665

Carbon-graphite fracture mechanics dependence on graphite crystallite structure, discussing crystal size effects on strength 11 p1674 A72-26812

Elastic inhomogeneous continuum stability dependence on internal stress tensors field and boundary conditions, noting application to composite materials 12 p1843 A72-27171

Elastic wave propagation and energy scattering in materials reinforced by inextensible fibers 12 p1881 A72-27252

Harmonic equation for antplane shear deformation of elastic composite materials with multiple circular inclusions 12 p1883 A72-27562

Micromechanics of deformed continua, discussing atomic structure effects on stress concentrations in composite materials, framed structures and grids 12 p1884 A72-27640

Fiber composites plastic flow and fracture, using plane strain model for analysis 12 p1884 A72-27730

Computer program to reduce automated multiaxial testing strain gage and applied loads data from tubular or flat specimens including fiber composites 12 p1877 A72-27999

High modulus fiber composite circular tube specimens multiaxial load testing, noting gripping methods to reduce transitional strains 12 p1886 A72-28000

Cocuring technique optimization for primary aircraft components composite materials, discussing mechanical and dimensional properties test data, production cost analysis and cure time 12 p1815 A72-28077

Numerically controlled composite tape laying machine, discussing production run simulation, raw material quality effect and control corrective devices 12 p1815 A72-28078

Composite materials fabrication, emphasizing high strength/stiffness to weight ratio as critical performance requirements 12 p1815 A72-28082

Fiber reinforced Mod 3 carbon-carbon composites mechanical and thermal properties comparison with polycrystalline bulk graphite 12 p1834 A72-28087

Aromatic polyimide binder for compression moldable high performance composites preparation with thermal curing to obtain good thermal-oxidative stability and toughness 12 p1834 A72-28090

Addition type polyimide-graphite fiber composites fabrication from monomeric reactant solutions to improve mechanical properties and thermal stability 12 p1834 A72-28091

Flexural strength of Pyco-bond polyacrylonitrile /PAN/ precursor carbon fiber substrates for carbon-carbon composite fabrication 12 p1835 A72-28092

Carbon-carbon composite material for high performance aircraft braking systems, noting weight savings and thermal characteristics improvements 12 p1835 A72-28093

Composite materials application to gas turbine fan guide vane fabrication, noting economic factors and prototypes performance in engine tests 12 p1815 A72-28100

Composite materials evaluation methods, discussing high quality photographs, radiography, laser holographic interferometry, thermographic fluorescent phosphors, liquid crystals and acoustic techniques 12 p1815 A72-28101

Long range transport aircraft structures and composite materials technology for airframe and engine systems 13 p1897 A72-28955 [AIAA PAPER 72-362]

Finite plane elastic buckling deformations of incompressible composite columns reinforced by straight parallel fibers 13 p2059 A72-29599

Dynamics of composite materials - ASME Conference, La Jolla, California, June 1972 13 p2060 A72-29690

Aircraft structures design and development with composite materials, considering materials characteristics relations to structural components dynamic response 13 p2060 A72-29691

Stress wave propagation and fracture in composites, discussing micromechanical and homogeneous-continuum theories 13 p2060 A72-29692

Directionally reinforced composites treated as homogeneous continuum with microstructure, deriving displacement equations of motion by Hamilton principle 13 p2060 A72-29694

Interacting continua theory for stress wave propagation in composites with microstructural stress and displacement fields, discussing elastic and viscoelastic materials behavior 13 p2060 A72-29695

Harmonic elastic wave propagation in composites with periodic structures by variational methods developed from crystal lattice studies 13 p2060 A72-29696

Elastic waves propagation in randomly inhomogeneous fiber reinforced or layered composites from perturbation methodology for electron and vibrational waves in disordered media 13 p2061 A72-29697

Increased volume fraction effect on transverse rupture strength and fracture toughness of hot pressed and annealed composites of polycrystalline magnesium oxide 13 p1980 A72-29828

Crystalline polymers behavior as multiphase composite solid, calculating supermolecular structures effects on stiffness properties 14 p2163 A72-30181

Failure phenomena relationship to kinetic equation for defect buildup from brittle fracture analysis of composite glass plastic in uniaxial eccentric tension 14 p2164 A72-30426

Thermomechanical erosion prediction for ablative, composite material, reentry nose tip applications and model development for heating, pressure and shear forces 14 p2171 A72-30827 [AIAA PAPER 72-299]

Composite materials stress analysis techniques, discussing strain gages, photoelastic coatings moire and holographic applications 14 p2167 A72-30861 [ASME PAPER 72-DE-6]

High modulus composites structural design applications, considering fatigue performance vs cost 14 p2167 A72-30866 [ASME PAPER 72-DE-24]

Thermal expansion of carbon-carbon composites as function of temperature and fiber orientation by dilatometric measurements 15 p2260 A72-31256

Epoxide resins for application in composite materials, discussing crosslinking reactions, temperature effects on cure, and electrical and physical properties 15 p2260 A72-31441

Mechanical properties of composite materials, discussing elastic deformation and failure modes 15 p2260 A72-31442

Composite materials for engineering component and structure design, considering mechanical properties and cost-effective performance 15 p2260 A72-31443

Dispersed particle shape effect on elastic behavior of magnesium oxide composites at low graphite concentrations 15 p2260 A72-31585

Tangential force distribution at fiber surface in composite material under tensile stress without displacement at fiber axis 15 p2260 A72-31743

Structural components design from fiber composites, noting computer programs for structural and stress analysis 15 p2328 A72-32128

Temperature effects on stress-strain diagram, tensile strength and creep properties of fiber-epoxy resin composites 15 p2260 A72-32137

Finite element method for discrete models of composite materials, discussing nonlinear dynamic problems 15 p2330 A72-32296

Carbon and graphite fiber reinforced composites elastic constants derived from ultrasonic immersion technique 15 p2261 A72-32503

Particulate composite model deformation and failure behavior under plane uniaxial compressive stress, using finite element method 15 p2258 A72-32556

Upper and lower bounds for complex elastic moduli of composite materials with isotropic linear viscoelastic phases behaving as homogeneous isotropic materials 16 p2468 A72-33199

Dynamic load tests for impact strength of ceramic composites with fiber reinforced alumina matrix, obtaining dynamic stress-strain curves 16 p2414 A72-33300

Steady state creep of composite material with discontinuous fibers, determining random function mean and variance for fiber stress distribution 16 p2412 A72-34115

Carbon fibers for composite materials reinforcement, discussing mechanical properties and economic factors 17 p2569 A72-34188

Variational methods for dispersion relations and elastic properties of composite materials. [ASME PAPER 71-APMW-21] 17 p2623 A72-34302

Constitutive equations for plane harmonic waves propagation in composite fiber reinforced elastic material 17 p2625 A72-34321

Approximate method for composite materials effective elastic moduli determination from uniform stress-

strain field or as second derivative of average strain energy 17 p2625 A72-34322

Results of preliminary studies of a bearingless helicopter rotor concept. [AHS PREPRINT 600] 17 p2489 A72-34490

Ballistic-damage-tolerant composite flight control components. [AHS PREPRINT 674] 17 p2626 A72-34514

Carbon fibre composites with ceramic and glass matrices. I - Discontinuous fibres. 17 p2570 A72-34668

A lattice model for stress wave propagation in composite materials. [ASME PAPER 72-APM-52] 17 p2627 A72-34778

Experimental investigation of the interlaminar shear properties of composite materials. [SESA PAPER 1985A] 17 p2631 A72-34824

Tridimensional textiles for composites. 17 p2571 A72-34935

The integration of composite structures into aircraft design. 17 p2492 A72-35281

Composite materials technology utilization in structural design, considering stiffness, strength, weight, fatigue properties, adhesive joining and structural reliability 17 p2633 A72-35283

Upper and lower bounds of effective thermal conductivity for statistically homogeneous composite materials, using variational principles 17 p2638 A72-35285

Observations of failure modes in carbon composite materials. 17 p2571 A72-35288

The transverse Poisson's ratio of composites. 17 p2571 A72-35289

Shear deformation in heterogeneous anisotropic plates. 17 p2633 A72-35294

Russian book on metal alloys structure and properties covering structural changes in solid bodies, metals atomic structure, diffusion, phase transformations and composite materials 17 p2568 A72-35446

Advanced materials: Composites and carbon; Proceedings of the Symposium, Chicago, Ill., April 26-28, 1971. 17 p2571 A72-35651

High strength alumina, boron, silicon carbide and graphite reinforcing fibers for composite materials 17 p2572 A72-35656

Carbon-carbon composite process and fabrication techniques, discussing heat treatment effects and physical properties correlation to material structure 17 p2561 A72-35666

Mechanical properties of carbon filament wound carbon matrix composite from tensile tests, noting reinforcement efficiency 17 p2573 A72-35669

Composite materials sum and product physical properties, considering magnetostrictive and piezoelectric interactions 18 p2717 A72-35996

The strength of fibre composites. 18 p2703 A72-36268

Coupled glass-fibre/polypropylene composite - An initial evaluation. 18 p2703 A72-36269

Improving the impact resistance of glass-fibre composites. 18 p2703 A72-36270

Composite materials crack propagation and failure modes leading to fracture instability, discussing maximum strength conditions and fatigue 18 p2703 A72-36394

Theory of elastic wave propagation in composite materials. 18 p2703 A72-36395

NASA research on refractory carbides, nitrides and borides, discussing electronic and defect structures, hot extrusion, uranium nitride, cermet for bearings and composite evaluation 18 p2701 A72-36594

Effect of fiber end, fiber orientation and spacing in composite materials. 18 p2738 A72-37086

The stress boundary value problem for plane strain deformations of an ideal fibre-reinforced material. 19 p2870 A72-37371

Thermal expansion at elevated temperatures. III - A hemispherical laminar composite of pyrolytic graphite, silicon carbide and its constituents between 300 and 800 K. 19 p2822 A72-37463

Calculation of residual stresses in wound materials produced by a layer-on-layer solidification process 19 p2872 A72-37532

Interferometric holography for bond inspection in aerospace composite materials and honeycomb structures 19 p2806 A72-37607

Holometric deformation measurement on carbon carbon biaxial test specimens. 19 p2822 A72-37616

Nondestructive testing of advanced composites. 19 p2799 A72-37669

Graphite-epoxy composites application to commercial transports for weight and cost reduction 19 p2873 A72-37680

Effectiveness of using composite materials directionally reinforced by hollow fibers 19 p2823 A72-38002

High modulus fiber composites development from viewpoint of reinforcement patterns and material properties 20 p2943 A72-38946

Strength factors of fiber reinforced composites under tension, compression, shear, bending and plane stress 20 p2944 A72-38947

RF shielding and electrical properties of boron and carbon fiber reinforced composites. 20 p2944 A72-38987

Multi-cycle plasma arc evaluation of oxidation inhibited carbon-carbon material for shuttle leading edges. [ASME PAPER 72-ENAV-26] 20 p2894 A72-39151

Theoretical model for acoustic emission relationship to fiber cracking during rising load tensile test on fiber reinforced composites 20 p2925 A72-39285

Composite materials; Meeting, 1st, Konstanz, West Germany, October 22, 23, 1970, Technical Reports 20 p2939 A72-39436

Boron and carbon fibers fabrication and properties for composite materials reinforcing elements, noting strength and stiffness dependence on stress orientation 20 p2944 A72-39437

Coating of fibers and the fabrication of fiber-reinforced composite materials 20 p2929 A72-39443

Fiber arrangements for one, two and three dimensional ideal composite materials, discussing fabrication processes 20 p2940 A72-39446

Laminar composite materials with special physical properties 20 p2940 A72-39451

Aluminum/plastic semifinished material - A new material for multiple applications 20 p2944 A72-39452

Processing of carbon/carbon composites - An overview. 21 p3072 A72-40552

Boron polyimide composite development. 21 p3072 A72-40553

Strength of S-glass fiber. 21 p3072 A72-40554

A multi-continuum theory for composite elastic materials. 21 p3072 A72-40676

Variational theorems for harmonic waves in elastic composites with periodic structures, considering wave propagation in layered and in fiber reinforced composites 21 p3119 A72-41101

Dynamic inelastic properties of materials. I - Damping characteristics of fiber composites. II - Representation of time dependent characteristics of metals. [ICAS PAPER 72-28] 21 p3069 A72-41153

Physical, mechanical and thermal characteristics of reimpregnated pyrolyzed carbon-carbon and graphite-graphite composites [ICAS PAPER 72-29] 21 p3073 A72-41154

Boron fiber reinforced composites technology assessment and utilization, stressing cost reduction [ICAS PAPER 72-30] 21 p2995 A72-41155

Investigation of the strength and deformability of thin composite materials of magnetic recorder type. I - Strength and deformability at elevated temperatures 21 p3073 A72-41707

Composite materials obtained by depositing boron layers under vacuum on aluminum sheets 21 p3190 A72-42646

Filament wound pressure vessel isotensoid theory, considering composite material as macroscopically homogeneous anisotropic continuum 22 p3238 A72-42838

Larmor radius and collisional effects on the dynamic stability of a composite medium. 22 p3212 A72-42990

Reinforcement of structural materials by long strong fibres. 22 p3241 A72-43026

German monograph - Contribution to the reinforcement of plastics with special allowance for the reinforcement and matrix materials. 22 p3197 A72-43078

Stress-rupture of simple S-glass/epoxy composites. 23 p3305 A72-43492

Fiber composite columns under compression. 23 p3344 A72-43494

Boundary value problems for concentrated forces acting inside semiinfinite anisotropic plate under plane stress, investigating failure modes of unidirectional composites 23 p3344 A72-43495

Book - Fracture: An advanced treatise. Volume 7 - Fracture of nonmetals and composites. 23 p3345 A72-43501

Theoretical approach to the fracture of two-phase glass-crystal composites. 23 p3306 A72-43560

A finite element stress analysis of a crack in a bi-material plate. 23 p3346 A72-43707

Boron-aluminum structural component for Shuttle. 24 p3458 A72-44890

The stress distribution near the tip of an array of screw dislocations piled-up against an inclusion. 24 p3460 A72-45694

Polyfluoroethylene-based composite materials mechanical properties, discussing strengthening mechanism of filler additions 24 p3417 A72-45731

Composite materials durability and strength estimations, using reliability theory for failure rate characteristic 24 p3418 A72-45733

Structural and strength characteristics of carbon materials, considering composites preparation and applications 24 p3418 A72-45748

COMPOSITE PROPELLANTS

Pure solid and composite propellants combustion theory based on laminarized solutions to energy and flow conservation equations 02 p0270 A72-11766

Composite propellant powder combustion velocities as function of pressure, discussing powder sensitivity, limiting kinetic stage changes and surface monovariant equilibrium 06 p0867 A72-17568

Combustion of composite solid propellants with ammonium perchlorate base and pyrolyzable binder, investigating perchlorate grain size, binder concentration and catalyst effects 06 p0867 A72-17574

Heterogeneous composite solid propellants ignition behavior under exposure to hot oxidizing gas, using gas phase model with species and energy radial diffusion 07 p1051 A72-19726

Burning rate of composite solid propellant charges, noting application in solid propellant pressure accumulators 09 p1411 A72-22893

Simple composite propellant modelled by ammonium perchlorate-wax mixtures, noting stoichiometric composition effects on explosive properties 09 p1373 A72-23142

Gamma radiation effects on composite propellants stability, investigating polyurethane, polybutadiene, silicone and polyisoprene binders mechanical properties 14 p2144 A72-30760

Composite and double base solid propellant rocket motors storage, considering ingredients and materials compatibility and ignition temperatures effects on spontaneous inflammation potential 14 p2144 A72-30761

Atmospheric humidity, temperature, vibrational and static loads effects on composite and double base rocket propellants strength and safety characteristics. 14 p2145 A72-30764

Internal reflection IR spectroscopy application to composite and double base propellants study, discussing merits as quality control technique 15 p2296 A72-32312

COMPOSITE STRUCTURES

NT LAMINATES

Graphite fiber composite fan blade design for subsonic turbfan engines, discussing weight and fatigue sensitivity reductions and performance test results [SAE PAPER 710771] 01 p0116 A72-10265

Matrix formulation of free-free modal synthesis procedures for dynamic analysis of composite structural systems, giving flow charts [SAE PAPER 710783] 01 p0137 A72-10274

Mechanical strength and performance of combined multicomponent bonded materials, including laminar, fiber, flake filled and metal matrix composites 01 p0093 A72-11086

Stress and failure analysis of glass-epoxy composite plate with circular hole under uniaxial tension by finite element method [SESA PAPER 1942] 02 p0248 A72-11517

Composite rotating sphere with concentric inhomogeneity of elastic constants and outer boundary free from tractions, calculating stress by digital computer 02 p0259 A72-12180

Bending stresses in composite shell at conical interface between metal and fiberglass reinforced plastic portions under internal pressure 02 p0298 A72-12683

Finite amplitude stress wave propagation behind shock in unidirectionally reinforced fiber matrix composites under impact loads 04 p0585 A72-14534

Carbon fiber reinforced composites properties and design limitations relative to elastic anisotropy in pump and fan applications 04 p0536 A72-14744

Glass fiber reinforced plastic composites design, strain limitation and creep fatigue properties for large structures 04 p0588 A72-15052

Stress distribution at hole in multilayer anisotropic shells of composite glass-plastic or cermet material 04 p0588 A72-15052

Metal-skin honeycomb composite structure design and manufacture for Concorde rudder, noting structural adhesive bonding in aircraft construction 04 p0589 A72-15090

Axially symmetric torsional waves in elastic circular composite cylinders, plotting dispersion diagrams 04 p0590 A72-15185

Compounded rotating disks stress-strain analysis from equilibrium and compatibility equations and boundary condition, comparing results with photoelastic and finite difference approximation 05 p0732 A72-15804

Cast telescope mirror design with light metallic structures, examining possibilities offered by composite high modulus fiber structures [ONERA, TP NO. 1022] 05 p0660 A72-15855

Composite multilayer fibrous shell structural design optimization, using nonlinear mathematical programming methods [ASME PAPER 71-WA/DE-12] 05 p0733 A72-15943

Torsional vibration induced by periodic circumferential shear force on composite circular cylinder with varying rigidity and density, obtaining solutions for various boundary conditions 05 p0740 A72-16727

Unidirectional carbon fiber composites effects and use of stress envelopes in aircraft structure design 05 p0681 A72-16997

Stress and displacement solutions to elastic deformation of homogeneous and composite anisotropic near cylindrical bodies, using Almansi algorithm 06 p0894 A72-17688

Interferometric holography application to photoelastic stress analysis of opaque anisotropic composite plates under static and dynamic transverse and in-plane loads 06 p0898 A72-18349

Composite propeller blades with carbon fiber reinforced plastics spar for hovercraft, presenting mechanical properties test data for different composite configurations 07 p0912 A72-19062

Composite elastic beams equations under initial stress, investigating flexural wave propagation and structural stability 07 p1090 A72-19733

Longitudinal elastic wave propagation along composite bar with conical sections and interface discontinuities in material properties, solving multiple reflection by finite difference method 08 p1245 A72-21606

Boron-epoxy structure repair technology based on titanium plugs and fiberglass, discussing equipment, graphical design and nondestructive tests 08 p1193 A72-21691

Composite filament wound boron-epoxy rocket motor combustion chamber design, fabrication and hydrostatic tests 08 p1177 A72-21692

Graphite fiber reinforcement of glass composite structure for increased cost effectiveness as compared to laminates and sandwich structures 08 p1193 A72-21694

Stability analysis of composite systems, applying scalar and vector Liapunov function approach to specific cases 09 p1290 A72-23091

Radial vibrations of isotropic homogeneous sphere and cylinder bonded to thin nonhomogeneous casting outside 10 p1557 A72-24406

Longitudinal vibrations of composite rod under concentrated impact forces at junctions between prismatic sections 10 p1557 A72-24627

Selective reinforcement with high strength boron filament to achieve cost effectiveness and weight savings for composite structures [AIAA PAPER 72-396] 11 p1731 A72-25417

Composite F-111 fuselage design, analysis and testing, considering graphite, boron and glass-epoxy and boron-aluminum systems 11 p1575 A72-25453

Uniaxial, biaxial and shear loading tests on filament wound carbon-carbon composite tubes and rings 11 p1670 A72-25458

Stress analysis of short beam bending of graphite fiber reinforced epoxy composites 11 p1671 A72-25464

Failure modes effect on compressive strength of boron-epoxy composites tested on coupons, honeycomb sandwich columns and beams 11 p1671 A72-25466

Acoustic emission analysis of deformation and fracture modes under straining of fiber glass-epoxy composite structures, including NOL rings and vessels 11 p1671 A72-25469

Stress concentrations around circular openings and failure criteria for orthotropic and anisotropic composite laminated plates subjected to uniaxial, biaxial and shear loading 11 p1732 A72-25474

Torsional stress analysis of rectangular beam composed of two elastic materials, using complex variable and conformal mapping 11 p1733 A72-25544

Plane unstable deformation and stability loss of incompressible laminated composites under highly elastic strains 12 p1880 A72-27229

Composite turbofan blades for high temperature applications, discussing weight reduction and design procedure 12 p1816 A72-28102

Energy method based approximate calculation for natural frequencies of single layer compound shells of revolution 12 p1886 A72-28144

A-4 Skyhawk horizontal stabilizer experimental graphite-epoxy composite construction, describing design, manufacturing and testing techniques [AIAA PAPER 72-358] 13 p2056 A72-28954

Mohr formulas construction for composite structures including frames and cylindrical and conical shells 13 p2058 A72-29460

Navy program for composites technology development in aircraft structures, discussing design, reliability and cost 14 p2073 A72-30860

Thermal expansion in simple solids and structural composites due to anharmonic vibrations, using atomic density model 15 p2322 A72-31257

Plane stress solution for thin walled cantilever beam with end load extended for beam width effects in composite orthotropic beam bending 16 p2463 A72-32841

Thermoelastic stress bounds in fiber reinforced composite beams of arbitrary cross section, examining conditions for applicability of elementary beam theory 16 p2464 A72-32915

Stresses induced by torsional vibration in twisted composite cylindrical shell of cylindrically aeolotropic materials for high and low frequencies 16 p2466 A72-33102

Optimal composite structures of multilayer spherical vessels in terms of elastic deformation under critical loads in thermal field 16 p2467 A72-33158

Plastic composite container cylindrical wall fabrication by two stage procedure combining radial and cross winding of glass fiber rovings 16 p2398 A72-33305

Nondestructive vibration tests of fatigue crack damage in composite structures, investigating glass reinforced epoxy and polyester laminates 16 p2414 A72-33318

Rotating disk with eccentric elliptic insert determining elastic field in inclusion by complex variable technique 16 p2427 A72-33790

Composite cylinder of helically wound fiber laminates, calculating torsional fracture strength with allowance for plastic deformation due to matrix distortion 16 p2472 A72-33949

Composite cylinders of helically wound fiber laminates, predicting burst fracture strength under internal pressure for comparison with experiment on epoxy-glass cylinders 16 p2472 A72-33950

Electric spark activated hot pressing application for sintered composite structures, noting process parameters optimization for superalloy powders 16 p2411 A72-34093

Application of boron/epoxy to the CH-54B Skycrane helicopter. [AHS PREPRINT 670] 17 p2491 A72-34510

Effect of end attachment on the strength of fiber reinforced composite cylinders. [SESA PAPER 1994A] 17 p2630 A72-34817

The integration of composite structures into aircraft design. 17 p2492 A72-35281

Data generation for engineering design with advanced composites. 17 p2571 A72-35653

Boron- and graphite-epoxy and boron-aluminum composites forming, processing and costs for aircraft structural materials 17 p2560 A72-35663

Composite sphere and cylinder vibrations, considering radial and rotary/torsional vibrations 18 p2735 A72-36756

Elastic stability theory of compressible and incompressible composite media 19 p2871 A72-37530

Determination of influence coefficients for composite structures by holographic interferometry. 19 p2873 A72-37614

Vibrations of elastically connected ring systems. 19 p2873 A72-37692

Oscillations, statics and transfer matrices of composite shells of revolution contacting elastic bases, using initial parameters method 19 p2876 A72-38156

Filament winding techniques for rotor blade applications. 19 p2808 A72-38165

Mandrel design for the filament winding process. 19 p2808 A72-38168

Statistical failure characteristics and probability evaluation of the static strength of structural components made of composite polymer materials 20 p2943 A72-38942

Influence of technological factors upon the mechanical reliability of composite-material structures 20 p2943 A72-38945

A plane contact problem of thermoelasticity for a composite rectangle 20 p2978 A72-39019

Pure bending of a rectangular plate made of heteromodelus material 20 p2978 A72-39020

Cracks and screw dislocation arrays in anisotropic bimaterial plates. 20 p2937 A72-39291

Longitudinal tensile failure of unidirectional fibrous composites. 20 p2944 A72-39789

Transverse tensile properties of an unbonded model composite. 20 p2941 A72-39790

Russian book - Plates strengthened by composite rings and elastic cover pieces. 21 p3116 A72-40385

Aircraft structures weight reduction through fiber-matrix composite materials, discussing anisotropic elastic and failure behavior of composite light shell structures [ICAS PAPER 72-38] 21 p3120 A72-41163

Bursting strength and toughness of wire reinforced composite tubes under uniaxial/hoop stress. 21 p3120 A72-41208

Bursting of wire reinforced composite tubes under biaxial tension stresses. 21 p3121 A72-41209

Method of calculating rotating disk of complex profile 21 p3127 A72-41701

Photoelastic study of stress concentration in perforated composite pipes under external pressure 22 p3233 A72-42064

Extensional vibration of a certain type of composite circular plate with a central hole. 22 p3240 A72-42879

The method of Muskhelishvili applied to coupled isotropic elastic plates 22 p3242 A72-43202

Stability of orthotropic stiffened composite plates. 23 p3352 A72-44109

Large deflection of rectangular orthotropic plates. 23 p3352 A72-44111

Action of a moving load on a composite shell with elastic filler 24 p3459 A72-45262

COMPOSITE WRAPPING

Fiberglass overwrapped Al alloy for space shuttle cryogenic hydrogen and oxygen tanks, noting weight reduction and impeding effect on cyclic loading induced crack growth rate 01 p0139 A72-10738

Residual temperature stresses and deformations during thermal treatment of thick walled glass fiber reinforced plastic wound cylinders and rings 08 p1194 A72-21755

Model filament wound epoxy composites. 19 p2808 A72-38164

High modulus fiber composites development from viewpoint of reinforcement patterns and material properties 20 p2943 A72-38946

Precise alignment and uniform distribution of fibres in a metal matrix. 24 p3413 A72-44898

COMPOSITES

U COMPOSITE MATERIALS

COMPOSITION [PROPERTY]

NT ATMOSPHERIC COMPOSITION

NT ATMOSPHERIC MOISTURE

NT ATOM CONCENTRATION

NT BODY COMPOSITION [BIOLOGY]

NT CARBON DIOXIDE CONCENTRATION

NT CHEMICAL COMPOSITION

NT CONCENTRATION [COMPOSITION]

NT GAS COMPOSITION

NT IONOSPHERIC COMPOSITION

NT LUNAR COMPOSITION

NT METEORIC COMPOSITION

NT METEOROID CONCENTRATION

NT MOISTURE CONTENT

NT PLANETARY COMPOSITION

NT PLASMA COMPOSITION

Physical properties of monocarbides of Zr, Nb and alloys in homogeneity range, explaining electronic structure relationship to composition changes

02 p0241 A72-11453

Magellanic Clouds kinematics, composition and other properties, discussing radio sources, atomic abundances, stellar luminosity limits, regional magnetic fields and polarization

03 p0424 A72-13252

Algorithmic calculation for composition changes due to nuclear reactions and convective mixing during stellar evolution

15 p2314 A72-32374

Superplasticity in two phase compositions based on refractory metal alloys, noting creep rate dependence on concentration and electroconductivity

16 p2405 A72-33094

Plotting of composition vs property curves for superconducting systems with a digital computer by the method of simplex arrays

22 p3191 A72-42813

COMPOUND HELICOPTERS

Marchetti SV-20-A twin engine winged commercial/utility helicopter, describing design details, on-board systems and payload accommodations

09 p1262 A72-22907

S-67 flight test program.
[AHS PREPRINT 653]

17 p2488 A72-34479

Flight investigation of design features of the S-67 winged helicopter.
[AHS PREPRINT 601]

17 p2488 A72-34485

Helicopter development, discussing articulated, rigid, tilt and stowed rotors, compound helicopters, rotor drives, flight control and avionics systems

24 p3369 A72-45558

COMPRESSED AIR

Arc-air method application to groove planing, cutting and beveling, describing manual, semiautomatic and full-automatic units

07 p0994 A72-18932

Gas mixture properties at high temperatures, pressures and densities, applying to thermal ionization of adiabatically compressed air

08 p1210 A72-20942

Solid combustibles flame spread rates in compressed atmospheres, noting dependence on oxygen concentration

14 p2170 A72-30340

Pressurized air assisted gas turbine fuel system, describing single stage centrifugal turbocompressor and rotary-lobe compressor designs and performance characteristics

18 p2694 A72-36043

COMPRESSED GAS

NT HIGH PRESSURE OXYGEN

Infinite homogeneous self gravitating compressed gas media nonlinear condensations, describing finite amplitude motion with asymptotic expansions

06 p0880 A72-17889

High performance shock tube using electromagnetically compressed and heated driver gas

07 p0965 A72-20559

Mathematical model for compressed gas convection into lower atmosphere with substantial density changes

10 p1563 A72-24778

Dielectric constant measurements of compressed gaseous and liquid oxygen for computing Clausius-Mossotti function

11 p1691 A72-26782

Gas compressibility measurements at high pressure and temperature using externally heated pressure vessels

12 p1889 A72-28106

Mathematical model for compressed gas thermal convection into lower atmosphere with substantial density changes

14 p2170 A72-30215

Two chamber adiabatic test compression system design with controlled throttle for high temperature nitrogen and nitrous oxide-type gases with exothermal reactions

18 p2676 A72-37189

COMPRESSIBILITY

Small dilatation and short time approximate constitutive equations for compressible nonlinear viscoelastic materials, using multiple integrals and kernel functions

01 p0137 A72-10319

Low strength polymeric materials specimen geometry and lateral constraints effects on isothermal compressibility by compression tests
[SESA PAPER 1935]

02 p0248 A72-11518

Lunar regolith powder weight density, compressibility and torsional strength determination at atmospheric pressure and He atmosphere

02 p0281 A72-12288

Liquid n-octane, n-decane and n-undecane densities and adiabatic/isothermal compressibilities from sound velocity measurements at high pressures and 30-140 C

02 p0261 A72-12829

Intermolecular interaction potential parameters determination from gas compressibility data based on equation of state in kinetic theory

05 p0692 A72-17068

Cs and Hg vapors compressibility factor in supercritical range as function of density, considering charged particles and atoms polarization interactions in ionized metal vapors

07 p1040 A72-18943

Lunar regolith powder weight density, compressibility and torsional strength determination at atmospheric pressure and He atmosphere

10 p1532 A72-23757

Mercury porosimetry for iron powders void and internal particle porosity change as function of compacting pressure, noting compressibility improvement by precompact and annealing

11 p1639 A72-25828

Gas compressibility measurements at high pressure and temperature using externally heated pressure vessels

12 p1889 A72-28106

Experimental data gathering, processing and presentation for materials enthalpy, heat capacity, thermal conductivity, compressibility and volume over wide pressure and temperature ranges

14 p2130 A72-30599

Angular distribution and intensity of light scattered by carbon dioxide near critical point, noting temperature dependence of isothermal compressibility and long range correlation length

16 p2422 A72-32945

A method of analysis for compressible viscoelastic solids.

18 p2736 A72-36936

COMPRESSIBILITY EFFECTS

Spiral grooves gas bearing theory, taking into account sliding and gas compressibility effects on load carrying capacity

02 p0236 A72-11585

Gas flow fluctuations near stagnation point on hot wall, taking into account laminar boundary layer compressibility effects

04 p0462 A72-15178

Supersonic turbulent boundary layer interaction with compression corner, noting static pressure distributions, flow visualization and schlieren photographs

05 p0610 A72-16976

Compressibility and total enthalpy difference effects on laminar free shear layer from numerical integration of equations of motion

05 p0653 A72-17011

Solar wind stream-stream interactions, studying time profiles, velocity variations, corotating spiral, increased pressure due to radial compression and zonal flow directions

06 p0872 A72-17443

Strength analysis of thin elastoplastic shell with allowance for compressibility, relating loads and moments to deformation of middle surface

08 p1246 A72-21712

Flying machine using reaction forces on body moving in compressible fluids within piston device equivalent to air pressure pump

08 p1108 A72-21798

Compressibility effects on straight through labyrinth seal performance in regenerative turbomachine

08 p1178 A72-21935

Fluid compressibility effect on nonstationary laminar flow within infinite cylindrical pipe

11 p1618 A72-26502

Integral equation for calculation of unsteady aerodynamic forces on helicopter lifting rotor blades, taking into account air compressibility
[ONERA, TP NO. 1081]

13 p1895 A72-29671

Nearly incompressible elastic solid compressibility effects theory, applying to annular wedge straightening, stretching and shearing and cylindrical tube telescopic shear problems

15 p2330 A72-32477

Finite bending of a compressible anisotropic rectangular block into a hyperbolic shell.

17 p2634 A72-35438

Elastic stability theory of compressible and incompressible composite media

19 p2871 A72-37530

Hysteresis curve equation for calculation of elastoplastic deformations caused by forced vibrations, taking into account medium compressibility and inertial forces

21 p3123 A72-41359

Characteristics of gas flows in diffusers at transonic velocities

21 p2994 A72-41698

Incompressible free shear layers instability, considering Reynolds number, velocity profile, disturbances and compressibility effects

22 p3167 A72-42579

Two-dimensional model for thermal compression.

22 p3136 A72-42868

Laser compression of matter to super-high densities - Thermonuclear /CTR/ applications.

23 p3294 A72-43262

Influence of steric effects and compressibility on nonlinear response to laser pulses and the diameters of self-trapped filaments.

23 p3296 A72-43873

COMPRESSIBLE BOUNDARY LAYER

Unsteady compressible free convection near infinite vertical flat plate with temperature and velocity variations in boundary layer

01 p0146 A72-11392

Compressible boundary layer flow problems, using weighted residuals method with exponentials in velocity and enthalpy approximations

02 p0204 A72-12258

Compressible turbulent boundary layer equations for flow on B wall of MHD accelerator, including electron thermal nonequilibrium and finite rate ionization

03 p0397 A72-13923

Generalized transformation of plane compressible and axisymmetric equation for self similar solutions of dissipative boundary layer for bodies with variable surface

04 p0510 A72-14468

Computerized calculations of turbulent shear layers with compressibility, heat transfer, three dimensionality or unsteady flow, using differential equation [ASME PAPER 71-WA/FE-8]

05 p0646 A72-15934

Integral computation for nonequilibrium compressible turbulent boundary layers using moment, momentum and skin friction equations
[ASME PAPER 71-WA/APM-12]

05 p0647 A72-15968

Inviscid variable density core flow in thin compressible boundary layer near stagnation point of smooth blunt body

05 p0601 A72-16216

Compressible turbulent boundary layer properties on porous cone at Mach 8, examining Crocco theory for flows with mass addition

05 p0602 A72-16536

Velocity profile shapes computation in supersonic compressible turbulent boundary layers with adverse pressure gradients, discussing data and theory discrepancy, curvature, and three dimensional effects

05 p0649 A72-16544

Steady two dimensional laminar compressible boundary layer of reacting gas mixture with surface vaporization and fuel injection, using integral method

07 p0967 A72-19129

Two dimensional compressible boundary layer turbulent velocity profile on adiabatic and isothermally cooled walls with zero pressure gradient

07 p0970 A72-20080

Compressible boundary layer flow past swept wavy wall with heat transfer and ablation, measuring pressure and temperature disturbances

07 p1101 A72-20247

Accuracy tests of Wang method for calculating three dimensional laminar compressible boundary layer flow equations

08 p1150 A72-21625

Compressible boundary layer stability at subsonic speeds, using orthogonalization calculation method

09 p1293 A72-22409

Mach number distribution along critical streamline in compressed layer in front of cylinder in supersonic flow

10 p1415 A72-23752

Rectilinear impulsive motion of compressible boundary layer on infinite plate, deriving integration method for differential equations of motion under energy dissipation neglect

10 p1465 A72-24203

Wind tunnel investigation of adiabatic compressible turbulent boundary layer in adverse and favorable pressure gradients at supersonic speed

10 p1468 A72-24421

Compressible turbulent boundary layer with arbitrary pressure gradients on solid or permeable surfaces, using extended mixing length theory

11 p1616 A72-25917

Dynamic and thermal laminar compressible boundary layers on flat plate, noting interaction of two quasi-steady flows
[ONERA, TP NO. 1068]

12 p1797 A72-27167

Energy supply calculation for two dimensional steady laminar compressible boundary layer flows with hypersonic hydrogen-air combustion

13 p2334 A72-31465

Energy equation for solution compressible laminar boundary layer generalized with orthogonal curvilinear coordinates

15 p2218 A72-32146

Numerical check on boundary layer equations asymptotic expansion solutions for Falkner-Skan reverse flow and unit Prandtl number compressible boundary layer with blowing

15 p2219 A72-32589

Sharp flat plate laminar, transitional and turbulent skin friction via finite difference integration of compressible boundary layer equations

15 p2180 A72-32596

Subsonic and supersonic steady two dimensional compressible turbulent boundary layer flow past wavy wall, presenting wall pressure and temperature distributions

16 p2341 A72-32828

Three dimensional compressible turbulent boundary layer growth prediction, deriving entrainment equation

tions from two dimensional incompressible flow relations
16 p2375 A72-32835

Small cross flow integral method for growth prediction of three dimensional compressible turbulent boundary layers on adiabatic walls
[AIAA PAPER 72-697] 16 p2345 A72-34046

Compressible boundary layer with normal pressure gradients, investigating quasi-similar, nonlinear in-tegro-differential equations properties at wall and sharp and blunt leading edges
[AIAA PAPER 72-696] 16 p2345 A72-34048

Transformations of the compressible boundary layer equations.
17 p2538 A72-34341

On the structure of hypersonic turbulent boundary layers.
17 p2540 A72-35188

On the extension of particular solutions of the energy equation of compressible turbulent boundary layers.
17 p2544 A72-35954

Structure of turbulent underexpanded jets expelled into a submerged space and into a slipstream
18 p2642 A72-36884

A study of the asymptotic behaviour of the external fringes of compressible, laminar boundary layers of a dissociating gas.
18 p2683 A72-36937

Solution of the equations of the compressible boundary layer (laminar, transition, turbulent/ by an implicit finite difference technique.
19 p2785 A72-37521

Hypersonic unsteady compressible boundary layer dependence on Prandtl number.
19 p2787 A72-38429

Compressible boundary-layer equations solved by the method of parametric differentiation.
20 p2914 A72-39614

The prediction of compressible turbulent boundary-layer flows with mass addition.
[ASME PAPER 72-HT-58] 20 p2914 A72-39658

Stewartson transformation correlating three dimensional compressible boundary layer growth on impulsive moving body, assuming small cross flow
21 p3047 A72-41782

Influence of wall temperature on heat transfer in a compressible three-dimensional turbulent boundary layer
23 p3248 A72-43694

A simple theory for the two-dimensional compressible turbulent boundary layer.
[ASME PAPER 72-FE-15] 23 p3280 A72-44062

COMPRESSIBLE FLOW

NT TRANSONIC FLOW

Equivalence laws and approximate equations for incompressible and compressible viscous flows in pipes with variable cross sections
01 p0051 A72-11256

Book on pressure probe methods for wind speed and direction covering incompressible and subsonic compressible flow pressures, temperature, etc
01 p0072 A72-11273

Compressible gas subsonic or transonic flow in front of obstacle, determining stagnation pressure with thermal relaxation time by numerical and wind tunnel methods
02 p0151 A72-12097

Compressible viscous flow between concentric fixed and rotating disks, comparing analog computer calculation with experiment on radial flow
02 p0203 A72-12099

Force and pressure distribution measurements on delta wing-body combination in compressible flow, investigating Reynolds number effect
[DGLR PAPER 71-118] 02 p0152 A72-12707

Two and three dimensional turbulent boundary layer development in incompressible and compressible flows, obtaining boundary layer equations similarity solutions via mixing length model
[DGLR PAPER 71-066] 02 p0206 A72-12719

High subsonic velocity aerodynamics boundary problem, transforming compressible flow to incompressible
03 p0307 A72-13238

Local skin friction evaluation in compressible flow, using incompressible Clauser charts and sublayer methods for adiabatic and nonadiabatic situations
03 p0341 A72-13614

Pressure distribution and compressible gas critical flow rate in constant cross section circular pipe with impermeable adiabatic wall from Frossel equations
04 p0511 A72-14640

Convergent conical nozzle shape effect on propulsive performance and compressible flow field internal characteristics
[ASME PAPER 71-WA/FE-3] 05 p0647 A72-15927

Navier-Stokes equations asymptotic solution for compressible weightless conducting fluid flow in plane channel with intense blowing from walls
05 p0648 A72-16219

High speed boundary layer flow three dimensional disturbances interaction with thermal and ablative response in adjacent surface material, considering laminar and turbulent compressible flows
[AIAA PAPER 72-93] 05 p0748 A72-16811

Hot-wire anemometers signals resolution into velocity-temperature fluctuations correlations in compressible flow with shear turbulence wakes
[AIAA PAPER 72-117] 05 p0664 A72-16822

Subsonic and transonic compressible potential flow over nonlifting hovering helicopter rotor blades, calculating flow field by three-dimensional nonlinear relaxation scheme
[AIAA PAPER 72-39] 05 p0607 A72-16901

Internal compressible spatially nonuniform ducted flow performance, defining diffuser efficiency, loss coefficient and static pressure rise coefficient
[AIAA PAPER 72-85] 05 p0652 A72-16960

Homogeneous compressible turbulence field with large amplitude and density fluctuations generated in subsonic wind tunnel by rapid mixing of hot and cold air streams
[AIAA PAPER 72-119] 05 p0652 A72-16980

Statistical equations for turbulent fluctuations of energy, concentration and rotation in compressible flows
06 p0797 A72-17557

Similitude solutions for turbulent boundary layers in compressible flow with pressure gradient and heat transfer at wall, obtaining velocity and enthalpy profiles
06 p0798 A72-17845

Compressible axisymmetric coaxial jets turbulent mixing in constant area duct, considering axial and radial pressure distributions
07 p0967 A72-19094

Surface friction coefficient dependence on Mach number and velocity gradients in adiabatic compressible laminar gas flow
08 p1107 A72-21311

Mixing length model for turbulent boundary layer in incompressible flow with fluid injection at wall, extending solution to compressible case
[ONERA, TP NO. 986] 09 p1294 A72-22818

German monograph on gas dynamic properties of turbulent subsonic compressible flow of ideal gas at insulator walls in MHD generator
10 p1517 A72-23771

Compressible flow measurement and loss prediction in radial vaneless diffuser in centrifugal compressor, using hot-wire anemometers
10 p1416 A72-23861

Laminar and turbulent compressible wall jet characteristics, obtaining density variation as function of velocity and Mach number at exit
11 p1618 A72-26593

Possible regimes and solutions for adiabatic one dimensional compressible gas flow in convergent and divergent ducts with friction
12 p1797 A72-27348

Heat transfer to surfaces in turbulent compressible gas flows with various boundary conditions
13 p2063 A72-28627

Two dimensional laminar compressible flow of electrically conducting gas at thermodynamic equilibrium and perpendicular to magnetic field lines
13 p2013 A72-29362

Tangential MHD discontinuity stability for ideally conducting compressible fluid in magnetic and gravitational fields
13 p2020 A72-30068

Velocity calculation from pitot tube pressure measurements in compressible two phase flow, taking into account droplet momentum loss
14 p2104 A72-30252

Laminar mixing zone calculated for two homogeneous compressible gas flows with pressure gradient, noting coincidence of velocity distribution for identical gas dynamic parameters
14 p2070 A72-31009

Heat transfer and longitudinal temperature distribution at Hartmann-Sprenger tube inlet calculated approximately on basis of boundary layer data in steady compressible flow
15 p2217 A72-31685

Isentropic perfect gas steady compressible flow finite element analysis through nonlinear equations linearization based on perturbation theory
15 p2217 A72-31719

Perfect gas unsteady compressible homentropic flow with zero spatial pressure gradient, deriving characteristic equations
15 p2218 A72-32324

Time dependent finite difference /fluid-in-cell/ method for supersonic aerodynamic problems concerning inviscid compressible flow with contact surface and shock discontinuities
16 p2342 A72-32884

Perturbation theory for equations of motion of electrically and thermally conducting viscous compressible flow in homogeneous magnetic field, calculating fluctuation modes
16 p2435 A72-33008

Wind tunnel ventilation duct aerodynamic stability analysis for incompressible and slightly compressible flow
16 p2378 A72-33439

Solution of the two-dimensional, unsteady, compressible Navier-Stokes equations using a second-order accurate numerical scheme.
17 p2538 A72-34646

Analysis and testing of compressible flow ejectors with variable area mixing tubes.
[ASME PAPER 72-FE-14] 17 p2485 A72-34968

Compressible swirling flow through convergent-divergent nozzles.
17 p2485 A72-34999

Downstream effects of discontinuous injection of foreign gases in inert laminar boundary layer flows.
17 p2542 A72-35632

Iterative calculation of a three-dimensional boundary layer and comparison with experiment
17 p2543 A72-35748

Expansion solution for subsonic compressible flow.
18 p2679 A72-36124

Compressible laminar wake behind a thin flat plate.
19 p2747 A72-38798

Heat transfer at reattachment of a compressible flow over a backward facing step with a suction slot.
20 p2885 A72-39626

Research planning in steady compressible flow aerodynamics, discussing projects on annular wings, shockless transonic airfoils and Smith panel method for three dimensional flow problems
[ICAS PAPER 72-01] 21 p2990 A72-41126

Axial velocity distribution and streamline boundary selection to derive two dimensional infinite duct shapes for inviscid irrotational compressible flows
[ICAS PAPER 72-08] 21 p2990 A72-41133

Determination of the parameters of a fluid in the neighborhood of the junction of wavefronts by the Legras method
22 p3165 A72-41927

Flow equations for axisymmetric compressible conical flow in Busemann nozzle, noting numerical method for integral lines construction for given Mach number
22 p3134 A72-42288

Performance and flow properties change through a rocket turbine by presence of solid particles.
24 p3361 A72-45206

Axisymmetric nozzles shape for thrust optimization, comparing maximum thrust circular arc and conical nozzles performances
24 p3365 A72-45784

COMPRESSIBLE FLUIDS

McNamee-Gibson displacement potential functions generalization to problems for compressible pore fluid in theory of consolidation or thermoelasticity
03 p0455 A72-14389

Book on fluid dynamics covering theories of perfect, viscous and compressible fluids, infinite and finite span wings, boundary layer flow, etc
04 p0462 A72-15357

Radial pressure distribution in laminar flow of compressible fluid between two coaxial disks from analog computer study
04 p0514 A72-15702

Finite element algorithm derived for partial differential equation system governing laminar three dimensional boundary layer flow of multicomponent compressible fluid
[AIAA PAPER 72-108] 05 p0604 A72-16817

Sonic boom signature by bicharacteristic method, correcting zeroth order /free stream/ characteristics to obtain solution to compressible fluid exact equations of motion
[AIAA PAPER 72-195] 05 p0652 A72-16907

Two dimensional flow of gas jet around dihedral obstacle, investigating screen proximity and fluid compressibility effects
06 p0799 A72-17912

Book on compressible fluid dynamics covering steady flow, shock waves and self similar motions
07 p0967 A72-19448

Normal axial impact of thin liquid filled elastic cylindrical shell with rigid bottom on compressible fluid half space surface
09 p1350 A72-22207

Book on ideal and real compressible fluid dynamics covering supersonic flow past airfoils and shock wave interaction with laminar boundary layer
09 p1295 A72-23045

Electromagnetic and plasma wave reflection at interface between moving dielectric medium and compressible plasma
09 p1364 A72-23243

Geometrical characterization of steady nondissipative compressible fluid flow described by first order partial differential equations system
09 p1295 A72-23366

Oblique magnetic fields effect on compressible conductive fluids motion in presence of thin foil, noting lift values in hyperlipitic and double hyperbolic cases
09 p1365 A72-23560

Steady compressible fluid flow and plane shock wave propagation in pipe bends, discussing parameter effects and boundary conditions
10 p1464 A72-23878

Velocity and magnetic field expressed by six scalar potentials from MHD equations system, noting compressible fluids flow
10 p1520 A72-24219

- Nonuniform vortex flow of compressible gas past cascade of plates, noting monochromatic pressure waves at harmonics of plate vibration frequency 10 p1418 A72-24538
- Linear impulsive spin down from rigid body rotational equilibrium of radiation penetrated opaque compressible fluid in circular cylinder 11 p1680 A72-25555
- Fluid compressibility effect on nonstationary laminar flow within infinite cylindrical pipe 11 p1618 A72-26502
- Hollow elastic momentless spherical shell translatory displacements in compressible fluid under nonstationary spherical wave 12 p1880 A72-27234
- Compressible anisotropic magnetoplasma filled cylindrical waveguide excitation by electric dipole, plotting electric field patterns as function of electron temperature and density 12 p1782 A72-27489
- Obliquely incident electromagnetic waves reflection and transmission by moving compressible plasma slab, applying field and wave-four vectors Lorentz transformations to wave equations 13 p2010 A72-28543
- Nonlinear transverse forced resonant oscillations in isotropic elastic body and ideally conducting compressible fluid flowing in external magnetic field 13 p2010 A72-28719
- High velocity water jet generation dynamics, deriving equations of motion for mathematical model with nozzle profiles and liquid compressibility approximations 14 p2093 A72-30180
- Steady flow of compressible heat conducting fluid, discussing effect of small transfer coefficient on isentropic sonic singularity in Laval nozzle 14 p2171 A72-30713
- Linear theory based analysis of compressible electroconductive fluid flow satisfying perfect gas equation in presence of thin profiles within quasi-aligned magnetic field 14 p2095 A72-30824
- Hodographic equations solution containing critical point for compressible fluid two dimensional flow, noting calculation of wing profiles and turbine engine cascades [ONERA, TP NO. 1048] 14 p2095 A72-30841
- Convective and radiative heat transfer in compressible gas boundary layer 16 p2343 A72-32995
- Radiation from a magnetic line source covered with an anisotropic warm plasma slab 17 p2587 A72-34386
- Effect of rotation on laminar compressible fluid flow in a vertical cylinder 17 p2539 A72-34972
- Unsteady motion of a compressible viscous fluid in a spherical layer 18 p2682 A72-36882
- Low-frequency wavelike process of deformation in a semifinite cylindrical shell immersed in a compressible fluid 19 p2877 A72-38157
- Conjugate-flow theory for heterogeneous compressible fluids, with application to non-uniform suspensions of gas bubbles in liquids 21 p3044 A72-40120
- Nonlinear transverse forced resonant oscillations in isotropic elastic body and ideally conducting compressible fluid flowing in external magnetic field 22 p3210 A72-42096
- Flow stability of ideal compressible and incompressible fluids, solving Navier-Stokes equation for rotating liquid with free boundary in gravitational field 22 p3165 A72-42151
- Calculation of two-dimensional flows in hydrodynamics and the heat-transfer of a viscous fluid 22 p3166 A72-42287
- Hydrodynamic fluid pressure on a shell during hydraulic impact 23 p3280 A72-43788
- Radiation properties of the semi-infinite vortex sheet 24 p3359 A72-44918
- Numerical analysis of natural frequency spectrum of plastic plate free vibrations in compressible inviscid fluid 24 p3459 A72-45003
- Jet pumps for compressible fluids at supersonic velocities 24 p3393 A72-45362
- COMPRESSING**
- Crococ-Lee theory extension to flow behavior prediction for two dimensional supersonic turbulent near wake behind bluff body during recompression 16 p2343 A72-33402
- Eigenfunction technique development to incorporate stress singularities at circumference of end planes into problem of solid cylinder compression between rough rigid stamps 17 p2633 A72-35403
- Study of reliability of Al-Au thermocompressions by measurement of resistance 18 p2668 A72-37105

- COMPRESSION BUCKLING**
- U BUCKLING**
- COMPRESSION LOADS**
- NT AXIAL COMPRESSION LOADS
- NT IMPACT LOADS
- Temperature and compressive loading cycles effects on high performance multilayer insulation materials and composites, discussing application to space shuttle orbiter 01 p0092 A72-10779
- Initial crack effect on slender column compression load carrying capacity, deflection and stress intensity factor 01 p0140 A72-10989
- Solid rectangular beams under bending tests, obtaining tension-compression stress-strain curves 01 p0141 A72-11002
- Equation of state for porous metals at high temperatures under strong shock compression, considering phase transitions 02 p0258 A72-11469
- Circular cylindrical shells buckling under edge compression at various boundary conditions, obtaining critical loads and wave number from Donnell equations 02 p0292 A72-12107
- Infinitely long orthotropic cylindrical shell partially filled with elastic media under compression load, determining local stability 02 p0299 A72-12688
- Substructure variations and crystal lattice periods dependence on compression stress in beryllium single crystals during plastic deformation due to base slip 03 p0376 A72-14018
- Stress concentration around circular hole in infinite semibrittle plate under omnidirectional tension at infinity or pressure at hole contour 03 p0452 A72-14127
- Stress-strain increment relations for materials with different compression and tension resistance under orthogonal loading 04 p0586 A72-15007
- Plates in uniaxial compression with various support conditions at unloaded boundaries, predicting behavior after buckling 04 p0591 A72-15288
- Temperature and compression rate effects on metal powder packing density, obtaining activation energy from Boltzmann equation 05 p0665 A72-16089
- Load or compression eccentricity effect on buckling and postbuckling behavior of flat plates, presenting stress distribution curves 05 p0737 A72-16116
- Equilibrium conditions of closed elastic spherical shell under uniform nearly critical compression loads, determining shell deformation in Hilbert spaces 05 p0739 A72-16587
- Bending tests of beam with different creep characteristics in tension and compression 06 p0899 A72-18639
- X ray study of structural changes in Ni single crystals during recrystallization process after uniaxial deformation under compression loads with high loading rates 06 p0834 A72-18744
- Elastic stability of laminated circular plate with rectangular anisotropy under in-plane compression forces along edge 07 p1090 A72-19693
- Critical stability and supercritical equilibrium behavior of compressed viscoelastic rod 07 p1091 A72-19761
- Stability loss of circular annular plate under compression, determining critical loads with inner edge free and outer edge hinged or clamped 07 p1092 A72-19900
- Elastic rods and rings stability under compression beyond elasticity limit, determining equilibrium branching characteristics near bifurcation point 07 p1095 A72-20314
- Rational parameters and reinforcement of stiffened laminar plates with instability tendencies under compression loads 08 p1243 A72-21236
- Critical values of compressive loads applied to mid-section of cylindrical shell weakened by circular holes 08 p1244 A72-21241
- Critical compressive stresses leading to instability of layer fastened to elastic half space 08 p1244 A72-21368
- Anisotropy effect on glass fiber reinforced plastics cyclic deformability and heating kinetics under cyclic tension compression loads 08 p1191 A72-21501
- Uniaxially stressed elastic/soft shells with fold formation during compressive strain, formulating equilibrium and boundary conditions for uniaxial region 08 p1247 A72-21812
- Axisymmetrically heated orthotropic multilayer cylindrical shell with shear sensitive couplings and elastic stiffener, investigating stability and critical force under compression 09 p1402 A72-22735

- Elastic and plastic buckling analysis of uniformly compressed rectangular plates, using Kantorovich method 09 p1408 A72-23556
- Piston exerting pressure on liquid filled cylinder, determining deformation state based on thin elastic orthotropic plate theory 10 p1556 A72-24266
- Random elastic modulus variability of building materials test pieces under compression and tensile loads 10 p1557 A72-24403
- Combined plasma and magnetic field cumulation due to heavy conducting liner implosion, noting compression parameters for plane and cylindrical bodies 10 p1523 A72-24723
- Stiffened panels initial buckling under longitudinal compression, presenting results obtained by numerical methods 10 p1558 A72-24843
- Flugge equations for circular cylindrical shells buckling under compression, considering Donnell theory limits, stress determination and boundary conditions 10 p1560 A72-25025
- Multilayer insulation apparent thermal conductivity measurement at low compressive loads, describing test calorimeter and experimental technique [AIAA PAPER 72-367] 11 p1670 A72-25392
- Longitudinal bending stability of hard polymer rods under compression load and creep 11 p1675 A72-26824
- Static stability of long cylindrical shells under external pressure, using Euler-Lagrange equations 12 p1880 A72-27228
- Stepwise compression loading effect on yield stress of carbon and alloy steels in cylindrical samples with end plane cylindrical notches filled with solid lubricant 12 p1831 A72-28237
- Analytical solution to difference stability equations, evaluating adequacy of difference scheme for circular cylindrical shell and rectangular hinged plate under compression 13 p2053 A72-28389
- Temperature effects on synthetic rubber sliding friction characteristics against smooth steel surfaces under compression loads in vacuum and air at 10-140 C 13 p1962 A72-28554
- Testing machine for synthetic plastic cylindrical specimens cyclic cophasal compression-torsion load tests, describing mechanical and hydraulic subsystems and testing techniques 13 p1938 A72-28559
- Optimal geometrical and physical properties of sandwich plates with rigid cores under compressive load, discussing critical stress and structural stability 15 p2322 A72-31359
- Real time focused image holographic interferometry for deformation recording in diffusively reflecting plate under compression 15 p2233 A72-31415
- Stress analysis of two coaxially conjugated elastic isotropic cylinders under compression loads in terms of Fourier-Bessel series 15 p2323 A72-31447
- Local buckling analysis for triangular-corrugated core sandwich panels in compression, noting buckling mode nodal line features 15 p2326 A72-31709
- Equilibrium equations and boundary conditions for elastic buckling of open cylindrical sandwich shell under compressive forces applied to freely supported edges 16 p2467 A72-33116
- Elastic buckling of simply supported sandwich panels with fiber reinforced laminated face plates and honeycomb cores subjected to uniform end loading 16 p2469 A72-33405
- Compressed initially bent Shanley column analyzed for geometric imperfection coupling and material behavior effects on critical time to creep collapse 16 p2474 A72-34131
- Plane-strain compression of rigid plastic material between flat platens, approximating frictional boundary conditions by entrapped viscous fluid lubricant 16 p2428 A72-34171
- Shear buckling of an elastically supported fiber 17 p2633 A72-35290
- Impression of pointed dies onto cross section circumference sections of semifinite cylindrical shell, solving shell theory equations without allowance for friction effects 19 p2872 A72-37557
- Equilibrium conditions of closed elastic spherical shell under uniform nearly critical compression loads, determining shell deformation in Hilbert spaces 19 p2872 A72-37558
- The plastic deformation behavior of Mo single crystals under compression 19 p2816 A72-37689
- Load capacity of tension-bent and compression-bent circular plates 19 p2877 A72-38161
- Buckling of circular cylindrical shells under compression. III - Solutions based on the Donnell type equations considering prebuckling edge rotations 19 p2878 A72-38299

Experimental creep buckling of circular cylindrical shell under uniform compression. 20 p2978 A72-38883

Large elastic deformations of an incompressible material heteroresistant to tensile and compressive strains 20 p2978 A72-39021

Experimental investigation of the stability of compressed heated three-layer plates beyond the proportional limit 20 p2981 A72-39920

Forced vibration solution and wind tunnel investigation of shallow cylindrical shells under moving pulsating pressure discontinuities, noting compression shock effects 21 p3122 A72-41352

Effect of inertial loading on the compression of powdered materials by a vibration process 21 p3061 A72-41369

Calculating the stability of centrally compressed thin-walled bars with various profiles 21 p3126 A72-41549

Nonlinear buckling of cylindrical shells. 22 p3236 A72-42607

Transport aircraft wing compression panel failure in bending test due to stringer interruptions, analyzing structural deficiency via column and beam bending theories 22 p3183 A72-42827

Fiber composite columns under compression. 23 p3344 A72-43494

Longitudinal compression of a three-layer plate with initial deflection and a physical nonlinearity of the middle layer /the filler/ 23 p3346 A72-43673

Strength and deformation characteristics of fibreglass under torsional and compressive shear loads, investigating temperature effects on elastic modulus 23 p3306 A72-43730

COMPRESSION TESTERS

U COMPRESSION TESTS

COMPRESSION TESTS

Constant stress and compression creep testing in vacuum conditions, describing simple spring loaded apparatus characteristics and performance 01 p0071 A72-11171

Low strength polymeric materials specimen geometry and lateral constraints effects on isothermal compressibility by compression tests [SESA PAPER 1935] 02 p0248 A72-11518

Al alloys compressed strips, determining anisotropy of toughness and crack sensitivity by tests 02 p0244 A72-12244

Uniform low temperature compression effect on accelerated aging of Duralumin specimens, noting Plateau due to Guinier-Preston zones 02 p0245 A72-12539

Stress concentration coefficients calculation at sharp cracks and notches for rods in tension, compression and combined bending and torsion 03 p0443 A72-13457

Unstable propagation and brittle fracture arrest in steels from double cantilever beam test under compression 05 p0677 A72-17107

Dynamic yielding of annealed and cold worked Fe-Ti alloy determined in shock compression tests 05 p0679 A72-17121

Stress-strain behavior of steel under elastic compression at 4.2 K, observing discontinuous twinning 07 p1020 A72-20413

Test procedures and apparatus for short and long term creep of polymer monofilaments under radial compression 08 p1194 A72-21758

Copper, zinc and aluminum mechanical properties comparison by cyclic and steady state compressive load tests, noting stress-strain curve relationship to strain rate 08 p1188 A72-21921

Al alloy and brass deformation compression tests inadequacy for friction determination and boundary agents, EP additives and hydrodynamic and solid lubricants evaluation 08 p1181 A72-22195

Plastic flow properties and stress measurement for metal working conditions with flat ring compression specimens and interfacial friction consideration 08 p1250 A72-22196

Compression creep in ordered binary and ternary ordered bcc Ni alloys investigated by transmission electron microscopy 11 p1667 A72-26937

Thin cylindrical shells prepared from fibreglass reinforced plastics under long term compression, investigating strain buildup nature during creep process 12 p1878 A72-27078

Uniaxial compressive stress apparatus for InSb investigation at low temperatures in large magnetic fields 13 p1959 A72-29753

Cyclic compressive fatigue cracking tests of prenotched fiber reinforced epoxy materials at low stress 16 p2414 A72-33319

Equipment for low cycle fatigue bending, torsion and tension-compression tests, considering design and performance 16 p2394 A72-33846

Prestrained and annealed elastic materials stress-strain relationship calculation in plastic range, compared with tensile and compression load tests results 16 p2472 A72-33948

A comparison between the tensile and compressive creep behaviour of an 11 per cent chromium steel. 19 p2814 A72-37222

Fatigue limits of cylindrical test pieces in rotative bending and in tension-compression, investigating strain gradient effect 19 p2875 A72-37788

Aluminum matrix composites fracture mechanism dependence on static loading conditions and reinforcing filament type, investigating failure modes in tension and compression tests 23 p3299 A72-43497

Characterization of four polymeric materials at strain rates from 0.0001 to 1000 per sec. 24 p3417 A72-44612

The effect of pre-strain on the yield behavior of vanadium. 24 p3413 A72-44721

Stress concentration coefficients calculation at sharp cracks and notches for engine parts in tension, compression and combined bending and torsion 24 p3458 A72-44932

COMPRESSION WAVES

Flames vibratory propagation appearance conditions at constant volume, considering expansion and compression waves amplitude 03 p0456 A72-13794

Stress concentration at circular holes in polyurethane plates under plane compression wave, obtaining interference fringes 03 p0451 A72-14121

Compression wave propagation from cylindrical cavity in weakly conducting magnetoelastic medium under unperturbed magnetic field 03 p0452 A72-14129

One-dimensional compression/expansion shock waves propagation in elastic nonheat conducting bodies, deriving differential equation for shock amplitude time rate of change 04 p0592 A72-15547

Suspended compression shock construction near supersonic point in plane nonuniform ideal gas flow by hodograph technique 05 p0600 A72-16213

Apollo 14 explosion seismic refraction data, showing lunar near surface regolith thickness and compressional wave velocity 09 p1390 A72-23495

Plane harmonic compression waves scattering by circular holes in thin elastic plate, calculating dynamic stresses concentration 10 p1554 A72-24179

Dynamic stress concentration around elliptical discontinuities in elastic medium, considering rigid and empty cavity scatterers for compression and vertically polarized shear incident waves [ASME PAPER 72-APM-D] 10 p1554 A72-24180

Unsteady laminar wall boundary layers formation within finite expansion or compression waves in tube with gas at rest 11 p1616 A72-25981

Magnetospheric equatorial compressional wave propagation to ground observed as transverse wave, noting plane of polarization 11 p1625 A72-26413

German monograph on wave expansion in gases with thermodynamic relaxation covering steady dispersed compression wave development in piston barrel for two component mixtures [DFVLR-SONDDR-184] 15 p2218 A72-31768

Effect of pore pressure on the velocity of compressional waves in low-porosity rocks. 18 p2685 A72-36031

Steady solutions of generalized Korteweg-de Vries equation for oscillatory solitary waves in dispersive media 21 p3089 A72-40197

COMPRESSIVE STRENGTH

Hat section stiffened compression panel of graphite/epoxy composite for space shuttle, discussing quality control procedures 01 p0139 A72-10736

Lime, cement, fly ash and sand combination airport pavement design and testing, discussing material structural and chemical properties, compressive strength, costs, etc 02 p0200 A72-12023

Hereditarily elastic body model with various tensile and compressive strengths, using elasticity theory with differing moduli 02 p0294 A72-12429

Heat treatable Al alloys tensile and compressive moduli of elasticities data from USAF programs, comparing to long-accepted typical values 03 p0378 A72-14175

Stress-strain increment relations for materials with different compression and tension resistance under orthogonal loading 04 p0586 A72-15007

Stress-strain tensor component relations for isotropic elastic bodies with different tension and compression resistance 04 p0586 A72-15008

Elasticity theory relations for material with tension- and compression-varying modulus of elasticity, representing elastic strain energy as quadratic form potential 04 p0586 A72-15009

Compressive strength of Cu-W fiber metal matrix composite as function of temperature, comparing to cermets 06 p0832 A72-18363

Compression strength theory for monodirectional reinforced homogeneous anisotropic and piecewise homogeneous composite materials, using microvolume stability loss failure mechanism 06 p0838 A72-18655

Residual stresses and geometrical imperfections effects on compressive strength of thin walled welded box columns 07 p1088 A72-19114

Crystalline ceramics compressive fracture strength and microhardness tests at room temperature, suggesting microplasticity role in failure mechanisms 09 p1334 A72-22388

Compressive strength of Ti alloy airframe skin stringer panels reinforced with B-Al composite by brazing [AIAA PAPER 72-359] 11 p1729 A72-25387

Failure modes effect on compressive strength of boron-epoxy composites tested on coupons, honeycomb sandwich columns and beams 11 p1671 A72-25466

Particulate fillers bulk effects on epoxy resin compositions flexural, compressive and tensile strengths and moduli 12 p1834 A72-28089

Compressive strength and stiffness improvement for crystalline thermoplastic polymers via solid glass sphere reinforcement 16 p2414 A72-33370

Strength of titania and aluminum silicate under combined stresses. 19 p2822 A72-37271

Tensile and compressive flow strength and work hardening behavior in maraging steels, attributing strength differential to nonlinear elastic interactions between interstitials and dislocations 20 p2939 A72-39306

Book - Metal matrix composites. 21 p3070 A72-41528

The effect of a thermal and ultrahigh vacuum environment on the strength of precompressed granular materials. 22 p3173 A72-42528

Investigation of the strength of construction materials for various principal-stress relations 23 p3349 A72-43955

Stability of an elastoplastic rod of varying resistance to tension and compression with allowance for the initial stresses 23 p3352 A72-44162

Compressive strength of Cu-W fiber metal matrix composite as function of temperature, comparing to cermets 24 p3416 A72-45750

COMPRESSOR BLADES

Metallographic and fractographic analyses of cracking in T53-L13 gas turbine engine compressor disks 01 p0085 A72-10816

Forged Inconel alloy 718 metal powder preforms for dense aircraft engine compressor rotor blades 02 p0233 A72-11441

Axial compressors lengthwise compaction and compression ratio increase per unit length by blade chords and clearances reduction and blades number proportional increase [DGLR PAPER 71-098] 02 p0271 A72-12740

Tip clearance effect on compressor blade aerodynamic characteristics, applying Bolyay analysis to low aspect ratio rectangular wing 02 p0153 A72-12825

Chaplygin compressibility law in calculation of flow characteristics around compressor blading of axial turbomachines 03 p0308 A72-13544

Periodic pressure fluctuations measurements on fixed blades of high power axial compressor, describing calibration and data acquisition methods [ONERA, TP NO. 967] 04 p0463 A72-15555

Axial flow multistage compressor design, discussing high speed flow measurements and Reynolds number and blade airfoil shape effect on aerodynamic performance 05 p0601 A72-16483

Stalled blade rows dynamic performance in terms of blade channel fluid inertia and surface boundary layer-caused time delay 05 p0602 A72-16487

- Flow visualization in supersonic axial compressor by short exposure schlieren photography of shock wave patterns in rotating annular cascade of compressor blades
[ONERA, TP NO. 1026] 05 p0708 A72-17192
- Milling, band grinding, final manual polishing and tumbler polishing effects on fatigue life and surface finish of steel compressor blades
06 p0824 A72-18651
- Subsonic unsteady aerodynamic pressures on blades of compressor wheel rotating freely in air stream
[ONERA, TP NO. 1077] 10 p1420 A72-24854
- Finite difference method application to axial flow compressors rotating stall nonlinear analysis, taking into account blade row characteristics
[ASME PAPER 72-GT-3] 11 p1568 A72-25606
- Jet flaps for high turning compressor cascades in incompressible axial flow, calculating blade pressure and jet slope distributions
[ASME PAPER 72-GT-16] 11 p1569 A72-25615
- Turbocompressor deceleration cascades blades surface roughness effects on boundary layer, noting pressure and velocity distributions
[ASME PAPER 72-GT-48] 11 p1570 A72-25640
- Radial inflow compressor feasibility, discussing blade loadings for various pressure ratios and efficiency of rotor and diffuser
[ASME PAPER 72-GT-52] 11 p1570 A72-25644
- Constraining U-shaped frames for blade edges protection during hydrojet shot blasting of compressor blades for gas turbine engines
11 p1642 A72-26819
- Gas turbine engine compressor blade and materials fatigue strength dependence on pressure under contact friction corrosion
12 p1831 A72-28244
- Compressor blade vibration indicator measurement by positioning one inductive sensor by rotor blades and another by toothed gear on rotor shaft
13 p1956 A72-28784
- Pressure measurement between compressor impeller blades during steady and transient operation, discussing system circuit diagram
13 p1957 A72-29139
- Influence of the angle of attack on the performance of high-deflection stator blades
17 p2484 A72-34889
- Flat beam linear vibration analysis from mode measurement and moire technique, applying to prototype turbine compressor blade
18 p2734 A72-36375
- Behavior of boundary layers on rough compressor blades
18 p2641 A72-36420
- Blade passage measurement with the aid of a graphite pin probe in the case of fluid flow engines
19 p2804 A72-38724
- Influence of viscosity on the characteristics of compressor bladings for supersonic flow conditions
20 p2963 A72-39912
- Erosion effects on gas turbine engine compressor blades due to dust ingestion, discussing means for alleviating performance and service life losses
[ICAS PAPER 72-02] 21 p3099 A72-41127
- Precision forged turbine and compressor blades
22 p3183 A72-42518
- In-flight and flight-line monitor system to detect foreign object damage in jet engines
22 p3179 A72-42690
- Failure and crack formation in gas turbine engine compressor disks under variable stresses from fatigue tests, considering safety factors
23 p3347 A72-43736
- Reduction of end losses in cascades of cambered blades
23 p3248 A72-44025
- Influence of revolutions on efficiency and characteristics of the rotating axial cascade of blades.
24 p3363 A72-45361
- COMPRESSOR EFFICIENCY**
- Axial compressors lengthwise compaction and compression ratio increase per unit length by blade chords and clearances reduction and blades number proportional increase
[DGLR PAPER 71-098] 02 p0271 A72-12740
- Supersonic axial flow shock-in-rotor type compressor performance tests, discussing factors responsible for low efficiency
05 p0601 A72-16481
- Turbojet engine compressor efficiency relationship to cascade characteristics diagram, using influence coefficients
07 p1054 A72-18995
- Radial inflow compressor feasibility, discussing blade loadings for various pressure ratios and efficiency of rotor and diffuser
[ASME PAPER 72-GT-52] 11 p1570 A72-25644
- German monograph - Computational and experimental investigations regarding the operational characteristics of a three-stage axial-flow compressor with high performance per stage
19 p2745 A72-37490
- Compressor exergetic efficiency calculation from gas exergy losses caused by pressure drop and cool-

ing, noting relations to isothermal, adiabatic and polytropic efficiencies
19 p2746 A72-37668

Optimal modes of operation of a centrifugal-compressor wheel with preswirling of the flow
24 p3364 A72-45622

COMPRESSOR ROTORS

Stroboscopic measurement of elastic untwisting angles of axial compressor rotor vanes under centrifugal and aerodynamic forces
01 p0143 A72-11371

Flow passage geometry optimization in compressor rotor design treated as boundary value problem with variational calculus solution
02 p0151 A72-12179

Supersonic axial flow shock-in-rotor type compressor performance tests, discussing factors responsible for low efficiency
05 p0601 A72-16481

Pressure sensor measurements of fluctuating aerodynamic forces on rotor blades related to compressor noise generation
[ASA PAPER H 6] 08 p1107 A72-21486

Flow measurement instrumentation for turbomachine rotors, noting telemetry type data transmission system with strain gauge pressure transducers for turbocompressor
[ASME PAPER 72-GT-55] 11 p1630 A72-25646

Noise generated by free flow turbulence incident on rotor or stator in axial flow fans and compressors, noting sound spectrum dependence
13 p0208 A72-29575

The bursting speed of a symmetrical conical disk with radial holes.
22 p3238 A72-42835

Analytical method for combining the interaction of inlet distortion and turbulence.
23 p3247 A72-43330

COMPRESSORS**NT CENTRIFUGAL COMPRESSORS****NT SUPERSONIC COMPRESSORS****NT TRANSONIC COMPRESSORS****NT TURBOCOMPRESSORS**

Coherent and incoherent structures of aerodynamic noise, analyzing compressor near field and hot jet IR emission source
[ONERA, TP NO. 983] 09 p1294 A72-22816

Aircraft fan and compressor noise generation mechanism, considering mass flow and lift forces fluctuations from rotor and stator airfoils
13 p0208 A72-29569

Compressor directivity determination at discrete frequencies by tone power separation from noise background, using Fourier analysis of sound pressure autocorrelation
13 p0208 A72-29572

Engine compressor face rake for flight test instrumentation F-14A/TF-30.
22 p3216 A72-42686

COMPTON EFFECT

Gas-Cerenkov detector for 10-100 MeV gamma rays based on conversion and Compton scattering in plastic scintillator
03 p0352 A72-13034

Gas heating by If radiation due to Compton scattering near quasars, Seyfert galaxies nuclei and pulsars
03 p0435 A72-13801

Air ionization, secondary electron emission and Compton currents at W-Be interfaces under Co 60 gamma radiation
03 p0403 A72-14083

Spontaneous and induced Compton scattering of high frequency waves by relativistic electrons in synchrotron sources
04 p0487 A72-14902

NGC 5128 X ray spectrum from sounding rocket and balloon observations, presenting inverse Compton models
04 p0568 A72-15372

Solar flare X-ray emission Compton backscattering from Fe lines examination
05 p0710 A72-16720

Synchro-Compton theory for variable compact components in extragalactic radio sources, suggesting stellar mass object collapse as energy source
08 p1233 A72-21181

Gamma ray spectrometer with antiCompton shield for OSO-7 spacecraft
08 p1167 A72-21515

Weak extragalactic X ray sources radio identification, suggesting production by inverse Compton losses of electrons from radio galaxies
09 p1377 A72-22988

Cosmic electrons energy spectrum between 1 and 25 GeV from balloon observations, noting Compton/synchrotron loss effects
[AD-745871] 09 p1377 A72-23001

X ray background radiation from discrete sources, considering inverse Compton mechanism in galaxies and intergalactic space and soft component origin
10 p1529 A72-23913

Induced Compton scattering and nonlinear electromagnetic wave propagation in laser beam focused plasma
10 p1522 A72-24605

Cygnus X-1 model with hard X rays from inverse Compton scattering of B star UV photons and IR synchrotron radiation from other component
10 p1530 A72-24944

Shock wave structure in radiation spectrum of photon-electron interaction via induced Compton effect
12 p1848 A72-27056

Galactic formation initiation mechanism with thermal instability in expanding universe, noting Compton scattering energy exchange ensuring gravitational instability dominance
13 p0209 A72-29086

High X ray luminosity associated with richest galaxy clusters, noting inverse Compton effect by relativistic electrons and bremsstrahlung from hot gas
13 p0240 A72-29412

Stimulated Compton scattering of laser radiation by electron plasma, determining electrons diffusion coefficient and velocity distribution function
13 p1972 A72-29987

X ray sources associated with galactic clusters resulting from relativistic electrons Compton scattering on microwave background radiation
17 p2599 A72-35072

Plasma electron velocity distributions determined from the polarization of free-free bremsstrahlung.
19 p2841 A72-38439

Linear and circular polarization of synchro-Compton radiation scattered by optically thin power law distribution of gyrating ultrarelativistic electrons
20 p2965 A72-39893

Non-thermal bremsstrahlung of fast electrons and flare of stars.
20 p2974 A72-39894

Compton scattering by thermal electrons in X-ray sources.
23 p3328 A72-43230

Shock wave structure in radiation spectrum of photon-electron interaction via induced Compton effect
24 p3431 A72-45709

COMPUTATION**NT ORBIT CALCULATION**

Optimal control computation for nonlinear hyperbolic partial differential system by gradient and quasi-linearization techniques, noting MHD, fluid flow and electromagnetic wave propagation
10 p1456 A72-24453

Computational technique for crack growth prediction in metal subjected to variable amplitude cyclic loading, taking into account yield zone ahead of crack tip
[ASME PAPER 71-MET-X] 11 p1735 A72-25876

Nonlinear control system optimal bang-bang controls computation, noting algorithm obtained by parameter optimization
11 p1577 A72-26666

Automatic switched Shuman filter for shock waves numerical computation, noting third and fourth order accurate finite difference schemes
11 p1619 A72-26668

COMPUTER COMPONENTS

Reliability program for SAAB 37 Viggen airborne computer, discussing prototype and components operating tests and failure rates
10 p1443 A72-23984

Medium scale integration /MSI/ modules for arithmetic section in small, medium and process computers, emphasizing carry-lookahead procedure
13 p1926 A72-30053

Cellular-array arithmetic unit with multiplication and division.
17 p2519 A72-34297

Storage tube figure display apparatus
21 p3034 A72-41251

Multiprogrammed virtual memory digital computer systems analysis and design, discussing component characteristics, operating system structure and mathematical description techniques
23 p3267 A72-43987

COMPUTER DESIGN

Signal flow graph theory based computer diagnosis using blocking gate approach, constructing algorithm for gates optimal locations determination for maximum faults distinguishability
02 p0184 A72-11479

STAR self testing and repairing fault tolerant digital computer for outerplanet exploration spacecraft, discussing architecture, reliability analysis, software and peripheral system automatic maintenance
02 p0184 A72-11482

Separate and nonseparate arithmetic error detecting and correcting codes for digital computer design, considering cost and effectiveness tradeoffs
02 p0184 A72-11483

Soviet progress and bibliography on fault tolerant digital computers design, emphasizing redundancy application to achieve high reliability
02 p0184 A72-11484

Ultrareliable fault-tolerant digital computer design with protective standby replacement and hybrid redundancy, presenting mathematical models for system reliability evaluation
02 p0185 A72-11487

- Three-failure-tolerant digital computer system design using adaptive majority voting in hardware and software for real time control application
02 p0185 A72-11488
- Distributed fault-tolerant aerospace digital computer design with duplicated central multiprocessor, triplicated memory and conventional redundancy local processors for error detection and correction
02 p0185 A72-11489
- Stellar attitude reference and navigation associative processor with high computational speed for radar approach control in ATC
02 p0256 A72-12033
- Microelectronic computer system with image data cross correlation generation for real time video pattern abstraction, discussing design and operating characteristics
03 p0329 A72-14178
- Planar coax micropackaging of minicomputers for aircraft navigation and military systems, noting environmental tests
05 p0632 A72-15772
- Digital system automated design and analysis developments covering interactive graphic computer aided design, gate level simulation, synthesis, partitioning, interconnection and fault test generation
06 p0778 A72-17471
- Interactive computerized design and programs for computer logic design block assignment to modules, comparing performance with manual solutions
06 p0778 A72-17472
- Minicomputers evolution, considering price reduction, performance improvement, operation simplification, and applications for data collection and transmission
06 p0780 A72-18179
- STARAN IV-X associative array processor for automation in ATC environment, considering air tracking, conflict prediction and resolution functions
10 p1442 A72-23818
- Fault tolerant redundancy for manned spacecraft computers considered as long term desirable solution from cost analysis
10 p1443 A72-23819
- Computer reliability in terms of design criteria to minimize faults incidence, discussing failures detection and correction, fault diagnosis and system maintenance
10 p1444 A72-23985
- Large scale integrated circuits for digital differential analyzers, giving operational specifications for shift registers, adders and integrators
10 p1448 A72-24276
- Homogeneous computing media, examining microelectronic fabrication, interconnection and control problems for MOSFET, bipolar transistors and IC structures
10 p1448 A72-24277
- Rapid data input system for Minsk 22 digital computers using photographic film read by photoelectric scanning system
10 p1445 A72-24495
- Reliable, economical and easily operated read-only magnetic core storage devices for control computers, discussing design features
10 p1445 A72-24639
- Russian papers on cybernetic systems accuracy and reliability covering error correction schemes, statistical analysis and computer design
11 p1599 A72-25426
- CAMAC modular digital data handling system for communication with computer, discussing compatibility and data acquisition in astronomy application
11 p1600 A72-25692
- Hale observatories computer system design for telescope control and data handling, using solid state techniques
11 p1601 A72-25696
- Digital correlators and correlometers operational and design characteristics
11 p1602 A72-26444
- Digital correlator systems design for nonstationary signals, presenting circuit diagrams for multichannel centering system and memory operation
11 p1602 A72-26445
- Design and production related cost reduction factors in universal digital computers fabrication
11 p1603 A72-26825
- Aerospace guidance multiprocessor with memory units attached to time-multiplexed data bus, predicting performance in terms of queueing theory, Markov process and simulation
12 p1786 A72-27433
- Book on coherent optical computers covering lens design, power sources, computation mathematics, modulation, detection, digital techniques and applications
15 p2203 A72-31499
- Parallel digital computer application to radar tracking data processing, discussing system design for efficiency maximization and performance, desensitization in traffic level fluctuation
15 p2203 A72-31781
- Array processor design for massive computation, discussing special purpose satellite computer for communication with main memory through multiple module access units
16 p2366 A72-33242
- Univac 1616 computer design featuring uses of 16-bit word technology, medium and large scale integration, and transistor-transistor logic
16 p2366 A72-33243
- Digital attitude and heading reference system computer for aircraft heading control, discussing design and performance features
16 p2367 A72-33244
- Univac 1832 multiprocessor avionics computer for airborne ASW, discussing input/output controllers and interfaces and IC design features
16 p2367 A72-33245
- Performance characteristics and design options for software controlled I/O processor for aerospace computer applications with high speed real time responses
17 p2521 A72-34702
- Process computer system design, discussing structural units, data flow coordination with storage, input/output channels and periphery coupling problems
17 p2523 A72-35443
- The SKC-2000 advanced aerospace computer.
17 p2523 A72-35578
- Advantages of MOS/LSI computers in avionics systems.
17 p2523 A72-35579
- High performance 16-bit computer organization.
17 p2523 A72-35580
- Modular avionics computer design concept to permit tailoring for diverse applications via microprogramming
17 p2524 A72-35581
- Techniques for generating highly reliable redundant systems.
18 p2663 A72-36309
- The AEG 60-50 process computer in special research field 55 at the Rhein-Westphalian Technische Hochschule at Aachen
18 p2664 A72-36680
- Computer adapted for Boolean functions analysis and synthesis, describing structure and method of design
18 p2664 A72-36792
- Error correction in redundant logic circuits without application of majority elements
19 p2769 A72-37758
- Future trends of airborne computers.
20 p2905 A72-39109
- Digital computer hierarchical structure based on tree model using request/service resources as nodes, examining parallel multiple-stream organizations effectiveness
20 p2906 A72-39735
- The possibility of constructing an algorithmically universal hybrid computer
21 p3024 A72-40177
- Microminiaturization, microprogramming, multiprocessing, and processing and memory module design technology of aerospace computers in different size ranges
21 p3025 A72-41113
- Digital filter realizations using a special-purpose stored-program computer.
23 p3267 A72-43815
- Multiprogrammed virtual memory digital computer systems analysis and design, discussing component characteristics, operating system structure and mathematical description techniques
23 p3267 A72-43987
- Innovative architecture; Annual International Conference, 6th, San Francisco, Calif., September 12-14, 1972, Digest of papers.
24 p3383 A72-45665
- Parallel Element Processing Ensemble /PEPE/ digital computer for real time radar data processing and control, discussing system design and applications
24 p3383 A72-45666
- Fault-tolerance experiments with the JPL STAR computer.
24 p3383 A72-45671
- A prognosis on fault-tolerant digital control systems.
24 p3383 A72-45672
- Reliability of modular computer systems with varying configuration and load requirements.
24 p3383 A72-45673
- COMPUTER GRAPHICS**
Pattern recognition by computerized local processing of binary matrix representations
01 p0018 A72-10476
- Symbol generation with black-and-white or color display devices and time shared computer for man-machine communication
01 p0034 A72-10484
- Diffraction theory of microwave holography, presenting computer aided imaging approach for alleviating optically reconstructed image distortion
01 p0068 A72-10707
- Operator interactive computer controlled electro-optical system for photographic image enhancement prior to target or pattern identification
01 p0070 A72-10869
- Computer controlled scintiscanning for pulmonary blood flow distribution, discussing real time data monitoring, contour plots and three dimensional and wall reflection maps
01 p0020 A72-11038
- Remote sensor data analysis using color TV display system and interactive graphics equipment on-line to IBM 360/44 computer
02 p0226 A72-11838
- Automatic device using tetragonal conducting film sheets to feed graphic information into computer
02 p0187 A72-12279
- Computer-aided interactive graphic displays for ATC, discussing subsystems, data processing flow and operational capabilities
02 p0257 A72-12420
- Aircraft design interactive computer graphics technique, using human decision input response to computer output information
02 p0300 A72-12733
- Automatized graphic information input into computer, using electric potential distribution introduced into conducting underlay sheet by current carrying drawing pen
03 p0326 A72-13093
- Storage oscilloscope interface for small computers, describing graphic display characteristics and line cursor and character generators
03 p0329 A72-14177
- Electromagnetic wave propagation in rectangular waveguide with periodic ferrite structure, presenting computer graphics for stop bandwidth vs magnetic field strength
05 p0627 A72-16342
- Digital system automated design and analysis developments covering interactive graphic computer aided design, gate level simulation, synthesis, partitioning, interconnection and fault test generation
06 p0778 A72-17471
- Interactive computer graphics design aids to IC mask layouts, discussing hardware and software techniques including IMP program
06 p0778 A72-17473
- Time shared electronically patched hybrid computer for design automation, discussing remote terminal graphics capabilities and simulation language compiler
06 p0778 A72-17476
- Computer graphics techniques, discussing hard and soft copy outputs, animation, man machine interactions and physical and biological applications
06 p0779 A72-17635
- Computer aided design in electronics, discussing interactive computing with time sharing teletype keyboards or CRT graphics and applications in IC, network analysis and optimization
06 p0780 A72-18236
- AS-11A stereoplotter computerized adaptation to stereo-modeling of SLAR terrain mapping
06 p0818 A72-18330
- Sounding rocket radio tracking systems with real time trajectory plotting, developing computer program for exoatmospheric trajectory determination
07 p0939 A72-19089
- Ventricular function determination by computer graphic techniques for increasing speed, accuracy, reliability and scope of angiocardigraphic analyses determining human heart dimensions
07 p0928 A72-19308
- Computer graphics system simulation of saccadic eye movement made for time optimal control behavior study, incorporating eye muscle characteristics
07 p0928 A72-19309
- Hybrid computer and graphics terminals for real time dynamic man machine interaction, discussing AM communication system simulation
07 p0951 A72-20335
- Computer interactive graphics for digital simulation of engineering fields modeled by partial differential equations boundary value problems
07 p0951 A72-20337
- Computerized dynamic simulation with graphic display of crystal plastic dislocation movement among random obstacles, emphasizing stress-strain, strain rate and thermal activation mechanisms
07 p1095 A72-20338
- Direct simulation Monte Carlo method for rarefied gas dynamics, discussing computer display units use for flow visualization
07 p0973 A72-20344
- Automatic device using tetragonal conducting film sheets to feed graphic information into computer
11 p1601 A72-25704
- Automatized graphic information input into computer, using electric potential distribution introduced into conducting underlay sheet by current carrying drawing pen
11 p1601 A72-25705
- Logic character generator for CRT text display and DEC PDP 8/S graphics
11 p1601 A72-26290

Interactive computer graphics with three dimensional real time CRT display of air combat maneuvers for fighter pilot training

11 p1613 A72-26291

Programming system for automatic plotting of mask patterns for ICs

12 p1791 A72-27551

Interactive computer graphics technique for structural analysis, aiding engineering decisions by CRT graphical and numerical information display

12 p1787 A72-27864

Modeling process for mathematical representation of mechanical problems, deriving design information in digital or graphic form

13 p2000 A72-28450

Smoothed wind fields generated from ATS 3 cloud motions measurements observed on computer display system

13 p1991 A72-28827

Schedule analysis computer program algorithms for waterfall bar chart display and commodity flow processing and graphing through network

15 p2203 A72-31696

Computer graphics for invariant torus behavior in four dimensional phase space, varying equation parameter over large intervals

15 p2263 A72-31758

Graphic color display adapted to traffic control for direct operator-computer dialogue, noting instruction repertoire, switching device and input devices

16 p2420 A72-32894

Computer printing device for improved image recording of binary and half tone synthesized amplitude holograms

16 p2390 A72-33084

Computerized angiographic heart geometry analysis for three dimensional ventricle models of man and dog, using Ta markers

16 p2354 A72-33424

Digital computer program for automatic processing of rocketsonde and radar digitized data, presenting graphical output from meteorological rocket soundings during 7 March 1970 solar eclipse

16 p2419 A72-33944

Use of digital computer graphics in gear design

17 p2520 A72-34338

Engine condition monitoring - The Pan Am approach: Phase II.

17 p2597 A72-35324

Symbol generators for the representation of switching circuits by data display devices according to the television principle

19 p2769 A72-37935

Method for transforming three-dimensional images on maps, plans, and other documents with the aid of an electronic computer

19 p2802 A72-38082

Computer-graphics studies of dipole-dipole collisions - Evidence for neutral collision complexes.

21 p3087 A72-40559

The airborne visual simulation as an electronic display.

21 p3010 A72-41410

A new concept of flight displays compatible with digital airborne computers.

21 p3012 A72-41426

Digital simulation for selection of extremal and lengthwise admissible paths on unidirectional computer graph

22 p3156 A72-42146

A general program for computer plotting of Mohr's circle.

22 p3156 A72-42608

Application of computer mathematics procedures for prediction of phase diagrams

22 p3191 A72-42812

Plotting of composition vs property curves for superconducting systems with a digital computer by the method of simplex arrays

22 p3191 A72-42813

Modeling a holographic process on a computer

23 p3287 A72-43531

COMPUTER METHODS

U COMPUTER PROGRAMS

COMPUTER PROGRAMMING

NT LANGUAGE PROGRAMMING

NT MICROPROGRAMMING

NT MULTIPROGRAMMING

NT ON-LINE PROGRAMMING

Flight training simulator programming, noting operation under real time executive

02 p0199 A72-11653

Miss distance simulation for SAM guided by proportional navigation, using ASIM programming language for digital computer

03 p0386 A72-13611

Sandwich beam design, deriving linear programming formulation suitable for computer treatment

04 p0590 A72-15191

Modal synthesis techniques for large structures dynamic analysis, presenting flow charts for computer programming

05 p0736 A72-16083

Deep space probe MULTIPAC data system computer repairable during flight via command and telemetry links by reprogramming failed unit

05 p0633 A72-16573

Programming systems for onboard unmanned deep space probe computers, describing Mariner and outer planet Grand Tour Programs

07 p0949 A72-19295

Interactive simulation language-8 for minicomputer and programming procedures for nonlinear differential equations solution, considering integration step size and computational accuracy and speeds

07 p0951 A72-20334

Real time computer simulation of command and control in transportation systems, detailing models, and programming technique and ATC controller effectiveness evaluation

07 p0952 A72-20363

Dynamic programming application to computer algorithm construction for elasticity theory two dimensional problems, solving boundary value problem for elliptic differential equation

08 p1243 A72-21235

Software reliability engineering, emphasizing looping, deadlocks and difficulties due to imperfect logic, and error causes

10 p1486 A72-24020

Analog and hybrid computers automated programming, setup and checking facilities for off and on-line program preparation and debugging

10 p1445 A72-24090

Analog computers application to resonance phenomena analysis in oscillating systems, describing programming of variable frequency harmonic oscillations

10 p1445 A72-24492

Programming and operations of astronomer data acquisition system using NOVA computer

11 p1601 A72-25699

Time shared computer systems output maximization via degenerate exponential distribution function modeling, noting reducibility to Markov processes

11 p1601 A72-25900

Programming system for automatic plotting of mask patterns for ICs

12 p1791 A72-27551

Data file optimal arrangement by programmed procedures formulated as combinatorial problem, using branch-and-bound method for solution

12 p1787 A72-28118

Critical examination of programming courses design and subject matter, emphasizing fundamental principles and algorithm construction

15 p2202 A72-31453

General purpose simulation system /GPSS/ to program discrete time dependent mathematical models related to transport and queueing processes

17 p2521 A72-34471

Computer programming languages, discussing system dependent and problem-oriented languages, ALGOL, FORTRAN and applicability ranges

17 p2523 A72-35444

Aerospace computer software validation and verification methods application to complex systems, discussing code execution and analysis tools, program diagnostics, cost and schedules

17 p2524 A72-35582

Finite word length effects on digital filter implementation.

18 p2663 A72-36303

FORTAN subroutines for plate bending and plane stress elements stiffness and geometric matrices generation, taking into account anisotropic properties and linear thickness variations

18 p2739 A72-37166

Programming method for computer analysis of linear passive circuits powered by voltage sources

19 p2777 A72-37311

Machine oriented language for modular computer programming, discussing subprogram composition, conditional addresses and description table structure

19 p2769 A72-38089

Digital programming techniques for maximum utility and flexibility in filament winding.

19 p2808 A72-38170

Electronic control systems flexible programming techniques based on interconnection design or on utilization of easily exchangeable program carriers

19 p2782 A72-38313

Data file optimal arrangement for retrieval by programmed procedures formulated as combinatorial problem, using branch-and-bound method for solution

19 p2770 A72-38619

Two dimensional microprogrammed cellular arrays logic organization and control structure for multifunctional digital subsystems

20 p2906 A72-39736

Modified Hestenes method of Lagrange multipliers for numerical iterative solution of mathematical programming problems in function minimizing noting improved convergence

21 p3074 A72-40226

Direct acquisition and processing of data in thermal tests with the aid of a programmable desk computer system

21 p3043 A72-41850

Code correcting asymmetric-error bursts during information exchange between computers

22 p3156 A72-42189

Standardized programming routine operations independent of problem and language for controlling computer program design, discussing advantages and applications

23 p3267 A72-43991

Programming for discrete events simulation models, discussing languages construction from general programming language building blocks

23 p3268 A72-44144

Optimal design of indeterminate truss using geometric programming.

23 p3354 A72-44256

Precompiler to simplify programming of celestial mechanics problems in TRIGMAN formula manipulation system, introducing data tube SERIES into FORTRAN program

24 p3442 A72-45242

Formulation of diurnal D-region models using a photochemical computer code and current reaction rates.

24 p3399 A72-45583

Computer programming for minimization of time required for retranslation with compilers, discussing finite state machine modeling with circulating page loose system

24 p3383 A72-45670

A prognosis on fault-tolerant digital control systems.

24 p3383 A72-45672

COMPUTER PROGRAMS

NT COMPILERS

NT COMPUTER SYSTEMS PROGRAMS

NT INPUT/OUTPUT ROUTINES

NT MACHINE-INDEPENDENT PROGRAMS

NT MULTIPLE OUTPUT PROGRAMS

NT OPERATING SYSTEMS [COMPUTERS]

NT SUBROUTINES

EEG parameters estimation and statistical uncertainty calculation by computer program

01 p0016 A72-10073

Weather map numerical analysis for Northern Hemisphere, describing program with flow field for geopotential value checking

01 p0094 A72-10196

Magnetic tape recorded flight data analysis by FORTRAN program

01 p0017 A72-10215

Large scale structural systems dynamic response analysis, discussing numerical techniques with emphasis on computer codes usage [SAE PAPER 710780]

01 p0137 A72-10272

Analog matrix, input data and procedure for AI frame and Cu-clad printed circuit board module thermal resistance analysis using ECAP program

01 p0035 A72-10380

Digital computer program high speed algorithm for high resolution images geometric correction, discussing application to ERTS return beam vidicon images

01 p0065 A72-10454

Microwave oriented circuit analysis program /MODMAN/ to handle nonlinear, time-varying, lumped and distributed elements in time domain, using transmission line modeling algorithm

01 p0045 A72-10687

Computer program for microwave circuit scattering matrix sensitivity, applying to stripline elliptic low pass filters and thin-film negative resistance transistor amplifier

01 p0034 A72-10688

REDAP 31 network analysis program for design of S-band phase shifter with P-I-N diodes for phase array antennas

01 p0040 A72-10689

Computer program for design optimization of three-stage wideband low-noise integrated microwave amplifier

01 p0041 A72-10690

Pattern recognition computer programs for transforming and characterizing input scene through successive layers of recognition cone

01 p0046 A72-10867

Computer programs for global disk and landmarks registration of cloud motions from satellite data for ocean weather monitoring applications

01 p0070 A72-10871

Linear and nonlinear material static and dynamic structural analysis using NASTRAN digital computer program with finite element approach

01 p0140 A72-10983

Finite element method extension using computer program for solving problems of elastic bodies in contact with stiffness method advantages

01 p0141 A72-11047

Fault-tolerant digital computer logic design for dynamic and interactive recovery with data integrity

after error, discussing hardware and software functions requirements

02 p0184 A72-11480

Hardware and software parallel digital computer system described by flow table model, calculating output hazard for unbounded line delay effects

02 p0185 A72-11490

Computer program for atmospheric effects on IR radiation, calculating transmission and radiance spectra for various remotely sensed atmospheric, path and target conditions

02 p0187 A72-11862

Composite rotating sphere with concentric inhomogeneity of elastic constants and outer boundary free from tractions, calculating stress by digital computer

02 p0259 A72-12180

Computer program for thermal stress and buckling analysis of nonuniformly heated segmented ring-stiffened cylindrical and conical shells

02 p0293 A72-12252

FAA air traffic control automation program, discussing en route stage, computer program, data processing and storage and terminal area navigation and display techniques

02 p0256 A72-12380

Digital computer programmed numerical calculation based on admittance method for torsional forced vibration spectra of masses and stress distribution in transmission system

02 p0271 A72-12435

Computer programs and program systems for IC synthesis, emphasizing models, analysis methods, optimized design and monolithic and hybrid IC configurations

02 p0197 A72-12668

Computer program for buckling loads of shallow stiffened eccentrically orthotropic sandwich shells [DGLR PAPER 71-109]

02 p0299 A72-12703

Plaque program for logic network wiring on IC box cards

03 p0327 A72-13167

Gaussian periodic data optimal smoothing, describing convolution kernel and computer program

03 p0381 A72-13200

Computer calculation for atmospheric total mass and seasonal redistribution from pressure and temperature field data, discussing error sources

03 p0348 A72-13480

Inductor design for minimum inductance at given dc level, using computer programs [IEEE PAPER 8,6]

03 p0332 A72-13759

Computer program for construction and integration of chemical reaction rate equations, applying to nitric oxide formation and decomposition

04 p0482 A72-14583

Solar system data processing system (SSDPS)/computer solution for major planetary masses from optical, radar and radio tracking data

04 p0575 A72-15034

Book on automated structural analysis covering computer oriented problem solving methods for trusses, plane and space frames, curved beams, etc

04 p0591 A72-15270

Computer storage hierarchy hardware influence on data base management systems software technology [IEEE PAPER 13,5]

04 p0598 A72-15712

Computer aided linear circuit design for network synthesis, analysis, optimization and data storage noting MARTHA program

05 p0639 A72-15785

Integrated data processing system organizational model methodology for individual firms, emphasizing interdependence on program groups

05 p0632 A72-15815

Mathematical analysis of Vuilleumier refrigerator, calculating internal pressures, temperatures and gas flow rates via computer program

05 p0745 A72-15886

Ni alloy stress rupture data correlation and extrapolation from computerized evaluations of time-temperature parameters relative abilities

05 p0670 A72-15905

Forming of 7075-T6 Al in high pressure environments, predicting fracture occurrence via finite element stress analysis computer programs and pressure dependent model

05 p0671 A72-15912

Numerical method for cylindrical microwave cavities calibration for plasma diagnostics, noting computer programs applicability for arbitrary electron density radial distributions

05 p0662 A72-16418

Airborne computer programmed adaptive optimal control for subsonic vehicle automatic landing with aerodynamic performance

05 p0685 A72-16430

Interplanetary spacecraft trajectory error analysis by closed form approximation to state transition matrix, enabling rapid estimation with computer program

05 p0718 A72-16443

Turbine blade local heat transfer coefficient calculation with digital computer program and naphthalene blade mass transfer in cascade flow

05 p0747 A72-16498

Computerized PCM data presentation and real-time monitoring system, presenting functional flow diagrams for computer program

05 p0633 A72-16677

Slat-airfoil combinations aerodynamics modeled by single point vortex to represent leading edge slat, discussing on-line computer graphics program

[AIAA PAPER 72-221]

05 p0603 A72-16798

Center of mass motion of spacecraft in central gravitational field, analyzing programming of size and position of elements in mass geometry leading to arbitrarily large displacements

05 p0731 A72-17032

Interactive computerized design and programs for computer logic design block assignment to modules, comparing performance with manual solutions

06 p0778 A72-17472

Interactive computer graphics design aids to IC mask layouts, discussing hardware and software techniques including IMP program

06 p0778 A72-17473

One dimensional analysis computer program for junction device modeling, exemplifying hf bipolar transistor Fermi statistics effect and velocity limitation in high current density

06 p0779 A72-17478

Computer aided steady state response analysis for nonlinear electric circuits with periodic input, using Newton algorithm with rapid convergence

06 p0779 A72-17480

Air transportation modal split analysis by computer simulation program for determining utilization of alternative travel modes between origins and destinations

06 p0905 A72-17973

MARS digital simulation model in GPSS for determining scheduled flight operations and maintenance resources effects on aircraft availability and usage rates

06 p0779 A72-17976

GERT simulation program as stochastic network analysis technique for modeling policies and processes in performance tests and checkout

06 p0780 A72-17977

GERTS II simulation program for graphically modeling and analyzing complex stochastic systems, discussing applications to assembly line, project management, conveyor and inventory systems

06 p0780 A72-17978

GPSS/360 interactive simulation program with report generator, selective output display and HELP blocks for model manipulation and real time viewing

06 p0780 A72-17980

Computer program for photometric orbital elements determination of eclipsing binary stars

06 p0883 A72-18022

FORTAN programs for calculating principal stresses, strains and directions from rosette readings

06 p0781 A72-18324

Complex systems calibration based on computer derived transfer function, discussing theory, Fortran calibration program, error analysis and applications

07 p0949 A72-18818

Computerized polycardiographic data processing covering 23 cardiac and respiratory characteristics, using rabbits data

07 p0926 A72-18868

Computer program for low temperature ablator nosetip shape change at angle of attack, comparing with supersonic wind tunnel tests on camphor models [AIAA PAPER 72-90]

07 p1098 A72-18952

Iterative and direct modification procedures for structural analysis matrix displacement method, discussing computer program implementation

07 p1089 A72-19329

Artificial intelligence applications for chemical inference, discussing modified heuristic DENDRAL computer program for cyclic structure and linear molecule identification

07 p0936 A72-19498

Artificial intelligence application to mass spectra interpretation, discussing heuristic Dendritic Algorithm based computer program to generate structural isomers

07 p0950 A72-19608

Nonlinear wave propagation of laser beams in absorbing fluid media, comparing computer model calculation results with experiment on liquid carbon disulfide cell

07 p1006 A72-19837

Statistical analysis of system component error propagation by digital simulation using Continuous System Modeling program, considering strapped down inertial guidance computer

07 p1033 A72-20347

Computer simulation prediction program for attitude disturbance torques for Tiros series spacecraft rotational motion control

07 p1086 A72-20361

Classification of mass spectra on computers (COM-SOC) for compound characterization of complex mix-

tures with geochemical and environmental applications

07 p0980 A72-20393

Closed type gas turbines heated with nuclear energy, calculating heat transmitter dynamic behavior with computer program

07 p1055 A72-20598

Meteorological effects on cosmic rays, deriving muon and pion intensity and meteorological coefficient formulas and computer calculation scheme

07 p1066 A72-20654

NASTRAN/NASA structural analysis program for computer stress analysis based on finite element method, noting vibration, acoustics, transient motion and random response applications

08 p1138 A72-21325

Boundary value solutions and computer programs for one dimensional laminar flame propagation equations

08 p1129 A72-22040

Sequential control using computer program for signal processing, noting machine tool, die casting, elevator and warehouse applications

09 p1290 A72-22240

DESAG computer program extension with graphic terminal to functional network conception and implantation

09 p1283 A72-23469

Hardware monitor and associated analysis programs to evaluate real time satellite command and control digital computer system performance

10 p1442 A72-23817

Metric tensors as alternate to coordinate transformation equations for computer program inputs in automatic problem formulation

10 p1443 A72-23923

Computer programmed instruction checklist for reliability and maintainability engineers requirements

10 p1443 A72-23981

Probabilistic methods application to software reliability analysis, deriving expressions for hazard, density, failure and reliability functions

10 p1486 A72-23983

Complex system mission worth optimization by redundancies discussing MISDGRAD computer program to evaluate cost-reliability for mission without maintenance

10 p1550 A72-23994

Software reliability engineering, emphasizing looping, deadlocks and difficulties due to imperfect logic, and error causes

10 p1486 A72-24020

Fifth order modified Runge-Kutta integration algorithm, presenting truncation error estimation method and computation procedure flow chart

10 p1505 A72-24091

Modified sweep variation method for optimal control programs, solving two point boundary value problem by linear perturbation technique

10 p1551 A72-24455

Avionics systems electrical interface connection design information document creation and dissemination, using EMPRENT computer program

10 p1453 A72-24864

Hail damage to aircraft, predicting metal surfaces dent depth and deformation shape with computer program

[AIAA PAPER 72-335]

Computerization of panel flutter boundary calculations with aerodynamic forces derived from linear three dimensional unsteady potential flow theory

11 p1731 A72-25424

Computer program for photometric orbital elements determination of eclipsing binary stars

11 p1718 A72-25958

Multilevel structural analysis for multilayered fiber-epoxy and metal matrix composites, using FORTRAN IV

11 p1601 A72-26033

Computer program for biowaste resistojet nozzle performance prediction, taking into account viscous effect at low Reynolds number

[AIAA PAPER 72-450]

Computer calculation for atmospheric total mass and seasonal redistribution from pressure and temperature field data, discussing error sources

11 p1623 A72-26250

Automatic search for Huffman sequential logic circuit breakdown detection sequence, using VEGA program through matrices and graphs utilization

11 p1612 A72-26549

FAA automated ATC system, discussing subsystems related to operational and nonoperational computer program components, data entry and display, communication, personnel and environments

11 p1684 A72-27000

Geometrically nonlinear structure elastic stress propagation, deformation and dynamic response under impact, using finite element matrix displacement method and computer programs

12 p1879 A72-27189

Plane Poiseuille flow Orr-Sommerfeld problem numerical solutions comparison and computer program implementation

12 p1797 A72-27192

- Modular computer program for digital transmission systems, applying to optimization of filters in multitransponder satellite and ground stations
12 p1786 A72-27323
- Computerized antenna array design, using Automated Engineering and Scientific Optimization Program
12 p1792 A72-27735
- Computer program to reduce automated multiaxial testing strain gage and applied loads data from tubular or flat specimens including fiber composites
12 p1787 A72-27999
- Computer program for gas turbine characteristics and influence coefficients calculation, allowing for cascade loss distribution during flow choking
12 p1862 A72-28151
- Dynamic electrocardiography with analog computer program to detect, count and classify atypical ventricular depolarization complexes
12 p1775 A72-28281
- Finite time element method for failure probability prediction in multiple load-path system with random loads, noting flow chart for suggested computer program
13 p2052 A72-28369
- Computer program analysis of errors in mutual orientation elements on aerial photographs with different lengthwise overlaps, discussing error minimization
13 p1955 A72-28497
- Algorithm and computer program to calculate low run multiple nomenclature production process optimal parameters
13 p1962 A72-28741
- Computer program in ALGOL 60 language for calculation of long blades twist in axial flow turbines and compressors
13 p1893 A72-28782
- LB 21 and space shuttle orbiter aerodynamic testing, discussing computer program supplanting reentry vehicle free flight aerodynamic testing
13 p1894 A72-28934
- Computer algorithms and programs for complex surface geometrical parameters calculation and discrete curve coordinates determination by interpolation
13 p1924 A72-29141
- Sky wave correction /Swanson/ model and computer program for real time propagation prediction for airborne OMEGA system
13 p1997 A72-29190
- Hardware and software integration of OMEGA and LORAN C and D receivers based on hyperbolic navigation systems compatibility
13 p1999 A72-29205
- Computerized calculation of wave dispersion curves for hot Maxwellian electron magnetoplasma, applying to upper hybrid and cyclotron frequencies
13 p2013 A72-29340
- Computer algorithm to calculate surfaces formed by equidistant conic sections, using successive approximation method
13 p1966 A72-29461
- Data acquisition, reduction, quick-look data and standard and special programs for ESRO 1A and B auroral particle satellite experiment
13 p1925 A72-29868
- Computer algorithms and programs contribution to aircraft structure operational reliability and fatigue life calculation
14 p2164 A72-30288
- Structural systems stability and natural frequency analysis eigenvalue problems solution by Sturm sequence method, using finite element technique
14 p2168 A72-30931
- Hollow elliptical waveguide numerical analysis by polygon approximation with computer program to obtain cutoff wavelength without Mathieu functions
14 p2087 A72-30943
- Book on extended surface thermal transfer covering heat exchanger design, convective transfer, radiation and computer programs
14 p2172 A72-30975
- Computer controlled ground truth station for environmental agricultural aerial photographic remote sensors data processing, discussing system components, printout format and computer program
15 p2213 A72-31249
- EHF double-drift IMPATT oscillator small and large signal behavior analysis with computer program, noting second harmonic tuning and single frequency operation possibilities
15 p2204 A72-31314
- Computerized determination of cryogenic gas behavior near vapor region, obtaining state equation coefficients from curve fitting program
15 p2334 A72-31580
- Schedule analysis computer program algorithms for waterfall bar chart display and commodity flow processing and graphing through network
15 p2203 A72-31749
- Structural mechanics computer programs compendium covering subject oriented information according to structure type, load environment and analytical models
15 p2328 A72-31771
- FORTTRAN IV program for small structure analysis with maximum 10 deg of indeterminacy
15 p2328 A72-31772
- Astronautical digital computing hardware and software trends and implications, considering data rates, reliability, LSI, speed-storage tradeoff, etc
15 p2203 A72-31822
- Computer program for symbolic network functions, using numerical algorithms for branches not represented by symbolic parameters
15 p2211 A72-31845
- SIDERAL program organization and computational method application to calculation of malfunction by drift of linear analog equipment
15 p2207 A72-31872
- Structural components design from fiber composites, noting computer programs for structural and stress analysis
15 p2328 A72-32128
- Molecular flux distribution in cylindrical vacuum chambers with various inlet and pumping configurations under assumption of Knudsen law validity, describing computer program
15 p2183 A72-32382
- Skewed wire antennas electric and magnetic near fields prediction from computer programs based on matrix inversion method
15 p2209 A72-32567
- Maxwell equations solution for electromagnetic field in circular cylindrical tubes, deriving recursion formulas for computer processing
16 p2364 A72-33668
- Mathematical model for magnetosphere surrounding rotating neutron star, noting computer programs for Maxwell and plasma equations solution
16 p2460 A72-33927
- Digital computer program for automatic processing of rocketsonde and radar digitized data, presenting graphical output from meteorological rocket soundings during 7 March 1970 solar eclipse
16 p2419 A72-33944
- Image enhancement by computer programs, discussing digital filtering, fast Fourier transform algorithm, data management and large matrix handling
17 p2520 A72-34404
- Pattern recognition computer programs for input data preprocessing with characterization and transformation through layered recognition cone
17 p2520 A72-34405
- Computer program algorithm for processing local landmark and cloud motion data recorded by satellite observation
17 p2520 A72-34410
- Simulation of an air cargo handling system
17 p2536 A72-34472
- Dexter - A one-dimensional code for calculating thermionic performance of long converters.
17 p2521 A72-34587
- The orbit of Cosmos 307 rocket and its use in atmospheric research.
17 p2545 A72-34632
- Computer thermal analysis of hybrid microcircuits.
17 p2521 A72-34679
- A computer system for structural design
17 p2522 A72-34743
- A method of realization of the functions of a program timer on a computer used in a spacecraft on-board equipment control system
17 p2522 A72-35028
- Computer program for the calculation of the thrust and of the firing data of internal cylindrical rocket burners with different profiles
17 p2523 A72-35417
- A computation method for the determination of thermodynamic values and performance data of rocket propellants, propellant charges for cannons, and ignition mixtures
17 p2596 A72-35418
- Aerospace computer software validation and verification methods application to complex systems, discussing code execution and analysis tools, program diagnostics, cost and schedules
17 p2524 A72-35582
- DC analysis of linearized electronic circuits with the aid of electronic computers
17 p2524 A72-35977
- Data structures and computational organization in digital image enhancement.
18 p2658 A72-36262
- Digital simulation of stiff linear dynamic systems.
18 p2663 A72-36315
- On the accuracy and application of the point matching method for shallow shells.
18 p2739 A72-37090
- Zero overhead testing relationship to software requirements, testing dynamic accuracies, LSI product types and function and parametric speeds related to product lines
18 p2664 A72-37109
- Three dimensional holographic interferometry program for study of fringes due to displacement or deformation
19 p2799 A72-37630
- Photometric observations from sounding rockets - Selection of horizontal sightings
19 p2789 A72-37784
- An integrated computer system for preliminary design of advanced aircraft.
19 p2749 A72-38112
- [AIAA PAPER 72-796]
19 p2750 A72-38112
- Computer program for automated design of long haul transport aircraft, discussing cost effectiveness of composite materials for aircraft structure
19 p2750 A72-38121
- [AIAA PAPER 72-794]
19 p2750 A72-38121
- Computerized finite element three dimensional stress analysis, taking into account mechanical and thermal stresses
19 p2878 A72-38649
- Computer program for numerical analysis of atmospheric fronts in lower troposphere based on models for spatial distribution of hydrothermal characteristic in air mass
19 p2829 A72-38771
- Computer program to simulate electromagnetic signal densities, data rates and power from land based radar transmitters as functions of time and location
20 p2902 A72-38992
- Visual aid-to-eye direct coupling, evaluating partial coherence effects on imagery optical performance by computer program
20 p2931 A72-39050
- A time-sharing computer program for defining human thermal comfort conditions in any atmosphere.
20 p2905 A72-39142
- [ASME PAPER 72-ENAV-33]
20 p2905 A72-39142
- General principles and detail similarities in visual pattern analysis by single neuron operation, computer programs and psychological perception
20 p2891 A72-39275
- Efficient computation of radiant-interchange configuration factors within the enclosure.
20 p2983 A72-39488
- Heat transfer coefficient measurement and thermal network analysis computer program for improving performance and reliability of microelectronic package/board and chip/substrate systems
20 p2908 A72-39497
- A digital simulation system for heat transfer modelled by ordinary and partial differential equations.
20 p2986 A72-39673
- [ASME PAPER 72-HT-25]
20 p2986 A72-39673
- Computer program for solar corona emission line polarization computation to interpret measurements in terms of coronal magnetic field direction
20 p2971 A72-39757
- Applicability of associative computers to parallel adaptive break down of telemetry information into discrete elements
21 p3014 A72-40316
- Computer simulation of a digital satellite communications link.
21 p3024 A72-40854
- Digraphs application to electronic linear networks analysis, developing computer program
21 p3024 A72-40992
- Network algebra simplification through computerized minimization of Boolean functions, describing FORTTRAN IV program
21 p3038 A72-41001
- Process computation systems, discussing translator programs for conversion of user programs into machine language
21 p3024 A72-41002
- System analysis for an airline operational environment through a computerized network simulation model.
21 p3025 A72-41077
- Book - A theory of supercritical wing sections, with computer programs and examples.
21 p2993 A72-41534
- Transient oscillator analysis of a high-pressure electrically excited CO laser.
22 p3184 A72-41970
- A general program for computer plotting of Mohr's circle.
22 p3156 A72-42608
- Error analysis of astronomical-geodetic network compensation methods, noting distortions minimization in polygon nodes by large blocs compensation with computers aid
22 p3173 A72-42721
- Cascade computer controlled system for LSI devices testing, considering interim buffer storage and programmable pattern generator
22 p3160 A72-42823
- Theoretical and practical comparison between two minute Doppler and short Doppler satellite position fix accuracy.
22 p3203 A72-42947
- Book - Thermal structural analysis programs: A survey and evaluation.
22 p3241 A72-43046
- Aircraft synthesis analysis program /ASAP/ for computerized aircraft design, enabling large number of trade-off studies for design optimization
23 p3250 A72-43454
- [SAWE PAPER 907]
23 p3250 A72-43454

- Mission analysis and performance program as part of computerized aircraft configuration synthesis process, describing interfaces with other system modules
[SAWE PAPER 909] 23 p3250 A72-43456
- Computerized weight data storage, recording and information system to aid in aerospace vehicle design
[SAWE PAPER 933] 23 p3266 A72-43473
- Aerospace vehicles preliminary design computer program to include cost, reliability, maintainability and safety parameters in addition to weight as performance determining factors
[SAWE PAPER 940] 23 p3342 A72-43480
- Application of an electronic computer to the calculation of the locking band in nonlinear phase-lock automatic frequency control systems
23 p3264 A72-43763
- An estimate of expected critical-path length in PERT networks.
23 p3308 A72-43806
- Spectral line identification computer program determining wavelength and equivalent line width for photometric measurements
23 p3267 A72-44029
- Aircraft structures shock and blast loading characteristics from internal detonation, comparing computer program results with available data
24 p3365 A72-44610
- Multipoint real time all-day computerized noise monitoring system for diagnostic evaluation of airport, discussing design and applications
24 p3387 A72-44684
- Relative position of the rib within the chest and its determination on living subjects with the aid of a computer program.
24 p3372 A72-44957
- The on-board computer of the Astronomical Netherlands Satellite [ANS].
24 p3382 A72-45163
- Spacecraft rendezvous trajectories and targeting maneuvers onboard sequential computation, taking into account maneuver constraints and state vector update information
24 p3450 A72-45172
- Low thrust constant acceleration trajectories for a Mercury orbit.
24 p3441 A72-45208
- Some experiences with the solution of potential flow in the plane cascade on the computer.
24 p3393 A72-45365
- Automatic software diagnostic package for airborne computer, using testing computer for decision making based on received data
24 p3383 A72-45669
- COMPUTER SIMULATION**
U COMPUTERIZED SIMULATION
COMPUTER STORAGE DEVICES
NT BUFFER STORAGE
NT CORE STORAGE
NT FLIP-FLOPS
NT MAGNETIC CORES
NT MAGNETIC DRUMS
NT MAGNETIC TAPES
NT RANDOM ACCESS MEMORY
NT REGISTERS [COMPUTERS]
NT SHIFT REGISTERS
Optics for data processing, discussing magneto-optic and holographic memories in computer systems
01 p0035 A72-11315
- Photosensitive magneto-optic films for large capacity computer memories
01 p0035 A72-11316
- Data holder made of three thin ferromagnetic coupled films for magneto-optic computer memory
01 p0035 A72-11317
- Digital holographic memory with acousto-optical deflection random access and automatic inscription
01 p0073 A72-11319
- Electronic deflection printer with holographic memory, using photosensitive device for textual recording
01 p0073 A72-11320
- Mathematical model for control process as adaptive memory tracker, discussing digital simulation
02 p0186 A72-11659
- Digital computer memory system for real time processing of air and naval traffic data, discussing logic design, time comparisons and optimum use
02 p0188 A72-12647
- Ferrite core memory for space flight devices, comparing 1 bit storage capacity power consumption with MOS cell
[DGLR PAPER 71-090] 02 p0196 A72-12734
- Computational time and computer storage requirements for discrete Kalman filter, comparing simultaneous and sequential types of measurement processing
02 p0198 A72-12806
- Logic functions for magnetic bubble devices based on interaction of circular magnetic domains in rare earth iron oxides, considering gates for dynamic memory
[IEEE PAPER 2,3] 03 p0327 A72-13753
- MnBi magnetic film optical memory system characteristics evaluation, considering laser power requirement, bit packing density and SNR
[IEEE PAPER 3,4] 03 p0332 A72-13754
- Ten million bit magnetic film computer memory, discussing design, fabrication, performance and cost per bit
[IEEE PAPER 11,1] 03 p0327 A72-13761
- Nondestructive readout in computer storage of plated wires on Permalloy film deposited substrates, testing design parameters effects on performance
[IEEE PAPER 11,2] 03 p0332 A72-13762
- Plated-wire computer memory using thin Permalloy film on W wire substrate, testing nondestructive and destructive readout characteristics
[IEEE PAPER 11,3] 03 p0327 A72-13763
- High speed easy rewrite read-only memory using plated wire with multilayered nondestructive readout magnetic thin film, testing performance
[IEEE PAPER 11,4] 03 p0332 A72-13764
- Destructive readout computer memory of wire substrate electrodeposited with two thin Permalloy layers separated by Cu
[IEEE PAPER 11,5] 03 p0332 A72-13765
- Holographic optical techniques application to bulk magnetic storage for high information density and memory capacity and fast random access
[IEEE PAPER 19,4] 03 p0361 A72-13776
- Mathematical model for design of plated-wire magnetic memory cell, considering drive requirement minimization as criterion
[IEEE PAPER 21,1] 03 p0328 A72-13777
- Coupled-film closed-easy-axis arrays for large capacity NDRO multiple-write bulk memory, discussing disturb mechanisms limitation on performance and design
[IEEE PAPER 21,9] 03 p0328 A72-13780
- Magnetic bubble repertory dialer memory design, noting bit storage capacity and random access
[IEEE PAPER 28,1] 03 p0328 A72-13782
- Functional speed measurements of propagating devices based on cylindrical domains in orthoferrites and garnets, noting storage capability
[IEEE PAPER 28,2] 03 p0333 A72-13783
- Storage oscilloscope interface for small computers, describing graphic display characteristics and line cursor and character generators
03 p0329 A72-14177
- Finite memory uncertain stochastic controller, developing optimal and suboptimal algorithms
03 p0329 A72-14181
- MOS Si-gate arrays for static, dynamic and programmable read-only memories, investigating information storage reliability
03 p0336 A72-14282
- Voltage contrast mode scanning electron microscopy application to defect and failure analysis of semiconductor memories
03 p0336 A72-14288
- Computer storage hierarchy hardware influence on data base management systems software technology
[IEEE PAPER 13,5] 04 p0598 A72-15712
- Bulk storage applications in Illiac 4 system, discussing Unicon 690 mass memory for Advanced Research Projects Agency network of telephone lines and interface message processors
[IEEE PAPER 23,4] 04 p0496 A72-15714
- Direct coupled circuits in memory cell prototype with normally-off GaAs MESFET at 4.2 K
05 p0638 A72-17096
- MnBi thin films as potential storage media within holographic optical memory system having write-in reference beam for readout
[CLEA PAPER 18,1] 07 p0950 A72-19399
- Associative memory model using neuron synaptic weight change for storing input disturbances
08 p1138 A72-20871
- Industrial applications of lasers, considering programmable machining, distance measurement, computer memories, communication, night clubs, machine shops, aircraft manufacture and tunnel boring machine alignment
08 p1182 A72-21207
- Adaptive statistical system with feedback loop for weather analysis and forecasting, examining learning process features
08 p1202 A72-22113
- Mass storage systems technologies covering magnetic recording, surface wave acoustics, magneto-optic beam addressing, magnetic bubbles, switchable resistances and IC memories
09 p1283 A72-23413
- Burn in technique in nonvolatile metal oxide semiconductor /MOS/ memory using ionizing radiation of reprogrammable electron beam
10 p1443 A72-23927
- Computer storage array of isolated electrodes imbedded between capacitor parallel plates, discussing read-write cycle time, expected performance and experimental techniques
10 p1443 A72-23933
- Semiconductor lasers with high energy electron pencil beam excitation for high capacity computer storage application
10 p1492 A72-24513
- Reliable, economical and easily operated read-only magnetic core storage devices for control computers, discussing design features
10 p1445 A72-24639
- Digital computer simulation of random processes specified by canonical expansion, discussing quantization steps for storage requirements reduction
11 p1600 A72-25432
- Design and operation of digital image recorder based on single stage intensifier and silicon target intensifier television camera tube coupled to large memory
11 p1631 A72-25685
- Optimal flexible ferrite keeper for ferromagnetic thin film memories performance improvement, noting requirements for high permeability, low loss factor and dielectric constant, etc
11 p1601 A72-25899
- Capacitive memory storage for filtration of repetitive pulse radio signals mixed with additive noise
11 p1598 A72-26734
- Integrated metal-nitride-oxide-silicon /MNOS/ semiconductor storage units characteristics, design and operation in FETs
12 p1791 A72-27574
- Holographic memory devices for bulk information recording, discussing use of image converter for brightness amplification and lithium niobate electro-optical deflector for beam switching
12 p1807 A72-27588
- Abstract family of multistorage tape acceptors and associated languages, discussing wedge operation and applications
12 p1787 A72-27675
- Parameterized daily profile characterization of global atmospheric conditions to minimize computer storage, discussing mathematical representations, wind, density and temperature profiles
13 p1989 A72-28806
- Memory and photoconductivity in CdSe polycrystals at 77 and 300 K, plotting photocurrent vs illumination levels
13 p2024 A72-30012
- Algorithm to transpose large matrices in excess of direct access computer memory for external sequential storage
15 p2203 A72-31748
- I-V characteristics of polarized and nonpolarized memory effects in GaAs thin films evaporated on tungsten substrates
15 p2292 A72-31869
- Holographic information storage survey, discussing hologram classification, characteristics, physical recording processes, and capacity-limiting factors
15 p2239 A72-32351
- Registers and digital circuits with FETs and integrated operational amplifiers to permit analog measurements storage for display on CRT oscilloscope
15 p2204 A72-32499
- Advances in LSI technology.
17 p2527 A72-34569
- An investigation of amorphous semiconductor memory devices utilizing thick film fabrication techniques.
17 p2527 A72-34682
- Plated wire associative memory elements.
17 p2523 A72-35172
- Error reduction in digitally generated holographic memories via parity sequence interlacing with true data sequence for spectrum shaping
19 p2796 A72-37581
- Optimal programming data distribution in digital computer storage devices, noting independent subprograms assembling
19 p2769 A72-38088
- A holographic memory recording matrix permitting real-time data modification.
20 p2922 A72-39037
- Binary information storage with bipolar transistors, tunnel diodes, MIS and glass semiconductors, considering Gunn effect devices application
20 p2905 A72-39425
- Amorphous semiconductors for optical memory and other devices.
20 p2961 A72-39707
- A new type of switching and memory effect by controlling the polarized field in semiconductor interface.
20 p2961 A72-39709
- Disk and toroidal solid state computer storage cell arrays without boundary cells, comparing read- and write-time characteristics with conventional organizations
20 p2910 A72-39966
- Dynamic error of storing voltages at capacitors in the storage channel of an integrator of variable structure
21 p3024 A72-40165
- An adaptive replacement algorithm for paged-memory computer systems.
23 p3266 A72-43420
- Design optimization of an integrated-circuit direct access memory unit
23 p3267 A72-43841
- Advanced optical storage techniques for computers
23 p3288 A72-43876

- Multiprogrammed virtual memory digital computer systems analysis and design, discussing component characteristics, operating system structure and mathematical description techniques 23 p3267 A72-43987
- COMPUTER SYSTEMS PROGRAMS**
 NT INPUT/OUTPUT ROUTINES
 NT OPERATING SYSTEMS [COMPUTERS]
 Hardware software firmware tradeoffs - IEEE Conference, Boston, September 1971 10 p1442 A72-23815
- Performance characteristics and design options for software controlled I/O processor for aerospace computer applications with high speed real time responses 17 p2521 A72-34702
- Optimal programming data distribution in digital computer storage devices, noting independent subprograms assembling 19 p2769 A72-38088
- Operational software for computerized process control, considering operations system, translator, supervision and auxiliary and service programs 21 p3024 A72-41000
- An adaptive replacement algorithm for paged-memory computer systems. 23 p3266 A72-43420
- COMPUTER TECHNIQUES**
 Computer generated Lame functions of first kind definable by polynomial coefficients and eigenvalues 01 p0093 A72-10005
- Voice quality improvement in He atmospheres by on-line segment dilation 01 p0101 A72-10158
- Large scale structural systems dynamic response analysis, discussing numerical techniques with emphasis on computer codes usage [SAE PAPER 710780] 01 p0137 A72-10272
- Crop discrimination with manual and automatic computerized side-looking radar imagery analysis for microtexture pattern recognition 01 p0065 A72-10451
- Aerial triangulation for optimum photogrammetric project parameters, discussing flight altitude, bridging distance and control points for computerized optimization 01 p0066 A72-10462
- Pattern recognition, invariance, redundancy and information reduction in computer aided image processing 01 p0034 A72-10475
- Primary component corrections for global cosmic ray variations from latitudinal expeditions, discussing adaptation to computer 01 p0118 A72-10584
- Computer image processing for photoreconnaissance, enhancement and calibration applications 01 p0070 A72-10870
- WINDCO interactive man-computer system for automated cloud motion tracking using precisely aligned digital ATS satellite pictures 01 p0070 A72-10872
- Computer aided biplane roentgen videometry system for dynamic circulatory structure studies including blood flow and heart volume determination 01 p0020 A72-11040
- NERVA fuel quality control, discussing planning, nondestructive tests, computer data acquisition and certification systems 02 p0258 A72-11552
- Field and test data analysis with time share computer, using Weibull probability plotting, hazard rates and least squares regression 02 p0185 A72-11555
- Straight line computer solution of Chaplygin equation, with application to high subsonic gas flow incident on airfoil with local supersonic zone 02 p0149 A72-11581
- Monte Carlo methods for hybrid computer solution of nonlinear parabolic partial differential equations with two spatial dimensions 02 p0186 A72-11657
- Circuit theory optimization techniques in computer aided electric circuits and devices design, discussing algorithms, sequential methods, convergence speed, topologies, system responses, etc 02 p0197 A72-11688
- Monochromatic electromagnetic field diffraction problems in homogeneous medium, presenting computer aided numerical analysis 02 p0171 A72-11690
- Computer enhancement of multispectral satellite-and air-photographs and imagery for earth resources 02 p0186 A72-11801
- Natural formations optical spectral reflectance optimal coding with speedy digital computer processing advantage for remote sensing of earth surface 02 p0187 A72-11811
- Computerized statistical identification of aerial photograph ground patterns, comparing elliptical boundary condition with minimum distance to mean classification models 02 p0187 A72-11842

- Digital computer mapping of terrain by clustering techniques, using color IR film emulsion layers as three band spectrometer 02 p0215 A72-11879
- Automatic soil type mapping, using multispectral remote sensing and computerized pattern recognition 02 p0215 A72-11881
- Soviet monograph on variable stars observation covering photographic photometry, photoelectric observation, image processing devices and computer techniques 02 p0279 A72-12122
- Computerized bias optimization of telemetry timing accuracy applied to Minuteman system 02 p0174 A72-12144
- Computerized series solution of relativistic motion of planet Mercury for Schwarzschild and isotropic coordinates 02 p0260 A72-12306
- Computer controlled telemetry data acquisition station, noting cost effectiveness 02 p0179 A72-12407
- Multiprogrammed digital computer controlled acquisition and processing of quasi-static analog transducer data during spacecraft environmental simulation tests 02 p0200 A72-12478
- Digital computer automated test equipment and procedures for remote sensors and electronics for scanning celestial sphere for X rays prior to spacecraft launch 02 p0200 A72-12479
- Radar detection and resolution, discussing computer analysis of interval modulated signal ambiguity properties and synthesis method 02 p0181 A72-12648
- Hybrid computer for solving complex problems in distributed parameter systems in terms of parabolic differential equations 02 p0188 A72-12655
- Computer investigation of three fluid electrical current sheet model, solving magnetic annular shock tube problem [SRL-TR-71-0021] 02 p0200 A72-12659
- Satellite orbit determination accuracy from radio interferometer tracking data containing systematic errors, using digital computer techniques on Symphonie transfer orbit [DFVLR-SONDDR-212] 02 p0182 A72-12744
- Weather forecasting, discussing statistical entropy, numerical and statistical methods and computer technology utilization 02 p0254 A72-12777
- Coarsely stabilized spacecraft-borne Michelson interferometer, obtaining high resolution by computerized spectrum reconstruction with fast Fourier transform 03 p0354 A72-13055
- Time shared performance test monitor function, operation and self repair of corporate feed array radars with computer control for long time internal reliability 03 p0321 A72-13165
- Computerized error function method of wreckage trajectory analysis in aircraft accident investigation, using fundamental equations of motion 03 p0309 A72-13250
- Computer based analysis of holography using ray tracing and wave front matching aberrations 03 p0358 A72-13433
- Computer modeling technique for electromagnetic scattering and radiation problems in resonance region employing thin wire electric field integral equation 03 p0328 A72-14028
- Digital computer solution for near field coupling between high and low gain antennas above conductive surface 03 p0323 A72-14029
- Computer aided intrasystem electromagnetic compatibility prediction programs, discussing mathematical models and program philosophies 03 p0328 A72-14039
- Automated electromagnetic pollution data acquisition systems for environmental ecology, discussing computer technique and data retrieval, analysis and storage 03 p0328 A72-14040
- Pioneer F and G space probe EMC specification limits, comparing computer analysis prediction and system test data 03 p0329 A72-14048
- Parameter regions for proper operation of multifilter phase lock loops used for demodulation by digital and analog computer techniques 03 p0339 A72-14194
- Approximate S-N fatigue testing/digital computer method for quasi-static boundary value problems in plasticity theory, applying to continuum models 03 p0453 A72-14210
- Orbit distributions of hypothetical comets from Jovian surface eruptions, calculating orbital elements with computer 03 p0439 A72-14240

- Computer solution to vector variational formulation of electromagnetic Maxwell equations for dielectrically loaded rectangular waveguide 03 p0335 A72-14249
- Computer analysis of linear electric circuits without restrictions on network topology and component composition, using system matrix 04 p0495 A72-14464
- Torsional vibrations of shaft with multiple flywheels, presenting computer generated graphs for vibration modes 04 p0584 A72-14517
- Far IR Fourier spectrometer with built-in real time digital computer for routine physical and chemical spectroscopy 04 p0520 A72-14523
- Computerized synoptic weather map forecasting of heavy snowfall in Colorado 04 p0542 A72-14685
- Computer technology projection in terms of cost and performance for future ATC system, determining data processing systems availability 04 p0496 A72-14834
- Extremal problems of natural vibration spectrum optimal control in mechanical systems with constraints, using mathematical programming methods 04 p0586 A72-15004
- Computer laser devices for logical operations, discussing analog-digital converter, gate circuits, bistable elements, flip-flop and shift register 04 p0496 A72-15141
- Book on automated structural analysis covering computer oriented problem solving methods for trusses, plane and space frames, curved beams, etc 04 p0591 A72-15270
- Computer servocontrolled granite stage and measuring microscope, discussing mechanical and optical construction, control electronics and applications 04 p0522 A72-15477
- Computer controlled automatic system for measuring electroconductivity and Hall effect in semiconductors, noting data acquisition instrumentation 04 p0496 A72-15534
- Computer aided Foldy-Wouthuysen canonical transformation on Dirac Hamiltonian with electromagnetic potentials included 04 p0496 A72-15627
- Multidimensional random hypersurfaces generation with given statistical properties on digital computer, using linear filter theory 04 p0540 A72-15628
- Flutter of thin homogeneous isotropic cylindrical panels from analog computer study 04 p0593 A72-15646
- Radial pressure distribution in laminar flow of compressible fluid between two coaxial disks from analog computer study 04 p0514 A72-15702
- United Air Lines computerized information retrieval system for message switching, flight planning and monitoring and aircraft parts inventory control [IEEE PAPER 23.3] 04 p0598 A72-15713
- Digital data reduction techniques for stellar spectrograms, discussing digital noise smoothing for SNR improvement 05 p0632 A72-15762
- Third order nonlinear van der Pol oscillating systems, discussing digital computer verification for existence of stable limit cycles in state space trajectory plots 05 p0639 A72-15806
- Book on computer applications to engineering analysis covering mathematical models, numerical techniques, program usage, programming and design 05 p0632 A72-16106
- Computer controlled production test system for airborne phased array modules, describing various measurement capabilities 05 p0637 A72-16417
- Low cost automated digitized measurement for microwave antenna feed power gain and relative phase, using computer facilities 05 p0637 A72-16420
- Synergic control of computer-manipulators, evaluating system 05 p0621 A72-16450
- Computer controlled vacuum optical calibration bench for astronomical satellites, describing pumping system 05 p0644 A72-16755
- Digital computer investigation of radio signals transmitted by Vener 7 during Venus soft landing, describing spectral analysis and telemetric data detection methods 05 p0630 A72-16770
- Computerized analytical model of two dimensional multicomponent airfoil in viscous subsonic flow [AIAA PAPER 72-2] 05 p0606 A72-16861
- Dither adaptive control technique application to constant fuel rate problem, illustrating with analog computer solution 06 p0792 A72-17308

- Development programs for ATC system improvement by digital computers and data displays applications 06 p0844 A72-17328
- Computerized photogrammetric terrain analysis and representation in three dimensional coordinates, discussing construction of digital terrain model 06 p0813 A72-17429
- Bubble chamber high energy particle tracks semiautomatic measuring device, using small on-line computer for data processing 06 p0813 A72-17438
- Computer search for optimum narrow band FM and PM systems bandpass filters, noting low index angle modulated signals 06 p0783 A72-17484
- Program system for computation of surface from set of data points, using piecewise polynomial functions 06 p0815 A72-17753
- Digital computer techniques for randomly excited n-degrees of freedom structural system response by discrete time series with output covariance 06 p0895 A72-17857
- Computer technological development effects on professional engineers education and work, considering impacts of computerized design, simulation, etc 06 p0780 A72-18235
- Computerized Eros II airborne collision avoidance time frequency system design, considering radio transmission, synchronization and ground stations 06 p0845 A72-18247
- Computerized modular automatic test equipment for commercial airliner avionics device performance, discussing data handling ability and cost effectiveness 06 p0796 A72-18250
- Nonlinear mechanical oscillation systems analysis by analog computer, exemplifying pendulum rotating about vertical axis 06 p0851 A72-18725
- Computer aided engineering - Conference, Waterloo, Canada, May 1971 07 p1024 A72-18776
- Engineering curves and surfaces representation by spline functions, discussing computerized approximation methods for algebraic, transcendental and transfer functions 07 p1024 A72-18777
- Hybrid computer method of nonstationary spectrum analysis of aircraft noise, applying to flyover and jet aircraft noise abatement under operational conditions 07 p0911 A72-18778
- Interpolation of function of two variables by surface splines method, solving linear equations system by digital computer 07 p1026 A72-19095
- Computers in biomedicine - Conference, University of Hawaii, January 1972 07 p0928 A72-19306
- Computerized EEG data acquisition and transmission system for large hospitals with multiple critical care patient monitoring units, noting telephone access from outside 07 p0928 A72-19307
- Real time computer aided mechanical testing and data analysis system for composites, confirming computer analysis by motion pictures of thin walled graphite/epoxy composite fracture 07 p0965 A72-19734
- Charpy impact test computerized data acquisition and analysis system using analog to digital converter 07 p1090 A72-19735
- Computerized estimation of deformation parameters for Sellars-Tegart equation relating stress, strain rate and temperature in creep and hot torsion testing of metals 07 p1090 A72-19736
- Heat transfer steady state and transient response problems nodal formulation and numerical solution on digital computer 07 p1101 A72-19918
- Interference rejection method for high speed analog to digital converters, noting application to on-line computer systems 07 p0948 A72-20386
- Multicarrier communications satellite signal power, center frequency and rms deviation computer controlled monitoring system with frequency shift radiometer principle 07 p0948 A72-20491
- Numerical analysis of passing screw dislocation arrays under stress for computerized work hardening model 07 p1097 A72-20556
- Cardiographic interpretation of computerized apexo-carotid diagram, using heart-motor pump comparison 07 p0934 A72-20607
- Computerized oesocardiogram for left auricle mechanical activity examination, comparing with catheterization technique 07 p0934 A72-20608
- IC technology review, considering computer applications and microelectronics prospects 08 p1142 A72-21843
- German monograph on computerized statistical analysis of Al alloy fatigue test data, considering welded samples and thin plates 08 p1188 A72-21848
- Soviet papers on digital computers application to reliability problems solution for recoverable, failing, controlled, redundant and electronic systems 08 p1179 A72-22051
- Computer aided administrative control systems development for industrial enterprises management, covering product manufacture 08 p1256 A72-22146
- Selection, arrangement and use of computers and peripheral equipment in automated administrative control management system within industrial enterprise 08 p1256 A72-22147
- Data transmission system design in computerized administrative control system for industrial enterprise management 08 p1257 A72-22148
- Industrial enterprises preparation for computerized administrative control systems introduction 08 p1257 A72-22149
- Hoghorn parabolic antenna design, presenting relations for dimensions, aperture field and radiation patterns calculation by computer 09 p1284 A72-22242
- Computer calculation of spectral brightness coefficients on aerial photographs, determining contrast features density gradients 09 p1308 A72-22484
- Partial load computation for axial flow compressor stages, describing computer method limitations 09 p1374 A72-22632
- Anthropotechnical aspects of aircraft taxiing guidance in airfield runway areas, suggesting computerized operational system 09 p1269 A72-22779
- Hybrid computing techniques in helicopter simulation, taking into account complex dynamic systems nonlinear effects 09 p1283 A72-22936
- Automatic computer-controlled system with laser technology for quality inspection of mass produced automobile master brake cylinders 09 p1319 A72-22979
- Computer processing of star meridian observations, concerning reduction to visible area, declinations, right ascensions and conversion 09 p1283 A72-23063
- Clinical reliability and normal variations of Frank ECG computer analysis by Smith-Hyde program for healthy and cardiac patients 09 p1272 A72-23274
- Automation of aerial photointerpretation based on application of photometric, microdensitometric and digital computer technology 09 p1313 A72-23308
- High resolution NMR spectrometer conversion from continuous wave to Fourier transform operation, permitting computer systems and pulse amplifiers use 09 p1316 A72-23408
- Three stage retinal model for visual monitoring method applied to computerized photointerpretation of aerial photographs 09 p1284 A72-23624
- Algorithm for automatic construction of finite element approximation to Laplace equation, noting convergence 10 p1502 A72-23719
- STARAN IV-X associative array processor for automation in ATC environment, considering air tracking, conflict prediction and resolution functions 10 p1442 A72-23818
- Instantaneous velocity vector determination in two dimensional flow by hot-wire anemometer and on-line digital computer technique 10 p1478 A72-23877
- Metric tensors as alternate to coordinate transformation equations for computer program inputs in automatic problem formulation 10 p1443 A72-23923
- Computer controlled electron beam machine for microcircuit fabrication, using digital technique capable of working on complex patterns 10 p1459 A72-23956
- Computerized and analytic techniques for estimating multiplexed systems output probability distribution, considering system effectiveness, reliability and survivability 10 p1486 A72-23977
- Hybrid computation interpolation procedure, using table of function values represented by two dimensional array stored in digital computer core memory 10 p1445 A72-24092
- System diagnosis based on ordered statistical samples, discussing Kolmogoroff-Smirnoff detector use for on-line computers in testing noisy systems 10 p1482 A72-24597
- Meteor trail radar operated under digital controller synchronization and programmed for alternate and simultaneous two orthogonal directions search 10 p1438 A72-24715
- Solid body elastic deformation potential energy and structure calculation on computer by finite element method and calculus of variations 10 p1559 A72-24924
- Configuration factors for radiative heat transfer analysis with partially occluded surfaces, defining areas by computer technique [AIAA PAPER 72-304] 11 p1742 A72-25238
- Digital computer calculation of complex electric networks described by mathematical models, calculating flow distribution 11 p1577 A72-25282
- Stellar photometric classification by comparing color indices to indices of standard stars with UPX-YZVS system, outlining computer method 11 p1715 A72-25294
- Rotating mirror image position sensor for high angular resolution optical tracking, discussing performance improvement by computer generated variable density spatial filter 11 p1591 A72-25312
- Computer analysis of shells bifurcation buckling, presenting graphical results [AIAA PAPER 72-352] 11 p1729 A72-25381
- Computer approximate computation of multidimensional normal distribution, examining error measure, random processes and correlation coefficient 11 p1676 A72-25429
- Lower bound estimates of error distributions for analog computer solutions of linear algebraic equations 11 p1600 A72-25433
- Automated echelle spectrograph data handling using computer control 11 p1716 A72-25693
- Rotating analyzer astronomical photopolarimeter automation by on-line computer control system 11 p1600 A72-25695
- Computer control data acquisition system for 46 meter radio telescope at Algonquin Observatory 11 p1631 A72-25697
- Computer controlled coude and Cassegrain scanner telescope spectrometers at McDonald Observatory, discussing design, instrument performance and computer program 11 p1632 A72-25698
- Computerized analysis of prismatic rectangular plate assemblies natural frequencies and initial buckling stresses 11 p1734 A72-25731
- Computer program for bifurcation buckling analysis of shells under collapse load, using strain energy methods and two dimensional finite difference grid 11 p1736 A72-25980
- Turbine aerodynamics research trends, covering engine cooling, high work factor turbines, pneumatic variable geometry and computer analysis 11 p1572 A72-26036
- Russian book on eclipsing binary stars covering limb darkening law, photometric eclipsing phases, computer applications and models 11 p1720 A72-26046
- Algorithm for moving object hologram synthesis with digital computer 11 p1633 A72-26365
- Computerized image analysis, establishing desirable scene characteristics for biomedical display in automated system 11 p1602 A72-26388
- Digital computer technique for computation of pulmonary mechanics parameters, using phasor method and Fourier series analysis of respiratory flow signals 11 p1587 A72-26620
- Computer assisted monitoring of ECG waveforms and heart sounds frequency spectra to detect bubble laden blood during decompression sickness 11 p1587 A72-26626
- Left ventricular volume time course from computer processing of video angiographic data based on X ray densitometry measurements 11 p1587 A72-26627
- Random sample comparison of computer program for ECG diagnoses and physicians readings 11 p1590 A72-26975
- Computer calculation of minimum weight ribbed plates under axial compression by random search method and linear programming 12 p1878 A72-27083
- Probability minimization and detection of errors in computerized analysis of civil engineering frameworks, noting graphical output advantages 12 p1786 A72-27190
- Electronic data processing for management information utilization 12 p1890 A72-27267
- Organizational changes due to electronic data processing /EDP/ introduction into INTERFLUG material-technical supply 12 p1890 A72-27273
- Heat conductivity differential equation solution by hydraulic model system, facilitating temperature values conversion into electrical quantities for hybrid computer 12 p1888 A72-27301

Menu selection for SKYLAB astronauts by computer technique based on mixed integer programming code, using measure of pleasure lists
12 p1769 A72-27442

Computer analysis of helicopter pilots eye movement patterns dependence on visual task skill and performance time
12 p1770 A72-27475

Reliability, quality and testing assurance in ATS F and G system, discussing computerized handling of spacecraft parts information
12 p1814 A72-27524

Analog measuring data transmission systems optimization by computers, noting improvement of dynamic response and linearity in digital systems
12 p1786 A72-27580

Four-phase radio continuum receiver with digital demodulation and signal integration for transfer into on-line computer, discussing calibration
12 p1793 A72-27808

Automatic ECG recording and analysis by electronic data processing equipment, discussing methods of data acquisition and transmission for routine diagnosis and prophylactic mass examinations
12 p1772 A72-27821

Interactive computer graphics technique for structural analysis, aiding engineering decisions by CRT graphical and numerical information display
12 p1787 A72-27864

Automated scanning spectroradiometer for color vision test stimuli and luminescence measurements, applying computer analysis of spectral data
12 p1811 A72-27944

Low cost real time computerized C 14 radiorespirometry telemetering system for monitoring human metabolism data during space missions
12 p1774 A72-28277

Competition criteria for chemical reactions selection in nonequilibrium computer calculations on combustion systems properties, noting seeded flames and rocket exhausts
13 p1912 A72-28548

Computerized reconstruction of orthogonal representations from cylindrical and conical mapped projections with known parameters and base
13 p1956 A72-28738

Computer calculation of second order curve segment discriminant in geometrical problem associated with aircraft lofting, assessing method accuracy
13 p1986 A72-28739

Computer and meteorological satellite effects on weather support for manned space missions, discussing Gemini 5 and Apollo 11 landing weather predictions and cloud climatology
13 p1989 A72-28804

Information theory approaches to air navigation, discussing ATC, collision avoidance and computer applications
13 p1996 A72-29013

Automatic real time processing of meteor radar echoes, using digital computers
13 p1924 A72-29033

Computer algorithm for plates and shells internal forces and moments and stress-strain state determination from strain gage data
13 p2058 A72-29144

Semiconductor devices series production process control and analysis by statistical procedures, noting computer controlled data acquisition system for silicon diodes production
13 p1965 A72-29166

Polynomial surface approximation to OMEGA sky wave corrections for small computer compatible with automatic receiver
13 p1925 A72-29187

Design characteristics and in-flight performance tests of computerized airborne OMEGA receiver, noting time independent one mile accuracy
13 p1997 A72-29188

Metal-dielectric-semiconductor junction transistor HF response analysis by digital computer, deriving switching time as function of impurity concentration and electrode voltage
13 p1932 A72-29294

Computer method of link formation in multiple nomenclature aircraft production lines, minimizing idle time
13 p1966 A72-29464

Digital computer estimates of random processes spectral density by statistical correlation method, calculating errors in numerical integration techniques
13 p1937 A72-29495

Moving sound sources spectral analysis techniques, discussing computer controlled one-third octave band and narrowband analysis
13 p2005 A72-29566

Surface pressure and vector wind fields computerized analysis from satellite radar radiometer simulation and conventional data
13 p1995 A72-29619

Simultaneous operation of digital computer units to reduce input times and prolong useful computer operation time
13 p1925 A72-29944

Kalman filter stability analysis by mathematical modeling, using floating point computer algorithm
13 p1934 A72-30000

Process computer technology, discussing data recognition, on-line open loop operation and system characteristics
13 p1926 A72-30051

Measuring tape recorder, properties and utilization for signal recording and processing, discussing digital computer techniques and compensation for interference effects
14 p2104 A72-30287

Subjective iterative group /SIG/ methodology in forecasting involving computer and computer related technology
14 p2174 A72-30450

Computer calculation of artificial satellite ephemerides from Smithsonian mean orbital elements, comparing observed and computed toponetric equatorial coordinates
14 p2087 A72-30480

Spectroscopic binary orbital elements calculated by FORTRAN IV computer programs, considering period, radial velocity Fourier coefficients and element improvement by least squares method
14 p2159 A72-30736

Computerized measurement and analysis of day-to-day variations of corrected orthogonal ECG and vectorcardiogram in normal subjects, using results as assessment standards
14 p2077 A72-30967

Low storage numerical solution of waveguide problem based on impulse analysis, using random walk technique to eliminate large matrix processing
15 p2194 A72-31542

Computer model study of FET with submicrometer gates, noting gain-bandwidth product increase with decreasing gate length
15 p2205 A72-31544

Data transmission developments, considering computer improvements, networks, routes and frequency multiplexed PCM system
15 p2195 A72-31619

Computer method of optimal turbomachine disk design, using local search techniques to determine disk minimum weight
15 p2328 A72-31746

Cantilever beam tapered linearly in horizontal and vertical planes, obtaining computer solution for free transverse vibration fundamental frequency and harmonics
15 p2328 A72-32022

Head-up display for aircraft three dimensional sky path observation during navigation and landing, discussing computer units, CRT and image generating subsystems
15 p2268 A72-32042

Real time holographic quasi-dynamic 3-D image display, discussing computerized synthetic hologram generator concept and system block diagram
15 p2237 A72-32054

Computerized analytical system for side-looking radar imagery interpretation by isodensitracer scanned density data multivariate analysis applied to environmental discrimination
15 p2198 A72-32064

Ku band radio interferometer for discrete radio sources mapping, discussing construction and incorporated PDP-8 computer for pointing, tracking, delay compensation and data analysis
15 p2207 A72-32107

Computer controlled random environment test systems for large scale off-line data analysis and reduction, using Fourier analyzer
15 p2204 A72-32609

Electronic display in future avionic systems, emphasizing computer techniques and digital data exchange systems
15 p2242 A72-32635

Computer technique to synthesize binary holograms for wave beams analysis in quasi-optical communication channels
15 p2242 A72-32674

Optimal state space synthesis of discrete linear computer controlled systems with quadratic cost function, using Liapunov, Pontryagin, and Bellman techniques
15 p2242 A72-32765

Digital computer studies of control loop parameters and configurations effects on performance of synchronous turbogenerator with two field windings
15 p2183 A72-32793

Passive and active electric circuit analysis by structural numbers method with computer time and space advantages, noting application to transistor circuits
16 p2370 A72-32851

Computerized analysis of overlapping Raman and IR spectral lines, describing routine for resolving complex spectrum into component lines via operator intervention
16 p2366 A72-33027

Nondestructive vibration analysis of mechanical structures, using digital computer technique for sound wave spectrum analysis
16 p2397 A72-33220

Computerized calculation of electronic circuit and equipment reliability and quality control, presenting task examples and printout form
16 p2368 A72-33347

Computer calculations of horizontal linear antenna impedance for multilayer plane stratified medium, using induced emf method
16 p2368 A72-33492

Biotelemetry and computer analysis techniques for steep states and wakefulness studies during aerospace flight
16 p2356 A72-33560

Computerized aircraft landing measurement system for civil airport, using optical, seismic and IR sensors
16 p2374 A72-33627

Algorithm for moving object hologram synthesis with digital computer
16 p2394 A72-33717

Serial ECG change detection and description in myocardial infarction survivors, using computer analysis to find best diagnostic discriminants from multiple criteria
16 p2357 A72-34008

Computerized photographic imagery analysis system with interactive operator controls for processing option selection in image enhancement prior to pattern identification
17 p2520 A72-34407

Comparison of computer-acquired performance data from several fixed spaced planar diodes
17 p2496 A72-34605

A computer system for structural design
17 p2522 A72-34743

Analysis of a control computer complex as a multiphase queueing system
17 p2522 A72-35030

Three-dimensional small-signal analysis of bipolar transistors
17 p2530 A72-35099

An automated gradient projection algorithm for optimal control problems
17 p2576 A72-35244

Digital computer investigation of radio signals transmitted by Venera 7 during Venus soft landing, describing spectral analysis and telemetric data detection methods
17 p2516 A72-35273

Process computer system design, discussing structural units, data flow coordination with storage, input/output channels and periphery coupling problems
17 p2523 A72-35443

Sizing new generation aircraft wire and circuit breakers utilizing computer techniques
17 p2498 A72-35568

Computer control of aircraft landing
17 p2578 A72-35950

Computer aided study of nondiffusive plane convection mixing of scalar field by isotropic turbulence of single velocity modes
18 p2678 A72-36017

Stochastic optimal path selection via N discrete points set, discussing probability distributions and computer requirements
18 p2672 A72-36055

Image processing by digital computer
18 p2663 A72-36247

Image restoration - The removal of spatially invariant degradations
18 p2658 A72-36257

Space-variant image motion degradation and restoration
18 p2658 A72-36258

Inverse filtering for linear shift-variant imaging systems
18 p2658 A72-36259

Electronically restored holographic data recording process for analog shape visualization with random access computer storage, discussing system design and capabilities
18 p2659 A72-36271

An analog computer technique for estimating sample times for digital simulation
18 p2663 A72-36305

Hybrid processing of empirical functions in mechanics
18 p2710 A72-36423

A new project of 8-cm radioheliograph
18 p2691 A72-36434

A new computer-assisted stereocomparator
18 p2664 A72-36499

The AEG 60-50 process computer in special research field 55 at the Rhein-Westphalian Technische Hochschule at Aachen
18 p2664 A72-36680

Automatic computation of exponentials, logarithms, ratios and square roots
18 p2705 A72-37021

Programming method for computer analysis of linear passive circuits powered by voltage sources
19 p2777 A72-37311

Computer method for plasticity theory boundary value problem for medium with unknown equations of state, using complex load simulating device
19 p2870 A72-37387

An automatic measuring and recording system for clinical electrooculography.

19 p2759 A72-37400

Some properties of iterative square-rooting methods using high-speed multiplication.

19 p2769 A72-37577

Cross-ambiguity function for a linear FM pulse compression radar.

19 p2764 A72-37868

Digital tracking with phased arrays.

19 p2765 A72-38261

Measurement transducers in industrial process control, discussing requirements for dynamic properties, stability, linearity and computer applications

19 p2803 A72-38315

Process control of the 100-meter telescope - Astronomical concept

19 p2803 A72-38485

Computer aided analysis of hologram optical elements for aberration and dispersion reduction and recording on thick media

20 p2922 A72-39036

Space shuttle terminal navigation with conventional navigation aids.

[AIAA PAPER 72-832]

20 p2950 A72-39095

Quadruple-redundancy management for fly-by-wire control system reliability, discussing analog circuit and digital computer voter/monitor techniques

[AIAA PAPER 72-884]

20 p2910 A72-39117

Square root least squares and filtering solutions for fixed point and interval smoothing problems, comparing computational stability and precision and computer requirements

[AIAA PAPER 72-877]

20 p2910 A72-39122

A simulation technique used in the development of a flight control system for an aerodynamically controlled missile.

[AIAA PAPER 72-858]

20 p2976 A72-39136

Memory requirements and computation times for implementing reduced consensus algorithms.

20 p2905 A72-39434

Computerized long term weather forecasting via mathematical modeling of atmospheric processes based on meteorological parameters worldwide observational data

20 p2948 A72-39939

A method of calculating the parameters of a linearized transistor model

21 p3027 A72-40475

A recursive least-squares approach to the on-line adaptive control problem.

21 p3037 A72-40640

A computational technique for optimal control problems having singular arcs.

21 p3037 A72-40641

Digital computer synthesis of Fourier holograms of transparencies, noting significance to digital filtering method development for optical signal processing

21 p3054 A72-40670

Digraphs application to electronic linear networks analysis, developing computer program

21 p3024 A72-40992

Process computation systems, discussing translator programs for conversion of user programs into machine language

21 p3024 A72-41002

Prediction displays based on the extrapolation method.

21 p3010 A72-41409

Human or computer control role in teleoperator remote control mechanisms, discussing control modes, sensing and transmission time delay problems

21 p3011 A72-41416

Computerized supervisory control for interpretation of subgoal statements from human operator to permit teleoperator interaction with environment without long time delay

21 p3011 A72-41417

A method for the development and optimization of controller-models for man-machine systems.

21 p3011 A72-41420

Computer-aided vector Taylor series approximation of fundamental matrix of ordinary first order differential equations with variable coefficients

21 p3076 A72-41785

Stability criterion and imaginary axis displacement for real roots determination of algebraic equations on analog computers

21 p3025 A72-41806

Variational formulation and computer solution for thermal boundary layer flow over flat plate in entrance region, assuming temperature dependent thermal conductivity and viscosity

22 p3156 A72-41959

Efficient computer decoding of pseudorandom radar signal codes.

22 p3153 A72-41978

Evolution of the electronic head-up display.

22 p3176 A72-42295

On the solution of non-linear simultaneous equations with particular reference to fluid-dynamics.

22 p3199 A72-42325

Objective-prism plates photometric computerized calibration method based on continuum energy dis-

tribution of standard stars within photographic plate field

22 p3177 A72-42376

Figl astrophysical observatory design and instrumentation, describing solar radiation insulation, computerized data reduction, area scanning photoelectric photometer and Cassegrain spectrograph

22 p3178 A72-42541

Digital computer technique and real time monitor software application to instrumentation data acquisition system, discussing design guidelines and gas turbine engine test example

22 p3156 A72-42681

Digital computer controlled testing equipment for separately driven coaxial gas turbine low and high pressure compressors, emphasizing reliability and flexibility in system design

22 p3157 A72-42682

Computer-operated data acquisition and control system for automatic diagnostic monitoring of propulsion research instrument

22 p3216 A72-42684

Development of a digital control system for a spacecraft propulsion test facility.

22 p3163 A72-42685

Nondestructive stability evaluation of large shell structures by direct computer controlled testing.

22 p3157 A72-42695

Computer control of the General Dynamics High Speed Wind Tunnel.

22 p3157 A72-42697

Transient test techniques for modal survey testing.

22 p3163 A72-42698

Best linear invariant estimation of Weibull parameters - Samples censored by time and truncated distributions.

22 p3199 A72-42969

Parallelized algorithms for computer solution of spanning tree, distance and path problems on cellular array of identical modules containing memory and combinational logic

22 p3157 A72-43023

A new approach to automatic scanning of contour maps.

22 p3174 A72-43024

An adaptive replacement algorithm for paged-memory computer systems.

23 p3266 A72-43420

The weight module - A keystone in the aircraft synthesis program.

[SAWE PAPER 912]

23 p3250 A72-43459

Computerized airframe manufacturing cost and weight analysis, using technique for detailed parts list generation from configuration concept as input

[SAWE PAPER 913]

23 p3293 A72-43460

L-1011 computerized weight reporting system present and future capabilities.

[SAWE PAPER 932]

23 p3251 A72-43472

Wideband pulsed-RF phase measurement.

23 p3270 A72-43575

Computer-controlled queuing system with service interruptions.

23 p3275 A72-43605

Utilization of computers in mechanical strength studies

23 p3345 A72-43644

The optimal control of merging aircraft - Implementation of the hybrid air traffic controller.

23 p3277 A72-43868

Characteristic curve formulas of cosmic objects and stellar focal images for photometric measurement processing on computer

23 p3267 A72-44030

Computer aided directivity measurements of large antennas in Fresnel zone

23 p3274 A72-44491

Improvement of an algorithm for the rejection of points in the solution of a mutual orientation problem on a digital computer

24 p3401 A72-44861

A method of computing numerically integrated stiffness matrices.

24 p3457 A72-44878

Point-to-point national data communication geostationary satellite system associated with computers, discussing organization, earth station equipment and technical and economical feasibility

24 p3380 A72-44975

Minicomputers application for long distance data transmission, noting multipurpose use of VT 1010/B computer in satellite operation program

24 p3382 A72-45391

Remotely controlled astronomical observatory telescope Cassegrain focus, evaluating computerized automated electronic system advantage over conventional instrument

24 p3405 A72-45543

The automatic computation of exponentials, logarithms, ratios, and square roots.

24 p3383 A72-45668

COMPUTERIZED CONTROL

U NUMERICAL CONTROL

COMPUTERIZED DESIGN

Tubular traveling wave antenna array for radar applications and microwave television transmitters, describing computer program for design

01 p0039 A72-10668

Computerized optimization procedure for microwave circuits without tuning elements, applying to high pass filter design

01 p0040 A72-10686

Computer program for microwave circuit scattering matrix sensitivity, applying to stripline elliptic low pass filters and thin-film negative resistance transistor amplifier

01 p0034 A72-10688

REDAP 31 network analysis program for design of S-band phase shifter with P-I-N diodes for phase array antennas

01 p0040 A72-10689

Computer program for design optimization of three-stage wideband low-noise integrated microwave amplifier

01 p0041 A72-10690

Circuit theory optimization techniques in computer aided electric circuits and devices design, discussing algorithms, sequential methods, convergence speed, topologies, system responses, etc

02 p0197 A72-11688

Computer aided circuit design and analysis, emphasizing algebra of structural numbers as synthesis technique without system structure restriction

02 p0186 A72-11693

High efficiency GaAs transferred electron device operation and microwave oscillator design by simple static I-V characteristics description for time domain computer simulation

02 p0193 A72-12230

Computer programs and program systems for IC synthesis, emphasizing models, analysis methods, optimized design and monolithic and hybrid IC configurations

02 p0197 A72-12668

Aircraft design interactive computer graphics technique, using human decision input response to computer output information

02 p0300 A72-12733

Self consistent junction circulator theory, considering lossless ferrite loaded symmetric n-port junction and numerical design procedures

03 p0330 A72-13232

Thin film optical waveguides using magneto-optic GdIG as substrate, discussing computerized design for propagation mode converter efficiency

03 p0332 A72-13755

Inductor design for minimum inductance at given dc level, using computer programs

03 p0332 A72-13759

Computerized design algorithm for ferrite core memory system, considering cross-temperature effect under worst driving conditions

03 p0327 A72-13766

Dc, ac and transient models of IC operational amplifier for computer aided circuit design and analysis applications

03 p0329 A72-14180

Computer simulation techniques in aerospace ground equipment design for maintenance testing of avionic systems

03 p0329 A72-14196

Numerical method and computerized design for feedback controller pulse transfer function in overall error criterion minimization, comparing results with sampled error method

03 p0329 A72-14355

Robust delta modulator configuration with minimal mean square error from signal statistics estimates, discussing design and performance by digital simulation

04 p0486 A72-14486

Wire antenna computer design to determine feed voltages for obtaining pattern synthesis and gain maximization, using matrix methods

04 p0495 A72-14492

Computer aided design of single tuned parametric amplifiers, stressing voltage gain-bandwidth product

04 p0497 A72-14715

Computer aided linear circuit design for network synthesis, analysis, optimization and data storage noting MARTHA program

05 p0639 A72-15785

One dimensional bipolar junction transistor, comparing charge control and regional mathematical models for suitability in device and circuit computerized analysis and design

05 p0636 A72-16359

Computer simulation in optimized 5-GHz Gunn diode oscillator design

05 p0633 A72-16360

Ten-stage electrostatic depressed collector designed with analog computer for improving klystron power conversion efficiency

05 p0637 A72-16365

Satellite attitude control with gimbaled reaction wheel digital system, discussing logic and compu-

terized design, implementation, fabrication and performance tests

05 p0726 A72-16458

Control system design computerized optimization technique based on high speed repetitive simulations and gradient minimization, considering application to reusable and expendable boost vehicles

[AIAA PAPER 72-98] 05 p0729 A72-16812

Digital system automated design and analysis developments covering interactive graphic computer aided design, gate level simulation, synthesis, partitioning, interconnection and fault test generation

06 p0778 A72-17471

Interactive computerized design and programs for computer logic design block assignment to modules, comparing performance with manual solutions

06 p0778 A72-17472

Interactive computer graphics design aids to IC mask layouts, discussing hardware and software techniques including IMP program

06 p0778 A72-17473

CIRCAL-2 general purpose on-line circuit design computer program featuring multiple analysis, text editing, network representation and user-program interaction optimization capabilities

06 p0778 A72-17474

Algebraic scheme describing electric element and subnetwork interconnection into networks by wiring operators having conversation capability with computer

06 p0778 A72-17475

Time shared electronically patched hybrid computer for design automation, discussing remote terminal graphics capabilities and simulation language compiler

06 p0778 A72-17476

Coordinated characterization and mathematical modeling for device, circuit and system designs and computer analysis, applying to bipolar transistor

06 p0778 A72-17477

One dimensional analysis computer program for junction device modeling, exemplifying hf bipolar transistor Fermi statistics effect and velocity limitation in high current density

06 p0779 A72-17478

Computer aided steady state response analysis for nonlinear electric circuits with periodic input, using Newton algorithm with rapid convergence

06 p0779 A72-17480

Hybrid computer aided design of thick electrostatic electron lenses by Laplace equation solution in terms of cylindrical harmonics, applying to CRT

06 p0779 A72-17481

Computer aided design in electronics, discussing interactive computing with time sharing teletype keyboards or CRT graphics and applications in IC, network analysis and optimization

06 p0780 A72-18236

High power L-band microminiaturized hybrid type integrated transistor amplifier design and realization by computer

06 p0785 A72-18314

Broadband parametric amplifier design using computerized optimization procedure based on Gauss-Newton iteration technique

06 p0786 A72-18376

Computer aided renormalized perturbation method for inhomogeneously loaded waveguide performance calculation

06 p0786 A72-18377

Aircraft preliminary design procedure with integrated performance simulation, using time sharing computer facility

07 p0913 A72-20353

Interactive graphics technique for design of single input linear feedback systems described by state equations or cascaded transfer functions

07 p0963 A72-20391

Closed type gas turbines heated with nuclear energy, calculating heat transmitter dynamic behavior with computer program

07 p1055 A72-20598

Computerized numerical nodal analysis of heat transfer away from bridgwire of electroexplosive device to meet all- and no-fire requirements

08 p1219 A72-20753

Hybrid computer synthesis and simulation algorithm for optimal discrete nonlinear filters, giving timing, accuracy and equipment requirement estimates

08 p1137 A72-20851

Computerized design and weight estimation of high voltage power conditioner for communication spacecraft

08 p1112 A72-21417

Automated minimum weight design of ring and stringer stiffened conical shells, using membrane theory for prebuckling analysis

08 p1245 A72-21599

Conjugate gradient method for computerized antenna radiation pattern synthesis using error functional minimization and iterative procedure

08 p1143 A72-21988

Digital computer prepared optimal controls setting diagrams for single loop, linear and concentrated parameter control circuit design

09 p1291 A72-23372

Computer aided design of linear time-invariant multivariable feedback control systems, given specifications in frequency domain in stability margin form

10 p1455 A72-23789

Hybrid computer aided synthesis of thick electrostatic electron lenses by Laplace equation solution in terms of cylindrical harmonics with gradient used in trajectory integration

10 p1509 A72-23940

Electron microscope interfaced computer for generating, registering and fabricating microelectronic device and circuit patterns

10 p1459 A72-23955

Transport aircraft fuselage computerized design, determining optimal structural distribution for strength and displacement constraints

[AIAA PAPER 72-330] 11 p1727 A72-25366

Computerized structural design of aerospace vehicle, stressing automated routines for finite element models generation

[AIAA PAPER 72-332] 11 p1727 A72-25367

Computer aided iterative design of nonlinear single loop control system with sinusoidal describing function and time response display capability

11 p1601 A72-26042

Computerized filter design, discussing frequency analysis and synthesis programs for quadrupole eigenmodes and transfer function

11 p1604 A72-26089

RF ion thruster for spacecraft propulsion, discussing tests and digital computer calculations to optimize design parameter

[AIAA PAPER 72-474] 11 p1709 A72-26205

Path connection algorithms for optimal IC layout on circuit board, using digital computer

11 p1607 A72-26784

Nonlinear mathematical dc models of planar transistors for computerized IC design and analysis obtained by continuity equation approximate solution

12 p1789 A72-27313

Hybrid computers application to digital communication systems design, using real time simulation

12 p1786 A72-27324

Computer aided thermomechanical design of mercury bombardment ion thrusters, involving heat transfer, vibration and stress analysis

[AIAA PAPER 72-431] 12 p1860 A72-27420

Dynamic systems as models for electronic measuring instruments computerized development and design

12 p1791 A72-27579

Computer aided circuit design by TRAPATT diode model consisting of nonlinear capacitance shunted by voltage- and current-controlled switch

12 p1791 A72-27672

Computerized antenna array design, using Automated Engineering and Scientific Optimization Program

12 p1792 A72-27735

Automatic control system synthesis by computer-aided version of grapho-analytical method

13 p1934 A72-28459

Large amplitude flight simulator for fighter design refinement, noting extensive computer commitment

13 p1938 A72-28757

Computerized synthesis technique for nonlinear feedback control systems, incorporating circle and Popov criteria

13 p1936 A72-29107

Computerized synthesis of wideband series stabilized tunnel diode amplifier based on distributed constant elements

13 p1931 A72-29286

Computerized optimal design by nonlinear programming for minimum weight elastic plates crossed with rigid ribs for vibrational loading to meet natural frequencies condition

14 p2165 A72-30576

Aerospace complex physical systems including human operator, discussing computerized design for behavior analysis by means of mathematical models

14 p2093 A72-30846

Computer designed optical integrating devices for semiconductor laser arrays, considering diode, collection, projection and zoom parameters

15 p2248 A72-32048

Computer aided thermal design of LSI module packs for forced convection air cooling, using modal conductance matrix method

16 p2368 A72-33195

Communication satellite modeling into subsystems to formulate parametric relationships among power, mass and cost, comparing computerized design alternatives

17 p2512 A72-34263

A broad-band wide-angle scan matching technique for large environmentally restricted phased arrays

17 p2513 A72-34353

Computer aided impedance matching of an interleaved waveguide phased array

17 p2525 A72-34373

Computed performance data for a thermionic converter having a CI-CVD-W emitter and a polycrystalline Nb collector

17 p2521 A72-34613

Computer thermal analysis of hybrid microcircuits

17 p2521 A72-34679

Computer-aided thermal design of LSI packages

17 p2527 A72-34681

An algorithm for the automatic synthesis of nearly optimal 2-level and/or combinational circuits

17 p2533 A72-35058

Design of simple control loops in the time domain by simulation of the hybrid mode

17 p2534 A72-35756

Pattern synthesis of linear arrays using Fourier coefficient matching

18 p2659 A72-36298

Design of digital filters using state-space realization

18 p2674 A72-36943

Design considerations of a 3.1-3.5 GHz GaAs FET feedback amplifier

19 p2771 A72-37269

Computerized design of electric filters with given frequency response, discussing attenuation characteristic approximation by Chebyshev method

19 p2776 A72-37307

Active controls - Changing the rules of structural design

19 p2748 A72-37681

Application of the computer to aerial design and development

19 p2773 A72-37873

A computerized system for the preliminary design of commercial airplanes

[AIAA PAPER 72-793] 19 p2749 A72-38110

A flutter optimization program for aircraft structural design

[AIAA PAPER 72-795] 19 p2876 A72-38111

An integrated computer system for preliminary design of advanced aircraft

[AIAA PAPER 72-796] 19 p2749 A72-38112

Computer program for automated design of long haul transport aircraft, discussing cost effectiveness of composite materials for aircraft structure

[AIAA PAPER 72-794] 19 p2750 A72-38121

Digital computer algorithm for electronic circuit calculations

19 p2774 A72-38422

Nonlinear programming in computerized electronic circuits design, discussing optimization methods and real time operation

19 p2782 A72-38578

Eigenfrequencies of monolithic filters

19 p2774 A72-38608

An improved design and measurement of attenuation characteristics of RF suppressors

20 p2902 A72-38997

Antenna pattern analysis for compatibility prediction

20 p2902 A72-39000

Computer simulation aided airborne attack missile launch system design for safe separation from carrier aircraft, discussing ejection and control systems design

[AIAA PAPER 72-828] 20 p2951 A72-39099

A variation-iteration technique for the design of wall-impedance waveguides

20 p2903 A72-39429

The optimum design of small nonuniformly spaced arrays

21 p3027 A72-40362

On the removal of blindness in phased antenna arrays by element positioning errors

21 p3027 A72-40363

Computerized design for cylindrical cage antenna, using polynomial approximation of current to reduce computer size and time requirements

21 p3028 A72-40511

Bubnov-Galerkin solutions to wire-antenna problems

21 p3032 A72-40631

Recent development on thermal design of spacecraft

21 p3115 A72-41125

Integration of aerospace vehicle performance and design optimization

[AIAA PAPER 72-948] 22 p3137 A72-42355

Aircraft synthesis analysis program /ASAP/ for computerized aircraft design, enabling large number of trade-off studies for design optimization

[SAWE PAPER 907] 23 p3250 A72-43454

An aerodynamics model applicable to the synthesis of conventional fixed-wing aircraft

[SAWE PAPER 908] 23 p3250 A72-43455

Mission analysis and performance program as part of computerized aircraft configuration synthesis process, describing interfaces with other system modules

[SAWE PAPER 909] 23 p3250 A72-43456

Wideband limitations of waveguide arrays

23 p3270 A72-43573

Digital filter realizations using a special-purpose stored-program computer

23 p3267 A72-43815

- An algorithm to obtain the steady state response of nonlinear periodic systems. 23 p3267 A72-43852
- Electric field distribution and strength and electron trajectories computations in designing electron optical display systems, using rectangular networks 23 p3291 A72-44312
- Aircraft/spacecraft design approach and performance data, considering space shuttle program 24 p3467 A72-45159
- Application of cascade and actuator disc theories to computer aided design of fans. 24 p3363 A72-45359
- ## COMPUTERIZED SIMULATION
- ### NT ANALOG SIMULATION
- ### NT DIGITAL SIMULATION
- Adaptive statistical prediction algorithm for character recognition by computer simulation involving handprinted numerals 01 p0034 A72-10472
- Feature classifying filter for pattern recognition system simulated on computer for line printed numerals 01 p0034 A72-10473
- Computer simulation of evoked cortical audio potentials in animals and humans, noting clinical application for hearing threshold measurements 01 p0016 A72-11324
- Lunar surface soil mechanical properties from computer simulation of Surveyor spacecraft observation data for each landing site, estimating cohesion 02 p0275 A72-11595
- Second order Markov process statistical model for gravity anomalies in local region, applying to error analysis in inertial navigation system computerized simulation 02 p0207 A72-11596
- Handling qualities simulation program for augmentor wing jet STOL research aircraft considering control devices design 02 p0154 A72-11654
- Hybrid computer simulation program used in development and software design validation of digital flight control system for Titan 3C space booster 02 p0186 A72-11655
- Aerodynamic multivariable function generation in real time simulation of high performance missile 02 p0186 A72-11656
- Plasma physics computer simulation of double stream and beam instabilities, wavelength nonlinearities and velocity distribution, using superparticle and Vlasov equation models 02 p0263 A72-11691
- Double 45 degree z cut KD P electro-optic Q switch simulation with programmable desk top computer, deriving extinction ratio dependence plot graphs 02 p0224 A72-11746
- Multispectral photographic data preprocessing and computerized simulation of ERTS data channel to make terrain maps, testing classification accuracy improvement possibility 02 p0215 A72-11880
- Computer simulation studies of hybrid pull-up bootstrap decoding algorithm, devising technique for efficient computational allocation and reliable identification of decoded data sections 02 p0187 A72-12154
- Fast Fourier transforms for digital matched filters in wideband radars, using computer simulation for word size and dynamic range relationship determination 02 p0188 A72-12398
- Stress corrosion crack initiation and propagation characteristics computerized simulation validity 02 p0295 A72-12480
- Simulation of complex systems - Conference, Tokyo, September 1971 02 p0188 A72-12654
- Hybrid computer simulation of spinning satellite dynamic behavior during flexible booms deployment and attitude control maneuvers, deriving equations of motion from Lagrange equations 02 p0286 A72-12658
- Miss distance simulation for SAM guided by proportional navigation, using ASIM programming language for digital computer 03 p0386 A72-13611
- Anhyseretic contact printing magnetization simulation by computer with Preisach diagram modified by Onsager field effect [IEEE Paper 14.2] 03 p0327 A72-13768
- Computerized simulation for AM radio receiver waveform performance degradation under pulsed interference 03 p0324 A72-14035
- Computer simulation techniques in aerospace ground equipment design for maintenance testing of avionics systems 03 p0329 A72-14196
- Simulation language for digital static checks for hybrid and analog computers 04 p0495 A72-14417
- Gunn diode large signal admittance dependence on bias and frequency, discussing computer simulation and broadband oscillator and amplifier design 04 p0497 A72-14712
- Nonrecursive and recursive adaptive equalizers for digital communication, discussing computerized simulation of performance 04 p0493 A72-15520
- Navier-Stokes equations numerical solution by computerized simulation for viscous channel flow with diaphragm orifice reducing cross section 04 p0513 A72-15644
- Lynden-Bell statistical mechanics predictions compared with most and least violently relaxed one dimensional self gravitating systems, using computer experiments 05 p0714 A72-16055
- Computerized simulation techniques for plasmas, discussing electrostatic particle model properties and implications 05 p0694 A72-16058
- Computer simulation in optimized 5-GHz Gunn diode oscillator design 05 p0633 A72-16360
- Turbulent heating in computer simulation of modified plasma two stream instability driven by relative electron-ion drifts across magnetic field 05 p0696 A72-16687
- Control system design computerized optimization technique based on high speed repetitive simulations and gradient minimization, considering application to reusable and expendable boost vehicles [AIAA Paper 72-98] 05 p0729 A72-16812
- Automated scheduling algorithm for aircraft from terminal area to touchdown, discussing system features and STOL air traffic computerized simulation [AIAA Paper 72-120] 05 p0688 A72-16905
- Fast time simulation application to ATC systems, discussing control action exercise within strategic/tactical spectrum 05 p0645 A72-16994
- Computerized man machine systems human factors research simulator, discussing application to railroad train operations 06 p0795 A72-17434
- Computerized simulation of high intensity beam charged particle trajectories in electromagnetic fields with rotational symmetry, applying to ion extraction 06 p0852 A72-17491
- Bearing estimation performance of monopulse tracking with passive linear arrays, using computer simulation for various integration times and input S/N ratios 06 p0774 A72-17809
- Automated ATC guidance technique for aircraft curved flight trajectories, describing flight profiles synthesizing algorithms and computerized simulation technique [AIAA Paper 72-121] 06 p0845 A72-17922
- Computer simulation applications - Conference, New York, December 1970 06 p0779 A72-17972
- Military aircraft operations and logistics computerized simulation for support and maintenance cost estimates 06 p0758 A72-17974
- ATC study by computerized simulation, using successive approximation models 06 p0845 A72-17975
- Lounge planning model for airport terminal design simulation, taking into account scheduled arrivals and departures, aircraft types, passenger number, gate assignments, etc 06 p0780 A72-17979
- Numerical experiments in collisionless stellar systems evolution by gravitational n-body calculations using computers 06 p0885 A72-18076
- Computer models for simulating self consistent collisionless stellar systems evolution under gravitational field 06 p0885 A72-18081
- Computer simulation data on pulsed IMPATT microwave oscillator performance improvement via double-drift diodes and second harmonic tuning 06 p0788 A72-18463
- Computer simulated data analysis procedure for improved resolution of optical instrument by integral equation numerical solution 06 p0840 A72-18738
- Aircraft safety enhancement by computer controlled flight simulator training of air crews, discussing Boeing 747 program 07 p0926 A72-18839
- ATC at single-runway airport analyzed by fast time simulation with high speed digital computers 07 p1032 A72-19064
- Computer graphics system simulation of saccadic eye movement made for time optimal control behavior study, incorporating eye muscle characteristics 07 p0928 A72-19309
- Computerized simulation from model of human pupillary motor behavioral response to light, accommodation and fusional inputs 07 p0928 A72-19310
- Electrical cardiac activity computer simulation model including biophysically faithful conduction system and electrocardiograms for high fidelity production 07 p0929 A72-19313
- Computer simulated phased arrays with randomly located elements, deriving peak sidelobe level for comparison with measurement 07 p0945 A72-19783
- Computerized simulation of two dimensional turbulent flow in Fourier space with random initial conditions on coefficients, discussing velocity, pressure and vorticity fields 07 p0971 A72-20084
- Computer simulation - Conference, Boston, July 1971 07 p0950 A72-20326
- Apollo manned mission real time ground support computer simulation for NASA flight controller training to maximize flight crew safety 07 p0933 A72-20329
- Stochastic simulation model for space shuttle fleet operations, using closed loop queueing system approach 07 p0965 A72-20330
- Integrated systems approach to computer simulation with functional modules to achieve control processor independent expansion and optimization 07 p0951 A72-20331
- Hybrid computer simulation for telemetry data collected during missile flight control system model post-flight verification and hardware performance analysis 07 p1085 A72-20332
- Bioelectric ECG and EEG signal analysis using hybrid computer techniques and parameter optimization for autocorrelation function modeling 07 p0933 A72-20333
- Hybrid computer and graphics terminals for real time dynamic man machine interaction, discussing AM communication system simulation 07 p0951 A72-20335
- Boeing 707 cockpit simulator with computer generated displays, moving area navigation map and ATC information 07 p1033 A72-20336
- Computerized dynamic simulation with graphic display of crystal plastic dislocation movement among random obstacles, emphasizing stress-strain, strain rate and thermal activation mechanisms 07 p1095 A72-20338
- Analog/hybrid simulation of noise effect on adaptive delta modulation system consisting of transmitter, receiver and error simulator 07 p0951 A72-20339
- Linear first order differential equation transient response computer simulation using transition matrix method 07 p1028 A72-20340
- Airfield surface system fast-time computer simulation model for airport planning systems analysis 07 p0965 A72-20341
- Air/ground interface simulation in GPSS/360 for passenger transfer between airport terminal and aircraft 07 p1106 A72-20342
- Nonlinear computerized simulation of air cushion vehicle dynamics, using bond graph techniques 07 p0913 A72-20343
- Direct simulation Monte Carlo method for rarefied gas dynamics, discussing computer display units use for flow visualization 07 p0973 A72-20344
- Aerospace systems radar target computer simulation model based on simple multiple reflector geometrical configuration 07 p0948 A72-20345
- Aircraft preliminary design procedure with integrated performance simulation, using time sharing computer facility 07 p0913 A72-20353
- Nonlinear model for computer simulation of human arterial system, using finite difference technique for pressure and flow calculations 07 p0934 A72-20357
- Computer simulation of empirical confidence limits for variance spectra, applying to Gaussian random noise data stochastic model 07 p0951 A72-20360
- Computer simulation prediction program for attitude disturbance torques for Tiros series spacecraft rotational motion control 07 p1086 A72-20361
- Computer simulation requirements for air and ground transportation system, emphasizing mathematical models capable of system performance relation to design parameters 07 p0952 A72-20362
- Real time computer simulation of command and control in transportation systems, detailing models, and programming technique and ATC controller effectiveness evaluation 07 p0952 A72-20363
- Computerized numerical calculation of muons production spectrum, angular distribution and Coulomb scattering in determining meteorological factors effects on cosmic rays 07 p1067 A72-20655
- Hybrid computer synthesis and simulation algorithm for optimal discrete nonlinear filters, giving

- timing, accuracy and equipment requirement estimates 08 p1137 A72-20851
- Hybrid Monte Carlo techniques with digital and analog computers and minimal interface, simulating random walks for partial differential equations solution 08 p1138 A72-21602
- Meteorological radar signal reflectivity probability and quantization error dependence on incoherent storage device parameters from computer simulation 08 p1201 A72-21995
- Hybrid computer simulation of cardiovascular system in biomedical engineering education 09 p1268 A72-22455
- Collisionless plasmas numerical simulation with weighted particles and periodically reconstructed distribution function, estimating diffusion rates 09 p1358 A72-22462
- ATC systems analysis by computerized real time environmental simulation, taking into account new aircraft types, navigation and supervision aids 09 p1348 A72-22782
- Computer simulation of crack tip atomic structure in diamond, relating covalent bond structure to dislocation nucleation and propagation likelihood 09 p1338 A72-22923
- Hybrid computing techniques in helicopter simulation, taking into account complex dynamic systems nonlinear effects 09 p1283 A72-22936
- Raman band rotational structure computer simulation, noting application to gaseous chlorine spectrum analysis 09 p1358 A72-23050
- Relativistic electron beam and ring phenomena calculation using plasma simulation program CYLRAD 10 p1518 A72-23958
- Bayesian analysis application to reliability and life parameter estimation for Weibull failure model, using Monte Carlo simulation 10 p1503 A72-23978
- Random access memory with single error correction circuitry, predicting failure, card and module removal rates by computer simulation 10 p1443 A72-23980
- Binary collision loaded-sphere molecular model for diatomic gases computer simulation, obtaining normal shock waves velocity, density and temperature profiles 10 p1466 A72-24297
- Mathematical statistics application to complex systems modeling, considering group method of data handling, simulation and regression methods 10 p1457 A72-24634
- Hydraulic transmission line equations for computer simulation of arterial circulatory systems 10 p1431 A72-24811
- Computer simulation for TRAPATT circuit response to periodic current impulse, noting avalanche diode microwave oscillation efficiency 10 p1458 A72-24935
- Digital computer simulation of random processes specified by canonical expansion, discussing quantization steps for storage requirements reduction 11 p1600 A72-25432
- Plasma beam cyclotron instability theory based on computer simulation, noting stabilizing effect due to Landau damping 11 p1693 A72-25562
- Dynamic modeling application to technological forecasting, discussing mathematical simulation for R and D management planning in project selection and budget allocation 11 p1748 A72-26284
- Hybrid computers application to digital communication systems design, using real time simulation 12 p1786 A72-27324
- Man computer weapons effectiveness and system test environment /WESTE/ instrumentation system with Decca navigation for simulated combat environmental flight tests 12 p1754 A72-27515
- Dynamical motion simulation facility for Symphonie satellite, using sensors, attitude control electronics and analog computer in closed loop system [DFVLR-SONDDR-201] 12 p1795 A72-27659
- Nonlinear fracture toughness determination via three point bending test simulation by elastic-plastic finite element computer program 12 p1830 A72-27731
- Galactic cluster lifetimes from observed age distribution comparison to evaporation times by numerical experiments with star cluster models 12 p1873 A72-27897
- Stability of encounterless self gravitating constant density system from computer experiment, using Fourier series expansions and Bessel functions 12 p1874 A72-27906
- Numerical experimentation in collisionless systems for Jeans instability, static self consistent models and spiral patterns 12 p1874 A72-27908
- Computer model for evolution of isolated rotating disks of stars, noting gravitational two stream dynamic instability for infinite double periodic stellar systems 12 p1874 A72-27909
- Spiral density wave structure persistence conditions determined from computer simulations of galaxies evolution, noting gravitational azimuthal and radial forces effects 12 p1874 A72-27910
- Computer simulation of plasmas by following actual orbits of particles interacting through electrostatic forces 12 p1852 A72-27914
- Computer models for collisionless stellar systems equations of motion, obtaining force from smoothed gravitational field 12 p1875 A72-27920
- Computer simulation of pulsed hydrofluoric acid laser pumped by chain reaction, investigating cavity and chemical parameters effects on laser pulse 12 p1826 A72-27938
- Cost effectiveness determination for different levels of reliability and maintainability of training aircraft, using computer simulation 13 p2067 A72-28355
- Theoretical and computer simulation of laminar interactions of plasmas with different mass and density, discussing piston-ion dynamics solutions 13 p2009 A72-28427
- F 2 layer parameter forecasting by computer based on series coefficients dependence on Wolf number 13 p1946 A72-28597
- Four dimensional atmospheric model providing global moisture, temperature, pressure and density profiles as attenuation model inputs for earth resources satellite mission simulation 13 p1989 A72-28805
- Automatic ceilometer systems for sky state reporting, discussing computerized cloud simulation model, instrumentation and data sampling 13 p1992 A72-28850
- Air Force Global Weather Central computer simulation of specific aircraft flight plans, using update weather information for specified route profile 13 p1924 A72-28873
- Monte Carlo simulation for imperfect second order hybrid phase locked loop in radio frequency interference and Gaussian noise backgrounds, employing digital computer simulation model 13 p1935 A72-29104
- Computerized simulation of single large amplitude whistler wave propagation in plasma, noting collisionless damping, oscillations and equilibrium 13 p2012 A72-29128
- Aerospace complex physical systems including human operator, discussing computerized design for behavior analysis by means of mathematical models 14 p2093 A72-30846
- Anisotropic homogeneous plasmas, deriving computer model to predict effects of circularly polarized parallel plasma waves in external uniform magnetic field direction on instabilities 14 p2140 A72-30938
- Aeroelasticity, discussing gust and maneuver load alleviation, flutter suppression, aircraft stability, computerized aeroelastic analysis, aeroelastic optimization, composite structures, etc 15 p2322 A72-31202
- Electron-optical parameters effect on GaP/Cs/dynode photomultipliers time response characteristics, describing computer simulation and pulse response measurement techniques 15 p2234 A72-31532
- Software models to test operating conditions of logic nets, discussing application to network faults diagnostics 15 p2203 A72-31749
- Computer simulation for performance of carbon dioxide laser heterodyne communication system with photoconductive n-type mercury-cadmium telluride detector/mixer 15 p2198 A72-32062
- ATC systems fast-time simulation, emphasizing importance of human operator performance realistic modeling 15 p2269 A72-32097
- Computerized Monte Carlo techniques for nonlinear error analysis of system behavior, using random number generators for input distribution simulation 15 p2264 A72-32184
- Computerized navigator training simulator for complete array of air navigation instruments, discussing design and human factors 15 p2214 A72-32208
- Computer simulation by Monte Carlo technique of particulate fluxes in divergent conical Knudsen cell orifices, considering specular reflection and surface diffusion effects 15 p2218 A72-32380
- Computer simulation of airborne gamma ray spectrometer with prescribed photopeak windows from flight over surfaces with arbitrary-dimension radiation sources 16 p2392 A72-33617
- Digital equilibrium temperature model for diurnal surface thermal and energy transfer simulation based on Myrup analog solution 16 p2419 A72-33942
- Hybrid computer simulation of cochlea mathematical model, noting nonlinear damping 16 p2359 A72-33971
- Digital computer controlled flight simulators for undergraduate pilot, electronic warfare, air-to-air combat and helicopter training 17 p2535 A72-34393
- General purpose simulation system /GPSS/ to program discrete time dependent mathematical models related to transport and queueing processes 17 p2521 A72-34471
- Simulation of an air cargo handling system 17 p2536 A72-34472
- Discrete vortex model numerical simulation of Onsager negative temperature instability for interacting line vortices two dimensional motions 17 p2538 A72-34871
- Particle interactions in real and numerically simulated plasmas, considering effects of macroparticles formation via idealized clustering 17 p2590 A72-35143
- The fitting, calibration, and validation of simulation models 17 p2523 A72-35226
- Verification of theory for plasma of finite-size particles 17 p2592 A72-35618
- A data collection and display system for a large-scale simulation 17 p2524 A72-35848
- Computerized simulation of ballistocardiograph subjective evaluation and objective manual measurements, correlating heart beat with ideal pattern 18 p2652 A72-36037
- Digital computer technique for ballistocardiography simulation, using distributed parameters for vessel segments in circulatory system model 18 p2652 A72-36038
- Practical problems and solutions in modeling physical systems with time-domain input-output measurements or specifications 18 p2663 A72-36327
- Frequency/temperature characteristics of Gunn devices 18 p2667 A72-36684
- Digital computer simulation of human systemic arterial pulse wave transmission - A nonlinear model 18 p2655 A72-37028
- Reliability assurance of space equipment components, discussing drift and failure modes, computerized simulation and thermal maps 18 p2743 A72-37127
- Transient characteristics of lumped-parameter delay lines 18 p2674 A72-37216
- Computerized statistical simulation of automatism of spontaneously active smooth muscle strip, neglecting individual cell spontaneous activity 19 p2757 A72-37949
- Results of a computer simulation of an arc plasma in a curved discharge tube 19 p2841 A72-38085
- A method for simulating wind conditions during atmospheric stagnation periods 20 p2947 A72-38965
- Computer program to simulate electromagnetic signal densities, data rates and power from land based radar transmitters as functions of time and location 20 p2902 A72-38992
- Experimental and simulation study results on the development of a planetary landing site selection system [AIAA PAPER 72-868] 20 p2951 A72-39131
- Computer simulation of the space shuttle orbiter environmental thermal control system [ASME PAPER 72-ENAV-12] 20 p2896 A72-39165
- An algorithm for linearly constrained adaptive array processing 20 p2904 A72-39777
- Simulation of torsional vibrations of rods without concentrated masses 21 p3116 A72-40167
- Computer simulation of RF-confinement of plasmas in an open-ended toroidal quadrupole 21 p3089 A72-40191
- Computer simulations of transport processes 21 p3024 A72-40247
- Using the quasi-homogeneity of differential equations in modeling physical systems 21 p3083 A72-40377
- Optimal single stage control law applicable to linear multivariable systems based on discrete-time analysis, discussing real time simulation on hybrid computer 21 p3037 A72-40637
- Unknown plant self organizing time optimal controller with variable switching surface and adaptation logic net, noting effectiveness by computer simulation 21 p3037 A72-40639
- Computer simulation of a digital satellite communications link 21 p3024 A72-40854

Light pulse propagation through clouds - Models and experiments.

21 p3063 A72-40857

Computer simulation of a digital satellite communications system utilizing TDMA and coherent quadruphase signalling.

21 p3020 A72-40895

System analysis for an airline operational environment through a computerized network simulation model.

21 p3025 A72-41077

The airborne visual simulation as an electronic display.

21 p3010 A72-41410

Computer simulation of retargeting procedure with closed form iterative solution and parameter optimization for nonlinear low thrust spacecraft guidance scheme

[AIAA PAPER 72-916]

21 p3082 A72-41561

The effect of membrane parameters on the properties of the nerve impulse.

22 p3140 A72-41936

Analytic expressions for electron energy transfer rates for nitrogen and oxygen vibrational excitation in ionosphere, applying to atmospheric and ionospheric computer modeling

22 p3168 A72-42001

Response of a seat-passenger system to impulsive loading.

22 p3151 A72-42766

Principles of modelling studies of fuel systems and hydraulic systems by electronic analog computers

22 p3157 A72-42922

Digital computer equipped facility for training simulators environmental simulation capability testing, describing electronics interface, control and display equipment

22 p3164 A72-42928

A simple method of hologram transmission by using random phase reference - Principle and computer simulation.

23 p3290 A72-43949

Berner simulation method /BERSIM/ based on lumping recurring combinations of operations into component subsystems representing specified transformations of input into output variables

23 p3267 A72-44143

Programming for discrete events simulation models, discussing languages construction from general programming language building blocks

23 p3268 A72-44144

Mathematical model for dynamics simulation of aircraft turboprop engines, using digital, analog and hybrid computers

23 p3327 A72-44288

Parametric instabilities and anomalous heating of plasmas near the lower hybrid frequency.

23 p3323 A72-44545

Respiratory control system benchmark simulation on hybrid computer for Cheyne-Stokes breathing, emphasizing equations for arterial and venous carbon dioxide and oxygen stores

23 p3268 A72-44551

Lockheed airline system simulation and aircraft scheduling models.

24 p3466 A72-44579

F 2 layer parameter forecasting by computer based on series coefficients dependence on Wolf number

24 p3398 A72-45097

Study of a viscous flow in rotating centrifugal impellers.

24 p3363 A72-45368

Nonlinear instability of Bernstein modes pumped by an electromagnetic wave.

24 p3430 A72-45571

Formulation of diurnal D-region models using a photochemical computer code and current reaction rates.

24 p3399 A72-45583

Computer simulation of the F-region seasonal anomaly.

24 p3400 A72-45586

COMPUTERS

NT AIRBORNE/SPACEBORNE COMPUTERS

NT ANALOG COMPUTERS

NT DIGITAL COMPUTERS

NT HYBRID COMPUTERS

NT SEQUENTIAL COMPUTERS

NT UNIVAC COMPUTERS

Computers - Conference, Las Vegas, November 1971

02 p0185 A72-11651

German book on control technology development covering historic periods, symbols and representations, stability, integral transformations, computers, servos, relays and multivariable systems, optimization, etc

08 p1145 A72-21478

Reliability statistics of third generation computer systems failure causes, emphasizing cumulative effects of hardware and software

10 p1444 A72-23986

Medium scale integration /MSI/ modules for arithmetic section in small, medium and process computers, emphasizing carry-lookahead procedure

13 p1926 A72-30053

Russian book on man and computer covering interaction systems technological capabilities, mathematical aspects and applications

15 p2188 A72-31272

COMSAT PROGRAM

Communication satellite technology progress survey, discussing Early Bird and Intelsat satellites and Comsat program

06 p0777 A72-18620

Solar cells testing and array performance evaluation for communication satellites at Comsat laboratories, noting electron irradiation and proton damage studies

12 p1759 A72-28044

CONCENTRATING

Biological phosphate origin through atmosphere-hydrosphere interrelations, discussing concentrative processes, dehydration mechanics and evaporation

05 p0617 A72-16129

CONCENTRATION [COMPOSITION]

NT ATMOSPHERIC MOISTURE

NT ATOM CONCENTRATION

NT CARBON DIOXIDE CONCENTRATION

NT MASCONS

NT METEOROID CONCENTRATION

NT MOISTURE CONTENT

Temperature, concentration and heat conductivity profiles of chemically reacting gas mixtures with thermal gradient, using classical transfer equations

01 p0023 A72-10489

Heavier-than-helium cosmic ray nuclei composition inferring galactic confinement of particles, path lengths and transit times

03 p0409 A72-13137

Stable molecules spatial concentration profiles in high intensity combustion chamber, using quartz sampling probe and gas chromatography

05 p0751 A72-17088

Absorbed oxygen concentration variation with depth in Nb during oxidation

07 p1022 A72-20555

Binary alloys concentration distribution determination in migrating liquid-solid plane phase interfaces range during crystallization

07 p1022 A72-20571

Laminar flow dispersion coefficient for curved tubes and channels determined by mathematical model, permitting concentration distribution computation

10 p1468 A72-24371

Carbon solubility in Nb at 1500-2150 C, determining saturation concentrations from electrical resistivity vs reaction time curves

11 p1662 A72-26740

Nonuniform concentration mechanism for observed drag reduction in flows with high molecular weight polymer additives, considering boundary layer with varying viscosity on sphere

13 p1942 A72-29113

Composition dependence of ultrasonic velocity in binary Mg base alloys measured by pulse method

14 p2143 A72-31030

Ionized and neutral specie concentration in rarefied hypersonic wake flow behind cone, using electrostatic and electron density probes

15 p2177 A72-31209

Concentration dependence of interdiffusion coefficient in binary metallic systems with continuous and bounded solid solutions

15 p2243 A72-31572

Composition dependence of density in NiTi and CoTi.

18 p2701 A72-36592

German monograph - A photometric method for measuring the concentration distribution in turbulent boundary layers

19 p2799 A72-37652

Concentration dependences and equilibrium values of the impurity distribution coefficients in bismuth telluride

19 p2845 A72-38177

Shrinkage concentration behavior of two phase systems /Co-Ni, Co-Fe, Fe-Ni, Fe-Cu/ in sintering correlated with diffusion parameters

19 p2808 A72-38280

Constitution and property relations regarding cermets and other multiphase materials

20 p2940 A72-39453

Concentration dependence of surface tension in solutions of surface-inactive polymers

21 p3072 A72-40079

Reagent concentration and temperature fluctuation effects on turbulent burning rate, noting temperature pulsations influence on energy balance

21 p3128 A72-40976

Electromechanical, photomechanical and concentration effects of impurities in semiconductors

21 p3098 A72-41677

Gaseous and particulate iodine in the marine atmosphere.

22 p3173 A72-42469

Gaseous and particulate bromine in the marine atmosphere.

22 p3173 A72-42470

Investigation of the formation of local concentrations near the critical liquid-gas point by the electron paramagnetic resonance

23 p3356 A72-43326

Influence of hydraulic extrusion on the composition and properties of the Nb3Sn compound

23 p3323 A72-43597

CONCENTRATORS

Electrochemical carbon dioxide concentrator materials compatibility to space shuttle life support environment, comparing with LiOH method

01 p0018 A72-10768

CONCENTRIC CYLINDERS

Free convective heat transfer measurement from solid copper inner cylinder to cylindrical casing

09 p1410 A72-22351

Radiant flux from finite cylindrical volume to coaxial screen calculated under quasi-homogeneous medium and arbitrary optical thickness assumptions

10 p1561 A72-23841

Small gap approximation for axial magnetic field effects on stability of nonrotationally symmetric disturbances in inviscid flow between concentric rotating cylinders

11 p1694 A72-25773

Viscous incompressible flow between two coaxial rotating circular cylinders with small uniform injection at inner cylinder, obtaining solution of Navier-Stokes equations

13 p1941 A72-28883

Nonlinear heat conduction in rarefied gases between concentric cylinders and spheres, using series expansion in terms of temperature difference for closed-form solution

13 p2064 A72-29118

Induced magnetic field effects on MHD flow between rotating coaxial /insulator/ cylinders, obtaining exact solution and graphical results

15 p2288 A72-32420

Stability of spiral flow and of the flow in a curved channel.

17 p2540 A72-35051

Composite sphere and cylinder vibrations, considering radial and rotatory/torsional vibrations

18 p2735 A72-36756

On the comparison of phase and multi-layer techniques for numerical solution of the scattering problems.

22 p3154 A72-42305

Numerical analysis of the natural convection in a porous medium between two concentric cylinders

22 p3244 A72-42640

Forced harmonic and random vibrations of concentric cylindrical shells immersed in acoustic fluids.

23 p3352 A72-44117

Turbulent flow of drag reducing fluids between concentric rotating cylinders.

24 p3393 A72-45254

CONCORDE AIRCRAFT

Concorde airworthiness certification, discussing ground and flight test programs for performance, flying qualities and structures fatigue properties evaluation

01 p0003 A72-10253

Concorde engine performance, reviewing control, reheat and exhaust systems

01 p0116 A72-10267

Concorde aircraft electrical power systems design, noting dc and emergency supplies and installation

03 p0311 A72-12910

French jet aircraft noise reduction research facilities, discussing in-flight and overly noise measurements, various silencer configurations and Concorde engine tests

03 p0406 A72-13680

Concorde supersonic transport hydraulic control systems, describing design features with emphasis on reliability

03 p0312 A72-13962

Meteorological information assistance for Concorde aircraft test flights, discussing high tropospheric turbulence and lower stratospheric temperature predictions and instruments

04 p0542 A72-14680

Upper atmospheric turbulence correlation to supersonic aircraft dynamics, noting Concorde contribution

04 p0542 A72-14681

Toulouse-Bretigny link involving ATC and flight simulators with Concorde cockpit replica

04 p0545 A72-15072

Metal-skin honeycomb composite structure design and manufacture for Concorde rudder, noting structural adhesive bonding in aircraft construction

04 p0589 A72-15090

Concorde airframe testing for thermal effects on structural strength and fatigue life, discussing facilities for flight conditions simulation

05 p0614 A72-17197

Aircraft safety factors, noting navigational and flight system in Concorde design

07 p0911 A72-18828

Concorde aerodynamic configuration R and D, discussing wing layout in terms of drag, stability, control and weight distribution characteristics

07 p0911 A72-19057

Cosmic radiation effects in Concorde prototype cabin, using photographic dosimeters for neutron dose measurement and nuclear emulsions for all charged particle recordings

07 p0927 A72-19241

Concorde aircraft systems reliability and safety flight and simulator testing, discussing operational and environmental conditions and maintenance procedures

07 p0965 A72-20309

Olympus engine flight testing for relighting and anti-icing, engine control and noise and vibration assessments in support of Concorde aircraft development

08 p1224 A72-21898

Concorde sonic boom measurement, discussing structural vibrational response

08 p1111 A72-21911

Pipe joint flexible metal seal development and testing for Concorde Olympus 593 under thermal and pressure cycling

08 p1178 A72-21938

Glass-vinyl retractable windshield visor development for Concorde aircraft, considering rain, hail and icing effects, strength and stiffness under aerodynamic loading and heating

09 p1261 A72-22900

Concorde aircraft optical transparency components design characteristics and reliability tests, noting visor, pilot forward windshield, flight deck side windows and cabin windows

12 p1753 A72-27012

Concord aircraft windshield panels bird impact resistance, noting effects of edge clamping width, ply thickness, composition and temperature

12 p1812 A72-27013

Stratospheric meteorological characteristics effects on Concorde supersonic flight performance, fuel consumption, dynamic behavior and passenger comfort

13 p1994 A72-28876

Concorde dynamic behavior from flight tests, discussing integrated design effects, wing, fin and elevon flutter, gust and runway response and engine surge effects

[AIAA PAPER 72-381] 13 p1897 A72-28958

Aircraft tires design and performance characteristics, considering VTOL and Concorde operating conditions

13 p1901 A72-30098

Concorde engines design for maintainability and reliability to reduce turnaround time, discussing diagnostic facilities and on-wing maintenance features

15 p2298 A72-32457

Concorde on-time operation as total management problem from design to airline operations, discussing techniques for in-flight failure diagnosis and onward reporting

15 p2181 A72-32460

Numerical prediction of the diffusion of exhaust products of supersonic aircraft in the stratosphere

19 p2748 A72-37824

Operating cost comparisons between Concorde and Boeing 707 and 747 aircraft, considering profitability

20 p2888 A72-39818

Concorde electrically signalled fly by wire control system with mechanical linkages for standby fail-safe redundancy

21 p2994 A72-41068

CONCRETES

Mechanical structure and component stress measurement by reinforced concrete, microconcrete, elastic and plastic models

18 p2733 A72-36370

Concrete airport pavement thickness determination methods comparison, noting design life dependence on safety factors

18 p2675 A72-36786

A ten-inch extensometer measuring small low-frequency strains.

21 p3052 A72-40234

CONDENSATES

Equipment and techniques for He sorption by condensed gas layers at 0.1 picotorr

09 p1364 A72-23227

Aitken condensation nuclei clouds microstructure and area contamination profiles, discussing small sources pollution and plumes polyfurfuration

[AIAA PAPER 71-1125] 11 p1628 A72-26989

Steam-condensate mixture boundary layer flow along curved body surface with arbitrary pressure gradient at low Mach number and constant physical properties

16 p2378 A72-33437

Experimental investigation of the combustion process of two-component heterogeneous condensed systems at low pressures

20 p2987 A72-40042

Influence of hygroscopic substances on the transparency of aerosols from combustion products of condensed systems

20 p2987 A72-40043

Sanitary-hygienic evaluation of the extraction method for water recycling in atmospheric moisture condensates

21 p3006 A72-40435

Investigation by the method of secondary ion-ion emission of the initial phase of the formation process of a silver vacuum condensate on a nickel substrate

21 p3068 A72-40960

Unsteady burning of reacting mixture of air and condensed-phase combustion products in closed variable volume, noting mathematical model for parameters calculation

21 p3128 A72-40977

Propagation of the front of an exothermic reaction in condensed mixtures whose components interact through a high-melting layer

22 p3245 A72-43177

CONDENSATION

Hydrogen condensation on tungsten as function of temperature, coverage and population of binding states, noting initial sticking coefficients variations

01 p0089 A72-11113

Electrically charged low mobility droplet production by water vapor condensation on to gaseous ions from aircraft static discharger

02 p0231 A72-12556

Sodium heat pipes sonic limit, describing vapor dissociation-recombination and homogeneous vapor condensation phenomena

[ASME PAPER 71-WA/HT-11] 05 p0743 A72-15871

Infinite homogeneous self gravitating compressed gas media nonlinear condensations, describing finite amplitude motion with asymptotic expansions

06 p0880 A72-17889

Two dimensional stability of condensed systems combustion, evaluating effects of heat transfer from combustion region

06 p0902 A72-17906

Water vapor condensation in centered rarefaction wave arising in supersonic flow around apex of obtuse angle

06 p0799 A72-17911

Hg vapor condensation on cooled vertical steel cylinder at 70-185 C, considering heat flux relation to saturated vapor/cooling surface temperature difference

06 p0903 A72-18190

Droplet growth on passivated hygroscopic condensation nuclei in device with controllable relative humidity

08 p1172 A72-22000

Quantum condensation in finite volume boson gas, using Bogoliubov quasi-expectation value method

10 p1563 A72-24676

Model for textural features and mineralogical composition of Ca and Al-rich inclusions in C3 chondrites during condensation in primitive solar nebula

14 p2157 A72-30585

Liquid film condensation of low pressure metal vapors on isothermal vertical flat plates, obtaining equations for heat transfer rate prediction

14 p2173 A72-31059

Spectroscopic analysis of condensations density and intensity variations in solar eruptive prominences, discussing hypothetical magnetic field effects

15 p2318 A72-32781

Method of characteristics application to supersonic jet and nozzle gas flow with allowance for equilibrium and nonequilibrium condensation

17 p2544 A72-35929

Condensed zinc particle size determined by a time discrete sampling apparatus.

20 p2913 A72-39608

Detection of crystals in CO2 jet plumes.

21 p3046 A72-41306

Laminar boundary layer at critical point of blunt body in molecular oxygen flow, noting wall influence on condensation

22 p3243 A72-42257

Lunar composition in terms of evolutionary mode based on inhomogeneous planetary accretion and high temperature condensation

24 p3439 A72-44977

Early stage condensation in planetary formation, discussing atomic and molecular reactions in interstellar space and earth outer atmosphere properties

24 p3444 A72-45452

Chemical effects in plasma condensation.

24 p3429 A72-45457

CONDENSATION PUMPS

Hydrogen evacuation with He condensation pump in ultrahigh vacuum region

06 p0795 A72-17698

Prepumped systems with ion sorption and titanium sublimation vacuum pumps for ultrahigh vacuum production

07 p0914 A72-19906

CONDENSATION TRAILS

U CONTRAILS

CONDENSER RADIATORS

U CONDENSERS [LIQUIFIERS]

U HEAT RADIATORS

CONDENSERS

Heat and mass transfer along axially conducting gas controlled heat pipes, discussing wall temperature profiles and condenser characteristics

[ASME PAPER 71-WA/HT-29] 05 p0745 A72-15882

CONDENSERS [LIQUIFIERS]

Water heat pipes transient thermal impedance, monitoring evaporator, vapor space and condenser temperature

[ASME PAPER 71-WA/HT-9] 05 p0743 A72-15869

Heat pipe operating conditions and evaporator, condenser and adiabatic parts, discussing fluid capillary transport for heat pipe calculation

05 p0750 A72-17047

CONDENSING

NT FILM CONDENSATION

Uncondensed components effects on heat transfer in condensation of nitrogen tetroxide partly in second dissociation stage, deriving heat of vaporization

01 p0145 A72-10494

Vaporization and condensation effects on Apollo 11 glass spherules from microbreccia samples, suggesting concentration gradients as result of impact event

11 p1723 A72-26522

Formation of clouds in a cooling interstellar medium.

19 p2854 A72-37231

Bulk viscosity coefficient and the second heat conduction coefficient near the critical condensation point

20 p2983 A72-39396

Mathematical model for surface tension induced thermocapillary fluid flow influence on conductive heat transfer through condensate film broken by non-wetting strips

[ASME PAPER 72-HT-H] 20 p2985 A72-39654

Three-phase heat transfer - Transient condensing and freezing from a pure vapor onto a cold horizontal plate - Analysis and experiment.

22 p3243 A72-41957

Exciton condensation in a momentum space under the action of optical pumping

22 p3185 A72-42161

CONDITIONED RESPONSES

U CONDITIONING [LEARNING]

CONDITIONING [LEARNING]

Respiration effects on human heart rate deceleration and biphasic cardiac response in aversive shock conditioning situation

01 p0010 A72-10195

Soviet book on physiology of conditioned reflexes covering brain and nervous system, tonic reflexes, functional models, inhibition localization, etc

01 p0011 A72-10295

Operant conditioning for producing gross motor responses, discussing application to physical medicine and rehabilitation with mentally retarded Downs syndrome children

04 p0478 A72-14706

Conditioned reflex as component of artificial conditioned-natural unconditioned reflex system controlling adaptive behavioral patterns, noting contribution to complex nervous activity understanding

04 p0476 A72-15582

Frontal lobe damage effect on conditional motor reflexes, communication capability and emotional behavior in baboon apes

04 p0476 A72-15583

Rapid ventilatory response in man at work on set for different standard starting commands, discussing relation to work load and conditioning process

05 p0619 A72-16788

Hologram data treatment comparison to human brain function, discussing recognition signals, Pavlovian qualities and intelligence function

06 p0768 A72-17997

Hypothalamic stimulation conditioned negative fear reflex in cats before/after neocortex isolation

07 p0920 A72-19859

Improperly controlled learning processes relationship to hypertonic blood pressure irregularities pathogenesis in rats, investigating negative emotional reactions effects

07 p0925 A72-20659

Entropy effect in two dimensional conditional reflex decision situations upon rats central nervous analysis-synthesis processes

07 p0925 A72-20661

Central nervous plasticity and stereotypy intercorrelation in conditional reflex two dimensional decision situations

07 p0925 A72-20662

Rod-cone interaction in human scotopic vision, presenting test flash threshold as function of conditioning flash interval

08 p1116 A72-21460

Soviet papers on human higher nervous activity physiology covering conditioned reflexes and adaptive behavior, neurotropic substance effects, mathematical and structural modeling, etc

08 p1118 A72-21834

Neurophysiological mechanisms responsible for conditioned reflexes, considering cells, reaction relationship to animal behavior, neuronal stimuli interactions, internal inhibitions and trace process reproduction

08 p1118 A72-21835

Conditioned reflex mechanisms responsible for regulation of emotions in higher order animal and human neurophysiology

08 p1118 A72-21837

- Conditioned reflex activity, discussing biological and nervous system, electric analog simulation and mathematical and structural modeling
08 p1127 A72-21842
- Conditioned stimuli presentation role in successive differentiation and inhibition limits in monkeys
13 p1902 A72-28644
- Passenger behavioral inaction in survivable aircraft accidents, suggesting maladaptive behavior counteraction by leadership and/or training
13 p1908 A72-28727
- Concentrated and extended learning effects on formation rate and retention degree of conditioned reflex during mice adaptation to high altitude hypoxia
13 p1903 A72-28770
- Unconditioned /muscular load stimulus/ and conditioned /metronome stimulus/ cardiac reflexes in hypnotic and alert states
16 p2353 A72-32991
- LF whole body vibration effects on rat escape conditioning in terms of frequency, amplitude and controls for noise and activation
16 p2357 A72-33868
- Reflex and conditional movement observation of central nervous system function restitution in Macaca mulatta monkeys with cortical lesions, studying pathological forced grasping
18 p2651 A72-36977
- Proteinase activity in different regions of the brain during development and inhibition of a conditioned passive-avoidance reflex
20 p2890 A72-38927
- Blood vessel reactions to natural defense and conditioned reflexes from plethysmography and blood pressure measurements, discussing cortical effects mechanisms
21 p3000 A72-40758
- Higher nervous activity of monkeys two years after the extirpation of the dorsolateral frontal cortex
21 p3001 A72-40803
- Effect of electrical excitation of various auditory analyzer levels on a conditioned motor reflex
21 p3001 A72-40805
- Evoked potentials of the primary auditory cortical zone produced by positive and inhibitive conditioned stimuli
21 p3001 A72-40806
- Role of the reticular formation of the mid-brain in the storage and recreation of a system of conditioned reflexes
21 p3001 A72-40809
- Critique of Pavlov conditioned reflex role in higher nervous activity and association principle role in psychical activity
21 p3001 A72-40811
- Electrophysiological analysis of defense reflex and unconditioned reaction and conditioned signal analyzers in nodal mechanisms of functional system /afferent synthesis, decision making, correction, etc/
21 p3004 A72-41675
- Development of a defensive conditioned reflex to a light stimulus after previous visual deprivation
23 p3257 A72-44078
- Age-induced long-term memory changes in animals
23 p3257 A72-44079
- Characteristics of conditioned reflexes to an ecologically adequate stimulus in hens
23 p3257 A72-44080
- CONDITIONS**
- NT ADIABATIC CONDITIONS
- NT CHRONIC CONDITIONS
- NT FLIGHT CONDITIONS
- NT KUTTA-JOUKOWSKI CONDITION
- NT LIPSCHITZ CONDITION
- NT NONEQUILIBRIUM CONDITIONS
- NT RUNWAY CONDITIONS
- CONDUCTING FLUIDS**
- Rankine vortex conducting gas rotating about cylinder axis, investigating magnetic field effects on transverse waves
01 p0106 A72-10132
- Momentum jet and electric discharge from same hole in plane wall bounding viscous incompressible conducting fluid, investigating flow field with similarity solutions
01 p0107 A72-10139
- MHD boundary layer calculation for conducting fluid along semiinfinite flat plate with transverse magnetic field, deriving momentum and kinetic energy integral equations
01 p0113 A72-11383
- Axissymmetric inviscid compressible transonic flow of electrically conducting, heat nonconducting gas in Laval nozzle in presence of meridional magnetic field, deriving equations for magnetic effects on dynamic flow characteristics
02 p0149 A72-11576
- Conducting fluid convective motion in earth core estimated from geomagnetic field and time derivative data at earth surface
02 p0220 A72-12087
- Upstream influence on MHD flow velocity by Rankine body moving parallel to uniform magnetic field in conducting fluid
03 p0394 A72-13153
- Conducting fluid steady MHD pipe flow under transverse magnetic field, obtaining mass flow rate
03 p0394 A72-13241
- Steady state turbulent solar magnetic fields dynamic evolution, considering weak random magnetic excitation in electrically conducting fluid under varying kinematic conditions
03 p0430 A72-13336
- Viscous electroconducting liquid two unidimensional Hartmann flows electromagnetic coupling under transverse magnetic field induction
03 p0396 A72-13790
- Self similar solutions for unsteady shear flows of conducting Newtonian fluids with rheological power law under transverse magnetic field
03 p0397 A72-13997
- Variational problem of conducting fluid flow in MHD channel at large magnetic Reynolds numbers at induction saturation
03 p0397 A72-13999
- Time and coordinate dependence of magnetic field for steady symmetric flows of compressible conducting fluid at large Reynolds numbers, investigating self excitation conditions
03 p0398 A72-14001
- Steady flow of viscous incompressible conducting fluid in rectangular channel with sectional walls under longitudinal external magnetic field, deriving velocity distribution
03 p0398 A72-14009
- Free convective motion of conducting fluid past vertical plate in uniform transverse magnetic field, determining optimum dimensions of heat exchangers
03 p0399 A72-14011
- Axissymmetric rotational motion of electrically conducting fluid between dielectric disks in crossed electric and magnetic fields
03 p0399 A72-14012
- Time dependent hydromagnetic oscillations in contained rotating conducting fluid under magnetic field, using interior boundary layer expansion
04 p0549 A72-15115
- Conducting incompressible fluid in laminar pipe flow under traveling magnetic field, investigating friction coefficient and energy balance
04 p0558 A72-15341
- Stationary viscous incompressible conducting fluid in conical flow, investigating diverging and converging electric current effects
04 p0558 A72-15342
- Inviscid incompressible conducting fluid motion under line sink in uniform strong magnetic field
04 p0550 A72-15343
- Magnetic field effect on heat transfer in steady plane laminar conducting incompressible viscoelastic liquid flow in channel with nonconducting walls
04 p0560 A72-15580
- Two dimensional axisymmetric surface waves motion in inviscid incompressible homogeneous electrically conducting fluid under uniform magnetic and electric fields, considering surface tension effects
04 p0560 A72-15744
- Navier-Stokes equations asymptotic solution for compressible weightless conducting fluid flow in plane channel with intense blowing from walls
05 p0648 A72-16219
- MHD convection in rotating electrically conducting viscous fluid layer within magnetic field, investigating linear stability
06 p0861 A72-18069
- Magnetohydrodynamic theory of spherical drop deformation and drag under axisymmetric current distribution in conducting viscous incompressible fluid
06 p0864 A72-18533
- Optimal control of hydromagnetic flow of electrically conducting fluid in equilibrium cylindrical configuration, using dynamic programming method
07 p1040 A72-18980
- Flow field induced by electric current jet in incompressible viscous conducting fluid, solving nonlinear momentum equation by series expansion procedure
07 p0967 A72-19504
- Nonuniform plane parallel plasma streams instability with/without magnetic field, comparing with conducting fluid
07 p1042 A72-19618
- Book on models of particles and moving conducting media covering generator electrodynamics, electron tubes, particle accelerators, plasma and electron beam simulation, ion propulsion, etc
07 p1036 A72-20203
- MHD dynamo model for incompressible real electrically conducting fluid unsteady flow
07 p1044 A72-20304
- Transverse hydromagnetic plane waves existence in uniformly heated electrically conducting fluid under temperature gradient and magnetic field
07 p1045 A72-20442
- Inviscid conducting gas steady one-dimensional MHD flow, using three-dimensional phase diagram for differential equations analysis
08 p1214 A72-21646
- Laminar MHD boundary layer lateral velocity component profile for conducting fluid injection at oblique incidence, considering drag force and pressure gradient effects
08 p1214 A72-21647
- Anisotropic conducting fluid flow in presence of traveling magnetic field, determining Hall effect via solution to electromagnetic field distribution boundary value problem
08 p1214 A72-21648
- Two dimensional MHD conducting fluid flow past insulating cylinder in presence of arbitrarily oriented magnetic field, determining lift and drag coefficients for small Hartmann numbers
09 p1359 A72-22533
- Hydrodynamic stability of electrically conducting hot viscous fluid surrounded by perfectly conducting rigid boundary in presence of magnetic field
09 p1365 A72-22825
- Perfectly conducting incompressible fluid motion past thin body in oblique field, discussing magnetic field influence on lift
09 p1365 A72-23559
- Oblique magnetic fields effect on compressible conductive fluids motion in presence of thin foil, noting lift values in hyperlipic and double hyperbolic cases
09 p1365 A72-23560
- Electrically conducting viscous incompressible fluid rotating with oscillating disk in magnetic field
09 p1366 A72-23575
- Electromagnetic coupling between one dimensional laminar flows of viscous conducting fluid in presence of magnetic field, noting static and dynamic efficiencies dependence on Hartmann number
10 p1519 A72-24065
- Steady state exact solutions of MHD equations for perfectly conducting self gravitating incompressible fluid, showing solutions existence for rotating planetary ellipsoid free liquid surface
10 p1539 A72-24328
- Conducting fluid laminar free convective flow over heated rotating horizontal plate in presence of strong magnetic field aligned with rotation vector
10 p1522 A72-24465
- Internal Alfvén gravity waves propagation in rotating Boussinesq inviscid adiabatic conducting fluid shear flow within transverse magnetic field, considering electromagnetic and Coriolis forces effects
10 p1511 A72-24470
- Joule dissipation effect on convective instability of current carrying fluid in magnetic field
10 p1522 A72-24533
- Interacting viscous conducting media flow in inclined channel in presence of transverse magnetic field, using Moiseev asymptotic method for steady flows with wavy interface
10 p1522 A72-24546
- Ohmic law generalization in electrodynamics for electrically conductive fluid medium in turbulent motion, taking into account Hall effect
10 p1524 A72-24931
- Magnetosphere neutral layer plasma conductivity determination from model of linear magnetic dipole in conducting fluid flow
11 p1622 A72-25945
- Hydromagnetic stability of isothermal stratified plasma atmosphere uniform flow over conducting liquid along magnetic field, discussing dispersion relation for static configuration
11 p1695 A72-26115
- General relativity equations solution for interaction of gravitational radiation and conducting fluids in magnetic field, noting energy absorption in specified depth surface layer
11 p1720 A72-26116
- Hydromagnetic stability of rotating nondissipative inviscid incompressible conducting fluid annulus permeated by radially varying magnetic field, considering axisymmetric and nonaxisymmetric disturbances
11 p1619 A72-26639
- Unsteady viscous incompressible electrically conducting fluid flow generated by porous disk rotation, investigating transverse magnetic field effect
12 p1851 A72-27305
- Oscillation periods of rotating perfectly conducting liquid column in presence of axial magnetic field and uniform current
12 p1851 A72-27534
- Nonlinear transverse forced resonant oscillations in isotropic elastic body and ideally conducting compressible fluid flowing in external magnetic field
13 p2010 A72-28719
- Effect of magnetic field superimposed on turbulent shear flow of electrically conducting fluid, discussing turbulent friction in plane flow
13 p2010 A72-28764
- Convective hydromagnetic stability of hot conducting fluid layer in magnetic field by Liapunov method
13 p2011 A72-28891
- Uniform vertical magnetic field effect on Ekman layer over horizontal plate at rest relative to rotating conducting liquid
13 p2011 A72-29006
- Two dimensional laminar compressible flow of electrically conducting gas at thermodynamic equilibrium and perpendicular to magnetic field lines
13 p2013 A72-29362

Nonstationary laminar zero-discharge MHD Couette flow produced by sudden movement of highly conductive plate in closed volume filled with conducting liquid

13 p2016 A72-29607

Slow viscous incompressible conducting fluid MHD flow between two nonparallel walls, obtaining velocity profile solution in power series for small Reynolds numbers

13 p2020 A72-30047

Tangential MHD discontinuity stability for ideally conducting compressible fluid in magnetic and gravitational fields

13 p2020 A72-30068

Linear theory based analysis of compressible electroconductive fluid flow satisfying perfect gas equation in presence of thin profiles within quasi-aligned magnetic field

14 p2095 A72-30824

Lighthill method for ohmic dissipation pulsation effect on sound field generated by turbulent flow of conducting fluid

14 p2141 A72-31001

Heat transfer in MHD boundary layer flow of conducting incompressible fluid with aligned magnetic field on flat plate at high Prandtl number

14 p2141 A72-31068

MHD Couette flow of electrically conducting viscous incompressible fluid in transverse magnetic field with time dependent suction or injection

15 p2286 A72-32396

Steady laminar MHD flow of viscous incompressible electrically conducting fluid between long concentric rotating porous cylinders under radial magnetic field

15 p2287 A72-32397

Asymptotic solution for inviscid conducting fluid flow past arbitrary wing profile in magnetic field

16 p2434 A72-32929

Perturbation theory for equations of motion of electrically and thermally conducting viscous compressible flow in homogeneous magnetic field, calculating fluctuation modes

16 p2435 A72-33008

Skin friction effects due to Hall currents in conducting unsteady slip flow over porous flat plate under transverse magnetic field

16 p2435 A72-33108

Precessional torque of conducting fluid as source of geodynamo action, noting oblate spheroidal experiment

16 p2385 A72-33341

MHD wave propagation and generation during spin-up of rotating viscous incompressible electrically conducting fluid

16 p2436 A72-33572

Plane vortex sheet in incompressible inviscid and finitely conducting fluids, investigating discontinuity in density and conductivity on hydromagnetic stability

16 p2438 A72-33842

Conducting fluid flow near neutral sheet in magnetic field, assuming cold polar wind plasma geomagnetic tail

16 p2438 A72-33930

Theoretical study of electromagnetic coupling in the forced oscillatory regime of two one-dimensional laminar flows of a viscous and electroconducting liquid in the presence of a transverse uniform magnetic field

17 p2587 A72-34281

On the motion of a perfectly conducting fluid past a thin body.

17 p2485 A72-35055

Motion of a sphere in an electrically conducting rotating fluid.

18 p2714 A72-36123

Solution of some mixed boundary value problems of conducting medium thermodynamics by the method of variable separation

18 p2715 A72-36802

Fast magnetoacoustic wave interaction with shock wave propagating in ideal electrically conducting gas, showing magnetic field stabilizing effect

18 p2711 A72-36812

Hydrodynamic stability of the gradient flow of a conducting fluid with a rheological power law in a transverse magnetic field

18 p2716 A72-36814

Steady flow of conducting fluid in MHD ball bearing clearance between two eccentric spheres, deriving load, friction moment and optimum operation mode

18 p2696 A72-36818

Self-similar separation flows in a laminar magnetohydrodynamic boundary layer during injection and suction

18 p2716 A72-36886

The influence of geostrophic force on the stability of an heterogeneous conducting fluid with a radial gravitational force.

18 p2683 A72-36933

Determination of the separation parameter of an incompressible magnetohydrodynamic boundary layer by applying the dimensionality theory

18 p2717 A72-37181

Classification of the magnetohydrodynamic motions of a rotating fluid

19 p2839 A72-37392

Multiplicity theorem for aligned steady MHD flows of inviscid perfectly conducting gas, assuming constant density along streamline

19 p2840 A72-37405

Hydrodynamic stability of periodic burning front for ideally conducting incompressible fluids in longitudinal or transverse magnetic field

19 p2882 A72-38457

Propagation of Alfvén-gravitational waves in a stratified perfectly conducting flow with transverse magnetic field.

19 p2843 A72-38791

Momentum transport by gravity waves in a perfectly conducting shear flow.

19 p2788 A72-38792

MHD instability of two dimensional laminar boundary layer in incompressible electrically conducting fluid along concave wall with periodic three dimensional disturbances

20 p2957 A72-39328

The linear stability of flow in a circular pipe in the presence of a strong transverse magnetic field.

20 p2958 A72-40018

Nonlinear transverse forced resonant oscillations in isotropic elastic body and ideally conducting compressible fluid flowing in external magnetic field

22 p3210 A72-42096

One dimensional steady conducting gas flow in nonaccelerating coordinate system under magnetic field, calculating pressure, density and temperature variations with boundary shock wave

23 p3281 A72-44265

Magnetohydrodynamic flow between parallel rotating disks. I - Influence of finite wall-conductance.

23 p3322 A72-44400

MHD Couette flow between conducting walls with heat transfer.

24 p3428 A72-44970

Linearized analysis of magnetohydrodynamic channel entrance flow.

24 p3430 A72-45573

On the unsteady magnetohydrodynamic flow over yawed infinite cylinder.

24 p3395 A72-45599

CONDUCTING MEDIA

U CONDUCTORS

CONDUCTION BANDS

Semiconducting crystal superconductivity in laser field by interaction between electron conduction band and light induced polarization

02 p0269 A72-12883

Electron plasma fluctuations in semiconductor with nonparabolic conduction band under external electric and magnetic fields

08 p1218 A72-21877

Emitter conduction bands with negative electron affinity energy from surface barrier lowering of Cs p-type semiconductors

10 p1526 A72-24351

Emitter conduction bands with negative electron affinity energy from surface barrier lowering of Cs p-type semiconductors

17 p2595 A72-34952

Plasma echo-type oscillations in n-type InSb semiconductor, noting conduction band nonparabolicity effects

21 p3098 A72-41687

Theory of Poole-Frenkel conduction in low-mobility semiconductors.

22 p3214 A72-42317

CONDUCTION ELECTRONS

Parallel and perpendicular magnetic field effects on optically injected electron-hole plasma diffusion in Ge from density measurement by infrared beam absorption technique

05 p0702 A72-17167

Lamb waves interaction with conduction electrons in piezosemiconductor, deriving dispersion equation for CdS wafers

06 p0865 A72-17393

Intraband multiphoton conduction-electron transfer probability in semiconductor under electromagnetic wave action in uniform magnetic field

08 p1216 A72-21066

Ion crystal plasma wave echoes from conduction electrons interaction with phonons in self consistent field

10 p1527 A72-24926

Temperature and charge carrier density dependence of conduction electron optical effective mass in semiconductor compounds

13 p2021 A72-28788

Average energy to form electron-hole pairs in GaP diodes with alpha particles.

20 p2908 A72-39564

Solid state physics experiment for conduction electrons effective mass determination in ultrapure n-type InSb by means of magnetophonon effect

21 p3096 A72-40203

CONDUCTIVE HEAT TRANSFER

Pyrolytic graphite heat conductivity coefficients in direction perpendicular to deposition surface at high temperatures

01 p0090 A72-10488

Temperature, concentration and heat conductivity profiles of chemically reacting gas mixtures with thermal gradient, using classical transfer equations

01 p0023 A72-10489

Hydraulic analogy application to heat conduction problems, considering seepage and network pipe flow models for complex heat flux phenomena representation

01 p0145 A72-11174

Controllable states insufficiency to characterize rigid heat conductors dependence on temperature fields in experimental materials measurements programs

01 p0146 A72-11389

Three dimensional heat conduction behavior in laminated composites calculated from continuum model using asymptotic developments

02 p0300 A72-11547

Differential nonstationary heat equations numerical solution for bladed gas turbine air cooled disk, taking into account cascade vertical temperature variation and coolant heating

02 p0301 A72-12251

Least squares and point matching techniques compared for solution of two dimensional steady state heat conduction problems with irregularly shaped boundaries

[ASME PAPER 71-HT-P] 02 p0302 A72-12318

Heat transfer through fabrics by convection, conduction, radiation and vaporization related to skin temperature and thermal injury

03 p0319 A72-13700

Heat conduction in vacuum insulated capillaries to prevent failure of level indicators and controllers based on condensation in evaporating cryogenic liquid

03 p0456 A72-13883

Conductive heat transfer from rib roughened surfaces in gas cooled reactor fuel elements

04 p0595 A72-14596

Heat conduction model of surface thermal history of moon as function of dust, anorthosite, basalt and dunite layers

04 p0571 A72-14598

Steady heat conduction boundary value problem solution by generalized Kantorovich method of reduction to ordinary differential equations

04 p0595 A72-14642

Nonlinear heat conduction equation explicit solution in combustion theory with allowance for gas dynamics model equation and resulting Cauchy problem solution

04 p0595 A72-14643

Steady heat conduction plane problem solution for infinitely long cylinder with constant surface thermal flux density and temperature

04 p0595 A72-14644

Hyperbolic and parabolic partial differential equations behavior comparison by studying point-to-point time optimal control for heat conduction and vibrating string motion

04 p0505 A72-14673

Initial viscous heat conducting gas dynamic state one dimensional decay problem solution, using kinetic theory with Boltzmann equation

04 p0512 A72-14982

Piecewise linear approximation of inverse nonstationary conductive heat transfer through unbounded plate with arbitrary temperature distribution and asymmetric boundary conditions

05 p0742 A72-15847

Zirconium carbide high temperature heat conductivity measurement by radial heat flux method combined with photographic technique

05 p0680 A72-15852

Similar unsteady one dimensional motion of viscous heat conducting gas due to sudden energy release at surface

[ASME PAPER 71-WA/HT-3] 05 p0743 A72-15864

Two dimensional stationary temperature fields determination in ribs, cylinders and pipes with temperature independent heat conductivity

05 p0746 A72-16188

Smooth curved metal surfaces thermal conductance at high vacuum, verifying contacting surfaces plastic deformation

[AIAA PAPER 72-20] 05 p0666 A72-16868

Relativistic hydrodynamics, considering Cauchy problem in fluid evolution, ideal isentropic fluids, electromagnetic field effect and viscous/heat conducting thermodynamic flow models

06 p0846 A72-17252

Steady heat conduction boundary value problems from complementary variational principles

06 p0902 A72-17780

Asymptotic developments in transonic flows, considering three dimensional flows near shock and plane viscous and heat conducting flow

06 p0756 A72-18105

Kubo type time correlation formulas for incompressible heat conducting fluids turbulent transport coefficients, establishing relation to cascade and closure-of-hierarchy methods

06 p0801 A72-18173

Conductive and radiative energy transfer in absorbing, emitting and conducting medium bounded by two black plates, using Milne-Eddington type absorption coefficient

06 p0903 A72-18187

Small parameter method application to quasi-linear problems solution in nonstationary heat conduction with substantial nonlinearities and weak perturbation, analyzing error

07 p1098 A72-18937

Sufficient conditions definition for existence of solution for heat conduction equation coupling to telegrapher equation

07 p1028 A72-19897

Solar corona structure and dynamics in context of energy transfer processes of dissipation, radiation, heat conduction and hydrodynamic expansion

07 p1078 A72-20006

Boundary conditions in steady and unsteady heat conduction for gas turbine rotors, using blade-disk temperature relation

08 p1222 A72-20944

Boundary conditions in heat conduction for nozzle blades with shrouds exposed to cooling air on one side

08 p1222 A72-20945

Steady heat conduction of cooled gas turbine hollow nozzle blades with gas temperature variation along cascade

08 p1223 A72-20948

Steady heat conduction solution for gas turbine shrouded blade and disk of hyperbolic profile with central hole

08 p1223 A72-20949

Numerical integration of unsteady heat conduction equations for gas turbine rotor with shrouded blades, using grid method

08 p1223 A72-20950

Steady heat conduction solution for intensified cooling of turbine rotor blade leading edge with holes and air channel

08 p1223 A72-20951

Unsteady temperature field and conductive heat accumulating properties of bodies with dihedral and polyhedral angles

08 p1251 A72-20954

Three dimensional nonstationary heat conduction of hollow circular cylinder in medium with different temperature

08 p1251 A72-20972

Conductive heat flux propagation rate in gases as function of absolute temperature

08 p1253 A72-21447

Green functions in heat conduction solutions for hollow cylinder with mixed boundary conditions

08 p1253 A72-21448

Nonuniform temperature distribution effect on heat conduction coefficient of hot-wire cell, using computerized net point method

08 p1166 A72-21449

Heat transfer in shield-vacuum thermal insulation layers at various temperatures and pressures, noting conductivity anisotropy

08 p1253 A72-21451

Conductive heat transfer equation solved by finite difference scheme with uniform rapid convergence

08 p1253 A72-21458

Finite difference method explicit solution of Cauchy problem for system of heat conduction differential equations

08 p1254 A72-21464

R function and variational methods solution for mixed boundary value problem of Laplace equation applied to stationary heat conduction and electrodynamic problems

08 p1209 A72-21704

Heat conduction, stress-strain state and thermoelectricity of massive bodies of revolution under nonuniform heating

09 p1400 A72-22709

German book on unsteady heat conduction and temperature field equalization covering mathematical treatment with Laplace transformations

09 p1412 A72-23175

Laser heating of plasma based on heat conduction mechanism of spherical thermal wave, taking into account nuclear fusion heat generation

09 p1365 A72-23551

One dimensional conductive and radiative heat transfer through gray medium bounded by two diffuse surfaces, noting solutions existence and uniqueness

09 p1412 A72-23586

Shape factors of heat conduction for fin arrangements with isothermal boundaries, using conformal mapping

09 p1412 A72-23688

Bounded plasma ionization instability inhomogeneity scale evaluation, assuming negligible electron energy losses due to heat conduction

10 p1517 A72-23844

Heat conduction and thermoelectricity in solids, discussing thermomechanical coupling, structural analysis and thermal stresses and deformations

[SMRT PAPER L 1/1] 10 p1556 A72-24394

Closed form solution for spherical and cylindrical wave propagation in laser conductively heated plasma, considering account of nuclear fusion energy recovery

10 p1522 A72-24721

Laser conductive heating of plasma with accounted nuclear fusion energy, assuming plane thermal wave

10 p1522 A72-24722

Discrete random walk heat conduction equation for thin layer with stepwise temperature change, comparing with parabolic and hyperbolic solutions

11 p1744 A72-25266

Heat conduction and radiative transfer equations of IR cooling by atomic O in thermosphere

11 p1622 A72-25848

Nucleate pool boiling three component heat flux theory, taking into account latent heat transport, molecular heat conduction and turbulent convection

11 p1746 A72-26539

Two heat conducting phases free boundary problem with temperature distribution within phases, proving existence and uniqueness theorems

12 p1836 A72-27124

Periodic liquid heating through infinite plate, taking into account temperature induced variation in heat capacity and conductivity

12 p1888 A72-27227

Heat conduction heating of plasma by high power ultrashort laser pulse incident on solid target, noting focusing and energy absorption role

12 p1852 A72-27622

Uniqueness and existence theorems for nonideal thermal contact between three dimensional solid parts in heat conduction theory, noting case of two dimensional body

12 p1889 A72-27996

Thin plates and coatings in thermal contact with standard, determining total emissivity by inverse methods of heat conduction

12 p1889 A72-28115

Conductive heat propagation with finite rate for semibound solid body under periodic surface temperature fluctuations dependent on relaxation time

12 p1890 A72-28174

Combined radiation-convection interaction for slow speed gas flow over flat plate, comparing with two dimensional and axisymmetric stagnation point geometries

13 p2064 A72-28631

Boundary layer approach to local potential solution of diffusion equations, applying to transpiration cooled half space and heat conduction in melting solid

13 p2064 A72-28885

Nonlinear differential energy equation of static state stellar atmospheres with radiation and heat conduction terms

13 p2036 A72-28890

Nonlinear heat conduction in rarefied gases between concentric cylinders and spheres, using series expansion in terms of temperature difference for closed-form solution

13 p2064 A72-29118

Three dimensional steady temperature field calculation for solid bodies under concentrated heat source, using flow kinetic heat conduction method

13 p2065 A72-29151

Adiabatic density perturbations damping by radiative viscosity and heat conductivity, taking into account plasma recombination in hot expanding Universe

14 p2148 A72-30202

Coordinate functions in Kantorovich variational method, noting application to stationary heat conduction boundary value problems

14 p2170 A72-30592

Thermosphere kinetic temperature diurnal variation from heat conduction equation periodic solution, determining heat sources from solar radiation atmospheric absorption

14 p2101 A72-30640

Temperature difference between steadily flowing fluid and solid sphere due to viscous dissipation determined for simultaneous conduction and radiation [DFVLR-SONDDR-220]

14 p2105 A72-30710

Steady flow of compressible heat conducting fluid, discussing effect of small transfer coefficient on isentropic sonic singularity in Laval nozzle

14 p2171 A72-30713

German book on heat transfer and fluid flow, covering heat conduction and temperature distribution in bodies of simple and complex geometries, fluid mechanics, etc

14 p2171 A72-30902

Orthogonal projection method for nonstationary heat conduction boundary value problem with thermal conductivity and specific heat as prescribed functions of position

14 p2126 A72-31049

Approximate solution of nonlinear boundary value problems in high temperature conductive heat transfer

14 p2174 A72-31161

Piecewise linear approximation of inverse nonstationary conductive heat transfer through unbounded plate with arbitrary temperature distribution and asymmetric boundary conditions

15 p2334 A72-31266

Classical and finite difference methods for diffusion and heat conduction problems

15 p2334 A72-31298

Heat conductivity equation solution for laminar gas flow in tubes, calculating temperature field and heat removal for molecular lasers with gas pumping

15 p2245 A72-31421

Stationary heat conduction between stagnant binary gas mixture and two constant temperature plane parallel walls for arbitrary Knudsen numbers

15 p2334 A72-31462

Exact nonlinear equation derived approximation for second order effects in thermoelectricity theory for isotropic and transversely isotropic heat conducting elastic materials

15 p2329 A72-32282

Self excited increasing thermal wave generation models, using hyperbolic wave heat conduction and thermoelectricity equations

15 p2336 A72-32285

Expansion formulas for Kampe de Fériet and radial wave functions application to heat conduction and quantum mechanics problems

15 p2336 A72-32398

Laser heating of two temperature plasma based on conductive heat transfer, taking into account nuclear fusion energy

16 p2434 A72-32876

Nonlinear thermoelasticity theory extension via entropy production inequality theorem, deriving expressions for stress tensor and heat conduction vector

16 p2465 A72-32980

Unsteady heat conduction in hollow cylinder suddenly heated by temperature field moving along outer and inner side surfaces

16 p2475 A72-33114

Heat conduction in infinite incompressible fluid with turbulent velocity field, deriving physically impossible growth in time of long-wavelength modes of average temperature

16 p2424 A72-33127

Statistical solution to unsteady heat conduction through flat multilayer insulating wall, using random walk method

16 p2477 A72-33407

Normal-mode expansion technique for unsteady radiative and conductive heat transfer in absorbing emitting isotropically scattering slab with reflective boundaries

16 p2478 A72-33438

Thermal resistance of planar semiconductor structures.

17 p2594 A72-34296

Transient thermal waves in the general theory of heat conduction with finite wave speeds. [ASME PAPER 72-APM-23]

17 p2636 A72-34794

To geometrized theory of hyperbolic heat conduction equation.

17 p2637 A72-35049

Minimum weight passive insulation requirements for hypersonic cruise vehicles.

17 p2638 A72-35256

Heat conduction in a turbulent magnetic field, with application to solar-wind electrons.

17 p2601 A72-35584

Laminar gas flow in narrow channels of constant and variable cross sections in the presence of heat transfer

17 p2543 A72-35807

Programmable computation method based on matrix formulation for numerical solution of differential equations in heat conduction and thermal stress problems

17 p2635 A72-35898

Self-similar motions of a viscous heat conducting gas during an abrupt energy release

18 p2683 A72-36894

Convergence and accuracy of three finite difference schemes for a two-dimensional conduction and convection problem.

18 p2741 A72-37170

Heterogeneously combust binary gas mixture ignition time as function of initial state and thermokinetic properties, noting heat conduction equations for fuel and oxidizer

19 p2879 A72-37358

An improved method for the solution of the heat equation in Chebyshev series.

19 p2879 A72-37370

Solution of the inverse heat conduction problem by using the regularization method to increase the peaks of the self-contraction function/Paterson's function/

19 p2880 A72-37753

Relativistic thermodynamics development based on invariant entropy concept, considering frictionless heat conduction and Carnot cycles

19 p2835 A72-37928

Solution of boundary value problems in heat conduction by the method of the successive averaging of a desired function

19 p2881 A72-38042

Determination of the temperature dependence of the thermophysical characteristics of solid materials by the method of successive approximations

19 p2881 A72-38044

Heat-conduction equations for multilayer shells

19 p2881 A72-38158

Thermal boundary equilibria in brittle bodies with heat conducting cracks under combined loads and temperature fields

19 p2877 A72-38198

Identification of parameters in nonlinear boundary conditions of distributed systems with linear fields

19 p2780 A72-38245

Heat conduction as mechanism for solar microwave bursts attenuation, noting effect of gyromagnetic absorption layers

19 p2852 A72-38497

Economical difference schemes for solving the heat-conduction equation in polar, cylindrical, and spherical coordinates

19 p2883 A72-38847

Inviscid non-monatomic interstellar gas radial flow, considering gravitational and heat conducting effects in stellar winds

20 p2967 A72-39193

Rotationally symmetric temperature distribution in region between two coaxial circular cones for isothermal and adiabatic conditions, solving heat conduction equation

20 p2983 A72-39329

Simple conduction model for theoretical steady-state heat pipe performance

20 p2984 A72-39607

Mathematical model for surface tension induced thermocapillary fluid flow influence on conductive heat transfer through condensate film broken by non-wetting strips

[ASME PAPER 72-HT-H]

20 p2985 A72-39654

Effect of wall conduction on the stability of a fluid in a rectangular region heated from below

[ASME PAPER 72-HT-G]

20 p2985 A72-39655

Analysis of real-gas and matrix-conduction effects in cyclic cryogenic regenerators

[ASME PAPER 72-HT-27]

20 p2986 A72-39672

Digital simulation of the SEI-1 static electrointegrator for solving heat-type equations

21 p3127 A72-40160

Analog model for two dimensional heat conduction equation, noting electrical networks for one dimensional difference equations solution

21 p3127 A72-40179

Electrical modeling of nonlinear problems of thermal engineering

21 p3128 A72-40182

Qualitative analysis of the linearization of quasi-linear problems of nonstationary heat conduction

21 p3129 A72-41055

Internal energy and conductive and frictional dissipation, mass, momentum and energy production as functions of density, entropy and geometric state variables

21 p3130 A72-41228

The problem of conductivity-type laser heating of two-temperature plasma, the nuclear fusion energy being taken into consideration, in the spherically symmetric case

21 p3093 A72-41480

Steady state or periodic solution to initial boundary value problems for heat conduction equation with nonlinear terms and boundary conditions

21 p3131 A72-41667

Radiant conduction heat transfer in semitransparent solid materials

22 p3243 A72-41955

Averaged equations for joint treatment of hydrodynamic expansion and conduction-type heating of plasma, the energy of nuclear fusion being taken into consideration. II - Spherical problem

22 p3211 A72-42630

Thermal design of hybrid modules and assemblies

22 p3161 A72-43172

Adiabatic density perturbations damping by radiative viscosity and heat conductivity, taking into account plasma recombination in hot expanding universe

23 p3333 A72-43231

Approximate optimal control solution to boundary value problem for one dimensional heat conduction equation, using Fredholm linear integral and degenerate kernels

23 p3274 A72-43526

Problem of the spatial localization of thermal disturbances in nonlinear heat-conduction theory

23 p3356 A72-43529

On the approximation of the thermal conductivity of rigid heat conductors as a Cauchy problem

23 p3356 A72-43721

One-dimensional shock waves in heat conducting materials with memory. I - Thermodynamics

23 p3314 A72-44341

Stability and oscillation characteristics of finite-element, finite-difference, and method of weighted residuals for transient two-dimensional heat conduction in structures

24 p3461 A72-44608

Determination of the radial heat conductivity of multilayer tubes for thermionic converters

24 p3461 A72-44875

Dual analysis for heat conduction problems by finite elements

24 p3461 A72-44877

Partial differential heat conduction equation for temperature distribution in rectangular plate, comparing with finite difference solution

24 p3465 A72-45268

CONDUCTIVITY METERS

NT ELECTRICAL CONDUCTIVITY METERS

Convective conductance meter for continuous measurement of outdoor exposed surface convection coefficient, using electrically heated plaques with known surface radiation properties

07 p0981 A72-18821

CONDUCTORS

NT AIRCRAFT ANTENNAS

NT ANTENNAS

NT CASSEGRAIN ANTENNAS

NT DIPOLE ANTENNAS

NT DIRECTIONAL ANTENNAS

NT ELECTRIC CONDUCTORS

NT ELECTRIC WIRE

NT ELECTROLYTES

NT EXPLODING WIRES

NT FLAT CONDUCTORS

NT HELICAL ANTENNAS

NT HORN ANTENNAS

NT ION EXCHANGE MEMBRANE ELECTROLYTES

NT LENS ANTENNAS

NT LOG PERIODIC ANTENNAS

NT LOG SPIRAL ANTENNAS

NT LOOP ANTENNAS

NT MICROWAVE ANTENNAS

NT MISSILE ANTENNAS

NT MOLTEN SALT ELECTROLYTES

NT MONOPOLE ANTENNAS

NT MONOPULSE ANTENNAS

NT OMNIDIRECTIONAL ANTENNAS

NT PARABOLIC ANTENNAS

NT PHOTOCONDUCTORS

NT RADAR ANTENNAS

NT RADIO ANTENNAS

NT SCHWARZSCHILD ANTENNAS

NT SLOT ANTENNAS

NT SPIRAL ANTENNAS

NT STEERABLE ANTENNAS

NT SUPERCONDUCTORS

NT THERMAL CONDUCTORS

NT TURNSTILE ANTENNAS

NT TWO REFLECTOR ANTENNAS

NT WAVEGUIDE ANTENNAS

NT YAGI ANTENNAS

Controllable states insufficiency to characterize rigid heat conductors dependence on temperature fields in experimental materials measurements programs

01 p0146 A72-11389

Closed rectangular cavity resonator with conducting walls, calculating differences of electromagnetic zero point fluctuation radiation pressure

02 p0260 A72-12434

Charged conductors in homogeneous collisionless magnetoactive plasma at hybrid frequencies, investigating antenna array quasi-electrostatic field one dimensional structure

08 p1138 A72-20746

Inhomogeneous plasma effect on helical slow wave systems approximated by anisotropically conducting plane

10 p1522 A72-24518

Reflection and transmission of plane E wave incident on moving conducting medium, discussing growing wave excitation

12 p1782 A72-27490

Ideally conducting and dielectric coaxial solids of revolution, investigating joint excitation by TM wave

15 p2209 A72-32658

CONES

NT ABLATIVE NOSE CONES

NT CIRCULAR CONES

NT CONICAL BODIES

NT NOSE CONES

NT ROCKET NOSE CONES

NT SLENDER CONES

Hypersonic source flow past wedges and cones, calculating flow nonuniformities effects on shock shape, velocity, pressure and density by perturbation analysis

01 p0033 A72-11394

Compressible turbulent boundary layer properties on porous cone at Mach 8, examining Crocco theory for flows with mass addition

05 p0602 A72-16536

Mass transfer effects on hypersonic turbulent boundary layer properties from profile measurements on porous cone

[AIAA PAPER 72-184]

05 p0650 A72-16839

Pressure distribution and force coefficients for cones at angles of incidence as function of Mach number, using extended method of equivalent axisymmetric bodies

10 p1417 A72-24028

Similarity method solution of differential equations of motion for supersonic laminar boundary near symmetry plane of cone at angle of incidence

10 p1418 A72-24326

Numerical solution for super-Alfvenic supersonic aligned MGD flow over cone with attached shock wave, obtaining surface pressure coefficients, current and vorticity distributions

10 p1418 A72-24463

Nose blunting, exposure time and initial temperature effects on axisymmetric bodies ablation surface cross hatching patterns, presenting test results on cones with various vertex angles

11 p1572 A72-26006

Weakly complete projecting convex cone, considering operators subalgebra representation

13 p1987 A72-29776

Numerical analysis of inviscid hypersonic flow characteristics in shock layer between bow shock and cone at angles of attack, taking into account laminar separated flow

14 p2069 A72-30328

Axisymmetric convergent cone profile synthesis to transform parallel flow at inlet to uniform sonic flow at outlet, examining solution convergence

15 p2177 A72-31206

Three dimensional elasticity boundary value problems solution via multidimensional Fourier transforms, applying to semiinfinite solid and hollow cones

15 p2324 A72-31481

Kinetic forming of conical Al component from solid cylindrical billet, analyzing forming and inertia stresses, impact velocity and displacement-time history

15 p2244 A72-31708

Exact boundary layer calculations for heat and mass transfer on cones at angle of attack, considering Mach number, enthalpy ratio and cross flow effects

15 p2337 A72-32591

Hypersonic boundary layer profiles upstream of transition point on cone surface from pitot surveys, heat transfer and wall pressure measurements and spark schlieren photographs

16 p2341 A72-32837

German monograph on supersonic flow past blunt sharp edged cones, comparing Van Dyke and method of characteristics results with schlieren photos and shadowgraphs

16 p2343 A72-33505

Aerodynamics of a slender cone with asymmetric nose bluntness at Mach 14

20 p2886 A72-39634

The effect of angle of attack on boundary-layer transition on cones

20 p2886 A72-39638

Wall interference effects on cone-cylinder pressure distribution in variable porosity trisonic wind tunnel as function of model blockage and Mach number

[AIAA PAPER 72-1010]

21 p3041 A72-41592

Experimental determination of asymmetry-induced trim angles of attack

[AIAA PAPER 72-1032]

21 p2993 A72-41605

Spin induced boundary layer distortion on rotating cone at supersonic speeds via spark shadowgraphs, correlating Magnus and normal force measurements with boundary layer configurations

[AIAA PAPER 72-967]

22 p3135 A72-42343

Wave propagation in a thin hollow cone by a finite element method

24 p3458 A72-44886

CONFERENCES

Parachutes and related technologies - Conference, London, September 1971

01 p0003 A72-10301

Papers on air piracy and international law based on McGill University Conference /October 1970/, covering legal problem solving, hijacking, etc

01 p0146 A72-10321

Ionospheric propagation - Conference, Kleinheubach, West Germany, October 1970

01 p0054 A72-10401

Photogrammetry - Conference, San Francisco, September 1971

01 p0065 A72-10448

Pattern recognition in biological and technical systems - Conference, Berlin, April 1970

01 p0017 A72-10463

Microwaves - Conference, Stockholm, August 1971, Volumes 1 and 2

01 p0035 A72-10626

Space shuttle materials - Conference, Huntsville, Alabama, October 1971, Volume 3

01 p0090 A72-10726

Nondestructive evaluation in aerospace, weapon systems and nuclear applications Conference, San Antonio, April 1971

01 p0075 A72-10801

Two dimensional digital pictorial signal processing - Conference, University of Missouri, Columbia, October 1971

01 p0069 A72-10865

Astronautical research - IAF Conference, Konstanz, West Germany, October 1970
01 p0130 A72-10926

Ultrasonics - Conference, London, September 1971
01 p0070 A72-11015

Power conditioning - IEEE Conference, California Institute of Technology, Pasadena, April 1971
01 p0007 A72-11051

Applied MHD and high temperature gas dynamics - Conference, Gdansk, Poland, May 1970
01 p0110 A72-11201

Educational satellites - Conference, Nice, France, May 1971, covering space communication, TV, performance, data handling, economics, etc
01 p0147 A72-11277

Microwaves and optical generation and amplification - Conference, Amsterdam, September 1970, covering microwave tubes, solid state devices and quantum electronics
01 p0044 A72-11278

Uranium plasmas - Conference, Atlanta, November 1971
01 p0099 A72-11326

Powder metallurgy - Conference, New York, July 1970, Volume 4, Processes, Volume 5, Materials and properties
02 p0239 A72-11426

Nonlinear mechanics and stability - Conference, Rome, February 1970
02 p0251 A72-11492

Quality control - Conference, Chicago, May 1971
02 p0304 A72-11551

Astronomy - Conference, University of Sydney, Australia, May 1971
02 p0276 A72-11639

Computers - Conference, Las Vegas, November 1971
02 p0185 A72-11651

Progress in radio science 1966-1969 - Conference, Ottawa, August 1969, Volume 3, radio waves and circuits and radio electronics
02 p0190 A72-11676

Heat transfer in low Reynolds number flow - ASME Conference, Washington, D.C., November 1971
02 p0301 A72-11722

Remote sensing of environment - Conference, University of Michigan, May 1971
02 p0207 A72-11776

Applied mechanics - Conference, University of Calgary, Canada, May 1971
02 p0292 A72-12001

Protection against accelerator and space radiation - Conference, Geneva, April 1971, Volume 1, Health physics
02 p0160 A72-12051

Telemetry - Conference, Washington, D.C., September 1971
02 p0173 A72-12126

Electronics and aerospace systems - IEEE Conference, Washington, D.C., October 1971
02 p0177 A72-12376

Telemetry applications in aerospace industry - ISA Conference, Las Vegas, May 1971
02 p0179 A72-12402

Electrical and electronic measurement and test instrument - Conference, Ottawa, June 1971
02 p0200 A72-12476

Static electrification - Conference, London, May 1971
02 p0260 A72-12551

Metal ductility and toughness - Conference, Kyoto, October 1971
02 p0246 A72-12557

Interstellar dust - IAU Conference, Jena, East Germany, August 1969
02 p0283 A72-12626

Radio aids to maritime and aerial navigation - Conference, Trieste, June 1971
02 p0257 A72-12640

Simulation of complex systems - Conference, Tokyo, September 1971
02 p0188 A72-12654

Weather prediction - Conference, Ostseebad Kuhlungsborn, East Germany, October 1969
02 p0253 A72-12776

Space astronomy techniques - Conference, Munich, August 1970
03 p0352 A72-13026

Medical primatology - Conference, New York, September 1969
03 p0313 A72-13068

Astronomy - IAU Conference, Brighton, England, August 1970
03 p0417 A72-13101

Ballistocardiography and clinical studies - Conference, Atlantic City, 2 May 1970
03 p0314 A72-13141

Systems, man and cybernetics - IEEE Conference, Anaheim, California, October 1971
03 p0318 A72-13161

Coronary heart disease - Conference, Frankfurt am Main, West Germany, January 1970
03 p0314 A72-13176

Physics of solar corona - NATO Conference, Athens, September 1970
03 p0421 A72-13201

General relativity and cosmology - Conference, Varenna, Italy, June-July 1969
03 p0426 A72-13265

Solar magnetic fields - Conference, College de France, Paris, August-September 1970
03 p0427 A72-13276

Mesospheric models - Conference, Frascati, Italy, July 1970
03 p0345 A72-13376

Magnetic bubble devices in memory hierarchies - IEEE Conference, Denver, April 1971
03 p0331 A72-13751

Fluid power - Conference, London, September 1970
03 p0312 A72-13960

Electromagnetic compatibility - IEEE Conference, Philadelphia, July 1971
03 p0323 A72-14027

Molecular beams - Conference, Cannes, June-July 1971
03 p0392 A72-14051

Nuclear and space radiation effects - Conference, University of New Hampshire, Durham, July 1971
03 p0402 A72-14076

Electronics and electrical engineering - IEEE Conference, Houston, April 1971
03 p0335 A72-14176

Reliability physics - IEEE Conference, Las Vegas, March-April 1971
03 p0335 A72-14276

Electronics - IEEE Conference, Chicago, October 1971
04 p0485 A72-14476

Distributed parameter systems control - Conference, Banff, Canada, June 1971
04 p0504 A72-14660

Biomechanics - Conference, Eindhoven, Netherlands, August 1969
04 p0477 A72-14703

Designing with composite materials - Conference, London, October 1971
04 p0536 A72-14742

Chemical evolution and life origin - Conference, Pont-a-Mousson, France, April 1970, Volume 1, Molecular evolution
04 p0467 A72-14751

Air transportation and society - AIAA/FAA Conference, Key Biscayne, June 1971
04 p0544 A72-14809

Ionosphere-magnetosphere interactions - Conference, New Delhi, February 1971
04 p0515 A72-14926

Astronomical constants - IAU Conference, Heidelberg, August 1970
04 p0574 A72-15025

Superconductivity - Conference, Stanford, California, August 1969
04 p0562 A72-15291

Electromagnetic wave theory - Conference, Tiflis, U.S.S.R., September 1971
04 p0488 A72-15376

Marine and aerospace engineering - Conference, Paris, May 1971
04 p0463 A72-15551

Submillimeter waves - Conference, New York, March-April 1970
04 p0532 A72-15590

Electronics research and engineering - IEEE Conference, Boston, November 1971
05 p0633 A72-15779

Satellite projects Azur, Dial and Heos - Conference, Bremen, West Germany, April 1971
05 p0714 A72-16134

External galaxies and quasars - IAU Conference, University of Uppsala, Sweden, August 1970
05 p0716 A72-16369

Automatic control in space - Conference, Dubrovnik, Yugoslavia, September 1971
05 p0724 A72-16427

Gas turbines - Conference, Tokyo, October 1971
05 p0601 A72-16480

Automatic control systems testing and evaluation - Conference, Saint Mary College of Maryland, August/September 1971
05 p0686 A72-16652

Phenomena in ionized gases - Conference, Oxford, England, September 1971
05 p0699 A72-17216

Relativistic fluid dynamics - Conference, Bressanone, Italy, June 1970
06 p0846 A72-17251

Cosmic ray physics - Conference, Moscow, USSR, October-November 1970
06 p0868 A72-17257

Radio technical capabilities and limitations of ATC systems - Conference, Washington, D.C., November 1971
06 p0844 A72-17326

Photo-optical instrumentation - Conference, Tokyo, June 1970
06 p0812 A72-17426

Quiescent plasmas - Conference, Elsinore, Denmark, September 1971
06 p0854 A72-17501

Vertebrates visual processes - Conference, University of Chile, Santiago, November-December, 1970
06 p0762 A72-17718

Computer simulation applications - Conference, New York, December 1970
06 p0779 A72-17972

Fluid mechanics - Conference, Kazimierz, Poland, September 1969, Parts 1 and 2
06 p0800 A72-18101

Anelasticity effects due to defects and phase transformations in solids - Conference, Lausanne, Switzerland, June 1970
06 p0830 A72-18291

AC-DC energy conversion - Conference, Milan, Italy, November 1970
06 p0785 A72-18307

Hf solid state and quantum electronic devices - Conference, Cornell University, August 1971
06 p0787 A72-18453

Solid lubrication - Conference, Denver, August 1971
06 p0823 A72-18583

Space for mankind benefit - Conference, Huntsville, November 1971
06 p0891 A72-18609

Nonlinear oscillations in mechanics - Conference, Kiev, U.S.S.R., August 1969
06 p0849 A72-18692

Environmental effects on aircraft and propulsion systems - Conference, Trenton, N.J., May 1971
07 p1052 A72-18751

Computer aided engineering - Conference, Waterloo, Canada, May 1971
07 p1024 A72-18776

Air safety - Conference, Mexico City, October 1971
07 p0911 A72-18827

Special steels - Conference, Nantes, France, May 1971
07 p1010 A72-18969

Laser engineering and applications - Conference, Washington, D.C., June 1971
07 p1002 A72-19207

Systems science - Conference, University of Hawaii, January 1972
07 p0949 A72-19270

Computers in biomedicine - Conference, University of Hawaii, January 1972
07 p0928 A72-19306

Astrophysics and general relativity - Conference, Brandeis University, Waltham, Massachusetts, June-July 1968
07 p1073 A72-19426

Transcript of conference on origins of life covering cosmic evolution, abundance and distribution of biologically important elements, earth and Mars atmosphere evolution, etc
07 p1074 A72-19450

Origins of life - Conference, Princeton, New Jersey, May 1967
07 p1074 A72-19451

Space law - IAF Conference, Konstanz, West Germany, October 1970
07 p1102 A72-19452

Biochronometry - NAS-NASA Conference, Friday Harbor, Washington, September 1969
07 p0918 A72-19526

Metallurgy and metal science - Conference, Moscow, May 1968
07 p1011 A72-19543

Multivariable technical control system - Conference, Dusseldorf, West Germany, October 1971
07 p0960 A72-19696

Solar-terrestrial physics - Conference, Leningrad, May 1970
07 p0977 A72-20004

Fluid mechanics - Conference, Rynia, Poland, September 1971
07 p0969 A72-20060

Transportation noises - Conference, University of Washington, Seattle, March 1969
07 p0931 A72-20162

Gyro technology - Conference, Kiel, Germany, May 1971
07 p0989 A72-20276

Computer simulation - Conference, Boston, July 1971
07 p0950 A72-20326

Nondestructive testing - Conference, Trieste, Italy, May 1971
07 p0991 A72-20420

Chronology of universe - Conference, Padua, Italy, November 1970
07 p1083 A72-20463

Special steels - Conference, Nantes, France, May 1971
07 p1021 A72-20482

Explosives and pyrotechnics - Conference, Philadelphia, September 1971
08 p1218 A72-20751

Nonlinear estimation theory and applications - Conference, San Diego, September 1971
08 p1143 A72-20843

Nondestructive testing techniques - ISA Conference, Chicago, October 1971
08 p1163 A72-20914

Physics - Conference, Bratislava, Czechoslovakia, May 1968
08 p1205 A72-20936

- Test pilots 1971 reports - Conference, Beverly Hills, California, September 1971 08 p1230 A72-21001
- Shock tubes - Conference, London, July 1971 [AD-736510] 08 p1148 A72-21013
- Metal working technology - Conference, Timisoara, Rumania, October 1971 08 p1173 A72-21026
- Nuclear science and power systems - IEEE-NASA-AEC Conference, San Francisco, November 1971 08 p1166 A72-21506
- D and E region winds over Europe - Conference, London, April 1971 08 p1159 A72-21526
- Atheromatosis, chest angina and arrhythmia - Conference, Brussels, October 1970 08 p1117 A72-21541
- Survival and flight equipment - Conference, Las Vegas, September 1971 08 p1109 A72-21560
- Plastics - Conference, Washington, D.C., February 1972 08 p1192 A72-21676
- Sonic booms - Conference, Houston, November 1970 08 p1110 A72-21901
- Fluid sealing - Conference, Coventry, England, March-April 1971 08 p1177 A72-21926
- Space applications of camera tubes - Conference, Paris, November 1971 08 p1169 A72-21951
- Corrosion testing - Conference, Toronto, June 1970 08 p1188 A72-22101
- Statistical methods in meteorology - Conference, Leningrad, September 1969 08 p1202 A72-22112
- Vibrations in rotating systems - Conference, London, February 1972 08 p1224 A72-22127
- Fluid power - Conference, University of Surrey, England, January 1971 08 p1113 A72-22151
- Metal forming - AIME Conference, Cleveland, October 1970 08 p1250 A72-22193
- Turbulence measurements in liquids - Conference, Rolla, Missouri, September 1969 09 p1292 A72-22301
- Geoscience electronics - IEEE Conference, Washington, D.C., August 1971 09 p1306 A72-22311
- D and E region ion chemistry - Conference, University of Illinois, Urbana, July 1971 09 p1274 A72-22352
- Ceramics in severe environments - Conference, North Carolina State University, Raleigh, December 1970 09 p1333 A72-22376
- Metal deposition - Conference, Vilnius, Lithuanian SSR, April 1971 09 p1318 A72-22526
- Superconductivity in d- and f-band transition metals - Conference, University of Rochester, New York, October 1971 09 p1367 A72-22551
- Man and technology in orientation and navigation Conferences, Essen, Germany, October 1971 09 p1348 A72-22776
- Simple and multiple electronic processes in X and XUV region - Conference, Paris, September 1970 09 p1356 A72-22826
- Background noise in active semiconductor devices - Conference, Toulouse, France, September 1971 09 p1286 A72-23101
- ATC tasks work load assessment - Conference, Darmstadt University of Technology, June 1971 09 p1270 A72-23126
- Space rescue - Conference, Konstanz, West Germany, October 1970 09 p1395 A72-23151
- Fiber composites mechanical properties - Conference, Teddington, England, November 1971 09 p1338 A72-23162
- Ordinary differential and functional equations - Conference, Kyoto, Japan, September 1971 09 p1341 A72-23251
- Photointerpretation - Conference, Dresden, Germany, September 1970, Parts 1 and 2 09 p1301 A72-23276
- Nonlinear dynamics of flight vehicle - Conference, University of Technology, Loughborough, England, March 1972 09 p1407 A72-23451
- Welded structures fatigue - Conference, Abington, England, July 1970 09 p1332 A72-23615
- Advances in welding processes - Conference, Abington, Cambridge, England, April 1970 09 p1319 A72-23626
- Decision and control including adaptive processes - IEEE Conference, Miami Beach, Florida, December 1971 10 p1454 A72-23776
- Hardware software firmware tradeoffs - IEEE Conference, Boston, September 1971 10 p1442 A72-23815
- Advances in metallography - Conference, Leoben, Austria, October 1970 10 p1493 A72-23822
- Internal flows - Conference, Salford, England, April 1971 10 p1415 A72-23853
- High energy astrophysics - Conference, Erice, Italy, May-June 1971 10 p1532 A72-23883
- Galactic nuclei - Conference, Vatican City, April 1970 10 p1533 A72-23894
- Electron, ion and laser beam technology - IEEE Conference, Boulder, Colorado, May 1971 10 p1517 A72-23926
- Reliability and maintainability - Conference, San Francisco, January 1972 10 p1485 A72-23972
- Structural mechanics in reactor technology - Conference, Berlin, Germany, September 1971 10 p1556 A72-24392
- Electromagnetic suspension - Conference, Southampton, England, July 1971 10 p1460 A72-24756
- Automatic meteorological stations - Conference, Potsdam, East Germany, March 1970 10 p1507 A72-25007
- Multiply charged heavy ion sources and accelerating systems - Conference, Gatlinburg, Tennessee, October 1971 10 p1516 A72-25026
- Meteorological observations and instrumentation - AMS Conference, San Diego, March 1972 10 p1507 A72-25076
- Temperate latitude sporadic E cause and structure - Conference, Utah State University, Logan, September 1971 10 p1477 A72-25151
- Composite materials testing and design - ASTM Conference, Anaheim, California, April 1971 11 p1670 A72-25452
- Upper atmosphere physics - Conference, Erice, Italy, June 1970, Volume 2 11 p1621 A72-25834
- Dynamical aspects of critical phenomena - Conference, Fordham University, New York, June 1970 11 p1701 A72-26022
- Physics - Conference, Evian, Haute-Savoie, France, May 1971 11 p1692 A72-26430
- Infrasonic research - Conference, Pullman, Washington and Moscow, Idaho, November 1970 11 p1627 A72-26508
- Diurnal rhythm and loss of sleep effects on human efficiency - Conference, Strasbourg, July 1970 11 p1580 A72-26676
- Refractory powder metallurgy - Conference, Reutte, Austria, June 1971, Volumes 1, 2, 3 and 4 11 p1642 A72-26826
- Electron microscopy and structure of materials - Conference, University of California, Berkeley, September 1971 11 p1666 A72-26926
- Numerical analysis applications - Conference, University of Dundee, Scotland, March 1971 11 p1679 A72-26953
- Optical transparencies - Conference, London, June 1971 12 p1752 A72-27001
- Vacuum technology - Conference, Boston, October 1971 12 p1805 A72-27034
- Applications of experimental and theoretical structural dynamics - Conference, University of Southampton, England, April 1972 12 p1882 A72-27337
- Outer solar system - AAS Conference, Seattle, June 1971 12 p1870 A72-27344
- Ionosphere - Conference, Kleinheubach, West Germany, September 1971 12 p1802 A72-27769
- Gravitational n body problem - IAU Conference, Cambridge, England, August 1970 12 p1872 A72-27890
- Solar cells - Conference, Toulouse, France, July 1970 12 p1755 A72-28001
- Radiation effects in semiconductors - Conference, State University of New York, Albany, August 1970 12 p1856 A72-28051
- Materials science - Conference, Los Angeles, April 1972 12 p1833 A72-28076
- Elastohydrodynamic lubrication - Conference, Leeds University, England, April 1972 12 p1816 A72-28107
- Aerospace medicine - Conference, Bal Harbour, Florida, May 1972 12 p1764 A72-28251
- Operations research and reliability - Conference, Turin, Italy, June-July 1969 13 p1961 A72-28351
- Stability in mechanics of continuous solids - Conference, University of Waterloo, Ontario, Canada, October 1970-September 1971 13 p2054 A72-28476
- X ray spectroscopy - Conference, Ivano-Frankovsk, Ukrainian SSR, February 1971 13 p1972 A72-28488
- Aerospace and aeronautical meteorology - AMS Conference, Washington, D.C., May 1972 13 p1988 A72-28801
- Circuit theory - Conference, University of Missouri, Rolla, May 1972 13 p1935 A72-29101
- OMEGA navigation system - Conference, Washington, D.C., November 1971 13 p1997 A72-29180
- MHD - Conference, Argonne, Illinois, March 1972 13 p1899 A72-29351
- Solar eclipse 1970 - Conference, Seattle, June 1971 13 p2041 A72-29526
- Noise and vibration control engineering - Conference, Purdue University, Indiana, July 1971 13 p2005 A72-29553
- Dynamics of composite materials - ASME Conference, La Jolla, California, June 1972 13 p2060 A72-29690
- Galactic astronomy - Conference, State University of New York, Stony Brook, June-July 1968, covering Galactic structure, spiral shape theories, star migration, etc 14 p2152 A72-30486
- Lunar geophysics - Conference, Houston, October 1971 14 p2153 A72-30501
- High temperature mechanical properties - Conference, Clermont-Ferrand, France, October 1970 14 p2116 A72-30526
- Metallic corrosion - Conference, Amsterdam, September 1969 14 p2117 A72-30534
- Rocket propellants, propulsive charges and explosives lifetime - Conference, Karlsruhe, Germany, September-October 1971 14 p2143 A72-30751
- Nonlinear oscillations theory application to electronics and electrical engineering - Conference, Kiev, August-September 1969 14 p2089 A72-31101
- International cooperation in space operations and exploration - AAS Conference, Washington, D.C., March 1971 14 p2175 A72-31135
- Electronics - Conference, Rome, March 1970 15 p2193 A72-31177
- Aviation and astronautics - Conference, Tel Aviv-Haifa, March 1972 15 p2177 A72-31201
- Relays - Conference, Oklahoma State University, Stillwater, April 1972 15 p2204 A72-31214
- Space activity in fields of ecology and earth resources - Conference, Rome, Italy, March 1972 15 p2220 A72-31226
- Thermal expansion - Conference, Corning, New York, October 1971 15 p2259 A72-31254
- Applied mathematics and mechanics - Conference, Mannheim, Germany, April 1971 15 p2323 A72-31451
- Scintillation and semiconductor counters - IEEE/AEC/NBS Conference, Washington, D.C., March 1972 15 p2233 A72-31529
- Ordinary differential equations - USN Conference, Washington, D.C., June 1971 15 p2262 A72-31751
- Astronautical engineering - Conference, Mar del Plata, Argentina, October 1969 15 p2320 A72-31801
- High power ultrasonics - Conference, Graz, Austria, September 1970 15 p2256 A72-31831
- Circuit theory - IEEE Conference, North Hollywood, April 1972 15 p2211 A72-31843
- Electro-optical systems design - Conference, New York, September 1971 15 p2247 A72-32026
- Space navigation - Conference, Orlando, Florida, March 1972 15 p2269 A72-32176
- Navigation for general aviation and navigation training - Conference, Atlanta, February-March 1972 15 p2271 A72-32201
- Total system approach to time scheduled aircraft operations - Conference, London, May 1972 15 p2339 A72-32451
- Electromagnetic hazards, pollution and environmental quality - Conference, Purdue University, Indiana, May 1972 15 p2209 A72-32563

- Environmental progress - Conference, New York, May 1972
15 p2191 A72-32601
- Electronic displays - Conference, London, February 1972
15 p2181 A72-32631
- Light scattering by fluids - Conference, France, July 1971
16 p2428 A72-32941
- Astronomy - Conference, University of Adelaide, Australia, December 1971
16 p2451 A72-33031
- Molecular beams - Conference, Cannes, France, June-July 1971
16 p2429 A72-33051
- Fluidics - Conference, Prague, June-July 1971
16 p2350 A72-33176
- Transportation - Conference, Washington, D.C., May-June 1972
16 p2347 A72-33180
- Reinforced plastics - Conference, Karlovy Vary, Czechoslovakia, May 1972
16 p2414 A72-33301
- Air transportation - SAE/AIAA/ASME Conference, Washington, D.C., May-June 1972
16 p2481 A72-33306
- Civil aviation safety - Conference, Beirut, Lebanon, November-December 1971
16 p2481 A72-33326
- Mathematical problems in geophysical sciences - Conference, Rensselaer Polytechnic Institute, Troy, New York, July 1970
16 p2384 A72-33335
- Explosives in engineering design - Conference, University of New Mexico, Albuquerque, March 1972
16 p2398 A72-33351
- Reinforced thermoplastics - Conference, El Segundo, California, March 1972
16 p2415 A72-33414
- Aerospace instrumentation - Conference, Cranfield Institute of Technology, England, March 1972
16 p2393 A72-33626
- Isotopic composition of primary cosmic radiation - Conference, Lyngby, Denmark, March 1971
16 p2446 A72-33726
- Electrocatalysis and fuel cells - Conference, Seattle, December 1970
16 p2351 A72-33876
- Cosmic plasma physics - Conference, Frascati, Italy, September 1971
16 p2459 A72-33901
- Creep in structures - Conference, Goteborg, Sweden, August 1970
16 p2411 A72-34110
- Two Dimensional Digital Signal Processing Conference, University of Missouri, Columbia, Mo., October 6-8, 1971, Proceedings.
17 p2520 A72-34401
- Institute of Electrical and Electronics Engineers, Southwestern Annual Conference and Exhibition, 24th, Dallas, Tex., April 19-21, 1972, Record.
17 p2514 A72-34413
- International Space Rescue Symposium, 4th, Brussels, Belgium, September 21, 1971, Proceedings.
17 p2620 A72-34426
- Annual Thermionic Conversion Specialist Conference, 10th, San Diego, Calif., October 4-6, 1971, Conference Record.
17 p2494 A72-34576
- Electronic Components Conference, 22nd, Washington, D.C., May 15-17, 1972, Proceedings.
17 p2527 A72-34676
- Institute of Electrical and Electronics Engineers, Region Six Conference, San Diego, Calif., April 19-21, 1972, Record.
17 p2528 A72-34701
- Shaping the future with plastics; Proceedings of the Thirtieth Annual Technical Conference, Chicago, Ill., May 15-18, 1972, Part 1.
17 p2570 A72-34712
- Regional Conference on Control Theory, University of Maryland, Baltimore, Md., August 23-27, 1971, Proceedings.
17 p2533 A72-34948
- Metabolism of the hypoxic and ischaemic heart; Proceedings of the Symposium, Geneva, Switzerland, June 14-17, 1971, Part 1.
17 p2501 A72-34976
- International Space Rescue Symposium, 2nd, Mar del Plata, Argentina, October 9, 1969, Proceedings.
17 p2622 A72-35549
- NAECON '72; Proceedings of the National Aerospace Electronics Conference, Dayton, Ohio, May 15-17, 1972.
17 p2493 A72-35551
- Heat Transfer and Fluid Mechanics Institute, 23rd, San Fernando Valley State College, Northridge, Calif., June 14-16, 1972, Proceedings.
17 p2542 A72-35631
- Advanced materials: Composites and carbon; Proceedings of the Symposium, Chicago, Ill., April 26-28, 1971.
17 p2571 A72-35651
- International Geological Congress, 24th, Montreal, Canada, August 21-30, 1972, Proceedings. Section 15 - Planetology.
17 p2614 A72-35676
- Electrical contacts - 1972; Proceedings of the Sixth International Conference on Electrical Contact Phenomena, Chicago, Ill., June 5-9, 1972.
18 p2664 A72-35979
- Statistical models and turbulence; Proceedings of the Symposium, University of California, La Jolla, Calif., July 15-21, 1971.
18 p2676 A72-36001
- Circulatory assist and ballistocardiographic studies; Proceedings of the Fifteenth Annual Meeting, Atlantic City, N.J., May 1, 1971.
18 p2648 A72-36032
- Gas turbine pumps; Proceedings of the Joint Conference, San Francisco, Calif., March 26, 27, 1972.
18 p2693 A72-36040
- Vibration technology: Balancing flexible rotors; Conference, Technische Universitat Berlin, Berlin, West Germany, March 23, 24, 1970, Summaries
18 p2731 A72-36064
- Electrical contacts - 1971; Proceedings of the Seventeenth Annual Holm Seminar on Electric Contact Phenomena, Chicago, Ill., October 13-15, 1971.
18 p2665 A72-36114
- Lunar Science Institute, Conference on Lunar Geophysics, Houston, Tex., October 18-21, 1971, Proceedings.
18 p2724 A72-36275
- Scanning the spectrum; Proceedings of the Tenth Annual Region 3 Convention, University of Tennessee, Knoxville, Tenn., April 10-12, 1972.
18 p2665 A72-36301
- Experimental mechanics in research and development; Proceedings of the International Symposium, University of Waterloo, Waterloo, Ontario, Canada, June 12-16, 1972. Volumes 1 & 2.
18 p2732 A72-36352
- Airports: Key to the air transportation system; Proceedings of the Conference, Atlanta Ga., April 14-16, 1971.
18 p2675 A72-36776
- Conference on Radio Receivers and Associated Systems, University College of Swansea, Swansea, Wales, July 4-6, 1972, Proceedings.
18 p2661 A72-36842
- Yugoslav Symposium on Physics of Ionized Gases, 6th, Miljevac, Yugoslavia, July 16-21, 1972, Proceedings.
18 p2713 A72-36951
- Southeastern Conference on Theoretical and Applied Mechanics, 5th, North Carolina State University and Duke University, Raleigh and Durham, N.C., April 16, 17, 1970, Proceedings.
18 p2736 A72-37051
- High reliability electronic components; International Conference, Toulouse, France, March 6-10, 1972, Proceedings
18 p2668 A72-37101
- International Microwave Symposium, Arlington Heights, Ill., May 22-24, 1972, Proceedings.
19 p2770 A72-37251
- Fall Powder Metallurgy Conference, Detroit, Mich., October 19-21, 1971, Proceedings.
19 p2815 A72-37591
- Engineering applications of holography; Proceedings of the Symposium, Los Angeles, Calif., February 16, 17, 1972.
19 p2797 A72-37601
- Joint Automatic Control Conference, 13th, Stanford University, Stanford, Calif., August 16-18, 1972, Preprints of Technical Papers.
19 p2779 A72-38226
- INTERKAMA 1971; International Congress with Exposition for Measurement Technology and Automation, 5th, Duesseldorf, West Germany, October 14-20, 1971, Reports
19 p2782 A72-38301
- Japan Congress on Materials Research, 15th, Tokyo, Japan, September 1971, Proceedings.
20 p2935 A72-38877
- EMC at the crossroads; International Electromagnetic Compatibility Symposium, Arlington Heights, Ill., July 18-20, 1972, Record.
20 p2901 A72-38976
- Electro-optics '72; Proceedings of the Second International Conference, Brighton, England, February 29-March 2, 1972.
20 p2921 A72-39026
- Interamerican Conference on Materials Technology, 3rd, Rio de Janeiro, Brazil, August 14-17, 1972, Proceedings.
20 p2936 A72-39201
- Acoustic emission; Proceedings of the Symposium, Bal Harbour, Fla., December 7, 8, 1971.
20 p2924 A72-39276
- Composite materials; Meeting, 1st, Konstanz, West Germany, October 22, 23, 1970, Technical Reports
20 p2939 A72-39436
- INTERNEPCON '71; Proceedings of the International Electronic Packaging and Production Conference, Brighton, Sussex, England, October 19-21, 1971.
20 p2908 A72-39490
- Magnetosphere-ionosphere interactions; Proceedings of the Advanced Study Institute, Dalseter, Norway, April 14-23, 1971.
20 p2917 A72-39526
- International Space Rescue Symposium, 1st, New York, N.Y., October 14, 1968, Proceedings.
20 p2977 A72-39550
- Conference on Solid State Devices, 3rd, Tokyo, Japan, September 1, 2, 1971, Proceedings.
20 p2960 A72-39701
- Annual Corporate Aircraft Safety Seminar, 17th, Washington, D.C., April 17, 18, 1972, Proceedings.
20 p2887 A72-39740
- Line formation in the presence of magnetic fields; Proceedings of the Conference, Boulder, Colo., August 30-September 2, 1971.
20 p2970 A72-39752
- Activation analysis in geochemistry and cosmochemistry; Proceedings of the Advanced Study Institute, Kjeller, Norway, September 7-12, 1970.
20 p2898 A72-39826
- NEWNAV Symposium, Frankfurt am Main, West Germany, October 5-7, 1971, Report. Volumes 1 & 2.
21 p3079 A72-40276
- Antennas; Specialists' Meeting, Darmstadt, West Germany, February 22-24, 1972, Reports
21 p3027 A72-40502
- Visual performance when using optical instruments; Symposium, Munich, West Germany, July 21-23, 1971, Technical Papers.
21 p3054 A72-40727
- Annual International Conference on Communications, 8th, Philadelphia, Pa., June 19-21, 1972, Conference Record.
21 p3016 A72-40851
- Israel Conference on Mechanical Engineering, 6th, Haifa, Israel, June 26, 27, 1972, Proceedings.
21 p3118 A72-40926
- Extension Seminar on High Temperature Strength of Metals, Kyoto, Japan, August 21, 1971, Preprints.
21 p3068 A72-41007
- Japan National Congress for Applied Mechanics, 20th, Tokyo, Japan, October 23, 24, 1970, Proceedings.
21 p3121 A72-41226
- Displays and controls; Proceedings of the Advanced Study Institute, Berchtesgaden, West Germany, March 15-26, 1971.
21 p3009 A72-41402
- Symposium on Foundations of Plasticity, Warsaw, Poland, August 29-September 2, 1972, Proceedings.
21 p3124 A72-41501
- High altitude physiology: Cardiac and respiratory aspects; Proceedings of the Symposium, London, England, February 17, 18, 1971.
22 p3143 A72-42583
- International Aerospace Instrumentation Symposium, 18th, Miami, Fla., May 15-17, 1972, Proceedings.
22 p3178 A72-42676
- Dynamic response of structures; Proceedings of the Symposium, Stanford University, Stanford, Calif., June 28, 29, 1971.
22 p3236 A72-42755
- Amorphous materials; Proceedings of the Third International Conference on the Physics of Non-crystalline Solids, University of Sheffield, Sheffield, England, September 14-18, 1970.
22 p3196 A72-42790
- Semiconductor/IC Processing and Production Conference, Anaheim, Calif., February 8-10, 1972 and New York, N.Y., June 13-15, 1972, Proceedings of the Technical Program.
22 p3160 A72-42822
- International Conference on Structural Safety and Reliability, Washington, D.C., April 9-11, 1969, Proceedings.
22 p3240 A72-42966
- International Interdisciplinary Cycle Research Symposium, 3rd, Noordwijk, Netherlands, August 22-28, 1971, Proceedings.
22 p3147 A72-42976
- Book - Thermal structural analysis programs: A survey and evaluation.
22 p3241 A72-43046
- National Electronic Packaging and Production Conference, Anaheim, Calif., February 8-10, 1972 and New York, N.Y., June 13-15, 1972, Proceedings of the Technical Program.
22 p3161 A72-43171
- Life sciences and space research X; Proceedings of the Fourteenth Plenary Meeting, Seattle, Wash., June 21-July 2, 1971.
23 p3253 A72-43381
- Symposium on Waves and Resonances in Plasmas, St. John's, Newfoundland, Canada, July 5-9, 1971, Proceedings.
23 p3319 A72-43511
- Asilomar Conference on Circuits and Systems, 5th, Pacific Grove, Calif., November 8-10, 1971, Record.
23 p3276 A72-43851

- The surface crack: Physical problems and computational solutions; Proceedings of the Winter Annual Meeting, New York, N.Y., November 26-30, 1972.
23 p3352 A72-44226
- Aircraft jet-engine control; Conference, Velešín, Czechoslovakia, June 12-16, 1972, Proceedings
23 p3326 A72-44276
- All-Union Conference on the Physics of Cosmic Rays, Tiflis, Georgian SSR, October 19-22, 1971, Proceedings
23 p3329 A72-44401
- The application of operational research to transport problems; Proceedings of the Conference, Sandefjord, Norway, August 14-18, 1972.
24 p3466 A72-44576
- Conference on Reliability Testing and Reliability Evaluation, The Hague, Netherlands, September 4-8, 1972, Proceedings.
24 p3405 A72-44651
- Aircraft fatigue: Design, operational and economic aspects.
24 p3366 A72-44726
- Symposium on the Morphology and Physics of Magnetospheric Substorms, Moscow, USSR, August 3, 1971, Proceedings.
24 p3395 A72-44846
- International Colloquium on Gasdynamics of Explosions and Reactive Systems, 3rd, Marseille, France, September 12-17, 1971, Proceedings.
24 p3461 A72-45016
- Atmospheric Flight Mechanics Conference, 2nd, Palo Alto and Moffett Field, Calif., September 11-13, 1972, Informal Papers.
24 p3361 A72-45326
- Conference on Fluid Machinery, 4th, Budapest, Hungary, September 11-16, 1972, Proceedings.
24 p3393 A72-45351
- From plasma to planet; Proceedings of the Twenty-First Nobel Symposium, Saltsjöbaden, Sweden, September 6-10, 1971.
24 p3444 A72-45451
- Astronomy from a space platform; Proceedings of the Symposium, Philadelphia, Pa., December 27, 28, 1971.
24 p3446 A72-45526
- Conference on Theoretical Ionospheric Models, Pennsylvania State University, University Park, Pa., June 14-16, 1971, Proceedings.
24 p3399 A72-45579
- Innovative architecture; Annual International Conference, 6th, San Francisco, Calif., September 12-14, 1972, Digest of papers.
24 p3383 A72-45665
- CONFIDENCE**
Obedience to rotation-indicating visual displays as a function of confidence in the displays.
17 p2510 A72-35943
- CONFIDENCE LIMITS**
Point estimate calculation of underlying distribution function for probability plot, developing confidence coefficient for Weibull model
02 p0252 A72-11557
- Inherent uncertainties in virial mass determinations of bound and unstable groups of galaxies, computing evolution tracks for different mass loss mechanisms and rates
07 p1072 A72-19341
- Computer simulation of empirical confidence limits for variance spectra, applying to Gaussian random noise data stochastic model
07 p0951 A72-20360
- Numerically exact nonlinear filter synthesis, describing confidence intervals for error performance statistical inferences
08 p1144 A72-20850
- Lower confidence bound for reliability and specifications for nonnormally distributed stress corrosion test data, using Weibull statistical distribution
08 p1189 A72-22102
- Confidence level determination in terms of reliability index /MTBF/ for MIL-STD-781 truncated sequential probability ratio tests
10 p1444 A72-23989
- Complex system represented by fault-free with independent components, calculating confidence interval for failure probability by moment method
10 p1444 A72-24018
- Eclipse analyses confidence in eclipsing binary photometric solutions, discussing consistency with stellar interior model density distributions and interactions between member stars
11 p1716 A72-25677
- Reliability lower confidence limit estimation for serial systems with failure in any subsystems resulting in overall failure
13 p1962 A72-28362
- Geomagnetic and meteorological elements lunar daily variation calculation by modified Chapman-Miller method, estimating confidence limits for parameters reliability
16 p2384 A72-32972
- Liquid scintillation counters application in search for relativistic quarks in cosmic rays, setting upper confidence limits on particle intensity
17 p2601 A72-35471
- Variation analysis and design of experiments as an aid to design quality assurance.
20 p2930 A72-39856
- A note on a comparison of confidence interval techniques in truncated life tests.
21 p3075 A72-40828
- Least squares estimation of cosmological model parameters, comparing confidence limits with Solheim trial method
21 p3109 A72-41440
- Upper limits on vertical fluxes of $1/3$ e and $2/3$ e charged quarks in cosmic rays from observations with scintillation counter telescope
21 p3101 A72-41450
- Probability of digital-data reception with a given confidence level under conditions of random radio noise
23 p3266 A72-44208
- Fundamentals of multivariate analysis - Linear regression.
23 p3310 A72-44394
- Charts for confidence limits and tests for failure rates.
23 p3294 A72-44395
- A survey and comparison of methods for determining confidence bounds on system reliability from subsystem data.
24 p3406 A72-44652
- Estimation, confidence intervals, and incentive plans for sequential three way decision procedures.
24 p3406 A72-44667
- Point and confidence interval estimates for acceleration and aging component probability distribution functions in accelerated life tests and reliability prediction
24 p3406 A72-44669
- CONFIGURATION MANAGEMENT**
Quality control function in configuration management, discussing hardware and software validity for decision formulation
02 p0304 A72-11553
- Configuration management on small production contracts for U.S. Government, including identification, control and accounting
03 p0460 A72-14204
- CONFIGURATIONS**
Configuration factors for radiative heat transfer analysis with partially occluded surfaces, defining areas by computer technique
11 p1742 A72-25238
- CONFORMAL MAPPING**
Hollow waveguide problem considering numerical solution with scalar field approximation, Green function and conformal transformation
02 p0191 A72-11692
- Circular network analysis by conformal mapping method, evaluating physical and geometric magnitudes in turbine driven machinery
04 p0461 A72-14514
- Torsion of hollow beam consisting of two homogeneous isotropic rods with different elastic properties and simply connected cross sections, solving by conformal mapping
04 p0586 A72-14992
- Conformal transformations applications to plane electromagnetic wave diffraction by infinitely conducting network, discussing energy distribution
04 p0490 A72-15410
- Hollow waveguide performance numerical solution review covering finite difference and element methods, polynomial approximation, point matching, integral equations and conformal transformation
06 p0784 A72-18237
- Biharmonic boundary value problems solution by summary representations method and conformal mapping for plane with two circular holes
08 p1242 A72-20906
- Plane potential flow problem for laminar boundary layer on rotating infinite cylindrical blade, using conformal coordinate transformation
08 p1108 A72-21614
- Friedmann cosmological models in terms of conformally invariant gravitation theory, noting two physically connected universe halves
10 p1541 A72-24474
- Green function for stress components in circumferentially loaded circular disk, noting conformal mapping for arbitrary shape
10 p1557 A72-24717
- Green function for stress components in straight edge loaded half plane disk, noting conformal mapping for arbitrary shape
10 p1558 A72-24718
- Hodograph method involving conformal mapping for turbomachine blade subsonic flow profile calculation
11 p1570 A72-25635
- Green function for stress distribution in plane shaped disk with edge loaded circular hole, noting conformal mapping for arbitrary shape
12 p1883 A72-27391
- Plane potential flow stability with respect to bounded and free hollow vortices, using conformal mapping method
13 p1941 A72-28716
- Aerodynamic profiles lift coefficient determination by empirical formula based on potential flow lines obtained by conformal mapping
13 p1894 A72-29132
- Torsion problem of solid rod with wing profile shaped cross section solved by conformal mapping and gamma function derivative, calculating maximum stresses and rigidities
15 p2327 A72-31741
- Two fluid cosmological model in conformal and conformally flat forms, deriving solutions in elementary functions
15 p2307 A72-31796
- Nonlinear equations systems iterative solution methods convergence, generalizing Varga matrix splitting technique to nonlinear mappings in Banach space
15 p2264 A72-32465
- Coefficients ratio modulus invariance of elliptic differential equation for conformal mapping of definition domain
16 p2417 A72-34011
- Hamiltonian system evolutionary stability via area preserving mapping, using Bartlett eigenvector method
17 p2547 A72-35108
- Application of conformal transformation to the variational method - Buckling loads of polygonal plates.
18 p2738 A72-37074
- An approximate method for solving problems involving separated flows past bodies
21 p2990 A72-41088
- Conformal mapping procedure for numerical generation of airfoils with local curvature singularities, presenting test problem results for zero trailing edge angle
21 p2992 A72-41259
- V-wings and diamond ring-wings of minimum induced drag.
21 p2992 A72-41263
- Conformal mapping for interaction of two dimensional flow of ideal fluid and injected counterflow with jet formation, calculating cavitation void dimensions
22 p3165 A72-42065
- Plane potential flow stability with respect to small perturbation flow of bounded and free hollow vortices, using conformal mapping method
22 p3165 A72-42093
- Versatile stretching of a disc shaped as a plane with elliptic aperture.
22 p3236 A72-42627
- Velocity space maps and transforms of tracking observations, for orbital trajectory state analysis.
24 p3440 A72-45135
- CONFORMAL TRANSFORMATIONS**
U CONFORMAL MAPPING
CONGENITAL ANOMALIES
Photopic spectral curves of relative luminous efficiency for congenital deficiencies of color vision, using optical bench, interference filters and Bachstein flicker photometer
03 p0316 A72-13935
- Familial cardiomyopathy detection by electrocardiography noting arrhythmias, ventricular hypertrophy, abnormal Q waves and intraventricular conduction defects
04 p0466 A72-14443
- Abnormal ECG in healthy man due to former disease, subclinical disease, congenital anomalies, hereditary disease or functional aberrations
07 p0924 A72-20574
- Color discrimination threshold determination for spectral sensitivity in subjects with congenital color vision disorders
13 p1903 A72-28763
- Echocardiography in the diagnosis of congenital mitral stenosis and in evaluation of the results of mitral valvotomy.
19 p2755 A72-37499
- The mitral apparatus - Functional anatomy of mitral regurgitation.
20 p2892 A72-39460
- The scoliosis of congenital heart disease.
24 p3370 A72-44560
- CONGENITAL CONDITIONS**
U CONGENITAL ANOMALIES
CONGRUENCES
Computational solutions of matrix problems over an integral domain.
21 p3076 A72-41315
- CONICAL BODIES**
NT SLENDER CONES
Lateral vibration of thin conical bar with clamped base and free tip, calculating characteristic modes and frequencies
01 p0138 A72-10509
- Area rule for change in lift/drag ratio of hypersonic delta wing due to conical body addition on compression side
02 p0151 A72-12270
- Mass addition distribution and gas injectant effects on heat transfer rates, transition locations and surface pressures of sharp cone
05 p0748 A72-16838

Radiation field from slot antennas on semiinfinite conducting cone surface, evaluating patterns for various cone angles, slot positions and azimuthal variations

06 p0781 A72-17342

Slot excited conical antenna, calculating first order diffraction coefficients by integral expressions for radiation field

06 p0781 A72-17343

Critical streamline length in axisymmetric and plane ideal gas flows past conical bodies as function of Mach number and form parameter

06 p0755 A72-17677

Supersonic near wake flow around blunt and sharp cones with trailing edge turbulent boundary layer

06 p0757 A72-18141

Radially conducting cone wave spectrum calculation for noncophasal excitation, noting circularly polarized TEM and elliptically polarized TM wave amplitudes

07 p0938 A72-19003

Frequency-independent multimode equiangular/conical spiral antenna with thick wires, calculating current distribution and radiation pattern by numerical program

07 p0939 A72-19187

Conical reflector microwave antenna design including subreflector with horn feed, presenting ray and physical optics analysis for radiation patterns

07 p0957 A72-19786

Conical gas film between rotating and vibrating conical rotor and nonmoving bearing, determining gas film stiffness and optimum angle

07 p0971 A72-20093

Flow structure between bow shock wave and blunted cone surface, studying internal shock waves by numerical solution via finite difference methods

07 p0910 A72-20108

Longitudinal elastic wave propagation along composite bar with conical sections and interface discontinuities in material properties, solving multiple reflection by finite difference method

08 p1245 A72-21606

Stress-strain curve determination for shear of twisted conical elastic bar, using torque and angle distribution

09 p1404 A72-22774

Static aerodynamic characteristics of bulbous based cone models and slender wings at subsonic speed, using magnetic suspension and balance system

10 p1461 A72-24769

Point source wave field diffraction on nontransparent circular cone, using steepest descent method and integral transformations

11 p1597 A72-26385

Longitudinal propagation of elastic disturbance in conical rod, discussing Young modulus, material density and periodic and impulsive stress

11 p1737 A72-26589

Shadowgraph photography method for supersonic air flow pattern around porous cone in uniform injection, noting pressure distribution dependence

12 p1752 A72-27986

Microwave breakdown calculation on symmetrically excited conical reentry vehicle based on variational technique, comparing with experimental data

13 p1916 A72-28536

Rarefied gas flow problems, discussing mean free path effects on sharp nosed conical and bluff bodies drag and heat transfer coefficients

15 p2218 A72-32314

Collection efficiency of conical and blunted axisymmetric power law bodies in hypersonic flight through dust clouds and of impact angle and velocity

15 p2180 A72-32580

Three dynamic conical bar theories, solving transient axisymmetric motion via method of characteristics

[ASME PAPER 72-APM-20] 17 p2581 A72-34797

Unified area rule for hypersonic and supersonic wing-bodies

17 p2485 A72-35251

Surface waves in the corrugated conical horn

17 p2517 A72-35387

Parameters influencing dynamic stability characteristics of Viking-type entry configurations at Mach 1.76

17 p2622 A72-35494

Elastic wave propagation in a rod of finite length with a variable cross section

20 p2978 A72-39321

Radiation characteristics of dielectric cones

20 p2904 A72-39773

Formation of a shock wave around a blunt conical body placed in a rarefied hypersonic flow

21 p2993 A72-41340

Viking configuration pitch damping derivatives as influenced by support interference and test technique at transonic and supersonic speeds

[AIAA PAPER 72-1012] 21 p3041 A72-41593

Telemetry acquisition of aerodynamic heat rates to conical, free-flight models at Mach 6 in an aeroballistic range

22 p3155 A72-42703

The bursting speed of a symmetrical conical disk with radial holes

22 p3238 A72-42835

Despun conical flight vehicles eccentric insulation mass properties history, deriving preflight and in-flight equations for weight, center of gravity coordinates and moments and products of inertia

[SAWE PAPER 938] 23 p3342 A72-43478

Axial-radar cross section of finite cones by the equivalent-current concept with higher-order diffraction

24 p3381 A72-45640

CONICAL FLARE

U CONES

CONICAL FLOW

Stationary viscous incompressible conducting fluid in conical flow, investigating diverging and converging electric current effects

[AD-740536] 04 p0558 A72-15342

Flow in gas lubricated conical bearings, considering analytical and numerical solutions for axisymmetric flow model with temperature dependent viscosity and dissipation coefficients

06 p0801 A72-18124

Hypersonic flow past final thickness delta wing, presenting conical flow equations with boundary value solution

06 p0757 A72-18128

Taylor series truncation method for steady supersonic inviscid gas flow past nonaxisymmetric conical bodies

09 p1295 A72-23498

Conical diffuser response to velocity distribution and turbulence intensity at inlet

10 p1416 A72-23858

Wide angle conical diffuser performance improvement by conical splitter vanes, considering static pressure recovery

10 p1416 A72-23860

Turbulent shear stress and kinetic energy characteristics of subsonic air flow in straight conical diffuser, using hot-wire anemometry measurements

10 p1416 A72-23862

Asymptotic solution for velocity distribution in viscous liquid axisymmetric flow in conical diffusers

14 p2070 A72-31006

Closed form solution to conical inviscid hypersonic flow over circular cone at zero angle of attack

17 p2486 A72-35433

Boundary layer and inviscid main stream interaction in asymmetric supersonic steady gas flow incident on circular cone at high Reynolds numbers

18 p2641 A72-36662

Boundary layer closure in the conical shock tube

19 p2788 A72-38431

Flow equations for axisymmetric compressible conical flow in Busemann nozzle, noting numerical method for integral lines construction for given Mach number

22 p3134 A72-42288

Singular points in conical flow streamline patterns, considering rotational and irrotational flows

22 p3135 A72-42580

Conical caret wings supersonic characteristics, examining flow transition from weak to strong attached shock waves

24 p3361 A72-45114

Hypersonic leading edge problem - Wedges and cones

24 p3364 A72-45778

CONICAL NOZZLES

Externally water cooled conical nozzle throat wall thickness design for high pressure and temperature argon flow medium

[DGLR PAPER 71-095] 02 p0299 A72-12702

Nozzle boundary layer effects on resistojets performance, presenting conical design model in heater stagnation conditions

03 p0405 A72-12973

Convergent conical nozzle shape effect on propulsive performance and compressible flow field internal characteristics

[ASME PAPER 71-WA/FE-3] 05 p0647 A72-15937

Swirling flow effects on annular conical diffuser performance in axial flow turbomachines, showing stagnation region and inner body diameter dependence

14 p2069 A72-30580

Computer simulation by Monte Carlo technique of particulate fluxes in divergent conical Knudsen cell orifices, considering specular reflection and surface diffusion effects

15 p2218 A72-32380

Air film cooling in a nonadiabatic wall conical nozzle

17 p2638 A72-35493

Optimal arrangement of conical nozzles in a segment of a partial supersonic turbine stage

20 p2963 A72-39913

Axisymmetric nozzles shape for thrust optimization, comparing maximum thrust circular arc and conical nozzles performances

24 p3365 A72-45784

CONICAL SCANNING

Conical scanning system for Pioneer Jupiter spacecraft pointing control, discussing signal processor, spacecraft dynamic behavior, system stability and error budget

15 p2320 A72-31791

CONICAL SHELLS

Initial interaction phase between thin shallow conical shell vibrating axisymmetrically and ideal incompressible fluid, determining hydrodynamic pressure effects

01 p0050 A72-10574

Static loads effect on natural vibrations of thin truncated conical shells by shallow shell theory, determining resonant frequency spectrum due to prestressing

01 p0142 A72-11362

Static and dynamic buckling behavior of clamped shallow conical shells under axisymmetric loads

02 p0291 A72-11963

Computer program for thermal stress and buckling analysis of nonuniformly heated segmented ring-stiffened cylindrical and conical shells

02 p0293 A72-12252

Beam theory application to cylindrical and conical shells bending, deriving flexibility functions from membrane equations

02 p0296 A72-12529

Elastic equilibrium in circular conical orthotropic shells of linearly variable thickness, investigating stresses under arbitrary loads

02 p0297 A72-12615

Truncated conical shell buckling under combined torsion and internal pressure load, discussing prebuckling stress conditions

02 p0298 A72-12666

Optimal temperature field s and stress-strain state in orthotropic conical and cylindrical shells subject to local heating

04 p0588 A72-15051

Elastic equilibrium of circular conical orthotropic shells with linearly varying thickness, determining real and complex roots of stress state characteristic equation

04 p0594 A72-15710

Circular conical orthotropic shells of linearly variable thickness loaded by distributed and concentrated forces and moments, analyzing stress-strain state by numerical methods

04 p0594 A72-15749

Power parameter determination in rotary swaging of thin conical shells, discussing radial contact stresses

05 p0666 A72-16628

Asymptotic solution to nonlinear Donnell equations of elastic conical shells, applied to buckling of frustum under axial load

06 p0893 A72-17303

Elasticity theory axisymmetric problem for hollow cone, analyzing stress-strain state and boundary value problem by asymptotic methods

07 p1093 A72-19980

Kirchhoff method application to asymptotic solution of plane wave diffraction on dielectric conical shells, calculating electromagnetic field vector

08 p1131 A72-20931

Ideal incompressible fluid sloshing under centrifugal force in partially filled conical cavity rotating at constant angular velocity

08 p1149 A72-21244

Conical foil radiation detectors sensitivity and time response, formulating time dependent thermal equations

08 p1166 A72-21433

Automated minimum weight design of ring and stringer stiffened conical shells, using membrane theory for prebuckling analysis

08 p1245 A72-21599

Temperature fields produced in viscoelastic cylindrical, conical and spherical shells by cyclic loads, calculating displacements from zero moment stress theory formulas

09 p1399 A72-22701

Stress-strain state of circular conical shell of linearly variable thickness within small elastoplastic deformation theory, assuming specific convective heat transfer at surface

09 p1401 A72-22722

Boundary value problems for buckling and initial postbuckling of clamped shallow spherical and conical thin walled sandwich shells under uniformly distributed hydrostatic pressure

[ASME PAPER 71-APM-YY] 10 p1554 A72-24182

Influence coefficients for circumferential stress resultants in long conical shell elements without edges interaction

10 p1555 A72-24192

Free flexural vibration of truncated conical shells, using Galerkin method and Donnell type basic equation

10 p1559 A72-25024

Viking conical aeroshell structural prototype design, analysis and testing, comparing buckling failure data with theoretical predictions

[AIAA PAPER 72-370] 11 p1725 A72-25395

- Lowest natural vibration frequencies of conical shell for various boundary conditions, using finite difference scheme 12 p1878 A72-27081
- Mixed variational formulation and finite element method for axisymmetric cylindrical, conical, spherical and ellipsoidal shells 12 p1879 A72-27195
- Elastic truncated thin conical shell response to dynamically applied axial force from numerical solution of nonlinear equations 12 p1881 A72-27244
- Ring stiffened truncated cone shells vibration mode tests, describing air and electrodynamic shakers and mobile noncontacting displacement sensitive sensor system 12 p1882 A72-27340
- Strain energy calculation for stability analysis of cylindrical and conical sandwich shells, using Euler-Poisson equations 12 p1885 A72-27975
- Acoustic pressure wave effect on motion of elastic conical shell fastened in rigid screen, using Timoshenko theory 13 p2055 A72-28772
- Mohr formulas construction for composite structures including frames and cylindrical and conical shells 13 p2058 A72-29460
- Truncated orthotropic conical shells thermostability at different temperature gradients, using Ritz method 14 p2163 A72-30193
- Nonlinear critical stability of truncated conical shell uniformly loaded by external hydrostatic pressure, using Bubnov-Galerkin method 16 p2470 A72-33412
- Exact analysis of a thick sandwich conical shell by forward integration. [ASME PAPER 71-APMW-20] 17 p2624 A72-34312
- Elastic wave propagation in a joined cylindrical-conical-cylindrical shell. [SESA PAPER 1983] 17 p2630 A72-34819
- Conical and cylindrical shell deformation with nonlinear one dimensional wave processes, describing algorithm for method of characteristics application 18 p2735 A72-36664
- Ritz method for truncated conical shell vibrations investigation, assuming deflection expanded in exponential power series 18 p2735 A72-36694
- Applications of holography to vibrations of segmented shells. 19 p2873 A72-37617
- Elasticity theory axisymmetric problem for hollow cones analyzing stress-strain state and boundary value problem by asymptotic methods 20 p2982 A72-40036
- Plane acoustic pressure wave effect on motion of thin elastic truncated conical shell fastened in rigid screen, using Timoshenko theory 21 p3116 A72-40263
- Equilibrium equation for unsteady creep of thin truncated conical shell under internal pressure, solving in successive time steps with Taylor series expansion 22 p3233 A72-42062
- Wave propagation in a truncated conical shell. 22 p3235 A72-42524
- Limiting equilibrium of shallow conical shells of variable thickness 23 p3348 A72-43787
- A finite element model for shells based on the discrete Kirchhoff hypothesis. 24 p3457 A72-44876

CONICS

- NT ELLIPSES
- NT HYPERBOLAS
- Computer algorithm to calculate surfaces formed by equidistant conic sections, using successive approximation method 13 p1966 A72-29461

CONJUGATE POINTS

- Short wave radio reception and signal path at magnetically conjugate point in Southern Hemisphere, using 40-110 msec delay times 01 p0028 A72-10592
- Soviet-French Project Omega for near space disturbance studies, using ground and balloon measurements at conjugate points 01 p0063 A72-11075
- Stability conditions for direct control systems in critical case, assuming pair of imaginary conjugated and zero characteristic numbers 04 p0538 A72-14623
- Algorithm selection for optimization solutions by finite, ad hoc, conjugate, Newton and restricted step methods 07 p1025 A72-18783
- Nocturnal F region electrodynamic drift at conjugate point sunrise time, discussing dynamo electrostatic field normal component change as cause of ionosphere vertical movement 09 p1297 A72-22576

Oscillation criteria for fourth order differential equation conjugate point location relationship in terms of existence of solution with two double zeros 11 p1678 A72-26159

Auroral conjugate points relative motion during substorms, showing existence of equatorward and poleward auroral arc systems 11 p1625 A72-26404

Predawn effect on hot and cold electrons at magnetoconjugate point in F 2 layer, discussing electron shock wave speed and thermal collisionless wave energy dissipation 11 p1628 A72-26916

Conjugate point photoelectron flux measurements in ionosphere during 7 March 1970 solar eclipse, using retarding potential analyzer onboard Nike-Tomahawk rocket 12 p1801 A72-27153

Whistler mode signals observation in conjugate region of 200 kHz broadcast station by satellite-borne narrow band receiver, considering field-aligned ducted and nonducted propagation 13 p1950 A72-29384

Heat resistant alloys conjugate phases extraction, separation and chemical analysis, discussing control of minor phases as precipitation products 13 p1978 A72-29443

Predawn airglow enhancement project, discussing magnetically conjugate photoelectron impact excitation observation and geophysical interpretation 14 p2098 A72-30147

Incoherent scatter and filter photometer search for 6300 A predawn enhancement by magnetically conjugate photoelectron impact excitation, comparing with ionospheric electron density 14 p2098 A72-30148

Cosmos 381 onboard ionospheric station signals received from magnetically conjugate region by ground wideband antennas 14 p2085 A72-30476

Theory of magnetically conjugate transport of cold plasma in the outer low-latitude ionosphere 17 p2548 A72-35218

Magnetospheric and ionospheric conjugate point phenomena as solar events manifestations via solar wind shock wave interaction with geomagnetic field 19 p2790 A72-37858

Simultaneous F-region conjugate point dawn effects at two mid-latitude stations. 20 p2916 A72-39234

Conjugate features of magnetospheric electron dynamics observed at balloon altitudes. 21 p3049 A72-41614

Auroral photometric observations at geomagnetically conjugate points. 22 p3169 A72-42020

Determination of optical transfer functions by Fourier transformation in spatially incoherent light 22 p3205 A72-42296

Coordinated observations of the magnetosphere - The development of a substorm. 22 p3171 A72-42410

Projective properties of holographic imaging. 24 p3401 A72-44767

CONJUGATES

- NT CONJUGATE POINTS
- F 2 region magnetic disturbances conjugacy mechanisms, considering vertical ionization profiles 08 p1155 A72-20801
- Conjugate unsteady problem of convective heat transfer for uniform flow over solid body with matching boundary conditions at interface 13 p2064 A72-28889
- Complex conjugate fourth order partial differential equations for circular cylindrical shells deformation, comparing accuracy with Fluegge, Morley and Novozhilov equations 15 p2331 A72-32559
- Rate of convergence of several conjugate gradient algorithms. 17 p2573 A72-34218
- Conjugate-flow theory for heterogeneous compressible fluids, with application to non-uniform suspensions of gas bubbles in liquids. 21 p3044 A72-40120
- Polak-Ribiere conjugate gradient algorithm modifications to eliminate minimization at each iteration for efficient implementation with convergence 22 p3198 A72-41931

CONNECTIONS

- U JOINTS [JUNCTIONS]
- CONNECTIVE TISSUE
- NT COLLAGENS
- Training effect on oxygen consumption in negative muscular work, considering connective tissue strengthening and muscle viscosity changes 03 p0315 A72-13676

CONNECTORS

- NT ELECTRIC CONNECTORS
- NT UMBILICAL CONNECTORS
- Coaxial connector standard interfaces for optimum microwave performance, discussing single connector reflection coefficient measurement equipment and procedures 01 p0041 A72-10693

CONNECTORS [ELECTRIC]

U ELECTRIC CONNECTORS

CONOIDS

U CONICAL BODIES

CONSCIOUSNESS

Soviet book on psychic phenomena and brain, covering cybernetics, dialectical materialist implications, consciousness, psychophysiology and cerebral neurodynamic structures 08 p1121 A72-22164

Human consciousness and choice role in biological control process automation to define differences between manual and automatic control systems 21 p3009 A72-41405

Some data on the interrelations of conscious and unconscious reactions 23 p3257 A72-44076

CONSECUTIVE EVENTS

Robert Bruce's spider problem extended - Reliability of adaptive experimental systems. 24 p3406 A72-44666

CONSEQUENT LAKES

U LAKES

CONSEQUENT STREAMS

U STREAMS

CONSEQUENT VALLEYS

U VALLEYS

CONSERVATION EQUATIONS

Pure solid and composite propellants combustion theory based on laminarized solutions to energy and flow conservation equations 02 p0270 A72-11766

Hugoniot analysis of shock disturbance propagation with steady velocity through composite material, deriving conservation equations 02 p0248 A72-11982

Air-augmented shrouded and ducted rocket secondary combustor performance parameter analysis based on one dimensional conservation equations 03 p0405 A72-13834

Conservation equations for blast waves one dimensional nonsteady flow field, considering Eulerian space and time profiles [ASME PAPER 71-WA/APM-1] 05 p0745 A72-15974

Time independent or periodic Hamiltonian conservative differential equations, studying open, oscillating, limited and abnormal trajectories [ONERA, TP NO. 1046] 06 p0877 A72-17661

Dimensionless parameter for thermodynamic state prediction in atmospheric pressure plasma jets, using conservation equations 06 p0862 A72-18188

Closed system equilibrium correlation functions relationships based on total momentum conservation, discussing application to solids or liquids electrical conductivity via nuclei dynamics 07 p1035 A72-19669

Steady rarefied gas flow around sphere with radial reflection of particles along normals, calculating gas dynamics variables of conservation equation 10 p1419 A72-24628

Regularizing time transformation for conservative systems reduction to normal coordinates, studying normal configurations existence in terms of Hamiltonian structural properties 13 p2002 A72-28714

Mass transfer effect on heat transfer to evaporating droplet, considering mass efflux shielding effect and forced convection flow field 14 p2172 A72-31051

Gas ionization buildup behind hypersonic shock waves, calculating onset point properties from plasma conservation and electron energy equations 16 p2434 A72-32902

Control volume method for finite amplitude shock front propagation in hyperelastic materials, solving steady state conservation equations 16 p2427 A72-33830

Conservation equations for wave and/or turbulence momentum and energy flux in interplanetary space shock vicinity, developing modifications for electron temperature calculations 16 p2459 A72-33913

Liquid fuel droplet transient combustion in supercritical hot stagnant oxidizing environment, solving conservation equations 17 p2636 A72-34903

Vapor pressure decrease rate during cooling agent introduction in semiclosed volume, determining pressure drop from energy and mass conservation equations 19 p2879 A72-37355

Thermodynamic parameters and reacting multicomponent mixture composition, using state equations and energy conservation equations for reaction kinetics 21 p3013 A72-40989

Averaged equations of laser heating of Z-pinch plasma the nuclear fusion energy being taken into consideration. 21 p3093 A72-41481

Accuracy of the conservation of the third adiabatic invariant of charged-particle motion in axisymmetric fields. II 22 p3217 A72-42209

- Asymptotic behavior of solutions of systems of conservative differential equations 23 p3308 A72-43693
- On the sufficiency of the energy criterion for the stability of certain nonconservative systems of the lower-load type. [ASME PAPER 72-APM-E] 23 p3350 A72-44052
- CONSERVATION LAWS**
- Integral conservation laws derivation for geostrophic zonal flow field disturbance, applying to flow stabilization 03 p0348 A72-13478
- Angular momentum conservation law compliance of generalized triple configuration model for spin-detonation nucleus, assuming transverse Chapman-Jouguet wave 03 p0342 A72-13734
- Tellegen theorem as energy conservation principle statement for energy exchange between elements in electric network 04 p0507 A72-15527
- Steady state operational characteristics of two-component heat pipes, applying mass and energy conservation laws and thermodynamic phase equilibrium relations [ASME PAPER 71-WA/HT-30] 05 p0745 A72-15883
- Transcendence of baryon number conservation law, discussing static black hole properties as final massive star collapse state 07 p1076 A72-19667
- Celestial mechanics considerations for many body problem with finite and infinite macroobjects motions correlation and conservation principles elucidation 08 p1236 A72-21641
- Two dimensional cascades supersonic exit flow field, using Oswatitsch method of characteristics and conservation laws [ASME PAPER 72-GT-49] 11 p1570 A72-25641
- Integral conservation laws derivation for geostrophic zonal flow field disturbance, applying to flow stabilization 11 p1623 A72-26248
- Baryon number nonexistence for static black holes and resulting baryonic conservation law transcendence and noninteraction with outside universe 12 p1848 A72-28152
- Conservation laws and symmetry properties of scalar tensor gravitational theories in terms of Einstein, von Freud, Moller and Komar extensions 12 p1847 A72-28153
- Equilibrium state stability in elastic conservative system, relating system postbuckling behavior to critical branching point 13 p2054 A72-28478
- Shock wave solutions of nonlinear hyperbolic system of conservation laws, considering case of zero viscosity 13 p1940 A72-28616
- Nonfriction vortices generation by jet flow in stationary fluid, using conservation of momentum principle 15 p2219 A72-32554
- Conservation laws related to energy release rates associated with cavity or crack rotation and expansion, discussing plastic stress distribution around cracks [ASME PAPER 72-APM-22] 17 p2580 A72-34795
- New demonstration of the adiabatic theorem for conservative systems in wave mechanics 18 p2711 A72-36473
- Recent extensions to Eulerian methods for numerical fluid dynamics. 18 p2682 A72-36803
- Einstein relativity principle incompatibility with conservation of angular momentum, discussing invariance of inertia reference systems and formulas for relative and absolute velocities 19 p2834 A72-37921
- Simplified conservation laws for finite-difference computations. 20 p2946 A72-39637
- On the energy and momentum conservation laws for linearized electromagnetic fields in a dispersive medium. 21 p3085 A72-41496
- Motion of a solid with a nonholonomic constraint around a fixed point in a conservative force field 23 p3313 A72-43800
- Explosive instability temporal development, noting linear damping role in nonlinear wave interaction under conservation laws of energy and momentum 23 p3282 A72-44318
- Angular momentum conservation laws formulation for Einstein field equations solution in general relativity, applying to Kerr metric 24 p3425 A72-44787
- CONSOLES**
- NT REMOTE CONSOLES
- The evolution of head-up displays. 20 p2925 A72-39333
- CONSOLIDATION**
- Melting atmosphere, atomizing media and consolidation techniques effects on Co base alloy powder products physical properties 02 p0240 A72-11436
- McNamee-Gibson displacement potential functions generalization to problems for compressible pore fluid in theory of consolidation or thermoelasticity 03 p0455 A72-14389
- CONSTANT SPEED PROPELLERS**
- U VARIABLE PITCH PROPELLERS
- CONSTANTS**
- NT GRAVITATIONAL CONSTANT
- NT PERCEPTUAL TIME CONSTANT
- NT SOLAR CONSTANT
- NT TIME CONSTANT
- Lunar elements and fundamental constants corrections from meridian observations for nodal period, determining corrections to solar mean anomaly and eccentricity 06 p0875 A72-17298
- Time constancy of physical constants in expanding universe, discussing light speed, Planck constant and electron and proton mass in context of Dirac hypothesis 16 p2425 A72-33517
- CONSTELLATIONS**
- NT CASSIOPEIA CONSTELLATION
- NT CENTAURUS CONSTELLATION
- NT CORONA BOREALIS CONSTELLATION
- NT CYGNUS CONSTELLATION
- NT ORION CONSTELLATION
- NT SAGITTARIUS CONSTELLATION
- NT SCORPIUS CONSTELLATION
- NT TAURUS CONSTELLATION
- CONSTITUTIONAL DIAGRAMS**
- U PHASE DIAGRAMS
- CONSTITUTIVE EQUATIONS**
- Small dilatation and short time approximate constitutive equations for compressible nonlinear viscoelastic materials, using multiple integrals and kernel functions 01 p0137 A72-10319
- Viscoelastic fluids continuum mechanical theory, discussing constitutive equation and tensor analysis [AD-736009] 02 p2023 A72-12004
- General equations of thick shells for arbitrary material and large deflections, considering thermodynamic and velocity damping properties 02 p0293 A72-12344
- Book on mathematical fluid dynamics covering viscous and ideal fluid motion, boundary theory, constitutive equations, hydrodynamics and kinematics 02 p2026 A72-12623
- Solid materials inelastic constitutive relations, developing internal variable thermodynamic formalism for microstructural rearrangements 03 p0446 A72-13710
- Linear viscoelastic solid defined by constitutive equations replacing bounded domain in time interval on real axis, deriving theorem regarding solution of second problem of limits 03 p0447 A72-13787
- First approximation of linear elastic shell theory using split constitutive equation of stress tensor 03 p0454 A72-14341
- Constitutive equations derivation for electrical conduction due to small deformation superposition, applying to deformed spherical shell current density determination 04 p0549 A72-15254
- Stress and strain approximate analysis for thin elastic shells by rational derivation of two dimensional differential and constitutive equations 04 p0592 A72-15506
- Discrete elasticity theory constitutive and motion equations, considering finite difference and partial differential equations 05 p0737 A72-16297
- Large deformations of incompressible isotropic materials with parabolic stress-strain relations, deriving constitutive equation from strain energy function 06 p0848 A72-17919
- Blood flow mathematical formulation, considering tissues constitutive equations, geometrical configurations, arterial wave propagation, etc 06 p0768 A72-17959
- Energy methods for nonlinear viscoelastic bodies based on constitutive relations affecting critical state in advanced creep 09 p1403 A72-22764
- Constitutive equations for materials with time dependent and time independent plasticity, applying to impact of identical bars 09 p1328 A72-22996
- Constitutive equations for bimodulus elastic materials, postulating rheological model based on anisotropy stress-strain laws 11 p1736 A72-25984
- Third order constitutive equations for transport coefficients in rarefied gases, using Chapman-Enskog theory 11 p1617 A72-26009
- Inferential structure of variational statements for equations of motion and constitutive relations, noting function space choice 11 p1690 A72-26554
- Nonlocal elasticity theory from global equilibrium and second thermodynamics laws, deriving constitutive equations from Clausius-Duhem inequality and Gibbs thermodynamics 11 p1738 A72-26721
- Constitutive equations for nonlocal theory of polar elastic dielectrics interaction with quasi-static electric field, using variational principle 11 p1738 A72-26723
- Constitutive equations for incremental stress-strain relations in elastoplastic media, noting plane stress and strain in isotropic materials 14 p2131 A72-30715
- Constitutive equations for multipolar solid with memory, deriving boundary conditions and free energy equation from first and second thermodynamics laws respectively 15 p2273 A72-31363
- Nonlinear creep, viscoelasticity and elastoplasticity boundary value problems, discussing matrix constitutive differential equation formulation and higher order numerical methods 15 p2326 A72-31712
- Constitutive equations of linear viscoelastic dielectrics, assuming small displacements, velocities and temperature independent memory functions 15 p2208 A72-32289
- Nonlinear anisotropic elastic constitutive equations for micromorphic and micropolar mixtures, investigating plane wave propagation via field equations with restricted coupling 15 p2278 A72-32446
- Constitutive and equilibrium equations for theory of thin shells with slowly varying curvature based on Novoshilov and Koiter assumptions 16 p2465 A72-33004
- Schaefer equilibrium and compatibility equations and Reissner constitutive equations for orthotropic cylindrical shells reduction to four simultaneous third-order equations 16 p2466 A72-33023
- Stress-strain diagrams for constant strain rates in shear of Ti from torsion test machine, deriving constitutive equation for dynamic overstress 16 p2405 A72-33197
- Stress and heat flux constitutive equations dependence on observer reference frame, considering field equation for temperature of gas at rest 16 p2478 A72-33526
- Constitutive equations for metallic creep analysis based on simultaneous strain hardening and crack propagation processes, calculating creep rupture time 16 p2408 A72-33589
- Onsager irreversibility theory extension to nonlinear constitutive relations and with allowance for inclusion of all thermodynamic variables 16 p2479 A72-33826
- Nonlocal fluid dynamics continuum theory with equilibrium and constitutive equations derived by generalizing Stokes Laws, noting steady channel and shear flow 16 p2379 A72-33832
- Energy theorems for creep constitutive relationships, discussing total deformation of body composed of elastic-creeping material with allowance for stress redistribution effects 16 p2473 A72-34118
- On a laminated orthotropic shell theory including transverse shear deformation. [ASME PAPER 72-APM-7] 17 p2629 A72-34807
- Theory of nonlinear viscoelasticity and its applications 17 p2631 A72-35109
- Constitutive equations to characterize rubberlike nonlinear viscoelastic materials under finite deformation stress, obtaining numerical solutions via finite difference technique 17 p2633 A72-35401
- Hypo-elastic dielectrics. I - Constitutive equations. II - Birefringence in simple shear. 18 p2720 A72-37043
- On strain energy and constitutive relations for alkali metals. 18 p2703 A72-37087
- Elasto-visco-plastic constitutive equations for quasi-static structures calculations. [ONERA, TP NO. 1089] 19 p2875 A72-37763
- Method of Lagrange multipliers for exploitation of the entropy principle. 19 p2825 A72-37842
- Muller entropy principle-imposed restrictions on thermodynamic and thermostatic constitutive relations for fluids in electromagnetic fields 19 p2834 A72-37843
- Constitutive equations and optical yielding of anisotropic perfectly plastic dielectrics. 19 p2878 A72-38799
- Constitutive equations and wave propagation of anisotropic perfectly plastic materials. 19 p2878 A72-38800
- Classical physics treatment combined with constitutive equations for local relativistic equivalence and material indifference principles 21 p3085 A72-41201
- Elastic isotropic material mechanical and thermal constitutive equations restrictions investigation to en-

- sure local stability under perturbations of deformation gradient and temperature field 21 p3120 A72-41203
- Constitutive equations and boundary value problems in discrete theory of elasticity, noting linear systems of prismatic rods and lattice type shells 21 p3123 A72-41390
- Constitutive equations of generalized Brandtl-Reuss theory of elastoplastic deformation, noting second order effects 21 p3124 A72-41506
- Non-linear elastic constitutive equations 21 p3125 A72-41514
- Extension of the Curie principle and constitutive relations for fluids with antisymmetric stress 22 p3166 A72-42311
- Line spring analysis model for long part-through surface cracks in walls of plate or shell structures, formulating constitutive laws 23 p3353 A72-44234

CONSTRAINTS

NT METEOROLOGICAL PARAMETERS

- Mechanical constraints effects on loose spherical metal particles sintering rates, considering one, two and three dimensional arrays 02 p0232 A72-11433
- Optimal design of elastic beams under alternative loads and constraints on generalized compliance and bending stiffness [AD-743419] 02 p0291 A72-11962
- Acceleration force simulation for altered weight effect on animal tolerance to restraint, discussing body mass loss, reduced lymphocyte count and disorientation 04 p0472 A72-14866
- Extremal problems of natural vibration spectrum optimal control in mechanical systems with constraints, using mathematical programming methods 04 p0586 A72-15004
- Necessary conditions for inequality-type mixed constraint optimal control, using abstract multiplier rule for Banach space of continuous and bounded measurable functions 04 p0506 A72-15201
- Computational algorithm for optimal control problem with variable terminal point constrained on state space surface, using iteration technique for satisfying transversality condition [ASME PAPER 71-WA/AUT-6] 05 p0640 A72-15957
- Controllability regions of linear steady system with two and three control constraints, presenting initial states set determination procedure 05 p0690 A72-16585
- Conjugate gradient iterative method for optimal control problems with state variable constraint, noting optimal trajectory cases 06 p0793 A72-17953
- Redundancy of Hamiltonian constraints in classical and Dirac quantum theories of gravitation, suggesting replacement by single integral-form condition 07 p1035 A72-20195
- Gyrostal inertial motion under nonholonomic constraint of mass center coincidence with fixed point 08 p1208 A72-21360
- Linear invariant solution to gyrostal motion under nonholonomic constraint 08 p1208 A72-21361
- Solutions existence and uniqueness for linear invariant relation to gyrostal motion under nonholonomic constraint 08 p1208 A72-21362
- Sensitivity comparison of equivalent open and closed loop optimal control systems, extending performance index formulas to instantaneous and isoperimetric constraints 10 p1456 A72-24456
- Lower and upper bounds for number of lattice points in simplex, using linear programming algorithm for generating feasible cutting patterns for paper reels 11 p1678 A72-26157
- Differential games extremal strategies with player control action subject to integral constraints 13 p2002 A72-28712
- Minimum weight elastic structure designs under dynamic loads with constraints on stress displacements and natural oscillation frequencies 13 p2062 A72-30009
- Stability loss condition for long rectangular cross section band from nonlinear elastic material with internal constraints, discussing critical loads and deformations 16 p2467 A72-33120
- Natural frequencies and dynamic response constraints in optimal structural design, considering mathematical programming aspects 18 p2739 A72-37167
- Optimal control of plant described by nonlinear hyperbolic equations with variable initial conditions of system, noting constraints on plant phase coordinates 19 p2777 A72-37343
- Controllability regions of linear steady system with two and three control constraints, presenting initial states set determination procedure 19 p2825 A72-37556

- Instability conditions for holonomic system with stationary constraints, applying to pendulum and to rectilinear motion of material point 20 p2955 A72-40033
- Linear estimation stochastic filtering and deterministic linear optimal regulation duality concept extension to problems with inequality constraints 21 p3074 A72-40228
- Relation between the first integrals of a non-holonomic mechanical system and a corresponding system freed of constraints 22 p3204 A72-41902
- Differential games extremal strategies with player control action subject to integral constraints 22 p3198 A72-42090
- First order constraints in three dimensional continuous elastic fibrous media and thin shells, presenting equilibrium equations 23 p3349 A72-43825

CONSTRICTIONS

- Heat transfer distribution in supersonic arc plasma constrictor of variable cross sectional area ducts, including pressure and compression shock front effects 14 p2141 A72-31071
- Collision periodic orbits calculation in restricted three body problem 20 p2973 A72-39885

CONSTRUCTORS

- Chest strapping-induced increased lung recoil pressure effects on maximal expiratory flow relation to lung surface compliance decrease 10 p1425 A72-24478
- S-64 Sky crane helicopter current and anticipated applications in commerce and industry, considering logging operations in ecologically sensitive or rugged areas, bridge construction, etc 16 p2348 A72-33185

CONSTRUCTION

- Nonmetallic material properties effects on structural design for reliability, considering molecular chain folding, polymer crystallization, entropic molecular segregation, adhesion and intermolecular forces 01 p0092 A72-10986
- Ti alloys for airframe shell construction based on room temperature strength, stiffness and densities comparison with Al alloys, stainless steel and Be data 03 p0373 A72-13615
- High strength Ti alloys for aircraft accessories structural materials, comparing room temperature physical properties of ultrahigh tensile steels and other alloys 03 p0373 A72-13617
- Endurance limit of construction materials under fast and thermal neutron irradiation in reactor channel 06 p0834 A72-18682
- Strength and plasticity characteristics of hardened multilayer structural steels, investigating layer thickness effect 07 p1013 A72-19746
- Nondestructive ultrasonic determination of defects in structural steel blanks 07 p0991 A72-20423
- Soviet handbook on vibration absorbing properties of construction materials under cyclic straining, covering energy dissipation and dynamic strength 08 p1185 A72-20975
- Large automated tape placement machine tool design and construction for laying up aircraft structures from composite materials 08 p1177 A72-21690
- Sign-variable nonisothermal plastic deformation and creep behavior of polycrystalline construction materials, taking into account Bauschinger effect 09 p1401 A72-22726
- Structural model application to construction material alternate stress description at elevated temperatures 09 p1401 A72-22727
- Short fiber reinforced thermoset composite materials for engineering construction, tabulating flexural properties and Charpy impact strengths 09 p1338 A72-23165
- Neutron irradiation effect on submicroporosity formation and redistribution in structural graphite 09 p1340 A72-23482
- Random elastic modulus variability of building materials test pieces under compression and tensile loads 10 p1557 A72-24403
- Recrystallized silicon carbide and reaction bonded silicon nitride as construction materials for gas turbine engine components, describing thermal and mechanical properties [ASME PAPER 72-GT-20] 11 p1673 A72-25619
- Metal matrix composites application to aircraft structures, describing design, analysis and fabrication of aircraft bulkhead with B-Al as main structural material 12 p1886 A72-28096
- Boron and carbon fiber reinforced plastics applications in aircraft and engine structural components, discussing dynamic and impact damping properties compared to conventional materials 13 p1982 A72-28555

- Neutron irradiation effects on structural materials brittle fracture initiation and propagation mechanisms, discussing residual elements influence on radiation defect stabilization 15 p2258 A72-32486

- Neutronically generated He irradiation effects on high temperature fracture of fcc, bcc and hcp structural metals and alloys 15 p2258 A72-32487

- Al alloys, high strength steels and Ti alloys in aircraft construction, reviewing prematerials in heavier than air vehicles 17 p2568 A72-35375

- Investigation of defects and damage in metallic materials by metallographic examinations 20 p2941 A72-39573

- Isothermal deformation behavior of structural metals in laboratory creep, relaxation and low cycle fatigue tests at high temperatures 21 p3119 A72-41009

- Sheet metal economics in aircraft construction based on strength/weight and stiffness/weight comparison of Al alloys and Ti alloys in relation to cost and structural weight considerations 21 p3060 A72-41071

- Reinforcement of structural materials by long strong fibres 22 p3241 A72-43026

- Investigation of the strength of construction materials for various principal-stress relations 23 p3349 A72-43955

- A comparison of the axial and reversed-torsional strain cycling low-cycle fatigue strength of several structural materials 23 p3304 A72-44397

CONSUMPTION

- NT FUEL CONSUMPTION
- NT OXYGEN CONSUMPTION
- NT WATER CONSUMPTION

CONTACT LENSES

- Autocollimating photokeratoscope for human in vivo corneal shape measurements for contact lens fitting and dioptric image examination 07 p0987 A72-19826

CONTACT POTENTIALS

- Local level filling and Fermi distribution in metal semiconductor contact as function of voltage and level location 09 p1372 A72-23355
- Contact potential difference effects on lubricant film thickness in electronic equipment joints, noting molecules orientation in electric field 13 p1930 A72-29052

CONTACT RESISTANCE

- Electrical resistance and thermal joint conductance measurements at perfect contact interfaces from electroplating, soldering and explosive bonding [AIAA PAPER 72-19] 05 p0666 A72-16859
- Sliding friction and normal force adhesion under ultrahigh vacuum environment, describing test apparatus for real time analysis via contact resistance measurement 08 p1176 A72-21436
- Electric contact phenomena in ultraclean and specifically contaminated metallic systems, noting resistance relationship to load curves and surface conditions 10 p1448 A72-24172
- Rough surfaces thermal contact resistance in vacuum for normal height distribution, discussing bolted joint nonuniform stress distribution effect [AIAA PAPER 72-281] 11 p1741 A72-25221
- Conduction electron phonon scattering effect on electrical resistance of metallic contacts during pressure welding 16 p2370 A72-33952
- Evaluation of testing methods for gold plated or gold clad contacts 18 p2664 A72-35984
- Pd-Al intermetallic compound contact materials 18 p2698 A72-35985
- 1972 seminar supplement to bibliography and abstracts on electrical contacts, circuit breakers and arc phenomena 18 p2664 A72-35986
- Electric contact phenomena in ultra clean and specifically contaminated systems 18 p2717 A72-36115
- Electric contact between metal and n-type semiconductor, investigating contact pressure effects on electron tunneling and phonon conductance to provide band structure 18 p2718 A72-36488
- Influence of a sinusoidal pressure variation on contact thermal resistances 22 p3244 A72-42644

- 18 p2664 A72-35986

- 18 p2717 A72-36115

- 18 p2718 A72-36488

- 22 p3244 A72-42644

CONTACTS (ELECTRIC)

U ELECTRIC CONTACTS

- CONTAINERS
- Nonlinear oscillations of liquid in movable conical containers, presenting approximate procedures for solving weight boundary value problem of eigenvalues 07 p0972 A72-20211

Statistical energy analysis of sound-structural interaction, considering sound transmission through complex walls and piping systems and fluid filled container vibrations

13 p2005 A72-29556

Air cargo intermodal and interline containers handling in warehouse storage, transportation and distribution, considering total pack and interlock requirements

16 p2372 A72-33174

Determination of the parameters of motion of a container and its load with allowance for their interaction during internal vibrational finishing operations

19 p2824 A72-37426

CONTAMINANTS

NT RADIOACTIVE CONTAMINANTS

NT TRACE CONTAMINANTS

Analysis methods for microsize atmospheric aerosols and particulate contaminants from natural and industrial sources, discussing electron microscopy, electron probes, X ray diffraction, etc [AIAA PAPER 71-1104]

01 p0067 A72-10550

Ultrastructural and morphometric studies of beryllium oxide-contaminated environment effect on monkey and dog lung tissue

07 p0925 A72-20686

Spacecraft critical surfaces protection from molecular and particulate contamination sources including gloves, tissues, and covering or packaging materials

12 p1768 A72-27042

Piezoelectric quartz crystal microbalance for material outgassing and optical element contaminant film measurements

12 p1806 A72-27043

Aviator breathing oxygen contaminant detector using gas chromatography and portable IR analyzer

12 p1773 A72-28253

Contaminant analysis in gaseous oxygen generated by chlorate candle combustion, using Draeger tubes

12 p1779 A72-28254

Spacecraft functional properties degradation due to surface contamination with outgassing vapors, discussing contaminant materials transport and sorption characteristics

23 p3254 A72-43619

CONTAMINATION

NT FUEL CONTAMINATION

NT SPACECRAFT CONTAMINATION

Planetary quarantine microbial contamination control, considering clean room concept and microbiologic barrier techniques

01 p0019 A72-10821

Nonsterile space flight hardware effects on planetary quarantine, evaluating contamination sources, design and mission parameters, cleanliness conditions and bioload

01 p0020 A72-10824

Terrestrial biosphere back contamination from outer space organisms, discussing microbiologic control and prevention requirements

01 p0020 A72-10825

Electron energy derivation from contaminated Langmuir probe, explaining E region high temperature

05 p0654 A72-16007

Distillation experiments showing volatility-caused amino acid contamination of commercially available aqueous hydrochloric acid

05 p0624 A72-16079

Clam seals comparison with elastomers, discussing aircraft use, contamination, inspection, corrosion and erosion, surface finish, service life and cost

08 p1179 A72-21941

Ta, Nb and La superconductivity, investigating surface contamination effects on electron tunneling characteristics

09 p1367 A72-22554

Electric contact phenomena in ultraclean and specifically contaminated metallic systems, noting resistance relationship to load curves and surface conditions

10 p1448 A72-24172

Optical mirrors contamination by condensation of outgassed spacecraft materials in vacuum under UV irradiation, describing test apparatus and results with various materials

11 p1637 A72-25208

Turbojet engine oil circuit contamination rate determination by spectrometric analysis, obtaining mathematical theory for data interpretation

11 p1703 A72-25567

Electrostatic and electron temperature probes compared during ionospheric rocket soundings, noting lower ionosphere discrepancies due to surface contamination

11 p1633 A72-26102

Cu surface contamination effect on hot crack susceptibility and weldability of Co based superalloys

13 p1965 A72-29419

Ta-W-Hf alloy mechanical properties impairment from oxygen contamination, noting hafnium dioxide precipitate in reaction zone

14 p2121 A72-30769

Electric contact phenomena in ultra clean and specifically contaminated systems.

18 p2717 A72-36115

Contact contamination - Formation of carbonaceous deposits on electrical contacts.

18 p2665 A72-36119

Apollo and terrestrial geochemical samples examination for indigenous amino acids distribution and optical configuration, stressing close monitoring of contamination sources

19 p2762 A72-37648

CONTEXT FREE LANGUAGES

Terminal context in context-sensitive grammars.

17 p2524 A72-35924

CONTINENTS

NT AFRICA

NT AUSTRALIA

Continental growth by island arc volcanism, observing Si, K, Rb, Ba, Sr and light rare earth element abundances

01 p0052 A72-10068

CONTINGENCY

Linear contingency method for elasticity theory of anisotropic plane with elliptic hole, deriving boundary value problems solutions

11 p1733 A72-25543

Human flexible processing accomplishment in speeded recognition task with visual stimulus dimension relevancy contingent upon other dimension stimuli values

13 p1911 A72-29832

CONTINUITY [MATHEMATICS]

Positive additive functionals of homogeneous processes with independent increments in phase space, considering continuity condition for process distribution Laplace transform

01 p0094 A72-11264

Symplectic structure of continuous system, constructing relativistic free vibrating cord without linearization

03 p0389 A72-13792

Continuity of probability distribution functions obtained by superposition

04 p0540 A72-15260

Layer potentials continuity in theory of vibrations of elastic medium

06 p0894 A72-17556

Uniqueness theorem for dynamic infinitesimal invariant theory of hereditary elasticity, defining conditions of continuity and positive determinability

08 p1246 A72-21708

Spectral continuity conditions of linear operator, noting application to elliptical operators approximation in separable Hilbert spaces

10 p1505 A72-24070

Markovian characteristics of time dependent excursions and independent incursions processes provided with limits to left and continuous to right, noting Poisson punctual process and Borel sets

10 p1505 A72-24114

Generalized solution regularity of arbitrary order quasi-linear elliptic equations, indicating continuity conditions of variational problems

13 p1987 A72-30001

Conditions for complete continuity of integral operators with stationary features in a space of continuous functions

23 p3307 A72-43224

First derivative discontinuities of space-time metric tensor in Einstein equations solution for nonisotropic and isotropic hypersurfaces, proving coordinate system existence for continuity

23 p3312 A72-43302

Analytic continuation of functions over infinite dimensional domains, covering Banach manifolds; hypoaalytical mappings, convexity and topology

24 p3418 A72-44827

CONTINUITY EQUATION

F region electron-ion gas dynamic model with stability dependence on periodic solutions convergence of continuity equations

08 p1153 A72-20725

Ionospheric electron concentrations and temperatures determined by time dependent continuity equations model during 11 September 1969 solar eclipse

09 p1390 A72-23518

Thermospheric atomic hydrogen concentration diurnal variations from time dependent continuity and diffusion equations, using Jacchia background atmosphere thermal and density structure formulas

13 p1953 A72-29806

Ionized and neutral atmospheres coupled ionospheric continuity and motion equations, discussing nonlinear force effects on F2 height and electron density

15 p2230 A72-32257

Continuity, motion and Maxwell equations for steady MHD flow under constant magnetic flux

17 p2588 A72-34765

Solution to a nonstationary continuity equation for disturbed ionospheric conditions

17 p2551 A72-35862

F region electron-ion gas dynamic model with stability dependence on continuity equations periodic solutions convergence

19 p2791 A72-38353

Transfer equations for stellar systems

23 p3338 A72-44035

Continuity equation for dynamic auroral ionospheric model relating electron density profiles to auroral arc brightness

24 p3400 A72-45589

CONTINUOUS RADIATION

Emitted light power of CW injection laser related to threshold current, electrical and thermal resistances and external quantum efficiency

01 p0079 A72-10325

CW power of single cavity multiple IMPATT diode oscillator at 9.1 GHz, comparing with moding of multiple device oscillators

01 p0038 A72-10649

X band power, bandwidth, efficiency and temperature performance of one watt CW microwave integrated avalanche diode oscillator

01 p0038 A72-10650

Completely sealed off room temperature CO laser system, discussing performance and continuous wave power

01 p0080 A72-10852

Irregular, spiral and elliptical galaxies radio continuum measurements at 1420 MHz, presenting positions flux densities and brightness distributions

01 p0131 A72-11005

Spiral galaxies radio continuum emission origin, discussing supernovae and relativistic electrons effects

01 p0131 A72-11006

Nuclear radiation enhancement of carbon dioxide laser performance, discussing low pressure CW and high pressure pulsed discharges

01 p0082 A72-11330

Rabbit and monkey corneal damage following CW carbon dioxide laser irradiation, discussing hazard level derivation

02 p0163 A72-12413

Dust continuous spectrum and Balmer line intensity ratio in Orion Nebula from slit spectroscopy observations

02 p0284 A72-12631

Solar corona X ray data from SOLRAD satellites, detailing spectral energy distribution, ionization balance, continuum radiation and line emission

03 p0410 A72-13219

Spectroscopic characteristics of continuous wave neutral argon laser using helium and chlorine for power enhancement

03 p0367 A72-13432

Excited IR fluorescence in gas compounds with negligible absorption, using CW carbon dioxide laser

03 p0367 A72-13554

CW longitudinal flow carbon monoxide chemical laser system analysis, discussing vibrational levels, population densities, excitation and relaxation processes and dynamic model

03 p0368 A72-13858

CW avalanche diode microwave oscillator frequency modulation, using injected rf signal

03 p0334 A72-14075

CW CO laser by discharging premixed carbon disulfide-oxygen flame, suggesting chemical pumping mechanism and flame laser possibility

04 p0529 A72-14589

High power CW gas dynamic laser mode-control experiment with unstable resonator at high Fresnel number, obtaining near and far field intensity distribution

04 p0529 A72-14605

Radiation intensity of CW argon ion laser with nonlinearly absorbing argon cell in cavity, showing pressure relation to amplification and absorption

04 p0530 A72-14658

CW 100 GHz Si IMPATT diodes with nearly abrupt junctions, discussing output power and dc and small signal analyses

04 p0502 A72-15594

Distributed unidirectional microwave IMPATT diode amplifier and CW tests for X and C band circuits

05 p0633 A72-15783

Vapor-grown GaAs transfer electron microwave oscillator, discussing design, fabrication and CW power conversion efficiency

05 p0637 A72-16366

Double heat sinking high power CW TRAPATT diode oscillators using integral metallic heat spreaders

06 p0784 A72-17788

Pulsed and CW solid state microwave oscillator EM noise as function of power level and locking parameters

06 p0788 A72-18465

FM/CW varactor Gunn diode oscillator powered subminiature IC radar altimeter design on homodyne principle for ultralight reliable minimum chance detection

06 p0819 A72-18473

High power efficiency CW Gunn devices design and fabrication, discussing GaAs preparation techniques and device physics

06 p0789 A72-18478

Medium power high gain, CW transferred electron microwave amplifiers at C band, describing bandwidth, saturation, intermodulation distortion and dynamic range characteristics

06 p0789 A72-18483

CW diffusion type chemical HF laser and two-vibrational level HF molecular models, analyzing laser performance
[AIAA PAPER 72-145] 07 p1000 A72-18955

FM-CW radar range measurement by carbon dioxide laser, considering laser output nonlinear variation due to frequency pulling/pushing and refractivity changes
07 p0940 A72-19205

Continuous TEM power from single longitudinal mode Nd-YAG laser pumped with tungsten-iodine lamp
07 p1004 A72-19235

Sound velocity and attenuation variations with magnetic field from ultrasonic continuous wave spectrometry
07 p0984 A72-19321

Pulsed and CW laser beam propagation through atmosphere
[CLEA PAPER 2,5] 07 p0942 A72-19380

CW gas laser operating in far IR, discussing water vapor excitation by dc discharges
07 p0946 A72-19961

Magneto-optical effect on CW radiation intensity of Ar laser with cell in magnetic field for various gain conditions
07 p1009 A72-20615

Physical and operating principles of CW heterojunction injection lasers at room temperature
08 p1181 A72-21056

Optimal continuous recording of amplitude-phase distributions on spatial carrier frequency for light wave modulation and optical antenna simulation
08 p1132 A72-21263

Continuous laser action in Nd-yttrium aluminum oxide rod, determining terminal state loss coefficient in stimulated emission
08 p1217 A72-21322

Planetary nebula IR continuum and line radiation from spectrophotometric observation relation to visual and radio wave data
08 p1235 A72-21387

Continuous chemical laser optimum optic axis position for maximum multimode power operation and intensity distribution
[AD-742961] 08 p1182 A72-21557

Thermal self disturbance effect on second harmonic generation in crystals and CW and pulsed lasers
08 p1184 A72-22034

Magnetic field effect on gain saturation in CW Ar laser associated with Zeeman splitting
08 p1184 A72-22036

Chemistry and performance characteristics of flash photolysis and microwave discharge initiated CW carbon disulfide/oxygen lasers
09 p1325 A72-23236

High resolution NMR spectrometer conversion from continuous wave to Fourier transform operation, permitting computer systems and pulse amplifiers use
09 p1316 A72-23408

CW X band Gunn microwave oscillators, measuring frequency variation relationship to ambient temperature
10 p1450 A72-24555

Semiconductor laser continuous emission conditions at room temperature, assuming output power drop with increasing current due to p-n junction heating
10 p1492 A72-24582

Low voltage transversely excited gas transport CW carbon dioxide laser, discussing construction and power output, gain and efficiency
11 p1646 A72-25304

Vortex discharge in Ar as optical pumping source for ionic crystal CW lasers, comparing efficiency with YAG-Nd crystal pumping
11 p1648 A72-26331

Exposure conditions and film processing parameters effects on sensitivity, diffraction efficiency and SNR of holograms recorded with continuous and pulsed radiation sources
11 p1637 A72-26796

Continuous He-Ne laser radiation power interferometry using Michelson interferometer with frequency doubler
12 p1819 A72-27051

Temperature distribution and heat dissipation calculations for CW and pulsed laser optical elements
12 p1824 A72-27873

Second harmonic conversion of CW YAG-Nd laser radiation on lithium metaniobate crystals, discussing conversion coefficient optimization
12 p1825 A72-27886

C and X band CW GaAs Schottky barrier IMPATT oscillators with nichrome as barrier metal, noting high power efficiency and low noise performance
12 p1793 A72-27966

Deep penetration welding and cutting with high power CW carbon dioxide lasers, describing experimental setup
13 p1965 A72-29422

Observed continuous solar spectrum intensity comparison with photospheric models, noting bend-off due to veiled line haze
13 p2047 A72-29734

CW Gunn oscillator cavity loading and bias voltage effects on external negative differential conductance
13 p1933 A72-29825

Thermal defocusing of high intensity continuous Ar laser radiation in absorbing medium with allowance for spherical aberrations
14 p2110 A72-30355

Lamb dip for 119 micron line of CW gas laser, noting decay constants due to pressure
14 p2110 A72-30424

CW oscillator model for laser amplifier, including nonlinear effect of gain saturation
14 p2111 A72-30896

Ar plasma radiation dispersion by plane grating, measuring ionic spectral lines and continuous spectrum intensity time variation
15 p2286 A72-32340

Galactic background continuous radiation observation at 15 GHz, determining brightness temperature and thermal radiation component
15 p2313 A72-32348

High power carbon dioxide lasers review covering CW, Q switched and pulsed atmospheric pressure lasers and various excitation techniques
16 p2399 A72-32848

CW dye laser output tuning by mirror-grating combination with interspersed output coupling element, noting orders of magnitude reduction of fluorescence background intensity
16 p2401 A72-33388

Coherent CW radiation by tunable GaAs injection laser in external dispersive cavity at 77 K, discussing monochromatic output spectral analysis by Fabry-Perot interferometer
16 p2401 A72-33393

Continuously burning optical discharge in Ar and Xe at atmospheric pressures, evaluating laser beam energy absorption, electron density and plasma temperature
16 p2402 A72-33691

Proton bombarded stripe geometry heterojunction lasers for 300 K CW operation compared with oxide insulated lasers
16 p2403 A72-33757

Second harmonic conversion of CW YAG-Nd laser radiation on lithium metaniobate crystals, discussing conversion coefficient optimization
16 p2404 A72-33995

CW argon ion laser characteristics at high steady discharge currents, discussing output limitation by low inversion utilization efficiency due to cavity mirrors optical degradation
16 p2404 A72-34035

Compact extragalactic nonthermal sources.
17 p2604 A72-34519

Welding with a CW YAG laser beam
17 p2563 A72-35181

Output fluctuations of CW-pumped Nd:YAG lasers.
17 p2564 A72-35345

The chromosphere in continuum emission observed at the total solar eclipse on 7 March 1970.
17 p2616 A72-35698

Frequency separation in structure of solar continuum radio bursts.
17 p2602 A72-35713

CW optically pumped tunable dye laser wavelength ranges, linewidth, mode purity, polarization and power output characteristics
17 p2565 A72-35947

Continuous arc generation in Ar via focused CW carbon dioxide TEA laser, inducing gas breakdown by focal volume preionization with single pulse
18 p2697 A72-36082

A 22 percent C.W. efficiency solid state microwave oscillator.
19 p2771 A72-37266

CW gasdynamic thermally excited and selectively pumped CO₂-N₂ mixing laser.
19 p2811 A72-38097

Calculations of gain and power output for a gasdynamic laser.
19 p2813 A72-38693

Air cooled CW 30 W carbon dioxide laser construction for technological applications, using radiation energy extraction through GeAs or GaAs plate
20 p2932 A72-39507

Utilization of photorecombination of radicals and atoms in continuous-wave lasers.
20 p2932 A72-39508

Influence of gas pressure in arc lamps on the pumping efficiency of CW garnet lasers.
20 p2933 A72-39513

High-power microwave amplifier using IMPATT diodes.
20 p2909 A72-39776

Experimental CW chemical laser studies.
[AIAA PAPER 72-712] 21 p3063 A72-40920

Thick target processes during hard X ray emission, noting electron bombardment during solar flare impulsive phase and white light flare optical continuum production
21 p3100 A72-41292

Broadband continua temporal behavior at type IV initial stages, recording by radio interferometers
21 p3101 A72-41296

Influence of the lowering of the ionization energy on the continuous radiation of an argon plasma
21 p3093 A72-41343

Statistical tests for spectral correlation analysis of continuum VHF radio emission fluctuations from noise storms
21 p3102 A72-41778

Wavelength tuning of an intracavity pumped CW mode-locked dye laser.
22 p3184 A72-41989

The Cygnus X-region. VII - Radio continuum search for a ring of filaments around the area.
22 p3225 A72-42390

A CW Gunn diode bistable switching element.
22 p3159 A72-42610

IR CW laser emission from arc generated flowing CO active medium, describing thermal dissociation of oxygen followed by carbon disulfide injection
22 p3185 A72-42615

Molecular vibration levels inversion ratios increase by vibrationally cold CO addition to CW CO chemical laser, observing R-branch emission lines
22 p3185 A72-42615

Approximate theory of the CW gasdynamic laser with an unstable resonator.
22 p3186 A72-42631

Multisectional CW gas dynamic laser output radiation density distribution control via transmitting mirror with variable reflection coefficient
22 p3186 A72-42632

Ultrasensitive response of a CW dye laser to selective extinction.
23 p3297 A72-44186

A wide-band Gunn-effect CW waveguide amplifier.
23 p3272 A72-44193

Elements of a theory of CW gasdynamic quantum generators.
23 p3297 A72-44225

Measurement of best time-delay resolution obtainable along east-west and north-south ionospheric paths.
24 p3381 A72-45637

Continuous He-He laser radiation intensity correlation function measurement, using Michelson interferometer and frequency doubler
24 p3412 A72-45704

Influence of a temperature dependent spectral absorption coefficient on radiative flux.
24 p3466 A72-45791

CONTINUOUS WAVE RADAR

FM/CW laser radar technique for smoke plume opacity remote measurement, discussing eye safety
[AIAA PAPER 71-1081] 01 p0080 A72-10539

Microwave hologram CW radar system, discussing theory and flight test imagery, optical processors and alignment procedures
02 p0171 A72-11819

Combined FM CW radar and radiometer at millimeter wavelengths, investigating objects signatures measurement
04 p0494 A72-15611

Sensitivity calibration of dual beam vertically pointing FM-CW radar, presenting antenna main lobe radiation patterns
06 p0776 A72-18443

Noncontacting measurements by miniature CW Doppler radar with semiconductor microwave generator
09 p1285 A72-22691

Meteor trail winds over Europe, discussing continuous wave radar observations and measurement errors with respect to height and time
10 p1474 A72-24708

Radio meteor winds determination in Southern Hemisphere from vertically emitted continuous wave radiation, considering diurnal variations and wind and turbulence effects
10 p1474 A72-24709

Continuous wave Doppler radar with microwave oscillator for ATC measurements and surveillance
12 p1789 A72-27403

A method of phase detection of the beat signal in FM-CW radar.
17 p2514 A72-34383

An application of correlation to radar systems.
19 p2764 A72-37927

CW radar system for tactical aircraft real time command, control and positioning, using combination of frequency and time multiplexing for range measurement
22 p3203 A72-42946

CONTINUOUS WAVES

U CONTINUOUS RADIATION

CONTINUUM FLOW

Continuum gas viscous performance, comparing two seal groove aspect ratio geometries
02 p0237 A72-12850

Continuum plasma turbulent boundary layer structure in shear flow, showing electron to ion saturation currents ratio decrease from laminar case
[AIAA PAPER 72-107] 07 p1040 A72-18953

Boundary layer ionization on flat plate and cylindrical plasma probes in high speed flow, considering ionized continuum flow and collisionless plasma
16 p2374 A72-32831

A semiempirical method for the evaluation of aerothermodynamic properties in the intermediate hypersonic flow regimes.
[ICAS PAPER 72-03] 21 p2990 A72-41128
Rarefied gas flow through a slit.
24 p3395 A72-45572

CONTINUUM MECHANICS
Balance laws of micromorphic theory for polycrystalline mixtures, granular composites and fluid suspensions involving motions with wavelength comparable to intrinsic discontinuities in materials
01 p0102 A72-10320
Continuum mechanics models of macroscopically inhomogeneous elastic medium with microstructure, using moment theory
02 p0288 A72-11608
Linear creep properties in continuous media for wide time-variable parameters range of instantaneous elastic deformation under simple loads
02 p0289 A72-11616
Thermoelasticity quasi-static, dynamic and coupled problems in continuum mechanics, discussing formulation and variational principles methods for solution
02 p0290 A72-11634
Viscoelastic fluids continuum mechanical theory, discussing constitutive equation and tensor analysis
[AD-736009] 02 p0203 A72-12004
Variational perturbation problem solution in power series form for elliptic functional description of elastic continuous medium state by Euler-Lagrange equations
02 p0259 A72-12233
Continuous solid medium electroelastic equations of state, finding solution by variational principles application
03 p0390 A72-13916
Soviet papers on elasticity and inelasticity covering deformable media mechanics, continuum mechanics, polymer materials, random inputs, stress concentration, ductility and crystallization temperature properties
03 p0453 A72-14205
Nonhomogeneous elastic structure with quasi-periodic coefficients, deriving mechanical model by continuum spectral theory
04 p0594 A72-15745
Continuous bodies incremental deformation and stability under initial stress, discussing relationships for elasticity constants and material stress tensors
[ASME PAPER 71-WA/APM-9] 05 p0734 A72-15970
Stability characteristics of finite difference schemes based on lumped-parameter model and numerical integrator for wave propagation in continuous media
05 p0735 A72-16081
Isotropic continuum model of elastic interaction of edge and screw dislocation with nearby inclusion
06 p0894 A72-17492
Spatio-temporal tensorial structure of fluid magnetodynamic equations in terms of electromagnetism and continuum mechanics
06 p0861 A72-18103
Finite element and finite difference formulations for solid continua by variational principles, including potential energy, complementary energy and Reissner principles
07 p1087 A72-18792
Matrices of fundamental solutions constructed for loading singularities and Green method in unbounded micropolar elastic continuum
07 p1095 A72-20243
Book on plasticity theory covering stress and strain as basic concepts of continuum mechanics, differential equations of motion, plastic flow, yield criteria, elastic-plastic equilibrium, plane strain, etc
08 p1244 A72-21477
Critique of paper on lower bounds on deformations of dynamically loaded rigid plastic continua
08 p1245 A72-21630
Impulse-energy tensor for heat flow-crossed continuum subjected to electromagnetic field, using energy balance and quantity of movement equations
09 p1351 A72-22673
Discrete elasticity concept based on analysis of material points, lines, surfaces or rigid bodies interconnected by hyperelastic continuous bodies
09 p1403 A72-22759
Continuum model for cylindrical and spherical elastic laminated composites deformation, using balance and constitutive equations
09 p1405 A72-22992
Book on tensor analysis and continuum mechanics covering strain, permutation and stress tensors, vector and tensor comparison, application to elasticity and shell theory, etc
09 p1406 A72-23000
Ritz method application to transformations and complementations of polygenetic force problems of mechanics
10 p1512 A72-24521
Book on continuous elements dynamics covering membrane, torsional, string and elastic beam vibration, four pole techniques, periodic forced motion and surface waves
10 p1557 A72-24674

Loose medium deformations and displacements fluctuations verification by statistical tests, noting inception information from autocorrelation and boundary conditions cross correlation functions
10 p1512 A72-24719
Classical boundary value problems in theory of thermal stresses in piecewise continuous anisotropic elastic bodies under coupling conditions
10 p1563 A72-24994
Statics, motion equations, deformation, dynamics and classification of Cosserat continua
10 p1513 A72-25000
Elastic inhomogeneous continuum stability dependence on internal stress tensors field and boundary conditions, noting application to composite materials
12 p1843 A72-27171
Book on finite element method application to boundary value problems, nonlinear continuum thermodynamics and thermoviscoelasticity
12 p1882 A72-27325
Flux functions and balance laws for linear momentum in continuum mechanics, deriving traction vector and differential equilibrium equation
12 p1846 A72-27570
Micromechanics of deformed continua, discussing atomic structure effects on stress concentrations in composite materials, framed structures and grids
12 p1884 A72-27640
Stability in mechanics of continuous solids - Conference, University of Waterloo, Ontario, Canada, October 1970-September 1971
13 p2054 A72-28476
Comparative study of lunar objects selenodetic coordinates catalogs based on continuous media deformation theory
13 p2037 A72-28987
Thermomechanical interactions between elastic waves and nonstationary temperature fields in solid continua, considering coupled and uncoupled theories
13 p2064 A72-29093
Stress wave propagation and fracture in composites, discussing micromechanical and homogeneous-continuum theories
13 p2060 A72-29692
Directionally reinforced composites treated as homogeneous continuum with microstructure, deriving displacement equations of motion by Hamilton principle
13 p2060 A72-29694
Interacting continua theory for stress wave propagation in composites with microstructural stress and displacement fields, discussing elastic and viscoelastic materials behavior
13 p2060 A72-29695
Orthogonality condition application to continuum mechanics systems with zero free energy, viscoelastic materials and chemical problems
14 p2130 A72-30419
Laminated plate continuum theory with microstructure, studying one dimensional harmonic wave propagation in infinite laminate
14 p2169 A72-31147
Kinematic equations derivation for traveling displacements field in Cosserat continuum by Lagrange formalism, noting analogy with Maxwell equations
15 p2274 A72-31474
Nonlinear Cosserat continuum theory of elasticity, discussing kinematics and stressed state as functions of angular velocity, acceleration, volume forces and moments
15 p2274 A72-31476
German monograph on theory of simple waves and application in continuum mechanics covering phase curves for quasi-linear autonomous system
15 p2275 A72-31505
Nonlinear thermoelasticity theory in terms of continuum mechanics terminology, assessing strain gradients and couple stresses effects on stress distribution
15 p2330 A72-32293
Gosiewski vorticity tensor formula generalization from moving unit vector associated with material point to vector field relative to moving continuum
16 p2423 A72-33112
Generalized continuum mechanics application to turbulent flows developing from unstable vortex wakes
16 p2377 A72-33143
Pulsars 0950 plus 08 and 1133 plus 16 flux density spectra measurements at 1.4-5.0 GHz, noting equivalent continuum break
16 p2456 A72-33477
Soviet book on continuum mechanics covering dynamic, thermodynamic and electrodynamic equations mechanic problems, three dimensional space, internal degrees of freedom, etc
16 p2425 A72-33578
Approximation of mathematical models for continuous media with many degrees of freedom, local structure and interactions, discussing parameters similarity conditions
16 p2425 A72-33586
Nonlocal fluid dynamics continuum theory with equilibrium and constitutive equations derived by

generalizing Stokes Laws, noting steady channel and shear flow
16 p2379 A72-33832
Discrete and continuous systems spurious solutions avoidance through Hamilton principle reciprocal form derivation of geometric compatibility conditions
[ASME PAPER 72-APM-54] 17 p2627 A72-34777
Physical determination of fields of displacements and their derivatives in continuous media.
[ASME PAPER 72-APM-15] 17 p2629 A72-34801
Continuous elastic systems flutter and divergence instability under nonconservative loading, determining slopes of loading-frequency curves
17 p2633 A72-35255
Nonequilibrium thermodynamics with rate equations as nonlinear solid mechanics foundation, noting viscoelastic, viscoplastic and plastic behavior
18 p2732 A72-36076
Analytical foundations of experimental mechanics - Trends in analytical mechanics.
18 p2732 A72-36354
Variational principle of linear differential equations.
18 p2705 A72-36717
On the role of density gradients in the continuum theory of mixtures.
18 p2712 A72-37076
Certain problems in continuum mechanics for a deformed body of variable mass
19 p2835 A72-38471
A multi-continuum theory for composite elastic materials.
21 p3072 A72-40676
Investigation of the self-oscillations of a continuous medium arising at a stability loss in operation steadiness
22 p3164 A72-41907
The oriented elastic continuum as a model for the magnetoelastic body.
22 p3206 A72-42525
Continuum and finite element branching studies of the circular plate.
22 p3235 A72-42603
Causality in the relativistic theory of elastic media in the three-dimensional case.
22 p3206 A72-42626
Incompressible continuous media three dimensional boundary problems solution by pure shear state analysis, discussing application to plasticity theory
23 p3314 A72-44222
Fracture of WC-Co from a continuum viewpoint.
24 p3413 A72-44815

CONTOURS
Fluid flow numerical solution by contour dynamics methodology with flow features resolution advantage.
01 p0049 A72-10227
Perspective effects on direction of rotation judgments, using figures with rectangular and trapezoidal contours
02 p0167 A72-11898
Noncoherent moire contour-sum contour-difference and vibration analysis of three dimensional objects using grid projection and offset camera
03 p0358 A72-13438
Two dimensional elasticity theory, discussing first, second and mixed boundary value problems solution in contour integral form
03 p0451 A72-14116
Inverse contour problem of approximating functions for compacts of positive logarithmic capacity in complex plane
12 p1836 A72-27070
Surface evaluation of airfoils via contouring.
19 p2806 A72-37605
Real time holographic contouring and coherent light interferometry of gear tooth surfaces.
19 p2797 A72-37606
Holography application in photogrammetric contour mapping, discussing topographic data acquisition, storage, retrieval and display problems
19 p2797 A72-37609
A new approach to automatic scanning of contour maps.
22 p3174 A72-43024
Rotating disks optimal design allowing for creep from additional coupling imposition and contour displacement
23 p3347 A72-43746

CONTRACT INCENTIVES
Multiple performance parameters related to single incentive scale for contract management
04 p0598 A72-15225

CONTRACT MANAGEMENT
Configuration management on small production contracts for U.S. Government, including identification, control and accounting
03 p0460 A72-14204
Multiple performance parameters related to single incentive scale for contract management
04 p0598 A72-15225

CONTRACT NEGOTIATION
Price and technical quality effectiveness in winning government R and D contracts
06 p0905 A72-17397

- Profit policy for defense contract negotiations relating to capital employed for cost reduction
09 p1413 A72-22237
- Work administration system for aerospace applications, considering contractual statements, corporate requirements, schedule accomplishment and cost effectiveness
[AIAA PAPER 72-244] 10 p1564 A72-24449
- Incentive contracts with price differential acceptance test plans to motivate producer to product improvement, defining admissible strategies in terms of risk limitation
13 p2066 A72-28354
- Cost-to-produce estimation consideration as design parameter in defense material contractual arrangement
17 p2639 A72-34462
- An operations research approach to solve complex and unstructured problems illustrated for the case of cost-plus-award fee contracts.
17 p2639 A72-35341
- Forecasting costs and completion dates for defense research and development contracts.
24 p3468 A72-45479

CONTRACTION

- Stresses in a welded diaphragm due to boundary contraction and normal uniform pressure.
[SESA PAPER 1811] 17 p2631 A72-34821

CONTRACTS

NT SUBCONTRACTS

CONTRACTS

- Wind direction rotation with altitude and time dependent downward phase propagation observed by vapor trail experiments, suggesting upward propagation of atmospheric waves
16 p2383 A72-32969
- SST contrails stratospheric dispersion by aircraft wake, atmospheric turbulence and exhaust gases temperature induced buoyancy
[AIAA PAPER 72-650] 16 p2388 A72-34084

CONTRAST

NT IMAGE CONTRAST

NT PHASE CONTRAST

- Detection and recognition of colored signal lights.
17 p2510 A72-35691

CONTROL

- Nonlinear control system optimal bang-bang controls computation, noting algorithm obtained by parameter optimization
11 p1577 A72-26666

- The foot as input device for control operation.
21 p3012 A72-41428

CONTROL BOARDS

- Meaningful shape coding for aircraft switch knobs.
17 p2510 A72-35944

- The evolution of head-up displays.
20 p2925 A72-39333

- Aircraft instrument panel redesign to alleviate crew task, proposing integral displays and controls for flight information
21 p3080 A72-40291

CONTROL DATA (COMPUTERS)

- Optimal operation assignment and data array storage allocation in data system consisting of central processing unit and peripheral computer controlling data flow
09 p1283 A72-23439

- Executive job handling program for operation with fault tolerant multiprocessor in real time control environment
10 p1442 A72-23816

CONTROL DEVICES

U CONTROL EQUIPMENT

CONTROL EQUIPMENT

NT CONTROL STICKS

NT CRYOSTATS

NT PRESSURE REGULATORS

NT PRESSURE SWITCHES

NT SPEED REGULATORS

NT TELEOPERATORS

NT THERMOSTATS

- Integrated electronics digital-analog solar cell array control unit, discussing circuit design and radiation hardening
01 p0042 A72-11059

- High pervance electron guns with control grids and low voltage beam modulation, considering design, operation, structural and control characteristics
02 p0189 A72-11562

- Papers on noise and vibration control covering acoustics in free space, outdoors, small enclosures and rooms, measurement, analysis and design problems
02 p0258 A72-12100

- Concorde supersonic transport hydraulic control systems, describing design features with emphasis on reliability
03 p0312 A72-13962

- Minicomputer use for terminal control and matching functions and data compression in data transmission systems
05 p0633 A72-16199

- Satellites and spacecraft flight control systems, discussing approaches for stationkeeping and orbit determination/correction
05 p0729 A72-16746

- Photomultiplier operation pulsed control in semiconductor circuit for background cosmic radiation noise error minimization in atmospheric shower station
06 p0811 A72-17294

- Combined delay and loss common-control queueing system, obtaining stationary state loss and waiting probabilities and waiting time distribution function
06 p0794 A72-18243

- Electrostatic rf ion thruster development, including power conditioning and control units
07 p1054 A72-19600

- Operational optimization of ion traps with dc amplifiers mounted on nonoriented earth satellite, proposing control circuit
07 p0993 A72-20664

- Soviet book on control system technology for flight vehicles covering production of mechanical, hydraulic, pneumatic, electric and electronic elements
08 p1179 A72-22024

- Three phase bidirectional pulsating flow hydraulic control system, discussing design, performance and applications
08 p1114 A72-22162

- Supervisory circuits in electronic data processing power supplies, describing inadmissible line voltages indication networks
10 p1445 A72-24818

- SECANT system of aircraft separation and control by nonsynchronous technique for midair collision avoidance
[SAE PAPER 720313] 11 p1683 A72-25577

- Hale observatories computer system design for telescope control and data handling, using solid state techniques
11 p1601 A72-25696

- Microwelding and microsoldering equipment control systems, discussing ac phase cut-off, dual pulse, dc and intermediate frequency units
11 p1639 A72-25810

- Airport lights systems control with thyristors, discussing light intensity regulation, command board design and insulation test equipment
12 p1794 A72-27401

- Semiconductor strain gage design and environmental performance for flight control systems
12 p1812 A72-27962

- Variable magnetic baffle as control device for Kaufman electron bombardment ion thrusters with hollow cathode
[AIAA PAPER 72-488] 13 p2027 A72-28949

- Ground station with control, communication and information processing centers, discussing automation, data transfer, system control and emergencies
[DGLR PAPER 72-007] 13 p1959 A72-28965

- AEROS research satellite control program, describing system objectives, operational testing, error analysis and command verification
[DGLR PAPER 72-023] 13 p1918 A72-28968

- Undesirable mechanical vibration control concepts for acoustic noise reduction, considering environment characteristics, attenuation degrees and passive and active control mechanisms
13 p2005 A72-29555

- Minimum weight phase change thermal control device for planetary descent probes, discussing test over various heat loads
[AIAA PAPER 72-287] 14 p2171 A72-30826

- Control equipment designs for phase error estimation of pulse sequences in multichannel magnetic recording systems
16 p2367 A72-33264

- A method of using a control computer in a system controlling onboard spacecraft equipment
17 p2522 A72-35027

- Polish aircraft industry production and fabrication techniques, discussing metal working, digital controlled machining and cost reduction
18 p2696 A72-37010

- Remote power control for aircraft generating and distribution systems.
18 p2648 A72-37034

- Equivalent circuits and oriented graphs for network analysis and synthesis of nonlinear transducers used in control systems
19 p2777 A72-37316

- Measurement transducers in industrial process control, discussing requirements for dynamic properties, stability, linearity and computer applications
19 p2803 A72-38315

- Quantitative aspects of reliability in process-control systems.
21 p3038 A72-40922

- Optimal linear inertia-free processing of meter readouts with allowance for control-equipment signals
24 p3403 A72-45316

- Use of oblique-cut lithium niobate in optical-beam control systems.
24 p3411 A72-45606

CONTROL MOMENT GYROSCOPES

- Gimbaled control moment gyro for Skylab telescope mount stringent pointing requirements, investigating normal and clamped operation modes and dynamic response of attitude control
01 p0097 A72-10382

- Stability and CMG wobble damping of flexible, spinning space stations.
[AIAA PAPER 72-888] 20 p2975 A72-39113

- Omega-Dot law for time optimum approximation of rotating satellites wobble damping with control moment gyroscopes, calculating wobble rates by energy sink method
24 p3453 A72-45777

CONTROL PANELS

U CONTROL BOARDS

CONTROL ROCKETS

- Flight test evaluation of a fluidically actuated monopropellant hydrazine roll control system.
[AIAA PAPER 72-975] 24 p3452 A72-45410

CONTROL SIMULATION

- Analog computer simulation of automatic control systems containing time delay element in feedback loop, evaluating errors
01 p0044 A72-10152

- Augmentor wing jet STOL research aircraft development progress report covering design, engine tests, performance prediction, control simulation and stability augmentation
[SAE PAPER 710757] 01 p0003 A72-10254

- Three-axis flight table with dc torque motors, discussing servo loops design and mechanical oscillations frequencies
02 p0257 A72-12541

- Airplane hydraulic control systems digital simulation, using method of characteristics for distributed parameter analysis of transmission line dynamics
[ASME PAPER 71-WA/FE-21] 05 p0615 A72-15928

- Dynamic test facility for Symphony satellite attitude control, discussing sun and earth sensors and analog computer for motion simulator
05 p0643 A72-16432

- Spherical air bearing supported test facility for satellite attitude control system performance testing, discussing motion simulator and automatic balancing system
05 p0643 A72-16435

- Kalman linear filtering technique for spinning satellite attitude restitution, evaluating reliability by model for simulation of measurements by sensors
[ONERA, TPN NO. 953] 05 p0724 A72-16436

- Three-axis attitude control and stabilization system for sounding rocket payload, discussing performance from simulation and ground test results
05 p0728 A72-16478

- Fast time simulation application to ATC systems, discussing control action exercise within strategic/tactical spectrum
05 p0645 A72-16994

- ATC at single-runway airport analyzed by fast time simulation with high speed digital computers
07 p1032 A72-19064

- Apollo manned mission real time ground support computer simulation for NASA flight controller training to maximize flight crew safety
07 p0933 A72-20329

- ATC system analysis by fast time arithmetic simulation techniques, describing ground model development
09 p1272 A72-23141

- Individual style differences between operators of simulated aircraft control
09 p1273 A72-23579

- Teleoperator manipulator for payload handling in space shuttle, noting design features and simulations of master-slave remote control system
[AIAA PAPER 72-238] 13 p1909 A72-29075

- Perturbation extremum controller with simple coincidence logic, discussing fluidic implementation and performance in simulated plant control
16 p2350 A72-33193

- An optimal model-following flight control system for manual control.
19 p2753 A72-38228

- Advanced fighter controls flight simulator for all-systems compatibility testing.
[AIAA PAPER 72-837] 20 p2911 A72-39090

- Reentry vehicle spiral descent terminal guidance, verifying concept feasibility through hybrid man-in-loop simulators
[AIAA PAPER 72-834] 20 p2950 A72-39093

- A simulation technique used in the development of a flight control system for an aerodynamically controlled missile.
[AIAA PAPER 72-858] 20 p2976 A72-39136

- High performance jet aircraft variable feel flight control systems for simulation of aerodynamic reaction forces proportional to dynamic pressure
21 p3039 A72-41069

- A model for analysing the coordination of manual movements.
21 p3010 A72-41413

- Control simulation models of three dimensional joint angle motions, including circle, ellipse and straight line trajectories and orientations in space 22 p3162 A72-42187
- Use of modeling and simulation methods in the design of gas turbine engine control systems 23 p3326 A72-44283
- Synthesis of the control systems of a two-shaft helicopter gas turbine engine 23 p3327 A72-44289
- Analog model of gas turbine engine control systems, using statistical estimates and flow rate, heat conduction and dynamic equations 23 p3327 A72-44293
- Nonlinear digital modeling of gas turbine propulsion units 23 p3327 A72-44294
- A simple algorithmic method for the simulation of a spacecraft with flexible appendages. 23 p3343 A72-44552
- Parametric optimization of the equivalent transfer function of a system with the aid of the error integral 24 p3387 A72-45700

CONTROL STABILITY

- Frequency conditions of absolute stability for closed automatic control system with nonlinear unsteady units 01 p0045 A72-10499
- Plasma column equilibrium position feedback control based on combination principle, analyzing system stability 01 p0109 A72-10502
- Closed linear systems optimal stabilization determining transfer function from Wiener Hopf equation 01 p0045 A72-10572
- Stability conditions for direct control systems in critical case, assuming pair of imaginary conjugated and zero characteristic numbers 04 p0538 A72-14623
- Stability control of rotating circular plates with edge slots and membrane stresses by finite element method [ASME PAPER 71-WA/AUT-2] 05 p0733 A72-15951
- Large launch vehicle attitude control system absolute stability mathematical model, using quadratic Liapunov function for exponential property description 05 p0728 A72-16475
- Controlled motion dynamics of spacecraft performing maneuvers, applying point transformation to third-order nonlinear system moving about center of mass in lateral motion 05 p0730 A72-17029
- Pulsed relay control system for stabilizing spacecraft orientation in flight, allowing for changes in characteristics of guidance sensor systems and slave mechanisms 05 p0731 A72-17031
- Optimal control algorithm for nonlinear stochastic systems ensuring probability-wise stability and minimum error, using Liapunov theory and dynamic programming 05 p0691 A72-17141
- Phase-plane analysis of transient response of on-off control system relative to sinusoidal inputs 06 p0795 A72-18714
- Algorithmic procedure in compensator design for hyperstable discrete model reference adaptive systems/MRAS/ 07 p1027 A72-19294
- German book on control technology development covering historic periods, symbols and representations, stability, integral transformations, computers, servos, relays and multivariable systems, optimization, etc 08 p1145 A72-21478
- Servomechanism with nonlinear static and Coulomb friction under autonomous operation, predicting stability boundaries by analog computer simulation 08 p1113 A72-22154
- Digital control system instability caused by introduction of floating point arithmetic in controller 09 p1341 A72-23096
- Stability regions of phase-locked AFC with nonlinear control circuit, describing system dynamics by differential equations 09 p1290 A72-23180
- Periodic motions stability of nonlinear control systems with energy consumption, using contact transformations 10 p1458 A72-25074
- Two stage magnetic operational amplifier transfer function, time constants and control stability conditions, using difference equation approach 11 p1605 A72-26466
- Mathematical model for hydraulic fatigue testing machine, analyzing nonlinear control stability of vibratory loading process 12 p1796 A72-27978
- Optimizing functional for combined control of dynamic control plant, synthesizing stabilization system for maximal transient damping 13 p1935 A72-28713

- Dynamic control stability on given time interval, using Liapunov-like functions and integral manifolds in quadratic forms 13 p2004 A72-29471
- Control optimization avoiding stability problem by integrating matrix Riccati equation 13 p1937 A72-30074
- Absolute stability of nonlinear automatic control systems based on root locus trajectories and Popov line hodographs 13 p1937 A72-30094
- Transmission line with feedback, deriving Nyquist stability from Mikhailov criterion with application to liquid fuel rocket model 17 p2621 A72-35100
- Absolute stability analysis of attitude control systems for large boosters. 17 p2622 A72-35489
- Rotating body linear dynamic control by complex transfer function approach with application to stability conditions for controlled gyro and homing missiles 17 p2583 A72-35528
- Stability and transient behavior of composite nonlinear systems. 17 p2534 A72-35530
- Fine guidance pointing stability of a 120-inch /3 meter/ large space telescope /LST/. [AIAA PAPER 72-853] 20 p2949 A72-39076
- Using the quasi-homogeneity of differential equations in modeling physical systems 21 p3083 A72-40377
- The influence of a prediction display on the human transfer characteristics. 21 p3012 A72-41432
- Investigation of the stability of a hydraulic servo motor with rigid feedback 22 p3139 A72-41858
- Constant coefficients for linearized flow rate equation of hydraulic throttle servodrive in closed circuit stability solution by Liapunov theorem 22 p3139 A72-41873
- Optimizing functional for combined control of dynamic control plant, synthesizing stabilization system for maximal transient damping 22 p3162 A72-42091
- Liapunov function method in control problems of distributed parameter systems /Survey/ 22 p3205 A72-42180
- Error incidence probability for system control reliability determination, assuming Markov process 22 p3162 A72-42183
- Design of controllers for open-loop unstable multivariable system using inverse Nyquist array. 23 p3275 A72-43609
- Regulator vector selection algorithm for largest estimate of exponential absolute control stability region based on Popov frequency condition reformulation 23 p3276 A72-43853
- Sufficient condition formulation for Lure type nonlinear continuous control system exponential absolute stability 23 p3309 A72-43854
- Regions of absolute ultimate boundedness for discrete-time systems. 23 p3309 A72-43857
- Recent results in convolution feedback systems. 23 p3276 A72-43861
- Synthesis of hyperstable discrete model reference adaptive systems. 23 p3276 A72-43867
- Determination and quality estimation of stability in discrete linear systems 24 p3386 A72-44722
- CONTROL STICKS**
- Influence of prolonged longitudinal accelerations on control habits 21 p3004 A72-41750
- CONTROL SURFACES**
- NT AERIAL RUDDERS
- NTAILERONS
- NT ELEVATORS [CONTROL SURFACES]
- NT FLAPS [CONTROL SURFACES]
- NT GUIDE VANES
- NT HORIZONTAL TAIL SURFACES
- NT JET FLAPS
- NT JET VANES
- NT LEADING EDGE SLATS
- NT SPLIT FLAPS
- NT SPOILERS
- NT TRAILING-EDGE FLAPS
- NT WING FLAPS
- Subsonic oscillating surface theory for wings with partial span controls, noting computer program rapidity [AIAA PAPER 72-61] 05 p0608 A72-16931
- Singular surfaces for time optimal control in zero sum differential games between two aircraft in three dimensional space, assuming spherical acceleration vectorgram 07 p1027 A72-19279
- Vibration analysis of shaft supported low aspect ratio control surfaces on guided rockets, using Rayleigh-Ritz method 07 p1097 A72-20602

- Approximate method for nonlinear differential equations of motion solution in flight dynamics, applying to control surface buzz and slender wing oscillations 09 p1262 A72-23453
- Control surface dynamic hinge moment coefficients estimation based on system state measurements from flight tests, using least squares criterion [AIAA PAPER 72-379] 11 p1730 A72-25403
- Utilization of wing and empennage volume for aircraft fuel tankage, presenting equations and charts for quick determination of available volume 11 p1576 A72-25811
- Modified gas dynamic functions of total momentum of plane boundary layer for arbitrarily oriented control surfaces and for stratified flows with potential layer 11 p1574 A72-26973
- Stress levels and fatigue in aircraft structures subjected to jet noise, noting stress calculation for skin panels and control surfaces 13 p1898 A72-29579
- Theoretical and experimental study of the pressure and heat-flux distributions on a control surface in the presence of a thick hypersonic turbulent boundary layer [ICAS PAPER 72-23] 21 p2991 A72-41148
- The sweepback effect in the subsonic region in the lower atmosphere and in the hypersonic region at high altitudes 24 p3359 A72-44983
- A study of dedicated control surfaces for direct sideforce control. 24 p3368 A72-45344
- CONTROL SYSTEMS**
- U CONTROL**
- CONTROL THEORY**
- Soviet papers on complex automatic control systems, covering elastic spacecraft stabilization, nonlinear dynamic systems controllability and random vibration spectra control 01 p0045 A72-10496
- Multidimensional variable structure systems synthesis for automatic optimization of inertialess technological plants in presence of constraints 01 p0045 A72-10498
- Controllability of dynamic systems with motion described by nonlinear differential equations 01 p0045 A72-10500
- Gradient method for optimization control system construction with cross couplings between channels 01 p0045 A72-10501
- Plasma column equilibrium position feedback control based on combination principle, analyzing system stability 01 p0109 A72-10502
- Ideally conducting plasma confined in vacuum by circularly polarized magnetic field, investigating MHD instabilities suppression by distributed automatic control system 01 p0109 A72-10503
- Aircraft pitching and yawing cross couplings compensation at high speed 01 p0005 A72-10506
- Reachable sets calculation for linear dynamical system control, suggesting iterative procedures for numerical approximations 01 p0034 A72-11124
- Estimation and control relations separation for discrete time stochastic systems, considering assumptions on linearity, criteria, information pattern, constraints and noise distributions 01 p0047 A72-11306
- Online identification on human describing function by iterative differential analyzer, noting application to man-machine systems and online adaptive control systems 02 p0169 A72-12661
- Stochastic linear-quadratic-Gaussian problem role in optimal closed loop control system design, emphasizing philosophy, modeling and problem formulation [AD-738763] 02 p0198 A72-12801
- Noninteracting decoupling control theory for linear constant multivariable systems, using dynamic feedback matrix compensators 02 p0198 A72-12802
- Linear regulator and servomechanism theories modification to account for fluctuation disturbances, obtaining deterministic controller design to maintain set point regulation or servotracking 02 p0198 A72-12803
- Bibliography on linear-quadratic-Gaussian problems covering quadratic criteria, state estimation, stochastic control, computations and applications 02 p0198 A72-12813
- Differential and difference equations approximate solutions in finite state machine form, developing adaptive gain changer model in aircraft stability control system 03 p0338 A72-13164
- Approximation method for determination of distributed parameter systems optimal control, considering state and control variable constraints 03 p0338 A72-13917

Distributed parameter systems control - Conference, Banff, Canada, June 1971

04 p0504 A72-14660

Distributed parameter control system optimal control problems, formulating existence with minimum norm technique

04 p0505 A72-14667

Discrete system high order optimality sufficient conditions and methods for singular and nonsingular controls study

04 p0505 A72-14996

Control system synthesis from transient process estimates with Liapunov functions, proposing optimality criteria based on Gaussian minimum constraint principle extension

04 p0505 A72-14997

Optimal control systems with terminal state constraints, presenting algorithm based on constraint-saddle conjugate gradient method for function minimization

04 p0506 A72-15111

Modal theory of state observers for control of multivariable time-invariant linear systems with plant matrices possessing distinct eigenvalues

04 p0507 A72-15529

Optimal control of linear systems /continuous and discrete/, using quadratic performance criterion

04 p0507 A72-15667

Analytical inversion of quasi-orthogonal matrix for Simpson method of state feedback gains calculation in multiloop linear mode control systems

05 p0639 A72-15807

Fluidic threshold logic application to fluidic control systems, comparing with AND-OR logic for number of elements and weight
[ASME PAPER 71-WA/FLCS-5]

05 p0615 A72-15918

Direct and inverse problems of sensitivity theory, discussing solvability conditions, search optimization and applicability in automatic control

05 p0640 A72-16206

Linear dynamic control system identification by local impulse response approximation, comparing with Goodman-Reswick model

05 p0641 A72-16319

Structure, controllability and synthesis of n-dimensional invariant systems under perturbation vector, using governing equations

05 p0641 A72-16352

Adaptive model following control systems design by hyperstability approach for flight control and simulation

05 p0613 A72-16956

Linear time-varying control systems with one feedback nonlinearity, determining combined time-frequency condition for stability

05 p0642 A72-17090

Optimal averaging of discontinuous processes with distributed parameters, taking into account random disturbances and measurement errors

05 p0683 A72-17130

Statistical solution of analytical design of optimal control system maintaining coarseness /universality/ with minimum quality loss

05 p0691 A72-17135

Optimal control synthesis for linear stochastic systems with random piecewise-continuous coefficients as function of time

05 p0683 A72-17139

Nonlinear optimal control problems with undetermined final time, using conjugate-gradient method

06 p0792 A72-17312

Control, prediction and risk optimization in scheduling problems with incomplete random information

06 p0793 A72-17729

Collection of papers on control systems theory and applications covering optimal control, final value control systems, discrete stochastic differential games, linear estimation, etc
[AD-738871]

06 p0793 A72-17952

Kalman-Bucy colored noise filtering discrete time results and continuous time linear minimum variance estimation by calculus of variations

06 p0793 A72-17955

Singular controls calculation based on Poisson brackets, applying to nuclear reactor

06 p0849 A72-18300

Autonomous threshold elements diagnostic tests and verification control, noting cascade, pyramidal and branching schemes

06 p0785 A72-18303

Frequency criterion of weak instability in nonlinear control systems

06 p0794 A72-18304

Optimal control systems synthesis with allowance for given reliability, finding extremal value of quality function with constraint on probability of fail-safe operation

06 p0794 A72-18305

German book on time variable multiparameter control systems covering reduction, canonical forms, decoupling, feedback stabilization, observers, inversion and multiloop synthesis

06 p0794 A72-18517

Stochastic optimal control for operations of plants with pure lag and two point estimate of performance index investigating systems stability

06 p0795 A72-18662

System properties of information patterns in complex hierarchical automatic control systems

07 p0949 A72-18927

Optimal control of distributed parameter systems with incomplete state information by dynamic programming and Liapunov methods

07 p1034 A72-18981

Stability analysis of steady control systems acted upon by random signal in single valued one dimensional nonlinearity form, using statistical linearization

07 p0959 A72-18989

Feasible solutions to automatic control problems satisfying multiple state and control variable inequality constraints, discussing algorithmic numerical implementation

07 p0959 A72-19281

Multivariable technical control system - Conference, Dusseldorf, West Germany, October 1971

07 p0960 A72-19696

Minimal order controller for decoupling of linear multivariable systems with low order control devices and reduced control effort

07 p0960 A72-19697

Model-following algorithm and equicontrollability in multivariable feedback control systems, considering application to decoupling problem

07 p0960 A72-19698

Linear dynamic control systems controllability and observability quality analysis and optimization, considering determinant, trace and maximal eigenvalue

07 p0960 A72-19699

Algebraic algorithm for reducing to state form multivariable control systems defined by linear constant differential operators

07 p0950 A72-19702

Frequency response design for interactive multivariable feedback control systems, using characteristic transfer functions

07 p0960 A72-19704

Linear time-invariant controllable plant, determining semiclosed loop nominally equivalent control realization for reduced sensitivity to plant parameter perturbations

07 p0961 A72-19705

Linear multivariable control system state observation by sampling with arbitrary but fixed distribution of sampling instants, emphasizing dual control by step functions

07 p0961 A72-19707

Model-following control for nonlinear multivariable plants, considering implicit algorithm solution and application to variable stability aircraft control synthesis

07 p0961 A72-19708

Two-variable second order system for multivariable systems predictive control, deriving algorithm for near time optimal control

07 p0961 A72-19709

Linear multivariable system design based on relationship between performance index parameters and optimal response in frequency domain, exemplifying gas turbine feedback controller design

07 p0961 A72-19710

Multivariable linear systems control structure via optimal control theory with quadratic criterion, permitting compensation for nonzero mean value and slowly varying perturbations

07 p0961 A72-19711

Quasi-time optimal control synthesis of two-control variable system by equivalent switching signum function method

07 p0961 A72-19712

Multivariable control systems, discussing effects of interaction vs noninteraction /decoupling/ on system performance and energy requirements

07 p0962 A72-19715

Optimal control on nonlinear multivariable plant with common constraint on control action, presenting linear programming algorithm

07 p0962 A72-19717

Optimal control of lumped and distributed parameter systems with time lag, considering approach with extrapolator insertion and suboptimal solution based on system dynamic equation

07 p0962 A72-19718

Nonlinear multivariable system optimal control with respect to time and fuel consumption, discussing Gauss-Newton and Davidson methods and application to geostationary satellite

07 p0962 A72-19719

Optimal control of linear multivariable plants with one or more quality criteria, considering control channels and game theory

07 p0962 A72-19720

Control theory of dynamic multiconnected systems with differential operators, time lags and hereditary components

07 p0962 A72-19721

Linear multivariable feedback control system design techniques

07 p0963 A72-19723

Optimal multivariable control systems theory, considering linear programming, maximum principle and differential games

07 p0963 A72-19724

Absolute stability region of linear portion of single loop automatic control system with one nonlinear element determined by frequency criteria

07 p0963 A72-19898

Optimal strategies for decision chain with controllable connections and finite number of states and decisions, deriving existence theorem

07 p1028 A72-19904

Stability requirement of gyro systems in generalized Thomson-Tait theory

07 p0989 A72-20277

Minimum dimensionality determination for control process stabilizing linear mechanical system equilibrium position, obtaining necessary and sufficient conditions

07 p1036 A72-20320

Control system stability with nonlinear feedback in steady equilibrium state

07 p0963 A72-20321

Self similar invariant group solutions to Bellman nonlinear partial differential equation for optimal correction problems of control systems motion with random disturbances

07 p0963 A72-20322

External disturbance accommodation in optimal control, based on characterization of waveform modes, applying to linear-quadratic regulator problem

07 p0963 A72-20591

Standard linear estimation and control problem with quadratic loss, optimizing information rate by minimizing total measurements number through Riccati equation singular solution

08 p1144 A72-20859

Automatic systems efficiency determination, using characteristic equation roots sensitivity with respect to system parameters changes

08 p1146 A72-22063

Controlled plants operation efficiency change prediction by analytic and probabilistic methods with data processing

08 p1180 A72-22064

Control synthesis equations for aircraft motion on phase space surface

09 p1261 A72-22208

Optimal and quasi-optimal automatic control systems synthesis by cross section method

09 p1290 A72-22489

Nonlinear systems controllers design based on Liapunov functions and time domain ratio criterion, presenting digital computer algorithm

09 p1290 A72-23090

Linear multivariable system stabilization by output feedback technique based on gradient approach

09 p1290 A72-23097

Linear time invariant multirate sampled data control systems characteristic equation simplification

09 p1290 A72-23099

Matrix notation for replacing vector analysis in control theory by introduction of differential operators similar to Hamiltonian operator

09 p1352 A72-23369

Numerical algorithm for optimal coefficient equations in analytical design of complex control plants

09 p1291 A72-23426

Optimal control synthesis for linear passive stationary plants with symmetrical coefficient matrices of minimized functional

09 p1291 A72-23431

Singular control problems calculation in trajectory optimization using sufficient conditions for control values set form

09 p1291 A72-23432

Discrete and continuous dynamic adaptation algorithms construction for extremal quality functional trajectory equations of adaptive control system

09 p1283 A72-23435

Hierarchical control structures aggregation and construction for class of complex systems

09 p1292 A72-23489

Decision and control including adaptive processes - IEEE Conference, Miami Beach, Florida, December 1971

10 p1454 A72-23776

Quadratic cost, nonlinear optimal adaptive stochastic control of linear plant and measurement models excited by white Gaussian noise and with unknown parameters

10 p1455 A72-23792

Systems analysis and mathematical modeling role in planning transportation networks from control theory viewpoint

10 p1442 A72-23796

Stochastic nonlinear system one-step optimal dual control instead of separation control policy for performance improvement

10 p1456 A72-23810

Terminal control solution in terms of finite dimensional minimization of convex function, applying to time optimal control and minimum energy problems

10 p1457 A72-24459

Dynamic logic control systems theory based on axiomatic concepts of models, deriving conditions for existence and uniqueness of solution for differential logic equations

10 p1457 A72-24636

Time optimal control system for linear plant with transfer functions containing zeros

10 p1458 A72-24999

Linear dynamic control system identification by local impulse response approximation, comparing with Goodman-Reswick model

10 p1458 A72-25073

Stochastic control theory application to flight problem, discussing aircraft identification and adaptive control over wide environmental range

10 p1458 A72-25146

Linear continuous time systems optimal dual control problem solution by reduction to partial differential equation in finite domain with suitable boundary conditions

10 p1458 A72-25170

Parameter identification method for mathematical extremal control model of complex structure for static plants based on regression analysis

10 p1458 A72-25192

Output voltage characteristics of single phase thyristor inverter based on pulse duration modulation with direct shaping of control pulses, considering harmonic coefficients

11 p1603 A72-25277

SCR trigger circuits design generating short control pulses for converters based on SCR elements, presenting circuit diagrams

11 p1603 A72-25280

Function space linear bounded phase coordinate control problems under regularity and normality conditions discussing solution existence and uniqueness conditions

11 p1608 A72-25322

Input-output stability of linear time invariant multivariable closed loop control systems

11 p1608 A72-25327

Structure, controllability and synthesis of n-dimensional invariant systems under perturbation vector, using governing equations

11 p1608 A72-25328

Control, prediction and risk optimization in scheduling problems with incomplete random information

11 p1608 A72-25331

Servo systems operational reliability analysis for variable intensity of fluctuating interference, discussing Markov process probability determination and Kolmogoroff equations solution

11 p1609 A72-25441

Russian papers on discrete control systems covering inertialess Markov objects, pulse amplitude and frequency modulation and statistical analysis

11 p1609 A72-25442

Continuous signals discrete values for analysis and synthesis of control systems with variable parameters, obtaining recurrent formulas and error estimate

11 p1609 A72-25445

Suboptimal feedback control law synthesis for nonlinear systems, using second order approximation to optimal control

11 p1610 A72-25872

Control theory application to nonlinear elastic analysis of trusses, partitioning structure into statically determinate stages

11 p1736 A72-25989

Book on sensitivity theory covering continuous and sampled data systems, linear, nonlinear and self exciting dynamic systems, optimal systems, large systems, controllability, etc

11 p1611 A72-26021

Rank correlation coefficient method for complex control plants parameters selection, applying to aircraft power system monitoring

11 p1612 A72-26442

Matrix and graphic test construction methods for optimal design of logic networks in automatic control systems

11 p1612 A72-26443

Control algorithm with variable structure for incomplete state information on third order system, using error and first derivative

12 p1794 A72-27674

Multiple function stochastic automata performance in environment with random control processes, showing improved learning rate

12 p1787 A72-27922

Multiple input automata with optimal response to any input set, using maximum mean gain as criteria for response selection

12 p1787 A72-27923

Variational problems in automatic control theory, presenting existence theorems for solution of boundary value problems for nonlinear differential equations with deviating argument

12 p1837 A72-27995

Second order systems time optimal control with delay, determining maximum number of switching points for control function

12 p1794 A72-28141

Automatic control system synthesis by computer-aided version of grapho-analytical method

13 p1934 A72-28459

Digital dynamics simulation of continuous controlled processes based on repeated integral transformation of differential equations

13 p1934 A72-28607

Variable structure automatic control relay system design with reduced insensitivity zone and given transient process requirements

13 p1935 A72-28612

Algorithmic method in ALGOL 60 for successive approximations of optimal control problems, discussing improved convergence

13 p1935 A72-28707

Differential games extremal strategies with player control action subject to integral constraints

13 p2002 A72-28712

Control parameters required for stabilization of motion in systems with nonholonomic couplings by dynamic programming method of summary representations

13 p2003 A72-29068

Russian papers on large adaptive control systems covering pattern recognition, statistical analysis, simulation, reliability, etc

13 p1936 A72-29153

Optimal viability of complex system with ambient medium interaction, using stochastic game theory

13 p1936 A72-29174

Signal system design with digital displays for deviation control in complex multiparameter technological processes, using algorithm to estimate efficiency

13 p1936 A72-29177

Singular controls calculation based on Poisson brackets, applying to nuclear reactor

13 p1937 A72-29440

Autonomous threshold elements diagnostic tests and verification control, noting cascade, pyramidal and branching schemes

13 p1934 A72-30071

Frequency criterion of weak instability in nonlinear control systems

13 p1937 A72-30072

Optimal control systems synthesis with allowance for given reliability, finding extremal value of quality function with constraint on probability of fail-safe operation

13 p1937 A72-30073

LF and HF oscillations in plasma-electron beam system, investigating instability control

14 p2137 A72-30310

Quasi-conservative optimal nonlinear self excited oscillation systems theory for automatic control, telemechanics and computer applications

14 p2133 A72-31130

Russian book on high precision servo systems synthesis covering combined feedback and open loop controls, accuracy improvement and root-mean-square errors minimization

15 p2210 A72-31273

Nonlinear microwave circuit feedback model analysis by describing function in control theory, applying to oscillator phase locking problem

15 p2210 A72-31355

Control theory of second order linear hyperbolic partial differential equations, discussing relation to harmonic and spectral analysis

15 p2263 A72-31757

Globally controllable nonlinear differential systems arising from linear system under perturbation

15 p2264 A72-31762

Controllable matched filter model for single circuit and twin circuit parametric converters

15 p2207 A72-31886

Single closed loop discontinuous control system, determining discrete correcting element parameters from linear inequalities

15 p2212 A72-32175

Infinite dimensional system optimal discrete-time feedback controller calculation by n-dimensional system approximation using recurrence relations with functional analysis

15 p2212 A72-32245

Automatic control theory trends /1950-1970/, discussing nonlinear, discontinuous and adaptive systems, optimization problems, Liapunov stability theory, etc

15 p2212 A72-32576

Transfer function estimates in random vibration test control, using digital techniques for rapid reduction of statistical errors

15 p2215 A72-32626

Digital computer studies of control loop parameters and configurations effects on performance of synchronous turbogenerator with two field windings

15 p2183 A72-32793

High speed deterministic adaptive controller for linear and nonlinear plants, identifying control law from state and input data by linear regression procedure

15 p2212 A72-32794

Sensitivity design of multiple input controller for dynamic optimization applied to linear systems with quadratic performance index

15 p2212 A72-32795

Limit cycle stability of third and higher order feedback systems predicted from negative slope of describing function

15 p2213 A72-32796

Numerical methods for Liapunov linear matrix equations solution in control systems analysis and design

15 p2265 A72-32798

Noninteractive compensation of linear multivariable control systems based on matrix block diagram technique

15 p2213 A72-32799

Discrete system feedback design based on complex number plane mapping, determining gain

15 p2213 A72-32800

State space approach to linear multivariable servomechanism problem, deriving controllability conditions and design procedure

15 p2213 A72-32801

Matrix Riccati equation solution method in optimal control theory, noting boundary conditions implementation

15 p2265 A72-32803

Observability conditions for nonlinear and unsteady linear systems, noting control systems design

16 p2371 A72-33092

Optimal invariant control system synthesis for inertial plants with nonminimal phases and random perturbation compensation

16 p2371 A72-33263

Computational difficulties reduction in optimal control and estimation problems, discussing controllability and observability

17 p2574 A72-34417

State dependent state variable feedback method to control multiple input multiple output nonlinear and/or time varying systems

17 p2532 A72-34420

Hingeless rotor - Experimental frequency response and dynamic characteristics with hub moment feedback controls.

17 p2489 A72-34494

[AHS PREPRINT 612] Constant voltage and constant emitter-temperature control schemes dynamics in thermionic reactor, showing closed loop responses to load changes, converter failures and reactivity perturbations

17 p2494 A72-34581

Optimal and quasi-optimal automatic control systems synthesis by cross section method

17 p2533 A72-34652

Regional Conference on Control Theory, University of Maryland, Baltimore, Md., August 23-27, 1971, Proceedings.

17 p2533 A72-34948

System theory on group manifolds and coset spaces.

17 p2575 A72-34949

Controllability, observability and optimal feedback control of affine hereditary differential systems.

17 p2533 A72-34950

The maximum principle and controllability of nonlinear equations.

17 p2533 A72-34951

Comparison principle and finite time stability of control systems.

17 p2581 A72-35052

An automated gradient projection algorithm for optimal control problems.

17 p2576 A72-35244

Finite group homomorphic sequential systems generalization from linear system theory, developing controllability, observability, minimality and realizability concepts

17 p2523 A72-35526

Stability of linear time-invariant distributed parameter single-loop feedback systems.

17 p2534 A72-35535

Optimal smoothing for continuous-time systems with multiple time delays.

17 p2534 A72-35536

Optimality conditions of second and higher orders for discrete systems, discussing functional minimization and Pontryagin maximum principle limitations

17 p2534 A72-35725

Voltage-conversion for incore-thermionic-reactors.

18 p2645 A72-36182

Effective dimensional reduction in the computation of linear, discrete, time-delay problems.

18 p2672 A72-36302

Dynamic verification of a digital flight control system.

18 p2673 A72-36336

Minimum fuel control of second order system in n-dimensional Euclidean space, examining Pontryagin maximum principle applicability

18 p2673 A72-36696

Hill-climbing controller for plants with any dynamics and rapid drifts.

18 p2673 A72-36819

Optimal control with partially specified input functions.

18 p2673 A72-36821

Maximum likelihood identification of time varying and random system parameters. 18 p2673 A72-36822

Optimal control laws for stochastic problems involving intentional errors, caution and probing 18 p2674 A72-36825

Modifications and extensions of the sequential gradient-restoration algorithm for optimal control theory. [AD-736265] 19 p2776 A72-37246

Choice of parameters for measuring devices in a closed-loop linear control system 19 p2777 A72-37319

The problem of encounter avoidance in linear differential games 19 p2824 A72-37377

Certain problems of the theory of hierarchical control systems 19 p2824 A72-37379

Mathematical model of class of complex control systems composed of structures obtained from aggregates of ordered sets and random operators 19 p2777 A72-37380

Extension of the frequency-type unconditional stability criterion of controlled systems with one nonlinear nonstationary element 19 p2777 A72-37431

French monograph - Contribution to the study of extremal control systems 19 p2778 A72-37487

Controllability regions of linear steady system with two and three control constraints, presenting initial states set determination procedure 19 p2825 A72-37556

Existence theorems for dynamical systems admissible controls for avoidance of given set of state spaces, considering control process governed by ordinary differential equations [ASME PAPER 72-AUT-C] 19 p2778 A72-37723

Variational method in the control system invariance problem 19 p2778 A72-37990

Optimization of control and observation processes in a dynamic system at random disturbances 19 p2778 A72-37991

Fluidics control technology applications to thrust reversal, turbine engine speed, pressure valves, nozzle and fuel flow, discussing life and reliability 19 p2849 A72-38050

Digital programming techniques for maximum utility and flexibility in filament winding. 19 p2808 A72-38170

Investigation of the structure of processes in discrete automatic control systems by the application of graph theory 19 p2779 A72-38180

The output control of linear time-invariant multivariable systems with unmeasurable arbitrary disturbances. 19 p2779 A72-38231

Dynamic programming technique for simultaneous measurement and dynamic control optimization for stochastic systems 19 p2779 A72-38233

Pontryagin Minimum Principle application to stochastic optimal control problems formulated around linear systems with Gaussian noise and general cost criteria 19 p2779 A72-38234

Optimal decentralized control of two coupled linear stochastic systems, introducing fake plant white noise for weak coupling effects compensation 19 p2779 A72-38236

Transfer-characterization and the unique realization of linear time-invariant multivariable systems. 19 p2780 A72-38238

Linear control system design with parameter uncertainties, using stochastic control approach based on minimization of state vector-dependent quadratic performance index expected value 19 p2780 A72-38239

Invariant poles feedback control of flexible, highly variable spacecraft. 19 p2869 A72-38240

Variable stability simulation techniques for nonlinear, rate dependent systems. 19 p2780 A72-38241

Transfer function concept extension to analytical representation of linear time-invariant plants and controllers with multiple inputs and outputs 19 p2780 A72-38242

Suboptimal stochastic control of a class of linear distributed parameter regulators. 19 p2780 A72-38243

Hyperstability concepts and their application to discrete control systems. 19 p2780 A72-38248

Control theory stability criteria applied to discrete time feedback systems, investigating numerical integration methods for initial value problems solution 19 p2826 A72-38250

Effects of incomplete adaptation and disturbance in adaptive control. 19 p2781 A72-38263

Design techniques for model-reference adaptive control systems. 19 p2781 A72-38266

Asymptotic series solution of optimal systems with small time-delay. 19 p2826 A72-38268

On-line identification of multivariable stochastic feedback systems. 19 p2781 A72-38270

A biased filter for linear discrete dynamic systems. 19 p2781 A72-38273

The dynamic modeling technique for obtaining closed-loop control laws for aircraft/aircraft pursuit-evasion problems. 19 p2753 A72-38276

Feedback loop equations and discrete measuring point methods for synthesis of optimal control systems with location dependent controlled variables 19 p2782 A72-38311

Adaptive control systems fundamental functions, principles, characteristics and applicability 19 p2782 A72-38312

Electronic control systems flexible programming techniques based on interconnection design or on utilization of easily exchangeable program carriers 19 p2782 A72-38313

Optimal control synthesis for linear passive stationary plants with symmetrical coefficient matrices of minimized functional 19 p2782 A72-38514

Singular control problems calculation in trajectory optimization using sufficient conditions for control values set form 19 p2782 A72-38515

Discrete and continuous dynamic adaptation algorithms construction for extremal quality functional trajectory equations of adaptive control system 19 p2770 A72-38518

Optimal strategies for control of a semi-Markovian process by a set of observers 19 p2770 A72-38584

The observability of unforced physical systems by linear non-sequential estimators in the validation of linear error analysis. [AIAA PAPER 72-876] 20 p2910 A72-39123

Riccati equation asymptotic theory, deriving a priori bound dependence on information and control energy rates and state dimensions 20 p2945 A72-39347

Problem of the analytical design of controllers for parabolic and hyperbolic equations 20 p2946 A72-39468

Integral equations of a multiport network with a digital control automaton 21 p3036 A72-40154

Inverse data transformation in control problems 21 p3036 A72-40156

Linear estimation stochastic filtering and deterministic linear optimal regulation duality concept extension to problems with inequality constraints 21 p3074 A72-40228

A recursive least-squares approach to the on-line adaptive control problem. 21 p3037 A72-40640

Modal control theory for distributed parameter systems with multienginevalue assignment implemented for one dimensional diffusion equation 21 p3037 A72-40642

Necessary conditions for optimality in a general class of non-linear mixed boundary value control problems. 21 p3037 A72-40644

Selection of an optimal control law for time-lag control systems subjected to random load disturbances 21 p3038 A72-40705

Optimal risk equation and solution existence and uniqueness of dual control problems with unknown parameter and additive disturbances 21 p3038 A72-40706

Absolute instability of nonlinear pulse-amplitude modulated control systems - Frequency criteria 21 p3038 A72-40707

Probability model and causal approach to failure mechanisms and reliability of control systems applied to IC 21 p3024 A72-40711

NERVA flight engine control system design. 21 p3083 A72-40764

Probabilistic approach to design of control systems. 21 p3038 A72-41232

Mass attraction reduction by integral control in spinning drag-free satellites. 21 p3115 A72-41304

Man machine system input via human controller output transformation, illustrating with spacecraft lateral position manual control problem 21 p3010 A72-41411

Lectures on theory of manual-vehicle control. 21 p3011 A72-41418

Some contributions to the theory of linear models describing the control behaviour of the human operation. 21 p3011 A72-41419

Second order optimality conditions for variable end time terminal control problems. 21 p3039 A72-41571

[AIAA PAPER 72-932] An algorithm in the gradient method for synthesis of nonlinear control systems 21 p3039 A72-41804

Compatible controllers for time-varying linear plants. 22 p3161 A72-41939

Fluidic implementation of a perturbation extremum controller. 22 p3139 A72-42050

Optimal controller design for parabolic type second-order linear stationary systems, discussing integro-differential equation solution possibility 22 p3162 A72-42079

Differential games extremal strategies with player control action subject to integral constraints 22 p3198 A72-42090

Linear dynamic control system synthesis methods based on aggregation and suboptimal control by decomposition, considering quadratic performance criterion 22 p3162 A72-42177

An application of the theory of Lie groups in the optimal control problem for linear dynamic systems with time-variable coefficients 22 p3162 A72-42181

Global asymptotic stability of two classes of control system with pulse-width and pulse-frequency modulation 22 p3162 A72-42184

Readjustment algorithm for searchless self adaptive control system with reference standard by direct Liapunov method 22 p3205 A72-42186

A control algorithm for the orbital reentry of a space vehicle 22 p3223 A72-42206

Variational method for invariance problem solution for optimal finite state of nonlinear dynamic systems under external disturbances 22 p3162 A72-42240

Optimal control of complex time lag systems with series connected lumped and distributed parameters described by linear differential equations 22 p3162 A72-42241

Mathematical methods of man machine control system synthesis, using homeostasis and functional compatibility principle 22 p3162 A72-42243

Equations of motion appropriate to the analysis of control configured vehicles. [AIAA PAPER 72-952] 22 p3137 A72-42353

On the convergence of difference approximations in distributed parameter optimal control problems. 22 p3162 A72-42486

Analog and digital automatic control systems for aerospace and process applications, discussing transfer function and state variable methods 22 p3162 A72-42714

Limitations on the synthesis of control systems in the case of incompletely accessible state variables 22 p3162 A72-42739

Control and estimation separation in stochastic optimization, discussing Wonham observer matrix reversibility and replacement in closed and closed-open loop systems 22 p3163 A72-42740

Attitude control of satellites using the solar radiation pressure. 22 p3231 A72-42871

Closed loop pulsed automatic control system, determining discrete correcting element parameters from linear equalities 22 p3163 A72-43009

LF and HF oscillations in plasma-electron beam system, investigating instability control 23 p3317 A72-43212

Infinite-time reachability of state-space regions by using feedback control. 23 p3274 A72-43538

Extension of analytical design techniques to multivariable feedback control systems. 23 p3274 A72-43539

Some numerical results using Kalaba's new approach to optimal control and filtering. 23 p3274 A72-43543

On discrete linear time-invariant systems with singular transition matrix. 23 p3275 A72-43545

An improved general algorithm for arbitrary pole assignment. 23 p3275 A72-43546

Polynomial operators for nonlinear systems analysis. 23 p3308 A72-43599

Stability bounds for nonlinear systems designed via frequency domain stability criteria. [ASME PAPER 72-AUT-L] 23 p3275 A72-43636

Optimal minimax regulation of a dynamic system. 23 p3276 A72-43860

Linearizing compensation for nonlinear control system transformation into linear system without ap-

proximation, discussing differential operator matrix definition and random noise effects
23 p3277 A72-43945

Controllability properties of right invariant nonlinear systems described by evolution differential equation in Lie group
23 p3309 A72-43981

A method for calculating canonic realizations for linear, unsteady, discrete systems
23 p3277 A72-43989

The inverse problem of optimal process theory and the synthesis of linear optimal systems in the case of restricted phase coordinates
23 p3277 A72-44008

Application of quadratic optimization to supersonic inlet control.
23 p3251 A72-44195

Basic considerations concerning the design of control systems
23 p3326 A72-44279

Nonlinear differential equations control systems, determining conditions for observability of initial state and vector of constant parameters extended from time-varying linear systems
23 p3310 A72-44548

A study of dedicated control surfaces for direct sideforce control.
24 p3368 A72-45344

Modelled time optimal control process investigation for system with relay components, noting Hausdorff maximum principle application for optimal linear control
24 p3386 A72-45389

Duality in problems of the calculus of variations and optimal control
24 p3419 A72-45390

Maximum principle and penalty function technique for flight optimization, noting optimal control for climbing flight
24 p3369 A72-45444

Man machine control system synthesis, noting quality criteria and estimates for weighting function coefficients of optimization potential
24 p3376 A72-45508

Invariant transformation of the control laws in ergatic systems
24 p3376 A72-45510

Formation of an optimizing functional in control systems
24 p3386 A72-45511

Selection of an optimizing functional in control system synthesis
24 p3387 A72-45512

Mathematical description of a human operator in ergatic control systems
24 p3376 A72-45514

Methodical aspects of studies of ergatic differential-game systems
24 p3376 A72-45517

Differential games problem of pursuit tracking solved by invariants theory, noting explicit laws of pursuer activity control
24 p3387 A72-45518

Analytical designing of regulators for second-order nonlinear systems
24 p3387 A72-45519

Man in a control circuit during an information game synthesis
24 p3377 A72-45520

Theoretical-experimental method for parametric synthesis of director-type control systems
24 p3377 A72-45522

CONTROL UNITS [COMPUTERS]

Integrated systems approach to computer simulation with functional modules to achieve control processor independent expansion and optimization
07 p0951 A72-20331

Reliable, economical and easily operated read-only magnetic core storage devices for control computers, discussing design features
10 p1445 A72-24639

CONTROL VALVES

Directional selector valves with proportional flow control under varying load conditions, discussing hydraulic spool valves design
03 p0312 A72-13963

Hydraulic servomechanism spool type control valve orifice flow characteristics, measuring mass flow for various spool determined port shapes
07 p0915 A72-20533

F-111 aircraft landing gear and speedbrake hydraulic system control by single dual-function valve, describing design features and performance characteristics
08 p1111 A72-21024

Loaded hydraulic cylinder response to step inputs in on-off servos with three position valves, considering cavitation effect on system natural frequency [ASME PAPER 72-AUT-A]
10 p1423 A72-25052

Constant pressure gradient valves static characteristics, describing approximate procedures for flow rate determination without allowance for hydrodynamic effects
13 p1899 A72-29134

L-1011 TriStar cartridge valves and manifolds, reservoirs and hydraulic service center design for speedy maintenance and servicing
14 p2073 A72-31050

CONTROLLABILITY

Controllability of dynamic systems with motion described by nonlinear differential equations
01 p0045 A72-10500

Handling qualities simulation program for augmentor wing jet STOL research aircraft considering control devices design
02 p0154 A72-11654

Structure, controllability and synthesis of n-dimensional invariant systems under perturbation vector, using governing equations
05 p0641 A72-16352

Controllability regions of linear steady system with two and three control constraints, presenting initial states set determination procedure
05 p0690 A72-16585

General aviation type light airplanes pilot workload during steep landing approach, comparing flight tested control response parameters with handling qualities criteria [AIAA PAPER 72-125]
05 p0613 A72-16941

Model-following algorithm and equicontrollability in multivariable feedback control systems, considering application to decoupling problem
07 p0960 A72-19698

Linear dynamic control systems controllability and observability quality analysis and optimization, considering determinant, trace and maximal eigenvalue
07 p0960 A72-19699

Global controllability of nonlinear differential systems during linear system perturbation, discussing controllable and uncontrollable parts splitting and null domain nature
11 p1608 A72-25323

Structure, controllability and synthesis of n-dimensional invariant systems under perturbation vector, using governing equations
11 p1608 A72-25328

Globally controllable nonlinear differential systems arising from linear system under perturbation
15 p2264 A72-31762

State space approach to linear multivariable servomechanism problem, deriving controllability conditions and design procedure
15 p2213 A72-32801

Computational difficulties reduction in optimal control and estimation problems, discussing controllability and observability
17 p2574 A72-34417

System theory on group manifolds and coset spaces.
17 p2575 A72-34949

Controllability, observability and optimal feedback control of affine hereditary differential systems.
17 p2533 A72-34950

The maximum principle and controllability of nonlinear equations.
17 p2533 A72-34951

Controllability of linear continuous systems with a time-variable delay.
17 p2534 A72-35532

Criteria for nonlinear systems controllability in terms of state variable analytic function and derivatives, implying strong accessibility for manifolds including Euclidean spaces
18 p2673 A72-36616

Controllability regions of linear steady system with two and three control constraints, presenting initial states set determination procedure
19 p2825 A72-37556

Some effects of bias errors in redundant flight control systems.
19 p2779 A72-38237

Flying experience with the SC1 research aircraft and the P1127 prototype at the Royal Aircraft Establishment, Bedford, England.
22 p3136 A72-42324

An analysis of aircraft lateral-directional handling qualities using pilot models.
22 p3137 A72-42347

Controllability properties of right invariant nonlinear systems described by evolution differential equation in Lie group
23 p3309 A72-43981

CONTROLLED ATMOSPHERES

NT CABIN ATMOSPHERES

NT INERT ATMOSPHERE

NT SPACECRAFT CABIN ATMOSPHERES

Normal and germ free rat antibody response to sheep erythrocyte inoculation in He-O atmosphere, analyzing microagglutinin and hemolysin titres [AD-736324]
04 p0471 A72-14861

Carburization of various irons in methane-hydrogen atmosphere at 750 C, comparing activity coefficients and solubility limits
04 p0533 A72-14978

Ti honeycomb brazing, discussing filler metals, furnace temperature and atmosphere control and use of protected graphite as furnace material
07 p0998 A72-20288

Respiration in altered gas environment for spontaneous breathing and voluntarily maintained pulmonary ventilation level conditions
08 p1120 A72-22077

Autonomous combustion of Al sphere in controlled atmospheres oxygen-argon, nitrogen and air, identifying products
10 p1562 A72-24238

Hypoxia effect on aircraft pilot performance, using Link GAT 1 trainer and controlled composition atmosphere under varied altitude conditions for simulated ILS landing approaches
12 p1776 A72-28310

Calculation procedures for some parameters of space suit gas medium supply systems
21 p3006 A72-40449

CONTROLLED FUSION

Controlled thermonuclear fusion for space propulsion, discussing magnetic-confinement and laser-plasma fusion engines
04 p0556 A72-14889

Collective self fields generated from intense electron beams for high energy positive particle acceleration and Astron hot plasma confinement for fusion control
10 p1523 A72-24788

Controlled nuclear fusion plasma stabilization by electrostatic forces, reducing applied magnetic field
11 p1694 A72-25791

Electron cyclotron drift instability linear theory application to controlled fusion and collisionless shocks, proving anomalous resistance to current flow normal to magnetic field
17 p2592 A72-35624

Pulsed power - A new technology for controlled thermonuclear fusion.
18 p2715 A72-36332

Laser power and pulse duration requirements for hot plasma production by flame propagation in solid DT targets for controlled thermonuclear fusion
20 p2931 A72-39354

Laser compression of matter to super-high densities - Thermonuclear /CTR/ applications.
23 p3294 A72-43262

Pulsed laser produced high temperature plasma for electric power generation by controlled nuclear fusion, discussing gas dynamic model
23 p3321 A72-43723

Fission and fusion propulsion for deep space missions, discussing gas and colloid core reactors, controlled fusion, MHD and laser plasma systems
24 p3423 A72-45168

CONTROLLED STABILITY

U CONTROL

U STABILITY

CONTROLLERS

NT SERVOMECHANISMS

NT SERVOMOTORS

Distributed impedance controller synthesis for stabilization of plane fluid flows, investigating Rayleigh-Taylor instability
01 p0050 A72-10504

Optimal limited state variable feedback controllers design for static and dynamic linear systems [AD-738770]
02 p0198 A72-12809

Finite memory uncertain stochastic controller, developing optimal and suboptimal algorithms
03 p0329 A72-14181

Amplifier amplitude characteristic nonlinearity effect on dynamic properties of autooscillatory temperature controller
07 p0981 A72-18926

Optimal controllers analytic design for linear steady controlled differential equations system
08 p1145 A72-21467

Mathematical models for hydraulic position servo, deriving time optimal controllers
08 p1113 A72-22156

Nonlinear systems controllers design based on Liapunov functions and time domain ratio criterion, presenting digital computer algorithm
09 p1290 A72-23090

Digital control system instability caused by introduction of floating point arithmetic in controller
09 p1341 A72-23096

Recursive minimum variance linear filter and controller for systems with white state-dependent noise
10 p1455 A72-23800

Digital controller simulation by analog means with independent gain adjustment of proportional, derivative and integral modes
10 p1445 A72-24093

Meteor trail radar operated under digital controller synchronization and programmed for alternate and simultaneous two orthogonal directions search
10 p1438 A72-24715

Solid state stepping motor drive controller to provide constant angular shaft velocity for scanner applications
13 p1933 A72-29767

Graphical design technique based on Nyquist plane construction using circle criterion for nonlinear systems controller synthesis
14 p2091 A72-30375

- Solid state dc power controller design functional requirements, considering system overcurrent protection, power control by low voltage signals, power output to load status, etc 15 p2182 A72-31219
- High speed deterministic adaptive controller for linear and nonlinear plants, identifying control law from state and input data by linear regression procedure 15 p2212 A72-32794
- Sensitivity design of multiple input controller for dynamic optimization applied to linear systems with quadratic performance index 15 p2212 A72-32795
- Modularized digital controller for closed loop systems using MOS, MSI and LSI components 17 p2521 A72-34703
- Digital controller for high pressure rocket engine. 18 p2721 A72-36335
- State-feedback-controllers and state-estimators design for roll-pitch-horizontal motions of helicopter near hover, using rotor dynamics model [AIAA PAPER 72-778] 19 p2752 A72-38137
- Mass attraction reduction by integral control in spinning drag-free satellites. 21 p3115 A72-41304
- Fluidic implementation of a perturbation extremum controller. 22 p3139 A72-42050
- Attitude control of satellites using the solar radiation pressure. 22 p3231 A72-42871
- The optimal control of merging aircraft - Implementation of the hybrid air traffic controller. 23 p3277 A72-43868
- Optimal synthesis of a two-parameter continuous controller for a jet engine with an afterburner 23 p3326 A72-44284
- Use of fluidic elements for jet engine controllers 23 p3327 A72-44290
- A digital model of jet engine hydraulic fuel controller 23 p3327 A72-44291
- Aerodynamic solar semipassive hybrid system for continuous three dimensional attitude control of axisymmetric satellite in near-earth orbits, discussing operation, design and optimization 24 p3450 A72-45146
- CONVAIR MILITARY AIRCRAFT**
U MILITARY AIRCRAFT
CONVECTION
NT FORCED CONVECTION
NT FREE CONVECTION
Hydrodynamic convective stability in catalytic chemical reaction with thermal and concentration coupling dependent on Lewis number 02 p0301 A72-12092
- Gravitational convection by magnetocaloric effect in incompressible nonconducting ferromagnetic fluid 03 p0457 A72-13993
- Mountain barrier and convective area minimum size determination for numerical forecasting models, reducing primitive equations system to advection difference equation 04 p0544 A72-15459
- MHD convection in rotating electrically conducting viscous fluid layer within magnetic field, investigating linear stability 06 p0861 A72-18069
- Nonlinear initial boundary value problem for time dependent convection-diffusion equation with ionization and recombination reactions 09 p1341 A72-22472
- Mathematical model for compressed gas convection into lower atmosphere with substantial density changes 10 p1563 A72-24778
- Plasma interchange instability and convection in gravitational field, showing viscosity and resistivity stabilization and critical Reynolds number 11 p1697 A72-26584
- Latitude dependent time variations of solar differential rotation and global activity distribution asymmetry, assuming large scale convection due to angular momentum transport 13 p2046 A72-29730
- Goldberg and Unno method application to microturbulent velocity determination in stellar atmosphere with convection 13 p2047 A72-29732
- Internal gravity waves and convective instability caused by liquid layer nonuniform vertical density distribution, noting error in thermal conductivity measurement near critical point 14 p2095 A72-31008
- German monograph on mass transport in thin fluid layers covering diffusion, convection, laminar flow rate distribution, flame ionization and gas chromatography measurements, etc 15 p2216 A72-31350
- Friction term formulation and convective instability in a shallow atmosphere. 18 p2706 A72-36633

Numerical treatment of a model of the hydromagnetic dynamo with a selected system of convection in the earth's core. 23 p3284 A72-43422

CONVECTION CLOUDS

NT CIRRUS CLOUDS

NT CUMULONIMBUS CLOUDS

NT STRATOCUMULUS CLOUDS

Thermodynamic conditions for the development of convective clouds and a method of forecasting the quantity of rainfall 22 p3202 A72-42953

Mathematical formulation of ice crystal formation and propagation mechanism in seeded supercooled convective clouds 23 p3311 A72-43722

CONVECTION CURRENTS

Drift shells and pitch angle evolution of energetic particle motion in magnetospheric model including convection electric field 01 p0117 A72-10077

Ionospheric horizontal drifts during large vertical convection of mid dip-latitude postmidnight F region, using spaced antenna measurements 01 p0052 A72-10087

Flowing plasma ionization density measurement by stagnation probe, comparing measured with calculated plasma sheath convection current values [AD-738692] 01 p0110 A72-11189

Mathematical two dimensional model of vertical wind shear near convective cloud in free atmosphere 06 p0840 A72-17622

Mass and energy exchange in tropical convective cloud systems from ATS cloud photographs 09 p1344 A72-22430

Clear air turbulence association with rapid temperature change over Bahrain, suggesting convectionally induced internal wave dissipation in inversion layer as turbulence mechanism 09 p1346 A72-23424

Convective plumes model with heat flux, layer depth and surface turbulence intensity as parameters [AD-745511] 09 p1347 A72-23655

Numerical simulation of three dimensional shape-preserving convective elements from buoyancy release in incompressible fluid, using Navier-Stokes equations 12 p1839 A72-27027

Two dimensional dynamic model numerical simulation for micro- and macrostructures of moist convective clouds, comparing to field observations 12 p1839 A72-27028

Heat and momentum transfer properties and storm propagation speed under steady convective overturning in shear, considering cumulonimbus convection scale of atmospheric motion 12 p1840 A72-27704

Developing cumulus clouds annihilation, considering ascending and descending spontaneous convective streams initiated by explosions 12 p1841 A72-27989

Mathematical model of atmospheric electric clouds, calculating electric charges and fields from convection and conductivity data 13 p1996 A72-30086

Isotropic conducting plasma dynamic behavior near rotating magnetized sphere, showing electric field-produced meridional convective currents 14 p2138 A72-30630

Temperature profile derivation for uppermost convection region of two solar convection zone models from finite amplitude convection theory 16 p2451 A72-33037

Random ionization waves convective instability in glow discharge positive column, calculating fluctuations spectrum as function of position along column for localized white noise source 16 p2437 A72-33747

Lunar local surface magnetic fields production mechanism, considering convection currents due to ionization of volcanic-ash-particle flow by electrogasdynamical model 17 p2614 A72-35586

Magnetospheric convection induced longitudinal or Fermi acceleration role in nighttime auroral particle flux production mechanism 17 p2601 A72-35592

Physical and numerical experiments on layered convection in a density-stratified fluid. 17 p2543 A72-35764

Russian book - Large-scale motions in the convective zones of stars and large planets. 21 p3104 A72-40462

Atmospheric model for numerical simulation of five minute oscillation field properties of solar granular convection-excited gravity waves 21 p3107 A72-41277

Injun 5 satellite measurements of magnetospheric convection electric fields via double probe technique, discussing substantiation withOGO 6 results 22 p3174 A72-42901

Developing cumulus clouds annihilation, considering ascending and descending spontaneous convective streams initiated by explosions 22 p3202 A72-43003

CONVECTIVE FLOW

Space-time correlations of convection turbulent velocities in smooth circular duct with longitudinal separations 01 p0049 A72-10038

Venus subcloud layer, investigating radiant heat transfer in convective lower atmosphere 01 p0128 A72-10370

Asymptotic methods application to differential equations in nonlinear solar convection theory at high Rayleigh number, noting discrepancy from numerical integration 02 p0276 A72-11644

Steady state convection in solar atmosphere outer layers, plotting physical parameters as functions of geometrical depth 02 p0276 A72-11645

Conducting fluid convective motion in earth core estimated from geomagnetic field and time derivative data at earth surface 02 p0220 A72-12087

Solar hydrodynamic dynamo theories concerning convective zone large scale velocity fields and magnetic activity cycle 03 p0433 A72-13360

Large scale alternating solar magnetic field generation by outer shell convective flow, constructing oscillator hydromagnetic dynamo model 05 p0715 A72-16232

Free convection flow along infinite vertical flat plate under periodically varying suction and with fluctuating plate temperature, analyzing mean velocity and temperature profiles 05 p0747 A72-16668

Geomagnetic dipole field kinematic reversals due to cyclonic convective cell distribution fluctuations in earth core 06 p0807 A72-17895

Thin solar convection zone relation to sunspot cycle, noting magneto-kinematical model 06 p0886 A72-18099

Weakly ionized plasma instability in strong nonuniform magnetic field with convective flow and steadily oscillating final state 06 p0865 A72-18543

Thermally induced convection flow characteristics in separated or wake formation regions over heated cylindrical surface submerged in water 07 p1100 A72-19630

Radial diffusion and convection capillary model for analysis of tissue protein concentration and colloidal osmotic pressure changes during transcapillary fluid movement 08 p1114 A72-20896

Laminar free convective flow of viscoelastic fluid past infinite porous plate 08 p1151 A72-21748

Eigenmodes growth rate in convectively unstable self gravitating gas sphere, using spherical harmonic series expansion and Laplace transforms 09 p1392 A72-23545

Statistical solution of steady natural turbulent convection at large Grashof numbers 10 p1465 A72-24103

Convective motions in rotating laterally heated annulus with contacting rigid lid, determining radial temperature difference for transition to vortex regime 10 p1506 A72-24420

Conducting fluid laminar free convective flow over heated rotating horizontal plate in presence of strong magnetic field aligned with rotation vector 10 p1522 A72-24465

Joule dissipation effect on convective instability of current carrying fluid in magnetic field 10 p1522 A72-24533

Binary stars convective zones reaction to periodic gravitational fluctuations due to stellar revolutions asynchronism, using incompressible fluid plane layer model 10 p1543 A72-24631

Main sequence, red giant and white dwarf stars convective envelopes evolution, discussing mixing length theory inadequacy 10 p1545 A72-24826

Diffusion with convection for parallel wall Couette flow, using Airy functions 11 p1618 A72-26591

Apollo 14 experiments to demonstrate flow patterns of convection and heat transfer in gases and liquids under weightlessness 13 p2035 A72-28614

Convection instability in viscous incompressible liquid layer with free boundaries under modulated external force field 13 p2064 A72-28723

Convective hydromagnetic stability of hot conducting fluid layer in magnetic field by Liapunov method 13 p2011 A72-28891

Directional dependence of sound wave emission by convective turbulence in solar atmosphere, considering cut-off frequency effects on transmitted acoustic spectrum 13 p2048 A72-29926

German book on heat transfer and fluid flow, covering heat conduction and temperature distribution in

bodies of simple and complex geometries, fluid mechanics, etc

14 p2171 A72-30902

Book on extended surface thermal transfer covering heat exchanger design, convective transfer, radiation and computer programs

14 p2172 A72-30975

Concentration stress convection in slow gas mixture flow due to density gradients, noting similarity to thermal stress convection

14 p2096 A72-31015

Integral method application to convective flows with axial diffusion, obtaining heat and mass transfer characteristics

14 p2096 A72-31058

Velocity and temperature profiles of plane Poiseuille flow with finite amplitude convection and longitudinal vortices, investigating uniform axial temperature gradient effect

14 p2173 A72-31063

Steady asymptotic suction profiles in free convection laminar boundary layer flows on heated vertical circular cylinder

14 p2096 A72-31070

Plane unsteady convective motion of viscous incompressible liquid in infinite horizontal vessel of rectangular cross section due to wall temperature fluctuations

14 p2174 A72-31157

Algorithmic calculation for composition changes due to nuclear reactions and convective mixing during stellar evolution

15 p2314 A72-32374

Magnetic field effect on finite amplitude convection in fluids complying with Boussinesq approximation, discussing maximum Nusselt number shift

16 p2452 A72-33039

Model for magnetospheric substorm growth phase, noting dayside magnetopause convection onset, geomagnetic tail configurational changes and breakup with auroral electrojet development

16 p2387 A72-33903

Convective clouds fluid dynamic numerical modeling, considering plumes, thermals and vortex rings formation

[AIAA PAPER 72-651]

16 p2419 A72-34083

Atomization of liquid droplets in a convective gas stream.

17 p2540 A72-35044

Viscous dissipation effects on unsteady free convective flow past an infinite, vertical porous plate with constant suction.

17 p2637 A72-35047

On the state of the geomagnetic field and its reversals.

17 p2548 A72-35323

Shock tube investigation of low-density heated fluid element dynamic reaction to reflected shock wave passage, noting similarity to atmospheric thermals

17 p2542 A72-35615

Fluid dynamics of convective stellar envelopes.

17 p2618 A72-35933

Computer aided study of nondiffusive plane convection mixing of scalar field by isotropic turbulence of single velocity modes

18 p2678 A72-36017

Convective cells formation in fluid unsteady flow between two horizontal rigid boundaries with time periodic temperature distribution

18 p2681 A72-36483

Nusselt number dependence on Rayleigh number for steady convection in porous medium, explaining heat transport abrupt change by breakdown of Darcy law

18 p2740 A72-36484

Numerical integration of nonlinear convective flow equations for arbitrary atmospheric temperature and wind profiles, discussing cloud streets formation

19 p2828 A72-37998

Inversion of a laminar boundary layer during the injection of CO₂ through a vertical porous surface under natural convection conditions

19 p2881 A72-38191

Coriolis force influence on convective stability in viscoelastic fluid layer heated from below, contrasting with rotation effects on ordinary viscous fluid

20 p2982 A72-39326

Branching theory application to convection and axisymmetric flow formation in internally heated self gravitating liquid filled sphere

20 p2915 A72-40030

Application of Tolubinskii's integral method to the solution of boundary value problems of nonstationary convective diffusion

21 p3129 A72-41056

Influence of intracellular convection on the oxygen release by human erythrocytes.

21 p3003 A72-41625

Magnetic field and suction effects on unsteady MHD free convection flow of conductive fluid around nonconductive porous flat plate

21 p3095 A72-41787

Diffusion toward a particle in the case of shear flow of a viscous liquid - Approximation of the diffusion boundary layer

22 p3165 A72-41910

Forced-convective-flow carbon monoxide laser.

22 p3184 A72-41968

Convection instability in viscous incompressible fluid layer with free boundaries under modulated external force field

22 p3243 A72-42099

Convective instability of a fluid in hydrodynamically connected vertical channels

22 p3166 A72-42260

Convective interaction in a partially-liquid-filled vertical vessel with heat influxes in its lateral and free surfaces and bottom

22 p3244 A72-42261

Stationary spherical vortices in a perfect fluid.

22 p3167 A72-42980

The breakup of liquid droplet columns by shock waves.

24 p3391 A72-45048

Effect of a flow with a stagnation point on the rate of variation of the total entropy of a fluid mixture

24 p3465 A72-45074

CONVECTIVE HEAT TRANSFER

Venusian atmosphere heat transfer processes, calculating radiant fluxes and convective motion model

01 p0127 A72-10364

Energy spectrum equations for steady state turbulent convection model based on Heisenberg statistical theory, noting application to convection in planetary and stellar atmospheres

01 p0146 A72-11311

Split-film anemometer probe determination of convective heat transfer coefficient azimuthal dependence in low Reynolds number flow over cylinders, discussing axial heat losses

02 p0224 A72-11725

Concentric spherical heat exchanger, showing heat transfer coefficient decrease with coolant flow rate increase

02 p0303 A72-12320

Nonstationary thermoelastic stress determination in hollow cylinder walls under convective heat transfer

03 p0443 A72-13459

Heat transfer through fabrics by convection, conduction, radiation and vaporization related to skin temperature and thermal injury

03 p0319 A72-13700

Forced convective heat transfer of laminar flow in curved channel with square cross section at constant wall heat flux

04 p0510 A72-14595

Pressure and convective heat transfer distribution at air inlet central body surface, reducing Navier-Stokes equations to partial differential equations with similar solutions

04 p0596 A72-14971

Metal-rich 1.19 solar mass main sequence star evolution to convection onset in core during He flash

04 p0577 A72-15283

Temperature fluctuation structure in turbulent wake behind heated circular cylinder, investigating thermal convection, production and diffusion

04 p0596 A72-15330

Thermal load effect on convective heat transfer in turbulent flow in circular duct

05 p0742 A72-15843

Multimoment solutions to convective heat transfer from sphere, discussing maximum drag coefficient and validity at all Knudsen numbers

[ASME PAPER 71-WA/HT-1]

05 p0743 A72-15863

Ablation performance of dielectric heat shields for planetary entry, testing diffuse reflectance by convective and radiative heating

[AIAA PAPER 72-89]

05 p0747 A72-16809

Film and convection cooling interaction and effect on wall cooling efficiency for gas turbine applications

[AIAA PAPER 72-8]

05 p0748 A72-16873

Graphite ablation in combined convective and radiative heating, considering mass and energy transfer effects

[AIAA PAPER 72-88]

05 p0750 A72-16954

Local or radiative-convective heat transfer coefficient determination at porous surface in presence of two dimensional temperature field, using temperature gradient method

05 p0751 A72-17070

Convective heat flow pressure and density measurements at surface of central body of air inlet with live point and axial symmetry

06 p0755 A72-17560

Convective conductance meter for continuous measurement of outdoor exposed surface convection coefficient, using electrically heated plaques with known surface radiation properties

07 p0981 A72-18821

Convective heat transfer coefficient for particles of arbitrary shape in flow at low Reynolds number, using equivalent radius method

07 p1098 A72-18985

Transient three dimensional natural convective modes in porous media as function of Rayleigh number

07 p1099 A72-19623

Forced convective heat transfer for laminar flow of Newtonian fluid inside noncircular duct, taking into account viscous dissipation and work compression

07 p1100 A72-19628

Correlation for Prandtl number effect on laminar forced convective heat transfer with secondary flow

07 p1100 A72-19629

Branching theory application to convection and axisymmetric flow formation in internally heated self gravitating liquid filled sphere

07 p0968 A72-19973

Axial arc column interaction with shock waves and high velocity gas flow effects in forced convection, proposing heat transfer theory

07 p1047 A72-20548

Laminar natural convection heat transfer from leading edge of isothermal plate under nonuniform gravity

[ASME PAPER 71-HT-CC]

08 p1250 A72-20875

Flow field model of convective heat transfer along reattachment surface in planar supersonic turbulent flow

[ASME PAPER 71-HT-W]

08 p1251 A72-20876

Free convection velocity fields measurements and stagnation point location around horizontal torus in air, using fine particle trajectories

[ASME PAPER 71-HT-X]

08 p1163 A72-20877

Convective heat transfer from human form, using cylindrical model and aluminum statue physical replica in oven and wind tunnel air flow studies

08 p1123 A72-20892

Calorimetric gage for convective and radiative wall heat flux measurements in Ar arc plasma

08 p1254 A72-21628

Heat and mass exchange in laminar boundary layer in air-carbon dioxide binary mixture under free convection on porous heated vertical surface

08 p1255 A72-21664

Free convective heat transfer measurement from solid copper inner cylinder to cylindrical casing

09 p1410 A72-22351

Electromagnetic field forces on finite conducting bodies, discussing heating rates and temperatures with ambient air convection and machine design recommendations

09 p1359 A72-22679

Convective heat transfer between jets produced by plasmamotors and heated substrate, showing independence of plasma flow rate

09 p1319 A72-23189

Jupiter atmosphere thermospheric temperature profile from heat conduction equation, noting radiative and convective transfer

09 p1393 A72-23658

Forced convection heat transfer for turbulent flow over flat surface with attached protrusion for varying Reynolds number and boundary layer thickness

10 p1561 A72-23882

Contact binary star systems model, considering superadiabatic energy transfer mechanism of convective envelope

10 p1550 A72-25199

Finite element method for boundary value radiative and convective heat transfer problems

[AIAA PAPER 72-274]

11 p1740 A72-25214

Laminar and turbulent convective heating distributions on delta wing space shuttle boosters with interference effects

[AIAA PAPER 72-315]

11 p1567 A72-25249

Convective cooling system design for Mach 6 hypersonic transport Al alloy airframe, using water glycol loop network

[AIAA PAPER 72-334]

11 p1574 A72-25369

Nucleate pool boiling three component heat flux theory, taking into account latent heat transport, molecular heat conduction and turbulent convection

11 p1746 A72-26539

Single continuous algebraic correlation equation for convective heat transfer in cross flow for wide Reynolds number range, considering applications to hot-wire anemometry

11 p1747 A72-26541

Forced heat convection from sphere immersed in inviscid fluid stream at small Peclet number, using matched asymptotic expansions

11 p1747 A72-26669

Finite difference calculations for structure of finite amplitude thermal convection within self gravitating fluid sphere with uniform heat release

12 p1889 A72-27715

Convective heat transfer for fluid flow on plate with internal heat sources in boundary layer, solving laminar-turbulent transition equations by difference method

12 p1889 A72-28138

Boundary layer theory for convective heat transfer of two dimensional film cooling systems in turbulent regime, noting momentum, enthalpy and concentration equations

13 p2063 A72-28630

Conjugate unsteady problem of convective heat transfer for uniform flow over solid body with matching boundary conditions at interface

13 p2064 A72-28889

Calculation method for steady convective heat transfer in single-flow motion of several media, deriving equation system for characteristic directions and compatibility conditions

13 p2066 A72-29943

Weather radar observations of Alps foothill region convective precipitation development and lifetime

13 p1996 A72-30088

Mathematical model for compressed gas thermal convection into lower atmosphere with substantial density changes

14 p2170 A72-30215

Mass exchange and thermal time scales for shell source burning binary components with deep outer convective layers, interpreting numerical results from analytical model

14 p2159 A72-30739

Convective heat transfer of sphere in rarefied gas subsonic flow, comparing calculation with measurement

14 p2071 A72-31023

Free convection effect on vertical porous insulation layer thermal conductivity in high pressure gas environment

14 p2172 A72-31057

Experimental setup and flow patterns for natural convective heat transfer from plate with arbitrary inclination

14 p2173 A72-31060

Mass entrainment products effect on radiative and convective heat transfer during decomposition of graphite blunt body in steady hypersonic flow of radiating air

14 p2174 A72-31158

Microelectronic devices liquid cooling by free and forced convection, investigating component size effects on heat transfer by boundary layer analysis and experiment

14 p2091 A72-31172

Thermal load effect on convective heat transfer in turbulent flow of viscous incompressible liquid in circular tube

15 p2334 A72-31262

Convective heat transfer in fully developed MHD channel flow between two parallel electrically conducting plates

15 p2335 A72-31636

Heat transfer to two dimensional laminar flow, calculating axial conduction and fluid preheating effects on adiabatic forced convection at low Peclet number

15 p2336 A72-32478

Convective and radiative heat transfer in compressible gas boundary layer

16 p2343 A72-32995

Rotation effect on total heat transport and cell size in solar convection zone

16 p2451 A72-33038

Capillary heat convective diffusion model of liquid layer sandwiched between two planes for calculating slag and metal movement rates

16 p2476 A72-33157

Wall and ambient temperature distribution effects on free convection heat transfer from nonisothermal vertical flat plate in temperature stratified medium for Prandtl number range

16 p2477 A72-33434

Thermal convective instability in semiinfinite constant temperature viscous fluid with lower boundary suddenly heated, calculating neutral stability curve and critical Rayleigh number

16 p2478 A72-33656

Radiative and convective heat transfer for stagnation point flow of emitting carbon dioxide and nitrogen gas mixture, assuming thermodynamic equilibrium in shock layer

17 p2636 A72-34470

Flow conditioning in electric discharge convection lasers

17 p2562 A72-34638

Heat transfer by free convection from a longitudinally vibrating vertical plate

17 p2637 A72-35045

Onset of convection near a suddenly heated horizontal wire

17 p2637 A72-35048

Danckwert liquid film surface layer renewal concept as refinement of Reynolds theory of correlation between convective heat transfer and momentum transfer

17 p2637 A72-35050

Lateral heat exchange in a thermocouple

17 p2498 A72-35513

Effects of vorticity, displacement speed and curvature on heat transfer with dissipation

17 p2638 A72-35747

Calculus of variations and finite difference method for combined free and forced convective heat transfer through vertical noncircular ducts, calculating Nusselt number

18 p2741 A72-36926

Heat transfer from a slowly rotating sphere.

18 p2741 A72-36934

Unsteady-state temperature distribution in a convecting fin of constant area.

18 p2741 A72-36935

Convergence and accuracy of three finite difference schemes for a two-dimensional conduction and convection problem.

18 p2741 A72-37170

Steady state heat transfer in one dimensional flow involving simultaneous convective and diffusive transport via finite difference formulation

18 p2741 A72-37171

Convective heat exchange of metastable liquid during suspension of boiling

19 p2881 A72-38037

Forced convection heat transfer from cylinders to water in cross flow, quantifying method of accounting for fluid property variation

19 p2881 A72-38397

Heat transfer during uniform injection on a vertical surface under conditions of combined free and forced convection

20 p2982 A72-39225

Heat emission from the lower faces of plane surfaces in the presence of a steady thermal flux under conditions of natural convection

20 p2982 A72-39322

Unsteady heat transfer and temperature for Stokesian flow about a sphere.

[ASME PAPER 72-HT-C] 20 p2983 A72-39482

Film boiling correlations for stable natural convection heat transfer for various heater substances and pressures

20 p2983 A72-39487

Use of an infrared-imaging camera to obtain convective heating distributions.

20 p2926 A72-39640

Stability of convective heat transfer through horizontal air layer heated from below and constrained internally by thin walled honeycomb panels

[ASME PAPER 72-HT-60] 20 p2985 A72-39656

Heat transfer by laminar natural convection in low aspect ratio cavities.

[ASME PAPER 72-HT-52] 20 p2985 A72-39661

Transient laminar free convection in closed spherical containers.

[ASME PAPER 72-HT-37] 20 p2986 A72-39669

A digital simulation system for heat transfer modelled by ordinary and partial differential equations.

[ASME PAPER 72-HT-25] 20 p2986 A72-39673

Investigation of the mesoscale convective processes during the forthcoming GARP implementation.

20 p2948 A72-39800

Influence of thermal instability on the convective heat transfer coefficient for flows past slender bodies of arbitrary configuration

20 p2987 A72-39914

Numerical experiment of radiative-convective equilibrium of the Martian atmosphere.

21 p3105 A72-40772

Laplace transformation for unsteady convective heat transfer with nonlinear and time dependent heat transfer coefficients, obtaining nonlinear integral equation solution

21 p3130 A72-41066

Multicomponent diffusion and heat transfer in flows of a chemically balanced ionized gas past bodies

21 p3047 A72-41658

Thermal state of selectively absorbing plane gas layer blown from porous plate into stabilized turbulent high temperature gas flow, considering radiative and convective heat transfer

21 p3131 A72-41672

Studies on the convective heat transfer from a rotating disk. VI - Experiment on the laminar mass transfer from a stepwise discontinuous naphthalene disk rotating in a uniform forced stream.

22 p3243 A72-41946

Numerical analysis of the natural convection in a porous medium between two concentric cylinders

22 p3244 A72-42640

Prediction of thermal-shock resistance during heating at very high rates.

22 p3241 A72-43000

German monograph - Cooling of geometrically simple bodies / flat plate, cylinder, sphere/ by convection and radiation.

22 p3244 A72-43062

Unsteady convective heat transfer in the initial section of a pipe with a smooth inlet

23 p3356 A72-43670

Nonstationary thermoelastic stress determination in hollow cylinder walls under convective heat transfer

24 p3458 A72-44934

Response of convectively controlled burning to nonlinear disturbances.

24 p3464 A72-45055

Thermal diffusion and convective stability. II - An analysis of the convected fluxes.

24 p3465 A72-45561

CONVENTIONS

Conventions on international responsibility for damage caused by space objects, studying UN juridical subcommittee resolution

08 p1255 A72-21076

Warsaw Air Transport Convention second revision by Guatemala Protocol of 8 March 1971, discussing provisions for air carrier liability

14 p2174 A72-30821

CONVERGENCE

Step-by-step algorithmic numerical solution for nonlinear Volterra integro-differential equation, considering convergence

01 p0093 A72-11105

Stiffness matrix method application to finite deformation theory, noting convergence through use of iterative interpolation in numerical calculations

02 p0298 A72-12667

Remes algorithm modification for linear approximation problem solution, discussing geometric interpretation and convergence

03 p0381 A72-13619

Summability and absolute convergence of Fourier series in large, proving theorems on boundedness of trigonometric polynomials integral norms sequence

03 p0382 A72-13947

Nonlinear elliptical equations first boundary value problem, presenting approximation capacity and convergence of straight line procedure

04 p0538 A72-14625

Convergence of iterative schemes for calculating stress state of thin shells with allowance for nonlinear terms in differential equilibrium equations

04 p0587 A72-15048

Matrix representation of nonlinear equation iterations based on polynomial methods, considering convergence and application to parallel computation

04 p0540 A72-15373

Asymptotically diagonal systems for variational expansions applied to elliptic partial differential equations, estimating convergence rate

04 p0540 A72-15374

Infinite series summation in terms of rapidly convergent definite integrals

05 p0682 A72-15808

Vibration mode shapes and frequencies determination by finite element method using consistent and lumped masses formulations in differential equation solution, considering convergence rate

[AD-739820] 05 p0736 A72-16086

Impulse motion convergence in game theory, considering control problems of pursuit involving escape and capture

05 p0690 A72-16583

Iterative process convergence in least squares and maximum likelihood methods of processing measurements in spacecraft trajectory control, space navigation and geodesy systems

05 p0633 A72-16761

Ordinary differential equations convergent solutions growth estimates, computing error function asymptotic growth rate

05 p0683 A72-17000

Finite difference schemes with splitting operator for mixed type differential equations systems, considering solutions stability and convergence properties

06 p0839 A72-18117

Convergent power series solution in powers of time for unsteady viscous flow near stagnation after impulsive motion of bluff body from vorticity distribution viewpoint

06 p0757 A72-18135

Waveguide integral equation numerical solution by moment method, suggesting algorithm for detecting and alleviating relative convergence behavior

[AD-745595] 06 p0775 A72-18368

Convergence conditions for Galerkin method, applying to boundary value problems of structural stability and critical buckling loads

07 p1025 A72-18798

Approximating trajectory solution to state constrained optimal control problems, discussing convergence

07 p0959 A72-19289

Stochastic approximation algorithm with nonstationary regression function for signal parameter estimation, considering convergence, mean square error bound and applications

07 p1027 A72-19291

Convergence and stability criteria of monotonic difference schemes for linear parabolic differential equations with interface boundary conditions

08 p1199 A72-21286

Conductive heat transfer equation solved by finite difference scheme with uniform rapid convergence

08 p1253 A72-21458

Convergence of random number sums of independent infinitesimal multidimensional stochastic step processes to generalized Poisson processes

09 p1340 A72-22423

Sundman power series convergence enhancement in three body problem by Poincare transformation

09 p1350 A72-22482

Stochastic approximation for identification of element with second order lag, noting convergence with optimum parameter

09 p1291 A72-23371

Ritz-Galerkin procedure used for nonlinear boundary value problems solution, noting convergence of perturbed Galerkin method

09 p1343 A72-23561

Algorithm for automatic construction of finite element approximation to Laplace equation, noting convergence

10 p1502 A72-23719

Steepest descent variable step-size algorithm with dynamic programming for mean square error adaptive equalizer, noting convergence

10 p1455 A72-23794

Topology of convergence precompact on locally convex space, defining p-infratunneled spaces by Banach-Dieudonne theorem

10 p1505 A72-24113

Nonlinear transformation for improper integral calculation, noting faster convergence than linear methods

10 p1506 A72-24997

Partial orderings applications to convergence of iterative methods for solution of linear equation systems involving positive definiteness or monotonicity

11 p1677 A72-25862

Curved cylindrical shell finite element with reduced stiffness matrix, noting convergence for symmetrical and unsymmetrical loading

11 p1735 A72-25896

Schlieren observation of generation and convergence of shock waves produced in He and Ar by capacitor bank discharge in parallel rail type device

11 p1695 A72-25921

Iterative formula for constructing Liapunov functions in convergent series form

12 p1836 A72-27073

Measured and mean convergences in topological vector spaces, considering Banach space

12 p1836 A72-27176

Convergence of plate bending eigenvalue solutions from conforming displacement finite elements based on thick plate free vibration conversion to isoperimetric variational problem

12 p1879 A72-27194

Iterative solution for linear and nonlinear dc networks with independent voltage sources, noting convergence conditions

12 p1794 A72-27398

Quadratic optimal control problem solution via multipliers method, generating minimizing convergent sequence of arcs

12 p1794 A72-27509

Classical isoperimetric problem approximation via multipliers method, generating minimizing convergent sequence of arcs

12 p1836 A72-27510

Convergence rate of epsilon algorithm, using Pade table and analytic functions

12 p1837 A72-27717

Laplace equation iterative solution for boundary value problems in structural hardening and heat resistance formulation, noting convergence

12 p1887 A72-28226

Algorithmic method in ALGOL 60 for successive approximations of optimal control problems, discussing improved convergence

13 p1935 A72-28707

Inverse variants of Galerkin-Krylov method, discussing convergence patterns of approximate solutions to boundary value problems

13 p1986 A72-29063

Elastic plates and shallow shells in finite deflection, obtaining iterative solution with good convergence for thermal stresses

15 p2324 A72-31488

Bairstow Method extension with restored convergence for multiple quadratic factors using interval arithmetic

15 p2262 A72-31631

Mixed triangular finite element model for plate bending problems including shear deformation effects, discussing error analysis and convergence

15 p2326 A72-31716

Gravity anomalies interpretation by iterative data processing, discussing convergence improvement

15 p2231 A72-32347

Nonlinear equations systems iterative solution methods convergence, generalizing Varga matrix splitting technique to nonlinear mappings in Banach space

15 p2264 A72-32465

Nonparametric probability density function modeling algorithms comparison for convergence rate and limit cycle stability relative to implementation ease

16 p2367 A72-33867

Rate of convergence of several conjugate gradient algorithms

17 p2573 A72-34218

Nonlinear generalizations of matrix diagonal dominance with application to Gauss-Seidel iterations

17 p2573 A72-34220

The numerical solution of hyperbolic systems using bicharacteristics.

17 p2574 A72-34449

On the numerical solution of elliptic partial differential equations by the method of lines.

17 p2575 A72-34647

Iterative process convergence in least squares and maximum likelihood methods of processing measurements in spacecraft trajectory control, space navigation and geodesy systems

17 p2523 A72-35264

A rapidly convergent iterative method for the solution of the generalised nonlinear least squares problem.

17 p2577 A72-35849

Convergence and accuracy of three finite difference schemes for a two-dimensional conduction and convection problem.

18 p2741 A72-37170

Note on the 'alpha'-constant stiffness method for the analysis of non-linear problems.

18 p2739 A72-37172

Strong convergence in the whole of an iteration process for ordinary differential equations

19 p2825 A72-37733

Convergence of a multipoint iteration method for solving nonlinear equations

19 p2826 A72-38215

Enlarging the region of convergence of Kalman filters that encounter nonlinear elongation of measured range.

20 p2907 A72-39121

[AIAA PAPER 72-879]

Plate convergence, transcurent faults, and internal deformation adjacent to Southeast Asia and the Western Pacific.

20 p2917 A72-39479

Iterative solution of nonlinear structural problems, using convergence criteria based on displacement quantities

20 p2946 A72-39625

Book - Weak convergence of measures: Applications in probability.

20 p2946 A72-39730

Numerical solution of quasi-conservative hyperbolic systems - The cylindrical shock problem.

21 p3043 A72-40101

Modified Hestenes method of Lagrange multipliers for numerical iterative solution of mathematical programming problems in function minimizing noting improved convergence

21 p3074 A72-40226

Initial-value methods in the theory of Fredholm integral equations. II.

21 p3075 A72-40550

A computational technique for optimal control problems having singular arcs.

21 p3037 A72-40641

Investigation of the convergence region boundary in a power series of functions of two complex variables

21 p3075 A72-41090

Convergence rate estimates for the sums of random values determined in a Markov chain with absorption

21 p3075 A72-41094

Convergence of the homogeneous linear approximation method in problems of plasticity theory of inhomogeneous bodies

22 p2322 A72-41911

Polak-Ribiere conjugate gradient algorithm modifications to eliminate minimization at each iteration for efficient implementation with convergence

22 p3198 A72-41931

On the convergence of difference approximations in distributed parameter optimal control problems.

22 p3162 A72-42486

Iteration process convergence improvement based on stiffness change expression as linear combination of two matrices in structural reanalysis

22 p3235 A72-42602

Extension of the range of convergence of precise iterative methods

22 p3200 A72-43133

Widely convergent method for finding multiple solutions of simultaneous nonlinear equations.

23 p3308 A72-43400

Optimisation of contraction-mapping algorithm for calculating optimal controls.

23 p3275 A72-43607

Iterative method of computing the limiting solution of the matrix Riccati differential equation.

23 p3275 A72-43610

A general theory of convergence for numerical methods.

24 p3419 A72-45300

Best finite elements distribution around a singularity.

24 p3420 A72-45786

CONVERGENT NOZZLES

Mass blocking of subsonic isentropic swirling flow through convergent axisymmetric nozzle, considering radial velocity component effect on vorticity

03 p0342 A72-13957

Convergent conical nozzle shape effect on propulsive performance and compressible flow field internal characteristics

05 p0647 A72-15937

CONVERGENT-DIVERGENT NOZZLES

Mean velocity and turbulent fluctuation distributions for sub- and supersonic jets in convergent nozzles, obtaining sound power spectra

[AIAA PAPER 72-157] 05 p0651 A72-16872

Laminar boundary layer velocity profiles in convergent nozzle incompressible swirling flow, considering boundary layer growth effects on free stream axial and tangential velocities

10 p1471 A72-25068

Axisymmetric convergent cone profile synthesis to transform parallel flow at inlet to uniform sonic flow at outlet, examining solution convergence

15 p2177 A72-31206

Two stream ejector propulsion performance, measuring nozzle geometry effect on discharge coefficient for 2-90 deg convergence angles

[ONERA, TP NO. 1050] 15 p2177 A72-31208

Supercritical pressure convergent nozzle performance prediction by time dependent method of characteristics solution to mixed flow problem, adapting Moretti-Abbott technique

[AIAA PAPER 72-680] 16 p2346 A72-34061

CONVERGENT-DIVERGENT NOZZLES

Axisymmetric inviscid compressible transonic flow of electrically conducting, heat nonconducting gas in Laval nozzle in presence of meridional magnetic field, deriving equations for magnetic effects on dynamic flow characteristics

02 p0149 A72-11576

Numerical solution for swirling ideal gas flow in Laval nozzle, determining swirling effects on nozzle performance

02 p0149 A72-11583

Liquid and solid particle trajectory calculation in two phase Laval nozzle flows, determining density, velocity and temperature

02 p0149 A72-11588

Euler and Lagrange methods of calculation for agglomeration of particles due to velocity drop disparities among particles in Laval nozzles

02 p0149 A72-11593

Transformation of differential equations describing interaction between electric arc and gas flow by taking temperature as independent variable, considering Laval nozzle example

03 p0344 A72-14392

Convergent-divergent nozzles thrust model measurement on supersonic aircraft afterbody

[ONERA, TP NO. 978] 05 p0642 A72-15856

Lax finite difference scheme application to transonic two dimensional Laval nozzle and supersonic blunt body flow with detached shock wave, considering inviscid thermally nonconducting

06 p0756 A72-18126

Plane irrotational flow of fluid with arbitrary thermodynamic properties in throat of Laval nozzle, solving flow equations

07 p0972 A72-20111

Mixed subsonic-supersonic flows solution for choked isentropic flow in convergent-divergent nozzle, comparing results with series solution

10 p1561 A72-23721

Numerical prediction of subsonic and supersonic flow through convergent-divergent nozzle

10 p1416 A72-23874

Plane transonic gas flows through Laval nozzle and symmetrical wedge-shaped profile, solving boundary value problem by reduction to singular integral equation

10 p1418 A72-24433

Electrothermal thruster supersonic convergent-divergent nozzle performance with lithium vapor propellant, predicting exhaust velocity by isentropic flow equations

[AIAA PAPER 72-453] 11 p1708 A72-26189

Transient flow induced in convergent-divergent nozzles by shock front impingement, investigating nozzle shape and Mach number effects on formation process of reflected shock

15 p2179 A72-32143

Transient flow induced by shock front impingement on Laval nozzles observed by schlieren method, noting time variations of temperature and pressure

15 p2179 A72-32144

Characteristic parameters of stationary supersonic plasma flow in magnetic de Laval nozzle calculated for collisional and collisionless cases, measuring ion saturation currents

15 p2285 A72-32268

Influence of contraction section shape and inlet flow direction on supersonic nozzle flow and performance.

17 p2483 A72-34204

Compressible swirling flow through convergent-divergent nozzles.

17 p2485 A72-34999

A contribution to the gas dynamics of oblique shocks with change of total enthalpy.

18 p2682 A72-36725

Analysis of a transonic flow in elliptic nozzles

18 p2642 A72-36898

Turbulent diffusion in Laval nozzle, studying mixing of weakly heated jet coaxial with main flow in subsonic flow region

20 p2913 A72-39368

Critical flow rate and pressure ratio for nitrogen flowing through convergent-divergent nozzle at stagnation conditions, emphasizing thermodynamic critical region

21 p3046 A72-41180

Nonsymmetric flow in Laval-type rocket nozzles, deriving formulae for optimum nozzle design with neutralized lateral forces and turning couples

24 p3359 A72-44675

CONVERTAPLANES

U/VSTOL AIRCRAFT CONVERTERS

Dc-dc converter input filter requirements and design for spacecraft power processing equipment

01 p0007 A72-11058

Electropneumatic converter for pneumatic pulse transformation into dc or ac signal, using corona discharge current

03 p0311 A72-13556

Self oscillating dc-to-dc converters performance and design, considering switching frequency, duty cycles, line and load regulation and peak-to-peak ripple

04 p0465 A72-14487

Regulated dc-to-dc converter for voltage step-up or step-down with input-output isolation, using bistable comparator output voltage control through encoder

04 p0465 A72-14488

Self oscillating dc-dc converter analysis and optimal design, modeling by single loop nonlinear feedback system

04 p0465 A72-14571

IC microcircuit for time-pulse voltage converter for conversion of dc voltage into electric pulses of length proportional to input signal

06 p0784 A72-17836

Flashlamp pumped dye-doped polymethyl methacrylate laser thermal and photochemical effects decrease and peak power output increase by light converter

07 p1002 A72-19206

Diode half wave rectifier for ac-to-dc signal conversion in electronic voltmeter

09 p1306 A72-22343

Quadratic logarithmic converter used with linear microammeter for decibel scale noise measurements

09 p1306 A72-22344

Voltage-frequency converter network design and operation, presenting circuit diagram

10 p1453 A72-24817

Condenser charging by dc-dc converter consisting of SCR series inverter, transformer and rectifier-filter circuit, considering power consumption

11 p1577 A72-25278

SCR trigger circuits design generating short control pulses for converters based on SCR elements, presenting circuit diagrams

11 p1603 A72-25280

Forward loop signal attenuation and phase shift diagrams for design of feedback amplifier and compensation network for dc flyback converter

13 p1899 A72-29110

Open circuit voltage transfer function synthesis to realize arbitrary real rational function in complex variable, using generalized positive impedance converter

15 p2211 A72-31847

Characterization of a bilateral DC converter as a DC transformer.

17 p2497 A72-34705

Generalised method of harmonic reduction in a.c.-d.c. converters by harmonic current injection.

18 p2648 A72-37209

On the performance and design of self-oscillating dc-to-dc converters.

19 p2754 A72-37850

A digital computer simulation model for an SCR dc to dc voltage converter.

19 p2754 A72-38267

Network analysis and frequency response of LF filter with distributed RC structure and voltage converter

22 p3158 A72-42120

CONVEXITY

Laser with convex-plane resonator and cross sectional variable mirror transmission, showing effective transverse mode selection and diffraction divergence

02 p0239 A72-12767

Convex figures in mathematical geodesy, applying function h for ellipse and ellipsoid of revolution

03 p0351 A72-14328

Conditional expectation and integral of random closed convexity in probability space

06 p0839 A72-17555

Reinforcing fiber frame incurvation influence on elasticity and thermal expansion coefficients of composite material

08 p1194 A72-21754

Adjustable structure model for parameter adaptive control, noting convexity of performance index function over evaluation interval

10 p1455 A72-23793

Weakly complete projecting convex cone, considering operators subalgebra representation

13 p1987 A72-29776

Ubiquitous convex groups of real vectorial space of infinite dimension, obtaining characterization via decomposition family concept

13 p1987 A72-29777

Dense convexes class characterization in real seminormalized space on basis of decomposition family concept

13 p1987 A72-29779

Boundary minorizing of the solution of an equation connected with the Signorini problem

18 p2704 A72-36466

Laser with convex-plane resonator and cross sectional variable mirror transmission, showing effective transverse mode selection and diffraction divergence

20 p2931 A72-39073

Differential equation solution existence in complete locally convex topological Hausdorff vector space defined by saturated seminorms

21 p3076 A72-41783

The branch and boundary method as a regular method of solving irregular problems of mathematical programming. I

22 p3198 A72-42188

Analytic continuation of functions over infinite dimensional domains, covering Banach manifolds, hypoanalytical mappings, convexity and topology

24 p3418 A72-44827

Duality in problems of the calculus of variations and optimal control

24 p3419 A72-45390

CONVOLUTION INTEGRALS

Isotropic incompressible turbulence numerical simulation, presenting algorithm for convolution sums calculation

02 p0205 A72-12367

Convolution type integral equations over arbitrary finite segment number with kernels, showing solvability in spaces, applications and correctness

02 p0294 A72-12430

Gaussian periodic data optimal smoothing, describing convolution kernel and computer program

03 p0381 A72-13200

Periodic integral convolution equations in elasticity theory and mathematical physics, demonstrating solution existence

05 p0739 A72-16589

Monte Carlo and convolution methods for statistical analysis of ladder filters, describing programs for determining attenuation probabilistic distribution as function of components dispersions

09 p1289 A72-23679

Radiographic image enhancement based on mathematical concepts of image convolution, Fourier transformation and spatial frequency filtering, discussing hardware and computer needs

10 p1481 A72-24322

Fourier transformations for convolution integral calculation in image distortion correction by ground visual observations of solar intensity distribution, noting successive approximations method

13 p2046 A72-29726

Periodic integral convolution equations in elasticity theory and mathematical physics, demonstrating solution existence

19 p2872 A72-37561

Recent results in convolution feedback systems.

23 p3276 A72-43861

CONVOLUTIONS [MATHEMATICS]

U CONVOLUTION INTEGRALS

CONVULSIONS

Functional development of the altitude convulsion mechanism in mice and rabbits /Research note/.

18 p2650 A72-36445

COOLANTS

NT ENGINE COOLANTS

Nonflammable coolants for Saturn instrument unit environmental control systems, considering component materials compatibility with selected dielectric fluids

01 p0091 A72-10769

Concentric spherical heat exchanger, showing heat transfer coefficient decrease with coolant flow rate increase

02 p0303 A72-12320

Coolant flow and heat transfer in rotating circular cylindrical enclosure, solving Navier-Stokes and energy equations by finite difference formulation

06 p0802 A72-18189

Transient processes in heat exchanger, allowing for coolant variable density

09 p1410 A72-22413

COOLING

NT AIR COOLING

NT EVAPORATIVE COOLING

NT FILM COOLING

NT GAS COOLING

NT LIQUID COOLING

NT QUENCHING [COOLING]

NT RADIANT COOLING

NT REGENERATIVE COOLING

NT SODIUM COOLING

NT SUPERCOOLING

NT SURFACE COOLING

NT SWEAT COOLING

NT THERMOELECTRIC COOLING

NT THERMOMAGNETIC COOLING

Logarithmic equation for iron meteorite cooling rate determination from kamacite bandwidths and Ni concentrations

01 p0126 A72-10102

Leg cooling effect improving tolerance to positive headward acceleration in sitting position

04 p0479 A72-15210

Radiative cooling effects on flow field and heat transfer behind reflected shock wave

[AD-737423] 04 p0597 A72-15338

Tangential blowing and wall cooling effects on axisymmetric models flow separation at Mach 6, comparing pressure distribution with Busemann formula

05 p0601 A72-16227

Unidirectionally and cross rolled Ti alloys elastic properties anisotropy during cooling, discussing Young modulus distribution

06 p0834 A72-18666

Gas kinetic cooling by absorption of carbon dioxide laser radiation, explaining by vibrational energy transfer and relaxation rates

07 p1000 A72-19046

Transistor power amplifier for 2.5 GHz range directional transmitters, noting cooling problems elimination

08 p1140 A72-21306

Si diode array vidicon for ground based and spaceborne planetary and stellar imaging, noting integration time, storage and slow scan capabilities extension through cooling

08 p1171 A72-21970

Growth rate of semiconductor epitaxial films obtained by forced cooling from liquid phase

09 p1372 A72-23360

Bending stress in oxygen pressurated Nb during oxidation, cooling, dissolution and annealing, using thin film model

11 p1658 A72-25853

Compact photomultiplier housing with controlled cooling, discussing temperature control and measurement

12 p1806 A72-27265

Heat transfer dynamics during cooling of thin vertical plates, observing boundary layer formation and motion

13 p2065 A72-29454

Charge carrier cooling in nonhomogeneous semiconductors by static electric field, plotting average electron temperature as function of current

14 p2142 A72-30362

X ray and metallographic analyses of Ni-Mo, Ni-Ta, Ni-Nb, Ni-Zr and Ni-Ti alloys crystallized at high cooling rates, observing metastable phases

14 p2115 A72-30405

Temperature distribution and heat dissipation calculations for CW and pulsed laser optical elements

16 p2403 A72-33982

Flat plate leading edge blunting and wall cooling effects on supersonic laminar flow ramp-induced separation

16 p2344 A72-34032

Rates of solidification of Apollo 11 basalt and Hawaiian tholeiite.

20 p2967 A72-39181

Cooling associated with minority carriers exclusion effect in semiconductors, discussing influence of electroconductivity and forbidden bandwidth

21 p3097 A72-40788

Elastomeric problems for multiply-connected plates with heat dissipation at both plane surfaces.

21 p3121 A72-41237

Peclet number, length/diameter ratio, Grashof number, Knudsen number, overheat ratio and yaw angle interaction effects in cylindrical hot-wire and hot-film probes cooling

21 p3057 A72-41620

Determination of the optimum concentration level of solar radiation in solar batteries with different types of cooling

22 p3140 A72-43189

Three dimensional temperature distribution of internally cooled hollow airfoil section turbine blades, deriving heat transfer equations for digital computation

23 p3325 A72-43667

Influence of the cooling rate after sintering on the structure and properties of the ZrGr₁Si₂5 cermet

23 p3303 A72-44014

COOLING FINNS

Optimal radiative capacity of star shaped radiator with mirror reflecting surfaces for vacuum cooling of elongated finned bodies

02 p0304 A72-12867

Radiator fins for cooling electronic equipment elements, calculating design parameters effects on heat transfer efficiency

05 p0746 A72-16198

Radiative heat transfer characteristics of optimal geometry radiating stainless steel fin

07 p1098 A72-18997

Straight fins with periodic base temperature variation, calculating design parameters effects on heat transfer rates, temperature distributions and efficiencies [ASME PAPER 72-HT-E]

20 p2983 A72-39484

- The effect of thermal conductivity and base-temperature depression on fin effectiveness. 20 p2983 A72-39489
- Temperature distribution and heat flux in infinite length rectangular and finite length cylindrical fins, examining validity of one dimensional approximation 22 p3243 A72-41961
- ### COOLING SYSTEMS
- Forced air cooling of cylindrical body with distributed thermal input, calculating temperature distribution and optimum mechanical dimensions for temperature rise minimization 02 p0189 A72-11560
- Radiative cooling system for nearly spherical or polyhedral bodies using radially attached diverging conical elements 02 p0304 A72-12863
- Thermal control methods for high density packaging, discussing cooling techniques for hybrid circuit consisting of semiconductor chips and/or thin film components 03 p0337 A72-14293
- Nerve structures localized cooling device using vacuum insulated closed circuit controlled cryogenic probe with cooling range of plus/minus 20 C 04 p0481 A72-15252
- Heat transfer rate prediction in cooling system design for gas turbines [AIAA PAPER 72-10] 05 p0707 A72-16865
- Two phase heat transfer in porous metal transpiration cooling system, comparing measured with calculated temperature distribution [AIAA PAPER 72-25] 05 p0749 A72-16916
- Gas turbine blade cooling channel hydraulic resistance calculation based on energy and continuity equations 05 p0707 A72-17061
- Porous cooling unsteady state problem approximation based on elementary thermal balance concept, solving differential equations by computerized Euler method 06 p0904 A72-18513
- Thermal radiative cooling system characteristics determination, taking into account surface material thermal conductivity and blackness degree dependence on temperature 10 p1561 A72-23840
- Capillary evaporation cooling system with water as working medium, measuring effectiveness in terms of heat flux density vs water consumption [DFVLR-SONDDR-112] 10 p1561 A72-24023
- Cooling system based on vaporization of solar cell preheated solution drawn through chamber with atomizing injector 10 p1422 A72-24314
- Experimental cold plates provided with heat pipes for thermal control of electronic equipment [AIAA PAPER 72-269] 11 p1740 A72-25210
- Heat pipe applications for waste heat rejection, cooling and temperature control in space shuttle, discussing design and performance [AIAA PAPER 72-272] 11 p1725 A72-25212
- Convective cooling system design for Mach 6 hypersonic transport Al alloy airframe, using water glycol loop network [AIAA PAPER 72-334] 11 p1574 A72-25369
- Thermodynamic coupling effects on temperature distribution, Nusselt number and cooling requirements in laminar nonisothermal pipe flow with coolant injection 11 p1745 A72-25734
- Energy capacity margin of heat absorbing liquid /water/ in cooling system, considering specific heat and maximum critical heat flux 11 p1747 A72-26969
- Test apparatus and technique for assessing Peltier thermoelectric cooling device operational characteristics 12 p1755 A72-27721
- Cryogenic microwave equipment for solids study provided with adiabatic demagnetization cooling system, noting relaxation time measurement in magnetic fields 12 p1796 A72-27856
- Boundary layer theory for convective heat transfer of two dimensional film cooling systems in turbulent regime, noting momentum, enthalpy and concentration equations 13 p2063 A72-28630
- Russian papers on cooled high temperature gas turbines covering engine theory and design, power plants development, heat transfer and air cooling systems 13 p2029 A72-29925
- Apollo 16 lunar surface magnetometer cooling system variable conductance heat pipe/radiator design and thermal performance [AIAA PAPER 72-271] 14 p2171 A72-30828
- Satellite sensor cooling systems, considering cryogenic heat pipes, sublimation, radiation cones and surface treatment 15 p2319 A72-31240
- Space simulation shrouds cryogenically cooled with liquid carbon dioxide, discussing automatic temperature control and operating cost savings 15 p2214 A72-32611
- Fusion reactor RF heating below 100 MHz, discussing coil structures and arcing and cooling problems in main fusion region 16 p2433 A72-32813
- Fabrication and testing of tungsten heat pipes for heat pipe cooled reactors. 17 p2636 A72-34596
- Performance of low pressure ratio ejectors for engine nacelle cooling. [SAE AIR 1191] 18 p2721 A72-36530
- Cryopump cooling requirements, refrigeration, design and vacuum application, considering Brayton, Claude, Stirling cycles and Joule-Thomson and regenerative processes 18 p2696 A72-36838
- Russian book - Optimization of thermal circuits of complex gas-turbine power plants 19 p2848 A72-37450
- Temperature field of a gas turbine rotor blade externally cooled by an air-liquid mixture 19 p2849 A72-38043
- A novel specimen stage permitting high-resolution electron microscopy at low temperatures. 21 p3051 A72-40218
- Design modeling of external and internal cooling systems for bodies exposed to high temperature gas flow, discussing operation similarity conditions 21 p3129 A72-41052
- Dimensionless pressure method to account for air density variations in gas turbine cooling system design 21 p3099 A72-41059
- Thermal energy dissipation in artificial antennas of large broadcasting transmitters studying cooling systems 23 p3278 A72-44311
- Experimental study of heat transfer during cooling of a high-temperature gas flow in a pipe. 23 p3357 A72-44539
- Heat release and resistance of the cylindrical heat exchangers of blades with a dual flow cooling system 24 p3434 A72-45625
- ### COORDINATE SYSTEMS
- #### U COORDINATES
- ### COORDINATE TRANSFORMATIONS
- Laser station coordinate and Geos B satellite position compensation with simultaneous optical and laser observations 02 p0219 A72-12045
- Coordinate transformation for decoupling equations for tangential electric and magnetic field propagation through series of uniform cylindrical layers with arbitrary properties 07 p0946 A72-19799
- Coordinate mapping for solutions of Einstein initial value problem for vacuum gravitational fields 09 p1350 A72-22471
- Correction procedures for spherical surface transformation on plane for high altitude aerial photographs 09 p1310 A72-22948
- Metric tensors as alternate to coordinate transformation equations for computer program inputs in automatic problem formulation 10 p1443 A72-23923
- Coordinate transformation equations derivation to determine third orthogonal velocity component from measurements at common point by two rotationally displaced laser Doppler velocimeter systems 11 p1629 A72-25308
- Holographic method of character recognition, describing transformation from real space Cartesian coordinates to characteristic space 12 p1846 A72-27955
- Regularizing time transformation for conservative systems reduction to normal coordinates, studying normal configurations existence in terms of Hamiltonian structural properties 13 p2002 A72-28714
- Three dimensional orthogonal coordinate system transformation by simultaneous independent small angle axes rotation using transformation matrix 16 p2424 A72-33249
- Coordinate perturbation and multiple scale techniques application to supersonic flow field around two dimensional wing and oscillations in closed tube 16 p2379 A72-33576
- Control function improvement method for flight dynamics variational problems solution, discussing dynamic programming, trajectories with uncontrolled elements and coordinate transformation 17 p2607 A72-35036
- Geocentric coordinates transformation from system related to mean pole and mean equator into instantaneous pole and instantaneous equator system, noting Cartesian coordinates 17 p2548 A72-35359
- Coordinate transformation for perturbation analysis of elastic structural system imperfections influence on elastic buckling 18 p2732 A72-36079
- Gravitation theory in terms of scalar and tensor field, noting Lyra general reference system transformations and scale invariance 18 p2711 A72-36713
- Influence of the reference catalog system on the coordinates of determined stars in zonal meridional observations 19 p2861 A72-37974
- Error analyses of Euler angle transformations arising in design of precision pointing systems, guidance sensors and instruments with gimbals [AIAA PAPER 72-851] 20 p2949 A72-39078
- Differential equation reduction via coordinate transformation to algebraic form for problems characterization in elastic shell Cosserat surface theory 21 p3119 A72-41103
- Projective properties of holographic imaging. 24 p3401 A72-44767
- On the use of a coordinate transformation for analysis of axisymmetric vibration of polar orthotropic annular plates. 24 p3457 A72-44883
- Hyperbolic space criterion for cosmological model based on axioms conforming to special and general theory of relativity, noting coordinate transformation 24 p3439 A72-44969
- The use of complex coordinates in the study of rotor dynamics. [AIAA PAPER 72-954] 24 p3369 A72-45413
- ### COORDINATES
- #### NT ASTRONOMICAL COORDINATES
- #### NT CARTESIAN COORDINATES
- #### NT GEOCENTRIC COORDINATES
- #### NT GEODETIC COORDINATES
- #### NT LAGRANGE COORDINATES
- #### NT PLANETOCENTRIC COORDINATES
- #### NT POLAR COORDINATES
- Laser station coordinate determination by geometrical method and satellite observations 02 p0219 A72-12046
- Covariance matrix of coordinate fluctuations of instantaneous radar center of reflection from set of scatterers 04 p0487 A72-15144
- Unified coordinate system for earth planetary distribution of F2 and sporadic E layer transmission parameters, suggesting geomagnetic longitude and modified magnetic inclination 08 p1153 A72-20726
- Mixmaster world model with arbitrarily moving matter, using coordinate system with matrix of reference point components of three dimensional metric tensor 08 p1237 A72-21714
- Dimensional analysis pi-theorem local generalization by Lie transformation group investigation, constructing local canonical coordinate systems to obtain factoring properties of certain functions 10 p1503 A72-23921
- Geomagnetic invariant coordinates and related field line parameters calculation via field model and fast numerical method 12 p1803 A72-27771
- Magnetic apex coordinate system for plasma density organization in low and middle latitude F2 region 13 p1951 A72-29395
- Coordinate functions in Kantorovich variational method, noting application to stationary heat conduction boundary value problems 14 p2170 A72-30592
- Time dependent orthogonal coordinate system rotation by unit vector along effective axis, obtaining angular velocity and effective angle interpretation 15 p2275 A72-31590
- Poisson equations solution in orthogonal curvilinear coordinate systems to allow Laplace and Helmholtz equations separability, applying to hydrodynamic, electrostatic, electromagnetic and MHD problems 15 p2278 A72-32249
- Exposure calibration, orientation and point coordinate distortions in aerial photographs from one or two camera stations 15 p2240 A72-32378
- Algorithms for photogrammetric model coordinates variance and covariance estimation, considering convergence properties 16 p2384 A72-33029
- Unified coordinate system for global distribution of F2 and sporadic E layer transmission parameters, suggesting geomagnetic longitude and modified magnetic inclination 19 p2791 A72-38354
- Harmonic frames of reference in Einstein's theory of gravitation 20 p2953 A72-39406
- Determination of the covariance matrix of the spatial coordinates of points of a geometrical model 24 p3397 A72-44867
- ### COORDINATION
- Eye-hand coordination modifiable parameters under optical distortion conditions, deriving quadratic equation for hand response adaptation 02 p0167 A72-11897
- ### COPILOTS
- ### U AIRCRAFT PILOTS
- ### COPOLYMERIZATION
- Acrylamide polymerization - New method for determining the oxygen content in blood. 24 p3376 A72-45376

COPOLYMERS

Carbonized and ion beam thinned polyacrylonitrile copolymer fibers examination by low angle electron scattering electromicroscopy technique
09 p1339 A72-23190

COPPER

Mechanical response of Al and Cu under complex strain histories conditions, using endochronic theory of viscoplasticity without yield surface
03 p0444 A72-13504

Cu single crystal fatigue life explanation by work hardening using statistical theory of slip
03 p0379 A72-14258

Annealing effects in plated -wire memory elements, investigating Cu and Permalloy interdiffusion at low temperatures by X ray diffraction and electron beam microprobe
04 p0503 A72-15715

Compressive strength of Cu-W fiber metal matrix composite as function of temperature, comparing to cermets
06 p0832 A72-18363

Composite plasma sprayed coatings of Cu, Ni and boron nitride, noting anfriction and wear characteristics
06 p0822 A72-18429

Cu electrical resistance and heat content oscillographic measurement, using high voltage pulse method
07 p0981 A72-18804

Coaxial plasmatron with central electrode composed of cylindrical Cu and W thermionic cathodes, noting thermal efficiency
08 p1214 A72-21455

Copper, zinc and aluminum mechanical properties comparison by cyclic and steady state compressive load tests, noting stress-strain curve relationship to strain rate
08 p1188 A72-21921

Corrosion effects evaluation from electrode potentials, noting copper pitting and weathering
08 p1189 A72-22108

Electron microscopic study of cyclically deformed Al, Cu, Al-Mg-Zn alloy and carbon steel dislocation structure
10 p1494 A72-23830

Critical aspect ratio of W fiber in copper matrix for stress rupture applications
11 p1654 A72-25482

Niobium diffusion into copper as function of time and temperature, obtaining rates by electrical resistance measurements
12 p1828 A72-27448

Three dimensional heat propagation problem of copper electrode destruction under concentrated heat flux with allowance for metal evaporation
12 p1890 A72-28175

Thermal effects on phase structure of welded joints of Al alloy with Cu addition
13 p1978 A72-29022

Cu surface contamination effect on hot crack susceptibility and weldability of Co based superalloys
13 p1965 A72-29419

Zr-Cu-Mo system phase diagram from microscopy, X ray analysis and mechanical tests, noting beta solid solution transformation into alpha, omega and beta phase mixtures
14 p2122 A72-30978

X ray photoelectron spectroscopic measurements of Fe and Cu valence states produced by ion sputtering reduction, applying to multiplet splitting and isoelectronic shifts
16 p2389 A72-33026

Fracture-surface energy model for Cu-W fiber metal matrix composites, using plastic flow analysis
16 p2470 A72-33613

Thermal conductivity of W wire reinforced Cu as function of W content
16 p2411 A72-34017

Plastic anisotropy quantitative calculation formula verified on Cu, Ni and Al, discussing physical sense of coefficients
18 p2735 A72-36475

L-S coupling interpretation of high-resolution LMM Auger spectra of Cu and Zn
19 p2846 A72-38597

High energy electrons monokinetic beam propagation in Cu and Al crystals, investigating critical voltage effect on contrast
21 p3069 A72-41342

The influence of grain and twin boundaries in fatigue cracking
21 p3069 A72-41350

Effect of grain size on the thermal diffusion of copper in aluminum
22 p3193 A72-43036

Inelastic effects during metal fatigue
22 p3195 A72-43156

Compressive strength of Cu-W fiber metal matrix composite as function of temperature, comparing to cermets
24 p3416 A72-45750

COPPER ALLOYS

NT BRASSES

NT BRONZES

Ordered Cu-Au alloy atomic order parameters, using field ion microscopy
04 p0560 A72-14548

Al-AlCu intermetallic unidirectionally solidified eutectic composite structure and heat treatment effects on room temperature tensile properties
05 p0676 A72-17104

Age hardened Al-Cu single crystal anisotropy from stress-strain curves, using plane strain compression tests
05 p0677 A72-17106

Cu contents effect on Ti-Cu alloys physical and mechanical properties, discussing beta phase decomposition during annealing
07 p1012 A72-19574

Interfacial dislocations and failure in tension of directionally solidified Al-Cu-Mg eutectic
07 p1016 A72-19937

Internal oxidation behavior of Cu-Cr-Si ternary alloys microstructure comparison with Cu-Si binary alloys, discussing oxide-matrix interface nucleation
07 p1021 A72-20439

Hydrogen embrittlement of stable austenitic Ni-Cu steel, observing intergranular decohesion in fractured specimens by microfractography, electron microscopy and X ray crystallography
07 p1021 A72-20485

Guinier-Preston zone nucleation and growth as function of vacancies in Al-Cu alloy
08 p1190 A72-22166

Fracture toughness tests on Al-Cu alloy plate, noting insensitivity to strain rate
09 p1328 A72-22913

X ray spectral analysis of Ti-Cu alloys electronic structure
09 p1329 A72-23043

Differential sputtering yield of Ni-Cu alloy solid solution bombarded by Ar ions
10 p1495 A72-24057

Micrographic observation of Al and Al-Cu intermetallic dendrites shape at birth in liquid of nearly eutectic composition
10 p1496 A72-24239

Sintering and aging effects on mechanical behavior of low carbon copper steel
10 p1488 A72-24696

Cold working effect on precipitation-recrystallization interaction in Cu-Ni-Zn alloy, discussing superposed strengthening mechanism during annealing
11 p1641 A72-26738

Cold working effect on Cu-Ni-Si-Mg and Cu-Ni-Si-Cr alloys age hardening behavior, presenting hardness and tensile strength vs aging time at 350 and 400 C
11 p1662 A72-26743

Quenched powder metallurgy of high strength-high conductivity wrought Cu-Zr and Cu-Zr-Cr alloys, using nitrogen atomization
13 p1974 A72-28659

Co-Cu alloy phase formation and separation morphology changes with temperature and anomalous diffusive X ray scattering in solid solutions
13 p1976 A72-28905

Martensitic transformation in Cu-Al-Ni alloy thin film, investigating gamma-prime phase substructure formation and crystal growth pattern
13 p1976 A72-28907

Cu-Al-Ni alloys single crystals internal friction temperature dependence during martensitic transformations
13 p1977 A72-28912

Chemical bond in Cu-Ti intermetallic phases, from X ray K absorption edges studies
13 p1981 A72-29914

Gamma-prime phase crystal structure in Cu-Al-Ni alloy from electron microscopic study, noting twinning and substructure during formation
14 p2115 A72-30406

Al-Cu alloy structural changes after long term natural aging by X ray diffraction analysis
14 p2115 A72-30413

Quenching rate and alloying element content effects on precipitation extent and corrosion resistance of Al-Cu alloys, discussing microstructure, chemical composition and mechanical properties
14 p2119 A72-30604

Structural decomposition and hardening of supersaturated Al-Cu, Al-Cu-Ag, Al-Zn, Cu-Sn and Cu-Ni-Co solid solutions
15 p2255 A72-31565

Al-Cu-Mg alloys room temperature age hardening, determining effects of tension load up to plastic deformation from measurements of mechanical properties and electrical resistance [DFVLR-SONDDR-188]
16 p2408 A72-33674

Crack propagation in Al-Cu-Mg alloy sheet under vibratory bending loads, noting crack length to loading cycles number relationship
16 p2408 A72-33677

Chill zone structures in Al-Cu alloys as function of heat sink, surface microprofile and liquid metal fluid flow
16 p2409 A72-33810

Amorphous structure analysis of sput quenched Cu-Zr noncrystalline phase, using electron microscopy
16 p2410 A72-33814

Study of certain features of the electronic structure of the ternary alloys Ni₃/Mn, Fe/ and Ni₃/Mn, Co/
17 p2568 A72-35518

Complexonometrical analysis of molybdenum aluminides and Cu-Mo alloys without preliminary separation of components
18 p2655 A72-36097

Mercury embrittlement of age-hardened Cu-1.9 wt pct cobalt and Cu-3.6 wt pct titanium
20 p2938 A72-39296

Thermoelastic martensite caused elastic vibration damping in Cu-Al-Ni alloy, observing shape memory effect
22 p3190 A72-42442

Heat-resistant copper-base alloys containing rare-earth and high-melting metals, characterized by high electrical conductivity
22 p3192 A72-42819

COPPER COMPOUNDS

NT COPPER OXIDES

NT COPPER SULFIDES

Laser induced chemical decomposition of copper maleate and fumarate and fragment reaction with low hydrocarbons, comparing with thermal heating
10 p1433 A72-23951

Effect of copper, cobalt and manganese salts on certain morphological-biochemical components of the blood in young sheep of the Hissar breed
20 p2893 A72-40075

COPPER YOUNG

Optical emission spectrum of Ba and CuO combustion products during nozzle expansion into vacuum
01 p0146 A72-11312

COPPER SULFIDES

Copper sulfide-cadmium sulfide single crystal photovoltaic heterojunctions, showing optically induced and thermal effects on short circuit current degradation
03 p0389 A72-13603

Photovoltaic effect and energy band model of solar cell cadmium-sulfide-copper-disulfide heterojunctions
12 p1855 A72-28007

Thin film Cu-CdS solar cell electrochemical plating potential and solution composition effects on copper sulfide surface layer formation and cell efficiency
12 p1855 A72-28008

Postdip heat treatment effects on thin film copper sulfide-cadmium sulfide junction solar cells spectral response, diode parameters and resistance
12 p1855 A72-28010

Recombination diffusion length of minority carriers in thin layer cuprous sulfide solar cells
12 p1856 A72-28011

Improved efficiency of cadmium sulfide-copper sulfide thin film solar cells, noting optimization of layer formation, gridding and encapsulation
12 p1756 A72-28016

Trapped charge effect on photovoltaic properties of copper sulfide-cadmium sulfide single crystal heterojunction in terms of tunneling by photocapacitance technique
15 p2294 A72-32520

Preparation and properties of nonheat-treated single crystal Cu₂S-CdS heterojunctions
17 p2595 A72-35331

Photovoltaic properties of single-crystal CdS-Cu₂S cells
22 p3214 A72-42457

CORDAGE

Axial cords effects on parachute drag and stability characteristics and opening time, discussing wind tunnel and balloon drop tests results
01 p0004 A72-10306

Parachute canopy fabrics and rigging lines cordage properties requirements, considering nylon, polypropylene, silk, cotton and nonwoven scrim-reinforced fabrics
01 p0005 A72-10314

CORDITE

U COLLOIDAL PROPELLANTS

U DOUBLE BASE PROPELLANTS

CORE FLOW

Flow characteristics of colloid core reactor rocket engine, studying two component vortex flows with solid to gas mass density ratios over 100 [AD-735527]
01 p0100 A72-11359

Multicellular viscous vortex core embedded in unsteady outer potential swirling flow, obtaining numerical solution
02 p0253 A72-11971

Thin liquid layer linear hydrodynamic stability in vertical rotating tube with core gas flow
02 p0303 A72-12353

Inviscid variable density core flow in thin compressible boundary layer near stagnation point of smooth blunt body
05 p0601 A72-16216

Spectral measurements of jet turbulence noise in core and annular mixing region, using subsonic test experiments [AIAA PAPER 72-158]
07 p0966 A72-18957

Aerodynamics of vortex chambers with symmetrical air injection, discussing core and end boundary layer flows interaction and momentum loss from end surfaces friction

09 p1260 A72-22676

Trailing vortex core decay with axial injection as function of momentum flux parameter

09 p1261 A72-23623

Fully developed laminar flows in ducts with secondary motions, considering annuli with rotating core, pipe with swirl generator and straight rectangular duct

10 p1463 A72-23865

Core axial density distribution in gas jets freely expanding into vacuum from double concentric orifices, using electron beam fluorescence technique

15 p2218 A72-32150

The intrinsic structure of turbulent jets

18 p2684 A72-37201

Boundary layer core flow model of concentrated columnar vortex interaction with plane solid nonrotating surface, applying to tornado interpretation

24 p3391 A72-45022

Frictionless core flow and friction layers at turbomachine walls and blades for real two dimensional cascade flow modeling

24 p3394 A72-45370

CORE SAMPLING

Lunik 16 core-tube soil sample petrology and chemical composition

01 p0126 A72-10107

Li, Be and B abundances in Apollo 11, 12 and 14 and Lunik 16 missions fine and core samples

03 p0414 A72-12903

Microscopic and electron microprobe analyses of silicate melt inclusions and glasses in lunar soil fragments from Lunik 16 core sample

09 p1379 A72-22255

Lithic and vitreous particles in Lunik 16 core tube samples from Mare Fecunditatis, discussing particle type proportions and petrological and mineralogical aspects

09 p1379 A72-22256

Thermoluminescent and luminescent properties of Apollo 12 lunar fines, core tube samples and rock chips

10 p1537 A72-24163

CORE STORAGE

Ferrite core memory for storage of Helios probe perisolar space data before transmission to telemetry system

11 p1601 A72-25806

CORES

NT EARTH CORE
NT HONEYCOMB CORES
NT LUNAR CORE
NT MAGNETIC CORES
NT REACTOR CORES

Mars internal structure models with chondrite as potential core-forming material, discussing absence of internal origin magnetic field

07 p1084 A72-20518

Zeta core for sandwich construction with rigidity-to-weight ratio comparable to honeycomb core, discussing elastic properties and cost

23 p3355 A72-44495

CORIOLIS EFFECT

Matrix calculation of forced atmospheric oscillations for Hall, Coriolis and Pedersen regions

01 p0053 A72-10090

Coriolis acceleration effects on flight of projectiles fired from earth surface, discussing horizontal and vertical velocities

01 p0132 A72-11050

Topography and Coriolis effects on Martian atmospheric circulation, incorporating low radiative time constant and large variations in analytical model

01 p0135 A72-11279

Navigators, pilots and airman trainees response to Coriolis accelerations, investigating nystagmus sensitivity coefficient relationship to motion sickness resistance

01 p0021 A72-11286

Coriolis force effect on axially symmetric body oscillating slowly along axis in rotating viscous fluid

05 p0610 A72-17081

Uniformly curved fluid conveying tube free vibration and stability, showing flow velocity, fluid pressure and Coriolis force effects on natural frequency

06 p0821 A72-17853

Rotational, centrifugal and Coriolis force effects on turbulent boundary layer development, discussing changes in structure and shear stress distribution

10 p1464 A72-23870

Atmospheric models of vertical structure of semidiurnal atmospheric gravitational tides, taking into account Coriolis force and vertical acceleration components

10 p1473 A72-24530

Shrouded propellers and rotor blades free vibrations determination by variational method, showing Coriolis effect on critical flutter speed

11 p1732 A72-25536

Alcohol ingestion effect on vestibular responses to angular acceleration and Coriolis stimulation, discussing nystagmus and subjective responses

14 p2082 A72-31090

Coriolis forces effect on bubbles trajectories in rotating containers, determining critical Reynolds number

17 p2537 A72-34209

New hubs for multi-bladed tail rotors.

[AHS PREPRINT 602] 17 p2489 A72-34491

Coriolis force influence on convective stability in viscoelastic fluid layer heated from below, contrasting with rotation effects on ordinary viscous fluid

20 p2982 A72-29326

Coriolis constants for prolate symmetric top molecules from gas phase Raman band contours observation, noting comparison with IR spectroscopy

22 p3209 A72-42719

Features of a speech signal during cumulative action of Coriolis accelerations

23 p3257 A72-44154

Residual drag torque on magnetically suspended rotating spheres.

23 p3315 A72-44540

CORK [MATERIALS]

Mechanical characteristics of natural and synthetic rubber, noting features of cork filled urethane

10 p1502 A72-24861

CORNEA

Rabbit and monkey corneal damage following CW carbon dioxide laser irradiation, discussing hazard level derivation

02 p0163 A72-12413

Autocollimating photokeratoscope for human in vivo corneal shape measurements for contact lens fitting and dioptric image examination

07 p0987 A72-19826

Keratoconus/noninflammatory conic protrusion of cornea/ diagnosis and rehabilitation in USAF flying personnel

12 p1768 A72-28331

Laser irradiations inhibitory effect on cornea vascularization after treatment with supranatural total extract

13 p1906 A72-29867

Spectral sensitivity after prolonged intense spectral light exposure of rhesus monkey corneas, demonstrating long term loss of cone photopigment response

21 p3000 A72-40739

Determination of corneal configuration by the measurement of its derivatives.

21 p3055 A72-40745

Unsteady state description of living corneal mass transport modes, elucidating cornea thickness control mechanism

21 p3001 A72-40912

Keratoconus incidence in USAF flying personnel, discussing diagnosis, etiology and therapy

24 p3378 A72-45663

CORNERS

Disk shaped frame corner stress under external load, using complex variables and conformal mapping

03 p0448 A72-13886

Integral methods application to turbulent corner flow problem, obtaining mean velocity profile first approximation for turbulent boundary layer with streamwise pressure gradient

[ASME PAPER 71-WA/FE-36] 05 p0646 A72-15921

Axisymmetric plane transonic flow past convex corner point, obtaining characteristics by mapping into hodograph plane

10 p1468 A72-24435

Distribution theory application to fixed end point problem in variational calculus for extremal containing corners, obtaining Euler equation

12 p1885 A72-27849

Three dimensional viscous flow near corner, constructing Stokes slow-flow solution

13 p1944 A72-30031

Supersonic ideal gas flow in corner formed by intersecting plates, using direct computation method for nonequilibrium flows with detached shock waves

14 p2071 A72-31021

Supersonic interaction effects on boundary layer flow structure in intersecting wedge corner at high Reynolds numbers from surface pressure measurements and oil flow visualization

16 p2341 A72-32830

A simple formula for the maximum stress in a twisted angle or channel.

22 p3240 A72-42894

Turbulent supersonic boundary layer flow in the neighborhood of a 90 deg corner.

24 p3361 A72-45204

CORONA BOREALIS CONSTELLATION

Type R Corona Borealis variable stars luminosity variations attributed to formation of carbon layer from He nuclear transformation process at stellar core-envelope boundary

08 p1231 A72-21086

CORONA DISCHARGES

U ELECTRIC CORONA

CORONAGRAPHS

Digitized SEC vidicon detector for OSO-H satellite coronagraph, describing optics

08 p1170 A72-21959

White light and XUV coronas on 7 March 1970 from rocket photographs, comparing with X ray, Lyman alpha, Fe XIV and IR eclipse photographs

13 p2031 A72-29542

Rocket-borne coronagraph photometry of solar corona during 7 March 1970 eclipse for streamer analysis

13 p2043 A72-29543

Mercury magnitude determination near superior conjunction with aid of coronagraph photography and photometric calibration

15 p2312 A72-32090

Space observations of the solar corona.

17 p2611 A72-35326

CORONARY CIRCULATION

Human cardiocirculatory responses to submaximal physiologically paced bicycle ergometry, recording prejection period, isovolumic contraction, left ventricular ejection and pulse transmission time

01 p0010 A72-10147

Coronary heart disease - Conference, Frankfurt am Main, West Germany, January 1970

03 p0314 A72-13176

Coronary angiography findings in 263 patients of different age groups compared with history of angina pectoris, risk factors and ECG at rest

03 p0314 A72-13177

Exercise ECG correlation to morphological patterns of selective cinecoronary arteriography and ventriculography, revealing significant information on occlusion and stenosis

03 p0314 A72-13178

Myocardial blood flow measurement value in ischemic heart disease assessment, discussing Xenon 133 injection into coronary arteries

03 p0315 A72-13179

Xenon 133 method for coronary blood flow measurement during exercise, noting unsuitability for patients with coronary disease

03 p0319 A72-13180

Coronary blood flow measurement in various hemodynamic conditions by argon technique, determining oxygen consumption and coronary vascular resistance

03 p0315 A72-13183

Clinical assessment of degree of obstruction from coronary arteriograms of ischemic and rheumatic heart patients

03 p0316 A72-13847

Human epicardial arterial circulation platelet aggregates role in sudden coronary death, discussing relation to atherosclerotic stenosis and acute thrombosis

05 p0616 A72-16013

Stellate ganglion stimulation and hypoxia effects on hemodynamics and coronary circulation in dogs, discussing myocardial oxygen consumption, sympathetic nerve vasoconstrictor effect and vasodilatory response

05 p0617 A72-16153

Reciprocal temperature changes in dogs during constant thermomodulation for coronary sinus blood flow measurement

06 p0769 A72-18197

Beta-adrenergic inhibitors effects on coronary blood flow and myocardial oxygen consumption of normal and coronary artery disease patients

08 p1118 A72-21549

Tachycardia role in coronary vascular bed hemodynamic response to severe exercise in dogs

10 p1426 A72-24483

Assessment of regional myocardial temperature changes effect on blood flow measurements by heated cross-thermocouples in dogs

10 p1432 A72-25071

Beta-adrenergic blocking effect on canine coronary and systemic hemodynamic adaptation during treadmill exercise

11 p1579 A72-25802

Hemodynamic variables relation to coronary blood flow and myocardial oxygen consumption during upright bicycle exercise

11 p1587 A72-26618

Left ventricular dynamic function in terms of internal diameter, pressure and flow in dogs at rest and during isoproterenol and metaraminol infusions

11 p1582 A72-26773

Acute hypoxia effects on dog coronary blood flow and cardiac function from cardiac beta-adrenergic and hemodynamics study

12 p1760 A72-27482

Clinical diagnosis of ST/T depression in resting ECG, noting coronary heart disease and left ventricular hypertrophy

12 p1772 A72-27733

Autonomic nervous system role in controlling coronary and cardiac responses to hypoxic hypoxia, measuring blood flow with Doppler ultrasonic flow transducer

12 p1767 A72-28313

Coronary system autoregulation patterns and mechanisms from coronary flow shift measurements during circumflex artery perfusion experiments in dogs

13 p1901 A72-28637

Cardiac stroke volume measurements during supine bicycle exercise and recovery period, using indicator-dilution technique

14 p2079 A72-30701

Platelet aggregates role in intramyocardial vessel circulation impedance in patients dying suddenly of coronary artery disease

15 p2186 A72-31770

Radiocardiography method for ventricular volume measurements, recording subclavian vein-injected radioisotope passage through cardiac cavities

15 p2190 A72-32495

Indicator dilution methods for ventricular volume measurements from washout curves, discussing intraventricular blood mixing uniformity

15 p2190 A72-32496

Mountain inhabitants cardiocirculatory adaptation to chronic hypoxia, studying coronary flow and myocardial oxygen consumption and efficiency

15 p2187 A72-32498

Cardiac performance and the coronary circulation of man in chronic hypoxia.

17 p2502 A72-34992

Studies of the influence of theophylline on the vasodilating action of different medications on the cerebral and coronary circulation of man

18 p2651 A72-36799

Coronary flow determination in experimental conditions with the use of radioactive xenon.

19 p2755 A72-37475

Coronary collateral circulation and myocardial blood flow reserve.

19 p2755 A72-37500

Temporal relation of the second heart sound to aortic flow in various conditions.

19 p2759 A72-38818

Coronary blood flow and myocardial metabolism in man at high altitude.

22 p3144 A72-42593

Anatomy of the coronary circulation at high altitude.

22 p3144 A72-42594

Cardiocirculatory adaptation to chronic hypoxia. II. Comparative study of myocardial metabolism of glucose, lactate, pyruvate and free fatty acids between sea level and high altitude residents.

22 p3148 A72-43022

Continuous recording of His bundle electrogram during selective coronary cineangiography in man.

23 p3255 A72-43813

Effects of coronary arteriography on myocardial blood flow.

23 p3256 A72-43933

The effect of hypoxia on the coronary blood flow in reserpinized dogs.

24 p3370 A72-44562

Clinicoarteriographic correlations in angina pectoris with and without myocardial infarction.

24 p3372 A72-45010

CORONAS

NT ELECTRIC CORONA

NT SOLAR CORONA

Long term galactic cosmic ray intensity modulation correlation to 5303 A coronal intensity during rising part of solar activity cycle

01 p0120 A72-10909

Stellar winds and breezes classification using energy flux and particles kinetic and thermal energies for criteria, noting coronal temperature effects

15 p2313 A72-32298

CORPUSCULAR RADIATION

NT BETA PARTICLES

NT CYCLOTRON RADIATION

NT ELECTRON BEAMS

NT ELECTRON PRECIPITATION

NT ELECTRON RADIATION

NT ION CYCLOTRON RADIATION

NT PRIMARY COSMIC RAYS

NT RADIATION BELTS

NT SOLAR CORPUSCULAR RADIATION

NT SOLAR COSMIC RAYS

NT SOLAR PROTONS

Latitude dependence of upper atmosphere corpuscular radiation intensity, analyzing sounding data from Indian Ocean area

01 p0118 A72-10369

Auroral absorption and DR currents development during magnetic storms, discussing corpuscular fluxes arrival from magnetospheric tail into lower ionosphere

01 p0059 A72-10619

Space environment simulator with ultrahigh vacuum chamber and UV and corpuscular radiation for material samples physical properties in-situ measurement

02 p0201 A72-12701

Heavier-than-helium cosmic ray nuclei composition inferring galactic confinement of particles, path lengths and transit times

03 p0409 A72-13137

Large-scale solar coronal magnetic field from optical and radio observations for corpuscular propagation in corona and interplanetary medium

03 p0432 A72-13346

High energy particle sources, taking into account cosmic ray sources, sun, artificial plasmas, interplanetary and planetary sources, interstellar space, supernovae, radio galaxies and quasars

07 p1059 A72-19428

Night source ionized component profiles in chemistry and aeronomy of D and E regions, considering scattered L alpha and beta emissions and corpuscular fluxes

07 p0936 A72-20038

Solar modulation process for galactic cosmic ray particle time variation, discussing interplanetary magnetic fields and plasma, energy losses from solar wind deceleration, etc

08 p1227 A72-21188

Microwave, X ray and corpuscular emission by gas discharges in coaxial plasma gun, measuring pressure and current distribution

09 p1362 A72-23212

Penetrating particles effect on low energy scintillation spectrometers sensitivity in various regions of magnetosphere

11 p1632 A72-25934

Corpuscular radiation intensity relationship to midlatitude mesosphere temperature from rocket and balloon sounding and ground measurements

13 p0209 A72-28603

Book on theory of fully ionized plasmas covering Coulomb systems equilibrium and nonequilibrium states, charged particle radiation and interactions with EM fields

13 p0211 A72-29098

Fuor luminosity phenomena due to thermal corpuscular radiation emitting energy sources

15 p2304 A72-31330

Magnetospheric geometry derivation from ISIS-1 observations of soft particles penetration into polar cap and auroral regions, discussing entry and energization mechanisms

15 p2227 A72-31953

Interplanetary particles intensity relationship with solar activity based on Heos A1 observations during 1969-1971

15 p2300 A72-31992

Interplanetary radiation types in terms of possible space flight hazards, discussing electromagnetic and corpuscular radiation, cosmic rays and radiation belts

16 p2446 A72-33553

The absolute vertical cosmic-ray muon intensity at sea level.

17 p2600 A72-35147

Meridional motion of a corpuscular entry region from observations of riometric absorption

17 p2551 A72-35864

The imaging properties of the positron camera

18 p2652 A72-36424

Radiation of charged particle moving uniformly in a nonstationary magnetoactive plasma

19 p2843 A72-38570

Corpuscular radiation intensity relationship to midlatitude mesosphere temperature from rocket and balloon soundings and ground measurements

24 p3435 A72-45103

CORRECTION

NT OPTICAL CORRECTION PROCEDURE

Dynamic pressure, downwash and pressure gradient corrections of wind tunnel model measurements, discussing displacement limit for adequate accuracy [DFVLR-SONDDR-214]

19 p2747 A72-38687

Corrections to star catalogues from satellite observations.

22 p3220 A72-41997

Aircraft noise duration correction for effective perceived noise level /EPNL/ computation, eliminating mathematical anomaly incurred by present FAA and ICAO prescribed method

22 p3139 A72-42909

CORRELATION

NT ANGULAR CORRELATION

NT AUTOCORRELATION

NT CORRELATION COEFFICIENTS

NT CORRELATION DETECTION

NT CROSS CORRELATION

NT DATA CORRELATION

NT SIGNAL ANALYSIS

NT STATISTICAL CORRELATION

Light emission intensity correlation functions associated with LF oscillations in beam plasma discharge

02 p0263 A72-11421

Correlation filters alignment for optical character recognition, discussing kinematic mounting and in position techniques

02 p0225 A72-11750

Spatial-temporal correlation functions of field due to electromagnetic waves backscattering from random inhomogeneities in extended layer

02 p0180 A72-12580

Relativistic plasma with particles interacting through electromagnetic field, constructing statistical description by reduced distribution functions and correlation patterns

03 p0395 A72-13626

Correlation functions of signal and noise at output of discrete channel, determining SNR or speech intelligibility

03 p0323 A72-13891

Closed system equilibrium correlation functions relationships based on total momentum conservation,

discussing application to solids or liquids electrical conductivity via nuclei dynamics

07 p1035 A72-19669

Correlation functions describing fluctuation of slow electromagnetic waves in plasma layer

08 p1212 A72-21065

Optimum decision rule for sync word location in binary data frame, noting sum maximization of correlation and energy correction terms

11 p1592 A72-25888

Correlations analysis method for homogeneous and inhomogeneous systems under external field based on BBGKY hierarchy and decomposition of reduced distribution functions

11 p1689 A72-26480

Single continuous algebraic correlation equation for convective heat transfer in cross flow for wide Reynolds number range, considering applications to hot-wire anemometry

11 p1747 A72-26541

Correlation function of depolarized finite collimated Gaussian laser beam in atmospheric turbulent medium

11 p1599 A72-26748

Two point correlation description of MHD plasma properties subject to electrothermal instability, calculating electron number density and temperature fluctuations

13 p2015 A72-29373

Sound transmission loss and diffraction measurements by combined correlation and Fourier techniques

13 p2006 A72-29768

Inhomogeneous viscoelastic shell stability, determining correlation functions for first approximations of sag, stress functions and critical time alterations

13 p2062 A72-29886

Relativistic plasma particle correlation function based on transverse electromagnetic field energy density treatment by enlarged Bogoliubov hypothesis

14 p2140 A72-30881

Nonlinear Boltzmann equation prediction of time correlation functions with long asymptotic time tails

15 p2278 A72-32307

Correlation functions of signal and noise at output of discrete channel, determining SNR or speech intelligibility

15 p2202 A72-32702

Binary gas mixture density correlation functions from initial value problem based on linearized Boltzmann equation for analysis of Rayleigh-Brillouin scattering

16 p2428 A72-32942

The two-particle correlation function in nonequilibrium statistical mechanics.

17 p2581 A72-35164

Correlation of noise-like emission reflected from a statistically uneven surface

17 p2583 A72-35543

Three point distribution function related to lower order functions for closure of hierarchy of equations for turbulent probability distribution functions

18 p2677 A72-36005

Free hot jet turbulence space-time correlation function measurement based on IR detection

18 p2680 A72-36468

Correlation between two base-station antennas affected by local scatterers and directions of incoming mobile radio waves.

18 p2661 A72-36846

Integral and correlation methods for separation and reattachment phenomena in aerodynamics, applying to turbulent boundary layer

19 p2786 A72-37762

Correlation analysis techniques to characterize acoustic emission pulses from Mg alloys, obtaining time varying spectra

20 p2924 A72-39281

Lowest order two particle correlation function solution to BBGKY hierarchy obtained via Green function with Fourier transform satisfying analyticity requirements for causality

20 p2956 A72-39725

Balescu-Guernsey-Lenard kinetic equation for homogeneous dilute electron gas extended to higher densities, specifying conditions for BBGKY hierarchy correlation functions solution

20 p2958 A72-39815

Short distance behaviour of the pair correlation function for classical plasmas.

21 p3091 A72-40570

Oxygen ion anticorrelation to molecular ion concentrations from OGO 6 observations in F 2 region

22 p3169 A72-42016

Diversity reception during radio wave scattering on statistically uneven surface, using geometrical optics method

22 p3153 A72-42084

Improved holographic matched filter systems for pattern recognition using a correlation method.

22 p3177 A72-42445

Applicability bounds for the equation describing the mean field in a discrete scattering medium with allowance for the correlation of the scatterers

22 p3155 A72-42660

On a resolution of the equations governing the second order correlation functions for an isotropic hydromagnetic turbulence. 22 p3212 A72-43100

Type of equations for the solution of some gravitational prospecting problems from the anomalies on a complex relief, using a correlation model 23 p3285 A72-43847

Whittaker method for astronomical observational data smoothing, noting correlation function for latitude weighting functions determination 24 p3447 A72-45677

CORRELATION COEFFICIENTS

Laser anemometer system for instantaneous velocity measurement in turbulent pipe flow, determining two point velocity correlation coefficients 01 p0071 A72-11169

Spatial correlation coefficients measurements on one-hop hf radio waves obliquely reflected from ionosphere for various antenna spacings 01 p0032 A72-11252

Correlation coefficients for galactic cosmic rays relation to solar activity indices in interplanetary space 02 p0273 A72-11937

Ionospheric D region electron concentration, deriving correlation coefficient expression with allowance for scattering layer electrons/molecules collisions 02 p0222 A72-12593

Correlation energy calculation for system of fermions by means of variational method 05 p0702 A72-16785

Geopotential and longitudinal and transverse wind components correlation coefficients in nonhomogeneous nonisotropic atmosphere 06 p0843 A72-18444

Isobaric correlation coefficient functions for wind and geopotential, describing relationship by two differential equations derived from geostrophic wind equations 09 p1344 A72-22432

Human tilt tolerance relation to aerobic capacity, weight, height and physical fitness, determining correlation coefficient between heart rate and orthostatic response 10 p1428 A72-23733

Frequency and angular correlation function relationship for signal scattering cross section of extensive bodies 10 p1436 A72-24586

Computer approximate computation of multidimensional normal distribution, examining error measure, random processes and correlation coefficient 11 p1676 A72-25429

Rank correlation coefficient method for complex control plants parameters selection, applying to aircraft power system monitoring 11 p1612 A72-26442

Correlation coefficients for galactic cosmic rays relationship to solar activity indices in interplanetary space 13 p2030 A72-29249

Mg filterheliogram comparison with Ca spectroheliogram, noting correlation coefficient between location and intensity of bright features on sun 13 p2045 A72-29708

Stochastic and deterministic relationships between random variables, noting correlation coefficient as measure of regression lines representation accuracy 22 p3178 A72-42449

Diurnal variation of the correlation of Pc 3 and Pc 4 micropulsation characteristics with magnetic activity. 23 p3286 A72-44524

CORRELATION DETECTION

Quantitative interpretation of correlation mask remote sensors UV, visible and IR spectral data, discussing beam transmittance attenuation by absorption, scattering and emission [ALAA PAPER 71-1061] 01 p0066 A72-10530

Coupled detection-estimation of Gauss-Markov processes in white Gaussian noise, deriving Bayes optimal recursive rules 06 p0775 A72-18388

Optimal radio signal processing system on background of correlated interference, calculating detection characteristics 07 p0937 A72-18850

Flame photometric detection of small concentrations of sulfur compounds in ambient air, describing spectrum scanning detector, rotating interference filter and correlation detector 10 p1480 A72-24101

IR measurement of hot jets turbulence intensity axial and transverse profiles, noting application to sound sources detection 10 p1563 A72-24656

Multifilter detection system with phase autocorrelator, discussing design based on correction detection probability vs mismatch between signal and filter central frequencies 11 p1597 A72-26315

Broadband correlation meter with multiplier using vacuum thermal converters for 1.5 KHz-15 MHz range and variable signal delay 13 p1961 A72-29920

Estimation-correlation principle application to harmonic signal receiver with unknown carrier frequency, using searching phase locked AFC circuit as estimation unit 15 p2202 A72-32667

Digital correlator for change detection in picture element processing with CDC 1700 computer to obtain spatial alignment accuracy 17 p2556 A72-35538

The theoretical amplification limit of modulation amplifiers with correlation detection 18 p2668 A72-37035

An application of correlation to radar systems. 19 p2764 A72-37927

Dyadic correlation function method for structured radar signal sidelobe suppression during reception, noting Walsh function role 21 p3020 A72-40901

Clear air turbulence detection possibility by optical laser radar and turbulent fluctuation correlations 23 p3264 A72-43898

Autocorrelation function of smooth steady random signal determination from consecutive derivative dispersions by MacLaurin, least squares and Taylor methods 24 p3380 A72-45317

CORRELATION FUNCTIONS

U. CORRELATION

CORRELATORS

NT. IMAGE CORRELATORS

Optimal filter and polarity coincidence correlator signal detection efficiency for arbitrary noise distribution 02 p0176 A72-12217

Multidimensional Gaussian distribution integrals evaluation for correlator analysis, discussing fix error probability and variance 03 p0387 A72-14189

Variance estimate of second order moment by nonlinear correlator in presence of additive amplitude and phase modulation and normal noise 07 p0939 A72-19021

Electronic correlator for plasma wave induced coherent signals cross correlation measurement, producing 1 microsecond time delays by automatically switching lumped circuit delay line 07 p0958 A72-20582

Synchronous detector technique for statistical properties improvement in phase comparison AM radio altimeter signal 11 p1633 A72-26304

Digital correlators and correlometers operational and design characteristics 11 p1602 A72-26444

Digital correlator systems design for nonstationary signals, presenting circuit diagrams for multichannel centering system and memory operation 11 p1602 A72-26445

Nonlinear resonating correlator with orthogonal filters, considering cut-off frequency of ergodic random process with constant power spectral density 14 p2090 A72-31125

Variable area modulation dual signal recording onto single input device for coherent optical correlators 15 p2249 A72-32165

Laguerre filters parameters choice for correlator input networks application, noting output SNR improvement 16 p2368 A72-33089

Comparative analysis of frequency response determination methods for searchless adaptive systems 21 p3038 A72-40709

Correlator with orthogonal filters for acoustic diagnostics, noting Laguerre functions variations in signal pairs autocorrelation 22 p3176 A72-42133

Real time correlator design and operation with signal delay at 40 Hz-20 kHz, using Stieltjes principle 22 p3176 A72-42244

Digital parallel correlator with LSI single-chip bipolar transistor construction, discussing triple diffusion process for p-n-p and p-n-p junctions 23 p3273 A72-44453

CORROSION

NT. CAVITATION CORROSION

NT. ELECTROCHEMICAL CORROSION

NT. FRETTING CORROSION

NT. FUEL CORROSION

NT. INTERGRANULAR CORROSION

NT. SCALE [CORROSION]

NT. STRESS CORROSION

Filiform corrosion of steel, magnesium and aluminum coated and uncoated surfaces in humid and corrosive atmospheres 04 p0536 A72-15735

Temperature effects on anodic polarization of Ti open surface and corrosion crevices, discussing critical potential relation to pitting 06 p0829 A72-17946

Adsorption, corrosion and hydrogen embrittlement effects on crack formation in quenched carbon steels in active media, using tensile stress-rupture tests 08 p1910 A72-22183

Environmental sensitivity effect on crack propagation rates in steels and Al and Ti alloys, discussing corrosion fatigue 10 p1499 A72-24899

Metallic corrosion - Conference, Amsterdam, September 1969 14 p2117 A72-30534

CORROSION PREVENTION

Corrosion and stress corrosion cracking prevention on space shuttle by materials selection 01 p0085 A72-10775

Rust inhibited chemically inert perfluorinated polymer greases for liquid fueled rocket engines, discussing lubricating and nonreactive properties under high pressure operating conditions 06 p0837 A72-18604

Fiberglass reinforced thermoplastics and thermosets for corrosive environments, noting composites performance increase by constituents change 12 p1833 A72-27404

Protective coatings for corrosion prevention of high strength steels under environmental conditions of humidity, salt fog, tap and salt water immersion 12 p1835 A72-28157

Hydrogen evolution and ferric iron corrosion inhibition by synergistic action of substituted thioamides and thioamides to minimize metal corrosion during acid cleaning 13 p1980 A72-29624

Fretting corrosion fatigue prevention by barrier approach, discussing test program and application to helicopter part fatigue life increase [AHS PREPRINT 672] 17 p2626 A72-34512

Austenitic steel stress corrosion prevention at high temperatures and pressures, investigating inhibitor adsorption properties from capacitance measurements and polarization curves 17 p2568 A72-35474

Thermionic converter heated by gasoline flame or heat pipe, describing materials protection against corrosion and furnace design and operation 18 p2644 A72-36165

Cathodic protection and hydrogen in stress corrosion cracking. 19 p2817 A72-37765

Thermochemical techniques application to corrosion protection of metallic powders, mechanical parts and tools, describing chromizing, chromaluminizing, tantaluminizing and niobiumizing processes [ONERA, TP NO. 1049] 19 p2817 A72-37769

Developments in the field of metallic diffusion protective layers employed against high-temperature corrosion 20 p2944 A72-39450

CORROSION RESISTANCE

NT. OXIDATION RESISTANCE

Book on vacuum brazing covering dissimilar metals joining, stress cracking, corrosion resistance, joint design, heat treatment and production engineering problems 01 p0073 A72-10165

Corrosion effect on mechanical properties of sintered powder iron and bronze parts, describing test procedure for corrosion resistance determination 02 p0241 A72-11459

Passivation velocity apparatus for testing Al-Mg alloy sensitivity to corrosion under voltage 02 p0246 A72-12599

Mo and C additives effects on austenite susceptibility to deformation martensite formation and steel resistance to hydroerosion 03 p0375 A72-13941

Titaniums sulfide initiation of pitting corrosion of Ti stabilized corrosion resistant Cr-Ni-Ti steels 03 p0379 A72-14367

Corrosion resistance of stainless steels in acid solutions, describing electrochemical cell for recording potential/current density and polarization curves 04 p0533 A72-15236

Wear, bending and corrosion resistance of stainless steels with Cr thermal vacuum diffused coating 04 p0535 A72-15661

Anodizing effect on corrosion fatigue strength of sheet duralumin under low and high bending stress 04 p0535 A72-15662

Potential change under pitting corrosion and repassivation on Cr-Ni steels alloyed with V, Si, Mo and Re 04 p0535 A72-15730

Ti surface oxide films ionic and electronic conductivity properties and correlation with crevice corrosion susceptibility in contact with polytetrafluoroethylene gaskets 04 p0535 A72-15732

Environmental effects on superalloy high temperature corrosion in gas turbines, noting blade surface temperature as critical factor [ASME PAPER 71-WA/CD-1] 05 p0704 A72-15945

Heat and corrosion resisting alloys development for gas turbine combustion liner, presenting microstructure of specimens after thermal shock test 05 p0675 A72-16494

Hydraulic fluids behavior under extreme temperature, pressure and filtration conditions, considering viscosity, wear and corrosion resistance 05 p0681 A72-17084

Ag addition effects on high strength Al-Zn-Mg-Cu alloys tensile properties and resistance to stress corrosion cracking

05 p0677 A72-17113

Fatigue and fatigue-corrosion properties of high strength stainless maraging martensitic structural and stainless austenitic steels

05 p0680 A72-17206

Solar cells with improved photoelectric efficiency, describing use of noncorroding Ti-Pd-Ag contacts, titanium oxide antireflection layer and welded cell joints

06 p0760 A72-17751

Dispersion strengthened Co alloys structural stability, tensile and creep rupture strengths and hot corrosion properties

06 p0829 A72-17829

Rust inhibited chemically inert perfluorinated polymer greases for liquid fueled rocket engines, discussing lubricating and nonreactive properties under high pressure operating conditions

06 p0837 A72-18604

Mn additions effects on austenitic stainless steels yield strength, work hardening characteristics, corrosion resistance and machinability

07 p1011 A72-19478

Austenitic stainless steel with improved corrosion resistance, yield strength and hot workability

07 p1011 A72-19487

High Cr ferritic steels intergranular and stress corrosion properties and resistance to sea water, organic and inorganic acids and acid mixtures

07 p0995 A72-19572

Hot corrosion resistant Pt-Al coating for high temperature aircraft engine Ni alloy components, presenting cyclic sulfidation and thermal shock test results

07 p1012 A72-19573

Boron addition effects on scaling resistance of Ni-Cr steel at high temperatures

07 p1012 A72-19738

Oxygen effect on structure and mechanical, technological and corrosive properties of stainless steel melted in open and vacuum furnaces

07 p1013 A72-19739

Prestress effect on stress corrosion resistance of fatigue precracked high strength steels

07 p1016 A72-19941

Corrosion resistance decrease and embrittlement in Ni-Mo cermet alloys after heat treatment from electrical resistance measurement

07 p1017 A72-19965

Fuel lubricity effects on aircraft engine fuel pump wear, discussing remedial use of corrosion inhibitors and change to noncorroding pump construction materials

08 p1222 A72-21450

Clam seals comparison with elastomers, discussing aircraft use, contamination, inspection, corrosion and erosion, surface finish, service life and cost

08 p1179 A72-21941

Thermodynamics of ceramic oxide corrosion by sulphur and oxygen bearing atmospheres, considering formation products and furnace refractory materials choice

09 p1333 A72-22377

Corrosion resistant fabrication methods in jumbo jetliners components to reduce maintenance and repair downtime, discussing clad wing and fuselage skins

10 p1487 A72-24025

Ti alloys fracture strength in air and sea water obtained by bending tests of notched specimens, noting stress corrosion resistance enhancement by Mo addition

10 p1499 A72-24891

Adhesive bonded clad Al corrosion penetration rates from accelerated tests [SAE PAPER 720344]

11 p1656 A72-25600

Mn content effect on mechanical properties and corrosion fatigue and stress corrosion cracking resistance of Al-Mg casting alloys

11 p1658 A72-25850

Fatigue and fatigue-corrosion properties of high strength stainless maraging, martensitic structural and stainless austenitic steels

11 p1660 A72-26141

Stainless steels sensitivity to pitting corrosion under sulfides action, measuring rupture potential

11 p1661 A72-26648

High temperature effects on stability, corrosion behavior, structure and protective effectiveness of Al coatings on Ni and Co alloys

11 p1664 A72-26852

Gas turbine engine compressor blade and materials fatigue strength dependence on pressure under contact friction corrosion

12 p1831 A72-28244

Paint coatings aging effect on D16T type alloy corrosion fatigue in NaCl solution, noting protective efficiency decrease

13 p1984 A72-29486

Iron content and stress level effect on flaking corrosion of Al alloy sheets, describing experimental technique

13 p1980 A72-29826

Ni-Mo-W alloys hardness rating and corrosion resistance to sulfuric and hydrochloric acids, discussing dispersion hardening, quenching and aging treatments

14 p2114 A72-30272

Superalloys properties and utilization at high temperatures, discussing chemical resistance, diffusion treatment, B and Zr action and grain size

14 p2116 A72-30527

Heat treatment and grain size effects on stress corrosion resistance and life duration of maraging steels, investigating crack initiation and propagation

14 p2117 A72-30539

Heat treatment hardening effect on stress corrosion resistance of ultrapure maraging and stainless steels, emphasizing hydrogen embrittlement

14 p2117 A72-30540

Anodic salt-chromate stress corrosion resistance test of Al-Zn-Mg alloys, noting time reduction and correlation with natural environment exposures

14 p2117 A72-30541

Quenching rate and alloying element content effects on precipitation extent and corrosion resistance of Al-Cu alloys, discussing microstructure, chemical composition and mechanical properties

14 p2119 A72-30604

Low carbon and nitrogen concentrations in chromium ferritic stainless steel obtained with gas rinsing at reduced pressure, noting weldability and corrosion resistance

14 p2119 A72-30606

Scandium alloys properties based on phase diagrams, noting corrosion resistance

15 p2289 A72-31186

Ti alloy initial H content effect on resistance to hot salt stress corrosion embrittlement and cracking, discussing annealing treatment influence

15 p2253 A72-31296

Ti-Al-V foil stress corrosion methanol cracking resistance improved by treatment with pentanedione, suggesting metal ions removal from protective film

15 p2253 A72-31297

Adhesive bonding of L-1011 body shell panels for improved fatigue strength and corrosion resistance

15 p2245 A72-32429

Tensile strength, toughness and corrosion resistance of dross aluminized carbon steel specimens under static, cyclic and impact loads

16 p2406 A72-33267

Al alloy welded seams corrosion fatigue strength increase by epoxy polymer coatings under cyclic tensile stresses

16 p2397 A72-33268

Porosity effect on mechanical properties, airtightness, corrosion resistance and moisture absorption of glass fiber reinforced plastics

16 p2414 A72-33270

Resin selection for manufacture of chemically resistant glass fiber reinforced polyesters, considering structural factors of chain for susceptibility to alkaline hydrolysis

16 p2414 A72-33304

Susceptibility of the NiCr 15 Fe chromium-nickel alloy /Remanit 1675 SEW and Thermax 1675/ to intercrystalline corrosion

17 p2566 A72-34396

Compatibility of brazed joints with potassium and vacuum.

17 p2567 A72-34938

Improvement of the anticorrosion properties of water-containing hydropurified diesel fuels with the aid of saltless additions

17 p2596 A72-35177

Stability and hot corrosion of aluminum coatings on the INCO 713C alloy and on cobalt alloys

18 p2701 A72-36595

Hot corrosion of experimental aluminum-coated cobalt-base alloys.

18 p2702 A72-36797

Contribution to the study of the stabilization of corrosion-resistant chromium-nickel austenitic steels

18 p2702 A72-37014

Active corrosion in aqueous solutions, discussing reactions, adsorption, intergranular attack, pitting, crevice corrosion and stress corrosion cracking

19 p2815 A72-37446

German monograph - Effect of molybdenum and degree of age hardening on the corrosion properties of maraging chromium steels

19 p2816 A72-37654

Effect of additions of Cu and Zr on stress corrosion cracking of Al-Mg alloys.

19 p2820 A72-38370

Effects of small amounts of additional elements on stress corrosion cracking of Al-Zn-Mg alloys. VI.

19 p2821 A72-38555

Electrochemical protection potential of metals and alloys in pitting, intergranular corrosion and stress corrosion cracking in presence of chlorides

21 p3065 A72-40087

Strain hardening of maraging steels in liquid nitrogen

22 p3187 A72-41867

Study of the properties of porous materials of nickel-molybdenum and nickel-chromium-molybdenum alloys

22 p3188 A72-42193

Effect of cyclic stress wave form on corrosion fatigue crack propagation in Al-Zn-Mg alloys.

22 p3194 A72-43043

Mechanical properties of heat and corrosion resistant nonmagnetic Ni-Cr-Nb spring alloys with W addition tested in aggressive and nitric acid base media

23 p3300 A72-43595

Measurement of stacking fault energy in CrMnNi austenitic steel by the method of extended nodes

24 p3415 A72-45397

CORROSION TESTS

NT SALT SPRAY TESTS

Corrosion effect on mechanical properties of sintered powder iron and bronze parts, describing test procedure for corrosion resistance determination

02 p0241 A72-11459

Passivation velocity apparatus for testing Al-Mg alloy sensitivity to corrosion under voltage

02 p0246 A72-12599

Corrosion fatigue cyclic crack growth rate above and below environmental threshold stress in steels as function of frequency and potentials, indicating hydrogen embrittlement

03 p0377 A72-14172

Vibrations effect on corrosion rate by experimental method, comparing reaction kinetics on two specimens with and without alternating stresses

04 p0591 A72-15237

Zr alloys hydride distribution after oxidation in steam at 550 C, discussing hydrogen uptake

04 p0534 A72-15362

Maraging steel laminates stress corrosion cracking behavior, showing composite base plate and weld structure influence on crack propagation reduction

04 p0534 A72-15569

Zr and Zr-Cr alloys corrosion behavior in steam, noting parabolic rate law breakaway point to linear rate

05 p0676 A72-16797

Ni corrosion by hydrogen sulfide, determining nickel sulfide scale chemical composition and crystallographic orientation by electron and X ray diffraction

06 p0828 A72-17606

Oxidation and hot corrosion tests of coated Ta and Ta based alloys between 800 and 1500 C in still air and in oxidizing gas stream

06 p0828 A72-17614

Hot corrosion of thoria dispersed nickel and thoria dispersed Ni-Cr alloy in high velocity gas stream of jet fuel combustion products

07 p1010 A72-18753

Nondestructive tests of welded joint heterogeneities and corrosion cavities by densitometric photometric differentiation of radiographs

07 p0995 A72-19674

Corrosion testing - Conference, Toronto, June 1970

08 p1188 A72-22101

Lower confidence bound for reliability and specifications for nonnormally distributed stress corrosion test data, using Weibull statistical distribution

08 p1189 A72-22102

Corrosion testing classification based on similarity between laboratory and operating conditions, emphasizing qualitative nature of accelerated tests

08 p1189 A72-22103

Laboratory metal corrosion testing, considering reasons, conditions and damage assessment

08 p1189 A72-22104

Electrochemical tests, noting electric potential, current and electrode impedance measurements for corrosion rate and oxidizing power evaluation

08 p1189 A72-22105

Corrosion effects evaluation from electrode potentials, noting copper pitting and weathering

08 p1189 A72-22108

Corrosion products X ray analysis using Powder Diffraction File, noting manual and computer searches

08 p1129 A72-22109

Corrosion tests by ellipsometer, discussing apparatus design and bare metal surface and thin film properties

08 p1172 A72-22110

Metal single crystals use for corrosion tests, noting anisotropy, adsorption, oxidation and pitting

08 p1189 A72-22111

Stress corrosion of uranium carbide ceramics in atmospheric environments containing water

09 p1335 A72-22399

Accelerated full scale aircraft turbine engine corrosion tests in controlled environment, simulating salt, high temperature and humidity conditions

10 p1528 A72-24320

[NACE PAPER 76]

Electrochemical and stress corrosion tests of Ti-Ni alloys in acidic chloride solutions at ambient and elevated temperatures

10 p1497 A72-24321

Tensile ligament instability model for stress corrosion crack propagation velocity in austenitized steel tempered at 750 F

10 p1499 A72-24888

- Adhesive bonded clad Al corrosion penetration rates from accelerated tests [SAE PAPER 720344] 11 p1656 A72-25600
- Hot corrosion effects on Inconel-700 and Inconel-X gas turbine rotor blades during burning of high sulfur concentration residual oil fuels [ASME PAPER 72-GT-87] 11 p1656 A72-25662
- Ti alloys hot salt stress corrosion cracking mechanism, discussing cold deformation and heat treatment effects, tensile tests, hydrogen analysis and microscope investigation 14 p2117 A72-30535
- Anodic salt-chromate stress corrosion resistance test of Al-Zn-Mg alloys, noting time reduction and correlation with natural environment exposures 14 p2117 A72-30541
- Microstructural changes relationship to corrosion susceptibility in ternary Al alloy obtained from stress corrosion cracking tests and electron metallography, noting precipitate-free region 14 p2118 A72-30542
- Automatic recording instrument for crack initiation time and breakdown curve for low carbon and stainless steel corrosion-fatigue tests under bending and tensile loads 16 p2394 A72-33849
- German monograph - Studies of high-temperature corrosion of cobalt and cobalt alloys with radioactive isotopes 19 p2816 A72-37657
- A study of the mechanical behaviors of austenitic stainless steels in the process of stress corrosion testing. 19 p2820 A72-38372
- Autoclaves for the study of the effects of deformation on the high temperature aqueous corrosion of metals. 21 p3039 A72-40216
- Analytical fracture mechanics application to stress corrosion cracking test methods for examining crack growth kinetics and time-to-failure 21 p3067 A72-40913
- Metallic corrosion testing in high velocity liquids 22 p3183 A72-42858
- German monograph - Influence of programmed welding cycle temperatures on the microstructure formation and corrosion behavior of austenitic corrosion-resistant steels. 22 p3195 A72-43075
- Influence of prior electrochemical history on the propagation of localized corrosion. 22 p3195 A72-43129
- CORRUGATED PLATES**
- Stiffness, stress and deformation analysis of discretely attached corrugated shear webs, using minimum potential energy and calculus of variations methods [AIAA PAPER 72-351] 11 p1728 A72-25380
- Plane plastic deformation during single pass rolling of corrugated metal sheet, determining stress-strain fields for first and second phases 13 p1964 A72-29148
- Local buckling analysis for triangular-corrugated core sandwich panels in compression, noting buckling mode nodal line features 15 p2326 A72-31709
- An experimental buckling study of skin-corrugated ring-stiffened curved panels. [SESA PAPER 1993A] 17 p2630 A72-34818
- A nonlinear problem of pure bending of a three-layer plate with a corrugated sheet filler 23 p3346 A72-43655
- CORRUGATED SHELLS**
- Axially compressed semi-sandwich corrugated ring-stiffened cylindrical shell crippling local buckling and general instability prediction by finite difference energy method [AIAA PAPER 72-138] 05 p0740 A72-16892
- Buckling strain effects on critical stresses in design of longitudinally corrugated shells for axial compression 15 p2333 A72-32680
- CORRUGATING**
- Dispersion equation of a corrugated elliptic waveguide 17 p2515 A72-34845
- Corrugated image screens advantages over flat screens, determining light intensity per corrugation, maximum viewing angle and reflection factor 21 p3055 A72-40743
- CORTICOSTEROIDS**
- NT ALDOSTERONE
- NT CORTISONE
- NT HYDROXYCORTICOSTEROID
- Short term response of insulin, glucose, growth hormone and corticosterone to acute vibration stress in rats 01 p0015 A72-11289
- Hypertrophic effects of chronic exercise on plasma corticosterone and adrenal cortex in rat 04 p0473 A72-15219
- Shock-induced fighting effect on pituitary adrenocorticotrophic hormone ACTH and adrenocortical steroids plasma concentration in rats, relating psychological stress to physiological function 05 p0617 A72-16080
- Adrenocortical steroids during acute exposure to environmental stresses, noting effects of injected cortisol removal, uptake and release 06 p0763 A72-17874
- Corticosterone content in blood plasma, cerebral cortex and skeletal muscles during hypoxia adaptation in rats 08 p1121 A72-22083
- Circadian adrenal periodicity of plasma corticosterone levels in man under random living schedule 09 p1265 A72-22643
- Human blood serum 11-oxy corticosteroid content after maximum stress exercise, noting heart rate and blood pressure changes 09 p1266 A72-22878
- Changes in the overall electrical activity of the mesencephalic reticular formation, the hippocampus, and the cerebral cortex under the influence of hydrocortisone and DOCA 20 p2890 A72-38929
- Unconjugated urinary corticosterone excretion in laboratory rats exposed to high pressure helium-oxygen environments. 24 p3374 A72-45656
- CORTISONE**
- Myocardial infarction stress effect on serum cortisol, plasma free fatty acid and urinary catecholamine levels 11 p1582 A72-26787
- Lysosomal enzymes of eye tissues during the action of hydrocortisone 22 p3141 A72-42279
- CORUNDUM**
- U ALUMINUM OXIDES
- COS-B SATELLITE**
- Celestial gamma rays arrival direction and energy spectra measurement and spectrum analysis using ESRO satellite COS-B data 03 p0408 A72-13029
- TD-1, HEOS-B and COS-B satellite-borne experiments, discussing X ray and gamma astronomy 04 p0582 A72-15690
- COSINE**
- U TRIGONOMETRIC FUNCTIONS
- COSMIC DUST**
- NT INTERPLANETARY DUST
- NT METEOROID DUST CLOUDS
- Oxygen isotope ratios in iron meteorites magnetite crust and cosmic spherules as indicators for atmospheric oxygen development 02 p0279 A72-12117
- Interstellar dust - IAU Conference, Jena, East Germany, August 1969 02 p0283 A72-12626
- Dust grain orientation parameter from Fokker-Planck equation, considering magnetic relaxation time, nearly spherical grains and oblate spheroids 02 p0283 A72-12627
- Dust grain existence at large distances from galactic plane by computing interstellar radiation field pressure effects on grains 02 p0283 A72-12629
- Dust continuous spectrum and Balmer line intensity ratio in Orion Nebula from slit spectroscopy observations [AD-745076] 02 p0284 A72-12631
- Extinction curves for Mie scattering by interstellar grains, including refractive index differences in vacuum UV for methane, ammonia and water ice absorption 02 p0284 A72-12633
- IR spectra of rock forming terrestrial and meteoritic silicates important in cosmic silicate dust 02 p0284 A72-12635
- Circumstellar dust formation hypothesis based on O stars mean circumstellar extinction, explaining Ca and Na abundance in interstellar gas 02 p0284 A72-12636
- Dust particle formation in circumstellar space accompanying star formation, discussing necessary and sufficient condition for grain escape by fragmentation 02 p0284 A72-12637
- Dust particle dynamical behavior during cloud collisions, discussing grain distribution in resultant cloud 02 p0284 A72-12638
- Diffuse galactic light absolute intensity interpretation, showing interstellar dust discrete cloud structure effect on grain properties determination 03 p0416 A72-13015
- Lunar ejecta and meteorites experiment, determining speed, direction, mass and flux density of cosmic dust particles 04 p0509 A72-15102
- Interstellar extinction curves for stellar far UV radiation, discussing required multicomponent interstellar dust model 05 p0720 A72-16717
- Interstellar dust distribution, nature and physicochemical and dynamic evolution, discussing star and galaxy observation, light diffusion, star reddening and IR sources 06 p0882 A72-17995
- MHz IR/OH sources, discussing M type Mira variables or M supergiants photospheric temperature and dust shell structure 07 p1069 A72-19075
- Dust particle composition and effect on light transmission in interstellar medium, discussing gas, magnetic fields, cosmic rays and background radiation 07 p1074 A72-19557
- Homogeneous anisotropic solutions of Einstein equations with cosmological term for universe with plane comoving frame filled with powder 09 p1352 A72-23361
- Gas and dust cloud evolution with allowance for dimensional finiteness and stellar evolution into red supergiant after hydrogen depletion 11 p1715 A72-25297
- Spectrophotometry of nebulosity associated Ae and Be stars, discussing age, circumstellar dust shells geometry and red stellar objects 11 p1720 A72-26114
- Lunar occultations of IRC plus 10216 for IR radiation distribution, deducing model of late type carbon star surrounded by thermally reemitting dust shell 11 p1721 A72-26123
- Ca and Na ionization equilibrium ratio in dust filled interstellar clouds, considering cosmic ray and charge transfer influence 13 p2040 A72-29405
- Proton accretion effect on circumstellar dust grains mass, noting impossibility of grain formation in H II region 13 p2048 A72-29790
- Stellar radiation and gravitational effects on neutral atoms and dust grains at large distances for various spectral type stars in schematic evolutionary galaxy 14 p2158 A72-30735
- Comet core ice particle dust cover failure conditions, noting critical dust matrix thickness relation to sun proximity 14 p2160 A72-30831
- Micrometeorite and cosmic dust flux rates for near earth orbit and interplanetary space from satellite and ground based measurements 15 p2309 A72-31955
- Coordinate system valid for Oppenheimer-Snyder spherical dust cloud collapse into black hole 16 p2452 A72-33046
- H I region molecular formation on interstellar dust grains, discussing nonequilibrium evaporation mechanism for adsorbed particles 16 p2452 A72-33128
- On the contribution of transition radiation from dust grains to the diffuse X-ray background. 17 p2600 A72-35314
- Quantum models for the lowest-order velocity-dominated solutions of irrotational dust cosmologies. 17 p2613 A72-35392
- Observations of planetary nebulae at 1.65 to 3.4 microns. 19 p2854 A72-37233
- Spherically symmetric system of radiating body surrounded by absorbing dust zone, investigating relativistic radiation pressure effects 19 p2859 A72-37893
- Microwave-analogy tests regarding light scattering at cosmic dust particles 19 p2804 A72-38507
- Heavy metal particle detection in noctilucent clouds by rocket experiments, using Pandora inflight shadowing technique 20 p2964 A72-39373
- Aluminum 26 and manganese 53 produced by solar-fare particles in lunar rock and cosmic dust 20 p2970 A72-39472
- Interstellar molecules and dense clouds. 20 p2970 A72-39600
- Dust particle sizes in cometary atmospheres and the heliocentric distance 20 p2970 A72-39726
- Solar coronal F component separation from K component by utilizing elongation dependence differences in scattering populations, computing F for wide range of parameters 21 p3106 A72-41041
- Balloon optical experiments in IR, visible, UV and X ray regions, considering in situ measurements of atmospheric composition, electric field and cosmic dust 21 p3049 A72-41613
- Interactions between stars and local dust formations 21 p3113 A72-41758
- Dark dust nebulae and bright H II clouds, considering light molecules, stellar birth region, radio and IR astronomy 22 p3220 A72-41995
- Internal dust effects on nebulae structure and spectrum, solving radiation transfer equation for spherical models with nonisotropic scattering 22 p3227 A72-42558
- COSMIC GASES**
- NT INTERPLANETARY GAS
- NT INTERSTELLAR GAS
- Electromagnetic radiation in universe, discussing relict radio emission, energy density, hot model isotropic extragalactic component isolation, intergalactic gas, radio sources and quasars 03 p0414 A72-14317

Thermodynamic models of gas-solid equilibria in cosmochemical systems containing H, O, Si, Mg, S, C, Cl and F

07 p1075 A72-19587

Big bang theory for age determination of galaxies, considering formation through gravitational instability and primeval gas velocity distribution fluctuations

07 p1084 A72-20470

Current-optical effects of anisotropic absorption of polarized and unpolarized light in rarefied cosmic media

10 p1525 A72-23763

Extragalactic clouds supersonic collisions with galactic gases, discussing high velocity neutral hydrogen gas result of recombination following post-shock surplus energy radiation

10 p1538 A72-24248

Intergalactic medium presence in clusters of galaxies from investigation of separation and size-separation ratio of double radio sources located inside and outside clusters

10 p1544 A72-24670

Quasars energy source and structure in terms of kinetic energy conversion to radiation in shock fronts of colliding gas clouds

10 p1544 A72-24671

Cosmic and solar wind abundance analysis for D and He-3 in protosolar gas, noting chemical equilibrium reaction role in D enrichment

12 p1868 A72-27216

Soft X-ray emission from intergalactic gas in the neighbourhood of the Galaxy.

19 p2855 A72-37345

Electromagnetic background radiation in universe, discussing relic radio emission, energy density, hot model isotropic extragalactic component isolation, intergalactic gas, radio sources and quasars

19 p2854 A72-38815

X-ray emission from intergalactic gas in the neighbourhood of galaxies.

20 p2964 A72-39240

Propagation of radiative shock waves in an inhomogeneous cosmic medium.

22 p3225 A72-42452

Equilibrium energy spectrum for the galactic cosmic electrons.

23 p3328 A72-43831

COSMIC NOISE

Substorm electron drift relationship to cosmic noise absorption on auroral zone morning side, calculating electron energy loss

01 p0063 A72-10918

Cosmic noise ionospheric absorption measurements with riometers, showing mid and low latitudinal variation

02 p0221 A72-12464

Sudden cosmic noise absorption from D region N-h profile during solar X ray flares on 13 April 1966

04 p0566 A72-14512

Planetary magnetic activity effects on hf cosmic noise absorption measurements at low and temperature latitudes

04 p0516 A72-14941

Book on radio wave propagation covering ground, tropospheric and ionospheric waves, atmospheric and cosmic noise, reflection, attenuation, signal distortion, space communication, etc

04 p0487 A72-15269

Rocket cosmic radio noise measurements at 1.16-2.40 MHz and 1600 km, confirming spectrum flatness

05 p0711 A72-15763

Photomultiplier operation pulsed control in semiconductor circuit for background cosmic radiation noise error minimization in atmospheric shower station

06 p0811 A72-17294

Diurnal, seasonal and solar cycle variations in cosmic noise absorption during 1957-1966, showing various ionospheric layers contribution

09 p1385 A72-22586

Cosmic background radiation temperature from interstellar CN band R branch absorption line in star zeta Ophiuchi spectrum

15 p2313 A72-32309

Cosmic microwave background radiation origin by energy dissipation associated with primordial chaotic universe

16 p2459 A72-33770

Characteristic features of ELF-noise spectra during the excitation of the earth-ionosphere resonator by cosmic sources

18 p2662 A72-36861

X-ray bremsstrahlung in the stratosphere and the auroral activity of January 21 and February 3, 1969

18 p2722 A72-36863

COSMIC PLASMA

Cosmic plasma phenomena in astrophysics, discussing distribution, ionospheric disturbances, magnetospheric waves, solar wind, etc

05 p0723 A72-17217

Radiative cooling induced thermal instability mechanism for condensation in astrophysical plasma

07 p1040 A72-19348

Scattering and scintillations of rf radiation from distant discrete astronomical sources as measure of interplanetary plasma irregularities

07 p1079 A72-20020

Ultrarelativistic cosmic plasma analysis of high density electron beams transport across strong magnetic fields with application to pulsar NP 0532 spectrum

07 p1064 A72-20634

Interplanetary plasma microinstabilities within framework of underlying electron-proton solar exosphere, discussing solar wind high beta effects

11 p1714 A72-26529

Ionized gas effect on interstellar space synchrotron emission, noting magnetic field orientation-dependent low frequency cut-off

14 p2156 A72-30559

Cosmic plasma physics - Conference, Frascati, Italy, September 1971

16 p2459 A72-33901

Cosmic plasma relations with laboratory plasmas within astrophysics, considering inhomogeneity, electrostatic double layers, filamentary structures and non-Maxwellian effects

16 p2438 A72-33902

Earth bow shock wave structure model based on development of strong density gradient in magnetic field-free cosmic plasma

16 p2387 A72-33935

On the physical nature of cosmic electromagnetic absorption. V - The Einstein-de Sitter cosmology with plasma coupled to radiation at non-relativistic temperature.

20 p2967 A72-39185

On the physical nature of cosmic electromagnetic absorption. VI - The Einstein-de Sitter cosmology with plasma coupled to radiation at relativistic temperature.

20 p2967 A72-39186

Electromagnetic wave dispersion in ionized cosmic medium for spatially flat Brans-Dicke cosmology

20 p2969 A72-39265

Frequency correlation measurement of pulsar spectral fine structure due to radio emission scattering by interstellar plasma

21 p3101 A72-41752

Turbulent plasma 'caldrons' in galactic nuclei

21 p3114 A72-41772

Effect of Thomson scattering on the emission spectrum of an optically semitransparent plasma

21 p3102 A72-41774

Transfer effects on X-ray lines in optically thick celestial sources.

24 p3435 A72-44843

COSMIC RADIATION

U COSMIC RAYS

COSMIC RADIO WAVES

U EXTRATERRESTRIAL RADIO WAVES

COSMIC RAY SHOWERS

Monte Carlo simulation on high energy cosmic ray propagation and multiplication in high altitude emulsion chamber observations, examining two-fire-ball and H-quantum models

01 p0121 A72-11123

Ultrahigh energy cosmic ray models indication of galactic origin and composition, based on energy spectrum flattening data

02 p0272 A72-11901

Hadrons in extensive air showers, predicting arrival time spectra from fireball and isobar-p ionization models for high energy interactions

03 p0409 A72-13147

Relativistic quark search by flash tube chamber in extensive air showers at ground level

03 p0410 A72-13149

High energy primary cosmic ray particle evidence from energetic air shower observation data analysis

03 p0413 A72-14097

Air shower cores or relativistic monopoles as sources of straight lightning, considering thundercloud conditions over ocean and land areas

03 p0350 A72-14100

Nuclear-electron cascades longitudinal evolution calculation in ionization calorimeter for primary nucleons and pions, using Monte Carlo method

06 p0811 A72-17260

Secondary cosmic ray shower charged particles angular distribution asymmetry in C-system and azimuthal plane related to single fireball formation

06 p0868 A72-17263

Energy spectrum, composition and anisotropy study of cosmic radiation from extensive air showers, using scintillation and Cerenkov detectors

06 p0870 A72-17277

Extensive air showers radio emission polarization, spatial distribution and electric field strength, noting geomagnetic mechanism effect

06 p0870 A72-17278

Electron and muon density fluctuations, trajectory distribution and azimuthal symmetry in cosmic ray air showers

06 p0870 A72-17279

Vertical extensive air showers at aircraft heights, constructing integral spectrum based on particle number

06 p0870 A72-17280

Primary cosmic radiation energy spectrum approximation from air showers, high-energy hadrons and Proton 4 data

06 p0870 A72-17281

Cosmic radiation high energy hadron component relation to extensive electron-photon showers, comparing sampling events based on multicore structure and total energy

06 p0870 A72-17282

Extensive air shower spectra based on electron and muon number

06 p0871 A72-17283

Extensive air shower characteristics and muon counts at different level observations relative to particle number and primary energy spectra

06 p0871 A72-17284

High energy cosmic ray interactions at one TeV, including X process, horizontal showers and muon pool showers

06 p0871 A72-17285

Energy spectrum of muon formed electromagnetic cascades in vertical cosmic radiation flux

06 p0871 A72-17287

Spectral calculations of electromagnetic and nuclear showers of cosmic ray muons interacting with substance

06 p0871 A72-17288

Muon densities in penetrating high energy particles, comparing with extensive atmospheric showers

06 p0871 A72-17289

Muon generated cascade showers in iron, using ionization calorimeter and hodoscope detectors

06 p0871 A72-17290

Cosmic ray showers age distribution, assuming composite nature of horizontal showers due to initiation by several primary showers

07 p1056 A72-18908

Spurious physical effects in penetrating cosmic ray showers resulting from momentum measurement errors

07 p1060 A72-19853

Semiautomatic stereophotographic processing of cosmic ray shower particle interaction data from Wilson chamber

07 p0988 A72-19865

High energy inelastic interactions in cosmic ray showers, using Wilson chamber

07 p1060 A72-19866

Extensive atmospheric showers and high energy transfer from interacting nucleons to electron photon cascades

07 p1060 A72-19867

Radiation measuring instruments assembly for extensive air showers and cosmic ray particle nuclear interactions at high energies

07 p0988 A72-19868

High energy gamma quanta point sources from extensive air showers Cerenkov flares records, finding flux limits of radio galaxy and pulsars

07 p1064 A72-20635

High energy hadrons time structure in extensive air showers, considering production of nucleon-antinucleon pairs in particle interactions

07 p1067 A72-20687

Measuring equipment for charged particles spatial distribution in cosmic ray showers, considering multi-axial and secondary young showers

08 p1226 A72-21077

Inelasticity fluctuations effect on cosmic ray showers development, proposing criteria for lateral electron distribution and relative abundance of hadrons and muons

10 p1529 A72-24213

Muon rich showers interpretation, allowing for combined influence of types I and II fluctuations

10 p1529 A72-24229

Cosmic ray experiment jet shower event with possible new particle existence

11 p1712 A72-25867

Cosmic ray showers age parameter change with density of penetrating component, using Geiger counters and scintillator system

12 p1864 A72-27720

Time structure of massive interacting particles with energies above 20 GeV near axes of cosmic ray showers of energy above 100 TeV

12 p1864 A72-27737

Astrophysical equipment for Cerenkov radiation measurement from atmospheric showers, discussing source of high energy gamma rays in galactic equator direction

14 p2146 A72-30201

Intensity and energy spectrum calculation of albedo electrons recorded in cosmic particle showers by gas discharge counters

14 p2105 A72-30629

Extensive air showers at zenith, measuring associated UHF radio pulses with optical Cerenkov emission receiver as trigger source

14 p2147 A72-30858

Lateral distribution, radiation spectra and pulse shapes calculated from mathematical models of cosmic ray showers radio emission, noting chemical composition of primary particle

15 p2230 A72-32262

Radio pulses from extensive air showers detected by antenna array with east-west oriented dipoles connected in parallel 16 p2444 A72-33036

Underground delayed shower particles small pulse events interaction analysis for muons and pions compared with quark behavior 16 p2450 A72-34140

Upper limit of the mean interaction path of cosmic protons generating extensive air showers 17 p2598 A72-34287

Study of high energy /25-10,000 GeV/ interactions with a multiplate cloud chamber using Monte Carlo simulations for energy calibration. 17 p2585 A72-34922

Temporal distribution of Cerenkov light from extensive air showers, discussing experimental setup and pulse shape 17 p2599 A72-35140

Analysis of geometry effects in the detection of Cerenkov light from extensive air showers. 17 p2599 A72-35141

Monte Carlo calculation of radial and time dependence of isophote diagrams for Cerenkov light in 0.1 to 1 TeV extensive air shower 17 p2599 A72-35142

Electron showers of high primary energy in lead. 17 p2585 A72-35472

High energy gamma ray sources search by Cerenkov radiation recording from extensive air showers, noting atmospheric transparency effects 19 p2850 A72-37805

Preliminary results of observations of the pulsar CP 1133 with the aid of a device for recording Cerenkov flares of extensive atmospheric showers 19 p2850 A72-37806

Pion exchange and the cosmic-ray nucleon cascade. 19 p2851 A72-37923

Extensive air showers and the sporadic decimeter radio emission of Jupiter 19 p2863 A72-38073

Astrophysical equipment for Cerenkov radiation measurement from atmospheric showers, discussing source of high energy gamma rays in galactic equator direction 23 p3328 A72-43226

High energy inelastic interactions in cosmic ray showers from Wilson chamber and ionization calorimeter observations, noting secondary particles occurrence dependence on primary energy 23 p3330 A72-44406

The EAS power spectrum at sea level for $N = 10$ million to 1 billion particles 23 p3330 A72-44418

EAS Cerenkov glow and the relation of shower strength to the primary-particle energy 23 p3330 A72-44419

Experiment for studying the pulse shape of Cerenkov emission at large distances from an extensive air shower 23 p3330 A72-44420

Angular distribution of extensive air showers in a range of large zenith angles 23 p3330 A72-44421

Energy spectrum and composition of primary cosmic radiation at energies from 50 to 5000 TeV 23 p3330 A72-44422

Investigation of EAS characteristics at sea level with the aid of the classical method and by the method of recording radio emission 23 p3330 A72-44423

Low-energy nucleons in extensive air showers 23 p3331 A72-44424

Certain characteristics of the muon and electron components of extensive air showers at mountain level 23 p3331 A72-44425

Muon component near the axis of an extensive air shower 23 p3331 A72-44426

Energy spectrum and angular distribution of cascades with an energy greater than 0.3 TeV, formed by cosmic muons 23 p3331 A72-44427

A study of the mechanisms of formation of penetrating particle groups by the spark calorimeter method 23 p3291 A72-44430

Fluctuations of the spatial distribution of the number of particles in showers generated by muons in heavy material 23 p3331 A72-44431

Behavior of the spatial distribution function of shower particles near the axis of a cascade shower 23 p3331 A72-44432

Angular distribution of high-energy cosmic-ray muons 23 p3331 A72-44434

S-system motion effect on angular distribution of secondary high energy particle cluster in showers formed by primary and neutral particles, considering nucleon collision line 23 p3331 A72-44436

COSMIC RAYS
NT COSMIC RAY SHOWERS
NT PRIMARY COSMIC RAYS

NT SECONDARY COSMIC RAYS
NT SOLAR COSMIC RAYS

Cosmic gamma rays at 0.3-3.7 MeV measured by NaT/Tl crystal detector 64-channel spectrometer on-board Cosmos 135 and 163 01 p0118 A72-10153

Book on solar and galactic cosmic rays covering collisions with matter, propagation through geomagnetic field and atmosphere and origin 01 p0118 A72-10170

Interstellar medium physical properties and distribution, discussing ionization heating by starlight, cosmic X rays and subcosmic rays 01 p0128 A72-10413

Primary component corrections for global cosmic ray variations from latitudinal expeditions, discussing adaptation to computer 01 p0118 A72-10584

Cosmic ray density distribution inside cosmic ray modulating spherical cone in solar wind, noting modulation depth quasi-periodic variation 01 p0119 A72-10606

Cosmic ray energetic spectrum variation from observed latitudinal effects during 1954-1962 solar activity cycle 01 p0119 A72-10607

Supernova Vela X and local remnants as origin of below 1000 GeV cosmic electrons, deducing existence at 10 to 15 GeV from muon poor showers 01 p0119 A72-10853

Balloon measurements for differential energy spectra of cosmic ray protons and He over half solar cycle 1965-1969, using Geiger tube hodoscope 01 p0119 A72-10876

Cosmic ray neutron leakage flux and energy spectrum measurements in 0.01-10 MeV range by OGO 6 satellite-borne neutron detector 01 p0119 A72-10877

North-south asymmetry of cosmic ray intensity dependence on interplanetary sector magnetic field sign, based on spherical harmonic analysis during several sector structure passages 01 p0120 A72-10908

Long term galactic cosmic ray intensity modulation correlation to 5303 A coronal intensity during rising part of solar activity cycle 01 p0120 A72-10909

Similarity models of interstellar loop structures, investigating magnetic field and energy losses effects and cosmic ray emission 01 p0131 A72-11011

Cosmic Li, Be and B nuclei charge and isotopic composition measured by particle telescopes, finding L/M ratio 01 p0121 A72-11200

Cosmic soft X ray and UV radiation sources, discussing transition radiation emission in interstellar space 01 p0121 A72-11211

Primeval fireball cosmic background radiation spectrum in homogeneous axisymmetric anisotropic world model including electron neutrino effects on expansion dynamics 01 p0121 A72-11339

High speed interstellar gas dynamic resonant hydromagnetic wave interaction with cosmic ray shocks 01 p0121 A72-11140

Cosmic and X ray irradiated quartz particles as contributor to interstellar extinction, discussing grain radiation damage measurements and absorption spectra in wavelengths of approximately 1600 Å to 20 micrometers 01 p0134 A72-11163

Extragalactic cosmic ray hypothesis plausibility from viewpoints of energy supply, acceleration process efficiency, galactic nucleus activity and intergalactic space 01 p0122 A72-11268

Galaxy source of ultrahigh energy cosmic rays, interpreting energy spectrum kinks as galactic to metagalactic radiation transition 01 p0122 A72-11270

Galactic cosmic ray-solar wind nonlinear interaction effects on solar wind geometry near and far from sun 02 p0272 A72-11917

Neutron cosmic ray spectrograph method of separating recorded data by energies, using statistical analysis of data combinations with different dead times 02 p0229 A72-11936

Correlation coefficients for galactic cosmic rays relation to solar activity indices in interplanetary space 02 p0273 A72-11937

Cosmic proton and neutron produced recoil proton energy spectra measurements along earth-moon-earth trajectory with nuclear emulsions aboard Zond 5 and 7 [CERN-71-16] 02 p0273 A72-12074

In-flight warming meter for solar and cosmic radiation dose equivalent measurements for radiological protection in SST aircraft 02 p0274 A72-12078

Cosmic ray exposure shutdown tracks in human tissue from solar minimum to maximum at SST flight level [CERN-71-16] 02 p0163 A72-12079

Galactic cosmic ray self trapping, discussing hydromagnetic wave velocity of ray propagation from sources 02 p0274 A72-12190

Cosmic ray neutrons angular distribution and energy spectrum at 3200 m altitude, using ionization calorimeter and proportional counters 02 p0275 A72-12828

Cosmic ray intensity long term modulation and 27 day recurrence relationship to solar activity 03 p0407 A72-12945

Cosmic X ray sources polarization, spectra and locations measurement, describing Skylark experiments and UK-5 satellite-borne instruments 03 p0409 A72-13042

Radio Astronomy Explorer Satellite data on solar bursts, interstellar medium ionized component distribution, cosmic rays and galactic halo magnetic fields 03 p0330 A72-13067

Pulsars formation rate and connection with supernovae and cosmic rays, discussing stellar magnetic field strength 03 p0421 A72-13134

Pulsar origin of cosmic rays, considering accelerated charged particles maximum energy 03 p0421 A72-13135

Neutron star surface structure and cooling calculations for pulsar cosmic ray production through surface material acceleration 03 p0421 A72-13136

Heavier-than-helium cosmic ray nuclei composition inferring galactic confinement of particles, path lengths and transit times 03 p0409 A72-13137

Diffuse cosmic background radiation measurements, emphasizing microwave and X ray spectra and excitation mechanism 03 p0409 A72-13138

Dispersion energy relation for ultrahigh energy nuclear reactions in cosmic ray emulsion 03 p0410 A72-13148

Nuclear radiation interference and damage effects in galactic and solar cosmic ray measurements during charged particle experiments by deep space missions 03 p0438 A72-14085

Fast particle interaction with intergalactic matter, discussing relaxation of power law cosmic ray spectra 04 p0570 A72-14553

Nonuniform solar wind velocity effect on interplanetary medium and on cosmic radiation, observing diurnal variations 04 p0567 A72-14928

Interstellar propagation of 2-8 Z galactic cosmic ray nuclei at 10-1000 MeV/nucleon, analyzing differential kinetic energy spectra 04 p0567 A72-15323

Cosmic ray induced radioactivity effects on diffuse gamma ray background measurement from 600 MeV proton irradiation experiment 04 p0567 A72-15324

Heavy nuclei enrichment in solar accelerated particles, discussing differential energy spectra, photospheric and coronal abundances, satellite observation and agreement with galactic cosmic rays 04 p0568 A72-15366

Li, Be and B production rate in interstellar gas by galactic cosmic rays from diffusion model of fast particles, accounting for He component 05 p0708 A72-15760

Fission origin of cosmic ray fossil tracks in augite achondrite high-uranium-concentration meteorite Angra dos Reis 05 p0714 A72-16078

Cosmic ray spectrum at nonrelativistic energy region, noting ionization loss effects 05 p0709 A72-16238

Atmospheric temperature effect on solar diurnal variation of muon component, considering asymptotic characteristics of cosmic ray anisotropy 05 p0709 A72-16257

Atmospheric neutron production by cosmic rays, calculating Cd-In ratio 05 p0662 A72-16258

Cosmic gamma radiation theoretical and experimental investigations, discussing sources, interactions with interstellar and intergalactic media, atmospheric backgrounds, balloon and satellite measurements, etc 05 p0709 A72-16328

Active solar regions effects on galactic cosmic ray intensity 05 p0710 A72-16526

Metagalactic gamma rays from relativistic electron bremsstrahlung interactions under assumption of single power law source 05 p0710 A72-16712

OGO-5 measurement of 10-200 MeV cosmic ray electron energy spectra, discussing quiet time flux intensity 05 p0720 A72-16719

European Space Research and Technology Center /ESTEC/ results in cosmic rays, ionospheric physics and surface physics 05 p0644 A72-16754

Scaling hypothesis testing by angular distributions from cosmic ray experiments 05 p0711 A72-17125

Constant cosmic spherule influx rate measured on quaternary deep sea sediments 05 p0722 A72-17153

Cosmic ray physics - Conference, Moscow, USSR, October-November 1970 06 p0868 A72-17257

Cosmic ray hadrons inelastic collision cross sections and partial K-neutral pion inelasticity factor in ionization calorimeter 06 p0868 A72-17262

High energy cosmic ray pions and nucleons interactions with atomic nuclei, using ionization calorimeter and spark chambers system 06 p0869 A72-17267

Cosmic ray particle high energy inelastic interactions, discussing pion and nucleon interaction angular and energy characteristics and muon production mechanism 06 p0869 A72-17270

Inelastic ionization cross section of cosmic ray hadrons with carbon nuclei at energies of 100 to 300 GeV 06 p0869 A72-17271

Off-ecliptic north-south anisotropies in cosmic radiation intensity during polar storm events 06 p0873 A72-17467

Semidiurnal lunar variation, solar and sidereal effects on cosmic radiation intensity, using zenith pointed particle telescopes 06 p0873 A72-17490

Cosmic ray muon intensity in interplanetary magnetic field, revealing sidereal variation due to motion of solar system relative to local galactic rotation frame 06 p0873 A72-17648

Cosmic ray exposure age of australites and far-east tektites, using C14 content as indication of terrestrial age 06 p0878 A72-17761

Pulsar produced cosmic rays energy spectrum, investigating light elements origin 06 p0874 A72-18161

Gas retention and cosmic ray exposure ages of lunar rock from Hadley Rille, using isotopic dilution method 06 p0888 A72-18268

Isolated pulsar or neutron star upper mass limit based on consideration of rotational energy by ejection of low energy cosmic rays or photons 06 p0891 A72-18508

Forbush decreases in galactic cosmic ray flux and associated vlf nighttime ionospheric propagation phenomena 07 p1056 A72-18900

Cosmic rays generation by charged particles acceleration in electromagnetic constant crossed fields during magnetic stars contraction to neutron star dimensions 07 p1056 A72-19042

Interstellar matter cooling and recombination after supernova ionization, comparing X ray and cosmic ray heating mechanisms 07 p1070 A72-19083

Solar modulated galactic cosmic rays radial gradient idealized model for comparable deceleration and convection effects 07 p1057 A72-19138

Radionuclides formation rate as function of depth in moon for bombardments by galactic cosmic ray particles and by solar protons 07 p1057 A72-19140

Cosmic radiation effects in Concorde prototype cabin, using photographic dosimeters for neutron dose measurement and nuclear emulsions for all charged particle recordings 07 p0927 A72-19241

Superconducting magnetic spectrometer for cosmic ray nuclei spectrum analysis, describing design, calibration and operation 07 p0983 A72-19315

Forbush decreases in cosmic radiation, discussing cosmic ray flow pattern deduction from anisotropies, modulation dependence on rigidity and theoretical models 07 p1058 A72-19355

Cosmic ray nuclei intensity and energy spectrum measurement in nuclear emulsions stack, noting no charge dependence in solar modulation process 07 p1059 A72-19582

Balloon measurement of low energy cosmic gamma ray flux, obtaining energy spectrum 07 p1059 A72-19585

Inelastic high energy multiple interactions between cosmic ray particles and atomic nucleus targets, using Wilson chamber and ionization calorimeter 07 p0988 A72-19864

Cosmic ray heavy nuclear component during solar activity minimum, using Cerenkov counters onboard Elektron satellites 07 p1060 A72-19872

Galactic cosmic ray modulation by interplanetary medium, including solar wind boundary problem 07 p1061 A72-20021

Low energy solar cosmic ray measurements in interplanetary space with Zond space probes, comparing to galactic cosmic rays 07 p1061 A72-20022

Pulsar production rate relationship to high energy cosmic ray origin and number density 07 p1081 A72-20059

Extragalactic origin of diffuse low energy cosmic gamma rays, using balloon-borne detector system 07 p1063 A72-20392

Cosmic ray muons integral energy spectrum and angular distribution at sea level represented by power law, using primary interaction model 07 p1063 A72-20475

Galactic cosmic ray particle intensity decrease relationship to low energy proton flux increase based on interplanetary Zond 3 and Venera probes measurements 07 p1063 A72-20626

Ionization loss effects on cosmic ray lifetime in galactic interstellar medium, noting dependence on particle energy 07 p1064 A72-20637

Interstellar gas role in cosmic ray yearly variations determined from solar short wave radiation induced gas ionization 07 p1065 A72-20640

Solar modulation of cosmic ray intensity in stratosphere, examining relationship to sunspots group number and heliographic latitudes over 11 year period 07 p1065 A72-20641

Solar wind magnetic fields characteristics relative to 11 year cosmic ray modulation in interplanetary space 07 p1065 A72-20642

Nonstationary and asymmetric cosmic ray modulation theory, discussing moving boundary problem and solar wind model with spherical singularity 07 p1065 A72-20643

Galactic cosmic ray modulation region evaluation from meteoroid orbit, velocity and radioactive dating data 07 p1065 A72-20644

Three dimensional cosmic ray anisotropy and density distribution at earth orbit and in interplanetary space with allowance for primary particle and nucleon energy spectrum 07 p1065 A72-20645

Solar active regions effects on galactic cosmic ray distribution and interplanetary magnetic field structure 07 p1065 A72-20646

Diurnal, sporadic and yearly variations in cosmic ray flux based on neutron component data, noting relation to solar activity cycles 07 p1066 A72-20647

Diffusion and stochastic variations of galactic cosmic rays in solar wind 07 p1066 A72-20648

Stratospheric cosmic ray short period variations at 30 km by spectral density method 07 p1066 A72-20653

Meteorological effects on cosmic rays, deriving muon and pion intensity and meteorological coefficient formulas and computer calculation scheme 07 p1066 A72-20654

Computerized numerical calculation of muons production spectrum, angular distribution and Coulomb scattering in determining meteorological factors effects on cosmic rays 07 p1067 A72-20655

Solar wind propagation limitations by galactic magnetic field and cosmic rays and solar system motion relative to interstellar gas 08 p1225 A72-20701

Atmospheric pressure, temperature, humidity and 200-mb level changes effects on cosmic ray neutron component intensity, using multifactorial regression analysis 08 p1225 A72-20702

Muon telescopes calibration for cosmic rays rigid component variations by data comparison with variable aperture telescope 08 p1162 A72-20720

High energy charged particles angular distribution measurements in equatorial region cosmic radiation above atmosphere by Proton 2 satellite 08 p1226 A72-20799

Solar modulation process for galactic cosmic ray particle time variation, discussing interplanetary magnetic fields and plasma, energy losses from solar wind deceleration, etc 08 p1227 A72-21188

Particle detector assembly for low energy heavy mass cosmic ray nuclei identification 08 p1167 A72-21508

Electron scattering effects on response of cosmic ray particle telescopes from pulse height and counting rate measurements 08 p1167 A72-21510

Models of galactic diffuse sources of soft cosmic X rays, estimating spectrum and intensity 08 p1228 A72-21650

TD-1 satellite mounted slow analysis camera with supervidicon image tube to observe cosmic ray tracks in spark chamber 08 p1170 A72-21961

Pion generation during collective interactions between nucleons of heavy cosmic ray nuclei, using Proton 4 satellite data 08 p1228 A72-22179

Nighttime D region ionization production by cosmic X rays from various celestial sources and galactic background 09 p1375 A72-22359

High energy cosmic ray hadrons energy measurement using glass scintillator ionization spectrometer 09 p1309 A72-22523

Tranquillity Base rocks irradiation depths and cosmic rays exposure ages from rare gases in samples, noting correlated variations in He 3/Ne 21 and Ar 38/Ne 21 due to shielding differences 09 p1377 A72-22596

MHD stability problems in radio galaxy structure and cosmic ray interaction with magnetic fields 09 p1386 A72-22751

Pulsars CP 0328 and NP 0531 twinkling explained by interstellar electron density fluctuations due to Alfvén wave passage and coupling of cosmic rays to interstellar gas 09 p1377 A72-22753

Interplanetary space three dimensional cosmic ray anisotropy from harmonic components of diurnal variations 09 p1377 A72-22926

Expression for annual modulation of diurnal variation from generalized cosmic ray anisotropy in space, applying to earth revolution induced modulation 09 p1377 A72-22927

Semidiurnal cosmic ray anisotropy, eliminating atmospheric effects and global isotropic variations in cosmic ray telescope 09 p1377 A72-22928

Space anisotropy responsible for solar semidiurnal variation of cosmic ray intensity studied with data from worldwide network of neutron monitor stations 09 p1377 A72-22929

Cosmic electrons energy spectrum between 1 and 25 GeV from balloon observations, noting Compton/synchrotron loss effects 09 p1377 A72-23001

German monograph on experimental search for quarks in cosmic ultraradiation, describing hodoscope for particle ionization measurement 09 p1378 A72-23100

TD-1A satellite functional description for stellar UV spectroscopy and solar and cosmic ray experiments, emphasizing attitude control subsystem 09 p1396 A72-23263

Galactic and universal theories of cosmic ray source mechanisms, energy requirements, particle composition, propagation through interstellar matter and acceleration in supernovae remnants 10 p1533 A72-23889

Skylark 904 sounding rocket cosmic X ray experiment, discussing detector and counter operation and data retrieval technique 10 p1529 A72-24198

Cosmic radiation effects and damage on solar cells, discussing shielding, stability improvement, space environments, minority carrier lifetime and photosensitivity spectral distribution 10 p1422 A72-24312

Radio continuum survey of spiral galaxies M51 and NGC 5195 for study of galactic magnetic field and cosmic rays origin and distribution 10 p1543 A72-24623

Cosmic ray proton and He nuclei differential energy spectra measurements by balloon-borne ionization spectrometer 11 p1712 A72-25881

Particle-proton total cross section from cosmic ray data on proton-air inelastic cross sections 11 p1712 A72-25884

Outer space and earth surface galactic cosmic ray intensity data correlation analysis for studying interplanetary magnetic field structure 11 p1713 A72-25936

Ionospheric detection of cosmic X rays by VLF links using nova sources 11 p1714 A72-26417

Radiogenic Ar 40/Ar 39 age and cosmic ray irradiation history of Apollo 15 anorthosite sample 15415, indicating Imbrian impact heating 12 p1862 A72-27111

Antiproton energy spectrum in cosmic rays from primary proton-interstellar hydrogen collision in two fireball model 12 p1863 A72-27186

Cosmogenic radionuclides pickup by cloud water and deposition in precipitation described by model 12 p1863 A72-27503

Time variable energy losses effects on cosmic ray nuclei composition, discussing fragmentation processes during heavy nuclei propagation through interstellar matter 12 p1864 A72-27692

Hydromagnetic wave scattering of high energy cosmic rays in highly ionized interstellar gas to confine cosmic rays to Milky Way

12 p1864 A72-27745

Sea level absolute vertical cosmic ray muon intensity from range spectrometer measurements within tropic zone

12 p1864 A72-28225

Russian book on geomagnetic field cosmic rays covering charged particle motion theory, extratroposphere currents, magnetosphere tail and solar wind effects, etc

12 p1864 A72-28345

Exponential functions model for D region vertical distribution of electron density profiles, taking into account solar X- and cosmic rays

13 p1945 A72-28581

Solar wind distortion of stellar anisotropy of galactic cosmic rays, associating annual particle density variation with earth revolution about sun

13 p2029 A72-28590

Cosmic ray diffusion in radial divergent flow of magnetic discontinuities in interplanetary plasma, discussing isotropy in presence of regular magnetic field

13 p2029 A72-28591

Meteor-induced magnetic effect on cosmic ray intensity for meteor streams with orbits normal or parallel to interplanetary magnetic field lines of force

13 p2029 A72-28592

Interstellar gas motions and density and temperature variations, discussing galactic structure, radiation fields and cosmic ray effects

13 p2038 A72-29009

Cosmic X ray background intensity and spectrum interpretation in terms of metagalactic origin within evolutionary cosmology framework

13 p2030 A72-29087

Galactic cosmic ray-solar wind nonlinear interaction effects on solar wind geometry near and far from sun

13 p2030 A72-29229

Neutron cosmic ray spectrograph method of separating recorded data by energies, using statistical analysis of data combinations with different dead times

13 p1957 A72-29248

Correlation coefficients for galactic cosmic rays relationship to solar activity indices in interplanetary space

13 p2030 A72-29249

Low energy relativistic cosmic ray electrons temporal intensity variations from IMP satellite measurements, considering correlation with solar activity

13 p2030 A72-29376

Self consistent model for cosmic ray propagation from sources in Galaxy toward earth, using H and He isotope interstellar spectra

13 p2031 A72-29409

Galactic cosmic ray anisotropy due to radial and diffusive streaming in direction of interplanetary magnetic field, using neutron monitor data

13 p1033 A72-29747

Galactic cosmic rays density distribution normal to solar equatorial plane and resultant semidiurnal anisotropy, comparing different methods results with experimental observations

13 p1033 A72-29807

Cosmic ray anomalous absorption height dependence on zenith distance in midlatitude ionosphere during solar flare emission from polarization study

14 p2146 A72-30461

Celestial sources investigation for high energy cosmic gamma rays with particular attention to Crab Nebula

14 p2147 A72-30560

Harmonic analysis of solar wind geometry and geomagnetic activity levels during even and odd cycles based on cosmic ray intensity variations for 1900-1969 period

14 p2147 A72-30651

Weber experiment gravitational signals correlation to solar and geomagnetic activity and cosmic ray intensity

14 p2160 A72-30886

Scaling hypothesis and limiting fragmentation mechanism for cosmic ray muon production, noting energy independent charge ratio

15 p2298 A72-31289

Cosmic ray irradiations study of gas rich meteoroid aubrites by track method, comparing with lunar soils

15 p2303 A72-31308

Transient North-South anisotropies in cosmic radiation intensity, noting occurrence during Forbush decreases

15 p2298 A72-31432

Cosmic ray density gradient perpendicular to ecliptic plane, noting component introduction into diurnal variation depending on sense and direction of interplanetary magnetic field

15 p2298 A72-31436

Cerenkov counter for astronomical observatory high energy cosmic ray experiments, discussing UV-reflecting paint, radiator and photomultiplier positioning improvements

15 p2234 A72-31536

Variable cosmic X ray source location determination, noting Crab pulsar as radio, optical, X ray and gamma source

15 p2298 A72-31599

Diffuse cosmic gamma ray flux density and energy spectrum observation at equatorial balloon altitude, discussing photon count, flux and spectra

15 p2299 A72-31924

Background spallation source errors in satellite measurements of diffuse cosmic X ray spectrum with crystal scintillators

15 p2300 A72-31986

Report to COSPAR on Australian space program covering earth atmosphere, cosmic and synchrotron radiation, X ray astronomy, weather satellites, deep space and sounding rockets

15 p2338 A72-32007

Report to COSPAR on Netherlands space research covering solar and stellar radiation, cosmic gamma and X rays, photometry and satellite geodesy

15 p2338 A72-32010

Nonionizing component of underground high energy cosmic radiation investigated with anticoincidence screen and counters, noting bremsstrahlung as photons source

15 p2301 A72-32232

Relativistic charged particles produced transition radiation as diffuse cosmic X rays source, discussing validity based on interstellar space energy density consideration

15 p2301 A72-32716

Distribution of high velocity hydrogen near Galactic center due to free-free emission from exploding hot gas or cosmic ray pressure

15 p2317 A72-32756

Magnetic field rapid dissipation induced by stochastic topology of lines of force, discussing implications for hydromagnetic turbulence, solar activity and cosmic ray diffusion

16 p2378 A72-33454

Interplanetary radiation types in terms of possible space flight hazards, discussing electromagnetic and corpuscular radiation, cosmic rays and radiation belts

16 p2446 A72-33553

Cosmic ray nuclei charge and isotope composition measurement, discussing data for Li, Be, B and 15-30Z nuclei

16 p2447 A72-33727

Cosmic ray isotopic data extraction via geomagnetic field, discussing magnetic effects on particle flux and finite resolution limitations of counters

16 p2447 A72-33728

Balloon flight observation of charge composition fine details and gross features of isotopic abundance in near relativistic cosmic rays

16 p2447 A72-33729

Heavy cosmic ray nuclei tracks in etched plastic sheets flown in satellites and balloons, discussing detector response as function of velocity

16 p2447 A72-33730

Cosmic ray nuclei isotope identification with cryogenic magnet plus plastic scintillators to measure charge composition and rigidity

16 p2447 A72-33732

Li, Be and B spallation reactions in galactic cosmic rays from observations of cross sections of energetic protons incident on C and O targets

16 p2447 A72-33734

Li, Be and B nuclei production via nuclear spallation reactions generated by Galactic cosmic ray bombardment of interstellar gas

16 p2448 A72-33737

Be isotopic ratio in galactic cosmic rays, noting mean interstellar hydrogen density and rays age

16 p2448 A72-33738

Nitrogen existence in galactic cosmic ray sources, considering formation from CNO cycle hydrogen and He burning and ejection from normal stars

16 p2448 A72-33739

Model for low energy galactic cosmic ray effects on young and F star Li abundance and H I region heating

16 p2448 A72-33740

Interstellar cosmic ray electron component and isotopic composition relations from positron observations

16 p2448 A72-33741

Diffusion propagation and source distribution effects on cosmic ray charge composition and anisotropy in galactic disk, considering nuclear fragmentation

16 p2448 A72-33742

Low energy cosmic ray deuteron and He 3 source spectra observation implications for adiabatic deceleration in solar cavity, discussing interstellar propagation

16 p2448 A72-33743

Supernova explosion mechanism and quantitative game for galactic chemical evolution, discussing relationship to cosmic rays

16 p2459 A72-33744

Neutron star acceleration of He, Fe and supernova debris into cosmic ray flux throughout Galaxy, discussing magnetic and superfluidity effects

16 p2448 A72-33745

Cosmic ray electron search and study, comparing near earth to interstellar spectrum

16 p2448 A72-33869

Galactic magnetic field origin and large scale instability associated with Galactic field and cosmic rays, discussing thermal instability in interstellar gas

16 p2460 A72-33922

Interplanetary magnetic field irregularities and shock effects associated with cosmic ray Forbush decreases

16 p2449 A72-33939

Diurnal cosmic ray neutron variation dependence on interplanetary magnetic field based on neutron monitor data

16 p2449 A72-33940

Observation of the diffuse cosmic gamma radiation in the 30-50-MeV region.

17 p2598 A72-34522

Test of scale invariance in pion production at high energies using cosmic ray primary nucleon and sea level muon intensities.

17 p2599 A72-34875

An improved measurement of the charge ratio of cosmic ray muons in the range 10-300 GeV/c.

17 p2599 A72-34920

Galactic cosmic rays anisotropy prediction as function of energy for various assumed source distributions and magnetic field configurations

17 p2599 A72-34924

Origin of the low energy diffuse cosmic X-ray flux.

17 p2599 A72-35071

The absolute vertical cosmic-ray muon intensity at sea level.

17 p2600 A72-35147

Disk-shaped diffusion model with inhomogeneous distribution of gas and heavy relativistic nuclei sources for galactic cosmic rays chemical composition

17 p2600 A72-35206

Cosmic-ray heating of low-density interstellar H II regions.

17 p2600 A72-35296

The stability of a self-gravitating, nonrotating gas layer with stellar, magnetic, and cosmic-ray components. I.

17 p2611 A72-35313

Brief survey of the problems of space radiobiology and radiation safety in space flights.

17 p2509 A72-35376

Characteristics of cosmic ray diurnal variation from Deep River neutron and meson data and temperature effects.

17 p2601 A72-35400

Liquid scintillation counters application in search for relativistic quarks in cosmic rays, setting upper confidence limits on particle intensity

17 p2601 A72-35471

Cosmic ray electron spectrum and its modulation near solar maximum.

17 p2601 A72-35583

Rigidity dependence of cosmic ray modulation function at 2-13 Gv from C-130 aircraft survey flights data

17 p2602 A72-35606

Auroral cosmic radio emission absorption mechanisms, considering ionization rate, recombination coefficient and collision frequency effects

17 p2602 A72-35865

Cosmic ray anisotropy and conditions in the interplanetary medium during a solar cycle

17 p2603 A72-35871

Argon 37/argon 39 activity ratios in meteorites and the spatial constancy of the cosmic radiation.

18 p2723 A72-36027

Pion generation during collective interactions between nucleons in heavy cosmic ray nuclei, using Proton 4 satellite data

18 p2721 A72-36235

North-south asymmetry in cosmic ray intensity increases before magnetic storms

18 p2722 A72-36851

Some aspects of cosmic ray differential spectrum measurements

18 p2722 A72-36852

The diurnal effect of the cosmic rays during the period 15 October 1965-30 June 1966. I - Method of analysis and statistical distribution.

18 p2722 A72-37159

The diurnal effect of the cosmic rays during the period 15 October 1965-30 June 1966. II - The equatorial cosmic-ray anisotropy and the interplanetary magnetic field.

18 p2722 A72-37160

The north-south anisotropy and the cosmic-ray radial gradient in the vicinity of the earth.

18 p2722 A72-37164

Detection of high-energy gamma rays from the Crab Nebula.

19 p2850 A72-37503

Solar flare composition and energy spectra of heavy nuclei from 1971 rocket observations comparing to cosmic ray abundances

19 p2850 A72-37509

Solar wind propagation limitations by galactic magnetic field and cosmic ray pressure and solar system motion relative to interstellar gas

19 p2851 A72-38329

Atmospheric pressure, temperature, humidity and 200-mb level changes effects on cosmic ray neutron component intensity, using multifactorial regression analysis

19 p2852 A72-38330

Muon telescopes calibration for cosmic rays hard component variations by data comparison with variable aperture standard telescope

19 p2803 A72-38348

On the acceleration of charged particles to cosmic ray energies.

19 p2852 A72-38483

Low energy cosmic particle and soft X ray photon produced nonthermal electrons effect on interstellar gas ionization and thermal energy equilibrium

19 p2867 A72-38508

Zenith angle dependence of the meteorological corrections coefficients for cosmic ray hard component.

19 p2852 A72-38632

Geomagnetic cutoffs for cosmic-ray protons for seven energy intervals between 1.2 and 39 Mev.

19 p2852 A72-38728

Cosmic ray muon sea level momentum spectra and charge ratios geomagnetic latitude dependence measurements by spark chamber technique

19 p2853 A72-38754

Anomalous increase in the total X-ray background at balloon altitude.

19 p2853 A72-38755

Cosmic-ray diffusion coefficient in interplanetary space.

19 p2853 A72-38756

Weak decay, branching ratio and decay probability of strongly interacting particle event observed by Niu in cosmic nuclear jet shower

19 p2853 A72-38808

On the physical nature of cosmic electromagnetic absorption. V - The Einstein-de Sitter cosmology with plasma coupled to radiation at non-relativistic temperature.

20 p2967 A72-39185

Observations of the radial gradient of galactic cosmic radiation over a solar cycle.

20 p2964 A72-39337

Energy spectrum and composition of pulsar-accelerated cosmic rays.

20 p2964 A72-39343

The muon flux of cosmic rays at sea level.

20 p2964 A72-39349

Composition of cosmic-ray nuclei at high energies.

20 p2965 A72-39716

Recent developments in the history of the nucleosynthesis of the solar system.

20 p2971 A72-39837

Three-dimensional cosmic ray anisotropy in interplanetary space. III, IV.

21 p3101 A72-41385

Upper limits on vertical fluxes of $1/3$ e and $2/3$ e charged quarks in cosmic rays from observations with scintillation counter telescope

21 p3101 A72-41450

Stratospheric balloons role in galactic cosmic radiation research with detection techniques for study of rate and heavy elements abundances and isotopic composition analysis

21 p3101 A72-41615

Inelasticity of cosmic neutron interactions in carbon

21 p3102 A72-41840

Nuclear particle fluxes and radioactive isotopes production rate distribution from cosmic rays data along orbits, calculating iron meteorite dimensions prior to atmosphere entry

22 p3220 A72-41919

Convection and diffusion transport equation of galactic cosmic ray electrons with energy loss and absorption allowance for supernova compressed halo models

22 p3217 A72-42210

Results of cosmic ray intensity measurements on the Venus-7 automatic station

22 p3218 A72-42213

Atmospheric effects on the surface cosmic ray meson intensity recorded in London.

22 p3218 A72-42369

The density of H₂ molecules in dark interstellar clouds.

22 p3224 A72-42385

Change in the eleven-year modulation at the time of the June 8, 1969, Forbush decrease.

22 p3172 A72-42424

Cosmogenic radionuclides in the Allende and Murchison carbonaceous chondrites.

22 p3225 A72-42466

Geometric factor of a cosmic ray detector - Equivalence of alternative analytical derivations.

22 p3178 A72-42647

Depth distributions of cosmic ray produced radionuclides in chondrites and achondrites, determining apelia from Al 26 activities

22 p3228 A72-42861

Solar wind noble gases and solar flare emitted Fe group nuclei energetic tracks in chondrite Weston, considering galactic cosmic ray generated tracks

22 p3228 A72-42863

Gamma radiation of Magellanic Clouds and metagalactic origin of cosmic rays.

23 p3328 A72-43264

Statistical analysis of Forbush decreases and the preceding increases in cosmic-ray intensity

23 p3328 A72-43354

East-west asymmetry of cosmic rays at the sea level in the range of geomagnetic latitudes from 50°N to 20°S

23 p3328 A72-43355

Variation of the cosmic-ray gradient during a solar activity cycle

23 p3328 A72-43374

All-Union Conference on the Physics of Cosmic Rays, Tiflis, Georgian SSR, October 19-22, 1971, Proceedings

23 p3329 A72-44401

High altitude cosmic ray pion and nucleon interaction characteristics at high energies, using spark chamber, Cerenkov absorption spectrometer and ionization calorimeter measurements

23 p3329 A72-44402

Multiple collisions and an optical model of the inelastic interaction between cosmic particles and nuclei

23 p3330 A72-44413

Energy spectra and angular distributions of cosmic ray muons with an energy of 2 to 10 TeV

23 p3331 A72-44428

A study of the vestigial records of cosmic rays in lunar rocks using a thick section technique.

23 p3341 A72-44459

Stopping rate of negative cosmic-ray muons near sea level.

23 p3332 A72-44501

Nature of the long-term and short-term modulations of cosmic-ray intensity.

23 p3332 A72-44521

Diffusion processes of cosmic rays with energies between 2 and 20 GV during Forbush decreases - The diurnal effect.

24 p3434 A72-44785

Exponential functions model for D region vertical distribution of electron density profiles, taking into account solar X- and cosmic rays

24 p3397 A72-45081

Solar wind distortion of stellar anisotropy of galactic cosmic rays, associating annual particle density variation with earth revolution about sun

24 p3435 A72-45090

Cosmic ray diffusion in radial divergent flow of magnetic discontinuities in interplanetary plasma, discussing isotropy in presence of regular magnetic field

24 p3435 A72-45091

Meteor-induced magnetic effect on cosmic ray intensity for meteor streams with orbits normal or parallel to interplanetary magnetic field lines of force

24 p3435 A72-45092

Charged and neutral cosmic rays radioactive isotope and momentum distribution measuring techniques in high energy particle astronomy observatories /HEAO/

24 p3404 A72-45540

COSMOGONY

U COSMOLOGY

COSMOLOGY

NT HUBBLE DIAGRAM

Interacting radio galaxies, considering dynamics of streaming through intergalactic medium and secondary radio structures origin

01 p0126 A72-10288

Radio source counts, cosmology and evolution in uniform model universes

01 p0127 A72-10323

Primeval fireball cosmic background radiation spectrum in homogeneous axisymmetric anisotropic world model including electron neutrino effects on expansion dynamics

01 p0121 A72-11139

Spatially homogeneous rotating and expanding universe models, deriving Lagrangian function from Einstein field equations

01 p0103 A72-11260

Antimatter existence on cosmological scale in universe, comparing calculated annihilation gamma ray spectrum with background observations

02 p0278 A72-11967

Spectroscopic He abundance in population II stars from viewpoint of big-bang cosmology, taking into account neutrino emission according to photon-neutrino coupling theory

02 p0281 A72-12303

Monte Carlo method application to meteor stream formation by meteor material ejection from comet nucleus, determining age of Draconids

02 p0282 A72-12333

Einstein light deflection by galaxy cluster gravitational field effect on extragalactic observations, explaining uniform background inhomogeneities

02 p0286 A72-12892

Galactic spiral arm structure theory, discussing density wave pattern and material objects concepts

03 p0418 A72-13105

He abundances in universe, discussing stellar structure and evolution, He production, variable stars and globular clusters H-R diagrams shape

03 p0418 A72-13112

Helium production in different cosmological models based on solar system, stars and nebulae observations and stellar evolution calculations

03 p0419 A72-13118

Pulsar origin of cosmic rays, considering accelerated charged particles maximum energy

03 p0421 A72-13135

Anisotropic universe model based on Einstein equations for metric with cosmological term

03 p0388 A72-13193

General relativity and cosmology - Conference, Varenna, Italy, June-July 1969

03 p0426 A72-13265

Gaseous general relativistic kinetic theory, detailing matter model, thermodynamics, cosmology and Einstein field equation completion with Liouville or Boltzmann equation

03 p0388 A72-13266

Relativistic cosmological model, showing relation to fluid dynamics in Newtonian theory and space-time dependence on causality condition

03 p0426 A72-13267

Astrophysical cosmology, discussing universe expansion, Robertson-Walker models, radio sources, quasars, cosmic X ray background, intergalactic media, etc

03 p0426 A72-13268

General relativity and cosmology of quasi-stellar objects, covering distances, red shifts and gravitational fields

03 p0426 A72-13270

Galactic formation theories, discussing hot big bang and Friedmann models, primordial fireball and Hubble diagram

03 p0426 A72-13271

Cosmological density fluctuations in hadron stage, examining relativistic free particle and high temperature hadron gas models

03 p0426 A72-13273

Cosmological gravity fourth-order equation system yielding geodesic lines, considering cylindrical and spherical universes

03 p0435 A72-13726

Optical search for Ryle-Neville radio sources, discussing cosmological model constraints and quasar and radio galaxies optical and radio luminosity functions

04 p0570 A72-14549

Galactic evolution and cosmology implications of primordial solar D/H ratio, discussing deuterium production mechanisms

04 p0574 A72-14980

Empirical dimensionless ratios between universal physical constants, supporting steady cosmological expanding universe model

04 p0574 A72-14983

Expanding rotating shearing Bianchi type IX universe, investigating rotation effects on singularity

04 p0549 A72-15290

Universe cluster expansion model, showing velocity dispersion increases from center to turnover radius

04 p0578 A72-15308

Quasar red shifts and spatial density with statistical approach, confirming cosmological distances and uniform distribution in accompanying space

04 p0580 A72-15452

Meteor observation and counting, discussing meteor stream formation along comet orbit

05 p0712 A72-15975

Asteroids origin, discussing Phaethon model, masses, distribution, fragmentation and disintegration

05 p0713 A72-15980

Cosmological models dynamics and structural evolution feedback from density inhomogeneities energy momentum tensor, using hf approximation

05 p0715 A72-16166

Cosmological evolution theories, discussing big bang theory, galactic evolution, quasars, pulsars, gravitational collapse, stellar evolution, supernovae, black holes, etc

05 p0716 A72-16311

Hubble parameter derivation for regions beyond local anisotropy, discussing cluster galaxies magnitude-red shift diagram

05 p0717 A72-16380

Extragalactic distance scales, discussing brightest galactic cluster member utilization as distance indicators

05 p0717 A72-16381

Cosmological evidence from radio galaxies and optical object counts, quasar red shifts and evolutionary properties

05 p0717 A72-16383

Quasar primordial He content prediction from primordial temperature fluctuations necessary for galaxy formation

05 p0717 A72-16384

Intergalactic matter and radiation relation to origin and evolution of universe

05 p0717 A72-16385

Black hole prediction in gravitational collapse of star and universe in terms of quantum principle, chemical mechanics and superspace dynamics

05 p0690 A72-16528

Periodic model of time evolving universe, examining stability of Einstein static solution to field equations 05 p0723 A72-17180

CP-noninvariance model of baryon interaction and charge asymmetry of universe, postulating kappa particle /neutral massive fermion/ 06 p0875 A72-17275

Perturbations in Godel universe, considering Einstein equations in relativistic cosmology 06 p0876 A72-17564

Quasar luminosity due to unique big bang in specific space-time region, considering Minkowskian geometry 06 p0878 A72-17669

Dissipative effects in universe expansion, considering damping of anisotropy in homogeneous cosmological models [AD-745836] 06 p0880 A72-17885

Restricted two body problem anamolistic and sideral orbital periods in coordinate and proper time, noting cosmological constant 06 p0884 A72-18035

Hadron era evolution, discussing equation of state, ultimate temperature, galactic formation and adiabatic exponent application to Friedman universes 06 p0886 A72-18096

Pulsar produced cosmic rays energy spectrum, investigating light elements origin 06 p0874 A72-18161

Elementary particle theory and field equations in cosmological spaces, using four dimensional conformal imbeddings 06 p0891 A72-18421

Particle creation by strong rapidly changing gravitational fields in gravitational collapse of heavy star and in initial singularity 07 p1068 A72-19000

Metric tensor components of isotropic inhomogeneous cosmological model obtained from Einstein equations 07 p1072 A72-19340

Equations of free particle motion, gas energy, distribution evolution and cosmic indeterminacy for Friedmann universe filled with uniform density and pressure ideal gas 07 p1074 A72-19429

Homogeneous isotropic Newtonian and Robertson-Walker cosmological models, discussing radiative transfer and optics 07 p1074 A72-19431

Parametric solution of Brans-Dicke cosmological equations for flat Friedmann type expanding universe for time, density, expansion parameter and scalar field 07 p1074 A72-19525

Exact cosmological solutions in Brans-Dicke scalar tensor theory, noting consequences for solar relativistic effects 07 p1075 A72-19584

Particle production and vacuum polarization, in anisotropic gravitational field, discussing energy momentum tensor values and collapse behavior 07 p1034 A72-19632

Pulsar production rate relationship to high energy cosmic ray origin and number density 07 p1081 A72-20059

Elemental nucleosynthesis, considering cosmological, stellar, galactic and solar system evolution and atomic nuclei energetic levels 07 p1083 A72-20466

Population II stars age determination by main sequence turnoff luminosity and other methods, noting cosmological and galactic evolution implications 07 p1083 A72-20468

Big bang theory for age determination of galaxies, considering formation through gravitational instability and primeval gas velocity distribution fluctuations 07 p1084 A72-20470

Astrophysical study of cosmological evolution, discussing evidence from radio source counts and quasar spatial distribution 07 p1084 A72-20471

Neutrino interactions in lepton era of universe and hot big bang cosmology according to proton-neutrino coupling theory 07 p1084 A72-20538

Lunar evolution theory, discussing terrestrial cluster dynamics during earth accumulation 08 p1231 A72-21129

Galactic clusters size determination from known red shift relation, discussing distribution inhomogeneities, evolution, universe expansion and Hubble constant correction 08 p1234 A72-21282

Radio galaxy and quasar evolution models derived by formalism for number of sources in universe at any instant of cosmic time 08 p1234 A72-21382

Book on physical cosmology development covering universe expansion, steady state, isotropy, Hubble constant, cosmic time scale, mass density, etc 08 p1236 A72-21480

Mixmaster world model with arbitrarily moving matter, using coordinate system with matrix of

reference point components of three dimensional metric tensor 08 p1237 A72-21714

Cosmological model with negative and positive mass particles, discussing cosmological term, gravitation shielding, red shift and interacting Vorontsov Veliaminov galaxies 09 p1379 A72-22202

Cosmological implications of radioactive decays study by Rutherford, suggesting evolving nonstatic universe 09 p1386 A72-22688

Thermodynamic quantities expression in terms of S matrix to formulate questions pertaining to statistical mechanics-particle physics boundary, applying to cosmology 09 p1355 A72-22750

Quasar 3C279 flux density variation measurement as evidence for alternate model to explain apparent expansion rate of 10c 09 p1387 A72-22976

Book on astronomy and cosmology covering big bang, steady state and oscillating universe theories, radio sources, galaxies, interstellar meteor relativity and extraterrestrial life 09 p1389 A72-23248

Homogeneous anisotropic solutions of Einstein equations with cosmological term for universe with plane comoving frame filled with powder 09 p1352 A72-23361

Galactic nuclei origins, evolution, observational evidence and activity relation to cosmological problems, examining Milky Way, spiral and radio galaxies and quasars 10 p1532 A72-23884

Galaxy and globular cluster ages in relation to Hubble constant, deceleration parameter and Friedmann expansion time 10 p1535 A72-23911

Cosmic epoch dependent evolution of radio sources with identified optical counterparts 10 p1535 A72-23912

Nonlinear hydrodynamic effects in dynamic motions of metagalactic turbulence in pre-Friedmann universe 10 p1536 A72-24141

Current lines of relativistic fluid investigated by Ehlers method, applying to MHD Godel type universes 10 p1520 A72-24220

Rotating gas and dust clouds as basis of ring and disk structures in celestial bodies 10 p1539 A72-24311

Gravitational collapse /black holes/ search in universe, noting application of optical astronomy and radiation detectors on satellites and rockets 10 p1541 A72-24407

Friedmann cosmological models in terms of conformally invariant gravitation theory, noting two physically connected universe halves 10 p1541 A72-24474

Cosmological models with astrophysical and geophysical properties by introducing particles mass field and dimensionless coupling constant in conformally invariant gravitational theory 10 p1541 A72-24475

Quasars as cosmological and local objects, considering red shift origin and optical and radio luminosities comparison with galaxies 10 p1541 A72-24522

Rapid perturbation growth conditions for expanding universe, discussing background density decrease with time 10 p1543 A72-24661

Zero-pressure universe model parameters from red shift and apparent magnitude data for clusters of galaxies 10 p1545 A72-24809

Red shift-absolute magnitude relation for uniform time-dependent universe expansion rate suggesting large scale clustering modifications based on light propagation model 10 p1545 A72-24810

Godel metric type MHD universes, using Maxwell and conservation equations 10 p1524 A72-24857

Hydrogen gas cloud gravitational contraction and fragmentation in expanding universe, noting cooling and massive stars formation 10 p1547 A72-24870

Radio methods for cosmological model testing, discussing radio telescope requirements, source sampling procedures and counts as basic cosmological data 10 p1549 A72-25054

Field and geodetic line equations for light rays in open and closed isotropic radiative universe model 10 p1549 A72-25059

Relativistic homogeneous anisotropic models analogs construction in Newtonian cosmology 11 p1716 A72-25711

Local and cosmological irreversibility and time anisotropy theories from thermodynamics, statistical

mechanics, astrophysics and quantum-relativity viewpoints 11 p1716 A72-25775

Galaxy formation process in expanding universe from study of hydrodynamic equations for rotating gaseous ellipsoid with uniform density 11 p1717 A72-25865

Newtonian hydrodynamic equations derived from scalar-tensor theory field equations for cosmic fluid nonlinear effects during galaxy formation 11 p1717 A72-25866

Restricted two body problem anamolistic and sideral orbital periods in general relativistic coordinate and proper time, noting cosmological constant 11 p1719 A72-25971

Cosmological origin of red shift in spectral lines of astronomic bodies, suggesting interpretation based on inelastic interactions between photons of essentially nonzero mass 11 p1723 A72-26507

Space-time model locally identical with Minkowski space in geometrical and causality features, implying non-Doppler red shift and cosmology 12 p1868 A72-27218

Velocity dominated singularities generalized to solutions of Einstein equations with irrotational perfect fluid sources within hydrodynamic cosmological models 12 p1870 A72-27410

Noncovariant gravitation theory field equations based on preferred reference frame applied to homogeneous isotropic cosmological model, finding conservation law for total energy 12 p1875 A72-28154

Finite particle propagator constructed by path integral method, deriving infinitesimal propagator in relativistic quantum mechanics from mass nature consideration in Machian cosmological sense 13 p2001 A72-28499

Conformally flat linear axial symmetry chronometrically invariant cosmological models, discussing various types of spaces realized during model evolution 13 p2036 A72-28759

Japanese cosmological studies covering evolutionary cosmology, astrophysics, relativity, nuclear physics and metagalactic phenomena 13 p2038 A72-29083

Expanding hot universe evolution from astrophysical cosmology point of view, emphasizing galaxy formation relation to state of matter and radiation in early universe 13 p2038 A72-29084

Gravitational instability and galaxy formation in expanding universe, considering primordial turbulence and density perturbations 13 p2038 A72-29085

Galactic formation initiation mechanism with thermal instability in expanding universe, noting Compton scattering energy exchange ensuring gravitational instability dominance 13 p2039 A72-29086

Cosmic X ray background intensity and spectrum interpretation in terms of metagalactic origin within evolutionary cosmology framework 13 p2030 A72-29087

Monte Carlo method application to meteor stream formation by meteor material ejection from comet nucleus, determining age of Draconids 13 p2039 A72-29217

Cosmological geodetic survey network construction via spacecraft tracking and laser beams, calculating power required for balloon satellite photography 13 p1922 A72-29631

Adiabatic density perturbations damping by radiative viscosity and heat conductivity, taking into account plasma recombination in hot expanding Universe 14 p2148 A72-30202

Expanding universe postulate vs tired light effect for cosmological red shift explanation, discussing possible tests 14 p2155 A72-30551

Universe evolution, discussing constituents, matter and antimatter, quasars and radio stars in various galaxies 14 p2157 A72-30623

Particular and general exact solutions of Einstein equations for matter filled space under assumption of spherically symmetric distribution of perfect fluid 15 p2305 A72-31343

Book on astronomy covering optical and radio telescopes properties and atmospheres of inner and outer planets, stellar lifetimes and evolution, galaxies, cosmology, etc 15 p2306 A72-31516

Flat homogeneous isotropic relativistic cosmological two fluid model, using Robertson-Walker metric 15 p2307 A72-31795

Two fluid cosmological model in conformal and conformally flat forms, deriving solutions in elementary functions 15 p2307 A72-31796

Nonhomologous expansion in modified Friedmann cosmological model, neglecting particle collisions 15 p2313 A72-32304

V/Vm insensitivity to red shift random shuffling based on luminosity function in Einstein-de Sitter cosmological model

15 p2314 A72-32375

Curved space cosmological bounds on time variation of gravitational constant in terms of Brans-Dicke theory for Friedmann expanding cosmologies

16 p2450 A72-32864

Book on stellar astronomy covering H-R diagram, solar system, nuclear energy sources, Milky Way Galaxy, quasars, cosmology, planetology, etc

16 p2453 A72-33275

Information propagation time direction of cosmological models in terms of conventional electrodynamic theory, contrasting with Wheeler-Feynman theory

16 p2424 A72-33286

Critique of papers on quasars covering theory of gravitational lens intensified bright compact objects

16 p2454 A72-33452

Magnitude redshift relation in flat Brans-Dicke cosmology, discussing gravitational constant effects on stellar evolution and galactic luminosity

16 p2455 A72-33471

Red shift observations for galactic studies, discussing Stephan Quintet in Pegasus, spiral galaxy expulsion evolutionary hypothesis and Andromeda velocity patterns

16 p2456 A72-33541

Radio sources with straight spectra and spectral index of 0.3, noting relationship to self absorption, electron energy distribution and cosmological evolution

16 p2457 A72-33685

Energy release mechanism during early universe expansion leading to distortion of relict black body spectrum, noting Comptonization effects

16 p2461 A72-34151

On galaxy formation from primeval universal turbulence.

17 p2606 A72-34574

The reddening, distance modulus, chemical composition and age of the galactic cluster NGC 752.

17 p2607 A72-34675

Cosmological models interpretation of extragalactic radio source counts

17 p2612 A72-35350

Quantum models for the lowest-order velocity-dominated solutions of irrotational dust cosmologies.

17 p2613 A72-35392

Faraday rotation in connection with Hoyle theory of intergalactic magnetic field existence in steady state cosmology, considering cosmological model with cosmic magnetic field

17 p2614 A72-35504

Closed rotating cosmologies containing matter described by the kinetic theory - Entropy production in the collision time approximation.

17 p2618 A72-35823

Thermal and gravitational instability in universe, obtaining equation for growth rate of density contrast

17 p2618 A72-35910

Conformally flat linear axisymmetric chronometrically invariant cosmological models, discussing various types of spaces realized during model evolution

18 p2724 A72-36237

Expanding universe models showing particle pairs annihilation at critical temperatures

18 p2725 A72-36525

Universe expansion induced electromagnetic wave backscattering absence in Robertson-Walker space-time as consequence of motion equations conformal invariance

18 p2711 A72-36711

Many-body forces and the effect of the matter distribution in the universe to the gravitational constant.

18 p2728 A72-36800

Book on classical relativity theory covering relativistic kinematics and mechanics, tensor calculus, electrodynamics, gravitational fields and effects, elastic continua mechanics, thermomechanics and cosmology

18 p2712 A72-36850

Book on quasars and pulsars covering nature, origin, life span, universe concept with motion as fundamental unit and space-time reciprocal relationship

18 p2729 A72-37023

On the ability of the luminosity-volume test to reveal the statistical evolution of the luminosity of quasi-stellar sources.

19 p2854 A72-37226

The correlation of redshift with magnitude and morphology in the coma cluster.

19 p2854 A72-37228

Rotatory perturbations in anisotropic cosmology

19 p2864 A72-38078

Weber coincidence experiments in terms of cosmological gravitational waves, noting inconsistency in radiated pulse energy estimate

19 p2866 A72-38491

Astronomical models for matter sources leading to galaxy formation, considering source nature and origin

19 p2867 A72-38505

German book - Relativistic astrophysics

19 p2868 A72-38721

Hamiltonian approach to the dynamics of expanding homogeneous universes in the Brans-Dicke cosmology.

19 p2869 A72-38807

On the physical nature of cosmic electromagnetic absorption. V - The Einstein-de Sitter cosmology with plasma coupled to radiation at non-relativistic temperature.

20 p2967 A72-39185

On the physical nature of cosmic electromagnetic absorption. VI - The Einstein-de Sitter cosmology with plasma coupled to radiation at relativistic temperature.

20 p2967 A72-39186

Faraday rotation by cosmic magnetic field in cosmology based on scalar-tensor theory of gravitation

20 p2969 A72-39264

Electromagnetic wave dispersion in ionized cosmic medium for spatially flat Brans-Dicke cosmology

20 p2969 A72-39265

Galaxy formation in generic dust filled anisotropic cosmology, analyzing density perturbations growth rate

20 p2972 A72-39872

Book - General relativity: Papers in honour of J. L. Synge.

20 p2954 A72-40001

Cosmological electrodynamics and gravitation theory, considering singularity, constraint, Mach, Olbers, arrow-of-time and tail problems

20 p2974 A72-40004

The Robertson-Walker cosmology and the Friedmann cosmology

20 p2975 A72-40071

The abundance of helium in the cosmos. I.

21 p3103 A72-40379

Interaction between weak gravitational waves and a gas

21 p3084 A72-40402

Construction of a general cosmological solution of the Einstein equations with a singularity with respect to time

21 p3103 A72-40403

Spatially homogeneous general relativistic Bianchi cosmological models with diagonal metrics, noting field equations simplicity

21 p3104 A72-40569

Weinberg model application to hot universe of weakly interacting particles at nonzero temperature, noting long range character

21 p3084 A72-40726

An upper limit on the neutrino rest mass.

21 p3088 A72-40830

Statistical studies of the evolution of extra-galactic radio sources. I, II, & III.

21 p3105 A72-41026

Gravitational radiation interaction with background fluid of collisionless particles with zero rest mass in homogeneous isotropic Friedmann universe

21 p3105 A72-41028

Quasar 3C 323.1 in rich compact galactic cluster Zw Cl 1545.1+2104, considering red shift, energy distribution and luminosity

21 p3107 A72-41268

Least squares estimation of cosmological model parameters, comparing confidence limits with Solheim trial method

21 p3109 A72-41440

Cosmological model radiation pressure and density calculation by red shift-stellar magnitude ratios from galactic observations

21 p3109 A72-41441

Inhomogeneous cosmological models in terms of impulse energy tensor, discussing coupled Einstein equations, gauge invariance and Lorentz gauge

21 p3110 A72-41442

On the cosmological equations in a universe with small scale condensations.

22 p3220 A72-41998

Hubble constant, Friedmann time and expanding universe limits from measurements of distances to furthest galaxies, considering quasar red shift cut-off

22 p3222 A72-42138

Universe evolution study from contemporary chemical composition of cosmic matter, noting concentration changes of protons, neutrons and He 4

22 p3222 A72-42140

Homogeneous stellar system with purely gravitational interactions, predicting oscillatory relaxation time

22 p3207 A72-42853

Exact expressions for the properties of the zero-pressure Friedmann models.

22 p3229 A72-42890

Book - Gravitation and cosmology: principles and applications of the general theory of relativity.

22 p3208 A72-43080

Shmidt cosmological hypothesis impact on geophysics, geochemistry and geology, discussing planetary evolution, initial earth temperature and gravitational differentiation

22 p3230 A72-43154

Adiabatic density perturbations damping by radiative viscosity and heat conductivity, taking into account plasma recombination in hot expanding universe

23 p3333 A72-43231

Faraday depolarization of extragalactic radio sources.

23 p3335 A72-43268

Einstein equations reduction to friction systems in homogeneous cosmological models, investigating Bianchi models isotropization and statistical analysis

23 p3335 A72-43301

Joining of two semiclosed worlds and a cosmological model of matter-antimatter asymmetry.

23 p3336 A72-43489

Generalization of the Taub-Kazner cosmological metric in the scalar-tensor gravitation theory.

23 p3313 A72-43500

The cosmological evolution of radio sources of large angular extent.

23 p3336 A72-43554

Quasars as images of Seyfert nuclei.

23 p3336 A72-43559

Galactic evolution - Program and initial results.

23 p3337 A72-43832

Quasar red shift relationship to cosmological distance, considering explanation in terms of gravitational and Doppler effects and unknown process

23 p3338 A72-43993

Radio galaxies and quasars observations cosmological interpretation, discussing radio source counts, spectral index and angular size relations to distance and expanding sources apparent motions

23 p3340 A72-44245

On irrotational Bianchi-type universes in the Brans-Dicke cosmology.

23 p3314 A72-44314

Gravitational emission in the scalar-tensor theory of gravitation

23 p3315 A72-44476

Particle production and vacuum polarization in anisotropic gravitational field, discussing energy momentum tensor values and collapse behavior

24 p3424 A72-44564

Hyperbolic space criterion for cosmological model based on axioms conforming to special and general theory of relativity, noting coordinate transformation

24 p3439 A72-44969

On the physical nature of cosmic neutrino absorption. I - Cosmological models with continuous creation. II - Cosmological models without continuous creation.

24 p3439 A72-44974

Stellar implosion, gas cloud collapse into white dwarf or neutron star and atomic hydrogen cloud collapse, considering effects of cosmic bodies at high velocities

24 p3439 A72-45017

Idealized homogeneous and nonisotropic cosmological models with electromagnetic and massless scalar fields, noting Einstein equations

24 p3442 A72-45246

Early stage condensation in planetary formation, discussing atomic and molecular reactions in interstellar space and earth outer atmosphere properties

24 p3444 A72-45452

Accretion processes leading to formation of meteorite parent bodies.

24 p3444 A72-45454

The structure and formation of comets.

24 p3445 A72-45464

Mathematical consequences of physical laws invariance hypothesis under space-time-dependent changes in unit length, discussing conformally covariant and cosmological theories interrelationship

24 p3447 A72-45626

COSMONAUTS

Radiation doses received by cosmonauts in manned Soyuz 3-9 from mission retrieved thermoluminescent glass dosimeters

02 p0168 A72-12075

COSMOS SATELLITES

NT INTERCOSMOS SATELLITES

UV airlow in 1304 A line of oxygen from Cosmos 215 satellite

01 p0053 A72-10362

Geomagnetic survey by Cosmos-49 satellite as international program, discussing data analysis and observation accuracy

02 p0219 A72-12082

Atmospheric density near 150 km altitude from Cosmos 316 orbital decay, noting density increases during geomagnetic storms

05 p0655 A72-16070

Integral and differential electron energy spectra in inner radiation belt from Cosmos 219 satellite observation

05 p0711 A72-16768

Intercosmos 4 solar radiation equipment, including Lyman, optical and X ray photometers, spectroheliographs, polarimeters and optical orientation system

07 p0986 A72-19643

Energetic gamma quantum flux recording from extragalactic source 3C 120 by Cosmos 251 and 264 satellites

07 p1076 A72-19803

Cosmos satellite measurements of high energy gamma quanta from Crab Nebula region, indicating excess flux association with Taurus constellation point source 07 p1064 A72-20636

Primary cosmic ray high energy gamma quanta flux measurements on Cosmos 208 satellite-borne instruments 08 p1225 A72-20798

Proton 2 and 4 and Cosmos 196 orientation by quick response algorithm from onboard three component magnetometer readings 08 p1240 A72-21138

Intercosmos 3 satellite vlf radiation and natural signals recording with circular antenna, whistler recorders, sonograms and spectroanalyzers 08 p1157 A72-21146

Excess radiation and primary cosmic ray intensity variations at 200-350 km during 1965-1969 solar cycle from Cosmos satellite data 08 p1227 A72-21156

Simultaneous measurements of ionospheric electrons number vertical distribution by incoherent ground radio wave scattering and coherent signals from Intercosmos 2 and Cosmos 321 satellites 11 p1628 A72-26918

Recoverable-observation Cosmos satellites, discussing launch frequency, recovery beacons, binary coded Morse code transmissions and flight duration relation to resolution 12 p1877 A72-27689

The orbit of Cosmos 307 rocket and its use in atmospheric research. 17 p2545 A72-34632

Upper atmosphere zonal winds speed vs local time from data based on Cosmos 316 orbit analysis 17 p2547 A72-35075

Integral and differential electron energy spectra in inner radiation belt from Cosmos 219 satellite observation 17 p2600 A72-35271

Energetic gamma quantum flux recording from radio galaxy 3C 120 by Cosmos 251 and 264 satellites 17 p2617 A72-35726

Proton 2 and 4 and Cosmos 196 orientation by high speed algorithm from onboard three component magnetometer readings 20 p2976 A72-39243

Intercosmos 3 satellite VLF radiation and natural signals recording with circular antenna, whistler recorders, sonograms and spectroanalyzers 20 p2903 A72-39251

Excess radiation and primary cosmic ray intensity variations at 200-350 km during 1965-1969 solar cycle from Cosmos satellite data 20 p2964 A72-39261

Spatial distribution of excess-radiation intensity at low altitudes 22 p3218 A72-42212

Investigation of the angular distribution of particles on the basis of Cosmos-219 satellite data 23 p3343 A72-44174

COSMOS 224 SATELLITE
Daylong nitrogen ion 3914 A emission profiles for average solar activity at 110-240 km heights from Cosmos 224 observations 23 p3282 A72-43357

COSMOS 381 SATELLITE
Cosmos 381 onboard ionospheric station signals received from magnetically conjugate region by ground wideband antennas 14 p2085 A72-30476

COSSERAT SURFACES
Linear elastic Cosserat continuum mixed boundary-initial value problem uniqueness theorem, using Kirchhoff proof in classical elastostatics 03 p0382 A72-14363

Statics, motion equations, deformation, dynamics and classification of Cosserat continua 10 p1513 A72-25000

Boundary value problems in dynamics of Cosserat infinite elastic medium with finite crack, noting couple stresses effect on dynamic stress concentration 14 p2164 A72-30299

Kinematic equations derivation for traveling displacements field in Cosserat continuum by Lagrange formalism, noting analogy with Maxwell equations 15 p2274 A72-31474

Nonlinear Cosserat continuum theory of elasticity, discussing kinematics and stressed state as functions of angular velocity, acceleration, volume forces and moments 15 p2274 A72-31476

Cosserat strip bending by singular shear stresses, normal stress dipoles and spin moments, confirming Saint Venant principle 15 p2324 A72-31484

Cosserat surface uniqueness theorem for non-homogeneous anisotropic thermoelastic shells small motions and temperature variations superposed on large deformation 16 p2465 A72-32981

Cosserat couple stresses theory application to time varying concentrated forces induced displacements in infinite elastic space 16 p2469 A72-33385

Nonlinear equations of discrete elastic Cosserat media from multipolar media equations, studying small rotation theory 16 p2425 A72-33591

Nonlinear theory of two dimensional and three dimensional discrete elastic Cosserat media, noting application to reinforced shells and lattice type structures 16 p2425 A72-33592

Elastic sandwich plates analysis with core layer as orthotropic Cosserat surface supporting force and moment stresses 16 p2471 A72-33787

Thick shell and oriented surface theories. 19 p2873 A72-37694

Differential equation reduction via coordinate transformation to algebraic form for problems characterization in elastic shell Cosserat surface theory 21 p3119 A72-41103

Symmetry transformations for thin elastic shells. 22 p3234 A72-42398

Equilibrium equations of sandwich shell element with weak core and thin membrane facings under large transverse normal and shear strains, showing analogy to Cosserat surface theory 23 p3351 A72-44103

Nonlinear sandwich shell and Cosserat surface theory. 23 p3351 A72-44107

COST ANALYSIS

Planetary quarantine cost and mission success constraints, formulating mathematical models for international goals and implementation systems 01 p0019 A72-10819

Experiment sensors impact on on-orbit vehicle configurations and operations in NASA program, synthesizing and cost analyzing common module sets 01 p0135 A72-10945

Delta and Thor/Agena satellite launch vehicles, discussing costs, performance and mission planning based on booster design flexibility, incorporating computer programmed strapdown inertial guidance 01 p0136 A72-10953

Variable speed constant frequency power generation equipment influence weapon system effectiveness, considering weight and cost 01 p0008 A72-11067

Human ejection vertebral injury data in aircraft accidents by cross reference to final medical diagnosis, considering costs and prevention for seat systems 02 p0167 A72-11714

Redundancy configuration effect on electronic system reliability, discussing MTBF and cost analysis 02 p0194 A72-12445

Relative cost comparisons of composite applications with conventional material components selected from F-111A supersonic fighter bomber 03 p0310 A72-14234

Computer technology projection in terms of cost and performance for future ATC system, determining data processing systems availability 04 p0496 A72-14834

Remote sensing with sounding rockets and balloons, discussing cost, mineralogical surveys, land use and hydrological assessments 05 p0654 A72-15756

Value engineering based cost data application to design of aircraft in production 06 p0906 A72-18435

Technological advances and program risks assessment by operations research and systems analysis techniques, applying to cost overruns and schedule slippages in weapon systems 07 p1106 A72-20270

Nonlinear filter dynamics for stochastic optimal control for quadratic cost functional, evaluating performance 08 p1145 A72-20866

Fault tolerant redundancy for manned spacecraft computers considered as long term desirable solution from cost analysis 10 p1443 A72-23819

Statistical-analytical cost models for spacecraft development and fabrication, taking into account various technical and management factors 10 p1564 A72-24026

Satellite long life assurance, investigating shuttle era spacecraft program cost relationship to mean time to failure [AIAA PAPER 72-225] 10 p1551 A72-24436

Product assurance cost aspects on high reliability space programs, discussing design, packaging, failure trends, acceptance testing and Apollo project [AIAA PAPER 72-247] 10 p1551 A72-24452

Space shuttle thermal protection refurbishment labor costs and techniques, noting motion studies results for maintenance tasks in terms of manpower and performance time [AIAA PAPER 72-374] 11 p1726 A72-25398

Business V/STOL aircraft economic viability based on cost benefit analysis and comparison with turbine powered aircraft [SAE PAPER 720334] 11 p1576 A72-25594

Aircraft transparencies from civil operator viewpoint, considering replacement cost of flight deck and cabin windows 12 p1753 A72-27005

Prager-Shield theory for optimal plastic design extended to multicomponent cost functions and load conditions, applying to fiber reinforced plate 12 p1881 A72-27243

Structural design, performance and costs of rigid or semirigid solar panels for geostationary satellites power supplies 12 p1758 A72-28034

Curing technique optimization for primary aircraft components composite materials, discussing mechanical and dimensional properties test data, production cost analysis and cure time 12 p1815 A72-28077

System reliability demonstration test cost minimization for one-shot electroexplosive device 13 p2024 A72-28367

New York-New Jersey megalopolis offshore jetport feasibility, considering noise, air-water pollution, land conservation, cost, etc 13 p1938 A72-28792

Cost analysis of high altitude meteorological network data with respect to research effectiveness and data reduction 13 p1990 A72-28820

Nuclear rocket for space tug, comparing performance and operational costs with chemical propulsion 13 p2000 A72-28926

TV network distribution systems cost, comparing video tape shipping, terrestrial interconnection with delay for time zones and indirect and direct satellite transmission [AIAA PAPER 72-552] 13 p1918 A72-28983

Complex systems optimization with respect to vector-valued cost function without prespecified constraints or criteria weighting, deriving algorithm for characteristic set of noninferior solutions 14 p0087 A72-30825

Navy program for composites technology development in aircraft structures, discussing design, reliability and cost [ASME PAPER 72-DE-3] 14 p2073 A72-30860

Cost analysis for solar cell space power systems, considering array area and module standardization 15 p2338 A72-32133

Maintenance processes planning in air transportation, discussing aircraft availability, cost analysis and production management 17 p2560 A72-35441

Production and test facilities availability effect on costs involved in obtaining item at required quality level, examining component rejects and defectives 18 p2670 A72-37133

Comparative analysis of the operative costs of large amphibious hovercraft 18 p2643 A72-37212

V/STOL - Selection and problems of the new medium 18 p2643 A72-37215

Solar array cost reduction. 19 p2754 A72-37642

Private aircraft ownership and use for family travel and pleasure, discussing costs, maintenance and operational problems [AIAA PAPER 72-812] 19 p2750 A72-38119

Operating cost comparisons between Concorde and Boeing 707 and 747 aircraft, considering profitability 20 p2888 A72-39818

S-3A aircraft weight control program organization and methods, considering cost and schedule performance [SAWE PAPER 906] 23 p3250 A72-43453

Computerized airframe manufacturing cost and weight analysis, using technique for detailed parts list generation from configuration concept as input [SAWE PAPER 913] 23 p3293 A72-43460

Aerospace vehicles preliminary design computer program to include cost, reliability, maintainability and safety parameters in addition to weight as performance determining factors [SAWE PAPER 940] 23 p3342 A72-43480

Space subsystems cost optimization technique for minimization of total spacecraft plus boost cost, studying orbital logistics spacecraft [SAWE PAPER 941] 23 p3342 A72-43481

Minimum operational costs of passenger and cargo transport aircraft, considering effects of flight distance, wind conditions and optimum speed and altitude 23 p3252 A72-44338

A systems analysis of subsonic versus supersonic jet travel. 24 p3466 A72-44580

Economic and operational aspects of fatigue - Figures of a Swiss ground attack/fighter aircraft. 24 p3367 A72-44742

Structural fatigue cost penalties in airline operations, considering inspection, maintenance and carrying capacity reduction 24 p3367 A72-44743

Structural fatigue cost in aircraft maintenance and repair, considering inspections, defect rectification, preventive modifications, replacements and NDT
24 p3367 A72-44744

Space shuttle design evolution for program cost minimization, discussing refurbishment, payload impact, management cost and mission specifications and objectives
24 p3450 A72-45171

Implications of new transport vehicles and cost analysis of supplying and maintaining a manned lunar laboratory.
24 p3441 A72-45209

The effect of space shuttle payload design techniques on total space program cost.
24 p3451 A72-45210

Cost prediction of space projects.
24 p3468 A72-45211

The space tug optimum cost evaluation.
24 p3468 A72-45212

Commercial space applications economics, discussing meteorological, navigational traffic control and communications satellites, nuclear waste disposal, space manufacturing, solar power generation, etc
24 p3441 A72-45216

COST EFFECTIVENESS

Precision photogrammetric techniques coordinated with classical geodetic surveys for moderate cost control surveys, discussing error sources
01 p0065 A72-10455

Aluminum stiffening structural sections selectively reinforced with boron/epoxy composite materials, discussing mechanical properties, cost effectiveness and stress distribution
01 p0139 A72-10737

Cost effective ship-based research balloon fleet for scientific experiments meeting stringent space research budget requirements
01 p0048 A72-10954

Guided weapon systems design under cost restrictive conditions, discussing conceptual design planning and performance tradeoffs against cost and reliability
01 p0147 A72-11155

Joint venture and international collaboration in guided weapon systems design, development and production, discussing cost sharing coordination between governments and contractors
01 p0147 A72-11156

Separate and nonseparate arithmetic error detecting and correcting codes for digital computer design, considering cost and effectiveness tradeoffs
02 p0184 A72-11483

NASA quality assurance program, discussing management planning, assessment, failure prevention and cost effectiveness
02 p0304 A72-11554

Hybrid system to process multispectral photographic data from aircraft and spacecraft sensors, assessing data quality, cost effectiveness and delay reduction
02 p0228 A72-11883

Modulation/demodulation techniques for optical one-gigabit/sec intersatellite data transmission link system, comparing per-unit data costs for system selection
02 p0174 A72-12142

Radar digital control system, discussing cost effectiveness, block levels, flexibility, tradeoffs, data management, decision making and future applications
02 p0178 A72-12395

Aircraft integrated data systems, discussing cost effectiveness, reliability and maintenance
03 p0327 A72-13417

Ten million bit magnetic film computer memory, discussing design, fabrication, performance and cost per bit
[IEEE PAPER 11.1] 03 p0327 A72-13761

Optimal air defense strategy with budgetary constraints, considering artillery, airborne interceptor and mobile surface to air missile effectiveness against penetrating enemy
03 p0459 A72-14197

Space operations cost effectiveness improvement by earth-to-orbit shuttle, discussing space utilization growth and economics
[SD-71-780] 05 p0724 A72-16048

Computerized modular automatic test equipment for commercial airliner avionics device performance, discussing data handling ability and cost effectiveness
06 p0796 A72-18250

NASA programs phased planning and quality assurance techniques, noting cost effectiveness
07 p1102 A72-19126

Communications and TV broadcasting antenna feeder cost-efficient designs, relating climatology, oscillation theory and structural aerodynamic stability
07 p0955 A72-19513

In-house R and D laboratory organization cost effectiveness evaluation methods, discussing supervisory, program and special appraisals, visiting committees and natural competition
07 p1105 A72-19551

Aerospace subsystem alternate designs and cost effectiveness evaluation and optimization, considering algorithm of three functions with minimal coupling
07 p1105 A72-19552

Linear programming procedure for efficiency and cost optimization in aerial survey mission
08 p1165 A72-21164

International TV broadcasting satellite system, discussing technical problems and cost effectiveness in competition with conventional TV systems
08 p1132 A72-21205

Graphite fiber reinforcement of glass composite structure for increased cost effectiveness as compared to laminates and sandwich structures
08 p1193 A72-21694

Fast IC signal delay time reduction by high packing density, discussing yield, power dissipation and cost problems
09 p1290 A72-22820

Emergency reentry manned spacecraft remedial concepts, mission constraints and system designs in terms of cost effectiveness
09 p1396 A72-23159

Decision theory and cost-benefit modeling application to large government funded systems development programs, discussing Bayesian techniques
10 p1564 A72-23993

Complex system mission worth optimization by redundancies discussing MISDGRAD computer program to evaluate cost-reliability for mission without maintenance
10 p1550 A72-23994

Cost effective nonstatistical procurement of VHF power transistors with high degree of confidence in reliability
10 p1447 A72-24014

Long time mission spacecraft computer reliability economics based on failure and step improvement costs evaluation
10 p1444 A72-24017

Cost efficiency and relative economic merits prediction for solar energy conversion systems
10 p1423 A72-24316

Human role in space shuttle on-orbit maintenance vs space station modules earth return, considering feasibility and cost effectiveness
[AIAA PAPER 72-229] 10 p1487 A72-24440

Econometric approach to space shuttle design for optimum operational redundancy levels, using payload-cost effectiveness criterion
[AIAA PAPER 72-242] 10 p1551 A72-24448

Work administration system for aerospace applications, considering contractual statements, corporate requirements, schedule accomplishment and cost effectiveness
[AIAA PAPER 72-244] 10 p1564 A72-24449

Cost effective innovations in space programs management, discussing communication, problem solving and reward and punishment
[AIAA PAPER 72-246] 10 p1564 A72-24451

Aircraft maintenance optimization, considering safety, reliability, punctuality and cost factors
10 p1422 A72-25108

Selective reinforcement with high strength boron filament to achieve cost effectiveness and weight savings for composite structures
[AIAA PAPER 72-396] 11 p1731 A72-25417

Organic and metal matrix composites physical and mechanical properties and application to spacecraft and missile components, considering cost effectiveness
11 p1674 A72-26233

Optimization of diagnostic tests for monitoring industrial system efficiency, obtaining compromise between costs and utilization
11 p1611 A72-26441

Industrial enterprise training expense planning in terms of staff productivity and work time
11 p1748 A72-26543

Cost effectiveness determination for different levels of reliability and maintainability of training aircraft, using computer simulation
13 p2067 A72-28355

Strike aircraft reliability prediction in cost effectiveness analyses, showing failure probability distribution with time
13 p1896 A72-28360

Cost effectiveness model for evaluating general aviation weather dissemination techniques, stressing design variables and time periods
13 p1994 A72-28871

Aircraft maintenance operations and personnel requirements planning for optimal economic effectiveness, formulating relations between work productivity, downtime and aircraft utilization
14 p2174 A72-30822

High modulus composites structural design applications, considering fatigue performance vs cost
[ASME PAPER 72-DE-24] 14 p2167 A72-30866

FRAM/failure rate appraisal machine/ concept and application for modular electronic and electromechanical assemblies environmental cycling tests, noting technical and economical effectiveness
14 p2093 A72-31169

Low cost optimal earth resources technology satellite station for satellite tracking and image data reception and recording
15 p2213 A72-31246

Composite materials for engineering component and structure design, considering mechanical properties and cost-effective performance
15 p2260 A72-31443

Management information system role in cost effective civil and military aircraft operations, discussing hardware modification and human resources and communication system adaptation
15 p2339 A72-32458

Major civil airport planning, discussing information gathering and processing for aviation demand, aircraft movements revenue and cost forecasts and pricing policy evaluation
16 p2481 A72-33327

Government regulations effects on local service airlines cost performance and growth strategies
16 p2481 A72-33374

Resource allocation for minimum cost launch vehicle assignment to space missions, using network and dynamic programming algorithm
16 p2482 A72-33498

Weapon system program choice for development in aerospace industry, considering cost effectiveness and ranking illustrated on stand-off tactical interdiction missiles
16 p2482 A72-33598

Military system and equipment Level of Repair optimization for minimum life cycle costs, considering weapon systems deployment, operation level and mobility requirements
16 p2482 A72-33793

Communication satellite modeling into subsystems to formulate parametric relationships among power, mass and cost, comparing computerized design alternatives
17 p2512 A72-34263

Linear programming procedure for efficiency and cost optimization in aerial survey mission
17 p2521 A72-34455

Multifunction microwave apertures - Concepts and potential.
17 p2531 A72-35574

Aerospace computer software validation and verification methods application to complex systems, discussing code execution and analysis tools, program diagnostics, cost and schedules
17 p2524 A72-35582

Production measuring equipment and techniques for quality control, emphasizing measurement accuracy, speed and cost effectiveness maximization
19 p2802 A72-38304

Design and manufacturing considerations in hermetic microcircuit enclosures.
20 p2908 A72-39495

Electronic packaging and LSI techniques cost efficient use in meeting weight, volume, reliability, circuit speed and thermal protection requirements
20 p2909 A72-39769

Burn-in technique cost effectiveness in semiconductor and IC reliability enhancement, noting failure rate relationship to operating time
20 p2909 A72-39770

The cost-effectiveness of advanced remote sensing systems.
21 p3131 A72-40864

System analysis for an airline operational environment through a computerized network simulation model.
21 p3025 A72-41077

Cost effective algorithm for optimal route aircraft scheduling for airlines by mixed integer multi-commodity flow technique and Dantzig-Wolfe decomposition
24 p3466 A72-44582

Optimal cost effective sequencing model for component reliability tests, applying to complex electronic equipment
24 p3467 A72-44654

Test facilities for aeropropulsion systems, emphasizing utilization, cost and technical advantages, aircraft inlet-engine systems compatibility and test types
[AIAA PAPER 72-1034] 24 p3388 A72-45401

COST ESTIMATES
Space vehicles development and fabrication cost estimation, deriving statistical-analytical formulas with allowance for technical complexity and learning factor
01 p0147 A72-11219

Military aircraft operations and logistics computerized simulation for support and maintenance cost estimates
06 p0758 A72-17974

Spacecraft mean time to failure/MTTF/ and launch success probability /LSP/ effects on annual satellite system costs
09 p1395 A72-22775

Optimal closed loop control of discrete stochastic nonlinear systems, obtaining solution by cost function in power series around deterministic trajectory
10 p1457 A72-24499

- V/STOL aircraft potential for short haul civil air traffic, discussing present technology and investment costs in comparison with advanced ground transportation systems
13 p1898 A72-30076
- Parametric cost estimating aids DOD in systems acquisition decisions.
17 p2639 A72-34461
- Cost-to-produce estimation consideration as design parameter in defense material contractual arrangement
17 p2639 A72-34462
- Economics of a new regional airport.
18 p2743 A72-36779
- Economic analysis of aeronautical communication system via satellite, noting cost estimates and annual charge per user
21 p3081 A72-40298
- Improving R & D management through prototyping.
21 p3132 A72-40970
- The Agena orbit transfer stage as an interim space tug.
24 p3451 A72-45195
- Cost prediction of space projects.
24 p3468 A72-45211
- Cost estimation for engineering proposals in competitive bidding, discussing cost variability quantification methods based on PERT assumptions
24 p3468 A72-45478
- Forecasting costs and completion dates for defense research and development contracts.
24 p3468 A72-45479
- COST REDUCTION**
- Helicopter elastomeric bearing rotors, discussing downtime and cost reduction, maintenance, endurance and inspection
01 p0073 A72-10150
- Production cost control and tracking, discussing design decision effects
[SAE PAPER 710747] 01 p0146 A72-10246
- Aircraft design producibility to reduce production cost and enhance product profitability, using joint engineering and manufacturing team
[SAE PAPER 710748] 01 p0074 A72-10247
- Space shuttle low density ablative thermal protection systems, emphasizing low cost refurbishment techniques
01 p0091 A72-10766
- European Space Research and Technology Center satellite project control system, describing critical path network analysis, work package cost control and project planning
02 p0304 A72-12035
- Post Apollo program, considering space shuttle design, operation, transportation and payload cost reduction, rocket developments and plans for Mars expedition
03 p0440 A72-13612
- Low cost large array of decoding magnetic switches with electrodeposited Au conductors and Permalloy memory elements featuring high output flux for low driving current
[IEEE PAPER 21.3] 03 p0328 A72-13778
- Low cost metal matrix composition fabrication techniques, considering plasma spraying and continuous casting
03 p0364 A72-14236
- Low cost large solid rocket boosters technology, discussing propellant, case material, insulation, nozzle ablatives and thrust vector control
04 p0565 A72-14435
- Collision avoidance systems and pilot warning instruments, minimizing cost by pilot detection, evaluation and avoidance execution
04 p0545 A72-14823
- Soviet air traffic service productivity increase and manpower saving by introduction of new airliner types
05 p0612 A72-16779
- Supplementary Aviation Information Display for ATC, discussing remote sensing capability and cost savings
06 p0845 A72-17424
- Reusable shuttle for cost reduction, including reusability rate, expanded orbit capabilities and flight frequency
06 p0906 A72-18171
- Minicomputers evolution, considering price reduction, performance improvement, operation simplification, and applications for data collection and transmission
06 p0780 A72-18179
- Combined inertial/radio navigation systems for cost reduction, noting superior accuracy of VOR and DME
06 p0846 A72-18286
- Statistical evaluation for forged jet engine parts tensile tests cost reduction, using regression analysis
07 p0995 A72-19484
- Naval aircraft optimal repair and replacement policies determination for operation cost minimization by dynamic programming
[AD-736094] 08 p1256 A72-21470
- Low cost 300 gallon fiber reinforced plastic aircraft wing fuel tank manufacturing technology
08 p1177 A72-21693
- Profit policy for defense contract negotiations relating to capital employed for cost reduction
09 p1413 A72-22237
- Combined educational and TV network satellite distribution system for public broadcasting service, discussing cost reduction techniques
10 p1435 A72-24035
- Cost reduction by integration of assurance technologies from complex systems development risk management model
[AIAA PAPER 72-245] 10 p1487 A72-24450
- Low cost meteorological sounding rocket evolution, including Arcas, Lokidart and Viper Dart systems for various altitude ranges
10 p1552 A72-25090
- Commercial applications of quiet light aircraft technology, discussing cost and noise reduction
[SAE PAPER 720339] 11 p1576 A72-25596
- Complementary metal oxide semiconductor applications, noting device power dissipation, high noise immunity, good switching speeds and cost reduction
11 p1701 A72-26386
- Complex bipolar IC logic circuits realization by economical high speed techniques using metal bonding or cells available in library
11 p1606 A72-26548
- Design and production related cost reduction factors in universal digital computers fabrication
11 p1603 A72-26825
- Structural weight optimization with piecewise concave cost functionals defined on set in Euclidean space for anisotropic cylindrical shells
12 p1881 A72-27254
- AMSAT-OSCAR-B series of radio communication satellite for worldwide use with low cost terminals in amateur and education services
[AIAA PAPER 72-521] 12 p1779 A72-27351
- Space shuttle cost savings from viewpoints of reusable system, launch rate, vehicle life and overall program
12 p1877 A72-27514
- Plywrap process for low cost automated fabrication of fiber reinforced plastic composites, noting applications from missile interstages to modular housing
12 p1815 A72-28081
- Graphite fiber with high tensile strength and modulus and good elongation at low cost for aerospace applications
12 p1834 A72-28084
- Surface integrity machining practices application to jet engines production, noting cost reduction and process selection and quality control improvement
[ASM PAPER W 72-27.2] 12 p1862 A72-28163
- Superplastic alloys based on Al, Cu, Zn, Mg, Ti and carbon or stainless steels, discussing macroscopic properties and manufacturing cost reduction
14 p2120 A72-30622
- Squeeze casting for precision shaping mechanical properties, surface finish and cost reduction in metal working
[ASME PAPER 72-DE-7] 14 p2108 A72-30862
- Inexpensive microwave high density channel filters to meet amplitude and phase requirements without external equalization
15 p2210 A72-31181
- Military systems cost reduction via civil avionics procurement techniques, discussing cost-reliability design criteria
15 p2338 A72-32215
- Space shuttle payload design for weight and cost reduction, discussing refurbishable modular design concept
15 p2321 A72-32317
- Space simulation shrouds cryogenically cooled with liquid carbon dioxide, discussing automatic temperature control and operating cost savings
15 p2214 A72-32611
- Cost-saving techniques in helicopter structural test methods, suggesting system simulation, component replacement time calculation and computer techniques
16 p2373 A72-33221
- Reusable two-stage meteorological rocket vehicle, discussing design, performance, second stage recovery technique and cost
17 p2619 A72-34185
- Space shuttle program, discussing configurational concepts, payload carrying capacity variants and cost reduction design changes
17 p2621 A72-34869
- Polish aircraft industry production and fabrication techniques, discussing metal working, digital controlled machining and cost reduction
18 p2696 A72-37010
- NASA program for low cost turbojet and turbofan engine fabrication for missile and light aircraft propulsion
19 p2848 A72-37637
- Solar array cost reduction.
19 p2754 A72-37642
- Graphite-epoxy composites application to commercial transports for weight and cost reduction
19 p2873 A72-37680
- Modular heat rejection system to accommodate widely varying thermal loads in space shuttles and future spacecraft, emphasizing commonality design philosophy for cost reduction
[ASME PAPER 72-ENAV-34] 20 p2976 A72-39144
- Variation analysis and design of experiments as an aid to design quality assurance.
20 p2930 A72-39856
- Low cost design of linear pulse stretcher circuit for short duration pulse time measurement in nuclear instrumentation and computing counters
21 p3033 A72-40997
- Boron fiber reinforced composites technology assessment and utilization, stressing cost reduction
[ICAS PAPER 72-30] 21 p2995 A72-41155
- Characterization and algorithm for optimal solution of stochastic linear programming to minimize cost
21 p3075 A72-41234
- Determination of the optimum concentration level of solar radiation in solar batteries with different types of cooling
22 p3140 A72-43189
- High strength bimetallic rivets produced by inertia welding Al-Ti alloy shank with pure Ti tail, noting weight and cost reduction for aerospace vehicle production
[SAWE PAPER 902] 23 p3293 A72-43452
- RAM - A concept for reducing space payload costs.
[SAWE PAPER 942] 23 p3343 A72-43482
- Logical groupings of preventive maintenance and replacement policies for stochastically failing items to reduce cost under continuous surveillance
24 p3406 A72-44653
- NASA space science, exploration and applications plans and policies in view of space shuttle capabilities, emphasizing cost reduction
24 p3440 A72-45162
- Study of shuttle-based systems for high-energy planetary missions.
24 p3441 A72-45189
- The Space Station Prototype Program - The development of a regenerative life support system for extended-duration missions.
24 p3375 A72-45193
- NASA's management concept for the Space Shuttle Program.
24 p3468 A72-45194
- Employee motivation programs as a means of cost reduction in aerospace industries.
24 p3468 A72-45221
- Manned and unmanned space-based astronomical observatory systems pros and cons, discussing experiment management complexity and cost reduction
24 p3447 A72-45546
- COSTS**
- NT AIRCRAFT PRODUCTION
NT AIRPLANE PRODUCTION COSTS
NT FREIGHT COSTS
- COUETTE FLOW**
- Heat transfer in rarefied Couette gas flow, obtaining reduced distribution function, macroscopic temperature profile and heat flux
03 p0456 A72-13242
- Supercritical stationary states of dissipative hydromagnetic rotating Couette flow between electrically insulating cylinders within axial magnetic field
04 p0554 A72-14405
- Maxwell boundary conditions method application in kinetic theory of gases, investigating linearized plane Couette flow
04 p0510 A72-14594
- Unsteady approach to nonisothermal flow theory for Couette flow, making general assumptions concerning rheological law and temperature dependence of fluidity
04 p0512 A72-14985
- Nonlinear disturbances of viscous flow in pipes and between rotating cylinders, considering Couette and Poiseuille flows
05 p0648 A72-16027
- Turbulent diffusion flame model in Couette flow, including wall effect
[AIAA PAPER 72-214] 05 p0748 A72-16856
- Incompressible fluid unsteady kinetic energy equation periodic solution for harmonic oscillation viscous dissipation influence on temperature field, considering Couette steady flow solution
05 p0750 A72-17007
- MHD Couette flow stochastic processes optimal control synthesis by dynamic programming
05 p0653 A72-17131
- Linearized hydrodynamic stability of viscoelastic fluid Couette flow in gravity field
06 p0798 A72-17778
- Plane Couette flow of incompressible non-Newtonian viscous fluid between parallel plates, using minimum entropy production variational principle
06 p0798 A72-17779
- Couette flow between eccentric cylinders with inner cylinder rotating, using least squares numerical method for partial differential equations solution
07 p0970 A72-20070
- Motion equations approximate solution for viscous fluid Couette flow instability caused by spiral symmetry vortices
09 p1295 A72-23073

- Temperature distributions in constant viscosity incompressible Couette flow with additional pressure gradients 11 p1743 A72-25262
- Diffusion with convection for parallel wall Couette flow, using Airy functions 11 p1618 A72-26591
- Incompressible viscoelastic isotropic fluid stability in Couette flow, discussing physical parameters effect on critical Reynolds number and cells shape of secondary flow 12 p1797 A72-27169
- Uniform suction effect at stationary plate on longitudinal and transverse velocities of plane Couette flow between parallel plates 13 p1941 A72-28884
- Nonstationary laminar zero-discharge MHD Couette flow produced by sudden movement of highly conductive plate in closed volume filled with conducting liquid 13 p2016 A72-29607
- Inviscid plane Couette flow infinitesimal instability as initial value problem, using distribution-theoretic approach 14 p2126 A72-30230
- Magnetic and electric field effects on steady state laminar MHD Couette flow of non-Newtonian fluids governed by Prandtl rheological law or Ostwald-de Waele power law 14 p2139 A72-30717
- MHD Couette flow of electrically conducting viscous incompressible fluid in transverse magnetic field with time dependent suction or injection 15 p2286 A72-32396
- Internal aerodynamic problem solution by kinetic equation for Couette and Poiseuille flows and heat transfer between plane plates 16 p2343 A72-33153
- The bounding theory of turbulence and its physical significance in the case of turbulent Couette flow. 18 p2677 A72-36006
- Flow problems solutions estimation by variational principles application, exemplifying by plane Couette and Poiseuille and axisymmetric pipe flow 18 p2679 A72-36391
- The forces on a flat plate in a Couette flow. 18 p2683 A72-36996
- Time dependent solution to motion and energy equations for unsteady laminar spherical Couette flow of incompressible constant viscosity fluid 18 p2684 A72-37055
- Combined finite element-weighted residuals method for linearized BGK Boltzmann kinetic theory equation, considering cylindrical Couette flow. 18 p2684 A72-37168
- Stability of the Couette rotatory motion of two-phase media 19 p2787 A72-38209
- Spectral theory of Taylor vortices. I - Structure of unstable modes. 19 p2788 A72-38550
- Kramer and Couette flows using the Bhatnagar-Gross-Krook model. 20 p2913 A72-39418
- Analytical and low-speed experimental diffusion-thermo effects in turbulent binary boundary layers. [ASME PAPER 72-HT-56] 20 p2985 A72-39660
- Nonstationary laminar zero-discharge MHD Couette flow produced by sudden movement of highly conductive plate in closed volume filled with conducting liquid 21 p3091 A72-40661
- MHD Couette flow between conducting walls with heat transfer. 24 p3428 A72-44970
- Turbulent flow of drag reducing fluids between concentric rotating cylinders. [CSME PAPER 71-52] 24 p3393 A72-45254
- COULOMB COLLISIONS**
- Coulomb logarithm for hot plasma viscosity coefficient in magnetic field by quantum mechanical unified theory 02 p0267 A72-12770
- Coulomb collisions nonlinear effects on Landau damping of weakly damped plasma electron wave 04 p0559 A72-15347
- Bound states and Coulomb interaction effects on thermodynamic properties of cesium plasma calculated on computer for different pressures and temperatures 05 p0693 A72-15838
- Secondary particles in pion-nucleon and coherent interactions, measuring momentum from multiple Coulomb scattering 06 p0870 A72-17272
- Computerized numerical calculation of muons production spectrum, angular distribution and Coulomb scattering in determining meteorological factors effects on cosmic rays 07 p1067 A72-20655
- Coulomb interactions within dense Boltzmann plasma in transition from ideal to nonideal state, proposing effective Coulomb pair cross section concept 10 p1517 A72-23834

- Random walk models replacing Fokker-Planck equation for many particle systems with Coulomb interactions 10 p1513 A72-25041
- Hydrogen negative ion electron detachment collision process cross section calculation using Coulomb trajectory impact-parameter method 14 p2135 A72-30884
- Waves and particles interaction in weakly turbulent collision-free Vlasov plasma under pure Coulomb interaction and zero magnetic field 14 p2140 A72-30937
- Bound states and Coulomb interaction of continuum particles effects on thermodynamic properties of cesium plasma calculated on computer for different pressures and temperatures 15 p2283 A72-31259
- Nonlinear current oscillations in a plasma diode 18 p2714 A72-36205
- Computer-graphics studies of dipole-dipole collisions - Evidence for neutral collision complexes. 21 p3087 A72-40559
- Coulomb-collision corrected ion-acoustic line profiles. 21 p3092 A72-40819
- COULOMB POTENTIAL**
- Strong coupling superconductors transition temperature derivation from Coulomb pseudopotential and Einstein-type phonon spectrum 03 p0402 A72-13672
- Radiative properties of charged particles moving in attractive Coulomb fields related to repulsive fields by symmetry relationships 12 p1848 A72-28155
- Statistical Coulomb potential and thermodynamic, kinetic and optical properties of nonideal dense plasma 12 p1853 A72-28173
- Air composition and thermodynamic properties at 12,000-25,000 K and 0.1-100 atm with allowance for Coulomb interaction effect on pressure and for ionization potential decrease 13 p2018 A72-29878
- Repulsive potential determination for alkali cations, halide anions and anisotropic molecules from scattering experiments and bond energy data 21 p3087 A72-40555
- Bond energy electrostatic potential calculation and equilibrium and rate constants prediction for alkali and halide ions association with neutrals 21 p3087 A72-40556
- Short distance behaviour of the pair correlation function for classical plasmas. 21 p3091 A72-40570
- Model potential calculations of lithium transitions. 24 p3426 A72-44808
- COUNTDOWN**
- Europa 2 launcher F 11 flight test review concerning countdown, flight plan and trajectory and organizational details 02 p0286 A72-12034
- COUNTERBALANCES**
- Spin dynamics model of space station with counterweight connected by multiple cables, using linearized motion equations [AIAA PAPER 72-172] 05 p0730 A72-16882
- COUNTERFLOW**
- Growth rates of unstable electromagnetic waves propagating perpendicularly to symmetric counterstreaming finite temperature plasmas 13 p2012 A72-29129
- Ethanol liquid fuel counterflow diffusion flame stabilization and thermal structure determination by interferometry 13 p1913 A72-29306
- Counterflow diffusion flame gas dynamic structure analysis in porous cylinder forward stagnation region, using surface and boundary layer approximations 15 p2336 A72-32310
- Conformal mapping for interaction of two dimensional flow of ideal fluid and injected counterflow with jet formation, calculating cavitation void dimensions 22 p3165 A72-42065
- COUNTERMEASURES**
- NT CHAFF
- NT ELECTRONIC COUNTERMEASURES
- NT JAMMING
- COUNTERS**
- NT CERENKOV COUNTERS
- NT ELECTRON COUNTERS
- NT NEUTRON COUNTERS
- NT NEUTRON SPECTROMETERS
- NT PARTICLE TELESCOPES
- NT PROPORTIONAL COUNTERS
- NT QUANTUM COUNTERS
- NT RADIATION COUNTERS
- NT SCINTILLATION COUNTERS
- NT SPARK CHAMBERS
- Electronic fringe counter with CdS cell photosensors, dc bridge and strip recorder for interferometric applications 12 p1792 A72-27762
- Digital pulse counter with delay line and tunnel diodes 17 p2529 A72-34760

- Method for calibration and verification of automatic liquidborne particle counter/light method. [SAE ARP 1192] 18 p2692 A72-36533
- COUNTERSINKING**
- Countersink boring machines with programmed digital control systems for precision spacing multiple hole drilling in extended aircraft engine components 11 p1642 A72-26816
- COUNTING**
- Counting theorems for random processes discretization in linear systems described by finite spectrum functions 17 p2534 A72-35776
- COUNTING CIRCUITS**
- NT SCALERS
- Incoherent optical system model with photodetectors governed by Laguerre counting statistics obtaining error probabilities for comparison with Poisson counting 06 p0776 A72-18394
- Noise resistance techniques for calculating linear signal interpolation errors in adaptive quantizers 13 p1931 A72-29268
- Multichannel clock with dekatrons using multiple crossover connector for program commutation and command pulse splitting 13 p1933 A72-29919
- A meter giving the number of overshoots of the realization of a steady random process 21 p3058 A72-41732
- COUPLED MODES**
- Electrostatic potential fluctuations spectrum in turbulent hot ion plasma confined between magnetic mirrors, investigating mode coupling, energy cascading and electron concentration 01 p0108 A72-10242
- MHD wave modes nonlinear coupling by quantum field approach with Hamiltonian formulation, applying to solar coronal heating 01 p0129 A72-10797
- Coupled thermoelasticity in infinite body with cavity, introducing Sommerfeld type scalar potential and temperature radiation conditions 02 p0259 A72-12236
- Rheological properties of Maxwell fluid-St Venant solid model for solids, noting slip lines direction during plastic flow 02 p0259 A72-12238
- Magnetospheric hydromagnetic waves propagation characteristics, discussing isotropic/poloidal and guided/toroidal modes coupling in conjunction with hydromagnetic wedge model 02 p0268 A72-12870
- Read avalanche diode noise theory, showing carrier current modulation and lf and hf noise coupling in non-linear regime 03 p0333 A72-13848
- Two mode lasers with photon intensity coupling near threshold treated by fluctuation theory detailing intensity, correlations and line widths 05 p0667 A72-16017
- Algebraic prediction formalism for ring laser mode coupling by phase modulation 05 p0668 A72-16566
- Coupled longitudinal and transverse plasma waves propagating normal to applied magnetic field, using three fluid model 05 p0700 A72-17230
- Mechanical system of elastically coupled bodies carrying identical vibrators, examining self synchronization behavior 06 p0850 A72-18713
- Coupled mode locking equations solved for homogeneously broadened lasers modulated near axial mode separation frequency 07 p1001 A72-19192
- Two mode coupling and frequency pulling in He-Ne laser without absorbing medium in resonator 08 p1183 A72-21728
- Nonlinear mode coupling in equations of motion for thin panel vibration as function of membrane stretching-bending energy ratio 09 p1408 A72-23465
- Coupled mode model for dynamic interaction between flexible rotary machines and elastic supporting structures [AIAA PAPER 72-375] 11 p1730 A72-25399
- Power transfer in optical fiber with nonuniform refractivity in mode propagation direction, using coupled mode theory 12 p1779 A72-27164
- Thermomechanical interactions between elastic waves and nonstationary temperature fields in solid continua, considering coupled and uncoupled theories 13 p2064 A72-29093
- Electron-ion modes parametric coupling in low pressure RF self sustained plasma discharge, noting plasma frequency emissions 14 p2138 A72-30399
- Nonlinear coupled cyclotron oscillators excitation by external sine wave force, analyzing amplitude/phase variation and negative absorption 14 p2132 A72-31115

Coupled electroelastic vibrations of piezoceramic cylinders from polycrystalline electrostriction theory, taking into account mechanical and dielectric losses 14 p2132 A72-31117

Nonlinear coupling of wave modes in cold magnetized plasma, applying to electrostatic wave transformation in connection with solar type 3 radiation 15 p2283 A72-31431

Coupled oscillations of inviscid homogeneous liquid with free surface under vacuum or gas filled space in elastic cylindrical container 15 p2217 A72-31472

Collisions role in nonlinear mode coupling and harmonic generation associated with electromagnetic wave in plasma, describing plasma electron distribution function by kinetic equation 15 p2195 A72-31679

Aerodynamic effects on circular-orbiting cylindrical satellites coupled librational motion, analyzing equilibrium configurations stability by linearized and Liapunov direct method 15 p2320 A72-31818

Preloaded thin walled open section elastic column dynamic stability under free longitudinal vibrations, deriving criterion for flexural and torsional vibrations nonlinear coupling 15 p2332 A72-32560

Lasing kinetics in coupled lasers pair, noting generation of steady state oscillations without relaxation 15 p2252 A72-32696

F region crossed field instability nonlinear theory based on energy transfer by mode coupling and absorption by linear damping with application to equatorial electrojet 16 p2384 A72-32976

Coupled mode equations derivation for wave interactions in plasmas, considering oscillations production and cold magnetized plasma 17 p2589 A72-34923

Flexible cable in uniform flow field, calculating coupling between longitudinal and transverse modes to obtain centripetal acceleration effects on tension 18 p2734 A72-36418

Normal mode formulation of spin wave-helicon wave interactions in ferromagnetic semiconductors. 18 p2718 A72-36452

Drude theory of electromagnetic waves in an inclined magnetic field. I - One-band model of charge carriers. 19 p2840 A72-37510

Theoretical study and demonstration of the coupling of modes of a resonant cavity by an electron beam 19 p2774 A72-38543

Parametric coupling of large amplitude pump wave to E layer plasma mode to explain auroral electrojet irregularities external production and control 19 p2793 A72-38746

Frequency stabilization of a gas laser using mode-interaction effects. 19 p2814 A72-38822

Laser action with coupled types of oscillations 20 p2931 A72-39319

Strongly coupled stress waves in heterogeneous plates. 20 p2980 A72-39616

Optical propagation in space-time-modulated media using many-space-scale perturbation theory. 21 p3014 A72-40142

Randomly coupled flexural and longitudinal vibrations of plates. 21 p3120 A72-41111

Mode-coupling effects in thin platelet semiconductor lasers. 21 p3064 A72-41381

Coupled fields in inhomogeneous warm plasmas with static pressure gradients. I. 22 p3210 A72-42313

Effect on entry vehicle dynamic stability of aerodynamic and mass asymmetry coupling. [AIAA PAPER 72-973] 22 p3231 A72-42338

Monochromatic plasma waves linear and nonlinear coupling, discussing I.F. modulation partial transfer /Luxembourg effect/ and application to ionospheric diagnostics 23 p3319 A72-43517

Beam port coupled waveguide antenna radiation patterns for uniform and cosine plus pedestal radiating aperture distribution, using coupled mode theory 23 p3264 A72-43602

Field components of coupled electromagnetic and electron acoustic waves in warm stratified plasmas, using first order wave equations and Heading embedded form 23 p3322 A72-44319

The coupled transverse vibrations of a spinning membrane disk with a central hub. 23 p3355 A72-44367

Buildup of oscillations in crossed-field backward-wave oscillators. 24 p3385 A72-44973

Motion of a rotationally symmetrical gyro with an arbitrary number of vessels containing liquid 24 p3395 A72-45578

COUPLERS
NT ANTENNA COUPLERS

NT COUPLING CIRCUITS
Regulating amplifier with optoelectronic coupler for sonar sea bed layer measurements 09 p1284 A72-22239

Laser beam periodic coupler design based on radiation property reciprocity theorem, suggesting use of reflecting layers and long wavelength gratings 23 p3288 A72-43888

COUPLING
NT CROSS COUPLING
NT GYROSCOPIC COUPLING
NT MICROWAVE COUPLING
NT OPTICAL COUPLING
NT THERMODYNAMIC COUPLING
Viscous electroconducting liquid two unidimensional Hartmann flows electromagnetic coupling under transverse magnetic field induction 03 p0396 A72-13790

Perturbation procedure for weakly coupled oscillators in connection with statistical mechanics ergodic problem and nonlinear interaction models 12 p1844 A72-27248

Random vibration of two multimodal mechanical systems with point coupling, obtaining power flow spectral density by statistical energy analysis 13 p2005 A72-29563

Magnetoelastic coupling existence between shearing stresses and linear deformation, noting influence on Poynting effect experimental results 13 p1980 A72-29782

Coupling of free electron and nitrogen vibrational temperature nonequilibrium in weakly ionized nozzle expansions of shock heated nitrogen [AIAA PAPER 72-683] 16 p2380 A72-34059

Mutual coupling of infinite periodic phased arrays of arbitrarily oriented dipoles, investigating dipole length, orientation and phase effects on current distribution 21 p3027 A72-40368

Coupling by slots in rectangular waveguides with arbitrary wall thickness. 22 p3159 A72-42752

A simple coupling between the electromagnetic and gravitational fields. 22 p3207 A72-42855

COUPLING CIRCUITS
Gunn diode microwave oscillator postcoupling to waveguide, deriving theory based on equivalent circuit for load impedance assessment 01 p0037 A72-10640

Coupled-film closed-easy-axis arrays for large capacity NDRO multiple-write bulk memory, discussing disturb mechanisms limitation on performance and design [IEEE PAPER 21.9] 03 p0328 A72-13780

Small arbitrary shape antennas with inner transmission line loading, showing efficiency without external matching circuit 04 p0501 A72-15432

Direct coupled circuits in memory cell prototype with normally-off GaAs MESFET at 4.2 K 05 p0638 A72-17096

Monopole antenna with lumped mutual coupling between driven and folded sections, noting staggered resonant frequencies and bandwidth broadening from input impedance analysis 06 p0782 A72-17355

Electronically scanned steerable antenna array design with interelement coupling, considering maximum gain and radiation pattern control 06 p0773 A72-17497

Top wall and multiple branch hybrid junction waveguide couplers for millimeter wavelengths, measuring insertion loss performance 06 p0787 A72-18378

One- and two-conductor transmission lines electromagnetically coupled to rocket, deriving current bounds in load impedances under incident plane monochromatic wave 07 p0956 A72-19556

External circuit coupling effects on dc anomalous resistivity in electron plasma oscillation 07 p1043 A72-19666

Normally off Si MESFET for simple dc coupled circuits, computing threshold voltage with two dimensional device model 08 p1141 A72-21426

German monograph on optimal design of HF band-pass filters with lumped elements, covering LC coupled two- and four-circuit systems 09 p1284 A72-22328

Coupled line microstrip circuit for high power and efficiency L and S band TRAPATT diode oscillators 10 p1450 A72-24307

Base resistance coupled transistorized multivibrator design characterized by superior frequency stability regardless of wide voltage fluctuation 13 p1934 A72-30017

Two cavity self exciting SHF microwave oscillator with resistance coupling through low Q-factor resonant diaphragm, noting frequency stability 14 p2090 A72-31121

Simplified equivalent circuit analysis for Gunn diode coupling to rectangular waveguide by inductive post, using perturbation approximation 15 p2205 A72-31353

Electromagnetic boundary value problem of two rectangular waveguides coupled by aperture radiating into free space, solving integral equation by moments method 15 p2205 A72-31357

Electromagnetic transient coupling between ungrounded loops for two layer conducting half space approximation of earth 16 p2388 A72-34007

Improved injection locking of microwave FM-oscillators. 19 p2771 A72-37262

K-band high power single-tuned IMPATT oscillator stabilized by hybrid-coupled cavities. 19 p2771 A72-37263

Optimal vascular pressure measurements with transducers located outside body with rigid and elastic tube couplings 19 p2760 A72-37757

A quasi-optical directional coupler. 20 p2907 A72-39222

Synthesis of passive matching two-ports with given apparent resistances. III 20 p2907 A72-39424

COUPLING COEFFICIENTS
Zinc oxide longitudinal acoustic microwave transducer, measuring untuned insertion loss and electroacoustic coupling constant 01 p0042 A72-10705

Nonlinear Landau damping and growth of finite amplitude cyclotron harmonic plasma waves in magnetic field, measuring coupling coefficients by calibrated interferometer 07 p1041 A72-19506

Mathematical model of weak coupling influence on damped harmonic oscillators with different eigenfrequencies applied to bounded plasma oscillations 11 p1698 A72-26600

Beam maser spectrometric measurements of normal, C-13 and O-18 formaldehyde transitions, determining coupling constants for all rotational transitions hyperfine structure 16 p2431 A72-33132

A contribution to the theory of finite antenna groups, taking into consideration radiation coupling 21 p3028 A72-40503

COUPLINGS
Metric swaged pipe coupling design and development for aircraft hydraulic systems, presenting fatigue test results 08 p1179 A72-21940

Mandelstam couplings theory for subdividing discrete mechanical system of three degrees of freedom gear transmission 09 p1409 A72-23614

Influence of coupling behavior on the quietness of multiply supported shaft systems 18 p2694 A72-36070

COVALENT BONDS
Chemical box model of energy storage in covalent bonds and nonequilibrium distributions in prebiological synthesis leading to macromolecules 04 p0482 A72-14755

Oxide spinels crystallographic structure determination, stability relationships, covalent bondings and physical properties 10 p1501 A72-24730

Dependence of the properties of monocarbides of group IV-V transition metals on carbon content 22 p3189 A72-42198

COVARIANCE
Discrete time square root Kalman filtering techniques, discussing computational requirements and covariance and information implementations 02 p0198 A72-12804

Covariance matrix of coordinate fluctuations of instantaneous radar center of reflection from set of scatterers 04 p0487 A72-15144

Error covariance matrix square root calculation in orbit determination from ground based observations 05 p0720 A72-16752

Error covariance matrix evaluation at end of orbit extrapolation in terms of state vectors at measurement, discussing computation and interpretation 05 p0720 A72-16753

Generalized matrix inverse application to dynamic system state vector estimation, determining covariance matrix for comparison with optimal Kalman type procedure 05 p0641 A72-17089

Lorentz transformation role in special to general relativity theory transition, noting neglect by Einstein and general covariance physical meaning exaggeration 06 p0848 A72-17991

Closed loop covariances prediction in reentry vehicle tracking and data compression, presenting simulation results 08 p1144 A72-20846

Dynamic system time varying parameters on-line estimation using adaptive extended Kalman filter based on predicted error covariance matrix alteration 08 p1144 A72-20847

- Sequential testing of actual and calculated error covariances consistency in recursive nonlinear estimators, noting method application to linear filters
08 p1197 A72-20857
- Maximum likelihood estimates of covariance parameters of time discrete nonstationary linear systems from residuals measurement of suboptimal sequential filter
08 p1145 A72-20865
- Power series solutions to transition and matrix covariance differential equations, obtaining truncation error bounds and polynomial approximations
09 p1341 A72-23093
- Optimum bounding filter design based on error covariance for Kalman-Bucy and Wiener filters with inexact known parameters, obtaining performance figure of merit
10 p1454 A72-23785
- Statistical analysis of MOS integrated circuits from initial data of electrophysical and geometric distribution laws and covariance matrix
10 p1449 A72-24289
- Nonthermal ultrarelativistic plasmas covariant analysis with quantum electrodynamics and Green function theory of nonequilibrium statistical mechanics, discussing electron-positron pair production and annihilation
10 p1525 A72-25100
- Covariant statistical mechanics equations system for distribution function of relativistic particles in steady external gravitational field, noting Vlasov equation as limiting case
13 p2035 A72-28465
- Local Lorentz transformation in chronometric invariants, demonstrating appropriate operation for general covariant tensors from tetrad formalism
14 p2130 A72-30218
- Algorithms for photogrammetric model coordinates variance and covariance estimation, considering convergence properties
16 p2384 A72-33029
- A sequential algorithm for covariance matrix calculations.
17 p2574 A72-34416
- A gradient method for estimating the covariational matrix of unknown parameters
17 p2523 A72-35039
- Optimal smoothing for continuous-time systems with multiple time delays.
17 p2534 A72-35536
- On discrete-time Kalman filter in singular case and a kind of pseudo-inverse of a matrix.
18 p2672 A72-36059
- Dynamic nonlinear system direct statistical analysis by Covariance Analysis Describing Function Technique with linearization, giving illustrative examples [AIAA PAPER 72-875]
20 p2905 A72-39124
- Finite range gravitation theory extension to generally covariant massive two-tensor field gravitation theory containing eight dynamically independent degrees of freedom
20 p2953 A72-39342
- Use of the three-dimensional covariance matrix in analyzing the polarization properties of plane waves.
23 p3315 A72-44518
- Determination of the covariance matrix of the spatial coordinates of points of a geometrical model
24 p3397 A72-44867
- Lorentz-covariant reference-tetrad theories of gravitation
24 p3425 A72-44913
- Mathematical consequences of physical laws invariance hypothesis under space-time-dependent changes in unit length, discussing conformally covariant and cosmological theories interrelationship
24 p3447 A72-45626
- On the gauge groups of linear conservative gravitational theories.
24 p3447 A72-45630
- COWELL METHOD**
U NUMERICAL INTEGRATION
CRAB NEBULA
Crab Nebula pulsar NP 0532 model for interaction and polarization of radio radiation with surrounding media
02 p0277 A72-11772
- Gamma ray astronomy, discussing energy spectrum, diffuse background flux, extragalactic origin and Crab Nebula emission
03 p0408 A72-13027
- Crab Nebula optical pulsar NP 0532 polarization minima delay mechanism, suggesting relativistic radiation from region orbiting relativistically around neutron star
03 p0434 A72-13553
- Galactic center region, Virgo and Crab Nebula gamma ray observations, measuring intensity and energy spectra
04 p0578 A72-15312
- Gamma ray absorption near Crab Nebula pulsar NP 0532 within beam model, discussing pair production in photon field
05 p0711 A72-17161
- Crab Nebula and Vela pulsar constant elastic energy density contours, discussing micro and macroquakes
06 p0886 A72-18095
- X ray pulsar observed near Crab Nebula by balloon-borne telescope, discussing identification with NP 0527 or NP 0532
07 p1070 A72-19122
- Crab Nebula pulsed X radiation from balloon flights, extracting pulsar profile
07 p1056 A72-19135
- Pulsars optical counterpart observation, noting Crab Nebula pulsar visual magnitude
07 p1080 A72-20050
- X ray power density spectrum observation of pulsars, detecting Crab Nebulae pulsar radiation
07 p1080 A72-20051
- Pulsed gamma ray emission measurement above 50 MeV from Crab Nebula pulsar with balloon-borne spark chamber
07 p1063 A72-20235
- Cosmos satellite measurements of high energy gamma quanta from Crab Nebula region, indicating excess flux association with Taurus constellation point source
07 p1064 A72-20636
- Steady state problem of energy spectrum of variable magnetic field accelerated electrons, considering synchrotron X ray emission of Crab pulsar and nebula
08 p1231 A72-21119
- Pulsar and quasar energy sources, discussing Crab nebula, rotating neutron stars and gravitational collapse role
08 p1233 A72-21208
- Crab pulsar optical pulse stability comparison to radio frequency output, noting negative results in search for polar precession
08 p1235 A72-21396
- Circular polarization measurements of Crab Nebula pulsar NP 0532, including main pulse leading and trailing edge components
09 p1394 A72-23675
- [AD-736711]
Pulsar electrodynamic properties, radiation mechanism, galactic distribution and pulse shape, period distribution and propagation characteristics, reviewing Crab Nebula pulsar features
10 p1533 A72-23888
- Massive rotating objects with magnetic fields in galactic nuclei, considering similarities between Crab Nebula and quasars
10 p1535 A72-23908
- Optical and X ray pulsars, discussing Crab pulsar, emission behavior, pulse intensity, periodicity, polarization properties and antenna emission, plasma maser and Chiu models
10 p1547 A72-24919
- Crab pulsar period speedup observed by optical timing on 26 October 1971, noting similarity to September 1969 event
11 p1724 A72-26573
- Crab Nebula pulsar X ray radiation pulses at 100-400 keV searched for via balloon flights with NaI detector
13 p2034 A72-29965
- Celestial sources investigation for high energy cosmic gamma rays with particular attention to Crab Nebula
14 p2147 A72-30560
- Crab Nebula X ray emission synchrotron model confirmation by sounding rocket polarimeter polarization detection data
14 p2156 A72-30565
- Trillion electron volt pulsed gamma rays from Crab Nebula pulsar NP 0532
14 p2156 A72-30566
- Crab pulsar LF radiation polarization parameters and pulse shapes, showing highly polarized precursor component
14 p2156 A72-30567
- Variable cosmic X ray source location determination, noting Crab pulsar as radio, optical, X ray and gamma source
15 p2298 A72-31599
- Interstellar absorption of Crab Nebula soft X ray from Aerobee rocket photographic scan, estimating average volume densities for H, O, Ne, Si and Mg
16 p2445 A72-33129
- Optical timing of the Crab pulsar, NP 0532.
17 p2605 A72-34535
- The structure of the Crab Nebula at 2.7 and 5 GHz.
19 p2855 A72-37340
- Detection of high-energy gamma rays from the Crab Nebula.
19 p2850 A72-37503
- Faraday rotation of linearly polarized radio waves from the Crab Nebula by the solar corona.
21 p3109 A72-41327
- Discovery of interstellar circular polarization in the direction of the Crab Nebula.
23 p3336 A72-43557
- Upper limit on the gravitational flux reaching the earth from the Crab pulsar.
23 p3337 A72-43874
- Low energy X-ray survey from the Crab Nebula to Cygnus.
24 p3435 A72-44842
- CRACK FORMATION**
U CRACK INITIATION
CRACK INITIATION
Tensile and fatigue tests on steel, brass and aluminum with starter cracks, showing relation of strength and ductility to crack propagation and stress cycles
01 p0083 A72-10392
- Metallographic and fractographic analyses of cracking in T53-L13 gas turbine engine compressor disks
01 p0085 A72-10816
- Fatigue crack initiation and growth in sharply notched mild steel, showing specimen size, geometry and loading effects on fatigue life
01 p0142 A72-11098
- Automatic device for thermal and thermomechanical fatigue tests of steel specimens, noting crack nucleation and growth by hardening due to lattice defects
02 p0200 A72-11996
- Stress corrosion crack initiation and propagation characteristics computerized simulation validity
02 p0295 A72-12480
- Metal ductile facies fracture study of cups formation from cracks by cleavage, noting roles of dislocations and inclusions
02 p0246 A72-12600
- Impurities effects on crack initiation and propagation in polymethyl methacrylate under laser pulsed radiation
02 p0250 A72-12689
- Fatigue crack onset and propagation from bending behavior of revolving flat specimens
03 p0445 A72-13594
- Hydrogen charging of iron-chrome-nickel austenitic stainless alloys, investigating crack initiation in Inconel 600
03 p0373 A72-13600
- Fatigue cracks nucleation in steel bearings subjected to cyclic contact stresses
03 p0377 A72-14020
- Ultrasonic fatigue at small strain amplitudes in Ti, developing solitary slip band microcracks
04 p0533 A72-14539
- Creep damage mechanics, considering fracture initiation and propagation and prior loadings effect [ASME PAPER 71-WA/MET-1] 05 p0732 A72-15908
- Anodic layer thickness effect on fatigue crack initiation and fracture mode in mono and polycrystalline aluminum
05 p0672 A72-16015
- Electrical analog to determine potential field distribution for crack growth monitoring of edge notched and compact tension specimens for current input and probe positions optimization
05 p0666 A72-16303
- Microfibrillar superlattice with vacancy defect and point dislocation in microcrack formation and propagation in nylon 6 fibers
05 p0681 A72-16308
- Crackline loaded edge crack stress corrosion specimen, investigating crack initiation and propagation
05 p0673 A72-16324
- Plate microcracking of ferrous martensites containing Mn, Cr and Ni, discussing austenite grain size variations
05 p0678 A72-17119
- Ductile fracture development in steel due to microcracks and pores formation
05 p0679 A72-17205
- Fatigue crack formation speed relationship to stress intensity factor, investigating crack propagation by fracture mechanics methods
06 p0895 A72-17810
- Slip band formation and crack initiation in Ti as function of cyclic loading frequency, considering plastic strain amplitude or distribution as causes [DFVLR-SONDDR-149]
06 p0832 A72-18425
- Gas turbine blades fatigue crack development and failure analysis under thermal cycling tests, considering chemical processes and thermal and mechanical stresses
06 p0898 A72-18550
- Thermally activated crystal microcrack initiation by fusion of leading and following dislocations
06 p0898 A72-18551
- Fractographic analysis of failure kinetics and crack formation in Al alloys, showing microfatigue intrusions and extrusions for various initial stress levels
06 p0834 A72-18653
- Ti influence on ductility of normalized low alloy steel, considering crack initiation and propagation
06 p0834 A72-18687
- Al-Mg alloy with Ti, Zr, Mo and B additions under tensile and impact loads, investigating mechanical properties, strength and crack formation
07 p0104 A72-19839
- Test equipment with variable deflection and twist for metal fatigue microcrack initiation and growth detection
07 p0987 A72-19849

Impurities and crystal lattice role in metal brittleness, discussing stress concentration and relaxation, crack initiation and plastic deformation

07 p1018 A72-20145

Crack initiation and propagation microscopic and phenomenological characteristics, discussing breakdown, plasticity and microcrack convergence

07 p1094 A72-20147

German monograph on fracture formation and behavior in Ni maraging steel under repeated stress alternations, considering Al and Ti effects on steel strength

08 p1190 A72-22172

Adsorption, corrosion and hydrogen embrittlement effects on crack formation in quenched carbon steels in active media, using tensile stress-rupture tests

08 p1190 A72-22183

Cracks interaction with other cracks or boundaries under tension, determining critical loads for rapid fracture initiation by optical measurement

09 p1404 A72-22914

Light beams diffraction patterns of thin plexiglass plate for load induced thickness variations, noting crack opening and edge sliding modes stress intensity factors

[ASME PAPER 71-APM-QQ] 10 p1553 A72-24178

Material testing by holographic interferometry, discussing application to early detection of delayed cracking, fatigue damage and bond imperfections

10 p1482 A72-24575

Fatigue crack initiation and growth in filament reinforced Al alloys, noting interface crack tip stress distribution effects

11 p1654 A72-25480

Crystal grain size effect on fracture initiation in mild steel under triaxial stress, using notch tests at low temperatures

11 p1657 A72-25756

Crack initiation detecting and recording instrument with optical strain gages for double shear fatigue tests of aircraft fasteners

11 p1632 A72-25823

Tensile stress effect on formation of suboxide needles, microcracks and oxide wedges during low temperature Nb oxidation

11 p1658 A72-25854

Ductile fracture development in steel due to microcracks and pores formation

11 p1660 A72-26140

Stress corrosion cracking mechanism of low carbon steels to explain transcrystalline brittle mechanical cracks development along grain boundaries

11 p1666 A72-26923

Mica glass ceramics mechanical properties and thermal shock behavior in terms of microstructural variables, discussing fracture propagation and secondary cracks formation

11 p1675 A72-26949

Impact fracture resistance of Cr-Mn-Si steel, investigating alloying effects on crack initiation and propagation

12 p1831 A72-28238

High temperature low cycle fatigue of alloys as process of crack nucleation and growth to ultimate failure

13 p2058 A72-29445

Model for metal fatigue fracturing, noting crack initiation and two stages of propagation, emphasizing experimental fractographic /electron microscopy/ research

13 p2061 A72-29773

Temperature effects on critical crack opening as fracture toughness criterion for medium strength steel, taking into account local plasticity and propagation resistance

14 p2118 A72-30590

Mill annealed Ti alloy fatigue at 600 F and room temperature, noting critical local stress for slip bands formation and cracking

14 p2120 A72-30611

Stress corrosion crack initiation and propagation for Ti alloy in sodium chloride solutions, noting anodic dissolution

15 p2253 A72-31295

Ultrasonic metal fatigue, discussing crack initiation and growth and frequency effects

15 p2256 A72-31837

Microcrack initiation and propagation in ductile metals at low cycle and ultrasonic frequencies, investigating fatigue fracture mechanism by scanning electron microscope

15 p2256 A72-31838

Neutron irradiation effects on structural materials brittle fracture initiation and propagation mechanisms, discussing residual elements influence on radiation defect stabilization

15 p2258 A72-32486

Dynamic analysis of transient impact response of finite crack opened by in-plane shear tractions

16 p2464 A72-32920

Testing method for materials exposed to explosive forming, noting applications in study of formability, heat treatment effects and crack initiation

16 p2391 A72-33235

Automatic recording instrument for crack initiation time and breakdown curve for low carbon and stainless steel corrosion-fatigue tests under bending and tensile loads

16 p2394 A72-33849

Understress and coxing cycles effect on deeply notched carbon steel fatigue behavior, emphasizing crack initiation and breakdown

16 p2472 A72-33947

Effects of thickness on fatigue crack initiation and growth in notched mild steel specimens.

17 p2627 A72-34747

Fatigue crack initiation and propagation in welded structures, considering low and high cyclic stresses, microstructure and environment effects

17 p2635 A72-35919

Filler wire composition effects on solidification cracking resistance in weldable Al-Zn-Mg alloy

18 p2699 A72-36426

Analysis of a partially cracked panel.

18 p2735 A72-36771

Breakdown of some transparent dielectrics under the action of neodymium and ruby lasers in free light emission modes

19 p2810 A72-37542

Crack toughness - Physical and technological significance

19 p2875 A72-37854

A device for recording acoustic signals of crack formation in brittle materials

19 p2802 A72-38018

Effect of notch root radius on the initiation and propagation of fatigue cracks.

20 p2981 A72-39960

Study of fatigue crack initiation from flaws using fracture mechanics theory.

20 p2981 A72-39961

Crack arrest and crack initiation in a titanium alloy.

20 p2942 A72-39962

The stress gradient as a cause for the manifestation of the scale effect in brittle fracture of materials

21 p3123 A72-41364

Stresses in bonded materials with a crack perpendicular to the interface.

21 p3124 A72-41396

Causes for the formation of internal discontinuities of the metal in forged blanks of turbine blades prepared from EI893 alloy

22 p3216 A72-42249

Criteria of fracture initiation from the view of fracture mechanics

22 p3239 A72-42857

Formation of defects in reflecting coatings under the action of high temperatures

22 p3197 A72-43193

Microscopic aspects of fracture in ceramics.

23 p3305 A72-43504

Theoretical approach to the fracture of two-phase glass-crystal composites.

23 p3306 A72-43560

A practical method for determining Dugdale model solutions for cracked bodies of arbitrary shape.

23 p3346 A72-43701

Path independent integrals to predict onset of crack instability in an elastic plastic material.

23 p3346 A72-43711

Al alloy sheet panel tests for cracks emanating from stress concentration areas at holes or cutout edge

23 p3347 A72-43713

Failure and crack formation in gas turbine engine compressor disks under variable stresses from fatigue tests, considering safety factors

23 p3347 A72-43736

Experimental and theoretical study of the fracture of sheet materials in the presence of cracks

23 p3349 A72-43958

Dynamic fracture criteria for ductile and brittle metals.

23 p3354 A72-44260

The direct study of crack formation in metals in a high-voltage electron microscope

24 p3401 A72-44717

Fracture mechanics development from Griffith to crack opening displacement /COD/ concept, discussing crack initiation and propagation, stress-strain characteristics and yield point

24 p3456 A72-44814

Development and present-day state of the fatigue-damage theories.

24 p3457 A72-44873

Method for applying a fatigue crack to impact test specimens made from tough materials.

24 p3417 A72-45765

CRACK PROPAGATION

Tensile and fatigue tests on steel, brass and aluminum with starter cracks, showing relation of strength and ductility to crack propagation and stress cycles

01 p0083 A72-10392

Electrochemical potential microstructure and stress intensity factor effect on aqueous stress corrosion crack propagation rate in high strength Ti alloy

01 p0085 A72-10776

Trapezoidal isoparametric and triangular singularity elements for crack tip elastic stress intensity factor for mesh having small number of degrees of freedom

01 p0140 A72-10992

Nonlinear effects due to crack front plastic yield and slow crack extension in energy release rate and fracture toughness calculations

01 p0140 A72-10993

Maraging and Ni steels stress corrosion cracking rates dependence on stress intensity factor, discussing measurements in salt and distilled water

01 p0086 A72-10995

Crack stability dependence on energy demand or release characteristics, discussing application to fracture tests analysis

01 p0141 A72-10996

Ti-Al-V alloy under vacuum fatigue tests, examining temperature and chemical environment effects on fatigue crack growth

01 p0087 A72-11034

Fatigue crack initiation and growth in sharply notched mild steel, showing specimen size, geometry and loading effects on fatigue life

01 p0142 A72-11098

Kinetic energy velocity and acceleration formulas of penny shaped crack propagation in brittle body under triaxial tensile stress

01 p0144 A72-11391

Acoustic emission monitoring of boron epoxy composite, showing crack extension characterization by emission bursts

02 p0249 A72-11993

Automatic device for thermal and thermomechanical fatigue tests of steel specimens, noting crack nucleation and growth by hardening due to lattice defects

02 p0200 A72-11996

Crack opening displacement concept for fracture toughness testing, presenting elastic and plastic notch tip stress and deformation relationships in plane strain

02 p0292 A72-12005

Newtonian quasi-static crack propagation theory application to nonlinear structures, considering slender beams, plates and circular cylindrical shells

02 p0292 A72-12029

Hardened steel inhibited crack propagation mechanism, observing striation in microstructure on fracture surface

02 p0243 A72-12212

Tension-compression cycling effects on fatigue crack growth in high strength alloys

02 p0294 A72-12469

[ASME PAPER 71-PVP-2] Stress corrosion crack initiation and propagation characteristics computerized simulation validity

02 p0295 A72-12480

High strength steels stress corrosion crack propagation velocity relationship to crack tip stress intensity

02 p0295 A72-12482

Impurities effects on crack initiation and propagation in polymethyl methacrylate under laser pulsed radiation

02 p0250 A72-12689

Elastoplastic material crack propagation behavior under arbitrary loading, introducing plastic zone, intensity and retardation factor concepts

02 p0300 A72-12726

[DGLR PAPER 71-111] Polycrystalline materials wedge crack growth enhancement by vacancy diffusion under creep failure conditions, considering grain boundary sliding mechanism

03 p0442 A72-12998

Strain gage measurements of stress intensity factor for crack propagation in fatigue cracked thin metal sheets

03 p0444 A72-13542

Crack propagation rates during bending fatigue tests on flat hardened steel as function of stress intensity and plasticity area

03 p0445 A72-13593

Fatigue crack onset and propagation from bending behavior of revolving flat specimens

03 p0445 A72-13594

Testing temperature effect on intergranular fracture propagation in steel sensitive to tempering brittleness

03 p0372 A72-13599

Yield stress effects at high strain rate on finite crack unsteady motion

03 p0446 A72-13705

Crack growth criteria, formulating nonlinear fracture mechanics theory

03 p0446 A72-13709

Griffith crack propagation in polymethyl methacrylate, examining stress changes by photoelastic method

03 p0380 A72-13719

Crack development in thin viscoelastic polymer plate, using two phase fracture model without Volterra principle

03 p0448 A72-13901

Grain orientation effect on fatigue crack propagation in notched test specimens cut from cold rolled prestressed annealed brass plate

03 p0375 A72-13934

Elastoplastic bodies with crack at tip, determining limiting loads and crack propagation from variational relations 03 p0451 A72-14117

Crack growth in elastoplastic and viscous media under cyclic loading 03 p0452 A72-14137

Stress-strain state of shallow shell with crack along principal curvature line, discussing membrane stresses in plates and spherical shells 03 p0453 A72-14140

High temperature fatigue crack growth studies by compliance calibration test method, evaluating temperature and cycle rates effects 03 p0339 A72-14169

Corrosion fatigue cyclic crack growth rate above and below environmental threshold stress in steels as function of frequency and potentials, indicating hydrogen embrittlement 03 p0377 A72-14172

Maraging steel laminates stress corrosion cracking behavior, showing composite base plate and weld structure influence on crack propagation reduction 04 p0534 A72-15569

Ti-Al-Mo-V alloy sustained load stress corrosion crack growth in salt and distilled water environments 04 p0534 A72-15570

Griffith fracture theory application to thermal crack propagation, computing stress-strain field and critical temperature [ASME PAPER 71-MET-N] 05 p0731 A72-15790

Fatigue crack propagation rates for aluminum alloy plates under mode I extensional loads and transverse mode II bending loads 05 p0732 A72-15793

Creep damage mechanics, considering fracture initiation and propagation and prior loadings effect [ASME PAPER 71-WA/MET-1] 05 p0732 A72-15908

Double cantilevered specimen crack growth, computing fracture surface energies from dynamical cleavage analysis 05 p0735 A72-16019

Fatigue crack growth rate testing in gaseous environments at nonambient pressure and temperature in test chamber 05 p0643 A72-16186

Subcritical crack extension in elastoplastic or viscoelastic plastic matrix, showing similar mathematical representations for fatigue crack propagation and creep rupture under sustained loads 05 p0737 A72-16302

Electrical analog to determine potential field distribution for crack growth monitoring of edge notched and compact tension specimens for current input and probe positions optimization 05 p0666 A72-16303

Crack growth dependence on applied high stress level cycle number, showing fatigue life inversely proportional to stress exponential function 05 p0673 A72-16304

Near tip strain criterion validity for ductile crack growth on specimen surface 05 p0673 A72-16307

Microfibrillar superlattice with vacancy defect and point dislocation in microcrack formation and propagation in nylon 6 fibers 05 p0681 A72-16308

High temperature low cycle fatigue of Cr-Mo-V steel, observing crack growth rate correlation with crack tip stress 05 p0673 A72-16321

Crackline loaded edge crack stress corrosion specimen, investigating crack initiation and propagation 05 p0673 A72-16324

Purity effect on fatigue crack growth in high strength steel at room temperature 05 p0674 A72-16325

Plastic zone formation and fatigue crack propagation rate during high cyclic bending of metals 05 p0674 A72-16326

Stress corrosion crack growth in air melted and vacuum arc remelted nickel maraging steel, using stress wave analysis technique 05 p0674 A72-16327

Automatic recording of crack length in slow fracture tests of flat high strength steel in water 05 p0741 A72-17087

Unstable propagation and brittle fracture arrest in steels from double cantilever beam test under compression 05 p0677 A72-17107

Hydrogen environment effects on fatigue crack growth rates in Ti-Al-V weldments over low ambient temperature range 05 p0678 A72-17116

Ductile fracture development in steel due to microcracks and pores formation 05 p0679 A72-17205

Cracks interactions with transversal and surface elastic waves, relating crack propagation threshold conditions to critical pulse duration 06 p0893 A72-17419

Fatigue crack formation speed relationship to stress intensity factor, investigating crack propagation by fracture mechanics methods 06 p0895 A72-17810

Crack propagation in presence of crack branching events in seminfinite nonhomogeneous elastic brittle plate under edge impact loading 06 p0896 A72-17914

Fiberglass reinforced plastics under constant strain rate, deriving failure models as random process for microscopic crack propagation 06 p0898 A72-18548

Solid bodies crack development theory, emphasizing crack tip fine and hyperrfine structures concepts and time dependent effects 06 p0898 A72-18554

Ti influence on ductility of normalized low alloy steel, considering crack initiation and propagation 06 p0834 A72-18687

Stress-strain state in elastic plane with small radial cracks and circular hole under hydrostatic tension 07 p1091 A72-19765

Stress-strain state relationship to crack development morphology in elastic strain region of austenitic steel sample under cyclic bending 07 p1013 A72-19769

Test equipment with variable deflection and twist for metal fatigue microcrack initiation and growth detection 07 p0987 A72-19849

Crack initiation and propagation microscopic and phenomenological characteristics, discussing breakdown, plasticity and microcrack convergence 07 p1094 A72-20147

Analytical model for surface fatigue crack configuration during propagation into thick plate under cyclic loading [AD-741575] 07 p1095 A72-20242

Fatigue strength and life estimation method for thick walled cylinders under pulsating internal pressure, using fracture mechanics crack propagation law [ASME PAPER 71-PVP-15] 08 p1244 A72-21482

Interaction between two noncoplanar parallel staggered elastic cracks with narrow spacing, calculating stress intensity required for crack propagation 09 p1397 A72-22250

Fracture mechanical analysis for stability criteria and propagation behavior of thermal stress cracks in brittle ceramics in severe thermal environments 09 p1333 A72-22382

Fatigue failure mechanism in short fiber reinforced plastics, determining crack growth rates under cyclic loading [PI PAPER 2] 09 p1336 A72-22539

Crack propagation in elastic layer under antiplane state of deformation for arbitrarily distributed shearing forces on crack surface 09 p1404 A72-22766

Energy balance criterion application to crack growth under cyclic fatigue loading, considering stress-strain behavior of plastic deformation energy 09 p1404 A72-22911

Brittle fracture dynamics, deriving motion equations and stability conditions of surface cracks under stress waves from energy balance and angular momentum conservation law 09 p1404 A72-22916

Fatigue striation formation and crack propagation mechanism in Al alloy films from electron microscope studies 09 p1328 A72-22917

Crack propagation in two dimensional geometry with isotropic homogeneous and linearly elastic properties under in-plane tension loading 09 p1405 A72-22921

Propagating crack properties characterization during fatigue cycling, using ultrasonic flaw detection and acoustic emission 09 p1310 A72-22922

Computer simulation of crack tip atomic structure in diamond, relating covalent bond structure to dislocation nucleation and propagation likelihood 09 p1338 A72-22923

Crack propagation and substructure formation near fatigue crack in austenitic stainless steel observed by X ray diffraction and replica electron microscopy 09 p1329 A72-23148

Fracture mechanics application to welded structures fatigue, using crack propagation law 09 p1409 A72-23616

Stress functions for anisotropic elastic body with uniformly propagating circumferential crack, considering axially orthotropic cylinder 10 p1553 A72-23744

Fatigue crack propagation theory based on linear accumulation of metallurgical damage in plastic region 10 p1553 A72-24098

Crack toughness tests of fiber composite laminates, using linear elastic fracture mechanics 10 p1500 A72-24258

Fatigue crack propagation in epoxy resin matrix reinforced with discontinuous metal fibers 10 p1501 A72-24261

Interaction diagram for mixed crack extension modes in unidirectional graphite-epoxy laminates from critical load test data 10 p1501 A72-24265

Fracture toughness expressions including nonlinear effects due to crack front plastic yield and possible crack extension prior to fracture instability [SMRT PAPER L 1/4] 10 p1497 A72-24396

Transmission electron microscope examination of deformation microstructures adjacent to fatigue cracks in Al alloys 10 p1497 A72-24823

Fatigue crack propagation relation to plasticized zone formation at crack tip in ferritic carbon steels and in Cr-Ni austenitic stainless steels 10 p1558 A72-24855

Mean stress effect on fatigue crack propagation rate in half inch thick Al alloy specimens of high and low fracture toughness 10 p1498 A72-24884

Notched bend test crack opening displacement gage for continuous measurement of apparent rotation axis and true displacement location at crack tip 10 p1483 A72-24885

Al alloy notch-bend and compact-tension specimens thickness and crack length effects on plane-strain fracture toughness test results 10 p1498 A72-24886

Tensile, plane strain fracture toughness and fatigue tests of high strength Al alloy cylinders, discussing unstable crack growth conditions 10 p1498 A72-24887

Tensile ligament instability model for stress corrosion crack propagation velocity in austenitized steel tempered at 750 F 10 p1499 A72-24888

Carbon steel fatigue crack propagation rate dependence on strength and stress history, discussing conditions for crack nonpropagation 10 p1499 A72-24889

Crack arrest in transversely loaded elastic plates from fracture mechanics combined with stress intensity factor for tensile and compression loads 10 p1499 A72-24890

Variational methods for approximate solutions to Fredholm integral equations describing stress intensity factors and plastic regions of Dugdale cracks [AD-744365] 10 p1558 A72-24892

Mathematical model for superonic crack propagation in cubic lattice, deriving velocity-applied stress relation 10 p1558 A72-24895

Crack shape and plastic energy dissipation rate relation to plate thickness and applied stress for penny-shaped crack in elastic plate 10 p1559 A72-24896

Approximate stress intensity factor for corner flaw emanating from quarter infinite solid edge, based on Smith solution for semicircular flaw 10 p1559 A72-24898

Environmental sensitivity effect on crack propagation rates in steels and Al and Ti alloys, discussing corrosion fatigue 10 p1499 A72-24899

Calibration procedure for crack length determination based on in test crack opening displacement monitoring 10 p1559 A72-24900

Stress corrosion crack paths in Al-Zn-Mg alloys, showing normal coincidence with grain boundaries 11 p1652 A72-25289

Fatigue crack initiation and growth in filament reinforced Al alloys, noting interface crack tip stress distribution effects 11 p1654 A72-25480

Ni fatigue crack propagation under low cyclic loads at high temperature in vacuum after annealing and mechanical treatment 11 p1655 A72-25497

Hardened steel inhibited crack propagation mechanism, observing striation in microstructure on fracture surface 11 p1656 A72-25710

Stationary and nonstationary random envelope processes digital simulation, presenting application to crack propagation under random loadings 11 p1686 A72-25730

High strength steel flat plates brake formability from bend tests on sheared edges specimens, noting Hutchinson method sensitivity for different crack propagation propensities materials 11 p1657 A72-25819

Metal stress corrosion crack propagation rate theory based on film rupture mechanism 11 p1735 A72-25852

Computational technique for crack growth prediction in metal subjected to variable amplitude cyclic loading, taking into account yield zone ahead of crack tip [ASME PAPER 71-MET-X] 11 p1735 A72-25876

High power ultrasonics in metal fatigue studies, considering crack propagation and slip patterns for high and low frequencies 11 p1639 A72-26053

Cyclic loads frequency and environmental effects on fatigue crack propagation rate, comparing theoretical results with Al alloy thin plates experimental data 11 p1663 A72-26802

Microstructural effects on high strength Mg, Al and Ti alloys stress corrosion crack growth in aqueous environments, discussing correlations relative to composition and preferred orientation 11 p1668 A72-26946

Mica glass ceramics mechanical properties and thermal shock behavior in terms of microstructural variables, discussing fracture propagation and secondary cracks formation 11 p1675 A72-26949

Water damage in glass fiber-polyester resin composites, discussing fiber debonding, crack propagation and water resistance 11 p1675 A72-26950

Two dimensional wave motion generated in prestressed body by crack extension, noting consistency with fracture criterion related to cohesive traction zones near crack tip 12 p1883 A72-27560

Fracture toughness of high strength alloys, discussing rocket motor cases, nondestructive test standards and subcritical crack growth 12 p1829 A72-27656

Cyclic stress ratio effects on stainless steel fatigue crack propagation at 1000 F, using linear elastic fracture mechanics 12 p1829 A72-27663

Engineering formula relating crack tip stress intensity coefficient to mechanical properties and structural element size 12 p1887 A72-28236

Impact fracture resistance of Cr-Mn-Steel, investigating alloying effects on crack initiation and propagation 12 p1831 A72-28238

Axisymmetric temperature problem with arbitrary load duration for disk-shaped crack fracture mechanics, using Fredholm equation with symmetrical kernel for temperature field determination 13 p2055 A72-28720

Plastic strains and crack growth in Al alloy under static and repeated static loading 13 p1977 A72-28915

High temperature low cycle fatigue of alloys as process of crack nucleation and growth to ultimate failure 13 p2058 A72-29445

Model for metal fatigue fracturing, noting crack initiation and two stages of propagation, emphasizing experimental fractographic /electron microscopy/ research 13 p2061 A72-29773

Ni-Cr-Ti steel aircraft structural element fatigue life calculation based on failure mechanism involving crack propagation 14 p2164 A72-30429

Stress relieving heat treatment for service failure prevention of stressed austenitic stainless steel components of high temperatures, noting cracking regulation by oxidation mechanism 14 p2117 A72-30538

Fatigue crack growth rate in precracked steel samples observed at 100 C by etching technique, noting flow stress and yield in plastic zone 14 p2119 A72-30608

Macroparametric, microstructural and general rationales methods for fatigue resistant materials, noting crack propagation and fracture mechanics 14 p2120 A72-30612

Binary Al alloys intermetallic phases effects on microcracks nucleation and propagation at 300 C in uniaxial tension, considering alloying elements influence on mechanical properties 14 p2124 A72-31036

Crack propagation in biaxially stressed and heat treated cylindrical pressure vessel observed by strain gage displacement measurement, noting effects of initial surface cracks 14 p2169 A72-31176

Stress corrosion crack initiation and propagation for Ti alloy in sodium chloride solutions, noting anodic dissolution 15 p2253 A72-31295

Longitudinal shear crack propagation after stability loss in infinite elastic medium, discussing wave diffraction at edges 15 p2327 A72-31734

Microcrack initiation and propagation in ductile metals at low cycle and ultrasonic frequencies, investigating fatigue fracture mechanism by scanning electron microscope 15 p2256 A72-31838

Neutron irradiation effects on structural materials brittle fracture initiation and propagation mechanisms, discussing residual elements influence on radiation defect stabilization 15 p2258 A72-32486

Ti alloy fracture strength determination by crack propagation observation in specimen center, noting

load-displacement curve construction from cyclic loading test 15 p2259 A72-32804

Crack depth measuring instrument for fatigue crack propagation study in notch tests, noting application at high temperatures 16 p2391 A72-33234

Temperature effect on fatigue crack growth in high strength annealed Ti-Al-V alloy in water, oxygen/hydrogen and vacuum environments 16 p2406 A72-33320

Constitutive equations for metallic creep analysis based on simultaneous strain hardening and crack propagation processes, calculating creep rupture time 16 p2408 A72-33589

Dynamic stress field solution to plane strain crack propagation in elastic body under general loading at constant and nonlinear extension rate 16 p2470 A72-33612

German papers on crack propagation in metal sheets, resonant vibration of cylindrical shells and stress concentration in plastic plates 16 p2470 A72-33676

Crack propagation in Al-Cu-Mg alloy sheet under vibratory bending loads, noting crack length to loading cycles number relationship 16 p2408 A72-33677

Uniformly propagating finite crack in elastic strip of finite width, using two dimensional dynamic equations of elasticity 16 p2471 A72-33831

Plastic deformation at a stably growing crack tip. 17 p2569 A72-34252

Strain energy release rate for radial cracks emanating from a pin loaded hole. 17 p2623 A72-34254

Crack opening displacement and the rate of fatigue crack growth. 17 p2565 A72-34255

Note on dynamic fracture toughness measurement. 17 p2566 A72-34257

Effects of thickness on fatigue crack initiation and growth in notched mild steel specimens. 17 p2627 A72-34747

Conservation laws related to energy release rates associated with cavity or crack rotation and expansion, discussing plastic stress distribution around cracks [ASME PAPER 72-APM-22] 17 p2580 A72-34795

Shape factors for nozzle corner cracks evaluated from epoxy-model pressure vessels. 17 p2630 A72-34814

Use of special gauges for determining crack growth rate in fatigue in the AU4G1 aluminium alloy 17 p2567 A72-34890

Fracture of cylindrical and spherical shells containing a crack. 17 p2634 A72-35645

Fatigue crack initiation and propagation in welded structures, considering low and high cyclic stresses, microstructure and environment effects 17 p2635 A72-35919

Griffith crack propagation through viscoelastic solid at under subcritical stresses, measuring growth rate for comparison with theory 18 p2733 A72-36366

Composite materials crack propagation and failure modes leading to fracture instability, discussing maximum strength conditions and fatigue 18 p2703 A72-36394

An atomistic study of cracks in diamond-structure crystals. 18 p2718 A72-36509

Fractographic lines in maraging steel - A link to fracture toughness. 18 p2700 A72-36584

A sandwiched layer of dissimilar material weakened by crack-like imperfections. 18 p2737 A72-37058

An improved Cranz-Schardin high-speed camera for two-dimensional photomechanics. 19 p2795 A72-37516

Creep rupture theory covering viscous and brittle scattered fractures and major crack growth 19 p2874 A72-37703

Investigation of the effect of some surface-active media on the variations in strength characteristics of steel U8 in a high strength state 19 p2817 A72-37738

Crack toughness - Physical and technological significance 19 p2875 A72-37854

On the fatigue crack propagation in polymeric materials. 20 p2943 A72-38886

Testing of hydrogen pressure or stress concentration induced crack propagation theory for steels based on decohesion mechanism 20 p2935 A72-39003

Environmental acceleration of fatigue-crack growth in a high-strength steel. 20 p2935 A72-39140

The octahedral shear strain theory and its relation to biaxial cumulative fatigue damage. 20 p2978 A72-39202

Creep-fatigue interaction interpretation for austenitic stainless steels from crack growth viewpoint, investigating time and cycle dependent failure at elevated temperature 20 p2937 A72-39213

Acoustic emission testing and microcracking processes. 20 p2924 A72-39277

Crack growth behavior correlation to acoustic emission signal amplitude distribution in high strength steel heat treated to different fracture toughness values 20 p2924 A72-39282

Effect of thickness and orientation on fatigue crack growth rate in 4340 steel. 20 p2937 A72-39294

Hydrogen gas effects on cleavage cracking in Ti-Al-Mo-V samples under static and cyclic loading 20 p2939 A72-39308

Possibility of determining the fracture toughness of materials on the basis of the form of static bend test fracture samples. 20 p2941 A72-39714

Review - Fatigue-crack propagation in metallic and polymeric materials. 20 p2980 A72-39793

Fatigue-crack propagation characteristics of aluminum alloys in thick sections. 20 p2942 A72-39951

Metal fatigue crack propagation under cyclic loads, assuming specific energy dissipation as material constant 20 p2981 A72-39953

Criteria for delayed fracture in solids and their experimental verification. 20 p2981 A72-39954

Stress intensity factors for transversely loaded elastic plates and their application to predictions of crack arrest. 20 p2981 A72-39956

Acoustic emissions and energy transfer during crack propagation. 20 p2981 A72-39957

Effect of notch root radius on the initiation and propagation of fatigue cracks. 20 p2981 A72-39960

Crack arrest and crack initiation in a titanium alloy. 20 p2942 A72-39962

Designing to avoid stress-corrosion and/or fatigue failures. [AICHE PAPER 15C] 21 p3116 A72-40125

Complex stress-intensity factors at bifurcated cracks. 21 p3117 A72-40675

Analytical fracture mechanics application to stress corrosion cracking test methods for examining crack growth kinetics and time-to-failure 21 p3067 A72-40913

Fatigue strength of overloaded stiffeners in cracked panels, evaluating stress intensity factor and overload coefficients for fatigue crack propagation via finite element method [ICAS PAPER 72-40] 21 p3120 A72-41165

Circular cracks in tension and torsion. 21 p3123 A72-41395

Stresses in bonded materials with a crack perpendicular to the interface. 21 p3124 A72-41396

Application of the variational principle to the solution of problems of crack theory in viscoelastic media 21 p3126 A72-41539

Crack tip stress field alteration via elastic pulses for changing crack trajectory or fracturing process termination, using polarization optical method 21 p3061 A72-41824

Fiber glass reinforced plastics elastoplastic behavior due to microcrack propagating across matrix, using elastic index of work done 22 p3232 A72-41943

Axisymmetric temperature problem with arbitrary load duration for disk-shaped crack fracture mechanics, using Fredholm equation with symmetrical kernel for temperature field determination 22 p3233 A72-42097

Fracture analysis for linear elastic material in antiplane strain, discussing fast moving cracks propagation, flint knapping and equations of motion 22 p3237 A72-42801

Brittle fracture under dynamic loading conditions. 22 p3239 A72-42848

Criteria of fracture initiation from the view of fracture mechanics 22 p3239 A72-42857

Brittle striation formation role in corrosion fatigue crack propagation mechanism in Al-Zn-Mg alloy from test in NaCl solution under reversed anodic-cathodic current 22 p3193 A72-43033

Effect of cyclic stress wave form on corrosion fatigue crack propagation in Al-Zn-Mg alloys. 22 p3194 A72-43043

Investigation of the kinetics of low-cycle fatigue of steels in a hydrogen atmosphere and in vacuum 22 p3195 A72-43161

Application of cylindrical samples to the determination of the resistance to crack propagation of materials 22 p3242 A72-43163

Combined mode crack extension in adhesive joints. 23 p3305 A72-43493

A crack stopper concept for filamentary composite laminates. 23 p3305 A72-43498

Microscopic aspects of fracture in ceramics. 23 p3305 A72-43504

Fracture mechanics of composites. 23 p3345 A72-43509

Theoretical approach to the fracture of two-phase glass-crystal composites. 23 p3306 A72-43560

Computer simulation of fracture spreading in a visco-elastic solid. 23 p3267 A72-43702

Crack opening displacement relationship to notch root contraction from fracture toughness tests, describing plastic deformation mechanism at notch tip 23 p3346 A72-43704

Crack propagation speed measurements with wedge loaded double cantilever beam of PMMA, calculating stress intensity, strain energy release rate and kinetic energy 23 p3346 A72-43709

Some preliminary observations on the extension of cracks under static loadings at elevated temperatures. 23 p3301 A72-43712

Experimental and theoretical study of the fracture of sheet materials in the presence of cracks 23 p3349 A72-43958

Fatigue fracture and crack propagation in aluminum alloys. II. 23 p3302 A72-43973

Electron fractography of fatigue failure and macrocrack propagation in dual phase Ti alloy during cyclic loading at minus 140 to plus 150 C. 23 p3303 A72-44097

The surface flaw in aircraft structures and related fracture mechanics analysis problems. 23 p3352 A72-44228

Surface flaws measurement devices and quasi-static fracture tests, discussing cyclic crack growth, elastic compliance derivative method and stress intensity equations 23 p3353 A72-44229

Measuring fracture toughness - A simplified approach using controlled crack propagation. 23 p3290 A72-44258

Dynamic fracture criteria for ductile and brittle metals. 23 p3354 A72-44260

Fatigue crack propagation in A514 base plate and welded joints. 23 p3354 A72-44309

Fatigue-crack growth in 20% cold-worked Type 316 stainless steel at elevated temperatures. 24 p3435 A72-44555

Effects of projectile damage on critical helicopter components. 24 p3454 A72-44609

Mean stress effects on fatigue crack propagation rate from tests at various temperatures, assuming initial, tensile and shear modes and final propagation stages 24 p3454 A72-44627

The fatigue strength under varying mean stress. 24 p3455 A72-44629

Polymer fatigue failure mechanism examination on constant deflection type testing machine, investigating applied stress and temperature effects on crack propagation rate 24 p3455 A72-44631

The direct study of crack formation in metals in a high-voltage electron microscope 24 p3401 A72-44717

Computation of post-yield behaviour in notch-bend and tension testpieces. 24 p3456 A72-44796

Plane-stress fracture toughness testing using a crack-line-loaded specimen. 24 p3456 A72-44810

Crack growth resistance in plane-stress fracture testing. 24 p3456 A72-44811

Plastic flow around an expanding crack. 24 p3456 A72-44812

Fracture mechanics development from Griffith to crack opening displacement (COD) concept, discussing crack initiation and propagation, stress-strain characteristics and yield point 24 p3456 A72-44814

Design against fatigue failure in thermoplastics. 24 p3457 A72-44816

Compliance calibrations of a contoured and face grooved double cantilever beam specimen. 24 p3413 A72-44817

Fatigue crack closure at positive stresses. 24 p3457 A72-44819

Development and present-day state of the fatigue-damage theories. 24 p3457 A72-44873

Stress-strain state in tension of orthogonally stiffened fiberglass-reinforced plastic with cracks in transversely stiffened layers 24 p3460 A72-45754

Method for applying a fatigue crack to impact test specimens made from tough materials. 24 p3417 A72-45765

CRACKING [FRACTURING]

Corrosion and stress corrosion cracking prevention on space shuttle by materials selection 01 p0085 A72-10775

Portable self contained ultrasonic field inspection equipment for nondestructive crack detection in T53 gas turbine compressor disks 01 p0076 A72-10814

Ductile tensile cracking macroscopic simulation with perforated pure Al specimens, determining fracture energy as function of hole size and pattern 01 p0086 A72-10987

Crack angle effect on high strength metals fracture toughness, using Al alloys and tool steel ASTM-type single edge notch tension specimens 01 p0086 A72-10988

Stress corrosion cracking of Cr-Ni austenitic stainless steel with Mo and Cu additions in boiling sulfuric medium 01 p0089 A72-11181

Al alloys compressed strips, determining anisotropy of toughness and crack sensitivity by tests 02 p0244 A72-12244

Hydrogen diffusivity and solubility in alpha-Ti alloys, considering absorption effect on stress corrosion cracking 02 p0244 A72-12481

Breakdown of three dimensional brittle medium weakened by concentric systems of interconnected circular cracks, using Fredholm integral equations 03 p0447 A72-13732

Elastic plate with two collinear thermally insulated cracks, calculating steady temperature field and stresses for uniform heat flux at infinity 03 p0450 A72-14112

Generalized epicyclic properties application to fracture mechanics, considering stress fields of constrained plastic zones around cracks in thin elastic plate 03 p0455 A72-14388

Grain boundary region constituents corrosion behavior and solution chemistry within stress corrosion cracks in Al alloys observed from pH changes 04 p0535 A72-15733

Critique of microstructure effect on strength, toughness and stress corrosion cracking susceptibility of metastable beta titanium alloy, discussing recrystallization conditions 05 p0679 A72-17122

Al sheet weld cracking, discussing hold-down, localized heating, welding speed and gap effects 06 p0820 A72-17702

Cr and U contents effect on high strength Cr-Mo-Va alloy steel sheet hot cracking susceptibility, using Huxley test method 06 p0820 A72-17704

Semibrittle tears and fractures by progressive cracking in metallic structures, discussing metal fatigue and environmental stress 06 p0897 A72-18297

Hydrogen cracking of high strength steels during cathode polarization in acidic media, investigating time to cracking variation with current density 07 p1013 A72-19770

Static hydrogen fatigue of high strength steels, deriving relationship between time to cracking and tensile stresses magnitude for cadmium-plated steel 07 p1014 A72-19774

Prestraining effect on stress corrosion resistance of fatigue precracked high strength steels 07 p1016 A72-19941

Precipitation hardened Ni-Al alloy mechanical properties, relating ductility and strength to precipitate caused inhibition of microcrack initiation and propagation 07 p1021 A72-20438

Gamma radiation effect on cracking and tensile strength of polycapromide /capron/ film 08 p1196 A72-21870

Thermocrossing and thermal stresses in packing rings of face-type mechanical seals under dry friction 08 p1177 A72-21927

Alloy composition, specimen stressing and surface conditions effects on stress corrosion cracking 08 p1189 A72-22106

Soviet book on corrosion cracking of carbon steels covering chemical composition, structure, mechanical properties, anode and cathode processes role and adsorption losses 08 p1190 A72-22163

Quenched and tempered Ni carbon steel retained austenite transformation and crack observation by X ray diffraction under low cycle fatigue testing 09 p1329 A72-23149

Ni carbon steel microstructure changes in retained austenite phase and crack observation during low cycle fatigue testing 09 p1330 A72-23150

Stress distribution determination for long isotropic elastic cylinder with strip crack on diametral plane by complex variable technique and Fredholm equation solution 09 p1409 A72-23574

Fatigue indicators with analytic or visual notched and cracked coupons techniques and strain multipliers for welded structures 09 p1316 A72-23620

Torsion of embedded infinite elastic circular cylindrical fiber with penny shaped crack, investigating breaking behavior from Fredholm integral equation iterative solution 10 p1553 A72-24094

Hexagonal metals stress corrosion cracking fractographs interpretation, noting striations as prominent feature of transgranular fractures 11 p1652 A72-25288

Acoustic emission monitoring of postweld heat treatment cracking in Rene 41 weldments, correlating relative crack susceptibility of different microstructures 11 p1653 A72-25345

Aerospace vehicle high tensile strength fasteners stress corrosion cracking and hydrogen embrittlement [AIAA PAPER 72-385] 11 p1653 A72-25407

Al alloys hand forgings fracture strength and stress corrosion characteristics from precracked specimens bending tests in air and sea water 11 p1658 A72-25833

Constrained zones and stress intensity factors in cracked thin elastic plates under combined tensile and shear loads 11 p1735 A72-25893

Fracture toughness anisotropy and crack sensitivity of Al alloys extruded bars notched cylindrical samples 11 p1659 A72-26130

Safe welding procedures for carbon manganese steels, noting hydrogen cracking association with hardening of heat affected zone 11 p1641 A72-26490

Stress-strain state determination for closed cracked cylindrical shell, using Fredholm integral equations 12 p1880 A72-27236

Al-Zn-Mg alloy tear resistance relationship to stress corrosion cracking from tear, tensile and corrosion tests 12 p1830 A72-27750

Ti alloys hot salt stress corrosion cracking mechanism, discussing cold deformation and heat treatment effects, tensile tests, hydrogen analysis and microscope investigation 14 p2117 A72-30535

Microstructural changes relationship to corrosion susceptibility in ternary Al alloy obtained from stress corrosion cracking tests and electron metallography, noting precipitate-free region 14 p2118 A72-30542

Finite element method with compliance equations determining energy release rates and stress intensity factors for complex crack configurations and loadings 14 p2168 A72-30908

Slip band blocking effect of disperse particles on crack suppression and creep rupture strength of intermetallic Al-Fe-Ni alloy 14 p2124 A72-31033

Elastic properties of media with cracks, discussing elastic anisotropy and crack distribution 15 p2327 A72-31733

Al-Zn-Mg alloys hot cracking during solidification, discussing chemical composition, Al purity, temperature, aging, dissolved gases and grain refining additives effects 15 p2256 A72-31774

Rotating bending fatigue limit correlation with non-propagating crack for steel specimens with hole 15 p2329 A72-32140

Neutron irradiation effects on structural materials brittle fracture initiation and propagation mechanisms, discussing residual elements influence on radiation defect stabilization 15 p2258 A72-32486

Nondestructive vibration tests of fatigue crack damage in composite structures, investigating glass reinforced epoxy and polyester laminates 16 p2414 A72-33318

Cyclic compressive fatigue cracking tests of prenotched fiber reinforced epoxy materials at low stress 16 p2414 A72-33319

Definition of the fatigue limit on the basis of the distribution of the resistance over the set of elementary volumes of which the sample is composed 17 p2565 A72-34196

Pressurized crack behavior in two-dimensional rocket motor geometries. 17 p2596 A72-34203

Buekner formulation combined with finite element method for arbitrary shaped cracked bodies stress intensity factors in framework of linear fracture mechanics 17 p2623 A72-34253

Catalytic dissociation, hydrogen embrittlement, and stress corrosion cracking. 17 p2566 A72-34256

Investigations aimed at eliminating the susceptibility to thermal cracking of the high corrosion resistant NiMo 30 nickel-molybdenum alloy /Remanit HB/ 17 p2559 A72-34394

Critical species in the transgranular stress corrosion cracking of titanium alloys in aqueous solutions. 17 p2567 A72-34733

An optical method for the determination of constrained zones at crack-tips. 18 p2733 A72-36368

Interface morphology development during stress corrosion cracking. I - Via surface diffusion. 18 p2700 A72-36583

Cathodic protection and hydrogen in stress corrosion cracking. 19 p2817 A72-37765

Thermal boundary equilibria in brittle bodies with heat conducting cracks under combined loads and temperature fields 19 p2877 A72-38198

Stress corrosion cracking of 18% Cr ferritic stainless steels. 19 p2820 A72-38300

Effect of additions of Cu and Zr on stress corrosion cracking of Al-Mg alloys. 19 p2820 A72-38370

A study of the mechanical behaviors of austenitic stainless steels in the process of stress corrosion testing. 19 p2820 A72-38372

The role of metal dissolution in the process of stress corrosion cracking of austenitic stainless steel. 19 p2821 A72-38374

Effects of small amounts of additional elements on stress corrosion cracking of Al-Zn-Mg alloys. VI. 19 p2821 A72-38555

An analytical approach to the non propagating crack problem using the finite element method. 20 p2977 A72-38882

Use of acoustic emission for the detection of weld and stress corrosion cracking. 20 p2925 A72-39283

Theoretical model for acoustic emission relationship to fiber cracking during rising load tensile test on fiber reinforced composites 20 p2925 A72-39285

Cracks and screw dislocation arrays in anisotropic bimaterial plates. 20 p2937 A72-39291

Gaseous hydrogen-induced cracking of Ti-5Al-2.5Sn. 20 p2937 A72-39292

Ni alloys weld testing for hot cracking resistance, describing vareststraint test method 21 p3060 A72-40848

Crack tip stress field alteration via elastic pulses for changing crack trajectory or fracturing process termination, using polarization optical method 21 p3061 A72-41824

On the application of the mixed finite element methods to the stress concentration problems of cylindrical shells with a circular cutout or a crack. 22 p3232 A72-41942

Some recent experimental investigations in stress-wave propagation and fracture. 22 p3237 A72-42768

German monograph - The causes of hot crack formation in welded joints of austenitic steel with 16 percent chromium and 16 percent nickel. 22 p3195 A72-43079

Differentiating stress corrosion cracking from hydrogen cracking of ferritic 18-8 stainless steels. 22 p3195 A72-43127

The effect of some electrolytes on the stress corrosion cracking of AISI 4340 steel. 22 p3195 A72-43128

Polycrystalline aluminum and magnesium oxide ceramics fracture strength, considering plastic deformation and twinning role in crack nucleation 23 p3305 A72-43505

Approximate stress-strain state determination in plate weakened by arbitrarily oriented rectilinear cracks and circular holes in elasticity theory 23 p3349 A72-43801

CRACKS

NT MICROCRACKS

NT SURFACE CRACKS

Initial crack effect on slender column compression load carrying capacity, deflection and stress intensity factor 01 p0140 A72-10989

Plane strain analysis of two bonded semiinfinite elastic media with different thermomechanical properties and cracks, calculating stress factors and maximum stress angles 01 p0140 A72-10990

Stress intensity factors for circular crack near surface of semiinfinite solid, considering pure beam bending and approximate thickness effect for plate deep surface flaw 01 p0140 A72-10991

Two-layered plane strain elastic cylinder with cracked inner bore under internal pressure loading,

obtaining stress intensity factors by finite element method 01 p0141 A72-10994

Thermal stresses, temperature distribution and displacement fields in elastic solid with spherical cavity and external crack 01 p0144 A72-11385

Residual buckling strength of Al alloy elastic column with fatigue crack [SESA PAPER 1914A] 02 p0288 A72-11511

Pressure vessels with cracks, formulating stress analysis for safety factors 03 p0443 A72-13452

Stress concentration coefficients calculation at sharp cracks and notches for rods in tension, compression and combined bending and torsion 03 p0443 A72-13457

Fracture mechanics of interfacial cracks between two bonded dissimilar anisotropic elastic half spaces, presenting two dimensional analysis of stress fields 03 p0446 A72-13707

Asymptotic methods for complex mixed problems of elasticity related to stress concentration in plates with cracks or inclusions 03 p0449 A72-14102

Circular disk with external radial cracks, obtaining limiting equilibrium stress-strain state through singular integral equation solution 03 p0451 A72-14115

Dual integral equations method application to elastic bodies with plane circular cracks in torsion 03 p0452 A72-14135

Cracked rectangular plates vibration and stability, computing eigenvalues, natural frequencies and moment distribution 04 p0583 A72-14448

Stress intensity and plane dilatational wave diffraction in elastic material with finite crack 04 p0583 A72-14459

Shear stress and stability of composite elastic double layer with plane circular crack under torsion 04 p0588 A72-15054

Three dimensional temperature distribution at thermally insulated crack in plate 04 p0593 A72-15658

Crack corrosion in metals and metal alloys, considering electrochemical reaction kinetics as function of oxygen concentration and pH 04 p0536 A72-15738

Boundary collocation method for estimating stress intensity factors for through-thickness interior crack in finite rectangular plate [ASME PAPER 71-MET-L] 05 p0732 A72-15794

Transient stress analysis for sudden twisting of penny-shaped crack in infinite elastic body under torsion, using integral transform [ASME PAPER 71-WA/APM-10] 05 p0734 A72-15969

Mass concept for moving crack, relating stress concentrations of elastic field with crack inertia 05 p0673 A72-16306

Optical interference technique for experimental stress analysis of cracked structures, obtaining crack shape relationship to stress intensity factor 05 p0666 A72-16322

Plastic stress and strain intensity factors for cracked plates in tensile fields 05 p0737 A72-16323

Mixed boundary value problem of infinite elastic plate with parabolic crack, obtaining solution by complex variable method 05 p0741 A72-17004

Brittle strength characteristics of construction materials with cracks calculated by graphical analysis procedure, considering state of limiting equilibrium 06 p0899 A72-18560

Limiting equilibrium of elastic half space with randomly oriented crack 07 p1092 A72-19780

Stress analysis of infinite plate with parallel cracks under symmetrical edge loads 07 p1092 A72-19781

Stress-strain state in tension of orthogonally stiffened fiberglass-reinforced plastic with cracks in transversely stiffened layers 07 p1094 A72-20128

Penny shaped interface crack between elastic layer and half space, calculating stress intensity factors and strain energy release rate for aluminum-epoxy combination 09 p1398 A72-22530

Stress intensity factor of crack near inclusion in infinite elastic plane, using numerical methods 09 p1398 A72-22531

Mixed boundary value problem for infinite parallel cracks row solved by reduction to Fredholm integral equation 09 p1398 A72-22534

Numerical solution of integral equations for dislocation densities and stress singularities associated with cracks and pile ups in bimetallic media 09 p1398 A72-22622

Electron fractographic investigation of fracture properties via removal of metal oxide film accumulated on crack surface during service life of steel structures 09 p1309 A72-22639

Stress and couple stress fields near antiplane shear crack tip, determining eigenfunctions to satisfy field equations and boundary conditions 09 p1402 A72-22744

Circumferential crack in closed shallow cylindrical shell under tension, computing stress singularities strength 09 p1404 A72-22915

Central crack in plane orthotropic rectangular sheet under tension, showing stress intensity factors dependence on geometric and elastic constants 09 p1404 A72-22915

Circumferential crack in cylindrical shell under torsion, presenting membrane and bending components of stress intensity factor ratio 09 p1404 A72-22918

Statistical crack length distribution of flaw sizes in steel parts during manufacturing 09 p1328 A72-22920

Authoradiographic study of stress intensity factor influence on hydrogen distribution at crack tips in Ti-Al-V alloy, using tritium doped salt water as corrosive medium [ONERA, TP NO. 1052] 10 p1496 A72-24234

Thermal stresses and displacements in elastic medium containing parallel circular cracks, using perturbation technique 10 p1560 A72-25045

Axisymmetric stress field in infinite homogeneous isotropic elastic solid with crack surrounding cylindrical cavity, solving elastic equilibrium equations 11 p1738 A72-26720

Mellin transforms for finite elastic disk radial crack stress intensity factor and energy formulae in terms of Fredholm equation solution, considering constant loading case 11 p1738 A72-26724

Crack and notch induced stress concentrations effect on steel mechanical properties at 20-293 K, using static and dynamic test methods 12 p1831 A72-28240

Boundary value problems in dynamics of Cosserat infinite elastic medium with finite crack, noting couple stresses effect on dynamic stress concentration 14 p2164 A72-30299

Elastic crack tip stress fields, considering weight function 15 p2322 A72-31347

Numerical solution of singular integral equations system for stress concentration in elastic plane with curvilinear crack 15 p2327 A72-31735

Displacement and stress field for elastic solid containing cruciform crack with unequal length arms 15 p2330 A72-32292

Elastic-plastic medium yield zone spread from penny shaped crack determined from continuous distribution of dislocations, noting system energy change 16 p2468 A72-33226

Stress analysis for brittle body with thermoinsulated crack under mechanical load and temperature field, noting limiting equilibrium equation 16 p2469 A72-33272

Stress analysis for circular disk with diametral crack under symmetric and antisymmetric loads, solving integral equations via factorization 16 p2469 A72-33273

The evaluation of the stress intensity factors for cracks subjected to tension, torsion, and flexure by an efficient numerical technique. [ASME PAPER 72-MAT-B] 17 p2631 A72-34966

A comparison of numerical methods for determining stress intensity factors. 17 p2631 A72-34973

Analysis of an inclined crack centrally placed in an orthotropic rectangular plate. 19 p2870 A72-37221

Asymmetric collinear internal cracks interaction evaluation by measuring diameter variation and shape distortion of caustic surface impinged upon by retarded laser radiation 19 p2870 A72-37224

Stability analysis of internal pressure loaded crack in adhesive layer bonding elastic plate to rigid base using energy and critical load intensity criteria 19 p2870 A72-37245

Criteria for valid plane strain fracture toughness testing dealing with straightness of fatigue crack front of metal specimens 20 p2981 A72-39958

Elastic analysis for a radial crack in a circular ring. 20 p2981 A72-39959

Photoelastic determination of mixed mode stress intensity factors. 20 p2981 A72-39963

The use of pre-cracked Charpy specimens to determine dynamic fracture toughness. 20 p2981 A72-39964

- Stress concentration around circular crack on interface between two bonded dissimilar isotropic elastic half spaces
20 p2982 A72-40020
- Crack tip vicinity stress generated by plane transient tension-stress wave diffraction, examining ductility effects on fracture modes
21 p3117 A72-40672
- Bent plates and shells equations and rupture modes, characterizing cracks and stress intensity
21 p3122 A72-41338
- Stress distribution at crack tips in elastic plate loaded by two concentrated opposite forces perpendicular to crack
21 p3123 A72-41389
- The stress intensity factors of a radial crack in a finite rotating elastic disc
21 p3124 A72-41397
- Stresses around an axial crack in a pressurized cylindrical shell
23 p3346 A72-43705
- A finite element stress analysis of a crack in a bi-material plate
23 p3346 A72-43707
- Stress distribution at defects in the form of rigid sharply-angled inclusions
23 p3349 A72-43952
- The torsion of a circular cylinder containing a symmetric array of edge cracks
23 p3350 A72-44048
- Stress-strain characterization of part-through crack in plate under tension in terms of stress intensity factor
23 p3352 A72-44227
- Numerical evaluation of elastic stress intensity factors by the boundary-integral equation method
23 p3353 A72-44233
- The importance of service inspection in aircraft fatigue
24 p3367 A72-44740
- A sandwich plate with a part-through and a debonding crack
24 p3456 A72-44813
- Pressure vessels with cracks, formulating stress analysis for safety factors
24 p3458 A72-44927
- Stress concentration coefficients calculation at sharp cracks and notches for engine parts in tension, compression and combined bending and torsion
24 p3458 A72-44932
- The effect of shear on a penny-shaped crack at the interface of an elastic half-space and a rigid foundation
24 p3459 A72-45250
- CRAFT**
U. VEHICLES
CRANES
Flying crane helicopters utilization in construction industry for materials transport and structural erection work, discussing technical and economic aspects
23 p3251 A72-43637
- CRANIUM**
NT. INTRACRANIAL CAVITY
Human craniocerebral trauma dependence on impact conditions, giving case histories
05 p0619 A72-16643
- CRASH INJURIES**
Fatal aviation accident human factors investigation by roentgenography, noting flight environment factors, injury pattern relation to aircraft design and victim identification
06 p0768 A72-17880
- Crashworthy upper torso restraint systems for general aviation, incorporating strap takeup devices
08 p1126 A72-21578
- Vertical drop rig test equipment for measuring shock attenuation of crash helmets, discussing shock absorption criteria for impact protection
11 p1584 A72-26016
- Analytical model for nonpenetrating impact caused head injuries, evaluating protective device effectiveness via energy absorption characteristics
15 p2191 A72-32602
- Aircraft crash landing induced acceleration effects on seated occupants, discussing energy absorber system dynamic response characteristics for injury protective devices
15 p2191 A72-32603
- Crash helmet performance prediction through maximum strain criteria, using brain injury biodynamic model
15 p2192 A72-32607
- Crash energy absorption for prevention of fatal injuries, considering human deceleration tolerance with respect to required energy absorber force-deflection relationship
15 p2192 A72-32630
- Aircraft accident in the Faroe Islands in 1970 - Observations from a medical point of view, with special reference to spinal fractures
17 p2508 A72-34556
- Blood serum enzymes activity changes in polytraumatized humans injured in automobile accidents
21 p3002 A72-41188

- Human tolerance limitations related to aircraft crashworthiness
22 p3151 A72-42765
- Response of a seat-passenger system to impulsive loading
22 p3151 A72-42766
- A study of USAF survival accidents 1 Jan. 1965-31 Dec. 1969
23 p3259 A72-43425
- CRASH LANDING**
Aircraft crash fire protection, using passenger compartment heat shield of fire-retardant polyisocyanurate foam and intumescent paint
03 p0310 A72-13484
- Antimisting kerosene fuels for aircraft crash fires reduction
07 p1050 A72-18837
- Emergency Life Saving Instant Exit system in aircraft fuselage for use after crash landing, discussing design and ground testing
08 p1109 A72-21583
- Pilot survival probabilities under various conditions of high performance aircraft takeoff and landing accidents, suggesting emergency action guidelines for pilot training
10 p1428 A72-23732
- Jet engine fuel modification to decrease fire hazard in survivable aircraft crashes
[ASME PAPER 72-GT-25] 11 p1702 A72-25621
- Safe aircraft fuels crashworthiness evaluation in terms of ignition susceptibility parameter, noting full scale crash environment simulation
[ASME PAPER 72-GT-27] 11 p1702 A72-25623
- Crash safe turbine fuel to reduce fire probability and severity during aircraft ground crash, investigating physical and chemical properties
[ASME PAPER 72-GT-28] 11 p1702 A72-25624
- General aviation crashworthy personnel restraint systems, discussing strap take-up devices, comfort, fit and ease of use
13 p1908 A72-28726
- Aircraft crash landing induced acceleration effects on seated occupants, discussing energy absorber system dynamic response characteristics for injury protective devices
15 p2191 A72-32603
- Deceleration attenuation effectiveness of airbag restraint systems compared with seat belt-shoulder harness for aircraft occupants crash protection
15 p2191 A72-32605
- CRASHES**
NT. CRASH LANDING
Test facility design for aircraft crashworthiness evaluation and improvement, considering survivable accident surrounding conditions, equipment and testing methods
[SAE PAPER 720323] 11 p1576 A72-25586
- Worldwide distress alarm, identification and position location system for downed aircraft, discussing GRAN feasibility tests
15 p2272 A72-32214
- A survey of rotary-wing aircraft crashworthiness
22 p3138 A72-42763
- CRATERING**
NT. PROJECTILE CRATERING
Phase composition changes, crater formation and metal ejection during erosion by pulsed laser beam
07 p1009 A72-20610
- Martian cratering by asteroid impact, discussing Palomar-Leiden asteroid statistics, Opik capture theory and evolutionary extrapolation limitations
10 p1531 A72-23705
- Martian crater obliteration theory, suggesting filling by dust deposition
10 p1531 A72-23706
- Lunar glass particle micrometeorite crater morphology, showing radial fracture and spallation zone relationships
13 p2036 A72-28755
- Mars doublet cratering by impacting meteoroid breakup due to stresses in gravitational field, using Monte Carlo simulation
14 p2149 A72-30317
- Glass lined microcraters on lunar rocks attributed to hypervelocity impact of extralunar particles
17 p2615 A72-35682
- CRATERS**
NT. LUNAR CRATERS
NT. METEORITE CRATERS
NT. TYCHO CRATER
Central peaked Martian crater distribution from Mariners 6 and 7 photographs, comparing south polar region to equator
03 p0440 A72-14310
- Radar observations of Martian craters and scarp during 1971 opposition
04 p0579 A72-15359
- Radar observation of Mars surface, noting rugged terrain and craters
04 p0579 A72-15360
- Thermomathematical model for calculating craters formed by short pulses in electro discharge machining
08 p1173 A72-21028

- Basalt plates craters produced by steel balls, noting profiles at normal and oblique impacts
08 p1232 A72-21153
- Rock type discrimination from ratioed airborne thermal IR scanner images of Pisgah Crater /California/
08 p1162 A72-22018
- Mars craters degradation and density regional variations from Mariner 6 and 7 imagery, using numerical scoring method
14 p2149 A72-30318
- Hellas-Hellepontos transition zone properties in origin model with impact and later isostatic subsidence
16 p2454 A72-33445
- Basalt plates craters produced by high velocity impact of steel spheres, noting profiles at normal and oblique angles
20 p2978 A72-39258
- CRAZING**
U. SURFACE CRACKS
CREATINE
Muscle metabolism during isometric exercise performed at constant force
21 p3005 A72-40425
- CREATININE**
Urine and plasma protein and creatinine measurements in acclimatized and unacclimatized men before, during and after high altitude ascent
10 p1426 A72-24482
- Nitrogen excretion as a measure of protein metabolism in man under different conditions of renal function
21 p3003 A72-41523
- CREEP ANALYSIS**
Finite element analysis of creep due to stress and strain in double edge notched plates and round bars
01 p0138 A72-10519
- Kink movement and cutting forest dislocation models of creep in thermally activated crystalline solids
01 p0140 A72-10857
- Creep strength analysis of heat resistant alloys under repeated unsteady loads
01 p0144 A72-11376
- Nonlinear boundary value problem of creep for isotropic bodies with random mechanical properties under random loads, calculating structural component reliability and service life
02 p0289 A72-11619
- Creep theory by rheonomic body interpretation as controlled system with unknown vectors at input and output, obtaining stress-strain curves for experimental verification
02 p0289 A72-11620
- Thin shell creep and plasticity analyses reduced to linear programming problem by functionals and finite difference equations
02 p0290 A72-11622
- Empirical power law application to secondary creep, steady state hot working and high temperature tensile or compressive yielding, discussing activation parameters interrelations
02 p0247 A72-12814
- Time effects on stress concentration around circular and elliptical holes in infinite plate with nonlinear creep
03 p0451 A72-14126
- Ti-Al-V room temperature creep, considering tensile and torsional loading, plastic deformation, stress relief and design limitations
03 p0377 A72-14171
- Validity hypothesis for total creep rate potential in strain-hardenable materials, discussing carbon steel torsion and tensile tests
04 p0586 A72-15006
- Nonlinear hereditary elasticity theory boundary value problem solution using complex potentials in successive approximation algorithm for stress concentration and nonlinear creep analysis
04 p0588 A72-15059
- Cyclic strain accumulation induced creep behavior prediction via plasticity model, considering non-homogeneous stress states
[ASME PAPER 71-APM-NN] 04 p0589 A72-15179
- Rheomobility effects in creep instability of rods with initial deflection, determining critical load by Ritz method
04 p0594 A72-15708
- Elastoplastic creep analysis for cylindrical pressure vessel structural response during cyclic thermal shock, internal pressure and extended high temperature loading
[ASME PAPER 71-WA/PVP-12] 05 p0732 A72-15911
- Steady and unsteady creep stages in porous body sintering and hot compacting, using three dimensional viscous flow theory
05 p0665 A72-16092
- Complex potentials for nonlinear elasticity, creep and small elastoplastic deformations, applying to stress concentration at curvilinear hole in infinite plane
05 p0742 A72-17183

Quasi-linearized solution to nonlinear Volterra equations in design of structures under creep deformations

06 p0897 A72-18318

High temperature creep of niobium alloy, obtaining creep limit, microhardness and gas analysis data

06 p0833 A72-18637

Creep and plastic deformation analysis of riveted joint elements using elastoplastic theory

07 p1087 A72-18982

Stress redistribution in statically indeterminate structures under creep, discussing effects on time to brittle fracture and service life determinations

07 p1088 A72-19259

Machine metals fatigue life, creep theory and stress and strain kinetics in severe environments, formulating physical equations

08 p1246 A72-21805

Compression creep mechanisms in ceramic materials at elevated temperatures by lattice dislocations, grain boundary sliding and stress directed diffusion

09 p1334 A72-22393

Metal creep fatigue analysis and life prediction by inelastic strain ranges partitioning into reversed tensile and compressive plasticity and creep components

09 p1406 A72-23198

Time and cycles to failure diagrams for strain rate and hold periods effects on high temperature metal creep fatigue in design analysis

09 p1407 A72-23199

Oxidation and substructural effects on low stress creep of Al near melting point

09 p1331 A72-23507

Moment stress-strain state of two layer circular cylindrical shells under creep conditions

11 p1733 A72-25542

Two dimensional reinforced plastic material anisotropic creep derivation from orthotropic plate time functions and stress tensor invariants

13 p2034 A72-28437

Work hardening-recovery model of dislocation creep, deriving multiaxial mechanical equation of states for strain/time relationship under arbitrary temperature-stress sequences

13 p2061 A72-29872

Activation energy of high temperature creep in Cr alloy with aluminum oxide, comparing with moving monovacancies in pure Cr

14 p2112 A72-30161

Metal creep activation energy determination during plastic deformation process, using temperature differential method

14 p2115 A72-30412

Flat Ti alloy sheet creep under variable loads at 300-400 C, comparing prediction with test data

14 p2116 A72-30434

Stress analysis of thick walled hollow viscoelastic circular cylinder enclosed in elastic shell and subjected to nonlinear creep conditions, noting temperature effects

14 p2165 A72-30439

Creep rate dependence on high temperature oxidation in austenitic steel, noting preformed oxide layer and environment cycling effects

14 p2117 A72-30537

Creep deformation transition theory in spherical shells, using generalized strain measure for asymptotic solution

14 p2169 A72-30999

Viscoelastic model for constitutive nonlinear creep law with combined strain and time hardening assumptions, evaluating material parameters for Al alloys

15 p2254 A72-31554

Unsteady torsional creep of multiply connected cylindrical rod with arbitrary cross section, calculating elliptic rod relaxation

15 p2327 A72-31744

Steady state creep theory for discontinuous fiber composites, considering rigid and creeping fibers and sliding interface

15 p2261 A72-32300

Orientation and elongation effects on grain boundary correction term in foil surface energy measurement by zero creep, using virtual work method

15 p2258 A72-32637

Recovery-work hardening model of steady state creep for Al, assuming equal internal and applied stress

15 p2259 A72-32642

Constitutive equations for metallic creep analysis based on simultaneous strain hardening and crack propagation processes, calculating creep rupture time

16 p2408 A72-33589

Maxwell rheological creep model verification by tensile tests on Mg alloy at 150 C under step loadings, treating thermodynamics of ideal creep

16 p2412 A72-34111

Creep tests on Cr martensite stainless steel, showing inapplicability of Garofalo equation for stress dependence of secondary creep rate during variable stress experiment

16 p2412 A72-34112

Rheological model for creep under intermittent square wave stress pulses, taking into account time dependent dislocation density

16 p2412 A72-34113

Elastic-plastic-viscous model for creep analysis of rheo-mobile materials, taking into account cracks and other defects

16 p2412 A72-34116

Energy theorems for creep constitutive relationships, discussing total deformation of body composed of elastic-creeping material with allowance for stress redistribution effects

16 p2473 A72-34118

Creep deformation upper bounds for smooth pipe bends under constant external bending moments, using energy method analysis

16 p2473 A72-34123

Numerical procedure for spherical and cylindrical shells creep behavior, taking into account stress redistribution due to interaction between elastic and creep strains

16 p2473 A72-34125

Instantaneous and time dependent solutions for thin rectangular plates nonlinear creep bending within framework of Karman theory

16 p2473 A72-34126

Contribution to the study of creep in thin permalloy films.

17 p2596 A72-35759

Relations between the experimental parameters describing the steady-state and transient creep.

18 p2732 A72-36343

Direct and indirect creep modelling technique in photoelasticity.

18 p2734 A72-36379

Analysis of primary creep of molybdenum at high temperatures.

18 p2700 A72-36580

Temperature effects on the strainrange partitioning approach for creep-fatigue analysis.

19 p2815 A72-37638

Mathematical relationships for primary, secondary and tertiary creep and their use in extrapolation of tensile creep data.

19 p2874 A72-37708

Form of the modified Orowan creep equation for a case in which the internal stress is due to dislocation-interactions.

20 p2978 A72-39008

Steady-state creep of shells of revolution in the case of the Tresca criterion

22 p3233 A72-42051

Equilibrium equation for unsteady creep of thin truncated conical shell under internal pressure, solving in successive time steps with Taylor series expansion

22 p3233 A72-42062

Determination of the regions of action of various creep mechanisms in ceramic materials

23 p3307 A72-43932

CREEP BUCKLING

Thin circular cylindrical shells under uniform axial compression loads, examining axially symmetrical creep buckling

02 p0296 A72-12531

Creep buckling of cylindrical finite two-layer shell under external hydrostatic pressure, considering rigidly clamped and hinged end conditions

03 p0444 A72-13574

Creep buckling of simply supported initially slightly curved column under variable axial load, describing deflection up to critical point

07 p1088 A72-19168

Second order deformation theory for axially held strut during thermal cycling at creep relaxation temperature, using galerkin method with assumed sine wave

16 p2473 A72-34124

Compressed initially bent Shanley column analyzed for geometric imperfection coupling and material behavior effects on critical time to creep collapse

16 p2474 A72-34131

Exact differential equation derived for optimal design of straight nonprismatic column subject to creep buckling

16 p2474 A72-34132

Imperfect circular cylindrical shells creep and elastic buckling under nonuniform external loads, solving ordinary differential equations via finite difference technique

16 p2474 A72-34133

Small nonaxisymmetric initial shape deviations effect on creep buckling and critical time of thin walled circular cylindrical shell in axial compression

16 p2474 A72-34134

Creep-buckling of flat rectangular plates when the creep exponent ranges from 3 to 7.

19 p2875 A72-37717

Creep buckling of slender or thin-walled structures, taking into account strain rate dependent time-hardening and elastic deformation effects

19 p2875 A72-37884

Experimental creep buckling of circular cylindrical shell under uniform compression.

20 p2978 A72-38883

Axissymmetric-multilobe creep buckling transition in thin walled circular cylindrical shells under uniformly distributed axial compressive load

22 p3239 A72-42844

CREEP DIAGRAMS

Automatic recording of cyclic creep and strain curves for metals under low cycle static tension

03 p0444 A72-13468

Nickel base alloy under axisymmetric tension compression tests, obtaining breaking load diagrams and fatigue and creep curves

06 p0833 A72-18638

Heat resistant metals long time creep prediction at low stresses or temperatures

06 p0834 A72-18668

Graph-analytic technique to plot Cr steel stress relaxation curve from primary and isochronous creep diagrams

16 p2472 A72-33848

A rational approach to creep design.

19 p2874 A72-37706

Elastic stiffness and ductility of refractory materials of long service life, noting creep diagrams and tensile strength

23 p3301 A72-43959

Automatic recording of cyclic creep and strain curves for metals under low cycle static tension

24 p3458 A72-44943

CREEP PROPERTIES

NT STEADY STATE CREEP

NT TENSILE CREEP

Nonlinear photoelasticity, elastoplasticity and creep problems studies by optical polarization methods, comparing transparent model and photoelastic coating techniques

02 p0289 A72-11613

Linear creep properties in continuous media for wide time-variable parameters range of instantaneous elastic deformation under simple loads

02 p0289 A72-11616

Time operator method in creep theory for orthotropic bodies, obtaining asymptotic solutions for laminar orthotropic rod and elastic plate vibration problems

02 p0289 A72-11617

Tube and hollow sphere revolving in thermal fluid under surface pressure load, obtaining stress-strain state and random temperature dependences of creep

02 p0289 A72-11618

Creep theory by rheonomic body interpretation as controlled system with unknown vectors at input and output, obtaining stress-strain curves for experimental verification

02 p0289 A72-11620

Heat resistant alloys thermal microstresses effect on creep and fatigue life under thermal cycling conditions

02 p0242 A72-11633

Metal fatigue mechanisms in subcreep temperature range, discussing response to cyclic loading including hardening, softening and inhomogeneous plastic strain development

02 p0295 A72-12496

Metal fatigue time and cycle dependent deformation and fracture mechanisms in creep range from cumulative damage law standpoint for lifetime prediction

02 p0295 A72-12497

Rheomobility and structural creep, correlating mobile, rigid, elastic, viscous and plastic models

02 p0297 A72-12612

Nonlinear creep of glass fabric-plastic composite under loading in uniaxial stressed state

02 p0250 A72-12676

Orthotropic glass fabric laminate creep under combined torsion and tension, describing test facility

02 p0250 A72-12677

Powder metallurgical tungsten fine wire creep behavior at 2100-3000 C, determining activation energy and stress dependence

03 p0370 A72-12996

Polycrystalline materials wedge crack growth enhancement by vacancy diffusion under creep failure conditions, considering grain boundary sliding mechanism

03 p0442 A72-12998

Screw connections high temperature behavior, discussing creep induced tension relaxation and cyclic loads long term tolerance

03 p0363 A72-13375

High temperature creep activation energies relationship to diffusion in TiC, ZrC and UC

03 p0371 A72-13461

CoO single crystal creep rate at different temperatures, stresses and oxygen pressures, noting slip occurrence

03 p0373 A72-13647

Pure metals creep or self diffusion activation energy from hot-hardness data, noting temperature and elastic modulus effects

03 p0375 A72-13931

Grain size and precipitate parameters effect on creep properties of Ni-Cr alloys

03 p0379 A72-14339

Composite materials testing with four point loading method, studying environmental and creep effects in flexure

04 p0537 A72-15091

Dislocation creep model for work hardening and recovery, deriving mechanical equation of states for various magnitudes and directions

04 p0589 A72-15160

Creep surface in Al alloy under combined tension and torsion, obtaining strain rate vectors from probes

04 p0590 A72-15195

High precision strain gage dynamometers design and testing at ONERA Modane test center, discussing accuracy limitation due to hysteresis and creep effects [ONERA, TP NO. 995]

05 p0642 A72-15859

Commercial alloy creep and rupture strength data correlation for predicting design creep properties [ASME PAPER 71-WA/MET-2] 05 p0671 A72-15907

Creep damage mechanics, considering fracture initiation and propagation and prior loadings effect [ASME PAPER 71-WA/MET-1] 05 p0732 A72-15908

Turbine casing components stresses in presence of creep, demonstrating calculation method validity for thick-walled structures by elastoplastic analogy

05 p0734 A72-15985

Mono- and polycrystalline Ni high temperature creep kinetics, investigating substructural changes

05 p0671 A72-16000

Steel sheet creep, plastic deformation and service life under temperature and stress cycles

06 p0899 A72-18558

Bending tests of beam with different creep characteristics in tension and compression

06 p0899 A72-18639

Aging creep theory application to anisotropic strain hardenable metals

06 p0900 A72-18680

Cu, Al and Pb bcc metals, investigating dislocation structure and creep characteristics change mechanism at transition from low to high temperature

07 p1014 A72-19822

Steady creep rate logarithm and creep limit obedience to normal distribution law

07 p1014 A72-19846

Diffusion creep influence on grain boundary-adjacent precipitate free zone formation in Ni-Cr alloys subjected to high temperature tensile and creep tests

07 p1021 A72-20437

Ni based superrefractory alloy high temperature fatigue tests, studying creep as function of stress load and frequency and temperature

07 p1022 A72-20487

Al single crystals relationship between stress, strain and dislocation density ring elevated temperature creep by direct observation of etch pits

08 p1185 A72-20990

Metals and alloys for aerospace applications, emphasizing creep and fatigue properties and oxidation resistance at high temperatures

08 p1185 A72-21171

Stress concentration near elliptic and square orifices in plates with nonlinear viscoelastic hereditary creep properties

08 p1244 A72-21242

Setup to determine sonic creep and acoustic fatigue in polymers under symmetrical and asymmetrical load cycles at sonic and ultrasonic oscillation frequencies

08 p1147 A72-21763

Additional vibrational loading effect on thin tubular glass fabric reinforced plastic samples creep under shear in reinforcement plane at 20-50 C

08 p1195 A72-21854

Fiberglass reinforced plastics creep characteristics under high strain rate loading-unloading conditions

08 p1195 A72-21855

Perforated flexible polymer plates stressed state problem with boundary conditions and viscoelastic and creep properties effects

08 p1248 A72-21861

Creep characteristics of unidirectional plastics reinforced by hollow glass fibers with insignificant capillary effect

08 p1196 A72-21868

Stoichiometry effect on high temperature creep in oxides, relating impurities, point defects concentration and diffusion

09 p1335 A72-22397

Polymers viscoelastic behavior during crosslinking reactions, deriving equations for creep response to step increase in crosslink density

09 p1336 A72-22521

Sign-variable nonisothermal plastic deformation and creep behavior of polycrystalline construction materials, taking into account Bauschinger effect

09 p1401 A72-22726

Stresses, strains and moments interrelationship in axisymmetrically loaded circular cylindrical shell under unsteady creep conditions

09 p1401 A72-22729

Creep properties in turbine disks of heat resistant alloy under plastic deformation due to nonstationary thermal conditions

09 p1401 A72-22730

Nonlinear creep characteristics of variably thick rotating disks under nonuniform heating conditions, determining critical rpm and temperature field and time to failure

09 p1402 A72-22731

Fatigue strength of heat resistant materials under thermal cyclic loads leading to sign variable plasticity and creep

09 p1402 A72-22732

Energy methods for nonlinear viscoelastic bodies based on constitutive relations affecting critical state in advanced creep

09 p1403 A72-22764

Extruded dispersion strengthened Mg-MgO alloys microstructure, discussing high temperature creep effect on dislocation structure changes

09 p1328 A72-22984

Papers on design for high temperature environments covering structural fatigue, creep interaction and ratcheting deformation and inelastic stress analysis

09 p1406 A72-23196

Creep ratcheting deformation and rupture damage from thermal transient stress cycle and constant membrane force under high temperature metal creep conditions

09 p1406 A72-23197

Mathematical model and inelastic stress analysis for metal creep-fatigue interaction and progressive deformation in breeder reactors operation

09 p1407 A72-23200

Surface defects absence after intergranular creep from Al bicrystals grain boundaries observation by transmission electron microscopy

10 p1495 A72-24084

High temperature creep behavior of sintered polycrystalline strontium zirconate as function of temperature, stress, grain size and strain level, using pure bending test method

10 p1497 A72-24275

Metal creep under multiaxial stress states, proposing technique for numerical stress analysis data collection [SMRT PAPER L 1/3]

10 p1556 A72-24395

Book on binary metal oxides covering non-stoichiometry, electrical conductivity, diffusion theory, point defects, high temperature creep and electrochemical transport properties

10 p1527 A72-25075

Elastic glass and Thorol fiber/epoxy matrix composite material creep tests, determining creep rate dependence on specimen geometry and stress state

11 p1672 A72-25481

Creep and low cycle fatigue dynamic behavior, noting stress concentration time dependence, strain hardening and local plastic deformations in dead annealed Al thin walled tubes

11 p1658 A72-25829

Cavitation by creep of Mg alloys, using density measurements and metallurgical examinations

11 p1661 A72-26650

Fe-Mo solid solutions transient creep behavior as function of applied stress, noting temperature effect

11 p1662 A72-26656

Turbine blade alloys vibrational fatigue and creep properties under high and low frequency axisymmetric loads at room and elevated temperatures

11 p1662 A72-26798

Statistical analysis of strain criteria and stochastic relations for Al alloy fatigue life and minimum creep rate at 175-250 C

11 p1663 A72-26800

Tungsten alloy wires strength, creep properties and fatigue limit, investigating fracture characteristics

11 p1663 A72-26807

Creep characteristics of weakly strain-hardenable alloy under variable tensile load and temperature conditions

11 p1663 A72-26808

Longitudinal bending stability of hard polymer rods under compression load and creep

11 p1675 A72-26824

High temperature creep properties of W-Re alloy under vacuum for thoria dispersion hardening from electron microscope and activation energy studies

11 p1665 A72-26863

Compression creep in ordered binary and ternary ordered bcc Ni alloys investigated by transmission electron microscopy

11 p1667 A72-26937

Thin cylindrical shells prepared from fiberglass reinforced plastics under long term compression, investigating strain buildup nature during creep process

12 p1878 A72-27078

Mathematical model to describe complete creep process in metal from hardening and brittle failure theories

12 p1828 A72-27322

Creep stability of bars and thin plates and shells for given loading force, considering instability criteria

13 p2054 A72-28481

Strain rate controlling mechanisms of superplastic deformation at various stresses and temperatures, considering vacancy and dislocation creep and grain boundary sliding

13 p1974 A72-28657

Reversed creep deformation behavior of metals, observing acceleration at high temperatures due to grain boundary sliding enhancement

13 p1978 A72-29444

Gamma irradiation effects on epoxy-diane resin creep and stress relaxation properties indicated by loaded specimens birefringence patterns

13 p1984 A72-29481

Rarefied gas flows effect on metals creep properties, examining molecular flow density distribution as function of specimen surface distance from nozzle

13 p1979 A72-29483

Flat Ti alloy sheet creep under variable loads at 300-400 C, comparing prediction with test data

14 p2116 A72-30434

Zirconium carbide creep characteristics and limit at 2450-2810 K, examining test conditions effects on parameters

14 p2116 A72-30435

Loading conditions effect on relaxation and creep in inhomogeneous hereditary elastoplastic polycrystalline materials

14 p2168 A72-30953

Russian papers on alloying and properties of heat resistant alloys covering creep, solid solution and dispersion hardening, chemical interactions and protective coatings

15 p2254 A72-31557

Metal hardening level evaluation on basis of volume dislocation structure from stress field of dislocation loops

15 p2254 A72-31562

Creep theory with anisotropic hardening compared to curves obtained from verification experiments with loading and unloading in steps

15 p2256 A72-31707

Nonlinear creep, viscoelasticity and elastoplasticity boundary value problems, discussing matrix constitutive differential equation formulation and higher order numerical methods

15 p2326 A72-31712

Oxide inclusions induced reductions in Nabarro-Herring creep and sintering rates of metals, discussing effect of inclusions diffusional mobility in metal matrix

15 p2257 A72-32112

Temperature effects on stress-strain diagram, tensile strength and creep properties of fiber-epoxy resin composites

15 p2260 A72-32137

Superplasticity in two phase compositions based on refractory metal alloys, noting creep rate dependence on concentration and electroconductivity

16 p2405 A72-33094

Al-Mg solid solution creep at 570-800 K, discussing creep rate controlling mechanism due to Mg atoms interactions with dislocations

16 p2407 A72-33442

Creep in structures - Conference, Goteborg, Sweden, August 1970

16 p2411 A72-34110

Unified description of structures behavior subject to elastic, creep and plastic deformations

16 p2473 A72-34117

Approximate method for reactions redistribution and displacements in statically indeterminate structures, using strain hardening hypothesis and creep power law

16 p2473 A72-34119

Heteroplastic materials creep characteristics from constant strain rate isothermal traction tests, deriving deformation functions for material behavior beyond elastic range

16 p2412 A72-34120

Three dimensional elastoviscoplastic theory for complex structures static-dynamic creep deformation under time varying stress and temperature fields, generalizing Odqvist-Hoff law

16 p2473 A72-34121

Microstructural damage effect on high temperature materials creep life, considering Robinson and Odqvist correlation laws

16 p2474 A72-34127

Lateral deflection of axially loaded imperfect bar under creep, solving nonlinear integrodifferential equations by quasi-linearization technique

16 p2474 A72-34130

Steels creep behavior relationship to stress-strain curve shape, defining creep resistance as function of strain hardening coefficient

16 p2412 A72-34146

Strengthening mechanism in metals during creep under variable stress for dislocation network structure studies

16 p2475 A72-34164

Differences in the creep characteristics at room temperature of steels with and without distinct yield point

17 p2566 A72-34397

Plane problem of thermal creep at high temperatures

17 p2636 A72-34473

Dislocation mechanisms in creep

17 p2635 A72-35921

Creep of different molybdenum alloys at high temperature and under strong stresses

18 p2698 A72-36144

Effect of low-pressure oxygen on the creep properties of W-25 pct Re. 18 p2700 A72-36581

A comparison between the tensile and compressive creep behaviour of an 11 per cent chromium steel. 19 p2814 A72-37222

Nonlinear physical dependence of reticular polymers and glass fiber reinforced plastics under conditions of diminishing creep 19 p2822 A72-37527

Structures and materials performance under creep and plastic deformation, discussing energy theorems implications 19 p2874 A72-37705

Phenomenology and engineering significance of creep recovery in heat resistant steels, stressing ductility and microstructural effects 19 p2816 A72-37707

The comparison of torsion and tension creep data for a 0.18 per cent carbon steel. 19 p2816 A72-37709

Creep damage role in governing elevated temperature strain cycling fatigue lives of heat resistant stainless steel and cobalt alloy 19 p2817 A72-37712

Combined stress creep of non-linear viscoelastic material. 19 p2822 A72-37714

Stress redistribution caused by creep in a thick walled circular cylinder under axial and thermal loading. 19 p2874 A72-37716

Creep delay in low-carbon steel at room temperature 19 p2818 A72-38011

Creep of porous nickel in oxidizing and neutral media 19 p2819 A72-38287

The effect of hydrostatic pressure on plastic deformation and creep of polycrystalline metals at elevated temperatures. 20 p2977 A72-38878

The influence of finite-deformations upon the creep behavior of circular plates. 20 p2980 A72-39693

Theoretical and experimental features and methods of creep. [ICAS PAPER 72-45] 21 p3069 A72-41170

Mechanism of high temperature creep of aluminum-magnesium solid solution alloys. 21 p3069 A72-41299

Low carbon steel S-N diagram for stresses ranging to fatigue limit, noting cyclic creep, macroplastic cyclic stress and fatigue failure 21 p3122 A72-41353

Microalloying effect on creep and stress rupture characteristics of hot rolled and annealed Mo alloys 21 p3070 A72-41355

Theoretical and experimental investigation of the relationship between plastic and creep deformation of structures. 21 p3124 A72-41509

Book - Metal matrix composites. 21 p3070 A72-41528

Determination of mosaic-block disorientations in the creep of aluminum by the method of low-angle X-ray scattering 23 p3299 A72-43341

Rotating disks optimal design allowing for creep from additional coupling imposition and contour displacement 23 p3347 A72-43746

Non-linear free vibration of a beam with time-dependent material properties. 23 p3355 A72-44374

High-temperature creep of polycrystalline chromium. 23 p3304 A72-44449

Estimates of creep-fatigue interaction in irradiated and unirradiated austenitic stainless steels. 24 p3412 A72-44554

High temperature creep activation energies relationship to diffusion in TiC, ZrC and UC 24 p3413 A72-44936

Contribution to the study of the creep behavior of 18 per cent-nickel maraging steel 24 p3415 A72-45600

A comparison of single-integral non-linear viscoelasticity theories. 24 p3460 A72-45695

Turbine casing components stresses in presence of creep, demonstrating calculation method validity for thick-walled structures by elastoplastic analogy 24 p3460 A72-45727

Creep strength analysis of heat resistant alloys under repeated unsteady loads 01 p0144 A72-11376

Ni base superalloy powder with refractory oxide particle dispersion, presenting high temperature creep, stress rupture, microstructure activation energy and processing history 02 p0240 A72-11442

Directional solidification of off-eutectic Al-Be alloy, obtaining ultimate strength, elastic modulus and concentration perturbation caused by freezing rate changes [AD-738212] 02 p0242 A72-11985

Creep rupture test program for Al alloys, circumventing parametric methods limitations by extrapolation procedure with graphical extension of isostress curves 03 p0378 A72-14174

Plastic strain and rupture characteristics of thin walled tubular Ni samples under complex loading and biaxial tension 04 p0588 A72-15058

Ni alloy stress rupture data correlation and extrapolation from computerized evaluations of time-temperature parameters relative abilities [ASME PAPER 71-WA/MET-4] 05 p0670 A72-15905

Waspaloy sheet creep rupture time dependent sensitivity to sharp-edged notches at 1000-1400 deg F, optimizing smooth and notched specimen yield strengths [ASME PAPER 71-WA/MET-3] 05 p0670 A72-15906

Commercial alloy creep and rupture strength data correlation for predicting design creep properties [ASME PAPER 71-WA/MET-2] 05 p0671 A72-15907

Subcritical crack extension in elastoplastic or viscoelastic-plastic matrix, showing similar mathematical representations for fatigue crack propagation and creep rupture under sustained loads 05 p0737 A72-16302

Directionally solidified Al-AlNi intermetallic eutectic alloy microstructural characteristics and effects on creep fracture 05 p0678 A72-17115

Book on refractory metals creep rupture behavior to high temperatures covering test procedures and data analysis for W, Re, Ta, Mo and Nb and alloys 06 p0828 A72-17725

Dispersion strengthened Co alloys structural stability, tensile and creep rupture strengths and hot corrosion properties 06 p0829 A72-17829

High temperature tests of creep rupture strength of W composite cast with heat resistant alloy coatings 06 p0829 A72-17947

Plastic deformation, creep rupture strength, endurance limit and service life of prestressed strain hardenable material 06 p0900 A72-18681

Stress rupture data from S glass composite matrix effectiveness tests, noting skewed lifetime distribution in statistical patterns 08 p1192 A72-21683

Ti, Zr, Mo, B and Mn additives effect on rupture characteristics of cast Al-Mg alloy under uniaxial tensile stress 09 p1328 A72-23033

Environment and grain size effect on steady state creep and creep rupture properties of Ni-W solid solution 09 p1331 A72-23381

Short time stress rupture test data correlation for design, using computerized time-temperature parametric methods [AIAA PAPER 72-327] 11 p1653 A72-25363

Photothermoelastic analysis of temperature and rupture stress in cryogenic tanker structures, using steel and plastic ship models 11 p1728 A72-25373

Critical aspect ratio of W fiber in copper matrix for stress rupture applications 11 p1654 A72-25482

Metallographic examination of stainless steel specimens exposed to long term creep rupture tests, noting carbides precipitation and stress induced grain boundary migration 11 p1658 A72-25832

High temperature Ni base alloys microstructure via transmission electron microscopy and electron diffraction contrast theory, predicting yield and creep strength 11 p1667 A72-26931

Individual melts stress rupture strength extrapolation based on limited number of tests, comparing results with parametric method 12 p1831 A72-28231

Gas turbine engine hot part equivalent tests duration determination by analytical method based on Larson-Miller parametric description of stress rupture strength 12 p1887 A72-28243

Stress rupture strength, short term strength, creep and heat resistance measurement arrangement for coated refractory materials at 1500-1700 C in air with radiative heating 12 p1796 A72-28248

Tensile, creep and creep rupture strength hot hardness tests for metallic and nonmetallic materials 13 p1958 A72-29442

Precipitated carbide role in Cr-Ni stainless steels high temperature properties and creep rupture strength 13 p1979 A72-29447

Hydrostatic pressure effect on tensile creep and creep rupture of polycrystalline metals at high temperatures 13 p2058 A72-29450

Creep rupture characteristics of alloy in uniaxial tension, considering transient, steady state and accelerated phases 13 p1981 A72-29890

Creep velocity and rupture strength calculated for tensile stress, noting high temperature tests of austenitic steel 14 p2121 A72-30697

Slip band blocking effect of disperse particles on crack suppression and creep rupture strength of intermetallic Al-Fe-Ni alloy 14 p2124 A72-31033

Nonlinear creep failure of imperfect sandwich structures under time variable loading, considering rod and cylindrical shell 15 p2324 A72-31490

Mo, W, Nb, Ti, V and N complex alloying to harden cast heat resistant austenitic steel, discussing phase composition and stress-rupture strength 15 p2254 A72-31563

Components creep-rupture life prediction for multiaxial stress from uniaxial test data, discussing crack initiation and propagation phases stress states 16 p2412 A72-34114

Brittle creep rupture process in beam subjected to simultaneous loading with bending moment and axial force 16 p2474 A72-34128

Book - Advances in creep design 19 p2874 A72-37701

Creep rupture under stress concentration. 19 p2874 A72-37702

Creep rupture theory covering viscous and brittle scattered fractures and major crack growth 19 p2874 A72-37703

Creep fracture theory investigating ratio of ultimate creep rupture time to latent failure under multiaxial states of stress 19 p2874 A72-37704

Physical and metallurgical factors causing embrittlement and creep rupture life reduction determined by tests, discussing crystal and grain boundary deformation and notch effects 19 p2874 A72-37711

Stress criterion for creep rupture in tubes under combined axial load and internal pressure, deriving stress concentration from high temperature tests 19 p2874 A72-37715

Plane stress rupture criterion for age hardening materials during plastic deformation, calculating resistance to shear and torsion of solid and hollow round bars 19 p2818 A72-38009

Inconel alloy 617 - A new high-temperature alloy. 19 p2821 A72-38388

Static and dynamic fatigue behavior of glass filament-wound pressure vessels at ambient and cryogenic temperatures. 19 p2823 A72-38832

Stress dependent cyclic creep rupture tests of Ti and Co-base alloys and stainless steel at 1300 F 20 p2938 A72-39305

Simple structures behavior under constant loads, considering low stress levels and creep rupture mechanism with internal damage affecting strain rate 21 p3117 A72-40673

Stainless steels high temperature creep rupture strength relationship to carbide precipitation morphology 21 p3069 A72-41013

The effect of alloying elements on creep rupture strength and microstructure of 12 percent chromium heat resisting steel. 21 p3069 A72-41014

Microalloying effect on creep and stress rupture characteristics of hot rolled and annealed Mo alloys 21 p3070 A72-41355

A new creep rupture testing machine with loading by tubular springs and electronic temperature control 22 p3164 A72-42860

Stress-rupture of simple S-glass/epoxy composites. 23 p3305 A72-43492

Heat treatment effectiveness criteria for thermomechanically strengthened steels, using creep rupture, fatigue, bending and tensile tests 23 p3300 A72-43643

Fiber reinforced metallic matrix composite under creep, discussing rigidity, stress distribution, rupture strength and failure time 23 p3306 A72-43727

Strain-rupture criteria for simple and complex loads 23 p3349 A72-43954

Creep resistance 01 p0084 A72-10748

U CREEP STRENGTH 01 p0086 A72-10979

CREEP RUPTURE STRENGTH

Larson-Miller parameter application to N6 base alloys creep rupture data, discussing extrapolation method limitations

Ni, Fe and Ti alloys creep rupture characteristics in high temperature, high pressure gaseous hydrogen and helium

- Al alloy rupturing analysis in complex stress state, noting sublimation and self diffusion values of activation energy in torsional to tensile state transition 23 p3301 A72-43957
- Creep and fracture of OT-4 titanium alloy in the temperature range from 400 to 550 C 23 p3302 A72-43960
- Materials creep behavior and elevated temperature design. 24 p3453 A72-44553
- Estimation of creep and fatigue behaviour under cyclic loading. 24 p3456 A72-44793
- Stepwise fatigue testing of high temperature alloy, noting strain hardening phenomena in prestressed samples 24 p3416 A72-45755

CREEP STRENGTH

- Low impulsive loading effect on strength creep resistance of polycrystalline Al at elevated temperatures 02 p0243 A72-12011
- Al-Mg-Si alloy fatigue, vibration creep and creep strength tests at room temperature, determining mean stress effects on fatigue strength and cumulative damage 02 p0297 A72-12536
- German monograph on Zn and Zn-Cu-Ti-Al alloy creep resistance under high loads covering grain boundary precipitation, rotation-shear hole and annealing 04 p0535 A72-15697
- Commercial alloy creep and rupture strength data correlation for predicting design creep properties [ASME PAPER 71-WA/MET-2] 05 p0671 A72-15907
- Mo- and Ta-base refractory alloys creep tests, determining interactions between creep strength, fatigue life and strain aging by fatigue vibration application 05 p0677 A72-17111
- High temperature creep of niobium alloy, obtaining creep limit, microhardness and gas analysis data 06 p0833 A72-18637
- Rutile creep resistant substructure recovery at 1000-1040 C, discussing stress relaxation mechanism due to dislocation walls or subgrain boundaries migration 07 p1023 A72-18800
- Time varying external pressure effect on creep collapse of long thin walled quasielliptic cylindrical shell, taking into account elastic deformation 08 p1245 A72-21612
- Ceramic fiber reinforced Ni base alloy for gas turbine blades, improving creep resistance at high temperatures 09 p1335 A72-22396
- Aligned fibrous composites microstructural parameters, showing fiber thickness effect on fracture, fabrication, matrix cracking, creep resistance and fatigue 09 p1338 A72-23163
- Tensile, creep and creep rupture strength hot hardness tests for metallic and nonmetallic materials 13 p1958 A72-29442
- Mo addition effect on high temperature creep resistance and diffusion activation energy of Nb alloys tested in torsion and tension at 1100-1500 C in vacuum 14 p2116 A72-30436
- Testing machine for creep resistance of foam plastics under simultaneous static and vibration loads 14 p2092 A72-30591
- Tensile properties from high temperature and room temperature tests of Ti alloys containing Ga correlated with creep resistance at 1000 F, noting activation energy 14 p2120 A72-30614
- Antiscratch properties of nitrided layers of creep-resisting steels at high temperatures 22 p3187 A72-41868
- Effect of overheating on the creep resistance of metastable alloys 23 p3301 A72-43927
- Investigation of the state of the structure of turbine-disk materials after operation 23 p3302 A72-43965

CREEP TESTS

- Magnetic transformation effect on creep behavior of fcc nickel-cobalt alloy compared with self diffusion data in Curie temperature vicinity 01 p0083 A72-10391
- Constant stress and compression creep testing in vacuum conditions, describing simple spring loaded apparatus characteristics and performance 01 p0071 A72-11171
- Sheet metal biaxial creep testing, using edge clamped circular diaphragm deflected by lateral hydrostatic pressure 03 p0373 A72-13649
- Creep rupture test program for Al alloys, circumventing parametric methods limitations by extrapolation procedure with graphical extension of isostress curves 03 p0378 A72-14174
- Ta-W-Hf alloy ultrahigh vacuum high temperature creep tests, showing deoxidation effect on creep behavior and early test stage oxygen-associated dynamic strain aging 05 p0674 A72-16392

- Directionally solidified Al-AlNi intermetallic eutectic composites creep tests, identifying time dependent fracture mechanism 05 p0678 A72-17114
- Book on refractory metals creep rupture behavior to high temperatures covering test procedures and data analysis for W, Re, Ta, Mo and Nb and alloys 06 p0828 A72-17725
- Combined tension-torsion creep testing of polymers, discussing equivalent stress and strain concept, testing apparatus and preliminary results for polythene 06 p0835 A72-17795
- Creep behavior during and immediately after loading of Nimonic 90 and H 46 Cr steel under various stresses, temperatures and rates 06 p0829 A72-17801
- Fatigue life and creep tests of refractory materials under programmed thermal cycling for different stress levels 06 p0831 A72-18351
- Bending tests of beam with different creep characteristics in tension and compression 06 p0899 A72-18639
- Thermocycling treatment influence on structural changes and strength in coarse grain Ni under creep tests 06 p0834 A72-18686
- Steady creep rates in Ni poly- and single crystals in presence of dislocation stresses 06 p0835 A72-18748
- Computerized estimation of deformation parameters for Sellars-Tegart equation relating stress, strain rate and temperature in creep and hot torsion testing of metals 07 p1090 A72-19736
- Oriented glass fiber reinforced plastics fatigue strength and creep under interlayer shear and compression 08 p1194 A72-21752
- Test procedures and apparatus for short and long term creep of polymer monofilaments under radial compression 08 p1194 A72-21758
- Creep test for microfailures of glass reinforced epoxy and polyester laminates immersed in water at ultimate flexural stress 09 p1336 A72-22537
- Discontinuous rigid or creeping fiber reinforced composite materials, predicting steady state creep behavior 09 p1338 A72-23167
- Eddy current extensometer for monitoring long term creep in diameter of pressurized tubular stainless steel specimens 11 p1613 A72-25821
- Creep tests for thermal preycling effect on time to failure and long term ductility of austenitic steel thin walled tubular samples 11 p1663 A72-26809
- Test conduct inaccuracies effect estimation for statistical spread of experimental creep rate and long term strength values 12 p1813 A72-27456
- Individual melts stress rupture strength extrapolation based on limited number of tests, comparing results with parametric method 12 p1831 A72-28231
- High temperature constant load creep tests on pure powder metallurgy W and tungsten-thoria alloy, discussing stress dependence 13 p1975 A72-28665
- High temperature steady state tensile creep behavior of Ni-W solid solutions, showing creep rate relation to stress and stacking fault energy 13 p1975 A72-28668
- High temperature contact creep tests in vacuum and in metal melts, noting adsorption effect on surfaces plastic deformation 13 p1963 A72-28768
- Polycrystalline microstructure changes of corundum during high temperature creep tests, using optical microscopy 13 p1983 A72-28775
- Al crystal block structure and size changes during creep evaluated by small-angle X ray scattering technique 13 p1977 A72-28909
- Zirconium carbide creep characteristics and limit at 2450-2810 K, examining test conditions effects on parameters 14 p2116 A72-30435
- Creep velocity and rupture strength calculated for tensile stress, noting high temperature tests of austenitic steel 14 p2121 A72-30697
- Mechanical vibrations effect on flow stress and strain rate from tensile and creep tests as function of amplitude 15 p2257 A72-31841
- Steady state creep measurements of lead-phosphor bronze discontinuous fiber composites under nonuniform deformation, comparing to fiber and matrix alone 15 p2261 A72-32299

- Nonlinear viscoelastic behavior of isotropic unoriented crystalline polyethylene terephthalate at 70-100 C, using creep, recovery and load tests 16 p2416 A72-33614
- Metal creep tests in thin walled ring shaped specimens for geometrical constancy under variable weights 16 p2472 A72-33850
- Maxwell rheological creep model verification by tensile tests on Mg alloy at 150 C under step loadings, treating thermodynamics of ideal creep 16 p2412 A72-34111
- Creep tests on Cr martensite stainless steel, showing inapplicability of Garofalo equation for stress dependence of secondary creep rate during variable stress experiment 16 p2412 A72-34112
- High vacuum and rarefied atmosphere creep apparatus. 17 p2536 A72-35846
- Dislocation mechanisms in creep. 17 p2635 A72-35921
- Direct and indirect creep modelling technique in photoelasticity. 18 p2734 A72-36379
- Comparison of experimental and theoretical thermal fatigue lives for five nickel-base alloys. 19 p2815 A72-37639
- Physical and metallurgical factors causing embrittlement and creep rupture life reduction determined by tests, discussing crystal and grain boundary deformation and notch effects 19 p2874 A72-37711
- Creep tests on 2-1/4 per cent chromium 1 per cent molybdenum steel in bainitic condition. 19 p2817 A72-37713
- Refractory materials cyclic elastoplastic tests under shear with holding creep, showing relationship between creep rate and recurrent static deformation 19 p2876 A72-38007
- Prediction of deformability and fracture processes for polymer materials 20 p2943 A72-38943
- Corundum polycrystalline microstructure changes during high temperature creep tests, using optical microscopy 21 p3072 A72-40269
- Isothermal deformation behavior of structural metals in laboratory creep, relaxation and low cycle fatigue tests at high temperatures 21 p3119 A72-41009
- Creep test diagrams plotted to estimate heat resistance for turbine blades design, predicting fatigue life with allowance for loading cycle form and duration 21 p3123 A72-41366
- Quadrisectional facility for studying creep and fatigue strength under deep freezing conditions 21 p3057 A72-41719
- A new creep rupture testing machine with loading by tubular springs and electronic temperature control 22 p3164 A72-42860
- Fiber reinforced metallic matrix composite under creep, discussing rigidity, stress distribution, rupture strength and failure time 23 p3306 A72-43727
- Fatigue life and creep tests of refractory materials under programmed thermal cycling for different stress levels 24 p3416 A72-45738
- CRESTATRONS**
U TRAVELING WAVE TUBES
- CREVASSES**
NT GLACIERS
- CREVICES**
U CRACKS
- CREWS**
NT FLIGHT CREWS
NT SPACECREWS
- CRIMPING**
U FOLDING
- CRITERIA**
NT STRUCTURAL DESIGN CRITERIA
Air traffic control systems efficiency evaluation, discussing measures for criteria conflict solution 09 p1270 A72-23128
- Adaptive equalization of data transmission rate in telephonic systems, considering criteria and iterative algorithms 18 p2661 A72-36790
- CRITICAL EXPERIMENTS**
Critical spherical symmetry benchmark experiment on gas core nuclear reactor using uranium hexafluoride 05 p0688 A72-16387
- Significance of the results of the ITR critical experiments for the calculation of an incore-thermionic reactor. 18 p2645 A72-36180
- Measurements with thermionic fuel elements in the ITR critical facility. 18 p2645 A72-36181
- CRITICAL FLICKER FUSION**
Flicker and flash threshold experiments, discussing flicker cut-off frequency and flash duration relations and visual sensitivity 07 p0926 A72-19028

Light variation threshold amounts for flicker and flickering pattern detection as function of variation frequency
09 p1269 A72-22615

Role of eye movements in the perception of apparent motion.
23 p3259 A72-43804

Sensitivity of the human ERG and VECF to sinusoidally modulated light.
23 p3258 A72-44383

CRITICAL FLOW

Laminar liquid flow stability in vertical slots under natural convection, showing critical layer level for nonstationary perturbations
02 p0202 A72-11591

Acoustic attenuation calculation for turbulent flow in rigid tubes, determining critical flow velocity dependence on wall roughness and sound wave frequency
03 p0340 A72-12954

Pressure distribution and compressible gas critical flow rate in constant cross section circular pipe with impermeable adiabatic wall from Frossel equations
04 p0511 A72-14640

Critical streamline length in axisymmetric and plane ideal gas flows past conical bodies as function of Mach number and form parameter
06 p0755 A72-17677

Mach number distribution along critical streamline in compressed layer in front of cylinder in supersonic flow
10 p1415 A72-23752

Infinitesimal centered disturbance effect on plane Poiseuille flow at supercritical Reynolds number, determining modulated wave as function of position and time
10 p1562 A72-24423

Critical discharge regimes of two phase steam/water mixture flow from nozzles, using counterpressure effect
11 p1619 A72-26674

Flow separation effects on critical lift of helicopter rotor, using blade angle of attack criterion
11 p1573 A72-26893

Atmospheric models for critical flux Richardson number prediction for turbulence maintenance in stratified flows
12 p1840 A72-27702

Linearization and perturbation procedures to calculate nonlinear effects in fluid stability problems with application to nonlinear critical layer
16 p2377 A72-33338

Critical flow rate and pressure ratio for nitrogen flowing through convergent-divergent nozzle at stagnation conditions, emphasizing thermodynamic critical region
21 p3046 A72-41180

Critical mass flow and nonequilibrium nozzle flow of vibrationally relaxing, ideal dissociating diatomic and singly ionizing monatomic gases, using steepest descent method
21 p3046 A72-41249

Interferograms of turbulent boundary layer separation in critical blowing of gas through porous plate, noting velocity and concentration profiles of blowing parameters
23 p3281 A72-44082

CRITICAL FREQUENCIES

F 1 layer appearance and critical frequencies average daily variations at Tsumeb, Southwest Africa, as function of sunspot cycle phase
01 p0055 A72-10428

Sporadic E layer reflection behavior measurements from two closely located stations, deriving drift direction and critical frequencies daily variation
01 p0055 A72-10431

Cross correlation characteristics of deviations in critical frequencies of F 2 region
01 p0059 A72-10594

Radio communication accuracy characteristics in calculation of maximum frequency, skip distance and emission angle by transmission curves for midlatitude ionosphere
01 p0028 A72-10600

F 2 layer critical frequency variations relation to solar radio flux intensity, using mathematical approximations
01 p0059 A72-10613

Time between noontime and evening maxima in F 2 layer critical frequency compared with evening maximum period, showing dependence on noontime solar zenith angle
01 p0059 A72-10615

Critical frequency computation for partially filled elliptical waveguide with dielectric rod
02 p0183 A72-12752

F 2 layer anomalies association with equatorial electrojet, investigating midday critical frequencies of sporadic E layer
04 p0515 A72-14932

Electrojet effects on critical frequencies in equatorial F region during magnetically quiet and disturbed days
04 p0516 A72-14936

Statistical analysis of low latitude F 2 layer disturbances associated with sudden commencement

type geomagnetic storms, investigating critical frequencies
04 p0516 A72-14937

Cut-off frequencies of degenerate LSE and LSM modes in rectangular waveguides containing dielectric layers in H plane
04 p0502 A72-15526

F 2 layer critical frequency deviations and negative disturbance zones during solar eclipse of 22 September 1968
05 p0657 A72-16264

Ionospheric storms features based on F2 critical frequency data, investigating magnetosphere during geomagnetic storms
06 p0810 A72-18280

Height-frequency characteristic forecasting for E layer at arbitrary time and point location, using solar angle zenith relationship
08 p1153 A72-20708

Auroral ionosphere radio self emission at supercritical frequencies from accelerated protons charge exchange effects, comprising radio bursts, storms and amplifications
08 p1153 A72-20713

Critical frequencies and geometrical parameters of parabolic model in oblique backscatter ionospheric sounding, using distance-frequency characteristics
08 p1154 A72-20732

F 2 layer diffuse reflections and critical frequencies increase on ionogram recordings during Northern Hemisphere nighttime magnetic storm of 2 December 1967, noting cosmic radio emission decrease
08 p1154 A72-20738

Ionogram electron density-height distributions for analysis of multiple cusp structure near E region critical frequency
08 p1156 A72-21101

F region disturbances, explaining critical frequency changes on basis of neutral winds, electrodynamic drift and temperature and chemical composition variation
08 p1158 A72-21222

Sporadic E layer critical frequency relationship to ionospheric wind direction for midlatitudes in summer period
10 p1472 A72-24079

F region critical frequencies deviation from median due to solar cycle phase, latitude and time, discussing short waves radio communications reliability
11 p1593 A72-26271

F 2 region critical radio frequencies forecasts from solar cycles, ionospheric disturbances data, latitude and annual and diurnal variations
11 p1594 A72-26272

Diurnal variations of F 2 region critical frequencies and quiet and perturbed ionosphere N/h_p profiles during solar cycle, estimating signal reflection altitudes
11 p1594 A72-26274

Sporadic E layer cyclic variations during solar activity cycle, noting time dependence of occurrence probability and critical frequency
11 p1623 A72-26281

Single pulse radio echo fading dependence on sporadic E layer critical and screening frequencies
11 p1595 A72-26282

Ionospheric multifrequency absorption measurement description by empirical expressions in terms of E layer critical frequency, solar activity and seasonal effects
13 p1952 A72-29667

Calculation of the critical frequencies of higher-order modes in a hollow elliptic waveguide
17 p2516 A72-34846

Analysis of the dispersion equation of a dual-layer elliptic waveguide for critical conditions
17 p2529 A72-34847

Height-frequency characteristic forecasting for E layer at arbitrary time and point location, using solar zenith angle relationship
19 p2790 A72-38336

Auroral ionosphere radio self emission at supercritical frequencies from accelerated protons charge exchange effects, comprising radio noise bursts, storms and amplifications
19 p2790 A72-38341

Critical frequencies and geometric parameters of parabolic ionosphere layer model in oblique backscatter sounding, using distance-frequency characteristics
19 p2791 A72-38360

F 2 layer spread reflections and critical frequencies increase on ionogram recordings during Northern Hemisphere nighttime magnetic storm of 2 December 1967, noting cosmic radio emission decrease
19 p2791 A72-38366

Regression-line studies of E-region seasonal anomaly.
19 p2794 A72-38863

Critical frequency computation for partially filled elliptical waveguide with dielectric rod
20 p2902 A72-39058

Geometrical dimensions and effective number of large scale ionospheric inhomogeneities by F 2 critical frequency variability analysis
23 p3283 A72-43360

Phenomena associated with very high power, high frequency F-region modification below the critical frequency.
24 p3400 A72-45596

CRITICAL LOADING

Imperfect nonlinear system elastic buckling critical load calculation by higher order approximation, using perturbation approach and discrete coordinate diagonalized system
01 p0136 A72-11035

Upset steel cylinders under axial compression loads, determining localized surface stress and strain critical values at fracture
01 p0141 A72-11032

Carrying capacity solutions for perforated circular plates of rigid plastic material by kinematic method
01 p0143 A72-11366

Local buckling and collapse of thin walled lipped channel beams under critical end moments
01 p0144 A72-11396

Spiral grooves gas bearing theory, taking into account sliding and gas compressibility effects on load carrying capacity
02 p0236 A72-11585

Fourier series terms number effect on sandwich plate critical shear stress calculation accuracy
02 p0294 A72-12438

Computer program for buckling loads of shallow stiffened eccentrically orthotropic sandwich shells [DGLR PAPER 71-109]
02 p0299 A72-12703

Anisotropic shell supercritical deformation, deriving formula for lower critical load for shallow orthotropic spherical segment under external pressure
03 p0447 A72-13729

Critical load and stability analysis for three layer orthotropic cylindrical shell with filler under nonuniform external pressure
03 p0448 A72-13906

Elastoplastic bodies with crack at tip, determining limiting loads and crack propagation from variational relations
03 p0451 A72-14117

Critical thermal loads during external and internal heating of annular channels, discussing curvature effect on density level in thermal flux during forced fluid motion
03 p0458 A72-14157

Elastoplastic stability of structural rods in unloadable systems, considering load carrying capacity increase by critical state onset delay
03 p0454 A72-14214

Herringbone grooved gas bearing load carrying capacity optimization, considering lubricant film thickness, groove width and length ratios and angle
04 p0527 A72-14915

Axissymmetric load influence on stability of eccentrically reinforced shells of revolution, determining critical loads and linear and nonlinear relations for moment-subcritical states
04 p0587 A72-15014

Cylindrical shell stability and load capacity at large plastic deformations under internal pressure
04 p0587 A72-15019

Critical load limit and stability of elastic isotropic and orthotropic cylindrical shells, using net-point method for end conditions
04 p0588 A72-15053

Rheomobility effects in creep instability of rods with initial deflection, determining critical load by Ritz method
04 p0594 A72-15708

Local plastic deformation relation to tangential shear stresses, deriving expressions to determine critical levels
05 p0734 A72-15982

Variable thickness shallow spherical shells of revolution axisymmetric loads carrying capacity, determining limit equilibrium through application of Tresca yield point concept
05 p0734 A72-15983

Laminated anisotropic imperfect circular cylindrical shells under axial compression, obtaining upper bound buckling load solution [AIAA PAPER 72-139]
05 p0740 A72-16893

Column axial load carrying capacity optimization vs structural weight, using finite element displacement method for buckling load, mode shape and strain energy density [AIAA PAPER 72-141]
05 p0740 A72-16894

Postbuckling collapse, end shortening, stiffness and ultimate load for geometrically imperfect simply supported plates with stress free edges
06 p0896 A72-17964

Critical loads for elastic buckling of monosymmetric beams and cantilevers
06 p0897 A72-17969

Approximate buckling load of orthotropic hyperbolic paraboloid metal shells, using energy approach
06 p0897 A72-17970

Deformability and strength of soft fiber reinforced plastics under biaxial tension, determining low temperature critical tensile stresses and elongation ratios
06 p0836 A72-18562

Nickel base alloy under axisymmetric tension compression tests, obtaining breaking load diagrams and fatigue and creep curves

06 p0833 A72-18638

Cyclic loading failure criteria based on plastic deformation energy concepts, considering material load carrying capacity

06 p0899 A72-18650

Load bearing capacity of shells of revolution, applying viscoplastic strain hardenable material model

06 p0899 A72-18656

Critical cleavage stresses dependence on ordering degree in Ni-Cr alloy

06 p0835 A72-18745

Optimal rigid-plastic limit load analysis of spherical shells under nonsymmetrical loadings, using SUMT and Rosenbrock method

07 p1087 A72-18791

Convergence conditions for Galerkin method, applying to boundary value problems of structural stability and critical buckling loads

07 p1025 A72-18798

Optimality criterion for beams and frames with segmentwise constant cross sections and alternative loading exceeding plastic load carrying capacity

07 p1088 A72-19119

Dynamic buckling of elastic shallow structures under periodic loading, determining critical load upper and lower bounds by energy method

07 p1090 A72-19731

Acoustic loads effect on carrying capacity and vibration stability of longitudinally stiffened cylindrical metal panels, investigating fatigue strength and stress-strain state

07 p1091 A72-19760

Critical stability and supercritical equilibrium behavior of compressed viscoelastic rod

07 p1091 A72-19761

Material anisotropy effect on stress-strain state and limiting load in plane plastic deformation

07 p1091 A72-19764

Stability loss of circular annular plate under compression, determining critical loads with inner edge free and outer edge hinged or clamped

07 p1092 A72-19900

Transverse anisotropy effect on collapse loads of plastic rotating disks and circular plates

07 p1093 A72-19946

Limit analysis of ductile fiber reinforced structures, obtaining critical load of composite sandwich ring

07 p1093 A72-19950

Freely supported three layer cylindrical panel stability and critical loads under combined uniform axial compression and transverse pressure

08 p1242 A72-20907

Local stability of thin walled isotropic elastic cylinder, deriving characteristic equations for critical load calculation

08 p1242 A72-20969

Critical values of compressive loads applied to mid-section of cylindrical shell weakened by circular holes

08 p1244 A72-21241

Critical compressive stresses leading to instability of layer fastened to elastic half space

08 p1244 A72-21368

Elastic filler rigidity effect on cylindrical glass fiber reinforced plastic shells stability loss and critical load value under axial compression

08 p1245 A72-21503

Deformability and carrying capacity of glass fiber-polymer composite thick walled rings under internal or external pressure

08 p1195 A72-21764

Elastic shell geometry and rigidity effects on critical load in pure bending within structurally orthotropic theory, taking into account reinforcing rib eccentricity

08 p1247 A72-21816

Tapered I-beams elastic twisting and flexural-torsional buckling, considering critical loads as function of taper ratio

08 p1249 A72-21924

Thermal buckling of parallelogram shaped plate under stationary temperature field and uniformly distributed forces, deriving critical load

09 p1402 A72-22733

Axisymmetrically heated orthotropic multilayer cylindrical shell with shear sensitive couplings and elastic stiffener, investigating stability and critical force under compression

09 p1402 A72-22735

Imperfection influence on nonlinear stability of long circular cylindrical shells subject to critical hydrostatic pressure

09 p1403 A72-22763

Energy methods for nonlinear viscoelastic bodies based on constitutive relations affecting critical state in advanced creep

09 p1403 A72-22764

Impact detonation mechanism in ammonium perchlorate mixtures with inflammable additions, determining critical detonation triggering stresses

09 p1373 A72-22890

Cracks interaction with other cracks or boundaries under tension, determining critical loads for rapid fracture initiation by optical measurement

09 p1404 A72-22914

Interaction diagram for mixed crack extension modes in unidirectional graphite-epoxy laminates from critical load test data

10 p1501 A72-24265

Critical compressive buckling and stability of straight beams under axial and transverse loads calculated by three unknowns methods

10 p1560 A72-25121

Asymmetrically stiffened elastic cylindrical shells under axial compression, calculating critical loads for various end conditions

11 p1733 A72-25541

Prestressed circular ring snap-through under continuously distributed or discrete torsional loads, determining critical torque by asymptotic solution

11 p1734 A72-25721

Computer program for bifurcation buckling analysis of shells under collapse load, using strain energy methods and two dimensional finite difference grid

11 p1736 A72-25980

Linear programming simplex method for static load limit of circular arch

11 p1739 A72-26921

Ultimate safe load estimates for stability of isotropic elastic materials

12 p1883 A72-27563

Linearized elastic equilibrium stability equations for orthotropic cylindrical shell under critical axial compression

12 p1885 A72-27970

Nonlinear stability and vibrations of shallow shells eccentrically stiffened by oblique angled ribs under critical loads

12 p1885 A72-27971

Axial compression stability critical load and buckling of cylindrical shells resting on Winklerian elastic base, using dynamic programming

12 p1885 A72-27972

Shallow spherical sandwich shells limiting equilibrium for material with different tension and compression yield stresses

12 p1885 A72-27974

Rib reinforced cylindrical shell supercritical post-buckling strains, allowing for geometrical surface deflection

12 p1885 A72-27976

Optimal weight and load capacity of ellipsoidal cylindrical shell of revolution of constant thickness with central circular hole under uniform internal pressure

12 p1885 A72-27977

Elastoplastic deformation effects on load bearing capacity of samples with stress concentrators under alternating cyclic loading, obtaining nomograms by digital computer

12 p1887 A72-28228

Cylindrical samples with deep circular hyperbolic notch, investigating cyclic inelastic strain induced stress redistribution effects on load bearing capacity

12 p1830 A72-28229

Nonlinear first order differential equation for carrying capacity of anisotropic circular plates, curved elongate disks and shallow shells of revolution

13 p2054 A72-28457

Canonical equations of motion for continuous elastic system, predicting critical buckling loads for unbounded deformation

13 p2054 A72-28482

Limiting load calculation for thin walled I-beam in oblique bending and torsion beyond elastic limit

13 p2055 A72-28734

Cylindrical shell stability with variable thickness and moderate length under distributed ring load and uniform pressure, determining critical load

13 p2058 A72-29459

Collapse loads of symmetrically tapered cantilever beams under uniformly distributed end shear, considering optimum tapering angle for minimum weight

13 p2059 A72-29596

Critical force instability analysis for rectangular plates with mixed boundary conditions, using deflection forms in Fourier series

14 p2165 A72-30575

Mill annealed Ti alloy fatigue at 600 F and room temperature, noting critical local stress for slip bands formation and cracking

14 p2120 A72-30611

Optimal geometrical and physical properties of sandwich plates with rigid cores under compressive load, discussing critical stress and structural stability

15 p2322 A72-31359

Filler influence on critical load and buckling zone size in circular elastic three layer ring under uniformly distributed vertical load in rigid cavity

15 p2328 A72-31745

Buckling strain effects on critical stresses in design of longitudinally corrugated shells for axial compression

15 p2333 A72-32680

Plastic deformation and limiting strain curves of Ti alloys in plane stressed state, comparing with yield and rupture conditions

15 p2259 A72-32684

Stability loss condition for long rectangular cross section band from nonlinear elastic material with internal constraints, discussing critical loads and deformations

16 p2467 A72-33120

Optimal composite structures of multilayer spherical vessels in terms of elastic deformation under critical loads in thermal field

16 p2467 A72-33158

Analytical solution of stress distribution and load endurance of perforated square plate supported at corners, comparing with photoelastic observations

16 p2470 A72-33410

Linear stability and critical stress formulas for isotropic cylindrical shells with stepwise variable wall thickness under torsion

16 p2470 A72-33411

Elastic-plastic systems under dynamic loadings, discussing compounded shakedown load solution by zero work and direct search methods

[ASME PAPER 71-APMW-27] 17 p2624 A72-34309

Improved bounds for buckling loads of tapered inelastic columns.

17 p2626 A72-34330

Stability of a beam on an elastic foundation subjected to a follower force.

17 p2626 A72-34331

Shear buckling of an elastically supported fiber.

17 p2633 A72-35290

Griffith crack propagation through viscoelastic solid at under subcritical stresses, measuring growth rate for comparison with theory

18 p2733 A72-36366

Symmetrical and antisymmetrical wrinkling of sandwich panels.

18 p2736 A72-37056

German monograph - A contribution to the clarification of the carrying characteristics of closed isotropic circular cylindrical shells

19 p2871 A72-37478

Load capacity of tension-bent and compression-bent circular plates

19 p2877 A72-38161

Configuration determination method for metal crystal superdislocation anchored at two points and under stress in sliding plane, calculating critical stress related to double source unlocking

20 p2978 A72-39005

The carrying capacity of frames under the influence of concentrated forces

20 p2981 A72-39919

Applicability of the Euler approach to investigate the strain stability of anisotropic nonlinearly elastic bodies under finite subcritical strains.

21 p3116 A72-40273

Transverse shear effect on thin shells collapse load, considering influence on Shapiro yield surfaces

21 p3121 A72-41213

Behavior of viscoelastic shallow spherical shells subjected to dynamic pressure.

21 p3122 A72-41245

Asymptotic analysis of the behavior of an elastic rod under aperiodic intense loading

21 p3127 A72-41670

Reissner nonlinear equations for stability analysis of shallow shells of revolution, noting critical loads range and error analysis

22 p3232 A72-41856

Experimental investigation of the carrying capacity in bending of steel box-section beams

22 p3232 A72-41870

Estimation of the effect of stress concentration in nonstationary loading regimes

22 p3232 A72-41922

Carrying capacity of thin-walled shells subjected to impulsive radial pressure loads

22 p3233 A72-42052

Stability of elastoplastic rod under external conservative and nonconservative forces, discussing nonconservative component effect and critical load magnitude

22 p3234 A72-42149

Elastic isotropic plates stability for nonlinear stress-strain relations, noting effect of deformation tensor invariant on critical load magnitude

22 p3234 A72-42275

Limit analysis and plastic design of structural elements of complex shape.

22 p3235 A72-42577

Peak load-impulse characterization of critical pulse loads in structural dynamics.

22 p3236 A72-42757

Aircraft structural design loads definition by mission analysis criteria, taking into account gust loads via power spectral density method

22 p3138 A72-42828

Aircraft structural safety criteria based on acceptable failure probability, determining critical load levels

22 p3138 A72-42829

ICAO structural airworthiness requirements relation to air transportation safety, considering maneuver and gust loads in terms of limit load concept 22 p3138 A72-42830

Buckling of circular cylindrical shells under axial compression. 22 p3239 A72-42840

Influence of the degree of strain-hardening and roughness of friction surfaces on wear rate and carrying capacity 22 p3183 A72-43157

Fiber composite columns under compression. 23 p3344 A72-43494

Limiting equilibrium of orthogonally coupled cylindrical shells 23 p3346 A72-43656

Minimum weight structural design, generalizing method for deriving sufficient optimality conditions with examples for specified maximum deflection and critical nonconservative loading parameters 23 p3347 A72-43719

Limiting equilibrium of shells of revolution and circular plates with allowance for shear stresses 23 p3348 A72-43789

Dynamic response of viscoelastic shallow spherical shells. 23 p3349 A72-43972

Post-buckling of axially compressed plates. 24 p3455 A72-44632

Free vibration frequencies and critical buckling loads for thin walled shells of revolution constructed out of layered or heterogeneous anisotropic materials 24 p3455 A72-44676

Plastic design of regular orthotropic grids with two adjacent edges fixed, free, or hinged. 24 p3456 A72-44794

Local plastic deformation relation to tangential shear stresses, deriving expressions to determine critical levels 24 p3460 A72-45724

Variable thickness shallow spherical shells of revolution axisymmetric loads carrying capacity, determining limit equilibrium through application of Tresca yield point concept 24 p3460 A72-45725

CRITICAL MACH NUMBER
U CRITICAL VELOCITY
U MACH NUMBER

CRITICAL MASS
Radiation pressure on quasar outer envelope material as cause of mass outflow for masses less than gravitational force-determined critical value 14 p2155 A72-30552

Critical experiment ITR - Methods of nuclear design calculation and theoretical interpretation of experimental data. 18 p2709 A72-36185

CRITICAL PATH METHOD
An estimate of expected critical-path length in PERT networks. 23 p3308 A72-43806

CRITICAL POINT
Nb-Ti alloy critical current density increase dependence on temperature, discussing evidence supporting rigidly pinned vortex lattice model 04 p0562 A72-15292

Monochromatic light beam propagation in optically nonhomogeneous medium containing matter in near critical state, determining exciting wave electric field strength 05 p0691 A72-16683

Lattice gas critical point and nonanalytical three dimensional models comparison with experimental data 05 p0691 A72-17062

Inviscid solar wind equations supersonic solutions existence domain from critical point boundary conditions 06 p0881 A72-17894

Nonanalytic equation of state formulation at critical point of fluid phase transformation 09 p1413 A72-23690

Equilibrium thermodynamics of critical points, discussing phase transition theory and scaling hypothesis for single component systems 10 p1562 A72-24400

Dynamical aspects of critical phenomena - Conference, Fordham University, New York, June 1970 11 p1701 A72-26022

Equilibrium state stability in elastic conservative system, relating system postbuckling behavior to critical branching point 13 p2054 A72-28478

Critical superconductivity currents measurement in niobium based U shaped and coiled wires within steady magnetic field 13 p2007 A72-30013

Clear air turbulence nonlinear generation mechanism based on finite amplitude periodic waves in stratified shear flow critical layers, considering buoyancy, viscosity and heat conduction effects 14 p2127 A72-30226

Hodographic equations solution containing critical point for compressible fluid two dimensional flow,

noting calculation of wing profiles and turbine engine cascades [ONERA, TP NO. 1048] 14 p2095 A72-30841

Internal gravity waves and convective instability caused by liquid layer nonuniform vertical density distribution, noting error in thermal conductivity measurement near critical point 14 p2095 A72-31008

Benzene isochoric specific heat curves along saturation line in biphasic and single phase states, noting variations near critical point 15 p2334 A72-31393

Angular distribution and intensity of light scattered by carbon dioxide near critical point, noting temperature dependence of isothermal compressibility and long range correlation length 16 p2422 A72-32945

Power spectrum of light scattered from surface waves thermally excited on carbon dioxide liquid-vapor interface near critical point 16 p2423 A72-32948

Monochromatic light beam propagation and scattering in optically nonhomogeneous medium containing matter in near critical state, determining exciting wave electric field strength 16 p2426 A72-33694

Critical point regularity conditions and asymptotic solutions to the time stationary, linearized, inhomogeneous solar wind flow problem. 17 p2599 A72-35095

Influence of cerium, lanthanum, neodymium, and boron on the critical points and the linear expansion coefficient of Kh17N2 steel 17 p2569 A72-35523

Analytical investigation of normal shock waves in water near the thermodynamic critical point. 17 p2543 A72-35635

Finite amplitude neutrally stable two dimensional disturbances in parallel flows for large Reynolds numbers, investigating phase shift across critical layer 19 p2786 A72-37572

Volume and enthalpy changes at critical point of condensed state, noting Ar enthalpy dependence on temperature 19 p2881 A72-38045

Bulk viscosity coefficient and the second heat conduction coefficient near the critical condensation point 20 p2983 A72-39396

Critical flow rate and pressure ratio for nitrogen flowing through convergent-divergent nozzle at stagnation conditions, emphasizing thermodynamic critical region 21 p3046 A72-41180

Elastic conservative structural systems stability with many degrees of freedom, discussing critical singular points effect 21 p3120 A72-41206

Holographic technique for investigation of critical phenomena in aniline-cyclohexane and triethylamine-water binary critical mixtures, noting phase transition visualization 21 p3056 A72-41219

Buildup of thermal equilibrium in a fluid near the critical point 22 p3242 A72-41882

Laminar boundary layer at critical point of blunt body in molecular oxygen flow, noting wall influence on condensation 22 p3243 A72-42257

Critical superconductivity currents measurement in niobium based U shaped and coiled wires within steady magnetic field 22 p3190 A72-42735

Investigation of the formation of local concentrations near the critical liquid-gas point by the electron paramagnetic resonance 23 p3356 A72-43326

Critical-point anomalies in the electron-paramagnetic-resonance linewidth and in the zero-field relaxation time of antiferromagnets. 24 p3432 A72-45674

CRITICAL PRESSURE
Hypersonic two component gas mixture nozzle flow with condensation or evaporation discontinuity, determining Pitot pressure limits 02 p0230 A72-12255

Pneumatic fluid power valve flow rate derivation in terms of flow passage effective area and critical pressure ratio 08 p1113 A72-22158

Nonlinear critical stability of truncated conical shell uniformly loaded by external hydrostatic pressure, using Bubnov-Galerkin method 16 p2470 A72-33412

CRITICAL REYNOLDS NUMBER
U CRITICAL VELOCITY
U REYNOLDS NUMBER

CRITICAL SPEED
U CRITICAL VELOCITY

CRITICAL STRESS
U CRITICAL LOADING

CRITICAL TEMPERATURE

Griffith fracture theory application to thermal crack propagation, computing stress-strain field and critical temperature [ASME PAPER 71-MET-N] 05 p0731 A72-15790

Order-disorder reaction in Ni-V, Ni-V-Nb and Ni-V-Ta alloys, estimating critical temperature 05 p0671 A72-15999

Cumulation-laser heating of D-T plasma for cylindrical wave, investigating pulse energy increase for critical temperature attainment from average value mathematical model 05 p0695 A72-16279

Critical temperature dependence of Nb-Al-Ge superconducting alloys on composition and heat treatment, discussing phase boundaries and electron state densities 07 p1049 A72-20154

Phase diagrams, superconducting properties and annealing critical temperature of Nb-Al-Ge alloys, establishing four phase peritectic equilibria 08 p1218 A72-21778

Nonlinear creep characteristics of variably thick rotating disks under nonuniform heating conditions, determining critical rpm and temperature field and time to failure 09 p1402 A72-22731

Ordering in fcc lattice ternary alloys with allowance for atoms interactions, noting phase transformation critical temperature and superlattices existence 13 p1976 A72-28691

Numerical solution to stabilization temperatures of supersonic boundary layer under intense surface cooling without constraints on disturbance wave number and Reynolds number 16 p2343 A72-33155

Numerical solution to Percus-Yevick equation and thermodynamic functions of dense gas in supercritical temperature range with Lenard-Jones potential 16 p2476 A72-33160

Stabilization of a superconducting modification of beryllium by an aluminum admixture 20 p2960 A72-39407

Recrystallization and polygonization conditions in high purity metals, noting critical temperature and additives effect 21 p3065 A72-40093

Phenomenological models of the electron-phonon interaction and the superconductivity criterion of metals 21 p3098 A72-41688

Determination of the critical temperatures of cylindrical shells of variable thickness 22 p3243 A72-42053

CRITICAL VELOCITY
Acoustic attenuation calculation for turbulent flow in rigid tubes, determining critical flow velocity dependence on wall roughness and sound wave frequency 03 p0340 A72-12954

External pressure effects on cantilever rotating shaft vibration, determining critical whirling speed as function of pressure and area distribution by energy method 07 p1096 A72-20528

Vibrations causes and degrees of freedom relationship in rotor machines at critical velocities, determining rotor imbalance from amplitude characteristics 08 p1243 A72-21232

Critical Reynolds numbers estimation for flows having velocity profile with point of inflection, discussing plane parallel flows stability energetic analysis 08 p1151 A72-21660

Transfer matrix and dynamic stiffness techniques application to critical speed analysis in rotating machinery 08 p1224 A72-22128

Laminar/turbulent boundary layer transition on parabolic wing profile in supersonic wind tunnel, noting critical Reynolds number increase with leading edge thickness 09 p1259 A72-22407

Nonlinear creep characteristics of variably thick rotating disks under nonuniform heating conditions, determining critical rpm and temperature field and time to failure 09 p1402 A72-22731

Continuously supported railroad track under axial compression forces and moving load, noting critical velocity for high speed trains 09 p1409 A72-23558

Shrouded propellers and rotor blades free vibrations determination by variational method, showing Coriolis effect on critical flutter speed 11 p1732 A72-25536

Gyroscopic effects on elastically supported high speed rotors, examining critical velocity and disturbance behavior via equations of motion 11 p1686 A72-25723

Critical shock wave velocity for ionization front propagation with photoionization of hydrogen by radiation, using pinch discharge tube measurements [AIAA PAPER 72-410] 11 p1706 A72-26161

Steady bifurcating time periodic solutions stability for flows in bounded domain with complex conjugate simple eigenvalues at critical Reynolds number

12 p1837 A72-27712

Incompressible boundary layer velocity profile on swept wings, comparing critical Reynolds number to straight wing value

13 p1894 A72-29639

Transient torsional vibration of asymmetric rotor with limited power supply near critical speed calculated by asymptotic method

16 p2463 A72-32874

Material damping effect on rotating system stability as function of critical angular velocity, using elastic continuum whirling shaft model

16 p2465 A72-32986

Coriolis forces effect on bubbles trajectories in rotating containers, determining critical Reynolds number

17 p2537 A72-34209

Fluid transition through critical value, considering self oscillation onset mode frequency

18 p2681 A72-36663

A comparison of initial velocities for dynamic instability of a shallow arch.

18 p2738 A72-37080

Influence of the structural format on the range of critical rotational speeds of rotors in aircraft engines

20 p2963 A72-39801

The critical velocity of gas-plasma interaction and its possible hetegonic relevance.

24 p3429 A72-45468

CROCCO METHOD

Loitsiankii parametric method application to universalize isothermal laminar boundary layer partial differential equations in Crocco variables

05 p0649 A72-16221

CROCCO-LEE THEORY

Crocco-Lee theory extension to flow behavior prediction for two dimensional supersonic turbulent near wake behind bluff body during recompression

16 p2343 A72-33402

CROP GROWTH

Sounding rockets in remote sensing programs for agricultural census and crop yield estimates in Argentina

02 p0228 A72-11854

Crop, soil and geological mapping from digitized multispectral satellite photography, discussing data processing requirements and surface features distinguishable from satellite altitudes

02 p0214 A72-11876

Action of a constant magnetic field on plant growth

17 p2503 A72-35006

CROP VIGOR

Southern corn leaf blight detectability by remote sensing based on pattern recognition technique application to multispectral color and IR photographic and scanner data

02 p0212 A72-11814

Spectral brightness coefficient and photodensity measurements for remote vegetation productivity sensing in visible band

15 p2222 A72-31396

Satellite earth resources remote sensing in visible, IR and microwave regions for plant disease and salinity evaluation

15 p2229 A72-32049

CROSS CORRELATION

Air pollution circulation patterns remote sensing, describing multispectral stereo image pairs digital cross correlation

[AIAA PAPER 71-1106]

01 p0067 A72-10551

Cross correlation characteristics of deviations in critical frequencies of F 2 region

01 p0059 A72-10594

Microelectronic computer system with image data cross correlation generation for real time video pattern abstraction, discussing design and operating characteristics

03 p0329 A72-14178

Cross correlation model for interpreting empirical results on binaural noise masking level differences in sinusoidal signal detection, comparing with equalization-cancellation model

04 p0550 A72-15296

White noise mean square sound pressure in turbulent flow in cylindrical duct, using cross correlation technique

[ASME PAPER 71-WA/FE-5]

05 p0647 A72-15936

Surface wave parametric signal processing, obtaining cross correlation of digitally coded input signals

05 p0631 A72-17074

Auto- and cross correlation functions for neuron reactions in vasomotor center to adequate stimulation of cats vestibular apparatus

06 p0762 A72-17673

Two-channel direction finding with point source emission and spaced antennas reception, investigating cross correlation and background noise interference effects on accuracy

07 p0938 A72-19007

Cross correlation identification of linear time varying processes based on pseudorandom sequences, presenting digital simulation results

07 p0948 A72-20390

Electronic correlator for plasma wave induced coherent signals cross correlation measurement, producing 1 microsecond time delays by automatically switching lumped circuit delay line

07 p0958 A72-20582

Cross correlation analysis of turbulent jet flow noise with pressure fluctuation as acoustic source

[ASA PAPER H 12]

08 p1150 A72-21488

Loose medium deformations and displacements fluctuations verification by statistical tests, noting inception information from autocorrelation and boundary conditions cross correlation functions

10 p1512 A72-24719

Antisymmetric pseudorandom signal performance in measurement of second order kernels in Volterra series representation of nonlinear system by cross correlation

10 p1439 A72-24805

Auto and cross correlation functions of combined binary pseudorandom sequences in digital space communication systems

10 p1439 A72-24907

PSK signal cross-correlated receiver output SNR in presence of random misalignments with respect to carrier frequency and arrival signal time

13 p1921 A72-29283

Solar magnetogram recorded mean photospheric magnetic field cross correlation with interplanetary magnetic field

13 p2049 A72-29935

Electromagnetic waves backscattering in magnetoactive plasma containing random inhomogeneities of electron density, calculating field spatial-time and cross correlation functions

14 p2086 A72-30789

Extended Huygens-Fresnel principle for mutual coherence /cross correlation/ function of finite optical beam propagation in turbulent medium

15 p2249 A72-32161

Direct correlation measurement of turbulent jet noise and flow by cross correlating narrow filtered input turbulence and output acoustic signals

[AIAA PAPER 72-640]

16 p2381 A72-34092

Recursive filtering techniques in space navigation, describing initialization procedure to account for state vector errors correlation

17 p2532 A72-34214

Time correlation functions for gases of linear molecules in a magnetic field.

17 p2589 A72-34894

Theoretical model prediction for matched filter selectivity and noise effects on strained object deformation in optical correlation applications, comparing results with experiments

21 p3053 A72-40611

Time scales and correlations in a turbulent boundary layer.

21 p3047 A72-41626

CROSS COUPLING

Aircraft pitching and yawing cross couplings compensation at high speed

01 p0005 A72-10506

Scattering diagram for mutual cross coupling between antennas in Fresnel zone

02 p0196 A72-12757

Digital computer solution for near field coupling between high and low gain antennas above conductive surface

03 p0323 A72-14029

Two center-fed feed-point displaced dipole antennas, calculating mutual impedance for various combinations of displacements and heights

04 p0501 A72-15433

Radiative coupling of fed and unfed adjacent antennas in navigation systems rotating beam circular arrays, deriving equivalent circuit via quadrupole theory

05 p0635 A72-16300

Multifrequency array antenna of interlaced open ended waveguide elements for L, S, and C bands, reducing mutual interaction by cross polarization

06 p0782 A72-17360

Frequency discriminator like two-channel device with greater sensitivity by crossed feedback, calculating variable frequency emf effect on operation

07 p0938 A72-18853

Mathematical model for multiple bearing supported isotropic undamped rotors with arbitrary stiffness and mass distribution, taking into account horizontal/vertical motion coupling

07 p1096 A72-20529

Trajectory properties of roots of characteristic equations with complex coefficients for two dimensional systems with feedforward and feedback cross couplings

08 p1200 A72-21768

Liquid propellants coupling effects on parallel stage space shuttle configuration structural dynamics, using forty degree of freedom analytical model

[AIAA PAPER 72-347]

11 p1725 A72-25376

Cross coupling in a five horn monopulse tracking system.

17 p2513 A72-34356

Combinational distortions and cross distortions in parametric microwave systems

19 p2768 A72-38665

Electromagnetic compatibility problem of RF oscillators and switching operations in power network as interference source, discussing transmission line shielding and coupling impedance

20 p2901 A72-38988

Analysis and prediction of coupling between collocated antennas.

20 p2902 A72-38999

Scattering diagram for mutual cross coupling between antennas in Fresnel zone

20 p2907 A72-39063

CROSS FAULTS

U GEOLOGICAL FAULTS

CROSS FLOW

Cross flow through in-line tube bank, investigating surface roughness effects on behavior by pressure drop, static pressure and skin friction distributions measurements

02 p0203 A72-12102

Turbulence intensity effects on mass transfer from cylinders in cross flow at various Reynolds numbers

[ASME PAPER 70-WA/HT-3]

02 p0205 A72-12312

Laminar three dimensional boundary layer nonequilibrium effects at hypersonic wing swept leading edge with intensively cooled surface, considering sweep induced crossflow effect

[VPIE-71-23]

02 p0152 A72-12422

Cross flow blown two dimensional stationary plasma arc deflection and temperature distribution as function of collisional drift velocity and electric field

03 p0397 A72-13921

Jet mixing flow from slotted source into longitudinal cross flow shown analogous to heat expansion in plane jets

05 p0648 A72-16220

Three dimensional hypersonic turbulent boundary layer under normal and longitudinal pressure gradients and cross flow along windward symmetry plane of body of revolution

[AIAA PAPER 72-186]

05 p0605 A72-16841

Turbulent jets interaction with cross flow, presenting longitudinal and transverse velocity, temperature and turbulence distributions

[AIAA PAPER 72-149]

05 p0651 A72-16870

Cross flow effect on lifting fan noise at subsonic blade tip speeds, analyzing radiation pattern change due to inlet flow distortion

[AIAA PAPER 72-128]

05 p0608 A72-16921

Wake instabilities and vortices spacing, position and strength behind slender cylindrical bodies at large incidence with subcritical cross flow Reynolds numbers

05 p0610 A72-17010

Durando model overprediction of deflected jet vortex strength in subsonic cross flow

08 p1151 A72-21631

Mixing length model for computing three dimensional turbulent boundary layers with small cross flow

[ONERA, TP NO. 985]

09 p1294 A72-22817

Fluid flow and heat transfer in tube bank with two cylinders in cross flow, determining static pressure, Nusselt number and drag coefficients

11 p1743 A72-25259

Secondary flow measurements in rotating ducts, obtaining pressure distributions and cross-flow velocities

[ASME PAPER 72-GT-17]

11 p1569 A72-25616

Fan-in-wing model noise due to cross flow generated in- and outflow distortions and unsteady rotor blade forces

[ASME PAPER 72-GT-92]

11 p1571 A72-25666

Single continuous algebraic correlation equation for convective heat transfer in cross flow for wide Reynolds number range, considering applications to hot-wire anemometry

11 p1747 A72-26541

Free stream turbulence effect on mass transfer from circular cylinder in cross flow as function of Schmidt and Reynolds numbers, using electrochemical measurement method

14 p2096 A72-31061

Steady state magnetically balanced cross flow arc, calculating flow and temperature fields and boundary shape under assumption of two independent variables

[AIAA PAPER 72-687]

16 p2439 A72-34055

A method for increasing thrust reverser utilization on STOL aircraft.

[AIAA PAPER 72-782]

19 p2752 A72-38141

Forced convection heat transfer from cylinders to water in cross flow, quantifying method of accounting for fluid property variation

19 p2881 A72-38397

Mathematical models for temperature profiles and heat transfer rates in two-stream and multistream cross flow heat exchanger

21 p3128 A72-40931

Evaluation of windward streamline effective cone boundary-layer analyses.

22 p3136 A72-42874

An experimental investigation of a jet issuing from a wing in crossflow. 24 p3362 A72-45332

CROSS RELAXATION

Carbon dioxide laser cross relaxation effects on hole burning process in Doppler broadened gain or absorption line 11 p1647 A72-26146

The effect of cross relaxation on the behavior of gas laser oscillators. 19 p2813 A72-38691

CROSS SECTIONS

Gradient method for optimization control system construction with cross couplings between channels 01 p0045 A72-10501

Optimal and quasi-optimal automatic control systems synthesis by cross section method 09 p1290 A72-22489

Rectangular and D-shaped cylinders pressure distribution and aerodynamic force measurements in two dimensional flow as function of cross sectional height/width ratio 10 p1419 A72-24840

Stokes flow about slender particle with nonuniform cross section under distributed force, obtaining solution to integral equation for twisted particle by perturbation scheme 12 p1798 A72-27834

Relative cross sections for gas phase photodetachment of electrons from amide and arsenide ions using ion cyclotron resonance spectrometer 13 p1914 A72-30064

Absolute cross sections for Werner band system excitation of molecular hydrogen by electron impact, discussing relative spectral response calibration 13 p2009 A72-30065

Cross section determination of proton production in collisions of electrons and hydrogen ions 14 p2134 A72-30801

Cross sections for dissociative excitation of hydrogen ions by electrons determined by coincident detection of protons and H atoms 14 p2134 A72-30804

Diatomic molecules dissociation investigation from effective cross section measurement of slow atomic negative ions formation by molecules collisions with fast ions and atoms 16 p2432 A72-34152

Optimal and quasi-optimal automatic control systems synthesis by cross section method 17 p2533 A72-34652

Pressure rise during combustion in semiclosed volume with reduced gas flow cross section in condensed system channel 19 p2879 A72-37354

The propagation of sound in a circular duct of continuously varying cross-sectional area. 22 p3207 A72-42911

Calculation of photoabsorption processes in helium. 24 p3426 A72-45012

Photoionization and photoabsorption cross sections for ionospheric calculations. 24 p3400 A72-45590

Cross section parameters for electron impact excitation, noting mathematical models for aeronautical users 24 p3400 A72-45591

CROSSED FIELD AMPLIFIERS

High power nitrogen-carbon dioxide cross beam electric discharge convection laser amplifier with rectangular channel 07 p1003 A72-19216

Minimum noise coefficients of M-type microwave beam amplifiers with crossed fields, taking into account delay system distributed losses 10 p1453 A72-24913

Carrier wave behavior in n-type GaAs slab under crossed dc electric and magnetic fields, investigating traveling space charge amplifier magnetic control 14 p2143 A72-30941

Magnetron crossed field amplifier multistage frequency multiplier HF field properties, obtaining numerical solutions for nonlinear governing equations 15 p2209 A72-32669

Russian book on microwave electronics covering linear-beam and cross-field backward and traveling wave amplifiers and oscillators, klystrons, masers, plasma devices, etc 17 p2532 A72-34650

CROSSED FIELDS

Steady laminar viscous conducting fluid flow in infinite rectangular channel in crossed electric and magnetic fields, deriving flow rate and potential distribution 03 p0398 A72-14008

Axisymmetric rotational motion of electrically conducting fluid between dielectric disks in crossed electric and magnetic fields 03 p0399 A72-14012

Ar gas dc discharge plasma characteristics in crossed electric and magnetic fields, examining equivalent pressure concept 04 p0556 A72-14945

Monograph on design and characteristics of rotating plasma device under crossed electric and magnetic fields, covering dynamic behavior of hydrogen puff 05 p0642 A72-15798

Cross-field current driven ion acoustic instability in two plasma devices, causing neutral sheet phenomena, anomalous dispersion and ion heating [AD-740261] 06 p0858 A72-17541

Cosmic rays generation by charged particles acceleration in electromagnetic constant crossed fields during magnetic stars contraction to neutron star dimensions 07 p1056 A72-19042

Two fluid MHD model for flat plasma condenser in crossed magnetic and alternating electric fields, calculating impedance and disturbed plasma parameters 09 p1360 A72-22953

Crossed fields effect on plasma injection in magnetic trap 09 p1363 A72-23220

Strong magnetic fields and electric current densities effects on acoustic oscillations and instability in stationary inhomogeneous low temperature plasma flow in crossed fields 10 p1517 A72-23838

Diamagnetic energy measurements on rotating plasma in crossed static electric and magnetic fields with short circuiting metal wall 10 p1519 A72-24097

Interaction solutions of steady crossed field MHD channel flows for perfect, singly ionizing monatomic and thermodynamically unspecified gases 10 p1523 A72-24789

Small scale sporadic E layer explained by means of cross field instability, proposing numerical solution based on realistic three dimensional perturbation 10 p1478 A72-25164

Three dimensional linear analysis of ionosphere cross field instability, noting potential as E region irregularities source 10 p1478 A72-25166

Neutron flux and energy spectra from crossed field acceleration model of plasma focus and z-pinch discharges 11 p1693 A72-25565

Trioplasmatron using crossed field hydrogen discharge between cold cathode and disk anode, noting pulse modulation applications 13 p1927 A72-28380

Plasma inhomogeneity in crossed electromagnetic field, comparing motion velocity to ion component transverse drift rate in polarized electric field 13 p2019 A72-29893

Plasma diffusion coefficient in crossed electric and magnetic fields, discussing lifetime in magnetic trap and expression for ion mobility 13 p2019 A72-29942

Dispersion equation derivation for HF electromagnetic waves in weakly ionized plasma in crossed fields, noting oscillation spectrum 13 p2020 A72-30048

F region crossed field instability nonlinear theory based on energy transfer by mode coupling and absorption by linear damping with application to equatorial electrojet 16 p2384 A72-32976

Nonlinear theory of crossed field and two stream instabilities of nonthermal plasma motions in equatorial electrojet 16 p2387 A72-33937

Two fluid MHD model to study cylindrical plasma condenser resonance properties in crossed axial magnetic and alternating electric fields 17 p2593 A72-35881

Two fluid MHD model for flat plasma condenser in crossed magnetic and alternating electric fields, calculating impedance and disturbed plasma parameters 17 p2593 A72-35882

A theoretical analysis of the acceleration of ions in axially symmetric crossed fields with an external source and sectioned electrodes 17 p2593 A72-35902

Calculation of the dependence of the charge density on the distribution of the potential in crossed symmetric electric and magnetic fields 17 p2593 A72-35903

On the influence of excited ions and crossed electric and magnetic fields on ionisation cross-sections. 18 p2714 A72-36956

Cross polarizing effects of a water film on a parabolic reflector at microwave frequencies. 21 p3027 A72-40375

Buildup of oscillations in crossed-field backward-wave oscillators. 24 p3385 A72-44973

CROSSLINKING

Polymers viscoelastic behavior during crosslinking reactions, deriving equations for creep response to step increase in crosslink density 09 p1336 A72-22521

Electron bombardment deposited polymer thin films electrical properties as function of formation current, noting increase in crosslinking and dangling bonds 12 p1788 A72-27277

Epoxide resins for application in composite materials, discussing crosslinking reactions, temperature effects on cure, and electrical and physical properties 15 p2260 A72-31441

CROSSTALK

NT IONOSPHERIC CROSS MODULATION AM/PM conversion and transfer in nonlinear signal transmission systems, calculating coefficients as function of multicarrier powers for intelligible crosstalk 12 p1782 A72-27554

Cross coupling in a five horn monopulse tracking system. 17 p2513 A72-34356

CROWDING

Crowding phenomenon effect on blood cell oxygen consumption, using Carotieson diver technique for polymorphonuclear leukocyte, lymphocyte and platelet measurements 12 p1763 A72-27842

CRUCIBLES

Oscillating torus shaped crucible viscometer, discussing oscillating viscous liquid fluid dynamic problem 04 p0522 A72-15480

CRUCIFORM WINGS

Supersonic flow around thin cruciform wing with antisymmetrical angle of attack distribution and horizontal plane with leading edge, considering flow separation at edges 10 p1420 A72-25118

The effects of protuberances and scaling parameters on the aerodynamic characteristics of an air-to-air cruciform missile. [ALAA PAPER 72-969] 22 p3231 A72-42342

CRUISING FLIGHT

Transonic air transport design, discussing wind tunnel tests, supercritical flow technology, sonic beam avoidance, cruising speed, operating costs and transport family development 03 p0310 A72-13487

Supercritical thick wing for structural weight reduction and increased cruise speeds flight tested on Navy T2-C aircraft [SAE PAPER 720320] 11 p1576 A72-25583

Propulsion system flexibility in V/STOL aircraft with one lift-cruise engine, discussing takeoff thrust requirements and cruise fuel consumption efficiency [ASME PAPER 72-GT-105] 11 p1576 A72-25670

High cruise altitude operational advantages for commercial transport aircraft utilizing technological innovations in structures, propulsion, controls, avionics and aerodynamics 13 p1996 A72-28875

Minimum weight passive insulation requirements for hypersonic cruise vehicles. 17 p2638 A72-35256

Energy management during the space shuttle transition. 24 p3452 A72-45347

CRUSTS

NT EARTH CRUST

NT LUNAR CRUST

CRYODEPOSITS

Mathematical model for radiative transfer properties of high albedo carbon dioxide and water cryodeposits on opaque substrate [ALAA PAPER 72-58] 05 p0749 A72-16929

CRYOGENIC EQUIPMENT

Heat conduction in vacuum insulated capillaries to prevent failure of level indicators and controllers based on condensation in evaporating cryogenic liquid 03 p0456 A72-13883

Nerve structures localized cooling device using vacuum insulated closed circuit controlled cryogenic probe with cooling range of plus/minus 20 C 04 p0481 A72-15252

Arterial and grooved wick cryogenic nitrogen heat pipe performance tests, comparing elevation sensitivity, priming and heat transfer characteristics [ASME PAPER 71-WA/HT-42] 05 p0745 A72-15889

Ball, globe, gate, butterfly, Y-type and safety-and-relief valves assessed for cryogenic applications 11 p1642 A72-26777

Cryogenic microwave equipment for solids study provided with adiabatic demagnetization cooling system, noting relaxation time measurement in magnetic fields 12 p1796 A72-27856

Mechanical seal for airborne Stirling cycle cryogenic refrigerator, noting He cross leaks and sealing faces galling and blistering [ASLE PREPRINT 72AM 16] 13 p1964 A72-28973

Satellite sensor cooling systems, considering cryogenic heat pipes, sublimation, radiation cones and surface treatment 15 p2319 A72-31240

Space shuttle umbilical systems for mating, connection and checkout of carrier assemblies and couplings for cryogenic, electrical, pneumatic and hydraulic services 15 p2213 A72-31695

Glass silvered Dewar for liquid helium without auxiliary shielding cryogenics, using surrounding annular space for radiation shielding 15 p2214 A72-32431

CRYOGENIC FLUID STORAGE

Varian HR-60 NMR spectrometer probe with Dewared insert for low temperature operation
15 p2240 A72-32435

A high-accuracy temperature stabilizing and control device also operating in the cryogenic range
19 p2804 A72-38645

Simplified theory for optimizing the design of a heat shield in an isochorically operated toroidal dewar.
19 p2805 A72-38843

Thermohydrodynamic conditions at the peak flux of horizontal heaters in superfluid liquid helium II at zero net mass flow.
20 p2984 A72-39647

Analysis of real-gas and matrix-conduction effects in cyclic cryogenic regenerators.
[ASME PAPER 72-HT-27] 20 p2986 A72-39672

Low-temperature part of a spectrometer for gigahertz-ultrasonics and ultrasonic paramagnetic resonance.
21 p3051 A72-40215

Reynolds number and drive power variation with Mach number, pressure and temperature in cryogenic wind tunnel
[AIAA PAPER 72-995] 21 p3040 A72-41581

Quadrisectional facility for studying creep and fatigue strength under deep freezing conditions
21 p3057 A72-41719

CRYOGENIC FLUID STORAGE

Space shuttle cryogenic tanks self evacuating multilayer insulation, evaluating thermal and dynamic performance
01 p0139 A72-10778

Discretely oriented thread reinforced polyurethane cryogenic foam insulation systems for liquid hydrogen fuel tanks
[MDAC-WD-1756] 01 p0092 A72-10981

Analytical model of thermal/structural optimization for long term storage cryogenic propellant systems
[AIAA PAPER 72-142] 05 p0691 A72-16881

ELDO launch vehicle cryogenic tanks fabrication, discussing Al alloy selection and mechanical properties at low temperatures, manufacturing processes and thermal insulation
09 p1318 A72-22690

Photothermoelastic analysis of temperature and rupture stress in cryogenic tanker structures, using steel and plastic ship models
[AIAA PAPER 72-344] 11 p1728 A72-25373

Storage and handling of cryogenics.
19 p2784 A72-38827

Zero-gravity thermal performance of the Apollo cryogenic gas storage system.
19 p2869 A72-38830

A thermal stratification model of a cryogenic tank at supercritical pressures.
19 p2883 A72-38845

Determination of the optimal parameters of high-pressure cryogenic fluid storage systems.
20 p2962 A72-39358

CRYOGENIC FLUIDS

NT FLOX
NT LIQUID HELIUM
NT LIQUID HYDROGEN
NT LIQUID NITROGEN
NT LIQUID OXYGEN
NT SOLIDIFIED GASES

Thermal modeling of space shuttle cryogenic turbopump, considering heat transfer for two-phase cryogen and gas impingement on turbine blades and rotating disks
[ASME PAPER 71-WA/HT-43] 05 p0664 A72-15890

Space and ground environments effect on cryogenic multilayer insulation materials, tabulating mechanical and thermophysical test data
[AIAA PAPER 72-286] 11 p1741 A72-25225

Cryogenic liquids cavitation erosion of plastic and cold-short metals at 77 K, determining vapor pressure effect
13 p1979 A72-29479

Space simulation shrouds cryogenically cooled with liquid carbon dioxide, discussing automatic temperature control and operating cost savings
15 p2214 A72-32611

Study of the solidification of cryogenic fluids by means of evacuation
19 p2881 A72-38039

Techniques for determining average density and related parameters in two-phase cryogenic flow systems.
19 p2805 A72-38835

Critical levitation loci for spheres on cryogenic fluids.
19 p2836 A72-38844

CRYOGENIC MAGNETS

Cu clad N8-Ti wire wound superconducting solenoids with large fields at 1.6-5.2 K
10 p1446 A72-23762

Cosmic ray nuclei isotope identification with cryogenic magnet plus plastic scintillators to measure charge composition and rigidity
16 p2447 A72-33732

Analysis of cryogenic suspensions for use in spacecraft
22 p3230 A72-42208

CRYOGENIC ROCKET PROPELLANTS

Space shuttle cryogenics technology, flight and ground operations, checkout, maintenance and safety
03 p0441 A72-13695

Slush, boiling methane and methane mixture characteristics, noting advantages as potential rocket, aircraft and motor vehicle fuels
04 p0564 A72-15542

Analytical model of thermal/structural optimization for long term storage cryogenic propellant systems
[AIAA PAPER 72-142] 05 p0691 A72-16881

Specific impulse, mass and propellant efficiency characteristics of miniature motors using cryogenic fuels for auxiliary rocket thrusters
07 p0914 A72-18983

Low thermal flux glass fiber composite over-wrapped tubing with metallic liners for leak free cryogenic propulsion plumbing systems
[AIAA PAPER 72-328] 11 p1637 A72-25364

Detonation and burning characteristics of liquid oxygen-liquid methane mixtures.
19 p2848 A72-38834

CRYOGENIC STORAGE

Space shuttle environmental temperature control-life support system program changes, discussing air cooled electronic equipment, cryogenic stores, crew size and mission duration
[ASME PAPER 72-ENAV-18] 20 p2895 A72-39159

Shadow shields for minimizing radiant heat transfer into cryogenic propellant tanks on interplanetary missions, predicting performance for comparison with scale model experiment
21 p3130 A72-41181

CRYOGENICS

High conductivity superfluid region in cryogenic liquid helium 4 bath with temperature gradient in equilibrium with saturating vapor
01 p0101 A72-10040

Cryogenically formed prestressed stainless steel glass fiber reinforced vessels, demonstrating structural performance for space shuttle life support oxygen/nitrogen high pressure gas tanks
01 p0139 A72-10770

Hot pressed Ti alloy powders, evaluating strength and toughness at cryogenic temperatures
02 p0240 A72-11439

Electron microscope examination of freeze-etched air-filled lung alveoli extracellular lining layer, discussing sample preparation techniques
05 p0623 A72-16787

Direct coupled circuits in memory cell prototype with normally-off GaAs MESFET at 4.2 K
05 p0638 A72-17096

Low temperature test facility for cryogenic and rocket materials under combined tension and torsion
06 p0797 A72-18648

Millimeter and submillimeter band frequency conversion in nonlinear bulk n-InSb semiconductor at liquid helium temperature
08 p1140 A72-21060

Positive pressure cooling of cryogenic baths of liquid nitrogen by helium gas addition for frequency shift of ruby laser
09 p1326 A72-23411

High strength quenched steel with high ductility at cryogenic temperatures and negligible cooling rate effects on plasticity during welding
11 p1660 A72-26136

Space simulation facility for one year SERT 2 mercury ion thruster testing, discussing cryogenic operation and electrical and thermal insulation
[AIAA PAPER 72-430] 11 p1613 A72-26174

Cryogenic Josephson junction magnetometer in magnetocardiography, discussing high ambient noise levels in unshielded environment
12 p1769 A72-27288

Al single crystals, investigating scale factor effects on stepwise deformation at 1.4 K
14 p2115 A72-30410

Computerized determination of cryogenic gas behavior near vapor region, obtaining state equation coefficients from curve fitting program
15 p2334 A72-31580

High pressure cryogenic hydraulically actuated valve for repeated sealing of liquid He-containing cell
15 p2183 A72-32436

Attachment for studying optical properties of highly cooled crystals in the vacuum ultraviolet region
17 p2555 A72-35309

Thermal effects in JFET and MOSFET devices at cryogenic temperatures.
18 p2666 A72-36453

Book - Advances in cryogenic engineering, Volume 17
19 p2883 A72-38826

Cryobiology phenomena and applications, considering mode of action of various substances for freezing injury protection
19 p2762 A72-38828

Theoretical analysis of a cryogenic gas bearing with a flexible damped support.
19 p2810 A72-38837

Unconstrained liquid mass /Leidenfrost phenomenon/ pool and forced convective film boiling at cryogenic temperature
19 p2883 A72-38841

Some contributions to energetics by the Lewis Research Center and a review of their potential non-aerospace applications.
[ASME PAPER 72-AERO-12] 22 p3245 A72-43148

CRYOPUMPING

Zone melting high vacuum facility with cryogenic pumping and residual gas carbon-containing components exclusion for ultrapure metals production
06 p0796 A72-17992

Cryogenic techniques for high vacuum differential pumping with low conductivity cooled channels and supersonic jet target
09 p1364 A72-23225

Zone melting high-vacuum system with cryogenic pumping for zone refining Zr
14 p2092 A72-30220

Cryopump cooling requirements, refrigeration, design and vacuum application, considering Brayton, Claude, Stirling cycles and Joule-Thomson and regenerative processes
18 p2696 A72-36838

CRYOSORPTION

CRYOSORPTION

CRYOSTATS

Helium cryostat for X ray studies of phase transformations and structural changes in single metal crystals
08 p1169 A72-21792

Cryostat for high resolution tensile measurements of thermally activated processes during plastic deformation
09 p1398 A72-22657

Superconducting magnetic suspension systems safety aspects, discussing relief valves for He boil-off, flowmeters, cryostat temperature monitors, power supply diodes and safety interlocks
10 p1462 A72-24774

CRYOTRONS

An algorithm for computer calculation of critical curves of longitudinal cryotrons
21 p3025 A72-40183

CRYSTAL DEFECTS

NT CRYSTAL DISLOCATIONS
NT EDGE DISLOCATIONS
NT FRENKEL DEFECTS
NT POINT DEFECTS
NT SCREW DISLOCATIONS
NT VACANCIES [CRYSTAL DEFECTS]

Electron microscopy and diffraction analysis of lattice imperfections of layered superconducting transition metal dichalcogenide intercalation complexes
01 p0113 A72-10019

High purity W ion irradiated in situ under ultrahigh vacuum at high temperature, examining depleted zone defect structure by field ion microscopy
02 p0242 A72-11909

Single crystal Si defect accumulation and transition to amorphous state under Xe, Ar, Ne, O and P ion irradiation, using EPR
02 p0269 A72-12884

Charge state effects on defect production mechanisms, configurations, mobility, annealing kinetics, interaction and dissociation in displacement damage in covalent semiconductors
03 p0403 A72-14077

Vitreous silica and silicon-silicon dioxide interface defect structure and behavior during ionizing or particle irradiation
03 p0403 A72-14081

Annealing defects in n-type silicon, observing anomalous heat treatment temperatures of A and E centers
04 p0560 A72-14529

Burst noise in bulk materials and transistors attributed to crystallographic defects, investigating gold addition effects
04 p0498 A72-15131

Low energy He ion bombardment effects on Ni alloy single crystal surface, observing defect structure with stacking faults, tangled dislocations and carbide precipitation
04 p0533 A72-15159

Impurities effect on microstructure alignment in unidirectionally solidified Al-AlNi eutectic intermetallic, noting fiberless region defects
05 p0679 A72-17123

Thermodynamic estimation of transition metal stacking fault energy, discussing relation to lattice stability and structural changes
05 p0679 A72-17149

FET devices stacking faults induced leakage currents, pinpointing critical processing steps by diagnostic X ray charts
06 p0782 A72-17364

Microvolume decohesion hypothesis for crystal lattice defects explaining metal fatigue under variable stresses
06 p0829 A72-17743

Anelasticity effects due to defects and phase transformations in solids - Conference, Lausanne, Switzerland, June 1970
06 p0830 A72-18291

Energy spectrum of radiation defects in proton bombarded n-type Si crystals from Hall effect and electroconductivity measurements 07 p1049 A72-19901

Transition metals and alloys electron structure and packing defect energy theory, discussing crystal atomic interactions and brittle breakdown 07 p1049 A72-20148

Neutron irradiation produced lattice disorder in Li doped float zone melted n-p type Si solar cells 08 p1216 A72-21182

Soviet papers on imperfections of crystalline structure effects on physical and mechanical properties of metals and alloys, covering radiation damage, microdeformations, X ray investigations, etc 08 p1187 A72-21785

Small impurity amounts effect on packing defect density and deformation energy in Ni 08 p1188 A72-21791

UV radiation effects on pyrolytic boron nitride lattice imperfections, using space environment simulator 09 p1336 A72-22404

Metal welded joints formation as diffusion intensification from atom jumps stimulation by phonons from atomic thermal vibrations or crystal defects generation 09 p1319 A72-22867

Maximum internal friction onset temperature and magnitude in Co as function of thermomechanical treatment and crystal lattice defects 09 p1329 A72-23035

Defects high temperature diffusion effect on Mossbauer spectral lines width and positions in crystals with quantum transfer between multiplet sublevels in fine structure 09 p1372 A72-23038

Burst noise relationship to Si crystal dislocations and defects near emitter-base junction and surface zone in bipolar transistors 09 p1286 A72-23106

Laser stimulated Raman scattering and IR absorption on crystal defects leading to atomic migration in solids 11 p1647 A72-26144

Lithium niobate crystal refractive index inhomogeneity influence on second harmonic generation from He-Ne laser 11 p1650 A72-26360

Statistical estimation method for brittle metals fracture strength, taking into account stress nonuniformities due to dislocation defects 11 p1738 A72-26803

Transparent dielectrics destruction by mode-locked laser ultrashort pulses, discussing filamentary defect presence indication of radiation self focusing 12 p1853 A72-27068

CdS thin film conductivity reactions to grain boundary and stacking faults, correlating grain size to mobility 12 p1856 A72-28012

Irradiated semiconductors defects theory, considering electronic structure in rigid lattice and lattice distortion near defects 12 p1856 A72-28052

Irradiation produced defects and electrical properties of n and p-type Si, discussing radiation damage due to neutron and ion implantation 12 p1857 A72-28058

Li defect interactions in electron irradiated n-type single crystal Si from electron paramagnetic resonance measurements 12 p1858 A72-28063

Introduction rate and annealing of defects produced in Li-diffused float zone n-type Si by 30 MeV electrons and fission neutrons 12 p1858 A72-28064

Electron energy threshold measurements in irradiated II-VI compounds interpreted in terms of damage on metal and chalcogenide sublattices 12 p1859 A72-28070

Lattice damage measurement of Cd ion implanted GaAs semiconductors by optical reflection and scanning electron microscope 12 p1859 A72-28075

Electron paramagnetic resonance investigation of III-V compound semiconductor crystals, observing large magnetic moments, heteropolar chemical bonding and impurities 13 p2021 A72-28572

Defect annealing in neutron irradiated Si by deep trap concentrations, using space charge limited current (SCLC) 13 p2022 A72-29630

Surface phase transformation during cavitation erosion in Co and Fe alloys, suggesting stacking fault energy effect on erosion resistance 14 p2119 A72-30603

Crystal lattice defects induced by cyclic straining in quenched Al-Zn alloy, noting fatigue effects on dislocations accumulation and grain boundary migration 14 p2120 A72-30610

Fcc metal defect structure due to ultrasonic fatigue observation via transmission electron microscopy for dislocations 15 p2256 A72-31836

Oxygen and nitrogen atoms effect on defects recovery in cold rolled Nb during annealing 16 p2406 A72-33208

Lithium niobate crystal refractive index inhomogeneity influence on second harmonic generation from He-Ne laser 16 p2403 A72-33713

EPR transitions of quadrupole interaction of cubic imperfections with ground-vibronic-state degeneracy /Jahn-Teller effect/ 16 p2431 A72-33725

Susceptibility of the NiCr 15 Fe chromium-nickel alloy /Remanit 1675 SEW and Therman 1675/ to intercrystalline corrosion 17 p2566 A72-34396

Application of the moving-slit X-ray automonochromatization method in structural studies of planar diodes and an attempt to correlate electrical properties with lattice defects. 17 p2595 A72-34749

Separation of iron and annealing-out of lattice defects in rapidly-solidified aluminum-iron alloys. I - Microstructure and properties of quenched samples. II - Tempering behavior 17 p2567 A72-35174

A dynamical theory for the contrast of perfect and imperfect crystals in the scanning electron microscope using backscattered electrons. 18 p2692 A72-36749

Detection of defects in semiconductor structures by means of recording the temperature and electric fields. 18 p2693 A72-37106

Measurement of carrier lifetime in the base of silicon diodes - Application to the control of manufacturing techniques. 18 p2669 A72-37108

Properties of 1 MeV electron-irradiated defect centers in p-type silicon. 19 p2844 A72-37687

Twinning faults in epitaxial films of germanium telluride and GeTe-SnTe alloys. 19 p2844 A72-37688

Quantum crystals in the single-particle picture. 19 p2844 A72-37943

Fracture of nonlinear KDP and LiNbO₃ crystals by ruby laser radiation 19 p2812 A72-38537

Experimental determination of the coefficients of radiantly stimulated diffusion of sulphur in cadmium sulfide 20 p2959 A72-38954

The interaction of lattice defects and grain boundaries. 20 p2962 A72-39996

Ti based beta alloy strain hardening and failure characteristics, emphasizing initial deformation phase and microdefect onset and development 21 p3071 A72-41716

Study of the composition of inclusions in synthetic diamond crystals by the local analysis method 22 p3196 A72-42155

Nature of radiation defects formed by ruby laser emission on the surface of solids 22 p3185 A72-42273

Determination of mosaic-block disorientations in the creep of aluminum by the method of low-angle X-ray scattering 23 p3299 A72-43341

Shock damaged zircon, corundum, rutile, monazite and quartz crystalline inclusions in Muong Nong-type indochinite /tektite/, noting production from detrital sedimentary materials as possible terrestrial origin 23 p3335 A72-43398

Contribution to the study of phenomena of ordering of defects in single crystals of alumina- or zirconia-base refractory materials 23 p3302 A72-44000

Changes in the physical properties of metals subjected to elastoplastic deformation 23 p3303 A72-44199

Investigation of radiation paramagnetic defects in alkaline-silicate glass subjected to the action of high quasi-hydrostatic pressures - Structure of hole defects 24 p3417 A72-45421

Transparent dielectrics destruction by mode-locked laser ultrashort pulses, discussing filamentary defect presence indication of radiation self focusing 24 p3432 A72-45721

Supermolecular structure artificial defects and bond strength influence on mechanical strength of pyrographite 24 p3418 A72-45761

CRYSTAL DISLOCATIONS

NT EDGE DISLOCATIONS
NT SCREW DISLOCATIONS

Metal crystals dislocations movements and interactions with dislocation dipole under applied cyclic stresses for various configurations and starting conditions, using numerical methods 01 p0113 A72-10208

Transmission electron microscopic investigation of heterogeneous nucleation of Al-Ag alloys metastable gamma prime phase, noting association with four dislocation types 01 p0083 A72-10209

Kink movement and cutting forest dislocation models of creep in thermally activated crystalline solids 01 p0140 A72-10857

Critique of theoretical and experimental findings on slip geometry in bcc metals, especially Fe-Si alloy single crystals 01 p0089 A72-11300

Metal ductile facies fracture study of cups formation from cracks by cleavage, noting roles of dislocations and inclusions 02 p0246 A72-12600

Tungsten carbide dislocation structures analysis by transmission electron microscopy, deriving Burger vectors from energy considerations and electron micrographs contrast 03 p0370 A72-12995

Resistive force on moving dislocations at low temperature in solids and crystal defect studies by ultrasonic methods, determining temperature dependence of mechanical properties 03 p0362 A72-13224

Dislocation substructure in fatigued Al and Ni polycrystals surface layer and interior due to high and low stress cycling, discussing stacking fault energy influence 04 p0534 A72-15577

Dislocation splitting and stacking fault energy variation during plastic deformation of TaC at 2200 C, using bending tests and microscope observations [ONERA, TP NO. 1005] 05 p0670 A72-15861

Basal dislocations determination in sapphire single crystals, using X ray transmission topography 05 p0701 A72-16018

Physical theory of plasticity, considering mathematical hypotheses and assumptions, single crystals dislocations and plastic deformation, polycrystals homogeneous strain analysis, slip theories, etc 06 p0896 A72-17962

Thermally activated crystal microcrack initiation by fusion of leading and following dislocations 06 p0898 A72-18551

Steady creep rates in Ni poly- and single crystals in presence of dislocation stresses 06 p0835 A72-18748

Cu, Al and Pb bcc metals, investigating dislocation structure and creep characteristics change mechanism at transition from low to high temperature 07 p0104 A72-19822

Interfacial dislocations and failure in tension of directionally solidified Al-Cu-Mg eutectic 07 p0106 A72-19937

Hardening mechanisms during plastic deformation of pure bcc metals, discussing stresses relation to fine structure and crystal dislocation paths 07 p0108 A72-20142

Rapidly and unidirectionally solidified Al alloys microstructure, discussing crystal dislocation origins and patterns 07 p0109 A72-20240

Computerized dynamic simulation with graphic display of crystal plastic dislocation movement among random obstacles, emphasizing stress-strain, strain rate and thermal activation mechanisms 07 p0109 A72-20240

Al single crystals relationship between stress, strain and dislocation density ring elevated temperature creep by direct observation of etch pits 08 p1185 A72-20990

Basal and prismatic crystal dislocations in Be, measuring critical resolved shear stress dependence on temperature at 300-500 K 08 p1185 A72-20991

Mo single crystal internal dislocational friction and ultrasound damping dependence on oscillation amplitude, exposure time and annealing temperature 08 p1185 A72-21073

Intermetallics and carbide forming additions of Cr, Ti, Ce, V and Nb for hardening of cold worked Mn rich steel from crystal dislocations growth 09 p1327 A72-22230

Compression creep mechanisms in ceramic materials at elevated temperatures by lattice dislocations, grain boundary sliding and stress directed diffusion 09 p1334 A72-22393

Nonbasal deformation modes activation in Czochralski sapphire and fine grained alumina polycrystals deformation, noting water weakening 09 p1335 A72-22395

Computer simulation of crack tip atomic structure in diamond, relating covalent bond structure to dislocation nucleation and propagation likelihood 09 p1338 A72-22923

Dislocation loops in thin W foil due to ion irradiation, using electron microscopic analysis 09 p1331 A72-23505

Dislocations distribution in Al single crystals observed by X ray topography, noting effects of critical work hardening with annealing and secondary recrystallization 10 p1495 A72-24068

Dislocation damping by point defects entrapment, calculating internal friction force rate dependence based on weak interactions continuum model 10 p1527 A72-24979

Multiphase Al alloys strengthening by dislocation substructures in repeated rolling and recovery cycles at elevated temperature

11 p1667 A72-26930

Udimet 500 alloy dislocation substructure and fracture surface topography during deformation to failure in low cycle fatigue at high temperatures

11 p1667 A72-26938

Te-doped GaAs injection laser, investigating crystal growth dislocations effects on output radiation-injection current characteristics

12 p1822 A72-27617

Crystals deformation and orientation effects on Al polygonization process, noting dislocation densities dependence on stress axis orientation

13 p1972 A72-28464

Strain rate controlling mechanisms of superplastic deformation at various stresses and temperatures, considering vacancy and dislocation creep and grain boundary sliding

13 p1974 A72-28657

Plastic deformation in bcc metal single crystals, discussing glide and work hardening, dislocations, core structure and atomic calculations

13 p2061 A72-29874

Heisenberg antiferromagnet with noncollinear sublattices and linear dislocation, considering coupled spin wave states and density

13 p2023 A72-29910

Mo single crystal weakening after hot rolling and annealing, showing decreased dislocation density and hardness recovery by electron microscopy

14 p2112 A72-30160

Phase precipitated helicoidal dislocations and vacancy-type stacking faults in aged austenite Fe-Ni-Ti alloy, using electron microscope diffraction contrast analysis

14 p2112 A72-30162

Dislocation substructures effect on relaxation and internal friction peak in cold rolled Mo single crystals after annealing

14 p2122 A72-30956

Ultrasound damping in Mg and Al alloys by structural grains and dislocation oscillations during work hardening, recrystallization and oversaturated solid solution decay

14 p2122 A72-30957

Crystal lattice and dislocation anharmonicities interdependence and stress-strain correlation in presence of interaction between ultrasonic waves of different frequencies

14 p2169 A72-30959

Internal friction and relaxation mechanisms in substructure hardened fcc alloys and bcc metals, presenting dislocation parameters for annealed and cold worked Fe alloys

14 p2122 A72-30960

Heat resistance improvement by interface dislocation, dispersion hardening and reinforcement of Mo, Fe, Ni and Al metals and alloys

15 p2254 A72-31560

Metal hardening level evaluation on basis of volume dislocation structure from stress field of dislocation loops

15 p2254 A72-31562

Metal fatigue tests at various frequencies to observe surface structure, dislocations in crack vicinity, plastic deformation and ultrasonic resonance techniques

15 p2257 A72-31839

Positron annihilation lifetimes and trapping probabilities for vacancies and dislocations in Al single crystal

15 p2258 A72-32228

Elastic dilatational field association with twist dislocation loop interaction with free surface of two phase system interface

15 p2331 A72-32504

Mobile dislocation density and strain rate sensitivity of bcc Fe-Ni alloys from deformation onset to high temperature plateau

15 p2258 A72-32639

Line and surface defect treatments of elastic media dislocation field, noting nonuniqueness with respect to Burgers and jump conditions

16 p2467 A72-33141

Interaction forces between two dislocations in infinite weakly anisotropic media with bcc crystal lattice elastic properties

16 p2424 A72-33146

Multiple plastic and viscoplastic potentials for single crystal and polycrystal with mean densities and mean lengths of dislocations as internal variables

16 p2470 A72-33615

Tensile deformation of Co single crystal in high temperature fcc phase, noting dislocations effect on work hardening

16 p2410 A72-33819

Somigliani dislocations effect in infinite elastic cylinder, determining stresses in form of eigenfunctions expansions

17 p2626 A72-34654

Transparent and opaque crystal surface fracture mechanism analogies under laser beam action, determining dislocation structure

17 p2562 A72-34664

The application of a dislocation model to the strain and temperature dependence of the strain hardening exponent n in the Ludwik-Hollomon relation between stress and strain in mild steels

18 p2701 A72-36589

Nucleation and growth of deformation twins in Mo-35 at. % Re alloy

18 p2702 A72-36748

Physics of strengthening mechanisms in crystalline solids

19 p2843 A72-37444

Electron microscope double contrast images to identify Burgers vectors of close packed metal crystal dislocations

19 p2846 A72-38590

Configuration determination method for metal crystal superdislocation anchored at two points and under stress in sliding plane, calculating critical stress related to double source unlocking

20 p2978 A72-39005

Formation of voids and dislocation loops in near-stoichiometric NiAl by aging at 700 to 900 C, and some effects on alloy properties

20 p2937 A72-39288

The effect of elastic anisotropy on dislocations in Ni₃Fe

20 p2937 A72-39293

Thermal unpinning of dislocations - Hasiguti peaks of internal friction

20 p2962 A72-39993

Interactions between dislocations or flux lines moving through hardened crystal, discussing distribution functions method applications to diffuse and localized obstacles

20 p2962 A72-39994

Crystal structure and shear strength of solids and imperfections in metals in framework of X ray diffraction and dislocation theory

20 p2942 A72-39998

Influence of dislocations in subgrains on the substructural hardening of aluminum

21 p3068 A72-40961

Dislocation pile-ups in periodic internal stresses

22 p3214 A72-42316

Measurement of the stacking-fault energy of gold using the weak-beam technique of electron microscopy

22 p3177 A72-42320

Hydrogen cold work peak measurements in Nb, showing hydrogen atoms-dislocations binding energy extent and temperature effects on internal friction

22 p3189 A72-42440

Dependence of changes in the electronic dislocation-braking force during superconducting transition on the stresses, temperature, and strain rate

23 p3312 A72-43315

Continual theory of dislocations and the theory of small elastoplastic deformations

23 p3345 A72-43584

Dislocation-substructure-strengthening and mechanical-thermal treatment of metals

23 p3304 A72-44299

Field-ion microscopic study of the interstitial plasticity of tungsten single crystals

23 p3304 A72-44484

Electron-microscope study on the recrystallization in technically pure aluminum

24 p3412 A72-44719

CRYSTAL FILTERS

Transient response of solid state YIG crystal dispersion filter, noting application to main radar bang generation with intrapulse frequency modulation

03 p0337 A72-14379

Microwave spectrometer crystal current leveler for broadband video detector and rotary wave attenuator control

04 p0524 A72-15541

Eigenfrequencies of monolithic filters

19 p2774 A72-38608

CRYSTAL GROWTH

NT CZOCHRALSKI METHOD

NT EPITAXY

Thermal treatment for delayed and reduced crystal grain growth during sintering of oxides, metals and alloys

02 p0232 A72-11431

Oxygen content and stoichiometry effects on metal carbides grain growth in liquid phase sintering, discussing carbide-metal interface solution reaction as rate controlling mechanism

02 p0240 A72-11434

Rolling workability of pure W single crystals grown by electron beam zone melting technique, discussing crack occurrence

03 p0374 A72-13718

Boundary segregate concentration during grain growth annealing of ultrapure Al as function of migration rate and distance

03 p0379 A72-14259

Carbon impurity effects on molybdenum ingot formation, detailing crystal growth, size reduction and length

04 p0533 A72-14987

Temperature, pressure and crystallization time effects on artificial diamond crystal growth of various morphological shapes

05 p0681 A72-16355

High temperature GaAs bipolar transistor n-p-n junction fabrication by vapor phase growth technique, considering I-V characteristics dependence on procedure

06 p0783 A72-17607

BiTe crystal critical growth rate calculation based on theory for diffusional supercooling of melt with excess Te

08 p2127 A72-21338

Guinier-Preston zone nucleation and growth as function of vacancies in Al-Cu alloy

08 p1190 A72-22166

Subgrain growth during annealing of rolled samples of Mo-Ti-C alloy and of single crystal Mo purified by electron beam zone melting

09 p1329 A72-23034

Laser reflection studies of surface morphology of growing or evaporating crystals

09 p1326 A72-23409

Ordered growth and etching of uranium and zirconium oxide-tungsten fiber refractory composites, using X ray diffraction and scanning electron microscopy

11 p1668 A72-26943

Crystal growth, physical and spectroscopic properties and laser performance of Nd and Ho doped crystals with apatite structure

12 p1825 A72-27927

Cubic SiC film growth rate on Si substrate by methyltrichlorosilane decomposition in hydrogen flow, noting dependence on mixture flow rate and temperature

12 p1860 A72-28114

Na additions effects on Si growth velocity and morphology in Al-Si alloys, considering coupled zone adsorption mechanism

13 p1975 A72-28664

Austenite grain growth characteristics of heat treated Ni maraging steel

13 p1976 A72-28673

Martensitic transformation in Cu-Al-Ni alloy thin film, investigating gamma-prime phase substructure formation and crystal growth pattern

13 p1976 A72-28907

Refractory compounds single crystals preparation, emphasizing hot pressing under high pressures

13 p1982 A72-30113

Metastable coesite crystal growth in highly strained quartz under 5-20 kb pressures and 450-900 C

14 p2099 A72-30322

Semiconductor gamma ray detectors development, using cadmium dichlorides, dibromides, diiodides and difluorides as doping agents in CdTe crystal growth

14 p2142 A72-30549

Molybdenum carbide needle formation, growth in kinetics and morphology Fe-C-Mo alloy from lattice parameters measurements

14 p2120 A72-30618

Surface energy effect on alloy structure formation, analyzing crystal growth and formation from supersaturated solutions

15 p2253 A72-31221

Single crystal scheelite material for Nd doped intermediate gain laser host substance, considering optimum growth conditions, lasing parameter and Nd concentration

15 p2292 A72-32030

Influence of twinned growth crystals on the texture of nickel work hardened in tension

18 p2702 A72-36703

Vapor grown solid state single crystal oxide thin films characteristics and synthesis by thermal vaporization, chemical vapor deposition and sputtering

19 p2843 A72-37443

Alpha aluminum oxide whiskers growth in presence of lead by vapor/liquid/solid phase mechanism in moist hydrogen at 1200-1400 C

19 p2823 A72-38279

Investigation of the viscosity and density of solution melts intended for growing yttrium-iron garnet [YIG]/single crystals

19 p2847 A72-38684

Influence of irradiation by 1.2-MeV electrons on the electrophysical properties of p-Si single crystals grown in a hydrogen atmosphere

21 p3098 A72-41686

Physical metallurgy of single crystals of high-melting and rare metals and alloys

22 p3191 A72-42807

Recrystallization and grain growth in titanium. I - Characterization of the structure

22 p3193 A72-43032

Growth rate of refractory oxide particles in nickel cermets

23 p3299 A72-43290

Cast heterophase Mo and alloys fracture strength and plastic characteristics, investigating crystal growth texture, orientation and substructure 23 p3301 A72-43741

Alpha aluminum whiskers growth in mullite ceramic composition following vapor-liquid-solid phase 23 p3303 A72-44152

Electron-microscope study on the recrystallization in technically pure aluminum. 24 p3412 A72-44719

New space processing experiments for the Skylab missions. 24 p3407 A72-45125

Growth kinetics of dispersed thorium in Ni and Ni-Cr alloys. 24 p3415 A72-45480

CRYSTAL LATTICES

NT BODY CENTERED CUBIC LATTICES

NT CLOSE PACKED LATTICES

NT CUBIC LATTICES

NT FACE CENTERED CUBIC LATTICES

Cation distribution observation over nonequivalent lattice sites in shocked orthopyroxene, noting Mg and Fe order-disorder 01 p0053 A72-10293

Action kinetics and radiation spectra of multiruby lasers, determining effect of crystal C axes angular orientation relative to ruby pairs geometrical axes 01 p0079 A72-10374

Metal powders sintering activation mechanism, considering heterogeneous metals particles diffusion flow, mutual solubility and crystal lattices distortion 02 p0232 A72-11432

Rolled metals and alloys with various lattice types and packing defect energies, showing elastic properties isotropy and Young modulus anisotropy 03 p0371 A72-13188

Nonstoichiometric vacancy order in vanadium monoxide from electron microscopy and diffraction patterns, proposing partial phase diagram 03 p0401 A72-13584

Zr and V linear thermal expansion coefficients explanation by alpha Zr hexagonal crystal lattice anisotropy 03 p0376 A72-13946

Substructure variations and crystal lattice periods dependence on compression stress in beryllium single crystals during plastic deformation due to base slip 03 p0376 A72-14018

Periodic lattice one-electron Green function calculation based on pseudopotential matrix element, applying to impurity levels in semiconductors 03 p0404 A72-14268

Proton and fluorine nuclear magnetic spin-lattice relaxations due to internal rotations in magnesium fluorosilicate hexahydrate 04 p0564 A72-15636

Face-centered orthorhombic martensite in Ti-V alloy, determining axial ratios and lattice parameters by transmission electron microscopy and X ray diffraction 05 p0676 A72-17102

Etch pit technique for titanium and zirconium crystal orientation determination, discussing etch pit locations and polycrystalline specimen goniomicroscopic observation 05 p0679 A72-17124

Thermodynamic estimation of transition metal stacking fault energy, discussing relation to lattice stability and structural changes 05 p0679 A72-17149

Microvolume decohesion hypothesis for crystal lattice defects explaining metal fatigue under variable stresses 06 p0829 A72-17743

Molybdenum disulfide and layer lattice materials lubricating mechanism and effectiveness from sulfur atoms strong polarization, using scanning electron microscope 06 p0822 A72-18157

Hardening mechanisms of interaction between superlattice dislocations and point defects in Ni-Al intermetallic compound mechanical properties strain rate and temperature dependence 06 p0832 A72-18420

Maraging steel embrittlement by titanium carbonylides lattices separation during cooling, suggesting rapid quenching and plastic deformation temperature reduction 07 p1012 A72-19677

Alloying additives effects on Ti and Zr resistivity, thermal expansion, crystal lattice parameters and polymorphous transformations temperatures 07 p1017 A72-19990

Impurities and crystal lattice role in metal brittleness, discussing stress concentration and relaxation, crack initiation and plastic deformation 07 p1018 A72-20145

Ultracure metals microimpurities determination from crystal lattice and atomic properties, comparing spectral analysis activation, mass spectrometric, thermophysical, recrystallization and kinetic methods 07 p1049 A72-20149

Quantum mechanical electron motion problem in binary alloy crystal lattice, discussing Bloch approximation, energy spectra, and third element admixture conductivity effects 07 p1049 A72-20150

Temperature dependence of strain rate sensitivity in low temperature deformation processes, considering inherent lattice conditions and impurity atoms effects 07 p1022 A72-20573

Mossbauer gamma radiation diffraction by Y-Fe garnet crystals with Mossbauer nuclei in magnetic and electric field nodes 08 p1217 A72-21767

Ti-Co intermediate phase transformations discussing lattice formation, intermetallics melting points and stoichiometric composition 08 p1187 A72-21783

Primary and secondary radiation damage to metals and alloys crystal lattices 08 p1187 A72-21786

German monograph on lattice and solid metal surface transport processes, discussing atom migration, activation energies, impurity atom diffusion, Kossel-Stranski model, etc 08 p1212 A72-22173

Maximum superconducting transition temperature estimation, discussing optimum resonant frequency for attractive interaction, umklapp electron scattering and lattice instabilities 09 p1367 A72-22553

Mossbauer lines diffusion broadening and weakening in crystals impurity atoms nuclear spectra 09 p1371 A72-23030

Va crystal lattice interatomic bonds and elastic and inelastic X ray scattering intensity calculation 09 p1329 A72-23042

Computation procedure for crystal lattice electrostatic strain energy derivatives 09 p1372 A72-23228

Oxide spinels crystallographic structure determination, stability relationships, covalent bondings and physical properties 10 p1501 A72-24730

Glass network physical properties model, using physical chemistry description of crystal structure without regularly repeating lattice 10 p1502 A72-24735

Ion crystal plasma wave echoes from conduction electrons interaction with phonons in self consistent field 10 p1527 A72-24926

Atomic radius ratios and lattice constants in intermetallic compounds Laves phases, presenting semistatistically calculated values for niobium diferride based on rigid sphere model 10 p1527 A72-24978

Lattice source interference method for detection of X ray diffraction in Al-Zn solid solutions, taking into account precipitation effects 10 p1499 A72-24981

Abrikosov vortex lattice in superconductors, calculating resonance linewidth and vacancy formation energy 11 p1699 A72-25718

Propulsion system based on ion tunneling through preferentially oriented metal crystal lattice [AIAA PAPER 72-480] 11 p1710 A72-26208

Impurity atoms effects on grain boundary motion velocity, considering interactions with metal lattice vacancies 11 p1662 A72-26655

Scandium substitution for lanthanum in lanthanum hexaboride crystal lattice, investigating effect on thermionic characteristics 12 p1854 A72-27309

Mica polymorph distribution among space groups from unit layer and stacking sequence characteristics 12 p1802 A72-27512

Angular annihilation photon distribution curves from positron-electron annihilation method for metallic phase interaction with crystal lattice in synthetic diamonds 12 p1833 A72-27764

Lattice disorder effects in ion implanted Si and compound semiconductors, using IR and EPR measurements 12 p1859 A72-28074

Phase composition and lattice constants of carbide films from vaporized Zr interaction on graphite surface at 1700 C 13 p1912 A72-28566

Al-Zn alloy supersaturated solid solution decomposition during aging, studying single crystal lattice characteristics via X ray diffusive scattering techniques 13 p1976 A72-28902

Electron microscopic and X ray analyses of ordering kinetics in Ni-Mo alloys, noting lattice type change and complex domain structure formation causes 14 p2115 A72-30409

Crystal lattice and dislocation anharmonicity interdependence and stress-strain correlation in presence of interaction between ultrasonic waves of different frequencies 14 p2169 A72-30959

Ti-Si system phase diagram and equilibrium states, noting crystal lattices and thermograms 14 p2123 A72-30986

Alloying effects on high temperature softening due to crystal lattice, stacking fault energy and decreased mobility interactions 15 p2254 A72-31564

Theoretical model for HF mechanical waves interaction with crystal lattices based on measurements of high amplitude ultrasonic waves attenuation in metal crystals 15 p2292 A72-31835

High amplitude ultrasonic stress waves effect on metals elastic and plastic deformation characteristics, verifying model for sound waves-lattice structure interactions 15 p2328 A72-31842

Electron microscopic investigation of slip processes during plastic deformation of WC-Co based cermets, observing WC grain boundary sliding and Co phase crystal lattice transformations 15 p2257 A72-32117

Coherent potential approximation generalization for disordered alloy systems, showing different results for propagator and locator formalisms in multiple site approximation [ONERA, TP NO. 1126] 15 p2293 A72-32229

Ti-Mo binary solid solution, investigating superconducting transition temperature, lattice instability and electron-to-atom ratio by calorimetric measurements 15 p2295 A72-32544

Lattice dynamical model for Cs vibration frequency distribution, specific heat and electrical and thermal resistivity calculations 16 p2441 A72-33584

Normal, highly conducting and ion-exchanging solid electrolytes structure and conductivity, with particular attention to rechargeable silver halid batteries 16 p2352 A72-33899

Theory of elastic wave propagation in composite materials. 18 p2703 A72-36395

A dynamical theory for the contrast of perfect and imperfect crystals in the scanning electron microscope using backscattered electrons. 18 p2692 A72-36749

On strain energy and constitutive relations for alkali metals. 18 p2703 A72-37087

Monte Carlo studies of the relaxation of vector end-to-end length in random-coil polymer chains. 20 p2898 A72-39599

Calculation of electronic Green functions using nonorthogonal basis functions - Application to crystals. 20 p2961 A72-39810

Mechanical twins formation process, distinguishing between deformation and strain and between crystal structure and lattice 20 p2961 A72-39991

Single and double shear invariant plane crystallographic theories for martensitic transformations, calculating lattice deformations by combined Bain and complementary shear strains 21 p3065 A72-40089

Vitrification in ternary diamond-like semiconductors 21 p3096 A72-40380

Electrodynamical analysis of superconducting vortices interaction with cylindrical cavities [pinning], calculating critical currents in type II superconductors in external magnetic field 21 p3096 A72-40416

Void lattice model for Mo physical properties and equilibrium lattice spacing determination, calculating defect Green function 21 p3066 A72-40623

Two-dimensional lattice orientation and three-dimensional crystallinity in carbon fibres. 21 p3073 A72-40687

Phenomenological models of the electron-phonon interaction and the superconductivity criterion of metals 21 p3098 A72-41688

Recombination and annihilation rates of interstitial atoms and vacancies in crystal lattices, taking account of diffusion 21 p3088 A72-41690

Electroconductivity anisotropy effect on transverse Dember effect angular dependence and spectral distribution in p-type CdSb lattice 21 p3098 A72-41693

Electron spin resonance of divalent Mn ion doped in thallous azide single crystals, investigating temperature effects on spin Hamiltonian parameters 22 p3192 A72-42716

Magnetic properties and texture of a thin strip of nickel-iron-molybdenum alloys 22 p3192 A72-43012

X-ray structural examination of phase transformations in the VT14 titanium alloy during heating 22 p3192 A72-43015

Recombinational luminescence of NaI-Tl single crystals excited in the A-band of activation absorption 23 p3323 A72-43342

Quantum impulse autocorrelation function of one dimensional harmonic crystal lattice, noting periodic time dependence at high and low temperatures

23 p3312 A72-43405

Phase diagrams from X ray analysis of rapidly crystallized Ni-Sn alloys, noting crystal lattices and phase transformation

23 p3300 A72-43648

Physicomechanical properties of titanium-tungsten solid alloys with deficiency of carbon in the carbide solid solution lattice

24 p3415 A72-45385

CRYSTAL OPTICS

Ruby and Nd lasers fundamental emission effects on excitation of stimulated Raman scattering in liquid and crystalline media by second harmonics

03 p0366 A72-13364

Laser pumping pulse shape effects on second harmonic emission waveform during nonlinear crystal excitation by ultrashort light pulse

03 p0366 A72-13368

Elastic wave velocities and polarization in planes of cubic crystals, plotting velocity curves

03 p0402 A72-13861

Optical birefringent networks synthesis, describing use of building blocks of polarizers, birefringent crystals and optical compensators

04 p0548 A72-14737

Spatial dispersion effects in crystal optics, obtaining dispersion law for normal waves in crystals via electromagnetic field tensor equations

04 p0548 A72-14739

Scintillator crystal system with monitoring streak camera for flash X ray burst time measurements

04 p0523 A72-15482

Integrated miniature guided wave optical transmission systems using crystals adapted to thin film nonlinear interaction and photolithographic technique

07 p1004 A72-19228

Vertically oriented double crystal attachment to vacuum X ray spectrograph for enhanced resolution of ionic solids and solutions molecular spectra

07 p0983 A72-19317

Multiplication and mixing of electromagnetic waves in optically nonlinear anisotropic crystal media

07 p1007 A72-20119

Pulse duration reduction with power gain during second harmonic generation by nonlinear crystal in Q switched buildup resonator

08 p1183 A72-21729

Thermal self disturbance effect on second harmonic generation in crystals and CW and pulsed lasers

08 p1184 A72-22034

Quartz crystals ultrasonic vibrations produced by laser beam, noting light modulation depth dependence on effective cross section and amplitude

09 p1322 A72-22415

Laser damage resistance properties of thin film multilayer antireflection coatings for quartz optics

09 p1326 A72-23348

Quantum yield of ruby crystals luminescence for excitation in UV region, noting Cr concentration effect

10 p1490 A72-24043

Electro-optical Fabry-Perot modulator with KDP and ADP crystals as optical resonators, determining modulation and frequency response characteristics

10 p1492 A72-24583

Light absorption by molecular crystals with dual zone of exciton states

12 p1847 A72-27226

Discrete ten stage system for laser beam deflection based on electro-optical effect in lithium niobate crystals

12 p1808 A72-27595

Absorption spectrum of Cr cations in magnesium aluminate spinel crystals excited by strong optical pumping

12 p1854 A72-27596

Longitudinal electro-optical effect in oblique cut lithium niobate crystal with minimum half wave voltage between incident beam and optical axis angle

12 p1855 A72-27603

Image conversion from 10.6 to 0.65 micron wavelength by nonlinear optical method in proustite crystal

12 p1821 A72-27604

Crystal characteristics of optical detectors for direct measurement of high power laser radiation

12 p1824 A72-27874

Crystal growth, physical and spectroscopic properties and laser performance of Nd and Ho doped crystals with apatite structure

12 p1825 A72-27927

He-Ne laser light modulation with lithium niobate crystals, noting lower light power and modulator volume requirements, better mechanical properties and lower thermal sensitivity

13 p1969 A72-29632

Ruby laser emission second harmonic generation effectiveness in organic polycrystals from comparison to lithium niobate

13 p1970 A72-29689

Harmonic elastic wave propagation in composites with periodic structures by variational methods developed from crystal lattice studies

13 p2060 A72-29696

Phononless lines shift and broadening and electron phonon interaction in lanthanum trifluoride-Nd crystal, obtaining temperature dependence of non-radiative transition probability

14 p2142 A72-30359

Free electron waves interaction with coherent laser light in crystalline medium, discussing quantum mechanical treatment and path integral approach

14 p2110 A72-30725

German monograph on optical transmission measurement interferometer with plane-parallel birefringent crystal plates covering plate combination selection based on interference pattern mathematics

15 p2233 A72-31525

Light signal modulation by traveling wave in circular waveguide with coaxial KDP crystal

15 p2207 A72-31881

Photochromic crystal materials erase mode recording characteristics measurement, using Ar laser for optical recording and readout

15 p2240 A72-32361

Liquid crystals synthesis, physical chemistry and material parameters effects on mesomorphic and electro-optical behavior

15 p2240 A72-32363

Crystal characteristics of optical detectors for direct measurement of high power laser radiation

16 p2403 A72-33983

Optical second harmonic generation and parametric oscillation.

17 p2594 A72-34566

Image pickup and display devices.

17 p2552 A72-34568

A graphite crystal polarimeter for stellar X-ray astronomy.

17 p2553 A72-34637

Attachment for studying optical properties of highly cooled crystals in the vacuum ultraviolet region

17 p2555 A72-35309

Low temperature interference filter design for atmospheric windows far IR photometers based on selective reststrahlen reflection of crystals

19 p2796 A72-37586

Use of generalized theory of optical diffraction for the study of second harmonic generation.

19 p2811 A72-37673

Optical communications in Japan.

19 p2766 A72-38602

Bandwidth and threshold calculations for angle-tuned parametric oscillators.

19 p2813 A72-38689

Electro-optic KTN /potassium tantalate niobate/ crystals for modulators, deflectors, phase shifters and polarization rotator devices

20 p2922 A72-39047

On diffraction and focusing in anisotropic crystals.

20 p2961 A72-39779

Recrystallized Al monocrystals applications to optics and X ray spectroscopy, describing preparation methods

21 p3065 A72-40085

Interferometric method for measuring electro-optic coefficients in crystals.

21 p3095 A72-40138

Boundary conditions in the exciton absorption region.

21 p3096 A72-40139

Anisotropy of Raman scattering by optical phonons in cubic zinc blende crystals, describing experimental arrangements

21 p3061 A72-40141

Raman scattering techniques applied to problems in solid state physics.

21 p3096 A72-40602

Discontinuities propagation in quasi-linear hyperbolic partial differential equation systems, noting MHD flow and crystal optics equations

22 p3204 A72-41905

Stress induced birefringence in an isolated and a shortcircuited KH2PO4 crystal.

23 p3324 A72-44322

Heterodyne, microwave bias and pyroelectric photon infrared detectors, noting mixed crystal photoconductive and photovoltaic detectors

23 p3291 A72-44392

Influence of a linear inhomogeneity of the refractive index of nonlinear crystals on second-harmonic generation.

24 p3411 A72-45604

Use of oblique-cut lithium niobate in optical-beam control systems.

24 p3411 A72-45606

Profile of a parametric luminescence line emitted by lithium niobate crystals.

24 p3432 A72-45614

Temperature and angular widths of the phase-matching curve of a lithium niobate crystal.

24 p3432 A72-45615

Periodic control of the emission from a ruby laser achieved by a Q switch utilizing the transverse electro-optical effect.

24 p3412 A72-45618

Quartz oscillator short term frequency instability lower limit estimation by calculating Q values and non-linearity and resonator parameter fluctuation effects

07 p0953 A72-19009

Phase locking loop synchronized quartz oscillator for integral frequency multiplication in wideband carrier frequency systems

07 p0954 A72-19174

Relaxation oscillator synchronized by quartz crystal between emitter and base of unijunction transistor, obtaining sinusoidal output by series-connected RC load

13 p1926 A72-28377

ADP or KDP crystal induced second harmonic emission from Ar laser resonator, noting crystal temperature effects on primary/secondary radiation phase synchronism

16 p2400 A72-33281

Fluctuations in a quantum frequency standard

23 p3271 A72-43842

Molecular crystals stationary Raman oscillators quantum model, deriving coupled nonlinear equations for excited modes polariton operators

24 p3409 A72-44912

CRYSTAL STRUCTURE

NT WIDMANSTATTEN STRUCTURE

Lunar basalts 10044 and 12021 Fe oxidation state in plagioclase and distribution in crystal structure, using Mossbauer spectroscopy

01 p0124 A72-10064

Polycrystalline Mo work function calculation from electron emission microscopy, determining crystallographic grain orientation effects

01 p0071 A72-11027

Morphology of poly-p-xylylene crystallized during polymerization from X ray measurements, electron and optical microscopy and differential thermal analysis

02 p0247 A72-11465

Crystal structure of alpha poly-p-xylylene films from electron microscopy and diffraction and X ray scattering

02 p0248 A72-11466

Twinning in alloys cubic superlattices, discussing crystal structure criteria

02 p0247 A72-12815

Tungsten carbide dislocation structures analysis by transmission electron microscopy, deriving Burger vectors from energy considerations and electron micrographs contrast

03 p0370 A72-12995

Allowed states of electronic complexes and impurity molecules in crystals determination in molecular orbital scheme of molecular electronic calculations

03 p0392 A72-13864

Grain orientation effect on fatigue crack propagation in notched test specimens cut from cold rolled prestressed annealed brass plate

03 p0375 A72-13934

Phase composition and structure of Be alloys containing Ru, Os, Rh or Ir, noting isomorphous beryllides existence

03 p0375 A72-13942

Vanadium carbide diffraction spectrum reflection intensity under Mo and CuK-alpha irradiation, showing crystalline structure and interatomic ionic interaction

04 p0533 A72-14618

Carbon impurity effects on molybdenum ingot formation, detailing crystal growth, size reduction and length

04 p0533 A72-14987

Uniaxial stress effect on monocrystalline niobium stannide superconducting transition temperature, considering crystal structure

04 p0562 A72-15293

Thermodynamic solids theory generalized for internal strains in perfect non-Bravais crystals, applying to trigonal Se and Te structure

04 p0562 A72-15470

Mono- and polycrystalline Ni high temperature creep kinetics, investigating substructural changes

05 p0671 A72-16000

Holocene Bahamian oolites examination by scanning electron and light microscopy, observing aragonite crystals morphology, orientation and modification by boring activities of endolithic algae

05 p0654 A72-16037

Ni-NiNb intermetallic unidirectional eutectic alloy crystal structure and high temperature behavior, considering mechanical twinning relationship to strain hardening and ductility

05 p0677 A72-17108

Crystal structures and martensitic transformation mechanism of TiNi, using X ray diffraction and electrical resistivity measurements

06 p0827 A72-17421

Earth gravitational potential, including surface density, crystal thickness, potential coefficients, contour maps and spherical harmonic expansion

06 p0877 A72-17657

Spectroluminescent and lasing properties of Nd ions in anisotropic scheelite crystal structures

07 p1007 A72-20121

Nb and Nb alloys mechanical properties during plastic deformation and heat treatment, discussing grain size, dislocation structure and substructural changes effects
07 p1018 A72-20144

Precipitation hardening of quenched superconducting Nb-Al alloys, examining polycrystalline and single crystal samples and intermetallic phases
07 p1050 A72-20155

Al and Al-Si alloy thermal expansion at low temperatures, noting near-eutectic crystalline composition
07 p1019 A72-20156

Latent image formation in radiographic emulsion of AgBr crystals dispersed in gelatin layer, considering crystal structure and X and gamma rays energy recording
07 p0991 A72-20242

Facility for electron microscopy of specimens in controlled environments, observing lattice structure in wet catalase crystals
07 p0993 A72-20586

Plasticity conditions of monocrystals of higher symmetry tetragonal system, using energy density and deformation relations
08 p1242 A72-20938

Nd-Dy alloy magnetic and structural properties over entire composition range
08 p1217 A72-21596

Helium cryostat for X ray studies of phase transformations and structural changes in single metal crystals
08 p1169 A72-21792

Electron wave attenuation technique for current transit determination through semiconducting films with various crystal structures
09 p1284 A72-22209

A-15 superconducting films preparation computer-aided method, noting alloying effects and crystal structure stability determinations applications
09 p1368 A72-22559

Oxidation and substructural effects on low stress creep of Al near melting point
09 p1331 A72-23507

Electron bombardment disordering of ordered Ni-Mn alloy along different crystallographic directions
10 p1514 A72-24075

Nonstoichiometry of beta and beta-two aluminas in epitaxial coexistence from crystallographic investigation
10 p1433 A72-24082

Crystal structure of iron-zirconium disulfide and cobalt-zirconium disulfide systems
10 p1496 A72-24089

Transverse negative differential conductivity in semiconductors, discussing effect of locations and shapes of energy surfaces in k-space and favorable crystal orientations
11 p1701 A72-25856

Russian book on powdered metals toxicity covering industrial dust, physiological effects, safety standards, electron configurations and crystalline structure
11 p1584 A72-26067

Carbon-graphite fracture mechanics dependence on graphite crystallite structure, discussing crystal size effects on strength
11 p1674 A72-26812

Crystal-morphology role in refraction of cold drawn polyethylene samples of varying lamellar thickness and density, relating elastic restoring force to crystal deformation
12 p1832 A72-27283

High purity Al single crystal orientation explained by Rowland transformation model, observing recrystallization grains
12 p1855 A72-27300

Correction to nonlinear refractivity calculation for cubic lattice crystal with allowance for higher induced multiples
12 p1855 A72-27300

Ni single crystal growth by Czochralski method, investigating growth rate, direction and initial structures effects on substructure
13 p1976 A72-28906

Martensitic transformation in Cu-Al-Ni alloy thin film, investigating gamma-prime phase substructure formation and crystal growth pattern
13 p1976 A72-28907

Al crystal block structure and size changes during creep evaluated by small-angle X ray scattering technique
13 p1977 A72-28909

Pyrochlore and perovskite preparation and structure in bismuth rhodium oxide system, discussing variable position parameter, occupancy factor and structure stability
13 p2022 A72-29375

Tin lead telluride rock salt structure solid solutions phase stability at 356-500 C, using room temperature lattice parameter measurements
13 p1913 A72-29750

X ray diffraction discovery of borides with yttrium chromium boride type orthorhombic structure
13 p1984 A72-29799

Normal modulus of elasticity of filamentary silicon nitride crystals with three orientations, calculating elastic plibilities
13 p1984 A72-30117

Gamma-prime phase crystal structure in Cu-Al-Ni alloy from electron microscopic study, noting twinning and substructure during formation
14 p1115 A72-30406

Electron microscopic and X ray analyses of ordering kinetics in Ni-Mo alloys, noting lattice type change and complex domain structure formation causes
14 p1115 A72-30409

Iron carbide single crystal growth texture due to anisotropy of interatomic interactions associated with oriented covalent Fe-C bonds
14 p1212 A72-30774

Heat treated light alloy bar deformation, temperature and time factor effects macrostructure and mechanical properties
14 p1214 A72-31038

Combined heat treatment and machining effects on Mg-Nd alloys structure and mechanical properties, noting strain hardening mechanism
14 p1215 A72-31042

Russian paper on intermetallic compounds covering structure, properties and applications of carbides, nitrides, oxides, phosphides, aluminides, antimonides, arsenides and chalcogenides
15 p2252 A72-31192

Interstitial phases, crystal structure and chemical bonds of titanium, vanadium and niobium carbides, comparing with transition metal carbides
15 p2252 A72-31195

Stoichiometric composition, crystal structure and chemical bond variations in Ta-O system
15 p2290 A72-31197

Liquid crystal structure, physical properties, discussing electronics applications and technical development trends
15 p2291 A72-31594

Fcc metal defect structure due to ultrasonic fatigue observation via transmission electron microscopy for dislocations
15 p2256 A72-31836

Superlattice structure and electron correlation of Co-Si system, using X ray and metallographic analyses
15 p2257 A72-32115

Crystallographic structure, phase transformations, Curie temperature and Faraday rotation of Ti-substituted MnBi films
15 p2294 A72-32522

Solid state physics - An overview.
17 p2594 A72-34561

Effects of disorientation of grains on the viscoplastic behavior of fcc polycrystals
17 p2634 A72-35407

Carbon fiber structure at graphitization temperatures to 3100 C in terms of surface energy and internal stress accounting for low shear strength
17 p2572 A72-35660

Work function dependence on crystal orientation for W with special emphasis to the variation near the /110/ orientation.
18 p2656 A72-36130

Work function change of tungsten /110/ planes as function of Mo coverage.
18 p2656 A72-36134

Crystal orientation effect on electron work function in chemical vapor deposited W layers on thermionic converter cylindrical emitters
18 p2717 A72-36142

Two-phase crystal structure microdeformation measurement by combined holographic interferometry and X ray diffraction
18 p2690 A72-36358

An atomistic study of cracks in diamond-structure crystals.
18 p2718 A72-36509

The structure of the metastable precipitates formed during ageing of an Al-Mg-Si alloy.
18 p2702 A72-36743

Changes of electrical and structural properties of Au thin films obtained by sputtering during the annealing process.
18 p2720 A72-36955

Directional dependence of the high-temperature thermal diffusivity of crystal-oriented pyrolytic graphite
18 p2704 A72-37180

Solution of the inverse heat conduction problem by using the regularization method to increase the peaks of the self-contraction function /Paterson's function/
19 p2880 A72-37753

Evidence of crystal structure in some sputtered MoS2 films.
19 p2823 A72-37897

Book - Amorphous semiconductors.
20 p2958 A72-38924

Electrical conductivity of pressed cadmium antimonide
20 p2959 A72-39218

X ray diffraction study of crystal structure of metastable phase in rapidly solidified Al-Zr alloys
20 p2939 A72-39307

Unidirectionally oriented pseudobinary eutectic solidification in ternary systems, investigating crystallographic and mechanical characteristics of ZrCuSi fibers embedded in Cu matrix
20 p2940 A72-39441

Elasticity of some mantle crystal structures. I - Pleonaste and hercynite spinel.
20 p2917 A72-39478

Phase transformations and exsolution in lunar and terrestrial calcic plagioclases.
20 p2970 A72-39480

Chemical and structural classification of Apollo 11 lunar rocks, showing lunar surface material temperature history and meteoritic component presence
20 p2900 A72-39842

Dynamic recrystallization occurrence during deformation at elevated temperatures, examining subgrain structure role in austenitic stainless steels
20 p2942 A72-39990

Mechanical twins formation process, distinguishing between deformation and strain and between crystal structure and lattice
20 p2961 A72-39991

Domain structures in metal crystals, investigating ordering in Ni-Mo alloys
20 p2962 A72-39997

Crystal structure and shear strength of solids and imperfections in metals in framework of X ray diffraction and dislocation theory
20 p2942 A72-39998

Habit plane interpretations of surface martensite transformation and orientation measurements compared with invariant plane strain /IPS/ theory
21 p3065 A72-40088

Phenocryst fabric in lunar basalt sample 12052 from the Ocean of Storms.
21 p3106 A72-41115

Crystallization and structure of hypereutectic iron-carbon-chromium alloys
21 p3071 A72-41788

Martian light sources generated by suspended crystals producing parhelic halo in atmosphere, noting randomly oriented and gravitationally arranged suspensions
22 p3223 A72-42142

Structons /close-neighbor arrangements/ stability and characteristics in anhydrous borate crystals and glasses containing bridging and nonbridging or tribonded oxygens
22 p3197 A72-42795

Crystal structures and transition temperatures of polymorphous metals, discussing mechanical properties, thermal conditions for deformation and metal working by pressure
22 p3190 A72-42803

Cast heterophase Mo and alloys fracture strength and plastic characteristics, investigating crystal growth texture, orientation and substructure
23 p3301 A72-43741

Dislocation-substructure-strengthening and mechanical-thermal treatment of metals.
23 p3304 A72-44299

A study of the effect of grain orientation misfit on the viscoplastic behavior of polycrystalline metals /fcc system/
24 p3414 A72-45251

Linear and nonlinear dielectric properties of crystals with tetrahedral structure
24 p3412 A72-45772

CRYSTAL SURFACES

Hydrogen condensation on tungsten as function of temperature, coverage and population of binding states, noting initial sticking coefficients variations
01 p0089 A72-11113

Reflection electron diffraction and ellipsometric studies of oxidation of niobium crystal surface, showing oxygen absorption in lattice and oxide film formation stages
07 p1017 A72-19944

Dynamics of flare formation by pulsed laser beam at surface of alkali halide crystals
07 p1007 A72-20124

Biaxial tension and combined tension-torsion induced initial yield surfaces and plastic deformation onset, using localized strain theory
08 p1195 A72-21852

German monograph on model concept for erosion mechanism involved in crystalline material surface bombardment covering particle elastic deformation during impact
09 p1397 A72-22324

Electron reflection mechanism and gas adsorption effect at W /001/ surface in energy range 1-10 eV
09 p1370 A72-22804

Methane, hydrogen and oxygen adsorption and displacement on crystal surface of W investigated by thermal desorption and work function changes
09 p1276 A72-22807

Laser reflection studies of surface morphology of growing or evaporating crystals
09 p1326 A72-23409

Dielectric and semiconductor crystals surface defects, considering electric polarization structures
10 p1525 A72-23761

- Oxygen chemisorption surface states effects on electrical conductivity of CdS single crystals and evaporated films 11 p1701 A72-25855
- Re single crystal LEED diffraction pattern, showing surface carbon structure 13 p2021 A72-28800
- Temperature dependent optical constants of Ti and W crystal surfaces cleaned by ion bombardment in ultrahigh vacuum 15 p2274 A72-31376
- Ferroelectric nature of superficial layer on barium titanate crystals from scanning electron microscope and optical observations 15 p2291 A72-31681
- Kinematic intensity recovery from LEED data of specular and nonspecular beams from Ni(111) surface, noting multiple scattering interference elimination 15 p2276 A72-31855
- Surface phonon appearance criteria associated with crystal surface gas adsorption, discussing entropy variation and colliding particle-crystal energy exchange 15 p2280 A72-31858
- Surface treatment effects on light and X ray irradiated surface photoconductivity of InSb semiconductor single crystals at liquid nitrogen temperature 15 p2292 A72-31866
- Elastic dilatational field association with twist disclination loop interaction with free surface of two phase system interface 15 p2331 A72-32504
- Grain orientation and nonmetallic inclusion distribution and identification by color etching of single crystal and polycrystalline Mo 16 p2407 A72-33532
- Deformed Cu-Au single crystal surface slip bands fine structure, determining separation distance between individual slip lines 16 p2408 A72-33774
- Fluorescence of anthracene single crystals whose surface is disturbed by an impurity 19 p2847 A72-38781
- Quenching of fluorescence and the photoeffect in anthracene crystals 19 p2847 A72-38782
- A LEED investigation of the chemisorption of nitrous oxide on a tungsten (100) surface 20 p2898 A72-39188
- Investigation of tantalum-compound films at the surface of acicular tungsten microcrystals 21 p3068 A72-40964
- Deformation mechanism of aluminum and zinc single crystals during low-temperature cavitation 22 p3192 A72-43019
- ### CRYSTALLINITY
- Weld solidification synthesis with crystalline organic materials, investigating substructure size, growth rate and thermal gradients 13 p1966 A72-29424
- Impurity concentration relationship to electrons and holes density and potential fluctuations in completely compensated crystalline semiconductors with randomly distributed donors and acceptors 13 p2024 A72-29993
- Crystalline polymers behavior as multiphase composite solid, calculating supermolecular structures effects on stiffness properties 14 p2163 A72-30181
- Nonlinear viscoelastic behavior of isotropic unoriented crystalline polyethylene terephthalate at 70-100 C, using creep, recovery and load tests 16 p2416 A72-33614
- Two-dimensional lattice orientation and three-dimensional crystallinity in carbon fibres 21 p3073 A72-40687
- Crystalline solids surfaces with catalysis, electronics and corrosive reactions, discussing slow electron diffraction, ionic field microscopy and Auger spectroscopy techniques for surface cleanliness measurement 23 p3324 A72-44461
- ### CRYSTALLITES
- Carbon-graphite fracture mechanics dependence on graphite crystallite structure, discussing crystal size effects on strength 11 p1674 A72-26812
- ### CRYSTALLIZATION
- #### NT RECRYSTALLIZATION
- Physicomechanical properties of metals at crystallization temperatures, considering density, viscosity, strength, hardness, elasticity and creep 03 p0378 A72-14219
- Temperature, pressure and crystallization time effects on artificial diamond crystal growth of various morphological shapes 05 p0681 A72-16355
- Fractional crystallization and crustal contamination roles in origin of quaternary basaltic magmas from Black Rock Desert Region in Utah 06 p0810 A72-18515
- Binary alloys concentration distribution determination in migrating liquid-solid plane phase interfaces range during crystallization 07 p1022 A72-20571
- Binary Al alloys with variable melting volume and liquid zone velocities, investigating crystallization during zone melting 07 p1022 A72-20572
- Free convection effect on plane crystallization front instability under conditions of phase transition, using method of small perturbations 08 p1151 A72-21661
- Noncrystalline Ge film preparation by rf sputtering onto substrate with explosive crystallization triggered by localized transient energy pulse at room temperature 09 p1369 A72-22625
- Electrical conductivity and thermal emf as function of temperature in CdSb, discussing energy spectrum and crystallization 09 p1372 A72-23479
- Differentiated igneous textures of Apollo 11 lunar ferrobalt samples, indicating fractional crystallization followed by crystal-liquid separation 10 p1537 A72-24157
- Crystallization sequence, petrology and mineralogy of Apollo 12 basalt sample 12009 10 p1537 A72-24160
- Refractory glass-ceramics forming systems characteristics and production, discussing crystallization factors 10 p1501 A72-24728
- Solid solutions of stabilized Zr in cubic form prepared from zirconium and yttrium oxide mixture by ammonia precipitation and heat treatment 11 p1660 A72-26486
- Crystallization experiments on Apollo 11 magmas of K and Rb-rich basalt, discussing plagioclase characteristics 11 p1723 A72-26523
- Ordered crystallization casting of Ni superalloys for turbine blades, using power down and high rate solidification processes 11 p1646 A72-26894
- Semiconductor layers alloying by directional crystallization of compressed melts doped by contact with Ag, Ge, Te, Al and Sb films 13 p2020 A72-28564
- Crystallization discontinuity and layer thickness in welded joints as function of overcooling and isotherm shape 13 p1963 A72-28922
- X ray and metallographic analyses of Ni-Mo, Ni-Ta, Ni-Nb, Ni-Zr and Ni-Ti alloys crystallized at high cooling rates, observing metastable phases 14 p2115 A72-30405
- Cr-N alloy phase diagram from thermal and X ray analysis, metallographic observation and hardness tests, noting melts crystallization 14 p2123 A72-30987
- Russian papers on light and nonferrous alloys structure and properties covering phase diagrams, alloying effects, reduction, crystallization and recrystallization, solid solutions decomposition, etc 14 p2123 A72-31027
- Primary crystallization of intermetallic compounds in Al alloy as function of high melting metal concentration and casting temperature 14 p2124 A72-31034
- Diffusion layer formation on metallic surfaces, discussing saturation, crystallization, phase structure, chemical reactions, thermal and contact conditions 15 p2255 A72-31571
- Crystal lattice disarrangement by melting In-Tl alloy, noting fcc and bcc metastable phases formation during rapid crystallization 16 p2441 A72-33536
- Apollo 14 Rb-Sr isotope rock sample data, relating isochron age to igneous crystallization time 17 p2607 A72-35073
- As-Te-Ge amorphous semiconductor film optical memory effect due to crystallization and reversion during exposure to pulsed laser beam, noting writing and erasing characteristics 20 p2961 A72-39708
- Experimental evidence against the role of selective volatilization on the lunar surface 21 p3013 A72-40452
- Detection of crystals in CO₂ jet plumes 21 p3046 A72-41306
- Phase compositions, impurity effects, crystallization and production of plastic W and Mo alloys and heat resistant W-based alloys 22 p3192 A72-42815
- Effect of the process of crystallization of the liquid phase under pressure on the properties of Silumin 22 p3192 A72-42959
- Contribution to the study of phenomena of ordering of defects in single crystals of alumina- or zirconia-base refractory materials 23 p3302 A72-44000
- Metastable growth patterns in some terrestrial and lunar rocks 23 p3339 A72-44133
- ### CRYSTALLOGRAPHY
- Tensor description of laser beam second harmonic generation in dc magnetic field, using group theory derivation of nonzero element relations for all crystallographical classes 03 p0365 A72-12963
- Selected microarea electron diffraction technique in high voltage electron microscopy, discussing applications in crystallography and metallurgy 04 p0523 A72-15490
- Tantalum and tungsten vanadium trioxide oxides crystallographic order ratio from diffraction spectrum intensities and overstructure lines disappearance 05 p0675 A72-16699
- Ti-Zr-O ternary alloys radiocrystallographic analysis, relating microstructure to composition and thermal treatment 06 p0827 A72-17569
- Ni corrosion by hydrogen sulfide, determining nickel sulfide scale chemical composition and crystallographic orientation by electron and X ray diffraction 06 p0828 A72-17606
- Oxide spinels crystallographic structure determination, stability relationships, covalent bondings and physical properties 10 p1501 A72-24730
- Light figure microscope construction for crystal grain orientation determination in metal specimens 11 p1632 A72-25759
- Electron-microscopic investigation of the development of a cellular structure in molybdenum during hydroextrusion 17 p2569 A72-35524
- X-ray spectra and electronic structure of titanium nitrides of limit composition and in the homogeneity range 19 p2821 A72-38406
- On Maxwell's equations in three-dimensional anisotropic periodic media - Tensor formulation of the problem and the N-beam approximation 20 p2962 A72-40019
- Single and double shear invariant plane crystallographic theories for martensitic transformations, calculating lattice deformations by combined Bain and complementary shear strains 21 p3065 A72-40089
- The effects of irradiation with protons on the crystallographic order of the compound BiTe₂Se 24 p3432 A72-45200
- ### CRYSTALS
- NT BICRYSTALS
- NT BRAVAIS CRYSTALS
- NT CREATINE
- NT CRYSTAL OSCILLATORS
- NT CRYSTALLITES
- NT DENDRITIC CRYSTALS
- NT IONIC CRYSTALS
- NT LIQUID CRYSTALS
- NT METAL CRYSTALS
- NT MIXED CRYSTALS
- NT PIEZOELECTRIC CRYSTALS
- NT POLYCRYSTALS
- NT QUARTZ CRYSTALS
- NT SINGLE CRYSTALS
- NT WHISKERS [SINGLE CRYSTALS]
- Temperature effects on crystalline solids adhesion, noting friction rise above seizure point 12 p1818 A72-28187
- Analogy between body force and inelastic strain gradient in all crystal systems. 24 p3459 A72-45247
- ### CSM
- #### U COMMAND SERVICE MODULES
- ### CUBIC LATTICES
- NT BODY CENTERED CUBIC LATTICES
- NT FACE CENTERED CUBIC LATTICES
- Twinning in alloys cubic superlattices, discussing crystal structure criteria 02 p0247 A72-12815
- Elastic wave velocities and polarization in planes of cubic crystals, plotting velocity curves 03 p0402 A72-13861
- Mathematical model for supersonic crack propagation in cubic lattice, deriving velocity-applied stress relation 10 p1558 A72-24895
- Solid solutions of stabilized Zr in cubic form prepared from zirconium and yttrium oxide mixture by ammonia precipitation and heat treatment 11 p1660 A72-26486
- Correction to nonlinear refractivity calculation for cubic lattice crystal with allowance for higher induced multipoles 12 p1855 A72-27620
- W addition effect on Co-Nb alloys, noting phase structure transformation from cubic to hexagonal due to mean electron density increase 12 p1829 A72-27642
- Angular force models with electron-ion interaction applied to bcc and fcc metals, calculating phonon dispersion curves for V, Nb and Ta 15 p2258 A72-32226
- EPR transitions of quadrupole interaction of cubic imperfections with ground-vibronic-state degeneracy /Jahn-Teller effect/ 16 p2431 A72-33725
- Cubic stabilized zirconia utilization as solid electrolyte in high temperature fuel cell system for efficient and economical energy conversion 16 p2352 A72-33894

Thermal conductivity of compact samples of cubic BN 19 p2823 A72-38408

On the splitting of dislocations in the diamond cubic lattice. 20 p2962 A72-39992

Anisotropy of Raman scattering by optical phonons in cubic zinc blende crystals, describing experimental arrangements 21 p3061 A72-40141

Electron paramagnetic resonance hyperfine spectral observation of double quantum transitions of Ti positive ions in strontium chloride single cubic crystal host 24 p3378 A72-45311

CUES

Reactions choice limiting cueing signals effect on reaction time, considering dependence on time interval between cueing and start signals 02 p0165 A72-12852

Oculomotor accommodation and convergence as distance perception cues, showing size perception change relation to glasses adaptation 06 p0765 A72-17411

Oculomotor cue-based distance perception, discussing glasses adaptation-caused accommodation and convergence changes in stereoscopic depth perception 06 p0765 A72-17414

Visual space geometry and perception experiments, demonstrating size-distance relations for various visual cues 07 p0926 A72-19031

Counteradaptation and cue discrepancy as perceptual adaptation basis, considering changes in registered and apparent distance of luminous object moving in dark 08 p1115 A72-20988

Vergence eye movements to pairs of disparity stimuli with shape selection cues. 18 p2651 A72-36612

Effects of visual cues on the standing body sway of males and females. 18 p2654 A72-36918

Supplementary cues and delayed-alternation performance of frontal monkeys. 20 p2892 A72-39372

Visually directed pointing as a function of target distance, direction, and available cues. 22 p3151 A72-42929

CUESTAS

U RIDGES

CULTIVATION

Bioengineering models of energy and mass exchange of algae under varying ambient conditions, noting mass cultivation possibility for oxygen regeneration in closed environments 20 p2893 A72-38959

Mathematical model of two-component alga-bacteria biocenosis 21 p2997 A72-40431

CULTURE TECHNIQUES

Microbiological examination of space hardware, discussing viable organisms neutralization buried inside solid materials, sampling procedures and culture media 01 p0019 A72-10820

Three dimensional organization of spherical colonies formed by L5178Y cells grown in soft agar cultures from light and scanning electron microscopy 01 p0015 A72-11039

Tobacco tissue cultures with Apollo 12 lunar material, determining endogenous sterols and fatty acids concentrations by gas chromatography and mass spectrometry 07 p0920 A72-19850

Modular microbiology laboratory design considerations and zero gravity experiments to investigate microbial culture systems behavior 12 p1765 A72-28280

Chlorella population age structure and cell requirements correlation with nutrient medium nitrogen and phosphorus absorption 13 p1909 A72-29311

Isolation of extremely halophilic carbohydrate-utilizing bacteria, using acid formation from various sugars as carbohydrate metabolism index 15 p2187 A72-32729

Isolation of a polyvalent bacteriophage for Escherichia coli, Klebsiella pneumoniae, and Aerobacter aerogenes. 19 p2755 A72-37650

Functional reliability of the biological component of a life support system 21 p2998 A72-40448

Determination of copper, iron, cobalt, nickel, and manganese in biological samples of vegetable origin 23 p3260 A72-43924

Lactate dehydrogenase from an extremely thermophilic bacillus. 23 p3259 A72-44450

Water-soluble insulin receptors from human lymphocytes. 24 p3373 A72-45375

CUMULATIVE DAMAGE

Glass fiber reinforced plastics irreversible cumulative damage under axial cyclic tension compression loads with heat production 08 p1191 A72-21500

Spectrometric oil analysis program /SOAP/ method for turbojet and helicopter transmissions damage monitoring and flight safety 09 p1319 A72-22933

Cumulative fatigue damage in Al-Zn-Mg alloy fillet welded joints, analyzing constant amplitude and programmed load fatigue test results 09 p1332 A72-23618

Data scatter reduction in Al-Zu-Mg welded specimens cumulative fatigue damage testing, noting fatigue life improvement by shot peening and static or dynamic prestressing 09 p1332 A72-23619

Reliability statistics of third generation computer systems failure causes, emphasizing cumulative effects of hardware and software 10 p1444 A72-23986

Fatigue crack propagation theory based on linear accumulation of metallurgical damage in plastic region 10 p1553 A72-24098

Statistical evaluation of welded airframe component fatigue damage increment during cyclic loading with constant force amplitude 10 p1559 A72-24922

Cumulative shock loading fatigue in solids, describing experimental setup and fracture morphologies 10 p1560 A72-25124

Two stress level cumulative fatigue damage prediction for glass fiber-epoxy laminates 11 p1670 A72-25462

Fatigue life cumulative damage prediction procedure for engineering metals subjected to complicated stress-strain histories, noting errors in average mean stress method 11 p1658 A72-25831

Cumulative damage and structural changes in friction contact areas of steel plates under cyclic pulsed loads, noting microhardness distribution and surface layers microstructure 12 p1818 A72-28191

Fatigue strength and cumulative damage in fiberglass-epoxy composite specimens under unsteady elastic bending loads, determining loading spectrum effect on service life 13 p1983 A72-28562

Cumulative damage probability in dynamic or static fatigue failure of brittle graphite materials as function of stress 16 p2414 A72-33321

A model of a nonlinear viscoelastic medium allowing for the effects of cumulative damage 19 p2871 A72-37528

Plasticity and rupture of heat-resistant materials subjected to a small number of cycles of simultaneous variation of temperature and load 19 p2818 A72-38006

On the cumulative fatigue damage of glass fiber reinforced plastics subjected to repeated tensile impact load. 20 p2943 A72-38888

The octahedral shear strain theory and its relation to biaxial cumulative fatigue damage 20 p2978 A72-39202

Fatigue cumulative damage in cases of rotating-bending and torsional multistep loading. 21 p3118 A72-40933

The accumulation of damage in a glass-reinforced plastic under tensile and fatigue loading. 22 p3196 A72-42456

Fracture mechanics and cumulative damage of simulated solid propellant under dynamic loads, obtaining low cycle fatigue curve 23 p3325 A72-43706

The cyclic plastic strain and cumulative fatigue damage - Fatigue damage caused by the stress below the fatigue limit. 24 p3454 A72-44628

Optimal fleet reliability under fatigue and chance overload in service. 24 p3365 A72-44656

Cumulative damage stochastic models and distributions of strength of steels and graphite. 24 p3412 A72-44673

Development and present-day state of the fatigue-damage theories. 24 p3457 A72-44873

Strength margin estimation in materials sustaining cumulative static and cyclic damage under thermocyclic loads 24 p3460 A72-45736

CUMULONIMBUS CLOUDS

Tropical disturbances effect on general atmospheric circulation, considering Hadley cell rising branch and cumulonimbus clouds heat release 07 p1029 A72-19096

A climatology of the potential vertical extent of giant cumulonimbus in some selected areas. 18 p2077 A72-36700

CUMULUS CLOUDS

Cumulus clouds vertical motion velocity spectra curves, turbulence dissipation rates and energy determination from aircraft measurements 06 p0842 A72-17941

Cumulus and stratocumulus ice crystal and nuclei concentrations, drop size distributions, glaciation differences and enhancement mechanisms 07 p1030 A72-19101

Discriminant analysis application to data on precipitation formation in convective cumulus clouds to relate process to surrounding atmosphere and cloud characteristics 08 p1201 A72-21993

Cumulus cloud microstructure measurement by single particle optical spectrometer, inferring transition from water to ice phase regions from droplet size and number distributions 09 p1307 A72-22444

One dimensional model for climatological evaluation of ice phase seeding for isolated cumulus cloud modification 09 p1345 A72-22448

GaAs lidar reflectance of fair weather cumulus clouds at 0.903 micron from aircraft observation 09 p1280 A72-23349

Developing cumulus clouds annihilation, considering ascending and descending spontaneous convective streams initiated by explosions 12 p1841 A72-27989

Averaged atmospheric IR counter radiation values in cumulus clouds, using statistical characteristics 14 p2099 A72-30249

Cumulus clouds vertical motion velocity spectra curves, turbulence dissipation rates and energy determination from aircraft measurements 16 p2418 A72-33782

Time dependent one dimensional numerical model of hail-bearing cumulus cloud, using microphysical process parameterization and exponential raindrop and hailstone size distributions 22 p3201 A72-42513

Developing cumulus clouds annihilation, considering ascending and descending spontaneous convective streams initiated by explosions 22 p3202 A72-43003

CURES

Epoxide resins for application in composite materials, discussing crosslinking reactions, temperature effects on cure, and electrical and physical properties 15 p2260 A72-31441

CURIE TEMPERATURE

Digital magnetic temperature transducer using permeability discontinuity at Curie temperature for high stability and reproducibility without calibration [IEEE PAPER 8,5] 03 p0332 A72-13758

Heisenberg ferromagnet thermodynamic properties in external magnetic field near Curie temperature, studying magnetization, susceptibility, entropy and magnetocaloric effect 08 p1217 A72-21520

Dielectric dispersion in SrSi filamentary single crystals as function of Curie temperature in If and shf range 09 p1367 A72-22422

Crystallographic structure, phase transformations, Curie temperature and Faraday rotation of Ti-substituted MnBi films 15 p2294 A72-32522

Magnetic balance for magnetic saturation measurement and determination of retained austenite, Curie temperature, permeability and martensite content 16 p2391 A72-33237

Formation of fluorine-containing solid solutions based on barium titanate 19 p2845 A72-38407

Extension of the Curie principle and constitutive relations for fluids with antisymmetric stress. 22 p3166 A72-42311

CURING

Curing technique optimization for primary aircraft components composite materials, discussing mechanical and dimensional properties test data, production cost analysis and cure time 12 p1815 A72-28077

Adhesives polymerization and rapid ambient temperature curing, using Co 60 gamma rays and electron beams 12 p1833 A72-28079

The effects of various cure cycles upon the viability of Bacillus subtilis var. niger spores within solid propellant. 18 p2652 A72-36437

CURL (VECTORS)

NT VORTICITY

CURRENT AMPLIFIERS

NT PHOTOMULTIPLIER TUBES

Minority carrier diffusion effect on current gain in miniature bipolar transistors 04 p0498 A72-15132

Voltage controlled low power current sources characteristics, discussing circuits, transistor and emitter resistance and operational amplifiers 13 p1900 A72-30052

Electron swarms in uniform electric fields, discussing anode current amplification/radial distribution and drift-diffusion equation

15 p2285 A72-32239

CURRENT DENSITY

Rocket-borne measurement of Birkeland ionospheric current density associated with auroral arc and electrojet

01 p0061 A72-10898

Meridional currents intensity in equatorial electrojet region, computing electric and magnetic fields

01 p0063 A72-10924

MHD channels magnetoacoustic and ionization instabilities effect on mean current density and electric field strength, determining effective electroconductivity and Hall parameter

01 p0110 A72-11208

Low energy and strong current density ion source using mesh grid extraction

02 p0266 A72-12491

Time harmonic electromagnetic wave diffraction by thin conducting circular disk at different media plane interface, calculating induced surface current density and scattering cross section

03 p0322 A72-13237

Minimum threshold current density of double heterojunction injection lasers

03 p0367 A72-13412

Plasma jet formation within high pressure discharges in air at atmospheric pressure, discussing electrode configuration, current density and accelerating magnetic field strength

03 p0396 A72-13662

Electric field intensity and pulsation spectra variation along rectangular channel in transverse magnetic field, noting current density changes

03 p0398 A72-14006

Magnetic field distribution in linear MHD channel for large Reynolds numbers, determining current density and longitudinal field component

03 p0398 A72-14010

MNOS transistors charge storage properties at high electric field strengths and current densities near gate insulator breakdown, determining reliable operating limits

03 p0336 A72-14277

Electrochemical machining electrode processes thermodynamic and kinetic characteristics, discussing temperature, electrolyte viscosity and flow rate and current density effects on metal removal rate

04 p0526 A72-14475

Current density nonlinear transient response and energy absorption of weakly ionized plasma under pulsed electric field

04 p0555 A72-14532

Constitutive equations derivation for electrical conduction due to small deformation superposition, applying to deformed spherical shell current density determination

04 p0549 A72-15254

Nb-Ti alloy critical current density increase dependence on temperature, discussing evidence supporting rigidly pinned vortex lattice model

04 p0562 A72-15292

NbN film superconducting properties measured as function of thickness, discussing transition temperature, critical current and magnetic field

04 p0562 A72-15294

Quasi-stationary pulsed discharge characteristics of nitrogen plasma as function of current density and pressure

05 p0693 A72-15839

Electrostatic surface and bulk ionization ion thrusters current densities for propulsive and working fluid utilization efficiency

05 p0705 A72-16772

Pulsed flat electrode erosion plasma accelerator, determining electric and magnetic fields distribution, current density and electron concentration

05 p0697 A72-16987

Injection laser threshold current density, radiation pattern and electric field distribution relation to layer thickness and dielectric constants, using waveguide theory

06 p0825 A72-17772

Abrikosov and Mendelssohn models of nonideal superconductors of second kind in transverse magnetic field, discussing Landau-Ginzburg parameters and critical current density

07 p1049 A72-20153

Precipitates dispersion and fluxoid pinning/critical current density/ in superconducting Nb-Hf alloy during aging, using transmission electron microscopy

07 p1020 A72-20409

Thermionic converter electrode performance of electron emission current density in terms of Cs arrival rate and surface temperature

07 p0915 A72-20568

Loading current density effect on normal lead styphnate ignition in primary explosive hot wire initiation, using capacitor discharge and constant current activation signals

08 p1218 A72-20752

Electron wave attenuation technique for current transit determination through semiconducting films with various crystal structures

09 p1284 A72-22209

Surface current density of perfectly conducting polygonal cylinders for axially polarized incident electromagnetic field

09 p1350 A72-22247

Nb-Al-Ge alloy superconductor deposits structure, transition temperature and critical current densities after preparation by triode sputtering and heat treatment

09 p1369 A72-22795

Pinning force of vortex lines and microstructural inhomogeneities in superconductors, using magnetization and critical current measurements

09 p1369 A72-22796

Steady state charged cylindrical electron-ion beam with high current in kinetics model framework, discussing densities proportionality and relativistic factor

09 p1360 A72-22951

Solid state sinusoidal signal generator based on current density oscillation effect in high resistivity p-type InSb with transmutation doping

09 p1288 A72-23191

Diode junction parameters and inverse saturation current measurements as function of current density and temperature

09 p1289 A72-23418

Strong magnetic fields and electric current densities effects on acoustic oscillations and instability in stationary inhomogeneous low temperature plasma flow in crossed fields

10 p1517 A72-23838

Nonlinear conductivity of plasma with FM electromagnetic wave propagation, proposing electronic current density calculation method

10 p1519 A72-24130

Relativistic electron beam injection into dense plasma, analyzing perturbed electric and magnetic fields and charge and current densities

10 p1521 A72-24353

Width of space charge layer of reverse-biased p-n junction in p-n-p-n structure effect on current density, mobile charge carriers and constituent transistors gain coefficients

10 p1526 A72-24584

Semiconductor measurement technology at extremely low currents, discussing dc characteristics and ac amplification

10 p1452 A72-24815

Evaporation, superficial diffusion and oxidation role in grain junctions electromigration phenomenon in binary Al crystals traversed by high density continuous current

10 p1498 A72-24860

Vacuum arc stationary cathode mechanism theoretical analysis, determining cathodic temperature and current density

10 p1524 A72-24930

Secondary diffraction from close edges on perfectly conducting bodies, representing scattered field by iterative surface current density replacement technique

10 p1440 A72-24938

Magnetic fields effect on anode heat losses in MPD accelerator arcs, noting minimal charge current density

[AIAA PAPER 72-502]

11 p1711 A72-26225

Ti alloys processability by electrochemical method, showing output rate and surface quality improvement from increased current density and electrolyte temperature

11 p1640 A72-26261

Ar laser levels population inversion dependence on current density, discharge tube pressure and magnetic flux

11 p1649 A72-26350

Third harmonic current density excitation by HF electric field in Lorentz plasma, calculating electron distribution function with unnormalized spherical harmonics and Fourier series

11 p1697 A72-26553

Electrode system for ventricular defibrillation, noting current density role and rounded edge effectiveness

11 p1588 A72-26628

Pulsed flat electrode erosion plasma accelerator, determining electric and magnetic fields distribution, current density and electron concentration

12 p1850 A72-27131

Transient current density in plasma subjected to pulsed electric field derived from Boltzmann transfer equation

12 p1850 A72-27278

Numerical analysis of surface current density distribution and electromagnetic fields of conducting body, noting radiation patterns of radial dipole and quarter wavelength monopole

13 p1916 A72-28541

Electrocardiography and magnetocardiography to determine flux and vortex sources respectively of heart electrical activity impressed current density

13 p1909 A72-28998

Double heterostructure injection lasers with narrow active regions, discussing threshold current densities, emission polar diagrams and optical field penetration into boundary regions

15 p2249 A72-32237

End effect in current response of highly negative cylindrical Langmuir probe in collisionless plasma flow, discussing use for ion temperature determination

15 p2288 A72-32418

Multifilamentary superconducting Nb-Sn composite wires in ductile metal matrix, determining transition temperature and critical current density

15 p2294 A72-32534

Ar laser levels population inversion dependence on current density, discharge tube pressure and magnetic flux

16 p2402 A72-33703

Relativistic electron beam injection into dense plasma, analyzing perturbed electric and magnetic fields and charge and current densities

17 p2589 A72-34954

Electrostatic surface ionization and electron bombardment ion thrusters current densities for propulsive and working fluid utilization efficiency

17 p2597 A72-35275

Steady state charged cylindrical electron-ion beam with high current in kinetic model framework, discussing densities proportionality and relativistic factor

17 p2593 A72-35880

The influence of magnetic pressure on the performance of a high-current discharge thermionic converter

18 p2646 A72-36195

Excitation and ionization processes in a low-voltage arc discharge

18 p2714 A72-36213

Current instabilities and constriction in thermionic converters

18 p2647 A72-36221

Gas shielded arc welding of Ni, discussing current density, energy, arc length and preheating temperature effects on welds porosity

18 p2695 A72-36427

Solid-body-surface and thin-layer analyses by the static method of secondary-ion mass spectroscopy

18 p2719 A72-36830

Green function for temporal electromagnetic plasma wave echoes oblique to external magnetic field, calculating current density and damping term

19 p2839 A72-37333

Instabilities in semiconductors with negative differential mobility.

19 p2844 A72-37465

Critical current periodicity of Josephson junction interferometers.

19 p2846 A72-38601

Determination of conduction anisotropies in semiconductors.

21 p3097 A72-40697

Temperature dependence of thermionic emission current density of Pt additive powdered zirconium carbide deposit on diode cathode working surface

21 p2997 A72-40801

OH maser sources parametric down-conversion, deriving nonlinear current densities, electron cyclotron wave damping and parametric gain coefficient

21 p3064 A72-41030

Effect of substrate temperature on electrical properties of amorphous germanium films.

23 p3324 A72-44069

Physical limits of semiconductor devices miniaturization for electronic computers, considering thermal energy dissipation, electrical resistance and high current density induced electromigration effects

23 p3273 A72-44332

Pressure, temperature, current density, and potential difference fluctuations in subsonic flow of combustion products plasma, noting steadiness, ergodicity and distribution functions

24 p3429 A72-45502

CURRENT DISTRIBUTION

Broadband dipole antenna design based on method of moments, noting VSWR and current distribution

01 p0043 A72-11241

Alternative derivation of Mei integral equation for numerical determination of current distribution along thin wire antennas

01 p0043 A72-11246

Dipole theory application to directional characteristics of Yagi antenna systems, assuming harmonic current distribution along radiating elements

02 p0193 A72-12221

Cascade connected electrode scheme for MHD applications, noting potential and current distributions and Hall voltage buildup

02 p0265 A72-12276

Induced current distribution in flat narrow conducting strip moving in inhomogeneous magnetic field, presenting current field and densities

03 p0311 A72-13564

Spreading currents in parabolic rotating coordinates, determining magnetic field components consistent with Laplace equation series expansion

03 p0311 A72-13565

Magnetoplasma with skin current characterized by current and electron temperature nonuniformity, analyzing instabilities for perturbations above ion gyrofrequency

03 p0396 A72-13713

Tunneling current calculation for free electrons subject to arbitrary one-electron potential, using Keldysh perturbation theory

03 p0404 A72-14266

Pinch-in effect due to emitter current distribution instability in transistors with emitter-stripe geometry

04 p0499 A72-15209

Ion-wave current instabilities theory, showing inhomogeneities generated by field aligned currents in collisionless plasma

04 p0559 A72-15350

Antenna synthesis problems for given radiation pattern, discussing stable method of solution for amplitude or phase current distribution

04 p0500 A72-15404

Phase-amplitude current distribution calculation for plane array and curvilinear radiator based on given amplitude radiation pattern

04 p0500 A72-15405

Synthesis of currents along linear antennas, reducing to solution of integral equation

04 p0500 A72-15406

Electromagnetic wave diffraction on infinite lattice of perfectly conducting arbitrary flat elements from numerical method, determining secondary field and strips current distribution

04 p0491 A72-15417

Admittance calculation for vertical monopole antenna driven by coaxial line, approximating current distribution by polynomial with complex coefficients

04 p0501 A72-15429

Transport processes in electrolytic solutions, considering current and potential distributions in localized corrosion

04 p0536 A72-15737

Conducting ground half space effects on dipole antenna input impedance computed by current distribution Fourier transform

06 p0781 A72-17353

Closed magnetic fields of helical ring currents on concentric spheres surrounded by semiconductor /Tornado trap/

06 p0863 A72-18405

Magnetic field stability in Tornado-2 trap as function of helical currents on concentric sphere

06 p0863 A72-18406

Magnetohydrodynamic theory of spherical drop deformation and drag under axisymmetric current distribution in conducting viscous incompressible fluid

06 p0864 A72-18533

Input resistance derivation for finite horizontal loops with uniform current distribution located above lossy half-space ground

06 p0777 A72-18737

Antenna radiation pattern synthesis, discussing current phase and amplitude distribution determination by iterative and quadratures solutions respectively

07 p0953 A72-19004

Linear array antenna radiation pattern synthesis for minimum sidelobe level outside of given intervals, calculating current distribution

07 p0953 A72-19005

Frequency-independent multimode equiangular/conical spiral antenna with thick wires, calculating current distribution and radiation pattern by numerical program

07 p0939 A72-19187

Rf excitation of external terminated longitudinal conductor axially parallel to rocket skin by transverse electromagnetic field, deriving currents in cable-connecting impedances

07 p0956 A72-19555

One- and two-conductor transmission lines electromagnetically coupled to rocket, deriving current bounds in load impedances under incident plane monochromatic wave

07 p0956 A72-19556

Current distribution in cylindrical parasitic antenna immersed in arbitrarily directed and polarized incident plane electromagnetic wave

[AD-743574] Transients determined for Cs vapor discharge phases, observing current fluctuations between steady states in negative resistance zone above 0.2 torr

07 p1046 A72-20517

Secondary gas flow effect on energy transfer distributions from plasma torches, obtaining radial distributions of current and energy flux

07 p1046 A72-20546

Parabolic antenna instantaneous phase center calculations, using radiation patterns from aperture field and current distribution methods

08 p1138 A72-20744

Switching characteristics of MOS channel transistors, solving nonlinear differential equations describing current and potential distribution

08 p1140 A72-21267

German monograph on electric arc behavior in narrow channel with plasma cooling by channel wall and

continuously decreasing current for switching applications

10 p1517 A72-23773

Avalanche carrier multiplication influence on semiconductor device p-n junction quality, discussing current distribution and I-V characteristics during avalanche breakdown

10 p1446 A72-23849

Current lines of relativistic fluid investigated by Ehlers method, applying to MHD Godel type universes

10 p1520 A72-24220

MOS transistor current fluctuation relation to capture centers surface density, energy position and gate potential, determining spectral amplitude distribution

10 p1449 A72-24284

Numerical solution for super-Alfvénic supersonic aligned MGD flow over cone with attached shock wave, obtaining surface pressure coefficients, current and vorticity distributions

10 p1418 A72-24463

Synthesis of linear antenna with integrated currents for specified ratio of antenna radiation to elementary radiator patterns

10 p1436 A72-24504

Current distribution approximation for toroidal antennas of small cross section under incident electromagnetic excitation

10 p1453 A72-25104

MPD thruster diagnostics and interpretation of electric current distribution, applying integral form of Maxwell equation for moving Hall probe

[AIAA PAPER 72-498] 11 p1711 A72-26221

Mass flow and current distribution in magnetic MPD accelerator thruster plumes calculated from meridional flow stream function equation

[AIAA PAPER 72-501] 11 p1696 A72-26224

Electrode gap current and temperature distributions during electrochemical precision processing of metals, studying gas and electrolyte flow

11 p1613 A72-26258

Induced current distribution in flat narrow conducting strip moving in inhomogeneous magnetic field, presenting current field and densities

11 p1691 A72-26751

Spreading currents in parabolic rotating coordinates, determining magnetic field components consistency with Laplace equation series expansion

11 p1607 A72-26752

Oscillation periods of rotating perfectly conducting liquid column in presence of axial magnetic field and uniform current

12 p1851 A72-27534

Input impedances and current distributions of cylindrical monopole antennas of various lengths in hot lossy plasma as function of plasma density

13 p2009 A72-28538

Current distribution over coaxial plasma gun outer electrode, attributing current concentration at electrode edge to accelerator cavity conductivity anisotropy

13 p2012 A72-29140

Linear nonequilibrium Faraday type MHD generator, predicting electrode configuration effects on voltage drops, axial leakages and current distribution

13 p1900 A72-29353

Time dependent and stationary two dimensional calculation of current and potential distributions in MHD generator preionizer and entrance region flow

13 p2013 A72-29358

Variable saturation of series LC circuit, discussing current response, ferromagnetic jump, symmetry and subharmonic oscillations

14 p2090 A72-31116

Oscillatory current characteristics of Stark ladder electron with weak LO phonon coupling in solids

15 p2293 A72-32218

Electron swarms in uniform electric fields, discussing anode current amplification/radial distribution and drift-diffusion equation

15 p2285 A72-32239

Narrow strongly radiating slot voltage distribution, investigating cavity coupling with integral equation

15 p2209 A72-32659

Thin circular loop antenna input admittance and current distribution calculation comparison

15 p2209 A72-32673

On the behavior of thin-wire antennas and scatterers arbitrarily located within a parallel-plate region

17 p2513 A72-34365

Theoretical analyses on Apollo lunar surface electrical properties experiment transmitter antenna

17 p2515 A72-34423

Distribution of current in centre-fed cylindrical dipole antennas with arbitrarily displaced feed points

17 p2526 A72-34517

Possible mechanism for CO₂-discharge current variation under the influence of laser radiation

17 p2562 A72-34840

Closed magnetic fields of helical ring currents on concentric spheres surrounded by conductor /Tornado trap/

17 p2588 A72-34855

Magnetic field stability in Tornado-2 trap as function of helical currents on concentric spheres

17 p2588 A72-34856

Motion of a sphere in an electrically conducting rotating fluid

18 p2714 A72-36123

Measurement of Hall mobility of current carriers in inhomogeneous semiconductor samples

18 p2720 A72-36964

Fourier series analysis of multielement circular loop antenna with arbitrary circumference for current distribution and self and mutual admittances

19 p2775 A72-38615

Flux vortices and transport currents in type II superconductors

20 p2961 A72-39809

Wave propagation on helical antennas

21 p3015 A72-40352

Mutual coupling of infinite periodic phased arrays of arbitrarily oriented dipoles, investigating dipole length, orientation and phase effects on current distribution

21 p3027 A72-40368

Bubnov-Galerkin solutions to wire-antenna problems

21 p3032 A72-40631

An expression for the distribution of current in asymmetrically driven antenna immersed in a dissipating medium

21 p3022 A72-41322

Electrodynamic mathematical model for electroconductivity of nonuniform plasma with Hall effect, calculating current distribution from Riemann problem solution

22 p3210 A72-41888

Antenna radiation patterns from statistical phase synthesis of antenna arrays, estimating directivity loss for in- and out-of-phase initial current distribution

23 p3265 A72-44203

CURRENT REGULATORS

Microwave spectrometer crystal current leveler for broadband video detector and rotary wave attenuator control

04 p0524 A72-15541

Ac and dc power regulation by switched capacitor, analyzing voltage spectrum for resistive load

07 p0958 A72-20389

Solid state dc power controller design functional requirements, considering system overcurrent protection, power control by low voltage signals, power output to load status, etc

15 p2182 A72-31219

German monograph - Investigations concerning a new frequency changer with 'forced' commutation for supplying power to one- or multiple phase consumers

19 p2753 A72-37482

Vapor deposition in vacuum under conditions of constant vapor flow with the aid of electron emission current control

20 p2954 A72-39694

CURRENT SHEETS

Wall friction effect on current sheet speed of magnetically driven shock tube, establishing steady state existence

01 p0105 A72-10027

Computer investigation of three fluid electrical current sheet model, solving magnetic annular shock tube problem

[SRL-TR-71-0021] 02 p0200 A72-12659

Electric field aligned sheet currents of low energy electrons and protons near auroral arc, obtaining magnetic signatures

03 p0349 A72-13516

Neutral current sheets in slow moving plasma with frozen-in magnetic field with null force line

03 p0438 A72-14070

Argon plasma transient axial flow and heating characteristics in pinched column of linear z-pinch device with collapsing current sheets conversion to axial streaming velocity

[AIAA PAPER 72-208] 05 p0696 A72-16886

Neutral current sheath formation from plane dipole magnetic field extension by plasma flow, discussing solar corona streamers and geomagnetic tail

07 p1039 A72-18914

Two dimensional model for plasma without magnetic field trapped near current sheet end in dipole magnetic field resembling geomagnetic tail

08 p1157 A72-21108

Current sheet velocity limitation in magnetically driven shock tube with plasma electrodes, examining wall ablation and friction and Hall current effects

[AIAA PAPER 72-409] 11 p1695 A72-26160

Solar flare and neutral sheet simulation by investigating behavior of plasma current through magnetic neutral point created by capacitor discharges

15 p2301 A72-32342

Solar flares induced magnetic field configurations, considering open and closed current sheets instabilities as flare sources

15 p2301 A72-32788

Shock wave generation by high current pulsed discharges, determining shock front velocity as function of magnetic pressure on current sheath

16 p2434 A72-32909

- On neutral sheets in the solar wind.
17 p2599 A72-35096
- Neutral current sheath formation from plane dipole magnetic field extension by plasma flow, discussing solar corona streamers and geomagnetic tail
20 p2957 A72-39380
- Magnetic neutral sheet model in terms of self consistency between current and tail field in reversal region
20 p2919 A72-39548
- Sweet's mechanism for the destruction of magnetic flux.
20 p2955 A72-40017
- Resonant interaction of an electrostatic wave with electrons in a current sheet.
22 p3169 A72-42008

CURRENT STABILIZERS**U CURRENT REGULATORS****CURTISS-WRIGHT MILITARY AIRCRAFT****U MILITARY AIRCRAFT****CURVATURE**

- Velocity profile shapes computation in supersonic compressible turbulent boundary layers with adverse pressure gradients, discussing data and theory discrepancy, curvature, and three dimensional effects
05 p0649 A72-16544
- Meridional curvature effect on thin walled cylindrical shell buckling under external constant directional lateral pressure
05 p0739 A72-16546
- Ground plane curvature effect on aperture admittance of waveguide fed axial slot on teflon coated metal cylinder for underdense plasma
06 p0771 A72-17354
- Transient calculation method for electric drive units described by first and second order differential equations, using special transformation for integral curve curvature determination
10 p1423 A72-24754
- Theorem of pursuit game with curvature constraints during two points motion in Euclidean space
11 p1675 A72-25320
- Time-space nonholonomic characteristics of curvature tensor for three dimensional physical space in gravitational and inertial fields
12 p1843 A72-27049
- Infinitesimally small slip bendings of sign-variable curved surface of revolution with parabolic boundary parallels
13 p2061 A72-29794
- Constitutive and equilibrium equations for theory of thin shells with slowly varying curvature based on Novoshilov and Koiter assumptions
16 p2465 A72-33004
- On the extension of particular solutions of the energy equation of compressible turbulent boundary layers.
17 p2544 A72-35954
- Recent results on the effect of longitudinal curvature on a laminar layer
18 p2685 A72-37213
- Effect of spherical spectacle lenses on the monochromatic aberration of the eye
21 p3007 A72-40746
- Conformal mapping procedure for numerical generation of airfoils with local curvature singularities, presenting test problem results for zero trailing edge angle
21 p2992 A72-41259
- German monograph - Three-dimensional boundary layers at curved walls.
22 p3167 A72-43051
- Second order boundary layer solutions on a curved surface.
[ASME PAPER 72-FE-21] 23 p3280 A72-44063
- Longitudinal curvature and displacement speed effects on incompressible laminar boundary layers.
24 p3393 A72-45249
- Time-space nonholonomic characteristics of curvature tensor for three dimensional physical space in gravitational and inertial fields
24 p3425 A72-45702

CURVE FITTING

- Curve and surface fitting with Schmidt potential functions, including polynomial and straight line fit
02 p0252 A72-12601
- Deschamps graphical method application to multiport waveguide junction scattering coefficient measurement with averaging and least square fitting for error reduction
06 p0787 A72-18379
- Refractivity measurement of pure hexagonal structure 2H SiC over visible range, determining birefringence from curve fitting of data to Cauchy dispersion equation
09 p3109 A72-22603
- Computerized determination of cryogenic gas behavior near vapor region, obtaining state equation coefficients from curve fitting program
15 p2334 A72-31580
- Best fitting triaxial ellipsoid representation of seleno-equipotential surface at Apollo 12 landing site based on observed local gravity and moon angular velocity
15 p2308 A72-31922

- Prior distributions fitted to observed reliability data.
22 p3182 A72-41980
- Characteristic curve formulas of cosmic objects and stellar focal images for photometric measurement processing on computer
23 p3267 A72-44030
- Limitations in the acquisition of nonlinear aerodynamic coefficients from free-oscillation data by means of the Chapman-Kirk technique.
24 p3362 A72-45336
- Computer algorithm for breakpoints and forcing functions determination for optimal curve fitting by piecewise differential approximation
24 p3419 A72-45632

CURVED BEAMS

- Curved beam finite elements comparison for structural vibration problems, obtaining ring natural frequencies
01 p0136 A72-10222
- Natural torsional vibrations of curved shafts, discussing oscillating system with varying flywheels
04 p0584 A72-14470
- Optimum thickness variation in annular strip /curved beam/ under bending moment at constant stress based on Mises-Hencky yield criterion
10 p1558 A72-24847
- Incremental growth of beams under combined direct load and cyclically varying curvature
11 p1735 A72-25897
- Thermal stresses in homogeneous isotropic and composite curved beams for temperature distribution in polynomial form with coefficients representing functions of two remaining coordinates
11 p1737 A72-26665
- Uniformly loaded parabolic arches lateral-torsional buckling, deriving governing linear differential equations from Clebsch-Kirchhoff equilibrium equations for thin curved bars
12 p1888 A72-28349
- Governing equation derivation for coupled extension, flexure and torsion in pretwisted curved beams of thin walled open section, using three dimensional elasticity
[ASME PAPER 72-APM-5] 17 p2630 A72-34809
- Finite element models with rigid displacement for nonrigid structure analysis, noting curved beam and shells
18 p2739 A72-37173
- Torsion and flexure of curved, thin-walled beams or tubes.
19 p2874 A72-37696
- Method of characteristic application to curved beam motion under pulse type loading, investigating photoelastic fringe patterns and pulse propagation
24 p3458 A72-44888

CURVED PANELS

- Cylindrical panel natural vibrations, describing motion of base with dynamic elasticity equations
11 p1733 A72-25539
- Resonant frequencies of two thin walled cylindrical panels connected by elastic filler, considering symmetric and asymmetric vibration modes
13 p2058 A72-29146
- Vibration analysis of cylindrical panels.
17 p2623 A72-34230
- An experimental buckling study of skin-corrugated ring-stiffened curved panels.
[SESA PAPER 1993A] 17 p2630 A72-34818
- Buckling of orthotropic, curved, sandwich panels subjected to edge shear loads.
18 p2735 A72-36770

CURVED SURFACES

- U CONTOURS**
- U SHAPES**
- U SURFACES**
- CURVES [GEOMETRY]**
- NT EPICYCLOIDS**
- Hilbert space filling curves for solutions of sets of nonlinear equations
09 p1340 A72-22244
- Phi-spatial filter method for straight or curved line geometric feature extraction of characters, using coherent optical system
12 p1820 A72-27494
- Computer calculation of second order curve segment discriminant in geometrical problem associated with aircraft lofting, assessing method accuracy
13 p1986 A72-28739
- Nonlinear algebraic transformation to determine straight line and second order curve intersection point in aircraft lofting problem
13 p1986 A72-28742
- Computer algorithms and programs for complex surface geometrical parameters calculation and discrete curve coordinates determination by interpolation
13 p1924 A72-29141

CUSHIONS

- Seat cushion evaluation for behavior during helicopter crash or aircraft ejection and spinal injury probability
08 p1126 A72-21577
- Combined hydrostatic suspension Hg cushion effects on gyrocompass response precision during irregular roll of platform
13 p1961 A72-30022

Dilatant suspensions impact energy absorbent properties, considering application to ejection seat cushions for occupant acceleration attenuation
15 p2191 A72-32604

CUSPS

- Occurrence of Pc 4, 5 micropulsation activity at the polar cusp.
22 p3171 A72-42411

CUT-OFF

- Nonlinear resonating correlator with orthogonal filters, considering cut-off frequency of ergodic random process with constant power spectral density
14 p2090 A72-31125
- Daily variation of electron and proton geomagnetic cutoffs calculated for Fort Churchill, Canada.
22 p3170 A72-42401

CUT-OUTS**U OPENINGS****CUTTERS****NT BLADES [CUTTERS]****NT DRILLS**

- Fully redundant hermetically sealed cable cutter for application to electroexplosive devices in space
08 p1221 A72-20775

CUTTING

NT METAL CUTTING

NT MILLING [MACHINING]

NT PLANING

NT SHEARING

NT SPARK MACHINING

- Plastics cutting and drilling with carbon dioxide IR laser beam, discussing economics and commercially available equipment
07 p0999 A72-20554
- Gas jet combination with laser for cutting operations, discussing laser characteristics, beam guiding mirror, lens, nozzle, nozzle gas and workpiece materials
09 p1320 A72-23629
- Oxygen jet-carbon dioxide laser beam cutting in mild and stainless steels, noting speed and material thickness limitations
09 p1321 A72-23639
- Lower and upper bounds for number of lattice points in simplex, using linear programming algorithm for generating feasible cutting patterns for paper reels
11 p1678 A72-26157
- Wear resistance of artificial and natural diamond grindstones in ruby cutting, noting tests for grain geometry and fabrication technique effects
12 p1814 A72-27765
- Deep penetration welding and cutting with high power CW carbon dioxide lasers, describing experimental setup
13 p1965 A72-29422
- Electrothermal cutting processes using a CO2 laser.
[IEEE PAPER TOD-71-118] 17 p2560 A72-35644

CW RADAR**U CONTINUOUS WAVE RADAR****CYANAMIDES**

- Nucleotides condensation in aqueous system in prebiotic conditions, investigating effects of imidazole, cyanamide and polyornithine
04 p0483 A72-14766

CYANIDES

NT CYANOGEN

NT HYDROGEN CYANIDES

- Cyanide and carbon molecules and isotopes electronic systems opacity probability distribution functions for stellar equilibrium model atmospheres calculations
03 p0416 A72-13012
- Rate constant for quenching of B /super 2/Sigma-plus state of CN radical as function of quenching collision relative velocity and total pressure in fluorescence cell
04 p0553 A72-15635
- Potassium cyanide effect on phospholipid exchange in rat brain and liver during histotoxic hypoxia as function of body temperature
05 p0618 A72-16357
- Intensity variations of CN photospheric and K line chromospheric network with time
05 p0718 A72-16505
- Turbulent micro and macromotion velocities in solar photosphere from CN molecule vibrational band line contours
07 p1077 A72-19810
- Bright point intensity distribution on CN spectroheliogram of sunspot penumbra on 4 July 1970
13 p2045 A72-29710
- Cosmic background radiation temperature from interstellar CN band R branch absorption line in star zeta Ophiuchi spectrum
15 p2313 A72-32309
- Turbulent micro and macromotion velocities in solar photosphere from CN molecule vibrational band line contours
17 p2617 A72-35735
- Formation of urea and guanidine by irradiation of ammonium cyanide.
23 p3262 A72-43569

CYANO COMPOUNDS**NT CYANAMIDES**

High precision rotational constants and transition frequencies in ground state interstellar molecule cyanoacetylene 01 p0023 A72-11147

CYANOGEN
Cyanogen induced phosphorylation of sugars in aqueous solution, discussing system prebiotic plausibility 04 p0483 A72-14771

A shock tube determination of the electronic transition moment of the CN red band system. 23 p3316 A72-44329

CYANOPHYTA
U BLUE GREEN ALGAE
CYANOSIS
The scoliosis of congenital heart disease. 24 p3370 A72-44560

CYBERNETICS
Mathematics for pattern recognition, discussing perceptrons, combinatorics and statistics, feature selection, cybernetic methods and fuzzy sets 01 p0034 A72-10465

Systems, man and cybernetics - IEEE Conference, Anaheim, California, October 1971 03 p0318 A72-13161

Laser coherent monochromatic light for cybernetics research in pattern classification, discussing fingerprints and letters 04 p0531 A72-15137

Hologram data treatment comparison to human brain function, discussing recognition signals, Pavlovian qualities and intelligence function 06 p0768 A72-17997

Soviet book on psychic phenomena and brain, covering cybernetics, dialectical materialist implications, consciousness, psychophysiology and cerebral neurodynamic structures 08 p1121 A72-22164

Russian papers on cybernetic systems accuracy and reliability covering error correction schemes, statistical analysis and computer design 11 p1599 A72-25426

Cybernetic equipment reliability and precision analysis from algorithmic, conversion and instrumental errors, surveying digital, analog and hybrid computers and converters 11 p1608 A72-25427

Cybernetic system effectiveness analysis with operations research and statistical theory based on stochastic treatment 11 p1608 A72-25428

Russian book on flight navigation cybernetics covering Doppler, astro and radio inertial schemes and satellite systems 12 p1843 A72-28344

Information lossless automata for unknown input sequences identification of arbitrary length, noting solvability conditions and application to automata superposition 16 p2366 A72-33087

Application of a learning recognition system for classification of game situations 19 p2769 A72-37422

Object code storage in the static portion of a short-time memory 19 p2759 A72-37423

Models of neurons reacting to input signal alternation in space and time 19 p2759 A72-37424

Neuron mathematical model synthesis from algorithms to construct neural networks and single threshold element in network form 19 p2759 A72-37425

General principles and detail similarities in visual pattern analysis by single neuron operation, computer programs and psychological perception 20 p2891 A72-39275

Preprocessing of nerve pulse sequences for analysis by digital computer 23 p3261 A72-44349

Problems of complex object modeling based on heuristic self-organization 24 p3376 A72-45509

CYCLES
NT ACTIVITY CYCLES [BIOLOGY]
NT BRAYTON CYCLE
NT CARNOT CYCLE
NT OTTO CYCLE
NT RANKINE CYCLE
NT SOLAR CYCLES
NT STIRLING CYCLE
NT STRESS CYCLES
NT SUNSPOT CYCLE
NT THERMODYNAMIC CYCLES
NT WORK-REST CYCLE
Long period pulsations of finite amplitude baroclinic wave, noting stable limit cycle for small friction effect 09 p1347 A72-23653

Energy balance equation for machine unit with rotating element, noting energy distribution in periodic and nonperiodic operation modes 22 p3181 A72-41857

CYCLIC ACCELERATORS
NT BETATRONS

NT BEVATRON
CYCLIC HYDROCARBONS
NT ANTHRACENE
NT CYCLOPROPANE
Polycyclic hydrocarbon molecules formation in cool stars atmospheres and gases ejected by supernovae and Seyfert galaxies, discussing Platt particles origin 02 p0284 A72-12634

Reversible photodimerization of polycyclic aromatic hydrocarbons as basis for optical information storage, discussing monomer and photodimer photosensitivity, thermal stability and refractive index specifications 09 p1314 A72-23331

CYCLIC LOADS
Temperature and compressive loading cycles effects on high performance multilayer insulation materials and composites, discussing application to space shuttle orbiter 01 p0092 A72-10779

Cast high temperature Ni base alloy Udimet 500 low cycle fatigue, determining total stress and strain range vs fatigue life at elevated temperatures 01 p0087 A72-11030

Analytic yield surface in work hardening including stress in transition range after load change /Bauschinger effect/ 01 p0144 A72-11388

Graphite-epoxy conductive polymers as fatigue damage indicators of structures under cyclic strain [SESA PAPER 1915] 02 p0287 A72-11509

Thermoplasticity problems of materials with time dependent mechanical properties, obtaining approximate plastic deformation under cyclic loading 02 p0291 A72-11638

Tension-compression cycling effects on fatigue crack growth in high strength alloys [ASME PAPER 71-PVP-2] 02 p0294 A72-12469

Metal fatigue mechanisms in subcreep temperature range, discussing response to cyclic loading including hardening, softening and inhomogeneous plastic strain development 02 p0295 A72-12496

Metal fatigue time and cycle dependent deformation and fracture mechanisms in creep range from cumulative damage law standpoint for lifetime prediction 02 p0295 A72-12497

Screw connections high temperature behavior, discussing creep induced tension relaxation and cyclic loads long term tolerance 03 p0363 A72-13375

Microinhomogeneous elastoplastic cyclically strain hardenable material under symmetric loading, calculating stress-strain relationship 03 p0443 A72-13453

Surface layers and aging influence on Bauschinger effect in profiled low carbon steel under low tension-compression load cycles 03 p0445 A72-13592

Secondary fatigue curves for determining service life of metal specimens under unsteady loads 03 p0445 A72-13592

Beta structure effect on cyclic fatigue strength in Ti alloy under various heat treatments 03 p0372 A72-13595

Scale factor and surface imbedded inserts effect on bending cyclic fatigue strength of nonhardened and roll hardened Al-Ti alloy 03 p0372 A72-13596

Crack growth in elastoplastic and viscous media under cyclic loading 03 p0452 A72-14137

Cyclic deformation and fatigue testing equipment and techniques for biaxial stress, stress concentration and pure bending 03 p0339 A72-14168

Corrosion fatigue cyclic crack growth rate above and below environmental threshold stress in steels as function of frequency and potentials, indicating hydrogen embrittlement 03 p0377 A72-14172

Rheological relations of moment-stress plasticity for steady and cyclic loads, using small elastoplastic strains 03 p0453 A72-14212

Elastoplastic circular plates optimum shakedown design under cyclic loading 04 p0585 A72-14613

Canonical form for boundary conditions of thin elastic shells with oscillating loads applied on edges 04 p0587 A72-15013

Titanium alloy microstructure effect on fatigue strength under symmetric bending load cycles in air and NaCl solution 04 p0535 A72-15663

Strength margin estimation in materials sustaining cumulative static and damage under cyclic thermal loads 05 p0735 A72-15994

Zircaloy plastic properties and fatigue fracture modes under strain controlled push-pull cyclic loads, noting plastic anisotropy changes for warm cross rolled and recrystallized materials 05 p0678 A72-17120

Cyclic loading effects on resistance to brittle fracture of low carbon structural steels, using crack with criterion 06 p0831 A72-18353

Slip band formation and crack initiation in Ti as function of cyclic loading frequency, considering plastic strain amplitude or distribution as causes [DFVLR-SONDDER-149] 06 p0832 A72-18425

Failure analysis of plastic materials susceptible to cyclic strain hardening under thermal load, considering residual stress concentration 06 p0898 A72-18547

Refractory and structural steels and Al alloys, obtaining low cyclic plastic deformation and breaking stress curves 06 p0898 A72-18549

Low cyclic failure resistance at elevated temperatures and static defects calculation based on fatigue and empirical endurance curves 06 p0898 A72-18555

Cyclic bending stress distribution in fir tree turbine blade root for arbitrary loading phase 06 p0899 A72-18629

Deformation kinetics and failure of refractory Nb and Mo base alloys in plastic state under low cyclic fatigue 06 p0833 A72-18631

Nb and Nb-Zr alloy tubular and sheet samples cyclic loading tests, determining heat treatment effects on notch sensitivity and fatigue strength 06 p0834 A72-18646

Two-mirror optical system to study energy dissipation in elastic systems subjected to cyclic straining and vibrations 06 p0819 A72-18649

Cyclic loading failure criteria based on plastic deformation energy concepts, considering material load carrying capacity 06 p0899 A72-18650

Plastic deformation fatigue theory extended to tests at stresses below elastic limit, explaining cyclic loading frequency effect on fatigue life 06 p0899 A72-18652

Fibrous composite materials experimental failure studies at high temperatures and cyclic loading 06 p0838 A72-18654

Titanium alloy durability under cyclic torsion in vacuum at various temperatures, investigating fatigue life and tensile strength 06 p0834 A72-18665

Thermostable and heat resistant steels and alloys vibration loading frequency effects on fatigues at high temperatures 06 p0834 A72-18688

Finite element method application to fracture mechanics problems of stress concentration and intensity factors and elastoplastic response to cyclic loading 07 p1088 A72-19130

Mechanical energy consumption effects of thermal dissipation and cyclic straining methods during sample life tests 07 p1089 A72-19260

Dynamic buckling of elastic shallow structures under periodic loading, determining critical load upper and lower bounds by energy method 07 p1090 A72-19731

Two and three dimensional quasi-static coupled thermal diffusivity problem for deformable body, determining physicochemical state of solid circular cylinder under cyclic loads 07 p1090 A72-19752

Stress-strain state relationship to crack development morphology in elastic strain region of austenitic steel sample under cyclic bending 07 p1013 A72-19769

Recrystallized and unrecrystallized deformed semfinished wrought Al alloy under cyclic and static loads, investigating macrofracture kinetics 07 p1014 A72-19840

Ductility and fracture of heat resistant steels at high temperatures and unsteady loading, estimating loading cycle effect on plastic strain buildup to failure 07 p1017 A72-20127

Analytical model for surface fatigue crack configuration during propagation into thick plate under cyclic loading [AD-741575] 07 p1095 A72-20242

Fatigue life gages to determine cumulative fatigue damage due to variable cyclic strain history on unmatched materials 08 p1163 A72-20915

Fatigue life gages planning and application to airplane cyclic fatigue test, describing automatic data acquisition system 08 p1163 A72-20916

Soviet handbook on vibration absorbing properties of construction materials under cyclic straining, covering energy dissipation and dynamic strength 08 p1185 A72-20975

Glass fiber reinforced plastics irreversible cumulative damage under axial cyclic tension compression loads with heat production 08 p1191 A72-21500

Anisotropy effect on glass fiber reinforced plastics cyclic deformability and heating kinetics under cyclic tension compression loads

08 p1191 A72-21501

Setup to determine sonic creep and acoustic fatigue in polymers under symmetrical and asymmetrical load cycles at sonic and ultrasonic oscillation frequencies

08 p1147 A72-21763

Fiberglass reinforced plastics creep characteristics under high strain rate loading-unloading conditions

08 p1195 A72-21855

Fiberglass reinforced plastics fatigue failure prediction based on test demonstrated correlation between static and cyclic strainability

08 p1195 A72-21856

Fatigue failure mechanism in short fiber reinforced plastics, determining crack growth rates under cyclic loading

[PIPAER 2]

09 p1336 A72-22539

Temperature fields produced in viscoelastic cylindrical, conical and spherical shells by cyclic loads, calculating displacements from zero moment stress theory formulas

09 p1399 A72-22701

Elastoplastic stressed state of multilayer cylinder during loading, unloading and cyclic loading processes

09 p1401 A72-22721

Energy balance criterion application to crack growth under cyclic fatigue loading, considering stress-strain behavior of plastic deformation energy

09 p1404 A72-22911

Tensile microstrain and cyclic loading behavior of carbon fiber reinforced plastic composites at elevated temperature

09 p1338 A72-23169

Fatigue fracture of polymethyl methacrylate at room temperature under uniaxial failure cyclic loading

09 p1339 A72-23244

Parametric instability of flat rectangular plates under periodic or shear sinusoidal in-plane boundary loads

09 p1408 A72-23463

Statistical evaluation of welded airframe component fatigue damage increment during cyclic loading with constant force amplitude

10 p1559 A72-24922

Ni fatigue crack propagation under low cyclic loads at high temperature in vacuum after annealing and mechanical treatment

11 p1655 A72-25497

Two dimensional elastoplastic finite element analysis of structural members under cyclic thermal-mechanical loadings

[ASME PAPER 72-GT-1]

11 p1734 A72-25604

Computational technique for crack growth prediction in metal subjected to variable amplitude cyclic loading, taking into account yield zone ahead of crack tip

[ASME PAPER 71-MET-X]

11 p1735 A72-25876

Theoretical fatigue test procedure for reliability analysis of machine parts, calculating fatigue probability in load carrying components

11 p1640 A72-26244

Cyclic loads frequency and environmental effects on fatigue crack propagation rate, comparing theoretical results with Al alloy thin plates experimental data

11 p1663 A72-26802

Plastic percentage reduction of area and elongation for circular cylindrical sample in tensile deformation, proposing stress analysis method for metallic sleeves under low cycle loads

11 p1738 A72-26810

Two coordinate oscillograph recording device with automatic reversing for stress-strain tests under static and cyclic loads

11 p1637 A72-26814

Ti alloys fatigue strength, stress concentration sensitivity and grain sizes effects at normal and high temperature under cyclic loads

11 p1663 A72-26821

Fatigue failure tests of low carbon Mn steel, analyzing structural damage under cyclic loads in relation to temperature curve

12 p1829 A72-27458

Fatigue testing machine for material behavior under elastoplastic bending loads with constant or smoothly varying programmed vibration frequency and amplitude

12 p1795 A72-27463

Cumulative damage and structural changes in friction contact areas of steel plates under cyclic pulsed loads, noting microhardness distribution and surface layers microstructure

12 p1818 A72-28191

Wear micromechanism in hard and brittle chromium steels under cyclic slide friction loads

12 p1818 A72-28194

Elastoplastic deformation effects on load bearing capacity of samples with stress concentrators under alternating cyclic loading, obtaining nomograms by digital computer

12 p1887 A72-28228

Material fatigue failure criterion during cyclic loading, noting energy dissipation and resonant frequency roles

12 p1888 A72-28250

Testing machine for synthetic plastic cylindrical specimens cyclic cophasal compression-torsion load tests, describing mechanical and hydraulic subsystems and testing techniques

13 p1938 A72-28559

Stress-service life relations for duralumin samples from impact and nonimpact tensile tests with cyclic axial loads, noting notch sensitivity

13 p1978 A72-29147

Steels shafts fatigue failure under cyclic loading and fretting corrosion, indicating fatigue strength increase through surface layer wear resistance augmentation

13 p1979 A72-29476

Borated steels strength under static bending, cyclic flexure and torsion and impact loads, correlating fatigue strength, residual stresses and core properties

13 p1979 A72-29477

Crystal lattice defects induced by cyclic straining in quenched Al-Zn alloy, noting fatigue effects on dislocations accumulation and grain boundary migration

14 p1210 A72-30610

Temperature effects on nonelastic behavior of turbine rotor disk for steady and cyclic loading, noting creep solutions, transient stress and plastic strain

14 p2167 A72-30906

FRAM /failure rate appraisal machine/ concept and application for modular electronic and electromechanical assemblies environmental cycling tests, noting technical and economical effectiveness

14 p2093 A72-31169

Ti alloy fracture strength determination by crack propagation observation in specimen center, noting load-displacement curve construction from cyclic loading test

15 p2259 A72-32804

Safe stress range for metal fatigue deformation preceding fracture under combined cyclic and steady push-pull loads

16 p2468 A72-33228

Load cycle frequency and time characteristic effects on plastics fatigue behavior, considering relaxation, retardation and internal damping induced heating effects

16 p2416 A72-34145

Definition of the fatigue limit on the basis of the distribution of the resistance over the set of elementary volumes of which the sample is composed

17 p2565 A72-34196

Fatigue life gages use in combination with strain multipliers in field applications with random ergodic cyclic strains

17 p2554 A72-34822

Steady state response of nonlinear beam under periodic loading, using finite element techniques for nonlinear differential equation

18 p2732 A72-36078

A mechanical pulsator for testing plastics with the capacity for adjusting cyclic and mean load during test

18 p2676 A72-37097

Measurement of the damping capacity and dynamic modulus of high-damping metals under direct cyclic stresses

19 p2795 A72-37460

Effect of the loading frequency on the fatigue strength of metals

19 p2818 A72-38012

Influence of the structure of VTZ-1 and VT-18 alloys on the fatigue strength for an asymmetrical loading cycle

19 p2819 A72-38017

Filament wound cylindrical pressure vessel design and development for operation under cyclic-loaded high hydraulic pressure in underwater environment

19 p2877 A72-38166

Effect of stress amplitude and number of vibration cycles on the damping decrement in metals

19 p2878 A72-38217

The octahedral shear strain theory and its relation to biaxial cumulative fatigue damage

20 p2978 A72-39202

Creep-fatigue interaction interpretation for austenitic stainless steels from crack growth viewpoint, investigating time and cycle dependent failure at elevated temperature

20 p2937 A72-39213

Fatigue tests at low cyclic loads of smooth and notched Ti alloy specimens, noting surface hardening effect on service life

20 p2941 A72-39580

Review - Fatigue-crack propagation in metallic and polymeric materials

20 p2980 A72-39793

Metal fatigue crack propagation under cyclic loads, assuming specific energy dissipation as material constant

20 p2981 A72-39953

Study of fatigue crack initiation from flaws using fracture mechanics theory

20 p2981 A72-39961

Stability and non-stationary vibration of columns under periodic loads

21 p3116 A72-40336

Influence of the cycling frequency and directional anisotropy on the fatigue strength of AMg6BM aluminum-alloy sheet

21 p3070 A72-41356

Comparison of the resistance to fracture of the K1c of the AK4-1T1, V95T1, and D16T aluminum alloys and VT8 and VT9 titanium alloys under static and cyclic loading

21 p3071 A72-41705

Allowance for the hysteresis behavior of a continuous medium in a complex state of stress under conditions of simple cyclic loading

21 p3127 A72-41711

Estimation of the effect of stress concentration in nonstationary loading regimes

22 p3232 A72-41922

Stress amplitude and hysteresis loop width changes in alpha Ti during cyclic work softening-work hardening with constant strain amplitude

22 p3189 A72-42438

Cyclic hardening of Al-Zn single crystals at constant plastic strain amplitude, observing similarity between fatigue hardening and work hardening

22 p3189 A72-42439

Influence of the cycling frequency on the fatigue and corrosion fatigue of steel samples with bushings

22 p3242 A72-43155

Inelastic effects during metal fatigue

22 p3195 A72-43156

Investigation of the kinetics of low-cycle fatigue of steels in a hydrogen atmosphere and in vacuum

22 p3195 A72-43161

Fracture mechanics and cumulative damage of simulated solid propellant under dynamic loads, obtaining low cycle fatigue curve

23 p3325 A72-43706

Dynamic model for microinhomogeneous elastoplastic medium under cyclic loads with varying amplitude

23 p3347 A72-43729

Fatigue test equipment for 293-233 K and 50-100 ton static or 25-50 ton cyclic loads, using Freon 22 as coolant

23 p3278 A72-43759

Elastoplastic computation of thin cylindrical shells under cyclic loading

23 p3348 A72-43786

Energy dissipation in metals during high-frequency fatigue tests. I

23 p3302 A72-43963

Energy dissipation in metals during high-frequency fatigue tests. II

23 p3302 A72-43964

Measuring fracture toughness - A simplified approach using controlled crack propagation

23 p3290 A72-44258

Development of a push-pull fatigue testing machine under high pressure, and the results of preliminary fatigue tests

24 p3401 A72-44630

Microinhomogeneous elastoplastic cyclically strain hardenable material under symmetric loading, calculating stress-strain relationship

24 p3458 A72-44928

Al and Al-Zr coating effects on heat resistant alloy turbine blades high temperature fatigue resistance under bending-torsion cyclic loads

24 p3415 A72-45732

Strength margin estimation in materials sustaining cumulative static and cyclic damage under thermocyclic loads

24 p3460 A72-45736

Cyclic loading effects on resistance to brittle fracture of low carbon structural steels, using crack width criterion

24 p3416 A72-45740

Ductility and fracture of heat resistant steels at high temperatures and unsteady loading, estimating loading cycle effect on plastic strain buildup to failure

24 p3416 A72-45753

CYCLING

U CYCLES

CYCLONES

Tropical hurricanes and storm outflow layer wind analyses from ATS 3 satellite data, noting cyclonic eddy asymmetric structure

03 p0384 A72-14144

Long wave radiation and surface friction effects on midlatitude cyclone development in eight-level primitive equation orographic model

03 p0385 A72-14229

Storm forecasts by meteorological satellites, describing TV monitoring of cyclones and hurricanes

05 p0683 A72-15978

Periodic aspects of nonphenemeral Euroatlantic blocking systems persistence, noting dominant role played by cyclonic vortices

05 p0684 A72-16794

Geomagnetic dipole field kinematic reversals due to cyclonic convective cell distribution fluctuations in earth core

06 p0807 A72-17895

Solar magnetic field regularities analogy with terrestrial cyclones instead of convection cells in vertical heat transport

07 p1074 A72-19558

Storm available potential energy generation and boundary layer frictional dissipation estimation in heat transfer from ocean to atmosphere within east coast cyclone

07 p0980 A72-20451

Conditional instability of second kind (CISK) model of surface cyclonic vorticity dependence on vertical distribution of latent heat release

12 p1838 A72-27019

Baroclinic instability formulation as initial value problem compared to normal mode studies, considering cyclone development in atmosphere

13 p1945 A72-28446

Relative vorticity and balanced height distributions from cloud velocities associated with cloud structure of extratropical cyclone over continental U.S.

16 p2419 A72-33945

Lunar and solar gravitational effects on earth atmosphere, describing latitudinal distribution of cyclone centers by momentum distribution of horizontal tide-generating forces

23 p3310 A72-43249

Satellite-observed Southern Hemisphere cloud vortices in relation to conventional observations.

23 p3285 A72-44145

CYCLOPROPANE

Differential neurophysiological and psychological effects of subanesthetic concentrations of cyclopropane, diethyl ether, methoxyflurane and ethrane in conscious man

04 p0480 A72-15220

Evidence for protonated cyclopropane intermediates in crossed-beam ion molecule reactions.

24 p3379 A72-45475

CYCLOTETRAMETHYLENE TETRAMINE

U HMX

CYCLOTETRAMETHYLENE TRINITRAMINE

U RDX

CYCLOTRON FREQUENCY

Electron cyclotron harmonics emission as function of electron plasma frequency in He reflex discharge, measuring electron densities

01 p0105 A72-10026

Circularly polarized microwave damping at electron cyclotron frequency in low density magneto cesium plasma, investigating power absorption coefficient and refractive index

04 p0555 A72-14853

Magnetospheric electron cyclotron and Langmuir plasma frequencies ratio determination from satellite observed electron and ion density data

05 p0659 A72-16765

Electromagnetic wave propagation and thermal spread in uniform magnetoplasma at electron-cyclotron resonance frequencies, discussing kinetic and multifluid theory

06 p0854 A72-17489

Fast electron-cyclotron wave excitation with infinite phase velocity along magnetic field in nonequilibrium electron plasma

06 p0862 A72-18402

Infinite uniform Vlasov plasma response to steady state transverse excitation, considering spatial electron cyclotron damping

06 p0864 A72-18539

Electrostatic wave instabilities at harmonics of electron cyclotron frequency in hot and cold anisotropic plasma with Maxwellian temperature distribution

07 p1039 A72-18824

Nonlinear Landau damping and growth of finite amplitude cyclotron harmonic plasma waves in magnetic field, measuring coupling coefficients by calibrated interferometer

07 p1041 A72-19506

Semiconductors cyclotron echo signals from dipole interactions of electrons with alternating magnetic fields, discussing frequency doubling and excitation mechanism

07 p1048 A72-19639

Magnetized large volume plasma heating by hf ring field at ion cyclotron frequency

08 p1215 A72-21727

Electromagnetic wave propagation obliquely incident on thermal inhomogeneous plasma at frequencies near second electron cyclotron harmonic

09 p1365 A72-23521

Collisional cyclotron instability nature in ionized gases in presence of Ramsauer effect

10 p1520 A72-24224

Pulsed RF hydrogen plasma heating in mirror machine near ion cyclotron frequency and harmonics

11 p1699 A72-26703

Computerized calculation of wave dispersion curves for hot Maxwellian electron magnetoplasma, applying to upper hybrid and cyclotron frequencies

13 p2013 A72-29340

Alouette 2 plasma resonances observation near ionospheric electron cyclotron frequency harmonics, interpreting frequency shift as wave dispersion effects

17 p2546 A72-34692

Fast electron cyclotron wave excitation with infinite phase velocity along magnetic field in nonequilibrium electron plasma

17 p2588 A72-34853

Magnetospheric electron cyclotron and Langmuir plasma frequencies ratio determination from satellite observed electron and ion density data

17 p2548 A72-35268

Weak electrostatic turbulence observation in earth bow shock magnetic field gradient, suggesting cyclotron drift instability role

23 p3342 A72-44523

Semiconductors cyclotron echo signals from dipole interactions with alternating magnetic fields, discussing frequency doubling and excitation mechanism

24 p3431 A72-44571

CYCLOTRON RADIATION

NT ION CYCLOTRON RADIATION

Hot magnetoplasmas cyclotron radiation, investigating thermal particle motion effects

01 p0107 A72-10142

Charged particles magnetic scattering on cyclotron instability waves of radiation belt plasma, estimating proton relaxation time

01 p0119 A72-10608

Fast cyclotron and synchrotron transverse waves noise measurement in electron flux, using resonator with homogeneous electric field

02 p0190 A72-11573

Ion acoustic and cyclotron harmonic plasma waves parametric excitation by hf electric field, measuring thresholds and growth rates agreeable with theory

06 p0861 A72-17827

High frequency heating of dense toroidal plasma by nonaxisymmetric ion cyclotron waves resonant excitation in closed magnetic trap

07 p1043 A72-19636

Cyclotron magnetoacoustic wave generation by planets and binary stars in circular orbits, deriving interstellar gas density variations

08 p1231 A72-21122

Electrostatic cyclotron harmonic waves propagation in inhomogeneous electron plasma slab, deriving RF electric field

14 p2138 A72-30397

Experimental investigation of electrostatic cyclotron harmonic waves excited in inhomogeneous plasma column with axial magnetic field by RF capacitor field

14 p2138 A72-30398

Electron beam amplifier based on fast cyclotron wave interaction with slow synchronous wave in axisymmetrical electrostatic field, discussing power efficiency increase

15 p2210 A72-32737

Ion acoustic, electron plasma and cyclotron harmonic waves parametric instabilities in magnetic field and applications to plasma heating

16 p2433 A72-32811

Turbulence of electrostatic electron cyclotron harmonic waves observed by Ogo 5.

17 p2549 A72-35599

Electron cyclotron drift instability linear theory application to controlled fusion and collisionless shocks, proving anomalous resistance to current flow normal to magnetic field

17 p2592 A72-35624

Instability of electromagnetic cyclotron harmonic waves in plasmas.

17 p2592 A72-35775

OH maser sources parametric down-conversion, deriving nonlinear current densities, electron cyclotron wave damping and parametric gain coefficient

21 p3064 A72-41030

Hamiltonian analysis of charged particle motion in the pulsar rotating magnetic field.

21 p3111 A72-41472

High frequency heating of dense toroidal plasma by nonaxisymmetric cyclotron waves resonant excitation in closed magnetic trap

24 p3427 A72-44568

CYCLOTRON RESONANCE

Higher order cyclotron harmonic resonance of electrons with electromagnetic wave propagation through collisionless magnetoplasma, deriving energy oscillation time period

01 p0105 A72-10023

Circularly polarized electromagnetic wave propagation through afterglow helium slab plasma near electron cyclotron frequency

02 p0266 A72-12653

Cyclotron resonance interaction between electromagnetic waves and nonthermal plasmas for Cauchy velocity distributions yielding algebraic dispersion equations

06 p0860 A72-17745

Low frequency drift instability in local electron cyclotron resonance produced plasma, discussing oscillation fundamental frequency characteristics, wave propagation, density and potential waves, etc

07 p1039 A72-18799

Electron cyclotron resonance in Penning ion source, measuring electron temperature from X ray emission spectra

10 p1516 A72-25029

Plasma beam cyclotron instability theory based on computer simulation, noting stabilizing effect due to Landau damping

11 p1693 A72-25562

Quiescent plasma production with axially homogeneous density distribution in skipping magnetic fields by electron cyclotron resonance discharge, noting high electron temperatures

12 p1851 A72-27400

MHD stability in Hg vapor discharge plasma excited by standing microwave near electron cyclotron resonance, discussing electron energy anisotropy effect on LF oscillations

13 p2017 A72-29618

Nonlinear coupled cyclotron oscillators excitation by external sine wave force, analyzing amplitude/phase variation and negative absorption

14 p2132 A72-31115

Investigation of two types of collisionless linear dampings of electromagnetic waves in a non-homogeneous magnetized plasma.

17 p2588 A72-34870

Collisional losses in a very-low-frequency duct associated with the lower-hybrid-resonance frequency.

17 p2517 A72-35608

Production of intense ion beams by high-frequency electric fields.

19 p2839 A72-37331

MHD stability in Hg vapor discharge plasma excited by standing microwave near electron cyclotron resonance, discussing electron energy anisotropy effect on LF oscillations

21 p3091 A72-40671

Differential equations for energy flow between electron beam and electromagnetic field, avoiding electron trajectory explicit calculation in nonlinear treatment of cyclotron resonance interaction

22 p3159 A72-42304

Investigation of interaction between Pc 1 and 2 and Pc 5 micropulsations at the synchronous orbit during magnetic storms.

22 p3171 A72-42412

Initial electron velocity and emitter surface roughness effects on oscillatory velocities dispersion in helical electron beams used in cyclotron resonance masers

22 p3208 A72-42664

Calculation of the parameters of a plasma accelerated in a high-frequency electric field and a static magnetic field

23 p3320 A72-43660

Rocket observation of topside resonances.

23 p3286 A72-44517

CYCLOTRONS

Low-frequency oscillations in a Penning-discharge plasma under conditions of a cyclotron ion source

21 p3095 A72-41682

CYGNUS CONSTELLATION

Temporal behavior, intensity fluctuations and energy spectrum of pulsating X ray source Cygnus X-1 from Uhuru observations

01 p0121 A72-11092

Cas A, Tau A, Cyg A and Orion Nebula absolute flux density measurements at centimeter wavelengths

04 p0578 A72-15313

High energy gamma rays from Cygnus region, using balloon flight measurements with spark chamber telescope

06 p0873 A72-17891

Scorpius X-1 and Cygnus X-1 pulsed radio emission search by sensitive de-dispersing technique

07 p1073 A72-19422

Cassiopeia A secular flux density decrease relative to Cygnus A and Taurus A at 1.4 and 3 GHz, discussing application to antennas and radio telescopes calibration

09 p1390 A72-23529

Soft X-rays from Cygnus X-2 and from Cygnus X-1 in eclipse/.

17 p2600 A72-35297

High energy gamma ray point sources in Cassiopeia and Cygnus regions, using extensive air shower Cerenkov flashes detection technique

23 p3329 A72-43941

CYLINDERS

High temperature and pressure detonation gas expansion as shock wave from cylindrical volume, calculating flow velocity, pressure and density

02 p0302 A72-12285

Plane electromagnetic wave diffraction on two cylinders with different radii, assuming infinite length and ideal conductivity

04 p0491 A72-15413

Two dimensional stationary temperature fields determination in ribs, cylinders and pipes with temperature independent heat conductivity

05 p0746 A72-16188

Gegenbauer /ultraspherical/ polynomials and Meijer G-functions for solution of heat production and diffu-

sion in cylinder with internal sources leading to axisymmetric temperature distribution

05 p0747 A72-16791

German monograph on steady flow past sphere and cylinder near wall, discussing drag, lift and flow visualization

08 p1108 A72-21950

Nonsymmetrical cylinders and valves under nonsymmetrical loading

08 p1113 A72-22157

Surface current density of perfectly conducting polygonal cylinders for axially polarized incident electromagnetic field

09 p1350 A72-22247

Two dimensional MHD conducting fluid flow past insulating cylinder in presence of arbitrarily oriented magnetic field, determining lift and drag coefficients for small Hartmann numbers

09 p1359 A72-22533

Temperature and thermal stress distribution in cylinder of finite length for mixed heating conditions

09 p1400 A72-22707

Elastoplastic stressed state of multilayer cylinder during loading, unloading and cyclic loading processes

09 p1401 A72-22721

Reynolds number and cylindrical spacing effect on Karman vortex street formation from smoke visualizations of single and tandem cylinder wakes

09 p1261 A72-22939

Plastic compression of short cylinders prepared from incompressible rigid-plastic material with variable vertical yield point distribution, deriving variational equation of plastic flow

09 p1406 A72-23183

Piston exerting pressure on liquid filled cylinder, determining deformation state based on thin elastic orthotropic plate theory

10 p1556 A72-24266

Rectangular and D-shaped cylinders pressure distribution and aerodynamic force measurements in two dimensional flow as function of cross sectional height/width ratio

10 p1419 A72-24840

Hydrodynamic field generated by sphere motion along viscous fluid filled cylinder axis beyond Stokes regime

10 p1470 A72-24852

Unsteady flow evolution at sphere and elliptical cylinder obtained by flow visualization techniques, showing streamline sequence dependence on angle of attack

12 p1797 A72-27469

Cylindrical samples with deep circular hyperbolic notch, investigating cyclic inelastic strain induced stress redistribution effects on load bearing capacity

12 p1830 A72-28229

Momentum consideration aided air resistance calculations for cylinder, discussing position effects

13 p1893 A72-28705

Dynamic thermo-magnetoelastic problems of long cylinder and infinite medium with hole under magnetic field, using variation method and Laplace transforms

13 p2056 A72-28882

Helium use to minimize deflection of modulated laser beam in measurement of free surface motion of expanding annular cylinder loaded by exploding wire

13 p1960 A72-29765

Momentum and energy equations for pool film boiling heat transfer from horizontal cylinder to saturated liquids, using integral boundary layer analysis

14 p2173 A72-31067

Definition of the fatigue limit on the basis of the distribution of the resistance over the set of elementary volumes of which the sample is composed

17 p2565 A72-34196

Development of transition in the wake of a cylinder perpendicular to a supersonic flow

17 p2484 A72-34769

Eigenfunction technique development to incorporate stress singularities at circumference of end planes into problem of solid cylinder compression between rough rigid stamps

17 p2633 A72-35403

Damping coefficient measurement for sound waves inside cylindrical tube closed at one end and excited at other end by loudspeaker

17 p2582 A72-35426

Axial-symmetric deformations of a rubber-like cylinder under initial stress.

18 p2738 A72-37081

An experimental study of the sensitivity to freestream turbulence of heat transfer in wakes of cylinders in crossflow.

19 p2787 A72-38396

Forced convection heat transfer from cylinders to water in cross flow, quantifying method of accounting for fluid property variation

19 p2881 A72-38397

An investigation of the flow around rectangular cylinders.

19 p2747 A72-38813

Breakdown of superfluidity for cylinders in saturated liquid helium II.

19 p2836 A72-38840

Wall interference effects on cone-cylinder pressure distribution in variable porosity trisonic wind tunnel as function of model blockage and Mach number

[AIAA PAPER 72-1010] 21 p3041 A72-41592

Base mounted cylinders effect on near wake of axisymmetric blunt base in supersonic flow

[AIAA PAPER 72-1013] 21 p2993 A72-41594

On the unsteady magnetohydrodynamic flow over yawed infinite cylinder.

24 p3395 A72-45599

CYLINDRICAL AFTERBODIES

U AFTERBODIES

U CYLINDRICAL BODIES

CYLINDRICAL ANTENNAS

Automatically retrodirective performance from circular arrays and circularly continuous aperture antennas, applying method to cylindrical antennas

01 p0043 A72-11248

Book on metallic and dielectric antennas covering planar, cylindrical and plasma types for symmetrical, dipole and ring excitations

04 p0497 A72-14612

Cylindrical grid-like antenna in anisotropic compressible homogeneous plasma, obtaining magnetic field effects on wave dispersion by numerical solution

04 p0488 A72-15306

Modes propagating inside tubular microwave antenna, studying canonical problems by asymptotic and modal techniques

04 p0301 A72-15430

Two-layer dielectric loaded cylindrical antenna with wall airgap, calculating radiation pattern by boundary value approach

06 p0775 A72-18240

Cylindrical antenna radiation resistance and total radiated power in weakly ionized plasma, considering electron collisional effects

07 p0944 A72-19592

Circular semiinfinite dielectric rod antenna, determining near- and far-zone fields, gain and beamwidth under excitation by HE/sub 11/ hybrid mode

07 p0956 A72-19782

Current distribution in cylindrical parasitic antenna immersed in arbitrarily directed and polarized incident plank electromagnetic wave

[AD-743574] 07 p0957 A72-19787

Toeplitz matrix in numerical solution of integral equation for cylindrical antenna and array, presenting rapid inversion algorithm by exploiting symmetry properties

[AD-743577] 07 p0957 A72-19795

Thin antenna hf time response from thin wire approximation and source gap model for integral equation solution

07 p0957 A72-19798

Impedance strip synthesis on symmetric cylindrical antenna excited by phased magnetic flux ring, determining radiation pattern for pure resistance conditions

08 p1131 A72-20932

Broadband cylindrical monopole antenna with adjustable quasi-distributed capacitive loading, comparing theoretical and experimental admittances

11 p1604 A72-25744

Local FM radio pulse scattering by cylinder and linear cylinder array in Kirchhoff approximation

13 p1914 A72-28407

Optimal directional gain and slope difference characteristics of cylindrical nonsuperdirectional slot antennas, relating sidelobe-main lobe radiation

13 p1927 A72-28408

Cylindrical antenna immersed in weakly ionized magnetoplasma, calculating steady magnetic field effect on electromagnetic and electroacoustic radiation resistances

16 p2434 A72-32860

Numerical analysis of boundary value problem for finite cylindrical dipole antenna of arbitrary orientation in magnetized plasma approximated by uniaxial medium

16 p2366 A72-34107

An electromagnetic analysis of a cylindrical homogeneous lens.

17 p2525 A72-34362

Distribution of current in centre-fed cylindrical dipole antennas with arbitrarily displaced feed points.

17 p2526 A72-34517

Cylindrical phased arrays - Beam scanning and sidelobe control.

17 p2531 A72-35573

Optimal distributions for semi-circular arrays of isotropic radiators.

18 p2666 A72-36330

Analysis and element pattern design of periodic arrays of circular apertures on conducting cylinders.

21 p3026 A72-40351

Computerized design for cylindrical cage antenna, using polynomial approximation of current to reduce computer size and time requirements

21 p3028 A72-40511

CYLINDRICAL BODIES

NT ROTATING CYLINDERS

Plane electromagnetic wave scattering by imperfectly conducting cylinder with radially inhomogeneous

dielectric coating, using phase shift method for evaluation

01 p0024 A72-10130

Multipole methods for electromagnetic scattering from conducting cylinder over dielectric half space, noting application to radar cross sections

01 p0030 A72-10842

Upset steel cylinders under axial compression loads, determining localized surface stress and strain critical values at fracture

01 p0141 A72-11032

Forced air cooling of cylindrical body with distributed thermal input, calculating temperature distribution and optimum mechanical dimensions for temperature rise minimization

02 p0189 A72-11560

Shock wave impact at flat/spherical end surface of cylindrical body in supersonic nitrogen flow, using pulsed ruby laser for shadow photography

02 p0151 A72-12280

Turbulence intensity effects on mass transfer from cylinders in cross flow at various Reynolds numbers [ASME PAPER 70-WA/HT-3]

02 p0205 A72-12312

Monatomic He-Ar binary gas mixtures heat transfer to cylinders in low Reynolds number flow, considering internal energy effects

02 p0303 A72-12358

Unstiffened cylinders natural frequency equations, determining modal density distribution and acoustic radiation efficiency

02 p0293 A72-12373

Two finite conducting cylinders radial vibrations in E polarized electromagnetic wave, detailing pressure distribution and resonance effects

02 p0262 A72-12877

Ductility relationship to plasticity characteristics in cylindrical steel samples with short notch under tension

03 p0443 A72-13458

Transition on plane plate in presence of vortices detached from cylinder in free flow

03 p0342 A72-13788

Cylindrical shafts with deep circumferential grooves, determining effective stress concentration under axial tension or bending

03 p0451 A72-14125

Cylindrical shaft with circumferential groove, obtaining approximate solution for stress concentration at groove contour under torsion

03 p0452 A72-14130

Cylindrical nuclear fueled capsules heat transfer gaps, determining dimensional changes with neutron radiographs

04 p0546 A72-14428

Steady heat conduction plane problem solution for infinitely long cylinder with constant surface thermal flux density and temperature

04 p0595 A72-14644

Hf electromagnetic wave scattering and diffraction by smooth dielectric cylinder and sphere based on Lorentz excitation theory

04 p0490 A72-15397

Plane electromagnetic wave diffraction by periodic lattice of long finite conductivity cylinders with arbitrary electric radius

04 p0491 A72-15414

Flutter of thin homogeneous isotropic cylindrical panels from analog computer study

04 p0593 A72-15646

Plane electromagnetic wave diffraction by infinite cylinder with unsteady impedance boundary conditions

05 p0627 A72-16409

Asymptotic solution to short wave diffraction by convex cylinder, constituting geometrical optic expansion and caustic curves for illuminated and shadow region

05 p0628 A72-16411

Wake instabilities and vortices spacing, position and strength behind slender cylindrical bodies at large incidence with subcritical cross flow Reynolds numbers

05 p0610 A72-17010

Steady two dimensional symmetric viscous flow past parabolic cylinder in uniform stream, correlating calculated nose skin friction with boundary layer theory

05 p0610 A72-17012

Partially insulated homogeneous cylinder temperature distribution from heat conductivity boundary value problem equations

05 p0751 A72-17142

Stress and displacement solutions to elastic deformation of homogeneous and composite anisotropic near cylindrical bodies, using Almansi algorithm

06 p0894 A72-17688

Nonheat treated extruded Mo alloy under tension and vacuum conditions at various temperatures, investigating cylindrical samples size effects on mechanical properties

06 p0833 A72-18635

Scattering properties of conducting cylindrical obstacle in rectangular waveguide, deriving scattered field integral representation via Green function

07 p0944 A72-19593

Thermally induced convection flow characteristics in separated or wake formation regions over heated cylindrical surface submerged in water
07 p1100 A72-19630

Thermoelastic waves diffraction steady state problems in multiply connected cylindrical and spherical surfaces, deriving scalar wave equations
07 p1094 A72-19986

Freely supported three layer cylindrical panel stability and critical loads under combined uniform axial compression and transverse pressure
08 p1242 A72-20907

Two dimensional two step difference scheme for shock wave interaction with cylinder in supersonic flow
08 p1150 A72-21443

Solid cylinder stress-strain state under thermal and mechanical loads, obtaining analytical solutions via flow theory based on Von Mises yield condition
09 p1401 A72-22723

Continuum model for cylindrical and spherical elastic laminated composites deformation, using balance and constitutive equations
09 p1405 A72-22992

Flat face cylinders in rarefied supersonic gas flow, investigating perturbed region evolution based on pitot tube method
10 p1415 A72-23751

Mach number distribution along critical streamline in compressed layer in front of cylinder in supersonic flow
10 p1415 A72-23752

Radiant flux from finite cylindrical volume to coaxial screen calculated under quasi-homogeneous medium and arbitrary optical thickness assumptions
10 p1561 A72-23841

Nonstationary radiative heat transfer between cylindrical body and ambient medium, determining regular heating condition region
10 p1561 A72-23842

Radial vibrations of isotropic homogeneous sphere and cylinder bonded to thin nonhomogeneous casting outside
10 p1557 A72-24406

Friction drag coefficient determination for cylindrical bodies in laminar and turbulent incompressible fluid flow
10 p1420 A72-25135

Separation flow field measurements for space shuttle cylindrical configurations in hypersonic streams, using pressure heat transfer and visualization techniques
[AIAA PAPER 72-294] 11 p1567 A72-25232

Fluid flow and heat transfer in tube bank with two cylinders in cross flow, determining static pressure, Nusselt number and drag coefficients
11 p1743 A72-25259

Laminar free convection about isothermal horizontal cylinders with constant heat flux, calculating velocity and temperature profiles
11 p1743 A72-25263

Shock wave impact at flat/spherical end surface of cylindrical body in supersonic nitrogen flow, using pulsed ruby laser for shadow photography
11 p1571 A72-25702

Acoustic and elastic HF waves propagation in nonuniform cylindrical waveguides, deriving asymptotic approximate solutions
11 p1686 A72-25726

Anisotropic cylindrical beam bending by transverse load in elastic plane, reducing to Almansi problem
11 p1736 A72-26091

Axial, circumferential and radial residual stresses calculation in polycrystalline coatings and cylindrical elements during surface layer removal by electrochemical processing
11 p1737 A72-26263

Stressed state induced in compound thick walled cylinder for testing residual tensile stresses effect on machine parts wear resistance
12 p1814 A72-27461

Blowing and suction effects on pulsations of isothermal turbulent jets propagating along porous cylinder
12 p1752 A72-28169

Unloading wave propagation in semiinfinite elastoplastic cylindrical rod for concave stress-strain diagram with no initial linear segment
13 p2053 A72-28388

Resonant frequencies of two thin walled cylindrical panels connected by elastic filler, considering symmetric and asymmetric vibration modes
13 p2058 A72-29146

Friction drag and heat transfer on long blunt-nosed cylinder in supersonic flow, determining location of transition zone as function of Mach number
13 p1895 A72-29642

Rigidity of developable surfaces with cylindrical connections and without plane domains, subjected to infinitesimally small bendings
13 p2061 A72-29793

Three dimensional axisymmetric problem for stressed state of elastic homogeneous cylindrical

orthotropic bodies of revolution, using method based on small parameters
13 p2062 A72-29948

Third order extension of perturbation method to solve Oseen equations for two dimensional steady viscous flow past cylindrical body at low Reynolds number
14 p2095 A72-30722

Pressure distribution and heat transfer in flow separation zone of cone tipped cylindrical body, using shadowgraph photography for flow visualization
14 p2070 A72-31005

Schlieren method for qualitative study of optical inhomogeneities produced by temperature field in cylindrical solid body
14 p2106 A72-31162

Unsteady torsional creep of multiply connected cylindrical rod with arbitrary cross section, calculating elliptic rod relaxation
15 p2327 A72-31744

Elastic wave diffraction on multiconnected cylindrical or spherical regions in nonsymmetric elasticity theory, determining constants of series solution
15 p2330 A72-32290

Linearized supersonic flow past harmonically vibrating cylindrical body, solving boundary value problem by cylindrical integral transformation
16 p2342 A72-32878

Unsteady heat conduction in hollow cylinder suddenly heated by temperature field moving along outer and inner side surfaces
16 p2475 A72-33114

Aerodynamic normal shock noise measurements on nose cylinder bodies in transonic flow
[AIAA PAPER 72-669] 16 p2346 A72-34068

Vibration analysis of cylindrical panels.
17 p2623 A72-34230

Cylindrical diode characteristics with sublimed electrode surfaces.
17 p2527 A72-34607

Electromagnetic waves on a conducting infinite cylinder in a magnetoionic medium.
17 p2517 A72-35399

Finite element analysis of the axisymmetric vibrations of cylinders.
17 p2634 A72-35409

Calculation of solar radiation incident on a cylindrical surface
17 p2498 A72-35515

Scattering of elastic waves by moving objects.
18 p2709 A72-36403

Resonant mode sound field radiated by nonuniform slender circular cross section free-free beams, using dipole array modeling
18 p2710 A72-36410

Transient mode of a flow in the plane wake of a thin plate or cylinder
18 p2642 A72-36899

Solution of the general heat transfer problem by the integral Tolubinskii method for a longitudinal flow past cylindrical bodies
18 p2742 A72-37182

Influence of a trailing vortex on friction pulsations in the near-wall region of the leading stagnation point of a cylinder in transverse flow
19 p2786 A72-38041

Plane and cylindrical electromagnetic waves diffraction on infinitely long cylindrical bodies, calculating induced currents, diffraction patterns and near fields
19 p2767 A72-38654

Plane TE polarized electromagnetic wave diffraction on infinite conducting cylinder in nonhomogeneous medium, calculating far field diffraction patterns
19 p2768 A72-38656

Microwave filter of interdigital or comb construction, calculating attenuation coefficient relationship to impedance of slabline with cylindrical inner conductor
21 p3032 A72-40628

Theory of laminar film condensation of flowing vapor.
21 p3128 A72-40950

Partial differential equation solution for plane electromagnetic wave diffraction by infinite dielectric cylinder of arbitrary cross section
21 p3085 A72-41199

Regime factor and stress concentration parameter for sudden heating of solid cylinders and disks, noting thermal stability criterion with allowance for statistical strength
21 p3123 A72-41361

Transverse magnetic field effect on unsteady incompressible laminar MHD boundary layer flow, noting cylindrical body oscillations in fluid
21 p3095 A72-41786

Temperature distribution and heat flux in infinite length rectangular and finite length cylindrical fins, examining validity of one dimensional approximation
22 p3243 A72-41961

Diffraction of an electromagnetic wave by a noninfinitely conductive cylindrical object of arbitrary cross section
22 p3153 A72-41991

Numerical solution to the Navier-Stokes equations in the problem of a gas flow past a stoke
22 p3166 A72-42252

New method for determining the distribution of delta-g anomalies for a sphere, horizontal cylinder, and vertical material half-line
22 p3173 A72-42574

Application of cylindrical samples to the determination of the resistance to crack propagation of materials
22 p3242 A72-43163

A note on the twisting deformation of a non-homogeneous shaft containing a circular crack.
23 p3346 A72-43708

The boundary layer of higher order at the stagnation line of a yawed cylinder in the case of strong suction or injection
23 p3249 A72-44297

The vortex street in the wake of a vibrating cylinder.
23 p3281 A72-44302

Scattering of obliquely incident waves by inhomogeneous fibers.
24 p3379 A72-44710

Ductility relationship to plasticity characteristics in cylindrical steel samples with short notch under tension
24 p3458 A72-44933

Three dimensional shock wave configurations in front of cylindrical body on supersonic wing or of fluid jet injected into main supersonic flow, examining high pressure gradient regions
24 p3361 A72-45113

Velocity-dependent multiple scattering by two thin cylinders.
24 p3381 A72-45641

CYLINDRICAL CHAMBERS

Coolant flow and heat transfer in rotating circular cylindrical enclosure, solving Navier-Stokes and energy equations by finite difference formulation
06 p0802 A72-18189

Cylindrical tube geometry and electrode separation effects on normal ionizing shock waves, showing speed proportional to azimuthal drive and axial magnetic fields
10 p1470 A72-24794

Molecular flux distribution in cylindrical vacuum chambers with various inlet and pumping configurations under assumption of Knudsen law validity, describing computer program
15 p2183 A72-32382

Boundary-layer effects on pressure variations in Ludwig tubes.
20 p2914 A72-39620

CYLINDRICAL SHELLS

Edge loaded cylindrical shells of resolution nonlinear axisymmetric deformation determination from asymptotic solution of Reissner equations, using multiple scale perturbation technique
01 p0136 A72-10031

Infinite slab, cylindrical or spherical shells with nonuniform heat generation sources and equal surface temperatures, obtaining maximum internal temperature from error bounds
01 p0145 A72-10511

Thin walled sandwich cylindrical shells under internal pressure, calculating elastic-plastic zone propagation
01 p0141 A72-11001

Natural vibrations of closed crosswise reinforced orthotropic circular cylindrical shells, using digital computer solution
01 p0142 A72-11363

Barrel shaped cylindrical shell stability and free vibrations under torque, evaluating distortion influence by small parameter method
01 p0142 A72-11364

Transient response of Al cylindrical shells to longitudinal impact, indicating wave front propagation at plate velocity
02 p0287 A72-11505

[SESA PAPER 1885] Computer algorithm of initial functions for elastic thick finite hollow axisymmetric cylinders under static conditions
02 p0288 A72-11604

Edge effect equations for stability, vibration and deflection of asymmetric three layer circular plate and cylindrical shell with filler
02 p0288 A72-11605

Tube and hollow sphere revolving in thermal flux under surface pressure load, obtaining stress-strain state and random temperature dependences of creep
02 p0289 A72-11618

Moving load effect on circular cylindrical shell in acoustic medium, discussing free axisymmetric vibration mode, shape and frequencies
02 p0290 A72-11627

Temperature fields and stresses in thin elastic non-ferromagnetic electrically conducting cylindrical shells heated by induction determined from heat source distribution and thin shell theory relations
02 p0290 A72-11631

Deformation, stress and singularity in cylindrical shells under concentrated circumferential loads, comparing with two dimensional elasticity and plate bending
02 p0291 A72-11662

Newtonian quasi-static crack propagation theory application to nonlinear structures, considering slender beams, plates and circular cylindrical shells
02 p0292 A72-12029

Circular cylindrical shells buckling under edge compression at various boundary conditions, obtaining critical loads and wave number from Donnell equations

02 p0292 A72-12107

Computer program for thermal stress and buckling analysis of nonuniformly heated segmented ring-stiffened cylindrical and conical shells

02 p0293 A72-12252

Liquid motion in circular cylinder with elastic bottom under longitudinal excitation, representing dynamic and kinematic free surface conditions as nonlinear equations

02 p0204 A72-12254

Unsteady supersonic aerodynamic forces on oscillating circular cylindrical shell calculated using linearized equation of potential flow

02 p0151 A72-12256

Vertical thin circular cylindrical shells partially or completely filled with stationary liquid, determining free vibration characteristics with finite element theory

02 p0293 A72-12371

Noncircular cylindrical shells dynamic analysis using transfer matrix method

02 p0293 A72-12372

Resonant and nonresonant sound transmission through cylinder walls, using statistical analysis

02 p0260 A72-12374

Stress analysis of pressurized ribbed cylindrical shell with intersecting reinforced circular hole under internal pressure

02 p0294 A72-12470

ASME PAPER 71-PVP-8] Isothermal analogy for thermal stress in cylindrical shells, presenting orthogonal coordinate boundary condition equations

02 p0294 A72-12471

ASME PAPER 71-PVP-18] Stress concentration in shallow cylindrical shell with circular hole under axial tension, torsion and internal pressure loading

02 p0295 A72-12472

Plastic collapse limit analysis for combined edge and pressure loading on circular cylindrical shells for Tresca yield condition

02 p0295 A72-12474

Improved finite difference solutions for stress in thin cylindrical shells, using Donnell assumptions

02 p0295 A72-12475

ASME PAPER 71-PVP-24] Beam theory application to cylindrical and conical shells bending, deriving flexibility functions from membrane equations

02 p0296 A72-12529

Thin circular cylindrical shells under uniform axial compression loads, examining axially symmetrical creep buckling

02 p0296 A72-12531

Highly elastic cylindrical layer reinforced with anisotropic shell, deriving stress-strain state and nonlinear elastic stability

02 p0299 A72-12687

Infinitely long orthotropic cylindrical shell partially filled with elastic media under compression load, determining local stability

02 p0299 A72-12688

Rupture induced perturbation loads in pressurized orthotropic circular cylindrical shells

02 p0299 A72-12704

Nonstationary thermoelastic stress determination in hollow cylinder walls under convective heat transfer

03 p0443 A72-13459

Creep buckling of cylindrical fin two-layer shell under external hydrostatic pressure, considering rigidly clamped and hinged end conditions

03 p0444 A72-13574

Thick walled rigid plastic cylinders under pressure, obtaining uniqueness and stability of finite deformation

03 p0446 A72-13706

Temperature field analysis in locally heated cylindrical shell for stressed state production with lowest elastic energy

03 p0456 A72-13733

Thermal stresses from inner surface temperature of micropolar hollow cylinder in static thermoelasticity problem with vanishing body loads

03 p0448 A72-13889

Plastic stability of cylindrical shells under combined internal pressure and axial compression loads

03 p0448 A72-13904

Critical load and stability analysis for three layer orthotropic cylindrical shell with filler under nonuniform external pressure

03 p0448 A72-13906

Curvilinear material anisotropy effects on temperature distributions of thin walled cylindrical shells of revolution

03 p0449 A72-13919

Compression wave propagation from cylindrical cavity in weakly conducting magnetoelastic medium under unperturbed magnetic field

03 p0452 A72-14129

Stress concentration at hypotrochoid hole in cylindrical shell under internal pressure and axial tensile stresses

03 p0453 A72-14138

Ductility and fracture of metallic thin walled tubular samples under complex stress of internal pressure and axial tension

03 p0454 A72-14215

Thermoviscoelastic stress analysis for hollow circular cylinder with reinforcing interlayer under pressure, axial tension and nonstationary temperature field

04 p0587 A72-15016

Cylindrical shell stability and load capacity at large plastic deformations under internal pressure

04 p0587 A72-15019

Random search method application to optimal design of closed circular cylindrical shells under axial compressive loading

04 p0587 A72-15020

Optimal temperature field and stress-strain state in orthotropic conical and cylindrical shells subject to local heating

04 p0588 A72-15051

Critical load limit and stability of elastic isotropic and orthotropic cylindrical shells, using net-point method for end conditions

04 p0588 A72-15053

Stress concentration around elliptic hole in infinitely long circular cylindrical shell under torsional loads

04 p0589 A72-15122

Perturbation solution for stress concentration around elliptic hole in cylindrical shell under torsional loading

04 p0589 A72-15123

Radiated pressure field in unbounded acoustic medium produced by pulsed elastic cylindrical circular shell

04 p0590 A72-15188

Optimal temperature fields in locally heated orthotropic cylindrical shells, determining rigidities effect

04 p0593 A72-15655

Steady state heat transfer problem solutions in living tissue modeled as cylindrical shells, discussing blood flow and temperature distributions in extremities

ASME PAPER 71-WA/HT-34] 05 p0745 A72-15885

Shell bending and Timoshenko-type theory to solve stresses of semiinfinite elastic circular cylindrical shells produced by radial pressure pulses

ASME PAPER 71-WA/APM-16] 05 p0733 A72-15964

Thin cylindrical shell bending deformation from axisymmetrical temperature distribution generated by narrow heating element

05 p0736 A72-16113

Slot length effect on buckling load of cylindrical shell with circular holes

05 p0739 A72-16543

Meridional curvature effect on thin walled cylindrical shell buckling under external constant directional lateral pressure

05 p0739 A72-16546

Intrusion of pointed dies into cross section circumference sections of semiinfinite cylindrical shell, solving shell theory equations without allowance for friction effects

05 p0739 A72-16586

Axially compressed semi-sandwich corrugated ring-stiffened cylindrical shell crippling local buckling and general instability prediction by finite difference energy method

ALAA PAPER 72-138] 05 p0740 A72-16892

Small deflection theory for dynamic elastic buckling of stringer-stiffened cylindrical shells under axial impact, discussing optimum stiffener geometry

05 p0742 A72-17248

Semiempirical stress analysis of cantilevered thin walled cylinder, obtaining local stresses via strain gages

SAE PAPER 720285] 06 p0893 A72-17324

Flutter of thin elastic circular cylindrical fluid filled shells, presenting potential flow theory for coupled hydrodynamic forces

06 p0894 A72-17763

Photoelastic analysis of cylindrical shells of revolution with one hemispheric closed end and reinforcing flanges at opposite end rim, examining boundary conditions effects

06 p0899 A72-18640

Rib reinforced cylindrical shells deformation under local load, examining stress-strain distribution

06 p0899 A72-18641

Cylindrical shell under internal pressure, detailing axial thermal stresses relaxation

06 p0900 A72-18669

Nonlinear resonance oscillations of flexible rod and elastic cylindrical shell under potential and nonpotential forces, investigating motion instability

06 p0900 A72-18704

Zero moment theory application to cylindrical shells with elliptical geometries under constant transverse loads

07 p1087 A72-18992

Axisymmetric deformation of infinite cylindrical shell under stress-strain state arising from internal pressure in statistically inhomogeneous Winklerian medium

07 p1088 A72-19258

Nonstationary thermal interaction between thermally inert circular disk in bounded cylinder with controlled temperature, describing control process by third order differential equation

07 p1098 A72-19263

Axially compressed cylindrical shells with axisymmetric imperfections, analyzing random buckling behavior and failure probability by statistical methods

07 p1089 A72-19689

Dynamic behavior of stiffened hollow viscoelastic cylinder and elastic shell-contained sphere, taking into account compressibility and internal pressure

07 p1090 A72-19751

Pulsed laser beam effect on residual stresses behavior in transverse weld on cylindrical shell

07 p0996 A72-19776

Semimomentless theory of closed cylindrical plastic shells subject to random gust loads, obtaining normal circumferential force, shear, transverse bending moment and shell thickness

07 p1092 A72-19851

Elastoplastic stressed state of thin cylindrical shells with circular hole, using small strain theory

07 p1092 A72-19896

Buckling of arbitrary open cylindrical shells, investigating noncircularity effect

07 p1093 A72-19949

Homogeneous laminar combustion in semienclosed cylindrical tube, relating stability to hydrodynamic and thermodynamic flow parameters longitudinal high frequency disturbances

07 p1101 A72-19988

Residual stresses effect on technical cohesive strength of welded cylindrical shell with surface defects, presenting plane strain fracture toughness determination method

07 p0997 A72-20131

Axially nonuniform thin cylindrical shells dynamic analysis, obtaining free flexural vibration characteristics by hybrid of finite element and classical shell theories

07 p1097 A72-20531

Three dimensional nonstationary heat conduction of hollow circular cylinder in medium with different temperature

08 p1251 A72-20972

Axial impact of semiinfinite elastic cylindrical shell filled with inviscid compressible fluid, obtaining equations of motion

08 p1149 A72-21166

Membrane and bending moment stresses distribution at elliptical hole in circular cylindrical shell, solving boundary value problems

08 p1243 A72-21234

Critical values of compressive loads applied to mid-section of cylindrical shell weakened by circular holes

08 p1244 A72-21241

Stability and postbuckling equilibrium of nearly cylindrical shells of revolution under axial compression

08 p1244 A72-21291

Green functions in heat conduction solutions for hollow cylinder with mixed boundary conditions

08 p1253 A72-21448

Fatigue strength and life estimation method for thick walled cylinders under pulsating internal pressure, using fracture mechanics crack propagation law

ASME PAPER 71-PVP-15] 08 p1244 A72-21482

Elastic filler rigidity effect on cylindrical glass fiber reinforced plastic shells stability loss and critical load value under axial compression

08 p1245 A72-21503

Time varying external pressure effect on creep collapse of long thin walled quasielliptic cylindrical shell, taking into account elastic deformation

08 p1245 A72-21612

Orthotropic hinged cylindrical shell stability under uniform external pressure, deriving linearized three dimensional differential equations

08 p1246 A72-21711

Elasticity theory method for nonlinear stress-strain relationships in thin anisotropic shells, discussing fiberglass reinforced cylindrical shell

08 p1247 A72-21810

Orthotropic circular cylindrical elastic shell vibration mode shape analysis by Vlasov equations, using asymptotic method

08 p1247 A72-21813

Variable wall thickness influence on axisymmetric vibrations frequencies and reduced masses of cylindrical elastic shell filled with ideal incompressible fluid

08 p1247 A72-21815

Successive approximations method for stress concentration problem at hole in cylindrical shell

08 p1247 A72-21818

Thin shell theory analysis of thin walled cylindrical shell necking phenomenon as tensile deformation nonuniformity

08 p1248 A72-21821

Additional vibrational loading effect on thin tubular glass fabric reinforced plastic samples creep under shear in reinforcement plane at 20-50 C

08 p1195 A72-21854

Composite viscous polymer cylindrical shells buckling modes under prolonged loading, taking into account initial imperfections 08 p1248 A72-21859

German monograph on bending theory extension for stress analysis of disks and cylindrical shells 09 p1397 A72-22333

Rotationally symmetrical cylindrical shell loaded by uniform pressure distribution along length, calculating quasi-steady viscoplastic flow under Huber-Mises condition 09 p1399 A72-22696

Temperature fields produced in viscoelastic cylindrical, conical and spherical shells by cyclic loads, calculating displacements from zero moment stress theory formulas 09 p1399 A72-22701

Temperature induced stresses and displacements in fiberglass reinforced plastic cylindrical shell 09 p1399 A72-22704

Thermal stress distribution in orthotropic cylindrical shell weakened by circular hole, obtaining general solution by small parameter method 09 p1400 A72-22715

Thermal stressed state determination for open thin walled cylindrical shells, using method of integral relations 09 p1400 A72-22716

Stresses, strains and moments interrelationship in axisymmetrically loaded circular cylindrical shell under unsteady creep conditions 09 p1401 A72-22729

Nonuniformly heated infinite elastic cylindrical shell stability under axial compression loads 09 p1402 A72-22734

Axisymmetrically heated orthotropic multilayer cylindrical shell with shear sensitive couplings and elastic stiffener, investigating stability and critical force under compression 09 p1402 A72-22735

Temperature and internal pressure effects on circular cylindrical shell stability under tension and compression, deriving critical temperature and loads 09 p1402 A72-22736

Imperfection influence on nonlinear stability of long circular cylindrical shells subject to critical hydrostatic pressure 09 p1403 A72-22763

Torsional behavior of twisted elastic orthotropic cylindrical shells after stability loss, using energy method 09 p1404 A72-22771

Circumferential crack in closed shallow cylindrical shell under tension, computing stress singularities strength 09 p1404 A72-22912

Circumferential crack in cylindrical shell under torsion, presenting membrane and bending components of stress intensity factor ratio 09 p1404 A72-22918

Perturbation analysis of nonlinear free flexural vibrations of circular cylindrical shell, using Donnell equations 09 p1405 A72-22998

Nonlinear random radial vibration of elastic cylindrical shell under load, using stochastic linearization and correlation analysis 09 p1409 A72-23606

Axially homogeneous stress and strain in anisotropic thin walled cylindrical shells, considering pure bending, stretching and twisting [ASME PAPER 71-APMW-4] 10 p1554 A72-24181

Dynamic response of pressurized thin walled circular cylindrical shell under initial biaxial stress and subjected to radial uniformly moving force, noting transient and steady state [ASME PAPER 71-APM-GGG] 10 p1554 A72-24186

Elasticity theory for unsymmetric deformation of nonhomogeneous anisotropic cylindrical shells, using Donnell equations 10 p1555 A72-24252

Thermal stress analysis of laminated alternate ply cylindrical shells under internal pressure, using Donnell equations 10 p1556 A72-24257

Partial differential equation for thin walled circular cylindrical shells, deriving solutions for displacement and stresses in terms of surface coordinates low degree polynomials 10 p1557 A72-24560

Tensile, plane strain fracture toughness and fatigue tests of high strength Al alloy cylinders, discussing unstable crack growth conditions 10 p1498 A72-24887

Intermediate length open noncircular cylindrical shells analysis based on Vlasov semimembrane theory 10 p1559 A72-24992

Flügge equations for circular cylindrical shells buckling under compression, considering Donnell theory limits, stress determination and boundary conditions 10 p1560 A72-25025

Cylindrical shell vibrations in incompressible inviscid fluid near free interface, calculating natural frequencies with Fourier transforms 10 p1471 A72-25130

Violation effect of moment equilibrium about normal in shell of revolution and helical shell theory, discussing distribution 10 p1560 A72-25171

Dynamic nonlinear elastic response of buckling sensitive cylindrical shells to lateral pressure loading, using numerical and computerized analysis [AIAA PAPER 72-357] 11 p1729 A72-25386

Asymmetrically stiffened elastic cylindrical shells under axial compression, calculating critical loads for various end conditions 11 p1733 A72-25541

Moment stress-strain state of two layer circular cylindrical shells under creep conditions 11 p1733 A72-25542

Curved cylindrical shell finite element with reduced stiffness matrix, noting convergence for symmetrical and unsymmetrical loading 11 p1735 A72-25896

Thermal stresses in cylindrical shell under moving hot spot with cooling effect of surrounding media 11 p1737 A72-26428

Viscoelasticity analysis of bending displacements in thin walled closed cylindrical shell loaded by moving moment 11 p1739 A72-26920

Bubnov-Galerkin method for dynamic stability of closed thin walled orthotropic cylindrical shell loaded by variable external pressure 11 p1739 A72-26977

Dynamic stability of rapidly heated shallow cylindrical shells, formulating nonlinear equations 12 p1877 A72-27076

Thin cylindrical shells prepared from fiberglass reinforced plastics under long term compression, investigating strain buildup nature during creep process 12 p1878 A72-27078

Nonlinear equilibrium equations and elastic stability of cylindrical shell weakened by circular hole 12 p1878 A72-27080

Mixed variational formulation and finite element method for axisymmetric cylindrical, conical, spherical and ellipsoidal shells 12 p1879 A72-27195

Static stability of long cylindrical shells under external pressure, using Euler-Lagrange equations 12 p1880 A72-27228

Two dimensional static solutions for cylindrical shells with nonhomogeneous boundary conditions, discussing numerical results for circular shell 12 p1880 A72-27230

Boundary surfaces during plastic buckling of hollow cylindrical shell under combined loading by external pressure and axial force 12 p1880 A72-27231

Stress-strain state determination for closed cracked cylindrical shell, using Fredholm integral equations 12 p1880 A72-27236

Dynamics snap-through instability existence conditions in nonlinear plane deformation of shallow circular cylindrical elastic shell under impulsive loading 12 p1880 A72-27241

Structural weight optimization with piecewise concave cost functionals defined on set in Euclidean space for anisotropic cylindrical shells 12 p1881 A72-27254

Fatigue failure criteria under combined stress conditions, considering complex form, thin and thick walled cylinders as test specimens 12 p1828 A72-27317

Hybrid cylindrical shell finite element, determining natural frequencies from equilibrium equations, stress functions stress-strain relationships and boundary force transfer matrices 12 p1882 A72-27339

Vibration of free and fluid loaded uniform or rib reinforced cylindrical shells, solving equations of motion for natural frequencies 12 p1882 A72-27341

Linearized elastic equilibrium stability equations for orthotropic cylindrical shell under critical axial compression 12 p1885 A72-27970

Axial compression stability critical load and buckling of cylindrical shells resting on Winklerian elastic base, using dynamic programming 12 p1885 A72-27972

Nonuniform heating effect on stability of eccentrically stiffened smooth cylindrical shells under combined loading 12 p1885 A72-27973

Strain energy calculation for stability analysis of cylindrical and conical sandwich shells, using Euler-Poisson equations 12 p1885 A72-27975

Rib reinforced cylindrical shell supercritical post-buckling strains, allowing for geometrical surface deflection 12 p1885 A72-27976

Optimal weight and load capacity of ellipsoidal cylindrical shell of revolution of constant thickness with central circular hole under uniform internal pressure 12 p1885 A72-27977

Stress distribution in circular cylindrical shell weakened by two identical holes on common generatrix 12 p1886 A72-27984

Closed thin circular cylindrical shells external pressure pulse and structural parameters effects on stability under dynamic loading 12 p1886 A72-28129

Circular cylindrical shell under distributed edge load along circular hole contour, calculating stress concentration by trigonometric series solution for shallow shell equation 12 p1886 A72-28130

Analytical solution to difference stability equations, evaluating adequacy of difference scheme for circular cylindrical shell and rectangular hinged plate under compression 13 p2053 A72-28389

Hemispherical elastic nonexpandable weightless film fastened along equator to inner wall of closed cylindrical vessel under hydrostatic pressure, determining film axisymmetric equilibrium shapes 13 p1940 A72-28392

Heating rate effects on residual stresses in thick walled cylinders produced by winding heated binder impregnated fiberglass tape on cold spool 13 p1982 A72-28553

Stability of transversely isotropic cylindrical shell with elastic filler under axial compression, deriving approximate equations for transverse shear stress effect 13 p2055 A72-28556

Internal pressure induced stresses, displacements and time-variable plasticity radii for thick walled fiber reinforced cylinder with hereditary elastic binder interlayers 13 p2055 A72-28557

Finite circular cylindrical shell under uniform pressure on outer rim, comparing stresses and displacements 13 p2055 A72-28624

Cylindrical shell stability with variable thickness and moderate length under distributed ring load and uniform pressure, determining critical load 13 p2058 A72-29459

Mohr formulas construction for composite structures including frames and cylindrical and conical shells 13 p2058 A72-29460

Tangential displacements of spherical and circular cylindrical shallow shells calculated from stress function 13 p2059 A72-29490

Joule heating power density in NbZr superconductor hollow cylinder, estimating temperature changes and instability locations 13 p2023 A72-29855

Dynamic behavior of thin walled semifinite elastic cylindrical shell with liquid under axial impact loads 13 p1943 A72-30008

Gravitational wave diffraction by liquid on surface of vertical circular cylindrical shells, determining velocity potentials 14 p2093 A72-30192

Shear strains and elastic anisotropy of transversely isotropic cylindrical shell with circular hole under uniform internal pressure, using shallow shell equations 14 p2165 A72-30438

Average stress and strain across thickness of liquid filled cylindrical elastic thin walled shell with rigid bottom under axial impact loads 14 p2166 A72-30698

Variational principle based Pian hybrid finite element procedure for static cylindrical shell analysis extended to plate and shell vibration 14 p2169 A72-31149

Cylindrical shell rectangular finite element from generalized independent strain functions and corresponding displacement functions 14 p2169 A72-31174

Stability analysis of thin walled circular cylindrical shell under shearing force action to one end, calculating buckling modes 15 p2324 A72-31483

Nonlinear creep failure of imperfect sandwich structures under time variable loading, considering rod and cylindrical shell 15 p2324 A72-31490

Elastic deformation of thin walled spherical and cylindrical shells and associated rings under external loads for small displacements 15 p2325 A72-31604

Deformation and stress in shells with discontinuous wall thickness variations, noting cylinder with ribs under internal pressure 15 p2326 A72-31705

Zero moment stress effect on modal density spectrum of fluctuating thin cylindrical shells and cylindrical panels 15 p2327 A72-31737

Stress concentrations in cylindrical shells with cutouts under uniformly distributed axial tensile load, presenting exact solution of differential equation 15 p2328 A72-32138

Singularities of cylindrical shell under concentrated twisting couple, investigating axial and circumferential deformations and shear stress distribution

15 p2329 A72-32139

Nearly incompressible elastic solid compressibility effects theory, applying to annular wedge straightening, stretching and shearing and cylindrical tube telescopic shear problems

15 p2330 A72-32477

Axially compressed cylindrical shells buckling behavior, deriving formula based on equivalent axisymmetric imperfections concept in terms of shell radius/thickness ratio

15 p2331 A72-32553

Complex conjugate fourth order partial differential equations for circular cylindrical shells deformation, comparing accuracy with Flugge, Morley and Novozhilov equations

15 p2331 A72-32559

Stress and displacement solution to Lamé problem for multilayer spherical vessels and cylindrical tubes in nonlinear elasticity theory

15 p2333 A72-32679

Differential equations for stress-strain state of circular cylindrical shell with circular holes resting on elastic base under external pressure

15 p2333 A72-32686

Nonlinear stress-strain-curvature problem applied to noncircular cylindrical membrane shell under lateral pressure

16 p2464 A72-32917

Membrane and bending stress analysis for thin circular cylindrical shells with elliptic hole

16 p2464 A72-32918

Vibrational frequency density analysis of thin spherical and cylindrical shells of revolution, using asymptotic integration method

16 p2464 A72-32935

Natural vibration frequency spectra of circular cylindrical and spherical shells of revolution, using Bessel function

16 p2465 A72-32936

Schaefer equilibrium and compatibility equations and Reissner constitutive equations for orthotropic cylindrical shells reduction to four simultaneous third-order equations

16 p2466 A72-33023

Stresses induced by torsional vibration in twisted composite cylindrical shell of cylindrically anisotropic materials for high and low frequencies

16 p2466 A72-33102

Equilibrium equations and boundary conditions for elastic buckling of open cylindrical sandwich shell under compressive forces applied to freely supported edges

16 p2467 A72-33116

Axisymmetrical stability loss in elastic cylindrical shell under longitudinal and transverse impact waves, discussing buckling and similarity parameter for simulation

16 p2468 A72-33159

Linear stability and critical stress formulas for isotropic cylindrical shells with stepwise variable wall thickness under torsion

16 p2470 A72-33411

German papers on crack propagation in metal sheets, resonant vibration of cylindrical shells and stress concentration in plastic plates

16 p2470 A72-33676

Resonant vibration of thin walled rods and stiffened plates and cylindrical shells, noting aircraft and rocket structures

16 p2471 A72-33679

Numerical procedure for spherical and cylindrical shells creep behavior, taking into account stress redistribution due to interaction between elastic and creep strains

16 p2473 A72-34125

Stable bifurcation mode prior to instability in thick walled cylindrical viscoplastic pressure vessel under internal hydrostatic pressure

16 p2474 A72-34129

Imperfect circular cylindrical shells creep and elastic buckling under nonuniform external loads, solving ordinary differential equations via finite difference technique

16 p2474 A72-34133

Small nonaxisymmetric initial shape deviations effect on creep buckling and critical time of thin walled circular cylindrical shell in axial compression

16 p2474 A72-34134

Matrix progression method analysis of free vibration problem for cantilever thin circular cylindrical elastic shells, using Flugge equations

16 p2475 A72-34173

Analysis of wave propagation in elastic cylindrical shells by the perturbation method.

17 p2623 A72-34307

Response of a ring-reinforced cylindrical shell, immersed in a fluid medium, to an axisymmetric step pulse.

[ASME PAPER 72-APM-8] 17 p2624 A72-34314

Energy transfer between flexural and extensional modes of cylindrical shells.

17 p2625 A72-34323

Spatial and temporal load pulse parameters for circular cylindrical shells /tubes/ dynamic plastic deformation

[ASME PAPER 72-APM-29] 17 p2628 A72-34790

Longitudinal impact of cylindrical shells with discontinuous cross-sectional area.

[ASME PAPER 72-APM-24] 17 p2628 A72-34793

Effect of end attachment on the strength of fiber reinforced composite cylinders.

[SESA PAPER 1994A] 17 p2630 A72-34817

Elastic wave propagation in a joined cylindrical-conical-cylindrical shell.

[SESA PAPER 1983] 17 p2630 A72-34819

Buckling of a circular cylindrical shell in axial compression and SS4 boundary conditions.

17 p2632 A72-35236

Equation for nonlinear vibrations of shells.

17 p2633 A72-35246

On the flutter of thin cylindrical shells conveying fluid.

17 p2634 A72-35415

Fracture of cylindrical and spherical shells containing a crack.

17 p2634 A72-35645

Conical and cylindrical shell deformation with nonlinear one dimensional wave processes, describing algorithm for method of characteristics application

18 p2735 A72-36664

Nonuniformly thick combined cylindrical shell vibrations, studying radial displacement, bending moment and shearing force

18 p2735 A72-36695

Radial vibration of a composite cylindrical shell subjected to a magnetic field.

18 p2711 A72-36753

On axisymmetric vibration in a transversely isotropic finite cylindrical shell acted upon by a magnetic field.

18 p2711 A72-36755

Numerical solution for the mean first-passage-time for snap-through of shells.

18 p2737 A72-37061

A proof of the accuracy of a set of simplified buckling equations for circular cylindrical elastic shells.

18 p2739 A72-37091

Thermal displacements and stresses in cylindrical shells due to instantaneous line heat sources.

19 p2870 A72-37272

Longitudinal impact on a thin cylindrical shell

19 p2870 A72-37321

Buckling of an elastic cylindrical shell during longitudinal impact against an obstacle

19 p2870 A72-37322

Further results on the stability of a finitely deformed thin cylindrical shell.

19 p2871 A72-37415

German monograph - A contribution to the clarification of the carrying characteristics of closed isotropic circular cylindrical shells

19 p2871 A72-37478

Synthesis of optimal cylindrical reinforced-plastic shells under external pressure and axial compression

19 p2872 A72-37534

Behavior of glass fiber reinforced plastic cylindrical shells under the action of external pressure pulses

19 p2872 A72-37538

Dynamic stability of axisymmetrically heated glass fiber reinforced cylindrical plastic shells which are coupled with elastic cylinders

19 p2872 A72-37539

Impression of pointed dies onto cross section circumference sections of semiinfinite cylindrical shell, solving shell theory equations without allowance for friction effects

19 p2872 A72-37557

Applications of holography to vibrations of segmented shells.

19 p2873 A72-37617

Loading rig in which axially compressed thin cylindrical shells buckle near theoretical values.

19 p2783 A72-37730

Shells of revolution free of bending under uniform axial loading.

19 p2876 A72-37886

Low-frequency wavelike process of deformation in a semiinfinite cylindrical shell immersed in a compressible fluid

19 p2877 A72-38157

Filament wound cylindrical pressure vessel design and development for operation under cyclic-loaded high hydraulic pressure in underwater environment

19 p2877 A72-38166

Stress analysis of shell junctions fabricated by the filament-winding method.

19 p2877 A72-38169

Buckling of circular cylindrical shells under compression. III - Solutions based on the Donnell type equations considering prebuckling edge rotations.

19 p2878 A72-38299

Post-critical deformations of a cylindrical shell subject to the action of external pressure and a temperature field

19 p2878 A72-38472

Experimental creep buckling of circular cylindrical shell under uniform compression.

20 p2978 A72-38883

Selection of optimal parameters of waffle structures from the condition of minimum weight

20 p2980 A72-39905

Determination of the natural frequencies of cylindrical shells of variable thickness

20 p2980 A72-39906

Dispersion of flexural waves in circular cylindrical shells.

20 p2982 A72-39975

Stresses in a circular cylindrical shell having two circular cutouts.

20 p2982 A72-40063

Dynamics of non-circular stiffened cylindrical shells.

21 p3116 A72-40333

Stability of a twisted orthotropic cylindrical shell with a jump-wise variable wall rigidity

21 p3118 A72-40815

Calculation of rib-reinforced minimum-weight cylindrical shells under external pressure by the random search method

21 p3119 A72-41099

Forced vibration solution and wind tunnel investigation of shallow cylindrical shells under moving pulsating pressure discontinuities, noting compression shock effects

21 p3122 A72-41352

Buckling of inelastic cylindrical shells under axial impact.

21 p3124 A72-41507

Stress distribution in a cylindrical shell with reinforced holes

21 p3126 A72-41542

Equilibrium and elastic deformation equations for closed cylindrical shells with arbitrary cross section and variable wall thickness

21 p3126 A72-41551

Calculation of the stress concentration at the joint between a cylindrical casing and a branch pipe for internal pressure

21 p3127 A72-41710

On the application of the mixed finite element methods to the stress concentration problems of cylindrical shells with a circular cutout or a crack.

22 p2332 A72-41942

Carrying capacity of thin-walled shells subjected to impulsive radial pressure loads

22 p2333 A72-42052

Determination of the critical temperatures of cylindrical shells of variable thickness

22 p2343 A72-42053

Cylindrical shells vibration under external forces with allowance for internal and external friction, obtaining harmonic influence functions in series form

22 p2333 A72-42056

Cylindrical shells of optimal torsional stiffness

22 p2333 A72-42112

Nonlinear buckling of cylindrical shells.

22 p2336 A72-42607

Nondestructive stability evaluation of large shell structures by direct computer controlled testing.

22 p3157 A72-42695

Dynamic behavior of thin walled semiinfinite elastic cylindrical shell with compressible liquid under axial impact loads

22 p3167 A72-42736

The dynamic plastic behavior of shells.

22 p2336 A72-42756

Stresses in a circular cylindrical shell with arbitrary holes.

22 p2338 A72-42837

Square edged semiinfinite circular cylindrical shell, deriving boundary value problem closed form solution based on Novozhilov complex form cylinder equations

22 p2338 A72-42839

Buckling of circular cylindrical shells under axial compression.

22 p2339 A72-42840

Axisymmetric-multilobe creep buckling transition in thin walled circular cylindrical shells under uniformly distributed axial compressive load

22 p2339 A72-42844

Buckling of integrally stiffened cylindrical shells - A review of experiment and theory.

22 p2339 A72-42846

Torsional vibration of an orthotropic cylindrical shell.

22 p3240 A72-42881

Nonlinear natural vibrations of rectangular plates and cylindrical panels

22 p3242 A72-43134

Nonaxisymmetric vibrations of arbitrarily thick circular cylindrical shells

23 p3345 A72-43624

Strength of a cylindrical shell of variable thickness located in a temperature field

23 p3346 A72-43653

Limiting equilibrium of orthogonally coupled cylindrical shells

23 p3346 A72-43656

- Stresses around an axial crack in a pressurized cylindrical shell. 23 p3346 A72-43705
- Refractory materials heat resistance criteria, taking into account hollow cylinder thermal stress distribution 23 p3306 A72-43738
- Ribbed cylindrical shells modeling method for stress-strain state and stability 23 p3347 A72-43745
- Longitudinal rib reinforced cylindrical shell under axial compression loads, determining equilibrium stability with approximation of transcendental equations 23 p3347 A72-43748
- Elastoplastic computation of thin cylindrical shells under cyclic loading 23 p3348 A72-43786
- Hydrodynamic fluid pressure on a shell during hydraulic impact 23 p3280 A72-43788
- Numerical determination of the stress concentration around a hole in a circular cylindrical shell 23 p3348 A72-43799
- The accuracy of Donnell's theory for very high harmonic loading on closed cylinders. 23 p3350 A72-44059
- Forced harmonic and random vibrations of concentric cylindrical shells immersed in acoustic fluids. 23 p3352 A72-44117
- Vibration characteristics of cylindrical shells with several axially equispaced constraints. 23 p3355 A72-44371
- Stress concentration of a cylindrical shell with one or two circular holes. 23 p3355 A72-44399
- Nonlinear theory for static analysis of moderately thick circular cylindrical shells under axisymmetric loads applied to pyrolytic graphite 24 p3454 A72-44603
- Parametric influences on the response of structural shells. 24 p3454 A72-44604
- Triangular facet finite element application in thin cylindrical shell analysis by displacement method 24 p3456 A72-44792
- Vibration of simply supported cylindrical shells with longitudinal stiffeners. 24 p3457 A72-44882
- Nonstationary thermoelastic stress determination in hollow cylinder walls under convective heat transfer 24 p3458 A72-44934
- Forced and free vibrations of shallow cylindrical shell in rectangular duct filled with ideal fluid 24 p3459 A72-45004
- Residual stresses effect on technical cohesive strength of welded cylindrical shell with surface defects, presenting plane strain fracture toughness determination method 24 p3408 A72-45757
- Mechanical behavior of fiber reinforced cylindrical shells. 24 p3461 A72-45783

CYLINDRICAL TANKS

- Navier-Stokes equations numerical solution for viscous incompressible fluid in circular cylinder with rotating top disk, computing secondary flow at Reynolds numbers to 400 06 p0802 A72-18526
- Harmonic functions system for resonant vibrations of liquid in elastic circular cylindrical tank, calculating shells surface pressure from equations of motion 13 p1940 A72-28394
- Crack propagation in biaxially stressed and heat treated cylindrical pressure vessel observed by strain gage displacement measurement, noting effects of initial surface cracks 14 p2169 A72-31176
- Hydraulic shock of incompressible heavy fluid in closed cylindrical tank under abrupt deceleration 15 p2219 A72-32685
- Fluid oscillations in a partially filled cylindrical tank with a spring supported elastic floor. 18 p2684 A72-37062
- The unit stress state in a cylindrical tank with a flat bottom and a partly cantilevered shell 20 p2979 A72-39594
- Unsteady axisymmetric flows of a liquid draining from a circular tank. 20 p2913 A72-39605
- Influence of discontinuity stresses on main propellant tankage of a space shuttle orbiter. 21 p3120 A72-41135
- [ICAS PAPER 72-10] Draining of a fluid from a rotating cylindrical tank. 21 p3046 A72-41307
- Free oscillations of a liquid rotating in a cylindrical vessel under conditions of weightlessness 22 p3165 A72-42251
- Convective interaction in a partially-liquid-filled vertical vessel with heat influxes in its lateral and free surfaces and bottom 22 p3244 A72-42261

CYLINDRICAL WAVES

- Electromagnetic cylindrical wave group aging properties, describing extragalactic red shift production mechanism 01 p0135 A72-11325
- Hydromagnetic cylindrical blast wave propagation in self gravitating polytropic gas, obtaining graphs for velocity, pressure, density and magnetic field distributions 02 p0264 A72-12181
- Cylindrical gravitational waves propagation modes in hot plasma subject to axial magnetic field, investigating instability conditions 03 p0388 A72-13025
- Cylindrical blast wave propagation in MGD, deriving closed-form solutions for line explosion in medium with constant pressure, density and axial magnetic field 03 p0400 A72-14391
- Cumulation-laser heating of D-T plasma for cylindrical wave, investigating pulse energy increase for critical temperature attainment from average value mathematical model 05 p0695 A72-16279
- Pulsed cylindrical converging shock wave generation in decreasing density medium by axial explosion-implosion discharge 05 p0700 A72-17233
- Coordinate transformation for decoupling equations for tangential electric and magnetic field propagation through series of uniform cylindrical layers with arbitrary properties 07 p0946 A72-19799
- Toroidal gravitational waves in general relativity, considering analog to imploding-exploding cylindrical waves, linear field equations and symmetric metric 08 p1210 A72-21922
- Self similar flow patterns due to cylindrical ionizing symmetrical strong shock and detonation wave propagation outwards into gas at rest 09 p1295 A72-23564
- Schlieren photographic investigation of shock wave propagation over narrow slit, noting cylindrical expansion wave origin at slit upstream edge 11 p1616 A72-25920
- Cylindrical elastic wave diffraction on semiinfinite screen, describing motion with displacement vector consistent with Lamé equation 11 p1688 A72-26380
- Electromagnetic cylindrical wave diffraction by linear emitter in parabolic cylinder with slots 13 p1917 A72-28709
- Dispersion equations and resonant absorption of plane and cylindrical surface waves in transition layer between plasmas, noting Langmuir oscillations 15 p2286 A72-32385
- Imploding spherical and cylindrical shocks, considering rear flow field with nonadiabatic isothermal flow and zero temperature gradient 16 p2376 A72-33009
- Propagation of spherical and cylindrical shock waves in an inhomogeneous atmosphere with allowance for back pressure 21 p3047 A72-41662
- Amplification of cylindrical electromagnetic waves reflected from a rotating body 23 p3262 A72-43307

CYLINDROIDS CYLINDRICAL BODIES

- Renal polycystoma - Incidence among flight personnel 19 p2756 A72-37877

CYTOCHROMES

- Evolutionary rate of cistrons in vertebrates, discussing hemoglobin and cytochrome c changes involving amino acid mutant substitution 02 p0158 A72-11762
- Cytochrome c X ray structure and molecular evolution rates, using amino acid sequence comparative data 02 p0158 A72-11763
- Zn concentration in chromatoid bodies of ribosome crystals in Entamoeba invadens, using absorption spectroscopy, electron microprobe and dithione staining techniques 15 p2186 A72-31725
- Evolutionary clock - Nonconstancy of rate in different species. 19 p2758 A72-38551
- Respiratory chain components correlation to tension production at various oxygen pressures in guinea pig ductus arteriosus, investigating light absorption changes 22 p3144 A72-42670

CYTOGENESIS

- Biological dosimetry in acute human irradiation from cytogenic study of peripheral blood and bone marrow 04 p0467 A72-14606

CYTOLOGY

- Chronic microwave irradiation effects on experimental animal blood forming systems, examining

peripheral blood count changes and nuclei and mitosis abnormalities in erythroblastic and lymphoid cells

- 02 p0158 A72-11708
- Soviet book on gravitation receptor covering evolution of structural, cytochemical and functional organization in invertebrates /statocyst/ and vertebrates /vestibular apparatus/ 03 p0316 A72-13850

Organ cell lysosomes polymorphic properties and formation by Golgi complex, discussing role in neurocyte structure restitution following gamma irradiation 14 p2075 A72-30594

Dynamics of secondary vacuole movement within cytoplasm of Tradescantia virginiana hair cells 15 p2186 A72-32350

Acute hypoxia of the myocardium - Ultrastructural changes. 17 p2501 A72-34982

Myocardial ultrastructure in acute and chronic hypoxia. 17 p2502 A72-34988

Cytologic aspect of RF radiation in the monkey. 19 p2758 A72-38709

Morphological changes in spinal cord neurons of animals due to the decreased intensity of supraspinal stimulation 21 p2998 A72-40580

CYTOPLASM

- Phylogenic origin of cytoplasmids from Cyanophyceae alga involved in endosymbiosis with colorless Cryptophyte 13 p1907 A72-29996
- Dynamics of secondary vacuole movement within cytoplasm of Tradescantia virginiana hair cells 15 p2186 A72-32350
- Cytoplasmic heredity theory linking mitochondria origin to bacteria 19 p2758 A72-38549
- RNA content in the cortex neurons in connection with the change in its function during the emergence of an animal from hypothermia 20 p2890 A72-38928
- CZOCHEWSKI METHOD**
- Ni single crystal growth by Czochralski method, investigating growth rate, direction and initial structures effects on substructure 13 p1976 A72-28906

D

D LINES

- Rb 87 line shift produced by rare buffer gases and molecular nitrogen measured from applied magnetic field magnitude and hyperfine structure of D lines 10 p1490 A72-24040
- Na atoms D line radiation excited in collisions with molecular gases, noting transfer cross section dependence on kinetic energy for given quantum number change 13 p2009 A72-30063
- Na-He atomic collisions induced D lines broadening, fine structure transitions cross sections and multipole polarization resonance levels relaxation 15 p2283 A72-32651
- Sodium D lines broadening and shift parameters under atomic H and He collisions effect, calculating low lying states interatomic potentials 15 p2317 A72-32772
- Space and time variations of the solar Na D line profiles. 17 p2616 A72-35697
- Upper atmospheric sodium and stratospheric warmings. 18 p2687 A72-36643
- A working model for sunspot umbrae. 18 p2727 A72-36740
- Sodium emission from the atmosphere during a solar eclipse. 19 p2793 A72-38857
- He-D3 spectroheliogram absorption features correlation with magnetic field regions and H alpha structures 21 p3108 A72-41279
- Study of the chromosphere in the D3He line during the eclipse of September 22, 1968 21 p3114 A72-41764

D REGION

- Midlatitude D layer observations during sunspot minimum, emphasizing atmospheric ionization and ozonospheric parameters 01 p0055 A72-10433
- Electron density profile determination in D region based on frequency dependence of radio waves absorption, discussing lower ionosphere anomalous ionization 01 p0059 A72-10595
- Electron concentration profiles in D region from radio wave partial reflection coefficients 01 p0028 A72-10614
- Differential phase shift and absorption measurements of partially reflected radio waves, providing

electron density and collision frequency data from 70-90 km

01 p0030 A72-10836

Equilibrium concentrations of negative ions in nighttime D region, comparing computations to mass spectrometric measurements

01 p0063 A72-10917

D region positive and negative ion chemistry review, noting dominant roles of water ion clusters, NO cation and hydrates

02 p0219 A72-11979

Ionospheric D region electron concentration, deriving correlation coefficient expression with allowance for scattering layer electrons/molecules collisions

02 p0222 A72-12593

Sunspot cycle 1958/70 effects on D region ionospheric absorption and stratospheric temperature measured by radiosonde

03 p0345 A72-12978

Global morphology of integrated product with respect to D and E regions electron concentration height and collision frequency

03 p0345 A72-12981

Oxygen, hydrogen and nitrogen constituents in mesosphere, investigating ionization process in D region at midlatitudes

03 p0346 A72-13379

Laboratory measurements of D region ion-molecule reactions using flowing afterglow system

03 p0347 A72-13388

Dissociative recombination coefficients of water vapor and nitric oxide in determining D region electron densities

03 p0347 A72-13389

Lower D region ion density measurement with paracathode blunt probe consisting of disk-shaped collector with guard ring at bottom

03 p0347 A72-13398

Positive ion composition in equatorial D region, investigating reaction kinetics

03 p0412 A72-13522

D region echo amplitude distribution, observing coherent scattering contribution

03 p0349 A72-13523

VLF phase regressions at sunrise related to variations of reflection coefficient in D region, using IENG data

04 p0485 A72-14465

Sudden cosmic noise absorption from D region N-h profile during solar X ray flares on 13 April 1966

04 p0566 A72-14512

Electron concentration and collisions number fluctuations effect on D region profiles based on radio waves partial reflection data

05 p0656 A72-16244

D region ionization by electron fluxes as explanation for latitudinal radio wave absorption

05 p0656 A72-16249

N/h/ electron concentration profile in ionospheric D layer by exponent of frequency dependence of radio wave absorption

05 p0627 A72-16401

VLF propagation and D region aeronomy model for vlf phase behavior predictions and observations during two solar eclipses

05 p0630 A72-16618

Two body ion-ion neutralization rates measurement by merged beam technique, considering D region reactions

06 p0805 A72-17465

Night source ionized component profiles in chemistry and aeronomy of D and E regions, considering scattered L alpha and beta emissions and corpuscular fluxes

07 p0936 A72-20038

Neutral species chemical reactions in D and E regions, taking into account effects of photodissociation and transport by horizontal and vertical flow and molecular diffusion

07 p0936 A72-20039

Sudden ionospheric perturbation effect on D region vertical distribution profiles, finding sixfold electron concentration increase at 75-80 km

08 p1154 A72-20729

D region extraionization and solar X-ray flux from vlf data, emphasizing solar spectral shape and use of continuity equation for ionization time history

08 p1227 A72-21116

D and E region winds over Europe - Conference, London, April 1971

08 p1159 A72-21526

Circulation motions in D and E regions, discussing planetary waves, tidal oscillations, gravity waves, turbulence and drift measurement

08 p1160 A72-21527

D region neutral gas winds, density changes and short wave radio absorption correlation, determining air mass flow rates from chaff fall rate measurements

08 p1160 A72-21532

D and E region ion chemistry - Conference, University of Illinois, Urbana, July 1971

09 p1274 A72-22352

Diatomic oxygen and carbon dioxide density profiles effects on photoionization rates in D region [AD-741091]

09 p1274 A72-22356

Nightglow evidence of precipitating energetic electrons in midlatitude nighttime D region based on intensity determination from satellite and rocket data

09 p1375 A72-22358

Nighttime D region ionization production by cosmic X rays from various celestial sources and galactic background

09 p1375 A72-22359

D and E regions positive ion chemistry based on E and F regions ion-molecule reaction rate constants comparison with laboratory measurement

09 p1275 A72-22360

D and E region ion chemistry reaction rate measurements, noting hydration, charge exchange and ion-atom interchanges

09 p1275 A72-22366

Effective electron loss rates in lower D region from ionization changes during solar X ray flares, noting water cluster ions destruction

09 p1376 A72-22369

D and E region electron density profile, investigating geographical, diurnal, seasonal and sunspot cycle variations

09 p1376 A72-22370

D and E regions electron densities measurement by incoherent scattering technique, noting sporadic E layer and echoes [AD-742616]

09 p1376 A72-22371

Synoptic measurement of midlatitude D region electron density diurnal and seasonal variations under quiet conditions, using differential absorption partial reflection experiment

09 p1376 A72-22372

D region positive ion and electron conductivities and densities measurement by parachute borne blunt probes during 1970-1971 winter anomaly

09 p1376 A72-22373

D region neutral gas winds, density variations and short wave absorption, determining correlation from ultraviolet chaff and absorption measurements at 2.83 MHz

09 p1277 A72-22374

D region negative ion reaction schemes, discussing reaction rates of nitrogen dioxide with hydrogen

09 p1275 A72-22592

NO ion production rate in D region in relation to electron densities

09 p1300 A72-23027

Neutral atmosphere effects on lower ionosphere, considering D region atomic oxygen, nitric oxide and water vapor and electron density distributions

10 p1474 A72-24712

Ionosphere composition and ion concentration measurements for D and E region, including aerodynamic and plasma dynamic effects

11 p1621 A72-25836

D region ionization by solar corpuscular streams, considering formation of charged particle concentration profiles

11 p1622 A72-25948

Daytime electron density profile in E and D regions from rocket lower ionosphere sounding, noting winter electromagnetic absorption anomaly

11 p1622 A72-26101

Solar X-rays absorption profiles and residual fluxes in D and E layers during 7 March 1970 eclipse from rocket measurements

12 p1863 A72-27146

Electron recombination loss coefficients and concentration profiles for D region during solar eclipses from rocket measurements

12 p1800 A72-27149

Disturbed D layer electron density profiles at high energy particle incidence, using partial reflection method

12 p1864 A72-27783

Exponential functions model for D region vertical distribution of electron density profiles, taking into account solar X- and cosmic rays

13 p1945 A72-28581

D region electron density profiles calculated as function of solar zenith angles, noting LF radio wave propagation

13 p1945 A72-28582

Upper atmosphere atomic oxygen distribution calculated for D and E region aeronomy problems solution

13 p1947 A72-28604

D region chemistry based on earth albedo effects from airborne radio sounding experiments, suggesting visible light energy flux role

13 p1950 A72-29342

Diurnal and seasonal variations of ionospheric absorption in D and E regions, discussing blanketing sporadic E presence effect

13 p1922 A72-29392

Solar flare flux effects on D region effective ion recombination coefficient decrease, discussing electron and negative ion densities

13 p1913 A72-29654

Radio waves field strength measurement and recording for D region behavior during partial solar eclipse of 25 February 1971

13 p1961 A72-30050

Partial reflection method to obtain D region electron density profiles and collision number

14 p2086 A72-30791

Atmospheric gravity waves effects in ionosphere, discussing F region traveling ionospheric disturbances, sporadic E layer and D region radar scattering

15 p2222 A72-31285

Long term A3 absorption associated with nuclear explosion caused artificial radiation belts, discussing electron precipitation role in D region ionization

15 p2299 A72-31933

Antarctic D region reflection heights from relative phase measurements on VLF transmissions at several phase locked frequencies, interpreting results by waveguide mode theory

15 p2200 A72-32105

Review of symposium on D region, upper polar ionosphere, magnetosphere and wave-particle interactions

15 p2229 A72-32251

Ion pair production rate and electron number density in ionospheric D region from ground based and rocket measurements, discussing two ion model

15 p2229 A72-32252

Rayleigh distribution of radio signals partially reflected from D region, noting amplitude fluctuations dependence on antenna radiation pattern

15 p2202 A72-32733

D region electron concentration and collision frequency with neutral molecules from radio waves backscattered by inhomogeneities in propagation medium

16 p2385 A72-33484

On the possibility of a simultaneous measurement of wind speed, wind direction, air density and air temperatures at heights which correspond to the upper D-region /max. 95 km/ with chaff cloud sensors.

17 p2545 A72-34631

Dispersive motions in the ionosphere.

17 p2546 A72-34696

An investigation of the ionospheric D region at sunrise. I - Time variations of ozone, metastable molecular oxygen, and atomic oxygen. II - Estimation of some photodetachment rates. III - Time variations of negative-ion and electron densities.

18 p2656 A72-36295

Photodetachment of electrons from major negative ions in the lower D region.

18 p2686 A72-36622

Possibility of estimating an energetic particle stream in the ionospheric D region at sunrise and under daytime conditions

18 p2688 A72-36858

Observations of D-region modifications at low and very low frequencies.

18 p2662 A72-37009

D region electron density profile determination based on LF link operating on one-hop ionospheric propagation of ordinary and quasi-transverse wave

18 p2689 A72-37163

Sudden ionospheric disturbance effect on D region vertical distribution profiles, finding sixfold electron concentration increase at 75-80 km

19 p2791 A72-38357

Ionospheric D region, a sensitive detector of hard X-rays of solar subflares.

19 p2852 A72-38628

D-region electron densities and collision frequencies from Faraday rotation and differential absorption measurements.

19 p2793 A72-38858

Laboratory positive and negative ion composition measurements compared with D region ion-molecule reaction observations

20 p2917 A72-39527

On the diurnal and seasonal variations of the D- and E-regions above Kjeller.

20 p2917 A72-39529

D region ion compositions model during quiet and intense PCA conditions associated with dissociative recombination and ion-ion neutralization

20 p2917 A72-39530

Theoretical investigation of nitric oxide and its role in D-region ionization.

20 p2918 A72-39531

Mid-latitude D-region ionization associated with the 'slot' in radiation belt electrons.

20 p2964 A72-39533

Recent work on ionospheric irregularities and drifts.

20 p2920 A72-39981

A high-frequency dynamic phase metering instrument for ionospheric research.

21 p3051 A72-40214

Electron and positive ion density altitude distributions in the equatorial D-region.

22 p3170 A72-42366

Partial reflections from a thin parabolic layer in the lower D-region.

22 p3170 A72-42374

D-region measurements with the differential-absorption, differential-phase partial-reflection experiments.

22 p3172 A72-42423

The effective recombination coefficient in the ionospheric D region
23 p3283 A72-43364

High power radio transmitter for structural investigation of ionospheric D and E regions by signal reflection and electron concentration profiles
23 p3263 A72-43378

Theoretical estimate of the effective recombination coefficient in the D region.
23 p3284 A72-43818

Exponential functions model for D region vertical distribution of electron density profiles, taking into account solar X- and cosmic rays
24 p3397 A72-45081

D region electron density profiles calculated as function of solar zenith angles, noting LF radio wave propagation
24 p3397 A72-45082

Upper atmosphere atomic oxygen distribution calculated for D and E region aeronomy problems solution
24 p3398 A72-45104

Theoretical models of the D-region.
24 p3399 A72-45580

The relationship of theory and experiment in the D-region.
24 p3399 A72-45581

Formulation of diurnal D-region models using a photochemical computer code and current reaction rates.
24 p3399 A72-45583

DAEMO [DATA ANALYSIS]
U DATA PROCESSING
U DATA REDUCTION
U DATA TRANSMISSION

DAMAGE
NT CUMULATIVE DAMAGE
NT IMPACT DAMAGE
NT METEORITIC DAMAGE
NT PROTON DAMAGE
NT RADIATION DAMAGE
NT RAIN IMPACT DAMAGE

Metal fatigue time and cycle dependent deformation and fracture mechanisms in creep range from cumulative damage law standpoint for lifetime prediction
02 p0295 A72-12497

Metal fatigue damage nondestructive detection, discussing inspection methods, equipment, advantages, limitations and test results
[AD-741977] 02 p0296 A72-12498

Cumulative damage in metal fatigue, suggesting unified theory applicable to stress or strain controlled conditions
03 p0442 A72-12922

An estimate of sonic boom damage to large windows.
17 p2623 A72-34234

Investigation of defects and damage in metallic materials by metallographic examinations
20 p2941 A72-39573

DAMPING
NT ELASTIC DAMPING
NT LANDAU DAMPING
NT VIBRATION DAMPING
NT VISCOUS DAMPING

Whirling elastic shaft-disk system, investigating interaction effects of external and linear/nonlinear material damping, elastic restoring forces and inertia forces
01 p0101 A72-10036

Dynamic damping coefficient extraction from reentry vehicle flight test telemetered lateral rate data
03 p0441 A72-13951

Nonsymmetrical aerodynamic damping moments on 10 deg cone at supersonic speeds and large angles of attack, comparing Newtonian theory prediction with wind tunnel test results
[AIAA PAPER 72-29] 05 p0609 A72-16947

Infinite uniform Vlasov plasma response to steady state transverse excitation, considering spatial electron cyclotron damping
[AD-737564] 06 p0864 A72-18539

Al alloy melts with Fe, Cr, Co and Ni, measuring kinematic viscosity by oscillatory-rotary method using logarithmic damping decrement
07 p1012 A72-19550

Angular velocity vector active damping during spin-up of electrically supported gyro with mass-unbalance readout, using Euler equations of motion
07 p0986 A72-19691

Elastic stability of laminated circular plate with rectangular anisotropy under in-plane compression forces along edge
07 p1090 A72-19693

Stellar atmosphere UV spectral line broadening by electron collision, radiative and classical damping
08 p1237 A72-21750

Liapunov functional stability analysis in structural dynamics problems including wave equations with nonlinear damping
09 p1407 A72-23457

Whistler damping factor dependence on magnetic field strength in geometrical optics approximation,

emphasizing nonlinear effects at low frequencies in ionospheric propagation
09 p1282 A72-23516

Sound waves radiative damping in isothermal atmosphere, discussing relaxation influence on model response to body force and chromosphere dissipation effect on oscillation
10 p1543 A72-24622

Chandlerian wobble period correlation to damping coefficient of earth polar motion for 10 yr intervals during 1900-1970
10 p1475 A72-24871

Dislocation damping by point defects entrainment, calculating internal friction force rate dependence based on weak interactions continuum model
10 p1527 A72-24979

Distributed elastic system discrete model mass, stiffness and damping matrices derivation from dynamic test response data
[AIAA PAPER 72-346] 11 p1728 A72-25375

Mathematical model of weak coupling influence on damped harmonic oscillators with different eigenfrequencies applied to bounded plasma oscillations
11 p1698 A72-26600

Solar curve of iron growth, noting damping dependence on excitation potentials
12 p1867 A72-27204

Adiabatic density perturbations damping by radiative viscosity and heat conductivity, taking into account plasma recombination in hot expanding Universe
14 p2148 A72-30202

Ionic collision effects on spatial ion wave echoes in single-ended Q machine plasma, noting echo peak amplitude damping
15 p2288 A72-32423

Damping perturbation of high order nonlinear autonomous Liapunov system, reducing system equations integration to quadratures via transformation to lower order quasi-linear nonautonomous system
16 p2422 A72-32938

Investigation of two types of collisionless linear dampings of electromagnetic waves in a non-homogeneous magnetized plasma.
17 p2588 A72-34870

Elastic stability of folded plate structures of triangular cross-section.
18 p2738 A72-37073

Fe-Ni-C alloys internal damping, martensitic structure and mechanical properties after quenching and tempering, discussing Mo and Cr additions
19 p2806 A72-37418

Stability of linear systems with constraint damping and integrals of the motion.
19 p2856 A72-37519

Elastic conservative structural systems stability with many degrees of freedom, discussing critical singular points effect
21 p3120 A72-41206

Adiabatic density perturbations damping by radiative viscosity and heat conductivity, taking into account plasma recombination in hot expanding universe
23 p3333 A72-43231

DAMPING FACTOR
U DAMPING
DAMPING IN PITCH
U DAMPING
U PITCH [INCLINATION]
DAMPING IN ROLL
U DAMPING
U ROLL
DAMPING IN YAW
U DAMPING
U YAW
DAMPING TESTS
Wind tunnel stability tests of aerodynamic pitch damping of aircraft model oscillating in two degrees of freedom
03 p0307 A72-13539

Test facility for vibrations damping study of structural elements in water flow based on frequency and amplitude measurement at various flow conditions
06 p0796 A72-18364

Interference between recrystallization and allotropic transformation of cold rolled and annealed Co investigated by internal damping measurements
11 p1661 A72-26649

Utilization of computers in mechanical strength studies
23 p3345 A72-43644

DAMPNESS
U MOISTURE CONTENT
DANGER
U HAZARDS
DARK ADAPTATION
Sensitization by annular surrounds, tracing early light and dark adaptation curves
03 p0317 A72-13936

Darkness enhancement measurement in intermittent light as function of flicker frequency, describing experimental assembly
06 p0762 A72-17605

Visual adaptation to light and dark in humans and animals, discussing cellular mechanisms
06 p0762 A72-17720

Human dark adaptometric visual threshold recovery and electroretinograms in response to double light flashes, using Fourier analysis of oscillatory potentials
07 p0916 A72-19024

Dark adaptation with logarithmically time decreasing background luminance, noting threshold time lag variation with rate of background change
07 p0930 A72-19827

Achromatic and chromatic thresholds during dark adaptation against varying background luminances, noting trend change at transition from cone to rod function
07 p0930 A72-19828

Temporal summation function form change during dark adaptation, noting relationship to change under other stimulus manipulations
09 p1269 A72-22616

Landolt ring radioactive plague night vision tester comparison with electroretinography and Goldmann-Weekers dark adaptometry apparatus from special tests of night blind patients
12 p1777 A72-28332

Five-component cyclic model of retinal photopigment kinetics for photochemical changes corresponding to rod adaptation in rat and man in dark
13 p1906 A72-29966

Consensual photopupil responses to light flashes recorded in full dark adaptation, noting bleaching and backgrounds effects
13 p1907 A72-29969

Human retinal rod rhodopsin bleaching and regeneration measurements, tracing dark adaptation curves
15 p2184 A72-31364

Dark adaptation studies of bleach-induced visual threshold rise and subsequent return to rhodopsin level
15 p2184 A72-31365

Lamellar structure and rhodopsin location in bleached and unbleached rod photoreceptor membranes of dark adapted frog retinas by X ray diffraction study
15 p2186 A72-32199

Model to account for visual responses to light flashes of dark adapted eye, discussing perceived brightness variation with intensity
18 p2651 A72-36611

Age dependence of changes in pupil diameter in the dark.
21 p3007 A72-40732

Localization and dynamic changes of glycogen in frog retina adapted to darkness or light, I, II.
23 p3258 A72-44377

Photopic and scotopic contributions to the human visually evoked cortical potential.
23 p3261 A72-44380

On a long-term temporal aspect of stereoscopic depth sensation.
23 p3258 A72-44381

Component analysis of electroretinogram in dark and light adapted sheep eye, noting rod and cone receptor potentials and transient and dc responses
23 p3261 A72-44382

DARKENING
NT LIMB DARKENING
Disturbance-induced lunar surface darkening due to soil photometric function changes resulting from particle rearrangement
13 p2037 A72-28994

DARKNESS
Sleep interruption, sleep deprivation and continuous darkness effects on circadian rhythms in human performance
11 p1581 A72-26685

DART TURBOPROP ENGINES
U TURBOPROP ENGINES
DASSAULT AIRCRAFT
Dassault Falcon 10 turboprop powered executive aircraft, attributing safe stall characteristics to wing design optimization
08 p1108 A72-21274

Wind tunnel testing of Dassault-Breguet-Dornier Alpha Jet twin engine trainer, emphasizing tests for wing-empennage flutter and jet induced interference effects
13 p1940 A72-30077

DATA ACQUISITION
Remote sensing photointerpretation tests, discussing film-filter combinations, image acquisition time, scale and detection accuracy
01 p0065 A72-10450

NERVA fuel quality control, discussing planning, nondestructive tests, computer data acquisition and certification systems
02 p0258 A72-11552

Small scale aerial photography use in regional agricultural survey, discussing equipment used, sampling techniques and data collection and interpretation
02 p0213 A72-11835

Hybrid system to process multispectral photographic data from aircraft and spacecraft sensors, assessing data quality, cost effectiveness and delay reduction
02 p0228 A72-11883

Geomagnetic survey by polar-orbiting OGO 2 and 4, discussing data acquisition and reduction results and accuracy

02 p0219 A72-12081

Computer controlled telemetry data acquisition station, noting cost effectiveness

02 p0179 A72-12407

Electrical and electronic measurement and test instrument - Conference, Ottawa, June 1971

02 p0200 A72-12476

Interim automatic scanning multichannel data acquisition system for environmental test laboratory, using programmable calculator

02 p0200 A72-12477

Multiprogrammed digital computer controlled acquisition and processing of quasi-static analog transducer data during spacecraft environmental simulation tests

02 p0200 A72-12478

Radar data automatic extraction, discussing azimuth quantization methods, moving window detection, coordinate measurement and ATCAS extractor

02 p0181 A72-12650

Wind tunnels measuring equipment and procedures and data acquisition and processing systems electronics, describing computerized real time data processing system

[DFVLR-SONDDR-156] 02 p0201 A72-12898

Real time ground control optimization of data acquisition of solar spectra scans from OSO 6

03 p0417 A72-13060

Automated electromagnetic pollution data acquisition systems for environmental ecology, discussing computer technique and data retrieval, analysis and storage

03 p0328 A72-14040

Single scan TV-radiography system for providing A-D converter analog signal for digital data acquisition, obtaining transfer functions

04 p0522 A72-15226

Industrial R and D data collection to relate idea dispositions by management to subjective evaluation, considering urgency, predictability and expected time horizon roles

04 p0598 A72-15455

Acquisition probability equation for navigation systems terrain correlation devices, using two different correlation algorithms

[AIAA PAPER 72-122] 05 p0688 A72-16974

Aeromagnetic surveying with airborne fluxgate magnetometer, discussing field data compilation and interpretation

06 p0812 A72-17373

Acquisition and processing of plasma fluctuation data using fast Fourier transform analog-digital spectral analysis technique

06 p0859 A72-17548

Meteorological satellites data gathering equipment including TV cameras, temperature humidity, ozone and radiation measuring devices, discussing data processing and evaluation for weather forecasting

[DGLR PAPER 71-131] 06 p0892 A72-18231

Self contained portable data acquisition system for marine, environmental and ecology research, using multiple analog recording and digital telemetry transmitter

06 p0797 A72-18613

Remote sensing for earth resources data, discussing sensors equipment and project organization and management

06 p0810 A72-18615

Computerized EEG data acquisition and transmission system for large hospitals with multiple critical care patient monitoring units, noting telephone access from outside

07 p0928 A72-19307

Charpy impact test computerized data acquisition and analysis system using analog to digital converter

07 p1090 A72-19735

Fatigue life gages planning and application to air-plane cyclic fatigue test, describing automatic data acquisition system

08 p1163 A72-20916

Multichannel automatic data acquisition and processing in ergonomic measurements of radar controller work from ECG, EOG, EMG and respiration

09 p1271 A72-23136

Reliability data collection methods, considering equipment initial design, breadboard models, prototype, production, acceptance, qualification, field installation and operation

10 p1443 A72-23975

Metal creep under multiaxial stress states, proposing technique for numerical stress analysis data collection

[SMRT PAPER I.1/3] 10 p1556 A72-24395

Data acquisition and reduction for model aerodynamics in superconductive magnetic suspension and balance of supersonic wind tunnel facility

10 p1461 A72-24766

Aerodynamic data acquisition with magnetic balance on wind tunnel model delta and AGARD G wing planforms and body of revolution

10 p1462 A72-24770

Mean wind direction determining circuit for meteorological data collecting system

10 p1484 A72-25018

Data acquisition and transfer efficiency and reliability in computerized automatic control systems for communications, listing probability and expectation criteria

11 p1600 A72-25436

Computer control data acquisition system for 46 meter radio telescope at Algonquin Observatory

11 p1631 A72-25697

Programming and operations of astronomer data acquisition system using NOVA computer

11 p1601 A72-25699

Camac modular instrumentation data handling system for interfacing to digital computers and hardware controllers, noting astronomical data acquisition application

11 p1601 A72-25700

Low cost radiation shield for thermistor deployment in atmospheric boundary layer, noting measurement accuracy relationship to data acquisition system

11 p1682 A72-26087

Analog measuring data transmission systems optimization by computers, noting improvement of dynamic response and linearity in digital systems

12 p1786 A72-27580

Low cost real time computerized C 14 radiorespirometry telemetering system for monitoring human metabolism data during space missions

12 p1774 A72-28277

Pacific Ocean meteorological data collection from military and civil aircraft in-flight reports, discussing computer processing for daily analysis and monthly and seasonal means

13 p1994 A72-28874

Parameter identification method using combined acceleration search /Partan/ and continuous parameter tracking techniques

13 p1935 A72-29102

Frequency response data identification technique using adaptive hybrid computer to improve quality and acquisition time

13 p1935 A72-29103

Semiconductor devices series production process control and analysis by statistical procedures, noting computer controlled data acquisition system for silicon diodes production

13 p1965 A72-29166

FAA airborne OMEGA development program covering signal monitoring, airborne data collection and system operational evaluation

13 p1998 A72-29195

Data acquisition, reduction, quick-look data and standard and special programs for ESRO 1A and B auroral particle satellite experiment

13 p1925 A72-29868

Process computer technology, discussing data recognition, on-line open loop operation and system characteristics

13 p1926 A72-30051

Experimental data gathering, processing and presentation for materials enthalpy, heat capacity, thermal conductivity, compressibility and volume over wide pressure and temperature ranges

14 p2130 A72-30599

Satellite IR telescopes in oceanography for data acquisition on ocean state, circulation, surface temperature, salinity, pollution, etc

15 p2221 A72-31238

European synchronous meteorological satellite system Meteosat, discussing mission, control and data acquisition

15 p2265 A72-31345

Data system in Eole satellites program, discussing balloon localization, UHF information transmission and reception, distance measurement and data acquisition

15 p2268 A72-31981

Integrated data acquisition and processing system for inlet-aircraft engine matching, considering all-digital, analog and hybrid approach

15 p2298 A72-32319

Digital recording techniques for airborne data acquisition, emphasizing laser beam holographic recorders

16 p2394 A72-33642

Serial PCM system for flight test data acquisition and reduction compared with Harrier system

16 p2364 A72-33644

Airborne flight test data acquisition system modular design to provide digital readings from monitoring transducers analog signal

16 p2364 A72-33645

Satellites use for position determination and data acquisition systems application to earth sciences and industry

17 p2603 A72-34398

Use of satellites for the transmission of meteorological data and the tracking of observation stations

17 p2603 A72-34399

Eole - The tracking and collection of data applicable to meteorology

17 p2622 A72-35718

The collection of data by geostationary meteorological satellites

17 p2622 A72-35719

Eole program for tracking and gathering information from drifting buoys at sea

17 p2617 A72-35720

A data collection and display system for a large-scale simulation.

17 p2524 A72-35848

Airlines and aircraft manufacturers requirements for airport pavement evaluation/data system, discussing relationships between strength, landing gear design, aircraft weight, range, etc

18 p2675 A72-36789

ATC services configuration with secondary surveillance radar and primary radar data acquisition system, discussing signal processing by automated decoder

21 p3080 A72-40288

Data acquisition, storage and processing, discussing data reduction by statistical coding, interpolation, prediction and parameter identification

21 p3014 A72-40322

The cost-effectiveness of advanced remote sensing systems.

21 p3131 A72-40864

Decision directed phase locked loops acquisition properties improvement technique for PCM bit synchronizer of random nonreturn to zero data

21 p3038 A72-40872

Hydrodynamic test tunnel for unsteady pressure and force measurements and hydrogen bubble flow visualization data acquisition

21 p3041 A72-41585

Direct acquisition and processing of data in thermal tests with the aid of a programmable desk computer system

21 p3043 A72-41850

Experiment design - An organized approach to data collection.

22 p3245 A72-41935

Digital computer technique and real time monitor software application to instrumentation data acquisition system, discussing design guidelines and gas turbine engine test example

22 p3156 A72-42681

Computer-operated data acquisition and control system for automatic diagnostic monitoring of propulsion research instrument

22 p3216 A72-42684

A near real time data acquisition/reduction facility for the Boeing wind tunnels.

22 p3164 A72-42699

Instrumentation systems design for extended bandwidth data acquisition, discussing problem areas in transducers, amplifiers and signal conditioning, data recording and playback

22 p3157 A72-42712

Automatic acquisition and tracking system for laser communication.

23 p3265 A72-44176

The intermittent small-scale structure of turbulence - Data-processing hazards.

23 p3282 A72-44305

Field reporting system for reliability analysis on telecommunication equipment.

24 p3384 A72-44657

Reliability, safety, maintainability and system effectiveness disciplines acquisition, processing, dissemination and exchange via Government-Industry Data Exchange Program and Failure Rate Data Program

24 p3467 A72-44660

Computer-aided binary code sequence selection for data acquisition system in PCM-TDMA satellite communication, evaluating performance and reliability

24 p3379 A72-44779

Streamflow forecasting project to assess feasibility of air and spaceborne remote sensed data acquisition application to watershed hydrological behavior prediction

24 p3398 A72-45215

Analysing vibration and shock data. I - Data acquisition and pre-processing.

24 p3382 A72-45287

Mariner Mars 1971 adaptive mission planning for scientific objectives flexibility based on planetary features observed, discussing plan change implementation

[AIAA PAPER 72-944] 24 p3444 A72-45439

DATA ADAPTIVE EVALUATOR/MONITOR

U DATA PROCESSING

U DATA REDUCTION

U DATA TRANSMISSION

DATA ANALYSIS

U DATA PROCESSING

U DATA REDUCTION

DATA COMPRESSORS

U DATA REDUCTION

U DATA TRANSMISSION

DATA CONTROL SYSTEMS

U DATA SYSTEMS

DATA CONVERSION ROUTINES

NT SUBROUTINES

DATA CONVERTERS

NT ANALOG TO DIGITAL CONVERTERS

NT BINARY TO DECIMAL CONVERTERS
NT DIGITAL TO ANALOG CONVERTERS
Decoder for delay-modulated digital data conversion to nonreturn to zero data, discussing time-phase ambiguity resolution capability in real time
01 p0025 A72-10331
Double ended scan converters for multisensor data display in radar, sonar and TV applications
02 p0193 A72-12394
Data transmission and distribution systems interface, using semiconductor technology in multiplexing, asynchronous data transfer, A-D and D-A data conversion and sensor signal conditioning
02 p0194 A72-12404
Decoding technique for delay modulated digital data conversion to NRZ/c/ data, describing logic implementation and timing diagrams
04 p0486 A72-14490
Automatic hydrometeorological stations standardized sensors, describing data converters for atmospheric pressure, precipitation, humidity and wind and water and soil temperature measurements
10 p1483 A72-25014
Gas flow direction measurement using flow to electric pulse converter
16 p2395 A72-33957
Circuit synthesis for random numbers probabilistic digital transducers reduced to synthesis of random binary signal converters, noting method description with Boolean functions
16 p2372 A72-34012
Converter of the Gray code to a conventional binary code
17 p2515 A72-34762
Time-optimal mathematical models operating with low-frequency pulse-frequency-modulated input information converted to an intermediate digital code
17 p2524 A72-35786
Book - Electromechanical system components.
20 p2890 A72-39811
Optimal invariant conversion of information from a turbine flow meter and a capacitive fuel gauge
21 p3058 A72-41801

DATA CORRELATION
NT SIGNAL ANALYSIS
Data correlation and annotation of earth resources remote survey pictorial records
01 p0065 A72-10453
Nb alloy silicide coating thickness data correlation by thermoelectric, metallographic and pointed micrometer techniques, discussing state of art in thickness control, penalties and substrate independence
01 p0075 A72-10750
Magnetoionospheric wave and particle phenomena correlation to convection electric fields in nightside magnetosphere during isolated substorms
01 p0062 A72-10904
Subsurface discontinuity detection by microwave radiometry, noting microwave temperature correlation with moisture patterns
02 p0209 A72-11792
Multispectral scanner data training sets size effect on correlation between soil reflectance and organic matter content obtained from ground truth
02 p0227 A72-11845
Cosmic ray decreases correlation to solar flare occurrence by epoch analysis of monitor data, proposing mechanism for explanation
03 p0412 A72-13528
Physical training effect on subjective rating of perceived exertion, investigating correlation with heart rate and blood lactate concentration
03 p0319 A72-13678
QRS amplitude relation to frontal QRS axis and heart-electrode distance, using 12-lead ECG
03 p0320 A72-13881
Magnesium alloys torsional vibration damping correlation with texture orientation resulting from fabrication method
03 p0375 A72-13930
Pure metals creep or self diffusion activation energy from hot-hardness data, noting temperature and elastic modulus effects
03 p0375 A72-13931
Tadjabkhsh method of meteorological data assimilation for numerical weather forecast analyses, testing validity under condition of one of three dependent variables being observed
03 p0384 A72-14141
Upper atmospheric turbulence correlation to supersonic aircraft dynamics, noting Concorde contribution
04 p0542 A72-14681
Ni alloy stress rupture data correlation and extrapolation from computerized evaluations of time-temperature parameters relative abilities
[ASME PAPER 71-WA/MET-4] 05 p0670 A72-15905
Commercial alloy creep and rupture strength data correlation for predicting design creep properties
[ASME PAPER 71-WA/MET-2] 05 p0671 A72-15907
Solar wind velocity correlation with 5303 A coronal intensity
05 p0710 A72-16523

Vhf waves transhorizonal propagation and day types correlation with sporadic E ionospheric layers in temperate zone, discussing wind shear theories
05 p0659 A72-16782
Surface layer humidity correlation to height of atmosphere emitting in IR spectral region, determining water vapor content by recording earth radiation angular distribution
06 p0808 A72-18046
Small gage thermocouples calibration procedure, noting data correlation with thermoelectric theory
07 p0984 A72-19326
Solar active regions properties observation, noting correlation with magnetic field, flares, sunspots, magnetic knots, pores, umbral flashes, etc
07 p1079 A72-20009
Solar surges /plasma ejections/ relation to spot groups and flares, correlating various observational data
07 p1063 A72-20294
Aircraft altitude two-loop feedback control system designed by compensation parameter variation technique, determining correlation between system sensitivity computations and observations
07 p0963 A72-20592
Central nervous plasticity and stereotypy intercorrelation in conditional reflex two dimensional decision situations
07 p0925 A72-20662
OGO-E plasmopause crossing correlation with ground observations of Pi geomagnetic micropulsations
08 p1159 A72-21223
Atmospheric surface layer meteorological elements representative values determination as optimal filtration problem, examining data correlation with errors in initial statistical characteristics
08 p1203 A72-22121
Suboptimal decision algorithm to correlate sensor data with stored tracks in real time track-while-scan surveillance system
10 p1441 A72-23780
Optimal tracking filter for processing sensor data of imprecisely determined origin in surveillance system by minimizing effects of correlation uncertainties
10 p1455 A72-23787
Chandlerian wobble period correlation to damping coefficient of earth polar motion for 10 yr intervals during 1900-1970
10 p1475 A72-24871
Sco X-1 simultaneous hard X ray and optical observations from balloon and ground correlating thermal X rays and optical emissions
10 p1530 A72-24949
Short time stress rupture test data correlation for design, using computerized time-temperature parametric methods
[AIAA PAPER 72-327] 11 p1653 A72-25363
Gas turbine engines emission data correlation based on combustor theoretical model, proposing correction factors for data reduction to standard test conditions
[ASME PAPER 72-GT-60] 11 p1704 A72-25651
Fixed point smoothing of sequentially correlated processes by extending filtering technique to simultaneous estimation of state and process noise contribution
11 p1610 A72-25871
Outer space and earth surface galactic cosmic ray intensity data correlation analysis for studying interplanetary magnetic field structure
11 p1713 A72-25936
Optical correlation technique, converting input data into area charts with binary valued density
12 p1820 A72-27495
Al-Zn-Mg alloy tear resistance relationship to stress corrosion cracking from tear, tensile and corrosion tests
12 p1830 A72-27750
Space-time correlation of field amplitude and phase in plane waveguide with statistically irregular boundary, using Born approximation and perturbation theory method
13 p1928 A72-28471
Hydrocarbon-air mixtures reaction in incident shock waves of pressure greater than 25 atmospheres, correlating with shock tube results
13 p2063 A72-28549
Analog and digital computers for automatic statistical analysis of unsteady random process recorded data, calculating correlation functions and expectancy
13 p1925 A72-29165
Digital computer synthesis of transparent object holograms, noting image discretization, two dimension Fourier transformations spectrum and digital data correlation with optical parameters
13 p1958 A72-29617
Neutron activation data for Ru, Os, Ir, Pt and Pu in iron meteorites, noting correlation
14 p2157 A72-30582
Weber experiment gravitational signals correlation to solar and geomagnetic activity and cosmic ray intensity
14 p2160 A72-30886

DATA LINKS
Correlated particle flux, magnetic field, electron intensity and niometer absorption measurements during recovery phase of polar magnetic substorm on 6 March 1970
15 p2226 A72-31946
Data correlation of jet noise total sound power and peak sideline overall sound pressure level for subsonic and supersonic convergent exhaust nozzles
[AIAA PAPER 72-643] 16 p2381 A72-34089
Velocity-pressure correlations in a homogeneous turbulence associated with a plane pure deformation
17 p2537 A72-34280
Self-consistent kinetic equations.
17 p2581 A72-35152
Geomagnetic storms correlation with chromospheric flare series and with central meridian passages of recurrent positive plages
18 p2723 A72-36087
Correlation between the reliability of silicon bipolar transistors and their excess background noise
18 p2669 A72-37110
Zenith angle dependence of the meteorological corrections coefficients for cosmic ray hard component.
19 p2852 A72-38632
The interpretation of ionospheric radio drift measurements. V - Demonstration of the point effect in time-averaged correlations and drift calculations.
19 p2794 A72-38862
Film boiling correlations for stable natural convection heat transfer for various heater substances and pressures
20 p2983 A72-39487
Correlation of irradiation data using activation fluences and irradiation temperature.
21 p3083 A72-40763
A study on the correlation between thermal fatigue and low-cycle fatigue at elevated temperatures.
21 p3119 A72-41008
Arbitrary length thin liquid film cooling mass transfer data correlation, accounting for film roughness and entrainment effects
22 p3243 A72-41960
Correlation of Magnus force data for slender spinning cylinders.
22 p3135 A72-42344

DATA HANDLING SYSTEMS
U DATA SYSTEMS
DATA LINKS
High stability and power IMPATT oscillator design for line-of-sight communication links, avoiding spurious resonances and mode jumping
01 p0037 A72-10645
Gunn and IMPATT diodes applications for microwave power oscillators and amplifiers in radio link equipment
01 p0042 A72-10711
Low noise phase locked power microwave sources for solid state radio links with 960 voice channels, discussing design
01 p0006 A72-10712
High data rate convolutional coding for space station telemetry links, considering sequential and cascaded Viterbi decoding
02 p0174 A72-12132
Modulation/demodulation techniques for optical one-gigabit/sec intersatellite data transmission link system, comparing per-unit data costs for system selection
02 p0174 A72-12142
Digital telemetry/communication laser link system design for operation at 1 gigabit/sec
02 p0174 A72-12143
Circuit design techniques used for wideband signal processing systems, considering 1000 MB/S microwave communication link
02 p0176 A72-12163
X band gallium arsenide field effect transistor, noting applications for radar receivers, microwave communication links and electronic countermeasures
02 p0193 A72-12184
Twisted shielded pair /TSP/ time division multiplexed data bus with standard interfaces for use in aerospace applications
02 p0194 A72-12405
Angle modulation distortions and measurements in broadband FM microwave links
04 p0485 A72-14466
High speed digital communication over space to earth satellite links by quadrature phase modulation, discussing modulator, receiver and system technology for maximizing data transfer
04 p0485 A72-14477
Tactical optical ground communication systems, discussing use of GaAs and carbon dioxide lasers and ultrawideband data links
04 p0485 A72-14482
Millimeter wave and laser space-to-space communication links comparison, considering ehf system based on size, weight, power consumption and communication parameters calculations
04 p0493 A72-15609
Europe-Africa geodetic link in spatial triangulation of passive Pigeon satellite, discussing laser telemetry operation
04 p0520 A72-15725

Space real time data links during processing of French D2 scientific satellite for hydrogen frequency bands investigation

05 p0628 A72-16447

Development programs for ATC system improvement by digital computers and data displays applications

06 p0844 A72-17328

Airline air/ground radio communications and data link service implementation for San Francisco-Hawaii center

06 p0770 A72-17337

Atmospheric attenuation due to rain based on links experiment and statistical study of equivalent precipitation for given path length and time percentage

07 p0939 A72-19188

Error coding techniques application to communication satellite links, discussing computer simulation results

07 p0948 A72-20495

Dynamic programming method application to signal processing components selection for cascaded communication links to satisfy overall gain and noise figure

09 p1281 A72-23415

Frequency bands for space-earth links in broadcasting satellite service, stressing application to educational television

10 p1435 A72-24032

Real time pilot reports via digital ground-air-ground data link, discussing encoding and processing equipment, meteorological codes and automatic real time weather forecasts

10 p1440 A72-25079

GaAs injection laser optical link assembly with silicon photodiode and optical transistor, noting applicability to optical data processing

11 p1648 A72-26328

Economic and social implications of Indian national satellite for television and telecommunication, noting data links need

[AIAA PAPER 72-583] 12 p1781 A72-27384

TE mode propagation properties in circular waveguide, determining communication link transmitting and receiving equipment requirements

12 p1784 A72-27795

Microwave radio link transmission loss Rayleigh-like long term distribution explained by two-path propagation model

12 p1784 A72-27796

Ground reflections effect on satellite transmission link fading characteristics, computing transmitter field intensity fluctuations as function of terrain profile elevation angle

12 p1785 A72-27800

Line-of-sight radio link attenuation by atmospheric precipitation and phase interference fading during multipath propagation in 7-15 GHz range

12 p1785 A72-27802

Surface wave devices signal processing for space communication, developing fast lock up spread spectrum communication link breadboard

13 p1920 A72-29106

Multimode fiber optics data transmission through high electrical noise environments for send-receive communication links

15 p2198 A72-32059

Electronic display in future avionics systems, emphasizing computer techniques and digital data exchange systems

15 p2242 A72-32635

Variable rate optical communication schemes over earth/space link neutralizing atmospheric turbulence effects

17 p2514 A72-34415

Operation of information satellites in an interference environment

17 p2515 A72-34518

Air/ground digital communications in airline operations

18 p2660 A72-36561

Time synchronized ranging system (TSRS) providing high-speed real-time two-way data link between community members

19 p2764 A72-37904

Flight-test experience in digital control of a remotely piloted vehicle

[AIAA PAPER 72-883] 20 p2889 A72-40059

Geostationary satellite system for air navigation via voice and data communication, discussing ground facilities and avionics

21 p3080 A72-40284

Automatic position reporting, ATC communication, weather information and message identification via digital ground-air-ground data link, discussing operational and maintenance requirements

21 p3080 A72-40286

Meteorological and takeoff and landing information transmission by proposed automated meteorological and information service, discussing air-ground data link

21 p3080 A72-40287

Computer simulation of a digital satellite communications link

21 p3024 A72-40854

Linear cross polarization and attenuation measurements on terrestrial link at 11 GHz correlated with rainfall information

21 p3017 A72-40855

Techniques for dealing with the effects of bad weather in satellite communications systems

21 p3017 A72-40856

Light pulse propagation through clouds - Models and experiments

21 p3063 A72-40857

Data link design for planetary video data transmission back to earth based on rate distortion theory generalization of information theory

21 p3019 A72-40891

Phase noise types in digital satellite communication links, discussing continuous binary phase shift keyed modulation systems with coherent detection

21 p3020 A72-40896

On the performance of digital communication systems with bandpass limiters. I - One-link system. II - Two-link system

23 p3265 A72-44181

DATA MANAGEMENT

Space shuttle orbiter flight instrumentation, data handling and communication requirements, discussing data gathering methods, crew displays, computer processing, recording and digital data bus telemetry

02 p0179 A72-12406

Scientific balloon data management system, discussing airborne and ground station equipment for telemetry, command and flight control

03 p0327 A72-13725

Systems analysis for equipment performance and data management in aerospace programs

03 p0460 A72-14199

ALSEP data management, describing processing facility characteristics and support activities

04 p0509 A72-15101

Computer storage hierarchy hardware influence on data base management systems software technology [IEEE PAPER 13.5]

04 p0598 A72-15712

Optimal operation assignment and data array storage allocation in data system consisting of central processing unit and peripheral computer controlling data flow

09 p1283 A72-23439

Polaris and Poseidon missile systems reliability assessment, discussing test programs, analytical techniques and data management

10 p1551 A72-24013

Weapon system reliability improvement through integrated maintenance data collection and evaluation system, considering maintenance organization and operation

13 p2067 A72-28368

NASA program for acquisition, analysis and dissemination of space propagation and interference data for space systems designers, operators and regulatory agencies

[AIAA PAPER 72-577] 13 p1918 A72-28985

Organization and management requirements for environmental testing laboratory from viewpoint of test results, data handling, analysis and test reporting

15 p2340 A72-32617

Texture measurements in earth resources data management system by automatic photointerpretation with analog and digital techniques, discussing data processing rate requirements

17 p2520 A72-34409

Integration of an automated onboard data management system with a manned spacecraft environmental thermal control and life support system

[ASME PAPER 72-ENAV-6] 20 p2896 A72-39171

DATA PROCESSING

NT BATCH PROCESSING

NT CENSORED DATA [MATHEMATICS]

NT DATA CORRELATION

NT DATA REDUCTION

NT DATA RETRIEVAL

NT DATA SMOOTHING

NT DATA STORAGE

NT KARHUNEN-LOEVE EXPANSION

NT OPTICAL DATA PROCESSING

NT PARALLEL PROCESSING [COMPUTERS]

NT SIGNAL ANALYSIS

NT SIGNAL PROCESSING

NT VOICE DATA PROCESSING

Radio astronomy technology developments, discussing antennas, receivers and data processing

01 p0047 A72-10417

Redundancy reduction method for multichannel spectrometer solar radio data processing, using least squares technique

01 p0128 A72-10418

Optimal inertialess transformation of output signals from several devices, noting method application to analog data processing systems

01 p0045 A72-10571

Pattern recognition computer programs for transforming and characterizing input scene through successive layers of recognition cone

01 p0046 A72-10867

Field and test data analysis with time share computer, using Weibull probability plotting, hazard rates and least squares regression

02 p0185 A72-11555

Associative array digital processors application to numerical solution of partial differential equations, illustrating methodology on weather forecasting equations

02 p0186 A72-11658

Remote sensor data analysis using color TV display system and interactive graphics equipment on-line to IBM 360/44 computer

02 p0226 A72-11838

Multispectral scanner data preprocessing to improve automated recognition by reducing atmospheric and sensor induced signal variability

02 p0227 A72-11841

Pattern recognition of multispectral scanner remote sensor data, using table look-up approach for processing simplicity and time reduction

02 p0227 A72-11846

Tissue equivalent plastic counter for radiation dose equivalent measurement in mixed radiation field, discussing data processing

02 p0163 A72-12070

ERTS multispectral scanner data telemetry decommutator/processor capable of decommutating five spectral bands of digital video data

02 p0175 A72-12162

Space and high altitude aerial photography agricultural ground data collection and processing for Arizona survey evaluation

02 p0220 A72-12200

ATS-F satellite short and long term data processing, detailing millimeter wave propagation experiment

02 p0177 A72-12384

Radar signal and data processing with digital techniques, using pipeline fast Fourier transform methods

02 p0188 A72-12397

Visual display systems for man-machine communications, discussing applications, data processing, hardware designs and human engineering

02 p0230 A72-12419

Computer-aided interactive graphic displays for ATC, discussing subsystems, data processing flow and operational capabilities

02 p0257 A72-12420

Multiprogrammed digital computer controlled acquisition and processing of quasi-static analog transducer data during spacecraft environmental simulation tests

02 p0200 A72-12478

Digital computer memory system for real time processing of air and naval traffic data, discussing logic design, time comparisons and optimum use

02 p0188 A72-12647

Radar data automatic extraction, discussing azimuth quantization methods, moving window detection, coordinate measurement and ATCAS extractor

02 p0181 A72-12650

German ground operation system for satellites and space probes, discussing telemetric data processing, handling and flow

[DGLR PAPER 71-123] 02 p0201 A72-12742

Computational time and computer storage requirements for discrete Kalman filter, comparing simultaneous and sequential types of measurement processing

02 p0198 A72-12806

Wind tunnels measuring equipment and procedures and data acquisition and processing systems electronics, describing computerized real time data processing system

[DFVLR-SONDDR-156] 02 p0201 A72-12898

Computer technology projection in terms of cost and performance for future ATC system, determining data processing systems availability

04 p0496 A72-14834

Solar system data processing system/SSDPS/computer solution for major planetary masses from optical, radar and radio tracking data

04 p0575 A72-15034

ALSEP data management, describing processing facility characteristics and support activities

04 p0509 A72-15101

Integrated data processing system organizational model methodology for individual firms, emphasizing interdependence on program groups

05 p0632 A72-15815

Ground based satellite control center data processing for Azur satellite, using automatic guidance

05 p0632 A72-16138

Geomagnetic field vector components measurement methods, considering data processing problems

06 p0812 A72-17371

Acquisition and processing of plasma fluctuation data using fast Fourier transform analog-digital spectral analysis technique

06 p0859 A72-17548

Kalman and linear numerical filtering, discussing data processing from wind tunnel and rocket flight tests

06 p0774 A72-17847

Earth resources technology satellite program, discussing mission requirements, payload, orbital characteristics, earth stations, data processing, system design and international features [DGLR PAPER 71-139] 06 p0892 A72-18230

Remote sensing possibilities by aerial photographic methods based on scanning, scatterometry, radiometer and vidicon systems, discussing ground resolution, data automation and satellite observation [DGLR PAPER 71-128] 06 p0818 A72-18234

Peak reading and thresholding in radar weather data processing, describing PPI map 06 p0843 A72-18440

Computerized polycardiographic data processing covering 23 cardiac and respiratory characteristics, using rabbits data 07 p0926 A72-18868

Aircraft engine test data processing by polynomial relations, assuming normal measurement error distribution 07 p0994 A72-18978

ERTS A and B satellite systems for multispectral imaging of earth surface, discussing sensors, operational control and data processing requirements and implementation 07 p1085 A72-19276

Computers in biomedicine - Conference, University of Hawaii, January 1972 07 p0928 A72-19306

Real time computer aided mechanical testing and data analysis system for composites, confirming computer analysis by motion pictures of thin walled graphite/epoxy composite fracture 07 p0965 A72-19734

Semiautomatic stereophotographic processing of cosmic ray shower particle interaction data from Wilson chamber 07 p0988 A72-19865

Direct broadcasting communication satellites, discussing frequency allocation, modulation and data processing systems 07 p0948 A72-20266

Satellite system and data processing center feasibility for carrying out meteorological surveys in Mediterranean area 07 p0993 A72-20605

Astronomical interpretation of dust particle data recorded by Pioneer spacecraft, suggesting sensor surface orientation role for error correction 08 p1232 A72-21149

Controlled plants operation efficiency change prediction by analytic and probabilistic methods with data processing 08 p1180 A72-22064

Meteorological measurements representativeness and analog discrete filters synthesis with optimal data processing and weighting function averaging procedures 08 p1203 A72-22123

Adaptive algorithms for dynamic systems observation based on extremal data processing systems construction 09 p1283 A72-22219

Multihole flow probe measurement data evaluation by multidimensional approximation of calibration curves and surfaces 09 p1260 A72-22631

Ground based ATC information processing systems analysis, considering controllers work load 09 p1348 A72-22778

Multichannel automatic data acquisition and processing in ergonomic measurements of radar controller work from ECG, EOG, EMG and respiration 09 p1271 A72-23136

Time series analysis of physiological and work study data in ATC tasks, using heart rate as strain indicator 09 p1271 A72-23137

Phased array radar systems synthesis based on life cycle cost minimization, taking into account high-speed digital data processing 09 p1280 A72-23374

Elevation angle and range error correction equations for satellite tracking data processing with assumed spherical tropospheric refractivity 09 p1281 A72-23510

Optimal tracking filter for processing sensor data of imprecisely determined origin in surveillance system by minimizing effects of correlation uncertainties 10 p1455 A72-23787

Electronics and data processing technology effects on radar state of art, discussing automated air traffic control surveillance systems 10 p1435 A72-24490

Mathematical statistics application to complex systems modeling, considering group method of data handling, simulation and regression methods 10 p1457 A72-24634

Meteor trail radar data processing for upper atmosphere research, proposing dissemination for dynamosphere synoptic exploration 10 p1438 A72-24716

Supervisory circuits in electronic data processing power supplies, describing inadmissible line voltages indication networks 10 p1445 A72-24818

Automatic telemetering meteorological stations and visual observation data processor control 10 p1507 A72-25020

Large data processing systems for requirements of meteorology, environmentalology, earth resources inventories and hydrology in 1980s 10 p1446 A72-25095

Military weather forecasting requirements by 1980, discussing decision making, data processing, satellite data, mission and terminal forecasts, display and computer flight planning 10 p1508 A72-25096

CAMAC modular digital data handling system for communication with computer, discussing compatibility and data acquisition in astronomy application 11 p1600 A72-25692

Hale observatories computer system design for telescope control and data handling, using solid state techniques 11 p1601 A72-25696

ATC system, discussing flight data and radar processing functions and terminal automation program 11 p1683 A72-25875

Sleep loss effect on reaction and movement times during information processing in step tracking task 11 p1580 A72-26680

Electronic data processing for management information utilization 12 p1890 A72-27267

Organizational changes due to electronic data processing /EDP/ introduction into INTERFLUG material-technical supply 12 p1890 A72-27273

Data processing in isolated crab biological strain receptor formed by muscle, transducer and encoder, noting pulse frequency modulation in encoding process 12 p1771 A72-27577

Floating point arithmetic operators with variable dynamic range and multiple precision, noting word method for numerical data processing in computation and process control 12 p1787 A72-27666

Automatic ECG recording and analysis by electronic data processing equipment, discussing methods of data acquisition and transmission for routine diagnosis and prophylactic mass examinations 12 p1772 A72-27821

Sensor measurements correlation to human visibility via sensor equivalent visibility /SEV/ concept, discussing data processing scheme 13 p1992 A72-28846

Pacific Ocean meteorological data collection from military and civil aircraft in-flight reports, discussing computer processing for daily analysis and monthly and seasonal means 13 p1994 A72-28874

Human flexible processing accomplishment in speeded recognition task with visual stimulus dimension relevancy contingent upon other dimension stimuli values 13 p1911 A72-29832

Global atmospheric circulation barotropic spectral model application to satellite asymptotic data continuous processing 14 p2127 A72-30258

Statistical data processing method for accuracy evaluation of satellite orbits parameters obtained from onboard measurements of two stars angular positions 14 p2151 A72-30454

Data processing method for optimal prediction of spacecraft orbital elements, using dynamic and quadratic programming 14 p2151 A72-30455

Experimental data gathering, processing and presentation for materials enthalpy, heat capacity, thermal conductivity, compressibility and volume over wide pressure and temperature ranges 14 p2130 A72-30599

Electronic data processing in airline material supplies operations, discussing procedural efficiency improvement through reduction of stochastic effects inherent in aircraft maintenance operations 14 p2174 A72-30823

Unitary and interdisciplinary information processing of remote satellite observations of earth resources, noting ground station requirement for Italy 15 p2222 A72-31253

Measurement data processing in celestial navigation based on least squares method, calculating errors correlation matrix 15 p2267 A72-31731

Astronautical digital computing hardware and software trends and implications, considering data rates, reliability, LSI, speed-storage tradeoff, etc 15 p2203 A72-31822

Integrated data acquisition and processing system for inlet-aircraft engine matching, considering all-digital, analog and hybrid approach 15 p2298 A72-32319

Gravity anomalies interpretation by iterative data processing, discussing convergence improvement 15 p2231 A72-32347

Digital control and data processing system to replace analog instrumentation in vibration test laboratories, discussing signal generation, data acquisition, storage and analysis 15 p2215 A72-32618

Global meteorological data analysis using Gram-Schmidt generated orthogonal polynomial base functions 15 p2266 A72-32719

Predictive model for human operator performance in short term visual information processing based on psychological research to obtain decision accuracy and response time 16 p2359 A72-33865

Digital computer program for automatic processing of rocketsonde and radar digitized data, presenting graphical output from meteorological rocket soundings during 7 March 1970 solar eclipse 16 p2419 A72-33944

Helicopter stability derivative extraction and data processing using Kalman filtering techniques [AHS PREPRINT 641] 17 p2490 A72-34501

Gradient methods of parameter estimation during the mathematical treatment of measurements 17 p2522 A72-35038

A gradient method for estimating the covariational matrix of unknown parameters 17 p2523 A72-35039

Digital image processing and interpretation of photographic film data. 18 p2690 A72-36319

Hybrid processing of empirical functions in mechanics 18 p2710 A72-36423

Application of electronic data processing airport analysis in airlines operations and for manufacturers. 19 p2747 A72-37277

An automatic data processing system for laser anemometers. 19 p2795 A72-37287

Phase detector data distortion in phase-lock loop receivers. 19 p2763 A72-37297

Generalized dynamic systems and process prediction 19 p2833 A72-37378

Optimal programming data distribution in digital computer storage devices, noting independent subprograms assembling 19 p2769 A72-38088

Real time telemetry processing systems, describing display features and limitations [AIAA PAPER 72-783] 19 p2752 A72-38142

Automated data processing and display capabilities of radiation measuring systems for surveillance, protection and control in nuclear research, medicine and power production 19 p2802 A72-38306

Man machine systems operational effectiveness augmentation through human factors engineering to enhance human operator capability for parallel data processing and decision making 19 p2761 A72-38308

Ground based optical astronomy developments, emphasizing faint objects positional observation, trigonometric parallaxes, data analysis and measuring techniques 19 p2865 A72-38477

Probability threshold of data element similarity as separation criterion for automatic multiparameter biomedical data classification 20 p2893 A72-38937

Astronomical interpretation of dust particle data recorded by Pioneer spacecraft, suggesting sensor surface orientation role for error correction 20 p2968 A72-39254

Comparison of information takeoff from a shadow-indication instrument by television and photographic techniques 20 p2928 A72-40049

Inverse data transformation in control problems 21 p3036 A72-40156

Reversible integrodifferentiator with automatic data input 21 p3024 A72-40162

Applicability of associative computers to parallel adaptive break down of telemetry information into discrete elements 21 p3014 A72-40316

Data acquisition, storage and processing, discussing data reduction by statistical coding, interpolation, prediction and parameter identification 21 p3014 A72-40322

Automatic air targets recognition via digital radar data processing, discussing methods for noise signals suppression 21 p3081 A72-40547

Automated area navigation with real time track computation, discussing information processing by on-board computer for immediate pilot instruction 21 p3081 A72-40683

Process computation systems, discussing translator programs for conversion of user programs into machine language 21 p3024 A72-41002

Direct acquisition and processing of data in thermal tests with the aid of a programmable desk computer system

21 p3043 A72-41850

Influence of dispersion on the accuracy of estimating the fatigue life from the results of accelerated investigations by the prefracture method.

22 p2322 A72-41928

A gradient method of expanding a group data handling method to new plants not studied by experiments

22 p3162 A72-42242

Applications of a technique for estimating aircraft states from recorded flight test data.

[AIAA PAPER 72-965] 22 p3138 A72-42360

Utilization of computers in mechanical strength studies

23 p3345 A72-43644

The intermittent small-scale structure of turbulence - Data-processing hazards.

23 p3282 A72-44305

Analysing vibration and shock data. I - Data acquisition and pre-processing.

24 p3382 A72-45287

Optimal linear inertia-free processing of meter readings with allowance for control-equipment signals

24 p3403 A72-45316

Extraterrestrial electromagnetic radiation and particle flux characteristics of low and medium energy, considering onboard spacecraft measuring instruments and data processing systems

24 p3404 A72-45398

Space astronomical observatory mission planning, analysis and operation and data utilization in terms of space and ground facility instruments and support subsystems

24 p3382 A72-45530

DATA PROCESSING EQUIPMENT

NT AIRBORNE/SPACEBORNE COMPUTERS

NT ANALOG COMPUTERS

NT COMPUTERS

NT DATA PROCESSING TERMINALS

NT DIGITAL COMPUTERS

NT HYBRID COMPUTERS

NT PRINTERS [DATA PROCESSING]

NT SEQUENTIAL COMPUTERS

NT UNIVAC COMPUTERS

Azur project data processing, noting problems with computational equipment intended for industrial operation

05 p0752 A72-16141

Real time pilot reports via digital ground-air-ground data link, discussing encoding and processing equipment, meteorological codes and automatic real time weather forecasts

10 p1440 A72-25079

Specification requirements for quality assurance of automated data processing systems based on hardware development procedures

11 p1602 A72-26791

Flow equations for floating body flowmeters, discussing density and viscosity effect, instrument characteristics and computer algorithms

14 p2104 A72-30484

Digital data processing equipment for continuous ECG analysis, noting analog to digital converter and amplitude distribution analysis

17 p2522 A72-34914

Development of coordinate signal transmission and data processing equipment for operation supervision in space travel

19 p2765 A72-38305

Russian book - Design principles for multiple-valued physical circuits.

21 p3027 A72-40386

DATA PROCESSING TERMINALS

Minicomputer use for terminal control and matching functions and data compression in data transmission systems

05 p0633 A72-16199

Visual display units as manifold input output devices in data processing systems, discussing structure, characteristics and applications

13 p1925 A72-29343

DATA PROCESSORS

U DATA PROCESSING EQUIPMENT

DATA READOUT SYSTEMS

U DATA SYSTEMS

U DISPLAY DEVICES

DATA RECORDERS

Vestibulometric swing to obtain measured doses of receptor stimulation in otolith apparatus and semicircular labyrinth ducts with simultaneous physiological data recording

06 p0769 A72-18200

Design and operation of digital image recorder based on single stage intensifier and silicon target intensifier television camera tube coupled to large memory

11 p1631 A72-25685

Long term high temperature test machine to record structural changes of materials

12 p1795 A72-27464

Analog and digital computers for automatic statistical analysis of unsteady random process recorded data, calculating correlation functions and expectancy

13 p1925 A72-29165

Digital theodolite for automatic angle measurement with photoelectric sensor and magnetic data recorder for computer use

16 p2394 A72-33800

Storage tube figure display apparatus

21 p3034 A72-41251

DATA RECORDING

Magnetic tape recorded flight data analysis by FORTRAN program

01 p0017 A72-10215

Fraunhofer hologram for recording square of modulus of far field radiation pattern due to mixture of known and unknown source distributions

02 p0224 A72-11548

Multiplex FM recording system parameters effect on system design, considering SNR, deviation ratio, wow and flutter, tape speed errors, crosstalk and FM filters

02 p0230 A72-12409

Iterative hysteretic model for calculating magnetization distribution in thin magnetic layer for digital recording systems

[IEEE PAPER 14,7] 03 p0328 A72-13769

Automatic zero suppression system for recording solar bursts time functions and data reduction without information loss

07 p0982 A72-19052

Electro-optic materials and fixing techniques for holographic recording and storage performance improvements

[CLEA PAPER 18,2] 07 p0950 A72-19400

Satellite time-of-day code generator for data recording time identification, using ICs mounted on thick film multilayer printed ceramic substrates

07 p0944 A72-19605

Turbulent heating arc plasma voltage and current digital measurement recording, computing time dependent resistivity

07 p1045 A72-20400

Solar cosmic ray flare recording in stratosphere in Murmansk and Antarctic regions during February-April 1969

07 p1066 A72-20649

Astronomical interpretation of dust particle data recorded by Pioneer spacecraft, suggesting sensor surface orientation role for error correction

08 p1232 A72-21149

AS type solar prominence kinematics of 10 September 1956, noting hyperbolic spiral knot motion from recorded data analysis

09 p1390 A72-23398

Imagewise electrostatic charge buildup in electron beam recording, determining trajectories by Runge-Kutta method

10 p1479 A72-23929

Structural Acoustic Monitor system for airframe structural proof testing, providing multichannel recording and aural monitoring of acoustic data derived from aircraft mounted accelerometers

10 p1459 A72-24146

Pulse amplitude system with finite data recording time, deriving transfer function for signal shaper

11 p1609 A72-25444

Holographic memory devices for bulk information recording, discussing use of image converter for brightness amplification and lithium niobate electro-optical deflector for beam switching

12 p1807 A72-27588

Acoustic holography Doppler effects due to sound source or receiver motion during recording process

13 p1958 A72-29615

Low cost optimal earth resources technology satellite station for satellite tracking and image data reception and recording

15 p2213 A72-31246

Data storage and retrieval by holographic techniques, noting parallel recording of complex function at Fourier transform plane

15 p2236 A72-32040

Variable area modulation dual signal recording onto single input device for coherent optical correlators

15 p2249 A72-32165

Photochromic crystal materials erase mode recording characteristics measurement, using Ar laser for optical recording and readout

15 p2240 A72-32361

Digital recording techniques for airborne data acquisition, emphasizing laser beam holographic recorders

16 p2394 A72-33642

Instantaneous velocity nonuniformity measurement of mechanism motion using phasemeters with magnetic data recording

16 p2395 A72-33963

Synchronizing electronic equipment for digital computers input graphic data recording fidelity improvement ensuring proper timing of set and reset pulses

16 p2367 A72-34018

Electronically restored holographic data recording process for analog shape visualization with random ac-

cess computer storage, discussing system design and capabilities

18 p2659 A72-36271

Laser beam scanning and recording in two dimensional pattern on silver halide, evaluating systems performance based on signal response, granularity and noise characteristics

20 p2930 A72-39040

Astronomical interpretation of dust particle data recorded by Pioneer spacecraft, suggesting sensor surface orientation role for error correction

20 p2968 A72-39254

Experimental investigation of a holographic system that records front surface detail from a scene moving at high velocities.

21 p3053 A72-40612

Acoustic holography Doppler effects due to sound source or receiver motion during recording process

21 p3054 A72-40668

High speed, high density digital recording.

22 p3175 A72-41933

Analog and digital data recording systems, discussing accuracy, versatility and cost factor tradeoffs in selecting equipment for given applications

22 p3155 A72-42707

Instrumentation systems design for extended bandwidth data acquisition, discussing problem areas in transducers, amplifiers and signal conditioning, data recording and playback

22 p3157 A72-42712

Broadband magnetic tape prediction recording of data modulated carrier MHz radio telemetry signals, applying to Aris, Mercury and Gemini programs

24 p3385 A72-45269

DATA REDUCTION

NT DATA SMOOTHING

Magnetic tape recorded flight data analysis by FORTRAN program

01 p0017 A72-10215

Planetary mass estimation from radar and optical observation data analysis of sun and planets [AD-737167]

01 p0127 A72-10292

Pattern recognition, invariance, redundancy and information reduction in computer aided image processing

01 p0034 A72-10475

Quantitative interpretation of correlation mask remote sensors UV, visible and IR spectral data, discussing beam transmittance attenuation by absorption, scattering and emission

[AIAA PAPER 71-1061] 01 p0066 A72-10530

Midlatitude ionospheric trough characteristics from computer analysis of Ariel 3 electron density data, correlating with geomagnetic phenomena

01 p0120 A72-10921

Geophysical satellites high resolution imaging systems data redundancy reduction, using Apollo 9 photographs for computerized statistical analysis of picture structure

02 p0226 A72-11837

Data compression and random noise effects on pattern recognition and picture quality of multispectral scanner data

02 p0227 A72-11840

Extended wavelength field spectroradiometry for multispectral scanner data interpretation in airborne observations

02 p0228 A72-11853

Multispectral photographic data preprocessing and computerized simulation of ERTS data channel to make terrain maps, testing classification accuracy improvement possibility

02 p0215 A72-11880

Geomagnetic survey by polar-orbitingOGO 2 and 4, discussing data acquisition and reduction results and accuracy

02 p0219 A72-12081

Geomagnetic survey by Cosmos-49 satellite as international program, discussing data analysis and observation accuracy

02 p0219 A72-12082

Real time programmable video data compression system for microwave transmission of ATS satellite pictures between acquisition station and central computer processing

02 p0173 A72-12128

Manual reduction of Faraday rotation observations of ionospheric electron density at low latitudes, comparing with computer ray trace analysis

02 p0221 A72-12462

Solar UV flux measurements by balloon-borne grating monochromator, using FM-FM analog and PCM telemetry systems for computerized data analysis

03 p0409 A72-13051

Lunar occultation light curve model for photoelectric data analysis, using least squares method

03 p0421 A72-13133

Book on random data analysis and measurement procedures covering physical systems dynamic response properties, random processes, statistical sampling, data acquisition and processing, etc

03 p0327 A72-13175

Solar spectra photographic recording technique, using spectra-spectroheliography method with data reduction
03 p0429 A72-13313

Past meteorological data assimilation in dynamical analysis, computing initial condition with time sequential data for error reduction
04 p0541 A72-14455

Various updating effects on meteorological data analysis accuracy, using balanced barotropic model
04 p0541 A72-14456

Numerical fluctuations minimization during luminosity functions and density evolution derivations from data subject to observational selection, applying to 3CR quasars
04 p0577 A72-15284

Globular clusters NGC 1851 and 2808, reducing plate material with iris photometer
05 p0711 A72-15761

Digital data reduction techniques for stellar spectrograms, discussing digital noise smoothing for SNR improvement
05 p0632 A72-15762

Adaptive variable length coding for efficient compression of spacecraft TV data of Grand Tour missions
06 p0771 A72-17401

Computer simulated data analysis procedure for improved resolution of optical instrument by integral equation numerical solution
06 p0840 A72-18738

Automatic zero suppression system for recording solar bursts time functions and data reduction without information loss
07 p0982 A72-19052

Channel coding/decoding schemes compatibility with TV data compressor for planetary missions in real time transmission
07 p0941 A72-19274

On-line digital computer system for real time interpretation and report generation of electrocardiograms from remote locations over switched telephone network
07 p0928 A72-19311

Charpy impact test computerized data acquisition and analysis system using analog to digital converter
07 p1090 A72-19735

Reduction principle validity in perturbed motion stability theory for near-critical systems with gyro horizon application
07 p1035 A72-19972

Geophysical data analysis for high latitude negative geomagnetic disturbances revealing geomagnetic pulsations during auroral arcs passage
08 p1155 A72-20809

Closed loop covariances prediction in reentry vehicle tracking and data compression, presenting simulation results
08 p1144 A72-20846

Taxonomy for incomplete data problems, developing unified analysis methods based on maximum likelihood estimate
08 p1199 A72-21199

Venus upper clouds composition from Mariner 5 occultation data analysis concerning temperature and pressure profiles, abundances, polarization characteristics, reflection and emission spectra
08 p1236 A72-21496

Graphical analysis of accelerated life test data on insulating fluids, capacitors, bearings and electronic devices, using inverse power law model
08 p1176 A72-21587

Discriminant analysis application to data on precipitation formation in convective cumulus clouds to relate process to surrounding atmosphere and cloud characteristics
08 p1201 A72-21993

Airborne radar measurement of 2.25 cm backscatter from sea surface, obtaining wind speed by computerized clustering data analysis techniques
09 p1296 A72-22312

Disk diameter errors due to wire thickness in reduction of visual planetary observations
09 p1311 A72-23062

Computer processing of star meridian observations, concerning reduction to visible area, declinations, right ascensions and conversion
09 p1283 A72-23063

AS type solar prominence kinematics of 10 September 1956, noting hyperbolic spiral knot motion from recorded data analysis
09 p1390 A72-23398

Data reduction for photographic catalog of AGK2-AGK3 stars in terms of random and systematic errors in plate constants
09 p1392 A72-23543

Compression of data from measurements in real time nonlinear estimation to reduce data processing requirements without performance deterioration, applying to reentry vehicle tracking
10 p1442 A72-23802

Satellite IR spectrometer sounding measurements reduction for atmospheric temperature profiles, ob-

taining coefficients by statistical regression and minimum information solutions
10 p1508 A72-25081

Wind profile measurements to 200 meters by acoustic echo sounder and Doppler shift, describing signal emission and data reduction
10 p1508 A72-25084

Gas turbine engines emission data correlation based on combustor theoretical model, proposing correction factors for data reduction to standard test conditions [ASME PAPER 72-GT-60]
11 p1704 A72-25651

Flow data reduction validity for supersonic axial compressors, presenting experimental results for rotating supersonic cascade [ASME PAPER 72-GT-100]
11 p1571 A72-25669

Photographic telescope Gautier used for photographs of moon together with stellar background, noting reduction method for lunar positions deduction
11 p1716 A72-25771

Statistical diagnosis of aeronautical systems reliability and maintenance, using Benzecri factorial analysis for data reduction
11 p1639 A72-25817

Weather stations data analysis with unequally spaced observations, considering errors and variance transfer functions
11 p1680 A72-26076

Atmospheric density variations from meteorological rocket soundings, discussing data reduction methods and error sources for bead thermistor and inflatable falling sphere instruments
11 p1626 A72-26473

Photographic position of comet Ikeya-Seki, presenting data reduction procedure
12 p1868 A72-27220

Computer program to reduce automated multi-axial testing strain gage and applied loads data from tubular or flat specimens including fiber composites
12 p1787 A72-27999

Data compression for spacecraft borne signal measurement, discussing nonlinear quantizing, histogram parameter extraction, and signal encoding [DFVLR-SONDDR-204]
13 p1921 A72-29346

Modified run-length encoding system for text and drawing documents to obtain higher data reduction ratio
13 p1922 A72-29349

Geomagnetic data testing by including monopole term in spherical harmonic reduction
13 p1951 A72-29394

Digital data processing techniques for aircraft engine noise data reduction, analyzing fan noise spectrum
13 p1925 A72-29840

Data acquisition, reduction, quick-look data and standard and special programs for ESR0 1A and B auroral particle satellite experiment
13 p1925 A72-29868

Solar X-ray data normalization, using conversion factors independent of incident photons spectrum
13 p2034 A72-29941

Earth resources survey systems, discussing benefits, ground truth problem, data analysis, experimental satellites, operational system, and developing countries needs and activities
14 p2175 A72-31142

Photointerpretation and computerized radiometric analysis of ERTS multispectral TV and scanner imagery of Israel
15 p2221 A72-31242

Vehicle orientation degrees of freedom remote measurement with mounted passive devices and polarization-modulated light, discussing data reduction and system accuracy
15 p2267 A72-31780

High-orbital satellite global photographs and TV pictures, discussing planetary geographical and topographical data interpretation
15 p2225 A72-31807

Pioneer spacecraft intermittent solar wind streams data temporal variations analysis to account for anomalous type 3 bursts
15 p2299 A72-31964

Eole satellite observed meteorological balloon data analysis, obtaining mean zonal velocity, meridional velocity and temperature vs latitude from statistical estimates
15 p2266 A72-31980

Satellite Prospero onboard micrometeoroid detector data analysis for near earth flux
15 p2310 A72-31987

Geopotential harmonics of fifteenth order obtained from decaying satellite orbits analysis
15 p2311 A72-32001

Antarctic ice sheet complex permittivity in VLF band from reduction of measurement data with buried dipole antenna under snow surface
15 p2200 A72-32104

Ku band radio interferometer for discrete radio sources mapping, discussing construction and incorporated PDP-8 computer for pointing, tracking, delay compensation and data analysis
15 p2207 A72-32107

Computer controlled random environment test systems for large scale off-line data analysis and reduction, using Fourier analyzer
15 p2204 A72-32609

Heat capacity data analysis for solid solutions of superconducting Nb-Ti system, investigating electronic structure
15 p2296 A72-32692

Global meteorological data analysis using Gram-Schmidt generated orthogonal polynomial basis functions
15 p2266 A72-32719

Radio sources position determination by lunar occultation, noting observation technique and data analysis method
16 p2453 A72-33287

Filtering polynomial technique to estimate wind, divergence and vertical motion profiles, suppressing random error effects
16 p2418 A72-33667

Graphic procedure for strength test data conversion from test temperature to design temperature based on equivalent damageability concept
16 p2411 A72-33847

Structural information model for data compression algorithm synthesis, using piecewise signal approximation
16 p2395 A72-33954

Filtering with perfectly correlated measurement noise.
17 p2533 A72-35240

Application of factorial analysis of correspondences to the compression of image signals
17 p2517 A72-35671

Experimental study of image coding by complex Haar and Hadamard transformations
17 p2518 A72-35673

Adaptive compression of prediction of differential coding images
17 p2518 A72-35674

Effective dimensional reduction in the computation of linear, discrete, time-delay problems.
18 p2672 A72-36302

Digital techniques for image data processing and analysis, discussing data sampling, conversion, computer implementation, image matching, etc
18 p2664 A72-36490

Holographic strain analysis using spline functions.
19 p2797 A72-37611

Quantitative data reduction with the use of fringe control techniques in conjunction with holographic interferometry.
19 p2797 A72-37612

Three dimensional flow field visualization, data acquisition and reduction via holography, noting applications in schlieren and interferometric techniques
19 p2798 A72-37620

Orientation of astrographs in observations and measurements
19 p2802 A72-37972

A generalized method for the identification of aircraft stability and control derivatives from flight test data.
19 p2753 A72-38260

Ground based optical astronomy developments, emphasizing faint objects positional observation, trigonometric parallaxes, data analysis and measuring techniques
19 p2865 A72-38477

Reduction principle validity in perturbed motion stability theory for near-critical systems with gyro horizon application
20 p2955 A72-40029

Simulation of the process of reducing the redundancy of multichannel telemetry information on a digital computer by the method of adaptive break down into discrete elements and associative sorting
21 p3014 A72-40313

Reduction of redundant multichannel telemetry information by the method of adaptive break down into discrete elements and associative sorting
21 p3014 A72-40315

Applicability of associative computers to parallel adaptive break down of telemetry information into discrete elements
21 p3014 A72-40316

Data acquisition, storage and processing, discussing data reduction by statistical coding, interpolation, prediction and parameter identification
21 p3014 A72-40322

Telemetric frame compression coefficient and shaping algorithm for spacecraft data processing systems for arbitrary number of active channels
21 p3014 A72-40326

A priori estimation of the quality of a data-compression system from the statistical characteristics of the sensors employed
21 p3024 A72-40328

Transmission efficiency of gas chromatography algorithmic data compression and coding for spacecraft atmosphere studies
21 p3053 A72-40549

Wind tunnel data correction for interference due to flow boundary constraints /wall effects/, acoustic and model support effects

21 p3043 A72-41640

Influence of dispersion on the accuracy of estimating the fatigue life from the results of accelerated investigations by the prefraction method.

22 p3232 A72-41928

Application of sample quantiles to the compression of telemetric transmission and statistical processing of medical information

22 p3150 A72-42221

Measurement system decomposition for aerodynamic coefficient estimation.

[AIAA PAPER 72-964]

22 p3177 A72-42345

Figl astrophysical observatory design and instrumentation, describing solar radiation insulation, computerized data reduction, area scanning photoelectric photometer and Cassegrain spectrograph

22 p3178 A72-42541

Transient test techniques for modal survey testing.

22 p3163 A72-42698

A near real time data acquisition/reduction facility for the Boeing wind tunnels.

22 p3164 A72-42699

The efficiency of the method of the least squares for adjusting observations with non-normal distributions

22 p3199 A72-42998

Metallic solid material transient displacement field measurement by moiré fringe photographic recording technique with computer program for data analysis

24 p3401 A72-44611

Factors affecting phase-change paint heat-transfer data reduction with emphasis on wall temperatures approaching adiabatic conditions.

[AIAA PAPER 72-1030]

24 p3389 A72-45407

A thermal mapping technique for shock tunnels and a practical data reduction procedure.

[AIAA PAPER 72-1031]

24 p3389 A72-45408

DATA RETRIEVAL

Bulk data storage and retrieval with scanning laser and electron beams, discussing spot formation focal sensitivity, noise, beam deflection, speed and media environment

[IEEE PAPER 19,2]

03 p0368 A72-13775

Corrosion products X ray analysis using Powder Diffraction File, noting manual and computer searches

08 p1129 A72-22109

Radiometric method for atmospheric moisture data retrieval above radiosonde hygrometer cut-off or during malfunction, inferring average moisture decrease through radiative transfer equation

09 p3107 A72-22441

Skyhawk 904 sounding rocket cosmic X ray experiment, discussing detector and counter operation and data retrieval technique

10 p1529 A72-24198

Data storage and retrieval by holographic techniques, noting parallel recording of complex function at Fourier transform plane

15 p2236 A72-32040

DATA SAMPLING

Transfer function compensation technique for processing sampled imagery data prior to recording on hard copy to remove degrading effect for quality improvement

01 p0046 A72-10873

Small scale aerial photography use in regional agricultural survey, discussing equipment used, sampling techniques and data collection and interpretation

02 p0213 A72-11835

Oscillographically measured semiconductor element I-V characteristics plotting optimization by considering measuring instrument and sampling signal shape and frequency effects on hysteresis

03 p0330 A72-12968

Closed-loop nonlinear sampled-data systems with constant and finite Hankel transformable distributed elements, deriving frequency domain stability criteria

04 p0504 A72-14662

Cyclic phenomena periodicity by expected mean square deviation statistical analysis of observational data samples, using null hypothesis and unequally spaced sample intervals

04 p0574 A72-14908

Adaptive control for linear discrete time stochastic systems with unknown gain parameters, considering open loop feedback optimal control using quadratic performance index

[AD-739126]

06 p0791 A72-17305

Parameter adaptive self organizing control of linear discrete time systems, presenting stochastic approximation algorithms for feedback systems identification

06 p0791 A72-17306

Image data coding by adaptive block classification and quantization of source output symbols, evaluating performance

06 p0772 A72-17402

Adaptive sampling of continuous measurement signals, calculating mean sampling rate

06 p0773 A72-17572

Stationary-nonstationary temporal sampling for synoptic meteorological networks, illustrating oceanic wind speed measurements

06 p0842 A72-18436

Complex sampling with cascaded triple input majority logic redundant systems, deriving failure probability

07 p0949 A72-19173

Linear multivariable control system state observation by sampling with arbitrary but fixed distribution of sampling instants, emphasizing dual control by step functions

07 p0961 A72-19707

Linear time invariant multirate sampled data control systems characteristic equation simplification

09 p1290 A72-23099

Difference equation inequalities in sampled data system stability analysis, discussing solution asymptotic behavior

09 p1342 A72-23252

Numerical linear interpolator design with ICs, noting application to digital filters and sampled data systems

09 p1289 A72-23677

Digital adaptive sampling, stressing implementation problem

10 p1455 A72-23799

Sampling theorem application to time varying systems, considering Hankel transform as example

11 p1675 A72-25293

Discrete time systems with periodic feedback gain, deriving stability conditions and Nyquist plot from linear operator spectral theory

11 p1608 A72-25318

Book on sensitivity theory covering continuous and sampled data systems, linear, nonlinear and self exciting dynamic systems, optimal systems, large systems, controllability, etc

11 p1611 A72-26021

Automatic ceilometer systems for sky state reporting, discussing computerized cloud simulation model, instrumentation and data sampling

13 p1992 A72-28850

Analysis of errors generated by Kotelnikov series representation of finite signals during quantization by delta functions, finite duration sampling and constant amplitude sampling

13 p1919 A72-29044

Data compression for spacecraft borne signal measurement, discussing nonlinear quantizing, histogram parameter extraction, and signal encoding

[DFVLR-SONDDR-204]

13 p1921 A72-29346

Sampling theorem with small truncation error for band limited signals, discussing applications to pulse transmission filter design

13 p1922 A72-29397

Space-averaged sound pressure measurement by sequentially sampled microphone arrays, considering scanning rate and rms detector time constants effect

13 p1958 A72-29565

Linear statistical forecasting with noncorrelated predictors by multiple regression equations, showing degradation dependence on sampled cross covariances

13 p1995 A72-29591

Signal discretization frequency upper bounds determination to satisfy prescribed level of mean square error in continuous signal restoration

13 p1925 A72-30021

PCM speech transmission systems, comparing pseudorandomly dithered quantization with fixed level method by intelligibility and subjective appreciation tests and statistical analysis

14 p2087 A72-30942

Jointly optimal filters for fixed range radar filter-sampler-filter system, determining impulse response function forms

15 p2207 A72-31793

Multidimensional asynchronous FM pulse systems stability, considering continuous linear part transmission matrix poles located on imaginary axis

15 p2212 A72-32172

Single closed loop discontinuous control system, determining discrete correcting element parameters from linear inequalities

15 p2212 A72-32175

Infinite dimensional system optimal discrete-time feedback controller calculation by n-dimensional system approximation using recurrence relations with functional analysis

15 p2212 A72-32245

Low pass sampling bandwidth selection for digital mechanization of matched filter bit-synchronizer combination, discussing data rate vs SNR performance

16 p2363 A72-33217

Independent random test values effective sample numbers for mean and variance distributions in meteorological and geophysical statistical tests

16 p2385 A72-33382

Standard and bilinear z transformation techniques for digital sampling filters block diagrams derivation

16 p2369 A72-33671

Exponential signal reconstruction sampling rate restriction derivation based on pole-zero cancellations in Z transform

16 p2365 A72-33756

State space technique application to discrete linear control systems synthesis, discussing time-optimal

and quadratic-cost problems, and pole assignment method

17 p2532 A72-34246

Sampled imagery transfer function compensation by inverse function, noting truncation effects on processing array SNR performance

17 p2521 A72-34412

Price adjusted single sampling with linear indifference.

17 p2560 A72-34943

Correlation functions and reconstruction error for quantized Gaussian signals transmitted over discrete memoryless channels.

17 p2516 A72-35333

Digital simulation for sampled electro-optical imaging system performance prediction and optimization

17 p2557 A72-35552

Investigation of data rate requirements for low visibility approach with a scanning beam landing guidance system.

17 p2578 A72-35562

An analog computer technique for estimating sample times for digital simulation.

18 p2663 A72-36305

Generalized multi-dimensional sampling theory and applications in optical systems.

18 p2672 A72-36333

Optimal minimal-order observers for discrete-time systems - A unified theory.

18 p2674 A72-37099

Linear stochastic system optimal measurement strategy and matched Kalman type filter computation via transformation into deterministic control problem

18 p2674 A72-37100

A method for generalized statistical studies of discrete information transmission systems

19 p2764 A72-37301

Measurement of three-dimensional refractive-index fields by holographic interferometry.

19 p2798 A72-37621

Structural-matrix methods for discrete automatic control system designs

19 p2779 A72-38185

Investigation of data rate requirements for low visibility approach with a scanning beam landing guidance system.

19 p2832 A72-38259

Book - Bayesian statistics: A review.

20 p2946 A72-39728

Optimal single stage control law applicable to linear multivariable systems based on discrete-time analysis, discussing real time simulation on hybrid computer

21 p3037 A72-40637

Bounded-input bounded-output stability of nonlinear discrete systems by a method of comparison.

21 p3037 A72-40645

Single and double sample Dodge-Romig lot tolerance percent defective /LTPD/ rectifying inspection plans, using standard tables

21 p3059 A72-40827

Multidimensional asynchronous FM sampled data systems stability, considering continuous linear part transfer matrix poles located on imaginary axis

22 p3162 A72-42080

Stability conditions and effective bandwidths of first and second degree pulsed phase locked AFC systems with proportionately integrating filter, using Z transform method

23 p3263 A72-43433

Moment sampling method as selfvalidating aircraft weight and balance accounting procedure

[SAWE PAPER 920]

23 p3251 A72-43467

Estimates of unknown parameter from quantized observations given as sequence of evenly distributed random values, noting optimal grouping equations for general distribution function

23 p3266 A72-44218

DATA SMOOTHING

Aerial multispectral scanner data determination with filtering and smoothing along flight line over extended areas, deriving algorithm for cloud-shadowed area detection

02 p0212 A72-11817

Optimal smoothing application to testing of inertial navigation systems, gyros and component failure detection during mission

02 p0258 A72-12810

Gaussian periodic data optimal smoothing, describing convolution kernel and computer program

03 p0381 A72-13200

Formant-coded voiced speech parameters smoothing and quantizing effects subjective evaluation, obtaining average quantization threshold levels

04 p0487 A72-15298

Sensitivity algorithms for finite memory batch processing smoother /Kalman filter/, applying to ship inertial velocity error estimation

05 p0686 A72-16572

Computing techniques for finite Fourier transform, applying to Poisson equation, interpolation and quadrature and data smoothing

07 p1025 A72-18784

Data scatter reduction in Al-Zu-Mg welded specimens cumulative fatigue damage testing, noting

fatigue life improvement by shot peening and static or dynamic prestressing

09 p1332 A72-23619

Data window for digital spectrum estimation of random data by fast Fourier transform techniques, noting bandwidth increase by various data smoothing sequences

10 p1439 A72-24804

Running average method of data smoothing effect on persistence tendency change in meteorological time series

10 p1507 A72-25004

Fixed point smoothing of sequentially correlated processes by extending filtering technique to simultaneous estimation of state and process noise contribution

11 p1610 A72-25871

Vertical deflections estimation with inertial navigation system, geodetic position and velocity reference and optimal data smoother, noting applicability to surveys from moving vehicles

12 p1843 A72-27634

Recursive updating of smoothing and filtering algorithms for discretely observed continuous dynamic linear systems

19 p2826 A72-38274

Square root least squares and filtering solutions for fixed point and interval smoothing problems, comparing computational stability and precision and computer requirements

[AIAA PAPER 72-877]

20 p2910 A72-39122

Linear system proper frequencies and vibration dampings obtained by mathematical smoothing of mechanical admittance measurements

22 p3241 A72-43093

Whittaker method for astronomical observational data smoothing, noting correlation function for latitude weighting functions determination

24 p3447 A72-45677

DATA STORAGE

Data holder made of three thin ferromagnetic coupled films for magneto-optic computer memory

01 p0035 A72-11317

Crimped films for object reconstruction and image storage, comparing performance to holographic films

01 p0073 A72-11318

FAA air traffic control automation program, discussing en route stage, computer program, data processing and storage and terminal area navigation and display techniques

02 p0256 A72-12380

ERTS-A orbital earth resources data utilization, describing user community size and character and central repository data center

02 p0305 A72-12381

Long life magnetic tape recorder for onboard data storage in space flights, discussing two motor tape transport and static memories for improved reliability [IEEE PAPER 12,4]

03 p0360 A72-13767

Magneto-optic storage density and read-write rate, discussing transducer cost, solid state injection lasers, holographic techniques and high activity data base applications

[IEEE PAPER 19,1]

03 p0361 A72-13774

Bulk data storage and retrieval with scanning laser and electron beams, discussing spot formation focal sensitivity, noise, beam deflection, speed and media environment

[IEEE PAPER 19,2]

03 p0368 A72-13775

Lf spectrum analysis instrumentation, describing stored data signals Fourier series parameters analog computation techniques

04 p0523 A72-15487

Computer storage hierarchy hardware influence on data base management systems software technology [IEEE PAPER 13,5]

04 p0598 A72-15712

Bulk storage applications in Illiac 4 system, discussing Unicon 690 mass memory for Advanced Research Projects Agency network of telephone lines and interface message processors

[IEEE PAPER 23,4]

04 p0496 A72-15714

Optical holographic storage in lithium niobate single crystals, noting erasability and rewritability

07 p0981 A72-18890

Electro-optic materials and fixing techniques for holographic recording and storage performance improvements

[CLEA PAPER 18,2]

07 p0950 A72-19400

Holographic information storage with reference wave modulation by Fabry-Perot interferometer, using two coherent sources

07 p0985 A72-19417

Reduced data storage requirement of synthetic aperture radar for target classification by fast Fourier transform

08 p1134 A72-21422

Meteorological radar signal reflectivity probability and quantization error dependence on incoherent storage device parameters from computer simulation

08 p1201 A72-21995

Reliability tests improvement by ergodic processes failure prediction and data storage for high reliability products manufactured in small numbers

08 p1180 A72-22067

Mass storage systems technologies covering magnetic recording, surface wave acoustics, magneto-optic beam addressing, magnetic bubbles, switchable resistances and IC memories

09 p1283 A72-23413

Automatic meteorological station MME-1 data storage and interrogation device for transmission to central station

10 p1445 A72-25019

Ferrite core memory for storage of Helios probe perisolar space data before transmission to telemetry system

11 p1601 A72-25806

Associative impulse analyzer for measurement of probability density functions in electronic memories

11 p1602 A72-26446

Data file optimal arrangement by programmed procedures formulated as combinatorial problem, using branch-and-bound method for solution

12 p1787 A72-28118

Data storage and retrieval by holographic techniques, noting parallel recording of complex function at Fourier transform plane

15 p2236 A72-32040

Diffraction theory for large storage capacity holographic random access memory design, discussing geometric optimization of detector array and storage plate

15 p2238 A72-32159

Holographic information storage survey, discussing hologram classification, characteristics, physical recording processes, and capacity-limiting factors

15 p2239 A72-32351

Magneto-optics materials for use in data storage, discussing quality evaluation based on figure of merit reflecting heat sensitivity and readout requirements

15 p2203 A72-32352

Undoped lithium niobate for holographic storage applications, reviewing physics and recording performance

15 p2239 A72-32353

Transition metal doped lithium niobate for holographic storage, measuring recording sensitivity, maximum diffraction efficiency and erase behavior

15 p2239 A72-32354

Recyclable holographic recording media performance parameters comparison to develop tradeoffs for storage and imaging applications

15 p2239 A72-32360

High contrast and sensitivity thermal erase cathodochromic sodalite for storage and display applications, measuring contrast ratio versus electron beam flux

15 p2240 A72-32362

Resolution of optical-memory matrices prepared from photochromatic materials when using a focused beam to record information

18 p2692 A72-36658

The L14-120GJ, a new bistable image storage tube

18 p2667 A72-36677

RF time domain nonreal time reflectometer operating as nanosecond radar with pulse spectrum lines reflections measured and stored for echo computation

19 p2770 A72-37256

Error reduction in digitally generated holographic memories via parity sequence interlacing with true data sequence for spectrum shaping

19 p2796 A72-37581

Data file optimal arrangement for retrieval by programmed procedures formulated as combinatorial problem, using branch-and-bound method for solution

19 p2770 A72-38619

A holographic memory recording matrix permitting real-time data modification.

20 p2922 A72-39037

Reading of holograms by a semiconductor injection laser.

20 p2933 A72-39518

As-Te-Ge amorphous semiconductor film optical memory effect due to crystallization and reversion during exposure to pulsed laser beam, noting writing and erasing characteristics

20 p2961 A72-39708

Some optical properties of liquid crystals

20 p2961 A72-39850

Modular navigation (MONA) dual channel automatic area navigation system, describing computer, flight data storage and control/display units

21 p3079 A72-40277

Data acquisition, storage and processing, discussing data reduction by statistical coding, interpolation, prediction and parameter identification

21 p3014 A72-40322

Photoanodic engraving process produced high bit density surface relief holograms on semiconductor crystals for data storage, retrieval and replication applications

21 p3054 A72-40614

Small-size phase holograms for binary data storage

21 p3058 A72-41744

Real time analog computation at light speed and rapid access data storage in optical data processing systems, considering coherent electro-optical instrumentation

22 p3180 A72-42713

Phototropic borosilicate glass optical density variation by exposure to UV or blue light, considering utilization for digital data storage and/or cathode ray tubes

22 p3180 A72-42941

Advanced optical storage techniques for computers.

23 p3288 A72-43876

DATA SYSTEMS

NASA/MSC Earth Resources Research Data Facility for remote sensing of geology, geography, agriculture, forestry, hydrology and oceanography

02 p0200 A72-11824

Army data analysis system for fixed and rotary wing aircraft flight testing, including airborne and computer controlled ground stations equipment

02 p0179 A72-12408

Helios solar probe mission, describing project management, data reception system, trajectory monitoring and international cooperation [DGLR PAPER 71-052]

02 p0284 A72-12720

Aircraft integrated data systems, discussing cost effectiveness, reliability and maintenance

03 p0327 A72-13417

Visual film, TV and optical data systems unified classification for performance criteria based on equation similar to ideal imaging system description by Rose

03 p0329 A72-14188

Aircraft integrated data systems application to flight safety analysis, engine performance monitoring, crew proficiency, autoland evaluation, operations and logistics

04 p0495 A72-14726

ALSEP central station data subsystem, discussing power conditioning unit and electric power subsystem

04 p0508 A72-15094

Computer storage hierarchy hardware influence on data base management systems software technology [IEEE PAPER 13,5]

04 p0598 A72-15712

Deep space probe MULTIPAC data system computer repairable during flight via command and telemetry links by reprogramming failed unit

05 p0633 A72-16573

DC 9 aircraft integrated data system simulator to facilitate interacting systems checking, input circuit integrity, performance degradation and calibration

06 p0796 A72-18284

Optimal operation assignment and data array storage allocation in data system consisting of central processing unit and peripheral computer controlling data flow

09 p1283 A72-23439

Rapid data input system for Minsk 22 digital computers using photographic film read by photoelectric scanning system

10 p1445 A72-24495

Large data processing systems for requirements of meteorology, environmentalology, earth resources inventories and hydrology in 1980s

10 p1446 A72-25095

Camac modular instrumentation data handling system for interfacing to digital computers and hardware controllers, noting astronomical data acquisition application

11 p1601 A72-25700

Parameterized daily profile characterization of global atmospheric conditions to minimize computer storage, discussing mathematical representations, wind, density and temperature profiles

13 p1989 A72-28806

Data system in Eole satellites program, discussing balloon localization, UHF information transmission and reception, distance measurement and data acquisition

15 p2268 A72-31981

Nomographic correction method for quantization error limited data systems, modifying root-summed-squared error analysis for non-Gaussian distribution

16 p2367 A72-33863

Russian book - Design principles for multiple-valued physical circuits.

21 p3027 A72-40386

Defense Documentation Center independent R and D data bank for evolution and maintenance of creative technology oriented defense industry

21 p3132 A72-40974

DATA TRANSMISSION

NT CHANNELS [DATA TRANSMISSION]

Wideband data transmission on group-band communication channels, using dual single-sideband modulation with basic transmission rate of 48 kbit/sec

01 p0024 A72-10113

Information feedback application to AM laser communication system, predicting multiplicative error, background shot noise and photon arrival fluctuation effects on continuous parameter transmission

01 p0025 A72-10326

Bit error rate estimation for narrow band digital communication in presence of atmospheric radio noise bursts

01 p0025 A72-10334

Reliable data transmission block coding techniques including burst error, fire, Reed-Solomon and product codes and majority decoding algorithm

01 p0025 A72-10335

Radio signals information capability estimation during propagation through electromagnetic fields, using pulse amplitude modulation 01 p0065 A72-10446

Methodological problems in unidimensional information transmission involving circular light identification tasks 01 p0013 A72-10718

Report on U.S. telecommunications telemetry information theory in period 1966-1969, discussing ionospheric and tropospheric data transmission 02 p0171 A72-11687

Format logic design for airborne memory controlled PCM telemetry multiplex digital and analog data system 02 p0187 A72-12130

Shock hardened delayed transmission pulse code modulated system for artillery projectile instrumentation with in-barrel and in-flight monitoring capability 02 p0175 A72-12155

Data transmission and distribution systems interface, using semiconductor technology in multiplexing, asynchronous data transfer, A-D and D-A data conversion and sensor signal conditioning 02 p0194 A72-12404

Digital telemetry data transmitter featuring triangular wave generator and signal mixer for reducing sensitivity to transmission path characteristics variations 02 p0179 A72-12415

High speed digital communication at millimeter wavelengths, discussing system requirements, digital computer use, transmission data rate and equipment development 04 p0485 A72-14481

Minicomputer use for terminal control and matching functions and data compression in data transmission systems 05 p0633 A72-16199

Adaptive variable length coding for efficient compression of spacecraft TV data of Grand Tour missions 06 p0771 A72-17401

Optical data transmission system with dielectric single-mode glass fiber waveguide, PCM semiconductor laser diode transmitter and avalanche photodiode receiver 06 p0774 A72-17770

Data transmitting dielectric light waveguide production problems, noting light scattering and absorption losses due to glass material impurities 06 p0825 A72-17774

Nationwide real time automated ATC system interconnected by data transmission links, discussing radar signal acquisition/transfer and computer complex 06 p0845 A72-18283

Computerized EEG data acquisition and transmission system for large hospitals with multiple critical care patient monitoring units, noting telephone access from outside 07 p0928 A72-19307

Laser communication systems for terrestrial and space data transmission, discussing line-of-sight requirements and atmospheric effects 07 p0947 A72-20225

Digital simulation for predicting performance of data communication networks with computerized switching centers, detailing space shuttle interior communication system 07 p0952 A72-20364

Human behavior analysis based on nine component functional brain model, discussing information transmission mechanism via nerve path channels 07 p0923 A72-20460

Meteorological geostationary satellite international program for earth cloud cover observation and meteorological data relays between ground stations as part of Global Atmospheric Research Program 08 p1241 A72-21204

Terrestrial surface observation from space platform, considering atmospheric effects, surface spectral properties and information resolution and transmission 08 p1170 A72-21965

Data transmission system design in computerized administrative control system for industrial enterprise management 08 p1257 A72-22148

Data transmission interference protection under extreme noise, using tolerance detectors with redundancy coding 09 p1278 A72-22851

Compression of data from measurements in real time nonlinear estimation to reduce data processing requirements without performance deterioration, applying to reentry vehicle tracking 10 p1442 A72-23802

Book on telemetry and remote control covering information theory, analog/digital techniques, signal transmission, data processing and coding, etc 10 p1436 A72-24550

Digital data transition tracking loop as practical implementation of optimum self bit synchronizer in Mariner spacecraft telemetry demodulators 10 p1437 A72-24687

Automatic remote transmitting meteorological station, discussing development, working principle, technological features and sensors 10 p1462 A72-25010

Automatic meteorological station MME-1 data storage and interrogation device for transmission to central station 10 p1445 A72-25019

Classification of automatic meteorological ground stations networks in populated areas, discussing required equipment, data transmission, real time operation and costs 10 p1507 A72-25021

Time division multiplexing system for asynchronous high data rate telemetry, discussing design features 10 p1440 A72-25061

Flow measurement instrumentation for turbomachine rotors, noting telemetry type data transmission system with strain gauge pressure transducers for turbocompressor [ASME PAPER 72-GT-55] 11 p1630 A72-25646

Data transmission bandwidth requirements compression for band-limited functions, investigating feasibility through analog signal routing 11 p1592 A72-25887

Phase shift methods for data transmission vestigial sideband signal generation, providing shaping functions by shift registers, weighting resistors, summing amplifiers and low pass filters 11 p1592 A72-25890

Video information transmission over planar and rectangular multimode waveguides under excitation by coherent light, calculating field distribution by geometrical optics approximation 11 p1633 A72-26330

Modular computer program for digital transmission systems, applying to optimization of filters in multitransponder satellite and ground stations 12 p1786 A72-27323

Analog measuring data transmission systems optimization by computers, noting improvement of dynamic response and linearity in digital systems 12 p1786 A72-27580

Voice digital data rate reduction technique by exploiting zero and one bits imbalance in PCM TDM bit stream output encoding, discussing hardware implementation 12 p1785 A72-27845

Error probabilities estimates for communication systems using orthogonal multiposition signals in information transmission, noting techniques applicability to diversity reception systems with self selection 13 p1918 A72-28893

Synchronization theory for digital data transmission with random changes in channel characteristics 14 p2085 A72-30333

PCM speech transmission systems, comparing pseudorandomly dithered quantization with fixed level method by intelligibility and subjective appreciation tests and statistical analysis 14 p2087 A72-30942

ATC operational systems, discussing global surveillance and voice and data communication between aircraft and earth station 14 p2129 A72-31141

Geostationary Intelsat satellite networks for retransmission of data received by earth resources satellites 15 p2221 A72-31243

Data transmission developments, considering computer improvements, networks, routes and frequency multiplexed PCM system 15 p2195 A72-31619

SSB signal generation without Nyquist filter or auxiliary equipment for PM modems in data transmission 15 p2195 A72-31620

Mars and Venus automatic station data transmission systems for surface and atmosphere studies, discussing relay and direct transmission modes 15 p2203 A72-31823

High speed facsimile transmission system based on LR70 laser scanner, presenting typical system output image 15 p2248 A72-32041

Generator for data transmission lines stochastic noise bursts simulation with statistically independent burst durations and intervals 15 p2201 A72-32475

Carrier synchronization and polyphase signal detection in digital communication network for high speed data transmission, deriving reconstructed noisy signal error probability 16 p2363 A72-33218

Noise stability of frequency-time adaptive transmission systems for discrete information, using resolving feedback circuits 16 p2363 A72-33266

Random multiple access data transmission systems with feedback for message confirmation and retransmission in event of errors, evaluating channel capacity 16 p2372 A72-33794

Data transmission systems with decision feedback in presence of burst noise, calculating statistical relations among received sequences as function of duration and spacing 16 p2372 A72-33795

A/D and D/A converter for color TV signal digital transmission over communication satellites, discussing system design features 17 p2524 A72-34262

Semiconductor optoelectronic devices, discussing light emitting indicator diodes, data display systems, photosensitive arrays and optical data transmission links 17 p2594 A72-34332

Correlation functions and reconstruction error for quantized Gaussian signals transmitted over discrete memoryless channels. 17 p2516 A72-35333

Video data transmission minimum channel capacity requirement calculation from rate distortion function of source with known probability distribution 18 p2657 A72-36253

The use of linear programming to design digital filters from impulse-response specifications. 18 p2663 A72-36304

Adaptive equalization of data transmission rate in telephonic systems, considering criteria and iterative algorithms 18 p2661 A72-36790

A method for generalized statistical studies of discrete information transmission systems 19 p2764 A72-37301

Transmission of a fluidic signal at intermediate distances. 19 p2754 A72-38046

A priori estimation of the quality of a data-compression system from the statistical characteristics of the sensors employed 21 p3024 A72-40328

Injection laser and light emitting diode techniques to transmit digital data in local distribution 21 p3018 A72-40869

Carrier phase jitter extraction method for VSB and SSB data transmission systems. 21 p3021 A72-40910

Dual mode - An efficient encoding method of nonsynchronous data signals on PCM. 21 p3023 A72-41827

Signal quality monitoring of computer data transmission. [ASME PAPER 72-AERO-1] 22 p3156 A72-43146

Phase modulated data transmission with partial pilot signals, interpolating reference demodulation signals at receiving end by maximum cross correlation 23 p3264 A72-43771

Flawless operation probability for information transmission reliability of electronic logic circuits with binary data inputs 23 p3271 A72-43784

Optimal filtration algorithms of Markov parameters of discrete time signals in digital data transmission system with background noise, using Gaussian probability density approximation 23 p3264 A72-44005

Monolithic quartz and ceramic bandpass filters for narrow band analog data transmission systems 23 p3273 A72-44347

Broad-band information transfer with the aid of laser-beam coupling fields 23 p3266 A72-44359

Point-to-point national data communication geostationary satellite system associated with computers, discussing organization, earth station equipment and technical and economical feasibility 24 p3380 A72-44975

Minicomputers application for long distance data transmission, noting multipurpose use of VT 1010/B computer in satellite operation program 24 p3382 A72-45391

DATING

U CHRONOLOGY

U TIME MEASUREMENT

DAWN CHORUS

VLF emissions during post breakup phase of polar substorm. 17 p2547 A72-35064

Simultaneous F-region conjugate point dawn effects at two mid-latitude stations. 20 p2916 A72-39234

DAYGLOW

Molecular nitrogen dayglow emission in F region, noting volume emission rates, integrated overhead intensities and solar activity effects 04 p0518 A72-14959

Equatorward motion of midday auroras during magnetospheric substorms, using all sky photographs 06 p0805 A72-17463

Molecular nitrogen photoelectron impact excitation of Herman-Kaplan upper electronic state, considering cascade contribution to low lying states in electron auroras and dayglow 06 p0806 A72-17647

Earth horizons nighttime, twilight and daytime visual observations from manned Soyuz spacecraft, discussing upper atmosphere emission layer structure and aureole development 08 p1158 A72-21148

Resonance scattering and direct photoelectron excitation contribution to molecular nitrogen first positive bands emission in day airglow from rocket measurements

13 p1953 A72-29808

Upper atmospheric Na abundance from daytime spectroscopic absorption measurement compared with twilight glow observation

16 p2383 A72-32970

Sodium emission from the atmosphere during a solar eclipse.

19 p2793 A72-38857

Earth horizons nighttime, twilight and daytime visual observations from manned Soyuz spacecraft, discussing upper atmosphere emission layer structure and aureole development

20 p2916 A72-39253

Dayglow nitrogen ion 3914 A emission profiles for average solar activity at 110-240 km heights from Cosmos 224 observations

23 p3282 A72-43357

Tilting-filter measurements in dayglow rocket photometry.

23 p3289 A72-43893

DAYTIME

Daytime and nighttime sporadic F layer regularities correlation with other ionospheric phenomena based on vertical sounding data

01 p0059 A72-10611

Latitudinal distribution of electron temperature in F 2 layer during summer daytime period of low solar activity from electron density profile geometrical parameters

05 p0656 A72-16248

Brightness profiles of earth daytime horizon from Soyuz spacecraft photographic photometry, deriving atmospheric scattering coefficient relation to optical thickness vertical distribution

06 p0808 A72-18040

Quarter thickness variation and particle temperature dependence on height and frequency in summer daytime F region

08 p1155 A72-20815

Dayside magnetosphere stably trapped radiation zone high latitude boundary determination from energetic electron intensity spatial distribution observation by Imp 3 satellite

11 p1713 A72-26106

Daytime and nighttime electron temperatures from topside resonances, using oblique echo theory

11 p1625 A72-26409

Daytime sky brightness and scattered light polarization, emphasizing atmospheric radiation field characteristics

13 p1945 A72-28516

Daytime 30 MHz PCA from satellite and riometer measurements, noting linear relationship to square root of integral and differential solar proton fluxes

13 p2030 A72-29339

Photodetachment of electrons from major negative ions in the lower D region.

18 p2686 A72-36622

Noctilucent clouds in daytime - Circumpolar particulate layers near the summer mesopause.

22 p3173 A72-42515

C [CURRENT]

U DIRECT CURRENT

C 9 AIRCRAFT

DC 9 aircraft integrated data system simulator to facilitate interacting systems checking, input circuit integrity, performance degradation and calibration

06 p0796 A72-18284

C 10 AIRCRAFT

Airline Propulsion Team approach to DC-10 aircraft power plant design for maximum operational effectiveness

[SAE PAPER 710778]

01 p0116 A72-10270

DC-10 nondestructive testing manual, detailing section/subject format, methods, planned area accessibility and aircraft maintenance

01 p0078 A72-11109

DC-10 aircraft automatic landing performance and failure assessment monitor system

08 p1204 A72-21003

Heat treatment and machining for distortion control of large Al alloy forgings for DC 10 aircraft

09 p1317 A72-22476

DC-10 aircraft structural design, flight handling characteristics and fatigue tests

09 p1262 A72-23446

DC 10 aircraft automatic flight guidance system, noting dual-dual fail-passive autoland

09 p1349 A72-23448

DC 10 aircraft wing stringers fabrication and processing, discussing stress relieving and stretch form contouring techniques, aging and tempering processes and flaw detection

[ASM PAPER W 72-31.3]

12 p1817 A72-28161

How United trains DC-10 pilots.

19 p2760 A72-37898

CHAVILLAND AIRCRAFT

The DHC-7, first generation transport category STOL - Particular design challenges.

19 p2750 A72-38115

AIAA PAPER 72-809

LAVAL NOZZLES

U CONVERGENT-DIVERGENT NOZZLES

DEACCLIMATIZATION

U ACCLIMATIZATION

DEACTIVATION

Bacteriophage synergistic inactivation by heat and ionizing radiation from kinetic model describing dose rate and temperature dependences

06 p0768 A72-18185

Na deactivation effect on carbon dioxide-nitrogen gas dynamic laser gain

07 p1008 A72-20564

Resonance theory of three body ion-atom association reactions in rare gases, estimating quasi-bound electron state population and deactivation cross section

09 p1356 A72-22792

Optimal temperature control for microbial inactivation by composite environment of heat and gamma radiation, using quadratic technique

18 p2649 A72-36313

Metastable atomic oxygen deactivation in upper atmosphere by inelastic collisions and by spontaneous irradiation, noting airglow intensity dependence on red lines irradiation

19 p2792 A72-38633

DEADWEIGHT

U STATIC LOADS

DEAFNESS

U AUDITORY DEFECTS

DEATH

Clinical death period and reanimation concepts, noting erroneous interpretations of irreversible histological alterations, revival attempt period and organism self reanimation potential

09 p1266 A72-22876

DEBRIS

NT SPACE DEBRIS

DEBUGGING

U CHECKOUT

DEBYE LENGTH

Ion and electron temperatures difference relaxation rate in uniform plasma, noting relationship to Debye length

02 p0267 A72-12769

Photoconductivity in depleted surface layer of quasi-monopolar semiconductors with arbitrary diffusion to Debye lengths ratio, noting n-type low resistance gallium arsenide

15 p2296 A72-32694

Instability of a weakly ionized plasma with respect to vibrations with wavelengths of the order of the Debye radius

22 p3213 A72-43104

DEBYE TEMPERATURE

U SPECIFIC HEAT

DECAMETRIC WAVES

Io modulation of Jupiter decametric emissions, using cyclotron magnetosphere model and coupling by whistler mode electromagnetic waves

01 p0125 A72-10084

Jupiter decameter radio burst possibility as indicator of high velocity fluxes and shock waves in solar wind

02 p0273 A72-11935

Solar U-type radio bursts in outer corona at 0.7 MHz related to magnetic bottle

03 p0406 A72-12937

Solar decameter and hectometer wavelength radio burst generation, examining dynamic spectra and source position as function of frequency and time

03 p0424 A72-13221

Jupiter decametric radio emission relation to solar wind, geomagnetic activity and shock waves causing Forbush decreases

03 p0436 A72-13820

Jovian decametric radiation observations, showing satellite Io relative position correlated to highest frequency

04 p0581 A72-15515

Collisionless shock wave interaction with particle stream in upper solar corona from decameter radio observation

05 p0708 A72-15764

X ray detection on Jupiter with actively collimated balloonborne scintillation counter, noting decametric emission due to electron precipitation

06 p0872 A72-17445

Astronomical model for Jovian decametric radio emission control by Io satellite based on two surface sources on planet and particle interaction with plasma

06 p0891 A72-18504

Maximum cut-off frequency of Io controlled Jovian decametric radiation as function of lambda coordinates

07 p1059 A72-19599

Three station interferometer observations of Jovian decametric burst at 18 MHz, discussing possible solar wind interference

12 p1871 A72-27743

Jupiter decameter radio bursts as indicator of high velocity fluxes and shock waves in solar wind

13 p2030 A72-29247

Transequatorial off-path propagation outside of great circle at decametric waves associated with forward scattering by field aligned irregularities in equatorial ionosphere

14 p2084 A72-30129

Jupiter decametric radiation modulation by photoelectron emission by satellite Io, describing future probe experimental test

14 p2156 A72-30558

Io effects on Jupiter decametric radio bursts, discussing ionosphere vs solid surface for required conductivity

16 p2455 A72-33465

Decametric radio identification of an extragalactic X-ray source.

17 p2604 A72-34520

The plasma physics of the Jovian decameter radiation.

17 p2605 A72-34539

The type IIIB burst - A precursor of decametre type III radio-burst.

20 p2965 A72-39882

Structure of Jupiter's decametric radio sources - Two-dimensional probability and flux studies, 1957-1970.

24 p3436 A72-44691

Thin ice crust, chondritic composition and ionosphere considerations for Io electrical conductivity and decametric radio emission modulation in unipolar inductor model

24 p3437 A72-44704

Linear polarization survey for galactic background radiation at 1415 MHz in North Polar Spur, Cetus Arc and Loop III, noting continuous maxima shift

24 p3438 A72-44835

DECARBONATION

Kinetics of carbothermal reduction of quartz under vacuum.

21 p3073 A72-40934

DECARBOXYLATION

Alpha amino acids proteinoids or thermal polymers enzyme activity, investigating hydrolytic activities and decarboxylation reactions

04 p0483 A72-14776

DECARBURIZATION

Decarburization kinetics of Nb wires with dissolved carbon in high temperature oxygen flow, monitoring electrical resistivity and CO partial pressure

15 p2244 A72-32113

Decarburization kinetics of low alloy ferritic steels in sodium.

22 p3194 A72-43042

DECAY

NT BIOLUMINESCENCE

NT CHEMILUMINESCENCE

NT ELECTROLUMINESCENCE

NT ELECTRON EMISSION

NT FIELD EMISSION

NT FLUORESCENCE

NT INCANDESCENCE

NT ION EMISSION

NT LIGHT EMISSION

NT LUMINESCENCE

NT LUNAR LUMINESCENCE

NT NEUTRON DECAY

NT NEUTRON EMISSION

NT NUCLEAR FISSION

NT OPTICAL RESONANCE

NT PARTICLE EMISSION

NT PHOSPHORESCENCE

NT PHOTOELECTRIC EFFECT

NT PHOTOELECTRIC EMISSION

NT PHOTOIONIZATION

NT PHOTOLUMINESCENCE

NT PHOTOPRODUCTION

NT PLASMA DECAY

NT RADIO EMISSION

NT RADIOACTIVE DECAY

NT SECONDARY EMISSION

NT SELF SUSTAINED EMISSION

NT SHOCK WAVE LUMINESCENCE

NT SOLAR RADIO BURSTS

NT SOLAR RADIO EMISSION

NT SPECTRAL EMISSION

NT STIMULATED EMISSION

NT THERMAL EMISSION

NT THERMIONIC EMISSION

NT THERMOLUMINESCENCE

NT X RAY FLUORESCENCE

Fourier transformation for natural abundance C 13 free induction decays of cyclic antibiotic valinomycin and K ion complex, noting chemical shift differences

13 p1913 A72-29862

DECAY RATES

NT ELECTRON DECAY RATE

Numerical analysis of radio echoes decay rate from randomly ionized meteor trails

01 p0130 A72-10913

Flutter equation approximate true damping or rate-of-decay solution by determinant iteration

01 p0142 A72-11133

Nitrogen dioxide producing chemiluminescent radiative and three-body recombination reaction at low pressures, determining airglow and oxygen atoms decay time by resonance fluorescence method

03 p0347 A72-13395

Supersaturated semiconductor solid solutions decay kinetic equations and time constants, noting free current carriers effect

04 p0561 A72-15081

Solar type 3 bursts from high resolution radio spectrographs, deriving coronal temperatures from decay times

06 p0876 A72-17576

White dwarf magnetic fields decay time scale for dipolar and toroidal configurations

06 p0876 A72-17581

Circular vortex rings with nonsimilar vorticity distributions submerged in inviscid stream, considering motion and decay by inner and outer asymptotic expansions matching

[AD-741267] 06 p0798 A72-17781

Incompressible microstretch fluid flow in rigidly bounded domain, deriving kinetic energy decay rate via linear model subject to entropy principle and boundary adherence condition

06 p0799 A72-17918

Quasi-particle decay rates by electron-electron scattering in superconductors, noting effect on states tunneling density

08 p1217 A72-21595

Single mode He-Ne laser output, predicting intensity correlation function form and decay time near threshold

[AD-742154] 09 p1324 A72-23081

Small scale wind shear effects on overdense and underdense radio meteor echoes, noting premature decay and scatter in decay time

10 p1440 A72-24952

Glass and carbon fiber reinforced plastic beam specimens dynamic moduli and loss factors determination from vibration frequency and decay rate measurements

13 p1984 A72-29095

Fast electron gun with subnanosecond switching times and 100 mA peak beam current for delayed coincidence studies of atomic decays

13 p1933 A72-29761

Electron beam excited P-15 phosphor 3900 A spectral component fast decay time measurement by delayed coincidence technique

13 p2000 A72-29762

GaAs doped Si light emitting diode as light source for optical timing system calibration, studying fast luminescent decay characteristics

13 p2000 A72-29763

Time invariance violation in charge asymmetry experiment, showing K-meson decay rate difference reversal from world to antiworld with particle unchanged

14 p2130 A72-30265

Lamb dip for 119 micron line of CW gas laser, noting decay constants due to pressure

14 p2110 A72-30424

Solar proton events end prediction from flux decay rates observation, noting particle energy effect on accuracy

15 p2301 A72-31999

High gain CW He-Xe laser transitions due to Xe 5d level long-lived decaying emission

15 p2250 A72-32301

Circularly polarized photon echo decay measurement as function of Cr concentration in ruby, noting relationships to temperature, pulse separation and external magnetic field

15 p2295 A72-32545

Weakly ionized nonequilibrium plasma flow from gas discharge tube positive column, obtaining electron temperature axial decay rate from energy equation

16 p2437 A72-33655

Decay rate coefficients at 250-370 K for three-body recombination kinetics of O and CO, considering CO, carbon dioxide and nitrogen as third body

17 p2511 A72-34736

The effect of wind shear gradients on underdense radio meteor decay times.

17 p2517 A72-35398

Further comparison of theory and experiment for decay of homogeneous turbulence.

17 p2542 A72-35629

Decay of isotropic turbulence generated by a mechanically agitated grid.

19 p2787 A72-38426

The effect of cross relaxation on the behavior of gas laser oscillators.

19 p2813 A72-38691

Weak decay, branching ratio and decay probability of strongly interacting particle event observed by Niu in cosmic nuclear jet shower

19 p2853 A72-38808

Effect of fluorescence observation geometry on lifetime measurement, including the development of an approximation to the detector collection efficiency integral.

23 p3288 A72-43884

On a long-term temporal aspect of stereoscopic depth sensation.

23 p3258 A72-44381

Decay of swirl in a straight pipe flow /with hub at the entrance/.

24 p3394 A72-45367

DECCA NAVIGATION

Man computer weapons effectiveness and system test environment /WESTE/ instrumentation system

with Decca navigation for simulated combat environmental flight tests

12 p1754 A72-27515

DECELERATION

NT SPIN REDUCTION

Ground test determination of design data for low supersonic high density air deployable deceleration systems, considering high strain rate effects on parachute materials

01 p0005 A72-10313

Decelerating MHD effect on rotational funnel flow excited by vortex line or radial converging currents

03 p0397 A72-13994

Perturbation solution of deceleration trajectory in ballistic reentry through rotating atmosphere with winds, assuming constant gravitational field and square law drag force

09 p1395 A72-22924

Decelerating motion of identical and independent water drops succession, determining drag coefficient as function of Reynolds number

10 p1465 A72-24104

Meteorite particle movement in earth atmosphere, discussing deceleration dependence on velocity, atmospheric density and surface evaporation reactive forces

14 p2152 A72-30493

Crash energy absorption for prevention of fatal injuries, considering human deceleration tolerance with respect to required energy absorber force-deflection relationship

15 p2192 A72-32630

Hydraulic shock of incompressible heavy fluid in closed cylindrical tank under abrupt deceleration

15 p2219 A72-32685

Angle of attack increase of an airfoil in decelerating flow.

18 p2641 A72-36773

Meteorite particle motion in earth atmosphere, discussing deceleration dependence on velocity, atmospheric density and surface evaporation reactive forces

19 p2864 A72-38322

German monograph - Pressure variation along a plane slender wedge and along a slender cone of revolution at decelerated flight in the supersonic range near sonic velocity.

22 p3136 A72-43074

DECIMETER WAVES

Reflected signal and receiver noise interference error in antenna temperature and calibration measurements by artificial moon method in centimeter and decimeter bands

08 p1142 A72-21726

Transistorized microwave amplifier/limiter for upper part of decimeter wave range, suggesting limitation in automatic gain control transistors

10 p1451 A72-24588

Jupiter - New evidence of long-term variations of its decimeter flux density.

21 p3107 A72-41274

Type 4 decimetric, moving and quasi-stationary groups described in terms of onset time lags for different frequencies and components

21 p3101 A72-41763

Quasi-periodic solar radio pulsations at decimetric wavelengths.

22 p3222 A72-42045

DECISION ELEMENTS

U LOGICAL ELEMENTS

DECISION MAKING

Avionics contribution to airspace decision making problems, considering navigation, surveillance radar, collision avoidance and ATC techniques

01 p0097 A72-10180

Production cost control and tracking, discussing design decision effects

[SAE PAPER 710747] 01 p0146 A72-10246

ATC system decision making problem and future technological and administrative improvements

02 p0255 A72-11718

Pollution and environmental quality remote sensing, describing five dimensional sensor/applications matrix for decision guidance

02 p0212 A72-11827

Project management mathematical models for task scheduling, resource allocation, information planning and decision making

06 p0905 A72-18067

Materials selection problems due to wide variety of new products, discussing technologically and economically optimal decisions on product design, development and future substitutions

06 p0906 A72-18255

Decision making under determinateness, risk and indeterminateness conditions

06 p0781 A72-18302

Digital decision directed suboptimal receiver design for random multipath channel communication with intersymbol interference, predicting performance for steady state probability of correct decision

07 p0941 A72-19272

R and D management policies choices with respect to Bayesian decision-theoretic model in simulated environments

07 p1105 A72-19553

Entropy effect in two dimensional conditional reflex decision situations upon rats central nervous analysis-synthesis processes

07 p0925 A72-20661

Central nervous plasticity and stereotypy intercorrelation in conditional reflex two dimensional decision situations

07 p0925 A72-20662

Group composition and n-dimensionality personality trait effects on decision and communication task efficiency in laboratory triads

08 p1125 A72-21200

Man machine decision making procedures for multicriterial aggregate estimates, using pairwise comparisons and linear programming

09 p1273 A72-23430

Robots /electromechanical systems with local computers and sensor controlling motors and effectors/ space application categories and operating and decision making requirements

10 p1458 A72-23777

Reliability decision making under uncertainty between alternative design approaches, using dynamic programming

10 p1504 A72-23995

Decision making models application to systems configuration, reliability, repair level and spares optimization and availability analysis

10 p1486 A72-24006

Apollo program management decisions based on reliability analysis, discussing incentive fees, testing optimization, engineering changes approval and flight readiness certification

10 p1486 A72-24007

Sleep loss and work-rest cycle effects on combat efficiency, considering psychomotor reactivity, vigilance and decision making capacity

11 p1588 A72-26688

Numerical algorithm for guaranteed minimax /max-min/ estimates for multistep decision making processes, using ALGOL 60

13 p1924 A72-28708

Decision diagrams use in logic analysis for aircraft maintenance schedule testing relative to operational reliability control

13 p1967 A72-30041

Management alternatives evaluation methodology for capital expenditures on large facilities in terms of competitive capability enhancement for aerospace contracts

15 p2340 A72-32615

Weapon system program choice for development in aerospace industry, considering cost effectiveness and ranking illustrated on stand-off tactical interdiction missiles

16 p2482 A72-33598

Altitude effects on decision making performance of cognitive, psychomotor and complex card sorting tasks

16 p2357 A72-34096

Quantitative evaluation for R and D resource allocation in terms of funding project priorities

19 p2884 A72-38024

Man machine systems operational effectiveness augmentation through human factors engineering to enhance human operator capability for parallel data processing and decision making

19 p2761 A72-38308

Book - Fundamentals of pattern recognition.

20 p2905 A72-39575

Behavioural characteristics of men in the performance of some decision-making task components.

20 p2898 A72-39805

Human operator decision making role in information presentation system determined by experiments using laboratory performance and test measures, field observation, electrical and biochemical measures

21 p3010 A72-41408

DECISION THEORY

NT STATISTICAL DECISION THEORY

Aircraft trajectory optimization for maximum profit as decisional problem under risk conditions, determining probabilities by Monte Carlo method

02 p0257 A72-12747

Decision error estimates applied to detection problem with digital radar, computing upper and lower bounds for error probability

05 p0632 A72-17093

Optimal strategies for decision chain with controllable connections and finite number of states and decisions, deriving existence theorem

07 p1028 A72-19904

Landing sequence strategy variations for individual ATC operators, indicating dependence on flight progress data variation, existing maneuvering conditions and controller personality traits

09 p1271 A72-21311

Decision and control including adaptive processes - IEEE Conference, Miami Beach, Florida, December 1971

10 p1454 A72-23776

Adaptive filter techniques application to maneuvering reentry vehicle tracking, using Wald sequential test, decision theory and stochastic approximation 10 p1509 A72-23779

Suboptimal decision algorithm to correlate sensor data with stored tracks in real time track-while-scan surveillance system 10 p1441 A72-23780

Decision theory and cost-benefit modeling application to large government funded systems development programs, discussing Bayesian techniques 10 p1564 A72-23993

Optimum decision rule for sync word location in binary data frame, noting sum maximization of correlation and energy correction terms 11 p1592 A72-25888

Interdiction bombing mission effectiveness model for bad and good weather aircraft type selection depending on weather conditions at target site 13 p1896 A72-28400

Statistical superoptimal search strategies of self-optimizing systems, applying to one dimensional step type and multiextremal problems 13 p1936 A72-29160

Multiple decision procedures, discussing location, scale parameters, discrete populations and multinomial and multivariate normal distributions in subset selection formulation 14 p2126 A72-30998

Linear control systems optimal synthesis using ALGOL program for digital computers minimizing error square integral 15 p2210 A72-31687

Orbit determination strategy, detailing optimization criterion correlation with measurement errors 15 p2307 A72-31817

Team size and decision rule in the performance of simulated monitoring teams. 21 p3008 A72-41016

Decision surface estimate of nonlinear system stability domain by Lie series method. 23 p3274 A72-43540

DECKS [FLOORS]
U FLOORS
DECLINATION

Magnetic declination effect on elevation control of F 2 layer maximum, considering east component of geomagnetic field from Capetown and Canberra observations 01 p0054 A72-10427

Geomagnetic field extrapolated spherical data for years 1600 to 1800 from declination and inclination analysis, giving Gaussian coefficients and errors 02 p0218 A72-11953

Declination, average pulse energy and pulse shape of weak pulsars, determining barycentric period 04 p0574 A72-14981

Computer processing of star meridian observations, concerning reduction to visible area, declinations, right ascensions and conversion 09 p1283 A72-23063

Star declinations from simultaneous observations at upper and lower culminations 09 p1388 A72-23064

Venus and Mars visible geocentric declinations from daytime observations with Wanschaff vertical circle compared to nighttime results 09 p1388 A72-23065

Poltava latitude changes derived from Boss catalog stars observations with Bamberg zenith telescope, deducing declination system from 12 year observation cycle 09 p1300 A72-23069

Geomagnetic field extrapolated spherical data for years 1600 to 1800 from declination and inclination analysis, giving Gaussian coefficients and errors 13 p1949 A72-29265

Comparison of the declinations of Talcott pair centers, obtained from latitude observations by ZTF-135 in Pulkovo, with certain catalogs 19 p2861 A72-37978

Declinations of bright and weak stars determined separately from observations in the upper and lower culminations by the Struve-Ertel vertical circle during 1955-1961 19 p2861 A72-37981

Declinations of the sun, Mercury, and Venus in the FK4 system as deduced from observations with the vertical circle of the Nikolaev Observatory during 1966-1967 19 p2861 A72-37983

DECODERS

Decoder for delay-modulated digital data conversion to nonreturn to zero data, discussing time-phase ambiguity resolution capability in real time 01 p0025 A72-10331

Convolutional coding and decoding techniques in communication systems, discussing distance properties, optimal decoder in memoryless channel, error probabilities and bit synchronization 01 p0025 A72-10336

Optimal metric programmable high speed sequential decoder for convolutional code deep space channels 01 p0026 A72-10340

Branch synchronizer for convolutional decoders, noting design adaptability to nonsystematic codes of different constraint lengths 02 p0188 A72-12410

Error correcting data decoder assembly for mission independent sequential decoding at all stations in deep space tracking network, discussing design and performance 07 p0949 A72-19298

Fast responding mark/space ratio decoder for use with slug Josephson interferometers, presenting circuit waveforms 07 p0992 A72-20580

Binary PSK signals optimized on minimax and quadratic criteria, noting design of coders and decoders on shift registers with external logic 13 p1914 A72-28415

ATC services configuration with secondary surveillance radar and primary radar data acquisition system, discussing signal processing by automated decoder 21 p3080 A72-40288

DECODING

Nonsystematic quick-look-in convolutional codes for sequential decoding in deep space channels 01 p0026 A72-10339

High speed decision sequential decoder design and tests for digital errors, white noise and real channels 01 p0026 A72-10341

Convolutional coding, Viterbi decoding and binary phase shift keying modulation for reliable communication on power limited satellite and space channels 01 p0026 A72-10342

Orthogonal convolutional coding with on-off signaling and Viterbi decoding for synchronous multiple access communication with bound bit error rate 01 p0026 A72-10343

Error correction techniques of convolutional coding with Viterbi maximum likelihood decoding for communications systems design, using computer simulation 01 p0026 A72-10344

High data rate convolutional coding for space station telemetry links, considering sequential and cascaded Viterbi decoding 02 p0174 A72-12132

Computer simulation studies of hybrid pull-up bootstrap decoding algorithm, devising technique for efficient computational allocation and reliable identification of decoded data sections 02 p0187 A72-12154

Low cost large array of decoding magnetic switches with electrodeposited Au conductors and Permalloy memory elements featuring high output flux for low driving current [IEEE PAPER 21.3] 03 p0328 A72-13778

Decoding technique for delay modulated digital data conversion to NRZ/c/ data, describing logic implementation and timing diagrams 04 p0486 A72-14490

FSK transmission experiments on uhf satellite link, noting threshold convolutional decoding contribution to SNR 06 p0773 A72-17599

Channel coding/decoding schemes compatibility with TV data compressor for planetary missions in real time transmission 07 p0941 A72-19274

TDMA satellite communication system with convolutional encoding and Viterbi decoding, evaluating data buffering and control configurations 07 p0941 A72-19297

Periodic, continuous and aperiodic white noise effects on human serial decoding performance, relating subjective and autonomic responses 12 p1775 A72-28289

Extractop model for time signal decoding for worldwide synchronization using Transit satellite system 15 p2199 A72-32078

Encoding and decoding of color information using two-dimensional spatial filtering. 17 p2556 A72-35537

Octal Reed-Solomon code to obtain decoding error probability approximation improvement over minimum distance bound 18 p2658 A72-36266

Efficient computer decoding of pseudorandom radar signal codes. 22 p3153 A72-41978

Q-ary output data transmission channel with burst errors, discussing burst-b distance measure and binary block code decoding algorithm for error correction 22 p3153 A72-41979

Communication systems with binary convolutional signal encoding and threshold decoding, discussing orthogonal checkout sums distribution for correct and erroneous synchronization 22 p3154 A72-42235

Linguistic message decoding algorithms for communication with extraterrestrial intelligences, considering unified procedure and key problems solutions 24 p3382 A72-45226

DECOMMUTATORS

ERTS multispectral scanner data telemetry decom-mutator/processor capable of decommutating five spectral bands of digital video data 02 p0175 A72-12162

DECOMPOSITION

NT GLYCOLYSIS
NT PHOTODECOMPOSITION
NT PHOTODISSOCIATION
NT PHOTOLYSIS
NT PROPELLANT DECOMPOSITION
NT RADIOLYSIS

Gaseous diethyl peroxide spontaneous ignition during decomposition in cylindrical vessel, investigating diluents and temperature effects on self heating 02 p0301 A72-12027

Fan shaped precipitate formation during supersaturated Al-Zr solid solution decomposition, discussing interpretation as grain boundary migration 02 p0247 A72-12820

Martensite first stage decomposition mechanism and kinetics during tempering of quenched Re steels with varying carbon concentration 08 p1187 A72-21779

Catalytic action of metal oxides on isopropylbenzene hydroperoxide decomposition in liquid phase 08 p1129 A72-22094

Laser induced chemical decomposition of copper maleate and fumarate and fragment reaction with low hydrocarbons, comparing with thermal heating 10 p1433 A72-23951

Polymers flammability tests for research, safety and acceptance purposes, noting ignition limits, decomposition and testing procedures 11 p1746 A72-26044

Population inversion in exothermal decomposition reactions of multiatomic molecules for chemical and collision laser systems 13 p1912 A72-28778

Al-Zn alloy supersaturated solid solution decomposition during aging, studying single crystal lattice characteristics via X ray diffusive scattering techniques 13 p1976 A72-28902

Ti alloy volume reduction during decomposition of metastable alpha-prime, alpha-two and beta phases after cooling from beta range 14 p2114 A72-30401

Decomposition mechanism of Cu, Ag and Au solid solutions in InAs single crystals, using isotopic radiography 14 p2143 A72-30961

Structural decomposition and hardening of supersaturated Al-Cu, Al-Cu-Ag, Al-Zn, Cu-Sn and Cu-Ni-Co solid solutions 15 p2255 A72-31565

Electron microscopic investigation of Al-Mn alloy precipitate structure and morphology after annealing induced decomposition 15 p2257 A72-32114

Hydrazine thrusters for space application. 21 p3098 A72-40123

Co-V solid solution decomposition by equilibrium phase precipitation at aging temperatures, using electron microscopic and X ray analysis 24 p3414 A72-45382

DECOMPRESSION
U PRESSURE REDUCTION
DECOMPRESSION SICKNESS

Asseptic bone necrosis pathology from radiographic studies in dogs with decompression sickness noting articular cartilage erosion and joint dysplasia and exostosis 06 p0764 A72-18786

Ultrasonic transducer monitoring of decompression-caused gas bubbles in rat thigh muscle tissue for decompression sickness time course development studies 07 p0921 A72-20183

Compression cycles effects on alveolar volumes of sea lions and dogs excised lungs, noting decompression sickness prevention by airways cartilaginous reinforcement 08 p1116 A72-21186

Decompression sickness treatment in USAF hyperbaric oxygen chambers 08 p1126 A72-21575

Computer assisted monitoring of ECG waveforms and heart sounds frequency spectra to detect bubble laden blood during decompression sickness 11 p1587 A72-26626

Central nervous system symptoms and simple bends in gas decompression sickness cases during USAF operational flying 12 p1775 A72-28283

Hyperbaric environment decompression effects on human blood and urine chemistry and hemostatic system, showing physiological parameter alteration in presence and absence of bends symptoms 14 p2081 A72-31087

Effects of nitrogen and helium upon pulmonary damage after rapid decompression to 2 torr. [AD-746093] 17 p2508 A72-34544

Influence of prolonged starvation on the frequency of occurrence of decompression-induced pulmonary hemorrhage.

17 p2508 A72-34545

Effects of vagotomy and increased blood pressure on the incidence of decompression-induced pulmonary hemorrhage.

18 p2650 A72-36446

Roentgenologic studies of the effects of rapid decompression and hypoxia on the gall bladder in cats.

19 p2758 A72-38705

Precordial monitoring for pulmonary gas embolism and decompression bubbles.

19 p2762 A72-38710

Case report on dive decompression induced maxillary sinus barotrauma due to sinus pressure buildup caused by ostium blockage

22 p3150 A72-42497

Interactions between gas bubbles and components of the blood - Implications in decompression sickness.

24 p3374 A72-45652

DECONDITIONING

Confinement, physical deconditioning and hypercapnia effects on human musculoskeletal protein by chromatographic method for quantifying urinary peptides and free amino acids
[AD-736665]

06 p0767 A72-17869

DECONTAMINATION

NT SPACECRAFT STERILIZATION

High and ultrahigh vacuum equipment and components selection, discussing gas-surface interactions, contamination and cleaning problems

19 p2835 A72-38391

Microflora accumulation prevention methods during spacecraft flight, noting bacterial filters for air purification and wiping with disinfectants for surface contamination reduction

24 p3376 A72-45213

High level cleanliness maintenance and contamination control for instrument unit ring guidance system in Saturn 5 launch vehicle

24 p3388 A72-45297

DECOUPLING

NT SPIN DECOUPLING

Noninteracting decoupling control theory for linear constant multivariable systems, using dynamic feedback matrix compensators

02 p0198 A72-12802

Minimal order precompensator with state feedback for decoupling linear time-invariant multivariable control system, discussing design parameters determination from linear equations

04 p0506 A72-15109

Minimal order controller for decoupling of linear multivariable systems with low order control devices and reduced control effort

07 p0960 A72-19697

Model-following algorithm and equicontrollability in multivariable feedback control systems, considering application to decoupling problem

07 p0960 A72-19698

Multivariable control systems, discussing effects of interaction vs noninteraction /decoupling/ on system performance and energy requirements

07 p0962 A72-19715

Hammerstein form nonlinear systems class invertibility and reproducibility criteria derivation, noting decoupling possibility by dynamic precompensation and nonlinear state feedback

10 p1502 A72-23781

Cosmic ray ionization rate for hydrogen calculated for ambipolar diffusion efficiency in decoupling magnetic flux from gas during cloud collapse with angular momentum

10 p1544 A72-24664

Decoupled formulation of vector wave equation in orthogonal curvilinear coordinates, applying to ferrite-filled and curved waveguide of general cross section

11 p1607 A72-26995

Plasma corona electron temperature decoupling from core of solid deuterium pellet heated in vacuum by convergent laser beams

16 p2433 A72-32810

Decoupling and synthesis of certain nonlinear systems.

19 p2827 A72-38275

Decoupling of linear discrete time systems by state variable feedback.

19 p2827 A72-38563

Prediction of near-field antenna coupling in the presence of obstacles.

20 p2902 A72-38998

Decoupling and diagonalization conditions determination for nonlinear multivariable time-varying differential equations system by state feedback, giving illustrative examples

23 p3275 A72-43611

DEEP DRAWING

German monograph on deep drawing of pre-hardened and partially annealed Al and Al alloys, noting anisotropy effect of bottom zone of plate samples

09 p1317 A72-22329

DEEP SPACE

NT INTERPLANETARY SPACE

NT INTERSTELLAR SPACE

Papers on planetary quarantine covering microbial survival in deep space, contamination by nonsterile flight hardware and sterilization

01 p0019 A72-10817

Microbial survivability in deep space environmental simulation experiments, describing aerospace ecology and panspermia avoidance

01 p0019 A72-10823

Power processing requirements for solar electric propulsion in deep space mission, noting use of electron bombardment ion thruster with hollow cathode

01 p0007 A72-11055

Automatic control of ESRO drag-free deep space probe for measuring Robertson matrix beta and gamma constants

[ONERA, TP NO. 952]

05 p0727 A72-16468

Deep space probe MULTIPAC data system computer repairable during flight via command and telemetry links by reprogramming failed unit

05 p0633 A72-16573

Future deep space missions, discussing exploration of interplanetary conditions outside ecliptic plane and solar system Grand Tour with outer planets flyby

07 p1068 A72-19059

Temperature effects on microorganism survival in deep space vacuum, using molecular sink test

09 p1265 A72-22641

Deep space navigation requirements for interplanetary missions /1978-1990/

15 p2269 A72-32178

DEEP SPACE NETWORK

Nonsystematic quick-look-in convolutional codes for sequential decoding in deep space channels

01 p0026 A72-10339

Optimal metric programmable high speed sequential decoder for convolutional code deep space channels

01 p0026 A72-10340

Phase locked loop bandwidth, acquisition time and SNR for Doppler tracking deep space communications for Venus and Jupiter probes

05 p0629 A72-16575

Error correcting data decoder assembly for mission independent sequential decoding at all stations in deep space tracking network, discussing design and performance

07 p0949 A72-19298

Trojan deep space communications systems, maintaining powerful relay satellites in equilibrium at Lagrangian points of earth, Mars and Venus orbits

10 p1548 A72-24975

Lunar radar measurement for remotely located clock time synchronization, discussing applications to deep space tracking, computer technique for time delay correction and accuracy

15 p2199 A72-32069

DEFECTS

NT AUDITORY DEFECTS

NT CRYSTAL DEFECTS

NT CRYSTAL DISLOCATIONS

NT EDGE DISLOCATIONS

NT FRENKEL DEFECTS

NT INCLUSIONS

NT POINT DEFECTS

NT SCREW DISLOCATIONS

NT SURFACE DEFECTS

NT VACANCIES [CRYSTAL DEFECTS]

NDT program for detectability changes of tight defects in Al as function of applied load

01 p0085 A72-10756

Coated Nb alloys as radiative thermal protection system skin materials for space shuttle, investigating flaw growth

01 p0085 A72-10757

Flat hole model for defect size definition from ultrasonic inspection as function of echo amplitude and depth

01 p0076 A72-10809

Metallurgical defects in hot extruded aluminum alloys, describing investigation methods and remedies

01 p0077 A72-11041

Al content caused defect in gas tungsten arc welded Hastelloy, using electron microprobe analysis

06 p0820 A72-17708

Low cyclic failure resistance at elevated temperatures and static defects calculation based on fatigue and empirical endurance curves

06 p0898 A72-18555

Supramolecular structure artificial defects influence on mechanical strength of pyrographite

07 p1024 A72-20136

Imperfection influence on nonlinear stability of long circular cylindrical shells subject to critical hydrostatic pressure

09 p1403 A72-22763

Statistical crack length distribution of flaw sizes in steel parts during manufacturing

09 p1328 A72-22920

Failure phenomena relationship to kinetic equation for defect buildup from brittle fracture analysis of composite glass plastic in uniaxial eccentric tension

14 p2164 A72-30426

IC reliability assessment based on defects and failure mechanisms analysis instead of MTBF estimations

14 p2091 A72-31166

Axially compressed cylindrical shells buckling behavior, deriving formula based on equivalent axisymmetric imperfections concept in terms of shell radius/thickness ratio

15 p2331 A72-32553

IAD-3 amplitude-phase impedance defectoscope.

19 p2805 A72-38765

Investigation of defects and damage in metallic materials by metallographic examinations

20 p2941 A72-39573

Bilateral version of an ultrasonic velocimetric method of defectoscopy.

21 p3057 A72-41721

The influence of production imperfections on design of optimum structures.

22 p3239 A72-42841

Asymmetric imperfections effect on spherical elastic shell buckling strength under uniform external pressure

23 p3351 A72-44104

DEFENSE COMMUNICATIONS SATELLITE

SYSTEM

British defense and civil communications satellite program, discussing Skynet, INTELSAT, ESRO and New Space Technology Program activities

[AIAA PAPER 72-548]

12 p1781 A72-27371

DEFENSE INDUSTRY

Profit policy for defense contract negotiations relating to capital employed for cost reduction

09 p1413 A72-22237

Defense Documentation Center independent R and D data bank for evolution and maintenance of creative technology oriented defense industry

21 p3132 A72-40974

Forecasting costs and completion dates for defense research and development contracts.

24 p3468 A72-45479

DEFENSE PROGRAM

Parametric cost estimating aids DOD in systems acquisition decisions.

17 p2639 A72-34461

Cost-to-produce estimation consideration as design parameter in defense material contractual arrangement

17 p2639 A72-34462

Defense system procurement evaluation before documentation release to industry, discussing improved specifications, competition, planning and data requirements

17 p2639 A72-34463

DEFINITION

Aircraft and spacecraft conceptual definitions in national and international law

11 p1749 A72-26561

DEFLAGRATION

Solid propellant reaction kinetics at gaseous fuel and catalyst-containing ammonium perchlorate interface, studying ignition and deflagration

07 p1051 A72-19367

Pure and doped ammonium perchlorate deflagration rate sensitivity due to sample temperature and environmental pressure changes

07 p1051 A72-19729

Wall effects on deflagration, combustion rate, and self and hot-point ignition temperature and delay

11 p1747 A72-26789

Comment on 'The deflagration of single crystals of ammonium perchlorate.'

19 p2848 A72-38873

Mach stem generation by colliding spherical pressure waves in spark ignited combustible gas, noting simultaneous deflagration wave characteristics

24 p3462 A72-45028

Low speed steady one dimensional flow models for monodisperse spray deflagration, considering homogeneous, heterogeneous and premixed combustion

24 p3464 A72-45054

DEFLATING

U INFLATABLE STRUCTURES

U PRESSURE REDUCTION

DEFLECTION

Axisymmetric circular membranes large deflections, solving nonlinear partial differential equations by iterative method in conjunction with finite difference approximations

02 p0296 A72-12526

Bimetallic rectangular plate with two interconnected layers of anisotropic and isotropic materials and large deflections in nonuniform pressure and temperature field

05 p0735 A72-16016

Deflection function for symmetrical bending of unloaded annular plate, constructing stiffness, mass and stability coefficient matrices by function manipulation

05 p0739 A72-16550

Large deflection microstructure continuum model for composite beam flexural wave propagation and free vibration, deriving equations of motion

[AIAA PAPER 72-140]

05 p0741 A72-16937

Large deflection of rectangular thin elastic plates with unsupported edges, using finite difference technique based on dynamic relaxation methods

06 p0895 A72-17799

Iterative solution for non-Levy rectangular plates with corner supports, assuming small deflection theory

06 p0896 A72-17966

Stress and deflection distribution for circular and elliptical toroidal shells under internal pressure from first order differential equations solutions

07 p1088 A72-19118

Pontryagin maximum principle application to minimum deflection of cantilever beam under own weight

10 p1558 A72-24880

Ring assembly with hinged cross section and uniform radial and transverse loads, determining deflection dependence on bulkheads and rigidity of supports

[AIAA PAPER 72-355]

11 p1729 A72-25384

Bending deflection calculation for laminated beams with layers of different rigidity

11 p1733 A72-25546

Coupled nonlinear equations of motion of large deflections of impacted helical springs, comparing with streak photographs

11 p1688 A72-26061

Static deflection effect on nonlinear spring mass system step function response, considering approximate calculation of oscillation period

11 p1688 A72-26372

Elastic-plastic analysis of large deflection of axisymmetrically loaded circular plates, using incremental theory

11 p1737 A72-26426

Large deflection of variable thickness square plate under uniform load, using strain energy method

11 p1737 A72-26588

Bending problem for circular three layer plate with rigid circular insert, studying deflection under bending moment

12 p1879 A72-27090

Dynamic deflection of elastic rectangular plate hinged to rigid base moving under sinusoidal pressure impulse action, noting base inertia effect

12 p1879 A72-27091

Vertical deflections estimation with inertial navigation system, geodetic position and velocity reference and optimal data smoother, noting applicability to surveys from moving vehicles

12 p1843 A72-27634

Large deflection calculation of circular and annular strain hardenable rigid plastic plates under axisymmetric load, using Kirchhoff-Love hypothesis and Tresca flow condition

14 p2165 A72-30440

Berger equation inconsistencies for large deflections of thin elastic plates with freely moveable edges

14 p2169 A72-31173

Random deflection function for taut string on elastic foundation subject to random loads, using invariant imbedding method and Fokker-Planck equations

15 p2273 A72-31311

Stress analysis and deflection equation for uniformly loaded and heated two layer clamped rectangular plate

15 p2322 A72-31362

Natural frequencies of beams with stepwise variable cross sections, approximating deflection shape by sectionwise representation of inertia load

15 p2323 A72-31454

Large amplitude deflections and induced stresses in uniformly pressure loaded circular plate on elastic foundation, using von Karman coupled nonlinear partial differential equations

15 p2331 A72-32558

Free and forced vibrations of two dimensional grids with simple and bridge-type boundary conditions, presenting closed form solutions for nodal deflections and moments

15 p2332 A72-32561

Singular perturbation methods for deflections, frequencies and eigenmodes of statically loaded or freely vibrating circular or annular membrane

16 p2467 A72-33106

Dynamic structural analysis of viscoplastic thin walled shells, noting time dependent profile of deflection

16 p2467 A72-33122

Deflection of plate on elastic support from equilibrium equations based on shell theory

16 p2472 A72-34015

Lateral deflection of axially loaded imperfect bar under creep, solving nonlinear integrodifferential equations by quasi-linearization technique

16 p2474 A72-34130

On the finite deflections of thin beams.

17 p2634 A72-35404

An asymptotic solution for the large deflection of a circular plate with a central hole.

18 p2732 A72-36081

Bending of rectangular plates of linearly varying thickness

18 p2736 A72-36991

Infinite plate with a supported reinforced circular hole.

18 p2738 A72-37071

Maximum deflection and bending moments of simply supported anisotropic rectangular plate under uniform transverse load, using double Fourier series

20 p2981 A72-39973

Analysis of static deflections by holographically recorded vibration modes.

22 p3177 A72-42397

Column buckling under random initial deformations influence, determining mean square nonstationary deflection by Green function technique

23 p3351 A72-44106

Large deflection of rectangular orthotropic plates.

23 p3352 A72-44111

DEFLECTORS

NT BLAST DEFLECTORS

In-line eight stage digital light deflector with prisms and polarization switch, using Pockels effect with transverse field.

07 p1003 A72-19222

Improvements in electro-optic circular-scan deflectors.

21 p3050 A72-40146

Optical considerations for an acoustooptic deflector.

23 p3288 A72-43885

DEFOCUSING

Isoplanatic instrument wave aberration determination, using longitudinal defocusing

03 p0360 A72-13563

Defocused confocal Fabry-Perot spherical interferometer for analysis of Q switched visible and near IR lasers longitudinal mode outputs

10 p1481 A72-24564

Beam-defocusing effect due to filament magnetic fields in electron guns of electron linear accelerators.

19 p2772 A72-37404

Differential effects of refractive errors and receptive field organization of central and peripheral ganglion cells.

19 p2756 A72-37826

Photographic processing method for solar activity macrostructural distributions determination, suppressing minor and sporadic formations by defocusing technique

23 p3340 A72-44239

DEFORMATION

NT AXIAL STRAIN

NT ELASTIC BENDING

NT ELASTIC BUCKLING

NT ELASTIC DEFORMATION

NT NUCLEAR DEFORMATION

NT PLASTIC DEFORMATION

NT STATIC DEFORMATION

NT TENSILE DEFORMATION

NT WAVE FRONT DEFORMATION

Edge loaded cylindrical shells of resolution nonlinear axisymmetric deformation determination from asymptotic solution of Reissner equations, using multiple scale perturbation technique

01 p0136 A72-10031

Gas saturated surface layer deformation in rolled Ti alloys as function of specimen thickness reduction

01 p0077 A72-11080

Stress analysis for transverse deformation of fiber reinforced composites

02 p0249 A72-11991

Stiffness matrix method application to finite deformation theory, noting convergence through use of iterative interpolation in numerical calculations

02 p0298 A72-12667

Elasticity tensor formulas for wave propagation, vibration and stability of deformed isotropic solids

03 p0448 A72-13887

Soviet papers on elasticity and inelasticity covering deformable media mechanics, continuum mechanics, polymer materials, random inputs, stress concentration, ductility and crystallization temperature properties

03 p0453 A72-14205

Stress concentration problems in two and three dimensional elastoplasticity, using Ilyushin small deformation theory

03 p0453 A72-14213

Constitutive equations derivation for electrical conduction due to small deformation superposition, applying to deformed spherical shell current density determination

04 p0549 A72-15254

Geometric displacements and space-time derivatives determining velocity and strain fields in solids under deformation

05 p0738 A72-16529

Axisymmetric deformation of infinite cylindrical shell under stress-strain state arising from internal pressure in statistically inhomogeneous Winklerian medium

07 p1088 A72-19258

Deformation rate and temperature effects on optimum strength and ductility of die forged and extruded Mo-Ti alloys

07 p1014 A72-19845

Test procedures and apparatus for short and long term creep of polymer monofilaments under radial compression

08 p1194 A72-21758

Creep ratchetting deformation and rupture damage from thermal transient stress cycle and constant membrane force under high temperature metal creep conditions

09 p1406 A72-23197

Metal matrix composites deformation and mechanical properties prediction from component phases information, examining interface role, residual stress effect and thermal degradation

10 p1553 A72-24176

Loose medium deformations and displacements fluctuations verification by statistical tests, noting information from autocorrelation and boundary conditions cross correlation functions

10 p1512 A72-24719

Confocal spherical laser resonator deformation analysis based on perturbation method, investigating forced oscillation

10 p1493 A72-25150

Stiffness, stress and deformation analysis of discretely attached corrugated shear webs, using minimum potential energy and calculus of variations methods

[AIAA PAPER 72-351]

11 p1728 A72-25380

Metal rolling speed effect on force and friction reduction by ultrasonic vibrations imposed on rollers, noting coefficient of friction dependence on deformation

12 p1814 A72-27645

Solids deformation resistance increased by active lubricants effects on coupled friction surfaces, noting damage localization to thin surface layers

12 p1817 A72-28181

Ridge dimensions determination and causes of self oscillation in solid surface layers deformation under sliding friction

12 p1817 A72-28182

Russian monograph on three dimensional deformable bodies stability covering linearized equations for subcritical deformations and strength analysis of low shear rigidity structures

12 p1888 A72-28337

Additional deformation work for splines forming in splined circular profiles pressing, deriving characteristic displacement velocity distribution equations

13 p1963 A72-28744

Comparative study of lunar objects selenodetic coordinates catalogs based on continuous media deformation theory

13 p2037 A72-28987

Magnetoelastic coupling existence between shearing stresses and linear deformation, noting influence on Poynting effect experimental results

13 p1980 A72-29782

Al single crystals, investigating scale factor effects on stepwise deformation at 1.4 K

14 p2115 A72-30410

Primary recrystallization in TD-nickel bars on sublight optical level identified by transmission electron microscopy examination of deformation and annealing substructures

14 p2119 A72-30601

Coarse grain transformation in TD-nickel bar subjected to deformation and annealing, noting abnormal growth caused by thermomechanical effects

14 p2119 A72-30602

Complex conjugate fourth order partial differential equations for circular cylindrical shells deformation, comparing accuracy with Fluegge, Morley and Novozhilov equations

15 p2331 A72-32559

Holographic interferometric measurement of materials time dependent deformation responses to various environmental influences, discussing CW and pulsed laser techniques and holographic microscopy

16 p2388 A72-32820

Ti comparison with Al for effects on Fe alloy deformation and fracture, discussing intergranular failure suppression

16 p2411 A72-33823

Second order deformation theory for axially held strut during thermal cycling at creep relaxation temperature, using galerkin method with assumed sine wave

16 p2473 A72-34124

Time and temperature independent permissible deformation limits as basis for dimensioning of cyclically and multiaxially stressed plastics structural components

16 p2416 A72-34147

A comparison of flow and deformation theories in a radially stressed annular plate.

[ASME PAPER 72-APM-44]

17 p2627 A72-34781

Numerical solution of problems of large deformations for spherical elastic shells

17 p2634 A72-35421

Fluid jets and droplets deformation in transverse supersonic two phase gas flow

17 p2544 A72-35932

On motions with a history of constant deformation

18 p2680 A72-36463

Holometric deformation measurement on carbon carbon biaxial test specimens.

19 p2822 A72-37616

- Three dimensional holographic interferometry program for study of fringes due to displacement or deformation 19 p2799 A72-37630
- Introduction of two resolving functions into the equations for nonshallow shells 20 p2979 A72-39405
- Single and double shear invariant plane crystallographic theories for martensitic transformations, calculating lattice deformations by combined Bain and complementary shear strains 21 p3065 A72-40089
- Autoclaves for the study of the effects of deformation on the high temperature aqueous corrosion of metals. 21 p3039 A72-40216
- Deformation microstructure of fine grained and plate-like structure two phase Ti alloys, noting plasticity decrease in beta phase presence 21 p3068 A72-40963
- Isothermal deformation behavior of structural metals in laboratory creep, relaxation and low cycle fatigue tests at high temperatures 21 p3119 A72-41009
- Pure Co single crystals allotropic transformation effects on deformation behavior, noting flow stress and work hardening rate relationship to history 22 p3193 A72-43034
- Isotropic materials nonlinear rheonomic behavior at small strains, deriving model structure deformation laws 23 p3345 A72-43623
- Changes in the physical properties of metals subjected to elastoplastic deformation 23 p3303 A72-44199
- Experimental characterization of yield induced by surface flaws. 23 p3353 A72-44230

DEGASSING

- Early catastrophic degassing of earth, considering mechanisms and times from volatiles abundances and distribution in atmosphere, hydrosphere and crust 03 p0350 A72-13744
- Surface oxide film effects on hydrogen liberation rate from Al and alloys in high vacuum at 20-450 C 05 p0675 A72-16627
- Nitrogen solubility, degassing kinetics and diffusion coefficients for Mo-N, W-N and Re-N systems for 1300-3050 C 11 p1663 A72-26841
- Equilibria and degassing kinetics in the systems Mo-N, W-N, and Re-N 18 p2701 A72-36596
- Lunar volcanic gas release rate estimation from orbiting Apollo spacecraft-borne mass spectrometer detection, noting atmospheric perturbation 19 p2868 A72-38736

DEGENERATIVE FEEDBACK
U NEGATIVE FEEDBACK
DEGRADATION

- NT THERMAL DEGRADATION
- Free radicals formation during elastomers mechanical degradation by grinding below and above glass transition point at liquid nitrogen and room temperatures 04 p0484 A72-15264
- Gold-Weisberg phonon kick and extended Longini field-inhibited diffusion degradation mechanisms for GaAs double heterostructure injection lasers, discussing experimental tests 09 p1325 A72-23088
- Cadmium sulfide solar cells stress analysis in relation to degradation caused by fabrication technology, discussing barrier layer formation process 12 p1757 A72-28020

DEGREES OF FREEDOM

- Autonomous Hamiltonian system with two degrees of freedom, investigating origin and periodic orbits stability with two time variable method 01 p0123 A72-10030
- Kinetic equation for gases with rotational degrees of freedom under equality of probabilities of direct and inverse transitions and stereoisomerism of molecules 01 p0050 A72-10350
- Trapezoidal isoparametric and triangular singularity elements for crack tip elastic stress intensity factor for mesh having small number of degrees of freedom 01 p0140 A72-10992
- Self sustained oscillations of mechanical system with infinite number of degrees of freedom, considering application to diffusion in porous medium 02 p0258 A72-11496
- Self-correcting incremental solution procedure for nonlinear structural mechanics, noting application to systems with many degrees of freedom 02 p0260 A72-12272
- Additive type composite oscillations in nonlinear damped vibratory system with two degrees of freedom, presenting modified Galerkin method 03 p0382 A72-13628
- Oscillation periods of single degree of freedom variable mass point, using stiffening hypothesis 03 p0390 A72-14220

Linear nongyroscopic conservative system stability from modified Lagrange equations of motion, using pseudo degree of freedom concepts and vibration method 03 p0362 A72-14394

Scattering function of ellipsoidal gas molecules with translational and rotational degrees of freedom 04 p0552 A72-14629

Macroscopic integrodifferential transport equations for gas mixture with internal degrees of freedom and chemical reactions from model kinetic equation 04 p0552 A72-14633

Hydrodynamic equations for non-Lagrangian statistical mechanical particle systems with three degrees of freedom under frictional and velocity dependent forces 04 p0512 A72-15202

Mean-square approximate estimator for standard deviation of natural frequency of two degrees of freedom spring systems, comparing with Monte Carlo simulation [ASME PAPER 71-WA/APM-7] 05 p0734 A72-15971

Single- and many degree of freedom nonlinear structural systems transient dynamic response by presentation of equations of motion, damping and restoring force functions 05 p0736 A72-16082

Triangular /KLI/ and quadrilateral /KQT/ thin shallow shell elements with 20 degrees of freedom, basing bending behavior on discrete Kirchhoff formulation 05 p0739 A72-16549

Three degrees of freedom motions of slender cones with slight compounded asymmetries in hypersonic flight wind tunnel stability tests [AIAA PAPER 72-28] 05 p0608 A72-16939

Digital computer techniques for randomly excited n-degrees of freedom structural system response by discrete time series with output covariance 06 p0895 A72-17857

Quasi-periodic n-degrees of freedom solutions to Hamiltonian systems with 2n plus 2 variables, noting applicability to planar three body problem 06 p0839 A72-17882

Forced vibrations and stability of one degree of freedom system with damping proportional to velocity, determining amplitude and phase resonance curves 06 p0901 A72-18710

Nonlinear self oscillation solution for systems with two degrees of freedom, comparing with harmonic linearization method for error of small parameter method 06 p0851 A72-18721

Thermal equilibrium fluctuations and Rayleigh light scattering in isotropic gyrotropic continuous medium with internal rotational degrees of freedom 07 p1034 A72-18909

Stellar motion in asymmetric galaxies with three degrees of freedom, using four dimensional surface of section mapping and stochastic measurement 07 p1034 A72-19072

Multiple elastic postbuckling path generation at coincident branching points for system with many degrees of freedom 07 p1087 A72-19113

Isotropic turbulence spectrum based on Heisenberg theory of viscosity limiting effect on fluid motion degrees of freedom, taking into account nonlinear inertial transfer term 07 p0968 A72-19671

Tactical missile controlled test vehicle flight test analysis by six-degree-of-freedom digital simulation 07 p1086 A72-20351

Vibrations causes and degrees of freedom relationship in rotor machines at critical velocities, determining rotor imbalance from amplitude characteristics 08 p1243 A72-21232

Pod-mounted jet engine follower force instability, analyzing two degrees of freedom system dynamics 09 p1374 A72-22938

Beecham-Kryloff-Bogoliubov approximation method application to n degree of freedom nonlinear systems, using averaged kinetic energy and virtual work terms in Lagrange equation 09 p1342 A72-23454

Single degree of freedom systems with nonlinear spring characteristics of skew symmetric form, discussing 1/2 subharmonic oscillation analysis by harmonic balance method 09 p1342 A72-23455

Multivariable probability density determination of random vibration systems with n degrees of freedom by Fokker-Planck equation 09 p1353 A72-23609

Mandelstam couplings theory for subdividing discrete mechanical system of three degrees of freedom gear transmission 09 p1409 A72-23614

Earth pointing rotating satellites attitude control system based on two-degree of freedom gyroscope, determining conditions for rotor spin axis fixation in inertial space 10 p1509 A72-24646

Power spectral density function parameters with random vibration applications, considering response spectra of multidegree of freedom linear systems [ASCE PREPRINT 1375] 10 p1560 A72-25189

Spacelike hypersurface conformally invariant three-geometry role in unconstrained dynamical degrees of freedom of gravitational field 11 p1691 A72-26706

Finite difference equations of motion for conservative and nonconservative dynamic systems with finite degrees of freedom, obtaining numerical solution by Hamilton principle 12 p1844 A72-27193

Natural vibration modes of coupled spring-mass nonlinear system with two degrees of freedom from stability analysis 12 p1844 A72-27245

Nonsymmetrical stellar motion in galaxies, finding number of isolating integrals in systems with three degrees of freedom from four dimensional mapping 12 p1874 A72-27911

Finite element method for calculating vibrations of thin rectangular plate with four degrees of freedom 13 p2000 A72-28466

Finite element method for in-plane free vibrations of shear wall type structures, noting rectangular plate elements with six degrees of freedom per node 13 p2057 A72-29092

Finite element displacement field with internal equilibrium application to nine degrees of freedom triangular bending element stiffness matrix calculation 14 p2168 A72-30930

Generalized Thomson-Tait-Chetaev stability theorem for n-degrees-of-freedom mechanical oscillating systems with virtual nonconservative displacement forces 15 p2274 A72-31456

Instability regions of vibratory system with two degrees of freedom under random parametric effect, calculating bounds by numerical and analytical methods 15 p2275 A72-31608

Distributed parameter system approximation by system with finite freedom degrees number, solving stability and vibration of elastic shells for eigenvalue densening case 15 p2327 A72-31739

Multidegree of freedom linear systems mean-square response to nonstationary random vibratory excitation, using staircase approximation to continuous intensity functions 15 p2331 A72-32552

Averaging and Ritz methods for solution approximation of nonlinear periodic and combined resonances in vibrating systems with multiple degrees of freedom 16 p2424 A72-33145

French book on thermodynamics of equilibrium and nonequilibrium composite systems covering entropy potentials for n degrees of freedom system 16 p2478 A72-33503

Approximation of mathematical models for continuous media with many degrees of freedom, local structure and interactions, discussing parameters similarity conditions 16 p2425 A72-33586

Application of statistical linearization techniques to nonlinear multidegree-of-freedom systems. [ASME PAPER 71-WA/APM-5] 17 p2624 A72-34315

Helicopter stability derivative extraction and data processing using Kalman filtering techniques. [AHS PREPRINT 641] 17 p2490 A72-34501

Freedoms retention determination eigenvalue analysis of complex structures large dynamic matrices deriving transformation vectors based on maximum swept volume deformation modes 17 p2576 A72-35253

The effects of damping on a non-linear system with two degrees of freedom. 18 p2709 A72-36080

The locking effect in an autooscillatory system with two degrees of freedom 19 p2783 A72-38580

Finite range gravitation theory extension to generally covariant massive two-tensor field gravitation theory containing eight dynamically independent degrees of freedom 20 p2953 A72-39342

Nonlinear system described by three generalized coordinates, noting dynamic response stability equivalence to two degrees of freedom system 20 p2953 A72-39553

Flight-mechanical analysis of various flight conditions of conventional aircraft. V - Mechanical foundations /Dynamics of the rigid body/ 21 p2994 A72-40175

Elastic conservative structural systems stability with many degrees of freedom, discussing critical singular points effect 21 p3120 A72-41206

Analysis of impact vibrations by delta-function method - Case of one degree-of-freedom system. I - Perfectly elastic collision. 21 p3121 A72-41238

A method and equipment for the investigation of spatial vibrations in rotating reductor unit components 22 p3182 A72-42129

Three-dimensional finite element analysis for fracture mechanics. 23 p3353 A72-44235

Equations for the general motion of a rocket in a resistant medium 24 p3452 A72-45448

DEHYDRATED FOOD

Biochemical and physiological evaluation of nourishment of subjects feeding on dehydrated products in test chamber with regenerative life support system, discussing metabolic data and hormone function 24 p3375 A72-45128

DEHYDRATION

Posthypoxic thirst and relative dehydration of rats after return from hypoxia to normoxia, measuring body weight and water intake 02 p0165 A72-12835

Energetical conditions of primeval biosynthesis and transdehydration feasibility on simplified present day templates 04 p0468 A72-14757

Energy transfer conditions of transdehydration reactions on primeval earth leading to transphosphorylation, transacylation and peptide synthesis 04 p0468 A72-14768

Biological phosphate origin through atmosphere-hydrosphere interrelations, discussing concentrative processes, dehydration mechanics and evaporation 05 p0617 A72-16129

Living organisms defense and preservation via refrigeration and vacuum combined use in lyophilization technique 12 p1769 A72-27293

DEICERS

Aircraft engine anti-icing tests and evaluation describing ground and airborne techniques [AIAA PAPER 72-162] 05 p0706 A72-16828

C-54 A/B aircraft engine air particle separator anti-ice system design features, manufacturing techniques and testing 07 p1053 A72-18769

USSR electric impulse de-icing system design. 18 p2648 A72-37033

DEICING SYSTEMS

U DEICERS

DEIMOS

Mars observation by Mariner 9, discussing TV pictures of surface, UV and IR spectroscopy of atmosphere, S band experiment and Phobos and Deimos studies 10 p1538 A72-24309

Blue filter polarimeter observations of Deimos and Phobos, discussing polarization-phase angle curve for Deimos dust surface layer 12 p1865 A72-27097

Phobos and Deimos orbital characteristics, noting related Martian physical properties determination 15 p2302 A72-31277

Navigational aspects of two impulse transfer initiated rendezvous with Deimos using modified Viking Monte Carlo error analysis program 15 p2269 A72-32177

Mars and its satellites as viewed by Mariner 9 17 p2607 A72-34752

Viewing Phobos and Deimos for navigating Mariner 9. [AIAA PAPER 72-927] 24 p3423 A72-45433

DEIONIZATION

Meteors radio echo duration dependence on electron attachment, photodetachment and turbulent and ambipolar diffusion deionization processes 09 p1383 A72-22502

Electron attachment, photodetachment and turbulent diffusion deionization effects on duration distribution of Geminid meteor radio echoes 09 p1384 A72-22512

Deionization mechanism of expanding plasma cloud produced by arc burning in vacuum, discussing charged particle concentration and ion thermal velocity 10 p1521 A72-24356

Deionization mechanism of expanding plasma cloud produced by arc burning in vacuum, discussing charged particle concentration and ion thermal velocity 17 p2589 A72-34956

DEKATRONS

U COUNTERS

DELAMINATING

Aircraft windshield reliability, discussing delamination, interface shear stress effects and analogy to metal fatigue 12 p1812 A72-27011

DELAY CIRCUITS

NT PHANTASTRONS

Spatially periodic coupled cavity slow wave structures for multibeam microwave tube stabilization without absorber 02 p0190 A72-11575

Thermal and electric fields interaction in LF integrated circuits design, applying thermal feedback loops to bandpass filter, delay circuit and Schmidt-trigger oscillator 10 p1448 A72-24280

Minimum noise coefficients of M-type microwave beam amplifiers with crossed fields, taking into account delay system distributed losses 10 p1453 A72-24913

Optimal delay control circuit adjustment by approximate calculation with quadratic error integral and ITAE criterion dependence on loop amplification 19 p2783 A72-38643

New active all-pass network with linear group delay. 20 p2910 A72-39431

Hybrid monostable delay circuit based on bipolar and low threshold voltage MOSFET transistor 20 p2910 A72-39788

Real time correlator design and operation with signal delay at 40 Hz-20 kHz, using Stieltjes principle 22 p3176 A72-42244

Signal frequency distortions in frequency-modulated oscillators with feedback delay 23 p3266 A72-44209

DELAY LINES

NT ACOUSTIC DELAY LINES

Pulsed ruby laser with complex mirror resonator including optical delay line, observing mode locking effects in emission dynamics 02 p0238 A72-12290

Active all-pass circuits transfer function and synthesis, including delay lines, phase correctors and wide-band phase shifter applications 03 p0338 A72-13169

Ultrasonic delay lines design and construction for 100-2000 MHz using evaporated CdS on sapphire and quartz and sputtered ZnO transducers 05 p0626 A72-16010

Emission dynamics of pulsed laser with optical delay line in resonator 08 p1181 A72-20797

Pulsed ruby laser with complex mirror resonator with optical delay line, observing mode locking effects in emission dynamics 10 p1488 A72-23764

Maximum transmission delay in microwave TWT delay lines as function of electron beam size, current, shape and velocity distribution 12 p1782 A72-27436

Voltage variable TWT delay line design, discussing electron beam velocity dispersion causes 12 p1782 A72-27437

Quasi-one dimensional spectral analysis of input signal by delay line circulator, discussing ring frequency characteristic influence on harmonic signal buildup efficiency 13 p1930 A72-29043

Transistorized electronic equipment with delay line for optimal filtration of PSK signals 13 p1930 A72-29047

Microwave pulse frequency shift and frequency modulation in YIG bar magnetostatic delay line with adiabatically varying parameters 13 p1923 A72-30095

Statistical analysis of random mismatched tapped delay line filters effect on binary phase shift keying pulse compression codes peak-to-sidelobe and SNR 15 p2196 A72-31792

Equivalent baseband and passband delay line and transversal equalizers derivation for linear modulation systems, obtaining relationship between tap coefficients 15 p2211 A72-31844

Search radar constant false alarm rate receiver circuit for background noise and clutter compensation, using matched dispersive delay lines flanking hard limiter 16 p2365 A72-33762

Set of steady states of a system composed of two delay lines and tunnel diodes 17 p2529 A72-34759

Digital pulse counter with delay line and tunnel diodes 17 p2529 A72-34760

Transient characteristics of lumped-parameter delay lines 18 p2674 A72-37216

Light pulse structure and bandwidth bounds in ruby laser with delay line inside variable effective length resonator 21 p3066 A72-40799

Self-excitation of oscillations in a system consisting of a delay line, inductance, and tunnel diodes 24 p3384 A72-44895

DELTA FUNCTION

Multidimensional Fourier transforms application to theoretical physics partial differential equations, using singular delta function for homogeneous equations general integral 07 p1027 A72-19436

Hall-Weaire tight binding Hamiltonian solution in cycle free approximation for band structures and delta functions of amorphous semiconductors 11 p1700 A72-25725

Analysis of errors generated by Kotelnikov series representation of finite signals during quantization by delta functions, finite duration sampling and constant amplitude sampling 13 p1919 A72-29044

Analysis of impact vibrations by delta-function method - Case of one degree-of-freedom system. I - Perfectly elastic collision. 21 p3121 A72-41238

DELTA LAUNCH VEHICLE

Delta and Thor/Agenda satellite launch vehicles, discussing costs, performance and mission planning based on booster design flexibility, incorporating computer programmed strapdown inertial guidance 01 p0136 A72-10953

DELTA MODULATION

Robust delta modulator configuration with minimal mean square error from signal statistics estimates, discussing design and performance by digital simulation 04 p0486 A72-14486

Optimum adaptive variable step size delta modulator-demodulator producing minimum error for Markov-Gaussian source 06 p0772 A72-17404

Analog/hybrid simulation of noise effect on adaptive delta modulation system consisting of transmitter, receiver and error simulator 07 p0951 A72-20339

Energy spectra of mixed discrete random processes in statistical multiplexing systems with pulse position, delta and pulse code modulation 13 p1919 A72-29054

Bandwidth economy for multiplexed digital signals. 21 p3020 A72-40897

DELTA WINGS

Supersonic and hypersonic flows with attached shock waves over delta wing at angle of attack, deriving unified theory for flow field 02 p0150 A72-12030

Area rule for change in lift/drag ratio of hypersonic delta wing due to conical body addition on compression side 02 p0151 A72-12270

Thin shock layer theory of lifting properties of reentry caret and flat delta wings and waveriders at high incidence angles and Mach number 02 p0152 A72-12345

Unsteady pressure distribution on harmonically oscillating circular cylindrical fuselage body with conical nose and delta wing with straight, cubic or sinusoidal leading edges 02 p0153 A72-12730

Symmetrically deformed delta wing in supersonic flow, considering leading edge flow separation induced vortices effects on downwash, pressure distribution and aerodynamic characteristics 04 p0463 A72-15741

Thermoelastic effect on flutter and vibration of built up delta wings with solid, stiffened and honeycomb/corrugated sandwich skins [AIAA PAPER 72-174] 05 p0740 A72-16834

Hypersonic flow past final thickness delta wing, presenting conical flow equations with boundary value solution 06 p0757 A72-18128

Delta wing configuration design with anhedral heat shield for high lift reentry in 6-20 Mach number range [AIAA PAPER 72-132] 09 p1259 A72-22501

Metallic materials for delta wing space shuttle configuration with metallic thermal protection system 10 p1498 A72-24876

Slender body theory for flow calculation past low aspect ratio delta wing with straight trailing edge, noting lifting vortices distribution 10 p1420 A72-25131

Laminar and turbulent convective heating distributions on delta wing space shuttle boosters with interference effects [AIAA PAPER 72-315] 11 p1567 A72-25249

Hypersonic gun tunnel balance and pressure measurements on sharp leading edge delta wings, comparing experimental coefficients and shock angles with predicted values 11 p1571 A72-25735

Fighter aircraft maneuverability, range and armament requirements, discussing canard vs delta configurations 11 p1577 A72-26657

Pressure distribution over delta wing with blunted edges at small angles of attack in hypersonic wind tunnel tests 14 p2071 A72-31022

Three dimensional boundary layer separation on slender bodies, delta wings and propulsion intake systems, reviewing computing techniques for interfering inviscid flow fields 16 p2341 A72-32826

Analytical method of characteristics to determine front shock and sonic boom due to flat delta wing with supersonic leading edges [DFVLR-SONDDR-205] 16 p2348 A72-33401

Finite difference method computation of multi-shocked three dimensional wing-body supersonic

flow fields with real gas effects, applying to delta winged space shuttle
[AIAA PAPER 72-702] 16 p2345 A72-34042
Rarefied hypersonic flow characteristics of delta wings and trailing edge spoilers.
17 p2485 A72-35229
Unified area rule for hypersonic and supersonic wing-bodies.
17 p2485 A72-35251
Development of the Saab-Scania Viggen.
19 p2748 A72-37749
Experimental investigations of separated flows on wing-body combinations with very slender wings at free-stream Mach numbers from 0.5 to 2.2.
[ICAS PAPER 72-25] 21 p2991 A72-41150
Quasi-homogeneous approximation for wing with curved subsonic leading edges at supersonic speeds.
[ICAS PAPER 72-54] 21 p2992 A72-41176
Delta wing separation can dominate shuttle dynamics.
[AIAA PAPER 72-976] 22 p3230 A72-42336

DEMAGNETIZATION

Magnetic properties and paleomagnetic data of Permian Cutler and Elephant Canyon formations in Utah, discussing thermal demagnetization and origin of stable magnetization
09 p1305 A72-23668
Cryogenic microwave equipment for solids study provided with adiabatic demagnetization cooling system, noting relaxation time measurement in magnetic fields
12 p1796 A72-27856
Investigation method for shock wave induced demagnetization in YIG, noting impact study of magnetic properties
13 p1959 A72-29757
Lunar breccia and crystalline rocks thermomagnetic magnetization characteristics, presenting alternating field and thermal demagnetization curves
14 p2154 A72-30507

DEMAND [ECONOMICS]

Utah-Colorado-New Mexico-Arizona regional air transportation study, assessing scheduled air carrier service demand for 1971-1990
07 p1102 A72-19178

DEMODULATION

Coherent demodulation of continuous phase binary FSK signals in additive white noise, determining error probability
02 p0174 A72-12135
Modulation/demodulation techniques for optical one-gigabit/sec intersatellite data transmission link system, comparing per-unit data costs for system selection
02 p0174 A72-12142
Harmonically modulated reflected light signals phase shift and demodulation, assuming single scattering
06 p0848 A72-18047
Four-phase radio continuum receiver with digital demodulation and signal integration for transfer into on-line computer, discussing calibration
12 p1793 A72-27808
Linear product demodulator for quadrature double sideband signal, evaluating channel noise and phase jitter effect on carrier
13 p1920 A72-29105
Baseband distortion caused by intermodulation in multicarrier FM systems.
17 p2512 A72-34266
Discrete-time demodulation of continuous-time signals.
17 p2516 A72-35332
Digital simulation for radio frequency interference and specular multipath effects on FM spread spectrum demodulation with feedback and phase lock loops
18 p2659 A72-36317
Variants of conventional FM demodulation having the aim of improving poor signal-to-noise ratios.
18 p2661 A72-36843
Complex detection - A waveform preserving technique for single-sideband demodulation.
18 p2661 A72-36844
Complex detection - A waveform preserving technique for single-sideband demodulation.
21 p3017 A72-40862
Phase locked feedback circuit for FM demodulation, discussing all digital circuit design and voltage controlled oscillator algorithm to avoid analog implementation problems
21 p3018 A72-40873
Phase modulated data transmission with partial pilot signals, interpolating reference demodulation signals at receiving end by maximum cross correlation
23 p3264 A72-43771

DEMODULATORS

NT MODEMS
NT PHASE LOCK DEMODULATORS
VI-F modulation/demodulation system performance prediction by atmospheric noise model, comparing results with measurements
01 p0025 A72-10327

Capacitor-fed parallel chopper as phase sensitive demodulator, discussing design, stability, linearity and wide dynamic frequency range
04 p0507 A72-15522

Optimum adaptive variable step size delta modulator-demodulator producing minimum error for Markov-Gaussian source
06 p0772 A72-17404

Statistical noise characteristics and conditional signal distribution function measurements at output of standard FM demodulator
09 p1277 A72-22570

Digital data transition tracking loop as practical implementation of optimum self bit synchronizer in Mariner spacecraft telemetry demodulators
10 p1437 A72-24687

Canonical equations for frequency demodulator using feedback, calculating harmonic distortion for sinusoidal modulating signal
11 p1593 A72-25891

Dicke radiometer for 100 meter radio telescope, discussing demodulator design with dc coupling for difference signal and individual switching phases
12 p1792 A72-27807

Direct-detection optical receivers for angle-modulated signals.
21 p3017 A72-40858

Reciprocal of normalized mean square error [MSE] and output SNR as performance measures in optimal and suboptimal demodulators
21 p3017 A72-40863

Threshold noise of an FM receiver at small signal-to-noise ratios
22 p3154 A72-42236

Statistical noise characteristics and conditional signal distribution function measurements at output of standard FM demodulator
24 p3379 A72-44749

DENDRITIC CRYSTALS

Micrographic observation of Al and Al-Cu intermetallics dendrites shape at birth in liquid of nearly eutectic composition
10 p1496 A72-24239

Solution kinetics of secondary phases in cast dendritic and nondendritic Mg-Zn and Mg-Zn-Zr alloys, using cylindrical and spherical diffusion models
15 p2257 A72-32119

DENSIFICATION

Dislocation slip motions as densification kinetics mechanism in refractory materials sintering process, discussing electron microscopic observations of partially sintered MgO and W compacts
11 p1643 A72-26834

DENSITOMETERS

NT MICRODENSITOMETERS
Ear densitograph for noninvasive cardiac performance measurements during physical activities, exercise tests, flight conditions and for critical patients long-term monitoring
11 p1582 A72-25500
Left ventricular volume time course from computer processing of video angiocardigraphic data based on X ray densitometry measurements
11 p1587 A72-26627
The use of infrared absorption to determine density of liquid hydrogen.
19 p2805 A72-38836

DENSITY [MASS/VOLUME]

NT ATMOSPHERIC DENSITY
NT GAS DENSITY
NT SPACE DENSITY
Anaerobic glycolysis and specific gravity of red blood cells in rats exposed to pure oxygen at 600 torr
01 p0015 A72-11297
Lunar regolith powder weight density, compressibility and torsional strength determination at atmospheric pressure and He atmosphere
02 p0281 A72-12288
Fiberglass reinforced plastics heat conductivity as function of porosity, reinforcement factor and density
02 p0250 A72-12686
Ti alloys for airframe shell construction based on room temperature strength, stiffness and densities comparison with Al alloys, stainless steel and Be data
03 p0373 A72-13615
Equilibrium rotating superdense baryons in general relativity theory, determining integral parameters /mass semiaxes quadrupole moment/ in angular velocity approximation
03 p0435 A72-13805

Globular clusters with inhomogeneous composition, deriving partial densities of masses
03 p0436 A72-13826

Lunar regolith powder weight density, compressibility and torsional strength determination at atmospheric pressure and He atmosphere
10 p1532 A72-23757

Transient strain in axially impacted hollow non-homogeneous cone with axially varying modulus of elasticity and density
03 p1555 A72-24195

Fe powder preform hot rolling, investigating mechanical properties, microstructure and internal oxidation resistance as function of final density
10 p1488 A72-24695

Calcium and phosphorus excretion relation to bone density changes in immobilized Macaca nemestrina monkeys
12 p1760 A72-27473

Lunar surface diurnal temperature variations calculation based on Apollo 12 lunar fines thermophysical properties and surface layer core-tube sample density
16 p2454 A72-33432

Laser compression of matter to super-high densities - Thermonuclear /CTR/ applications.
23 p3294 A72-43262

DENSITY [NUMBER/VOLUME]

NT ELECTRON DENSITY [CONCENTRATION]
NT ELECTRON DENSITY PROFILES
NT ELECTRON DISTRIBUTION
NT ION DENSITY [CONCENTRATION]
NT IONOSPHERIC ELECTRON DENSITY
NT IONOSPHERIC ION DENSITY
NT MAGNETOSPHERIC ELECTRON DENSITY
NT MAGNETOSPHERIC ION DENSITY
NT MAGNETOSPHERIC PROTON DENSITY
NT METEOROID CONCENTRATION
NT PACKING DENSITY
NT PARTICLE DENSITY [CONCENTRATION]
NT PLASMA DENSITY
NT PROTON DENSITY [CONCENTRATION]
NT SPACE DENSITY

Finite difference calculus development of method to express thermodynamic limit of statistical-mechanical average as power series in number density, noting advantages and applicability
21 p3087 A72-40562

Photoanodic engraving process produced high bit density surface relief holograms on semiconductor crystals for data storage, retrieval and replication applications
21 p3054 A72-40614

DENSITY [RATE/AREA]

U FLUX DENSITY

DENSITY DISTRIBUTION

Nonhomogeneous fluid geostrophic flow, establishing relationship between velocity and density fields
01 p0051 A72-11230

Fabry-Perot interferometer for studying spatial distribution of plasma electron concentration, discussing resolution using solid state gas laser light source
02 p0223 A72-11403

Relativistic nonlinear gravitational instability theory for hydrodynamical system of equations applicable to early cosmic expansion, deriving density perturbations associated with rotational and gravitational waves
02 p0275 A72-11524

Explosion induced plane shock wave propagation in gas medium with exponential density distribution, determining gas flow behavior by difference approximation method
02 p0201 A72-11578

Nighttime lower ionospheric electron density distribution models for vertically polarized radio wave propagation parameters
02 p0173 A72-12112

Linear electron density distribution along faint meteor trail, discussing radio echo time-amplitude characteristics and ionization curve
02 p0282 A72-12335

Flame propagation and overdense heating in laser beam created plasma, calculating density and temperature profiles by one dimensional continuum hydrodynamic theory
02 p0238 A72-12363

Upper atmosphere ozone, aerosol and neutral constituent density profiles estimation by recursive filtering algorithm for satellite observation data
02 p0222 A72-12811

Diffusion flames turbulence measurements by microphones, hot wire probes, Pitot tubes and photodiodes, evaluating density fluctuations by indirect methods
02 p0303 A72-12854

Gravitational fields of giant planets in hydrostatic equilibrium, solving equations for linear and quadratic density distributions
03 p0436 A72-13818

NDT for detecting density variation, local anomalies regions and completeness of copper-infiltrated W powder rocket nozzle inserts
03 p0364 A72-14025

Two dimensional molecular dynamics digital simulation of Ar liquid-vapor interface at triple point, yielding strongly oscillatory density profile
03 p0393 A72-14263

Earth mantle and core density using Monte Carlo models compared with lunar structure from crust and seismology data, noting planetological contrast
04 p0571 A72-14616

Lagrange method extended to method of characteristics for solving first order hyperbolic partial differential equations, applying to ionospheric ion density distribution
04 p0539 A72-14885

Cosmological models dynamics and structural evolution feedback from density inhomogeneities energy momentum tensor, using hf approximation
05 p0715 A72-16166

- Concentration profile equations for finite length flat vertical plate moving in viscous incompressible fluid
05 p0650 A72-16783
- Laser schlieren measurement of density gradients in laminar hypersonic boundary layer interacting with corner expansion wave in shock tunnel
[AIAA PAPER 72-75] 05 p0606 A72-16879
- Homogeneous compressible turbulence field with large amplitude and density fluctuations generated in subsonic wind tunnel by rapid mixing of hot and cold air streams
[AIAA PAPER 72-119] 05 p0652 A72-16980
- Upper atmosphere density fluctuations associated with solar activity and local time values, using Cosmos 14 satellite drag data
05 p0659 A72-17037
- Pulsed cylindrical converging shock wave generation in decreasing density medium by axial explosion-implosion discharge
05 p0700 A72-17233
- Solar wind structure from long lived inhomogeneities in corona, allowing for velocity, density and temperature perturbations
06 p0872 A72-17444
- Temperature and density fluctuations in photosphere from Fe and Mg line intensities, noting variations due to granulation in solar atmosphere model
06 p0876 A72-17579
- Vertical gravity gradient measurements for areal density contrast exploration in gravity surveys and prospecting applications
06 p0809 A72-18147
- Spectrographic measurement of electron temperature and ion density profiles in cesium plasma thermionic converter
06 p0862 A72-18309
- Vertical density gradients as source of two stream instability irregularities in radio aurora theory
07 p0976 A72-19164
- Stellar dynamical and density wave theories for spiral pattern persistence in Galaxy with differential rotation
07 p1074 A72-19430
- Radiative cooling effects in absorbing-emitting gas behind reflected shock waves, using expansion procedure in small density ratio across shock front
[AD-738781] 07 p0967 A72-19503
- Small scale phase space density granulations/clumps/ in turbulent plasma due to fluctuating electric field
07 p1041 A72-19510
- Point explosion in cosmic spheroid with exponential density distribution, observing shock wave propagation along symmetry axis direction
07 p1075 A72-19583
- Pulsar distance determination from electron density distribution in line of sight estimated from frequency dispersion measures
07 p1080 A72-20054
- Rf excitation produced plasma instability, considering density fluctuation and drive frequency introduction by amplitude modulation
07 p1045 A72-20441
- Gas density distributions in argon and carbon dioxide supersonic jets with low angular divergence in vacuum, using Laval supersonic nozzle
07 p0973 A72-20512
- Hf potential effect on high amplitude waves propagation in magnetoactive plasma plane layer, noting particle density distribution
08 p1212 A72-21211
- D region neutral gas winds, density variations and short wave absorption, determining correlation from ultralight chaff and absorption measurements at 2.83 MHz
09 p1277 A72-22374
- Transient processes in heat exchanger, allowing for coolant variable density
09 p1410 A72-22413
- Snow-plough model of plasma acceleration for determining time dependence, gas density distribution and energy transfer
09 p1359 A72-22819
- Interstellar gas streaming velocity due to galactic spiral density waves, deriving mathematical expressions for Oort constant and differential galactic rotation nodes from Lin theory
09 p1391 A72-23538
- Schlieren optics for visualization and differentiation of density gradients with color and brightness distinctions, applying to supersonic flow through tandem grid
09 p1316 A72-23669
- Supersonic axisymmetric turbulent jet density fluctuations measurement by single beam schlieren system, using preheater to reduce jet static/ambient temperature difference
10 p1466 A72-24292
- Linear initial value problem of partially mixed cylindrical wake in uniformly stratified fluid, obtaining exact solutions for density and velocity distributions
10 p1466 A72-24299
- Vertical air density gradient in stratosphere as function of altitude
10 p1472 A72-24489
- Earth gravity anomalies sources depth, testing hypothesis of density variations origin
10 p1472 A72-24523
- Shock wave passage through curved interface from low to high density medium, showing interaction dependence on density ratio
10 p1469 A72-24541
- Density fluctuations and ion acoustic two stream instability characteristics of RF generated plasma derived from electromagnetic scattering at 24 GHz
10 p1523 A72-24800
- Spiral galaxy density wave maintenance mechanism from rotating disk star-gas system model description of stellar birth and disintegration effects
10 p1547 A72-24869
- Radial density profiles and emittance for nitrogen ion beams from Penning-type cyclotron ion source with hot filament
10 p1516 A72-25028
- Luminous filaments model of density condensations optically thick to ionizing radiation in planetary nebulae
10 p1550 A72-25197
- Probability density distributions for distance from arbitrary point to randomly distributed weather stations
11 p1592 A72-25767
- Atmospheric density variations from meteorological rocket soundings, discussing data reduction methods and error sources for bead thermistor and inflatable falling sphere instruments
11 p1626 A72-26473
- Electromagnetic wave transformation and absorption in Ar plasma with nonmonotonic longitudinal density distribution
11 p1699 A72-26758
- Conventional and explosive compacting effect on density distribution in green briquettes, investigating normal and shear stresses
11 p1643 A72-26830
- Fog and cloud microstructure and density distributions from directional light scattering coefficient/halo indicatrix/
11 p1683 A72-26883
- Neutral atmospheric density profiles measurements in lower thermosphere by satellite-borne accelerometers, noting longitudinal variations at high latitudes
13 p1948 A72-28833
- Infinite plane plates sound radiation due to bending waves interactions with density and stiffness fluctuations in material
13 p2004 A72-29094
- Linear electron density distribution along faint meteor trail, discussing radio echo time-amplitude characteristics and ionization curve
13 p2039 A72-29219
- Rarefied gas flows effect on metals creep properties, examining molecular flow density distribution as function of specimen surface distance from nozzle
13 p1979 A72-29483
- Relative brightnesses along solar radius from density photometry of corona at eclipses
13 p2046 A72-29715
- Concentration profile derivation for fluid flow near rotating disk with chemical reactions, considering concentration gradient and barodiffusion effects
13 p1944 A72-30049
- Adiabatic density perturbations damping by radiative viscosity and heat conductivity, taking into account plasma recombination in hot expanding Universe
14 p2148 A72-30202
- Lunar gravitational field expansion coefficients C20 and C22 calculation, using Cassini equator inclination and radial bulk density distribution
14 p2149 A72-30213
- Spiral structure density wave model of inner parts of Galaxy, calculating density, potential and velocity perturbation and dispersion in gas and stars
14 p2161 A72-30914
- Concentration stress convection in slow gas mixture flow due to density gradients, noting similarity to thermal stress convection
14 p2096 A72-31015
- Galactic tidal interactions, computing mass loss for hyperbolic collisions and giant system formation from density distribution models
14 p2161 A72-31043
- Out-of-plane density distribution and in-plane velocity distribution measurements from low energy helium scattering inelastically from 550 K silver
15 p2276 A72-31861
- Orbiting satellite environment and self contamination, calculating pressure, density and condensation rates and adsorption layers on critical surfaces
15 p2321 A72-31870
- Nighttime molecular nitrogen and oxygen number density profiles at 130-220 km over Sardinia from ESRO mass spectrometer measurements
15 p2226 A72-31938
- Core axial density distribution in gas jets freely expanding into vacuum from double concentric orifices, using electron beam fluorescence technique
15 p2218 A72-32150
- Superconducting to normal transition field as function of temperature for Ta with thin surface layer variable density impurities
15 p2293 A72-32241
- Spiral galaxy density wave damping by induced large-scale shock in interstellar medium
15 p2315 A72-32718
- Inner solar corona electron density distribution as function of heliographic latitude, longitude and radial distance from K-coronameter polarization-brightness data
15 p2318 A72-32786
- Shock tube diaphragm rupture effect on density distribution in rarefaction wave as function of time, using mirror laser interferometer measurement
16 p2390 A72-33161
- Transonic plane flow past wavy wall during choked wind tunnel operation, calculating flow velocity from Mach-Zehnder interferometer measured density distribution
16 p2378 A72-33508
- Mass flow rate and mean density measurements in separated laminar boundary layers with large transverse density gradients, analyzing density difference effects on instability
16 p2379 A72-33571
- Internal waves in sheeted thermocline with finite discontinuities in density profile formulating eigenvalue problem as homogeneous Fredholm integral equation
16 p2386 A72-33573
- Langmuir wave coupling in inhomogeneous plasma due to combined density gradient and external HF electric field
16 p2436 A72-33654
- Perturbation methods for density stratified viscous flow past flat plate, using boundary layer and low Reynolds number approximations
[AIAA PAPER 72-646] 16 p2381 A72-34086
- Microwave absorption by longitudinally inhomogeneous plasma, noting waveguide excitation in homogeneous region
17 p2588 A72-34859
- Influence of the diurnal effect in the atmospheric density distribution on the braking of a satellite
17 p2546 A72-35032
- Cosmic-ray heating of low-density interstellar H II regions.
17 p2600 A72-35296
- Screen equidensities in aerial photograph interpretation
17 p2555 A72-35337
- Experimental and two-dimensional computational study of end losses from a theta pinch.
17 p2592 A72-35628
- Density distribution in a high-pressure gas jet measured by laser-induced gas breakdown.
17 p2486 A72-35630
- Physical and numerical experiments on layered convection in a density-stratified fluid.
17 p2543 A72-35764
- Galactic spiral structure temporal decay based on density waves hypothesis
17 p2619 A72-35955
- Current instabilities and constriction in thermionic converters
18 p2647 A72-36221
- The structure of the Coma cluster of galaxies.
19 p2854 A72-37229
- German monograph - Investigation of electron beam welding with particular consideration of the mean power density and the radial power density distribution in the beam cross section
19 p2807 A72-37658
- Propagation and growth of shock waves in inhomogeneous fluids.
19 p2787 A72-38430
- Density wave detection by local hydrogen gas and young stars radial velocities comparison with Lin theory of galactic spiral structure
19 p2866 A72-38494
- Intercloud atomic H gas density distribution from 21 cm line width variations with galactic longitude
19 p2867 A72-38512
- Effect of concentration gradient on composition of sampled gas. II - Experimental verification.
19 p2805 A72-38870
- Earth density, surface wave velocity and other properties calculation from model consistent with physical and petrological mantle theories
20 p2917 A72-39475
- Parametric excitation of Bernstein waves in inhomogeneous magneto-plasmas.
21 p3089 A72-40187
- Measurements of gradients of gravity in mines.
21 p3048 A72-40500
- Nonaxisymmetrical disturbances effect on stability of cylindrical fluid flow with exponential density variation in radial direction and axial and azimuthal velocities
21 p3045 A72-40682
- Propagation of magnetohydrodynamic shock waves in a medium with diminishing density
21 p3094 A72-41653

- A calculated hydrogen distribution in the exosphere.
22 p3168 A72-42004
- D-region measurements with the differential-absorption, differential-phase partial-reflection experiments.
22 p3172 A72-42423
- The estimation of masses of individual galaxies in clusters of galaxies.
22 p3227 A72-42551
- Theory of thermal fluctuations in nonequilibrium systems
22 p3206 A72-42659
- A method of estimating the excess electron density in random irregularities embedded in the ionosphere.
22 p3173 A72-42883
- Possibility of determining the three-dimensional distribution of a plasma with the aid of an SHF resonator
22 p3214 A72-43122
- Adiabatic density perturbations damping by radiative viscosity and heat conductivity, taking into account plasma recombination in hot expanding universe
23 p3333 A72-43231
- Lunar gravitational field expansion coefficients C20 and C22 calculation, using Cassini equator inclination and radial bulk density distribution
23 p3334 A72-43243
- The effect of meteoric ion processes on radio studies of meteoroids.
23 p3336 A72-43558
- The negative space-charge density distribution and the potential distribution in a Penning discharge cell
23 p3324 A72-44211
- Diffusion coefficients measurement in solid and liquid Al, discussing experimental techniques and temperature dependence
23 p3304 A72-44300
- Density distribution of the radiation passing through a scattering medium from a bounded source
24 p3424 A72-44634
- Small disturbances propagation effect on self similar flow due to point explosion in medium with density varying according to distance from center
24 p3390 A72-44786
- ### DENSITY MEASUREMENT
- #### NT X RAY DENSITY MEASUREMENT
- Double Langmuir probe, microwave cavity and upper hybrid frequency measurements of plasma density in hydrogen, helium, neon and argon
01 p0110 A72-11190
- Multifrequency interferometer for inhomogeneous plasma density soundings, determining time dependence, spatial distribution and plasma layer size
02 p0263 A72-11413
- Point density measurement and crack detection in P/M green compacts with interconnected porosity by pneumatic tests, noting application to quality control
02 p0233 A72-11458
- Digital picture processing techniques for increased detail resolution, applying equidensity film methods [DFVLR-SONDDR-170]
02 p0229 A72-12018
- Low temperature plasma electron density measurements using ruby laser light scattering method
02 p0264 A72-12210
- Liquid n-octane, n-decane and n-undecane densities and adiabatic/isothermal compressibilities from sound velocity measurements at high pressures and 30-140 C
02 p0261 A72-12829
- Direct display plasma density and temperature meter, using floating double probe method
04 p0520 A72-14533
- Disk pump driven fluid layer device for density stratified water channel flow measurements, using hydrogen bubble technique
04 p0509 A72-15118
- High resolution electron microscope observation of voids in amorphous Ge films, noting density dependence on substrate temperature
04 p0562 A72-15152
- Upper atmospheric density measurements accuracy from triaxial accelerometer instrumented inflated falling sphere
04 p0519 A72-15156
- Low inertia instrument for ozone density measurement in atmosphere near ground
04 p0525 A72-15624
- Polarographic method for simultaneous measurement of wall gradients of velocity and of concentration in unsteady laminar or steady turbulent flow
06 p0797 A72-17558
- Convective heat flow pressure and density measurements at surface of central body of air inlet with live point and axial symmetry
06 p0755 A72-17560
- Interplanetary plasma electron and proton density fluctuation measurements by space probes and from radio sources scintillation spectra, noting agreement with power-law irregularity spectrum
06 p0881 A72-17901
- Low energy per pulse high repetition rate laser radar capabilities for atmospheric density measurement above 30 km
06 p0775 A72-18093
- Shock tube experimental techniques for studying fast processes coupled to shock wave propagation in

- reactive gases, describing pressure, density and temperature measurement methods
06 p0800 A72-18120
- Alpha iron lattice dilation by titanium, measuring densities and lattice parameters
07 p1016 A72-19942
- Atmospheric turbulence, wind velocity, temperature and density measurements at 90-250 km, using explosive contaminants release from Skylark rockets
07 p0979 A72-20265
- Turbulent wake of slender cone at Mach 12.5, measuring density and temperature fluctuations simultaneously
10 p1479 A72-24080
- [AIAA PAPER 72-118]
Low temperature plasma electron density measurements using ruby laser light scattering method
11 p1693 A72-25706
- Liquid Rb and Cs density and thermal expansion measurements near fusion point, discussing temperature dependence and gamma ray irradiation method
11 p1746 A72-26237
- Atmospheric neutral density measurement near 400 km during daytime by microphone density gage on OGO 6
11 p1625 A72-26407
- Rocket-borne mass spectrometer tested in high velocity molecular beam facility for thermospheric atomic oxygen density measurement
11 p1634 A72-26422
- Cavitation by creep of Mg alloys, using density measurements and metallurgical examinations
11 p1661 A72-26650
- Lunar topsoil density variations from Lunik and Surveyor radio wave, alpha and gamma scattering data, discussing Lunik 13 and Surveyor 7 landing sites
11 p1724 A72-26909
- Upper atmosphere density measurement techniques used by Sputnik 3 and San Marco 1 and 2 satellites
12 p1802 A72-27683
- Point density measurement in gas jets by flow visualization based on Raman spectrum lines proportionality
13 p1959 A72-29670
- [ONERA, TP NO. 1080]
Liquid and two phase liquid-gaseous hydrogen density determination via dielectric constant measurement by open-ended microwave cavity
14 p2103 A72-30197
- Ionospheric rotational temperature and density measurement, using fluorescence produced by rocket-borne electron beam gun
14 p2106 A72-30974
- Nighttime molecular nitrogen and oxygen number density profiles at 130-220 km over Sardinia from ESRO mass spectrometer measurements
15 p2226 A72-31938
- Ionospheric molecular oxygen density measurements during solar grazing ray absorption experiment on Ariel 3 satellite
15 p2226 A72-31950
- Ionospheric neutral density profile measurement by ultrasensitive triaxial electrostatic force rebalance accelerometer onboard Cannon Ball 2
15 p2227 A72-31962
- Upper atmosphere density from orbital drag on Cannon Ball II and Musket Ball satellites
15 p2227 A72-31963
- Solar radiation absorption measurements in 2150 A region as function of altitude to obtain oxygen and ozone densities
16 p2384 A72-32975
- Mass flow rate and mean density measurements in separated laminar boundary layers with large transverse density gradients, analyzing density difference effects on instability
16 p2379 A72-33571
- Electron-optical methods of investigating inhomogeneities in rarefied gases.
17 p2552 A72-34515
- Measurements of molecular oxygen in the thermosphere.
17 p2546 A72-34694
- Composition dependence of density in NiTi and CoTi.
18 p2701 A72-36592
- Determination of the plasma density in a collisionless plasma.
18 p2717 A72-37041
- Techniques for determining average density and related parameters in two-phase cryogenic flow systems.
19 p2805 A72-38835
- Calibration procedure to correct for the effects of dielectric containers in microwave plasma density measurements.
21 p3056 A72-41377
- Some topside electron density measurements from Ariel III satellite during the geomagnetic storm of 25-27 May 1967.
22 p3169 A72-42017
- Full-range solution for the measurement of thin-film surface densities with proton-excited X rays.
24 p3431 A72-44715

DEOXIDIZING

- Steel cleanliness conditions for formation and decantation of inclusions due to deoxidation during production up to solidification
03 p0371 A72-13198
- Ta-W-Hf alloy ultrahigh vacuum high temperature creep tests, showing deoxidation effect on creep behavior and early test stage oxygen-associated dynamic strain aging
05 p0674 A72-16392
- V, Nb and Ta deoxidizing capability in liquid Fe from oxide phase formation identification by electronographic and X ray analyses
07 p1011 A72-19545
- Influence of boron on the structure and properties of electron-beam melted molybdenum
24 p3414 A72-45380

DEOXYRIBONUCLEIC ACID

- Photochemical reactions in pyrimidine base of DNA after UV irradiation, relating mutagenic and lethal effect to dimerization
04 p0467 A72-14608
- Biological effects of unfocused laser radiation on DNA and RNA synthesis and cell activities in thymine dependent E. coli strain
04 p0477 A72-14610
- DNA primary structure variability relation to origin and evolution, discussing taxon scale in existing animal, plant and microorganism systems
04 p0470 A72-14792
- DNA-RNA molecular hybridization testing of chronon theory of circadian timekeeping in protozoa cells
07 p0920 A72-19542
- Evolutionary significance of primary amino acid or nucleotide base sequences of DNAs within various phylogenetic groups
12 p1759 A72-27160

DEPENDENCE

NT SPATIAL DEPENDENCIES

NT TIME DEPENDENCE

DEPOLMENT

- American and European solar generator technology development review, discussing roll-up arrays, flexible panels, and stowage and deployment system components
12 p1756 A72-28005

DEPOLARIZATION

- Hydrometeors linear depolarization ratios measurements by monostatic lidar, using different size water drops and ice crystal clouds
01 p0095 A72-10830
- Electrostrictively induced stimulated Brillouin light scattering effect on atmospheric depolarization, obtaining solutions for steady state and transient conditions
03 p0367 A72-13429
- Polarization electric field and depolarization current measurements in plasma flows along toroidal solenoid with diverter
06 p0853 A72-17387
- Stokes Q branch fundamental vibrational Raman light scattering cross sections and depolarization ratio measurement for molecular gases
07 p1038 A72-20292
- Sintered prepolarized perovskite type ferroelectric ceramics adiabatic depolarization and energy conversion under shock wave action
10 p1422 A72-24128
- Correlation function of depolarized finite collimated Gaussian laser beam in atmospheric turbulent medium
11 p1599 A72-26748
- Interferometer investigations of Cassiopeia linear polarization at centimeter wavelengths, explaining results by source model incorporating Faraday depolarization
12 p1865 A72-27094
- Dynamic electrocardiography with analog computer program to detect, count and classify atypical ventricular depolarization complexes
12 p1775 A72-28281
- Rat vena porta muscle cells spontaneous activity intensified by direct current depolarization and inhibited by hyperpolarization, noting effects of calcium and sodium ions
13 p1902 A72-28638
- Functional organization and neurophysiological mechanisms of return corticothalamic system in anesthetized cats, showing axon terminal presynaptic depolarization
13 p1902 A72-28762
- Linear polarization and depolarization observation of quasar red shift explained as Faraday dispersion in or near source
15 p2313 A72-32365
- Singly scattered radiation in weakly inhomogeneous turbulent plasma for incidence angles greater than critical angle, calculating backscattered wave depolarization from radiative transport equation
15 p2288 A72-32425
- Lunar radar backscattering measurement of 0.86 cm circularly polarized radiation, noting echo polarization ratio and depolarization variations with incidence angle
19 p2868 A72-38735

Faraday depolarization of extragalactic radio sources. 23 p3335 A72-43268

Comparison of the vectors of the ventricular depolarization and repolarization of man during immersion in a standing position 24 p3372 A72-44924

The effect of the subsurface on the depolarization of rough-surface backscatter. 24 p3380 A72-45635

DEPOLARIZERS
U DEPOLARIZATION

DEPOSITION
NT ANODIZING
NT ELECTRODEPOSITION
NT ELECTROPLATING
NT VACUUM DEPOSITION
NT VAPOR DEPOSITION

Fluid dynamical study of accretion process with gravitating point source motion through adiabatic gas, applying to galaxies 01 p0126 A72-10289

Limited three body problem applied to planetary angular momentum increment due to accretion of particles in heliocentric orbits, discussing planet rotation laws 02 p0282 A72-12330

Noncoagulating polydisperse aerosol deposition from two dimensional turbulent boundary layer and fully developed turbulent pipe flows [AIAA PAPER 72-81] 05 p0650 A72-16806

Detonation deposited coatings, determining adhesive strength as function of coating thickness and process technological parameters 14 p2107 A72-30432

Accretionary processes in the early solar system - An experimental approach. 17 p2618 A72-35836

Geochemically and geophysically consistent model of lunar accretion process to explain initial temperature distribution 18 p2725 A72-36291

Solution of the problem of the unsteady motion of a mixture in a flat duct using a quasi-homogeneous model with allowance for deposition on the walls 19 p2788 A72-38589

Sand deposition due to wind action in Martian craters, comparing to terrestrial analogs 20 p2969 A72-39389

DEPOSITS
NT CRYODEPOSITS

DEPRESSURIZATION
U PRESSURE REDUCTION

DEPRIVATION
NT SENSORY DEPRIVATION
NT SLEEP DEPRIVATION

Space environment weightlessness induced perceptual deprivation, considering hand-eye coordination, visual judgments and motion and time perception 16 p2355 A72-33549

DEPTH MEASUREMENT
Water depth attenuation coefficients and bottom reflectance characteristics from large area multispectral scanner measurements for discharge and concentrations monitoring 02 p0211 A72-11812

Radar instrument for measuring snow density, water content, layer depth and inhomogeneity based on snow cover electrical properties effects on echo characteristics 06 p0805 A72-17591

Sea depth determination in coastal waters based on solar reflection aerial photographs interpretation, presenting formula as function of swell parameters 09 p1303 A72-23307

Capacitance depth gage for thin liquid films thickness measurement, noting application to interface waves amplitude and frequency measurements 09 p1316 A72-23410

Profiling technique with scanning electron microscope to obtain depth information on single small specimen micrograph 10 p1481 A72-24240

DEPTH PERCEPTION
U SPACE PERCEPTION

DERIVATION CALCULUS
U DIFFERENTIAL CALCULUS

DESCENT
NT PARACHUTE DESCENT
DESCENT TRAJECTORIES
NT REENTRY TRAJECTORIES

Terrain clearance during descent and approach of aircraft under radar control, discussing optimum profile, ATC, nav aids and rules 01 p0097 A72-10183

Optimal control algorithm for spacecraft descent in atmosphere at speed near escape velocity, using game theory 01 p0135 A72-10298

Explicit analytic guidance technique for hyperbolic approach phases of lunar and interplanetary spacecraft trajectories from first order solution for perturbed planet centered trajectory [AIAA PAPER 72-15] 07 p1032 A72-18944

Perturbation solution of deceleration trajectory in ballistic reentry through rotating atmosphere with winds, assuming constant gravitational field and square law drag force 09 p1395 A72-22924

Landing control algorithm using onboard digital computer for spacecraft hyperbolic velocity reentry, discussing simulation test results 11 p1684 A72-26898

Probability for spore sterilization by aerodynamic heating, considering straight line and decaying circular orbital Mars entry trajectories 16 p2461 A72-34165

Synthesis of a nonlinear law for spacecraft motion control in the earth's atmosphere 17 p2621 A72-35201

Wind velocity and some Venusian surface characteristics monitored by the 'Venera-7' automatic inter-planetary station 17 p2610 A72-35210

Reentry vehicle spiral descent terminal guidance, verifying concept feasibility through hybrid man-in-loop simulators [AIAA PAPER 72-834] 20 p2950 A72-39093

DESERT ADAPTATION
Natural acclimatization to work in severe heat. 17 p2508 A72-34550

New data on physiological adaptations to arid zones 17 p2504 A72-35021

DESERTS
Multistage resource inventory and analysis program combining remote sensing techniques and ecological principles in California Desert pilot area, discussing photointerpretation and ground truthing 02 p0210 A72-11802

Clear sky atmospheric thermal radiation from all-wave radiation and air temperature measurements, showing diurnal and desert condition induced deviations from empirical formula 12 p1840 A72-27706

Prebiotic thymidine phosphorylation at 65 C by urea-phosphate mixtures in simulated desert conditions 15 p2185 A72-31629

DESICCANTS
Development of a desiccant CO2 adsorbent tailored for shuttle application. [ASME PAPER 72-ENAV-11] 20 p2896 A72-39166

DESICCATORS
Heat pipe evaporation zone length based on desiccation length calculations for various capillary cross sections and thermal loads 05 p0743 A72-15853

DESIGN OF EXPERIMENTS
U EXPERIMENTAL DESIGN

DESORPTION
Hydrogen and nitrogen desorption phenomena associated with a stainless steel 304 low energy electron diffraction /LEED/ and molecular beam assembly. 19 p2762 A72-38023

Chemisorption of CO on tungsten /100/ - Combined flash desorption and electron stimulated desorption study. I. 22 p3152 A72-42297

Effects of simulated space vacuum on bacterial cells. 23 p3254 A72-43395

Backscattering of desorbed gas molecules from spacecraft 23 p3284 A72-43618

DESPINNING
U SPIN REDUCTION

DESTABILIZATION
Rotor components vibration destabilizing effects on dual spin spacecraft dynamics, considering turbulent liquid sloshing in Intelsat 4 propellant tank 07 p0973 A72-20488

Destabilization and aging mechanisms for ionic conductivity decrease in stabilized zirconia type electrolytes, discussing yttria stabilization 16 p2361 A72-33895

On the destabilizing effect in a non-conservative system with slight internal and external damping. 21 p3124 A72-41483

DESTRUCTION
Missile destruct systems explosive transmission line manifolds, discussing designs for high reliability under severe environmental conditions 08 p1221 A72-20782

DESTRUCTIVE TESTS
Automatic testing machine for mechanical properties of metals under static loading 06 p0796 A72-18365

Mechanical energy consumption effects of thermal dissipation and cyclic straining methods during sample life tests 07 p1089 A72-19260

Ti-Al-V alloy biaxial yield strength improvement by combined texture and age hardening, using hydroburst tests 07 p1011 A72-19482

System reliability demonstration test cost minimization for one-shot electroexplosive device 13 p2024 A72-28367

Surface flaws measurement devices and quasi-static fracture tests, discussing cyclic crack growth, elastic compliance derivative method and stress intensity equations 23 p3353 A72-44229

Automatic testing machine for mechanical properties of metals under static loading 24 p3389 A72-45751

DESULFURIZING
Desulfurization of cobalt, nickel, and their eutectic carbon alloys during noncrucible zone melting in vacuum 23 p3300 A72-43647

DESYNCHRONIZED SLEEP
U RAPID EYE MOVEMENT STATE

DETECTION
NT AIRCRAFT DETECTION
NT CORRELATION DETECTION
NT FOREST FIRE DETECTION
NT HIGH ALTITUDE NUCLEAR DETECTION
NT RADAR DETECTION
NT SIGNAL DETECTION
NT TARGET RECOGNITION

DETECTORS
Some space instruments for the study of micrometeoroids. 17 p2558 A72-35940

DETERIORATION
Detection of structural deterioration and associated airline maintenance problems. [SAWE PAPER 918] 23 p3293 A72-43465

DETERMINANTS
Flutter equation approximate true damping or rate-of-decay solution by determinant iteration 01 p0142 A72-11133

Pade table for formal power series with notation for extension to Laurent series, relating algebraic theory to bigradient determinants and numerical analysis algorithms 11 p1676 A72-25501

Determinant with first and second kind Bessel functions elements, presenting zeros estimates 12 p1836 A72-27072

A modernized specialized computer for evaluating determinants 21 p3036 A72-40161

Mathematical spectra theory application to matrix eigenvalue problem, obtaining explicit form of determinant characteristic polynomial by numerical methods 21 p3076 A72-41781

DETERMINATION
U MEASUREMENT

DETONABLE GAS MIXTURES
Detonation waves in gas mixtures, liquids and solids, presenting wave equations for real gases 03 p0456 A72-13687

Variation of the rate of divergent spherical detonations in strict propane-oxygen-nitrogen and acetylene-oxygen-nitrogen mixtures as a function of the radial abscissa - Influence of the dilution in the inert state 17 p2635 A72-34283

Influence of water vapor on the normal flame velocity of a methane-air mixture at high pressures 19 p2882 A72-38459

Quasi-onedimensional analysis of gaseous free detonations. 21 p3044 A72-40194

Determination of the detonation velocity of isoatomic mixtures 24 p3462 A72-45032

Heat addition to supersonic flow by shock induced combustion studied by spherical and conical projectiles shot into explosive gas mixtures 24 p3360 A72-45038

One dimensional theory of electric discharge detonation effects in flame propagation within square duct with combustible gas mixture, applying to electrochemical pulse jet engine 24 p3464 A72-45064

DETONATION
Confined small diameter PETN, RDX and tetryl columns longitudinal detonations, using focused Q switched ruby laser 03 p0367 A72-13604

Angular momentum conservation law compliance of generalized triple configuration model for spin-detonation nucleus, assuming transverse Chapman-Jouguet wave 03 p0342 A72-13734

Combustible fuel-air mixture laminar and turbulent flame propagation mathematical model, with reference to detonation and prevention 03 p0456 A72-13876

Chemical reaction delayed effect on triple shock front confluence point trajectory in detonations, developing qualitative detonation cell model 06 p0904 A72-18530

Direct detonation of insensitive PETN, RDX and tetryl explosives with Q switched ruby laser radiation 08 p1220 A72-20771

Potassium chlorate/red phosphorus mixtures sensitivity tests for initiation by electrostatic discharge, heating and impact 08 p1221 A72-20776

Detonating cut-off pyrotechnic chain of explosive devices for stage separation involving primers, relays and fuses

08 p1221 A72-20777

Impact detonation mechanism in ammonium perchlorate mixtures with inflammable additions, determining critical detonation triggering stresses

09 p1373 A72-22890

One dimensional pulsating detonations calculation with induction zone kinetics, obtaining Chapman-Jouguet steady solution profiles

11 p1745 A72-25983

Detonation deposited coatings, determining adhesive strength as function of coating thickness and process technological parameters

14 p2107 A72-30432

Variation of the rate of divergent spherical detonations in strict propane-oxygen-nitrogen and acetylene-oxygen-nitrogen mixtures as a function of the radial abscissa - Influence of the dilution in the inert state

17 p2635 A72-34283

Condensed liquid explosive detonation pressure from free surface velocity measurement, noting pressure curve dependence on charge diameter and wall thickness

24 p3463 A72-45036

DETONATION WAVES

Blast wave techniques for exothermic processes in relation to propulsion systems, using shock or detonation tubes, point explosions, reflected shocks and implosion vessels

[AD-737415]

01 p0117 A72-10939

Detonation waves collision in variable gas medium with plane, cylindrical or spherical obstruction, determining gas parameters behind reflected shock wave

02 p2021 A72-11579

Hydromagnetic cylindrical blast wave propagation in self gravitating polytropic gas, obtaining graphs for velocity, pressure, density and magnetic field distributions

02 p0264 A72-12181

High temperature and pressure detonation gas expansion as shock wave from cylindrical volume, calculating flow velocity, pressure and density

02 p0302 A72-12285

Detonation waves in gas mixtures, liquids and solids, presenting wave equations for real gases

03 p0456 A72-13687

Tunguska explosion of 30 June 1908, determining air waves propagation velocity

03 p0438 A72-13981

Cylindrical blast wave propagation in MGD, deriving closed-form solutions for line explosion in medium with constant pressure, density and axial magnetic field

03 p0400 A72-14391

Three dimensional transverse wave structure effect on detonation wave and Chapman-Jouguet gross properties, using planar model

04 p0510 A72-14410

Conservation equations for blast waves one dimensional nonsteady flow field, considering Eulerian space and time profiles

[ASME PAPER 71-WA/APM-1]

05 p0745 A72-15974

Explosive shock loading effect on materials mechanical properties, describing test equipment

06 p0797 A72-18659

Cylindrically symmetric blast wave generated by infinitely long line explosion in cold and homogeneous gas rotating rigidly within self gravitational field

07 p1070 A72-19134

Detonation propagation through tubes coated with thin liquid fuel films, considering boundary layer displacement effect on propagation speed, pressure ratio and reaction zone length

07 p1100 A72-19728

Gas motion behind plane detonation wave orthogonal to free surface, solving Goursat problem for perturbed region

07 p0969 A72-19979

Two dimensional detonation wave structure and propagation calculated numerically, comparing to exact solutions

07 p0971 A72-20086

Blast and detonation wave phenomena applications in war and peace, discussing hypervelocity launchers, shock tubes and explosive weapons

08 p1146 A72-21014

Nonisentropic flow behavior behind propagating self similar blast wave

[AD-745485]

08 p1252 A72-21260

Ignition time delay measurement between leading shock front and hydroxyl emission onset in two phase detonation of decane-oxygen

08 p1255 A72-22041

Chemionization in oxyhydrogen plasma detonation waves

08 p1129 A72-22045

German monograph on pulsed laser induced spherical unsteady blast waves in stationary and flowing gases

09 p1325 A72-23161

Self similar flow patterns due to cylindrical ionizing symmetrical strong shock and detonation wave propagation outwards into gas at rest

09 p1295 A72-23564

High temperature and pressure detonation gas expansion as shock wave from cylindrical volume, calculating flow velocity, pressure and density

10 p1561 A72-23759

Blast wave propagation in uniform or gravitationally stratified media, using Brinkley-Kirkwood shock propagation theory

10 p1471 A72-25069

Seismic wave prediction from high altitude nuclear detonation, using ground reflected spherical shock parameters

11 p1627 A72-26519

Pure metals bulk modulus pressure dependence from detonation generated shock wave data, using empirical relations between propagation velocity and material flow rate

11 p1662 A72-26741

Self similar blast waves propagation, studying flow field in terms of shock front velocity and ambient atmospheric density variation ahead of front

[AD-745816]

12 p1889 A72-27832

Detonation wave generation in gas discharge plasma by pulsed electrical discharge

14 p2137 A72-30313

Vorticity jump across stationary MHD discontinuity generalization from gas dynamics problem, noting results validity for shock and detonation waves

16 p2435 A72-33011

Liquid and solid explosives detonation, initiation and shock interaction with inert materials for precision work

16 p2476 A72-33352

Explosive charge design to drive metal by detonation in terms of impulse, acceleration and final velocity, using Gurney model

16 p2398 A72-33355

Measurement of the characteristic times of detonation-wave formation in a tube filled with an acetylene-air mixture

18 p2676 A72-35999

Detonation and burning characteristics of liquid oxygen-liquid methane mixtures.

19 p2848 A72-38834

Experimental investigation of the detonation properties of hydrogen-oxygen and hydrogen-nitric oxide mixtures at initial pressures up to 40 atmospheres.

19 p2883 A72-38875

Gas motion behind plane detonation wave orthogonal to free surface, solving Goursat problem for perturbed region

20 p2915 A72-40035

Detonation shock wave study of liquid fuel droplets in gaseous oxidizing agent flow, using schlieren and scanning photography

20 p2962 A72-40044

Characteristics of models of detonation spinning in various combustible media

20 p2987 A72-40045

Quasi-one-dimensional analysis of gaseous free detonations.

21 p3044 A72-40194

Performance and limitations of shock tubes with imploding detonation drivers.

21 p3128 A72-40767

Position of the transition point through the sonic velocity behind the detonation front

21 p3045 A72-40987

Experimental investigation of pressure profiles in a helical shock wave irregularly reflected in plexiglass cylinders

21 p3045 A72-40988

Measurements of the local velocity of shock and detonation waves by schlieren interferometry of Doppler-shifted laser light.

22 p3178 A72-42455

Equimolar oxyhydrogen detonation wave behavior near pressure limit, considering unsteadiness caused by tube length

22 p3244 A72-42485

Detonation wave generation in gas discharge plasma by pulsed electrical discharge

23 p3318 A72-43215

Initiation of a detonation by a laser beam focused in a gaseous medium

24 p3410 A72-45026

Combustion product gas dynamic motion effects on detonation front propagation, discussing reacting blast wave and finite kinetic rate models and asymptotic results

24 p3391 A72-45027

Mach stem generation by colliding spherical pressure waves in spark ignited combustible gas, noting simultaneous deflagration wave characteristics

24 p3462 A72-45028

Instabilities in the reaction zones of detonation waves.

24 p3462 A72-45029

Shock wave velocity, combustion front and pressure measurements of unstable detonations in propane-oxygen-nitrogen mixtures, comparing with double discontinuity theory

24 p3462 A72-45030

Chapman-Jouguet surface characteristics in flow field behind steady gaseous detonation wave, using schlieren photography

24 p3462 A72-45031

Smoked foil observation technique for transient behavior produced by perturbing equilibrium configuration detonation waves

24 p3462 A72-45033

Propagation of blast waves in a combustible gas.

24 p3462 A72-45034

Divergent cylindrical detonation of nitromethane

24 p3463 A72-45037

Method of measuring the fine structure of detonation fronts in solid explosives.

24 p3463 A72-45039

Approximate equations of the flow behind a detonation with lateral confinement

24 p3463 A72-45041

Two-phase detonations with bimodal drop distributions.

24 p3463 A72-45052

Theoretical analysis of a rotating two-phase detonation in liquid rocket motors.

24 p3433 A72-45053

DETONATORS

Secondary explosive spark detonators design and performance, determining ambient pressure variations effects on firing characteristics

08 p1219 A72-20758

Pulsed carbon dioxide laser welding of miniature explosive detonators

08 p1221 A72-20778

Automated detonator production facility features, describing modernization program

08 p1221 A72-20780

Initiation mechanisms for explosive materials and experiments for hazard evaluation, discussing subdetonation reactions and mathematical models of explosive processes

16 p2442 A72-33353

Hot wire and exploding bridgwire detonators, design characteristics, handling safety and hazard situations

16 p2442 A72-33358

DEUTERIDES

High temperature heating of plasma by ultrashort laser pulses focused onto lithium deuteride, noting various diagnostic methods

12 p1851 A72-27581

Laser pulse heating of plasma, predicting efficiency enhancement by addition of heavy element impurities or deuterides to solid target surface

12 p1852 A72-27621

DEUTERIUM

Galactic evolution and cosmology implications of primordial solar D/H ratio, discussing deuterium production mechanisms

04 p0574 A72-14980

Temperature dependence of scattering cross sections for cold and hot neutrons colliding with oxygen and deuterium molecules

08 p1211 A72-21872

Jupiter spectral observations, discussing presence of deuterated methane in atmosphere and comparison with solar spectra for telluric features identification

10 p1539 A72-24347

Chemical laser with deuterium and nitrogen fluorides mixture, examining excited molecules emission spectra

11 p1649 A72-26351

High temperature deuterium plasma production by laser heating of gas filled cylindrical tube, optimizing pulse duration and configuration

12 p1849 A72-27059

Cosmic and solar wind abundance analysis for D and He-3 in protosolar gas, noting chemical equilibrium reaction role in D enrichment

12 p1868 A72-27216

Total energy distributions of field emitted electrons from tungsten as function of coverage by hydrogen and deuterium, observing elastic and inelastic spectrum

15 p2275 A72-31851

Metastable /2S/ atoms production by electron impact induced dissociative excitation of molecular deuterium, measuring total cross section via Lyman alpha flux

15 p2282 A72-32645

Plasma corona electron temperature decoupling from core of solid deuterium pellet heated in vacuum by convergent laser beams

16 p2433 A72-32810

Chemical laser with deuterium and nitrogen fluorides mixture, examining excited molecules emission spectra

16 p2402 A72-33704

Jupiter atmosphere methane deuterium/hydrogen ratio estimate from exchange reaction and temperature studies

20 p2968 A72-39242

Flame structure and flame reaction kinetics. VII - Reactions of traces of heavy water, deuterium and carbon dioxide added to rich hydrogen + nitrogen + oxygen flames.

24 p3378 A72-44920

DEUTERIUM COMPOUNDS

NT DEUTERIDES

NT HEAVY WATER

Self pulsed electrically initiated HF and DF chemical laser with high pulse repetition frequency gain switched operation
06 p0826 A72-18458

HD absorption spectrum measurements in vacuum UV region for Rydberg states and ionization energy determination
16 p2431 A72-33583

Pulse energy and temporal/spatial distribution of carbon dioxide laser pumped by energy transfer from vibrationally excited DF produced by deuterium-fluorine chain reaction
22 p3185 A72-42617

DEUTERIUM OXIDES
U HEAVY WATER

DEUTERIUM PLASMA
Nuclear fusion by laser radiation, discussing plasma heating mechanisms and limitations in DD reaction production
04 p0557 A72-15172

Cumulation-laser heating of D-T plasma for cylindrical wave, investigating pulse energy increase for critical temperature attainment from average value mathematical model
05 p0695 A72-16279

Nuclear microfusion energy recovery threshold increase during laser pulse heating process of D-T plasma
05 p0695 A72-16280

Spectral analysis of light reflected from Nd laser produced deuterium plasma, observing Doppler shift
07 p1039 A72-18888

Laser heating and fusion energy recovery of D-T plasma by mechanical-magnetic cumulation, considering cylindrical wave system
09 p1365 A72-23553

Mathematical model for deuterium slab solid and plasma under laser pulses irradiation, noting shock wave propagation and slab acceleration
[AIAA PAPER 72-721] 16 p2439 A72-34027

Laser-beam-scattering measurement of ion temperature in a theta-pinch plasma and evidence for thermonuclear reactions.
19 p2840 A72-37548

Deuterium-tritium heating to thermonuclear temperatures by means of ion-ion collisions in the presence of intense laser radiation.
21 p3094 A72-41632

Nanosecond and picosecond laser-produced CD2 plasmas.
24 p3427 A72-44709

High temperature deuterium plasma production by laser heating of gas filled cylindrical tube, optimizing pulse duration and tube configuration
24 p3431 A72-45712

DEUTERON IRRADIATION
N-p silicon solar cells damage at room temperature by proton and deuteron irradiation, considering particle mass and energy functions and illuminating light wavelength effects
04 p0561 A72-14574

DEUTERONS
Proton elastic scattering by deuterons in backward hemisphere, examining normal and center of mass scattering angle and differential cross section
04 p0551 A72-14437

Low energy cosmic ray deuteron and He 3 source spectra observation implications for adiabatic deceleration in solar cavity, discussing interstellar propagation
16 p2448 A72-33743

DEVELOPERS (PHOTOGRAPHY)
U PHOTOGRAPHIC DEVELOPERS

DEVITRIFICATION
U CRYSTALLIZATION

DEWAR SYSTEMS
U CRYOGENIC EQUIPMENT

DH 112 AIRCRAFT
Economic and operational aspects of fatigue - Figures of a Swiss ground attack/fighter aircraft.
24 p3367 A72-44742

DH 121 AIRCRAFT
Trident aircraft air-system interrogator airborne first line test apparatus for electrical components malfunction diagnosis
06 p0796 A72-18154

Quiet RTOL /reduced takeoff and landing/ short haul aircraft cost comparison with Trident 3 aircraft up to design range stage length
15 p2180 A72-31320

DHC 5 AIRCRAFT
Buffalo photographic aircraft for oil slick remote sensing, using aerial cameras and thermal IR scanner
05 p0658 A72-16600

Augmentor wing design for Buffalo STOL aircraft, discussing operational principle and wind tunnel test results
21 p2994 A72-40684

DIABATIC PROCESSES
U HEAT TRANSFER

DIAGNOSIS
Clinical electrocardiography diagnostic capability, discussing phase plane cardiogram sensitivity to aberrations in QRS contours
01 p0017 A72-10148

Thermovisors /recording IR detectors/ development, discussing application to biomedical investigations and disease diagnostics
01 p0022 A72-11293

Myokinase activity determination as diagnostic test for human myocardial infarction, comparing to creatine phosphokinase activity test
05 p0618 A72-16388

Image processing of diagnostic echocardiogram by ultrahigh speed analog to digital converter interfacing digital computer
07 p0928 A72-19312

Clinical response to nitroglycerin therapy correlation with coronary angiography as diagnostic test for coronary artery disease in patients with chest pain
07 p0920 A72-19993

Reliability of electroencephalography as diagnostic method from specialists interpretation of curve morphological features, discussing normal and pathological record evaluation
08 p1124 A72-21000

Picoscale blood diagnostic device for red and white cell count, noting piston principle electronic operation
09 p1272 A72-23257

ECG, physical exercise and drug use in diagnosis and aeromedical evaluation of supraventricular arrhythmias, presenting case histories of pilots with wandering cardiac pacemakers
10 p1428 A72-23741

Serum petidase activity determination as enzymatic diagnostic test for myocardial infarction
11 p1579 A72-25851

Random sample comparison of computer program for ECG diagnoses and physicians readings
11 p1590 A72-26975

Heart and circulatory system functional diagnostics, discussing ECG, blood pressure, X ray, phonocardiographical and pulmonary examinations
12 p1760 A72-27271

Automatic ECG recording and analysis by electronic data processing equipment, discussing methods of data acquisition and transmission for routine diagnosis and prophylactic mass examinations
12 p1772 A72-27821

Objective evaluation of main rheoencephalogram parameter for disturbed brain blood circulation
12 p1773 A72-28218

Frontal sinus hematoma incidence in flying personnel and scuba divers, discussing diagnosis and clinical treatment
12 p1765 A72-28275

ECG diagnostics for arrhythmia assessment in flying personnel flight fitness examination
12 p1775 A72-28294

Keratoconus /noninflammatory conic protrusion of cornea/ diagnosis and rehabilitation in USAF flying personnel
12 p1768 A72-28331

Serial ECG change detection and description in myocardial infarction survivors, using computer analysis to find best diagnostic discriminants from multiple criteria
16 p2357 A72-34008

Diagnostic errors in draft age patients, noting doctor, examination methods, disease type and patient factors and psychosomatic disturbance detection
16 p2359 A72-34149

Methods for measuring the HF oscillation frequency in ultrasound pulses of equipment for diagnostic ultrasonography.
19 p2759 A72-37399

Echocardiography in the diagnosis of congenital mitral stenosis and in evaluation of the results of mitral valvotomy.
19 p2755 A72-37499

Description of an easy and simplified test for electromyographic diagnosis of latent spasmophilia in flight personnel
19 p2760 A72-37878

Renin in differential diagnosis of hypertension.
19 p2757 A72-38144

Analysis of intracavitary electrocardiograms through a saline bridge in the diagnosis of cardiac arrhythmias.
24 p3370 A72-44559

Automatic software diagnostic package for airborne computer, using testing computer for decision making based on received data
24 p3383 A72-45669

DIAGRAMS
NT BENDING DIAGRAMS
NT CIRCUIT DIAGRAMS
NT CREEP DIAGRAMS
NT HERTZSPRUNG-RUSSELL DIAGRAM
NT NYQUIST DIAGRAM
NT PHASE DIAGRAMS
NT S-N DIAGRAMS
NT STRESS-STRAIN DIAGRAMS

Wyld diagram method extended to turbulence decay, considering operators expressed as integrals with kernels
19 p2785 A72-37469

Energy flow diagrams.
24 p3369 A72-44686

DIAL SATELLITE
Satellite projects Azur, Dial and Heos - Conference, Bremen, West Germany, April 1971
05 p0714 A72-16134

German-French DIAL aeronomy satellite project, describing geocoronal radiation, electron density and equatorial electrojet measurements
10 p1535 A72-24029

DIAL aeronomy satellite design and operational features, describing in-flight behavior
10 p1551 A72-24030

DIAMAGNETISM
Solar wind perturbations downstream of moon outside of diamagnetic cavity, considering lunar surface magnetized areas as possible sources
07 p1057 A72-19144

Diamagnetic enhancement of magnetic susceptibility of amorphous semiconductors, considering mobility states and paramagnetic Van Vleck reduction
09 p1373 A72-23508

Diamagnetic energy measurements on rotating plasma in crossed static electric and magnetic fields with short circuiting metal wall
10 p1519 A72-24097

Equilibrium configurations of Vlasov plasmas carrying a current component along an external magnetic field.
19 p2839 A72-37332

DIAMANT LAUNCH VEHICLE
Launch center for solid-liquid propellant rocket probes, Diamant and Europa 2, describing payload preparation hall
[DGLR PAPER 72-0137] 13 p1939 A72-28962

DIAMETERS
The determination of the diameter of Io from its occultation of beta Scorpii C on May 14, 1971.
24 p3436 A72-44700

Spline functions application to approximation theory problem of determining diameters of subspaces and manifolds in Banach space
24 p3419 A72-45548

DIAMINES
NT GUANIDINES

DIAMOND WINGS
U LOW ASPECT RATIO WINGS
U SWEPT WINGS

DIAMONDS
Second order electro-optic effect in diamond, discussing birefringence due to dispersion and random residual strains
[AD-736674] 02 p0260 A72-12545

Semiconductors with diamond and zincblende structures, calculating dielectric function by empirical pseudopotential method
03 p0405 A72-14270

X ray topography of natural diamond, showing impurity platelet distribution, slip depth, temperature and stress conditions after plastic deformation
05 p0702 A72-16020

Temperature, pressure and crystallization time effects on artificial diamond crystal growth of various morphological shapes
05 p0681 A72-16355

Room temperature IR absorption spectra of B alloyed powdered synthetic diamonds
07 p1050 A72-20253

Computer simulation of crack tip atomic structure in diamond, relating covalent bond structure to dislocation nucleation and propagation likelihood
09 p1338 A72-22923

Angular annihilation photon distribution curves from positron-electron annihilation method for metallic phase interaction with crystal lattice in synthetic diamonds
12 p1833 A72-27764

Wear resistance of artificial and natural diamond grindstones in ruby cutting, noting tests for grain geometry and fabrication technique effects
12 p1814 A72-27765

Electron microscope study of hard alloy surface layer formation characteristics during diamond grinding with electrolysis
12 p1814 A72-27766

Thermal flux on contact area and temperature distribution on specimen surface during diamond grinding
12 p1814 A72-27767

Synthetic diamond single crystals, investigating impurities and inclusions effects on ferromagnetic properties and heat resistance
12 p1833 A72-27768

Diamond powder lattice parameter changes during fast electron irradiation at various temperatures, discussing crystal defect stability and neutron irradiation comparison
13 p1983 A72-28760

Role of an electric field in the diffusion mechanism of the graphite-to-diamond phase transformation
19 p2823 A72-38405

On the splitting of dislocations in the diamond cubic lattice.
20 p2962 A72-39992

Study of the composition of inclusions in synthetic diamond crystals by the local analysis method
22 p3196 A72-42155

DIAPHRAGM [ANATOMY]

ECG P-wave-like deflections caused by strong diaphragmatic action potentials in obese woman with fever and erysipelas

13 p1908 A72-28569

Electromyographic investigation of diaphragm cross contraction following spinal cord section in cats, noting diaphragm motoneurons excitation by breathing center pulses

22 p3142 A72-42281

DIAPHRAGMS

Sheet metal biaxial creep testing, using edge clamped circular diaphragm deflected by lateral hydrostatic pressure

03 p0373 A72-13649

DIAPHRAGMS [MECHANICS]

Cavity resonator thermal stabilization, using gas pressure controlled membrane

02 p0196 A72-12698

Open ended parallel plate waveguide, calculating radiation pattern variation with diaphragm dimension

07 p0945 A72-19663

Heat transfer to casing in axial clearance space between nozzle diaphragm and turbine wheel

12 p1861 A72-28134

Shock tube diaphragm rupture effect on density distribution in rarefaction wave as function of time, using mirror laser interferometer measurement

16 p2390 A72-33161

A method of calculating acoustic resonance phenomena generated by the unsteadiness of singular pressure losses in the pipes

17 p2580 A72-34279

Stresses in a welded diaphragm due to boundary contraction and normal uniform pressure.

17 p2631 A72-34821

Rectangular aperture diaphragm dimension determination for ring laser resonator principal transverse mode selection and higher modes suppression

20 p2933 A72-39510

DIASTOLE

Beta-adrenergic and vagal blockage altered autonomous control effects on left ventricular function in conscious dogs, noting heart rate, stroke volume and end-diastolic and end-systolic diameters

02 p0163 A72-12090

Fluid mechanics of left ventricle model with mitral and aortic valves, showing ring vortex relation to diastole and closure

11 p1589 A72-26775

Physiological evaluation of diastole mechanism in rat hypertrophied myocardium as function of heart rate, Ca ion concentrations and temperature

13 p1901 A72-28521

Coronary heart disease discriminatory factors from comparison with healthy controls, noting diastolic hypertension significance

15 p2183 A72-31282

Automated constant cuff-pressure system to measure average systolic and diastolic blood pressure in man.

17 p2507 A72-34298

Left ventricular dynamics during handgrip.

19 p2755 A72-37243

Relationship of pulmonary artery to left ventricular diastolic pressures in acute myocardial infarction.

20 p2892 A72-39461

DIATOMIC GASES

Mars atmosphere diatomic oxygen upper limit abundance, using high dispersion spectroscopic data from 1969 apparition

04 p0569 A72-14498

Master equation for vibrational relaxation of diatomic dilute gases, discussing restrictions on experimental initial conditions and scattering cross sections

04 p0553 A72-15634

Binary collision loaded-sphere molecular model for diatomic gases computer simulation, obtaining normal shock waves velocity, density and temperature profiles

10 p1466 A72-24297

Molecular diffusion laser gain determination from interaction kinetics between diatomic and cold working gases, examining annihilation processes

10 p1491 A72-24360

Diatomic-monatomic molecular gas mixtures oscillation and rotation energies relaxation equations, taking into account transport and chemical reaction processes

14 p2083 A72-30327

Generalized phase shift effect on classical limit of rotational excitation collision cross sections related to transport properties of diatomic gas molecules

16 p2428 A72-32925

Diatomic gas flow behind blast wave, discussing vibrational nonequilibrium effects and solution of governing equations via characteristics method

16 p2378 A72-33440

Molecular diffusion laser gain determination from interaction kinetics between diatomic and cold working gases, examining annihilation processes

17 p2563 A72-34959

German monograph - Solution of the boundary layer equations for chemically reacting gases by a collocation method.

22 p3167 A72-43071

DIATOMIC MOLECULES

Missing solar UV opacity from band adsorption coefficient comparison between photospheric diatomic molecules and metals and hydrogen

04 p0579 A72-15327

Diatomic molecules forbidden transitions moments, Franck-Condon factors and lifetimes, calculating CO Cameron system intensity by perturbation theory

05 p0692 A72-16750

Adiabatic-nuclei theory application to diatomic molecules excitation by electron impact, approximating fixed nuclei phase shifts dependence on internuclear separation

06 p0852 A72-17826

Large diatomic and polyatomic molecules formation from big radicals in interstellar medium, noting association reaction role

06 p0891 A72-18506

Chemical reactions in shock waves, discussing diatomic molecules dissociation and combustion processes

08 p1148 A72-21016

Molecular rotation stimulation and deactivation of diatomic molecule addition to monatomic gas, discussing energy exchange in rarefied gas flow

08 p1211 A72-21656

Post-threshold translational energy dependence of endoergic cross sections for vibrational excitation and reactive scattering of diatomic molecules by atomic or molecular impact

09 p1357 A72-22858

Attractive well potential effects on vibrational transition probability during atom-diatom molecule collinear collision

10 p1514 A72-24335

Chemical lasers diatomic and multiatomic molecules dissociation in nonequilibrium conditions, discussing vibrational energy exceeding gas temperature

11 p1646 A72-25713

Model potential method for calculating positively charged diatomic sodium molecular ions potential energy curves and resonance charge transfer cross sections

12 p1848 A72-28350

Diatomic carbon negative ion search in HD 201626 and solar spectra, noting rotational lines coincidence with absorption features

13 p2038 A72-29010

Quantum mechanical calculation of interaction potential energy surface role in vibrational excitation of diatomic molecules

14 p2134 A72-30750

Diatomic molecules partition functions derivation by classical and quantum mechanical theories for simple harmonic oscillator and square-well potential

15 p2280 A72-31693

Diatomic molecular vibrational excitation and dissociation effects on imploding shock waves, comparing shock tube data to prediction

15 p2192 A72-32148

Tabulation of diatomic molecular lines observed in sunspot spectra with rotation branch, quantum number and vibration band

15 p2316 A72-32750

Vibrational energy transfer probabilities for inelastic collisions between diatomic molecules, considering system represented by harmonic oscillators coupled by time dependent interaction potential

16 p2431 A72-33582

Hydrogen and hydrocarbon diatomic molecules and cations rotational state upper limits determination, noting potential energy functions

16 p2432 A72-34098

Diatomic molecules dissociation investigation from effective cross section measurement of slow atomic negative ions formation by molecules collisions with fast ions and atoms

16 p2432 A72-34152

Rates of interaction of vibrationally excited hydroxyl $v = 9$ with diatomic and small polyatomic molecules.

17 p2511 A72-35648

Electron transmission spectroscopy - Core-excited resonances in diatomic molecules.

17 p2586 A72-35771

Tunable Raman excitation and vibrational relaxation in diatomic molecules.

17 p2586 A72-35802

Monte Carlo trajectory calculations of the three-body recombination and dissociation of diatomic molecules.

19 p2838 A72-38805

Calculation of intensities of vibration-rotation of a diatomic molecule by the factorization method

21 p3087 A72-40471

Photoelectrically observed diatomic carbon absorption lines in sunspot spectra for two energy bands

21 p3108 A72-41284

Diatomic carbon lines search in sunspot umbras spectrum from solar telescope observations

21 p3108 A72-41285

Diatomic molecular dissociation in pure gas and mixtures with inert diluent, expressing as set of coupled quadratically nonlinear differential equations

22 p3208 A72-42400

[AICHE PAPER 6B] Electric dipole moment of diatomic molecules by configuration interaction. IV.

24 p3426 A72-44870

Transport properties of a gas of diatomic molecules. V - GPS calculation of the rotational relaxation time of the Ar-N₂ system.

24 p3427 A72-45307

DICHLORIDES

Dichlorodifluoromethane-fluorine flame structure, taking samples by molecular beam sampling system for analysis by mass spectrometry

02 p0303 A72-12483

DICHOTOMIES

Stochastic time varying patterns classification by Kalman filter, discussing optimum dichotomizer with supervised learning

12 p1790 A72-27498

DICHROISM

Circular and linear dichroism for the near infrared.

23 p3289 A72-43899

DICHROMATES

U CHROMATES

DICKE RADIOMETERS

Dicke-type microwave radiometer for daily measurements of 2800 MHz solar flux, discussing antenna system and dynamic range

04 p0522 A72-15163

Dicke radiometer for 100 meter radio telescope, discussing demodulator design with dc coupling for difference signal and individual switching phases

12 p1792 A72-27807

DICKE TYPE RADIOMETERS

U DICKE RADIOMETERS

DIELECTRIC CONSTANT

U DIELECTRIC PROPERTIES

DIELECTRIC MATERIALS

U DIELECTRICS

DIELECTRIC PERMEABILITY

Dielectric permeability tensor operator for surface wave-electron beam interaction in relativistic nonuniform plasma stream with cylindrical geometry

09 p1359 A72-22769

Electromagnetic wave diffraction on ideally conducting homogeneous bodies of revolution with arbitrary complex permittivity and permeability, using variables separation method

13 p1920 A72-29279

DIELECTRIC POLARIZATION

Dielectric and semiconductor crystals surface defects, considering electric polarization structures

10 p1525 A72-23761

Dielectric constant measurements of compressed gaseous and liquid oxygen for computing Clausius-Mossotti function

11 p1691 A72-26782

Influence of the polarity of the dispersive medium on the structure and properties of plastic lubricants

17 p2571 A72-35176

Mathematical model for dielectrics with time dependent polarization, noting relaxation time distribution function

21 p3085 A72-41074

DIELECTRIC PROPERTIES

NT PERMITTIVITY

Temperature compensated high dielectric constant material, discussing low loss at microwave frequencies, reproducibility and mechanical properties

01 p0044 A72-11308

Radiative heat transfer across vacuum gap between two closely spaced metal bodies with arbitrary dielectric properties, solving Maxwell equations

02 p0300 A72-11672

Low loss reactive wall rectangular and circular waveguides with periodic dielectric structures for millimeter wave and high power applications

02 p0190 A72-11678

Dielectric surface waveguides for millimeter and optical wavelength applications, discussing technologies, materials, fabrication and measurement

02 p0191 A72-11683

Lunar soil dielectric constant and loss-tangent and electrical resistivity measurement by Q meter method, noting resemblance to dense terrestrial rock powders

02 p0281 A72-12287

Surface moisture effect on dielectric properties of ultrafine barium titanate particulates of varying particle size

02 p0269 A72-12416

Dielectric properties of high purity polycrystalline barium titanate, observing temperature effects as function of heat treatment

02 p0269 A72-12417

Amorphous semiconductors dielectric properties based on randomly distributed local electron states in disordered solids, crystalline impurities and polymer aggregates

02 p0269 A72-12450

Alkali halide crystals optical dc dielectric strength determination, using carbon dioxide laser induced breakdown threshold data

03 p0368 A72-13607

Semiconductors with diamond and zincblende structures, calculating dielectric function by empirical pseudopotential method

03 p0405 A72-14270

Weakly divergent beam propagation of electromagnetic waves in statistically inhomogeneous nonlinear medium with dielectric constant dependence, using small perturbation method

05 p0625 A72-15818

Equivalent dielectric properties of infinite two dimensional periodic metal tape structures in presence of electromagnetic waves propagating in various directions

05 p0628 A72-16410

Injection laser threshold current density, radiation pattern and electric field distribution relation to layer thickness and dielectric constants, using waveguide theory

06 p0825 A72-17772

Bulk semiconductor material complex microwave conductivity and dielectric constant measurements by cavity perturbation techniques

06 p0786 A72-18371

Thin film resistors and capacitors design, considering stability, power, size, film thickness, parasitic inductance capacitance and resistance and dielectric loss properties

06 p0790 A72-18573

Quantum optics analysis of light propagation and photon flux fluctuations in medium with random dielectric constant inhomogeneities

07 p0938 A72-18912

End holes effects on dielectric constant measurement of long glass tubes by cylindrical microwave resonant cavity

08 p1164 A72-20940

Dielectric dispersion in SrSi filamentary single crystals as function of Curie temperature in lf and shf range

09 p1367 A72-22422

Lunar soil dielectric constant and loss-tangent and electrical resistivity measurement by Q meter method, noting resemblance to dense terrestrial rock powders

10 p1532 A72-23756

Gamma ray radiation effects on epoxy resin electric properties, studying electric insulation and arc resistances and dielectric breakdown strength

10 p1502 A72-25149

Optimal flexible ferrite keeper for ferromagnetic thin film memories performance improvement, noting requirements for high permeability, low loss factor and dielectric constant, etc

11 p1601 A72-25899

Dielectric and optical constants of p-type GaSb single crystals, interpreting singularities by energy bands diagram

11 p1689 A72-26485

Dielectric constant measurements of compressed gaseous and liquid oxygen for computing Clausius-Mossotti function

11 p1691 A72-26782

Coupled electroelastic vibrations of piezoceramic cylinders from polycrystalline electrostriction theory, taking into account mechanical and dielectric losses

14 p2132 A72-31117

Contaminated Langmuir probes LF admittance measurements in mercury vapor plasma, considering dielectric relaxation in insulating layers

15 p2241 A72-32516

Optical second harmonic generation and parametric oscillation.

17 p2594 A72-34566

Possible field expansions in open waveguides and resonators

17 p2515 A72-34829

Determination of the dielectric constants of microwave-striplines

17 p2530 A72-35429

Focusing of intense electromagnetic waves in ducts with saturating nonlinearity.

18 p2659 A72-36293

UHF and microwave dielectric properties of an amorphous semiconductor.

18 p2718 A72-36311

Series solution for electromagnetic wave propagation in radially and axially nonuniform media - Geometrical-optics approximation.

18 p2712 A72-37024

Model random medium with two kinds of dielectric layers stacked in arbitrary proportions, calculating electromagnetic wave propagation characteristics by transmission line analogy

19 p2767 A72-38613

Vector wave solution of light beam propagating along lenslike medium.

20 p2903 A72-39266

Quantum optics analysis of light propagation and photon flux fluctuations in medium with random dielectric constant inhomogeneities

20 p2932 A72-39378

Stationary expressions for scattering coefficients of rectangular waveguides with dielectric plugs constituting a finite planar array.

21 p3027 A72-40371

Dielectric slab surrounding medium gain effects on bound modes amplification via estimation of evanescent surface wave interactions in optical waveguide by perturbation theory

21 p3062 A72-40605

Partial differential equation solution for plane electromagnetic wave diffraction by infinite dielectric cylinder of arbitrary cross section

21 p3085 A72-41199

Calibration procedure to correct for the effects of dielectric containers in microwave plasma density measurements.

21 p3056 A72-41377

Reflection and refraction of radio waves from the ionosphere in presence of time-varying irregularities.

22 p3154 A72-42302

Analytical model for a polarizable medium at radio and lower frequencies.

22 p3155 A72-42467

Dielectric dispersion of irradiated BaTiO₃ near the phase transition.

22 p3215 A72-42934

Physical and electrical properties of thin-film barium titanate prepared by RF sputtering on silicon substrates.

22 p3215 A72-42999

Weakly divergent beam propagation of electromagnetic waves in statistically inhomogeneous nonlinear medium with dielectric constant dependence, using small perturbation method

23 p3263 A72-43426

Exact solution of the equations of molecular optics for refraction and reflection of an electromagnetic wave on a semi-infinite dielectric.

23 p3313 A72-43803

Longitudinal dielectric tensor for an electron gas in a uniform magnetic field.

23 p3321 A72-43808

The pressure dependence of the E2 reflectivity peak and of the dielectric constant in III-V semiconductors.

23 p3324 A72-44321

Scattering of obliquely incident waves by inhomogeneous fibers.

24 p3379 A72-44710

Propagation of the mutual coherence of optical waves in a random medium.

24 p3424 A72-44711

Degenerate electron gas self energy approximation by dielectric function, calculating quasi-particle and plasmaron properties

24 p3428 A72-44797

The effect of the subsurface on the depolarization of rough-surface backscatter.

24 p3380 A72-45635

Linear and nonlinear dielectric properties of crystals with tetrahedral structure

24 p3412 A72-45772

DIELECTRICS

NT RADOME MATERIALS

Plane electromagnetic wave scattering by imperfectly conducting cylinder with radially inhomogeneous dielectric coating, using phase shift method for evaluation

01 p0024 A72-10130

Dielectric cone feeds design for microwave antennas, presenting radiation patterns

01 p0029 A72-10675

Hertzian dipole radiation with impulsive currents in nondispersive dielectric half space

01 p0030 A72-10841

Multipole methods for electromagnetic scattering from conducting cylinder over dielectric half space, noting application to radar cross sections

01 p0030 A72-10842

Dielectric loaded cavity or waveguide slot antennas for telemetry applications, describing design and fabrication

02 p0192 A72-12157

Critical frequency computation for partially filled elliptical waveguide with dielectric rod

02 p0183 A72-12752

Plane electromagnetic wave reflection and transmission at moving boundary between two dielectric media

03 p0321 A72-13091

Axisymmetric rotational motion of electrically conducting fluid between dielectric disks in crossed electric and magnetic fields

03 p0399 A72-14012

Amorphous polymer dielectric luminescence and destruction under Q switched laser radiation with subthreshold power and picosecond pulses

03 p0369 A72-14071

Polarization and stress tensor characteristics as function of interaction between mechanical, thermal and electromagnetic processes in elastic isotropic dielectrics

03 p0390 A72-14103

Semiconductor-thermoplastic-dielectric hybrid IC's reliability, discussing interelement adhesive bonding properties and thermally induced strains effects

03 p0337 A72-14294

Dielectric materials for antenna system radomes, discussing electromagnetic wave propagation and climatic factors effects

03 p0381 A72-14362

Parallel polarized electromagnetic waves scattering by radially inhomogeneous isotropic dielectric cylinders, computing scattered field coefficients by Fourier least squares fit technique

04 p0485 A72-14413

Dielectric siphons, using weak polarization force density exerted on insulating dielectric liquids by nonuniform electric field

04 p0520 A72-14416

Book on metallic and dielectric antennas covering planar, cylindrical and plasma types for symmetrical, dipole and ring excitations

04 p0497 A72-14612

Dielectrophoresis force measurements and wedge shaped capacitor separation properties in satellite zero gravity conditions

04 p0549 A72-14988

Bandwidth widening of waveguide H-plane Y-circulator with cylindrical ferrite post coated by dielectric sleeve

04 p0499 A72-15244

Lens waveguides characteristics, analyzing Gaussian beams propagation through periodic system of thin plane-parallel nonlinear dielectric plates

04 p0489 A72-15389

Hf electromagnetic wave scattering and diffraction by smooth dielectric cylinder and sphere based on Lorentz excitation theory

04 p0490 A72-15397

Conical logarithmic foil type spiral antenna, presenting model of wavelength lenses used in dielectric rod antennas

04 p0500 A72-15408

Electrodynamical theory of artificial dielectrics based on rigorous solution for diffraction on system scattering elements consisting of periodical gratings formed by thin metallic strips

04 p0490 A72-15412

Electromagnetic surface field propagation on dielectric wedge excited by line source, using steepest descent method

04 p0491 A72-15419

Electromagnetic traveling plane wave diffraction from arbitrary angled dielectric wedge, investigating surface currents on walls

04 p0491 A72-15420

Thermal conductivity cell for dielectric materials powdered samples and thermal diffusivity and conductivity measurements, using line heat source principle

04 p0523 A72-15493

Cut-off frequencies of degenerate LSE and LSM modes in rectangular waveguides containing dielectric layers in H plane

04 p0502 A72-15526

Semiconductor-dielectric system for controlling space charge and valley population redistribution by external field

05 p0702 A72-16201

Bandwidth properties and design of shielded asymmetrical striplines filled by dielectric

05 p0636 A72-16340

Characteristic impedance formulas for rectangular waveguides with dielectric slab, discussing interference filter design application

05 p0627 A72-16343

Scattering of arbitrarily impinging monochromatic electromagnetic waves by thin infinitely long isotropic, dielectric and metal rods of elliptic cross section

05 p0628 A72-16412

High frequency electric field backscattering by plane electromagnetic wave incident on perfectly conducting sphere with radially inhomogeneous dielectric coating

05 p0630 A72-16621

E-plane dielectric slabs symmetrical loading effects on horn aperture efficiency enhancement from far field calculation [AD-738714]

06 p0781 A72-17347

Optimal design of directive dielectric loaded circular waveguide antenna for parabolic reflectors and radar detection

06 p0782 A72-17356

Heating dynamics of transparent dielectrics exposed to pulsed laser beam operating in free laser mode

06 p0825 A72-17697

Exact linear dielectric operator for stratified plasma streams with velocity gradients for diagnostics with electromagnetic waves

06 p0861 A72-17748

Data transmitting dielectric light waveguide production problems, noting light scattering and absorption losses due to glass material impurities

06 p0825 A72-17774

Two-layer dielectric loaded cylindrical antenna with wall airgap, calculating radiation pattern by boundary value approach

06 p0775 A72-18240

Parallel plate waveguide radiation into dielectric or plasma layer, using Hilbert formulation

06 p0791 A72-18734

Hollow and dielectric loaded waveguide modes solution, comparing finite element and finite dif-

ference methods based on coefficient matrices and computing time considerations

07 p0952 A72-18793

Dielectric substrate layer surface wave parasitic resonance effects on microstripline waveguide conductor

07 p0958 A72-18855

Metal clad dielectric slab waveguide for integrated optics, obtaining dispersion equation solution and propagation modes from simplified model

07 p0940 A72-19229

Linear and circular birefringence of low loss single mode glass fiber dielectric optical waveguide as function of length

07 p0940 A72-19232

Electromagnetic scattering of square pulse from lossy dielectric slab mounted on perfectly conducting planar ground surface

07 p0945 A72-19660

Circular semiinfinite dielectric rod antenna, determining near- and far-zone fields, gain and beamwidth under excitation by HE/sub 11/ hybrid mode

07 p0956 A72-19782

Wideband dual mode dielectric loaded horn antenna, discussing structure and radiation patterns

07 p0957 A72-19793

Circular and rectangular waveguide excited dielectric spheres as antenna feed, noting gain and polarization linearity

07 p0957 A72-19796

Anisotropic grounded dielectric or plasma layer motion effects on magnetic or electric current line source radiation patterns

07 p0946 A72-19802

Laser flare luminosity front displacements and atom density at surfaces of transparent dielectrics as function of pulse intensities

07 p1007 A72-20123

Kirchhoff method application to asymptotic solution of plane wave diffraction on dielectric conical shells, calculating electromagnetic field vector

08 p1131 A72-20931

Phased directional surface wave splitters and microwave and integrated optics elements based on single mode, dielectric and rectangular waveguides

08 p1131 A72-20935

Dielectric sulfur activated liquids for high productivity electroerosive machining of steels and metallic carbides, comparing with petroleum

08 p1174 A72-21034

Pulse energy and heat distribution in dielectric and metal during electroerosive machining

08 p1174 A72-21035

Heat exchange effects in thermal diffusivity measurements in dielectrics by plane temperature wave method, applying to rock and mineral studies

08 p1251 A72-21095

Electromagnetic wave propagation along open rectangular dielectric waveguide, deriving dispersion equations for surface waves propagation constants

08 p1136 A72-21739

Electromagnetic and plasma wave reflection at interface between moving dielectric medium and compressible plasma

09 p1364 A72-23243

Material dispersion contribution to signal envelope delay distortion in weakly guiding dielectric optical fiber waveguides

09 p1314 A72-23340

Energy transfer optimization in electromagnetic wave transmission through dispersive dielectric media

09 p1365 A72-23522

Gunn domain oscillations suppression by dielectric surface loading of transversely thin GaAs diodes

10 p1526 A72-24305

Wide rectangular low loss metal waveguide with dielectric layer on opposite walls, noting attenuation based on eigenwaves

10 p1451 A72-24585

Electromagnetic wave diffraction by dielectric steps in waveguides, calculating microwave scattered field by modified residue calculus technique

10 p1451 A72-24593

Microwaves propagation through circular waveguide partially filled with lossless cold electron plasma dielectric, presenting computed dispersion curves for waveguide and plasmaguide modes

10 p1522 A72-24677

Anomalous refraction maxima in bidirectional plane polarized radiant flux transmittances of roughened dielectric surfaces

[AIAA PAPER 72-302] 11 p1742 A72-25236

Multimode dielectric slab waveguide power coupling due to core-cladding interface irregularities, obtaining power distribution and radiation losses

11 p1603 A72-25270

Dielectrics breakdown under ultrashort neodymium laser pulses at fundamental and second harmonic frequencies

11 p1647 A72-25719

Microwave two reflector rectangular backfire antenna with dielectric surface wave structure as waveguide prolongation, obtaining far field radiation pattern

11 p1604 A72-25749

Linear antenna in anisotropic plasma with ion depletion, calculating reactance change due to surrounding dielectric layer thickness

11 p1593 A72-25949

Laser induced transparent dielectrics surface fracture mechanism determination based on electron microscopic photograph analysis and disturbed specular reflection under predischARGE conditions study

11 p1648 A72-26333

Thermoelastic stresses in solid transparent isotropic homogeneous dielectric under self-focused laser beam

11 p1648 A72-26334

Multilayer dielectric reflective coatings performance in solid state laser pumping systems

11 p1649 A72-26345

Ceramic dielectrics capacitors, considering perovskites and barium titanate physicochemical properties

11 p1702 A72-26545

Constitutive equations for nonlocal theory of polar elastic dielectrics interaction with quasi-static electric field, using variational principle

11 p1738 A72-26723

Ni powder artificial dielectric in waveguide transverse magnetic field, noting nonreciprocal nature of microwave attenuation and phase shift

11 p1607 A72-26786

Transparent dielectrics destruction by mode-locked laser ultrashort pulses, discussing filamentary defect presence indication of radiation self focusing

12 p1853 A72-27068

Surface wave propagation mechanism on dielectric bodies noting compatibility with physical properties involved with optical cables for commercial transmission systems

12 p1782 A72-27556

Solid state laser resonator inhomogeneous dielectric and mirror elements matching effects on Q factor and output power

12 p1822 A72-27609

Transparent dielectric surface photoelectric emission current under laser pulse illumination, noting correlation to surface treatment and damage threshold

12 p1822 A72-27613

Launching horn effect on radiation pattern of dielectric cone feeds, proposing wide angle sidelobe reduction via absorbent sheath

12 p1791 A72-27669

Metal-dielectric-semiconductor junction transistor HF response analysis by digital computer, deriving switching time as function of impurity concentration and electrode voltage

13 p1932 A72-29294

Plane and circular dielectric waveguides with thermal losses, considering transverse wave numbers behavior behind cut-off value and dispersion equations solution

14 p2086 A72-30797

Solar cells insulating dielectrics breakdown tests in dilute Ar plasma at positive bias voltages to 20 kV

14 p2140 A72-30926

Dielectric waveguide X band telemetry system for remote power and multiplexing applications in noisy electromagnetic pulse environment

14 p2087 A72-31047

Electron work function for metallic sphere and thin film on dielectric substrate as function of radius, thickness and dielectric constant

15 p2290 A72-31222

Magnetoelastic effects in elastic dielectric analysis based on continuum with single magnetic moment, noting magnetically saturated material

15 p2274 A72-31482

Constitutive equations of linear viscoelastic dielectrics, assuming small displacements, velocities and temperature independent memory functions

15 p2208 A72-32289

Epitaxial YIG film separated from conductive plane by thin dielectric layer, considering magnetostatic propagation dispersion and insertion loss

15 p2294 A72-32502

Ideally conducting and dielectric coaxial solids of revolution, investigating joint excitation by TM wave

15 p2209 A72-32658

Ferrite and dielectric element waveguide phase shifters with rectangular hysteresis loop, deriving differential phase and attenuation constants for wave propagation

15 p2202 A72-32662

Bidirectional optical scattering from dielectric materials of various pigmentation and surface roughnesses, obtaining cross section data to determine angular, spectral and polarization behavior

16 p2427 A72-33839

Natural frequencies of a cylindrical microwave cavity containing a coaxial cylindrical dielectric sample

17 p2513 A72-34334

The behavior of electromagnetic fields at edges. Integral equation for electromagnetic wave scattering by thin dielectric ring

17 p2526 A72-34379

Dielectric breakdown in electrical insulators used in thermionic converters.

17 p2496 A72-34593

Thermal analysis of high performance devices mounted on dielectric substrates.

17 p2527 A72-34677

Electron currents injected through dielectrics

17 p2529 A72-34753

Theory for the excitation of SHF elastic waves by multiple-film transducers / Allowance for the influence of metallic and dielectric layers/

17 p2529 A72-34843

Hollow dielectric waveguide for distributed feedback lasers.

17 p2564 A72-35346

Engineering approach to the design of tapered dielectric-rod and horn antennas.

17 p2530 A72-35362

Circular waveguides lined with artificial anisotropic dielectrics.

17 p2530 A72-35468

Propagation mode and scattering loss of a two-dimensional dielectric waveguide with gradual distribution of refractive index.

17 p2530 A72-35469

Ultrasonic wave generation in solids using transducer composed of high rigidity dielectric /polypropylene/ between two electrodes

18 p2691 A72-36402

Propagation of an electromagnetic shock discontinuity in a non-linear isotropic material.

18 p2712 A72-36992

Hypo-elastic dielectrics. I - Constitutive equations. II - Birefringence in simple shear.

18 p2720 A72-37043

Application of statistical methods to the study of the rigidity of a dielectric

18 p2720 A72-37116

An artificial dielectric lens suitable for high power applications.

18 p2671 A72-37148

Breakdown of some transparent dielectrics under the action of neodymium and ruby lasers in free light emission modes

19 p2810 A72-37542

Formation of fluorine-containing solid solutions based on barium titanate

19 p2845 A72-38407

Electrical properties of thick-film barium titanate dielectrics produced by flame spraying.

19 p2846 A72-38616

Paraxial electromagnetic wave packets diffraction on thin conducting periodic structures and dielectric plate, noting packet width and phase front curvature changes

19 p2767 A72-38653

Constitutive equations and optical yielding of anisotropic perfectly plastic dielectrics.

19 p2878 A72-38799

The lightning arrestor-connector - A new concept in system electrical protection.

20 p2889 A72-38989

Critical frequency computation for partially filled elliptical waveguide with dielectric rod

20 p2902 A72-39058

Amplification of acoustic surface waves under transverse magnetic field in coupled intrinsic semiconductor-piezoelectric systems.

20 p2960 A72-39703

Laser-induced damage in transparent dielectrics - The relationship between surface damage and surface plasmas.

21 p3062 A72-40241

Radiation patterns of dielectric antenna of size comparable to radiator wavelength in air, discussing narrow band and broadband configurations

21 p3030 A72-40528

Dielectric coating effects on millimeter wave diffraction pattern of gratings, noting sharp anomalous dips in transmission intensity for P and S polarizations

21 p3031 A72-40604

Mathematical model for dielectrics with time dependent polarization, noting relaxation time distribution function

21 p3085 A72-41074

Deposition of dielectric films on the electrodes of an electrostatic gyroscope

21 p3059 A72-41814

Liquid dielectrics specific heat determination by adiabatic calorimeter with monotonic heating

21 p3059 A72-41819

Radiation patterns of wideband horn antenna loaded by dielectric belt, noting satellite and terrestrial radio relay applications

21 p3036 A72-41832

Radiation of electron bunches passing through a dielectric plate in a waveguide

21 p3036 A72-41842

Diffraction of an electromagnetic wave by a noninfinitely conductive cylindrical object of arbitrary cross section

22 p3153 A72-41991

Diffraction by an infinite corner reflector transversely loaded by concentric dielectric slabs.

22 p3159 A72-42301

Diffraction of plane electromagnetic wave at a corrugated dielectric surface

22 p3155 A72-42662

- Velocity-dependent multiple scattering by two thin cylinders. 24 p3381 A72-45641
- Radiation from an open-ended waveguide with extended dielectric loading. 24 p3381 A72-45643
- Transparent dielectrics destruction by mode-locked laser ultrashort pulses, discussing filamentary defect presence indication of radiation self focusing 24 p3432 A72-45721

DIENCEPHALON

- Nervous respiratory disorder in patients with diencephalic and vegetative vascular syndromes, discussing arterial hypoxemia development and resulting oxygen insufficiency 02 p0160 A72-12012
- Changes of the catecholamine content in the brain of albino rats under overstrain caused by running in a rotating drum 19 p2757 A72-38034

DIES

- Eccentric circular ring elastic contact with rigid symmetric dies under equal diametrically opposite loads 05 p0738 A72-16329
- Intrusion of pointed dies into cross section circumference sections of semiinfinite cylindrical shell, solving shell theory equations without allowance for friction effects 05 p0739 A72-16586
- Dynamic contact problems of die or bandage on elastic layer surface or cylinder, analyzing vibrationally induced elastic waves 10 p1558 A72-24779
- Die-casting machine design trends, considering uses of elbow lever and hydraulic systems and programmed control 16 p2399 A72-34142
- Fabrication of shaping cermet elements of die-casting molds for plastics by the hydrostatic pressing method 22 p3182 A72-42199

DIESEL ENGINES

- Mathematical model of nitric oxide formation by fuel droplet burning above fuel critical pressure, applying to diesel engine operations 17 p2511 A72-34901
- Improvement of the anticorrosion properties of water-containing hydropurified diesel fuels with the aid of saltless additions 17 p2596 A72-35177

DIETHYL ETHER

- Differential neurophysiological and psychological effects of subanesthetic concentrations of cyclopropane, diethyl ether, methoxyflurane and ethrane in conscious man 04 p0480 A72-15220

DIETS

- Apollo 14 food system, describing new items, improvements in production methods, packaging and preparation with emphasis on rehydratable foods 02 p0166 A72-11706
- Biochemical and physiological effects of Apollo flight diet, noting no significant variations in serum electrolytes, endocrine values, body fluids and hematologic parameters 02 p0167 A72-11707
- Protein-rich food substitute from microalgae cultures for human nutrition, describing experimental production, protein value determination, special diets and food shortage relief 06 p0768 A72-18159
- Gaseous nitrogen production in humans under steady-state conditions, relating expired nitrogen minute volume increase after protein consumption to possible gastrointestinal and metabolic effects 08 p1122 A72-20882
- Dietary lipid effect on platelet adhesion and aggregation, blood coagulation and fibrinolysis and relation to atherosclerosis and thrombosis 08 p1117 A72-21543
- Blood lipid levels and dietary habits in atherosclerotic and healthy subjects, showing lipid and glucose metabolism disturbance increase in coronary cases 08 p1117 A72-21546
- Dietary and pharmacological treatment of atherogenic hyperlipidemias from lipid-sugar balance and drug efficacy studies 08 p1117 A72-21547
- Menu selection for SKYLAB astronauts by computer technique based on mixed integer programming code, using measure of pleasure lists 12 p1769 A72-27442
- Dihydroxyacetone (DHA) as nutrient in growing rats diet, showing unsuitability of regenerated DHA-containing formose mixtures for space crew diets 16 p2354 A72-33371
- Weightlessness effects on calcium and electrolyte metabolism from measurements during Gemini 7 flight, using dietary control and excreta collection techniques 16 p2355 A72-33552

- Rat pulmonary lipid metabolism during feeding and fasting from studies of lung lecithin half life after C-14/1/palmitate and H-3/U/glucose injection 18 p2651 A72-36573
- Dietary regulation of fatty acid synthesis in rat liver and hepatic autotransplants. 19 p2757 A72-38147
- Relationship of sodium deprivation to +Gz acceleration tolerance. 24 p3377 A72-45653

DIFFERENCE EQUATIONS

- Difference analog of nonlinear hydrodynamic boundary value problem from Navier-Stokes steady state theory 01 p0050 A72-10576
- Elliptic and parabolic partial differential difference equations solution using modified random walk Monte Carlo technique 01 p0093 A72-10858
- Thin shell creep and plasticity analyses reduced to linear programming problem by functionals and finite difference equations 02 p0290 A72-11622
- Difference schemes for first and third order Poisson equation in polar, cylindrical and spherical coordinates 02 p0252 A72-11735
- Difference schemes for continuous computation of supersonic steady gas flows with internal compression shock waves 02 p0150 A72-11737
- Nonstationary temperature field determination in stream turbine casing-connector nozzle by difference method based on heat balances, comparing results with electric analog studies 02 p0303 A72-12534
- Differential and difference equations approximate solutions in finite state machine form, developing adaptive gain changer model in aircraft stability control system 03 p0338 A72-13164
- Elasticity theory Lamé difference equations system solved by two-step iteration procedure based on Samarskii regularization 03 p0447 A72-13727
- Matricial difference schemes based on numerical methods characterized by approximations for integrating stiff systems of differential equations 04 p0540 A72-15375
- Mountain barrier and convective area minimum size determination for numerical forecasting models, reducing primitive equations system to advection difference equation 04 p0544 A72-15459
- Group velocity and numerical error propagation in partial differential and finite difference equations of gas dynamics [AIAA PAPER 72-153] 05 p0652 A72-16952
- Elasticity theory equations for orthotropic plate bending, derived from combination variational and difference-differential procedures 05 p0741 A72-17144
- Nonlinear difference schemes for quasi-linear transfer equation in gas dynamics and shock wave computations 07 p0971 A72-20085
- Stability and local error of difference formulas derived from characteristic polynomial for first order ordinary differential equation solution 07 p1028 A72-20472
- First boundary value problem solution of nonlinear Poisson equation in rectangular region by finite difference equations approximation 08 p1198 A72-20902
- Two dimensional two step difference scheme for shock wave interaction with cylinder in supersonic flow 08 p1150 A72-21443
- Difference equation inequalities in sampled data system stability analysis, discussing solution asymptotic behavior 09 p1342 A72-23252
- Explicit difference schemes for hydrodynamic equations with no stability condition constraints on time step 09 p1295 A72-23491
- Linear difference equations solved by indefinite Z transformations technique using Cramer rule for simultaneous algebraic equations 11 p1678 A72-26664
- Inverse eigenvalue problem numerical solution for matrices and difference and differential equations, obtaining algorithms for parameters estimation 11 p1679 A72-26955
- Analytical solution to difference stability equations, evaluating adequacy of difference scheme for circular cylindrical shell and rectangular hinged plate under compression 13 p2053 A72-28389
- Spectral stability characteristics of difference schemes for hyperbolic differential equations in gas dynamics involving triangular and tetragonal bases 15 p2178 A72-31444

- Liapunov functions for nonlinear autonomous difference equations stability analysis, defining difference gradient, principal sum and definite sum 15 p2265 A72-32802
- Difference scheme for initial value problem of one dimensional Vlasov equation for collisionless electron plasma with homogeneous ion background 16 p4434 A72-33006
- Recursive bootstrap maximum likelihood estimators algorithms for identification of process modeled by stable linear difference equation under additive output measurement noise 18 p2672 A72-36056
- A through-type counting method for two-dimensional and spatial supersonic flows. II 18 p2642 A72-36810
- Sufficient conditions for two stage stochastic optimal control difference approximation by finite dimensional extremum problem sequences 19 p2777 A72-37318
- Conservative difference schemes for linear and nonlinear problems of mathematical physics, discussing gas dynamics and magnetogasdynamics problems requirements 19 p2833 A72-37383
- Structure of absolutely approximating and absolutely correct difference schemes 19 p2824 A72-37384
- Large particle method differential approximations in difference equation schemes for gas dynamics problems, discussing viscous effects and solution stability 19 p2745 A72-37385
- Numerical methods of solving weather forecasting problems 19 p2828 A72-37386
- Analysis of discrete automatic control systems with variable parameters by the method of orthogonal expansions. I, II 19 p2778 A72-37438
- A stability theory for perturbed difference equations. 19 p2826 A72-38249
- Economical difference schemes for solving the heat-conduction equation in polar, cylindrical, and spherical coordinates 19 p2883 A72-38847
- Numerical gas dynamic calculations by difference method with two moving curve families, noting water mass impact on plane solid wall 19 p2789 A72-38851
- Difference schemes with a divergent operator for a general system of second-order hyperbolic equations 19 p2828 A72-38854
- Fractional steps method of difference schemes for approximate numerical solution of parabolic and elliptic initial boundary value problems 20 p2945 A72-39327
- Analog model for two dimensional heat conduction equation, noting electrical networks for one dimensional difference equations solution 21 p3127 A72-40179
- Classes of uniqueness of solutions to a boundary value problem in an infinite layer for systems of linear difference-differential equations 21 p3074 A72-40257
- Necessary and sufficient conditions for the absolute asymptotic stability of linear systems of differential equations with constant delay 22 p3198 A72-42143
- Asymptotic method for nonlinear wave systems of periodic structure 22 p3155 A72-42657
- Achievement of given motion by impulse correction under arbitrary disturbances/difference models/ 23 p3313 A72-44044
- Application of the 'vanishing viscosity' method to improve stability conditions for higher-accuracy difference schemes used with the heat-conduction equation 23 p3356 A72-44046
- A difference method for plane problems in magnetoelastodynamics. [ASME PAPER 72-APM-A] 23 p3321 A72-44051
- On an augmentation of the error made by numerical treatment of second-order conservative point transformations 24 p3419 A72-45071
- Straightforward difference scheme for nonlinear parabolic equations in polar coordinates 24 p3420 A72-45649

DIFFERENTIAL ALGEBRA

- U DIFFERENTIAL CALCULUS
U MATRICES [MATHEMATICS]

DIFFERENTIAL AMPLIFIERS

- Acceleration measurement by reference mass displacement in spherical cavity, considering triaxial accelerometer with capacitive sensors and differential amplifier 22 p3175 A72-41929

DIFFERENTIAL ANALYZERS
U ANALOG COMPUTERS

DIFFERENTIAL CALCULUS

Network sensitivity analysis emphasizing first, higher and mixed higher derivatives computation and iterative synthesis techniques

02 p0197 A72-12114

Flight mechanics derivative transformations by matrix methods for changing coordinate or independent variable systems

05 p0612 A72-16706

Holomorphic rational functions involving error bounds without derivatives solution by numerical differentiation procedure

14 p2126 A72-30709

Signal with bounded spectrum, obtaining higher derivatives by reduction to stationary random process filtering problem solvable with Kolmogorov-Wiener and Kalman-Bucy techniques

15 p2207 A72-32171

Necessary and sufficient conditions for differentiable non-scalar-valued functions to attain extrema

19 p2826 A72-38244

Computer algorithm for breakpoints and forcing functions determination for optimal curve fitting by piecewise differential approximation

24 p3419 A72-45632

DIFFERENTIAL EQUATIONS

NT BIHARMONIC EQUATIONS

NT BLASIUS EQUATION

NT BURGER EQUATION

NT CHANDRASEKHAR EQUATION

NT DUFFING DIFFERENTIAL EQUATION

NT ELLIPTIC DIFFERENTIAL EQUATIONS

NT FALKNER-SKAN EQUATION

NT FOKKER-PLANCK EQUATION

NT GAUSS EQUATION

NT LAME WAVE EQUATIONS

NT LIOUVILLE EQUATIONS

NT PARABOLIC DIFFERENTIAL EQUATIONS

NT PARTIAL DIFFERENTIAL EQUATIONS

NT POISSON EQUATION

NT VLASOV EQUATIONS

NT VORTICITY EQUATIONS

Integrability of rotating satellite differential equation of motion in axially symmetric gravitational field

01 p0122 A72-10008

Concentration distribution in turbulent flow as function of velocity field, deriving differential equations from characteristic functionals to describe diffusion process

01 p0049 A72-10190

Kalman filtering process digital simulation by numerical integration of matrix differential equations describing linear system random process model and optimal filter

01 p0024 A72-10225

Differential equations derived for elastic-plastic behavior of rotationally symmetric shells, approximating in finite difference forms and solved by elimination method

01 p0138 A72-10394

Controllability of dynamic systems with motion described by nonlinear differential equations

01 p0045 A72-10500

Stochastic differential equations vector solution by two-time method, applying to random harmonic oscillators and wave propagation in random media

01 p0093 A72-10510

Step-by-step algorithmic numerical solution for nonlinear Volterra integro-differential equation, considering convergence

01 p0093 A72-11105

Sixth order nonlinear differential equation isolated equilibrium point stability determination, constructing Liapunov function

01 p0094 A72-11125

Book on integral transforms for solving ordinary and partial differential equations in applied mathematics covering Laplace, Fourier and Hankel transforms

01 p0094 A72-11274

Redundancy with repair for system mean time to first failure, presenting differential equation coefficients for Markov process

02 p0236 A72-11556

Asymptotic methods application to differential equations in nonlinear solar convection theory at high Rayleigh number, noting discrepancy from numerical integration

02 p0276 A72-11644

Aerodynamic behavior of thin jet-flapped airfoil, investigating integrodifferential equation solution

02 p0149 A72-11669

Uniformly and asymptotically stable solutions to linear Volterra integrodifferential equation system, discussing Liapunov stability

02 p0252 A72-11997

Differential equations solution for turbulent two dimensional jet flows bounded by parallel planes

02 p0156 A72-12000

Soviet book on theory of differential equations with deviating argument covering step methods, existence and uniqueness theorems, solutions stability, approximations, etc

02 p0252 A72-12124

Stability properties of functional differential system solutions, discussing Liapunov functions construction

02 p0252 A72-12173

Micropolar elastic theory axial symmetric problems, deriving differential equations for elastic potential and half space

02 p0260 A72-12239

Half range differential approximation for spherically symmetric radiative transfer in concentric spheres with and without internal heat sources

02 p0302 A72-12259

Contact stress between half plane and elastic cover plate, reducing problem to Prandtl type integrodifferential equation with Hilbert kernel

02 p0294 A72-12433

Optimal trajectory in phase space, deriving differential motion equations with Euler-Lagrange method

02 p0199 A72-12880

Bogoliubov-Mitropolski-Hale integral manifold theorem for perturbed nonlinear differential equations, using generalized variation of parameters formula

03 p0381 A72-12907

Airfoil theory singular integrodifferential equation reduction to integral equations with quasi-regular and regular kernels, applying to jet flapped wing problem

03 p0381 A72-12987

Differential and difference equations approximate solutions in finite state machine form, developing adaptive gain changer model in aircraft stability control system

03 p0338 A72-13164

Faraday rotation as perturbation for analytic solution of system of differential equations for line formation in inhomogeneous magnetic fields

03 p0427 A72-13295

Nonlinear differential second order equation system development for gyroscopic coupling of forced nonlinear oscillators

03 p0389 A72-13631

Nonhomogeneous media electrodynamics with varying permittivity and permeability, solving nonstationary equations by differential operators

03 p0389 A72-13654

Electric and magnetic field scattering on ellipsoidal inhomogeneities in circular waveguides from integrodifferential equation derived expressions

03 p0322 A72-13735

Small parameter linear differential systems approximate solution, noting Liapunov reduction as particular case

03 p0389 A72-13785

Simple wave interaction solutions for nonlinear plane k-waves of nonelliptic quasi-linear differential equations using Riemann invariants

03 p0389 A72-13885

Solution stability of linear differential equations systems with harmonic coefficients, using Jordan canonical forms and perturbation method

03 p0382 A72-13918

Differential equations of motion for stable member of three-axis gyro stabilized platform

03 p0387 A72-14190

Periodic solution existence for second order differential equation

03 p0382 A72-14250

Nth order linear differential inequalities reduction to first order, permitting Chaplygin theorem infinite applicability limit and solution by quadratures

03 p0382 A72-14313

Rotational symmetry solutions to differential equations of stationary barotropic or axisymmetric incompressible flow

03 p0344 A72-14345

Reproduction by substitutions of ordinary differential equations integrable in elementary and special functions

03 p0383 A72-14373

Transformation of differential equations describing interaction between electric arc and gas flow by taking temperature as independent variable, considering Laval nozzle example

03 p0344 A72-14392

Mass service process differential equations with losses, annihilation and multiplication processes, demonstrating unique solution existence

04 p0538 A72-14627

Steady heat conduction boundary value problem solution by generalized Kantorovich method of reduction to ordinary differential equations

04 p0595 A72-14642

Nonlinear differential equations systems solution by A-stable numerical integration techniques

04 p0539 A72-14732

Gyroscopy precession equations over infinite time interval from conditions based on solutions to differential equations with small parameters at derivatives

04 p0521 A72-15001

Shooting method and contraction mapping application to existence-uniqueness theorem derivation for numerical solution of second order delay differential equations boundary value problems

04 p0539 A72-15042

Modified quasi-linearization algorithm for solving nonlinear two-point boundary value problems based on performance index and cumulative error in differential equations

04 p0539 A72-15045

Closure approximation in hierarchy stochastic differential operator equations in statistical mechanics

04 p0540 A72-15257

Matricial difference schemes based on numerical methods characterized by approximations for integrating stiff systems of differential equations

04 p0540 A72-15375

Feld modification for integrodifferential equation solution for voltage on exponentially narrow waveguide slit, discussing further changes in method

04 p0501 A72-15409

Iterative method to solve planetary boundary layer differential equations, overcoming difficulties of previous approaches

04 p0519 A72-15460

Stress and strain approximate analysis for thin elastic shells by rational derivation of two dimensional differential and constitutive equations

[AD-745612] 04 p0592 A72-15506

Differential equations of motion construction from given manifold, determining functional minimization of solution

04 p0550 A72-15544

One-dimensional compression/expansion shock waves propagation in elastic nonheat conducting bodies, deriving differential equation for shock amplitude time rate of change

04 p0592 A72-15547

Book on similarity laws and modeling covering dimensional analysis, transformations, differential equations, gas flows and nonequilibrium processes

04 p0513 A72-15675

Third order nonlinear van der Pol oscillating systems, discussing digital computer verification for existence of stable limit cycles in state space trajectory plots

05 p0639 A72-15806

Stationary nonlinear dynamic systems identification, using modified differential approximation technique

[ASME PAPER 71-WA/AUT-11]

Superposable and self-superposable MGD flows from nonlinear differential equations, considering entropy, flow velocity and magnetic field strength

05 p0694 A72-16030

Differential equations systems formulation and numerical integration in gravitational problem of stellar n-bodies, discussing close approaches

05 p0713 A72-16052

Vibration mode shapes and frequencies determination by finite element method using consistent and lumped masses formulations in differential equation solution, considering convergence rate

[AD-739820] 05 p0736 A72-16086

Thermal stresses in thin symmetrically heated disk with time and temperature dependent mechanical properties, deriving integrodifferential equation defining stress function

05 p0740 A72-16624

Minimum weight panel designs subject to supersonic flutter constraint, approximating governing differential equations by difference equations

[AIAA PAPER 72-170] 05 p0741 A72-16908

Ordinary differential equations convergent solutions growth estimates, computing error function asymptotic growth rate

05 p0683 A72-17000

Optimal control of systems described by stochastic differential equations with delayed argument, using Kozhevnikov mean principle

05 p0683 A72-17140

Elasticity theory equations for orthotropic plate bending, derived from combination variational and difference-differential procedures

05 p0741 A72-17144

Longitudinal instability of electron beams interacting with passive resonator, considering Landau damping influence by linear differential equations of motion solution

05 p0701 A72-17243

Liapunov functions generation, using auxiliary functional differential equations table for invariance determination

06 p0838 A72-17378

Necessary and sufficient equilibrium stability conditions for differential equations systems with quasi-homogeneous right sides

06 p0838 A72-17382

Integro-differential initial value problem solution, differentiating for time variable and integrating for space variable

06 p0838 A72-17383

Backward differentiation formulas application to differential algebraic equations, obtaining efficient algorithm as compared to Gear-Nordsieck method

06 p0779 A72-17479

Nonlinear differential equation of second order, investigating integrability criteria

06 p0838 A72-17553

Ordinary differential equations with highest derivatives multiplied by small parameters, discussing initial value problems and use of implicit function theorem methods

06 p0839 A72-17628

Time independent or periodic Hamiltonian conservative differential equations, studying open, oscillating, limited and abnormal trajectories

[ONERA, TP NO. 1046] 06 p0877 A72-17661

Soviet book on qualitative methods in celestial mechanics covering differential equations of motion averaging schemes, Newton type convergence method, three body problems, etc

06 p0879 A72-17821

Ordinary differential equation eigenvalues, presenting method based on interior zeros of one parameter solutions to second order equation with one endpoint boundary condition

06 p0839 A72-17883

Discrete stochastic differential games with quadratic payoff function, deriving deterministic, randomized and game optimal control strategies

06 p0793 A72-17956

Spectral properties of differential displacement equations system describing natural vibrations of shell of revolution with m waves along parallel

06 p0897 A72-17990

Numerical integration of N-body problem in integrodifferential equations, using integrals as constraints and for correction application in least squares procedure

06 p0885 A72-18074

Finite difference schemes with splitting operator for mixed type differential equations systems, considering solutions stability and convergence properties

06 p0839 A72-18117

Differential equations describing dynamic behavior of unsteady plane exothermic reaction front in gasless system

06 p0903 A72-18204

Stochastic differential equations for a posteriori probability distribution in problems of Markov process parameter estimation, adaptive filtering and signal detection

06 p0794 A72-18301

Perturbation theorems proving for nonlinear systems of differential equations with integral solution of linearized equation

06 p0840 A72-18739

Numerical algorithm for Galerkin solutions of nonlinear ordinary differential equations in dynamic system applications

07 p1025 A72-18785

Second order differential equations system solution in convergent integrals, describing solution limit in vector form as special case of linear system solution property

07 p1026 A72-18815

Algorithm for constructing linear and nonlinear differential and algebraic equations of state variables of nonlinear electronic circuits

07 p0958 A72-18846

Differential equations system with right side dependent on constant parameters, obtaining approximate numerical solution by maximum principle of control theory

07 p1026 A72-18967

Differential equation initial value problem solution error bounds construction by interval arithmetic to guarantee exact solution inclusion

07 p1026 A72-18968

Sensitivity functions for differential equations describing aircraft perturbed motion, noting dependence on time derivatives, system parameters and coordinates

07 p1032 A72-18977

Book on asymptotic behavior and stability in ordinary differential equations covering linear and nonlinear systems, Liapunov and analytical-topological methods

07 p1026 A72-19184

Real time near optimal closed loop control solution to fixed time nonlinear differential game by periodically updating to two point boundary value problem

07 p1027 A72-19278

Singular surfaces for time optimal control in zero sum differential games between two aircraft in three dimensional space, assuming spherical acceleration vectogram

07 p1027 A72-19279

Singular perturbation of absolute stability of Lure-Postnikov nonlinear systems described by differential equations with small parameters at higher derivatives

07 p1027 A72-19293

Averaging techniques for nonlinear integral and integrodifferential equations, considering standard equations with and without rapid and slow variables, asymptotic series application to unsolved problems

07 p1027 A72-19609

Algebraic algorithm for reducing to state form multivariable control systems defined by linear constant differential operators

07 p0950 A72-19702

Control theory of dynamic multiconnected systems with differential operators, time lags and hereditary components

07 p0962 A72-19721

Multiple point boundary value problem with linear integrodifferential equation simplification

07 p1028 A72-19983

Asymptotic method applications to differential equations solution construction and stability analysis and to stochastic systems

07 p1028 A72-20206

Interactive simulation language-8 for minicomputer and programming procedures for nonlinear differential equations solution, considering integration step size and computational accuracy and speeds

07 p0951 A72-20334

Linear first order differential equation transient response computer simulation using transition matrix method

07 p1028 A72-20340

Stability and local error of difference formulas derived from characteristic polynomial for first order ordinary differential equation solution

07 p1028 A72-20472

Transcendental series solution of Chini-Painleve nonlinear differential equations describing vehicle and meteorite oscillation during planetary atmospheric entry

07 p0964 A72-20594

Goodman-Lance method of adjoints extension for solving boundary value problems of nonlinear differential equation systems

08 p1197 A72-20786

Coefficients estimation in nonlinear differential equations by direct integration followed by unconstrained nonlinear programming

08 p1197 A72-20854

Class of homogeneous polynomial solutions to differential equations of motion of elastic body

08 p1242 A72-20912

Perturbed motion differential equations for stability and integration problems in mechanics

08 p1205 A72-20964

Switching characteristics of MOS channel transistors, solving nonlinear differential equations describing current and potential distribution

08 p1140 A72-21267

Transformation of integrodifferential equation of motion of heavy solid body about fixed point

08 p1207 A72-21341

Polynomial solutions to integrodifferential equation of motion of solid body with fixed point for Lagrange conditions

08 p1207 A72-21342

Algebraic invariant relation of integrodifferential equation of motion of solid body about fixed point for Hess conditions, proving uniqueness

08 p1207 A72-21344

Solutions existence for algebraic invariant relation to integrodifferential equation of motion of solid body about fixed point in trigonometric and exponential polynomials class

08 p1207 A72-21346

Solutions existence for nonlinear invariant relation to integrodifferential equations of motion of solid body about fixed point

08 p1207 A72-21347

Solutions existence conditions for integrodifferential equation of motion of solid body about fixed point

08 p1207 A72-21349

Integrodifferential equation exponential solutions for body motion about fixed point

08 p1208 A72-21353

Nonlinear differential equations system stability conditions for arbitrary initial perturbations of zero solution, using Liapunov functions

08 p1199 A72-21461

Ordinary linear differential equation boundary value problem solution in form of asymptotic series in powers of small parameter

08 p1199 A72-21462

Finite difference method explicit solution of Cauchy problem for system of heat conduction differential equations

08 p1254 A72-21464

Operator approach solution to boundary value problems with infinite defect for differential equations with deviating argument, considering Fredholm alternative validity and compressed mappings application

08 p1199 A72-21465

Optimal controllers analytic design for linear steady controlled differential equations system

08 p1145 A72-21467

Nonlinear system of differential equations for gravity perturbation on geometrical form of thin axisymmetric cavity in heavy fluid

08 p1151 A72-21705

Asymptotic method solution for boundary value problems for nonlinear differential equations describing transonic and slow supersonic flow past thin bodies

08 p1108 A72-21709

Orthotropic hinged cylindrical shell stability under uniform external pressure, deriving linearized three dimensional differential equations

08 p1246 A72-21711

Differential equation solution for plane self focusing and one dimensional self modulation of waves interacting in nonlinear media

08 p1209 A72-21718

Asymptotic almost periodic differential equations solved by introducing semiseparated conditions concept

09 p1340 A72-22246

Ordinary differential operators eigenvalues calculation, noting numerical integration scheme for initial value problem

09 p1340 A72-22461

Power series solutions to transition and matrix covariance differential equations, obtaining truncation error bounds and polynomial approximations

09 p1341 A72-23093

Ordinary differential and functional equations - Conference, Kyoto, Japan, September 1971

09 p1341 A72-23251

Functional analysis techniques for existence of holonomic solutions to linear differential equation systems with singular points

09 p1342 A72-23254

Equivalence of integral equation form and infinite system of linear equations with eigenvalue localization, applying to linear ordinary differential equations

09 p1342 A72-23367

Matrix notation for replacing vector analysis in control theory by introduction of differential operators similar to Hamiltonian operator

09 p1352 A72-23369

Filtration and extrapolation of multivariable random processes described by linear differential equations system, examining adaptive filter synthesis

09 p1283 A72-23436

Differential equations solutions stability for physical discrete systems with delayed argument, impact excitation, variable mass or structure, disturbances or weak couplings

09 p1343 A72-23601

Applied nonlinear mechanics problems solutions by variable scale method, choosing transformations for linearization of differential equations

09 p1343 A72-23602

Dynamic systems stability problems, differential equations linearization and random processes

09 p1343 A72-23603

Increased accuracy cubic spline approximation to two-point boundary value problems for differential equation, noting truncation error

10 p1502 A72-23722

Near optimal closed loop control laws for fixed time pursuit-evasion differential game between two aircraft in vertical plane, using dynamic modeling

10 p1421 A72-23805

Differential equations similarity analysis, using Lie infinitesimal contact transformation group as search method for other possible transformation groups

10 p1503 A72-23922

Third order nonlinear differential equation invariants use to obtain integrable forms

10 p1504 A72-24053

Lie transformations for perturbed canonical system of differential equations solution, proposing parameter square root series development for resonance problems of celestial mechanics

10 p1536 A72-24119

Perturbation method for stability boundaries of Hill equation with three independent parameters

10 p1505 A72-24190

Markov processes for local diffusions defined by second order differential operator delta with Holder coefficients on manifold

10 p1505 A72-24201

Structural design systematology of statics and dynamics numerical approximate procedures based on variational principles and differential equations [SMRT PAPER M 7/4]

10 p1505 A72-24397

Differential games with deviation from encounter, considering strategies for continuous, programmed and discontinuous controlled motion onto given set

10 p1511 A72-24426

Analog simulation of hyperbolic differential equations with split boundary conditions, comparing to digital solutions to nonlinear flow

10 p1445 A72-24454

Dynamic logic control systems theory based on axiomatic concepts of models, deriving conditions for existence and uniqueness of solution for differential logic equations

10 p1457 A72-24636

Approximate model to reduce differential equation order for linear system of series connected elementary aperiodic components with different time constants

10 p1457 A72-24753

Transient calculation method for electric drive units described by first and second order differential equations, using special transformation for integral curve curvature determination

10 p1423 A72-24754

Boundary value problems for overdetermined elliptical systems of differential equations with arbitrary sized rectangular matrix

10 p1506 A72-24777

Statistical linearization of stochastic differential equations for optimal terms in mean square distance

10 p1506 A72-24993

Freely supported rectangular plate flexure under arbitrarily distributed load, obtaining differential equations solution in trigonometric polynomials

10 p1559 A72-24996

Oscillation modes and stability region of harmonic oscillators with homogeneous nonlinear rheological differential equations of motion

10 p1513 A72-24998

Optimal control of linear stochastic feedback systems described by functional differential equations

10 p1458 A72-25145

Predictor-corrector method for stiff linear differential equations, considering truncation error estimation and system stability

11 p1675 A72-25272

Nonlinear differential equations cycle properties and frequency, using Leray-Schauder theorem for cycle existence proof

11 p1675 A72-25325

Sufficient conditions for existence, uniqueness and finite-dimensional approximation of solution to first order infinite-dimensional vector differential equation

11 p1676 A72-25357

Geometric interpretation of solution existence for nonlinear ordinary differential equations with linear and nonlinear boundary conditions, analyzing funnel of solutions

11 p1676 A72-25503

Asymptotic behavior of unperturbed linear and nonlinear perturbed functional differential equations

11 p1677 A72-25524

Accuracy improvement of nonlinear systems phase trajectories graphic construction, noting second order ordinary differential equations solution

11 p1733 A72-25547

Characteristic finite difference method for solution of two dimensional wave equation represented by one parameter differential systems

11 p1677 A72-25863

Minimum time thrust start-up of nuclear rocket as optimal control problem with integrodifferential constraints, using Pontryagin maximum principle and calculus of variations

11 p1685 A72-25870

Equilibrium stability of hyperelastic bodies under finite strain, deriving differential equations and boundary conditions of critical equilibrium states

11 p1686 A72-25916

Linearization and Liapunov stability analysis of nongyroscopic holonomic conservative dynamic differential equations system

11 p1677 A72-25979

Oscillation criteria for fourth order differential equation conjugate point location relationship in terms of existence of solution with two double zeros

11 p1678 A72-26159

Finite difference approximation of eigenvalues of singular differential operators in Hilbert space

11 p1678 A72-26556

Inverse eigenvalue problem numerical solution for matrices and difference and differential equations, obtaining algorithms for parameters estimation

11 p1679 A72-26955

Error bounds relationship to norm in approximate numerical solutions of initial value problems for ordinary differential equations

11 p1679 A72-26957

Linear multistep methods with variable matrix coefficients for asymptotic numerical integration of ordinary differential equations system

11 p1679 A72-26960

High order explicit Runge-Kutta method for linear autonomous systems of differential equations, using interpolation formulas integration

11 p1680 A72-26962

Laplace-Carson transform solution for integrodifferential equation of motion for droplet suspended in viscous gas slipstream

12 p1796 A72-27093

Equation difference minimization techniques for ordinary nonlinear differential equations approximate periodic solution generation, noting error bounding procedure validity

12 p1836 A72-27240

Heat conductivity differential equation solution by hydraulic model system, facilitating temperature values conversion into electrical quantities for hybrid computer

12 p1888 A72-27301

Gravitational many body problem differential equation system formulation and numerical integration

12 p1874 A72-27902

Neuron networks dynamic behavior in terms of linear differential equations for membrane potential changes and neuron threshold

12 p1772 A72-27925

Variational problems in automatic control theory, presenting existence theorems for solution of boundary value problems for nonlinear differential equations with deviating argument

12 p1837 A72-27995

Lie group theory application to linear differential equations of motion with variable parameters, considering flight vehicle example

12 p1847 A72-28127

Flight vehicle motion described by linear differential equations with variable parameters, discussing programmed optimal control solution by functional analysis

12 p1755 A72-28128

Thin circular plate free vibrations with mixed boundary conditions from differential equations for vibration modes of circular isotropic plate in dimensionless polar coordinates

13 p2053 A72-28395

Iterative solution of coupled nonlinear differential equations under boundary conditions for flow and heat transfer of Rivlin-Ericksen fluid between rotating parallel disks

13 p1986 A72-28881

Nonlinear differential energy equation of static state stellar atmospheres with radiation and heat conduction terms

13 p2036 A72-28890

Homogeneous difference schemes stability for ordinary differential equation of arbitrary order with discontinuous coefficients, analyzing positive definite operators class

13 p1986 A72-29076

Coefficient stability of homogeneous difference schemes using irregular networks for fourth order differential equation with discontinuous coefficients

13 p1986 A72-29081

Transfer function of polynomial discrete linear pulse systems for differential equation solution

13 p1936 A72-29269

Stochastic differential equations for a posteriori probability distribution in problems of Markov process parameter estimation, adaptive filtering and signal detection

13 p1937 A72-29441

Harmonic functions skew derivative problem reduction to study of integrodifferential equation by constraints imposition on boundary condition coefficients

13 p1987 A72-29469

Differential systems perturbation method by association with easy-to-integrate reduced system, applying to nonlinear mechanics

13 p1987 A72-29780

Calculation method for steady convective heat transfer in single-flow motion of several media, deriving equation system for characteristic directions and compatibility conditions

13 p2066 A72-29943

K-order differential equation solution obtained for system of polynomial functions for shallow spherical shell under uniform pressure, using Bubnov-Galerkin and collocation methods

13 p2062 A72-29947

System of equations derived for unsteady temperature field of arbitrary multilayer shell, using polynomial expression as temperature approximation for shell thickness

13 p2066 A72-29949

Gradient catastrophe /solution derivative discontinuity/ occurrence time for quasi-linear hyperbolic differential equations describing elastic string oscillations

14 p2130 A72-30194

Differential equations for shallow orthotropic shells with variable thickness obtained by Bubnov-Galerkin variational method, presenting error assessment

14 p2163 A72-30195

Spectral properties of differential displacement equations system describing natural vibrations of shell of revolution with m waves along parallel

14 p2163 A72-30217

Localized point centered initial disturbances effects on marginally unstable plane parallel flow, presenting differential equations solution for nonlinear response

14 p2094 A72-30366

Linear stiff differential equations subdominant solutions, developing numerical integration algorithm

14 p2126 A72-30525

Eigenvalues examination for self adjoint singular differential operators in Hilbert space by finite difference methods

14 p2126 A72-30619

Polynomial spline function for approximate solution of Cauchy problem for nonlinear differential equations of order n

14 p2126 A72-30716

Higher order differential equations solutions for viscoelastic stress-strain functional relationships, recommending Runge-Kutta integration technique

14 p2168 A72-30929

Axissymmetric celestial bodies equilibrium shapes in post-Newtonian approximation of general relativity using integrodifferential equation

14 p2161 A72-31077

Vectorial differential equations in potential theory, discussing Fredholm alternative in normalized spaces, generalized harmonic vector fields, Poisson equation and Robins-Praeger problem

15 p2261 A72-31452

Nonlinear differential equations of motion of complex configuration, developing stable solution method

15 p2261 A72-31489

Centers and foci composition of united trajectories of two autonomous scalar second order differential equations

15 p2262 A72-31551

Nonlinear creep, viscoelasticity and elastoplasticity boundary value problems, discussing matrix constitutive differential equation formulation and higher order numerical methods

15 p2326 A72-31712

Ordinary differential equations - USN Conference, Washington, D.C., June 1971

15 p2262 A72-31751

Small change sensitivity of autonomous neutral functional differential equations in neighborhood of equilibrium point

15 p2263 A72-31752

Boundary value problem solution uniqueness relation to existence for nonlinear differential equations of arbitrary order satisfying solution compactness condition

15 p2263 A72-31753

Dissipative systems of ordinary differential equations concepts extension to functional and partial differential equations

15 p2263 A72-31754

Generalized differential system for Hamiltonian, Hermitian and corresponding symmetric nonreal linear matrix differential equations systems

15 p2263 A72-31756

Variational calculus methods for periodic solutions of autonomously perturbed Hamiltonian systems of differential equations

15 p2263 A72-31759

Boundary value problems for discrete spectrum of nonlinear ordinary differential operators on unbounded intervals

15 p2263 A72-31760

Linear differential equations solution symmetry properties, using Lie algebraic methods and finite dimensional linear systems theory

15 p2264 A72-31761

Globally controllable nonlinear differential systems arising from linear system under perturbation

15 p2264 A72-31762

Linear autonomous differential equations finite time stability theory, extending to systems driven by white noise

15 p2264 A72-31764

Second order delay differential equations, investigating oscillatory behavior of stable and unstable equations solutions and nonoscillatory solution existence

15 p2264 A72-31765

Special boundary value problems solution method for Mathieu differential equation, transforming Mathieu equation to Hill differential equation via Fourier series expansion

15 p2264 A72-32468

Differential equations for stress-strain state of circular cylindrical shell with circular holes resting on elastic base under external pressure

15 p2333 A72-32686

Optimal control of observation processes, formulating solvability conditions in terms of ordinary differential equations

16 p2370 A72-32927

Liapunov function application to stability of unperturbed motion of differential equations with respect to part of variables

16 p2422 A72-32940

Completeness proof for linear elasticity theory set of three harmonic functions based on theory of linear differential equations with constant coefficients

16 p2466 A72-33018

Differential boundary value problem solution by FORTRAN program using finite difference method

16 p2416 A72-33524

Variational principle by imposing time-independent spatial variation on hypothetical system governed by differential equation

16 p2416 A72-33664

Differential equations system solution satisfying dual integral equations, noting biomechanics applications

16 p2417 A72-33828

Existence and uniqueness theorems for Cauchy problem solution for linear singular integrodifferential operator equation

16 p2417 A72-34010

Exact differential equation derived for optimal design of straight nonprismatic column subject to creep buckling

16 p2474 A72-34132

Stability of a class of systems of nonlinear differential equations

17 p2574 A72-34348

- Criterion for unique periodic solution of perturbed Liénard equation for small amplitude periodic perturbation 17 p2574 A72-34400
- Self-adjusting hybrid schemes for shock computations. 17 p2575 A72-34648
- Coefficient criterion of stability for Liapunov indices in a two dimensional linear system 17 p2575 A72-34774
- Application of a limit theorem to solutions of a stochastic differential equation. 17 p2575 A72-34866
- Dissipative periodic process theory for application to elasticity and distributed parameter and hereditary systems defined by partial and functional differential equations 17 p2575 A72-34867
- Single point and multipoint methods for numerical integration of differential equations, discussing solution efficiency improvement via automatic step selection 17 p2576 A72-35040
- Numerical integration of ordinary differential equations in a real-time modeling procedure 17 p2576 A72-35041
- To geometrized theory of hyperbolic heat conduction equation. 17 p2637 A72-35049
- Independent variable transformations for stepwise solution of differential equations of motion power series expansions, considering convergence radius 17 p2609 A72-35105
- Controllably periodic perturbations of autonomous systems. 17 p2576 A72-35200
- Real and definite processes in complete probabilized space, showing Markov process as solution of stochastic differential equation 17 p2576 A72-35420
- Equivalent predictions of the circle criterion and an optimum quadratic form for a second-order system. 17 p2577 A72-35534
- On the choice of boundary conditions for integration of transfer equations. 17 p2577 A72-35695
- Structure of a family of trajectories in the neighborhood of a singular point of a first-order differential equation of degree two 17 p2577 A72-35723
- Book - Riccati differential equations 17 p2577 A72-35798
- Relationship between finite differences and quadratures of a Green's function for a second-order ordinary differential operator 17 p2577 A72-35803
- Investigation of a solution to an almost everywhere multidimensional mixed problem of a class of second-order hyperbolic equations with a nonlinear operator-containing right side 17 p2577 A72-35841
- Investigation of a strongly generalized solution to a multidimensional mixed problem of a class of second-order hyperbolic equations with a nonlinear operator-containing right side 17 p2577 A72-35843
- The first Cauchy-Goursat problem of a hyperbolic-type equation degenerating at the boundary and having singular coefficients at the degeneration line 17 p2577 A72-35844
- Lyapunov functionals for a class of delay-differential systems. 18 p2709 A72-36052
- Steady state response of nonlinear beam under periodic loading, using finite element techniques for nonlinear differential equation 18 p2732 A72-36078
- On the algebraic structure of a class of solvable quantum problems. 18 p2711 A72-36514
- A basic theorem in the computation of ellipsoidal error bounds. 18 p2705 A72-36602
- Linear homogeneous system of differential equations as model for perturbation problems including functions with retarded and/or advanced arguments 18 p2705 A72-36614
- A singular multi-parameter eigenvalue problem in second order ordinary differential equations. 18 p2705 A72-36615
- Nonzero solutions of boundary value problems for second order ordinary and delay-differential equations. 18 p2705 A72-36617
- Boundary value problems for second order, ordinary differential equations involving a parameter. 18 p2705 A72-36619
- Second order differential guidance game, formulating strategy for optimal feedback control 18 p2673 A72-36660
- Shell of revolution natural vibration spectrum, investigating moment and momentless type systems of differential equations 18 p2735 A72-36665
- Variational principle of linear differential equations. 18 p2705 A72-36717
- Phase-plane solution for the electrostatic field of an ionospheric satellite. 18 p2728 A72-36950
- A-stable, accurate averaging of multistep methods for stiff differential equations. 18 p2705 A72-37019
- Maximal contraction points of autonomous nonlinear system phase trajectories, using van der Pol differential equations 18 p2674 A72-37149
- A numerical method for coupled differential equations. 18 p2705 A72-37174
- Infinite systems of stochastic differential equations arising in optimal nonlinear filtering theory 19 p2824 A72-37323
- A posteriori error bounds for approximate solutions of linear second-order ordinary differential equations. 19 p2824 A72-37372
- Trajectories behavior and finite time stability of differential equations system, using Liapunov techniques 19 p2833 A72-37375
- The problem of encounter avoidance in linear differential games 19 p2824 A72-37377
- Asymptotic solution of a second-order linear differential system 19 p2824 A72-37382
- Structure of absolutely approximating and absolutely correct difference schemes 19 p2824 A72-37384
- Large particle method differential approximations in difference equation schemes for gas dynamics problems, discussing viscous effects and solution stability 19 p2745 A72-37385
- Flow equations for flat plate turbulent boundary layer with Reynolds, continuity and energy components, deriving semiempirical differential equation for turbulence scale 19 p2785 A72-37471
- Closed system of differential equations derived for kinematic characteristics of nonstationary turbulent flow in pressurized smooth pipe 19 p2785 A72-37473
- Strong convergence in the whole of an iteration process for ordinary differential equations 19 p2825 A72-37733
- A certain property of standard Fredholm-type nonlinear integro-differential equations 19 p2825 A72-38178
- A characteristic problem for a hyperbolic-type equation degenerating at the boundary 19 p2825 A72-38187
- Problem of the eigenvalues of certain unbounded and nonsymmetrical operators and their applications to ordinary differential equations 19 p2825 A72-38195
- The Dirichlet problem of the Poisson integrodifferential equation 19 p2825 A72-38208
- Control theory stability criteria applied to discrete time feedback systems, investigating numerical integration methods for initial value problems solution 19 p2826 A72-38250
- Lyapunov functions for quadratic differential equations with applications to adaptive control. 19 p2826 A72-38264
- Investigation of the stability of solutions of second-order differential equations with periodic coefficients by the differential invariant method 19 p2827 A72-38467
- Approximate integration of a nonlinear system of differential equations with time lag 19 p2827 A72-38468
- One realization of Liapunov's method for integrating linear equations 19 p2827 A72-38469
- Filtration and extrapolation of multidimensional random processes described by linear differential equations system, examining adaptive filter synthesis 19 p2770 A72-38519
- Differential equations for digital model of linear quadrupole, discussing digital simulation of analog radio equipment circuits 19 p2775 A72-38659
- Solution of a boundary value problem for a class of nonlinear ordinary differential equations by the method of successive approximations 20 p2945 A72-39463
- Asymptotic behavior of solutions of boundary value problems for systems of linear ordinary differential equations with a small parameter by the derivative 20 p2945 A72-39464
- Coincidence of the mapping point with the slip plane in the modified differential descent method 20 p2946 A72-39470
- Group properties of ordinary linear second-order differential equations 20 p2946 A72-39471
- A modified gradient technique for solving boundary and initial value problems. 20 p2946 A72-39618
- A digital simulation system for heat transfer modelled by ordinary and partial differential equations. [ASME PAPER 72-HT-25] 20 p2986 A72-39673
- Variability of solutions to higher-order time-lag linear differential equations 20 p2947 A72-39864
- Solution to the encounter avoidance problem in a linear differential game 20 p2947 A72-39865
- Local Vogt-Russell theorem confirmation by linear approximation for stellar structure nonlinear differential equations, discussing equilibrium model local uniqueness and stellar stability 20 p2973 A72-39888
- An integro-differential equation approach to acoustic scattering from fluid-immersed elastic bodies. 21 p3083 A72-40102
- Assessment of the errors of a version of the hybrid quasi-analog system due to errors in quantization in time in the solution of systems of ordinary differential equations 21 p3024 A72-40158
- A hybrid quasi-analog system for solving boundary value problems 21 p3024 A72-40159
- Stability of solutions to the Hill equation with an operator coefficient having a negative mean value 21 p3074 A72-40256
- Using the quasi-homogeneity of differential equations in modeling physical systems 21 p3083 A72-40377
- Russian book - Mechanics of deformable one-dimensional bodies of variable length. 21 p3116 A72-40387
- Linear distributed parameter systems modal analysis and design for low sensitivity optimal feedback control, using linear differential operators 21 p3037 A72-40646
- Numerical stabilization of the differential equations of Keplerian motion. 21 p3106 A72-41050
- Characteristic equation coefficients of monodromy matrix for linear system of second order homogeneous differential equations with periodic coefficients 21 p3075 A72-41092
- A method for solving Cauchy problems for systems of differential equations with rational coefficients 21 p3075 A72-41093
- General solution of a system of differential equations with an irregular singular point 21 p3075 A72-41095
- Differential equation reduction via coordinate transformation to algebraic form for problems characterization in elastic shell Cosserat surface theory 21 p3119 A72-41103
- Nonlinear differential equation periodic solution approximation by pseudo-linear representation of nonlinear terms effects on single harmonic, using describing function matrix method 21 p3076 A72-41314
- Differential equation solution existence in complete locally convex topological Hausdorff vector space defined by saturated semiorms 21 p3076 A72-41783
- Computer-aided vector Taylor series approximation of fundamental matrix of ordinary first order differential equations with variable coefficients 21 p3076 A72-41785
- Instability of the characteristic indices of systems of linear differential equations with almost periodic coefficients 22 p3197 A72-41853
- Trajectory deviation conditions in second order linear differential escape game, using Pontryagin principle 22 p3204 A72-41903
- Time evaluation of discontinuity occurrence in solutions of boundary problems for second-order hyperbolic quasi-linear systems 22 p3198 A72-41912
- A note on algebraic differential equations whose coefficients are entire functions of finite order. 22 p3198 A72-41948
- Invariant solutions of the differential equations of the uniform motion of a Hooke medium 22 p3233 A72-42058
- Necessary and sufficient conditions for the absolute asymptotic stability of linear systems of differential equations with constant delay 22 p3198 A72-42143
- Approximate solution, in generalized functions, to integral and integrodifferential equations with difference kernels 22 p3198 A72-42145
- Differential equations for heat transfer in turbulent boundary layer flow of incompressible fluid with constant thermophysical characteristics 22 p3166 A72-42253
- Algorithm for identification of unsteady dynamic objects described by linear differential equation, noting quasi-optimal system operation 22 p3205 A72-42290
- Differential equations for energy flow between electron beam and electromagnetic field, avoiding electron

trajectory explicit calculation in nonlinear treatment of cyclotron resonance interaction

22 p3159 A72-42304

Diatomic molecular dissociation in pure gas and mixtures with inert diluent, expressing as set of coupled quadratically nonlinear differential equations [AICHE PAPER 6B]

22 p3208 A72-42400

Asymptotic method for nonlinear wave systems of periodic structure

22 p3155 A72-42657

Variable-step truncation error estimates for Runge-Kutta methods of order 4 or less.

22 p3199 A72-42746

Linear multistep methods for a class of functional differential equations.

22 p3199 A72-42774

Vertical asymptotes and bounds for certain solutions of a class of second order differential equations.

22 p3199 A72-42914

Second order differential equations with general boundary conditions.

22 p3199 A72-42915

Differential equation for maximum beam deflections in transverse bending based on trapezoidal rule

22 p3240 A72-42958

German monograph - Stability conditions for a linear homogeneous ordinary differential equation of second order with stochastic parameter excitation.

22 p3199 A72-43055

German monograph - Iterative algorithms for ordinary differential equations and their suitability for parallel processing by means of symbol manipulation.

22 p3200 A72-43063

Widely convergent method for finding multiple solutions of simultaneous nonlinear equations.

23 p3308 A72-43400

Reduction principle application to solution stability of system of differential equations in critical cases, noting instability of free gyroscope in gimbal suspension

23 p3287 A72-43416

Numerical integration of nonlinear differential equations in nonlinear circuits analysis, obtaining information on unsteady processes from calculation with controlled level time quantization step

23 p3269 A72-43444

Control of jump parameter systems with discontinuous state trajectories.

23 p3275 A72-43547

Formal solution of a system of differential equations of fractional rank with an irregular singular point

23 p3308 A72-43579

Representation of the solution of a nonlinear differential equation in the form of a path integral

23 p3308 A72-43580

Nonlinear mechanics perturbation method for Liapunov functions construction, noting application to nonlinear differential equations

23 p3308 A72-43582

Decoupling and diagonalization conditions determination for nonlinear multivariable time-varying differential equations system by state feedback, giving illustrative examples

23 p3275 A72-43611

A method for partitioning the phase space into regions with constant-sign increments of phase coordinates

23 p3275 A72-43780

Infinitely distant points of a differential equation

23 p3309 A72-43846

Linear inequalities and P matrices, with applications to stability of nonlinear systems.

23 p3309 A72-43859

A priori bounds and upper and lower solutions for nonlinear second-order boundary-value problems.

23 p3309 A72-43980

Controllability properties of right invariant nonlinear systems described by evolution differential equation in Lie group

23 p3309 A72-43981

Differential pursuit games with nonlinear evading player and linear pursuer, considering determination of initial states

23 p3277 A72-44001

Cauchy problem for abstract Love equations

23 p3309 A72-44042

Boundary value problems for multidimensional hyperbolic equations with degeneration

23 p3310 A72-44487

Nonlinear differential equations control systems, determining conditions for observability of initial state and vector of constant parameters extended from time-varying linear systems

23 p3310 A72-44548

The growth of entire solutions of differential equations of finite and infinite order.

24 p3418 A72-44725

Differential equations of motion of two mutually perturbing bodies, noting series expansion of perturbation function for close commensurability of mean motions

24 p3437 A72-44761

Spinor differential equation of generalized unperturbed Kepler motion, using motor method and Lie algebra

24 p3442 A72-45238

Integrodifferential equations for curved walls effect on laminar boundary layer characteristics, noting wall friction, layer thickness and transverse pressure

24 p3394 A72-45447

On zeros of solutions of the second-order linear differential equation with retardation.

24 p3419 A72-45577

A numerical integration method useful for studying ionospheric phenomena.

24 p3399 A72-45582

A priori estimates at the boundary for solving second-order elliptic integrodifferential equations

24 p3420 A72-45648

Comparison of linear and Riccati equations used to solve optimal control problems.

24 p3420 A72-45776

DIFFERENTIAL GEOMETRY

NT LIE GROUPS

NT RIEMANN MANIFOLD

NT SPINOR GROUPS

NT TENSOR ANALYSIS

Nonlinear closed loop system reduction of differential trajectory sensitivity to continuous variations or external disturbance

09 p1340 A72-22245

Differential geometry of reductive homogeneous spaces with invariant affine connections, identifying geodesic lines with subgroup trajectories of space motions

09 p1340 A72-22295

Differential geometric methods to extend linear system theory to nonlinear classes, considering differential equations, controllability, optimal control, stochastic processes and bilinear system problems

10 p1503 A72-23788

Differential geometry extremal problem of holomorphic embedding of complex curves in Kaehler manifold with constant holomorphic curvature, using Riemann surface moduli theory

10 p1506 A72-24862

Caratheodory classical thermodynamics formulation presented in mathematically rigorous form by differential geometry and topology methods

18 p2741 A72-36508

DIFFERENTIAL INTERFEROMETRY

Transient phase object high sensitivity measurement by He-Ne laser beam transmission through differential interferometer and signal detection with p-i-n photodiode

15 p2235 A72-31784

Differential stress-holo-interferometry. [SESA PAPER 1989A]

17 p2554 A72-34816

A differential interferometer and its application to heat and mass transfer measurements.

[ASME PAPER 72-HT-12]

20 p2927 A72-39683

A laser interferometer for combustion, aerodynamics and heat transfer studies.

24 p3402 A72-44950

DIFFERENTIAL OPERATORS

U DIFFERENTIAL EQUATIONS

U OPERATORS [MATHEMATICS]

DIFFERENTIAL PRESSURE

Fluidic wind sensor measurements from low threshold to high velocities, noting wind angle resolution from output differential pressure signal

10 p1484 A72-25083

High precision electrostatic feedback transducer for very low differential pressure measurement in gas media, suggesting low pressure standard role [RAE-TR-71022]

16 p2394 A72-33638

An improved pressure-sphere anemometer.

22 p3178 A72-42596

DIFFERENTIAL THERMAL ANALYSIS

Ta-Co system phase diagram from differential thermal, X ray, and microstructural analyses, determining composition, temperature, structural type and lattice constant

03 p0374 A72-13740

Apollo 11 lunar fines behavior and gas evolution characteristics from high vacuum differential thermal analysis and mass spectroscopy

04 p0569 A72-14504

Data uncertainties effects on thermal analysis, discussing Monte Carlo method combination with sensitivity analysis

[AIAA PAPER 72-60]

05 p0749 A72-16930

Equilibrium diagram of Cr-Va alloy produced by arc melting under Ar atmosphere, using high temperature differential thermal analysis

07 p1019 A72-20160

Nb-Ga system equilibrium phase diagram determination by differential thermal, tempering microstructural and X ray analysis techniques, discussing various compounds formation temperatures and characteristics

07 p1050 A72-20161

Thermal decomposition kinetics of tetramethylene tetranitramine beta HMX from differential thermal analysis and activation energy calculation

08 p1219 A72-20755

Differential thermal analysis for electrical insulation thermal degradation and thermogram shape, combining equations for required life line

09 p1339 A72-23271

Ce-N alloys phase diagram from durometric, X ray, metallographic and differential thermal analyses

14 p2123 A72-30991

Temperature measuring instrument with thermocouple for differential thermal analysis equipment used in phase diagram construction

14 p2106 A72-30995

Derivative graph method of thermal analysis for lubricating oils

17 p2571 A72-35180

X ray and differential thermal analysis for phase diagrams of binary alloys of samarium oxides and gadolinium oxides with calcium oxides, noting solid solutions formation

23 p3304 A72-43250

X ray, microstructural and differential thermal analysis for binary Zr alloys, noting formation of ternary phases and solid solutions

23 p3300 A72-43588

Phase transformations in chromium-titanium compounds.

24 p3413 A72-44922

DIFFERENTIATORS

A differential-integral amplitude-time converter of nanosecond-range pulses

19 p2771 A72-37305

Reversible integrodifferentiator with automatic data input

21 p3024 A72-40162

DIFFRACTION

NT ELECTRON DIFFRACTION

NT FRESNEL DIFFRACTION

NT NEUTRON DIFFRACTION

NT PULSE DIFFRACTION

NT WAVE DIFFRACTION

NT X RAY DIFFRACTION

Spherical aberration effect on far field Fraunhofer diffraction for circular aperture illuminated by quasi-monochromatic partially space coherent light

01 p0103 A72-11188

High frequency diffraction problems, using matrix formulation in spectral domain

04 p0489 A72-15396

Fabry-Perot open resonators, determining eigenvectors, resonant frequencies and diffraction losses by asymptotic perturbation method

04 p0502 A72-15436

Stationary functionals for introducing eigenfunctions in diffraction theory of electrodynamic systems

08 p1133 A72-21372

Constrained-impedance eigenfunctions, using projection method for field expansion in diffraction problems

15 p2202 A72-32661

Interference measurement techniques for small phase difference changes, noting diffraction and noise effects as limiting factors

15 p2243 A72-32769

Analysis of antennas on finite circular cylinders with conical or desk end caps.

17 p2525 A72-34361

Complex resonant frequencies calculation in external diffraction problems for arbitrary shaped bodies, noting Green function poles correspondence to eigenvalue zeros of integral equation

19 p2767 A72-38652

Expansion of diffracted electromagnetic fields in eigenfunctions of the d'Alembert operator

23 p3312 A72-43335

DIFFRACTION GRATINGS

U GRATINGS [SPECTRA]

DIFFRACTION PATHS

Ground wave propagation over spherical earth, considering land-sea and homogeneous paths

10 p1438 A72-24740

DIFFRACTION PATTERNS

Ti alloys omega phase transformations by cryogenic cooling of bcc beta phase, interpreting electron diffraction pattern change in terms of displacement type reactions

01 p0082 A72-10204

NDT holographic interference pattern technique to determine Advanced Test Reactor fuel element swage joint tightness

01 p0078 A72-11110

Projected interference fringes in holographic interferometry for large surface movements measurements

02 p0231 A72-12544

Nonstoichiometric vacancy order in vanadium monoxide from electron microscopy and diffraction patterns, proposing partial phase diagram

03 p0401 A72-13584

Interference fringes production from binary stars focal images obtained with Lallemand electronic camera

03 p0435 A72-13798

Longitudinal and transverse wave diffraction on cavities, investigating field pattern by dynamic photoelasticity method with flat models

03 p0452 A72-14131

Vanadium carbide diffraction spectrum reflection intensity under Mo and CuK-alpha irradiation, showing crystalline structure and interatomic ionic interaction

04 p0533 A72-14618

Thin amplitude dynamic holograms diffraction efficiency, showing dependence on interference pattern, modulation depth, radiation intensity and material properties

04 p0521 A72-14659

Geometric optics method accuracy in design of dual-mirror antenna illumination system, noting diffraction effects and near field influence

04 p0499 A72-15242

Asymmetrical profile calculation of spherical multiple wave interference patterns at finite distance with nonparallel mirror Fabry-Perot interferometer

05 p0662 A72-16193

Slot excited conical antenna, calculating first order diffraction coefficients by integral expressions for radiation field

06 p0781 A72-17343

Long E-plane sectoral horn, deriving complex reflection coefficient from aperture by geometrical diffraction theory

06 p0781 A72-17346

Radio waves arrival angles distribution function in Fraunhofer diffraction zone upon plane wave normal incidence on inhomogeneous scattering layer

07 p0938 A72-19017

Displacement and profile diffractographic measurement using changes in far field diffraction patterns of slit aperture between test and reference object [CLEA PAPER 11,5]

07 p0984 A72-19390

Diffractographic dimensional measurement, discussing profile determination from diffraction patterns [CLEA PAPER 11,5]

07 p0984 A72-19391

Vibrational amplitude measurement of diffuse surface by modulation of projected fringes in optical field

07 p0985 A72-19407

Hologram interference fringe relationship to nonlinearity of simple oscillations

07 p0987 A72-19836

Physical analysis of photoelastic interferometry and holography, considering retardation, isochromac and isopachic fringe systems and model materials

08 p1166 A72-21330

Vibration measurement based on moire pattern fringes motion due to line gratings respective displacement, noting high accuracy and resolution

09 p1315 A72-23388

Light beams diffraction patterns of thin plexiglass plate for load induced thickness variations, noting crack opening and edge sliding modes stress intensity factors

10 p1553 A72-24178

Transitional ferrite phase formation in Fe-Cr-Ni alloy evidenced on electron micrographs and diffraction patterns

11 p1657 A72-25760

Superhigh frequency electromagnetic waves diffraction by conducting screen circular aperture with phase change by dielectric disk and multiple internal reflections, noting patterns and backscattering apparatus

11 p1597 A72-26371

Holographic recording systems stabilization with intermittent exposure control for interference patterns fidelity

12 p1806 A72-27263

Diffraction efficiency of phase holograms formed by surface deformation of light sensitive dichromated gelatin films

12 p1808 A72-27600

Laser irradiance modulation effect on high error fringes brightness in time average hologram reconstruction, noting exposure time increase

12 p1809 A72-27682

Lens MTF calculation in presence of diffraction patterns via image mathematical model construction yielding Fourier transform

12 p1810 A72-27937

Dispersive optical imaging systems for chromatic aberration correction, considering broadband holographic reconstruction and generation, optical information processing and diffraction pattern achromatization

12 p1811 A72-27950

Retina visual acuity testing by zero and first order moire fringes, using square-wave amplitude gratings

12 p1772 A72-27953

Holographic system stability tested by diffraction efficiency-exposure curves obtained in real time from probing holograms sequence, emphasizing temperature effects

13 p1956 A72-28685

X ray diffraction patterns of aging nimonic alloys, noting effects of atomic volume difference between precipitation phase and matrix

13 p1976 A72-28766

Re single crystal LEED diffraction pattern, showing surface carbon structure

13 p2021 A72-28800

Artificial compensation holograms for complex optical objective substitution, using interference fringe image technique

13 p1958 A72-29513

Interference method for gas laser phase front measurements based on comparison with radiation shifted in mirror plane

13 p1970 A72-29681

Experimental development by holography of three dimensional moire fringes for very large deformations study

13 p1960 A72-29781

Holographic diffraction grating production by impressing interference fringes with photographic procedure, using two laser beams

14 p2105 A72-30579

Holographic interferometry for strain measurements in bodies, obtaining frozen interference fringes for stressed plane mechanical component via double exposure

14 p2105 A72-30840

Spectrometer entrance slit diffraction effects on observed fast beam spectral line width

15 p2280 A72-31383

Diffraction analysis of Fabry-Perot interferometer with metal mirror gratings for oblique incident polarized plane electromagnetic wave reception

15 p2233 A72-31413

Absolute intensity LEED spectra for clean Ni surfaces, discussing measurement uncertainties

15 p2276 A72-31854

Clean Ge crystal surface oxidation process investigation by LEED and conductivity measurements

15 p2292 A72-31868

Diffraction theory for large storage capacity holographic random access memory design, discussing geometric optimization of detector array and storage plate

15 p2238 A72-32159

Laser interference fringe jitter due to wavelength instability, suggesting pulse shape blurring intensity variation control by flat or large-angle wedge beam splitter

15 p2249 A72-32166

Transient high voltage and electric field measurement with electro-optical fringe pattern method employing pulsed laser Kerr system polarimeter

15 p2240 A72-32434

Diffraction of electromagnetic waves by a two-dimensional aperture with arbitrary cross-sectional shape

17 p2514 A72-34385

Electron diffraction patterns of previously deformed Ti-Nb alloy containing unequal populations of omega phase variants, noting anisotropy

17 p2566 A72-34673

Electro-optical torque sensor based on slit aperture produced diffraction patterns [SESA PAPER 1925-II]

17 p2553 A72-34813

Application of dispersion techniques to molecular band intensity measurements. I - Principles of 'fringe shift' and 'fringe slope' band analysis procedures.

17 p2586 A72-35832

Fringe shift and slope analysis of interferometric spectrogram formed by NO-gamma system spectral band

17 p2586 A72-35833

Holographic interferometry analyzed from the point of view of moire patterns.

18 p2690 A72-36362

Double exposure holographic recording of rapidly changing object via mode locked ruby laser generated interference pattern

19 p2796 A72-37580

Method of stationary phase for analysis of fringe functions in hologram interferometry.

19 p2796 A72-37582

Quantitative data reduction with the use of fringe control techniques in conjunction with holographic interferometry.

19 p2797 A72-37612

Displacement field analysis via holographic interferogram, measuring fringe pattern shift due to change of observation direction through double exposure hologram

19 p2797 A72-37613

A general theory of polarization holography and its application to photoelastic analysis.

19 p2799 A72-37627

Three dimensional holographic interferometry program for study of fringes due to displacement or deformation

19 p2799 A72-37630

Use of generalized theory of optical diffraction for the study of second harmonic generation.

19 p2811 A72-37673

Plane and cylindrical electromagnetic waves diffraction on infinitely long cylindrical bodies, calculating induced currents, diffraction patterns and near fields

19 p2767 A72-38654

Plane TE polarized electromagnetic wave diffraction on infinite conducting cylinder in nonhomogeneous medium, calculating far field diffraction patterns

19 p2768 A72-38656

Determination of three orthogonal displacement components from one double exposure hologram.

20 p2927 A72-39847

Anomalous line broadening in the low temperature X-ray diffraction pattern of niobium.

20 p2942 A72-39989

Fresnel-like interference on an ion-wave decay in a plasma.

21 p3089 A72-40200

Electro-optical noncontracting torque sensor, using slit diffraction pattern technique

21 p3051 A72-40231

Edge effect improved fringe definition on high contrast film by pseudo-solarization for polariscopes in photoelastic stress analysis

21 p3052 A72-40232

A method for directly determining surface strain fields using diffraction gratings.

21 p3052 A72-40236

X ray diffraction patterns of aging nimonic alloys, noting effects of atomic volume difference between precipitation phase and matrix

21 p3065 A72-40267

Multiple mirror astronomical telescope using laser source light collimated with central Cassegrain system, presenting expected diffraction patterns

21 p3052 A72-40378

Dielectric coating effects on millimeter wave diffraction pattern of gratings, noting sharp anomalous dips in transmission intensity for P and S polarizations

21 p3031 A72-40604

Diffraction of electromagnetic plane waves by infinite slit perforated in a conducting screen with finite thickness.

21 p3022 A72-41267

An investigation of the ground diffraction pattern of radio waves reflected by the ionosphere.

22 p3154 A72-42362

Surface distortion and strain fields visualization by grating produced diffraction patterns, discussing different detection techniques

22 p3234 A72-42391

Noise-cancelling signal difference method for optical velocity measurements.

22 p3177 A72-42394

German monograph - A hologram interferometer for the determination of amplitude and phase of optical excitation in diffraction patterns.

22 p3181 A72-43056

Full-field surface-strain and displacement analysis of three-dimensional objects by speckle interferometry.

23 p3349 A72-43984

A neoteric interferometer for use in holographic photoelasticity.

23 p3290 A72-43985

Phase correlation between two sources formed on a diffusing surface - Application to the human retina

23 p3261 A72-44379

Time variations in the far-field diffraction patterns of spatial modes from electron-beam-pumped semiconductor lasers.

24 p3409 A72-44712

Method of characteristic application to curved beam motion under pulse type loading, investigating photoelastic fringe patterns and pulse propagation

24 p3458 A72-44888

Focusing properties of converging-beam holograms.

24 p3405 A72-45602

DIFFRACTION PROPAGATION

Secondary diffraction from close edges on perfectly conducting bodies, representing scattered field by iterative surface current density replacement technique

10 p1440 A72-24938

Diffraction coefficients of scalar field for higher order edges and vertices, noting far field behavior of boundary layer expansion

11 p1617 A72-26158

Emission of density modulated electron flux passing over diffraction structures formed by half planes and combs with oblique teeth, discussing optimum emitted power conditions

12 p1793 A72-27858

Holograms with high diffraction efficiency, describing bleaching experiments and SNR measurements in reconstructed image

12 p1810 A72-27887

Diffraction of plane waves scattered by impedance structures in anisotropic medium, noting wedge shaped region with cold plasma under external magnetic field

14 p2086 A72-30809

Kirchhoff-Fresnel diffraction field fluctuation at plane screen aperture in turbulent atmosphere

16 p2425 A72-33487

Holograms with high diffraction efficiency, describing bleaching experiments and SNR measurements in reconstructed image

16 p2395 A72-33996

Simplified method of calculating microwave diffraction loss over spherical earth.

18 p2660 A72-36517

- Wave-guiding properties of stripe-geometry double heterostructure injection lasers. 18 p2698 A72-36981
- Plane electromagnetic wave diffraction on thin ribbons grating, discussing scattered field singularities for E polarized waves 19 p2769 A72-38850
- Diffraction of plane electromagnetic wave at a corrugated dielectric surface 22 p3155 A72-42662

DIFFRACTION TELESCOPES

U SPECTROSCOPIC TELESCOPES

DIFFRACTOMETERS

- Centroid shift of diffraction line due to X ray diffractometer geometry in stress measurement 04 p0547 A72-14527
- Diffractographic dimensional measurement, discussing profile determination from diffraction patterns [CLEA PAPER 11.5] 07 p0984 A72-19391
- Low power X ray diffractometer with multiwire proportional counter detector array for remote mineralogical analysis of lunar, planetary or asteroid soils detector array 08 p1167 A72-21507
- A diffraction transducer for vibration analysis. 17 p2626 A72-34722
- Optical diffractometer with laser beam having approximately uniform transverse intensity distribution 21 p3051 A72-40210

DIFFUSE RADIATION

- Objects optical granularity in diffuse coherent light, noting similarity to image formation in diffuse incoherent light 01 p0073 A72-11313
- Diffusely illuminated objects holographic reconstruction with suppressed granularity by incoherent superposition of reconstruction waves longitudinal modes, describing experimental setup 02 p0229 A72-12116
- Absorption spectrum of atomic Ca trapped in solid hydrocarbons, comparing with diffuse interstellar band at 4430 Å 02 p0284 A72-12632
- Diffuse reflection of point source /flare/ light emission for cold dwarf star seminfinit plane parallel atmosphere, calculating polarization 02 p0285 A72-12831
- Galactic disk component of diffuse X radiation from unresolved red dwarf flare stars 03 p0408 A72-12993
- Diffuse galactic light absolute intensity interpretation, showing interstellar dust discrete cloud structure effect on grain properties determination 03 p0416 A72-13015
- Diffuse gravitational background radiation in universe, assuming gravitational field fluctuations macroscopic nature and Einstein equations applicability 03 p0417 A72-13095
- Diffuse cosmic background radiation measurements, emphasizing microwave and X ray spectra and excitation mechanism 03 p0409 A72-13138
- Cosmic ray induced radioactivity effects on diffuse gamma ray background measurement from 600 MeV proton irradiation experiment 04 p0567 A72-15324
- Aerial photographic determination of sea state, using reflection at water surface of natural light diffuse component radiated by sky-sun combination 04 p0525 A72-15563
- Light diffuse transmission and reflection by semiinfinite atmosphere with four term scattering indicatrix 06 p0884 A72-18029
- Models of galactic diffuse sources of soft cosmic X rays, estimating spectrum and intensity 08 p1228 A72-21650
- Planetary atmosphere diffuse radiation from limb side, applying to Mars atmospheric emission 08 p1238 A72-21832
- Nonuniform non-Lambertian diffusely scattering surface optical transfer characteristics and initial irradiance distribution inside sphere, discussing spherical harmonic moment measurement 09 p1309 A72-22610
- Spectrum studies of extragalactic diffuse background radiation fields consisting of X ray and thermal or microwave background 10 p1529 A72-23914
- Satellite photometric observation of diffuse celestial sources such as Milky Way, zodiacal light and gegenschein 10 p1546 A72-24863
- Diffuse gravitational background radiation in universe, assuming gravitational field fluctuations macroscopic nature and Einstein equations applicability 11 p1716 A72-25703
- Helios solar probe-borne zodiacal light photometer for diffuse light measurements in interplanetary space 11 p1632 A72-25805
- Light diffuse transmission and reflection by semiinfinite atmosphere with four term scattering indicatrix 11 p1719 A72-25965

Diffuse galactic light observation, suggesting emanation from discrete sources 11 p1720 A72-26113

Spatial noise in holographic images of diffusely scattering objects with allowance for recording apparatus resolving capacity 12 p1810 A72-27871

Laboratory simulation of diffuse reflectivity from plane parallel cloudy planetary atmosphere, comparing to theory 12 p1796 A72-27947

Elliptical and barred spiral Markarian galaxies, discussing starlike and diffuse spectra dependence on morphology 15 p2304 A72-31327

Diffuse cosmic gamma ray flux density and energy spectrum observation at equatorial balloon altitude, discussing photon count, flux and spectra 15 p2299 A72-31924

Diffuse X ray emission from galaxy interarm region, suggesting population of unresolvable low luminosity sources as emission model 16 p2445 A72-33138

Spatial noise in holographic images of diffusely scattering objects with allowance for recording apparatus resolving capacity 16 p2395 A72-33980

Observation of the diffuse cosmic gamma radiation in the 30-50-MeV region. 17 p2598 A72-34522

Galactic ridge of discrete diffuse X ray sources, calculating intensity in terms of scale height and radial gradient 17 p2598 A72-34523

Origin of the low energy diffuse cosmic X-ray flux. 17 p2599 A72-35071

On the contribution of transition radiation from dust grains to the diffuse X-ray background. 17 p2600 A72-35314

A multiple-scattering model of the diffuse component of lunar radar echoes. 20 p2903 A72-39473

A longitude survey of radio recombination lines from the diffuse interstellar medium. 22 p3227 A72-42552

Calculation of stellar and diffuse radiation for a plane-parallel seminfinit model of the Galaxy 23 p3338 A72-44027

Phase correlation between two sources formed on a diffusing surface - Application to the human retina 23 p3261 A72-44379

Light spectral width and constant frequency shift during spontaneous diffusion in ideal gas for fixed photon wave 23 p3315 A72-44479

Approximate formulas for the intensity of diffuse reflected emission from a seminfinit atmosphere 24 p3448 A72-45685

DIFFUSERS

- Two dimensional diffusers flow patterns with laminar boundary layer entry, investigating wall shape and vanes effects with water table test facility 02 p0204 A72-12231
- Boundary layer suction intensity and slot location effects on performance of curvilinear annular diffuser for various Mach and Reynolds numbers 03 p0308 A72-13736
- Intermittency factor of diffuser flow boundary layer with positive pressure gradient, using hot wire anemometers and multichannel analyzer 04 p0461 A72-14411
- Diffuser for altitude simulation in rocket motor operation, featuring film cooling with water inflow by motor exhaust gas ejector action 05 p0704 A72-16004
- Boundary layer growth measurements in optimum annular diffusers, discussing pressure recovery and mean total pressure loss [AIAA PAPER 72-86] 05 p0604 A72-16807
- Mach 2.65 axisymmetric mixed-compression inlet system diffuser and boundary layer bleed system performance estimates confirmed by tests [AIAA PAPER 72-45] 05 p0609 A72-16959
- Equilibrium turbulent flow of incompressible fluid in plane diffusers, taking into account channel cross section including viscous sublayer 06 p0801 A72-18144
- Incompressible fluid near equilibrium turbulent flow velocity distribution through plane diffuser, taking into account upstream conditions 07 p0972 A72-20115
- Flow analysis and dimensioning data for parallel walled radial diffusers, stating flow separation criterion 09 p1260 A72-22629
- Centrifugal turboengine diffuser with high enlargement area compared with logarithmic spiral types, discussing boundary layers, secondary flow, shapes and aerodynamic parameters 10 p1463 A72-23747
- Pressure recovery calculation for subsonic adiabatic air flow through diffusers with tail pipes, assuming turbulent inlet boundary layer 10 p1415 A72-23855

Low speed performance and boundary layer growth in optimal annular diffuser with uniform center body diameter and conically diverging wall 10 p1415 A72-23856

Turbulent boundary layer growth measurement on annular diffuser containing free vortex swirl 10 p1416 A72-23857

Conical diffuser response to velocity distribution and turbulence intensity at inlet 10 p1416 A72-23858

Wind tunnel diffuser design for separated region spread reduction based on egg box principle 10 p1416 A72-23859

Wide angle conical diffuser performance improvement by conical splitter vanes, considering static pressure recovery 10 p1416 A72-23860

Turbulent shear stress and kinetic energy characteristics of subsonic air flow in straight conical diffuser, using hot-wire anemometry measurements 10 p1419 A72-24545

Diffuser performance and idling characteristics in shock tube at Mach 8, discussing pressure recovery factor laminar and transition flows in boundary layer 10 p1419 A72-24545

Flow fields and inviscid core of two dimensional diffuser with fluid extraction on diverging walls, describing streamline patterns, stagnation region and stall conditions [ASME PAPER 72-GT-2] 11 p1568 A72-25605

Cascade technology for centrifugal compressor vanned diffuser design, comparing performance results with conventional diffuser data [ASME PAPER 72-GT-39] 11 p1569 A72-25633

Radial inflow compressor feasibility, discussing blade loadings for various pressure ratios and efficiency of rotor and diffuser [ASME PAPER 72-GT-52] 11 p1570 A72-25644

Hydraulic vortex amplifiers with and without diffusers, discussing supply pressure and liquid viscosity effects on system performance 11 p1578 A72-26980

Swirling flow effects on annular conical diffuser performance in axial flow turbomachines, showing stagnation region and inner body diameter dependence 14 p2069 A72-30580

Asymptotic solution for velocity distribution in viscous liquid axisymmetric flow in conical diffusers 14 p2070 A72-31006

Swirling flows vortex breakdown in nozzles, diffusers and combustion chambers, considering analogy to boundary layer separation 18 p2641 A72-36385

Improving diffuser performance by artificial means. 20 p2885 A72-39624

The effect of entrance configuration on local heat-transfer coefficients in subsonic diffusers. [ASME PAPER 72-HT-34] 20 p2986 A72-39670

Flow quality improvements in a blowdown wind tunnel using a multiple shock entrance diffuser. [AIAA PAPER 72-1002] 21 p3041 A72-41587

Characteristics of gas flows in diffusers at transonic velocities 21 p2994 A72-41698

Influence of tangential fluid injection on the performance of two-dimensional diffusers. [ASME PAPER 72-FE-16] 23 p3280 A72-44064

DIFFUSION

- NT AMBIPOLAR DIFFUSION
- NT ATMOSPHERIC DIFFUSION
- NT ELECTRON DIFFUSION
- NT GASEOUS DIFFUSION
- NT IONIC DIFFUSION
- NT MAGNETIC DIFFUSION
- NT MOLECULAR DIFFUSION
- NT PARTICLE DIFFUSION
- NT PLASMA DIFFUSION
- NT SELF PROPAGATION
- NT SPECIES DIFFUSION
- NT SURFACE DIFFUSION
- NT THERMAL DIFFUSION
- NT TURBULENT DIFFUSION
- Magnetic transformation effect on creep behavior of fcc nickel-cobalt alloy compared with self diffusion data in Curie temperature vicinity 01 p0083 A72-10391
- Markov processes for local diffusions defined by second order differential operator delta with Holder coefficients on manifold 10 p1505 A72-24201
- Electromagnetic properties of semiconductor diffusion films, using impedance measurements 11 p1700 A72-25779
- Diffusion with convection for parallel wall Couette flow, using Airy functions 11 p1618 A72-26591
- Diffusion kinetics and thermodynamic characteristics of solid phase interactions in systems cobalt-transition metal carbides 13 p1981 A72-30104
- Classical and finite difference methods for diffusion and heat conduction problems 15 p2334 A72-31298

- Diffusion effects on stellar surface chemical composition, emphasizing solar atmosphere conditions
15 p2305 A72-31342
- German monograph on mass transport in thin fluid layers covering diffusion, convection, laminar flow rate distribution, flame ionization and gas chromatography measurements, etc
15 p2216 A72-31350
- Zr and V alpha and beta stabilizing element effects on phase boundaries in arc fused Ti-Al alloy studied by diffusion layer method
19 p2817 A72-37754
- Study of the diffusing properties of the retina - Application to the optical system of the eye
21 p3007 A72-40736
- Al alloy rupturing analysis in complex stress state, noting sublimation and self diffusion values of activation energy in torsional to tensile state transition
23 p3301 A72-43957
- DIFFUSION BONDING**
U DIFFUSION WELDING
DIFFUSION COEFFICIENT
- Nonlocal theory of electrostatic trapped particle instability in collisionless toroidal plasma, estimating particle mode nonlinear diffusion coefficient
01 p0108 A72-10239
- Heat treatment, quenching and aging caused metastable and stable alpha and beta structures effects on nitrogen diffusion rate in Ti alloy during nitriding
02 p0244 A72-12248
- Hydrogen diffusivity and solubility in alpha-Ti alloys, considering absorption effect on stress corrosion cracking
02 p0244 A72-12481
- Photoresonance cesium plasma development and decay, determining density spatial-temporal behavior and recombination and polar diffusion coefficients by probe measurements
03 p0396 A72-13664
- Free oxygen content and diffusion coefficient in adrenalectomized rat skeletal muscles after physical strain
03 p0317 A72-13991
- Alloying and heat treatment ordering effect on hydrogen diffusion coefficients, penetrability and solubility in Pd-Ag alloys
03 p0376 A72-14016
- Diffusion rate of diluted drag reducing polymers in turbulent boundary layer
03 p0343 A72-14319
- Planetary boundary layer mixing length flow hypothesis with dependence on Reynolds tangential stress permitting turbulent diffusion coefficient maximum values computation
04 p0519 A72-15458
- Atomic and molecular hydrogen mixture viscosity measurement, considering mutual diffusion coefficients, collision cross sections and interaction potentials
04 p0553 A72-15637
- Hydrodynamic asymptotic characteristics of autocorrelation function for molecule velocity in classical liquid, obtaining Lagrangian diffusion coefficient
05 p0692 A72-16684
- C 14 diffusion coefficients in W and W-Re alloys single crystals at 1500-1800 C, discussing tracer activation energy and frequency factor
05 p0676 A72-16731
- Electron beam interaction with collisionless plasma, obtaining beam spatial distribution function from velocity diffusion coefficient measurement
06 p0858 A72-17540
- Brownian particle sedimentation rate and diffusion coefficient determination by holographic double exposure interferometry
06 p0816 A72-17982
- Plasma ambipolar diffusion coefficient and electron density determination from thermal density fluctuations cross spectrum based on Langmuir probe measurements
06 p0864 A72-18536
- Nitrogen interaction with Ni-based melts at 1600 C, noting absorption rate dependence on nitrogen diffusion rates and melt viscosities
07 p1011 A72-19546
- Magnetospheric trapped particle diffusion coefficients and acceleration in earth radiation belts
07 p1062 A72-20035
- Hydrogen plasma generation by microwave field in magnetic-mirror device due to electron cyclotron resonance, measuring transverse diffusion coefficient dependence on magnetic field
07 p1046 A72-20506
- Self diffusion coefficients of carbon and oxygen in dolomite
07 p0937 A72-20520
- Thermal conductivity and thermal diffusion coefficients determination for plane plate heated unilaterally from above under fourth kind boundary conditions
08 p1252 A72-21313
- Winds velocity, direction and diffusion coefficients over Heiss Island from artificial luminous clouds observations
08 p1160 A72-21534
- Diurnal and seasonal variation of ambipolar diffusion coefficient in meteor trail zone within upper atmosphere
08 p1238 A72-21888
- Vertical macroturbulence diffusion coefficient and Na 22 and Be 7 flux from stratosphere to troposphere estimated using ground level measurements and two layer model
09 p1376 A72-22416
- Mossbauer lines diffusion broadening and weakening in crystals impurity atoms nuclear spectra
09 p1371 A72-23030
- Diffusion coefficient and distribution of Ti atoms in thin Al film from electric current vs time curves for oxidation of solid solution
09 p1329 A72-23036
- Heat treatment produced metastable and stable alpha and beta structures effects on nitrogen diffusion rate in Ti alloy during nitriding
11 p1660 A72-26134
- Nitrogen solubility, degassing kinetics and diffusion coefficients for Mo-N, W-N and Re-N systems for 1300-3050 C
11 p1663 A72-26841
- High temperature solubility and diffusion coefficient of nitrogen in rhenium
12 p1827 A72-27138
- Niobium diffusion into copper as function of time and temperature, obtaining rates by electrical resistance measurements
12 p1828 A72-27448
- Density function for lower troposphere vertical turbulence diffusion coefficient derived from atmosphere radiometric probe data
13 p2029 A72-28456
- Cation self diffusion coefficients in potassium oxide-strontium oxide-silicon dioxide glass, using radioactive tracers and sequential etching technique
13 p1912 A72-28625
- Interdiffusion studies in bcc phase of Zr-Ti alloy, using geoscan electron microprobe
13 p1973 A72-28653
- Electron probe microanalysis of Mo-Pd system diffusion at 1000-1600 C, measuring chemical diffusion coefficient as function of temperature, concentration and activation energy
13 p1978 A72-29221
- Plasma diffusion coefficient in crossed electric and magnetic fields, discussing lifetime in magnetic trap and expression for ion mobility
13 p2019 A72-29942
- Tungsten-rhenium alloys and tungsten self diffusion coefficient temperature dependence investigation, noting Re addition effects
14 p2114 A72-30402
- Whistler waves amplification in magnetosphere, obtaining particles pitch angle and energy diffusion coefficients and one dimensional Fokker-Planck equation
15 p2194 A72-31427
- Concentration dependence of interdiffusion coefficient in binary metallic systems with continuous and bounded solid solutions
15 p2243 A72-31572
- Light elements production from primary cosmic rays spallation in interstellar gas, noting diffusion coefficient of relativistic particles in galaxy
15 p2301 A72-32754
- C diffusion mobility and coefficients in W-Mo steels gamma and alpha phases, discussing ionization effect on activation energy increase
16 p2408 A72-33538
- Anomalous diffusion coefficient of axially decaying RF discharge collisional plasma under instability mode suppressed by feedback technique
16 p2437 A72-33657
- Effects of junction depth on the radiation damage of silicon solar cells.
17 p2594 A72-34388
- Transverse diffusion and conductivity coefficients for a three-dimensional magnetized equilibrium plasma.
17 p2592 A72-35379
- New measurement and evaluation method for the determination of the diffusion coefficient of hydrogen in solid metals
18 p2692 A72-36841
- Determination of upper atmosphere parameters by measuring the ambipolar diffusion coefficient by the method of meteor trail radar observations
18 p2688 A72-36862
- The determination of diffusion coefficient for Na in dc arc plasma by measurements of intensity distribution of emitted light.
18 p2716 A72-36959
- Self-diffusion of cobalt in the ternary system Co-Ni-Fe
19 p2814 A72-37416
- Oxygen diffusion coefficient variation with temperature observed during dissolution in alpha-zirconium, noting oxygen content effect on oxygen atom elementary jump length
19 p2817 A72-37795
- Diffusion cooling in neon, argon, and krypton afterglow plasmas.
19 p2841 A72-38378
- Markovian plasma turbulence model to obtain convergent perturbation series for diffusion coefficient via trajectories in particle propagator
19 p2841 A72-38442
- Cosmic-ray diffusion coefficient in interplanetary space.
19 p2853 A72-38756
- Diffusion effects in solids caused by radiation exposure, calculating diffusion coefficients of additions and defects
20 p2958 A72-38952
- Experimental determination of the coefficients of radiantly stimulated diffusion of sulphur in cadmium sulfide
20 p2959 A72-38954
- Interdiffusion in nickel-molybdenum and palladium-molybdenum systems
20 p2939 A72-39315
- Estimation of the turbulent diffusion coefficient and of the vertical wind velocity component from the distribution of natural radioactivity
20 p2964 A72-39320
- The mechanisms of diffusion in metals and alloys.
20 p2962 A72-39999
- Diffusion in the system K2O-SrO-SiO2. IV - Mobility model, electrostatic effects, and multicomponent diffusion.
21 p3097 A72-40935
- Emitter-dip model of diffusion anomalies of n-p-n Si HF transistors doped with B and P
21 p3035 A72-41489
- Influence of a variable electric field on the diffusion of ions in a gas
21 p3086 A72-41676
- Diffusion toward a particle in the case of shear flow of a viscous liquid - Approximation of the diffusion boundary layer
22 p3165 A72-41910
- Isotope effect measurements application to determination of sodium diffusion mechanism and rate in sodium silicate glass
22 p3196 A72-42794
- Grain size and temperature effects on Cr and Al diffusion coefficients and mobility in Ni-20Cr and thorium dispersed NiCr alloys from measurement at 1038-1200 C
22 p3193 A72-43028
- German monograph - Determination of the diffusion coefficient of hydrogen in the binary iron-nickel system at 25 and 58 C.
22 p3194 A72-43057
- Diffusion coefficients measurement in solid and liquid Al, discussing experimental techniques and temperature dependence
23 p3304 A72-44300
- Influence of weak disturbances on the operation of a gas laser with a homogeneous working-transition line
23 p3297 A72-44467
- DIFFUSION EFFECT**
U DIFFUSION
DIFFUSION ELECTRODES
- Teflon-bonded hydrophobic gas diffusion electrode performance prediction by mathematical treatment of flooded catalyst agglomerate model
16 p2352 A72-33892
- DIFFUSION FLAMES**
- Diffusion flames turbulence measurements by microphones, hot wire probes, Pitot tubes and photodiodes, evaluating density fluctuations by indirect methods
02 p0303 A72-12854
- Supersonic diffusion flame in duct configuration to study mixing with combustion of two parallel methane and air flows
03 p0405 A72-13545
- NO formation in spherical diffusion flames around hydrocarbon fuel drops burning in air [WSCI PAPER 71-29]
04 p0482 A72-14582
- Soot oxidation rate from diffusion flame measurements extrapolated for gas turbine combustion chambers
05 p0747 A72-16368
- Sound effect on diffusion flames, presenting vortex model
05 p0747 A72-16701
- Turbulent diffusion flame model in Couette flow, including wall effect [AIAA PAPER 72-214]
05 p0748 A72-16856
- Nonuniform potential and dissipation flow structure of turbulent diffusion flame front at high Reynolds numbers
06 p0902 A72-18104
- Ionic winds with restricted entrainment and gauze electrode, considering diffusion flame aeration in combustion systems
07 p1037 A72-19372
- Particle formation rates in thermal decomposition of acetylene in diffusion flame, noting activation energy
07 p1099 A72-19373
- Flow phenomena, mixing and stability of high speed enclosed multijet turbulent diffusion flames fed by propane and air
10 p1563 A72-25139

- Ethanol liquid fuel counterflow diffusion flame stabilization and thermal structure determination by interferometry 13 p1913 A72-29306
- Counterflow diffusion flame gas dynamic structure analysis in porous cylinder forward stagnation region, using surface and boundary layer approximations 15 p2336 A72-32310
- The turbulence diffusion in free jets and flames 18 p2740 A72-36245
- Topler schlieren study of diffusion flame structure of plane laminar hydrogen-air jets in rectangular channel with vortex generators 19 p2879 A72-37365
- Burke-Shumann-Zeldovich model for aerodynamic characteristics of straight jet laminar diffusion flames, considering free, semibounded and slipstream types 19 p2882 A72-38460
- Optical measurements in a pulsating flame. [ASME PAPER 72-HT-8] 20 p2926 A72-39679
- Effect of the temperature on the burn-out of hydrogen diffusion flames in a supersonic flow in a closed channel 21 p3129 A72-40983
- Experiments on methods for improved fuel ignition in scramjet combustion systems. [ICAS PAPER 72-15] 21 p3099 A72-41140
- Radiation intensity of a steady flame above a burning fluid 22 p3243 A72-42166
- German monograph - Turbulence behavior and degree of nonmixing of jets and jet flames. 22 p3245 A72-43077
- Measurement of the velocity distribution in the boundary layer over a flat plate with a diffusion flame. 24 p3464 A72-45062
- Diffusion flame in homologous turbulent shear flows. 24 p3395 A72-45564
- DIFFUSION PUMPS**
- In-line high vacuum conductance valve with attached diffusion pump for shock tube evacuation 13 p1959 A72-29758
- DIFFUSION THEORY**
- Self sustained oscillations of mechanical system with infinite number of degrees of freedom, considering application to diffusion in porous medium 02 p0258 A72-11496
- Thermodynamic equilibrium variational theory for multiphase systems subject to nonhydrostatic stress, considering diffusion and phase transformations 03 p0455 A72-12908
- Carbon-oxygen reaction kinetic limitations on carbon ablation rate, discounting diffusional transport limits above 1650 K 03 p0457 A72-13955
- Diffusion model applicability to lateral transport in terrestrial and lunar exospheres, using kinetic theory 07 p1056 A72-18902
- Monograph on diffusion couple technique for Ti-Al system interdiffusion phenomena, discussing layer growth, phase development, grain boundary diffusion mechanism, mass transport, etc. 07 p1011 A72-19267
- Temperature distribution in composite media with internal heat generation, solving diffusion equation via Vodka type orthogonality relationship 07 p1100 A72-19626
- Radial diffusion and convection capillary model for analysis of tissue protein concentration and colloidal osmotic pressure changes during transcapillary fluid movement 08 p1114 A72-20896
- BiTe crystal critical growth rate calculation based on theory for diffusional supercooling of melt with excess Te 08 p1217 A72-21338
- Probabilistic derivation of quantum mechanics wave equations for Brownian motion and spatial-temporal diffusion 10 p1505 A72-24071
- Book on binary metal oxides covering non-stoichiometry, electrical conductivity, diffusion theory, point defects, high temperature creep and electrochemical transport properties 10 p1527 A72-25075
- X ray diffusion by thin films under grazing incidence, using reciprocity theorem 11 p1689 A72-26484
- Streamlines and fluid diffusion determination for axisymmetric irrotational and rotational flows in ducted propellers, noting conformal mapping of arbitrarily shaped domain onto rectangle 12 p1751 A72-27168
- Point defects investigation in Si and Ge by diffusion techniques, precipitation from supersaturated solid solutions, quenching from high temperatures and plastic deformation 12 p1856 A72-28053
- Boundary layer approach to local potential solution of diffusion equations, applying to transpiration cooled half space and heat conduction in melting solid 13 p2064 A72-28885

- Critical analysis of Mouthaan-Susskind diffusion theory for magnetron diode electron transport, noting theoretical results discrepancy with experimental data 13 p1931 A72-29289
- Quasi-linear diffusion theory for axisymmetric toroidal plasma, considering normal modes and energy conservation 15 p2287 A72-32413
- Capillary heat convective diffusion model of liquid layer sandwiched between two planes for calculating slag and metal movement rates 16 p2476 A72-33157
- Disk-shaped diffusion model with inhomogeneous distribution of gas and heavy relativistic nuclei sources for galactic cosmic rays chemical composition 17 p2600 A72-35206
- Singularities of nonstationary solutions to the equation of diffusion in a gravitational field. I, II 18 p2687 A72-36655
- On the role of density gradients in the continuum theory of mixtures. 18 p2712 A72-37076
- Influence of isothermic reaction levels on the diffusion growth of compounds with a binary equilibrium diagram 19 p2817 A72-37792
- Role of an electric field in the diffusion mechanism of the graphite-to-diamond phase transformation 19 p2823 A72-38405
- Experimental facility and diffusion technique for measuring turbulence characteristics during hydrocarbon fuels burning in air streams 23 p3287 A72-43658
- Diffusion processes of cosmic rays with energies between 2 and 20 GV during Forbush decreases - The diurnal effect. 24 p3434 A72-44785
- High order terms diffusion equation derivation for strong fluctuating flows by random walk method, discussing phenomenological analogy with equations of motion 24 p3390 A72-44994
- Mixed, nonequilibrium and coherent diffusion in stationary media with intense energy sources, noting finite speed of light effects 24 p3428 A72-45057
- Resonant diffusion in the presence of strong plasma turbulence. 24 p3430 A72-45567
- DIFFUSION WELDING**
- Metal matrix fabrication processes, considering plasma sprayed and diffusion bonded tapes and consolidated sheet material 01 p0074 A72-10733
- Continuous seam diffusion bonding application to Ti and superalloys lap, butt and T joints production [SME PAPER AD 71-264] 01 p0076 A72-10970
- Forging techniques and applications for YF-12A aircraft Ti alloy bulkhead production, considering diffusion bonding and die shimming 04 p0527 A72-14914
- Diffusion welding of cast and wrought Udimet 700 superalloy gas turbine engine components, discussing interfacial grain boundary migration and microstructural homogeneity effects on weld joint quality 07 p0997 A72-19998
- Vacuum hot press diffusion welding of nickel-chromium-thorium dioxide sheet, describing specimen preparation, welding procedure and welded joints photomicrographic microstructure 07 p0997 A72-20002
- Metal welded joints formation as diffusion intensification from atom jumps stimulation by phonons from atomic thermal vibrations or crystal defects generation 09 p1319 A72-22867
- Diffusion bonding compared to other processes, discussing mechanical properties, metallurgical condition, fatigue, pressure, temperature and production problems 09 p1320 A72-23633
- Diffusion bonded joints tensile strength determination from ultrasonic pulse echo and attenuation measurements, discussing contamination and SNR effects 10 p1485 A72-23814
- Ti alloy sheets diffusion brazing, describing chemical cleaning, auxiliary metal cladding, heating and pressure augmented fusion processes involved in high quality joints production 10 p1497 A72-24658
- Interdiffusion of tight contact welded ring Ti-W pairs at high temperature, using X ray analysis and electron beam techniques 10 p1497 A72-24785
- Thick steel plate diffusion welding in air with dead-weight loading and autogenous surface cleaning 11 p1637 A72-25343
- Solid state joining in gas turbine engines, discussing diffusion bonding, friction welding and coextrusion metal bonding [ASME PAPER 72-GT-74] 11 p1639 A72-25656
- Sintered Mo diffusion weld strength dependence on contact surface flatness and smoothness 11 p1644 A72-26847

- Mechanical properties of thick Be plate produced by diffusion bonding of thin sheets from ingot material 13 p1973 A72-28655
- NAND gate logic transistor circuit design, layout, fabrication and electrical parameters, noting base and resistors diffusion welding 17 p2530 A72-35069
- Electrolytic and nonelectrolytic diffusion methods for protective coatings production from gas, liquid or solid phase, discussing wear resistance enhancement in boridized steels 20 p2929 A72-39449
- Ti fabrication advances in forging, diffusion bonding, hot forming, chemical milling and laser cutting 21 p3061 A72-41335
- Diffusion bonded columbium panels for the shuttle heat shield. 24 p3406 A72-44889
- DIFFUSIVITY**
- Inspiration time correction factor for pulmonary diffusing capacity measurement by single breath method 01 p0015 A72-11259
- Jacketed tubular chemical reactor optimal startup control, presenting distributed maximum principle for diffusional parameter system 02 p0301 A72-12093
- Hydrogen diffusivity in Fe with cavities at room temperature calculated by mathematical model and numerical methods 03 p0378 A72-14256
- Kinetic data analysis of internal oxidation in dilute Ni-Be alloys, deriving activation energy and diffusivity of oxygen in Ni 07 p1021 A72-20435
- Thermal conductivity, diffusivity and specific heat of lunar soil and basalt analogs, using Luna 16 samples 10 p1532 A72-23753
- Tangential and radial eddy diffusivity effects on nonsymmetric turbulent diffusion in plain impervious tube as function of Schmidt number 14 p2096 A72-31069
- Simultaneous determination of the thermokinetic characteristics of solids by a variable regime method 17 p2638 A72-35749
- Stability of Al₃Mg₂ particles against diffusive coagulation in aluminum-magnesium alloys 23 p3301 A72-43649
- DIFLUORIDES**
- NT CALCIUM FLUORIDES
- DIFLUORO COMPOUNDS**
- NT POLYTETRAFLUOROETHYLENE
- Dichlorodifluoromethane-fluorine flame structure, taking samples by molecular beam sampling system for analysis by mass spectrometry 02 p0303 A72-12483
- DIGESTIVE SYSTEM**
- NT GASTROINTESTINAL SYSTEM
- NT INTESTINES
- NT MOUTH
- NT PANCREAS
- NT TEETH
- Incorporation of methionine-S 35 in the proteins of the digestive organs of rabbits under the action of radiation and vibration 21 p2998 A72-40440
- Role of the hypothalamus and limbic system in the regulation of the motor and secretory functions of the digestive apparatus 21 p3000 A72-40754
- Behavior concept formulation for visceral systems, considering digestive system data and extension from motor function concepts 24 p3370 A72-44586
- DIGITAL COMMAND SYSTEMS**
- Radar digital control system, discussing cost effectiveness, block levels, flexibility, tradeoffs, data management, decision making and future applications 02 p0178 A72-12395
- Countersink boring machines with programmed digital control systems for precision spacing multiple hole drilling in extended aircraft engine components 11 p1642 A72-26816
- Time of delay signal information addition to OMEGA worldwide VLF navigation system by digital code applicable for clock resetting and timing for automatic data recording 15 p2199 A72-32077
- Flight-test experience in digital control of a remotely piloted vehicle. [AIAA PAPER 72-883] 20 p2889 A72-40059
- Digital command system second-order subcarrier tracking loop performance. 21 p3038 A72-40870
- Qualitative investigation of nonlinear pulse systems by the point mapping method 23 p3277 A72-44006
- The use of minimum order state observers in digital flight-control systems. 24 p3382 A72-45343
- DIGITAL COMMUNICATION**
- U PULSE COMMUNICATION
- DIGITAL COMPUTERS**
- NT SEQUENTIAL COMPUTERS

General purpose electronic modular units for human factors research instrumentation, considering digital and analog computers, logic modules and interface and auxiliary equipment

01 p0048 A72-10569

Linear and nonlinear material static and dynamic structural analysis using NASTRAN digital computer program with finite element approach

01 p0140 A72-10983

Fault-tolerant digital computer logic design for dynamic and interactive recovery with data integrity after error, discussing hardware and software functions requirements

02 p0184 A72-11480

Mathematical reliability modeling for fault tolerant digital computers, summarizing error masking and standby sparing reliability equations

02 p0184 A72-11481

Separate and nonseparate arithmetic error detecting and correcting codes for digital computer design, considering cost and effectiveness tradeoffs

02 p0184 A72-11483

Soviet progress and bibliography on fault tolerant digital computers design, emphasizing redundancy application to achieve high reliability

02 p0184 A72-11484

Ultrareliable fault-tolerant digital computer design with protective standby replacement and hybrid redundancy, presenting mathematical models for system reliability evaluation

02 p0185 A72-11487

Three-failure-tolerant digital computer system design using adaptive majority voting in hardware and software for real time control application

02 p0185 A72-11488

Distributed fault-tolerant aerospace digital computer design with duplicated central multiprocessor, triplicated memory and conventional redundancy local processors for error detection and correction

02 p0185 A72-11489

Hardware and software parallel digital computer system described by flow table model, calculating output hazard for unbounded line delay effects

02 p0185 A72-11490

Associative array digital processors application to numerical solution of partial differential equations, illustrating methodology on weather forecasting equations

02 p0186 A72-11658

Digital computer memory system for real time processing of air and naval traffic data, discussing logic design, time comparisons and optimum use

02 p0188 A72-12647

Digital computers data output alphanumeric display by commercially available TV sets, describing system design

03 p0355 A72-13075

Radar signal processing by digital computer modeling, presenting apparent target splitting probability and azimuth estimate distribution for shifting window target detectors

03 p0326 A72-14361

High speed digital communication at millimeter wavelengths, discussing system requirements, digital computer use, transmission data rate and equipment development

04 p0485 A72-14481

On-line digital spectrum analysis based on fast Fourier transform algorithm, exemplifying by plasma density fluctuations correlation

04 p0496 A72-15488

Minicomputer use for terminal control and matching functions and data compression in data transmission systems

05 p0633 A72-16199

Planetary disturbing function expansion, using classical binomial or Laplace series methods on large scale digital computer with Poisson program

06 p0878 A72-17665

Minicomputers evolution, considering price reduction, performance improvement, operation simplification, and applications for data collection and transmission

06 p0780 A72-18179

Man computer dialogue, considering human factors effects on interaction course

07 p0927 A72-19128

On-line digital computer system for real time interpretation and report generation of electrocardiograms from remote locations over switched telephone network

07 p0928 A72-19311

Image processing of diagnostic echocardiogram by ultrahigh speed analog to digital converter interfacing digital computer

07 p0928 A72-19312

Computational mean square error due to roundoff in digital filters implemented on fixed point computers

07 p1033 A72-20346

Hybrid Monte Carlo techniques with digital and analog computers and minimal interface, simulating random walks for partial differential equations solution

08 p1138 A72-21602

Digital image processing for TV camera noise suppression and photometric and geometric distortions calibration and rectification

08 p1172 A72-21977

Soviet papers on digital computers application to reliability problems solution for recoverable, failing, controlled, redundant and electronic systems

08 p1179 A72-22051

Hardware monitor and associated analysis programs to evaluate real time satellite command and control digital computer system performance

10 p1442 A72-23817

STARAN IV-X associative array processor for automation in ATC environment, considering air tracking, conflict prediction and resolution functions

10 p1442 A72-23818

Digital computers application as filters in launch vehicles and high performance aircraft attitude control systems, estimating number of computer operations

10 p1444 A72-24031

Rapid data input system for Minsk 22 digital computers using photographic film read by photoelectric scanning system

10 p1445 A72-24495

Mean square error and functional state prediction algorithm for plants controlled by automatic system containing digital computer

11 p1600 A72-25439

Design and production related cost reduction factors in universal digital computers fabrication

11 p1603 A72-26825

Analog and digital computers for automatic statistical analysis of unsteady random process recorded data, calculating correlation functions and expectancy

13 p1925 A72-29165

Time response analysis for digital computer speed evaluation

13 p1925 A72-29270

Digital computer estimates of random processes spectral density by statistical correlation method, calculating errors in numerical integration techniques

13 p1937 A72-29495

Digital computer synthesis of transparent object holograms, noting image discretization, two dimension Fourier transformations spectrum and digital data correlation with optical parameters

13 p1958 A72-29617

Measuring tape recorder, properties and utilization for signal recording and processing, discussing digital computer techniques and compensation for interference effects

14 p2104 A72-30287

Aircraft inertial navigation system, discussing mode selection unit, digital computer and control display for operator communication with system

15 p2267 A72-31596

Linear control systems optimal synthesis using ALGOL program for digital computers minimizing error square integral

15 p2210 A72-31687

Parallel digital computer application to radar tracking data processing, discussing system design for efficiency maximization and performance, desensitization in traffic level fluctuation

15 p2203 A72-31781

Astronautical digital computing hardware and software trends and implications, considering data rates, reliability, LSI, speed-storage tradeoff, etc.

15 p2203 A72-31822

Reliability-maximizing digital computer synthesis based on multiple redundant network design, discussing majority structure distribution optimization technique

15 p2203 A72-32174

Programmable digital differential analyzer for connection to digital computer, discussing dynamical problem solution and real time systems simulation capability

15 p2204 A72-32387

Ultrasonic flaw detector data analysis, discussing digital computer interface and encoders

16 p2397 A72-33202

Digital attitude and heading reference system computer for aircraft heading control, discussing design and performance features

16 p2367 A72-33244

Fixed point computer mean square errors in multiplication as function of number of digital order

16 p2367 A72-33959

Synchronizing electronic equipment for digital computers input graphic data recording fidelity improvement ensuring proper timing of set and reset pulses

16 p2367 A72-34018

Analysis of a control computer complex as a multiphase queuing system

17 p2522 A72-35030

Texture synthesis by image processing equipment consisting of digital computer and input/output unit, noting image signatures of constant parameter areas

17 p2555 A72-35338

Process computer system design, discussing structural units, data flow coordination with storage, input/output channels and periphery coupling problems

17 p2523 A72-35443

High performance 16-bit computer organization.

17 p2523 A72-35580

Modular avionics computer design concept to permit tailoring for diverse applications via microprogramming

17 p2524 A72-35581

Digital image processing and interpretation of photographic film data.

18 p2690 A72-36319

Optimal programming data distribution in digital computer storage devices, noting independent subprograms assembling

19 p2769 A72-38088

Digital computer algorithm for electronic circuit calculations

19 p2774 A72-38422

Future trends of airborne computers.

[ALAA PAPER 72-895] 20 p2905 A72-39109

Two dimensional microprogrammed cellular arrays logic organization and control structure for multifunctional digital subsystems

20 p2906 A72-39736

A hybrid quasi-analog system for solving boundary value problems

21 p3024 A72-40159

Computer simulations of transport processes.

21 p3024 A72-40247

A new concept of flight displays compatible with digital airborne computers.

21 p3012 A72-41426

Digital-computer analysis of electron guns for cathode-ray tubes by taking into account initial thermal velocities.

21 p3088 A72-41834

Transient test techniques for modal survey testing.

22 p3163 A72-42698

Reliability-maximizing digital computer synthesis based on redundant network design, discussing majority structure optimal allocation technique

22 p3157 A72-43008

Information theory application for structural complexity measure of microelectronic logic circuits for digital computers, noting elements standardization for design quality criteria

23 p3269 A72-43441

Multiprogrammed virtual memory digital computer systems analysis and design, discussing component characteristics, operating system structure and mathematical description techniques

23 p3267 A72-43987

Improvement of an algorithm for the rejection of points in the solution of a mutual orientation problem on a digital computer

24 p3401 A72-44861

Automatic complex control systems with digital computer application for optimal control of production systems, selecting optimality criterion from hierarchically distributed local criteria

24 p3387 A72-45513

Parallel Element Processing Ensemble (PEPE)/digital computer for real time radar data processing and control, discussing system design and applications

24 p3383 A72-45666

DIGITAL DATA

Decoder for delay-modulated digital data conversion to nonreturn to zero data, discussing time-phase ambiguity resolution capability in real time

01 p0025 A72-10331

Coding for analog and digital data transmission over channels with noiseless and noisy feedback links

02 p0197 A72-11680

Low loss wideband circular wave guide bend characteristics and branching filters for millimeter wave large capacity digital transmission

02 p0190 A72-11682

Format logic design for airborne memory controlled PCM telemetry multiplex digital and analog data system

02 p0187 A72-12130

High density digital tape recorder with combined phase encoded digital electronics and helical scan video transport

02 p0229 A72-12152

Twisted shielded pair (TSP) time division multiplexed data bus with standard interfaces for use in aerospace applications

02 p0194 A72-12405

Digital telemetry data transmitter featuring triangular wave generator and signal mixer for reducing sensitivity to transmission path characteristics variations

02 p0179 A72-12415

Optimization methods in digital data transmission systems, discussing equalization circuits for base band channel using metallic lines

02 p0182 A72-12691

Noise reduction in pulse width modulated converters with rms voltage values digital readout, using active or passive filters methods

03 p0331 A72-13557

Soviet book on statistical theory of digital data transmission through parallel channels covering optimal and suboptimal reception systems under signal fading and interference

03 p0323 A72-13968

Decoding technique for delay modulated digital data conversion to NRZ/c/ data, describing logic implementation and timing diagrams

04 p0486 A72-14490

Surface wave parametric signal processing, obtaining cross correlation of digitally coded input signals

05 p0631 A72-17074

Spatial digital transform coding of color images using three primary color data planes

06 p0772 A72-17403

Solar Fraunhofer line profiles determination by digital data recording double-pass spectrophotometer, presenting observed atomic Ni and Fe lines intensity distributions

06 p0884 A72-18028

Earth science and technical applications of multispectral photography and digital image processing techniques

08 p1166 A72-21334

VHF remote control anemometer network with digital receiving station for wind measurement and gale warning system

10 p1463 A72-25013

Real time pilot reports via digital ground-air-ground data link, discussing encoding and processing equipment, meteorological codes and automatic real time weather forecasts

10 p1440 A72-25079

Design and operation of digital image recorder based on single stage intensifier and silicon target intensifier television camera tube coupled to large memory

11 p1631 A72-25685

CAMAC modular digital data handling system for communication with computer, discussing compatibility and data acquisition in astronomy application

11 p1600 A72-25692

Radar echo maximum intensity display by digital comparator with shift register video signals storage in National Severe Storms Laboratory

11 p1591 A72-25762

Solar Fraunhofer line profiles determination by digital data recording double-pass spectrophotometer, presenting observed atomic Ni and Fe lines intensity distributions

11 p1719 A72-25964

Digital computer synthesis of transparent object holograms, noting image discretization, two dimension Fourier transformations spectrum and digital data correlation with optical parameters

13 p1958 A72-29617

Optical communications with FDM digital data channels, examining signal optimal reception and noise stability

14 p2084 A72-30331

Digital FM signal receiver with postdetector integration, determining error probability as function of input SNR and noise stability

14 p2084 A72-30332

Synchronization theory for digital data transmission with random changes in channel characteristics

14 p2085 A72-30333

Magnetosphere thermal plasma densities determination from hydromagnetic whistler digital sonograms and modified normalized dispersion curves

15 p2283 A72-31430

Filtering and hard-limiting effects on digital FM signals power spectra, using Postl direct method

15 p2194 A72-31543

Error probability distribution of digital data magnetic recording in computer drum memory

16 p2367 A72-33262

Digital computer program for automatic processing of rocketsonde and radar digitized data, presenting graphical output from meteorological rocket soundings during 7 March 1970 solar eclipse

16 p2419 A72-33944

The precision-processing subsystem for the Earth Resources Technology Satellite.

18 p2674 A72-36497

Cloud liquid water content measurement via digital radar system, presenting two dimensional display of storm system characteristics

21 p3077 A72-40250

Elimination of an ambiguity in the reading of digital computational devices

21 p3035 A72-41810

High speed, high density digital recording.

22 p3175 A72-41933

Analog and digital data recording systems, discussing accuracy, versatility and cost factor tradeoffs in selecting equipment for given applications

22 p3155 A72-42707

Probability of digital-data reception with a given confidence level under conditions of random radio noise

23 p3266 A72-44208

Error probability estimates in two channel diversity reception systems of digital data transmission with allowance for fading correlation and incomplete signal separation

24 p3379 A72-44751

Effects of bandlimiting on the coherent detection of PSK, ASK and FSK signals.

24 p3380 A72-44900

DIGITAL FILTERS

Optimal frequency domain design of two dimensional low pass finite impulse response digital filters by linear programming

01 p0046 A72-10868

Statistical long term speech spectrum analysis and perceptual evaluation, using digital bandpass filter technique

02 p0171 A72-11666

Fast Fourier transforms for digital matched filters in wideband radars, using computer simulation for word size and dynamic range relationship determination

02 p0188 A72-12398

Time and frequency domain properties of orthogonal nonrecursive binomial sequences, discussing digital filters synthesis

03 p0381 A72-13408

Optimal digital Kalman filtering for systems with continuous input noise by autocorrelation function matching [ASME PAPER 71-WA/AUT-21]

05 p0640 A72-15952

Coefficient rounding effect in digital filters using floating point arithmetic

05 p0633 A72-16576

Noise contaminated pulse signal transit time measurement by receiver using digital filters

07 p0939 A72-19051

Computational mean square error due to roundoff in digital filters implemented on fixed point computers

07 p1033 A72-20346

Digital filter synthesis for radar signal processing applications, discussing frequency sampling method extension with advantage of known waveform and reduced computations

08 p1146 A72-21916

Filtration and extrapolation of multivariable random processes described by linear differential equations system, examining adaptive filter synthesis

09 p1283 A72-23436

Numerical linear interpolator design with ICs, noting application to digital filters and sampled data systems

09 p1289 A72-23677

Digital MTI detection filter using on-line adaptive procedure for adjustment

10 p1456 A72-23804

System methodology application to filter design for inertial reference unit calibration in digital test station for FB-111 aircraft navigation system

10 p1456 A72-23820

Digital computers application as filters in launch vehicles and high performance aircraft attitude control systems, estimating number of computer operations

10 p1444 A72-24031

Surface acoustic wave technology in communication systems, discussing analog and digital matched filters and navigation, ATC and collision avoidance applications

10 p1483 A72-24940

Linear multiple section binary filters analysis and synthesis, discussing mesh functions spectra for signal measurement in automatic control systems

11 p1612 A72-26452

Modular computer program for digital transmission systems, applying to optimization of filters in multitransponder satellite and ground stations

12 p1786 A72-27323

Sampling theorem with small truncation error for band limited signals, discussing applications to pulse transmission filter design

13 p1922 A72-29397

Filtering and hard-limiting effects on digital FM signals power spectra, using Postl direct method

15 p2194 A72-31543

Adjacent channel discrimination enhancement in Gray-scale binary coded two dimensional array, using checkerboard filter for pattern noise suppression

15 p2238 A72-32162

Shift register implemented binary transversal filter type digital pulse waveform generators truncation and approximation error spectrum analysis via inverse Fourier transform

16 p2362 A72-32854

Standard and bilinear z transformation techniques for digital sampling filters block diagrams derivation

16 p2369 A72-33671

Recursive digital MTI radar filter design in z plane, detailing spectrum rolloff and flat passband in amplitude response

16 p2369 A72-33758

Fast computational techniques for generalized two dimensional Wiener filtering.

17 p2532 A72-34402

Image enhancement by computer programs, discussing digital filtering, fast Fourier transform algorithm, data management and large matrix handling

17 p2520 A72-34404

Frequency domain design of two-dimensional finite impulse response digital filters.

17 p2532 A72-34406

On structures for nonrecursive digital filters.

17 p2516 A72-35221

Finite word length effects on digital filter implementation.

18 p2663 A72-36303

The use of linear programming to design digital filters from impulse-response specifications.

18 p2663 A72-36304

Mathematical methods for improving the significance of scintigrams

18 p2652 A72-36425

Design of nonrecursive digital moving-target-indicator radar filters.

18 p2667 A72-36687

Design of digital filters using state-space realization.

18 p2674 A72-36943

Evaluation of the basis parameters of a frequency-code receiver with a generalized differential circuit

19 p2771 A72-37304

An application of correlation to radar systems.

19 p2764 A72-37927

Frequency detection with digital resonators without damping

19 p2773 A72-37939

Predictive filtering of multi-channel time series records with application to Doppler radar data.

19 p2781 A72-38272

Square root least squares and filtering solutions for fixed point and interval smoothing problems, comparing computational stability and precision and computer requirements [AIAA PAPER 72-877]

20 p2910 A72-39122

Transformation of reactive ladders into digital circuits.

20 p2910 A72-39427

Effects of finite register length in digital filtering and the fast Fourier transform.

20 p2904 A72-39780

Digital filters with cyclically variable coefficients

21 p3025 A72-40221

Quantization error of the coefficients in digital filters with N shift sequences

21 p3025 A72-40223

Microwave filter of interdigital or comb construction, calculating attenuation coefficient relationship to impedance of slabline with cylindrical inner conductor

21 p3032 A72-40628

Digital computer synthesis of Fourier holograms of transparencies, noting significance to digital filtering method development for optical signal processing

21 p3054 A72-40670

Frequency-sampling and transversal digital filter equalizers optimal design from specified unit impulse time response, using linear programming algorithm

21 p3033 A72-40900

Digital filter realizations using a special-purpose stored-program computer.

23 p3267 A72-43815

Digital filter design using observers.

23 p3276 A72-43864

Optimal filtration algorithms of Markov parameters of discrete time signals in digital data transmission system with background noise, using Gaussian probability density approximation

23 p3264 A72-44005

Optimal equalization of discrete signals passed through a random channel.

23 p3265 A72-44178

Linear filtration of random signals based on the criterion of maximum signal-to-noise ratio

23 p3273 A72-44215

Analysing vibration and shock data. I - Data acquisition and pre-processing.

24 p3382 A72-45287

DIGITAL INTEGRATORS

High resolution digital integrator design based on second order differences

07 p0963 A72-20388

Large scale integrated circuits for digital differential analyzers, giving operational specifications for shift registers, adders and integrators

10 p1448 A72-24276

Additive noise effect on accuracy of integrating digital voltmeters using pulse frequency and pulse time converters

16 p2370 A72-33955

A differential-integral amplitude-time converter of nanosecond-range pulses

19 p2771 A72-37305

DIGITAL NAVIGATION

Digital solid state altitude encoder for ATC transponder reporting, covering Gray and Gillham codes [SAE PAPER 720314]

11 p1630 A72-25578

Operational advantages of low cost VLF/OMEGA digital navigation system for various aircraft types

13 p1998 A72-29196

Digital autopilot for SKYLAB orbital assembly attitude control during docking, discussing jet selection logic, inter-axis dependence and onboard computer

15 p2269 A72-32183

Error analysis for digital avionics system involving Doppler navigation by intermittent scanning of single beam multimode radar, noting optimum statistical data processing

15 p2271 A72-32204

DIGITAL RADAR SYSTEMS

Radar digital control system, discussing cost effectiveness, block levels, flexibility, tradeoffs, data management, decision making and future applications

02 p0178 A72-12395

- Splash detection radar digital signal processing by off-line computer using wideband video recorder
02 p0178 A72-12399
- Decision error estimates applied to detection problem with digital radar, computing upper and lower bounds for error probability
05 p0632 A72-17093
- Stanford pulse Doppler radar and digital data acquisition system for meteor trail wind measurements
10 p1438 A72-24711
- Radar sequential detector for digital processing of signal masked by noise, determining false alarm and detection probabilities and mean test duration
10 p1439 A72-24908
- Optimal selectivity digital recorders for meteor trails radar observations, considering input process quantization rate and spectral width selection
13 p1929 A72-29031
- Automatic real time processing of meteor radar echoes, using digital computers
13 p1924 A72-29033
- Cloud liquid water content measurement via digital radar system, presenting two dimensional display of storm system characteristics
21 p3077 A72-40250
- Investigations on the use of a Kalman filtering method in tracking systems for air traffic control. [ICAS PAPER 72-43]
21 p3082 A72-41168
- DIGITAL SIMULATION**
- Kalman filtering process digital simulation by numerical integration of matrix differential equations describing linear system random process model and optimal filter
01 p0024 A72-10225
- Large signal nonlinear modeling and digital simulation of microwave transistor power amplifier and GaAs Gunn relaxation oscillator
01 p0041 A72-10691
- Digital simulation of general atmospheric circulation via spatial finite difference dense grid, considering surface properties and pressure distribution maps
02 p0252 A72-11652
- Mathematical model for control process as adaptive memory tracker, discussing digital simulation
02 p0186 A72-11659
- Human postural control system dynamic model, discussing stick man pitch axis dynamics digital simulation and difficulties in linearizing equations of motion
03 p0318 A72-13163
- Digital computer simulation of rarefied gas molecular beam-rough metal surface interaction
03 p0392 A72-14057
- Different pair potentials for simulating vacancy in Al, discussing program planning for relaxations calculation around vacancy to effect computing time reduction
03 p0378 A72-14253
- Two dimensional molecular dynamics digital simulation of Ar liquid-vapor interface at triple point, yielding strongly oscillatory density profile
03 p0393 A72-14263
- Robust delta modulator configuration with minimal mean square error from signal statistics estimates, discussing design and performance by digital simulation
04 p0486 A72-14486
- Gaussian envelope microwave pulse generation using absorption p-i-n diode modulator, predicting performance by digital simulation
04 p0498 A72-14718
- Free molecular flow heat transfer to rough surface, discussing surface/molecule interaction model for digital simulation
[ASME PAPER 71-WA/HT-8] 05 p0743 A72-15868
- Airplane hydraulic control systems digital simulation, using method of characteristics for distributed parameter analysis of transmission line dynamics
[ASME PAPER 71-WA/FE-21] 05 p0615 A72-15928
- Quasi-steady continuous process adaptive optimal control, discussing algorithms and model for sensitivity matrix calculation and digital simulation for strategy
05 p0640 A72-16200
- Numerical simulations of three dimensional homogeneous isotropic turbulence at wind tunnel Reynolds numbers, solving Navier-Stokes equations for incompressible flow
05 p0649 A72-16685
- Linear system digital simulation by matrix exponentiation with generalized hold order algorithm for accuracy improvement at less computer time
06 p0839 A72-17630
- Book on discrete event computer simulation for complex systems synthesis and analysis covering random numbers use, languages, and interactive man machine applications
06 p0779 A72-17812
- Air transportation modal split analysis by computer simulation program for determining utilization of alternative travel modes between origins and destinations
06 p0905 A72-17973
- MARS digital simulation model in GPSS for determining scheduled flight operations and maintenance resources effects on aircraft availability and usage rates
06 p0779 A72-17976
- GERT simulation program as stochastic network analysis technique for modeling policies and processes in performance tests and checkout
06 p0780 A72-17977
- GERTS II simulation program for graphically modeling and analyzing complex stochastic systems, discussing applications to assembly line, project management, conveyor and inventory systems
06 p0780 A72-17978
- GPSS/360 interactive simulation program with report generator, selective output display and HELP blocks for model manipulation and real time viewing
06 p0780 A72-17980
- Non-supervised learning algorithm steady state behavior for multicategory pattern classification by analysis and digital computer simulations
06 p0780 A72-18256
- Plasma density inhomogeneity effects on beam-plasma instability and Landau damping from digital simulation using charge sheet model
06 p0865 A72-18541
- Phase lock loop receiving system digital simulation for estimating mean time to indicate lock and probability distribution function for wide SNR range
07 p0939 A72-19065
- Digital simulation for steady state and transient thermal responses of LSI with metal within substrate, considering computer time cost
07 p0954 A72-19176
- Quasi-time optimal nonlinear controller for steerable antennas or telescopes in target acquisition or slew mode, predicting performance by digital simulation
07 p0959 A72-19288
- FORTAN digital simulation of ATC radar beacon system making possible computer generated movie display
07 p0950 A72-19301
- Atmospheric heating and kinetic cooling nonlinear effects on IR carbon dioxide laser beam propagation, comparing digital simulation results with geometrical optics
[CLEA PAPER 2.6] 07 p0942 A72-19381
- Ion heating in high Mach number oblique collisionless shock waves, noting role of two-ion beam instability from digital simulation
07 p1043 A72-19665
- Numerical simulation of gas atom scattering from solid surface and satellite drag coefficient calculation
07 p0910 A72-20106
- Partial differential equation language /PDEL/ for batch and interactive digital simulation of PDE models
07 p0951 A72-20327
- Interactive simulation language-8 for minicomputer and programming procedures for nonlinear differential equations solution, considering integration step size and computational accuracy and speeds
07 p0951 A72-20334
- Computer interactive graphics for digital simulation of engineering fields modeled by partial differential equations boundary value problems
07 p0951 A72-20337
- Statistical analysis of system component error propagation by digital simulation using Continuous System Modeling program, considering strapped down inertial guidance computer
07 p1033 A72-20347
- Monte Carlo digital simulation of probabilistic buckling behavior of indeterminate structure under initial stresses due to random geometric lack-of-fit
07 p1095 A72-20348
- Tactical missile controlled test vehicle flight test analysis by six-degree-of-freedom digital simulation
07 p1086 A72-20351
- Digital simulation model of N helicopter formation flight characterized by close aircraft spacing, parallel flight vector and low bandwidth external forcing functions
07 p0913 A72-20354
- Digital simulation of two dimensional or marginally turbulent three dimensional flows by discretization and numerical integration, noting Galerkin method efficiency in avoiding errors
07 p0951 A72-20355
- Numerical simulation of atmospheric turbulence in planetary boundary layer due to wind shear and/or unstable thermal stratification, noting buoyancy and planetary rotation effects
07 p1031 A72-20359
- Digital simulation for predicting performance of data communication networks with computerized switching centers, detailing space shuttle interior communication system
07 p0952 A72-20364
- Cross correlation identification of linear time varying processes based on pseudorandom sequences, presenting digital simulation results
07 p0948 A72-20390
- On-line digital computer maximum likelihood estimate of Earth atmosphere profile ahead of flight vehicle using discrete measurements of density, temperature and pressure
[AD-739472] 08 p1156 A72-20853
- Combined signal detection and trajectory estimation functions optimization application to Monte Carlo simulation for trajectory moving across two dimensional grid
08 p1144 A72-20858
- Spurious target generation due to hard limiting in pulse compression radars with three phase coded signals superposed at input, comparing with digital simulation
08 p1134 A72-21416
- Digital simulation of human cardiovascular system, noting blood pressure control by physiological reflexes
08 p1125 A72-21475
- Numerical simulation of two dimensional and marginal three dimensional turbulent flows, discussing variable eddy viscosity model, discretization, numerical integration and Galerkin methods
08 p1200 A72-21492
- Maximum likelihood estimation for Weibull distribution parameters from multicensored samples by Monte Carlo simulation
08 p1200 A72-21589
- Radio system operational reliability analysis by mathematical methods with use of digital computer, discussing statistical modeling algorithm
08 p1143 A72-22065
- Digital computer simulation of circulatory and respiratory systems interaction model for oxygen and carbon dioxide gas exchange between pulmonary blood and alveolar air
09 p1268 A72-22456
- Galerkin method for numerical simulation of incompressible boundary flows in box geometries with periodic and free slip conditions, noting Taylor-Green vortex decay
09 p1294 A72-22941
- ATC system analysis by fast time arithmetic simulation techniques, describing ground model development
09 p1272 A72-23141
- Space shuttle flight crew/computer interface display and control functional requirements optimization by real time digital simulation
[ALAA PAPER 72-226] 10 p1460 A72-24437
- Digital computer simulation of random processes specified by canonical expansion, discussing quantization steps for storage requirements reduction
11 p1600 A72-25432
- Stationary and nonstationary random envelope processes digital simulation, presenting application to crack propagation under random loadings
11 p1686 A72-25730
- PCM and FDM/FM systems noise and signal distortion analysis by digital simulation with FORTRAN language based on fast Fourier transform
11 p1601 A72-26043
- Modular computer program for digital transmission systems, applying to optimization of filters in multitransponder satellite and ground stations
12 p1786 A72-27323
- Russian book on random signal generation covering ultralow and audio frequency spectra, random number and pseudorandom signals simulation and automatic control
12 p1786 A72-28347
- Digital dynamics simulation of continuous controlled processes based on repeated integral transformation of differential equations
13 p1934 A72-28607
- Mathematical model for numerical simulation of warm fog modification by seeding hygroscopic particles, taking into account turbulent diffusion and horizontal wind advection
13 p1992 A72-28844
- Extremal correlation algorithm for automatic control of two image congruent superposition, using digital simulation and statistical trial techniques
13 p1924 A72-29161
- Statistical analysis for single airport ATC digital simulation using Poisson distribution law, calculating optimal number of channels
13 p1996 A72-29179
- MHD power generators analytical modeling by digital technique for prediction of performance and efficiency as function of size and operating conditions
[AD-741173] 13 p1900 A72-29355
- Aircraft and other vehicle simulators for training crews, discussing evolution of needs, digital techniques, and visual and physiological experiences
14 p2092 A72-30844
- ATC procedures training by digital radar simulators, taking into account geographic terrain, radar, wind and aircraft characteristics and flight plans
15 p2214 A72-32098
- Algorithms for incorporating electromagnetic field into plasma numerical simulation to explain unwanted noise generation rates
15 p2288 A72-32421
- Theory of the dynamic vibration neutralizer with motion-limiting stops.
[ASME PAPER 71-APMW-14] 17 p2625 A72-34317
- Digital simulation for sampled electro-optical imaging system performance prediction and optimization
17 p2557 A72-35552

- Design of simple control loops in the time domain by simulation of the hybrid mode 17 p2534 A72-35756
- Numerical simulation studies of two-dimensional turbulence. I - Models of statistically steady turbulence. 17 p2543 A72-35765
- Numerical simulations of three dimensional isotropic turbulence in incompressible fluid at low wind tunnel Reynolds numbers 18 p2677 A72-36007
- Space-variant image motion degradation and restoration. 18 p2658 A72-36258
- An analog computer technique for estimating sample times for digital simulation. 18 p2663 A72-36305
- Digital simulation of stiff linear dynamic systems. 18 p2663 A72-36315
- Digital simulation for radio frequency interference and specular multipath effects on FM spread spectrum demodulation with feedback and phase lock loops 18 p2659 A72-36317
- Electron-relaxation effects in transferred-electron devices revealed by new simulation method. 18 p2667 A72-36689
- Digital simulations of effects of two-antenna interference on space vehicle guidance. 19 p2830 A72-37292
- Electron bunching and output gap interaction in broad-band klystrons. 19 p2772 A72-37566
- An investigation of vehicle dependent aspects of terminal area ATC operation. 19 p2832 A72-38256
- A digital computer simulation model for an SCR dc to dc voltage converter. 19 p2754 A72-38267
- Differential equations for digital model of linear quadrupole, discussing digital simulation of analog radio equipment circuits 19 p2775 A72-38659
- An iterative array which can represent the rotation and translation of objects. 20 p2905 A72-39422
- A digital simulation system for heat transfer modelled by ordinary and partial differential equations. [ASME PAPER 72-HT-25] 20 p2986 A72-39673
- Modeling a hybrid quasi-analog system on a computer 21 p3023 A72-40157
- Digital simulation of the SEI-1 static electrointegrator for solving heat-type equations 21 p3127 A72-40160
- Simulation of the process of reducing the redundancy of multichannel telemetry information on a digital computer by the method of adaptive break down into discrete elements and associative sorting 21 p3014 A72-40313
- Digital simulation for selection of extremal and lengthwise admissible paths on unidirectional computer graph 22 p3156 A72-42146
- Development and evaluation of an energy-oriented guidance logic for air combat models. [AIAA PAPER 72-949] 22 p3137 A72-42354
- Book - Computer simulation of dynamic systems. 22 p3157 A72-43081
- Output-feedback control law for randomly distributed multivariable system. 23 p3275 A72-43608
- Digital-computer simulation of the motion of a walking machine 23 p3278 A72-44002
- A digital model of jet engine hydraulic fuel controller 23 p3327 A72-44291
- Determination of the operational transfer functions of a gas turbine engine on a digital computer 23 p3327 A72-44292
- Nonlinear digital modeling of gas turbine propulsion units 23 p3327 A72-44294
- Determination of the statistical characteristics of a turbine stage and a group of turbine stages 23 p3328 A72-44295
- Simulation procedure for mission and maintenance planning of an air force wing. 24 p3365 A72-44663
- Jet stream formation from uniform distribution of grains in similar elliptical orbits, discussing models with numerical simulation 24 p3445 A72-45461
- On the power law for the kinetic energy spectrum of large scale atmospheric flow. 24 p3398 A72-45483
- Effect of envelope limiting in pulse-compression moving-target-indicator radar systems. 24 p3380 A72-45575
- Hybrid computer simulation program used in development and software design validation of digital flight control system for Titan 3C space booster 02 p0186 A72-11655
- Multichannel high-speed high-density digital recorder, describing tape transport and signal system 02 p0187 A72-12151
- Digital IC of ECL series without temperature compensation, discussing emitter coupled logic circuits interconnection methods 02 p0197 A72-12669
- Wireless electronic time distributing system, investigating integrable digital receiver circuit and frequency bandwidths 02 p0197 A72-12696
- Digital videomagnetograph providing real time display of line of sight component of solar magnetic fields 03 p0356 A72-13281
- All digital IC FM discriminator design, computing output SNR above threshold 04 p0486 A72-14489
- Single scan TV-radiography system for providing A-D converter analog signal for digital data acquisition, obtaining transfer functions 04 p0522 A72-15226
- Recovered carrier phase ambiguity resolution in four-phase PSK digital satellite communications system 06 p0772 A72-17409
- Digital system automated design and analysis developments covering interactive graphic computer aided design, gate level simulation, synthesis, partitioning, interconnection and fault test generation 06 p0778 A72-17471
- Digital loaded-line phase shifters for phased array antennas, discussing lossy microstrips effects and P-I-N diode switching shortcomings in design requirements 07 p0954 A72-19048
- Digital speech detector with increased voice signal and reduced noise sensitivity for satellite capacity improvement 07 p0939 A72-19067
- In-line eight stage digital light deflector with prisms and polarization switch, using Pockels effect with transverse field 07 p1003 A72-19222
- Digital decision directed suboptimal receiver design for random multipath channel communication with intersymbol interference, predicting performance for steady state probability of correct decision 07 p0941 A72-19272
- Digital system for wideband Gaussian noise generation using simultaneously generated PN-sequence with analog summation of independent binary waveforms 07 p0941 A72-19284
- Digital differential analyzers number comparison in realization of direction cosine, Euler angle and quaternion attitude algorithms 07 p0949 A72-19296
- On-line equalization of digital communication channels, discussing extended discrete Kalman filter use as adaptive equalizer 08 p1131 A72-20855
- Operational ternary computer random access memory, describing capacity and access and conversion times 08 p1138 A72-20872
- Range sidelobe suppression technique for Barker type phase reversal codes in digital processor for pulse compression 08 p1133 A72-21404
- Digitized SEC vidicon detector for OSO-H satellite coronagraph, describing optics 08 p1170 A72-21959
- Book on digital and analog monolithic IC systems, covering manufacturing methods, component design, MOS logic, arithmetic, error correction, codes, applications, etc 09 p1286 A72-23044
- Digital control system instability caused by introduction of floating point arithmetic in controller 09 p1341 A72-23096
- Digital lightning goniometry for flash locations at great distances by atmospheric and whistlers analysis 09 p1304 A72-23471
- Subminiature TV camera using hybrid packaging techniques and digital circuitry for full EIA composite video output format and 450 TV/RH resolution capability 09 p1316 A72-23599
- Digital controller simulation by analog means with independent gain adjustment of proportional, derivative and integral modes 10 p1445 A72-24093
- Dynamic logic control systems theory based on axiomatic concepts of models, deriving conditions for existence and uniqueness of solution for differential logic equations 10 p1457 A72-24636
- Meteor trail radar operated under digital controller synchronization and programmed for alternate and simultaneous two orthogonal directions search 10 p1438 A72-24715
- Digital signal analyzer design based on fast Fourier transform algorithm shift register coupled with single flow-through arithmetic unit 10 p1446 A72-25062
- Optimal control design for digital guidance system, conducting efficiency and reliability analyses 11 p1600 A72-25437
- Error correlation technique to ensure reliability of discrete automatically controlled digital systems inputs, noting lower redundancy requirement 11 p1600 A72-25438
- Narrow pulse optical communication digital systems with PPM and on-off keying, investigating timing error effects on bit error probabilities 11 p1592 A72-25885
- Deterministic methods to calculate quantization error in digital control system 11 p1610 A72-25976
- Solar proton event classification system with index of three digits representing proton flux, absorption and sea level neutron monitor response measurements 11 p1714 A72-26425
- Digital correlators and correlometers operational and design characteristics 11 p1602 A72-26444
- Digital correlator systems design for nonstationary signals, presenting circuit diagrams for multichannel centering system and memory operation 11 p1602 A72-26445
- Digital precision measurement of thermocouple thermal emf at 200-1000 C, examining block diagram 11 p1634 A72-26457
- Digital indicators design and logic circuits employing gas discharge tubes and illuminated and synthesizing indicators 11 p1605 A72-26458
- Vibrating string accelerometer sea gravity meter with electronics for digital readout, discussing performance tests 11 p1635 A72-26499
- Hybrid computers application to digital communication systems design, using real time simulation 12 p1786 A72-27324
- Mathematical model for digital systems reliability, determining probability of success and of various failure modes 13 p1923 A72-28356
- Analytical expression for digital element transfer function derived with Laplace transforms 13 p1927 A72-28413
- Digital precision frequency synthesizers constructed on IC logic modules without using LC filters, analyzing restrictive factors 13 p1930 A72-29050
- Signal system design with digital displays for deviation control in complex multiparameter technological processes, using algorithm to estimate efficiency 13 p1936 A72-29177
- Dynamic motion analysis of digital servo system with proportional bang-bang control by trajectory mapping on phase plane 15 p2211 A72-31895
- Time division demultiplexing technique using two channel simulation of twenty-four channel digital optical PCM communication system 15 p2200 A72-32163
- Digital control and data processing system to replace analog instrumentation in vibration test laboratories, discussing signal generation, data acquisition, storage and analysis 15 p2215 A72-32618
- Electronic display in future avionics systems, emphasizing computer techniques and digital data exchange systems 15 p2242 A72-32635
- Hybrid LSI logic modules for aerospace. 17 p2527 A72-34683
- Digital pulse counter with delay line and tunnel diodes 17 p2529 A72-34760
- Digital data processing equipment for continuous ECG analysis, noting analog to digital converter and amplitude distribution analysis 17 p2522 A72-34914
- Digital controller for high pressure rocket engine. 18 p2721 A72-36335
- Dynamic verification of a digital flight control system. 18 p2673 A72-36336
- Electromagnetic compatibility enhancement during functional integration and operation of transmitters and receivers in digital communication systems 20 p2901 A72-38983
- Interference performance degradation to digital systems. 20 p2901 A72-38984
- Analog computer simulation for PCM-FM and four-phase DPSK digital radio receivers susceptibility to interference sources 20 p2905 A72-38985
- Digital p-i-n diode microwave drive amplifier design guidelines, discussing sharp switching pulses and short circuit protection features 20 p2904 A72-39734

DIGITAL SYSTEMS

NT DIGITAL NAVIGATION
NT DIGITAL RADAR SYSTEMS

- Design and flight experience with a digital fly-by-wire control system using Apollo guidance system hardware on an F-8 aircraft.
[AIAA PAPER 72-881] 20 p2889 A72-40060
- Modeling a hybrid quasi-analog system on a computer 21 p3023 A72-40157
- Topological analysis of the sensitivity of a digital system 21 p3036 A72-40222
- Russian book - Design principles for multiple-valued physical circuits. 21 p3027 A72-40386
- Susceptibility measurements on PCM-FM and four phase differential PSK digital receivers simulated on analog computer 21 p3016 A72-40852
- Feedback quantization noise effects on differential PCM systems, showing SNR relation to noise optimized prediction 21 p3017 A72-40860
- Hybrid digital transmission systems based on optical fiber waveguides and analog repeaters, noting YAG laser light modulation by phase shift keyed sub-carrier 21 p3018 A72-40868
- Near optimum digital phase locked loops. 21 p3038 A72-40871
- Decision directed phase locked loops acquisition properties improvement technique for PCM bit synchronizer of random nonreturn to zero data 21 p3038 A72-40872
- Phase locked feedback circuit for FM demodulation, discussing all digital circuit design and voltage controlled oscillator algorithm to avoid analog implementation problems 21 p3018 A72-40873
- The mathematical synthesis and analysis of fluid logic networks. 22 p3161 A72-42049
- Evolution of the electronic head-up display. 22 p3176 A72-42295
- Digital computer technique and real time monitor software application to instrumentation data acquisition system, discussing design guidelines and gas turbine engine test example 22 p3156 A72-42681
- Digital data system with real time displays and multiprocessing capability for multitest of aircraft structure with operational manpower reduction, assessing performance 22 p3163 A72-42696
- Analog and digital automatic control systems for aerospace and process applications, discussing transfer function and state variable methods 22 p3162 A72-42714
- Discrete address beacon system /DABS/ development for surveillance and ground-air communications in support of ATC automation 22 p3204 A72-43151
- Regions of absolute ultimate boundedness for discrete-time systems. 23 p3309 A72-43857
- Synthesis of hyperstable discrete model reference adaptive systems. 23 p3276 A72-43867
- Bistable trigger stages composed of digital multiplexer with IC logic modulus replacing NAND or NOR circuits 23 p3267 A72-43990
- Digital parallel correlator with LSI single-chip bipolar transistor construction, discussing triple diffusion process for n-p-n and p-n-p junctions 23 p3273 A72-44453
- DIGITAL TECHNIQUES**
- Two dimensional digital pictorial signal processing - Conference, University of Missouri, Columbia, October 1971 01 p0069 A72-10865
- Digital fast transform methods application to satellite image processing, comparing with nontransform algorithms 02 p0227 A72-11843
- Digital picture processing techniques for increased detail resolution, applying equidensity film methods [DFVLR-SONDDR-170] 02 p0229 A72-12018
- Radar signal digital processing for replacing analog circuitry, discussing rf signal representation, sidelobe reduction, coherent processors and filter design 02 p0178 A72-12396
- Radar signal and data processing with digital techniques, using pipeline fast Fourier transform methods 02 p0188 A72-12397
- Optics and electronics of digitized birefringent filter solar magnetograph to isolate magnetic sensitive lines 03 p0357 A72-13287
- Simulation language for digital static checks for hybrid and analog computers 04 p0495 A72-14417
- Digital measurement of pulsed laser energy, using planar vacuum photodiode detector with photocurrent capacitive integration and voltmeter display 04 p0530 A72-14921
- Telemetry systems with discrete compression-expansion function, calculating noise stability improvement as compared to linear and nonlinear signal conversion operations 04 p0487 A72-15000
- Nonrecursive and recursive adaptive equalizers for digital communication, discussing computerized simulation of performance 04 p0493 A72-15520
- Digital data reduction techniques for stellar spectrograms, discussing digital noise smoothing for SNR improvement 05 p0632 A72-15762
- Digital sine wave generator, discussing advantages over conventional RC and LC oscillators due to superior phase constancy 05 p0634 A72-15814
- Low cost automated digitized measurement for microwave antenna feed power gain and relative phase, using computer facilities 05 p0637 A72-16420
- Nonlinear and digital synthesis of computerized optimal control systems for long-life orbital stations and laboratories 05 p0724 A72-16434
- Fourier, Hadamard and Karhunen-Loeve transformations for digital speech processing, comparing bit rate requirements 06 p0772 A72-17405
- Computerized photogrammetric terrain analysis and representation in three dimensional coordinates, discussing construction of digital terrain model 06 p0813 A72-17429
- Automatic digital detection of fluctuating Rice-distributed signals in presence of Gaussian noise, using M-out-of-N threshold detection criteria 07 p0947 A72-20194
- Turbulent heating arc plasma voltage and current digital measurement recording, computing time dependent resistivity 07 p1045 A72-20400
- Digital computer numerical procedure to solve dynamo theory MHD equations for earth nucleus, using combination of Fourier and finite difference methods for integration 08 p1155 A72-20810
- Discrete-time nonlinear estimators digital implementations by computerized Monte Carlo method, comparing with alternative techniques 08 p1145 A72-20864
- ATC radar performance monitoring, considering advances in radar signal processing and digital display techniques 08 p1134 A72-21525
- Image photon counting technique using digital accumulation of individual events registered by high gain image intensifier and TV camera and stored in on-line computer 08 p1170 A72-21960
- Iterative algorithm for digital adaptive null steering of RF antenna arrays, demonstrating feasibility by computer simulation 09 p1289 A72-23416
- Digital adaptive sampling, stressing implementation problem 10 p1455 A72-23799
- Computer controlled electron beam machine for microcircuit fabrication, using digital technique capable of working on complex patterns 10 p1459 A72-23956
- Auroral spectrophotometric measurements in /S-I/ region and of O I line /5577/, discussing digital recording and computer averaging techniques 10 p1474 A72-24745
- Data window for digital spectrum estimation of random data by fast Fourier transform techniques, noting bandwidth increase by various data smoothing sequences 10 p1439 A72-24804
- Phase noise and transient times for binary quantized digital phase locked loops in white Gaussian noise 11 p1592 A72-25886
- Discrete automatic monitoring and measuring systems with discrete random sequence and continuous process reconstructed output signals, deriving probability criteria for reading frequency determination 11 p1611 A72-26438
- Digital computer technique for computation of pulmonary mechanics parameters, using phasor method and Fourier series analysis of respiratory flow signals 11 p1587 A72-26620
- Digital pulse programmer with saturation burst sequence for pulsed nuclear magnetic resonance spectroscopy 12 p1806 A72-27125
- Digital adaptive echo cancellation mathematical technique for voice circuits derived from satellite transmission [AIAA PAPER 72-539] 12 p1780 A72-27362
- Four-phase radio continuum receiver with digital demodulation and signal integration for transfer into on-line computer, discussing calibration 12 p1793 A72-27808
- Modeling process for mathematical representation of mechanical problems, deriving design information in digital or graphic form 13 p2000 A72-28450
- Digital evoked brain potential detector using multichannel amplitude analyzers 13 p1908 A72-28645
- OMEGA receiver with digital solid state circuits for remote unmanned platform positioning, discussing ship to shore tests and design features 13 p1925 A72-29184
- Digital microwave power measuring device with automatic range selection 13 p1931 A72-29267
- Digital data processing techniques for aircraft engine noise data reduction, analyzing fan noise spectrum 13 p1925 A72-29840
- ECG amplifier and cardiachometer for exercise studies, using digital algorithm for heart rate computation and ECG signal preprocessing for R wave detection 14 p2080 A72-30707
- Book on coherent optical computers covering lens design, power sources, computation mathematics, modulation, detection, digital techniques and applications 15 p2203 A72-31499
- Digital communication system for analog signal transmission by digital modulation techniques, presenting detection schemes 15 p2201 A72-32565
- Transfer function estimates in random vibration test control, using digital techniques for rapid reduction of statistical errors 15 p2215 A72-32626
- Digital phase locked loop realization for near-optimum demodulation of continuous-time FM signal using stochastic estimation theory 16 p2362 A72-33213
- Low pass sampling bandwidth selection for digital mechanization of matched filter bit-synchronizer combination, discussing data rate vs SNR performance 16 p2363 A72-33217
- DAMIEN III digital magnetic tape recording system for aircraft flight test data acquisition, discussing components 16 p2393 A72-33629
- Digital recording techniques for airborne data acquisition, emphasizing laser beam holographic recorders 16 p2394 A72-33642
- Discrete representation of continuous time signals and sequences by digital means, using frequency warping function 16 p2365 A72-33753
- Digital theodolite for automatic angle measurement with photoelectric sensor and magnetic data recorder for computer use 16 p2394 A72-33800
- Digital equilibrium temperature model for diurnal surface thermal and energy transfer simulation based on Myrup analog solution 16 p2419 A72-33942
- Time variable pulse front fluctuations effect on random error in digital pulse duration measurements 16 p2395 A72-33953
- Two Dimensional Digital Signal Processing Conference, University of Missouri, Columbia, Mo., October 6-8, 1971, Proceedings. 17 p2520 A72-34401
- Automated cloud tracking using precisely aligned digital ATS pictures. 17 p2521 A72-34411
- Fourier transform of two-dimensional signals. II 17 p2516 A72-35185
- Discrete-time demodulation of continuous-time signals. 17 p2516 A72-35332
- Digital methods of frequency measurement - A comparison. 17 p2530 A72-35363
- Digital correlator for change detection in picture element processing with CDC 1700 computer to obtain spatial alignment accuracy 17 p2556 A72-35538
- Digital technique for automatic change detection in aerial reconnaissance side-looking radar imagery, discussing image correlators 17 p2557 A72-35554
- DC analysis of linearized electronic circuits with the aid of electronic computers 17 p2524 A72-35977
- Picture coding via linear transformation and quantization on subpictures with applications to monochromatic image processing 18 p2658 A72-36254
- Recent developments in digital image processing at the image processing laboratory at the Jet Propulsion Laboratory. 18 p2658 A72-36255
- Image restoration - The removal of spatially invariant degradations. 18 p2658 A72-36257

- Inverse filtering for linear shift-variant imaging systems. 18 p2658 A72-36259
- Role of recursive estimation in statistical image enhancement. 18 p2658 A72-36260
- Data structures and computational organization in digital image enhancement. 18 p2658 A72-36262
- Digital image enhancement heuristic, superresolution and positive restoration techniques, providing bibliography. 18 p2658 A72-36264
- Generalized multi-dimensional sampling theory and applications in optical systems. 18 p2672 A72-36333
- Measurements of ultrasonic velocities using a digital averaging technique. 18 p2691 A72-36401
- Digital techniques for image data processing and analysis, discussing data sampling, conversion, computer implementation, image matching, etc. 18 p2664 A72-36490
- The image-processing system for the Earth Resources Technology Satellite. 18 p2674 A72-36496
- A digital portable line-drawing rectifier. 18 p2692 A72-36500
- Construction, analysis, and design of FM digital devices for controlling and measuring rapidly varying quantities. 19 p2776 A72-37303
- Digital programming techniques for maximum utility and flexibility in filament winding. 19 p2808 A72-38170
- Digital tracking with phased arrays. 19 p2765 A72-38261
- Process control of the 100-m telescope - Digital control. 19 p2803 A72-38486
- Numerical integration of gamma ray photopeak digital data from nondestructive activation analysis. 20 p2899 A72-39834
- Thermal imaging with pyroelectric IR detector arrays, discussing signal processing by digital technique to eliminate voltage offset variations effects in preamplifiers. 20 p2928 A72-39968
- Integral equations of a multipoint network with a digital control automaton. 21 p3036 A72-40154
- Assessment of the errors of a version of the hybrid quasi-analog system due to errors in quantization in time in the solution of systems of ordinary differential equations. 21 p3024 A72-40158
- A modernized specialized computer for evaluating determinants. 21 p3036 A72-40161
- An algorithm for computer calculation of critical curves of longitudinal cryotrons. 21 p3025 A72-40183
- Present status of self-contained navigation systems combining Doppler velocity sensors and attitude/heading references. 21 p3079 A72-40282
- Optical direct detection using avalanche devices. 21 p3018 A72-40867
- Digital processing for motion compensation in high resolution airborne synthetic aperture radar imagery in presence of simultaneous longitudinal, lateral and vertical maneuvers. 21 p3022 A72-41076
- Effect of single-bit digitization in adaptive array control loops. 21 p3034 A72-41085
- High precision stellar electrophotometer design, using two channel single photoamplifier photometer and digital computer for statistical atmospheric noise damping. 21 p3056 A72-41447
- Application of digital techniques to the measurement of PCM signal power. 22 p3155 A72-42705
- A new approach to automatic scanning of contour maps. 22 p3174 A72-43024
- Digitally pressure-scanned Fabry-Perot interferometer for studying weak spectral lines. 23 p3289 A72-43891
- Integrating digital voltmeter - Operating principles and accuracy. 24 p3403 A72-45275
- DIGITAL TO ANALOG CONVERTERS**
- Reconstruction errors, quantization noise and channel bandwidth in high order digital to analog conversion. 06 p0779 A72-17783
- Magnetic-transistor master oscillator with digital analog converter as programmer for needed output voltage frequency shifts. 07 p0946 A72-19959
- Digital analog converter output voltage variation coefficient derivation, obtaining operational error

- statistical characteristics estimates and elements parameter. 11 p1602 A72-26447
- Phase metering information converters with digital analog computation, discussing analysis of prototype semiconductor model with ten-digit binary codes. 11 p1602 A72-26449
- A/D and D/A converter for color TV signal digital transmission over communication satellites, discussing system design features. 17 p2524 A72-34262
- Magnetic and transistorized magnetic digital-to-analog converters. 17 p2529 A72-34768
- DIGITAL TRANSDUCERS**
- Apodized interdigital transducers acoustic surface wave front distortion, describing perturbation and compensation method. 03 p0360 A72-13602
- Digital magnetic temperature transducer using permeability discontinuity at Curie temperature for high stability and reproducibility without calibration [IEEE PAPER 8,5]. 03 p0332 A72-13758
- Log-periodic interdigital transducer design to obtain wide bandwidth for acoustic surface waves. 06 p0784 A72-18241
- Weighted acoustic surface wave dispersive microwave filter apodized interdigital array design modification for phase error correction to reduce distortion. 06 p0787 A72-18380
- Interdigital acoustic surface wave transducer impedance characteristics calculation from equivalent circuit, demonstrating effectiveness on delay lines [AD-743552]. 09 p1316 A72-23421
- Surface waves generation and absorption by interdigital transducer with uniform finger spacing, discussing parallel equivalent circuit derived in weak coupling approximation. 13 p1960 A72-29769
- High resolution angular velocity measurement by high speed digital transducer feeding photosensor pick-up pulses into pulse shaping circuit. 14 p2103 A72-30199
- Fluidic digital logic devices vs electromechanical-electronic equivalents, describing Coanda effect application to bistable jet amplifiers /flip-flops/ as switching or memory devices. 15 p2182 A72-31218
- Circuit synthesis for random numbers probabilistic digital transducers reduced to synthesis of random binary signal converters, noting method description with Boolean functions. 16 p2372 A72-34012
- Analysis of piezoelectric thin-film transducers for elastic surface waves. 19 p2804 A72-38607
- Use of rotated electrodes for amplitude weighting in interdigital surface-wave transducers. 22 p3178 A72-42619

DIGITALIS

- Arrhythmias relation to coronary artery disease, discussing conduction defects, sudden death prodromata and prevention and digitalis as antiarrhythmic agent. 02 p0157 A72-11476
- Myocardial infarction effects on drug tolerance and hemodynamic changes due to digitalis doses, discussing toxic arrhythmias. 08 p1115 A72-21082

DIGITIZERS

- U ANALOG TO DIGITAL CONVERTERS**
- DIGITS**
- NT BINARY DIGITS**
- Mathematical model for digit summation task search time distribution dependence on size of visual display with randomly arranged three digit numbers. 24 p3374 A72-44558

DIHEDRAL ANGLE

- Unsteady temperature field and conductive heat accumulating properties of bodies with dihedral and polyhedral angles. 08 p1251 A72-20954
- Primary velocities distribution in two dimensional turbulent boundary layer inside dihedral. 12 p1797 A72-27179
- Wind tunnel investigation of supersonic air flow behavior on rotatable right dihedral formed by two plane plates with sharp edges. 13 p1894 A72-29636
- Initial dihedral wing-body interaction for supersonic leading edges, determining expansion of velocity potential on root chord. 14 p2069 A72-30365
- V-wings and diamond ring-wings of minimum induced drag. 21 p2992 A72-41263

DIHEDRAL EFFECT**U LATERAL STABILITY****DILATATION****U STRETCHING****DILATATIONAL WAVES**

- Stress intensity and plane dilatational wave diffraction in elastic material with finite crack. 04 p0583 A72-14459

DILATOMETERS**U EXTENSOMETERS****DILATOMETRY**

- Two electrical transducer techniques for dilatometric study of quenched-in point defects. 07 p0993 A72-20589
- Continuous volume-temperature dilatometer measurement of small liquid samples in biological application. 13 p1959 A72-29752
- Correctness of boundary conditions in the method of measuring the heat exchange coefficient by the rate of the thermal deformation of samples. 19 p2881 A72-38038
- Dilatometric studies of volume compression effect during aging of nimonic alloy showing linear dependence of matrix lattice constant on gamma prime phase. 21 p3068 A72-40957

DILUTIONS

- Gaseous diethyl peroxide spontaneous ignition during decomposition in cylindrical vessel, investigating diluents and temperature effects on self heating. 02 p0301 A72-12027

DILUTION

- Indicator dilution methods for ventricular volume measurements from washout curves, discussing intraventricular blood mixing uniformity. 15 p2190 A72-32496
- Variation of the rate of divergent spherical detonations in strict propane-oxygen-nitrogen and acetylene-oxygen-nitrogen mixtures as a function of the radial abscissa - Influence of the dilution in the inert state. 17 p2635 A72-34283

DIMENSIONAL ANALYSIS

- Book on similarity laws and modeling covering dimensional analysis, transformations, differential equations, gas flows and nonequilibrium processes. 04 p0513 A72-15675
- Minimum dimensionality determination for control process stabilizing linear mechanical system equilibrium position, obtaining necessary and sufficient conditions. 07 p1036 A72-20320
- Similarity theory for turbulently stratified fluid with horizontal and vertical dimensionalities analysis, discussing Karman constant dependence. 07 p1031 A72-20698
- Algebraic dimensional analysis developed algorithm to generate optimized dimensionless products set associated with physical phenomenon, using matrix methods. 10 p1443 A72-23916
- Similarity analysis group theory methods application to dimensional analysis, discussing incompressible fluid mechanics case. 10 p1503 A72-23917
- General dimensional analysis as extension of conventional /restricted/ dimensional analysis of physical phenomena, using progressive homogeneity law and fundamental magnitudes. 10 p1503 A72-23918
- Dimensional analysis proportionalities method parallel to formal similitude method for accelerative mechanics problems. 10 p1503 A72-23919
- Pi-theorem alternative formulation, defining independent dimensionless products in terms of universal constants, governing equations and initially and additionally specified physical quantities. 10 p1503 A72-23920
- Dimensional analysis pi-theorem local generalization by Lie transformation group investigation, constructing local canonical coordinate systems to obtain factoring properties of certain functions. 10 p1503 A72-23921
- Dimensional analysis and similarity theories application to biological organisms relationships between body size and metabolism. 11 p1585 A72-26074
- German book on principles and applications of similarity theory in physical-technical research covering coherent dimensional units and invariance principle, physical dimensions, etc. 15 p2218 A72-31900
- Similarity theory for turbulence in stratified fluid from horizontal and vertical dimensional analysis approach, discussing Karman constant dependence. 20 p2948 A72-39013
- Quasi-one-dimensional analysis of gaseous free detonations. 21 p3044 A72-40194
- Scale analysis of atmospheric large-scale motions in low latitudes. 23 p3311 A72-44241
- Book - Dimensional analysis and group theory in astrophysics. 23 p3341 A72-44500
- Parametric influences on the response of structural shells. 24 p3454 A72-44604
- Investigations on the stability of the characteristic of radial flow fans. 24 p3363 A72-45356

DIMENSIONAL MEASUREMENT

Kr 85 clouds released by instantaneous point sources, measuring speed, height, short period concentrations, crosswind and downwind concentration integrations and dimensions

01 p0095 A72-10828

Large steerable radio reflectors profile measurement with laser system, describing instrument design, accuracy and modifications

02 p0238 A72-12113

Gas lasers application to precise length measurements via absorbing medium resonance determined wavelength

04 p0530 A72-14734

Diffraction optical dimensional measurement, discussing profile determination from diffraction patterns

[CLEA PAPER 11,5] Laser interferometers for displacement, length, gas refractivity, laser wavelength and relative object position measurements

07 p0984 A72-19391

[CLEA PAPER 15,1] Photometric monitoring of film thickness of stacked structures for high strength and laser flux resistance

07 p1049 A72-20126

Measurement accuracy and reliability of photogrammetric methods in stereoscopic height determinations of wooded areas

09 p1312 A72-23284

Atmospheric constituents dimension, composition and dynamics from optical radar echo observation of laser light scattering

11 p1592 A72-25849

TV microscopic system for on-line measurement of cat omentum microvessels diameter relative to heart action

11 p1587 A72-26621

Nondestructive technique for continuous recording of thickness or contour profiles, using mechanical probes

13 p2000 A72-29760

Pulse distortion and amplitude smear calculation for electron beam measurements of distance from space vehicles to deployable structure measurements on space vehicles

14 p2103 A72-30198

Mercury diameter measurement by photoelectric Hertzprung method during transit on 9 May 1970

15 p2312 A72-32091

Ultrasonic range finder

17 p2553 A72-34763

Electromagnetic thickness measurement on the AWACS radome.

24 p3384 A72-44901

DIMENSIONAL STABILITY

NT SHELL STABILITY

NT STRUCTURAL STABILITY

Presintering effects on dimensional change of iron powder compacts, using dilatometric, thermogravimetric, differential thermal analyses and resistivity measurements

02 p0233 A72-11461

Dimensional stability and micromechanical properties of materials for use in OAO, investigating residual stresses, creep properties and stress relaxation

[AIAA PAPER 72-325] Fast response thermal compensation system for gas laser resonator length and frequency stabilization, discussing fabrication and design calculation

12 p1822 A72-27607

Carboxy-terminated polybutadiene/ammonium perchlorate base solid propellants aging properties under long time storage conditions at 243-353 K, considering mechanical, dimensional and combustion properties

14 p2145 A72-30763

DIMENSIONLESS NUMBERS

NT GRASHOF NUMBER

NT HARTMANN NUMBER

NT LEWIS NUMBERS

NT MACH NUMBER

NT NUSSELT NUMBER

NT PECLET NUMBER

NT PRANDTL NUMBER

NT RAYLEIGH NUMBER

NT REYNOLDS NUMBER

NT RICHARDSON NUMBER

NT SCHMIDT NUMBER

NT SIMILARITY NUMBERS

NT STANTON NUMBER

Dimensionless numbers system selection for generalizing I-V characteristics of thermionic heat converters

01 p0006 A72-10492

Biological tissue heat transport dimensionless parameters for steady state and transient analysis of homeotherm thermoregulation

04 p0472 A72-14864

Empirical dimensionless ratios between universal physical constants, supporting steady cosmological expanding universe model

04 p0574 A72-14983

Dimensionless parameter for thermodynamic state prediction in atmospheric pressure plasma jets, using conservation equations

06 p0862 A72-18188

Solid body motion with fixed point in central Newtonian force field, classifying angular velocity vector hodograph as function of dimensionless parameters

08 p1208 A72-21363

Algebraic dimensional analysis developed algorithm to generate optimized dimensionless products set associated with physical phenomenon, using matrix methods

10 p1443 A72-23916

Pi-theorem alternative formulation, defining independent dimensionless products in terms of universal constants, governing equations and initially and additionally specified physical quantities

10 p1503 A72-23920

Biological similarity theory for numerical relationships of morphometric and physiometric organization in mammals, using allometric growth equations and body weight correlations

10 p1432 A72-25098

Dimensionless thermal contact conductance parameter for determination of interstitial thermal control materials effectiveness for metallic junctions [AIAA PAPER 72-284]

11 p1741 A72-25224

Screw type axial flow pump impellers pressure losses generalization by dimensionless coefficient in Euler number form

12 p1752 A72-28139

Dimensionless heat transfer equations of reacting media in chemical equilibrium, using Lewis-Semenov criterion

12 p1889 A72-28140

DIMENSIONS

NT DIAMETERS

NT FILM THICKNESS

NT HEIGHT

NT SCALE HEIGHT

NT TARGET THICKNESS

NT THICKNESS

DIMERIZATION

Reversible photodimerization of polycyclic aromatic hydrocarbons as basis for optical information storage, discussing monomer and photodimer photosensitivity, thermal stability and refractive index specifications

09 p1314 A72-23331

DIMERS

Absorption effects of dimers of water molecule in atmosphere, using spectroscopic and maser measurements

03 p0348 A72-13400

Dimer formation effect on thermal diffusion factor at low temperatures for krypton-argon system

03 p0391 A72-13749

Spectroscopic moments of molecular collision induced far IR and Raman spectra, stressing gas dimers contribution

09 p1276 A72-22859

DIMETHYLHYDRAZINES

Effect of neurohomologous phospholipids associated with other substances on experimental intoxication by asymmetrical dimethylhydrazine. II - Biochemical aspects of the pyridoxine-phospholipid association

21 p3009 A72-41195

DIMPLING

Dimpling behavior of metal plate with mode I edge crack, relating flaw depth, applied stress level and crack tip plastic zone

05 p0673 A72-16305

DIODES

NT AVALANCHE DIODES

NT CESIUM DIODES

NT GERMANIUM DIODES

NT JUNCTION DIODES

NT PARAMETRIC DIODES

NT PHOTODIODES

NT PLASMA DIODES

NT THERMIONIC DIODES

NT TUNNEL DIODES

NT VARACTOR DIODES

Planar Gunn effect devices for microwave oscillators, discussing impedance matching and diode conductivity profile effect on output power

01 p0028 A72-10628

High power Q-band pulsed Gunn diode microwave oscillator constructed from thin GaAs sandwich layers grown by vapor phase epitaxy

01 p0036 A72-10630

Microwave oscillator detector Gunn diode as inexpensive alarm device for Doppler radar application

01 p0028 A72-10642

Magnetic field effect on Gunn diode oscillator frequency and output power, discussing strong field domain

02 p0196 A72-12885

High intensity ionizing gamma ray pulsed radiation effects on Gunn diode microwave oscillator failure modes

03 p0334 A72-14089

Gunn diode large signal admittance dependence on bias and frequency, discussing computer simulation and broadband oscillator and amplifier design

04 p0497 A72-14712

Frequency response and I-V characteristics of metal/chalcohalogenide glass/metal diode structures

04 p0498 A72-15079

Book on transistors in pulse circuits covering switching diodes and circuits, multivibrators, blocking oscillators, etc

05 p0640 A72-16288

Computer simulation in optimized 5-GHz Gunn diode oscillator design

05 p0633 A72-16360

Hysteresis loops during breakdown in reverse bias segment of p-PbS point contact diodes I-V curves

05 p0638 A72-17177

Gunn diode microwave oscillator thermal resistance reduction for increased output power and efficiency

07 p0958 A72-20685

Two terminal semiconductor strain tensor based on evaporated piezoelectric layer for modulation of forward I-V characteristics of thin film diode

08 p1164 A72-20925

Light emitting diodes for efficient conversion of electrical energy into electromagnetic radiation, discussing photometry, electrical injection, electroluminescence, design and applications

08 p1141 A72-21430

Solid state microwave power amplifier with unidirectional transmission line loaded by negative resistance diode series, calculating large signal characteristics

08 p1142 A72-21558

Magnetodiode model of intrinsic semiconductor slab under Lorentz force and double injection inducing ambipolar drift and carrier redistribution

08 p1142 A72-21746

Barrier capacitance effect on transient characteristics of light diodes, obtaining time dependence of p-n junction volume charge voltage and recombination emission intensity

09 p1284 A72-22211

Diode half wave rectifier for ac-to-dc signal conversion in electronic voltmeter

09 p1306 A72-22343

Solid state microwave devices, discussing varactor, varistor, tunnel, Gunn, IMPATT and TRAPATT diodes and power transistors characteristics and applications

09 p1285 A72-22567

Noise of high electric field biased gallium arsenide diodes, calculating LF power spectrum

09 p1288 A72-23123

HF thermal noise in single and double injection space charge limited solid state diodes

09 p1288 A72-23124

Bulk effect diodes combination with YIG elements to provide oscillator operation up to 18 GHz, discussing design, circuit diagrams and performance

10 p1448 A72-24037

Gunn domain oscillations suppression by dielectric surface loading of transversely thin GaAs diodes

10 p1526 A72-24305

Wideband microwave device with diode and single component correction circuits Q factors measurement from frequency dependence of input traveling wave coefficients

10 p1453 A72-24918

Thermal diode heat pipe for advanced thermal control flight experiment, discussing engineering model analysis, design, fabrication and test

11 p1739 A72-25205

[AIAA PAPER 72-260] Microwave power transistors and active two terminal devices performance, describing representative applications

11 p1607 A72-26983

Broadband diode phase shifter design, discussing switched and loaded line, reflection and lumped element high pass and low pass circuits

11 p1607 A72-26992

Epitaxial InP diode for high efficiency circuit controlled microwave oscillator, discussing solution growth technique, layers electrical properties and I-V performance

12 p1854 A72-27162

Static and impedance characteristics and equivalent circuit of p-n-p-n inductance diode, using ambipolar diffusion length

12 p1790 A72-27499

Optical interaction of inhomogeneously excited semiconductor injection laser diodes, noting power efficiency increase with inhomogeneity

12 p1822 A72-27606

Integral diode cell for solar arrays compared with bypass configuration, discussing design, advantages and electrical performance test data

12 p1757 A72-28031

Critical analysis of Muthaana-Susskind diffusion theory for magnetron diode electron transport, noting theoretical results discrepancy with experimental data

13 p1931 A72-29289

GaAs doped Si light emitting diode as light source for optical timing system calibration, studying fast luminescent decay characteristics

13 p2000 A72-29763

Charged particle inertial-electrostatic containment in spherical diode gas discharge gap, measuring flux radial and energy distributions

13 p1933 A72-29915

Gunn diode active region thickness, free electron mobility/concentration, structure and contacts, including treatment of GaAs

13 p1934 A72-30036

Transmission lines with nonlinear capacitance semiconductor diodes, investigating electromagnetic traveling and standing waves instabilities and self amplitude modulation

14 p2086 A72-30795

Microwave semiconductor diode technology review and development prospects in terms of fabrication processes and materials

14 p2088 A72-30834

Relay circuits malfunction due to interactions between coil induced currents and diode coil shunts, discussing circuit design and operating conditions

15 p2204 A72-31217

Nodal equations derivation for lumped circuit representation of Gunn diode with steadily propagating domain under steady state and transient conditions

15 p2205 A72-31317

Simplified equivalent circuit analysis for Gunn diode coupling to rectangular waveguide by inductive post, using perturbation approximation

15 p2205 A72-31353

Transverse magnetic field effects on n-type GaAs Gunn diodes microwave power, coherence and dynamic I-V characteristics [ONERA, TP NO. 1051]

15 p2207 A72-31884

GaAs Gunn diode LSA operation mode in multiloop circuit to extend high frequency limit

15 p2207 A72-31888

Gunn diode elements design, operation, performance, efficiency, heat dissipation, lifetime and applications as microwave oscillators

15 p2208 A72-32500

Emitted phonon spectrum effects on detected signal response in superconducting Sn diodes, noting deviation from linearity

15 p2209 A72-32541

Microwave diode switch operating at 35 GHz for spin lattice relaxation time measurement, discussing insertion loss, and rise and decay times characteristics

16 p2369 A72-33623

Avalanche generation process interpretation for nontransit frequency oscillations association with current runaway in bulk InP microwave diode oscillators

16 p2369 A72-33755

Frequency stabilized self-oscillating microwave up-converter with transferred electron diodes, noting maximum power output and bandwidth

16 p2369 A72-33764

Nonlinear characteristics of semiconductor diode multiplier circuits for frequency converters

16 p2370 A72-33951

Thermionic energy conversion with a Ba-Cs diode

17 p2496 A72-34603

Device for ac induction measurements in air, using the Gauss effect in germanium semiconductor diodes

17 p2529 A72-34767

New measurement method of Gunn-diode impedance

17 p2529 A72-35000

Thermal noise in double injection diodes operating in the insulator regime

18 p2667 A72-36979

Measurement of carrier lifetime in the base of silicon diodes - Application to the control of manufacturing techniques

18 p2669 A72-37108

The effects of X-ray irradiation on MAS diodes

21 p3032 A72-40695

Injection laser and light emitting diode techniques to transmit digital data in local distribution

21 p3018 A72-40869

Light emitting diodes (LED) materials characteristics, heterojunction band structures and optical spectral ranges, considering application to information processing

21 p3035 A72-41649

Snap-off diodes for avalanche generators step pulse output rise time steepening, describing circuit diagram and time-volt-ampere characteristics

21 p3035 A72-41650

Generation of infrared radiation in a metal-to-metal point-contact diode at synthesized frequencies of incident fields - A high-speed broad-band light modulator

22 p3157 A72-41971

Low temperature characteristics of the Gunn diode

22 p3159 A72-42307

A CW Gunn diode bistable switching element

22 p3159 A72-42610

Static and dynamic characteristics of double-injection currents in p'-n-n' diode structures with deep impurities and nonideally injecting junctions

23 p3268 A72-43346

Local-oscillator-circuit optimisation for minimum distortion in double-balanced modulators

23 p3270 A72-43603

Impedance of a unipolar semiconductor diode under conditions of space-charge limited current with allowance for recombination

23 p3270 A72-43630

GaAs light emitting diodes intensity fluctuations measurements at .025-20 kHz

23 p3297 A72-44190

A single-tuned oscillator circuit for Gunn diode characterizations

23 p3272 A72-44194

Solid state microwave devices, discussing varactor, varistor, tunnel, Gunn, IMPATT, and TRAPATT diodes and power transistors characteristics and applications

24 p3384 A72-44746

Noise properties of the injection-limited Gunn diode

24 p3385 A72-44962

DIOPHANTINE EQUATION

Approximation of functions with diophantine conditions by polynomials with integral coefficients

03 p0382 A72-13948

DIOXIDES

NT CARBON DIOXIDE

NT COESITE

NT HYDROGEN PEROXIDE

NT QUARTZ

NT SILICON DIOXIDE

DIPHOSPHATES

NT ADENOSINE DIPHOSPHATE (ADP)

DIPOLE ANTENNAS

Earth surface roughness effects on vertical Hertz dipole electromagnetic field reflection

01 p0027 A72-10447

Hertzian dipole radiation with impulsive currents in nondispersive dielectric half space

01 p0030 A72-10841

Radiation patterns of symmetrical dipoles or small apertures on perfectly conducting sphere, using dyadic Green function analysis

01 p0030 A72-10844

Design, construction and testing of wideband circularly polarized dipole antenna suitable for ionospheric research

01 p0043 A72-11235

Broadband dipole antenna design based on method of moments, noting VSWR and current distribution

01 p0043 A72-11241

Mutual microwave coupling effects on element VSWR in linear dipole log periodic antenna array

01 p0043 A72-11242

Dipole theory application to directional characteristics of Yagi antenna systems, discussing harmonic current distribution along radiating elements

02 p0193 A72-12221

Center fed full wave dipole antenna with feed points displaced transverse to dipole axis, considering radiation patterns, electrical properties and power gain

02 p0177 A72-12325

Book on metallic and dielectric antennas covering planar, cylindrical and plasma types for symmetrical, dipole and ring excitations

04 p0497 A72-14612

Iterative synthesis of dipole antenna array for maximum directivity radiation pattern, considering amplitude-phase distributions

04 p0499 A72-15142

Signal fluctuation effect on directional properties of multidipole receiving antenna, calculating radiation pattern

04 p0499 A72-15143

Space charge layer /ion sheath/ effects on impedance of lf transmitting electric dipole in ionospheric plasma

04 p0490 A72-15399

Two center-fed feed-point displaced dipole antennas, calculating mutual impedance for various combinations of displacements and heights

04 p0501 A72-15433

Time domain analysis of wire antennas including straight, vee and zigzag dipoles

04 p0502 A72-15448

Active loop-dipole antennas with height reduction properties at resonance, deriving input impedance power gain and radiation patterns

04 p0502 A72-15519

Frequency response of passive dipole antennas fed by transistor circuit, investigating power gain, bandwidth and voltage SWR

04 p0503 A72-15670

Log periodic dipole antenna design with loop elements, discussing radiation patterns and resistance, efficiency, polarization and gain

04 p0503 A72-15673

Electrical properties of unbalanced center-fed non-planar dipole antenna, discussing radiation patterns and resistance, power gain, aperture and efficiency

04 p0503 A72-15674

Vertical dipole antenna design for CW Doppler radar midair collision avoidance system

05 p0629 A72-16571

Conducting ground half space effects on dipole antenna input impedance computed by current distribution Fourier transform

06 p0781 A72-17353

Microwave attenuation due to ohmic losses in periodic linear arrays of metallic cylinders, ribbons and slots in metallic ground plane

06 p0786 A72-18372

Balun-fed open sleeve dipole in front of metallic reflector for 225-400 MHz band operation, investigating radiation pattern and gain

07 p0957 A72-19794

Electron temperature effects on radiation fields and resistance of short electric dipole antenna embedded in hot uniaxial plasma

08 p1215 A72-21991

Power integral method for electric and magnetic dipole antennas vlf/elf radiation patterns in cold magnetoplasma, emphasizing focusing effects of refractive index surface

09 p1279 A72-23009

Radiation pattern of spacecraft dipole antenna mounted on conducting finite length cone calculated by superposition of radiated and diffracted waves

09 p1282 A72-23524

Log periodic dipole antenna design parameters effects on bidirectional radiation pattern

09 p1282 A72-23571

Dipole antenna near electric field, basing calculation method on integral equation for antenna surface charge distribution function

10 p1451 A72-24579

Radiation pattern of longitudinal magnetic dipole near circular cylinder parallel to flat screen

10 p1453 A72-24903

Nonlinear sheath admittance, currents and charges associated with high peak voltage drive on VLF-ELF dipole antenna moving in ionosphere

11 p1599 A72-26769

Active loop dipole aerials with height reduction properties at resonance, investigating transistor configurations in loop monopole aerial

12 p1792 A72-27699

Iterative method for synthesis of reflector antenna array of dipole elements to provide given radiation pattern, obtaining impedance matching values

13 p1926 A72-28372

Dipole antenna radiation patterns in sinusoidally space-time periodic media

13 p1915 A72-28531

Fourier transform solution for fields from current dipole element radiating in free space

13 p1916 A72-28540

Numerical analysis of surface current density distribution and electromagnetic fields of conducting body, noting radiation patterns of radial dipole and quarter wavelength monopole

13 p1916 A72-28541

Radiation patterns of linear equidistant fishbone-type dipole antenna array fed by long symmetrical transmission line

13 p1930 A72-29056

Bandwidth log-periodic dipole array radiation pattern and impedance characteristics as function of design parameters

15 p2208 A72-32390

Log periodic dipole antenna input impedance and gain characteristics derivation via periodically loaded line theory and Poynting vector method, discussing separation angle effect

15 p2208 A72-32473

Mathematical analysis of feed point displacement effects on linear dipole antennas, investigating radiation properties

16 p2362 A72-32852

Numerical analysis of boundary value problem for finite cylindrical dipole antenna of arbitrary orientation in magnetized plasma approximated by uniaxial medium

16 p2366 A72-34107

Distribution of current in centre-fed cylindrical dipole antennas with arbitrarily displaced feed points

17 p2526 A72-34517

Antenna array analysis of arbitrarily-located, parallel center-fed dipoles with terminals in a common plane

18 p2666 A72-36328

A short-wave rotating antenna for 500-kW transmitter output

18 p2666 A72-36676

Log periodic dipole antenna systems for ILS localizers, noting reduced sensitivity to snow and ice

19 p2830 A72-37279

Dipole antenna radiation in homogeneous plasma layer magnetized by normal uniform magnetic field, calculating radiation pattern

19 p2768 A72-38661

The effect of asymmetry on toroidal hydromagnetic waves in a dipole field

20 p2957 A72-39230

A numerical solution for the near and far fields of an annular ring of magnetic current

21 p3015 A72-40354

Gain of arrays of dipoles with a ground plane

21 p3027 A72-40364

Mutual coupling of infinite periodic phased arrays of arbitrarily oriented dipoles, investigating dipole length, orientation and phase effects on current distribution

21 p3027 A72-40368

On the relationship between classical and matrix design methods for arrays of wire antennas.

21 p3027 A72-40373

Constrained optimization of the gain of an array of thin wire antennas.

21 p3027 A72-40374

A contribution to the theory of finite antenna groups, taking into consideration radiation coupling

21 p3028 A72-40503

Theoretical and experimental investigations, conducted with the aid of a plate containing holes, concerning the simulation of a statistically arranged antenna group

21 p3028 A72-40505

Design and investigations regarding a phase-controlled dipole group with radiation input

21 p3028 A72-40508

The effect of amplitude and phase tolerances on the phase characteristics of dipole arrays

21 p3028 A72-40512

Combination of sum and difference diagrams of a dipole group in front of a parabolic reflector for a two-plane monopulse method

21 p3029 A72-40517

Active transistorized directional dipole VHF receiving antennas for ATC and mobile applications and field intensity measurement

21 p3030 A72-40527

New combination of logarithmic-periodic dipole antennas for the short wave range

21 p3031 A72-40537

Series-dipole antenna design based on Ehrenspect short backfire antenna mirror method, noting small dimensions and cost reduction

21 p3031 A72-40539

Bubnov-Galerkin solutions to wire-antenna problems.

21 p3032 A72-40631

An expression for the distribution of current in asymmetrically driven antenna immersed in a dissipating medium.

21 p3022 A72-41322

Admittance measurements of a 36-m dipole antenna in the topside ionosphere.

22 p3153 A72-42007

DIPOLE MOMENTS

NT ELECTRIC MOMENTS

NT MAGNETIC MOMENTS

Trapped particle motion response to collapsing dipole moment in secularly varying geomagnetic field

07 p1058 A72-19158

Secular geomagnetic dipole moment decrease effect on inner proton belt proton energy distribution, comparing with radial diffusion influences

07 p1058 A72-19159

Spectroscopic moments of molecular collision induced far IR and Raman spectra, stressing gas dimers contribution

09 p1276 A72-22859

Dipole moment expression for Rayleigh scattering field from finite closed perfectly conducting body irradiated by LF plane electromagnetic wave

10 p1434 A72-23720

Aeros satellite magnetic properties, describing measurement procedures for component induced disturbance fields, dipole moments and eddy currents

13 p1940 A72-30080

Dipole moment derivative of triatomic hydrogen ion electronic ground state, considering fundamental spectrum observation in hydrogen gas in local thermodynamic equilibrium

22 p3209 A72-42720

The effect of change in the geomagnetic dipole moment on the rate of the earth's rotation.

23 p3285 A72-43819

Electric dipole moment of diatomic molecules by configuration interaction. IV.

24 p3426 A72-44870

DIPOLARS

Metal crystals dislocations movements and interactions with dislocation dipole under applied cyclic stresses for various configurations and starting conditions, using numerical methods

01 p0113 A72-10208

Electromagnetic potentials excited by dipole oscillator moving in homogeneous uniformly drifting medium, analyzing frequency spectrum and finite dimensions effect on higher harmonics

08 p1135 A72-21736

Electromagnetic waves scattering by uniformly moving objects in free space, considering two dimensional monopoles and dipoles

09 p1282 A72-23523

Electromagnetic processes computation in circuits with SHF currents by reduction to integral equation, using dipoles system representation

13 p1937 A72-29945

Relaxation methods of magnetic and acoustic spectroscopy for studies of gravitational and inertial

dipoles and quadrupoles in molecules and nuclei of solid bodies

14 p2143 A72-30963

Fourier-Bessel superposition and Laplace transformation methods for surface displacement produced by time dependent dipole in elastic half space, noting buried dipole case

19 p2876 A72-37887

Double-dipole exciter for the primary focus of the 100-m radio telescope Effelsberg

21 p3029 A72-40518

DIRAC EQUATION

Relativistic treatment of Dirac-Hestenes and Maxwell equations

13 p1987 A72-29787

Poincare noninvariance of Stigma equation as alternative to Dirac equation for spin one-half finite mass particles

15 p2280 A72-31519

Time constancy of physical constants in expanding universe, discussing light speed, Planck constant and electron and proton mass in context of Dirac hypothesis

16 p2425 A72-33517

DIRECT CURRENT

Vhf dc-dc conversion and regulation in low MHz range, discussing power loss reduction

01 p0007 A72-11057

Dc-dc converter input filter requirements and design for spacecraft power processing equipment

01 p0007 A72-11058

Series inverter silicon controlled rectifier 2800 watt dc power supply, noting high efficiency, low weight and stable voltage regulation

01 p0008 A72-11064

Aircraft hybrid electrical power systems, describing variable frequency generation and high voltage dc distribution

01 p0009 A72-11068

Kubo bulk electrical conductivity of two dimensional guiding center plasma in strong dc magnetic field

02 p0263 A72-11966

Three-axis flight table with dc torque motors, discussing servo loops design and mechanical oscillations frequencies

02 p0257 A72-12541

Dc excited argon laser anode oscillation noise, discussing relation to ballast resistance, suppression conditions and current fluctuation frequency response to laser fluctuation

02 p0239 A72-12826

Electropneumatic converter for pneumatic pulse transformation into dc or ac signal, using corona discharge current

03 p0311 A72-13556

Inductor design for minimum inductance at given dc level, using computer programs

[IEEE PAPER 8,6] 03 p0332 A72-13759

Dc feedback controlled constant voltage transformer, comparing with ferroresonant regulator

[IEEE PAPER 17,2] 03 p0311 A72-13771

Dc flow through p-n junction by modified Melehy force field method, discussing space charge variation in depletion layer

03 p0338 A72-13866

EMC improvement with least sacrifice of power efficiency in designing dc/dc converters and switching voltage regulators

03 p0312 A72-14049

Self oscillating dc-to-dc converters performance and design, considering switching frequency, duty cycles, line and load regulation and peak-to-peak ripple

04 p0465 A72-14487

Regulated dc-to-dc converter for voltage step-up or step-down with input-output isolation, using bistable comparator output voltage control through encoder

04 p0465 A72-14488

Nonparabolic n-InSb semiconductors, presenting microwave conductivity dc field induced anisotropy

04 p0560 A72-14543

Self oscillating dc-dc converter analysis and optimal design, modeling by single loop nonlinear feedback system

04 p0465 A72-14571

Photoelectrically excited electrons diffusion and dc effect in ZnO single crystals, calculating drift mobility and lifetime product

05 p0667 A72-16158

AC-DC energy conversion - Conference, Milan, Italy, November 1970

06 p0785 A72-18307

Ac and dc power regulation by switched capacitor, analyzing voltage spectrum for resistive load

07 p0958 A72-20389

Bulk conductors dc field distribution applications to electrical resistivity measurements and nondestructive testing

07 p0998 A72-20461

Battery powered dc integrated circuit for temperature regulation in small experimental animals, using thermistor probes and heating pads

08 p1114 A72-20895

Kilowatt rotary dc-dc power transformer in modular sections for spacecraft applications, discussing electrical and mechanical designs and characteristics

08 p1112 A72-21414

Pulse width modulated regulating dc-to-dc converter with small number of transistors to improve circuit reliability

10 p1452 A72-24680

Power supply for magnetic suspension system, using controlled rectifier and dc power amplifier circuits

10 p1461 A72-24767

Condenser charging by dc-dc converter consisting of SCR series inverter, transformer and rectifier-filter circuit, considering power consumption

11 p1577 A72-25278

Push-pull magnetic amplifier circuit operation as variable polarity dc source for electroplating applications

11 p1603 A72-25279

Nonlinear mathematical dc models of planar transistors for computerized IC design and analysis obtained by continuity equation approximate solution

12 p1789 A72-27313

Iterative solution for linear and nonlinear dc networks with independent voltage sources, noting convergence conditions

12 p1794 A72-27398

Rat vena porta muscle cells spontaneous activity intensified by direct current depolarization and inhibited by hyperpolarization, noting effects of calcium and sodium ions

13 p1902 A72-28638

Analog simulation of Josephson superconducting junctions dc characteristics for two mixed microwave frequencies, discussing signal detection sensitivity improvement

13 p2021 A72-28648

HF follower currents effect on dc arc I-V characteristics, indicating use of HF follower arc for quasi-steady arc power control

13 p2017 A72-29645

N region capture centers effects on small signal impedance in p-n diode structure during passage of strong dc current

13 p1933 A72-29977

Dc arc plasma, investigating applied magnetic field, trace elements and gap spacing effects on spectral line intensity spatial distribution

14 p2139 A72-30783

Narrow band retuned dc pumped amplifier-filter design based on diffron, considering electron beam interaction

14 p2088 A72-30798

Regenerative semiconductor parametric amplifier under dc through p-n junction, analyzing nonlinear phenomena

14 p2090 A72-31124

Solid state dc power controller design functional requirements, considering system overcurrent protection, power control by low voltage signals, power output to load status, etc

15 p2182 A72-31219

Temperature and electric field profiles in two TRAPATT diode structures in nonoscillatory state under dc bias, comparing geometrical limitations on diamond heat sinks

15 p2205 A72-31316

Phase transitions effect on dc electrical resistance of barium titanate investigated for yttrium-doped polycrystals and for reduced single crystals

15 p2294 A72-32483

High voltage dc arc interrupter for use in high power pulse generators and switching application in high voltage dc power transmission system

15 p2201 A72-32569

Langmuir probe dc and second harmonic characteristics measuring system, describing switching circuitry

16 p2392 A72-33608

Linear negative feedback dc current magnetic transducers for telemetry input signals, discussing operation principles and design

16 p2370 A72-33862

Characterization of a bilateral DC converter as a DC transformer.

17 p2497 A72-34705

Dc power supply for military electronics applications, describing circuit design for well regulated and filtered output dc voltage from various ac or dc sources

17 p2497 A72-34708

RF augmentation in CO2 closed-cycle dc electric-discharge convection lasers.

17 p2565 A72-35818

Controlled dc to dc converter for a space-qualified thermionic-reactor.

18 p2644 A72-36170

Feedback circuitry for dc amplifiers voltage drift compensation, discussing performance criteria in terms of residual offset voltage, system stability, correction and measurement time

18 p2671 A72-37150

On the performance and design of self-oscillating dc-to-dc converters. 19 p2754 A72-37850

A digital computer simulation model for an SCR dc to dc voltage converter. 19 p2754 A72-38267

Measurements of plasma velocity distributions in free-burning dc arcs up to 2160 A. 20 p2958 A72-39644

Linear analog to pulsewidth converter insertion into control loop in dc/dc regulators for space applications to permit high sampling frequencies 21 p2997 A72-41081

DIRECT LIFT CONTROLS

Direct lift control feasibility for integration into F-14A automatic carrier landing system (ACLS), using moving-base six-degree-of-freedom simulation [AIAA PAPER 72-873] 20 p2951 A72-39127

Test of direct lift control in the case of the experimental aircraft DFVLR-HFB 320 20 p2888 A72-39934

DIRECT POWER GENERATORS

NT ALKALINE BATTERIES

NT FUEL CELLS

NT HYDROGEN OXYGEN FUEL CELLS

NT MAGNETOHYDRODYNAMIC GENERATORS

NT METAL AIR BATTERIES

NT PHOTOELECTRIC GENERATORS

NT RADIOISOTOPE BATTERIES

NT SOLAR CELLS

NT THERMIONIC CONVERTERS

NT THERMOELECTRIC GENERATORS

NT ZINC-OXYGEN BATTERIES

EMC improvement with least sacrifice of power efficiency in designing dc/dc converters and switching voltage regulators 03 p0312 A72-14049

High efficiency solar electricity converters utilizing wave-like properties of radiation interacting with absorber-converter elements, discussing cost and fabrication advantages [ASME PAPER 71-WA/SOL-1] 05 p0614 A72-15891

DIRECTIONAL FINDERS (RADIO)

U RADIO DIRECTION FINDERS

DIRECTIONAL ANTENNAS

NT DIPOLE ANTENNAS

NT HELICAL ANTENNAS

NT HORN ANTENNAS

NT LENS ANTENNAS

NT LOG PERIODIC ANTENNAS

NT LOOP ANTENNAS

NT PARABOLIC ANTENNAS

NT RADAR ANTENNAS

NT SLOT ANTENNAS

NT STEERABLE ANTENNAS

NT TWO REFLECTOR ANTENNAS

NT YAGI ANTENNAS

Directional ionosonde aeriels and instrumentation for ionospheric reflection angle of arrival measurements 01 p0053 A72-10091

X-band linear phased array tracking antenna with digital phase shifters and beam steering, evaluating beamwidth, gain and direction error 01 p0028 A72-10663

Multimode feeds development for offset Cassegrain tracking antennas 01 p0040 A72-10678

Moderate gain superdirective antenna arrays design based on backfire principle, using parasitic elements 01 p0040 A72-10685

Nozzle shaped antenna for synchronous satellite, obtaining radiation patterns 01 p0043 A72-11245

Dipole theory application to directional characteristics of Yagi antenna systems, assuming harmonic current distribution along radiating elements 02 p0193 A72-12221

Equiphasic radiating apertures maximum directivity under nonaxial orientation conditions, discussing limitation dependence on illumination law for major and lateral lobes 02 p0194 A72-12570

Antenna sidelobe radiation probability assessment for directional gain 03 p0333 A72-13832

Iterative synthesis of dipole antenna array for maximum directivity radiation pattern, considering amplitude-phase distributions 04 p0499 A72-15142

Signal fluctuation effect on directional properties of multipole receiving antenna, calculating radiation pattern 04 p0499 A72-15143

Highly directional circular array antennas radiation characteristics calculation, showing sidelobe size dependence on aperture angle 04 p0499 A72-15240

Optimal design of directive dielectric loaded circular waveguide antenna for parabolic reflectors and radar detection 06 p0782 A72-17356

Bearing estimation performance of monopulse tracking with passive linear arrays, using computer simulation for various integration times and input S/N ratios 06 p0774 A72-17809

Optimum directional arrays design with linear programming simplex method generation of point elements excitation 06 p0774 A72-17855

Ground based Doppler navigation system for wide range elevation and azimuth aircraft approach guidance, using linear directive antenna array for conical surface definition 06 p0845 A72-18183

Linear antenna synthesis for minimum sidelobe level, eliminating superdirectivity effect 07 p0956 A72-19567

Ionospheric drifts measurement by small base diversity reception method, investigating dependence on receiving antennas orientation 08 p1154 A72-20731

Homogeneous polarization diagrams synthesis for entire radiation pattern of single reflector pencil beam antenna, noting radiator aperture misalignment effect 08 p1138 A72-20933

Phased directional surface wave splitters and microwave and integrated optics elements based on single mode, dielectric and rectangular waveguides 08 p1131 A72-20935

Maximum likelihood estimate of carrier frequency and arrival direction of radio signals in background noise for large aperture antennas 08 p1133 A72-21373

Reciprocity theorem for antenna directivity pattern measurement of optical superheterodyne receiver for carbon dioxide laser radiation 08 p1140 A72-21376

Optimum directive gain of circular Taylor patterns for planar aperture antenna design 08 p1143 A72-21987

Ionospheric and magnetic disturbances effects on short wave radio links, using directional antennas and 1.5-24 MHz frequencies 11 p1594 A72-26279

Received signal spectrum gravity center and effective antenna centers of airborne Doppler velocimeter in horizontal flight 11 p1606 A72-26730

Autotracking antenna effect on dual spin spacecraft nutational stability, using averaging, eigenvalues and digital simulation techniques [AIAA PAPER 72-571] 12 p1876 A72-27379

Receiving and transmitting antennas directional gain effect on microwave long distance tropospheric propagation 12 p1783 A72-27632

Directivity characteristics of scannable planar antenna arrays, illustrating grating lobes presence effect 13 p1928 A72-28527

Optimum aperture distributions for radiation pattern shaping for arbitrary superdirectivity ratio in antenna design 13 p1915 A72-28528

A synthesis of array antennas for high directivity and low sidelobes. 17 p2525 A72-34354

Cross coupling in a five horn monopulse tracking system. 17 p2513 A72-34356

A millimeter wave receiving antenna with an omnidirectional or directional scannable azimuth pattern and a directional vertical pattern. 17 p2525 A72-34364

The monopole slot - A small broad-band unidirectional antenna. 17 p2525 A72-34367

Relationship between antenna synthesis for a given radiation pattern and the synthesis of spatial signal processing systems 17 p2515 A72-34832

Steerable directional VHF antenna design for radio interferometric tracking and ranging of Symphonie satellite [DFVLR-SONDDR-222] 17 p2536 A72-35432

Radiation pattern determination for an antenna receiving random signals 17 p2517 A72-35540

Application of the Volterra series to the analysis and design of an angle track loop. 19 p2830 A72-37283

Ionospheric drifts measurement by small base diversity reception method, investigating dependence on receiving antennas orientation 19 p2791 A72-38359

Selection of an optimal design for a spacecraft antenna system 21 p3025 A72-40311

Spacecraft antenna feeder channel parameter control in flight 21 p3026 A72-40319

Certain problems in designing highly directional spacecraft antennas 21 p3026 A72-40325

Experimental investigation regarding Archimedean spiral antennas for the L-band, and radiator groups constructed from them whose radiation directions are controlled by a conduction matrix 21 p3028 A72-40510

The effect of amplitude and phase tolerances on the phase characteristics of dipole arrays 21 p3028 A72-40512

Integral equation and optics methods for far field radiation characteristics calculation of plane antennas with arbitrary reflector-source configurations 21 p3029 A72-40522

Radiation pattern and gain of reflector antenna with adjusting ring, discussing directivity and bandwidth 21 p3031 A72-40540

Side and back lobe structures of directive antennas. 21 p3020 A72-40903

A directional antenna represented by a system of two wires positioned on the generatrix of a relief impedance cylinder 21 p3033 A72-40942

Linear antenna synthesis for minimum sidelobe level, eliminating superdirectivity effect 22 p3158 A72-42085

Radiation field of a plane aperture in an inhomogeneous stratified medium over a large-radius sphere 22 p3155 A72-42654

Influence of the phase-amplitude distribution of the field in the aperture of an antenna on its directional properties 23 p3270 A72-43773

Antenna radiation patterns from statistical phase synthesis of antenna arrays, estimating directivity loss for in- and out-of-phase initial current distribution 23 p3265 A72-44203

Linear antenna directivity loss for fluctuating signal reception, noting effects of signal to noise ratio and antenna length 23 p3265 A72-44204

Discrete-antenna synthesis theory in the case of uniform approximation to a given radiation pattern 23 p3266 A72-44213

Computer aided directivity measurements of large antennas in Fresnel zone 23 p3274 A72-44491

Coupled active parallel doublets network within external electromagnetic field at receiving station, investigating decoupling function between radiating elements 24 p3382 A72-45771

DIRECTIONAL CONTROL

NT THRUST VECTOR CONTROL

Spacecraft soft orbital rendezvous guidance involving orbital transfer maneuver for velocity vector directional coincidence to reduce terminal relative velocity 05 p0729 A72-16757

Electro-optical multiple transit laser beam deflection system using KDP crystals and quadrupolar electrode arrangements 07 p1000 A72-19011

Helicopter maneuverability factors, discussing flight direction change ability, acceleration limitations and rotor thrust requirements [AHS PREPRINT 640] 17 p2490 A72-34500

Spacecraft soft orbital rendezvous guidance involving orbital transfer maneuver for velocity vector directional coincidence to reduce terminal relative velocity 17 p2622 A72-35260

An analysis of aircraft lateral-directional handling qualities using pilot models. 22 p3137 A72-42347

Regulator vector selection algorithm for largest estimate of exponential absolute control stability region based on Popov frequency condition reformulation 23 p3276 A72-43853

DIRECTIONAL STABILITY

NT GYROSCOPIC STABILITY

Hovercraft internal and external aerodynamic forces, discussing control, suspension, yawing moments, directional and roll stability and random surface performances 09 p1260 A72-22824

Analysis of a lateral-directional airframe/propulsion system interaction of a Mach 3 cruise aircraft. [AIAA PAPER 72-961] 22 p3137 A72-42348

DIRECTIVITY

Short backfire antenna directivity determination from plane conduction reflection coefficient 02 p0192 A72-12111

Equiphasic radiating apertures maximum directivity under nonaxial orientation conditions, discussing limitation dependence on illumination law for major and lateral lobes 02 p0194 A72-12570

Satellite tracking radio interferometer with 1 deg sec directional accuracy, discussing low noise level and precise time allocation requirements [DGLR PAPER 71-125] 02 p0182 A72-12738

Low energy gamma ray telescope with active honeycomb collimator and anticoincidence detector, describing directivity techniques for galactic sources 03 p0408 A72-13030

Balloon-borne galactic X ray detection unit, obtaining high directivity with honeycomb collimator and angular resolution with solar sensor
03 p0353 A72-13043

Radio astronomical observation of two local sources associated with unipolar sunspot group 275 and bipolar group 282, investigating emission directivity and brightness temperature
04 p0572 A72-14636

Antenna arrays performance optimization, emphasizing directivity and signal to noise power ratio
04 p0499 A72-15301

Gravitational radiation detector angular dependence, obtaining directivity pattern
05 p0656 A72-16184

Rectangular planar antenna array directivity from constituent linear arrays of dipoles or isotropic elements, using Forman method
06 p0782 A72-17358

Hansen-Woodyard condition applicability in continuous linear array design for increased directivity with optimal excitation
06 p0775 A72-18238

Improved circuit theory for linear antenna array design, obtaining maximum directivity and corresponding current distributions and driving-point voltages and currents
07 p0958 A72-20193

Radiative heat transfer spectral, temperature and directional dependence on interacting opaque surfaces system properties, testing models with accounted non-gray character
[AIAA PAPER 72-306] 11 p1742 A72-25240

Subsonic jet noise directivity prediction from acoustic pressure measurements
11 p1706 A72-26041

Directivity characteristics of scannable planar antenna arrays, illustrating grating lobes presence effect
13 p1928 A72-28527

Directivity pattern accuracy effects on angular coordinate determination by scanning active optical radars
16 p2362 A72-33188

Thermal emissivity and directivity for V groove and rectangular cavities, optimizing geometry and surface properties for maximum focusing of emitted energy
[ASME PAPER 72-HT-L] 20 p2984 A72-39651

Mathematical models for radiative heat transfer prediction in real enclosures, noting directional characteristics of heat exchanging surfaces
[ASME PAPER 72-HT-K] 20 p2984 A72-39652

Statistically dilute antenna groups with enhanced minimum distance between elements
21 p3028 A72-40504

Focus field and horn exciter regarding parabolic antennas with small f/D-ratio
21 p3029 A72-40523

Spatial measurement of the magnetic field direction in plasma.
21 p3094 A72-41633

High power monopulse laser with a stabilized spectrum and radiation directivity close to that of diffraction
24 p3410 A72-45422

DIRECTORIES
U INDEXES [DOCUMENTATION]

DIRECTORS [ANTENNA ELEMENTS]
Short backfire antenna directivity determination from plane conduction reflection coefficient
02 p0192 A72-12111

Rectangular planar antenna array directivity from constituent linear arrays of dipoles or isotropic elements, using Forman method
06 p0782 A72-17358

The loop antenna with director arrays of loops and rods.
17 p2526 A72-34378

DIRICHLET PROBLEM
Quasi-linear parabolic equations, investigating conditions for Cauchy-Dirichlet problem solution
03 p0383 A72-14380

Second and third degree harmonic interpolation formulas for given point in bounded simply connected n-dimensional region, indicating approximate solution of Dirichlet problem
04 p0538 A72-14727

Dirichlet problem reduction to boundary value problem via invariant imbedding techniques and Fredholm integral equation method
04 p0540 A72-15632

Laplace equation internal Dirichlet and Neumann boundary value problems solution procedure for thermal potential of steady temperature field
07 p1098 A72-18988

Dirichlet and Volterra problem with prescribed singularities for plane with rectilinear boundary slits, applying to fluid mechanics
07 p0971 A72-20092

Poisson equation boundary value problems summary representation formulas for three layer annular sector with Dirichlet or Neumann conditions
08 p1205 A72-20963

Laplace operator eigenvalue computation for simply connected region with homogeneous Dirichlet and Neumann boundary conditions and finite difference problem
09 p1340 A72-22296

Algorithms for eigenvalue spectrum determination in Dirichlet and Neumann problems for Helmholtz equation in configuration domains
12 p1847 A72-27985

First eigenvalue and first eigenfunction properties of linear elliptic partial differential equation in variational form with discontinuous coefficients, considering Dirichlet problem
16 p2416 A72-33502

Stability of difference schemes for elliptic equations in terms of the Dirichlet boundary conditions
18 p2705 A72-36801

The Dirichlet problem of the Poisson integrodifferential equation
19 p2825 A72-38208

Calculation of a plane stationary temperature field in the presence of a heat source
20 p2987 A72-39915

A regularity theorem for linear second order elliptic divergence equations.
22 p3198 A72-41947

Dirichlet series in eigenvalues of boundary value problems for an arbitrary second-degree elliptic differential operator
23 p3309 A72-44043

DIRIGIBLES
U AIRSHIPS

DISCHARGE COEFFICIENT
Nd glass absorption of flash pump emission energies with varying discharge parameters, Xe pressure and glass thickness
08 p1184 A72-22030

Electron densities and drift velocities dependence on macroscopic discharge parameters in positive column of He-Cd laser
10 p1493 A72-25048

Discharge coefficients of centrifugal screw-type swirl injector with helical channel, calculating drag and surface geometry effects
11 p1712 A72-26970

Discharge and pressure recovery coefficients of blocked gas flow in curvilinear channel with guide vanes, minimizing losses and separation at convex wall
11 p1574 A72-26971

Fluid discharge rate relationship to space fraction for fluidized layers in reactor
13 p1943 A72-29786

Two stream ejector propulsion performance, measuring nozzle geometry effect on discharge coefficient for 2-90 deg convergence angles
[ONERA, TP NO. 1050] 15 p2177 A72-31208

DISCHARGE TUBES
U GAS DISCHARGE TUBES

DISCHARGERS
NT STATIC DISCHARGERS
Nanosecond solid dielectric discharger fired by Q switched ruby laser for commutation of coaxial line forming high amplitude voltage pulses
07 p1008 A72-20509

DISCONTINUITY
NT SHOCK DISCONTINUITY
Electromagnetic wave transformation at moving boundary discontinuity with reactive parameters in dispersive medium by Lagrangian field equations
04 p0489 A72-15388

Infinitely long rectangular waveguide discontinuity problem, calculating reflection and transmission coefficients of wave propagation
04 p0491 A72-15428

Anisotropic plasma rotational discontinuity theory, considering parallel and perpendicular components of plasma pressure and magnetic induction
05 p0695 A72-16074

Axisymmetric bodies with discontinuous curvature in transonic flow, calculating surface pressure distribution
[AIAA PAPER 72-137] 05 p0606 A72-16891

Optimal averaging of discontinuous processes with distributed parameters, taking into account random disturbances and measurement errors
05 p0683 A72-17130

Photothermoelastic analysis of shrinkage stresses near discontinuity in fiber composite material, relating matrix cracking to fiber packing
06 p0835 A72-17800

Contact discontinuity motion past slender body of revolution in shock tube, solving unsteady supersonic flow problem by method of integral transformation
07 p0909 A72-20072

Inviscid relaxing gas flow through tube with variable cross sectional area, deriving governing equation for weak discontinuity amplitude evolution
07 p0970 A72-20073

Space-time relationship derivation to estimate traveling time of discontinuities running against magnetosphere in unperturbed solar wind
08 p1153 A72-20714

Numerical solutions of linear and nonlinear hydrostatic primitive equations for frontogenesis forced by

nondivergent horizontal wind, noting discontinuities prediction
09 p1347 A72-23651

Relaxation analysis of discontinuities in axisymmetric rotating actuator disk flow
[ASME PAPER 72-GT-26] 11 p1569 A72-25622

Coefficient stability of homogeneous difference schemes using irregular networks for fourth order differential equation with discontinuous coefficients
13 p1986 A72-29081

Tangential MHD discontinuity stability for ideally conducting compressible fluid in magnetic and gravitational fields
13 p2020 A72-30068

Millimeter wave scattering at turbulent density discontinuities in plasma from electrodeless inductive discharge
14 p2136 A72-30174

Waveguide model for calculating microstrip discontinuities and T-junctions wave impedances, using orthogonal series procedure
15 p2201 A72-32470

Discontinuity problems in optimal control of systems describable by ordinary differential equations, deriving Weierstrass optimality conditions
16 p2371 A72-32939

Discontinuities in a collisionless plasma flow having a strong magnetic field.
18 p2717 A72-37042

Boundary value problem for degenerate equations with discrete coefficients
19 p2824 A72-37317

Space-time relationship derivation to estimate traveling time of discontinuities running against magnetosphere in unperturbed solar wind
19 p2791 A72-38342

Atmospheric transmittance measurements time and spatial representativeness optimization by allowing for fog element caused discontinuities
20 p2947 A72-38971

An experimental investigation of the formation of vortices behind the isosceles triangular cross-sectional obstacles protruding from the plane wall.
21 p2992 A72-41246

Propagation of two-dimensional strong discontinuity waves in an elastic-viscoplastic medium.
21 p3124 A72-41503

Propagation of viscous fluid jets in a medium with a density discontinuity
21 p3047 A72-41666

Time evaluation of discontinuity occurrence in solutions of boundary problems for second-order hyperbolic quasi-linear systems
22 p3198 A72-41912

Acoustic transmission and reflection by a shear discontinuity separating hot and cold regions.
23 p3315 A72-44373

DISCOVERER SATELLITES
U.S. reconnaissance satellites development, discussing RAND project, Agena, Discoverer, Samos and Midas
12 p1876 A72-27109

DISCOVERING
U EXPLORATION

DISCRETE FUNCTIONS
Estimation and control relations separation for discrete time stochastic systems, considering assumptions on linearity, criteria, information pattern, constraints and noise distributions
01 p0047 A72-11306

German monograph on maximum principle application to optimum control of discrete problem
02 p0197 A72-11741

Discrete time square root Kalman filtering techniques, discussing computational requirements and covariance and information implementations
02 p0198 A72-12804

Discrete time systems unknown parameter identification, considering unified error function minimization approach
04 p0506 A72-15106

Discrete variable approach for stress wave propagation in axisymmetric layered elastic-plastic solids
04 p0593 A72-15626

Discrete stochastic differential games with quadratic payoff function, deriving deterministic, randomized and game optimal control strategies
06 p0793 A72-17956

Differential equations solutions stability for physical discrete systems with delayed argument, impact excitation, variable mass or structure, disturbances or weak couplings
09 p1343 A72-23601

Optimal closed loop control of discrete stochastic nonlinear systems, obtaining solution by cost function in power series around deterministic trajectory
10 p1457 A72-24499

Transfer function of polynomial discrete linear pulse systems for differential equation solution
13 p1936 A72-29269

Multiple decision procedures, discussing location, scale parameters, discrete populations and multinomial and multivariate normal distributions in subset selection formulation
14 p2126 A72-30998

Discrete representation of continuous time signals and sequences by digital means, using frequency warping function

16 p2365 A72-33753
Discrete and continuous systems spurious solutions avoidance through Hamilton principle reciprocal form derivation of geometric compatibility conditions
[ASME PAPER 72-APM-54] 17 p2627 A72-34777
Discrete vortex model numerical simulation of Onsager negative temperature instability for interacting line vortices two dimensional motions

17 p2538 A72-34871
On discrete-time Kalman filter in singular case and a kind of pseudo-inverse of a matrix.

18 p2672 A72-36059
Recursive updating of smoothing and filtering algorithms for discretely observed continuous dynamic linear systems

19 p2826 A72-38274
Correlation and indeterminate functions of signals with discrete frequency-time structure, noting linear frequency modulation of signal element

19 p2768 A72-38669
Response of discrete linear systems to forcing functions with inequality constraints.

20 p2910 A72-39604
Reduced order observers design for optimal control of linear discrete time stochastic systems, considering velocity-aided tracking filter

23 p3276 A72-43856
Regions of absolute ultimate boundedness for discrete-time systems.

23 p3309 A72-43857

DISCRIMINATION

NT BRIGHTNESS DISCRIMINATION
NT SENSORY DISCRIMINATION
NT TACTILE DISCRIMINATION
NT VISUAL DISCRIMINATION

DISCRIMINATORS

All digital IC FM discriminator design, computing output SNR above threshold

04 p0486 A72-14489

Multichannel IC spike height discriminator for separating electrical activity of neural units recorded with microelectrode

04 p0481 A72-15223

Frequency discriminator like two-channel device with greater sensitivity by crossed feedback, calculating variable frequency emf effect on operation

07 p0938 A72-18853

Probability density functions for output process in frequency discriminator under action of additive mixture of fluctuating radio signal and random noise

13 p1914 A72-28411

Frequency discriminator use for range measurements with FM radar systems, deriving reflecting target distance relationship to output voltage

13 p1918 A72-28892

Delay-lock discriminator to measure spatial delay time of noiselike signal received by two spaced antennas

14 p2088 A72-30336

Book on phase locked and frequency feedback systems covering FM and multiple loop principles, limiter-discriminator operation, phase detection techniques, etc

15 p2210 A72-31500

An irregular signal phase discriminator

21 p3033 A72-40943

DISEASES

NT AEROSINUSITIS
NT ANEMIAS
NT ARTERIOSCLEROSIS
NT ARTHRITIS
NT ASTHMA
NT ATAXIA
NT ATELECTASIS
NT CANCER
NT CARBON MONOXIDE POISONING
NT CYANOSIS
NT EDEMA
NT ENCEPHALITIS
NT EPILEPSY
NT FIBROSIS
NT HEADACHE
NT HEART DISEASES
NT INFARCTION
NT INFECTIOUS DISEASES
NT KIDNEY DISEASES
NT LEAD POISONING
NT LEUKEMIAS
NT MARCOLEPSY
NT PARKINSON DISEASE
NT PULMONARY LESIONS
NT RADIATION SICKNESS
NT RESPIRATORY DISEASES
NT TACHYCARDIA
NT THROMBOPENIA
NT TOOTH DISEASES
NT TUBERCULOSIS
NT TUMORS
NT UROLITHIASIS

Intestinal disaccharidosis and autoinfection occurrence in guinea pigs and rats under magnetic field effect, noting Escherichia population changes

05 p0622 A72-16647

DISHES

U PARABOLIC REFLECTORS

DISILICIDES

Titanium disilicide oxidation mechanism at various temperatures, discussing surface quality effect, growth rate and protective mechanism

03 p0369 A72-12925

Antioxidation coatings of Ta and Ta alloys for high temperature long term operation, emphasizing sintered molybdenum disilicide

11 p1663 A72-26840

Disilicide coated Ta-W alloy system oxidation behavior at 927-1482 C, using thermogravimetric, X ray diffraction and electron microprobe analyses

14 p2121 A72-30771

Interaction of titanium diboride with titanium disilicide and silicon at high temperatures

19 p2819 A72-38284

DISINTEGRATION

Rat tissue autolysis rate during hypokinesia, discussing relation to free amino acid background changes

05 p0619 A72-16648

Numerical solution of disintegration and surface stability of gas bubbles under nonspherical free oscillation

08 p1149 A72-21295

DISKS

Elastic shaft bonded to dissimilar elastic disk, considering torsion problem

04 p0583 A72-14449

Steady laminar boundary layer generated by vortex over fixed coaxial disk, solving governing equations by numerical integration

12 p1798 A72-27833

Axisymmetric rotating flow past a circular disk.

17 p2540 A72-35190

DISKS [SHAPES]

NT ACTUATOR DISKS

NT ROTATING DISKS

Elastic quadrant shaped disk loaded on horizontal and vertical edges, determining stress values at arbitrary points

02 p0259 A72-12235

Circularly symmetrical disks with circular hole and loaded by pressure at edges, calculating linear and power-law strain hardening

02 p0297 A72-12535

Disk shaped frame corner stress under external load, using complex variables and conformal mapping

03 p0448 A72-13886

Axisymmetric Reissner-Sagoci problem in linear micropolar elasticity for stress and displacement under load applied by rigid circular disk

03 p0448 A72-13890

Axisymmetric rotational motion of electrically conducting fluid between dielectric disks in crossed electric and magnetic fields

03 p0399 A72-14012

Unitary stress state and deformations in rotating axisymmetric disk, using function applicable to axisymmetric pipes

04 p0584 A72-14471

Electrochemical thinning of metal disks for electron microscopic thin foils preparation

04 p0527 A72-15492

Disk stretching under tensile stresses, determining stress at arbitrary point in half band form connected with quadrant

05 p0737 A72-16294

Thermal stresses in thin symmetrically heated disk with time and temperature dependent mechanical properties, deriving integrodifferential equation defining stress function

05 p0740 A72-16624

Nonstationary thermal interaction between thermally inert circular disk in bounded cylinder with controlled temperature, describing control process by third order differential equation

07 p1098 A72-19263

Rupture strength of disk with surface crack under concentrated loads, applying integral equation to stressed state

07 p1092 A72-19777

German monograph on bending theory extension for stress analysis of disks and cylindrical shells

09 p1397 A72-22333

Book on plastic analysis and plate, shell and disk theories and design covering stress-strain concepts, laws and theorems

10 p1553 A72-23749

Hydrodynamic forces in sinusoidal vibrations of disk in water channel with toroidal vorticity wake pattern, applying results to flapping wing mechanics

10 p1471 A72-25129

Hyperboloidal profile circular disk stress distribution induced by thermal pulse nonuniform temperature field

11 p1739 A72-26979

Stress concentration in infinite elastic isotropic disk with circular hole under internal tensile loading

12 p1882 A72-27320

Green function for stress distribution in plane shaped disk with edge loaded circular hole, noting conformal mapping for arbitrary shape

12 p1883 A72-27391

Galactic disk systems relaxation time due to particle encounters, discussing validity of Boltzmann-Vlasov equation

12 p1872 A72-27894

Cyclic nonisothermal plastic deformation of ductile disk, verifying experimentally with turbine disk of heat resistant alloys

13 p2053 A72-28398

Nonlinear first order differential equation for carrying capacity of anisotropic circular plates, curved elongate disks and shallow shells of revolution

13 p2054 A72-28457

Notch stress concentration in disk with elastic core under tension, using finite element method

13 p2060 A72-29600

Disks with inclined face, investigating effects of joint between hub and disk face on stress-strain state

14 p2164 A72-30430

German monograph - Computation of the stress condition in homogeneous anisotropic discs with the aid of an integral equation method

19 p2873 A72-37660

Stresses and strains in the plastic range in an annular disk due to steady-state radial temperature variation.

21 p3121 A72-41210

Diffraction of an elastic wave at a disk

21 p3127 A72-41669

The stretching of a disc shaped as a semi-infinite plate with half-elliptic edge sector.

22 p3236 A72-42628

Disk fillets stressed state, determining concentration coefficient and bearing capacity effect

23 p3347 A72-43747

DISLOCATIONS [MATERIALS]

NT CRYSTAL DISLOCATIONS

NT EDGE DISLOCATIONS

NT SCREW DISLOCATIONS

Plastic flow material transport during sintering, considering dislocation nucleation mechanism

02 p0232 A72-11429

Dislocations forces during sintering of loose and cold-pressed metal powders, using photoelasticity for stress estimation and electron microscopy for defects structure

02 p0232 A72-11430

Elastoplastic deformation in medium with initial dislocations and temperature field, expressing kinetic stress and distortion tensors by Hamiltonian derivatives

02 p0290 A72-11630

Computer model of dislocation motion acted on by viscous drag through point obstacle array for tensile stress and shock deformation tests

[AD-737978] 04 p0584 A72-14528

Ultrasonic bond formation between soft fcc metals, observing dislocation processes

04 p0526 A72-14837

Dislocation creep model for work hardening and recovery, deriving mechanical equation of states for various magnitudes and directions

04 p0589 A72-15160

Flux lines interaction with dislocations in twisted superconducting niobium single crystals, measuring flux gradient and dislocation arrangement

06 p0830 A72-18055

Borrmann X ray topographic examination of dislocation structures, discussing geometric effects on linear defects image width

07 p0989 A72-20158

Transparent and opaque materials fracture mechanism analogies under laser beam action, determining dislocation structure

08 p1185 A72-22093

Somigliani dislocations effect in infinite elastic cylinder, determining stresses in form of eigenfunctions expansions

09 p1398 A72-22491

Numerical solution of integral equations for dislocation densities and stress singularities associated with cracks and pile ups in bimetallic media

09 p1398 A72-22622

Magnetization and elastic stresses effect on Ni dislocations movement due to domain wall interactions

09 p1371 A72-22866

Electron microscopic study of cyclically deformed Al, Cu, Al-Mg-Zn alloy and carbon steel dislocation structure

10 p1494 A72-23830

Impurities effects on stress corrosion and work hardening induced dislocation structures in stainless steels, considering stacking fault energy relationship

10 p1496 A72-24231

Internal friction peak in fresh tempered martensite from Fe-Ni-C alloy cooled to 77 K, suggesting hypothetical carbon atoms interactions with mobile dislocations

10 p1496 A72-24232

High temperature sintering induced dislocations in refractory materials, studying material and diffusion transport processes

10 p1496 A72-24244

Plane and antiplane elasticity boundary value problems reduced to integral equations by dislocation

layers, noting closed form solutions for half and whole space

10 p1557 A72-24561

Dislocation structure analysis in ferromagnetic materials by magnetic techniques, discussing methods based on magnetization curve static properties and magnetic relaxation phenomena

10 p1487 A72-24574

Dislocation velocity-stress relationship in plastically deformed Al at room temperature, noting entropy term in Gibbs free energy equation

11 p1661 A72-26652

Nb-Ti alloy elasticity modulus temperature dependence, considering foreign atoms interactions with dislocations

11 p1662 A72-26737

Statistical estimation method for brittle metals fracture strength, taking into account stress nonuniformities due to dislocation defects

11 p1738 A72-26803

Dislocation slip motions as densification kinetics mechanism in refractory materials sintering process, discussing electron microscopic observations of partially sintered MgO and W compacts

11 p1643 A72-26834

Dislocation structure and strength of Ti at low and intermediate temperatures, investigating strain, grain size and interstitial solute hardening

11 p1666 A72-26927

Electron microscope observed dislocation splitting in bent thin tantalum carbide sheet, analyzing results in terms of strain rate law and carbon diffusion model

11 p1669 A72-26948

High temperature dislocation rearrangement in lightly cold deformed Nb as function of time and temperature, using etch pit technique for evaluation

12 p1827 A72-27136

Elastic fields of dislocation loop in two phase material consisting of isotropic elastic half spaces

12 p1884 A72-27567

Friction force electron component for superconductor dynamic dislocation at various temperatures and propagation rates

13 p2021 A72-28901

Dislocations with Burgers vector during Zr single crystals deformation at different temperatures, examining shear plane foils by electron microscope

13 p1978 A72-29223

Work hardening-recovery model of dislocation creep, deriving multiaxial mechanical equation of states for strain/time relationship under arbitrary temperature-stress sequences

13 p2061 A72-29872

Mobile point defects interaction with moving dislocation in inelastic solid bodies, considering energy dissipation due to impurity relaxation

14 p2169 A72-30954

Energy losses due to hysteresis friction during oscillations of dislocations in elastic field of point defect in solids, discussing temperature and amplitude effects

14 p2121 A72-30955

Dislocation motions as internal friction mechanism in solids due to medium frequency acoustic waves, considering motional energy transfer to thermal phonons and lattice vibrations

15 p2292 A72-31833

Silicon dislocation density relationship to solar cell current loss at low temperature, presenting temperature-diffusion length and I-V characteristics

15 p2183 A72-32132

Nitride precipitate platelets and dislocation loops formation in Nb-N alloys during aging at 535 C from electron microscope observations of structural changes

16 p2405 A72-32999

Elastic-plastic medium yield zone spread from penny shaped crack determined from continuous distribution of dislocations, noting system energy change

16 p2468 A72-33226

Dislocation mechanisms in creep

17 p2635 A72-35921

The effect of dislocation tangles on superconducting properties

18 p2719 A72-36746

Three dimensional holographic interferometry program for study of fringes due to displacement or deformation

19 p2799 A72-37630

Form of the modified Orowan creep equation for a case in which the internal stress is due to dislocation-interactions

20 p2978 A72-39008

The temperature dependence of the friction stress for basal dislocations in beryllium in the range 300-500 K

20 p2935 A72-39191

Dislocation motion as a source of acoustic emission

20 p2924 A72-39280

On the splitting of dislocations in the diamond cubic lattice

20 p2962 A72-39992

Line integral expressions along line singularity loop for elastic strain and curvature, observing plastic dislocations, distortions and rotations

21 p3125 A72-41511

Disclinations theory described by plastic and elastic distortions, considering line singularity and dislocation loop

21 p3125 A72-41513

Modified Gilman equation relating dislocation velocity to applied effective stress shown in agreement with stress relaxation experiments on Ti

22 p3189 A72-42436

DISORIENTATION

Disorientation and related experiences reported by pilots flying several aircraft types, comparing with previous reports

01 p0021 A72-11288

Disorientation in naval aircraft accidents from psychophysiological and environmental factors, suggesting flight scheduling and training improvements

08 p1126 A72-21574

Case report of fighter pilot disorientation episode during night flying exercise, suggesting psychological stress factor

11 p1584 A72-26019

Brief vestibular disorientation test technique for assessment of potential nonpilot airborne specialists or naval flight officers

12 p1773 A72-28256

Obedience to rotation-indicating visual displays as a function of confidence in the displays

17 p2510 A72-35943

Relation between a pilot's sensory perception of linear accelerations and the aircraft motion

24 p3377 A72-45654

DISPERSING

Laminar flow dispersion coefficient for curved tubes and channels determined by mathematical model, permitting concentration distribution computation

10 p1468 A72-24371

Fraunhofer single beam holography application to gas/liquid mixture high velocity flow cross section determination, observing liquid component effects on droplet dispersion composition

24 p3405 A72-45624

DISPERSION

Dispersion characteristics and frequency stabilization of 0.63 micron laser in magnetic field

02 p0180 A72-12583

Normal mode solutions for bounded systems from linear dispersion roots, discussing plasma waves and instabilities and damping effects in Q machines

06 p0858 A72-17537

Tungsten dispersion strengthening by hafnium nitride covapor deposition, discussing effects of matrix microstructure and dispersoids number, size and spacing variations

07 p1019 A72-20366

Air pollutants lateral dispersion coefficient determination from turbulence intensity, presenting formula for wind direction frequency distribution function

09 p1344 A72-22436

Focused light beam intensity fluctuations measurement during passage through turbulent atmosphere, discussing random walks effects on dispersion

16 p2364 A72-33494

Spin stabilization dispersive effect on marginally stable bodies due to precession rate, comparing analytical results with aeroballistic range measurements

24 p3362 A72-45340

DISPERSION PRECIPITATION HARDENING U PRECIPITATION HARDENING

DISPERSIONS

NT AEROSOLS

NT COLLOIDAL PROPELLANTS

NT COLLOIDS

NT FOG

NT LIQUID-GAS MIXTURES

NT NUCLEAR EMULSIONS

NT PHOTOGRAPHIC EMULSIONS

NT SMOKE

Holes dispersion hardening in sintered metal powder, discussing dispersed particle effects

02 p0233 A72-11446

Coextrusion of metal powder and ceramic dispersions clad alloyed Al as function of cartridge density and reactor core length

02 p0233 A72-11456

Optimum dispersion time and size particle determination for zirconium diboride powder grinding in vibrating mill, using gas flow rate method

13 p1967 A72-30101

Dispersed particle shape effect on elastic behavior of magnesium oxide composites at low graphite concentrations

15 p2260 A72-31585

Influence of the polarity of the dispersive medium on the structure and properties of plastic lubricants

17 p2571 A72-35176

Pulsation rates of continuous and discrete components of dispersed flow

20 p2915 A72-40047

DISPLACEMENT

Crack opening displacement concept for fracture toughness testing, presenting elastic and plastic notch tip stress and deformation relationships in plane strain

02 p0292 A72-12005

Shells finite element analysis, discussing inplane and normal displacements interpolation schemes and convergence rates

02 p0296 A72-12532

Displacement equations for rotating cylinder of revolution with stress on boundary corresponding to centrifugal force

03 p0445 A72-13625

Geometric displacements and space-time derivatives determining velocity and strain fields in solids under deformation

05 p0738 A72-16529

Equilibrium equations solution for displacements of inhomogeneous isotropic elastic media

05 p0739 A72-16588

Statistical analysis of piezoelectric transducer voltage-displacement characteristic, determining linearity deviations magnitude

09 p1317 A72-23676

Loose medium deformations and displacements fluctuations verification by statistical tests, noting inception information from autocorrelation and boundary conditions cross correlation functions

10 p1512 A72-24719

Virtual displacement application to nonholonomic systems with arbitrary constraints to derive Lagrange and Appell equations of motion

10 p1513 A72-24995

Finite element generalization of plate displacement functions to shell analysis, using strain energy tensor concept

10 p1560 A72-25187

Impact probe displacement effects in supersonic turbulent boundary layer in terms of Mach number profiles

11 p1572 A72-26005

Cantilever beam transverse vibrations induced by time varying linear displacements of clamped end under external loads, taking into account internal energy dissipation

11 p1738 A72-26797

Rigid body model for nonholonomic kinematic linkages of tangentially sliding nonrolling bearings, noting virtual displacements and mechanical work

12 p1845 A72-27539

Elastodynamics three dimensional problems formulation using displacement potential functions

12 p1883 A72-27544

Uniqueness of solutions to displacement problem for unbounded bodies in linear elastodynamics

12 p1884 A72-27564

Stokes-Helmholtz decomposition role in displacement potentials derivation in elasticity

12 p1884 A72-27569

Tangential displacements of spherical and circular cylindrical shallow shells calculated from stress function

13 p2059 A72-29490

Finite element displacement field with internal equilibrium application to nine degrees of freedom triangular bending element stiffness matrix calculation

14 p2168 A72-30930

Cylindrical shell rectangular finite element from generalized independent strain functions and corresponding displacement functions

14 p2169 A72-31174

Approximate values for elastic body stresses and displacements based on finite element method and virtual displacements and minimum potential energy principles equivalence

15 p2323 A72-31477

Singular integral representations of displacement and rotation vectors for homogeneous isotropic centrosymmetric body, using Nowacki couple stress theory of thermoelasticity

16 p2465 A72-32984

Limit displacement or solids parameters optimization for perfectly locking bodies, presenting mathematical models based on extremum energy theorems

16 p2423 A72-33104

Radial vibrations and plane wave propagation in elastic deforming sphere with superimposed time dependent displacement field

16 p2467 A72-33117

Cosserat couple stresses theory application to time varying concentrated forces induced displacements in infinite elastic space

16 p2469 A72-33385

Physical determination of fields of displacements and their derivatives in continuous media

[ASME PAPER 72-APM-15] 17 p2629 A72-34801

Nonuniformly thick combined cylindrical shell vibrations, studying radial displacement, bending moment and shearing force

18 p2735 A72-36695

Equilibrium equations solution for displacements of inhomogeneous isotropic elastic media

19 p2872 A72-37560

Displacement field analysis via holographic interferogram, measuring fringe pattern shift due to change of observation direction through double exposure hologram

19 p2797 A72-37613

Iterative solution of nonlinear structural problems, using convergence criteria based on displacement quantities 20 p2946 A72-39625

Impulsive loading in structural plasticity, obtaining displacement bounds via deformation theory based on extremum paths 22 p3337 A72-42759

Rotating disks optimal design allowing for creep from additional coupling imposition and contour displacement 23 p3347 A72-43746

A new variational principle for finite elastic displacements. 23 p3350 A72-44047

Equilibrium and stress resultant displacement equations of thin rings based on virtual work principle, stressing warping and twisting moments 23 p3351 A72-44101

Transfer matrix approach for determining stresses and displacements in elastostatics of laminated composites [ASCE PREPRINT 1674] 23 p3351 A72-44105

Triangular facet finite element application in thin cylindrical shell analysis by displacement method 24 p3456 A72-44792

DISPLACEMENT MEASUREMENT

Projected interference fringes in holographic interferometry for large surface movements measurements 02 p0231 A72-12544

Optical interference measurement of various shaped elastic plates deflection and application to thermal stress problems 02 p0300 A72-12824

Nonperiodically moving object holographic interferometry by time-averaging method, considering single exposure technique advantage over multiple exposure in thermal deformation observation 03 p0357 A72-13373

Excited Hg atom and electron concentration measurement behind shock front in nonstationary plasma by continuous displacement recording of interference bands 03 p0357 A72-13374

Separation measurement between two distant partially reflecting parallel surfaces using Michelson interferometer 03 p0358 A72-13435

Axial and radial displacements determination in rotor center of gravity for gyroscope with elastic suspension 03 p0360 A72-13560

Displacement and profile diffractographic measurement using changes in far field diffraction patterns of slit aperture between test and reference object [CLEA PAPER 11,5] 07 p0984 A72-19390

Laser interferometers for displacement, length, gas refractivity, laser wavelength and relative object position measurements [CLEA PAPER 15,1] 07 p1005 A72-19396

Displacement measuring instrument based on holographic interferometry using He-Ne laser with split beam for interference fringes on photographic plate 07 p0987 A72-19848

Mathematical model of capacitive transducer for displacement measurement in open mesh grid structures 08 p1163 A72-20918

Industrial applications of lasers, considering programmable machining, distance measurement, computer memories, communication, night clubs, machine shops, aircraft manufacture and tunnel boring machine alignment 08 p1182 A72-21207

Displacement measurement of weight center of light beam transmitted through turbulent atmosphere 08 p1135 A72-21734

Notched bend test crack opening displacement gage for continuous measurement of apparent rotation axis and true displacement location at crack tip 10 p1483 A72-24885

Self balancing ac bridge with double conversion of unbalance-signal and low capacitance sensor for displacement measurement 11 p1634 A72-26459

Mechanical and electrical methods of measuring vibration rates, displacements, accelerations and time derivatives, examining magnetoelectric and piezoelectric sensors characteristics 11 p1635 A72-26462

Involuntary head movement and helmet motion displacements during human centrifuge runs to 6 Gz from photographic recordings 12 p1766 A72-28288

Positive acceleration force-produced displacements of helmet-attached reticle in front of left eye 12 p1777 A72-28330

Crack propagation in biaxially stressed and heat treated cylindrical pressure vessel observed by strain gage displacement measurement, noting effects of initial surface cracks 14 p2169 A72-31176

Time-average holography with thin phase recording materials, obtaining characteristic function solution for sinusoidal vibration and constant velocity motion 15 p2235 A72-31614

Rotor displacement measurement of electrostatic gyroscope by capacitive sensor using spherical electrode 15 p2236 A72-31899

Coherent light signal optoelectronic processing techniques application to engineering components displacement measurement and vibration amplitude real time imaging 15 p2238 A72-32168

An improved method for obtaining the general-displacement field from a holographic interferogram. 17 p2553 A72-34721

A diffraction transducer for vibration analysis. 17 p2626 A72-34722

Optical path meter for contactless measurement of body mechanical deflection 17 p2556 A72-35442

Displacement measurement from double-exposure laser photographs. 17 p2564 A72-35751

Holographic interferometry analyzed from the point of view of moire patterns. 18 p2690 A72-36362

High speed accelerometers to determine test platform tilt and translational motion displacements, discussing instrument configurations without gyroscopes [AIAA PAPER 72-818] 20 p2923 A72-39105

Note on displacements in accelerating disks of variable thickness. 20 p2980 A72-39690

Determination of three orthogonal displacement components from one double exposure hologram. 20 p2927 A72-39847

Transducing techniques for displacements in picometer-mm range into electrical signals 21 p3051 A72-40202

Application of holography in high-temperature displacement measurements. 21 p3052 A72-40235

Surface distortion and strain fields visualization by grating produced diffraction patterns, discussing different detection techniques 22 p3234 A72-42391

Rigid-body motions and strain-displacement equations of curved shell finite elements. 22 p3240 A72-42892

Crack opening displacement relationship to notch root contraction from fracture toughness tests, describing plastic deformation mechanism at notch tip 23 p3446 A72-43704

Experimental investigation of displacements and stresses in a rod during impact loading 23 p3448 A72-43795

Full-field surface-strain and displacement analysis of three-dimensional objects by speckle interferometry. 23 p3349 A72-43984

A neoteric interferometer for use in holographic photoelasticity. 23 p3290 A72-43985

Carotid displacement pulse first time derivative recording as noninvasive technique for heart function assessment 24 p3370 A72-44561

Metallic solid material transient displacement field measurement by moire fringe photographic recording technique with computer program for data analysis 24 p3401 A72-44611

Measurement of small strain amplitudes in internal friction experiments by means of a laser interferometer. 24 p3402 A72-44947

Relative position of the rib within the chest and its determination on living subjects with the aid of a computer program. 24 p3372 A72-44957

General index for the assessment of cardiac function. 24 p3372 A72-45011

Operational dynamics of inductive and capacitive differential circuits of small-displacement transducers 24 p3403 A72-45314

Rapid radial displacement of a toroidal plasma filament by a transverse magnetic field 24 p3429 A72-45506

DISPLAY DEVICES

NT ANEMOMETERS

NT APPROACH INDICATORS

NT FLOW DIRECTION INDICATORS

NT GYRO HORIZONS

NT HEAD-UP DISPLAYS

NT HOT-FILM ANEMOMETERS

NT HOT-WIRE ANEMOMETERS

NT PLAN POSITION INDICATORS

NT POSITION INDICATORS

NT RADARSCOPES

NT RADIO DIRECTION FINDERS

NT SPACECRAFT POSITION INDICATORS

NT SPEED INDICATORS

NT TACHOMETERS

NT WIND VANES

Legibility of cold cathode, side illumination and straight projection electronic digital displays under varying ambient light and viewing positions 01 p0016 A72-10118

Symbol generation with black-and-white or color display devices and time shared computer for man-machine communication 01 p0034 A72-10484

Automated radar terminal system /ARTS/ for monitoring and tracking all aircraft within radar range, displaying identification, altitude and ground speed information to air traffic controller 01 p0098 A72-10960

Human factors engineering of aircraft cockpit data entry keyboards on area navigation control and display units 01 p0020 A72-11138

Electronic displays for attack aircraft, discussing subsystems, simulation technique and pilot role [DFVLR-SONDDR-140] 02 p0225 A72-11756

Narrow beam millimeter wave radiometer with real-time TV display for terrain mapping, analyzing contours blurring caused by antenna pattern and output integration 02 p0191 A72-11821

Remote sensor data analysis using color TV display system and interactive graphics equipment on-line to IBM 360/44 computer 02 p0226 A72-11838

Moving window displays for IR scanner signals, producing images on magnetic video tape 02 p0228 A72-11852

Airborne pictorial navigation systems for visual indication of aircraft position in addition to digital readout 02 p0256 A72-12106

FAA air traffic control automation program, discussing en route stage, computer program, data processing and storage and terminal area navigation and display techniques 02 p0256 A72-12380

Double ended scan converters for multisensor data display in radar, sonar and TV applications 02 p0193 A72-12394

Visual display systems for man-machine communications, discussing applications, data processing, hardware designs and human engineering 02 p0230 A72-12419

Computer-aided interactive graphic displays for ATC, discussing subsystems, data processing flow and operational capabilities 02 p0257 A72-12420

Tactical ATC display system for airport surveillance, precision approach and landing and operator/aircraft/machine operations by using terminal Area Surveillance Radar 02 p0230 A72-12421

Digital computers data output alphanumeric display by commercially available TV sets, describing system design 03 p0355 A72-13075

Flight display systems current state and future developments, discussing dual attitude indicators and automatic chart systems CRTs, engine displays and malfunction warning systems 03 p0357 A72-13423

Concurrent and terminal display exposure effects on perceptual adaptation for localizing movements with displacing prism 03 p0319 A72-13878

Storage oscilloscope interface for small computers, describing graphic display characteristics and line cursor and character generators 03 p0329 A72-14177

Visual film, TV and optical data systems unified classification for performance criteria based on equation similar to ideal imaging system description by Rose 03 p0329 A72-14188

Moving display visibility effect on pilot tracking performance, discussing dependence on illumination intensity and color 04 p0477 A72-14445

Cockpit information for pilot and flight crew as key to transport aircraft accident prevention, discussing cockpit layout and displays in terms of flight safety requirements 04 p0464 A72-14813

Three color optical pyrometer with microsecond resolution time based on three-wavelength double ratio method, displaying temperature/time relationship on cathode ray oscilloscope 04 p0522 A72-15476

Visual display IR spectrometer for pulsed transversely excited carbon dioxide laser, tabulating observed wavelengths [AD-740011] 04 p0524 A72-15540

Visible displays of millimeter and submillimeter wave images for all-weather ground surveillance, discussing image conversion [AD-736578] 04 p0494 A72-15612

Holographic multicolor moving map display using photoresist recording and He-Cd laser 05 p0660 A72-15787

Alphanumeric data representation by TV receivers, describing coding device and gate system for video signal generation 05 p0634 A72-15813

Display device for engine rotational speed nonuniformity parameters indication on oscilloscope without supplementary computation 05 p0662 A72-16125

Development programs for ATC system improvement by digital computers and data displays applications 06 p0844 A72-17328

Airborne traffic display system using beacon and radar surveillance network and ground computer processing 06 p0844 A72-17329

Supplementary Aviation Information Display for ATC, discussing remote sensing capability and cost savings 06 p0845 A72-17424

Stereoscopic projection screens for three dimensional image display, discussing classification by diffusing properties, surface types and applications 06 p0814 A72-17440

Computer graphics techniques, discussing hard and soft copy outputs, animation, man machine interactions and physical and biological applications 06 p0779 A72-17635

Linear airspeed and runway rate field displays, measuring initial response latencies, control reversals and root mean square tracking errors 06 p0845 A72-17717

Holography utilization effectiveness in three dimensional image displays, information storage, image multiplication and recording, interferometry, coding, lens corrosion, pattern recognition, etc 06 p0816 A72-17951

GPSS/360 interactive simulation program with report generator, selective output display and HELP blocks for model manipulation and real time viewing 06 p0780 A72-17980

FORTAN digital simulation of ATC radar beacon system making possible computer generated movie display 07 p0950 A72-19301

Boeing 707 cockpit simulator with computer generated displays, moving area navigation map and ATC information 07 p1033 A72-20336

Computerized dynamic simulation with graphic display of crystal plastic dislocation movement among random obstacles, emphasizing stress-strain, strain rate and thermal activation mechanisms 07 p1095 A72-20338

Direct simulation Monte Carlo method for rarefied gas dynamics, discussing computer display units use for flow visualization 07 p0973 A72-20344

ATC radar performance monitoring, considering advances in radar signal processing and digital display techniques 08 p1134 A72-21525

Statistical analysis of cockpit simulator data on altimetry display for commercial aircraft 08 p1168 A72-21573

Optimal solutions for apportionment between automatic and manual flight control, considering number and types of displays required 09 p1348 A72-22783

Star sky simulation in testing and training stands, using spherical mirror, collimator and imbedded spheres 09 p1310 A72-22949

Sailplane computer displaying rate of climb simultaneously with airspeed for pilot determination of best strategy for local upcurrent-downcurrent conditions 09 p1316 A72-23550

Optical properties of nematic and cholesteric liquid crystals, noting application for visualization and display systems 09 p1373 A72-23598

Profiling technique with scanning electron microscope to obtain depth information on single small specimen micrograph 10 p1481 A72-24240

On-line analog display system for cardiovascular functions and beat-by-beat cardiac output derived from single aortic blood flow measurement 10 p1430 A72-24375

Space shuttle flight crew/computer interface display and control functional requirements optimization by real time digital simulation 10 p1460 A72-24437 [AIAA PAPER 72-226]

Electronic production of shifting grid pattern displays featuring variable spatial frequency, temporal frequency and modulation depth 10 p1433 A72-25184

Pilot warning systems for visual midair collision avoidance, noting reaction to imminent threats, scanning patterns and display sector size effects [SAE PAPER 720312] 11 p1583 A72-25576

Flight tests of combination flight director displayed and attitude command control system effect on at-

titude command control system effect on general aviation aircraft handling qualities during ILS approach [SAE PAPER 720316] 11 p1575 A72-25580

Pulse operated multichannel annunciator system for pilot warning of aircraft systems malfunctions, describing circuit design 11 p1630 A72-25593 [SAE PAPER 720333]

Computer aided iterative design of nonlinear single loop control system with sinusoidal describing function and time response display capability 11 p1601 A72-26042

Logic character generator for CRT text display and DEC PDP 8/S graphics 11 p1601 A72-26290

Interactive computer graphics with three dimensional real time CRT display of air combat maneuvers for fighter pilot training 11 p1613 A72-26291

Integrated display system design with navigation update, weapon delivery, reconnaissance, bomb damage assessment, threat and terrain avoidance capabilities for multicrew military aircraft 11 p1684 A72-26292

Data display techniques in man operated automatic control system, assessing information volume versatility and operability 11 p1585 A72-26451

Electroluminescent matrix display system with amorphous semiconductor threshold switches for isolation and memory, discussing performance and address waveforms 12 p1788 A72-27239

Interactive computer graphics technique for structural analysis, aiding engineering decisions by CRT graphical and numerical information display 12 p1787 A72-27864

Smoothed wind fields generated from ATS 3 cloud motions measurements observed on computer display system 13 p1991 A72-28827

Man machine system to repackage weather information for easy assimilation, considering computer driven keyboard CRT displays 13 p1924 A72-28872

Signal system design with digital displays for deviation control in complex multiparameter technological processes, using algorithm to estimate efficiency 13 p1936 A72-29177

Small aircraft navigation over 10-400 mile course segments by raw OMEGA phase information dc presentation on conventional ID-249 course deviation indicator 13 p1999 A72-29201

Visual display units as manifold input output devices in data processing systems, discussing structure, characteristics and applications 13 p1925 A72-29343

Three grid LEED-Auger display system for electron emission from solids at low primary beam energies 13 p1932 A72-29751

Alphanumeric characters for small TV type raster displays, describing legibility experiment for character height optimization 13 p1911 A72-29821

Exercise cardiograph with heart rate display on beat to beat basis, R wave recognition circuit and noise linear filtering efficiency 14 p2082 A72-31092

Compensatory tracking task performance with continuous error information feedback via visual, auditory or electrocutaneous displays 14 p2083 A72-31152

Target and surrounding nontarget stimuli size differences effect on visual search time for displays with large fields 14 p2083 A72-31153

White background noise intensity effects on human visual target detection performance considering display difficulty levels, target location, detection time and error 14 p2083 A72-31156

Aircraft inertial navigation system, discussing mode selection unit, digital computer and control display for operator communication with system 15 p2267 A72-31596

Schedule analysis computer program algorithms for waterfall bar chart display and commodity flow processing and graphing through network 15 p2203 A72-31696

Head-up display for aircraft three dimensional sky path observation during navigation and landing, discussing computer units, CRT and image generating subsystems 15 p2268 A72-32042

Real time holographic quasi-dynamic 3-D image display, discussing computerized synthetic hologram generator concept and system block diagram 15 p2237 A72-32054

Azimuth display of attenuation instrument used with weather radar to measure rain induced attenuation over slant paths 15 p2207 A72-32101

Direct display plasma density and temperature meter with Langmuir probe for ionospheric observation 15 p2231 A72-32338

High contrast and sensitivity thermal erase cathodochromic sodalite for storage and display applications, measuring contrast ratio versus electron beam flux 15 p2240 A72-32362

Registers and digital circuits with FETs and integrated operational amplifiers to permit analog measurements storage for display on CRT oscilloscope 15 p2204 A72-32499

Electronic displays - Conference, London, February 1972 15 p2181 A72-32631

Aircraft electronic display for pilot precise control in complex tasks, discussing clarity, stability and readability of CRT images 15 p2181 A72-32632

Civil helicopter electronic display requirements contrasted with fixed wing aircraft 15 p2182 A72-32633

Electronic displays with weapon aiming sensors in aircraft navigator-attack systems 15 p2273 A72-32634

Electronic display in future avionic systems, emphasizing computer techniques and digital data exchange systems 15 p2242 A72-32635

Aircraft CRT electronic displays discussing operational flexibility versus control and monitor complexities, economics, reliability and human factors 15 p2182 A72-32636

Graphic color display adapted to traffic control for direct operator-computer dialogue, noting instruction repertoire, switching device and input devices 16 p2420 A72-32894

Auditory display in dual-axis compensatory tracking task, discussing performance measures in terms of squared error integral and human operator describing functions 16 p2359 A72-33866

Stimulus complexity and the EEG - Differential effects of the number and the variety of display elements. 17 p2507 A72-34248

Semiconductor optoelectronic devices, discussing light emitting indicator diodes, data display systems, photosensitive arrays and optical data transmission links 17 p2594 A72-34332

Image pickup and display devices. 17 p2552 A72-34568

A data collection and display system for a large-scale simulation. 17 p2524 A72-35848

Obedience to rotation-indicating visual displays as a function of confidence in the displays. 17 p2510 A72-35943

Electronically restored holographic data recording process for analog shape visualization with random access computer storage, discussing system design and capabilities 18 p2659 A72-36271

Nematic liquid crystals application to monochromatic or multicolor display devices based on vertical phase elastoelectric deformation effect 18 p2719 A72-36679

Recent research applicable to the design of electronic displays. 18 p2653 A72-36902

Symbol generators for the representation of switching circuits by data display devices according to the television principle 19 p2769 A72-37935

Video signals generation from binary data and mixing with analog information from cameras or tape recorders for simultaneous display on cathode ray tubes 19 p2769 A72-37936

Automated data processing and display capabilities of radiation measuring systems for surveillance, protection and control in nuclear research, medicine and power production 19 p2802 A72-38306

Visual information electronic display systems from human factors engineering viewpoint, discussing intelligibility optimization in terms of human vision physiological characteristics 19 p2803 A72-38309

Incoherent radiation imaging system analysis from detector-display characteristics, target response function and noise characteristics 20 p2922 A72-39044

Modular navigation /MONA/ dual channel automatic area navigation system, describing computer, flight data storage and control/display units 21 p3079 A72-40277

Aircraft instrument panel redesign to alleviate crew task, proposing integral displays and controls for flight information 21 p3080 A72-40291

Corrugated image screens advantages over flat screens, determining light intensity per corrugation, maximum viewing angle and reflection factor
21 p3055 A72-40743

Proximity and direction of arrangement in numeric displays.
21 p3008 A72-41017

Error search reading tasks to investigate practical applicability of blinking display coding techniques, noting reading speed reduction compared to steady display
21 p3008 A72-41018

Storage tube figure display apparatus
21 p3034 A72-41251

Temporal and spatial characteristics of selective encoding from visual displays.
21 p3009 A72-41255

Displays and controls; Proceedings of the Advanced Study Institute, Berchtesgaden, West Germany, March 15-26, 1971.
21 p3009 A72-41402

Display device layout based on human operator manual control information requirements consideration, discussing functional categories, motion compatibility, indicators relation and integration
21 p3009 A72-41404

Prediction role in execution of manual control with display device to aid human operator adaptation
21 p3010 A72-41406

Display device design and human operator training based on visual and auditory sensation and perception principles, emphasizing fitting between man and information
21 p3010 A72-41407

Prediction displays based on the extrapolation method.
21 p3010 A72-41409

The airborne visual simulation as an electronic display.
21 p3010 A72-41410

Problems arising in the transfer of training from simulated to real control systems.
21 p3010 A72-41412

Manual workload determination by control characteristics, control-display relationships, demands for dexterity and sensitivity and speed and accuracy requirements
21 p3010 A72-41414

Man machine system functions and display and control role descriptions by flow diagrams, giving examples of keying and task in guided weapon system
21 p3011 A72-41415

The design of a nonlinear multi-parameter model for the human operator.
21 p3011 A72-41421

A new concept of flight displays compatible with digital airborne computers.
21 p3012 A72-41426

A psychologist's laboratory approach to a human factors problem.
21 p3012 A72-41430

Results of the investigation of different extrapolation displays.
21 p3012 A72-41431

The influence of a prediction display on the human transfer characteristics.
21 p3012 A72-41432

Human operator dynamics for aural compensatory tracking.
22 p3149 A72-41950

Digital data system with real time displays and multiprocessing capability for multitask of aircraft structure with operational manpower reduction, assessing performance
22 p3163 A72-42696

Interactions of signal and background variables in visual processing.
22 p3152 A72-42931

Electric field distribution and strength and electron trajectories computations in designing electron optical display systems, using rectangular networks
23 p3291 A72-44312

Mathematical model for digit summation task search time distribution dependence on size of visual display with randomly arranged three digit numbers
24 p3374 A72-44558

A sight simulation technique using TV-screen perspective correction for restricted maneuver flight missions
24 p3388 A72-45298

DISPLAY SYSTEMS
U DISPLAY DEVICES
DISPOSAL
NT WASTE DISPOSAL
DISSIPATION
NT ENERGY DISSIPATION
NT OHMIC DISSIPATION
Asymptotic stability of mechanical system with two mathematical pendulums and rod subjected to axial follower, correcting aerodynamic and dissipative forces
12 p1847 A72-27979

Dissipative systems of ordinary differential equations concepts extension to functional and partial differential equations
15 p2263 A72-31754

DISSIPATORS
U DISSIPATION
DISSOCIATION
NT AUTOIONIZATION
NT GAS DISSOCIATION
NT PHOTODISSOCIATION
NT THERMAL DISSOCIATION
Triatomic hydrogen positive ions dissociation at 410, 510 and 550 keV in molecular hydrogen gas, measuring atoms yield as function of target thickness
01 p1014 A72-11148

Chemical lasers diatomic and multiatomic molecules dissociation in nonequilibrium conditions, discussing vibrational energy exceeding gas temperature
11 p1646 A72-25713

Diatomic molecules dissociation investigation from effective cross section measurement of slow atomic negative ions formation by molecules collisions with fast ions and atoms
16 p2432 A72-34152

Dissociation of molecular ions formed by charge exchange in an in-line tandem mass spectrometer.
19 p2763 A72-38801

Monte Carlo trajectory calculations of the three-body recombination and dissociation of diatomic molecules.
19 p2838 A72-38805

Chemical reaction rates for dissociation and exchange in nonisothermal plasma from molecular energy level occupation investigation
20 p2957 A72-39018

DISSOLUTION
U DISSOLVING
DISSOLVING
Dynamics of dissolution of gas bubbles or pockets in tissues.
18 p2655 A72-37027

The role of metal dissolution in the process of stress corrosion cracking of austenitic stainless steel.
19 p2821 A72-38374

DISSYMMETRY
U ASYMMETRY
DISTANCE
NT DEBYE LENGTH
NT MISS DISTANCE
NT MISSILE RANGES
NT RADAR RANGE
NT RADIO RANGE
NT RANGE AND RANGE RATE TRACKING
NT REENTRANCE RANGE
Distance effects on radio interferometric measurement accuracy, discussing single error source influence on total error
02 p0182 A72-12708

Pulsar distance determination from electron density distribution in line of sight estimated from frequency dispersion measures
07 p1080 A72-20054

Probability density distributions for distance from arbitrary point to randomly distributed weather stations
11 p1592 A72-25767

DISTANCE MEASURING EQUIPMENT
NT ALTIMETERS
NT GEODIMETERS
NT LASER RANGE FINDERS
NT OPTICAL RANGE FINDERS
NT RADIO ALTIMETERS
NT RANGE FINDERS
Pulsed Doppler radar loss of detection probability due to echo signal misalignment, discussing distance measurement refinement by interpolation
02 p0179 A72-12571

VOR, Direct Measuring Equipment and TACAN polar coordinate radio navigation systems history, improvements and future development
02 p0257 A72-12646

High accuracy laser reflector telemetric measurement for earth-moon distance variation in time by correlation method
04 p0495 A72-15727

Distance estimation for supernova remnants and H II regions from H I absorption measurements
05 p0712 A72-15770

Extragalactic distance scales, discussing brightest galactic cluster member utilization as distance indicators
05 p0717 A72-16381

Operational requirements for VORTAC system improvements, including precision VOR, navigation broadcast, DME capacity and CAS signals synchronization
06 p0845 A72-17336

Combined inertial/radio navigation systems for cost reduction, noting superior accuracy of VOR and DME
06 p0846 A72-18286

French Geole satellite system for geodetic survey, discussing frequency selection, antenna problems, distance measuring equipment and instrument errors
08 p1158 A72-21206

Area navigation systems, discussing VOR/DME, Doppler and inertial systems, CRT displays, data links, etc
08 p1204 A72-21523

Geodetic optical distance measuring instruments with electro-optical polarization modulators, comparing characteristics of four possible configurations
09 p1314 A72-23336

Extragalactic eclipsing binaries parallax determination by Gaposchkin method, noting application to distance determination of nearby galaxies
10 p1549 A72-25057

Two-laser optical distance measuring instrument with atmospheric refractivity correction, noting accuracy
11 p1646 A72-25305

Solar chromosphere double limb effect attributed to instrument, discussing application to height measurement
11 p1717 A72-25905

Aircraft distance measuring equipment with VOR radio receivers and ground station transponder for pulse interrogation
12 p1842 A72-27105

Laser tracking measurements of distance to light reflector mounted on Lunokhod 1, describing equipment and procedure
12 p1825 A72-27888

Pulse distortion and amplitude smear calculation for electron beam measurements of distance from space vehicles to deployable structure measurements on space vehicles
14 p2103 A72-30198

Galactic supernova remnants radio frequency absorption line observations, deriving distances, radio luminosity function and distribution
14 p2158 A72-30726

Pulsars distance computation, considering period-luminosity relationship and uncertainties inherent in dispersion measure /DM/ method
14 p2159 A72-30738

H II regions radial velocities in Carina arms from Fabry-Perot interferometric H alpha measurements, determining early stars distances from spectroscopic and photoelectric observations
14 p2159 A72-30740

Earth chord length determinations, using synchronous photographic satellite observations with simultaneous topocentric distance data from laser measurement
14 p2103 A72-31076

Data system in Eole satellites program, discussing balloon localization, UHF information transmission and reception, distance measurement and data acquisition
15 p2268 A72-31981

Negligible intergalactic matter model, deriving distance-red shift relation and comparing to acceleration parameter of homogeneous model
16 p2455 A72-33470

Solid state modular ground based distance measuring equipment /DME/ receiver for en route aircraft navigation and landing
16 p2420 A72-33521

Laser tracking measurements of distance to light reflector mounted on Lunokhod 1, describing equipment and procedure
16 p2404 A72-33997

Integrated inertial-VOR-DME or inertial-TACAN navigation system, presenting slant range and bearing adjustment procedure via least squares method
16 p2421 A72-34136

Ultrasonic range finder
17 p2553 A72-34763

Ranging signals for aeronautical satellite systems
17 p2516 A72-35220

Configuration and flight test of the only operational Air Force area navigation system.
17 p2578 A72-35557

Updating inertial navigation systems with VOR/DME information.
20 p2950 A72-39083

Navigation satellite system based on triangular distance measurement between two satellites and aircraft, noting simplification of air- and satellite-borne equipment requirements
21 p3080 A72-40285

Space Shuttle landing navigation using precision distance measuring equipment.
24 p3421 A72-44637

DISTANCE PERCEPTION
U SPACE PERCEPTION
DISTILLATION
Distillation experiments showing volatility-caused amino acid contamination of commercially available aqueous hydrochloric acid
05 p0624 A72-16079

Pressure effects on molten metals reactions with ambient atmosphere during purification by distillation, obtaining impurities concentration ratio via Langmuir relative volatility rule
07 p0997 A72-20287

DISTILLATION EQUIPMENT

Compression distillation unit design and development for integrated water and waste management system onboard spacecraft, describing reliability and performance tests

[ASME PAPER 72-ENAV-1] 20 p2897 A72-39176

DISTORTION

- NT FLOW DISTORTION
- NT SIGNAL DISTORTION
- NT SURFACE DISTORTION

Optical distortion induced by heated windows in high power laser systems, deriving figures of merit for window materials

02 p0237 A72-11470

Eye-hand coordination modifiable parameters under optical distortion conditions, deriving quadratic equation for hand response adaptation

02 p0167 A72-11897

Holographic image structure spatial filtering resulting from nonlinear distortions in hologram recording

10 p1479 A72-24048

DISTRIBUTED AMPLIFIERS

Balanced negative feedback circuits for reducing nonlinear distortions in distributed gain power amplifiers

02 p0193 A72-12223

Nonlinear stochastic systems stability conditions description by Volterra integral equation, applying to distributed parameter feedback control system with nonlinear amplifier of random gain

04 p0504 A72-14663

Distributed unidirectional microwave IMPATT diode amplifier and CW tests for X and C band circuits

05 p0633 A72-15783

DISTRIBUTION (PROPERTY)

- NT ANGULAR DISTRIBUTION
- NT ANTENNA RADIATION PATTERNS
- NT BOLTZMANN DISTRIBUTION
- NT CHARGE DISTRIBUTION
- NT CURRENT DISTRIBUTION
- NT DIFFRACTION PATTERNS
- NT ELECTRON DENSITY PROFILES
- NT ELECTRON DISTRIBUTION
- NT ENERGY DISTRIBUTION
- NT FLOW DISTRIBUTION
- NT FORCE DISTRIBUTION
- NT FREQUENCY DISTRIBUTION
- NT HOLE DISTRIBUTION [ELECTRONICS]
- NT HOLE DISTRIBUTION [MECHANICS]
- NT INTERFERENCE LIFT
- NT ION DISTRIBUTION
- NT LOAD DISTRIBUTION [FORCES]
- NT MASS DISTRIBUTION
- NT MOMENT DISTRIBUTION
- NT NEUTRON DISTRIBUTION
- NT PRESSURE DISTRIBUTION
- NT RADIAL DISTRIBUTION
- NT RADIATION DISTRIBUTION
- NT SIDELOBES
- NT SPATIAL DISTRIBUTION
- NT SPECTRAL ENERGY DISTRIBUTION
- NT STAR DISTRIBUTION
- NT STRESS CONCENTRATION
- NT TEMPERATURE DISTRIBUTION
- NT VELOCITY DISTRIBUTION
- NT VERTICAL DISTRIBUTION

Solute dispersion distribution over tube cross section with flowing solvent, comparing with Gaussian distribution

10 p1466 A72-24330

DISTRIBUTION FUNCTIONS

Redistribution function of line radiation during scattering without atom velocity restriction

01 p0104 A72-10093

Electrostatic wave-particle interactions in inhomogeneous collisionless plasma, calculating resonant distribution function, charge densities and trapping periods

01 p0107 A72-10136

Higher moment Vlasov equations of collisionless fully ionized plasma for studying solar wind proton thermal anisotropy, heat flux and distribution function

01 p0119 A72-10880

Galaxy clusters stability, obtaining mass distribution function from combined virial theorem and mass to light ratios

01 p0131 A72-11003

Point estimate calculation of underlying distribution function for probability plot, developing confidence coefficient for Weibull model

02 p0252 A72-11557

Jacketed tubular chemical reactor optimal startup control, presenting distributed maximum principle for diffusional parameter system

02 p0301 A72-12093

Linear viscoelasticity theory dynamic functions, deriving delay and relaxation times distribution functions in polymers

02 p0293 A72-12211

Feedback control dynamic system described by linear differential equation with random coefficients, calculating parameters distribution effect on behavior precision

02 p0197 A72-12339

Solar magnetic field vector distribution in quiescent prominence plasma with components both along and perpendicular to long axis

03 p0432 A72-13350

Relativistic plasma with particles interacting through electromagnetic field, constructing statistical description by reduced distribution functions and correlation patterns

03 p0395 A72-13626

Low pressure glow cathode triodes gas discharges, determining electron energy distribution function in double layer by probe measurements

03 p0400 A72-14349

Self consistent kinetic equations for evolution of particle distribution functions and wave intensity spectra of relativistic spatially homogeneous multispecies plasma in ambient magnetic field

04 p0553 A72-14401

Aerospace reliability methods, discussing distribution functions, sampling, accelerated life testing and case histories of space electric rocket and microthruster power conditioner tests

04 p0526 A72-14441

Shock wave structure in monatomic gases, using Fokker-Planck model for particle collisions and Mott-Smith distribution for shock front

04 p0512 A72-15162

Whistler instability of electron plasmas with non-Maxwellian velocity distribution function

05 p0698 A72-17015

Chapman-Enskog method modification for gas flow Prandtl boundary layer zero approximation distribution function construction, applying Mises transform to Boltzmann equation

05 p0653 A72-17209

Laminar leading edge of collisionless plasma perpendicular shock structure and distribution functions, considering instability calculations

05 p0654 A72-17227

Coupled equations for collision amplitudes in three body system involving particle redistribution

06 p0851 A72-17391

Ion distribution function oscillations in first order ionic waves of single ended Q device, noting plasma confinement in static magnetic field

06 p0855 A72-17507

Electrostatic waves perturbed distribution function behavior in presence of forced oscillations, considering Maxwellian ion and electron plasma waves excited by dipole

06 p0855 A72-17508

Non-Maxwellian plasma response to acoustic wave propagation in single ended Q device, investigating ion distribution function

06 p0855 A72-17509

Wave exciting grid-plasma interaction in single ended Q device, determining ion velocity distribution function

06 p0855 A72-17510

Perturbed density and ion velocity distribution functions of grid-excited ion acoustic waves in collisionless plasma in single ended Q device

06 p0855 A72-17511

Wake behind obstacle immersed in plasma flow of single ended Q-machine, using experiment as diagnostic of ion distribution function

06 p0856 A72-17526

Electron beam interaction with collisionless plasma, obtaining beam spatial distribution function from velocity diffusion coefficient measurement

06 p0858 A72-17540

Electrostatic energy analyzer for local ion velocity distribution function measurement in double ended Q machine plasma column

06 p0814 A72-17551

Plasma conductivity dependence on electron velocity distribution function in distorted Maxwellian form

06 p0860 A72-17690

Stellar velocity distribution functions in nonrotating clusters, considering encounter multiplicity effects and dissipation increase from masses dissipation

06 p0883 A72-18024

Boltzmann integrals for inelastic collisions and radiative processes in stationary monatomic plasma, using Grad 8-moment approximation of particles momentum distribution functions

06 p0861 A72-18174

Magnetic effects on Lorentz plasma collision processes, calculating electron distribution function in presence of strong arbitrarily oriented magnetic and weak electric fields

06 p0864 A72-18535

Radio waves arrival angles distribution function in Fraunhofer diffraction zone upon plane wave normal incidence on inhomogeneous scattering layer

07 p0938 A72-19017

Steady creep rate logarithm and creep limit obedience to normal distribution law

07 p1014 A72-19846

Kinetic theory and nonequilibrium distribution functions of reacting gases with simultaneous reactions

07 p1035 A72-20114

Stability of steady large amplitude whistler wave supported by weak electrostatic waves in collisionless magnetoplasma, constructing distribution function via Vlasov equation solution

08 p1213 A72-21258

Feedback control dynamic system described by linear differential equation with random coefficients, calculating parameters distribution effect on behavior precision

08 p1146 A72-21554

Fine structure of energy distribution function for electron beam interacting with plasma

08 p1215 A72-21722

System reliability improvement by redundancy, noting independence of distribution law type

08 p1180 A72-22057

Reliability theory distribution function construction for failure analysis in physical processes, considering mechanical system service life and living organisms life span

08 p1180 A72-22062

Ideal gas many particle distribution functions in microspace from solution of chain of integrodifferential equations

09 p1354 A72-22220

Air pollutants lateral dispersion coefficient determination from turbulence intensity, presenting formula for wind direction frequency distribution function

09 p1344 A72-22436

Collisionless plasmas numerical simulation with weighted particles and periodically reconstructed distribution function, estimating diffusion rates

09 p1358 A72-22462

Second derivative measurement of Langmuir probe characteristics for electron energy distribution functions in nonstationary plasmas by sample and hold technique

09 p1359 A72-22654

Safety factor distribution function for plastic collapse of structure with random resistance members, discussing variance-expected value ratio

09 p1406 A72-23075

Schwarzschild solution to Vlasov equation for velocity distribution function of self gravitating stellar system

10 p1535 A72-24112

Statistical analysis of MOS integrated circuits from initial data of electrophysical and geometric distribution laws and covariance matrix

10 p1449 A72-24289

Chapman-Enskog method modification for gas flow Prandtl boundary layer zero approximation distribution function construction, applying Mises transform to Boltzmann equation

11 p1614 A72-25332

Trapped particle induced frequency shift in response of electrostatic wave to adiabatic and sudden excitations, obtaining distribution functions and nonlinear dispersion relation

11 p1693 A72-25566

Linear viscoelasticity theory dynamic functions, deriving delay and relaxation times distribution functions in polymers

11 p1734 A72-25709

Collisional distributions in mirror plasmas, using successive approximation technique for Fokker-Planck equation lowest eigenvalue and eigenmode

11 p1694 A72-25792

Time shared computer systems output maximization via degenerate exponential distribution function modeling, noting reducibility to Markov processes

11 p1601 A72-25900

Stellar velocity distribution functions in nonrotating clusters, considering encounter multiplicity effects and dissipation increase from masses dissipation

11 p1719 A72-25960

Narrow band process signal model for phase and amplitude difference distribution densities of alternating period compensation system output signal

11 p1596 A72-26310

Correlations analysis method for homogeneous and inhomogeneous systems under external field based on BBGKY hierarchy and decomposition of reduced distribution functions

11 p1689 A72-26480

Two dimensional characteristic and distribution functions of monomode laser radiation random processes with nonlinear optics application

11 p1651 A72-26716

Nonlinear interactions between synthesized plasma positive and negative ion beams, discussing effect on individual velocity distribution functions

12 p1849 A72-27058

Random vibratory processes and envelopes distributions interrelationship, tabulating probability density functions and moments

12 p1846 A72-27725

Distribution theory application to fixed end point problem in variational calculus for extremal containing corners, obtaining Euler equation

12 p1885 A72-27849

Strong field electromagnetic wave interactions with anisotropic plasmas, considering electron velocity distribution function

13 p2009 A72-28449

Covariant statistical mechanics equations system for distribution function of relativistic particles in steady external gravitational field, noting Vlasov equation as limiting case

13 p2035 A72-28465

Particle size distribution functions reconstruction from scattered radiation data, discussing accuracy and applicability of small angle, spectral transparency and complete indicatrix methods

13 p1955 A72-28514

Critique of paper on error distributions in air navigation, noting inappropriateness of Gaussian distribution

13 p1996 A72-29015

Frequency distribution changes of energy deposited in short pathlengths as function of energy degradation of primary proton beam

13 p2004 A72-29425

Inviscid plane Couette flow infinitesimal instability as initial value problem, using distribution-theoretic approach

14 p2126 A72-30230

Mars surface normal albedo distribution function from red light photometry data

14 p2152 A72-30489

High momentum transfer collisions importance for anisotropic part of distribution function in Lorentz and single component plasmas

14 p2134 A72-30802

Cosmic objects and phenomena frequency distribution functions monotone decrease with respect to importance, considering star clusters, binaries, lunar craters, solar activity, etc

14 p2160 A72-30912

Massive stars velocity distribution function in clusters, determining escape rate and energy dissipation

15 p2305 A72-31339

Anisothermal magnetoplasma with non-Maxwellian particle distribution function, calculating ac electrical conductivity collisional factor from convergent classical kinetic equation

15 p2287 A72-32410

Thermal molecular jets mixing produced by Knudsen effusion from porous wall, obtaining Boltzmann equation approximate solution by moment method via assumed distribution function

16 p2429 A72-33055

Plasma stability in field of longitudinal monochromatic wave, examining satellites excitation by Langmuir wave

16 p2437 A72-33693

Low pressure He and Ne discharge generated positive plasma column potential, determining electron concentration from electron energy distribution functions

16 p2437 A72-33746

Particle scattering due to Rosenbluth-Post convective plasma loss-cone instability distribution function

17 p2587 A72-34189

A one-dimensional harmonic oscillator in quantum mechanics with a nonnegative distribution function in the phase space

17 p2579 A72-34198

Statistical mechanics of magneto-active plasma.

17 p2590 A72-35144

Self-consistent kinetic equations.

17 p2581 A72-35152

On the size distribution of turbulent elements in the earth's magnetosphere.

17 p2549 A72-35717

Equilibrium distribution of chemical species in a reacting gas mixture

17 p2512 A72-35808

Distribution function for free electrons in a molecular-nitrogen plasma.

17 p2593 A72-35891

Non-analytic character of the shear-tensor distribution function in incompressible turbulence.

18 p2678 A72-36012

The influence of a nonequilibrium electron distribution function near the cathode and fractional coverage on the characteristics of a thermionic emission converter in the arc mode

18 p2647 A72-36220

Application of statistical methods to the study of the rigidity of a dielectric

18 p2720 A72-37116

Mars surface normal albedo distribution function from red light photometry data

19 p2864 A72-38318

Atmospheric turbulence induced optical effects due to refractive index fluctuations, solving Maxwell equations for instantaneous intensity distribution function

20 p2948 A72-39055

Mathematical model for dielectrics with time dependent polarization, noting relaxation time distribution function

21 p3085 A72-41074

Particle collisions integral in Boltzmann equation for arbitrary distribution function, with particular attention to two dimensional flows

22 p3205 A72-42266

Pair-correlation and angular distribution functions calculations for one and two dimensional amorphous structures

22 p3197 A72-42797

Estimation and prediction of Gumbel and Frechet distribution parameters, noting statistical decision in tests, sequential analysis and graphical procedures

22 p3199 A72-42968

The efficiency of the method of the least squares for adjusting observations with non-normal distributions

22 p3199 A72-42998

Particle distribution function evolution effect on turbulent plasma heating by wave interaction, considering stochastic heating of ions

23 p3318 A72-43314

Investigation of the applicability of different laws of extremal-value statistics to the approximation of empirical distributions of maximum wind velocities

23 p3310 A72-43535

Asymptotic methods of calculating the effectiveness of one variant procedure of selecting operational subchannels in an adaptive multichannel communications system

23 p3266 A72-44207

Study of high-energy hadron interactions by the nuclear photoemulsion method

23 p3330 A72-44416

Behavior of the spatial distribution function of shower particles near the axis of a cascade shower

23 p3331 A72-44432

Statistical noise characteristics and conditional signal distribution function measurements at output of standard FM demodulator

24 p3379 A72-44749

Pressure, temperature, current density, and potential difference fluctuations in subsonic flow of combustion products plasma, noting steadiness, ergodicity and distribution functions

24 p3429 A72-45502

Experimental determination of the distribution rule for the time of failure-free operator action in the tracking mode (with pursuit)

24 p3377 A72-45521

Investigation of the variable stars WR-96, GR-29, and WR-96 J2

24 p3448 A72-45682

Nonlinear interactions between synthesized plasma positive and negative ion beams, discussing effect on individual velocity distribution functions

24 p3431 A72-45711

DISTRIBUTION MOMENTS

NT STANDARD DEVIATION

NT VARIANCE [STATISTICS]

Distribution moments mathematical method for partially coherent light beam propagation through random phase screens in linear and nonlinear media

02 p0181 A72-12589

Wind shear third and fourth moments and distribution function in atmospheric boundary layer, emphasizing longitudinal turbulent velocity vertical variations

13 p1993 A72-28860

First and second moment of an optical wave propagating in a random medium - Equivalence of the solution of the Dyson and Bethe-Salpeter equation to that obtained by the Huygens-Fresnel principle.

17 p2580 A72-34290

Statistical self-similarity and inertial subrange turbulence.

18 p2678 A72-36021

DISTURBANCE THEORY

U PERTURBATION THEORY

DISTURBANCES

Finite amplitude disturbances effect on plane Poiseuille flow hydrodynamic stability, presenting numerical method for solving parabolic partial differential equations derived from Navier-Stokes equation

10 p1468 A72-24422

Infinitesimal centered disturbance effect on plane Poiseuille flow at supercritical Reynolds number, determining modulated wave as function of position and time

10 p1562 A72-24423

Disturbance-induced lunar surface darkening due to soil photometric function changes resulting from particle rearrangement

13 p2037 A72-28994

Liapunov functions and integral inequalities for study of finite time stability of motion, noting small parameter system subjected to continuous disturbances

13 p2004 A72-29496

Spreading of a turbulent disturbance.

17 p2541 A72-35249

Three-dimensional disturbances in the boundary layer along a concave wall

22 p3165 A72-42111

DISTURBING FUNCTIONS

Near resonance due to commensurability between Jupiter-Saturn mean motions, discussing effect on planetary system secular disturbing function

06 p0877 A72-17659

Planetary disturbing function expansion, using classical binomial or Laplace series methods on large scale digital computer with Poisson program

06 p0878 A72-17665

External disturbance accommodation in optimal control, based on characterization of waveform modes, applying to linear-quadratic regulator problem

07 p0963 A72-20591

Book on perturbation theory in celestial mechanics, covering disturbing function, Lagrange method and Delaunay theory

09 p1389 A72-23246

Velocity perturbation functions in linear theory for bounded stream flow past slender profile

14 p2070 A72-31018

DISULFIDES

NT CARBON DISULFIDE

Cold pressed powdered boron nitride, Mo, W, Nb disulfides and diselenides, investigating thermal dissociation in He by X ray analysis

03 p0380 A72-13551

Erichmanite /natural osmium disulfide/ chemical analysis and X ray data, noting osmium abundance

03 p0351 A72-14369

Crystal structure of iron-zirconium disulfide and cobalt-zirconium disulfide systems

10 p1496 A72-24089

Thermal vacuum tests of rhenium disulfide decomposition as function of temperature at 800-1200 C, using thermogravimetric method

13 p2023 A72-29649

DITHERS

Dither adaptive control technique application to constant fuel rate problem, illustrating with analog computer solution

06 p0792 A72-17308

DIURESIS

Isolation stress effect on micturition circadian rhythm and diuresis occurrence in unrestrained chimpanzee under entrained and free running conditions [AD-739468]

07 p0921 A72-20180

Renal clearance studies of left atrial distention effect in dog, indicating antidiuretic hormone inhibition mechanism of diuresis

12 p1763 A72-27828

Water immersion tests to study body fluid balance disturbances during weightlessness, observing diuretic reflex control of blood volume

16 p2355 A72-33551

Vasopressin /antidiuretic hormone/ role in central vascular volume and fluid balance maintenance during continuous positive pressure breathing in dogs

17 p2505 A72-35917

DIURNAL RHYTHMS

U CIRCADIAN RHYTHMS

DIURNAL VARIATIONS

Diurnal and seasonal variations of scintillations in short wave radio signals of earth satellites and spacecraft

01 p0053 A72-10359

F 1 layer appearance and critical frequencies average daily variations at Tsumeb, Southwest Africa, as function of sunspot cycle phase

01 p0055 A72-10428

Sporadic E layer reflection behavior measurements from two closely located stations, deriving drift direction and critical frequencies daily variation

01 p0055 A72-10431

Daily, annual and long term ionosscatter and sporadic E variations above Europe, using hf propagation measurements

01 p0055 A72-10432

Daytime and nighttime sporadic F layer regularities correlation with other ionospheric phenomena based on vertical sounding data

01 p0059 A72-10611

Precipitated electron energy latitude and time variations from auroral-height measurement during IQSY, using meridian scanning photometers

01 p0120 A72-10896

Upper atmosphere neutral oxygen density diurnal variations from incoherent scatter and satellite drag data, noting deviations from Jacchia static diffusion model predictions

01 p0062 A72-10911

Twelve hour light-dark-dark cycle phase shift effects on monkey feeding behavior and serial task performance

02 p0157 A72-11703

Diurnal and seasonal changes in occurrence frequency of rapid phase fluctuations in vlf received at Franz Josef Land correlated with geophysical observations

02 p0172 A72-11922

F 2 region maximum electron density level height and molecular temperature diurnal variations at equatorial latitudes from Ibadan station data

02 p0218 A72-11941

Magnetosphere model for low energy cosmic ray proton propagation mode to synchronous orbit satellite, calculating geomagnetic cutoffs and penetration regions [AD-741079]

02 p0274 A72-12453

- Beacon satellite transmission determination of ionosphere total electron content, describing equivalent slab thickness and diurnal, seasonal and solar cycle behavior02 p0221 A72-12460
- Sporadic E layer shielding frequency correlation to limiting reflection frequency calculated by diurnal data from nine ground stations02 p0221 A72-12522
- Chapman uniform electrical conductivity core model for geomagnetic disturbance daily variations due to solar wind, noting error in analysis02 p0222 A72-12794
- Sudden enhancement and decrease of elf atospherics, investigating diurnal variations for frequencies03 p0321 A72-13090
- Geomagnetic field and interplanetary plasma parameters daily variations correlation, taking into account corrections for storm time effects03 p0348 A72-13511
- Tornado and funnel cloud comparison in seasonal and diurnal distributions, air mass instability, tropospheric vertical wind shear and geographical distribution03 p0385 A72-14231
- Vlf phase regressions at sunrise related to variations of reflection coefficient in D region, using IENGFDATA04 p0485 A72-14465
- Quiet day diurnal variability of equatorial geomagnetic field H component related to ionospheric dynamics04 p0515 A72-14878
- Nonuniform solar wind velocity effect on interplanetary medium and on cosmic radiation, observing diurnal variations04 p0567 A72-14928
- Ionospheric electron content over New Delhi, observing seasonal and solar cycle variations of diurnal changes04 p0515 A72-14930
- Electronic collision frequency relationship with radio frequency in F region, investigating height, diurnal and seasonal variations04 p0516 A72-14933
- Diurnal and seasonal variations of F region irregularities drift and anisotropy parameters during IQSY from aerial fading records, noting magnetic activity effect04 p0517 A72-14955
- Ionospheric absorption measurements at 2.2 MHz by vertical incidence pulse sounding method, observing diurnal and seasonal variations04 p0518 A72-14965
- Ionospheric radio absorption, observing diurnal and seasonal variations and sunspot numbers and solar flares effects04 p0518 A72-14966
- Lunar mass spectrometer experiment, determining global distributions and diurnal variations of lunar atmosphere04 p0509 A72-15103
- Diurnal phase and amplitude variations of long radio waves at great distances, explaining sunrise and sunset fadings04 p0492 A72-15443
- Saccadic eye movements significance for jet pilots, noting saccade rate diurnal fluctuations and alcohol and tranquilizer negative effects05 p0616 A72-15800
- Power spectra of ionospheric electron content fluctuations from 6 year continuous records, noting gravity wave and seasonal daily variations05 p0655 A72-16066
- Atmospheric temperature effect on solar diurnal variation of muon component, considering asymptotic characteristics of cosmic ray anisotropy05 p0709 A72-16257
- Daytime ionogram corrections for underlying ionization in absence of X-trace of sporadic E layer05 p0657 A72-16265
- Magnetic perturbations in near polar region and morning-night sectors of auroral oval as function of current sources and modulation by universal time05 p0657 A72-16276
- Arctic polar region geomagnetic perturbations during IQSY, noting diurnal variations05 p0658 A72-16278
- Latitudinal, diurnal, seasonal and solar cycle variations in vhf-uhf scintillation producing irregularities in F layer electron density05 p0630 A72-16617
- Diurnal variation of lower ionosphere, analyzing nature and behavior of absorption long range variations over solar activity cycle05 p0660 A72-17182
- F 1 layer diurnal and seasonal model for medium to high latitudes, comparing calculated and observed electron density diurnal variations06 p0804 A72-17458
- Semidiurnal lunar variation, solar and sideral effects on cosmic radiation intensity, using zenith pointed particle telescopes06 p0873 A72-17490
- Ionospheric electron content diurnal and latitudinal variations from differential Faraday effect, discussing solar elevation and geophysical mechanisms06 p0805 A72-17640
- Ionospheric disturbance in American zone during IGY-IGC, showing latitudinal, annual and diurnal solar variations effects and regional geomagnetic anomaly06 p0806 A72-17641
- Electron density distribution inhomogeneities from vhf Faraday rotation measurements, noting diurnal, seasonal, sunspot cycle and geomagnetic activity effects06 p0806 A72-17642
- Venus 8.2 mm radio emission dependence on sun-light phase angle, considering implications regarding day/night atmospheric temperature variations06 p0884 A72-18031
- Ozone observation and daily and seasonal variations at Cologne, noting longitudinal variations for monthly means06 p0808 A72-18146
- Meteorological satellites and Gemini and Apollo earth photographs, showing annual and diurnal oceanographic, hydrologic and geologic dynamic features06 p0810 A72-18614
- F 2 ionization distribution diurnal variations from airborne ionosonde measurements during June-July 1966 over Tamarassat meridian, correlating magnetic activity with wind variations06 p0810 A72-18731
- PE sub s harmonic components diurnal and seasonal variations and latitudinal dependence, investigating relationship to drift velocity in E region06 p0811 A72-18749
- Diurnal temperature variations in lunar surface layer from Apollo 12 samples, comparing with Apollo 11 samples and IR measurements07 p1068 A72-18874
- Geoelectric field strengths deduction from mid-frequency slopes on diurnal incidence plot of pc 1 hydromagnetic whistlers07 p0974 A72-18904
- Wind, pressure and temperature diurnal and semidiurnal variations to 30 km altitude over tropical western Pacific, considering atmospheric model based on linearized equations of motion07 p1029 A72-19099
- Exosphere geocoronal hydrogen density, vertical structure and diurnal variability from Lyman spectra observational data, discussing polar wind origins07 p0978 A72-20041
- Diurnal, sporadic and yearly variations in cosmic ray flux based on neutron component data, noting relation to solar activity cycles07 p1066 A72-20647
- F region ionization anomalous evening enhancement, discussing seasonal variations, solar activity and geomagnetic coordinates maximum in Yakutsk08 p1153 A72-20707
- Slip effect in diurnal phase and amplitude cycles of vlf signals in lower ionosphere due to wave interference at transmitting point08 p1130 A72-20710
- Polar latitude sporadic E layer diurnal variations with appearance dependence on cutoff frequency08 p1130 A72-20727
- Eastern and western polar electrojets intensity diurnal variations with respect to universal time08 p1154 A72-20740
- Diurnal fluctuations in radio echo producing ionospheric region horizontal scale and height, discussing dependence on solar position08 p1131 A72-20819
- Solar wind flux velocity diurnal variations relation to magnetic activity index based on Mariner 2 and 4, Pioneer 6 and Vela satellites data08 p1226 A72-20821
- Horizontal neutral winds meridional component from incoherent scatter measurements of F region ionization drifts, noting diurnal variations08 p1156 A72-21098
- Ionospheric drift patterns diurnal, seasonal and solar cycle variations from synoptic measurements over east Siberia by closely spaced receivers, using Briggs similar fades method08 p1160 A72-21530
- Satellite orbital inclination change due to rotating upper atmosphere with day-to-night density variation, deriving resonance conditions08 p1241 A72-21640
- Seasonal and diurnal variations of earth albedo from turbidity measurements, showing lower atmosphere moisture effect08 p1237 A72-21799
- Diurnal and beat-to-beat variation factors in vectorcardiograms, noting respiratory movements, electrode location shift, skin-electrode impedance and heart electrical center mobility08 p1127 A72-21849
- Diurnal and seasonal variation of ambipolar diffusion coefficient in meteor trail zone within upper atmosphere08 p1238 A72-21888
- North-south ionospheric movements at low latitude station, investigating diurnal and seasonal velocity variations from cross correlation and similar fades time delays measurements08 p1136 A72-21981
- Upper atmospheric oxygen red line diurnal variations and midnight minimum, noting emission relation to kinetic temperature in magnetic storm09 p1296 A72-22234
- Midlatitude auroral zone positive ion mass spectrometer observations in E region, noting diurnal variation and sporadic E events09 p1375 A72-22364
- D and E region electron density profile, investigating geographical, diurnal, seasonal and sunspot cycle variations09 p1376 A72-22370
- Synoptic measurement of midlatitude D region electron density diurnal and seasonal variations under quiet conditions, using differential absorption partial reflection experiment09 p1376 A72-22372
- Diurnal, seasonal and solar cycle variations in cosmic noise absorption during 1957-1966, showing various ionospheric layers contribution09 p1385 A72-22586
- Diurnal phase anomaly in upper atmospheric density and temperature inferred from satellite drag and incoherent scattering observations09 p1298 A72-22590
- Interplanetary space three dimensional cosmic ray anisotropy from harmonic components of diurnal variations09 p1377 A72-22926
- Expression for annual modulation of diurnal variation from generalized cosmic ray anisotropy in space, applying to earth revolution induced modulation09 p1377 A72-22927
- Semidiurnal cosmic ray anisotropy, eliminating atmospheric effects and global isotropic variations in cosmic ray telescope09 p1377 A72-22928
- Space anisotropy responsible for solar semidiurnal variation of cosmic ray intensity studied with data from worldwide network of neutron monitor stations09 p1377 A72-22929
- Day, night and sunset mesospheric nitric oxide concentrations during polar cap absorption from rocket measurements of cation composition and charged particle densities09 p1300 A72-23026
- Free nutations of earth from 1904-1941 latitude observations at Pulkovo, noting diurnal variations with almost identical amplitudes09 p1388 A72-23058
- Earth free diurnal nutation parameters comparison based on determinations from latitude observations at various observations09 p1388 A72-23059
- Orionid meteor head echoes variations with diurnal radiant motion compared to Perseid meteors09 p1389 A72-23395
- Atmospheric models of vertical structure of semidiurnal atmospheric gravitational tides, taking into account Coriolis force and vertical acceleration components10 p1473 A72-24530
- Lower ionospheric structure, discussing electron production, loss and transport effects and diurnal variations10 p1473 A72-24703
- Sporadic E layer variations monitoring in 50 MHz band, examining diurnal, seasonal, magnetic and meteoroid showers relationships of oblique incidence paths10 p1441 A72-25152
- Venus 8.2 mm radio emission dependence on sun-light phase angle, considering implications for day/night atmospheric temperature variations11 p1719 A72-25967
- Declinational component of geomagnetic lunar tide diurnal variations, noting effects of electric currents induced in oceans11 p1622 A72-26103
- Low latitude geomagnetic field diurnal variations caused by solar wind associated component, noting evening side depression11 p1713 A72-26109
- Diurnal variations of F 2 region critical frequencies and quiet and perturbed ionosphere N/h/ profiles during solar cycle, estimating signal reflection altitudes11 p1594 A72-26274
- Time and space characteristics of F scattering, investigating maximum appearance probability, intensity and seasonal and diurnal variations11 p1595 A72-26280
- Atmospheric density annual and diurnal variations in lower ionosphere, from satellite radar tracking data, considering drag coefficient modeling and orbit determination techniques11 p1625 A72-26410
- Human performance dependence on time of day, discussing circadian and physiological rhythms relation and environmental change effects11 p1580 A72-26677

Sleep deprivation effects relation to work duration, time of day, circadian rhythm, memory function, task performance, environmental factors, drug use and age
11 p1580 A72-26678

Human functional level performance characteristics, noting relationship between spontaneous rhythm diurnal variations in psychic and physical performance
11 p1589 A72-26691

Clear sky atmospheric thermal radiation from all-wave radiation and air temperature measurements, showing diurnal and desert condition induced deviations from empirical formula
12 p1840 A72-27706

Adcock direction finder errors due to diurnal and sporadic ionospheric variations and tilting layers effects on reflected signal
12 p1804 A72-27780

Sporadic E layer structure and dynamics diurnal and seasonal variations from ionosondes frequency and drift measurements
12 p1804 A72-27781

Earth atmosphere boundary layer nonstationary problems, considering diurnal changes of meteorological fields and nonperiodic evolution of elements from wind variations
12 p1841 A72-27988

Diurnal and annual temperature variations at 30-60 km from statistical analysis of rocketsonde data, obtaining solar radiation errors magnitude
13 p1947 A72-28829

Rocket sounding of ozone diurnal variations in upper stratosphere and lower mesosphere
13 p1947 A72-28831

Daily difference analysis of magnitude, vertical and latitudinal structure of irregular mesospheric wind variations due to gravity waves
13 p1948 A72-28832

Diurnal and seasonal changes in occurrence frequency of rapid phase fluctuations in VLF received at Franz Josef Land correlated with geophysical observations
13 p1920 A72-29234

Vertical concentration profile and diurnal variations of N and NO vs solar activity from satellite horizon airglow experiment
13 p1948 A72-29237

F 2 region maximum electron density level height and molecular temperature diurnal variations at equatorial latitudes from Ibadan station data
13 p1949 A72-29253

Daily variations in E region horizontal drift at Thumba/India, showing daytime westward and nighttime eastward drifts
13 p1949 A72-29275

Diurnal changes in gas exchange and metabolic rate under normal and inverted day-night schedule conditions, studying human adaptation to shifted schedule
13 p1904 A72-29318

Sleep deprivation effects on diurnal urine potassium excretion, showing individual circadian rhythm variations
13 p1904 A72-29320

Meteorological-astronomical diurnal and seasonal environmental rhythm simulation for psychological stresses alleviation in long term space missions
13 p1910 A72-29322

Atmospheric oxygen concentration latitudinal and diurnal variations from incoherent scatter and satellite drag data, noting compatibility with Jacchia model
13 p1951 A72-29389

Diurnal variability of atmospheric refraction index at UHF in boundary layer for various weather types during summer-fall season
13 p1995 A72-29590

Ionospheric absorption measurement by 1F mode field strength recording with A3 circuit at 6 MHz, noting diurnal and seasonal variations
13 p1952 A72-29660

Thermospheric atomic hydrogen concentration diurnal variations from time dependent continuity and diffusion equations, using Jacchia background atmosphere thermal and density structure formulas
13 p1953 A72-29806

Range and frequency spread F diurnal and seasonal variations at magnetic equatorial station Thumba, noting geomagnetic activity effect
14 p2097 A72-30130

Seasonal features of nocturnal 6300 Å emission variation and decay coefficient in nightglow related to recombination coefficient for F layer ionization
14 p2097 A72-30132

Hydroxyl emission bands intensity, and vibrational and rotational temperatures sporadic and harmonic components in seasonal and diurnal variations
14 p2098 A72-30142

Mars upper cover temperature, representing diurnal variations at different areographic latitudes as harmonic series
14 p2148 A72-30207

Thermosphere kinetic temperature diurnal variation from heat conduction equation periodic solution, determining heat sources from solar radiation at-mospheric absorption
14 p2101 A72-30640

Solar proton flare prediction, examining diurnal rotation of axis connecting two stable spots and change in horizontal gradient of spots magnetic field
14 p2147 A72-30649

Lower ionospheric seasonal anomaly in electron density levels, noting diurnal and latitudinal characteristics at various heights
14 p2102 A72-30653

Auroral sporadic E layer diurnal distribution correlation to charged particle integral flux diurnal variations observed by satellite in winter, noting Kp index effect
14 p2102 A72-30655

Solar X-ray flux daily changes before and after proton flare, using zero-epoch superposition method
14 p2148 A72-30911

Computerized measurement and analysis of day-to-day variations of corrected orthogonal ECG and vectorcardiogram in normal subjects, using results as assessment standards
14 p2077 A72-30967

Cosmic ray density gradient perpendicular to ecliptic plane, noting component introduction into diurnal variation depending on sense and direction of interplanetary magnetic field
15 p2298 A72-31436

Diurnal variations of micropulsation activity polarization parameters in horizontal plane, describing experimental technique
15 p2230 A72-32258

Geomagnetic activity index Ap correlation with daily magnetic variations during quiet sun year 1964
15 p2230 A72-32260

Near IR airglow observation by sound rocket to determine layer height diurnal variation and rocket axis zenith angle
15 p2231 A72-32328

Semidiurnal variation in O I 5577 Å nightglow due to lunar tidal dynamics effect in E and F regions
16 p2383 A72-32971

Geomagnetic and meteorological elements lunar daily variation calculation by modified Chapman-Miller method, estimating confidence limits for parameters reliability
16 p2384 A72-32972

Two layer model for diurnal temperature variations analysis for radiative heat transfer between lower atmosphere and underlying layer
16 p2417 A72-33293

Lunar surface diurnal temperature variations calculation based on Apollo 12 lunar fines thermophysical properties and surface layer core-tube sample density
16 p2454 A72-33432

Diurnal cosmic ray neutron variation dependence on interplanetary magnetic field based on neutron monitor data
16 p2449 A72-33940

Digital equilibrium temperature model for diurnal surface thermal and energy transfer simulation based on Myrup analog solution
16 p2419 A72-33942

Lunar semidiurnal variations of the geomagnetic field determined from the 2.5-min data scalings
17 p2545 A72-34691

Influence of the diurnal effect in the atmospheric density distribution on the braking of a satellite
17 p2546 A72-35032

Characteristics of cosmic ray diurnal variation from Deep River neutron and meson data and temperature effects
17 p2601 A72-35400

Equatorial anomaly changes caused by ionospheric disturbances, noting diurnal variations of magnetic storm effect
17 p2551 A72-35868

Whistler activity in central Europe during the period of increasing solar activity from 1964 to 1968
18 p2657 A72-36230

A theoretical study of the diurnal wind variations in the planetary boundary layer
18 p2706 A72-36645

Solar cosmic ray anisotropy 27-day variations during IGY from global network stations neutron component data
18 p2722 A72-36876

The diurnal effect of the cosmic rays during the period 15 October 1965-30 June 1966. I - Method of analysis and statistical distribution.
18 p2722 A72-37159

The diurnal effect of the cosmic rays during the period 15 October 1965-30 June 1966. II - The equatorial cosmic-ray anisotropy and the interplanetary magnetic field.
18 p2722 A72-37160

Nocturnal and semiannual variations of the intensity of 5577 Å emission of atomic oxygen.
19 p2789 A72-37511

F region ionization anomalous evening enhancement, discussing seasonal variations, solar activity effects and maximum value dependence on geomagnetic latitude and longitude
19 p2790 A72-38335

Slip effect in diurnal phase and amplitude cycles of VLF signals in lower ionosphere due to wave interference at transmitting point
19 p2765 A72-38338

Polar latitude sporadic E layer diurnal variations with appearance dependence on cut-off frequency
19 p2766 A72-38355

Easterly and westerly polar electrojets intensity diurnal variations with respect to universal time and geo- and heliophysical phenomena
19 p2791 A72-38368

Diurnal variation of the H+ flux between the ionosphere and the plasmasphere.
19 p2793 A72-38759

Lunar magnetic variations at Trelew/Argentina.
19 p2794 A72-38860

OH airglow IR observation from high altitude sites with bandpass filter, noting average spatial and diurnal fluctuations
19 p2794 A72-38861

Diurnally varying neutral wind effects on lower F region ionization distribution, noting Appleton anomaly disappearance time
19 p2794 A72-38865

Quiet day daily geomagnetic field variability associated with equatorial ionospheric upheavals, noting longitudinal extent
19 p2794 A72-38869

Psychological tests for diurnal variations of human visual discrimination threshold by varying test object illumination level
20 p2891 A72-38931

Crop surface albedo measurements, taking into account cloudiness, zenith angle and day period effects
20 p2915 A72-38970

The influence of vertical motions on the diurnal variations of temperature and density in the thermosphere.
20 p2916 A72-39236

The interpretation of surface equatorial magnetic daily variations on disturbed days.
20 p2916 A72-39238

Formation of auroral patches in the midday sector during a substorm.
20 p2916 A72-39239

On the diurnal and seasonal variations of the D- and E-regions above Kjeller.
20 p2917 A72-39529

Morphologic maps of pulsating aurora for late afternoon and evening geomagnetic sector near Tromsø during 1967-1969
20 p2918 A72-39540

Properties of low energy particle impacts in the polar domain in the dawn and dayside hours.
20 p2964 A72-39541

Plasmapause nightside, dayside and bulge positive ion concentration measurements with OGO 5 mass spectrometer compared with magnetospheric convection model
20 p2919 A72-39544

Diurnal variation in energy balance microclimate across coastal beach, noting surface moisture effect
21 p3078 A72-40468

Three-dimensional cosmic ray anisotropy in interplanetary space. III, IV.
21 p3101 A72-41385

Detection of whistler mode signals from VLF transmitter in Australia.
21 p3023 A72-41386

Diurnal and seasonal behavior of discrete white clouds on Mars.
21 p3110 A72-41454

DP-2 mode daily magnetic variation in polar cap based on magnetic and auroral records, noting relationship to magnetospheric substorms
22 p3168 A72-42005

Daily variation of electron and proton geomagnetic cutoffs calculated for Fort Churchill, Canada.
22 p3170 A72-42401

Falls of meteorites in Germany: Temporal distribution of the falls and deductions with regard to their origin - Hypotheses concerning the origin of the meteorites as well as further falls and findings in Germany
22 p3227 A72-42542

The sunspot cycle and solar and lunar daily variations in H.
22 p3228 A72-42882

Earth atmosphere boundary layer nonstationary problems, considering diurnal changes of meteorological fields and nonperiodic evolution of elements from wind variations
22 p3202 A72-43002

Mars upper cover temperature, representing diurnal variations at different areographic latitudes as harmonic series
23 p3333 A72-43237

Human prolactin - 24-hour pattern with increased release during sleep.
23 p3316 A72-43977

Diurnal variation of the correlation of Pc 3 and Pc 4 micropulsation characteristics with magnetic activity.
23 p3286 A72-44524

Diffusion processes of cosmic rays with energies between 2 and 20 GV during Forbush decreases - The diurnal effect.

24 p3434 A72-44785

DIVERGENCE

Atmospheric deviations of ageostrophic wind in jet stream domain, using dimensionless vector characteristics

02 p0255 A72-12787

Kalman filter divergence due to errors, applying to orbital navigation

02 p0198 A72-12805

Divergence prevention in decision directed adaptive recursive estimators in relation to error covariance

06 p0792 A72-17307

Autoparametric excitation in relation to divergence and flutter of autonomous mechanical cantilever systems under nonpotential circulatory forces

06 p0851 A72-18726

Centered Gaussian process oscillations /Brownian motion/, obtaining divergence rate in sequence of finite partitions

10 p1504 A72-24054

Linear mechanical elastic systems divergence with infinitely large frequency onset, noting discrete cantilever beam under nonconservative forces

[ASME PAPER 71-APM-DDD] 10 p1555 A72-24189

Planetary divergence field estimation via Lagrangian tracers and Eole experimental balloons data, developing spatial analysis method

15 p2266 A72-31952

A regularity theorem for linear second order elliptic divergence equations.

22 p3198 A72-41947

DIVERGENT NOZZLES

Thermal and I-V characteristics of dc plasmatron with vortex stabilized arc, interelectrode insert and diverging arc channel for various nozzle diameters

05 p0694 A72-15854

Gas density distributions in argon and carbon dioxide supersonic jets with low angular divergence in vacuum, using Laval supersonic nozzle

07 p0973 A72-20512

Thermal and I-V characteristics of dc plasmatron with vortex stabilized arc, interelectrode insert and diverging arc channel for various nozzle diameters

15 p2283 A72-31271

Computer simulation by Monte Carlo technique of particulate fluxes in divergent conical Knudsen cell orifices, considering specular reflection and surface diffusion effects

15 p2218 A72-32380

Effects of heat addition in divergent nozzles with application to MPD thrusters.

17 p2635 A72-34213

DIVERTERS

Plasma density profiles by microwave interferometry technique in Sirius stellarator diverter for two magnetic field configurations and injection methods

04 p0555 A72-14619

Plasmoids interaction in diverter magnetic field, investigating integral electron capture intensity

09 p1362 A72-23205

Plasma flows interaction with plasma cylinder in diverter magnetic field, investigating plasma dynamics with electric probes, plasmoscope and mass spectrograph

09 p1362 A72-23210

Confinement time of plasma injected in magnetic field of racetrack with diverter, noting plasma equilibrium in toroidal magnetic field

22 p3213 A72-43106

DIVIDERS

Wide dynamic range analog multiplier with variable transconductance divider in operational transistor amplifier feedback path

11 p1603 A72-25742

DIVIDING [MATHEMATICS]

Cellular-array arithmetic unit with multiplication and division.

17 p2519 A72-34297

DIVING [UNDERWATER]

Human mental and psychomotor performance measurements in compressed oxygen-helium atmosphere pressure chamber for dive between 100 and 1500 feet

02 p0166 A72-11701

Diving operations medical aspects significance for manned planetary surface exploration in high density atmospheres, considering protective clothing, breathing apparatus and gas mixtures, etc

12 p1769 A72-27415

Biotelemetry system for EEG monitoring of free swimming diver at 15 meter depth, discussing power requirements, antenna design and signal attenuation

12 p1770 A72-27478

Frontal sinus hematoma incidence in flying personnel and scuba divers, discussing diagnosis and clinical treatment

12 p1765 A72-28275

Bradycardia diving reflex to apneic face immersion related to physical exercise

17 p2506 A72-35964

Case report on dive decompression induced maxillary sinus barotrauma due to sinus pressure buildup caused by ostium blockage

22 p3150 A72-42497

DNA

U DEOXYRIBONUCLEIC ACID

DO-31 AIRCRAFT

Anthropotechnical aspects of V/STOL aircraft control, discussing instrument and control systems concepts based on development and flight tests of experimental Do-31 VTOL aircraft

09 p1270 A72-22784

DOCKING

U SPACECRAFT DOCKING

DOCUMENTATION

Avionics systems electrical interface connection design information document creation and dissemination, using EMPRENT computer program

10 p1453 A72-24864

Defense system procurement evaluation before documentation release to industry, discussing improved specifications, competition, planning and data requirements

17 p2639 A72-34463

Defense Documentation Center independent R and D data bank for evolution and maintenance of creative technology oriented defense industry

21 p3132 A72-40974

DOCUMENTS

NT ABSTRACTS
NT BIBLIOGRAPHIES
NT DRAWINGS
NT HANDBOOKS
NT MANUALS
NT TEXTBOOKS
NT TEXTS

DOGHOUSES

U PROTUBERANCES

DOLOMITE [MINERAL]

Self diffusion coefficients of carbon and oxygen in dolomite

07 p0937 A72-20520

DOMAIN WALL

Incompressible microstretch fluid flow in rigidly bounded domain, deriving kinetic energy decay rate via linear model subject to entropy principle and boundary adherence condition

06 p0799 A72-17918

Magnetization and elastic stresses effect on Ni dislocations movement due to domain wall interactions

09 p1371 A72-22866

Raman scattering techniques applied to problems in solid state physics.

21 p3096 A72-40602

DOMAINS

NT MAGNETIC DOMAINS

Order-disorder transition cooling effects on V carbide superlattice domain structure, using electron and optical microscopy

03 p0370 A72-12997

Closed solution to Gunn effect field domain formation and propagation, using approximate I-V curve and method of characteristics

04 p0563 A72-15503

Incompressible microstretch fluid flow in rigidly bounded domain, deriving kinetic energy decay rate via linear model subject to entropy principle and boundary adherence condition

06 p0799 A72-17918

DOMES [STRUCTURAL FORMS]

NT RADOMES

Stability of a dome rigidly clamped over its edge under uniform external pressure

17 p2635 A72-35806

DOMINANCE

NT EYE DOMINANCE

DONNELL EQUATIONS

Circular cylindrical shells buckling under edge compression at various boundary conditions, obtaining critical loads and wave number from Donnell equations

02 p0292 A72-12107

Asymptotic solution to nonlinear Donnell equations of elastic conical shells, applied to buckling of frustum under axial load

06 p0893 A72-17303

Free flexural vibration of truncated conical shells, using Galerkin method and Donnell type basic equation

10 p1559 A72-25024

Flugge equations for circular cylindrical shells buckling under compression, considering Donnell theory limits, stress determination and boundary conditions

10 p1560 A72-25025

The accuracy of Donnell's theory for very high harmonic loading on closed cylinders.

23 p3350 A72-44059

DONOR MATERIALS

Electron irradiation effects on Li doped silicon solar cells, noting changes in donor concentration and defects formation

12 p1757 A72-28022

DOPING [ADDITIVES]

U ADDITIVES

DOPPLER EFFECT

Neutral gas wind effect on Doppler shifts in frequency spectrum of atmospheric gravity waves in F region with resultant phase altitude dependence alteration

01 p0054 A72-10426

Clutter suppression by amplitude weighted pulse trains in coherent radar, obtaining optimum weights and signal-to-clutter gain as function of Doppler frequency

01 p0030 A72-10789

Spectral analyses of Mira-type variable stars near light maximum, discussing empirical curve of growth, Doppler velocity, damping constant and electron pressures

01 p0129 A72-10792

Orbital elements and onboard transmitter frequency drift of active satellite from Doppler and angle data recorded at single receiving station

02 p0171 A72-11664

Spectral broadening in laser Doppler velocimeter, showing identity of wave vectors spread for incident and detected fields and scattering center finite volumetric stay

02 p0229 A72-12094

Frequency variations from uniformly moving source in homogeneous and inhomogeneous isotropic plasmas, calculating source-to-transmitted-wave group velocity ratio from Doppler curves slopes

02 p0264 A72-12120

Nonlinear theory of cascaded two-way coherent spacecraft tracking system model, obtaining steady state probability density functions of phase and Doppler error

02 p0174 A72-12137

Source motion effects on Doppler period variations of high velocity pulsars, considering first and second time derivatives

02 p0281 A72-12309

Sacramento Peak magnetograph, discussing modified Doppler-Zeeman analyzer for separate measurements of circularly polarized line displacement

03 p0356 A72-13284

Magnetic field and turbulence in sunspots, studying local variations of saturation and Doppler broadening

03 p0428 A72-13297

Optical excitation of divergent alkali atomic beam by radiation absorption, deriving absorption coefficient for line broadening and/or Doppler effect

03 p0393 A72-14062

Photomultiplier signal for water axial velocity in glass pipe, providing turbulent liquid flow information and laser Doppler velocimeter evaluation

04 p0520 A72-14438

Earth gravity field representation by simple layer potential from Doppler tracking of satellites

04 p0514 A72-14565

Radio propagation from transmitter moving through irregular stationary ionospheric plasma, obtaining fluctuation dispersions for Faraday rotation angle and rate, phase, Doppler shift and refractions

04 p0489 A72-15395

Frequency domain representation of Doppler invariant FM signal defining matched pulse compression filter

04 p0507 A72-15693

Doppler ultrasonic probe phonocardiography for human cardiovascular velocity measurement, showing normal tracings and aging effects

05 p0617 A72-16154

Doppler cardiometry determination of human cardiovascular velocities in patients with heart diseases, discussing impaired left ventricular function detection

05 p0617 A72-16155

Lunar gravity measurements via Apollo 14 Doppler radio tracking over 100 kilometer band during low periapsis altitude orbits, relating to surface features

05 p0722 A72-17126

Small radar equivalent surface measurements by Doppler differentiation between signal in target and parasitic echoes

06 p0775 A72-18193

Spectral analysis of light reflected from Nd laser produced deuterium plasma, observing Doppler shift

07 p1039 A72-18888

Doppler broadening elimination in red Balmer line of atomic hydrogen at 6563 A by high resolution saturation spectroscopy

07 p1037 A72-19132

F and G dwarf stars synthetic spectra and colors computation from chemical abundance, Doppler broadening velocity and damping constant

07 p1071 A72-19181

Spontaneous emission from driven Doppler broadened gas of two level atoms radiating into free space, predicting power spectrum

07 p0940 A72-19194

Micron sized particle velocity relaxation measurement in shock wave, using laser Doppler methods

07 p1005 A72-19389

Two channel high resolution spectrometric measurements of plasma velocity from intrinsic radiation in optical range by Doppler effect

07 p1044 A72-19885

Laser applications in metrology and geodesy, discussing use of beam directionality for alignment purposes, interference patterns and interferometry, modulated light methods, optical Doppler methods, etc 07 p1007 A72-20222

European local geodetic datum centering by Doppler measurements of navigation and geodetic satellites [DFVLR-SONDDR-139] 07 p1033 A72-20273

Laser Doppler velocimeter signals statistical properties, examining bandwidth, counting time and input SNR effects on zero crossing counter output fluctuations rms value 07 p0990 A72-20370

Laser induced line narrowing effects in coupled Doppler broadened transitions within standing wave field 07 p1039 A72-20682

Internal asynchronous modulation of multifrequency He-Ne laser with Doppler broadened transition line 08 p1181 A72-20793

Moving plasma heating by fast large amplitude hf magnetoacoustic wave, noting Doppler effect resonance splitting 08 p1212 A72-21070

Local and integral ionospheric electron concentrations and horizontal gradients effects on reduced Doppler frequency shift difference along satellite orbit 08 p1132 A72-21144

Coherent radar pulse train clutter performance prediction for targets with range acceleration effects on Doppler response 08 p1133 A72-21405

Sky wave backscattering with narrow beam antenna coupled with signal modulations and Doppler shift as means of sea state observation and environmental monitoring 08 p1134 A72-21493

Sectoral radio measurement of meteor trail drifts with If radar signals, determining Doppler shift sign and period 08 p1238 A72-21887

Velocity measurement by Doppler light scattering due to particle finite residence time, estimating ambiguity and noise effects on turbulent spectra of frequency fluctuation 09 p1305 A72-22302

Two dimensional laser Doppler forward and backscatter velocimetry in turbulent flows, applying to four inch pipe 09 p1305 A72-22303

Radar data statistical evaluation, emphasizing mean Doppler shift for aircraft radial velocity calculation 09 p1278 A72-22897

CO Cameron system band intensity from measurements of equivalent widths of resolved rotational lines, using Doppler growth curve for line strength conversion 10 p1514 A72-24095

Coherent and noncoherent modes of optical beating in laser Doppler velocity measurement using light scattered from single and multiple particles 10 p1481 A72-24412

Finite rest masses of wave quanta in material media, discussing dispersion and Einstein formulas equivalence, Doppler effect, gravitational red shift and radio photon trajectories 10 p1512 A72-24790

Doppler spectral width of radar signal reflected from sea surface as function of illuminated region dimensions, waviness scale and emission factors 10 p1439 A72-24904

Uncertainty functions side maxima for phase manipulated signals with low sidelobe levels in autocorrelation functions, noting Doppler frequency shift effect 10 p1440 A72-24916

Atmospheric isotropic turbulence kinetic energy dissipation and wind spectra estimation from Doppler spectra of precipitation particle velocities 10 p1507 A72-25001

Wind profile measurements to 200 meters by acoustic echo sounder and Doppler shift, describing signal emission and data reduction 10 p1508 A72-25084

Coordinate transformation equations derivation to determine third orthogonal velocity component from measurements at common point by two rotationally displaced laser Doppler velocimeter systems 11 p1629 A72-25308

Satellite orbit tracking data accuracy estimation by partial differentiation, using Doppler and interferometer methods 11 p1593 A72-26097

Carbon dioxide laser cross relaxation effects on hole burning process in Doppler broadened gain or absorption line 11 p1647 A72-26146

Received signal spectrum gravity center and effective antenna centers of airborne Doppler velocimeter in horizontal flight 11 p1606 A72-26730

Instantaneous and continuous blood flow velocity measurement by Doppler ultrasonic flowmeter using transcutaneous and implanted probes 11 p1589 A72-26778

Ionospheric HF Doppler dispersion during 7 March 1970 solar eclipse, noting traveling ionospheric disturbance 12 p1801 A72-27157

Research measurement error determination for two frequency Doppler measurement of artificial satellites 12 p1782 A72-27532

Frequency modulation demodulation technique for turbulence velocity measurements by laser Doppler velocimeter [AD-744534] 12 p1809 A72-27836

Laser Doppler-type remote sensor for wind velocity and atmospheric turbulence measurements 13 p1956 A72-28859

Ground satellite control station network, including tracking stations for measuring Doppler effect with IRIS receivers [DGLR PAPER 72-009] 13 p1938 A72-28960

Velocimeter design for MHD boundary layer flow velocity measurement, using Doppler frequency shift of laser light scattered from added macroscopic particles 13 p1957 A72-29360

Luminosity variation of star in circular orbit around extreme Kerr black hole due to Doppler effects and gravitational field light focusing 13 p2041 A72-29416

Vibration stability and interference transfer function of onboard transponder with phase lock AFC used in Doppler system for measuring spacecraft trajectory parameters 13 p1958 A72-29456

Acoustic holography Doppler effects due to sound source or receiver motion during recording process 13 p1958 A72-29615

Sunspots, Doppler shifts, geophysical changes and statistical evaluation of diffuse objects motion in sun, discussing solar magnetic fields and 22 year cycle 13 p2044 A72-29701

Doppler laser velocimeter and hot-wire anemometer readings in cylinder wake compared, describing instrument caused spectrum broadening effects neutralization method 13 p1960 A72-29889

Medical monitoring system for enclosed men, using ultrasonic Doppler-cardiography for heart rate determination 14 p2078 A72-30384

Venera satellite parachute probe method for Doppler measurement of Venus atmosphere wind velocity and turbulence 14 p2151 A72-30466

Meter and decimeter wave reflected signals distribution and surface backscattering patterns effective beamwidth investigation by method based on Doppler effect 14 p2086 A72-30792

Photon correlation spectrometer for laboratory wind tunnel measurement of laser Doppler signals backscattered from dust particles 14 p2111 A72-30854

Noncoherent isotropic scattering in plane parallel finite layer, considering Doppler line broadening 15 p2273 A72-31331

Zeeman triplet with unsplit upper level formation in isothermic atmosphere under magnetic field, considering Doppler and Lorentz frequency profiles of transitions 15 p2304 A72-31332

Doppler carrier frequency shift measurement accuracy, finding relationships in errors for coherent and noncoherent pulse trains 15 p2195 A72-31657

Computational method for determining numerical values of relativity by two-way Doppler radio tracking and ranging data from planetary orbiting spacecraft 15 p2310 A72-31978

Optical, mechanical and electrical arrangements of laser Doppler velocimeter, presenting Doppler signals displays and three dimensional gas velocity profiles in vortex region 15 p2236 A72-32044

Laser Doppler velocimetry system design for optical measurement of intrablade flow velocity in turbomachinery 15 p2237 A72-32045

Laser Doppler velocimeter designs for atmospheric applications, discussing illuminating techniques, SNR, performance comparison and system selection 15 p2237 A72-32051

VLF wave normal direction measurement during propagation through ionosphere by Doppler technique, using rocket-borne receivers 15 p2201 A72-32332

Radiation source motion at superluminal speed in vacuum, defining conditions for Vavilov-Cerenkov and Doppler effects 15 p2279 A72-32767

Gaussian beam laser Doppler velocimeter system under high scattering center concentrations and steady

flow conditions, deriving noise spectral densities and SNR 16 p2390 A72-33210

Generalized radar equations derivation to obtain Doppler frequency shift and variance in Fresnel zone due to target movement 16 p2365 A72-33765

Laser Doppler anemometer for three dimensional liquid and gas flow velocity measurements in water tunnels 16 p2396 A72-34158

Satellite beacons observations from 1964 to 1970. 17 p2547 A72-35125

Two channel high resolution spectrometric measurements of plasma velocity from intrinsic radiation in optical range by Doppler effect 17 p2590 A72-35133

A laser velocimeter for Reynolds stress and other turbulence measurements. 17 p2555 A72-35235

HF electrostatic wave instability induced in plasma by electron beam, noting resonant frequency Doppler shift 17 p2591 A72-35369

Doppler shift of solar photospheric spectral lines related to downward motions over plages 17 p2617 A72-35705

A relative performance analysis of atmospheric laser Doppler velocimeter methods. 17 p2558 A72-35949

Optical polarization effects in a gas laser. 18 p2697 A72-36487

Design of nonrecursive digital moving-target-indicator radar filters. 18 p2667 A72-36687

A historical survey of the application of the Doppler principle for radio navigation. 19 p2830 A72-37276

An automatic data processing system for laser anemometers. 19 p2795 A72-37287

Fluid mechanics anemometry based on laser light frequency modulation /Doppler effect/, describing measurement of extensions of vortices and oscillations in flow boundary layers 19 p2801 A72-37394

Doppler effect characteristics and applications to artificial satellite tracking, considering computer program in orbit parameter calculations 19 p2765 A72-38172

Doppler Q switching in a single-mode CO₂ laser by a rotating mirror. 19 p2812 A72-38594

Local and integral ionospheric electron concentrations and horizontal gradients effects on reduced Doppler frequency shift difference along satellite orbit 20 p2903 A72-39249

The Mueller matrix for scattering - Including the effects of interference. 20 p2970 A72-39754

Determination of the orbits of artificial satellites by the integrated Doppler effect method 20 p2974 A72-40023

A unified analysis on laser Doppler velocimeters. 21 p3061 A72-40211

Fabry-Perot spectrometer adjustment for the compensation of Doppler shift from rapidly rotating and rapidly flowing sources. 21 p3053 A72-40607

Acoustic holography Doppler effects due to sound source or receiver motion during recording process 21 p3054 A72-40668

Electron impact effects on Ba I, Ba II and Sr I selected spectral line Doppler widths calculated for laser-generated plasmas for chemical release simulation 21 p3092 A72-40821

Noise-cancelling signal difference method for optical velocity measurements. 22 p3177 A72-42394

Measurements of the local velocity of shock and detonation waves by schlieren interferometry of Doppler-shifted laser light. 22 p3178 A72-42455

Uniform moving source radiated sound field from equivalent stationary source distribution via transformation based on retarded-time position and Doppler frequency shift 22 p3205 A72-42461

Fluid velocity measurement of oscillatory flow generated from vortex shedding by laser Doppler system, discussing frequency tracker design, continuous detection problem and application 22 p3178 A72-42677

Laser Doppler velocimeter operating in forward- and back-scatter modes for supplementing wind tunnel flow field measurements in subsonic, transonic and supersonic regimes 22 p3179 A72-42678

Cylindrical waveguide with density modulated electron beam pumped by external electromagnetic field, considering Doppler effect conditions in beam radiation spectrum 23 p3265 A72-44157

A differential laser Doppler velocity meter employing a Fabry-Perot interferometer

23 p3292 A72-44472

Laser frequency measurement by comparison with stable molecular oscillator Doppler shift produced by reflection of UHF modulated coherent optical signal

24 p3411 A72-45425

Generation of plasma oscillation by beam-plasma interaction.

24 p3430 A72-45574

DOPPLER NAVIGATION

Geometry and latitude/longitude differentials approximations for position fixing by Doppler signals and earth satellites

01 p0097 A72-10182

Closed form solution for Doppler satellite navigation for arbitrary orbits with ellipsoid Earth model and straight path signal transmission

05 p0686 A72-16561

Flight navigation technology current state and development trends, discussing transition from Doppler to inertial systems, use of computers and satellites, collision avoidance, etc

05 p0687 A72-16737

All-weather landing aids for civil VTOL aircraft and helicopters, discussing Doppler and inertial navigations, instrument landing systems and ground visibility improvement

05 p0688 A72-16780

Ground based Doppler navigation system for wide range elevation and azimuth aircraft approach guidance, using linear directive antenna array for conical surface definition

06 p0845 A72-18183

Microwave Doppler scanning landing guidance system with radar beam comparison and signal format simplification suggestion

06 p0846 A72-18398

Area navigation systems, discussing VOR/DME, Doppler and inertial systems, CRT displays, data links, etc

08 p1204 A72-21523

VOR and Doppler VOR ground station equipment based on reliable solid state radio transmitters and signal generating devices for aircraft navigation

12 p1779 A72-27104

Russian book on flight navigation cybernetics covering Doppler, astro and radio inertial schemes and satellite systems

12 p1843 A72-28344

Doppler navigation system suitability for area navigation, discussing routes versatility, accuracy and continuous velocity vector sensor

15 p2271 A72-32203

Error analysis for digital avionics system involving Doppler navigation by intermittent scanning of single beam multimode radar, noting optimum statistical data processing

15 p2271 A72-32204

Autonomous navigation systems, discussing Doppler navigation, inertial platforms and onboard computers

21 p3079 A72-40283

Ground-based Doppler navigation waveguide slot antenna design for optimal directional multilobe reception from aircraft

21 p3028 A72-40509

Theoretical and practical comparison between two minute Doppler and short Doppler satellite position fix accuracy.

22 p3203 A72-42947

DOPPLER RADAR

Microwave oscillator detector Gunn diode as inexpensive alarm device for Doppler radar application

01 p0028 A72-10642

Doppler system with navigation radar device, computer unit and data transmitter for continuous recording of aircraft position and speed

02 p0258 A72-12749

CAT detection by airborne laser Doppler radar and ground based ultrasensitive microwave Doppler radar methods

04 p0543 A72-14822

Pulse and Doppler microwave radars comparison with respect to accuracy of moving targets velocity measurements and power characteristics

05 p0661 A72-16034

Vertical dipole antenna design for CW Doppler radar midair collision avoidance system

05 p0629 A72-16571

Phase locked loop bandwidth, acquisition time and SNR for Doppler tracking deep space communications for Venus and Jupiter probes

05 p0629 A72-16575

Low noise Ku band klystron oscillators for Doppler radar, discussing FM noise induced frequency deviation, spurious modulation and countermeasures

07 p0954 A72-19049

Atmospheric lee waves three dimensional structures through high sensitivity Doppler radar measurements based on backscatter from refractive index inhomogeneities

07 p1029 A72-19100

Criterion for estimating radar capability to resolve two targets with differential motion, noting application to synthetic aperture radars and Doppler filters

08 p1134 A72-21424

Spectrum shape of Doppler radar return from two dimensional random rough surface model using helmholtz integral approach and Kirchhoff approximation

09 p1277 A72-22314

Noncontacting measurements by miniature CW Doppler radar with semiconductor microwave generator

09 p1285 A72-22691

CW carbon dioxide laser Doppler radar for remote measurement of atmospheric wind velocity and turbulence, obtaining Doppler signal via homodyned radiation scattered by airborne particles

09 p1315 A72-23407

Stanford pulse Doppler radar and digital data acquisition system for meteor trail wind measurements

10 p1438 A72-24711

Ionospheric weather index in terms of ionization irregularities at given time and place derived from continuous steep incidence HF Doppler soundings

11 p1627 A72-26518

Continuous wave Doppler radar with microwave oscillator for ATC measurements and surveillance

12 p1789 A72-27403

East African low level cross equatorial air current exploration, using light aircraft-borne Doppler radar wind finding equipment

12 p1840 A72-27703

Generalized radar equations derivation to obtain Doppler frequency shift and variance in Fresnel zone due to target movement

16 p2365 A72-33765

Simple Doppler radar using the CL8630 Gunn effect oscillator for the observation of small rotating objects.

17 p2524 A72-34245

Microwave Doppler radar spectrum-based design parameters.

17 p2515 A72-34422

Filtering with perfectly correlated measurement noise.

17 p2533 A72-35240

A geopotential model /APL 5.0-1967/ determined from satellite Doppler data at seven inclinations.

18 p2685 A72-36029

Hybrid and pyrotechnic IR flare generated plasma effects on dual frequency Doppler range measurement system, discussing diagnostics and contamination concentration analysis

18 p2660 A72-36339

Measurement of aerosol motion and wind velocity in the lower troposphere by Doppler optical radar.

18 p2706 A72-36638

Radar meteorology in the Soviet Union - 1970.

18 p2707 A72-36719

A test of the effect of satellite spin on two-way Doppler range-rate measurements.

19 p2830 A72-37278

Predictive filtering of multi-channel time series records with application to Doppler radar data.

19 p2781 A72-38272

Present status of self-contained navigation systems combining Doppler velocity sensors and attitude/headings references.

21 p3079 A72-40282

Detection of Doppler radio signals on a receiver with an additive noise blip number counter

21 p3022 A72-41116

Measurements of air motion in regions of clear air turbulence using high-power Doppler radar.

24 p3421 A72-44978

DORMANT VEGETATION

U VEGETATION

DORNIER AIRCRAFT

Wind tunnel testing of Dassault-Breguet-Dornier Alpha Jet twin engine trainer, emphasizing tests for wing-empennage flutter and jet induced interference effects

13 p1940 A72-30077

DORSAL SECTIONS

High threshold afferents role in dorsal surface potential formation in cat spinal cord

13 p1905 A72-29327

A possible anatomical basis for descending control of impulse transmission through the dorsal horn.

21 p2998 A72-40578

DOSAGE

NT RADIATION DOSAGE

Apparatus for programmed oral administration of drugs to large primates in altered environments.

18 p2654 A72-36921

DOSE

U DOSAGE

DOSIMETERS

NT THRESHOLD DETECTORS [DOSIMETERS]

Polycarbonate merits as visual solid detector in high energy radiation dosimetry

02 p0162 A72-12066

In-flight warning meter for solar and cosmic radiation dose equivalent measurements for radiological protection in SST aircraft

02 p0274 A72-12078

Cosmic radiation effects in Concorde prototype cabin, using photographic dosimeters for neutron dose measurement and nuclear emulsions for all charged particle recordings

07 p0927 A72-19241

Dosimetric characteristics of CdS semiconductor detectors and photoresistors for gamma rays recording

16 p2390 A72-33076

Iridium and tantalum foils for spaceflight neutron dosimetry.

17 p2558 A72-35901

New cancer therapy treatment techniques using space dosimetric concepts.

24 p3374 A72-45112

DOUBLE BASE PROPELLANTS

NT DOUBLE BASE ROCKET PROPELLANTS

Surface ignition behavior of M2 double base propellant, analyzing reaction kinetics

10 p1528 A72-25142

Double base solid propellants life determination from accelerated aging tests at elevated temperatures, discussing surface properties effect on weight loss and autocatalytic decomposition

14 p2144 A72-30757

Insulation and bonding materials effects on double base solid propellants stability, using vacuum reactivity testing technique

14 p2145 A72-30766

Double base propellant nitroglycerin interactions with inhibition materials cellulose acetate and ethyl cellulose, noting time and temperature effects

14 p2145 A72-30767

Internal reflection IR spectroscopy application to composite and double base propellants study, discussing merits as quality control technique

15 p2296 A72-32312

DOUBLE BASE ROCKET PROPELLANTS

Cast double base propellant rocket motors safe storage and service life assessment, examining environmental storage conditions and accelerated temperature effects

14 p2144 A72-30758

Composite and double base solid propellant rocket motors storage, considering ingredients and materials compatibility and ignition temperatures effects on spontaneous inflammation potential

14 p2144 A72-30761

Atmospheric humidity, temperature, vibrational and static loads effects on composite and double base rocket propellants strength and safety characteristics

14 p2145 A72-30764

Contribution to the discussion of mixed-mode propulsion and reusable one-stage-to-orbit vehicles

24 p3450 A72-45191

DOUBLE PRECISION ARITHMETIC

Cellular-array arithmetic unit with multiplication and division.

17 p2519 A72-34297

DOUBLE SIDEBAND TRANSMISSION

Linear product demodulator for quadrature double sideband signal, evaluating channel noise and phase jitter effect on carrier

13 p1920 A72-29105

DOUGLAS MILITARY AIRCRAFT

U MILITARY AIRCRAFT

DOVAP

U DOPPLER EFFECT

DOWN-CONVERTERS

Microstrip double down-converter receiver in civil satellite earth stations for reduced interface problems, increased reliability and minimum initial cost

03 p0334 A72-14074

DOWNTIME

Helicopter elastomeric bearing rotors, discussing downtime and cost reduction, maintenance, endurance and inspection

01 p0073 A72-10150

Concorde engines design for maintainability and reliability to reduce turnaround time, discussing diagnostic facilities and on-wing maintenance features

15 p2298 A72-32457

DOWNWASH

Supercooled and warm fog dispersion technology, considering air heating, helicopter downwash and seeding methods

04 p0543 A72-14812

Downwash behind lifting surface related to loading in ideal incompressible gas by equations of motion linearization

07 p0908 A72-19110

Rotary wing and VTOL aircraft induced downwash effects on ground personnel, considering injuries, body heat loss, work capability impairment and sound pressure effects

14 p2072 A72-30425

Dynamic pressure, downwash and pressure gradient corrections of wind tunnel model measurements, discussing displacement limit for adequate accuracy

19 p2747 A72-38687

Downwash distribution at surface of rectangular planform wings with prescribed subsonic aerodynamic loading for various aspect ratios

19 p2747 A72-38809

- Evaluation of the downwash integral for rectangular planforms by the BAC subsonic lifting-surface method. 19 p2747 A72-38810
- DRACONID METEORIODS**
 Monte Carlo method application to meteor stream formation by meteor material ejection from comet nucleus, determining age of Draconids 02 p0282 A72-12333
 Spectrographic, photometric and chemical identification of Giacobinid /Draconid/ meteoroids, noting compositional similarity to carbonaceous and olivine-bronzite chondrites 23 p3336 A72-43600
- DRAFTING [DRAWING]**
 Automatized graphic information input into computer, using electric potential distribution introduced into conducting underlay sheet by current carrying drawing pen 03 p0326 A72-13093
 Automatized graphic information input into computer, using electric potential distribution introduced into conducting underlay sheet by current carrying drawing pen 11 p1601 A72-25705
- DRAFTING MACHINES**
 Computers and automatic drafting machines as aids in artwork production for printed circuits 19 p2809 A72-38307
 Computation and automatic drawing of the contour lines of functions of two independent variables 23 p3310 A72-44362
- DRAG**
 NT AERODYNAMIC DRAG
 NT FRICTION DRAG
 NT INTERFERENCE DRAG
 NT MINIMUM DRAG
 NT PRESSURE DRAG
 NT SATELLITE DRAG
 NT SUPERSONIC DRAG
 NT VISCOUS DRAG
 NT WAVE DRAG
 Motion of asymmetric body of revolution in rotating liquid, calculating drag on ellipsoid 02 p0204 A72-12175
 Area rule for change in lift/drag ratio of hypersonic delta wing due to conical body addition on compression side 02 p0151 A72-12270
 Power law bodies lift and drag coefficients interrelationship under Newtonian nonaffine similarity laws, presenting rules for equivalent transformations identification 02 p0151 A72-12273
 Jet aircraft brake parachute loads under engine wake, evaluating velocity and drag coefficient influences 02 p0155 A72-12504
 Gas-metal surface interactions effect on aerodynamic lift and drag coefficients in free molecular flow 03 p0342 A72-14059
 Multimoment solutions to convective heat transfer from sphere, discussing maximum drag coefficient and validity at all Knudsen numbers [ASME PAPER 71-WA/HT-1] 05 p0743 A72-15863
 Heat transfer, drag and lift coefficients for free molecular flow over concave surfaces, describing Monte Carlo simulation technique [ASME PAPER 71-WA/HT-17] 05 p0744 A72-15876
 Magnetohydrodynamic theory of spherical drop deformation and drag under axisymmetric current distribution in conducting viscous incompressible fluid 06 p0864 A72-18533
 Conical and spherical nose shapes effects on drag and static stability at Mach 10 07 p0908 A72-19695
 Two dimensional MHD conducting fluid flow past insulating cylinder in presence of arbitrarily oriented magnetic field, determining lift and drag coefficients for small Hartmann numbers 09 p1359 A72-22533
 Decelerating motion of identical and independent water drops succession, determining drag coefficient as function of Reynolds number 10 p1465 A72-24104
 Fluid flow and heat transfer in tube bank with two cylinders in cross flow, determining static pressure, Nusselt number and drag coefficients 11 p1743 A72-25259
 Discharge coefficients of centrifugal screw-type swirl injector with helical channel, calculating drag and surface geometry effects 11 p1712 A72-26970
 Equilibrium diabatic Ekman layer geostrophic drag, heat and mass transfer coefficients, presenting velocity and temperature profiles 14 p2100 A72-30346
 Rarefied gas flow problems, discussing mean free path effects on sharp nosed conical and bluff bodies drag and heat transfer coefficients 15 p2218 A72-32314
 Residual drag torque on magnetically suspended rotating spheres. 23 p3315 A72-44540

- DRAG BALANCE**
 U AERODYNAMIC BALANCE
 U LIFT DRAG RATIO
- DRAG CHUTES**
 Jet aircraft brake parachute loads under engine wake, evaluating velocity and drag coefficient influences 02 p0155 A72-12504
- DRAG COEFFICIENT**
 U AERODYNAMIC COEFFICIENTS
 U AERODYNAMIC DRAG
- DRAG DEVICES**
 NT AERODYNAMIC BRAKES
 NT DRAG CHUTES
 NT LEADING EDGE SLATS
 NT SPLIT FLAPS
 NT SPOILERS
 NT TRAILING-EDGE FLAPS
 NT WING FLAPS
 TU-154 lift and drag augmenting devices for takeoff and landing characteristics improvement 03 p0310 A72-13472
 Flight test of direct side force control by rudder deflection and asymmetrical drag on T-33 airplane, noting use in dive bombing 12 p1754 A72-27520
- DRAG EFFECT**
 U DRAG
- DRAG MEASUREMENT**
 Drag and lift experimental determination for low aspect ratio rectangular wings with blunt trailing edges at Mach numbers 0.5-2.2 [DGLR PAPER 71-114] 02 p0152 A72-12712
 Microaccelerometer for satellite drag measurement and compensating thrust control 06 p0892 A72-18260
 Body drag measurement in low density supersonic gas stream in various Knudsen number ranges 08 p1166 A72-21409
 Spanwise velocity distribution effect on drag measurement of short struts in two dimensional turbulent airstreams 10 p1417 A72-23881
 Optical TV scanning for wind tunnel model position detection in magnetic suspension system for sphere low density drag measurements [ONERA, TP NO. 988] 10 p1461 A72-24764
 Spheres drag coefficient measurements in laminar flow as function of Reynolds number, using wind tunnel model magnetic suspension system 10 p1419 A72-24772
 High temperature skin friction meter design for drag measurements, using motor-transducer air core assembly 12 p1812 A72-27959
 Roughened and smooth spherical wind sensors lift and drag, calculating aerodynamic coefficient spectra from velocity 13 p1894 A72-29620
 Sting-free measurements of sphere drag in laminar flow. 21 p2989 A72-40110
- DRAG REDUCTION**
 Diffusion rate of diluted drag reducing polymers in turbulent boundary layer 03 p0343 A72-14319
 Suppressed turbulent diffusion of drag reducing polymer solution in turbulent boundary layer, measuring concentration with laser-phototransistor unit [AD-737467] 03 p0343 A72-14321
 Flat plate in turbulent shear flow polymer solution, predicting maximum drag reduction with interactive layer concept 03 p0343 A72-14322
 Hydrodynamic resistance reduction for bodies moving under water, analyzing dynamic equations of viscous incompressible fluid 04 p0514 A72-15703
 Spinning drag-free satellite trapping control phenomenon due to proof mass effect on translation controller design 05 p0725 A72-16445
 Wave drag reduction by antisymmetric wing and body arrangement, discussing application to transport aircraft at supersonic speeds 05 p0602 A72-16534
 Base pressure drag reduction on rectangular wings with blunt trailing edges from low speed wind tunnel measurements [DFVLR-SONDDR-219] 10 p1419 A72-24842
 Nonuniform concentration mechanism for observed drag reduction in flows with high molecular weight polymer additives, considering boundary layer with varying viscosity on sphere 13 p1942 A72-29113
 Drag reducing polymers influence on velocity gradients at wall for turbulent pipe flow, observing viscous sublayer thickening 16 p2379 A72-33574
 Minimum ballistic factor missile shapes. 19 p2746 A72-37522
 Turbulent flow of drag reducing fluids between concentric rotating cylinders. [CSME PAPER 71-52] 24 p3393 A72-45254
- DRAGULATORS**
 U DRAG DEVICES

- DRAINAGE**
 Unsteady axisymmetric flows of a liquid draining from a circular tank. 20 p2913 A72-39605
 Draining of a fluid from a rotating cylindrical tank. 21 p3046 A72-41307
- DRAINING**
 U DRAINAGE
- DRAWINGS**
 Modified run-length encoding system for text and drawing documents to obtain higher data reduction ratio 13 p1922 A72-29349
- DREAMS**
 Physiology of sleep phases and dreams, discussing data on highly organized and interacting neurohumoral mechanisms exhibiting alternating forms of brain bioelectric activity 08 p1118 A72-21838
- DRIFT**
 Mathematical model for computation of electronic circuit drift reliability and circuit production yields, discussing operational parameter allowance 14 p2091 A72-31165
- DRIFT [INSTRUMENTATION]**
 Extremal system with second control loop for search signal frequency regulation to optimize primary loop operation, determining system dynamic errors under random drift 02 p0197 A72-12340
 Equivalent harmonic solutions for systematic drift of astatic gyroscope about outer gimbal axis with base under random angular vibrations 02 p0231 A72-12564
 Wide gap spark chamber feeding technique for compensation of charged particle track drift due to avalanches 07 p0988 A72-19956
 Extremal system with second control loop for search signal frequency regulation to optimize primary loop operation, determining system dynamic errors under random drift 08 p1146 A72-21555
 MOSFET for input impedance measuring amplifier, discussing input stage temperature drift and protection from overvoltage 10 p1482 A72-24599
 Extremal feedback control system operation with integral PFM in extremum drift mode, determining equations of motion and steady state regime 11 p1610 A72-25449
 Gyro drift detection and isolation for redundant inertial measuring unit configuration of Carousel V system 15 p2270 A72-32190
 Feedback circuitry for dc amplifiers voltage drift compensation, discussing performance criteria in terms of residual offset voltage, system stability, correction and measurement time 18 p2671 A72-37150
 Optimum aiding of inertial navigation systems using air data. [AIAA PAPER 72-847] 20 p2950 A72-39082
 Some results of calibrating CG-2 gravimeters /Sharpe/ by the tilt method. 21 p3053 A72-40499
- DRIFT RATE**
 Electron and ion drift rate effect on floating double probe characteristics in Maxwellian plasmas 02 p0266 A72-12768
 Weakly turbulent plasma wave system, obtaining drift solution for stationary distribution stability 03 p0394 A72-13274
 Cross flow blown two dimensional stationary plasma arc deflection and temperature distribution as function of collisional drift velocity and electric field 03 p0397 A72-13921
 Plasma sheath drift origin of hot ions in modified Penning discharge 04 p0551 A72-14439
 Small scale F region irregularities at Varanasi, plotting horizontal drift velocities and directions, axial ratios and orientations and rms random velocity values histograms 04 p0517 A72-14954
 Electron drift speed and multiplication rate in pulsed Ar positive column in axial electric field 04 p0553 A72-15669
 Altitude dependent vertical drift velocity of small scale ionospheric inhomogeneities, using correlation of signal time lag scanning in frequency domain 05 p0657 A72-16270
 Structure and movements of E region inhomogeneities, describing ionospheric drift velocities and directions for different seasons 05 p0660 A72-17178
 Solar radio spike bursts, discussing categorization by high time resolution dynamic spectra and drift 06 p0876 A72-17578
 Human visual system multiple channels sensitivity to patterns at low luminance or high drift rates, noting retinal ganglion cells selective sensitivity 06 p0761 A72-17602

- PE sub s harmonic components diurnal and seasonal variations and latitudinal dependence, investigating relationship to drift velocity in E region
06 p0811 A72-18749
- Magnetosphere If electric fields influence on trapped radiation region particle behavior, considering magnetic drift rates
07 p1062 A72-20036
- Drift waves propagation in ionized plasma, considering drift rate, ion sound phase velocity and effect of impurities
07 p1045 A72-20444
- Growth rate and boundary of drift dissipative instability in plasma under linear theta pinch conditions
07 p1045 A72-20477
- Seasonal variation in ionospheric horizontal drift velocities under normal E and sporadic E conditions for middle latitudes
08 p1157 A72-21115
- Solar magnetic fields forced latitudinal drift rate due to differential rotation, taking into account turbulent friction and pressure forces
09 p1382 A72-22286
- Drift angle effect on rolling wheel pneumatic tire lateral and angular deformation amplitudes, deriving formula for reaction forces
09 p1351 A72-23176
- Test stand for rolling wheel with pneumatic tire at variable drift angles, deriving kinematic parameters and elasticity coefficients from static and dynamic tests
09 p1351 A72-23177
- Momentum transfer theory for ion drift velocity in multicomponent gas mixture at arbitrary electric field strengths
10 p1519 A72-24096
- Electron densities and drift velocities dependence on macroscopic discharge parameters in positive column of He-Cd laser
10 p1493 A72-25048
- Neutral gas velocity distribution, transverse drift velocity, particle and energy densities in column under free fall conditions, considering wastage by ionization processes
11 p1698 A72-26645
- Microwave time of flight method for measuring electron drift velocity in GaAs semiconductors
12 p1855 A72-27667
- Radial bearing placed on journal of Cardan suspension, investigating ball dimension errors effect on gyro drift rate
13 p1962 A72-28385
- Virtual height dependence of ionospheric F region parameters including angular divergence of reflected radio waves, heterogeneity coefficient and random and drift motions velocity
13 p1948 A72-29038
- HF electrostatic instabilities driven by electron-ion relative drift velocity across external magnetic field for inhomogeneous plasma, noting Landau damping role
16 p2433 A72-32809
- Geomagnetic field line tracing by plasma clouds produced by Ba vapor release, noting different ion drift rates and directions
16 p2384 A72-32977
- Free electrons-laser interaction induced electron forward drift and dc current generation, deriving drift velocity by nonrelativistic classical and quantum mechanical theories
16 p2402 A72-33397
- Ion concentration inhomogeneities in the ionosphere at an altitude of 600 km
17 p2547 A72-35207
- Similarity method to compute ionosphere drift velocity and direction from radio sounding data
19 p2792 A72-38640
- Direct measurements of plasma drift velocities at high magnetic latitudes.
19 p2793 A72-38757
- Drift instabilities in an inhomogeneous collisionless plasma
20 p2957 A72-39355
- Geomagnetic DP-2 variation base level from F region electron drift velocity measurements in equatorial electrojets
22 p3169 A72-42013
- Equatorial ionosphere irregularities vertical drift velocity calculation, showing agreement with incoherent scatter results
22 p3170 A72-42370
- Electron density and temperature in microwave plasmas at higher pressures.
22 p3211 A72-42479
- Drift velocities, diffusion coefficients, and temperatures of photoions in argon, nitrogen, and oxygen
22 p3209 A72-42926
- On the drift velocity of electrons in a gas.
22 p3212 A72-42996
- Surface drift vibrations of a weakly ionized plasma
22 p3212 A72-43102
- Synchronous observations of lower-ionospheric wind conditions in Dushanbe and at the equator
23 p3285 A72-44166
- Current induced drift rate of plasma electrons in electric and magnetic fields, noting electron velocities in turbulent heating of plasma
24 p3429 A72-45507
- Current-driven drift wave instability in a sheared magnetic field.
24 p3430 A72-45570
- DRILLING**
Pulsed Nd laser drilling and welding of metal, metal-semiconductor and semiconductor elements, discussing bond penetration and character, mechanical strength and I-V characteristics
03 p0363 A72-13860
- Drill hole heat transfer upon hot liquid injection into productive layer, enhancing oil extraction process effectiveness
04 p0594 A72-14515
- Moving heat source model of temperature profile and thermal stress propagation for laser drilled holes in alumina ceramic material
07 p0994 A72-19211
- Thermal distortion insensitive TEM mode beam of hf YAG laser for high precision drilling machine
07 p1004 A72-19236
- Laser microdrilling of synthetic ruby, sapphire, silicon and ferrite materials, showing hole parameters dependent on focal length, beam power and pulse rate
07 p0997 A72-20200
- Plastics cutting and drilling with carbon dioxide IR laser beam, discussing economics and commercially available equipment
07 p0999 A72-20554
- Carbon dioxide laser radiation interaction with solids, applying to fused quartz drilling
09 p1323 A72-22904
- Luna 16 automatic probe drilling experiment, obtaining lunar rocks physicochemical properties for comparison with terrestrial rocks
11 p1613 A72-25938
- Countersink boring machines with programmed digital control systems for precision spacing multiple hole drilling in extended aircraft engine components
11 p1642 A72-26816
- Commercially available laser systems applications to welding, drilling, scribing and other machining operations
11 p1652 A72-26984
- Nd glass laser drilling and welding applications and tests on materials to evaluate feasibility and operational advantages, identifying optimal pulse energies and durations
15 p2244 A72-32028
- Electron beam welding, machining and drilling, discussing technical and economic factors
16 p2399 A72-33540
- Effects of environment on formation of finished surface in drilling aluminum and aluminum alloys.
21 p3060 A72-40936
- DRILLS**
High angular velocity device design problems, considering gyroscopes, ultracentrifuges, yarn-spinning textile machinery and dental drill
19 p2809 A72-38544
- DRINKING**
Calorimetric measurements of human body temperature and of hot saline solution drinking effects on sweating rate
09 p1267 A72-23440
- Calorimetric study of sweating man response to drinking hot saline solution as function of temperature, volume and salinity of ingested liquid
09 p1267 A72-23441
- DRIVES**
Soviet book on hydraulics, hydraulic machines and hydraulic drives covering fluid dynamics, pipe flows, jet pumps, turbines, bladed transmissions, etc
04 p0466 A72-15247
- Dynamic processes of electric drive system with electromagnetic clutch modeled by analog computer element with logical input-output relation
10 p1423 A72-24755
- DROGUE PARACHUTES**
U DRAG CHUTES
DROGUES
U TOWED BODIES
DRONE AIRCRAFT
NT TARGET DRONE AIRCRAFT
DRONE HELICOPTERS
U HELICOPTERS
DRONE VEHICLES
NT TARGET DRONE AIRCRAFT
Remotely manned vehicles (RMV) application in aerial warfare, considering anti-aircraft defenses lethality increase, equipment costs and role of man during combat mission
13 p1896 A72-28451
- DROP SIZE**
Rain droplet size distribution effects on microwave attenuation at millimeter wavelengths, comparing calculation with measurement
01 p0027 A72-10406
- Hydrometeors linear depolarization ratios measurements by monostatic lidar, using different size water drops and ice crystal clouds
01 p0095 A72-10830
- Visibility relationships to atmospheric liquid water content in fog derived from fog drop size distribution model
01 p0096 A72-11281
- Shock wave damping and droplet atomization function of relaxation zone in noncombustible two phase gas-liquid mixtures
02 p0202 A72-11592
- Coacervate drops oxidoreductases and stability in primitive prebiological systems, using polyphenol oxidase-carbohydrate-histone-quinones
04 p0469 A72-14784
- Polydisperse spray device with controllable drop size distribution for two phase detonation research
04 p0509 A72-15486
- Cumulus and stratocumulus ice crystal and nuclei concentrations, drop size distributions, glaciation differences and enhancement mechanisms
07 p1030 A72-19101
- IR radiation radiative transfer calculation for selected spectral intervals due to various model cloud droplet size distribution
07 p0980 A72-20456
- Droplet growth on passivated hygroscopic condensation nuclei in device with controllable relative humidity
08 p1172 A72-22000
- Rain droplets growth by collision and coalescence during fall through sheared air flow, discussing discrepancies between calculated and experimental collision efficiencies
11 p1619 A72-26642
- Theoretical and measured rainfall attenuation of millimeter waves, correlating attenuation coefficients, rain rate and drop size distributions
12 p1785 A72-27803
- Quasi-steady state combustion theories compared with observations of hydrocarbon fuel droplet and flame zone diameters, noting underestimation of burning rate
13 p2063 A72-28545
- Cloud statistics stratification by climatological regime, month and time of day, extending simulation to drop size distributions and liquid water content
13 p1989 A72-28808
- Coastal and inland fog microphysical features, discussing visibility, liquid water content, drop size distributions and haze droplet concentrations
13 p1991 A72-28842
- Airborne electrostatic probe for cloud droplet size measurement, calculating flow distribution and particle trajectories
16 p2390 A72-33150
- On depolarization of visible light from water clouds for a monostatic lidar.
18 p2706 A72-36646
- Stability of a liquid film in a lateral gas flow and the size of droplets during the breaking of the film
20 p2987 A72-39925
- Investigation of the coagulation and breaking of droplets of comparable dimensions in an electric field
20 p2956 A72-40038
- Two-phase detonations with bimodal drop distributions.
24 p3463 A72-45052
- Erosion of materials under drip impact loads, determining wear rate dependence on drop size, impact velocity and material properties
24 p3460 A72-45723
- DROP TESTS**
Ribbon parachutes drop tests at Mach 0.57-1.70, measuring opening shock loads and functioning time sequence
01 p0004 A72-10312
- Liquid nitrate ester sensitivity and dissolved water desensitization, using thermal initiation and drop weight impact tests
09 p1373 A72-23145
- DROP WEIGHT TESTS**
U DROP TESTS
DROPS [LIQUIDS]
NT RAINDROPS
Laser light scattering by fuel droplets in flame combustion zone, measuring intensity distribution with contactless optical probe
01 p0066 A72-10495
- Fluid droplet collapse in two phase gas flows, noting time dependence
01 p0145 A72-10573
- Electrically charged low mobility droplet production by water vapor condensation on to gaseous ions from aircraft static discharger
02 p0231 A72-12556
- Acoustic wave excitation in water droplet with giant pulse radiation from Q switched laser, noting diffraction effects on laser power density requirement
03 p0367 A72-13372
- Bipropellant fuel droplets combustion in oxidizing atmospheres from spherico-symmetrical nonconvective quasi-steady state model, discussing supercritical pressures and forced convection probability
04 p0596 A72-15273
- Erosion of materials under drip impact loads, determining wear rate dependence on drop size, impact velocity and material properties
05 p0734 A72-15981

Physical processes of fluids atomization in electric field, discussing droplet surface instability and boundary values of surface tension coefficient

05 p0667 A72-17185

Magnetohydrodynamic theory of spherical drop deformation and drag under axisymmetric current distribution in conducting viscous incompressible fluid

06 p0864 A72-18533

Two phase flow model of water droplets velocity in air stream, using Fresnel biprism and laser differential scheme

07 p1000 A72-18940

Droplets coalescence in clouds, considering microturbulence effects due to laminar shear flow

07 p1030 A72-19102

Cavitation phenomena role in liquid drop impact erosion of steam turbine blades leading edges

07 p0967 A72-19262

Flame temperatures, composition profiles and burning rates in liquid n-heptane droplet and sphere combustion

07 p1051 A72-19362

Hydrodynamic characteristics of freely falling water droplets in air, establishing relationships among Reynolds, Laplace and Bond criteria

07 p1030 A72-19854

Cavity formation and drop transfer time correlation with welding current in powder covered /submerged/ arc welding, using high speed X ray photography

07 p0998 A72-20396

Electromagnetic wave diffraction on arbitrary spheres, calculating scattering cross sections and attenuation by four water droplets

08 p1131 A72-20789

Temperature and concentration fields of liquid solution droplets during unsteady vaporization process in high temperature gas media

08 p1252 A72-21308

Maximum volatile solute vaporization escape prior to droplet solidification during metal vapor chemical release process

08 p1128 A72-21618

Large drops coalescence, investigating approach rate dependence on electric field strength and distance

08 p1201 A72-21998

Supercooled water drops freezing by contact nucleation with AgI and silicate particles, determining effective temperature in updraft wind tunnel experiments

09 p1345 A72-22445

Supercooled cloud water droplets in free fall shattered by shock waves measuring ice crystal formation probability

09 p1345 A72-22446

Surface tension determination at immiscible liquids or liquid-gas phase interfaces by capillary rise measurement of droplet

09 p1294 A72-22678

Decelerating motion of identical and independent water drops succession, determining drag coefficient as function of Reynolds number

10 p1465 A72-24104

Liquid rocket LF unsteady transient behavior calculation from droplet evaporation and combustion parameters

10 p1528 A72-24644

Interior and exterior hydrodynamics of spherical droplet submerged in unbounded arbitrary velocity field, including effects of surface active agents

10 p1470 A72-25042

Breakup of accelerating liquid drops in gas dynamic flow, presenting unified theory for acceleration and aerodynamic effects

11 p1619 A72-26641

Venus lower atmosphere enhanced microwave attenuation explained by water vapor and droplet layer, calculating mass density distributions

11 p1724 A72-26762

Laplace-Carson transform solution for integrodifferential equation of motion for droplet suspended in viscous gas slipstream

12 p1796 A72-27093

Liquid droplets behavior in high velocity gas jets, deriving fluid flow model solutions near symmetry axis and for liquid-gas boundary layer

[DFVLR-SONDDR-200] 13 p1941 A72-29003

Velocity calculation from pitot tube pressure measurements in compressible two phase flow, taking into account droplet momentum loss

14 p2104 A72-30252

Mass transfer effect on heat transfer to evaporating droplet, considering mass efflux shielding effect and forced convection flow field

14 p2172 A72-31051

Liquid drop evaporation in stagnant environment at high temperature and pressure, noting gas phase nonideal behavior effects

14 p2173 A72-31066

Lifetime nomogram for evaporating drop at vapor combustion, applying thermomechanical and aerodynamic decay to jet engine combustion chamber

[DFVLR-SONDDR-203] 16 p2477 A72-33422

Mathematical model of nitric oxide formation by fuel droplet burning above fuel critical pressure, applying to diesel engine operations

17 p2511 A72-34901

Liquid fuel droplet transient combustion in supercritical hot stagnant oxidizing environment, solving conservation equations

17 p2636 A72-34903

Atomization of liquid droplets in a convective gas stream.

17 p2540 A72-35044

Fluid jets and droplets deformation in transverse supersonic two phase gas flow

17 p2544 A72-35932

In-line holography of reacting liquid sprays

19 p2798 A72-37619

Heat transfer in water droplets and its role in the calculation of highly stressed injection coolers

[DFVLR-SONDDR-196] 20 p2911 A72-39075

The behavior of two-phase systems during adiabatic expansion

20 p2953 A72-39595

Experimental investigation of the influence of acoustic oscillations on the evaporation intensity of liquid droplets

20 p2987 A72-40037

Investigation of the coagulation and breaking of droplets of comparable dimensions in an electric field

20 p2956 A72-40038

Approximate determination of the change in the aerosol distribution spectrum in a Venturi coagulator tube

20 p2928 A72-40039

Detonation shock wave study of liquid fuel droplets in gaseous oxidizing agent flow, using schlieren and scanning photography

20 p2962 A72-40044

Interaction between the droplets of a polydispersed condensate in a nozzle flow

20 p2915 A72-40046

Diffusive and radiative effects on vaporization times of drops in film boiling.

21 p3130 A72-41185

Electro-optical design and performance parameters of polluted air liquid droplet size distribution measurement by pulsed junction diode laser light external scattering

22 p3179 A72-42680

The breakup of liquid droplet columns by shock waves.

24 p3391 A72-45048

Model for shock wave propagation through gas-liquid drop medium based on liquid phase atomization by boundary layer stripping

24 p3391 A72-45049

A theoretical model for the combustion of droplets in super-critical conditions and gas pockets.

24 p3463 A72-45050

Chemical aspects in the shock initiation of fuel droplets.

24 p3433 A72-45051

DROSOPHILA

Phase resetting behavior of circadian rhythm of pupal eclosion in fruitfly populations

07 p0918 A72-19529

Phase shifting effect of light on circadian rhythm and photoreceptive pigment location in Drosophila in postpupation stages

07 p0919 A72-19536

Ecdysone harmonic control of Drosophila circadian rhythms and synchronizing mechanisms, discussing light stimulation and neurohormone secretion

07 p0919 A72-19537

Viruslike particles in salivary glands, muscles and nerves of normal and gamma irradiated Drosophila melanogaster, showing age dependent infection

08 p1116 A72-21198

Natural aging and radiation-induced life shortening in Drosophila melanogaster.

24 p3373 A72-45279

DROWSINESS

U SLEEP

DRUG THERAPY

U CHEMOTHERAPY

DRUGS

NT ADRENERGICS

NT ANTIADRENERGICS

NT ANTIBIOTICS

NT ANTICHOLINERGICS

NT ANTIIDIARETICS

NT ANTIIRADIATION DRUGS

NT CENTRAL NERVOUS SYSTEM STIMULANTS

NT CHOLINERGICS

NT CORTISONE

NT CYCLOPROPANE

NT DIGITALIS

NT EPINEPHRINE

NT HEMOSTATICS

NT INSULIN

NT MORPHINE

NT MOTION SICKNESS DRUGS

NT NARCOTICS

NT NEMBUTAL [TRADEMARK]

NT NORADRENALINE

NT NOREPINEPHRINE

NT PENICILLIN

NT PENTOBARBITAL SODIUM

NT RESERPINE

NT SEDATIVES

NT STIMULANT

NT TRANQUILIZERS

NT VASOCONSTRICTOR DRUGS

Wake-sleep cycle importance in military service, considering drugs effects on wakefulness

07 p0922 A72-20383

Medication effects on pilot performance, covering tranquilizers, sedatives, antibiotics, stimulants, antihistamine and hypotension drugs

13 p1909 A72-28750

Apparatus for programmed oral administration of drugs to large primates in altered environments.

18 p2654 A72-36921

DRY FRICTION

Martensite and solid Cr-containing inclusion effects on wear resistance of cermet steel during dry friction with R18 steel

05 p0665 A72-16095

Modified PV criterion for self lubricated dry bearings, observing bearing length and diameter effect on steady state temperature

06 p0823 A72-18594

Low pressure gauge with compensation of dry friction forces in servomechanism with respect to mean value

07 p0982 A72-18929

Friction coefficient, standard wear and surface layer temperature of seal for dry friction pairs in jet engines, investigating crystal lattice parameters

07 p0996 A72-19768

Thermocracking and thermal stresses in packing rings of face-type mechanical seals under dry friction

08 p1177 A72-21927

Wear mechanism of lead-bronze dry sliding in air on hardened steel ring

11 p1638 A72-25510

Structural energy loss mechanisms, considering hysteresis, edge damping of panels, acoustic losses, dry friction, multilayer sandwich damping, etc

12 p1882 A72-27342

Sliding dry friction of hard refractory metals and ceramics, discussing surface changes as function of load, sliding speed, temperature and mechanical properties

12 p1817 A72-28184

The dry wear behaviour of porous cobalt.

18 p2696 A72-36795

The stability of a uniaxial gyrostat under conditions of dry friction in the stabilization and precession axes

21 p3059 A72-41813

DRY HEAT

Space flight hardware sterilization, considering dry heat and chemical destruction

01 p0019 A72-10822

Spore survival in dry heat sterilization as function of water activity, indicating entropy-molecular stability relationship

04 p0475 A72-15259

Dry heat resistance of bacillus spores on spacecraft metal surfaces for different pressures, atmospheres and materials

04 p0475 A72-15261

DRYING

NT DEHYDRATION

DRYING APPARATUS

NT DESICCATORS

DTA [ANALYSIS]

U DIFFERENTIAL THERMAL ANALYSIS

DTMB-111 GROUND EFFECT MACHINE

U GROUND EFFECT MACHINES

DTMB-430 GROUND EFFECT MACHINE

U GROUND EFFECT MACHINES

DUAL SPIN SPACECRAFT

Spin-axis attitude stability in torque-free environment of dual spin spacecraft with energy losses in both bodies

[AIAA PAPER 72-16] 05 p0730 A72-16964

Analog simulation of dual-spin satellite dynamics and control, emphasizing Hughes gyrostat spacecraft

07 p1086 A72-20352

Rotor components vibration destabilizing effects on dual spin spacecraft dynamics, considering turbulent liquid sloshing in Intelsat 4 propellant tank

07 p0973 A72-20488

Equations of motion for structural flexibility influence on dual spin spacecraft dynamic response, noting elastic deformations and rotation rates coupling

[AIAA PAPER 72-348] 11 p1725 A72-25377

Intelsat 4 nutation dynamics and gyrostat stabilization technique for precision pointing in international telecommunication, discussing damper and fuel sloshing

[AIAA PAPER 72-537] 12 p1780 A72-27360

Autotracking antenna effect on dual spin spacecraft nutational stability, using averaging, eigenvalues and digital simulation techniques

[AIAA PAPER 72-571] 12 p1876 A72-27379

Synchronous communication satellites body stabilized three axis attitude control superiority over dual spin techniques, emphasizing single large pitch momentum wheel configuration with magnetic torquing

[AIAA PAPER 72-572] 12 p1876 A72-27380

Stability of linear systems with constraint damping and integrals of the motion.

19 p2856 A72-37519

Dual spin spacecraft simulation on three axis air bearing ball in atmosphere testing propellant tank dissipation and spacecraft stability in autotrack mode [AIAA PAPER 72-860] 20 p2911 A72-39108

Stability of dual spin spacecraft containing tracking payloads. [AIAA PAPER 72-890] 20 p2975 A72-39111

Attitude stability of a dual-spin satellite with a large flexible solar array. [AIAA PAPER 72-887] 20 p2975 A72-39114

Nutational stability of a dual-spin satellite under the influence of applied reaction torques. [AIAA PAPER 72-885] 20 p2976 A72-39116

Effect of bearing flexibility on dual-spin satellite attitude stability. 21 p3115 A72-41303

OSO pointing accuracy improvement through dual spin stabilization, discussing OSO design evolution 1962-72 24 p3449 A72-45145

DUCTED BODIES

MHD generator duct external loop electric current maximization by working material resistivity tensor optimal distribution 10 p1521 A72-24434

DUCTED FANS

Variable pitch ultrahigh bypass ratio ducted fan engine design for STOL transport aircraft [ASME PAPER 72-GT-61] 11 p1704 A72-25652

Fan engine compressor noise measurement by spinning mode synthesizer for use in duct liner optimization 13 p2028 A72-29574

Noise generated by free flow turbulence incident on rotor or stator in axial flow fans and compressors, noting sound spectrum dependence 13 p2028 A72-29575

DUCTED FLOW

NT KNUDSEN FLOW

Space-time correlations of convection turbulent velocities in smooth circular duct with longitudinal separations 01 p0049 A72-10038

Plasma temperature and seed atom concentration in MHD generator ducts and combustion chambers by optical measurements, discussing boundary layer thickness, optical density, etc 01 p0072 A72-11218

Optically thin radiation effects on local heat transfer in gas flow narrow duct thermal entrance region, presenting Nusselt number variations terms for uniform and parabolic velocity profiles 02 p0303 A72-12321

Sound propagation in acoustic ducts with shear flow and wall lining by Ritz-Galerkin technique 04 p0511 A72-14848

Sound attenuation in lined rectangular ducts with uniform steady flow, considering aircraft engine noise reduction 04 p0565 A72-15267

Aerodynamic noise interference generated by fluid flow in acoustically lined ducts 04 p0462 A72-15268

Thermal load effect on convective heat transfer in turbulent flow in circular duct 05 p0742 A72-15843

Average stagnation pressure measurement in low velocity ducted gas flow with nonuniform velocity profiles, discussing mathematical technique and computer program [ASME PAPER 71-WA/PUR-1] 05 p0645 A72-15910

Incompressible laminar flow in conduit with arbitrary cross section, time varying pressure gradient and initial velocity, constructing finite series solution by orthonormalizing procedure [ASME PAPER 71-WA/FE-22] 05 p0646 A72-15927

White noise mean square sound pressure in turbulent flow in cylindrical duct, using cross correlation technique [ASME PAPER 71-WA/FE-5] 05 p0647 A72-15936

Incompressible turbulent flow in parallel-plate channel with one porous bounding wall, using velocity slip model [ASME PAPER 71-WA/FE-1] 05 p0647 A72-15939

General MHD duct flow problems solution using machine transformation and finite difference technique supplemented by successive overrelaxation [ASME PAPER 71-WA/APM-15] 05 p0694 A72-15965

Explicit finite difference procedure to solve time averaged equations of motion for unstalled turbulent duct flows in coordinate system approximating real flow streamlines [AIAA PAPER 72-43] 05 p0651 A72-16878

Sound propagation within and radiated from annular duct flow, measuring acoustic distributions for single and multimode excitations [AIAA PAPER 72-197] 05 p0691 A72-16924

Internal compressible spatially nonuniform ducted flow performance, defining diffuser efficiency, loss coefficient and static pressure rise coefficient [AIAA PAPER 72-85] 05 p0652 A72-16960

Boron containing solid propellant combustion efficiency and fuel-air ratio determination from particle

laden plume nonequilibrium effects in ducted subsonic flow [AIAA PAPER 72-36] 05 p0750 A72-16972

Viscous incompressible flow in straight duct, relating duct wall drag, axial pressure gradient, flux rate and cross sectional area 05 p0653 A72-17002

Moderate Hartmann number MHD duct flow with applied transverse magnetic field, using numerical methods 06 p0859 A72-17619

Turbulent velocity field calculation for rectilinear duct with noncircular cross section, using integral transformation and dimensionless velocity ratio 06 p0800 A72-18110

Compressible axisymmetric coaxial jets turbulent mixing in constant area duct, considering axial and radial pressure distributions 07 p0967 A72-19094

Forced convective heat transfer for laminar flow of Newtonian fluid inside noncircular duct, taking into account viscous dissipation and work compression 07 p1100 A72-19628

Unsteady laminar viscous incompressible electrically conducting flow between nonconducting parallel flat plates with applied constant magnetic field 07 p1044 A72-20245

Small samples acoustic transmission loss measurement with constant energy flow in small duct 08 p1206 A72-21296

Numerical analysis of capture area ratio effect on shock wave propagation from free stream into moving flowing duct 08 p1150 A72-21619

Supersonic and subsonic jet flows coexistence in constant section duct, analyzing pressure on walls and in fluid and schlieren visualization [ONERA, TP NO. 976] 09 p1294 A72-22813

Secondary flows effect on turbulent longitudinal velocity distribution in square ducts, using Navier-Stokes and continuity equations 10 p1463 A72-23864

Fully developed laminar flows in ducts with secondary motions, considering annuli with rotating core, pipe with swirl generator and straight rectangular duct 10 p1463 A72-23865

Pseudoviscous method application to computation of supersonic flow of inviscid ideal gas through two dimensional or annular axisymmetric ducts 10 p1417 A72-23876

Two dimensional shock wave interaction with bends in rectangular duct, showing far wall Mach reflection 10 p1464 A72-23879

Shock wave propagation in ducts with abrupt area expansion, discussing vortices generation and wave diffraction and reflection effects on ducted flow 10 p1464 A72-23880

Equation of isovolumetric fluid pulsed and potential flow in convergent duct solved by perturbation method 10 p1465 A72-24118

Transverse shear flow stability analysis based on disturbance energy balance determination, applying to ducted and jet stream boundary layer flows 10 p1469 A72-24531

Secondary flow measurements in rotating ducts, obtaining pressure distributions and cross-flow velocities [ASME PAPER 72-GT-17] 11 p1569 A72-25616

Dynamic response of MHD flow under impulsive pressure gradient, obtaining approximate analytic solutions for conduits of arbitrary cross sections by complex variable approach 11 p1695 A72-26039

Perturbation velocity corrections for eccentric model position and different air flow ducting in rectangular wind tunnels [DFVLR-SONDDER-191] 11 p1573 A72-26581

Possible regimes and solutions for adiabatic one dimensional compressible gas flow in convergent and divergent ducts with friction 12 p1797 A72-27348

Enhanced turbulent diffusion of nitrous oxide in parallel wall duct with obstructions for high Reynolds numbers 12 p1797 A72-27536

Measurement of spatially coherent and incoherent structure of axial compressor-generated noise modes propagating in duct [ONERA, TP NO. 1045] 12 p1861 A72-28049

Thermal load effect on convective heat transfer in turbulent flow of viscous incompressible liquid in circular tube 15 p2334 A72-31262

Inverse Laval problem of three dimensional subsonic and supersonic flows in nozzles and ducts of variable cross section in terms of asymptotic series 16 p2342 A72-32930

Pressure, shear stress and yaw angle measurements in flow through aircraft intake S-shaped ducts with turbulent boundary layer at entry, noting vortex generation 16 p2377 A72-33403

Memories of longitudinal fluctuations of velocity in a smooth circular duct 17 p2539 A72-34907

Unsteady flow at the junction of a branched duct. 17 p2539 A72-34971

Sound attenuation in acoustically lined circular ducts in the presence of uniform flow and shear flow. 17 p2582 A72-35411

Sound propagation in duct shear layers. 17 p2582 A72-35413

Acoustic refraction and attenuation in cylindrical and annular ducts. 17 p2582 A72-35414

Transmission of sound in ducts with thin shear layers - Convergence to the uniform flow case. 18 p2710 A72-36405

Calculus of variations and finite difference method for combined free and forced convective heat transfer through vertical noncircular ducts, calculating Nusselt number 18 p2741 A72-36926

Incompressible potential flow solution for axisymmetric body-duct configurations. 18 p2683 A72-36940

On the use of the Preston tube in elliptical ducts. 18 p2676 A72-37094

Pressure loss and heat transmission in cylindrical ducts [ONERA, TP NO. 1057] 19 p2880 A72-37768

Solution of the problem of the unsteady motion of a mixture in a flat duct using a quasi-homogeneous model with allowance for deposition on the walls 19 p2788 A72-38589

Secondary flows in ducts of square cross-section. 19 p2789 A72-38795

Interaction between two streams of incompressible fluids in flat duct, using Chaplygin method of singular points 20 p2913 A72-39370

Boundary-layer effects on pressure variations in Ludwig tubes. 20 p2914 A72-39620

Optimization of acoustic linings in presence of wall shear layers. 21 p3083 A72-40334

Axial velocity distribution and streamline boundary selection to derive two dimensional infinite duct shapes for inviscid irrotational compressible flows [ICAS PAPER 72-08] 21 p2990 A72-41133

Probability distribution of velocities and temperatures near a wall 23 p3279 A72-43696

Frequency response of ducts in the shape of a truncated cone 23 p3279 A72-43697

Experimental study of the plane deformation of a homogeneous turbulence 23 p3280 A72-43822

Developing laminar and turbulent duct flow with chemical reaction. 24 p3378 A72-45061

DUCTED PROPELLERS

U SHROUDED PROPELLERS

DUCTED ROCKET ENGINES

Air-augmented shrouded and ducted rocket secondary combustor performance parameter analysis based on one dimensional conservation equations 03 p0405 A72-13834

Boron reaction characteristics in ducted rockets under varying primary chamber conditions detailing various gaseous propellants effects 15 p2296 A72-32311

DUCTILITY

Nb alloys bend ductility at various temperatures, showing silicide coatings and electron beam and gas tungsten arc welding effects on mechanical properties 01 p0083 A72-10284

Brazed joints shear strength and ductility tests, discussing deformation, hardness, corrosion, irradiation, structure and microanalysis 01 p0074 A72-10285

Tensile and fatigue tests on steel, brass and aluminum with starter cracks, showing relation of strength and ductility to crack propagation and stress cycles 01 p0083 A72-10392

Ductility enhancement in directionally solidified Ni base Mar-M200 alloy by Hf additions increasing gamma-gamma prime eutectic 01 p0089 A72-11104

Metal ductility and toughness - Conference, Kyoto, October 1971 02 p0246 A72-12557

High strength low alloy type ferrite pearlite steel microstructural and compositional variations effect on work hardening, ductility and impact toughness 02 p0246 A72-12558

Superalloys ductility and workability improvements without sacrificing elevated temperature strength for aircraft engine applications 02 p0246 A72-12561

Inconel 718 welding techniques, investigating microfissuring, impact strength, penetration and ductility 02 p0246 A72-12774

Ductility relationship to plasticity characteristics in cylindrical steel samples with short notch under tension 03 p0443 A72-13458

Ductility and fracture of metallic thin walled tubular samples under complex stress of internal pressure and axial tension
03 p0454 A72-14215

Substitutional dynamic strain aging effects on Fe-Nb alloys mechanical properties, attributing ductility reduction to work hardening and strain rate effects
04 p0534 A72-15576

Near tip strain criterion validity for ductile crack growth on specimen surface
05 p0673 A72-16307

Tensile ductile-brittle transition temperature and slip mechanism of thoriated Cr, comparing with unalloyed Cr
05 p0678 A72-17117

Ductile fracture development in steel due to microcracks and pores formation
05 p0679 A72-17205

Carbon effects on strength, ductility, brittle transitions and plastic strains of tungsten at high temperatures
06 p0833 A72-18634

Ti influence on ductility of normalized low alloy steel, considering crack initiation and propagation
06 p0834 A72-18687

Ductility and fracture of heat resistant steels at high temperatures and unsteady loading, estimating loading cycle effect on plastic strain buildup to failure
07 p1017 A72-20127

Grain size and carbon content effects on recrystallized Mo wire ductility at room and low temperatures
11 p1657 A72-25758

VT22 high strength Ti alloy beta phase decomposition kinetics under heat treatment, noting omega and alpha phases formation effect on ductility
11 p1660 A72-26133

Ductile type fracture after heat treatment of VT3-1 Ti alloy with Al, Mo, Cr and Fe additives investigated by electron microscopy and tensile tests
11 p1660 A72-26135

High strength quenched steel with high ductility at cryogenic temperatures and negligible cooling rate effects on plasticity during welding
11 p1660 A72-26136

Fe effect on plasticity and ductility of dispersion hardened Ni alloys with various quantities of Nb and Ti at cryogenic temperature
11 p1660 A72-26137

Ductile fracture development in steel due to microcracks and pores formation
11 p1660 A72-26140

Ferritic stainless weld metal ductility, investigating yield and fracture stresses after heat treatment
11 p1661 A72-26494

Alpha Zr tensile properties tests noting strain aging effects on strain rate, work hardening and ductility anomalies
11 p1661 A72-26595

Creep tests for thermal preycling effect on time to failure and long term ductility of austenitic steel thin walled tubular samples
11 p1663 A72-26809

Grain boundary network of allotropic phase change for ductility enhancement in Fe-Ta alloys
11 p1668 A72-26941

Cyclic nonisothermal plastic deformation of ductile disk, verifying experimentally with turbine disk of heat resistant alloys
13 p2053 A72-28398

Ta alloys fusion weld ductility, discussing welding parameters, alloy components, interstitial impurities and weldment microstructure effects
15 p2244 A72-31775

High temperature strength and ductility study of hot working behavior of steels, using hot impact tension tests
16 p2406 A72-33316

Room temperature ductility of different types of molybdenum after differing annealing
18 p2698 A72-36155

German monograph - Improvement of the ductility characteristics of flash butt welding joints involving carbon steels by pulse normal annealing and hot heading in the welding machine
19 p2807 A72-37659

Phenomenology and engineering significance of creep recovery in heat resistant steels, stressing ductility and microstructural effects
19 p2816 A72-37707

The grain-size-dependences of the failure mode and ductility transition temperatures of melted chromium and tungsten.
20 p2935 A72-39139

Elevated temperature ductility minimum in Hastelloy alloy X.
20 p2938 A72-39304

Correlation of irradiation data using activation fluences and irradiation temperature.
21 p3083 A72-40763

Influence of the test temperature on the fracture energy of graphite
21 p3074 A72-41714

Elastic stiffness and ductility of refractory materials of long service life, noting creep diagrams and tensile strength
23 p3301 A72-43959

Dynamic fracture criteria for ductile and brittle metals.
23 p3354 A72-44260

Plastic flow around an expanding crack.
24 p3456 A72-44812

Ductility relationship to plasticity characteristics in cylindrical steel samples with short notch under tension
24 p3458 A72-44933

Boron and carbon contents effect on elastic properties strength and ductility of electron beam melted Mo-B alloys
24 p3414 A72-45381

Ductility and fracture of heat resistant steels at high temperatures and unsteady loading, estimating loading cycle effect on plastic strain buildup to failure
24 p3416 A72-45753

DUCTS
NT ACOUSTIC DUCTS
NT AIR DUCTS
Rectangular and triangular duct entrance region laminar flow pressure losses from velocity profiles and integral energy equation
04 p0512 A72-15194

Intercomponent complex annular ducts design for gas turbine engines
10 p1416 A72-23872

Path arrangement optimization method for fluid distribution network with separable and concave cost function, using simplex method in nonlinear programming
13 p2053 A72-28423

Hydraulic duct transfer function determination for prediction of liquid-fuel engine space launcher LF vibrations, investigating incompressible flow rate modulation by deformable walls
24 p3392 A72-45117

DUFFING DIFFERENTIAL EQUATION
Duffing type quasi-linear differential equation system, obtaining ultrasubharmonic resonance by small parameter and harmonic balance methods for comparison with analog computer solutions
01 p1011 A72-10034

Quasi-periodic solution of nonlinear differential system in case of resonance, concerning Duffing equation
05 p0682 A72-16120

Galerkin method for subharmonic solutions of Duffing differential equation, noting error estimation
14 p2126 A72-31102

Switching curves and lobesweeping in origin seeking time optimal control for Duffing oscillator, using Pontryagin maximum principle
19 p2777 A72-37373

Non-stationary random vibration of non-linear structures.
21 p3125 A72-41517

DUMMIES
Impact tests on anthropomorphic dummies for protection effectiveness evaluation of lap belt, Air Force shoulder harness-lap belt and airbag-lap belt restraints [AD-741530]
12 p1769 A72-27471

Human body or dummy mechanical impedance calculation by acceleration measurement at two point reference system with circular spring supporting mass
15 p2192 A72-32608

DUMPING
Transversely excited high pressure carbon dioxide laser cavity dumping with reproducible time delay between current excitation and gain-switched laser pulses
16 p2403 A72-33844

DUNGEYS WIND SHEAR MECHANISM
U WIND SHEAR
DUOPLASMATRONS
Duoplasmatron as negative hydrogen ion source to study geometrical and electrical parameters effects on beam and analyze composition, energy spectrum and emittance
10 p1518 A72-23963

DURABILITY
Soviet book on structural shape effects of machine parts on durability, covering production, gear transmissions shafts, axles, threaded joints, etc.
03 p0364 A72-13966

Composite materials durability and strength estimations, using reliability theory for failure rate characteristic
05 p0680 A72-15991

Titanium alloy durability under cyclic torsion in vacuum at various temperatures, investigating fatigue life and tensile strength
06 p0834 A72-18665

Aviation fuels and additives effect on steel endurance limit at room temperature
13 p1980 A72-29487

Chemical composition, powder particle size, porosity and heat treatment effects on sulfurized iron graphite cermets durability
13 p1984 A72-30118

Combined reliability and durability estimation for machines and devices under working conditions with the use of indicators of service life consumption
19 p2808 A72-38219

Composite materials durability and strength estimations, using reliability theory for failure rate characteristic
24 p3418 A72-45733

DURATION
U TIME
DUST
NT COSMIC DUST
NT INTERPLANETARY DUST
NT LUNAR DUST
NT METEOROID DUST CLOUDS
NT TERRESTRIAL DUST BELT
Dusty inlet air filtering in aircraft turbine engines, discussing engine operation, dust and filter characteristics
05 p0704 A72-16179

Martian dust storm depth determination from carbon dioxide absorption and abundance observation on Mars by earth based spectroscopy
06 p0890 A72-18348

Dust content effect on heat transfer in hypervelocity wind tunnels, discussing gas flow pattern distortion due to interaction with particles
08 p1253 A72-21453

Carbon dioxide and dust effect on Martian atmospheric temperatures from time dependent calculations
12 p1865 A72-27033

Air dust erosive damage to helicopter gas turbine engine parts, discussing inertial rotorless filtering systems
13 p2026 A72-28786

Dust influx into upper atmosphere above 30 km determined from laser radar measurement
16 p2386 A72-33610

Approximate determination of the change in the aerosol distribution spectrum in a Venturi coagulator tube
20 p2928 A72-40039

Steady flow past body fixed in uniform flow of dusty gas, obtaining velocity distribution
21 p2989 A72-40195

The effect of cloud scattering on the absorption of solar radiation by atmospheric dust.
22 p3201 A72-42512

Solar system thin disk form planet formation in equatorial plane from nebula dust component, discussing gravitational effects and mass increase rate
23 p3335 A72-43261

DUST COLLECTORS
Hot water ejector application to environmental control, considering noise suppression, air and gas purification and dust particles precipitation
10 p1460 A72-24491

Collection efficiency of conical and blunted axisymmetric power law bodies in hypersonic flight through dust clouds and of impact angle and velocity
15 p2180 A72-32580

DWARF STARS
NT SUBDWARF STARS
NT WHITE DWARF STARS
Diffuse reflection of point source /flare/ light emission for cold dwarf star semiinfinite plane parallel atmosphere, calculating polarization
02 p0285 A72-12831

Galactic disk component of diffuse X radiation from unresolved red dwarf flare stars
03 p0408 A72-12993

Spectrographic observation of hot OB subdwarf HD 149382
03 p0435 A72-13799

Stellar evolution in close binary systems, discussing post main sequence stage, hydrodynamical processes and dwarf binaries
03 p0437 A72-13868

F and early G dwarf stars atmospheric models and line data, deriving temperatures, abundances and gravities
04 p0577 A72-15282

F and G dwarf stars synthetic spectra and colors computation from chemical abundance, Doppler broadening velocity and damping constant
07 p1071 A72-19181

K3-M2 dwarf space motions in solar neighborhood analyzed for sun motion
07 p1073 A72-19347

Metal lines and dwarf stars study by photoelectric photometry based on narrow passbands
10 p1538 A72-24230

Sequential three color photometry of dwarf cepheid DY Pegasi, noting smooth color variation with phase
15 p2314 A72-32370

Kinematics of faint M stars near the north galactic pole, and the mass density in the solar neighbourhood.
19 p2855 A72-37341

H and K emission intensity and line width dependence on stars age and luminosity, discussing dwarf stars and giants
19 p2866 A72-38503

Non-thermal bremsstrahlung of fast electrons and flare of stars.
20 p2974 A72-39894

Radiation pressure supported stars, degenerate dwarfs, neutron stars and black holes high energy observations from space platforms 24 p3446 A72-45536

DYADICS

Dyadic Green functions for cylindrical circular or rectangular waveguides with moving isotropic homogeneous media 10 p1440 A72-25046
Dyadic correlation function method for structured radar signal sidelobe suppression during reception, noting Walsh function role 21 p3020 A72-40901

DYES

Laser pumped organic dye laser frequency-time characteristics, noting noncoincidence of amplification and photon density maxima 02 p0238 A72-12118
Dye penetrant surface defect indications on 2014-T6 Al gas metal arc weldments heat affected zone, considering minimization by arc stabilization and caustic etch time reduction 02 p0236 A72-12775
Tunable multiple wavelength organic dye laser using optical feedback through partially transparent mirrors 03 p0367 A72-13443
Passively mode locked Rhodamine 6G dye laser, obtaining frequency tuning with intracavity Fabry-Perot filter and transform limited duration picosecond pulses 03 p0368 A72-13605
Superradiative properties of high gain flashlamp-pumped dye laser amplifier, determining small signal amplification as function of pumping power and frequency 03 p0369 A72-14393
Emission spectrum and intensity variation of organic dye solutions excited by nitrogen laser pulsed radiation 04 p0529 A72-14655
Dye laser monochromatic coherent light wavelength tuning with minimized optical cavity degradation and without external optics 04 p0531 A72-15502
Organic dye lasers radiation nonlinear interaction with alkali metals spark discharge plasma, showing angular and spectral broadening 04 p0532 A72-15573
Rhodamine 6G dye laser tuning by variable birefringence filter using lead lanthanum zirconate titanate electrooptic ceramics for wavelength selection 07 p1002 A72-19203
Flashlamp pumped dye-doped polymethyl methacrylate laser thermal and photochemical effects decrease and peak power output increase by light converter 07 p1002 A72-19206
Transient gain measurements on laser dyes of flashlamp pumped rhodamine 6G-ethanol solutions with air and nitrogen 07 p1002 A72-19208
Dye laser system with narrow linewidth oscillator, transverse mode selector, power amplifier and nitrogen pumping, noting 50 kw and 5 nsec pulse generation capability 07 p1002 A72-19209
Pulsed dye lasers logarithmic detector circuit with two ultrafast photodiodes, eliminating intensity variations problem 07 p1005 A72-19415
Repetitive dye laser with monochromatic beam of tunable wavelength, noting spectroscopic applications 07 p1009 A72-20588
Optimum lasing conditions and spectral characteristics of organic dye lasers at 3,100-11,000 Å 07 p1009 A72-20613
Wavelength tunable dye laser pumped by dual pulse lamps with Fabry-Perot interferometer in resonator 07 p1009 A72-20614
Organic dyes molecular photodecay effect on output and power losses of laser activated by flash pump white light 08 p1184 A72-22029
Rhodium solution laser emission pulse characteristics relation to pumping energy distribution over container end surface 08 p1184 A72-22048
Absorption spectra and detection sensitivity enhancement by organic dye laser quenching with broadband cavity 09 p1323 A72-22601
Tunable dye laser system with narrow band filter for Raman spectroscopy of gases 09 p1326 A72-23351
Fast coaxial flash lamp pumped liquid dye laser /I.D.I./ for photolysis and biophysical and biochemical applications 09 p1326 A72-23406
Experimentally produced vortex ring structure and stability, using dye and hydrogen bubble techniques for flow field, ring velocity and growth rate observations 10 p1466 A72-24327

Laser emission in near IR by flash lamp pumped fluorescent dyes, presenting oscillograms 11 p1651 A72-26505
Thin polymer film bleachable dye switches for Q switched laser to achieve high power single pulse radiation 12 p1822 A72-27612
Quasi-stationary supersonic plasma flare generation by lamp-pumped rhodamine laser, studying shock wave structure by high speed cinematography 12 p1825 A72-27882
Organic dye desensitization of bleached AgBr phase holograms against printout darkening by Ar ion laser light 12 p1811 A72-27949
Plasma spectral absorption coefficients determination by organic dye laser with tunable radiation frequency 13 p2015 A72-29504
Energy conversion efficiency of xanthene dye laser pumped by mode-locked Nd-glass laser second harmonic, discussing effect of excited molecules transition to triplet state 13 p1970 A72-29686
Superradiant laser emission from organic dyes rhodamine 6G and B with coaxial flashlamp pumping source, relating input threshold energy to dye concentration 13 p1971 A72-29864
Wide tuning range organic dye laser design, using nitrogen laser line as transverse pumping source 13 p1971 A72-29869
Xenon filled coaxial pulse tube for pumping organic dye solutions, obtaining intensive light flashes 13 p1971 A72-29923
Small spectral width emission from dye laser with interference filter and quartz plate Fabry-Perot interferometer for spectroscopic investigations 14 p2110 A72-30674
Flashlamp pumped tunable narrowband traveling wave dye ring laser, stabilizing emission frequency by intracavity Fabry-Perot etalon 14 p2110 A72-30675
Electrical pumping discharge confined by liquid wall of vortex channel in dye laser solution 15 p2251 A72-32528
Short flash characteristics of spiral pumping lamp for dye laser 16 p2400 A72-33079
Surface crack detection in ferrous and nonferrous metals, glass, ceramics and plastics by water-washable dye penetrants process 16 p2397 A72-33239
Rhodamine 6G photodegradation resistance improvement in cooled solid matrices of polymethylmethacrylate, investigating time and temperature dependence of bleaching by linearly polarized lasers 16 p2401 A72-33386
Wavelength tunable UV dye laser pumped by the fourth harmonic of Nd:YAG laser. 19 p2810 A72-37407
Continuously tunable dye laser to obtain output wavelength variation by changing pump laser beam incidence angle on prism lateral face 20 p2933 A72-39563
Energy absorption mechanisms of thin film optical waveguide surface in contact with low index dyes 21 p3050 A72-40147
Transition metal complex organic dye solution for Nd-glass laser Q-switching and mode locking, noting high photochemical stability 21 p3062 A72-40244
Pulsed monochromatic laser with toluene, xylene, ethanol, isomyl alcohol and dimethylformamide solutions of organic dyes, discussing wavelength variations and power outputs 21 p3064 A72-41736
Optical elements of a laser-pumped dye laser 21 p3064 A72-41737
Wavelength tuning of an intracavity pumped CW mode-locked dye laser. 22 p3184 A72-41989
Deposition of finishes and dyes in materials dried using microwave heating. 22 p3183 A72-42480
A new optical PCM communication system 22 p3186 A72-42939
Use of light transformers in organic dye lasers 23 p3295 A72-43413
Evanescent-field-pumped dye laser. 23 p3296 A72-43816
Ultrasensitive response of a CW dye laser to selective extinction. 23 p3297 A72-44186
Fluorescent organic dyes solutions for Nd:YAG laser output performance improvement 23 p3297 A72-44191
Flashlamp-pumped dye lasers for investigations of the upper atmosphere. 24 p3409 A72-44948

DYNAMIC CHARACTERISTICS

NT AERODYNAMIC DRAG
NT AERODYNAMIC STABILITY
NT AIRCRAFT STABILITY
NT ATTITUDE STABILITY

NT BOUNDARY LAYER STABILITY
NT COMBUSTION STABILITY
NT CONTROL STABILITY
NT DIRECTIONAL STABILITY
NT DRAG
NT DYNAMIC PRESSURE
NT DYNAMIC STABILITY
NT FLAME STABILITY
NT FLOW CHARACTERISTICS
NT FLOW DISTRIBUTION
NT FLOW STABILITY
NT FLOW VELOCITY
NT FREQUENCY STABILITY
NT FRICTION DRAG
NT GYROSCOPIC STABILITY
NT HOVERING STABILITY
NT INTERFERENCE DRAG
NT INTERFERENCE LIFT
NT JET LIFT
NT LATERAL STABILITY
NT LIFT
NT LONGITUDINAL STABILITY
NT MAGNETOHYDRODYNAMIC STABILITY
NT MINIMUM DRAG
NT MOTION STABILITY
NT PRESSURE DRAG
NT ROTARY STABILITY
NT ROTOR LIFT
NT SATELLITE DRAG
NT SPACECRAFT STABILITY
NT SUPERSONIC DRAG
NT TRANSIENT RESPONSE
NT VISCOS DRAG
NT WAVE DRAG
NT ZERO LIFT
Dynamical behavior classification for three bodies moving in plane under mutual gravitational influence 01 p0123 A72-10015
Nighttime ionosphere dynamical behavior, discussing motions effect on OI emission intensity 01 p0063 A72-10919
Coaxial flow gaseous core nuclear reactor system dynamic analysis, developing mathematical model and equations solution by computer program 01 p0100 A72-11352
Nonautonomous systems periodic solutions through Liapunov functions construction, considering application to nth-order dynamic systems forced oscillations 02 p0251 A72-11498
Dynamic characteristics of turbomotor simulator supported on gas lubricated foil bearings of reduced length with starting and stopping unaided by external pressurization 02 p0235 A72-11538
Human operator dynamic characteristics measurement, using pseudorandom binary signals and mathematical models in closed loop control system 02 p0169 A72-12660
Sound reflection by dense doubly periodic grating parallel to rigid baffle, describing asymptotic characteristics by double lattice virtual mass including mirror image 03 p0387 A72-12914
Neighboring optimal feedback control for multiinput nonlinear dynamical systems with discontinuous control, applying to minimum time satellite attitude acquisition problem solution 03 p0338 A72-13407
Dynamic damping coefficient extraction from reentry vehicle flight test telemetered lateral rate data 03 p0441 A72-13951
Logic networks with hydraulic elements, considering dynamic qualities of hydraulic transmission system 03 p0312 A72-13965
Soviet book on gyroscopic systems and inertial guidance instruments, emphasizing system motion under various dynamic conditions and systematic errors 03 p0362 A72-14167
Thin walled elastic axisymmetric fluid filled tanks under longitudinal vibrations, determining dynamic characteristics 04 p0586 A72-15011
Dynamic negative differential conductivity in bulk semiconductors, analyzing relation to impulse responses 04 p0562 A72-15129
Dynamic analysis of vertical rotor rotating in elastic sliding bearings, analyzing precession stability and self oscillation zone 04 p0594 A72-15748
Dynamic characteristics of buoyant low altitude clouds formed by solid rocket motor launches, determining initial temperature by motion pictures combined with conservation equations [ASME PAPER 71-WA/FE-33] 05 p0724 A72-15923
Stationary nonlinear dynamic systems identification, using modified differential approximation technique [ASME PAPER 71-WA/AUT-11] 05 p0682 A72-15955
Probabilistic output analysis of dynamic nonlinear system with random characteristics by functional Volterra series 05 p0641 A72-16315

Silicate glasses fatigue in dynamic and static tests, discussing fracture stress dependence on time of loading 05 p0681 A72-16422

Nonlinear control systems of vehicles angular orientation, investigating dynamic properties by method of harmonic linearization 05 p0727 A72-16474

Approximations and bifurcations in flight dynamic system, investigating singular point motion over trajectory during partition process 05 p0611 A72-16582

Jet flap type exhaust flows acoustic and fluid dynamic characteristics, measuring sound power output and noise spectra for various configurations [AIAA PAPER 72-130] 05 p0608 A72-16920

Optimal design of dynamic system with universality for series of maneuvers with various degrees of informativeness, considering flight mechanics of limited power engine system 06 p0848 A72-18299

Dynamic system optimal design with various degrees of maneuver parameters information, considering space flight mechanics problem of payload maximization for limited propulsive power 06 p0849 A72-18306

Dynamic properties of turbine wheels under bending vibrations, classifying resonant frequencies on basis of vibration modes 06 p0899 A72-18644

Gas turbine blades dynamics characteristics determination, investigating vibrational stresses, thermal cycles, alloy physicomechanical properties and coatings effects 06 p0900 A72-18683

Artificial biped locomotion dynamic equilibrium, representing mathematical model by two nonlinear differential equations with variable coefficients 06 p0769 A72-18703

Amplifier amplitude characteristic nonlinearity effect on dynamic properties of autooscillatory temperature controller 07 p0981 A72-18926

Dynamic behavior of stiffened hollow viscoelastic cylinder and elastic shell-contained sphere, taking into account compressibility and internal pressure 07 p1090 A72-19751

Nonlinear computerized simulation of air cushion vehicle dynamics, using bond graph techniques 07 p0913 A72-20343

Sliding bearing structural features and materials effects on running and friction behavior at contact surface 07 p0998 A72-20524

Closed type gas turbines heated with nuclear energy, calculating heat transmitter dynamic behavior with computer program 07 p1055 A72-20598

Air flow turbulent behavior and dynamic characteristics dependence on underlying surface roughness variations 07 p1031 A72-20695

Dynamic characteristics and nonlinear oscillations of liquid in spherical shell of revolution, modifying Lukovskii approximation method 08 p1148 A72-20962

Dynamic characteristics of strongly damped pendulum, assessing vibrations effects on vertical determination accuracy 08 p1206 A72-20974

Soviet handbook on vibration absorbing properties of construction materials under cyclic straining, covering energy dissipation and dynamic strength 08 p1185 A72-20975

Dynamic equivalence between vehicles with motor-driven constant speed rotor under bearing friction and freely spinning torque free rotor, deriving equations of motion 08 p1108 A72-21174

All-moving tail plane parameters influence on glider static and dynamic characteristics, discussing lateral and longitudinal stability, maneuverability and pilot induced oscillations 08 p1110 A72-21632

Minimal dynamic systems invariant Borel probabilistic measure with metric space and topological entropy equality 08 p1210 A72-22187

Hydraulic amplification of electric step motor torque, discussing system dynamic characteristics 09 p1263 A72-22689

Finite difference analysis of dynamic deformation of thin elastoplastic shells of revolution under intense heating 09 p1401 A72-22728

Quasi-harmonic vibrations of dynamic system with arbitrary number of degrees of freedom and finite number of discrete nonlinearities, using Van der Pol method 09 p1352 A72-23178

Nonlinear dynamic motion response analysis of flight vehicles typified by continuously changing vibration damping and frequency 09 p1262 A72-23452

Zaidenberg correlation method for nonlinear systems dynamic properties under random excitation, determining statistically equivalent linearized terms for equations of motion 09 p1353 A72-23607

Statics, motion equations, deformation, dynamics and classification of Cosserat continua 10 p1513 A72-25000

Static and dynamic analysis of legged planetary instrument landers, taking into account structural flexibility, elastic-plastic gear load characteristics and soil properties [AIAA PAPER 72-371] 11 p1725 A72-25396

Helicopter rotor blades bending vibrations, examining scale effects, dynamic similarity and natural frequencies via series of Legendre polynomials [AD-745569] 11 p1734 A72-25733

Probabilistic output analysis of dynamic nonlinear system with random characteristics by functional Volterra series 11 p1610 A72-25798

Mathematical model for dynamic yield point dependence in strain rate based on similarity and dimensionality theories and Weierstrass theorem 13 p2054 A72-28458

Digital dynamics simulation of continuous controlled processes based on repeated integral transformation of differential equations 13 p1934 A72-28607

Fourier transforms for linear systems transient time and frequency characteristics, using discrete functional values for initial information 13 p1985 A72-28675

Analog dynamic model of tracked air cushion vehicle for high speed ground transportation systems 13 p1896 A72-28704

Concorde dynamic behavior from flight tests, discussing integrated design effects, wing, fin and elevator flutter, gust and runway response and engine surge effects [AIAA PAPER 72-381] 13 p1897 A72-28958

Hydraulic test facility for dynamic characteristics of potentiometric pressure sensors with connecting lines of various geometries, shaping pressure pulse signal by electromagnetic valve 13 p1957 A72-29135

Turboprop engines dynamic parameters experimental determination by rpm transient response to instantaneous fuel supply changes 13 p2027 A72-29137

Optimal design of dynamic system with universality for series of maneuvers with various degrees of informativeness, considering flight mechanics of limited power engine system 13 p2052 A72-29439

Dynamic behavior of thin walled semiinfinite elastic cylindrical shell with liquid under axial impact loads 13 p1943 A72-30008

Steady motion of dense electron beam in rarefied phonon plasma along magnetic field, analyzing polarization effects 14 p2136 A72-30305

Dynamic behavior of long-period oscillations of surface wave type in system of inhomogeneous ion beams moving in dense plasma along magnetic field 14 p2136 A72-30307

Adaptive radiometer dynamic properties and parameters optimization based on minimum mean square error criterion 14 p2088 A72-30373

Single degree of freedom nonlinear mechanical system vibration characteristics calculation by averaging procedure, taking into account energy dissipation 16 p2424 A72-33279

The controllable twist rotor performance and blade dynamics. [AHS PREPRINT 614] 17 p2488 A72-34483

Hingeless rotor - Experimental frequency response and dynamic characteristics with hub moment feedback controls. [AHS PREPRINT 612] 17 p2489 A72-34494

Reactor core length, externally configured thermionic converter. 17 p2495 A72-34589

The dynamic stress-strain behavior in torsion of 1100-O aluminum subjected to a sharp increase in strain rate. [ASME PAPER 72-APM-6] 17 p2629 A72-34808

Investigation of the damping features of a pressure regulator 17 p2559 A72-34916

Dynamic characteristics of electrical measuring instruments and transducers, discussing static calibration curve, dynamic tests and parameters determination 17 p2557 A72-35757

Stability of the dynamic parameters of a transistor in a small signal mode superimposed on a static injection mode 17 p2596 A72-35801

Approximations yielding closed equations for isotropic turbulence compared to laboratory and computer experiments, emphasizing Langevin type model equation for velocity 18 p2677 A72-36008

Unbalanced shafts vibration and stability characteristics, considering elastic and damping properties of sliding bearings oil films 18 p2731 A72-36069

Dynamics and control of an incore-thermionic-reactor in the power region. 18 p2644 A72-36174

The dynamic characteristics of clamped rectangular plates of orthotropic material. 18 p2737 A72-37067

Experimental determination of viscoelastic characteristics 18 p2740 A72-37211

Generalized dynamic systems and process prediction 19 p2833 A72-37378

Complex systems dynamics and stability problems, deriving equations of motion and boundary conditions from principle of least action 19 p2784 A72-37388

French monograph - Linear estimation of the parameters of multidimensional dynamic systems and statistical validation of the model - Applications to process identification 19 p2778 A72-37486

Approximations and bifurcations in flight dynamic system, investigating singular point motion over trajectory during partition process 19 p2748 A72-37553

The output control of linear time-invariant multivariable systems with unmeasurable arbitrary disturbances. 19 p2779 A72-38231

Liapunov theory application to stability analysis of large scale dynamic systems, developing methods for vector Liapunov functions construction 19 p2781 A72-38262

Dynamic behavior of nonlinear power amplifiers in stable and injection-locked modes. 19 p2773 A72-38293

Measurement transducers in industrial process control, discussing requirements for dynamic properties, stability, linearity and computer applications 19 p2803 A72-38315

Experimental technique for determination of roller bearing preload to optimize dynamic characteristics and minimize operating temperature 19 p2810 A72-38650

Hamiltonian approach to the dynamics of expanding homogeneous universes in the Brans-Dicke cosmology. 19 p2869 A72-38807

The study on dynamical behavior of fiberglass reinforced plastics (FRP) by dynamical mechanical model. 20 p2943 A72-38887

Atmospheric flow turbulent behavior and dynamic characteristics dependence on underlying surface roughness variations 20 p2948 A72-39010

Dynamic models for hydraulic machine parts, discussing resonant properties of one degree of freedom system and dynamic characteristics of nonlinear parametric systems 20 p2953 A72-39421

Dynamic characteristics of composite laminates. 20 p2979 A72-39558

Dynamic characteristics of hot-wire anemometers with glass-coated thermistors 21 p3050 A72-40132

F-111A inlet nozzle dynamic distortion diagnostics for airframe-propulsion integration based on flight and transonic wind tunnel tests [ICAS PAPER 72-18] 21 p2991 A72-41143

Ground and torque relation to swivel angle and lateral displacement of wheel rim plane, using string model for tire 21 p2996 A72-41260

Entropy criterion in the estimation of the dynamic quality of automatic control systems 21 p3039 A72-41803

A form of the translational dynamical equations for relative motion in systems of many non-rigid bodies. 22 p3205 A72-42113

Dynamic characteristics, stability and steady state accuracy for orbital gyroscope with digital control, noting bit density requirements of onboard computer. 22 p3202 A72-42207

Dynamic behavior of thin walled semiinfinite elastic cylindrical shell with compressible liquid under axial impact loads 22 p3167 A72-42736

The dynamic viscoelastic properties of some non-crystalline metals. 22 p3214 A72-42792

Dynamic aspects of Fokker F-28 aircraft design. 22 p3138 A72-42831

Simple analyses for the non-symmetric dynamic expansion of cylindrical cavities. 22 p3240 A72-42893

Dynamic behavior of M-4S rocket devices for strap-on booster separation and nose cone and flare deployment 22 p3232 A72-43143

Steady motion of dense electron beam in rarefied phonon plasma along magnetic field, analyzing polarization effects 23 p3317 A72-43207

Dynamic behavior of long-period oscillations of surface wave type in system of inhomogeneous ion beams moving in dense plasma along magnetic field 23 p3317 A72-43209

Inverse problems of the dynamics of a ponderous solid with one fixed point 23 p3312 A72-43219

Rotating aerospace vehicles dynamic balance error terms due to despin masses misalignment and aerodynamic effects [SAWE PAPER 930] 23 p3342 A72-43470

Analytical design of adaptive systems with stabilized dynamic characteristics 23 p3276 A72-43783

Amplitude-phase-frequency characteristics of a high-rpm centrifugal pump 23 p3294 A72-44021

Investigation of the dynamic characteristics of the speed governor of a hydropneumatic feed drive 23 p3253 A72-44022

DYNAMIC CONTROL

Reachable sets calculation for linear dynamical system control, suggesting iterative procedures for numerical approximations 01 p0034 A72-11124

Noninteracting decoupling control theory for linear constant multivariable systems, using dynamic feedback matrix compensators 02 p0198 A72-12802

Large linear time invariant dynamic control system optimum simplified model based on performance index connecting feedback errors 04 p0506 A72-15113

Stability-instability criterion of time varying linear systems, using canonical form of differential equations [ASME PAPER 71-WA/AUT-20] 05 p0682 A72-15953

Optimal dynamic system design for maneuvers with complete statistical information applied to limited power space flight 05 p0641 A72-16313

Fixed level intersection by two stationary ergodic independent random processes in observation time for dynamic control sampling and reliability estimation 05 p0641 A72-16316

Linear dynamic control system identification by local impulse response approximation, comparing with Goodman-Reswick model 05 p0641 A72-16319

Optimal allocation and guidance for linear time varying interception and rendezvous problems of dynamic deterministic or stochastic systems 05 p0686 A72-16558

Generalized matrix inverse application to dynamic system state vector estimation, determining covariance matrix for comparison with optimal Kalman type procedure 05 p0641 A72-17089

German book on time variable multiparameter control systems covering reduction, canonical forms, decoupling, feedback stabilization, observers, inversion and multiloop synthesis 06 p0794 A72-18517

Axiomatic determination of dynamic logic control systems based on Moore automaton elements and combined continuous and finite models 06 p0781 A72-18660

Numerical algorithm for Galerkin solutions of nonlinear ordinary differential equations in dynamic system applications 07 p1025 A72-18785

Dynamic control system parameters optimization for series of maneuvers under different degrees of informability 07 p0959 A72-19652

Linear dynamic control systems controllability and observability quality analysis and optimization, considering determinant, trace and maximal eigenvalue 07 p0960 A72-19699

Control theory of dynamic multiconnected systems with differential operators, time lags and hereditary components 07 p0962 A72-19721

Krylov-Bogoliubov asymptotic method for oscillation analysis in time lag systems under pulse inputs 08 p1206 A72-20970

Deviation accumulation conditions and maximum dynamic error of linear automatic control system under perturbation, including theorem for Bellman equation 08 p1146 A72-22177

Angular rigidity of support shaft elastic suspension of dynamically adjustable gyroscopes 09 p1307 A72-22348

Discrete and continuous dynamic adaptation algorithms construction for extremal quality functional trajectory equations of adaptive control system 09 p1283 A72-23435

Optimal estimates for nonlinear dynamic systems with time delay, using calculus of variations 10 p1454 A72-23784

Minimax feedback control of uncertain discrete time dynamic systems with set description, using dynamic programming 10 p1456 A72-23806

Dynamic logic control systems theory based on axiomatic concepts of models, deriving conditions for existence and uniqueness of solution for differential logic equations 10 p1457 A72-24636

Linear dynamic control system identification by local impulse response approximation, comparing with Goodman-Reswick model 10 p1458 A72-25073

Optimality conditions for dynamic control systems, considering multidimensional singular controls and state space transformations 11 p1608 A72-25324

Optimal dynamic system design for maneuvers with complete statistical information applied to limited power space flight 11 p1610 A72-25796

Fixed level intersection by two stationary ergodic independent random processes in observation time for dynamic control sampling and reliability estimation 11 p1610 A72-25799

Book on sensitivity theory covering continuous and sampled data systems, linear, nonlinear and self exciting dynamic systems, optimal systems, large systems, controllability, etc 11 p1611 A72-26021

Optimizing functional for combined control of dynamic control plant, synthesizing stabilization system for maximal transient damping 13 p1935 A72-28713

Dynamic control stability on given time interval, using Liapunov-like functions and integral manifolds in quadratic forms 13 p2004 A72-29471

Control design for dynamic /vibratory/ loading of high speed rotating machinery, discussing rotor, bearing span and support stiffness and coupling centering [ASME PAPER 72-DE-39] 14 p2167 A72-30872

Dynamic motion analysis of digital servo system with proportional bang-bang control by trajectory mapping on phase plane 15 p2211 A72-31895

Parameter estimation in dynamic biological control systems based on multicompartmental input-output behavior 15 p2192 A72-32766

Automatic systems design for monitoring dynamic control systems, noting feedback control system performance prediction based on subsystems characteristics 16 p2371 A72-33085

Uniaxial gyrostabilizer dynamic control system based on degenerate equations neglecting small time constant terms 16 p2421 A72-33961

Rotating body linear dynamic control by complex transfer function approach with application to stability conditions for controlled gyro and homing missiles 17 p2583 A72-35528

Closed loop dynamics of in-core thermionic reactor systems 18 p2644 A72-36173

Design of model-reference adaptive control systems using Liapunov functions 18 p2672 A72-36326

Hill-climbing controller for plants with any dynamics and rapid drifts 18 p2673 A72-36819

Experimental investigation of an astronaut maneuvering scheme 18 p2655 A72-37026

Astroelasticity in design and analysis of flexible space vehicles, presenting dynamics and control considerations 18 p2738 A72-37082

Optimal avoidance control to transfer dynamic system from initial to terminal state in maxmin distance problem [ASME PAPER 72-AUT-D] 19 p2778 A72-37724

Variational method in the control system invariance problem 19 p2778 A72-37990

Optimization of control and observation processes in a dynamic system at random disturbances 19 p2778 A72-37991

Dynamic programming technique for simultaneous measurement and dynamic control optimization for stochastic systems 19 p2779 A72-38233

Transfer-characterization and the unique realization of linear time-invariant multivariable systems 19 p2780 A72-38238

Discrete and continuous dynamic adaptation algorithms construction for extremal quality functional trajectory equations of adaptive control system 19 p2770 A72-38518

Nonautonomous phase system of equations with a small parameter, containing invariant tori and rough homoclinic curves 19 p2828 A72-38579

Trajectory synthesis of optimal control 21 p3037 A72-40704

Optimizing functional for combined control of dynamic control plant, synthesizing stabilization system for maximal transient damping 22 p3162 A72-42091

Linear dynamic control system synthesis methods based on aggregation and suboptimal control by decomposition, considering quadratic performance criterion 22 p3162 A72-42177

An application of the theory of Lie groups in the optimal control problem for linear dynamic systems with time-variable coefficients 22 p3162 A72-42181

Variational method for invariance problem solution for optimal finite state of nonlinear dynamic systems under external disturbances 22 p3162 A72-42240

Optimal random disturbance intensity control of dynamic systems, minimizing error with respect to observed and controlled plant coordinates 23 p3274 A72-43221

Infinite-time reachability of state-space regions by using feedback control 23 p3274 A72-43538

Decision surface estimate of nonlinear system stability domain by Lie series method 23 p3274 A72-43540

On discrete linear time-invariant systems with singular transition matrix 23 p3275 A72-43545

The dynamics and control of Eulerian turbomachines. [ASME PAPER 72-AUT-S] 23 p3279 A72-43633

Optimal minimax regulation of a dynamic system 23 p3276 A72-43860

Differential pursuit games with nonlinear evading player and linear pursuer, considering determination of initial states 23 p3277 A72-44001

The inverse problem of optimal process theory and the synthesis of linear optimal systems in the case of restricted phase coordinates 23 p3277 A72-44008

Parametric optimization of the equivalent transfer function of a system with the aid of the error integral 24 p3387 A72-45700

DYNAMIC LOADS

NT AERODYNAMIC LOADS

NT BLAST LOADS

NT CYCLIC LOADS

NT GUST LOADS

NT IMPACT LOADS

NT LANDING LOADS

NT ROLLING CONTACT LOADS

NT SHOCK LOADS

NT THRUST LOADS

NT TRANSIENT LOADS

NT VIBRATORY LOADS

NT WING LOADING

Numerical method for wave propagation and dynamic stresses in viscoelastic cylinders under internal and external loads 01 p0144 A72-11375

Creep strength analysis of heat resistant alloys under repeated unsteady loads 01 p0144 A72-11376

Static and dynamic load measurements for stress-strain behavior and load-time characteristics of aerodynamic decelerator canopy fabrics, using metal foil strain gages 02 p0287 A72-11507

Moving load effect on circular cylindrical shell in acoustic medium, discussing free axisymmetric vibration mode, shape and frequencies 02 p0290 A72-11627

Beams and plates resting on elastic base with loads moving along line or strip, calculating wave processes based on half space dynamic model 02 p0290 A72-11629

Static and dynamic buckling behavior of clamped shallow conical shells under axisymmetric loads 02 p0291 A72-11963

Dynamic and plastic behavior of mild steel and Al wide beams and rectangular flat plates 02 p0291 A72-11964

Low impulsive loading effect on strength creep resistance of polycrystalline Al at elevated temperatures 02 p0243 A72-12011

Straight beams and rectangular frames stress-strain calculation under pulsed loading, taking into account shock waves finite propagation velocity and internal damping 02 p0300 A72-12855

One dimensional heat insulated structure under dynamic loads, showing thermoviscoelastic effects on spontaneous heating and stress-strain state 03 p0444 A72-13460

Gear transmission systems statistical characteristics under dynamic loads, noting normal Gaussian curve for operating conditions

04 p0585 A72-14614

Minimum weight design of perfectly plastic continuous sandwich beams with two equal spans for movable loads

04 p0593 A72-15647

Dynamic overstressing and annealing effects on fatigue life of convoluted metal bellows, using dynamic model and strain gage measurements

05 p0742 A72-17245

Similarity solution for nonlinear viscoplastic semi-infinite rod under constant velocity impact

07 p1088 A72-19115

Dynamic buckling of elastic shallow structures under periodic loading, determining critical load upper and lower bounds by energy method

07 p1090 A72-19731

Bounds for impulsively loaded plastic structures, considering fixed end beam with uniform velocity distribution

07 p1093 A72-19947

Failure analysis probability for structures excited by randomly varying dynamic loads, comparing Gaussian and filtered Poisson processes

07 p1093 A72-19948

Critique of paper on lower bounds on deformations of dynamically loaded rigid plastic continua

08 p1245 A72-21630

Impurities and temperature effects on microdeformation of Mo single crystals under dynamic loads

08 p1188 A72-21789

Dynamic radial vibrations and stresses in thick circular annulus of nonisotropic elastic material, using Hankel transform

08 p1246 A72-21793

Dynamic buckling of shallow circular cylindrical hinged panel under axial compression

08 p1249 A72-22087

Dynamic buckling and plate to shell transition of thick spherical caps under large amplitude axisymmetric flexural vibrations

08 p1249 A72-22135

Discrete model of dynamic forces between teeth of single stage transmission with parallel gear axes

09 p1404 A72-22772

Continuously supported railroad track under axial compression forces and moving load, noting critical velocity for high speed trains

09 p1409 A72-23558

Dynamic shear modulus and damping of polystyrene composites filled with glass, salt and foam, including skin effect correction

10 p1500 A72-24260

Viscoelasticity analysis of bending displacements in thin welded closed cylindrical shell loaded by moving moment

11 p1739 A72-26920

Natural and associated transverse vibrations of elastic beam under uniformly distributed moving load

12 p1879 A72-27092

Dynamics snap-through instability existence conditions in nonlinear plane deformation of shallow circular cylindrical elastic shell under impulsive loading

12 p1880 A72-27241

Elastic truncated thin conical shell response to dynamically applied axial force from numerical solution of nonlinear equations

12 p1881 A72-27244

Closed thin circular cylindrical shells external pressure pulse and structural parameters effects on stability under dynamic loading

12 p1886 A72-28129

Surface finishing effects on steel sensitivity to stress concentration under variable loads, emphasizing diamond smoothing and roller technique

12 p1831 A72-28246

Optimal design of elastic structures, emphasizing stability and response under applied static and dynamic loads

13 p2054 A72-28487

Shallow spherical shells axisymmetric vibrations under time varying loads, discussing transverse shear and rotatory inertia effects in terms of Fourier-Bessel series

13 p2056 A72-28880

Unsteady loading effects in high temperature fatigue tests of refractory alloys for turbine blades, noting steady and programmed notch tests

13 p1980 A72-29494

Minimum weight elastic structure designs under dynamic loads with constraints on stress displacements and natural oscillation frequencies

13 p2062 A72-30009

Atmospheric turbulent characteristics and velocity longitudinal component intensity profiles, applying to dynamic wind loads computation

14 p2127 A72-30264

Refractory material blade alloys fatigue life up to 950 C under nonstationary loading, noting log-normal law distribution

14 p2116 A72-30428

Flat Ti alloy sheet creep under variable loads at 300-400 C, comparing prediction with test data

14 p2116 A72-30434

Equations of motion and free vibration for trusswork structures under nonperiodic dynamic loads, calculating longitudinal and transverse end forces

15 p2322 A72-31360

Dynamic input to cargo in turbojet aircraft studied during C141 and C5A flights, discussing instrumentation, test procedures, data reduction processes and results

15 p2181 A72-32625

Rotating shaft bending vibrations under harmonically varying transverse load and periodic parametrically exciting axial force, using linearized theory of small displacements

16 p2463 A72-32877

Elastic-viscoplastic solution for deformation of impulsively loaded strain rate sensitive steel rings

16 p2464 A72-32916

Dynamic load tests for impact strength of ceramic composites with fiber reinforced alumina matrix, obtaining dynamic stress-strain curves

16 p2414 A72-33300

Elastic-plastic systems under dynamic loadings, discussing compounded shakedown load solution by zero work and direct search methods

[ASME PAPER 71-APMW-27]

17 p2624 A72-34309

Response of a ring-reinforced cylindrical shell, immersed in a fluid medium, to an axisymmetric step pulse

[ASME PAPER 72-APM-8]

17 p2624 A72-34314

Stability of a beam on an elastic foundation subjected to a follower force

17 p2626 A72-34331

Dynamic buckling of shallow circular cylindrical hinged panel under axial compression

17 p2626 A72-34665

Dynamically loaded elastic, viscous, plastic and rigid, viscoplastic structures instantaneous mode responses definitions and characterization by variational criteria with isometric constraints

[ASME PAPER 72-APM-17]

17 p2628 A72-34799

On the transient response of a closed spherical shell to a local radial impulse

18 p2739 A72-37089

Investigation of the snap-through of rigidly clamped shallow spherical shells under the action of a dynamic stepped load

19 p2877 A72-38163

Computer solution of dynamic problems for bending of beams and thin plates beyond the elastic limit under alternating loads

19 p2877 A72-38194

Effect of the structure of carbon steels on their dynamic properties during dynamic loading

21 p3067 A72-40923

A quadratic programming approach to the impulsive loading analysis of rigid plastic structures

21 p3120 A72-41205

Behavior of viscoelastic shallow spherical shells subjected to dynamic pressure

21 p3122 A72-41245

On the collision of a cold elastic plate with a hot elastoplastic plate

21 p3124 A72-41482

Elastic wave energy absorption in structures under dynamic loads, noting fatigue fracturing decrease with energy transfer into damping medium

21 p3126 A72-41540

Buckling of plates and cylindrical panels under the action of axial dynamic compression

22 p2332 A72-41923

Extremum principles for a class of dynamic rigid-plastic problems

22 p2325 A72-42522

On the formation of plastic adiabatic bands in a thin tube subjected to a dynamic torsion

22 p2326 A72-42638

Minimum weight elastic structure designs under dynamic loads with nonlinear constraints on stress displacements and natural oscillation frequencies

22 p2326 A72-42737

The dynamic plastic behavior of shells

22 p2326 A72-42756

Peak load-impulse characterization of critical pulse loads in structural dynamics

22 p2326 A72-42757

Impulsive loading in structural plasticity, obtaining displacement bounds via deformation theory based on extremum paths

22 p2327 A72-42759

Response of a seat-passenger system to impulsive loading

22 p3151 A72-42766

Brittle fracture under dynamic loading conditions

22 p2329 A72-42848

Dynamic loading of a fluid-filled spherical shell

22 p3240 A72-42891

Liapunov method extension to dynamically loaded elastically end-restrained columns stability and frames forced vibration boundedness problems

[ASCE PREPRINT 1639]

23 p3352 A72-44110

Dynamic response of circular plates to pulse loads

23 p3354 A72-44254

A finite element model for shells based on the discrete Kirchhoff hypothesis

24 p3457 A72-44876

Method of characteristic application to curved beam motion under pulse type loading, investigating photoelastic fringe patterns and pulse propagation

24 p3458 A72-44888

One dimensional heat insulated structure under dynamic loads, showing thermoviscoelastic effects on spontaneous heating and stress-strain state

24 p3458 A72-44935

Action of a moving load on a composite shell with elastic filler

24 p3459 A72-45262

DYNAMIC MODELS

Bond graph methods for assembling structural dynamic models from component models, using ENPORT programs for simulation or analysis

[SAE PAPER 710781]

01 p0137 A72-10273

Large structural systems dynamic mathematical models, predicting eigenvalue and eigenvector with statistical analysis

[SAE PAPER 710785]

01 p0137 A72-10276

Torsion problem of inhomogeneous anisotropic viscoelastic rod transformation, using area variation coefficient for modeling

01 p0138 A72-10582

Dynamic model for estimating Bayesian recursive images by linear Kalman filtering

01 p0046 A72-10866

Electrical and nuclear propulsion plasma containment problems, discussing simulation experiments and scaling devices feasibility

01 p0117 A72-10938

Energy spectrum equations for steady state turbulent convection model based on Heisenberg statistical theory, noting application to convection in planetary and stellar atmospheres

01 p0146 A72-11311

Planetary nebulae dynamic models, incorporating expanding shell thermal histories and thermal stability in terms of high temperature evolutionary phase

02 p0276 A72-11667

Critique of self similar solutions for physical property models of laminar boundary layer separation due to adverse pressure gradients, noting viscosity-enthalpy relation

02 p0204 A72-12265

Search radar performance environmental model using clutter and interference returns

02 p0178 A72-12389

Rigid plastic circular plate dynamic model with yield time delay, discussing residual deflection as function of load duration

02 p0293 A72-12426

Hereditarily elastic body model with various tensile and compressive strengths, using elasticity theory with differing moduli

02 p0294 A72-12429

Rheomobility and structural creep, correlating mobile, rigid, elastic, viscous and plastic models

02 p0297 A72-12612

Aeroelastic models construction for flutter analysis of aircraft design, noting error risk reduction

[DGLR PAPER 71-082]

02 p0299 A72-12722

Hard sphere liquid Bernal model with cell method extension, determining liquid argon behavior near melting

03 p0388 A72-13151

Human postural control system dynamic model, discussing stick man pitch axis dynamics digital simulation and difficulties in linearizing equations of motion

03 p0318 A72-13163

Finite element discrete model for large aspect ratio wing transverse vibrations, using inhomogeneous elements with various stiffness-length relations

03 p0442 A72-13189

Relativistic cosmological model, showing relation to fluid dynamics in Newtonian theory and space-time dependence on causality condition

03 p0426 A72-13267

Dynamic modeling of stratospheric and mesospheric circulation and thermal structure

03 p0346 A72-13382

Molecular collision model, comparing generalized phase shift approximation method with classical trajectory calculations for rotational inelasticity

03 p0391 A72-13857

CW longitudinal flow carbon monoxide chemical laser system analysis, discussing vibrational levels, population densities, excitation and relaxation processes and dynamic model

03 p0368 A72-13858

Liquid propellant rocket abort fireball model, specifying heat flux as function of time

03 p0457 A72-13953

Impulsive spatial interaction model between monoenergetic molecular beam and rough isotropic rigid metal surface in free molecule flow

03 p0392 A72-14058

Linear dynamic system sensitivity models simplification conditions application to adaptive nonsearching system synthesis algorithms

04 p0505 A72-14999

- Spatial motion of two thread-coupled bodies along satellite circular orbit, discussing system equilibrium position stability and phase trajectories
04 p0582 A72-15003
- Holographic measurement of red blood cell rotation in orifice flow, transforming orientation into form distribution data
04 p0479 A72-15140
- External biodynamic models for human mechanical response to various environmental forces, emphasizing injury mechanisms
[AD-736985] 04 p0481 A72-15266
- Convergent-divergent nozzles thrust model measurement on supersonic aircraft afterbody
[ONERA, TP NO. 978] 05 p0642 A72-15856
- Modeling techniques for fluid line transients, considering heat transfer and viscous dissipation
[ASME PAPER 71-WA/FE-9] 05 p0646 A72-15933
- Aircraft ejection simulation by human thoraco-lumbar spine flexion dynamic model, using strength of materials theory and shear effects for curved elastic beam
[ASME PAPER 71-WA/BHF-7] 05 p0620 A72-15947
- Varying energy and gamma /quasi-steady/ models for point source blast waves from high speed solids impact, comparing 1100-0-aluminum shock decay data
05 p0736 A72-16101
- Aircraft steering dynamics model with translational and rotational equations, considering zero sideslip and acceleration and lift bank angle transfer functions
05 p0611 A72-16112
- Thin elastic shell postbuckling behavior from asymptotic integration solution for differential equations, permitting dynamic effect modeling
05 p0738 A72-16425
- Turbulent wake calculations with eddy viscosity model, predicting velocity profiles and displacement thicknesses
05 p0603 A72-16538
- Sound effect on diffusion flames, presenting vortex model
05 p0747 A72-16701
- Fluctuating flow in idealized model of turbulent shear layer composed of many discrete two dimensional vortices, analyzing noise generation
[AIAA PAPER 72-155] 05 p0609 A72-16955
- Plasma models of topside ionosphere, investigating electrostatic wave propagation
05 p0698 A72-17022
- General relativistic kinetic theory of gases, discussing microscopic model, space-time, self-consistent Einstein-Maxwell-Liouville equations and irreversible processes
06 p0847 A72-17255
- Relativistic heat propagation models, considering hyperbolic system of partial differential equations, momentum-energy tensor for ideal fluid and classical Fourier law
06 p0847 A72-17256
- Multiple production processes hydrodynamic-type models validated by high energy particle collision collective interactions
06 p0869 A72-17265
- Increased Reynolds number simulation with roughness set on aircraft model in transonic flow, investigating flow separation by parietal visualization technique
06 p0758 A72-17846
- Thin solar convection zone relation to sunspot cycle, noting magneto-kinematical model
06 p0886 A72-18099
- Round-off error analysis in numerical solutions of finite element equations in dynamic models
07 p1025 A72-18796
- CW diffusion type chemical HF laser and two-vibrational level HF molecular models, analyzing laser performance
[AIAA PAPER 72-145] 07 p1000 A72-18955
- Model-following algorithm and equicontrollability in multivariable feedback control systems, considering application to decoupling problem
07 p0960 A72-19698
- F region electron-ion gas dynamic model with stability dependence on periodic solutions convergence of continuity equations
08 p1153 A72-20725
- Biased estimator as alternative to linear unbiased estimator for dynamic system model states and parameters optimization and regulation, noting squared errors sum
08 p1144 A72-20852
- Optimal filtering for state estimation of nonlinear dynamic models observed with discrete noisy observations by retaining second order terms in series approximation
08 p1145 A72-20863
- Rheological model of reticular polymers and glass fiber reinforced plastics based on stress-strain relationship during damped creep elastic deformation
08 p1191 A72-21499
- Durando model overprediction of deflected jet vortex strength in subsonic cross flow
08 p1151 A72-21631
- Hydrodynamic models and computational schemes optimization in statistical weather forecasting
08 p1202 A72-22114
- Dynamic model of night time hydroxyl rotational temperature variations from airborne and ground measurements
09 p1298 A72-22587
- Structural model application to construction material alternate stress description at elevated temperatures
09 p1401 A72-22727
- Monostable three output fluid amplifier models with curved walls in turbulent jet flow, comparing wall design in dynamic and static tests
09 p1263 A72-22931
- Two dimensional dynamic model for background noise generation in bipolar transistors, using equivalent circuit
09 p1286 A72-23105
- Near optimal closed loop control laws for fixed time pursuit-evasion differential game between two aircraft in vertical plane, using dynamic modeling
10 p1421 A72-23805
- Coupled mode model for dynamic interaction between flexible rotary machines and elastic supporting structures
[AIAA PAPER 72-375] 11 p1730 A72-25399
- Solid body model for electric arc acceleration in thermionic cathode rail accelerator, discussing plasma mass effects
[AIAA PAPER 72-412] 11 p1706 A72-26162
- Dynamic modeling application to technological forecasting, discussing mathematical simulation for R and D management planning in project selection and budget allocation
11 p1748 A72-26284
- Magnetosphere fast electron precipitation investigated by simulation experiments with model created by plasma stream interaction with dipole magnetic field
11 p1714 A72-26531
- Nonregular oceanic level fluctuations dependence on atmospheric pressure and tangential wind stress, deriving fluctuation spectrum from linear hydrodynamic model
11 p1682 A72-26882
- Stochastic dynamic prediction of meteorological fields in deterministic and indeterminate atmosphere
12 p1838 A72-27020
- Two dimensional dynamic model numerical simulation for micro- and macrostructures of moist convective clouds, comparing to field observations
12 p1839 A72-27028
- Ergodic boundary in initial conditions space for turbulent two dimensional flow, explaining phenomenon in terms of negative temperatures for point vortex model
12 p1797 A72-27183
- Molecular dynamic techniques for simulating one dimensional shock wave motion in three dimensional solid, using rare gas solid model
12 p1881 A72-27282
- Local heating effect of electrical resistance gages measuring strain across thickness of plane photoelastic Araldite models
12 p1807 A72-27316
- Impulse and kinetic momentum equations for dynamics of variable mass solid using mechanical model
12 p1846 A72-27543
- Dynamic systems as models for electronic measuring instruments computerized development and design
12 p1791 A72-27579
- Thermodynamic limiting relations between physical measurement accuracy and measurement performance energy dissipation, considering equilibrium and nonequilibrium dynamic models
13 p2003 A72-28761
- Pulmonary oxygen transport dynamic model representing lung gas-side airway and alveolar regions and blood-side capillary bed
13 p1909 A72-28996
- Liquid droplets behavior in high velocity gas jets, deriving fluid flow model solutions near symmetry axis and for liquid-gas boundary layer
[DFVLR-SONDDR-200] 13 p1941 A72-29003
- Window response to sonic booms, establishing upper bounds by mechano-acoustical network modeling of one and two degree of freedom dynamic systems
13 p2057 A72-29091
- Corrections to collision induced vibration transition probability calculated from three dimensional semiclassical model
13 p2009 A72-30062
- Radiative-dynamic model for static stability of rotating atmospheres, deriving mean equilibrium value of Richardson number in troposphere
14 p2127 A72-30341
- Linear mathematical model for twin shaft gas turbine with isolated turbocompressor, calculating dynamic constants as function of operational modes
14 p2146 A72-30581
- Molecular band model for inhomogeneous radiating gases nonuniform transfer paths based on single collision broadened spectral line growth
14 p2135 A72-30891
- CW oscillator model for laser amplifier, including nonlinear effect of gain saturation
14 p2111 A72-30896
- Plasma containment in toroidal systems investigated on basis of fluid model containing inertia, momentum transfer, ionic collisions and thermal conductivity effects
15 p2285 A72-32273
- Mechanical models in thermoelasticity associated with boundary problems of classical physical fields with postulated laws of variation and periodicity
15 p2330 A72-32288
- Hill model for myocardium activity, taking into account contractile state variations and characteristic force-velocity curve
15 p2187 A72-32492
- Laser ignition and combustion of boron particles, developing oxide coating and droplet burning models for low and high temperature stages respectively
15 p2296 A72-32582
- Prediction models for dynamic environment experienced by cargo during air and rail transportation
15 p2339 A72-32610
- Aeroelastic model response comparison to amplitudes of sectional and linear wind tunnel models, indicating incorrectness of direct scaling
16 p2342 A72-32904
- Supermolecular scale microscopic dynamic model for solid body macroscopic friction and wear effects
16 p2398 A72-33367
- Lattice dynamical model for Cs vibration frequency distribution, specific heat and electrical and thermal resistivity calculations
16 p2441 A72-33584
- Baysian recursive linear Kalman filtering technique for image estimation with noise background elimination, proposing time invariant dynamic model to provide stationary statistics
17 p2520 A72-34403
- Impact crater formation at intermediate velocities.
[ASME PAPER 72-MAT-C] 17 p2631 A72-34967
- Analysis and testing of compressible flow ejectors with variable area mixing tubes.
[ASME PAPER 72-FE-14] 17 p2485 A72-34968
- On the structure of hypersonic turbulent boundary layers.
17 p2540 A72-35188
- The fitting, calibration, and validation of simulation models.
17 p2523 A72-35226
- Salutation threshold velocity simulation by dynamic model with terrestrial and Martian surface applications, using particle trajectory equations for near ground-atmosphere interface
17 p2614 A72-35637
- Turbulence model equations for calculation of supersonic and hypersonic flows, representing Reynolds stresses and turbulent heat flux vector in terms of eddy viscosity
17 p2543 A72-35639
- Laboratory model information relating to modeled geophysical phenomena, noting magnetosphere study from plasma physics experiments
17 p2551 A72-35904
- Magnetic dipole field interaction with plasma flow ions, noting qualitative model of solar wind flow past magnetosphere
17 p2593 A72-35905
- Two-mass system as human body dynamic model in ballistocardiography, outlining transfer function parameter computation procedure
18 p2652 A72-36039
- Two dimensional recursive filter for Bayesian estimate of pictorial data represented by dynamic model of random field with exponential autocorrelation
18 p2658 A72-36261
- Theory of elastic wave propagation in composite materials.
18 p2703 A72-36395
- Determination of the motion of a model, possessing a mass and a viscoelastic element, for a given harmonic law of motion of the vibrating support
19 p2871 A72-37427
- The dynamic modeling technique for obtaining closed-loop control laws for aircraft/aircraft pursuit-evasion problems.
19 p2753 A72-38276
- F region electron-ion gas dynamic model with stability dependence on continuity equations periodic solutions convergence
19 p2791 A72-38353
- A theoretical solution of the Lockhart and Martinelli flow model for calculating two-phase flow pressure drop and hold-up.
19 p2787 A72-38392
- A critical examination of the validity of simplified models for radiant heat transfer analysis.
19 p2882 A72-38399

- The mechanics of an organized wave in turbulent shear flow. III - Theoretical models and comparisons with experiments. 19 p2789 A72-38794
- Strong shock propagation through decreasing density. 19 p2789 A72-38796
- The study on dynamic behavior of fiberglass reinforced plastics /FRP/ by dynamical mechanical model. 20 p2943 A72-38887
- The matrix fatigue behaviour of fibre composites subjected to repeated tensile loads - Application to B/Al6061 composites. 20 p2936 A72-39208
- Turbulence in dynamic models of the atmosphere. 20 p2948 A72-39357
- Dynamic models for hydraulic machine parts, discussing resonant properties of one degree of freedom system and dynamic characteristics of nonlinear parametric systems 20 p2953 A72-39421
- Nonperiodic oceanic level fluctuations dependence on atmospheric pressure and tangential wind stress, deriving fluctuation spectrum from linear hydrodynamic model 20 p2948 A72-39569
- Monte Carlo studies of the relaxation of vector end-to-end length in random-coil polymer chains. 20 p2898 A72-39599
- An analysis of heat transfer in turbulent pipe flow with variable properties. [ASME PAPER 72-HT-59] 20 p2985 A72-39657
- The calculation of low-Reynolds-number phenomena with a two-equation model of turbulence. [ASME PAPER 72-HT-20] 20 p2914 A72-39688
- Karman vortex street in a uniform shear flow. 21 p2992 A72-41247
- Machine elements vibration parameters from dynamic model of planetary gears, noting energy spectrum, correlation and amplitude distribution functions. 22 p3182 A72-42132
- Stability of the Martian atmosphere. 22 p3224 A72-42292
- Machine code for finite difference solution of wake vortex governing equations and far flow field prediction in trailing vortices, developing turbulent energy model [AIAA PAPER 72-989] 22 p3134 A72-42326
- Book - Computer simulation of dynamic systems. 22 p3157 A72-43081
- The parameters of a two-mass oscillatory system in which one of the masses is acted upon by a complex working resistance 23 p3312 A72-43352
- Lumped parameter model description of distributed parameter fluid dynamic systems by bond graph techniques [ASME PAPER 72-AUT-J] 23 p3279 A72-43634
- Descriptive model of the turbulent motion of an isovolumetric fluid 23 p3279 A72-43699
- A practical method for determining Dugdale model solutions for cracked bodies of arbitrary shape. 23 p3346 A72-43701
- Dynamic model for microinhomogeneous elastoplastic medium under cyclic loads with varying amplitude 23 p3347 A72-43729
- Application of a time-dependent boundary-layer analysis to the problem of dynamic stall. 23 p3249 A72-44058
- Line spring analysis model for long part-through surface cracks in walls of plate or shell structures, formulating constitutive laws 23 p3353 A72-44234
- Dynamic model compensation algorithm accuracy for sequential estimation of time history of lunar satellite acceleration due to modeled surface mascons effects 24 p3440 A72-45139
- Continuity equation for dynamic auroral ionospheric model relating electron density profiles to auroral arc brightness 24 p3400 A72-45589
- DYNAMIC MODULUS OF ELASTICITY**
- Oxygen effect on dynamic elastic modulus of titanium-oxygen alloys by density and longitudinal ultrasonic wave velocity measurements 01 p0083 A72-10393
- Al wrought alloys dynamic elasticity modulus and Poisson ratio dependence on temperature, using ultrasonic measurement method 07 p1019 A72-20239
- Glass and carbon fiber reinforced plastic beam specimens dynamic moduli and loss factors determination from vibration frequency and decay rate measurements 13 p1984 A72-29095
- Measurement of the damping capacity and dynamic modulus of high-damping metals under direct cyclic stresses. 19 p2795 A72-37460
- Vibration measurements of temperature dependent dynamic moduli of Al/resin/Al sandwich bars with cyanocrylate adhesives 21 p3118 A72-40720
- DYNAMIC PRESSURE**
- Cooled miniature pneumometric probes for high temperature gases dynamic or stagnation pressure and velocity measurement 01 p0072 A72-11213
- Lunar induced and permanent magnetism, discussing solar wind dynamic pressure effects and Apollo data 03 p0418 A72-13109
- Plane steady flow of two viscous fluids in contact, presenting normal and tangential pressure 04 p0510 A72-14513
- Jet noise simple-source theory experimental verification, determining relation of measured sound power and jet pressure levels of turbojet engine 06 p0867 A72-17856
- Characteristic overpressure concept for sonic bangs effect on structures and dynamic magnification factor engineering formula 06 p0758 A72-17858
- Dynamic pressure, downwash and pressure gradient corrections of wind tunnel model measurements, discussing displacement limit for adequate accuracy [DFVLR-SONDDR-214] 19 p2747 A72-38687
- Thermally controlled entry guidance for shuttle. [AIAA PAPER 72-831] 20 p2951 A72-39096
- Hydrodynamic fluid pressure on a shell during hydraulic impact 23 p3280 A72-43788
- Condensed liquid explosive detonation pressure from free surface velocity measurement, noting pressure curve dependence on charge diameter and wall thickness 24 p3463 A72-45036
- DYNAMIC PROGRAMMING**
- High order optimality conditions of singular controls, considering Pontryagin maximum principle, Bellman dynamic programming and functional analysis 01 p0044 A72-10297
- Discrete-time linear quadratic stochastic control system with perfect measurements of state, obtaining optimal solution by dynamic programming 02 p0198 A72-12808
- Linear time optimal control system with retardations in controls, discussing controllability, existence and uniqueness, synthesis techniques and dynamic programming [AD-737927] 03 p0338 A72-13406
- Weak solutions of degenerate partial differential equation of dynamic programming, investigating relation to value function of stochastic optimal control problem 03 p0382 A72-13701
- MHD Couette flow stochastic processes optimal control synthesis by dynamic programming 05 p0653 A72-17131
- Minimal energy stochastic controller design for electrically driven vehicles, using dynamic programming 06 p0795 A72-17304
- Dynamic programming for optimal stochastic control problem with Gaussian shot noise involving parabolic or elliptic differential equation in unbounded domain, discussing iterative solution and quasi-linearization 07 p1027 A72-19292
- Minimax optimal control problems with incomplete information, using dynamic programming and phase space location measurements 07 p0963 A72-19970
- Dynamic programming application to computer algorithm construction for elasticity theory two dimensional problems, solving boundary value problem for elliptic differential equation 08 p1243 A72-21235
- Naval aircraft optimal repair and replacement policies determination for operation cost minimization by dynamic programming [AD-736094] 08 p1256 A72-21470
- Dynamic programming method application to signal processing components selection for cascaded communication links to satisfy overall gain and noise figure 09 p1281 A72-23415
- Steepest descent variable step-size algorithm with dynamic programming for mean square error adaptive equalizer, noting convergence 10 p1455 A72-23794
- Reliability decision making under uncertainty between alternative design approaches, using dynamic programming 10 p1504 A72-23995
- Resonant frequency and vibration modes of variable cross section bar in elastic medium under transversal force, noting dynamic programming combined with optimization principle 12 p1845 A72-27538
- Control parameters required for stabilization of motion in systems with nonholonomic couplings by dynamic programming method of summary representations 13 p2003 A72-29068
- Dynamic programming for optimal statistical control of self adaptive systems with fixed learning experiments, noting structural constraints for suboptimality 13 p1965 A72-29178
- Data processing method for optimal prediction of spacecraft orbital elements, using dynamic and quadratic programming 14 p2151 A72-30455
- Minimum weight hinged and unhinged cantilever truss design as variational problem, using dynamic programming method 14 p2166 A72-30690
- Optimal segment boundaries with composite order function in piecewise approximation chosen by dynamic program in scalar state variable, noting uniqueness properties 15 p2262 A72-31634
- Dynamic optimization procedure for bivalent knapsack problem solution involving large number of variables 15 p2203 A72-31750
- Control function improvement method for flight dynamics variational problems solution, discussing dynamic programming, trajectories with uncontrolled elements and coordinate transformation 17 p2607 A72-35036
- Multilevel hierarchical structural design optimization, proposing component by component ascent method of dynamic programming 17 p2533 A72-35171
- Russian book on numerical methods in optimal control systems theory covering functional extremum, dynamic programming, control synthesis and statistical linearization of nonlinear systems 17 p2533 A72-35458
- Dynamic programming technique for simultaneous measurement and dynamic control optimization for stochastic systems 19 p2779 A72-38233
- Minimax technique in optimal control problems with incomplete information on phase vector, using dynamic programming and system position measurement refinements 20 p2911 A72-40027
- A stochastic automata theoretical approach to dynamic programming. 22 p3199 A72-42633
- Optimal control of stochastic systems with continuous and discontinuous random disturbances, obtaining problem solution conditions for linear system via dynamic programming 23 p3276 A72-43782
- A computational successive improvement scheme for adaptive optimal control processes. 23 p3268 A72-44549
- Dynamic programming and the optimum design of rotating disks. 23 p3356 A72-44550
- Lockheed airline system simulation and aircraft scheduling models. 24 p3466 A72-44579
- DYNAMIC PROPERTIES**
- U DYNAMIC CHARACTERISTICS**
- DYNAMIC RESPONSE**
- NT TRANSIENT RESPONSE**
- Large scale structural systems dynamic response analysis, discussing numerical techniques with emphasis on computer code usage [SAE PAPER 710780] 01 p0137 A72-10272
- Gimballed control moment gyro for Skylab telescope mount stringent pointing requirements, investigating normal and clamped operation modes and dynamic response of attitude control 01 p0097 A72-10382
- Dynamic response of infinitely wide perfectly flexible foil bearings to small sinusoidal tensile variations [ASME PAPER 71-LUB-20] 02 p0235 A72-11540
- Feedback control dynamic system described by linear differential equation with random coefficients, calculating parameters distribution effect on behavior precision 02 p0197 A72-12339
- Extremal system with second control loop for search signal frequency regulation to optimize primary loop operation, determining system dynamic errors under random drift 02 p0197 A72-12340
- Dust particle dynamical behavior during cloud collisions, discussing grain distribution in resultant cloud 02 p0284 A72-12638
- Book on random data analysis and measurement procedures covering physical systems dynamic response properties, random processes, statistical sampling, data acquisition and processing, etc 03 p0327 A72-13175
- Chordwise bending vibrations and flutter of thin isotropic rectangular plates, considering static and dynamic responses 03 p0443 A72-13404

Plate under projectile impact, calculating motion response due to random initial velocity distribution over surface by stochastic model 03 p0447 A72-13852

N-wave dynamic magnification factors for sonic bangs response on complicated structures 04 p0464 A72-14849

Semiinfinite elastic solid response to arbitrary axially directed line load, transforming simultaneous partial differential equations by Hankel transforms [ASME PAPER 71-APMW-1] 04 p0589 A72-15180

Shock response of simply supported sandwich beam with viscoelastic core, using four element model for dynamic shear properties 04 p0591 A72-15274

Rigid body general motion dynamic effects due to acceleration of arbitrary order, using Samov-Mangeron recursive formulas 04 p0551 A72-15746

Infinitely long Euler-Bernoulli damped periodic aluminum beam with elastic springs, determining distance for steady state sinusoidal response to spatial decay 05 p0736 A72-16111

Circle moving under fluid dynamic and gravitational forces in viscous incompressible flow, describing dynamic interaction by numerical method [AIAA PAPER 72-111] 05 p0604 A72-16819

Finite periodic beam response to turbulent boundary layer pressure field fluctuation, using transfer matrix technique [AIAA PAPER 72-171] 05 p0650 A72-16832

Plane symmetrical exothermic reaction center dynamic behavior, deriving system nonlinear transfer function-pressure pulse and unit mass heat release relationships [AIAA PAPER 72-67] 05 p0750 A72-16934

Helicopter rotor blade response to random loads treated by theory of linear dynamic systems with time-varying coefficients [AIAA PAPER 72-169] 05 p0613 A72-16940

Linear time-varying system under modulated signal excitation, obtaining quasi-stationary response by separable system approximation with parameter optimization 06 p0771 A72-17379

Validity proof of asymptotic methods in oscillation theory of one dimensional nonlinear dynamic systems described by hyperbolic and parabolic differential equations 06 p0839 A72-17681

Regularization theorems for epsilon solutions to Bellman functions in optimal quick response problems 06 p0847 A72-17728

Digital computer techniques for randomly excited n-degrees of freedom structural system response by discrete time series with output covariance 06 p0895 A72-17857

Random vibrations nonlinear theory, investigating nonlinear systems response to random excitation via Markov processes modeling 06 p0896 A72-17961

X band IMPATT and Gunn oscillator, calculating injection lock time, modulation bandwidth, noise and FM suppression and dynamic response 06 p0788 A72-18471

Airloads and structural integrity flight testing /U.S. Air Force/, noting dynamic response, fatigue tests and temperature data acquisition 06 p0759 A72-18490

Infinite uniform Vlasov plasma response to steady state transverse excitation, considering spatial electron cyclotron damping [AD-737564] 06 p0864 A72-18539

Dynamic response predictions of fluidically controlled pulsatile hydraulic flow and pressure generator for biomedical systems 07 p0914 A72-18820

Motion dynamics of aircraft-autopilot closed loop system under influence of atmospheric turbulence and electric circuitry thermal noise 07 p0911 A72-18990

Suboptimal Kalman filter design for system state estimation in presence of plant dynamics uncertainties and measurements noise, optimizing tradeoff between sensitivity and estimation error 07 p0959 A72-19302

Periodically supported beams acoustically induced vibration response based on equivalent structural wavelength definition [ASA PAPER E 14] 07 p1089 A72-19330

Phase locked AFC system, calculating phase detector response effects on dynamic properties 07 p0943 A72-19524

Pinned-free beam response to transient support excitation, using pinned-pinned beam model parameters 07 p1096 A72-20526

Fluid oscillator temperature sensor, noting fast dynamic response and application in high temperature environments 08 p1164 A72-20926

Feedback control dynamic system described by linear differential equation with random coefficients, calculating parameters distribution effect on behavior precision 08 p1146 A72-21554

Extremal system with second control loop for search signal frequency regulation to optimize primary loop operation, determining system dynamic errors under random drift 08 p1146 A72-21555

Dynamic response index /DRI/ minimization for personnel aircraft emergency catapult escape systems to reduce injury probability 08 p1112 A72-21576

Nonlinear dynamic response of deformable solids under time and space dependent thermal and mechanical loads determined by finite element method 08 p1248 A72-21822

Transfer matrix and dynamic stiffness techniques application to critical speed analysis in rotating machinery 08 p1224 A72-22128

Polynomial filter design with three layer RC distributed elements and operational amplifiers, investigating active elements effects on response 09 p1290 A72-23354

Dynamic response of pressurized thin walled circular cylindrical shell under initial biaxial stress and subjected to radial uniformly moving force, noting transient and steady state [ASME PAPER 71-APM-GGG] 10 p1554 A72-24186

Turbulence generated sound due to interaction with sound absorbent liners, investigating dynamic process via rigid boundary model with homogeneous array of circular orifices or pistons 10 p1511 A72-24424

Dynamic processes of electric drive system with electromagnetic clutch modeled by analog computer element with logical input-output relation 10 p1423 A72-24755

Nonlinear dynamic response of single elastic cables with low initial tension, examining free and forced vibrations with incremental deformations theory 10 p1560 A72-25185

Asymptotic dynamic response of infinite beam on elastic foundation to randomly moving load 11 p1727 A72-25292

Regularization theorems for epsilon solutions to Bellman functions in optimal quick response problems 11 p1608 A72-25330

Dynamic deflections and bending moments of simply supported Bernoulli-Euler beam under traveling mass loads [AIAA PAPER 72-338] 11 p1728 A72-25371

Distributed elastic system discrete model mass, stiffness and damping matrices derivation from dynamic test response data [AIAA PAPER 72-346] 11 p1728 A72-25375

Equations of motion for structural flexibility influence on dual spin spacecraft dynamic response, noting elastic deformations and rotation rates coupling [AIAA PAPER 72-348] 11 p1725 A72-25377

Dynamic nonlinear elastic response of buckling sensitive cylindrical shells to lateral pressure loading, using numerical and computerized analysis [AIAA PAPER 72-357] 11 p1729 A72-25386

Heterogeneous shear deformation effect on dynamic response of laminated plates for various local elastic deformation and interface conditions [AIAA PAPER 72-398] 11 p1731 A72-25419

Direct numerical integration scheme for viscoelastoplastic response of isotropic axisymmetric shells under impulsive loads [AIAA PAPER 72-400] 11 p1731 A72-25421

Aerodynamic lag effects on wing bending dynamic response at supersonic speeds, noting application to stress estimation under gust loads 11 p1572 A72-25922

Dynamic response of MHD flow under impulsive pressure gradient, obtaining approximate analytic solutions for conduits of arbitrary cross sections by complex variable approach 11 p1695 A72-26039

Hydraulic feedback servomechanism for dynamic response characteristics control, discussing design parameters and fluid properties influence on system performance 11 p1578 A72-26981

Geometrically nonlinear structure elastic stress propagation, deformation and dynamic response under impact, using finite element matrix displacement method and computer programs 12 p1879 A72-27189

Elastic truncated thin conical shell response to dynamically applied axial force from numerical solution of nonlinear equations 12 p1881 A72-27244

Closed form solution for dynamic response of infinite plate with elastic foundation and damping under arbitrary initial conditions and load distribution 12 p1883 A72-27559

Analog measuring data transmission systems optimization by computers, noting improvement of dynamic response and linearity in digital systems 12 p1786 A72-27580

Modified Van der Pol wave motion oscillator model for prediction of aortic dynamic response to negative g impact accelerations 12 p1765 A72-28271

Averaging technique for nonlinear viscoelastic dynamic problems, considering forced oscillations of oscillator with weakly nonlinear hereditary elastic characteristics 13 p2054 A72-28551

Window response to sonic booms, establishing upper bounds by mechano-acoustical network modeling of one and two degree of freedom dynamic systems 13 p2057 A72-29091

Solid propellants burning rate dynamic response to rapid pressure changes, discussing equations applicability to combustion extinction prediction as function of pressure decay rate 13 p2065 A72-29304

Aircraft structures design and development with composite materials, considering materials characteristics relations to structural components dynamic response 13 p2060 A72-29691

Transients analysis for nonlinear branched dynamic systems by integral manifold and small parameter method 13 p2007 A72-29997

Hovercraft heaving response to regular head or following seas, determining dependency on craft natural frequency and damping, wave frequency and cushion platform 14 p2071 A72-30254

Complex elastic systems natural frequencies computation from measured dynamic response to harmonic excitation, applying to helicopter and transport aircraft 14 p2164 A72-30326

Dynamic response of thin circular arches to in-plane forced excitation under cyclic symmetric and unsymmetric support movement 14 p2169 A72-31175

Spherical cap dynamic buckling under impulsive loading, comparing prediction by energy criterion with experiment using spray deposited explosive 15 p2323 A72-31405

Elastic shell initial stress effects on dynamic response in all free vibration modes, considering transverse shear and normal strains 15 p2328 A72-32021

Multidegree of freedom linear systems mean-square response to nonstationary random vibratory excitation, using staircase approximation to continuous intensity functions 15 p2331 A72-32552

Dynamic response and buckling mode of elastically supported circular plates with initial tension under arbitrary surface load 15 p2332 A72-32578

Single degree of freedom system displacement response exceedance of given level under nonstationary random excitation, considering aircraft flight through turbulent region with variable intensity 15 p2279 A72-32592

Low speed wind tunnel investigation of vortex formation effect on angle section columns galloping response, varying stiffness and damping characteristics 15 p2332 A72-32594

Aircraft crash landing induced acceleration effects on seated occupants, discussing energy absorber system dynamic response characteristics for injury protective devices 15 p2191 A72-32603

Chamois leather mechanical response, comparing stress relaxation and frequency response characteristics to human skin for applications in anthropometric dummy construction 15 p2191 A72-32606

Holographic interferometric measurement of materials time dependent deformation responses to various environmental influences, discussing CW and pulsed laser techniques and holographic microscopy 16 p2388 A72-32820

Time domain analysis of long thin bar antenna response to gravitational signals, estimating sensitivity limit via noise background analysis 16 p2423 A72-33013

Forced vibrations of thick homogeneous anisotropic elastic sphere, studying dynamic response to uniformly distributed internal and external pressure 16 p2424 A72-33147

Instrumentation for space-time correlated measurement of explosion induced dynamic effects, discussing framing cameras, flash X-ray systems, pin switches and piezoresistive gages 16 p2392 A72-33360

Presupposition, aim and methods for teaching transducer technology to users and designers, reviewing transducer static and dynamic performance characteristics and classifications 16 p2393 A72-33632

Response of a ring-reinforced cylindrical shell, immersed in a fluid medium, to an axisymmetric step pulse. [ASME PAPER 72-APM-8] 17 p2624 A72-34314

Calculation of correlation matrices for linear systems subjected to nonwhite excitation. [ASME PAPER 71-APMW-10] 17 p2625 A72-34316

Determination of airfoil and rotor blade dynamic stall response.

[AHS PREPRINT 613] 17 p2490 A72-34495

Spatial and temporal load pulse parameters for circular cylindrical shells /tubes/ dynamic plastic deformation

[ASME PAPER 72-APM-29] 17 p2628 A72-34790

Structural system response to white noise excitation, deriving integral equation for first passage time-density function via Markov process model

[ASME PAPER 72-APM-11] 17 p2629 A72-34805

An approximate analysis of non-linear non-conservative systems subjected to step function excitation.

17 p2582 A72-35412

On the prediction of acceleration response of air cushion vehicles to random seaways and the distortion effects of the cushion inherent in scale models.

[AIAA PAPER 72-598] 18 p2642 A72-36538

Behavior of spherical balloons in wind shear layers.

18 p2643 A72-36963

Viscoelastic fluid lines dynamic behavior, considering viscosity, stress-strain relaxation times and compressibility effects in transfer functions derivation for pressure-velocity relations

18 p2684 A72-37077

Nonstationary parametric response of a nonlinear column.

18 p2738 A72-37079

Natural frequencies and dynamic response constraints in optimal structural design, considering mathematical programming aspects

18 p2739 A72-37167

Book - An introduction to engineering systems.

20 p2945 A72-38925

Attitude dynamics of a three-axis stabilized satellite with a large flexible solar array.

[AIAA PAPER 72-857] 20 p2976 A72-39137

Nonlinear system described by three generalized coordinates, noting dynamic response stability equivalence to two degrees of freedom system

20 p2953 A72-39553

Dynamic snap-buckling of shallow arches under inclined loads.

20 p2980 A72-39617

Flight-mechanical analysis of various flight conditions of conventional aircraft. V. - Mechanical foundations /Dynamics of the rigid body/

21 p2994 A72-40175

Forced motion of isotropic and transversely isotropic viscoelastic Timoshenko beams using measured material.

21 p3116 A72-40331

Geometric criterion for the design of a non-oscillatory dynamical system.

21 p3037 A72-40647

Rigid aircraft longitudinal dynamic response to random atmospheric turbulence, defining spectral gust alleviation factors in terms of mass scale and damping ratio parameters

21 p2996 A72-41641

Response of a seat-passenger system to impulsive loading.

22 p3151 A72-42766

Dynamic response of circular plates to pulse loads.

23 p3354 A72-44254

Parametric influences on the response of structural shells.

24 p3454 A72-44604

Response of shallow spherical shells to pulse pressure loads.

24 p3454 A72-44605

Mapping of large dynamic deflections of structures.

24 p3454 A72-44606

Technique for measuring damping properties of thin viscoelastic layers.

24 p3402 A72-44885

Linear theory of a solid propellant rocket motor with modulated exhaust

24 p3433 A72-45116

Roll dynamic behavior of a very slender reentry vehicle.

24 p3452 A72-45348

DYNAMIC STABILITY

NT AERODYNAMIC STABILITY

NT AIRCRAFT STABILITY

NT ATTITUDE STABILITY

NT BOUNDARY LAYER STABILITY

NT COMBUSTION STABILITY

NT CONTROL STABILITY

NT DIRECTIONAL STABILITY

NT FLAME STABILITY

NT FLOW STABILITY

NT FREQUENCY STABILITY

NT GYROSCOPIC STABILITY

NT HOVERING STABILITY

NT LATERAL STABILITY

NT LONGITUDINAL STABILITY

NT MAGNETOHYDRODYNAMIC STABILITY

NT MOTION STABILITY

NT ROTARY STABILITY

NT SPACECRAFT STABILITY

Galaxy clusters stability, obtaining mass distribution function from combined virial theorem and mass to light ratios

01 p0131 A72-11003

Stability theory invariance principle extension to generalized dynamical systems, considering problems in thermoelasticity, viscoelasticity and distributed nonlinear networks

02 p0251 A72-11497

Circular cylindrical sandwich panel and rectangular sandwich plates dynamic stability under periodic external loads derived from mathematical model

02 p0298 A72-12664

Rotating star global axisymmetric dynamic stability, deriving local criteria by variational principle

03 p0417 A72-13021

Poppet valve design with flow force compensation for high pressure oil hydraulic systems, discussing dynamic stabilization

03 p0312 A72-13964

Nonlinear oscillations stochastic instability in dynamic systems, discussing nonequilibrium statistical mechanics

03 p0390 A72-14316

Linearized continuous baroclinic atmospheric model, discussing stability for planetary vorticity gradient

04 p0541 A72-14452

Gradient-recombination current instability in high resistance compensated semiconductors

04 p0561 A72-15084

Dynamic systems stability under periodic impulsive parametric excitation, deriving simple closed-form analytic stability criteria for special cases from general theory

[ASME PAPER 71-WA/APM-19] 05 p0733 A72-15961

Continuous media stationary motion stability using initial boundary value problem of partial differential equations in perturbations

[ASME PAPER 71-WA/APM-17] 05 p0647 A72-15963

Encounterless one-dimensional constant density self gravitating system stability for symmetric disturbances, using analytic treatment and computer experiments

05 p0713 A72-16054

Magnetic damping comparison with internal viscous damping effect on circulatory elastic system equilibrium stability

05 p0689 A72-16061

Liapunov direct method based approaches to hybrid dynamical systems stability, applying to attitude stability of flexible earth pointing satellite

[AIAA PAPER 72-18] 05 p0729 A72-16867

Forebody blowing induced dynamic instability effect on slender cones at hypersonic speeds, presenting theory based on unsteady imbedded Newtonian flow concepts

[AIAA PAPER 72-31] 05 p0607 A72-16919

Three degrees of freedom motions of slender cones with slight compounded asymmetries in hypersonic flight wind tunnel stability tests

[AIAA PAPER 72-28] 05 p0608 A72-16939

Dynamic stability of controlled spacecraft with liquid propellant rocket engines, considering acceleration and braking sections of trajectory

05 p0730 A72-17027

Onboard equipment layout effect on dynamic stability against liquid propellant sloshing in spacecraft

05 p0730 A72-17028

Dynamic stabilization of transverse Kelvin-Helmholtz instability driven by nonuniform plasma motion, using ac electric field near ion cyclotron frequency

06 p0857 A72-17531

Nonlinear solid body system rotating and oscillating parts effect on spatial vibration stability, deriving excitation-natural frequencies relationship

06 p0850 A72-18711

Sufficient conditions for asymptotic stability and instability for elastic systems with dissipation, using Liapunov direct method

07 p1026 A72-18809

System parameters random step changes effect on nonlinear system steady vibration stability

07 p1088 A72-19172

Acoustic loads effect on carrying capacity and vibration stability of longitudinally stiffened cylindrical metal panels, investigating fatigue strength and stress-strain state

07 p1091 A72-19760

Lf convective oscillations in polytropic atmospheres within strong magnetic field, considering stability of quasi-adiabatic and quasi-isothermal motions

07 p1082 A72-20376

Stability of electron beam injected into magnetospheric plasma at small and high altitudes

07 p0979 A72-20377

Dynamic stabilization of MHD instabilities in plasma column by multipole hf fields, analyzing dispersion equation

07 p1045 A72-20479

Transmission locked differentials and variable ratio drive improvement effect on engine driven machine high speed performance and stability

08 p1113 A72-22097

Nova outbursts hydrodynamic processes, studying mass loss mechanism based on direct shock wave ejection and pulsational instability

09 p1382 A72-22283

Pod-mounted jet engine follower force instability, analyzing two degrees of freedom system dynamics

09 p1374 A72-22938

Forced vibrations of two-mass system with damping through inelastic collisions, determining periodic motions stability regions with allowance for elastic coupling and friction

09 p1352 A72-23179

Dynamic systems stability problems, differential equations linearization and random processes

09 p1343 A72-23603

Parametric dynamic stability equations and boundary conditions for thin walled open cross section beam under axial load, taking into account longitudinal deformation effect

[ASME PAPER 71-APM-LL] 10 p1554 A72-24184

Stability criteria for continuous dynamic system under parametric excitation derived by Liapunov direct method, using time dependent functionals and Rayleigh operators quotients

[ASME PAPER 71-APM-EEE] 10 p1510 A72-24187

Upper bounds on lumped and continuous dynamic systems motion under loads and perturbations, discussing structure stability conditions

[ASME PAPER 71-APMW-3] 10 p1554 A72-24188

Dynamic stability of spinning bodies with elastic rods and rigid symmetric rotors parallel to axis

10 p1552 A72-24645

Bubnov-Galerkin method for dynamic stability of closed thin walled orthotropic cylindrical shell loaded by variable external pressure

11 p1739 A72-26977

Dynamic stability of rapidly heated shallow cylindrical shells, formulating nonlinear equations

12 p1877 A72-27076

Approximation for mechanical system equilibrium perturbation anharmonic analysis based on Fourier series with real multiplication factors of fundamental pulsation

12 p1845 A72-27542

Structural system dynamic instability regions determination by finite element and conjugate gradient methods

12 p1884 A72-27847

Stability of encounterless self gravitating constant density system from computer experiment, using Fourier series expansions and Bessel functions

12 p1874 A72-27906

Computer model for evolution of isolated rotating disks of stars, noting gravitational two stream dynamic instability for infinite double periodic stellar systems

12 p1874 A72-27909

Baroclinic long wave dynamic instability in Kochin two layer frontal model, extending Richardson number range in absence of beta effect

12 p1841 A72-27987

Perfect and imperfect plastic column buckling, describing bifurcation and stability theory for elastic-plastic and rigid-plastic bodies

13 p2054 A72-28480

Canonical equations of motion for continuous elastic system, predicting critical buckling loads for unbounded deformation

13 p2054 A72-28482

Numerical analysis methods for solution stability of reduced field equations describing perturbed motion of body under nonconservative loads

13 p2001 A72-28485

Dynamic stability of doubly curved planar rectangular shallow shell, using method of summary representation

13 p2057 A72-29066

Gravitational instability and galaxy formation in expanding universe, considering primordial turbulence and density perturbations

13 p2038 A72-29085

Hingeless blades flap-lag oscillations linear stability characteristics in hovering flight, examining precone, elastic and pitch-lag coupling and induced inflow aerodynamic effects

14 p2072 A72-30289

Stability conditions for damped single degree of freedom oscillator system under stationary narrow-band random excitation, obtaining approximate solution by perturbation method

14 p2131 A72-30718

Finite element method application to dynamic stability of thin plates and shells, noting nuclear reactor structural analysis

[SMRT PAPER M 2/1] 14 p2166 A72-30723

Near-solar mass star secular stability during gravitational contraction and main sequence phases, considering static and quasi-static models

14 p2158 A72-30734

Periodic two-parameter solution families of dynamic systems having first integral, showing stability and bifurcation existence criteria relationships to dimensionality and Hamiltonian systems

15 p2261 A72-31309

Rotating neutron stars stability and radial pulsations by energy method, allowing for relativistic effects 15 p2304 A72-31335

Generalized Thomson-Tait-Chetaev stability theorem for n-degrees-of-freedom mechanical oscillating systems with virtual nonconservative displacement forces 15 p2274 A72-31456

Stochastic atmospheric density fluctuations effect on circular-orbiting satellite roll-yaw oscillations stability 15 p2319 A72-31457

Dynamic stability of elastic systems under broad-band random excitation, presenting solution for straight rod under axial pulsating forces via perturbation method 15 p2274 A72-31460

Wheel balancing by static and dynamic trial method, using Churchill Mark 3 apparatus 15 p2213 A72-31635

Longitudinal shear crack propagation after stability loss in infinite elastic medium, discussing wave diffraction at edges 15 p2327 A72-31734

Linearized stability analysis of collapsing uniform nonrotating oblate gaseous spheroid, noting subcondensation growth rate dependence on shape and size 15 p2313 A72-32364

Preloaded thin walled open section elastic column dynamic stability under free longitudinal vibrations, deriving criterion for flexural and torsional vibrations nonlinear coupling 15 p2332 A72-32560

Material damping effect on rotating system stability as function of critical angular velocity, using elastic continuum whirling shaft model 16 p2465 A72-32986

German monograph on rotating nonround shafts stability under torsion, obtaining equations of motion solution via convergent double series expansion 16 p2469 A72-33399

Effect of lagging pitching moment on re-entry vehicle dynamic stability. 17 p2619 A72-34202

Stability analysis of a pinned-end beam undergoing non-linear free vibration. 17 p2623 A72-34236

Stability and control dynamics of helicopter hovering with heavy sling load, analyzing maneuvers for minimal excitation of pendulous motion [AHS PREPRINT 630] 17 p2489 A72-34488

Exact solution for dynamic oscillations of re-entry bodies. 17 p2622 A72-35231

Mode stability in a gas laser with nonlinear selection losses 17 p2563 A72-35304

The stability of a self-gravitating, nonrotating gas layer with stellar, magnetic, and cosmic-ray components. I. 17 p2611 A72-35313

Vibrational stability of supermassive stars stabilized dynamically by a uniform or differential rotation 17 p2613 A72-35461

Parameters influencing dynamic stability characteristics of Viking-type entry configurations at Mach 1.76. 17 p2622 A72-35494

Unbalanced shafts vibration and stability characteristics, considering elastic and damping properties of sliding bearings oil films 18 p2731 A72-36069

On the inflection point instability of a stratified Ekman boundary layer. 18 p2687 A72-36631

State equation for superdense stars treated as perfect degenerate tachyon gas, noting dynamic stability for arbitrarily large central densities 18 p2726 A72-36715

A comparison of initial velocities for dynamic instability of a shallow arch. 18 p2738 A72-37080

Studies of hydrodynamic events in stellar evolution. II - Dynamic instabilities in stellar envelopes. 19 p2854 A72-37234

Stability analysis of internal pressure loaded crack in adhesive layer bonding elastic plate to rigid base using energy and critical load intensity criteria 19 p2870 A72-37245

Some problems concerning stability in the presence of small random disturbances 19 p2833 A72-37324

Dynamic stability of axisymmetrically heated glass fiber reinforced cylindrical plastic shells which are coupled with elastic cylinders 19 p2872 A72-37539

Existence and bifurcation conditions of singular point consisting of focus fused from ordinary trajectories, investigating dynamic system stability 19 p2834 A72-37565

Stability considerations for a gas-lubricated tilting pad bearing. II - Analytical refinements and stability data. [ASME PAPER 72-1-LUB-G] 19 p2807 A72-37697

Stability characteristics of floating bush bearings. [ASME PAPER 71-LUB-9] 19 p2807 A72-37698

Stability theory for a star with a toroidal magnetic field 19 p2863 A72-38062

Effects of nuclear reactions on the stability of degenerate stars. 19 p2864 A72-38100

Hydrodynamic model calculations for dynamically unstable supermassive stars. 19 p2866 A72-38490

Nonlinear oscillations stochastic instability in dynamic systems, discussing nonequilibrium statistical mechanics 19 p2836 A72-38814

Slowly rotating relativistic stars. VI - Stability of the quasi-radial modes. 20 p2966 A72-38909

The stability of a coupled wave-turbulence system in a parallel shear flow. 20 p2948 A72-39797

A theorem of the Liapunov theorem type for the stability of a multidimensional system 20 p2954 A72-39866

Stability and non-stationary vibration of columns under periodic loads. 21 p3116 A72-40336

Instability of rotational and gravitational modes of oscillation. 21 p3078 A72-40773

Simply supported column dynamic stability under axial periodic load, discussing external viscous damping effect 21 p3121 A72-41242

Stationary motions of a triaxial body and their stabilities. 21 p3109 A72-41334

Methods of studying three-dimensional problems of stability in the presence of highly elastic strains 21 p3126 A72-41538

Experimental determination of asymmetry-induced trim angles of attack. 21 p2993 A72-41605

Model studies of plate and shell stability 22 p3233 A72-42055

Airborne towed cargo carrying bodies dynamic stability for single-point suspension system, using linearized small perturbation analysis [AIAA PAPER 72-986] 22 p3136 A72-42328

Bi-planar wind tunnel free flight test and instrumentation for difference between nonplanar and planar dynamic stability of blunt and sharp half cones, providing angular documentation [AIAA PAPER 72-983] 22 p3163 A72-42331

Effect on entry vehicle dynamic stability of aerodynamic and mass asymmetry coupling. [AIAA PAPER 72-973] 22 p3231 A72-42338

The dynamics of the ascending flight of sounding rockets [ONERA, TP NO. 1056] 22 p3231 A72-42582

Taylor instability in the shock layer on a Jovian atmosphere entry probe. 22 p3136 A72-42873

Larmor radius and collisional effects on the dynamic stability of a composite medium. 22 p3212 A72-42990

Baroclinic long wave dynamic instability in Kochin thin layer frontal model, noting beta effect on wave disturbances 22 p3202 A72-43001

German monograph - Stability conditions for a linear homogeneous ordinary differential equation of second order with stochastic parameter excitation. 22 p3199 A72-43055

A stability analysis for tethered aerodynamically shaped balloons. 23 p3250 A72-43332

Input delay influence on dynamic stability of potential finite automata in transition between two states, noting logic circuits synthesis based on Boolean algebra 23 p3274 A72-43350

Spin stabilized ballistic air-to-ground or ground-to-ground rocket, discussing dynamic stability-impact error relationship [SAWE PAPER 928] 23 p3342 A72-43468

Analytical design of adaptive systems with stabilized dynamic characteristics 23 p3276 A72-43783

Dynamic buckling of axially stiffened imperfect cylinders under axial impulse. 24 p3453 A72-44602

DYNAMIC STRUCTURAL ANALYSIS

Large scale structural systems dynamic response analysis, discussing numerical techniques with emphasis on computer codes usage [SAE PAPER 710780] 01 p0137 A72-10272

Bond graph methods for assembling structural dynamic models from component models, using ENPORT programs for simulation or analysis [SAE PAPER 710781] 01 p0137 A72-10273

Matrix formulation of free-free modal synthesis procedures for dynamic analysis of composite structural systems, giving flow charts [SAE PAPER 710783] 01 p0137 A72-10274

Direct-iterative eigensolution technique for simultaneous determination of structural system lowest frequencies and modal patterns, using reduced generalized coordinates and Stodola-Vianello method [SAE PAPER 710784] 01 p0137 A72-10275

Large structural systems dynamic mathematical models, predicting eigenvalue and eigenvector with statistical analysis [SAE PAPER 710785] 01 p0137 A72-10276

Statistical variance of eigenvalues and eigenvectors in random structure dynamic analysis by component mode synthesis [SAE PAPER 710786] 01 p0137 A72-10277

Linear and nonlinear material static and dynamic structural analysis using NASTRAN digital computer program with finite element approach 01 p0140 A72-10983

Resonant vibration and stresses of dynamically nonuniform annular cascade under aerodynamic interaction of alternating different blades 01 p0143 A72-11368

Self-correcting incremental solution procedure for nonlinear structural mechanics, noting application to systems with many degrees of freedom 02 p0260 A72-12272

Noncircular cylindrical shells dynamic analysis using transfer matrix method 02 p0293 A72-12372

Statistical linearization approach to determine approximate instantaneous correlation matrices of nonlinear structure response to nonwhite excitation 02 p0298 A72-12663

Dynamic structural analysis by finite element method, describing error bounds for eigenvalue analysis by elimination of variables 03 p0442 A72-13401

Two dimensional boundary value problem in elasticity for rectangular prism vibrations, considering dynamic stress and frequency characteristics 03 p0449 A72-13908

Dynamic stress concentration at circular hole generated by plane bending wave propagation in thin plate, analyzing dependence on vibration frequency 03 p0453 A72-14139

Dynamic analysis of shallow shells with doubly-curved triangular finite element, investigating natural frequencies, mode shapes and convergence 04 p0585 A72-14844

Computational efficiency of minimization algorithm for solving eigenvalue problem arising from dynamic structural analysis by finite element method 04 p0585 A72-14845

Conforming rectangular and triangular finite elements for plate free vibrations analysis in bending 04 p0585 A72-14846

N-wave dynamic magnification factors for sonic bangs response on complicated structures 04 p0464 A72-14849

Dynamic theory of thin elastic beams under large deflection, taking into account shear deformation and axial stress resultants [ASME PAPER 71-APM-EE] 04 p0590 A72-15183

Double cantilevered specimen crack growth, computing fracture surface energies from dynamical cleavage analysis 05 p0735 A72-16019

Single- and many degree of freedom nonlinear structural systems transient dynamic response by presentation of equations of motion, damping and restoring force functions 05 p0736 A72-16082

Modal synthesis techniques for large structures dynamic analysis, presenting flow charts for computer programming 05 p0736 A72-16083

Dynamic matrix analysis of vibrating three dimensional frame structures, comparing discrete and continuous mass systems 06 p0897 A72-17971

Two dimensional dynamic thermal stresses in Al plate, allowing for Newtonian surface heat transfer 06 p0899 A72-18642

Axially nonuniform thin cylindrical shells dynamic analysis, obtaining free flexural vibration characteristics by hybrid of finite element and classical shell theories 07 p1097 A72-20531

Snapping process dynamics of shallow elastic hinged cylindrical panel of rectangular platform under gaseous, liquid and solid loads 08 p1242 A72-21228

Frequency dependent condensation method for vibration problems in structural dynamics, presenting results for spring-mass system with six degrees of freedom 08 p1250 A72-22143

Two independent damping systems impact vibration analysis from solution of equations of motion by Laplace transformation 09 p1399 A72-22695

Three dimensional dynamic analysis of multilayered orthotropic viscoelastic plates, taking into account skin effect [AD-739806] 09 p1405 A72-22995

Liapunov functional stability analysis in structural dynamics problems including wave equations with nonlinear damping

09 p1407 A72-23457

Structural design systematology of statics and dynamics numerical approximate procedures based on variational principles and differential equations

[SMRT PAPER M 7/4] 10 p1505 A72-24397

Book on continuous elements dynamics covering membrane, torsional, string and elastic beam vibration, four pole techniques, periodic forced motion and surface waves

10 p1557 A72-24674

Literature review of structural safety, treating load, strength, dynamic structural and structural reliability analyses and design aspects

10 p1560 A72-25174

Distributed elastic system discrete model mass, stiffness and damping matrices derivation from dynamic test response data

[AIAA PAPER 72-346] 11 p1728 A72-25375

Liquid propellants coupling effects on parallel stage space shuttle configuration structural dynamics, using forty degree of freedom analytical model

[AIAA PAPER 72-347] 11 p1725 A72-25376

Spacecraft structural dynamics, design and testing, using Fourier transform and analog vibration simulation

[AIAA PAPER 72-349] 11 p1728 A72-25378

Dynamical torsion theory of rods deduced from linear elasticity equations, using averaging technique

11 p1736 A72-25987

Modal damping matrix off diagonal terms measurement in viscous damping exploration for dynamic analysis of linear structures

11 p1736 A72-25988

Geometrically nonlinear structure elastic stress propagation, deformation and dynamic response under impact, using finite element matrix displacement method and computer programs

12 p1879 A72-27189

Dynamic relaxation critical damping estimation in terms of mass dependent load vector concept involving vibration and Rayleigh principle

12 p1844 A72-27197

Finite element equations for hybrid coordinate dynamic analysis of interconnected rigid bodies with elastic flexible appendages for use in spacecraft simulation

12 p1876 A72-27257

Applications of experimental and theoretical structural dynamics - Conference, University of Southampton, England, April 1972

12 p1882 A72-27337

Matrix methods in structural dynamics, discussing frequency response, normal mode, Fourier, Newmark, difference and Houbolt methods

12 p1882 A72-27338

Structural energy loss mechanisms, considering hysteresis, edge damping of panels, acoustic losses, dry friction, multilayer sandwich damping, etc

12 p1882 A72-27342

Dynamic properties of thermosetting plastic composites unidirectionally reinforced by high elastic moduli boron and carbon fiber for aircraft structural applications

12 p1882 A72-27343

Strain work per unit time for static and dynamic pressing processes, taking into account inertial forces

13 p1966 A72-29466

Dynamics of composite materials - ASME Conference, La Jolla, California, June 1972

13 p2060 A72-29690

Directionally reinforced composites treated as homogeneous continuum with microstructure, deriving displacement equations of motion by Hamilton principle

13 p2060 A72-29694

Asymptotic solutions to dynamic problems of thermoelasticity estimation under homogeneous boundary conditions

13 p2062 A72-30067

Finite element method application to dynamic stability of thin plates and shells, noting nuclear reactor structural analysis

[SMRT PAPER M 2/1] 14 p2166 A72-30723

Bending deflections of rectangular plates with laminated orthotropic layers analysis by finite element displacement, comparing with carbon fiber reinforced plastic structures

14 p2167 A72-30905

Structural systems stability and natural frequency analysis eigenvalue problems solution by Sturm sequence method, using finite element technique

14 p2168 A72-30931

Honeycomb sandwich beams dynamic analysis by finite element method with three degrees of freedom per discrete element, obtaining flexural, in-plane and shearing modes

14 p2169 A72-31146

Variational principle based Pian hybrid finite element procedure for static cylindrical shell analysis extended to plate and shell vibration

14 p2169 A72-31149

Dynamic structural analysis of system formed by engine, variable ratio differential and working machine, calculating differential ratio for constant shaft rotation speed

15 p2182 A72-31609

Dynamic boundary value problems for elastic materials with microstructure reduction to tensor equations of motion subject to initial and boundary conditions

15 p2329 A72-32283

Uniqueness, existence and smoothness theorems for elliptic dynamic boundary problems in elasticity theory

15 p2329 A72-32286

Complex structures dynamic analysis by component mode technique, treating modal characteristics as random variables

15 p2331 A72-32555

Flutter instability control in continuous elastic system via feedback

16 p2463 A72-32843

First mode ultraharmonics in nonlinear beam vibration with various boundary conditions and structural properties

16 p2463 A72-32845

Dynamic analysis of transient impact response of finite crack opened by in-plane shear tractions

16 p2464 A72-32920

Finite element method application to nonlinear dynamic problems exemplified by study of plastic deformation behavior of cylindrical billet under impact of heavy rigid body

16 p2466 A72-33019

Dynamic structural analysis of viscoplastic thin walled shells, noting time dependent profile of deflection

16 p2467 A72-33122

Dynamic stress field solution to plane strain crack propagation in elastic body under general loading at constant and nonlinear extension rate

16 p2470 A72-33612

Resonant vibration of thin walled rods and stiffened plates and cylindrical shells, noting aircraft and rocket structures

16 p2471 A72-33679

Theory of the dynamic vibration neutralizer with motion-limiting stops.

[ASME PAPER 71-APMW-14] 17 p2625 A72-34317

Helicopters vibration reduction through fuselage nodalization, discussing analysis method and dynamic scale model and full scale flight test results

[AHS PREPRINT 611] 17 p2489 A72-34487

Free vibrations analysis of linear aerodynamic conservative structures in elastic range by finite element method, applying to transient or random forced responses calculation

17 p2626 A72-34742

Wave propagation in a viscoelastic fiber subjected to transverse impact.

[ASME PAPER 72-APM-27] 17 p2570 A72-34791

Dynamically loaded elastic, viscous, plastic and rigid, viscoplastic structures instantaneous mode responses definitions and characterization by variational criteria with isometric constraints

[ASME PAPER 72-APM-17] 17 p2628 A72-34799

Structural system response to white noise excitation, deriving integral equation for first passage time-density function via Markov process model

[ASME PAPER 72-APM-11] 17 p2629 A72-34805

Nonlinear panel response from a turbulent boundary layer.

17 p2632 A72-35228

Freedoms retention determination eigenvalue analysis of complex structures large dynamic matrices deriving transformation vectors based on maximum swept volume deformation modes

17 p2576 A72-35253

Invariant imbedding and optimum beam design with displacement constraints.

17 p2634 A72-35406

A comparison of approximate methods for solving non-conservative problems of elastic stability.

17 p2634 A72-35410

Bending and vibration of multilayered sandwich plates, presenting static and dynamic analysis method

17 p2635 A72-35976

An approximate theoretical study of the dynamic plastic behavior of shells.

18 p2732 A72-36077

Geometric concepts for microstructure change processes dynamics, considering time variation determination of system topological and metrical properties and particle size distribution evolution

18 p2718 A72-36397

Bounds on the extremal eigenvalues of the finite element stiffness and mass matrices and their spectral condition number.

18 p2705 A72-37202

Vibration of a stiffened ring considered as a cyclic structure.

18 p2739 A72-37205

Solution manifolds for dynamic elasticity equations corresponding to the action of a concentrated load

19 p2878 A72-38213

Bending vibrations of finite length prismatic bar moved in longitudinal direction through tubelike supports, using variational technique

20 p2979 A72-39332

Dynamic strength of tangentially wound toothed blade roots

20 p2979 A72-39586

Response of discrete linear systems to forcing functions with inequality constraints.

20 p2910 A72-39604

The use of pre-cracked Charpy specimens to determine dynamic fracture toughness.

20 p2981 A72-39964

Dynamics of non-circular stiffened cylindrical shells.

21 p3116 A72-40333

Russian book - Mechanics of deformable one-dimensional bodies of variable length.

21 p3116 A72-40387

Dynamic stress concentration of notched strips.

21 p3117 A72-40715

A quadratic programming approach to the impulsive loading analysis of rigid plastic structures.

21 p3120 A72-41205

Simply supported column dynamic stability under axial periodic load, discussing external viscous damping effect

21 p3121 A72-41242

Stress differentiation procedure for screen technique studies in dynamic photoelasticity, giving expressions for elastic modulus and Poisson coefficient

21 p3123 A72-41363

Extremum principles for a class of dynamic rigid-plastic problems.

22 p3235 A72-42522

Dynamic response of structures; Proceedings of the Symposium, Stanford University, Stanford, Calif., June 28, 29, 1971.

22 p3236 A72-42755

Peak load-impulse characterization of critical pulse loads in structural dynamics.

22 p3236 A72-42757

Impulsive loading in structural plasticity, obtaining displacement bounds via deformation theory based on extremum paths

22 p3237 A72-42759

Structural dynamics and aeroelasticity analysis of space shuttle, covering vibration modes, thermal protection system dynamics, ground winds, flutter, buffet and noise

22 p3237 A72-42761

Analysis of the transient response of shell structures by numerical methods.

22 p3237 A72-42762

Response of linear and nonlinear continuous structures subject to random excitation and the problem of high-level excursions.

22 p3241 A72-42970

Structural mass properties mathematical modeling for dynamic structural analysis, describing matrix notation for finite element methods application

23 p3344 A72-43484

Liapunov method extension to dynamically loaded elastically end-restrained columns stability and frames forced vibration boundedness problems

[ASCE PREPRINT 1639] 23 p3352 A72-44110

Dynamic fracture criteria for ductile and brittle metals.

23 p3354 A72-44260

Dynamic buckling of axially stiffened imperfect cylinders under axial impulse.

24 p3453 A72-44602

Mapping of large dynamic deflections of structures.

24 p3454 A72-44606

Dynamic blast loads on preheated and prestressed thin plates.

24 p3454 A72-44607

The damping properties of elastically supported sandwich plates.

24 p3458 A72-44915

Structural problems of the helios solar probe.

24 p3449 A72-45122

DYNAMIC TESTS

Shock precompression effect on dynamic fracture strength of steel and Al alloy, investigating crack initiation and growth

04 p0533 A72-14541

Dynamic deceleration anthropomorphic dummy tests of general aviation occupant lap belt/shoulder harness restraint systems

[SAE PAPER 720325] 11 p1583 A72-25588

Structural evaluations and dynamic testing of solar electric propulsion components, surveying power conditioning panel modal frequencies by holographic interferometry technique

[AIAA PAPER 72-442] 13 p1899 A72-28941

Stress-strain diagrams for constant strain rates in shear of Ti from torsion test machine, deriving constitutive equation for dynamic overstress

16 p2405 A72-33197

Statistical correlation techniques applied to jet aircraft autoland system dynamic ground tests with simulated dynamic and aerodynamic characteristics

16 p2420 A72-33641

Dynamic characteristics of electrical measuring instruments and transducers, discussing static calibration curve, dynamic tests and parameters determination 17 p2557 A72-35757

Design analysis and performance characteristics of a circular test base. [AIAA PAPER 72-845] 20 p2911 A72-39084

Dynamic and static characteristics of jet engine simulators 23 p3327 A72-44286

DYNAMICS

Dynamical aspects of critical phenomena - Conference, Fordham University, New York, June 1970 11 p1701 A72-26022

Soviet book on continuum mechanics covering dynamic, thermodynamic and electrodynamic equations mechanic problems, three dimensional space, internal degrees of freedom, etc 16 p2425 A72-33578

Russian book - Dynamics and acoustics of machines. 22 p3182 A72-42126

Mechanical systems generalization using multilinear transformations and multiple index system flow formalism 24 p3424 A72-44624

DYNAMO THEORY

Oscillatory hydromagnetic dynamo model of variable sign large scale solar magnetic field, using Benard convective cell with Coriolis velocity disturbance 01 p0128 A72-10585

Criticism of cyclonic reversal mechanism and dynamo theory for solar 22-year cycle, proposing penetrating magnetic and general field theory 02 p0276 A72-11641

Dynamo theory MHD equations numerical solution, showing rapid variation of electromagnetic field, hydrodynamic velocities and earth core magnetic moment 02 p0217 A72-11933

Geomagnetic dynamo theory postulating magnetic field by self excitation due to electric currents within earth core 02 p0220 A72-12086

Geomagnetism theory of dynamos in homogeneous fluid masses, considering Rikitake self reversing, kinematic and hydromagnetic dynamo problems 02 p0220 A72-12088

Solar hydrodynamic dynamo theories concerning convective zone large scale velocity fields and magnetic activity cycle 03 p0433 A72-13360

Solar magnetic field and solar cycle dynamo theory based on mean field MHD 03 p0433 A72-13361

Large scale solar magnetic field dynamo model in terms of force-free constituents series, deducing periodic solution by eigenvalue method 03 p0433 A72-13362

Small amplitude velocity waves turbulent distribution in infinite medium, demonstrating kinematic dynamo regeneration 04 p0573 A72-14906

Large scale alternating solar magnetic field generation by outer shell convective flow, constructing oscillator hydromagnetic dynamo model 05 p0715 A72-16232

Electrical conduction in orthogonal coordinates from nondipole geomagnetic field effect on conductivity tensor of ionospheric dynamo region 05 p0657 A72-16260

Nighttime ionospheric dynamo current modulation due to galactic X ray ionization, observing diurnal sidereal time variation in geomagnetic field 07 p1056 A72-18898

Dynamo action of magnetohydrodynamic fluid motions with two dimensional periodicity 07 p1042 A72-19611

MHD dynamo model for incompressible real electrically conducting fluid unsteady flow 07 p1044 A72-20304

Digital computer numerical procedure to solve dynamo theory MHD equations for earth nucleus, using combination of Fourier and finite difference methods for integration 08 p1155 A72-20810

Earth precession as origin of geomagnetic field, discussing dynamo theory and core electroconductivity 10 p1472 A72-24524

Dynamo theory of magnetic stars, proposing symmetrical rotator as alternative to skew rotator 10 p1546 A72-24833

Solar magnetic field variation during solar rotation from sunspot observations, noting similarity to magnetic stars and behavior as quadrupole magnetic rotator 12 p1871 A72-27746

Dynamo theory MHD equations numerical solution, showing rapid variation of electromagnetic field, hydrodynamic velocities and earth core magnetic moment 13 p1949 A72-29245

E and F regions plasma horizontal drift measurements by oblique incidence incoherent scatter radar system, suggesting solar semidiurnal tidal oscillation dynamo action 13 p2031 A72-29386

Solar cycle dynamo theory and Babcock and Leighton model inadequacies, considering alternative theory based on deep magnetic field 13 p2046 A72-29729

Parker dynamo theory failure in explanation for galactic magnetic field origin and form, noting reasons 13 p2050 A72-29957

Turbulent plasma dynamo mechanisms of magnetic field origin in astrophysics, noting Steenbeck and Parker theories 14 p2162 A72-31150

Earth core hydromagnetic oscillations with respect to geomagnetic secular variation time scales and role in dynamo process-produced geomagnetic field 15 p2222 A72-31279

Geomagnetic substorm magneto-ionospheric effect, discussing electric field transmission, magnetic field variations and currents flowing in dynamo region 15 p2230 A72-32259

Alpha effect solar dynamo model magnetic field and velocity expansion in spherical harmonics, solving mean field induction equation 15 p2316 A72-32755

Kinematic dynamo theory of electric currents flow in earth liquid core, discussing model, field electrodynamics and hydromagnetic dynamo 16 p2385 A72-33340

Precessional torque of conducting fluid as source of geodynamo action, noting oblate spheroidal experiment 16 p2385 A72-33341

Turbulent dynamo theory based on functional analysis, noting equation with variational derivatives of characteristic functional 16 p2427 A72-34155

A physical mechanism for the production of solar flares. 17 p2608 A72-35088

On the state of the geomagnetic field and its reversals. 17 p2548 A72-35323

Dynamo instability and feedback in a stochastically driven system. 18 p2678 A72-36013

A kinematic theory of large magnetic Reynolds number dynamos. 19 p2833 A72-37248

The generation of magnetic fields in astrophysical bodies. IX - A solar dynamo based on horizontal shear. 20 p2966 A72-38910

Lagrangian approach to kinematic-dynamo equations for astrophysical bodies, obtaining variational principle for eigenvalue computation 20 p2966 A72-38911

The Nyquist criterion for kinematic-dynamo action. 20 p2956 A72-38912

Spherical kinematic dynamo models with asymmetric magnetic fields based on mean field electrodynamics and on nearly axisymmetric limit 20 p2954 A72-39875

One dimensional migratory dynamo model for alpha effect turbulence controlled by increasing magnetic field, considering oscillatory antisymmetric solutions relation to solar cycle 20 p2972 A72-39877

Mathematical model of earth liquid core dynamo mechanism for magnetic field maintenance based on simple motions with spherical harmonic form 21 p3048 A72-40400

Numerical treatment of a model of the hydromagnetic dynamo with a selected system of convection in the earth's core. 23 p3284 A72-43422

The effect of change in the geomagnetic dipole moment on the rate of the earth's rotation. 23 p3285 A72-43819

Dynamo theory for lunar magnetic field based on hypothetical thermal convection in rotating moon core analogous to earth 23 p3341 A72-44448

DYNAMOMETERS

High precision strain gage dynamometers design and testing at ONERA Modane test center, discussing accuracy limitation due to hysteresis and creep effects [ONERA, TP NO. 995] 05 p0642 A72-15859

Automated microdynamometer for thin plastic specimens microtension tests with continuous microscopic observation and automatic diagram plotting 11 p1633 A72-26288

Automatic remote mechanical system parameter control by electrical elements, introducing rigidity for mass sensitive measurement in dynamometry 16 p2370 A72-33956

DYNAMOS

U ROTATING GENERATORS

DYNODES

Model of dynodes system with random electron-hole pairs number, calculating equations for mean fluxes transport and correlated noise fluctuations 09 p1280 A72-23116

Electron-optical parameters effect on GaP/Cs/dynode photomultipliers time response characteristics, describing computer simulation and pulse response measurement techniques 15 p2234 A72-31532

Ceramic envelope electron multiplier design with hemispherically shaped dynodes, discussing electron optics, photosensitivity and applications 15 p2234 A72-31533

DYSON THEORY

First and second moment of an optical wave propagating in a random medium - Equivalence of the solution of the Dyson and Bethe-Salpeter equation to that obtained by the Huygens-Fresnel principle. 17 p2580 A72-34290

DYSPROSIUM

Nd-Dy alloy magnetic and structural properties over entire composition range 08 p1217 A72-21596

Some new Dy II identifications in the solar spectrum. 17 p2616 A72-35696

E

E LAYERS

U E REGION

E REGION

NT SPORADIC E LAYER

Thermally excited E layer tidal winds based on UV radiation as thermal source, using isothermal atmosphere model 01 p0055 A72-10429

Equatorial E region short wave oblique incidence propagation experiment showing transmitted impulse delay increase with frequency decrease 01 p0056 A72-10437

Ray path and absorption calculation for mf and hf radio wave oblique propagation through model ionosphere in nighttime, noting E region ionization role 02 p0184 A72-12875

Global morphology of integrated product with respect to D and E regions electron concentration height and collision frequency 03 p0345 A72-12981

Solar X-ray control of E and sporadic E layers during November 1966-July 1968, discussing blanketing frequency 03 p0413 A72-13535

Thumba night time equatorial E region electron density profiles from rocket-borne Langmuir probe experiments 04 p0517 A72-14957

Magnetic latitude effect on wave dispersion in drifts and random movements of ionization irregularities in E region, suggesting charged particle precipitation role 04 p0518 A72-14964

Electron energy derivation from contaminated Langmuir probe, explaining E region high temperature 05 p0654 A72-16007

Structure and movements of E region inhomogeneities, describing ionospheric drift velocities and directions for different seasons 05 p0660 A72-17178

If instability mode in partly ionized plasma due to electron temperature gradient aligned perpendicular to magnetic field, applying to E and F regions [AD-737931] 06 p0804 A72-17460

Night source ionized component profiles in chemistry and aeronomy of D and E regions, considering scattered L alpha and beta emissions and corpuscular fluxes 07 p0936 A72-20038

Neutral species chemical reactions in D and E regions, taking into account effects of photodissociation and transport by horizontal and vertical flow and molecular diffusion 07 p0936 A72-20039

Height-frequency characteristic forecasting for E layer at arbitrary time and point location, using solar angle zenith relationship 08 p1153 A72-20708

Ionogram electron density-height distributions for analysis of multiple cusp structure near E region critical frequency 08 p1156 A72-21101

Seasonal variation in ionospheric horizontal drift velocities under normal E and sporadic E conditions for middle latitudes 08 p1157 A72-21115

D and E region winds over Europe - Conference, London, April 1971 08 p1159 A72-21526

Circulation motions in D and E regions, discussing planetary waves, tidal oscillations, gravity waves, turbulence and drift measurement 08 p1160 A72-21527

Harmonic analysis of E layer drift measurements by closely spaced receiver method combined with on-line analog computer 08 p1160 A72-21529

Steady nonlinear waves propagation along ring electron beam axis analogous to ionospheric F layer 08 p1215 A72-21723

D and E region ion chemistry - Conference, University of Illinois, Urbana, July 1971

09 p1274 A72-22352
D and E regions positive ion chemistry based on E and F regions ion-molecule reaction rate constants comparison with laboratory measurement

09 p1275 A72-22360
Midlatitude auroral zone positive ion mass spectrometer observations in E region, noting diurnal variation and sporadic E events

09 p1375 A72-22364
E region ion density and composition determination by incoherent scatter radar measurement
[AD-742618]

09 p1375 A72-22365
D and E region ion chemistry reaction rate measurements, noting hydration, charge exchange and ion-atom interchanges

09 p1275 A72-22366
D and E region electron density profile, investigating geographical, diurnal, seasonal and sunspot cycle variations

09 p1376 A72-22370
D and E regions electron densities measurement by incoherent scattering technique, noting sporadic E layer and echoes
[AD-742616]

09 p1376 A72-22371
Regular tidal winds and irregular gravity waves domination of E region transport processes

10 p1477 A72-25161
Three dimensional linear analysis of ionosphere cross field instability, noting potential as E region irregularities source

10 p1478 A72-25166
Ionosphere composition and ion concentration measurements for D and E region, including aerodynamic and plasma dynamic effects

11 p1621 A72-25836
Nighttime E region electron density variation effects on MF and HF radio wave propagation, discussing ionospheric absorption detection experiments

11 p1593 A72-26070
Daytime electron density profile in E and D regions from rocket lower ionosphere sounding, noting winter electromagnetic absorption anomaly

11 p1622 A72-26101
E and F region apparent and true drifts over magnetic equator correlated to solar activity, comparing electron density sensitivity to geomagnetic range

11 p1623 A72-26104
Magnetic field line connection between F region irregularities causing scintillation and ionospheric conditions inducing spread E

11 p1625 A72-26405
Lunar variations of Peruvian electrojet, analyzing E region electron drift and geomagnetic field H component data

11 p1626 A72-26415
E layer effective recombination coefficient determination from solar flare enhanced electron density and solar X-ray flux measurements and ionospheric relaxation time constant evaluation

11 p1627 A72-26766
Solar X-rays absorption profiles and residual fluxes in D and E layers during 7 March 1970 eclipse from rocket measurements

12 p1863 A72-27146
Ionosonde observations and Faraday rotation measurements of E and F region total electron content during two solar eclipses

12 p1801 A72-27154
Beamed radio waves interaction in E and F1 regions propagation, noting beam width and field amplitude changes caused by defocusing

13 p1945 A72-28579
Upper atmosphere atomic oxygen distribution calculated for D and E region aeronomy problems solution

13 p1947 A72-28604
Daily variations in E region horizontal drift at Thumba/India, showing daytime westward and nighttime eastward drifts

13 p1949 A72-29275
E and F regions plasma horizontal drift measurements by oblique incidence incoherent scatter radar system, suggesting solar semidiurnal tidal oscillation dynamo action

13 p2031 A72-29386
Diurnal and seasonal variations of ionospheric absorption in D and E regions, discussing blanketing sporadic F presence effect

13 p1922 A72-29392
F region ionosonde observations to reconstruct ionizing X ray and far UV radiation source distribution over solar disk during March 1970 total solar eclipse

13 p2044 A72-29552
F region electron density distortion at magnetic equator by Sq current system, noting dependence on alpha coefficient profiles

13 p1952 A72-29663
E region drift velocity estimates from amplitude and phase measurements of pulsed radio waves reflected from lower ionosphere

13 p1923 A72-29664

Ionospheric multifrequency absorption measurement description by empirical expressions in terms of E layer critical frequency, solar activity and seasonal effects

13 p1952 A72-29667
E region electron collision frequency vertical distribution by ground measurement of radio wave absorption, using electron concentration data obtained by rocket-borne interferometer

14 p2100 A72-30462
Photochemical model of N and NO distribution based on E region ion composition

15 p2226 A72-31916
Ion chemistry and heating of daytime ionosphere E and lower F regions, calculating neutral atmosphere densities, ion production rates and solar EUV radiation absorption

15 p2192 A72-32253
Semidiurnal variation in O I 5577 A nightglow due to lunar tidal dynamics effect in E and F regions

16 p2383 A72-32971
Dispersive motions in the ionosphere.

17 p2546 A72-34696
Nonlinear saturation of 'type I' irregularities in the equatorial electrojet.

18 p2685 A72-35990
Height-frequency characteristic forecasting for E layer at arbitrary time and point location, using solar zenith angle relationship

19 p2790 A72-38336
Parametric coupling of large amplitude pump wave to E layer plasma mode to explain auroral electrojet irregularities external production and control

19 p2793 A72-38746
Regression-line studies of E-region seasonal anomaly.

19 p2794 A72-38863
On the diurnal and seasonal variations of the D- and E-regions above Kjeller.

20 p2917 A72-39529
Electron-density increase in the E layer below an artificial barium cloud.

20 p2920 A72-39983
Geomagnetic DP-2 variation base level from E region electron drift velocity measurements in equatorial electrojets

22 p3169 A72-42013
An investigation of the ground diffraction pattern of radio waves reflected by the ionosphere.

22 p3154 A72-42362
Different conductivities effect in ionospheric E layer of polar cap regions, noting electric current along high latitude magnetic field force lines

23 p3283 A72-43370
High power radio transmitter for structural investigation of ionospheric D and E regions by signal reflection and electron concentration profiles

23 p3263 A72-43378
Beamed radio waves interaction in E and F1 regions propagation, noting beam width and field amplitude changes caused by defocusing

24 p3397 A72-45079
Upper atmosphere atomic oxygen distribution calculated for D and E region aeronomy problems solution

24 p3398 A72-45104
Mean dissociative and effective recombination coefficients of E region, discussing charged particle reactions effect on model formation

24 p3399 A72-45584

EAR

NT COCHLEA
NT EARDRUMS
NT LABYRINTH
NT MIDDLE EAR
NT SEMICIRCULAR CANALS
NT VESTIBULES

Distensibility and stress relaxation characteristics of capacitance and resistance vessels of isolated rabbit ear as function of basal tone

04 p0473 A72-15124
Various work-rest cycles and environmental temperature effects on body temperature, determining external auditory canal and core temperature relationship

08 p1123 A72-20886
Ear site body temperature measurement relation to radiant heating of scalp and upper face

12 p1768 A72-28333
Thermal relationship between tympanic membrane and hypothalamus in conscious cat and monkey.

17 p2499 A72-34344
The physiology of hearing. I - The middle and the inner ear

EAR PRESSURE TEST

Simulated sonic boom effect on tracking performance and autonomic response, noting heart rates, skin conductance and startle reflex

06 p0767 A72-17868

EAR PROTECTORS

Earplugs effect on passenger speech reception and intelligibility in rotary wing aircraft, noting protection against noise annoyance, fatigue and deafening

01 p0022 A72-11294

Flight helmet optimal fitting technique, using automatic recording audiometer and noise source for acoustic leakage detection

04 p0479 A72-14873
Aircraft noise protective earplug design, employing perforated and slit modifications for additional protection without tympanic membrane pressure excess risk

07 p0933 A72-20187
USAF V-51R noise protector earplugs modification to allow for pressure equalization during aircraft climb and descent

12 p1774 A72-28276
Earplugs effectiveness for narrow band white noise real-ear attenuation and wearability

16 p2358 A72-33325

EARDRUMS

Aircraft noise protective earplug design, employing perforated and slit modifications for additional protection without tympanic membrane pressure excess risk

07 p0933 A72-20187
Myogenic and eardrum evoked auditory potentials and cortical responses to 0.2 millisecond voltage pulse acoustic stimuli

20 p2891 A72-38932

EARLY APOLLO SURFACE EXPERIMENTS

PACKAGE

U EASEP

EARLY STARS

NT PROTOSTARS

NT T TAURI STARS

Radiative, segregation and evaporation processes of ice particles surrounding early type stars of Orion association, justifying ice particle model for dust grains

01 p0129 A72-10794
Early O and Of spectroscopic and photometric data, evaluating atmospheric properties, surface gravities and temperature scales

01 p0131 A72-11009
IR point source Becklin star spectrum consistent with highly reddened early-type supergiant with weak absorption masked by low resolution

01 p0133 A72-11094
Small Magellanic Cloud NGC 371 region photometric studies for cepheids period-luminosity relations, noting domination by young supergiant stars

03 p0425 A72-13258
Interstellar absorption in Perseus OB 2 association direction from UBVY-beta photometry of early type stars in four fields

03 p0438 A72-13875
F and early G dwarf stars atmospheric models and line data, deriving temperatures, abundances and gravities

04 p0577 A72-15282
Early type supergiant far UV spectrum observations, showing broad absorption feature near 1720 A

04 p0578 A72-15315
Equilibrium temperatures of interstellar grains around early stars, discussing dependency on grain size and stellar distance

06 p0875 A72-17297
Early type stars photoelectric spectra obtained with Mariner 9 UV spectrometer, obtaining resonant line features and spectral energy distribution

06 p0890 A72-18347
Model atmosphere and spectral analysis for two early B-type supergiant stars, deducing stellar mass and evolutionary phase

07 p1070 A72-19085
Rapid rotation effect on weak and intermediate strength early type stellar radiation spectral absorption lines

09 p1390 A72-23527
Galactic nucleus evolutionary processes, considering mass ejection from newly formed massive stars, gas concentration toward center, kinetic energy exchange and stellar collisions

10 p1535 A72-23907
IR and optical observations of cluster surrounding Herbig Be type star BD plus 40.4124, noting extreme youth of group

11 p1721 A72-26122
H II regions radial velocities in Carina arms from Fabry-Perot interferometric H alpha measurements, determining early stars distances from spectroscopic and photoelectric observations

14 p2159 A72-30740
Average interstellar electron and early star density in Galactic disk, examining hot stars ionizing photons and H II regions photoionization

14 p2161 A72-31044
Early B stars with normal helium abundances and small rotational velocities, deducing gravity from H lines and ESW stark broadening

15 p2316 A72-32751
Meridian circulation with rapid differential rotation in radiative stellar envelopes.

17 p2605 A72-34532
Photometric study of the open cluster NGC 2232.

18 p2728 A72-36742
Early star absolute magnitude from equivalent H gamma and delta line widths and Balmer hydrogen series line

19 p2859 A72-37908

Galactic structure at galactic longitudes from 230 to 355 deg on the basis of photoelectric UVB H beta photometry of 55 southern open star clusters
19 p2867 A72-38513

Structure and motions in the Carina spiral feature.
20 p2973 A72-39880

Mechanical equilibrium equation of nongray stellar matter, approximating electron pressure vs temperature in early stellar atmospheres
21 p3109 A72-41435

The dynamical effects of stellar mass loss on diffuse nebulae.
22 p3224 A72-42380

EARTH (PLANET)

Early catastrophic degassing of earth, considering mechanisms and times from volatiles abundances and distribution in atmosphere, hydrosphere and crust
03 p0350 A72-13744

Earth compartmentalization by meridians and parallels, discussing structuralization and latitude-longitude dissymmetry
03 p0350 A72-13800

Earth limb radiance measurements inversion, yielding temperature distribution as function of altitude in real atmospheres
03 p0384 A72-14146

High temperature thermal properties of solid and liquid metals and rocks and minerals, discussing earth heat balance and measurement methods for heat capacity and conductivity
04 p0596 A72-14653

Unified coordinate system for earth planetary distribution of F2 and sporadic E layer transmission parameters, suggesting geomagnetic longitude and modified magnetic inclination
08 p1153 A72-20726

Lunar evolution theory, discussing terrestrial cluster dynamics during earth accumulation
08 p1231 A72-21129

Free nutations of earth from 1904-1941 latitude observations at Pulkovo, noting diurnal variations with almost identical amplitudes
09 p1388 A72-23058

Earth free diurnal nutation parameters comparison based on determinations from latitude observations at various observations
09 p1388 A72-23059

Earth chord length determinations, using synchronous photographic satellite observations with simultaneous topocentric distance data from laser measurement
14 p2103 A72-31076

Electromagnetic transient coupling between ungrounded loops for two layer conducting half space approximation of earth
16 p2388 A72-34007

Unified coordinate system for global distribution of F2 and sporadic E layer transmission parameters, suggesting geomagnetic longitude and modified magnetic inclination
19 p2791 A72-38354

EARTH ALBEDO

Earth radiation climatology, noting qualitative agreement between calculated and satellite measured outgoing radiation data with allowance for inaccuracies due to albedo levels overrating
01 p0095 A72-10958

Rocket-borne apparatus for X ray measurement in 25 to 200 keV range, noting primary diffuse component and earth albedo spectral analyses
02 p0231 A72-12448

Bidirectional reflectance at several wavelengths from moonlit earth observations by airglow photometer on OGO-4 satellite
03 p0433 A72-13428

Time variations of zonal averages of albedo and absorbed solar radiation derived from brightness data of digitized satellite pictures
03 p0385 A72-14228

Solar radiation angular field structure from upper atmospheric boundary scattering, taking into account underlying surface albedo fluctuations
06 p0807 A72-17942

Seasonal and diurnal variations of earth albedo from turbidity measurements, showing lower atmosphere moisture effect
08 p1237 A72-21799

Earth albedo neutrons energy and angular distributions, suggesting neutron source of inner radiation belt trapped protons
11 p1712 A72-25880

ESRO satellites solar array performance under orbital environmental conditions, discussing radiation damage and earth albedo effects
12 p1759 A72-28047

D region chemistry based on earth albedo effects from airborne radio sounding experiments, suggesting visible light energy flux role
13 p1950 A72-29342

Solar radiation angular field structure from upper atmospheric boundary scattering, taking into account underlying surface albedo fluctuations
16 p2386 A72-33783

Sea surface albedo for short wave solar radiation in terms of sun altitude and atmospheric transmittance, noting wind and surface roughness effects
18 p2687 A72-36642

Solar radiant energy reflection and absorption by cloud layers
21 p3049 A72-41795

EARTH ATMOSPHERE

NT ARTIFICIAL RADIATION BELTS
NT CHEMOSPHERE
NT D REGION
NT E REGION
NT EXOSPHERE
NT F REGION
NT FREE ATMOSPHERE
NT INNER RADIATION BELT
NT IONOSPHERE
NT LOWER ATMOSPHERE
NT LOWER IONOSPHERE
NT MAGNETOPAUSE
NT MAGNETOSPHERE
NT MESOPAUSE
NT MESOSPHERE
NT MIDLATITUDE ATMOSPHERE
NT OUTER RADIATION BELT
NT OZONOSPHERE
NT PROTON BELTS
NT RADIATION BELTS
NT SPORADIC E LAYER
NT THERMOSPHERE
NT TROPOPAUSE
NT TROPOSPHERE
NT UPPER IONOSPHERE

Radiative heat transfer equilibrium in Earth, Venus and Mars atmospheres, taking into account interaction with ground
01 p0058 A72-10561

Air law concept as totality of legal regulations related to atmosphere use by flying devices, discussing relation to international environmental protection
01 p0147 A72-11107

World Weather Watch and Global Atmospheric Research Program remote sensing applications, considering weather prediction and modification, atmosphere pollution monitoring and global atmosphere mathematical modeling and simulation
02 p0208 A72-11784

Cloud streeting in earth atmosphere, discussing satellite observations and theoretical formation mechanisms
04 p0541 A72-14457

Optical angle of refraction through earth mean atmosphere determination by three models of refractivity and iterative methods
04 p0515 A72-14884

Solar radiation effects on earth atmosphere with MR-12 and M-100 meteorological rockets launched at onset of chromospheric flare, noting atmospheric parameters measurements
04 p0580 A72-15453

Solar effects contradictory relationships with earth atmosphere, discussing geomagnetic disturbance, annual variations, stratospheric transport and high energy particles
05 p0656 A72-16233

Moment of inertia of earth atmosphere relative to earth axis of rotation
06 p0808 A72-18038

Environmental forces effects on gravity oriented satellites attitude dynamics, considering earth atmosphere aerodynamic and solar radiation forces effects
07 p1085 A72-19060

Transcript of conference on origins of life covering cosmic evolution, abundance and distribution of biologically important elements, earth and Mars atmosphere evolution, etc
07 p1074 A72-19450

Solar-terrestrial physics - Conference, Leningrad, May 1970
07 p0977 A72-20004

On-line digital computer maximum likelihood estimate of Earth atmosphere profile ahead of flight vehicle using discrete measurements of density, temperature and pressure
08 p1156 A72-20853

Planetary atmospheres composition diversity, discussing evolution of Mars, Venus, earth and Jupiter from primitive solar nebula
08 p1119 A72-22012

Turbulent earth atmosphere optical inhomogeneities determination from solar limb image characteristics in motion pictures of solar disk edge
09 p1305 A72-22233

Steady state global climatic model for earth-atmosphere-ocean system, discussing perturbations effect on stability
09 p1343 A72-22426

Moment of inertia of earth atmosphere relative to earth axis of rotation
11 p1622 A72-25974

Earth atmosphere boundary layer nonstationary problems, considering diurnal changes of meteorologi-

cal fields and nonperiodic evolution of elements from wind variations
12 p1841 A72-27988

Russian papers on solar activity effects on earth atmosphere and biosphere covering climate, vegetation, animals and man
12 p1763 A72-28206

Jupiter, Saturn and earth atmospheric circulation seasonal variation data analogies, noting factors governing planetary atmospheric temperature
13 p2048 A72-29813

Meteoritic particle movement in earth atmosphere, discussing deceleration dependence on velocity, atmospheric density and surface evaporation reactive forces
14 p2152 A72-30493

Venus and earth atmospheres dissimilarity from radio astronomy and space probes observations
14 p2158 A72-30695

Report to COSPAR on Australian space program covering earth atmosphere, cosmic and synchrotron radiation, X ray astronomy, weather satellites, deep space and sounding rockets
15 p2338 A72-32007

Report to COSPAR on Indian space program covering organizations, ground station facilities, atmosphere and astronomy studies and international collaborations
15 p2338 A72-32012

Monte Carlo treatment of Lyman-alpha radiation in a plane-parallel atmosphere.
17 p2598 A72-34538

Russian book on atmosphere studies covering determination of periodic variations in meteorological elements to assess seasonal pressure, temperature and wind variations
17 p2546 A72-34975

Synthesis of a nonlinear law for the control of spacecraft motion in the atmosphere of the earth
17 p2621 A72-35202

Earth and Mars - Evolution of atmospheres and surface temperatures.
17 p2613 A72-35395

Book - The earth's atmosphere
17 p2550 A72-35797

Terrestrial and solar atmospheres general circulations from laboratory experiments on rotating cylinders filled with differentially heated fluids, noting solar equatorial acceleration
17 p2551 A72-35941

Meteoritic particle motion in earth atmosphere, discussing deceleration dependence on velocity, atmospheric density and surface evaporation reactive forces
19 p2864 A72-38322

The determination of the vertical structure of the atmosphere from satellite measurements
19 p2792 A72-38700

Ammonia photolysis and the role of ammonia in chemical revolution.
20 p2898 A72-39375

Apollo 16 far-ultraviolet camera/spectrograph - Earth observations.
21 p3105 A72-40600

Brightness temperature of the terrestrial sky at 2.66 GHz.
22 p3173 A72-42516

Earth atmosphere boundary layer nonstationary problems, considering diurnal changes of meteorological fields and nonperiodic evolution of elements from wind variations
22 p3202 A72-43002

Lunar and solar gravitational effects on earth atmosphere, describing latitudinal distribution of cyclone centers by momentum distribution of horizontal tide-generating forces
23 p3310 A72-43249

Isothermal atmosphere inhomogeneities effects on electromagnetic cascade electrons integral energy spatial distribution
23 p3331 A72-44433

Early stage condensation in planetary formation, discussing atomic and molecular reactions in interstellar space and earth outer atmosphere properties
24 p3444 A72-45452

A practical evaluation of earth-backscatter simulation and an estimate of the HF ground-scatter coefficient.
24 p3380 A72-45636

EARTH AXIS

Terrestrial pole motion components, discussing variations in Chandler wobble period and sidereal motion direction and average annual motion along ellipse
07 p0976 A72-19815

Prime geocentric meridian longitudes and UT, discussing position in terrestrial rectangular coordinates in relation to earth pole motion
07 p0976 A72-19816

Chandlerian wobble period correlation to damping coefficient of earth polar motion for 10 yr intervals during 1900-1970
10 p1475 A72-24871

Geocentric coordinates transformation from system related to mean pole and mean equator into instantaneous

- ous pole and instantaneous equator system, noting Cartesian coordinates 17 p2548 A72-35359
- Terrestrial pole motion components, discussing variations in Chandler wobble period and sidereal motion direction and average annual motion along ellipse 17 p2549 A72-35740
- Prime geocentric meridian longitudes and UT, discussing position in terrestrial rectangular coordinates in relation to earth pole motion 17 p2549 A72-35741
- The Chandlerian wobble from 1900 to 1970. 18 p2727 A72-36731
- EARTH CORE**
- Dynamo theory MHD equations numerical solution, showing rapid variation of electromagnetic field, hydrodynamic velocities and earth core magnetic moment 02 p0217 A72-11933
- Spiral geometry and distribution of global geomagnetic anomalies, discussing ideal liquid motion between concentric spherical surfaces of earth sub-core and core radii 02 p0218 A72-11952
- Geomagnetic dynamo theory postulating magnetic field by self excitation due to electric currents within earth core 02 p0220 A72-12086
- Conducting fluid convective motion in earth core estimated from geomagnetic field and time derivative data at earth surface 02 p0220 A72-12087
- Chapman uniform electrical conductivity core model for geomagnetic disturbance daily variations due to solar wind, noting error in analysis 02 p0222 A72-12794
- Earth mantle and core density using Monte Carlo models compared with lunar structure from crust and seismology data, noting planetological contrast 04 p0571 A72-14616
- Excess secular change in ecliptic obliquity in relation to earth internal motion due to mantle-core coupling 04 p0575 A72-15028
- Viscosity calculation of earth core at inner and outer boundary, using Andrade formula 06 p0807 A72-17760
- Digital computer numerical procedure to solve dynamo theory MHD equations for earth nucleus, using combination of Fourier and finite difference methods for integration 08 p1155 A72-20810
- Earth precession as origin of geomagnetic field, discussing dynamo theory and core electroconductivity 10 p1472 A72-24524
- Changes in total magnetic energy stored outside earth core accompanying earth dipole field decrease over 60 years period from paleomagnetic measurement 11 p1623 A72-26108
- Dynamo theory MHD equations numerical solution, showing rapid variation of electromagnetic field, hydrodynamic velocities and earth core magnetic moment 13 p1949 A72-29245
- Spiral geometry and distribution of global geomagnetic anomalies, discussing ideal liquid motion between concentric spherical surfaces of earth sub-core and core radii 13 p1949 A72-29264
- Earth core hydromagnetic oscillations with respect to geomagnetic secular variation time scales and role in dynamo process-produced geomagnetic field 15 p2222 A72-31279
- Kinematic dynamo theory of electric currents flow in earth liquid core, discussing model, field electrodynamics and hydromagnetic dynamo 16 p2385 A72-33340
- Planetary waves in terms of geomagnetic secular variation due to earth core fluid oscillation under MHD forces, using thick shell model 16 p2385 A72-33342
- Mathematical model of earth liquid core dynamo mechanism for magnetic field maintenance based on simple motions with spherical harmonic form 21 p3048 A72-40400
- Numerical treatment of a model of the hydromagnetic dynamo with a selected system of convection in the earth's core. 23 p3284 A72-43422
- The effect of change in the geomagnetic dipole moment on the rate of the earth's rotation. 23 p3285 A72-43819
- EARTH CRUST**
- Continental growth by island arc volcanism, observing Si, K, Rb, Ba, Sr and light rare earth element abundances 01 p0052 A72-10068
- Earth planetary structure from gravitational information, discussing crust, mantle, gravity anomalies, satellite and ground observation methods and improved earth model 04 p0519 A72-15075
- Volcanic basalt geochemistry in Afar Triple Junction, suggesting relation to crustal thinning and melting zone shallowing under rift 05 p0658 A72-16722
- Fractional crystallization and crustal contamination roles in origin of quaternary basaltic magmas from Black Rock Desert Region in Utah 06 p0810 A72-18515
- Spectral distribution characteristics of geomagnetic field mean intensity variations, relating longitudinal specific resistance and integral conductivity of top rock layer 09 p1296 A72-22236
- Plane stratified earth crust parameters determination from dispersion curve of Rayleigh surface waves fundamental tone 09 p1304 A72-23488
- Microorganisms effects on oxygen and compounds cycles, leading to changes in oxygen distribution in earth crust, hydrosphere, atmosphere and biomass 09 p1267 A72-23592
- Earth electrical parameters measurement by radio wave methods involving electromagnetic propagation along or reflection from surface, considering penetration depth, earth stratification and surface inhomogeneities 10 p1474 A72-24737
- Autocorrelation functions of anomalous magnetic field and earth crust structure of central portion of Arctic Ocean, using sliding energy spectrum method 13 p1946 A72-28589
- Attenuation rate of electromagnetic waves for dominant ELF and VLF modes of earth crust waveguide 15 p2200 A72-32110
- Earth crust waveguide three layer model for electromagnetic wave propagation, showing mode relation to absorption conditions 16 p2362 A72-33074
- Autocorrelation functions of anomalous magnetic field and earth crust structure of central portion of Arctic Ocean, using sliding energy spectrum method 24 p3397 A72-45089
- EARTH CURRENTS**
- U TELLURIC CURRENTS**
- EARTH ENVIRONMENT**
- Remote sensing of environment - Conference, University of Michigan, May 1971 02 p0207 A72-11776
- Radar and radiometric millimeter wave signal systems in near earth environment for remote detection purposes 04 p0494 A72-15610
- Aerial photography interpretation for studies of natural environment and resources 09 p1312 A72-23277
- Large data processing systems for requirements of meteorology, environmental, earth resources inventories and hydrology in 1980s 10 p1446 A72-25095
- Book on earth environment covering atmospheric structure, terrestrial magnetic field, solar radiation, micrometeorites, ionosphere and van Allen belts 10 p1478 A72-25173
- Short and long range contributions of NASA space program to life quality improvement, discussing land and crop surveys, communications and environment modification 11 p1748 A72-26098
- Space applications benefits through international cooperation, emphasizing environmental problems 14 p2175 A72-31143
- Cartographic and environmental surveys by Skylab orbiting stations and ERTS satellite using panoramic and mapping cameras and laser altimeter 15 p2232 A72-31247
- Coastal environment remote sensing from satellite and aircraft imaging platforms for geological, oceanographic and ecological investigations 15 p2232 A72-32622
- Canadian program for global environmental and world resources monitoring system, discussing management, technology and user interface [AIAA PAPER 72-742] 18 p2742 A72-36548
- One fluid solar wind model prediction from corona base density and temperature for parameters at earth 19 p2853 A72-38733
- EARTH FIGURE**
- U GEODESY**
- EARTH HYDROSPHERE**
- Terrestrial biosphere back contamination from outer space organisms, discussing microbiologic control and prevention requirements 01 p0020 A72-10825
- Space TV images use in hydrothermal temperature discontinuity front location, examining cloud cover distributions over Sea of Japan 02 p0214 A72-11872
- Chesapeake Bay aquatic ecosystems observations, using satellite remote sensing multispectral photography and imagery 02 p0215 A72-11885
- Automated photometric wetland mapping using aerial color film microdensitometric analysis and computer techniques 02 p0215 A72-11886
- Biochemical functions of organisms in evolution of biosphere, discussing redox reactions, elementary compositions and metal compounds role in photosynthesis 04 p0470 A72-14796
- Soviet book on gravitational effects on animal evolution covering land and aqueous conditions adaptation and weightlessness in space 06 p0763 A72-17818
- Joint ocean-atmosphere model response to solar zenith angle seasonal variation, noting snow cover and ocean surface effects on lower troposphere warming 11 p1620 A72-25766
- Russian papers on solar activity effects on earth atmosphere and biosphere covering climate, vegetation, animals and man 12 p1763 A72-28206
- Solar activity effects in magnetosphere and ionosphere relation to geomagnetic activity and biospheric development, noting 11 year geomagnetic perturbation cycles 12 p1805 A72-28209
- Solar activity effects on biospheric processes for biological and physicochemical systems in unsteady state, considering maximum effects on man at certain electromagnetic wave frequencies 12 p1773 A72-28211
- Solar activity effects on biosphere processes, discussing radiation-induced molecular activation mechanisms in water and biological plasma calcium ion concentration changes 12 p1763 A72-28213
- Effect of aerosol variation on radiance in the earth's atmosphere-ocean system. 17 p2547 A72-35194
- EARTH MANTLE**
- Earth mantle and core density using Monte Carlo models compared with lunar structure from crust and seismology data, noting planetological contrast 04 p0571 A72-14616
- Excess secular change in ecliptic obliquity in relation to earth internal motion due to mantle-core coupling 04 p0575 A72-15028
- Earth planetary structure from gravitational information, discussing crust, mantle, gravity anomalies, satellite and ground observation methods and improved earth model 04 p0519 A72-15075
- Earth mantle shear velocity model derived from S waves travel time gradient direct measurement, disregarding deep depth lateral homogeneity assumption 04 p0519 A72-15578
- Southern Great Basin upper Cenozoic high Sr87/Sr86 and Sr/Rb ratio basalt initial composition, showing mantle material derivation 05 p0655 A72-16043
- Earth density, surface wave velocity and other properties calculation from model consistent with physical and petrological mantle theories 20 p2917 A72-39475
- Elasticity of some mantle crystal structures. I - Pleonaste and hercynite spinel. 20 p2917 A72-39478
- EARTH MOTION**
- Excess secular change in ecliptic obliquity in relation to earth internal motion due to mantle-core coupling 04 p0575 A72-15028
- Earth motion nutations, considering external forces effects from sun and moon 04 p0575 A72-15030
- Earth nutation tables, comparing precession-nutations and tidal potential 04 p0575 A72-15031
- Earth precession constant correction, considering Fricke catalogs 04 p0576 A72-15039
- Earth gravity field, movement and temporal form variation determination by satellite tracking, long base interferometry or lunar observation 04 p0520 A72-15723
- Variations of the earth's gravity field due to the free nutation. 17 p2544 A72-34272
- Perturbation theory for torsional earth oscillations - Second approximation 17 p2548 A72-35475
- EARTH MOVEMENTS**
- NT EARTHQUAKES**
- Satellite photographs of Himalayan-Indian Ocean tectonic patterns, showing major left and right lateral shear belts as evidence of wrench movements 05 p0655 A72-16040
- Earth Love waves and toroidal oscillations attenuation, presenting frequency dependent model of internal friction 09 p1299 A72-22801
- Earth velocity through microwave background, discussing absolute and relative motion, inertial frame and distant matter distribution and Mach principle 14 p2157 A72-30624
- Relation between tectonic processes on the earth and moon 19 p2860 A72-37958

Continuous natural background sources of microseismic motions due to atmospheric and ocean loading, wind, flowing water and local disturbances [AIAA PAPER 72-819] 20 p2915 A72-39104

EARTH ORBITAL RENDEZVOUS
Optimal terminal rendezvous as a stochastic differential game problem. 19 p2869 A72-37284

EARTH ORBITING SPACE STATIONS
U FOSS
EARTH ORBITS
NT APOGEES
NT PERIGEEES
Parameters affecting communication and rescue time constraints for emergency astronaut return from low earth orbits 09 p1395 A72-23155

Gas dynamics of steady rotating azimuthally dependent solar wind under magnetic field influence, calculating azimuthal distribution of radial velocity near earth orbit 13 p2034 A72-29960

Mars observations during 1971 opposition, noting south pole phenomena relation to Martian atmosphere changes 15 p2306 A72-31600

Capture resonance of asteroid 1685 Toro by earth due to gravitational interaction at close encounters 15 p2307 A72-31721

Micrometeorite and cosmic dust flux rates for near earth orbit and interplanetary space from satellite and ground based measurements 15 p2309 A72-31955

Terrestrial and lunar orbital and rotational motion behavior, discussing kinematic theory and ground and space vehicle based observation techniques 19 p2865 A72-38479

Performance optimization of satellite semipassive aerodynamic attitude controller for near-earth orbits, considering damping time and pointing error [AIAA PAPER 72-923] 21 p3082 A72-41567

Analysis of the possibility of planetary escape by means of the solar sail 22 p3230 A72-43072

Unique charts for space missions. 24 p3422 A72-44644

Discrepancy between Brown theory and Griffith values for lunar perigee and node mean motions partial derivatives with respect to moon mean motion 24 p3442 A72-45241

EARTH PLANETARY STRUCTURE
Earth planetary structure from gravitational information, discussing crust, mantle, gravity anomalies, satellite and ground observation methods and improved earth model 04 p0519 A72-15075

Linear inverse problem of coefficient matrix eigenvectors, implying surface waves and free oscillations for earth structure 08 p1159 A72-21495

Internal structure dynamics of earth, moon and planets, showing density variation and bulk modulus as function of pressure with correction of Bullen hypothesis 16 p2461 A72-34176

Russian book - Physics of the earth and planets: Figures and internal structure 19 p2856 A72-37474

Lava tubes of the Cave Basalt, Mount St. Helens, Washington. 19 p2790 A72-38296

Russian book - Hydrodynamic evolution model of the earth. 21 p3103 A72-40461

Measurements of gradients of gravity in mines. 21 p3048 A72-40500

EARTH RADIATION
U TERRESTRIAL RADIATION

EARTH RESOURCES
NT DESERTS
NT FARM CROPS
NT FORESTS
NT GLACIERS
NT GRANITE
NT LAKES
NT LAVA
NT RIVERS
NT ROCKS
NT SANDS
NT SHALES
NT VEGETATION
IR remote scanning of natural resources, discussing thermal to optical image conversion on photographic film 02 p0208 A72-11781

Environmental analysis of Lake Tahoe Basin from small scale multispectral aerial imagery, discussing color enhancement usefulness for interpretation and management of natural resources 02 p0210 A72-11800

Computer enhancement of multispectral satellite- and air-photographs and imagery for earth resources 02 p0186 A72-11801

NASA/MSC Earth Resources Research Data Facility for remote sensing of geology, geography, agriculture, forestry, hydrology and oceanography 02 p0200 A72-11824

Natural resources multispectral remote sensing for natural emergencies, discussing various imaging techniques 02 p0212 A72-11828

Soviet aerial survey techniques for natural resources data, discussing photograph interpretation, fast aerospotometers, data processing and multispectrum cameras 02 p0216 A72-11888

Satellite communication regional and domestic applications, discussing educational, earth resources, geological survey, environmental and maritime uses 04 p0487 A72-15073

Thermal IR imaging remote sensing device for aerial earth resource surveys, noting hydrogeology, volcanology, forest fire and geothermal region detection and ice sheet study applications 06 p0807 A72-17789

Soviet book on terrestrial studies by satellite observation covering meteorology, hydrology, oceanography, geomorphology, geobotanics, geography, pedology, atmospheric physics and TV and photographic analysis 06 p0810 A72-18523

United Nations proposals concerning legal principles for use of natural resources of celestial bodies and ocean floor 07 p1103 A72-19464

French space applications program for telecommunications, meteorology, natural resources survey and air/sea traffic control 08 p1256 A72-21201

Earth science and technical applications of multispectral photography and digital image processing techniques 08 p1166 A72-21334

Aerial photography interpretation for studies of natural environment and resources 09 p1312 A72-23277

Photointerpretation methods for earth resources and geological studies, discussing quantitative photographic techniques, automation and digital evaluation methods 09 p1302 A72-23292

Short and long range contributions of NASA space program to life quality improvement, discussing land and crop surveys, communications and environment modification 11 p1748 A72-26098

United Nations FAO interest in remote sensing techniques application to agricultural, forestry and fisheries resources survey and management 15 p2220 A72-31228

Photointerpretation and computerized radiometric analysis of ERTS multispectral TV and scanner imagery of Israel 15 p2221 A72-31242

Spaceborne and airborne remote sensing methods and applications for earth resources observation 15 p2221 A72-31245

Geographical interpretations of ESSA and Nimbus weather satellite pictures for earth resources applications, noting ERTS project 15 p2221 A72-31248

Report to COSPAR on French space program covering ionospheric and magnetospheric physics, meteorology, earth resources and exobiology 15 p2337 A72-32003

Gases and vapors spectral signatures application in correlation spectroscopy and interferometry for aerospace monitoring of earth resources and pollution 16 p2393 A72-33630

Balloon nacelle for terrain photography from very high altitudes 24 p3403 A72-45229

EARTH RESOURCES PROGRAM

Data correlation and annotation of earth resources remote survey pictorial records 01 p0065 A72-10453

EROS program thematic mapping system for binary graphic overlays of open water, snow and ice, reflective IR vegetation and human works 01 p0066 A72-10460

NASA earth resources satellite R and D program for acquiring data on agriculture, forestry, geography, geology, hydrology, mineralogy and marine resources 01 p0063 A72-10949

Earth resources information systems using satellite and aerial IR terrain photography and ground teams for international cooperation, emphasizing timber inventory 01 p0063 A72-10950

IR scanner for Indian land areas and oceans thermal mapping, using satellite-borne multispectral photography 02 p0225 A72-11777

Multistage resource inventory and analysis program combining remote sensing techniques and ecological principles in California Desert pilot area, discussing photointerpretation and ground truthing 02 p0210 A72-11802

Natural formations optical spectral reflectance optical coding with speedy digital computer processing advantage for remote sensing of earth surface 02 p0187 A72-11811

Remote sensing of Indian resources, investigating Englemann Spruce beetle infestation, topographic features and potential mineral areas 02 p0213 A72-11848

Earth Resources Survey /ERS/ program personnel training and education, discussing trainee selection, knowledge categories and training methods for remote sensing 02 p0304 A72-11855

RADAM /Radar Amazon/ side-looking radar imagery and multiband aerial photography for mineral, vegetation, soil and water resources mapping in Brazil 02 p0216 A72-11890

Frequency allocation for space research, radio astronomy, time signal and earth resources exploration, reviewing allowable power flux density and emitter power 02 p0177 A72-12386

CNES airborne remote sensing of earth resources comparison with classical photodetection methods, discussing application to oceanography, geology, agriculture, hydrology and human activities 06 p0803 A72-17385

Earth resources applications of multispectral remote sensing techniques for airborne and satellite-borne imaging systems, discussing microwave radiometer augmentation of visual and IR data 06 p0813 A72-17430

Remote sensing for earth resources data, discussing sensors equipment and project organization and management 06 p0810 A72-18615

International legal aspects of earth resources survey from space 07 p1104 A72-19467

International cooperation in space law problems, considering space communication systems, geostationary orbits use, frequency band allocation, world weather watch and earth resources survey programs 07 p1105 A72-19475

NASA space station activities, describing Skylab missions and capabilities in physical and life sciences, earth resources surveying and technology experimentation 09 p1395 A72-22935

Aerial photography and photogrammetry objectives and requirements for natural resources surveys 09 p1304 A72-23312

Skylab earth resources experiment package, examining crew tasks [AIAA PAPER 72-234] 10 p1472 A72-24444

NASA Earth Resources Survey program review, discussing satellite and aircraft observation application to agriculture, geology, hydrology, geography, oceanography and environment pollution 12 p1877 A72-27688

Four dimensional atmospheric model providing global moisture, temperature, pressure and density profiles as attenuation model inputs for earth resources satellite mission simulation 13 p1989 A72-28805

Earth resources survey systems, discussing benefits, ground truth problem, data analysis, experimental satellites, operational system, and developing countries needs and activities 14 p2175 A72-31142

Space activity in fields of ecology and earth resources - Conference, Rome, Italy, March 1972 15 p2220 A72-31226

United Nations activity in international space program for earth resources and environmental pollution surveillance by satellites 15 p2220 A72-31227

Radiation measurements and thermal IR and photographic imaging techniques in meteorology and earth resources survey applications 15 p2221 A72-31241

Unitary and interdisciplinary information processing of remote satellite observations of earth resources, noting ground station requirement for Italy 15 p2222 A72-31253

Norwegian report to COSPAR on space scientific activities and application program, including satellite geodesy and earth resources research 15 p2338 A72-32009

Satellite earth resources remote sensing in visible, IR and microwave regions for plant disease and salinity evaluation 15 p2229 A72-32049

Texture measurements in earth resources data management system by automatic photointerpretation with analog and digital techniques, discussing data processing rate requirements 17 p2520 A72-34409

Operational earth observation systems and resources management - A global program. [AIAA PAPER 72-735] 18 p2725 A72-36539

Orbiting space laboratories for earth resources program, discussing satellites and Skylab missions and international cooperation [AIAA PAPER 72-741] 18 p2742 A72-36547

Canadian program for global environmental and world resources monitoring system, discussing management, technology and user interface [AIAA PAPER 72-742] 18 p2742 A72-36548

The cost-effectiveness of advanced remote sensing systems. 21 p3131 A72-40864

Remote sensing of earth resources by microwave radiometry. 24 p3402 A72-45107

EARTH RESOURCES SURVEY AIRCRAFT

Multichannel multispectral scanner system for NASA C-130 earth resources aircraft, describing electronic equipment and calibration sources 01 p0048 A72-10946

NASA/MSC earth observation aircraft program radar scatterometers, presenting system evaluation 02 p0172 A72-11849

Operational earth observation systems and resources management - A global program. [AIAA PAPER 72-735] 18 p2725 A72-36539

EARTH RESOURCES TECHNOLOGY SATELLITES

ERTS satellite return beam vidicon TV system and multispectral scanner images, describing photogrammetric and cartographic evaluations 01 p0065 A72-10449

ERTS satellite image processing for multispectral scanning system, discussing distortion from geometrical properties 01 p0066 A72-10458

Systems approach to space technology application, covering Global Atmospheric Research Program and Earth Resources Technology Satellites 01 p0146 A72-10952

Artificial satellites for earth resources and environmental contamination control, discussing remote sensing physical problems and earth surface radiative characteristics 02 p0207 A72-11778

Environments susceptibility to low resolution imaging for land-use mapping, relating landscapes spatial frequency distributions to expected ERTS resolutions 02 p0210 A72-11796

High altitude aircraft and Apollo 9 multispectral photography and simulated ERTS-A imagery evaluation, comparing with ground observations in Arizona 02 p0210 A72-11799

ERTS return beam vidicon system geometric calibration for high resolution photoimage maps cartographic referencing and register, discussing optical and electronic distortion sources 02 p0225 A72-11818

ERTS return beam vidicon imagery simulation, predicting resolvability of ground targets as function of target size, contrast, spectral distribution and radiance level 02 p0226 A72-11833

Information content in simulated ERTS space photographs as function of various levels of image resolution 02 p0212 A72-11834

ERTS-A satellite geometric and radiometric received image errors, presenting detection and correction with digital algorithms 02 p0171 A72-11847

ERTS multispectral scanner data telemetry decommutator/processor capable of decommutating five spectral bands of digital video data 02 p0175 A72-12162

ERTS-A orbital earth resources data utilization, describing user community size and character and central repository data center 02 p0305 A72-12381

Earth resources technology satellite program, discussing mission requirements, payload, orbital characteristics, earth stations, data processing, system design and international features [DGLR PAPER 71-139] 06 p0892 A72-18230

NASA space applications program review, discussing potential of communication, navigation and earth observation satellites 06 p0893 A72-18610

Remote sensing history and techniques, describing ERTS instrumentation for earth science studies 07 p0976 A72-19177

ERTS A and B satellite systems for multispectral imaging of earth surface, discussing sensors, operational control and data processing requirements and implementation 07 p1085 A72-19276

Return beam vidicon multispectral camera system for ERTS A and B, describing camera system design and performance characteristics in terms of ERTS mission purpose 07 p0986 A72-19601

Performance tests of return beam vidicon multispectral television camera system for ERTS program 07 p0986 A72-19657

ERTS program, discussing orbit selection and sensor equipment 07 p1085 A72-20305

NASA ERTS and Skylab programs review, presenting information on spacecraft design, orbits, attitudes,

sensors, image characteristics, data handling and processing, etc 10 p1539 A72-24323

Earth resources survey systems, discussing benefits, ground truth problem, data analysis, experimental satellites, operational system, and developing countries needs and activities 14 p2175 A72-31142

European space program for remote sensing techniques application, noting earth resources survey satellites 15 p2220 A72-31229

Space technology development effect on meteorology progress, discussing earth resources technology satellites and meteorological satellites 15 p2220 A72-31234

Geostationary Intelsat satellite networks for retransmission of data received by earth resources satellites 15 p2221 A72-31243

Low cost optimal earth resources technology satellite station for satellite tracking and image data reception and recording 15 p2213 A72-31246

Cartographic and environmental surveys by Skylab orbiting stations and ERTS satellite using panoramic and mapping cameras and laser altimeter 15 p2232 A72-31247

The image-processing system for the Earth Resources Technology Satellite. 18 p2674 A72-36496

The precision-processing subsystem for the Earth Resources Technology Satellite. 18 p2674 A72-36497

Operational earth observation systems and resources management - A global program. [AIAA PAPER 72-735] 18 p2725 A72-36539

Orbiting space laboratories for earth resources program, discussing satellites and Skylab missions and international cooperation [AIAA PAPER 72-741] 18 p2742 A72-36547

ERTS-borne return beam vidicon camera using high resolution TV sensors coaligned to view identical scene in different spectral bands 19 p2795 A72-37576

Earth resources technology satellites /ERTS/ program requirements, considering coverage, spectral characteristics, system performance, photographic interpretation and information extraction 24 p3398 A72-45115

High resolution multispectral camera system for ERTS A & B. 24 p3402 A72-45182

The role of the United Nations in earth resources satellites. 24 p3468 A72-45185

EARTH ROTATION

Altitude dependent superrotation of earth upper atmosphere, using nonlinear continuity, momentum conservation and state equations of gas dynamics 01 p0052 A72-10076

Earthquake excitation of Chandler wobble in earth rotation 03 p0351 A72-14365

Earth rotational direction and speed effects on terrestrial circumnavigation relativistic time, suggesting clock paradox empirical proof 06 p0849 A72-18381

Uniform time systems relevance to precise astronomical observations and accurate determination of irregularities in earth rotation, outlining proposals for time signals 07 p1032 A72-19068

Lateral refraction dependence on earth rotation and correction formula for angle measurement errors in class I triangulation 09 p1299 A72-22946

Short period terms in earth rotation rate and polar motion, considering data truncation effects on periodograms 10 p1475 A72-24872

Moment of inertia of earth atmosphere relative to earth axis of rotation 11 p1622 A72-25974

Aperture synthesis of ring antenna arrays radiation pattern using earth rotation 11 p1597 A72-26710

Oceanic and atmospheric flow geostrophic adjustment by means of gravity-inertial wave propagation from initially imbalanced regions 15 p2222 A72-31278

Superrotation of the upper atmosphere. 20 p2916 A72-39336

Fundamental geodetic parameters of the earth's figure and the structure of the earth's gravity field derived from satellite data. 21 p3048 A72-40494

On the diffusion of the perturbing toroidal magnetic field from the core to the mantle. 21 p3048 A72-40501

Instability of rotational and gravitational modes of oscillation. 21 p3078 A72-40773

Role of the swarm of satellite-particles on the origination of the earth's rotation 22 p3220 A72-41916

Upper limit of the torque of the solar wind on the earth. 22 p3219 A72-42427

The effect of change in the geomagnetic dipole moment on the rate of the earth's rotation. 23 p3285 A72-43819

Earth precession, nutation, polar axis displacement and rotation period reduction, discussing solid core existence within liquid core, elasticity and polar displacement 23 p3341 A72-44462

EARTH SATELLITES

NT AEROS SATELLITE

NT ALOUETTE SATELLITES

NT APPLICATIONS TECHNOLOGY SATELLITES

NT BEACON SATELLITES

NT COMMUNICATION SATELLITES

NT COS-B SATELLITE

NT COSMOS SATELLITES

NT DISCOVERER SATELLITES

NT EARTH RESOURCES TECHNOLOGY SATELLITES

NT ELEKTRON SATELLITES

NT ENVIRONMENTAL RESEARCH SATELLITES

NT EOLE SATELLITES

NT EOSS

NT ESRO SATELLITES

NT ESSA SATELLITES

NT EXPLORER SATELLITES

NT GEODETIC SATELLITES

NT GEOPHYSICAL SATELLITES

NT HEOS B SATELLITE

NT HEOS SATELLITES

NT INTELSTAT SATELLITES

NT INTERCOSMOS SATELLITES

NT METEOROLOGICAL SATELLITES

NT MIDAS SATELLITES

NT MOLNIYA SATELLITES

NT MOON

NT NAVIGATION SATELLITES

NT NAVSTAR SATELLITES

NT NIMBUS SATELLITES

NT OAO

NT OGO

NT OGO-A

NT OGO-B

NT OGO-D

NT OGO-E

NT OSO

NT OSO-G

NT OSO-H

NT PAGEOS SATELLITE

NT PAS

NT PROTON SATELLITES

NT RADIO ASTRONOMY EXPLORER SATELLITE

NT RELAY SATELLITES

NT SAN MARCO SATELLITE

NT SIRIO SATELLITE

NT SYMPHONIE SATELLITES

NT SYNCHRONOUS METEOROLOGICAL SATELLITE

NT SYNCOM SATELLITES

NT TIROS SATELLITES

NT TRANSIT SATELLITES

NT UHURU SATELLITE

NT VENERA SATELLITES

Vacuum chamber simulation of solar radiation effects on space satellites and components at 300-400 miles, using short arc xenon lamps 05 p0643 A72-16386

Earth satellite plane periodic oscillations damping with respect to center of mass in orbital plane during motion on elliptical Kepler orbit 05 p0730 A72-17030

Angular position of sun disoriented artificial earth satellites with angular velocities not exceeding 0.5 deg/sec, using harmonic analysis of magnetometric data 05 p0631 A72-17033

Mathematical model of solar radiation pressure effects on earth satellite orbit 08 p1237 A72-21643

Earth shadow effects on light artificial satellite orbital motion 13 p2051 A72-28440

Earth satellite orbit motion in terms of probability densities and distributions for large populations and single satellites 15 p2307 A72-31692

Determination of the orientation of ionospheric irregularities causing scintillation of signals from earth satellites. 19 p2794 A72-38866

EARTH SHAPE

U GEODESY

EARTH SURFACE

Earth surface thermal radio emission measurements by UHF radiometry onboard Cosmos 243 satellite,

showing brightness profiles of water, ice and land areas
01 p0053 A72-10363

Earth surface roughness effects on vertical Hertz dipole electromagnetic field reflection
01 p0027 A72-10447

Magnetosphere transmittance for fast magnetosonic waves, considering refraction, reflection and earth surface intersection
01 p0058 A72-10587

Artificial satellites for earth resources and environmental contamination control, discussing remote sensing physical problems and earth surface radiative characteristics
02 p0207 A72-11778

Airborne remote sensing of earth surface physical properties, using panchromatic and IR black and white, true color and IR false color photography
02 p0208 A72-11782

Soyuz 6 multispectral aerogeophysical measurements of Usturt plateau and Caspian and Aral Seas, discussing remote sensing information yield on earth water/land and atmosphere properties
02 p0208 A72-11785

Thermal IR remote sensing of surface geothermal heat flow, presenting nighttime heat budget equation based on solar and geothermal energy
02 p0208 A72-11786

Earth surface feature recognition with IR imagery, evaluating Meteor satellite data
02 p0213 A72-11836

Natural formation interpretation from spectrophotometric measurements of underlying earth surface from manned spacecraft Soyuz 7 and Soyuz 9
02 p0228 A72-11887

Meteorological precipitation and earth surface under cloud characteristics from airborne microwave radiation measurements using millimeter and centimeter waves
02 p0216 A72-11889

Earth surface remote sensing with thermal IR radiation, investigating uncovered soils with heat balance equations under various weather conditions and times of day
02 p0172 A72-12017

Magnetic survey worldwide earth coverage by land, sea and airplane measurements data
02 p0220 A72-12085

Satellite measurements of tropospheric and earth surface state parameters for long term numerical weather forecasting, discussing data fluctuations
02 p0255 A72-12789

Soviet book on ground wave radio propagation at medium and long wavelengths covering field strength calculations over plane and spherical earth, soil conductivity, etc
03 p0323 A72-13950

Mars surface topographic characteristics relationship to earth features, using Mariner 6 and 7 photographs
04 p0569 A72-14501

Microwave radiometer and scatterometer sensing for earth surface and subsurface measurements
06 p0815 A72-17784

Multispectral TV camera systems for satellite recording of earth surface electromagnetic radiation at separate wavelengths
06 p0817 A72-18232

Atmospheric effects on remotely sensed earth surface signature recognition, considering scattering, absorption and emission effects
06 p0809 A72-18233

Elliptically polarized ionospheric source generation of short period geomagnetic disturbances at earth surface
08 p1153 A72-20719

Terrestrial surface observation from space platform, considering atmospheric effects, surface spectral properties and information resolution and transmission
08 p1170 A72-21965

Molodenski integral equation for gravitational field calculation at point M on earth surface as function of neighboring region astronomical geodetic measurements
09 p1299 A72-22675

Radio propagation over slightly roughened curved earth surface, using perturbation method and Taylor series in model calculation
10 p1439 A72-24743

Outer space and earth surface galactic cosmic ray intensity data correlation analysis for studying interplanetary magnetic field structure
11 p1713 A72-25936

Overlap emissivity of atmospheric carbon dioxide and water vapor for computer simulated earth surface temperature calculations
11 p1628 A72-26986

Ground surface shadow bands observations during 7 March 1970 solar eclipse by photoelectric detection, indicating atmospheric turbulence effect
12 p1800 A72-27142

Relations between normal mode radio propagation parameters and properties of earth-lower ionosphere isotropic waveguide, allowing for geomagnetic field
13 p1945 A72-28583

Total precipitable water in atmosphere vertical column relation to surface humidity from measurements at desert, coastal and maritime sites
13 p1989 A72-28812

Soyuz 9 spectrophotometry of earth surface features, comparing manned spacecraft-obtained and conventional spectrographs
14 p2100 A72-30464

Satellite observation of earth surface, discussing remote sensing techniques application in pollution control and ecology
15 p2319 A72-31232

Magnetic dipole or small current loop over homogeneous flat earth, calculating transient electromagnetic field for airborne remote sensing
15 p2224 A72-31672

High-orbital satellite global photographs and TV pictures, discussing planetary geographical and topographical data interpretation
15 p2225 A72-31807

Aircraft laser radar measurements of atmospheric backscattering coefficients for cloud and underlying surface studies
15 p2266 A72-31908

Skylab radar altimeter for earth surface features remote sensing with high range resolution mode for ocean wave height determination
15 p2236 A72-31995

Earth surface layer potential density from gravity anomalies combined with satellite Doppler observations
16 p2382 A72-32888

Balloon-nacelle for small scale photography and multispectral photometric ground measurements, describing automatic adjustment device for photographic lens diaphragm
16 p2349 A72-33633

Earth and Mars - Evolution of atmospheres and surface temperatures.
17 p2613 A72-35395

Geometric similitude of lunar and terrestrial craters.
17 p2615 A72-35681

Simplified method of calculating microwave diffraction loss over spherical earth.
18 p2660 A72-36517

The potentialities of space technology in relation to oceanography and surface meteorology.
19 p2790 A72-37924

Elliptically polarized ionospheric source generation of short period geomagnetic disturbances at earth surface
19 p2791 A72-38347

Propagation of internal acoustic-gravity waves around a spherical earth.
19 p2793 A72-38748

Deformation of the earth by surface loads.
20 p2916 A72-39335

A contribution to the numerical treatment of the electromagnetic field /H-polarization/ in horizontally non-homogeneous models of the earth.
21 p3048 A72-40498

Earth surface and background wind effects on mesoscale and large scale meteorological processes in free stably stratified atmosphere
21 p3078 A72-41794

A method of calculating meteorological elements for mesoscale processes
24 p3420 A72-44633

Determination of refraction in the propagation of electromagnetic waves at the earth's surface
24 p3379 A72-44865

Relations between normal mode radio propagation parameters and properties of earth-lower ionosphere isotropic waveguides, taking into account geomagnetic field
24 p3397 A72-45083

Exact localization of isolated points on earth surface with Geole system satellite observation, noting applications in geodetic survey, geodynamics and geophysics
24 p3398 A72-45228

EARTH TIDES

Methane absorption stabilized 30 meter laser strain meter with Fabry-Perot geometry for earth tide, nuclear explosion and free earth oscillation observation
14 p2109 A72-30323

The theory of motion of the horizontal pendulum with a Zoellner suspension and some indications for the instrumental design.
21 p3084 A72-40495

EARTH-MARS TRAJECTORIES

Optimal transfer trajectories between Earth and Mars presented as functions of idealized Hohmann transfer approximation
07 p1077 A72-19824

Mariner 4 trajectory relation to proposed location of bow wave caused by solar wind interaction with Mars ionosphere, noting planet orbit aberration effects
09 p1385 A72-22581

Gradient method and Euler equations application to low thrust earth-to-Mars spacecraft orbital transfer trajectory optimization
13 p2034 A72-28438

Mars 3 probe design and mission details, covering trajectory correction lander separation, engine start-up, aerodynamic braking and dust storm data
14 p2151 A72-30477

Mars Viking 1975 mission objectives and navigation activities from trans-Mars injection through post-landing stationkeeping phase, considering trajectory dispersions
15 p2269 A72-32180

Minimum energy trajectory and propellant consumption considerations for launch windows to Mars and Venus planets with Grand Tour mission possibilities
23 p3336 A72-43553

Evaluation of optical data for Mars approach navigation.
24 p3422 A72-44646

EARTH-MOON SYSTEM

Geodetic applications of earth-moon laser ranging, discussing methods, accuracy, equipment, experiments and station characteristics
02 p0207 A72-11698

Earth motion nutations, considering external forces effects from sun and moon
04 p0575 A72-15030

High accuracy laser reflector telemetric measurement for earth-moon distance variation in time by correlation method
04 p0495 A72-15727

Transportable lunar ranging with neodymium glass laser and Coude optical system, noting geophysical applications [CLEA PAPER 9,6]
07 p0943 A72-19388

Earth and moon chemical composition differences based on model of lunar formation from circumterrestrial swarm of particles and larger objects
07 p1077 A72-19820

Terrestrial dust belt particles origin, character and trapped time from observations of earth-moon system libration points
08 p1229 A72-20839

Earth-moon system gravitational effect on Venera automatic interplanetary stations motion away from earth
08 p1239 A72-22086

Meteorite flux at lunar surface as function of position and earth-moon distance, applying to crater counting
10 p1531 A72-23703

Earth-moon distance measurement by laser ranging methods, discussing retroreflectors, light collectors, time interval measuring devices and moon ranging stations
13 p2037 A72-28993

Earth-moon system periodic orbits calculation by modified quasi-linearization combined with particular solutions method, using restricted three body model
14 p2149 A72-30232

Observational bias source in lunar transient events correlation with perigee and tidal stresses, using statistical analysis for 1947-1967 period
14 p2150 A72-30324

Lunar research bibliography covering earth-moon system, moon motion, gravitational field, structure, thermal history, composition, photometry, spacecraft exploration, etc
14 p2155 A72-30521

Earth-moon system mass from ratio of solar mass to sum of terrestrial and lunar masses, discussing solar attraction effects and radar distance measurements
15 p2306 A72-31598

Apollo 15 orbital science payload instruments for exploring lunar origin and evolution to relate to earth history
15 p2310 A72-31984

Lunar rock nature and properties from Apollo samples, discussing crust, Fra Mauro, interior, chronology, surface processes and earth-moon environment
15 p2314 A72-32376

Earth-moon system gravitational effect on Venera automatic interplanetary stations motion away from earth
17 p2606 A72-34655

Earth and moon chemical composition differences based on model of lunar formation, from circumterrestrial swarm of particles and larger objects
17 p2618 A72-35745

Generalization of the sphere of interaction for the restricted four-body problem
20 p2975 A72-40073

Long term stability of earth and lunar orbiters - Theory and analysis. [AIAA PAPER 72-936]
21 p3112 A72-41574

Celestial mechanics principles application to geostationary satellites in equatorial plane and in earth-moon system libration points, considering Jupiter and Saturn stationary satellites
22 p3222 A72-42141

- Lunar crater origins due to external impact of particles moving within earth-moon gravitational dipole during earliest history stage
22 p3226 A72-42538
- Earth geophysical effects due to tidal capture of moon from direct orbit, discussing volcanism, atmosphere and hydrosphere origins and biological evolution
22 p3226 A72-42539
- Origin and evolution of the earth-moon system.
22 p3227 A72-42540
- Detection of earthward flow of keV protons in the geomagnetic tail at lunar distances.
23 p3333 A72-44532

EARTH-MOON TRAJECTORIES

- Cosmic proton and neutron produced recoil proton energy spectra measurements along earth-moon-earth trajectory with nuclear emulsions aboard Zond 5 and 7 [CERN-71-16]
02 p0273 A72-12074
- First order asymptotic matching computational technique for calculation of perturbed moon-centered hyperbola parameters in earth-moon trajectory
11 p1720 A72-25996
- Spacecraft free fall trajectory calculation, using numerical optimization procedure based on Hamilton principle for two point boundary value problems
16 p2460 A72-34021
- Shuttle flight opportunities between stations orbiting the earth and moon.
21 p3108 A72-41302
- Analysis of the Radio Astronomy Explorer lunar orbit mission.
[AIAA PAPER 72-940]
24 p3444 A72-45437

EARTH-VENUS TRAJECTORIES

- Minimum energy trajectory and propellant consumption considerations for launch windows to Mars and Venus planets with Grand Tour mission possibilities
23 p3336 A72-43553

EARTHQUAKES

- Earthquake excitation of Chandler wobble in earth rotation
03 p0351 A72-14365
- Elastic dislocation theory of Chandler wobble excitation by earthquakes
09 p1299 A72-22802
- Time dependent power spectral density function for first passage probabilities in nonstationary random processes in civil engineering involving earthquakes and wind
10 p1514 A72-25188
- Constant stress effect on propagation velocity of elastic waves in three dimensional body, considering earth crust and earthquake prediction applications
15 p2329 A72-32284
- Three dimensional seismic monitoring system developed from inertial guidance gyroscopes and accelerometers, noting pole shift observation, tilting during earth tides and earthquakes forecasting
[AIAA PAPER 72-840]
20 p2923 A72-39088

EASEP

- Apollo 11 EASEP nickel resistance thermometer lunar surface data, presenting unshadowed equivalent brightness temperature and thermal parameters and emission directional dependence
12 p1869 A72-27330

EATING

- Twelve hour light-dark-dark cycle phase shift effects on monkey feeding behavior and serial task performance
02 p0157 A72-11703

EBERT SPECTROMETERS

- Solar spectrum measurements at 2100-3200 Å by Aerobee rocket mounted Ebert-Fastie spectrometer with LiF diffusion plates
13 p2040 A72-29408
- Exit slit mirror system in rocket-borne scanning Ebert grating spectrometer, discussing imaging properties and required adjustments
21 p3053 A72-40606

EBULLITION

U BOILING

ECCENTRIC ORBITS

- Criticism of artificial satellite theory for small eccentricities
01 p0123 A72-10016
- Satellite in eccentric Keplerian orbit transgressing Roche limit about rigid sphere, considering time dependent evolution problem with various centrifugal and tidal forces
01 p0134 A72-11145
- Statistical analysis of eccentricity changes in nearly parabolic comets, showing data samples relation to Bernoulli random variable with two different unknown parameters
07 p1072 A72-19339
- Stellar perturbations of eccentric orbits of long period comets
07 p1081 A72-20232
- Hill variable modification of Brouwer satellite theory algorithm for simplified orbital element and perturbation calculations and orbital eccentricity generalization
08 p1237 A72-21749

- Satellite coordinates calculation for arbitrary inclinations and orbit eccentricity below Laplace limit
10 p1543 A72-24633
- Interplanetary spacecraft transfer maneuver for hyperbolic trajectory change into eccentric orbit, using aerodynamic drag to obtain nearly circular orbit
14 p2151 A72-30471
- Asteroids and comets orbit perturbation equations for small eccentricity values
14 p2161 A72-31080

- Collapsed objects absence in eccentric binary star systems and nonevidence of black holes formation effect on multiple line binaries
18 p2729 A72-36983

- Undisturbed eccentric anomaly difference as the independent variable in the perturbation differential equations.
19 p2856 A72-37520

- Ephemeris of a highly eccentric orbit - Explorer 28.
20 p2968 A72-39194

- Interaction between attitude libration and orbital motion of a rigid body in a near Keplerian orbit of low eccentricity.
20 p2968 A72-39197

- A two-parameter survey of periodic orbits in the restricted problem of three bodies.
21 p3106 A72-41049

- Quasi-periodic orbits about the translunar libration point.
[AIAA PAPER 72-935]
21 p3112 A72-41573

- Critical inclinations and eccentricities concepts for N planet problem, applying results to general three body problem
24 p3442 A72-45239

ECCENTRICITY

- Load or compression eccentricity effect on buckling and postbuckling behavior of flat plates, presenting stress distribution curves
05 p0737 A72-16116

- Lunar elements and fundamental constants corrections from meridian observations for nodal period, determining corrections to solar mean anomaly and eccentricity
06 p0875 A72-17298

- Orbital eccentricity and angular momentum management scheme stability for satellite large attitude maneuver followed by trim maneuver sequence
11 p1719 A72-25978

- Perturbation velocity corrections for eccentric model position and different air flow ducting in rectangular wind tunnels
[DFVLR-SONDR-191]
11 p1573 A72-26581

- Flow between eccentric rotating cylinders.
[ASME PAPER 72-LUB-J]
19 p2786 A72-37699

- Invalidity of Neptune predicted position derivation from perturbations on Uranus via method neglecting eccentricity
21 p3111 A72-41474

- Despun conical flight vehicles eccentric insulation mass properties history, deriving preflight and in-flight equations for weight, center of gravity coordinates and moments and products of inertia
[SAWE PAPER 938]
23 p3342 A72-43478

ECHELETTE GRATINGS

- High spectral resolution UV space astronomy spectrographs with echelle gratings
03 p0354 A72-13052

- Ruling defects of echelle diffraction gratings for far IR high luminosity spectrometers
05 p0689 A72-16192

- Transmission and passband properties of polyethylene echelle gratings and combined filters for long wave IR spectrum
08 p1210 A72-22038

- Automated echelle spectrograph data handling using computer control
11 p1716 A72-25693

- Astronomical spectroscopy using ultraviolet resolution single Fabry-Perot interferometer in tandem with echelle Hilger monochromator
12 p1811 A72-27942

- Pressure-scanned echelle grating plus Fabry-Perot stellar spectrophotometer.
21 p3053 A72-40609

- Optical properties of transmission echelle high-pass filters.
21 p3055 A72-40823

ECHELON FAULTS

U GEOLOGICAL FAULTS

ECHO SUPPRESSORS

- Digital adaptive echo cancellation mathematical technique for voice circuits derived from satellite transmission
[AIAA PAPER 72-539]
12 p1780 A72-27362

ECHOES

- NT ANGELS
NT AURORAL ECHOES
NT CLUTTER
NT LUNAR ECHOES
NT LUNAR RADAR ECHOES
NT RADAR ECHOES
NT RADIO ECHOES
NT SIGNAL REFLECTION
NT VENUS RADAR ECHOES

- Perturbation theory, saturation and relaxation effects in electron and ion plasma wave echoes
05 p0699 A72-17220

- Electron plasma wave echoes experimental investigation, discussing amplitude decay under plasma and random noise influence
06 p0858 A72-17538

- Ion crystal plasma wave echoes from conduction electrons interaction with phonons in self consistent field
10 p1527 A72-24926

- IF amplifier automatic gain control (AGC) for ultrasonic pulse echo measurements
11 p1633 A72-26055

- External magnetic field effect on two frequency quadrupole spin echo in polycrystalline specimen
13 p1915 A72-28473

- Green function for temporal electromagnetic plasma wave echoes oblique to external magnetic field, calculating current density and damping term
19 p2839 A72-37333

- Macroscopic photon echo polarization and radiation intensity in Cr ion doped ruby laser stimulated by coherent light pulses
19 p2814 A72-38780

- Plasma echo-type oscillations in n-type InSb semiconductor, noting conduction band nonparabolicity effects
21 p3098 A72-41687

- Absolute accuracy of the pulse-echo overlap method and the pulse-superposition method for ultrasonic velocity.
23 p3313 A72-44114

ECLIPSES

NT LUNAR ECLIPSES

NT SOLAR ECLIPSES

- Soviet book on compact binary stellar systems with globular components covering disk darkening, eclipsing, absolute dimensions and masses, etc
08 p1229 A72-20910

- Negative search for post-eclipse brightening of Io and Europa satellites in 1970 based on single beam photometric observation
10 p1532 A72-23714

- Soft X-rays from Cygnus X-2 and from Cygnus X-1 in eclipse.
17 p2600 A72-35297

- Compact expressions for maximum and minimum eclipse durations of spacecraft circular orbit, presenting numerical data as aid to spacecraft design
19 p2862 A72-38021

- The equilibrium potential of a magnetospheric satellite in an eclipse situation.
23 p3168 A72-42003

- The physical properties of the Jovian atmosphere inferred from eclipses of the Galilean satellites. II - 1971 apparition.
24 p3435 A72-44689

ECLIPSING BINARY STARS

- UBV photometric studies of eclipsing variable R Canis Majoris confirming primary component as FIV star, discussing ordinary semidetached system possibility
01 p0129 A72-10793

- Eclipsing variable star EQ Taurus photoelectric brightness variation observations in B and V light
03 p0433 A72-13488

- Eclipsing variable system AW Peg spectrophotometric data, examining spectral line geometries and intensities and atmospheric conditions
03 p0439 A72-14244

- Photoelectric observations in different colors of eclipsing variable TX Cancri, presenting tables
05 p0723 A72-17199

- Eclipsing variable binary AI Draconis BV photoelectric observations, using wideband filters
06 p0882 A72-18007

- Computer program for photometric orbital elements determination of eclipsing binary stars
06 p0883 A72-18022

- Interferometric observations of emission of radio eclipsing binaries beta Persei and beta Lyrae at 2965 and 8085 MHz
07 p1082 A72-20289

- Photoelectric observation of eclipsing contact binary 44 i Bootis period changes
09 p1391 A72-23534

- Hyades member star BD plus 16.516 deg described as late evolution product of binary system with mass exchange and loss through planetary nebula phase
10 p1543 A72-24618

- Visual observations of eclipsing period elements of nova-like variable V Sagittae for estimate of total magnitude of uneclipsed binary
10 p1545 A72-24829

- Simultaneous observations of radio flares from beta Persei on 25-25 January 1972 at 2.8, 3.7 and 11.1 cm, noting spectral characteristics difference from quasi-steady component
10 p1547 A72-24945

- Radio emission variations of eclipsing binary stars beta Persei and beta Lyrae tabulated
10 p1547 A72-24946

Extragalactic eclipsing binaries parallax determination by Gaposchkin method, noting application to distance determination of nearby galaxies
10 p1549 A72-25057

Close binary stars system model for totally eclipsing AW UMa light curves and line profiles, noting very low mass ratio
10 p1550 A72-25195

Eclipse analyses confidence in eclipsing binary photometric solutions, discussing consistency with stellar interior model density distributions and interactions between member stars
11 p1716 A72-25677

Secondary component of eclipsing binary beta Lyrae as massive main sequence star in rapid nonuniform motion, refuting black hole suggestion
11 p1717 A72-25869

Computer program for photometric orbital elements determination of eclipsing binary stars
11 p1718 A72-25958

Russian book on eclipsing binary stars covering limb darkening law, photometric eclipsing phases, computer applications and models
11 p1720 A72-26046

UBV photometric properties and probability of discovery in blue light of detached close binaries models
12 p1867 A72-27214

X ray emitting component Centaurus X-3 mass limit in close eclipsing binary system with regard to Roche lobe principle
14 p2156 A72-30569

Eclipsing binary WZ Sge observation for light curves with 3-sec time resolution, noting amplitude variation similarity to other cataclysmic variables
15 p2314 A72-32368

Photoelectric photometry of binary VV Pup with 3-sec time resolution, suggesting qualitative model from eclipses identification
15 p2314 A72-32369

Emission line star WRA 795 as optical counterpart of Cen X-3 occulting binary system
16 p2456 A72-33474

Uhuru satellite data on periodic pulsating X ray source in Hercules, interpreting intensity variations as occulting binary star system effect
16 p2446 A72-33475

The limb darkening problem in eclipsing binaries.
17 p2612 A72-35382

Narrow-band photoelectric photometry of the peculiar Wolf-Rayet eclipsing binary CV Serpens.
17 p2617 A72-35732

Period changes in eclipsing variables. II - The system VW Cephei.
18 p2723 A72-36084

The primary spectrum of the eclipsing binary LR Centauri.
19 p2856 A72-37505

On the optical search for Centaurus X-3.
19 p2856 A72-37506

Spectrophotometric study of eclipsing-variable system components. I
19 p2858 A72-37811

Eclipsing and spectroscopic binary beta Persei radio star, suggesting X ray source nature
19 p2851 A72-37889

Extent of information that can be obtained from the luminosity loss curves of eclipsing systems with extended atmospheres
19 p2860 A72-37953

A statistical method for the determination of the rate of changes of period for eclipsing binaries.
20 p2974 A72-39892

Secondary fluctuations in the light curve of epsilon Aur.
20 p2974 A72-39898

Photoelectric observations of the 1971-eclipse of 32 Cyg.
20 p2974 A72-39900

Effect of a temporal shift in the min II of eclipsing binaries
20 p2975 A72-40072

Stratification of the emission in the envelope of a Wolf-Rayet type eclipsing binary V444 Cyg
21 p3113 A72-41759

Eclipsed binary brightness curve determination by least squares method, using weighted gravity center point observations
21 p3113 A72-41760

Photometric elements of corpuscular unstable AH Vir eclipsing binary at 4400 and 5600 A, comparing stellar gas stream and solar chromosphere densities
23 p3338 A72-44028

Proper motions of 122 eclipsing variables
24 p3448 A72-45688

ECLIPTIC

Excess secular change in ecliptic obliquity in relation to earth internal motion due to mantle-core coupling
04 p0575 A72-15028

Mission analysis of Helios spacecraft swingby past Venus to acquire extraecliptic trajectory
[AIAA PAPER 72-50]
05 p0721 A72-16951

Off-ecliptic north-south anisotropies in cosmic radiation intensity during polar storm events
06 p0873 A72-17467

Interplanetary shock wave inclination to ecliptic plane dependence on chromospheric flare and earth projection heliolatitude differences
06 p0884 A72-18027

Interplanetary shock wave inclination to ecliptic plane dependence on chromospheric flare and earth projection heliolatitude differences
11 p1719 A72-25963

Hydrodynamic approximation for solar wind nonuniformity in ecliptic plane, noting linear disturbances caused by nonuniform velocity of plasma flow from corona
13 p2029 A72-28577

Earth capture of dust particles moving in ecliptic plane heliocentric orbits, using three gravitational bodies analysis
14 p2153 A72-30494

Earth capture of dust particles moving in ecliptic plane heliocentric orbits, using three gravitational bodies analysis
19 p2864 A72-38323

A determination of the motion of the ecliptic.
23 p3337 A72-43833

Hydrodynamic approximation for solar wind nonuniformity in ecliptic plane, noting linear disturbances caused by nonuniform velocity of plasma flow from corona
24 p3435 A72-45077

ECLOGITE

Pb and Sr isotopic composition measurements on eclogites from South Africa
05 p0658 A72-16551

ECOLOGICAL SYSTEMS

U ECOLOGY

ECOLOGY

NT COASTAL ECOLOGY

Microbial survivability in deep space environmental simulation experiments, describing aerospace ecology and panspermia avoidance
01 p0019 A72-10823

Grasslands mapping for ecosystem analysis, determining spectroradiance/reflectance characteristics by aerial and satellite-borne multispectral scanner imagery, aerial and ground photography and spectrometry
02 p0208 A72-11783

Phyto-ecological approach to remote sensing of man made ecosystems, comparing vegetation and landscapes in Old and New Worlds
02 p0210 A72-11797

Multistage resource inventory and analysis program combining remote sensing techniques and ecological principles in California Desert pilot area, discussing photointerpretation and ground truthing
02 p0210 A72-11802

Forest vegetation distributional and statistical parameters ecological analysis by multiband remote sensing in areas devoid of ground control
02 p0212 A72-11815

Chesapeake Bay aquatic ecosystems observations, using satellite remote sensing multispectral photography and imagery
02 p0215 A72-11885

Wideband spectrum utilization above 10 GHz for high speed digital communications and ecological monitoring
02 p0176 A72-12182

Automated electromagnetic pollution data acquisition systems for environmental ecology, discussing computer technique and data retrieval, analysis and storage
03 p0328 A72-14040

Book on aerial photoecology covering aerial survey images interpretation, processing and printing operations and economic considerations
04 p0514 A72-14572

Ecogenesis of volcanic island of Surtsey after 1967 lava eruption, discussing terrestrial and marine littoral and sublittoral biomes
04 p0473 A72-14916

Self contained portable data acquisition system for marine, environmental and ecology research, using multiple analog recording and digital telemetry transmitter
06 p0797 A72-18613

Biotelemetry applications in medicine, animal experiments and ecology, including ergonomics, internal bleeding detection, fetal monitoring, animal brain implantations, animal movement tracking, etc
07 p0931 A72-19916

Cellular evolution investigation using molecular biology, microbial physiology and ecology
08 p1119 A72-22011

Aerial photography for rural soil mapping, considering geographic, ecologic and agricultural production interpretation
09 p1301 A72-23279

Ecological study of damp wasteland according to seasons and with various photographic emulsions
09 p1303 A72-23293

ECONOMIC FACTORS

Space flight ecology and physiology, discussing atmospheric temperatures and radiation, biological effects of acceleration, deceleration and weightlessness and physiological stresses
11 p1584 A72-26018

Space activity in fields of ecology and earth resources - Conference, Rome, Italy, March 1972
15 p2220 A72-31230

International programs for simultaneous ecological study via remote sensing techniques, discussing European and Italian space programs
15 p2319 A72-31232

Satellite observation of earth surface, discussing remote sensing techniques application in pollution control and ecology
15 p2319 A72-31232

Airborne remote sensing missions and instrumentation to investigate Penobscot River water ecology for thermal, chemical and solid pollutants
15 p2221 A72-31252

Commercial transport aircraft engine technology contribution to world air transportation, considering social and ecological compatibility with community
16 p2348 A72-33314

Characteristics of conditioned reflexes to an ecologically adequate stimulus in hens
23 p3257 A72-44080

ECONOMIC ANALYSIS

Short-short haul STOL network economics for commuter ports in Detroit region, estimating service demand, aircraft number and maintenance costs
03 p0459 A72-13696

Price/demand/cost economic aspects of carbon fiber reinforced plastics composites in aero-engine applications
04 p0536 A72-14743

Economically optimal operation of protection circuit for plant subject to stationary random process, determining failure rate of plant
04 p0496 A72-14995

Book on electrochemical machining covering metallurgical effects, electrolytes, tool design, rotating surfaces and operating costs
06 p0821 A72-17819

Cost efficiency and relative economic merits prediction for solar energy conversion systems
10 p1423 A72-24316

Econometric approach to space shuttle design for optimum operational redundancy levels, using payload-cost effectiveness criterion
[AIAA PAPER 72-242]
10 p1551 A72-24448

Economic interpretation of dual variables in linear fractional programming, noting coherence of marginal pricing
14 p2087 A72-30714

Economic analysis of satellite network construction program, suggesting Italian national center formation for space exploration
15 p2319 A72-31231

Economic analysis of aeronautical communication system via satellite, noting cost estimates and annual charge per user
21 p3081 A72-40298

Technical and economic processes representation of radioelectronic equipment synthesis optimization using elementary random magnitudes involving output parameters deterioration rates and fabrication tolerances
23 p3269 A72-43442

ECONOMIC FACTORS

Land pollution remote sensing, discussing economic and political impact in terms of land use, transportation, energy supplies and recreational opportunities
[AIAA PAPER 71-1039]
01 p0057 A72-10523

Ti-Al-V alloy powders electrically activated pressure sintering /spark sintering/, considering mechanical properties and economic factors
02 p0240 A72-11428

Economic evaluation of airport fog dispersal methods in the U.S., including crushed dry ice and liquid propane
04 p0542 A72-14677

ATC technology impact on flight operations and public value of aviation, discussing microwave landing system economic aspects
04 p0544 A72-14810

Time/frequency collision avoidance systems, discussing operating principle and economic aspects for airlines and general aviation
04 p0544 A72-14816

Route charges system for Europe, stressing financial necessity
04 p0597 A72-15071

TV programs direct broadcasting by satellites, discussing frequency range, amplitude vs frequency modulation, satellite stabilization and economic aspects
04 p0494 A72-15678

Space operations cost effectiveness improvement by earth-to-orbit shuttle, discussing space utilization growth and economics
[SD-71-780]
05 p0724 A72-16048

German commercial airports adaptation to traffic development, considering economic factors
05 p0643 A72-16187

Water based offshore and floating island airports planning and construction, discussing economic, technical and social aspects

05 p0644 A72-16695

Airport financing, discussing funds, long term planning, commercial principles, private enterprise, loans and revenue

05 p0753 A72-16698

Management enhancement of researchers motivation in times of economic uncertainty, stressing security related aspects of employment

06 p0905 A72-17396

Price and technical quality effectiveness in winning government R and D contracts

06 p0905 A72-17397

Space shuttle program evaluation, discussing national economic benefits relative to aerospace industry employment, domestic production, balance of trade, etc

06 p0893 A72-18612

Laser technology applications, considering economic factors in terms of market oriented products

07 p1105 A72-19554

Laser beam welding operational and economic aspects, discussing comparative merits vs conventional welding techniques in terms of quality, speed, depth and power limitations

07 p0998 A72-20397

Plastics cutting and drilling with carbon dioxide IR laser beam, discussing economics and commercially available equipment

07 p0999 A72-20554

Space shuttle, tug and orbital station transportation system benefits and applications, noting European economic implications

08 p1229 A72-20977

Economic factors influence on reliability optimization of complex radio systems and elements

08 p1143 A72-22066

Development trends in airborne man machine flight control, discussing optimal division between human pilot and machine in relation to total system performance and economic factors

09 p1270 A72-22781

Fixed wing agricultural aircraft, comparing different designs in terms of performance, safety, handling and economic efficiency

09 p1262 A72-22940

Image scale selection for topographic map revision in orthophotograph production considering economics and suitability

09 p1311 A72-22968

Space shuttle orbiter vehicle structural design configurations development and evaluation with respect to overall system weight and program cost

[ALAA PAPER 72-373] 11 p1726 A72-25397

Flight crew training programs cost and quality, emphasizing safety and flight simulator application

11 p1590 A72-26998

European passenger aircraft Airbus program, discussing various configurations performance, economic factors and technical support

12 p1753 A72-27108

Economic and social implications of Indian national satellite for television and telecommunication, noting data links need

[ALAA PAPER 72-583] 12 p1781 A72-27384

STOL, VTOL and V/STOL air transportation systems development, characteristics and requirements, presenting economic forecast

12 p1754 A72-27661

Composite materials application to gas turbine fan guide vane fabrication, noting economic factors and prototypes performance in engine tests

12 p1815 A72-28100

Aerospace technology economic and social effects, relating U.S. space expenditures and gross national product

14 p2174 A72-30682

Quiet RTOL /reduced takeoff and landing/ short haul aircraft cost comparison with Trident 3 aircraft up to design range stage length

15 p2180 A72-31320

Economics of material cutting and removal by plasma torches, presenting cutting rates as function of plate thickness for different materials

15 p2243 A72-31321

Low cost flight simulator for general aviation pilot training, containing IFB instrumentation and turbulence injection device

15 p2214 A72-32211

Airport capacity and air traffic congestion effects on airport operations in terms of time and costs

15 p2339 A72-32454

VTOL short haul transportation applications discussing concept evolution and economic factors

16 p2480 A72-33181

Dallas/Fort Worth airport planning and construction economics impact on community economy and life style

16 p2373 A72-33307

Airport and air transportation benefits and costs to community and industry, considering institutional, environmental and economic issues

16 p2373 A72-33308

Airport economic and social impact on environs in terms of community development

16 p2373 A72-33309

Short haul air transportation system economic and political problems, noting community acceptance and passenger service standards

16 p2481 A72-33310

Commercial airport and air transport service economic impacts on business and industrial communities

16 p2481 A72-33312

Aero engines and propulsion systems development contribution to air transport economics and regularity, considering environmental factors

16 p2443 A72-33313

Technical and economic aspects of explosive metal fabrication, considering requirements for close tolerances, nonsymmetrical shapes, large size workpieces and unusual material properties

16 p2398 A72-33354

Electron beam welding, machining and drilling, discussing technical and economic factors

16 p2399 A72-33540

Carbon fibers for composite materials reinforcement, discussing mechanical properties and economic factors

17 p2569 A72-34188

Advantages of MOS/LSI computers in avionics systems.

17 p2523 A72-35579

Air transport developments effects on economy and environment, discussing government power to control airport use and location and air pollution

17 p2639 A72-35952

Economics of a new regional airport.

18 p2743 A72-36779

Factors to be considered in airline scheduling.

19 p2883 A72-37745

STOL-based short haul transportation feasibility for airport congestion alleviation from airline viewpoint, discussing system requirements, economic factors and safety

[ALAA PAPER 72-807] 19 p2750 A72-38120

Economic impact of applying advanced technologies to transport airplanes.

[ALAA PAPER 72-758] 19 p2751 A72-38128

Space technological advance effects on human extraterrestrial, scientific, economic and sociological progresses

19 p2867 A72-38545

Operating cost comparisons between Concorde and Boeing 707 and 747 aircraft, considering profitability

20 p2888 A72-39818

Advanced technology applications to present and future transport aircraft.

[ALAA PAPER 72-759] 20 p2888 A72-40051

ILS replacement by microwave landing system, considering landing phase range from acquisition to touchdown, terminal approach handling by airborne navigation system and economic advantages

21 p3081 A72-40294

Public policy, regulatory controls, market strategies and systems economics considerations for future U.S. domestic communication satellite system

21 p3132 A72-40865

Sheet metal economics in aircraft construction based on strength/weight and stiffness/weight comparison of Al alloys and Ti alloys in relation to cost and structural weight considerations

21 p3060 A72-41071

Short haul intercity air transportation systems requirements for successful competition with lower cost ground modes

[ICAS PAPER 72-16] 21 p2995 A72-41141

Hypersonic transports commercial applications, examining economic and noise and air pollution aspects

[ICAS PAPER 72-32] 21 p2995 A72-41157

Economic considerations for low-traffic satellite earth stations.

21 p3022 A72-41320

Economic and social aspects of commercial aviation at supersonic speeds.

[ICAS PAPER 72-51] 21 p2996 A72-41851

Flying crane helicopters utilization in construction industry for materials transport and structural erection work, discussing technical and economic aspects

23 p3251 A72-43637

Book - Electronic integrated systems design.

23 p3274 A72-44475

Lockheed airline system simulation and aircraft scheduling models.

24 p3466 A72-44579

A systems analysis of subsonic versus supersonic jet travel.

24 p3466 A72-44580

Airports planning for West Germany, discussing geographical air traffic patterns, economic and noise aspects

[DGLR PAPER 72-034] 24 p3387 A72-44614

Airline operational problems from traffic volume increase, discussing flight safety, passenger comfort, schedule adherence and economy aspects

[DGLR PAPER 72-037] 24 p3467 A72-44618

Space structures and materials technology utilization and transfer to world economic and social problems, considering thermal control, NDT, systems analysis and design

24 p3407 A72-45154

Economic materials processing in orbiting spacecraft under zero gravity conditions, emphasizing single crystal electronic materials and high purity biologicals

24 p3407 A72-45157

Military aircraft construction, design and economic requirements, discussing fighter payloads, armament efficiency and fire control systems

24 p3369 A72-45450

ECONOMICS

NT DEMAND [ECONOMICS]

Monograph on electron beam welding covering space charge effect, equipment, metallurgical and mechanical aspects, production engineering, economics and applications

01 p0073 A72-10167

Civil aviation air transportation contributing factors to American economy, considering disposable income, airline fares and time-trend variable

02 p0304 A72-11721

Economics in electromagnetic field measurement surveys for siting of earth stations operating in shared frequency bands at 4 and 6 GHz, considering interference detection

03 p0324 A72-14044

Soviet look on air transport economics covering efficiency and control improvement, maintenance, work and wages, tariffs, cost and revenues, etc

03 p0459 A72-14098

Interflug national economic control system, discussing objectives, costs, labor, science and technology, material and price management plans

05 p0753 A72-16778

Radio communication system optimization from viewpoints of global synthesis, including economics and partial synthesis based on noise stability, precision and reliability

08 p1136 A72-21845

Book on IATA organization and functions, discussing international aviation history, conference machinery, enforcement of conference resolutions, air transportation economics, public corporations, etc

10 p1564 A72-23846

Long time mission spacecraft computer reliability economics based on failure and step improvement costs evaluation

10 p1444 A72-24017

Business V/STOL aircraft economic viability based on cost benefit analysis and comparison with turbine powered aircraft

[SAE PAPER 720334] 11 p1576 A72-25594

Book on world airlines economic regulation, analyzing multilateral international agreements, national aviation interests and competitive situation

11 p1748 A72-25923

Book on air transportation, covering history, government agencies roles in economic and safety regulation of air carriers, accounting, financial and legal aspects, etc

12 p1891 A72-28205

Aeronautical communication satellite technical and economic survey, considering wave propagation, noise, aircraft antennas and VHF and UHF links

15 p2193 A72-31180

Commercial airlines aircraft selection factors, considering size, range, economics, traffic, runway quality, maintenance and operating costs, reliability and cargo handling

16 p2348 A72-33333

ICAO assistance to member states in various transport airports and navigation facilities economics including accounting and financial statistics

16 p2481 A72-33334

EDDIES

U VORTICES

EDDY CURRENTS

Crossing points computed curves from metal sheet response to pulsed eddy currents, suggesting independent lift-off distance variation possibility

05 p0666 A72-17049

X ray, ultrasonic and eddy current nondestructive testing of aircraft structure for maintenance and special problems

07 p0994 A72-18840

Electric field in flow of medium with tensor conductivity due to Hall effect, studying eddy currents structure in magnetic field variation region

07 p1044 A72-20316

Electric eddy currents formation during thermal acceleration of inviscid quasi-linear plasma in profiled channel

08 p1215 A72-21654

Eddy current extensometer for monitoring long term creep in diameter of pressurized tubular stainless steel specimens

11 p1613 A72-25821

Eddy current sensor for mechanical vibration measurements, describing circuit design for stable and reliable operation at 30 MHz

13 p1930 A72-29051

- Aeros satellite magnetic properties, describing measurement procedures for component induced disturbance fields, dipole moments and eddy currents
13 p1940 A72-30080
- Turbine blade trailing edge wall thickness measurement by phase sensitive eddy current technique
16 p2397 A72-33201
- Possibility of using the eddy-current method to measure the local magnetization of an object.
19 p2805 A72-38761
- A new circuit for the contactless thickness measurement with the aid of pulse-excited LC measuring circuits
20 p2927 A72-39696
- The magnetic field of eddy currents above a surface crack in metal with excitation of them by an applied inductor.
21 p3057 A72-41722
- Analysis of noise immunity of two-channel eddy-current flaw detector.
21 p3057 A72-41723
- EDDY DIFFUSION**
U TURBULENT DIFFUSION
- EDDY VISCOSITY**
- Finite difference schemes for surface and planetary boundary layer solutions using grid spacings proportional to mixing length and eddy viscosity
03 p0386 A72-14337
- Turbulent wake calculations with eddy viscosity model, predicting velocity profiles and displacement thicknesses
05 p0603 A72-16538
- Pressure gradient effect on mixing length for equilibrium turbulent boundary layers, calculating eddy viscosity
[AIAA PAPER 72-213] 05 p0651 A72-16855
- Turbulent boundary layer model with eddy viscosity representation of inner wall region for cases with suction or injection, presenting wall shear calculation method
07 p0973 A72-20248
- Lin parameter and eddy viscosity of atmospheric vortex streets, using TIROS and Gemini data
08 p1200 A72-21621
- Kinematic eddy viscosity for incompressible two dimensional turbulent flow, obtaining Navier-Stokes equations and conditions for equilibrium and nonequilibrium boundary layers
15 p2216 A72-31470
- Mixing length theory derivation of barotropic planetary boundary layer profiles for geostrophic wind deviations, Reynolds stress, eddy viscosity and turbulent kinetic energy dissipation
15 p2224 A72-31675
- Turbulent mixing layers analytical and experimental mean velocity profiles, discussing Goetler eddy viscosity theory
16 p2374 A72-32832
- Double hierarchy in repeated cascade theory of turbulence.
24 p3390 A72-44997
- EDEMA**
- Hemodynamics, pulmonary gas exchange and circulatory responses to high altitude in subjects with previous history of high altitude pulmonary edema
02 p0156 A72-11422
- Hyperbaric oxygen exposure effect on cardiovascular system in rats, discussing pulmonary edema relation to hypertensive left ventricular failure
07 p0921 A72-20182
- Thyroid glands iodine concentrations, blood proteins and morphological changes in rats with acute hypoxic hypoxia and pulmonary edema
07 p0924 A72-20620
- EDGE DISLOCATIONS**
- Slip line field for plane strain extrusion of strain hardening material, calculating shear stress
03 p0363 A72-13708
- Ultrasonic fatigue at small strain amplitudes in Ti, developing solitary slip band microcracks
04 p0533 A72-14539
- Plastic flow stress around dislocations on Ni-Al intermetallic cube and octahedral cross slip systems
05 p0678 A72-17118
- Isotropic continuum model of elastic interaction of edge and screw dislocation with nearby inclusion
06 p0894 A72-17492
- Plastic deformation of solid body in terms of slip dislocations displacement rate
06 p0894 A72-17687
- Low temperature slip discontinuity and strength of pure Al crystals as function of strain rate
06 p0831 A72-18355
- Slip band formation and crack initiation in Ti as function of cyclic loading frequency, considering plastic strain amplitude or distribution as causes
[DFVLR-SONDDR-149] 06 p0832 A72-18425
- Infinite elastic solid deformation in antiplane strain mode, discussing corresponding strain model with continuous distribution of slipping edge dislocations
09 p1405 A72-22919
- Various restrain dislocation distributions effect on mechanical twinning behavior in purified Nb single crystals
10 p1497 A72-24824
- Transitional microstructure of machined surface layer due to built-up edge disintegration
11 p1638 A72-25508
- High power ultrasonics in metal fatigue studies, considering crack propagation and slip patterns for high and low frequencies
11 p1639 A72-26053
- Dislocation bands in electrolytically hydrogen charged fcc Ni-Co alloy, describing band structure in terms of band axis and planes and Burgers vector
11 p1669 A72-26947
- Mill annealed Ti alloy fatigue at 600 F and room temperature, noting critical local stress for slip bands formation and cracking
14 p2120 A72-30611
- Slip band blocking effect of disperse particles on crack suppression and creep rupture strength of intermetallic Al-Fe-Ni alloy
14 p2124 A72-31033
- Electron microscopic investigation of slip processes during plastic deformation of WC-Co based cermets, observing WC grain boundary sliding and Co phase crystal lattice transformations
15 p2257 A72-32117
- Deformed Cu-Au single crystal surface slip bands fine structure, determining separation distance between individual slip lines
16 p2408 A72-33774
- Similarity solutions to nonlinear equations of motion of n dislocations group in slip plane under stress
18 p2719 A72-36745
- Edge and screw dislocations induced stress fields in isotropic medium, using Kauderer nonlinear elasticity theory
23 p3345 A72-43622
- Low temperature slip discontinuity and strength of pure Al crystals as function of strain rate
24 p3416 A72-45742
- EDGE LOADING**
- Edge loaded cylindrical shells of resolution nonlinear axisymmetric deformation determination from asymptotic solution of Reissner equations, using multiple scale perturbation technique
01 p0136 A72-10031
- Elastic quadrant shaped disk loaded on horizontal and vertical edges, determining stress values at arbitrary points
02 p0259 A72-12235
- Circularly symmetrical disks with circular hole and loaded by pressure at edges, calculating linear and power-law strain hardening
02 p0297 A72-12535
- Variable cross section elastic stringer end loaded longitudinal force transmission to stiffened elastic plate
03 p0444 A72-13465
- Homogeneous isotropic thin elastic shells under forces along edge and with faces free of tractions, deriving refined interior equilibrium equations
03 p0447 A72-13882
- Skew plates buckling with different edge support conditions, presenting Rayleigh-Ritz method results for various combinations of side ratio, skew angle and loadings
04 p0584 A72-14509
- Large deflection of rectangular thin elastic plates with unsupported edges, using finite difference technique based on dynamic relaxation methods
06 p0895 A72-17799
- Crack propagation in presence of crack branching events in semiinfinite nonhomogeneous elastic brittle plate under edge impact loading
06 p0896 A72-17914
- Elastic stability of laminated circular plate with rectangular anisotropy under in-plane compression forces along edge
07 p1090 A72-19693
- Stress analysis of infinite plate with parallel cracks under symmetrical edge loads
07 p1092 A72-19781
- Stability loss of circular annular plate under compression, determining critical loads with inner edge free and outer edge hinged or clamped
07 p1092 A72-19900
- Method of images solution for stress systems in rectangular plate under general self equilibrant edge tractions
07 p1095 A72-20244
- Stress-strain state of circular three layer laminar plates freely supported at circumference and loaded at edge
09 p1399 A72-22694
- Stress analysis of isotropic linearly elastic square plate of constant thickness loaded by concentrated forces at edges
09 p1399 A72-22698
- Bending theory of homogeneous isotropic micropolar cantilever beam loaded by moments at edges
09 p1399 A72-22700
- Green function for stress components in circumferentially loaded circular disk, noting conformal mapping for arbitrary shape
10 p1557 A72-24717
- Green function for stress components in straight edge loaded half plane disk, noting conformal mapping for arbitrary shape
10 p1558 A72-24718
- Flexural vibration of rectangular orthotropic plates with clamped, simply supported and/or free edges, presenting solution method for coupled characteristic equation pairs
11 p1735 A72-25737
- Green function for stress distribution in plane shaped disk with edge loaded circular hole, noting conformal mapping for arbitrary shape
12 p1883 A72-27391
- Circular cylindrical shell under distributed edge load along circular hole contour, calculating stress concentration by trigonometric series solution for shallow shell equation
12 p1886 A72-28130
- Thick rectangular plate stress functions under linear tensile forces application to longitudinal edges and resultant forces application to transverse edges
13 p2055 A72-28735
- Stress-strain state of elastic rectangular plate under arbitrary edge forces on displacements
13 p2058 A72-29458
- Stress analysis in circular disk loaded along circumference, noting results identity for stress presentation by Fourier series, Poisson integral and Green function
16 p2470 A72-33593
- Three dimensional photoelastic analysis of edge loaded ring reinforced rotating shells with zero bending, assuming pure membrane stress field
18 p2733 A72-36365
- Buckling of orthotropic, curved, sandwich panels subjected to edge shear loads.
18 p2735 A72-36770
- Uniformly loaded thin elastic isotropic circular plate with partly clamped and simply supported edges, determining deflection via solution of biharmonic differential equation
20 p2979 A72-39331
- Singular stress concentration at sharp edge of wedge in contact with half plane in elastostatics
21 p3119 A72-41104
- Numerical solution of bending stresses in elastic cantilever plates under surface and edge loads, noting boundary layer, load concentration and sweep back effects
22 p3236 A72-42609
- Variable cross section elastic stringer end loaded longitudinal force transmission to stiffened elastic plate
24 p3458 A72-44940
- EDGES**
NT LEADING EDGES
NT SHARP LEADING EDGES
NT TRAILING EDGES
- Taylor type antenna radiation distribution for aperture edge behavior realization in E or H planes
07 p0945 A72-19785
- The behavior of electromagnetic fields at edges.
17 p2513 A72-34357
- EDUCATION**
NT ASTRONAUT TRAINING
NT FLIGHT TRAINING
NT PILOT TRAINING
NT SPACE FLIGHT TRAINING
- Earth Resources Survey (ERS)/ program personnel training and education, discussing trainee selection, knowledge categories and training methods for remote sensing
02 p0304 A72-11855
- Educational programs for increasing public interest in space program benefits, describing summer teacher workshop on Apollo lunar and Skylab space station missions
06 p0906 A72-18623
- Educational and social applications of communication and meteorological satellite data dissemination, discussing learning and teaching model development
06 p0777 A72-18624
- Education and training of personnel for photointerpretation, discussing psychological, physiological and methodological aspects of aerial photointerpretation
09 p1272 A72-23298
- Industrial enterprise training expense planning in terms of staff productivity and work time
11 p1748 A72-26543
- AMSAT-OSCAR-B series of radio communication satellite for worldwide use with low cost terminals in amateur and education services
[AIAA PAPER 72-521] 12 p1779 A72-27351
- Fixed and broadcast communication satellites for educational information dissemination in U.S., discussing commercial, multipurpose domestic and hybrid systems
[AIAA PAPER 72-523] 12 p1779 A72-27352
- Critical examination of programming courses design and subject matter, emphasizing fundamental principles and algorithm construction
15 p2202 A72-31453
- Presupposition, aim and methods for teaching transducer technology to users and designers, reviewing

transducer static and dynamic performance characteristics and classifications

16 p2393 A72-33632

SkyLab project participation by students to stimulate interest in science and technology, giving winning experiment proposals

24 p3467 A72-45158

EDUCATIONAL TELEVISION

Educational satellites - Conference, Nice, France, May 1971, covering space communication, TV, performance, data handling, economics, etc

01 p0147 A72-11277

ATS-F educational TV experiment in India, discussing domestic communication satellite development and nationwide coverage problems

02 p0278 A72-11960

Satellite communication regional and domestic applications, discussing educational, earth resources, geological survey, environmental and maritime uses

04 p0487 A72-15073

Space communication application for information, education and cultural exchange, noting need for international cooperation

07 p1104 A72-19473

Frequency bands for space-earth links in broadcasting satellite service, stressing application to educational television

10 p1435 A72-24032

Technical standards for educational and community TV by satellite, considering picture quality requirement, modulations, SNR, threshold and fade margin, and channel width

10 p1435 A72-24034

Combined educational and TV network satellite distribution system for public broadcasting service, discussing cost reduction techniques

10 p1435 A72-24035

Ground and satellite based TV broadcasting compared in terms of economic, political and pedagogical implications to solve educational problems in developing countries

12 p1891 A72-27662

NASA ATS F/G satellites for educational TV broadcasting in foreign countries, discussing technologies and case histories

15 p2196 A72-31829

EEG [ELECTROENCEPHALOGRAMS]

U ELECTROENCEPHALOGRAPHY

EFFECTIVENESS

NT COST EFFECTIVENESS

NT SYSTEM EFFECTIVENESS

Stochastic models of human performance effectiveness functions reliability and correctability from error data generated by tracking and vigilance tasks

10 p1429 A72-24001

EFFECTORS

U CONTROL EQUIPMENT

EFFERENT NERVOUS SYSTEMS

Discharge patterns in motor nerve fibers during human voluntary muscle contractions

01 p0013 A72-10624

Spinal reflexes through electric stimulation of gastrocnemius and soleus human leg muscles, attributing increased tendon reflex amplitudes to gamma motoneurons hyperactivation

04 p0467 A72-14704

Short and long term mental and physical work effects on central nervous system and motor apparatus in young people

04 p0474 A72-15230

Bioelectric activity study of cat and dog cerebral intercentral relations during various motor activities and poses

04 p0474 A72-15231

Human arm muscle motor neuron reflex response to rectangular pulse excitation of ulnar nerve

04 p0476 A72-15587

Cat and rabbit middle ear muscles contraction by electric stimulation of motor nerves, noting sound transmission reduction

08 p1115 A72-21136

Cat middle ear muscles motor units twitch tension and contraction time in response to motor neuron threshold stimulation

08 p1116 A72-21137

Dynamic orthosympathetic control of cardiovascular system, studying efferent element link between autonomic vasomotor and cardiac centers and effector cells

08 p1118 A72-21548

Energetic motor activity rule hypothesis for physiological mechanisms of certain ontogenesis patterns, suggesting motor activity as excess anabolism induction factor

09 p1264 A72-22225

Functional organization of monkey cortical efferent zones in distal forelimb muscle control from intracortical microstimulation studies, showing stimulation thresholds distribution

09 p1267 A72-23582

Peripheral afferent input to monkey cortical efferent zones of distal forelimb muscle control, using single microelectrode for intracranial stimulation and cellular discharge recording

09 p1267 A72-23583

Vasomotor efferent effects on rabbit lung posterior lobe blood content in response to electrical stimulation of vagus nerve peripheral ends

09 p1268 A72-23693

Efferent vestibular activity in response to horizontal plane rotary stimulation in frog, showing efferent relations between both ears

10 p1426 A72-25099

Electromyogram and myogram responses in phasic stretch reflex under prestrain conditions as index of fusimotor activity level in normal humans

11 p1588 A72-26632

Neuronal mechanisms of muscular motor activity control, analyzing cerebrum-motoneuron connections, spinal potentials, monosynaptic responses and depolarization

13 p1907 A72-29981

Human spinal segment functional state before voluntary movement during water immersion, using H-reflex for spinal cord motoneuron excitability evaluation

14 p2073 A72-30255

Human and animal central nervous system repair processes for brain damage caused motor function disturbances

14 p2078 A72-31100

Multilevel motion control

17 p2504 A72-35018

Servo action in human voluntary movement

18 p2654 A72-36999

Russian book - Mechanisms of descending control of spinal cord activities

21 p2998 A72-40577

Morphological changes in spinal cord neurons of animals due to the decreased intensity of supraspinal stimulation

21 p2998 A72-40580

Synaptic suprasegmental control mechanisms of spinal cord motor neurons

21 p2999 A72-40584

Influence of a preceding afferent stimulation on the pyramidal activation of spinal motor neurons

21 p2999 A72-40588

Role of pyramidal and extrapyramidal components of cortically-induced efferent stimuli in the mechanism of cortical motor activity coordination

21 p2999 A72-40591

Synchronization in the work of motor neurons during arbitrary motor activity of various types

21 p2999 A72-40595

Role of efferent influences of temporo-rhinencephalic cerebral structures in pre-adjustment alterations of spinal motor neuron excitability

21 p2999 A72-40596

Role of the hypothalamus and limbic system in the regulation of the motor and secretory functions of the digestive apparatus

21 p3000 A72-40754

Cortical metabolism regulation and effector systems of the adaptation process

21 p3000 A72-40760

Role of afferent and efferent connections in the formation and reproduction of trace processes in man

21 p3001 A72-40807

Patterns of spontaneous and reflexly-induced activity in phrenic and intercostal motoneurons

21 p3003 A72-41462

Effects of physical exercise on spinal reflectivity in man

21 p3003 A72-41524

Respiration control mechanism ensuring adaptation to power requirements and chemical environment maintenance in tissues, considering brain stem location

24 p3371 A72-44600

EFFICIENCY

NT COMBUSTION EFFICIENCY

NT COMPRESSOR EFFICIENCY

NT ENERGY CONVERSION EFFICIENCY

NT NOZZLE EFFICIENCY

NT POWER EFFICIENCY

NT PROPELLER EFFICIENCY

NT PROPULSIVE EFFICIENCY

NT THERMODYNAMIC EFFICIENCY

NT TRANSMISSION EFFICIENCY

Multidimensional function extremum for sectioned resonator type gyroamplifier efficiency optimization

08 p1172 A72-22050

Controlled plants operation efficiency change prediction by analytic and probabilistic methods with data processing

08 p1180 A72-22064

Low energetic efficiency of semiconductor microwave scanning converters for radio images of fog obscured objects

13 p1932 A72-29297

EFFLUENTS

Trajectory and flow properties of submerged heated effluents discharging into moving waterway

[AIAA PAPER 72-79] 05 p0659 A72-16912

Mass spectrometer sampling system for measuring effluent concentrations downwind of stacks at various positions in turbulent flow within atmospheric simulation facility

[AIAA PAPER 72-649] 17 p2536 A72-35478

Detection of waste water effluents and of their surface spread in the English channel, the North sea and the Baltic sea, through determination of the surface temperature of the sea by means of infrared air pictures taken by satellites

24 p3398 A72-45223

EFFUSIVES

NT LAVA

EGGS

Effects of combined O-G simulation and hypergravity on eggs of the nematode, *Ascaris suum*. [DFVLR-SONDDR-225]

17 p2499 A72-34547

The influence of clinostat rotation on the fertilized amphibian egg.

18 p2649 A72-36435

Inert gas effects on embryonic development.

22 p3145 A72-42744

EIGENFUNCTIONS

U EIGENVECTORS

EIGENSTATES

U EIGENVECTORS

EIGENVALUES

Computer generated Lamé functions of first kind definable by polynomial coefficients and eigenvalues

01 p0093 A72-10005

Overdetermined collocation method change into Ritz-Galerkin method for applications to boundary value problems with eigenvalues

01 p0093 A72-10122

Direct-iterative eigensolution technique for simultaneous determination of structural system lowest frequencies and modal patterns, using reduced generalized coordinates and Stodola-Vianello method [SAE PAPER 710784]

01 p0137 A72-10275

Large structural systems dynamic mathematical models, predicting eigenvalue and eigenvector with statistical analysis

[SAE PAPER 710785] 01 p0137 A72-10276

Statistical variance of eigenvalues and eigenvectors in random structure dynamic analysis by component mode synthesis

[SAE PAPER 710786] 01 p0137 A72-10277

Ferrite-loaded waveguide Y-junction field mode identification by eigenvalue phase-frequency characteristics measurement, applying to millimeter wave circulator synthesis

01 p0041 A72-10697

Aperture and pattern space factors relationship for vector fields of rectangular and circular apertures, investigating characteristic functions

[AD-742948] 01 p0043 A72-11240

Complex structures mass and stiffness matrices reduction by automatic condensation, calculating lowest eigenfrequencies and eigenmodes of substitute systems

[DGLR PAPER 71-108] 02 p0299 A72-12721

Dynamic structural analysis by finite element method, describing error bounds for eigenvalue analysis by elimination of variables

03 p0442 A72-13401

Spherical harmonics method utilization in radiative transfer calculations, describing characteristic equations roots determination technique

03 p0389 A72-13795

Toroidal oscillations of spherical planetary models, presenting regular eigenfunction form near center

03 p0352 A72-14381

Nonconservative stability problems, obtaining eigenvalues with adjoint variational methods

[AD-742170] 04 p0583 A72-14446

Cracked rectangular plates vibration and stability, computing eigenvalues, natural frequencies and moment distribution

04 p0583 A72-14448

Computational efficiency of minimization algorithm for solving eigenvalue problem arising from dynamic structural analysis by finite element method

04 p0585 A72-14845

Sufficient criteria for MHD stability derived from lowest eigenvalue bounds of Sturm-Liouville problem

04 p0557 A72-15168

Open resonators stability analysis, describing integral equations eigenfunctions and eigenvalues short wave asymptotic expansions

04 p0502 A72-15435

Complex eigenvalues computation for vlf wave propagation in spherical earth-ionosphere waveguide

04 p0492 A72-15442

Resonance degeneration removal in earth-ionosphere spherical cavity resonator, calculating eigenfrequencies by perturbation method

04 p0492 A72-15444

Modal theory of state observers for control of multivariable time-invariant linear systems with plant matrices possessing distinct eigenvalues

04 p0507 A72-15529

Continuous linear elastic systems characteristic vibrations differential operator eigenvalues lower bounds calculation, obtaining Green integral operator first invariant upper bound via stress function

04 p0540 A72-15706

Thin circular flat plate simply supported at three points on circumference, obtaining vibration mode shapes and eigenvalues

05 p0738 A72-16532

- Bounds on condition number for irregular meshes of finite elements expressed in terms of extremal eigenvalues of element matrices
[AD-739416] 05 p0682 A72-16540
- Plane Poiseuille flow stability from Orr-Sommerfeld equation solution by Chebyshev polynomials expansion and QR matrix eigenvalue algorithm
05 p0653 A72-17009
- Optimal linear multivariable control systems design with prescribed eigenvalues, presenting method for corresponding weighting matrix elements
06 p0792 A72-17315
- Algorithm for selective computation of large structural modifications effect on eigenmodes of linear structure
06 p0895 A72-17848
- Ordinary differential equation eigenvalues, presenting method based on interior zeros of one parameter solutions to second order equation with one endpoint boundary condition
06 p0839 A72-17883
- Eigenvalue sensitivity in optimal feedback control systems with state estimation
07 p0962 A72-19716
- Asymptotic eigenvalue density estimates for edge-hinged thin elastic rectangular shell, determining shell stability linear equation solution conditions
07 p1095 A72-20324
- Single mode laser line width calculation by reduction to non-Hermitian eigenvalue problem using Fokker-Planck equation
07 p1008 A72-20440
- Natural oscillation frequencies of piecewise homogeneous L-shaped membranes, determining eigenvalues of second order elliptical differential operator
08 p1241 A72-20903
- Torsional bending vibrations mode shapes of space frame with variable elastic and mass characteristics, determining eigenvalue error limits
08 p1205 A72-20957
- Local stability of thin walled isotropic elastic cylinder, deriving characteristic equations for critical load calculation
08 p1242 A72-20969
- Trajectory properties of roots of characteristic equations with complex coefficients for two dimensional systems with feedforward and feedback cross couplings
08 p1200 A72-21768
- Optimal gradient minimization scheme for finite element eigenvalue and eigenvector problems, including effect of round-off errors and termination criterion
08 p1200 A72-22140
- Laplace operator eigenvalue computation for simply connected region with homogeneous Dirichlet and Neumann boundary conditions and finite difference problem
09 p1340 A72-22296
- Ordinary differential operators eigenvalues calculation, noting numerical integration scheme for initial value problem
09 p1340 A72-22461
- Linear time invariant multirate sampled data control systems characteristic equation simplification
09 p1290 A72-23099
- Equivalence of integral equation form and infinite system of linear equations with eigenvalue localization, applying to linear ordinary differential equations
09 p1342 A72-23367
- Rayleigh-Ritz method supplement for optimal evaluation of eigenvalue bounds for semibounded self adjoint operators
09 p1353 A72-23484
- Numerical computation of bilateral bounds for arbitrary vectorial and tensorial field quantities of elastic bodies eigenvalue states, applying to thin rectangular plate
09 p1409 A72-23566
- Natural axisymmetric vibration of thin elastic shell of revolution, deriving eigenvalues convergence to spectrum lower bound by asymptotic method
10 p1557 A72-24429
- Ground effect wing vehicles stability in forward motion, deriving characteristic equations by linear analysis
10 p1421 A72-24844
- Vibration of simply supported rectangular plate with unidirectional linear thickness variation, using perturbation technique for eigenvalue problem derived by Galerkin method
11 p1735 A72-25739
- Complex square stochastic matrix spectral inverse, examining nonzero eigenvalues on unit circle
11 p1677 A72-26152
- Finite difference approximation of eigenvalues of singular differential operators in Hilbert space
11 p1678 A72-26556
- Inverse eigenvalue problem numerical solution for matrices and difference and differential equations, obtaining algorithms for parameters estimation
11 p1679 A72-26955
- Simultaneous iteration for eigenvalue problem numerical solution by mutually orthogonal trial vectors close to required eigenvectors, applying to flutter analysis and Markov chains
11 p1679 A72-26959
- Eigenfunctions, eigenvalues and microwave attenuation constants in square and rectangular waveguides with rounded corners
11 p1607 A72-26994
- Convergence of plate bending eigenvalue solutions from conforming displacement finite elements based on thick plate free vibration conversion to isoperimetric variational problem
12 p1879 A72-27194
- Steady bifurcating time periodic solutions stability for flows in bounded domain with complex conjugate simple eigenvalues at critical Reynolds number
12 p1837 A72-27712
- Viscous flow stability between two rotating nonconcentric cylinders, obtaining approximate solution to eigenvalue problem by perturbation method
12 p1799 A72-27846
- Algorithms for eigenvalue spectrum determination in Dirichlet and Neumann problems for Helmholtz equation in configuration domains
12 p1847 A72-27985
- Finite difference approximation and Fourier analysis to determine mechanical system eigenfrequency, studying string and membrane vibration
12 p2000 A72-28417
- Difference scheme application to Laplace operator eigenvalues determination for regions composed of rectangles, using summary representation formulas
13 p1986 A72-29082
- Neumann problem for eigenvalues with homogeneous boundary conditions, using R-functions for complex-type regions
13 p1987 A72-29792
- Complex eigenvalues of frequency for Laplace tidal equation with negative equivalent depth, noting unstable modes role in solar differential rotation
14 p2100 A72-30344
- Eigenvalues examination for self adjoint singular differential operators in Hilbert space by finite difference methods
14 p2126 A72-30619
- Structural systems stability and natural frequency analysis eigenvalue problems solution by Sturm sequence method, using finite element technique
14 p2168 A72-30931
- Green operator first invariant upper bound for free oscillations eigenvalue upper limit, exemplifying for quadratic plate with two free and two clamped edges
15 p2274 A72-31459
- Elastic body stress concentration problem formulation as singular integral operator eigenvalue problem for half space
15 p2323 A72-31478
- Wall-impedance waveguide propagation constant determination from Rayleigh-Schrodinger power expansion of perturbed eigenvalues
15 p2194 A72-31549
- Eigenvalue equation, orthogonality theorem and wear eigenfunction expansion for boundary value coupling of second order Sturm-Liouville systems
15 p2262 A72-31588
- Time-average holography with thin phase recording materials, obtaining characteristic function solution for sinusoidal vibration and constant velocity motion
15 p2235 A72-31614
- Modified Rayleigh-Ritz method to obtain lower bounds of eigenvalues, applying to uniform cantilever column buckling
15 p2275 A72-31710
- Distributed parameter system approximation by system with finite freedom degrees number, solving stability and vibration of elastic shells for eigenvalue densening case
15 p2327 A72-31739
- Three resonant mode waveguide circulator adjustment with eigenvalues associated to resonant field patterns
15 p2208 A72-32388
- Random matrix spectra of eigenvalues in terms of Wigner set for statistical description of heavy nuclei energy levels
15 p2282 A72-32449
- First eigenvalue and first eigenfunction properties of linear elliptic partial differential equation in variational form with discontinuous coefficients, considering Dirichlet problem
16 p2416 A72-33502
- Internal waves in sheeted thermocline with finite discontinuities in density profile formulating eigenvalue problem as homogeneous Fredholm integral equation
16 p2386 A72-33573
- Free vibrations of elastic plate with random properties - The eigenvalue problem.
17 p2623 A72-34228
- Finite length inhomogeneous elastic rod free vibration, deriving asymptotic expressions for eigenvalues and eigenfunctions
17 p2625 A72-34320
- Block five diagonal matrices and the fast numerical solution of the biharmonic equation.
17 p2574 A72-34446
- Freedoms retention determination eigenvalue analysis of complex structures large dynamic matrices deriving transformation vectors based on maximum swept volume deformation modes
17 p2576 A72-35253
- Eigenvalues and eigenvectors for solutions to the radiative transport equation.
17 p2576 A72-35259
- Eigenfunction technique development to incorporate stress singularities at circumference of end planes into problem of solid cylinder compression between rough rigid stamps
17 p2633 A72-35403
- A method for selection of significant terms in the assumed solution in a Rayleigh-Ritz analysis.
17 p2634 A72-35408
- Local potential concept based variational method for eigenvalue problems of disturbance damping or amplification in stability analysis
17 p2583 A72-35641
- Poiseuille flow linear spatial stability in rigid pipe under infinitesimal disturbances, obtaining propagation modes eigenvalues
18 p2681 A72-36481
- On the algebraic structure of a class of solvable quantum problems.
18 p2711 A72-36514
- A singular multi-parameter eigenvalue problem in second order ordinary differential equations
18 p2705 A72-36615
- Flute modes in a plasma in the presence of nonuniform electric fields.
18 p2717 A72-37162
- Contribution to the theoretical study of the distribution of the emittance along the walls of an antiradiating cell
18 p2742 A72-37199
- Bounds on the extremal eigenvalues of the finite element stiffness and mass matrices and their spectral condition number.
18 p2705 A72-37202
- Viscosity effect on hypersonic flow field near slender body, discussing eigenvalue solutions for two and three dimensional flow around triangular plate
19 p2745 A72-37393
- A characteristic problem for a hyperbolic-type equation degenerating at the boundary
19 p2825 A72-38187
- Problem of the eigenvalues of certain unbounded and nonsymmetrical operators and their applications to ordinary differential equations
19 p2825 A72-38195
- Linear dynamic systems parameter identification via optimal input design, noting eigenfunction dependence on positive self adjoint operator
19 p2781 A72-38271
- Waveguides of arbitrary cross section by solution of a nonlinear integral eigenvalue equation.
19 p2773 A72-38292
- Complex resonant frequencies calculation in external diffraction problems for arbitrary shaped bodies, noting Green function poles correspondence to eigenvalue zeros of integral equation
19 p2767 A72-38652
- Continuum eigenmodes of an inhomogeneous plasma.
20 p2956 A72-39015
- Finite difference boundary value method for solving one-dimensional eigenvalue equations.
21 p3074 A72-40107
- Determination of accurate potential strengths to yield specified eigenvalues of the radial Schrodinger equation.
21 p3086 A72-40109
- Eigenvalues associated with balanced hybrid modes expressed in closed form to derive conical scalar horn antenna far field radiation patterns
21 p3032 A72-40630
- Modal control theory for distributed parameter systems with multieigenvalue assignment implemented for one dimensional diffusion equation
21 p3037 A72-40642
- Characteristic equation coefficients of monodromy matrix for linear system of second order homogeneous differential equations with periodic coefficients
21 p3075 A72-41092
- General solution of a system of differential equations with an irregular singular point
21 p3075 A72-41095
- Eigenvalue numerical solution for dispersion relation and propagation characteristics of nonlocal drift waves in cylindrical plasma based on two fluid model
21 p3093 A72-41495
- Mathematical spectra theory application to matrix eigenvalue problem, obtaining explicit form of determinant characteristic polynomial by numerical methods
21 p3076 A72-41781
- Asymptotic behavior of the eigenvalues and eigenfunctions of the Sturm-Liouville operator with a complex-valued polynomial potential.
22 p3198 A72-41854
- Double water-bag model stability for plane one dimensional stellar system, computing eigenfrequencies and eigenfunctions
22 p3224 A72-42384

Eigenvalue spectrum translation and frequency shifting by inertia and stiffness matrix modifications in iteration techniques

22 p3207 A72-42850

Second order differential equations with general boundary conditions.

22 p3199 A72-42915

Baroclinic long wave dynamic instability in Kochin two layer frontal model, noting beta effect on wave disturbances

22 p3202 A72-43001

Approximate calculation of a cavity resonator for n given initial natural frequencies

23 p3269 A72-43449

An improved general algorithm for arbitrary pole assignment.

23 p3275 A72-43546

Lower and upper bounds for the lowest characteristic value of the elastically supported membrane

23 p3347 A72-43717

Dirichlet series in eigenvalues of boundary value problems for an arbitrary second-degree elliptic differential operator

23 p3309 A72-44043

Integration scheme for two-dimensional impulsive waves in a linear acoustic medium.

23 p3314 A72-44250

On the use of a coordinate transformation for analysis of axisymmetric vibration of polar orthotropic annular plates.

24 p3457 A72-44883

Preliminary design of a sailplane wing for dynamic gust loads

24 p3368 A72-44992

A method of determining the eigenfrequencies of closed circular conical plates in the Vlasov-Mustari hypothesis

24 p3459 A72-45441

Best finite elements distribution around a singularity.

24 p3420 A72-45786

EIGENVECTORS

Warm inhomogeneous plasma models perturbation analysis, computing high frequency oscillation and eigenfrequencies and eigenfunctions formulas

01 p0106 A72-10134

Large structural systems dynamic mathematical models, predicting eigenvalue and eigenvector with statistical analysis

[SAE PAPER 710785] 01 p0137 A72-10276

Statistical variance of eigenvalues and eigenvectors in random structure dynamic analysis by component mode synthesis

[SAE PAPER 710786] 01 p0137 A72-10277

Elastic strip stresses and displacements, using eigenfunctions with coefficients determined by variational principles

[ASME PAPER 71-APMW-24] 04 p0589 A72-15181

Fabry-Perot open resonators, determining eigenvectors, resonant frequencies and diffraction losses by asymptotic perturbation method

04 p0502 A72-15436

Multiple completeness characteristics of eigenvectors and adjoint vectors of polynomial operator packets in separable Hilbert space

08 p1198 A72-21096

Stationary functionals for introducing eigenfunctions in diffraction theory of electrodynamic systems

08 p1133 A72-21372

Linear inverse problem of coefficient matrix eigenvectors, implying surface waves and free oscillations for earth structure

08 p1159 A72-21495

Optimal gradient minimization scheme for finite element eigenvalue and eigenvector problems, including effect of round-off errors and termination criterion

08 p1200 A72-22140

Somigliani dislocations effect in infinite elastic cylinder, determining stresses in form of eigenfunctions expansions

09 p1398 A72-22491

Stress and couple stress fields near antiplane shear crack tip, determining eigenfunctions to satisfy field equations and boundary conditions

09 p1402 A72-22744

Boltzmann neutron transport equation solution for homogeneous slabs and spheres, noting dominant critical eigenfunction existence and total flux boundedness, continuity and positivity

09 p1358 A72-23072

Positive to quasi-stochastic matrix reduction by similar variation method, determining largest characteristic number and eigenvector

09 p1343 A72-23490

Eigenfunction transform investigation of wedge diffraction of scalar pulse wave in three space dimensions, analyzing Green function

11 p1591 A72-25359

Simultaneous iteration for eigenvalue problem numerical solution by mutually orthogonal trial vectors close to required eigenvectors, applying to flutter analysis and Markov chains

11 p1679 A72-26959

Eigenfunctions, eigenvalues and microwave attenuation constants in square and rectangular waveguides with rounded corners

11 p1607 A72-26994

Eigenstate field parameter bounds in elastomechanics natural vibration problems

13 p2059 A72-29598

Localized electronic states size near mobility edge in semiconductor, considering eigenfunction behavior in random lattice problem

14 p2143 A72-30878

Eigenvalue equation, orthogonality theorem and wear eigenfunction expansion for boundary value coupling of second order Sturm-Liouville systems

15 p2262 A72-31588

Time-average holography with thin phase recording materials, obtaining characteristic function solution for sinusoidal vibration and constant velocity motion

15 p2235 A72-31614

Constrained-impedance eigenfunctions, using projection method for field expansion in diffraction problems

15 p2202 A72-32661

Bending of clamped skew plate under uniform loading, using Gaydon-Shepard eigenfunction expansion method

16 p2463 A72-32836

First eigenvalue and first eigenfunction properties of linear elliptic partial differential equation in variational form with discontinuous coefficients, considering Dirichlet problem

16 p2416 A72-33502

Finite length inhomogeneous elastic rod free vibration, deriving asymptotic expressions for eigenvalues and eigenfunctions

17 p2625 A72-34320

Block five diagonal matrices and the fast numerical solution of the biharmonic equation.

17 p2574 A72-34446

Somigliani dislocations effect in infinite elastic cylinder, determining stresses in form of eigenfunctions expansions

17 p2626 A72-34654

Hamiltonian system evolutionary stability via area preserving mapping, using Bartlett eigenvector method

17 p2547 A72-35108

Eigenvalues and eigenvectors for solutions to the radiative transport equation.

17 p2576 A72-35259

Flat plate withdrawal at high speed from quiescent liquid baths, calculating velocity profile via boundary condition transformation and eigenfunction expansion method

18 p2678 A72-36122

Recent results on the effect of longitudinal curvature on a laminar layer

18 p2685 A72-37213

An eigenfunction method for solving the second boundary-value problem in the theory of elasticity

19 p2877 A72-38182

Expansion of a theory of elasticity operator in a series of eigenfunctions

20 p2979 A72-39467

General solution of a system of differential equations with an irregular singular point

21 p3075 A72-41095

Method of eigenfunctions in problems of thermoelasticity and electroelasticity

21 p3122 A72-41348

Asymptotic behavior of the eigenvalues and eigenfunctions of the Sturm-Liouville operator with a complex-valued polynomial potential. I

22 p3198 A72-41854

On the perturbation method in the stability analysis of continuous systems.

22 p3206 A72-42842

Existence and uniqueness theorems of elliptic equations with eigenfunction exponential decrease at infinity and 2m order self adjoint differential operator in n -dimensional Euclidean space

23 p3307 A72-43223

Expansion of diffracted electromagnetic fields in eigenfunctions of the d'Alembert operator

23 p3312 A72-43335

The use of bar buckling eigenfunctions in the stability analysis of clamped skew plates.

23 p3355 A72-44456

Poorly founded systems of equations in astronomical practice and methods for their solution

24 p3437 A72-44760

Current-driven drift wave instability in a sheared magnetic field.

24 p3430 A72-45570

A three-dimensional model of thermosphere dynamics. I - Heat input and eigenfunctions. II - Tidal waves. III - Planetary waves.

24 p3400 A72-45594

EIKONAL EQUATION

Laser beam induced thermal blooming in absorbing gases from combined fluid dynamics and eikonal geometric optics theory, considering wind effects

09 p1352 A72-23333

Eikonal distorted wave analysis of inelastic electron-atom collisions at intermediate energies application to electron impact induced atomic hydrogen 2s and 2p states excitation

15 p2282 A72-32646

EINSTEIN EQUATIONS

Inertial-gravitational mass ratio in classical and quantum case, proving equivalence principle non-validity for Brans-Dicke gravitation theory compared to Einstein theory

01 p0102 A72-10861

Einstein gravitational field equations plane-front parallel ray wave exact solutions generalization to f - g gravity theory equations exact solutions

02 p0260 A72-12375

Diffuse gravitational background radiation in universe, assuming gravitational field fluctuations macroscopic nature and Einstein equations applicability

03 p0417 A72-13095

Anisotropic universe model based on Einstein equations for metric with cosmological term

03 p0388 A72-13193

Gaseous general relativistic kinetic theory, detailing matter model, thermodynamics, cosmology and Einstein field equation completion with Liouville or Boltzmann equation

03 p0388 A72-13266

Perturbations in Godel universe, considering Einstein equations in relativistic cosmology

06 p0876 A72-17564

Energy complex in general relativity in form of tetrahedral gravitational theory, including solutions to Einstein equations

06 p0849 A72-18419

Metric tensor components of isotropic inhomogeneous cosmological model obtained from Einstein equations

07 p1072 A72-19340

Tensor analysis of electromagnetic energy localization in space, generating gravitational field and space curvature via equation to Einstein tensor

07 p1035 A72-19685

Einstein and Einstein-Maxwell equations solutions by zero coupling transformations

09 p1349 A72-22201

Coordinate mapping for solutions of Einstein initial value problem for vacuum gravitational fields

09 p1350 A72-22471

Gravitational radiation from isolated material source in terms of van der Burg solution to Einstein field equations

09 p1352 A72-23359

Homogeneous anisotropic solutions of Einstein equations with cosmological term for universe with plane comoving frame filled with powder

09 p1352 A72-23361

Linear theories of gravitational fields, discussing Lorentz invariant approximation use to obtain Einstein equations approximation

09 p1352 A72-23386

Integrability and identity relations for Newman-Penrose formalism equations in spinor description, assuming Einstein equations validity for vacuum

10 p1510 A72-24105

Asymmetric Einstein equations with impulse-energy tensor in canonical form derived from variational principle, defining space-time continuum as pseudo-Riemann manifold

10 p1510 A72-24120

Einstein field equation representing static fluids in general relativity, obtaining all solutions with degenerate Weyl tensor

10 p1511 A72-24349

Finite rest masses of wave quanta in material media, discussing dispersion and Einstein formulas equivalence, Doppler effect, gravitational red shift and radio photon trajectories

10 p1512 A72-24790

Gravitational quadrupole radiation derivation from Einstein equations integration by successive approximation and variable separation procedures

10 p1513 A72-25167

Diffuse gravitational background radiation in universe, assuming gravitational field fluctuations macroscopic nature and Einstein equations applicability

11 p1716 A72-25703

Velocity dominated singularities generalized to solutions of Einstein equations with irrotational perfect fluid sources within hydrodynamic cosmological models

12 p1870 A72-27410

Particular and general exact solutions of Einstein equations for matter filled space under assumption of spherically symmetric distribution of perfect fluid

15 p2305 A72-31343

Einstein relativity principle incompatibility with conservation of angular momentum, discussing invariance of inertia reference systems and formulas for relative and absolute velocities

19 p2834 A72-37921

Book - General relativity: Papers in honour of J. L. Synge.

20 p2954 A72-40001

Einstein theories of special and general relativity, taking into account physical concepts relation to mathematical formalism, equivalence principle, field equations and gravitational waves
20 p2954 A72-40002

Poincare, Lorentz and Einstein contributions to relativity theory construction according to Whittaker, discussing influence on contemporary scientists
20 p2954 A72-40003

Exact solutions of the Einstein-Maxwell equations for an accelerated charge.
20 p2955 A72-40008

Construction of a general cosmological solution of the Einstein equations with a singularity with respect to time
21 p3103 A72-40403

Inhomogeneous cosmological models in terms of impulse energy tensor, discussing coupled Einstein equations, gauge invariance and Lorentz gauge
21 p3110 A72-41442

Hydrostatic pressure effects on atomic configuration based on principle of equivalence related to Einstein gravitational equations
22 p3205 A72-42459

Approximate solutions of the relativistic gravitational field equations to describe clusters of galaxies.
22 p3229 A72-42993

Einstein equations reduction to friction systems in homogeneous cosmological models, investigating Bianchi models isotropization and statistical analysis
23 p3335 A72-43301

First derivative discontinuities of space-time metric tensor in Einstein equations solution for nonisotropic and isotropic hypersurfaces, proving coordinate system existence for continuity
23 p3312 A72-43302

Natural rotation of bodies in Einstein's theory of gravitation
23 p3313 A72-44038

Angular momentum conservation laws formulation for Einstein field equations solution in general relativity, applying to Kerr metric
24 p3425 A72-44787

Idealized homogeneous and nonisotropic cosmological models with electromagnetic and massless scalar fields, noting Einstein equations
24 p3442 A72-45246

EJECTION
NT STELLAR MASS EJECTION
EJECTION INJURIES

Human ejection vertebral injury data in aircraft accidents by cross reference to final medical diagnosis, considering costs and prevention for seat systems
02 p0167 A72-11714

Aircraft ejection simulation by human thoraco-lumbar spine flexion dynamic model, using strength of materials theory and shear effects for curved elastic beam
[ASME PAPER 71-WA/BHF-7] 05 p0620 A72-15947

Emergency and test ejections with Martin-Baker seats, discussing fatality and injury causes and seat reliability
08 p1112 A72-21565

Dynamic response index /DRI/ minimization for personnel aircraft emergency catapult escape systems to reduce injury probability
08 p1112 A72-21576

Seat cushion evaluation for behavior during helicopter crash or aircraft ejection and spinal injury probability
08 p1126 A72-21577

Chemically strengthened glass for eject-through frangible canopy design in aircraft emergency escape systems, noting protection against ejection injuries
12 p1813 A72-27016

Ejection injuries from U.S. Navy aircraft, discussing statistical distribution of vertebral, shoulder, arm/hand, knee, leg, head and face injuries
12 p1774 A72-28273

A study of USAF survival accidents 1 Jan. 1965-31 Dec. 1969.
23 p3259 A72-43425

EJECTION SEATS

SR-71 aircraft ejection seat, obtaining ejection survival rate from case histories
08 p1112 A72-21562

Emergency and test ejections with Martin-Baker seats, discussing fatality and injury causes and seat reliability
08 p1112 A72-21565

Emergency systems for helicopter crew and passenger survivability improvement, discussing use of ejection seats, extraction systems parachute bail-out and shaped explosive charges
08 p1109 A72-21581

Lockheed ADP SR-1 ejection seat system for safe aircrew recovery under zero-zero, high Mach and altitude conditions, describing escape experiences with SR-71 aircraft
13 p1896 A72-28701

Dilantant suspensions impact energy absorbent properties, considering application to ejection seat cushions for occupant acceleration attenuation
15 p2191 A72-32604

EJECTORS

Ejector nozzle design criteria, analyzing primary/secondary flow interactions and diameter, spacing and temperature ratio effects
[AIAA PAPER 72-46] 05 p0609 A72-16963

Approximation method for gas ejection calculation, assuming zero mixer flow velocity and ejection coefficient and suction side optimum operation for uniform pressure distribution
08 p1107 A72-21320

Hot water ejector application to environmental control, considering noise suppression, air and gas purification and dust particles precipitation
10 p1460 A72-24491

Russian book on theory of ramjet and rocket ramjet engines covering supersonic diffuser operational principles and design, nozzle, combustion chamber and ejector
12 p1862 A72-28346

Two stream ejector propulsion performance, measuring nozzle geometry effect on discharge coefficient for 2-90 deg convergence angles
[ONERA, TP NO. 1050] 15 p2177 A72-31208

Analysis and testing of compressible flow ejectors with variable area mixing tubes.
[ASME PAPER 72-FE-14] 17 p2485 A72-34968

Performance of low pressure ratio ejectors for engine nacelle cooling.
[SAE AIR 1191] 18 p2721 A72-36530

Low pressure gas ejector operation with cylindrical mixing chamber, discussing design procedure with compression rate and ejection coefficient calculation
19 p2746 A72-37667

Throttle characteristics and mixing chamber geometry effects on low pressure gas ejector operation, noting air flow and pressure rates in air ejectors
22 p3133 A72-41859

Jet pumps for compressible fluids at supersonic velocities.
24 p3393 A72-45362

EKMAN LAYER
U BOUNDARY LAYER TRANSITION
ELASTIC ANISOTROPY

Anisotropic elasticity effects on plane shock wave propagation for arbitrary loading directions in plate impact experiments
04 p0585 A72-14538

Carbon fiber reinforced composites properties and design limitations relative to elastic anisotropy in pump and fan applications
04 p0536 A72-14744

Monocrystals elastic anisotropy effects on polycrystalline sinter matrix minimum porosity, thermal conductivity, mechanical and elastic properties, thermal stress resistance and Hugoniot elastic limit
08 p1186 A72-21441

Phonon limited mean free path in Cd by limiting point method, proposing model with elastic anisotropy
08 p1217 A72-21592

Dynamic radial vibrations and stresses in thick circular annulus of nonisotropic elastic material, using Hankel transform
08 p1246 A72-21793

Stress functions for anisotropic elastic body with uniformly propagating circumferential crack, considering axially orthotropic cylinder
10 p1553 A72-23744

Crack toughness tests of fiber composite laminates, using linear elastic fracture mechanics
10 p1500 A72-24258

Linear equations relating elastic compliance coefficients of anisotropic two-phase fiber reinforced composites
10 p1556 A72-24262

Elastic finite element analysis for stress distribution in gripped thin walled tubular anisotropic three dimensional composite specimens
11 p1731 A72-25457

Anisotropic cylindrical beam bending by transverse load in elastic plane, reducing to Almansi problem
11 p1736 A72-26091

Microhardness anisotropy of hardened and aged Be single crystal as function of purity
13 p1978 A72-29023

Quasi-longitudinal and quasi-transverse plane wave propagation in anisotropic elastic-plastic solids, approximating Be single crystal behavior
14 p2163 A72-30176

Shear strains and elastic anisotropy of transversely isotropic cylindrical shell with circular hole under uniform internal pressure, using shallow shell equations
14 p2165 A72-30438

Forced vibrations of thick homogeneous anisotropic elastic sphere, studying dynamic response to uniformly distributed internal and external pressure
16 p2424 A72-33147

Thermal circular and radial stresses in elastic orthotropic cylinders with anisotropic expansion coefficients
19 p2872 A72-37535

A universal connexion for waves in anisotropic media.
19 p2875 A72-37840

The effect of elastic anisotropy on dislocations in Ni3Fe.
20 p2937 A72-39293

Causality in the relativistic theory of elastic media in the three-dimensional case.
22 p3206 A72-42626

Two-dimensional problem of elasticity theory for an anisotropic inhomogeneous wedge
24 p3459 A72-45263

ELASTIC BARS

Longitudinal stress pulse amplification during propagation along tapered elastic bars in direction of decreasing cross section
[SESA PAPER 1894] 02 p0287 A72-11504

Optimal design of elastic beams under alternative loads and constraints on generalized compliance and bending stiffness
[AD-743419] 02 p0291 A72-11962

Rigid mass impact against viscoelastic bar of finite length, investigating longitudinal waves propagation and interaction
02 p0298 A72-12682

Two dimensional boundary value problem in elasticity for rectangular prism vibrations, considering dynamic stress and frequency characteristics
03 p0449 A72-13908

Elastic strip stresses and displacements, using eigenfunctions with coefficients determined by variational principles
[ASME PAPER 71-APMW-24] 04 p0589 A72-15181

Composite elastic beams equations under initial stress, investigating flexural wave propagation and structural stability
07 p1090 A72-19733

Elastic rods and rings stability under compression beyond elasticity limit, determining equilibrium branching characteristics near bifurcation point
07 p1095 A72-20314

Coupled motions of rotating free solid body and elastic rod torsional bending vibrations with precession and forced vibrations from energy exchange
08 p1205 A72-20959

Nonlinear plane bending of thin elastic rectilinear bar guide elements under concentrated force and torque
09 p1397 A72-22350

Stress-strain curve determination for shear of twisted conical elastic bar, using torque and angle distribution
09 p1404 A72-22774

Dynamic stability of spinning bodies with elastic rods and rigid symmetric rotors parallel to axis
10 p1552 A72-24645

Book on continuous elements dynamics covering membrane, torsional, string and elastic beam vibration, four pole techniques, periodic forced motion and surface waves
10 p1557 A72-24674

Natural and associated transverse vibrations of elastic beam under uniformly distributed moving load
12 p1879 A72-27092

Orbital and rotational motion stability of solid body containing elastic rods and fluid-filled cavity
13 p2002 A72-28715

Torsional waves far-field structure in infinite elastic rod of elliptical cross section, using perturbation method
13 p2057 A72-29004

Stability of compressed elastic rod with continuously varying stiffness, deriving solution via influence function
14 p2166 A72-30691

Variational principle for boundary value problem of elastic-plastic torsion of circular bars under quasi-static finite deformation
16 p2464 A72-32914

Optimal plane elastic trusses under alternative loads, designing for smallest total volume of bars with upper stress bound
16 p2466 A72-33017

Strain rate history effects on stress incremental wave front propagation in elastic bars, considering Taylor-Karman-Rakhmatulin theory
16 p2466 A72-33103

Axisymmetric impact of compactible rods subjected to finite deformations.
21 p3117 A72-40455

Buckling of elastic bars with varying stiffness and nonideal boundary conditions.
21 p3118 A72-40932

Comparison of experimental and numerical results concerning a hollow photoelastic bar with a slot subjected to torsion
21 p3122 A72-41337

Effect of the rate of pulsed heating of a bar on the magnitude of the thermoelastic stresses
21 p3126 A72-41548

Calculating the stability of centrally compressed thin-walled bars with various profiles
21 p3126 A72-41549

Orbital and rotational motion stability of rigid body containing elastic rods and fluid-filled cavity
22 p3204 A72-42092

A note on the twisting deformation of a non-homogeneous shaft containing a circular crack.

23 p3346 A72-43708

Spline transformation of independent variable for free transverse vibration of elastic bars with piecewise constant rigidity, calculating resonant frequencies

23 p3348 A72-43793

Infinite rectangular elastic bar surface mass distribution effects on harmonic wave propagation modes, obtaining approximate solution by expanding displacement as power series

23 p3352 A72-44123

ELASTIC BENDING

Statically indeterminate and determinate elastic beams optimal design for maximum-minimum deflection under distributed load

04 p0590 A72-15192

Saint Venant problem for orthotropic almost cylindrical beams, investigating elongation, bending due to couple and transversal loads and torsion due to torque

04 p0594 A72-15747

Hingeless rotor helicopter blade steady state response with nonuniform inflow and elastic blade bending

[AIAA PAPER 72-65]

05 p0741 A72-16933

Elasticity theory equations for orthotropic plate bending, derived from combination variational and difference-differential procedures

05 p0741 A72-17144

Reinforcing fiber frame incurvation influence on elasticity and thermal expansion coefficients of composite material

08 p1194 A72-21754

Elastic rectangular plate instability in pure bending along two perpendicular directions solved by Karman nonlinear equation reduction to partial differential equations integration

08 p1247 A72-21817

Linear uncoupled quasi-static thermoelasticity theory for thermal bending of nonuniformly heated parallelogram-shaped plates

09 p1400 A72-22710

Glass content and temperature effects on fabric reinforced plastic laminates static behavior, analyzing tensile and bending strength and elastic moduli

10 p1501 A72-24660

Upper yield stress effect on bending and torsion, noting relationship to strain rate

11 p1659 A72-25894

Anisotropic cylindrical beam bending by transverse load in elastic plane, reducing to Almansi problem

11 p1736 A72-26091

Viscoelasticity analysis of bending displacements in thin walled closed cylindrical shell loaded by moving moment

11 p1739 A72-26920

Third approximation solution to elastic bending equilibrium equations of Vekua plate theory in form of holomorphic functions

12 p1880 A72-27237

Fatigue testing machine for material behavior under elastoplastic bending loads with constant or smoothly varying programmed vibration frequency and amplitude

12 p1795 A72-27463

Boussinesq solution for elastic surface deflection due to continuous pressure with polynomial distribution over triangular area

12 p1884 A72-27568

Fatigue strength and cumulative damage in fiberglass-epoxy composite specimens under unsteady elastic bending loads, determining loading spectrum effect on service life

13 p1983 A72-28562

Elastic bending of rectangular continuous orthotropic plate with variable rigidities and elastic foundation coefficients for discontinuous boundary conditions along one edge

16 p2467 A72-33118

Bending and torsional mode deformations of two dimensional elastic wing under sinusoidal and random gust

16 p2469 A72-33229

Load capacity of tension-bent and compression-bent circular plates

19 p2877 A72-38161

Plane bending problems in the theory of elasticity for nonhomogeneous solids

19 p2877 A72-38162

Elastoplastic axisymmetric bending of a clamped circular plate under the action of a conically-distributed variable load

20 p2978 A72-39022

Improved method for determining shear stresses and checking the strength of circular cylinders in transverse bending

23 p3349 A72-43968

Compliance calibrations of a contoured and face grooved double cantilever beam specimen.

24 p3413 A72-44817

ELASTIC BODIES

Perturbed vibrational motion in isotropic elastic solid, using nonlinear Truesdell equations

01 p0101 A72-10039

Group matrix representation theory application to elastic spacecraft stabilization

01 p0135 A72-10497

Finite element method extension using computer program for solving problems of elastic bodies in contact with stiffness method advantages

01 p0141 A72-11047

Natural vibrations and resonant stresses of turbomachine blade rings and elastic bodies with cyclic symmetry, noting paradoxical frequency decrease

01 p0143 A72-11369

Thermal stresses, temperature distribution and displacement fields in elastic solid with spherical cavity and external crack

01 p0144 A72-11385

Affine similarity in static problems with mixed boundary conditions for inhomogeneous anisotropic linearly and nonlinearly elastic and viscoelastic and elastoplastic bodies

02 p0288 A72-11607

Elastic stability of body under conservative loads, deriving energy criterion with thermodynamic laws

02 p0292 A72-12003

Hereditarily elastic body model with various tensile and compressive strengths, using elasticity theory with differing moduli

02 p0294 A72-12429

Surface subsidence in semiinfinite resilient elastic solid mass supporting annular load distributed over circular ring

02 p0297 A72-12616

Static isotropic elastic body first and second boundary value problems solutions for inside and outside m dimensional sphere

02 p0300 A72-12876

Elastic bodies deformations theory, formulating boundary value problems

03 p0443 A72-13451

Double forces distribution over elastic body surface from Lamé equation describing static defects, discussing Kupradse potential and sources corresponding to plane dislocations and cracks

03 p0444 A72-13501

Elasticity tensor formulas for wave propagation, vibration and stability of deformed isotropic solids

03 p0448 A72-13887

Dual integral equations method application to elastic bodies with plane circular cracks in torsion

03 p0452 A72-14135

Statistical methods of stress and reliability analyses of elastic systems under random external loads

03 p0453 A72-14206

Closed quasi-linear cubic theory of viscoelasticity for bodies with force and moment physical nonlinearity

03 p0454 A72-14218

Homogeneous first order solutions to Lamé equations in statistical elasticity theory, yielding harmonic surface displacement for elastic body

03 p0454 A72-14371

Multipurpose optimal design of elastic structures with piecewise uniform cross section for load states and prescribed stiffness by energy methods

[AD-743418]

03 p0455 A72-14386

Infinite elastic-plastic beam impact by semiinfinite elastic rod, computing strain-time profiles

04 p0583 A72-14447

Elastic shaft bonded to dissimilar elastic disk, considering torsion problem

04 p0583 A72-14449

Stress-strain tensor component relations for isotropic elastic bodies with different tension and compression resistance

04 p0586 A72-15008

Statically indeterminate and determinate elastic beams optimal design for maximum-minimum deflection under distributed load

04 p0590 A72-15192

One-dimensional compression/expansion shock waves propagation in elastic nonheat conducting bodies, deriving differential equation for shock amplitude time rate of change

04 p0592 A72-15547

Transient stress analysis for sudden twisting of penny-shaped crack in infinite elastic body under torsion, using integral transform

[ASME PAPER 71-WA/APM-10]

05 p0734 A72-15969

Continuous bodies incremental deformation and stability under initial stress, discussing relationships for elasticity constants and material stress tensors

[ASME PAPER 71-WA/APM-9]

05 p0734 A72-15970

Nonlinear self excited oscillations in uniformly distributed oscillators interacting with traveling transverse or surface waves of elastic body

06 p0849 A72-18698

Combined rotational motions of free solid and coupled elastic bodies oscillations around center of mass with nutation passive dampers

06 p0850 A72-18707

Mechanical system of elastically coupled bodies carrying identical vibrators, examining self synchronization behavior

06 p0850 A72-18713

Stress-strain state determination in elastic parallelepiped by net point method and matrix filtering

07 p1091 A72-19754

Elastic body dynamics partial differential equations transformation into boundary value problem for Monge-Ampere equation

07 p1095 A72-20218

Class of homogeneous polynomial solutions to differential equations of motion of elastic body

08 p1242 A72-20912

Liquid fuel elastic rocket motion stability in supersonic flight, using vibration and thrust vector control equations for dynamic properties description

08 p1241 A72-21633

Elastic stability of nonlinearly elastic anisotropic body analyzed via variational principles in three dimensional theory

08 p1246 A72-21707

Stable equilibrium conditions for linear elastic body, using Reissner functional

08 p1248 A72-21819

Homogeneous linear approximations in uncoupled problems of thermoradiative elasticity and plasticity of solid body under nonuniform heating and radioactive radiation

09 p1401 A72-22720

Rayleigh type transverse surface wave existence in continuous elastic body with nonlocal interaction

09 p1403 A72-22748

Thermal diffusion in solids subject to deformation, using classical elasticity theory body force analogy for variational and reciprocal theorems

09 p1403 A72-22757

Discrete elasticity concept based on analysis of material points, lines, surfaces or rigid bodies interconnected by hyperelastic continuous bodies

09 p1403 A72-22759

Energy methods for nonlinear viscoelastic bodies based on constitutive relations affecting critical state in advanced creep

09 p1403 A72-22764

Random vibration of linearly elastic lumped mass systems containing, nonlinear damping to ideal stationary Gaussian white noise excitation

09 p1408 A72-23460

Numerical computation of bilateral bounds for arbitrary vectorial and tensorial field quantities of elastic bodies eigenvibration states, applying to thin rectangular plate

09 p1409 A72-23566

Nonlinear elasticity theory variational principles modification for finite deformation of elastic body

10 p1557 A72-24428

Classical boundary value problems in theory of thermal stresses in piecewise continuous anisotropic elastic bodies under coupling conditions

10 p1563 A72-24994

Asymptotic dynamic response of infinite beam on elastic foundation to randomly moving load

11 p1727 A72-25292

Coupled mode model for dynamic interaction between flexible rotary machines and elastic supporting structures

[AIAA PAPER 72-375]

11 p1730 A72-25399

Elastic body transverse impact against vibrating rectangular plate with allowance for rotatory inertia and shearing forces, using wave equation

11 p1732 A72-25532

Equilibrium stability of hyperelastic bodies under finite strain, deriving differential equations and boundary conditions of critical equilibrium states

11 p1686 A72-25916

Surface waves propagation in inhomogeneous elastic body, deriving wave equations asymptotic solutions

11 p1689 A72-26384

Variational minimum principle for two elastic bodies frictionless contact, discussing Hertzian and non-Hertzian normal half space problems

11 p1690 A72-26667

Mellin transforms for finite elastic disk radial crack stress intensity factor and energy formulae in terms of Fredholm equation solution, considering constant loading case

11 p1738 A72-26724

Three dimensional nonlinearly elastic anisotropic body with arbitrary elastic potential examined for large initial deformations, considering stress-strain state

12 p1877 A72-27077

Finite element equations for hybrid coordinate dynamic analysis of interconnected rigid bodies with elastic flexible appendages for use in spacecraft simulation

12 p1876 A72-27257

Dead load static stability of elastic solids in terms of zero moment condition of Beatty theory

12 p1883 A72-27557

Stress intensity factor of Griffith crack in elastic solid opened by thin symmetric wedge, using triple integral equations

12 p1883 A72-27558

Uniqueness of solutions to displacement problem for unbounded bodies in linear elastodynamics

12 p1884 A72-27564

- Elastic rod system stationary vibrations under combinational parametric resonance due to internal energy dissipation, using matrix method
12 p1885 A72-27969
- Velocity behavior of shear waves propagating in uniaxially prestressed isotropic elastic body
12 p1886 A72-27982
- Perfect and imperfect plastic column buckling, describing bifurcation and stability theory for elastic-plastic and rigid-plastic bodies
13 p2054 A72-28480
- Optimal design of elastic structures, emphasizing stability and response under applied static and dynamic loads
13 p2054 A72-28487
- Nonlinear transverse forced resonant oscillations in isotropic elastic body and ideally conducting compressible fluid flowing in external magnetic field
13 p2010 A72-28719
- Variational principles for linearized dynamic and static problems of elastic incompressible bodies for highly elastic initial deformations
13 p2059 A72-29499
- Wiener Hopf integral equation for problem of smooth stamp impression into elastic wedge face, solving by gamma and hypergeometric functions
13 p2059 A72-29500
- Notch stress concentration in disk with elastic core under tension, using finite element method
13 p2060 A72-29600
- Variational form to determine equations and boundary conditions for elastic isotropic homogeneous nonferromagnetic body subjected to external load, temperature and electromagnetic field actions
13 p2061 A72-29797
- Three dimensional axisymmetric problem for stressed state of elastic homogeneous cylindrical orthotropic bodies of revolution, using method based on small parameters
13 p2062 A72-29948
- Gradient catastrophe /solution derivative discontinuity/ occurrence time for quasi-linear hyperbolic differential equations describing elastic string oscillations
14 p2130 A72-30194
- Random deflection function for taut string on elastic foundation subject to random loads, using invariant imbedding method and Fokker-Planck equations
15 p2273 A72-31311
- Tapered elastic rod transient behavior under end impact due to mass striking, computing fixed end stress, struck end velocity and impact time duration
15 p2323 A72-31404
- Approximate values for elastic body stresses and displacements based on finite element method and virtual displacements and minimum potential energy principles equivalence
15 p2323 A72-31477
- Elastic body stress concentration problem formulation as singular integral operator eigenvalue problem for half space
15 p2323 A72-31478
- Schaefer stress representation for elastokinetics of linearly elastic isotropic homogeneous body under small deformations and torsions
15 p2324 A72-31486
- Rough surface elastic bodies stress calculation, using asymptotic method of boundary conditions
15 p2327 A72-31736
- Filler influence on critical load and buckling zone size in circular elastic three layer ring under uniformly distributed vertical load in rigid cavity
15 p2328 A72-31745
- Exact nonlinear equation derived approximation for second order effects in thermoelasticity theory for isotropic and transversely isotropic heat conducting elastic materials
15 p2329 A72-32282
- Dynamic boundary value problems for elastic materials with microstructure reduction to tensor equations of motion subject to initial and boundary conditions
15 p2329 A72-32283
- Thermal stresses in plane elasticity for doubly connected regions, considering temperature distribution, stress state problem formulation and nonconcentric annulus
15 p2329 A72-32287
- Elastic longitudinal or shear wave scattering by movable rigid sphere embedded in elastic solid, showing inverse Rayleigh limit dependence
16 p2423 A72-32988
- Forced vibrations of thick homogeneous anisotropic elastic sphere, studying dynamic response to uniformly distributed internal and external pressure
16 p2424 A72-33147
- Sudden heating-induced deflection of rectangular plate fitted into equal sized excavation in elastic foundation with relatively very low thermal conductivity
16 p2475 A72-33148
- Uniqueness principle application to construction of gravitational field generated by complex of elastic bodies for mass tensor
16 p2424 A72-33366
- Energetic boundedness conditions for internal work of deformation in elastic isotropic body
16 p2470 A72-33527
- Equations of motion for small vibrations superposed on time depending deformation of elastic body, discussing acoustic wave propagation
16 p2425 A72-33590
- Dynamic stress field solution to plane strain crack propagation in elastic body under general loading at constant and nonlinear extension rate
16 p2470 A72-33612
- Finite length inhomogeneous elastic rod free vibration, deriving asymptotic expressions for eigenvalues and eigenfunctions
17 p2625 A72-34320
- The plane solution for anisotropic elastic wedges under normal and shear loading.
[ASME PAPER 72-APM-13] 17 p2629 A72-34802
- Continuous elastic systems flutter and divergence instability under nonconservative loading, determining slopes of loading-frequency curves
17 p2633 A72-35255
- Thermo-elastic interactions in an infinite elastic solid due to a concentrated transient heat source.
18 p2735 A72-36754
- Solution of the impact problem of an elastic body and a rigid obstacle by the source-sink method
18 p2736 A72-36811
- A method of analysis for compressible viscoelastic solids.
18 p2736 A72-36936
- Independent moving vibrational /acoustic/ source-induced wave losses during friction of two elastic bodies
18 p2696 A72-36966
- Variational principles of the nonlinear theory of elasticity - Case of superposition of a small deformation on a finite deformation.
19 p2872 A72-37559
- Asymptotic method application to wave propagation in nonlinearly elastic rods, describing displacement field by perturbation series
19 p2875 A72-37885
- Electrostatic, reticular vorticity, turbulence effects and equivalences with tensional and spectral elastic fields.
20 p2953 A72-39419
- On the choice of a reference state in the application of Hamilton's principle in elastodynamics.
20 p2979 A72-39420
- Polymoment homogeneous solution characteristics in the theory of elasticity for design calculations
20 p2979 A72-39587
- An integro-differential equation approach to acoustic scattering from fluid-immersed elastic bodies.
21 p3083 A72-40102
- Applicability of the Euler approach to investigate the strain stability of anisotropic nonlinearly elastic bodies under finite subcritical strains.
21 p3116 A72-40273
- Russian book - Mechanics of deformable one-dimensional bodies of variable length.
21 p3116 A72-40387
- Methods of studying three-dimensional problems of stability in the presence of highly elastic strains
21 p3126 A72-41538
- Nonlinear transverse forced resonant oscillations in isotropic elastic body and ideally conducting compressible fluid flowing in external magnetic field
22 p3210 A72-42096
- Stress distribution in a homogeneous elastic sphere containing a penny shaped crack of prescribed shape.
23 p3354 A72-44268
- Elastic bodies deformations theory, formulating boundary value problems
24 p3458 A72-44926
- Analogy between body force and inelastic strain gradient in all crystal systems.
24 p3459 A72-45247
- The effect of shear on a penny-shaped crack at the interface of an elastic half-space and a rigid foundation.
24 p3459 A72-45250
- Unsteady longitudinal viscoelastic vibrations of a rod of variable thickness at small values of time
24 p3459 A72-45265
- Castiglano variational theorem for algebraic equation solution of thermal stresses determination in elastic parallelepiped, using Maxwell stress functions as cosine binomial series
24 p3459 A72-45267
- ELASTIC BUCKLING**
- Imperfect nonlinear system elastic buckling critical load calculation by higher order approximation, using perturbation approach and discrete coordinate diagonalized system
01 p0136 A72-10035
- Residual buckling strength of Al alloy elastic column with fatigue crack
[SESA PAPER 1914A] 02 p0288 A72-11511
- Plane discrete elastic lattice plates buckling, presenting plane and bending state of force equations
03 p0444 A72-13502
- Static perturbation technique functional form for postbuckling equilibrium path analysis by asymptotic approximation, noting relationship to Koiter method
05 p0742 A72-17244
- Small deflection theory for dynamic elastic buckling of stringer-stiffened cylindrical shells under axial impact, discussing optimum stiffener geometry
05 p0742 A72-17248
- Asymptotic solution to nonlinear Donnell equations of elastic conical shells, applied to buckling of frustum under axial load
06 p0893 A72-17303
- Critical loads for elastic buckling of monosymmetric beams and cantilevers
06 p0897 A72-17969
- Approximative buckling load of orthotropic hyperbolic paraboloid metal shells, using energy approach
06 p0897 A72-17970
- Multiple elastic postbuckling path generation at coincident branching points for system with many degrees of freedom
07 p1087 A72-19113
- Dynamic buckling of elastic shallow structures under periodic loading, determining critical load upper and lower bounds by energy method
07 p1090 A72-19731
- Dynamic buckling and plate to shell transition of thick spherical caps under large amplitude axisymmetric flexural vibrations
08 p1249 A72-22135
- Elastic and plastic buckling analysis of uniformly compressed rectangular plates, using Kantorovich method
09 p1408 A72-23556
- Finite element structural analysis for local buckling stresses in flat plates, panels and thin walled columns, deriving elastic and geometric stiffness matrices
[AIAA PAPER 72-354] 11 p1729 A72-25383
- Dynamic nonlinear elastic response of buckling sensitive cylindrical shells to lateral pressure loading, using numerical and computerized analysis
[AIAA PAPER 72-357] 11 p1729 A72-25386
- Rib reinforced cylindrical shell supercritical post-buckling strains, allowing for geometrical surface deflection
12 p1885 A72-27976
- Equilibrium state stability in elastic conservative system, relating system postbuckling behavior to critical branching point
13 p2054 A72-28478
- Structural approach to elastic stability in buckling problems, simplifying deformation concepts and loading condition definition
13 p2054 A72-28479
- Finite plane elastic buckling deformations of incompressible composite columns reinforced by straight parallel fibers
13 p2059 A72-29599
- Combined axial compression and shear deformation effect on elastic columns buckling behavior, evaluating third order polynomials eigenvalues by computerized Newton-Raphson technique
14 p2168 A72-30934
- Dynamic response and buckling mode of elastically supported circular plates with initial tension under arbitrary surface load
15 p2332 A72-32578
- Perturbation scheme for branching analysis of post-buckling behavior in elastic spherical shells
16 p2465 A72-33001
- Edge-loaded rectangular plate buckling behavior in elastoplastic range between proportional limit and yield point
16 p2466 A72-33020
- Equilibrium equations and boundary conditions for elastic buckling of open cylindrical sandwich shell under compressive forces applied to freely supported edges
16 p2467 A72-33116
- Axisymmetrical stability loss in elastic cylindrical shell under longitudinal and transverse impact waves, discussing buckling and similarity parameter for simulation
16 p2468 A72-33159
- Thin walled elastic structures optimization by overall and local buckling coincidence, discussing compression column design
16 p2468 A72-33200
- Elastic buckling of simply supported sandwich panels with fiber reinforced laminated face plates and honeycomb cores subjected to uniform end loading
16 p2469 A72-33405
- Imperfect circular cylindrical shells creep and elastic buckling under nonuniform external loads, solving ordinary differential equations via finite difference technique
16 p2474 A72-34133
- Magnetoelastic buckling of beams and thin plates of magnetically soft material.
[ASME PAPER 72-APM-35] 17 p2624 A72-34311
- Dynamic buckling of shallow circular cylindrical hinged panel under axial compression
17 p2626 A72-34665

Monograph - The elastic flexural-torsional buckling of beam-columns by discrete element techniques

17 p2634 A72-35548

Coordinate transformation for perturbation analysis of elastic structural system imperfections influence on elastic buckling

18 p2732 A72-36079

Clamped flat skew plates stability under inplane stresses in terms of oblique components, calculating elastic buckling coefficients via energy method

18 p2736 A72-36931

Symmetrical and antisymmetrical wrinkling of sandwich panels.

18 p2736 A72-37056

Internal buckling of a laminated medium.

18 p2737 A72-37059

Application of conformal transformation to the variational method - Buckling loads of polygonal plates.

18 p2738 A72-37074

A proof of the accuracy of a set of simplified buckling equations for circular cylindrical elastic shells.

18 p2739 A72-37091

Buckling of an elastic cylindrical shell during longitudinal impact against an obstacle

19 p2870 A72-37322

Continuum and finite element branching studies of the circular plate.

22 p3235 A72-42603

Fiber composite columns under compression.

23 p3344 A72-43494

Asymmetric imperfections effect on spherical elastic shell buckling strength under uniform external pressure

23 p3351 A72-44104

Column buckling under random initial deformations influence, determining mean square nonstationary deflection by Green function technique

23 p3351 A72-44106

ELASTIC COLLISIONS

U ELASTIC SCATTERING

ELASTIC CONSTANTS

U ELASTIC PROPERTIES

ELASTIC CYLINDERS

Two-layered plane strain elastic cylinder with cracked inner bore under internal pressure loading, obtaining stress intensity factors by finite element method

01 p0141 A72-10994

Computer algorithm of initial functions for elastic thick finite hollow axisymmetric cylinders under static conditions

02 p0288 A72-11604

Axially symmetric torsional waves in elastic circular composite cylinders, plotting dispersion diagrams

04 p0590 A72-15185

Elastic analysis of circular cylinders with stress singularities from boundary discontinuities, mixed displacement and axial load conditions [ASME PAPER 71-WA/APM-18]

05 p0733 A72-15962

Eccentric circular ring elastic contact with rigid symmetric dies under equal diametrically opposite loads

05 p0738 A72-16329

Resonant frequency, phase velocities and dispersion curves for wave propagation in isotropic elastic cylinders

06 p0895 A72-17854

Numerical approximation of Pochhammer-Chree longitudinal vibration modes in elastic cylinders by quadratic spline functions

07 p1087 A72-18797

Local stability of thin walled isotropic elastic cylinder, deriving characteristic equations for critical load calculation

08 p1242 A72-20969

Snapping process dynamics of shallow elastic hinged cylindrical panel of rectangular planform under gaseous, liquid and solid loads

08 p1242 A72-21228

Somigliani dislocations effect in infinite elastic cylinder, determining stresses in form of eigenfunctions expansions

09 p1398 A72-22491

Fundamental vibrations of long circular cylinder made of micropolar elastic solid, discussing dispersion equations

09 p1398 A72-22620

Wave propagation in bonded discretely inhomogeneous elastic cylindrical rods, including longitudinal and radial motions

09 p1409 A72-23563

Stress distribution determination for long isotropic elastic cylinder with strip crack on diametral plane by complex variable technique and Fredholm equation solution

09 p1409 A72-23574

Dynamic contact problems of die or bandage on elastic layer surface or cylinder, analyzing vibrationally induced elastic waves

10 p1558 A72-24779

Algebraic equations for displacement and stress vectors at faces and interfaces of elastic multilayered cylinders and infinite wedges, using matrix method

12 p1884 A72-27565

Vibrations and plane wave propagation in laminated elastic plates and cylinders, noting finite element method for conical shells

[AIAA PAPER 72-406]

13 p2056 A72-28959

Series solution for coaxial spherical cavity effect on torsional stress of finite length elastic circular cylinder

13 p2059 A72-29491

Thermal stresses in elastic cylinder for variable linear expansion coefficient and temperature, noting welded seam between two constant temperature cylinders

13 p2059 A72-29492

Dynamic contact problems of stamps bands oscillation on elastic layer surface or cylinder, analyzing vibrationally induced elastic waves

14 p2163 A72-30223

Stress analysis of two coaxially conjugated elastic isotropic cylinders under compression loads in terms of Fourier-Bessel series

15 p2323 A72-31447

Coupled oscillations of inviscid homogeneous liquid with free surface under vacuum or gas filled space in elastic cylindrical container

15 p2217 A72-31472

Thermoelastic stress analysis of stamps bands oscillation heated along helix, calculating stress function for given surface temperature distribution

15 p2333 A72-32687

Strain energy method for finite deformation of solid and tubular cylinders of incompressible isotropic elastic material, noting torsional and tensile tests on natural rubber

16 p2468 A72-33198

Somigliani dislocations effect in infinite elastic cylinder, determining stresses in form of eigenfunctions expansions

17 p2626 A72-34654

Elastic cylindrical antenna detection relationship to gravitational radiation sources

17 p2584 A72-35914

Fluid oscillations in a partially filled cylindrical tank with a spring supported elastic floor.

18 p2684 A72-37062

Propagation and attenuation of harmonic waves in a viscoelastic circular cylinder.

18 p2738 A72-37070

Axial-symmetric deformations of a rubber-like cylinder under initial stress.

18 p2738 A72-37081

Thermal circular and radial stresses in elastic orthotropic cylinders with anisotropic expansion coefficients

19 p2872 A72-37535

Dynamic stability of axisymmetrically heated glass fiber reinforced cylindrical plastic shells which are coupled with elastic cylinders

19 p2872 A72-37539

Propagation of Rayleigh waves on visco-elastic cylindrical surfaces placed in a magnetic field.

22 p3207 A72-42876

On the propagation of Love type waves in an infinite cylinder with rigidity and density varying linearly with the radial distance.

22 p3207 A72-42878

Reflection of pulses at the interface between an elastic rod and an elastic half-space.

23 p3314 A72-44119

Free vibrations of thick, layered cylinders having finite length with various boundary conditions.

24 p3425 A72-44884

ELASTIC DAMPING

Maximum logarithmic decrement vs frequency of damped oscillation of elastic thin beam including internal and viscous resistance

01 p0144 A72-11384

Alloying, thermal and mechanical treatment effects on Mg alloys damping properties under elastic vibrations, showing test results consistency with materials microdeformation theory

05 p0671 A72-15987

Forced transverse vibration damping of end loaded elastic cantilever beam, determining hysteresis loop contour from resonance curves

06 p0900 A72-18673

Torsional oscillation damping in circular rods coated with viscoelastic material as function of resonant frequency

07 p1087 A72-18924

Free oscillations frequencies and mode shapes determination of two parallel elastically coupled rods of variable cross section, applying Bubnov-Galerkin iterative method

08 p1243 A72-21231

Angular rigidity of support shaft elastic suspension of dynamically adjustable gyroscope

09 p1307 A72-22348

Higher order forces effect on shock absorbing systems of masses interconnected by elastic and damping members of aircraft landing gears

09 p1318 A72-22861

Slip contact joint frictional damping of vibration of beam on elastic support

09 p1408 A72-23464

Motion and stable equilibrium position of horizontal rotor with nonlinear elastic and internal damping properties, discussing stress-strain-time relations of shaft filaments

09 p1409 A72-23613

Dynamic shear modulus and damping of polystyrene composites filled with glass, salt and foam, including skin effect correction

10 p1500 A72-24260

Damping additions for plates using constrained thin viscoelastic sheets and metallic layers

11 p1688 A72-26063

Closed form solution for dynamic response of infinite plate with elastic foundation and damping under arbitrary initial conditions and load distribution

12 p1883 A72-27559

Axial compression stability critical load and buckling of cylindrical shells resting on Winklerian elastic base, using dynamic programming

12 p1885 A72-27972

Vibratory effects of disturbances transmitted from vehicle to viscoelastic vibroprotective damping coating in presence and absence of resonance

13 p2055 A72-28558

Torsional vibration damping in circular rods coated with viscoelastic material, noting technique effectiveness at certain resonant frequencies

13 p2058 A72-29209

Elastic damping of spin stabilized space stations nutational oscillations induced by time-variant moments of inertia

15 p2319 A72-31458

Material damping effect on rotating system stability as function of critical angular velocity, using elastic continuum whirling shaft model

16 p2465 A72-32986

A comparison of approximate methods for solving non-conservative problems of elastic stability.

17 p2634 A72-35410

Equipment vibration isolation principles, discussing damping, viscoelastic materials and shock absorbers

18 p2731 A72-35992

The effect of an elastic edge restraint on the forced vibration of a rectangular plate.

18 p2737 A72-37066

A certain generalization of the hysteresis loop contour equations to the case of an asymmetric cycle

19 p2876 A72-38003

Thermoelastic martensite caused elastic vibration damping in Cu-Al-Ni alloy, observing shape memory effect

22 p3190 A72-42442

The damping properties of elastically supported sandwich plates.

24 p3458 A72-44915

Alloying, thermal and mechanical treatment effects on Mg alloys damping properties under elastic vibrations, showing test results consistency with materials microdeformation theory

24 p3415 A72-45729

ELASTIC DEFORMATION

NT ELASTIC BENDING

NT ELASTIC BUCKLING

Human spine elastic deformation due to bending stresses, presenting statistical data on caudocephalad acceleration effects in vertebral column injuries

01 p0016 A72-10111

Stokes and Love integral representations for elastodynamic displacement fields in elastic solid deduced by potential theory method

01 p0138 A72-10513

Trapezoidal isoparametric and triangular singularity elements for crack tip elastic stress intensity factor for mesh having small number of degrees of freedom

01 p0140 A72-10992

Stroboscopic measurement of elastic untwisting angles of axial compressor rotor vanes under centrifugal and aerodynamic forces

01 p0143 A72-11371

Thermal stresses, temperature distribution and displacement fields in elastic solid with spherical cavity and external crack

01 p0144 A72-11385

Geometrical method in nonlinear shell theory for supercritical elastic deformation determination, considering stability loss and dynamics problems

02 p0289 A72-11612

Linear creep properties in continuous media for wide time-variable parameters range of instantaneous elastic deformation under simple loads

02 p0289 A72-11616

Elastoplastic deformation in medium with initial dislocations and temperature field, expressing kinetic stress and distortion tensors by Hamiltonian derivatives

02 p0290 A72-11630

Deformation, stress and singularity in cylindrical shells under concentrated circumferential loads, comparing with two dimensional elasticity and plate bending

02 p0291 A72-11662

- Elastic strain effects in ball bearing supports on motion of gyroscope Cardan suspension
02 p0231 A72-12565
- Finite element formulation for nonlinear large deflection elastic analysis of displacements and stresses in thin plate structures
02 p0298 A72-12657
- Elastic bodies deformations theory, formulating boundary value problems
03 p0443 A72-13451
- Deformation kinetics relationship to scale effect in notched samples during elastoplastic loading phase
03 p0443 A72-13455
- Double forces distribution over elastic body surface from Lamé equation describing static defects, discussing Kupradse potential and sources corresponding to plane dislocations and cracks
03 p0444 A72-13501
- Stresses due to initial elastic deformations in orthotropic thin plate strip, expressing Dirac function by Fourier series and integral
03 p0444 A72-13505
- Axisymmetric Reissner-Sagoci problem in linear micropolar elasticity for stress and displacement under load applied by rigid circular disk
03 p0448 A72-13890
- Variable-modulus isotropic material finite elastic deformation, deriving two dimensional stress concentration by dual series expansion
03 p0452 A72-14132
- Stress channelling in transversely isotropic elastic composites, comparing classical theory with ideal fiber reinforced composite plane deformation theory
03 p0455 A72-14385
- Displacements in nonhomogeneous elastic layer, investigating uniformly distributed load surface settling behavior dependence on layer depth relationship to loaded area width
03 p0455 A72-14387
- Nonlinear elastoplastic deformations of flexible shells of revolution, calculating stress concentration at circular hole in spherical shell
04 p0588 A72-15049
- Closed form equations for constrained torsion of turbine blades, estimating elastic twist and cross sectional depilation on analog computer
04 p0589 A72-15166
- Elastic strip stresses and displacements, using eigenfunctions with coefficients determined by variational principles
[ASME PAPER 71-APMW-24] 04 p0589 A72-15181
- Dynamic theory of thin elastic beams under large deflection, taking into account shear deformation and axial stress resultants
[ASME PAPER 71-APM-EE] 04 p0590 A72-15183
- Uniform circular plates axisymmetric elastic deformation under various static loadings and boundary conditions, solving flexural equilibrium equations
04 p0590 A72-15184
- Continuous bodies incremental deformation and stability under initial stress, discussing relationships for elasticity constants and material stress tensors
[ASME PAPER 71-WA/APM-9] 05 p0734 A72-15970
- First and second order moduli of elasticity for finitely deformed elastic materials, deriving acceleration waves propagation condition and growth equation
05 p0735 A72-16028
- Tensor calculus theorem application to elastic isotropic materials finite deformation, considering acceleration waves propagation and moduli of elasticity
05 p0735 A72-16029
- Rectangular variable thickness plate deflection under uniform lateral pressure, solving nonlinear partial differential equations with variable coefficients by iterative procedure
05 p0738 A72-16533
- Variational principles for elasticity theory problem of three dimensional linearly elastic incompressible anisotropic body with highly elastic deformations
05 p0741 A72-17143
- Inverse periodic plane deformation of isotropic elastoplastic surface with infinite series of curvilinear holes
05 p0741 A72-17146
- Thermoelasticity equations for thermal shock effect on freely supported circular plate, describing deformation and temperature field interactions
05 p0741 A72-17147
- Isotropic continuum model of elastic interaction of edge and screw dislocation with nearby inclusion
06 p0894 A72-17492
- Stress and displacement solutions to elastic deformation of homogeneous and composite anisotropic near cylindrical bodies, using Almansi algorithm
06 p0894 A72-17688
- Critical review on data accuracy of maximum principal elastic stresses and deflections of thin initially flat square isotropic plates under uniform normal pressure
06 p0894 A72-17796
- Hollow rubber impact absorber stiffness and deformation characteristics derivation by classical elasticity theory, noting accuracy
06 p0895 A72-17797
- Green-Naghdi nonlinear thermodynamics of elastic-plastic deformation at finite strain, discussing relationship to nonisothermal theory
06 p0896 A72-17921
- Large elastic deformation problems analysis by incremental finite element technique, using variational principles
07 p1087 A72-18782
- Classical elasticity displacement problem solution by integral equation method based on Betti tensor counterpart of Green procedure in potential theory
07 p1026 A72-18813
- Stress-strain state relationship to crack development morphology in elastic strain region of austenitic steel sample under cyclic bending
07 p1013 A72-19769
- Minimum weight design of elastic sandwich beam with segmentwise constant stiffness under displacement and stress constraints, using iterative solution and finite element analysis
[AD-745488] 07 p1092 A72-19825
- Stress-strain behavior of steel under elastic compression at 4.2 K, observing discontinuous twinning
07 p1020 A72-20413
- Nonlinear theory of thin walled open elastic beams with deformations by large cross sectional rotation, using potential energy principle
07 p1096 A72-20430
- Elastohydrodynamic lubrication of soft elastic-deformed contact surfaces, determining lubricant film thickness as function of inlet and outlet parameters
07 p0998 A72-20530
- Elastic-plastic deformation of thin membrane shells
08 p1244 A72-21290
- Rheological model of reticular polymers and glass fiber reinforced plastics based on stress-strain relationship during damped creep elastic deformation
08 p1191 A72-21499
- Time varying external pressure effect on creep collapse of long thin walled quasielliptic cylindrical shell, taking into account elastic deformation
08 p1245 A72-21612
- Strength analysis of thin elastoplastic shell with allowance for compressibility, relating loads and moments to deformation of middle surface
08 p1246 A72-21712
- Nonlinear viscoelastic body model for stress relaxation of amorphous linear polymers below vitrification temperature for various deformations, temperatures and deformation speeds
08 p1194 A72-21751
- Residual temperature stresses and deformations during thermal treatment of thick walled glass fiber reinforced plastic wound cylinders and rings
08 p1194 A72-21755
- Contact problem of semiinfinite plate deflection on linearly deformed half space with depth dependent elasticity modulus
08 p1247 A72-21808
- Stress-deformation effects on gasket joint of metal seals at high pressures
08 p1178 A72-21933
- German monograph on model concept for erosion mechanism involved in crystalline material surface bombardment covering particle elastic deformation during impact
09 p1397 A72-22324
- Thin walled Bourdon tube manometric spring deformation analysis by Ritz method in second approximation
09 p1397 A72-22349
- Axisymmetric deformation of hollow elongated elastic ellipsoid, using Lamé equilibrium equations
09 p1400 A72-22708
- Stress-strain state of circular conical shell of linearly variable thickness within small elastoplastic deformation theory, assuming specific convective heat transfer at surface
09 p1401 A72-22722
- Boundary value problems in micropolar theory of elasticity, obtaining displacement and rotation vectors from singular integral equations
09 p1402 A72-22745
- Crack propagation in elastic layer under antiplane state of deformation for arbitrarily distributed shearing forces on crack surface
09 p1404 A72-22766
- Elastic dislocation theory of Chandler wobble excitation by earthquakes
09 p1299 A72-22802
- Magnetization and elastic stresses effect on Ni dislocations movement due to domain wall interactions
09 p1371 A72-22866
- Infinite elastic solid deformation in antiplane strain mode, discussing corresponding strain model with continuous distribution of slipping edge dislocations
09 p1405 A72-22919
- Continuum model for cylindrical and spherical elastic laminated composites deformation, using balance and constitutive equations
09 p1405 A72-22992
- Drift angle effect on rolling wheel pneumatic tire lateral and angular deformation amplitudes, deriving formula for reaction forces
09 p1351 A72-23176
- Linear theory of elasticity application to wave propagation in homogeneous isotropic material with deformable microstructure, presenting approximate solution method
09 p1353 A72-23552
- Elastoplastic deformation of Zn single crystals under uniaxial tensile loads, noting critical stresses relationship to current pulses
10 p1553 A72-23766
- Elasticity theory for unsymmetric deformation of nonhomogeneous anisotropic cylindrical shells, using Donnell equations
10 p1555 A72-24252
- Piston exerting pressure on liquid filled cylinder, determining deformation state based on thin elastic orthotropic plate theory
10 p1556 A72-24266
- Nonlinear elasticity theory variational principles modification for finite deformation of elastic body
10 p1557 A72-24428
- Solid body elastic deformation potential energy and structure calculation on computer by finite element method and calculus of variations
10 p1559 A72-24924
- Nonlinear dynamic response of single elastic cables with low initial tension, examining free and forced vibrations with incremental deformations theory
10 p1560 A72-25185
- Impact-produced deformations in nonlinear viscoelastic rod of finite length, studying pulse propagation as nonlinear boundary value problem
11 p1685 A72-25353
- Equations of motion for structural flexibility influence on dual spin spacecraft dynamic response, noting elastic deformations and rotation rates coupling
[AIAA PAPER 72-348] 11 p1725 A72-25377
- Heterogeneous shear deformation effect on dynamic response of laminated plates for various local elastic deformation and interface conditions
[AIAA PAPER 72-398] 11 p1731 A72-25419
- Variational equations of motion for three layered laminated sandwich beam vibrations, assuming small elastic deformations and axial and bending motion
[AIAA PAPER 72-399] 11 p1731 A72-25420
- Torsional stress analysis of rectangular beam composed of two elastic materials, using complex variable and conformal mapping
11 p1733 A72-25444
- Nonlinear elastic suspension system with two spring pairs in parallel, measuring nondimensional load versus deflection curve and frequency response
11 p1736 A72-26007
- Resultant material and spatial energy propagation vectors for waves of small amplitude superposed on large static deformation in elastic materials
12 p1879 A72-27123
- Geometrically nonlinear structure elastic stress propagation, deformation and dynamic response under impact, using finite element matrix displacement method and computer programs
12 p1879 A72-27189
- Plane unstable deformation and stability loss of incompressible laminated composites under highly elastic strains
12 p1880 A72-27229
- Dynamics snap-through instability existence conditions in nonlinear plane deformation of shallow circular cylindrical elastic shell under impulsive loading
12 p1880 A72-27241
- Harmonic equation for antiplane shear deformation of elastic composite materials with multiple circular inclusions
12 p1883 A72-27562
- Stokes-Helmholtz decomposition role in displacement potentials derivation in elasticity
12 p1884 A72-27569
- Elastoplastic deformation effects on load bearing capacity of samples with stress concentrators under alternating cyclic loading, obtaining nomograms by digital computer
12 p1887 A72-28228
- Canonical equations of motion for continuous elastic system, predicting critical buckling loads for unbonded deformation
13 p2054 A72-28482
- Uniaxial elastic deformation pressure effects on electronic conduction in tetrahedrally bonded amorphous semiconducting thin films as function of temperature
13 p2021 A72-28574
- Room temperature uniaxial tension tests for elastic deformation of steel samples, showing quadratic stress-strain function
13 p1977 A72-29008
- Elastic deformation and rigidity of rectangular, circular and elliptic gimbals for gyroscope suspension
13 p1957 A72-29272
- Boussinesq problem for homogeneous viscoelastic half space governed by deformation law of typical body under concentrated or sinusoidal loads
13 p2062 A72-30092

Elastic deformations of porous Cu, Mo and W fiber materials after pressing and sintering due to residual stress relaxation

14 p2106 A72-30151

Transverse strain coefficient for steel box-section beam under tension, presenting test values for deformations before and beyond elastic limit

14 p2166 A72-30692

Berger equation inconsistencies for large deflections of thin elastic plates with freely moveable edges

14 p2169 A72-31173

Hingeless elastic helicopter blades coupled flap-lag motion under quasi-steady aerodynamic loads, reducing equations of motion to coupled nonlinear differential equations

15 p2180 A72-31211

Mechanical properties of composite materials, discussing elastic deformation and failure modes

15 p2260 A72-31442

Transverse impacts of hard cones on elastic membranes for various apex angles, using high speed photography

15 p2323 A72-31445

Schaefer stress representation for elastokinetics of linearly elastic isotropic homogeneous body under small deformations and torsions

15 p2324 A72-31486

Elastic deformation of thin walled spherical and cylindrical shells and associated rings under external loads for small displacements

15 p2325 A72-31604

High amplitude ultrasonic stress waves effect on metals elastic and plastic deformation characteristics, verifying model for sound waves-lattice structure interactions

15 p2328 A72-31842

Displacement and stress field for elastic solid containing cruciform crack with unequal length arms

15 p2330 A72-32292

Thin walled elastic shells stability under finite deformations, deriving equilibrium conditions and constitutive equations

15 p2330 A72-32464

Nearly incompressible elastic solid compressibility effects theory, applying to annular wedge straightening, stretching and shearing and cylindrical tube telescopic shear problems

15 p2330 A72-32477

Stress and displacement solution to Lamé problem for multilayer spherical vessels and cylindrical tubes in nonlinear elasticity theory

15 p2333 A72-32679

Elastic-viscoplastic solution for deformation of impulsively loaded strain rate sensitive steel rings

16 p2464 A72-32916

Reversible instantaneous deformations and internal energy in viscoelastic incompressible fluids, using Oldroyd and De Witt hydrodynamic models

16 p2376 A72-32937

Strain energy methods for stability of finitely deformed elastic membranes under conservative loading

16 p2465 A72-33002

Yield conditions formulation restrictions for large elastoplastic deformations, discussing isotropic and anisotropic hardening

16 p2396 A72-33024

Radial vibrations and plane wave propagation in elastic deforming sphere with superimposed time dependent displacement field

16 p2467 A72-33117

Stability loss condition for long rectangular cross section band from nonlinear elastic material with internal constraints, discussing critical loads and deformations

16 p2467 A72-33120

Line and surface defect treatments of elastic media dislocation field, noting nonuniqueness with respect to Burgers and jump conditions

16 p2467 A72-33141

Optimal composite structures of multilayer spherical vessels in terms of elastic deformation under critical loads in thermal field

16 p2467 A72-33158

Small disturbance behavior in laminar boundary layer on elastic surface experiencing deformation under perturbing pressure, noting surface resilience effect

16 p2377 A72-33164

Strain energy method for finite deformation of solid and tubular cylinders of incompressible isotropic elastic material, noting torsional and tensile tests on natural rubber

16 p2468 A72-33198

Equilibrium equation for elastic deformation effect on free electricity redistribution in thin electroconductive shells

16 p2469 A72-33271

Energetic boundedness conditions for internal work of deformation in elastic isotropic body

16 p2470 A72-33527

Equations of motion for small vibrations superposed on time depending deformation of elastic body, discussing acoustic wave propagation

16 p2425 A72-33590

Shock wave propagation in incompressible elastic Mooney-Rivlin material for arbitrary homogeneous strain state

16 p2426 A72-33788

Rotating disk with eccentric elliptic insert determining elastic field in inclusion by complex variable technique

16 p2427 A72-33790

Unified description of structures behavior subject to elastic, creep and plastic deformations

16 p2473 A72-34117

Energy theorems for creep constitutive relationships, discussing total deformation of body composed of elastic-creeping material with allowance for stress redistribution effects

16 p2473 A72-34118

Inflation pressure caused deformations of thin toroidal shells, discussing wrinkle development due to pressure reduction

[ASME PAPER 72-APM-32] 17 p2628 A72-34787

Dynamically loaded elastic, viscous, plastic and rigid, viscoplastic structures instantaneous mode responses definitions and characterization by variational criteria with isometric constraints

[ASME PAPER 72-APM-17] 17 p2628 A72-34799

Flexure of micropolar elastic beams.

17 p2631 A72-35056

Conical and cylindrical shell deformation with nonlinear one dimensional wave processes, describing algorithm for method of characteristics application

18 p2735 A72-36664

On the two-dimensional deformation of a semi-infinite porous elastic medium.

18 p2736 A72-36929

Bending of rectangular plates of linearly varying thickness

18 p2736 A72-36991

Forced axisymmetric response of fluid filled spherical shells.

18 p2684 A72-37063

Heat production effects in general linearized thermoviscoelasticity theory, deriving equations of motion, state and energy and boundary conditions for intensely strained objects

19 p2871 A72-37526

Elastic stability theory of compressible and incompressible composite media

19 p2871 A72-37530

Anisotropic circular cylinder stress analysis under uniaxial load, calculating elastic deformation

19 p2872 A72-37536

Variational principles of the nonlinear theory of elasticity - Case of superposition of a small deformation on a finite deformation.

19 p2872 A72-37559

Aluminium, II - A review of deformation properties of high purity aluminium and dilute aluminium alloys.

19 p2818 A72-37832

Regularities in the deformation and failure of commercial iron in a complex stress state under low-temperature conditions

19 p2818 A72-38005

Low-frequency wavelike process of deformation in a seminfinite cylindrical shell immersed in a compressible fluid

19 p2877 A72-38157

Theory for transverse vibrations of beams during elastoplastic deformations

19 p2877 A72-38179

Post-critical deformations of a cylindrical shell subject to the action of external pressure and a temperature field

19 p2878 A72-38472

Spherelike deformations of a balloon.

19 p2878 A72-38716

Features of deformation and stress distribution in a laminated plastic

20 p2944 A72-38948

Large elastic deformations of an incompressible material heteroresistant to tensile and compressive strains

20 p2978 A72-39021

Deformation of the earth by surface loads.

20 p2916 A72-39335

Axisymmetric impact of compactible rods subjected to finite deformations.

21 p3117 A72-40455

A multi-continuum theory for composite elastic materials.

21 p3072 A72-40676

On the asymptotically spherical deformations of arbitrary membranes of revolution fixed along an edge and inflated by large pressures - A nonlinear boundary layer phenomenon.

21 p3118 A72-40840

Time dependent deformation of isotropic viscoelastic materials, discussing rectilinear shear, circular cylinder torsion, spiral shear of layer and conical layer torsion

21 p3119 A72-41075

Hysteresis curve equation for calculation of elastoplastic deformations caused by forced vibrations, taking into account medium compressibility and inertial forces

21 p3123 A72-41359

Epoxy-thiocol binder viscoelastic deformation under short and long term loads, noting stress-strain linearity limit

21 p3073 A72-41360

Constitutive equations of generalized Brandt-Reuss theory of elastoplastic deformation, noting second order effects

21 p3124 A72-41506

Theory of slow elastic-plastic deformation of polycrystalline metals with micro-stresses as latent variables descriptive of the state of the material.

21 p3124 A72-41508

Line integral expressions along line singularity loop for elastic strain and curvature, observing plastic dislocations, distortions and rotations

21 p3125 A72-41511

Calculation of sandwich shells of revolution at large elastic-plastic deflections.

21 p3125 A72-41512

Disclinations theory described by plastic and elastic distortions, considering line singularity and dislocation loop

21 p3125 A72-41513

Nonlinear equilibrium equations for hinged flat circular and spherical membranes under large axisymmetric elastic deformations due to internal pressure

21 p3125 A72-41516

Book - Analysis of plates.

21 p3125 A72-41530

Multilayer shell theories with allowance for transverse shear and transverse normal deformation of layers, noting viscoelastic material and anisotropic shallow shells

21 p3125 A72-41537

Methods of studying three-dimensional problems of stability in the presence of highly elastic strains

21 p3126 A72-41538

Equilibrium and elastic deformation equations for closed cylindrical shells with arbitrary cross section and variable wall thickness

21 p3126 A72-41551

Asymptotic analysis of the behavior of an elastic rod under aperiodic intense loading

21 p3127 A72-41670

Allowance for the hysteresis behavior of a continuous medium in a complex state of stress under conditions of simple cyclic loading

21 p3127 A72-41711

Solution for shallow shells of revolution with allowance for large deflections by the method of integral relations

22 p3232 A72-41869

Stress-strain state of an isotropic half-plane with an elliptic hole, deformed by concentrated loads

22 p3233 A72-42057

Stress-strain state at holes in plates in the case of asymmetric buckling modes

22 p3233 A72-42059

Analogs between linearized and linear problems in elasticity theory in the case of uniform initial states

22 p3233 A72-42061

Elastic isotropic plates stability for nonlinear stress-strain relations, noting effect of deformation tensor invariant on critical load magnitude

22 p3234 A72-42275

On the effect of the form of the strain energy function on the solution of a boundary-value problem in finite elasticity.

22 p3236 A72-42606

The application of the finite element displacement method to problems of elastoplastic deformation.

22 p3238 A72-42832

Optimization of the range of elastic behavior of unidirectional composites by prestraining.

22 p3194 A72-43041

Continual theory of dislocations and the theory of small elastoplastic deformations

23 p3345 A72-43584

Experimental analysis of the stress distribution in the vicinity of a nonwelded rigid circular inclusion in the interior of a plate stressed in monoaxial tension

23 p3346 A72-43691

Nonlinear thin elastic plate deformation differential relations and static boundary conditions along contour, verifying theory by bending experiment on rectangular plate

23 p3348 A72-43791

Elastic and plastic deformations in torsional moment loaded rod, noting successive approximation for stress functions

23 p3348 A72-43794

Reissner-Sagoci problem for seminfinite elastic solid stress and displacement determination, discussing generalization to nonhomogeneous media with circular part under axisymmetric twisting

23 p3314 A72-44266

Computation of post-yield behaviour in notch-bend and tension testpieces.

24 p3456 A72-44796

Elastic bodies deformations theory, formulating boundary value problems

24 p3458 A72-44926

Deformation kinetics relationship to scale effect in notched samples during elastoplastic loading phase

24 p3458 A72-44930

- Pure antiplane stress and equilibrium of isotropic elastic beams, considering suspended cylinders 24 p3459 A72-44989
- ELASTIC MEDIA**
- Plane strain analysis of two bonded semiinfinite elastic media with different thermomechanical properties and cracks, calculating stress factors and maximum stress angles 01 p0140 A72-10990
- Continuum mechanics models of macroscopically inhomogeneous elastic medium with microstructure, using moment theory 02 p0288 A72-11608
- Wave propagation in nonlocal isotropic elastic medium of ordinary kinematic structure with energy density as functional of displacement gradient field 02 p0288 A72-11609
- Variational perturbation problem solution in power series form for elliptic functional description of elastic continuous medium state by Euler-Lagrange equations 02 p0259 A72-12233
- Elastic continuous media nonlinear models approximation, obtaining Euler-Lagrange functions 02 p0259 A72-12234
- Homogeneous isotropic elastic medium free vibration in unbounded space, obtaining relativistic relations in wave field from mathematical model 03 p0389 A72-13425
- Fracture mechanics of interfacial cracks between two bonded dissimilar anisotropic elastic half spaces, presenting two dimensional analysis of stress fields 03 p0446 A72-13707
- Continuous solid medium electroelastic equations of state, obtaining solution by variational principles application 03 p0390 A72-13916
- Anisotropic media elastoplastic behavior, developing plastic deformation theory from stress-strain relationships for linearly elastic media 03 p0454 A72-14216
- Linear elastic Cosserat continuum mixed boundary-initial value problem uniqueness theorem, using Kirchhoff proof in classical elastostatics 03 p0382 A72-14363
- Stress intensity and plane dilatational wave diffraction in elastic material with finite crack 04 p0583 A72-14459
- Semiinfinite elastic solid response to arbitrary axially directed line load, transforming simultaneous partial differential equations by Hankel transforms [ASME PAPER 71-APMW-1] 04 p0589 A72-15180
- Nonhomogeneous elastic structure with quasi-permeable coefficients, deriving mechanical model by continuum spectral theory 04 p0594 A72-15745
- Equilibrium equations solution for displacements of inhomogeneous isotropic elastic media 05 p0739 A72-16588
- Layer potentials continuity in theory of vibrations of elastic medium 06 p0894 A72-17556
- Matrices of fundamental solutions constructed for loading singularities and Green method in unbounded micropolar elastic continuum 07 p1095 A72-20243
- Stress intensity factor of crack near inclusion in infinite elastic plane, using numerical methods 09 p1398 A72-22531
- Tensionless contact area between beam and elastic half space determined by approximate technique 09 p1398 A72-22623
- Thermal stress-strain state analysis of nonlinear elastic medium by small parameter method 09 p1400 A72-22717
- Crack propagation in elastic layer under antiplane state of deformation for arbitrarily distributed shearing forces on crack surface 09 p1404 A72-22766
- Infinite elastic solid deformation in antiplane strain mode, discussing corresponding strain model with continuous distribution of slipping edge dislocations 09 p1405 A72-22919
- One dimensional shock wave propagation in inhomogeneous elastic materials, showing wave amplitude behavior dependence on critical jump in strain gradient 09 p1405 A72-22990
- Homogeneous isotropic elastic medium thermoelasticity equations based on variational principles noting definite integrals solutions by means of delayed potentials 09 p1406 A72-23070
- Stress concentration in elastic composite reinforced by two dimensional continuous parallel fiber array with one broken fiber 09 p1339 A72-23172
- Stress wave reflection and transmission at interfaces between homogeneous isotropic linear elastic materials 09 p1353 A72-23501
- Coupling of interstitial liquid and porous elastic medium deformation, calculating solidification by numerical integration of partial differential equations system of I-lame type 10 p1465 A72-24116
- Dynamic stress concentration around elliptical discontinuities in elastic medium, considering rigid and empty cavity scatterers for compression and vertically polarized shear incident waves 10 p1554 A72-24180
- Thermal stresses and displacements in elastic medium containing parallel circular cracks, using perturbation technique 10 p1560 A72-25045
- Distributed elastic system discrete model mass, stiffness and damping matrices derivation from dynamic test response data 11 p1728 A72-25375
- Constitutive equations for bimodulus elastic materials, postulating rheological model based on anisotropy stress-strain laws 11 p1736 A72-25984
- Axissymmetric stress field in infinite homogeneous isotropic elastic solid with crack surrounding cylindrical cavity, solving elastic equilibrium equations 11 p1738 A72-26720
- Resultant material and spatial energy propagation vectors for waves of small amplitude superposed on large static deformation in elastic materials 12 p1879 A72-27123
- Elastic inhomogeneous continuum stability dependence on internal stress tensors field and boundary conditions, noting application to composite materials 12 p1843 A72-27171
- Screw dislocation with free surface interaction in inhomogeneous elastic medium with continuously varying elastic moduli 12 p1881 A72-27253
- Equations of motion for oriented and multipolar discrete elastic media, noting elements formed by sets of free material points 12 p1845 A72-27394
- Resonant frequency and vibration modes of variable cross section bar in elastic medium under transversal force, noting dynamic programming combined with optimization principle 12 p1845 A72-27538
- Ultimate safe load estimates for stability of isotropic elastic materials 12 p1883 A72-27563
- Plane longitudinal displacement wave reflection from fixed surface in micropolar elastic half space, presenting reflection laws and amplitude ratios for specific cases 13 p2056 A72-29001
- Boundary value problems in dynamics of Cosserat infinite elastic medium with finite crack, noting couple stresses effect on dynamic stress concentration 14 p2164 A72-30299
- Instrument to determine steady and unsteady stress state of elastic fluids in viscometric flow, noting rheological measurements in solved polymers 14 p2094 A72-30421
- Magnetoelastic effects in elastic dielectric analysis based on continuum with single magnetic moment, noting magnetically saturated material 15 p2274 A72-31482
- Thermal stress and temperature distribution in rigidly bounded elastic half-space, taking into account coupling effects 15 p2325 A72-31637
- Elastic properties of media with cracks, discussing elastic anisotropy and crack distribution 15 p2327 A72-31733
- Longitudinal shear crack propagation after stability loss in infinite elastic medium, discussing wave diffraction at edges 15 p2327 A72-31734
- Numerical solution of singular integral equations system for stress concentration in elastic plane with curvilinear crack 15 p2327 A72-31735
- Displacement and stress field for elastic solid containing cruciform crack with unequal length arms 15 p2330 A72-32292
- Nonlinear elastic material approximation by piecewise linear material with linear boundary value problems, discussing isotropic case based on singular surfaces theory 15 p2330 A72-32295
- Nonlinear anisotropic elastic constitutive equations for micromorphic and micropolar mixtures, investigating plane wave propagation via field equations with restricted coupling 15 p2278 A72-32446
- Elastic dilatational field association with twist disclination loop interaction with free surface of two phase system interface 15 p2331 A72-32504
- Incompressible elastico-viscous liquid steady state laminar source flow between stationary infinite porous disks, noting Reynolds number effects 15 p2219 A72-32512
- Antiplane shear wave diffraction by two coplanar Griffith cracks in infinite isotropic homogeneous elastic medium 16 p2464 A72-32919
- Linearly elastic, transversely isotropic multilayer system, presenting stress and stability problem for two dimensional strain states 16 p2466 A72-33022
- Displacements, rotations and stresses equilibrium equations solution for plane micropolar elastic half space, using exponential Fourier transforms 16 p2466 A72-33105
- Line and surface defect treatments of elastic media dislocation field, noting nonuniqueness with respect to Burgers and jump conditions 16 p2467 A72-33141
- Cosserat couple stresses theory application to time varying concentrated forces induced displacements in infinite elastic space 16 p2469 A72-33385
- Nonlinear equations of discrete elastic Cosserat media from multipolar media equations, studying small rotation theory 16 p2425 A72-33591
- Nonlinear theory of two dimensional and three dimensional discrete elastic Cosserat media, noting application to reinforced shells and lattice type structures 16 p2425 A72-33592
- Shock wave propagation in incompressible elastic Mooney-Rivlin material for arbitrary homogeneous strain state 16 p2426 A72-33788
- Control volume method for finite amplitude shock front propagation in hyperelastic materials, solving steady state conservation equations 16 p2427 A72-33830
- Prestrained and annealed elastic materials stress-strain relationship calculation in plastic range, compared with tensile and compression load tests results 16 p2472 A72-33948
- Magnetized deformable media in general relativity. 17 p2584 A72-35911
- Mechanical structure and component stress measurement by reinforced concrete, microconcrete, elastic and plastic models 18 p2733 A72-36370
- Mathematical model and simulation for contact problems involving elastic half spaces and viscoelastic and friction effects 18 p2734 A72-36371
- Propagation mechanism of tensor wave in solid elastic body due to impact. 18 p2734 A72-36377
- Microrinhomogeneous elastic media with moduli tensor as coordinate random function, investigating stress and strain tensors 18 p2735 A72-36668
- On the two-dimensional deformation of a semi-infinite porous elastic medium. 18 p2736 A72-36929
- Equilibrium equations solution for displacements of inhomogeneous isotropic elastic media 19 p2872 A72-37560
- Vibrations of elastically connected ring systems. 19 p2873 A72-37692
- A universal connexion for waves in anisotropic media. 19 p2875 A72-37840
- Fourier-Bessel superposition and Laplace transformation methods for surface displacement produced by time dependent dipole in elastic half space, noting buried dipole case 19 p2876 A72-37887
- Applicability of the small parameter method to the estimation of stresses in nonhomogeneous elastic media 19 p2876 A72-38153
- Rayleigh wave effects in an elastic half-space. 20 p2980 A72-39615
- Stress concentration around circular crack on interface between two bonded dissimilar isotropic elastic half spaces 20 p2982 A72-40020
- Stress functions in three-dimensional elastodynamics. 21 p3117 A72-40677
- Stresses around one hole or two holes subjected to internal pressures in semi-infinite or infinite medium. 21 p3118 A72-40717
- Another boundary value problem of the linear theory of elasticity in regions with a fractionally-grained boundary 21 p3119 A72-41091
- Linear equilibrium stability relationship to wave propagation through elastic medium, considering Hadamard theorem proofs 21 p3085 A72-41102
- Connexions between the moduli for anisotropic elastic materials. 21 p3119 A72-41107
- Force-time investigations for the elastic impact between a rigid sphere and a thin layer. 21 p3121 A72-41212
- Optimal compression of constant-thickness media in a plane stress state 21 p3123 A72-41391
- Nonpolar thermodynamics of thermoelastic differential materials in terms of deformation gradient, temperature and Clausius-Duhem constraints 21 p3131 A72-41478
- Propagation of two-dimensional strong discontinuity waves in an elastic-viscoplastic medium. 21 p3124 A72-41503

- Invariant solutions of the differential equations of the uniform motion of a Hooke medium
22 p3233 A72-42058
- The oriented elastic continuum as a model for the magnetoelectric body.
22 p3206 A72-42525
- Causality in the relativistic theory of elastic media in the three-dimensional case.
22 p3206 A72-42626
- Fracture analysis for linear elastic material in antiplane strain, discussing fast moving cracks propagation, flint knapping and equations of motion
22 p3237 A72-42801
- First order constraints in three dimensional continuous elastic fibrous media and thin shells, presenting equilibrium equations
23 p3349 A72-43825
- Series solution of the three-dimensional elasticity problem of a layer.
23 p3350 A72-44049
- Modified Hellinger-Reissner variational method applicable to harmonic waves moving normal to fiber reinforced layered elastic composite, tabulating eigenfrequencies
23 p3351 A72-44061
- Integration scheme for two-dimensional impulsive waves in a linear acoustic medium.
23 p3314 A72-44250
- Thermoelastic contact problem of an elastic layer resting on an elastic foundation.
23 p3354 A72-44269
- Acceleration waves in orthotropic elastic materials.
23 p3354 A72-44342
- Investigation of the characteristics of turbulent air flow in a channel with elastic walls
24 p3393 A72-45257
- Plane thermoelastic one-dimensional waves in an inhomogeneous medium with allowance for connectedness
24 p3459 A72-45266
- ELASTIC MODULUS**
U MODULUS OF ELASTICITY
ELASTIC PLATES
- Stress tensor asymmetry effects on stress concentration at curvilinear holes in elastic plates under tension
02 p0289 A72-11611
- Nonlinear deflections and radial surface stresses in thin elastic circular glass plates with coaxial rings
02 p0249 A72-12418
- Contact stress between half plane and elastic cover plate, reducing problem to Prandtl type integrodifferential equation with Hilbert kernel
02 p0294 A72-12433
- Stress distribution for anisotropic elastic plate containing two or more arbitrary elliptical holes
02 p0298 A72-12674
- Optical interference measurement of various shaped elastic plates deflection and application to thermal stress problems
02 p0300 A72-12824
- Variable cross section elastic stringer end loaded longitudinal force transmission to stiffened elastic plate
03 p0444 A72-13465
- Plane discrete elastic lattice plates buckling, presenting plane and bending state of force equations
03 p0444 A72-13502
- Stress concentration around reinforced curvilinear hole in elastic infinite plate, discussing ring reinforcement rigidity effects
03 p0447 A72-13730
- Asymptotic methods for complex mixed problems of elasticity related to stress concentration in plates with cracks or inclusions
03 p0449 A72-14102
- Approximate solution for stress concentration near oval shaped hole in nonlinearly elastic plate, using small parameter and boundary perturbation methods
03 p0449 A72-14105
- Stress concentration near free hole in circular thick compressed plate, using plane elasticity theory
03 p0450 A72-14107
- Elastic plate with two collinear thermally insulated cracks, calculating steady temperature field and stresses for uniform heat flux at infinity
03 p0450 A72-14112
- Elastic plates with moduli of elasticity variable in tension and compression, deriving plane stress-strain relations
03 p0451 A72-14118
- Infinite elastic isotropic multiply connected plate, determining stress-strain state by asymmetric stress tensors and moment stresses
03 p0451 A72-14119
- Stress concentration at circular holes in polyurethane plates under plane compression wave, obtaining interference fringes
03 p0451 A72-14121
- Displacements in nonhomogeneous elastic layer, investigating uniformly distributed load surface settling behavior dependence on layer depth relationship to loaded area width
03 p0455 A72-14387
- Generalized epicycloid properties application to fracture mechanics, considering stress fields of constrained plastic zones around cracks in thin elastic plate
03 p0455 A72-14388
- Optimum variable thickness reinforcement around circular hole in flat elastic sheet under radial tension
04 p0583 A72-14463
- Forced vibrations of elastic plate with infinite series of identical circular holes, discussing elastic wave diffraction and stresses at/near holes
04 p0587 A72-15017
- Shear stress and stability of composite elastic double layer with plane circular crack under torsion
04 p0588 A72-15054
- Flexible elastic plate nonlinear vibration response and noise transmission from turbulent boundary layer by Monte Carlo technique, discussing subsonic and supersonic flow regions
05 p0651 A72-16850
- Mixed boundary value problem of infinite elastic plate with parabolic crack, obtaining solution by complex variable method
05 p0741 A72-17004
- Large deflection of rectangular thin elastic plates with unsupported edges, using finite difference technique based on dynamic relaxation methods
06 p0895 A72-17799
- Crack propagation in presence of crack branching events in seminfinite nonhomogeneous elastic brittle plate under edge impact loading
06 p0896 A72-17914
- Mean square error and bound on relative error for Reissner plate theory, including shear deformation effect
07 p1087 A72-18812
- Equivoluminal vibration modes of multipolar elastic plate with traction free faces
07 p1089 A72-19646
- Moment stresses and deflections of rigidly clamped hinged and simply supported square elastic plates beyond elastic limit, deriving equilibrium and strain compatibility equations
07 p1091 A72-19759
- Stress-strain state in elastic plate with small radial cracks and circular hole under hydrostatic tension
07 p1091 A72-19765
- Finite element method for elastic plastic sandwich plates analysis, presenting Lagrange multipliers interpretation
07 p1093 A72-19951
- Boundary conditions for unsteady flow fields bounded by incompressible elastic thick plane wall fixed to rigid surface
07 p0972 A72-20113
- Contact problem of semiinfinite plate deflection on linearly deformed half space with depth dependent elasticity modulus
08 p1247 A72-21808
- Plane wave propagation in laminated reinforced elastic plates with difference-differential equations analysis
08 p1247 A72-21809
- Elastic rectangular plate instability in pure bending along two perpendicular directions solved by Karman nonlinear equation reduction to partial differential equations integration
08 p1247 A72-21817
- Stress analysis of isotropic linearly elastic square plate of constant thickness loaded by concentrated forces at edges
09 p1399 A72-22698
- Linear uncoupled quasi-static thermoelasticity theory for thermal bending of nonuniformly heated parallelogram-shaped plates
09 p1400 A72-22710
- Trapezoidal plate thermoelasticity problem for various thermal load distributions, solving Poisson equation for sectorial annular region
09 p1400 A72-22711
- Stressed state of circular elastic plate with prestiffed equiaxial disk
09 p1406 A72-23181
- Mixed boundary elasticity solutions for plane with cuts on real axis, using hyperelliptic Riemann surface
10 p1553 A72-23768
- Plane harmonic compression waves scattering by circular holes in thin elastic plate, calculating dynamic stresses concentration
10 p1554 A72-24179
- Maximum dynamic to static deflection ratio for thermally induced vibrations of elastic beams and plates, considering damping and axial load effects [ASME PAPER 71-APM-UU]
10 p1554 A72-24185
- Crack arrest in transversely loaded elastic plates from fracture mechanics combined with stress intensity factor for tensile and compression loads
10 p1499 A72-24890
- Crack shape and plastic energy dissipation rate relation to plate thickness and applied stress for penny-shaped crack in elastic plate
10 p1559 A72-24896
- Constrained zones and stress intensity factors in cracked thin elastic plates under combined tensile and shear loads
11 p1735 A72-25893
- Infinite elastic thick plate with loads symmetrical to axis of revolution and middle plane, analyzing stress functions, Fourier-Bessel expansion and photoelastic experiment
11 p1626 A72-26427
- Dynamic deflection of elastic rectangular plate hinged to rigid base moving under sinusoidal pressure impulse action, noting base inertia effect
12 p1879 A72-27091
- Approximate theory for high frequency elastic plate vibrations in terms of thickness mode expansion
12 p1881 A72-27251
- Stress concentration in infinite elastic isotropic disk with circular hole under internal tensile loading
12 p1882 A72-27320
- Vibrations and plane wave propagation in laminated elastic plates and cylinders, noting finite element method for conical shells
13 p2056 A72-28959
- Plane stressed state of elastic rectangular plate solved by method of summary representations
13 p2057 A72-29067
- Stress-strain state of elastic rectangular plate under arbitrary edge forces on displacements
13 p2058 A72-29458
- Unsteady spherical shock wave effect on thin infinite elastic plate covering acoustic semispace, using integral transformation method
13 p1943 A72-29946
- Rigid smooth body pressing into elastic plate surface subjected to cylindrical bending, discussing contact problem and transverse shear strain
13 p2062 A72-29950
- Computerized optimal design by nonlinear programming for minimum weight elastic plates crossed with rigid ribs for vibrational loading to meet natural frequencies condition
14 p2165 A72-30576
- Thin elastic plates finite displacement flexure behavior, using piecewise linear finite element incremental stiffness technique
14 p2168 A72-30933
- Berger equation inconsistencies for large deflections of thin elastic plates with freely moveable edges
14 p2169 A72-31173
- Real time focused image holographic interferometry for deformation recording in diffusively reflecting plate under compression
15 p2233 A72-31415
- Elastic plates and shallow shells in finite deflection, obtaining iterative solution with good convergence for thermal stresses
15 p2324 A72-31488
- Contact problems for elastic semiplane reinforced with symmetric and asymmetric loaded elastic stiffeners
15 p2329 A72-32281
- Buckling behavior of simply supported elastic folded plate structures without and with transverse stiffeners under symmetrical and asymmetrical uniform vertical loads
15 p2332 A72-32562
- Rigidity effect of reinforcing rings on stressed state of physically nonlinear perforated elastic plates
15 p2333 A72-32683
- Thin elastic isotropic plates and shells thickness variation for rigidity functional stationary value, reducing problem to stress-strain state equations simultaneous solution
15 p2333 A72-32688
- Homogeneous differential equations of elastic rectangular plates with linear thickness variation, using Gran Olsson solution
16 p2471 A72-33682
- Elastic sandwich plates analysis with core layer as orthotropic Cosserat surface supporting force and moment stresses
16 p2471 A72-33787
- Uniformly propagating finite crack in elastic strip of finite width, using two dimensional dynamic equations of elasticity
16 p2471 A72-33831
- Deflection of plate on elastic support from equilibrium equations based on shell theory
16 p2472 A72-34015
- Free vibrations of elastic plate with random properties - The eigenvalue problem.
17 p2623 A72-34228
- On the extension of an infinite elastic plate containing an axisymmetric hole.
[ASME PAPER 72-APM-G]
17 p2624 A72-34313
- On natural vibrations and waves in laminated orthotropic plates.
[ASME PAPER 72-APM-14]
17 p2581 A72-34803
- Interaction between free oil jets and plates of various profiles
17 p2539 A72-34915
- Nonlinear panel response from a turbulent boundary layer.
17 p2632 A72-35228

Thickness-punch size ratio effects on stress state response of elastic plates and beams in flat contact under symmetric loads due to rigid punches
18 p2734 A72-36378

Sonic boom duration effects on thin circular elastic plate transient axisymmetric vibration via Hankel and Laplace transforms
18 p2734 A72-36409

Variational principle based three dimensional elasticity theory of micropolar anisotropic sandwich plates, considering transverse shear and strains and rotatory inertia
18 p2737 A72-37057

Classical plate theory for variable-thickness isotropic elastic axisymmetric circular plates in partial contact with each other and with rigid smooth surfaces of revolution
18 p2738 A72-37072

Application of conformal transformation to the variational method - Buckling loads of polygonal plates.
18 p2738 A72-37074

Stability analysis of internal pressure loaded crack in adhesive layer bonding elastic plate to rigid base using energy and critical load intensity criteria
19 p2870 A72-37245

Elastic impact on a three-layer plate in the presence of concentrated masses and nonlinear restraints
19 p2877 A72-38159

Uniformly loaded thin elastic isotropic circular plate with partly clamped and simply supported edges, determining deflection via solution of biharmonic differential equation
20 p2979 A72-39331

Stress intensity factors for transversely loaded elastic plates and their application to predictions of crack arrest.
20 p2981 A72-39956

Plane strain bending of laminated fibre-reinforced plates.
20 p2982 A72-40021

Free vibrations of finite element plates subjected to complex middle-plane force systems.
21 p3116 A72-40330

Stress distribution at crack tips in elastic plate loaded by two concentrated opposite forces perpendicular to crack
21 p3123 A72-41389

On the collision of a cold elastic plate with a hot elasto-plastic plate.
21 p3124 A72-41482

Mixed finite element analysis of elasto-plastic plates in bending.
21 p3124 A72-41502

Stress concentration around curvilinear holes in plates according to Reissner's theory
21 p3126 A72-41543

Weight minimization for elastic circular plates of variable thickness under uniformly distributed load with given stress function conditions
22 p3232 A72-41896

Model studies of plate and shell stability
22 p3233 A72-42055

Elastic isotropic plates stability for nonlinear stress-strain relations, noting effect of deformation tensor invariant on critical load magnitude
22 p3234 A72-42275

Bending of a rectangular plate with a clamped edge and an internal symmetric cut
22 p3234 A72-42291

Numerical solution of bending stresses in elastic cantilever plates under surface and edge loads, noting boundary layer, load concentration and sweep back effects
22 p3236 A72-42609

Extensional vibration of a certain type of composite circular plate with a central hole.
22 p3240 A72-42879

The method of Muskhelishvili applied to coupled isotropic elastic plates
22 p3242 A72-43202

Nonlinear thin elastic plate deformation differential relations and static boundary conditions along contour, verifying theory by bending experiment on rectangular plate
23 p3348 A72-43791

Approximate stress-strain state determination in plate weakened by arbitrarily oriented rectilinear cracks and circular holes in elasticity theory
23 p3349 A72-43801

Dynamic response of circular plates to pulse loads.
23 p3354 A72-44254

Non-linear flexural vibration of orthotropic skew plates.
23 p3355 A72-44375

Stress distributions in a semi-infinite plate with a row of circular holes.
23 p3355 A72-44398

Variable cross section elastic stringer end loaded longitudinal force transmission to stiffened elastic plate
24 p3458 A72-44940

Numerical analysis of natural frequency spectrum of plastic plate free vibrations in compressible inviscid fluid
24 p3459 A72-45003

Action of a moving load on a composite shell with elastic filer
24 p3459 A72-45262

ELASTIC PROPERTIES

NT AEROELASTICITY
NT AEROTHERMOELASTICITY
NT ANELASTICITY
NT DYNAMIC MODULUS OF ELASTICITY
NT ELASTOPLASTICITY
NT HYDROELASTICITY
NT MAGNETOSTRICTION
NT MODULUS OF ELASTICITY
NT PHOTOELASTICITY
NT PHOTOVISCOELASTICITY
NT PROPORTIONAL LIMIT
NT THERMOELASTICITY
NT THERMOVISCOELASTICITY
NT VISCOELASTICITY

Bone tissue elastic behavior based on Voigt model of two phase composite material, using ultrasonically determined hydroxyapatite elastic moduli
01 p0136 A72-10112

Griffith crack stress intensity factor and crack face displacement in elastic solid, detailing symmetrical, antisymmetrical and point body force distributions
01 p0136 A72-10185

Saint Venant problem solutions of cylindrical beam in linear theory of micropolar elasticity in terms of three functions
01 p0137 A72-10318

Hydroxyapatite isotropic and anisotropic elastic properties compared with experimentally observed anisotropic behavior of bone
01 p0018 A72-10625

Thick overlay elastic rectangular microwave guides, investigating layer thickness effect, energy partition and higher modes
01 p0042 A72-10706

Three dimensional problems in stability, elasticity and plasticity theory for isotropic, anisotropic and inhomogeneous bodies, noting applications to machine construction, civil engineering, geophysics, etc
02 p0288 A72-11602

Two dimensional contact problems solutions for nonclassical elastic regions for layer and strip
02 p0288 A72-11603

Nonclassical shell theory development from three dimensional boundary value problems solution in elasticity theory
02 p0288 A72-11606

Three dimensional elasticity mixed boundary value problems associated with Laplace equation in half space, including slotted regions and stamp contact solutions
02 p0289 A72-11610

Winding fiber reinforced plastics, investigating fiber curvature effects on elastic constants and tensile strength optimization
02 p0248 A72-11626

Composite rotating sphere with concentric inhomogeneity of elastic constants and outer boundary free from tractions, calculating stress by digital computer
02 p0259 A72-12180

Micropolar elastic theory axial symmetric problems, deriving differential equations for elastic potential and half space
02 p0260 A72-12239

Crack notched three point loaded bend specimens plain strain fracture toughness determination, showing relation between elastic work and stress intensity factor
03 p0442 A72-12960

Rolled metals and alloys with various lattice types and packing defect energies, showing elastic properties isotropy and Young modulus anisotropy
03 p0371 A72-13188

Ritz approximation to two dimensional strain elasticity and heat flow boundary value problems, considering piecewise linear and cubic functions for complete triangulation
03 p0381 A72-13620

French book on thin elastic structures vibration, describing antivibrational devices and rotating machines balancing
03 p0445 A72-13682

Temperature field analysis in locally heated cylindrical shell for stressed state production with lowest elastic energy
03 p0456 A72-13733

Stress distribution at contour of connected region in plane elasticity solved for half plane and circle
03 p0449 A72-13909

Polarization and stress tensor characteristics as function of interaction between mechanical, thermal and electromagnetic processes in elastic isotropic dielectrics
03 p0390 A72-14103

Two dimensional elasticity theory, discussing first, second and mixed boundary value problems solution in contour integral form
03 p0451 A72-14116

Soviet papers on elasticity and inelasticity covering deformable media mechanics, continuum mechanics, polymer materials, random inputs, stress concentration, ductility and crystallization temperature properties
03 p0453 A72-14205

Bi-harmonic stress and displacement potentials for two dimensional boundary problems in elasticity theory, using Galerkin method
03 p0453 A72-14207

Bi-harmonic problem of displacements in plane theory of elasticity, analyzing stress-strain state by iterative solution in series form
03 p0454 A72-14312

Torsion of hollow beam consisting of two homogeneous isotropic rods with different elastic properties and simply connected cross sections, solving by conformal mapping
04 p0586 A72-14992

Stress-strain tensor component relations for isotropic elastic bodies with different tension and compression resistance
04 p0586 A72-15008

Nonlinear hereditary elasticity theory boundary value problem solution using complex potentials in successive approximation algorithm for stress concentration and nonlinear creep analysis
04 p0588 A72-15059

Elastic stiffener bonded to elastic half plane with different mechanical properties, reducing governing integral equation to infinite system of linear algebraic equations
[ASME PAPER 71-APM-TT] 04 p0589 A72-15182

Fiber reinforced composites with transversely isotropic constituents, discussing various mathematical models for elastic constants calculation
04 p0590 A72-15189

Dynamic boundary value problem for elastic half space with rotational concentrated moment of variable magnitude, using Fourier and Laplace transforms
04 p0591 A72-15198

Continuous linear elastic systems characteristic vibrations differential operator eigenvalues lower bounds calculation, obtaining Green integral operator first invariant upper bound via stress function
04 p0540 A72-15706

Elastic stress field in hollow circular cylindrical anisotropic body under surface tractions expressed as Fourier series
[ASME PAPER 71-WA/APM-13] 05 p0734 A72-15967

Elastic boundary value problems static and geometric field parameters pointwise upper and lower bounds, determining solution coefficients by error energy minimization
05 p0735 A72-16062

Elastically supported cantilever stability with continuous lateral restraint under uniform distributed axial load, developing boundary conditions
05 p0737 A72-16118

Asymmetric micropolar elasticity plane problem, solving equilibrium equations with Fourier transformation for displacements, rotation and stresses
05 p0737 A72-16296

Discrete elasticity theory constitutive and motion equations, considering finite difference and partial differential equations
05 p0737 A72-16297

Plane theory of elasticity for infinite triangular wedge with notched apex, reducing problem to non-homogeneous Hilbert problem
05 p0737 A72-16301

Mass concept for moving crack, relating stress concentrations of elastic field with crack inertia
05 p0673 A72-16306

Periodic integral convolution equations in elasticity theory and non-mathematical physics, demonstrating solution existence
05 p0739 A72-16589

Elasticity theory three-dimensional axisymmetric problem reduction to two-dimensional analytical function boundary value problem
05 p0739 A72-16591

Variational principles for elasticity theory problem of three dimensional linearly elastic incompressible anisotropic body with highly elastic deformations
05 p0741 A72-17143

Elasticity theory equations for orthotropic plate bending, derived from combination variational and difference-differential procedures
05 p0741 A72-17144

Subgroup structure of symmetry group g of stress tensor for stored energy function in hyperelasticity
06 p0893 A72-17302

Fiber pull-out from elastic matrix, calculating shear stress and load distribution dependence on elastic properties and fiber length
06 p0897 A72-18152

Dog mesentery terminal venous microvessel distensibility characteristics from response to arterial and venous pressure changes

06 p0765 A72-18196

Elastic constants measurement using vibrating wire strain gages on diametrically loaded circular disk and ring specimens

06 p0818 A72-18325

Temperature and deformation velocity effects on elasticity and tensile strength of Mo and Nb alloys

06 p0833 A72-18636

Elastic systems nonlinear oscillations with moving inertial loads, noting standing waves superposition

06 p0901 A72-18706

Dual stress, strain and displacement formulations of linear finite element elasticity, showing Finzi stress function applicability

07 p1087 A72-18780

Limiting equilibrium of elastic half space with randomly oriented crack

07 p1092 A72-19780

Elastic equilibrium of infinite wedge with apical asymmetric notch, reducing to Hilbert problem for holomorphic vectors

07 p1093 A72-19976

Elasticity theory axisymmetric problem for hollow cone, analyzing stress-strain state and boundary value problem by asymptotic methods

07 p1093 A72-19980

Cold brittleness of transition metal alloys with bcc lattices, discussing elastic characteristics, packing defects energy, plastic deformation and rhodium admixture

07 p1018 A72-20143

Stressed state of infinite isotropic plate weakened by curvilinear hole with elastic plug, using asymptotic integration method

07 p1094 A72-20212

Maximum stress concentration in two dimensional elasticity theory for half plane and circle as function of contour distribution, using Cauchy-Buniakovskii inequality in Banach space

07 p1095 A72-20325

Heat treatment effect on elastic properties of steel clad material for devices in sulfuric acid, discussing structural changes and optimal conditions

07 p1020 A72-20415

Perturbation solution to nonlinear nonuniform torsion of thin walled open elastic beams with strain hardening dependent on torque-rotation behavior

07 p1096 A72-20431

Interatomic force model for elastic properties of alpha quartz and alkali halides generalized for specified structure under arbitrary pressure

07 p0980 A72-20519

Sphere unsteady motion in viscoelastic liquids, noting falling-ball technique use for elastic parameters determination

07 p0973 A72-20549

Elastic properties of bonded orthotropic layer plates, finding good agreement with fiberglass reinforced plastic laminates

07 p1097 A72-20596

Elasticity and potential theory axisymmetric problems solution for sphere and spherical cavity, constructing x-analytic functions for boundary surfaces

08 p1242 A72-20908

Torsional bending vibrations mode shapes of space frame with variable elastic and mass characteristics, determining eigenvalue error limits

08 p1205 A72-20957

Axisymmetric elasticity theory problems for stress-strain state of space with spherical incision, obtaining solutions with p-analytic functions

08 p1242 A72-20960

Dynamic programming application to computer algorithm construction for elasticity theory two dimensional problems, solving boundary value problem for elliptic differential equation

08 p1243 A72-21235

Stress concentration and elastohereditary values at curvilinear hole in fiberglass reinforced plastic plate under bending moment

08 p1243 A72-21237

Integral operators functions approximation for elasticity and materials aging equations, noting transcendental functions in solutions

08 p1243 A72-21239

Lattice type structures as discrete elasticity problem, determining potential of thin rods connecting rigid nodes pairs from equations of motion and constitutive equations

08 p1244 A72-21302

Tensile strength estimation for two dimensional composite with brittle matrix and randomly orientated discontinuous elastic fibrous reinforcement

08 p1244 A72-21324

Projective geometry method for elastic curve shape of equilibrium-state thin rod subject to end forces

08 p1209 A72-21365

Bending and torsion of thin isotropic rod with identical principal rigidities in bending, writing elastic curve equation in cylindrical coordinate system

08 p1209 A72-21367

Critical compressive stresses leading to instability of layer fastened to elastic half space

08 p1244 A72-21368

Uniqueness theorem for dynamic infinitesimal invariant theory of hereditary elasticity, defining conditions of continuity and positive determinability

08 p1246 A72-21708

Reinforcing fiber frame incurvation influence on elasticity and thermal expansion coefficients of composite material

08 p1194 A72-21754

Elasticity theory doubly periodic problem for unbounded anisotropic plate weakened by system of identical arbitrary holes with self balanced loads

08 p1246 A72-21807

Elasticity theory method for nonlinear stress-strain relationships in thin anisotropic shells, discussing fiberglass reinforced cylindrical shell

08 p1247 A72-21810

Heavy falling body elastic impact against circular plate center analyzed by Timoshenko type wave equation

08 p1247 A72-21814

Interaction between two noncoplanar parallel staggered elastic cracks with narrow spacing, calculating stress intensity required for crack propagation

09 p1397 A72-22250

German monograph on optimum principle for numerical representation of surfaces, discussing association with elasticity theory extremal requirements

09 p1340 A72-22319

German monograph on finite element method for elastic impact at half space, analyzing elasticity and inertia effects on energy absorption and contact time

09 p1397 A72-22338

Penny shaped interface crack between elastic layer and half space, calculating stress intensity factors and strain energy release rate for aluminum-epoxy combination

09 p1398 A72-22530

Potential equations and singularities methods comparison for two dimensional flow field cascades and stress distribution elasticity theories

09 p1260 A72-22627

Thermoelastic disturbance wave front propagation in elastic half space after thermal shock at surface

09 p1399 A72-22705

Axisymmetrically heated orthotropic multilayer cylindrical shell with shear sensitive couplings and elastic stiffener, investigating stability and critical force under compression

09 p1402 A72-22735

Micropolar elasticity plane problem singular solution based on stress equations and elastic potentials methods, discussing thermal stress concentration

09 p1402 A72-22743

Boundary value problems in micropolar theory of elasticity, obtaining displacement and rotation vectors from singular integral equations

09 p1402 A72-22745

Optimization of load-carrying elastic lattice structures designed on prescribed surface

09 p1402 A72-22746

Discrete elasticity concept based on analysis of material points, lines, surfaces or rigid bodies interconnected by hyperelastic continuous bodies

09 p1403 A72-22759

Crack propagation in two dimensional geometry with isotropic homogeneous and linearly elastic properties under in-plane tension loading

09 p1405 A72-22921

Book on tensor analysis and continuum mechanics covering strain, permutation and stress tensors, vector and tensor comparison, application to elasticity and shell theory, etc

09 p1406 A72-23000

Plane shock wave propagation in polytropic plastic body with elastic unloading properties, deriving closed form solution for time dependent stepwise decreasing load

09 p1353 A72-23554

Hartman-Olech theorem to prove asymptotic stability of mechanical system with nonlinear elastic characteristic, analyzing differential equations of motion

09 p1343 A72-23612

Gruneisen tensor relationship to elastic and thermal properties of anisotropic quartz fiber-phenolic composite

10 p1500 A72-24251

Macroscopic elastic constants of three dimensional multilaminar composites with anisotropic layers, assuming stress and displacement continuity

10 p1555 A72-24256

Plane and antiplane elasticity boundary value problems reduced to integral equations by dislocation layers, noting closed form solutions for half and whole space

10 p1557 A72-24561

Linear elastic fracture mechanics extension to fiber reinforced plastic composite laminates, noting dependence on homogeneous mode validity

[AIAA PAPER 72-384]

11 p1730 A72-25406

Elastic constants and bond stress distribution for discontinuous fiber-reinforced three dimensional composite subjected to uniaxial tension

[AIAA PAPER 72-397]

11 p1731 A72-25418

Asymmetric three layer beam design for elastic impact, proposing functional equation integration by computer method

11 p1732 A72-25531

Longitudinal and transverse vibrations and transient response of elastically coupled nonlinear mechanical system

11 p1732 A72-25534

Cylindrical panel natural vibrations, describing motion of base with dynamic elasticity equations

11 p1733 A72-25539

Linear contingency method for elasticity theory of anisotropic plane with elliptic hole, deriving boundary value problems solutions

11 p1733 A72-25543

Elastic constants of dilute Mo-Re alloys with bcc structure, determining randomly distributed point defects low concentration effects with T-matrix method

11 p1656 A72-25724

Be elastic constants at 25-300 C, using ultrasonic pulse technique

11 p1657 A72-25774

Elastic r-value variation in Ti sheet from direct measurement of width and thickness strains

11 p1659 A72-25895

Dynamical torsion theory of rods deduced from linear elasticity equations, using averaging technique

11 p1736 A72-25987

Control theory application to nonlinear elastic analysis of trusses, partitioning structure into statically determinate stages

11 p1736 A72-25989

Elasticity theory dynamic equations solutions concentrated near longitudinal or transverse wave beams propagating in inhomogeneous isotropic space

11 p1689 A72-26383

Speed and mechanical work measurements during knee bending and immediate or delayed leg extension exercise, showing muscle elastic potential energy utilization

11 p1587 A72-26615

Nonlocal elasticity theory from global equilibrium and second thermodynamics laws, deriving constitutive equations from Clausius-Duhem inequality and Gibbs thermodynamics

11 p1738 A72-26721

Constitutive equations for nonlocal theory of polar elastic dielectrics interaction with quasi-static electric field, using variational principle

11 p1738 A72-26723

Electrical and thermal conductivity, elastic properties and resistance to bending of porous tungsten in porosities region

11 p1665 A72-26868

Bending of unbounded plate coupled to elastic isotropic half space with vertical and horizontal springs, calculating contact stresses by double Fourier transforms

12 p1878 A72-27082

Symmetric discrete elastic conservative structural systems stability boundary estimation through reduction to linear equation recursive solution, using perturbation method

12 p1880 A72-27242

Crystal-morphology role in refraction of cold drawn polyethylene samples of varying lamellar thickness and density, relating elastic restoring force to crystal deformation

12 p1832 A72-27283

Stress boundary value problems for infinite wedges in linear elasticity theory solved by Mellin transforms

12 p1883 A72-27561

Elastic fields of dislocation loop in two phase material consisting of isotropic elastic half spaces

12 p1884 A72-27567

Added elastic load tests for thoracic elastance change effects on human response to carbon dioxide inhalation, using rebreathing technique

12 p1762 A72-27726

Nonresonant mode and nutation damping of rotational-vibrational motion of free solid body with elastic elements

12 p1846 A72-27968

Iterative solution existence for elastic equilibrium problem of thin plates and shells near boundary layer

12 p1886 A72-27997

Stress-strain state in pure bending for infinite elastic strip with circular central hole, using integral Fourier transforms

13 p2053 A72-28390

Stress calculation in inflexible overlapping cemented joint of orthotropic layers, taking into account joining geometry and elastic properties anisotropy

13 p1962 A72-28396

Singular moment stress homogeneous solutions of plane problem with semiinfinite cut in elasticity theory

13 p2056 A72-28773

Series representations of p-analytic functions in Legendre functions of first and second kind, applying to axisymmetric problems solution in elasticity theory

13 p2057 A72-29079

Mars and moon cores elastic properties inferred from hydrostatic equilibrium based on observed data for total mass, radius and moment of inertia

13 p2048 A72-29809

Axisymmetric geometry and load finite element structural analysis of isotropic elastic materials for parametric and optimization studies

13 p2062 A72-29875

Microinhomogeneous solid bodies elastic fields and effective moduli calculation method within framework of random field theory, using singular approximation

13 p2062 A72-29884

Two dimensional boundary value problems of elasticity for simply connected noncanonical domains, using small parameter method

13 p2062 A72-29952

Minimum weight elastic structure designs under dynamic loads with constraints on stress displacements and natural oscillation frequencies

13 p2062 A72-30009

Shock waves internal structure in gas of elastic spheres, solving nonlinear Boltzmann equation

13 p1944 A72-30029

Modified finite element method application to plane elastic area elementary triangles strained and stressed state description by polynomial algebraic expressions and harmonic functions

14 p2163 A72-30188

Elastic effects in metal hardness testing with blunt indenter, considering indentation in rigid plastic manner

14 p2113 A72-30268

Elastic crack tip stress fields, considering weight function

15 p2322 A72-31347

Nonlinear Cosserat continuum theory of elasticity, discussing kinematics and stressed state as functions of angular velocity, acceleration, volume forces and moments

15 p2274 A72-31476

Three dimensional elasticity boundary value problems solution via multidimensional Fourier transforms, applying to semiinfinite solid and hollow cones

15 p2324 A72-31481

Dispersed particle shape effect on elastic behavior of magnesium oxide composites at low graphite concentrations

15 p2260 A72-31585

Elastic properties of media with cracks, discussing elastic anisotropy and crack distribution

15 p2327 A72-31733

First boundary value problem solution for circle in static elasticity theory using Fredholm equation and source-sink method

15 p2328 A72-31849

Papers on elasticity and thermoelasticity covering contact problems, stress effects on elastic wave propagation velocity, self excited thermal waves, diffraction, nonlinear thermoelasticity, etc

15 p2329 A72-32280

Uniqueness, existence and smoothness theorems for elliptic dynamic boundary problems in elasticity theory

15 p2329 A72-32286

Plasticity, elastic relaxation and stress-strain relation characterization for Schofield-Scott Blair media, using nonequilibrium thermodynamics method

15 p2331 A72-32482

Carbon and graphite fiber reinforced composites elastic constants derived from ultrasonic immersion technique

15 p2261 A72-32503

Large amplitude deflections and induced stresses in uniformly pressure loaded circular plate on elastic foundation, using von Karman coupled nonlinear partial differential equations

15 p2331 A72-32558

Static boundary value problem of axisymmetric elasticity for elastic isotropic media with small energy contribution to potential due to moment effects

16 p2464 A72-32934

Completeness proof for linear elasticity theory set of three harmonic functions based on theory of linear differential equations with constant coefficients

16 p2466 A72-33018

Interaction forces between two dislocations in infinite weakly anisotropic media with bcc crystal lattice elastic properties

16 p2424 A72-33146

Inverse transformations in mathematical models of elasticity and plasticity problems reducible to biharmonic equation

16 p2468 A72-33163

Nb-Mo alloys elastic constants anomalous temperature dependence, proposing phase changes role and relationship to neutron diffraction and specific heat

16 p2405 A72-33167

Elastic-plastic-viscous model for creep analysis of rheo-mobile materials, taking into account cracks and other defects

16 p2412 A72-34116

Variational methods for dispersion relations and elastic properties of composite materials.

[ASME PAPER 71-APMW-21] 17 p2623 A72-34302

Russian book on metal fatigue and inelasticity covering structural inhomogeneities, static and dynamic loading, failure mechanisms, deformation, temperature effects and test methods

17 p2566 A72-34649

On the introduction of potential functions in linear elasticity

17 p2627 A72-34773

Dissipative periodic process theory for application to elasticity and distributed parameter and hereditary systems defined by partial and functional differential equations

17 p2575 A72-34867

Elastic behavior of multilayered bidirectional composites.

17 p2632 A72-35234

Elastic vibrations in roller bearings. I - The rotating mass is balanced with respect to its own rotation axis

17 p2561 A72-35894

Ultrasonic tests for incipient fatigue, hardness and elastic constants-tensile strength relationship in metals

18 p2690 A72-36125

Ultrasonic velocity measurement of elastic constants of Al-Al3Ni unidirectionally solidified eutectic.

18 p2701 A72-36591

On axisymmetric vibration in a transversely isotropic finite cylindrical shell acted upon by a magnetic field.

18 p2711 A72-36755

Hypo-elastic dielectrics. I - Constitutive equations. II - Birefringence in simple shear.

18 p2720 A72-37043

A sandwiched layer of dissimilar material weakened by crack-like imperfections.

18 p2737 A72-37058

Wave propagation in half plane consisting of two joined elastic quarter planes under in-plane disturbances normal to free surface, obtaining stresses at interface

18 p2738 A72-37069

Infinite plate with a supported reinforced circular hole.

18 p2738 A72-37071

A non-linear integral-type theory of inelasticity for transversely isotropic materials.

18 p2738 A72-37075

Nonstationary parametric response of a nonlinear column.

18 p2738 A72-37079

On strain energy and constitutive relations for alkali metals.

18 p2703 A72-37087

Experimental determination of viscoelastic characteristics

18 p2740 A72-37211

Point-loaded discs and blocks applicable to tensile testing of brittle materials.

19 p2870 A72-37223

An initial value method for dual integral equations.

19 p2824 A72-37413

Linear physical and nonlinear geometric formulation of design problem for prestressed rubber parts based on elasticity theory in terms of assembly requirements

19 p2871 A72-37428

Thermal expansion at elevated temperatures. III - A hemispherical laminar composite of pyrolytic graphite, silicon carbide and its constituents between 300 and 800 K.

19 p2822 A72-37463

Periodic integral convolution equations in elasticity theory and mathematical physics, demonstrating solution existence

19 p2872 A72-37561

Elasticity theory three-dimensional axisymmetric problem reduction to two dimensional analytic function boundary value problem

19 p2872 A72-37563

German monograph - Computation of the stress condition in homogeneous anisotropic discs with the aid of an integral equation method

19 p2873 A72-37660

Mixed boundary value problem in the theory of elasticity for a half-space with circular lines of separation between boundary conditions

19 p2876 A72-38152

Method of sources for solving axisymmetrical problems in the theory of elasticity

19 p2877 A72-38202

Solution manifolds for dynamic elasticity equations corresponding to the action of a concentrated load

19 p2878 A72-38213

Elastic constants of niobium-molybdenum alloys in the temperature range -190 to +100 C.

19 p2821 A72-38591

Energy propagation in a Cauchy elastic material.

19 p2878 A72-38718

Large elastic deformations of an incompressible material heteroresistant to tensile and compressive strains

20 p2978 A72-39021

Tensile and compressive flow strength and work hardening behavior in maraging steels, attributing strength differential to nonlinear elastic interactions between interstitials and dislocations

20 p2979 A72-39467

Elasticity of some mantle crystal structures. I - Pleonaste and hercynite spinel.

20 p2917 A72-39478

Beams on bilinear elastic foundations.

20 p2980 A72-39692

Thin elastic rings subjected to radial load sets

[ASME PAPER 71-WA/DE-2] 20 p2980 A72-39812

Elastic analysis for a radial crack in a circular ring.

20 p2981 A72-39959

Elasticity theory axisymmetric problem for hollow cones analyzing stress-strain state and boundary value problem by asymptotic methods

20 p2982 A72-40036

Stress induced martensitic transformation relationship to shape memory effect compared with superelasticity, transformation plasticity and reversible linear change

21 p3065 A72-40091

Electrical modeling of the plane problem of elasticity theory in terms of stresses

21 p3116 A72-40164

Singular moment stresses in homogeneous solutions of plane problem with semiinfinite cut within elasticity theory

21 p3116 A72-40274

Another boundary value problem of the linear theory of elasticity in regions with a fractionally-grained boundary

21 p3119 A72-41091

Elastic isotropic material mechanical and thermal constitutive equations restrictions investigation to ensure local stability under perturbations of deformation gradient and temperature field

21 p3120 A72-41203

Six dimensional vector space of stresses in elastic piecewise linear material divided into separate regions having different linear stress-strain relation

21 p3122 A72-41345

Method of eigenfunctions in problems of thermoelasticity and electroelasticity

21 p3122 A72-41348

Constitutive equations and boundary value problems in discrete theory of elasticity, noting linear systems of prismatic rods and lattice type shells

21 p3123 A72-41390

Stresses in bonded materials with a crack perpendicular to the interface.

21 p3124 A72-41396

The stress intensity factors of a radial crack in a finite rotating elastic disc.

21 p3124 A72-41397

On the plastic behaviour of time dependent materials - Theoretical and experimental investigation.

21 p3124 A72-41504

Non-linear elastic constitutive equations.

21 p3125 A72-41514

Experimental investigation of the elastic characteristics of composite bearings in turbine machinery for the purpose of increasing their efficiency and reliability during nonlinear vibrations of the rotor

22 p3181 A72-41860

Quasi-regularity of infinite systems in problems of two-dimensional elasticity theory for doubly connected domains

22 p3233 A72-42063

Integral equations and transformations in application to problems of elasticity theory

22 p3236 A72-42625

Minimum weight elastic structure designs under dynamic loads with nonlinear constraints on stress displacements and natural oscillation frequencies

22 p3236 A72-42737

The dynamic viscoelastic properties of some non-crystalline metals.

22 p3214 A72-42792

Effects of non-homogeneity on the stresses in a rotating cylinder.

22 p3240 A72-42877

Stress-strain state induced by local physicochemical transformations in a layer

22 p3242 A72-43164

Plane problem of elasticity theory for known normal and tangential stress tensor components at boundary of simply connected region, calculating stress concentration

23 p3344 A72-43353

Edge and screw dislocations induced stress fields in isotropic medium, using Kauderer nonlinear elasticity theory

23 p3345 A72-43622

Construction of the solution of a two-dimensional mixed boundary value problem for an arbitrary doubly connected region

23 p3345 A72-43629

Bearing supports elasticity effect on pendulum vibration of rigid rotating shaft with disk, noting vibrational frequencies relation to resonant frequencies

23 p3293 A72-43668

Elastic stiffness of AT-2 and AT-3 titanium alloys and their welds at high and low temperatures

23 p3302 A72-43966

A new variational principle for finite elastic displacements.

23 p3350 A72-44047

- On the solution of plane, orthotropic elasticity problems by an integral method. [ASME PAPER 72-APM-BB] 23 p3350 A72-44056
- Stability and vibration of transversely isotropic beams under initial stress. 23 p3350 A72-44057
- The elastic analysis of the part-circular surface flow problem by the alternating method. 23 p3353 A72-44232
- Numerical evaluation of elastic stress intensity factors by the boundary-integral equation method. 23 p3353 A72-44233
- Nonlinear elastic torsion analysis for aerospace materials. 23 p3354 A72-44251
- Zeta core for sandwich construction with rigidity-to-weight ratio comparable to honeycomb core, discussing elastic properties and cost. 23 p3355 A72-44495
- The calculation of elastic tanks partially filled with liquids for prediction of the Pogo effect. 24 p3392 A72-45152
- Boron and carbon contents effect on elastic properties strength and ductility of electron beam melted Mo-B alloys. 24 p3414 A72-45381

ELASTIC SCATTERING

- Laser radar application to air pollution measurement, discussing techniques and instrumentation utilizing elastic, Raman and fluorescence scattering [AIAA PAPER 71-1056] 01 p0028 A72-10527
- Electrical conductivities dependence on assumed values of elastic collision cross sections of electrons with neutral and charged particles in low temperature plasma. 01 p0110 A72-11205
- Low energy phase shifts for elastic scattering of electrons by Li and Na. 03 p0391 A72-13745
- Radiation damage in MgO, ZnO and magnesium difluoride, considering energy dependence and roles of radiolysis and elastic collisions. 03 p0404 A72-14088
- Elastic scattering without dissociation of nitrogen molecular ions by noble gas targets in 0.3-3 keV range, analyzing energy loss. 03 p0393 A72-14357
- Heuristic theory of positron-helium elastic scattering phase shifts and cross sections. 03 p0393 A72-14399
- Proton elastic scattering by deuterons in backward hemisphere, examining normal and center of mass scattering angle and differential cross section. 04 p0551 A72-14437
- Random method to solve basic rarefied gas/Boltzmann equation, applying to elastic collisions. 04 p0551 A72-14518
- Intermolecular potentials determination by inverting phase shifts obtained from high resolution measurements of protons differential elastic scattering by rare gas atoms. 04 p0552 A72-14577
- Measuring apparatus for differential cross sections of charge transfer and elastic scattering of atomic projectiles by gas targets. 04 p0553 A72-15539
- Small distance range anisotropic intermolecular interaction potentials for carbon dioxide and nitrogen oxide from beams elastic scattering data. 06 p0852 A72-17983
- Quasi-elastic scattering differential cross section for nonpolarized IR radiation in electron plasma of semiconductors in strong elastic fields. 09 p1366 A72-22210
- Elastic singlet p wave phase shift calculation for electron scattering by H atom and He cation, using time dependent Hartree-Fock perturbation theory. 09 p1355 A72-22786
- Va crystal lattice interatomic bonds and elastic and inelastic X ray scattering intensity calculation. 09 p1329 A72-23042
- Low energy elastic scattering cross section measurements for helium-nitrogen system, using two collimated aerodynamically intensified crossed molecular beams. 10 p1515 A72-24338
- Reduced mass and asymmetry differences effects on elastic collision integrals and thermal diffusion factors for isotopic hydrogen molecules. 10 p1515 A72-24340
- Elastic, inelastic and reactive scattering experiments with low, high and intermediate energy molecular beams. 11 p1691 A72-25675
- Elastic and one-phonon inelastic scattering of monoenergetic He atoms from cleaved LiF crystal surface. 15 p2281 A72-31862
- Redistribution of resonance radiation. 1 - The effect of collisions. 17 p2605 A72-34534
- Absolute differential cross sections of electrons elastically scattered on neon atom. 18 p2713 A72-36952

- Analysis of pion-helium scattering for the pion charge form factor. 19 p2837 A72-37922
- Elastic scattering of 600-MeV protons from H, D, He-3, and He-4. 19 p2837 A72-38025
- Nonelastic interactions of nucleons and pi mesons with complex nuclei at energies below 3 GeV. 19 p2837 A72-38027
- Interpretation of experimental differential elastic scattering cross section for H⁺/+ Ne. 20 p2956 A72-39721
- Application of the Harris-Nesbet method to a dipole coupling potential. 21 p3083 A72-40103
- Cross sections calculations for electron-oxygen scattering using the polarized orbital close coupling theory. 21 p3087 A72-40472
- Angular distribution of electrons elastically scattered from N₂. 21 p3088 A72-40777
- Elastic electron-neutral interaction in argon in the vicinity of the Ramsauer minimum. 22 p3211 A72-42642
- Light scattering studies in amorphous media. 22 p3206 A72-42798
- Coherent/incoherent elastic/inelastic neutron scattering in amorphous solids, presenting neutron intensity and correlation functions. 22 p3206 A72-42799
- Multifireball theory of particle production in inelastic high energy interactions, using elastic scattering amplitude for inelastic processes model. 23 p3316 A72-44412
- Electron scattering by molecules with and without vibrational excitation. IV - Elastic scattering and excitation of the first vibrational level for N₂ and CO at 20 eV. 24 p3427 A72-45304
- Electron scattering by molecules with and without vibrational excitation. V - Elastic scattering and non-resonant vibrational excitation of N₂ at 30-83 eV. 24 p3427 A72-45305

ELASTIC SHEETS

- Elastic unbounded homogeneous layer separation from half plane under normal load pressures, determining contact area with base for elastic moduli relationships. 08 p1243 A72-21233
- Longitudinal and transverse waves propagation and decay in elastic membranes with allowance for coupling effects, using Hadamard method. 16 p2465 A72-32983
- Stress concentration in elastic layer with circular slot analyzed by reducing mixed boundary value problem to initial condition problem via invariant imbedding. 16 p2471 A72-33827

ELASTIC SHELLS

- Differential equations derived for elastic-plastic behavior of rotationally symmetric shells, approximating in finite difference forms and solved by elimination method. 01 p0138 A72-10394
- Wave propagation in thin elastic shells by similar formation of shell and nonlinear elasticity theories equations. 01 p0142 A72-11197
- Temperature fields and stresses in thin elastic non-ferromagnetic electrically conducting cylindrical shells heated by induction determined from heat source distribution and thin shell theory relations. 02 p0290 A72-11631
- Acoustic field hf asymptotic characteristics after sound transmission through elastic shell, using integro-differential equations system. 03 p0388 A72-12917
- Homogeneous isotropic thin elastic shells under forces along edge and with faces free of tractions, deriving refined interior equilibrium equations. 03 p0447 A72-13882
- First approximation of linear elastic shell theory using split constitutive equation of stress tensor. 03 p0454 A72-14341
- Mathematical models of elastic shells and rods, discussing virtual work, operator classifications, deformations and constitutive equations. 03 p0454 A72-14344
- Pressure field calculations for random vibrations in wide class of elastic shells containing acoustic medium, discussing turbulent boundary layer-caused pulsations. 04 p0586 A72-15010
- Thin walled elastic axisymmetric fluid filled tanks under longitudinal vibrations, determining dynamic characteristics. 04 p0586 A72-15011
- Iteration method error estimates for thin elastic shell basic stressed state and simple fringe effect relation to boundary stressed state. 04 p0586 A72-15012
- Canonical form for boundary conditions of thin elastic shells with oscillating loads applied on edges. 04 p0587 A72-15013

Nonlinear elastoplastic deformations of flexible shells of revolution, calculating stress concentration at circular hole in spherical shell. 04 p0588 A72-15049

Critical load limit and stability of elastic isotropic and orthotropic cylindrical shells, using net-point method for end conditions. 04 p0588 A72-15053

Radiated pressure field in unbounded acoustic medium produced by pulsed elastic cylindrical circular shell. 04 p0590 A72-15188

Stress and strain approximate analysis for thin elastic shells by rational derivation of two dimensional differential and constitutive equations [AD-745612]. 04 p0592 A72-15506

Shell bending and Timoshenko-type theory to solve stresses of semiinfinite elastic circular cylindrical shells produced by radial pressure pulses [ASME PAPER 71-WA/APM-16]. 05 p0733 A72-15964

Stress state of variable thickness long elastic shallow shell in bending and torsion, applying equations to large turbine blades. 05 p0735 A72-15986

Thin elastic shell postbuckling behavior from asymptotic integration solution for differential equations, permitting dynamic effect modeling. 05 p0738 A72-16425

Equilibrium conditions of closed elastic spherical shell under uniform nearly critical compression loads, determining shell deformation in Hilbert spaces. 05 p0739 A72-16587

Flutter of thin elastic circular cylindrical fluid filled shells, presenting potential flow theory for coupled hydrodynamic forces. 06 p0894 A72-17763

Thin walled elastic isotropic shallow shell with thermal boundary conditions, obtaining thermoelastic solution in series form. 06 p0899 A72-18657

Shallow elastic shell under periodic distributed torque loading, investigating static stability enhancement through nonlinear boundary value problem periodic solutions. 06 p0900 A72-18697

Nonlinear resonance oscillations of flexible rod and elastic cylindrical shell under potential and nonpotential forces, investigating motion instability. 06 p0900 A72-18704

Optimal rigid-plastic limit load analysis of spherical shells under nonsymmetrical loadings, using SUMT and Rosenbrock method. 07 p1087 A72-18791

Oscillations and acoustic emission by interacting elastic shells in connecting medium, using quadratures with Green function. 07 p1034 A72-18922

Dynamic behavior of stiffened hollow viscoelastic cylinder and elastic shell-contained sphere, taking into account compressibility and internal pressure. 07 p1090 A72-19751

Stress-strain state of unclamped thin elastic zero curvature shell under three component surface load and tangential boundary forces. 07 p1095 A72-20313

Asymptotic eigenvalue density estimates for edge-hinged thin elastic rectangular shell, determining shell stability linear equation solution conditions. 07 p1095 A72-20324

Wave propagation in hollow elastic/viscoplastic sphere under impact load, assuming Mises condition, isotropic hardening and incompressibility. 07 p1096 A72-20429

Axial impact of semiinfinite elastic cylindrical shell filled with inviscid compressible fluid, obtaining equations of motion. 08 p1149 A72-21166

Uniaxially stressed elastic/soft shells with fold formation during compressive strain, formulating equilibrium and boundary conditions for uniaxial region. 08 p1247 A72-21812

Orthotropic circular cylindrical elastic shell vibration mode shape analysis by Vlasov equations, using asymptotic method. 08 p1247 A72-21813

Variable wall thickness influence on axisymmetric vibrations frequencies and reduced masses of cylindrical elastic shell filled with ideal incompressible fluid. 08 p1247 A72-21815

Elastic shell geometry and rigidity effects on critical load in pure bending within structurally orthotropic theory, taking into account reinforcing rib eccentricity. 08 p1247 A72-21816

Normal axial impact of thin liquid filled elastic cylindrical shell with rigid bottom on compressible fluid half space surface. 09 p1350 A72-22207

Stress-strain state produced by asymmetric physical and thermal loads in thin orthotropic viscoelastic shells of revolution. 09 p1399 A72-22702

Axisymmetric deformation of hollow elongated elastic ellipsoid, using Lamé equilibrium equations. 09 p1400 A72-22708

Thermal insulations in form of thin shells of revolution with rigid external and elastic internal layers resting on rigid core
09 p1400 A72-22713

Nonuniformly heated infinite elastic cylindrical shell stability under axial compression loads
09 p1402 A72-22734

Torsional behavior of twisted elastic orthotropic cylindrical shells after stability loss, using energy method
09 p1404 A72-22771

Rotationally symmetric stress and strain distribution in anisotropic elastic shells of revolution
[AD-745622] 09 p1405 A72-22944

Nonlinear random radial vibration of elastic cylindrical shell under load, using stochastic linearization and correlation analysis
09 p1409 A72-23606

Natural axisymmetric vibration of thin elastic shell of revolution, deriving eigenvalues convergence to spectrum lower bound by asymptotic method
10 p1557 A72-24429

Direct numerical integration scheme for viscoelastoplastic response of isotropic axisymmetric shells under impulsive loads
[AIAA PAPER 72-400] 11 p1731 A72-25421

Asymmetrically stiffened elastic cylindrical shells under axial compression, calculating critical loads for various end conditions
11 p1733 A72-25541

Hollow elastic momentless spherical shell translatory displacements in compressible fluid under nonstationary spherical wave
12 p1880 A72-27234

Elastic truncated thin conical shell response to dynamically applied axial force from numerical solution of nonlinear equations
12 p1881 A72-27244

Structural effects of meridian imperfections in symmetrically loaded elastic thin shell of revolution
12 p1881 A72-27255

Linearized elastic equilibrium stability equations for orthotropic cylindrical shell under critical axial compression
12 p1885 A72-27970

Acoustic pressure wave effect on motion of elastic conical shell fastened in rigid screen, using Timoshenko theory
13 p2055 A72-28772

Oscillations and acoustic emission by interacting elastic shells in connecting medium, using quadratures with Green function
13 p2004 A72-29208

Inhomogeneous viscoelastic shell stability, determining correlation functions for first approximations of sag, stress functions and critical time alterations
13 p2062 A72-29886

Dynamic behavior of thin walled semiinfinite elastic cylindrical shell with liquid under axial impact loads
13 p1943 A72-30008

Stress analysis of thick walled hollow viscoelastic circular cylinder enclosed in elastic shell and subjected to nonlinear creep conditions, noting temperature effects
14 p2165 A72-30439

Average stress and strain across thickness of liquid filled cylindrical elastic thin walled shell with rigid bottom under axial impact loads
14 p2166 A72-30698

Distributed parameter system approximation by system with finite freedom degrees number, solving stability and vibration of elastic shells for eigenvalue densening case
15 p2327 A72-31739

Elastic shell initial stress effects on dynamic response in all free vibration modes, considering transverse shear and normal strains
15 p2328 A72-32021

Thin walled elastic shells stability under finite deformations, deriving equilibrium conditions and constitutive equations
15 p2330 A72-32464

Preloaded thin walled open section elastic column dynamic stability under free longitudinal vibrations, deriving criterion for flexural and torsional vibrations nonlinear coupling
15 p2332 A72-32560

Natural frequency distribution theory of thin elastic shells under random vibrations in wideband field
15 p2332 A72-32677

Thin elastic isotropic plates and shells thickness variation for rigidity functional stationary value, reducing problem to stress-strain state equations simultaneous solution
15 p2333 A72-32688

Longitudinal, transverse and bending waves propagation in elastic shells, using Hadamard method within linear shell theory
16 p2465 A72-32982

Perturbation scheme for branching analysis of postbuckling behavior in elastic spherical shells
16 p2465 A72-33001

Linear theory for spirally sinusoidal stress distributions in elastic helicoidal shells applied to pure bending problem
16 p2465 A72-33003

Matrix progression method analysis of free vibration problem for cantilever thin circular cylindrical elastic shells, using Flugge equations
16 p2475 A72-34173

Analysis of wave propagation in elastic cylindrical shells by the perturbation method.
17 p2623 A72-34307

Contact pressure between an elastic spherical shell and a rigid plate.
[ASME PAPER 72-APM-31] 17 p2628 A72-34788

Numerical solution of problems of large deformations for spherical elastic shells
17 p2634 A72-35421

Elastic momentless shell completely filled with ideal incompressible liquid, detailing small steady free vibrations
18 p2681 A72-36667

Radial vibration of a composite cylindrical shell subjected to a magnetic field.
18 p2711 A72-36753

A proof of the accuracy of a set of simplified buckling equations for circular cylindrical elastic shells.
18 p2739 A72-37091

Equilibrium conditions of closed elastic spherical shell under uniform nearly critical compression loads, determining shell deformation in Hilbert spaces
19 p2872 A72-37558

Complex transforms method for Timoshenko theory of elastic shells, deriving transverse shear strain equations for shallow shells
19 p2876 A72-38154

Zero-moment reinforced axisymmetric shells
19 p2876 A72-38155

Heat-conduction equations for multilayer shells
19 p2881 A72-38158

Dispersion of flexural waves in circular cylindrical shells.
20 p2982 A72-39975

Stresses in a circular cylindrical shell having two circular cutouts.
20 p2982 A72-40063

Finite element large deflection analysis of elastic-plastic shells of revolution subjected to axisymmetric loading.
20 p2982 A72-40064

Plane acoustic pressure wave effect on motion of thin elastic truncated conical shell fastened in rigid screen, using Timoshenko theory
21 p3116 A72-40263

Differential equation reduction via coordinate transformation to algebraic form for problems characterization in elastic shell Cosserat surface theory
21 p3119 A72-41103

Buckling of inelastic cylindrical shells under axial impact.
21 p3124 A72-41507

Influence of elastic constants on the stability margins and weight characteristics of fiberglass-reinforced shells
22 p3196 A72-41864

Symmetry transformations for thin elastic shells.
22 p3234 A72-42398

Dynamic behavior of thin walled semiinfinite elastic cylindrical shell with compressible liquid under axial impact loads
22 p3167 A72-42736

Rotatory vibration of a thick spherical shell of isotropic non-homogeneous elastic material.
22 p3240 A72-42880

Torsional vibration of an orthotropic cylindrical shell.
22 p3240 A72-42881

Dynamic loading of a fluid-filled spherical shell.
22 p3240 A72-42891

First order constraints in three dimensional continuous elastic fibrous media and thin shells, presenting equilibrium equations
23 p3349 A72-43825

Theory of thin elastic shells applied to pipe bends subjected to bending and internal pressure.
24 p3456 A72-44795

Stress state of variable thickness long elastic shallow shell in bending and torsion, applying equations to large turbine blades
24 p3460 A72-45728

ELASTIC STABILITY
U DAMPING
ELASTIC STRENGTH
U PROPORTIONAL LIMIT
ELASTIC SYSTEMS

Whirling elastic shaft-disk system, investigating interaction effects of external and linear/nonlinear material damping, elastic restoring forces and inertia forces
01 p0101 A72-10036

Axial and radial displacements determination in rotor center of gravity for gyroscope with elastic suspension
03 p0360 A72-13560

Multimass multiply branched multistage elastic systems natural frequencies and oscillation modes, presenting algorithm and iterative calculation procedure
03 p0449 A72-13913

Magnetic damping comparison with internal viscous damping effect on circulatory elastic system equilibrium stability
05 p0689 A72-16061

Two-mirror optical system to study energy dissipation in elastic systems subjected to cyclic straining and vibrations
06 p0819 A72-18649

Vibration simulation of elastohysteretic systems on analog computers using photocurrent-voltage relationship of polycrystalline photoresistors
06 p0900 A72-18674

Nonlinear elastic systems with distributed parameters, obtaining single frequency mode random oscillations solution of boundary value problem by asymptotic method and Markov process
06 p0850 A72-18700

Sufficient conditions for asymptotic stability and instability for elastic systems with dissipation, using Liapunov direct method
07 p1026 A72-18809

Linear mechanical elastic systems divergence with infinitely large frequency onset, noting discrete cantilever beam under nonconservative forces
[ASME PAPER 71-APM-DDD] 10 p1555 A72-24189

Varied states superimposed on finite elements in discrete elasticity, noting small oscillations superposition on arbitrary motion of elastic system
12 p1845 A72-27393

Equilibrium state stability in elastic conservative system, relating system postbuckling behavior to critical branching point
13 p2054 A72-28478

Structural approach to elastic stability in buckling problems, simplifying deformation concepts and loading condition definition
13 p2054 A72-28479

Canonical equations of motion for continuous elastic system, predicting critical buckling loads for unbounded deformation
13 p2054 A72-28482

Complex elastic systems natural frequencies computation from measured dynamic response to harmonic excitation, applying to helicopter and transport aircraft
14 p2164 A72-30326

Dynamic stability of elastic systems under broadband random excitation, presenting solution for straight rod under axial pulsating forces via perturbation method
15 p2274 A72-31460

The elastic stability of two-parameter nonconservative systems.
[ASME PAPER 72-APM-43] 17 p2627 A72-34782

Coordinate transformation for perturbation analysis of elastic structural system imperfections influence on elastic buckling
18 p2732 A72-36079

Higher vibration modes by matrix iteration.
18 p2736 A72-36772

Elastically supported dry two degrees of freedom tuned gyroscopes, analyzing open-loop transfer function for characteristic errors
19 p2794 A72-37280

The effects of discrete masses and elastic supports on continuous beam natural frequencies.
21 p3116 A72-40335

ELASTIC WAVES
NT AERODYNAMIC NOISE
NT AIRCRAFT NOISE
NT BAROCLINIC WAVES
NT CAPILLARY WAVES
NT COHERENT ACOUSTIC RADIATION
NT COMPRESSION WAVES
NT DETONATION WAVES
NT DILATATIONAL WAVES
NT ELECTROSTATIC WAVES
NT ENGINE NOISE
NT GRAVITY WAVES
NT IONIC WAVES
NT JET AIRCRAFT NOISE
NT LAMB WAVES
NT LOVE WAVES
NT MACH CONES
NT MAGNETOACOUSTIC WAVES
NT MAGNETOELASTIC WAVES
NT MAGNETOHYDRODYNAMIC STABILITY
NT MAGNETOHYDRODYNAMIC WAVES
NT MICROSEISMS
NT NOISE [SOUND]
NT NORMAL SHOCK WAVES
NT OBLIQUE SHOCK WAVES
NT P WAVES
NT PHONON BEAMS
NT PHONONS
NT PLASMA WAVES
NT POLARIZED ELASTIC WAVES
NT RAYLEIGH WAVES
NT RIEMANN WAVES
NT ROCKET ENGINE NOISE
NT S WAVES
NT SEISMIC WAVES
NT SHOCK WAVES
NT SONIC BOOMS
NT SOUND WAVES

- NT STRESS WAVES
 NT THERMAL NOISE
 NT TOLLMEIN-SCHLICHTING WAVES
 NT ULTRASONIC RADIATION
- Finite element method for determining transient response of box-type structure to traveling sonic pressure wave
 01 p0136 A72-10219
- Initial strains effect on propagation rate of elastic waves, applying finite deformation theory
 01 p0138 A72-10581
- One dimensional elastoplastic wave propagation symposia review emphasizing elastoviscoplastic media, jet penetration into half space and polymer tests by transverse impact
 02 p0290 A72-11628
- Flames vibratory propagation appearance conditions at constant volume, considering expansion and compression waves amplitude
 03 p0456 A72-13794
- Elastic wave velocities and polarization in planes of cubic crystals, plotting velocity curves
 03 p0402 A72-13861
- Kirchhoff diffraction theory of scalar and electromagnetic waves application to elastic media, discussing Huygens principle, elastic waves tensor potential and Fresnel and Fraunhofer diffraction
 04 p0548 A72-14740
- Forced vibrations of elastic plate with infinite series of identical circular holes, discussing elastic wave diffraction and stresses at/near holes
 04 p0587 A72-15017
- First and second order moduli of elasticity for finitely deformed elastic materials, deriving acceleration waves propagation condition and growth equation
 05 p0735 A72-16028
- Tensor calculus theorem application to elastic isotropic materials finite deformation, considering acceleration waves propagation and moduli of elasticity
 05 p0735 A72-16029
- Monograph on head-on collision of combustion wave with shock wave and rarefaction wave covering gas dynamics, interactions, reflection process, etc
 05 p0746 A72-16046
- Laser schlieren measurement of density gradients in laminar hypersonic boundary layer interacting with corner expansion wave in shock tunnel
 [AIAA PAPER 72-75] 05 p0606 A72-16879
- Cracks interactions with transversal and surface elastic waves, relating crack propagation threshold conditions to critical pulse duration
 06 p0893 A72-17419
- Free flexural wave propagation in doubly periodic structures, obtaining natural frequencies
 06 p0894 A72-17764
- Water vapor condensation in centered rarefaction wave arising in supersonic flow around apex of obtuse angle
 06 p0799 A72-17911
- Crab Nebula and Vela pulsar constant elastic energy density contours, discussing micro and macroquakes
 06 p0886 A72-18095
- Elastic wave fields reconstruction from measurements over transducer array, stressing ultrasonic imaging system development
 07 p0986 A72-19647
- Thermoelastic waves diffraction steady state problems in multiply connected cylindrical and spherical surfaces, deriving scalar wave equations
 07 p1094 A72-19986
- Longitudinal plane harmonic elastic wave scattering and stress concentration at rough circular hole boundary in thin isotropic plate
 08 p1243 A72-21230
- Longitudinal elastic wave propagation along composite bar with conical sections and interface discontinuities in material properties, solving multiple reflection by finite difference method
 08 p1245 A72-21606
- Spherical wave functions in analysis of infinite systems of algebraic equations describing elastic wave diffraction in sequence of spherical cavities
 08 p1246 A72-21706
- Dynamic contact problems of die or bandage on elastic layer surface or cylinder, analyzing vibrationally induced elastic waves
 10 p1558 A72-24779
- Thermoelastic waves propagation in homogeneous isotropic medium under external generic forces and with distributed heat sources
 11 p1734 A72-25676
- Acoustic and elastic HF waves propagation in nonuniform cylindrical waveguides, deriving asymptotic approximate solutions
 11 p1686 A72-25726
- Schlieren photographic investigation of shock wave propagation over narrow slit, noting cylindrical expansion wave origin at slit upstream edge
 11 p1616 A72-25920
- Unsteady laminar wall boundary layers formation within finite expansion or compression waves in tube with gas at rest
 11 p1616 A72-25981
- Russian papers on mathematical problems of wave propagation and diffraction theory, covering elastic and short waves and point sources
 11 p1688 A72-26377
- Cylindrical elastic wave diffraction on semiinfinite screen, describing motion with displacement vector consistent with Lamé equation
 11 p1688 A72-26380
- Longitudinal propagation of elastic disturbance in conical rod, discussing Young modulus, material density and periodic and impulsive stress
 11 p1737 A72-26589
- Elastic wave propagation and energy scattering in materials reinforced by inextensible fibers
 12 p1881 A72-27252
- Longitudinal elastic impact wave propagation along branched thin rods, using Timoshenko theory
 12 p1881 A72-27256
- Antisymmetry principle for solving equation of elastic surface wave caused by waveguide
 12 p1845 A72-27392
- Acceleration waves propagation in elastic-plastic strain hardening rate independent solids, obtaining solution for discontinuity change in strength in homogeneously prestressed medium
 12 p1846 A72-27729
- Acoustic pressure wave effect on motion of elastic conical shell fastened in rigid screen, using Timoshenko theory
 13 p2055 A72-28772
- Torsional waves far-field structure in infinite elastic rod of elliptical cross section, using perturbation method
 13 p2057 A72-29004
- Thermomechanical interactions between elastic waves and nonstationary temperature fields in solid continua, considering coupled and uncoupled theories
 13 p2064 A72-29093
- Harmonic elastic wave propagation in composites with periodic structures by variational methods developed from crystal lattice studies
 13 p2060 A72-29696
- Elastic waves propagation in randomly inhomogeneous fiber reinforced or layered composites from perturbation methodology for electron and vibrational waves in disordered media
 13 p2061 A72-29697
- Dynamic contact problems of stamps bands oscillation on elastic layer surface or cylinder, analyzing vibrationally induced elastic waves
 14 p1263 A72-30223
- Lunar seismogram characteristics interpretation in terms of Gold-Soter powder layer theory, taking into account elastic wave scattering by surface undulations
 14 p2154 A72-30506
- Ultrasonic wave propagation in single crystals, discussing linear elastic wave attenuation, anisotropic interactions, particle displacement polarization and energy flux deviation
 15 p2292 A72-31834
- Theoretical model for HF mechanical waves interaction with crystal lattices based on measurements of high amplitude ultrasonic waves attenuation in metal crystals
 15 p2292 A72-31835
- Constant stress effect on propagation velocity of elastic waves in three dimensional body, considering earth crust and earthquake prediction applications
 15 p3239 A72-32284
- Elastic wave diffraction on multiconnected cylindrical or spherical regions in nonsymmetric elasticity theory, determining constants of series solution
 15 p2330 A72-32290
- Plane wave dispersion and nonlocal elasticity equations linearization, demonstrating continuum treatment of lattice dynamics
 15 p2330 A72-32445
- Elastic wave scattering by moving slab, calculating reflection and transmission coefficients for various incidence angles, frequencies and motion velocities
 15 p2219 A72-32476
- Nondispersive guidance structure for acoustic surface waves due to velocity reduction of thin conducting strip on piezoelectric substrate
 15 p2278 A72-32506
- Longitudinal, transverse and bending waves propagation in elastic shells, using Hadamard method within linear shell theory
 16 p2465 A72-32982
- Shock tube diaphragm rupture effect on density distribution in rarefaction wave as function of time, using mirror laser interferometer measurement
 16 p2390 A72-33161
- Elastic wave diffraction by rigid ellipsoid, deriving scattering cross section for incident P wave from integral equation solution
 16 p2426 A72-33659
- Transient elastic wave propagation in circular cylinder during sudden torsional shear stress application to end surface, noting surface particle velocity and stress
 16 p2426 A72-33660
- Sonic boom induced pressure wave propagation and attenuation in water, comparing ballistic range measurements with theoretical predictions
 [AIAA PAPER 72-654] 16 p2349 A72-34080
- Acoustic edge scattering of elastic surface waves
 17 p2579 A72-34227
- Variational methods for dispersion relations and elastic properties of composite materials
 [ASME PAPER 71-APMW-21] 17 p2623 A72-34302
- Guided elastic wave propagation near curved surfaces and in nonconstant thickness layers, discussing asymptotic solution and applications to Love, Rayleigh and Lamb waves
 [ASME PAPER 72-APM-00] 17 p2580 A72-34306
- High-frequency ultrasonic devices
 17 p2526 A72-34564
- Longitudinal pulses propagation in straight hollow circular elastic tubes, presenting strain-time records
 [ASME PAPER 72-APM-10] 17 p2629 A72-34806
- WKB large frequency expansion solution for elastic waves propagating into inhomogeneous elastic medium with harmonic periodicity, using perturbation method
 [ASME PAPER 72-APM-3] 17 p2630 A72-34810
- Elastic wave propagation in a joined cylindrical-conical-cylindrical shell
 [SESA PAPER 1983] 17 p2630 A72-34819
- Theory for the excitation of SHF elastic waves by multiple-film transducers / Allowance for the influence of metallic and dielectric layers/
 17 p2529 A72-34843
- Propagation mechanism of tensor wave in solid elastic body due to impact
 18 p2734 A72-36377
- Theory of elastic wave propagation in composite materials
 18 p2703 A72-36395
- Scattering of elastic waves by moving objects
 18 p2709 A72-36403
- Reflection and refraction of elastic waves in edge-impacted rectangular plates
 18 p2737 A72-37065
- A study of thermoelastic waves by the method of characteristics
 18 p2737 A72-37068
- Wave-front singularities for two-dimensional anisotropic elastic waves
 18 p2739 A72-37175
- Bending waves diffraction and scattering by mass impedance loadings of infinite plane plate, considering point load and semiinfinite rib arrays
 18 p2739 A72-37203
- Effect of electrode thickness on the frequency response of a piezoelectric transducer
 18 p2693 A72-37218
- A note on the low frequency diffraction of elastic waves by a Griffith crack
 19 p2870 A72-37414
- A device for recording acoustic signals of crack formation in brittle materials
 19 p2802 A72-38018
- Analysis of piezoelectric thin-film transducers for elastic surface waves
 19 p2804 A72-38607
- Martin-Ludford gas expansion into vacuum, investigating rarefaction wave penetration and flow characteristics
 19 p2788 A72-38715
- Constitutive equations and wave propagation of anisotropic perfectly plastic materials
 19 p2878 A72-38800
- Elastic wave propagation in a rod of finite length with a variable cross section
 20 p2978 A72-39321
- Boundary-layer effects on pressure variations in Ludwig tubes
 20 p2914 A72-39620
- Steady solutions of generalized Korteweg-de Vries equation for oscillatory solitary waves in dispersive media
 21 p3089 A72-40197
- Plane acoustic pressure wave effect on motion of thin elastic truncated conical shell fastened in rigid screen, using Timoshenko theory
 21 p3116 A72-40263
- Variational theorems for harmonic waves in elastic composites with periodic structures, considering wave propagation in layered and in fiber reinforced composites
 21 p3119 A72-41101
- Elastic wave energy absorption in structures under dynamic loads, noting fatigue fracturing decrease with energy transfer into damping medium
 21 p3126 A72-41540
- Diffraction of an elastic wave at a disk
 21 p3127 A72-41669
- Crack tip stress field alteration via elastic pulses for changing crack trajectory or fracturing process termination, using polarization optical method
 21 p3061 A72-41824
- Rarefaction wave generation by solar wind shock wave interaction with magnetosphere, noting geomagnetic field weakening during magnetic storm
 22 p3217 A72-41894

- Bending waves propagation through flat plate forming rigid sound bridge between two parallel plates, calculating energy transfer at LF oscillations
22 p3234 A72-42128
- Finite difference theory for Lamé equations of elastic waves propagation in two dimensional body under mixed boundary conditions
22 p3234 A72-42144
- Wave propagation in a truncated conical shell.
22 p3235 A72-42524
- Dynamic photoelasticity application to periodic/vibrating and pulse/stress wave fields, considering loading rate effect on material fringe value
22 p3237 A72-42767
- Some recent experimental investigations in stress-wave propagation and fracture.
22 p3237 A72-42768
- Reflection of pulses at the interface between an elastic rod and an elastic half-space.
23 p3314 A72-44119
- A new concept for correcting the attenuation effects in a shock tube.
24 p3388 A72-44985
- Plane thermoelastic one-dimensional waves in an inhomogeneous medium with allowance for connectedness
24 p3459 A72-45266
- Thermoelastic waves propagation in homogeneous isotropic medium, considering potential functions
24 p3460 A72-45598
- ELASTICITY**
U ELASTIC PROPERTIES
ELASTICIZERS
U PLASTICIZERS
ELASTODYNAMICS
NT ELASTIC DAMPING
NT ELASTOHYDRODYNAMICS
Book on uniqueness theorems in linear elasticity covering three and two dimensional elastostatics, whole and half spaces, mixed boundary value problems, elastodynamics, etc
01 p0136 A72-10003
- Perturbed vibrational motion in isotropic elastic solid, using nonlinear Truesdell equations
01 p0101 A72-10039
- Stokes and Love integral representations for elastodynamic displacement fields in elastic solid deduced by potential theory method
01 p0138 A72-10513
- Linear viscoelasticity theory dynamic functions, deriving delay and relaxation times distribution functions in polymers
02 p0293 A72-12211
- Elasticity theory Lamé difference equations system solved by two-step iteration procedure based on Samarski regularization
03 p0447 A72-13727
- Infinitely long Euler-Bernoulli damped periodic aluminum beam with elastic springs, determining distance for steady state sinusoidal response to spatial decay
05 p0736 A72-16111
- Mathematical modeling of discrete nonconservative dynamic elastic systems for finite sensitivity, using Liapunov stability
06 p0840 A72-18320
- Solution uniqueness in physically nonlinear viscoelasticity dynamic theory
08 p1195 A72-21761
- Nonstable oscillating motions positive measure set in dynamic system with noncompact phase space, considering elastically rebounded falling sphere on horizontal plate
08 p1210 A72-22188
- Linear viscoelasticity theory dynamic functions, deriving delay and relaxation times distribution functions in polymers
11 p1734 A72-25709
- Elastodynamics three dimensional problems formulation using displacement potential functions
12 p1883 A72-27544
- Uniqueness of solutions to displacement problem for unbounded bodies in linear elastodynamics
12 p1884 A72-27564
- Eigenstate field parameter bounds in elastomechanics natural vibration problems
13 p2059 A72-29598
- Boundary value problems in dynamics of Cosserat infinite elastic medium with finite crack, noting couple stresses effect on dynamic stress concentration
14 p2164 A72-30299
- Schaefer stress representation for elastokinetics of linearly elastic isotropic homogeneous body under small deformations and torsions
15 p2324 A72-31486
- Nonlinearity effects on finite amplitude, plane uniform oblique shock wave reflection, using inviscid gas analogous solution techniques
16 p2426 A72-33661
- Uniformly propagating finite crack in elastic strip of finite width, using two dimensional dynamic equations of elasticity
16 p2471 A72-33831
- Elastic vibrations in roller bearings. 1 - The rotating mass is balanced with respect to its own rotation axis
17 p2561 A72-35894
- On the dynamic response of an infinite Bernoulli-Euler beam.
18 p2735 A72-36758
- Book on classical relativity theory covering relativistic kinematics and mechanics, tensor calculus, electrodynamics, gravitational fields and effects, elastic continua mechanics, thermomechanics and cosmology
18 p2712 A72-36850
- Some properties pertaining to the stability of circulatory systems.
18 p2737 A72-37060
- Oscillatory flow of a viscous fluid in a flexible walled two dimensional channel.
18 p2684 A72-37064
- Astroelasticity in design and analysis of flexible space vehicles, presenting dynamics and control considerations
18 p2738 A72-37082
- An eigenfunction method for solving the second boundary-value problem in the theory of elasticity
19 p2877 A72-38182
- A technique for numerical solution of boundary value problems in the plane theory of elasticity by the finite-difference method
19 p2878 A72-38204
- Proof of existence theorems for the principal dynamic problems of thermoelasticity
20 p2978 A72-39317
- On the choice of a reference state in the application of Hamilton's principle in elastodynamics.
20 p2979 A72-39420
- Stress functions in three-dimensional elastodynamics.
21 p3117 A72-40677
- Diffraction of an elastic wave at a disk
21 p3127 A72-41669
- Invariant solutions of the differential equations of the uniform motion of a Hooke medium
22 p3233 A72-42058
- Analogies between linearized and linear problems in elasticity theory in the case of uniform initial states
22 p3233 A72-42061
- Three dimensional thermoelastodynamic theory for elastic beams, deriving nonlinear motion equations by combined expansion and variational methods
22 p3235 A72-42523
- Dynamic photoelasticity application to periodic/vibrating and pulse/stress wave fields, considering loading rate effect on material fringe value
22 p3237 A72-42767
- Elastodynamic theory of natural symmetrical vibrations of sandwich plates, assuming filler motion and layer displacements governed by Lamé and Kirchhoff equations
23 p3348 A72-43790
- A difference method for plane problems in magnetoelastodynamics.
23 p3321 A72-44051
- [ASME PAPER 72-APM-A] Drag spectra of simple structures in turbulence.
23 p3281 A72-44102
- ELASTOHYDRODYNAMICS**
Full lubrication characteristics, discussing pressure pump, viscosity, MHD, volume elasticity, centrifugal and rheodynamic techniques
03 p0365 A72-14299
- Isothermal elastohydrodynamic theory for full range of pressure-viscosity coefficient, considering film thickness effect
06 p0821 A72-17805
- Elastohydrodynamic lubrication of soft elastic-deformed contact surfaces, determining lubricant film thickness as function of inlet and outlet parameters
07 p0998 A72-20530
- Elastohydrodynamic lubrication - Conference, Leeds University, England, April 1972
12 p1816 A72-28107
- Reciprocating O ring seal sliding friction behavior prediction by elastohydrodynamic theory, noting dwell time, acceleration rate and previous deceleration effects
12 p1816 A72-28110
- Shear modulus of liquids at elastohydrodynamic lubrication pressures.
21 p3059 A72-40688
- ELASTOMERS**
NT THIOPLASTICS
Helicopter elastomeric bearing rotors, discussing downtime and cost reduction, maintenance, endurance and inspection
01 p0073 A72-10150
- Adhesive materials based on room temperature vulcanizing silicone elastomers for space shuttle vehicle reusable surface insulation bonding
01 p0075 A72-10763
- Elastomeric protective coating requirements from existing electrochemical metallic corrosion theories
03 p0364 A72-14238
- Free radicals formation during elastomers mechanical degradation by grinding below and above glass transition point at liquid nitrogen and room temperatures
04 p0484 A72-15264
- Internal strain measurement in solid elastomeric materials by radioactive implant method using pinhole camera or multichannel collimator
07 p0992 A72-20583
- Liquid polysulfide rubber, discussing fabrication method and physical properties
07 p1024 A72-20603
- Clam seals comparison with elastomers, discussing aircraft use, contamination, inspection, corrosion and erosion, surface finish, service life and cost
08 p1179 A72-21941
- Elastomeric silicone ablator heat shields thermal characteristics from NASA Planetary Atmosphere Experiments Test vehicle earth atmosphere entry measurements
13 p2064 A72-28953
- Silicone based elastomers acoustic excitation damping properties at 213-423 K, discussing testing technique and results at 200-1000 Hz
13 p1957 A72-29090
- Experimental determination of ultrasonic wave velocities in plastics, elastomers, and syntactic foam as a function of temperature.
18 p2703 A72-36415
- Use of a loaded silicon elastomer for insulation of channel multipliers of onboard electrons
18 p2670 A72-37140
- Isolator elastomers properties, discussing spring isolators, combination springs and pneumatic systems
19 p2806 A72-37550
- The fracture energy and some mechanical properties of a polyurethane elastomer.
19 p2823 A72-38450
- Recent developments in silicone elastomers for macroencapsulation.
20 p2944 A72-39492
- Elastomers fracture strength and failure modes under tension, tearing, ozone cracking, fatigue and abrasive wear associated with viscous resistance energy losses
23 p3305 A72-43506
- Molecular mechanical aspects of the isothermal rupture of elastomers.
23 p3305 A72-43507
- ELASTOPLASTICITY**
Differential equations derived for elastic-plastic behavior of rotationally symmetric shells, approximating in finite difference forms and solved by elimination method
01 p0138 A72-10394
- Thin walled sandwich cylindrical shells under internal pressure, calculating elastic-plastic zone propagation
01 p0141 A72-11001
- Affine similarity in static problems with mixed boundary conditions for inhomogeneous anisotropic linearly and nonlinearly elastic and viscoelastic and elastoplastic bodies
02 p0288 A72-11607
- Nonlinear photoelasticity, elastoplasticity and creep problems studies by optical polarization methods, comparing transparent model and photoelastic coating techniques
02 p0289 A72-11613
- Plate buckling elastoplastic process derivation allowing for secondary plastic deformation onset, examining stress discontinuity at overloading and unloading zones boundary
02 p0289 A72-11614
- One dimensional elastoplastic wave propagation symposia review emphasizing elastoviscoplastic media, jet penetration into half space and polymer tests by transverse impact
02 p0290 A72-11628
- Inhomogeneous microstructure elastoplastic medium, examining strain and work in plastic deformation
02 p0293 A72-12427
- Elastoplastic problem of stress concentration in orthotropic plate with circular hole under balanced biaxial tension of infinity
02 p0293 A72-12428
- Anisotropic and compressible work hardening materials three dimensional elastoplastic flow quasi-linear theory, deriving boundary integral equations
02 p0296 A72-12530
- Three layer plates elastoplastic stability, describing breakdown conditions by five differential equations with five unknown variables
02 p0299 A72-12690
- Elastoplastic material crack propagation behavior under arbitrary loading, introducing plastic zone, intensity and retardation factor concepts
02 p0300 A72-12726
- [DGLR PAPER 71-111] Microinhomogeneous elastoplastic cyclically strain hardenable material under symmetric loading, calculating stress-strain relationship
03 p0443 A72-13453
- Thermal stress concentration at circular heat-insulated hole in plate with elastoplastic strains, assuming temperature independent mechanical properties
03 p0445 A72-13575
- Optimal shape calculation for partially elastic and elastoplastic column under conservative load based on static stability criterion
03 p0447 A72-13851

Elastoplastic stress distribution in thin spherical metallic shells with cylindrical branch pipe under internal pressure

03 p0448 A72-13905

Elastic-plastic stress-strain analysis of beams with uniform cross section under combined loadings by finite element method

03 p0449 A72-13975

Elastoplastic bodies with crack at tip, determining limiting loads and crack propagation from variational relations

03 p0451 A72-14117

Crack growth in elastoplastic and viscous media under cyclic loading

03 p0452 A72-14137

Stress concentration problems in two and three dimensional elastoplasticity, using Ilyushin small deformation theory

03 p0453 A72-14213

Elastoplastic stability of structural rods in unloadable systems, considering load carrying capacity increase by critical state onset delay

03 p0454 A72-14214

Infinite elastic-plastic beam impact by semiinfinite elastic rod, computing strain-time profiles

04 p0583 A72-14447

Elastoplastic circular plates optimum shakedown design under cyclic loading

04 p0585 A72-14613

Elastoplastic body random vibration analysis by statistical linearization, obtaining free elastic vibration mode shapes and damping constants

04 p0586 A72-15005

Stress-strain increment relations for materials with different compression and tension resistance under orthogonal loading

04 p0586 A72-15007

Discrete variable approach for stress wave propagation in axisymmetric layered elastic-plastic solids

04 p0593 A72-15626

Error bounds on elastic-plastic strain wave measurements, considering one dimensional wave propagation in semiinfinite bar

[ASME PAPER 71-MET-W]

05 p0731 A72-15789

Elastoplastic creep analysis for cylindrical pressure vessel structural response during cyclic thermal shock, internal pressure and extended high temperature loading

[ASME PAPER 71-WA/PVP-12]

05 p0732 A72-15911

Turbine casing components stresses in presence of creep, demonstrating calculation method validity for thick-walled structures by elastoplastic analogy

05 p0734 A72-15985

Subcritical crack extension in elastoplastic or viscoelastic-plastic matrix, showing similar mathematical representations for fatigue crack propagation and creep rupture under sustained loads

05 p0737 A72-16302

Inverse periodic plane deformation of isotropic elastoplastic surface with infinite series of curvilinear holes

05 p0741 A72-17146

Complex potentials for nonlinear elasticity, creep and small elastoplastic deformations, applying to stress concentration at curvilinear hole in infinite plate

05 p0742 A72-17183

Green-Naghdi nonlinear thermodynamics of elastic-plastic deformation at finite strain, discussing relationship to nonisothermal theory

06 p0896 A72-17921

Stress concentrations at circular holes and inclusions in elastoplastic strain hardening plate under tension and shear

06 p0897 A72-18316

Elastic-plastic strain measurement on flat steel surfaces by moiré gratings, using electroluminescent source and crossing jig

06 p0818 A72-18323

Stationary small elastoplastic longitudinal forced vibrations of rods with internal resonance obtaining asymptotic solution of nonlinear partial differential equations

06 p0900 A72-18676

Small elastoplastic cyclic strain effects on internal friction and energy dissipation in metals during vibrations

06 p0834 A72-18679

Error analysis of finite element solutions for elastic-plastic sandwich plates

07 p1086 A72-18779

Creep and plastic deformation analysis of riveted joint elements using elastoplastic theory

07 p1087 A72-18982

Finite element method application to fracture mechanics problems of stress concentration and intensity factors and elastoplastic response to cyclic loading

07 p1088 A72-19130

Elastoplastic stressed state of thin cylindrical shells with circular hole, using small strain theory

07 p1092 A72-19896

Shock wave propagation and structure in elastoplastic material with translational work hardening, obtaining closed system of discontinuity equations

07 p1093 A72-19977

Circular elastoplastic beam under combined torsion and tension via Mindlin elastic model for materials with microstructure, taking into account work hardening

07 p1097 A72-20534

Book on plasticity theory covering stress and strain as basic concepts of continuum mechanics, differential equations of motion, plastic flow, yield criteria, elastic-plastic equilibrium, plane strain, etc

08 p1244 A72-21477

Strength analysis of thin elastoplastic shell with allowance for compressibility, relating loads and moments to deformation of middle surface

08 p1246 A72-21712

Necking instability in rectangular elastoplastic plate under biaxial tension, obtaining condition for equilibrium bifurcation by variational method

09 p1398 A72-22532

Elastoplastic stressed state of multilayer cylinder during loading, unloading and cyclic loading processes

09 p1401 A72-22721

Finite difference analysis of dynamic deformation of thin elastoplastic shells of revolution under intense heating

09 p1401 A72-22728

Elastoplastic analysis of unidirectional filament reinforced boron/aluminum and boron/epoxy composites under longitudinal loading, using finite element techniques

10 p1555 A72-24254

Direct numerical integration scheme for viscoelastoplastic response of isotropic axisymmetric shells under impulsive loads

[AIAA PAPER 72-400]

11 p1731 A72-25421

Two dimensional elastoplastic finite element analysis of structural members under cyclic thermal-mechanical loadings

[ASME PAPER 72-GT-1]

11 p1734 A72-25604

Upper yield stress effect on elastoplastic behavior of mild steel in bending and torsion, noting relationship to strain rate

11 p1659 A72-25894

Elastic-plastic analysis of large deflection of axisymmetrically loaded circular plates, using incremental theory

11 p1737 A72-26426

Fatigue testing machine for material behavior under elastoplastic bending loads with constant or smoothly varying programmed vibration frequency and amplitude

12 p1795 A72-27463

Acceleration waves propagation in elastic-plastic strain hardening rate independent solids, obtaining solution for discontinuity change in strength in homogeneously prestressed medium

12 p1846 A72-27729

Nonlinear fracture toughness determination via three point bending test simulation by elastic-plastic finite element computer program

12 p1830 A72-27731

Elastoplastic deformation effects on load bearing capacity of samples with stress concentrators under alternating cyclic loading, obtaining nomograms by digital computer

12 p1887 A72-28228

Variational solution to axisymmetric problem of rigid stamp quasi-static impression into elastoplastic half space

13 p2053 A72-28387

Unloading wave propagation in semiinfinite elastoplastic cylindrical rod for concave stress-strain diagram with no initial linear segment

13 p2053 A72-28388

Closed form solutions for one dimensional nonlinear waves in strain rate-sensitive elastoplastic material, describing dispersed wave motion behind propagating shock front

14 p2164 A72-30298

Elastoplastic equilibrium theorems for solid subjected to variable external effects, considering perfectly plastic and arbitrary hardening materials

14 p2165 A72-30574

Constitutive equations for incremental stress-strain relations in elastoplastic media, noting plane stress and strain in isotropic materials

14 p2131 A72-30715

Finite element method for nonlinear analysis of nuclear reactor structures, noting elasticity, viscoelasticity and elastoplasticity problems

[SMRT PAPER M 2/2]

14 p2166 A72-30724

Loading conditions effect on relaxation and creep in inhomogeneous hereditary elastoplastic polycrystalline materials

14 p2168 A72-30953

Elastoplastic stress concentration near elliptic hole in plate loaded in smallest axis direction

15 p2325 A72-31606

Nonlinear creep, viscoelasticity and elastoplasticity boundary value problems, discussing matrix constitutive differential equation formulation and higher order numerical methods

15 p2326 A72-31712

Stress-strain state of spherical body in centrally symmetric temperature field, noting elastoplastic interface and continuity conditions

15 p2327 A72-31742

Variational principle for boundary value problem of elastic-plastic torsion of circular bars under quasi-static finite deformation

16 p2464 A72-32914

Edge-loaded rectangular plate buckling behavior in elastoplastic range between proportional limit and yield point

16 p2466 A72-33020

Yield conditions formulation restrictions for large elastoplastic deformations, discussing isotropic and anisotropic hardening

16 p2396 A72-33024

Elastoplastic torsion of homogeneous and inhomogeneous torus segments of arbitrary cross section, noting plastic bands propagation with increasing torque

16 p2467 A72-33119

Elastic-plastic medium yield zone spread from penny shaped crack determined from continuous distribution of dislocations, noting system energy change

16 p2468 A72-33226

Temperature dependent elastoplastic wing assemblies and continua analysis via matrix displacement method

16 p2471 A72-33791

Three dimensional elastoviscoplastic theory for complex structures static-dynamic creep deformation under time varying stress and temperature fields, generalizing Odqvist-Hoff law

16 p2473 A72-34121

Growth of an acceleration wave in an elastoplastic isotropic medium undergoing finite deformation

17 p2580 A72-34277

The hodograph transformation in plastic waves with discontinuous loading conditions

[ASME PAPER 71-APMW-12]

17 p2624 A72-34308

Elastic-plastic systems under dynamic loadings, discussing compounded shakedown load solution by zero work and direct search methods

[ASME PAPER 71-APMW-27]

17 p2624 A72-34309

Elastic-plastic medium with doubly periodic square array of circular cylindrical voids, obtaining finite element solution for uniaxial deformation by variational principle

[ASME PAPER 72-APM-36]

17 p2628 A72-34784

Elastoplastic bending of rectangular plates with large deflection

[ASME PAPER 72-APM-34]

17 p2628 A72-34785

On uniqueness in ideally elastoplastic problems in case of nonassociated flow rules

[ASME PAPER 72-APM-33]

17 p2628 A72-34786

Determination of the unloading boundary in transverse impact of an elastic-plastic string

[ASME PAPER 72-APM-12]

17 p2629 A72-34804

Finite element analysis of elastoplastic structures with temperature dependent mechanical properties

17 p2631 A72-34947

Elastoplastic structural analysis from design viewpoint, discussing load limits and stability estimates based on large deformation assumption

17 p2632 A72-35113

Elasto-visco-plastic constitutive equations for quasi-static structures calculations

[ONERA, TP NO. 1089]

19 p2875 A72-37763

Refractory materials cyclic elastoplastic tests under shear with holding creep, showing relationship between creep rate and recurrent static deformation

19 p2876 A72-38007

Theory for transverse vibrations of beams during elastoplastic deformations

19 p2877 A72-38179

Computer solution of dynamic problems for bending of beams and thin plates beyond the elastic limit under alternating loads

19 p2877 A72-38194

An analytical approach to the non propagating crack problem using the finite element method

20 p2977 A72-38882

Elastoplastic axisymmetric bending of a clamped circular plate under the action of a conically distributed variable load

20 p2978 A72-39022

Finite element large deflection analysis of elastic-plastic shells of revolution subjected to axisymmetric loading

20 p2982 A72-40064

Combined tension-torsion elastic-plastic waves as propagating singular surfaces

21 p3121 A72-41244

Stress-strain state of thin circular perforated Cu plate under uniform tensile load, showing applicability of small elastoplastic finite deformation theory

21 p3122 A72-41351

On the collision of a cold elastic plate with a hot elasto-plastic plate

21 p3124 A72-41482

Mixed finite element analysis of elasto-plastic plates in bending

21 p3124 A72-41502

Constitutive equations of generalized Brandt-Reuss theory of elastoplastic deformation, noting second order effects 21 p3124 A72-41506

Convergence of the homogeneous linear approximation method in problems of plasticity theory of inhomogeneous bodies 22 p3232 A72-41911

Fiber glass reinforced plastics elastoplastic behavior due to microcrack propagating across matrix, using elastic index of work done 22 p3232 A72-41943

Stress concentration at an elliptic hole in an elastoplastic body 22 p3233 A72-42060

Stability of elastoplastic rod under external conservative and nonconservative forces, discussing non-conservative component effect and critical load magnitude 22 p3234 A72-42149

The application of the finite element displacement method to problems of elastoplastic deformation. 22 p3238 A72-42832

Stress concentration around a circular hole in an elastoplastic medium under the action of a temperature field and omnidirectional tension 23 p3344 A72-43418

Continual theory of dislocations and the theory of small elastoplastic deformations 23 p3345 A72-43584

Equilibrium equations and deformation of elastoplastic thin isotropic cylindrical shell with circular hole, noting nonlinear partial differential equations for plate displacements 23 p3345 A72-43587

Path independent integrals to predict onset of crack instability in an elastic plastic material. 23 p3346 A72-43711

Dynamic model for microinhomogeneous elastoplastic medium under cyclic loads with varying amplitude 23 p3347 A72-43729

Elastoplastic computation of thin cylindrical shells under cyclic loading 23 p3348 A72-43786

Stability of an elastoplastic rod of varying resistance to tension and compression with allowance for the initial stresses 23 p3352 A72-44162

Changes in the physical properties of metals subjected to elastoplastic deformation 23 p3303 A72-44199

Elasto-plastic stress analysis - A generalization for various constitutive relations including strain softening. 24 p3457 A72-44880

Microinhomogeneous elastoplastic cyclically strain hardenable material under symmetric loading, calculating stress-strain relationship 24 p3458 A72-44928

Equation of state relating time variations of stress and strain in elastoplastic material under tension 24 p3459 A72-45069

Some extremal properties and energy theorems for inelastic materials and their relationship to the deformation theory of plasticity. 24 p3460 A72-45692

On dual energy theorems for a class of elastoplastic problems due to G. Maier. 24 p3460 A72-45693

Turbine casing components stresses in presence of creep, demonstrating calculation method validity for thick-walled structures by elastoplastic analogy 24 p3460 A72-45727

ELASTOSTATICS

Book on uniqueness theorems in linear elasticity covering three and two dimensional elastostatics, whole and half spaces, mixed boundary value problems, elastodynamics, etc 01 p0136 A72-10003

Linear elastic Cosserat continuum mixed boundary-initial value problem uniqueness theorem, using Kirchhoff proof in classical elastostatics 03 p0382 A72-14363

Tensile load elastostatic transfer from rectangular cross section web to two infinite parallel sheets, deriving Cauchy type integral equation for adhesive bond force density 07 p1095 A72-20241

Plane elastostatic problem of stress concentration near flat interface inclusion in bonded dissimilar materials 09 p1405 A72-22997

Volume averages of stress and strain changes induced by Poisson ratio variation in boundary value problems of three dimensional classical elastostatics 12 p1884 A72-27566

A technique for numerical solution of boundary value problems in the plane theory of elasticity by the finite-difference method 19 p2878 A72-38204

Singular stress concentration at sharp edge of wedge in contact with half plane in elastostatics 21 p3119 A72-41104

Dependence of linear elasticity solutions on the elastic constants. II - Dependence on the shear modulus in elastostatics. 21 p3119 A72-41106

Methods of studying three-dimensional problems of stability in the presence of highly elastic strains 21 p3126 A72-41538

Plane elastostatic analysis of V grooved rectangular plates notch angle and specimen geometry effects on stress intensity factors and fracture toughness measurements 23 p3346 A72-43703

Transfer matrix approach for determining stresses and displacements in elastostatics of laminated composites [ASCE PREPRINT 1674] 23 p3351 A72-44105

ELDO LAUNCH VEHICLE

Organization, management, contract placement and financing of CECLES/ELDO European multinational program for launcher development 01 p0146 A72-10947

Industrial challenge of European space R and D programs, discussing ELDO Europa I launcher vehicle and ESRO-HEOS satellite technological problems 01 p0146 A72-10948

ELDO launch vehicle cryogenic tanks fabrication, discussing Al alloy selection and mechanical properties at low temperatures, manufacturing processes and thermal insulation 09 p1318 A72-22690

ELECTRA AIRCRAFT

Unpredicted structural vibration in Comet and Electra aircraft, Graf Zeppelin dirigible, missile antennas, etc 02 p0292 A72-12002

ELECTRETS

Ammonia beam maser with electret focuser providing semipermanent molecular separation under high vacuum for use in relaxation studies 01 p0081 A72-11187

Capacitive electret pressure sensors calibration for interior measurements in turbine engines, jets and exhaust nozzles 09 p1310 A72-22815

Properties of the electrostatic field of a system of annular electrets and possibilities of its application for focusing in molecular generators 19 p2804 A72-38538

ELECTRIC ANALOGIES

U ANALOGIES

ELECTRIC APPLIANCES

U ELECTRIC EQUIPMENT

ELECTRIC ARCS

NT MERCURY ARCS

Heat transfer from augmented flames and plasma jets based on magnetically rotated arcs, measuring transfer rate as function of electromagnetic torque 02 p0301 A72-12031

Anode heat flux for cascade atmospheric Ar arc of Maecker type, checking anode heat transfer model validity 02 p0302 A72-12266

Transformation of differential equations describing interaction between electric arc and gas flow by taking temperature as independent variable, considering Laval nozzle example 03 p0344 A72-14392

Thermal and I-V characteristics of dc plasmatron with vortex stabilized arc, interelectrode insert and diverging arc channel for various nozzle diameters 05 p0694 A72-15854

Electric arc in submerged gas jet, investigating laminar combustion zone extent, thermal layer radius and electric field strength 06 p0861 A72-17903

Approximate solution to Elenbass-Geller equation of arc electric and radiation characteristics as function of thermal conductivity by Galerkin method 07 p1043 A72-19879

Axial arc column interaction with shock waves and high velocity gas flow effects in forced convection, proposing heat transfer theory 07 p1047 A72-20548

German monograph on electric arc behavior in narrow channel with plasma cooling by channel wall and continuously decreasing current for switching applications 10 p1517 A72-23773

Solid body model for electric arc acceleration in thermionic cathode rail accelerator, discussing plasma mass effects [AIAA PAPER 72-412] 11 p1706 A72-26162

HF follower currents effect on dc arc I-V characteristics, indicating use of HF follower arc for quasi-steady arc power control 13 p2017 A72-29645

Electric arc plasma, predicting elements addition and electron density alteration effects on radial temperature distribution 14 p2139 A72-30778

Electric arc plasma, investigating reaction energy effects on radial temperature distribution 14 p2139 A72-30779

Dc arc plasma, investigating applied magnetic field, trace elements and gap spacing effects on spectral line intensity spatial distribution 14 p2139 A72-30783

Spectrochemical trace analyses in electric arc plasma, examining external magnetic field effects on spectral line intensity variation 14 p2139 A72-30784

Thermal and I-V characteristics of dc plasmatron with vortex stabilized arc, interelectrode insert and diverging arc channel for various nozzle diameters 15 p2283 A72-31271

Gas shielded strip electrode welding and cladding, discussing electric arc behavior, weld bead penetration depth, drop transfer speed, weld microstructure, etc 15 p2243 A72-31324

Numerical results of carbon dioxide-nitrogen-water gas dynamic laser comparison with arc-driven supersonic laser in gas dynamic mode 15 p2250 A72-32517

High voltage dc arc interrupter for use in high power pulse generators and switching application in high voltage dc power transmission system 15 p2201 A72-32569

Fusion reactor RF heating below 100 MHz, discussing coil structures and arcing and cooling problems in main fusion region 16 p2433 A72-32813

Steady state magnetically balanced cross flow arc, calculating flow and temperature fields and boundary shape under assumption of two independent variables [AIAA PAPER 72-687] 16 p2439 A72-34055

Energy transfer of thermal coupled radiation with turbulent convection in electric arcs in atmospheric air plasma [AIAA PAPER 72-685] 16 p2480 A72-34057

Atmospheric organic vapor effects on electric contact erosion, deriving showering arc duration, gap breakdown, arc number and energy 18 p2665 A72-36118

1970-1971 Holm Seminar supplement to bibliography and abstracts on electrical contacts, circuit breakers and arc phenomena. 18 p2665 A72-36120

The determination of diffusion coefficient for Na in dc arc plasma by measurements of intensity distribution of emitted light. 18 p2716 A72-36959

German monograph - Behavior of an electric arc produced by an exploding wire in a granular medium 19 p2834 A72-37483

Measurements of plasma velocity distributions in free-burning dc arcs up to 2160 A. 20 p2958 A72-39644

A system of disc-stabilized dc arc and solution nebulization device for the investigation of multicomponent plasmas. 21 p3039 A72-40213

Ar plasma diagnostics from stabilized arc emission spectra, noting thermodynamic equilibrium in central zone of arc channel 22 p3209 A72-41880

ELECTRIC BATTERIES

NT ALKALINE BATTERIES

NT METAL AIR BATTERIES

NT NICKEL CADMIUM BATTERIES

NT SILVER CADMIUM BATTERIES

NT STORAGE BATTERIES

NT ZINC-OXYGEN BATTERIES

Rechargeable oxygen electrode research program for hydrogen oxygen fuel cells and metal-oxygen batteries, discussing KOH solutions effects 04 p0466 A72-14675

Positive electrode materials for high energy density batteries with Li negative electrode, calculating discharge emf for various salts 06 p0760 A72-17575

Thermoelectric cooling battery performance of solar cell system, determining low temperature current requirements under various thermal loads 10 p1423 A72-24317

Hydrazine fuel cell development, electrochemical problems and applications, noting batteries with air oxidant 16 p2351 A72-33886

Normal, highly conducting and ion-exchanging solid electrolytes structure and conductivity, with particular attention to rechargeable silver halide batteries 16 p2352 A72-33899

Parallel operation of the solar generator and battery on the Symphonie satellite 18 p2648 A72-36681

ELECTRIC BRIDGES

Square wave source gated detector bridge for precise resistance measurement, discussing design and performance, and application in Pt resistance thermometry 06 p0785 A72-18244

Bridge circuit to minimize parasitic electrical disturbances in resistance strain gage measurements of dynamic stresses in impact tests 06 p0819 A72-18672

Self balancing ac bridge with double conversion of unbalance-signal and low capacitance sensor for displacement measurement

11 p1634 A72-26459

Antoniou bridge type gyrator circuit stability, showing sensitivity to resistors ratio variations

12 p1792 A72-27698

Two fluid model application to microbridges between superconductors, investigating superconducting particles number time variation possibility

13 p2023 A72-29789

Small temperature variation measurement by temperature sensor switching, using multipoint electronic automatic recording bridge with polarized relay

16 p2395 A72-33967

A six-phase bridge rectifier circuit with a reduced number of controlled rectifiers and a rigid external characteristic during high-level regulation

19 p2774 A72-38585

Electric model of bridging losses and optimal insulation layer thickness for small size resistance strain gages

21 p3056 A72-41367

Application of N equalizing and compensating signals in a single-cell reciprocal magnetoelectric transducer

24 p3386 A72-45315

ELECTRIC CHARGE

NT ELECTRIC DIPOLES

NT ELECTROSTATIC CHARGE

NT ION CHARGE

NT SPACE CHARGE

NT TRAVELING CHARGE

Electromechanical coupling and acoustic impedance response in piezoelectric transducer with diffusion under fixed charge

11 p1636 A72-26590

Nonlinear sheath admittance, currents and charges associated with high peak voltage drive on VLF-ELF dipole antenna moving in ionosphere

11 p1599 A72-26769

Scaling hypothesis and limiting fragmentation mechanism for cosmic ray muon production, noting energy independent charge ratio

15 p2298 A72-31289

The ignited mode of cesium thermionic diode. II - The charge influence on the volt-ampere characteristics.

18 p2647 A72-36211

Quantum fields interaction with classical sources on Schwarzschild background, noting mass, charge and angular momentum as sole measurable quantum numbers of black hole

18 p2726 A72-36716

Cosmic ray muon sea level momentum spectra and charge ratios geomagnetic latitude dependence measurements by spark chamber technique

19 p2853 A72-38754

ELECTRIC CHOPPERS

Capacitor-fed parallel chopper as phase sensitive demodulator, discussing design, stability, linearity and wide dynamic frequency range

04 p0507 A72-15522

Electromechanical filter with attenuation poles consisting of multi-mode vibrators.

21 p3036 A72-41828

ELECTRIC CIRCUITS

U CIRCUITS

ELECTRIC COILS

NT MAGNETIC COILS

Weakly damped Alfvén ion-cyclotron waves and fast magnetoacoustic waves in infinite plasma cylinder inserted into current bearing finite coil

07 p1046 A72-20516

Relay circuits malfunction due to interactions between coil induced currents and diode coil shunts, discussing circuit design and operating conditions

15 p2204 A72-31217

Application of N equalizing and compensating signals in a single-cell reciprocal magnetoelectric transducer

24 p3386 A72-45315

ELECTRIC CONDUCTORS

Plane electromagnetic wave scattering by imperfectly conducting cylinder with radially inhomogeneous dielectric coating, using phase shift method for evaluation

01 p0024 A72-10130

Automatic device using tetragonal conducting film sheets to feed graphic information into computer

02 p0187 A72-12279

Diffraction of plane electromagnetic waves of arbitrary orientation and incidence on triangular grid of cylindrical conductors

02 p0183 A72-12753

Induced current distribution in flat narrow conducting strip moving in inhomogeneous magnetic field, presenting current field and densities

03 p0311 A72-13564

Compression wave propagation from cylindrical cavity in weakly conducting magnetoelectric medium under unperturbed magnetic field

03 p0452 A72-14129

MHD squeeze film lubrication between electrically conducting parallel plates, showing graphically approach time under magnetic field in free space

05 p0665 A72-16031

Thin film conductors, distributed film resistors and capacitors design and associated IC layout to form functional arrays

06 p0790 A72-18574

Radially conducting cone wave spectrum calculation for noncophasal excitation, noting circularly polarized TEM and elliptically polarized TM wave amplitudes

07 p0938 A72-19003

Ideally conducting convex body mean differential monostatic scattering cross section, considering wavelength to body dimensions ratio

07 p0938 A72-19018

Nd-YAG laser system generating gold conductor patterns on ceramic substrates, using numerical control system for Si production

07 p1002 A72-19213

Rf excitation of external terminated longitudinal conductor axially parallel to rocket skin by transverse electromagnetic field, deriving currents in cable-connecting impedances

07 p0956 A72-19555

One- and two-conductor transmission lines electromagnetically coupled to rocket, deriving current bounds in load impedances under incident plane monochromatic wave

07 p0956 A72-19556

Bulk conductors dc field distribution applications to electrical resistivity measurements and nondestructive testing

07 p0998 A72-20461

Plane electromagnetic wave reflection from conducting convex cylinder in radially inhomogeneous absorbing medium, deriving equations for beam trajectories calculation

08 p1131 A72-20742

Surface current density of perfectly conducting polygonal cylinders for axially polarized incident electromagnetic field

09 p1350 A72-22247

Dipole moment expression for Rayleigh scattering field from finite closed perfectly conducting body irradiated by LF plane electromagnetic wave [AD-742573]

10 p1434 A72-23720

Plane electromagnetic wave diffraction on ideally conducting convex body of large electrical dimensions, obtaining Maxwell equations asymptotic solution

10 p1436 A72-24577

Phase velocity and Landau damping of ion acoustic waves propagating through plasma boundary layer at conducting sphere or cylinder based on two fluid model

10 p1523 A72-24746

Secondary diffraction from close edges on perfectly conducting bodies, representing scattered field by iterative surface current density replacement technique

10 p1440 A72-24938

Automatic device using tetragonal conducting film sheets to feed graphic information into computer

11 p1601 A72-25704

Induced current distribution in flat narrow conducting strip moving in inhomogeneous magnetic field, presenting current field and densities

11 p1691 A72-26751

Radar backscattering cross section and power of conducting cylindrical spacecraft in compressible electron-ion plasma environment

12 p1779 A72-27173

Electronic heating test arrangement for high temperature testing of metals and electrically conducting ceramics in vacuum, describing temperature control systems

12 p1796 A72-28249

Electromagnetic wave diffraction on ideally conducting homogeneous bodies of revolution with arbitrary complex permittivity and permeability, using variables separation method

13 p1920 A72-29279

Electric field and volume charge density distribution in bipolar conductivity semiconductor with recombination instability

15 p2291 A72-31392

Convective heat transfer in fully developed MHD channel flow between two parallel electrically conducting plates

15 p2335 A72-31636

Space charge electron flow between parallel conducting walls, developing relativistic method for potential and field distribution time variation

15 p2279 A72-32510

The behavior of electromagnetic fields at edges.

17 p2513 A72-34357

Conducting body radar scattering control by reactive loading, discussing field pattern synthesis for real current with least mean-square approximation

17 p2513 A72-34358

Averaged boundary conditions for a grid consisting of nonparallel and nonrectilinear conductors positioned on a nonplanar surface

17 p2529 A72-34830

Closed magnetic fields of helical ring currents on concentric spheres surrounded by conductor/Tornado trap/

17 p2588 A72-34855

Electromagnetic waves on a conducting infinite cylinder in a magnetoelectric medium.

17 p2517 A72-35399

Plane electromagnetic waves diffraction at arbitrary orientation and incidence on triangular grid of cylindrical conductors

20 p2902 A72-39059

Scattering of electromagnetic pulse waves by conducting wedge in an uniaxially anisotropic medium.

20 p2903 A72-39269

The relationship between the thick film conductor and substrate and its influence on conductor properties.

20 p2908 A72-39494

Radiation patterns of an antenna near a conducting strip.

21 p3015 A72-40365

Diffraction of electromagnetic plane waves by infinite slit perforated in a conducting screen with finite thickness.

21 p3022 A72-41267

Diffraction of an electromagnetic wave by a noninfinitely conductive cylindrical object of arbitrary cross section

22 p3153 A72-41991

Radar cross sections of conducting bodies of revolution, noting electric/magnetic polarizability tensors in L.F. Rayleigh scattering

24 p3381 A72-45639

ELECTRIC CONNECTORS

Papers on microwave advances covering precision coaxial connectors, O-type linear beam devices, electron dynamics and energy conversion and junction circulators

03 p0424 A72-13229

Microwave precision coaxial connectors in terms of dimensional specifications, material properties, surface characteristics and other parameters for transmission standards effects

03 p0330 A72-13230

Laminate materials, sockets and connectors for cost-effective high temperature accelerated life testing of IC

03 p0336 A72-14283

Refractory metal multilevel interconnection systems, comparing materials fabrication, yield and circuit performance with diffused Si planar runs and polycrystalline Si films

05 p0636 A72-16362

Semipermanent and permanent pressure connections in electronic systems, discussing design and performance evaluation

06 p0791 A72-18580

Permanent electric connections by alloy and solid phase bonding and fusion welding, considering surface contamination, interface contact, activation energy and connection stability

06 p0822 A72-18581

Reliable interconnections for U.S. Army avionics, determining best technique for terminating flat conductor cables with electrical connectors

10 p1447 A72-24012

Silicon solar cell interconnectors design for 5-10 years mission life, considering launch induced vibration stresses and thermal cycling stresses during mission

12 p1758 A72-28037

Friction and wear of electroplated hard gold deposits for connectors

18 p2693 A72-35981

The lightning arrester-connector - A new concept in system electrical protection.

20 p2889 A72-38989

ELECTRIC CONTACTS

Solar cells with improved photoelectric efficiency, describing use of noncorroding Ti-Pd-Ag contacts, titanium oxide antireflection layer and welded cell joints

06 p0760 A72-17751

Papers on thin film and semiconductor IC and contact and connection technology

06 p0790 A72-18570

Electrical contacts conduction principles, considering circuit voltage, current, variable resistance and resistive, mechanical, heating and adhesive properties

06 p0791 A72-18578

Switching contacts performance principles, noting inductive energy role in electrical breakdown voltage determination

06 p0791 A72-18579

Semipermanent and permanent pressure connections in electronic systems, discussing design and performance evaluation

06 p0791 A72-18580

Electric contact phenomena in ultraclean and specifically contaminated metallic systems, noting re-

sistance relationship to load curves and surface conditions
10 p1448 A72-24172

Delayed pulse echo and through-transmission ultrasonic techniques for nondestructive inspection and quality control of braze bonds in high current electric contact assemblies
10 p1487 A72-24173

Electron distribution near semiconductor-metal contact, discussing current carriers quantum properties effects
13 p2021 A72-28679

Electrical contacts - 1972; Proceedings of the Sixth International Conference on Electrical Contact Phenomena, Chicago, Ill., June 5-9, 1972.
18 p2664 A72-35979

Tribological properties of gold for electric contacts.
18 p2693 A72-35980

Friction, wear and noise of slip ring and brush contacts for synchronous satellite use.
18 p2693 A72-35982

Evaluation of gold electrodeposits for use in dry circuit applications.
18 p2664 A72-35983

Evaluation of testing methods for gold plated or gold clad contacts.
18 p2664 A72-35984

Pd-Al intermetallic compound contact materials.
18 p2698 A72-35985

1972 seminar supplement to bibliography and abstracts on electrical contacts, circuit breakers and arc phenomena.
18 p2664 A72-35986

Electrical contacts - 1971; Proceedings of the Seventeenth Annual Holm Seminar on Electric Contact Phenomena, Chicago, Ill., October 13-15, 1971.
18 p2665 A72-36114

Electric contact phenomena in ultra clean and specifically contaminated systems.
18 p2717 A72-36115

Nondestructive ultrasonic inspection of braze bonds in high current electrical contact assemblies.
18 p2695 A72-36116

The testing of contact materials for slip rings and brushes for space application.
18 p2698 A72-36117

Atmospheric organic vapor effects on electric contact erosion, deriving showering arc duration, gap breakdown, arc number and energy
18 p2665 A72-36118

Contact contamination - Formation of carbonaceous deposits on electrical contacts.
18 p2665 A72-36119

1970-1971 Holm Seminar supplement to bibliography and abstracts on electrical contacts, circuit breakers and arc phenomena.
18 p2665 A72-36120

The effect of contacts on microwave emission from InSb.
19 p2844 A72-37728

Installation for the simultaneous measurement of the functional properties of sliding contacts
20 p2928 A72-39936

Influence of fluctuations on the electromagnetic properties of Josephson tunneling contacts
22 p3208 A72-43124

Investigation of the nature of photostimulated exoelectronic emission during the friction of precision contacts
22 p3183 A72-43158

Properties of a superconducting point contact contained in a resonator
23 p3324 A72-44221

ELECTRIC CONTROL

Electrical control of fixation and erasure of holographic patterns in ferroelectric materials
07 p0981 A72-18880

Optimal test conditions in magneto-optical control by electrical system for subsurface defects detection, obtaining tangential magnetic field on carbon steel plates
07 p0991 A72-20421

Automatic remote mechanical system parameter control by electrical elements, introducing rigidity for mass sensitive measurement in dynamometry
16 p2370 A72-33956

A six-phase bridge rectifier circuit with a reduced number of controlled rectifiers and a rigid external characteristic during high-level regulation
19 p2774 A72-38585

Concorde electrically signalled fly by wire control system with mechanical linkages for standby fail-safe redundancy
21 p2994 A72-41068

Electrical components in gas turbine control systems.
22 p3216 A72-42521

Electrohydraulic stand for vibration strength testing, discussing system design, specifications, frequency-amplitude characteristics and applications
23 p3278 A72-43760

ELECTRIC CORONA

Positive corona streamers interactions with cloud droplets atomized from water and glycerin solution, discussing atmospheric significance
06 p0841 A72-17823

Powder concentration effects on corona particle charging efficiency of aerosols for electrogasdynamic generators
06 p0760 A72-18335

Plasma corona electron temperature decoupling from core of solid deuterium pellet heated in vacuum by convergent laser beams
16 p2433 A72-32810

ELECTRIC CURRENT

NT ALTERNATING CURRENT

NT ARC DISCHARGES

NT AURORAL ELECTROJET

NT BEAM CURRENTS

NT DIRECT CURRENT

NT EDDY CURRENTS

NT ELECTRIC ARCS

NT ELECTRIC CORONA

NT ELECTRIC DISCHARGES

NT ELECTRIC SPARKS

NT ELECTRODELESS DISCHARGES

NT ELECTROJETS

NT EQUATORIAL ELECTROJET

NT GAS DISCHARGES

NT GLOW DISCHARGES

NT HIGH CURRENT

NT IONOSPHERIC CURRENTS

NT LIGHTNING

NT LOW CURRENTS

NT MERCURY ARCS

NT PENNING DISCHARGE

NT RADIO FREQUENCY DISCHARGE

NT RING CURRENTS

NT RING DISCHARGE

NT TELLURIC CURRENTS

NT THRESHOLD CURRENTS

NT TOROIDAL DISCHARGE

Plasma hydrodynamic Buneman current instability under strong electric field, considering nonlinear stage in one dimensional case
01 p0105 A72-10024

Acoustic instability of plasma with current under equilibrium ionization and moderate neutral gas pressures
01 p0109 A72-10485

MHD instabilities of plasma with current, using two fluid model in crossed magnetic-electric fields
01 p0109 A72-10486

Rocket-borne measurement of particle fluxes and currents in auroral arc, determining pitch-angle distribution of electron and proton energies
01 p0120 A72-10897

Geomagnetic dynamo theory postulating magnetic field by self excitation due to electric currents within earth core
02 p0220 A72-12086

Affined RC or RL networks, investigating real and equal or imaginary, conjugate and inverse voltage and current transmittances
02 p0197 A72-12240

Electrostatic charging mechanisms leading to streaming current generation in moving fluids, considering initial discharge, electrode change and mobility charging current
02 p0261 A72-12553

Computer investigation of three fluid electrical current sheet model, solving magnetic annular shock tube problem
02 p0200 A72-12659

Spatial distribution of total magnetic vector and of electric currents in unipolar sunspot
03 p0428 A72-13300

Solar proton flare connection with strong electric currents, discussing net magnetic flux changes and electric conductivity and field strength
03 p0410 A72-13326

Spreading currents in parabolic rotating coordinates, determining magnetic field components consistent with Laplace equation series expansion
03 p0311 A72-13565

Intense pulsed electron beam production by current flow through narrow gap filled with plasma
03 p0396 A72-13656

Gamma and neutron radiation effects on bipolar transistor current gain response predicted from multiple linear regression analysis
03 p0335 A72-14091

Metal-insulator-metal tunneling junction, calculating effect of localized impurity states in barrier on tunneling current
03 p0404 A72-14267

Pulsed current changes in positive column of He and Ne discharges, observing gradient and electron concentration transient behavior
03 p0399 A72-14348

Gradient-recombination current instability in high resistance compensated semiconductors
04 p0561 A72-15084

Stationary viscous incompressible conducting fluid in conical flow, investigating diverging and converging electric current effects
04 p0558 A72-15342

Magnetospheric current effects on geomagnetic field structure, noting electron and proton precipitation into auroral zone
05 p0657 A72-16275

Current drainage from dilute plasma to high voltage probe via holes in Kapton H polyimide film, quartz and fluorinated ethylene propylene type C
05 p0696 A72-16815

Current reversal effect on anodic aluminum oxide film prepared in phosphate electrolyte, using electron microscope and isotopic labeling
05 p0667 A72-17056

Stationary plasma flow interaction with axisymmetric spatially periodic magnetic field in presence of Hall effect, determining electric currents structure
05 p0701 A72-17241

Static high pressure spherical plasma probe theories verification, showing saturation currents and I-V characteristics agreement with calculated values
06 p0853 A72-17416

Thermal and electrical characteristics of plasmatrons with interelectrode partition and distributed air supply, determining efficiency dependence on current
07 p1040 A72-18996

Flow field induced by electric current jet in incompressible viscous conducting fluid, solving nonlinear momentum equation by series expansion procedure
07 p0967 A72-19504

Transport phenomena theory for semiconductors in strong electric fields, examining negative differential conductivity and nonmonotonic current behavior
07 p1048 A72-19637

Electrodynamics and magnetoelasticity nonlinear Emden-Fowler equation solutions, considering heavy current carrying filaments equilibrium and boundary value problems
07 p1035 A72-19975

Cavity formation and drop transfer time correlation with welding current in powder covered /submerged/ arc welding, using high speed X ray photography
07 p0998 A72-20396

Electrolyte flow rate, electric current intensity and tool electrode shape influence on surface finish quality in precision electrochemical machining
08 p1175 A72-21044

Thermostimulated autophotocurrent emission from Cr-alloyed p-type GaAs electrode, determining spectral distribution and light and electric field effects on current
08 p1216 A72-21071

Transverse and longitudinal current fluctuations in degenerate nonparabolic semiconductors in strong electric field
08 p1216 A72-21074

Thyristors junction area current rise time extension, discussing emitter field regional delay times as function of p-n-p structural properties
08 p1140 A72-21266

Asymptotic expressions for electromagnetic field and currents induced in unbounded dense plasma by relativistic electron beam passage
08 p1215 A72-21721

Electrochemical tests, noting electric potential, current and electrode impedance measurements for corrosion rate and oxidizing power evaluation
08 p1189 A72-22105

Thermal and electric flow analogy application to heat transfer determination on basis of three dimensional model
09 p1410 A72-22628

Current carrier flow parameter fluctuations associated with steady state transport noise in semiconductor devices, considering generation-recombination processes, drift, diffusion and dielectric relaxation
09 p1288 A72-23125

Contractible current loop model for radius variations, induction current, temperature and inertia center velocity in plasmoid interacting with axially symmetric magnetic field
09 p1361 A72-23202

Single helix magnetic field with axial current, discussing field lines rotatory transformation and magnetic well and shear effect on plasma behavior
09 p1363 A72-23216

Double helix magnetic field in longitudinal and axial current fields of stellarators, noting rotatory transformation and shear of field lines
09 p1363 A72-23217

MHD generator duct external loop electric current maximization by working material resistivity tensor optimal distribution
10 p1521 A72-24434

Alloy p-n-p junction transistor diffusion capacity variation with emitter current as function of temperature at 80-320 K
10 p1451 A72-24558

Declinational component of geomagnetic lunar tide diurnal variations, noting effects of electric currents induced in oceans
11 p1622 A72-26103

Radial small-signal gain profile measurement in carbon dioxide laser discharge tube explained by axial gas temperature increase with discharge current
11 p1647 A72-26145

Current flow across double layer plasma in SERT 2 type hollow cathode ion thruster, using Langmuir probes
[AIAA PAPER 72-418]

11 p1706 A72-26168

MPD thruster diagnostics and interpretation of electric current distribution, applying integral form of Maxwell equation for moving Hall probe
[AIAA PAPER 72-498] 11 p1711 A72-26221

Solar current flow penetration to 1 AU in interplanetary medium, discussing inhibition of field line reconnection across neutral sheet 11 p1714 A72-26528

Spreading currents in parabolic rotating coordinates, determining magnetic field components consistency with Laplace equation series expansion 11 p1607 A72-26752

Nonlinear sheath admittance, currents and charges associated with high peak voltage drive on VLF-ELF dipole antenna moving in ionosphere 11 p1599 A72-26769

Theory of magnetotail elongation based on magnetosphere neutral layer drift notion due to electric current from trapped charge carriers inside surrounding plasma sheath 12 p1802 A72-27770

Plasma heating by HF electrostatic instabilities excitation with current across external magnetic field, estimating turbulence, ion collision frequencies and ion heating rates 13 p2009 A72-28426

Pulse plasma injector accelerating circuit resistance dependence on time and current amplitude calculated from current oscillograms 13 p2010 A72-28733

Hall currents effect on unsteady MHD flow of electrically conducting fluid past flat plate imbedded in uniform external transverse magnetic field 13 p2012 A72-29225

Electrothermal instability analysis for MHD generator, considering electron thermal conduction and wall boundaries effects for cases with current parallel or perpendicular to walls 13 p2014 A72-29366

Fluctuating electric current induced magnetic field effects on long wave nonequilibrium plasma instability associated with large scale closed cycle MHD generators 13 p2014 A72-29370

Weakly ionized plasma decay within cylinder with electrically conducting walls in presence of longitudinal magnetic field, determining electric current dependence on cylinder length 13 p2016 A72-29603

Plasma current layer formation due to electric field directed along magnetic field neutral line 13 p2017 A72-29699

Thin wire parallel to interface between two homogeneous half spaces, deriving transmission current wave propagation constant from boundary value problem solution 15 p2200 A72-32108

Electromagnetic gain mechanisms with required energy supplied by static currents and magnetic fields in homogeneous plasmas 16 p2434 A72-32853

Voltage and current generalized immittance converter realization, using with current conveyor for simulation 16 p2367 A72-32856

Free electrons-laser interaction induced electron forward drift and dc current generation, deriving drift velocity by nonrelativistic classical and quantum mechanical theories 16 p2402 A72-33397

CW argon ion laser characteristics at high steady discharge currents, discussing output limitation by low inversion utilization efficiency due to cavity mirrors optical degradation 16 p2404 A72-34035

Conducting body radar scattering control by reactive loading, discussing field pattern synthesis for real current with least mean-square approximation 17 p2513 A72-34358

Undamped photocurrent fluctuations in CdSe single crystals 18 p2718 A72-36348

Equilibrium configurations of Vlasov plasmas carrying a current component along an external magnetic field. 19 p2839 A72-37332

Boundary conditions in the presence of Hall current or finite ion Larmor radius effects. 19 p2839 A72-37338

Short-circuit current in silicon solar cells - Dependence on cell parameters. 19 p2753 A72-37567

Photocathode relative sensitivity spatial distribution as function of wavelength, noting maximum shift from photoeffect contribution to photomultiplier current 19 p2800 A72-37821

The temperature dependence of the critical current of a double Josephson junction. 19 p2846 A72-38556

Effect of the filling of the capture levels with increasing current on the formation of negative resistance under double injection conditions 19 p2846 A72-38574

Electrodynamics and magnetoelasticity nonlinear Emden-Fowler equation solutions, considering current

carrying heavy filaments equilibrium and boundary value problems 20 p2955 A72-40032

Electrodynamic analysis of superconducting vortices interaction with cylindrical cavities [pinning], calculating critical currents in type II superconductors in external magnetic field 21 p3096 A72-40416

Force free fields in type II superconductors. 21 p3096 A72-40573

Current and voltage waveform measurements with sampling oscilloscope and capacitive voltage-divide probe to verify TRAPATT diode oscillator theoretical model 21 p3032 A72-40635

Weakly ionized plasma decay within cylinder with electrically conducting walls in presence of longitudinal magnetic field, determining electric current dependence on cylinder length 21 p3091 A72-40657

A theoretical investigation on the generation current in silicon p-n junctions under reverse bias. 21 p3097 A72-40703

A method to calculate electric currents in quiescent prominences. 21 p3108 A72-41282

Voltage generalized-impedance converter synthesis with RC circuits for obtaining current transfer function proportional to square of s with application to filter design 22 p3140 A72-42303

Self-consistent description of the magnetotail current system. 22 p3172 A72-42429

Current noise and conductance-temperature characteristics of thin discontinuous Pt films on glass substrate interpreted by quantum mechanical electron tunneling model 22 p3214 A72-42453

Generation threshold of anomalous resistance for longitudinal currents in the magnetosphere 23 p3284 A72-43379

Transport phenomena theory for semiconductors in strong electric fields, examining negative differential conductivity and nonmonotonic current behavior 24 p3427 A72-44569

Axial-radar cross section of finite cones by the equivalent-current concept with higher-order diffraction. 24 p3381 A72-45640

ELECTRIC DIPOLES

Conducting half space electric dipole model of radio propagation through earth at 1-10 MHz 01 p0033 A72-11254

Electromagnetic wave scattering and diffraction on lattice of dipole vibrators 04 p0491 A72-15415

Reciprocity theorems in electromagnetic theory concerned with radio transmitting and receiving point interchange for electric dipole sources 05 p0625 A72-16008

Elf/vlf radiation resistance of finite electric dipole oriented at arbitrary angle in cold uniform magnetoplasma, deriving general integral expression 07 p1039 A72-18823

Electron temperature effects on radiation fields and resistance of short electric dipole antenna embedded in hot uniaxial plasma 08 p1215 A72-21991

Power integral method for electric and magnetic dipole antennas vlf/elf radiation patterns in cold magnetoplasma, emphasizing focusing effects of refractive index surface 09 p1279 A72-23009

Compressible anisotropic magnetoplasma filled cylindrical waveguide excitation by electric dipole, plotting electric field patterns as function of electron temperature and density 12 p1782 A72-27489

Human torso surface mathematical model to determine equivalent heart dipole and quadrupole locations for ECG measurements 13 p1908 A72-28571

Electrophysiologic data acquisition by multiple dipole type of inverse electrocardiographic procedure based on model data, noting favorable and unfavorable dipole array configuration 13 p1909 A72-28997

Green function solution for electric field intensity in space due to electric dipole at another point under boundary conditions on surface of revolution 13 p1921 A72-29341

The electromagnetic field generated by an electric dipole in a spherical cavity immersed in a nonlinear plasma 17 p2588 A72-34746

Electric dipole radiation at VLF in a uniform warm magneto-plasma. 19 p2840 A72-37833

Computer-graphics studies of dipole-dipole collisions - Evidence for neutral collision complexes. 21 p3087 A72-40559

Radiation from an electric dipole in anisotropic media. 24 p3424 A72-44706

Electric dipole moment of diatomic molecules by configuration interaction. IV. 24 p3426 A72-44870

The transient electromagnetic response of a spherical shell of arbitrary thickness. 24 p3381 A72-45638

ELECTRIC DISCHARGES

NT ARC DISCHARGES

NT ELECTRIC ARCS

NT ELECTRIC CORONA

NT ELECTRIC SPARKS

NT ELECTRODELESS DISCHARGES

NT GAS DISCHARGES

NT GLOW DISCHARGES

NT LIGHTNING

NT MERCURY ARCS

NT PENNING DISCHARGE

NT RADIO FREQUENCY DISCHARGE

NT RING DISCHARGE

NT TOROIDAL DISCHARGE

Momentum jet and electric discharge from same hole in plane wall bounding viscous incompressible conducting fluid, investigating flow field with similarity solutions 01 p0107 A72-10139

VLF noise spectra in earth-ionosphere cavity due to thunderstorm discharges, noting resonance level splitting by geomagnetic field 01 p0028 A72-10598

Electrodischarge and electrochemical machining applications in continuous repetitive production of aircraft jet engine components 01 p0078 A72-11150

Electrostatic charging mechanisms leading to streaming current generation in moving fluids, considering initial discharge, electrode change and mobility charging current 02 p0261 A72-12553

Dc excited argon laser anode oscillation noise, discussing relation to ballast resistance, suppression conditions and current fluctuation frequency response to laser fluctuation 02 p0239 A72-12826

Plasma jet formation within high pressure discharges in air at atmospheric pressure, discussing electrode configuration, current density and accelerating magnetic field strength 03 p0396 A72-13662

Stepped-leader theory in cloud-to-ground electrical discharges, estimating step-length for different electrical fields by equivalence to electron avalanche transition 04 p0543 A72-14880

Electrostatic field changes in vertical intracloud discharges, discussing positive streamers and return strokes 04 p0543 A72-14881

Pulsed chemical laser started by transverse electrical discharge, observing output energy dependence on fluorine compound used 04 p0530 A72-14974

Electronic system for electrodischarge machining, considering thyristor spark control and circuitry design for automatic feed down and short circuit clearance 04 p0502 A72-15530

Explosive erosion in Al, Cu, W and Pb electrodes during high current spark discharges, using time resolved photography 05 p0692 A72-16032

Carbon dioxide laser pumping at atmospheric pressure by electron beam controlled electrical discharge, discussing measured electrical and laser properties 07 p0999 A72-18875

Laser action in pulsed transverse discharge initiated chemical reactions forming hydrogen and deuterium halides, noting production of previously unobserved transitions 07 p0999 A72-18879

Laser action in carbon monoxide vibrational-rotational bands produced by electrical excitation of carbon monoxide-nitrogen-oxygen-helium mixtures following expansion in supersonic nozzle 07 p1001 A72-19047

Geomagnetic phenomena associated with auroras and magnetic storms, investigating analog modeling experiment by stationary electrical discharges under laboratory conditions 07 p0980 A72-20457

Transients determined for Cs vapor discharge phases, observing current fluctuations between steady states in negative resistance zone above 0.2 torr 07 p1046 A72-20517

Thermomathematical model for calculating craters formed by short pulses in electro discharge machining 08 p1173 A72-21028

Electrical erosion efficiency of metal working under increased pressure in discharge gap in air and water 08 p1174 A72-21029

Technological characterization of electric discharge machines by metal removal rate, volumetric electrode wastage and machined surface roughness 08 p1174 A72-21031

Electroerosion machining with optimal control of electrical parameters, number of passes and electrode

wear, using nonlinear programming and critical path method
08 p1174 A72-21032

Electric discharge carbon dioxide laser performance in terms of optical beam quality, electrical efficiency and gas utilization
10 p1489 A72-23943

Charged and neutral particles radial distribution across positive isothermal plasma column in high current discharges
10 p1521 A72-24355

Electric discharge plasma generator consisting of concentric or parallel electrodes mounted on titanium hydride coated heat resistant ceramic disk
10 p1521 A72-24365

Diaphragmless electrothermal shock tube for collision in preheated Ar, using RF plasma heater
10 p1459 A72-24410

Electrical discharge machining of zirconium diboride, considering operations and tooling requirements
[AIAA PAPER 72-329] 11 p1637 A72-25365

Normal ionizing shock waves characteristics in He under varying conditions of magnetic field strength, discharge current and gas pressure
11 p1694 A72-25789

Hollow cathode discharge effects on throttled electron bombardment ion thruster performance, considering discharge region diameter and length and baffle aperture area
[AIAA PAPER 72-421] 11 p1706 A72-26169

Electrostatic ion thruster theoretical model, deriving ionization rate density as function of discharge current
[AIAA PAPER 72-432] 11 p1707 A72-26175

Solid teflon pulsed plasma thruster quasi-steady and short pulse discharge operations, discussing propulsion system performance and erosion behavior
[AIAA PAPER 72-459] 11 p1709 A72-26195

Plasma diagnostics of inductively coupled RF Hg discharge in RIT-10 ion thruster
[AIAA PAPER 72-472] 11 p1709 A72-26203

Kinetics and cavity intensity models for output characteristics of pulsed electric discharge carbon dioxide lasers
12 p1820 A72-27287

Point discharge current and precipitation effect on atmospheric potential gradient vertical profile
12 p1839 A72-27501

Nonlinear model of ionization instability of MHD generators, assuming discharge structure with alternating layers of high and low electrical conductivity
13 p2014 A72-29371

Vacuum gap discharge conditions as function of electron beam parameters and metal vapor pressure
13 p2017 A72-29611

Current breaks due to capacitor discharges in W and Mo wires, noting duration proportional to wire mass
13 p2007 A72-29980

Electroexplosive devices firing energy parameters determination by capacitor discharge system providing exponential pulses terminated at adjustable width
14 p2143 A72-30200

Detonation wave generation in gas discharge plasma by pulsed electrical discharge
14 p2137 A72-30313

Pulsed Ar plasma temperature and charged particle concentration obtained as functions of elapsed discharge time by spectroscopic observation
14 p2139 A72-30780

Laser emission from pulsed transverse electric discharge in supersonic nozzle downstream region gas dynamic cooled mixture
15 p2245 A72-31385

Transversely excited pulsed carbon dioxide-nitrogen-helium laser with electrical discharge determined optimum partial pressure
15 p2249 A72-32236

Solar flare and neutral sheet simulation by investigating behavior of plasma current through magnetic neutral point created by capacitor discharges
15 p2301 A72-32342

Electrical pumping discharge confined by liquid wall of vortex channel in dye laser solution
15 p2251 A72-32528

Transverse electric discharge pulsed carbon dioxide laser, measuring refractivity time history by interferometry for comparison with prediction
15 p2251 A72-32537

Shock wave generation by high current pulsed discharges, determining shock front velocity as function of magnetic pressure on current sheath
16 p2434 A72-32909

Discharge stabilization in closed cycle carbon dioxide electric discharge convection lasers by aerodynamic, RF power and tandem techniques
[AIAA PAPER 72-723] 16 p2404 A72-34026

Flow conditioning in electric discharge convection lasers.
17 p2562 A72-34638

Charged and neutral particles radial distribution across positive isothermal plasma column in high current discharges
17 p2589 A72-34955

Electric discharge plasma generator consisting of concentric or parallel electrodes mounted on titanium hydride coated heat resistant ceramic disk
17 p2589 A72-34964

Electrical CO mixing gas dynamic laser.
[AIAA PAPER 72-725] 17 p2564 A72-35483

Initial-boundary-value problem of the formation of an electrical discharge in a flow.
17 p2592 A72-35627

RF augmentation in CO₂ closed-cycle dc electric-discharge convection lasers.
17 p2565 A72-35818

Excitation modes and operating characteristics of electric discharge convection lasers
[AIAA PAPER 72-722] 17 p2565 A72-35962

Arc mode thermionic converter at low cesium vapor pressures
18 p2647 A72-36216

Influence of an electrical discharge in a flame on the propagation of the flame
18 p2740 A72-36244

Electron density measurements in early stage of the high current pulsed discharge.
18 p2716 A72-36957

High power pulsed HCN laser.
19 p2811 A72-37583

Electric discharge concept to uncouple electron density from temperature for production of stable uniform electric laser discharges
19 p2812 A72-38596

Influence of plasma kinetic processes on electrically excited CO₂ laser performance.
19 p2812 A72-38598

Recent international development in non-traditional machining processes - EDM, ECM, LBM, EBM.
20 p2928 A72-39203

Energy characteristics of the laser action in rhodamine 6G pumped by a pinched discharge.
20 p2933 A72-39512

Free fall column theory allowing for 'neutral gas reduction' by ionization processes, and application of this theory to noble gas ion lasers
21 p3090 A72-40488

Investigation of the structure of a high-current discharge in a lithium plasma
22 p3209 A72-41878

Some characteristics of an electron-beam induced discharge in a vacuum
22 p3208 A72-43123

Detonation wave generation in gas discharge plasma by pulsed electrical discharge
23 p3318 A72-43215

Electrical discharge-produced explosions aboard supertankers during cleaning operation and electrostatic charging of supersonic aircraft during passage through heavy rain, noting water drop disintegration
24 p3368 A72-44979

One dimensional theory of electric discharge detonation effects in flame propagation within square duct with combustible gas mixture, applying to electrochemical pulse jet engine
24 p3464 A72-45064

Electronic energy transfer phenomena in rare gases.
24 p3429 A72-45310

ELECTRIC ENERGY STORAGE

MNOS transistors charge storage properties at high electric field strengths and current densities near gate insulator breakdown, determining reliable operating limits
03 p0336 A72-14277

Quasi-steady MPD propulsion systems for astronomical applications, describing electric energy storage bank, mass supply system, accelerator and operation principle
09 p1374 A72-22934

Electrohydraulic and electromagnetic metal forming, using capacitor stored energy conversion into hydraulic shock waves or magnetic pressure to deform sheet metal components, pipes, etc
15 p2243 A72-31323

ELECTRIC EQUIPMENT

Soviet book on electrical equipment and instrumentation of An-24 aircraft covering power sources, control, safety systems, engine, flight and navigation instruments and autopilot
05 p0615 A72-16400

Shielding procedures to control electromagnetic interference /EMT/ in design and operating electric equipment
10 p1452 A72-24813

Space shuttle umbilical systems for mating, connection and checkout of carrier assemblies and couplings for cryogenic, electrical, pneumatic and hydraulic services
15 p2213 A72-31695

ELECTRIC EQUIPMENT TESTS

Trident aircraft air-system interrogator airborne first line test apparatus for electrical components malfunction diagnosis
06 p0796 A72-18154

Airport lights systems control with thyristors, discussing light intensity regulation, command board design and insulation test equipment
12 p1794 A72-27401

ELECTRIC FIELD STRENGTH

MHD channels magnetoacoustic and ionization instabilities effect on mean current density and electric field strength, determining effective electroconductivity and Hall parameter
01 p0110 A72-11208

Magnetosonic perturbations caused by ideally conducting sphere expansion in cold plasma, determining electric field and magnetic induction time dependences
02 p0217 A72-11939

Coastline effect on electric field strength of geomagnetic micropulsations
03 p0344 A72-12977

Transverse photoconductivity and dark I-V characteristics of n-GaAs compensated with Cr in high electric field at room temperature
03 p0401 A72-13586

Soviet book on ground wave radio propagation at medium and long wavelengths covering field strength calculations over plane and spherical earth, soil conductivity, etc
03 p0323 A72-13950

Electric field intensity and pulsation spectra variation along rectangular channel in transverse magnetic field, noting current density changes
03 p0398 A72-14006

MNOS transistors charge storage properties at high electric field strengths and current densities near gate insulator breakdown, determining reliable operating limits
03 p0336 A72-14277

Dielectrophoresis force measurements and wedge shaped capacitor separation properties in satellite zero gravity conditions
04 p0549 A72-14988

Plasma ion collision transport analogy with turbulent velocity space momentum transfer, explaining confined plasma runaway electron absence in strong electric fields
04 p0560 A72-15469

Electric field strength, radiated power and radial temperature distribution measurements in high pressure Ar cascade arc
05 p0695 A72-16156

Electric field distribution in waveguide-slot radiator, describing measurement technique
05 p0635 A72-16333

Monochromatic light beam propagation in optically nonhomogeneous medium containing matter in near critical state, determining exciting wave electric field strength
05 p0691 A72-16683

Plane magnetized plasma layer interaction with hf electromagnetic field, showing electric field strength and direction dependence on ion acoustic-Alfven velocity ratio
05 p0697 A72-16982

Extensive air showers radio emission polarization, spatial distribution and electric field strength, noting geomagnetic mechanism effect
06 p0870 A72-17278

Magnetic and electric field intensities measurement with charged particle beams in coaxial high temperature plasma sources
06 p0863 A72-18415

Geoelectric field strengths deduction from mid-frequency slopes on diurnal incidence plot of pc 1 hydromagnetic whistlers
07 p0974 A72-18904

Large drops coalescence, investigating approach rate dependence on electric field strength and distance
08 p1201 A72-21998

Electric field voltage effect on dispersion of electrostatically atomized liquids and hydrocarbon fuels with and without gamma irradiation
09 p1350 A72-22546

Momentum transfer theory for ion drift velocity in multicomponent gas mixture at arbitrary electric field strengths
10 p1519 A72-24096

Average electric field and power density of electromagnetic wave scattered from rough layer with plane interface, calculating scattering cross sections
10 p1512 A72-24744

Linear electron acceleration mechanism in plasma, showing polarization fluctuations in diode under strong electric field
11 p1699 A72-26761

Plane magnetized plasma layer interaction with HF electromagnetic field, showing electric field strength and direction dependence on ion acoustic-Alfven velocity ratio
12 p1850 A72-27126

Magnetosonic perturbations caused by ideally conducting sphere expansion in cold plasma, determining electric field and magnetic induction time dependences
13 p1949 A72-29251

Green function solution for electric field intensity in space due to electric dipole at another point under boundary conditions on surface of revolution
13 p1921 A72-29341

- Electroacoustomagnetic and Hall effects in semiconductors within strong electric field involving phonon production by supersonic electron drift
13 p2022 A72-29437
- Resonant irradiation effect on cesium discharge plasma, charge density, electron temperature and electric field strength
13 p2017 A72-29610
- Beta-conductive method improvement for semiconductor electric field intensity measurement by pulsed electron beam
15 p2238 A72-32240
- Optical measurements of electric fields turbulence level in gun plasma, noting compatibility with spatial Landau damping
15 p2287 A72-32409
- Hydrogen atom ground state ionization probability derivation as function of electric field strength and distance to metal surface
15 p2279 A72-32699
- Monochromatic light beam propagation and scattering in optically nonhomogeneous medium containing matter in near critical state, determining exciting wave electric field strength
16 p2426 A72-33694
- Magnetic and electric field intensities measurement with charged particle beams in coaxial high temperature plasma sources
17 p2588 A72-34864
- A nomogram for determining the phase difference of an elliptically polarized wave
18 p2663 A72-37219
- Pulsar properties correlation with radially oscillating coherent plasma of electron-positron pair production by strong electric field around central object
19 p2859 A72-37892
- High level E-field susceptibility measurement problems and techniques.
20 p2906 A72-38981
- Ionospheric and magnetospheric electric field strength measurements in auroral and polar cap regions by Ba ion cloud and double floating probe techniques
20 p2918 A72-39543
- Resonant irradiation effect on Cs discharge plasma charge density, electron temperature and electric field strength
21 p3091 A72-40664
- The field strength conditions for measuring the carrier lifetime in semiconductor crystals by the light flash method
21 p3098 A72-41487
- Electric field intensity distribution function for thermoelectronic emission from hot cathodes in low temperature plasma, using Richardson Formula
21 p3094 A72-41656
- A measurement of ionospheric electric fields at high latitude.
22 p3169 A72-42015
- Effect of radiation polarization on hologram quality
22 p3176 A72-42107
- Theory of Poole-Frenkel conduction in low-mobility semiconductors.
22 p3214 A72-42317
- Induction effect of slowly decaying ring current, estimating electric field strength by model consisting of earth dipole and symmetric ring
22 p3172 A72-42430
- Disequilibria created by an electric field in a nitrogen plasma
23 p3321 A72-43695
- Electric field distribution and strength and electron trajectories computations in designing electron optical display systems, using rectangular networks
23 p3291 A72-44312
- Geomagnetic tail magnetic and electric fields U1.F, V1.F and E1.F fluctuations, considering relationship to substorm processes
24 p3397 A72-44857
- ELECTRIC FIELDS**
- Internal electrostatic field effect on ion separation in expanding pulsed laser produced plasmas
01 p0105 A72-10021
- Plasma hydrodynamic Buneman current instability under strong electric field, considering nonlinear stage in one dimensional case
01 p0105 A72-10024
- Oblique electromagnetic wave propagation modes in anisotropic ionized stratified medium, investigating electric field and polarization components
01 p0106 A72-10133
- Strong ionizing shock waves production in hydrogen and deuterium gases, measuring plasma electron temperature, axial electric field and density and magnetic field compression
01 p0108 A72-10237
- Isolated magnetospheric substorms model, explaining electric field origin, cold plasma flow, magnetic field lines and particle phenomena
01 p0060 A72-10889
- Parallel electric field evidence near auroral ionosphere deduced from low energy particles, energy spectra and angular distribution
01 p0061 A72-10895
- Magnetoionospheric wave and particle phenomena correlation to convection electric fields in nightside magnetosphere during isolated substorms
01 p0062 A72-10904
- Electric field induced splitting of drift shells composed of trapped particles, taking into account non-dipole field components to lowest order
01 p0062 A72-10905
- Meridional currents intensity in equatorial electrojet region, computing electric and magnetic fields
01 p0063 A72-10924
- Tropospheric layer structures effect on long range vhf radio communication, calculating wave modes at attenuation rate and electric field patterns
01 p0032 A72-11238
- Thermal conductivity, electrical conductivity, viscosity and diffusivity of ionized gas-solid suspension in electric field, using transport equations and particle interaction potentials
01 p0111 A72-11332
- Electron beam interaction with electromagnetic waves in longitudinal interaction devices during focusing by homogeneous magnetic and periodic electrostatic fields
02 p0189 A72-11564
- Spectrum analysis of synchronous recordings of Pi 1 irregular pulsations and auroral brightness at Sogra for ionospheric electric fields
02 p0216 A72-11923
- Vertical distribution of ionospheric and magnetospheric electric fields, estimating Joule heating
02 p0220 A72-12324
- Electrohydrodynamic ideal incompressible fluid flow in flat and circular channels, determining electric potential and field distribution
02 p0266 A72-12431
- Hall effect and conductivity dependence on applied electric field in multivalley semiconductor for power dependent intervalley scattering time
02 p0269 A72-12887
- Radiation pattern from open ended parallel plate waveguide with arbitrary electric or magnetic aperture field distribution, using Wiener Hopf technique
03 p0331 A72-13409
- Adiabatic charged particle orbits in magnetic null sheet with transverse electric and added normal magnetic fields
03 p0348 A72-13512
- Electric field aligned sheet currents of low energy electrons and protons near auroral arc, obtaining magnetic signatures
03 p0349 A72-13516
- Vertical motions of midlatitude F 2 layer during magnetospheric substorms, investigating electric field distribution
03 p0349 A72-13519
- Linear electron acceleration mechanism in plasma, showing polarization fluctuations in diode under strong electric field
03 p0395 A72-13573
- Electric field effects on electromagnetic wave packet motion in anisotropic nonlinear medium with electro-optical effect
03 p0322 A72-13737
- Dielectric siphons, using weak polarization force density exerted on insulating dielectric liquids by nonuniform electric field
04 p0520 A72-14416
- Three terminal voltage-tunable Gunn effect microwave oscillator, discussing depletion depth and electric field control modes for frequency
04 p0496 A72-14479
- Current density nonlinear transient response and energy absorption of weakly ionized plasma under pulsed electric field
04 p0555 A72-14532
- H beta satellites observation in presence of oscillating electric field associated with plasma turbulence [A72-741085]
04 p0555 A72-14576
- Hf electric field influence on electron drift instability and slow ion-acoustic waves for inhomogeneous magnetized plasma stabilization
04 p0555 A72-14617
- Light wave electric field Franz-Keldysh effect on GaAs absorption edge, using electroabsorbance, electroreflectance and photoconductivity spectrum and internal photoeffect analysis
04 p0561 A72-14621
- Nonuniform sinusoidal electric field anomalous influence on ion motion in gas with allowance for ion-atom collisions
04 p0547 A72-14622
- Stepped-leader theory in cloud-to-ground electrical discharges, estimating step-length for different electric fields by equivalence to electron avalanche transition
04 p0543 A72-14880
- Electrostatic field changes in vertical intracloud discharges, discussing positive streamers and return strokes
04 p0543 A72-14881
- Ar gas dc discharge plasma characteristics in crossed electric and magnetic fields, examining equivalent pressure concept
04 p0556 A72-14945
- Electron heating by oscillating electric field in presence of steady magnetic field, solving Boltzmann transport equation for electron velocity distribution in plasma
04 p0556 A72-14947
- Ionospheric plasma drift instability, showing electric and magnetic fields, electron density and temperature effects
04 p0517 A72-14956
- Nonuniform radial electric field effects on low beta magnetized plasma column stability from numerical analysis for weakly collisional regime
04 p0557 A72-15023
- Electric or magnetic field tangential components at ground-air interface, discussing secondary electromagnetic sources
04 p0492 A72-15438
- Closed solution to Gunn effect field domain formation and propagation, using approximate I-V curve and method of characteristics
04 p0563 A72-15503
- Electron drift speed and multiplication rate in pulsed Ar positive column in axial electric field
04 p0553 A72-15669
- Two dimensional axisymmetric surface waves motion in inviscid incompressible homogeneous electrically conducting fluid under uniform magnetic and electric fields, considering surface tension effects
04 p0560 A72-15744
- Monograph on design and characteristics of rotating plasma device under crossed electric and magnetic fields, covering dynamic behavior of hydrogen puff
05 p0642 A72-15798
- Transverse electric field in ionosphere and magnetosphere during inhomogeneities consisting of fast electrons
05 p0656 A72-16246
- Charged particle acceleration by nonstationary sinusoidal electric fields in earth magnetosphere based on mathematical model
05 p0709 A72-16256
- Lower ionospheric currents fields, determining Hall conductivity and geomagnetic lines of force slope effects
05 p0657 A72-16266
- High frequency electric field backscattering by plane electromagnetic wave incident on perfectly conducting sphere with radially inhomogeneous dielectric coating
05 p0630 A72-16621
- Pulsed flat electrode erosion plasma accelerator, determining electric and magnetic fields distribution, current density and electron concentration
05 p0697 A72-16987
- Electron heating model in perpendicular collisionless plasma shock waves based on electron trapping by turbulent electric field
05 p0697 A72-17014
- Physical processes of fluids atomization in electric field, discussing droplet surface instability and boundary values of surface tension coefficient
05 p0667 A72-17185
- Parametric plasma instability in hf electric field and constant magnetic field, noting longitudinal plasma oscillations growth
05 p0700 A72-17234
- Polarization electric field and depolarization current measurements in plasma flows along toroidal solenoid with diverter
06 p0853 A72-17387
- Interplanetary magnetic field fluctuations correlation with trapped particles redistribution, deriving magnetospheric electric field properties
06 p0875 A72-17468
- Quiescent large volume collisionless He and Ar plasma generation via hf electric fields, noting low cost
06 p0854 A72-17504
- Dynamic stabilization of transverse Kelvin-Helmholtz instability driven by nonuniform plasma motion, using ac electric field near ion cyclotron frequency
06 p0857 A72-17531
- Injection laser threshold current density, radiation pattern and electric field distribution relation to layer thickness and dielectric constants, using waveguide theory
06 p0825 A72-17772
- Electric field rise times of first and subsequent lightning return strokes, discussing waveform oscillograms
06 p0841 A72-17822
- Pulsed and hf electric field effects on ionizing particle recording in nuclear and photographic emulsions
06 p0816 A72-17833
- Piezoresonance modulation of IR amplitude in GaAs crystal by electric field at single, doubled and quadrupled frequencies
06 p0866 A72-17843
- Boltzmann equation solution analysis for Maxwell-Lorentz gas in electric field, discussing conditions for electron velocity distribution isotropic part evolution towards Maxwellian distribution
06 p0861 A72-18162
- Electrostatic field calculation for magnetron/injection electron gun with wedge shaped cathode
06 p0826 A72-18404

Interelectrode gas-filled gap electron avalanche formation effects in weak electric field, calculating ionization coefficient

06 p0863 A72-18411

Electric field induced ionizing potential waves in dense gas, describing avalanching electron gas breakdown into filaments by fluid dynamic and Maxwell field equations

06 p0864 A72-18534

Electrostatic focusing field inhomogeneity/gradients/ effects on high frequency electron-wave interaction processes in linear beam backward wave oscillator tube

07 p0952 A72-18845

Ion-electron collisions effect on ion cloud motion in magnetoactive plasma immersed in uniform external electric field

07 p1055 A72-18894

Electroconductivities and electrostatic field structure within equatorial electrojet, observing vertical distribution

07 p1056 A72-18896

Small scale phase space density granulations/clumps/ in turbulent plasma due to fluctuating electric field

07 p1041 A72-19510

Weak LF electric field influence on circadian rhythms of human rectal temperature and activity

07 p0918 A72-19531

Transport phenomena theory for semiconductors in strong electric fields, examining negative differential conductivity and nonmonotonic current behavior

07 p1048 A72-19637

Strong electric field recombinational domains in semiconductors with mobile holes and electrons during band-band illumination or double injection

07 p1048 A72-19638

Coordinate transformation for decoupling equations for tangential electric and magnetic field propagation through series of uniform cylindrical layers with arbitrary properties

07 p0946 A72-19799

Magnetosphere LF electric fields influence on trapped radiation region particle behavior, considering magnetic drift rates

07 p1062 A72-20036

Electric field measurements in ionosphere and magnetosphere by double probe and electron and ion drift techniques

07 p0978 A72-20042

Ionosphere electric field sources, magnitudes, relation to currents and effects on ionization distributions and electron density irregularities

07 p0978 A72-20043

Structural interactions between magnetosphere and ionosphere in terms of electrostatic field associated with plasma temperature difference

07 p0979 A72-20046

Electric field in flow of medium with tensor conductivity due to Hall effect, studying eddy currents structure in magnetic field variation region

07 p1044 A72-20316

Interplanetary origin of magnetospheric electric fields responsible for polar magnetic disturbances

07 p0979 A72-20382

Bulk conductors dc field distribution applications to electrical resistivity measurements and nondestructive testing

07 p0998 A72-20461

Radio wave alternating electric field heating of ionospheric plasma electrons with density increase below 200 km and decrease at F layer maximum

08 p1152 A72-20703

Charged conductors in homogeneous collisionless magnetoactive plasma at hybrid frequencies, investigating antenna array quasi-electrostatic field one dimensional structure

08 p1138 A72-20746

Transverse and longitudinal current fluctuations in degenerate nonparabolic semiconductors in strong electric field

08 p1216 A72-21074

Electron plasma fluctuations in semiconductor with nonparabolic conduction band under external electric and magnetic fields

08 p1218 A72-21877

Quasi-elastic scattering differential cross section for nonpolarized IR radiation in electron plasma of semiconductors in strong elastic fields

09 p1366 A72-22210

Light modulation by exciton electric absorption in thin high impedance recrystallized CdTe films within strong electric fields, showing spectral distribution curves

09 p1366 A72-22419

Plasma emitter shape determination in accelerating electric field for charged particle flux production

09 p1358 A72-22490

Two fluid MHD model to study cylindrical plasma condenser resonance properties in axial magnetic and alternating electric fields

09 p1360 A72-22952

Ball lightning theory based on thin conducting ladder networks and three dimensional fine particle structures formation in electric fields

09 p1346 A72-22963

Turbulent LF electric field fluctuations relationship with disturbed F region, spread F and scintillations of radio stars and satellites

09 p1300 A72-23025

Noise of high electric field biased gallium arsenide diodes, calculating LF power spectrum

09 p1288 A72-23123

German monograph on radiation characteristics of planar systems in aperture plane of parallel plate waveguide, obtaining relationship between electric and magnetic fields

10 p1434 A72-23775

Hydrogen atom emission spectrum calculation in uniform rotating electric field, applying to charged particles collisions and Stark broadening of plasma H lines

10 p1514 A72-24039

Relativistic electron beam injection into dense plasma, analyzing perturbed electric and magnetic fields and charge and current densities

10 p1521 A72-24353

Ionospheric and magnetospheric electric field measurements by rocket, satellite or balloon-borne electrostatic probes or by plasma drift methods

10 p1473 A72-24529

Electric field profile in n-type GaAs layer biased above transferred electron threshold for small signal amplifier operation

10 p1450 A72-24554

Dipole antenna near electric field, basing calculation method on integral equation for antenna surface charge distribution function

10 p1451 A72-24579

Sporadic E layer altitude and density variations caused by lunar influences, using model for electrostatic field and wind shear effects

10 p1478 A72-25163

Electron density maxima position relationship to wind profiles in sporadic E layer with electric fields and vertical ion motion

10 p1530 A72-25165

Semiconductor film impedance vs resistivity in free space electric field

11 p1700 A72-25778

Sunspots contact region charged particles acceleration by plasma flow induced electric field, noting Fermi type mechanism

11 p1695 A72-26107

Anomalous plasma heating by laser irradiation with superimposed electric field oscillating near plasma frequency

11 p1696 A72-26326

Radial profiles of ionized He flux and protons in magnetosphere, taking into account charge exchange processes and fluctuating electrostatic fields

11 p1624 A72-26397

Geomagnetic Sq current electric field mapping into lower atmosphere, calculating equipotential surfaces

11 p1626 A72-26416

Third harmonic current density excitation by HF electric field in Lorentz plasma, calculating electron distribution function with unnormalized spherical harmonics and Fourier series

11 p1697 A72-26553

Geomagnetic activity index response time to fluctuations in interplanetary electric field azimuthal component, relating to magnetosphere average energy content

11 p1627 A72-26670

Constitutive equations for nonlocal theory of polar elastic dielectrics interaction with quasi-static electric field, using variational principle

11 p1738 A72-26723

Pulsed flat electrode erosion plasma accelerator, determining electric and magnetic fields distribution, current density and electron concentration

12 p1850 A72-27131

Transient current density in plasma subjected to pulsed electric field derived from Boltzmann transfer equation

12 p1850 A72-27278

Turbulent plasma electric field energy density spectrum from statistical mechanics investigation based on canonical formalism for electron plasma

12 p1851 A72-27387

Cascade ionization of air by RF electric fields and intense laser pulses, solving Boltzmann equation for electron distribution

12 p1848 A72-27390

Tropical thunderstorm precipitation current variations due to lightning produced atmospheric electric field changes, considering charged raindrops turbulent diffusion

12 p1839 A72-27502

Inertial sensing principles interrelationship, stressing electric and magnetic procedures

12 p1809 A72-27788

Analytic models of large scale electric fields in atmosphere, considering geomagnetic Sq current in lower atmosphere and inner magnetosphere

12 p1804 A72-27790

Upper atmosphere electric fields derived from ionosphere-earth electric potential measurements following solar flare activity

12 p1804 A72-27805

Room temperature time of flight electron and hole mobility and trapping time measurements in zinc selenides as function of electric field

12 p1855 A72-27835

Electric field nature required for DP current system development in disturbed high latitude ionosphere, discussing F 2 region ionization drift

13 p1946 A72-28596

Qualitative microscopic model for biologic postsynaptic membrane with tunneling chemical bonds, noting selective ionic conductivity as function of electric field

13 p1909 A72-28769

West German-United States Barium Ion Cloud Project meteorological support at Wallops Station, discussing magnetospheric magnetic and electric fields

13 p1947 A72-28802

Contact potential difference effects on lubricant film thickness in electronic equipment joints, noting molecules orientation in electric field

13 p1930 A72-29052

Electrostatic field and electron trajectories calculation for focusing optoelectronic systems formed by interacting electrodes positioned on conducting surface

13 p2004 A72-29070

Spectrum analysis of synchronous recordings of Pi 1 irregular pulsations and auroral brightness at Sogra for ionospheric electric fields

13 p1948 A72-29235

Electrode boundary layer electrical breakdown mechanism with allowance for steep temperature gradients at surface, considering Joule heating or electrostatic field effect as causes

13 p2013 A72-29361

Plasma wave measurements duringOGO-5 dayside magnetosphere polar cusp encounters, discussing ULF magnetic field wave levels and VLF electric field amplitude ranges

13 p1950 A72-29380

Polar thermospheric wind calculation from convection electric field measurements in polar cap ionosphere, using simple ionospheric model

13 p1950 A72-29385

He ions motion normal to magnetic field under induced electric field, analyzing resonance mechanism

13 p2016 A72-29606

Plasma current layer formation due to electric field directed along magnetic field neutral line

13 p2017 A72-29699

Time varying magnetospheric electric field spatial distribution effect on plasmasphere temporal evolution, considering fine structure due to periodic gusts in convection electric field

13 p1953 A72-29804

Positively and negatively charged plasma components thermodynamic density fluctuations effect on ionospheric and magnetospheric slowly varying electric fields measurement

13 p1953 A72-29810

Electric field excited stable auroral red arc time dependent behavior, noting inconsistency with satellite and ground observation of 6300 A emission for electron energy

13 p1953 A72-29812

Density and electric field oscillations of plasma in stellarator, considering magnetic field strength effect, stabilization by ionic collisions and energy pumping mechanism

13 p2019 A72-29985

Ion-acoustic oscillations effect on turbulent plasma electric conductivity within weak external electric field

13 p2019 A72-29990

Airplane-borne cylindrical field mill type instrument to record atmospheric electric field

13 p1961 A72-30085

Microscopic processes within high energy ion acceleration in laser-produced plasmas, discussing transient electric field role

14 p2136 A72-30178

Charge carrier cooling in nonhomogeneous semiconductors by static electric field, plotting average electron temperature as function of current

14 p2142 A72-30362

Near field effects on pulsar particle acceleration, relating electric and magnetic field magnitudes

14 p2156 A72-30568

Ionosphere heating effects produced by transverse electric field, discussing strong nighttime source

14 p2100 A72-30631

Magnetospheric and ionospheric potential electric fields, using variational process based on transverse/longitudinal conductivity ratios in plasma

14 p2100 A72-30633

Magnetospheric electric fields estimation from electron fluxes intensity on early daylight side

14 p2102 A72-30660

Magnetic and electric field effects on steady state laminar MHD Couette flow of non-Newtonian fluids governed by Prandtl rheological law or Ostwald-de Waele power law

14 p2139 A72-30717

Gravitational radiation generation and detection, discussing Weber detector, interaction with electric and magnetic fields and gravitational astronomy

15 p2273 A72-31287

Temperature and electric field profiles in two TRAPATT diode structures in nonoscillatory state under dc bias, comparing geometrical limitations on diamond heat sinks

15 p2205 A72-31316

Joint photon-count probability distribution measurement of electric field amplitude correlation function for random-Gaussian light fields produced by laser beam scattering

15 p2280 A72-31378

Electric field and volume charge density distribution in bipolar conductivity semiconductor with recombination instability

15 p2291 A72-31392

Solar event-related ionospheric horizontal electric fields derived from balloon measurement of mid-European and equatorial ionosphere potentials

15 p2223 A72-31556

High electric field effects on I-V characteristics of Te-As-Ge-Si type chalcogenide thin film, noting Poole-Frenkel emission and electron tunneling roles

15 p2291 A72-31641

Electric field projections in contrast to voltage as working quantity for frontal plane ECG leads

15 p2188 A72-31766

Electric and magnetic fields fluctuations in region between shock wave front and magnetosphere boundary, noting resulting energy dissipation

15 p2225 A72-31902

Electron pressure effect on lunar wake shape and size, calculating electric field created by charge separation

15 p2308 A72-31925

Thermodynamic plasma density fluctuation induced electric noise field measurement as means to determine plasma density and electron and ion temperatures

15 p2284 A72-31943

Whistlers noise frequency and minimum group time delay determined from model magnetosphere and from measurement, noting precision effect on electric field calculation accuracy

15 p2198 A72-31947

Back surface electric field Si cell characteristics and fabrication using alloyed-through contact process

15 p2182 A72-32130

Electron swarms in uniform electric fields, discussing anode current amplification/radial distribution and drift-diffusion equation

15 p2285 A72-32239

Skewed wire antennas electric and magnetic near fields prediction from computer programs based on matrix inversion method

15 p2209 A72-32567

Electron beam amplifier based on fast cyclotron wave interaction with slow synchronous wave in axisymmetrical electrostatic field, discussing power efficiency increase

15 p2210 A72-32377

HF electric field effect on ultrasound wave propagation in semiconductor, noting amplification factor dependence on electron heating

15 p2279 A72-32739

Azimuthal electric fields role in toroidal plasma transport properties based on kinetic theory for collision dominated regime

16 p2432 A72-32806

Nightside magnetosphere convection electric field from motions of whistler ducts within plasmasphere, considering interplanetary magnetic field theta component

16 p2382 A72-32960

Electric and magnetic field effects on auroras formation, noting similarity with thermonuclear reactor plasma

16 p2456 A72-33518

Particle and energy fluxes across magnetic field in axisymmetric toroidal magnetic traps and plasmas with weak collisions, calculating radial electric field

16 p2440 A72-34153

Report on photo-sheath calculations for the satellite GEOS.

17 p2553 A72-34629

Plasma emitter shape determination in accelerating electric field for charged particle flux production

17 p2588 A72-34653

Real height variations of the ionospheric F2-layer above some pairs of geomagnetically conjugate stations.

17 p2545 A72-34689

Relativistic electron beam injection into dense plasma, analyzing perturbed electric and magnetic fields and charge and current densities

17 p2589 A72-34954

Solution of the Boltzmann equation for a fully ionized plasma in an oscillatory electric field and a steady magnetic field. V - Explicit solution for a homogeneous plasma in a high-frequency electric field.

17 p2589 A72-35057

Auroral electron acceleration by longitudinal electric field due to protons defreezing above ionosphere

17 p2550 A72-35852

A theoretical analysis of the acceleration of ions in axially symmetric crossed fields with an external source and sectioned electrodes

17 p2593 A72-35902

Calculation of the dependence of the charge density on the distribution of the potential in crossed symmetric electric and magnetic fields

17 p2593 A72-35903

A new source for the large-scale electric fields in the magnetosphere.

18 p2686 A72-36623

Quasi-linear theory of plasmas situated in a weak UHF electric field and a constant magnetic field

18 p2715 A72-36654

Electric fields in MHD channels in the case of anisotropic and nonuniform conductivity

18 p2716 A72-36817

Phase-plane solution for the electrostatic field of an ionospheric satellite.

18 p2728 A72-36950

Detection of defects in semiconductor structures by means of recording the temperature and electric fields.

18 p2693 A72-37106

Flute modes in a plasma in the presence of nonuniform electric fields.

18 p2717 A72-37162

Production of intense ion beams by high-frequency electric fields.

19 p2839 A72-37331

Variation of the longitudinal electric field by the internally modulated beam in a He-Ne laser.

19 p2810 A72-37408

Instabilities in semiconductors with negative differential mobility.

19 p2844 A72-37465

The effect of contacts on microwave emission from InSb.

19 p2844 A72-37728

Infrared dispersion of second-order electric susceptibilities in semiconducting compounds.

19 p2844 A72-37944

Radio wave alternating electric field heating of ionospheric plasma electrons with density increase below 200 km and decrease at F layer maximum

19 p2790 A72-38331

Role of an electric field in the diffusion mechanism of the graphite-to-diamond phase transformation

19 p2823 A72-38405

Properties of the electrostatic field of a system of annular electrets and possibilities of its application for focusing in molecular generators

19 p2804 A72-38538

A satellite survey of vector electric fields in the ionosphere at frequencies of 10 to 500 hertz. I - Isotropic, high-latitude electrostatic emissions.

19 p2768 A72-38742

A satellite survey of vector electric fields in the ionosphere at frequencies of 10 to 500 hertz. II - The electric component of ELF hiss.

19 p2768 A72-38743

A satellite survey of vector electric fields in the ionosphere at frequencies of 10 to 500 hertz. III - Low-frequency equatorial emissions and their relationship to ionospheric turbulence.

19 p2768 A72-38744

Kinetic theory of density fluctuations in a magnetized collision-dominated plasma in an electric field.

19 p2792 A72-38745

A small ELF electric field probe.

20 p2921 A72-38994

On the theory of electrical conductivity in semiconducting thin films under a high electric field.

20 p2959 A72-39216

Radial penetration of a hot plasma associated with a large-scale electric field in the magnetosphere, and some related problems.

20 p2916 A72-39228

Electrostatic, reticular vorticity, turbulence effects and equivalences with tensional and spectral elastic fields.

20 p2953 A72-39419

Radiation from a particle in static electric and magnetic fields.

20 p2956 A72-39459

Control of high-field domain in GaAs by the field effect and its application to functional devices.

20 p2960 A72-39706

Single-cycle electron acceleration in focused laser fields.

20 p2934 A72-39720

Investigation of the coagulation and breaking of droplets of comparable dimensions in an electric field

20 p2956 A72-40038

Characteristics of the low temperature effect of an electric field on the sensitivity of photographic emulsions

21 p3053 A72-40391

He ions motion normal to magnetic field under induced electric field, analyzing resonance mechanism

21 p3091 A72-40660

Determination of conduction anisotropies in semiconductors.

21 p3097 A72-40697

Formation of intense charged particle beams in a current-carrying plasma.

21 p3092 A72-40834

Diffusion in the system K2O-SrO-SiO2. IV - Mobility model, electrostatic effects, and multicomponent diffusion.

21 p3097 A72-40935

Interaction of a steady plasma flow with a dipole magnetic field in the presence of a radial electric field.

21 p3093 A72-41388

Balloon optical experiments in IR, visible, UV and X ray regions, considering in situ measurements of atmospheric composition, electric field and cosmic dust

21 p3049 A72-41613

Plasma heating by large-amplitude, low-frequency electric fields.

21 p3094 A72-41630

Group properties and invariant solutions of electric-field equations in the case of nonlinear Ohm's laws

21 p3086 A72-41654

Computer-aided numerical solution for electric field structure of rod and plate, calculating field distortion by rod antennas and near lightning rod

21 p3086 A72-41671

Influence of a variable electric field on the diffusion of ions in a gas

21 p3086 A72-41676

Scattering by a cylindrical semiconductor rod of anisotropic permittivity perpendicular to the electric field in a rectangular waveguide.

21 p3023 A72-41836

Experimental investigation of the effect of an electric field on a laminar flame

22 p3243 A72-41889

Longitudinal magnetospheric currents contribution to auroral electrojet from satellite observation data, noting magnetosphere electric field excitation of meridional Pedersen and Hall currents

22 p3169 A72-42225

Equations of plane potential electrohydrodynamic flow, noting jet and quasi-one dimensional flows of charged particles in curvilinear electrostatic field

22 p3210 A72-42269

Polar-cap electric field distributions related to the interplanetary magnetic field direction.

22 p3172 A72-42432

Fundamental transverse electric field /TE-sub 0/ mode selection for thin-film asymmetric light guides.

22 p3186 A72-42622

Injun 5 satellite measurements of magnetospheric convection electric fields via double probe technique, discussing substantiation withOGO 6 results

22 p3174 A72-42901

Measurement of nonthermal oscillations at the plasma frequency and its harmonics in a magnetized arc plasma, using the high-frequency Stark effect.

22 p3212 A72-42916

Determination of characteristic magnitudes of toroidal electrostatic analyzers - Application to the optimization of analyzers used in space physics

22 p3180 A72-42935

On the drift velocity of electrons in a gas.

22 p3212 A72-42996

Wave propagation in plasma modulated by external electric field, noting dispersion equation for coupled waves and instability conditions

22 p3212 A72-43101

Motion of plasmoids in a multipole magnetic field of toroidal configuration

22 p3214 A72-43120

Influence of nonuniformities of the built-in field on the collection efficiency of a semiconductor photocell

22 p3140 A72-43190

Numerical simulation of the relaxation of a beam of charged particles in a strong electric field

23 p3315 A72-43530

Calculation of the parameters of a plasma accelerated in a high-frequency electric field and a static magnetic field

23 p3320 A72-43660

Analysis of the electric field distribution in a rectangular waveguide with a flat transverse inhomogeneity

23 p3272 A72-44141

Quasi-linear theory for the low-frequency instability of a plasma placed in a weak SHF electric field

23 p3321 A72-44172

Method for solving the problem of radiation in an anisotropic plasma

23 p3321 A72-44220

On mechanical response of a non-uniform piezoelectric transducer under the influence of a body-force.

23 p3291 A72-44316

Electric field orientation, magnetic field strength and high voltage pulse delay effects on spark chamber track displacement from true particle trajectory

23 p3291 A72-44441

Parametric instabilities and anomalous heating of plasmas near the lower hybrid frequency.

23 p3323 A72-44545

Transport phenomena theory for semiconductors in strong electric fields, examining negative differential conductivity and nonmonotonic current behavior
24 p3427 A72-44569

Strong electric field recombinational domains in semiconductors with mobile holes and electrons during band-band illumination or double injection
24 p3431 A72-44570

Electric field variations during substorms - OGO-6 measurements.
24 p3396 A72-44854

Electric field nature for DP current system development in disturbed high latitude ionosphere, discussing F 2 region ionization drift
24 p3398 A72-45096

Transformation of trapped charged particles to transit particles under the influence of a high-frequency electric field
24 p3429 A72-45494

Current induced drift rate of plasma electrons in electric and magnetic fields, noting electron velocities in turbulent heating of plasma
24 p3429 A72-45507

ELECTRIC FILTERS
NT BANDPASS FILTERS
NT CRYSTAL FILTERS
NT DIGITAL FILTERS
NT ELECTROMAGNETIC WAVE FILTERS
NT INFRARED FILTERS
NT LINEAR FILTERS
NT LOW PASS FILTERS
NT MICROWAVE FILTERS
NT OPTICAL FILTERS
NT RADAR FILTERS
NT RADIO FILTERS
NT TRACKING FILTERS
NT ULTRAVIOLET FILTERS
NT WAVEGUIDE FILTERS

Dc-dc converter input filter requirements and design for spacecraft power processing equipment
01 p0007 A72-11058

Frequency domain representation of Doppler invariant FM signal defining matched pulse compression filter
04 p0507 A72-15693

Filter configuration for detecting pulse excitation smaller than kT, noting SNR and resolving time
05 p0631 A72-17075

Meteorological measurements representativeness and analog discrete filters synthesis with optimal data processing and weighting function averaging procedures
08 p1203 A72-22123

Telecommunications ultrasonic resonators, electromechanical and piezoelectric filters and microacoustic surface elastic wave devices
09 p1281 A72-23468

Monte Carlo and convolution methods for statistical analysis of ladder filters, describing programs for determining attenuation probabilistic distribution as function of components dispersions
09 p1289 A72-23679

Active notch filter circuits for extending accelerometers frequency response to near resonance, presenting error analysis of mismatching components
12 p1808 A72-27639

Transistorized electronic equipment with delay line for optimal filtration of PSK signals
13 p1930 A72-29047

Multidimensional non-Gaussian signals filtration in presence of time correlated noise with discrete values of argument
13 p1937 A72-29638

Nonstationary fluctuation signal analysis into predetermined frequency band by passing digitized information through resonant LCR filter mathematical analog
16 p2362 A72-32855

Laguerre filters parameters choice for correlator input networks application, noting output SNR improvement
16 p2368 A72-33089

Computerized design of electric filters with given frequency response, discussing attenuation characteristic approximation by Chebyshev method
19 p2776 A72-37307

Frequency response optimization of electric filters, modulators and impedance matching circuits using minimax criterion, noting nonlinear programming sequence
19 p2771 A72-37310

Transmission of two partially time coincident linearly frequency modulated signals through limiter-filter system, noting distortion and satellite signals generation
19 p2766 A72-38419

RC gyrator filters frequency characteristics stability analysis, noting elements sensitivity as function of frequency and Q value
19 p2774 A72-38421

A method of calculating the lag of the phase photoelectric installation of a time service
21 p3058 A72-41769

Electromechanical filter with attenuation poles consisting of multi-mode vibrators.
21 p3036 A72-41828

Network analysis and frequency response of LF filter with distributed RC structure and voltage converter
22 p3158 A72-42120

Correlator with orthogonal filters for acoustic diagnostics, noting Laguerre functions variations in signal pairs autocorrelation
22 p3176 A72-42133

ELECTRIC FUSES
Fast acting nonmechanical self healing mercury fuse for high current circuit protection
03 p0335 A72-14203

ELECTRIC GENERATORS
NT AC GENERATORS
NT ALKALINE BATTERIES
NT DIRECT POWER GENERATORS
NT DYNAMOMETERS
NT FUEL CELLS
NT HYDROGEN OXYGEN FUEL CELLS
NT MAGNETOHYDRODYNAMIC GENERATORS
NT METAL AIR BATTERIES
NT PHOTOELECTRIC GENERATORS
NT RADIOISOTOPE BATTERIES
NT ROTATING GENERATORS
NT SOLAR CELLS
NT SOLAR GENERATORS
NT THERMIONIC CONVERTERS
NT THERMOELECTRIC GENERATORS
NT TURBOGENERATORS
NT ZINC-OXYGEN BATTERIES

Power conditioning requirements and tradeoff considerations for space shuttle, warning against central power conversion use on orbiter and booster vehicles
01 p0007 A72-11052

Aircraft hybrid electrical power systems, describing variable frequency generation and high voltage dc distribution
01 p0009 A72-11068

Lunar Roving Vehicle navigation subsystem power converter design, discussing circuits, performance and voltage regulators and preregulators
01 p0009 A72-11069

German Research and Test Institute for Aero- and Astronautics 1970 report covering flow mechanics, power conversion, aerospace medicine, atmospheric physics, etc
01 p0048 A72-11151

Nuclear energy value to society, stressing usefulness for electric power generation and marine propulsion
03 p0387 A72-14376

Powder concentration effects on corona particle charging efficiency of aerosols for electrogasdynamic generators
06 p0760 A72-18335

Aircraft electric power generation history, noting aircraft performance effect on electrical system design
07 p0914 A72-20201

Radiation efficiency of electric power-energy conversion during pulsed discharge in Xe tube
11 p1651 A72-26364

Radiovoltaic generator energy conversion by thin film solar cells, noting performance dependence on semiconductor band gap and radioisotope characteristics
12 p1757 A72-28021

Microwave power generation via semiconductor devices, discussing circuit problems due to negative resistance
14 p2088 A72-30832

Total weight estimates of electric power supply system for transport vehicles involving power generators and primary electrical network with distribution system
16 p2350 A72-32997

Five channel recording instrument for energy dissipation evaluation in electric machines from thermal emf measurements
16 p2392 A72-33284

Radiation efficiency of electric power-energy conversion during pulsed discharge in Xe tube
16 p2403 A72-33716

Si p-n junction solar cell fill factor for electric power available to load, noting discrepancy between calculated and measured values due to recombination
17 p2494 A72-34264

Internal engine generator application to commercial transport aircraft.
17 p2498 A72-35566

Electrogasdynamic generator nonlinear internal resistance determination as function of flow parameters and model geometry via boundary conditions formulation
18 p2643 A72-35998

Liquid or solid propellant hot gas turbines as power source for hydraulic and electrical energy
18 p2648 A72-36558

Generalised method of harmonic reduction in a.c.-d.c. converters by harmonic current injection.
18 p2648 A72-37209

Effect of electrical generator parameters on transient suppressors.
19 p2753 A72-37291

ELECTRIC IGNITION
Turboprop electric igniter climatic test problems and equipment for assessing quality control
07 p0954 A72-19112

Loading current density effect on normal lead stynthane ignition in primary explosive hot wire initiation, using capacitor discharge and constant current activation signals
08 p1218 A72-20752

Computerized numerical nodal analysis of heat transfer away from bridgewire of electroexplosive device to meet all- and no-fire requirements
08 p1219 A72-20753

Fast rise high current constant trigger circuit for electroexplosive devices, using flat two-conductor transmission line to minimize inductance
08 p1219 A72-20761

Aerospace type electroexplosive devices gross sensitivity to short damped rf energy burst
08 p1220 A72-20765

Pulsed metallic-plasma generators.
20 p2958 A72-39781

ELECTRIC IMPULSES
U ELECTRIC PULSES

ELECTRIC LEADS
U ELECTRIC WIRE

ELECTRIC MOMENTS
Electromagnetic wave scattering characteristics at arbitrarily configured body with dimensions smaller than primary field wavelength, determining electric and magnetic moments
02 p0181 A72-12595

Electric multipole moments calculation by quasi-static method for homogeneous quasi-neutral oblate plasmoid during resonance
13 p2020 A72-30014

Electric multipole moments calculation by quasi-static method for homogeneous quasi-neutral oblate plasma spheroid during electromagnetic interaction under resonance conditions
22 p3212 A72-42729

ELECTRIC MOTORS
NT SYNCHRONOUS MOTORS
NT TORQUE MOTORS

Numerical analysis method for performance prediction of linear induction machines including liquid metal MHD pumps and generators and linear motors
13 p1900 A72-29365

Solid state stepping motor drive controller to provide constant angular shaft velocity for scanner applications
13 p1933 A72-29767

Structural design and electrical drive mechanism of helicopter hoist for rescue operations
13 p1912 A72-30097

German monograph on small variable-speed motors with high impulse performance, considering asynchronous cage type, dc shunt type and pneumatic motors
15 p2182 A72-31325

Solid and composite rotor induction motors, comparing predicted characteristics based on analytical and numerical analyses
15 p2182 A72-31779

Five channel recording instrument for energy dissipation evaluation in electric machines from thermal emf measurements
16 p2392 A72-33284

Gyroscope drive systems, discussing various ac and dc electric motor types and switching and control circuits
16 p2396 A72-34135

Book - Electromechanical system components.
20 p2890 A72-39811

Electrical components in gas turbine control systems.
22 p3216 A72-42521

ELECTRIC NETWORKS
Active RC circuit with grounded capacitors capable of functioning as differentiator, bridge, inductance simulator, bandpass filter and oscillator
03 p0337 A72-14354

Computer analysis of linear electric circuits without restrictions on network topology and component composition, using system matrix
04 p0495 A72-14464

Low sensitivity distributed-active bandpass network with effective use of capacitance to save space and weight
04 p0506 A72-15307

Network formulations of electromagnetic fields in moving dispersive plasma media by equivalent parameter representation
04 p0490 A72-15400

Orthogonal 2-port network impedance transforming properties and applications to harmonic oscillators and filters
04 p0502 A72-15521

Tellegen theorem as energy conservation principle statement for energy exchange between elements in electric network
04 p0507 A72-15527

Electric network scattering matrix and associated incident and reflected wave variables concepts applications in linear optimal control problem

04 p0507 A72-15528

Computer aided linear circuit design for network synthesis, analysis, optimization and data storage noting MARTHA program

05 p0639 A72-15785

Two dimensional network class port behavior equivalence to three layer structures of linear passive isotropic materials based on depth and surface properties analysis

06 p0793 A72-17595

Harmonic oscillations sum conversion by two terminal pair network with complex nonlinearity

07 p0956 A72-19565

Digital computer calculation of complex electric networks described by mathematical models, calculating flow distribution

11 p1577 A72-25282

Computer program for symbolic network functions, using numerical algorithms for branches not represented by symbolic parameters

15 p2211 A72-31845

Passive and active electric circuit analysis by structural numbers method with computer time and space advantages, noting application to transistor circuits

16 p2370 A72-32851

Total weight estimates of electric power supply system for transport vehicles involving power generators and primary electrical network with distribution system

16 p2350 A72-32997

Determination of linear circuit sensitivity to circuit parameter changes in the equations of state variables

19 p2777 A72-37312

Electronic circuit for linearizing the transfer function of a photographic plate used in mass-spectrometry.

20 p2925 A72-39428

Airport power supply system to meet increased load terminal demands, describing main and emergency standby network layout and equipment

24 p3388 A72-45272

ELECTRIC POTENTIAL

NT BIOELECTRIC POTENTIAL.

NT CONTACT POTENTIALS

NT COULOMB POTENTIAL

NT LOW VOLTAGE

NT PHOTOVOLTAGES

NT SPIKE POTENTIALS

Dember-Hall voltage ratio for low magnetoconcentration in intrinsic semiconductor

01 p0113 A72-10044

Electrostatic potential fluctuations spectrum in turbulent hot ion plasma confined between magnetic mirrors, investigating mode coupling, energy cascading and electron concentration

01 p0108 A72-10242

Potential and ion charge distribution in proximity to conducting sphere moving in low density collisionless ion-electron plasma

01 p0109 A72-10371

Affined RC or RL networks, investigating real and equal or imaginary, conjugate and inverse voltage and current transmittances

02 p0197 A72-12240

Electrohydrodynamic ideal incompressible fluid flow in flat and circular channels, determining electric potential and field distribution

02 p0266 A72-12431

Room temperature nonaqueous organic solvent electrochemical cell, producing open-circuit potential of 4.5 V

03 p0311 A72-12924

Automatized graphic information input into computer, using electric potential distribution introduced into conducting underlay sheet by current carrying drawing pen

03 p0326 A72-13093

Transient response of negatively biased Langmuir probes for planar and cylindrical plasma sheaths under large amplitude pulsed potentials [AD-739787]

03 p0361 A72-13924

Optimum manned spacecraft electrical power distribution voltage and frequency selection, discussing corona, radiation and safety

03 p0313 A72-14187

Field modification for integrodifferential equation solution for voltage on exponentially narrow waveguide slit, discussing further changes in method

04 p0501 A72-15409

Potential change under pitting corrosion and repassivation on Cr-Ni steels alloyed with V, Si, Mo and Re

04 p0535 A72-15730

Transport processes in electrolytic solutions, considering current and potential distributions in localized corrosion

04 p0536 A72-15737

Electrical analog to determine potential field distribution for crack growth monitoring of edge notched and compact tension specimens for current input and probe positions optimization

05 p0666 A72-16303

Switching contacts performance principles, noting inductive energy role in electrical breakdown voltage determination

06 p0791 A72-18579

Electrode potential gradients during dimensional electrochemical treatment of Ni and Ni based alloys

08 p1175 A72-21041

Low level current operation in insulated gate FET, obtaining analytical expression for voltage

08 p1142 A72-21744

Alkali antimonide photocathodes photoelectric yield / quantum efficiency / relation to reversible variation of surface potential, noting critical current density temperature dependence

08 p1171 A72-21968

Electrochemical tests, noting electric potential, current and electrode impedance measurements for corrosion rate and oxidizing power evaluation

08 p1189 A72-22105

Corrosion effects evaluation from electrode potentials, noting copper pitting and weathering

08 p1189 A72-22108

Microwave induced dc voltages across unbiased Josephson tunnel junctions, showing power spectra dependence on magnetic field

09 p1367 A72-22458

Ionospheric potential and thunderstorm activity annual variations during 1959-70 solar cycle from radiosonde measurements in free atmosphere

09 p1301 A72-23265

Metal probe potentials during mechanical displacement along surface of n-region of forward biased Si diode

09 p1288 A72-23362

Statistical analysis of piezoelectric transducer voltage-displacement characteristic, determining linearity deviations magnitude

09 p1317 A72-23676

Automatized graphic information input into computer, using electric potential distribution introduced into conducting underlay sheet by current carrying drawing pen

11 p1601 A72-25705

Retarding potential analyzer errors and performance degradation due to grid plane potential depressions

11 p1634 A72-26411

Charge carrier density, neutral gas density, electric potential and electron temperature profiles in cylindrical diffusion column, considering electron pressure

11 p1698 A72-26646

Calorimeter calibration for laser energy and power measurements in terms of electrical energy based on voltage, resistance and frequency standards

11 p1652 A72-26781

Upper atmosphere electric fields derived from ionosphere-earth electric potential measurements following solar flare activity

12 p1804 A72-27805

High frequency potential effect on fast transverse magnetic waves along plasma layer bounded by two conducting plates

12 p1785 A72-27855

Varactor broken voltage-capacitance curve due to uncompensated impurities concentration change at p-n junction

13 p1926 A72-28379

Laplace transformation for mechanical response of piezoelectric composite transducer under action of thermal field and electric potential, noting time dependent modulus of elasticity

13 p1955 A72-28621

Experimental investigation of toroidal discharge electrostatic potential fluctuations in turbulently heated plasma, discussing correlation with effective conductivity

13 p2012 A72-29122

Weak ion-acoustic quasi-shock wave propagation in collisionless plasma, determining long time behavior of precursor ion stream reflected by electrostatic potential

13 p2012 A72-29125

Linear nonequilibrium Faraday type MHD generator, predicting electrode configuration effects on voltage drops, axial leakages and current distribution

13 p1900 A72-29353

Characteristic functions of potential distribution on sphere with longitude dependent conductivity for application to ionosphere electrodynamics

14 p2101 A72-30644

Narrow strongly radiating slot voltage distribution, investigating cavity coupling with integral equation

15 p2209 A72-32659

Plasma accumulation in electrostatic potential well produced by electron space charges, determining diocotron instability as function of electron plasma and gyrofrequency ratio

16 p2434 A72-32819

Voltage and current generalized immittance converter realization, using with current conveyor for simulation

16 p2367 A72-32856

Voltages induced in superconductors in the absence of transport currents.

18 p2719 A72-36744

Calculation of electrostatic potential distribution in semiconductor's contact region during passage of injecting into blocking contact due to illumination.

19 p2846 A72-38626

Electrochemical protection potential of metals and alloys in pitting, intergranular corrosion and stress corrosion cracking in presence of chlorides

21 p3065 A72-40087

Effects of Landau damping on nonlinear wave modulation in plasma.

21 p3089 A72-40189

Current and voltage waveform measurements with sampling oscilloscope and capacitive voltage-divide probe to verify TRAPATT diode oscillator theoretical model

21 p3032 A72-40635

Potential measurement and stabilization of an isolated target using electron beams.

21 p3087 A72-40700

Influence of prior electrochemical history on the propagation of localized corrosion.

22 p3195 A72-43129

Comparison of microwave-induced constant-voltage steps in Pb and Sn Josephson junctions.

23 p3323 A72-43272

Capacitance voltage characteristics instability of metal-aluminum oxide-silicon dioxide-silicon (MAOS) structures, suggesting polarization effect in layer formed during deposition and annealing

23 p3324 A72-44070

The negative space-charge density distribution and the potential distribution in a Penning discharge cell

23 p3324 A72-44211

ELECTRIC POWER

L-band Gunn oscillator using nonsinusoidal device voltage /switching mode/, comparing efficiency and output power with sinusoidal mode

01 p0036 A72-10635

Variable speed constant frequency power generation equipment influence weapon system effectiveness, considering weight and cost

01 p0008 A72-11067

Concorde aircraft electrical power systems design, noting dc and emergency supplies and installation

03 p0311 A72-12910

Ac and dc electric power transient test equipment satisfying MIL-STD-704A requirements

03 p0312 A72-14038

Aircraft electric power equipment transient voltage and EMC limits specifications

03 p0312 A72-14043

ALSEP central station data subsystem, discussing power conditioning unit and electric power subsystem

04 p0508 A72-15094

High efficiency solar electricity converters utilizing wave-like properties of radiation interacting with absorber-converter elements, discussing cost and fabrication advantages

[ASME PAPER 71-WA/SOL-1] 05 p0614 A72-15891

Pollution free electrical power generation from solar energy, discussing microwave transmission to earth, power shortages, thermal pollution and solar cell manufacture cost

[ASME PAPER 71-WA/SOL-2] 05 p0614 A72-15892

Kilowatt rotary dc-dc power transformer in modular sections for spacecraft applications, discussing electrical and mechanical designs and characteristics

08 p1112 A72-21414

High power series voltage regulators, discussing power hybrid microelectronic design techniques

08 p1112 A72-21415

Calorimeter calibration for laser energy and power measurements in terms of electrical energy based on voltage, resistance and frequency standards

11 p1652 A72-26781

Stacked TRAPATT diodes oscillator with microstripline circuit to obtain 1 kw peak power at 1 GHz

12 p1788 A72-27163

High electric power output Si solar cell development, discussing increased energy conversion efficiency

12 p1757 A72-28026

One-wavelength MHD induction generator operated on NaK flow system with various excitation conditions, calculating magnetic flux density and power by Fourier series

13 p1900 A72-29364

Silicon solar energy conversion for electrical power generation on spacecraft.

17 p2494 A72-34186

Cylindrical Cs thermionic converter with unique emitter and five collectors, measuring I-V characteristics to determine emitter work function, ignition voltage and electric power

18 p2646 A72-36191

Airborne equipment electric power supply standards to provide characteristics limits for compatibility with ground support systems

[SAE AS 1212] 18 p2648 A72-36535

Electric power generation by thermionic converters, discussing physical principles of operation and technology utilization in communications, meteorology, geophysics, oceanography and space exploration

20 p2890 A72-39940

Low temperature characteristics of the Gunn diode.

22 p3159 A72-42307

ELECTRIC POWER CONVERSION

- U ELECTRIC GENERATORS
- ELECTRIC POWER PLANTS**
- NT NUCLEAR POWER PLANTS
 - NASA closed cycle MHD facility for power generation, discussing system components, design and operation [AIAA PAPER 72-103] 05 p0616 A72-16936
 - Large-scale concentration and conversion of solar energy. 18 p2643 A72-36075
 - Airport power supply system to meet increased load terminal demands, describing main and emergency standby network layout and equipment 24 p3388 A72-45272

ELECTRIC POWER SUPPLIES

- NT SPACECRAFT POWER SUPPLIES
- Aircraft electrical power systems design dependence on latitude, minimum weight requirement, reliability degree, environmental conditions and acceleration 13 p1899 A72-28693
- Permanent manned lunar stations electrical power systems, discussing nuclear energy, solar cells and electrochemical power cells 15 p2214 A72-31814
- Total weight estimates of electric power supply system for transport vehicles involving power generators and primary electrical network with distribution system 16 p2350 A72-32997
- Push-pull transistor amplifier fed from two different voltage power supplies, noting power efficiency improvement 22 p3158 A72-42115

ELECTRIC POWER TRANSMISSION

- Optimum manned spacecraft electrical power distribution voltage and frequency selection, discussing corona, radiation and safety 03 p0313 A72-14187
- Remote power control for aircraft generating and distribution systems. 18 p2648 A72-37034
- Progress in the efficiency of free-space microwave power transmission. 22 p3140 A72-42481

ELECTRIC PROPULSION

- NT ARC JET ENGINES
- NT ELECTROMAGNETIC PROPULSION
- NT ELECTROSTATIC PROPULSION
- NT ION PROPULSION
- NT PLASMA PROPULSION
- NT SOLAR ELECTRIC PROPULSION
- Electrical and nuclear propulsion plasma containment problems, discussing simulation experiments and scaling devices feasibility 01 p0117 A72-10938
- Power processing requirements for solar electric propulsion in deep space mission, noting use of electron bombardment ion thruster with hollow cathode 01 p0007 A72-11055
- Solar electric low thrust unmanned Mercury orbiter missions, considering spacecraft subsystems and ballistic and swingby trajectories [AIAA PAPER 72-425] 11 p1721 A72-26170
- Parallel rail solid fuel pulsed electric microthruster performance, noting mathematical model for mass ablation and plasma acceleration mechanism [AIAA PAPER 72-458] 11 p1708 A72-26194
- Optimization criteria for electric feeding in quasi-steady MPD thruster, discussing energy storage bank characteristics determination [AIAA PAPER 72-462] 11 p1709 A72-26197
- Solar electric propulsion upper stage for multiple space exploration missions, discussing spacecraft performance, configurations and program plans [AIAA PAPER 72-464] 11 p1709 A72-26199
- Electric propulsion spacecraft design for ion thruster systems testing with circular solar cells array as gyroscopic stable platform [AIAA PAPER 72-466] 11 p1578 A72-26200
- Solar electric propulsion application to comet and asteroid rendezvous and docking CARD missions with sample return [AIAA PAPER 72-470] 11 p1722 A72-26201
- ESRO electric propulsion systems R and D, discussing various concepts in terms of weight, cost, thrust level, efficiency, simplicity, exhaust velocity and development potential [AIAA PAPER 72-478] 11 p1710 A72-26207
- Electric propulsion systems assessment for military spacecraft, discussing ion, colloid, pulsed and quasi-steady plasma thrusters [AIAA PAPER 72-493] 11 p1711 A72-26217
- Solar electric propulsion subsystem performance tested on breadboard model, noting electrical power conversion, command, thrust vector control and propellant supply [AIAA PAPER 72-507] 11 p1711 A72-26227
- Solar electric propulsion for satellite transport into geostationary orbit, discussing launchers, energy supply, electrostatic ion thruster and mass/power ratio [AIAA PAPER 72-505] 12 p1860 A72-27422

- Ion thruster module design for primary electric propulsion systems, discussing optical configurations, discharge chamber, control and performance tests [AIAA PAPER 72-508] 12 p1860 A72-27423
- Model for mercury vapor electron bombardment ion thruster hollow cathodes operation and effects on thrust subsystem performance predictability [AIAA PAPER 72-420] 13 p2026 A72-28936
- Encounter trajectory design for solar electric propulsion rendezvous with low mass celestial bodies, noting target characteristics [AIAA PAPER 72-424] 13 p2036 A72-28939
- Encounter sequences determination techniques for multitarget flyby and rendezvous missions to asteroids and comets by spacecraft using solar electric propulsion [AIAA PAPER 72-429] 13 p2037 A72-28940
- Structural evaluations and dynamic testing of solar electric propulsion components, surveying power conditioning panel modal frequencies by holographic interferometry technique [AIAA PAPER 72-442] 13 p1899 A72-28941
- Solar array degradation effect on electric propulsion spacecraft performance, presenting power allocation strategy during mission [AIAA PAPER 72-444] 13 p2037 A72-28943
- Solar electric multimission spacecraft /SEMMS/ concept, investigating Mariner, Viking and TOPS technologies applicability to postulated mission/science objectives [AIAA PAPER 72-469] 13 p2026 A72-28946
- Nonchemical space propulsion systems for lunar and planetary flights, discussing fission, fusion and electric rockets 15 p2297 A72-31810
- Electrostatic ion thruster and hydrazine monopropellant systems for communication satellites, noting weight savings 17 p2596 A72-34265
- Thermionic reactor electric propulsion system requirements. 18 p2720 A72-36167
- Propulsive performance of a 30 kW arc-jet thruster stabilized by vortex and magnetic forces. 19 p2848 A72-37925

ELECTRIC PULSES

- Hertzian dipole radiation with impulsive currents in nondispersive dielectric half space 01 p0030 A72-10841
- Reactive two terminal pair network synthesis for shaping sawtooth current pulses in inductive load for given input function 02 p0193 A72-12222
- Photoelectric transducer with electric pulses as measure of rotating disk angle of turn, discussing design and measurement accuracy 05 p0662 A72-16124
- Peak parametric envelope calculation for hf pulse transients 06 p0773 A72-17571
- IC microcircuit for time-pulse voltage converter for conversion of dc voltage into electric pulses of length proportional to input signal 06 p0784 A72-17836
- Noise contaminated pulse signal transit time measurement by receiver using digital filters 07 p0939 A72-19051
- Unipolar pulsed plasma accelerator, describing trigatron circuit design for generation of 100 kA unipolar current pulses of 35 microsec duration 07 p1040 A72-19316
- Nanosecond solid dielectric discharger fired by Q switched ruby laser for commutation of coaxial line forming high amplitude voltage pulses 07 p1008 A72-20509
- Pulse energy and heat distribution in dielectric and metal during electroerosive machining 08 p1174 A72-21035
- Mass and energy balance for electrode wire fusion in pulsed current MIG /metal inert gas/ welding, discussing pulse duration and amplitude requirements and shielding gas composition effect 09 p1321 A72-23644
- IMPATT diode junction temperature measurement with accuracy from breakdown voltage by pulse techniques 10 p1449 A72-24304
- Electrically excited carbon dioxide-nitrogen laser using high repetition rate discharge pulses from pin electrode array transverse to supersonic flow 11 p1647 A72-26147
- Transient current density in plasma subjected to pulsed electric field derived from Boltzmann transfer equation 12 p1850 A72-27278
- High resolution angular velocity measurement by high speed digital transducer feeding photosensor pick-up pulses into pulse shaping circuit 14 p2103 A72-30199
- Electric current pulses effect on Zn monocrystals plastic deformation before brittle rupture, noting critical normal stresses increase 14 p2115 A72-30411

Short signal pulse shaping based on phase and amplitude selective properties of distributed parametric amplifiers operating under nonlinear conditions 14 p2090 A72-31112

Electrical breakdown of hexane investigated by high voltage nanosecond pulses, noting electron avalanche and streamer processes in time lag 15 p2278 A72-32244

Mathematical model for fast transverse glow discharges for pumping high pressure gas lasers, noting short rise time of applied voltage pulse 16 p2399 A72-33012

Gas flow direction measurement using flow to electric pulse converter 16 p2395 A72-33957

Toroidal plasma spectroscopic investigation from current pulse start to afterglow, noting electron temperature and density radial distributions and energy balance 17 p2591 A72-35373

Electron density measurements in early stage of the high current pulsed discharge. 18 p2716 A72-36957

USSR electric impulse de-icing system design. 18 p2648 A72-37033

Temperature-time characteristics of pulse-loaded temperature-measuring resistors 20 p2926 A72-39571

Response of the average pressure acting on the surface of an emitting circular transducer due to different reflecting objects. 21 p3055 A72-40948

Low cost design of linear pulse stretcher circuit for short duration pulse time measurement in nuclear instrumentation and computing counters 21 p3033 A72-40997

Computation of the shape and velocity of a nerve pulse 22 p3149 A72-42156

Holograms of spark discharges excited by nanosecond electric pulses 22 p3181 A72-43112

Experiment for studying the pulse shape of Cerenkov emission at large distances from an extensive air shower 23 p3330 A72-44420

ELECTRIC REACTORS

NT SATURABLE REACTORS

ELECTRIC RELAYS

- Self excited oscillations and transient responses of spacecraft stabilization relay system with delayed feedback, analyzing time delay effects in actuator circuit 08 p1241 A72-21170
- German book on control technology development covering historic periods, symbols and representations, stability, integral transformations, computers, servos, relays and multivariable systems, optimization, etc 08 p1145 A72-21478
- Variable structure automatic control relay system design with reduced insensitivity zone and given transient process requirements 13 p1935 A72-28612
- Relays - Conference, Oklahoma State University, Stillwater, April 1972 15 p2204 A72-31214
- Reduced voltage relay operation in aircraft high voltage ac power systems, describing RLC circuit theory, laboratory test arrangement and performance measurements 15 p2204 A72-31215
- Relay circuits malfunction due to interactions between coil induced currents and diode coil shunts, discussing circuit design and operating conditions 15 p2204 A72-31217
- Contactless relay circuits employing a branched-core magnetic modulator with second-harmonic output 19 p2771 A72-37302
- Electric relay spring design for miniaturization, deriving relation between length and thickness to minimize fiber stress under constant contacting force 19 p2775 A72-38617
- Book - Electromechanical system components. 20 p2890 A72-39811
- Switches for high-frequency channels 21 p3026 A72-40317
- Modelled time optimal control process investigation for system with relay components, noting Hausdorff maximum principle application for optimal linear control 24 p3386 A72-45389
- A near-time-optimal control circuit with a large number of relay elements 24 p3387 A72-45699

ELECTRIC ROCKET ENGINES

- NT ARC JET ENGINES
- NT ELECTROSTATIC ENGINES
- NT ELECTROTHERMAL ENGINES
- NT ION ENGINES
- NT PLASMA ENGINES
- NT RESISTOJET ENGINES

- Pulsed electric microthruster with solid fuel feed system, noting electrode geometry effects on performance and ablation patterns [AIAA PAPER 72-210] 05 p0705 A72-16799
- Electrodynamic thrusters for flight vehicle propulsion, reviewing design, efficiency and performance 08 p1224 A72-21669
- Test facility for electric microthrusters, describing microbalance for thrust and propellant mass flow rate measurement 09 p1292 A72-23404
- Magnetic field and polar region geometry effects on hollow cathode thruster performance of Kaufman electric engine [AIAA PAPER 72-417] 11 p1706 A72-26167
- Electric thruster for orbit and attitude control of nonspinning geostationary communications satellite [AIAA PAPER 72-436] 11 p1727 A72-26178
- Multimission and engine performance requirements for solar electric spacecraft propulsion stage configurations, considering launch vehicle compatibility integration payload and environmental extreme effects [AIAA PAPER 72-465] 11 p1712 A72-26325
- ELECTRIC SPARKS**
- High temperature U plasma generation at near gas core reactor conditions by sliding spark discharge into capillary channel lined with sintered uranium dioxide 01 p0112 A72-11338
- Specific quantitative trace analysis technique for solids using spark source mass spectrometry 03 p0361 A72-13849
- Explosive erosion in Al, Cu, W and Pb electrodes during high current spark discharges, using time resolved photography 05 p0692 A72-16032
- Sonic boom simulation devices and techniques, including wind tunnels, ballistic ranges, spark discharges and shock tubes 08 p1147 A72-21906
- Absorption spectra and plasma of laser spark in hydrogen, studying electron and atoms temperature and concentrations time variations 10 p1491 A72-24359
- Ignition energy measurement by nanosecond electric sparks produced by transmission line method, recording voltage pulses onto spark gap 10 p1563 A72-25138
- Nonprotein amino acids from spark discharges, comparing with Murchison meteorite amino acids 12 p1778 A72-27749
- Spark discharge light source for shock wave multiple exposure schlieren photography, describing pulse separator and spark trigger circuits 15 p2240 A72-32437
- Electric spark activated hot pressing application for sintered composite structures, noting process parameters optimization for superalloy powders 16 p2411 A72-34093
- Absorption spectra and plasma of laser spark in hydrogen, studying electron and atoms temperature and concentrations time variations 17 p2562 A72-34958
- Investigation of electrical processes in high frequency condensed-spark generators 22 p3139 A72-42169
- Holograms of spark discharges excited by nanosecond electric pulses 22 p3181 A72-43112
- ELECTRIC STIMULI**
- Visual cortex neuron responses to light flashes under hypothalamic and reticular electric stimulation in rats 02 p0158 A72-11758
- Neurosecretory cell functional activity of supraoptic and paraventricular hypothalamic nuclei in rats after electrical stimulation of midbrain reticular formation 02 p0158 A72-11759
- Vestibular nuclei bulbar complex evoked potentials under visceral and somatic nerves electric stimulation in anesthetized cats 02 p0164 A72-12512
- Hippocampus electric activity and cardiac rhythms variations responses to various intensity electric stimulation of central gray matter 02 p0165 A72-12881
- Blink reflexes in man during sleep and wakefulness, discussing electromyographically recorded orbicularis oculi mono- and polysynaptic responses to electrical stimuli 04 p0474 A72-15250
- Analgesic electrical stimulation in rat brainstem with other sensory modes unaffected 04 p0475 A72-15361
- Cerebral neurons population electric stimulation effect on deep sleep duration in Parkinsonism patients 04 p0476 A72-15585
- Thermal stability variations in blood serum protein after electrical stimulation of rabbit hypothalamic structures 07 p0920 A72-19649

- Cat and rabbit middle ear muscles contraction by electric stimulation of motor nerves, noting sound transmission reduction 08 p1115 A72-21136
- Cat middle ear muscles motor units twitch tension and contraction time in response to motor neuron threshold stimulation 08 p1116 A72-21137
- Functional organization of monkey cortical efferent zones in distal forelimb muscle control from intracortical microstimulation studies, showing stimulation thresholds distribution 09 p1267 A72-23582
- Vasomotor efferent effects on rabbit lung posterior lobe blood content in response to electrical stimulation of vagus nerve peripheral ends 09 p1268 A72-23693
- Lenticular conditioning-shock stimulation effect on cat visual cortex response to light stimuli, noting lateral gyrus photically evoked potential amplitude increase 11 p1578 A72-25801
- Electrode system for ventricular defibrillation, noting current density role and rounded edge effectiveness 11 p1588 A72-26628
- Cat and rat cardiac and cardiovascular reflexes response to electric pulse stimulation of sensorimotor cerebral cortex 12 p1761 A72-27647
- Cat auditory cortex neurons response to auditory and medial geniculate body electrical stimulation 12 p1761 A72-27651
- Neuronal spike activity changes in rabbit visual and sensorimotor neocortex and hippocampus during EEG activation 13 p1902 A72-28643
- Contractile responses of guinea pig, rat and human isolated ventricular myocardium to increased stimulation frequency 13 p1907 A72-30044
- Electric stimulation of rabbit brain limbic formations /claustrum, amygdala, hippocampus/, showing effect on emotional response motor and vegetative components 14 p2076 A72-30668
- Cat cerebellum cortex evoked response impulses interaction during stimulation of hypothalamus and peripheral nerves 14 p2076 A72-30669
- Cerebral cortex electric shock stimulation effects on phrenic nerve discharges in bivatogomized and curarized cats 14 p2077 A72-30842
- Cat bulbar respiratory neuron discharge modification by single electric shock stimulation of cerebral cortex 14 p2077 A72-30843
- Succinic dehydrogenase activity in rabbit eye ciliary epithelium during electric stimulation of hypothalamus, using histochemical techniques 14 p2078 A72-31099
- Long term weightlessness-induced physiological response normalization by muscle bioelectrostimulation, muscular tissue energy load increase and mineral metabolism stabilization 16 p2354 A72-33543
- Response-dependent electric shock punishment schedule preference during response sequence in food-deprived pigeons 16 p2357 A72-33773
- Neuroinhibition in the regulation of emesis 18 p2650 A72-36449
- Vicarious influence effect on eliciting pain in individuals subjected to previously reported nonpainful electric shocks 18 p2654 A72-36916
- Electrical stimulation of vestibular nuclei - Effects on light-evoked activity of lateral geniculate nucleus neurones 19 p2758 A72-38220
- Proteinase activity in different regions of the brain during development and inhibition of a conditioned passive-avoidance reflex 20 p2890 A72-38927
- Device for eliminating the artifact of electrical stimulation when recording evoked pulse activity of neurons 20 p2893 A72-38938
- Role of pyramidal and extrapyramidal components of cortically-induced efferent stimuli in the mechanism of cortical motor activity coordination 21 p2999 A72-40591
- Effect of electrical excitation of various auditory analyzer levels on a conditioned motor reflex 21 p3001 A72-40805
- Analysis of the activity evoked in the cerebellar cortex by stimulation of the visual pathways 21 p3003 A72-41460
- Unresponsiveness of pial precapillary vessels to catecholamines and sympathetic nerve stimulation 22 p3140 A72-41934
- Modulating effect of limbic brain formations on the blood system 22 p3142 A72-42282

- Reactions of auditory cortex neurons to geniculocortical fiber stimulation 22 p3145 A72-42723
- Effect of a polarizing current on the activity of neurons of the respiratory center 22 p3145 A72-42725
- Biological system transfer-function extraction using swept-frequency and correlation techniques 22 p3151 A72-42773
- The effect of electrical stimulation of the olfactory bulbs on the behaviour of cats and on the electrical activity of the neo- and archepaleocortex 22 p3147 A72-42960
- Lung volume changes of people in antithoracic position in hospital beds for control, exercising and muscle electric-stimulated groups 23 p3256 A72-43918
- Metabolic changes in healthy humans caused by prolonged bed rest in horizontal position, noting prevention by physical exercises and electric muscle stimulation 23 p3260 A72-43921
- Changes in the impulse activity of cortical neurons during selective reinforcement of a chosen range of their interspike intervals 23 p3257 A72-44087
- Neuronal and focal reactions of the parietal associative cortex to various peripheral stimuli 23 p3257 A72-44089
- Responses of anterior suprasylvian gyrus neurons to peripheral stimuli of different modalities 23 p3257 A72-44090
- Post-synaptic potentials of motor neurons of the facial nerve nucleus evoked by afferent and corticofugal pulse stimulation 23 p3257 A72-44091
- Elaboration of steady changes in the firing rate of cortical neuron populations 24 p3370 A72-44587
- Eye movements evoked by collicular stimulation in the alert monkey 24 p3371 A72-44906
- ELECTRIC STRAIN GAGES**
- U STRAIN GAGES**
- ELECTRIC SWITCHES**
- NT CRYOTRONS**
- NT THERMOSTATS**
- P-I-N diodes power handling characteristics in high power solid state TR switches 01 p0042 A72-10708
- Single and double channel laser triggered 1-3 MV switches design in high pressure gas, noting low jitter and built-in voltage isolation 04 p0532 A72-15532
- Six channel integrated MOS switch, discussing MOS transistor operation and circuits structure 09 p1288 A72-23663
- Four-terminal Si controlled switches, discussing negative resistance and linear amplification I-V characteristics and applications in oscillators and modulators 20 p2907 A72-39274
- Book - Electromechanical system components 20 p2890 A72-39811
- Switches for high-frequency channels 21 p3026 A72-40317
- ELECTRIC TERMINALS**
- Laminate materials, sockets and connectors for cost-effective high temperature accelerated life testing of IC 03 p0336 A72-14283
- Algebraic scheme describing electric element and subnetwork interconnection into networks by wiring operators having conversation capability with computer 06 p0778 A72-17475
- DESMAG computer program extension with graphic terminal to functional network conception and implantation 09 p1283 A72-23469
- ELECTRIC WELDING**
- NT ARC WELDING**
- NT ELECTRON BEAM WELDING**
- NT GAS TUNGSTEN ARC WELDING**
- NT PLASMA ARC WELDING**
- Beryllium joining by resistance welding, electron beam welding, dip brazing and braze welding 06 p0820 A72-17701
- Spot and seam welding of Cr ferritic stainless steel thin sheets, discussing electric current loading in relation to sheet thickness and contact pressure 07 p0995 A72-19575
- Ti structures controlled path resistance welding, discussing welded joints metallographic and mechanical properties 07 p0996 A72-19996
- Mass and energy balance for electrode wire fusion in pulsed current MIG /metal inert gas/ welding, discussing pulse duration and amplitude requirements and shielding gas composition effect 09 p1321 A72-23644
- FSRO findings on optimal resistance welding of solar cell interconnections for silver coated metals and pure silver 12 p1814 A72-28030

Flexible solar cell array module design technique, discussing electric welding procedure and equipment parameters effects on breaking strength and reliability 12 p1758 A72-28036

Automatic electrostatic contour welding of IC microcircuit metallic casings, using contact and electrode voltage feedback signals 13 p1963 A72-28921

Gas shielded strip electrode welding and cladding, discussing electric arc behavior, weld bead penetration depth, drop transfer speed, weld microstructure, etc 15 p2243 A72-31324

Joining plastic foils with the aid of high-frequency welding 20 p2930 A72-39942

The versatility of resistance welding machines for joining boron/aluminum composites. 21 p3060 A72-40847

ELECTRIC WIRE
NT EXPLODING WIRES
 Equivalent circuits and characteristics of multiwire and small active transistorized antennas including unipoles, loops, Franklin arrays and mast antennas 02 p0191 A72-11685

Au-Al wire bond, discussing intermetallic phase formation under elevated temperature treatments and reliability design limitations 03 p0364 A72-14284

Time domain analysis of wire antennas including straight, vee and zigzag dipoles 04 p0502 A72-15448

Strength analysis of hyperboloidal electric wire joint designs, expressing stress as function of contact loads 05 p0616 A72-17059

Radar cross section computation and contours map for thin straight wire, noting resonant peak and interference null variations with frequency and aspect ratio 06 p0771 A72-17351

Frequency-independent multimode equiaxial/conical spiral antenna with thick wires, calculating current distribution and radiation pattern by numerical program 07 p0939 A72-19187

German monograph on Frenkel defect structures in thin gold wire at high electron irradiation dose, using electrical resistance measurements 09 p1354 A72-22325

Thin wall airframe wire insulation relative thermal life and temperature rating evaluation procedure using Arrhenius plot 09 p1339 A72-23270

Avionics systems electrical interface connection design information document creation and dissemination, using EMPRENT computer program 10 p1453 A72-24864

Temperature control and measurement in electric wire annealing for standard Pt/Pt-10 Rh thermocouples 13 p1960 A72-29766

Current breaks due to capacitor discharges in W and Mo wires, noting duration proportional to wire mass 13 p2007 A72-29980

Thin wire parallel to interface between two homogeneous half spaces, deriving transmission current wave propagation constant from boundary value problem solution 15 p2200 A72-32108

Multifilamentary superconducting Nb-Sn composite wires in ductile metal matrix, determining transition temperature and critical current density 15 p2294 A72-32534

Sizing new generation aircraft wire and circuit breakers utilizing computer techniques. 17 p2498 A72-35568

On the relationship between classical and matrix design methods for arrays of wire antennas. 21 p3027 A72-40373

Constrained optimization of the gain of an array of thin wire antennas. 21 p3027 A72-40374

Electromagnetic-wave propagation along a horizontal wire above ground. 21 p3015 A72-40633

Propagation constants of electromagnetic waves along an infinitely long conducting wire in a general magnetoplasma. 21 p3092 A72-41266

ELECTRIC WIRING
U ELECTRIC WIRE
U WIRING
ELECTRICAL BREAKDOWN
U ELECTRICAL FAULTS
ELECTRICAL CONDUCTIVITY
U ELECTRICAL RESISTIVITY
ELECTRICAL CONDUCTIVITY METERS
 Electrical conductivity of shock wave produced Xe plasma measured by probe, noting dependence on Mach number 15 p2284 A72-31583

A new circuit for the contactless thickness measurement with the aid of pulse-excited I.C. measuring circuits 20 p2927 A72-39696

ELECTRICAL ENERGY
U ELECTRIC POWER
ELECTRICAL ENGINEERING
 Electronics and electrical engineering - IEEE Conference, Houston, April 1971 03 p0335 A72-14176

Mechanical and electrical techniques unification, discussing systems and balances 15 p2211 A72-31873

Scanning the spectrum; Proceedings of the Tenth Annual Region 3 Convention, University of Tennessee, Knoxville, Tenn., April 10-12, 1972 18 p2665 A72-36301

ELECTRICAL FAULTS
NT SHORT CIRCUITS
 Ultrasonic excitation induced vibration measurement for detecting incipient electrical breakdown in transducers, using laser-Michelson interferometer 01 p0081 A72-11018

High peak power LSA epitaxial GaAs diode relaxation oscillator breakdown under neutron irradiation 01 p0044 A72-11309

Irredundant multiple output combinational logic network fault detection and diagnosis theorems derivation from structural models in labeled direct graph form 02 p0184 A72-11478

Alkali halide crystals optical dc dielectric strength determination, using carbon dioxide laser induced breakdown threshold data [AD-737913] 03 p0368 A72-13607

Sequential faults examination on three-phase distribution transformer, suggesting protection scheme modifications 03 p0313 A72-14186

Avalanche injected current relationship to emitter-base junction breakdown damage in planar n-p-n gated transistors 03 p0336 A72-14279

Microcircuit failures due to electrical overstress, covering current density, thermally induced burn-out, junction shorts and second breakdown with nonuniform heat flow 03 p0336 A72-14290

Microwave breakdown prediction models for antenna system in ionized reentry environment 04 p0486 A72-14531

Avalanche breakdown voltage of Gaussian Si planar p-n junctions for design and impurity diffusion evaluation 04 p0561 A72-15126

Hysteresis loops during breakdown in reverse bias segment of p-PbS point contact diodes I-V curves 05 p0638 A72-17177

Voltage breakdown of microwave antennas, discussing ionization rates in hot air and breakdown suppression by electron flow 06 p0783 A72-17739

Trident aircraft air-system interrogator airborne first line test apparatus for electrical components malfunction diagnosis 06 p0796 A72-18154

Neutron irradiation induced material degradation and circuit failure in high power GaAs Gunn diode oscillator operating in LSA relaxation mode 06 p0788 A72-18472

Switching contacts performance principles, noting inductive energy role in electrical breakdown voltage determination 06 p0791 A72-18579

Electrical breakdown in reverse biased semiconductor p-n junctions involving Zener effect and avalanche mechanisms 07 p1048 A72-19821

Transistor damage by electrostatic discharges, noting charge stored by humans and protection techniques 08 p1140 A72-21064

Secondary breakdown effects on hf power transistor amplifier electrical characteristics, describing operation limits 09 p1288 A72-23364

N fail-safe logics for circuit fault restoration, comparing with failure probability of majority voting scheme and quadded logic 09 p1283 A72-23420

IMPATT diode junction temperature measurement with accuracy from breakdown voltage by pulse techniques 10 p1449 A72-24304

Dielectrics breakdown under ultrashort neodymium laser pulses at fundamental and second harmonic frequencies 11 p1647 A72-25719

Onboard localization of aircraft electrical equipment failures, using list checkout, automatic indication and dynamic programming method 11 p1578 A72-26895

P-n junction diodes fabricated by ion implantation doping, calculating I-V characteristics for comparison with measured breakdown voltages 12 p1789 A72-27312

Boron doped n-type Si planar diode and n-p-n epitaxial planar Si transistor junctions investigating

hydrostatic pressure effects on static characteristics and breakdown voltage 12 p1789 A72-27314

Fault detecting sequences construction based on input-output sequences observation in sequential circuits with shift registers as memory elements 12 p1794 A72-27496

Microwave breakdown calculation on symmetrically excited conical reentry vehicle based on variational technique, comparing with experimental data 13 p1916 A72-28536

Electrode boundary layer electrical breakdown mechanism with allowance for steep temperature gradients at surface, considering Joule heating or electrostatic field effect as causes 13 p2013 A72-29361

Solar cells insulating dielectrics breakdown tests in dilute Ar plasma at positive bias voltages to 20 kV 14 p2140 A72-30926

Electrical breakdown of hexane investigated by high voltage nanosecond pulses, noting electron avalanche and streamer processes in time lag 15 p2278 A72-32244

High intensity sound effects on electronic equipment and components in aircraft noise environment, noting whisker diode and printed circuit board damage 15 p2209 A72-32621

Electric measurement and defect localization in monolithic IC elements by incorporating test structures 15 p2212 A72-32759

Physical phenomena limitations on MOS IC miniaturization, considering gate oxide breakdown, drain source punch through, doping fluctuations, power dissipation and metal migration 16 p2370 A72-34102

Breakdown in argon and nitrogen under the influence of a 0.35-micron picosecond laser pulse. 17 p2564 A72-35508

Atmospheric organic vapor effects on electric contact erosion, deriving showering arc duration, gap breakdown, arc number and energy 18 p2665 A72-36118

Charge injection into the gate dielectric of MOS transistors during junction avalanche. 18 p2668 A72-37104

Application of statistical methods to the study of the rigidity of a dielectric 18 p2720 A72-37116

Miniaturized IC semiconductor device fabrication and failure under electrical load, using scanning electron microscope 21 p3035 A72-41492

ELECTRICAL IMPEDANCE
NT CONTACT RESISTANCE
NT ELECTRICAL RESISTANCE
NT LC CIRCUITS
NT REACTANCE
NT SKIN RESISTANCE
 Microwave Gunn oscillator frequency modulation in quenched domain mode, calculating signal admittance as function of bias voltage and amplitude 01 p0035 A72-10224

Gunn diode microwave oscillator postcoupling to waveguide, deriving theory based on equivalent circuit for load impedance assessment 01 p0037 A72-10640

Self admittance and radiation conductance characteristics of stripline feed slots in waveguide walls 01 p0029 A72-10683

Punch-through transit time negative resistance semiconductor device utilizing injection from Schottky barrier, deriving small signal theory for microwave impedance 01 p0042 A72-10787

First order admittance of coaxially driven infinite monopole antenna, obtaining Green function expansion 01 p0043 A72-11247

Metal-semiconductor-metal Schottky barrier microwave diode impedance and shot noise calculation 02 p0191 A72-11894

Ion transit time effects on plasma sheath RF admittance, using equivalent circuits for representation in low and high frequency ranges 03 p0394 A72-13150

Rectangular slot antennas radiation through inhomogeneous plasma layer with dielectric window, obtaining input admittances by fields modal expansion 04 p0554 A72-14412

Gunn diode large signal admittance dependence on bias and frequency, discussing computer simulation and broadband oscillator and amplifier design 04 p0497 A72-14712

Space charge layer /ion sheath/ effects on impedance of lf transmitting electric dipole in ionospheric plasma 04 p0490 A72-15399

Reflection from aperture of long F-plane sectoral horn antenna, determining electrical impedance by asymptotic diffraction theory 04 p0501 A72-15424

Admittance calculation for vertical monopole antenna driven by coaxial line, approximating current distribution by polynomial with complex coefficients

04 p0501 A72-15429

Linear antenna input admittance calculation, computing excitation integral by field expansion in Legendre functions

04 p0501 A72-15431

Two center-fed feed-point displaced dipole antennas, calculating mutual impedance for various combinations of displacements and heights

04 p0501 A72-15433

Full wave solution for vertically polarized wave propagation over rough variable impedance surface by Fourier transform

04 p0492 A72-15437

Active loop-dipole antennas with shielded reduction properties at resonance, deriving input impedance power gain and radiation patterns

04 p0502 A72-15519

Orthogonal 2-port network impedance transforming properties and applications to harmonic oscillators and filters

04 p0502 A72-15521

Impedance determination for symmetrical spherical probes and spacecraft housing with flat screen separation, using partial capacitance formula

05 p0662 A72-16268

TEM modes characteristics in shielded stripline with four internal strips, tabulating characteristic impedances at different line parameters

05 p0636 A72-16339

Wideband tunnel diode amplifier design, discussing circulator off-band impedance characteristics improvement through voltage standing wave ratio suppression network

05 p0638 A72-16594

Ray-optical calculation of modes scattered by obstacle in two dimensional waveguide or duct with weakly inhomogeneous medium and nonvanishing surface impedance walls

05 p0630 A72-16622

Electromagnetic plane wave diffraction by infinite slit in screen with surface impedance, deriving field and transmission coefficient by asymptotic numerical solution

06 p0771 A72-17352

Conducting ground half space effects on dipole antenna input impedance computed by current distribution Fourier transform

06 p0781 A72-17353

Monopole antenna with lumped mutual coupling between driven and folded sections, noting staggered resonant frequencies and bandwidth broadening from input impedance analysis

06 p0782 A72-17355

Longitudinal and transverse nonresonant slots on waveguide, calculating susceptance, conductance, reflectance and transmittance as function of wavenumber

07 p0952 A72-18843

Corrugated surface wave antenna design with low sidelobe level radiation pattern, finding relief modulated impedance parameters

07 p0955 A72-19514

Rf excitation of external terminated longitudinal conductor axially parallel to rocket skin by transverse electromagnetic field, deriving currents in cable-connecting impedances

07 p0956 A72-19555

Cylindrical antenna radiation resistance and total radiated power in weakly ionized plasma, considering electron collisional effects

07 p0944 A72-19592

Ground plane absorption coefficient effects on admittance of slot antenna radiating into warm lossy plasma

07 p0957 A72-19797

IMPATT diode thermal resistance measurement from heat diffusion effect on small signal impedance of p-n junction

07 p0958 A72-20684

Schwartz method application to stripline fields and impedance calculations for different cross sections and internal conductor dimensions

08 p1133 A72-21370

Linear IC amplifier analysis by admittance parameters of equivalent two terminal pair network as function of frequency, temperature and supply voltage

09 p1285 A72-22342

Excess, shot and channel thermal noises performance-limiting effects on junction FETs in high input impedance applications, considering minimization method

09 p1287 A72-23111

Input impedance of plane antenna immersed in plasma within magnetic field and propagating sheath waves

10 p1520 A72-24132

Quadrupole probe theory for hot collisionless isotropic plasma, noting impedance dependence on electron temperature at resonance and optimum dimension relationship to Debye length

10 p1523 A72-24798

Bipolar insulated gate FET IC buffer driver, discussing input and output interface capacitance and impedance characteristics and application to transistor-transistor logic

11 p1603 A72-25269

Broadband cylindrical monopole antenna with adjustable quasi-distributed capacitive loading, comparing theoretical and experimental admittances

11 p1604 A72-25744

Lumped-distributed active network function sensitivity formulas in terms of immittance parameters

11 p1610 A72-25747

Semiconductor film impedance vs resistivity in free space electric field

11 p1700 A72-25778

Linear antenna in anisotropic plasma with ion depletion, calculating reactance change due to surrounding dielectric layer thickness

11 p1593 A72-25949

Finite and infinite number element phased array antennas, deriving active impedance, element pattern and power gain

11 p1593 A72-26096

Transistorized amplifier input elements design for biopotentials recording, providing minimum noise at high input impedance

11 p1585 A72-26468

Conversion losses as function of signal power and circuit impedance in narrow band triode frequency converter under large amplitude operating conditions

11 p1598 A72-26733

Spherical probe impedance characteristics in isotropic plasma predicted by hydrodynamic theory compared to experimental results

11 p1699 A72-26768

Nonlinear sheath admittance, currents and charges associated with high peak voltage drive on VLF-ELF dipole antenna moving in ionosphere

11 p1599 A72-26769

Static and impedance characteristics and equivalent circuit of p-n-p-n inductance diode, using ambipolar diffusion length

12 p1790 A72-27499

Electrical components of cardiac and skeletal muscle impedance, calculating rectangular stimulating current mean value

13 p1908 A72-28461

Input impedances and current distributions of cylindrical monopole antennas of various lengths in hot lossy plasma as function of plasma density

13 p2009 A72-28538

N region capture centers effects on small signal impedance in p-n-n diode structure during passage of strong dc current

13 p1933 A72-29977

Wall-impedance waveguide propagation constant determination from Rayleigh-Schrodinger power expansion of perturbed eigenvalues

15 p2194 A72-31549

Open circuit voltage transfer function synthesis to realize arbitrary real rational function in complex variable, using generalized positive impedance converter

15 p2211 A72-31847

Waveguide model for calculating microstrip discontinuities and T-junctions wave impedances, using orthogonal series procedure

15 p2201 A72-32470

Contaminated Langmuir probes LF admittance measurements in mercury vapor plasma, considering dielectric relaxation in insulating layers

15 p2241 A72-32516

Constrained-impedance eigenfunctions, using projection method for field expansion in diffraction problems

15 p2202 A72-32661

Thin circular loop antenna input admittance and current distribution calculation comparison

15 p2209 A72-32673

Voltage and current generalized immittance converter realization, using with current conveyor for simulation

16 p2367 A72-32856

Longitudinal and transverse electromagnetic wave penetration into semifinite collisional plasma with fractionally accommodating boundary, obtaining reflection coefficient and surface impedance

16 p2435 A72-33449

Determining electrical ground constants from the mutual impedance of small coplanar loops

17 p2514 A72-34371

Theoretical analyses on Apollo lunar surface electrical properties experiment transmitter antenna

17 p2515 A72-34423

Application of the impedance treatment to diffraction problems for a rectangular waveguide

17 p2529 A72-34848

New measurement method of Gunn-diode impedance

17 p2529 A72-35000

Two sided error estimates for electrodynamic impedance, admittance and scattering matrices in diffraction theory

18 p2657 A72-36104

German monograph - Measurement of 'oscillation impedances' and optimization of frequency noise effects of microwave-semiconductor oscillators tunable over a wide frequency range

19 p2772 A72-37477

Electron bunching and output gap interaction in broad-band klystrons

19 p2772 A72-37566

Experimentally observed admittance properties of the semiconductor-insulator-semiconductor /SiS/ diode

19 p2772 A72-37568

Electric dipole radiation at VLF in a uniform warm magneto-plasma

19 p2840 A72-37833

Inductive post influence in perfectly conducting waveguides, calculating shunt impedance with allowance for spatial harmonics effect

19 p2766 A72-38413

A large-signal theory for current-driven frequency multipliers

19 p2775 A72-38609

Fourier series analysis of multielement circular loop antenna with arbitrary circumference for current distribution and self and mutual admittances

19 p2775 A72-38615

Electromagnetic compatibility problem of RF oscillators and switching operations in power network as interference source, discussing transmission line shielding and coupling impedance

20 p2901 A72-38988

Small-signal admittance of the insulator-n type-gallium-arsenide interface region

20 p2909 A72-39775

The determination of active array impedance with multielement waveguide simulators

21 p3026 A72-40357

Microwave filter of interdigital or comb construction, calculating attenuation coefficient relationship to impedance of slabline with cylindrical inner conductor

21 p3032 A72-40628

An expression for the distribution of current in asymmetrically driven antenna immersed in a dissipating medium

21 p3022 A72-41322

Admittance measurements of a 36-m dipole antenna in the topside ionosphere

22 p3153 A72-42007

Voltage generalized-impedance converter synthesis with RC circuits for obtaining current transfer function proportional to square of s with application to filter design

22 p3140 A72-42303

Frequency dependent deep level trap admittance and field effect transcapacitance of p-n junctions calculated by truncated space charge approximation

22 p3161 A72-43086

Junction circulator shunt conductance and susceptance-slope parameter calculation by constituent resonator input admittance formation, describing quarter wave mode operation

23 p3270 A72-43604

Impedance of a unipolar semiconductor diode under conditions of space-charge limited current with allowance for recombination

23 p3270 A72-43630

Frequency-variable semiconductor-oscillator in the microwave region

23 p3272 A72-43948

Theory of magnetically tunable band-pass filters

23 p3273 A72-44360

ELECTRICAL INSULATION

MNOS transistors charge storage properties at high electric field strengths and current densities near gate insulator breakdown, determining reliable operating limits

03 p0336 A72-14277

Arrhenius model and graphical methods for temperature accelerated life tests in electrical insulation systems

04 p0500 A72-15364

Nonconducting samples preparation for scanning electron microscope, using carbon as coating material

07 p0992 A72-20578

Thin wall airframe wire insulation relative thermal life and temperature rating evaluation procedure using Arrhenius plot

09 p1339 A72-23270

Differential thermal analysis for electrical insulation thermal degradation and thermogram shape, combining equations for required life line

09 p1339 A72-23271

Gamma ray radiation effects on epoxy resin electric properties, studying electric insulation and arc resistances and dielectric breakdown strength

10 p1502 A72-25149

Electrical measurement of moisture effects on adhesive bond strength, insulation resistance and hydrophilicity of cast epoxy and organosilicon adhesives

12 p1833 A72-27449

Solar cells insulating dielectrics breakdown tests in dilute Ar plasma at positive bias voltages to 20 kV

14 p2140 A72-30926

Metal-insulator-metal tunnel junctions, investigating effect of nonparabolic band structure energy-momentum relation on I-V characteristics
16 p2370 A72-34101

Implications of ceramic-insulator irradiation results for thermionic reactor design.
17 p2496 A72-34592

Dielectric breakdown in electrical insulators used in thermionic converters.
17 p2496 A72-34593

Effect of neutron spectra on the swelling of ceramic insulators and implications for thermionic reactor design.
18 p2703 A72-36146

Use of a loaded silicon elastomer for insulation of channel multipliers of onboard electronics
18 p2670 A72-37140

Mercury Hall ion engine principles and design, discussing plasma ion acceleration, mercury evaporation and ionization and acceleration channel electrical and thermal insulation
20 p2963 A72-39937

ELECTRICAL LEADS

U ELECTRIC CONDUCTORS

ELECTRICAL MEASUREMENT

NT POLAROGRAPHY

Electrical and electronic measurement and test instrument - Conference, Ottawa, June 1971
02 p0200 A72-12476

Czech FET properties in low temperature region, measuring static characteristics, electrical parameters and noise levels at 4.2-296 K
02 p0195 A72-12670

Portable electronic wattmeter for nonsinusoidal waveform low power factor circuit measurement, discussing design, calibration and applications [IEEE PAPER 8,2]
03 p0332 A72-13757

Ac and dc electric power transient test equipment satisfying MIL-STD-704A requirements
03 p0312 A72-14038

Electrical measurements on capillary-fed colloid thruster with Zener diode-like I-V characteristic and constant propellant mass flow rate
04 p0565 A72-15204

Semiconductor slab electroconductivity measurement based on circularly polarized microwave propagation in circular waveguide
04 p0502 A72-15533

Computer controlled automatic system for measuring electroconductivity and Hall effect in semiconductors, noting data acquisition instrumentation
04 p0496 A72-15534

Dispersion characteristics of laminated cylindrical dielectric waveguide in millimeter band, noting application to permittivity measurement
05 p0627 A72-16341

Turbulent heating arc plasma voltage and current digital measurement recording, computing time dependent resistivity
07 p1045 A72-20400

Ionospheric and magnetospheric electric field measurements by rocket, satellite or balloon-borne electrostatic probes or by plasma drift methods
10 p1473 A72-24529

Semiconductor measurement technology at extremely low currents, discussing dc characteristics and ac amplification
10 p1452 A72-24815

High tension exciter output voltage measurement based on cathode ray oscilloscope and high voltage probe, stressing calibration procedure [SAE AIR 1092]
11 p1604 A72-26028

Russian papers on automatic monitoring and electrical measurement methods covering optical systems, control devices, diagnostic test optimization, bionic applications, etc
11 p1611 A72-26435

Monotypic signal rejection by connecting line insertion to sensor and central electrical measuring device input galvanic decoupling
11 p1611 A72-26440

Mechanical and electrical methods of measuring vibration rates, displacements, accelerations and time derivatives, examining magnetolectric and piezoelectric sensors characteristics
11 p1635 A72-26462

Oscillating membrane pressure gage for direct electrical measurements of fast and large pressure variations, noting insensitivity to interference
11 p1636 A72-26700

Atmospheric electricity measurements at Waldorf observatory during 7 March 1970 solar eclipse
12 p1799 A72-27139

Low noise power level measurement at microwave frequencies, noting Nyquist equation applicability and cooled-to-uncooled element connections effects in receivers
12 p1779 A72-27175

Niobium diffusion into copper as function of time and temperature, obtaining rates by electrical resistance measurements
12 p1828 A72-27448

Electrical measurement of moisture effects on adhesive bond strength, insulation resistance and hydrophilicity of cast epoxy and organosilicon adhesives
12 p1833 A72-27449

Measurement circuit for temperature dependence of thermal emf and electrical conductivity in thermoelectric materials
12 p1807 A72-27452

Thermostat for electrical measurements of high resistance materials in air up to 1200 C
13 p1957 A72-29274

Critical superconductivity currents measurement in niobium based U shaped and coiled wires within steady magnetic field
13 p2007 A72-30013

Low power TTL IC in plastic and hermetic packages tested for reliability via critical dc parameters measurement in initial and post-stress states
14 p2091 A72-31168

RF receiver predetection SNR measurement from average postdetection signal-plus-noise and noise-only voltages, tabulating computed results
15 p2196 A72-31782

Excess white noise source in photomultiplier as function of temperature from voltage, intensity and ion pulse measurements, noting effect on photon counting statistics
15 p2207 A72-32238

Beta-conductive method improvement for semiconductor electric field intensity measurement by pulsed electron beam
15 p2238 A72-32240

Transient high voltage and electric field measurement with electro-optical fringe pattern method employing pulsed laser Kerr system polarimeter
15 p2240 A72-32434

Langmuir probe susceptibility- and conductance-voltage measurements via in-phase and quadrature component plots as function of applied dc potential
15 p2241 A72-32515

Electric measurement and defect localization in monolithic IC elements by incorporating test structures
15 p2212 A72-32759

Equipment for nondestructive measurements of the resistivity of semiconductor epitaxial layers by the three-point probe technique
17 p2557 A72-35755

Dynamic characteristics of electrical measuring instruments and transducers, discussing static calibration curve, dynamic tests and parameters determination
17 p2557 A72-35757

A new instrument for the measurement of low dynamic torque.
18 p2692 A72-36820

Study of reliability of Al-Au thermocompressions by measurement of resistance
18 p2668 A72-37105

Hall and resistance measurements on single crystal HgTe-InTe alloy systems for high pressure phases in terms of conduction state, band structure and impurity effects
19 p2844 A72-37464

A measuring method for MOST transconductance and its variation.
19 p2773 A72-37901

An elegant method for measuring MOST drain-source conductance in the saturated current region.
19 p2773 A72-37902

Crack depth measurement with surface waves.
19 p2809 A72-38569

The use of an electrical induction method for determining the physical condition of a ground steel surface.
19 p2805 A72-38762

Measurements of the field-effect and effective mobilities in MOS transistors.
20 p2907 A72-39272

A new circuit for the contactless thickness measurement with the aid of pulse-excited I.C measuring circuits
20 p2927 A72-39696

Potential measurement and stabilization of an isolated target using electron beams.
21 p3087 A72-40700

Thermally-stimulated current from the gold acceptor trapping level in silicon.
21 p3097 A72-40996

Measurement of substrate impurity profile of MIS field-effect transistors.
21 p3035 A72-41488

Facility for measuring and recording the electrical resistance of metallic samples during mechanical tests
21 p3043 A72-41718

Application of digital techniques to the measurement of PCM signal power.
22 p3155 A72-42705

Critical superconductivity currents measurement in niobium based U shaped and coiled wires within steady magnetic field
22 p3190 A72-42735

Injun 5 satellite measurements of magnetospheric convection electric fields via double probe technique, discussing substantiation with OGO 6 results
22 p3174 A72-42901

Measurement of surface leakage currents in a semiconductor photoelectric converter
22 p3140 A72-43188

Standardization of resistance and capacitance elements nonlinearity measurement procedure, proposing constant amplitude supply voltage
24 p3386 A72-45392

Permittivity measurement of nonmagnetic materials samples in waveguide systems with an unknown movable reflecting load
24 p3404 A72-45504

ELECTRICAL PROPERTIES

NT CAPACITANCE
NT CARRIER MOBILITY
NT CHARGE DISTRIBUTION
NT CONTACT RESISTANCE
NT DIELECTRIC PROPERTIES
NT ELECTRIC MOMENTS
NT ELECTRICAL IMPEDANCE
NT ELECTRICAL RESISTANCE
NT ELECTRICAL RESISTIVITY
NT ELECTRON MOBILITY
NT ELECTROSTRICTION
NT FERROELECTRICITY
NT HOLE MOBILITY
NT INDUCTANCE
NT IONOSPHERIC CONDUCTIVITY
NT LC CIRCUITS
NT MAGNETORESISTIVITY
NT PERMITTIVITY
NT PHOTOCONDUCTIVITY
NT PHOTOVOLTAIC EFFECT
NT PIEZOELECTRICITY
NT PLASMA CONDUCTIVITY
NT POLARIZATION CHARACTERISTICS
NT PYROELECTRICITY
NT REACTANCE
NT SKIN RESISTANCE
NT SUPERCONDUCTIVITY

Carbon dioxide laser electrical plasma properties from probe and techniques, discussing effects of electron energy distributions, dissociation and N, He and Xe additions
01 p0079 A72-10514

CW and pulsed InP transferred electron microwave oscillators, discussing fabrication techniques and electrical properties
01 p0036 A72-10633

Electrical properties of subsonic argon plasma stream seeded with uranium hexafluoride, using electrostatic probe
01 p0111 A72-11334

Preparation and electrical properties of thin cadmium antimonide and arsenide layers, comparing to single crystal films
02 p0268 A72-12281

Center fed full wave dipole antenna with feed points displaced transverse to dipole axis, considering radiation patterns, electrical properties and power gain
02 p0177 A72-12325

Dual-gate MOS transistor structure, operational principles and electrical characteristics, noting suitable properties for use in low noise microwave amplifier
03 p0330 A72-12969

Continuous solid medium electroelastic equations of state, obtaining solution by variational principles application
03 p0390 A72-13916

MIS semiconductors radiation-hardening mechanisms and radiation effects on electrical properties and degradation
03 p0405 A72-14281

Electric and photoelectric properties of CdTe films, describing solar cells preparation
04 p0465 A72-14593

Bulk type variable resistors with properties controlled by composition during fabrication, evaluating inorganic binders with optimal properties
05 p0701 A72-15754

Heating effect on potassium bichromate-saturated anodic aluminum oxide electrical characteristics, discussing surface conductivity and capacity and solution pH
05 p0667 A72-17052

Holographic Ice Survey System for down looking radar probing and measurement of sea ice and glaciers, discussing ice electrical properties and system design
06 p0814 A72-17590

Radar instrument for measuring snow density, water content, layer depth and inhomogeneity based on snow cover electrical properties effects on echo characteristics
06 p0805 A72-17591

Electrical contacts conduction principles, considering circuit voltage, current, variable resistance and resistive, mechanical, heating and adhesive properties
06 p0791 A72-18578

Carbon dioxide laser pumping at atmospheric pressure by electron beam controlled electrical discharge, discussing measured electrical and laser properties

07 p0999 A72-18875

Thermal and electrical characteristics of plasmatrons with interelectrode partition and distributed air supply, determining efficiency dependence on current

07 p1040 A72-18996

Low and high pass, bandpass and bandstop active filters, tabulating cut-off frequencies, thermal stability, impedance, power dissipation and voltage specifications

07 p0955 A72-19248

Nonequilibrium chemistry effects on electrical properties of solid propellant rocket motors turbulent afterburning exhaust plumes, describing free electron sources

07 p0935 A72-19359

Thermodynamic and electrical properties of tantalum nitride powders and thin films for semiconductor IC technology

07 p1049 A72-19935

Electronic characteristics of real CDS surfaces in room atmosphere and ultrahigh vacuum

07 p1050 A72-20458

Optical and electrical characteristics of gas discharge plasma in pulsed radiation sources as function of power dissipation

07 p1047 A72-20611

Hf and shf power transistor gain, efficiency and electrical characteristics for wideband linear amplifiers

08 p1139 A72-21051

Operational and equivalent circuit characteristics of low noise hf and shf transistors in wideband amplifiers

08 p1139 A72-21052

Lunar and terrestrial soil thermal and electrical properties measurement in vacuum and He atmospheres

08 p1232 A72-21150

Fast neutron radiation damage to glass ceramics and amorphous semiconductors electrical properties

09 p1336 A72-22405

Recrystallization effects on thin ZnTe film structure, electrical and optical properties

09 p1367 A72-22421

Anisotropic electrical properties and void structure of amorphous Ge, discussing low- and high-field resistivity measurement in planar and transverse directions

09 p1371 A72-22873

Reactivity evaporated titanium nitride resistors for thin film microcircuits, discussing nitrogen gas pressure and substrate temperature effects on electrical properties during evaporation

09 p1286 A72-22902

Secondary breakdown effects on hf power transistor amplifier electrical characteristics, describing operation limits

09 p1288 A72-23364

Temperature dependence of Ge solubility in CdSb single crystals from microstructural observations and measurements of microhardness and electrical properties

09 p1372 A72-23480

Ferrites electrical conductivity variations with time caused by cations distribution modification after cooling

10 p1525 A72-24121

Chemisorbed oxygen effect on electrical properties of monocrystalline cadmium sulfide thin plates with high resistivity

10 p1525 A72-24211

Tempering effects on weakly doped n-InSb electrical properties at 77 K, discussing diffusion and activation energies in reversible/irreversible defect change processes

10 p1526 A72-24242

Hybrid neuristor transmission lines with planar p-n-p-n semiconductor structures, discussing development, testing and electrical parameters

10 p1448 A72-24281

Zinc oxide as refractory material, discussing optical, elastic and electro- and photoconductivity properties

10 p1501 A72-24732

Earth electrical parameters measurement by radio wave methods involving electromagnetic propagation along or reflection from surface, considering penetration depth, earth stratification and surface inhomogeneities

10 p1474 A72-24737

Book on semiconductors covering electrical properties, energy band structure, impurities, epitaxial growth, silicon dioxide, surface properties, p-n junctions and measurement techniques

10 p1528 A72-25123

Gamma ray radiation effects on epoxy resin electric properties, studying electric insulation and arc resistances and dielectric breakdown strength

10 p1502 A72-25149

Heterojunction p-GaAs-n-ZnSe diodes electrical and photovoltaic properties, showing space charge limited current effects

11 p1606 A72-26624

Electron bombardment deposited polymer thin films electrical properties as function of formation current, noting increase in crosslinking and dangling bonds

12 p1788 A72-27277

Proton and electron radiation effects on silicon solar cells electric and photovoltaic properties, determining damage coefficients via minority carriers diffusion length measurement

12 p1759 A72-28045

Monoenergetic electrons and low energy protons radiation damage effect on Si solar cell electrical and optical properties

12 p1759 A72-28046

Irradiation produced defects and electrical properties of n and p-type Si, discussing radiation damage due to neutron and ion implantation

12 p1857 A72-28058

Annealing behavior of electrical properties and photoluminescence spectra in electron irradiated n-type GaAs semiconductors

12 p1859 A72-28068

Carrier concentration Hall mobility and photoconductivity in n- and p-type CdTe after neutron and electron bombardment

12 p1859 A72-28072

Double doping effect on electrical properties of Te and Hg doped and Te and In doped CdSb single crystals

13 p2020 A72-28565

Instrument to measure thermodynamic, electrical and optical properties of gases and liquids, describing thermostat for 83-923 K range

13 p1956 A72-28633

Electrical characterization of GaAs by Hall and magnetoresistance measurements, analyzing temperature dependence of carrier concentration

13 p2024 A72-30034

Lunar surface profile, subsurface features and electrical properties measurement for Apollo 17 coherent radar and optical recording system

14 p2085 A72-30512

Chalcogenide semiconductor compounds of b-subgroup transition elements, discussing binary system diagrams, stoichiometric composition and electrical properties

15 p2290 A72-31193

Pulsed IMPATT diode oscillators RF oscillations growth rate and frequency shift behavior during build-up period, comparing equivalent circuit derived electrical properties with measurements

15 p2208 A72-32472

Mars integrated radio temperature relation to blanket electrical properties for 1971 opposition, assuming Martian soil properties independence from depth and temperature

15 p2315 A72-32730

Manufacturing process for glass fiber chopped strand mats, discussing physical and electrical properties and applications to filament winding

16 p2414 A72-33303

Flame retardant glass reinforced thermoplastic polyester Celanex processing and performance, considering flammability, and electrical/mechanical properties

16 p2415 A72-33420

Piezosemiconductor crystals acoustoelectric surface domain waveguide effect for classical and transverse surface waves

16 p2441 A72-33596

Application of the moving-slit X-ray atomochromatization method in structural studies of planar diodes and an attempt to correlate electrical properties with lattice defects.

17 p2595 A72-34749

Determination of the excess air coefficient with the aid of electrical properties in the case of laminar flames of gaseous fuels

17 p2636 A72-34931

Investigation of the dependence of the electrical characteristics of a 'Fotovolta'-type high-voltage matrix photoconverter on the radiation intensity and temperature

17 p2498 A72-35511

French monograph - Experimental characterization and analysis of the effect of ionizing radiation on the electrical properties of MOS transistors

17 p2531 A72-35650

Studies of physical-mechanical properties of monocrystalline molybdenum and tungsten and electrical characteristics of TIC/thermionic converter

18 p2698 A72-36154

Laboratory studies on seismic and electrical properties of the moon.

18 p2724 A72-36282

Interdependence of the commutation and memorization effects and the thermal behavior in a series of chalcogenide glasses

18 p2718 A72-36344

Changes of electrical and structural properties of Au thin films obtained by sputtering during the annealing process.

18 p2720 A72-36955

Electrical changes in the surface region of chalcogenide glasses.

19 p2822 A72-37454

Thickness dependence of the electrical transport properties of germanium films.

19 p2844 A72-37685

Electrical and thermoelectrical effects in GaAs-InAs solid solutions

19 p2844 A72-37752

Yagi-Uda helical antenna array with moderate gain and compact mechanical design, determining electrical characteristics

19 p2773 A72-37941

Influence of heat treatment on the properties of Cr-SiO cermet thin films

19 p2844 A72-37948

Electronic control systems for industrial applications, discussing electrical and mechanical properties, circuit reliability and mechanical design features

19 p2782 A72-38314

Electrical properties and fabrication details of integral diode matrices with controllable avalanche breakdown produced from zone melted silicon under temperature gradient

19 p2774 A72-38416

Electrical properties of thick-film barium titanate dielectrics produced by flame spraying.

19 p2846 A72-38616

RF shielding and electrical properties of boron and carbon fiber reinforced composites.

20 p2944 A72-38987

Lunar and terrestrial soil thermal and electrical properties measurement in vacuum and He atmospheres

20 p2968 A72-39255

Anisotropic electrical properties of amorphous germanium.

20 p2960 A72-39457

Installation for the simultaneous measurement of the functional properties of sliding contacts

20 p2928 A72-39936

Apparatus for measurement and automatic graphical recording of variations of electrical characteristics of a metal-insulator-semiconducting structure

21 p3051 A72-40209

Output power saturation with increasing discharge current in powerful argon CW lasers

21 p3062 A72-40404

Space applications of Fabry-Perot modulator as alternative to mechanical devices, presenting optical and electrical performance data for different temperatures

21 p3055 A72-40824

Pressure dependence of electrical characteristics of semiconductor sensors using deformation potential for mechanical stress detection and measurement

21 p3056 A72-41109

The effect of membrane parameters on the properties of the nerve impulse.

22 p3140 A72-41936

Antifurcation and electrical properties of WSe₂-NbSe₂ quasi-binary alloys

23 p3299 A72-43292

Changes in the physical properties of metals subjected to elastoplastic deformation

23 p3303 A72-44199

Preswitching electrical properties, 'forming,' and switching in amorphous chalcogenide alloy threshold and memory devices.

24 p3385 A72-45270

Electrical characteristics of a CO laser discharge plasma

24 p3411 A72-45500

ELECTRICAL RESISTANCE

NT CONTACT RESISTANCE

NT LC CIRCUITS

NT SKIN RESISTANCE

Positive and negative deviations of linear electrical resistance of d-transition metals at high temperatures as function of Debye temperature and Fermi level

02 p0242 A72-12006

Gradient-recombination current instability in high resistance compensated semiconductors

04 p0561 A72-15084

N-port resistive network synthesis involving use of vectors, cones, bilinear inequalities and matrices

05 p0639 A72-15801

Electrical resistance, Hall coefficient and magnetic susceptibility of transition metal nitrides at low and room temperatures

06 p0827 A72-17386

Organism blood volume and losses determination by measuring human body electrical resistance, noting unsatisfactory results

06 p0768 A72-17994

Square wave source gated detector bridge for precise resistance measurement, discussing design and performance, and application in Pt resistance thermometry

06 p0785 A72-18244

Vacancy effects on residual electrical resistance of binary ordering fcc lattice alloys as function of composition and annealing temperature

06 p0832 A72-18422

Electrical contacts conduction principles, considering circuit voltage, current, variable resistance and resistive, mechanical, heating and adhesive properties 06 p0791 A72-18578

Input resistance derivation for finite horizontal loops with uniform current distribution located above lossy half-space ground 06 p0777 A72-18737

Structural changes, mechanical properties, electrical resistance and lattice constant during aging of Al alloys containing Mg, Li and Mn 06 p0834 A72-18743

Cu electrical resistance and heat content oscillographic measurement, using high voltage pulse method 07 p0981 A72-18804

Minimum charging resistance in relaxation generators for spark machining as function of supply voltage, using thyristor and voltage source circuit model 07 p0956 A72-19594

Structure, hardness, density, and electrical resistance of binary alloys V-Ti, V-Cr, V-Al and V-Sn 07 p1013 A72-19741

Temperature dependence of electrical resistance and thermal conductivity in duralumin quenched at 77 K 07 p1022 A72-20663

Electrical resistance and thermal conductivity dependence on temperatures in duralumin quenched at 77 K 07 p1022 A72-20666

Deposition of Ni-B coatings with specified electrical resistance onto fiberglass cloth reinforced plastics 09 p1318 A72-22528

Piezoresistance magnitude and temperature dependence changes of electron irradiated n-type silicon due to oxygen vacancy complex /A center/ 09 p1372 A72-23239

Niobium carbide resistors properties, investigating temperature dependence of electrical resistance and thermal stability 09 p1331 A72-23483

Schottky barrier crystal microwave video diodes design and fabrication to maximize burnout resistance and dynamic range for given detection sensitivity 10 p1450 A72-24553

Test assembly design for microstructural studies of metal and alloy fatigue in vacuum during heating, describing electrical resistance measurement and stroboscopic illumination 11 p1612 A72-25492

Be foil electrical resistance change during and after pulsed laser irradiation and annealing 12 p1853 A72-27067

Local heating effect of electrical resistance gages measuring strain across thickness of plane photoelastic Araldite models 12 p1807 A72-27316

Pulse plasma injector accelerating circuit resistance dependence on time and current amplitude calculated from current oscillograms 13 p2010 A72-28733

Distributed base resistance effect on stripline geometry transistor input characteristic, using equivalent circuit with pseudo-junction having high saturation current 13 p1930 A72-29059

Thermostat for electrical measurements of high resistance materials in air up to 1200 C 13 p1957 A72-29274

Nonlinear harmonic analysis of reflex klystrons with high electron conduction, using average method in second approximation 13 p1931 A72-29290

CW Gunn oscillator cavity loading and bias voltage effects on external negative differential conductance 13 p1933 A72-29825

Ta thermal conductivity and electric resistance at various temperatures 13 p1981 A72-29897

Impurities effect on platinum resistance thermometers temperature reading accuracy, presenting empirical formula for approximate error estimate as function of operational conditions 13 p1960 A72-29906

Phase transitions effect on dc electrical resistance of barium titanate investigated for yttrium-doped polycrystals and for reduced single crystals 15 p2294 A72-32483

Sensor design and principles for atomic oxygen concentration measurement in dissociated gases, using Ag thin film electrical resistance change during oxidation 16 p2390 A72-33162

Conduction electron phonon scattering effect on electrical resistance of metallic contacts during pressure welding 16 p2370 A72-33952

Electrogasdynamics generator nonlinear internal resistance determination as function of flow parameters and model geometry via boundary conditions formulation 18 p2643 A72-35998

Physical-mechanical properties of beryllium oxide and investigation of its electrical resistance under irradiation in a reactor 18 p2703 A72-36147

Si MOSFET elementary channel resistances before saturation onset from one dimensional theory, investigating current noise 18 p2668 A72-37037

Effect of temperature on the base resistance and the noise factor of a bipolar junction transistor. 19 p2773 A72-37848

A measuring method for MOST transconductance and its variation. 19 p2773 A72-37901

An elegant method for measuring MOST drain-source conductance in the saturated current region. 19 p2773 A72-37902

Effect of plasma resistance on electron temperature measurement by means of an electrostatic probe. 19 p2804 A72-38593

A precise method for measuring low-frequency small-signal conductance parameters of an MOS transistor. 20 p2907 A72-39273

High speed logic circuit interconnecting transmission line matching by nonlinear resistance, recommending use of Schottky diodes 20 p2909 A72-39737

Conductance associated with interface states in MOS tunnel structures. 21 p3032 A72-40701

Electric model of bridging losses and optimal insulation layer thickness for small size resistance strain gages 21 p3056 A72-41367

Facility for measuring and recording the electrical resistance of metallic samples during mechanical tests 21 p3043 A72-41718

Current noise and conductance-temperature characteristics of thin discontinuous Pt films on glass substrate interpreted by quantum mechanical electron tunneling model 22 p3214 A72-42453

Generation threshold of the anomalous resistance for longitudinal currents in the magnetosphere 23 p3284 A72-43379

Junction circulator shunt conductance and susceptance-slope parameter calculation by constituent resonator input admittance formation, describing quarter wave mode operation 23 p3270 A72-43604

Electric resistance and enthalpy of molybdenum and tungsten 23 p3272 A72-44167

Physical limits of semiconductor devices miniaturization for electronic computers, considering thermal energy dissipation, electrical resistance and high current density induced electromigration effects 23 p3273 A72-44332

Optical properties of thin cesium films over the wavelength range from 0.3 to 0.9 microns and their electrical resistance 24 p3426 A72-44801

Standardization of resistance and capacitance elements nonlinearity measurement procedure, proposing constant amplitude supply voltage 24 p3386 A72-45392

Be foil electrical resistance change during and after pulsed laser irradiation and annealing 24 p3432 A72-45720

ELECTRICAL RESISTIVITY

NT IONOSPHERIC CONDUCTIVITY

NT MAGNETORESISTIVITY

NT PHOTOCONDUCTIVITY

NT PLASMA CONDUCTIVITY

NT SUPERCONDUCTIVITY

Thermal conductivity, electrical resistivity, Lorentz ratio and thermopower of Ti, Al and Ni alloys for aerospace structures over 4-300 K range 01 p0113 A72-10173

Tungsten heat capacity, electrical resistivity and thermal radiation measurement over 2000-3600 K range by pulse heating technique 01 p0082 A72-10174

Lunar soil dielectric constant and loss-tangent and electrical resistivity measurement by Q meter method, noting resemblance to dense terrestrial rock powders 02 p0281 A72-12287

Chapman uniform electrical conductivity core model for geomagnetic disturbance daily variations due to solar wind, noting error in analysis 02 p0222 A72-12794

Stainless steel electrodes resistive and capacitive properties in contact with saline solutions of various concentrations and over extensive frequency range and current densities 03 p0318 A72-12953

Niobium-oxygen-nitrogen system solid solution, noting gas composition effects on hardness and electrical resistivity 03 p0369 A72-12958

Lunar electrical conductivity model, determining vacuum transient response to time varying spatially uniform magnetic field 03 p0434 A72-13508

Thermocouple efficiency with respect to Thomson effect and electric resistivity temperature dependence 03 p0360 A72-13651

Short range order and nucleation of long range order in Ni-rich Ni-Nb alloys, observing electrical resistivity changes dependence on solute concentration 03 p0379 A72-14338

Mathematical model for two-stream instability induced anomalous resistivity and heating in plasma with equal initial electron and ion temperatures in static electric field 04 p0554 A72-14402

Small pressure difference measurement in gas flow, using transducer based on liquid electrical conductivity measurement 04 p0523 A72-15483

Aging effect on duraluminum electrical resistivity alteration at low temperature plastic deformation 05 p0679 A72-17181

Higher harmonics in lunar transfer functions for surface magnetic field tangential components, discussing lunar electrical conductivity models 06 p0875 A72-17448

Si MOSFET substrate resistivity effect on surface state noise spectra 06 p0783 A72-17609

Thermal conductivity, electrical resistivity, emissivity and specific heat of polycrystalline vanadium under electron bombardment heating at 1200 to 1800 K 06 p0828 A72-17613

Bulk semiconductor material complex microwave conductivity and dielectric constant measurements by cavity perturbation techniques 06 p0786 A72-18371

Exponential conduction increase of semiconductors in strong magnetic fields, determining three dimensional random network resistance with percolation theory 07 p1047 A72-18918

Third harmonic generation in Ge induced by conduction nonlinearity during bulk heating of charge carriers by microwave fields 07 p1047 A72-19023

Alloying additives effects on Ti and Zr resistivity, thermal expansion, crystal lattice parameters and polymorphous transformations temperatures 07 p1017 A72-19990

Quantum mechanical electron motion problem in binary alloy crystal lattice, discussing Bloch approximation, energy spectra, and third element admixture conductivity effects 07 p1049 A72-20150

Turbulent heating arc plasma voltage and current digital measurement recording, computing time dependent resistivity 07 p1045 A72-20400

Bulk conductors dc field distribution applications to electrical resistivity measurements and nondestructive testing 07 p0998 A72-20461

Resistivity, thermoelectric power and magnetoresistance of carbon fibers derived from heat treated polyacrylonitrile 07 p1024 A72-20550

Integral relations derivation for stationary and nonstationary potential motions in cases of zero and infinite conductivity, applying to wave expansion in cylindrical waveguide 08 p1212 A72-20966

Matsevityi nonlinear resistances method for contact heat exchange boundary value problems of fourth kind 08 p1252 A72-21319

Carbon fibers elastic modulus inference from electrical conductivity inverse correlation with sound propagation rates 08 p1191 A72-21498

Temperature effects on electrical conductivity and transport mechanisms in sapphire from measurements under protection against surface and gas phase conduction 09 p1335 A72-22400

Solid state sinusoidal signal generator based on current density oscillation effect in high resistivity p-type InSb with transmutation doping 09 p1288 A72-23191

Lunar soil dielectric constant and loss-tangent and electrical resistivity measurement by Q meter method, noting resemblance to dense terrestrial rock powders 10 p1532 A72-23756

Electrical resistivity restoration in Van Arke type Zr deformed by lamination at 78 K attributed to point defects elimination 10 p1495 A72-24085

Temperature dependence of emf coefficient Hall constant and conductivity in solid and liquid phases of InSe semiconductor during melting 10 p1526 A72-24267

MHD generator duct external loop electric current maximization by working material resistivity tensor optimal distribution 10 p1521 A72-24434

Magnetic properties, electrical resistivity and hardness of vacuum melted Ni-Fe-Ta alloys 11 p1655 A72-25512

Transition from metallic to activation conductivity in doped semiconductors, noting activation energy dependence on compensation degree 11 p1700 A72-25720

Semiconductor film impedance vs resistivity in free space electric field

11 p1700 A72-25778

Carbon solubility in Nb at 1500-2150 C, determining saturation concentrations from electrical resistivity vs reaction time curves

11 p1662 A72-26740

Technological parameters effects on resistance values dispersion of thick film resistors, reviewing stability test performance

12 p1788 A72-27274

CdS thin film conductivity reactions to grain boundary and stacking faults, correlating grain size to mobility

12 p1856 A72-28012

Te single crystal electrical resistivity and Hall coefficient effects of electron irradiation, suggesting point defects and dislocations interaction

12 p1859 A72-28073

Burgers binary and Shkarofsky multiple collision theory numerical application to electrical conductivity in partially ionized solar magnetoplasma

13 p2018 A72-29714

Ti-Mo-Ni system polythermal section microstructure, hardness, resistivity and thermal expansion characteristics

14 p2112 A72-30153

Apollo 11 and 12 lunar surface rocks electrical conductivity at 300-1200 K in vacuum, Ar, He and He-hydrogen atmospheres, noting large hysteresis above 500 C

14 p2155 A72-30518

Nickel-trinickel alumide-trinickel niobiumide system polythermal cross sections from X ray and microstructural analysis, noting electrical resistivity increase with Al content

14 p2123 A72-30988

Yttrium alloys isoperiodic lines, solidus isotherms, equal hardness lines and resistivity presented diagrammatically

15 p2289 A72-31185

MOS transistor injection level dependent theory, calculating drain region saturation conductance by iterative procedure

15 p2205 A72-31318

High resistance n-type InP crystals electrical conductivity and photoconductivity characteristics at 80 K, discussing photosensitivity spectral distribution and temperature dependence

15 p2290 A72-31371

Dynamic spin disorder effect on electrical and thermal conductivity, noting low resonant frequency in metal atom magnon spectrum

15 p2290 A72-31388

Electrical conductivity, reluctance and Hall effect of n-type semiconductors determined at extremely low temperatures

15 p2291 A72-31389

High microwave voltage effects on p-n junction conductance under inverse dc bias, noting role of hole generation and accumulation by impact ionization

15 p2206 A72-31643

Electrical conductivity in mesosphere and upper stratosphere from rocket sounding by blunt probe technique, suggesting electron density profiles dependence on dissociative recombination variations

15 p2228 A72-31972

CdTe single crystals photoplastic characteristics, detailing illumination effect on yield stress and resistivity

15 p2294 A72-32501

Langmuir probe susceptibility- and conductance-voltage measurements via in-phase and quadrature component plots as function of applied dc potential

15 p2241 A72-32515

Thin film superconductors conductivity evaluation above transition temperature through renormalization of impurity-scattering vertex by pair fluctuation effect inclusion

15 p2295 A72-32540

Lattice dynamical model for Cs vibration frequency distribution, specific heat and electrical and thermal resistivity calculations

16 p2441 A72-33584

Equipment for nondestructive measurements of the resistivity of semiconductor epitaxial layers by the three-point probe technique

17 p2557 A72-35755

The effect of dislocation tangles on superconducting properties.

18 p2719 A72-36746

The Rayleigh-Taylor problem with a vertical magnetic field, including the effects of Hall current and resistivity.

19 p2839 A72-37339

Emissivity and electrical resistivity of tungsten-yttrium oxide cermet as function of composition at 1200-3200 K

19 p2819 A72-38286

Influence of impurities on the high-temperature electrical conductivity of CdTe crystals

19 p2847 A72-38677

Relation between diffusion and defect formation rates in silicon detectors exposed to gamma radiation

20 p2959 A72-38956

Exponential conduction increase of semiconductors in strong magnetic fields, determining three dimensional random network resistance with percolation theory

20 p2960 A72-39384

Measurement of melting point and electrical resistivity /above 3600 K/ of tungsten by a pulse heating method.

20 p2941 A72-39722

Calculation of electronic Green functions using nonorthogonal basis functions - Application to crystals.

20 p2961 A72-39810

Determination of conduction anisotropies in semiconductors.

21 p3097 A72-40697

Metal fiber composites electrical resistivity as function of fiber volume proportion, evaluating vacuum cast Cu/W

21 p3073 A72-41373

Matthiessen rule on binary alloy electrical resistivity temperature derivative, discussing data deviations in substitutional alloys after quenching, radiation damage and plastic deformation

22 p3189 A72-42298

Physical and electrical properties of thin-film barium titanate prepared by RF sputtering on silicon substrates.

22 p3215 A72-42999

Bi-Sb alloys for magneto-thermoelectric and thermomagnetic cooling.

22 p3215 A72-43089

Electrical resistivity changes in nichrome films sintering of various thickness with different heat treatment conditions, noting heat stability and thermal shock tests

23 p3292 A72-43280

Effect of substrate temperature on electrical properties of amorphous germanium films.

23 p3324 A72-44069

Magnetohydrodynamic flow between parallel rotating disks. I - Influence of finite wall-conductance.

23 p3322 A72-44400

The lunar conductivity profile and the nonuniqueness of electromagnetic data inversion.

24 p3436 A72-44693

Thin ice crust, chondritic composition and ionosphere considerations for Io electrical conductivity and decametric radio emission modulation in unipolar inductor model

24 p3437 A72-44704

Relationship between the electrical resistivity and solute concentration in the solid solution of tantalum-hydrogen system.

24 p3412 A72-44718

An apparatus for measuring the Hall effect of high-resistivity materials in alternating electric and magnetic fields

24 p3405 A72-45698

ELECTRICALLY SUSPENDED GYROSCOPES

U ELECTROSTATIC GYROSCOPES

ELECTRICITY

NT ALTERNATING CURRENT

NT ATMOSPHERIC ELECTRICITY

NT AURORAL ELECTROJETS

NT ELECTROJETS

NT EQUATORIAL ELECTROJET

NT GEOELECTRICITY

NT IONOSPHERIC CURRENTS

NT STATIC ELECTRICITY

NT TELLURIC CURRENTS

Book on electricity and electronics for aerospace vehicles covering theoretical foundations, measuring instruments, batteries, generators, motors, radio receivers and transmitters, navigation equipment, autopilots, etc

15 p2182 A72-31511

ELECTRIFICATION

Static electrification - Conference, London, May 1971

02 p0260 A72-12551

Solids static electrification models based on solid state physics, considering contact, deformation and cleavage charging processes

02 p0269 A72-12552

Frictional electrification from supersonic particle impact, determining particle charge and concentration, body intercepting area and velocity variations with speed

02 p0261 A72-12555

ELECTRO-OPTICAL EFFECT

Second order electro-optic effect in diamond, discussing birefringence due to dispersion and residual strains

[AD-736674]

02 p0260 A72-12545

Electric field effects on electromagnetic wave packet motion in anisotropic nonlinear medium with electro-optical effect

03 p0322 A72-13737

Book on lasers and applications covering theories of light, polarization, coherence, resonators, mirrors, modes, electro-optical effect, communication, holography, etc

06 p0827 A72-18524

Electro-optical multiple transit laser beam deflection system using KDP crystals and quadrupolar electrode arrangements

07 p1000 A72-19011

Rhodamine 6G dye laser tuning by variable birefringence filter using lead lanthanum zirconate titanate electrooptic ceramics for wavelength selection

07 p1002 A72-19203

In-line eight stage digital light deflector with prisms and polarization switch, using Pockels effect with transverse field

07 p1003 A72-19222

Electro-optical Q switching of solid state laser sources without linear energy polarization in optical resonator

09 p1326 A72-23422

Current-optical effects of anisotropic absorption of polarized and unpolarized light in rarefied cosmic media

10 p1525 A72-23763

Intracavity modulation of ruby laser with frequency near neighboring axial oscillations frequency difference, describing Q switch based on transverse electro-optical effect in KDP crystal

10 p1490 A72-24047

Electro-optical Fabry-Perot modulator with KDP and ADP crystals as optical resonators, determining modulation and frequency response characteristics

10 p1492 A72-24583

Photoelastic analysis of piezooptical and rheological properties of anisotropic composite glass plastics

10 p1557 A72-24626

Nonlinear interaction between circular coherent light and modulating electromagnetic waves in presence of quadratic electrooptical effect, noting frequency shift

10 p1493 A72-24912

Holographic memory devices for bulk information recording, discussing use of image converter for brightness amplification and lithium niobate electro-optical deflector for beam switching

12 p1807 A72-27588

Discrete ten stage system for laser beam deflection based on electro-optical effect in lithium niobate crystals

12 p1808 A72-27595

Longitudinal electro-optical effect in oblique cut lithium niobate crystal with minimum half wave voltage between incident beam and optical axis angle

12 p1855 A72-27603

Carbon dioxide-helium-nitrogen mixture laser, comparing GaAs, CdSe, CdS and CdTe electro-optical crystals suitability for radiation modulation at 20.6 microns

12 p1822 A72-27610

Ruby laser electro-optical modulator with low modulation voltage, discussing layout, operating principle and laser energy characteristics

12 p1822 A72-27611

Electro-optical processing of phased array signal reception, using electron beam addressing system with potassium deuterium phosphate target crystal

12 p1785 A72-27954

Liquid crystals synthesis, physical chemistry and material parameters effects on mesomorphic and electro-optical behavior

15 p2240 A72-32363

Electro-optical torque sensor based on slit aperture produced diffraction patterns

[SESA PAPER 1925-II]

17 p2553 A72-34813

Active Q switching technique for producing high laser power in a single longitudinal mode.

19 p2811 A72-37845

Superposition method for potential distribution in plane tetraode field with unipotential and bipotential grids, noting electro-optical effect in cylindrical lenses

19 p2776 A72-38667

Pulse generator for modulation of a low-voltage Pockels cell.

20 p2933 A72-39525

Electro-, magneto- and acousto-optical methods for laser Q-switching, discussing physical and operational principles

22 p3186 A72-42942

Book - Introduction to optical electronics.

23 p3295 A72-43650

Stimulated entropy /temperature/ scattering and its influence on stimulated Mandelstam-Brillouin scattering

23 p3297 A72-44478

Periodic control of the emission from a ruby laser achieved by a Q switch utilizing the transverse electro-optical effect.

24 p3412 A72-45618

ELECTRO-OPTICAL PHOTOGRAPHY

Operator interactive computer controlled electro-optical system for photographic image enhancement prior to target or pattern identification

01 p0070 A72-10869

Generalized quantum yield for sensitivity of photoelectric devices, considering multistage image converter and photomultiplier

02 p0223 A72-11411

- Ultrahigh speed electro-optical cameras with exposure times of several picoseconds, using bipplanar image converter, electron multiplier and Kerr cell
06 p0812 A72-17415
- Satellite-borne multispectral photographic line-scan system with direct optoelectrical signal conversion for photogrammetric and cartographic applications
06 p0815 A72-17757
- Spectroscope model design using ruby laser highly monochromatic light pulses, electro-optical scanning and high speed photography to study atmospheric gases absorption spectra
09 p1322 A72-22205
- Electron-optical system with electro- and magneto-static lenses, ensuring large image reduction for producing printed microcircuits
10 p1482 A72-24589
- Zeiss /Jena/ stereoplanigraph design and operation to obtain purely optical projection for object reconstruction, discussing human operator replacement by objective electro-optical system
16 p2394 A72-33870
- Computerized photographic imagery analysis system with interactive operator controls for processing option selection in image enhancement prior to pattern identification
17 p2520 A72-34407
- Electro-optical TV technique with laser source illumination to provide engineering metrology and NDT procedure resembling real time holographic interferometry
20 p2930 A72-39038
- Optical system parameters for electrophotographic print quality, discussing aberration effect on image optical density
21 p3059 A72-41818
- Image intensifier systems and their applications to astronomy.
22 p3181 A72-42989
- Future giant-aperture orbital space telescope design based on active optics and electro-optical techniques, discussing laser interferometry and precise servomechanisms roles
24 p3405 A72-45544
- ELECTRO-OPTICS**
Double 45 degree z cut KD P electro-optic Q switch simulation with programmable desk top computer, deriving extinction ratio dependence plot graphs
02 p0224 A72-11746
- Soviet book on electro-optical devices for space vehicles orientation and navigation covering vertical plotters and sun, planet and star trackers
02 p0256 A72-12125
- Scattering media visibility improvement analysis, using theoretical evaluations and experimental electro-optical measurement techniques in fog and underwater
02 p0253 A72-12644
- Ultrahigh speed holographic camera for three-dimensional photographs and interferograms, using ruby laser output
04 p0522 A72-15139
- Wideband electro-optic FM of laser light for optical communication, discussing modulator design, construction and testing
[AIAA PAPER 72-177]
05 p0631 A72-16961
- Quantum optics analysis of light propagation and photon flux fluctuations in medium with random dielectric constant inhomogeneities
07 p0938 A72-18912
- Performance characteristics of electro-optical material cadmium telluride for intracavity modulator of carbon dioxide lasers
07 p1003 A72-19223
- Electro-optic materials and fixing techniques for holographic recording and storage performance improvements
[CLEA PAPER 18,2]
07 p0950 A72-19400
- Strain biased transparent ferroelectric electro-optic ceramics for coherent transducers /page composers/ for holographic memories and optical data processing
[CLEA PAPER 18,6]
07 p0950 A72-19401
- Carbon dioxide lasers and GaAs electro-optical crystals 110-MHz bandwidth with coupling modulation technique
07 p1005 A72-19413
- Energy level and V-I characteristics of solid state heterojunction devices, discussing diodes, transistors, thyristors and optoelectronic structures
08 p1139 A72-21054
- Optoelectronic elements for information system applications, discussing photomultipliers, photodiodes, photoresistors, avalanche and photoparametric diodes response and bandwidth characteristics
08 p1169 A72-21844
- Regulating amplifier with optoelectronic coupler for sonar sea bed layer measurements
09 p1284 A72-22239
- Geodetic optical distance measuring instruments with electro-optical polarization modulators, comparing characteristics of four possible configurations
09 p1314 A72-23336
- Thin organosilicon films for integrated optical circuits and devices, discussing transparency and loss characteristics and refractive index control
09 p1314 A72-23339
- Holographic technique development review, discussing current and future applications and unsolved problems
09 p1315 A72-23375
- Muller matrix derivation for microwave light modulation studies in quasi-homogeneous magneto-optical and electro-optical media, taking into account finite light speed
10 p1493 A72-24914
- Programmed electro-optical systems of multichannel solar spectrometer for ground observations of X ray and EUV emission regions
11 p1630 A72-25680
- Russian book on satellite-borne electro-optical IR radiometers design for celestial bodies spectral radiance and energy distribution measurement
11 p1634 A72-26376
- Optimal parameters of electro-optical signal processor for phased array antennas, noting optical subsystem correspondence to optoacoustical spectrum analyzer
13 p1926 A72-28374
- Electro-optical regenerative assembly with p-n-p structure, emphasizing positive feedback and I-V characteristics
13 p1933 A72-29976
- Design data of guided wave structures for electro-optical modulation, evaluating propagation wave numbers, attenuation rate, phase modulation rate and dispersion characteristic
15 p2246 A72-31667
- Electro-optical media for initial light radiation frequency shift maximum, analyzing circular light/modulating wave interactions
15 p2197 A72-31880
- Electro-optical systems design - Conference, New York, September 1971
15 p2247 A72-32026
- Unmodulated solar radiation effect on electro-optical photoreceptors voltage sensitivity, noting photomultipliers and silicon photodiodes
15 p2237 A72-32121
- Transient high voltage and electric field measurement with electro-optical fringe pattern method employing pulsed laser Kerr system polarimeter
15 p2240 A72-32434
- Q switched laser operation with electro-optic switch mechanism, measuring initial photon number per mode of Nd-glass and Nd-YAG lasers
16 p2399 A72-33014
- Electro-optical Q switch synchronized by laser radiation for nanosecond light pulse shaping with energy dependent triggering
16 p2400 A72-33082
- Book - Semiconductor diode lasers
17 p2563 A72-35300
- A horizon sensor with a bolometer and electro-optical modulators
17 p2556 A72-35385
- Digital simulation for sampled electro-optical imaging system performance prediction and optimization
17 p2557 A72-35552
- Flight tests correlation with mathematical models to predict electro-optical viewing systems capability for military missions
17 p2557 A72-35553
- Single-crystal, electro-optic shutter for Q-switching lasers emitting unpolarized radiation.
18 p2698 A72-36698
- Electronic and optical phenomena in semiconductor.
19 p2844 A72-37445
- Multiplexing behavior of electrooptically Q-switched lasers.
19 p2813 A72-38692
- Electro-optics '72: Proceedings of the Second International Conference, Brighton, England, February 29-March 2, 1972.
20 p2921 A72-39026
- Electro-optic KTN /potassium tantalate niobate/ crystals for modulators, deflectors, phase shifters and polarization rotator devices
20 p2922 A72-39047
- An application of atmospheric light scattering for contrast analysis in electro-optical detection systems.
20 p2923 A72-39056
- FOSS - A dynamic six degree-of-freedom environmental simulator for evaluation of electro-optical guidance systems.
20 p2911 A72-39135
- Quantum optics analysis of light propagation and photon flux fluctuations in medium with random dielectric constant inhomogeneities
20 p2932 A72-39378
- Radio astronomical event visible image generation by electro-optical processing comparing SNR performance and electronic complexity with conventional technique
20 p2904 A72-39787
- Interferometric method for measuring electro-optic coefficients in crystals.
21 p3095 A72-40138
- Improvements in electro-optic circular-scan deflectors.
21 p3050 A72-40146
- Electro-optical noncontracting torque sensor, using slit diffraction pattern technique
21 p3051 A72-40231
- Optoelectronic speed control for replacing mechanical gear drives for precisely variable shaft speed ratios
21 p2997 A72-40259
- Optical communication with distant spacecraft, discussing electro-optical transducers, light sources and receivers
21 p3014 A72-40321
- Microelectronics developments and limitations, considering bipolar IC, metal-dielectric-semiconductor structures and optoelectronic communication links
21 p3033 A72-40940
- IR night vision instruments range calculation, taking into account atmospheric optics and electro-optical image converter characteristics
21 p3059 A72-41816
- Electro-optical design and performance parameters of polluted air liquid droplet size distribution measurement by pulsed junction diode laser light external scattering
22 p3179 A72-42680
- Real time analog computation at light speed and rapid access data storage in optical data processing systems, considering coherent electro-optical instrumentation
22 p3180 A72-42713
- A fast opto-electronic transducer
22 p3180 A72-42944
- Nimbus limb radiometer, Apollo fine sun sensor, and Skylab multispectral scanner.
23 p3288 A72-43882
- Noise characteristics of a digital system of light-beam deflection
24 p3410 A72-45323
- Time dependence of laser characteristics on external HF modulation of parameters by mirror oscillation and electrooptical and acoustooptical effects, noting laser mode locking
24 p3410 A72-45416
- Use of oblique-cut lithium niobate in optical-beam control systems.
24 p3411 A72-45606
- ELECTROACOUSTIC TRANSDUCERS**
NT MICROPHONES
Equivalent circuit model for electroacoustic surface microwave transducer, discussing radiation properties determination from excitation fields distribution
01 p0041 A72-10704
- Zinc oxide longitudinal acoustic microwave transducer, measuring untuned insertion loss and electroacoustic coupling constant
01 p0042 A72-10705
- Pulse compression of radar signals by ultrasonic liquid delay line, stressing wideband damped electroacoustic transducers construction
01 p0044 A72-11321
- Power generation and low noise amplification devices development during past decade, considering avalanche diodes, transferred electron and acoustoelectric devices and microwave transistors
07 p0952 A72-18825
- Micrometeorite flux observed by rocket-borne electroacoustic transducers
15 p2308 A72-31931
- One path ultrasonic flowmeter using electroacoustic feedback.
17 p2556 A72-35427
- IAD-3 amplitude-phase impedance deftoscopes.
19 p2805 A72-38765
- ELECTROACOUSTIC WAVES**
Electroacoustic magnetic and Hall effects in semiconductors in strong electric field involving phonon production by supersonic electron drift
03 p0401 A72-13088
- Current source generated electromagnetic and electroacoustic wave propagation through homogeneous, isotropic compressible electron-ion plasma, using two fluid continuum theory
04 p0554 A72-14510
- Electromagnetic and electroacoustic near zone fields of linear antenna in plasma measured by diagnostic probe
05 p0700 A72-17232
- Electroacoustomagnetic and Hall effects in semiconductors within strong electric field involving phonon production by supersonic electron drift
13 p2022 A72-29437
- Cylindrical antenna immersed in weakly ionized magnetoplasma, calculating steady magnetic field effect on the radiative and electroacoustic radiation resistances
16 p2434 A72-32860
- Sound propagation in ionized gases and electroacoustic effect.
21 p3085 A72-40993
- Coupled fields in inhomogeneous warm plasmas with static pressure gradients. I.
22 p3210 A72-42313
- Effects of pseudosonic and electroacoustic waves on the radiation of a plasma-coated spherical antenna.
24 p3386 A72-45645

ELECTROCARDIOGRAPHY

Human patients with chest pain and normal ECG, examining diagnostic value of graded exercise test, history and lipid levels with coronary arteriography data

01 p0010 A72-10146

Clinical electrocardiography diagnostic capability, discussing phase plane cardiogram sensitivity to aberrations in QRS contours

01 p0017 A72-10148

HIS bundle electrocardiography for arrhythmia studies, discussing conducting tissue potential recording, ventricular delay and block site determination and electrophysiological effects of drugs

02 p0157 A72-11473

Canine and human ventricular myocardium microelectrophysiologic studies of postextrasystolic T wave change relation to cellular repolarization and contractile potentiation magnitude

02 p0157 A72-11474

Arrhythmias relation to coronary artery disease, discussing conduction defects, sudden death prodromata and prevention and digitalis as antiarrhythmic agent

02 p0157 A72-11476

ECG telemetry systems parameters, discussing manufacturers specifications and standardized laboratory performance test data

02 p0169 A72-12139

Human pulse wave propagation velocity measurement, using biotelemetry system of photoresistance sensors and endoscopic bulbs connected to electrocardiograph

02 p0169 A72-12519

Physical exercise effect on ECG atrial recovery wave duration and magnitude in humans with A-V blocks

02 p0166 A72-12891

Age related diminutions in ballistocardiographic and electrocardiographic amplitudes, observing relation to heart position lateralization and size reduction

03 p0314 A72-13144

Exercise ECG correlation to morphological patterns of selective cinecoronary arteriography and ventriculography, revealing significant information on occlusion and stenosis

03 p0314 A72-13178

QRS amplitude relation to frontal QRS axis and heart-electrode distance, using 12-lead ECG

03 p0320 A72-13881

Familial cardiomyopathy detection by electrocardiography noting arrhythmias, ventricular hypertrophy, abnormal Q waves and intraventricular conduction defects

04 p0466 A72-14443

Exercise ECG multichannel radio telemetry equipment, discussing sources of malfunction and unreliability and remedial procedures

05 p0621 A72-16610

Electrocardiography telemetry system for intense radiation environment, describing electrode and transmitter implantation in monkey and heart signal transmission and reception

05 p0623 A72-16678

Electrocardiographic age trends in adult healthy populations, discussing diagnostic implications and overweight, exercise and latent coronary artery disease influence

06 p0761 A72-17425

Airline pilot postexercise electrocardiograms, showing S-T segment depression correlation to subsequent coronary heart disease

06 p0768 A72-17881

On-line digital computer system for real time interpretation and report generation of electrocardiograms from remote locations over switched telephone network

07 p0928 A72-19311

Electrical cardiac activity computer simulation model including biophysically faithful conduction system and electrocardiograms for high fidelity production

07 p0929 A72-19313

Biomedical transducers for NASA space program, discussing spray-on electrodes and telemetering for ECG respiration and body temperature

07 p0931 A72-19917

Coronary artery disease and vessel involvement severity predictions from electrocardiographic and vectorcardiographic patterns of anterior wall myocardial infarction

07 p0931 A72-19994

ECG evidence of myocardial ischemia in patients without arteriographic evidence of coronary artery disease, studying myocardial oxygen supply

07 p0920 A72-19995

ECG and VCG in diagnosis of myocardial infarction and QRS changes

07 p0920 A72-20174

Bioelectric ECG and EEG signal analysis using hybrid computer techniques and parameter optimization for autocorrelation function modeling

07 p0933 A72-20333

Abnormal ECG in healthy man due to former disease, subclinical disease, congenital anomalies, hereditary disease or functional aberrations

07 p0924 A72-20574

Atypical ECG of sportsmen, considering repolarization disorders due to ischemia, lesion, excitability and conduction signs

07 p0924 A72-20575

Pulsatile blood pressure and ECG in squirrel monkeys, considering catheter electromanometer system and implanted arterial cannulas long stability

08 p1124 A72-20900

Vectorcardiographic and ECG diagnosis of left anterior hemiblock combined with complete right bundle branch block, discussing coexisting myocardial infarction influence

08 p1127 A72-21850

Cardiac cycle intervals measurement with multibeam cathode oscilloscope synchronized with multichannel polycardiographic automatic recording machine

09 p1272 A72-23192

Clinical reliability and normal variations of Frank ECG computer analysis by Smith-Hyde program for healthy and cardiac patients

09 p1272 A72-23274

Mathematical, physical and engineering aspects of electro- and magnetocardiography, noting heart field nondipolar properties and heart vector determination difficulties

09 p1273 A72-23414

ECG, physical exercise and drug use in diagnosis and aeromedical evaluation of supraventricular arrhythmias, presenting case histories of pilots with wandering cardiac pacemakers

10 p1428 A72-23741

QRS wave detectors for arrhythmia and hemodynamic data analysis, using standardized FM magnetic tape containing various artifacts for evaluation

11 p1582 A72-25499

Positive acceleration effects on human cardiovascular system during centrifuge tests, studying ECG changes in terms of cardiac rhythm, heart rate and wave parameters

11 p1584 A72-26015

Computer assisted monitoring of ECG waveforms and heart sounds frequency spectra to detect bubble laden blood during decompression sickness

11 p1587 A72-26626

Gabor-Nelson myocardium electrical activity model for mathematical construction of vectorcardiogram from ECG for comparison of various lead systems

11 p1588 A72-26629

Random sample comparison of computer program for ECG diagnoses and physicians readings

11 p1590 A72-26975

Triglyceridemia relation to age, relative weight and ischemic cardiopathy probability from ECG, anthropometry and lipid and glucid metabolism studies

12 p1759 A72-27238

Heart and circulatory system functional diagnostics, discussing ECG, blood pressure, X ray, phonocardiographic and pulmonary examinations

12 p1760 A72-27271

Clinical diagnosis of ST/T depression in resting ECG, noting coronary heart disease and left ventricular hypertrophy

12 p1772 A72-27733

Automatic ECG recording and analysis by electronic data processing equipment, discussing methods of data acquisition and transmission for routine diagnosis and prophylactic mass examinations

12 p1772 A72-27821

Dynamic electrocardiography with analog computer program to detect, count and classify atypical ventricular depolarization complexes

12 p1775 A72-28281

Stress vectorcardiography quantitative analysis of ECG response to treadmill exercise test to establish diagnosis criteria for coronary heart disease

12 p1775 A72-28282

ECG diagnostics for arrhythmia assessment in flying personnel flight fitness examination

12 p1775 A72-28294

ECG P-wave-like deflections caused by strong diaphragmatic action potentials in obese woman with fever and erysipelas

13 p1908 A72-28569

Human torso surface mathematical model to determine equivalent heart dipole and quadrupole locations for ECG measurements

13 p1908 A72-28571

Electrophysiologic data acquisition by multiple dipole type of inverse electrocardiographic procedure based on model data, noting favorable and unfavorable dipole array configuration

13 p1909 A72-28997

Electrocardiography and magnetocardiography to determine flux and vortex sources respectively of heart electrical activity impressed current density

13 p1909 A72-28998

Piloting aptitude evaluation from ECG during hypoxia, considering right intraventricular conduction and ventricular repolarization anomalies

13 p1906 A72-29857

Cardiovascular and respiratory changes in dogs exposed to acute overheating, relating ECG changes to adrenergic and hypoxia effects

14 p2074 A72-30382

Lower body decompression effects on ECG, showing heart rate increase, R and T amplitude changes and heart electric axis displacement

14 p2074 A72-30383

ECG amplifier and cardiotelemetry for exercise studies, using digital algorithm for heart rate computation and ECG signal preprocessing for R wave detection

14 p2080 A72-30707

Computerized measurement and analysis of day-to-day variations of corrected orthogonal ECG and vectorcardiogram in normal subjects, using results as assessment standards

14 p2077 A72-30967

Electric field projections in contrast to voltage as working quantity for frontal plane ECG leads

15 p2188 A72-31766

Cardiac cycle length /RR interval/ and QT interval mathematical relationship from ECG obtained during exercise and recovery periods

15 p2187 A72-32747

Serial ECG change detection and description in myocardial infarction survivors, using computer analysis to find best diagnostic discriminants from multiple criteria

16 p2357 A72-34008

Digital data processing equipment for continuous ECG analysis, noting analog to digital converter and amplitude distribution analysis

17 p2522 A72-34914

Some preliminary observations on the correlation of the high frequency /acceleration/ direct-body ballistocardiogram with the apex cardiogram, carotid pulse and their derivatives

18 p2649 A72-36036

'VI-like' and 'aVF-like' leads for continuous electrocardiographic monitoring

19 p2759 A72-37244

A system for the mass examination of electrocardiograms

19 p2760 A72-37853

Prognostic value of an electrocardiographic sign in acute myocardial infarction

19 p2756 A72-37871

Relation of the electrocardiogram to hemodynamic alterations in pulmonary embolism

19 p2759 A72-38816

Vectorcardiographic and electrocardiographic differentiation between cor pulmonale and anterior wall myocardial infarction

21 p3001 A72-40769

The Macruz index and its clinical evaluation in electrocardiography with regard to the selection and control of air crews

21 p3009 A72-41193

Potassium chloride test for electrocardiogram evaluation in flight personnel medical appraisal

21 p3012 A72-41747

Yield of ischaemic exercise electrocardiograms in relation to exercise intensity in a normal population

22 p3151 A72-42900

A rapid assay of dipolar and extradiapolar content in the human electrocardiogram

23 p3259 A72-43811

The standard 12-lead scalar electrocardiogram - An assessment of left ventricular performance

23 p3255 A72-43812

Continuous recording of His bundle electrogram during selective coronary cineangiography in man

23 p3255 A72-43813

Continuous ECG monitoring method /scattergram/ for arrhythmia pattern recognition in intensive care units

23 p3260 A72-43938

Use of implantable telemetry systems for study of cardiovascular phenomena

23 p3260 A72-43996

Analysis of intracavitary electrocardiograms through a saline bridge in the diagnosis of cardiac arrhythmias

24 p3370 A72-44559

H-V intervals in left bundle-branch block - Clinical and electrocardiographic correlations

24 p3374 A72-45690

Clinical and anatomic implications of intraventricular conduction blocks in acute myocardial infarction

24 p3374 A72-45691

ELECTROCATALYSTS

Monograph on fuel cells covering thermodynamics, electrode polarization principles, electrocatalysis, system requirements, operational principles and applications

10 p1423 A72-24700

Electrocatalysis and fuel cells - Conference, Seattle, December 1970

16 p2351 A72-33876

Electrochemical oxidation and classification of fuel cells according to electrolyte, electrode, fuel, catalyst and temperature

16 p2351 A72-33877

- Hydrocarbon oxidation and catalysis on Pt fuel cell electrodes, using electrochemical methods with isotopic exchange and gas chromatography 16 p2361 A72-33878
- Metal catalyst theory for electrocatalysis in alkaline hydrogen oxygen fuel cells, using Tafel equation 16 p2351 A72-33880
- Cubic sodium tungsten bronze electrocatalytic activity increase for oxygen reduction by traces of Pt 16 p2361 A72-33883
- Organic catalysts for oxygen reduction, discussing phthalocyanines, Pfeiffer complexes and porphyrins 16 p2361 A72-33884
- Teflon-bonded hydrophobic gas diffusion electrode performance prediction by mathematical treatment of flooded catalyst agglomerate model 16 p2352 A72-33892

ELECTROCHEMICAL CELLS

- NT ALKALINE BATTERIES
- NT ELECTRIC BATTERIES
- NT FUEL CELLS
- NT HYDROGEN OXYGEN FUEL CELLS
- NT METAL AIR BATTERIES
- NT NICKEL CADMIUM BATTERIES
- NT SILVER CADMIUM BATTERIES
- NT STORAGE BATTERIES
- NT ZINC-OXYGEN BATTERIES
- Room temperature nonaqueous organic solvent electrochemical cell, producing open-circuit potential of 4.5 V 03 p0311 A72-12924
- Electrochemical energy cells for biological telemetry equipment, noting mercury cell use in implanted heart pacemakers 07 p0914 A72-19914
- Permanent manned lunar stations electrical power systems, discussing nuclear energy, solar cells and electrochemical power cells 15 p2214 A72-31814
- Electrochemical development of high energy batteries using organic solvents, organic cathode depolarizers and fused salts 16 p2351 A72-33888
- Mass and energy balance in air cooled matrix type phosphoric acid cell, noting operational reliability and construction 16 p2351 A72-33889
- Current-voltage and specific power-energy relationships for high temperature electrochemical cells with alkali metal anodes and chalcogen or halogen cathodes 16 p2352 A72-33900

ELECTROCHEMICAL CORROSION

- Electrochemical potential microstructure and stress intensity factor effect on aqueous stress corrosion crack propagation rate in high strength Ti alloy 01 p0085 A72-10776
- Electrochemical crevice corrosion process of Ti in hot concentrated chloride solution, discussing temperature, set potential and surface treatment 03 p0374 A72-13714
- Elastomeric protective coating requirements from existing electrochemical metallic corrosion theories 03 p0364 A72-14238
- Corrosion resistance of stainless steels in acid solutions, describing electrochemical cell for recording potential/current density and polarization curves 04 p0533 A72-15236
- Transport processes in electrolytic solutions, considering current and potential distributions in localized corrosion 04 p0536 A72-15737
- Crack corrosion in metals and metal alloys, considering electrochemical reaction kinetics as function of oxygen concentration and pH 04 p0536 A72-15738
- Stress corrosion crack tip electrochemical reactions simulation on Ti and alloy surfaces, using modified rotating disk apparatus with pH measurement 04 p0536 A72-15739
- Pitting and film deposits with organic fluid by electrolysis and fluid flow, discussing electrokinetically produced corrosion [ECS PAPER 88] 07 p1010 A72-18802
- Electrochemical tests, noting electric potential, current and electrode impedance measurements for corrosion rate and oxidizing power evaluation 08 p1189 A72-22105
- Electrochemical and stress corrosion tests of Ti-Ni alloys in acidic chloride solutions at ambient and elevated temperatures [NACE PAPER 30] 10 p1497 A72-24321
- German monograph - Influence of programmed welding cycle temperatures on the microstructure formation and corrosion behavior of austenitic corrosion-resistant steels. 22 p3195 A72-43075
- Influence of prior electrochemical history on the propagation of localized corrosion. 22 p3195 A72-43129
- Corrosion and electrochemical properties of Kh15N5i2T and Kh15N4AM3 oxidized steels 23 p3303 A72-44099

ELECTROCHEMICAL MACHINING

- Electrodischarge and electrochemical machining applications in continuous repetitive production of aircraft jet engine components 01 p0078 A72-11150
- Electrochemical machining electrode processes thermodynamic and kinetic characteristics, discussing temperature, electrolyte viscosity and flow rate and current density effects on metal removal rate 04 p0526 A72-14475
- Electrochemical thinning of metal disks for electron microscopic thin foils preparation 04 p0527 A72-15492
- Book on electrochemical machining covering metallurgical effects, electrolytes, tool design, rotating surfaces and operating costs 06 p0821 A72-17819
- Metal structure effect on anodic dissolution and surface microgeometry formation during electrochemical machining 08 p1175 A72-21040
- Electrolyte flow rate, electric current intensity and tool electrode shape influence on surface finish quality in precision electrochemical machining 08 p1175 A72-21044
- Anodic dissolution of metals during electrochemical precision processing, studying electrolyte composition and flow and mixing rates 11 p1640 A72-26255
- Electrochemical metal precision processing, discussing steels carbon content, surface purity, electrolyte anion composition and anode potential 11 p1640 A72-26256
- Electrolyte temperature, pH and mixing rate effects on anodic dissolution of steels and brass in electrochemical precision processing, using thermokinetic data processing 11 p1640 A72-26257
- Electrode gap current and temperature distributions during electrochemical precision processing of metals, studying gas and electrolyte flow 11 p1613 A72-26258
- Metal surface layer and microetching process along grain boundaries during electrochemical precision processing, verifying steel microcrack depths with mathematical model 11 p1640 A72-26260
- Ti alloys processability by electrochemical method, showing output rate and surface quality improvement from increased current density and electrolyte temperature 11 p1640 A72-26261
- Electrochemical precision metal processing accuracy, analyzing electrode gap size and surface nonuniformities effects on prescribed configuration 11 p1640 A72-26262
- Axial, circumferential and radial residual stresses calculation in polycrystalline coatings and cylindrical elements during surface layer removal by electrochemical processing 11 p1737 A72-26263
- Residual stresses and stress relaxation determination in electrochemical galvanic coating with automatic strain curve plotter 11 p1613 A72-26264
- Recent international development in non-traditional machining processes - EDM, ECM, LBM, EBM. 20 p2928 A72-39203

ELECTROCHEMICAL OXIDATION

- Soviet papers on anodic oxidation of metals covering aluminum and zirconium oxides, oxide films, anion sorption capacity, chemical composition, structure and physicochemical properties 05 p0667 A72-17050
- Electrochemical oxidation and classification of fuel cells according to electrolyte, electrode, fuel, catalyst and temperature 16 p2351 A72-33877
- Hydrocarbon oxidation and catalysis on Pt fuel cell electrodes, using electrochemical methods with isotopic exchange and gas chromatography 16 p2361 A72-33878
- Raney Pd-Ag catalysts for methanol oxidation in alkaline electrolyte in fuel cells 16 p2361 A72-33879
- Alloying component effect on Pt catalytic activity in anodic oxidation of methanol for fuel cells 16 p2361 A72-33881
- Sintered WC effects on fuel cell electrochemical oxidation in acid electrolytes, analyzing hydrogen, hydrazine, formaldehyde, acetaldehyde, formic acid and carbon monoxide fuels 16 p2351 A72-33882
- Hydrazine fuel cell development, electrochemical problems and applications, noting batteries with air oxidant 16 p2351 A72-33886
- Hydrocarbon electrochemical oxidation kinetics for fuel cells at low temperature, considering adsorption and bond cleavage 16 p2361 A72-33891
- Effect of chloride on the anodic dissolution of titanium in methanolic solutions. 21 p3013 A72-40842

On some aspects of low-temperature and anodic oxidation of metals and semiconductors. 21 p3067 A72-40914

ELECTROCHEMISTRY

- NT ELECTROLYSIS
- Electrochemical carbon dioxide concentrator materials compatibility to space shuttle life support environment, comparing with LiOH method 01 p0018 A72-10768
- Electrode potential gradients during dimensional electrochemical treatment of Ni and Ni based alloys 08 p1175 A72-21041
- Electrochemical techniques for time averaged turbulent velocity gradient and components of fluctuating velocity gradient at solid surface 09 p1306 A72-22305
- Russian papers on electrochemical treatment of metals covering anode and cathode processes, electromechanical precision processing of machine parts and wear resistant electrolytic alloys 11 p1640 A72-26254
- Metal-air fuel cell systems characteristics, noting electrochemical processes in zinc-air systems 16 p2352 A72-33897
- The reduction of chlorine on carbon in AlCl3-KCl-NaCl melts. 21 p3013 A72-40843
- Chemistry of grain boundaries and its relation to intergranular corrosion of austenitic stainless steel. 22 p3195 A72-43126

ELECTROCONDUCTIVITY

- Impurity, surrounding gas and pressure effects on organic semiconducting material electrical conductivity, discussing carrier origin and number, and measurement techniques 01 p0113 A72-10125
- Planar Gunn effect devices for microwave oscillators, discussing impedance matching and diode conductivity profile effect on output power 01 p0028 A72-10628
- Electrical conductivities dependence on assumed values of elastic collision cross sections of electrons with neutral and charged particles in low temperature plasma 01 p0110 A72-11205
- MHD channels magnetoacoustic and ionization instabilities effect on mean current density and electric field strength, determining effective electroconductivity and Hall parameter 01 p0110 A72-11208
- Thermal conductivity, electrical conductivity, viscosity and diffusivity of ionized gas-solid suspension in electric field, using transport equations and particle interaction potentials 01 p0111 A72-11332
- Graphite-epoxy conductive polymers as fatigue damage indicators of structures under cyclic strain [SESA PAPER 1915] 02 p0287 A72-11509
- Kubo bulk electrical conductivity of two dimensional guiding center plasma in strong dc magnetic field 02 p0263 A72-11966
- Electrical conductivity of pyrographite at high temperatures along and across deposition plane, using optical pyrometer measurements 02 p0251 A72-12860
- Hall effect and conductivity dependence on applied electric field in multivalley semiconductor for power dependent intervalley scattering time 02 p0269 A72-12887
- Immersion-type electroconductivity probe for anisotropic plasmas, calculating Hall coefficient 03 p0397 A72-13922
- Potentials, currents and velocity variation of rotating conducting disk system in liquid metal medium under uniform longitudinal magnetic field 03 p0397 A72-13996
- Dynamic and electromagnetic characteristics of MHD flow in square tube with walls differing in electroconductivity within oblique transverse magnetic field 03 p0398 A72-14007
- Ambipolar diffusion influence on MHD generator electrical conductivity, discussing plasma radiation, electron escape generator geometry and efficiency and ignition temperature range 04 p0554 A72-14404
- Temperature dependence of quantizing thin films electroconductivity in case of scattering at neutral impurities 04 p0561 A72-15078
- Constitutive equations derivation for electrical conduction due to small deformation superposition, applying to deformed spherical shell current density determination 04 p0549 A72-15254
- Semiconductor slab electroconductivity measurement based on circularly polarized microwave propagation in circular waveguide 04 p0502 A72-15533
- Computer controlled automatic system for measuring electroconductivity and Hall effect in semiconductors, noting data acquisition instrumentation 04 p0496 A72-15534

Ti surface oxide films ionic and electronic conductivity properties and correlation with crevice corrosion susceptibility in contact with polytetrafluoroethylene gaskets

04 p0535 A72-15732

Electrical conduction in orthogonal coordinates from nondipole geomagnetic field effect on conductivity tensor of ionospheric dynamo region

05 p0657 A72-16260

Plasma perturbations and destabilization in curved magnetic field due to electronic electrical conductivity finiteness

06 p0860 A72-17684

Hopping electroconductivity of n-type GaS single crystals, observing frequency dependence

06 p0866 A72-18181

Electroconductivities and electrostatic field structure within equatorial electrojet, observing vertical distribution

07 p1056 A72-18896

Electroconductivity, thermal conductivity and diffusivity, specific heat and emissivities of Ti at 1000-1700 K

07 p1010 A72-18935

Closed system equilibrium correlation functions relationships based on total momentum conservation, discussing application to solids or liquids electrical conductivity via nuclei dynamics

07 p1035 A72-19669

Electrical conductivity of nonideal low temperature plasma as function of metallization densities, applying to semiconductors and mercury vapor systems

07 p1043 A72-19880

Electroconductivity distribution and vertical gradients in photospheric layers of solar active region, using approximate model

07 p1082 A72-20293

Magnetoelastic vibrations of thin conducting plate in magnetic field, solving electrodynamic equations

07 p1095 A72-20315

Unsteady flow of viscous incompressible electrically conducting fluid past infinite nonconducting plate within uniform transverse magnetic field

08 p1212 A72-21079

Temperature controller with linear time variation for semiconductors thermally stimulated conductivity and thermoluminescence measurements at 90-300 K operating range

08 p1166 A72-21438

Turbulized combustion product plasma electrical conductivity, noting temperature dependent variation

08 p1214 A72-21649

Electrical conductivity relationship to phase composition in thin CdTe films deposited on mica bases and annealed in Cd vapor

09 p1367 A72-22420

Cathodic processes in Al electrodeposition from ethyl pyridine bromide electrolyte, discussing phase equilibrium and electrical conductivity dependence on solution composition

09 p1318 A72-22529

Electromagnetic field forces on finite conducting bodies, discussing heating rates and temperatures with ambient air convection and machine design recommendations

09 p1359 A72-22679

Microscopic perturbations of metals electron density complex dynamic matrix, deriving electroconductivity and kinetic coefficients

09 p1329 A72-23039

Dielectric tensor for electromagnetic waves in weakly inhomogeneous anisotropic media, taking into account permittivity and conductivity fluctuations

09 p1280 A72-23230

Flat electrically conducting screen with periodic filamentary structure as possible analog converter of electromagnetic field information

09 p1291 A72-23433

Electrical conductivity and thermal emf as function of temperature in CdSb, discussing energy spectrum and crystallization

09 p1372 A72-23479

Electrically conducting viscous incompressible fluid rotating with oscillating disk in magnetic field

09 p1366 A72-23575

Nonstabilized Ni-P thin films electrical conductivity at 50-280 C, using mass spectrographic, thermal differential, X ray diffraction and electron microdiffraction analyses

10 p1495 A72-24076

Linear anisotropic composites with periodic spatial structure, determining elastic moduli and electrical conductivity variational bounds

10 p1556 A72-24346

Earth precession as origin of geomagnetic field, discussing dynamo theory and core electroconductivity

10 p1472 A72-24524

Book on binary metal oxides covering non-stoichiometry, electrical conductivity, diffusion theory, point defects, high temperature creep and electrochemical transport properties

10 p1527 A72-25075

Oxygen chemisorption surface states effects on electrical conductivity of CdS single crystals and evaporated films

11 p1701 A72-25855

Nonideal dense plasma properties, discussing electrostatic shielding, many particle clusters, phase transitions, metallization and electrical conductivity [AIAA PAPER 72-414]

11 p1695 A72-26164

Electrical and thermal conductivity, elastic properties and resistance to bending of porous tungsten in porosities region

11 p1665 A72-26868

Aircraft windscreen design, discussing high impact strength glass, electroconductive film, transparency service life and weight reduction

12 p1753 A72-27006

Electrical conductivity measurement of dense nonideal Cs plasma at high pressure and temperatures

12 p1849 A72-27057

Vapor annealing effect on vacuum evaporator CdSe thin films electroconductivity as function of pressure and temperature

12 p1854 A72-27249

Vacuum deposition process relation to thin metal film properties, discussing current conducting mechanism

12 p1854 A72-27275

Electromagnetic plane field cumulation by heavy conducting shells implosion with quasi-relativistic velocity, solving Maxwell equations by characteristics method

12 p1851 A72-27396

Measurement circuit for temperature dependence of thermal emf and electrical conductivity in thermoelectric materials

12 p1807 A72-27452

CdS thin film conductivity reactions to grain boundary and stacking faults, correlating grain size to mobility

12 p1856 A72-28012

Uniaxial elastic deformation pressure effects on electronic conduction in tetrahedrally bonded amorphous semiconducting thin films as function of temperature

13 p2021 A72-28574

Experimental investigation of toroidal discharge electrostatic potential fluctuations in turbulently heated plasma, discussing correlation with effective conductivity

13 p2012 A72-29122

Weakly ionized plasma decay within cylinder with electrically conducting walls in presence of longitudinal magnetic field, determining electric current dependence on cylinder length

13 p2016 A72-29603

Lunar core-crust conductivity models compatibility with lunar surface field/interplanetary magnetic field transfer function from Apollo 12 magnetometer data

14 p2153 A72-30502

Lunar interior temperature profile estimation from electrical conductivity distribution based on forsteritic olivine composition

14 p2153 A72-30505

Lunar interior electrical conductivity from surface magnetic field measurements by Apollo magnetometers, calculating temperature profile for olivine moon model

14 p2154 A72-30508

Apollo 11 and 12 lunar surface rocks electrical conductivity at 300-1200 K in vacuum, Ar, He and He-hydrogen atmospheres, noting large hysteresis above 500 C

14 p2155 A72-30518

Earth electrical conductivity radial distribution effect on solar quiet day geomagnetic field variations

14 p2103 A72-30666

Linear theory based analysis of compressible electroconductive fluid flow satisfying perfect gas equation in presence of thin profiles within quasi-aligned magnetic field

14 p2095 A72-30824

Phase diagrams of Hf-Ce and Hf-Er alloys, plotting hardness and electroconductivity curves

15 p2289 A72-31188

Clean Ge crystal surface oxidation process investigation by I.E.D and conductivity measurements

15 p2292 A72-31868

Relativistic electron ring oscillations in circular waveguide with allowance for walls finite conductivity, noting radiative instability at subcritical frequencies

15 p2210 A72-32738

Superplasticity in two phase compositions based on refractory metal alloys, noting creep rate dependence on concentration and electroconductivity

16 p2405 A72-33094

Fillers effect on polytetrafluoroethylene friction properties, electroconductivity and thermal conductivity, noting friction coefficient reduction by laminar filler structures

16 p2413 A72-33269

Equilibrium equation for elastic deformation effect on free electricity redistribution in thin electroconductive shells

16 p2469 A72-33271

Conductance measurements for metal oxide-amorphous silicon junctions, showing temperature dependent tunneling

16 p2442 A72-33620

Normal, highly conducting and ion-exchanging solid electrolytes structure and conductivity, with particular attention to rechargeable silver halide batteries

16 p2352 A72-33899

Plasma motion relation to magnetic field line motion for imperfect electroconductivity, noting comparison with total particle drift distance

16 p2439 A72-33931

The perturbation of alternating geomagnetic fields by three-dimensional conductivity inhomogeneities

17 p2354 A72-34350

Determining electrical ground constants from the mutual impedance of small coplanar loops

17 p2514 A72-34371

Magnetohydrodynamic flow in the region of a conductivity discontinuity at the wall

17 p2587 A72-34460

Electrical conductivity of nonideal low temperature plasma as function of metallization densities, applying to semiconductors and mercury vapor systems

17 p2590 A72-35129

Temperature dependence of electrical and thermal conductivity for transition metals at 20 to 1200 C, noting periodic variations associated with atomic structures periodicity

17 p2568 A72-35519

Structure, electrical conductivity and electron transport mechanisms in chalcogenide glasses

17 p2596 A72-35750

Satellite measurements of the moon's magnetic field - A preliminary report

18 p2724 A72-36287

Combined Rayleigh and Kelvin instability of a Hall plasma with a vertical magnetic field

18 p2715 A72-36502

Fast magnetoacoustic wave interaction with shock wave propagating in ideal electrically conducting gas, showing magnetic field stabilizing effect

18 p2711 A72-36812

Lunar electrical conductivity

18 p2729 A72-37000

New efficient method for calculating hot electron effects applied to n-Ge

19 p2844 A72-37686

Effect of evaporation of the volatile component on the electrical properties of CdSb

19 p2845 A72-38402

Plasma velocity, ion density and electrical conductivity from electron density and temperature and electromagnetic field profile measurements in Ar plasma inverse pinch

19 p2841 A72-38437

Electrically conducting plane screen with periodic filamentary structure as possible analog converter of electromagnetic field information

19 p2782 A72-38516

Photoconductivity and electroconductivity spectral distributions in glassy cadmium silicon germanium arsenide semiconductors at 300 K related to quantum mechanism

19 p2847 A72-38682

Electroconductivity, thermal emf and Hall coefficient for single crystals of Bi-Sb alloys with Cd, In and Sn additions

19 p2847 A72-38683

motion

20 p2891 A72-38935

Lunar temperature profiles from electrical conductivity profile of olivine single crystal as lunar interior material representative sample

20 p2967 A72-39179

On the theory of electrical conductivity in semiconducting thin films under a high electric field

20 p2959 A72-39216

Electrical conductivity of pressed cadmium antimonide

20 p2959 A72-39218

Temperature dependence of electroconductivity and photosensitivity in CdS films

20 p2959 A72-39223

Electrical conductivity of tungsten trioxide /W(O₃)/

21 p3096 A72-40198

Study of the conductivity of the motor neuron membrane during supraspinal stimulation

21 p2999 A72-40585

Weakly ionized plasma decay within cylinder with electrically conducting walls in presence of longitudinal magnetic field, determining electric current dependence on cylinder length

21 p3091 A72-40657

Cooling associated with minority carriers excitation effect in semiconductors, discussing influence of electroconductivity and forbidden bandwidth

21 p3097 A72-40788

Electroconductivity anisotropy effect on transverse Demer effect angular dependence and spectral distribution in p-type CdSb lattice

21 p3098 A72-41693

Electrodynamical mathematical model for electroconductivity of nonuniform plasma with Hall effect, cal-

culating current distribution from Riemann problem solution 22 p3210 A72-41888

The moon's thermal state and an interpretation of the lunar electrical conductivity distribution. 22 p3226 A72-42531

Heat-resistant copper-base alloys containing rare-earth and high-melting metals, characterized by high electrical conductivity 22 p3192 A72-42819

Landau dispersion equations for oscillations damping of bounded electron plasma, noting application to plasma cylinder in conducting tube 23 p3319 A72-43410

Thermal and electrical conductivities, thermal expansion and specific heat of commercial graphite obtained by precipitation of methane pyrolysis products on hot surface 23 p3306 A72-43689

Disequilibria created by an electric field in a nitrogen plasma 23 p3321 A72-43695

Application of a strongly doped semiconductor model to the study of thermodynamic and conductivity properties 24 p3432 A72-45068

Electrical conductivity measurement of dense nonideal Cs plasma at high pressure and temperatures 24 p3431 A72-45710

ELECTROCUTANEOUS COMMUNICATION

Compensatory tracking task performance with continuous error information feedback via visual, auditory or electrocutaneous displays 14 p2083 A72-31152

ELECTRODE FILM BARRIERS

Deposition of dielectric films on the electrodes of an electrostatic gyroscope 21 p3059 A72-41814

ELECTRODELESS DISCHARGES

High stability electrodeless discharge lamps with less than 0.1 percent intensity variation, discussing construction and quality control procedures 04 p0509 A72-15485

Zeeman patterns and energy level Lande g factors from spectrograms of As ion electrodeless discharge tubes in presence of 24,025 G magnetic field 07 p0987 A72-19832

Population inversion in plasma via colliding waves generated by symmetric electrodeless electromagnetic shock tube 08 p1147 A72-21304

Rare gas ion laser excited by electrodeless microwave discharges, noting external magnetic field effects on output 11 p1651 A72-26571

Titanium nitride powder obtained by hydrogen reduction of titanium tetrachloride in nitrogen flow heated in microwave electrodeless discharge 13 p1967 A72-30111

Millimeter wave scattering at turbulent density discontinuities in plasma from electrodeless inductive discharge 14 p2136 A72-30174

Attachment length as stability criterion for bluff-body stabilized electrodeless arc, showing linear dependence on flow velocity ratio to power density 15 p2336 A72-32406

ELECTRODEPOSITION

NT ELECTROPLATING

Destructive readout computer memory of wire substrate electrodeposited with two thin Permalloy layers separated by Cu [IEEE PAPER 11,5] 03 p0332 A72-13765

Thin film formation techniques including evaporation, sputtering, anodization, chemical vapor deposition, electrodeposition and sintering, discussing surface scattering, tunneling, Schottky emission and conduction mechanisms 06 p0790 A72-18571

Adherent solid lubricant films electrochemical deposition, noting method application to metal forming techniques 06 p0824 A72-18606

Dispersion strengthening of electrolytically deposited nickel-aluminum oxide alloys, comparing tensile tests to theoretical values 08 p1186 A72-21442

Metal deposition - Conference, Vinyus, Lithuanian SSR, April 1971 09 p1318 A72-22526

Cathodic processes in Al electrodeposition from ethyl pyridine bromide electrolyte, discussing phase equilibrium and electrical conductivity dependence on solution composition 09 p1318 A72-22529

Evaluation of gold electrodeposits for use in dry circuit applications. 18 p2664 A72-35983

Study of tungsten and molybdenum coatings obtained by arc discharge in a vacuum 19 p2808 A72-38186

ELECTRODERMAL RESPONSE

U GALVANIC SKIN RESPONSE

ELECTRODES

NT ANODES

NT CATHODES

NT CELL CATHODES

NT COLD CATHODE TUBES

NT COLD CATHODES

NT DIFFUSION ELECTRODES

NT DYNODES

NT HOLLOW CATHODES

NT HOT CATHODES

NT ION SELECTIVE ELECTRODES

NT PHOTOCATHODES

NT PHOTOMULTIPLIER TUBES

NT PLASMA ELECTRODES

NT THERMIONIC CATHODES

NT TUBE ANODES

NT TUBE CATHODES

NT TUBE GRIDS

Electron work function and electrode physicochemical properties and surface temperature on boundary layer formation and thickness at electrodes in MHD channel 01 p0009 A72-11206

Cascade connected electrode scheme for MHD applications, noting potential and current distributions and Hall voltage buildup 02 p0265 A72-12276

Stainless steel electrodes resistive and capacitive properties in contact with saline solutions of various concentrations and over extensive frequency range and current densities 03 p0318 A72-12953

Plasma jet formation within high pressure discharges in air at atmospheric pressure, discussing electrode configuration, current density and accelerating magnetic field strength 03 p0396 A72-13662

Rechargeable oxygen electrode research program for hydrogen oxygen fuel cells and metal-oxygen batteries, discussing KOH solutions effects 04 p0466 A72-14675

Explosive erosion in Al, Cu, W and Pb electrodes during high current spark discharges, using time resolved photography 05 p0692 A72-16032

Ten-stage electrostatic depressed collector designed with analog computer for improving klystron power conversion efficiency 05 p0637 A72-16365

Pulsed electric microthruster with solid fuel feed system, noting electrode geometry effects on performance and ablation patterns [AIAA PAPER 72-210] 05 p0705 A72-16799

Positive electrode materials for high energy density batteries with Li negative electrode, calculating discharge emf for various salts 06 p0760 A72-17575

Ionic winds with restricted entrainment and gauze electrode, considering diffusion flame aeration in combustion systems 07 p1037 A72-19372

Biomedical transducers for NASA space program, discussing spray-on electrodes and telemetering for ECG respiration and body temperature 07 p0931 A72-19917

Multiple-wire spark counter characteristics for alpha particle detection, discussing electrodes surface finish and gas filling 08 p1164 A72-20941

Technological characterization of electric discharge machines by metal removal rate, volumetric electrode wastage and machined surface roughness 08 p1174 A72-21031

Optimization for maximum productivity of electric spark machining with vibrating electrode, noting erosion product removal difficulties 08 p1174 A72-21033

Electrode potential gradients during dimensional electrochemical treatment of Ni and Ni based alloys 08 p1175 A72-21041

Electrolyte flow rate, electric current intensity and tool electrode shape influence on surface finish quality in precision electrochemical machining 08 p1175 A72-21044

Reference electrode area and floating potential influence in Langmuir probe measurements of plasma density and temperature 09 p1311 A72-23229

Electrode vertex angle effect on fused weld bead geometry related to plate thickness in tungsten inert gas /TIG/ welding 09 p1320 A72-23634

Direct single electrode measurement of carbon dioxide partial pressure in liquids and gases, using pH changes due to gas diffusion 09 p1317 A72-23671

Computer storage array of isolated electrodes imbedded between capacitor parallel plates, discussing read-write cycle time, expected performance and experimental techniques 10 p1443 A72-23933

Monograph on fuel cells covering thermodynamics, electrode polarization principles, electrocatalysis, system requirements, operational principles and applications 10 p1423 A72-24700

Electrochemical precision metal processing accuracy, analyzing electrode gap size and surface nonuniformities effects on prescribed configuration 11 p1640 A72-26262

Electrode system for ventricular defibrillation, noting current density role and rounded edge effectiveness 11 p1588 A72-26628

Lifetime limitations of ion extraction systems for electron bombardment ion thrusters due to sputter erosion of electrode by ion beam [AIAA PAPER 72-477] 12 p1860 A72-27421

Silicon solar cells IR reflectance improvement by reflecting back electrode, obtaining 10 percent efficiency increase 12 p1758 A72-28032

Three dimensional heat propagation problem of copper electrode destruction under concentrated heat flux with allowance for metal evaporation 12 p1890 A72-28175

Thermal-to-electric power conversion efficiency of nonequilibrium MHD generator with Cs seeded noble gases, considering electrode configuration and gas dynamic effects 13 p1900 A72-29356

Electrode boundary layer electrical breakdown mechanism with allowance for steep temperature gradients at surface, considering Joule heating or electrostatic field effect as causes 13 p2013 A72-29361

Electrode design and implantation method for chronic experiments, discussing information loss factor elimination 14 p2078 A72-30393

Surface electrode position effect on electromyogram recording of electrical activity during repeated biceps and triceps brachii contractions 15 p2190 A72-32489

Surface electrode distance, area and pressure effects on electromyogram recording of large skeletal muscle electrical activity during defined muscular tensions 15 p2190 A72-32490

Metal-air batteries with alternately polarizable oxygen electrodes, discussing current state of technology 16 p2350 A72-33670

Electrodes converting hydrogen, methanol or oxygen for use in fuel cells with alkaline electrolyte, using Ag-Pd, Ni, Si and C catalysts 16 p2351 A72-33885

Rechargeable high energy density battery with Al and Cl electrodes and molten aluminum chloride-alkali chloride eutectic electrolyte 16 p2352 A72-33896

Impurities and additives effects on electrode properties in Cs vapor thermionic converter, noting coadsorption model for Cs-W-O surface 17 p2496 A72-34598

Investigation of the properties of electrode materials made on the basis of high-melting-point compounds and alloys 18 p2698 A72-36136

Local thermionic emission from bare and covered surfaces of cermetelectrodes. 18 p2646 A72-36193

Effect of electrode thickness on the frequency response of a piezoelectric transducer 18 p2693 A72-37218

'VI-like' and 'aVF-like' leads for continuous electrocardiographic monitoring. 19 p2759 A72-37244

Investigation of the transport of electrode metal during welding in a carbon dioxide atmosphere 19 p2810 A72-38588

The aluminum electrode in AlCl3-alkali-halide melts. 21 p3013 A72-40844

Use of rotated electrodes for amplitude weighting in interdigital surface-wave transducers. 22 p3178 A72-42619

ELECTRODISSOLUTION

Effect of chloride on the anodic dissolution of titanium in methanolic solutions. 21 p3013 A72-40842

ELECTRODYNAMICS

NT ELECTROHYDRODYNAMICS

NT ELECTROMECHANICS

NT QUANTUM ELECTRODYNAMICS

Nonhomogeneous media electrodynamics with varying permittivity and permeability, solving nonstationary equations by differential operators 03 p0389 A72-13654

Ultrasonic flaw detector pulse transducers operation using electrodynamic and capacitance receivers 03 p0361 A72-13987

R-function theory application for solution of boundary value problems in electrodynamics, considering field behavior at infinity 04 p0488 A72-15377

Electrodynamical theory of artificial dielectrics based on rigorous solution for diffraction on system scattering elements consisting of periodical gratings formed by thin metallic strips 04 p0490 A72-15412

Electrodynamic vibration exciters with interchangeable heads for environmental vibration testing

05 p0644 A72-16596

Electrodynamics of ionosphere and magnetosphere, discussing irregularities, red arc and auroral thermosphere density and temperature changes

06 p0809 A72-18279

Complex transmission coefficient of waveguide with two arbitrarily spaced infinitely thin plane parallel inhomogeneities, using Galerkin method for single-parameter approximation of electrodynamic problem

07 p0938 A72-19002

Electrodynamics and magnetoelasticity nonlinear Emden-Fowler equation solutions, considering heavy current carrying filaments equilibrium and boundary value problems

07 p1035 A72-19975

Magnetosphere theory of pulsar electrodynamics, discussing unipolar inductor with iron sphere having uniform magnetization parallel to rotation axis

07 p1080 A72-20058

Book on models of particles and moving conducting media covering generator electrodynamics, electron tubes, particle accelerators, plasma and electron beam simulation, ion propulsion, etc

07 p1036 A72-20203

Magnetoelastic vibrations of thin conducting plate in magnetic field, solving electrodynamic equations

07 p1095 A72-20315

Moment of forces on spacecraft with low angular velocities in variable magnetic field, using electrodynamic equations

08 p1240 A72-21140

Stationary functionals for introducing eigenfunctions in diffraction theory of electrodynamic systems

08 p1133 A72-21372

R function and variational methods solution for mixed boundary value problem of Laplace equation applied to stationary heat conduction and electrodynamic problems

08 p1209 A72-21704

Comb type slow wave structures properties outside passband, obtaining dispersion and field distribution expressions by electrodynamic analysis

08 p1135 A72-21738

Nocturnal F region electrodynamic drift at conjugate point sunrise time, discussing dynamic electrostatic field normal component change as cause of ionosphere vertical movement

09 p1297 A72-22576

Pulsar electrodynamic properties, radiation mechanism, galactic distribution and pulse shape, period distribution and propagation characteristics, reviewing Crab Nebula pulsar features

10 p1533 A72-23888

Upper atmospheric dynamics and electrodynamic processes for evaluation of meteor trail radar observations in synoptic meteorology

10 p1473 A72-24702

Ohmic law generalization in electrodynamics for electrically conductive fluid medium in turbulent motion, taking into account Hall effect

10 p1524 A72-24931

Russian book on electrodynamic plasma acceleration covering charged particles motion in electromagnetic field and pulsed, MHD, steady and Hall accelerators

12 p1853 A72-28341

Characteristic functions of potential distribution on sphere with longitude dependent conductivity for application to ionosphere electrodynamics

14 p2101 A72-30644

Ionosphere radio wave propagation from fluid plasma wave and magnetically nonpermeable medium electrodynamics studies

15 p2193 A72-31281

Information propagation time direction of cosmological models in terms of conventional electrodynamic theory, contrasting with Wheeler-Feynman theory

16 p2424 A72-33286

Soviet book on continuum mechanics covering dynamic, thermodynamic and electrodynamic equations mechanic problems, three dimensional space, internal degrees of freedom, etc

16 p2425 A72-33578

Generalization of basic equations of aerodynamics and electrodynamics.

17 p2539 A72-35043

Variational and probabilistic methods for multiphase media, noting applications in electrodynamics, nonlinear plasticity and mechanics

17 p2632 A72-35110

Stochastic electrodynamics based on zero electromagnetic field motion, deriving Schroedinger equation and electromagnetic model of gravitation

17 p2584 A72-35912

Two sided error estimates for electrodynamic impedance, admittance and scattering matrices in diffraction theory

18 p2657 A72-36104

Book on classical relativity theory covering relativistic kinematics and mechanics, tensor calculus, electrodynamics, gravitational fields and effects,

elastic continua mechanics, thermomechanics and cosmology

18 p2712 A72-36850

Moment of forces on spacecraft with low angular velocities in variable magnetic field, using electrodynamic equations

20 p2976 A72-39245

Cosmological electrodynamics and gravitation theory, considering singularity, constraint, Mach, Olbers, arrow-of-time and tail problems

20 p2974 A72-40004

Electrodynamics and magnetoelasticity nonlinear Emden-Fowler equation solutions, considering current carrying heavy filaments equilibrium and boundary value problems

20 p2955 A72-40032

Electrodynamic analysis of superconducting vortices interaction with cylindrical cavities (pinning), calculating critical currents in type II superconductors in external magnetic field

21 p3096 A72-40416

Electrodynamic effects of Jupiter's satellite Io.

21 p3104 A72-40483

Russian book - Introduction to nonlinear electrodynamics.

22 p3204 A72-42076

Chaplygin gas flow equation for thin conducting plate hydrodynamic and electrodynamic equations, noting special theory of relativity

23 p3312 A72-43404

Problem of error estimation during solution of internal boundary value problems in microwave electrodynamics

23 p3265 A72-44201

ELECTRODYNAMOMETERS

U DYNAMOMETERS

ELECTROENCEPHALOGRAPH

U ELECTROENCEPHALOGRAPHY

ELECTROENCEPHALOGRAPHY

Multichannel topography of human scalp alpha EEG potential fields

01 p0016 A72-10072

EEG parameters estimation and statistical uncertainty calculation by computer program

01 p0016 A72-10073

EEG and electrooculogram recording of chimpanzee sleep, noting rapid eye movement stages

01 p0009 A72-10074

EEG phase asymmetry fluctuations relation to respiration rhythm in subjects from pneumograms during rest, mental activity, hypnosis and sleep

05 p0620 A72-17214

Short-term memory and electrographic effective and trace processes relationship from visual and Rolandian cortical regions activity and Tarkhanov galvanocutaneous reaction

06 p0764 A72-17993

Factor analysis of frontal and occipital brain regions EEG indices interzonal variability, relating autocorrelation function parameters to neuron ensembles force level

06 p0764 A72-18057

EEG discharges virtual dipolar sources computation, using mathematical model with homogeneous spherical conductive medium to simulate human head

06 p0769 A72-18201

EEG study of cortical aftereffects to peripheral stimulation in cats

07 p0915 A72-18866

Uniform visual field influence on electroencephalographic alpha rhythm in man, discussing ocular fixation, visual attention and vigilance change effects

07 p0916 A72-19040

Occipital electroencephalographic response to slowly repeated aperiodic light flashes, discussing alpha wave and rhythmic afteractivity amplitude changes

07 p0916 A72-19041

Phase relations between alpha waves in EEG and automated rhythmic motoric activity as function of subject behavioral activity and thalamic pacemaker zones

07 p0916 A72-19109

Computerized EEG data acquisition and transmission system for large hospitals with multiple critical care patient monitoring units, noting telephone access from outside

07 p0928 A72-19307

Circadian rhythms variations for sleep, EEG, temperature and activity in monkeys, indicating acrophase, amplitude and level regulation

07 p0918 A72-19528

Isolation stress effect on circadian rhythmic patterns of EEG activity during sleep-wake and sleep cycles in unrestrained chimpanzee

07 p0921 A72-20181

Bioelectric ECG and EEG signal analysis using hybrid computer techniques and parameter optimization for autocorrelation function modeling

07 p0933 A72-20333

Human cortical auditory evoked response to speech and sound effects, relating EEG interhemispheric wave amplitude asymmetry to stimulus meaningfulness

08 p1115 A72-20984

Reliability of electroencephalography as diagnostic method from specialists interpretation of curve morphological features, discussing normal and pathological record evaluation

08 p1124 A72-21000

Comparative EEG characteristics of frontal and occipital human brain cortex, relating psychophysiological and neurophysiological factors

08 p1116 A72-21196

Isolated specific color dependent waveforms of visual evoked response to strong colored lights relating luminance and wave amplitude changes

09 p1267 A72-23500

Orienting response indication by EEG alpha rhythm desynchronization in relation to visual stimulation intensity

11 p1585 A72-26238

EEG measurement of sleep behavior patterns, discussing sleep stages, temporal patterns, circadian rhythm, intrasleep process stability and age factor

11 p1580 A72-26679

Jet aircraft noise effect on sleeping EEG and subsequent waking performance, showing presence of carry-over effects

12 p1770 A72-27474

Biotelemetry system for EEG monitoring of free swimming diver at 15 meter depth, discussing power requirements, antenna design and signal attenuation

12 p1770 A72-27478

Human electrophysiological changes during perceptual isolation from EEG, EMG, vertical eye movements and electrodermal measurements

12 p1771 A72-27484

Electrocorticograph monitoring of central nervous system state in dogs reanimated by artificial blood circulation after prolonged clinical death by drowning

12 p1764 A72-28215

EEG recording and analysis by analog technique as means of studying human responses to hyperventilation

12 p1767 A72-28312

Deep brain structure biopotential correlations during man sleep development, using electrosubcorticalograms

13 p1901 A72-28634

Neuronal spike activity changes in rabbit visual and sensorimotor neocortex and hippocampus during EEG activation

13 p1902 A72-28643

Adaptation period to inverted work-rest cycle observed with encephalograph, noting effect of brain bioelectric activity circadian rhythms stability

13 p1904 A72-29315

EEG diurnal rhythms during 72 hour insomnia, considering adaptation to altered work-rest cycle in subjects with stable and unstable brain activity rhythms

13 p1904 A72-29319

ECG heart rate recording of helicopter instructor pilots during flight training tasks, administrative work, automobile driving and eating

14 p2082 A72-31097

Human brain sensorimotor region EEG dependence on proprioceptive influence, instruction for active movement and preparation passive movement of hand

16 p2353 A72-32992

Occipital EEG activity during fluctuations of perception under stabilized image and simplified stimulus conditions.

17 p2506 A72-34247

Stimulus complexity and the EEG - Differential effects of the number and the variety of display elements.

17 p2507 A72-34248

Cortico-visceral studies of spinal cord reticular formation stimulation and destruction effects on electroencephalogram, cardiac activity and interoceptive glycemic reflexes

21 p3000 A72-40757

Electrophysiological analysis of limbic-reticular interaction during the orientating reflex

23 p3257 A72-44081

Ensemble characteristics of the human visual evoked response - Periodic and random stimulation.

24 p3374 A72-44575

ELECTROEROSION

U SPARK MACHINING

ELECTROEXPLOSIVE DEVICES

U INITIATORS [EXPLOSIVES]

ELECTROGENERATORS

U ELECTRIC GENERATORS

ELECTROHYDRAULIC CONTROL

U ELECTRIC CONTROL

U HYDRAULIC CONTROL

ELECTROHYDRAULIC FORMING

Electrohydraulic and electromagnetic metal forming, using capacitor stored energy conversion into hydraulic shock waves or magnetic pressure to deform sheet metal components, pipes, etc

15 p2243 A72-31323

ELECTROHYDRODYNAMICS

Ion oscillation theory for electrostatic dynamic channel Poiseuille and Hagen-Poiseuille type flows, using transport and dispersion equations in various ionized media

01 p0111 A72-11214

Electrohydrodynamic ideal incompressible fluid flow in flat and circular channels, determining electric potential and field distribution
02 p0266 A72-12431

Discontinuities in electrohydrodynamics, discussing surface charge generation at shock front and shock wave structure determination
05 p0690 A72-16580

Electrofluid-dynamic wind tunnel velocity augmentation by enthalpy addition during expansion at constant static pressure and temperature for aerospace vehicles flight conditions simulation
[AIAA PAPER 72-166] 05 p0645 A72-16831

Powder concentration effects on corona particle charging efficiency of aerosols for electrogasdynamic generators
06 p0760 A72-18335

Multiplex electrohydraulic system for aircraft fly by wire actuators with majority voting and pressure logic, discussing frequency response and environmental tests
08 p1113 A72-22152

Incompressible fluid jet propagation beyond charged particle source exit section, investigating electrohydrodynamic interaction parameter
10 p1522 A72-24549

Electrogasdynamic generator nonlinear internal resistance determination as function of flow parameters and model geometry via boundary conditions formulation
18 p2643 A72-35998

Weak waves, characteristics, and the problem of flows past slender profiles in electrohydrodynamics
18 p2716 A72-36896

Discontinuities in electrohydrodynamics, discussing surface charge generation at shock front and shock wave structure determination
19 p2834 A72-37551

Dynamics of stratified liquids in the presence of space charge.
19 p2788 A72-38432

Equations of plane potential electrohydrodynamic flow, noting jet and quasi-one dimensional flows of charged particles in curvilinear electrostatic field
22 p3210 A72-42269

ELECTROJETS

NT AURORAL ELECTROJETS
NT EQUATORIAL ELECTROJET

Geomagnetic field and AU/AL index variations with UT during international quiet days at high latitudes interpreted as electrojet diurnal redistribution
02 p0217 A72-11930

Eastern and western polar electrojets intensity diurnal variations with respect to universal time
08 p1154 A72-20740

Polar magnetic substorm generation through ionospheric current intensification in westward electrojet localized region, noting interplanetary magnetic field role
08 p1159 A72-21494

AU and AL indices variations effect on geomagnetic field during international quiet days at high latitudes interpreted as electrojet diurnal redistribution
13 p1948 A72-29242

Potential waves generation by transverse current in ionospheric electrojet region, discussing lower hybrid resonance domain
15 p2232 A72-32732

ELECTROKINETICS

Pitting and film deposits with organic fluid by electrolysis and fluid flow, discussing electrokinetically produced corrosion
[ECS PAPER 84] 07 p1010 A72-18802

Turbulent flow velocity and pressure fluctuations mean square values measurement by electrokinetic probe based on electrical properties of double metal-fluid interface layer
10 p1480 A72-24204

Kinetics of impact-radiative ionization and recombination
23 p3318 A72-43296

ELECTROLUMINESCENCE

Electroluminescent image converter with positive optical feedback, investigating steady state bistable operation mode stability
02 p0193 A72-12341

Light emitting diodes for efficient conversion of electrical energy into electromagnetic radiation, discussing photometry, electrical injection, electroluminescence, design and applications
08 p1141 A72-21430

Electroluminescent image converter with positive optical feedback, investigating steady state bistable operation mode stability
08 p1143 A72-21947

Noise in optical output of small area electroluminescent GaAs diffused junction diodes, comparing with theoretical shot noise limit
09 p1286 A72-23087

Temperature effects on blood electroluminescence, relating luminescence peaks to protein and lipid molecular structure changes
09 p1268 A72-23694

Electroluminescent matrix display system with amorphous semiconductor threshold switches for isolation and memory, discussing performance and address waveforms
12 p1788 A72-27239

Near junction doping characteristics of p-n GaP red emitting diodes by scanning electron microscope correlated with electrical and electroluminescent measurements
15 p2208 A72-32521

Coherent orange emission and bright electroluminescence from indium gallium phosphides vapor grown p-n junction laser diodes
15 p2251 A72-32532

Semiconductor quadrupole optical links consisting of electroluminescent diode and photoreceptor, discussing operation and design principles
17 p2594 A72-34333

Minority-carrier trapping and the luminescence time response of semiconductors.
19 p2844 A72-37946

ELECTROLUMINESCENT LAMPS
U ELECTROLUMINESCENCE
U LUMINAIRES

ELECTROLYSIS

Pitting and film deposits with organic fluid by electrolysis and fluid flow, discussing electrokinetically produced corrosion
[ECS PAPER 84] 07 p1010 A72-18802

Dislocation bands in electrolytically hydrogen charged fcc Ni-Co alloy, describing band structure in terms of band axis and planes and Burgers vector
11 p1669 A72-26947

Electrochemical conditions for separation of gamma prime phase from heat resistant Ni alloys by electrolysis
12 p1828 A72-27446

Electron microscope study of hard alloy surface layer formation characteristics during diamond grinding with electrolysis
12 p1814 A72-27766

Integrated water vapor electrolysis oxygen generator and hydrogen depolarized carbon dioxide concentrator development.
[ASME PAPER 72-ENAV-7] 20 p2896 A72-39170

Six-month test program of two water electrolysis systems for spacecraft cabin oxygen generation.
[ASME PAPER 72-ENAV-5] 20 p2896 A72-39172

Electrolytic and nonelectrolytic diffusion methods for protective coatings production from gas, liquid or solid phase, discussing wear resistance enhancement in boridized steels
20 p2929 A72-39449

Regeneration of oxygen from carbon dioxide and water.
24 p3375 A72-45183

ELECTROLYTE METABOLISM

Antinatriuretic effect of acute thoracic and abdominal inferior vena cava constriction on arterial pressure, renal hemodynamics and electrolyte excretion
02 p0157 A72-11660

Active Na-K transport and passive permeability temperature adaptation in ground squirrel erythrocytes
04 p0475 A72-15546

Body thermal stress, local heating and arterial occlusion effects on sweat electrolyte content
07 p0929 A72-19437

Cardiovascular and respiratory responses to intraarterial injection of K and Na ions in dogs for peripheral receptor site determination
07 p0921 A72-20177

Aortic constriction and release effects on kidney glomerulotubular balance in saline- and water-loaded dogs, studying sodium reabsorption changes
08 p1115 A72-21084

Multihour immersion effects on blood plasma protein and electrolyte concentration in trained and untrained subjects
12 p1770 A72-27480

Sleep deprivation effects on diurnal urine potassium excretion, showing individual circadian rhythm variations
13 p1904 A72-29320

Hypokinesia effect on fluid and electrolyte metabolism change patterns in rabbits from blood plasma studies
14 p2075 A72-30389

Potassium, sodium and calcium ion distribution in skeletal muscle subcellular organelles, discussing lipid, protein and nucleic acid binding
14 p2076 A72-30670

Electroretinographic illumination potentials dependence on extracellular chloride ion concentration in isolated frog retina
15 p2186 A72-32491

Weightlessness effects on calcium and electrolyte metabolism from measurements during Gemini 7 flight, using dietary control and excreta collection techniques
16 p2355 A72-33552

Effect of Acetazolamide /Diamox/ at different dose levels on survival time of rats under acute hypoxia and

on Na/+/K/+/ATP-ase activity of rat tissue microsomes.
17 p2499 A72-34546

Changes of intracellular myocardial electrolytes in experimental hypertension.
17 p2501 A72-34984

Ion alterations during myocardial ischemia.
17 p2502 A72-34994

Interrelationship of hemodynamic alterations of valvular heart disease and renal function - Influences on renal sodium reabsorption.
19 p2756 A72-37872

Sweat depression during controlled hyperthermia in man - Effects on the sweat rate and sweat electrolytes
20 p2892 A72-39591

Respiratory effects of hypochloremic alkalosis and potassium depletion in the dog.
21 p2997 A72-40418

Effects of simulated high altitude on renin-aldosterone and Na homeostasis in normal man.
21 p3005 A72-40422

Excitation contraction correlates in true ischemia.
23 p3255 A72-43814

Capillary circulation as a regulator of sodium reabsorption and excretion.
23 p3257 A72-43995

Increased fluid turnover and the activity of the renin-angiotensin system under various experimental conditions.
23 p3257 A72-43997

Metabolism of angiotensin II in sodium depletion and hypertension in humans.
23 p3257 A72-43998

Intracellular potassium in cells of the distal tubule.
24 p3373 A72-45231

Relationship of sodium deprivation to +Gz acceleration tolerance.
24 p3377 A72-45653

Response to daily lower body negative pressure /I.B.NP/ exposure -/70mm Hg/, with emphasis on plasma renin activity, sodium and potassium excretion.
24 p3377 A72-45658

ELECTROLYTES

NT ION EXCHANGE MEMBRANE ELECTROLYTES
NT MOLTEN SALT ELECTROLYTES

Electrochemical machining electrode processes thermodynamic and kinetic characteristics, discussing temperature, electrolyte viscosity and flow rate and current density effects on metal removal rate
04 p0526 A72-14475

Transport processes in electrolytic solutions, considering current and potential distributions in localized corrosion
04 p0536 A72-15737

Current reversal effect on anodic aluminum oxide film prepared in phosphate electrolyte, using electron microscope and isotopic labeling
05 p0667 A72-17056

Book on electrochemical machining covering metallurgical effects, electrolytes, tool design, rotating surfaces and operating costs
06 p0821 A72-17819

High temperature and ZrO2 ceramic electrolyte effects on ionic partial conductivity and fuel cells longevity
06 p0760 A72-18337

Electrolyte flow rate, electric current intensity and tool electrode shape influence on surface finish quality in precision electrochemical machining
08 p1175 A72-21044

Anodic dissolution of metals during electrochemical precision processing, studying electrolyte composition and flow and mixing rates
11 p1640 A72-26255

Electrochemical metal precision processing, discussing steels carbon content, surface purity, electrolyte anion composition and anode potential
11 p1640 A72-26256

Electrolyte temperature, pH and mixing rate effects on anodic dissolution of steels and brass in electrochemical precision processing, using thermokinetic data processing
11 p1640 A72-26257

Floodrode gap current and temperature distributions during electrochemical precision processing of metals, studying gas and electrolyte flow
11 p1613 A72-26258

Metal surface smoothing during electrochemical dissolution prior to polishing, involving electrolyte diffusion processes or semiconductor oxide film formation
11 p1640 A72-26259

Ti alloys processability by electrochemical method, showing output rate and surface quality improvement from increased current density and electrolyte temperature
11 p1640 A72-26261

Electrolyte hydrostatic pressure measurement in limited volume biological compartments by fluid filled glass micropipette used in microtransducer capacity
11 p1587 A72-26623

Sintered WC effects on fuel cell electrochemical oxidation in acid electrolytes, analyzing hydrogen,

hydrazine, formaldehyde, acetaldehyde, formic acid and carbon monoxide fuels

16 p2351 A72-33882

Cubic stabilized zirconia utilization as solid electrolyte in high temperature fuel cell system for efficient and economical energy conversion

16 p2352 A72-33894

Destabilization and aging mechanisms for ionic conductivity decrease in stabilized zirconia type electrolytes, discussing yttria stabilization

16 p2361 A72-33895

Normal, highly conducting and ion-exchanging solid electrolytes structure and conductivity, with particular attention to rechargeable silver halide batteries

16 p2352 A72-33899

Thermal conductivity measurements of nickel-cadmium aerospace cells. II - Component conductivities.

21 p2997 A72-40841

The effect of some electrolytes on the stress corrosion cracking of AISI 4340 steel.

22 p3195 A72-43128

Thermal diffusion annealing improved Ni-B composite electrolytic coatings with uniform B distribution over bulk matrix

23 p3303 A72-44012

The problem of decontaminating and preserving drinking water in spacecraft water supply systems

24 p3375 A72-45121

ELECTROLYTIC CELLS

Electrochemical oxidation and classification of fuel cells according to electrolyte, electrode, fuel, catalyst and temperature

16 p2351 A72-33877

Quinones as reversible redox couples for rechargeable cathodes, noting air regeneration capacity in organic electrolytes

16 p2352 A72-33898

Isobar-isothermal potentials, entropy and formation heat of chromium silicides from thermoelectromotive force measurements of high temperature galvanic elements

23 p3298 A72-43286

Regeneration of oxygen from carbon dioxide and water.

24 p3375 A72-45183

ELECTROLYTIC GRINDING

U ELECTROCHEMICAL MACHINING

ELECTROLYTIC POLARIZATION

Monograph on fuel cells covering thermodynamics, electrode polarization principles, electrocatalysis, system requirements, operational principles and applications

10 p1423 A72-24700

The aluminum electrode in AlCl₃-alkali-halide melts.

21 p3013 A72-40844

ELECTROLYTIC POLISHING

U ELECTROPOLISHING

ELECTROMAGNETIC ABSORPTION

NT AURORAL ABSORPTION

NT PHOTOABSORPTION

NT POLAR CAP ABSORPTION

NT ULTRAVIOLET ABSORPTION

NT X RAY ABSORPTION

Transparent fused silica wall irradiation induced optical absorption and heat deposition in nuclear light bulb engine

01 p0103 A72-11356

Lower ionospheric nighttime absorption as ionization processes indicator, discussing relationship to geomagnetic activity

02 p0216 A72-11921

Nighttime ionospheric radio wave propagation, determining geomagnetic latitude variations effects on absorption and reflection

02 p0218 A72-11944

Midlatitude ionospheric radio wave absorption measurements, using radio astronomical polarization method

02 p0172 A72-11945

Cosmic noise ionospheric absorption measurements with riometers, showing mid and low latitudinal variation

02 p0221 A72-12464

Nighttime hf radio wave field intensity measurement and absorption observation by narrow band receiver

02 p0184 A72-12874

Ray path and absorption calculation for mf and hf radio wave oblique propagation through model ionosphere in nighttime, noting E region ionization role

02 p0184 A72-12875

Sunspot cycle 1958/70 effects on D region ionospheric absorption and stratospheric temperature measured by radiosonde

03 p0345 A72-12978

Sudden cosmic noise absorption from D region N-h profile during solar X ray flares on 13 April 1966

04 p0566 A72-14512

Light wave electric field Franz-Keldysh effect on GaAs absorption edge, using electroabsorption, electroreflectance and photoconductivity spectrum and internal photoeffect analysis

04 p0561 A72-14621

Planetary magnetic activity effects on hf cosmic noise absorption measurements at low and temperate latitudes

04 p0516 A72-14941

Ionospheric absorption measurements at 2.2 MHz by vertical incidence pulse sounding method, observing diurnal and seasonal variations

04 p0518 A72-14965

Ionospheric radio absorption, observing diurnal and seasonal variations and sunspot numbers and solar flares effects

04 p0518 A72-14966

Anomalous changes in ionospheric radio absorption during winter at midlatitudes, investigating diurnal and seasonal variations and stratospheric warming

04 p0518 A72-14967

Laser light beam attenuation, considering turbulent pulsation effects in closed channel fluid flow axial region

04 p0530 A72-14989

Electromagnetic absorption heating in cold randomly inhomogeneous plasma, discussing consequences of thermal particle motion neglect

04 p0489 A72-15393

Vibration-rotation double resonance transitions in symmetrical top molecules in millimeter range under chopped laser radiation

04 p0532 A72-15615

D region ionization by electron fluxes as explanation for latitudinal radio wave absorption

05 p0656 A72-16249

Radio wave absorption during oblique propagation through ionosphere from vertical measurements, using rhombic antenna at 25 MHz

05 p0657 A72-16267

Slant incident electromagnetic wave absorption in linear plasma layers due to field swelling in resonance region

05 p0627 A72-16403

Diurnal variation of lower ionosphere, analyzing nature and behavior of absorption long range variations over solar activity cycle

05 p0660 A72-17182

Data transmitting dielectric light waveguide production problems, noting light scattering and absorption losses due to glass material impurities

06 p0825 A72-17774

Narrow light beam attenuation and scattering characteristics in turbid medium as function of distance from source from transport equation solution

06 p0774 A72-17938

Ionospheric absorption and atmospheric planetary scale waves fluctuations correlation

06 p0808 A72-18090

Neutral interstellar hydrogen atoms mean volume density from Lyman alpha absorption and radio measurements in solar region

06 p0886 A72-18098

Light beam time stationary multifocal structure in medium with Kerr type nonlinearity, relating maximum energy density and absorption coefficients

07 p0944 A72-19635

Coupled coherent and incoherent excitons motion effect on optical absorption line shape, deriving diffusion equation from density matrix equation of motion

07 p1035 A72-19672

Ground plane absorption coefficient effects on admittance of slot antenna radiating into warm lossy plasma

07 p0957 A72-19797

Optically pumped semiconductor lasers, discussing two photon absorption, emission from compounds and mixed crystals and smooth frequency variation

07 p1006 A72-20118

Plasma diagnostics using carbon dioxide laser absorption and interferometry, comparing electron densities with shock data

07 p1008 A72-20565

Plane electromagnetic wave reflection from conducting convex cylinder in radially inhomogeneous absorbing medium, deriving equations for beam trajectories calculation

08 p1131 A72-20742

Electromagnetic wave diffraction on arbitrary spheres, calculating scattering cross sections and attenuation by four water droplets

08 p1131 A72-20789

Steady phase direction at time of electromagnetic wave transmission from one isotropic absorbing medium to another

08 p1132 A72-21221

Optical absorption in UV and IR of proton bombarded potassium chloride at liquid nitrogen temperature attributed to trapped protons

08 p1211 A72-21249

Wind and density measurements by small sounding rockets, comparing results with ground observed radio wave absorption diurnal variations

08 p1160 A72-21531

D region neutral gas winds, density changes and short wave radio absorption correlation, determining air mass flow rates from chaff fall rate measurements

08 p1160 A72-21532

Temperature dependence of intrinsic light absorption band edge characteristics in p-type InSb

09 p1366 A72-22213

D region neutral gas winds, density variations and short wave absorption, determining correlation from ultralight chaff and absorption measurements at 2.83 MHz

09 p1277 A72-22374

Diurnal, seasonal and solar cycle variations in cosmic noise absorption during 1957-1966, showing various ionospheric layers contribution

09 p1385 A72-22586

Light absorptivity measurement in low loss liquid with interferometer based on refractivity dependence on temperature change due to absorption

09 p1309 A72-22602

Atmospheric refraction effects on IR far field irradiance distribution based on model of nonlinear interaction including absorption, transverse flow and vibrational relaxation effects

09 p1350 A72-22607

Electronic transition between energy bands as explanation for two optical absorption maxima in rare earth metals

09 p1369 A72-22609

Random gravitational plane wave metric effect on electromagnetic wave mean value, noting light dispersion and attenuation

09 p1351 A72-22682

Neutral density glass collimating absorption lens for ideally uniform laser beams production

09 p1315 A72-23347

Current-optical effects of anisotropic absorption of polarized and unpolarized light in rarefied cosmic media

10 p1525 A72-23763

French monograph on riometer measurement of abnormal ionospheric absorption, noting nighttime events association with F region lacunae

10 p1472 A72-23848

Internal Q switching and long time delay emission in electron beam excited p-type and n-type GaAs lasers, indicating optical absorption traps

10 p1489 A72-23947

High intensity laser radiation absorption in plasma produced from thick metal targets and thin Au foil

10 p1490 A72-23967

Ionization kinetics influence on light absorption zone behind plane stationary shock wave in hydrogen

10 p1467 A72-24358

Daytime electron density profile in E and D regions from rocket lower ionosphere sounding, noting winter electromagnetic absorption anomaly

11 p1622 A72-26101

Ionospheric radio wave absorption and intensity calculation, using vertical sounding data and riometric measurements

11 p1594 A72-26278

Light absorption and scattering factors in whole blood related to hemoglobin concentration, discussing oxygen saturation, cardiac output and pathological conditions

11 p1588 A72-26630

Evanescent photons absorption and emission in light excited molecules fluorescence

11 p1691 A72-26745

Electromagnetic wave transformation and absorption in Ar plasma with nonmonotonic longitudinal density distribution

11 p1699 A72-26758

Light absorption by molecular crystals with dual zone of exciton states

12 p1847 A72-27226

Dual resonant cavity absorption cell composed of Fabry-Perot interferometers excited by microwave sources, observing spectroscopic double resonance effects

12 p1806 A72-27264

Power resonance and frequency stabilization of gas laser with nonlinear absorption cell, considering He-Ne laser with Fabry-Perot resonator

12 p1820 A72-27584

Gas laser with strong absorption saturation to obtain high peak power and frequency self stabilization by generation of quasi-traveling wave in resonator

12 p1820 A72-27585

Radio attenuation by rain at 37 GHz using sun as source compared with sky emission observations, noting apparent absorber temperature effect

12 p1783 A72-27665

Intergalactic extinction relationship to large galactic clusters from statistical analysis of fourth and fifth Zwicky catalogs

12 p1872 A72-27759

Ionospheric absorption measurements during sunspot cycle at fixed frequencies, noting monthly and seasonal variations

12 p1804 A72-27782

Light propagation patterns in absorbing and scattering medium with radiation density dependent optical properties

13 p2002 A72-28510

Upper atmosphere particle flux density determined from nocturnal electromagnetic absorption caused by

geomagnetic storms, noting ionization process time lag in lower ionosphere
13 p1945 A72-28580

Ionospheric radio adsorption measuring device with readout data convenient for visual and computer processing, discussing block and circuit diagrams
13 p1955 A72-28602

Wave equations and photon absorption cross section of relativistic electron in magnetic field, taking into account relativistic energies
13 p2002 A72-28647

Electromagnetic wave absorption in warm homogeneous plasma under static magnetic field parallel to surface, taking into account plasma-vacuum boundary conditions
13 p2012 A72-29123

Lower ionospheric nighttime absorption as ionization processes indicator, discussing relationship to geomagnetic activity
13 p1948 A72-29233

Nighttime ionospheric radio wave propagation, determining geomagnetic latitude variations effects on absorption and reflection
13 p1949 A72-29256

Midlatitude ionospheric radio wave absorption measurements, using radio astronomical polarization method
13 p1920 A72-29257

Diurnal and seasonal variations of ionospheric absorption in D and E regions, discussing blanketing sporadic E presence effect
13 p1922 A72-29392

Enhanced indirect optical absorption measurement in AlAs and GaP with energy denominator variation for direct band gap evaluation
13 p2022 A72-29627

Optical weak absorption measurements in amorphous semiconductors AsS, GeAs and GeSbSe, showing dependence on band gap localized states
13 p2022 A72-29629

Ionospheric absorption measurement by 1F mode field strength recording with A3 circuit at 6 MHz, noting diurnal and seasonal variations
13 p1952 A72-29660

Ionospheric multifrequency absorption measurement description by empirical expressions in terms of E layer critical frequency, solar activity and seasonal effects
13 p1952 A72-29667

IR absorption coefficients in air at 6000-8500 K and 40-95 atm, interpreting absorption due to free-free electron transitions in neutral particle fields
13 p2006 A72-29676

Steady state laser mode locking with saturable absorber, describing pulse shape and amplitude as function of quantity of absorbing medium
14 p2111 A72-30793

Ionospheric radio waves absorption and stratosphere temperature variations with respect to season and sunspot cycles, examining 1963-5 winter anomaly
15 p2195 A72-31555

IR absorbent effects on evaporographic image contrast performance based on photometric study, presenting color photographs
15 p2188 A72-31615

Physical interpretation of electromagnetic waves attenuation function HF singularity during diffraction over spherical surface, applying to short wave diffraction in tropospheric model
15 p2195 A72-31651

Photon loss coefficients and gain measurement in CdS electron beam pumped lasers, noting absorption mechanism and efficiency
15 p2246 A72-31668

Long term A3 absorption associated with nuclear explosion caused artificial radiation belts, discussing electron precipitation role in D region ionization
15 p2299 A72-31933

Attenuation rate of electromagnetic waves for dominant E1,F and V1,F modes of earth crust waveguide
15 p2200 A72-32110

Air pressure effects on absorption dependence at IR wavelengths, using water vapor transmittance windows
15 p2202 A72-32657

Born approximation for resonance bremsstrahlung emission and photon absorption cross sections at electron-ion scattering, solving multiparticle problem
15 p2279 A72-32697

Earth crust waveguide three layer model for electromagnetic wave propagation, showing mode relation to absorption conditions
16 p2362 A72-33074

Mathematical models for radio attenuation in ice by electromagnetic absorption and reflection from interfaces, noting radar tracking
16 p2363 A72-33290

Field distribution and absorption coefficient calculations for normal incidence of extraordinary electromagnetic wave on linear plasma layer in hybrid resonance region
16 p2363 A72-33480

Narrow light beam attenuation and scattering characteristics in turbid medium as function of distance from source from transport equation solution
16 p2426 A72-33779

On the winter anomaly of ionospheric absorption.
17 p2546 A72-34695

The magnetic control of the lower ionospheric absorption at lower latitudes.
17 p2546 A72-34697

Ionization kinetics influence on light absorption zone behind plane stationary shock wave in hydrogen
17 p2539 A72-34957

Linear transformation and absorption of electromagnetic waves in plasma
17 p2591 A72-35165

Saturated absorption in optically pumped semiconductor lasers
17 p2563 A72-35303

Determination of electron concentration profiles in the lower ionosphere from the absorption at several frequencies
17 p2551 A72-35863

Height of the region of principal auroral radio-wave absorption in the presence of a sporadic E layer
17 p2519 A72-35869

Laser IR radiation attenuation in natural and artificial fogs, noting dependence on particle size distribution
18 p2697 A72-36102

Sunspot control of ionospheric absorption.
18 p2686 A72-36231

Vibrational relaxation of the bending mode of shock-heated CO2 by laser-absorption measurements.
18 p2697 A72-36562

Signal reflection height seasonal variations effect on radio waves absorption estimation from vertical ionospheric sounding
18 p2662 A72-36881

Amplitude limits to the theory of resonant absorption in cold plasmas.
18 p2716 A72-36960

Absorption of the 4- to 6-millimeter wavelength band in the atmosphere.
18 p2689 A72-36961

Attenuation of X rays in interstellar space.
19 p2852 A72-38600

D-region electron densities and collision frequencies from Faraday rotation and differential absorption measurements.
19 p2793 A72-38858

Atmospheric pressure, density and scale height calculated from H Lyman-alpha absorption allowing for the variation in cross-section with wavelength.
19 p2793 A72-38859

An ultra-broadband probe for RF radiation measurements.
20 p2921 A72-38993

On the physical nature of cosmic electromagnetic absorption. V - The Einstein-de Sitter cosmology with plasma coupled to radiation at non-relativistic temperature.
20 p2967 A72-39185

On the physical nature of cosmic electromagnetic absorption. VI - The Einstein-de Sitter cosmology with plasma coupled to radiation at relativistic temperature.
20 p2967 A72-39186

Light attenuation coefficient measurement in water of various turbidity with AR and Kr lasers, interpreting results by Mie scattering theory
20 p2931 A72-39270

Antiferromagnetic dispersion, absorption and light scattering in NiO and other face centred cubic crystals.
20 p2960 A72-39458

Spectral characteristics of a single-frequency argon laser with an absorbing film.
20 p2932 A72-39509

On the diurnal and seasonal variations of the D- and E-regions above Kjeller.
20 p2917 A72-39529

HF absorption of electromagnetic field in ionized oxygen plasma as function of dc discharge current
20 p2958 A72-39969

Energy absorption mechanisms of thin film optical waveguide surface in contact with low index dyes
21 p3050 A72-40147

Numerical analysis of microwave heat generation in disc-shaped Luneberg lenses.
21 p3032 A72-40627

Populating excited states of incoherent atoms using coherent light.
21 p3088 A72-40778

Measurements of enhanced absorption of electromagnetic waves and effective collision frequency due to parametric decay instability.
21 p3092 A72-40829

Resonance absorption of laser emission by methane behind the shock front
21 p3063 A72-40986

Magneto-microwave free-carrier absorption in germanium in the Faraday configuration.
21 p3097 A72-41379

Absorption of an obliquely incident extraordinary wave in a weakly inhomogeneous plasma in the hybrid resonance region
21 p3095 A72-41694

Solar radiant energy reflection and absorption by cloud layers
21 p3049 A72-41795

The effect of cloud scattering on the absorption of solar radiation by atmospheric dust.
22 p3201 A72-42512

Noncoherent scattering probabilistic formulation in terms of mean intensity averaged over absorption profile and mean scatterings number required for photon escape
22 p3206 A72-42559

Respiratory chain components correlation to tension production at various oxygen pressures in guinea pig ductus arteriosus, investigating light absorption changes
22 p3144 A72-42670

Influence of nonuniformities of the built-in field on the collection efficiency of a semiconductor photocell
22 p3140 A72-43190

Gas absorption lines detection based on multiple light passage through absorbing medium during generation process, noting radiation spectra of neodymium glass laser
23 p3295 A72-43305

Wave attenuation during plasma propagation, discussing particle collisions, absorption effect on geometric optics and linear mode coupling in cold magnetized plasma
23 p3320 A72-43519

Absorption profile of a planetary atmosphere - A proposal for a scattering independent determination.
23 p3289 A72-43889

Ultrasensitive response of a CW dye laser to selective extinction.
23 p3297 A72-44186

Stimulated entropy /temperature/ scattering and its influence on stimulated Mandelstam-Brillouin scattering
23 p3297 A72-44478

Photoionization and photoabsorption cross sections of CO2 at 584 Å.
23 p3317 A72-44519

Quadruple conjugate pair observations of the sudden commencement absorption event on June 17, 1965.
23 p3286 A72-44526

Light beam time stationary multifocal structure in medium with Kerr type nonlinearity, relating maximum energy density and absorption coefficients
24 p3408 A72-44567

Upper atmosphere particle flux density determined from nocturnal electromagnetic absorption caused by geomagnetic storms, noting ionization process time lag in lower ionosphere
24 p3397 A72-45080

Ionospheric radio absorption measuring device with readout data convenient for visual and computer processing, discussing block and circuit diagrams
24 p3402 A72-45102

Wave and polarization equations for short coherent light pulses transmission in linear amplifying and absorbing media, noting single pulse formation in lasers
24 p3410 A72-45420

Attenuation of ruby laser radiation in the boundary layer of the atmosphere during the temperature-dependent variations of the wavelength
24 p3411 A72-45424

Investigation wave transformation and absorption by a plasma in the upper hybrid frequency range
24 p3429 A72-45491

Nonlinear instability of Bernstein modes pumped by an electromagnetic wave.
24 p3430 A72-45571

Control of laser pulse duration by nonlinear absorption in semiconductors.
24 p3411 A72-45605

ELECTROMAGNETIC COMPATIBILITY
Electromagnetic compatibility - IEEE Conference, Philadelphia, July 1971
03 p0323 A72-14027

Pulse coded processing system EMC performance measurement, considering CW and pulsed interference effects and application to ATC radar beacon system transponders
03 p0324 A72-14033

Mathematical modeling methodology for communication receiver life cycle EMC decisions, considering analysis and prediction problems with emphasis on nonlinear circuits and systems
03 p0324 A72-14034

Computer aided intrasystem electromagnetic compatibility prediction programs, discussing mathematical models and program philosophies
03 p0328 A72-14039

Aircraft electric power equipment transient voltage and EMC limits specifications
03 p0312 A72-14043

EMC criteria for sharing frequency bands between communication satellite and terrestrial microwave radio relay systems
03 p0324 A72-14045

Time discrimination utilization in EMC, considering automatic position telemetering system using time division technique

03 p0325 A72-14047

Pioneer F and G space probe EMC specification limits, comparing computer analysis prediction and system test data

03 p0329 A72-14048

EMC improvement with least sacrifice of power efficiency in designing dc/dc converters and switching voltage regulators

03 p0312 A72-14049

Electromagnetic compatibility system design checklist, noting usefulness to project personnel [SAE AIR 1221]

11 p1604 A72-26026

EMC at the crossroads; International Electromagnetic Compatibility Symposium, Arlington Heights, Ill., July 18-20, 1972, Record.

20 p2901 A72-38976

Electromagnetic compatibility and interference problems of radar altimeters, collision avoidance systems and air and marine mobile satellite communication equipment in 1600 MHz region

20 p2901 A72-38977

Sensor selection for electromagnetic instrumentation system with sufficient sensitivity and bandwidth to demonstrate electroexplosive device compliance with MIL-E-6051D specified safety margin

20 p2962 A72-38979

Probability density - A new approach to system electromagnetic compatibility testing of digital circuits.

20 p2906 A72-38980

Electromagnetic compatibility enhancement during functional integration and operation of transmitters and receivers in digital communication systems

20 p2901 A72-38983

Electromagnetic compatibility problem of RF oscillators and switching operations in power network as interference source, discussing transmission line shielding and coupling impedance

20 p2901 A72-38988

Some new methods of performing low frequency EMC measurements.

20 p2921 A72-38995

Collision avoidance system electromagnetic compatibility with radar altimeters designed for 1600 MHz aeronavigation band

21 p3018 A72-40881

Book - EMI prediction and analysis techniques.

22 p3156 A72-43198

ELECTROMAGNETIC CONTROL

U ELECTROMAGNETS

U REMOTE CONTROL

ELECTROMAGNETIC DEDUCTION

U MAGNETIC INDUCTION

ELECTROMAGNETIC FIELDS

NT FAR FIELDS

Radio signals information capability estimation during propagation through electromagnetic fields, using pulse amplitude modulation

01 p0065 A72-10446

Earth surface roughness effects on vertical Hertz dipole electromagnetic field reflection

01 p0027 A72-10447

Reflector antennas with very high front-to-back ratio - Theory and experiments on models.

01 p0029 A72-10673

Subsurface electromagnetic fields of current carrying cable line source on flat earth conducting half space, considering mine rescue operations

01 p0060 A72-10840

Soviet book on electromagnetic fields and waves covering propagation in anisotropic media, waveguides and cavity resonators, diffraction interactions, etc

01 p0031 A72-11200

Microwave measurements of plasma parameters in medium pressure gas discharges in absence of constant magnetic field and in weak electromagnetic field

01 p0072 A72-11215

Monochromatic electromagnetic field diffraction problems in homogeneous medium, presenting computer aided numerical analysis

02 p0171 A72-11690

Null electromagnetic field propagation in general relativity, applying to Stokes parameters definitions for monochromatic light

02 p0259 A72-12178

Closed rectangular cavity resonator with conducting walls, calculating differences of electromagnetic zero point fluctuation radiation pressure

02 p0260 A72-12434

He-Ne laser active medium excitation and resonator geometry effects on TEM wave field

02 p0239 A72-12520

Electromagnetic fields calculation in one dimensional resonator with moving boundaries, considering orthogonal dynamic modes

02 p0195 A72-12591

Charged particle motion in pulsar electromagnetic fields, discussing coherent synchrotron radiation and charge bunching

03 p0438 A72-13874

Antenna arrays near-field radiation pattern prediction, using Harrington matrix methods

03 p0323 A72-14030

Spatial dispersion effects in crystal optics, obtaining dispersion law for normal waves in crystals via electromagnetic field tensor equations

04 p0548 A72-14739

Electromagnetic fields produced by quasi-stationary gravitational collapse of uniformly rotating current carrying relativistic thin disk

04 p0579 A72-15321

R-function theory application for solution of boundary value problems in electrodynamics, considering field behavior at infinity

04 p0488 A72-15377

Light transmission in medium with random inhomogeneities in Markov random process approximation, obtaining short wave field statistical characteristics

04 p0488 A72-15380

Nonlinear phenomena in transition region through resonance of dense inhomogeneous plasma in alternating electromagnetic field

04 p0489 A72-15390

Electromagnetic fields and energy flow lines in waveguide bifurcations with arbitrary passive terminations

04 p0489 A72-15392

Network formulations of electromagnetic fields in moving dispersive plasma media by equivalent parameter representation

04 p0490 A72-15400

Electromagnetic surface field propagation on dielectric wedge excited by line source, using steepest descent method

04 p0491 A72-15419

Self consistent theory of waves in fluctuating plasma, discussing Klimontovich-Maxwell electromagnetic field equations uniqueness solution and kinetic equation

04 p0493 A72-15449

Semiconductor-dielectric system for controlling space charge and valley population redistribution by external field

05 p0702 A72-16201

Monograph on semiclassical gas laser theory covering electromagnetic fields, atomic polarization, multimode theory, traveling- and standing-wave laser principles, collision effects, etc

05 p0668 A72-16398

Inverse electromagnetic field problem for one dimensional resonator, determining size change from intrinsic mode

05 p0627 A72-16408

HF electromagnetic field spectrum in one dimensional plasma cavity in pressure balance for arbitrary density

05 p0696 A72-16604

Transport coefficients of electron gas in electromagnetic field, using Grad thirteen moment method

05 p0697 A72-17005

Electromagnetic and electroacoustic near zone fields of linear antenna in plasma measured by diagnostic probe

05 p0700 A72-17232

Stability of weakly ionized homogeneous plasma placed in weak microwave field and in constant magnetic field, expressing growth increments of longitudinal waves

06 p0861 A72-17902

Cosmic rays generation by charged particles acceleration in electromagnetic constant crossed fields during magnetic stars contraction to neutron star dimensions

07 p1056 A72-19042

Scattering properties of conducting cylindrical obstacle in rectangular waveguide, deriving scattered field integral representation via Green function

07 p0944 A72-19593

Tensor analysis of electromagnetic energy localization in space, generating gravitational field and space curvature via equation to Einstein tensor

07 p1035 A72-19685

Taylor type antenna radiation distribution for aperture edge behavior realization in E or H planes

07 p0945 A72-19785

Kinetic equations for laser active medium disturbances and electromagnetic field modes in cavities with losses

07 p1006 A72-20117

Spectral distributions of laser emission as dynamic variables of electromagnetic field modes and active medium excitations, using perturbation theory

07 p1007 A72-20120

High performance shock tube using electromagnetically compressed and heated driver gas

07 p0965 A72-20559

Altitude dependence of vlf field of vertical electrical dipole in spherical waveguide of radially inhomogeneous ionosphere and earth, using Sommerfeld integral representations

08 p1130 A72-20736

Kirchhoff method application to asymptotic solution of plane wave diffraction on dielectric conical shells, calculating electromagnetic field vector

08 p1131 A72-20931

Electromagnetic field around thin linear receiving antenna by superposition of incident wave with antenna scattered field, deriving differential equations solution for field lines

08 p1132 A72-21327

Schwartz method application to stripline fields and impedance calculations for different cross sections and internal conductor dimensions

08 p1133 A72-21370

Asymptotic expressions for electromagnetic field and currents induced in unbounded dense plasma by relativistic electron beam passage

08 p1215 A72-21721

Electromagnetic potentials excited by dipole oscillator moving in homogeneous uniformly drifting medium, analyzing frequency spectrum and finite dimensions effect on higher harmonics

08 p1135 A72-21736

Group and symmetry theory application to degenerate mode splitting in magnetron cavity systems with electromagnetic fields disturbances

08 p1142 A72-21740

Transverse electromagnetic field and electron velocity vectors during rectangular pulse incidence on ionization front moving at light speed, describing steady state encounter region

08 p1136 A72-21741

Impulse-energy tensor for heat flow-crossed continuum subjected to electromagnetic field, using energy balance and quantity of movement equations

09 p1351 A72-22673

Electromagnetic field forces on finite conducting bodies, discussing heating rates and temperatures with ambient air convection and machine design recommendations

09 p1359 A72-22679

Gas discharge plasma detection characteristics, examining electron and ion densities and collision rates dependence on electromagnetic field frequency and amplitude

09 p1361 A72-22956

Fixed frequency or wideband real time measurements of microwave reflection and transmission coefficients and fields in open or closed structures

09 p1289 A72-23425

Flat electrically conducting screen with periodic filamentary structure as possible analog converter of electromagnetic field information

09 p1291 A72-23433

Near field characteristics of solid state laser frequency converters emission, determining medium transluence during single pulse excitation of organic phosphors

10 p1490 A72-24052

Electromagnetic field interaction with nonconducting polarizable and magnetizable continuum from theory based on total impulse energy tensor, deriving force density from relativistic balance approximation

10 p1510 A72-24124

Adiabatic transition experimental implementation by molecular beam irradiating field frequency variation

10 p1491 A72-24210

Classical laser theory, investigating anharmonic oscillators interaction with electromagnetic field in resonant cavity

[AD-740404]

10 p1492 A72-24603

1.TE solutions of relativistic Boltzmann equation in presence of external electromagnetic field

10 p1513 A72-24856

Radiative displacement of molecular beam sidebands by spatiotemporal modulation of irradiating RF field

10 p1492 A72-24858

Travel time effects on electron motion in HF electromagnetic fields, reviewing phase focusing and achromatic electron lens development

10 p1513 A72-24976

Plasma column stabilization by constant longitudinal inhomogeneous magnetic and rotating HF electromagnetic fields, noting application to plasma convective instabilities

11 p1694 A72-25786

Electromagnetic wave field effects on cold magnetoactive plasma potential oscillations, solving dispersion equation for sub-ion gyroscopic frequencies

12 p1849 A72-27066

Electromagnetic plane field cumulation by heavy conducting shells implosion with quasi-relativistic velocity, solving Maxwell equations by characteristics method

12 p1851 A72-27396

Linearly and circularly polarized electromagnetic field effective scattering areas relationships, considering radar reflection in reverse direction

12 p1783 A72-27629

Numerical accuracy of electromagnetic field spherical wave expansions, considering horn antenna radiation pattern

12 p1791 A72-27670

Magnetic storm strength ELF electromagnetic field effects on rabbits, dogs and bacteria, discussing changes in EEG, ECG and blood characteristics 12 p1763 A72-28214

Russian book on electrodynamic plasma acceleration covering charged particles motion in electromagnetic field and pulsed, MHD, steady and Hall accelerators 12 p1853 A72-28341

Nonequilibrium carrier distribution in drift junction transistor, considering base region hindering field effect on transit time, current gain cut-off and frequency response 13 p1926 A72-28371

Strong field electromagnetic wave interactions with anisotropic plasmas, considering electron velocity distribution function 13 p2009 A72-28449

Plasma ionization traveling disturbances velocity and spatial structure in strong electromagnetic waves field 13 p1915 A72-28469

Fourier transform solution for fields from current dipole element radiating in free space 13 p1916 A72-28540

Numerical analysis of surface current density distribution and electromagnetic fields of conducting body, noting radiation patterns of radial dipole and quarter wavelength monopole 13 p1916 A72-28541

Beamed radio waves interaction in E and F 1 regions propagation, noting beam width and field amplitude changes caused by defocusing 13 p1945 A72-28579

ELF and VLF waves propagation, deriving ionospheric field stable solutions by modified matrix multiplication technique for vertical geomagnetic field and large local refractivity 13 p1921 A72-29337

Kinetic equations derived for electromagnetic field inside cavity with resonance medium and external source, determining sensitivity thresholds, gain factors and spectral compositions 13 p1969 A72-29677

Variational form to determine equations and boundary conditions for elastic isotropic homogeneous nonferromagnetic body subjected to external load, temperature and electromagnetic field actions 13 p2061 A72-29797

Plasma inhomogeneity in crossed electromagnetic field, comparing motion velocity to ion component transverse drift rate in polarized electric field 13 p2019 A72-29893

Randomized electromagnetic field propagation through uniform medium, deriving autocorrelation and intensity fluctuation spectrum expressions 13 p2007 A72-30124

Kinetic model for electromagnetic field fluctuations in bounded isotropic plasma half space with specular reflection of electrons at boundary 14 p2135 A72-30170

Three layer atmospheric model for neutral gas motion-produced ionosphere and magnetosphere currents, electromagnetic field and charged particle concentration perturbations 14 p2100 A72-30632

Single point thunderstorm ranging method based on two radio frequencies field intensity spectral components ratio 14 p2129 A72-30639

Relativistic plasma particle correlation function based on transverse electromagnetic field energy density treatment by enlarged Bogoliubov hypothesis 14 p2140 A72-30881

High microwave voltage effects on p-i-n junction conductance under inverse dc bias, noting role of hole generation and accumulation by impact ionization 15 p2206 A72-31643

Magnetic dipole or small current loop over homogeneous flat earth, calculating transient electromagnetic field for airborne remote sensing 15 p2224 A72-31672

Optical pulse wave field longitudinal and transverse statistical correlations during propagation in turbulent atmosphere 15 p2198 A72-32061

Optically pumped magnetometer error, predicting atomic g-factor modification by nonresonant RF field 15 p2239 A72-32335

Algorithms for incorporating electromagnetic field into plasma numerical simulation to explain unwanted noise generation rates 15 p2288 A72-32421

Wave packet theory application to multimode laser cavity electromagnetic/optical/field analysis 15 p2251 A72-32649

Magnetron crossed field amplifier multistage frequency multiplier HF field properties, obtaining numerical solutions for nonlinear governing equations 15 p2209 A72-32669

Plasma column formation by interaction with rotating HF electromagnetic field and longitudinal constant magnetic field 16 p2433 A72-32815

Pulsar rotating electromagnetic field vectors classification for magnetosphere models 16 p2450 A72-32866

Electromagnetic field in MHD generator active zone approximated by cruciform plate, calculating secondary fields from Helmholtz equation 16 p2435 A72-33283

Maxwell equations solution for electromagnetic field in circular cylindrical tubes, deriving recursion formulas for computer processing 16 p2364 A72-33668

The perturbation of alternating geomagnetic fields by three-dimensional conductivity inhomogeneities. 17 p2545 A72-34350

The behavior of electromagnetic fields at edges. 17 p2513 A72-34357

Analysis of an optical beam waveguide consisting of a tapered lens-like medium and its applications. 17 p2580 A72-34382

Laplace equation to generate stationary electromagnetic vacuum fields, generalizing from Papapetrou-Majumdar class of static fields 17 p2580 A72-34425

Electromagnetic characteristics of MHD channels with nonconducting walls at finite magnetic Reynolds numbers 17 p2587 A72-34456

Time evolution of a rotating black hole immersed in a static scalar field. 17 p2605 A72-34536

The electromagnetic field generated by an electric dipole in a spherical cavity immersed in a nonlinear plasma 17 p2588 A72-34746

Possible field expansions in open waveguides and resonators 17 p2515 A72-34829

Averaged boundary conditions for a grid consisting of nonparallel and nonrectilinear conductors positioned on a nonplanar surface 17 p2529 A72-34830

Weak electromagnetic fields around a rotating black hole. 17 p2612 A72-35391

Multiphoton ionization of atomic hydrogen in the presence of an intense electromagnetic field. 17 p2586 A72-35827

Magnetized deformable media in general relativity. 17 p2584 A72-35911

Stochastic electrodynamics based on zero electromagnetic field motion, deriving Schroedinger equation and electromagnetic model of gravitation 17 p2584 A72-35912

On the behavior of the electromagnetic field with crests 17 p2584 A72-35913

Anomalous motion of radiating particles in strong fields. 18 p2713 A72-36712

Voltagess induced in superconductors in the absence of transport currents. 18 p2719 A72-36744

Wave propagation and dispersion in space-time periodic media. 18 p2663 A72-37208

Muller entropy principle-imposed restrictions on thermodynamic and thermodynamic constitutive relations for fluids in electromagnetic fields 19 p2834 A72-37843

Altitude dependence of VLF field of vertical electric dipole in spherical waveguide of radially inhomogeneous ionosphere and earth, using Sommerfeld integral representations 19 p2766 A72-38364

Plasma velocity, ion density and electrical conductivity from electron density and temperature and electromagnetic field profile measurements in Ar plasma inverse pinch 19 p2841 A72-38437

Electrically conducting plane screen with periodic filamentary structure as possible analog converter of electromagnetic field information 19 p2782 A72-38516

A general method for integrating the Schroedinger equation with a singular right-hand side in a homogeneous and constant electromagnetic field 19 p2843 A72-38855

Maxwell electromagnetic field theory review, emphasizing relationship between integral forms of Faraday and Ampere laws in conventional space and time concepts 20 p2904 A72-39778

Integral equation for electromagnetic field in diffuse boundary plasma, noting anomalous skin effect 21 p3090 A72-40409

A contribution to the numerical treatment of the electromagnetic field /H-polarization/ in horizontally non-homogeneous models of the earth. 21 p3048 A72-40498

Determination of the form of the capture area of a receiving antenna on the basis of energy streamlines 21 p3030 A72-40525

Transit time heating in stochastic electromagnetic fields. 21 p3092 A72-41222

On the energy and momentum conservation laws for linearized electromagnetic fields in a dispersive medium. 21 p3085 A72-41496

Russian book - Introduction to nonlinear electrodynamics. 22 p3204 A72-42076

Electromagnetic field, polarization and population inversion equations for spiked emission operation analysis in single mode laser 22 p3184 A72-42153

Differential equations for energy flow between electron beam and electromagnetic field, avoiding electron trajectory explicit calculation in nonlinear treatment of cyclotron resonance interaction 22 p3159 A72-42304

Bessel series solution to electromagnetic field and pulse function of cylindrical conducting screen located in monochromatic plane wave 22 p3155 A72-42667

A simple coupling between the electromagnetic and gravitational fields. 22 p3207 A72-42855

Expansion of diffracted electromagnetic fields in eigenfunctions of the d'Alembert operator 23 p3312 A72-43335

Electromagnetic induction in a half-space with a cylindrical inhomogeneity. 23 p3284 A72-43423

Diffraction of a plane wave by a ribbon grating in the case of short wavelengths 23 p3264 A72-43527

Influence of the phase-amplitude distribution of the field in the aperture of an antenna on its directional properties 23 p3270 A72-43773

Cylindrical waveguide with density modulated electron beam pumped by external electromagnetic field, considering Doppler effect conditions in beam radiation spectrum 23 p3265 A72-44157

Microwave generation with high energy electrons in magnetic undulator with transverse electromagnetic field, calculating frequency distribution of undulator radiation 23 p3265 A72-44158

The active field in an irregular slow-wave structure in the presence of a dynamic relative slip between the wave and the particle clusters 23 p3316 A72-44161

Polarization of the central field of a wave reflected from the ionosphere 23 p3265 A72-44173

Spectral characteristics of the scattering field of a uniformly traveling and rotating impedance cylinder 23 p3265 A72-44202

Field components of coupled electromagnetic and electron acoustic waves in warm stratified plasmas, using first order wave equations and Heading embedded form 23 p3322 A72-44319

Temperature of a free plasma filament in a high-frequency field at high pressures 23 p3322 A72-44464

Field expressions for a circular loop antenna in terms of a new set of functions. 24 p3379 A72-44707

Some features of the behavior of an intense light beam in a nonideal gas. 24 p3411 A72-45609

Electromagnetic wave field effects on cold magnetoactive plasma potential oscillations, solving dispersion equation for sub-ion gyroscopic frequencies 24 p3431 A72-45719

Coupled active parallel doublets network within external electromagnetic field at receiving station, investigating decoupling function between radiating elements 24 p3382 A72-45771

ELECTROMAGNETIC INTERACTIONS
NT PLASMA-ELECTROMAGNETIC INTERACTION

Soviet book on electromagnetic fields and waves covering propagation in anisotropic media, waveguides and cavity resonators, diffraction interactions, etc 01 p0031 A72-11200

Electron beam interaction with electromagnetic waves in longitudinal interaction devices during focusing by homogeneous magnetic and periodic electrostatic fields 02 p0189 A72-11564

Crab Nebula pulsar NP 0532 model for interaction and polarization of radio radiation with surrounding media 02 p0277 A72-11772

Elliptic equations solutions for electromagnetic effect in MHD rectangular channels using relationship to Laplace equations 03 p0397 A72-13995

Digital computer solution for near field coupling between high and low gain antennas above conductive surface 03 p0323 A72-14029

Radiative coupling of fed and unfed adjacent antennas in navigation systems rotating beam circular arrays, deriving equivalent circuit via quadrupole theory 05 p0635 A72-16300

Atom interactions with rf field, using quantum mechanical interpretation in terms of photons 07 p1038 A72-20433

Electromagnetic coupling between one dimensional laminar flows of viscous conducting fluid in presence of magnetic field, noting static and dynamic efficiencies dependence on Hartmann number 10 p1519 A72-24065

Electromagnetic field interaction with nonconducting polarizable and magnetizable continuum from force based on total impulse energy tensor, deriving force density from relativistic balance approximation 10 p1510 A72-24124

Dynamic processes of electric drive system with electromagnetic clutch modeled by analog computer element with logical input-output relation 10 p1423 A72-24755

Nonlinear interaction between circular coherent light and modulating electromagnetic waves in presence of quadratic electrooptical effect, noting frequency shift 10 p1493 A72-24912

Nonrelativistic quantum concept of electromagnetic field interaction with charged microparticles 11 p1692 A72-26093

Four-photon parametric frequency selection within broad stimulated emission lines during coherent light interaction, considering dye solution laser pumping 11 p1648 A72-26335

Electromagnetic wave interaction with irrotational moving fluid based on Maxwell equations and Minowski constitutive relation, noting flow velocity effects on scattering 11 p1689 A72-26471

Mode coupling effects on radio wave partial reflection from lower ionosphere at vertical incidence, using matrix perturbation analysis 11 p1599 A72-26764

Beamed radio waves interaction in E and F I regions propagation, noting beam width and field amplitude changes caused by defocusing 13 p1945 A72-28579

Periodic motions of weakly interacting modes in solid state lasers, using active matter pellet-resonator model 13 p1969 A72-29517

Electromagnetic field-two level atoms coherent interactions, using semiclassical approximation 15 p2250 A72-32305

Therapeutic electromedical equipment hazards due to electromagnetic interaction, considering implantation and simulation of human body 15 p2191 A72-32572

Theoretical study of electromagnetic coupling in the forced oscillatory regime of two one-dimensional laminar flows of a viscous and electroconducting liquid in the presence of a transverse uniform magnetic field 17 p2587 A72-34281

Electrons and photons interaction with relic radiation, establishing high energy gamma rays energy and intensity attenuation length 17 p2600 A72-35145

Structure of the power-law spectra of relativistic electrons in a turbulent plasma 17 p2593 A72-35907

Analysis and prediction of coupling between collocated antennas 20 p2902 A72-38999

Stellar energy-loss rates in a convergent theory of weak and electromagnetic interactions 20 p2972 A72-39868

Dielectric slab surrounding medium gain effects on bound modes amplification via estimation of evanescent surface wave interactions in optical waveguide by perturbation theory 21 p3062 A72-40605

Resonant interaction of an electrostatic wave with electrons in a current sheet 22 p3169 A72-42008

Electromagnetic waves interaction with transverse waves of thin piezoelectric plate in waveguide, noting transformation into acoustic waves 23 p3312 A72-43407

Book - Introduction to optical electronics 23 p3295 A72-43650

Experimental investigation of electromagnetic cascades at an energy greater than 20 GeV 23 p3291 A72-44444

Beamed radio waves interaction in E and F I regions propagation, noting beam width and field amplitude changes caused by defocusing 24 p3397 A72-45079

ELECTROMAGNETIC INTERFERENCE

NT ATMOSPHERICS
NT BLACKOUT [PROPAGATION]
NT COSMIC NOISE
NT CROSSTALK
NT DAWN CHORUS
NT ELECTROMAGNETIC NOISE
NT HISS

NT IONOSPHERIC CROSS MODULATION
NT IONOSPHERIC NOISE
NT IONOSPHERICS
NT JAMMING
NT RADIO FREQUENCY INTERFERENCE
NT SHOT NOISE
NT SUDDEN ENHANCEMENT OF ATMOSPHERICS
NT THERMAL NOISE
NT WHISTLERS
NT WHITE NOISE

Statistical model for communication probability estimate based on signal-to-interference and SNR criteria

01 p0031 A72-10997
Interference control in microwave circuit design, discussing coupling element, antenna terminals, radiated interference susceptibility and electromagnetic environments

02 p0189 A72-11558
Double reference beam holograms, evaluating interference effects of misalignment on image reconstruction

02 p0225 A72-11749
Receiver performance characteristics and failure mechanism in presence of interference, discussing measurement methods for interference susceptibility

02 p0192 A72-12150
Random errors in arrival time measurements of sinusoidal radio signal under noise and pulse interference

03 p0323 A72-13893
Pulse coded processing system EMC performance measurement, considering CW and pulsed interference effects and application to ATC radar beacon system transponders

03 p0324 A72-14033
Book on EMI test instrumentation and automatic measuring systems covering shielded enclosures, emission and susceptibility antennas and spectrum analyzers

04 p0486 A72-14611
Optical interference technique for experimental stress analysis of cracked structures, obtaining crack shape relationship to stress intensity factor

05 p0666 A72-16322
Two-channel direction finding with point source emission and spaced antennas reception, investigating cross correlation and background noise interference effects on accuracy

07 p0938 A72-19007
Biological radar clutter control by adaptive systems techniques, developing computer simulation for angel tolerance from bird electromagnetic characteristics

07 p0942 A72-19305
Frequency allocation effectiveness and mutual interference calculation for adjacent geostationary communication satellites

07 p0943 A72-19563
Adjacent channel interference effects in multicarrier telephony FM communications system

07 p0948 A72-20493
Minimum frequency separation between avionics receivers and transmitters for acceptable interference level

08 p1131 A72-20929
Potential noise stability of wideband communications systems during discrete signal reception on combined background of quasi-white noise and spectrally lumped interference

09 p1277 A72-22569
Data transmission interference protection under extreme noise, using tolerance detectors with redundancy coding

09 p1278 A72-22851
Constant false alarm rate signal processors for several electromagnetic interference types, using distribution-free methods and maximum likelihood estimation in radar target detection

10 p1437 A72-24683
Shielding procedures to control electromagnetic interference /EMT/ in design and operating electric equipment

10 p1452 A72-24813
Electromagnetic interference measurement by wide dispersion type spectrum analyzer electronically tuned over octave frequency range

11 p1632 A72-26027
[SAE AIR 1255]
Circuits for electromagnetic interference reduction in broadband solid state radio transmitters, discussing balanced transistor amplifier

15 p2209 A72-32564
Mathematical models for electromagnetic interference in electronic equipment, discussing nonlinear circuit analysis

15 p2201 A72-32568
Interfering beams amplitude modulation, applying optical heterodyne techniques

15 p2202 A72-32676
Random errors in arrival time measurements of sinusoidal radio signal under noise and pulse interference

15 p2202 A72-32704

Electron interferometer based on second order interference effects from laser modulated electron beam, applying quantum mechanical analysis

16 p2402 A72-33398
Error rate of phase-shift keying in the presence of discrete multipath interference.

17 p2516 A72-35334
Optimal predistortion efficiency for multiplicative disturbances in radio signal transmitting channel, noting Rayleigh distribution of signal fluctuations

17 p2518 A72-35778
Design of band-limited signal with no intersymbol interference - An extension of sampling function

19 p2767 A72-38606
Frequency sharing between broadcast satellites and tropospheric scatter systems.

20 p2901 A72-38978
Interference suppression design of switching circuits utilizing slewing rates.

20 p2906 A72-38982
Interference performance degradation to digital systems.

20 p2901 A72-38984
Minimisation of the solar array generated electrical interference on the GEOS satellite.

20 p2889 A72-38990
Radar EMI to voice communication receivers.

20 p2902 A72-38991
Gain averages as criteria for antenna EMC performance.

20 p2902 A72-39001
The Mueller matrix for scattering - Including the effects of interference.

20 p2970 A72-39754
Influence of polarization of laser fields on nonlinear interference effects

21 p3062 A72-40405
Satellite adjacent-channel interference due to multicarrier transponder operation.

21 p3020 A72-40892
Convolution noise and distortion in FDM/FM systems.

21 p3020 A72-40893
Impulse noise in FM receivers in the presence of adjacent channel interference and thermal noise.

21 p3020 A72-40894
Frequency allocation effectiveness and mutual interference calculation for adjacent geostationary communication satellites

22 p3153 A72-42081
August solar activity and its geophysical effects.

22 p3174 A72-42982
Book - EMI prediction and analysis techniques.

22 p3156 A72-43198
Determination of the optical thickness of polymer fracture surface layers from interference phenomena.

23 p3307 A72-44317
Potential noise stability of wideband communications systems during discrete signal reception on combined background of quasi-white noise and spectrally lumped interference

24 p3379 A72-44748
Rotating black holes - Separable wave equations for gravitational and electromagnetic perturbations.

24 p3439 A72-45014

ELECTROMAGNETIC MEASUREMENT
NT ELECTROMAGNETIC NOISE MEASUREMENT

Electromagnetic wave propagation anomalies over sea, comparing calculated and measured field strengths based on simultaneous refractivity vertical distribution measurement

01 p0026 A72-10405
Resonance rail line scattering range using flat parallel conductor transmission line for radar cross section measurement

01 p0032 A72-11251
Automated electromagnetic pollution data acquisition systems for environmental ecology, discussing computer technique and data retrieval, analysis and storage

03 p0328 A72-14040
Economics in electromagnetic field measurement surveys for siting of earth stations operating in shared frequency bands at 4 and 6 GHz, considering interference detection

03 p0324 A72-14044
Five component electromagnetic field station to record geomagnetic field magnetic and electric components variations

05 p0643 A72-16253
Impedance determination for symmetrical spherical probes and spacecraft housing with flat screen separation, using partial capacitance formula

05 p0662 A72-16268
Microwave antenna efficiency measurement by integrated isotropic levels comparison, featuring elimination of error due to specular ground reflections

05 p0637 A72-16421
Automatic measurements of wideband antenna radiation characteristics, using microwave generators linked with analyzers

06 p0775 A72-18194

- Magnetic and electric field intensities measurement with charged particle beams in coaxial high temperature plasma sources
06 p0863 A72-18415
- Interferometric measurement at 1415 MHz of radio telescope paraboloidal antenna radiation pattern, using cosmic radio sources with known flux density as signal source
07 p0945 A72-19789
- High resolution measurement of microwave refraction including arrival and fire angles on short line-of-sight tropospheric paths
07 p0946 A72-19790
- Electromagnetic velocity and flow measurements techniques application to cardiovascular patients, discussing utilization problems
09 p1272 A72-23275
- Radio receiver-transmitter system for synchronous heterodyne signal detection of 6 GHz band electromagnetic channel pulsed response, discussing operational principles and accuracy
09 p1280 A72-23353
- Fixed frequency or wideband real time measurements of microwave reflection and transmission coefficients and fields in open or closed structures
09 p1289 A72-23425
- Papers on electromagnetic probing in geophysics covering ground wave propagation, rough surface effects, geocrustal electric properties, HF radio backscatter from sea, etc
10 p1438 A72-24736
- Earth electrical parameters measurement by radio wave methods involving electromagnetic propagation along or reflection from surface, considering penetration depth, earth stratification and surface inhomogeneities
10 p1474 A72-24737
- Rough surface effects on EM reflection for electromagnetic probing in geophysics, using Rayleigh and Kirchhoff methods
10 p1512 A72-24738
- Electrical loss measurements in superconducting magnets at 60 Hz for Nb-Sn ribbon and Nb-Ti cable and multifilament coils
10 p1460 A72-24760
- Electromagnetic position sensor for magnetically supported model in wind tunnel, discussing design, operation principles and performance
10 p1462 A72-24773
- Electromagnetic interference measurement by wide dispersion type spectrum analyzer electronically tuned over octave frequency range
11 p1632 A72-26027
- Radio waves field strength measurement and recording for D region behavior during partial solar eclipse of 25 February 1971
13 p1961 A72-30050
- Microwave measurements on high permittivity materials with slotted waveguides excited in E mode
15 p2207 A72-31894
- Antarctic ice sheet complex permittivity in VLF band from reduction of measurement data with buried dipole antenna under snow surface
15 p2200 A72-32104
- Microwave antenna near field apparent image and phase-amplitude distribution measurement with photocontrolled semiconductor panel
15 p2209 A72-32672
- Electromagnetic transient coupling between ungrounded loops for two layer conducting half space approximation of earth
16 p2388 A72-34007
- The interpretation of ionospheric radio drift measurements. IV - The effects of signal coupling among spaced sensor channels.
17 p2515 A72-34699
- Magnetic and electric field intensities measurement with charged particle beams in coaxial high temperature plasma sources
17 p2588 A72-34864
- Measurement of Hall mobility of current carriers in inhomogeneous semiconductor samples
18 p2720 A72-36964
- Some problems of electromagnetic induction in the equatorial electrojet region. II - The analysis of magnetic and telluric variations at Zaria, Nigeria.
19 p2789 A72-37772
- Slotted-line measurement of insertion loss in three-port ferrite junction circulator.
19 p2775 A72-38636
- Complex analysis of satellite data for electromagnetic emission measurements in the radio, infrared and optical wavelength ranges
19 p2829 A72-38770
- Sensor selection for electromagnetic instrumentation system with sufficient sensitivity and bandwidth to demonstrate electroexplosive device compliance with MIL-E-6051D specified safety margin
20 p2962 A72-38979
- High level E-field susceptibility measurement problems and techniques.
20 p2906 A72-38981
- Some new methods of performing low frequency EMC measurements.
20 p2921 A72-38995
- Prediction of near-field antenna coupling in the presence of obstacles.
20 p2902 A72-38998
- Application of an agar-agar chamber for the study of electromagnetic waves in an inhomogeneous medium.
21 p3015 A72-40359
- Determination of the radiation characteristics of aircraft antennas in flight
21 p3030 A72-40534
- A measurement of ionospheric electric fields at high latitude.
22 p3169 A72-42015
- Electromagnetic thickness measurement on the AWACS radome.
24 p3384 A72-44901
- Wideband antenna test facility.
24 p3389 A72-45554
- An apparatus for measuring the Hall effect of high-resistivity materials in alternating electric and magnetic fields
24 p3405 A72-45698
- ELECTROMAGNETIC NOISE**
NT ATMOSPHERICS
NT COSMIC NOISE
NT DAWN CHORUS
NT HISS
NT IONOSPHERIC NOISE
NT IONOSPHERICS
NT SHOT NOISE
NT SUDDEN ENHANCEMENT OF ATMOSPHERICS
NT THERMAL NOISE
NT WHISTLERS
NT WHITE NOISE
- RF intrinsic and up or down-converted modulation noise mutual relationship with application to IMPATT diode oscillators
01 p0035 A72-10114
- Synchrotron radiation from incoming auroral electrons based on Schwinger equation, accounting for hf backscatter sounder noise
01 p0060 A72-10839
- Unlocked multimode He-Ne lasers If noise, discussing different modes intensity fluctuations mutual correlations
01 p0080 A72-10850
- Notch noise loading tests on predetection tape recording of FM carriers, showing noise power ratio dependence on record level and bias levels and output equalization
02 p0175 A72-12146
- Dc excited argon laser anode oscillation noise, discussing relation to ballast resistance, suppression conditions and current fluctuation frequency response to laser fluctuation
02 p0239 A72-12826
- Read avalanche diode noise theory, showing carrier current modulation and lf and hf noise coupling in nonlinear regime
03 p0333 A72-13848
- Electromagnetic noise and effects on communication systems, considering statistical parameters definition and measurements
03 p0324 A72-14036
- Composite incidental man-made radio noise data correlation to envelope statistic transformation hypothesis based on vlf airborne measurements of metropolitan area noise
03 p0324 A72-14041
- Impulse noise reproduction for temporary threshold shift and impulse noise measurements, considering rise time, frequency response and limitations of tape recorders
04 p0521 A72-14847
- Stark contours of hydrogen spectral lines in turbulent plasma with high noise level due to hf Langmuir oscillations
04 p0557 A72-14986
- Burst noise in bulk materials and transistors attributed to crystallographic defects, investigating gold addition effects
04 p0498 A72-15131
- Avalanche transit time diodes noise mechanisms and performance in microwave amplifier, oscillator and mixer applications
04 p0500 A72-15302
- Rocket cosmic radio noise measurements at 1.16-2.40 MHz and 1600 km, confirming spectrum flatness
05 p0711 A72-15763
- Optimal nonlinear logical filters for noise protection of space vehicle servosystems
05 p0726 A72-16460
- Noise parameters of space communication systems ground receiving antennas, considering noise effects on gain and radiation patterns
06 p0783 A72-17499
- Pulsed and CW solid state microwave oscillator EM noise as function of power level and locking parameters
06 p0788 A72-18465
- Noise contaminated pulse signal transit time measurement by receiver using digital filters
07 p0939 A72-19051
- Schottky barrier and n-n heterojunction diodes hf noise, considering ideality factor effect
07 p0955 A72-19358
- Waveguide cavity Gunn microwave power amplifiers, predicting maximum small signal gain and FM and AM noise performance
07 p0958 A72-19921
- Analog/hybrid simulation of noise effect on adaptive delta modulation system consisting of transmitter, receiver and error simulator
07 p0951 A72-20339
- Meteorological radar measurements, noting missile tracking radio interferometer noise due to stochastic refractive ray bending and associated multipath conditions
08 p1136 A72-21978
- Cavity resonator frequency detuning effects on FM and AM noise in cavity stabilized Gunn microwave oscillator
09 p1285 A72-22651
- Data transmission interference protection under extreme noise, using tolerance detectors with redundancy coding
09 p1278 A72-22851
- Noise in optical output of small area electroluminescent GaAs diffused junction diodes, comparing with theoretical shot noise limit
09 p1286 A72-23087
- Microbarrier mechanisms of 1/f noise for resistive materials and semiconductor devices
09 p1280 A72-23102
- Two dimensional dynamic model for background noise generation in bipolar transistors, using equivalent circuit
09 p1286 A72-23105
- Burst noise relationship to Si crystal dislocations and defects near bipolar emitter-base junction and surface zone in bipolar transistors
09 p1286 A72-23106
- Au-Si n and Al-Si p diodes noise operating in avalanche with charges injected by radiation
09 p1287 A72-23113
- Avalanche diode background noise in linear and nonlinear regimes, emphasizing source dependence on oscillation level
09 p1287 A72-23117
- Background noise in amplification and oscillation in Si and GaAs avalanche diodes
09 p1287 A72-23119
- Optimal correlating detector of fluctuating two frequency radar signals in unknown random noise
10 p1436 A72-24515
- Fixed point smoothing of sequentially correlated processes by extending filtering technique to simultaneous estimation of state and process noise contribution
11 p1610 A72-25871
- Ogo-5 observation of lower hybrid resonance noise, bursts, VLF hiss and whistlers near plasmopause during large magnetic storm
11 p1624 A72-26399
- Noise immunity and code sequence rejection probability in real multifrequency communications systems with multipositional frequency shift keying
11 p1598 A72-26729
- Multiplicative noise envelope distribution for ionospheric scatter channel from single and diversity radio reception, noting meteor trails effects on electromagnetic wave propagation
12 p1782 A72-27627
- Linear product demodulator for quadrature double sideband signal, evaluating channel noise and phase jitter effect on carrier
13 p1920 A72-29105
- Subtraction circuit design for impulse noise elimination at front end of aircraft oriented OMEGA navigation system receiver
13 p1999 A72-29204
- Avalanche photodiode optical detector noise amplitude distribution as function of operating conditions
13 p1971 A72-29924
- Dielectric waveguide X band telemetry system for remote power and multiplexing applications in noisy electromagnetic pulse environment
14 p2087 A72-31047
- Aeronautical communication satellite technical and economic survey, considering wave propagation, noise, aircraft antennas and VHF and UHF links
15 p2193 A72-31180
- Sense coil geometry and drive waveform effects on low level flux gate magnetometers sensor noise
15 p2233 A72-31507
- Multimode fiber optics data transmission through high electrical noise environments for send-receive communication links
15 p2198 A72-32059
- Algorithms for incorporating electromagnetic field into plasma numerical simulation to explain unwanted noise generation rates
15 p2288 A72-32421
- Generator for data transmission lines stochastic noise bursts simulation with statistically independent burst durations and intervals
15 p2201 A72-32475
- Incoherent receiver noise stability in multichannel system with channel frequency separation, deriving formula for receiver error probability
15 p2209 A72-32668

Electron beam modulation by SHF noise signal in plasma-beam system

15 p2289 A72-32698

Interference measurement techniques for small phase difference changes, noting diffraction and noise effects as limiting factors

15 p2243 A72-32769

Error probabilities in digital communication systems subject to mixture of man made or natural impulsive and Gaussian noise

16 p2365 A72-34106

Correlation of noise-like emission reflected from a statistically uneven surface

17 p2583 A72-35543

Intraocular noise - Origin and characteristics.

18 p2651 A72-36605

German monograph - Measurement of 'oscillation impedances' and optimization of frequency noise effects of microwave-semiconductor oscillators tunable over a wide frequency range

19 p2772 A72-37477

Man-made electromagnetic noise in southern California and southern Nevada.

19 p2764 A72-37869

Measurements of the laser linewidth due to quantum phase and quantum amplitude noise above and below threshold. I.

19 p2811 A72-38084

I-V characteristics of electric noise generated by flame between double probe electrodes during coke particle burning in air flow

19 p2882 A72-38458

Exponentially weighted noncoherent integration of pulsed signals in the presence of Gaussian noise and random impulse noise.

19 p2767 A72-38623

Error probability for multilevel PAM transmission with intersymbol interference, Gaussian and impulsive noise.

21 p3019 A72-40888

Impulse noise in FM receivers in the presence of adjacent channel interference and thermal noise.

21 p3020 A72-40894

Type 3 solar burst distinction from auroral type high pass noise via spectrum analysis

22 p3222 A72-42043

Influence of modulating /multiplicative/ noise on signal processing in a phased-array-antenna/receiver system

23 p3265 A72-44205

Effectiveness of certain easily realized rank detection algorithms for noise-masked signals

23 p3266 A72-44216

Geomagnetic tail magnetic and electric fields ULF, VLF and ELF fluctuations, considering relationship to substorm processes

24 p3397 A72-44857

ELECTROMAGNETIC NOISE MEASUREMENT

Atmospheric radio noise measurement by two methods for quasi-peak value, noting good correlation between techniques

01 p0031 A72-10923

Fast cyclotron and synchrotron transverse waves noise measurement in electron flux, using resonator with homogeneous electric field

02 p0190 A72-11573

Quadratic logarithmic converter used with linear microammeter for decibel scale noise measurements

09 p1306 A72-22344

Noise measurements of AM and FM microwave generators and amplifiers in nonlinear regime

10 p1452 A72-24643

The detection of unreliable contacts by noise measurements.

18 p2720 A72-37111

FM receiver noise figure measurement - A simplified method.

22 p3155 A72-42704

Accuracy of measuring the noise figure of microwave two-ports

23 p3273 A72-44313

ELECTROMAGNETIC PROPAGATION

U ELECTROMAGNETIC WAVE TRANSMISSION

ELECTROMAGNETIC PROPERTIES

NT ABSORPTIVITY
NT BIREFRINGENCE
NT BRIGHTNESS
NT COLOR
NT DICHROISM
NT ELECTRICAL PROPERTIES
NT ELECTROMAGNETIC ABSORPTION
NT FARADAY EFFECT
NT KERR MAGNETOOPTICAL EFFECT
NT LUMINOSITY
NT MAGNETIC PROPERTIES
NT OPACITY
NT OPTICAL PROPERTIES
NT OPTICAL REFLECTION
NT PHOSPHORESCENCE
NT PHOTOCONDUCTIVITY
NT PHOTOELASTICITY
NT PHOTOELECTRIC EFFECT
NT PHOTOELECTRIC EMISSION
NT PHOTOIONIZATION

NT PHOTOVISCOELASTICITY

NT PHOTOVOLTAIC EFFECT

NT RADIANCE

NT REFLECTANCE

NT REFRACTIVITY

NT SKY BRIGHTNESS

NT STELLAR LUMINOSITY

NT TRANSLUCENCE

NT TRANSMISSIVITY

NT TRANSMITTANCE

NT TRANSPARENCY

NT TURBIDITY

Electromagnetic-thermal properties of lunar surface

layers for radio communication around moon

04 p0577 A72-15121

Electromagnetic properties of semiconductor diffusion films, using impedance measurements

11 p1700 A72-25779

Influence of fluctuations on the electromagnetic properties of Josephson tunneling contacts

22 p3208 A72-43124

ELECTROMAGNETIC PROPULSION

Current and future rocket and spacecraft propulsion systems based on chemical propellants, nuclear thermoelectric, electrostatic and electromagnetic power generators

05 p0705 A72-16743

Effects of heat addition in divergent nozzles with application to MPD thrusters.

17 p2635 A72-34213

ELECTROMAGNETIC PULSES

Transverse electromagnetic field and electron velocity vectors during rectangular pulse incidence on ionization front moving at light speed, describing steady state encounter region

08 p1136 A72-21741

Relativistic shock propagation and search for electromagnetic pulses from supernovae, plotting kinetic energy factor vs external mass fraction

11 p1721 A72-26126

Single pulse radio echo fading dependence on sporadic E layer critical and screening frequencies

11 p1595 A72-26282

Frequency modulation and transient effects in resonant propagation of coherent light pulses

12 p1826 A72-27939

Electromagnetic pulsed radiation fields effects on monkeys and dogs behavior and blood chemistry, noting biological hazard absence

14 p2078 A72-30423

Radio pulses from extensive air showers detected by antenna array with east-west oriented dipoles connected in parallel

16 p2444 A72-33036

RF time domain nonreal time reflectometer operating as nanosecond radar with pulse spectrum lines reflections measured and stored for echo computation

19 p2770 A72-37256

Pulse propagation in a magnetoplasma. I - Longitudinal propagation.

19 p2843 A72-38751

Scattering of electromagnetic pulse waves by conducting wedge in an uniaxially anisotropic medium.

20 p2903 A72-39269

A simple, low power, multiple pulse NMR spectrometer.

21 p3056 A72-41005

Spectral analysis of microwave pulses by a ferrite transducer

22 p3158 A72-42119

Parabolic approximation of spatially bounded square and Lorentz two dimensional light pulse propagation in homogeneous isotropic linear medium without dispersion

23 p3313 A72-43682

Electromagneto-acoustic non-destructive testing in the Soviet Union.

24 p3408 A72-45291

ELECTROMAGNETIC PUMPS

Numerical analysis method for performance prediction of linear induction machines including liquid metal MHD pumps and generators and linear motors

13 p1900 A72-29365

ELECTROMAGNETIC RADIATION

NT AIRGLOW

NT BLACK BODY RADIATION

NT BREMSSTRAHLUNG

NT CERENKOV RADIATION

NT COHERENT ELECTROMAGNETIC RADIATION

NT COHERENT LIGHT

NT COMET TAILS

NT CYCLOTRON RADIATION

NT DAYGLOW

NT DECAMETRIC WAVES

NT DECIMETER WAVES

NT ELECTROMAGNETIC PULSES

NT EXTRATERRESTRIAL RADIO WAVES

NT FAR INFRARED RADIATION

NT FAR ULTRAVIOLET RADIATION

NT GALACTIC RADIO WAVES

NT GAMMA RAY BEAMS

NT GAMMA RAYS

NT GEGENSCHEIN

NT GEOCORONAL EMISSIONS

NT H WAVES

NT INFRARED RADIATION

NT LIGHT [VISIBLE RADIATION]

NT LIGHT BEAMS

NT LONG WAVE RADIATION

NT LYMAN ALPHA RADIATION

NT LYMAN BETA RADIATION

NT MICROWAVE EMISSION

NT MICROWAVES

NT MILLIMETER WAVES

NT MONOCHROMATIC RADIATION

NT NEAR INFRARED RADIATION

NT NEAR ULTRAVIOLET RADIATION

NT NIGHTGLOW

NT NONEQUILIBRIUM RADIATION

NT PHONON BEAMS

NT PHOTON BEAMS

NT PLANETARY RADIATION

NT POLARIZED ELECTROMAGNETIC RADIATION

NT POLARIZED LIGHT

NT RADIO BURSTS

NT RADIO EMISSION

NT RADIO WAVES

NT SHORT WAVE RADIATION

NT SKY RADIATION

NT SKY WAVES

NT SOLAR RADIO BURSTS

NT SOLAR RADIO EMISSION

NT SOLAR X-RAYS

NT SOMMERFELD WAVES

NT SUBMILLIMETER WAVES

NT SUNLIGHT

NT SYNCHROTRON RADIATION

NT TERRESTRIAL RADIATION

NT THERMAL RADIATION

NT TWILIGHT GLOW

NT ULTRAVIOLET RADIATION

NT X RAYS

NT ZODIACAL LIGHT

Electromagnetic cylindrical wave group aging properties, describing extragalactic red shift production mechanism

01 p0135 A72-11325

Passive electric microwave probe with balancing capacitance for studying waveguide fields at high microwave power levels in radiative plasma accelerators

02 p0223 A72-11418

Electromagnetic plane stress wave generation by capacitor bank for transient loading of photoelastic models along straight and curved boundaries [SESA PAPER 1907A]

02 p0199 A72-11503

Quasi-static surface waves at Maxwellian plasma boundary with diffuse electron scattering, considering plasma electromagnetic oscillations

02 p0266 A72-12577

Second harmonic emission from plasma hybrid resonance region during electromagnetic wave normal incidence on nonhomogeneous magnetoactive plasma layer

02 p0180 A72-12578

Plane electromagnetic wave diffraction on magnetoactive plasma cylinder, using energy method and particle scattering model

02 p0183 A72-12754

Cascaded annular lens systems for focusing electromagnetic waves, noting advantages of axicon

03 p0388 A72-12967

Electron emission in strong electromagnetic waves within quantum electrodynamics, discussing energy losses and electron pair production

03 p0415 A72-13003

Solar magnetic field measurements using electromagnetic radiation, atmospheric structure [MHD effects] and energy equipartition

03 p0427 A72-13277

Electric field effects on electromagnetic wave packet motion in anisotropic nonlinear medium with electro-optical effect

03 p0322 A72-13737

Soviet monograph on electron flux nonlinear interaction with slow electromagnetic waves in TWT, discussing output power and efficiency increase

03 p0333 A72-13949

Computer modeling technique for electromagnetic scattering and radiation problems in resonance region employing thin wire electric field integral equation

03 p0328 A72-14028

Electromagnetic radiation in universe, discussing relic radio emission, energy density, hot model isotropic extragalactic component isolation, intergalactic gas, radio sources and quasars

03 p0414 A72-14317

Electromagnetic solitary waves /solitons/, noting medium macroscopic motion absence and parametric pulse generation

04 p0489 A72-15387

Self focusing of electromagnetic waves in isotropic plasma, investigating nonlinear relaxation processes

04 p0489 A72-15391

Electromagnetic radiation modulators in millimeter and submillimeter wave range using gas-discharge plasma magneto-optical effects in alternating magnetic field

05 p0625 A72-15826

Energetic solar flare particles release from sun, describing satellite observations of solar electromagnetic radiation 05 p0710 A72-16522

Energy spectrum of muon formed electromagnetic cascades in vertical cosmic radiation flux 06 p0871 A72-17287

Phase and group velocity of electromagnetic waves in drifting uniaxial magnetoplasma, obtaining dispersion relation from Maxwell and plasma equations 06 p0853 A72-17349

Dual integral equations solutions to electromagnetic wave diffraction at plane conducting slotted screen 06 p0773 A72-17689

Conversion effectiveness of oscillations induced by electron beam in bound anisotropic plasma into electromagnetic emission 06 p0860 A72-17700

Electromagnetic radiation in uniformly moving homogeneous medium obtained by transformation and four dimensional Green function method 06 p0847 A72-17712

Transient effects due to electromagnetic cascades in Pb during Cu wall passage in ionization calorimeter 07 p0988 A72-19871

Multiplication and mixing of electromagnetic waves in optically nonlinear anisotropic crystal media 07 p1007 A72-20119

Spectral distribution of electromagnetic radiation emitted by charge moving in gravitational field of spherically symmetric black holes 07 p1081 A72-20226

Geomagnetic variations propagation theory for LF electromagnetic and Alfvén waves diffraction at stratified earth in thin gyrotopical ionosphere 08 p1130 A72-20711

Plane electromagnetic wave reflection from conducting convex cylinder in radially inhomogeneous absorbing medium, deriving equations for beam trajectories calculation 08 p1131 A72-20742

Minuteman HERO /hazards of electromagnetic radiation to ordnance/ preflight testing, describing ordnance monitoring system based on fiber optic data links 08 p1220 A72-20767

Quasi-periodic ionospheric electron density fluctuations effects on electromagnetic waves propagation, noting effect on surface recordings as geomagnetic variations 08 p1156 A72-20824

Comb type slow wave structures properties outside passband, obtaining dispersion and field distribution expressions by electrodynamic analysis 08 p1135 A72-21738

Electromagnetic field radiation from linearly and sinusoidally variable thickness layered structures under plane wave and concentrated source excitations 08 p1137 A72-21986

Electrostatic plasma wave conversion into electromagnetic waves, calculating dispersion relation at all wavelengths for perpendicular propagation mode 08 p1137 A72-21989

Physical optics approximation study of gravitational waves effect on electromagnetic propagation, noting unobservability of local scintillation effect 09 p1351 A72-22683

Short laser pulses for plasma heating, considering turbulent heating mechanisms, neutron yield and electromagnetic radiation 09 p1364 A72-23444

Clinical effects on atrio-ventricular pacing system of electromagnetic weapon detector systems used for air passenger screening at airports in air hijacking prevention efforts 10 p1428 A72-23740

Plane electromagnetic wave diffraction on ideally conducting convex body of large electrical dimensions, obtaining Maxwell equations asymptotic solution 10 p1436 A72-24577

Electromagnetic wave diffraction by dielectric steps in waveguides, calculating microwave scattered field by modified residue calculus technique 10 p1451 A72-24593

Electromagnetic wave propagation in weakly nonstationary plasma, determining variations of wave amplitudes and polarization characteristics 10 p1523 A72-24782

Electromagnetic wave propagation and absorption in weakly inhomogeneous plasma layer, calculating conditions for transformation into plasma wave 10 p1523 A72-24799

Wave equation derivation for electromagnetic and gravitational radiations in Schwarzschild field, obtaining third order corrections for scalar waves 10 p1514 A72-25168

Perturbation theory for electromagnetic radiation in weakly anisotropic magnetoplasma, calculating Green function for delta function source oriented parallel to static magnetic field 12 p1783 A72-27668

Numerical description of electromagnetic radiation from open-ended flanged waveguides, giving truncation

corrected expressions for field behavior in aperture perimeter vicinity 13 p1915 A72-28520

Obliquely incident electromagnetic waves reflection and transmission by moving compressible plasma slab, applying field and wave-four vectors Lorentz transformations to wave equations 13 p2010 A72-28543

Parametric decay instability of Langmuir and acoustic plasma waves induced by incident electromagnetic wave near plasma frequency, noting application to ionospheric instabilities 13 p2012 A72-29126

Martian ionosphere electromagnetic wave propagation characteristics for E, F1 and F2 models, calculating refractive index for zero and nonzero collision frequencies 13 p1922 A72-29474

Electromagnetic wave propagation in weakly nonstationary plasma, determining variation with time and polarization plane rotation 14 p2136 A72-30219

Kinetic instability bursts during heating of electron plasma in cylindrical resonator with standing electromagnetic waves 14 p2136 A72-30308

Electromagnetic emission in universe, discussing background radiation spectrum, extragalactic source brightness, intergalactic gas and energy density 14 p2152 A72-30479

Electromagnetic and gravitational waves emission by superlight sources in vacuum, considering multiparticle and form factor cut-off effect 14 p2130 A72-30625

Standardization of microwave irradiation experiments on animals, discussing power density level evaluations and local vs whole-body irradiation effects 14 p2080 A72-30746

Epitaxial film system parameters determination based on variational technique of computing electromagnetic waves reflectance and transmissivity in semiconductor structures 14 p2142 A72-30811

Carrier wave propagation at semiconductor surface with electron drift, discussing solid state traveling wave amplifier design 15 p2290 A72-31288

Quasar electromagnetic radiation emission in terms of general relativistic coupling between gravitational field and charged particle radiation field 15 p2306 A72-31592

Collisions role in nonlinear mode coupling and harmonic generation associated with electromagnetic wave in plasma, describing plasma electron distribution function by kinetic equation 15 p2195 A72-31679

Electromagnetic hazards, pollution and environmental quality - Conference, Purdue University, Indiana, May 1972 15 p2209 A72-32563

Ultrabroadband probe design for microwave radiation intensity measurement in harmful exposure study 15 p2191 A72-32574

Narrow strongly radiating slot voltage distribution, investigating cavity coupling with integral equation 15 p2209 A72-32659

Cylindrical antenna immersed in weakly ionized magnetoplasma, calculating steady magnetic field effect on electromagnetic and electroacoustic radiation resistances 16 p2434 A72-32860

Variable amplitude and phase velocity electromagnetic traveling wave field distribution in diverging MHD induction machine channel with liquid metal flow 16 p2435 A72-33282

Electromagnetic radiation frequency spectrum and mean power from accelerated magnetic dipoles in circular and Keplerian orbits, noting implications for pulsars 16 p2453 A72-33285

Induced electron emission dependence on polarization, frequency and intensity of second wave incident on electron with anomalous magnetic moment 16 p2424 A72-33365

Interplanetary radiation types in terms of possible space flight hazards, discussing electromagnetic and corpuscular radiation, cosmic rays and radiation belts 16 p2446 A72-33553

Nonionizing electromagnetic radiation effects in biological systems, discussing microwave penetration, therapeutic warming, light scattering in tissues and medical instrument applications 16 p2359 A72-33754

Microwave radiation - Biophysical considerations and standards criteria. 17 p2507 A72-34299

Diffraction of a plane electromagnetic wave on an anisotropic half-plane in free space and in a plane waveguide 17 p2515 A72-34828

Investigation of two types of collisionless linear dampings of electromagnetic waves in a nonhomogeneous magnetized plasma. 17 p2588 A72-34870

Some comments on the generation of electromagnetic traveling and standing waves for inductive acceleration of plasmas [DFVLR-SONDDR-209] 17 p2589 A72-34895

Cerenkov instability and VLF emissions generated outside the plasmopause. 17 p2547 A72-35063

VLF emissions during post breakup phase of polar substorm. 17 p2547 A72-35064

Linear transformation and absorption of electromagnetic waves in plasma 17 p2591 A72-35165

Calculation of sum-frequency electromagnetic waves emitted by a multilayer nonlinear plate 17 p2516 A72-35168

Electromagnetic waves on a conducting infinite cylinder in a magnetoionic medium. 17 p2517 A72-35399

Solution to a boundary value problem in the theory of diffraction of electromagnetic waves at a circular hole in a plane screen between two media 17 p2518 A72-35724

The electromagnetic radiation near the ion plasma frequency emitted by a turbulently heated plasma. 18 p2715 A72-36598

Electromagnetic radiation and scattering from loaded bodies of revolution of arbitrary shape, calculating plane wave scattering from apertures in cylinders and hemispheres 18 p2662 A72-36927

Green function for temporal electromagnetic plasma wave echoes oblique to external magnetic field, calculating current density and damping term 19 p2839 A72-37333

Electromagnetic and space charge disturbance transmission and reflection at plasma boundary and oblique incidence, discussing isotropic Vlasov plasma 19 p2839 A72-37336

Geomagnetic variations propagation theory for LF electromagnetic and Alfvén waves diffraction at stratified earth in thin gyrotopical ionosphere 19 p2765 A72-38339

Electromagnetic self induced vibrations in homogeneous unbounded electron beam moving with time dependent velocity, noting longitudinal and transverse wave generation 19 p2842 A72-38527

Cytologic aspect of RF radiation in the monkey. 19 p2758 A72-38709

Complex analysis of satellite data for electromagnetic emission measurements in the radio, infrared and optical wavelength ranges 19 p2829 A72-38770

German Book - Introduction into nonlinear optics, Volume I 19 p2813 A72-38775

Electromagnetic background radiation in universe, discussing relic radio emission, energy density, hot model isotropic extragalactic component isolation, intergalactic gas, radio sources and quasars 19 p2854 A72-38815

Computer program to simulate electromagnetic signal densities, data rates and power from land based radar transmitters as functions of time and location 20 p2902 A72-38992

Plane electromagnetic wave diffraction on magnetoactive plasma cylinder, using energy method and particle scattering model 20 p2902 A72-39060

The detection of gravitational waves by electromagnetic oscillators. 20 p2974 A72-40024

LF circularly polarized electromagnetic waves /helicons/ resonance crystal plates, deriving magnetoresistivity and Hall coefficient 21 p3066 A72-40624

A charged particle in the field of a transverse electromagnetic plane wave - A group-theoretical analysis. 21 p3084 A72-40722

Excitation of electromagnetic waves in a plasma by a relativistic electron beam 21 p3092 A72-40787

Slow electromagnetic waves in antiferromagnetics near the point of transition to the ferromagnetic phase 21 p3098 A72-41685

Radiation of an oscillator moving parallel with the interface of two media 21 p3036 A72-41843

Radiation of an oscillating charge in a three-dimensional periodically inhomogeneous medium 21 p3023 A72-41844

Study of the thermal self-focusing of electromagnetic waves in a plasma 22 p3211 A72-42652

Numerical integration of integral equation for phased array radiation modeled by impedance filaments in conductive plane, noting excitation by magnetic flux 22 p3159 A72-42663

Electromagnetic emission during the development of a hydrodynamic beam instability in a bounded plasma 22 p3213 A72-43115

Kinetic instability bursts during heating of electron plasma in cylindrical resonator with standing electromagnetic waves

23 p3317 A72-43210

Electromagnetic waves interaction with transverse waves of thin piezoelectric plate in waveguide, noting transformation into acoustic waves

23 p3312 A72-43407

Low frequency oscillations of cesium and mercury vapor plasmas, noting intensity distribution, radiation pattern and polarization characteristics of microwave emission

23 p3319 A72-43411

Electromagnetic radiation modulators in millimeter and submillimeter wave range using gas-discharge plasma magneto-optical effects in alternating magnetic field

23 p3319 A72-43434

Energy measurement of primary particles from shower formation in solids, discussing ultrasonic waves generation in metal plates and electromagnetic waves excitation in ferrites

23 p3291 A72-44437

State of the art in the detection of intelligent extraterrestrial signals.

24 p3441 A72-45190

Extraterrestrial electromagnetic radiation and particle flux characteristics of low and medium energy, considering onboard spacecraft measuring instruments and data processing systems

24 p3404 A72-45398

Self-consistent electromagnetic waves in relativistic Vlasov plasmas.

24 p3430 A72-45569

Profile of a parametric luminescence line emitted by lithium niobate crystals.

24 p3432 A72-45614

Electron bremsstrahlung from hot plasma in the presence of strong magnetic field.

24 p3431 A72-45627

Effects of pseudosonic and electroacoustic waves on the radiation of a plasma-coated spherical antenna.

24 p3386 A72-45645

ELECTROMAGNETIC SCATTERING

NT HALOS

NT IONOSPHERIC F-SCATTER PROPAGATION

NT LIGHT SCATTERING

NT MICROWAVE SCATTERING

NT MIE SCATTERING

NT RAMAN SPECTRA

NT RAYLEIGH SCATTERING

NT THOMSON SCATTERING

NT X RAY SCATTERING

Redistribution function of line radiation during scattering without atom velocity restriction

01 p0104 A72-10093

Atomic models of velocity noncorrelated radiation line scattering with frequency redistribution at large distance from atmosphere

01 p0104 A72-10094

Plane electromagnetic wave scattering by imperfectly conducting cylinder with radially inhomogeneous dielectric coating, using phase shift method for evaluation

01 p0024 A72-10130

Analog FM multiplex signal intermodulation formula based on time-variable electromagnetic waves tropospheric scatter propagation

01 p0027 A72-10411

Multipole methods for electromagnetic scattering from conducting cylinder over dielectric half space, noting application to radar cross sections

01 p0030 A72-10842

Modified Born approximation for electromagnetic backscattering cross section from turbulent plasmas, noting attenuation leading to saturation and cross-polarization

01 p0031 A72-10846

Electromagnetic wave scattering from rough surfaces by Kirchhoff approach and small perturbation method, discussing validity near grazing angle

01 p0032 A72-11249

Bidirectional scattering of electromagnetic waves from rough surfaces in plane of incidence restricted only by tangent plane approximation, comparing with other models

02 p0170 A72-11467

Ionospheric spread-F mechanism as electromagnetic wave scattering on electron density inhomogeneities, calculating characteristic dependence of height interval on operational frequency

02 p0216 A72-11920

Spatial-temporal correlation functions of field due to electromagnetic waves backscattering from random inhomogeneities in extended layer

02 p0180 A72-12580

Electromagnetic wave scattering characteristics at arbitrarily configured body with dimensions smaller than primary field wavelength, determining electric and magnetic moments

02 p0181 A72-12595

Gaussian electromagnetic wave beam diffraction and scattering problems solutions by optics formula

application to beam transformation through optical systems

02 p0261 A72-12603

Scattering diagram for mutual cross coupling between antennas in Fresnel zone

02 p0196 A72-12757

Quasi-ergodicity condition of dynamic electromagnetic scattering diagram of flying object in terms of amplitude or phase elements

02 p0183 A72-12765

Electromagnetic wave scattering by electron charge density fluctuations in plane waveguide with magnetoactive plasma, showing cross section spectrum function of plasma properties

02 p0183 A72-12766

Nonstationary radiation transfer with one dimensional anisotropic scattering, deriving Bessel function expressions for quantum exit from semiinfinite medium

02 p0262 A72-12830

Spectral distribution of radiation arising from nonlinear Thomson scattering of strong electromagnetic wave by ultrarelativistic electrons

03 p0390 A72-13017

Strong circularly polarized electromagnetic wave scattering by plasma electron as function of amplitude and magnetic field with radiation reaction

03 p0321 A72-13077

Electric and magnetic field scattering on ellipsoidal inhomogeneities in circular waveguides from integrodifferential equation derived expressions

03 p0322 A72-13735

Computer modeling technique for electromagnetic scattering and radiation problems in resonance region employing thin wire electric field integral equation

03 p0328 A72-14028

Tropospheric forward electromagnetic scatter propagation path loss prediction by modified Yeh method with empirically derived correction function

03 p0323 A72-14031

Reciprocity relations for electromagnetic waves scattered by isolated, stratified and composite anisotropic obstacles

04 p0547 A72-14535

Pulsar radiation scattering in interstellar medium, using Gaussian spatial autocorrelation function

04 p0577 A72-15281

Short wave asymptotic formulas for shadow zone of plane diffraction, discussing asymptotic solutions for field from point source

04 p0489 A72-15386

Hf electromagnetic wave scattering and diffraction by smooth dielectric cylinder and sphere based on Lorentz excitation theory

04 p0490 A72-15397

Conformal transformations applications to plane electromagnetic wave diffraction by infinitely conducting network, discussing energy distribution

04 p0490 A72-15410

Plane electromagnetic wave diffraction on two cylinders with different radii, assuming infinite length and ideal conductivity

04 p0491 A72-15413

Electromagnetic wave scattering and diffraction on lattice of dipole vibrators

04 p0491 A72-15415

Numerical solution for diffraction on conducting finite and infinite lattice of cylinders with circumferential cross section

04 p0491 A72-15416

Electromagnetic wave diffraction on infinite lattice of perfectly conducting arbitrary flat elements from numerical method, determining secondary field and strips current distribution

04 p0491 A72-15417

Diffraction anomaly from infinitely extended strip grating solution by successive approximation technique combination with singular integral equation

04 p0491 A72-15418

Electromagnetic traveling plane wave diffraction from arbitrary angled dielectric wedge, investigating surface currents on walls

04 p0491 A72-15420

Reflection from aperture of long E-plane sectoral horn antenna, determining electrical impedance by asymptotic diffraction theory

04 p0501 A72-15424

Hf backscattering of plane electromagnetic wave at oblique incidence on conducting circular metallic disk, noting polarization dependence on angle

04 p0493 A72-15524

Ray statistics of electromagnetic wave scattering in homogeneous isotropic turbulent medium with ellipsoidal inhomogeneities of refractive index, using Fokker-Planck equation

05 p0626 A72-16243

Plane electromagnetic wave diffraction by infinite cylinder with unsteady impedance boundary conditions

05 p0627 A72-16409

Scattering of arbitrarily impinging monochromatic electromagnetic waves by thin infinitely long isotropic, dielectric and metal rods of elliptic cross section

05 p0628 A72-16412

High frequency electric field backscattering by plane electromagnetic wave incident on perfectly conducting sphere with radially inhomogeneous dielectric coating

05 p0630 A72-16621

Ray-optical calculation of modes scattered by obstacle in two dimensional waveguide or duct with weakly inhomogeneous medium and nonvanishing surface impedance walls

05 p0630 A72-16622

Nonlinear wave coupling, scattering and radiation in plasmas for diagnostics application

05 p0699 A72-17221

Spectral calculations of electromagnetic and nuclear showers of cosmic ray muons interacting with substance

06 p0871 A72-17288

Electromagnetic wave scattering from curved rough surfaces and transmission through turbulent medium, obtaining solution by spatial Fourier transform of three transfer functions product

06 p0771 A72-17340

Electromagnetic wave scattering by underdense plasma layer, considering perturbation calculation for Gaussian, sech squared and parabolic density distribution

06 p0853 A72-17350

Ground and atmospheric scattered radiation discrimination by ground modulation based on chopper signal frequency analysis, considering feasibility from airborne tests results

06 p0814 A72-17587

Interplanetary scintillation of two pulsars, discussing scattering and amplitude modulation of incident radiation propagated through interstellar medium

07 p1069 A72-19073

Scattering properties of conducting cylindrical obstacle in rectangular waveguide, deriving scattered field integral representation via Green function

07 p0944 A72-19593

Electromagnetic scattering of square pulse from lossy dielectric slab mounted on perfectly conducting planar ground surface

07 p0945 A72-19660

Electromagnetic field around thin linear receiving antenna by superposition of incident wave with antenna scattered field, deriving differential equations solution for field lines

08 p1132 A72-21327

Soviet book on Riemann-Hilbert problem method in electromagnetic waves theory, covering wave diffraction, scattering and propagation, waveguides and open resonators

08 p1137 A72-22021

Relation for detector-aperture size for spatially coherent detection with dependent scattering applied to realistic laser radar signal signatures

09 p1278 A72-22618

Electromagnetic scattering by ungrounded conducting sphere above ground plane, calculating If ground wave backscatter

09 p1279 A72-22905

Electromagnetic wave scattering by arbitrarily oriented circular ice cylinders, deriving far field intensities for linearly polarized incident waves

09 p1280 A72-23341

Background medium anisotropy effect on electromagnetic waves scattering from ionospheric irregularities, calculating scattered power by Green function

09 p1282 A72-23519

Electromagnetic waves scattering by uniformly moving objects in free space, considering two dimensional monopoles and dipoles

09 p1282 A72-23523

Electromagnetic wave scattering on inhomogeneities by Born approximation, estimating maximum error for small correlation radius

10 p1436 A72-24503

Average electric field and power density of electromagnetic wave scattered from rough layer with plane interface, calculating scattering cross sections

10 p1512 A72-24744

Secondary diffraction from close edges on perfectly conducting bodies, representing scattered field by iterative surface current density replacement technique

10 p1440 A72-24938

Electromagnetic wave interaction with irrotational moving fluid based on Maxwell equations and Minkowski constitutive relation, noting flow velocity effects on scattering

11 p1689 A72-26471

Ionospheric scattered wave propagation mode and weak echo delay explained by analysis-derived model

11 p1597 A72-26570

Position and minimum scattering algorithms for narrow band signal source received by spaced receivers forming antenna arrays with large separations

11 p1598 A72-26715

Circularly polarized ultrashort radio wave reflection from lunar and planetary surfaces, determining angular scattering spectrum

11 p1599 A72-26908

- Radiation propagation in optically thin anisotropic noncrystalline media, obtaining explicit formulas for Stokes parameters of transmitted and scattered radiation 12 p1865 A72-27052
- Stimulated monochromatic electromagnetic wave scattering derived from analysis of nonlinear interactions in magnetoactive plasma 12 p1849 A72-27063
- Multiplicative noise envelope distribution for ionospheric scattering channel from single and diversity radio reception, noting meteor trails effects on electromagnetic wave propagation 12 p1782 A72-27627
- Linearly and circularly polarized electromagnetic field effective scattering areas relationships, considering radar reflection in reverse direction 12 p1783 A72-27629
- Plane monochromatic electromagnetic wave scattering by rotating metallic cylinder, noting frequency shift dependence on cylinder translational motion velocity 13 p1914 A72-28370
- Particle size distribution functions reconstruction from scattered radiation data, discussing accuracy and applicability of small angle, spectral transparency and complete indicatrix methods 13 p1955 A72-28514
- Numerical calculation of electromagnetic scattering properties of two dimensional bodies with arbitrary cross section, considering TM polarization of excitation and fields mode matching 13 p1916 A72-28534
- Ionospheric spread-F mechanism as electromagnetic wave scattering on electron density inhomogeneities, calculating characteristic dependence of height interval on operational frequency 13 p1948 A72-29232
- Strong circularly polarized electromagnetic wave scattering by plasma electron with radiation reaction, determining cross section as function of amplitude and magnetic field strength 13 p2015 A72-29427
- Electromagnetic waves scattering by underdense plasmas, examining intermittency phenomenon due to mixing between turbulent inner and outer inviscid wake 13 p1922 A72-29473
- Millimeter wave scattering at turbulent density discontinuities in plasma from electrodeless inductive discharge 14 p2136 A72-30174
- Electromagnetic waves backscattering in magnetoactive plasma containing random inhomogeneities of electron density, calculating field spatial-time and cross correlation functions 14 p2086 A72-30789
- Electromagnetic wave propagation in nondispersing media with spatial-time fluctuations of dielectric permittivity, calculating scattered field by perturbation method 14 p2086 A72-30796
- Noncoherent isotropic scattering in plane parallel finite layer, considering Doppler line broadening 15 p2273 A72-31331
- Electromagnetic single scattering near critical point in inhomogeneous optical medium with variable refractivity, discussing reflected light effect and Poynting vector reduction to Bragg conditions 15 p2279 A72-32693
- Solar radiation anisotropic nonconservative scattering in semiinfinite atmosphere, calculating plane and spherical albedo by exponential kernel approximation 16 p2446 A72-33463
- Pulsar pulse broadening due to multiple scattering by interstellar medium, finding exponential decay time constant relation to rms broadening of angular size 16 p2457 A72-33686
- Solar radiation absorption and scattering by particles in atmosphere, emphasizing absorption/backscatter ratio explanation 16 p2388 A72-34023
- Scattering of electromagnetic waves from an inhomogeneous magnetoplasma column moving in the axial direction. 17 p2587 A72-34359
- On the behavior of thin-wire antennas and scatterers arbitrarily located within a parallel-plate region. 17 p2513 A72-34365
- Integral equation for electromagnetic wave scattering by thin dielectric ring 17 p2526 A72-34379
- Book - Angular scattering functions for spheroids 17 p2582 A72-35457
- Scattering characteristics of a cross-junction of oversized waveguides. 18 p2660 A72-36486
- Influence of interstellar discontinuities on the shape of radio pulses from pulsars 18 p2726 A72-36652
- Influence of an interface on the spectrum of incoherently reflected waves 18 p2661 A72-36657
- Universe expansion induced electromagnetic wave backscattering absence in Robertson-Walker spacetime as consequence of motion equations conformal invariance 18 p2711 A72-36711
- Electromagnetic radiation and scattering from loaded bodies of revolution of arbitrary shape, calculating plane wave scattering from apertures in cylinders and hemispheres 18 p2662 A72-36927
- High level atmospheric refraction of electromagnetic waves as function of elevation and meteorological element vertical stratification 19 p2764 A72-37349
- Black hole rotational energy extraction by super-radiant scattering with impinging wave amplification and by floating particle orbits with zero net radiation reaction 19 p2857 A72-37720
- Scattering resonances of electromagnetic wave by an infinite plane grating with reflector. 19 p2767 A72-38612
- Scattering diagram for mutual cross coupling between antennas in Fresnel zone 20 p2907 A72-39063
- Dynamic electromagnetic scattering pattern of flying object, constructing quasi-ergodicity condition to compute standard statistical descriptions for recognition 20 p2903 A72-39071
- Electromagnetic wave scattering by electron charge density fluctuations in plane waveguide with magnetoactive plasma, showing cross section spectrum function of plasma properties 20 p2903 A72-39072
- Scattering of electromagnetic pulse waves by conducting wedge in an uniaxially anisotropic medium. 20 p2903 A72-39269
- Linear and circular polarization of synchro-Compton radiation scattered by optically thin power law distribution of gyrating ultrarelativistic electrons 20 p2965 A72-39893
- Scattering from inhomogeneous cylindrically symmetric lenses with a line infinity in the index of refraction. 21 p3050 A72-40148
- Scattering by a cylindrical semiconductor rod of anisotropic permittivity perpendicular to the electric field in a rectangular waveguide. 21 p3023 A72-41836
- On the comparison of phase and multi-layer techniques for numerical solution of the scattering problems. 22 p3154 A72-42305
- Infrared observations of the moon and their interpretation. 22 p3225 A72-42527
- Application of multiple-scattering theory to the derivation of kinetic equations for waves in a weakly turbulent plasma 22 p3212 A72-42665
- Gamma ray scattering asymmetries of Fe 57 nucleus, discussing hyperfine structure and conjugate spin transition 22 p3209 A72-42924
- Radiation from a free electron interacting with a circularly polarized laser pulse. 23 p3296 A72-43875
- Calculation of stellar and diffuse radiation for a plane-parallel semiinfinite model of the Galaxy. 23 p3338 A72-44027
- Spectral characteristics of the scattering field of a uniformly traveling and rotating impedance cylinder 23 p3265 A72-44202
- Scattering of obliquely incident waves by inhomogeneous fibers. 24 p3379 A72-44710
- The effect of the subsurface on the depolarization of rough-surface backscatter. 24 p3380 A72-45635
- The transient electromagnetic response of a spherical shell of arbitrary thickness. 24 p3381 A72-45638
- Velocity-dependent multiple scattering by two thin cylinders. 24 p3381 A72-45641
- Radiation propagation in optically thin anisotropic noncrystalline media, obtaining explicit formulas for Stokes parameters of transmitted and scattered radiation 24 p3425 A72-45705
- Stimulated monochromatic electromagnetic wave scattering derived from analysis of nonlinear interactions in magnetoactive plasma 24 p3431 A72-45716
- ELECTROMAGNETIC SHIELDING**
NT RADIO FREQUENCY SHIELDING
 Active shielding against radiation in space using charged particle deflection by electric and magnetic fields [CFRN-71-16] 02 p0258 A72-12076
 Shielding and semitransparent sporadic F layer fine structure characteristics from sporadic observations data analysis 02 p0222 A72-12523
- Semiconductor devices potential interference and biological exposure hazards in microwave leakage field, considering shielding and filtering methods for reducing susceptibility 03 p0320 A72-14032
- TEM modes characteristics in shielded stripline with four internal strips, tabulating characteristic impedances at different line parameters 05 p0636 A72-16339
- Bandwidth properties and design of shielded asymmetrical striplines filled by dielectric 05 p0636 A72-16340
- Pulsed voltage oscillator for nanosecond range operation under pressure in nitrogen-filled tank as conducting shield 07 p0946 A72-19957
- Shielding procedures to control electromagnetic interference /EMT/ in design and operating electric equipment 10 p1452 A72-24813
- Electronic equipment shielding against electromagnetic radiation and circuit protection against unwanted electrical signals 15 p2209 A72-32570
- The shielding effect of metallic spherical envelopes with respect to very short EM waves and pulses 17 p2530 A72-35223
- RF shielding and electrical properties of boron and carbon fiber reinforced composites. 20 p2944 A72-38987
- Reduction of temperature difference in shielding pipes for light-beam transmission. 20 p2903 A72-39267
- ELECTROMAGNETIC SHOCK TUBES**
U SHOCK TUBES
ELECTROMAGNETIC SPECTRA
 NT BALMER SERIES
 NT D LINES
 NT ELECTRONIC SPECTRA
 NT FRAUNHOFER LINES
 NT H ALPHA LINE
 NT H BETA LINE
 NT H GAMMA LINE
 NT H LINES
 NT INFRARED SPECTRA
 NT K LINES
 NT LINE SPECTRA
 NT LYMAN SPECTRA
 NT MICROWAVE SPECTRA
 NT PASCHEN SERIES
 NT RADIO SPECTRA
 NT RAMAN SPECTRA
 NT RYDBERG SERIES
 NT SOLAR SPECTRA
 NT STELLAR SPECTRA
 NT TELLURIC LINES
 NT UVB SPECTRA
 NT ULTRAVIOLET SPECTRA
 NT VIBRATIONAL SPECTRA
 NT X RAY SPECTRA
 Radio galaxies spectra and red shifts observed with Lick 120 inch telescope 08 p1235 A72-21393
 Statistical analysis of photocounts of arbitrary spectral profile Gaussian light, discussing two incoherent beams superposition 15 p2277 A72-32231
 Microwave Doppler radar spectrum-based design parameters. 17 p2515 A72-34422
 RF time domain nonreal time reflectometer operating as nanosecond radar with pulse spectrum lines reflections measured and stored for echo computation 19 p2770 A72-37256
- ELECTROMAGNETIC WAVE FILTERS**
 NT INFRARED FILTERS
 NT MICROWAVE FILTERS
 NT OPTICAL FILTERS
 NT RADAR FILTERS
 NT ULTRAVIOLET FILTERS
 NT WAVEGUIDE FILTERS
 Fabry-Perot interferometer application as filter with transmission windows at regular intervals in wave numbers to detect Raman scattered radiation from atmospheric gases [AIAA PAPER 71-1078] 01 p0067 A72-10537
 X ray pulse spectra measurement from Z-pinch plasma focus devices, describing Ross filter system with silicon diode detector capable of nanosecond time resolution 04 p0524 A72-15537
 German monograph on narrow band mechanical filter design, using resonant circuit and coupled four terminal network analogy 09 p1284 A72-22326
 Detectors for deterministic signals in noise with rational spectral density, considering analog filter for continuous input sampling and discrete filter for point sampling 10 p1436 A72-24511
 Tunable wide field birefringent element /filter magnetograph/ to separate polarized magnetic signal from selected spectral line width 13 p2045 A72-29706
- ELECTROMAGNETIC WAVE TRANSMISSION**
 NT DOUBLE SIDEBAND TRANSMISSION

NT HALOS
 NT IONOSPHERIC F-SCATTER PROPAGATION
 NT IONOSPHERIC PROPAGATION
 NT LIGHT SCATTERING
 NT LIGHT TRANSMISSION
 NT MICROWAVE ATTENUATION
 NT MICROWAVE TRANSMISSION
 NT MULTIPATH TRANSMISSION
 NT RADAR TRANSMISSION
 NT RADIO ATTENUATION
 NT RADIO TRANSMISSION
 NT SCATTER PROPAGATION
 NT SHORT WAVE RADIO TRANSMISSION
 NT SINGLE SIDEBAND TRANSMISSION
 NT TELEVISION TRANSMISSION
 NT TRANSEQUATORIAL PROPAGATION

Higher order cyclotron harmonic resonance of electrons with electromagnetic wave propagation through collisionless magnetoplasma, deriving energy oscillation time period

01 p0105 A72-10023

Scattering cross section of electromagnetic wave by collisionless plasma perpendicular to applied magnetic field

01 p0105 A72-10025

Oblique electromagnetic wave propagation modes in anisotropic ionized stratified medium, investigating electric field and polarization components

01 p0106 A72-10133

Ordinary electromagnetic waves propagating in plasma, calculating thermal and particle collisional corrections with moment approach

01 p0107 A72-10140

Electromagnetic wave line-of-sight propagation based on geometrical optics for different refractivity profiles above sea, noting earth surface reflection role

01 p0026 A72-10404

Electromagnetic wave propagation anomalies over sea, comparing calculated and measured field strengths based on simultaneous refractivity vertical distribution measurement

01 p0026 A72-10405

VLF electromagnetic wave perturbations in transpolar propagation, noting time dependent behavior of polar cap absorption effects

01 p0056 A72-10441

Spacecraft-ground communications system, discussing electromagnetic wave propagation and frequency bands

01 p0027 A72-10445

Energy and momentum transfer between fields and particles in plasma crossed by transverse electromagnetic wave, investigating MHD stability

01 p0109 A72-10884

Nonlinear skin effects in gas discharge and semiconductor plasmas during electromagnetic wave propagation and dissipation, obtaining wave amplitude and carrier temperature dependence on reflection parameters

01 p0102 A72-10974

Electromagnetic waves diffusion by space-time fluctuations in plasma electron density [ONFERA, TP NO. 1043]

01 p0110 A72-11180

Soviet book on electromagnetic fields and waves covering propagation in anisotropic media, waveguides and cavity resonators, diffraction interactions, etc

01 p0031 A72-11200

Strong linearly polarized electromagnetic wave propagation in overdense plasmas, considering relativistic electron velocities and nonlinear penetration effect [AD-736322]

01 p0111 A72-11226

Nonreciprocal guiding devices for electromagnetic surface waves, noting large bandwidth and nonrectilinear polarization of alternating magnetic field

01 p0044 A72-11323

Electromagnetic wave propagation perpendicular to applied uniform magnetic field in relativistic plasma, deriving dispersion relation for stability criterion

02 p0264 A72-12024

Null electromagnetic field propagation in general relativity, applying to Stokes parameters definitions for monochromatic light

02 p0259 A72-12178

Normal electromagnetic wave propagation in randomly inhomogeneous medium in presence of superrefraction, deriving phase fluctuation spectra by perturbation method

02 p0180 A72-12587

Markov chain successive approximation method for electromagnetic wave propagation in medium with random large discontinuities, using scalar parabolic equation

02 p0181 A72-12588

Electromagnetic wave reflection and transmission by stratified multilayered parallelly moving plasma media, using propagation matrices

02 p0182 A72-12652

Circularly polarized electromagnetic wave propagation through afterglow helium slab plasma near electron cyclotron frequency

02 p0266 A72-12653

Diffraction of plane electromagnetic waves of arbitrary orientation and incidence on triangular grid of cylindrical conductors

02 p0183 A72-12753

Nonducted vlf wave propagation near plasmapause during whistlers based on diffusive equilibrium and collisionless models for magnetospheric electron density distribution

02 p0222 A72-12873

Right handed circularly polarized electromagnetic wave propagation in hot inhomogeneous plasma, deriving local dispersion equation by WKB methods

03 p0393 A72-12949

Penetration depth of hf electromagnetic waves in weakly ionized plasma, considering nonlinearity effect on ionization balance

03 p0394 A72-13085

Plane electromagnetic wave reflection and transmission at moving boundary between two dielectric media

03 p0321 A72-13091

Time harmonic electromagnetic wave diffraction by thin conducting circular disk at different media plane interface, calculating induced surface current density and scattering cross section

03 p0322 A72-13237

Plasma conductivity frequencies, including electromagnetic wave propagation in alternating field and scattered light intensities

03 p0396 A72-13653

Dielectric materials for antenna system radomes, discussing electromagnetic wave propagation and climatic factors effects

03 p0381 A72-14362

Relativistic equations of motion of charged particle interacting with plane electromagnetic wave propagating at arbitrary angle to uniform magnetic field for magnetosphere model

04 p0554 A72-14406

Parallel polarized electromagnetic waves scattering by radially inhomogeneous isotropic dielectric cylinders, computing scattered field coefficients by Fourier least squares fit technique

04 p0485 A72-14413

Current source generated electromagnetic and electroacoustic wave propagation through homogeneous, isotropic compressible electron-ion plasma, using two fluid continuum theory

04 p0554 A72-14510

Electromagnetic wave propagation across external magnetic field in contraststreaming thermally anisotropic plasmas, investigating plasma stability

04 p0556 A72-14942

Inhomogeneous nonstationary medium caused electromagnetic wavefront phase disturbance reduction in holography by averaging

04 p0522 A72-15381

Average ray direction and mean square deviation formula for electromagnetic wave propagation in random inhomogeneous medium suited for calculation by ray tracing program

04 p0488 A72-15382

WKB type solution for electromagnetic wave propagation in circularly cylindrical coordinate system with rho-dependent refractivity, using Bessel function

04 p0488 A72-15384

Electromagnetic wave transformation at moving boundary discontinuity with reactive parameters in dispersive medium by Lagrangian field equations

04 p0489 A72-15388

Electromagnetic wave propagation and stability in inhomogeneous collisionless plasma under static magnetic field

04 p0490 A72-15401

Plane electromagnetic wave diffraction by periodic lattice of long finite conductivity cylinders with arbitrary electric radius

04 p0491 A72-15414

Electromagnetic wave reflection from region with variable drift velocity and polarization of waves propagating in nonuniformly moving medium, applying to isotropic plasma

04 p0491 A72-15421

Electromagnetic wave propagation in plane and spherical waveguide channels with conducting lower wall, investigating transverse wave spectrum dependence on curvature and boundary conditions

04 p0492 A72-15441

Magnetoionic mode reciprocity for oblique incident electromagnetic wave propagation through birefringent stratified media

04 p0492 A72-15445

Plane harmonic electromagnetic wave diffraction by conducting parallel half planes in uniaxially anisotropic media

04 p0492 A72-15447

Weakly divergent beam propagation of electromagnetic waves in statistically inhomogeneous nonlinear medium with dielectric constant dependence, using small perturbation method

05 p0625 A72-15818

Maxwell equation spinor formulation for Schwarzschild gravitational field effects on spherical electromagnetic waves propagation

05 p0689 A72-16165

Electromagnetic wave propagation in rectangular waveguide with periodic ferrite structure, presenting computer graphics for stop bandwidth vs magnetic field strength

05 p0627 A72-16342

Book on electromagnetic waves in moving magnetoplasmas covering propagation in infinite and bounded plasmas subject to magnetic fields for nonrelativistic and relativistic velocities

05 p0695 A72-16396

Equivalent dielectric properties of infinite two dimensional periodic metal tape structures in presence of electromagnetic waves propagating in various directions

05 p0628 A72-16410

Electromagnetic wave transmission and reflection by semiinfinite moving anisotropic plasma with parallel static magnetic field, considering incident H wave

05 p0696 A72-16623

Geomagnetic pulsations correlation with h type ionospheric sporadic echoes, considering effects on electromagnetic disturbances transmission

05 p0659 A72-16725

Multifrequency plane, spherical and beam waves propagation, calculating temporal frequency spectra in turbulent atmosphere

06 p0771 A72-17339

Electromagnetic wave scattering from curved ground surfaces and transmission through turbulent medium, obtaining solution by spatial Fourier transform of three transfer functions product

06 p0771 A72-17340

Electromagnetic plane wave diffraction by infinite slit in screen with surface impedance, deriving field and transmission coefficient by asymptotic numerical solution

06 p0771 A72-17352

Nonlinear amplitude distribution of electromagnetic wave propagating in plasma near hybrid resonance frequencies

06 p0771 A72-17390

Electromagnetic wave propagation and thermal spread in uniform magnetoplasma at electron-cyclotron resonance frequencies, discussing kinetic and multifield theory

06 p0854 A72-17489

Waveform distortion of strong field amplitude modulated plane electromagnetic wave propagating in anisotropic plasma

06 p0862 A72-18338

Refraction of electromagnetic wave with electric field perpendicular to applied magnetic field in anisotropic plasma cylinder cross section

07 p1046 A72-20507

Correlation functions describing fluctuation of slow electromagnetic waves in plasma layer

08 p1212 A72-21065

Steady phase direction at time of electromagnetic wave transmission from one isotropic absorbing medium to another

08 p1132 A72-21221

Polarization corrections for normal electromagnetic waves passing from homogeneous to nonhomogeneous anisotropic medium

08 p1135 A72-21735

Electromagnetic wave propagation along open rectangular dielectric waveguide, deriving dispersion equations for surface waves propagation constants

08 p1136 A72-21739

Quantizing magnetic field effect on electromagnetic wave propagation in multivalley n-type Si and Ge and PbTe semiconductors

08 p1218 A72-21878

Soviet book on Riemann-Hilbert problem method in electromagnetic waves theory, covering wave diffraction, scattering and propagation, waveguides and open resonators

08 p1137 A72-22021

Transmission and passband properties of polyethylene echelette gratings and combined filters for long wave IR spectrum

08 p1210 A72-22038

Effective transmission coefficient increase for Langmuir and electromagnetic waves passing through density barrier via perturbation transport by resonant electrons

08 p1216 A72-22090

Cylindrically guided hybrid TE and TM electromagnetic wave reflection and transmission from Maxwell equations and boundary value problems solution

09 p1278 A72-22605

Random gravitational plane wave metric effect on electromagnetic wave mean value, noting light dispersion and attenuation

09 p1351 A72-22682

Layer-like atmosphere discontinuities effects on earth-space communications, noting electromagnetic waves alteration and reflection by grazing incidence

09 p1279 A72-22898

Dielectric tensor for electromagnetic waves in weakly inhomogeneous anisotropic media, taking into account permittivity and conductivity fluctuations

09 p1280 A72-23230

Time dependent parallel and cross polarized electromagnetic pulse propagation in magnetoionic medium for normal incidence

09 p1280 A72-23231

Electromagnetic and plasma wave reflection at interface between moving dielectric medium and compressible plasma

09 p1364 A72-23243

Modulated electromagnetic wave transmission in dispersive medium with cubic nonlinearity, discussing solitary wave and instabilities in two-wave interaction

09 p1352 A72-23475

Electromagnetic wave propagation obliquely incident on thermal inhomogeneous plasma at frequencies near second electron cyclotron harmonic

09 p1365 A72-23521

Energy transfer optimization in electromagnetic wave transmission through dispersive dielectric media

09 p1365 A72-23522

Nonlinear conductivity of plasma with FM electromagnetic wave propagation, proposing electronic current density calculation method

10 p1519 A72-24130

FM electromagnetic wave propagation in Lorentzian plasma, taking into account harmonic generations effect

10 p1520 A72-24209

Electromagnetic wave propagation perpendicular to magnetic field in two-component warm plasma, obtaining dispersion relations for transverse waves

10 p1520 A72-24350

Electromagnetic waves penetration through magnetized plasma into lower hybrid resonance region examined in geometrical optics approximation

10 p1521 A72-24352

Optimal control computation for nonlinear hyperbolic partial differential system by gradient and quasi-linearization techniques, noting MHD, fluid flow and electromagnetic wave propagation

10 p1456 A72-24453

Induced Compton scattering and nonlinear electromagnetic wave propagation in laser beam focused plasma

10 p1522 A72-24605

Intensity dependent propagation characteristics of circularly polarized high power laser radiation in dense electron plasma, calculating energy losses

10 p1522 A72-24607

Laboratory electromagnetic scale modelling for studying geophysical and propagation boundary value problems

10 p1512 A72-24741

Inhomogeneous rarefied plasma, investigating non-local, linear and nonlinear effects on electromagnetic wave reflection and transmission

11 p1694 A72-25717

Plane and uniform heterogeneous electromagnetic waves reflection, observing Goos-Hanchen and Imbert effects

11 p1597 A72-26482

Electromagnetic wave transformation and absorption in Ar plasma with nonmonotonic longitudinal density distribution

11 p1699 A72-26758

Radiation propagation in optically thin anisotropic noncrystalline media, obtaining explicit formulas for Stokes parameters of transmitted and scattered radiation

12 p1865 A72-27052

Gage for solids and liquids moisture content measurement based on phase shift of UHF electromagnetic wave propagating through tested material, noting specimen thickness optimization

12 p1807 A72-27466

Radiation patterns of circular loop antenna in isotropic compressible plasma, discussing far fields for electromagnetic and electron plasma waves

12 p1790 A72-27491

VLF and LF electromagnetic ground wave propagation between points on smooth curved lunar surface surrounded by free space or cold isotropic plasma

12 p1783 A72-27635

Equivalent atmospheric turbulence models concept for structure function behavior of electromagnetic wave propagation, noting dependence on model characteristics

12 p1841 A72-27946

Russian papers on light scattering covering electromagnetic propagation in turbid media, transport equation solution methods, unsteady scattering, spectral line radiation and nonlinear phenomena

13 p2001 A72-28501

Obliquely incident electromagnetic waves reflection and transmission by moving compressible plasma slab, applying field and wave-four vectors Lorentz transformations to wave equations

13 p2010 A72-28543

Electromagnetic wave propagation in cylindrical plasma column of electrons and ions with and without applied uniform magnetic field in absence of collisions

13 p2010 A72-28681

Electromagnetic cylindrical wave diffraction by linear emitter in parabolic cylinder with slots

13 p1917 A72-28709

Growth rates of unstable electromagnetic waves propagating perpendicularly to symmetric counterstreaming finite temperature plasmas

13 p2012 A72-29129

Electromagnetic wave diffraction on ideally conducting homogeneous bodies of revolution with arbitrary complex permittivity and permeability, using variables separation method

13 p1920 A72-29279

Penetration depth of HF electromagnetic waves in weakly ionized plasma, considering nonlinearity effect on ionization balance

13 p2015 A72-29435

Randomized electromagnetic field propagation through uniform medium, deriving autocorrelation and intensity fluctuation spectrum expressions

13 p2007 A72-30124

Strong LF electromagnetic wave propagation in semiconductors with inelastic scattering of current carriers by optical phonons, calculating harmonics reflection coefficients

14 p2142 A72-30361

Electromagnetic waves propagation in inhomogeneous moving cold electron plasma without external magnetic field and collisions, investigating dynamical effects

14 p2086 A72-30790

Electromagnetic wave propagation in nondispersing media with spatial-time fluctuations of dielectric permittivity, calculating scattered field by perturbation method

14 p2086 A72-30796

Two counter streaming plasmas with anisotropic temperatures, deriving instability condition for ordinary mode electromagnetic propagation perpendicular to external magnetic field

14 p2140 A72-30935

Design data of guided wave structures for electrooptical modulation, evaluating propagation wave numbers, attenuation rate, phase modulation rate and dispersion characteristic

15 p2246 A72-31667

Precision frequency standards practical utility under field operating conditions, discussing propagation effects due to atmospheric and frequency parameters

15 p2199 A72-32066

Thin wire parallel to interface between two homogeneous half spaces, deriving transmission current wave propagation constant from boundary value problem solution

15 p2200 A72-32108

Mathematical model for modified ordinary electromagnetic wave propagation in presence of two cold counterstreaming plasma electron beams, noting instability regions and growth rate

15 p2286 A72-32274

Electromagnetic waves penetration through conducting gasket used to protect sensitive devices in aircraft, investigating field strength variation with distance from gasket

15 p2202 A72-32571

Plane electromagnetic wave diffraction on periodic arbitrary profile array, presenting near and far field asymptotic characteristics

15 p2202 A72-32660

Earth crust waveguide three layer model for electromagnetic wave propagation, showing mode relation to absorption conditions

16 p2362 A72-33074

Longitudinal and transverse electromagnetic wave penetration into semifinite collisional plasma with fractionally accommodating boundary, obtaining reflection coefficient and surface impedance

16 p2435 A72-33449

Field distribution and absorption coefficient calculations for normal incidence of extraordinary electromagnetic wave on linear plasma layer in hybrid resonance region

16 p2363 A72-33480

Monochromatic electromagnetic wave reflection and transmission at oblique incidence on sharp plasma boundary of moving ionization source

16 p2363 A72-33481

Electromagnetic wave propagation in uniform and nonuniform plasmas with enough strength to cause relativistic electron velocities, considering linear polarization and nonlinear penetration effects

16 p2438 A72-33926

Electromagnetic waves attenuation and phase velocity correction in polycrystals with anisotropic crystal distribution

16 p2365 A72-34013

Gaussian electromagnetic radiation beam propagation in turbulent medium, calculating broadening dependence on outer scale by modified Karman spectrum characterization

17 p2580 A72-34291

An electromagnetic analysis of a cylindrical homogeneous lens

17 p2525 A72-34362

Invariant imbedding in time-varying homogeneous nondispersive media

17 p2513 A72-34366

Electromagnetic wave propagation and wave-vector diagram in space-time periodic media

17 p2514 A72-34381

Diffraction of electromagnetic waves by a two-dimensional aperture with arbitrary cross-sectional shape

17 p2514 A72-34385

Wave propagation in a stratified turbulent magnetized plasma. I

17 p2587 A72-34516

Effective transmission coefficient increase for Langmuir and electromagnetic waves passing through density barrier via perturbation transport by resonant electrons

17 p2588 A72-34661

Application of a limit theorem to solutions of a stochastic differential equation

17 p2575 A72-34866

Electromagnetic waves penetration through magnetized plasma into lower hybrid resonance region examined in geometrical optics approximation

17 p2589 A72-34953

VLF wave propagation and its interaction with the magnetoplasma

17 p2516 A72-35357

Circular waveguides lined with artificial anisotropic dielectrics

17 p2530 A72-35468

Instability of electromagnetic cyclotron harmonic waves in plasmas

17 p2592 A72-35775

Local characteristics of ray propagation in an inhomogeneous anisotropic ionosphere

18 p2686 A72-36229

Focusing of intense electromagnetic waves in ducts with saturating nonlinearity

18 p2659 A72-36293

Propagation of an electromagnetic shock discontinuity in a non-linear isotropic material

18 p2712 A72-36992

Series solution for electromagnetic wave propagation in radially and axially nonuniform media - Geometrical-optics approximation

18 p2712 A72-37024

Propagation of electromagnetic waves in a rarefied plasma situated in an alternating magnetic field

18 p2717 A72-37177

Dispersion curves of mixing mode between electrostatic and electromagnetic waves propagating perpendicularly to ambient magnetic field for hydrogen plasma with Maxwellian velocity profile

19 p2839 A72-37335

Drude theory of electromagnetic waves in an inclined magnetic field. I - One-band model of charge carriers

19 p2840 A72-37510

Parametric excitation of electromagnetic waves

19 p2834 A72-37718

Transmission and reflection of an electromagnetic wave incident normally on a plasma half-space

19 p2840 A72-37726

Waveguides of arbitrary cross section by solution of a nonlinear integral eigenvalue equation

19 p2773 A72-38292

Application of dual integral equations to the problem of electromagnetic wave diffraction by a thin conducting ribbon

19 p2766 A72-38526

Model random medium with two kinds of dielectric layers stacked in arbitrary proportions, calculating electromagnetic wave propagation characteristics by transmission line analogy

19 p2767 A72-38613

Numerical solution to the problem of propagation of ELF electromagnetic waves in the lower ionosphere

19 p2767 A72-38651

Paraxial electromagnetic wave packets diffraction on thin conducting periodic structures and dielectric plate, noting packet width and phase front curvature changes

19 p2767 A72-38653

Plane and cylindrical electromagnetic waves diffraction on infinitely long cylindrical bodies, calculating induced currents, diffraction patterns and near fields

19 p2767 A72-38654

Plane TE polarized electromagnetic wave diffraction on infinite conducting cylinder in nonhomogeneous medium, calculating far field diffraction patterns

19 p2768 A72-38656

Pulse propagation in a magnetoplasma. I - Longitudinal propagation

19 p2843 A72-38751

Plane electromagnetic wave diffraction on thin ribbons grating, discussing scattered field singularities for E polarized waves

19 p2769 A72-38850

Plane electromagnetic waves diffraction at arbitrary orientation and incidence on triangular grid of cylindrical conductors

20 p2902 A72-39059

Electromagnetic wave dispersion in ionized cosmic medium for spatially flat Brans-Dicke cosmology

20 p2969 A72-39265

On diffraction and focusing in anisotropic crystals

20 p2961 A72-39779

Electromagnetic-wave propagation along a horizontal wire above ground. 21 p3015 A72-40633

Dispersion equations solved for electron and ion cyclotron waves propagating perpendicularly to magnetic field in plasma 21 p3091 A72-40656

Radiation of EM waves with Walsh-function time variation - Preliminary results. 21 p3020 A72-40902

Partial differential equation solution for plane electromagnetic wave diffraction by infinite dielectric cylinder of arbitrary cross section 21 p3085 A72-41199

Propagation constants of electromagnetic waves along an infinitely long conducting wire in a general magnetoplasma. 21 p3092 A72-41266

Diffraction of electromagnetic plane waves by infinite slit perforated in a conducting screen with finite thickness. 21 p3022 A72-41267

Electromagnetic wave propagation in a moving sinusoidal stratified turbulent plasma medium. 21 p3093 A72-41323

Book - Terrestrial propagation of long electromagnetic waves. 21 p3023 A72-41532

Radiative transport analysis of electromagnetic propagation in isotropic plasma turbulence. 21 p3094 A72-41634

Propagation of electromagnetic disturbances and the stability of stationary states in media with a nonlinear Ohm's law 21 p3086 A72-41651

Diffraction of an electromagnetic wave by a noninfinitely conductive cylindrical object of arbitrary cross section 22 p3153 A72-41991

A problem of electromagnetic wave propagation in a moving plane stratified medium 22 p3155 A72-42653

Diffraction of plane electromagnetic wave at a corrugated dielectric surface 22 p3155 A72-42662

Variation of tropospheric slant-path attenuation in the UK at 11.75 and 17 GHz. 22 p3155 A72-42751

Propagation of electromagnetic waves in a weakly ionized warm magnetoplasma. 22 p3155 A72-42991

German monograph - Electromagnetic wave propagation inside a paraboloid of revolution subjected to different types of excitation. 22 p3156 A72-43070

Weakly divergent beam propagation of electromagnetic waves in statistically inhomogeneous nonlinear medium with dielectric constant dependence, using small perturbation method 23 p3263 A72-43426

Exact solution of the equations of molecular optics for refraction and reflection of an electromagnetic wave on a semi-infinite dielectric. 23 p3313 A72-43803

Circular waveguide in an anisotropic medium 23 p3264 A72-44156

Method for solving the problem of radiation in an anisotropic plasma 23 p3321 A72-44220

Ray optics applications to electromagnetics and other disciplines, discussing matrix representation for wavefront curvature and field computation simplification via transformations 23 p3314 A72-44331

Circularly polarized waves in magnetoplasmas containing negative ions. 23 p3323 A72-44533

Book - The effects of the turbulent atmosphere on wave propagation. 24 p3379 A72-44650

Electromagnetic-wave propagation in a random nonlinear dispersive medium. 24 p3379 A72-44784

Determination of refraction in the propagation of electromagnetic waves at the earth's surface 24 p3379 A72-44865

Measurement of best time-delay resolution obtainable along east-west and north-south ionospheric paths. 24 p3381 A72-45637

Electromagnetic propagation from flanged waveguide, studying diffraction, radiation patterns and reflection/modal coefficients 24 p3381 A72-45642

Radiation from an open-ended waveguide with extended dielectric loading. 24 p3381 A72-45643

Reflection and transmission of electromagnetic waves by a moving inhomogeneous medium. 24 p3381 A72-45644

Radiation propagation in optically thin anisotropic noncrystalline media, obtaining explicit formulas for Stokes parameters of transmitted and scattered radiation 24 p3425 A72-45705

ELECTROMAGNETIC WAVES U ELECTROMAGNETIC RADIATION

ELECTROMAGNETICS U ELECTROMAGNETISM

ELECTROMAGNETISM

NT MAGNETOSTATICS

Electromagnetic wave theory - Conference, Tiflis, U.S.S.R., September 1971 04 p0488 A72-15376

Spatio-temporal tensorial structure of fluid magnetodynamic equations in terms of electromagnetism and continuum mechanics 06 p0861 A72-18103

ELECTROMAGNETS

NT HIGH FIELD MAGNETS

NT SUPERCONDUCTING MAGNETS

Electromagnetic suspension - Conference, Southampton, England, July 1971 10 p1460 A72-24756

Automatic electromagnetic suspensions using tuned RLC saturable reactor control 10 p1460 A72-24761

Electromagnetic remote model positioning sensing system for wind tunnels with magnetic suspension, using differential transformer action 10 p1461 A72-24762

ELECTROMECHANICAL DEVICES

Electromechanical nose wheel steering system for general aviation aircraft ground maneuverability improvement, describing design 01 p0006 A72-10963

Synchros as electromechanical function generators and receivers for analog computers, examining errors in standard resolvers operation 03 p0328 A72-13841

Man machine systems in navigation, discussing problems of integrating man with high speed and high capacity electromechanical systems with allowance for human weaknesses and abilities 09 p1269 A72-22777

Electromechanical system for wire drive along stellar right ascension of meridian circle of Odessa Astronomical Observatory 09 p1311 A72-23061

Robots /electromechanical systems with local computers and sensor controlling motors and effectors/ space application categories and operating and decision making requirements 10 p1458 A72-23777

Transient calculation method for electric drive units described by first and second order differential equations, using special transformation for integral curve curvature determination 10 p1423 A72-24754

Dynamic processes of electric drive system with electromagnetic clutch modeled by analog computer element with logical input-output relation 10 p1423 A72-24755

Electromechanical coupling and acoustic impedance response in piezoelectric transducer with diffusion under fixed charge 11 p1636 A72-26590

Electromechanical redundant activating mechanism for F-4 aircraft dual tandem hydraulic power servo, noting application to fly by wire control 14 p2072 A72-30422

FRAM /failure rate appraisal machine/ concept and application for modular electronic and electromechanical assemblies environmental cycling tests, noting technical and economical effectiveness 14 p2093 A72-31169

Method and equipment for checking chronometers by one-second timing radio signals under field conditions 19 p2795 A72-37346

Electromechanical measurement systems using analog transducers with ohmic resistance, electric and magnetic fields and digital/frequency and stochastic outputs 19 p2800 A72-37755

Pulsed operation mode of acoustic system of damper-piezovibrator-layer load connected into electrical circuit of thyatron generator 19 p2805 A72-38764

Book - Electromechanical system components. 20 p2890 A72-39811

Electro-osmotic energy conversion in the glass/n-propanol system. 21 p2997 A72-41384

Electromechanical filter with attenuation poles consisting of multi-mode vibrators. 21 p3036 A72-41828

An inertially balanced servo. 23 p3311 A72-43866

ELECTROMECHANICS

Metal wear mechanism during electromechanical processing explained by configurational localization model 05 p0665 A72-16094

Electromechanical machining metal removal mechanism based on configurational localization model, relating wear processes to electron exchange and free energy margin decrease 07 p0996 A72-19989

Optimal parameters selection for natural vibrations maximum damping rate, applying method to two mass electromechanical system 11 p1686 A72-25533

Electromechanical, photomechanical and concentration effects of impurities in semiconductors 21 p3098 A72-41677

ELECTROMIGRATION

Grain boundary migration measurements in bicrystalline Al under intense electric field, using optical microscope 01 p0089 A72-11182

Anodized aluminum metallization for reducing electromigration induced failure modes in silicon wafers 03 p0365 A72-14286

Evaporation, superficial diffusion and oxidation role in grain junctions electromigration phenomenon in binary Al crystals traversed by high density continuous current 10 p1498 A72-24860

Physical limits of semiconductor devices miniaturization for electronic computers, considering thermal energy dissipation, electrical resistance and high current density induced electromigration effects 23 p3273 A72-44332

ELECTROMOTIVE FORCES

NT PONDEROMOTIVE FORCES

Positive electrode materials for high energy density batteries with Li negative electrode, calculating discharge emf for various salts 06 p0760 A72-17575

Frequency discriminator like two-channel device with greater sensitivity by crossed feedback, calculating variable frequency emf effect on operation 07 p0938 A72-18853

Anomalous Hall effect of polarized electrons spin-orbit interactions in semiconductors, involving emf appearance in electric field and polarized light 07 p1048 A72-19642

Thomson autooscillatory systems synchronization and small external sinusoidal emf effect with hard and soft bounding of amplitude deviations 08 p1142 A72-21769

Alternating Josephson effect and junctions applications to radiation generators and detectors, electromotive force regulators, oscillators, mixers and noise thermometers 09 p1370 A72-22799

Electrical conductivity and thermal emf as function of temperature in CdSb, discussing energy spectrum and crystallization 09 p1372 A72-23479

Temperature dependence of emf coefficient Hall constant and conductivity in solid and liquid phases of InSe semiconductor during melting 10 p1526 A72-24267

Digital precision measurement of thermocouple thermal emf at 200-1000 C, examining block diagram 11 p1634 A72-26457

Measurement circuit for temperature dependence of thermal emf and electrical conductivity in thermoelectric materials 12 p1807 A72-27452

Steel components contact fatigue kinetics measurement by emf increase of inductive sensor 12 p1887 A72-28245

Dispersion equation determining periodic structures natural modes propagation constants, using induced electromotive and magnetomotive forces method 15 p2195 A72-31655

Five channel recording instrument for energy dissipation evaluation in electric machines from thermal emf measurements 16 p2392 A72-33284

Temperature dependence of the thermal electromotive force and of the Nerst-Ettingshausen effect in nickel-cobalt alloys 22 p3187 A72-41855

Theoretical interpretation of emf generation between noncompressed parts of bimetallic junction traversed by shock wave, taking into account radiation pressure of phonon gas 22 p3207 A72-43050

Isobar-isothermal potentials, entropy and formation heat of chromium silicides from thermoelectromotive force measurements of high temperature galvanic elements 23 p3298 A72-43286

Changes in the physical properties of metals subjected to elastoplastic deformation 23 p3303 A72-44199

Anomalous Hall effect of polarized electrons spin-orbit interactions in semiconductors, involving emf appearance in electric field and polarized light 24 p3431 A72-44573

ELECTROMYOGRAMS

U ELECTROMYOGRAPHY

ELECTROMYOGRAPHS

U ELECTROMYOGRAPHY

ELECTROMYOGRAPHY

Optimum cylindrical handle size determination by muscle electromyography, considering gripping task, routine performance and fatigue test 01 p0017 A72-10119

Human and monkey muscle tonic vibration reflex response to vibratory stimulation dependent on frequency range, electromyograph discharge interval length, etc 02 p0163 A72-12250

Electromyographic determination of muscular compliance during arm movements, using on-line analog computer
04 p0478 A72-14708

Frog and rabbit sciatic nerve afferent impulse recordings during prolonged sinusoidal vibration of foot
04 p0474 A72-15235

Electromyogram study of antagonist muscles reactions to Achilles tendon percussion or whole body sudden motion via test stand jerking
07 p0915 A72-18864

Electromyogram and myogram responses in phasic stretch reflex under prestrain conditions as index of fusimotor activity level in normal humans
11 p1588 A72-26632

Dynamic bioelectric impedance level of tissue area between active electromyograph electrodes related to human skeletal muscle fatigue
13 p1905 A72-29332

Surface electrode position effect on electromyogram recording of electrical activity during repeated biceps and triceps brachii contractions
15 p2190 A72-32489

Surface electrode distance, area and pressure effects on electromyogram recording of large skeletal muscle electrical activity during defined muscular tensions
15 p2190 A72-32490

Description of an easy and simplified test for electromyographic diagnosis of latent spasmodia in flight personnel
19 p2760 A72-37878

The silent period in man during muscle lengthening produced by loading
20 p2892 A72-39590

Synchronization in the work of motor neurons during arbitrary motor activity of various types
21 p2999 A72-40595

Electromyographic investigation of diaphragm cross contraction following spinal cord section in cats, noting diaphragm motoneurons excitation by breathing center pulses
22 p3142 A72-42281

ELECTRON ACCELERATORS

NT BETATRONS

Linear electron acceleration mechanism in plasma, showing polarization fluctuations in diode under strong electric field
03 p0395 A72-13573

Nonlinear nonlaminar 3D electron motion calculation through output cavity of klystron amplifier by Green function
04 p0497 A72-14697

Steady state problem of energy spectrum of variable magnetic field accelerated electrons, considering synchrotron X ray emission of Crab pulsar and nebula
08 p1231 A72-21119

Linear electron acceleration mechanism in plasma, showing polarization fluctuations in diode under strong electric field
11 p1699 A72-26761

Beam-defocusing effect due to filament magnetic fields in electron guns of electron linear accelerators.
19 p2772 A72-37404

The heating of the solar plasma due to microwave phenomena correlated with type II meter bursts.
22 p3222 A72-42041

Electron and plasma particle acceleration by moving pulsed laser, noting appearance of fast particles, hard radiation and neutrons
23 p3295 A72-43312

ELECTRON ATTACHMENT

Electron attachment rate determination by combined photographic and radar observation of meteors
01 p0128 A72-10601

Meteors radio echo duration dependence on electron attachment, photodetachment and turbulent and ambipolar diffusion deionization processes
09 p1383 A72-22502

Meteor method for determining errors in rate measurement of electron attachment to neutral air particles based on nonexistent recombination, turbulent diffusion and photodetachment
09 p1383 A72-22503

Nighttime radar method of meteor radio echo observation to determine electron attachment rate to neutral air particles
09 p1383 A72-22504

Radio echo determination of meteor body distribution by mass with allowance for electron attachment and overestimated nighttime values
09 p1383 A72-22505

Photometric parameters of Leonid meteor ionized trail and turbulent diffusion in M zone, determining electron attachment rate
09 p1384 A72-22510

Electron attachment, photodetachment and turbulent diffusion deionization effects on duration distribution of Geminid meteor radio echoes
09 p1384 A72-22512

Electron attachment rate relation to altitude in radar observation of meteor trails
09 p1384 A72-22513

Oxygen molecule electron affinity role in ion chemistry of lower ionosphere, noting binding energy of ground state
17 p2585 A72-34260

Emitter conduction bands with negative electron affinity energy from surface barrier lowering of Cs p-type semiconductors
17 p2595 A72-34952

The capacitances of aniso-type heterojunctions with continuously varying energy band gap and electron affinity in the transition region.
18 p2719 A72-36944

Low-temperature measurements of the three-body electron-attachment coefficient in O₂.
19 p2837 A72-37545

Electron attachment and compound formation in flames. V - Negative ion formation in flames containing chromium and potassium.
22 p3244 A72-42717

Determination of the coefficient of electron attachment to particles of meteor material
23 p3339 A72-44169

ELECTRON AVALANCHE

Transient radiation effects on silicon diodes in avalanche breakdown, considering voltage regulating diode response and temperature compensating junction effects
03 p0334 A72-14090

Avalanche injected current relationship to emitter-base junction breakdown damage in planar n-p-n gated transistors
03 p0336 A72-14279

Stepped-leader theory in cloud-to-ground electrical discharges, estimating step-length for different electric fields by equivalence to electron avalanche transition
04 p0543 A72-14880

Avalanche breakdown voltage of Gaussian Si planar p-n junctions for design and impurity diffusion evaluation
04 p0561 A72-15126

IMPATT diode avalanche region microwave self oscillation mechanism explanation by cavity resonator and feedback theories
06 p0787 A72-18383

Interelectrode gas-filled gap electron avalanche formation effects in weak electric field, calculating ionization coefficient
06 p0863 A72-18411

Electric field induced ionizing potential waves in dense gas, describing avalanching electron gas breakdown into filaments by fluid dynamic and Maxwell field equations
06 p0864 A72-18534

Electrical breakdown in reverse biased semiconductor p-n junctions involving Zener effect and avalanche mechanisms
07 p1048 A72-19821

Laser induced surface damage probability as function of power density, suggesting electron avalanche breakdown as cause
09 p1324 A72-23083

Avalanche carrier multiplication influence on semiconductor device p-n junction quality, discussing current distribution and I-V characteristics during avalanche breakdown
10 p1446 A72-23849

Radioisotope camera based on electron avalanche in liquid Xe, noting spatial and energy resolution advantages over existing gamma ray cameras
15 p2234 A72-31537

Low white noise voltage theory of avalanche diode extended to small multiplication M values and unequal hole and electron avalanche ionization coefficients
15 p2206 A72-31642

Electrical breakdown of hexane investigated by high voltage nanosecond pulses, noting electron avalanche and streamer processes in time lag
15 p2278 A72-32244

Avalanche generation process interpretation for nontransit frequency oscillations association with current runaway in bulk InP microwave diode oscillators
16 p2369 A72-33755

Influence of carrier diffusion on the intrinsic response time of semiconductor avalanches.
18 p2717 A72-36083

Charge injection into the gate dielectric of MOS transistors during junction avalanche.
18 p2668 A72-37104

A fast, high repetition rate avalanche transistors pulser for capacitive loads.
20 p2907 A72-39435

ELECTRON BEAM WELDING

Monograph on electron beam welding covering space charge effect, equipment, metallurgical and mechanical aspects, production engineering, economics and applications
01 p0073 A72-10167

Refractory alloy weldability and brazing, discussing manual and automatic tungsten arc and electron beam processes and fillers
01 p0075 A72-10752

Electron beam welding with filler metal, describing spot and butt welding applications
06 p0819 A72-17498

Beryllium joining by resistance welding, electron beam welding, dip brazing and braze welding
06 p0820 A72-17701

Electron beam welding of W-base alloy to Ta-base alloy, avoiding Re induced embrittlement by pure Mo transition piece
06 p0821 A72-17710

Electron beam welding induced secondary X rays observation with pinhole X ray movie camera to determine beam-metal interactions during penetration
07 p0997 A72-20003

Vacuum welding by electron beam bombardment, discussing electron gun arrangements with plane-radial, plane-linear and linear electron beams
08 p1176 A72-21049

Automatic electron beam welding machine for small components, discussing design, performance and inspection methods
09 p1321 A72-23637

Nucleation mechanism for weld solidification in electron beam and tungsten-inert gas welding processes
09 p1332 A72-23641

Electron beam welding focus effect on fusion zone penetration in thick austenitic stainless steel
09 p1321 A72-23643

Electron beam welding, discussing problem areas, equipment trends and industrial needs
10 p1485 A72-23966

Electron beam machine for thin metal plates welding and cutting under space conditions, noting design features and performance
11 p1639 A72-25809

Soft and out-of-vacuum electron beam welding system for high productivity, describing characteristics
16 p2397 A72-33224

Electron beam welding, machining and drilling, discussing technical and economic factors
16 p2399 A72-33540

Aluminum alloys electron beam weldability, considering precleaning, welding speed, voltage, pre- and post-weld heat treatments effects
17 p2561 A72-35799

German monograph - Investigation of electron beam welding with particular consideration of the mean power density and the radial power density distribution in the beam cross section
19 p2807 A72-37658

Influence of boron on the structure and certain properties of electron-beam melted molybdenum
20 p2939 A72-39313

A radiographic technique using an electron beam welder.
20 p2929 A72-39340

Automatic hermetic-sealing systems for semiconductor devices prepared by electron-beam welding
22 p3158 A72-42124

Electron beam diameter measurement technique and welding technology review, describing experimental apparatus
22 p3183 A72-42448

New space processing experiments for the Skylab missions.
24 p3407 A72-45125

ELECTRON BEAMS

Two dimensional scanning electron beam pumped laser, describing production of coherent emission
01 p0079 A72-10522

Relativistic electron beams in plasma, considering electrostatic instability conditions and critical currents
01 p0109 A72-10975

Thermonuclear microbomb ignition with intense relativistic electron beams for rocket propulsion, discussing achievable exhaust velocities and system optimization
01 p0117 A72-11222

Nonaxisymmetric tubular spiral electron beam interaction with fast waves in cylindrical waveguide within longitudinal magnetic field
02 p0170 A72-11563

Electron beam interaction with electromagnetic waves in longitudinal interaction devices during focusing by homogeneous magnetic and periodic electrostatic fields
02 p0189 A72-11564

Complete suppression of one signal in dual frequency mode of TWT operation, showing electron beam current and accelerating potential dependence on signal amplitude
02 p0189 A72-11565

Two stage M-type amplifier with two electron beams and stepwise variation of cathode, calculating gain in linear approximation
02 p0189 A72-11569

M-type amplifier operation with two electron beams and staggered dual section cathode
02 p0190 A72-11570

Periodic magnetic field effects at gun cathode on electron beam focusing stability under nonoptimal conditions
02 p0190 A72-11572

Absorbed doses at various depths in water target exposed to charged pions, muons and electron beams, using Monte Carlo program [CERN-71-16]
02 p0162 A72-12063

Ionic focusing of electron beam in transverse gas flow, using air, argon and helium

02 p0261 A72-12764

Relativistic beam equilibria above 10,000 amps, considering axial, diffuse, sharp boundary and azimuthal current models

02 p0267 A72-12840

Frequency spectrum analysis of electromagnetic self radiation from plasma interacting with high energy electron beam

03 p0393 A72-13082

Papers on microwave advances covering precision coaxial connectors, O-type linear beam devices, electron dynamics and energy conversion and junction circulators

03 p0424 A72-13229

Transverse fields effects on electron dynamics and energy conversion in O-type linear beam devices of traveling wave amplifiers

03 p0330 A72-13231

Book on microwave electronics covering electron beam microwave devices and solid state microwave oscillators and amplifiers

03 p0331 A72-13233

Intense pulsed electron beam production by current flow through narrow gap filled with plasma

03 p0396 A72-13656

Rolling workability of pure W single crystals grown by electron beam zone melting technique, discussing crack occurrence

03 p0374 A72-13718

Bulk data storage and retrieval with scanning laser and electron beams, discussing spot formation focal sensitivity, noise, beam deflection, speed and media environment

03 p0368 A72-13775

Low energy electron beam irradiation of aluminum-silicon nitride-silicon structures for elimination of bias polarization effects on I-V characteristics

03 p0402 A72-13865

Thin electrostatically self focusing electron streams in mercury vapor, analyzing energy distributions of ions and electrons ejected radially from beam

04 p0554 A72-14407

Wavelength tuning effect on lasing threshold in electron beam pumped GaAs lasers as function of current density and voltage

04 p0528 A72-14545

Electron beam interaction with bunched solid state plasma, deriving slow wave dispersion relations

04 p0561 A72-15080

One dimensional collisionless plasma instability driven by cold electron beam, determining limits from beam trapping

04 p0559 A72-15353

CW millimeter wave power generation with spiraling electron beams, investigating energy spread effects on performance limitation

05 p0636 A72-16363

Ion charge composition in plasma-electron beam system in strong longitudinal magnetic field, noting multiply charged ions production under high temperature conditions

05 p0701 A72-17235

Longitudinal instability of electron beams interacting with passive resonator, considering Landau damping influence by linear differential equations of motion solution

05 p0701 A72-17243

Self induced electron beam collapse prevention by external magnetic field, determining required field strength by scaling law based on simple orbit model

06 p0854 A72-17418

Ion acoustic wave excitation in plasma by modulated energetic electron beam, compared with grid excitation

06 p0856 A72-17519

Plasma wave growth from large diameter electron beam interaction with quiet collisionless unmagnetized discharge plasma, measuring linear dispersion properties

06 p0858 A72-17539

Electron beam interaction with collisionless plasma, obtaining beam spatial distribution function from velocity diffusion coefficient measurement

06 p0858 A72-17540

Conversion effectiveness of oscillations induced by electron beam in bounded anisotropic plasma into electromagnetic emission

06 p0860 A72-17700

Electron paths and spread velocities in helical beams of adiabatic M-type electron gun used in masers at cyclotron resonance

06 p0826 A72-18403

Contraststreaming electron beams instability in finite length one dimensional system with stationary neutralizing ion background, analyzing electrostatic waves space/time development by numerical simulation

06 p0865 A72-18540

Plasma density inhomogeneity effects on beam-plasma instability and Landau damping from digital simulation using charge sheet model

06 p0865 A72-18541

Carbon dioxide laser pumping at atmospheric pressure by electron beam controlled electrical discharge, discussing measured electrical and laser properties

07 p0999 A72-18875

Electron beam induced dissociative excitation of vacuum UV emission from atomic nitrogen multiplets, using normal incidence monochromator and pulse counting techniques

07 p1036 A72-18925

Colliding plasmas transverse instabilities, investigating ion dynamic and electron beam induced return currents effects

07 p1041 A72-19508

Stability of electron beam injected into magnetospheric plasma at small and high altitudes

07 p0979 A72-20377

Electrostatic oscillations of multivelocity electron streams in hot inhomogeneous plasma

07 p1046 A72-20502

Spark source generated electron beam interaction with plasma in uniform magnetic field, estimating HF longitudinal oscillation power

07 p1046 A72-20504

Ultrarelativistic cosmic plasma analysis of high density electron beams transport across strong magnetic fields with application to pulsar NP 0532 spectrum

07 p1064 A72-20634

High energy electron beam interaction with dense plasma, investigating unstable waves growth by numerical methods

08 p1213 A72-21259

Design and operation of scanning laser based on exciting electron beam directional variation, discussing laser characteristics for various operating modes

08 p1182 A72-21268

Temperature distribution and zone melting in carbon thin films heated by electron beam, using Sn crystal indicators

08 p1253 A72-21446

Electron beam interaction with bounded homogeneous plasma layer natural oscillations, using collisionless kinetic equation

08 p1215 A72-21720

Asymptotic expressions for electromagnetic field and currents induced in unbounded dense plasma by relativistic electron beam passage

08 p1215 A72-21721

Fine structure of energy distribution function for electron beam interacting with plasma

08 p1215 A72-21722

Steady nonlinear waves propagation along ring electron beam axis analogous to ionospheric E layer

08 p1215 A72-21723

Microwave signals detection with virtual cathode in klystron repeller by electrons screening at velocity modulated electron beam

08 p1136 A72-21766

Betatron electron beam evaluation for flaw detection in laminated materials by radiographic and radiometric methods

08 p1177 A72-21774

Resonator dielectric waveguide structure in electron beam pumped semiconductor laser, noting reduction of diffraction losses and of laser action threshold

08 p1184 A72-22089

German monograph on electron beam focusing in partial pressure analyzer with two compartment ion source, eliminating residual gas-filament interaction

09 p1306 A72-22318

High power electron beam pumped nitrogen super-radiant laser with 60 kW output

09 p1323 A72-22624

Dielectric permeability tensor operator for surface wave-electron beam interaction in relativistic nonuniform plasma stream with cylindrical geometry

09 p1359 A72-22769

Optimum pressure and field conditions for intense relativistic electron beam transport in longitudinal magnetic field

09 p1360 A72-22870

Steady state charged cylindrical electron-ion beam with high current in kinetics model framework, discussing densities proportionality and relativistic factor

09 p1360 A72-22951

Star stellarator model for hot electron plasma production by steady electron beam injection in closed magnetic traps

09 p1363 A72-23219

Electron beam and plasma nonlinear interactions, noting scattering zone, amplitude oscillation maximum, longitudinal velocity and relaxation patterns

10 p1517 A72-23760

Electron, ion and laser beam technology - IEEE Conference, Boulder, Colorado, May 1971

10 p1517 A72-23926

Burn in technique in nonvolatile metal oxide semiconductor /MOS/ memory using ionizing radiation of reprogrammable electron beam

10 p1443 A72-23927

Imagewise electrostatic charge buildup in electron beam recording, determining trajectories by Runge-Kutta method

10 p1479 A72-23929

Vesicular films in electron and laser beam recording suitable for computer output microfilm duplication and graphic arts

10 p1488 A72-23930

Wide bandwidth electron beam analog recorder and reproducer, using signal processing electronics and silver halide film

10 p1479 A72-23931

High dose rate electron beam irradiation using telescoping drift tube for flash X ray machine

10 p1509 A72-23935

Spectroscopic techniques for high temperature materials research program, studying light emission from plasmas generated by intense electron beam

10 p1518 A72-23937

Electron microbeam testing for large microcircuit arrays, using analog voltage signal injection into isolated contact and digital voltmeter readout

10 p1446 A72-23938

Frequency characteristics of traveling wave deflection system for wideband CRT deflector, improving sensitivity by low beam accelerating voltage

10 p1446 A72-23939

Gas laser excitation by relativistic electron beam pulse axial propagation through optical cavity, studying mechanism through timing and pressure dependence measurements

10 p1489 A72-23946

Computer controlled electron beam machine for microcircuit fabrication, using digital technique capable of working on complex patterns

10 p1459 A72-23956

Relativistic electron beam and ring phenomena calculation using plasma simulation program CYLRAD

10 p1518 A72-23958

Low transverse energy, high nugamma electron beam propagation characteristics, reviewing transport, compression and combination beam-handling concepts

10 p1518 A72-23959

Intense relativistic electron beam-plasma interactions in finite cavities, calculating neutral gas charge production and gas breakdown times

10 p1518 A72-23960

Ion acceleration by relativistic electron-beam-formed plasma, explaining ion energy dependence on neutral gas pressure by potential well model

10 p1518 A72-23961

Quiescent steady state plasma production by beam-plasma discharges in uniform magnetic fields, showing plasma density fluctuation relation to Penning effect

10 p1519 A72-24022

Gas rotation temperature measurement by means of high energy electron beam probe with allowance for secondary electrons

10 p1480 A72-24222

Relativistic electron beam injection into dense plasma, analyzing perturbed electric and magnetic fields and charge and current densities

10 p1521 A72-24353

Semiconductor lasers with high energy electron pencil beam excitation for high capacity computer storage application

10 p1492 A72-24513

Temperature dependence of internal quantum efficiency of spontaneous emission as function of beam voltage in electron beam excited p-type GaAs

10 p1526 A72-24559

Collective self fields generated from intense electron beams for high energy positive particle acceleration and Astron hot plasma confinement for fusion control

10 p1523 A72-24788

Heavy ion acceleration from strong electron beam in metallic plasma obtained with ruby laser and positive voltage pulses

10 p1524 A72-25034

Magnetic mirrors for highly stripped heavy ions production in hot electron plasmas by low voltage high current electron beam

10 p1524 A72-25035

Hydrogen, deuterium, helium, nitrogen and argon ion production and acceleration by intense pulsed relativistic electron beam

10 p1517 A72-25037

Electron beam fluorescence method for normal shock wave velocity distribution in Ar-He mixtures

11 p1615 A72-25556

Spatial distribution of electron beam excited plasma wave spectrum, determining wavenumber, amplitude and frequency by incoherent microwave scattering

11 p1693 A72-25564

Longitudinal electromagnetic wave excitation in restricted plasma by relativistic electron beam injection, determining increments, frequency distribution and width of spectra

12 p1849 A72-27064

High current relativistic electron beam properties, noting application in thermonuclear synthesis and accelerators

12 p1788 A72-27250

Electron beam velocity distribution function fine structure for plasma-beam discharge in hydrogen within longitudinal magnetic field

12 p1850 A72-27261

- Maximum transmission delay in microwave TWT delay lines as function of electron beam size, current, shape and velocity distribution 12 p1782 A72-27436
- Voltage variable TWT delay line design, discussing electron beam velocity dispersion causes 12 p1782 A72-27437
- Stimulated laser emission in vacuum UV by liquid Xe excitation with electron beam, determining threshold current density, radiation divergence and line half width 12 p1820 A72-27582
- Ruby laser coherent light scattering by cylindrical electron beam under longitudinal magnetic field 12 p1820 A72-27586
- Many element GaAs and CdS semiconductor laser achieving high power output by electron beam pumping 12 p1822 A72-27616
- Multielement electron beam pumped semiconductor laser using emitting GaAs disks with vapor deposited dielectric mirror coatings 12 p1824 A72-27876
- Electro-optical processing of phased array signal reception, using electron beam addressing system with potassium dideuterium phosphate target crystal 12 p1785 A72-27954
- Adhesives polymerization and rapid ambient temperature curing, using Co 60 gamma rays and electron beams 12 p1833 A72-28079
- Signal propagation along homogeneous drifting electron beam focused by strong magnetic field, obtaining phase velocity and space charge density 13 p1914 A72-28373
- Surface charge density in thermoplastic recording, showing potential-relief modulation dependence on frequency, scanning rate and electron beam properties 13 p1954 A72-28402
- Kinetic approximation for bounded electron beam stability in plasma situated in magnetic field, deriving instability increments and dispersion relations 13 p2010 A72-28578
- O-type synchronous electron beam waves interaction with electro-dynamically structured traveling wave, noting linear gain dependence on beam current and magnetic field 13 p1931 A72-29291
- Frequency spectrum analysis of electromagnetic self radiation from plasma interacting with high energy electron beam 13 p2015 A72-29432
- Vacuum gap discharge conditions as function of electron beam parameters and metal vapor pressure 13 p2017 A72-29611
- Three grid I.EED-Auger display system for electron emission from solids at low primary beam energies 13 p1932 A72-29751
- Electron beam excited P-15 phosphor 3900 A spectral component fast decay time measurement by delayed coincidence technique 13 p2000 A72-29762
- High purity aluminum-aluminum oxide reversible oxidation, discussing mechanism based on electron charging due to beam 13 p1980 A72-29827
- Electron beam-helicons interaction in semiconductor plasma, determining instabilities onset conditions for unbounded system 14 p2141 A72-30172
- Pulse distortion and amplitude smear calculation for electron beam measurements of distance from space vehicles to deployable structure measurements on space vehicles 14 p2103 A72-30198
- Steady motion of dense electron beam in rarefied phonon plasma along magnetic field, analyzing polarization effects 14 p2136 A72-30305
- I.F. and HF oscillations in plasma-electron beam system, investigating instability control 14 p2137 A72-30310
- CdS crystals lasing in air at atmospheric pressure and room temperature by low voltage electron beam pumping through Ni film 15 p2245 A72-31319
- Dispersion relationship for electrostatic instability associated with electron beam trapped in magnetic mirror of magnetosphere, taking into account nonuniformity of magnetic field 15 p2283 A72-31434
- Photon loss coefficients and gain measurement in CdS electron beam pumped lasers, noting absorption mechanism and efficiency 15 p2246 A72-31668
- Kinematic intensity recovery from I.EED data of specular and nonspecular beams from Ni(111) surface, noting multiple scattering interference elimination 15 p2276 A72-31855
- Beta-conductive method improvement for semiconductor electric field intensity measurement by pulsed electron beam 15 p2238 A72-32240
- Monochromatic plasma wave excitation by cold electron beam, obtaining instability maximum amplitude and oscillation period 15 p2285 A72-32270
- Mathematical model for modified ordinary electromagnetic wave propagation in presence of two cold counterstreaming plasma electron beams, noting instability regions and growth rate 15 p2286 A72-32274
- Mach 26 shock wave in nitrogen investigated by electron beam fluorescence technique, determining population distribution among rotational states 15 p2281 A72-32404
- Electron beam-plasma system oscillation spectrum control through modulation by external HF signal, discussing theory and experimental verification 15 p2289 A72-32671
- Electron beam modulation by SHF noise signal in plasma-beam system 15 p2289 A72-32698
- Electron beam amplifier based on fast cyclotron wave interaction with slow synchronous wave in axisymmetrical electrostatic field, discussing power efficiency increase 15 p2210 A72-32737
- HF radiation in type 3 burst sources, discussing amplification by proton and electron streams 15 p2316 A72-32753
- Quasi-linear approximation of absorption of oscillations excited by electron beam in nonuniform plasma, noting electron distribution change with heating under magnetic field 16 p2432 A72-32807
- Quantum mechanics framework for electron movement perpendicular to intense magnetic field, predicting energy broadening with time for initially monoenergetic electron beam 16 p2422 A72-32881
- Plasma wave excitation by monoenergetic relativistic electron beam, investigating beam-plasma wave synchronism during instability development 16 p2434 A72-32912
- Electron interferometer based on second order interference effects from laser modulated electron beam, applying quantum mechanical analysis 16 p2402 A72-33398
- Infinite cross section electron beam interaction with infinite turbulent plasma slab with finite thickness 16 p2438 A72-33837
- Ultrarelativistic electrons beam steady injection into plasma filled half space, using weak turbulence theory for assumed beam excited oscillations interaction 16 p2440 A72-34156
- Electron-optical methods of investigating inhomogeneities in rarefied gases. 17 p2552 A72-34515
- Resonator dielectric waveguide structure in electron beam pumped semiconductor laser, noting reduction of diffraction losses and of laser action threshold 17 p2562 A72-34660
- Electron trajectories and spread velocities in helical beams of adiabatic M-type electron gun used in masers at cyclotron resonance 17 p2562 A72-34854
- Emission of coherent microwave radiation from a relativistic electron beam propagating in a spatially modulated field. 17 p2589 A72-34874
- Relativistic electron beam injection into dense plasma, analyzing perturbed electric and magnetic fields and charge and current densities 17 p2589 A72-34954
- HF electrostatic wave instability induced in plasma by electron beam, noting resonant frequency Doppler shift 17 p2591 A72-35369
- Electron transmission spectroscopy - Core-excited resonances in diatomic molecules. 17 p2586 A72-35771
- Excitation of a long-pulse CO2 laser with a short-pulse longitudinal electron beam. 17 p2565 A72-35815
- Steady state charged cylindrical electron-ion beam with high current in kinetic model framework, discussing densities proportionality and relativistic factor 17 p2593 A72-35880
- Model improvements for thermionic diode plasmas. 18 p2715 A72-36218
- Pulsed power - A new technology for controlled thermonuclear fusion. 18 p2715 A72-36332
- Observation of satellite modes in a beam-plasma instability. 18 p2715 A72-36600
- Beam-defocusing effect due to filament magnetic fields in electron guns of electron linear accelerators. 19 p2772 A72-37404
- Photon count circuit conjugation with photomultiplier for spectrometric measurement of lines emitted by atomic barium jet excited by slow electron beam 19 p2799 A72-37671
- Plasma heating by fast electrons, and nonthermal X rays during solar flares 19 p2851 A72-38063
- Quantum yield variations of Nd ion activated glass as function of electron beam energy and intensity, noting nuclear particles effect on laser radiation 19 p2823 A72-38205
- Evaluation of rotational temperature at high vibrational temperature in electron beam fluorescence technique. 19 p2803 A72-38434
- Nonlinear interaction of a small cold beam and a plasma. II. 19 p2841 A72-38444
- Electromagnetic self induced vibrations in homogeneous unbounded electron beam moving with time dependent velocity, noting longitudinal and transverse wave generation 19 p2842 A72-38527
- Theoretical study and demonstration of the coupling of modes of a resonant cavity by an electron beam 19 p2774 A72-38543
- A design method for the electron beams of TWT's. 19 p2775 A72-38610
- Triode electron gun design for narrow electron beam under highly convergent lens action, using field emission source 19 p2775 A72-38611
- Possibility for buildup of laser radiation scattered by an electron beam 19 p2812 A72-38662
- Discontinuous generation of ultrahigh frequency oscillations during a plasma-beam interaction 19 p2768 A72-38664
- Influence of different types of oscillations on ion heating in plasma-beam discharges. 19 p2843 A72-38820
- Electron beam focusing by ions in transverse gas flows, considering air, argon and helium residuals 20 p2952 A72-39070
- Recent international development in non-traditional machining processes - EDM, ECM, LBM, EBM. 20 p2928 A72-39203
- Generation of controllable light pulses in an electron-beam-pumped laser. 20 p2933 A72-39514
- Application of the Monte-Carlo method to the calculations of the configuration of a heat source whose material is subjected to the action of electron beams. 21 p3127 A72-40135
- Suppression of instabilities in a beam-plasma system by a modulation of the electron beam. 21 p3089 A72-40199
- Electron beam evaporator with multiple source suitable for use in ultrahigh vacuum, noting control of evaporation rate 21 p3051 A72-40205
- The beam-plasma discharge laser 21 p3062 A72-40406
- Contribution to nonlinear theory of electron-beam kinetic instability in a plasma 21 p3090 A72-40408
- Potential measurement and stabilization of an isolated target using electron beams. 21 p3087 A72-40700
- Excitation of electromagnetic waves in a plasma by a relativistic electron beam 21 p3092 A72-40787
- Three-dimensional pattern of instability development during the interaction between a modulated electron beam and a plasma 21 p3092 A72-40800
- The possibility of producing plasma regions at thermonuclear fusion conditions in a supersonic flow by means of high power electron beam. 21 p3092 A72-41224
- High energy electrons monokinetic beam propagation in Cu and Al crystals, investigating critical voltage effect on contrast 21 p3069 A72-41342
- Experimental determination of ion density trapped by electron beam. 21 p3034 A72-41463
- Electron beam visualization in hypersonic air flows. [AIAA PAPER 72-1017] 21 p3042 A72-41596
- External high-frequency modulation of an electron beam and heating of plasma ions in the case of beam-plasma instability in the magnetic trap 21 p3095 A72-41678
- Suppression of oscillations in a plasma-beam system by modulation of low frequency signals 21 p3095 A72-41681
- Differential equations for energy flow between electron beam and electromagnetic field, avoiding electron trajectory explicit calculation in nonlinear treatment of cyclotron resonance interaction 22 p3159 A72-42304
- Effect of increasing beam voltage on the internal quantum efficiency of spontaneous emission in electron-beam-excited p-type GaAs. 22 p3185 A72-42308
- Measurement of the stacking-fault energy of gold using the weak-beam technique of electron microscopy. 22 p3177 A72-42320

Electron beam diameter measurement technique and welding technology review, describing experimental apparatus

22 p3183 A72-42448

Superradiant laser excitation at 3371 Å in molecular nitrogen second positive band system by high energy electron beam, noting 6 nsec pulse outputs to 24 MW

22 p3186 A72-42623

Development of nonlinear oscillations in the interaction between a modulated electron beam and a plasma

22 p3211 A72-42651

Initial electron velocity and emitter surface roughness effects on oscillatory velocities dispersion in helical electron beams used in cyclotron resonance masers

22 p3208 A72-42664

Injection of an electron beam into a plasma bounded by a conducting casing

22 p3213 A72-43105

Noncoherent excitation of plasma vibrations by an almost monoenergetic relativistic beam

22 p3213 A72-43114

Electromagnetic emission during the development of a hydrodynamic beam instability in a bounded plasma

22 p3213 A72-43115

Some characteristics of an electron-beam induced discharge in a vacuum

22 p3208 A72-43123

Steady motion of dense electron beam in rarefied phonon plasma along magnetic field, analyzing polarization effects

23 p3317 A72-43207

LF and HF oscillations in plasma-electron beam system, investigating instability control

23 p3317 A72-43212

Interaction between a plasma and an electron-beam modulated by low-frequency oscillations

23 p3318 A72-43309

Stimulated emission with pumping by a pulsed electron beam formed in a direct discharge

23 p3295 A72-43319

Excitation of potential oscillations in a plasma by a flow of phased oscillators

23 p3319 A72-43401

The velocity distribution of electrons in beams formed by high-perveance three-electrode guns

23 p3319 A72-43402

Compression of high current relativistic electron beams using converging magnetic fields

23 p3315 A72-43525

Plasma-beam interaction in limited geometry: Temperature effects

23 p3321 A72-43700

Diffusion of a filament of gas injected into a supersonic free jet

23 p3280 A72-43947

Cylindrical waveguide with density modulated electron beam pumped by external electromagnetic field, considering Doppler effect conditions in beam radiation spectrum

23 p3265 A72-44157

Electron impact ionization of ions trapped in a hollow electron beam

23 p3316 A72-44343

Utilization of a composite resonator for improving the monochromaticity of a semiconductor laser with electron-beam excitation

23 p3297 A72-44468

Time variations in the far-field diffraction patterns of spatial modes from electron-beam-pumped semiconductor lasers

24 p3409 A72-44712

Buildup of oscillations in crossed-field backward-wave oscillators

24 p3385 A72-44973

Kinetic approximation for confined electron beam stability in plasma situated in magnetic field, deriving instability increments and dispersion relations

24 p3428 A72-45078

Electron-beam flow visualization - Applications in the definition of configuration aerothermal characteristics

[AIAA PAPER 72-1016]

24 p3404 A72-45405

Generation of plasma oscillation by beam-plasma interaction

24 p3430 A72-45574

Cadmium sulfide single crystals suitable for electron-beam-pumped lasers

24 p3432 A72-45607

Longitudinal electromagnetic wave excitation in restricted plasma by relativistic electron beam injection, determining increments frequency distribution and width of spectra

24 p3431 A72-45717

ELECTRON BOMBARDMENT

Non-Boltzmann molecular nitrogen vibrational distribution in aurora during electron bombardment as function of altitude

02 p0221 A72-12456

Apparatus for emission spectroscopic studies on high density molecular jets excited by slow electron bombardment

03 p0392 A72-14054

Maximum propellant utilization in electron bombardment ion thruster for space applications

04 p0564 A72-14432

Mercury electron bombardment ion thrusters research program, discussing mission requirements, size, propulsion type and beam current range

04 p0565 A72-14434

Rocket-borne mass spectrometer with helium cooled electron bombardment ion source to reduce gas-wall interactions effects

04 p0524 A72-15538

Ni-Cr thick films triode sputtering technique with temperature control by low-energy electron bombardment heating, presenting phase diagram

05 p0675 A72-16393

Optical radiation from plasma discharge of electron bombardment mercury ion thruster, discussing electron temperature and primary electron fraction

[AIAA PAPER 72-205]

05 p0706 A72-16851

Hollow cathode neutralizer for electron bombardment ion thruster, discussing performance from SERT II flight

[AIAA PAPER 72-207]

05 p0706 A72-16853

Electron bombardment ion engines scaling laws, considering electron energy, current density, propellant properties and magnetic flux density

07 p1054 A72-19602

Critical magnetic flux indications of microanomalous plasma diffusion in electron bombardment ion engines

07 p1054 A72-19614

Ar plasma in ion engine discharge chamber with primary and Maxwell electron bombardment, discussing ion production probabilities in perturbed and unperturbed cases

08 p1223 A72-21209

Electron bombardment SERT II ion thruster operation using Xe, Kr, Ar, Ne, He, nitrogen and carbon dioxide

10 p1528 A72-23964

Electron bombardment type simplified ion source with magnetic field induction by filament heating current, discussing design and characteristics

10 p1518 A72-23965

Electron bombardment disordering of ordered Ni-Mn alloy along different crystallographic directions

10 p1514 A72-24075

Ion sources for high temperature operation based on electron bombardment and beam-plasma interactions

10 p1516 A72-25031

Hollow cathode discharge effects on throttled electron bombardment ion thruster performance, considering discharge region diameter and length and baffle aperture area

[AIAA PAPER 72-421]

11 p1706 A72-26169

Electron bombardment ion thruster ESKA 18-P thrust measurements by critically loaded columns suspension instrument and simultaneous beam diagnostics by electrostatic probes

[AIAA PAPER 72-433]

11 p1707 A72-26176

Dished accelerator grids design, fabrication and operation in electron bombardment ion thruster, studying ion extraction capability and discharge chamber performance

[AIAA PAPER 72-486]

11 p1710 A72-26212

Electron bombardment ion thruster performance characteristics with variable magnetic baffle and hollow cathode

[AIAA PAPER 72-489]

11 p1710 A72-26214

Chemical ionizing mass spectrometry with electron bombardment of reactant gas, discussing plasma chromatography

11 p1590 A72-26389

Work hardening and recrystallization grain structure of sintered and electron bombardment melted Ta after annealing

11 p1644 A72-26839

Electron bombardment deposited polymer thin films electrical properties as function of formation current, noting increase in crosslinking and dangling bonds

12 p1788 A72-27277

Lifetime limitations of ion extraction systems for electron bombardment ion thrusters due to sputter erosion of electrode by ion beam

[AIAA PAPER 72-477]

12 p1860 A72-27421

Intensified electron bombarded Si camera tube performance in low light level TV systems, predicting sensor resolution vs irradiance characteristics

12 p1810 A72-27934

Electron bombardment effects on transport properties and carrier lifetime degradation of Li doped Si solar cells

12 p1856 A72-28024

Carrier concentration Hall mobility and photoconductivity in n- and p-type CdTe after neutron and electron bombardment

12 p1859 A72-28072

Model for mercury vapor electron bombardment ion thruster hollow cathodes operation and effects on thrust subsystem performance predictability

[AIAA PAPER 72-420]

13 p2026 A72-28936

Variable magnetic baffle as control device for Kaufman electron bombardment ion thrusters with hollow cathode

[AIAA PAPER 72-488]

13 p2027 A72-28949

Characteristics of nonredundant auxiliary and prime propulsion power processors for electron bombardment ion thruster in communication satellites, discussing modular transistorized and SCR systems

[AIAA PAPER 72-518]

Refractory metals vacuum melting for ingot production and purification in arc and electron bombardment furnaces

14 p2107 A72-30531

Thermonuclear microexplosion ignition by bombarding dense target with intense relativistic electron beam, noting energy requirement reduction by self magnetic beam field

16 p2433 A72-32814

Metal fracture by electron pulse generated stress waves, noting intergranular fracture mechanism

16 p2472 A72-33845

Multielement electron beam pumped semiconductor laser using emitting GaAs disks with vapor deposited dielectric mirror coatings

16 p2404 A72-33985

Parametric optimization of a cylindrical converter with a molybdenum emitter and niobium collector

17 p2497 A72-34610

Single crystal disk substrate design with electron bombardment heating for LEED and Auger electron spectroscopy studies in ultrahigh vacuum

17 p2553 A72-34642

Certain characteristics of an electron-pumped pulsed laser of small dimensions

17 p2562 A72-34839

Electrostatic surface ionization and electron bombardment ion thrusters current densities for propulsive and working fluid utilization efficiency

17 p2597 A72-35275

On the contribution of transition radiation from dust grains to the diffuse X-ray background

17 p2600 A72-35314

Ion-thruster propellant utilization

17 p2597 A72-35490

Luminescence behavior of single-crystal semiconductor compounds under electron bombardment

17 p2596 A72-35721

The effects of electron bombardment on the noise properties of field effect transistors

18 p2666 A72-36322

Some results of studies of cathode luminescence in cerium-activated glass

19 p2845 A72-38190

Nickel single crystal target ionization by high voltage electron beam bombardment, using flight time mass spectroscopic analysis

19 p2835 A72-38666

Thick target processes during hard X ray emission, noting electron bombardment during solar flare impulsive phase and white light flare optical continuum production

21 p3100 A72-41292

ELECTRON BUNCHING

Line splitting in emission near plasma frequency in drift pair solar radio bursts, considering causes by model involving electrons bunching through solar corona

02 p0276 A72-11646

Hypotheses for excess background radiation at 200-500 km, suggesting single high energy electrons or electron clusters

07 p1064 A72-20638

Nonlinear plasma oscillations effect on electron bunching in microwave devices, noting space charge waves of finite amplitude

14 p2089 A72-31106

One dimensional Maxwellian electron plasma simulation by electron bunches, describing Landau damping of wave initially excited in medium and nonlinear effects of trapping

15 p2284 A72-31678

Solar stationary type 4 radio bursts caused by gyromagnetic radiation of bunched electrons

16 p2449 A72-33920

Electron bunching and output gap interaction in broad-band klystrons

19 p2772 A72-37566

Radiation of electron bunches passing through a dielectric plate in a waveguide

21 p3036 A72-41842

ELECTRON CAPTURE

Average energy electron capture coefficient dependence on air density, temperature and altitude under gamma radiation

01 p0059 A72-10599

Plasma electron density depletion by electron attaching gas introduction, deriving electrostatic probe technique

02 p0264 A72-12261

Cyclohexylamine determination in aqueous solutions of sodium cyclamate by electron capture gas chromatography

07 p0935 A72-19488

Silicon-silicon dioxide system, investigating effect of heating in dry and moist He on capture-center and recombination parameters by thermal and pyrolytic techniques

08 p1216 A72-21068

Plasmoids interaction in diverter magnetic field, investigating integral electron capture intensity
09 p1362 A72-23205

Fast iodine ions charge exchange in dense carbon dioxide supersonic jet, determining electron capture cross sections by least squares method
10 p1516 A72-25036

Photoemission from tetracene organic semiconductors due to electron capture defect ionization by excitons
11 p1700 A72-25785

Thermonuclear detonation and reimplosion of dense stellar cores, studying beta-processes effect on post-detonation evolution
13 p2044 A72-29625

Atomic hydrogen 3s state destruction by impact on nitrogen, argon and hydrogen molecules, considering collisional ionization and electron capture mechanisms
14 p2134 A72-30883

Thermally stimulated current measurement application to Ag doped Si semiconductor for energy level and electron capture cross section determination
16 p2441 A72-32859

Be 7 destruction via nuclear decay instigated by atomic electron capture in interstellar medium, considering Ar 37, Ca 41, Ti 44, V 49, Cr 51, Mn 53 and Fe 54
16 p2447 A72-33736

Production of intense ion beams by high-frequency electric fields
19 p2839 A72-37331

Evidence for radiative electron capture by fast, highly stripped heavy ions
23 p3316 A72-44073

Determination of electron and hole capture rates in nickel-doped germanium using photomagnetolectric and photoconductive methods
24 p3432 A72-45388

ELECTRON CLOUDS

HF radio waves scattering by spherical electron cloud with Gaussian density distribution
09 p1282 A72-23515

Variable radio structure model using relativistic electron cloud outbursts in stationary magnetic field tubes for faster than light velocities
10 p1536 A72-24139

The equilibrium and the pulsation frequency spectrum of an electron cloud of spherical and cylindrical symmetry
19 p2867 A72-38571

ELECTRON COLLISIONS

U ELECTRON SCATTERING

ELECTRON COUNTERS

Oxygen ionization and ion mobility measurements in air by open proportional counting chamber with electron counter and exoelectron emitter
09 p1305 A72-22203

Multichannel area stellar photometer using photosensitive cell array for individual photoelectron counting, applying to autoguidance
11 p1631 A72-25690

Intensity and energy spectrum calculation of albedo electrons recorded in cosmic particle showers by gas discharge counters
14 p2105 A72-30629

ELECTRON DECAY RATE

Electron lifetime in earth radiation belt due to resonant scattering with hiss vlf radiation
05 p0711 A72-17045

Effective electron loss rates in lower D region from ionization changes during solar X ray flares, noting water cluster ions destruction
09 p1376 A72-22369

Low-temperature measurements of the three-body electron-attachment coefficient in O2
19 p2837 A72-37545

ELECTRON DENSITY [CONCENTRATION]

NT ELECTRON DENSITY PROFILES

NT IONOSPHERIC ELECTRON DENSITY

NT MAGNETOSPHERIC ELECTRON DENSITY

Line radiation from theta pinch with oscillatory ion and electron density applied to solar spectral studies
01 p0106 A72-10098

Collisionless plasma shock wave measurements in magnetic field, determining plasma temperature and free electron densities
01 p0108 A72-10236

Electromagnetic waves diffusion by space-time fluctuations in plasma electron density
[ONERA, TP NO. 1043] 01 p0110 A72-11180

Electron density microwave measurements in helium-neon laser plasma, discussing population inversion during glow discharge
01 p0081 A72-11216

Excited state and electron densities in noble and atmospheric gas plasmas created by alpha particle induced ion irradiation, discussing plasma kinetic processes and superimposed electric field effects
01 p0112 A72-11335

Fabry-Perot interferometer for studying spatial distribution of plasma electron concentration, discussing resolution using solid state gas laser light source
02 p0223 A72-11403

Fabry-Perot interferometer employing gas laser for plasma bursts electron concentrations measurements at 3.39 micron wavelength
02 p0223 A72-11404

FM homodyne phase meter with klystron oscillator for measuring plasma electron concentration, presenting block diagrams of meter, detector and oscillator
02 p0223 A72-11414

Free electron density, electron temperature and gas ionization during shock wave propagation in Ar-filled shock tube from microwave radiation measurements
02 p0263 A72-12020

Pulsar distances and energy from assumed interstellar electron density, considering nonplausibility of associations with supernovae
02 p0278 A72-12047

Interferometric photoelectric scans of interstellar Ca I 4226 line for stars with interstellar Ca II K-lines, discussing deduced electron densities
02 p0280 A72-12197

Low temperature plasma electron density measurements using ruby laser light scattering method
02 p0264 A72-12210

Plasma electron density depletion by electron attaching gas introduction, deriving electrostatic probe technique
02 p0264 A72-12261

Linear electron density distribution along faint meteor trail, discussing radio echo time-amplitude characteristics and ionization curve
02 p0282 A72-12335

Electron and population densities in inhomogeneous nonequilibrium plasmas with photoabsorption, using radiative transport equation
02 p0266 A72-12441

Electromagnetic wave scattering by electron charge density fluctuations in plane waveguide with magnetoactive plasma, showing cross section spectrum function of plasma properties
02 p0183 A72-12766

Emission nebulae in Magellanic Clouds observed at 408 MHz, calculating electron density and total mass
02 p0285 A72-12796

Solar coronal monochromatic optical emission, inferring electron density and ionization or temperature distributions and variations with time
03 p0422 A72-13208

Excited Hg atom and electron concentration measurement behind shock front in nonstationary plasma by continuous displacement recording of interference bands
03 p0357 A72-13374

Theta pinch plasma electron density with high time resolution by side-on interferometry at 10.6 microns
03 p0396 A72-13670

Electron-ion recombination and ambipolar diffusion disruption of electron density in cryogenic helium plasma, using cavity resonator measurements
03 p0399 A72-14067

Pulsed current changes in positive column of He and Ne discharges, observing gradient and electron concentration transient behavior
03 p0399 A72-14348

Collisional radiative recombination applicability to time dependent electron density decay in helium afterglow before reaching quasi-steady state
04 p0555 A72-14579

Plasma diagnostic technique using three-mirror He-Ne laser interferometer for electron concentration measurement
04 p0555 A72-14654

Solar K corona intensity and electron density determination from photographs without eclipse
04 p0574 A72-14924

Ground state energy of interacting electrons for entire density range from two-point Padé approximation
04 p0549 A72-15229

German monograph on spectroscopic investigation of Cs plasma electron density and temperature and excited atom density in various operational states of thermionic converter
04 p0560 A72-15699

Electron density and diffusion measurements in ionized air in front of strong shock wave with resonant microwave probe and electromagnetic induction technique
05 p0648 A72-16211

Continuously burning optical discharge in Ar and Xe at atmospheric pressures, evaluating laser beam energy absorption, electron density and plasma temperature
05 p0669 A72-16679

Electron density and temperature fluctuations coupled through Ohm law for ionizable medium, applying to MHD generators and MPD arc thrusters
[AIAA PAPER 72-101] 05 p0706 A72-16813

Pulsed flat electrode erosion plasma accelerator, determining electric and magnetic fields distribution, current density and electron concentration
05 p0697 A72-16987

Shock wave deceleration and boundary layer mass loss effects on electron density and ionization levels of air in shock tube
05 p0700 A72-17225

Electron and muon density fluctuations, trajectory distribution and azimuthal symmetry in cosmic ray air showers
06 p0870 A72-17279

Electrons spatial and temporal response in collisionless plasma to externally applied voltage pulse
06 p0856 A72-17522

Interplanetary plasma electron and proton density fluctuation measurements by space probes and from radio sources scintillation spectra, noting agreement with power-law irregularity spectrum
06 p0881 A72-17901

Electron content measurement for low latitude station obtained at sunspot maximum by Syncom 3, observing seasonal variation and winter anomaly effect
06 p0874 A72-18089

Plasma ambipolar diffusion coefficient and electron density determination from thermal density fluctuations cross spectrum based on Langmuir probe measurements
06 p0864 A72-18536

Radio emission of galactic clusters at 1.4 and 2.7 GHz, computing mean electron density and hydrogen gas mass
07 p1075 A72-19577

Interstellar cloud properties based on electron concentration integral along line of sight from pulsar radiation measurements
07 p1080 A72-20053

Transient plasma diagnostics using carbon dioxide laser interferometry and absorption for electron density and temperature determination
07 p1008 A72-20557

Plasma diagnostics using carbon dioxide laser absorption and interferometry, comparing electron densities with shock data
07 p1008 A72-20565

Multimode cavity for simultaneous oxygen/argon plasma excitation and electron density measurements, noting gas pressure effect
08 p1213 A72-21323

Fluctuating signal propagation in plane laminar medium acting as spatial frequency filter, determining electron density distribution curvature radius in plasma layers
08 p1135 A72-21732

Pulsars CP 0328 and NP 0531 twinkling explained by interstellar electron density fluctuations due to Alfvén wave passage and coupling of cosmic rays to interstellar gas
09 p1377 A72-22753

Microscopic perturbations of metals electron density complex dynamic matrix, deriving electroconductivity and kinetic coefficients
09 p1329 A72-23039

Interferometric measurements of time dependent electron density in Xe pinched plasma laser, showing laser lines due to transitions in triply ionized species
09 p1366 A72-23700

Supersonic Ar, He and molecular nitrogen jets, determining electron temperature and concentration and atomic state population in shock waves region by spectroscopic measurement
10 p1517 A72-23837

Electron densities and drift velocities dependence on macroscopic discharge parameters in positive column of He-Cd laser
10 p1493 A72-25048

Impurities effect on level density of electron gas within strong magnetic field, discussing included self energy
11 p1693 A72-25526

Low temperature plasma electron density measurements using ruby laser light scattering method
11 p1693 A72-25706

Pulsed plasma thruster arc electron density measurement by Mach-Zehnder interferometer and He-Ne laser, determining exhaust ion temperature and total charge
[AIAA PAPER 72-463] 11 p1709 A72-26198

SID coincident with solar photon burst, showing vertical variations of electron concentration
11 p1713 A72-26269

Noontime N/h profiles forecasts and annual variation in F region, relating solar activity levels to vertical distribution of electron concentration
11 p1594 A72-26277

Explorer 35 observations of solar wind electron density and temperature, noting anisotropy direction correlation with magnetic field vector alignment
11 p1713 A72-26392

Pulsed flat electrode erosion plasma accelerator, determining electric and magnetic fields distribution, current density and electron concentration
12 p1850 A72-27131

CO-He laser vibrational population distribution and small signal gain measurements, comparing with prediction based on V-V anharmonic exchange relaxation
12 p1827 A72-28222

Electron density effect on microwave scattering from turbulent plasma, observing change from volume to surface scattering at critical density value
13 p2012 A72-29130

Linear electron density distribution along faint meteor trail, discussing radio echo time-amplitude characteristics and ionization curve

13 p2039 A72-29219

Mars atmospheric temperature, pressure and electron density from radio occultation measurement with Mariner 6 and 7, noting frozen carbon dioxide in middle atmosphere

13 p2039 A72-29335

Ionization stabilization in MHD generators by sensing electron density perturbation with linear feedback into nonequilibrium plasma

13 p2014 A72-29369

Two point correlation description of MHD plasma properties subject to electrothermal instability, calculating electron number density and temperature fluctuations

13 p2015 A72-29373

Electron density and temperature measurement from scattering of laser radiation in plasma within axisymmetric toroidal magnetic mirror machine

13 p2017 A72-29609

Temperature dependent electron density of state and dc resistivity of disordered binary alloys, using single band thermal disorder model

13 p2022 A72-29626

Predicting electron density for type 3 solar burst excitation by LF satellite radio observations

13 p2032 A72-29723

Discharge tube geometry effects on sensitivity of plasma electron density measurement by cylindrical cavity resonators

13 p2018 A72-29822

Enhanced damping of electrostatic wave primary mode due to combination scattering from plasma electron density oscillations

13 p2018 A72-29854

Impurity concentration relationship to electrons and holes density and potential fluctuations in completely compensated crystalline semiconductors with randomly distributed donors and acceptors

13 p2024 A72-29993

Equiatomic ordered, bcc TiFe and TiNi electron density in outer energy band from X ray K emission spectra

13 p1981 A72-30006

Gunn diode active region thickness, free electron mobility/concentration, structure and contacts, including treatment of GaAs

13 p1934 A72-30036

Microwave interferometry as plasma diagnostic technique to measure electron densities in partially ionized dense gases

14 p2103 A72-30177

Hypersonic missile trail conductivity measurement on ballistic test stand, calculating electron concentration decrease

14 p2069 A72-30312

Electric arc plasma, predicting elements addition and electron density alteration effects on radial temperature distribution

14 p2139 A72-30778

Comparative electron density measurements in positive low pressure He discharge column with Langmuir probes and microwave interferometer and cavity

14 p2105 A72-30808

Electronic density measurement in ionized Cs vapor by observation of fundamental series lines mixture, comparing to Stark widening theory based profiles

14 p2134 A72-30852

Free electrons in condensed matter under high pressure, calculating number with Thomas-Fermi statistical model

15 p2305 A72-31338

Cs plasma electron density radial distributions from resonance absorption in discharge tube

15 p2286 A72-32302

Rocket released artificial Cs plasma clouds in upper atmosphere, measuring electron density by HF radar observation

15 p2231 A72-32330

Glow mode electron plasma source for space chamber, measuring electron density and temperature for comparison with back diffusion sources

15 p2286 A72-32339

Precursor photoionization production of ionization onset point equivalent electron number densities, calculating phenomenon occurrence Mach number

15 p2281 A72-32407

Electron density fluctuation measurements in hypervelocity projectile hypersonic turbulent wakes, showing power spectra

15 p2242 A72-32584

Solar Fe XIII IR lines intensity ratio at 10747 and 10798 Å, deriving electron density as function of dilution factor with allowance for proton impact effect

15 p2318 A72-32784

Inner solar corona electron density distribution as function of heliographic latitude, longitude and radial distance from K-coronameter polarization-brightness data

15 p2318 A72-32786

Weak H beta emission at 26 deg galactic latitude, noting derived electron density agreement with pulsar data

16 p2455 A72-33460

Low pressure He and Ne discharge generated positive plasma column potential, determining electron concentration from electron energy distribution functions

16 p2437 A72-33746

Low density and pressure air plasma electron density simultaneous measurements by Langmuir and RF capacitance probes

16 p2438 A72-33836

Electron density measurements in bow shock stagnation and conical afterbody regions during blunt body atmospheric reentry, using flush mounted electrostatic probes

[AIAA PAPER 72-694]

16 p2345 A72-34047

Viscous shock layer analysis application to blunt nosed reentry vehicle plasma layer nonequilibrium flow species distribution, considering electron density

[AIAA PAPER 72-689]

16 p2346 A72-34053

Three dimensional electron density fluctuations scattering spectra in Mach 16 spherical projectile turbulent wakes from fine wire electron collection probe measurements

[AIAA PAPER 72-673]

16 p2432 A72-34066

Plasma electron density measurements using flat plate and semifocal millimeter wave Fabry-Perot interferometers

[AIAA PAPER 72-672]

16 p2440 A72-34067

The influence of the electron temperature and other parameters on the electron density of a cesium plasma in a thermionic converter.

17 p2497 A72-34611

The possibility of single-valued determination of electron concentration from results of phase measurements

17 p2585 A72-35031

A model for drift pair and hook burst emission from the solar corona.

17 p2617 A72-35712

Galactic nebulae electron temperature and density from forbidden line emissions interpreted in terms of transition probabilities and collision strengths

18 p2723 A72-36090

Work function theory for Cs-W and Cs-O-W.

18 p2656 A72-36133

Prediction of electron concentration reductions in re-entry flow fields due to electrophilic liquid and water injection.

[AIAA PAPER 72-670]

18 p2730 A72-36537

Transition from sheath-convection to saturation-current behaviour of a Langmuir probe in a flowing plasma.

18 p2715 A72-36688

Electron density measurements in early stage of the high current pulsed discharge.

18 p2716 A72-36957

Density of the solar corona from occultations of NP 0532.

19 p2855 A72-37242

An appraisal of the single Langmuir probe technique in the study of afterglow plasmas.

19 p2840 A72-37456

Forbidden line intensities in cesium plasmas.

19 p2840 A72-37776

Nonlinear theory of density fluctuations in turbulent plasmas.

19 p2841 A72-38443

Measurement of electron concentration in the plasma of a pulsed erosion-type accelerator

19 p2843 A72-38535

Kinetic theory of density fluctuations in a magnetized collision-dominated plasma in an electric field.

19 p2792 A72-38745

Electromagnetic wave scattering by electron charge density fluctuations in plane waveguide with magnetoactive plasma, showing cross section spectrum function of plasma properties

20 p2903 A72-39072

Calculation of electronic Green functions using nonorthogonal basis functions - Application to crystals.

20 p2961 A72-39810

Electron density and temperature measurement from laser radiation scattering in plasma within axisymmetric toroidal magnetic mirror machine

21 p3091 A72-40663

The measurement of the local electron density by means of direct reading microwave interferometer.

21 p3056 A72-41220

Coronagraphic observations of an enhanced coronal region. II - Temperature and density structure through the enhanced region.

21 p3108 A72-41288

H 157 alpha recombination line from H I region before NGC 2024 radio source, considering average electron concentration and line origin

21 p3102 A72-41776

The derivation of temperature gradient and electron density maps from EUV spectroheliograms.

22 p3222 A72-42036

Electron density and temperature in microwave plasmas at higher pressures.

22 p3211 A72-42479

Equiatomic ordered bcc TiFe and TiNi electron density in outer energy band from X ray K emission spectra

22 p3190 A72-42733

Electronic density and temperature deduced from the observation of the cone of resonance of an antenna in a magnetoplasma

22 p3212 A72-43049

Measurement of the electronic density in a hollow cathode discharge working with argon

22 p3181 A72-43098

A study of the electronic and gasdynamic parameters of a hypersonic wake behind models moving in argon

22 p3168 A72-43111

Hypersonic missile trail conductivity measurement on ballistic test stand, calculating electron concentration decrease

23 p3247 A72-43214

Diffusive spreading of weak plasma discontinuities in the presence of two kinds of positive ion

23 p3283 A72-43363

Free electrons and holes concentration calculated for quadratic dispersion law in doped semiconductors without degeneration, noting additive atoms effect

23 p3324 A72-43849

Energy spectrum and composition of primary cosmic radiation at energies from 50 to 5000 TeV

23 p3330 A72-44422

A Lecher wire microwave interferometer for measurements of electron density and electron temperature in a flowing transient plasma.

23 p3292 A72-44543

Excitation mechanisms in the argon-ion spectrum at near laser conditions and temperatures and densities in a hollow cathode argon-arc discharge.

24 p3428 A72-44807

Electrical characteristics of a CO laser discharge plasma

24 p3411 A72-45500

ELECTRON DENSITY PROFILES

Lindauer electron density profile for maximum F layer over sunspot cycle using frequency dependent radio ground echo in satellite ionograms

01 p0054 A72-10421

Electron density profile determination in D region based on frequency dependence of radio waves absorption, discussing lower ionosphere anomalous ionization

01 p0059 A72-10595

Phase difference measurement between magnetoionic components returned from lower ionosphere due to pulsed radio signal, obtaining electron density profiles

01 p0063 A72-10914

Electron density measurements for traveling ionospheric disturbances by Thomson scatter technique using Faraday rotation

01 p0031 A72-10922

Solar wind electron density variations, discussing radio source interplanetary scintillation and angular distribution measurements at various distances from sun

02 p0277 A72-11902

Night sky upper ionospheric electron concentration perturbations during magnetic storm, noting latitudinal distribution

02 p0217 A72-11940

Loran C system time tick transmission delay during solar eclipse of 7 March 1970, discussing atmospheric electron density effects

03 p0322 A72-13533

Sudden cosmic noise absorption from D region N-h profile during solar X ray flares on 13 April 1966

04 p0566 A72-14512

Plasma electron density profiles from Tonks-Dattner resonance frequencies for plane parallel and cylindrical columns

04 p0554 A72-14530

Interstellar electron density and magnetic field fluctuations effects on Faraday rotation and signal dispersion measure in radio band

04 p0487 A72-14901

Thumba night time equatorial E region electron density profiles from rocket-borne Langmuir probe experiments

04 p0517 A72-14957

Electron concentration and collisions number fluctuations effect on D region profiles based on radio waves partial reflection data

05 p0656 A72-16244

Numerical method for cylindrical microwave cavities calibration for plasma diagnostics, noting computer programs applicability for arbitrary electron density radial distributions

05 p0662 A72-16418

Electron density profiles as function of position in enhanced coronal region from Ni XV and Fe XIII emission lines observation

05 p0719 A72-16517

Electron density and temperature temporal and radial profiles in megawatt MPD-arc thruster exhaust, using Thomson scattering technique
[AIAA PAPER 72-209] 05 p0707 A72-16887

Temperature inhomogeneity effect on plasma column microwave resonant behavior in presence of axial magnetic field, ascribing spectral shifts to electron density and temperature profiles changes
06 p0854 A72-17417

Electron density distribution inhomogeneities from vhf Faraday rotation measurements, noting diurnal, seasonal, sunspot cycle and geomagnetic activity effects
06 p0806 A72-17642

Ionospheric effects of solar flares, considering flare spectrum below 10 A, flare X-rays relationship to sudden ionospheric disturbances and electron density profiles
06 p0874 A72-18087

Ionospheric electron density profiles and time variation of electron production rate for X-ray flare of 30 January 1968, observing decrease in effective recombination coefficient
06 p0874 A72-18088

Quantum efficiency at 6300 and 6364 A of recombination mechanism in nighttime F layer, obtaining ionospheric electron density profiles
07 p0974 A72-18893

Comparative IR schlieren and interferometry techniques for measuring electron density profiles from refractive index effects of rotationally symmetric plasmas
07 p0986 A72-19613

Lower ionospheric electron density profile determination at high latitudes from riometric observations, discussing cosmic radio emission absorption representation
08 p1225 A72-20730

Multicomponent meteoritic composition effects on meteor trails radio wave reflections, obtaining ionospheric electron concentration distribution
08 p1131 A72-20805

Radio absorption in lower ionosphere obtained from vertical distribution of electron density and production rates from solar protons energy spectrum
08 p1226 A72-20816

Ionogram electron density-height distributions for analysis of multiple cusp structure near E region critical frequency
08 p1156 A72-21101

Nighttime and sunrise period ionospheric electron density profiles with respect to time after sunset and solar zenith angle
08 p1226 A72-21102

Neutral wind influence on lower ionosphere nighttime electron and NO ion density profiles
08 p1157 A72-21112

Ionospheric electron density nighttime changes as function of local time, height and latitude during geomagnetic storms
08 p1157 A72-21113

Local and integral ionospheric electron concentrations and horizontal gradients effects on reduced Doppler frequency shift difference along satellite orbit
08 p1132 A72-21144

Geometric optics approximation for rf wave forward and backscatter characteristics by spherical overdense clouds for several electron density distributions
[AD-739797] 08 p1136 A72-21980

Xenon plasma produced in cascaded arcs, investigating spectral line widths, temperature and electron density profiles, transition probabilities and I-V characteristics
09 p1364 A72-23392

HF radio waves scattering by spherical electron cloud with Gaussian density distribution
09 p1282 A72-23515

VI.F waves propagation dependence on ionospheric horizontal electron density gradients associated with midlatitude depression from FR-1 satellite observation
10 p1472 A72-24060

Microwave equipment for electron density profiles determination used in ionization relaxation start study of shock induced Ar plasma
10 p1519 A72-24067

Simultaneous rocket observation of wind shear and electron density profile in lower ionosphere, noting sporadic E layer formation
10 p1477 A72-25154

Temporal variations of sporadic E layer blanketing frequency, virtual height and occurrence rate, calculating electron density profiles and tidal wind influence
10 p1441 A72-25162

Nonequilibrium partially ionized viscous shock layer on blunt body, determining electron temperature and electron-ion density profiles
11 p1744 A72-25560

Daytime electron density profile in E and D regions from rocket lower ionosphere sounding, noting winter electromagnetic absorption anomaly
11 p1622 A72-26101

Magnetospheric equator plane electron density profiles determination from plasmopause whistlers observed in UK
11 p1626 A72-26421

Vertical electron concentration and temperature profiles at 80-170 km measured by rocket launched on 10 July 1969 at Volgograd
11 p1628 A72-26917

Electron recombination loss coefficients and concentration profiles for D region during solar eclipses from rocket measurements
12 p1800 A72-27149

Electron density profiles calculation from ionograms, obtaining equivalent delay caused by ionization below minimum plasma frequency
12 p1802 A72-27307

W addition effect on Co-Nb alloys, noting phase structure transformation from cubic to hexagonal due to mean electron density increase
12 p1829 A72-27642

F region mean electron density profile seasonal and solar cycle dependence, using Chapman function for nighttime F layer description
12 p1803 A72-27775

Disturbed D layer electron density profiles at high energy particle incidence, using partial reflection method
12 p1864 A72-27783

Exponential functions model for D region vertical distribution of electron density profiles, taking into account solar X- and cosmic rays
13 p1945 A72-28581

D region electron density profiles calculated as function of solar zenith angles, noting LF radio wave propagation
13 p1945 A72-28582

Latitudinal and diurnal development of seasonal anomaly in upper ionosphere from Alouette 1 data, discussing vertical electron density profiles
13 p1946 A72-28594

Night sky upper ionospheric electron concentration perturbations during magnetic storm, noting latitudinal distribution
13 p1949 A72-29252

OSO-6 Mg X spectroheliogram data for corona electron density map construction during 7 March 1970 solar eclipse period
13 p2031 A72-29529

Partial reflection method to obtain D region electron density profiles and collision number
14 p2086 A72-30791

Average interstellar electron and early star density in Galactic disk, examining hot stars ionizing photons and H II regions photoionization
14 p2161 A72-31044

Interferometric investigation of impurities effects on electron density distribution in ionization-relaxation zone behind shock waves in monatomic gas
15 p2215 A72-31213

Ionospheric electron density measurement by radio propagation method, recording traveling ionospheric disturbance effect and sporadic E strata thicknesses
15 p2223 A72-31438

Model Martian atmosphere, investigating effects of departures from electron density profile spherical symmetry on radio wave phase shift in bistatic radar occultation experiment
15 p2194 A72-31440

Equatorial ionospheric vertical electron density profiles measurement by rocket-borne phase measuring swept RF probe with dc biased sensor, comparing data with ionograms
15 p2226 A72-31940

Electrical conductivity in mesosphere and upper stratosphere from rocket sounding by blunt probe technique, suggesting electron density profiles dependence on dissociative recombination variations
15 p2228 A72-31972

Nighttime F region vertical velocity estimation, using electron density profiles vs true height
15 p2231 A72-32267

Plasma electron density profile reflection coefficient frequency-dependent amplitude and phase determination by measuring time response to fast-rising voltage pulse
16 p2437 A72-33767

Ring current effect on magnetospheric electron density profiles derived from plasmopause whistlers.
17 p2600 A72-35368

Electron profiles during negative magnetic bays in the auroral zone
17 p2551 A72-35860

Calculations of electron-profile disturbances in the F region during the passage of a neutral wave
17 p2551 A72-35861

Determination of electron concentration profiles in the lower ionosphere from the absorption at several frequencies
17 p2551 A72-35863

Influence of horizontal electron-concentration gradients on the magnitude of the maximum usable frequency and the trajectory of radio wave propagation in the ionosphere
17 p2519 A72-35878

ELECTRON DIFFRACTION

UHF radio signals refraction angles and group delay times for biexponential model of ionospheric electron density profile
18 p2657 A72-36101

Possibility of estimating an energetic particle stream in the ionospheric D region at sunrise and under daytime conditions
18 p2688 A72-36858

D region electron density profile determination based on LF link operating on one-hop ionospheric propagation of ordinary and quasi-transverse wave
18 p2689 A72-37163

Lower ionospheric electron density profile determination at high latitudes from riometric observations, proposing cosmic radio emission absorption representation
19 p2791 A72-38358

Plasma velocity, ion density and electrical conductivity from electron density and temperature and electromagnetic field profile measurements in Ar plasma inverse pinch
19 p2841 A72-38437

Comparison between observed and numerically calculated atmospheric gravity waves in the F-region.
19 p2794 A72-38864

Local and integral ionospheric electron concentrations and horizontal gradients effects on reduced Doppler frequency shift difference along satellite orbit
20 p2903 A72-39249

Isotropically and anisotropically polarized He-Ne lasers output dependence on longitudinal magnetic fields, noting electron density radial redistribution in gas discharge plasma
20 p2932 A72-39411

Characteristics of interplanetary electron inhomogeneities according to observations in the period from 1967 to 1969
21 p3114 A72-41765

Electron and positive ion density altitude distributions in the equatorial D-region.
22 p3170 A72-42366

Magnetically symmetric detection of the mid-latitude electron density trough by Ariel 3 satellite.
22 p3170 A72-42372

Measurement of the electron density distribution in plasmas from the bending of a gas laser beam.
22 p3211 A72-42396

A method for determining the electron density distribution about the F2 peak of the ionosphere.
22 p3174 A72-42992

Theoretical study and wind tunnel simulation of the electrical phenomena of reentry
22 p3231 A72-43092

Group delay times of magnetoeionic components for horizontal electron density profiles in magnetic meridian plane, noting comparison with ionospheric sounding data
23 p3283 A72-43361

High power radio transmitter for structural investigation of ionospheric D and E regions by signal reflection and electron concentration profiles
23 p3263 A72-43378

Exponential functions model for D region vertical distribution of electron density profiles, taking into account solar X- and cosmic rays
24 p3397 A72-45081

D region electron density profiles calculated as function of solar zenith angles, noting LF radio wave propagation
24 p3397 A72-45082

Latitudinal and diurnal development of seasonal anomaly in upper ionosphere from Alouette 1 data, discussing vertical electron density profiles
24 p3398 A72-45094

Continuity equation for dynamic auroral ionospheric model relating electron density profiles to auroral arc brightness
24 p3400 A72-45589

ELECTRON DETECTORS

U ELECTRON COUNTERS

ELECTRON DIFFRACTION

Ti alloys omega phase transformations by cryogenic cooling of bcc beta phase, interpreting electron diffraction pattern change in terms of displacement type reactions
01 p0082 A72-10204

Nonstoichiometric vacancy order in vanadium monoxide from electron microscopy and diffraction patterns, proposing partial phase diagram
03 p0401 A72-13584

Selected microarea electron diffraction technique in high voltage electron microscopy, discussing applications in crystallography and metallurgy
04 p0523 A72-15490

Reflection electron diffraction and ellipsometric studies of oxidation of niobium crystal surface, showing oxygen absorption in lattice and oxide film formation stages
07 p1017 A72-19944

Reflection mode high energy electron diffraction study of titanium carbide single crystal surfaces in ultrahigh vacuum environment
07 p1019 A72-20408

Carbon dioxide absorption kinetics on monocrystalline Mo from Auger spectrometry and slow electrons diffraction

10 p1525 A72-24137

Metal adhesive forces to clean Fe surface measured with LEED and Auger emission spectroscopy, noting binding energy correlation to oxygen

10 p1497 A72-24821

Emission of density modulated electron flux passing over diffraction structures formed by half planes and combs with oblique teeth, discussing optimum emitted power conditions

12 p1793 A72-27858

Low energy electron diffraction structures due to CO and oxygen adsorption on clean Re surfaces produced by Ar ion bombardment at 20 to 920 C

13 p2020 A72-28522

Electron diffraction study of transformation twin rotations in Fe-Ni martensites, showing foil plane uncertainty effect with respect to image plane

13 p1975 A72-28666

Re single crystal LEED diffraction pattern, showing surface carbon structure

13 p2021 A72-28800

Si phase identification in super alpha Ti alloys, using electron transmission microscopy and diffraction analyses

14 p2120 A72-30616

Absolute intensity LEED spectra for clean Ni surfaces, discussing measurement uncertainties

15 p2276 A72-31854

Debye-Waller factors measurement for Mo and Cr surfaces near normal incidence based on LEED

15 p2292 A72-31857

Single crystal disk substrate design with electron bombardment heating for LEED and Auger electron spectroscopy studies in ultrahigh vacuum

17 p2553 A72-34642

Electron diffraction patterns of previously deformed Ti-Nb alloy containing unequal populations of omega phase variants, noting anisotropy

17 p2566 A72-34673

Hydrogen and nitrogen desorption phenomena associated with a stainless steel 304 low energy electron diffraction/LEED and molecular beam assembly

19 p2762 A72-38023

Solid surface geometry, atomic composition and electronic structure observations, discussing Auger spectroscopy, field ion microscopy and electron diffraction and scattering techniques

19 p2803 A72-38389

Crystalline solids surfaces with catalysis, electronics and corrosive reactions, discussing slow electron diffraction, ionic field microscopy and Auger spectroscopy techniques for surface cleanliness measurement

23 p3324 A72-44461

Oxidation of W/110/1 - LEED study of the oxide formation at 1000 K

24 p3378 A72-44952

ELECTRON DIFFUSION

Ambipolar diffusion influence on MHD generator electrical conductivity, discussing plasma radiation, electron escape generator geometry and efficiency and ignition temperature range

04 p0554 A72-14404

High energy cosmic ray electrons anisotropy, considering diffusion from discrete source model

04 p0568 A72-15510

Photoelectrically excited electrons diffusion and dc effect in ZnO single crystals, calculating drift mobility and lifetime product

05 p0667 A72-16158

Electron density and diffusion measurements in ionized air in front of strong shock wave with resonant microwave probe and electromagnetic induction technique

05 p0648 A72-16211

Relativistic electron pitch-angle diffusion driven by oblique lf whistler-mode turbulence in collisionless plasma immersed in static magnetic field

05 p0699 A72-17024

Vlf wave excitation during sudden storm commencement, causing magnetosphere trapped energetic electrons to diffuse and precipitate into lower ionosphere

06 p0803 A72-17451

Diffused electron and ion currents through grid anode of cesium thermionic diode, determining electron temperature and potential distribution in electrode gap

08 p1113 A72-21747

Electromagnetic plasma accelerator with electron drift and diffusion towards anodes, neutral gas ionization and extended ion acceleration zone

09 p1361 A72-22955

Magnetic field effect on threshold pressure reduction for He and Ar gas breakdown by carbon dioxide laser radiation, taking into account inhibition of radial electron diffusion

[AD-741539]

09 p1365 A72-23493

Minority carrier diffusion length in liquid epitaxial GaP, noting dependence on dominant impurity and

substrate growth orientation from Schottky diode photocurrent technique

10 p1526 A72-24551

Alloy p-n-p junction transistor diffusion capacity variation with emitter current as function of temperature at 80-320 K

10 p1451 A72-24558

Critical analysis of Mouthaan-Susskind diffusion theory for magnetron diode electron transport, noting theoretical results discrepancy with experimental data

13 p1931 A72-29289

Energetic electron intrusion into inner radiation zone during and after 2 September 1966 geomagnetic storm, noting radial diffusion role

17 p2601 A72-35596

Pitch-angle diffusion of radiation belt electrons within the plasmasphere

17 p2602 A72-35597

Spectral dependence of diffusion in a magnetized plasma

17 p2592 A72-35623

Initial-boundary-value problem of the formation of an electrical discharge in a flow

17 p2592 A72-35627

Electromagnetic plasma accelerator with electron drift and diffusion towards anodes, neutral gas ionization and extended ion acceleration zone

17 p2593 A72-35884

Diffusion cooling in neon, argon, and krypton afterglow plasmas

19 p2841 A72-38378

Radiation belt electron lifetimes and removal through pitch angle diffusion by plasmaspheric whistler waves in cyclotron harmonics

20 p2918 A72-39532

Electron diffusion across a shock wavefront in metals

22 p3208 A72-43184

Equilibrium energy spectrum for the galactic cosmic electrons

23 p3328 A72-43831

Velocity distribution function and balance parameters of electrons in a nonisothermal argon plasma at degrees of ionization from 0.000000001 to 0.01

24 p3428 A72-44968

ELECTRON DISTRIBUTION

NT ELECTRON DENSITY PROFILES

Electrostatic waves in longitudinally magnetized plasmas with random electron charge distribution and applied magnetic field, finding phase characteristics

01 p0106 A72-10128

Electron correlation effects on low temperature thermodynamics of amorphous semiconductors, predicting Curie law magnetic susceptibility and equilibrium electronic specific heat dependence on temperature

04 p0562 A72-15153

Langmuir wave-caused electron plasma distribution function deformation, discussing particle trapping effects

06 p0858 A72-17542

Longitudinal electron plasma waves interaction with electron distribution, investigating energy transfer

06 p0858 A72-17543

Magnetic effects on Lorentz plasma collision processes, calculating electron distribution function in presence of strong arbitrarily oriented magnetic and weak electric fields

06 p0864 A72-18535

Pulsar distance determination from electron density distribution in line of sight estimated from frequency dispersion measures

07 p1080 A72-20054

Energy operator diagonalization of interacting valence electrons in semiconductor and metal models

09 p1352 A72-23356

Flat plate Langmuir probe measurement of electron temperature in plasma with elliptically anisotropic velocity distribution, discussing probe orientation effects

09 p1366 A72-23578

Inelasticity fluctuations effect on cosmic ray showers development, proposing criteria for lateral electron distribution and relative abundance of hadrons and muons

10 p1529 A72-24213

Ionized plasma electron velocity distribution function relaxation numerical calculation to validate local Maxwellian form during transport process

11 p1693 A72-25523

Angular distribution of electrons at output of specimen observed by electron microscope, examining resolution problem for thin objects

11 p1635 A72-26483

Third harmonic current density excitation by HF electric field in Lorentz plasma, calculating electron distribution function with unnormalized spherical harmonics and Fourier series

11 p1697 A72-26553

F region parameters relationship to night sky optical emission, considering electron distribution produced by dissociative recombination

12 p1802 A72-27308

Electron distribution near semiconductor-metal contact, discussing current carriers quantum properties effects

13 p2021 A72-28679

Global electron concentration disturbances in low and middle latitude F 2 during magnetic storm

14 p2100 A72-30635

Magnetospheric quasi-stationary pinch effect and filamentary structure due to electron streams parallel to geomagnetic field lines

14 p2103 A72-30664

Collisions role in nonlinear mode coupling and harmonic generation associated with electromagnetic wave in plasma, describing plasma electron distribution function by kinetic equation

15 p2195 A72-31679

Anisotropic electron pitch angle distributions at synchronous altitude due to wave-particle scattering and ionospheric acceleration along field lines

15 p2299 A72-31961

Electron swarms in uniform electric fields, discussing anode current amplification/radial distribution and drift-diffusion equation

15 p2285 A72-32239

Quasi-linear approximation of absorption of oscillations excited by electron beam in nonuniform plasma, noting electron distribution change with heating under magnetic field

16 p2432 A72-32807

Interstellar OH maser size determination, discussing scattering by inhomogeneities in electron distribution

16 p2456 A72-33473

Experimental evidence of an electron temperature enhancement in the wake of an ionospheric satellite

17 p2545 A72-34633

Separatrix shape, presence and position and electron lifetime and space charge in helical Tornado trap magnetic field

17 p2588 A72-34857

High latitude observation of precipitating electron spikes by polar orbiter OGO 4 satellite, noting population dependence on local trapping limit

17 p2601 A72-35591

Distribution function for free electrons in a molecular-nitrogen plasma

17 p2593 A72-35891

The Maxwellization of electrons in Cs-plasma of a low-voltage arc discharge

18 p2715 A72-36215

The influence of a nonequilibrium electron distribution function near the cathode and fractional coverage on the characteristics of a thermionic emission converter in the arc mode

18 p2647 A72-36220

Angular distribution measurements of photoemitted electrons for InAs by means of magnetic field

19 p2843 A72-37406

The equilibrium and the pulsation frequency spectrum of an electron cloud of spherical and cylindrical symmetry

19 p2867 A72-38571

Influence of solar flux and the equatorial electrojet on the diurnal development of the latitude distribution of total electron content in the 'equatorial anomaly'

19 p2794 A72-38868

Russian book on electron configuration model of condensed matter based on Hubbard model covering physicochemical properties of transition metals, alloys and compounds

21 p3066 A72-40348

Angular distribution of electrons elastically scattered from N₂

21 p3088 A72-40777

On the drift velocity of electrons in a gas

22 p3212 A72-42996

Kinetic equation for electron distribution in high temperature laser plasma, calculating nonequilibrium conditions for strong field and plasma parameters

23 p3318 A72-43323

Electron distribution fluctuation in two level system of unstable electron gas, noting periodic time dependence of population

23 p3319 A72-43406

Ion acoustic instability in collisionless shocks

23 p3320 A72-43522

Certain characteristics of the muon and electron components of extensive air showers at mountain level

23 p3331 A72-44425

Behavior of the spatial distribution function of shower particles near the axis of a cascade shower

23 p3331 A72-44432

Velocity distribution function and balance parameters of electrons in a nonisothermal argon plasma at degrees of ionization from 0.000000001 to 0.01

24 p3428 A72-44968

Mathematical model for secondary electron production fall-off, calculating ionization cross section from electron distribution

24 p3400 A72-45592

ELECTRON EMISSION

NT FIELD EMISSION

NT PHOTOELECTRIC EMISSION

NT SECONDARY EMISSION

Electron cyclotron harmonics emission as function of electron plasma frequency in He reflex discharge, measuring electron densities 01 p0105 A72-10026

Periodic solar flare modulation by pulsating structure, attributing radiation to synchrotron radiation emitted by electrons in magnetic flux tube embedded in solar corona 02 p0274 A72-12412

Solid state colloidal plasma physics, discussing statistical ionization mechanics, electron emission and recombination, rocket exhausts, MHD generation, metal vapors electrostatic precipitation, etc 02 p0267 A72-12842

Electron emission in strong electromagnetic waves within quantum electrodynamics, discussing energy losses and electron pair production 03 p0415 A72-13003

Exoelectronic emission method for examining deformation induced structural changes and interactions with ambient medium of metals and alloys surfaces 07 p0989 A72-20157

Thermally stimulated autophotocurrent emission from Cr-alloyed p-type GaAs electrode, determining spectral distribution and light and electric field effects on current 08 p1216 A72-21071

Oxygen adsorption effects on Mo orientation contrasts and emission image under electron microscope 10 p1513 A72-24875

Cesium contact ion thruster, investigating carburized thoriated tungsten filaments electron emission under ion bombardment [ALAA PAPER 72-440] 11 p1707 A72-26181

Three grid LEED-Auger display system for electron emission from solids at low primary beam energies 13 p1932 A72-29751

Work functions of dilute W alloys from vacuum emission vehicle and thermionic microscope measurements, noting additives effect 14 p2120 A72-30613

Electron work function for metallic sphere and thin film on dielectric substrate as function of radius, thickness and dielectric constant 15 p2290 A72-31222

Photomultiplier negative electron affinity emitter materials photosensitivity performance, considering Cs-activated GaP and applications for low light level detection 15 p2291 A72-31531

Ion density and electron acceleration region location from satellite-borne solar flare X-ray measurements 15 p2302 A72-32790

Galaxy M87 X ray source origin, suggesting hot plasma thermal emission or ejected relativistic electrons interacting with intergalactic magnetic or radiation fields 16 p2452 A72-33135

Induced electron emission dependence on polarization, frequency and intensity of second wave incident on electron with anomalous magnetic moment 16 p2424 A72-33365

Electron spectroscopy for chemical analysis /ESCA/ technique for nondestructive elemental analysis of lunar and terrestrial minerals 16 p2454 A72-33447

N2 positive and N2+/ band systems and the energy spectra of auroral electrons. 17 p2545 A72-34634

Electron currents injected through dielectrics 17 p2529 A72-34753

Parametric emission of relativistic electron clusters in a waveguide with a layered dielectric filling 17 p2529 A72-34850

Solar thermal radio burst temperature and emission measure determination from flux spectrum, noting consistency with radio observation 17 p2608 A72-35090

Thermodynamic analysis of metal surfaces covered by electropositive adsorbates. 18 p2656 A72-36126

Plasma immersion probe measurements of electron work function. 18 p2690 A72-36127

Electron work function change of interstitial compounds of the 4a and 5a metals in dependence on the nonmetal content. 18 p2656 A72-36129

Crystal orientation effect on electron work function in chemical vapor deposited W layers on thermionic converter cylindrical emitters 18 p2717 A72-36142

On the radiation of discontinuous gold films by electric current transmission. 18 p2718 A72-36349

Dependence of emission on work function variation in metals under tension 18 p2699 A72-36350

Vapor deposition in vacuum under conditions of constant vapor flow with the aid of electron emission current control 20 p2954 A72-39694

Electron spectroscopic investigation of solid surfaces chemical composition and atomic binding states

and structure, discussing methods of inducing electron emission 20 p2927 A72-39695

Fabrication and accelerated life tests of self sustained electron emission cathode with Cr film vapor deposition on Cu disk base 21 p2997 A72-40790

Temperature dependence of thermionic emission current density of Pt additive powdered zirconium carbide deposit on diode cathode working surface 21 p2997 A72-40801

Field emission from carbon fibres - A new electron source. 22 p3208 A72-41966

Physicochemical investigation of the thermionic emission properties of metals and alloys 22 p3191 A72-42811

Field-emission microscopy of tungsten coated with a silicon oxide film 24 p3432 A72-44892

ELECTRON ENERGY

NT ELECTRON STATES

Higher order cyclotron harmonic resonance of electrons with electromagnetic wave propagation through collisionless magnetoplasma, deriving energy oscillation time period 01 p0105 A72-10023

Quiet solar corona thermal emission flux at 169 MHz, showing constant brightness and electron temperatures during cycle 01 p0123 A72-10045

Topside electron density profile from empirical relation between ionospheric slab thickness and mean gradient temperature in F region, using Saint Santin scatter data 01 p0052 A72-10085

Electron energy equation and recombination radiation loss for atomic radiating optically thin plasmas, using Kramers-Unsold approximation 01 p0106 A72-10097

Strong ionizing shock waves production in hydrogen and deuterium gases, measuring plasma electron temperature, axial electric field and density and magnetic field compression [AD-734469] 01 p0108 A72-10237

Narrow-band type 4 bursts behavior comparison with synchrotron radiation in media with refractive index less/equal unity, determining magnetic field and electron energy 01 p0118 A72-10415

Ion and electron temperature increases by friction heating between neutral gas winds and plasma in ionosphere 01 p0054 A72-10424

Average energy electron capture coefficient dependence on air density, temperature and altitude under gamma radiation 01 p0059 A72-10599

Solar wind two component model with protons collisionless beyond ten solar radii, discussing effects of variable electron temperature 01 p0119 A72-10879

Stable red arc 6300 A emission calculation from satellite electron temperature and density data during geomagnetic storms 01 p0061 A72-10893

Auroral electron flux and energy spectrum observations by synchronous ATS 5 and polar OV-1-17 satellites 01 p0061 A72-10894

Precipitated electron energy latitude and time variations from auroral-height measurement during IQSY, using meridian scanning photometers 01 p0120 A72-10896

Rocket-borne measurement of particle fluxes and currents in auroral arc, determining pitch-angle distribution of electron and proton energies 01 p0120 A72-10897

Ionospheric F region heating by hf transmitter, obtaining electron temperature maps and heating/cooling time constants 01 p0062 A72-10910

Substorm electron drift relationship to cosmic noise absorption on auroral zone morning side, calculating electron energy loss 01 p0063 A72-10918

Electron thermal boundary layer effects on Langmuir probe measurements in subsonic cold plasma flow 01 p0071 A72-11191

Free electron density, electron temperature and gas ionization during shock wave propagation in Ar-filled shock tube from microwave radiation measurements 02 p0263 A72-12020

Electron temperature profile across nonequilibrium stagnation point boundary layer in partially ionized gas, investigating charged particles interaction with body in ionosphere 02 p0262 A72-12268

Nonlinear discrete radio source spectra deviations from power law at 10-5000 MHz, considering low energy relativistic electron excess 02 p0281 A72-12305

Auroral electron precipitation modulation dependence on energy explained by resonance at rebound frequency 02 p0222 A72-12598

Ion and electron temperatures difference relaxation rate in uniform plasma, noting relationship to Debye length 02 p0267 A72-12769

Wall double layer temperature and plasma oscillations effect on electron energy distribution in low discharge plasma column 03 p0394 A72-13192

Electric field aligned sheet currents of low energy electrons and protons near auroral arc, obtaining magnetic signatures 03 p0349 A72-13516

Electron temperature measurements in ionospheric isotropic nonequilibrium plasma by electrostatic probes and radar backscatter 03 p0349 A72-13520

Plasma beam production with Penning type discharge, demonstrating anisotropic electron temperature 03 p0395 A72-13566

Magnetoplasma with skin current characterized by current and electron temperature nonuniformity, analyzing instabilities for perturbations above ion gyrofrequency 03 p0396 A72-13713

Upper atmosphere He, Ne, Na and K atoms collisions with molecular oxygen, determining ejected electron energy during fast Na, K, Rb and Cs ionization for meteor phenomena modeling 03 p0438 A72-13980

Low energy electrons anisotropic flux impulsive precipitations in structured aurora explained by potential difference along geomagnetic field lines of force 03 p0350 A72-14272

Low pressure glow cathode triodes gas discharges, determining electron energy distribution function in double layer by probe measurements 03 p0400 A72-14349

Thin electrostatically self focusing electron streams in mercury vapor, analyzing energy distributions of ions and electrons ejected radially from beam 04 p0554 A72-14407

Electron energy distribution in carbon dioxide laser mixtures under lasing and nonlasing conditions 04 p0528 A72-14540

Relaxation time estimation for electron velocity relative to dilute vortex core array in rotating neutron superfluid, applying to pulsar slowdown rate 04 p0571 A72-14590

Magnetospheric heat flux effect on height variation of electron and ion temperatures and ion composition in topside ionosphere 04 p0515 A72-14929

Electron heating by oscillating electric field in presence of steady magnetic field, solving Boltzmann transport equation for electron velocity distribution in plasma 04 p0556 A72-14947

Ground state energy of interacting electrons for entire density range from two-point Padé approximation 04 p0549 A72-15229

Windowless ultrahigh vacuum photoelectron spectrometer for high resolution studies of gas-metal surface reactions, measuring electron energy levels 04 p0523 A72-15489

Velocity dependence of ionization cross section of Ar, Kr and Xe during thermal energy metastable neon atoms impact, obtaining secondary electron ejection efficiency 04 p0553 A72-15640

German monograph on spectroscopic investigation of Cs plasma electron density and temperature and excited atom density in various operational states of thermionic converter 04 p0560 A72-15699

Collisional radiative model of population densities of metastable electron levels of orthohelium in low pressure rf helium plasma 05 p0694 A72-15998

Electron energy derivation from contaminated Langmuir probe, explaining E region high temperature 05 p0654 A72-16007

Electron temperature measurement error elimination with radio frequency Langmuir probe in low density plasma, measuring floating potential 05 p0694 A72-16049

Nighttime polar atmospheric structure and temperature variations due to gas kinetic and electron energy changes 05 p0656 A72-16240

Latitudinal distribution of electron temperature in F 2 layer during summer daytime period of low solar activity from electron density profile geometrical parameters 05 p0656 A72-16248

OGO-5 measurement of 10-200 MeV cosmic ray electron energy spectra, discussing quiet time flux intensity 05 p0720 A72-16719

Integral and differential electron energy spectra in inner radiation belt from Cosmos 219 satellite observation 05 p0711 A72-16768

Electron density and temperature fluctuations coupled through Ohm law for ionizable medium, applying to MHD generators and MPD arc thrusters [AIAA PAPER 72-101] 05 p0706 A72-16813

Optical radiation from plasma discharge of electron bombardment mercury ion thruster, discussing electron temperature and primary electron fraction [AIAA PAPER 72-205] 05 p0706 A72-16851

Electron density and temperature temporal and radial profiles in megawatt MPD-arc thruster exhaust, using Thomson scattering technique [AIAA PAPER 72-209] 05 p0707 A72-16887

Electron heating in weakly ionized collisionless beam plasma discharge as function of neutral gas pressure and plasma column length 05 p0697 A72-16986

Electron heating model in perpendicular collisionless plasma shock waves based on electron trapping by turbulent electric field 05 p0697 A72-17014

Electron temperature gradient instability in collisionless shocks propagating across magnetic field 05 p0700 A72-17228

Temperature inhomogeneity effect on plasma column microwave resonant behavior in presence of axial magnetic field, ascribing spectral shifts to electron density and temperature profiles changes 06 p0854 A72-17417

Lf instability mode in partly ionized plasma due to electron temperature gradient aligned perpendicular to magnetic field, applying to E and F regions [AD-737931] 06 p0804 A72-17460

Parametric excitation of ion-acoustic waves in Q machine plasma, controlling electron temperature by amplitude modulated rf heating 06 p0855 A72-17513

Ion acoustic waves instability from electron-ion temperature difference in homogeneous collisional ionized plasma, using fluid equations perturbation analysis 06 p0856 A72-17524

Electron temperature fluctuations associated with drift-type instability in Q device, discussing plasma diagnostic techniques 06 p0857 A72-17530

Single ended Q machine Ba plasma probe measurements of ion temperatures perpendicular to magnetic field, electron temperatures and plasma densities and potentials 06 p0859 A72-17550

Plasma conductivity dependence on electron velocity distribution function in distorted Maxwellian form 06 p0860 A72-17690

Solar wind model of electrons, protons and alpha particles velocity and temperature differences dependence on distance from sun 06 p0873 A72-18025

Boltzmann equation solution analysis for Maxwell-Lorentz gas in electric field, discussing conditions for electron velocity distribution isotropic part evolution towards Maxwellian distribution 06 p0861 A72-18162

Spectrographic measurement of electron temperature and ion density profiles in cesium plasma thermionic converter 06 p0862 A72-18309

Electron energy distribution in carbon monoxide lasers, considering excitation effects on exchange processes, power transfer to vibration levels and vibrationally excited molecules influence 07 p0999 A72-18883

Systematic increase in auroral electrons mean energy with total precipitated energy 07 p1058 A72-19151

Cylindrical mirror electron energy analyzer, discussing theory, operation and design parameters [AD-745599] 07 p0984 A72-19322

Energy spectrum of primary cosmic ray electrons at 2-200 GeV, using balloon-borne counter telescope with gas Cerenkov counter 07 p1059 A72-19578

Dispersion relation for uhf drift waves in nonuniform plasma with cold electrons drift through stationary ions, deriving plasma stability conditions 07 p1042 A72-19612

Multichannel modular spectrometer with electrostatic analyzers for low energy electron and proton flux measurement 07 p0988 A72-19954

Spectrometers with electrostatic analyzers alternating with shielding and suppressing gratings for low energy electron flux measurement 07 p0988 A72-19955

Transient plasma diagnostics using carbon dioxide laser interferometry and absorption for electron density and temperature determination 07 p1008 A72-20557

Ionospheric electron concentration and temperature as function of solar zenith angle from rocket sounding 08 p1154 A72-20734

Energy and angular distributions of electrons released during ion atom collisions from energy spectra studies, discussing autoionization transitions 08 p1210 A72-20836

Steady state problem of energy spectrum of variable magnetic field accelerated electrons, considering synchrotron X ray emission of Crab pulsar and nebula 08 p1231 A72-21119

Transverse electromagnetic field and electron velocity vectors during rectangular pulse incidence on ionization front moving at light speed, describing steady state encounter region 08 p1136 A72-21741

Diffused electron and ion currents through grid anode of cesium thermionic diode, determining electron temperature and potential distribution in electrode gap 08 p1113 A72-21747

Electron temperature effects on radiation fields and resistance of short electric dipole antenna embedded in hot uniaxial plasma 08 p1215 A72-21991

Single and double probe measurements of electron temperatures in flames, discussing difficulties in obtaining reliable I-V characteristics 08 p1129 A72-22043

Second derivative measurement of Langmuir probe characteristics for electron energy distribution functions in nonstationary plasmas by sample and hold technique 09 p1359 A72-22654

H Balmer lines H alpha/H beta ratios as electron temperature indicators in nonequilibrium plasmas 09 p1359 A72-22666

Solar wind properties and discontinuity characteristics, describing particle densities, wind speed, magnetic field level and near earth electron and ion temperatures 09 p1377 A72-22756

Inhomogeneous superconductors and proximity effects, calculating conditions for vortex lattice pinning energy as increasing function of magnetic field and temperature 09 p1370 A72-22798

Electron reflection mechanism and gas adsorption effect at W /001/ surface in energy range 1-10 eV 09 p1370 A72-22804

Electron energy distribution and losses existence limit at Langmuir paradox pressures in gas discharge, hypothesizing wall mechanism of electron collisions 09 p1361 A72-22958

Cosmic electrons energy spectrum between 1 and 25 GeV from balloon observations, noting Compton/synchrotron loss effects [AD-745871] 09 p1377 A72-23001

Ionospheric electron concentrations and temperatures determined by time dependent continuity equations model during 11 September 1969 solar eclipse 09 p1390 A72-23518

Supersonic Ar, He and molecular nitrogen jets, determining electron temperature and concentration and atomic state population in shock waves region by spectroscopic measurement 10 p1517 A72-23837

Bounded plasma ionization instability inhomogeneity scale evaluation, assuming negligible electron energy losses due to heat conduction 10 p1517 A72-23844

Low transverse energy, high nu/gamma electron beam propagation characteristics, reviewing transport, compression and combination beam-handling concepts 10 p1518 A72-23959

High pressure CO and N plasmas production by uncoupling electron temperature from number density, measuring electron-ion recombination rates 10 p1518 A72-23962

Interaction forces between monovalent metal crystals determined from electrons quantified energy variations 10 p1525 A72-24136

Ar/He plasma acoustic wave properties, expressing phase velocity and damping as function of ion-electron temperature ratio and relative species densities 10 p1520 A72-24300

Emitter conduction bands with negative electron affinity energy from surface barrier lowering of Cs p-type semiconductors 10 p1526 A72-24351

Absorption spectra and plasma of laser spark in hydrogen, studying electron and atoms temperature and concentrations time variations 10 p1491 A72-24359

Equatorial sporadic E sudden disappearance associated with magnetic field depressions, noting irregularities and electron velocities role 10 p1475 A72-24956

Electron cyclotron resonance in Penning ion source, measuring electron temperature from X ray emission spectra 10 p1516 A72-25029

Nonequilibrium partially ionized viscous shock layer on blunt body, determining electron temperature and electron-ion density profiles 11 p1744 A72-25560

Thomson scattering of electromagnetic wave in plasma and ionosphere for studying electron and ion temperatures 11 p1621 A72-25838

Penetrating particles effect on low energy scintillation spectrometers sensitivity in various regions of magnetosphere 11 p1632 A72-25934

Solar wind model of electrons, protons and alpha particles velocity and temperature differences dependence on distance from sun 11 p1713 A72-25961

Russian book on transition metals and alloys electron structure and electronic properties covering paramagnetism, positron annihilation, magnetic transformations and electron heat capacity 11 p1659 A72-26069

Electrostatic and electron temperature probes compared during ionospheric rocket soundings, noting lower ionosphere discrepancies due to surface contamination 11 p1633 A72-26102

Explorer 35 observations of solar wind electron density and temperature, noting anisotropy direction correlation with magnetic field vector alignment 11 p1713 A72-26392

Daytime and nighttime electron temperatures from topside resonances, using oblique echo theory 11 p1625 A72-26409

Artificial heating of lower ionosphere in controlled experiment, measuring electron temperature increase by radar backscatter system 11 p1625 A72-26412

Electron temperature determination from rate of ionization due to collisions between electrons and neutral particles in plasma 11 p1697 A72-26586

Charge carrier density, neutral gas density, electric potential and electron temperature profiles in cylindrical diffusion column, considering electron pressure 11 p1698 A72-26646

Electron energy, mobility and bremsstrahlung in weakly ionized nonisothermal plasmas, using Kogan approximation 11 p1698 A72-26647

Plasma beam production with Penning type discharge, demonstrating anisotropic electron temperature 11 p1699 A72-26753

Mercury vapor physicochemical processes kinematics in shock tube, determining electron gas energy balance equations and atom-atom collision cross sections 11 p1699 A72-26760

Ionospheric and neutral atmospheric temperature profile, composition and electron density and energy measurements by MR-12 rocket 11 p1628 A72-26905

Vertical electron concentration and temperature profiles at 80-170 km measured by rocket launched on 10 July 1969 at Volgograd 11 p1628 A72-26917

Electron heating in weakly ionized collisionless beam plasma discharge as function of neutral gas pressure and plasma column length 12 p1850 A72-27130

Averaged equations for laser heating of two temperature plasma with allowance for nuclear fusion energy, noting inequality of ion and electron temperature 12 p1851 A72-27395

Quiescent plasma production with axially homogeneous density distribution in skipping magnetic fields by electron cyclotron resonance discharge, noting high electron temperatures 12 p1851 A72-27400

Spatial and time dependence of electron velocity in short channel microwave FET, using Monte Carlo method 12 p1790 A72-27434

Peak electron energy spectra during auroral substorm from high energy resolution balloon X ray measurements 12 p1804 A72-27787

Electron energy threshold measurements in irradiated II-VI compounds interpreted in terms of damage on metal and chalcogenide sublattices 12 p1859 A72-28070

Strong field electromagnetic wave interactions with anisotropic plasmas, considering electron velocity distribution function 13 p2009 A72-28449

Wave equations and photon absorption cross section of relativistic electron in magnetic field, taking into account relativistic energies 13 p2002 A72-28647

Friction force electron component for superconductor dynamic dislocation at various temperatures and propagation rates 13 p2021 A72-28901

Heating mechanisms in laser pulse produced plasma from electron temperature and reflectivity measurements 13 p2011 A72-28999

- Two point correlation description of MHD plasma properties subject to electrothermal instability, calculating electron number density and temperature fluctuations
13 p2015 A72-29373
- Low energy relativistic cosmic ray electrons temporal intensity variations from IMP satellite measurements, considering correlation with solar activity
13 p2030 A72-29376
- Homogeneous plasma column generation by HF generator, probing for electron temperature and charged particle concentration
13 p2015 A72-29507
- Electron density and temperature measurement from scattering of laser radiation in plasma within axisymmetric toroidal magnetic mirror machine
13 p2017 A72-29609
- Resonant irradiation effect on cesium discharge plasma, charge density, electron temperature and electric field strength
13 p2017 A72-29610
- MHD stability in Hg vapor discharge plasma excited by standing microwave near electron cyclotron resonance, discussing electron energy anisotropy effect on LF oscillations
13 p2017 A72-29618
- Transverse magnetic field effect on electron temperature and energy distribution and spectral lines of gas discharge plasma
13 p2017 A72-29635
- Electron temperature and emission measures during solar X-ray flares, studying effects of gradual and rapid radiation flux increases
13 p2032 A72-29722
- Three grid LEED-Auger display system for electron emission from solids at low primary beam energies
13 p1932 A72-29751
- Electric field excited stable auroral red arc time dependent behavior, noting inconsistency with satellite and ground observation of 6300 Å emission for electron energy
13 p1953 A72-29812
- Satellite-borne low energy electron and proton spectrometer for measuring auroral electron and proton spectra
13 p1960 A72-29841
- Electron temperature radial dependence in two fluid models of solar wind, noting unrealistic assumption of heat conduction dominated electron gas energy equation
13 p2034 A72-29961
- Daytime F region inverse relationship between electron density and temperature, determining energy input profile and thermal flux
14 p2097 A72-30127
- Auroral spectroscopic and excitation processes, discussing atomic oxygen production, emission ratios and electron energy spectrum, UV and IR emissions, composition and temperature measurements
14 p2098 A72-30138
- Electron energy distribution, ions mass spectral composition and spatial charge concentration of currentless photoresonant Ce plasma obtained by associative ionization
14 p2136 A72-30175
- Kinetic instabilities during electron plasma heating in HF field of cylindrical resonator, discussing electron energy distribution function effect
14 p2137 A72-30309
- Charge carrier cooling in nonhomogeneous semiconductors by static electric field, plotting average electron temperature as function of current
14 p2142 A72-30362
- Flux densities, electron energies and brightness temperature determination from radio telescope observations of galactic sources and nonthermal radiation
14 p2155 A72-30553
- Intensity and energy spectrum calculation of albedo electrons recorded in cosmic particle showers by gas discharge counters
14 p2105 A72-30629
- Ionospheric electrons and neutral particles temperature and concentration profiles explained by electron gas cooling due to atomic hydrogen excitation, calculating heat flow
14 p2101 A72-30641
- Magnetized nonuniform plasmas, discussing description to all orders in electron and ion temperatures of waves by operator method
14 p2139 A72-30879
- Solar proton flare induced X ray bursts maximum flux, total radiated energy, electron temperature and emission from satellite measurements
14 p2160 A72-30910
- Total energy distributions of field emitted electrons from tungsten as function of coverage by hydrogen and deuterium, observing elastic and inelastic spectrum
15 p2275 A72-31851
- Absolute intensity LEED spectra for clean Ni surfaces, discussing measurement uncertainties
15 p2276 A72-31854
- Debye-Waller factors measurement for Mo and Cr surfaces near normal incidence based on LEED
15 p2292 A72-31857
- Surface contamination effect on electron temperature measurement using rocket-borne Langmuir probe in lower ionosphere
15 p2236 A72-31926
- Geomagnetic field aligned electron anisotropies at high latitudes for energies 1 and 6 keV observed by ESRO satellite, noting two regions of maximum occurrence frequency
15 p2226 A72-31928
- Correlated particle flux, magnetic field, electron intensity and riometer absorption measurements during recovery phase of polar magnetic substorm on 6 March 1970
15 p2226 A72-31946
- Rocket-observed energetic electron flux association with ground recorded plasmasphere whistler in terms of gyroresonant wave-particle interaction
15 p2198 A72-31948
- Steady state electron mean energy variation between parallel plates in Ar and He calculated by Monte Carlo simulation for comparison
15 p2285 A72-32222
- Electronic energy band structures for alpha and gamma phase Ce, using exchange potential and plane wave method
15 p2293 A72-32227
- HF electric field effect on ultrasound wave propagation in semiconductor, noting amplification factor dependence on electron heating
15 p2279 A72-32739
- Interplanetary high energy electron flux association with solar flares from HEOS-A1 data
15 p2302 A72-32792
- Plasma corona electron temperature decoupling from core of solid deuterium pellet heated in vacuum by convergent laser beams
16 p2433 A72-32810
- Gas ionization buildup behind hypersonic shock waves, calculating onset point properties from plasma conservation and electron energy equations
16 p2434 A72-32902
- Low energy outer zone electrons high latitude boundary variation with interplanetary magnetic field direction and with geomagnetic activity from Alouette and Explorer data
16 p2382 A72-32957
- Charge carrier motion in semiconductor with electron interactions, considering heating in presence of negligible electric field
16 p2441 A72-33278
- Weakly ionized nonequilibrium plasma flow from gas discharge tube positive column, obtaining electron temperature axial decay rate from energy equation
16 p2437 A72-33655
- Radio sources with straight spectra and spectral index of 0.3, noting relationship to self absorption, electron energy distribution and cosmological evolution
16 p2457 A72-33685
- Low pressure He and Ne discharge generated positive plasma column potential, determining electron concentration from electron energy distribution functions
16 p2437 A72-33746
- Probe temperature, shape and size effects on electron energy distribution measurements for positive plasma column of low pressure He and Ne discharges
16 p2437 A72-33750
- Conservation equations for wave and/or turbulence momentum and energy flux in interplanetary space shock vicinity, developing modifications for electron temperature calculations
16 p2459 A72-33913
- Electron-ion heating in high beta perpendicular collisionless shock waves by plasma cylinder magnetic compression using theta pinch
16 p2439 A72-33936
- Coupling of free electron and nitrogen vibrational temperature nonequilibrium in weakly ionized nozzle expansions of shock heated nitrogen
16 p2380 A72-34059
- [AIAA PAPER 72-683]
Measurement of the electron work function in binary and ternary transition metal-nonmetal systems.
17 p2595 A72-34602
- The influence of the electron temperature and other parameters on the electron density of a cesium plasma in a thermionic converter.
17 p2497 A72-34611
- Experimental evidence of an electron temperature enhancement in the wake of an ionospheric satellite.
17 p2545 A72-34633
- N2 positive and N2+/+ band systems and the energy spectra of auroral electrons.
17 p2545 A72-34634
- Emitter conduction bands with negative electron affinity energy from surface barrier lowering of Cs p-type semiconductors
17 p2595 A72-34952
- Absorption spectra and plasma of laser spark in hydrogen, studying electron and atoms temperature and concentrations time variations
17 p2562 A72-34958
- Integral and differential electron energy spectra in inner radiation belt from Cosmos 219 satellite observation
17 p2600 A72-35271
- Runaway electrons in toroidal plasma investigation by thick target bremsstrahlung measurement, noting energy distribution and runaway rate estimates
17 p2591 A72-35370
- Toroidal plasma spectroscopic investigation from current pulse start to afterglow, noting electron temperature and density radial distributions and energy balance
17 p2591 A72-35373
- Electron temperature in the Martian ionosphere.
17 p2613 A72-35499
- Cosmic ray electron spectrum and its modulation near solar maximum.
17 p2601 A72-35583
- On the stability of obliquely propagating whistlers.
17 p2517 A72-35600
- Whistler side-band growth due to nonlinear wave-particle interaction.
17 p2517 A72-35601
- Nonequilibrium energy constants associated with large-amplitude electron whistlers.
17 p2517 A72-35620
- On the temperature of the helium emission regions in the solar atmosphere.
17 p2616 A72-35699
- Auroral electron energy spectra at high latitudes from polar auroral arcs luminosity profile examination
17 p2550 A72-35853
- Electron energy distribution and losses existence limit at Langmuir paradox pressures in gas discharge, hypothesizing wall mechanism of electron collisions randomization
17 p2593 A72-35887
- Distribution function for free electrons in a molecular-nitrogen plasma.
17 p2593 A72-35891
- Galactic nebulae electron temperature and density from forbidden line emissions interpreted in terms of transition probabilities and collision strengths
18 p2723 A72-36090
- Analytical description of thermionic converter phenomena, assuming position linearity of interelectrode electron energy distribution and local thermodynamic equilibrium in cesium plasma near collector
18 p2646 A72-36200
- Arc discharge transition from diffusion to arc mode, presenting theory on I-V characteristics negative resistance section and on hysteresis causes
18 p2714 A72-36207
- Nonequilibrium relaxation phenomena in the near-emitter region of the thermionic converter.
18 p2647 A72-36209
- Atmospheric model synthesis of observed electron temperatures and concentrations in tropical ionosphere during 8 March 1970 magnetic storm, noting F2 region features
18 p2686 A72-36296
- Numerical and shock tube experiments for variation of bound electron temperature and nonequilibrium chemical and radiative relaxation behind normal shock waves in air, using atom-molecule collision model
18 p2681 A72-36564
- Turbulent heating of electrons and ions in a collisionless shock wave.
18 p2715 A72-36599
- Time-resolved diagnostic method for hydrogen plasmas.
18 p2716 A72-36949
- Temperature dependence of the electron thermal conductivity in rare gas plasmas.
18 p2716 A72-36958
- Measurements of MeV-electrons during the recovery-phase of a polar magnetic substorm on March 6, 1970.
19 p2789 A72-37409
- Energy loss of fast electrons and positrons in a plasma.
19 p2840 A72-37727
- Design considerations in the measurement of electron temperature in the ionosphere.
19 p2801 A72-37926
- Quantum yield variations of Nd ion activated glass as function of electron beam energy and intensity, noting nuclear particles effect on laser radiation
19 p2823 A72-38205
- Ionospheric electron concentration and temperature as function of solar zenith angle from rocket sounding
19 p2791 A72-38362
- Plasma velocity, ion density and electrical conductivity from electron density and temperature and electromagnetic field profile measurements in Ar plasma inverse pinch
19 p2841 A72-38437
- Effect of plasma resistance on electron temperature measurement by means of an electrostatic probe.
19 p2804 A72-38593
- Explorer 35 observation of geomagnetic tail low energy electrons, noting plasma sheet extension to lunar distance and correlation with solar wind
19 p2853 A72-38737

An evaluation of the intensity of Cerenkov radiation from auroral electrons with energies down to 100 eV.
19 p2792 A72-38741

Cosmic-ray diffusion coefficient in interplanetary space.
19 p2853 A72-38756

A new method for in situ electron temperature determinations from plasma wave phenomena.
19 p2793 A72-38758

A helium-neon laser active element with a metallic inner wall surface.
19 p2814 A72-38785

Electron temperature and density determination from RF impedance probe measurements in the lower ionosphere.
20 p2916 A72-39229

Measurements of electron detection efficiencies in solid state detectors.
20 p2925 A72-39401

High latitude variations of F-region electron temperature.
20 p2918 A72-39535

Interstellar gas electron temperature determination from recombination line spectra observations along galactic ridge
20 p2971 A72-39858

Non-thermal bremsstrahlung of fast electrons and flare of stars.
20 p2974 A72-39894

Temperature and emission measure deduced by coronal visible lines.
20 p2974 A72-39896

Electron density and temperature measurement from laser radiation scattering in plasma within axisymmetric toroidal magnetic mirror machine
21 p3091 A72-40663

Resonant irradiation effect on Cs discharge plasma charge density, electron temperature and electric field strength
21 p3091 A72-40664

MHD stability in Hg vapor discharge plasma excited by standing microwave near electron cyclotron resonance, discussing electron energy anisotropy effect on LF oscillations
21 p3091 A72-40671

Measurement of the electron temperature of small 3-cm radio bursts /Research note/.
21 p3100 A72-41291

Solar soft X-rays and solar activity. II - Observational assessment of the role of the type III acceleration mechanism in establishment of the soft X-ray source volume.
21 p3101 A72-41294

Influence of inelastic electron-energy losses on the development of ionization instability in a plasma
22 p3209 A72-41877

Anode heat transfer for a flowing argon plasma at elevated electron temperature.
22 p3210 A72-41952

Analytic expressions for electron energy transfer rates for nitrogen and oxygen vibrational excitation in ionosphere, applying to atmospheric and ionospheric computer modeling
22 p3168 A72-42001

Geomagnetic DP-2 variation base level from E region electron drift velocity measurements in equatorial electrojets
22 p3169 A72-42013

Nonadiabatic condition effects on ultrarelativistic electron energy losses in geomagnetic trap in remote magnetosphere regions
22 p3218 A72-42224

Effect of increasing beam voltage on the internal quantum efficiency of spontaneous emission in electron-beam-excited p-type GaAs.
22 p3185 A72-42308

Energy degradation calculation for electron interaction with carbon dioxide molecules, discussing relationship with Mariner UV data
22 p3171 A72-42421

Electron impact excitation cross sections and energy degradation in CO.
22 p3172 A72-42422

Electron density and temperature in microwave plasmas at higher pressures.
22 p3211 A72-42479

Direct measurement of diffusion cooling in an afterglow plasma.
22 p3212 A72-42918

Electronic density and temperature deduced from the observation of the cone of resonance of an antenna in a magnetoplasma
22 p3212 A72-43049

Pulse discharge plasma in Ar with gas ionization level near unity, noting plasma cylinder parameters, electron temperature and I-V characteristics
22 p3212 A72-43103

Molecular gas presence effect on electron energy balance in atomic gases, noting inelastic collisions loss factor in heated Ar plasma containing nitrogen molecules
22 p3213 A72-43110

Electron-energy distribution in a low-temperature plasma
22 p3213 A72-43118

Kinetic instabilities during electron plasma heating in HF field of cylindrical resonator, discussing electron energy distribution function effect
23 p3317 A72-43211

Calculation of the parameters of a plasma accelerated in a high-frequency electric field and a static magnetic field
23 p3320 A72-43660

Equilibrium energy spectrum for the galactic cosmic electrons.
23 p3328 A72-43831

Variation with electron velocity powers of electron collision frequency and energy transport coefficients in weakly ionized plasmas - Earth's lower ionosphere.
23 p3285 A72-43994

Glow discharge in rare-gas and metal vapour mixture. I - Distribution functions and kinetic coefficients in He-Cd mixture discharge.
23 p3322 A72-44320

Isothermal atmosphere inhomogeneities effects on electromagnetic cascade electrons integral energy spatial distribution
23 p3331 A72-44433

A Lecher wire microwave interferometer for measurements of electron density and electron temperature in a flowing transient plasma.
23 p3292 A72-44543

Detection of interplanetary electrons from 18 keV to 1.8 MeV during solar quiet times.
23 p3333 A72-44546

Origin of 200-keV interplanetary electrons.
23 p3333 A72-44547

Excitation mechanisms in the argon-ion spectrum at near laser conditions and temperatures and densities in a hollow cathode argon-arc discharge.
24 p3428 A72-44807

Dissociative attachment in carbon dioxide.
24 p3427 A72-45303

Electronic energy transfer phenomena in rare gases.
24 p3429 A72-45310

Current induced drift rate of plasma electrons in electric and magnetic fields, noting electron velocities in turbulent heating of plasma
24 p3429 A72-45507

Sunrise effects on the latitudinal variations of topside ionospheric densities and scale heights.
24 p3399 A72-45552

ELECTRON FLUX

U ELECTRONS

U FLUX (RATE)

ELECTRON FLUX DENSITY

Auroral electron flux and energy spectrum observations by synchronous ATS 5 and polar OV-1-17 satellites
01 p0061 A72-10894

Farley-Buneman instability nonlinear development mechanism in equatorial electrojet, noting turbulent vertical electron flux role
01 p0062 A72-10901

Fast cyclotron and synchrotron transverse waves noise measurement in electron flux, using resonator with homogeneous electric field
02 p0190 A72-11573

Solar wind 10-9900 eV electron flux, evaluating energy transport in plasma rest frame
03 p0412 A72-13507

Ionospheric photoelectron fluxes and motions simulated by Monte Carlo technique, including transport effects, elastic and inelastic collisions and energy losses
03 p0412 A72-13517

Soviet monograph on electron flux nonlinear interaction with slow electromagnetic waves in TWT, discussing output power and efficiency increase
03 p0333 A72-13949

Upper atmosphere supplementary electron flux data relationship to geomagnetic disturbance obtained from high altitude balloon experiments
05 p0709 A72-16236

D region ionization by electron fluxes as explanation for latitudinal radio wave absorption
05 p0656 A72-16249

Electron flux and energy spectra measurements at 200-600 km altitude by Cerenkov counters onboard Proton 1 and 2
05 p0709 A72-16254

Additional high energy electrons flux detection in upper atmosphere after magnetic perturbations
05 p0710 A72-16525

OGO-5 measurement of 10-200 MeV cosmic ray electron energy spectra, discussing quiet time flux intensity
05 p0720 A72-16719

Extensive air shower spectra based on electron and muon number
06 p0871 A72-17283

Photoelectron flux measurement of intensities of plasma lines in radar incoherent scatter spectrum by uhf radar
06 p0874 A72-18732

Charged particles observations on 21 December 1968 by Explorer 40 and from ground, noting auroral light primary energy influx by precipitation band of electron intensities
09 p1299 A72-23005

Differential photoelectron flux in lower ionosphere during 7 March 1970 solar eclipse observed by Nike-Apache rockets
09 p1378 A72-23012

Differential photoelectron fluxes at 560 km altitude observed by OVI-18 satellite on 22 March 1969, noting latitudinal variation
09 p1378 A72-23013

Model of dynodes system with random electron-hole pairs number, calculating equations for mean fluxes transport and correlated noise fluctuations
09 p1280 A72-23116

Emission of density modulated electron flux passing over diffraction structures formed by half planes and combs with oblique teeth, discussing optimum emitted power conditions
12 p1793 A72-27858

Low energy relativistic cosmic ray electrons temporal intensity variations from IMP satellite measurements, considering correlation with solar activity
13 p2030 A72-29376

Interplanetary electrons quiet-time intensity increases, considering trans-earth-orbital modulating region due to solar wind transport of photospheric field lines
13 p2030 A72-29377

Proton and electron fluxes limits in synchronous orbit, investigating local time dependence
13 p2031 A72-29393

Absorption coefficient of H-He plasma measured in temperature and electron density range of inverse bremsstrahlung and photoionization absorption
15 p2284 A72-31522

Low energy electron flux in magnetosphere, discussing relation to geophysical phenomena, solar wind, interplanetary magnetic field and charged particle longitudinal drift trajectories
15 p2225 A72-31903

Quasi-periodical intensity pulsations in trapped and precipitating electrons in earth outer radiation belt
15 p2299 A72-31914

Space charge electron flow between parallel conducting walls, developing relativistic method for potential and field distribution time variation
15 p2279 A72-32510

Stratospheric model for bremsstrahlung X ray relation emission to auroral electron flux, considering photon energy release in scintillation counters
17 p2551 A72-35872

Results of cosmic ray intensity measurements on the Venus-7 automatic station
22 p3218 A72-42213

Daily variation of electron and proton geomagnetic cutoffs calculated for Fort Churchill, Canada.
22 p3170 A72-42401

Solar-wind and interplanetary electron measurements on the Apollo 15 subsatellite.
22 p3218 A72-42403

Esro 1 /Aurora/ satellite electron intensity measurements, explaining disparities between different experiments by detectors low-energy thresholds difference
22 p3173 A72-42648

Rocket measurements of electron influx during a major magnetic storm with type A aurora.
23 p3332 A72-44515

Electron polar cap and the boundary of open geomagnetic field lines.
23 p3286 A72-44522

ELECTRON GAS

Cathode and anode temperatures effect on effective heat of condensation of electrons at anode for particular current density and different cesium vapor pressures
02 p0156 A72-12858

Hall effect mobility dependence on dispersion law in degenerate electron gas on semiconductor surface
02 p0270 A72-12890

Mercury vapor physicochemical processes kinematics in shock tube, determining electron gas energy balance equations
03 p0395 A72-13572

Transport coefficients of electron gas in electromagnetic field, using Grad thirteen moment method
05 p0697 A72-17005

Neutron star and white dwarf strong magnetic field generation mechanism involving thermodynamic equilibrium states of electron gas
05 p0723 A72-17162

F region electron-ion gas dynamic model with stability dependence on periodic solutions convergence of continuity equations
08 p1153 A72-20725

Impurities effect on level density of electron gas within strong magnetic field, discussing included self energy
11 p1693 A72-25526

Electron gas in superstrong magnetic fields of gravitationally collapsed objects outer region, noting Wigner transition to ordered structure
11 p1699 A72-26704

Ionospheric electrons and neutral particles temperature and concentration profiles explained by electron

- gas cooling due to atomic hydrogen excitation, calculating heat flow
14 p2101 A72-30641
- Degenerate electron gas magnetic properties implications for metals, white dwarfs and neutron stars, discussing nonmagnetic state for thermal equilibrium
14 p2158 A72-30728
- Reversible thermodynamic cycle of chemical to electric energy conversion with electron gas as working body, discussing Gibbs-Helmholtz equations
16 p2350 A72-32994
- Charge carrier motion in semiconductor with electron interactions, considering heating in presence of negligible electric field
16 p2441 A72-33278
- Equations of state and equilibrium for electron gas in strong magnetic field, discussing effects in pulsar crusts and atmospheres
16 p2460 A72-33929
- Constants of the linearized motion of Vlasov-plasmas.
17 p2590 A72-35158
- Nonstationary electron-ion gas distribution in the ionosphere
18 p2689 A72-36878
- Landau orbital ferromagnetism appearance likelihood in white dwarf stars, noting temperature requirements of noninteracting electron gas
19 p2859 A72-37891
- Neutron-rich nuclei in a Fermi gas
19 p2837 A72-38060
- F region electron-ion gas dynamic model with stability dependence on continuity equations periodic solutions convergence
19 p2791 A72-38353
- Balescu-Guernsey-Lenard kinetic equation for homogeneous dilute electron gas extended to higher densities, specifying conditions for BBGKY hierarchy correlation functions solution
19 p2791 A72-38353
- The heating of the solar plasma due to microwave phenomena correlated with type II meter bursts.
22 p3222 A72-42041
- The threshold of disintegration of nuclei in a degenerate electron-neutron gas
22 p3209 A72-42963
- Electron distribution fluctuation in two level system of unstable electron gas, noting periodic time dependence of population
23 p3319 A72-43406
- Longitudinal dielectric tensor for an electron gas in a uniform magnetic field.
23 p3321 A72-43808
- Calculation of transport coefficients of a non-Lorentzian plasma
23 p3321 A72-43821
- Equilibrium energy spectrum for the galactic cosmic electrons.
23 p3328 A72-43831
- Degenerate electron gas self energy approximation by dielectric function, calculating quasi-particle and plasmon properties
24 p3428 A72-44797
- Superhigh-frequency heating of a plasma and longitudinal electron heat conductivity in a magnetic field
24 p3429 A72-45492
- ### ELECTRON GUNS
- High perveance electron guns with control grids and low voltage beam modulation, considering design, operation, structural and control characteristics
02 p0189 A72-11562
- Periodic magnetic field effects at gun cathode on electron beam focusing stability under nonoptimal conditions
02 p0190 A72-11572
- Electron paths and spread velocities in helical beams of adiabatic M-type electron gun used in masers at cyclotron resonance
06 p0826 A72-18403
- Electrostatic field calculation for magnetron/injection/ electron gun with wedge shaped cathode
06 p0826 A72-18404
- Vacuum welding by electron beam bombardment, discussing electron gun arrangements with plane-radial, plane-linear and linear electron beams
08 p1176 A72-21049
- Low energy scanning electron beam gun with retarding field mode for microelectronic device evaluation
10 p1446 A72-23936
- Rectifier tube cathode as colloid thruster electron gun type neutralizer, discussing efficiency and accelerated life tests
11 p1711 A72-26228
- Fast electron gun with subnanosecond switching times and 100 mA peak beam current for delayed coincidence studies of atomic decays
13 p1933 A72-29761
- Electron trajectories and spread velocities in helical beams of adiabatic M-type electron gun used in masers at cyclotron resonance
17 p2562 A72-34854
- Beam-defocusing effect due to filament magnetic fields in electron guns of electron linear accelerators.
19 p2772 A72-37404
- A design method for the electron beams of TWT's.
19 p2775 A72-38610
- Triode electron gun design for narrow electron beam under highly convergent lens action, using field emission source
19 p2775 A72-38611
- Drift of amplification factor and its effects in a tri-electrode electron gun.
21 p3033 A72-40995
- Digital-computer analysis of electron guns for cathode-ray tubes by taking into account initial thermal velocities.
21 p3088 A72-41834
- Trajectory equations of laminar electron flow in exponential magnetic field, calculating electrode shapes of magnetron injection electron gun
21 p3088 A72-41835
- Pulsed atmospheric-pressure carbon-dioxide laser initiated by a cold-cathode glow-discharge electron gun.
22 p3186 A72-42753
- The velocity distribution of electrons in beams formed by high-perveance three-electrode guns
23 p3319 A72-43402
- ### ELECTRON IMPACT
- High resolution RF linear mass spectrometer for separation of ions formed by electron impact on organic molecules
01 p0064 A72-10043
- Electron scattering off atoms, diatomic and polyatomic molecules in impact spectroscopy, applying simple group theory
02 p0262 A72-11913
- Atomic oxygen coupled electron excitation and ionization by electron-atom and atom-atom collisions in nonequilibrium relaxation zone behind shock wave
02 p0207 A72-12896
- Electron impact broadening of ionized Be and Ba lines in electric shock tube plasma, measuring electron density and temperatures
03 p0393 A72-13020
- Vibrational population of molecular nitrogen electronic states in normal auroras, examining electron impact and cascade contributions
03 p0349 A72-13524
- Quantum mechanical calculations of autoionization structure in ionization of Ba positive ions by electron impact
03 p0391 A72-13746
- Electron impact Stark broadening of ionized chlorine lines in pulsed arc plasma using laser interferometric and spectroscopic measurements
03 p0396 A72-13748
- Water vapor laser pumping by upper lasing level excitation through direct electron impact, explaining mechanism by model
04 p0529 A72-14587
- Dissociative excitation of CO and metastable fragments by electron impact on carbon dioxide, investigating cross sections
06 p0803 A72-17447
- Molecular nitrogen photoelectron impact excitation of Herman-Kaplan upper electronic state, considering cascade contribution to low lying states in electron auroras and dayglow
06 p0806 A72-17647
- Adiabatic-nuclei theory application to diatomic molecules excitation by electron impact, approximating fixed nuclei phase shifts dependence on internuclear separation
06 p0852 A72-17826
- Excitation and ionization cross sections and rate coefficients of hydrogen-like ions by electron and proton impact in Bethe-Born approximation
06 p0852 A72-18052
- Scattering cross section for excited oxygen atoms production by electron impact dissociation of molecular oxygen
07 p1037 A72-18964
- Electron impact induced fragmentations of o-, m- and p-hydroxyalkylphenones and trimethylsilyl/TMS/ ether derivatives, using high resolution mass spectrometry, metastable defocusing and deuterium labeling
07 p0936 A72-19499
- Electron impact induced fragmentation of alkyl-N-/1-phenylethyl/-carbamates of primary, secondary and tertiary alcohols, using deuterium labeling and high resolution mass spectrometry
07 p0936 A72-19500
- Electron impact cross section and energy deposition in molecular hydrogen, using generalized oscillator strength in Born-Bethe approximation
07 p1038 A72-20567
- Differential and integral scattering cross sections for helium excitation by electron impact from ground state to 2/super 1/S state
07 p1038 A72-20679
- Vacuum UV excitation cross sections measurement by electron impact on nitric oxide, tabulating threshold energies and transition probabilities
09 p1357 A72-22857
- Electron impact excitation of nitric oxide in vacuum UV, measuring absolute cross sections for emission features
10 p1515 A72-24341
- Differential and total ionization cross sections of multielectron atoms by electron and proton impact
10 p1515 A72-24602
- Merging beams study of positive ion ionization by electron impact for atomic He, N and O
11 p1692 A72-26658
- Boltzmann distribution of nitrogen ions according to rotational energy levels in nitrogen ionization by slow electrons impact
12 p1847 A72-27050
- Electron impact excitation spectrum of molecular oxygen, investigating angular behavior of differential scattering cross sections and energy dissipation
12 p1848 A72-27851
- Electron impact induced aurone epoxides fragmentation, discussing ion formation, intermediates, thermal rearrangement and mass spectra
13 p1913 A72-29775
- Absolute cross sections for Werner band system excitation of molecular hydrogen by electron impact, discussing relative spectral response calibration
13 p2009 A72-30065
- Predrawn airflow enhancement project, discussing magnetically conjugate photoelectron impact excitation observation and geophysical interpretation
14 p2098 A72-30147
- Incoherent scatter and filter photometer search for 6300 A predrawn enhancement by magnetically conjugate photoelectron impact excitation, comparing with ionospheric electron density
14 p2098 A72-30148
- Atomic hydrogen collisional and radiative transition rates, computing excitation and ionization cross sections
14 p2133 A72-30564
- Hydrogen negative ion electron detachment collision process cross section calculation using Coulomb trajectory impact-parameter method
14 p2135 A72-30884
- Metastable /2S/ atoms production by electron impact induced dissociative excitation of molecular deuterium, measuring total cross section via Lyman alpha flux
15 p2282 A72-32645
- Eikonal distorted wave analysis of inelastic electron-atom collisions at intermediate energies application to electron impact induced atomic hydrogen 2s and 2p states excitation
15 p2282 A72-32646
- Electron impact low energy cross sections for transitions between highly excited states, obtaining upper bound via quantal impact parameter theory
15 p2315 A72-32715
- High energy resolution spectrometric measurement of relative emission cross section for electron impact excited molecular nitrogen second positive system bands
16 p2428 A72-32922
- Dissociative excitation of vacuum ultraviolet emission features by electron impact on molecular gases. III- CO2.
17 p2585 A72-34734
- Vibrational excitation in N2 by electron impact in the 15-35-eV region.
19 p2837 A72-37546
- Linear momentum transfer effects in molecular dissociation produced by electron impact.
21 p3087 A72-40557
- Cross sections for the excitation of Ar II laser lines in electron-ion collisions.
21 p3063 A72-40725
- Electron impact effects on Ba I, Ba II and Sr I selected spectral line Doppler widths calculated for laser-generated plasmas for chemical release simulation
21 p3092 A72-40821
- Energy and angular distributions of secondary electrons resulting from ionizing collisions of electrons with helium and krypton.
21 p3088 A72-41493
- Interpolation formulae for the electron impact excitation of ions in the H-, He-, Li-, and Ne-sequences.
22 p3224 A72-42379
- Electron deposition in water vapor, with atmospheric applications.
22 p3171 A72-42420
- Electron impact excitation cross sections and energy degradation in CO.
22 p3172 A72-42422
- Kinetics of impact-radiative ionization and recombination
23 p3318 A72-43296
- Electron impact ionization of ions trapped in a hollow electron beam.
23 p3316 A72-44343
- Excitation of vacuum ultraviolet radiation by electron impact on carbon monoxide - Some unresolved questions near threshold.
24 p3379 A72-45313
- Cross section parameters for electron impact excitation, noting mathematical models for aeronautical users
24 p3400 A72-45591

Boltzmann distribution of nitrogen ions according to rotational energy levels in nitrogen ionization by slow electrons impact

24 p3427 A72-45703

ELECTRON INTENSITY U ELECTRON FLUX DENSITY **ELECTRON INTERACTIONS** U ELECTRON SCATTERING **ELECTRON IONIZATION** U IONIZATION **ELECTRON IRRADIATION**

Thermoluminescent phosphorus films irradiation by electrons with energies up to 15 keV in vacuum chamber

01 p0114 A72-10372

Fused silica optical transmittance at elevated temperatures during high energy electron bombardment, noting optical absorption at short wavelengths

01 p0103 A72-11357

Rocket measurement of highly collimated short duration bursts of auroral electrons, comparing with existing auroral models

03 p0349 A72-13515

Low energy electron beam irradiation of aluminum-silicon nitride-silicon structures for elimination of bias polarization effects on I-V characteristics

03 p0402 A72-13865

Li-containing solar cell damage and recovery characteristics measurement under 1-MeV electron irradiation, deriving diffusion-length damage coefficient

03 p0312 A72-14092

Isothermal annealing measurements of zero-phonon line luminescence at 0.97 eV in electron irradiated Si, obtaining activation energy

04 p0560 A72-14546

Electron irradiation effects on MOS structures at vlf, considering inversion layer cut-off frequency and surface state density

06 p0865 A72-17610

Vacancy supersaturation effect on enhanced precipitation by high flux electron irradiation in stainless steel

07 p1033 A72-20410

Artificial magnetosphere interaction with 8 keV electrons in hydrogen plasma beam simulating solar wind, noting penetration caused by boundary instability

08 p1156 A72-20823

German monograph on Frenkel defect structures in thin gold wire at high electron irradiation dose, using electrical resistance measurements

09 p1354 A72-22325

High dose rate electron beam irradiation using telescoping drift tube for flash X ray machine

10 p1509 A72-23935

Laboratory irradiation tests with van de Graaff generator for simulation of spacecraft components radiation damage due to high energy space protons and electrons

12 p1863 A72-27552

Heat treatment and electron irradiation tests for spatial reliability of CdS and CdTe thin film solar cells, noting photovoltaic properties

12 p1756 A72-28019

Electron irradiation effects on Li doped silicon solar cells, noting changes in donor concentration and defects formation

12 p1757 A72-28022

Li dopant radiation damage inhibiting effect on electron irradiated n-type silicon, discussing EPR and photoconductivity experimental results

12 p1856 A72-28023

Solar cells testing and array performance evaluation for communication satellites at Comsat laboratories, noting electron irradiation and proton damage studies

12 p1759 A72-28044

Monoenergetic electrons and low energy protons radiation damage effect on Si solar cell electrical and optical properties

12 p1759 A72-28046

Electron irradiation of Li doped Ge at low temperatures, measuring Hall effect and minority carriers diffusion length

12 p1857 A72-28055

Phonon scattering and induced energy levels in electron irradiated Sb doped Ge in n to p-type conversion region, measuring thermal conductivity and Hall effect

12 p1857 A72-28057

Li defect interactions in electron irradiated n-type single crystal Si from electron paramagnetic resonance measurements

12 p1858 A72-28063

Introduction rate and annealing of defects produced in Li-diffused float zone n-type Si by 30 MeV electrons and fission neutrons

12 p1858 A72-28064

Electron irradiation of n-type Si or Te doped GaAs, determining carrier removal rate, mobility changes and annealing characteristics

12 p1858 A72-28067

Annealing behavior of electrical properties and photoluminescence spectra in electron irradiated n-type GaAs semiconductors

12 p1859 A72-28068

IR absorption bands in mechanically and chemically polished GaAs single crystals irradiated with varying neutron and electron doses

12 p1859 A72-28069

Electron radiation damage and edge emission of cadmium telluride, presenting cathodoluminescence spectra

12 p1859 A72-28071

Te single crystal electrical resistivity and Hall coefficient effects of electron irradiation, suggesting point defects and dislocations interaction

12 p1859 A72-28073

Diamond powder lattice parameter changes during fast electron irradiation at various temperatures, discussing crystal defect stability and neutron irradiation comparison

13 p1983 A72-28760

Radiation effects measurement on neutron, proton and electron irradiated Li-drifted Si detectors by IR response technique, comparing characteristics with photovoltage effect

15 p2234 A72-31538

Radiation damage effects in Li compensated Si nuclear particle detectors induced by irradiation with electrons, protons and fast neutrons

15 p2291 A72-31539

Transient 10 MeV electron radiation effects on RF power and recovery time of GaAs Schottky barrier IMPATT diodes

16 p2370 A72-33766

Auroral electron acceleration by longitudinal electric field due to protons defreezing above ionosphere

17 p2550 A72-35852

Study of point defects produced in aluminum by tempering and irradiation with electrons

18 p2702 A72-36705

Properties of 1 MeV electron-irradiated defect centers in p-type silicon.

19 p2844 A72-37687

One MeV electron irradiation of new technology silicon solar cells.

19 p2754 A72-37777

Electron abundance equilibrium as factor in biological effectiveness of proton beam irradiation of animals

21 p2998 A72-40450

Influence of irradiation by 1.2-MeV electrons on the electrophysical properties of p-Si single crystals grown in a hydrogen atmosphere

21 p3098 A72-41686

Development of phosphorescence during ruby irradiation

23 p3323 A72-43412

ELECTRON MASS

Temperature and charge carrier density dependence of conduction electron optical effective mass in semiconductor compounds

13 p2021 A72-28788

Time constancy of physical constants in expanding universe, discussing light speed, Planck constant and electron and proton mass in context of Dirac hypothesis

16 p2425 A72-33517

Solid state physics experiment for conduction electrons effective mass determination in ultrapure n-type InSb by means of magnetophonon effect

21 p3096 A72-40203

ELECTRON MICROSCOPES

Tungsten carbide dislocation structures analysis by transmission electron microscopy, deriving Burger vectors from energy considerations and electron micrographs contrast

03 p0370 A72-12995

Defective IC device glass surface passivation effects on scanning electron microscope analysis

03 p0365 A72-14287

Voltage contrast mode scanning electron microscopy application to defect and failure analysis of semiconductor memories

03 p0336 A72-14288

Zener diode surface and bulk breakdown mechanisms by scanning electron microscopy, discussing microplasma noise

03 p0336 A72-14289

Selected microarea electron diffraction technique in high voltage electron microscopy, discussing applications in crystallography and metallurgy

04 p0523 A72-15490

Electrochemical thinning of metal disks for electron microscopic thin foils preparation

04 p0527 A72-15492

Electron microscope examination of freeze-etched air-filled lung alveoli extracellular lining layer, discussing sample preparation techniques

05 p0623 A72-16787

Electron microscopy for structure study of anodic aluminum oxides prepared by various methods, comparing electrograms of oxides after heating, boiling and filling with water

05 p0624 A72-17054

CdTe condensed films hexagonal modification and twinning boundaries birefringence reflection, using electron microscope and diffraction analysis

07 p1047 A72-18856

Scanning electron microscope for metal matrix composite materials structure examination, emphasizing matrix behavior, filament under load and interface

07 p1011 A72-19485

Nonconducting samples preparation for scanning electron microscope, using carbon as coating material

07 p0992 A72-20578

Facility for electron microscopy of specimens in controlled environments, observing lattice structure in wet catalase crystals

07 p0993 A72-20586

Limiting resolution of reconstructed image of focused hologram in electron microscopes as function of aberration and spatial coherence

08 p1166 A72-21380

Morphology and physicomechanical properties of carbonized polyacrylonitrile fibers by scanning electron microscopy, discussing macro and microdefects effects on strength characteristics

08 p1195 A72-21762

Electron microscopic investigation of niobium-oxygen alloys with Zr and Hf additions, measuring oxygen solubility

08 p1187 A72-21787

Electron microscopy application to dynamic wear studies of Ni on Ni surface and subsurface topography and microstructure in nitrogen atmosphere

08 p1179 A72-21943

Routine method for ultrathin carbon support film production for electron microscopy, noting mechanical stability and strength

08 p1172 A72-22020

Transmission electron microscope investigation of Al-Mg-Si alloy precipitation, showing Guinier-Preston zone visibility due to matrix elastic strain introduction

09 p1328 A72-22983

Photoemission electron microscopy application to refractory metals and nonmetallic materials, discussing image formation and contrast enhancement problems

10 p1493 A72-23823

Graphite morphology in metallic materials from scanning electron micrographs, discussing sulfur contents effect in tempered cast iron

10 p1500 A72-23825

Electron microscope interfaced computer for generating, registering and fabricating microelectronic device and circuit patterns

10 p1459 A72-23955

Profiling technique with scanning electron microscope to obtain depth information on single small specimen micrograph

10 p1481 A72-24240

Transmission electron microscope examination of deformation microstructures adjacent to fatigue cracks in Al alloys

10 p1497 A72-24823

Oxygen adsorption effects on Mo orientation contrasts and emission image under electron microscope

10 p1513 A72-24875

Dark field electron microscopy with small annular zone of objective lens to reduce chromatic aberration effects on resolution

11 p1633 A72-26322

Angular distribution of electrons at output of specimen observed by electron microscope, examining resolution problem for thin objects

11 p1635 A72-26483

Fractographic study of stress corrosion fractures of low carbon steels with electron microscope

11 p1666 A72-26924

Electron microscopy and structure of materials - Conference, University of California, Berkeley, September 1971

11 p1666 A72-26926

Transmission and scanning electron microscope observations of Nb-Hf alloys fracture morphology, noting precipitate free zone

11 p1667 A72-26934

Compression creep in ordered binary and ternary ordered bcc Ni alloys investigated by transmission electron microscopy

11 p1667 A72-26937

High voltage electron microscope applications to materials reactions in gaseous environments, exemplifying by stress corrosion morphology in stainless steel, Al-Zn-Mg and Ti-Al

11 p1668 A72-26945

Lunar and terrestrial pyroxenes phase structure electron microscopic investigation, using ion-thinned samples

11 p1725 A72-26952

Electron microscope study of commercial Ni superalloys, discussing intermetallic compound and carbide precipitation hardening

12 p1827 A72-27137

In situ measurement of objective lens data for high resolution electron microscope, using Bragg reflex images of crystallites with known orientation

12 p1807 A72-27528

Electron microscope study of hyperoxia-induced pathogenetic ultrastructural changes in rat lung

12 p1761 A72-27531

Primary recrystallization in TD-nickel bars on sublight optical level identified by transmission electron microscopy examination of deformation and annealing substructures 14 p2119 A72-30601

Work functions of dilute W alloys from vacuum emission vehicle and thermionic microscope measurements, noting additives effect 14 p2120 A72-30613

Si phase identification in super alpha Ti alloys, using electron transmission microscopy and diffraction analyses 14 p2120 A72-30616

Solid surface inspection by X ray diffraction, electron microscopy and chemical techniques 14 p2131 A72-30693

Electron microscope study of precipitated fines of austenitic steel containing V and N, noting heat treatment effect on fcc crystal structure 15 p2254 A72-31523

Ferroelectric nature of superficial layer on barium titanate crystals from scanning electron microscope and optical observations 15 p2291 A72-31681

As-quenched and aged form of omega phase in Ti-Nb alloys investigated by electron microscopy and X ray diffraction 16 p2410 A72-33818

Electron microscopy at 3 million volts 17 p2535 A72-34199

Experiments on the phase contrast transfer functions of a superconducting lens 17 p2594 A72-34284

Electron-microscopic investigation of the development of a cellular structure in molybdenum during hydroextrusion 17 p2569 A72-35524

Fractography of fiber reinforced metal composites. 17 p2560 A72-35654

A dynamical theory for the contrast of perfect and imperfect crystals in the scanning electron microscope using backscattered electrons. 18 p2692 A72-36749

Freeze etching techniques in electron microscopic investigations of biological cells molecular structure 18 p2653 A72-36829

Quantitative microstructural measurements by room temperature photoemission electron microscopy, discussing relief contrast, edge effect, resolution and information depth 18 p2719 A72-36831

Physical parameters and structure of microwave power transistors, noting scanning electron microscope analysis of fine structure 18 p2671 A72-37144

Electron microscope double contrast images to identify Burgers vectors of close packed metal crystal dislocations 19 p2846 A72-38590

A versatile ultrahigh vacuum scanning electron microscope. 21 p3051 A72-40217

A novel specimen stage permitting high-resolution electron microscopy at low temperatures. 21 p3051 A72-40218

Microscopic and electron-microscopic investigation of the catalysis of ammonium perchlorate combustion 22 p3216 A72-43186

Scanning electron microscope stereophotographic picture synthesis from sequential holographic recording of three dimensional objects 23 p3290 A72-43904

The direct study of crack formation in metals in a high-voltage electron microscope 24 p3401 A72-44717

Review and forecast of electron microscope studies of membrane systems in terms of fundamental problems of biomedical research and molecular biology 24 p3371 A72-44869

Application of a field-emission microscope to the investigation of the work function of tungsten coated with a thin layer of silicon oxide and with tantalum 24 p3432 A72-44891

Field-emission microscopy of tungsten coated with a silicon oxide film 24 p3432 A72-44892

ELECTRON MICROSCOPY

U ELECTRON MICROSCOPES

ELECTRON MOBILITY

Electron motion equations for threshold input signal of M type amplifiers with secondary emission cathode in interaction space 02 p0190 A72-11571

Electron and ion drift rate effect on floating double probe characteristics in Maxwellian plasmas 02 p0266 A72-12768

Hf electric field influence on electron drift instability and slow ion-acoustic waves for inhomogeneous magnetized plasma stabilization 04 p0555 A72-14617

Plasma shock wave oscillation profile dependence on ion and electron friction and viscosity 04 p0555 A72-14620

Nonlinear nonlaminar 3D electron motion calculation through output cavity of klystron amplifier by Green function 04 p0497 A72-14697

Electron drift speed and multiplication rate in pulsed Ar positive column in axial electric field 04 p0553 A72-15669

Quantum mechanical electron motion problem in binary alloy crystal lattice, discussing Bloch approximation, energy spectra, and third element admixture conductivity effects 07 p1049 A72-20150

Transport theory Boltzmann equation and Monte Carlo methods applied to semiconductor negative differential mobility calculation 10 p1526 A72-24398

Travel time effects on electron motion in HF electromagnetic fields, reviewing phase focusing and achromatic electron lens development 10 p1513 A72-24976

Electron energy, mobility and bremsstrahlung in weakly ionized nonisothermal plasmas, using Kogan approximation 11 p1698 A72-26647

Microwave time of flight method for measuring electron drift velocity in GaAs semiconductors 12 p1855 A72-27667

Room temperature time of flight electron and hole mobility and trapping time measurements in zinc selenides as function of electric field 12 p1855 A72-27835

LF oscillations and electron drift in frozen plasma under strong electromagnetic radiation, deriving formulas for coupled Alfvén and spiral waves 13 p2035 A72-28593

Gunn diode active region thickness, free electron mobility/concentration, structure and contacts, including treatment of GaAs 13 p1934 A72-30036

Spread F association with ionospheric tilts due to total electron content drift, using incoherent scatter radar 15 p2230 A72-32261

Radiative transfer equation application to ionospheric photoelectrons transport, predicting photoelectrons angular distribution and escape flux 16 p2444 A72-32963

Charge carrier motion in semiconductor with electron interactions, considering heating in presence of negligible electric field 16 p2441 A72-33278

Free electrons-laser interaction induced electron forward drift and dc current generation, deriving drift velocity by nonrelativistic classical and quantum mechanical theories 16 p2402 A72-33397

Normal and hypoxic myocardium mitochondrial metabolism process, studying electron transport system 17 p2501 A72-34978

Electron cyclotron drift instability linear theory application to controlled fusion and collisionless shocks, proving anomalous resistance to current flow normal to magnetic field 17 p2592 A72-35624

Acceleration stress tolerance dependence on electron or ion transport across cell surface activation energy barrier, studying rat survival times 18 p2650 A72-36448

Studies of the electron transport chain of extremely halophilic bacteria. VII - Solubilization properties of menadiene reductase. 19 p2755 A72-37649

On the drift velocity of electrons in a gas. 22 p3212 A72-42996

LF oscillations and electron drift in frozen plasma under strong electromagnetic radiation, deriving formulas for coupled Alfvén and spiral waves 24 p3440 A72-45093

ELECTRON MULTIPLIERS

U PHOTOMULTIPLIER TUBES

ELECTRON OPTICS

Frequency contrast characteristics derivation method with devices for determining transfer functions of objectives and film, using electron-optical bench 02 p0229 A72-12171

High resolution electrons image intensifier for particle spectrographs, using channel plate, scintillator and fiber optics 04 p0524 A72-15536

Charged particle motion equations for fifth order spherical aberration of quadrupole-octupole lens with arbitrary electrode and pole shapes 05 p0638 A72-16989

Hybrid computer aided design of thick electrostatic electron lenses by Laplace equation solution in terms of cylindrical harmonics, applying to CRT 06 p0779 A72-17481

Electron tube present and future applications as oscillators, high power and hf amplifiers and optoelectronic converters 06 p0784 A72-17775

Three element einzel and asymmetric voltage lenses for electron optics, calculating focal lengths and spherical aberrations based on potential distribution inside equidiameter coaxial cylinders 07 p0992 A72-20585

Hybrid computer aided synthesis of thick electrostatic electron lenses by Laplace equation solution in terms of cylindrical harmonics with gradient used in trajectory integration 10 p1509 A72-23940

Third order aberration coefficients of electron trajectories for two tube electrostatic lenses 10 p1510 A72-23941

Electron image projection system using converter tube technique for microcircuit lithography, discussing performance tests and design changes 10 p1447 A72-23957

Rotationally symmetrical electromagnetic lenses of electron mirror and cathode lens type 10 p1513 A72-24977

Submillimeter plane waves formation by quasi-optical line and diverging lens with phase front adjustment 11 p1598 A72-26719

Electrostatic field and electron trajectories calculation for focusing optoelectronic systems formed by interacting electrodes positioned on conducting surface 13 p2004 A72-29070

Electron-optical parameters effect on GaP/Cs/dynode photomultipliers time response characteristics, describing computer simulation and pulse response measurement techniques 15 p2234 A72-31532

Ceramic envelope electron multiplier design with hemispherically shaped dynodes, discussing electron optics, photosensitivity and applications 15 p2234 A72-31533

Electron-optical methods of investigating inhomogeneities in rarefied gases. 17 p2552 A72-34515

The effect of atmospheric turbulence on the error of an optoelectronic angle sensor. 17 p2554 A72-34941

Microwave and optoelectronic devices performance and component reliability, considering varactors, p-i-n, avalanche and Gunn diodes, ICs, FETs, light emitters and liquid crystals 18 p2720 A72-37137

Reliability of semiconductor optoelectronic components - Analysis of the long-term behavior 18 p2670 A72-37138

An arrangement for studying the time characteristics of injection lasers 21 p3064 A72-41738

Electric field distribution and strength and electron trajectories computations in designing electron optical display systems, using rectangular networks 23 p3291 A72-44312

ELECTRON ORBITALS

Integrals for atomic wave functions of Slater orbitals, obviating numerical snags by Euler transformation 02 p0262 A72-11980

Lyman alpha radiation emission cross sections due to H/2p and H/2s formation in protons and hydrogen atoms collisions with hydrogen molecules 07 p1038 A72-20678

Inner shell ionized atoms, discussing orbital electron rearrangement processes based on shakeoff events and radiative Auger transition 09 p1356 A72-22834

Multiconfigurational interactions in atoms with incomplete electron shells, identifying K-alpha satellite emission lines 09 p1357 A72-22837

Electronic configuration effect on wetting characteristics of hard material mixed crystals, investigating transition metals carbides, nitrides and oxides 11 p1665 A72-26873

Orbiting electron magnetic susceptibility derivation from many band Hamiltonian using Bloch representation to avoid decoupling transformation ambiguity 15 p2282 A72-32547

Oxygen atom electron affinity calculation by symmetry-adapted pair correlation approximation, using pseudonatural orbitals (PSNO) technique 15 p2282 A72-32644

A simple, radially correlated ground state wavefunction for two electron atoms. 17 p2586 A72-35828

ELECTRON OSCILLATIONS

Higher order cyclotron harmonic resonance of electrons with electromagnetic wave propagation through collisionless magnetoplasma, deriving energy oscillation time period 01 p0105 A72-10023

Electrostatic oscillations of multivelocity electron streams in hot inhomogeneous plasma 07 p1046 A72-20502

Langmuir electron oscillation excitation by ion beam at velocity exceeding average electron thermal velocity in plasma formed by residual gas ionization 07 p1046 A72-20505

Effective transmission coefficient increase for Langmuir and electromagnetic waves passing through

- density barrier via perturbation transport by resonant electrons 08 p1216 A72-22090
- Higher harmonics intensities dependence on fundamental of electron oscillation in beam generated plasma 10 p1524 A72-24920
- Spectral intensity distribution of vibrational electron interaction with strong coupling during polymerization of monomer cyanine dye and dimer molecules 15 p2280 A72-31410
- Relativistic electron ring oscillations in circular waveguide with allowance for walls finite conductivity, noting radiative instability at subcritical frequencies 15 p2210 A72-32738
- Effective transmission coefficient increase for Langmuir and electromagnetic waves passing through density barrier via perturbation transport by resonant electrons 17 p2588 A72-34661
- The equilibrium and the pulsation frequency spectrum of an electron cloud of spherical and cylindrical symmetry 19 p2867 A72-38571
- ELECTRON PARAMAGNETIC RESONANCE**
- Impurity-related color centers and electron-hole traps in quartz by electron spin resonance and thermoluminescence observations 02 p0207 A72-11598
- Radical concentrations in gamma irradiated poly(ethylene 2,6-naphthalene dicarboxylate) by ESR spectrum analysis 10 p1433 A72-23847
- Li dopant radiation damage inhibiting effect on electron irradiated n-type silicon, discussing EPR and photoconductivity experimental results 12 p1856 A72-28023
- EPR for point defects produced in Si by fast neutron irradiation, emphasizing damage cluster model 12 p1858 A72-28060
- Electron paramagnetic resonance investigation of III-V compound semiconductor crystals, observing large magnetic moments, heteropolar chemical bonding and impurities 13 p2021 A72-28572
- EPR transitions of quadrupole interaction of cubic imperfections with ground-vibronic-state degeneracy /Jahn-Teller effect/ 16 p2431 A72-33725
- Electron paramagnetic resonance of radiation damage in a lunar rock. 17 p2609 A72-35098
- Ferromagnetic and paramagnetic resonance spectra of lunar material - Apollo 12. 18 p2724 A72-36276
- Classical nonlinear electronic relaxation oscillators as EPR and NMR signal detectors, reconstructing resonance lines from absorption induced oscillator waveform changes 18 p2662 A72-36993
- Electronic and nuclear magnetic resonances of the oxygen and hydrogen labile negative molecular ions. 20 p2956 A72-39189
- Electron spin resonance of gamma-irradiated poly(ethylene 2,6-naphthalene dicarboxylate). 20 p2898 A72-39400
- Electron paramagnetic resonance spectrum of vanadyl acetylacetonate dissolved in liquid crystal or isotropic solvent 21 p3013 A72-41177
- Resonant interaction of an electrostatic wave with electrons in a current sheet. 22 p3169 A72-42008
- Electron spin resonance of divalent Mn ion doped in thallous azide single crystals, investigating temperature effects on spin Hamiltonian parameters 22 p3152 A72-42716
- Laser magnetic resonance of the O₂ molecule using the 337-micron HCN laser. 22 p3209 A72-42896
- Investigation of the formation of local concentrations near the critical liquid-gas point by the electron paramagnetic resonance 23 p3356 A72-43326
- Electron paramagnetic resonance hyperfine spectral observation of double quantum transitions of Ti positive ions in strontium chloride single cubic crystal host 24 p3378 A72-45311
- Investigation of radiation paramagnetic defects in alkaline-silicate glass subjected to the action of high quasi-hydrostatic pressures - Structure of hole defects 24 p3417 A72-45421
- Critical-point anomalies in the electron-paramagnetic-resonance linewidth and in the zero-field relaxation time of antiferromagnets. 24 p3432 A72-45674
- ELECTRON PATHS**
- U ELECTRON TRAJECTORIES**
- ELECTRON PHONON INTERACTIONS**
- Dynamic equations for nonequilibrium stationary state superconductors with electron-phonon and electron-electron inelastic collisions 03 p0401 A72-13089
- Quasi-static measurement and electron phonon interpretation of specific heat of metals at low temperature 03 p0456 A72-13843
- Jahn-Teller Hamiltonian for triplet electron state coupling to phonon vibrations in cubic symmetry 03 p0404 A72-14264
- Radio signal electron-phonon detector design and experimental realization, considering requirements for minimum transduction and surface wave propagation loss 05 p0626 A72-16281
- Semiconductors theory for multivalley energy spectrum and multivalued equilibrium distribution of carriers during electron phonon interactions 07 p1048 A72-19641
- Electron phonon coupling in tight-binding approximation for phonon frequency renormalization and transition metal superconductivity coupling constant computation 09 p1368 A72-22555
- BCS theory for transition metals and alloys superconductivity, discussing electron phonon coupling, transition temperatures and Cooper pair fluctuations 09 p1368 A72-22556
- Electron phonon coupling and IR optical constants relationship to superconductivity in transition metals 09 p1369 A72-22566
- Transistor LF flicker background noise generation mechanism in terms of bulk effect due to temperature fluctuation or phonon electron interactions 09 p1286 A72-23107
- Transition series oxides metal-insulator phase transition based on electron phonon interaction model 11 p1701 A72-26024
- Thermal conduction anomalies and electron phonon interaction in thin metallic sheet at low temperatures 12 p1888 A72-27182
- Dynamic equations for superconductors with electron-phonon and electron-electron inelastic collisions, investigating nonequilibrium stationary states 13 p2022 A72-29438
- Reflectivity of metals at high temperatures based on Drude theory and electron-phonon scattering, detailing temperature dependence and optical constants 14 p2129 A72-30183
- Phononless lines shift and broadening and electron phonon interaction in lanthanum trifluoride-Nd crystal, obtaining temperature dependence of non-radiative transition probability 14 p2142 A72-30359
- Oscillatory current characteristics of Stark ladder electron with weak LO phonon coupling in solids 15 p2293 A72-32218
- Emitted phonon spectrum effects on detected signal response in superconducting Sn diodes, noting deviation from linearity 15 p2209 A72-32541
- In-Ti alloys electron phonon interaction and superconductivity electron tunneling examined by sum rule and mass defect theory 15 p2295 A72-32543
- Conduction electron phonon scattering effect on electrical resistance of metallic contacts during pressure welding 16 p2370 A72-33952
- Anisotropy and strong-coupling effects on the critical-magnetic-field curve of elemental superconductors. 18 p2719 A72-36710
- Transport coefficient of multi-layer film of semiconductors. 19 p2843 A72-37401
- Transport phenomena in an electron-phonon system in strong magnetic fields at low temperatures 20 p2953 A72-39310
- Extension of Eliashberg's theory to type-II superconductors. 21 p3096 A72-40574
- Phenomenological models of the electron-phonon interaction and the superconductivity criterion of metals 21 p3098 A72-41688
- Influence of the properties of the materials on junction tunnelling characteristics. 22 p3214 A72-42454
- Dependence of changes in the electronic dislocation-braking force during superconducting transition on the stresses, temperature, and strain rate 23 p3312 A72-43315
- Semiconductors theory for multivalley energy spectrum and multivalued equilibrium distribution of carriers during electron phonon interactions 24 p3431 A72-44572
- ELECTRON PHOTON CASCADES**
- Energy transfer to electron-photon component during hadron interaction in lead, using ionization calorimeter 06 p0869 A72-17268
- Cosmic radiation high energy hadron component relation to extensive electron-photon showers, comparing sampling events based on multicore structure and total energy 06 p0870 A72-17282
- High energy muon energy and angular distributions from electron-photon cascades, using emulsion chamber with X ray films 06 p0871 A72-17286
- Muon generated cascade showers in iron, using ionization calorimeter and hodoscopic detectors 06 p0871 A72-17290
- Transient effect in electron-photon shower on readings of ionization chamber and scintillation counter 06 p0871 A72-17291
- Extensive atmospheric showers and high energy transfer from interacting nucleons to electron photon cascades 07 p1060 A72-19867
- Electron photon cascade energy measurement by photometering blackened spots on X ray films 07 p0988 A72-19870
- Study of high energy /25-10,000 GeV/ interactions with a multiplate cloud chamber using Monte Carlo simulations for energy calibration. 17 p2585 A72-34922
- Electron showers of high primary energy in lead. 17 p2585 A72-35472
- Inverse bremsstrahlung caused fast cascade of electrons with Boltzmann energy distribution to explain laser induced gas breakdown via plasma heating 20 p2934 A72-39645
- Energy spectrum and angular distribution of cascades with an energy greater than 0.3 TeV, formed by cosmic muons 23 p3331 A72-44427
- Fluctuations of the spatial distribution of the number of particles in showers generated by muons in heavy material 23 p3331 A72-44431
- Isothermal atmosphere inhomogeneities effects on electromagnetic cascade electrons integral energy spatial distribution 23 p3331 A72-44433
- ELECTRON PLASMA**
- Electron cyclotron harmonics emission as function of electron plasma frequency in He reflex discharge, measuring electron densities 01 p0105 A72-10026
- Plasma waves maximum radiation temperatures near fundamental and second harmonic electron frequency 02 p0265 A72-12308
- Strong circularly polarized electromagnetic wave scattering by plasma electron as function of amplitude and magnetic field with radiation reaction 03 p0321 A72-13077
- Bulk recombination effects on nonstationary pinching and collapse of electron-hole plasma by magnetic field in crystal 03 p0401 A72-13581
- Collision integral for classical electron plasma, concerning Born-Bogoliubov-Green-Kirkwood-Yvon equations for long range interaction potential and motions of multiple particles 03 p0399 A72-14069
- Density waves propagation and amplification in p-InSb electron-hole plasmas, investigating dependence on frequency and injection level 04 p0561 A72-14851
- Whistler instability of electron plasmas with non-Maxwellian velocity distribution function 05 p0698 A72-17015
- Perturbation theory, saturation and relaxation effects in electron and ion plasma wave echoes 05 p0699 A72-17220
- Electrostatic waves perturbed distribution function behavior in presence of forced oscillations, considering Maxwellian ion and electron plasma waves excited by dipole 06 p0855 A72-17508
- Electron plasma wave echoes experimental investigation, discussing amplitude decay under plasma and random noise influence 06 p0858 A72-17538
- Langmuir wave-caused electron plasma distribution function deformation, discussing particle trapping effects 06 p0858 A72-17542
- Longitudinal electron plasma waves interaction with electron distribution, investigating energy transfer 06 p0858 A72-17543
- Electrostatic hf wave propagation in one dimensional collisionless plasma, describing electron trapping and oscillations and resonance-produced sidebands 06 p0858 A72-17544
- Statistical hf electron heating at oscillating plasma boundary with acceleration of double Langmuir layer 06 p0860 A72-17691
- Fast electron-cyclotron wave excitation with infinite phase velocity along magnetic field in nonequilibrium electron plasma 06 p0862 A72-18402
- External circuit coupling effects on dc anomalous resistivity in electron plasma oscillation 07 p1043 A72-19666

Velocity space instability in hot electron plasma created by adiabatic compression in pulsed magnetic mirror, observing radiation bursts below electron cyclotron frequency during compression [AD-740408] 08 p1213 A72-21257

Electron plasma fluctuations in semiconductor with nonparabolic conduction band under external electric and magnetic fields 08 p1218 A72-21877

Numerical solution of theta pinch in electron-hole plasma of Ge semiconductor under surface recombination as contactless method of current carrier injection 08 p1218 A72-22178

Quasi-elastic scattering differential cross section for nonpolarized IR radiation in electron plasma of semiconductors in strong elastic fields 09 p1366 A72-22210

Electrostatic longitudinal waves propagation and detection in isotropic collisionless hot electron plasma, calculating Landau dispersion curve and damping 09 p1359 A72-22794

Q factor over temperature range of microwave resonator coupled with drifting indium antimonide plasma 09 p1285 A72-22895

Electron plasma oscillations distribution upstream from earth bow shock, evaluating OGO-E plasma wave detector data 09 p1300 A72-23019

Star stellarator model for hot electron plasma production by steady electron beam injection in closed magnetic traps 09 p1363 A72-23219

Intensity dependent propagation characteristics of circularly polarized high power laser radiation in dense electron plasma, calculating energy losses 10 p1522 A72-24607

Variational and statistical methods for adiabatic electron plasma with self consistent field interaction in terms of Lagrange, Hamilton and Liouville formalization 12 p1850 A72-27185

Turbulent plasma electric field energy density spectrum from statistical mechanics investigation based on canonical formalism for electron plasma 12 p1851 A72-27387

Thermal electron relativistic streaming effects on electromagnetic instability in magnetoplasmas 12 p1851 A72-27389

Electron wave sideband frequencies and wave-trapped electron oscillations as cause of plasma instability 12 p1851 A72-27430

Radiation patterns of circular loop antenna in isotropic compressible plasma, discussing far fields for electromagnetic and electron plasma waves 12 p1790 A72-27491

Pulsed Si p-n junction mesoplasma dynamic I-V characteristics explained by mechanism based on hot carrier annihilation 12 p1853 A72-28113

Nonlinearity effect on electron plasma wave dispersion relation, using numerical simulation and theoretical analysis by perturbation expansion and Hamilton variational principle 13 p2011 A72-29121

Computerized calculation of wave dispersion curves for hot Maxwellian electron magnetoplasma, applying to upper hybrid and cyclotron frequencies 13 p2013 A72-29340

Stimulated Compton scattering of laser radiation by electron plasma, determining electrons diffusion coefficient and velocity distribution function 13 p1972 A72-29987

Kinetic instability bursts during heating of electron plasma in cylindrical resonator with standing electromagnetic waves 14 p2136 A72-30308

Kinetic instabilities during electron plasma heating in HF field of cylindrical resonator, discussing electron energy distribution function effect 14 p2137 A72-30309

Electrostatic cyclotron harmonic waves propagation in inhomogeneous electron plasma slab, deriving RF electric field 14 p2138 A72-30397

Electromagnetic waves propagation in inhomogeneous moving cold electron plasma without external magnetic field and collisions, investigating dynamo-optical effects 14 p2086 A72-30790

Nonlinear interaction of resonant plasma oscillations with nonresonant wave pulse, using water bag model of electron plasma 14 p2140 A72-30936

One dimensional Maxwellian electron plasma simulation by electron bunches, describing Landau damping of wave initially excited in medium and nonlinear effects of trapping 15 p2284 A72-31678

Sounding rocket experiment on nonlinear interaction between two electron plasma waves and ion

acoustic wave in ionosphere to investigate artificial realization feasibility 15 p2231 A72-32333

Glow mode electron plasma source for space chamber, measuring electron density and temperature for comparison with back diffusion sources 15 p2286 A72-32339

Ion acoustic and guided electron plasma waves excitation by grid antenna produced LF signals in cylindrical plasma column 15 p2289 A72-32650

Plasma accumulation in electrostatic potential well produced by electron space charges, determining diocotron instability as function of electron plasma and gyrofrequency ratio 16 p2434 A72-32819

Difference scheme for initial value problem of one dimensional Vlasov equation for collisionless electron plasma with homogeneous ion background 16 p2434 A72-33006

Fast electron cyclotron wave excitation with infinite phase velocity along magnetic field in nonequilibrium electron plasma 17 p2588 A72-34853

Solution of the Boltzmann equation for a fully ionized plasma in an oscillatory electric field and a steady magnetic field. V - Explicit solution for a homogeneous plasma in a high-frequency electric field. 17 p2589 A72-35057

Kinetic equations with radiation effects. 17 p2590 A72-35155

Nonlinear collisional excitation of plasma waves. 17 p2591 A72-35372

Detection of solar-wind electron plasma frequency fluctuations in an oblique nonlinear magnetohydrodynamic wave. 17 p2602 A72-35610

Water bag model application to one dimensional inhomogeneous two-stream collisionless electron plasma stability computation, noting electrostatic modes 17 p2592 A72-35619

Sideband growth in nonlinear Landau wave-particle interaction. 19 p2838 A72-37327

Electron-plasma-wave shocks in a bounded plasma. 19 p2840 A72-37719

Plasma electron velocity distributions determined from the polarization of free-free bremsstrahlung. 19 p2841 A72-38439

A general method for integrating the Schroedinger equation with a singular right-hand side in a homogeneous and constant electromagnetic field 19 p2843 A72-38855

The self-consistent test-particle approach to relativistic kinetic theory. 20 p2955 A72-40013

Pinch effect in a germanium electron-hole plasma 21 p3096 A72-40414

Coupled fields in inhomogeneous warm plasmas with static pressure gradients. I. 22 p3210 A72-42313

Nuclear reactions in a degenerate electron-nuclear plasma 22 p3209 A72-42964

Electromagnetic disturbances within a degenerate electron plasma in a quantizing magnetic field 22 p3212 A72-43010

Kinetic instability bursts during heating of electron plasma in cylindrical resonator with standing electromagnetic waves 23 p3317 A72-43210

Kinetic instabilities during electron plasma heating in HF field of cylindrical resonator, discussing electron energy distribution function effect 23 p3317 A72-43211

Frequency dependent antenna impedance characteristics in ionospheric plasma, discussing anisotropic and isotropic electron plasmas, loop antennas, resonance rectification and ion effects 23 p3319 A72-43512

Damping of finite-amplitude electron plasma waves in a collisionless plasma. 23 p3321 A72-44075

Field components of coupled electromagnetic and electron acoustic waves in warm stratified plasmas, using first order wave equations and Heading embedded form 23 p3322 A72-44319

ELECTRON PRECIPITATION

Synchrotron radiation from incoming auroral electrons based on Schwinger equation, accounting for hf backscatter sounder noise 01 p0060 A72-10839

Outer zone energetic electron precipitation, elf whistler and plasmopause location measurements by polar satellite OV-3-3 instruments 01 p0120 A72-10890

Precipitated electron energy latitude and time variations from auroral-height measurement during IQSY, using meridian scanning photometers 01 p0120 A72-10896

Auroral electron precipitation modulation dependence on energy explained by resonance at rebound frequency 02 p0222 A72-12598

Middy oval, cusp region and polar cap auroral electron precipitation at low magnetic activity, presenting intensity vs altitude profiles for nitrogen ion line emissions 03 p0350 A72-13531

Bremsstrahlung X rays from electron precipitation associated with discrete vlf emissions, recording wave-particle experiment near plasmopause with balloon-borne counters in Antarctica 03 p0413 A72-13536

Low energy electrons anisotropic flux impulsive precipitations in structured aurora explained by potential difference along geomagnetic field lines of force 03 p0350 A72-14272

Magnetic latitude effect on wave dispersion in drifts and random movements of ionization irregularities in E region, suggesting charged particle precipitation role 04 p0518 A72-14964

Magnetospheric current effects on geomagnetic field structure, noting electron and proton precipitation into auroral zone 05 p0657 A72-16275

X ray detection on Jupiter with actively collimated balloonborne scintillation counter, noting decametric emission due to electron precipitation 06 p0872 A72-17445

Vlf wave excitation during sudden storm commencement, causing magnetosphere trapped energetic electrons to diffuse and precipitate into lower ionosphere 06 p0803 A72-17451

Auroral zone vlf hiss and associated low energy electron precipitation in polar magnetosphere [AD-736327] 06 p0804 A72-17456

Sounding rocket observations of magnetic field aligned electron pitch angle distributions coincident with auroral precipitation band northern boundary 06 p0804 A72-17457

Auroral zone electron precipitation events before and at negative magnetic bays onset, presenting balloon recordings of bremsstrahlung X-rays intensity 06 p0808 A72-18092

Vlf auroral hiss comparison with low energy electron precipitation, using Ogo 4 data 07 p1058 A72-19149

Systematic increase in auroral electrons mean energy with total precipitated energy 07 p1058 A72-19151

Polar orbiting satellite ESRO-1A 1-13 keV electron measurements compared to bottomside ionosonde measurements for auroral particle precipitation and F region electron density 08 p1226 A72-21099

High energy electron precipitation events in auroral zone X rays, showing exponential daytime and flat nighttime energy spectra 08 p1226 A72-21110

Model calculation for electron production rates due to photoionization and particle precipitation below 100 km at midlatitude during solar minimum and maximum years 09 p1375 A72-22357

Nightglow evidence of precipitating energetic electrons in midlatitude nighttime D region based on intensity determination from satellite and rocket data 09 p1375 A72-22358

Rocket sounding of auroral zone F region low energy electron precipitation and excitation and ionization processes 09 p1298 A72-22585

Charged particles observations on 21 December 1968 by Explorer 40 and from ground, noting auroral light primary energy influx by precipitation band of electron intensities 09 p1299 A72-23005

Magnetospheric electrons precipitation into ionosphere due to conjugate conductivity asymmetry caused by wind induced ions vertical redistribution, using atmospheric model 10 p1530 A72-24791

Magnetosphere fast electron precipitation investigated by simulation experiments with model created by plasma stream interaction with dipole magnetic field 11 p1714 A72-26531

Electron precipitation in upper atmosphere at midlatitudes from positive ionized nitrogen molecules electrophotometric observation and night airglow and geomagnetic field measurements 12 p1802 A72-27302

Ionospheric irregularities-magnetospheric parameters relationship from satellite scintillation measurement, noting use as indirect electron precipitation indicator 12 p1803 A72-27772

Auroral particle precipitation /keV electrons and protons/ morphology from ESRO 1A particle spectrometer measurement, discussing particle populations in day and night magnetospheres 12 p1864 A72-27786

Magnetosheath electron precipitation effect on dayside auroral oval plasma density and conductivity, relating precipitation heat flux to solar wind energy density

13 p1950 A72-29381

Photoelectron precipitation induced dissociation of atmospheric nitrogen molecules during moderate solar activity

14 p2102 A72-30659

Quasi-periodical intensity pulsations in trapped and precipitating electrons in earth outer radiation belt

15 p2299 A72-31914

Long term A3 absorption associated with nuclear explosion caused artificial radiation belts, discussing electron precipitation role in D region ionization

15 p2299 A72-31933

Auroral electrojet polarization model, considering ionospheric Hall and Pedersen conductance maximum due to precipitation from electron plasma sheet inner edge

[AD-745672] 16 p2444 A72-32961

Thermospheric composition variations in south polar regions during magnetically quiet periods fromOGO-6 observations, considering atmospheric heating by electron precipitation cyclic variations

16 p2383 A72-32964

High latitude observation of precipitating electron spikes by polar orbiterOGO 4 satellite, noting population dependence on local trapping limit

17 p2601 A72-35591

Low energy auroral electron precipitation associated ELF noise band observation by polar-orbiting satellite INJUN 5

17 p2517 A72-35593

Pitch-angle diffusion of radiation belt electrons within the plasmasphere.

17 p2602 A72-35597

Precipitation dynamics and energy spectrum of auroral electrons in the midnight sector during a magnetospheric substorm

17 p2550 A72-35854

Airborne optical measurement comparison with satellite observation for auroral emissions and particle precipitation at noon, suggesting electron precipitation role

19 p2868 A72-38738

Local-time survey of plasma at low altitudes over the auroral zones.

19 p2792 A72-38739

Polar upper ionosphere morphology above E layer, discussing effects of winds, field aligned currents and electron precipitation

20 p2918 A72-39534

Properties of low energy particle impacts in the polar domain in the dawn and dayside hours.

20 p2964 A72-39541

High latitude particle precipitation and source regions in the magnetosphere.

20 p2964 A72-39542

Auroral electron and proton distribution in magnetosphere and precipitation pattern from satellite, rocket and ground based observations

20 p2920 A72-39976

Auroral space-time regularities relationship to magnetospheric variations, precipitating electron fluxes, magnetic tail formation and substorms

20 p2920 A72-39977

On the classification of high-latitude auroras.

20 p2920 A72-39979

Conjugate features of magnetospheric electron dynamics observed at balloon altitudes.

21 p3049 A72-41614

Occurrence of Pc 4, 5 micropulsation activity at the polar cusp.

22 p3171 A72-42411

Rocket measurements of electron influx during a major magnetic storm with type A aurora.

23 p3332 A72-44515

Quadruple conjugate pair observations of the sudden commencement absorption event on June 17, 1965.

23 p3286 A72-44526

ELECTRON PRESSURE

Spectral analyses of Mira-type variable stars near light maximum, discussing empirical curve of growth, Doppler velocity, damping constant and electron pressures

01 p0129 A72-10792

Charge carrier density, neutral gas density, electric potential and electron temperature profiles in cylindrical diffusion column, considering electron pressure

11 p1698 A72-26646

Electron pressure effect on lunar wake shape and size, calculating electric field created by charge separation

15 p2308 A72-31925

Mechanical equilibrium equation of nongray stellar matter, approximating electron pressure vs temperature in early stellar atmospheres

21 p3109 A72-41435

Molecular abundances and gas-to-electron pressure ratios as function of temperatures and pressures in solar composition gaseous mixture of late type stellar atmospheres

21 p3110 A72-41446

ELECTRON PROBES

Electron microprobe analysis of plagioclase points and pyroxene grains of Apollo 15415 anorthositic genesis rock

02 p0282 A72-12411

Electron microprobe analysis of Lunik 16 basalt fragments, noting similarity to Apollo 11 and 12 igneous rocks

09 p1379 A72-22252

Microscopic and electron microprobe analyses of silicate melt inclusions and glasses in lunar soil fragments from Lunik 16 core sample

09 p1379 A72-22255

Optical petrographic, electron microprobe and single crystal X ray diffraction analysis of basaltic and monomineralic soil fragments of Lunik 16 core sample from Sea of Fertility

09 p1379 A72-22257

Electron microprobe analyses of Lunik 16 mare basalt fragment G37 with high Al and low Mg content, discussing fragments G46 and G51

09 p1380 A72-22260

Electron microprobe analysis of chromian spinels from Apollo 14 rocks indicating crystallization from high aluminum low iron magma

12 p1865 A72-27113

Electron microprobe analysis of solute segregation near grain boundaries in Al-Zn-Mg alloy after quenching and aging heat treatment

13 p1973 A72-28652

Electron probe microanalysis of Mo-Pd system diffusion at 1000-1600 C, measuring chemical diffusion coefficient as function of temperature, concentration and activation energy

13 p1978 A72-29221

Low energy electron spectroscopy measurement of thin oxide layer growth on Al surface, noting oxidation uniformity dependence on residual gas water content

15 p2276 A72-31859

Spin effects on satellite-borne cylindrical probe electron density measurements, considering satellite wake and geomagnetic field effects

16 p2389 A72-32962

Three dimensional electron density fluctuations scattering spectra in Mach 16 spherical projectile turbulent wakes from fine wire electron collection probe measurements

[AIAA PAPER 72-673]

16 p2432 A72-34066

Amplitude and phase space potential oscillations measurements with hot electron probe in collisional Cs plasma compared with linear drift wave theory

21 p3093 A72-41376

ELECTRON RADIATION

NT BETA PARTICLES

NT ELECTRON BEAMS

Solar electrons and protons measurements in interplanetary space and in magnetotail, noting access to north polar cap

[AD-744404]

07 p1058 A72-19156

Electron wave attenuation technique for current transit determination through semiconducting films with various crystal structures

09 p1284 A72-22209

Proton and electron radiation effects on silicon solar cells electric and photovoltaic properties, determining damage coefficients via minority carriers diffusion length measurement

12 p1759 A72-28045

Interplanetary electrons quiet-time intensity increases, considering trans-earth-orbital modulating region due to solar wind transport of photospheric field lines

13 p2030 A72-29377

Solar relativistic electrons and particle events spectra during 1967-1969 from IMP-4 observations

13 p1033 A72-29746

Spiral galaxies radio sources spectral components, noting relativistic electrons radiation and luminosity-surface brightness diagram

14 p2148 A72-30203

Auroral electron spectrum space-time dynamics during magnetospheric substorms, using X ray bremsstrahlung balloon data

14 p2101 A72-30637

Simulated Nimbus orbital electron, proton and UV radiation effects on wide bandpass glass and narrow bandpass thin film interference filters and fused silicas

15 p2277 A72-32157

Relativistic electron ring oscillations in circular waveguide with allowance for walls finite conductivity, noting radiative instability at subcritical frequencies

15 p2210 A72-32738

Cosmic ray electron search and study, comparing near earth to interstellar spectrum

16 p2448 A72-33869

Solar stationary type 4 radio bursts caused by gyromagnetic radiation of bunched electrons

16 p2449 A72-33920

Electron processes in nonrelativistic electron streams against stationary ion background as wave packet envelope deformation in space and time

21 p3094 A72-41652

Radiation of electron bunches passing through a dielectric plate in a waveguide

21 p3036 A72-41842

Spiral galaxies radio sources spectral components, noting relativistic electrons radiation and luminosity-surface brightness diagram

23 p3333 A72-43232

Summary of latent effects in long term survivors of whole body irradiations in primates.

23 p3254 A72-43393

Radiation from a free electron interacting with a circularly polarized laser pulse.

23 p3296 A72-43875

ELECTRON RECOMBINATION

NT RADIATIVE RECOMBINATION

Generation-recombination model of large signal silicon transistor operating in IC microwatt range

02 p0188 A72-11521

Bulk recombination effects on nonstationary pinching and collapse of electron-hole plasma by magnetic field in crystal

03 p0401 A72-13581

Solar coronal total dielectronic recombination coefficient simple relationships for isoelectronic sequences of H, He, Ne, K-Ni and Li-F, Na-A and Cu-Kr

05 p0718 A72-16510

Strong electric field recombinational domains in semiconductors with mobile holes and electrons during band-band illumination or double injection

07 p1048 A72-19638

He ionization and excitation in optically thick solar prominences, considering recombination excitation for observed triplet-level populations at 5000-10,000 K electron temperature

08 p1231 A72-21123

Electron and hole recombination at deep impurity centers during nonequilibrium current carriers excitation by Nd-glass laser light in p- and n-type germanium

09 p1322 A72-22214

Reversible threshold switching in amorphous semiconductor alloys by carrier transport and recombinative electron injection

12 p1854 A72-27431

Disturbed ionospheric electron and ion kinetics, detailing dissociative recombination as regulating process for temporal evolution

14 p2102 A72-30654

Correlation measurements of LF current noise and frequency fluctuations in Gunn oscillators, emphasizing generation-recombination noise component

14 p2088 A72-30916

Electrical conductivity in mesosphere and upper stratosphere from rocket sounding by blunt probe technique, suggesting electron density profiles dependence on dissociative recombination variations

15 p2228 A72-31972

Possibility of the occurrence of alternating current in a circuit with a semiconductor sample exhibiting a recombinational instability

19 p2846 A72-38449

Strong electric field recombinational domains in semiconductors with mobile holes and electrons during band-band illumination or double injection

24 p3431 A72-44570

ELECTRON SCATTERING

Electron layer precession under magnetic field in background plasma, noting density effect on instability

01 p0107 A72-10144

Nonconservative radiative transfer in spherically symmetric system, calculating linearly polarized electron scattering atmosphere

01 p0102 A72-11127

Electrical conductivities dependence on assumed values of elastic collision cross sections of electrons with neutral and charged particles in low temperature plasma

01 p0110 A72-11205

Electron scattering off atoms, diatomic and polyatomic molecules in impact spectroscopy, applying simple group theory

02 p0262 A72-11913

Viscous friction effects on phonon-electron interactions and dislocation velocity by deformation measurement of metallic crystals under pulsating magnetic fields

02 p0243 A72-12169

Quasi-static surface waves at Maxwellian plasma boundary with diffuse electron scattering, considering plasma electromagnetic oscillations

02 p0266 A72-12577

Global morphology of integrated product with respect to D and E regions electron concentration height and collision frequency

03 p0345 A72-12981

Spectral distribution of radiation arising from nonlinear Thomson scattering of strong electromagnetic wave by ultrarelativistic electrons

03 p0390 A72-13017

Dynamic equations for nonequilibrium stationary state superconductors with electron-phonon and electron-electron inelastic collisions

03 p0401 A72-13089

Resonance electron spectrometry experiments on electron collisions involving vibrational excitation, deactivation and attachment in molecular oxygen

03 p0347 A72-13391

- Late twilight airglow vacuum UV spectra from sounding rocket observation, noting conjugate-point electron excitation role in O I emissions
03 p0350 A72-13525
- Low energy phase shifts for elastic scattering of electrons by Li and Na
03 p0391 A72-13745
- Rotational excitation of polyatomic molecule by electron collision attributed to polarization and electrostatic forces
04 p0552 A72-14852
- Bremsstrahlung emission by auroral electrons in upper atmosphere and penetration in lower atmosphere, comparing calculation with balloon measurement
04 p0566 A72-14879
- Electronic collision frequency relationship with radio frequency in F region, investigating height, diurnal and seasonal variations
04 p0516 A72-14933
- Rectangular pulse propagation through inhomogeneous medium as plasma diagnostics, investigating electron collisions effect on signal distortion
04 p0556 A72-14946
- Nonideality effects on Coulomb gas conductivity by finding conductivity due to electron scattering at atoms, solving kinetic equation of three component plasma model
05 p0694 A72-15850
- Electron concentration and collisions number fluctuations effect on D region profiles based on radio waves partial reflection data
05 p0656 A72-16244
- Electron lifetime in earth radiation belt due to resonant scattering with hiss vlf radiation
05 p0711 A72-17045
- Half wavelength antenna radiation admittance into warm lossy two layer plasma half space, using effects of slot width and electron collision frequency
06 p0781 A72-17348
- Longitudinal hf oscillations in homogeneous magnetoactive plasma by fast monoenergetic electron excitation
06 p0853 A72-17389
- Boltzmann kinetic equation with electron-electron collision coefficients for isothermal weakly ionized cesium-argon plasma, using nodal point method
06 p0860 A72-17695
- Conformal electron interactions in biopolymer and hypermolecular biological systems, discussing calcium ions effects, enzyme activity, muscle contractions and information theory
07 p0915 A72-18803
- Ion-electron collisions effect on ion cloud motion in magnetoactive plasma immersed in uniform external electric field
07 p1055 A72-18894
- State density singularities elimination in inhomogeneous superconductors by electron interactions nonuniformities, resulting in tunnel junction current-voltage characteristic fluctuation
07 p1047 A72-18919
- Cylindrical antenna radiation resistance and total radiated power in weakly ionized plasma, considering electron collisional effects
07 p0944 A72-19592
- Semiconductors cyclotron echo signals from dipole interactions of electrons with alternating magnetic fields, discussing frequency doubling and excitation mechanism
07 p1048 A72-19639
- Electrons and ionized impurities interaction in thin quantizing layers, discussing donor activation energy and kinetic characteristics
07 p1048 A72-19640
- Anomalous Hall effect of polarized electrons spin-orbit interactions in semiconductors, involving emf appearance in electric field and polarized light
07 p1048 A72-19642
- Mg ion excitation by electron collision in solar chromosphere studies, calculating scattering cross sections
07 p1081 A72-20234
- Differential and integral scattering cross sections for helium excitation by electron impact from ground state to 2/super 1/S state
07 p1038 A72-20679
- Electron scattering effects on response of cosmic ray particle telescopes from pulse height and counting rate measurements
08 p1167 A72-21510
- Quasi-particle decay rates by electron-electron scattering in superconductors, noting effect on states tunneling density
08 p1217 A72-21595
- Maximum superconducting transition temperature estimation, discussing optimum resonant frequency for attractive interaction, umklapp electron scattering and lattice instabilities
09 p1367 A72-22553
- Elastic singlet p wave phase shift calculation for electron scattering by H atom and He cation, using time dependent Hartree-Fock perturbation theory
09 p1355 A72-22786
- Electron reflection mechanism and gas adsorption effect at W /001/ surface in energy range 1-10 eV
09 p1370 A72-22804
- Weak extragalactic X ray sources radio identification, suggesting production by inverse Compton losses of electrons from radio galaxies
09 p1377 A72-22988
- Carbonized and ion beam thinned polyacrylonitrile copolymer fibers examination by low angle electron scattering electromicroscopy technique
09 p1339 A72-23190
- Electron beam and plasma nonlinear interactions, noting scattering zone, amplitude oscillation maximum, longitudinal velocity and relaxation patterns
10 p1517 A72-23760
- Radio recombination lines broadening in hydrogen by electron collisions, using Baranger impact theory
10 p1435 A72-24142
- Relativistic heavy ion in plasma, calculating energy loss based on electron scattering and momentum transfers
10 p1515 A72-24344
- Stellar evolution from precarbon-burning contraction to presupernova stage with and without neutrino production by electron neutrino interaction
10 p1545 A72-24825
- Strong pitch angle scattering of energetic electrons in presence of electrostatic waves due to ion cyclotron instability above midlatitude ionospheric trough region
11 p1714 A72-26398
- Quasi-projection operators for calculating electron resonances in multitarget scattering tested on He ion autoionization system
12 p1847 A72-27385
- Many electron pseudopotential method for electron-atom scattering, calculating singlet s wave and p wave phase shifts
12 p1848 A72-27429
- Strong circularly polarized electromagnetic wave scattering by plasma electron with radiation reaction, determining cross section as function of amplitude and magnetic field strength
13 p2015 A72-29427
- Dynamic equations for superconductors with electron-phonon and electron-electron inelastic collisions, investigating nonequilibrium stationary states
13 p2022 A72-29438
- Oblique radio wave propagation through horizontally stratified ionosphere, considering electron collisions effects, reflection behavior and coupling levels
13 p1923 A72-29657
- Electron-ion collision frequency and conductivity of non-Debye plasma formed in high pressure discharge from Ar, Kr and Xe tubes
13 p2018 A72-29891
- Dense isothermal plasma heating due to electron and ion scattering on turbulent pulsations of electric field oscillations
13 p2019 A72-29916
- E region electron collision frequency vertical distribution by ground measurement of radio wave absorption, using electron concentration data obtained by rocket-borne interferometer
14 p2100 A72-30462
- Free electron waves interaction with coherent laser light in crystalline medium, discussing quantum mechanical treatment and path integral approach
14 p2110 A72-30725
- Cross section determination of proton production in collisions of electrons and hydrogen ions
14 p2134 A72-30801
- Cross sections for dissociative excitation of hydrogen ions by electrons determined by coincident detection of protons and H atoms
14 p2134 A72-30804
- Hydrogen negative ion electron detachment collision process cross section calculation using Coulomb trajectory impact-parameter method
14 p2135 A72-30884
- Nonideality effects on Coulomb gas conductivity by finding conductivity due to electron scattering at atoms, solving kinetic equation of three component plasma model
15 p2283 A72-31269
- Kinematic intensity recovery from LEFD data of specular and nonspecular beams from Ni/111/ surface, noting multiple scattering interference elimination
15 p2276 A72-31855
- Electron production cross section during He atom ionization by proton impact, noting peak existence for electrons near incident proton velocities
15 p2281 A72-32220
- Eikonal distorted wave analysis of inelastic electron-atom collisions at intermediate energies application to electron impact induced atomic hydrogen 2s and 2p states excitation
15 p2282 A72-32646
- Magnetoactive plasma transverse waves propagation near electron gyrofrequency harmonics, taking into account electron collisions and relativistic effects
15 p2289 A72-32734
- Gas phase photodetachment of electron from selenide ion, determining affinity and spin-orbit coupling constant for SeH negative ion
16 p2360 A72-33580
- Pion-electron conjugation and twist angles determination in biphenyls via Raman intensity, comparing with hypsochromic UV shift of Suzuki method
16 p2431 A72-33585
- Calculation procedure involving wave function for vibrational correction to electron scattering cross section of hydrogen molecule in Born approximation
17 p2585 A72-34261
- Electrons and photons interaction with relic radiation, establishing high energy gamma rays energy and intensity attenuation length
17 p2600 A72-35145
- Wave-wave interactions due to scattering by electrons.
17 p2591 A72-35162
- Ion-ion correlation effects on electron-nucleus neutrino bremsstrahlung.
18 p2723 A72-36089
- A dynamical theory for the contrast of perfect and imperfect crystals in the scanning electron microscope using backscattered electrons.
18 p2692 A72-36749
- Absolute differential cross sections of electrons elastically scattered on neon atom.
18 p2713 A72-36952
- Polarization effects during electron scattering in the gravitational field of a rotating source
18 p2712 A72-36967
- Vibrational excitation in N2 by electron impact in the 15-35-eV region.
19 p2837 A72-37546
- Yields of gamma rays emitted following capture of negative muons by Si28 and Mg24.
19 p2837 A72-38026
- The incoherent scattering of radiation from a high temperature plasma.
19 p2842 A72-38523
- Kinetic theory of density fluctuations in a magnetized collision-dominated plasma in an electric field.
19 p2792 A72-38745
- Electron-electron collision induced anomalous Hall effect in ferromagnetic d metals at low temperatures
20 p2959 A72-39309
- State density singularities elimination in inhomogeneous superconductors by electron interactions nonuniformities, resulting in tunnel junction I-V characteristic fluctuation
20 p2960 A72-39385
- Electron loss in atom-molecule collisions.
21 p3087 A72-40473
- Linear momentum transfer effects in molecular dissociation produced by electron impact.
21 p3087 A72-40557
- Extension of Eliashberg's theory to type-II superconductors.
21 p3096 A72-40574
- Solar coronal F component separation from K component by utilizing elongation dependence differences in scattering populations, computing F for wide range of parameters
21 p3106 A72-41041
- Chou-Tien nonplane-parallel solution to transfer equation for radiation scattering by free electrons in stellar spherical atmosphere by regional averaging procedure
21 p3109 A72-41434
- Effect of Thomson scattering on the emission spectrum of an optically semitransparent plasma
21 p3102 A72-41774
- Electron impact excitation cross sections and energy degradation in CO.
22 p3172 A72-42422
- Elastic electron-neutral interaction in argon in the vicinity of the Ramsauer minimum
22 p3211 A72-42642
- Compton scattering by thermal electrons in X-ray sources.
23 p3328 A72-43230
- Equatorial UV airglow azimuthal variations from spinning rocket measurements, attributing origin to electron collision excited atomic hydrogen 1,2man alpha emission
23 p3282 A72-43263
- Variation with electron velocity powers of electron collision frequency and energy transport coefficients in weakly ionized plasmas - Earth's lower ionosphere.
23 p3285 A72-43994
- Spectral composition and phase function of plane monochromatic light wave scattering by electrons in high temperature plasma
23 p3322 A72-44465
- Parasitic pitch angle diffusion of radiation belt particles by ion cyclotron waves.
23 p3333 A72-44527
- Semiconductors cyclotron echo signals from dipole interactions with alternating magnetic fields, discussing frequency doubling and excitation mechanism
24 p3431 A72-44571
- Anomalous Hall effect of polarized electrons spin-orbit interactions in semiconductors, involving emf appearance in electric field and polarized light
24 p3431 A72-44573
- Theoretical interpretation of the optical and electron scattering spectra of polyatomic molecules. III - N2O

and the discovery of resonant phenomena in the B region at 6.8 eV.

24 p3426 A72-45301

Dissociative attachment in carbon dioxide.

24 p3427 A72-45303

Electron scattering by molecules with and without vibrational excitation. IV - Elastic scattering and excitation of the first vibrational level for N₂ and CO at 20 eV.

24 p3427 A72-45304

Electron scattering by molecules with and without vibrational excitation. V - Elastic scattering and non-resonant vibrational excitation of N₂ at 30-83 eV.

24 p3427 A72-45305

Possible explanation of non-power-law radio spectra of cosmic radio sources.

24 p3446 A72-45477

ELECTRON SOURCES

Supernova Vela X and local remnants as origin of below 1000 GeV cosmic electrons, deducing existence at 10 to 15 GeV from muon poor showers

01 p0119 A72-10853

Near earth interplanetary electron source detection related to coronal site type 3 bursts, using 80 MHz radioheliograph observations

16 p2445 A72-33044

RF discharge gap in cascaded plasma limiters, using tritium igniter as reliable electron priming source

18 p2715 A72-36451

Triode electron gun design for narrow electron beam under highly convergent lens action, using field emission source

19 p2775 A72-38611

Field emission from carbon fibres - A new electron source.

22 p3208 A72-41966

ELECTRON SPIN

Surface effects on paramagnetic metals spin susceptibility models, including random-phase-approximation equation derivation and induced magnetic moment calculation

15 p2295 A72-32549

Dynamics of the optical-pumping cycle of F centers in alkali halides - Theory and application to detection of electron-spin and electron-nuclear-double-spin resonance in the relaxed-excited state.

18 p2719 A72-36709

Electron spin resonance of divalent Mn ion doped in thallous azide single crystals, investigating temperature effects on spin Hamiltonian parameters

22 p3152 A72-42716

ELECTRON SPIN RESONANCE

U ELECTRON PARAMAGNETIC RESONANCE ELECTRON STATES

Excited state and electron densities in noble and atmospheric gas plasmas created by alpha particle induced ion irradiation, discussing plasma kinetic processes and superimposed electric field effects

01 p0112 A72-11335

Amorphous semiconductors dielectric properties based on randomly distributed local electron states in disordered solids, crystalline impurities and polymer aggregates

02 p0269 A72-12450

Vibrational population of molecular nitrogen electronic states in normal auroras, examining electron impact and cascade contributions

03 p0349 A72-13524

Allowed states of electronic complexes and impurity molecules in crystals determination in molecular orbital scheme of molecular electronic calculations

03 p0392 A72-13864

Jahn-Teller Hamiltonian for triplet electron state coupling to phonon vibrations in cubic symmetry

03 p0404 A72-14264

Hydrogen 2p and 2s states formation during 1-25 keV atomic collisions with rare gases from Lyman alpha radiation cross section measurement

05 p0693 A72-17168

Molecular nitrogen photoelectron impact excitation of Herman-Kaplan upper electronic state, considering cascade contribution to low lying states in electron auroras and dayglow

06 p0806 A72-17647

Electron states in glassy amorphous semiconductors, constructing trial wave functions for valence band

06 p0866 A72-18180

State density singularities elimination in inhomogeneous superconductors by electron interactions nonuniformities, resulting in tunnel junction current-voltage characteristic fluctuation

07 p1047 A72-18919

Critical temperature dependence of Nb-Al-Ge superconducting alloys on composition and heat treatment, discussing phase boundaries and electron state densities

07 p1049 A72-20154

Resonance theory of three body ion-atom association reactions in rare gases, estimating quasi-bound electron state population and deactivation cross section

09 p1356 A72-22792

Ta and W X ray spectra fine structure measurement, providing electron states density in unoccupied regions of energy bands of solids

09 p1370 A72-22842

Rare earth elements outer electrons X ray and UV photoemission spectra interpretation by multiplet splitting of final state

09 p1371 A72-22844

Soft X ray emission spectra from Al-Nb and Al-Pd alloys, deducing electron state density near Al ions

09 p1371 A72-22848

Ti, Zr and Hf hcp-bcc phase transformation isochromat spectroscopic investigation, noting fine structures to confirm electron state density

09 p1371 A72-22849

Excitation and relaxation of upper laser state in carbon dioxide discharge from Q spoiled pulse-produced fluorescence measurements

09 p1326 A72-23577

Supersonic Ar, He and molecular nitrogen jets, determining electron temperature and concentration and atomic state population in shock waves region by spectroscopic measurement

10 p1517 A72-23837

Nd-glass amplifier gain saturation by 1.06 micron light pulses determined by two laser states lifetimes and degeneracies and thermalization rates

12 p1792 A72-27752

Combined photon and particle diffusion of two level system with ground and excited atomic states and photon emission-formed radiation field

13 p2001 A72-28509

Localized electronic states size near mobility edge in semiconductor, considering eigenfunction behavior in random lattice problem

14 p2143 A72-30878

Atomic hydrogen 3s state destruction by impact on nitrogen, argon and hydrogen molecules, considering collisional ionization and electron capture mechanisms

14 p2134 A72-30883

Binary systems phase diagrams qualitative and quantitative analysis based on free atoms electron state energy ratios, formulating solid solubility criterion

14 p2123 A72-30994

Superlattice structure and electron correlation of Co-Sn system, using X ray and metallographic analyses

15 p2257 A72-32115

Amorphous semiconductors theories, discussing electron states and transport properties in terms of Cohen, Mott and Gubanov models

15 p2293 A72-32234

Rutile titanium dioxide molecular orbital energy level diagram deduction from X ray emission and absorption band spectra, noting Ti and O states roles

15 p2295 A72-32539

Oxygen atom electron affinity calculation by symmetry-adapted pair correlation approximation, using pseudonatural orbitals (PSNO) technique

15 p2282 A72-32644

Sodium D lines broadening and shift parameters under atomic H and He collisions effect, calculating low lying states interatomic potentials

15 p2317 A72-32772

Carbon monoxide oxidation reactions temperature dependence, correlating high to low temperature results via transition state theory

16 p2360 A72-33511

Hydrogen and hydrocarbon diatomic molecules and cations rotational state upper limits determination, noting potential energy functions

16 p2432 A72-34098

Intramolecular interactions and vibronic spectra of polyatomic molecules. IV - Electronic relaxations: Configurational and relaxational spectra - The four-level arrangement

19 p2838 A72-38778

State density singularities elimination in inhomogeneous superconductors by electron interactions nonuniformities, resulting in tunnel junction I-V characteristic fluctuation

20 p2960 A72-39385

Calculation of electronic Green functions using nonorthogonal basis functions - Application to crystals.

20 p2961 A72-39810

Ground and low-lying excited electronic states of FeH.

21 p3096 A72-40563

Two band superconductor state density vs energy, noting energy spectrum extremal points

21 p3098 A72-41697

Photoelectron energy distributions from clean polycrystalline W, observing surface state

22 p3190 A72-42477

Photoemission from surface states on tungsten.

22 p3190 A72-42478

Theoretical interpretation of the optical and electron scattering spectra of polyatomic molecules. III - N₂O and the discovery of resonant phenomena in the B region at 6.8 eV.

24 p3426 A72-45301

ELECTRON SWEEPING

U SWEEP FREQUENCY

ELECTRON TELESCOPES

U PARTICLE TELESCOPES

ELECTRON TEMPERATURE

U ELECTRON ENERGY

ELECTRON TRAJECTORIES

I-V characteristics and bandwidth properties of distributed emission amplifier within magnetic field, analyzing averaged electron trajectories and hf potential distribution

02 p0189 A72-11568

Electron paths and spread velocities in helical beams of adiabatic M-type electron gun used in masers at cyclotron resonance

06 p0826 A72-18403

Third order aberration coefficients of electron trajectories for two tube electrostatic lens

10 p1510 A72-23941

Electrostatic field and electron trajectories calculation for focusing optoelectronic systems formed by interacting electrodes positioned on conducting surface

13 p2004 A72-29070

Electron trajectories and spread velocities in helical beams of adiabatic M-type electron gun used in masers at cyclotron resonance

17 p2562 A72-34854

Trajectory equations of laminar electron flow in exponential magnetic field, calculating electrode shapes of magnetron injection electron gun

21 p3088 A72-41835

Differential equations for energy flow between electron beam and electromagnetism field, avoiding electron trajectory explicit calculation in nonlinear treatment of cyclotron resonance interaction

22 p3159 A72-42304

Optimal gyroresonator control in electric oscillating field by HF magnetic Lorentz force in terms of relativistic electron trajectory drifts

23 p3290 A72-44200

Electric field distribution and strength and electron trajectories computations in designing electron optical display systems, using rectangular networks

23 p3291 A72-44312

Thermal conductivity of superconducting layer in intermediate stage with Andreev electron excitation trajectories in magnetic field, using Green function and impurity distribution technique

23 p3325 A72-44486

ELECTRON TRANSFER

Transferred electron microwave oscillators /three-level and LSA relaxation types/ and amplifiers /reflection and traveling wave types/ fabrication, technology and performance capabilities

01 p0035 A72-10627

Transferred electron microwave oscillator devices with n-n-n structure by liquid phase epitaxy, reducing high resistance layer in interfaces and crystal defects

01 p0036 A72-10629

Liquid phase epitaxial GaAs transferred electron microwave oscillators with high dc to rf conversion efficiencies dependent on frequencies

01 p0036 A72-10631

Bulk InP three level transferred electron microwave oscillators, observing current-controlled instabilities and operation modes

01 p0036 A72-10632

CW and pulsed InP transferred electron microwave oscillators, discussing fabrication techniques and electrical properties

01 p0036 A72-10633

High efficiency transferred electron microwave oscillators operated in short LSA mode, noting pulse-operated diode power appearance time delay behavior

01 p0036 A72-10634

Supercritically doped transferred electron microwave amplifiers stabilization mechanisms, considering cathode contact, anode diffusion current and active region temperature gradient roles

01 p0036 A72-10636

Hydrogen diffusion, electron transfer and density distribution in Ta as function of temperature and field strength

02 p0242 A72-12009

High efficiency GaAs transferred electron device operation and microwave oscillator design by simple static I-V characteristics description for time domain computer simulation

02 p0193 A72-12230

Photochemical electron transfer evolution models, noting titanium and zinc oxides as photosensitizers

04 p0484 A72-14777

Vapor-grown GaAs transfer electron microwave oscillator, discussing design, fabrication and CW power conversion efficiency

05 p0637 A72-16366

InP transferred electron microwave oscillators, observing higher efficiency than IMPATT and GaAs devices

06 p0784 A72-18063

Transferred electron effect in GaAs, presenting three level solid state microwave oscillator advantages

06 p0866 A72-18454

Transferred electron microwave oscillators design for various peak and average power levels, considering tradeoff between operating mode and device configuration

06 p0789 A72-18475

Medium power high gain, CW transferred electron microwave amplifiers at C band, describing bandwidth, saturation, intermodulation distortion and dynamic range characteristics

06 p0789 A72-18483

Large signal analysis of stabilized supercritically doped transferred electron microwave amplifiers, considering diffusion and lattice temperature effects

06 p0790 A72-18484

Power generation and low noise amplification devices development during past decade, considering avalanche diodes, transferred electron and acoustoelectric devices and microwave transistors

07 p0952 A72-18825

Electromechanical machining metal removal mechanism based on configurational localization model, relating wear processes to electron exchange and free energy margin decrease

07 p0996 A72-19989

Hydrogen protons and atoms interaction with hydrogen and nitrogen molecules, showing electron transfers agreement with Franck-Condon principle

08 p1210 A72-20835

Intraband multiphoton conduction-electron transfer probability in semiconductor under electromagnetic wave action in uniform magnetic field

08 p1216 A72-21066

Noise characteristics and mechanisms in avalanche diodes and transferred electron devices

09 p1287 A72-23115

Supercritical CW GaAs transferred electron broadband reflection amplifier power gain and noise figure at 34 GHz

10 p1449 A72-24301

Thermal energy reaction rates determination for partial charge transfer chemical reactions, comparing with electron transfer efficiencies

10 p1514 A72-24336

Electric field profile in n-type GaAs layer biased above transferred electron threshold for small signal amplifier operation

10 p1450 A72-24554

Lower ionospheric structure, discussing electron production, loss and transport effects and diurnal variations

10 p1473 A72-24703

Multiaxis radial circuits for transferred electron microwave oscillator performance optimization to obtain wideband CW amplification, discussing LSA tests

11 p1604 A72-25745

High efficiency CW performance of InP transferred electron microwave oscillator with anomalous I-V characteristics temperature dependence

11 p1604 A72-25750

IMPATT diode and transferred electron Gunn devices for systems applications, comparing thermal noise and physical properties

12 p1788 A72-27295

Electron transfer frequencies and triplet-triplet transition spectra of polyphenyl compound molecule scintillators for UV lasers, using chaotic phase method

13 p1968 A72-29509

IR absorption coefficients of oxygen atom and molecule fields due to free-free electron transfers at specific elastic scattering cross sections

15 p2274 A72-31409

High efficiency X band pulse operation of transferred electron oscillator in hybrid mode, noting high material quality and optimum impedance match

15 p2206 A72-31548

Frequency stabilized self-oscillating microwave up-converter with transferred electron diodes, noting maximum power output and bandwidth

16 p2369 A72-33764

Structure, electrical conductivity and electron transport mechanisms in chalcogenide glasses

17 p2596 A72-35750

Electron-relaxation effects in transferred-electron devices revealed by new simulation method.

18 p2667 A72-36689

Excitation of nanosecond waves on positive columns.

19 p2838 A72-37328

Equations for electron and high-energy photon transfers in magnetic fields

19 p2837 A72-38059

Effects of magnetic field on electron transport properties in gallium arsenide.

20 p2960 A72-39704

Convection and diffusion transport equation of galactic cosmic ray electrons with energy loss and absorption allowance for supernova compressed halo models

22 p3217 A72-42210

Theory of microwave amplification with electron transfer

23 p3269 A72-43550

Charge, direction and temperature dependence of semiconductor electrotransmission in dc field, considering metals diffused in Ge, Se, Te, Si, BiTe, GaAs and InAs

23 p3324 A72-43642

ELECTRON TRANSITIONS

Phosphorus absolute transition probabilities determination from P I and P II lines strength measurement, using gas-driven shock tube

01 p0104 A72-11111

High precision rotational constants and transition frequencies in ground state interstellar molecule cyanoacetylene

01 p0023 A72-11147

Solar corona atomic states radiative and collisional transitions, inferring radiative recombination cross section from bound-free absorption coefficient

03 p0422 A72-13203

Ruby laser radiation nonlinear absorption by azulene solutions derived by taking into account two-photon transitions for comparison with measurement

03 p0366 A72-13367

Solar coronal total dielectronic recombination coefficient simple relationships for isoelectronic sequences of H, He, Ne, K-Ni and Li-F, Na-A and Cu-Kr

05 p0718 A72-16510

High power tunable IR gas lasers based on anharmonic molecules vibrational-rotational transitions excitation at gas pressures of 10 atm

06 p0825 A72-17786

Neutral B I vacuum UV spectra from hollow cathode light source, remeasuring electron transitions to higher accuracy

06 p0852 A72-17896

OH ground state transition frequency measurement, using beam maser spectrometer

07 p1006 A72-19423

Metastable argon-carbon dioxide dissociation and electronic excitation of carbon monoxide or oxygen

07 p1037 A72-19496

Optically pumped gas lasers with electron transitions to molecular excited state and resonant absorption lines

07 p1006 A72-19634

Auroral emission rates for various transitions from cross section data and secondary electron spectra measurements

08 p1227 A72-21114

Atomic, ion and electron transition pulsed gas discharge lasers, considering power efficiency factors, vacuum UV region and gas density

08 p1182 A72-21644

Time dependent progress of vibrational-rotational transitions in hydrogen-fluorine chemical laser investigated by oscillography with IKM-1 monochromator

08 p1183 A72-21715

Electronic transition between energy bands as explanation for two optical absorption maxima in rare earth metals

09 p1369 A72-22609

Tabulation of calculated rotational line intensities relative to integrated vibration-rotation band intensity for various electron transitions of nitrous oxide

09 p1276 A72-22665

Simple and multiple electronic processes in X and XUV region - Conference, Paris, September 1970

09 p1356 A72-22826

Optical and inner shell X ray transitions in highly ionized Cu, Fe and Ti observed from point plasma source generated in linear vacuum discharge

09 p1360 A72-22833

Inner shell ionized atoms, discussing orbital electrons rearrangement processes based on shakeoff events and radiative Auger transition

09 p1356 A72-22834

Photoabsorption and simple and multiple excitations of rare gases internal atomic layers under X ray action, relating electron transition and relaxed core energies

09 p1357 A72-22836

Molecular X ray emission spectra interpretation based on singly ionized states observation by photoelectron spectroscopy and transition probability calculation

09 p1357 A72-22838

Nonlinear effects in optical pumping of Ne transition by laser line

10 p1491 A72-24109

Positive ions excitation cross sections calculated for proton impact induced transitions among fine structure states

10 p1543 A72-24619

Fine structure and IR transmission functions of carbon dioxide absorption bands at high pressure and temperature, calculating transition lines strength and position

11 p1620 A72-25275

Electronic model for low temperature transition in magnetite with nonintegral average electron number on site

11 p1701 A72-26023

Population inversion through metastable ion formation by atomic inner shell electrons photoionization, determining effectiveness relationship to emission source plasma composition

11 p1648 A72-26332

Electron gas in superstrong magnetic fields of gravitationally collapsed objects outer region, noting Wigner transition to ordered structure

11 p1699 A72-26704

Quantum beats in transitions from levels subject to optical cascades

12 p1847 A72-27184

Optical interband transition energies in Ni and Ni based alloys, measuring light conductivity at various spectral energies

13 p1976 A72-28904

IR absorption coefficients in air at 6000-8500 K and 40-95 atm, interpreting absorption due to free-free electron transitions in neutral particle fields

13 p2006 A72-29676

Stable single frequency operation of molecular laser using carbon dioxide-helium mixture, ensuring vibrational-rotational transition by special selection of active element parameters

13 p1970 A72-29682

Kinetic equation of repeatedly ionized plasma from hyperbolic diffusion method, calculating direct transitions between excited ion states

13 p2008 A72-29895

SiO transitions radiative lifetimes and absolute oscillator strengths from RKR Franck-Condon factors

13 p2008 A72-30054

Corrections to collision induced vibration transition probability calculated from three dimensional semiclassical model

13 p2009 A72-30062

Atomic hydrogen collisional and radiative transition rates, computing excitation and ionization cross sections

14 p2133 A72-30564

Spectral line profile of optical transition spontaneous radiation during resonance with strong field on adjacent transition

14 p2110 A72-30781

Hydrogen molecule highly excited electronic levels, developing transition probabilities estimation method

14 p2135 A72-30888

Graphite band structure investigated by secondary electron emission, observing electron transitions to higher excited states

15 p2260 A72-31856

High power carbon dioxide laser produced dense He plasma, comparing experimental and theoretical Stark profile of forbidden and allowed transitions

15 p2285 A72-32223

Electron impact low energy cross sections for transitions between highly excited states, obtaining upper bound via quantal impact parameter theory

15 p2315 A72-32715

Mercuric chloride, bromide and iodide gas phase UV absorption spectra, discussing correlation with intermolecular charge transfer transitions

16 p2360 A72-32926

Beam maser spectrometric measurements of normal, C-13 and O-18 formaldehyde transitions, determining coupling constants for all rotational transitions hyperfine structure

16 p2431 A72-33132

Russian papers on physical processes in lasers covering mode locking regime, pinch discharge, electronic transitions in diatomic molecules and laser control

16 p2400 A72-33295

Pulsed emission at pulse front in molecular hydrogen, deuterium and nitrogen at near IR electronic transitions, analyzing spectral, temporal and energy characteristics

16 p2401 A72-33298

Carbon monoxide oxidation reactions temperature dependence, correlating high to low temperature results via transition state theory

16 p2360 A72-33511

Forced oscillations in a circuit with a nonlinear p-n junction capacitance

17 p2533 A72-34756

Magnetic dipole matrix elements for atomic transitions between Zeeman levels at microwave frequencies

17 p2585 A72-35769

Emission spectra of comet tail carbon monoxide molecular ion indicating constant or slowly varying electron transition moment

17 p2618 A72-35826

The capacitances of aniso-type heterojunctions with continuously varying energy band gap and electron affinity in the transition region.

18 p2719 A72-36944

Electronic and optical phenomena in semiconductor.

19 p2844 A72-37445

Observability of hyperfine structure and Lamb, nuclear-volume shifts in $1s_{n1}-1s_{n1}$ transitions of helium-like ions.

19 p2837 A72-37544

Forbidden line intensities in cesium plasmas.

19 p2840 A72-37776

Effect of atomic polarizability on low-energy free-free radiative transitions.

19 p2837 A72-37839

Infrared dispersion of second-order electric susceptibilities in semiconducting compounds.

19 p2844 A72-37944

Evaluation of rotational temperature at high vibrational temperature in electron beam fluorescence technique.

19 p2803 A72-38434

L-S coupling interpretation of high-resolution LMM Auger spectra of Cu and Zn.

19 p2846 A72-38597

IR emission of nitrogen layer heated by reflected shock wave, noting absorption cross sections under free-free electron transitions in neutral particle fields.

19 p2835 A72-38776

Radiative lifetimes for some resonance transitions of Fe I and Fe II in the region between 2300 Å and 3050 Å, and the application to iron abundance determinations in the sun and in the QSO PHL 938.

20 p2966 A72-38915

Emission and absorption RF recombination lines of interstellar neutral atomic H and He, discussing electron transition processes in nebula.

20 p2975 A72-40070

Calculation of intensities of vibration-rotation of a diatomic molecule by the factorization method.

21 p3087 A72-40471

Cross sections calculations for electron-oxygen scattering using the polarized orbital close coupling theory.

21 p3087 A72-40472

Atomic, ion and electron transition pulsed gas discharge lasers, considering power efficiency factors, vacuum UV region and gas density.

21 p3064 A72-41301

Dependence of the properties of monocarbides of group IV-V transition metals on carbon content.

22 p3189 A72-42198

Dependence of changes in the electronic dislocation-braking force during superconducting transition on the stresses, temperature, and strain rate.

23 p3312 A72-43315

Indirect transitions and absorption in the mid-IR region of the spectrum in SbSBr crystals.

23 p3323 A72-43337

Negative resistance, transit time and limited space charge accumulation modes of semiconductor devices operation with electron transitions.

23 p3272 A72-44138

A shock tube determination of the electronic transition moment of the CN red band system.

23 p3316 A72-44329

Influence of weak disturbances on the operation of a gas laser with a homogeneous working-transition line.

23 p3297 A72-44467

Electronic excitation of N₂ and dissociative excitation of O₂ by proton impact.

23 p3317 A72-44520

Laser-source spectroscopy. II - Experimental study of line broadening for the 00 1-/10 0, 02 0/ transition of CO₂ disturbed by N₂: Application of the theory of Anderson, Tsao, and Cornette to the calculation of pure and N₂-disturbed CO₂ linewidths.

23 p3298 A72-44535

Optically pumped gas lasers with electron transitions to molecular excited state and resonant absorption lines.

24 p3408 A72-44566

Model potential calculations of lithium transitions.

24 p3426 A72-44808

Electron paramagnetic resonance hyperfine spectral observation of double quantum transitions of Ti positive ions in strontium chloride single cubic crystal host.

24 p3378 A72-45311

ELECTRON TUBES

NT CAMERA TUBES

NT CATHODE RAY TUBES

NT CELESTROPE

NT IMAGE DISSECTOR TUBES

NT IMAGE ORTHICONS

NT KLYSTRONS

NT MAGNETRONS

NT MICROWAVE OSCILLATORS

NT MICROWAVE TUBES

NT ORTHICONS

NT PICTURE TUBES

NT PLANOTRONS

NT RETURN BEAM VIDICONS

NT THERMIONIC DIODES

NT TRAVELING WAVE TUBES

NT VACUUM TUBE OSCILLATORS

NT VACUUM TUBES

NT VIDICONS

Submillimeter waves development, discussing materials research, lasers, semiconductor and electron tube sources, system components and applications in space communication, imagery, metrology and sensing.

04 p0550 A72-15591

Frequency characteristics theory for two-stage electron tube microwave amplifiers coupled by transmission line on order of wavelength.

05 p0634 A72-15827

Electron tube present and future applications as oscillators, high power and hf amplifiers and optoelectronic converters.

06 p0784 A72-17775

IR image tube with electronic scanning and pyroelectric target for uncooled operation at ambient temperature, noting wideband spectral sensitivity.

08 p1171 A72-21966

High dose rate electron beam irradiation using telescoping drift tube for flash X ray machine.

10 p1509 A72-23935

A sealed, sectionalized million-V X-ray tube.

19 p2776 A72-38767

ELECTRON TUNNELING

Equivalent circuit models in semiconductor transport for thermal, optical, Auger-impact and tunneling recombination-generation-trapping processes.

[AD-740495] 03 p0401 A72-13585

Tunneling current calculation for free electrons subject to arbitrary one-electron potential, using Keldysh perturbation theory.

03 p0404 A72-14266

Metal-insulator-metal tunneling junction, calculating effect of localized impurity states in barrier on tunneling current.

03 p0404 A72-14267

Electron tunneling probabilities through slowly varying potential energy barrier with potential holes evaluated by T scattering matrix interaction formalism.

04 p0563 A72-15471

State density singularities elimination in inhomogeneous superconductors by electron interactions nonuniformities, resulting in tunnel junction current-voltage characteristic fluctuation.

07 p1047 A72-18919

Quasi-particle decay rates by electron-electron scattering in superconductors, noting effect on states tunneling density.

08 p1217 A72-21595

Ta, Nb and La superconductivity, investigating surface contamination effects on electron tunneling characteristics.

09 p1367 A72-22554

Thin film tunnel triode using p-type amorphous semiconductors to achieve injected current amplification.

10 p1451 A72-24624

Electron tunneling into amorphous InSb and GaSb films, discussing effects of temperature, voltage, coevaporation doping and Cu and Au diffusion.

10 p1527 A72-24874

High electric field effects on I-V characteristics of Te-As-Ge-Si type chalcogenide thin film, noting Poole-Frenkel emission and electron tunneling roles.

15 p2291 A72-31641

Superconductivity, temperature and tunneling effects in low carrier density semiconductor systems /tin, germanium and indium tellurides, lanthanum triselenide and strontium titanium oxide/.

15 p2293 A72-32325

One electron and Josephson tunneling in superconductors in terms of energy level concepts.

15 p2293 A72-32326

In-Tl alloys electron phonon interaction and superconductivity electron tunneling examined by sum rule and mass defect theory.

15 p2295 A72-32543

Conductance measurements for metal oxide-amorphous silicon junctions, showing temperature dependent tunneling.

16 p2442 A72-33620

Metal-insulator-metal tunnel junctions, investigating effect of nonparabolic band structure energy-momentum relation on I-V characteristics.

16 p2370 A72-34101

Electric contact between metal and n-type semiconductor, investigating contact pressure effects on electron tunneling and phonon conductance to provide band structure.

18 p2718 A72-36488

State density singularities elimination in inhomogeneous superconductors by electron interactions nonuniformities, resulting in tunnel junction I-V characteristic fluctuation.

20 p2960 A72-39385

Nonequilibrium phenomena in electron tunneling in normal metal-insulator-metal junctions.

21 p3096 A72-40343

Tunneling generation, relaxation, and tunneling detection of hole-electron imbalance in superconductors.

21 p3097 A72-40774

Effects of tunneling on an IMPATT oscillator.

21 p3034 A72-41382

Current noise and conductance-temperature characteristics of thin discontinuous Pt films on glass substrate interpreted by quantum mechanical electron tunneling model.

22 p3214 A72-42453

Influence of the properties of the materials on junction tunneling characteristics.

22 p3214 A72-42454

ELECTRON-ION RECOMBINATION

NT RADIATIVE RECOMBINATION

Electron-ion recombination and ambipolar diffusion disruption of electron density in cryogenic helium plasma, using cavity resonator measurements.

03 p0399 A72-14067

Electron-ion recombination rate measurements in flowing afterglow, using sampling mass spectrometer and floating double probe.

06 p0851 A72-17318

Hollow cylindrical cathode discharge sustaining potential reduction and recombination probability increase from transverse magnetic field and rising pressure and plasma density.

09 p1361 A72-22957

High pressure CO and N plasmas production by uncoupling electron temperature from number density, measuring electron-ion recombination rates.

10 p1518 A72-23962

Electron recombination loss coefficients and concentration profiles for D region during solar eclipses from rocket measurements.

12 p1800 A72-27149

Low altitude electron-ion dissociative recombination and ion-ion neutralization coefficients during PCA event from ESRO rocket flights data.

13 p2032 A72-29653

Si p-n junction solar cell fill factor for electric power available to load, noting discrepancy between calculated and measured values due to recombination.

17 p2494 A72-34264

Transverse magnetic field effects on cylindrical hollow cathode discharge voltage-current characteristics, noting sustaining potential and recombination probability changes.

17 p2593 A72-35886

Theoretical estimate of the effective recombination coefficient in the D region.

23 p3284 A72-43818

Measurement of the rate coefficient for the recombination of He+ with electrons.

23 p3315 A72-43869

Dissociative recombination at elevated temperatures. I - Experimental measurements in krypton afterglows.

23 p3316 A72-44346

Electron-ion recombination in a helium plasma produced by laser.

24 p3428 A72-44799

ELECTRONIC AMPLIFIERS

U AMPLIFIERS

ELECTRONIC CONTROL

Narrow band electrically controlled interferential polarization filter with fine tuning capability for solar physical research, discussing design and operation.

03 p0357 A72-13369

Pulsed injection laser current pulse height, width and rise time controls, comparing use of tube, transistor and SCR discharge circuits.

04 p0528 A72-14420

Computer servocontrolled granite stage and measuring microscope, discussing mechanical and optical construction, control electronics and applications.

04 p0522 A72-15477

AEROS scientific satellite attitude control system, considering control and measuring electronics, axis and spin control coils and spin stabilization.

04 p0503 A72-15649

Spacecraft precision off-on attitude control by pure jet torquing, using electronics based on control system idealized model.

05 p0726 A72-16459

Analytical design of pulse width modulated systems with time constant and delay for electronic control, using Z transform.

10 p1457 A72-24458

Single engine aircraft-borne weather radar with electronically scanned steerable phased array antenna [SAE PAPER 720315].

11 p1591 A72-25579

Miniaturized electronic system for controlling methanol concentration in aqueous electrolyte during fuel cell operation.

12 p1755 A72-27723

High voltage solar array technology, studying power conditioning control system design and array-space plasma interactions.

[AIAA PAPER 72-443] 13 p1899 A72-28942

Solid state stepping motor drive controller to provide constant angular shaft velocity for scanner applications.

13 p1933 A72-29767

Ac voltage squaring with semiconductor power amplifier based on electronic servo principle and feedback circuit.

16 p2370 A72-33958

Electronic temperature-flattening of thermionic reactors.

18 p2644 A72-36172

Electronic control systems flexible programming techniques based on interconnection design or on utilization of easily exchangeable program carriers.

19 p2782 A72-38313

Electronic control systems for industrial applications, discussing electrical and mechanical properties, circuit reliability and mechanical design features.

19 p2782 A72-38314

Process control of the 100-meter telescope - Astronomical concept 19 p2803 A72-38485

Four-terminal Si controlled switches, discussing negative resistance and linear amplification I-V characteristics and applications in oscillators and modulators 20 p2907 A72-39274

Control circuit for a power supply of a laser pump lamp. 20 p2933 A72-39524

Electronic simulator for calculating effective temperatures in the establishment of climatological procedures 21 p3077 A72-40166

Optoelectronic speed control for replacing mechanical gear drives for precisely variable shaft speed ratios 21 p2997 A72-40259

Calculation of the electronic readjustment of a tunnel-diode oscillator by a varactor 22 p3159 A72-42246

German monograph - A search procedure for electronic radar. 22 p3156 A72-43054

A near-time-optimal control circuit with a large number of relay elements 24 p3387 A72-45699

ELECTRONIC COUNTERMEASURES

NT CHAFF

X band gallium arsenide field effect transistor, noting applications for radar receivers, microwave communication links and electronic countermeasures 02 p0193 A72-12184

Low noise Ku band klystron oscillators for Doppler radar, discussing FM noise induced frequency deviation, spurious modulation and countermeasures 07 p0954 A72-19049

Solid state phased arrays for ECM applications. 17 p2531 A72-35569

YIG filter banks for ECM and communications. 19 p2772 A72-37523

ELECTRONIC EQUIPMENT

NT AVALANCHE DIODES

NT CRYOTRONS

NT ELECTRONIC FILTERS

NT ELECTRONIC MODULES

NT ELECTRONIC PACKAGING

NT ELECTRONIC RECORDING SYSTEMS

NT ELECTRONIC TRANSDUCERS

NT FIELD EFFECT TRANSISTORS

NT GALLIUM ARSENIDE LASERS

NT GERMANIUM DIODES

NT JUNCTION DIODES

NT JUNCTION TRANSISTORS

NT METAL OXIDE SEMICONDUCTORS

NT MICROMODULES

NT MINIATURE ELECTRONIC EQUIPMENT

NT MIS [SEMICONDUCTORS]

NT NEURISTORS

NT PARAMETRIC DIODES

NT PHOTODIODES

NT PHOTOTRANSISTORS

NT PHOTOVOLTAIC CELLS

NT RUBY LASERS

NT SEMICONDUCTOR DEVICES

NT SEMICONDUCTOR LASERS

NT SILICON TRANSISTORS

NT SOLID STATE DEVICES

NT SOLID STATE LASERS

NT SPACECRAFT ELECTRONIC EQUIPMENT

NT THERMISTORS

NT THYRISTORS

NT TRANSISTOR AMPLIFIERS

NT TRANSISTORS

NT VARACTOR DIODES

NT VARISTORS

Ultrasonic bonding tip design for densely wired electronic circuit boards, analyzing standing wave phenomena and resonant frequency [SAE PAPER 710789] 01 p0074 A72-10279

Multichannel multispectral scanner system for NASA C-130 earth resources aircraft, describing electronic equipment and calibration sources 01 p0048 A72-10946

Telemetry standards for transmitting, receiving and signal processing equipment at missile test ranges 02 p0176 A72-12164

Electronic equipment and calibration procedures for 86 MHz radio interferometer providing synchronized astronomical observations 02 p0194 A72-12576

Book on microwave electronics covering electron beam microwave devices and solid state microwave oscillators and amplifiers 03 p0331 A72-13233

Portable electronic wattmeter for nonsinusoidal waveform low power factor circuit measurement, discussing design, calibration and applications [IEEE PAPER 8.2] 03 p0332 A72-13757

Miniature refrigerators design for electronic devices, noting application to IR detectors cooling 03 p0313 A72-14366

Electronic system for electrodischarge machining, considering thyristor spark control and circuitry

design for automatic feed down and short circuit clearance 04 p0502 A72-15530

Electronic chronometer design problems, describing quartz clock components and temperature and voltage variation effect on accuracy 04 p0525 A72-15572

Radiator fins for cooling electronic equipment elements, calculating design parameters effects on heat transfer efficiency 05 p0746 A72-16198

Electronic computing wind vane for meteorological support during atmospheric diffusion studies 06 p0843 A72-18449

Electronic imaging devices in astronomy, describing TV readout image tubes 07 p0985 A72-19580

Quartz crystal oscillator device for continuous monitoring and controlling thin film thickness in optical and electronic applications, noting temperature effects on crystal oscillating frequency 07 p0990 A72-20284

Electronic correlator for plasma wave induced coherent signals cross correlation measurement, producing 1 microsecond time delays by automatically switching lumped circuit delay line 07 p0958 A72-20582

Electronic cameras to record and measure weak stars 1000-11000 A, noting atmospheric turbulence suppression and night sky brightness reduction 08 p1170 A72-21962

European Special Space Tug electronic subsystem requirements, considering strapdown inertial measuring unit, remote sensors, computer and fail-safe backup system 09 p1396 A72-23258

Dormant aerospace electronic system sedentary or nonoperating failure rate analysis by prediction technique 10 p1447 A72-24008

Electronics and data processing technology effects on radar state of art, discussing automated air traffic control surveillance systems 10 p1435 A72-24490

Electronic production of shifting grid pattern displays featuring variable spatial frequency, temporal frequency and modulation depth 10 p1433 A72-25184

Experimental cold plates provided with heat pipes for thermal control of electronic equipment [AIAA PAPER 72-269] 11 p1740 A72-25210

Engine ignition electronic system for triggering detonators in Aeros aeronomy satellite blastoff and release devices, discussing prototypes acceptance tests 11 p1610 A72-25803

Criterion selection and minimum margin search for optimization of complex electronic circuit parameters described by mathematical models 11 p1612 A72-26736

Dynamic systems as models for electronic measuring instruments computerized development and design 12 p1791 A72-27579

Electronic fringe counter with CdS cell photosensors, dc bridge and strip recorder for interferometric applications 12 p1792 A72-27762

Petron high voltage hybrid junction field effect J-FET/ devices for direct replacement of vacuum tubes in unchanged circuits 13 p1928 A72-28431

Method to obtain optimal efficiency gyroamplifier circuits with short waveguide selector by prior grouping of electronic oscillators 13 p1928 A72-28799

Transistorized electronic equipment with delay line for optimal filtration of PSK signals 13 p1930 A72-29047

Contact potential difference effects on lubricant film thickness in electronic equipment joints, noting molecules orientation in electric field 13 p1930 A72-29052

French quality assurance of electronic components, discussing organizational links with international bodies 14 p2174 A72-30848

Mathematical model for computation of electronic circuit drift reliability and circuit production yields, discussing operational parameter allowance 14 p2091 A72-31165

Book on electricity and electronics for aerospace vehicles covering theoretical foundations, measuring instruments, batteries, generators, motors, radio receivers and transmitters, navigation equipment, autopilots, etc 15 p2182 A72-31511

Liquid crystal structure, physical properties, discussing electronics applications and technical development trends 15 p2291 A72-31594

Mathematical models for electromagnetic interference in electronic equipment, discussing nonlinear circuit analysis 15 p2201 A72-32568

Electronic equipment shielding against electromagnetic radiation and circuit protection against unwanted electrical signals 15 p2209 A72-32570

Therapeutic electromedical equipment hazards due to electromagnetic interaction, considering implantation and simulation of human body 15 p2191 A72-32572

High intensity sound effects on electronic equipment and components in aircraft noise environment, noting whisker diode and printed circuit board damage 15 p2209 A72-32621

Electronic displays - Conference, London, February 1972 15 p2181 A72-32631

Electronic circuit reliability prediction model with statistical dependence for detailed failure modes 16 p2371 A72-33345

Computerized calculation of electronic circuit and equipment reliability and quality control, presenting task examples and printout form 16 p2368 A72-33347

Synchronizing electronic equipment for digital computers input graphic data recording fidelity improvement ensuring proper timing of set and reset pulses 16 p2367 A72-34018

Electronic Components Conference, 22nd, Washington, D.C., May 15-17, 1972, Proceedings. 17 p2527 A72-34676

Dc power supply for military electronics applications, describing circuit design for well regulated and filtered output dc voltage from various ac or dc sources 17 p2497 A72-34708

Radiation-hardened components, circuits and systems. 18 p2665 A72-36308

High reliability electronic components; International Conference, Toulouse, France, March 6-10, 1972, Proceedings 18 p2668 A72-37101

Standardization and quality assurance of electronic devices on the national and European levels 18 p2743 A72-37129

European co-ordination activities with particular reference to the Space Components Co-ordination Committee. 18 p2743 A72-37130

Qualification procedure for high reliability electronic part requirements for noncontinuous production 18 p2744 A72-37134

A time-frequency high performance collision avoidance system. [ONERA, TP NO. 1091] 19 p2830 A72-37764

Book - Solid state electronic devices. 20 p2907 A72-39024

Space shuttle environmental temperature control-life support system program changes, discussing air cooled electronic equipment, cryogenic stores, crew size and mission duration [ASME PAPER 72-ENAV-18] 20 p2895 A72-39159

Digraphs application to electronic linear networks analysis, developing computer program 21 p3024 A72-40992

Drift of amplification factor and its effects in a tri-electrode electron gun. 21 p3033 A72-40995

Effect of feedback and protective circuits on the reliability of electronic equipment 22 p3158 A72-42118

Implementation status of the Omega Navigation System. 22 p3203 A72-42945

Technical and economic processes representation of radioelectronic equipment synthesis optimization using elementary random magnitudes involving output parameters deterioration rates and fabrication tolerances 23 p3269 A72-43442

Stochastic coder electronic circuit for random numbers conversion into electrical voltages and vice versa, noting compactness and low cost 23 p3273 A72-44460

Book - Electronic integrated systems design. 23 p3274 A72-44475

ELECTRONIC EQUIPMENT TESTS

Electrical and electronic measurement and test instrument - Conference, Ottawa, June 1971 02 p0200 A72-12476

Digital computer automated test equipment and procedures for remote sensors and electronics for scanning celestial sphere for X rays prior to spacecraft launch 02 p0200 A72-12479

Computer simulation techniques in aerospace ground equipment design for maintenance testing of avionic systems 03 p0329 A72-14196

Low temperature liquid bath tests for IC environmental reliability, monitoring wire bonding, metallization, surface contamination, sealing and die bonding 03 p0337 A72-14296

- Computerized modular automatic test equipment for commercial airliner avionics device performance, discussing data handling ability and cost effectiveness
06 p0796 A72-18250
- Autonomous threshold elements diagnostic tests and verification control, noting cascade, pyramidal and branching schemes
06 p0785 A72-18303
- Low energy scanning electron beam gun with retarding field mode for microelectronic device evaluation
10 p1446 A72-23936
- Electron microbeam testing for large microcircuit arrays, using analog voltage signal injection into isolated contact and digital voltmeter readout
10 p1446 A72-23938
- Power transistor thermal cycling ratings and fatigue testing under operating conditions
10 p1447 A72-24011
- Spacecraft electronic equipment design criteria for maintainability and installation, discussing mockup zero g demonstration tests of new packaging concepts [AIAA PAPER 72-235]
10 p1487 A72-24445
- Onboard localization of aircraft electrical equipment failures, using list checkout, automatic indication and dynamic programming method
11 p1578 A72-26895
- Integral diode cell for solar arrays compared with bypass configuration, discussing design, advantages and electrical performance test data
12 p1757 A72-28031
- OMEGA receiver with digital solid state circuits for remote unmanned platform positioning, discussing ship to shore tests and design features
13 p1925 A72-29184
- Autonomous threshold elements diagnostic tests and verification control, noting cascade, pyramidal and branching schemes
13 p1934 A72-30071
- Software models to test operating conditions of logic nets, discussing application to network faults diagnostics
15 p2203 A72-31749
- Multi-environment reliability test program for airborne electronic systems under simulated temperature, humidity, vibration and shock conditions
15 p2215 A72-32616
- Electric measurement and defect localization in monolithic IC elements by incorporating test structures
15 p2212 A72-32759
- Survey of current component reliability problems and methods for prevention.
18 p2668 A72-37102
- Zero overhead testing relationship to software requirements, testing dynamic accuracies, LSI product types and function and parametric speeds related to product lines
18 p2664 A72-37109
- Department of Defense Reliability Analysis Center.
18 p2676 A72-37131
- High burnout gallium arsenide Schottky barrier diodes.
19 p2770 A72-37259
- High level E-field susceptibility measurement problems and techniques.
20 p2906 A72-38981
- Design, operation and testing of integrated STOL flight control system, noting approach accuracy and passenger comfort improvement
21 p3080 A72-40292
- A survey of the costs of hermetic packaging and testing microcircuits.
22 p3161 A72-43175
- Optimal cost effective sequencing model for component reliability tests, applying to complex electronic equipment
24 p3467 A72-44654
- Ranking the reliability of two designs by Monte Carlo techniques.
24 p3383 A72-44655
- An interactive approach for the generation and verification of test sequences in a logic system
24 p3382 A72-44662
- The problems of reliability growth and demonstration with military electronics.
24 p3384 A72-44670
- ELECTRONIC FILTERS**
- FM communication system multifilter phase lock loop state equations derivation from phase model, predicting noise improvement characteristics by analog and digital simulation
01 p0044 A72-10328
- Noise reduction in pulse width modulated converters with rms voltage values digital readout, using active or passive filters methods
03 p0331 A72-13557
- Orthogonal 2-port network impedance transforming properties and applications to harmonic oscillators and filters
04 p0502 A72-15521
- Five layer resonant transparent semiconductor device structures for microwave amplifiers, reactive elements, low current rectifiers and filters
08 p1139 A72-21059
- Polynomial filter design with three layer RC distributed elements and operational amplifiers, investigating active elements effects on response
09 p1290 A72-23354
- Binary split phase FSK signal noncoherent detection by multiple predetection filtering, noting probability of error per bit
10 p1437 A72-24686
- Transfer function sensitivity characteristics comparison of doubly terminated LC filters with active cascade and inductance simulation schemes
10 p1452 A72-24801
- Computerized filter design, discussing frequency analysis and synthesis programs for quadrupole eigenmodes and transfer function
11 p1604 A72-26089
- Multifilter detection system with phase autocorrelator, discussing design based on correction detection probability vs mismatch between signal and filter central frequencies
11 p1597 A72-26315
- Electronic filters realization by error function minimization, discussing parameter space algorithmic search and complex plane optimization methods
11 p1606 A72-26550
- Signal filtration algorithms and parameter estimation in additive non-Gaussian noise background by conditional Markov process theory
12 p1783 A72-27633
- Nonlinear resonating correlator with orthogonal filters, considering cut-off frequency of ergodic random process with constant power spectral density
14 p2090 A72-31125
- Binomial electronic filter design for nonnegative impulse transient response to obtain fast rise times via in-line pole-zero configuration
18 p2672 A72-36053
- Near optimum digital phase locked loops.
21 p3038 A72-40871
- Voltage generalized-immittance converter synthesis with RC circuits for obtaining current transfer function proportional to square of s with application to filter design
22 p3140 A72-42303
- An approach for generation of second order RC-active filters.
23 p3276 A72-43863
- ELECTRONIC LEVELS**
- U ELECTRON ENERGY**
- U ENERGY LEVELS**
- ELECTRONIC MODULES**
- NT MICROMODULES**
- Analog matrix, input data and procedure for AI frame and CU-clad printed circuit board module thermal resistance analysis using ECAP program
01 p0035 A72-10380
- General purpose electronic modular units for human factors research bioinstrumentation, considering digital and analog computers, logic modules and interface and auxiliary equipment
01 p0048 A72-10569
- Microwave module circuit design for airborne phased array radar with distributed power generation, reception and phase shift functions, considering performance, reliability and cost
01 p0028 A72-10660
- Integrated receiver module for satellite transponders, including tunnel diode amplifier, Schottky barrier mixer, Gunn oscillator and low pass filter
01 p0041 A72-10701
- Floating point cellular logic multiplier with variable dynamic range suitable for scientific satellites, missiles, desk calculators and cellular computers
04 p0499 A72-15208
- Cellular electronic logic circuit planar array representing objects inertial motion, applying to traffic control, image processing and artificial intelligence
06 p0779 A72-17496
- Computerized modular automatic test equipment for commercial airliner avionics device performance, discussing data handling ability and cost effectiveness.
06 p0796 A72-18250
- S band module with Gunn diode oscillators in series connection used as phased array radar 250 W power sources with efficient heat sink
06 p0789 A72-18476
- Integrated systems approach to computer simulation with functional modules to achieve control processor independent expansion and optimization
07 p0951 A72-20331
- Single-channel-per-voice-carrier transmission system application to data communication and small earth station operation, discussing modular design and performance
07 p0948 A72-20494
- Medium scale integration (MSI) modules for arithmetic section in small, medium and process computers, emphasizing carry-lookahead procedure
13 p1926 A72-30053
- Electric power supply systems for satellites, discussing packaging standardization of electronic circuits modules
13 p1900 A72-30096
- FRAM /failure rate appraisal machine/ concept and application for modular electronic and elec-
- tromechanical assemblies environmental cycling tests, noting technical and economical effectiveness
14 p2093 A72-31169
- Heat flux nondestructive inspection methods for laminate and sandwich structures and electronic components
15 p2232 A72-31322
- Computer aided thermal design of LSI module packs for forced convection air cooling, using modal conductance matrix method
16 p2368 A72-33195
- Mathematical model for reliability analysis of modularly redundant electronic systems with unequal failure rates for operating and standby units
16 p2398 A72-33344
- Airborne flight test data acquisition system modular design to provide digital readings from monitoring transducers analog signal
16 p2364 A72-33645
- Computer thermal analysis of hybrid microcircuits.
17 p2521 A72-34679
- Hybrid LSI logic modules for aerospace.
17 p2527 A72-34683
- Modularized digital controller for closed loop systems using MOS, MSI and LSI components
17 p2521 A72-34703
- Microelectronic module application to LSI set for implementation of digital filters, division and square root operations, polynomials, matrix computations, etc
17 p2522 A72-34704
- Modular avionics computer design concept to permit tailoring for diverse applications via microprogramming
17 p2524 A72-35581
- Numerical control component insertion for missile IC electronic module, tabulating producer-user survey data for designs usage and machine tools
17 p2532 A72-35923
- Millimeter-wave solid-state exciter-modulator-amplifier module for gigabit data-rate.
19 p2771 A72-37267
- An all solid-state MIC transmit-receive module.
19 p2771 A72-37268
- Production of prototype hybrid micro-electronic modules using thin film substrates.
20 p2908 A72-39493
- Missile guidance electronic packaging and module design for circuit protection against X rays, gamma radiation and nuclear blast damages
20 p2909 A72-39766
- Disk and toroidal solid state computer storage cell arrays without boundary cells, comparing read- and write-time characteristics with conventional organizations
20 p2910 A72-39966
- TCE-71A area navigation system based on modular design with provision for 20 waypoints parameter storage, describing computer, control display and automatic data entry units
21 p3079 A72-40278
- Parallelized algorithms for computer solution of spanning tree, distance and path problems on cellular array of identical modules containing memory and combinational logic
22 p3157 A72-43023
- Bistable trigger stages composed of digital multiplexer with IC logic modulus replacing NAND or NOR circuits
23 p3267 A72-43990
- Reliability of modular computer systems with varying configuration and load requirements.
24 p3383 A72-45673
- ELECTRONIC PACKAGING**
- Thermal control methods for high density packaging, discussing cooling techniques for hybrid circuit consisting of semiconductor chips and/or thin film components
03 p0337 A72-14293
- Circuit application consideration in selecting design, materials, processes and packaging for IC component reliability
03 p0337 A72-14295
- Variable conductance heat pipe technology for overcoming thermal resistance barrier in electronic package design
04 p0596 A72-15227
- Planar coax micropackaging of minicomputers for aircraft navigation and military systems, noting environmental tests
05 p0632 A72-15772
- Subminiature TV camera using hybrid packaging techniques and digital circuitry for full EIA composite video output format and 450 TV/HR resolution capability
09 p1316 A72-23599
- Failure mode control in plastic packaged IC for screening and quality assurance
10 p1447 A72-24010
- Spacecraft electronic equipment design criteria for maintainability and installation, discussing mockup zero g demonstration tests of new packaging concepts [AIAA PAPER 72-235]
10 p1487 A72-24445

- Schottky barrier gate FET design, device packaging and low noise characteristics 12 p1788 A72-27294
- Automatic electrostatic contour welding of IC microcircuit metallic casings, using contact and electrode voltage feedback signals 13 p1963 A72-28921
- Electric power supply systems for satellites, discussing packaging standardization of electronic circuits modules 13 p1900 A72-30096
- Low power TTL IC in plastic and hermetic packages tested for reliability via critical dc parameters measurement in initial and post-stress states 14 p2091 A72-31168
- Screen printed large thick film multilayer interconnection board assemblies for electronic packaging, discussing fabrication and feasibility 16 p2368 A72-33194
- Advances in LSI technology. 17 p2527 A72-34569
- A study of the heat flow and thermal instabilities in high power hybrid integrated circuits. 17 p2527 A72-34678
- Computer-aided thermal design of LSI packages. 17 p2527 A72-34681
- Failure analysis of plastic and ceramic packaged IC, describing plastic encapsulants chemical removal and radiographic failure detection procedures 17 p2528 A72-34707
- Monoplastic solid encapsulant for p-n-p and p-n-p silicon planar passivated signal transistors 17 p2528 A72-34715
- Plastic packages for complex microcircuits. 17 p2528 A72-34717
- Numerical control component insertion for missile IC electronic module, tabulating producer-user survey data for designs usage and machine tools 17 p2532 A72-35923
- Report on Flip Chip and Beam Lead bonding for electronic circuits. 18 p2666 A72-36528
- [SAE AIR 1141] Calculation of the temperature field of a heated zone of complex form consisting of a chassis and built-in components 18 p2742 A72-37187
- INTERNEPCON '71; Proceedings of the International Electronic Packaging and Production Conference, Brighton, Sussex, England, October 19-21, 1971. 20 p2908 A72-39490
- Design and manufacturing considerations in hermetic microcircuit enclosures. 20 p2908 A72-39495
- Heat transfer coefficient measurement and thermal network analysis computer program for improving performance and reliability of microelectronic package/board and chip/substrate systems 20 p2908 A72-39497
- Missile guidance electronic packaging and module design for circuit protection against X rays, gamma radiation and nuclear blast damages 20 p2909 A72-39766
- Electronic packaging techniques in housing spaceborne computer, digital telemetry and other microelectronics for protection against severe aerospace environment 20 p2909 A72-39767
- Weight saving, vibration proofing and heat dissipating techniques in avionics packaging, considering B-1 bomber electronic multiplexing system example 20 p2909 A72-39768
- Electronic packaging and LSI techniques cost efficient use in meeting weight, volume, reliability, circuit speed and thermal protection requirements 20 p2909 A72-39769
- Automatic hermetic-sealing systems for semiconductor devices prepared by electron-beam welding 22 p3158 A72-42124
- National Electronic Packaging and Production Conference, Anaheim, Calif., February 8-10, 1972 and New York, N.Y., June 13-15, 1972, Proceedings of the Technical Program. 22 p3161 A72-43171
- Thermal design of hybrid modules and assemblies. 22 p3161 A72-43172
- Fine line multilayer system packaging using hybrid thick film processing and materials 22 p3161 A72-43174
- A survey of the costs of hermetic packaging and testing microcircuits. 22 p3161 A72-43175
- Hermetic sealing of electronic subsystems with plastics 23 p3294 A72-44142
- A means of reducing custom LSI interconnection requirements. 23 p3273 A72-44454
- Calculation of the temperature field in a ventilated cassette-type radio electronic device 24 p3386 A72-45324
- ELECTRONIC PHOTOGRAPHY**
U ELECTRO-OPTICAL PHOTOGRAPHY
- ELECTRONIC RECORDING SYSTEMS**
Electronic system for continuous automatic recording of internal friction and modulus of elasticity at high temperatures 12 p1807 A72-27462
- Electronic imaging devices for astronomy from a space platform. 24 p3404 A72-45542
- ELECTRONIC SIGNAL MEASUREMENT**
U SIGNAL MEASUREMENT
- ELECTRONIC SPECTRA**
Inner and outer belt electron differential energy spectra from Cosmos 228 satellite data, discussing fluxes of precipitating and quasi-captured particles 02 p0272 A72-1916
- Nonthermal electron spectra hardness limit during flash phase of solar flares fromOGO-5 observation 04 p0566 A72-14561
- Ordering degree effect on elementary excitation spectrum gaps in nonideally ordered solid systems, obtaining Green functions for valence and conduction electrons calculations 10 p1527 A72-24982
- Inner and outer belt electron differential energy spectra from Cosmos 228 satellite data, discussing fluxes of precipitating and quasi-captured particles 13 p2030 A72-29228
- Vibrational analysis of electronic absorption spectra of 3-methyldiazirine and 3-methyl-d3-diazirine in vapor phase 18 p2657 A72-36566
- The decay characteristics of models of solar hard X-ray bursts. 22 p3217 A72-42040
- Origin of 200-keV interplanetary electrons. 23 p3333 A72-44547
- ELECTRONIC STRUCTURE**
U ATOMIC STRUCTURE
- ELECTRONIC SWITCHES**
U SWITCHING CIRCUITS
- ELECTRONIC TRANSDUCERS**
Electropneumatic converter for pneumatic pulse transformation into dc or ac signal, using corona discharge current 03 p0311 A72-13556
- Magneto-optic storage density and read-write rate, discussing transducer cost, solid state injection lasers, holographic techniques and high activity data base applications [IEEE PAPER 19,1] 03 p0361 A72-13774
- Ultrasonic flaw detector pulse transducers operation using electrodynamic and capacitance receivers 03 p0361 A72-13987
- Photoelectric transducer with electric pulses as measure of rotating disk angle of turn, discussing design and measurement accuracy 05 p0662 A72-16124
- Continuous transducer measurement of left ventricular wall thickness in open chest dogs, adapting mutual inductance coil technique 08 p1124 A72-20897
- Capacitance gap sensor with logarithmic output response and adjustment for minimum error 10 p1482 A72-24641
- Pneumatic thermistor transducer to measure steep ejection time interval between cardiac volume pulse upstroke start and maximum rise rate occurrence 11 p1588 A72-26633
- Correcting electronic transducer for rapidly changing temperature measurement, discussing design peculiarities for superior metrological characteristics 13 p1961 A72-30024
- High precision electrostatic feedback transducer for very low differential pressure measurement in gas media, suggesting low pressure standard role [RAE-TR-71022] 16 p2394 A72-33638
- Performance improvement of amplitude-constrained minimum-variance controller by minimising sum of variance. 20 p2911 A72-39772
- Acceleration measurement by reference mass displacement in spherical cavity, considering triaxial accelerometer with capacitive sensors and differential amplifier 22 p3175 A72-41929
- Spectral analysis of microwave pulses by a ferrite transducer 22 p3158 A72-42119
- Electronic devices with Rayleigh ultrasonic acoustic surface wave excitation for storage, recognition and separation of electrical signals usually requiring computerized operation 23 p3314 A72-44148
- ELECTRONICS**
Electronics and aerospace systems - IEEE Conference, Washington, D.C., October 1971 02 p0177 A72-12376
- Electronics and electrical engineering - IEEE Conference, Houston, April 1971 03 p0335 A72-14176
- Electronics - IEEE Conference, Chicago, October 1971 04 p0485 A72-14476
- Electronics research and engineering - IEEE Conference, Boston, November 1971 05 p0633 A72-15779
- Geoscience electronics - IEEE Conference, Washington, D.C., August 1971 09 p1306 A72-22311
- Electronic circuits statistical optimization with Monte Carlo procedure, discussing methods and algorithms for accelerating evolutionary modeling 10 p1452 A72-24638
- Bell lifting rotor systems, examining company contributions in electronics and avionics 10 p1421 A72-24877
- Electronics - Conference, Rome, March 1970 15 p2193 A72-31177
- Book - Topics in solid state and quantum electronics 17 p2594 A72-34560
- Institute of Electrical and Electronics Engineers, Region Six Conference, San Diego, Calif., April 19-21, 1972, Record. 17 p2528 A72-34701
- NAECON '72; Proceedings of the National Aerospace Electronics Conference, Dayton, Ohio, May 15-17, 1972. 17 p2493 A72-35551
- Scanning the spectrum; Proceedings of the Tenth Annual Region 3 Convention, University of Tennessee, Knoxville, Tenn., April 10-12, 1972. 18 p2665 A72-36301
- Book - Introduction to optical electronics. 23 p3295 A72-43650
- ELECTRONOGRAPHY**
Astrometric measurements of visual binaries by electronographic method, using Lallemand camera 03 p0415 A72-13002
- Electronographic photography of 3C 173 radio source and stars in same field 04 p0574 A72-14975
- Electron microscopy for structure study of anodic aluminum oxides prepared by various methods, comparing electrograms of oxides after heating, boiling and filling with water 05 p0624 A72-17054
- Electronography in space astronomy, discussing use of Lallemand electronic camera as photon receptor onboard balloons or rockets 08 p1170 A72-21963
- Electronic imaging devices for astronomy from a space platform. 24 p3404 A72-45542
- ELECTRONS**
NT CONDUCTION ELECTRONS
NT FREE ELECTRONS
NT HIGH ENERGY ELECTRONS
NT HOT ELECTRONS
NT PHOTOELECTRONS
- Ion production rates during electron-flux-atmosphere interactions based on atmospheric models with different energy and angular distributions 01 p0059 A72-10597
- Spontaneous and induced Compton scattering of high frequency waves by relativistic electrons in synchrotron sources 04 p0487 A72-14902
- Relative cross sections for gas phase photodetachment of electrons from amide and arsenide ions using ion cyclotron resonance spectrometer 13 p1914 A72-30064
- Electron trapping data in neutron irradiated high purity Si, using space charge limited current measurements 15 p2294 A72-32514
- Interstellar cosmic ray electron component and isotopic composition relations from positron observations 16 p2448 A72-33741
- Electron and proton acceleration in the outer magnetosphere regions during polar substorms 18 p2688 A72-36866
- Semiempirical method for determining electron wave-function parameters in solids 20 p2959 A72-38955
- ELECTROPHORESIS**
Dielectrophoresis force measurements and wedge shaped capacitor separation properties in satellite zero gravity conditions 04 p0549 A72-14988
- Erythrocyte hemolysate cataphoresis studies of human hemoglobin changes during stepwise adaptation to high mountain conditions 09 p1266 A72-22880
- Macaca nemestrina monkey organ tissue concentrations of lactic dehydrogenase (LDH), creatine phosphokinase and aldolase, with electrophoretic determination of LDH isozymes 13 p1906 A72-29861
- Platelet electrophoretic mobility response to adenosine diphosphate (ADP) in patients with coronary artery disease 15 p2183 A72-31283
- ELECTROPHOTOMETERS**
Soviet monograph on variable stars observation covering photographic photometry, photoelectric ob-

servation, image processing devices and computer techniques

02 p0279 A72-12122

Upper atmosphere twilight optical inhomogeneities relation to noctilucent clouds, using electrophotometry methods

06 p0807 A72-17933

Combined photoelectric-photographic and plethysmographic technique for continuous measurement of rabbit ear vein diameter and tissue volume changes

09 p1273 A72-23443

Metal lines and dwarf stars study by photoelectric photometry based on narrow passbands

10 p1538 A72-24230

Photoelectric scans of M supergiant alpha Ori and carbon stars from 3400 to 11,000 Å, obtaining dominant spectral features

10 p1548 A72-24967

Photoelectric observation of beta Scorpii occultation by Jovian satellite Io, noting Fresnel diffraction effects

10 p1548 A72-24969

Multichannel area stellar photometer using photosensitive cell array for individual photoelectron counting, applying to autoguidance

11 p1631 A72-25690

Secondary scattered light component of tropospheric twilight from electrophotometric observations, comparing with upper atmospheric scattering

13 p1954 A72-30070

Narrow-band photoelectric photometry of the peculiar Wolf-Rayet eclipsing binary CV Serpentis.

17 p2617 A72-35732

Procedure for the calibration of photoelectronic components in the IR spectral range

18 p2693 A72-37005

Rocket-borne Cassegrain optic stellar electrophotometer for early star observations in 1300-2000 Å region

19 p2796 A72-37585

Photoelectric photometry of close visual binaries

19 p2866 A72-38499

Design and testing of a nine-channel photometer

19 p2804 A72-38500

The employment of a novel Quantacron photomultiplier for increasing the sensitivity of older flame photometers in the near IR

20 p2927 A72-39697

Signal-to-noise ratio of a photodetector with a virtual cathode

21 p3055 A72-40802

High precision stellar electrophotometer design, using two channel single photomultiplier photometer and digital computer for statistical atmospheric noise damping

21 p3056 A72-41447

Figl astrophysical observatory design and instrumentation, describing solar radiation insulation, computerized data reduction, area scanning photoelectric photometer and Cassegrain spectrograph

22 p3178 A72-42541

A photoelectric study of Messier 81.

22 p3229 A72-42975

The physical properties of the Jovian atmosphere inferred from eclipses of the Galilean satellites. II - 1971 apparition.

24 p3435 A72-44689

ELECTROPHOTOMETRY

Photoelectric UVB photometry for galactic cluster NGC 7039 region stars, discussing MK spectral classifications and peculiar A stars

10 p1545 A72-24827

Lunar eclipse of 25 September 1965, observing penumbra densities and isophotes in B and V spectral regions by photoelectric photometry

14 p2161 A72-30915

Mercury diameter measurement by photoelectric Hertzprung method during transit on 9 May 1970

15 p2312 A72-32091

Photoelectric photometry of binary VV Pup with 3-sec time resolution, suggesting qualitative model from eclipses identification

15 p2314 A72-32369

Photoelectric transit observations of Saturn and Mars, showing culmination in universal ephemerides time

19 p2862 A72-37987

Pressure-scanned echelle grating plus Fabry-Perot stellar spectrophotometer.

21 p3053 A72-40609

Triaxial mount for electrophotometric observations of satellites during their transit into the shadow of the earth

23 p3290 A72-44040

ELECTROPHYSICS

NT ELECTRO-OPTICS

NT MOLECULAR ELECTRONICS

Influence of irradiation by 1.2-MeV electrons on the electrophysical properties of p-Si single crystals grown in a hydrogen atmosphere

21 p3098 A72-41686

ELECTROPHYSIOLOGY

HIS bundle electrocardiography for arrhythmia studies, discussing conducting tissue potential recording, ventricular delay and block site determination and electrophysiological effects of drugs

02 p0157 A72-11473

Canine and human ventricular myocardium microelectrophysiological studies of postextrasystolic T wave change relation to cellular repolarization and contractile potentiation magnitude

02 p0157 A72-11474

Receptor activity control from clinical physiological and electrophysiological observation data analysis, noting central nervous system role and feedback and self adaptation capabilities

02 p0157 A72-11543

Fish electroreceptor system morphology, physiology and evolution, considering electric current action, peripheral coding activity and central subsystems

02 p0157 A72-11545

Spinal reflexes through electric stimulation of gastrocnemius and soleus human leg muscles, attributing increased tendon reflex amplitudes to gamma motoneurons hyperactivation

04 p0467 A72-14704

Neuroelectric signal recognition system with computerized compensation for variations due to small random changes, slow trends and interference potentials

04 p0481 A72-15253

Human male gonadotropin secretion relation to sleep stages, using electrophysiologic recordings and radioimmunoassay techniques

05 p0620 A72-17128

Electrophysiology for auditory temporal masking mechanism study of cat cochlear nucleus and inferior colliculus single neurons

05 p0620 A72-17175

Electrophysiological responses to maximum exercise in healthy humans from polarcardiographic display of heart vector changes

07 p0916 A72-18891

Electrophysiological, neurophysiological, metabolic, vegetative, psychological, chemical and pathological aspects of sleep, noting disturbance and wakefulness mechanisms for various clinical disorders

09 p1264 A72-22223

Multichannel oscillograph for real time biomedical studies of LF physiological processes

09 p1270 A72-22881

Mathematical, physical and engineering aspects of electro- and magnetocardiography, noting heart field nondipolar properties and heart vector determination difficulties

09 p1273 A72-23414

Peripheral afferent input to monkey cortical efferent zones of distal forelimb muscle control, using single microelectrode for intracranial stimulation and cellular discharge recording

09 p1267 A72-23583

Single lateral geniculate neuron recording during receptive field-centered flashing spot variations for intensity response function comparison with optic neurons in cats

10 p1427 A72-25177

Human electrophysiological changes during perceptual isolation from EEG, EMG, vertical eye movements and electrodermal measurements

12 p1771 A72-27484

Electrical components of cardiac and skeletal muscle impedance, calculating rectangular stimulating current mean value

13 p1908 A72-28461

Functional organization and neurophysiological mechanisms of return corticothalamic system in anesthetized cats, showing axon terminal presynaptic depolarization

13 p1902 A72-28762

Electrophysiologic data acquisition by multiple dipole type of inverse electrocardiographic procedure based on model data, noting favorable and unfavorable dipole array configuration

13 p1909 A72-28997

Electrocardiography and magnetocardiography to determine flux and vortex sources respectively of heart electrical activity impressed current density

13 p1909 A72-28998

Lower body decompression effects on ECG, showing heart rate increase, R and T amplitude changes and heart electric axis displacement

14 p2074 A72-30383

Electric field projections in contrast to voltage as working quantity for frontal plane ECG leads

15 p2188 A72-31766

Weightlessness effects on animal voluntary motor activity and wakefulness from brain and muscle area electrical activity recordings during ballistic flight

16 p2355 A72-33548

An automatic measuring and recording system for clinical electro-oculography.

19 p2759 A72-37400

Role of afferent and efferent connections in the formation and reproduction of trace processes in man

21 p3001 A72-40807

Patterns of spontaneous and reflexly-induced activity in phrenic and intercostal motoneurons.

21 p3003 A72-41462

Morphological and electrophysiological analysis of afferent receptor connections in cerebellar cortex, discussing fast conducting, diffuse reticular and inferior olive fiber paths

21 p3004 A72-41674

Electrophysiological analysis of defense reflex and unconditioned reaction and conditioned signal analyzers in nodal mechanisms of functional system /afferent synthesis, decision making, correction, etc/

21 p3004 A72-41675

Electrophysiological investigation of the excitation and inhibition processes in the auditory cortex

22 p3148 A72-43165

Electrophysiological analysis of limbic-reticular interaction during the orientating reflex

23 p3257 A72-44081

Preprocessing of nerve pulse sequences for analysis by digital computer

23 p3261 A72-44349

Comparison of the vectors of the ventricular depolarization and repolarization of man during immersion in a standing position

24 p3372 A72-44924

ELECTROPLATING

Electrical resistance and thermal joint conductance measurements at perfect contact interfaces from electroplating, soldering and explosive bonding [AIAA PAPER 72-19]

05 p0666 A72-16859

Cermet coating with enhanced microhardness by Ni electroplating with fine corundum particles, presenting optimum electrolytes

09 p1318 A72-22527

Push-pull magnetic amplifier circuit operation as variable polarity dc source for electroplating applications

11 p1603 A72-25279

Thin film Cu-Cd solar cell electrochemical plating potential and solution composition effects on copper sulfide surface layer formation and cell efficiency

12 p1855 A72-28008

ELECTROPOLISHING

Metal surface smoothing during electrochemical dissolution prior to polishing, involving electrolyte diffusion processes or semiconductor oxide film formation

11 p1640 A72-26259

ELECTRORETINOGRAPHY

Conduction velocity groups in cat optic nerve from antidromic responses recorded in peripheral retina and area centralis

03 p0315 A72-13621

Eye movement control device for electronystagmography, describing construction, line drawing and basic circuits

03 p0319 A72-13724

Retinal ganglion cell spikes timing in mammalian retina, using electroretinography and computer analysis

06 p0762 A72-17721

Human dark adaptometric visual threshold recovery and electroretinograms in response to double light flashes, using Fourier analysis of oscillatory potentials

07 p0916 A72-19024

Intraelectroretinographic analysis of light signal spatial summation at different retinal nerve levels in frogs

11 p1585 A72-26454

Landolt ring radioactive plaque night vision tester comparison with electroretinography and Goldmann-Weekers dark adaptometry apparatus from special tests of night blind patients

12 p1777 A72-28332

Electroretinographic illumination potentials dependence on extracellular chloride ion concentration in isolated frog retina

15 p2186 A72-32491

Electroretinographic evidence for a photopic system in the rat.

17 p2500 A72-34878

Intraocular noise - Origin and characteristics.

18 p2651 A72-36605

The electrical activity of the isolated frog retina in buffered chloride-deficient Ringer's solution

22 p3147 A72-42987

Component analysis of electroretinogram in dark and light adapted sheep eye, noting rod and cone receptor potentials and transient and dc responses

23 p3261 A72-44382

Sensitivity of the human ERG and VECG to sinusoidally modulated light.

23 p3258 A72-44383

ELECTROSEISMIC EFFECT

U ELECTRIC CURRENT

U SEISMIC WAVES

ELECTROSLAG REFINING

Electroslag and vacuum remelted maraging steel rolling contact, investigating fatigue life as function of lubricant film thickness/surface roughness ratio

12 p1816 A72-28109

Lower oxide mechanism in reduction-oxidation reactions during Ti steels electrosmelting with slag and gas phases

14 p2112 A72-30158

ELECTROSTATIC CHARGE

Solids static electrification models based on solid state physics, considering contact, deformation and cleavage charging processes

02 p0269 A72-12552

Electrostatic charging mechanisms leading to streaming current generation in moving fluids, considering initial discharge, electrode change and mobility charging current

02 p0261 A72-12553

Size determination for stationary space charge clouds in streaming media from theoretical model of tanks filled with electrostatically chargeable inflammable fluids

02 p0261 A72-12554

Electrically charged low mobility droplet production by water vapor condensation on to gaseous ions from aircraft static discharger

02 p0231 A72-12556

Fluidic devices electrostatic modulation, verifying jet deflection analytical model by experimental results

07 p0913 A72-18819

Imagewise electrostatic charge buildup in electron beam recording, determining trajectories by Runge-Kutta method

10 p1479 A72-23929

Controlled nuclear fusion plasma stabilization by electrostatic forces, reducing applied magnetic field

11 p1694 A72-25791

Thunderstorms physical mechanisms of charge generation and separation, considering correlation between lightning and precipitation

13 p1995 A72-29873

Electrostatic charge on an aircraft and lightning striking the aircraft

21 p2994 A72-40171

Static electricity in fueling of supajets.

21 p3040 A72-41375

Upper limits on vertical fluxes of 1/3 e and 2/3 e charged quarks in cosmic rays from observations with scintillation counter telescope

21 p3101 A72-41450

Electrical discharge-produced explosions aboard supertankers during cleaning operation and electrostatic charging of supersonic aircraft during passage through heavy rain, noting water drop disintegration

24 p3368 A72-44979

ELECTROSTATIC ENGINES

Electrostatic surface and bulk ionization ion thrusters current densities for propulsive and working fluid utilization efficiency

05 p0705 A72-16772

Electrostatic ion thruster and hydrazine monopropellant systems for communication satellites, noting weight savings

17 p2596 A72-34265

Electrostatic surface ionization and electron bombardment ion thrusters current densities for propulsive and working fluid utilization efficiency

17 p2597 A72-35275

ELECTROSTATIC EROSION

U SPARK MACHINING

ELECTROSTATIC FIELDS

U ELECTRIC FIELDS

ELECTROSTATIC GYROSCOPES

Angular velocity vector active damping during spin-up of electrically supported gyro with mass-unbalance readout, using Euler equations of motion

07 p0986 A72-19691

Multidimensional function extremum for sectioned resonator type gyroamplifier efficiency optimization

08 p1172 A72-22050

Rotor displacement measurement of electrostatic gyroscope by capacitive sensor using spherical electrode

15 p2236 A72-31899

USAF development of electrostatic gyros for inertial air navigation, noting flight tests and associated airborne digital computer

17 p2578 A72-35558

Deposition of dielectric films on the electrodes of an electrostatic gyroscope

21 p3059 A72-41814

Development and testing of a precise marine electrostatic gyroscope.

24 p3401 A72-44638

ELECTROSTATIC PLASMA

U PLASMAS [PHYSICS]

ELECTROSTATIC PRECIPITATORS

Particle mass monitor system based on piezoelectric microbalance combined with electrostatic precipitator collector, considering applications to air quality monitoring, laboratory aerosol research, process control, etc

[AIAA PAPER 71-1100] 01 p0067 A72-10548

ELECTROSTATIC PROBES

Nonisothermal theory of electrostatic probe in weakly ionized plasma, giving I-V characteristics

01 p0108 A72-10238

Double Langmuir probe, microwave cavity and upper hybrid frequency measurements of plasma density in hydrogen, helium, neon and argon

01 p0110 A72-11190

Electron thermal boundary layer effects on Langmuir probe measurements in subsonic cold plasma flow

01 p0071 A72-11191

Plasma electron density depletion by electron attaching gas introduction, deriving electrostatic probe technique

02 p0264 A72-12261

Plasma ion temperature and neutral collision frequency determination by Langmuir probes

02 p0264 A72-12262

Transient response of negatively biased Langmuir probes for planar and cylindrical plasma sheaths under large amplitude pulsed potentials

[AD-739787] 03 p0361 A72-13924

Electron energy derivation from contaminated Langmuir probe, explaining E region high temperature

05 p0654 A72-16007

Electron temperature measurement error elimination with radio frequency Langmuir probe in low density plasma, measuring floating potential

05 p0694 A72-16049

Current collection characteristics of flush mounted electrostatic probes on sharp flat plate in ionized hypersonic flows

05 p0696 A72-16814

Plasma ambipolar diffusion coefficient and electron density determination from thermal density fluctuations cross spectrum based on Langmuir probe measurements

06 p0864 A72-18536

Multichannel modular spectrometer with electrostatic analyzers for low energy electron and proton flux measurement

07 p0988 A72-19954

Spectrometers with electrostatic analyzers alternating with shielding and suppressing gratings for low energy electron flux measurement

07 p0988 A72-19955

Collisionless ion beam plasma simulation of ionospheric plasma with Langmuir interpretation of density and frequency agreement

07 p1044 A72-20367

Potential distribution in positive ion sheath around plane Langmuir probe immersed in plasma

08 p1215 A72-22074

Second derivative measurement of Langmuir probe characteristics for electron energy distribution functions in nonstationary plasmas by sample and hold technique

09 p1359 A72-22654

Reference electrode area and floating potential influence in Langmuir probe measurements of plasma density and temperature

09 p1311 A72-23229

Flat plate Langmuir probe measurement of electron temperature in plasma with elliptically anisotropic velocity distribution, discussing probe orientation effects

09 p1366 A72-23578

Ionospheric and magnetospheric electric field measurements by rocket, satellite or balloon-borne electrostatic probes or by plasma drift methods

10 p1473 A72-24529

Electrostatic and electron temperature probes compared during ionospheric rocket soundings, noting lower ionosphere discrepancies due to surface contamination

11 p1633 A72-26102

Langmuir probe techniques for plasma measurement in ion thruster hollow cathode discharge configurations

[AIAA PAPER 72-416] 11 p1706 A72-26166

Electron bombardment ion thruster ESKA 18-P thrust measurements by critically loaded columns suspension instrument and simultaneous beam diagnostics by electrostatic probes

[AIAA PAPER 72-433] 11 p1707 A72-26176

Plasma ion temperature determination by measuring transient current to cylindrical Langmuir probe under collision free conditions

[AD-739815] 12 p1851 A72-27399

Cylindrical electrostatic analyzers in rocket and satellite instruments for space low energy charged particles measurements

13 p1960 A72-29842

Comparative electron density measurements in positive low pressure He discharge column with Langmuir probes and microwave interferometer and cavity

14 p2105 A72-30808

Surface contamination effect on electron temperature measurement using rocket-borne Langmuir probe in lower ionosphere

15 p2236 A72-31926

Direct display plasma density and temperature meter with Langmuir probe for ionospheric observation

15 p2231 A72-32338

End effect in current response of highly negative cylindrical Langmuir probe in collisionless plasma flow, discussing use for ion temperature determination

15 p2288 A72-32418

Symmetrical and asymmetrical electrostatic probes for RF plasma discharge data, describing feedback

network, stabilization, generation and electron temperature profiles

15 p2288 A72-32509

Langmuir probe susceptance- and conductance-voltage measurements via in-phase and quadrature component plots as function of applied dc potential

15 p2241 A72-32515

Contaminated Langmuir probes LF admittance measurements in mercury vapor plasma, considering dielectric relaxation in insulating layers

15 p2241 A72-32516

Airborne electrostatic probe for cloud droplet size measurement, calculating flow distribution and particle trajectories

16 p2390 A72-33150

Langmuir probe dc and second harmonic characteristics measuring system, describing switching circuitry

16 p2392 A72-33608

Low density and pressure air plasma electron density simultaneous measurements by Langmuir and RF capacitance probes

16 p2438 A72-33836

Electrostatic flush disk and cylindrical probe construction and electron density data during atmospheric reentry from beryllium sphere experiments

[AIAA PAPER 72-691] 16 p2346 A72-34051

The geometric factor of a cylindrical plate electrostatic analyzer.

17 p2553 A72-34639

Application of the floating-potential probe for studies of low-frequency oscillations in a plasma

17 p2588 A72-34755

Measurements of the plasma sheath capacitance using a simple tunnel diode oscillator.

17 p2558 A72-35847

Probe measurements of a cesium plasma in a simulated thermionic energy converter.

18 p2647 A72-36206

Transition from sheath-convection to saturation-current behaviour of a Langmuir probe in a flowing plasma.

18 p2715 A72-36688

Determination of the plasma density in a collisionless plasma.

18 p2717 A72-37041

An appraisal of the single Langmuir probe technique in the study of afterglow plasmas.

19 p2840 A72-37456

Mathematical model for perfectly absorbing spherical Langmuir probe in collisionless plasma, obtaining plasma density and ion temperature

19 p2842 A72-38524

Exact solution of the problem of measuring the parameters of a dense plasma with the aid of a spherical probe

19 p2842 A72-38534

Fixed-bias floating double-probe technique with simple Langmuir-probe characteristics.

19 p2804 A72-38592

Effect of plasma resistance on electron temperature measurement by means of an electrostatic probe.

19 p2804 A72-38593

Effect of angle of incidence on the response of cylindrical electrostatic probes at supersonic speeds.

20 p2926 A72-39602

A technique for recording Langmuir probe characteristics in afterglow plasmas.

21 p3051 A72-40212

Measurement of ionic parameters of a cesium plasma with the help of a grid probe with a cooled collector

22 p3211 A72-42645

Method of solving boundary-value problems for a Langmuir probe in a dense plasma

22 p3213 A72-43119

ELECTROSTATIC PROPULSION

NT ION PROPULSION

Current and future rocket and spacecraft propulsion systems based on chemical propellants, nuclear thermoelectric, electrostatic and electromagnetic power generators

05 p0705 A72-16743

Electrostatic rf ion thruster development, including power conditioning and control units

07 p1054 A72-19600

Electrostatic ion thruster theoretical model, deriving ionization rate density as function of discharge current

[AIAA PAPER 72-432] 11 p1707 A72-26175

Electrostatic rocket exhaust materials deposits effects on solar cells optical, thermal and electrical performance characteristics, using optical thin film theory

[AIAA PAPER 72-447] 11 p1578 A72-26184

Duration test and performance of annular colloid thruster, noting specific impulse increase and electrostatic vectoring

[AIAA PAPER 72-483] 11 p1710 A72-26209

ELECTROSTATIC SHIELDING

Active shielding against radiation in space using charged particle deflection by electric and magnetic fields [CERN-71-16] 02 p0258 A72-12076

Spectrometers with electrostatic analyzers alternating with shielding and suppressing gratings for low energy electron flux measurement 07 p0988 A72-19955

Transistor damage by electrostatic discharges, noting charge stored by humans and protection techniques 08 p1140 A72-21064

Nonideal dense plasma properties, discussing electrostatic shielding, many particle clusters, phase transitions, metallization and electrical conductivity [AIAA PAPER 72-414] 11 p1695 A72-26164

Shielded silicon gate complementary MOS integrated circuit. 24 p3385 A72-44972

ELECTROSTATIC WAVES

Similarity theory for electrostatic and magnetic collisionless shocks at zero ion temperature, using numerical simulation results 01 p0106 A72-10029

Electrostatic waves in longitudinally magnetized plasmas with random electron charge distribution and applied magnetic field, finding phase characteristics 01 p0106 A72-10128

Electrostatic wave-particle interactions in inhomogeneous collisionless plasma, calculating resonant distribution function, charge densities and trapping periods 01 p0107 A72-10136

Monochromatic waves propagating in uniform magnetoplasma, considering resonant interaction with electrostatic approximation 01 p0107 A72-10138

Periodic inhomogeneous plasma electrostatic waves, considering dispersion relation and longitudinal oscillations 01 p0107 A72-10141

Diffuse plasma resonances in space interpreted by wave-particle nonlinear interaction in weakly turbulent plasma, considering electrostatic electron cyclotron wave instability 02 p0265 A72-12366

Longitudinal electrostatic waves in perpendicular collisionless plasma shock, investigating stability 05 p0698 A72-17021

Plasma models of topside ionosphere, investigating electrostatic wave propagation 05 p0698 A72-17022

Dispersion relation for electrostatic plasma waves propagation at frequencies near electron cyclotron harmonics in warm magnetoplasma, determining refractive index curves 05 p0698 A72-17023

Electrostatic shift and broadening of Landau resonance by particle-wave interaction in turbulent plasmas 05 p0700 A72-17231

Electrostatic waves perturbed distribution function behavior in presence of forced oscillations, considering Maxwellian ion and electron plasma waves excited by dipole 06 p0855 A72-17508

Electrostatic wave propagation and damping in thermally ionized collisionless alkali plasma, determining electron and ion densities, electron temperature and ion distribution function 06 p0856 A72-17521

Langmuir wave-caused electron plasma distribution function deformation, discussing particle trapping effects 06 p0858 A72-17542

Electrostatic hf wave propagation in one dimensional collisionless plasma, describing electron trapping and oscillations and resonance-produced sidebands 06 p0858 A72-17544

Electrostatic field excitation in plasma layer by plane transverse electromagnetic wave as function of incident angle 06 p0862 A72-18339

Contrastreaming electron beams instability in finite length one dimensional system with stationary neutralizing ion background, analyzing electrostatic waves space/time development by numerical simulation 06 p0865 A72-18540

Electrostatic wave instabilities at harmonics of electron cyclotron frequency in hot and cold anisotropic plasma with Maxwellian temperature distribution 07 p1039 A72-18824

Electrostatic oscillations of multiveLOCITY electron streams in hot inhomogeneous plasma 07 p1046 A72-20502

Electrostatic oscillations enhancement in magnetized plasma by hf electromagnetic waves, noting detection by light scattering 07 p1046 A72-20539

Electrostatic ion wave Landau damping in magnetic field of Ar plasma QP machine 08 p1213 A72-21250

Stability of steady large amplitude whistler wave supported by weak electrostatic waves in collisionless magnetoplasma, constructing distribution function via Vlasov equation solution 08 p1213 A72-21258

Electrostatic ion wave stability in electrodynamic channel flow from approximate numerical solution of dispersion equations 08 p1211 A72-21305

Electrostatic plasma wave conversion into electromagnetic waves, calculating dispersion relation at all wavelengths for perpendicular propagation mode 08 p1137 A72-21989

Electrostatic longitudinal waves propagation and detection in isotropic collisionless hot electron plasma, calculating Landau dispersion curve and damping 09 p1359 A72-22794

Large amplitude electrostatic ion acoustic shock production by superposing pulsed photoionized plasma slab on dc background 09 p1360 A72-22871

Stable large amplitude high Mach number ion acoustic shocks in collisionless plasma, obtaining electron density as function of time 09 p1364 A72-23445

Electron-neutral collisions effects on wavelength and damping of electrostatic waves propagation in Ar and He plasmas 10 p1525 A72-25143

Grid produced LF electrostatic perturbations propagation and damping in near isothermal plasma, discussing ion ballistic contributions to ion acoustic waves 11 p1692 A72-25520

Trapped particle induced frequency shift in response of electrostatic wave to adiabatic and sudden excitations, obtaining distribution functions and nonlinear dispersion relation 11 p1693 A72-25566

Strong pitch angle scattering of energetic electrons in presence of electrostatic waves due to ion cyclotron instability above midlatitude ionospheric trough region 11 p1714 A72-26398

Plasma parametric instabilities excitation by radio waves in ionosphere, noting LF ionic and HF electrostatic wave growth 11 p1628 A72-26767

Parametric decay instability of Langmuir and acoustic plasma waves induced by incident electromagnetic wave near plasma frequency, noting application to ionospheric instabilities 13 p2012 A72-29126

Enhanced damping of electrostatic wave primary mode due to combination scattering from plasma electron density oscillations 13 p2018 A72-29854

Isolated finite amplitude electrostatic oscillations production in thin plasma layer between two parallel metallic surfaces in magnetic field 14 p2136 A72-30302

Electrostatic cyclotron harmonic waves propagation in inhomogeneous electron plasma slab, deriving RF electric field 14 p2138 A72-30397

Experimental investigation of electrostatic cyclotron harmonic waves excited in inhomogeneous plasma column with axial magnetic field by RF capacitor field 14 p2138 A72-30398

Lagrangian complex amplitude derivation for monochromatic electrostatic wave in unmagnetized collisionless plasma, investigating nonlinear Landau damping effects on instability 14 p2140 A72-30399

Nonlinear coupling of wave modes in cold magnetized plasma, applying to electrostatic wave transformation in connection with solar type 3 radiation 15 p2283 A72-31431

Dispersion relationship for electrostatic instability associated with electron beam trapped in magnetic mirror of magnetosphere, taking into account nonuniformity of magnetic field 15 p2283 A72-31434

HF electrostatic instabilities driven by electron-ion relative drift velocity across external magnetic field for inhomogeneous plasma, noting Landau damping role 16 p2433 A72-32809

Langmuir wave coupling in inhomogeneous plasma due to combined density gradient and external HF electric field 16 p2436 A72-33654

Kinetic theory of waves in hot, low density plasma. 17 p2591 A72-35161

HF electrostatic wave instability induced in plasma by electron beam, noting resonant frequency Doppler shift 17 p2591 A72-35369

Turbulence of electrostatic electron cyclotron harmonic waves observed by Ogo 5. 17 p2549 A72-35599

Dispersion curves of mixing mode between electrostatic and electromagnetic waves propagating perpen-

dicularly to ambient magnetic field for hydrogen plasma with Maxwellian velocity profile 19 p2839 A72-37335

A satellite survey of vector electric fields in the ionosphere at frequencies of 10 to 500 hertz. I - Isotropic, high-latitude electrostatic emissions. 19 p2768 A72-38742

Low frequency electrostatic waves in a turbulent plasma. 21 p3092 A72-41221

Resonant interaction of an electrostatic wave with electrons in a current sheet. 22 p3169 A72-42008

Isolated finite amplitude electrostatic oscillations production in thin plasma layer between two parallel metallic surfaces in magnetic field 23 p3317 A72-43204

Plasma frequency, hybrid frequency and harmonic gyrofrequency electron resonances due to electrostatic waves in ionosphere observed with topside sounders aboard rockets and satellites 23 p3263 A72-43513

Stationary solitary, snoidal and sinusoidal ion acoustic waves. 23 p3320 A72-43520

Wave growth in a strongly turbulent plasma. 24 p3430 A72-45568

ELECTROSTATICS

Electrostatic analyzer for very low energy particles, calculating trajectories 03 p0392 A72-14055

Electrostatic field calculation for magnetron/injection/electron gun with wedge shaped cathode 06 p0826 A72-18404

Electrostatic focusing field inhomogeneity/gradients/ effects on high frequency electron-wave interaction processes in linear beam backward wave oscillator tube 07 p0952 A72-18845

Electric field voltage effect on dispersion of electrostatically atomized liquids and hydrocarbon fuels with and without gamma irradiation 09 p1350 A72-22546

Computation procedure for crystal lattice electrostatic strain energy derivatives 09 p1372 A72-23228

Electrostatic adhesive devices for zero-g intra/extravehicular activities, noting applications to astronaut and cargo maneuvering, worksite restraint, tool and equipment tiedown, etc 10 p1431 A72-24650

Ion and electron temperature ratios in hot plasma, discussing energy relaxation, heating and cooling effects and electrostatic confinement by ambipolar diffusion 10 p1524 A72-25032

Electrostatic force for rotational torque production, applying to motor design 11 p1603 A72-25743

Ultrasonic wave generation in solids using transducer composed of high rigidity dielectric/polypropylene/ between two electrodes 18 p2691 A72-36402

Solution of mixed boundary value problems in heterogeneous media for multiply connected regions of complex shape by a structural method 20 p2946 A72-39469

Weak electrostatic turbulence observation in earth bow shock magnetic field gradient, suggesting cyclotron drift instability role 23 p3342 A72-44523

Radar observations of equatorial spread F in a region of electrostatic turbulence. 23 p3286 A72-44528

ELECTROSTRICTION

Electrostrictively induced stimulated Brillouin light scattering effect on atmospheric depolarization, obtaining solutions for steady state and transient conditions [AD-736316] 03 p0367 A72-13429

Coupled electroelastic vibrations of piezoelectric cylinders from polycrystalline electrostriction theory, taking into account mechanical and dielectric losses 14 p2132 A72-31117

ELECTROTHERMAL ENGINES

NT ARC JET ENGINES
NT PLASMA ENGINES
NT RESISTOJET ENGINES

Electrically heated thermal decomposition hydrazine thrusters, discussing propellant supply pressures compatibility and thrust levels [AIAA PAPER 72-451] 11 p1708 A72-26188

Electrothermal thruster supersonic convergent-divergent nozzle performance with lithium vapor propellant, predicting exhaust velocity by isentropic flow equations [AIAA PAPER 72-453] 11 p1708 A72-26189

ELEKTRON SATELLITES

Earth outer radiation belt and unstable radiation zone dynamics during IQSY magnetically quiet and disturbed period based on Elektron-series satellite data 22 p3218 A72-42211

ELEKTRON 4 SATELLITE

Positive H, HE and O ions in exosphere from mass spectrometers mounted on Elektron 4 satellite
01 p0053 A72-10368

ELEMENT ABUNDANCE

U ABUNDANCE

ELEMENTARY EXCITATIONS

NT EXCITONS
NT MAGNONS
NT PHONON BEAMS
NT PHONONS
NT PLASMONS

Quasi-particle decay rates by electron-electron scattering in superconductors, noting effect on states tunneling density
08 p1217 A72-21595

Ordering degree effect on elementary excitation spectrum gaps in nonideally ordered solid systems, obtaining Green functions for valence and conduction electrons calculations
10 p1527 A72-24982

ELEMENTARY PARTICLE INTERACTIONS

NT ELECTRON CAPTURE

NT MESON-NUCLEON INTERACTIONS

NT NUCLEON-NUCLEON INTERACTIONS

Free atoms and radicals elementary reactions, passing parent molecules through electrodeless rf or microwave discharge at various pressures and temperatures
03 p0320 A72-13392

CP-noninvariance model of baryon interaction and charge asymmetry of universe, postulating kappa particle /neutral massive fermion/
06 p0875 A72-17275

Book on theory of fully ionized plasmas covering Coulomb systems equilibrium and nonequilibrium states, charged particle radiation and interactions with EM fields
13 p2011 A72-29098

The self-consistent test-particle approach to relativistic kinetic theory.
20 p2955 A72-40013

ELEMENTARY PARTICLES

NT ALPHA PARTICLES
NT ANTINEUTRONS
NT ANTIPARTICLES
NT ANTIPROTONS
NT BARYONS
NT BETA PARTICLES
NT BOSONS
NT CONDUCTION ELECTRONS
NT DEUTERONS
NT ELECTRONS
NT FAST NEUTRONS
NT FERMIONS
NT FREE ELECTRONS
NT GRAVITONS
NT HADRONS
NT HIGH ENERGY ELECTRONS
NT HOT ELECTRONS
NT LEPTONS
NT LIGHT BEAMS
NT MESONS
NT NEUTRINOS
NT NEUTRON BEAMS
NT NEUTRONS
NT NUCLEONS
NT PHOTOELECTRONS
NT PHOTONS
NT PIONS
NT POSITRONS
NT PROTONS
NT QUARKS
NT RECOIL PROTONS
NT SOLAR PROTONS
NT TACHYONS
NT THERMAL NEUTRONS

Duality concept in elementary particle physics, discussing pion-nucleon scattering, amplitude exchange degeneracy, Regge poles and Veneziano models
05 p0692 A72-17077

Elementary particle theory and field equations in cosmological spaces, using four dimensional conformal imbeddings
06 p0891 A72-18421

Cosmic ray experiment jet shower event with possible new particle existence
11 p1712 A72-25867

ELEVATION ANGLE

Target azimuth and elevation estimation by four beam cluster, analyzing angle estimation accuracy as function of SNR by computerized Monte Carlo simulation
07 p0941 A72-19304

Multipath angle error reduction using multiple radar target signal processor with angle tracking of wave fronts
08 p1134 A72-21408

Elevation angle and range error correction equations for satellite tracking data processing with assumed spherical tropospheric refractivity
09 p1281 A72-23510

FM/CW interferometric ionosonde used for interferometric direction finding, computing incident azimuth and elevation from baseline array phase differences
09 p1281 A72-23514

GMD-1 tracking system for mesoscale wind data, minimizing elevation angle errors in jet stream CAT program by upwind release of rawinsonde
10 p1508 A72-25080

HF backscatter pulse signal incidence elevation angle measurements based on amplitude ratio of two antennas with different vertical patterns
12 p1783 A72-27779

SHF signal propagation through troposphere at low elevation angles, comparing fading measurements in winter and summer
15 p2194 A72-31550

Circumzenithal instrument for latitude and longitude determination and star transits observation through almucantar
15 p2238 A72-32122

A nomogram for look angles to geostationary satellites.
19 p2869 A72-37298

Directional far IR emission from sunlit lunar surface, determining brightness temperature as function of observer and sun elevation angles and surface parameters
22 p3226 A72-42537

Multimoded components wavefront arrival angle from measurements of signal induced in linear array, discussing numerical calculation from linear equation solution and polynomial roots
23 p3264 A72-43601

ELEVATIONS [DRAWINGS]

U DRAWINGS

ELEVATORS [CONTROL SURFACES]

Aircraft flight characteristics for landing approach by spoiler-elevator deflection coupling, considering pitch, flight path angle and speed
16 p2343 A72-33423

ELLIPSES

Free flexural vibrations of an elliptical plate with simply supported edge.
23 p3352 A72-44121

ELLIPSOIDS

Motion of asymmetric body of revolution in rotating liquid, calculating drag on ellipsoid
02 p0204 A72-12175

Convex figures in mathematical geodesy, applying function h for ellipse and ellipsoid of revolution
03 p0351 A72-14328

Scattering function of ellipsoidal gas molecules with translational and rotational degrees of freedom
04 p0552 A72-14629

Stress-strain state of thin ellipsoidal shell with central stiffened hole, using small elastoplastic deformation theory
04 p0588 A72-15050

Optimization problems in gravitational attraction, considering homogeneous ellipsoids interaction and free particle simple harmonic motion
06 p0851 A72-18740

Loxodrome and geodetic line azimuths relationship on ellipsoid of revolution
08 p1158 A72-21159

Axissymmetric deformation of hollow elongated elastic ellipsoid, using Lamé equilibrium equations
09 p1400 A72-22708

Ellipsoidal plasmoid equilibrium revolution frequency and potential energy and stability in external hf fields
09 p1362 A72-23204

Galaxy formation process in expanding universe from study of hydrodynamic equations for rotating gaseous ellipsoid with uniform density
11 p1717 A72-25865

Mixed variational formulation and finite element method for axisymmetric cylindrical, conical, spherical and ellipsoidal shells
12 p1879 A72-27195

Elastic wave diffraction by rigid ellipsoid, deriving scattering cross section for incident P wave from integral equation solution
16 p2426 A72-33659

Approximate calculation of the magnitude of the momentum during the passage of a material particle past an elongated homogeneous biaxial ellipsoid
17 p2618 A72-35812

Numerical analysis of three dimensional steady laminar free convection boundary layer due to heated ellipsoid, solving flow equations
19 p2881 A72-38394

Approximate calculation of the magnitude of the momentum during the passage of a material particle past an elongated homogeneous biaxial ellipsoid
17 p2618 A72-35812

Numerical analysis of three dimensional steady laminar free convection boundary layer due to heated ellipsoid, solving flow equations
19 p2881 A72-38394

ELLIPSOMETERS

Reflection electron diffraction and ellipsometric studies of oxidation of niobium crystal surface, showing oxygen absorption in lattice and oxide film formation stages
07 p1017 A72-19944

Corrosion tests by ellipsometer, discussing apparatus design and bare metal surface and thin film properties
08 p1172 A72-22110

ELLIPTIC DIFFERENTIAL EQUATIONS

Ellipsometric characterization of oxide films obtained by heat treatment of Al in air and vacuum, noting interface disruption due to gamma crystal penetration into coated metal
10 p1495 A72-24078

Cs adsorption on W and Ti observed by combination of ellipsometry, Auger spectroscopy and surface potential difference measurements, noting sticking coefficient and coverage
16 p2442 A72-33833

Ellipsometry for the study of equilibrium cesium adsorption.
17 p2552 A72-34599

ELLIPTIC DIFFERENTIAL EQUATIONS

Elliptic and parabolic partial differential difference equations solution using modified random walk Monte Carlo technique
01 p0093 A72-10858

Elliptic equations solutions for electromagnetic effect in MHD rectangular channels using relationship to Laplace equations
03 p0397 A72-13995

Rotationally symmetric force free magnetic field boundary value problem, using linear elliptic differential equation
03 p0400 A72-14352

Rotationally symmetric static incompressible infinite conducting plasma elliptic differential equation reduction to boundary value problem
03 p0400 A72-14353

Nonlinear elliptical equations first boundary value problem, presenting approximation capacity and convergence of straight line procedure
04 p0538 A72-14625

Asymptotically diagonal systems for variational expansions applied to elliptic partial differential equations, estimating convergence rate
04 p0540 A72-15374

Regularity of nonuniqueness solutions of degenerate elliptic-parabolic partial differential equations systems without compactness requirement for associated differential quadratic form
06 p0839 A72-17627

Elliptic restricted three body problem, using motion anomaly as independent variable
06 p0877 A72-17654

Triangular points linear stability in elliptic restricted three body problem, determining exponents by convergent iteration method
06 p0878 A72-17664

Numerical methods for parabolic, hyperbolic and elliptic flows in fluid mechanics and heat transfer, considering finite element method
07 p1097 A72-18795

Dynamic programming for optimal stochastic control problem with Gaussian shot noise involving parabolic or elliptic differential equation in unbounded domain, discussing iterative solution and quasi-linearization
07 p1027 A72-19292

Axissymmetric potential theory boundary value problems for iterative elliptic differential equation in rectangle and half strip
08 p1198 A72-20961

Boundary points regularity for second order elliptic equation with continuous coefficients
08 p1198 A72-21165

Dynamic programming application to computer algorithm construction for elasticity theory two dimensional problems, solving boundary value problem for elliptic differential equation
08 p1243 A72-21235

Coordinate sequences construction method for complex regions and various boundary conditions, deriving closed form solution to elliptical equation
08 p1200 A72-21702

Finite element method for approximate solution of elliptic partial differential equations on unbounded domains, proving error bounds
11 p1675 A72-25271

Russian book on approximate solutions of boundary value problems covering elliptic differential equations and Ritz, moment, straight lines and probability modeling methods
11 p1677 A72-26065

Error bounds for finite element methods and approximation with piecewise polynomials for elliptical differential equations solution
11 p1679 A72-26956

Asymptotic approximation methods for boundary layers in singular perturbation theory for linear elliptic partial differential equations in two independent variables
13 p1940 A72-28425

Generalized solution regularity of arbitrary order quasi-linear elliptic equations, indicating continuity conditions of variational problems
13 p1987 A72-30001

Uniqueness, existence and smoothness theorems for elliptic dynamic boundary problems in elasticity theory
15 p2329 A72-32286

First eigenvalue and first eigenfunction properties of linear elliptic partial differential equation in varia-

tional form with discontinuous coefficients, considering Dirichlet problem

16 p2416 A72-33502

Coefficients ratio modulus invariance of elliptic differential equation for conformal mapping of definition domain

16 p2417 A72-34011

Finite element method matrices in least squares approximation and elliptic partial differential equations, discussing numerical stability properties

17 p2573 A72-34219

Book - Approximation of elliptic boundary-value problems

17 p2574 A72-34622

On the numerical solution of elliptic partial differential equations by the method of lines.

17 p2575 A72-34647

Existence of multiple solutions for nonlinear elliptic boundary value problems.

17 p2575 A72-34936

Solvability of the first boundary value problem of higher-order elliptic quasi-linear equations with discontinuous and rapidly increasing Orlicz-class coefficients

17 p2577 A72-35842

Stability of difference schemes for elliptic equations in terms of the Dirichlet boundary conditions

18 p2705 A72-36801

Boundary value problem for degenerate equations with discrete coefficients

19 p2824 A72-37317

Modified Ritz method to find optimum boundaries to elliptic systems governed by Laplace or Poisson equation

19 p2826 A72-38246

A boundary value problem for a mixed-type equation with two perpendicular parabolic-degeneration lines

19 p2828 A72-38630

Fractional steps method of difference schemes for approximate numerical solution of parabolic and elliptic initial boundary value problems

20 p2945 A72-39327

Solution of a problem with a skew derivative in a half-space for certain elliptical equations

20 p2945 A72-39393

Book - Functional analysis and approximation theory in numerical analysis.

20 p2946 A72-39729

Solutions to certain elliptic equations, which are positive in the vicinity of an isolated singular point

20 p2947 A72-39867

Limiting equation for solving a boundary value problem in a multilayer domain

21 p3074 A72-40258

A regularity theorem for linear second order elliptic divergence equations.

22 p3198 A72-41947

Functional method investigations of imbedding theorems for random weight spaces of high order irregular elliptic equations with uniform boundary conditions

23 p3307 A72-43222

Existence and uniqueness theorems of elliptic equations with eigenfunction exponential decrease at infinity and 2m order self adjoint differential operator in n-dimensional Euclidean space

23 p3307 A72-43223

Estimates of derivative solutions of linear non-homogeneous elliptic-type equations of arbitrary order near the domain boundary in the L2 metric

23 p3309 A72-44041

Riemann boundary value problem with a shift in multiply connected regions for quasi-linear elliptic systems of equations

24 p3419 A72-45260

ELLIPTIC FUNCTIONS

Variational perturbation problem solution in power series form for elliptic functional description of elastic continuous medium state by Euler-Lagrange equations

02 p0259 A72-12233

Unified design charts for communication systems filter networks with inverse Chebyshev and elliptic function responses

06 p0787 A72-18400

Autonomous two body system described by nonlinear differential equations of motion, obtaining free relative vibration solution in terms of elliptic functions

06 p0849 A72-18694

Boundary value problem solution for first order elliptic system on plane

09 p1341 A72-22488

Spectral continuity conditions of linear operator, noting application to elliptical operators approximation in separable Hilbert spaces

10 p1505 A72-24070

Regularized first order algorithm for ideal resonance problem in solar system, considering solution in terms of elliptic functions

20 p2968 A72-39199

Exact expressions for the properties of the zero-pressure Friedmann models.

22 p3229 A72-42890

The superharmonic functions in the axiomatics of M. Brelot associated with a degenerate elliptical operator

24 p3418 A72-44825

A priori estimates at the boundary for solving second-order elliptic integrodifferential equations

24 p3420 A72-45648

ELLIPTIC INTEGRALS

U ELLIPTIC FUNCTIONS

ELLIPTICAL CYLINDERS

Gravity effects of infinite homogeneous elliptical cylinder segment

03 p0351 A72-14330

Zero moment theory application to cylindrical shells with elliptical geometries under constant transverse loads

07 p1087 A72-18992

Time varying external pressure effect on creep collapse of long thin walled quasielliptic cylindrical shell, taking into account elastic deformation

08 p1245 A72-21612

Microwave attenuation factor of TE and TM modes in hollow conducting elliptical waveguides, using first order perturbation formula for calculation

10 p1451 A72-24594

Torsional waves far-field structure in infinite elastic rod of elliptical cross section, using perturbation method

13 p2057 A72-29004

Harmonic waves propagation in infinite transversely isotropic cylinder with elliptic cross section, obtaining solution in terms of Mathieu functions

14 p2163 A72-30190

Unsteady torsional creep of multiply connected cylindrical rod with arbitrary cross section, calculating elliptic rod relaxation

15 p2327 A72-31744

Laplace equation for homogeneous magnetic field perturbation by superconducting elliptical cylinder and by two parallel circular cylinders

23 p3313 A72-43779

ELLIPTICAL ORBITS

NT APHELIONS

NT APOGEES

NT INTERPLANETARY TRANSFER ORBITS

NT PERIGEEES

NT PERIHELIONS

NT TRANSFER ORBITS

Transfer from high elliptical to circular orbit, using successive spacecraft braking maneuvers in planetary atmosphere with incomplete information

01 p0130 A72-10927

Precessing elliptical orbits stability in Schwarzschild field

04 p0571 A72-14559

Plane periodic oscillations of solid body on elliptic orbit, characterizing stability of motion equations periodic solutions

04 p0582 A72-14632

Extremum of satellite orbit perigee or apogee height in Hohmann transfer

05 p0713 A72-16006

Satellite attitude estimation on elliptic orbits by Kalman filters with periodic coefficients, demonstrating efficiency by earth pointing satellite using different instrumentation noise models

05 p0685 A72-16442

Earth satellite plane periodic oscillations damping with respect to center of mass in orbital plane during motion on elliptical Kepler orbit

05 p0730 A72-17030

Spin stabilized axisymmetric probe attitude deviation due to solar pressure in elliptic orbits

06 p0892 A72-17655

Nonspinning satellite earth-pointing attitude control for elliptic orbits using active regulation of pitch moment of inertia

08 p1204 A72-21605

Three body problem study of satellite capture by planets in elliptical orbits, deriving orbital elements in terms of mass ratio and planetary orbit eccentricity

12 p1865 A72-27096

Optimum elliptic orbit characteristics of planetary artificial satellite based on earth-planet-earth flight

14 p2151 A72-30472

Numerical integration method with recurrent power series for motion and variational equations of elliptic restricted three body problem

19 p2862 A72-38019

Improved criteria for hyperbolic-elliptic motion in the general three-body problem.

21 p3109 A72-41333

Analytic partial derivatives for estimating low-thrust parameters.

22 p3231 A72-42865

Jet stream formation from uniform distribution of grains in similar elliptical orbits, discussing models with numerical simulation

24 p3445 A72-45461

ELLIPTICAL POLARIZATION

Magnetoinic component with fluctuating elliptical polarization during wave reflection from F 2 layer, discussing suppression mechanism

01 p0028 A72-10593

Large amplitude linearly or elliptically polarized Alfvén wave propagation parallel to magnetic field, calculating nonlinear Landau damping rate

01 p0111 A72-11227

Elliptical polarization and depolarization coefficients for monochromatic radio waves reflected from F 2 ionosphere using Stokes parameters

05 p0656 A72-16241

Receiver arrangement for polarization selection based on multiplication of heterodyne-converted and amplified signals taken from dual-input antenna receiving elliptically polarized field

05 p0635 A72-16332

Polarization changes with distance from microwave antenna in near and intermediate zones for circularly and elliptically polarized fields in square and rectangular apertures

05 p0635 A72-16335

Elliptically polarized ionospheric source generation of short period geomagnetic disturbances at earth surface

08 p1153 A72-20719

Transfer of polarized radiation in a stellar atmosphere.

17 p2605 A72-34533

Polarization offset angle effect on isochromatic fringe visibility of holographic photoelasticity recordings, noting reference beam ellipticity adjustment

18 p2733 A72-36360

A nomogram for determining the phase difference of an elliptically polarized wave

18 p2663 A72-37219

Elliptically polarized ionospheric source generation of short period geomagnetic disturbances at earth surface

19 p2791 A72-38347

ELLIPTICITY

Rotating earth oblateness and equator ellipticity influence on near-equatorial synchronous satellite behavior, using nonlinear mechanics asymptotic method

03 p0436 A72-13835

ELONGATION

Saint Venant problem for orthotropic almost cylindrical beams, investigating elongation, bending due to couple and transversal loads and torsion due to torque

04 p0594 A72-15747

A simple method for determination of the elongation before reduction of area using a 100-deg cone indentation

18 p2676 A72-37098

EMBOLISMS

NT AEROEMBOLISM

Precordial monitoring for pulmonary gas embolism and decompression bubbles.

19 p2762 A72-38710

Relation of the electrocardiogram to hemodynamic alterations in pulmonary embolism.

19 p2759 A72-38816

EMBRITTEMENT

Electron beam welding of W-base alloy to Ta-base alloy, avoiding Re induced embrittlement by pure Mo transition piece

06 p0821 A72-17710

High pressure hydrogen effects on austenitic stainless steel embrittlement, determining yield, tensile and fracture strength

07 p1011 A72-19479

Maraging steel embrittlement by titanium carbonitrides lattices separation during cooling, suggesting rapid quenching and plastic deformation temperature reduction

07 p1012 A72-19677

Long-time isothermal temper embrittlement in Ni-Cr-Mo-V steels, noting tensile ductility decrease and intergranular fracture

07 p1015 A72-19932

Environmental hydrogen embrittlement of Ti-Al alloy as function of test displacement rate and microstructure variation

07 p1016 A72-19933

Corrosion resistance decrease and embrittlement in Ni-Mo cermet alloys after heat treatment from electrical resistance measurement

07 p1017 A72-19965

Transition metals and alloys electron structure and packing defect energy theory, discussing crystal atomic interactions and brittle breakdown

07 p1049 A72-20148

Hydrogen embrittlement of stable austenitic Ni-Cu steel, observing intergranular decohesion in fractured specimens by microfractography, electron microscopy and X ray crystallography

07 p1021 A72-20485

Adsorption, corrosion and hydrogen embrittlement effects on crack formation in quenched carbon steels in active media, using tensile stress-rupture tests

08 p1190 A72-22183

Fe-Ni-C alloy mixed austeno-martensitic microstructure embrittlement, investigating mechanical properties after thermomechanical treatment

10 p1495 A72-24087

- Aerospace vehicle high tensile strength fasteners stress corrosion cracking and hydrogen embrittlement [AIAA PAPER 72-385] 11 p1653 A72-25407
- Carbon and oxygen distribution and content effects on Mo mechanical properties and embrittlement 11 p1666 A72-26878
- Chromium stainless steel fatigue life reduction due to embrittlement in gaseous hydrogen atmosphere at room temperature, noting alleviating effect of atmosphere contaminants 13 p1979 A72-29484
- Dispersion hardening/aging/ effect on embrittlement of Ni base alloys in cold worked pipes during heat treatment 15 p2255 A72-31569
- Catalytic dissociation, hydrogen embrittlement, and stress corrosion cracking. 17 p2566 A72-34256
- Relation between hydrogen embrittlement and the formation of hydride in the group V transition metals. 18 p2700 A72-36578
- Strain rate, stress concentration and temperature effects on hydrogen environment embrittlement of metals 19 p2816 A72-37640
- Physical and metallurgical factors causing embrittlement and creep rupture life reduction determined by tests, discussing crystal and grain boundary deformation and notch effects 19 p2874 A72-37711
- Effect of residual elements on radiation strengthening in iron alloys, pressure vessel steels, and welds. 20 p2937 A72-39289
- Mercury embrittlement of age-hardened Cu-1.9 wt pct cobalt and Cu-3.6 wt pct titanium. 20 p2938 A72-39296
- Microcracks observed in hydrogenated niobium foil. 21 p3069 A72-41300
- Investigation of the kinetics of low-cycle fatigue of steels in a hydrogen atmosphere and in vacuum 22 p3195 A72-43161
- EMBRYOLOGY**
- Alpha-L-fucosidase, beta- and alpha-D-galactosidases and alpha-D-mannosidase activity changes in human placenta at various embryogenesis phases 02 p0163 A72-12294
- Histological examination of transverse acceleration stress effect on inner ear development of gestating rat embryos 07 p0923 A72-20446
- Energetic motor activity rule hypothesis for physiological mechanisms of certain ontogenesis patterns, suggesting motor activity as excess anabolism induction factor 09 p1264 A72-22225
- Embryogenesis of fertile chicken eggs in pure oxygen at reduced pressure 09 p1265 A72-22642
- Sperry neuronal specificity hypothesis for nerve cell connections formation between eye and brain during embryonic development, proposing systems matching theory 17 p2504 A72-35070
- Intravascular injection and histology studies of human embryonic and fetal choroidal vasculature development 19 p2755 A72-37398
- EMBRYOS**
- Inert gas effects on embryonic development. 22 p3145 A72-42744
- EMERGENCIES**
- Natural resources multispectral remote sensing for national emergencies, discussing various imaging techniques 02 p0212 A72-11828
- Emotional aspects of pilot performance under high stress in emergency situations, discussing psychophysiological training methods 05 p0623 A72-17098
- Psychophysiological potentials of pilots in simulated emergency situations, investigating motor reaction time, signal selection time, error number and type and processed information amount and rate 06 p0769 A72-18199
- Parameters affecting communication and rescue time constraints for emergency astronaut return from low earth orbits 09 p1395 A72-23155
- Lunar landing mission escape and rescue concepts, considering emergencies during earth orbit, translunar, lunar orbit, surface and rendezvous, transearth and earth reentry phases 09 p1396 A72-23157
- Terminal guidance systems and techniques application to manned space flight rescue operations, discussing emergency location and rescue spacecraft communication and guidance 09 p1396 A72-23158
- Emergency reentry manned spacecraft remedial concepts, mission constraints and system designs in terms of cost effectiveness 09 p1396 A72-23159
- Pilot survival probabilities under various conditions of high performance aircraft takeoff and landing accidents, suggesting emergency action guidelines for pilot training 10 p1428 A72-23732
- Magnetic compass use in instrument flight conditions, suggesting emergency procedures during aircraft system failures 15 p2238 A72-32212
- Flight mechanics aspects in space transportation system for international rescue, analyzing potential crises situations requiring emergency action 24 p3451 A72-45217
- EMERGENCY LIFE SUSTAINING SYSTEMS**
- Dynamic response index (DRI) minimization for personnel aircraft emergency catapult escape systems to reduce injury probability 08 p1112 A72-21576
- Lockheed ADP SR-1 ejection seat system for safe aircrew recovery under zero-zero, high Mach and altitude conditions, describing escape experiences with SR-71 aircraft 13 p1896 A72-28701
- Disposable emergency oxygen mask for air passengers based on continuous flow, phase dilution principle, describing altitude chamber tests with human subjects to study physiological responses 13 p1908 A72-28702
- Long range planning for the development of space flight emergency systems. 17 p2620 A72-34428
- EMISSION**
- NT BIOLUMINESCENCE
- NT CHEMILUMINESCENCE
- NT ELECTROLUMINESCENCE
- NT ELECTRON EMISSION
- NT FIELD EMISSION
- NT FLUORESCENCE
- NT HYDROXYL EMISSION
- NT INCANDESCENCE
- NT ION EMISSION
- NT LIGHT EMISSION
- NT LUMINESCENCE
- NT LUNAR LUMINESCENCE
- NT MICROWAVE EMISSION
- NT NEUTRON EMISSION
- NT OPTICAL RESONANCE
- NT PARTICLE EMISSION
- NT PHOSPHORESCENCE
- NT PHOTOELECTRIC EFFECT
- NT PHOTOELECTRIC EMISSION
- NT PHOTOIONIZATION
- NT PHOTOLUMINESCENCE
- NT RADIO BURSTS
- NT RADIO EMISSION
- NT SECONDARY EMISSION
- NT SELF SUSTAINED EMISSION
- NT SHOCK WAVE LUMINESCENCE
- NT SOLAR RADIO BURSTS
- NT SOLAR RADIO EMISSION
- NT SPECTRAL EMISSION
- NT SPONTANEOUS EMISSION
- NT STIMULATED EMISSION
- NT THERMAL EMISSION
- NT THERMIONIC EMISSION
- NT THERMOLUMINESCENCE
- NT X RAY FLUORESCENCE
- EMISSION SPECTRA**
- Spectral distribution of total continuous emission coefficient for LTE hydrogen plasma over 8000-16,000 K and 400-15,000 A ranges, observing Stark broadening 01 p0108 A72-10175
- Spiral galaxies radio continuum emission origin, discussing supernovae and relativistic electrons effects 01 p0131 A72-11006
- CH Cygni spectrum analysis in activity phase, discussing blue continuum, emission and UV absorption lines, radial velocity and stratification effects 01 p0131 A72-11008
- He emission line star G61-29, discussing spectral features and proper motion limits on maximum distance 01 p0133 A72-11095
- Cosmic soft X ray and UV radiation sources, discussing transition radiation emission in interstellar space 01 p0121 A72-11121
- Pulse widths formed by relativistic beaming pulsars effect on emission spectra 01 p0133 A72-11130
- Optical emission spectrum of Ba and CuO combustion products during nozzle expansion into vacuum 01 p0146 A72-11312
- Uranium arc plasma visible and near UV emission coefficients as function of U partial pressure and corresponding temperatures 01 p0112 A72-11337
- Uranium and tungsten plasmas emission and absorption properties at shock tube generated pressures of 3-48 atm and temperatures of 7,000-12,000 K 01 p0112 A72-11339
- High speed photographs of plasma emission spectra in UV and soft X radiation spectrum regions, discussing theory, design and operation of facilities 02 p0223 A72-11408
- Mountaintop high resolution spectral observations of diffuse isotropic submillimeter atmospheric and sky emission 02 p0274 A72-12194
- Active and quiet solar atmosphere models from OSO satellite data, presenting emission lines and continua from abundant elements 03 p0423 A72-13215
- Solar active regions and flares X ray spectroscopic data, observing ionized silicon emission lines 03 p0423 A72-13217
- Submillimeter wave stratospheric emission spectra measurement by aircraft- or balloon-borne phase modulated Fourier spectrometry, noting SNR and small errors 03 p0348 A72-13399
- Spectrum of low modulation frequencies of He-Ne laser radiation produced by motion of external reflector of matched and unmatched three-mirror resonators 03 p0368 A72-13666
- Fe XI to XV emission lines from transitions and isoelectronic spectra in manganese, chromium and vanadium 03 p0391 A72-13750
- Apparatus for emission spectroscopic studies on high density molecular jets excited by slow electron bombardment 03 p0392 A72-14054
- Wolf-Rayet type stars emission line variations from outer convective zone opening and matter ejection 03 p0439 A72-14243
- Emission spectrum and intensity variation of organic dye solutions excited by nitrogen laser pulsed radiation 04 p0529 A72-14655
- Molecular nitrogen dayglow emission in F region, noting volume emission rates, integrated overhead intensities and solar activity effects 04 p0518 A72-14959
- Markarian galaxies photometric observations, presenting emission line intensities and UV magnitudes 04 p0578 A72-15309
- Photoluminescence of Er cations in CdS, observing group I co-dopants sensitizing behavior and broad-band emission spectra 04 p0563 A72-15472
- Optical spectra of compact objects, reviewing emission line spectra of quasars 05 p0716 A72-16372
- Spectral energy distributions of peculiar galaxies and quasars by photoelectric spectrometry, observing emission lines strength 05 p0716 A72-16373
- Horizontally averaged nonthermal velocities determination in lower solar chromosphere, observing Doppler widths of weak rare earth emission lines in H and K wings 05 p0718 A72-16504
- Electron density profiles as function of position in enhanced coronal region from Ni XV and Fe XIII emission lines observation 05 p0719 A72-16517
- Quasar photoionization and emission line spectra, determining radiation/gas density 05 p0720 A72-16713
- Emission spectra of exploding copper wires in air and vacuum in IR, UV, visible and vacuum UV regions 05 p0691 A72-16991
- Terrestrial atmospheric effects on quasar red shift measurements, considering night sky emission lines and atmospheric window size limits 05 p0723 A72-17159
- Vertical extensive air showers at aircraft heights, constructing integral spectrum based on particle number 06 p0870 A72-17280
- Emission line of neutral carbon in solar spectrum at 1993.6 A from balloon-borne spectrography 06 p0876 A72-17566
- Atomic hydrogen 6300 A forbidden line emission altitude and intensity during predawn enhancement, using rotating photometer 06 p0806 A72-17644
- Be stars emission line profile broadening due to surrounding gaseous ring in circular motion according to Kepler law 06 p0880 A72-17892
- Spectral characteristics of Ar ion laser emission for determination of stability region, mode sequence and beat signal levels 06 p0826 A72-18009
- Temporal characteristics of emission line broadening in lasers with dispersive resonators for Nd ion activated phosphate glasses and disordered crystals 06 p0826 A72-18011
- Surface layer humidity correlation to height of atmosphere emitting in IR spectral region, determining water vapor content by recording earth radiation angular distribution 06 p0808 A72-18046
- Van der Waal broadening of shock excited emission lines at 5000 K for astrophysical applications 06 p0852 A72-18053

Ionospheric scintillations relationship to airglow emission spectrum at 6300 Å

07 p0974 A72-18895

Laser quantum theory for single mode steady state emission fluctuations and instability region with high density of excited atoms

07 p0999 A72-18910

Gas laser emission fluctuations of total radiation energy, polarized field components and line widths in longitudinal magnetic field

07 p0999 A72-18911

Spectral composition of emitted radiation, emissivity and absorptivity of Venus atmosphere at high temperatures

07 p1068 A72-18933

Spontaneous emission from driven Doppler broadened gas of two level atoms radiating into free space, predicting power spectrum

07 p0940 A72-19194

Spectral characteristics and small signal gains of carbon monoxide laser, using optimum gas compositions

07 p1003 A72-19218

Neodymium-glass laser emission spectral and temporal correlations during Q switching by rotating prisms and passive shutter

07 p1006 A72-19633

Synchrotron emission source identification from spectral index dependence on frequency

07 p1059 A72-19807

Carbon like spectra and ground energy levels of Sc, Ti and V ions in 16-22 Å range, using vacuum spark source

07 p1037 A72-19833

Spectral distributions of laser emission as dynamic variables of electromagnetic field modes and active medium excitations, using perturbation theory

07 p1007 A72-20120

Galactic nucleus IR measurements in terms of forbidden NE II emission line at 12.8 microns

07 p1081 A72-20229

Coronal condensation of 10 September 1970, observing iron and calcium emission lines

07 p1082 A72-20297

Pulse rate and pumping power effects on emission spectra and I-V characteristics of multielement GaAs injection lasers

08 p1181 A72-20796

Emission dynamics of pulsed laser with optical delay line in resonator

08 p1181 A72-20797

Tago-Sato-Kosaka comet isophote picture of 5 February 1970, noting tail composition, photographic magnitude and emission spectrum

08 p1229 A72-20831

Shock wave properties in RR Lyra type star atmospheres, discussing high temperature region structure behind wave front and emission line profiles

08 p1229 A72-20841

Auroral emission rates for various transitions from cross section data and secondary electron spectra measurements

08 p1227 A72-21114

Spectroscopic observations and classification of luminous galactic nuclei with broad emission lines, discussing gas density, velocity and outflow and electron scattering

08 p1234 A72-21279

IR spectral emittance measurement with airborne spectrometer for geological mapping over Pisgah Crater/California

08 p1162 A72-22017

Nd smooth pulsed laser action with narrow spectral line and emission amplification from Nd doped phosphate and silicate glass rods

08 p1183 A72-22027

Nd glass absorption of flash pump emission energies with varying discharge parameters, Xe pressure and glass thickness

08 p1184 A72-22030

Wolf-Rayet stars identification in spiral galaxy M33/NGC 598/ from narrow band interference filter photographs, tabulating apparent magnitudes and emission indexes

09 p1382 A72-22281

Chemical bond effect on K emission spectrum of oxygen and fluorine

09 p1275 A72-22522

Pseudo-hemispherical properties applied to radiative transfer in absorbing-emitting medium involving specular directional surfaces

09 p1351 A72-22671

Multiconfigurational interactions in atoms with incomplete electron shells, identifying K-alpha satellite emission lines

09 p1357 A72-22837

Molecular X ray emission spectra interpretation based on singly ionized states observation by photoelectron spectroscopy and transition probability calculation

09 p1357 A72-22838

X ray emission bands related to K line intensity for iron group transition metals, using orthogonalized plane wave method

09 p1370 A72-22840

Rare earth elements outer electrons X ray and UV photoemission spectra interpretation by multiplet splitting of final state

09 p1371 A72-22844

Al alloys solid binary solution soft X ray emission spectra interpretation by rigid band and virtual bound state models

09 p1371 A72-22847

Soft X ray emission spectra from Al-Nb and Al-Pd alloys, deducing electron state density near Al ions

09 p1371 A72-22848

Pulsating polar auroral line emission spectra observation at 3914 and 5577 Å by rocket-borne photometers

09 p1301 A72-23262

Photoelectric Fabry-Perot measurements of M8 and M42 nebulae H alpha and forbidden N II emission lines profiles, determining temperatures and turbulent motions

09 p1390 A72-23528

Relative intensity of solar XUV emission lines of Li isoelectronic sequence ions, taking into account transitional collision strengths

09 p1391 A72-23532

Seyfert galaxies emission, absorption, IR and optical spectral characteristics, suggesting model with sharp forbidden and Balmer line outer region and broad wing core

10 p1532 A72-23885

Seyfert, N-type, compact and radio galaxies spectroscopic properties, noting two dwarf emission line galaxies as possible young galactic nuclei

10 p1534 A72-23896

Radio-emitting and radio-quiet quasar optical emission and absorption line spectra

10 p1534 A72-23897

Intense IR radiation from galaxies central regions, comparing power levels with galactic nuclei optical and radio emission

10 p1534 A72-23899

Hydrogen atom emission spectrum calculation in uniform rotating electric field, applying to charged particles collisions and Stark broadening of plasma H lines

10 p1514 A72-24039

CO Cameron system band intensity from measurements of equivalent widths of resolved rotational lines, using Doppler growth curve for line strength conversion

10 p1514 A72-24095

Electron impact excitation of nitric oxide in vacuum UV, measuring absolute cross sections for emission features

[AD-742536] 10 p1515 A72-24341

High resolution observation of stratospheric submillimeter thermal emission spectrum by helium-cooled InSb electron bolometer on board Comet 2E aircraft

10 p1476 A72-25023

WR hot stars CIII, NIV and OV emission spectra structure associated with excitation of 2pn and pd ion configurations

10 p1549 A72-25169

Iron emission spectrum in phase transformations and recrystallization study of austenitic and carbon steels under high temperature hardening

11 p1655 A72-25496

Paschen beta emission line equivalent width variation in IR spectra of omicron Ceti

11 p1716 A72-25679

Four-photon parametric frequency selection within broad stimulated emission lines during coherent light interaction, considering dye solution laser pumping

11 p1648 A72-26335

Laser emission spectrum broadening due to saturable dye filter bleaching, discussing amplitude and phase modulation contributions

11 p1649 A72-26341

Chemical laser with deuterium and nitrogen fluorides mixture, examining excited molecules emission spectra

11 p1649 A72-26351

Injection laser pulsed emission mode effect on spectral characteristics

11 p1650 A72-26359

Cometary spectra analysis, noting resonance fluorescence mechanism of emissions

11 p1722 A72-26433

Alpha particles effect on carbon dioxide laser output power and emission spectra, using uranium acetate as radioactive source

11 p1651 A72-26552

Emission spectra of exploding copper wires in air and vacuum in IR, UV, visible and vacuum UV regions

12 p1843 A72-27134

HD 4180 shell H lines width variations comparison with Be stars, noting thirty year period emission decrease followed by outer shell absorption

12 p1867 A72-27213

Instantaneous and averaged emission spectra of injection laser under spontaneous pulsation as function of operation mode and photon distribution

12 p1824 A72-27875

Multielement electron beam pumped semiconductor laser using emitting GaAs disks with vapor deposited dielectric mirror coatings

12 p1824 A72-27876

High temperature gaseous disperse flow radiation spectra photoelectric recording by DFS-8 spectrograph

12 p1812 A72-28116

Electron structure of Al atoms in alloys with transition metals obtained from emission spectra

13 p1973 A72-28492

Angular spectrum of second harmonic generation during two frequency interactions in KDP laser

13 p1969 A72-29524

Inner corona spectral data of 7 March 1970 solar eclipse, noting line half widths and emission line origin area relationship

13 p2042 A72-29535

Fourier transform spectrometer observation of IR coronal emission lines during 7 March 1970 solar eclipse from high altitude aircraft

13 p2042 A72-29538

Photographic polarimeter measurement of linear polarization of coronal emission lines during 7 March 1970 solar eclipse

13 p2043 A72-29547

Spectral radio observations of 7 March 1970 solar eclipse, noting McMath plages intense activity source flux characteristics and weaker source bremsstrahlung emission

13 p2044 A72-29551

Electron temperature and emission measures during solar X-ray flares, studying effects of gradual and rapid radiation flux increases

13 p2032 A72-29722

Vanadium emission spectra studies of energy band structure in vanadium silicides, showing p-subzone splitting

13 p1980 A72-29798

Upper atmosphere mm emission spectrum from aircraft observation, comparing with rocket and ground based data

13 p1923 A72-29963

Auroral emission spectrum intensity ratios for IBC 2 system observed via aircraft flown digital multichannel photometer

14 p2097 A72-30137

Auroral spectroscopic and excitation processes, discussing atomic oxygen production, emission ratios and electron energy spectrum, UV and IR emissions, composition and temperature measurements

14 p2098 A72-30138

Hydroxyl emission bands intensity, and vibrational and rotational temperatures sporadic and harmonic components in seasonal and diurnal variations

14 p2098 A72-30142

K beta emission spectrum of metallic Cr, discussing structural X ray analysis revealed cubic structure

14 p2116 A72-30414

Fe light emission for simulated meteor conditions, measuring ionization and spectral emission cross sections for Fe reactions with nitrogen and oxygen for 350-2000 eV

14 p2156 A72-30562

Small spectral width emission from dye laser with interference filter and quartz plate Fabry-Perot interferometer for spectroscopic investigations

14 p2110 A72-30674

Solar spectrum Mg I multiplet lines hyperfine structures, examining emission lines with Fabry-Perot and Fourier transform spectrometers

14 p2158 A72-30730

Interstellar medium physical conditions from 21 cm hydrogen emission line observations in direction of pulsars, using 25 meter Dwingeloo radiotelescope

14 p2159 A72-30744

Plasma emission spectrum of circulating and sealed carbon dioxide molecular laser, discussing concentration dependencies

14 p2110 A72-30786

First positive and first negative nitrogen emission excitation kinetic mechanisms, investigating shock tube measurements of nonequilibrium radiation

14 p2134 A72-30837

Calibrated thermal emission spectra under extreme temperature, surface reststrahlen and cloud conditions from Nimbus 4 IR spectroscopy

15 p2223 A72-31510

Submillimeter isotropic background limits of stratosphere emission spectrum, using aircraft-borne Michelson interferometer and Rollin far IR detector

15 p2265 A72-31626

Jovian synchrotron emission measurements by radioheliograph at 80 MHz, passing square law detector outputs through RC integrators

15 p2307 A72-31799

Graphite band structure investigated by secondary electron emission, observing electron transitions to higher excited states

15 p2260 A72-31856

Rocket-borne spectrometric measurement of small solar flare O VII and Ne IX resonance lines and 5 keV X-ray continuum emission, analyzing data via nonisothermal model

15 p2300 A72-31990

- Jupiter atmospheric greenhouse effect modeled by two layer emission, deriving temperatures from non-gray step function approximation of IR absorption 15 p2312 A72-32096
- K and L lines of X ray emission spectra of Ti in alloys with Nb, noting atomic structure change during alloy formation 15 p2259 A72-32701
- Hydroxyl emission sources classification from observed main line polarization and satellite lines 15 p2315 A72-32710
- High energy resolution spectrometric measurement of relative emission cross section for electron impact excited molecular nitrogen second positive system bands 16 p2428 A72-32922
- High resolution spectroscopic studies of high density molecular beam production and emission spectrum excitation, using Ebert-Fastie vacuum spectrometer 16 p2430 A72-33059
- K2 III star Arcturus far UV chromospheric emission line spectrum observation with rocket-borne spectrometer, identifying hydrogen L alpha and O I 16 p2453 A72-33136
- OSO 1 observation of 300 second oscillation in solar transition region and coronal extreme UV emission line intensity 16 p2453 A72-33137
- Coherent emission lines in visible spectrum from triply ionized Er in barium yttrium fluoride, discussing energy level transitions associated with various lines 16 p2401 A72-33387
- Planetary nebula M2-9 spectrum analysis, discussing IR excess, internal motions and Fe II emission lines 16 p2455 A72-33459
- Emission line star WRA 795 as optical counterpart of Cen X-3 occulting binary system 16 p2456 A72-33474
- Quasars and emission line objects red shift distribution using power spectrum analysis method 16 p2457 A72-33625
- High resolution radio observation of H II region W 51, noting compact components with emission measures agreement with recombination line data non-LTE analysis 16 p2457 A72-33684
- Energy level population and emission spectrum of C IV ion in planetary nebula with radiative excitation 16 p2458 A72-33688
- Chemical laser with deuterium and nitrogen fluorides mixture, examining excited molecules emission spectra 16 p2402 A72-33704
- Injection laser pulsed emission mode effect on spectral characteristics 16 p2403 A72-33712
- Instantaneous and averaged spiking emission spectra of injection laser under spontaneous pulsation as function of oscillation mode and photon distribution 16 p2404 A72-33984
- Flowing air glow discharge near IR emission spectrum as function of pressure, noting atomic lines 16 p2427 A72-34097
- Energy release mechanism during early universe expansion leading to distortion of relict black body spectrum, noting Comptonization effects 16 p2461 A72-34151
- Spectral characteristics of hot stars with emission lines, discussing Ba, Of, P Cygni, Wolf-Rayet and B type supergiant stars 16 p2462 A72-34183
- Photoionization models for the emission-line regions of quasi-stellar and related objects. 17 p2605 A72-34527
- ESRO 2 satellite observation of solar X-ray emission from active limb prominence, obtaining temperatures and emission measures as function of time 17 p2608 A72-35085
- Solar thermal radio burst temperature and emission measure determination from flux spectrum, noting consistency with radio observation 17 p2608 A72-35090
- Helium and H alpha emission relationship observation in 11 February 1970 solar flare from photometric reduction of filtergrams 17 p2599 A72-35117
- A comparison between the emission-line galaxies NGC 5253 and NGC 5408. 17 p2611 A72-35310
- Calibration of the flux density of Cassiopeia A and Cygnus A in the range 300-9375 MHz. 17 p2617 A72-35728
- Synchrotron emission source identification from spectral index dependence on frequency 17 p2602 A72-35731
- Narrow-band photoelectric photometry of the peculiar Wolf-Rayet eclipsing binary CV Serpentis. 17 p2617 A72-35732
- Ionization mechanisms for quiescent prominence He II 4686 line emission under coronal UV radiation and high temperature conditions 17 p2618 A72-35737
- Emission spectra of comet tail carbon monoxide molecular ion indicating constant or slowly varying electron transition moment 17 p2618 A72-35826
- The classification of transitions between levels of principal quantum numbers 3 and 4 in Fe IX to XVI and Mn VIII to XV. 17 p2586 A72-35834
- Galactic nebulae electron temperature and density from forbidden line emissions interpreted in terms of transition probabilities and collision strengths 18 p2723 A72-36090
- Bright nebulae near concentrations of high-velocity gas. 19 p2856 A72-37504
- Adhesion and transfer of PTFE to metals studied by Auger Emission Spectroscopy. 19 p2807 A72-37646
- Solar radio burst time profiles comparison with H alpha line emission curves for corresponding flares, noting neutral hydrogen emission relation to electrons acceleration 19 p2850 A72-37802
- Continuous emission localization in solar flare nuclei 19 p2850 A72-37814
- Certain results of a study of the emission-frequency stability of gas lasers at 0.63, 1.5, 3.39, and 9.6 micron wavelengths 19 p2814 A72-38786
- Emission lines and optical continuum of Seyfert radio galaxy 3C 120 from spectrophotometric scans 20 p2965 A72-38905
- Hot star with broad H lines with weak variable central emission, noting Ca II and He I 20 p2966 A72-38920
- Laser quantum theory for single mode emission fluctuations and instability region with high density of excited atoms, noting self consistent field effects 20 p2931 A72-39376
- Gas laser emission fluctuations of total radiation energy, polarized field components and line widths in longitudinal magnetic field 20 p2931 A72-39377
- Stellar emission and absorption line spectra formation in presence of magnetic field interpreted by radiative transfer equation solution, considering dwarf stars observation 20 p2956 A72-39753
- Computer program for solar corona emission line polarization computation to interpret measurements in terms of coronal magnetic field direction 20 p2971 A72-39757
- Emission and absorption line spectra of type I supernovae after luminosity maximum interpreted by heating and ionization mechanisms in shell and intensity computation 20 p2973 A72-39886
- Temperature and emission measure deduced by coronal visible lines. 20 p2974 A72-39896
- Quartz and calcite spectral emission polarization calculation from Fresnel equation, comparing results with field measurements with broadband IR radiometer 21 p3097 A72-40603
- Coronagraphic observations of an enhanced coronal region. II - Temperature and density structure through the enhanced region. 21 p3108 A72-41288
- Observations of sources of maser radio emission with an angular resolution of 0.0002 sec 21 p3101 A72-41751
- Stratification of the emission in the envelope of a Wolf-Rayet type eclipsing binary V444 Cyg 21 p3113 A72-41759
- Effect of Thomson scattering on the emission spectrum of an optically semitransparent plasma 21 p3102 A72-41774
- Ar plasma diagnostics from stabilized arc emission spectra, noting thermodynamic equilibrium in central zone of arc channel 22 p3209 A72-41880
- Nonpeaked emission of a ruby laser with frequency tuning and selection 22 p3184 A72-42103
- Spectrum of stimulated emission in a resonator with plane mirrors 22 p3184 A72-42154
- Molecular vibration levels inversion ratios increase by vibrationally cold CO addition to CW CO chemical laser, observing R-branch emission lines 22 p3185 A72-42615
- The emission-line spectrum of Cygnus A. 23 p3334 A72-43251
- Dayglow nitrogen ion 3914 A emission profiles for average solar activity at 110-240 km heights from Cosmos 224 observations 23 p3282 A72-43357
- Tilting-filter measurements in dayglow rocket photometry. 23 p3289 A72-43893
- Spectrophotometry of the comet Tago-Sato-Kosaka 1969 IX 23 p3339 A72-44168
- A shock tube determination of the electronic transition moment of the CN red band system. 23 p3316 A72-44329
- Generation spectrum kinetics of a photodissociative iodine laser 23 p3297 A72-44480
- Neodymium-glass laser emission spectral and temporal correlations during Q switching by rotating prisms and passive shutter 24 p3408 A72-44565
- A further high-resolution search for Fe XXV line emission from Scorpius X-1. 24 p3438 A72-44838
- Interpretation of X-ray emission bands of AIII-BV compounds 24 p3432 A72-44914
- Rhodamine laser emission spectral band control by plane parallel plates and polarizing prisms, noting band widening by resonator loss modulation with Fabry-Perot interferometer 24 p3410 A72-45418
- Possible explanation of non-power-law radio spectra of cosmic radio sources. 24 p3446 A72-45477

EMISSION

- Human skin thermal radiation properties, presenting data on reflection, emission, transmission and complex refraction [ASME PAPER 71-WA/HT-37] 05 p0620 A72-15888
- Thermal conductivity, electrical resistivity, emissivity and specific heat of polycrystalline vanadium under electron bombardment heating at 1200 to 1800 K 06 p0828 A72-17613
- Spectral composition of emitted radiation, emissivity and absorptivity of Venus atmosphere at high temperatures 07 p1068 A72-18933
- Emissivity calculation for radiant heat flux from isothermal gas mixture of hydrocarbon fuel combustion products 10 p1561 A72-23839
- Sea foam emission and reflection characteristics at microwave frequencies from radiometric measurements, correlating data as functions of frequency and angle 10 p1475 A72-24749
- Overlap emissivity of atmospheric carbon dioxide and water vapor for computer simulated earth surface temperature calculations 11 p1628 A72-26986
- Thin plates and coatings in thermal contact with standard, determining total emissivity by inverse methods of heat conduction 12 p1889 A72-28115
- Reflectivity-emissivity relationship for isothermal atmosphere with coherent scattering and continuous absorption, generalizing for noncoherent case with line opacity 14 p2131 A72-30890
- Mean emissivity of a luminous flame - Spray combustion of liquid fuel. 18 p2740 A72-36148
- Emissivity and electrical resistivity of tungsten-yttrium oxide cermets as function of composition at 1200-3200 K 19 p2819 A72-38286
- Influence of the structure on the emissivity of aluminum-chromium-phosphate coatings at high temperatures 21 p3072 A72-40383
- Study of the dependence of the spectral and integral radiation properties of bodies on the surface roughness. 23 p3357 A72-44538

EMISSOGRAPHS

- U ACTINOMETERS
- U RECORDING INSTRUMENTS

EMITTANCE

- Graphite, Mo, Ta and W thermal radiation total emittance measurement in 1200-2400 K range, evaluating recorded data by computer program 02 p0243 A72-12101
- Fine scale surface oxide film roughness effects on metal substrate-oxide film system hemispherical emittance 02 p0303 A72-12319
- Thermal emittance measuring methods for solids at temperatures above 1500 K, discussing emittance dependence on surface characteristics 06 p0818 A72-18253
- Apollo lunar fine samples total emittance as function of temperature, using spectral emittance measurement technique 09 p1388 A72-23028
- Radial density profiles and emittance for nitrogen ion beams from Penning-type cyclotron ion source with hot filament 10 p1516 A72-25028
- Monte Carlo random walk methods for directional emittance of one dimensional absorbing-scattering slab with reflecting boundaries, considering refractive index, optical thickness and albedo [AIAA PAPER 72-309] 11 p1743 A72-25243

EMITTERS

- Contribution to the theoretical study of the distribution of the emittance along the walls of an antiradiating cell 18 p2742 A72-37199
- Effect of polarization on the apparent emittance of rectangular groove cavities. 20 p2954 A72-39629
- The universal high temperature emissometer. [ASME PAPER 72-HT-1] 20 p2926 A72-39675
- Mathematical model for moving radiometer system for reflected solar radiation measurement, discussing instrument time constant effect on surface emittance variations reproduction 20 p2927 A72-39795

EMITTERS

- NT THERMIONIC CATHODES
- NT THERMIONIC EMITTERS
- Pinch-in effect due to emitter current distribution stability in transistors with emitter-stripe geometry 04 p0499 A72-15209
- Thyristors junction area current rise time extension, discussing emitter field regional delay times as function of p-n-p-n structural properties 08 p1140 A72-21266
- Small signal microwave transistors design with arsenic and phosphorus diffused emitters, comparing performance in terms of power gain-bandwidth product, maximum frequency and noise figure 08 p1142 A72-21743
- Emitter conduction bands with negative electron affinity energy from surface barrier lowering of Cs p-type semiconductors 10 p1526 A72-24351
- Photomultiplier negative electron affinity emitter materials photosensitivity performance, considering Cs-activated GaP and applications for low light level detection 15 p2291 A72-31531
- Radio phase interferometers for emitter position location, predicting polarization mismatch errors effects on accuracy 15 p2206 A72-31777
- Minimum elements number on discrete two dimensional hologram with constant distance between emitters, considering reduction of matrix elements 15 p2242 A72-32665
- Emitter conduction bands with negative electron affinity energy from surface barrier lowering of Cs p-type semiconductors 17 p2595 A72-34952
- Initial electron velocity and emitter surface roughness effects on oscillatory velocities dispersion in helical electron beams used in cyclotron resonance masers 22 p3208 A72-42664

EMOTIONAL FACTORS

- Fainting prevention in flying personnel, discussing constitutional susceptibility, health irregularities, alcohol, heavy smoking, lack of sleep, emotions and medical histories 03 p0316 A72-13722
- Human coagulating and anticoagulating blood system changes due to emotional stress during parachute jumps, noting plasma recalcification time increase 04 p0474 A72-15233
- Emotional aspects of pilot performance under high stress in emergency situations, discussing psychophysiological training methods 05 p0623 A72-17098
- Crew members handling of emotionally disturbed aircraft passengers 07 p0926 A72-18836
- Hyperventilation relationship with spasmodophilia, noting psychoemotional cause and neuromuscular excitability 07 p0922 A72-20384
- Improperly controlled learning processes relationship to hypertonic blood pressure irregularities pathogenesis in rats, investigating negative emotional reactions effects 07 p0925 A72-20659
- Evoked cortical potentials changes from emotional visual word stimuli stress under amyxil anticholinesterase drug influence 08 p1116 A72-21194
- Conditioned reflex mechanisms responsible for regulation of emotions in higher order animal and human neurophysiology 08 p1118 A72-21837
- Psychiatric preventive intervention in emotional crisis situations during patients aeromedical evacuation and transportation, discussing personnel shortage 10 p1429 A72-23743
- Electric stimulation of rabbit brain limbic formations /claustrum, amygdala, hippocampus/, showing effect on emotional response motor and vegetative components 14 p2076 A72-30668
- Social and emotional crises with respect to isolation, confinement and group dynamics of astronaut crews during long duration space flight 16 p2354 A72-33545

Increase in skeletal muscle performance during emotional stress in man. 17 p2500 A72-34942

Limbico-neocortical, cardiovascular and hormonal system vegetative shifts associated with emotional behavior response, presenting neurogenic stress model for animals 22 p3148 A72-43166

Nervous-emotional stress as a problem of modern work physiology 22 p3148 A72-43170

EMOTIONS

- Negative and positive emotional states influence on blood cholesterol and arterial pressure levels in dogs, suggesting common subcortical genesis of atherosclerosis and hypertension 09 p1264 A72-22498
- Psychological and physiological parameters correlation for astronaut functional state relation to emotional tension level during ground and flight tests 16 p2356 A72-33563
- Negative /painful/ stimulus cessation relation to emotionally positive zone activation in rat brain during self stimulation experiments 20 p2892 A72-39410

EMPLOYEE RELATIONS

Frankfurt Airport air traffic controller opinion survey of attitudes toward work and working environment 09 p1271 A72-23138

EMULSIONS

NT NUCLEAR EMULSIONS

NT PHOTOGRAPHIC EMULSIONS

ENCAPSULATING

- Fluorinated ethylene propylene encapsulated N/P Si solar cells, investigating simulated micrometeoroid exposure effects on I-V performance in shock tube 01 p0006 A72-10381
- Multielectrode piezoelectric chip ultrasonic transducer, sampling and readout techniques for radioisotope encapsulation testing 01 p0069 A72-10810
- Hf and microwave hybrid circuits encapsulation, discussing hermetic seals formation 05 p0634 A72-16182
- Plastic encapsulated transistors and IC moisture resistance tests for reliability under laboratory and field conditions 06 p0782 A72-17363
- Semiconductor device IC encapsulation, thermal design, stress analysis, testing and applications 06 p0791 A72-18577
- IC plastic encapsulation reliability problems related to die stability, wire bond and package moisture integrity 11 p1606 A72-26546
- Encapsulation influence on Gunn effect devices from circuit analysis of wideband tunable transferred electron microwave oscillators 12 p1790 A72-27440
- Improved efficiency of cadmium sulfide-copper sulfide thin film solar cells, noting optimization of layer formation, gridding and encapsulation 12 p1756 A72-28016
- Reliability tests on miniature ceramic capacitors encapsulated by epoxy-novolac block polymer compounds 13 p1919 A72-29061
- Monoplastic solid encapsulant for n-p-n and p-n-p silicon planar passivated signal transistors 17 p2528 A72-34715
- Evaluation of plastic materials for semiconductor encapsulation. 17 p2570 A72-34716
- The detection of unreliable contacts by noise measurements. 18 p2720 A72-37111
- On the measurement of mechanical tension in plastic encapsulated devices by means of piezo-resistance. 18 p2669 A72-37112
- Losses in high-voltage transformers encapsulated by epoxy resins. 18 p2669 A72-37113
- Reliability of integrated circuits with plastic encapsulation 18 p2669 A72-37114
- Recent developments in silicone elastomers for macroencapsulation. 20 p2944 A72-39492
- Hermetic sealing of electronic subsystems with plastics 23 p3294 A72-44142

ENCEPHALITIS

Influence of rhythmical photostimulation on lower-order monkeys with hyperkinesia of post-encephalitic origin 20 p2890 A72-38930

ENCLOSURES

Efficient computation of radiant-interchange configuration factors within the enclosure. 20 p2983 A72-39488

The use of simple three-dimensional acoustic finite elements for determining the natural modes and frequencies of complex shaped enclosures. 22 p3206 A72-42464

ENCODERS

U CODERS

ENCODING

U CODING

ENCOUNTERS

- Binary systems formation probability during triple encounters, observing dependence on system/potential energy ratio 03 p0435 A72-13809
 - Encounter trajectory design for solar electric propulsion rendezvous with low mass celestial bodies, noting target characteristics [AIAA PAPER 72-424] 13 p2036 A72-28939
 - Encounter sequences determination techniques for multitarget flyby and rendezvous missions to asteroids and comets by spacecraft using solar electric propulsion [AIAA PAPER 72-429] 13 p2037 A72-28940
 - The problem of encounter avoidance in linear differential games 19 p2824 A72-37377
 - Impulse motion encounter in game theory, considering control problems of pursuit involving escape and capture 19 p2825 A72-37554
 - Solution to the encounter avoidance problem in a linear differential game 20 p2947 A72-39865
 - Mariner spacecraft 1973 for flyby Venus and encounter Mercury, discussing launch and arrival conditions and aiming zones selection to maximize science return [AIAA PAPER 72-942] 21 p3113 A72-41578
- ENDFIRE ARRAYS
- NT YAGI ANTENNAS
 - Anomalous wave nulls and relation to endfire surface wave radiation on phased arrays of TEM waveguides with metallic fences perpendicular to ground plane 07 p0945 A72-19788
- ENDOCRINE GLANDS
- NT ADRENAL GLAND
 - NT GONADS
 - NT PANCREAS
 - NT PARATHYROID GLAND
 - NT PITUITARY GLAND
 - NT THYROID GLAND
 - Hypoxic hypothermia effects on endocrine organs phospholipid metabolism during chronic hypoxic hypoxia 02 p0165 A72-12516
- ENDOCRINE SECRETIONS
- NT ALDOSTERONE
 - NT HORMONES
 - NT HYDROXYCORTICOSTEROID
 - NT INSULIN
 - NT PITUITARY HORMONES
 - NT THYROXINE
 - Hypokinesia effects on neurosecretory system of rat hypothalamus and hypophysis, noting increased antidiuretic hormone contents in blood 05 p0618 A72-16634
 - Work-rest schedules endocrine and metabolic effects on aircrews during 50 hour flight missions in C-141 aircraft, using urinary test techniques [AD-740992] 10 p1428 A72-23737
 - Role of the hypothalamus and limbic system in the regulation of the motor and secretory functions of the digestive apparatus 21 p3000 A72-40754
- ENDOCRINE SYSTEMS
- Central cooling and warming effects of preoptic/anterior hypothalamic region on thermoregulatory activity of neuroendocrine, cardiovascular and neuromuscular systems 03 p0313 A72-13070
 - Blood serum proteins thermal stability in patients with vegetative vascular and neuroendocrine syndromes, discussing ATP effects 09 p1266 A72-22877
 - Neuroendocrine responses in microwave radiation exposed rats, correlating thyroid and thyrotropic activity 12 p1767 A72-28321
 - Hippocampus morphology and physiology in relationship to emotion and memory mechanisms, time links, visceral activity and motivations and endocrine control 16 p2353 A72-33099
 - Seasonal rhythms of endocrine system in hibernating mammals, discussing central and peripheral biological clocks in relation to hypothalamus and pancreas/thyroid gland 16 p2353 A72-33099
 - Morpho-functional changes in the endocrine system during oxygen starvation 21 p2998 A72-40447
- ENDOCRINOLOGY
- Shock-induced fighting effect on pituitary adrenocorticotrophic hormone ACTH and adrenocor-

tical steroids plasma concentration in rats, relating psychological stress to physiological function
05 p0617 A72-16080

ENDOGENOUS CONDITIONS
U PHYSIOLOGY
ENDOLYMPH
Mathematical model for semicircular canal dynamic response to angular acceleration, emphasizing role of perilymph over endolymph in cupula displacement
07 p0917 A72-19491
Vestibular, auditory, acceleration and altitude decompression testing of pilot following endolymphatic shunt surgery for Menieres disease
12 p1771 A72-27485
The vestibular apparatus. I - The physics and physiology of the otoliths and the semicircular canals
22 p3146 A72-42787

ENDOTHELIUM
Albino rats spinal cord capillaries ultrastructure upon hypothermy, noting endothelial cells sinking to lower levels from microscopic observation
12 p1760 A72-37304

ENDURANCE
Screening test for physical fitness on bicycle ergometer, comparing endurance indices derived from heart rate, oxygen consumption, oxygen debt and work rate measurements
01 p0010 A72-10212
Plastic deformation, creep rupture strength, endurance limit and service life of prestressed strain hardenable material
06 p0900 A72-18681
Endurance limit of construction materials under fast and thermal neutron irradiation in reactor channel
06 p0834 A72-18682
Fatigue properties of Ni-Al-W alloy with gamma-prime matrix, noting high endurance limit/yield strength ratio at room temperature
11 p1661 A72-26653

ENERGY ABSORPTION
NT AURORAL ABSORPTION
NT ELECTROMAGNETIC ABSORPTION
NT MOLECULAR ABSORPTION
NT PHOTOABSORPTION
NT POLAR CAP ABSORPTION
NT SOLAR ABSORPTION
NT THERMAL ABSORPTION
NT THERMALIZATION [ENERGY ABSORPTION]
NT ULTRAVIOLET ABSORPTION
NT X RAY ABSORPTION
Crack stability dependence on energy demand or release characteristics, discussing application to fracture tests analysis
01 p0141 A72-10996
Radiant heat attenuation of W seeded hydrogen aerosol at high pressure and temperature for gas core nuclear rocket propellant application
01 p0112 A72-11340
Current density nonlinear transient response and energy absorption of weakly ionized plasma under pulsed electric field
04 p0555 A72-14532
Cross section geometry and deformation effects on rods vibration damping, determining surface layer energy absorbing properties for longitudinal and torsional oscillations
05 p0735 A72-15988
Continuously burning optical discharge in Ar and Xe at atmospheric pressures, evaluating laser beam energy absorption, electron density and plasma temperature
05 p0669 A72-16679
Energy absorption measurements of ion heating by ion-acoustic waves in ion streaming plasma
06 p0856 A72-17518
GaAs, injection lasers with homojunctions and single and double heterostructures, observing energy dependence of internal optical losses due to band-to-band absorption
07 p1006 A72-19823
Thermal diffusivity and heat capacity measurement by temperature vs time curve shape by laser pulse absorption, using thermocouple
07 p1101 A72-19890
Nd glass absorption of flash pump emission energies with varying discharge parameters, Xe pressure and glass thickness
08 p1184 A72-22030
Light modulation by exciton electron absorption in thin high impedance recrystallized CdTe films within strong electric fields, showing spectral distribution curves
09 p1366 A72-22419
Absorbing sphere model for ion-ion recombination upper limit thermal energy reaction rate and total cross section energy dependence
10 p1515 A72-24342
Fracture energy and deformation of unidirectionally and randomly oriented lamellar Al-Cu eutectics from surface microstructure studies
10 p1499 A72-24893
Energy absorbing seat design for light aircraft, describing development and static and dynamic testing [SAE PAPER 720322]
11 p1583 A72-25585

Upper atmosphere /thermosphere/ physical variations, discussing diffusive equilibrium, energy absorption and heat transfer
11 p1621 A72-25842
General relativity equations solution for interaction of gravitational radiation and conducting fluids in magnetic field, noting energy absorption in specified depth surface layer
11 p1720 A72-26116
Heat conduction heating of plasma by high power ultrashort laser pulse incident on solid target, noting focusing and energy absorption role
12 p1852 A72-27622
Energy absorption inelastic surface mechanisms effect on I-V characteristics profile for bounded semiconductors with negative differential conductivity
13 p2023 A72-29991
Aircraft crash landing induced acceleration effects on seated occupants, discussing energy absorber system dynamic response characteristics for injury protective devices
15 p2191 A72-32603
Dilant suspensions impact energy absorbent properties, considering application to ejection seat cushions for occupant acceleration attenuation
15 p2191 A72-32604
Crash energy absorption for prevention of fatal injuries, considering human deceleration tolerance with respect to required energy absorber force-deflection relationship
15 p2192 A72-32630
Thermal conductivity and heat capacity measurement by temperature vs time curve shape by laser pulse absorption, using thermocouple
17 p2637 A72-35138
Effect of optical constants on the energy distribution in homogeneous particles illuminated by a parallel beam of light
19 p2812 A72-38216
Influence of different types of oscillations on ion heating in plasma-beam discharges
19 p2843 A72-38820
Energy absorbing characteristics of rigid urethane foams
20 p2943 A72-38885
One-to-one telescope with pressurized Ar gas for nanosecond and picosecond laser output pulse sensitive detection via gas breakdown and energy absorption
21 p3062 A72-40618
Elastic wave energy absorption in structures under dynamic loads, noting fatigue fracturing decrease with energy transfer into damping medium
21 p3126 A72-41540
Resonances in the collisionless heating of a plasma by transit time magnetic pumping
21 p3094 A72-41631
Electron density and temperature in microwave plasmas at higher pressures
22 p3211 A72-42479
An assessment of energy absorbing devices for prospective use in aircraft impact situations
22 p3237 A72-42764
Influence of the polarization of incident radiation on the distribution of the energy absorbed in a particle
24 p3424 A72-44621
Cross section geometry and deformation effects on rods vibration damping, determining surface layer energy absorbing properties for longitudinal and torsional oscillations
24 p3460 A72-45730

ENERGY BANDS
NT BLOCH BAND
NT CONDUCTION BANDS
NT FORBIDDEN BANDS
Mixed zincblende ternary and quaternary alloys, comparing empirical pseudopotential and dielectric model methods for energy gap calculation
03 p0404 A72-14262
N- and p-type semiconductors energy band structure bending near interface
05 p0702 A72-16197
Electronic transition between energy bands as explanation for two optical absorption maxima in rare earth metals
09 p1369 A72-22609
Franck-Condon phonon displacement effects on mobility edge and energy gap in disordered materials
09 p1357 A72-22986
Energy operator diagonalization of interacting valence electrons in semiconductor and metal models
09 p1352 A72-23356
Fermi level and scattering phase function nomograms for semiconductors with parabolic and isotropic energy bands, noting charge transfer effects
11 p1700 A72-25781
Dielectric and optical constants of p-type GaSb single crystals, interpreting singularities by energy bands diagram
11 p1689 A72-26485
Photovoltaic effect and energy band model of solar cell cadmium-sulfide-copper-disulfide heterojunctions
12 p1855 A72-28007

ENERGY BUDGETS
P-n thin film solar cell based on thermally and electrochemically stable II-IV semiconductors with graded energy gaps
12 p1756 A72-28013
Photoelectric properties of cadmium telluride thin film solar cells, discussing energy gap temperature dependence, work function and current variations anomalies
12 p1756 A72-28018
Enhanced indirect optical absorption measurement in AlAs and GaP with energy denominator variation for direct band gap evaluation
13 p2022 A72-29627
Vanadium emission spectra studies of energy band structure in vanadium silicides, showing p-subzone splitting
13 p1980 A72-29798
Nonequilibrium plasma wave scattering cross section dependence on energy bands shape and field orientation in semiconductors
13 p2023 A72-29992
Equiatomic ordered, bcc TiFe and TiNi electron density in outer energy band from X ray K emission spectra
13 p1981 A72-30006
Two band model explanation of Hall effect in dirty type-II transition metal superconductors near upper critical field, noting interband impurity scattering role
15 p2295 A72-32542
The capacitances of aniso-type heterojunctions with continuously varying energy band gap and electron affinity in the transition region
18 p2719 A72-36944
Superconducting energy gaps and transition temperatures of disordered cadmium and zinc films
19 p2844 A72-37690
Structure of the energy bands of titanium, hafnium, and tantalum monocarbides
20 p2939 A72-39311
Ultrasonic evidence against multiple energy gaps in superconducting niobium
22 p3190 A72-42476
Equiatomic ordered bcc TiFe and TiNi electron density in outer energy band from X ray K emission spectra
22 p3190 A72-42733

ENERGY BUDGETS
NT ATMOSPHERIC HEAT BUDGET
Mercury vapor physicochemical processes kinematics in shock tube, determining electron gas energy balance equations
03 p0395 A72-13572
Heat transfer in thermal entrance region with turbulent flow between parallel plates, solving energy equation by difference methods
07 p1099 A72-19622
Exact and approximate expressions derived for energy content of vertical air column extending from earth surface to stratosphere
07 p0977 A72-19856
Clear air intermittent turbulence energy budget from aircraft data, obtaining turbulence parameters along aircraft path through application of electronic filters
09 p1344 A72-22437
Impulse-energy tensor for heat flow-crossed continuum subjected to electromagnetic field, using energy balance and quantity of movement equations
09 p1351 A72-22673
Energy balance criterion application to crack growth under cyclic fatigue loading, considering stress-strain behavior of plastic deformation energy
09 p1404 A72-22911
Mass and energy balance for electrode wire fusion in pulsed current MIG /metal inert gas/ welding, discussing pulse duration and amplitude requirements and shielding gas composition effect
09 p1321 A72-23644
Transverse shear flow stability analysis based on disturbance energy balance determination, applying to ducted and jet stream boundary layer flows
10 p1469 A72-24531
German papers on human body energy balance and temperature control covering energy conversion processes, chemical secretions, muscle activity, etc
11 p1584 A72-26071
Internal gravity waves effects on energy budgets and vertical angular momentum transport over mountainous terrain in southwestern U.S. from handheld camera pictures on Apollo 9
11 p1682 A72-26472
Mercury vapor physicochemical processes kinematics in shock tube, determining electron gas energy balance equations and atom-atom collision cross sections
11 p1699 A72-26760
Oscillations of spacecraft with on-off attitude control under constant perturbation moment, calculating energy expenditures for desired orientation maintenance
14 p2162 A72-30459
Mass and energy balance in air cooled matrix type phosphoric acid cell, noting operational reliability and construction
16 p2351 A72-33889

Solar chromosphere-corona transition region structure and energy balance calculation by static planar model compared with XUV resonance line observations

17 p2608 A72-35083

The response of a turbulent boundary layer to a step change in surface roughness. II - Rough-to-smooth.

17 p2540 A72-35191

Influence of the transverse distribution of pumping on the energetics and the profile of thermo-optical distortions in a rhodamine 6G laser

17 p2563 A72-35302

Toroidal plasma spectroscopic investigation from current pulse start to afterglow, noting electron temperature and density radial distributions and energy balance

17 p2591 A72-35373

Radiant interchange among suspended particles and its effect on thermal relaxation in gas-particle mixtures.

[DFVLR-SONDDR-210] 17 p2638 A72-35643

Chromospheric structure, magnetic field configuration, radiative transfer and energy balance relationship to solar prominences formation from corona

17 p2616 A72-35693

Calculation of the development of a turbulent boundary layer in the presence of an equally turbulent external field - Experimental verification

18 p2680 A72-36469

Hydrostatic oxygen burning in stars. II.

19 p2854 A72-37236

Diurnal variation in energy balance microclimate across coastal beach, noting surface moisture effect

21 p3078 A72-40468

Fluid flow across balance surface moving at constant velocity relative to coordinate system, calculating energy balance of turbojet engine

21 p3099 A72-40814

Reagent concentration and temperature fluctuation effects on turbulent burning rate, noting temperature pulsations influence on energy balance

21 p3128 A72-40976

Physical and chemical identification methods for biochemical reactions and energy balance of muscular contraction and shaking

21 p3003 A72-41469

Energy balance equation for machine unit with rotating element, noting energy distribution in periodic and nonperiodic operation modes

22 p3181 A72-41857

Energy flow diagrams.

24 p3369 A72-44686

ENERGY CONVERSION

Macroscopic metal crystal plastic deformation applications to aircraft and spacecraft materials production, considering internal friction and energy conversion into strain energy and heat

01 p0071 A72-11020

Vhf dc-dc conversion and regulation in low MHz range, discussing power loss reduction

01 p0007 A72-11057

Optimal conditions for energy conversion in MHD generator, observing ion seeding effect on plasma temperature

01 p0009 A72-11207

Papers on microwave advances covering precision coaxial connectors, O-type linear beam devices, electron dynamics and energy conversion and junction circulators

03 p0424 A72-13229

Transverse fields effects on electron dynamics and energy conversion in O-type linear beam devices of traveling wave amplifiers

03 p0330 A72-13231

Energy conversions and mean vertical motions in high latitude summer mesosphere and lower thermosphere, observing reaction kinetics

03 p0346 A72-13380

Power supply and converters for satellite and spacecraft, discussing fuel cells, radioisotopes, nuclear reactors, etc

05 p0615 A72-16745

AC-DC energy conversion - Conference, Milan, Italy, November 1970

06 p0785 A72-18307

Solar energy conversion as pollution-free power source, discussing silicon solar cells, power transmission techniques, satellite solar power stations and system control and guidance

06 p0893 A72-18625

TWT amplifier converter design with semiconductors and magnetics to achieve voltage regulation and high power efficiency for TOPS spacecraft

08 p1111 A72-21412

Kilowatt rotary dc-dc power transformer in modular sections for spacecraft applications, discussing electrical and mechanical designs and characteristics

08 p1112 A72-21414

Electrostatic plasma wave conversion into electromagnetic waves, calculating dispersion relation at all wavelengths for perpendicular propagation mode

08 p1137 A72-21989

Averaging process in thermodynamic systems energy transformation description

09 p1410 A72-22635

Sintered prepolarized perovskite type ferroelectric ceramics adiabatic depolarization and energy conversion under shock wave action

10 p1422 A72-24128

Selective surfaces and coatings for solar energy conversion systems, discussing semiconductor photoconverters, white-black surfaces, cooling systems and optimal optical properties

10 p1422 A72-24315

Cost efficiency and relative economic merits prediction for solar energy conversion systems

10 p1423 A72-24316

Pulse width modulated regulating dc-to-dc converter with small number of transistors to improve circuit reliability

10 p1452 A72-24680

Longitudinal plasma oscillations nonlinear instability due to energy transformation into harmonics and subharmonics

11 p1695 A72-25795

German papers on human body energy balance and temperature control covering energy conversion processes, chemical secretions, muscle activity, etc

11 p1584 A72-26071

Thermodynamics of human body metabolism, discussing energy conversion calorimetric measurements, body size, food intake, age, sex, endocrine and nervous effects

11 p1584 A72-26072

Human body biochemical energy conversion processes during muscular activity, discussing nutrition, circulation and respiration roles

11 p1585 A72-26075

Jet compression role in high temperature mechanical energy conversion heat exchanger based on ejector principle

12 p1755 A72-27724

Radiovoltaic generator energy conversion by thin film solar cells, noting performance dependence on semiconductor band gap and radioisotope characteristics

12 p1757 A72-28021

Schottky diode microwave down-converter conversion loss calculation as function of image terminal with consideration of barrier capacitance, series resistance and voltage drop

14 p2088 A72-30586

Mechanical oscillator model for experimental investigation of multistage electrical frequency multipliers subharmonic transient oscillations, considering energy flow under constant and/or phase modulated excitation

14 p2131 A72-30719

Reversible thermodynamic cycle of chemical to electric energy conversion with electron gas as working body, discussing Gibbs-Helmholtz equations

16 p2350 A72-32994

Russian book on magnetogasdynamic flow theory and calculations covering plasma flows and energy conversion in MHD channels of dc generator

16 p2438 A72-33873

Silicon solar energy conversion for electrical power generation on spacecraft.

17 p2494 A72-34186

Thermionic energy conversion with a Ba-Cs-diode.

17 p2496 A72-34603

Effect of chronic hypoxia on the kinetics of energy transformation in heart mitochondria.

17 p2502 A72-34993

Large-scale concentration and conversion of solar energy.

18 p2643 A72-36075

Vibrationally excited nitrogen in upper atmosphere

18 p2688 A72-36865

Sweet's mechanism for the destruction of magnetic flux.

20 p2955 A72-40017

Chemical energy transformation to mechanical energy and heat in muscles during exercise, considering energy sources for contraction, oxidations, glycolysis and alactic anaerobic mechanism

21 p3003 A72-41470

The impact of aerospace technology on energy conversion in the 70's.

[ASME PAPER 72-AERO-11] 22 p3140 A72-43147

Some contributions to energetics by the Lewis Research Center and a review of their potential non-aerospace applications.

[ASME PAPER 72-AERO-12] 22 p3245 A72-43148

Gravitational radiation from charged black holes.

23 p3336 A72-43499

Signal-to-energy conversion function in the photometry of solar soft X-radiation with broad-band detectors.

23 p3329 A72-44238

Mathematical model for life support system optimization in terms of reduced mass minimization as quality criteria for energy conversion and metabolic processes

24 p3375 A72-45133

ENERGY CONVERSION EFFICIENCY

Liquid phase epitaxial GaAs transferred electron microwave oscillators with high dc to rf conversion efficiencies dependent on frequencies

01 p0036 A72-10631

High efficiency transferred electron microwave oscillators operated in short LSA mode, noting pulse-operated diode power appearance time delay behavior

01 p0036 A72-10634

L-band Gunn oscillator using nonsinusoidal device voltage /switching mode/, comparing efficiency and output power with sinusoidal mode

01 p0036 A72-10635

Radiative noise effect on threshold current, output power and quantum yield of injection laser, evaluating noise loss factor

04 p0531 A72-15077

High efficiency solar electricity converters utilizing wave-like properties of radiation interacting with absorber-converter elements, discussing cost and fabrication advantages

[ASME PAPER 71-WA/SOL-1] 05 p0614 A72-15891

Charged aerosols for efficient power transduction in power conversion devices, deriving optimum particle radius to number of charges ratio for various operating conditions

06 p0760 A72-17422

Conversion effectiveness of oscillations induced by electron beam in bounded anisotropic plasma into electromagnetic emission

06 p0860 A72-17700

Solar cells with improved photoelectric efficiency, describing use of noncorroding Ti-Pd-Ag contacts, titanium oxide antireflection layer and welded cell joints

06 p0760 A72-17751

InP transferred electron microwave oscillators, observing higher efficiency than IMPATT and GaAs devices

06 p0784 A72-18063

Cesium plasma thermionic converters, discussing performance and efficiency improvement by governing electron transport in interelectrode space and cation generation

06 p0760 A72-18308

Optically pumped indium-gallium-arsenides laser coherent emission at room temperature, measuring total power conversion efficiency

[AD-737941] 07 p0999 A72-18882

Quantum efficiency at 6300 and 6364 Å of recombination mechanism in nighttime F layer, obtaining ionospheric electron density profiles

07 p0974 A72-18893

Lamp pumped IR solid state laser obtaining 20 W output and 4 percent efficiency from transition of Ho ion in sensitized YAG

07 p1004 A72-19234

Thermionic converter electrode performance of electron emission current density in terms of Cs arrival rate and surface temperature

07 p0915 A72-20568

Light emitting diodes for efficient conversion of electrical energy into electromagnetic radiation, discussing photometry, electrical injection, electroluminescence, design and applications

08 p1141 A72-21430

Quantum yield of ruby crystals luminescence for excitation in UV region, noting Cr concentration effect

10 p1490 A72-24043

Semiconductor air-air heat pumps with solar cell feed current, determining hot air flow temperature effects and energy conversion efficiency

10 p1423 A72-24319

Polarization characteristics and losses of anisotropic laser resonators composed of arbitrary number of mirrors

10 p1492 A72-24364

Temperature dependence of internal quantum efficiency of spontaneous emission as function of beam voltage in electron beam excited p-type GaAs

10 p1526 A72-24559

Huffman sequence synthesis by z transform zero pattern selection to obtain high energy for given peak amplitude, noting signal ambiguity functions

10 p1437 A72-24679

High conversion efficiency microwave second harmonic generator using negative resistance nonlinearity of n-type GaAs

11 p1591 A72-25741

IR radiation generation by Raman scattering and difference frequency mixing with Q switched Nd-YAG laser, noting peak power and photon conversion efficiency

11 p1647 A72-26149

Carbon monoxide quantum yield measurements of carbon dioxide photolysis by radiation at 1470 and 1500-1670 Å

11 p1590 A72-26423

Conversion losses as function of signal power and circuit impedance in narrow band triode frequency converter under large amplitude operating conditions

11 p1598 A72-26733

Effect of pumping radiation absorption by electron-excited molecules on organic compounds lasing efficiency

12 p1825 A72-27883

Thin film Cu-CdS solar cell electrochemical plating potential and solution composition effects on copper sulfide surface layer formation and cell efficiency

12 p1855 A72-28008

- Low photon IR photovoltaic response of CdS-metal junction, noting energy conversion efficiency 12 p1855 A72-28009
- Improved efficiency of cadmium sulfide-copper sulfide thin film solar cells, noting optimization of layer formation, gridding and encapsulation 12 p1756 A72-28016
- High electric power output Si solar cell development, discussing increased energy conversion efficiency 12 p1757 A72-28026
- Energy conversion efficiency of xanthene dye laser pumped by mode-locked Nd-glass laser second harmonic, discussing effect of excited molecules transition to triplet state 13 p1970 A72-29686
- Conversion efficiency and polarization behavior of Gunn diodes in resonant cavities, using I-V characteristics 13 p1937 A72-29866
- Plasma source efficiency with active element positioned between two plane parallel pumping elements 15 p2246 A72-31423
- Si solar cell efficiency in synchronous orbit radiation field increase via improvement in diffusion profile, low resistivity material and diode characteristics 15 p2183 A72-32131
- Radiation efficiency of electric power-energy conversion during pulsed discharge in Xe tube 16 p2403 A72-33716
- Cubic stabilized zirconia utilization as solid electrolyte in high temperature fuel cell system for efficient and economical energy conversion 16 p2352 A72-33894
- Effect of pumping radiation absorption by electron-excited molecules on organic compounds lasing efficiency 16 p2404 A72-33992
- Second harmonic conversion of CW YAG-Nd laser radiation on lithium metaniobate crystals, discussing conversion coefficient optimization 16 p2404 A72-33995
- Polarization characteristics and losses of anisotropic laser resonators composed of arbitrary number of mirrors 17 p2563 A72-34963
- Thermionic converters efficiency in commercial power generation applications, considering lifetime, reliability and cost 18 p2646 A72-36192
- Thermionic performance of fluoride CVD tungsten-niobium converter. 19 p2754 A72-37781
- Energy characteristics of the laser action in rhodamine 6G pumped by a pinched discharge. 20 p2933 A72-39512
- Electro-osmotic energy conversion in the glass/n-propanol system. 21 p2997 A72-41384
- High-intensity X-ray spectra and stimulated emission from laser plasmas. 22 p3210 A72-41990
- Effect of increasing beam voltage on the internal quantum efficiency of spontaneous emission in electron-beam-excited p-type GaAs. 22 p3185 A72-42308
- Progress in the efficiency of free-space microwave power transmission. 22 p3140 A72-42481
- Influence of nonuniformities of the built-in field on the collection efficiency of a semiconductor photocell 22 p3140 A72-43190
- Internal to total energy relation dependence on deformation time in impulsive loading of homogeneous free rod, noting energy conversion efficiency 23 p3344 A72-43338
- Influence of revolutions on efficiency and characteristics of the rotating axial cascade of blades. 24 p3363 A72-45361
- A method for estimation of axial turbomachinery stage characteristics on the basis of experimentally obtained data with a runner tested in a free blow-out aerodynamical scheme. 24 p3363 A72-45364
- Flow analysis in the axial-flow compressor impeller with meridional stream acceleration. 24 p3394 A72-45371
- front, considering distributed and lumped-parameter models 01 p0029 A72-10692
- Substorm electron drift relationship to cosmic noise absorption on auroral zone morning side, calculating electron energy loss 01 p0063 A72-10918
- Nonlinear effects due to crack front plastic yield and slow crack extension in energy release rate and fracture toughness calculations 01 p0140 A72-10993
- Crack stability dependence on energy demand or release characteristics, discussing application to fracture tests analysis 01 p0141 A72-10996
- Similarity models of interstellar loop structures, investigating magnetic field and energy losses effects and cosmic ray emission 01 p0131 A72-11011
- Split-film anemometer probe determination of convective heat transfer coefficient azimuthal dependence in low Reynolds number flow over cylinders, discussing axial heat losses 02 p0224 A72-11725
- Nonlinearity effects on two dimensional steady supersonic dissipative flow governed by Navier-Stokes equations, obtaining expressions for flows past thin airfoil and wedge 02 p0203 A72-11976
- Lunar soil dielectric constant and loss-tangent and electrical resistivity measurement by Q meter method, noting resemblance to dense terrestrial rock powders 02 p0281 A72-12287
- Concentric spherical heat exchanger, showing heat transfer coefficient decrease with coolant flow rate increase 02 p0303 A72-12320
- Anelastic solid energy dissipation linear memory models based on viscoelasticity theory, applied to earth and metals experimental data and dynamic loading problems 02 p0294 A72-12447
- Epoxy- and polyimide-graphite composites electrical dissipation factor and capacitance measurements as guide to molding quality, describing equipment 02 p0250 A72-12609
- Electron emission in strong electromagnetic waves within quantum electrodynamics, discussing energy losses and electron pair production 03 p0415 A72-13003
- Fatigue breakdown and energy dissipation dependence on stress during bending of cylindrical steel and iron specimens 03 p0372 A72-13589
- Cyclic deformation and energy dissipation during fatigue breakdown in steels under tension-compression and torsion 03 p0372 A72-13590
- High temperature properties of composite contact stack composed of alternating thermal flux sensors and heaters, determining heat conductivity and energy dissipation 03 p0458 A72-14160
- Kinetic energy losses due to liquid-to-solid phase transformation in heated two-component flow ascending in tube 03 p0342 A72-14161
- Ionization waves linear theory for low pressure noble gas strong current column, showing self excitation limit and temperature dependence of energy loss rate 03 p0400 A72-14351
- Elastic scattering without dissociation of nitrogen molecular ions by noble gas targets in 0.3-3 keV range, analyzing energy loss 03 p0393 A72-14357
- Azur satellite temperature control system for protection against internal heat dissipation and external thermal loads due to earth radiation and albedo 04 p0582 A72-15651
- Heat losses in oil wells hot liquid injections, modifying Oroveanu approximation method for exact solution 04 p0597 A72-15743
- Modeling techniques for fluid line transients, considering heat transfer and viscous dissipation [ASME PAPER 71-WA/FE-9] 05 p0646 A72-15933
- Energetic electrons absorption cross sections in weakly ionized atomic oxygen gas, showing energy losses through excitation 05 p0655 A72-16071
- Spin-axis attitude stability in torque-free environment of dual spin spacecraft with energy losses in both bodies [AIAA PAPER 72-16] 05 p0730 A72-16964
- Rotating dumbbell shaped satellites orientation optimization by system of jets, calculating energy losses 05 p0731 A72-17043
- Optimal hf triode oscillation tripler with allowance for power limitation by thermal losses on plate and grid electrodes 05 p0638 A72-17184
- Potential around moving test particle in quiescent plasma, discussing energy loss, transport properties and gravitational analog 06 p0859 A72-17549
- Dissipative effects in universe expansion, considering damping of anisotropy in homogeneous cosmological models [AD-745836] 06 p0880 A72-17885
- Turbulent energy dissipation rate statistical characteristics above 1000 m from radar measurements, discussing atmospheric boundary layer quantities 06 p0841 A72-17940
- Cumulus clouds vertical motion velocity spectra curves, turbulence dissipation rates and energy determination from aircraft measurements 06 p0842 A72-17941
- Incompressible fluid turbulent flow variational principles, discussing Malkus principle for maximum dissipation rate and minimum entropy production principle for convective and dissipative systems 06 p0800 A72-18116
- Flow in gas lubricated conical bearings, considering analytical and numerical solutions for axisymmetric flow model with temperature dependent viscosity and dissipation coefficients 06 p0801 A72-18124
- Extragalactic radio sources, discussing galactic radiation, quasars, nonthermal emissions, energy dissipation and spectrum analysis 06 p0886 A72-18172
- Thermal behavior of electron and ion gases in ionosphere, analyzing heat gain, transfer, loss and conductivity terms of energy equation 06 p0809 A72-18278
- Dissipative magnetic parameters measurement in ferrite and insertion loss measurement in waveguide Y-circulators below microwave resonance 06 p0786 A72-18367
- Thin film resistors and capacitors design, considering stability, power, size, film thickness, parasitic inductance capacitance and resistance and dielectric loss properties 06 p0790 A72-18573
- Two-mirror optical system to study energy dissipation in elastic systems subjected to cyclic straining and vibrations 06 p0819 A72-18649
- Flexural, longitudinal and torsional vibration damping of various size rods, taking into account surface layer energy loss 06 p0900 A72-18675
- Energy dissipation of vibrating structures in complex stress state, using generalized stresses and strains as coordinates 06 p0900 A72-18677
- Polymers mechanical losses temperature-frequency dependence, using nonlinear viscoelastic theory 06 p0838 A72-18678
- Small elastoplastic cyclic strain effects on internal friction and energy dissipation in metals during vibrations 06 p0834 A72-18679
- Sufficient conditions for asymptotic stability and instability for elastic systems with dissipation, using Liapunov direct method 07 p1026 A72-18809
- Mechanical energy consumption effects of thermal dissipation and cyclic straining methods during sample life tests 07 p1089 A72-19260
- Mathematical model for dissipative dual-spin satellite analysis, making use of high speed rotor symmetry to permit quasi-holonomic transformation 07 p1085 A72-19280
- Field approach to gravitation accounting for energy release and nonthermal radiation occurrence in pulsars and quasars 07 p1075 A72-19576
- Electromagnetic scattering of square pulse from lossy dielectric slab mounted on perfectly conducting planar ground surface 07 p0945 A72-19660
- GaAs, injection lasers with homojunctions and single and double heterostructures, observing energy dependence of internal optical losses due to band-to-band absorption 07 p1006 A72-19823
- Solar energy sources and dissipation and emission mechanisms, considering radiant flux of convection zone and photosphere and solar variabilities 07 p1078 A72-20005
- Ruby laser emission losses for free lasing modes and threshold and above threshold pumping 07 p1007 A72-20122
- Energy dissipation associated with transverse vibrations of sandwich metallic samples with damping coatings 07 p1094 A72-20135
- Storm available potential energy generation and boundary layer frictional dissipation estimation in heat transfer from ocean to atmosphere within east coast cyclone 07 p0980 A72-20451

ENERGY CONVERTERS

U DIRECT POWER GENERATORS

ENERGY DENSITY

U FLUX DENSITY

ENERGY DISSIPATION

X-type pseudoshock at high Mach number compared with lambda-type pseudoshock, discussing loss at duct center by leading shock wave 01 p0050 A72-10397

Cloud energy dissipation coefficient determination by ruby laser device, applying to water content and liquid particle concentration, vapor cloud and aerosol concentration 01 p0094 A72-10562

Microwave propagation on nonlinear transmission lines by examination of energy dissipation in shock

One dimensional nonlinear waves propagation in dissipative gas, obtaining exact solutions by method of separation of variables

07 p0973 A72-20500

Optical and electrical characteristics of gas discharge plasma in pulsed radiation sources as function of power dissipation

07 p1047 A72-20611

Ionization loss effects on cosmic ray lifetime in galactic interstellar medium, noting dependence on particle energy

07 p1064 A72-20637

Planetary bodies mass and energy losses as indications of eruptive evolution, discussing mean densities, geological processes scale and volcanic activities

08 p1228 A72-20829

Heat transfer in laminar and turbulent Newtonian fluid flow in narrow channels with allowance for temperature dependence of viscosity and energy dissipation

08 p1148 A72-20955

Soviet handbook on vibration absorbing properties of construction materials under cyclic straining, covering energy dissipation and dynamic strength

08 p1185 A72-20975

Photographic observations of W particle clusters high velocity impact against polystyrene, paraffin and W targets for energy dissipation in meteorite impact simulations

08 p1232 A72-21152

Continuous laser action in Nd-yttrium aluminum oxide rod, determining terminal state loss coefficient in stimulated emission

08 p1217 A72-21322

Transcendent Si power rectifier with high current and power dissipation capacity, discussing design, fabrication and performance tests

08 p1111 A72-21413

Black body X ray sources creation due to neutron stars rotational energy dissipation by strain hysteresis in crust

09 p1382 A72-22284

Secondary flow types and measurement in axial flow compressor cascades, discussing energy losses

09 p1260 A72-22633

Secondary losses reduction procedure in axial flow turbine stages, using boundary layer fences on blades profile suction side

09 p1374 A72-22634

Fast IC signal delay time reduction by high packing density, discussing yield, power dissipation and cost problems

09 p1290 A72-22820

Electron energy distribution and losses existence limit at Langmuir paradox pressures in gas discharge, hypothesizing wall mechanism of electron collisions

09 p1361 A72-22958

Cosmic electrons energy spectrum between 1 and 25 GeV from balloon observations, noting Compton/synchrotron loss effects

09 p1377 A72-23001

Modulated electromagnetic wave transmission in dispersive medium with cubic nonlinearity, discussing solitary wave and instabilities in two-wave interaction

09 p1352 A72-23475

Meteor trail photoobservations for atmospheric small scale turbulence vertical profile, determining eddy minima velocities and turbulent energy dissipation in M zone

09 p1393 A72-23650

Lunar soil dielectric constant and loss-tangent and electrical resistivity measurement by Q meter method, noting resemblance to dense terrestrial rock powders

10 p1532 A72-23756

German monograph on losses in gear pumps, discussing leakage, mechanical and hydraulic losses, measurement techniques and equipment, etc

10 p1422 A72-23774

Bounded plasma ionization instability inhomogeneity scale evaluation, assuming negligible electron energy losses due to heat conduction

10 p1517 A72-23844

Relativistic heavy ion in plasma, calculating energy loss based on electron scattering and momentum transfers

10 p1515 A72-24344

Human body calorimetry with water cooled garment for dynamic and continuous recording of heat dissipation from surface over extended time

10 p1431 A72-24485

Intensity dependent propagation characteristics of circularly polarized high power laser radiation in dense electron plasma, calculating energy losses

10 p1522 A72-24607

Electrical loss measurements in superconducting magnets at 60 Hz for Nb-Sn ribbon and Nb-Ti cable and multifilament coils

10 p1460 A72-24760

Darlington method in dissipative systems studies, representing R-functions as fractionally linear transforms with coefficients matrix function

10 p1512 A72-24780

Crack shape and plastic energy dissipation rate relation to plate thickness and applied stress for penny-shaped crack in elastic plate

10 p1559 A72-24896

Post-Newtonian approximation for calculation of energy and angular momentum radiated in form of gravitational waves by two point particles system, noting masses in hyperbolic Kepler orbit

10 p1547 A72-24933

Atmospheric isotropic turbulence kinetic energy dissipation and wind spectra estimation from Doppler spectra of precipitation particle velocities

10 p1507 A72-25001

Periodic motions stability of nonlinear control systems with energy consumption, using contact transformations

10 p1458 A72-25074

Frequency distribution of ionospheric horizontal winds vertical shear, noting altitude independence, turbulence and viscous energy dissipation

10 p1477 A72-25157

Multimode dielectric slab waveguide power coupling due to core-cladding interface irregularities, obtaining power distribution and radiation losses

11 p1603 A72-25270

Quasi-continuous charge carrier traps in molecular single crystals associated with polarization energy dissipation

11 p1700 A72-25782

Resistojet performance models for investigating energy losses in hydrogen, ammonia, methane and carbon dioxide nozzle flows

[AIAA PAPER 72-455]

11 p1708 A72-26191

Magnetic fields effect on anode heat losses in MPD accelerator arcs, noting minimal charge current density

11 p1711 A72-26225

Semiconductor injection laser with distributed radiative loss, calculating radiation line shape and width and quantum efficiency

11 p1648 A72-26329

Mode properties and energy losses for unstable laser resonator with curved and sharp edged mirrors

11 p1648 A72-26336

Complementary metal oxide semiconductor applications, noting device power dissipation, high noise immunity, good switching speeds and cost reduction

11 p1701 A72-26386

Midlatitude stable auroral red arcs observation from OVI-10, showing generation at plasmopause due to turbulent dissipation of ring current energy

11 p1624 A72-26401

Cantilever beam transverse vibrations induced by time varying linear displacements of clamped end under external loads, taking into account internal energy dissipation

11 p1738 A72-26797

Nonadiabatic and atmosphere induced energy losses as causes of proton capture in geomagnetic field

11 p1715 A72-26915

Predawn effect on hot and cold electrons at magnetoconjugate point in F 2 layer, discussing electron shock wave speed and thermal collisionless wave energy dissipation

11 p1628 A72-26916

Elastic wave propagation and energy scattering in materials reinforced by inextensible fibers

12 p1881 A72-27252

Ionization and associated energy loss effects on particles acceleration in solar atmosphere, emphasizing Fermi mechanisms

12 p1863 A72-27303

Structural energy loss mechanisms, considering hysteresis, edge damping of panels, acoustic losses, dry friction, multilayer sandwich damping, etc

12 p1882 A72-27342

Temperature distribution and dissipation effects on compressible isothermal atmosphere I. amb waves vertical structure

12 p1839 A72-27504

Laser with unstable telescopic resonator and large radiation loss, calculating energy characteristics and power efficiency

12 p1821 A72-27590

Time variable energy losses effects on cosmic ray nuclei composition, discussing fragmentation processes during heavy nuclei propagation through interstellar matter

12 p1864 A72-27692

Wave packet group velocity concept interpretation and application, considering propagation in dissipative media

12 p1783 A72-27719

Turbulence model based on transport equations for Reynolds stress tensor and energy dissipation rate, deriving simplified version for boundary layer flows

12 p1798 A72-27830

Electron impact excitation spectrum of molecular oxygen, investigating angular behavior of differential scattering cross sections and energy dissipation

12 p1848 A72-27851

Temperature distribution and heat dissipation calculations for CW and pulsed laser optical elements

12 p1824 A72-27873

Elastic rod system stationary vibrations under combinational parametric resonance due to internal energy dissipation, using matrix method

12 p1885 A72-27969

Flow velocity fluctuation intensity relationship to turbulent energy dissipation based on Kolmogoroff similarity hypothesis

12 p1799 A72-28133

Turbine nozzle vanes edge losses dependence on profile edge thickness, allowing flow velocity variation

12 p1861 A72-28135

Energy dissipation for turbulent flow in turbine blades guide vanes calculated with allowance for effects of Reynolds number and turbulence intensity

12 p1752 A72-28137

Statistical methods for friction and wear processes noting Rayleigh distribution of wear particles, surface dispersion velocity, energy dissipation and friction force

12 p1818 A72-28186

Material fatigue failure criterion during cyclic loading, noting energy dissipation and resonant frequency roles

12 p1888 A72-28250

ALSEP seismic records from Apollo 12 lunar module and Apollo 13 rocket stage impact, showing ringing phenomenon due to sphere curvature-caused energy dissipation

13 p2035 A72-28618

Thermodynamic limiting relations between physical measurement accuracy and measurement performance energy dissipation, considering equilibrium and nonequilibrium dynamic models

13 p2003 A72-28761

Profile losses at turbine rotor blade in unsteady gas flow from experimental data analysis, noting effect of turbulence caused by trailing edge wakes

13 p1893 A72-28783

Thermal storage type resistojets design for satellite attitude control, discussing heat loss minimization

13 p2026 A72-28927

Low energy Cs ion beam energy loss during traverse through near-thermal equilibrium Cs plasma as function of plasma density, comparing measurements with theoretical predictions

13 p2011 A72-29000

Nb superconducting resonant cavities application to linear accelerator and RF particle separator structures in GHz region for wall energy loss reduction

13 p1922 A72-29348

Random phase approximation for nonlinear theory of MHD nonequilibrium plasma steady turbulent regime, noting ionization level rise by energy dissipation

13 p2013 A72-29359

Frequency distribution changes of energy deposited in short pathlengths as function of energy degradation of primary proton beam

13 p2004 A72-29425

Thermal flux distribution in sectioned plasmatron channel with supersonic Ar plasma injection, discussing energy dissipation

13 p2017 A72-29634

Sunspot energy deficit relation to model depth, deriving facular model with two dimensional radiative transfer analysis

13 p2045 A72-29712

Alfven wave transmission in sunspot umbral magnetic flux tube, noting standing progressive waves and energy dissipation in facular regions

13 p2049 A72-29937

Velocity distribution downstream of nonuniform single and multiple smoothing screens, presenting theory based on energy losses and flow direction changes

13 p1940 A72-30100

HF transverse resonant vibrations of annular Al plates with polychlorovinyl and polyamide base coatings, noting damping and strain relationship to energy dissipation

14 p2164 A72-30427

Schottky diode microwave down-converter conversion loss calculation as function of image terminal with consideration of barrier capacitance, series resistance and voltage drop

14 p2088 A72-30586

Plane and circular dielectric waveguides with thermal losses, considering transverse wave numbers behavior behind cut-off value and dispersion equations solution

14 p2086 A72-30797

Heat losses due to spacecraft installation discontinuities on aluminized Mylar multilayer insulation, predicting blanket performance

[AIAA PAPER 72-285]

14 p171 A72-30829

Finite element method with compliance equations determining energy release rates and stress intensity factors for complex crack configurations and loadings

14 p2168 A72-30908

French monograph on flow near rotor blade tips, discussing three dimensional circulation and boundary layer effects, energy losses, velocity and pressure distributions, etc

14 p2069 A72-30950

- Mobile point defects interaction with moving dislocation in inelastic solid bodies, considering energy dissipation due to impurity relaxation 14 p2169 A72-30954
- Energy losses due to hysteresis friction during oscillations of dislocations in elastic field of point defect in solids, discussing temperature and amplitude effects 14 p2121 A72-30955
- Deflection and energy dissipation of thin cascade profiles in transonic flow for given pressure distribution, noting boundary layers and separated flow 15 p2178 A72-31501
- Transistorized microwave amplifiers with dissipative equalizing networks, describing transistor equivalent circuit 15 p2206 A72-31659
- Electric and magnetic fields fluctuations in region between shock wave front and magnetosphere boundary, noting resulting energy dissipation 15 p2225 A72-31902
- Exact solutions for plane thermoelastic and magnetothermoelastic wave frequency equations, determining specific loss extremum values 15 p2336 A72-32447
- Ionization energy loss of relativistic heavy nuclei for close collisions as function of charge, computing Born approximation corrections via Mott exact cross section 15 p2282 A72-32647
- Vela pulsar speedup explanation by corequake release of elastic energy stored within solid neutron lattice 16 p2450 A72-32869
- Single degree of freedom nonlinear mechanical system vibration characteristics calculation by averaging procedure, taking into account energy dissipation 16 p2424 A72-33279
- Five channel recording instrument for energy dissipation evaluation in electric machines from thermal emf measurements 16 p2392 A72-33284
- Energy and momentum losses of high temperature gas flow through externally cooled tube, solving laminar flow differential equations numerically on digital computer 16 p2378 A72-33430
- Charged particle energy dissipation in cold collisional plasma, discussing collisions effect on power spectrum 16 p2436 A72-33651
- Stellar magnetic oblique rotator internal motion field construction by perturbation technique estimating energy dissipation and turbulent viscosity 16 p2458 A72-33721
- Cosmic microwave background radiation origin by energy dissipation associated with primordial chaotic universe 16 p2459 A72-33770
- Turbulent energy dissipation rate statistical characteristics above 1000 m from radar measurements, discussing atmospheric boundary layer quantities 16 p2418 A72-33781
- Cumulus clouds vertical motion velocity spectra curves, turbulence dissipation rates and energy determination from aircraft measurements 16 p2418 A72-33782
- Temperature distribution and heat dissipation calculations for CW and pulsed laser optical elements 16 p2403 A72-33982
- Physical phenomena limitations on MOS IC miniaturization, considering gate oxide breakdown, drain source punch through, doping fluctuations, power dissipation and metal migration 16 p2370 A72-34102
- Energy release mechanism during early universe expansion leading to distortion of relic black body spectrum, noting Comptonization effects 16 p2461 A72-34151
- Plasma-ion beam nonlinear interaction for beam velocity exceeding electrons thermal velocity, noting plasma heating and beam energy dissipation 16 p2440 A72-34154
- Combustion instability oscillations damping in rocket motors by short nozzles, calculating acoustic losses 17 p2635 A72-34233
- Conservation laws related to energy release rates associated with cavity or crack rotation and expansion, discussing plastic stress distribution around cracks [ASME PAPER 72-APM-22] 17 p2580 A72-34795
- Dissipative periodic process theory for application to elasticity and distributed parameter and hereditary systems defined by partial and functional differential equations 17 p2575 A72-34867
- Viscous dissipation effects on unsteady free convective flow past an infinite, vertical porous plate with constant suction. 17 p2637 A72-35047
- Onset of convection near a suddenly heated horizontal wire. 17 p2637 A72-35048
- A physical mechanism for the production of solar flares. 17 p2608 A72-35088
- On neutral sheets in the solar wind. 17 p2599 A72-35096
- Mode stability in a gas laser with nonlinear selection losses 17 p2563 A72-35304
- Propagation mode and scattering loss of a two-dimensional dielectric waveguide with gradual distribution of refractive index. 17 p2530 A72-35469
- Soft collision plasma scattering function, conductivity and particle energy loss from simplified Fokker-Planck collision model 17 p2592 A72-35621
- Effects of vorticity, displacement speed and curvature on heat transfer with dissipation. 17 p2638 A72-35747
- Electron energy distribution and losses existence limit at Langmuir paradox pressures in gas discharge, hypothesizing wall mechanism of electron collisions randomization 17 p2593 A72-35887
- Possible refinement of the lognormal hypothesis concerning the distribution of energy dissipation in intermittent turbulence. 18 p2678 A72-36018
- The Apollo 15 lunar heat-flow measurement. 18 p2724 A72-36285
- Book - Annual review of fluid mechanics, Volume 4 18 p2679 A72-36382
- Independent moving vibrational /acoustic/ source-induced wave losses during friction of two elastic bodies 18 p2696 A72-36966
- Losses in high-voltage transformers encapsulated by epoxy resins. 18 p2669 A72-37113
- Measurement of the damping capacity and dynamic modulus of high-damping metals under direct cyclic stresses. 19 p2795 A72-37460
- Energy loss of fast electrons and positrons in a plasma. 19 p2840 A72-37727
- Approximate calculation of the maximum efficiency of an O-type oscillator with a resonance delay system in the presence of losses 19 p2774 A72-38412
- Unsteady weakly nonlinear waves in a multicomponent plasma with allowance for weak dissipation 19 p2842 A72-38528
- Atmospheric boundary layer turbulence modeling, considering terrain roughness effects, vertical mixing, high frequency spectra, energy dissipation rate and vertical component variance 19 p2828 A72-38557
- Aircraft measurements of dissipation of turbulent kinetic energy. 19 p2829 A72-38561
- Slowly rotating relativistic stars. VI - Stability of the quasi-radial modes. 20 p2966 A72-38909
- Analysis of effects of fluid energy dissipation on spinning satellite control dynamics. [AIAA PAPER 72-886] 20 p2976 A72-39115
- Photographic observations of W particle clusters high velocity impact against polystyrene, paraffin and W targets for energy dissipation in meteorite impact simulations 20 p2969 A72-39257
- Measurements of electron detection efficiencies in solid state detectors. 20 p2925 A72-39401
- Weight saving, vibration proofing and heat dissipating techniques in avionics packaging, considering B-1 bomber electronic multiplexing system example 20 p2909 A72-39768
- Stellar energy-loss rates in a convergent theory of weak and electromagnetic interactions. 20 p2972 A72-39868
- Metal fatigue crack propagation under cyclic loads, assuming specific energy dissipation as material constant 20 p2981 A72-39953
- Plasma low density regions caused by Langmuir turbulence, discussing energy dissipation of long wave oscillations and wave collapse 21 p3090 A72-40410
- Thermoelastic problems for multiply-connected plates with heat dissipation at both plane surfaces. 21 p3121 A72-41237
- An expression for the distribution of current in asymmetrically driven antenna immersed in a dissipating medium. 21 p3022 A72-41322
- Resonant frequency, fatigue and energy dissipation relations for endurance limit determination in Al alloy specimens under vibrational loads 21 p3070 A72-41368
- Influence of the test temperature on the fracture energy of graphite 21 p3074 A72-41714
- Influence of inelastic electron-energy losses on the development of ionization instability in a plasma 22 p3209 A72-41877
- Evanescent and internal gravity wave propagation effects on atmospheric dynamics, considering momentum transfer, energy dissipation and turbulence 22 p3168 A72-41964
- Convection and diffusion transport equation of galactic cosmic ray electrons with energy loss and absorption allowance for supernova compressed halo models 22 p3217 A72-42210
- Nonadiabatic condition effects on ultrarelativistic electron energy losses in geomagnetic trap in remote magnetosphere regions 22 p3218 A72-42224
- Energy degradation calculation for electron interaction with carbon dioxide molecules, discussing relationship with Mariner UV data 22 p3171 A72-42421
- Variation of the output of radioluminescence of organic scintillators with energy loss and the number of charges of ionizing particles 22 p3180 A72-42938
- Molecular gas presence effect on electron energy balance in atomic gases, noting inelastic collisions loss factor in heated Ar plasma containing nitrogen molecules 22 p3213 A72-43110
- Elastomers fracture strength and failure modes under tension, tearing, ozone cracking, fatigue and abrasive wear associated with viscous resistance energy losses 23 p3305 A72-43506
- Flow and energy loss distribution in annular stator nozzle cascades with cylindrical blade profiles of different twist, measuring flow exit angle along blade span 23 p3248 A72-43664
- Flow parameters and geometric factors effect on wake structure behind nozzle cascades with cooling air ejection through blade trailing edges, evaluating energy losses due to flow mixing process 23 p3248 A72-43665
- Filler quantity and type effects on mechanical energy losses in polymers, discussing molecular interaction and chemical bond influences 23 p3306 A72-43731
- Relationship between the dissipative properties of a vibrational system and its amplitude-phase-frequency characteristics 23 p3313 A72-43785
- Energy dissipation in metals during high-frequency fatigue tests. I 23 p3302 A72-43963
- Energy dissipation in metals during high-frequency fatigue tests. II 23 p3302 A72-43964
- Reduction of end losses in cascades of cambered blades 23 p3248 A72-44025
- Thermal energy dissipation in artificial antennas of large broadcasting transmitters studying cooling systems 23 p3278 A72-44311
- Plastic flow around an expanding crack. 24 p3456 A72-44812
- Energy releases in the upper atmosphere during geomagnetic disturbances. 24 p3396 A72-44847
- Mixed, nonequilibrium and coherent diffusion in stationary media with intense energy sources, noting finite speed of light effects 24 p3428 A72-45057
- A determination of thermal diffusivity under transient conditions 24 p3465 A72-45067
- Electron scattering by molecules with and without vibrational excitation. IV - Elastic scattering and excitation of the first vibrational level for N₂ and CO at 20 eV. 24 p3427 A72-45304
- Kinetics, spectrum, and specific loss properties of radiation emitted by rhodamine 6G in the case of pumping by a self-constricting discharge 24 p3410 A72-45417
- Alloying, thermal and mechanical treatment effects on Mg alloys damping properties under elastic vibrations, showing test results consistency with materials microdeformation theory 24 p3415 A72-45729
- Energy dissipation associated with transverse vibrations of sandwich metallic samples with damping coatings 24 p3461 A72-45760
- The influence of static stresses on the dissipation of energy due to forced oscillations. 24 p3461 A72-45767

ENERGY DISTRIBUTION

NT SPECTRAL ENERGY DISTRIBUTION

- High efficiency reflector antennas, discussing secondary subreflector for feed energy redistribution 01 p0039 A72-10671
- Wave propagation in nonlocal isotropic elastic medium of ordinary kinematic structure with energy density as functional of displacement gradient field 02 p0288 A72-11609

Linear energy transfer distribution for negative pions beams in human tissue, calculating relative biological efficiency and oxygen enhancement ratio [CERN-71-16] 02 p0162 A72-12064

Absolute UV calibration of rocket photometers used to update OAO calibration for determining energy distribution of reference stars 03 p0355 A72-13065

Wall double layer temperature and plasma oscillations effect on electron energy distribution in low discharge plasma column 03 p0394 A72-13192

Disturbance evolution on zonal flow background in baroclinic atmosphere with given wind profile, determining average-time energy distribution 03 p0383 A72-13479

Thin electrostatically self focusing electron streams in mercury vapor, analyzing energy distributions of ions and electrons ejected radially from beam 04 p0554 A72-14407

Electron energy distribution in carbon dioxide laser mixtures under lasing and nonlasing conditions 04 p0528 A72-14540

Energy equipartition among unequal masses in galactic nuclei and gravitating systems, discussing time scale for dynamical evolution 04 p0570 A72-14552

Trapped particles induced by fluctuating magnetospheric electric and magnetic fields, calculating radial diffusion and energy distribution and time variations 04 p0566 A72-14723

Conformal transformations applications to plane electromagnetic wave diffraction by infinitely conducting network, discussing energy distribution 04 p0490 A72-15410

Integral equations derived for single and composite radio signals with maximum energy concentration in given time interval or frequency band 05 p0625 A72-15824

Rarefied gases thermal energy diffusion model, using radiative transfer electrical network analog [ASME PAPER 71-WA/HT-4] 05 p0743 A72-15865

Vlasov equation stability properties of collisionless plasma and stellar gas, removing energy variation difficulties with multiple water bag model 05 p0694 A72-16060

CW millimeter wave power generation with spiraling electron beams, investigating energy spread effects on performance limitation 05 p0636 A72-16363

Damping of lateral oscillatory processes by end terminal displacement compensation, noting spring energy 05 p0691 A72-17132

Cosmic radiation high energy hadron component relation to extensive electron-photon showers, comparing sampling events based on multicore structure and total energy 06 p0870 A72-17282

High energy muon energy and angular distributions from electron-photon cascades, using emulsion chamber with X ray films 06 p0871 A72-17286

LF instability mode in partly ionized plasma due to electron temperature gradient aligned perpendicular to magnetic field, applying to E and F regions [AD-737931] 06 p0804 A72-17460

Electrostatic energy analyzer for local ion velocity distribution function measurement in double ended Q machine plasma column 06 p0814 A72-17551

Plasma conductivity dependence on electron velocity distribution function in distorted Maxwellian form 06 p0860 A72-17690

Ionization mechanism for low voltage neon plasma arcs, determining non-Maxwellian energy distribution effects and excited atoms collisions role 06 p0862 A72-18333

Energy complex in general relativity in form of tetrahedral gravitational theory, including solutions to Einstein equations 06 p0849 A72-18419

Electron energy distribution in carbon monoxide lasers, considering excitation effects on exchange processes, power transfer to vibration levels and vibrationally excited molecules influence 07 p0999 A72-18883

Plasma turbulent heating effectiveness by longitudinal ion current in mirror machine, determining hot ion lifetime and energy distribution function 07 p1039 A72-18913

Equations of free particle motion, gas energy, distribution evolution and cosmic indeterminacy for Friedmann universe filled with uniform density and pressure ideal gas 07 p1074 A72-19429

Magnetic bremsstrahlung energy straggling and radiation reaction, calculating particle and emitted photon distribution 07 p1037 A72-19668

Energy and angular distributions of electrons released during ion atom collisions from energy spectra studies, discussing autoionization transitions 08 p1210 A72-20836

Pulse energy and heat distribution in dielectric and metal during electroerosive machining 08 p1174 A72-21035

Fine structure of energy distribution function for electron beam interacting with plasma 08 p1215 A72-21722

UV absorption measurements across Saturn disk at 3300-4800 Å, considering rings and distribution in short wave region 08 p1238 A72-21829

Second derivative measurement of Langmuir probe characteristics for electron energy distribution functions in nonstationary plasmas by sample and hold technique 09 p1359 A72-22654

IR emission at 2.7 microns from carbon dioxide-molecular nitrogen mixture flow, noting energy redistribution 09 p1357 A72-22854

Electron energy distribution and losses existence limit at Langmuir paradox pressures in gas discharge, hypothesizing wall mechanism of electron collisions 09 p1361 A72-22958

Pulsed laser sensitizer using multiple imaging technique to retrieve average energy distribution from photographic plate optical density 09 p1325 A72-23346

Micrometeoroid simulation by accelerated microparticles bombardment of metal targets, discussing energy partition as function of impact velocity 09 p1409 A72-23667

Laser beams cross-sectional power distribution measurement by spinning disk scanner, using dual beam oscilloscope for laser beam profile display 10 p1489 A72-23949

Earth albedo neutrons energy and angular distributions, suggesting neutron source of inner radiation belt trapped protons 11 p1712 A72-25880

Mass, momentum and energy distribution measurement in quasi-steady MPD discharge, obtaining velocity vector profiles [AIAA PAPER 72-497] 11 p1696 A72-26220

Disturbance evolution on zonal flow background in baroclinic atmosphere with given wind profile, determining average-time energy distribution 11 p1682 A72-26249

Near and far field energy and power density distributions of multi-transverse mode double discharge TEA laser beam 11 p1651 A72-26671

Triple stellar system evolution and disintegration, discussing energy partitioning and initial velocity effects on stability 12 p1865 A72-27095

Energy distribution in plasma jet as function of capacitance and energy of storage elements and storage circuit inductance 13 p2015 A72-29452

Statistical method of Pearson moments applied to temperature regimes effects on ruby laser output energy distribution 13 p1968 A72-29506

Transverse magnetic field effect on electron temperature and energy distribution and spectral lines of gas discharge plasma 13 p2017 A72-29635

Energy flux intensity in selectively radiating gas nonisothermal layer from radiant transfer equation and mathematical model 13 p2066 A72-29898

Charged particle inertial-electrostatic containment in spherical diode gas discharge gap, measuring flux radial and energy distributions 13 p1933 A72-29915

Solar coronal magnetic field structure and energy content from synoptic data analysis, noting differential rotation effects 13 p2050 A72-29938

Daytime F region inverse relationship between electron density and temperature, determining energy input profile and thermal flux 14 p2097 A72-30127

Electron energy distribution, ions mass spectral composition and spatial charge concentration of currentless photoresonant Ce plasma obtained by associative ionization 14 p2136 A72-30175

Kinetic instabilities during electron plasma heating in HF field of cylindrical resonator, discussing electron energy distribution function effect 14 p2137 A72-30309

Maximum ion energy dependence on radiation density in laser plasma 14 p2137 A72-30315

Electromagnetic emission in universe, discussing background radiation spectrum, extragalactic source brightness, intergalactic gas and energy density 14 p2152 A72-30479

Solar wind thermal properties from positive component energy distribution observation by ESRO Heos 1 satellite 15 p2298 A72-31518

Total energy distributions of field emitted electrons from tungsten as function of coverage by hydrogen and deuterium, observing elastic and inelastic spectrum 15 p2275 A72-31851

Energy and angular distribution of hydrogen and rare gas ions backscattered from polycrystalline metal surfaces 15 p2276 A72-31852

Energy equation for solution compressible laminar boundary layer generalized with orthogonal curvilinear coordinates 15 p2218 A72-32146

Steady state electron mean energy variation between parallel plates in Ar and He calculated by Monte Carlo simulation for comparison 15 p2285 A72-32222

Acceleration and recombination effects on ion energy spectra, discussing energy distributions of hydrogen, zirconium, lithium, and deuterium ions in laser plasmas 16 p2428 A72-32910

High and medium energy molecular beam detection for large dispersion angle collision cross sections determination, using photographic plates 16 p2389 A72-33060

Face centered solid crystal cell spatial distribution effect on body surface-reflected molecular beam intensity distribution 16 p2430 A72-33066

Elastic-plastic medium yield zone spread from penny shaped crack determined from continuous distribution of dislocations, noting system energy change 16 p2468 A72-33226

Probe temperature, shape and size effects on electron energy distribution measurements for positive plasma column of low pressure He and Ne discharges 16 p2437 A72-33750

Particle and energy fluxes across magnetic field in axisymmetric toroidal magnetic traps and plasmas with weak collisions, calculating radial electric field 16 p2440 A72-34153

Velocity-pressure correlations in a homogeneous turbulence associated with a plane pure deformation 17 p2537 A72-34280

Entropy and chemical change. I - Characterization of product /and reactant/ energy distributions in reactive molecular collisions: Information and entropy deficiency. 17 p2511 A72-34738

Field variations of perfect fluid in axisymmetric stationary universe within general relativity theory concept, noting energy extremal properties for rotating stars 17 p2607 A72-34921

Runaway electrons in toroidal plasma investigation by thick target bremsstrahlung measurement, noting energy distribution and runaway rate estimates 17 p2591 A72-35370

Electron temperature in the Martian ionosphere. 17 p2613 A72-35499

A universal power characteristic of a high-temperature solar heat source 17 p2498 A72-35516

Nonequilibrium energy constants associated with large-amplitude electron whistlers. 17 p2517 A72-35620

Electron energy distribution and losses existence limit at Langmuir paradox pressures in gas discharge, hypothesizing wall mechanism of electron collisions randomization 17 p2593 A72-35887

Analytical description of thermionic converter phenomena, assuming position linearity of interelectrode electron energy distribution and local thermodynamic equilibrium in cesium plasma near collector 18 p2646 A72-36200

Nonequilibrium relaxation phenomena in the near-emitter region of the thermionic converter. 18 p2647 A72-36209

Systematic approach to study energy and information flow through measuring system in experimental mechanics, using transducer model 18 p2690 A72-36356

Stress state and velocity fluctuations in a perturbed boundary layer 18 p2680 A72-36464

Energy variation curves for direct flare radiation and reflection from eruptive star atmosphere, discussing color variations 19 p2858 A72-37808

Effect of optical constants on the energy distribution in homogeneous particles illuminated by a parallel beam of light 19 p2812 A72-38216

Tungusk meteorite explosion energy values for various altitudes from investigation of shock wave propagation in variable density atmosphere 19 p2864 A72-38321

Plasma turbulent heating effectiveness by longitudinal ion current in mirror machine, determining hot ion lifetime and energy distribution function 20 p2957 A72-39379

- Energy balance equation for machine unit with rotating element, noting energy distribution in periodic and nonperiodic operation modes 22 p3181 A72-41857
- Objective-prism plates photometric computerized calibration method based on continuum energy distribution of standard stars within photographic plate field 22 p3177 A72-42376
- Photoelectron energy distributions from clean polycrystalline W, observing surface state 22 p3190 A72-42477
- Electron-energy distribution in a low-temperature plasma 22 p3213 A72-43118
- Kinetic instabilities during electron plasma heating in HF field of cylindrical resonator, discussing electron energy distribution function effect 23 p3317 A72-43211
- Maximum ion energy dependence on radiation density in laser plasma 23 p3318 A72-43218
- Integral equations derived for single and composite radio signals with maximum energy concentration band in given time interval or frequency 23 p3263 A72-43432
- Velocity, enthalpy and turbulent energy distributions calculation for plane wake behind flat body by asymptotic solution based on turbulence theory 23 p3249 A72-44083
- Glow discharge in rare-gas and metal vapour mixture. I - Distribution functions and kinetic coefficients in He-Cd mixture discharge. 23 p3322 A72-44320
- Ultrahigh energy gamma quanta families detection by airborne emulsion chamber at 500-2500 m altitude, calculating energy distribution distortion by Monte Carlo method 23 p3329 A72-44403
- Isothermal atmosphere inhomogeneities effects on electromagnetic cascade electrons integral energy spatial distribution 23 p3331 A72-44433
- Influence of the polarization of incident radiation on the distribution of the energy absorbed in a particle 24 p3424 A72-44621
- Focusing characteristics of CO₂ laser beam. 24 p3409 A72-44776
- Chemical explosion energy distribution between gases and propelled mass, discussing momentum and kinetic energy transfer 24 p3463 A72-45040
- Approximate equations of the flow behind a detonation with lateral confinement 24 p3463 A72-45041
- Investigation of the uniformity of neodymium-glass laser emission 24 p3410 A72-45419
- Linear corrector for laser beam intensity distribution transformation into random distribution with rectangular envelope, noting uniform energy distribution result of spatial fluctuations averaging 24 p3411 A72-45608
- Increase in the ratio of the energy of ultrashort laser pulses to the energy of the background radiation. 24 p3411 A72-45613
- ENERGY EXCHANGE**
- U ENERGY TRANSFER**
- ENERGY LEVELS**
- NT ATOMIC ENERGY LEVELS
- NT ELECTRON STATES
- NT GROUND STATE
- NT INTERMOLECULAR FORCES
- NT MOLECULAR ENERGY LEVELS
- Binary alloys ground state energy and superstructures, examining bcc and fcc Ising model systems with first and second neighbor interactions 01 p0083 A72-10210
- Wall stabilized Ar arc plasma, investigating Boltzmann equilibrium existence between spectral energy levels 02 p0264 A72-12025
- Energy levels and mean life measurements of Cl ions at 500-2800 A using beam-foil spectra technique 02 p0170 A72-12547
- Atomic data for UV and X ray astronomy, considering atomic wave functions and energy levels, radiative transition probabilities and electron-ion collision cross sections 03 p0420 A72-13125
- Neon lower laser level spontaneous emission double resonance phenomena, discussing depopulation rates and resonance line profile changes 04 p0531 A72-15138
- Photon radiative exit from scattering isothermal atmosphere containing atoms with two energy levels 06 p0848 A72-18051
- Semiconductor device physical behavior, discussing energy levels, impurity conduction, p-n junction capacitance and bipolar and unipolar transistor I-V characteristics 06 p0790 A72-18575
- Kinetic model for gas dynamic laser energy extraction from carbon dioxide-nitrogen-helium mixture, predicting gain, saturation and pulse length 07 p1001 A72-19195
- Zeeman patterns and energy level Lande g factors from spectrograms of As ion electrodeless discharge tubes in presence of 24,025 G magnetic field 07 p0987 A72-19832
- Energy level and V-I characteristics of solid state heterojunction devices, discussing diodes, transistors, thyristors and optoelectronic structures 08 p1139 A72-21054
- Scattered light coherence in optically thin vapors and ideal gases in energy level crossing experiment formulated in terms of autocorrelation function 08 p1206 A72-21294
- Radiation induced extrinsic photoconductivity in Li doped Si, examining localized energy levels in forbidden gap 09 p1372 A72-23238
- Local level filling and Fermi distribution in metal semiconductor contact as function of voltage and level location 09 p1372 A72-23355
- Charged particles effect on plasma negative ions, examining Stark effect in energy level 11 p1693 A72-25714
- Transverse negative differential conductivity in semiconductors, discussing effect of locations and shapes of energy surfaces in k-space and favorable crystal orientations 11 p1701 A72-25856
- Quantum beats in transitions from levels subject to optical cascades 12 p1847 A72-27184
- Recombination parameters in low resistivity gamma irradiated n-type Ge, obtaining energy levels and temperature dependence of electron and hole capture probabilities 12 p1857 A72-28056
- Phonon scattering and induced energy levels in electron irradiated Sb doped Ge in n to p-type conversion region, measuring thermal conductivity and Hall effect 12 p1857 A72-28057
- Photoelectric emission usefulness for investigation of energy parameters and optical transitions of semiconductor surfaces 15 p2276 A72-31865
- One electron and Josephson tunneling in superconductors in terms of energy level concepts 15 p2293 A72-32326
- Random matrix spectra of eigenvalues in terms of Wigner set for statistical description of heavy nuclei energy levels 15 p2282 A72-32449
- Paramagnetic phase induced moment system containing substitutional impurities, calculating mode energies by Green function method in random phase approximation 15 p2295 A72-32546
- Thermally stimulated current measurement application to Ag doped Si semiconductor for energy level and electron capture cross section determination 16 p2441 A72-32859
- Quantum mechanics framework for electron movement perpendicular to intense magnetic field, predicting energy broadening with time for initially monoenergetic electron beam 16 p2422 A72-32881
- Coherent emission lines in visible spectrum from triply ionized Er in barium yttrium fluoride, discussing energy level transitions associated with various lines 16 p2401 A72-33387
- Energy difference measurement between 2S and 2P levels of multiply charged O 16 positive ion, using Stark quenching technique 16 p2432 A72-33768
- The geometric factor of a cylindrical plate electrostatic analyzer. 17 p2553 A72-34639
- Experimental evidence for stationary population inversions of atomic levels in an expanding hydrogen plasma [DFVLR-SONDDR-213] 17 p2589 A72-34898
- Recombination continuum in a lithium plasma spectrum 22 p3210 A72-42171
- Electron distribution fluctuation in two level system of unstable electron gas, noting periodic time dependence of population 23 p3319 A72-43406
- ENERGY LOSSES**
- U ENERGY DISSIPATION**
- ENERGY METHODS**
- NT BERNSTEIN ENERGY PRINCIPLE
- NT STRAIN ENERGY METHODS
- Energy-momentum tensor for radiation and radiative viscosity in optically thick matter having Thomson scattering with photon absorption and emission processes 01 p0129 A72-10798
- Rotation and mass inclusion into study of energy barriers location effects on thermonuclear reaction dynamics 02 p0262 A72-11981
- Elastic stability of body under conservative loads, deriving energy criterion with thermodynamic laws 02 p0292 A72-12003
- Temperature field analysis in locally heated cylindrical shell for stressed state production with lowest elastic energy 03 p0456 A72-13733
- Potential energy principle in equilibrium stability problems for flexible extendable thread, using Liapunov method 03 p0390 A72-14208
- Multipurpose optimal design of elastic structures with piecewise uniform cross section for load states and prescribed stiffness by energy methods [AD-743418] 03 p0455 A72-14386
- Fundamental frequency calculation method for bars and plates with arbitrary fixity of rotations, discussing buckling and vibration with realistic boundary conditions 04 p0591 A72-15275
- Castigliano theorem in energy method, considering global static constraints and restriction for generalized force variables reduction through integration 05 p0732 A72-15803
- Distortional energy theory for predicting failure of orthotropic materials exposed to three dimensional stress state [ASME PAPER 71-WA/DE-13] 05 p0732 A72-15942
- Elastic boundary value problems static and geometric field parameters pointwise upper and lower bounds, determining solution coefficients by error energy minimization 05 p0735 A72-16062
- Finite element and finite difference formulations for solid continua by variational principles, including potential energy, complementary energy and Reissner principles 07 p1087 A72-18792
- Critical Reynolds numbers estimation for flows having velocity profile with point of inflection, discussing plane parallel flows stability energetic analysis 08 p1151 A72-21660
- Energy methods for nonlinear viscoelastic bodies based on constitutive relations affecting critical state in advanced creep 09 p1403 A72-22764
- Spiral flow stability between rotating and sliding cylinders, using modified energy theory based on assumption of disturbance invariance along preferred spiral direction 10 p1466 A72-24298
- Terminal control solution in terms of finite dimensional minimization of convex function, applying to time optimal control and minimum energy problems 10 p1457 A72-24459
- Energy method for boundary conditions of beam vibrations under linear viscoelastic stress-strain law, deriving uniqueness, boundedness and stability theorems 12 p1885 A72-27848
- Energy method based approximate calculation for natural frequencies of single layer compound shells of revolution 12 p1886 A72-28144
- Hydromagnetic channel flow stability computation via energy method, solving eigenvalue problem by direct forward numerical integration 15 p2283 A72-31212
- Spherical cap dynamic buckling under impulsive loading, comparing prediction by energy criterion with experiment using spray deposited explosive 15 p2323 A72-31405
- Static boundary value problem of axisymmetric elasticity for elastic isotropic media with small energy contribution to potential due to moment effects 16 p2464 A72-32934
- Limit displacement or solids parameters optimization for perfectly locking bodies, presenting mathematical models based on extremum energy theorems 16 p2423 A72-33104
- Energy theorems for creep constitutive relationships, discussing total deformation of body composed of elastic-creeping material with allowance for stress redistribution effects 16 p2473 A72-34118
- Creep deformation upper bounds for smooth pipe bends under constant external bending moments, using energy method analysis 16 p2473 A72-34123
- An energy technique for use in the vibration testing of complex structures. 17 p2626 A72-34720
- A comparison of numerical methods for determining stress intensity factors. 17 p2631 A72-34973
- Clamped flat skew plates stability under inplane stresses in terms of oblique components, calculating elastic buckling coefficients via energy method 18 p2736 A72-36931

Stellar evaporation in globular clusters passing through galactic plane, considering gravitational perturbation increase of total energy within system
21 p3107 A72-41269

On the sufficiency of the energy criterion for the stability of certain nonconservative systems of the follower-load type
[ASME PAPER 72-APM-E] 23 p3350 A72-44052

Supersonic aircraft energy turns
23 p3252 A72-44196

Vibration of simply supported cylindrical shells with longitudinal stiffeners
24 p3457 A72-44882

Optimal guidance for the space shuttle transition
24 p3422 A72-45186

Some extremal properties and energy theorems for inelastic materials and their relationship to the deformation theory of plasticity
24 p3460 A72-45692

On dual energy theorems for a class of elastic-plastic problems due to G. Maier
24 p3460 A72-45693

Omega-Dot law for time optimum approximation of rotating satellites wobble damping with control moment gyroscopes, calculating wobble rates by energy sink method
24 p3453 A72-45777

ENERGY OF FORMATION

Bond dissociation energy of aluminum monoxide, tabulating flame compositions and temperatures
07 p1051 A72-19363

Average energy to form electron-hole pairs in GaP diodes with alpha particles
20 p2908 A72-39564

ENERGY REQUIREMENTS

Extragalactic cosmic ray hypothesis plausibility from viewpoints of energy supply, acceleration process efficiency, galactic nucleus activity and intergalactic space
01 p0122 A72-11268

Energy dependence of solar proton-proton reaction, generating p-p wave function from Schroedinger equation
05 p0718 A72-16501

Optimum duration of human circadian cycle with respect to energy cost during work hours, relating normal cycle change to prolonged space mission stresses
05 p0619 A72-16639

Minimal energy stochastic controller design for electrically driven vehicles, using dynamic programming
06 p0795 A72-17304

Multivariable control systems, discussing effects of interaction vs noninteraction/decoupling/on system performance and energy requirements
07 p0962 A72-19715

Non-LTE effects on mechanical heating in gray atmosphere applied to nonradiative energy input estimates for solar chromosphere from negative hydrogen ion emission
08 p1235 A72-21391

Small impurity amounts effect on packing defect density and deformation energy in Ni
08 p1188 A72-21791

Galactic and universal theories of cosmic ray source mechanisms, energy requirements, particle composition, propagation through interstellar matter and acceleration in supernovae remnants
10 p1533 A72-23889

Speed and mechanical work measurements during knee bending and immediate or delayed leg extension exercise, showing muscle elastic potential energy utilization
11 p1587 A72-26615

Energy cost/oxygen consumption/prediction for treadmill and various levels terrain walking at two speeds under three different pack loads
14 p2080 A72-30706

Thermonuclear microexplosion ignition by bombarding dense target with intense relativistic electron beam, noting energy requirement reduction by self magnetic beam field
16 p2433 A72-32814

The fracture energy of a glass fibre composite
17 p2570 A72-34670

USSR electric impulse de-icing system design
18 p2648 A72-37033

An explicit automatic terminal energy management guidance technique for space shuttle
[AIAA PAPER 72-833] 20 p2950 A72-39094

Metabolic energy requirements for pushing loaded handcars, measuring expenditure during treadmill and outdoor asphalt circuit walking
21 p3005 A72-40419

Solar wind models of energy transport mechanisms and nonthermal heating requirements, comparing predictions with spacecraft observation
21 p3100 A72-40484

Energy management during the space shuttle transition
24 p3452 A72-45347

ENERGY SOURCES

Magnitude and distribution of stresses produced by external energy sources in thick plate
04 p0593 A72-15657

Elemental synthesis and energy sources in stellar evolution, hydrogen, helium and advanced burning stages, p-p cycle, e process and nuclear equilibrium
06 p0876 A72-17585

Power generation for electrical, thermal and transportation needs, considering technology use for air, noise, thermal, water and nuclear pollution reduction
06 p0761 A72-18627

Electrochemical energy cells for biological telemetry equipment, noting mercury cell use in implanted heart pacemakers
07 p0914 A72-19914

Structure and evolution of radio galaxies and quasars, considering luminosity-sustaining energy source, emission mechanism, variability and mean activity time
07 p1083 A72-20469

Synchro-Compton theory for variable compact components in extragalactic radio sources, suggesting stellar mass object collapse as energy source
08 p1233 A72-21181

Geomagnetic field inflation during magnetic storm main phase, considering energy sources and injected proton plasma radial velocity
10 p1472 A72-24274

Quasars energy source and structure in terms of kinetic energy conversion to radiation in shock fronts of colliding gas clouds
10 p1544 A72-24671

Fuor luminosity phenomena due to thermal corpuscular radiation emitting energy sources
15 p2304 A72-31330

Limited energy source operational time comparison for continuous and pulse mode operations
15 p2196 A72-31785

Liquid or solid propellant hot gas turbines as power source for hydraulic and electrical energy
18 p2648 A72-36558

Approximation of energy generation and nucleosynthesis during hydrostatic carbon burning in massive stars, noting neutrino-dominated evolution effects
22 p3228 A72-42562

Energy sources for extragalactic explosive phenomena in galactic nuclei and quasars, considering gravitation and double radio sources
24 p3439 A72-45018

Mixed, nonequilibrium and coherent diffusion in stationary media with intense energy sources, noting finite speed of light effects
24 p3428 A72-45057

Effect of a line energy source at the boundary of a supersonic flow
24 p3361 A72-45187

ENERGY SPECTRA

NT ELECTRONIC SPECTRA

NT NEUTRON SPECTRA

Balloon measurements for differential energy spectra of cosmic ray protons and He over half solar cycle 1965-1969, using Geiger tube hodoscope
[AD-745870] 01 p0119 A72-10876

Cosmic ray neutron leakage flux and energy spectrum measurements in 0.01-10 MeV range by OGO 6 satellite-borne neutron detector
01 p0119 A72-10877

Trapped protons low energy differential spectra from polar orbiting Injun 5 satellite measurements, suggesting radiation belts impulsive acceleration mechanism
01 p0120 A72-10891

Auroral electron flux and energy spectrum observations by synchronous ATS 5 and polar OV-17 satellites
01 p0061 A72-10894

Parallel electric field evidence near auroral ionosphere deduced from low energy particles, energy spectra and angular distribution
01 p0061 A72-10895

Extraterrestrial gamma ray flux contribution to total 0.7-4.5 MeV radiation at various latitudes by balloon sounding
01 p0120 A72-11007

Temporal behavior, intensity fluctuations and energy spectrum of pulsating X ray source Cygnus X-1 from Uhuru observations
01 p0121 A72-11092

Cygnus X-6 soft X ray source location, presenting polycarbonate pulse-height spectrum and counter response to different model source energy spectra
01 p0121 A72-11096

Pulsar NP 0532 pulsed hard X ray energy spectrum measurement, using balloon sounding data
01 p0134 A72-11160

Galaxy source of ultrahigh energy cosmic rays, interpreting energy spectrum kinks as galactic to metagalactic radiation transition
01 p0122 A72-11270

Energy spectrum equations for steady state turbulent convection model based on Heisenberg statistical theory, noting application to convection in planetary and stellar atmospheres
01 p0146 A72-11311

Sea waves energy spectra from optical Fourier analysis of ocean photographs under particular skylight irradiance
02 p0211 A72-11809

Ultrahigh energy cosmic ray models indication of galactic origin and composition, based on energy spectrum flattening data
02 p0272 A72-11901

Inner and outer belt electron differential energy spectra from Cosmos 228 satellite data, discussing fluxes of precipitating and quasi-captured particles
02 p0272 A72-11916

Epithermal neutrons energy spectra in atmospheric equilibrium layers at 57 geomagnetic N, noting agreement with experimental error limits
02 p0273 A72-11918

Anomalous magnetic and gravitational fields energy spectra model, examining autocorrelation functions changes
02 p0217 A72-11932

Neutron cosmic ray spectrograph method of separating recorded data by energies, using statistical analysis of data combinations with different dead times
02 p0229 A72-11936

Solar proton flux and energy spectra from 1968-1969 ESRO 2 satellite measurements, detailing 18 November 1968 event
[CERN-71-16] 02 p0273 A72-12073

Electron temperature profile across nonequilibrium stagnation point boundary layer in partially ionized gas, investigating charged particles interaction with body in ionosphere
02 p0262 A72-12268

Rocket-borne apparatus for X ray measurement in 25 to 200 keV range, noting primary diffuse component and earth albedo spectral analyses
02 p0231 A72-12448

Cosmic ray neutrons angular distribution and energy spectrum at 3200 m altitude, using ionization calorimeter and proportional counters
02 p0275 A72-12828

Antiproton flux energy spectrum in Galactic interstellar space, discussing flux peak
03 p0408 A72-13005

Gamma ray astronomy, discussing energy spectrum, diffuse background flux, extragalactic origin and Crab Nebula emission
03 p0408 A72-13027

Celestial gamma rays arrival direction and energy spectra measurement and spectrum analysis using ESRO satellite COS-B data
03 p0408 A72-13029

Major sources of background counts for collimation gamma ray detector, measuring radiation direction and energy spectrum from balloon altitudes
03 p0352 A72-13032

Inner radiation belt proton source and loss processes, obtaining flux intensities, energy spectrums and radial distributions
03 p0412 A72-13513

Cosmic ray energy changes in interplanetary space by model for solar X-ray bursts
03 p0413 A72-13534

Soviet book on calms and storms in upper atmosphere covering energy variations, auroras, geomagnetic storms, weather forecasting, etc
03 p0350 A72-13967

Fast particle interaction with intergalactic matter, discussing relaxation of power law cosmic ray spectra
04 p0570 A72-14553

Nonthermal electron spectra hardness limit during flash phase of solar flares from OGO-5 observation
04 p0566 A72-14561

CAT inducing atmospheric conditions effects on SST flight, discussing turbulence in convective clouds and kinetic energy spectra of atmospheric motions
04 p0543 A72-14693

Galactic center region, Virgo and Crab Nebula gamma ray observations, measuring intensity and energy spectra
04 p0578 A72-15312

Interstellar propagation of 2-8 Z galactic cosmic ray nuclei at 10-1000 MeV/nucleon, analyzing differential kinetic energy spectra
04 p0567 A72-15323

Nuclear charge composition and energy spectra measurement for hydrogen, helium and medium nuclei in 12 April 1969 solar particle event
04 p0567 A72-15325

Heavy nuclei enrichment in solar accelerated particles, discussing differential energy spectra, photospheric and coronal abundances, satellite observation and agreement with galactic cosmic rays
04 p0568 A72-15366

Primary cosmic ray electrons energy spectrum measurements, using balloon-borne absorption spectrometer
04 p0568 A72-15509

Primary cosmic ray proton energy spectrum in 50 Ge V to 300 Te V range, using Proton 1, 2 and 3 satellite-borne counters
05 p0709 A72-16231

Galactic high energy electron differential spectrum, estimating spatial distribution and random magnetic field intensity
05 p0709 A72-16237

Cosmic ray spectrum at nonrelativistic energy region, noting ionization loss effects
05 p0709 A72-16238

- Electron flux and energy spectra measurements at 200-600 km altitude by Cerenkov counters onboard Proton 1 and 2 05 p0709 A72-16254
- Neutron energy spectrum of radiative pion captured by carbon 12, using gamma and neutron counters 05 p0692 A72-16688
- OGO-5 measurement of 10-200 MeV cosmic ray electron energy spectra, discussing quiet time flux intensity 05 p0720 A72-16719
- Long time variations of proton energy spectra in inner radiation belt during solar cycle 05 p0710 A72-16767
- Integral and differential electron energy spectra in inner radiation belt from Cosmos 219 satellite observation 05 p0711 A72-16768
- Particle multiplicity and momentum spectra for high energy inelastic nuclear interactions in Wilson chamber with polyethylene target 06 p0868 A72-17261
- Inelasticity factor dependence on particle energy spectra to explain nucleon flux calculations and Proton satellite data, considering scattering cross sections 06 p0869 A72-17264
- Multilayer X ray chamber for gamma quanta energy spectrum determination by primary photon impact and absorber calorimetric methods 06 p0869 A72-17266
- Energy spectrum, composition and anisotropy study of cosmic radiation from extensive air showers, using scintillation and Cerenkov detectors 06 p0870 A72-17277
- Primary cosmic radiation energy spectrum approximation from air showers, high-energy hadrons and Proton 4 data 06 p0870 A72-17281
- Extensive air shower characteristics and muon counts at different level observations relative to particle number and primary energy spectra 06 p0871 A72-17284
- Energy spectrum of muon formed electromagnetic cascades in vertical cosmic radiation flux 06 p0871 A72-17287
- Energy spectra of positive ion bursts on lunar night side from Apollo 12 and 14 Alsep suprathermal ion detectors data 06 p0872 A72-17462
- Scintillation crystal light yield dependence on emission energy in particle flux measurements with semiconductor spectrometer 06 p0816 A72-17835
- Pulsar produced cosmic rays energy spectrum, investigating light elements origin 06 p0874 A72-18161
- Gas laser emission fluctuations of total radiation energy, polarized field components and line widths in longitudinal magnetic field 07 p0999 A72-18911
- Systematic increase in auroral electrons mean energy with total precipitated energy 07 p1058 A72-19151
- Low energy gamma radiation spectrum from galactic center region, using balloon altitude observation 07 p1059 A72-19420
- Energy spectrum of primary cosmic ray electrons at 2-200 GeV, using balloon-borne counter telescope with gas Cerenkov counter 07 p1059 A72-19578
- Cosmic ray nuclei intensity and energy spectrum measurement in nuclear emulsions stack, noting no charge dependence in solar modulation process 07 p1059 A72-19582
- Balloon measurement of low energy cosmic gamma ray flux, obtaining energy spectrum 07 p1059 A72-19585
- Semiconductors theory for multivalley energy spectrum and multivalued equilibrium distribution of carriers during electron phonon interactions 07 p1048 A72-19641
- Isotropic turbulence spectrum based on Heisenberg theory of viscosity limiting effect on fluid motion degrees of freedom, taking into account nonlinear inertial transfer term 07 p0968 A72-19671
- Energy spectrum of radiation defects in proton bombarded n-type Si crystals from Hall effect and electroconductivity measurements 07 p1049 A72-19901
- Quantum mechanical electron motion problem in binary alloy crystal lattice, discussing Bloch approximation, energy spectra, and third element admixture conductivity effects 07 p1049 A72-20150
- Atmospheric kinetic and temperature energy spectral balances in thermally stratified turbulent flow without shear 07 p0980 A72-20454
- Cosmic ray muons integral energy spectrum and angular distribution at sea level represented by power law, using primary interaction model 07 p1063 A72-20475
- Primary cosmic rays energy spectrum at .100-1000 TeV from Proton 4 satellite data 07 p1064 A72-20629
- Primary cosmic ray particles disappearance and proton spectrum slope rise in 1 TeV energy region from Proton satellites data 07 p1064 A72-20630
- Primary cosmic rays alpha particles and protons energy spectra similarity and intensity difference at .05 to 1.6 TeV, using Proton satellites data 07 p1064 A72-20631
- Three dimensional cosmic ray anisotropy and density distribution at earth orbit and in interplanetary space with allowance for primary particle and nucleon energy spectrum 07 p1065 A72-20645
- Solar cosmic ray energy spectrum from calculation of secondary emission neutron component generation multiplicities 08 p1225 A72-20723
- Energy and angular distributions of electrons released during ion atom collisions from energy spectra studies, discussing autoionization transitions 08 p1210 A72-20836
- High energy electron precipitation events in auroral zone X rays, showing exponential daytime and flat nighttime energy spectra 08 p1226 A72-21110
- Steady state problem of energy spectrum of variable magnetic field accelerated electrons, considering synchrotron X ray emission of Crab pulsar and nebula 08 p1231 A72-21119
- High resolution rocket-borne X ray spectrometer with cooled lithium drifted semiconductor detectors for measuring differential X ray energy spectrum of SCO XR-1 08 p1168 A72-21518
- Gamma radiation source energy and activity determination for radiometric flaw detection in steel 08 p1177 A72-21775
- Post-threshold translational energy dependence of endoergic cross sections for vibrational excitation and reactive scattering of diatomic molecules by atomic or molecular impact 09 p1357 A72-22858
- Energy spectrum and decay of random two dimensional vorticity distributions at large Reynolds number [AD-740486] 09 p1294 A72-22943
- Cosmic electrons energy spectrum between 1 and 25 GeV from balloon observations, noting Compton/synchrotron loss effects [AD-745871] 09 p1377 A72-23001
- Electrical conductivity and thermal emf as function of temperature in CdSb, discussing energy spectrum and crystallization 09 p1372 A72-23479
- Scaling of energy spectrum of particles emitted in high energy nucleon-nucleon collisions 10 p1529 A72-24527
- Fully developed turbulence spectrum of incompressible viscoelastic fluids 10 p1469 A72-24534
- Neutron flux and energy spectra from crossed field acceleration model of plasma focus and z-pinch discharges 11 p1693 A72-25565
- Space charge limited current theory of thin film organic semiconductor systems, investigating energy spectrum of traps and free carrier capture kinetics 11 p1700 A72-25783
- Cosmic ray proton and He nuclei differential energy spectra measurements by balloon-borne ionization spectrometer 11 p1712 A72-25881
- Switch detector output random process energy spectrum and autocorrelation function, noting distortion reduction by proper parameter choice 11 p1605 A72-26317
- Energy spectra of multiply charged ions formed in laser beam interaction with plasma, noting recombination process role 12 p1849 A72-27065
- Antiproton energy spectrum in cosmic rays from primary proton-interstellar hydrogen collision in two fireball model 12 p1863 A72-27186
- Peak electron energy spectra during auroral substorm from high energy resolution balloon X ray measurements 12 p1804 A72-27787
- Energy spectra of mixed discrete random processes in statistical multiplexing systems with pulse position, delta and pulse code modulation 13 p1919 A72-29054
- Mathematical random fluctuation models for noise and energy spectra of pulsed processes during current passage through semiconductors 13 p2021 A72-29064
- Inner and outer belt electron differential energy spectra from Cosmos 228 satellite data, discussing fluxes of precipitating and quasi-captured particles 13 p2030 A72-29228
- Epithermal neutrons energy spectra in atmospheric equilibrium layers at 57 geomagnetic N, noting agreement with experimental error limits 13 p2030 A72-29230
- Anomalous magnetic and gravitational fields energy spectra model, examining autocorrelation functions changes 13 p1949 A72-29244
- Neutron cosmic ray spectrograph method of separating recorded data by energies, using statistical analysis of data combinations with different dead times 13 p1957 A72-29248
- Inner Van Allen zone proton energy spectrum at 30-300 MeV from ESO 2 satellite measurements 13 p2031 A72-29383
- Energy and time characteristics of Raman scattering by benzene in laser cavity as function of medium thickness and cavity length 13 p1969 A72-29523
- Solar X ray burst analysis from individual Jantata/energy and time recordings by Lunokhod 1 spectrometer 13 p2032 A72-29700
- Multiplicative factors for energy scale corrections of OSO-3 ion chamber for solar X-ray monitoring 13 p1033 A72-29748
- Satellite-borne low energy electron and proton spectrometer for measuring auroral electron and proton spectra 13 p1960 A72-29841
- ESRO 1A satellite observations of trapped and precipitated proton energy spectrum as function of invariant latitude on 8 March 1970 14 p2146 A72-30141
- Absolute intensity LEED spectra for clean Ni surfaces, discussing measurement uncertainties 15 p2276 A72-31854
- Diffuse cosmic gamma ray flux density and energy spectrum observation at equatorial balloon altitude, discussing photon count, flux and spectra 15 p2299 A72-31924
- Lunik 14 spacecraft radio signal reflection from lunar surface, showing energy spectrum dependence on surface roughness 15 p2202 A72-32655
- Atmospheric energy spectra from two dimensional synoptic scales applicable to pressure or geopotential surface variables 15 p2266 A72-32721
- Acceleration and recombination effects on ion energy spectra, discussing energy distributions of hydrogen, zirconium, lithium, and deuterium ions in laser plasmas 16 p2428 A72-32910
- HEAO experiment proposal for Be to Sn flux and energy spectra and Be to Fe isotopic composition of galactic primary cosmic rays 16 p2447 A72-33733
- N2 positive and N2+/+ band systems and the energy spectra of auroral electrons. 17 p2545 A72-34634
- Long term variations of proton flux and energy spectra in inner radiation belt during solar cycle 17 p2600 A72-35270
- Integral and differential electron energy spectra in inner radiation belt from Cosmos 219 satellite observation 17 p2600 A72-35271
- Cosmic ray electron spectrum and its modulation near solar maximum. 17 p2601 A72-35583
- Further comparison of theory and experiment for decay of homogeneous turbulence. 17 p2542 A72-35629
- Auroral electron energy spectra at high latitudes from polar auroral arcs luminosity profile examination 17 p2550 A72-35853
- Precipitation dynamics and energy spectrum of auroral electrons in the midnight sector during a magnetospheric substorm 17 p2550 A72-35854
- Structure of the power-law spectra of relativistic electrons in a turbulent plasma 17 p2593 A72-35907
- Theoretical studies of the flux and energy spectrum of gamma radiation from the sun. 18 p2721 A72-35993
- Nonthermal solar X-ray bursts origin in non-Maxwellian electron fluxes interactions with surrounding plasma, reviewing energy spectra 18 p2721 A72-36093
- Energy spectrum of interplanetary-plasma discontinuities 18 p2715 A72-36653
- Negative temperatures in two dimensional vortex motion. 18 p2681 A72-36669
- Some aspects of cosmic ray differential spectrum measurements 18 p2722 A72-36852
- Latitudinal energy distribution of geomagnetic disturbances 18 p2688 A72-36868

Galactic gamma-radiation between 200 MeV and 10 GeV.

18 p2722 A72-37008

Solar flare composition and energy spectra of heavy nuclei from 1971 rocket observations comparing to cosmic ray abundances

19 p2850 A72-37509

Observations of the solar wind with the European satellite Heos-1

19 p2850 A72-37785

Solar cosmic ray energy spectrum from calculation of secondary emission neutron component production multiplicities

19 p2852 A72-38351

Azimuthal propagation of low-energy solar-flare protons as observed from spacecraft very widely separated in solar azimuth.

19 p2852 A72-38726

Several observations of low-energy solar-proton spectra and possible interpretations.

19 p2852 A72-38727

Studies of outer belt and slot region protons at low altitudes.

19 p2853 A72-38740

An evaluation of the intensity of Cerenkov radiation from auroral electrons with energies down to 100 eV.

19 p2792 A72-38741

Cosmic ray muon sea level momentum spectra and charge ratios geomagnetic latitude dependence measurements by spark chamber technique

19 p2853 A72-38754

Cosmic-ray diffusion coefficient in interplanetary space.

19 p2853 A72-38756

Energy spectrum and composition of pulsar-accelerated cosmic rays.

20 p2964 A72-39343

Gas laser emission fluctuations of total radiation energy, polarized field components and line widths in longitudinal magnetic field

20 p2931 A72-39377

Composition of cosmic-ray nuclei at high energies.

20 p2965 A72-39716

Energy spectrum of small scale solar magnetic fields.

20 p2971 A72-39765

A balloon search for extraterrestrial high energy gamma-rays in the northern hemisphere.

20 p2965 A72-39876

Estimation of the mass composition and energy spectrum of a plasma jet from a conical pulsed accelerator

21 p3089 A72-40134

Spectrum of P Cygni in 1968-1969.

21 p3110 A72-41445

Energy and angular distributions of secondary electrons resulting from ionizing collisions of electrons with helium and krypton.

21 p3088 A72-41493

Two band superconductor state density vs energy, noting energy spectrum extremal points

21 p3098 A72-41697

Quasi-two dimensional turbulence model of energy spectra and potential enstrophy transfer in synoptic large scale quasi-horizontal atmospheric motions

21 p3049 A72-41793

Machine elements vibration parameters from dynamic model of planetary gears, noting energy spectrum, correlation and amplitude distribution functions

22 p3182 A72-42132

Equilibrium energy spectrum for the galactic cosmic electrons.

23 p3328 A72-43831

Energy spectrum and composition of primary cosmic radiation at energies from 50 to 5000 TeV

23 p3330 A72-44422

Energy spectrum and angular distribution of cascades with an energy greater than 0.3 TeV, formed by cosmic muons

23 p3331 A72-44427

Energy spectra and angular distributions of cosmic ray muons with an energy of 2 to 10 TeV

23 p3331 A72-44428

Device for studying the photonuclear interaction of superhigh-energy muons

23 p3291 A72-44440

Primary cosmic ray nucleon spectrum from sea-level muon spectrum and scaling hypothesis parameters.

23 p3332 A72-44458

Rocket measurements of electron influx during a major magnetic storm with type A aurora.

23 p3332 A72-44515

Detection of interplanetary electrons from 18 keV to 1.8 MeV during solar quiet times.

23 p3333 A72-44546

Origin of 200-keV interplanetary electrons.

23 p3333 A72-44547

Semiconductors theory for multivalley energy spectrum and multivalued equilibrium distribution of carriers during electron phonon interactions

24 p3431 A72-44572

Behavior of outer radiation zone and a new model of magnetospheric substorm.

24 p3396 A72-44850

Determination of the energy spectrum of the initial process in an amplitude gate subjected to the action of a random signal

24 p3380 A72-44897

Double hierarchy in repeated cascade theory of turbulence.

24 p3390 A72-44997

Possible explanation of non-power-law radio spectra of cosmic radio sources.

24 p3446 A72-45477

On the power law for the kinetic energy spectrum of large scale atmospheric flow.

24 p3398 A72-45483

Energy spectra of Cs⁺ ions scattered by the surface of a tungsten single crystal

24 p3429 A72-45501

Energy spectra of multiply charged ions formed in laser beam interaction with plasma, noting recombination process role

24 p3431 A72-45718

ENERGY STORAGE

NT ELECTRIC ENERGY STORAGE

NT HEAT STORAGE

Acousto-optical extraction of energy stored in pulsed He-Ne laser cavity, using modulator with piezoelectric transducer at light-ultrasound interaction region

01 p0081 A72-11322

Magnetic storm effects on neutral atmospheric composition above 400 km, discussing energy deposition

03 p0349 A72-13518

Chemical box model of energy storage in covalent bonds and nonequilibrium distributions in prebiological synthesis leading to macromolecules

04 p0482 A72-14755

Structural lipids role in accumulating light energy during prebiological evolution, using conductance studies in lipid-chlorophyll-water system

04 p0468 A72-14779

Acceleration equations for plasma injectors with capacitive and inductive energy storage elements

05 p0697 A72-16985

Geomagnetic tail role in magnetospheric substorms, discussing solar wind energy storage, magnetic merging process and plasma sheet origin

07 p0977 A72-20032

Fiber toughening mechanisms in continuous filament unidirectionally reinforced composites with elastoplastic matrices, discussing tensile energy storage in debonded region

11 p1671 A72-25463

Flight mechanics of point with limited power propulsion system and energy storage unit, investigating variational maximum payload problem with singular control optimization

11 p1727 A72-25932

Changes in total magnetic energy stored outside earth core accompanying earth dipole field decrease over 60 years period from paleomagnetic measurement

11 p1623 A72-26108

Optimization criteria for electric feeding in quasi-steady MPD thruster, discussing energy storage bank characteristics determination

[AIAA PAPER 72-462]

11 p1709 A72-26197

Coaxial plasma source energetic characteristics, establishing plasmoid energy linear dependence on battery stored energy

11 p1699 A72-26754

Acceleration equations for plasma injectors with capacitive and inductive energy storage elements

12 p1850 A72-27129

Coaxial integrated pulse generator and gas laser with double transmission line for energy storage, noting design parameters selection

12 p1823 A72-27700

Energy distribution in plasma jet as function of capacitance and energy of storage elements and storage circuit inductance

13 p2015 A72-29452

Energy storage in chromospheric magnetic flux ropes in solar flares, discussing kink perturbation instability suppression

13 p2049 A72-29936

High energy storage laser material Nd-doped silicate oxyapatite refractivity temperature dependence characteristics measurement

15 p2249 A72-32167

Stored energy function for multiaxial stress state in rubberlike materials from tensile data based on Valanis-Landel theory

16 p2472 A72-33838

Electrochemical development of high energy batteries using organic solvents, organic cathode depolarizers and fused salts

16 p2351 A72-33888

Changes in energy stores in the hypoxic heart.

17 p2501 A72-34985

Numerical calculation of energy storage, wave dispersion and propagation in waveguides of periodic resonator chains at high frequencies

18 p2657 A72-36105

Temperature change direct measurement and annealing experiment via differential power analysis to

determine stored energy release in metal plastic flow during compression

24 p3405 A72-44613

ENERGY STORAGE DEVICES

U ENERGY STORAGE

ENERGY TRANSFER

NT COUPLING CIRCUITS

Energy and momentum transfer between fields and particles in plasma crossed by transverse electromagnetic wave, investigating MHD stability

01 p0109 A72-10884

Satellite solar power stations, considering energy conversion, microwave generators and beam transfer to earth

02 p0155 A72-11770

Carbon dioxide and hydrogen mixtures in shock tube, noting rotational- and translational-vibrational energy transfer role from relaxation time measurement

02 p0203 A72-12028

Mathematical model for radiation damage cross section linear energy transfer dependence, explaining experimental values of relative biological effectiveness [CERN-71-16]

02 p0160 A72-12052

Linear energy transfer distribution for negative pions beams in human tissue, calculating relative biological efficiency and oxygen enhancement ratio [CERN-71-16]

02 p0162 A72-12064

Linear energy transfer response of polyvinyltoluene plastic scintillator, presenting data on quality factor and radiation dose equivalent determinations in mixed radiation field [CERN-71-16]

02 p0168 A72-12071

Temperature dependent gas internal diatomic laminar heat transfer, investigating continuity, energy, momentum for two dimensional flow between heated parallel plates [ASME PAPER 71-HT-N]

02 p0302 A72-12317

Isotropic turbulence energy transport approximation by local differential equation analogous to Fokker-Planck equation, noting Kolmogoroff distribution for infinite Reynolds number

02 p0205 A72-12449

Boundary layers nonlinear resonant instability, investigating Tollmien-Schlichting wave triads interactions with energy transfer from primary shear flow to disturbance

03 p0340 A72-13160

Flutter problem wing-air flow energy exchange at instability limit, obtaining vibration mode shapes from homogeneous boundary value problem analog model

03 p0442 A72-13191

Coronal magnetic fields effects on energy and mass flux from lower solar atmosphere levels into corona, discussing plasma instabilities, solar flares, radio bursts, etc

03 p0422 A72-13206

Solar wind 10-9900 eV electron flux, evaluating energy transport in plasma rest frame

03 p0412 A72-13507

Energy transfer rate from photoelectrons to thermal electrons, presenting function of three independent variables

03 p0413 A72-13532

Aluminum intergranular entropy estimation, neglecting coupling between atomic vibrations

03 p0376 A72-13969

Northern Hemisphere mean zonal flow across arbitrary horizontal surfaces, evaluating vertical transports of kinetic energy

04 p0541 A72-14454

Magnetic and gravitational energy release by resistive MHD instabilities responsible for solar flares

04 p0571 A72-14578

Solar energy exchange by thermal radiation, investigating monochromatic emission factors at 0.3-15 micron

04 p0596 A72-14702

Energetical conditions of primeval biosynthesis and transdehydration feasibility on simplified present day templates

04 p0468 A72-14757

Energetic excitation of precursor compounds in gaseous phase for models of primordial atmospheres in thermodynamic equilibrium

04 p0552 A72-14759

Energy transfer conditions of transdehydration reactions on primeval earth leading to transphosphorylation, transacylation and peptide synthesis

04 p0468 A72-14768

Electron-ion-plasmon-photon interactions and energy exchange mechanism in plasma-field/laser pulse/systems

04 p0557 A72-15155

Nitrogen to carbon dioxide vibrational energy transfer time measurement in gas dynamic laser

04 p0531 A72-15352

Electromagnetic fields and energy flow lines in waveguide bifurcations with arbitrary passive terminations

04 p0489 A72-15392

Tellegen theorem as energy conservation principle statement for energy exchange between elements in electric network

04 p0507 A72-15527

Carbon dioxide-carbon monoxide vibrational energy transfer rate at 730-2325 K from measurements following heating in shock tube
04 p0553 A72-15641

Similar unsteady one dimensional motion of viscous heat conducting gas due to sudden energy release at surface
[ASME PAPER 71-WA/HT-3] 05 p0743 A72-15864

Longitudinal wave interaction and excitation by plasma instability in equatorial electrojet, considering energy transfer mechanism
05 p0656 A72-16242

Nuclear microfusion energy recovery threshold increase during laser pulse heating process of D-T plasma
05 p0695 A72-16280

High pressure gas lasers excitation, determining energy introduction and space charge stability
05 p0668 A72-16415

Ultrahigh enthalpy gas generation by steady multicomponent flow process with kinetic energy transfer from low molecular weight gas to higher weight working medium
[AIAA PAPER 72-167] 05 p0750 A72-16979

Energy transfer to electron-photon component during hadron interaction in lead, using ionization calorimeter
06 p0869 A72-17268

K-neutral pion inelasticity factor measurement for nucleon interactions in carbon corresponding to primary neutron energy transferred to pions
06 p0869 A72-17269

Longitudinal electron plasma waves interaction with electron distribution, investigating energy transfer
06 p0858 A72-17543

Quasi-biennial modulation of kinetic energy transfer in stratosphere, comparing with hemispheric energy, eddy transports and tropical zonal wind and temperature
06 p0841 A72-17632

SNR expressions for image transmission through turbid medium, showing quality dependence on energy transfer, contrast frequency and sensor phonon illumination level
06 p0774 A72-17936

Conductive and radiative energy transfer in absorbing, emitting and conducting medium bounded by two black plates, using Milne-Eddington type absorption coefficient
06 p0903 A72-18187

Closure approximation for energy transfer mechanism of stationary locally isotropic turbulence in inertial and dissipation ranges
06 p0802 A72-18545

Spacecraft incipient failure detection, stressing acoustic energy release techniques
07 p0964 A72-18829

Electron energy distribution in carbon monoxide lasers, considering excitation effects on exchange processes, power transfer to vibration levels and vibrationally excited molecules influence
07 p0999 A72-18883

Energy transfer rates and spectral line inhomogeneity of narrow band oscillation phosphate glass and inorganic liquid lasers with Nd
07 p1004 A72-19227

Isotropic turbulence spectrum based on Heisenberg theory of viscosity limiting effect on fluid motion degrees of freedom, taking into account nonlinear inertial transfer term
07 p0968 A72-19671

Extensive atmospheric showers and high energy transfer from interacting nucleons to electron photon cascades
07 p1060 A72-19867

Energy transport within stellar structure, discussing radiative transfer and opacity relationship to mean free path of radiation
07 p1078 A72-19924

Solar corona structure and dynamics in context of energy transfer processes of dissipation, radiation, heat conduction and hydrodynamic expansion
07 p1078 A72-20006

Basic thermodynamic efficiency relationships for irreversible processes under all system circumstances, introducing high grade energy concept
07 p1101 A72-20543

Secondary gas flow effect on energy transfer distributions from plasma torches, obtaining radial distributions of current and energy flux
07 p1046 A72-20546

Electron impact cross section and energy deposition in molecular hydrogen, using generalized oscillator strength in Born-Bethe approximation
07 p1038 A72-20567

Coupled motions of rotating free solid body and elastic rod torsional bending vibrations with precession and forced vibrations from energy exchange
08 p1205 A72-20959

Dimensional metal working by material erosion involving stereomechanical energy transmission to surface of nonrigid mechanical body
08 p1173 A72-21027

Atmosphere hydrodynamic simulation model for cascade energy transfer in turbulent flow, using Euler gyro equations
08 p1158 A72-21190

Molecular rotation stimulation and deactivation of diatomic molecule addition to monatomic gas, discussing energy exchange in rarefied gas flow
08 p1211 A72-21656

Energy and momentum removal from troposphere and lower atmosphere by mountain lee wave breaking, discussing effects on atmospheric circulation evolution and maintenance
08 p1203 A72-22167

Mass and energy exchange in tropical convective cloud systems from ATS cloud photographs
09 p1344 A72-22430

High energy UV solar radiation transfer by stratospheric aerosols to biosphere, considering radiation injury to human lung
09 p1298 A72-22662

Snow-plough model of plasma acceleration for determining time dependence, gas density distribution and energy transfer
09 p1359 A72-22819

Book on heat transfer by thermal radiation, covering black body radiation, electromagnetic theory, energy exchange, Monte Carlo solution, and absorbing and emitting media
09 p1411 A72-23046

General structure steady state response under harmonic forcing in internal resonance relation, noting inertial nonlinearity effects on autoparametric interactions and energy flow
09 p1408 A72-23462

Energy transfer optimization in electromagnetic wave transmission through dispersive dielectric media
09 p1365 A72-23522

Laser heating and fusion energy recovery of D-T plasma by mechanical-magnetic cumulation, considering cylindrical wave system
09 p1365 A72-23553

One dimensional conductive and radiative heat transfer through gray medium bounded by two diffuse surfaces, noting solutions existence and uniqueness
09 p1412 A72-23586

Bent lever equilibrium and relativistic mass for point body in motion, introducing von Laue energy flow inertia into d'Alembert principle
10 p1505 A72-24074

Gravitational field angular momentum transfer analogy with Einstein gravitational energy transfer in general relativity
10 p1511 A72-24246

Shock response of two constituent composites /Elkonites/, predicting Hugoniot states with allowance for thermal energy transfer
10 p1556 A72-24259

Kinematic impact theory for inertial motion of rigid bodies of revolution and energy flow through wire grid
10 p1512 A72-24520

Energy transfer in thermally developing laminar gas flows with radiative interaction, using total band absorptance model
[AD-745475] 10 p1563 A72-25043

Contact binary star systems model, considering superadiabatic energy transfer mechanism of convective envelope
10 p1550 A72-25199

Charged particle thermodynamics in ionosphere, considering energy exchange due to collisions or thermal conductivity
11 p1621 A72-25837

Abundance in cold stellar atmospheres, noting effect on atmospheric thermal stratification and energy transfer from molecular spectra
11 p1722 A72-26432

Spacecraft propulsion based on electric energy extraction from solar wind or energy transfer from ground via plasma arcs
11 p1712 A72-26779

Resultant material and spatial energy propagation vectors for waves of small amplitude superposed on large static deformation in elastic materials
12 p1879 A72-27123

Potential or gravitational energy in Newtonian physics based on Maxwell definition, noting energy transfer
12 p1843 A72-27187

Vorticity and energy transfer equations for subsonic jet impingement on flat plate, noting turbulent jet effect on friction factor
12 p1799 A72-28171

Explicit numerical modeling method for dynamics of dense high temperature laser-produced plasmas, discussing time scale for energy transfer from electrons to ions
13 p2009 A72-28424

Galactic formation initiation mechanism with thermal instability in expanding universe, noting Compton scattering energy exchange ensuring gravitational instability dominance
13 p2039 A72-29086

Rod antenna near field energy flow direction and intensity characterization by time independent and dependent components of Poynting vector
13 p1932 A72-29398

Statistical energy analysis of sound-structural interaction, considering sound transmission through complex walls and piping systems and fluid filled container vibrations
13 p2005 A72-29556

Nonradial oscillations and energy transport in non-magnetic stationary rotating stellar wind in local theory limit
13 p2033 A72-29725

Subauroral red arcs formation mechanism involving magnetosphere-ionosphere energy conduction and lower atmosphere neutral composition changes due to turbulent mixing
13 p1952 A72-29802

Radiative energy transfer through gray gas layer between black concentric spheres at different temperatures
13 p2066 A72-30055

Solar rotation effects on solar wind magnetic energy transport by magnetic shear stress near sun
14 p2147 A72-30557

Momentum and energy equations for pool film boiling heat transfer from horizontal cylinder to saturated liquids, using integral boundary layer analysis
14 p2173 A72-31067

Small parameter method for analysis of encounter waves nonlinear self oscillations in ring gas laser, noting periodic energy transfer
14 p2111 A72-31104

Energy supply calculation for two dimensional steady laminar compressible boundary layer flows with hypersonic hydrogen-air combustion
15 p2334 A72-31465

Dislocation motions as internal friction mechanism in solids due to medium frequency acoustic waves, considering motional energy transfer to thermal phonons and lattice vibrations
15 p2292 A72-31833

Microcalorimetric investigation of energy transfer from atomic and molecular hydrogen beams to various surfaces at liquid helium temperatures and ultrahigh vacuum conditions
15 p2281 A72-31863

Atmospheric sound absorption prediction based four-gases composition and energy transfer mechanisms, comparing results with experiments at different humidities
15 p2277 A72-32020

Spherical, cylindrical or plane piston motion in nonuniform medium with radiative energy transfer, obtaining approximate analytic solutions and temperature profile behind shock front
15 p2336 A72-32394

Electromagnetic gain mechanisms with required energy supplied by static currents and magnetic fields in homogeneous plasmas
16 p2434 A72-32853

F region crossed field instability nonlinear theory based on energy transfer by mode coupling and absorption by linear damping with application to equatorial electrojet
16 p2384 A72-32976

Numerically computed momentum and energy accommodation coefficients and angular distributions of gas molecules reflected from solid crystalline surfaces applied to satellite drag calculation
16 p2430 A72-33065

Aerodynamic coefficients determination from momentum and energy exchange between low velocity molecular jet and solid surfaces, describing time of flight measurement technique
16 p2390 A72-33069

Photographic-oscillographic study of discharges in atmospheric pressure helium-carbon dioxide mixtures, discussing discharge paths nonuniformity and energy input maximization
16 p2435 A72-33391

French book on thermodynamics of equilibrium and nonequilibrium composite systems covering entropy potentials for n degrees of freedom system
16 p2478 A72-33503

Vibrational energy transfer probabilities for inelastic collisions between diatomic molecules, considering system represented by harmonic oscillators coupled by time dependent interaction potential
16 p2431 A72-33582

SNR expressions for image transmission through turbid medium, showing quality dependence on energy transfer, contrast frequency and sensor phonon illumination level
16 p2426 A72-33777

Solar wind expansion analysis with allowance for interaction with neutral interstellar matter, discussing kinetic energy loss due to EUV ionization of interstellar gas
16 p2449 A72-33910

Digital equilibrium temperature model for diurnal surface thermal and energy transfer simulation based on Myrup analog solution
16 p2419 A72-33942

- Energy transfer of thermal coupled radiation with turbulent convection in electric arcs in atmospheric air plasma
[AIAA PAPER 72-685] 16 p2480 A72-34057
- Energy transfer between flexural and extensional modes of cylindrical shells. 17 p2625 A72-34323
- Rotational excitation of rigid rotor in argon-nitrogen system, measuring energy transfer moments by particle-body and perturbation technique 17 p2585 A72-34740
- One-dimensional wave pulses in steel-epoxy composites. [SESA PAPER 1945] 17 p2631 A72-34823
- Excitation of molecular vibration on collision - Simultaneous vibrational and rotational transitions in hydrogen + argon at high collision velocities. 17 p2585 A72-35467
- On the extension of particular solutions of the energy equation of compressible turbulent boundary layers. 17 p2544 A72-35954
- Q values from lunar seismic record measurements indicating separation of scattering and real loss parameters effects on energy propagation, discussing geophysical models 18 p2724 A72-36288
- Observation of satellite modes in a beam-plasma instability. 18 p2715 A72-36600
- Energetic and topological effects in surface chemical reactions, considering intermolecular dispersion and dipole forces and chemisorption 18 p2657 A72-36828
- Self-similar motions of a viscous heat conducting gas during an abrupt energy release 18 p2683 A72-36894
- Black hole rotational energy extraction by super-radiant scattering with impinging wave amplification and by floating particle orbits with zero net radiation reaction 19 p2857 A72-37720
- Energy exchange processes in solar flares, noting initial derivation of energy from changing magnetic fields within solar atmosphere 19 p2850 A72-37782
- Influence of plasma kinetic processes on electrically excited CO₂ laser performance. 19 p2812 A72-38598
- Energy propagation in a Cauchy elastic material. 19 p2878 A72-38718
- Book - Energy metabolism of human muscle. 20 p2893 A72-39700
- Acoustic emissions and energy transfer during crack propagation. 20 p2981 A72-39957
- Determination of the form of the capture area of a receiving antenna on the basis of energy streamlines 21 p3030 A72-40525
- Wave energy exchanger for hybrid propulsion system. [ICAS PAPER 72-47] 21 p3100 A72-41172
- Elastic wave energy absorption in structures under dynamic loads, noting fatigue fracturing decrease with energy transfer into damping medium 21 p3126 A72-41540
- Energy transfer in vibration damping of pendulum with elastic suspension, noting periodic regimes and transient oscillations 21 p3086 A72-41547
- Analytic expressions for electron energy transfer rates for nitrogen and oxygen vibrational excitation in ionosphere, applying to atmospheric and ionospheric computer modeling 22 p3168 A72-42001
- A simple quadrature method for computing laminar boundary layers. 22 p3165 A72-42110
- Bending waves propagation through flat plate forming rigid sound bridge between two parallel plates, calculating energy transfer at LF oscillations 22 p3234 A72-42128
- Differential equations for energy flow between electron beam and electromagnetic field, avoiding electron trajectory explicit calculation in nonlinear treatment of cyclotron resonance interaction 22 p3159 A72-42304
- Comparison of solar-flare energy estimates made by analytical and numerical techniques. 22 p3219 A72-42426
- Multiple scattering of bending waves by random inhomogeneities. 22 p3235 A72-42460
- The moon's thermal state and an interpretation of the lunar electrical conductivity distribution. 22 p3226 A72-42531
- Pulse energy and temporal/spatial distribution of carbon dioxide laser pumped by energy transfer from vibrationally excited DF produced by deuterium-fluorine chain reaction 22 p3185 A72-42617
- Influence of the intermodal exchange on the wall heat flow in a gas possessing internal energy 22 p3244 A72-42641

- Criteria of fracture initiation from the view of fracture mechanics 22 p3239 A72-42857
- Compression of high current relativistic electron beams using converging magnetic fields. 23 p3315 A72-43525
- Variation with electron velocity powers of electron collision frequency and energy transport coefficients in weakly ionized plasmas - Earth's lower ionosphere. 23 p3285 A72-43994
- Ionization calorimeter for neutral pion production investigation in high energy hadrons interaction, noting energy transfer identity for nucleon and pion interactions 23 p3330 A72-44409
- Temperature change direct measurement and annealing experiment via differential power analysis to determine stored energy release in metal plastic flow during compression 24 p3405 A72-44613
- Energy flow diagrams. 24 p3369 A72-44686
- Shock waves role in coronal heating, solar wind and energy and material transfer to earth and in solar system 24 p3439 A72-45019
- Chemical explosion energy distribution between gases and propelled mass, discussing momentum and kinetic energy transfer 24 p3463 A72-45040
- Response of convectively controlled burning to nonlinear disturbances. 24 p3464 A72-45055
- Electronic energy transfer phenomena in rare gases. 24 p3429 A72-45310

ENGINE CONTROL

- NT ROCKET ENGINE CONTROL
- NT TURBOJET ENGINE CONTROL
- Concorde engine performance, reviewing control, reheat and exhaust systems [SAE PAPER 710775] 01 p0116 A72-10267
- Soviet book on gas turbine engines control systems design based on similarity theory, determining optimal controller formula from engine parameters 02 p0271 A72-12543
- Aircraft power plant management, discussing integration of intake, engine and exhaust system from control standpoint 03 p0405 A72-13418
- Olympus engine flight testing for relighting and anti-icing, engine control and noise and vibration assessments in support of Concorde aircraft development 08 p1224 A72-21898
- Transient characteristics and steady state off-design operation of mixed and unmixed type turbofan engines, noting peculiarities in control characteristics 09 p1374 A72-22626
- Optimal control of two shaft gas turbine engine in helicopter, using cybernetic equipment 09 p1374 A72-22862
- Propulsion control systems design for military and commercial V/STOL aircraft, considering power management performance with minimum weight and maximum reliability and maintainability [ASME PAPER 72-GT-79] 11 p1705 A72-25659
- Fluidics - A potential technology for aircraft engine control. 19 p2849 A72-38047
- A fluidic sensor for closed loop engine acceleration control. 19 p2849 A72-38049
- Fluidics control technology applications to thrust reversal, turbine engine speed, pressure valves, nozzle and fuel flow, discussing life and reliability 19 p2849 A72-38050
- NERVA flight engine control system design. 21 p3083 A72-40764
- Synthesis problems of optimum quick-response engine control systems 22 p3216 A72-42190
- Electrical components in gas turbine control systems. 22 p3216 A72-42521
- Basic considerations concerning the design of control systems 23 p3326 A72-44279
- Thermodynamic cycle parameter effects on bypass turbofan jet engine fuel consumption and performance under various flight conditions and engine ratings 23 p3326 A72-44281
- Use of modeling and simulation methods in the design of gas turbine engine control systems 23 p3326 A72-44283
- Optimal synthesis of a two-parameter continuous controller for a jet engine with an afterburner 23 p3326 A72-44284
- Planning and management requirements for aircraft jet engine control system research and development 23 p3294 A72-44285
- Synthesis of the control systems of a two-shaft helicopter gas turbine engine 23 p3327 A72-44289
- Use of fluidic elements for jet engine controllers 23 p3327 A72-44290

- Analog model of gas turbine engine control systems, using statistical estimates and flow rate, heat conduction and dynamic equations 23 p3327 A72-44293
- Nonlinear digital modeling of gas turbine propulsion units 23 p3327 A72-44294
- ENGINE COOLANTS
- Differential nonstationary heat equations numerical solution for bladed gas turbine air cooled disk, taking into account cascade vertical temperature variation and coolant heating 02 p0301 A72-12251
- Aircraft engines high pressure turbine guide vanes air cooling by internal insert, analyzing thermal stresses [AIAA PAPER 72-7] 05 p0707 A72-16866
- Turbine blade row coolant flow velocity, injection location and temperature effects on kinetic energy output [AIAA PAPER 72-12] 05 p0707 A72-16866
- Low conductivity insulating coating /graded thermal barrier/ to cool gas turbine engine with high pressure ratio and inlet temperature [AIAA PAPER 72-361] 11 p1669 A72-25389
- Turbine aerodynamics research trends, covering engine cooling, high work factor turbines, pneumatic variable geometry and computer analysis 11 p1572 A72-26036
- Heat generation sources in high speed cylindrical roller bearings for gas turbine oil cooler design 12 p1816 A72-28111
- ENGINE DESIGN
- NT ROCKET ENGINE DESIGN
- Propulsion system optimization for commercial transport aircraft design under Advanced Transport Technology study, considering impact on aircraft gross weight [SAE PAPER 710760] 01 p0115 A72-10257
- Advanced technology air transports propulsion system requirements, considering design, engine performance and reliability, maintenance, airline problems, noise and pollution control [SAE PAPER 710761] 01 p0115 A72-10258
- Solid rocket on-off and acceleration control, discussing motor concepts, thrust modulation and potential technology applications [SAE PAPER 710767] 01 p0116 A72-10262
- Graphite fiber composite fan blade design for subsonic turbofan engines, discussing weight and fatigue sensitivity reductions and performance test results [SAE PAPER 710771] 01 p0116 A72-10265
- Small three spool, reverse and mixed flow turbofan engine for business jets, discussing fuel consumption reduction, thermodynamic performance, efficiency and maintainability [SAE PAPER 710776] 01 p0116 A72-10268
- Aircraft power plant design and installation influence on operational effectiveness, discussing manufacturers and operators cooperation for reliability and maintainability enhancement [SAE PAPER 710777] 01 p0116 A72-10269
- Airline Propulsion Team approach to DC-10 aircraft power plant design for maximum operational effectiveness [SAE PAPER 710778] 01 p0116 A72-10270
- CF6 high bypass ratio turbofan engine design improvements for fuel consumption, thrust/weight ratio, starting, noise level, smoke emission, maintenance, monitoring and accessory replacement [SAE PAPER 710779] 01 p0117 A72-10271
- PT6 and JT15D gas turbine aircraft engines development and service experience 02 p0271 A72-11699
- Q/STOL jet aircraft engines design for low noise levels, describing takeoff thrust, bypass ratio and turbine stages 02 p0271 A72-12501
- Disk shaped lift engine providing additional thrust during takeoff and transition phases of V/STOL aircraft, returning to ground by jet after task accomplishment 02 p0272 A72-12900
- Propulsion twin spool power plant design and dimensioning with selective high pressure cut-off for supersonic aircraft with part of flight in subsonic range [DFVLR-SONDDR-169] 03 p0406 A72-13608
- NASA Quiet Engine experimental program for jet aircraft noise reduction, discussing aerodynamic and acoustic evaluation and tests of three fans 03 p0406 A72-13679
- GE CF6-50 high-bypass two-spool engine development, discussing configuration, installation, endurance tests and various failures 03 p0406 A72-13681
- Aircraft air breathing propulsion technology, discussing two-place aircraft, turbofan power plants, helicopter engines and V/STOL, CTOL, subsonic transports and supersonic aircraft 04 p0565 A72-14825
- Jet aircraft noise reduction, discussing engine design modifications 04 p0465 A72-15167

Soviet book on thermal and gas dynamic design of gas turbines in aircraft and liquid propellant rocket engines, covering three dimensional flows, temperature distribution, component cooling, etc
04 p0565 A72-15246

Aircraft noise measurement units and methods, discussing engine design for noise reduction
05 p0611 A72-16026

High intensity combustion chamber design for gas turbine of jet engine, considering primary, secondary and dilution zones
05 p0705 A72-16491

Aircraft gas turbine engine and components post-war development in Japan
05 p0705 A72-16499

Aircraft and reusable spacecraft propulsion systems current status and future development, discussing noise and exhaust emission problems, V/STOL bypass and fan engines, ramjets, etc
05 p0705 A72-16735

Turbine rotating disk hyperbolic thickness critical profile by radial displacement solution
06 p0894 A72-17794

Gas turbine engine inlet solid particle separator designed as integral engine part, discussing semirverse flow superiority
07 p1052 A72-18755

Inlet duct and turbofan engine compatibility without stalling and surge conditions obtained by design optimization and wind tunnel testing
07 p1052 A72-18761

Manufacturer viewpoint on aircraft engine safe introduction into airline service, discussing JT9D engine design for 747 aircraft
07 p1053 A72-18830

Influence coefficients method accuracy for design and adjustment of gas turbines, engines and parts
07 p1054 A72-18998

Hybrid rocket engine design, operation and performance, discussing optimum liquid and solid fuel combinations
07 p1055 A72-20303

Astafan turbofan engine with variable pitch fan rotor blades for thrust variation, discussing gearbox and core engine design
07 p1055 A72-20459

Commercially available aircraft turbofan engines specifications, describing design features and performance characteristics
07 p1055 A72-20625

Soviet civil gas turbine engines construction and performance, noting relatively high specific fuel consumption
08 p1223 A72-21275

Intercomponent complex annular ducts design for gas turbine engines
10 p1416 A72-23872

STOL and V/STOL transport aircraft design requirements consideration based on common propulsion and lift engine types use, noting fan lift solution superiority
10 p1421 A72-24865

T63/250 engine program current status, covering turboshaft helicopter engine and fixed wing aircraft powerplant models and applications
[SAE PAPER 720350] 11 p1703 A72-25601

Two spool geared fan jet engine design and development for general aviation, discussing performance, reliability and ecological aspects
[SAE PAPER 720351] 11 p1703 A72-25602

High bypass ratio JT15D-1 turbofan engine design and development testing
[SAE PAPER 720352] 11 p1703 A72-25603

Small radial inflow turbines for space applications, considering blade-shroud clearance, blade loading and exit diffuser design
[ASME PAPER 72-GT-42] 11 p1704 A72-25636

Variable pitch ultrahigh bypass ratio ducted fan engine design for STOL transport aircraft
[ASME PAPER 72-GT-61] 11 p1704 A72-25652

Supersonic turbine stator and rotor blading design corrected for boundary layer displacement thickness, discussing limitations due to normal shock wave at flow separation
[ASME PAPER 72-GT-63] 11 p1571 A72-25653

Integral and remote powered lift fan engines design for large civilian VTOL transports
[ASME PAPER 72-GT-65] 11 p1704 A72-25654

Propulsion system design for military VTOL aircraft, emphasizing subsonic cruise to maximum thrust ratio and exhaust downwash characteristics
[ASME PAPER 72-GT-73] 11 p1704 A72-25655

Design considerations in selecting geometries for high pressure ratio single stage centrifugal compressors
[ASME PAPER 72-GT-91] 11 p1571 A72-25665

Mixing parameter design of high loading spray type combustor for lift jet engine, using primary zone
[ASME PAPER 72-GT-99] 11 p1705 A72-25668

Steady state radial inlet pressure distortion index for axial flow compressor, examining radial velocity, continuity equation and mathematical model
[ASME PAPER 72-GT-109] 11 p1571 A72-25673

Hydrogen resistojet design and testing with Re heat exchanges, noting appropriate power efficiency and exhaust velocity for synchronous communication satellites orbital transfer
[AIAA PAPER 72-449] 11 p1708 A72-26186

Design and performance characteristics of ion thruster feed system components including high voltage isolator, liquid Hg flowmeter and W vaporiser
[AIAA PAPER 72-487] 11 p1710 A72-26213

Computer aided thermomechanical design of mercury bombardment ion thrusters, involving heat transfer, vibration and stress analysis
[AIAA PAPER 72-431] 12 p1860 A72-27420

Ion thruster module design for primary electric propulsion systems, discussing optical configurations, discharge chamber, control and performance tests
[AIAA PAPER 72-508] 12 p1860 A72-27423

Turbomeca Astafan geared fan engine with axial centrifugal compressor design, specifications and performance
12 p1861 A72-27748

Gas turbine units with constant pressure cycle, discussing design and optimization method
12 p1862 A72-28149

Russian book on theory of ramjet and rocket ramjet engines covering supersonic diffuser operational principles and design, nozzle, combustion chamber and ejector
12 p1862 A72-28346

Design and tests of dual deflectable beam strip ion thruster, noting application to two axes satellite attitude control and stationkeeping
[AIAA PAPER 72-494] 13 p2027 A72-28951

Russian papers on cooled high temperature gas turbines covering engine theory and design, power plants development, heat transfer and air cooling systems
13 p2029 A72-29925

Stage removal and addition effect on multistage axial compressor for application in engine design
15 p2179 A72-31706

Integrated data acquisition and processing system for inlet-aircraft engine matching, considering all-digital, analog and hybrid approach
15 p2298 A72-32319

RB 211 three-shaft turbofan engine for L-1011 airliner, describing design for noise reduction
15 p2298 A72-32428

Concorde engines design for maintainability and reliability to reduce turnaround time, discussing diagnostic facilities and on-wing maintenance features
15 p2298 A72-32457

Commercial transport aircraft engine technology contribution to world air transportation, considering social and ecological compatibility with community
16 p2348 A72-33314

Jet aircraft gas turbine engine technology impact on safety, reliability, airline profitability and international trade
16 p2443 A72-33315

NASA/General Electric joint development of low noise propulsion technology, describing demonstrator engine A design, components development and aerodynamic/acoustic performance evaluation
[AIAA PAPER 72-657] 16 p2443 A72-34077

F-100 and F-401 turbofan engine design and development for F-15 and F-14, discussing impingement cooling, Ti alloys, powder metallurgy and metal composites, etc
17 p2597 A72-34390

Lynx helicopter RS 360 turboshaft engine, describing modular design for maintainability
17 p2597 A72-34927

NASA program for low cost turbojet and turbofan engine fabrication for missile and light aircraft propulsion
19 p2848 A72-37637

Low pressure gas ejector operation with cylindrical mixing chamber, discussing design procedure with compression rate and ejection coefficient calculation
19 p2746 A72-37667

Pulsed-jet engine of Messerschmitt-Boelkow-Blohm without valve flaps
19 p2849 A72-38031

Influence of the structural format on the range of critical rotational speeds of rotors in aircraft engines
20 p2963 A72-39801

Quiet engine design for V/STOL and reduced takeoff and landing /RTOL/ aircraft, discussing various engine noise sources, countermeasures and tolerance levels
20 p2963 A72-39819

Russian book - The ASH-62IR engine /4th enlarged edition/.
21 p3098 A72-40463

Iterative solution to aerodynamic design of axial flow compressors used in turbojet engines, calculating meridional velocity distribution
21 p3099 A72-40930

Dimensionless pressure method to account for air density variations in gas turbine cooling system design
21 p3099 A72-41059

Theoretical and experimental study of a dual-mode ramjet /flight range from Mach 3.5 to 7/
[ICAS PAPER 72-24] 21 p3099 A72-41149

The simulation of high pressure hydrogen/oxygen rocket engines.
[AIAA PAPER 72-1027] 21 p3042 A72-41606

Elements of the theory of gas-turbine-unit designs
21 p3100 A72-41700

Engine selection for specific aircraft design and mission, considering bypass and pressure ratios and turbine temperature effects on performance and weight
[SAWE PAPER 910] 23 p3250 A72-43457

IL-62 aircraft propulsion system design and installation details, operational surveillance system and maintenance operations
23 p3325 A72-43639

Determination of the efficiency and range of application of turbines with velocity stages with the aid of the complex power coefficient
23 p3325 A72-43666

Basic dimensionless geometrical relations for the combustion chambers of aircraft gas turbine engines
23 p3325 A72-43674

Contribution to the determination of the characteristics of a gas turbine engine for a helicopter and to the choice of the throttling law
23 p3326 A72-44277

Basic considerations concerning the design of control systems
23 p3326 A72-44279

Design features of Soyuz life support and launch escape systems and Vostok rocket booster stage
23 p3343 A72-44335

Gas turbine wheel design analysis, presenting procedures for estimating revolution rates, blade numbers and component configurations effects on wheel weight for prescribed stresses
24 p3460 A72-45737

ENGINE FAILURE

STOL aircraft roll moment control possibility for externally-blown jet flap due to engine failure
02 p0154 A72-11700

Lubrication system filtration effects on rolling element bearing life and extended mean time to failure of gas turbine engines
07 p1052 A72-18754

Aircraft gas turbine engine monitoring for failure prevention, evaluating condition through spectrum analysis and real time correlation techniques
07 p1053 A72-18766

Engine out flight training safety, recommending certification requirements or training procedures changes
07 p0911 A72-18834

Attack helicopters engine failure problems, discussing flight test results in transition from powered high speed flight to autorotational flight
08 p1108 A72-21011

Russian book on aircraft engine reliability covering defects, fractures and failure analysis, service life prediction, production deficiencies and operational conditions
11 p1706 A72-26068

Hydraulic transmission for driving helicopter tail rotor, noting compensatory system for engine failure
12 p1755 A72-27862

Russian book - The ASH-62IR engine /4th enlarged edition/.
21 p3098 A72-40463

Signal classification through quasi-singular detection with applications in mechanical fault diagnosis.
22 p3158 A72-41976

ENGINE INLETS

Dusty inlet air filtering in aircraft turbine engines, discussing engine operation, dust and filter characteristics
05 p0704 A72-16179

Turbine inlet temperature sensor for gas turbine engines, using noble metal thermoelements with high signal level
[SAE PAPER 720160] 06 p0812 A72-17322

Simulated testing of turbojet engine ingestion of missile exhaust, determining design criteria for aircraft engine inlets from altitude chamber test data
07 p1052 A72-18758

Turbine inlet gas temperature limiting systems design and operation in turboprop engines, describing blocking mechanism, delaying element and altitude compensation
12 p1861 A72-27863

Integrated data acquisition and processing system for inlet-aircraft engine matching, considering all-digital, analog and hybrid approach
15 p2298 A72-32319

Engine inlet total pressure distortion effects on multistage axial compressor and turbojet/turbofan engine performance and stability, considering inlet-engine compatibility
[ICAS PAPER 72-19] 21 p2991 A72-41144

Calculation of the recirculation flow of VTOL lift engines.
[ICAS PAPER 72-42] 21 p3099 A72-41167

Installation caused flow distortion and its effect on noise from a fan designed for turbofan engines.
[AIAA PAPER 72-1006] 21 p2993 A72-41590

Axissymmetric jet stretcher diffuser performance for ramjet engine inlet configurations, testing at angles of attack and supersonic flow velocities
[AIAA PAPER 72-1024] 21 p2993 A72-41602

Wall porosity and angle of attack effects on jet stretcher flow field for supersonic engine inlet testing, using three dimensional method of characteristics [AIAA PAPER 72-1025] 21 p3042 A72-41603

Full-scale inlet/engine testing at high maneuvering angles at transonic velocities. 21 p3042 A72-41604 [AIAA PAPER 72-1026]

Analytical method for combining the interaction of inlet distortion and turbulence. 23 p3247 A72-43330

ENGINE MONITORING INSTRUMENTS

Flight display systems current state and future developments, discussing dual attitude indicators and automatic chart systems CRTs, engine displays and malfunction warning systems 03 p0357 A72-13423

Aircraft integrated data systems application to flight safety analysis, engine performance monitoring, crew proficiency, autoland evaluation, operations and logistics 04 p0495 A72-14726

Display device for engine rotational speed nonuniformity parameters indication on oscilloscope without supplementary computation 05 p0662 A72-16125

Aircraft gas turbine engine monitoring for failure prevention, evaluating condition through spectrum analysis and real time correlation techniques 07 p1053 A72-18766

Engine condition monitoring - The Pan Am approach: Phase II. 17 p2597 A72-35324

Automated airborne recording system to obtain data on aircraft engines, subsystems and operational performance, considering cost and economic benefits [AIAA PAPER 72-752] 19 p2802 A72-38126

In-flight and flight-line monitor system to detect foreign object damage in jet engines. 22 p3179 A72-42690

ENGINE NOISE

NT ROCKET ENGINE NOISE

Jet aircraft turbofan engine fan compressor noise reduction by acoustic linings, giving R and D results [BAS PAPER 71 SA6] 01 p0115 A72-10223

Aircraft engine noise effects in airport vicinities, discussing measurement scales, turbofan sources, noise reduction and future air traffic 02 p0154 A72-12022

Air breathing propulsion systems for reducing engine noise level, discussing stoichiometric gas turbine engines, V/STOL propfans and variable-geometry supersonic inlet and exhaust nozzles 03 p0406 A72-13486

Aircraft industry noise reduction efforts to meet FAA requirements for CTOL and STOL aircraft, emphasizing turbofan and compressor noise suppression and/or attenuation 04 p0565 A72-14820

Turbojet engine noise causes and reduction techniques, noting U.S. antinoise standards 04 p0465 A72-14925

Sound attenuation in lined rectangular ducts with uniform steady flow, considering aircraft engine noise reduction 04 p0565 A72-15267

Jet engine silencing plug nozzle suppressor configurations acoustic and thrust performance measurements [AIAA PAPER 72-160] 05 p0706 A72-16826

Army aircraft gas turbine engines pollution potential evaluation program, considering smoke emission, noise and invisible pollutants 07 p1053 A72-18772

Engine fan-compressor maximum noise reduction for given aircraft configuration by acoustic linings on nacelle inlet and exhaust walls 07 p1054 A72-19268

JT8D engine exhaust noise field, considering internal noise sources contribution from exhaust duct sound pressure measurements 07 p1054 A72-19331

Turbojet and turbofan engines noise signatures and sonic boom effects, discussing frequency spectra, atmospheric attenuation and noise suppression systems 07 p0912 A72-20163

Acoustical theory application to jet engine noise reduction, developing mathematical model for blade shock wave spacing in noise generation process 07 p1055 A72-20542

Turbofan engine trends for short haul conventional and STOL aircraft, considering variable pitch fans, reduction gears, thrust reversal and noise and environmental pollution [ASME PAPER 72-GT-86] 11 p1705 A72-25661

NASA quiet engine program, discussing noise reduction technology for subsonic civil transport aircraft propulsion system [ASME PAPER 72-GT-96] 11 p1705 A72-25667

Open-air jet engine test stand for flame stabilization, jet and compressor noise studies, noting provisions for rapid installation changes 12 p1795 A72-27416

Bibliography on noise control covering surface transportation, machinery and aircraft noise, industrial criteria, biodynamics, legislation and measurement 13 p2006 A72-29588

Digital data processing techniques for aircraft engine noise data reduction, analyzing fan noise spectrum 13 p1925 A72-29840

Lift fan blade interaction discrete frequency noise, discussing potential and viscous interactions relation to rotor-stator spacing 15 p2297 A72-32019

Low noise aircraft-engine configuration feasibility, discussing turbofan engine noise reduction 15 p2181 A72-32322

NASA/General Electric joint development of low noise propulsion technology, describing demonstrator engine A design, components development and aerodynamic/acoustic performance evaluation [AIAA PAPER 72-657] 16 p2443 A72-34077

Effect on supersonic jet noise of nozzle plenum pressure fluctuations. 17 p2597 A72-35243

NASA R and D programs for quiet STOL aircraft and engines development 18 p2721 A72-36503

Combustion noise generation by burning fuel-air mixtures induced pressure fluctuations as result of time variable heat release rate due to turbulence 18 p2741 A72-36505

Aircraft noise problem in piston engine to turbofan jumbo jet transports, discussing need for noise reduction research [AIAA PAPER 72-815] 19 p2750 A72-38117

Turbulent combustion induced noise, discussing scaling rules for sound power and directional characteristics of radiated sound 20 p2984 A72-39557

Quiet engine design for V/STOL and reduced takeoff and landing (RTOL) aircraft, discussing various engine noise sources, countermeasures and tolerance levels 20 p2963 A72-39819

NASA Quiet Engine program R and D on conventional takeoff and landing subsonic cruise aircraft engine noise [ICAS PAPER 72-48] 21 p3100 A72-41173

Installation caused flow distortion and its effect on noise from a fan designed for turbofan engines. [AIAA PAPER 72-1006] 21 p2993 A72-41590

NASA's quiet engine programs. 22 p3217 A72-43152

Experiment of supersonic air intake buzz. 23 p3249 A72-44496

Tone noise from rotor/stator interactions in high speed fans. 24 p3433 A72-44917

ENGINE PARTS

High pressure gaseous hydrogen effect on space shuttle main engine components alloys under static loads, using surface flawed flat plate PTC samples 01 p0085 A72-10774

Electrodischarge and electrochemical machining applications in continuous repetitive production of aircraft jet engine components 01 p0078 A72-11150

Jet engine component overhaul procedures for fatigue damage repair, detailing distressed metal removal, replacement and welding techniques 02 p0271 A72-12499

Aircraft gas turbine engine and components postwar development in Japan 05 p0705 A72-16499

Influence coefficients method accuracy for design and adjustment of gas turbines, engines and parts 07 p1054 A72-18998

Statistical evaluation for forged jet engine parts tensile tests cost reduction, using regression analysis 07 p0995 A72-19484

Diffusion welding of cast and wrought Udimet 700 superalloy gas turbine engine components, discussing interfacial grain boundary migration and microstructural homogeneity effects on weld joint quality 07 p0997 A72-19998

Recrystallized silicon carbide and reaction bonded silicon nitride as construction materials for gas turbine engine components, describing thermal and mechanical properties [ASME PAPER 72-GT-20] 11 p1673 A72-25619

Countersink boring machines with programmed digital control systems for precision spacing multiple hole drilling in extended aircraft engine components 11 p1642 A72-26816

Boron and carbon fiber reinforced plastics applications in aircraft and engine structural components, discussing dynamic and impact damping properties compared to conventional materials 13 p1982 A72-28555

Air dust erosive damage to helicopter gas turbine engine parts, discussing inertial rotorless filtering systems 13 p2026 A72-28786

Aircraft engine components fatigue life assessment under small cycle temperature conditions, including temperature field and stress-strain determination in critical spot 14 p2145 A72-30279

Radiographic measurement of gas turbine components during response to thrust changes, using linear accelerator for X ray generation 14 p2092 A72-30620

Aircraft gas turbine engine Ni base alloy disks and shafts thermomechanical treatment, considering yield strength and high and low cycle fatigue resistance 16 p2406 A72-33299

Russian book - Production of the principal elements and units of aircraft engines 17 p2560 A72-35456

Stress concentration coefficients calculation at sharp cracks and notches for engine parts in tension, compression and combined bending and torsion 24 p3458 A72-44932

ENGINE STARTERS

Airstart flight testing for single engine fighter/attack aircraft, including flight conditions, windmilling, fuel flows, gas temperature, ignition and acceleration 06 p0868 A72-18496

Onboard and ground based hydraulic starter systems design, construction and operation for aircraft turbine engines 08 p1224 A72-21484

Hydraulic starter systems for aircraft turbine engines, examining operation loads and fluid supply and pressure requirements 11 p1702 A72-25284

Low-explosive actuated mechanical devices to actuate switches and valves, sever cables or bolts, dispensing fluids, inflating bags or starting engines 16 p2442 A72-33359

The starting of turbine engines in helicopters. [AHS PREPRINT 662] 17 p2597 A72-34509

ENGINE TESTING LABORATORIES

Arnold Engineering Development Center turbine engine testing facilities and techniques for flight conditions and environment simulation, air/fuel flow and thrust measurement, etc [ASME PAPER 71-WA/GT-8] 05 p0642 A72-15901

Aircraft engine anti-icing tests and evaluation describing ground and airborne techniques [AIAA PAPER 72-162] 05 p0706 A72-16828

Open-air jet engine test stand for flame stabilization, jet and compressor noise studies, noting provisions for rapid installation changes 12 p1795 A72-27416

ENGINE TESTS

NT COLD FLOW TESTS

NT SPACE ELECTRIC ROCKET TESTS

Augmentor wing jet STOL research aircraft development progress report covering design, engine tests, performance prediction, control simulation and stability augmentation [SAE PAPER 710757] 01 p0003 A72-10254

Ten mlb concentric tubes biowaste resistojel thrust performance for hydrogen, water, methane, carbon dioxide and biopropellant mixtures, discussing vibration, shock and acceleration tests [SAE PAPER 710769] 01 p0116 A72-10263

Graphite fiber composite fan blade design for subsonic turbofan engines, discussing weight and fatigue sensitivity reductions and performance test results [SAE PAPER 710771] 01 p0116 A72-10265

Thermal shock fatigue tests on aircraft gas turbine engine inlet nozzles, showing cracks as function of material 01 p0143 A72-11373

NASA Quiet Engine experimental program for jet aircraft noise reduction, discussing aerodynamic and acoustic evaluation and tests of three fans 03 p0406 A72-13679

GE CF6-50 high-bypass two-spool engine development, discussing configuration, installation, endurance tests and various failures 03 p0406 A72-13681

Automated jet engine development facility, discussing assembly and test area and computer controlled operation [ASME PAPER 71-WA/GT-6] 05 p0642 A72-15899

USAF small gas turbine test complex, discussing machinery, equipment, simulated testing, altitude chambers and instrumentation [ASME PAPER 71-WA/GT-7] 05 p0642 A72-15900

Jet engine test facilities for JT9D experimental and production models [ASME PAPER 71-WA/GT-12] 05 p0642 A72-15904

F-14 Tomcat test program for hydraulic systems, spinning, low speed performance, stalling, afterburning turbofan engines, in-flight refueling and automatic telemetry equipment 06 p0758 A72-17582

Fighter/attack aircraft turbojet and turbofan engines testing with/without afterburners 06 p0868 A72-18495

Airstart flight testing for single engine fighter/attack aircraft, including flight conditions, windmilling, fuel flows, gas temperature, ignition and acceleration 06 p0868 A72-18496

Catapult steam ingestion test of turbofan engines in A-7 aircraft, correlating compressor stall occurrences with temperature increase rate in distorted region 07 p1052 A72-18760

Circumferential inlet pressure distortion index derivation for high hub-tip ratio multistage axial flow compressor from one dimensional isentropic flow expressions 07 p1053 A72-18762

Aircraft engine test data processing by polynomial relations, assuming normal measurement error distribution 07 p0994 A72-187978

Hybrid rocket engine design, operation and performance, discussing optimum liquid and solid fuel combinations 07 p1055 A72-20303

Temperature measurements of axial gas turbine rotor for start-up heating and cooling tests 08 p1223 A72-20953

Accelerated full scale aircraft turbine engine corrosion tests in controlled environment, simulating salt, high temperature and humidity conditions [NACE PAPER 76] 10 p1528 A72-24320

Dynamic model of high bypass ratio turbofan engines for L-1011 wind tunnel flutter test program [AIAA PAPER 72-376] 11 p1703 A72-25400

Cessna 210 aircraft electrically driven hydraulic power pack for landing gear system, noting engine and flight tests [SAE PAPER 720327] 11 p1577 A72-25589

High bypass ratio JT15D-1 turbofan engine design and development testing [SAE PAPER 720352] 11 p1703 A72-25603

Four stage gas turbine, measuring blade surface roughness and profile changes effects on flow characteristics and efficiency [ASME PAPER 72-GT-34] 11 p1704 A72-25630

Electric propulsion spacecraft design for ion thruster systems testing with circular solar cells array as gyroscopic stable platform [AIAA PAPER 72-466] 11 p1578 A72-26200

RF ion thruster for spacecraft propulsion, discussing tests and digital computer calculations to optimize design parameter [AIAA PAPER 72-474] 11 p1709 A72-26205

Ion thruster performance calibration investigating double ion content, back ingestion, beam spreading and propellant flow rate [AIAA PAPER 72-475] 11 p1709 A72-26206

Cs contact ion microthrusters, neutral fraction measurements, analytical methods and testing procedures [AIAA PAPER 72-495] 11 p1711 A72-26218

Prime 30 cm ion thruster power conditioning and control system development, integration and testing [AIAA PAPER 72-509] 12 p1860 A72-27424

Composite materials application to gas turbine fan guide vane fabrication, noting economic factors and prototypes performance in engine tests 12 p1815 A72-28100

Gas turbine engine hot part equivalent tests duration determination by analytical method based on Larson-Miller parametric description of stress rupture strength 12 p1887 A72-28243

Rocket engines simulated high altitude testing, using multiple stage ejector augmented supersonic diffuser system 13 p1938 A72-28692

Design and tests of dual deflectable beam strip ion thruster, noting application to two axes satellite attitude control and stationkeeping [AIAA PAPER 72-494] 13 p2027 A72-28951

Two stage solid propellant sounding rocket, discussing engine design, operation and tests 13 p2052 A72-29859

Procedure for the continuous sampling and measurement of gaseous emissions from aircraft turbine engines. [SAE ARP 1256] 18 p2721 A72-36532

The S4MA hypersonic wind tunnel - Its use for tests of ramjet engines with supersonic combustion of hydrogen 19 p2783 A72-37823

Blade passage measurement with the aid of a graphite pin probe in the case of fluid flow engines 19 p2804 A72-38724

Axisymmetric jet stretcher diffuser performance for ramjet engine inlet configurations, testing at angles of attack and supersonic flow velocities [AIAA PAPER 72-1024] 21 p2993 A72-41602

Wall porosity and angle of attack effects on jet stretcher flow field for supersonic engine inlet testing, using three dimensional method of characteristics [AIAA PAPER 72-1025] 21 p3042 A72-41603

Full-scale inlet/engine testing at high maneuvering angles at transonic velocities. [AIAA PAPER 72-1026] 21 p3042 A72-41604

Characteristics of an ejector-type engine simulator for STOJ. model testing. [AIAA PAPER 72-1028] 21 p3042 A72-41607

Digital computer technique and real time monitor software application to instrumentation data acquisition system, discussing design guidelines and gas turbine engine test example 22 p3156 A72-42681

Digital computer controlled testing equipment for separately driven coaxial gas turbine low and high

pressure compressors, emphasizing reliability and flexibility in system design 22 p3157 A72-42682

High response two-transducer pressure measurement for evaluating nonuniform and unsteady inlet flow distortion effects on supersonic jet engine stability and performance 22 p3216 A72-42683

Development of a rocket propulsion system with 500 kgf vacuum thrust for liquid hydrogen/liquid fluorine 23 p3325 A72-43620

Experience with the NRC 10 ft. x 20 ft. V/STOL propulsion tunnel - Some practical aspects of V/STOL engine model testing. 23 p3278 A72-44247

Aircraft gas turbine engine controllers and fuel pump testing under extreme fuel temperatures, noting cavitation characteristics 23 p3327 A72-44287

Mathematical model for dynamics simulation of aircraft turboprop engines, using digital, analog and hybrid computers 23 p3327 A72-44288

Development and testing of a radioisotope-fueled thruster for spacecraft propulsion. 24 p3434 A72-45178

Experimental performance of coaxial injectors in thrust-variable LO2/GH2-rocket engines. 24 p3434 A72-45181

The development of GH2/GO2-pulse mode rocket engines in the thrust range of 6,660-9,340 N /1,500-2,100 lbs/. 24 p3434 A72-45207

Test facilities for aeropropulsion systems, emphasizing utilization, cost and technical advantages, aircraft inlet-engine systems compatibility and test types [AIAA PAPER 72-1034] 24 p3388 A72-45401

ENGINEERING

Book on computer applications to engineering analysis covering mathematical models, numerical techniques, program usage, programming and design 05 p0632 A72-16106

Computer aided engineering - Conference, Waterloo, Canada, May 1971 07 p1024 A72-18776

ENGINEERING DEVELOPMENT

U PRODUCT DEVELOPMENT

ENGINEERING MANAGEMENT

Utility function construction for engineering plants quality criteria 09 p1413 A72-22216

Technological forecasting in venture analysis and planning for long-term growth objectives, engineering project selection and resource allocation [ASME PAPER 72-DE-26] 14 p2174 A72-30868

S-3A aircraft weight control program organization and methods, considering cost and schedule performance [SAWE PAPER 906] 23 p3250 A72-43453

Cost estimation for engineering proposals in competitive bidding, discussing cost variability quantification methods based on PERT assumptions 24 p3468 A72-45478

ENGINEERING TEST REACTORS

Measurements with thermionic fuel elements in the ITR critical facility. 18 p2645 A72-36181

ENGINES

NT AIR BREATHING ENGINES

NT ALGOL ENGINE

NT ARC JET ENGINES

NT BOOSTER ROCKET ENGINES

NT CONTROL ROCKETS

NT DIESEL ENGINES

NT DUCTED ROCKET ENGINES

NT ELECTRIC ROCKET ENGINES

NT ELECTROSTATIC ENGINES

NT ELECTROTHERMAL ENGINES

NT GAS TURBINE ENGINES

NT HELICOPTER ENGINES

NT HOT WATER ROCKET ENGINES

NT HYBRID PROPELLANT ROCKET ENGINES

NT HYDRAZINE ENGINES

NT HYDROGEN OXYGEN ENGINES

NT INTERNAL COMBUSTION ENGINES

NT ION ENGINES

NT JET ENGINES

NT LIQUID PROPELLANT ROCKET ENGINES

NT MICROROCKET ENGINES

NT NUCLEAR ENGINE FOR ROCKET VEHICLES

NT NUCLEAR ROCKET ENGINES

NT PISTON ENGINES

NT PLASMA ENGINES

NT PULSED JET ENGINES

NT PULSEJET ENGINES

NT RAMJET ENGINES

NT ROCKET ENGINES

NT SOLID PROPELLANT ROCKET ENGINES

NT SUPERSONIC COMBUSTION RAMJET ENGINES

NT TURBINE ENGINES

ENTHALPY

NT TURBOFAN ENGINES

NT TURBOJET ENGINES

NT TURBOPROP ENGINES

ENGRAVING

Photoanodic engraving process produced high bit density surface relief holograms on semiconductor crystals for data storage, retrieval and replication applications 21 p3054 A72-40614

ENHANCEMENT

U AUGMENTATION

ENLARGING

U EXPANSION

ENSKOG-CHAPMAN THEORY

U CHAPMAN-ENSKOG THEORY

ENSTATITE

Enstatite chondrite Abec isotopic ratios of Gd, Sm and Eu comparison with terrestrial samples 16 p2457 A72-33566

ENTHALPY

Plasma source with arc stabilized by supersonic air stream, measuring enthalpy, heat flux and potential distribution 01 p0048 A72-10491

Thermodynamic properties of gases at high temperatures, tabulating composition, enthalpy, entropy and thermal conductivity of combustion products with ion seeding 01 p0145 A72-11202

Partial molar enthalpy measurement of oxygen mixture in substoichiometric Zr at 1300 C, using Tian-Calvet microcalorimeter 02 p0170 A72-12167

Compressible boundary layer flow problems, using weighted residuals method with exponentials in velocity and enthalpy approximations 02 p0204 A72-12258

Heat transfer in rectangular annular channel during external heating under supercritical pressure, discussing thermal flux, mass flow rates and enthalpy 03 p0457 A72-14152

Contact surface turbulent mixing instability in free piston high enthalpy shock tunnel waves with test air and argon gases 05 p0644 A72-16548

Electrofluid-dynamic wind tunnel velocity augmentation by enthalpy addition during expansion at constant static pressure and temperature for aerospace vehicles flight conditions simulation [AIAA PAPER 72-166] 05 p0645 A72-16831

Ultrahigh enthalpy gas generation by steady multicomponent flow process with kinetic energy transfer from low molecular weight gas to higher weight working medium [AIAA PAPER 72-167] 05 p0750 A72-16979

Compressibility and total enthalpy difference effects on laminar free shear layer from numerical integration of equations of motion 05 p0653 A72-17011

Binary and ternary alloys of Cr and Fe with Ni, determining interaction coefficient and molar enthalpy for Cr at 1600 C by mass spectrometry 05 p0676 A72-17103

Burning gunpowder surface reactions relative to temperature, chemical enthalpy and acoustic waves of pressure, velocity and density 05 p0751 A72-17211

Enthalpy measurements of niobium silicides at 1200-2200 K by mixing method, using isothermic calorimeter 06 p0833 A72-18431

Radiative cooling effect on enthalpy distribution in air behind incident shock waves produced in explosively driven shock tubes 06 p0904 A72-18529

Cu electrical resistance and heat content oscillographic measurement, using high voltage pulse method 07 p0981 A72-18804

Alpha Ti plastic deformation behavior below 700 K, determining activation area and enthalpy as functions of stress and temperature 08 p1186 A72-21247

Calorimetric measurement of dissolution heat and partial enthalpy limit of Ga in Sn at 969 K 10 p1526 A72-24237

Levitation calorimetry for solid and liquid Mo enthalpy measurement, calculating specific heat and heat of fusion 10 p1496 A72-24243

Vanadium enthalpy and heat of fusion measurement with massive copper calorimeter 10 p1497 A72-24784

Enthalpy measurements of allotrop transformation of Co alloys during hcp-fcc transition with additive elements 10 p1498 A72-24850

Burning gunpowder surface reactions relative to temperature, chemical enthalpy and acoustic waves of pressure, velocity and density 11 p1744 A72-25337

Boundary layer theory for convective heat transfer of two dimensional film cooling systems in turbulent regime, noting momentum, enthalpy and concentration equations 13 p2063 A72-28630

- Vanadium enthalpy and heat of fusion measurement using massive copper calorimeter with isothermal jacket 14 p2113 A72-30222
- Experimental data gathering, processing and presentation for materials enthalpy, heat capacity, thermal conductivity, compressibility and volume over wide pressure and temperature ranges 14 p2130 A72-30599
- Sudden freeze approximation for fluid flow systems relaxation time at constant enthalpy and pressure 17 p2542 A72-35633
- A contribution to the gas dynamics of oblique shocks with change of total enthalpy. 18 p2682 A72-36725
- Enthalpy and heat capacity of boron carbide at temperatures ranging from 273 to 2600 K 18 p2704 A72-37191
- Temperature probes for flows at high enthalpy [ONERA, TP NO. 1074] 19 p2800 A72-37767
- Volume and enthalpy changes at critical point of condensed state, noting Ar enthalpy dependence on temperature 19 p2881 A72-38045
- Temperature distribution in hot wires in high-enthalpy low-density flows [DFVLR-SONDRD-216] 19 p2804 A72-38685
- Total enthalpy measurement from blunt body gas cap emission in arc-heated wind tunnels - Results and application. [AIAA PAPER 72-1021] 21 p2993 A72-41599
- Enthalpy and specific heat of tantalum carbide over the temperature range from 273 to 3600 K 22 p3187 A72-41890
- Velocity, enthalpy and turbulent energy distributions calculation for plane wake behind flat body by asymptotic solution based on turbulence theory 23 p3249 A72-44083
- Electric resistance and enthalpy of molybdenum and tungsten 23 p3272 A72-44167
- ENTIRE FUNCTIONS**
- Infinite series summation in terms of rapidly convergent definite integrals 05 p0682 A72-15808
- Real rational function Cauchy index computed from integral functions of polynomial coefficients and signature of infinite class of matrices 07 p1026 A72-18817
- Time optimal control of distributed systems with random properties, considering n integral relations and flying wing vehicle torsional vibration problems 10 p1421 A72-24427
- Limiting value of the lower indicator, and lower bounds for integral functions with positive zeros 20 p2947 A72-39863
- A note on algebraic differential equations whose coefficients are entire functions of finite order. 22 p3198 A72-41948
- The growth of entire solutions of differential equations of finite and infinite order. 24 p3418 A72-44725
- ENTRAINMENT**
- Ionic winds with restricted entrainment and gauge electrode, considering diffusion flame aeration in combustion systems 07 p1037 A72-19372
- Entrainment interface evolution in turbulent flow, examining surface slope discontinuities and curvature and overall speed of advance 10 p1467 A72-24332
- Axisymmetric turbulent jets local entrainment rate as function of axial distance from nozzle exit, using Ricou-Spalding porous wall technique 10 p1481 A72-24425
- Dislocation damping by point defects entrainment, calculating internal friction force rate dependence based on weak interactions continuum model 10 p1527 A72-24979
- Three dimensional compressible turbulent boundary layer growth prediction, deriving entrainment equations from two dimensional incompressible flow relations 16 p2375 A72-32835
- The intrinsic structure of turbulent jets. 18 p2684 A72-37201
- ENTRENCHED STREAMS**
- U STREAMS**
- ENTROPY**
- Thermodynamic properties of gases at high temperatures, tabulating composition, enthalpy, entropy and thermal conductivity of combustion products with ion seeding 01 p0145 A72-11202
- Pressure drop relation to entropy production in viscous low velocity adiabatic pipe flow, showing analogy with Oswatitsch theorem 01 p0051 A72-11255
- Weather forecasting, discussing statistical entropy, numerical and statistical methods and computer technology utilization 02 p0254 A72-12777
- Aluminum intergranular entropy estimation, neglecting coupling between atomic vibrations 03 p0376 A72-13969

- Superposable and self-superposable MGD flows from nonlinear differential equations, considering entropy, flow velocity and magnetic field strength 05 p0694 A72-16030
- Plane Couette flow of incompressible non-Newtonian viscous fluid between parallel plates, using minimum entropy production variational principle 06 p0798 A72-17779
- Incompressible fluid turbulent flow variational principles, discussing Malkus principle for maximum dissipation rate and minimum entropy production principle for convective and dissipative systems 06 p0800 A72-18116
- Entropy effect in two dimensional conditional reflex decision situations upon rats central nervous analysis-synthesis processes 07 p0925 A72-20661
- Minimal dynamic systems invariant Borel probabilistic measure with metric space and topological entropy equality 08 p1210 A72-22187
- Shock wave profile equation derivation based on minimal entropy rate variational principle for stationary irreversible processes, using local potential for Boltzmann type equation 09 p1295 A72-23473
- Probability density functions shape estimation by deterministic heuristic and entropy maximization algorithms 10 p1442 A72-23798
- Bayes analysis application to Weibull distribution parameters estimation, using entropy concept for figure of merit to assess reliability analysis 10 p1444 A72-23987
- Small scale flow and surface effects in multiphase media hydromechanics, obtaining entropy production in mixture for interphase transformations characterization 10 p1468 A72-24430
- Chernikov approximation for general relativistic thermodynamics nonstationary equations of heat transfer, thermal and viscous stresses and entropy balance 12 p1844 A72-27188
- Lunar rock and mineral shock melting and vaporization from hypervelocity meteoroid impacts, calculating entropy, phase changes and thermal equilibrium 14 p2155 A72-30520
- Nonlinear thermoelasticity theory extension via entropy production inequality theorem, deriving expressions for stress tensor and heat conduction vector 16 p2465 A72-32980
- Entropy waves effect on gas pressure oscillations during powder combustion in semiclosed volume, noting resonant frequencies equation 16 p2475 A72-33096
- French book on thermodynamics of equilibrium and nonequilibrium composite systems covering entropy potentials for n degrees of freedom system 16 p2478 A72-33503
- Entropy and chemical change. I - Characterization of product /and reactant/ energy distributions in reactive molecular collisions: Information and entropy deficiency. 17 p2511 A72-34738
- On the first-exursion probability in stationary narrow-band random vibration. II. [ASME PAPER 72-APM-16] 17 p2628 A72-34800
- Closed rotating cosmologies containing matter described by the kinetic theory - Entropy production in the collision time approximation. 17 p2618 A72-35823
- Caratheodory classical thermodynamics formulation presented in mathematically rigorous form by differential geometry and topology methods 18 p2741 A72-36508
- Method of Lagrange multipliers for exploitation of the entropy principle. 19 p2825 A72-37842
- Muller entropy principle-imposed restrictions on thermodynamic and thermostatic constitutive relations for fluids in electromagnetic fields 19 p2834 A72-37843
- Relativistic thermodynamics development based on invariant entropy concept, considering frictionless heat conduction and Carnot cycles 19 p2835 A72-37928
- Propagation and growth of shock waves in inhomogeneous fluids. 19 p2787 A72-38430
- Pressure propagation rate relation to local sound speed in unsteady anisentropic gas flow with particle-varying specific entropy 19 p2788 A72-38564
- Black hole physics compatibility with thermodynamics second law formulation based on black hole area as entropy measure 21 p3085 A72-41216
- A non-equilibrium thermodynamic theory of simple materials based on a single-integral thermodynamic functional. 21 p3124 A72-41505
- Entropy criterion in the estimation of the dynamic quality of automatic control systems 21 p3039 A72-41803

- Entropy and simple waves in multidimensional gas flow. 22 p3166 A72-42314
- Isobar-isothermal potentials, entropy and formation heat of chromium silicides from thermoelectromotive force measurements of high temperature galvanic elements 23 p3298 A72-43286
- Stimulated entropy /temperature/ scattering and its influence on stimulated Mandelstam-Brillouin scattering 23 p3297 A72-44478
- Necessary conditions for steady state in radiation - Matter interaction and the role of entropy. 24 p3461 A72-44806
- Effect of a flow with a stagnation point on the rate of variation of the total entropy of a fluid mixture 24 p3465 A72-45074
- Information theory and statistical mechanics applications to thermodynamics, discussing entropy and superiority of Georgian to Kelvin temperature scale 24 p3465 A72-45372
- Some reflections on the nature of entropy, irreversibility and the second law of thermodynamics. 24 p3465 A72-45628
- ENUMERATION**
- Algorithms for combinatorial problem optimal solution based on implicit enumeration method, applying to assembly line balancing 12 p1837 A72-28117
- ENVELOPES**
- Peak parametric envelope calculation for hf pulse transients 06 p0773 A72-17571
- Consequences of the Stromgren's theorem for radiative envelope stars. 18 p2728 A72-36760
- Studies of hydrodynamic events in stellar evolution. II - Dynamic instabilities in stellar envelopes. 19 p2854 A72-37234
- Mixing between stellar envelope and core in advanced phases of evolution. IV - Effect of superadiabaticity in convective envelope. 23 p3335 A72-43486
- Effect of envelope limiting in pulse-compression moving-target-indicator radar systems. 24 p3380 A72-45575
- ENVIRONMENT MODELS**
- ATS F/G spacecraft thermal control design verification by chamber thermal balance tests and performance prediction mathematical model of earth viewing module and orbital environment 12 p1877 A72-27527
- Mathematical expression for pilot incapacitation applied to data from high stress/short duration encounters with environmental problems 12 p1775 A72-28284
- ENVIRONMENT POLLUTION**
- NT AIR POLLUTION**
- NT WATER POLLUTION**
- Land pollution remote sensing, discussing economic and political impact in terms of land use, transportation, energy supplies and recreational opportunities [AIAA PAPER 71-1039] 01 p0057 A72-10523
- Environmental pollution sensing by vibrational laser Raman scattering probe measuring species constituency and temperature, discussing fluorescence, scattering cross sections and band shape [AIAA PAPER 71-1084] 01 p0067 A72-10541
- Spaceborne Fourier interference spectrometer for environmental pollutant sensor, discussing IR detection systems, instrument servo, data reduction and handling systems and optical tolerance [AIAA PAPER 71-1108] 01 p0067 A72-10552
- Miniaturized magnetic mass spectrometer for trace contaminants continuous monitoring and control, discussing applications to closed atmospheric systems in spacecraft and undersea environments [AIAA PAPER 71-1122] 01 p0068 A72-10558
- Laser fluorosensor for remote environmental probing, considering applications to oil slick mapping, locating lignin sulphate pollution sources and hydrologic monitoring of tracer dye dispersal [AIAA PAPER 71-1121] 01 p0080 A72-10559
- Air law concept as totality of legal regulations related to atmosphere use by flying devices, discussing relation to international environmental protection 01 p0147 A72-11107
- Artificial satellites for earth resources and environmental contamination control, discussing remote sensing physical problems and earth surface radiative characteristics 02 p0207 A72-11778
- Pollution and environmental quality remote sensing, describing five dimensional sensor/applications matrix for decision guidance 02 p0212 A72-11827
- METROMEX field project to investigate inadvertent weather modification by urban-industrial effects and man-made precipitation changes 03 p0384 A72-13636
- Automated electromagnetic pollution data acquisition systems for environmental ecology, discussing

computer technique and data retrieval, analysis and storage
03 p0328 A72-14040

Pollution free electrical power generation from solar energy, discussing microwave transmission to earth, power shortages, thermal pollution and solar cell manufacture cost
[ASME PAPER 71-WA/SOL-2] 05 p0614 A72-15892

Remote sensing methods applications to environmental protection, discussing microwave, radar, IR, optical and acoustical active and passive methods
[DGLR PAPER 71-132] 06 p0809 A72-18229

Solar energy conversion as pollution-free power source, discussing silicon solar cells, power transmission techniques, satellite solar power stations and system control and guidance
06 p0893 A72-18625

Power generation for electrical, thermal and transportation needs, considering technology use for air, noise, thermal, water and nuclear pollution reduction
06 p0761 A72-18627

National Environmental Policy Act /PL 91-190/ impact on Army aircraft turbine engine development in terms of performance, additional cost and time
07 p1053 A72-18773

Space and atmosphere contamination by industrial wastes, aircraft and spacecraft exhaust and radioactive waste disposal, considering legal safeguards
07 p1104 A72-19466

Classification of mass spectra on computers /COM-SOC/ for compound characterization of complex mixtures with geochemical and environmental applications
07 p0980 A72-20393

Ultrastructural and morphometric studies of beryllium oxide-contaminated environment effect on monkey and dog lung tissue
07 p0925 A72-20686

Turboprop engine trends for short haul conventional and STOL aircraft, considering variable pitch fans, reduction gears, thrust reversal and noise and environmental pollution
[ASME PAPER 72-GT-86] 11 p1705 A72-25661

Acoustical environment pollution control, considering noise annoyance effects due to industry and construction, surface and air traffic, alarm devices, radio and TV, etc
13 p2067 A72-29554

United Nations activity in international space program for earth resources and environmental pollution surveillance by satellites
15 p2220 A72-31227

Satellite observation of earth surface, discussing remote sensing techniques application in pollution control and ecology
15 p2319 A72-31232

Gases and vapors spectral signatures application in correlation spectroscopy and interferometry for aerospace monitoring of earth resources and pollution
16 p2393 A72-33630

Potential applications of NASA-developed technology to problems of the environment.
[ASME PAPER 72-ENAV-23] 20 p2895 A72-39154

Aircraft gas turbine engines environmental effects, considering thermal radiation, acoustic emissions and exhaust gases in relation to propulsion system design parameters
23 p3328 A72-44296

ENVIRONMENT SIMULATION
NT ACOUSTIC SIMULATION
NT ALTITUDE SIMULATION
NT SPACE ENVIRONMENT SIMULATION
NT THERMAL SIMULATION
NT WEIGHTLESSNESS SIMULATION

Laboratory simulation of Jovian atmospheric reactions, observing amino nitriles formation
04 p0572 A72-14764

Acceleration force simulation for altered weight effect on animal tolerance to restraint, discussing body mass loss, reduced lymphocyte count and disorientation
04 p0472 A72-14866

Stress corrosion crack tip electrochemical reactions simulation on Ti and alloy surfaces, using modified rotating disk apparatus with pH measurement
04 p0536 A72-15739

Condenser microphones sensitivity and frequency response characteristics measurement at normal and elevated atmospheric pressures in hyperbaric chamber air and He-air environments
06 p0766 A72-17808

R and D management policies choices with respect to Bayesian decision-theoretic model in simulated environments
07 p1105 A72-19553

Lunar laser reflectors specifications and fabrication procedures, discussing lunar environment simulator and optical test equipment, techniques and results
07 p0947 A72-20261

Astronaut training obtained visually in lunar module simulator via film, spacecraft models and landing site relief models as sources for complex TV system
08 p1147 A72-21335

ATC systems analysis by computerized real time environmental simulation, taking into account new aircraft types, navigation and supervision aids
09 p1348 A72-22782

Venus probes thermal insulation materials development and testing under simulated Venus atmospheric conditions
[AIAA PAPER 72-368] 11 p1744 A72-25393

Safe aircraft fuels crashworthiness evaluation in terms of ignition susceptibility parameter, noting full scale crash environment simulation
[ASME PAPER 72-GT-27] 11 p1702 A72-25623

Simulated gravity environment tests of vertical jump features, recording work performed, body center of gravity upward velocity, potential and kinetic energy changes
12 p1770 A72-27479

Man computer weapons effectiveness and system test environment /WESTE/ instrumentation system with Decca navigation for simulated combat environmental flight tests
12 p1754 A72-27515

Mathematical model for numerical simulation of warm fog modification by seeding hygroscopic particles, taking into account turbulent diffusion and horizontal wind advection
13 p1992 A72-28844

Multiscale numerical model for local weather development simulation, noting forecasting for long distance air travel
13 p1993 A72-28857

Meteorological-astronomical diurnal and seasonal environmental rhythm simulation for psychological stresses alleviation in long term space missions
13 p1910 A72-29322

Surface pressure and vector wind fields computerized analysis from satellite radar radiometer simulation and conventional data
13 p1995 A72-29619

Environmental chamber simulation to show terrestrial microorganisms survival under Jovian atmospheric conditions
15 p2183 A72-31293

Multi-environment reliability test program for airborne electronic systems under simulated temperature, humidity, vibration and shock conditions
15 p2215 A72-32616

Spacecraft boom deployment dynamics environmental simulation and testing for preflight system reliability evaluation
15 p2321 A72-32627

Materials characteristics relevance for USAF technology, discussing processing conditions, environment simulation, real time techniques, ultrasonic and X ray inspection methods, etc
16 p2404 A72-32823

A method for simulating wind conditions during atmospheric stagnation periods.
20 p2947 A72-38965

Computer program to simulate electromagnetic signal densities, data rates and power from land based radar transmitters as functions of time and location
20 p2902 A72-38992

FOSS - A dynamic six degree-of-freedom environmental simulator for evaluation of electro-optical guidance systems.
[AIAA PAPER 72-862] 20 p2911 A72-39135

Simulation in plasma wind tunnels of the environmental conditions for sounding rocket experiments
20 p2912 A72-39928

Application of an agar-agar chamber for the study of electromagnetic waves in an inhomogeneous medium.
21 p3015 A72-40359

Digital computer equipped facility for training simulators environmental simulation capability testing, describing electronics interface, control and display equipment
22 p3164 A72-42928

A sight simulation technique using TV-screen perspective correction for restricted maneuver flight missions
24 p3388 A72-45298

A practical evaluation of earth-backscatter simulation and an estimate of the HF ground-scatter coefficient.
24 p3380 A72-45636

ENVIRONMENT SIMULATORS
NT SOLAR SIMULATORS
NT SPACE SIMULATORS

Hailstone impact simulator for prediction of hail damage to aircraft structures, presenting data on damage to flat metal sheets and spherical caps
[AIAA PAPER 72-163] 05 p0645 A72-16957

Cascade wind tunnel and water table determination for trajectories and velocities of suspended particles in fluid flow through axial compressor stage
07 p0907 A72-18756

Night Carrier Landing Trainer flight and carrier environment simulator for A-7 aircraft pilot training, discussing performance predictions from computer data analysis
07 p0927 A72-19137

Hailstone impact simulator for aircraft damage prediction in testing prospective structural designs
13 p1938 A72-28855

USAF aerospace medical research on human capabilities as limiting factor in defense systems development, discussing environmental simulators and human test facilities
21 p3008 A72-40973

ENVIRONMENTAL CHAMBERS
U TEST CHAMBERS

ENVIRONMENTAL CONTROL
Nonflammable coolants for Saturn instrument unit environmental control systems, considering component materials compatibility with selected dielectric fluids
01 p0091 A72-10769

Mathematical models for man-machine control behavior in biodynamic environments including manual control performance and interface elements
03 p0318 A72-13162

Short haul operating systems in air transportation environments, discussing terminal vs cruise configurations, costs and noise abatement
03 p0309 A72-13422

Supercooled and warm fog dispersion technology, considering air heating, helicopter downwash and seeding methods
04 p0543 A72-14812

Facility for electron microscopy of specimens in controlled environments, observing lattice structure in wet catalase crystals
07 p0993 A72-20586

Malfunction detection for space station environmental/thermal control and life support system, using onboard computer
[AIAA PAPER 72-241] 10 p1423 A72-24447

Hot water ejector application to environmental control, considering noise suppression, air and gas purification and dust particles precipitation
10 p1460 A72-24491

Lungs fibrosis and cancer caused by asbestos fibers inhalation, noting environment control for protection against workers health hazards
11 p1583 A72-25548

Pilots seating active and passive isolation from I.F vibrations in helicopters and jet aircrafts, discussing human factors and dynamic environment
13 p1910 A72-29558

Private and governmental regulatory aspects of environmental noise abatement and control, discussing legal efforts and trends at local, state and federal levels
15 p2340 A72-32614

Aero engines and propulsion systems development contribution to air transport economics and regularity, considering environmental factors
16 p2443 A72-33313

U.S. federal regulation on occupational noise exposure control for hearing loss prevention, discussing noise measurement, reduction and periodic tests
16 p2358 A72-33324

Optimal temperature control for microbial inactivation by composite environment of heat and gamma radiation, using quadratic technique
18 p2649 A72-36313

Canadian program for global environmental and world resources monitoring system, discussing management, technology and user interface
[AIAA PAPER 72-742] 18 p2742 A72-36548

Environmental considerations in airport development.
18 p2743 A72-36778

What's new in airport planning.
18 p2675 A72-36780

Space station prototype environmental/thermal control and life system - A current overview.
[ASME PAPER 72-ENAV-35] 20 p2894 A72-39143

Development of a laboratory prototype spraying flash evaporator.
[ASME PAPER 72-ENAV-28] 20 p2894 A72-39149

Design criteria for the modular space station environmental control and life support system selection.
[ASME PAPER 72-ENAV-25] 20 p2894 A72-39152

Space station atmospheric revitalization system design, covering temperature, humidity, carbon dioxide, contaminant and oxygen generation and composition control and vehicle configuration
[ASME PAPER 72-ENAV-24] 20 p2894 A72-39153

Environmental control and life support subsystem conceptual design studies for shuttle launched 6-12 man crew modular space station
[ASME PAPER 72-ENAV-22] 20 p2895 A72-39155

Significant factors in environmental and thermal control/life support system design for space shuttle orbiter
[ASME PAPER 72-ENAV-21] 20 p2895 A72-39156

Optimal shuttle research applications module /RAM/ environmental control and life support system for sortie missions
[ASME PAPER 72-ENAV-20] 20 p2895 A72-39157

Comparative evaluation of environmental control and life support systems for the space shuttle orbiter.
[ASME PAPER 72-ENAV-19] 20 p2895 A72-39158

Space shuttle environmental temperature control-life support system program changes, discussing air cooled electronic equipment, cryogenic stores, crew size and mission duration
[ASME PAPER 72-ENAV-18] 20 p2895 A72-39159

- Modular environmental control/life support system design for low cost shuttle launched space station, evaluating humidity, carbon dioxide, water and waste management [ASME PAPER 72-ENAV-17] 20 p2895 A72-39160
- Computer simulation of the space shuttle orbiter environmental thermal control system. [ASME PAPER 72-ENAV-12] 20 p2896 A72-39165
- Integration of an automated onboard data management system with a manned spacecraft environmental thermal control and life support system. [ASME PAPER 72-ENAV-6] 20 p2896 A72-39171
- Effects of environment on formation of finished surface in drilling aluminum and aluminum alloys. 21 p3060 A72-40936
- Theoretical model, laboratory experiments and in situ measurements by instrumented sailplane for investigating cloud and precipitation formation physics relationship to atmospheric pollutants cleansing 23 p3311 A72-44263
- R and D on environmental and thermal control/life support system application to lunar base mission, discussing reliability and food regeneration 24 p3375 A72-45164
- The role of the United Nations in earth resources satellites. 24 p3468 A72-45185
- The Space Station Prototype Program - The development of a regenerative life support system for extended-duration missions. 24 p3375 A72-45193
- High level cleanliness maintenance and contamination control for instrument unit ring guidance system in Saturn 5 launch vehicle 24 p3388 A72-45297
- ENVIRONMENTAL ENGINEERING**
- Acoustic echo sounder as real time monitor of airport environmental meteorological parameters 01 p0103 A72-11137
- Environmental research with instrumented aircraft, discussing application to operational forecasting and weather modification experiments in hurricanes and tropical convective clouds 04 p0542 A72-14682
- Remote sensing methods applications to environmental protection, discussing microwave, radar, IR, optical and acoustical active and passive methods [DGI R PAPER 71-132] 06 p0809 A72-18229
- Environmental effects on aircraft and propulsion systems - Conference, Trenton, N.J., May 1971 07 p1052 A72-18751
- Collaboration of World Health Organization and various international astronomical organizations for space technology applications to man-environment relationships and medical and communication sciences 07 p0933 A72-20300
- Sonic boom research facilities and techniques, emphasizing applicability to other environmental problems 09 p1262 A72-23317
- Aircraft pilot seating protection from dynamic environment by active vibration isolation, discussing human frequency response characteristics 11 p1585 A72-26391
- Environmental effects on aircraft structure operational reliability, discussing failure removal and protective coating lifetime 14 p2072 A72-30285
- Environmental progress - Conference, New York, May 1972 15 p2191 A72-32601
- Si solar cell design for high power/weight ratio and extreme environmental operating conditions, describing technological innovations for reliability and efficiency enhancement 19 p2754 A72-37780
- Potential applications of NASA-developed technology to problems of the environment. [ASME PAPER 72-ENAV-23] 20 p2895 A72-39154
- Mathematical model for MOS transistor circuit analysis, noting parameters measurement and environmental effects representation 20 p2909 A72-39783
- Acoustic pressure and sound intensity levels and noise annoyance international standards for civil aircraft noise reduction 20 p2888 A72-39803
- Ground humidity and wind velocity effects on terrestrial scintillation, considering adiabatic temperature stratification factor 21 p3007 A72-40738
- Techniques for dealing with the effects of bad weather in satellite communications systems. 21 p3017 A72-40856
- Flying personnel auditory defects caused by environmental conditions, discussing aircraft noise, vibrations and atmospheric pressure effects 21 p3002 A72-40924
- ENVIRONMENTAL LABORATORIES**
- EOSS - A dynamic six degree-of-freedom environmental simulator for evaluation of electro-optical guidance systems. [AIAA PAPER 72-862] 20 p2911 A72-39135

ENVIRONMENTAL RESEARCH SATELLITES

- Satellite communication regional and domestic applications, discussing educational, earth resources, geological survey, environmental and maritime uses 04 p0487 A72-15073
- NASA developed geostationary weather and environmental satellite for launch in 1973, discussing ground station equipment, antenna system and data collection service 23 p3343 A72-43551

- Weather satellites - Their role in the application of environmental services to the marine industries. 24 p3420 A72-44648

ENVIRONMENTAL TEMPERATURE**U AMBIENT TEMPERATURE****ENVIRONMENTAL TESTS****NT COLD WEATHER TESTS****NT CORROSION TESTS****NT HIGH TEMPERATURE TESTS****NT LOW TEMPERATURE TESTS****NT SALT SPRAY TESTS****NT UNDERWATER TESTS**

- Monograph on stress corrosion failure, covering threshold stresses, fracture mechanics, electrochemical processes, hydrogen embrittlement, corrosion, various steels and alloys, environmental effects, etc 01 p0082 A72-10166

- Interim automatic scanning multichannel data acquisition system for environmental test laboratory, using programmable calculator 02 p0200 A72-12477

- Low temperature liquid bath tests for IC environmental reliability, monitoring wire bonding, metallization, surface contamination, sealing and die bonding 03 p0337 A72-14296

- Microorganism life in extreme high temperature, PH and solute concentration environments, noting salt effect on enzyme activity 04 p0471 A72-14801

- Composite materials testing with four point loading method, studying environmental and creep effects in flexure 04 p0537 A72-15091

- External biodynamic models for human mechanical response to various environmental forces, emphasizing injury mechanisms [AD-736985] 04 p0481 A72-15266

- Ti-Al-Mo-V alloy sustained load stress corrosion crack growth in salt and distilled water environments 04 p0534 A72-15570

- Planar coax micropackaging of minicomputers for aircraft navigation and military systems, noting environmental tests 05 p0632 A72-15772

- Fatigue crack growth rate testing in gaseous environments at nonambient pressure and temperature in test chamber 05 p0643 A72-16186

- Environmental tests on carbon fiber Vulcan air-brake flap, including thermal cycling, sustained loading, immersion, corrosion and lightning strike tests 05 p0681 A72-16998

- Plastic encapsulated transistors and IC moisture resistance tests for reliability under laboratory and field conditions 06 p0782 A72-17363

- JT15D turbofan engine antiicing system development, discussing icing test program and results 07 p1053 A72-18769

- C-54 A/B aircraft engine air particle separator anti-ice system design features, manufacturing techniques and testing 07 p1053 A72-18769

- Turboprop electric igniter climatic test problems and equipment for assessing quality control 07 p0954 A72-19112

- Environmental hydrogen embrittlement of Ti-Al alloy as function of test displacement rate and microstructure variation 07 p1016 A72-19933

- Lunar and terrestrial soil thermal and electrical properties measurement in vacuum and He atmospheres 08 p1232 A72-21150

- Sounding rocket payloads environmental testing, discussing test techniques for shock, vibration, temperature, humidity, pressure, contamination, corrosion effects during handling, storage, launch, flight and recovery 08 p1241 A72-21173

- Adverse environmental effects on epoxy composites resin-glass interface properties, investigating epoxy-compatible silanes contribution to composite performance 08 p1194 A72-21696

- Climatic load effects on carrying capacity of thick walled glass reinforced polymer rings with residual stresses 08 p1195 A72-21765

- Ceramics in severe environments - Conference, North Carolina State University, Raleigh, December 1970 09 p1333 A72-22376

- Silicon nitride ceramics resistance to thermal shock and stress in severe environments 09 p1334 A72-22386

- Sonic booms effects on domestic and wild animals, discussing field and laboratory findings 09 p1267 A72-23322

- Field and laboratory sonic boom simulators, noting required characteristics 09 p1292 A72-23323

- Environment and grain size effect on steady state creep and creep rupture properties of Ni-W solid solution 09 p1331 A72-23381

- Thermal shock and temperature cycling environmental testing, discussing military specifications, components thermal lag characteristics, environmental test chambers and various cooling methods 10 p1459 A72-24144

- Environmental sensitivity effect on crack propagation rates in steels and Al and Ti alloys, discussing corrosion fatigue 10 p1499 A72-24899

- Space and ground environments effect on cryogenic multilayer insulation materials, tabulating mechanical and thermophysical test data [AIAA PAPER 72-286] 11 p1741 A72-25225

- Organic matrices in structural composites, considering mechanical behavior, processability and properties in adverse environments 11 p1674 A72-26230

- High voltage electron microscope applications to materials reactions in gaseous environments, exemplifying by stress corrosion morphology in stainless steel, Al-Zn-Mg and Ti-Al 11 p1668 A72-26945

- Performance and environmental tests of large lightweight solar array unit, measuring structural members displacements with electro-optical instruments [AIAA PAPER 72-569] 12 p1755 A72-27377

- ATS F Environmental Measurements Experiment package for synchronous altitude space environment and electromagnetic-ionospheric interactions studies 12 p1795 A72-27525

- Semiconductor strain gage design and environmental performance for flight control systems 12 p1812 A72-27962

- Solar cells array design and assembly techniques, discussing tests for Esro satellites aerospace environments 12 p1758 A72-28033

- Protective coatings for corrosion prevention of high strength steels under environmental conditions of humidity, salt fog, tap and salt water immersion 12 p1835 A72-28157

- Parotid fluid 17-hydroxycorticosteroid level relation to hyperthermia stress at various heat levels during thermal environmental testing 12 p1768 A72-28335

- Materials selection for contact and clearance type seals for various environment conditions [ASLE PREPRINT 72AM 23] 13 p1964 A72-28975

- Soviet wind tunnel for power plant-environment interactions studies, discussing working sections velocity distributions calibration 13 p1939 A72-29644

- Explosives life limitation due to aging phenomena, discussing chemical and physical processes and environmental effects 14 p2143 A72-30752

- FRAM /failure rate appraisal machine/ concept and application for modular electronic and electromechanical assemblies environmental cycling tests, noting technical and economical effectiveness 14 p2093 A72-31169

- Computerized analytical system for side-looking radar imagery interpretation by isodensitracer scanned density data multivariate analysis applied to environmental discrimination 15 p2198 A72-32064

- Irradiation system for animal and human subjects exposure to controlled microwave radiation in environmental tests 15 p2191 A72-32573

- Computer controlled random environment test systems for large scale off-line data analysis and reduction, using Fourier analyzer 15 p2204 A72-32609

- Prediction models for dynamic environment experienced by cargo during air and rail transportation 15 p2339 A72-32610

- Low temperature environmental chamber for F-111 proof load testing, describing components of cold air forced convection recirculation system with liquid nitrogen injection 15 p2214 A72-32612

- Lunar roving vehicle qualification program to meet performance specifications under lunar conditions, describing testing procedures and project management techniques 15 p2214 A72-32613

- Multi-environment reliability test program for airborne electronic systems under simulated temperature, humidity, vibration and shock conditions 15 p2215 A72-32616

- Organization and management requirements for environmental testing laboratory from viewpoint of test results, data handling, analysis and test reporting 15 p2340 A72-32617

Dynamic input to cargo in turbojet aircraft studied during C141 and C5A flights, discussing instrumentation, test procedures, data reduction processes and results
15 p2181 A72-32625

Spacecraft boom deployment dynamics environmental simulation and testing for preflight system reliability evaluation
15 p2321 A72-32627

Temperature effect on fatigue crack growth in high strength annealed Ti-Al-V alloy in water, oxygen/hydrogen and vacuum environments
16 p2406 A72-33320

Helicopter/ship dynamic interface testing for launch and recovery capabilities under sea environment conditions, discussing visual landing aids, wind, visibility and ship motions
[AHS PREPRINT 650] 17 p2491 A72-34505

Cythere capsule for irradiation of experimental fuel elements under geometric and thermal conditions representative of thermionic converters
17 p2579 A72-34619

Experimental determination of the aeroacoustic environmental about a slender cone.
[AIAA PAPER 72-706] 17 p2486 A72-35482

Blood oxygenating ability of helium- and argon-oxygen environments relative to air, using alveolar gas equation to predict arterial oxygen pressure
18 p2649 A72-36438

The effects of environment on the elevated temperature fatigue behavior of nickel-base superalloy single crystals.
18 p2700 A72-36587

Electrical changes in the surface region of chalcogenide glasses.
19 p2822 A72-37454

Lunar and terrestrial soil thermal and electrical properties measurement in vacuum and He atmospheres
20 p2968 A72-39255

Changes in the wear resistance of polymer surface layers in aggressive and biologically active media
21 p3072 A72-40081

USAF aerospace medical research on human capabilities as limiting factor in defense systems development, discussing environmental simulators and human test facilities
21 p3008 A72-40973

Inert gas effects on embryonic development.
22 p3145 A72-42744

Thermal balance in man during 24 hours in a controlled environment
22 p3145 A72-42747

Influence of a preliminary exposure to carbon monoxide on the development of hypokinetic disturbances in albino rats
23 p3255 A72-43909

Fatigue behavior of a titanium 8Al-1Mo-1V alloy in a dry argon environment.
23 p3304 A72-44261

ENVIRONMENTS

NT AEROSPACE ENVIRONMENTS

NT CHROMOSPHERE

NT CISLUNAR SPACE

NT DEEP SPACE

NT EARTH ENVIRONMENT

NT EXTRATERRESTRIAL ENVIRONMENTS

NT HIGH ALTITUDE ENVIRONMENTS

NT HIGH GRAVITY ENVIRONMENTS

NT HIGH TEMPERATURE ENVIRONMENTS

NT INNER RADIATION BELT

NT INTERPLANETARY SPACE

NT INTERSTELLAR SPACE

NT IONOSPHERE

NT JUPITER ATMOSPHERE

NT LOW TEMPERATURE ENVIRONMENTS

NT LOWER IONOSPHERE

NT LUNAR ATMOSPHERES

NT LUNAR ENVIRONMENT

NT MAGNETOPAUSE

NT MAGNETOSPHERE

NT MARS ATMOSPHERE

NT MARS ENVIRONMENT

NT MESOPAUSE

NT MESOSPHERE

NT MIDLITUDE ATMOSPHERE

NT PLANETARY ATMOSPHERES

NT PLANETARY ENVIRONMENTS

NT ROTATING ENVIRONMENTS

NT SOLAR ATMOSPHERE

NT SPACECRAFT ENVIRONMENTS

NT STELLAR ATMOSPHERES

NT THERMAL ENVIRONMENTS

Friction and adhesive and abrasive wear of ceramics, discussing effect of environmental water and hydrocarbons
15 p2260 A72-32129

ENZYME ACTIVITY

NT FERMENTATION

Hypophysectomy in rats, resulting in prolonged red blood cell survival due to oxygen consumption decrease and altered erythrocyte enzymatic processes
01 p0010 A72-10075

Starvation effects on male rats, mice and guinea pigs hepatic drug metabolism, discussing ethylmorphine, p-nitroanisole and aniline
01 p0015 A72-11262

Alpha-L-fucosidase, beta- and alpha-D-galactosidases and alpha-D-mannosidase activity changes in human placenta at various embryogenesis phases
02 p0163 A72-12294

High altitude hypoxia effects on rat myocardium lactic dehydrogenase isozyme complement and anoxic tolerance
02 p0165 A72-12834

Alpha amino acids proteinoids or thermal polymers enzyme activity, investigating hydrolytic activities and decarboxylation reactions
04 p0483 A72-14776

Biochemical processes and structures interrelation, using nucleoprotein coacervate models and ribonuclease and polynucleotide phosphorylase enzymes
04 p0469 A72-14783

Coacervate drops oxidoreductases and stability in primitive prebiological systems, using polyphenol oxidase-carbohydrate-histone-quinones
04 p0469 A72-14784

Primitive earth model of ion selective enzymatic asymmetric synthetic membrane for accelerated nutrients and metabolites transfer studies
04 p0469 A72-14787

Microorganism life in extreme high temperature, PH and solute concentration environments, noting salt effect on enzyme activity
04 p0471 A72-14801

Serum enzyme activity changes response to constant test exercise, discussing relation to maximum oxygen uptake
04 p0472 A72-14897

Plasma renin activity during supine physical exercise as function of salt loading
04 p0480 A72-15214

Catalytic action in organic catalyst predecessors of contemporary enzymes, discussing polymers of alpha-amino acids and hydrogen cyanide
05 p0624 A72-16128

Myokinase activity determination as diagnostic test for human myocardial infarction, comparing to creatine phosphokinase activity test
05 p0618 A72-16388

Conformal electron interactions in biopolymer and hypermolecular biological systems, discussing calcium ions effects, enzyme activity, muscle contractions and information theory
07 p0915 A72-18803

Kinetics of heat inactivation of phosphoglycerate kinase in soluble fraction from hydrogenomonas facilis
07 p0922 A72-20237

Effect of salt on activity, stability and allosteric properties of catabolic threonine deaminase from extremely halophilic bacteria
09 p1275 A72-22535

Ribonuclease molecule damage and enzyme activity under UV irradiation and repeated freezing and thawing
09 p1274 A72-23594

Parenterally introduced protein hydrolyzates and aminopeptidase influence on human pancreas enzyme secretion activity
09 p1268 A72-23595

In vitro measurements of oxygen tension effect on teleost and amphibian retinal lactate dehydrogenase activity, discussing acetazolamide produced hypoxia effects
10 p1424 A72-23729

Pressure sensitivity of Na-K-Mg ATPase activity from rat intestine, investigating inhibiting effects of oxygen, nitrogen and helium tension increases
10 p1424 A72-23731

Thermolabile triose phosphate isomerase in psychrophilic Clostridium at moderate temperatures
10 p1426 A72-24750

Serum petidase activity determination as enzymatic diagnostic test for myocardial infarction
11 p1579 A72-25851

UV light production of free radicals in proteins and model compounds in vacuum and low temperatures, using EPR techniques
12 p1778 A72-27223

Heart enzyme activity under experimental myocardial ischemia in rabbits determined for blood, left and right ventricles and atrium
13 p1901 A72-28463

Cardiac membrane pain sensitivity in vagotomized cats under sensitizing acetylcholine influence during reduced cholinesterase activity
13 p1905 A72-29329

Epithelial follicle and mast cell role in peroxidase activity of thyroid gland during experimental burn development
13 p1905 A72-29330

Urease-active colloidal organo-complex extraction from Dublin clay loam soil, describing filtration procedure
13 p1913 A72-29399

Mechanical vibration induced physiological changes in rats, determining plasma Ca, Mg and inorganic phosphate concentration and xanthine oxidase activity response to frequency and g-levels
13 p1910 A72-29560

Macaca nemestrina monkey organ tissue concentrations of lactic dehydrogenase /LDH/, creatine phosphokinase and aldolase, with electrophoretic determination of LDH isozymes
13 p1906 A72-29861

Enzyme activity and ascorbic acid concentration as index of rat thyroid gland tissue functional activity during hyperthermia
14 p2077 A72-31098

Succinic dehydrogenase activity in rabbit eye ciliary epithelium during electric stimulation of hypothalamus, using histochemical techniques
14 p2078 A72-31099

Physiological effects on prolonged weightlessness in dogs aboard Cosmos 110 biosatellite, emphasizing body weight loss and enzyme activity and bone tissue mineral concentration changes
16 p2354 A72-33547

Effect of Acetazolamide /Diamox/ at different dose levels on survival time of rats under acute hypoxia and on Na⁺/K⁺-ATPase activity of rat tissue microsomes.
17 p2499 A72-34546

Magnetic field effects in enzymes, tissue respiration and some metabolism characteristics of an intact organism
17 p2503 A72-35003

Dipeptidyl aminopeptidase. I - Application in sequencing of peptides.
17 p2511 A72-35167

Studies of the electron transport chain of extremely halophilic bacteria. VII - Solubilization properties of menadiene reductase.
19 p2755 A72-37649

Hypocapnic hypoxia effects on blood coagulation and fibrinolysis
19 p2756 A72-37880

Renin in differential diagnosis of hypertension.
19 p2757 A72-38144

Peripheral venous renin activity during 70 deg tilt and lower body negative pressure.
19 p2758 A72-38703

Proteinase activity in different regions of the brain during development and inhibition of a conditioned passive-avoidance reflex
20 p2890 A72-38927

Variation of the acetylcholine content and of the cholinesterase activity in the blood under muscular strain
20 p2891 A72-38934

The resonance mechanism of the biological action of vibration
20 p2897 A72-39409

Effects of simulated high altitude on renin-aldosterone and Na homeostasis in normal man.
21 p3005 A72-40422

Blood serum enzymes activity changes in polytraumatized humans injured in automobile accidents
21 p3002 A72-41188

Effect of hypoxia and physical activity on plasma enzyme levels in man.
21 p3003 A72-41522

Lysosomal enzymes of eye tissues during the action of hydrocortisone
22 p3141 A72-42279

Succinic and lactic dehydrogenases activities in homogenates from myocardial tissues of guinea pigs, rabbits and dogs in high altitude environments
22 p3144 A72-42592

Hypoxic acclimation effects on rats heart, liver and kidney mitochondria, measuring cytochrome oxidase and succinic dehydrogenase activities
22 p3144 A72-42673

Increased fluid turnover and the activity of the renin-angiotensin system under various experimental conditions.
23 p3257 A72-43997

Metabolism of angiotensin II in sodium depletion and hypertension in humans.
23 p3257 A72-43998

Lactate dehydrogenase from an extremely thermophilic bacillus.
23 p3259 A72-44450

Influence of elevated partial oxygen pressure on the sympathetic-adrenal and acetyl-choline systems
24 p3371 A72-44595

In vivo hemolysis due to hyperoxia - Role of H2O2 accumulation.
24 p3374 A72-45651

Response to daily lower body negative pressure /LBNP/ exposure /-70mm Hg/, with emphasis on plasma renin activity, sodium and potassium excretion.
24 p3377 A72-45658

ENZYMES

NT CATALASE

NT CHOLINESTERASE

NT COENZYME

NT LYSOZYME

NT OXIDASE

Dipeptidyl aminopeptidase I preparation from beef spleen and rat liver, discussing contamination with catheptic carboxypeptidase C and Ser-Met dipeptidase
07 p0935 A72-18906

Thromboelastographic study of renin and angiotensin effect on blood clotting system of anesthetized and unanesthetized dogs
08 p1121 A72-22095

ENZYMOMOLOGY

Liver and muscle type isozymes of DPN-linked glycerol-3-P dehydrogenase in chickens in terms of tissue distribution, ontogeny and avian evolution
12 p1759 A72-27161

EOLE SATELLITES

Planetary divergence field estimation via Lagrangian tracers and Eole experimental balloons data, developing spatial analysis method
15 p2266 A72-31952

Eole satellite observed meteorological balloon data analysis, obtaining mean zonal velocity, meridional velocity and temperature vs latitude from statistical estimates
15 p2266 A72-31980

Data system in Eole satellites program, discussing balloon localization, UHF information transmission and reception, distance measurement and data acquisition
15 p2268 A72-31981

Eole - The tracking and collection of data applicable to meteorology
17 p2622 A72-35718

Eole program for tracking and gathering information from drifting buoys at sea
17 p2617 A72-35720

FOR [RENDEZVOUS]

U EARTH ORBITAL RENDEZVOUS

EOSS

Zero gravity earth orbital cloud physics facility requirements and design concepts, noting experiments feasibility relative to astronaut performance
13 p1990 A72-28815

EPHEMERIDES

NT PLANET EPHEMERIDES

Solar eclipse timings by photoelectric, photographic and visual observation for comparison of Newcombe sun tables and improved lunar ephemeris reference systems
13 p2041 A72-29527

Star catalog zero-point improvement by Bessel method modification for lunar observation data reduction
14 p2149 A72-30210

Computer calculation of artificial satellite ephemerides from Smithsonian mean orbital elements, comparing observed and computed topocentric equatorial coordinates
14 p2087 A72-30480

Ephemerides determination improvement of celestial bodies with nonperiodic trajectories, relating different observatories measurements
17 p2607 A72-35042

Ephemeris of a highly eccentric orbit - Explorer 28.
20 p2968 A72-39194

Terminal orbit of comet 1937 V /Finsler/
22 p3220 A72-41917

Star catalog zero-point improvement by Bessel method modification for lunar observation data reduction
23 p3333 A72-43240

Compilation of azimuth tables for the North star /for the tropical zone/
24 p3438 A72-44866

EPHEMERIS TIME

Nighttime laser ranging of French reflector for Soviet Lunokhod, discussing universal-ephemeris time difference determination
05 p0721 A72-16771

Ephemeris time, lunar orbital elements and FK4 equinox correction from the observations of the moon by the method of equal altitudes.
17 p2603 A72-34274

Nighttime laser ranging of French reflector for Soviet Lunokhod, discussing universal-ephemeris time difference determination
17 p2611 A72-35274

New measurements of circular polarization and an ephemeris for the variable white dwarf G195-19.
17 p2611 A72-35298

EPICARDIUM

Human epicardial arterial circulation platelet aggregates role in sudden coronary death, discussing relation to atherosclerotic stenosis and acute thrombi.
05 p0616 A72-16013

Baboon heart endocardial structure dynamic behavior, comparing left ventricle septum and epicardium contractile force and intramyocardial pressure changes
15 p2187 A72-32748

EPICYCLOIDS

Generalized epicycloid properties application to fracture mechanics, considering stress fields of constrained plastic zones around cracks in thin elastic plate
03 p0455 A72-14388

EPILEPSY

Cerebral blood flow and metabolic changes during wakefulness, sleep, coma and epileptic seizures in terms of homeostatic mechanisms
16 p2356 A72-33558

EPINEPHRINE

NT NOREPINEPHRINE

Epinephrine and norepinephrine effects on cerebral blood circulation volume and oxygen tension in tissues
02 p0165 A72-12517

Ground and flying activity endurance training effect on urinary excretion of noradrenaline and adrenaline
04 p0478 A72-14868

Adrenaline and noradrenaline metabolic stages and production mechanism under various physiological and pathological conditions, noting application to flight emotional stress detection
21 p3002 A72-41196

EPITAXY

Transferred electron microwave oscillator diodes with n-n structure by liquid phase epitaxy, reducing high resistance layer in interfaces and crystal defects
01 p0036 A72-10629

High power Q-band pulsed Gunn diode microwave oscillator constructed from thin GaAs sandwich layers grown by vapor phase epitaxy
01 p0036 A72-10630

Liquid phase epitaxial GaAs transferred electron microwave oscillators with high dc to rf conversion efficiencies dependent on frequencies
01 p0036 A72-10631

Epitaxial layer preparation on GaSb single crystal by liquid phase method, discussing crystal orientation effects
03 p0402 A72-13859

High purity epitaxial GaAs frequency response, determining heterodyne detection in millimeter and submillimeter regimes
04 p0563 A72-15613

Growth rate of semiconductor epitaxial films obtained by forced cooling from liquid phase
09 p1372 A72-23360

Epitaxy and vacancy structure of TiSe with type B8 ordering
10 p1495 A72-24077

Nonstoichiometry of beta and beta-two aluminas in epitaxial coexistence from crystallographic investigation
10 p1433 A72-24082

Minority carrier diffusion length in liquid epitaxial GaP, noting dependence on dominant impurity and substrate growth orientation from Schottky diode photocurrent technique
10 p1526 A72-24551

Liquid phase epitaxy GaAs growth in rotary reactors from Ga solution, noting thickness, doping uniformity, reproducibility and surface morphology
10 p1526 A72-24556

Book on semiconductors covering electrical properties, energy band structure, impurities, epitaxial growth, silicon dioxide, surface properties, p-n junctions and measurement techniques
10 p1528 A72-25123

Epitaxial InP diode for high efficiency circuit controlled microwave oscillator, discussing solution growth technique, layers electrical properties and I-V performance
12 p1854 A72-27162

Epitaxial and textured Pb films on mica and glass, using reflection electron diffraction, etching and optical microscopy for structure study
12 p1854 A72-27289

K band Read avalanche diodes fabricated by epitaxial deposition and diffusion processes, measuring capacitance-voltage characteristics and oscillator power efficiency
12 p1790 A72-27441

Pulse generation in planar Gunn devices of epitaxially grown GaAs layers, measuring current reduction by domain nucleation
12 p1791 A72-27671

Epitaxial GaAs carrier concentration profile, deep traps detection and properties determination, using Schottky barrier on semiconductors
13 p2024 A72-30035

Solar photosensitive elements prepared p-type GaAs liquid epitaxy on n-type GaAs substrate, measuring dark and light I-V characteristics and spectral response
14 p2142 A72-30225

Epitaxial film system parameters determination based on variational technique of computing electromagnetic waves reflectance and transmissivity in semiconductor structures
14 p2142 A72-30811

Gallium aluminum arsenide light emitting diode thin structures grown on GaP substrates by liquid phase epitaxial method
15 p2290 A72-31381

Epitaxial YIG film separated from conductive plane by thin dielectric layer, considering magnetostatic propagation dispersion and insertion loss
15 p2294 A72-32502

Gallium arsenide-aluminum gallium arsenide double heterostructure wafer fabrication, describing reproducible liquid phase epitaxial growth
15 p2250 A72-32518

Equipment for nondestructive measurements of the resistivity of semiconductor epitaxial layers by the three-point probe technique
17 p2557 A72-35755

Structure and properties of transition layers formed in the epitaxy process.
18 p2718 A72-36340

Behavior of epitaxial bipolar transistors in the strong injection regime
18 p2668 A72-37103

Twinning faults in epitaxial films of germanium telluride and GeTe-SnTe alloys.
19 p2844 A72-37688

Low capacitance high speed lead tin telluride photodiodes via liquid phase epitaxial growth, discussing frequency response to Nd-YAG and carbon dioxide lasers
22 p3159 A72-42620

Interpretation of steady-state surface photovoltage measurements in epitaxial semiconductor layers.
22 p3215 A72-43087

X-band silicon double-drift IMPATT diodes using multiple epitaxy.
23 p3273 A72-44334

EPITHELIUM

Mitotic index and aberrant mitose frequency in mice corneal and intestinal epithelial cells exposed to 50-630 MeV protons, estimating relative biological efficiency coefficients
02 p0161 A72-12055

Myoepithelial mechanism of high frequencies pulsatile discharge of human sweat glands
07 p0930 A72-19444

Mitosis duration and mitotic activity diurnal rhythms in esophageal epithelium of rats given thyroxine
07 p0924 A72-20623

Epithelial follicle and mast cell role in peroxidase activity of thyroid gland during experimental burn development
13 p1905 A72-29330

Succinic dehydrogenase activity in rabbit eye ciliary epithelium during electric stimulation of hypothalamus, using histochemical techniques
14 p2078 A72-31099

EPOCHS

U TIME MEASUREMENT

EPOXIDES

U EPOXY COMPOUNDS

EPOXY COMPOUNDS

Electron impact induced aurore epoxides fragmentation, discussing ion formation, intermediates, thermal rearrangement and mass spectra
13 p1913 A72-29775

A method of improving the physicochemical properties of filled epoxy compounds by treatment in an ultrasonic field
19 p2823 A72-38184

EPOXY RESINS

High temperature strength degradation of graphite and boron reinforced epoxy composites after room temperature aging
01 p0090 A72-10728

Lightning protective coatings for boron/epoxy composite materials, discussing high current damage mechanisms, simulation facility and test results on aluminum foils, meshes, etc
01 p0092 A72-10783

Unidirectional glass/graphite fiber-epoxy resin composite, discussing fabrication and performance tests for mechanical properties
01 p0092 A72-10971

Minimum weight web-core sandwich panels under axial compression loads, presenting numerical results for boron-epoxy and graphite-epoxy composites
01 p0142 A72-11131

Graphite-epoxy conductive polymers as fatigue damage indicators of structures under cyclic strain [SESA PAPER 1915]
02 p0287 A72-11509

Stress and failure analysis of glass-epoxy composite plate with circular hole under uniaxial tension by finite element method
02 p0248 A72-11517

Acoustic emission monitoring of boron epoxy composite, showing crack extension characterization by emission bursts
02 p0249 A72-11993

Epoxy- and polyimide-graphite composites electrical dissipation factor and capacitance measurements as guide to molding quality, describing equipment
02 p0250 A72-12609

Epoxy and polyester resin fatigue fracture tests for cyclic stress and moisture effects
08 p1192 A72-21680

Thermal and mechanical properties of randomly reinforced fiber/resin composites including boron/epoxy, Thorne/epoxy and S glass/epoxy materials
08 p1192 A72-21682

Carbon/epoxy composite reinforced plastic materials feasibility for application to aircraft landing gear wheel fabrication
08 p1193 A72-21686

Graphite reinforced epoxy stiffeners for variable geometry fuel tank to meet light weight requirement, discussing billet fabrication, assembly and installation
08 p1176 A72-21688

Boron-epoxy structure repair technology based on titanium plugs and fiberglass, discussing equipment, graphical design and nondestructive tests
08 p1193 A72-21691

Composite filament wound boron-epoxy rocket motor combustion chamber design, fabrication and hydrostatic tests
08 p1177 A72-21692

Alcyclic dicarboxylic anhydride structure effects on cured epoxidized novolac resin physical and chemical properties
08 p1193 A72-21695

Adverse environmental effects on epoxy composites resin-glass interface properties, investigating epoxy-compatible silanes contribution to composite performance
08 p1194 A72-21696

Water effect at epoxy resin-steel interface on adhesive bond strength as function of vitrification temperature
08 p1196 A72-21863

Carbon fiber reinforced epoxy resin composites, testing fracture behavior in flexural and shear modes under static, fatigue and creep loading
09 p1334 A72-22389

Creep test for microfailures of glass reinforced epoxy and polyester laminates immersed in water at ultimate flexural stress
09 p1336 A72-22537

Fiber orientation effects on physical properties of carbon fiber-epoxy resin composites
[PIPAER 3] 09 p1337 A72-22540

Carbon fiber reinforced epoxy resin composites fracture toughness dependence on fiber strength, diameter, volume fraction, modulus, fiber/matrix interface strength and temperature
09 p1337 A72-22544

Epoxy resin tensile specimen fabrication and testing, discussing factors controlling data scatter
09 p1337 A72-22650

Tensile strength of notched carbon and glass fiber reinforced epoxy resin composites as function of crack size
10 p1500 A72-24253

Elastoplastic analysis of unidirectional filament reinforced boron/aluminum and boron/epoxy composites under longitudinal loading, using finite element techniques
10 p1555 A72-24254

Stress wave surfaces in graphite fiber-epoxy matrix anisotropic plates under transverse impact forces, using Mindlin approximation theory
10 p1555 A72-24255

Fatigue crack propagation in epoxy resin matrix reinforced with discontinuous metal fibers
10 p1501 A72-24261

S glass/epoxy composites strength retention properties under long duration tensile load, proposing use of stress rupture data for reliable safe structural design
10 p1501 A72-24263

Interaction diagram for mixed crack extension modes in unidirectional graphite-epoxy laminates from critical load test data
10 p1501 A72-24265

Gamma ray radiation effects on epoxy resin electric properties, studying electric insulation and arc resistances and dielectric breakdown strength
10 p1502 A72-25149

Colaminated boron-polyimide film effect on strength of graphite fiber-epoxy resin composite double lap bolted joints
[AIAA PAPER 72-382] 11 p1730 A72-25405

Fatigue strength characteristics of boron-epoxy reinforced Al stringers for helicopter airframe
[AIAA PAPER 72-392] 11 p1574 A72-25413

Boron-epoxy reinforced Ti tubular truss for application to space shuttle booster thrust structure, evaluating performance
[AIAA PAPER 72-393] 11 p1730 A72-25414

Boron-epoxy reinforced composite metal shear web design for space shuttle orbiter main engine thrust beam structure
[AIAA PAPER 72-395] 11 p1726 A72-25416

Boron-epoxy composite design for aircraft structures, discussing materials variations, strength prediction inadequacies and full scale tests
11 p1670 A72-25454

Two stress level cumulative fatigue damage prediction for glass fiber-epoxy laminates
11 p1670 A72-25462

Failure modes effect on compressive strength of boron-epoxy composites tested on coupons, honeycomb sandwich columns and beams
11 p1671 A72-25466

Embedded strain gage technique for subsurface tensile testing of boron-epoxy composites
11 p1671 A72-25467

Acoustic emission analysis of deformation and fracture modes under straining of fiber glass-epoxy composite structures, including NOI rings and vessels
11 p1671 A72-25469

Elastic glass and Thornel fiber/epoxy matrix composite material creep tests, determining creep rate dependence on specimen geometry and stress state
11 p1672 A72-25481

Experimental weave pattern for three dimensional continuously woven fiber glass reinforced composite fabric impregnated with epoxy resin
[SAE PAPER 720340] 11 p1673 A72-25597

Fracture surface energy and acoustic emission of boron fiber-epoxy resin composite, using linear elastic fracture mechanics and compliance variation methods
11 p1674 A72-25858

Electrical measurement of moisture effects on adhesive bond strength, insulation resistance and hydrophilicity of cast epoxy and organosilicon adhesives
12 p1833 A72-27449

Particulate fillers bulk effects on epoxy resin compositions flexural, compressive and tensile strengths and moduli
12 p1834 A72-28089

Graphite fiber-epoxy composite systems development for F-5 aircraft landing gear door, speed brake, leading and trailing edge flaps and horizontal stabilizer
12 p1835 A72-28097

Fatigue strength and cumulative damage in fiberglass-epoxy composite specimens under unsteady elastic bending loads, determining loading spectrum effect on service life
13 p1983 A72-28562

Plasticizers and modifiers effect on epoxy polymers structure from electron microscopy and IR spectroscopy, observing chemical reactions between aliphatic resin and hardening agent
13 p1983 A72-28689

A-4 Skyhawk horizontal stabilizer experimental graphite-epoxy composite construction, describing design, manufacturing and testing techniques
[AIAA PAPER 72-358] 13 p2056 A72-28954

Gamma irradiation effects on epoxy-diane resin creep and stress relaxation properties indicated by loaded specimens birefringence patterns
13 p1984 A72-29481

Epoxide resins for application in composite materials, discussing crosslinking reactions, temperature effects on cure, and electrical and physical properties
15 p2260 A72-31441

One dimensional wave pulse propagation, attenuation and dispersion in uniaxially reinforced steel-epoxy resin composites
15 p2325 A72-31528

Temperature effects on stress-strain diagram, tensile strength and creep properties of fiber-epoxy resin composites
15 p2260 A72-32137

Acoustic emission from carbon fiber-epoxy composite during continuous tensile stress cycling
16 p2413 A72-32868

Al alloy welded seams corrosion fatigue strength increase by epoxy polymer coatings under cyclic tensile stresses
16 p2397 A72-33268

Adhesion effects on tensile and thermal expansion properties of aluminum oxide particles filled epoxy-urethane polymer at ambient and liquid nitrogen temperatures
16 p2415 A72-33415

Application of boron/epoxy to the CH-54B Sky crane helicopter.
[AHS PREPRINT 670] 17 p2491 A72-34510

Shape factors for nozzle corner cracks evaluated from epoxy-model pressure vessels.
17 p2630 A72-34814

Failure mechanism for carbon fibers in epoxy novolac matrices under tensile loads
17 p2633 A72-35286

Improving the impact resistance of glass-fibre composites.
18 p2703 A72-36270

Stress wave propagation observation in rigid high modulus epoxy polymer by slow motion photography, noting photoelastic properties and viscosity effect
18 p2734 A72-36380

Studies on flame-resistant epoxy resin - Pyrolysis of tetra-brominated epoxy resin and flame-resistant mechanism.
18 p2704 A72-36519

Losses in high-voltage transformers encapsulated by epoxy resins.
18 p2669 A72-37113

Some results of an experimental study of stress distribution at monofilament tips
19 p2822 A72-37529

Model filament wound epoxy composites.
19 p2808 A72-38164

Machining boron-epoxy composites.
19 p2809 A72-38386

Fatigue behavior of glass filament-wound epoxy composites in water.
21 p3072 A72-40246

Epoxy-thiocol binder viscoelastic deformation under short and long term loads, noting stress-strain linearity limit
21 p3073 A72-41360

Stress-rupture of simple S-glass/epoxy composites.
23 p3305 A72-43492

Mechanics of failure of fibrous composites.
23 p3345 A72-43508

EQUATIONS OF MOTION
NT EULER EQUATIONS OF MOTION
NT HYDRODYNAMIC EQUATIONS

NT KINEMATIC EQUATIONS
NT KINETIC EQUATIONS
NT NAVIER-STOKES EQUATION
NT REYNOLDS EQUATION

Integrability of rotating satellite differential equation of motion in axially symmetric gravitational field.
01 p0122 A72-10008

Solution of N planets equations of motion around sun with recurrent power series in time
01 p0123 A72-10014

Human body dynamics, discussing configuration, modeling techniques, kinematics, equations of motions and various limb motions examples
01 p0016 A72-10110

Brownian motion kinetic equation from Boltzmann equation for two component neutral gas by simultaneous expansion in density and mass ratios
01 p0050 A72-10233

Gravitational potential tensor and equations of motion of relativistic mechanics for isolated system of masses
01 p0127 A72-10345

Controllability of dynamic systems with motion described by nonlinear differential equations
01 p0045 A72-10500

Solar wind plasma spherically symmetrical outflow allowing for equations of motion of velocity components, discussing interplanetary field and single fluid MHD
02 p0278 A72-11914

Computerized series solution of relativistic motion of planet Mercury for Schwarzschild and isotropic coordinates
02 p0260 A72-12306

Hybrid computer simulation of spinning satellite dynamic behavior during flexible booms deployment and attitude control maneuvers, deriving equations of motion from Lagrange equations
02 p0286 A72-12658

Book on celestial mechanics covering Hamiltonian systems and equations of motion for three body problem
02 p0285 A72-12857

Optimal trajectory in phase space, deriving differential motion equations with Euler-Lagrange method
02 p0199 A72-12880

Howe gyroscope mounted on fixed base, deriving equations of motion with Laplace method
03 p0359 A72-13558

Stellar systems existence with positive total energy, using numerical integration of equations of motion for members of Orion Trapezium
03 p0435 A72-13808

Mass changes in restricted quasi-circular variable mass three body problem with particle equations of motion having Jacobi integral
03 p0436 A72-13828

Differential equations of motion for stable member of three-axis gyro stabilized platform
03 p0387 A72-14190

Relativistic equations of motion of charged particle interacting with plane electromagnetic wave propagating at arbitrary angle to uniform magnetic field for magnetosphere model
04 p0554 A72-14406

Plane periodic oscillations of solid body on elliptic orbit, characterizing stability of motion equations periodic solutions
04 p0582 A72-14632

Self adaptive controlled robot velocipedist, discussing speed control and equations of motion
04 p0505 A72-14984

Invariant manifolds in rigid body motion about fixed point, considering Euler-Poinsot, Lagrange-Poinsot and Kovalevskia cases
04 p0549 A72-15197

Differential equations of motion construction from given manifold, determining functional minimization of solution
04 p0550 A72-15544

Single- and many degree of freedom nonlinear structural systems transient dynamic response by presentation of equations of motion, damping and restoring force functions
05 p0736 A72-16082

Motion equations of constrained split fairing for avoiding contamination of sounding rocket payload environment by uncontained explosive actuation device
05 p0724 A72-16102

Gyrostad translational rotational motion equations in canonical form without trigonometric expressions in Hamiltonian
05 p0724 A72-16164

Discrete elasticity theory constitutive and motion equations, considering finite difference and partial differential equations
05 p0737 A72-16297

Equations of motion for stable member of three axis gyro stabilized platform for inertial navigation, including friction, inertia and torque motor effects
05 p0662 A72-16557

Explicit finite difference procedure to solve time averaged equations of motion for unstalled turbulent

duct flows in coordinate system approximating real flow streamlines
[AIAA PAPER 72-43] 05 p0651 A72-16878

Spin dynamics model of space station with counterweight connected by multiple cables, using linearized motion equations
[AIAA PAPER 72-172] 05 p0730 A72-16882

Sonic boom signature by bicharacteristic method, correcting zeroth order [free stream] characteristics to obtain solution to compressible fluid exact equations of motion
[AIAA PAPER 72-195] 05 p0652 A72-16907

Large deflection microstructure continuum model for composite beam flexural wave propagation and free vibration, deriving equations of motion
[AIAA PAPER 72-140] 05 p0741 A72-16937

Charged particle motion equations for fifth order spherical aberration of quadrupole-octupole lens with arbitrary electrode and pole shapes
05 p0638 A72-16989

Compressibility and total enthalpy difference effects on laminar free shear layer from numerical integration of equations of motion
05 p0653 A72-17011

Spacecraft banking control during reentry, deriving dynamic equations of angular motion
05 p0730 A72-17026

Equations of motion for oscillating heavy symmetrical gyroscope with cylindrical cavity partially filled with inviscid incompressible liquid
05 p0664 A72-17145

Longitudinal instability of electron beams interacting with passive resonator, considering Landau damping influence by linear differential equations of motion solution
05 p0701 A72-17243

Variational principles in general relativity, deriving Einstein field equations and equations of motion for charged and uncharged self gravitating fluids
06 p0847 A72-17254

Spinning satellite with rigid central body and flexible appendages, deriving equations of motion and Liapunov stability
06 p0892 A72-17652

Triaxial space station orbit around oblate earth, presenting equations of motion, Hamiltonian and integration methods
06 p0878 A72-17663

Soviet book on qualitative methods in celestial mechanics covering differential equations of motion varying schemes, Newton type convergence method, three body problems, etc
06 p0879 A72-17821

N-body problem equations of motion numerical integration methods supplemented by two body perturbation description and coordinate and time transformations
06 p0885 A72-18072

N-body gravitational problem numerical integration treatment of close approaches, using transformations for eliminating differential equations of motion singularities
06 p0885 A72-18079

Reactive solid or fuel combustion, deriving equations for movement and deformation of reaction front during oxidant diffusion through ash mantle
06 p0902 A72-18155

Autonomous two body system described by nonlinear differential equations of motion, obtaining free relative vibration solution in terms of elliptic functions
06 p0849 A72-18694

Sensitivity functions for differential equations describing aircraft perturbed motion, noting dependence on time derivatives, system parameters and coordinates
07 p1032 A72-18977

Equations of free particle motion, gas energy, distribution evolution and cosmic indeterminacy for Friedmann universe filled with uniform density and pressure ideal gas
07 p1074 A72-19429

Third-order resonance during oscillations of Hamiltonian system of nonlinearly coupled oscillators, obtaining equations of motion and phase portraits
07 p1035 A72-19978

Existence and branching of analytical solutions to equations describing oscillatory-rotatory motions of system of two pendulums with different masses
07 p1036 A72-20217

Elastic body dynamics partial differential equations transformation into boundary value problem for Monge-Ampere equation
07 p1095 A72-20218

Two coupled lasers theory, obtaining fields equations of motion
[AD-739802] 07 p1009 A72-20681

Class of homogeneous polynomial solutions to differential equations of motion of elastic body
08 p1242 A72-20912

Perturbed motion differential equations for stability and integration problems in mechanics
08 p1205 A72-20964

Dynamical equivalence between vehicles with motor-driven constant speed rotor under bearing friction

and freely spinning torque free rotor, deriving equations of motion
08 p1108 A72-21174

Motion equations order reduction for solid body with fixed point
08 p1207 A72-21340

Transformation of integrodifferential equation of motion of heavy solid body about fixed point
08 p1207 A72-21341

Polynomial solutions to integrodifferential equation of motion of solid body with fixed point for Lagrange conditions
08 p1207 A72-21342

Motion of body similar to Lagrange gyroscope, using Kolmogoroff theorem
08 p1207 A72-21343

Algebraic invariant relation of integrodifferential equation of motion of solid body about fixed point for Hess conditions, proving uniqueness
08 p1207 A72-21344

Solutions existence for algebraic invariant relation to integrodifferential equation of motion of solid body about fixed point in trigonometric and exponential polynomials class
08 p1207 A72-21346

Solutions existence for nonlinear invariant relation to integrodifferential equations of motion of solid body about fixed point
08 p1207 A72-21347

Solutions existence conditions for integrodifferential equation of motion of solid body about fixed point
08 p1207 A72-21349

Integrodifferential equation exponential solutions for body motion about fixed point
08 p1208 A72-21353

Goriachev-Chaplygin solution to gyroscopic motion of body around fixed point for periodic motion
08 p1208 A72-21355

Fourth algebraic integral in Kovalevskaya solution of rotating body motion about fixed point regarding angular momentum components
08 p1208 A72-21357

Asymptotically uniform motions of heavy solid body with fixed point, assuming moving hodograph intersections with Staudé cone
08 p1208 A72-21358

Motion equations of gyrostat with nonholonomic constraint under gravitational force
08 p1208 A72-21359

Gyrostat inertial motion under nonholonomic constraint of mass center coincidence with fixed point
08 p1208 A72-21360

Linear invariant solution to gyrostat motion under nonholonomic constraint
08 p1208 A72-21361

Solutions existence and uniqueness for linear invariant relation to gyrostat motion under nonholonomic constraint
08 p1208 A72-21362

Small perturbation stability of discontinuous solution of equations of motion for solid fuel combustion processes
08 p1253 A72-21463

Book on plasticity theory covering stress and strain as basic concepts of continuum mechanics, differential equations of motion, plastic flow, yield criteria, elastic-plastic equilibrium, plane strain, etc
08 p1244 A72-21477

Ritz-Galerkin process applied to coupled differential equations of motion of pretwisted tapered cantilever turbine blade vibrating in flexure
08 p1244 A72-21483

Hypersonic vehicles lateral dynamics during great circle flight, using linearized equations of motion and Newtonian theory for stability derivatives estimation
08 p1110 A72-21603

One dimensional atmospheric turbulent diffusion model and semiempirical equation, considering jumplike changes in particle velocity
08 p1201 A72-21999

Control synthesis equations for aircraft motion on phase space surface
09 p1261 A72-22208

Two independent damping systems impact vibration analysis from solution of equations of motion by Laplace transformation
09 p1399 A72-22695

Numerical integration of primitive equations for barotropic atmosphere, using spherical polar coordinates
09 p1346 A72-22809

Numerical solution of thermal shock equations for incompressible fluid with free convection and of motion equations in gravitational force field
09 p1410 A72-22882

Brittle fracture dynamics, deriving motion equations and stability conditions of surface cracks under stress waves from energy balance and angular momentum conservation law
09 p1404 A72-22916

Motion equations approximate solution for viscous fluid Couette flow instability caused by spiral symmetry vortices
09 p1295 A72-23073

Approximate method for nonlinear differential equations of motion solution in flight dynamics, applying to control surface buzz and slender wing oscillations
09 p1262 A72-23453

Nonlinear mode coupling in equations of motion for thin panel vibration as function of membrane stretching-bending energy ratio
09 p1408 A72-23465

Rectilinear motions in three body problem with null live forces constant, using inequality deduced from virial theorem
09 p1392 A72-23542

Zaidenberg correlation method for nonlinear systems dynamic properties under random excitation, determining statistically equivalent linearized terms for equations of motion
09 p1353 A72-23607

Hartman-Olech theorem to prove asymptotic stability of mechanical system with nonlinear elastic characteristic, analyzing differential equations of motion
09 p1343 A72-23612

Equations of motion for discrete structure fluid, discussing equilibrium pressure and fluid-wall interaction effects
09 p1296 A72-23691

Ion trajectories equations of motion solution for E x B type mass separator, presenting curves for mass species dispersion inside separator channel
10 p1509 A72-23942

Initially axially stressed Timoshenko beam equations of motion derived from three dimensional theories, discussing buckling loads and vibration frequencies
10 p1555 A72-24191

Rectilinear impulsive motion of compressible boundary layer on infinite plate, deriving integration method for differential equations of motion under energy dissipation neglect
10 p1465 A72-24203

Similarity method solution of differential equations of motion for supersonic laminar boundary near symmetry plane of cone at angle of incidence
10 p1418 A72-24236

Equations of motion with gravitational radiation reaction terms for gravitating system as source of asymptotically flat space
10 p1511 A72-24416

Flight vehicle angular velocity measurement by accelerometers, deriving equations of motion
10 p1481 A72-24497

Virtual displacement application to nonholonomic systems with arbitrary constraints to derive Lagrange and Appell equations of motion
10 p1513 A72-24995

Oscillation modes and stability region of harmonic oscillators with homogeneous nonlinear rheological differential equations of motion
10 p1513 A72-24998

Statics, motion equations, deformation, dynamics and classification of Cosserat continua
10 p1513 A72-25000

Equations of motion of steady viscous fluid flow in three dimensional boundary layer on walls of axial flow compressors and turbines, obtaining velocity field
10 p1420 A72-25120

Equations of motion for structural flexibility influence on dual spin spacecraft dynamic response, noting elastic deformations and rotation rates coupling
[AIAA PAPER 72-348] 11 p1725 A72-25377

Variational equations of motion for three layered laminated sandwich beam vibrations, assuming small elastic deformations and axial and bending motion
[AIAA PAPER 72-399] 11 p1731 A72-25420

Extremal feedback control system operation with integral PFM in extremum drift mode, determining equations of motion and steady state regime
11 p1610 A72-25449

Cylindrical panel natural vibrations, describing motion of base with dynamic elasticity equations
11 p1733 A72-25539

Coupled nonlinear equations of motion of large deflections of impacted helical springs, comparing with streak photographs
11 p1688 A72-26061

Inferential structure of variational statements for equations of motion and constitutive relations, noting function space choice
11 p1690 A72-26554

Complete and simplified equations of motion for rate gyro installed in flight vehicle, taking into account bearing torques
[DFVLR-SONDDR-190] 11 p1635 A72-26580

Equations of motion for torsional vibrations in system with nonlinear elastic term and variable moments of inertia, noting analog computer simulation
11 p1739 A72-26982

Laplace-Carson transform solution for integrodifferential equation of motion for droplet suspended in viscous gas slipstream
12 p1796 A72-27093

Finite difference equations of motion for conservative and nonconservative dynamic systems with finite

degrees of freedom, obtaining numerical solution by Hamilton principle 12 p1844 A72-27193

Equations of motion for oriented and multipolar discrete elastic media, noting elements formed by sets of free material points 12 p1845 A72-27394

Numerical integration for many body systems equations of motion, noting Monte Carlo and Boltzmann moment methods for large systems 12 p1873 A72-27895

Computer models for collisionless stellar systems equations of motion, obtaining force from smoothed gravitational field 12 p1875 A72-27920

Lie group theory application to linear differential equations of motion with variable parameters, considering flight vehicle example 12 p1847 A72-28127

Flight vehicle motion described by linear differential equations with variable parameters, discussing programmed optimal control solution by functional analysis 12 p1755 A72-28128

Harmonic functions system for resonant vibrations of liquid in elastic circular cylindrical tank, calculating shells surface pressure from equations of motion 13 p1940 A72-28394

Atmospheric motion equations numerical integration, presenting conservative finite difference approximation for quasi-uniform spherical grids derived from regular polyhedrons 13 p1985 A72-28445

General relativity equation of motion for spherically symmetric surface layer of ideal gas under central gravitational field 13 p2035 A72-28646

Magnetogasdynamics intrinsic equations, determining geometrical and mechanical characteristics of axisymmetric and meridional plane motions 13 p2010 A72-28682

Equations of motion and phase trajectory analysis for resonant oscillations of beam-pendulum system 13 p2003 A72-28721

Quadrature solution for variable mass point motion under perturbing force in trajectory plane normal to velocity vector 13 p2003 A72-28725

Acoustic pressure wave effect on motion of elastic conical shell fastened in rigid screen, using Timoshenko theory 13 p2055 A72-28772

Solar wind plasma spherically symmetrical outflow allowing for equations of motion of velocity components, discussing interplanetary field and single fluid MHD 13 p2039 A72-29226

Directionally reinforced composites treated as homogeneous continuum with microstructure, deriving displacement equations of motion by Hamilton principle 13 p2060 A72-29694

Hypervelocity impact parameters calculated from shock wave equations of motion, discussing viscosity effect on velocity and stress distributions 14 p2164 A72-30297

Error sources in numerical integration of spacecraft equations of motion in solar and planetary gravitational fields, suggesting methods for improving accuracy 14 p2151 A72-30453

Equations of motion for incompressible viscous fluid thin layer on cylinder outer side under gravity, calculating wave number, phase velocity and film thickness 14 p2094 A72-30699

Cooperative direction changing isomer movement on polymer chain lattice describing equations derivation procedure 14 p2125 A72-30962

Approximate periodic solution of satellite equation of motion based on Schwarzschild metric integration, noting relativistic effects 14 p2162 A72-31108

Rectangular plate nonlinear lumped-parameter model for large displacement amplitudes, deriving differential equations of motion via Hamilton principle and Euler equations 14 p2169 A72-31148

Equations of motion and free vibration for trusswork structures under nonperiodic dynamic loads, calculating longitudinal and transverse end forces 15 p2322 A72-31360

Nonlinear differential equations of motion of complex configuration, developing stable solution method 15 p2261 A72-31489

Numerical integration of equations of motion in finite element methods, investigating explicit methods stability 15 p2326 A72-31717

Equations of motion for contactless suspension gyroscope in force field 15 p2235 A72-31726

Partial differential equations of motion for nonlinear mechanical systems solved by Lanczos formula, discussing prismatic cylinder oscillations under uniformly distributed transverse load 15 p2275 A72-31729

Ionized and neutral atmospheres coupled ionospheric continuity and motion equations, discussing nonlinear force effects on F2 height and electron density 15 p2230 A72-32257

MHD instabilities growth rates from diffuse linear pinch equations of motion solution 15 p2287 A72-32416

Lorentz-covariant procedure for equations of structure and motion of particles represented by singularities in Einstein relativistic field theory 16 p2422 A72-32880

Liapunov function application to stability of unperturbed motion of differential equations with respect to part of variables 16 p2422 A72-32940

Perturbation theory for equations of motion of electrically and thermally conducting viscous compressible flow in homogeneous magnetic field, calculating fluctuation modes 16 p2435 A72-33008

Mechanical system nonlinear perturbation effect on equations of motion solutions, deriving boundedness and stability conditions via inequality theorems 16 p2423 A72-33101

Equations of motion for damped vibrating system excited by periodic impulsive forces, calculating minimum residual vibration amplitude and force transmitted to foundation 16 p2423 A72-33121

German monograph on rotating nonround shafts stability under torsion, obtaining equations of motion solution via convergent double series expansion 16 p2469 A72-33399

Equations of motion for small vibrations superposed on time depending deformation of elastic body, discussing acoustic wave propagation 16 p2425 A72-33590

Barium cloud striations deformation in ionosphere explained by equations of motion for plasma cloud thin bar model, discussing pinch effect 16 p2387 A72-33907

Sea level wind and pressure data adjustment to governing dynamical equations by numerical variational analysis, using Sasaki matching technique 16 p2419 A72-33941

Continuity, motion and Maxwell equations for steady MHD flow under constant magnetic flux 17 p2588 A72-34765

Certain motions of micropolar fluids 17 p2538 A72-34771

Three dynamic conical bar theories, solving transient axisymmetrical motion via method of characteristics [ASME PAPER 72-APM-20] 17 p2581 A72-34797

Independent variable transformations for stepwise solution of differential equations of motion power series expansions, considering convergence radius 17 p2609 A72-35105

The flow caused by the differential rotation of a right circular cylindrical depression in one of two rapidly rotating parallel planes. 17 p2540 A72-35189

Russian book - Calculation and analysis of flight-vehicle motion: Engineering handbook 17 p2492 A72-35451

Mathematical solution to equations of turbulent motion in viscous fluids asymptotic to strange attractors 18 p2678 A72-36015

Motion integrals conservation under Hamiltonian function variations, examining gyroscope equations of motion with parameter disturbances 18 p2711 A72-36666

Universe expansion induced electromagnetic wave backscattering absence in Robertson-Walker spacetime as consequence of motion equations conformal invariance 18 p2711 A72-36711

Similarity solutions to nonlinear equations of motion of n dislocations group in slip plane under stress 18 p2719 A72-36745

Plate vibrations and layer potentials 18 p2736 A72-37001

Motion stability of inertial navigation gyroscope system with gyro horizon compass, noting constant and time dependent coefficients of motion equations 19 p2830 A72-37320

Complex systems dynamics and stability problems, deriving equations of motion and boundary conditions from principle of least action 19 p2784 A72-37388

Numerical solution of the problem of the motion of a circular cylinder in a viscous fluid flow 19 p2784 A72-37395

Determination of the motion of a model, possessing a mass and a viscoelastic element, for a given harmonic law of motion of the vibrating support 19 p2871 A72-37427

The motion of a vortex filament with axial flow 19 p2786 A72-37598

Numerical integration method with recurrent power series for motion and variational equations of elliptic restricted three body problem 19 p2862 A72-38019

Third integral of equations of motion in axisymmetric potential field, noting Jeans theorem for phase density in star system 19 p2863 A72-38068

Equations of motion in the linear approximation. 19 p2835 A72-38174

Integration of equations of motion for nonconservative holonomic systems with pulsed coupling forces 19 p2825 A72-38192

Gravitational spin interaction. 19 p2835 A72-38425

A method of realizing servo links imposed on a mechanical system. I 19 p2835 A72-38587

The mechanics of an organized wave in turbulent shear flow. III - Theoretical models and comparisons with experiments. 19 p2789 A72-38794

Method of characteristics for nonlinear equations of perturbed motion of fluid near contact point between shock and diffraction waves 20 p2912 A72-39023

Third-order resonance during oscillations of Hamiltonian system of nonlinearly coupled oscillators, obtaining equations of motion and phase portraits 20 p2956 A72-40034

The theory of motion of the horizontal pendulum with a Zoellner suspension and some indications for the instrumental design. 21 p3084 A72-40495

Stress functions in three-dimensional elastodynamics. 21 p3117 A72-40677

The behaviour of the solutions of the equations of motion of a mechanical system, with a parameter occurring as a coefficient of each derivative. 21 p3084 A72-40812

Numerical stabilization of the differential equations of Keplerian motion. 21 p3106 A72-41050

A method of numerical integration for trajectories with variational equations. [AIAA PAPER 72-910] 21 p3111 A72-41557

Equations of motion for the variable mass flow-variable exhaust velocity rocket. [AIAA PAPER 72-912] 21 p3112 A72-41559

Integrals of the motion for optimal trajectories in atmospheric flight. [AIAA PAPER 72-931] 21 p3112 A72-41570

Interactions between stars and local dust formations 21 p3113 A72-41758

Numerical analysis of wave processes in a three-layer strip with rigid filler 22 p2322 A72-41872

Relation between the first integrals of a non-holonomic mechanical system and a corresponding system freed of constraints 22 p3204 A72-41902

Invariant solutions of the differential equations of the uniform motion of a Hooke medium 22 p2323 A72-42058

Dynamic equations integration with constraint factors, discussing Hamilton-Jacobi method applicability conditions 22 p3205 A72-42100

Quadrature solution for variable mass point motion under perturbing force in trajectory plane normal to velocity vector 22 p3205 A72-42101

Finned missiles nonlinear rolling motion characteristics at large angles of attack, solving differential equation of motion by global nonlinear least squares method [AIAA PAPER 72-980] 22 p3134 A72-42333

Helicopter rotor blade flapping motion stability, applying perturbation technique to linear equations of motion for different advance ratios and Lock numbers [AIAA PAPER 72-955] 22 p3137 A72-42351

Equations of motion appropriate to the analysis of control configured vehicles. [AIAA PAPER 72-952] 22 p3137 A72-42353

Applications of a technique for estimating aircraft states from recorded flight test data. [AIAA PAPER 72-965] 22 p3138 A72-42360

The dynamical effects of stellar mass loss on diffuse nebulae. 22 p3224 A72-42380

Simple thickness modes for laminated composite materials. 22 p2325 A72-42465

Three dimensional thermoelastodynamic theory for elastic beams, deriving nonlinear motion equations by combined expansion and variational methods 22 p2325 A72-42523

The dynamics of the ascending flight of sounding rockets [ONERA, TP NO. 1056] 22 p2321 A72-42582

Steady state equations of motion, equilibrium shape and stability derivatives of elastic airplanes evaluated with finite element methods. 22 p3138 A72-42845

- Rigid-body motions and strain-displacement equations of curved shell finite elements. 22 p3240 A72-42892
- Theory of a gyrohorizon compass with an azimuthally free casing of the sensitive element. 23 p3287 A72-43585
- Equations of motion of nonlinear nonholonomic mechanical systems of variable mass with impulsive constraint factors. 23 p3313 A72-43848
- The topology of the regularized integral surfaces of the 3-body problem. 23 p3309 A72-43982
- Stabilization of the motion of certain nonlinear systems by a linear approximation. 23 p3313 A72-44045
- Scattering of acoustical waves by a prolate spheroidal obstacle. 23 p3313 A72-44118
- Differential equations of motion of two mutually perturbing bodies, noting series expansion of perturbation function for close commensurability of mean motions. 24 p3437 A72-44761
- High order terms diffusion equation derivation for strong fluctuating flows by random walk method, discussing phenomenological analogy with equations of motion. 24 p3390 A72-44994
- Study of dynamic and thermal processes during steady motion of a viscous gas. 24 p3390 A72-44996
- The concept of reference loci applied to four-body dynamics. 24 p3440 A72-45137
- Relative equilibrium positions and their stability for a general gyrostat-satellite in a circular orbit. 24 p3449 A72-45142
- About the first integrals of the generalized problem of translatory-rotary motion of rigid bodies. 24 p3442 A72-45235
- Spinor differential equation of generalized unperturbed Kepler motion, using motor method and Lie algebra. 24 p3442 A72-45238
- The large Reynolds number - Asymptotic theory of turbulent boundary layers. 24 p3392 A72-45248
- Equations of motion of a viscous fluid with relaxation properties. 24 p3393 A72-45256
- Application of plane fixed equations of motion to reentry vehicle flight analysis. 24 p3452 A72-45345
- Perturbation methods in atmospheric flight mechanics. 24 p3368 A72-45350
- Equations for the general motion of a rocket in a resistant medium. 24 p3452 A72-45448
- Inertial effects in motion driven by hydrodynamic fluctuations. 24 p3430 A72-45560
- On the unsteady magnetohydrodynamic flow over yawed infinite cylinder. 24 p3395 A72-45599
- ### EQUATIONS OF STATE
- #### NT HUGONIOT EQUATION OF STATE
- FM communication system multifilter phase lock loop state equations derivation from phase model, predicting noise improvement characteristics by analog and digital simulation. 01 p0044 A72-10328
- Controllable states insufficiency to characterize rigid heat conductors dependence on temperature fields in experimental materials measurements programs. 01 p0146 A72-11389
- Equation of state for porous metals at high temperatures under strong shock compression, considering phase transitions. 02 p0258 A72-11469
- Plasma state variables diagnosis using laser light scattering. 02 p0263 A72-11697
- Extended Thomas-Fermi isolated atom model for pulsar outermost crust magnetic field effects, using pressure-density equations of state. 02 p0277 A72-11903
- Seigel state equation validity limit application to isentropic hydrogen and nitrogen steady and unsteady flow expansions at high pressure. 02 p0206 A72-12597
- State space method application to power servomechanism analysis, discussing transition matrices and state equations. 03 p0338 A72-13645
- Continuous solid medium electroelastic equations of state, obtaining solution by variational principles application. 03 p0390 A72-13916
- Equation of state for matter at 10-500 trillion g/cc, applying to baryon matter and neutron stars. 04 p0571 A72-14557
- Dislocation creep model for work hardening and recovery, deriving mechanical equation of states for various magnitudes and directions. 04 p0589 A72-15160
- Adaptive control algorithm with disturbance prediction for solution of deterministic and stochastic optimization problems of linear equation of state and quadratic performance criteria. 05 p0639 A72-15759
- Hadron era evolution, discussing equation of state, ultimate temperature, galactic formation and adiabatic exponent application to Friedman universes. 06 p0886 A72-18096
- Algorithm for constructing linear and nonlinear differential and algebraic equations of state variables of nonlinear electronic circuits. 07 p0958 A72-18846
- Optimal strategies for decision chain with controllable connections and finite number of states and decisions, deriving existence theorem. 07 p1028 A72-19904
- Stellar structure calculation by real gas equation of state, considering He abundances and solar lines of ionizable metal atoms. 07 p1078 A72-19925
- Interactive graphics technique for design of single input linear feedback systems described by state equations or cascaded transfer functions. 07 p0963 A72-20391
- Equation of state data of solids from shock vaporization, using spectroscopic technique. 09 p1351 A72-22856
- Thermodynamic properties of high temperature and density hydrogen, using Rowlinson equation of state. 09 p1412 A72-23234
- Nonanalytic equation of state formulation at critical point of fluid phase transformation. 09 p1413 A72-23690
- State sensitivity functions in aircraft parameter identification for lateral dynamics under aileron deflection from model response and in-flight test data. 10 p1421 A72-23807
- Equations of state for ultrahigh densities, obtaining relativistic statistical thermodynamics description of hadronic interactions. 10 p1533 A72-23891
- Model for I/O channel traffic in computer systems, obtaining closed solution for stationary probabilities of state. 10 p1446 A72-25148
- Nonlinear differential energy equation of static state stellar atmospheres with radiation and heat conduction terms. 13 p2036 A72-28890
- Expanding hot universe evolution from astrophysical cosmology point of view, emphasizing galaxy formation relation to state of matter and radiation in early universe. 13 p2038 A72-29084
- Work hardening-recovery model of dislocation creep, deriving multiaxial mechanical equation of states for strain/time relationship under arbitrary temperature-stress sequences. 13 p2061 A72-29872
- Mathematical model for magnetized solar wind with one fluid MHD and polytropic state equations, calculating magnetic field variables at earth. 13 p2034 A72-29958
- Computerized determination of cryogenic gas behavior near vapor region, obtaining state equation coefficients from curve fitting program. 15 p2334 A72-31580
- Equations of state and equilibrium for electron gas in strong magnetic field, discussing effects in pulsar crusts and atmospheres. 16 p2460 A72-33929
- State equation for superdense stars treated as perfect degenerate tachyon gas, noting dynamic stability for arbitrarily large central densities. 18 p2726 A72-36715
- Computer method for plasticity theory boundary value problem for medium with unknown equations of state, using complex load simulating device. 19 p2870 A72-37387
- Elasto-visco-plastic constitutive equations for quasi-static structures calculations. 19 p2875 A72-37763
- [ONERA, TP NO. 1089] Numerical calculation of third virial coefficient in equation of state of real gases eliminating errors associated with substitution of integration infinite integral. 19 p2838 A72-38462
- A generalized virial equation of state and its application to vapor-liquid equilibria at low temperatures. 19 p2883 A72-38838
- Introduction of two resolving functions into the equations for nonshallow shells. 20 p2979 A72-39405
- General relativity equations for hydrostatic equilibrium of spherical distribution of mass combined with equations of state for highly relativistic neutron star central regions. 20 p2955 A72-40011
- Two phase stellar structure with polytropic equations of state for shell and core, calculating configuration mass, radius and energy. 21 p3102 A72-40098
- Existence theorems in multidimensional problems of optimization with distributed and boundary controls. 21 p3074 A72-40548
- Thermodynamic parameters and reacting multicomponent mixture composition, using state equations and energy conservation equations for reaction kinetics. 21 p3013 A72-40989
- Extended Kalman filter application to delayed systems for state and time delay estimation, discussing two nonlinear estimators. 21 p3039 A72-41553
- [AIAA PAPER 72-902] Equation of state of a mixture of nonequid chemically reacting gases. 22 p3152 A72-41881
- Caloric state equation for isentropes and temperature calculation of nonequid Cs plasma produced in high density vapors by shock wave compression. 23 p3318 A72-43320
- Linear electronic networks analysis and synthesis via equations of variable states, noting structural features of circuits without component related degeneration. 23 p3271 A72-43844
- Equation of state relating time variations of stress and strain in elastoplastic material under tension. 24 p3459 A72-45069
- ### EQUATORIAL ELECTROJET
- Farley-Buneman instability nonlinear development mechanism in equatorial electrojet, noting turbulent vertical electron flux role. 01 p0062 A72-10901
- Meridional currents intensity in equatorial electrojet region, computing electric and magnetic fields. 01 p0063 A72-10924
- Equatorial ionospheric drift measurements and relation to electrojet from H component geomagnetic field variations. 02 p0221 A72-12459
- Sporadic E disappearance due to temporary reversal of equatorial electrojet current, observing horizontal geomagnetic field component. 03 p0345 A72-12999
- Three frequency radar spectral measurements of two stream and gradient plasma instabilities in equatorial electrojet as function of wavelength. 03 p0349 A72-13521
- F 2 layer anomalies association with equatorial electrojet, investigating midday critical frequencies of sporadic E layer. 04 p0515 A72-14932
- Electrojet effects on critical frequencies in equatorial F region during magnetically quiet and disturbed days. 04 p0516 A72-14936
- Longitudinal wave interaction and excitation by plasma instability in equatorial electrojet, considering energy transfer mechanism. 05 p0656 A72-16242
- Equatorward motion of midday auroras during magnetospheric substorms, using all sky photographs. 06 p0805 A72-17463
- Electroconductivities and electrostatic field structure within equatorial electrojet, observing vertical distribution. 07 p1056 A72-18896
- Wave propagation effects on irregularities observation in equatorial electrojet, presenting velocity profile and typical ray path. 09 p1300 A72-23024
- Lunar variations of Peruvian electrojet, analyzing E region electron drift and geomagnetic field H component data. 11 p1626 A72-26415
- Tropical sporadic E reflections and vertical plasma instabilities as function of equatorial electrojet and electron drift ratio based on ionogram observations. 16 p2382 A72-32867
- F region crossed field instability nonlinear theory based on energy transfer by mode coupling and absorption by linear damping with application to equatorial electrojet. 16 p2384 A72-32976
- Dawn and dusk ionospheric conductivity gradients effects on equatorial electrojet, deriving vertical currents existence. 16 p2385 A72-33377
- Nonlinear theory of crossed field and two stream instabilities of nonthermal plasma motions in equatorial electrojet. 16 p2387 A72-33937
- Nonlinear saturation of 'type I' irregularities in the equatorial electrojet. 18 p2685 A72-35990
- Low latitude equatorial electrojet analysis based on three dimensional electric field equation for ionosphere and magnetosphere. 18 p2687 A72-36854

Some problems of electromagnetic induction in the equatorial electrojet region. II - The analysis of magnetic and telluric variations at Zaria, Nigeria.

19 p2789 A72-37772

Influence of solar flux and the equatorial electrojet on the diurnal development of the latitude distribution of total electron content in the 'equatorial anomaly'.

19 p2794 A72-38868

The interpretation of surface equatorial magnetic daily variations on disturbed days.

20 p2916 A72-39238

Geomagnetic DP-2 variation base level from E region electron drift velocity measurements in equatorial electrojets

22 p3169 A72-42013

The equatorial electrojet according to measurements from the Cosmos 321 satellite

23 p3328 A72-43369

EQUATORIAL ORBITS

NT STATIONARY ORBITS

Scintillation effects on synchronous satellite communications systems at 250 MHz in equatorial region, discussing diversity techniques and composite diffraction refraction theory [ALAA PAPER 72-178]

05 p0631 A72-16906

Liapunov stability of circular equatorial motions of light bodies in Kerr gravitational field of massive rotating body, using geodesic lines equations

08 p1210 A72-22071

Frequency shift and mode shapes for equatorial vibrations of flexible boom on spin stabilized satellite, applying to thermal flutter resonance and nutational stability

15 p2320 A72-31803

Permanent rotations of an equatorial satellite in the geomagnetic field

19 p2869 A72-37437

First order theory of satellite orbit determination with time difference data for synchronous equatorial spacecraft, applying to VLBI experiments with ATS-3 [ALAA PAPER 72-924]

21 p3112 A72-41568

Small oscillations of gravity gradient satellite in circular near-equatorial orbit, discussing operational efficiency of magnetic damping systems

22 p3230 A72-42223

On the utilization of thermonuclear propulsion for an upper stage of the Europa III launcher

24 p3424 A72-45227

EQUATORS

NT MAGNETIC EQUATOR

Equatorial E region short wave oblique incidence propagation experiment showing transmitted impulse delay increase with frequency decrease

01 p0056 A72-10437

Equatorial sporadic E sudden disappearance associated with magnetic field depressions, noting irregularities and electron velocities role

10 p1475 A72-24956

Equatorial Faraday rotation measurements for night ionospheric electron density peak structures during equinoctial months, using ATS-C geostationary satellite radiation

10 p1476 A72-24958

Semiannual equatorial wind oscillations in upper stratosphere and lower mesosphere dependence on temperature variations in high and middle latitudes

14 p2099 A72-30259

Blanketing sporadic E layer latitude seasonal variations near geographic equator, noting spread F occurrence and solar cycle effects

15 p2231 A72-32265

Infrared and radar maps of the lunar equatorial region.

18 p2725 A72-36289

Equatorial stratospheric waves induced by diabatic heat sources.

22 p3201 A72-42508

Accuracy of the determination of the zero points of a fundamental catalog from observations of major and minor planets

24 p3447 A72-45676

EQUILIBRIUM

Axisymmetric MHD equilibria with elliptical cross sections and flat current profile, obtaining criterion for stability to localized modes by numerical computation

09 p1361 A72-23047

Book on structural analysis covering statically indeterminate structures, force and displacement methods, flexibility and stiffness matrices, strain energy, virtual work, energy theorems, etc

15 p2325 A72-31517

Stability analysis of gyrostad satellites possible equilibria under gravitational torques, considering inertia, equilibrium and angular momentum parameters

15 p2321 A72-32586

Instability conditions for holonomic system with stationary constraints, applying to pendulum and to rectilinear motion of material point

20 p2955 A72-40033

Instability of the equilibrium position of a multi-dimensional system consisting of 'neutrally' unstable subsystems

21 p3126 A72-41546

The equilibrium configuration of a slowly rotating mass of liquid in the presence of a poloidal magnetic field.

23 p3322 A72-44306

EQUILIBRIUM DIAGRAMS

U PHASE DIAGRAMS

EQUILIBRIUM EQUATIONS

Homogeneous isotropic thin elastic shells under forces along edge and with faces free of tractions, deriving refined interior equilibrium equations

03 p0447 A72-13882

Potential energy principle in equilibrium stability problems for flexible extendable thread, using Liapunov method

03 p0390 A72-14208

MHD equilibrium equations for axially asymmetric finite beta toroidal plasma with diffuse boundaries

04 p0556 A72-14854

Convergence of iterative schemes for calculating stress state of thin shells with allowance for nonlinear terms in differential equilibrium equations

04 p0587 A72-15048

Asymmetric micropolar elasticity plane problem, solving equilibrium equations with Fourier transformation for displacements, rotation and stresses

05 p0737 A72-16296

Equilibrium equations solution for displacements of inhomogeneous isotropic elastic media

05 p0739 A72-16588

Equilibrium equations for thin walled shallow paraboloid shell of revolution, solving boundary value problem for edge fastened loaded circular planform region

07 p1091 A72-19757

Moment stresses and deflections of rigidly clamped hinged and simply supported square elastic plates beyond elastic limit, deriving equilibrium and strain compatibility equations

07 p1091 A72-19759

Variational principle in equilibrium and stability theory of rotating bodies under magnetic and thermal fields, explaining spiral branch number in galaxies

07 p1077 A72-19806

Anisotropic equilibrium solution to Vlasov equation for high beta theta pinch plasma column

07 p1045 A72-20478

Euler-Lagrange equation construction to obtain phenomenological description of quasi-equilibrium systems in metrics, noting solution coincidence with Onsager equations

07 p1102 A72-20665

Stable equilibrium conditions for linear elastic body, using Reissner functional

08 p1248 A72-21819

Axisymmetric deformation of hollow elongated elastic ellipsoid, using Lamé equilibrium equations

09 p1400 A72-22708

Micropolar thermoelasticity steady state axisymmetric problem solution from equilibrium equations, considering uniform surface temperature and surface heat doublet cases

09 p1403 A72-22749

Bent lever equilibrium and relativistic mass for point body in motion, introducing von Laue energy flow inertia into d'Alembert principle

10 p1505 A72-24074

Stability loss in thin convex shells of revolution under axisymmetric stress, obtaining integrals for equilibrium equations

10 p1557 A72-24630

LTE solutions of relativistic Boltzmann equation in presence of external electromagnetic field

10 p1513 A72-24856

Violation effect of moment equilibrium about normal in shell of revolution and helical shell theory, discussing distribution

10 p1560 A72-25171

Time dependent solutions of Tokamak equilibrium equations for plasma diffusive processes

11 p1694 A72-25787

Equilibrium stability of hyperelastic bodies under finite strain, deriving differential equations and boundary conditions of critical equilibrium states

11 p1686 A72-25916

Nonlocal elasticity theory from global equilibrium and second thermodynamics laws, deriving constitutive equations from Clausius-Duhem inequality and Gibbs thermodynamics

11 p1738 A72-26721

Chemical and ionizational equilibrium equations of heterogeneous gas mixture composition with allowance for condensed phase ionization

11 p1747 A72-26965

Nonlinear equilibrium equations and elastic stability of cylindrical shell weakened by circular hole

12 p1878 A72-27080

Equilibrium equations of infinite strip with circular hole, using plane multiply connected domain method for stress field

12 p1878 A72-27087

Third approximation solution to elastic bending equilibrium equations of Vekua plate theory in form of holomorphic functions

12 p1880 A72-27327

Hybrid cylindrical shell finite element, determining natural frequencies from equilibrium equations, stress functions stress-strain relationships and boundary force transfer matrices

12 p1882 A72-27339

Flux functions and balance laws for linear momentum in continuum mechanics, deriving traction vector and differential equilibrium equation

12 p1846 A72-27570

Iterative solution existence for elastic equilibrium problem of thin plates and shells near boundary layer

12 p1886 A72-27997

Ca and Na ionization equilibrium ratio in dust filled interstellar clouds, considering cosmic ray and charge transfer influence

13 p2040 A72-29405

Elastoplastic equilibrium theorems for solid subjected to variable external effects, considering perfectly plastic and arbitrary hardening materials

14 p2165 A72-30574

Nonlinear equilibrium, stability and vibration equations of shallow sandwich shells with isotropic outer layer and rigid compressible filler obtained by variational method

14 p2166 A72-30700

Slender rotating body aeroelastic behavior under inertial, gravitational, thrust, servocontrol, elastic and aerodynamic forces, presenting equilibrium equations in matrix form

15 p2319 A72-31210

Equilibrium equations for boundary value problems in Vekua theory with moments allowance for plate with circular hole under bending and torsion

15 p2333 A72-32682

Constitutive and equilibrium equations for theory of thin shells with slowly varying curvature based on Novoshilov and Kolter assumptions

16 p2465 A72-33004

Schaefer equilibrium and compatibility equations and Reissner constitutive equations for orthotropic cylindrical shells reduction to four simultaneous third-order equations

16 p2466 A72-33023

Displacements, rotations and stresses equilibrium equations solution for plane micropolar elastic half space, using exponential Fourier transforms

16 p2466 A72-33105

Equilibrium equations and boundary conditions for elastic buckling of open cylindrical sandwich shell under compressive forces applied to freely supported edges

16 p2467 A72-33116

Equilibrium equation for elastic deformation effect on free electricity redistribution in thin electroconductive shells

16 p2469 A72-33271

Stress analysis for brittle body with thermoinsulated crack under mechanical load and temperature field, noting limiting equilibrium equation

16 p2469 A72-33272

Nonlocal fluid dynamics continuum theory with equilibrium and constitutive equations derived by generalizing Stokes Laws, noting steady channel and shear flow

16 p2379 A72-33832

Equations of state and equilibrium for electron gas in strong magnetic field, discussing effects in pulsar crusts and atmospheres

16 p2460 A72-33929

Deflection of plate on elastic support from equilibrium equations based on shell theory

16 p2472 A72-34015

The equilibrium configuration of the gaseous component of the Galaxy.

17 p2611 A72-35312

Variational principle in equilibrium and stability theory of rotating bodies under magnetic and thermal fields, explaining spiral branch number in galaxies

17 p2617 A72-35730

Variational principles of the nonlinear theory of elasticity - Case of superposition of a small deformation on a finite deformation.

19 p2872 A72-37559

Equilibrium equations solution for displacements of inhomogeneous isotropic elastic media

19 p2872 A72-37560

Thick shell and oriented surface theories.

19 p2873 A72-37694

Convergence of a simple iteration scheme in equilibrium problems of flexible plates

19 p2877 A72-38201

Ionisation equilibrium and line intensities for an X-ray heated H I gas.

19 p2852 A72-38509

The equilibrium and the pulsation frequency spectrum of an electron cloud of spherical and cylindrical symmetry

19 p2867 A72-38571

General relativity equations for hydrostatic equilibrium of spherical distribution of mass combined with equations of state for highly relativistic neutron star central regions

20 p2955 A72-40011

- Linear equilibrium stability relationship to wave propagation through elastic medium, considering Hadamard theorem proofs 21 p3085 A72-41102
- Mechanical equilibrium equation of nongray stellar matter, approximating electron pressure vs temperature in early stellar atmospheres 21 p3109 A72-41435
- Nonlinear equilibrium equations for hinged flat circular and spherical membranes under large axisymmetric elastic deformations due to internal pressure 21 p3125 A72-41516
- Equilibrium equations for given stress concentration in circular and annular plates under tensile loads with different yield points in tension and compression 21 p3126 A72-41545
- Equilibrium and elastic deformation equations for closed cylindrical shells with arbitrary cross section and variable wall thickness 21 p3126 A72-41551
- Steady state or periodic solution to initial boundary value problems for heat conduction equation with nonlinear terms and boundary conditions 21 p3131 A72-41667
- Differential rotation of polytropic stellar models by structural equilibrium equations, disproving Porfiriev theory 21 p3114 A72-41775
- Convergence of the homogeneous linear approximation method in problems of plasticity theory of inhomogeneous bodies 22 p3232 A72-41911
- Equilibrium equation for unsteady creep of thin truncated conical shell under internal pressure, solving in successive time steps with Taylor series expansion 22 p3233 A72-42062
- Multilayer shells structural analysis via equilibrium equations transformation into system of equivalent equations 22 p3238 A72-42836
- The method of Muskhelishvili applied to coupled isotropic elastic plates 22 p3242 A72-43202
- Equilibrium equations for vortex lines with allowance for interaction with boundary of ideal superconductor, calculating extremum values of magnetic field 23 p3312 A72-43316
- Equilibrium equations and deformation of elastoplastic thin isotropic cylindrical shell with circular hole, noting nonlinear partial differential equations for plate displacements 23 p3345 A72-43587
- Limiting equilibrium of shallow conical shells of variable thickness 23 p3348 A72-43787
- First order constraints in three dimensional continuous elastic fibrous media and thin shells, presenting equilibrium equations 23 p3349 A72-43825
- Equilibrium and stress resultant displacement equations of thin rings based on virtual work principle, stressing warping and twisting moments 23 p3351 A72-44101
- Equilibrium equations of sandwich shell element with weak core and thin membrane facings under large transverse normal and shear strains, showing analogy to Cosserat surface theory 23 p3351 A72-44103
- Nonlinear sandwich shell and Cosserat surface theory 23 p3351 A72-44107
- Stability of orthotropic stiffened composite plates 23 p3352 A72-44109
- A method for balancing geopotential and wind fields 24 p3420 A72-44765
- Pure antiplane stress and equilibrium of isotropic elastic beams, considering suspended cylinders 24 p3459 A72-44989
- Relative equilibrium positions and their stability for a general gyrostat-satellite in a circular orbit 24 p3449 A72-45142
- A linear asymptotic theory for anisotropic shells 24 p3460 A72-45473
- EQUILIBRIUM FLOW**
- NT FROZEN EQUILIBRIUM FLOW**
- Equilibrium shear flow of stratified brine in cyclically continuous rectangular tank, discussing stable density region erosion by turbulent layers, Richardson numbers, transition layer and entrainment 01 p0051 A72-11228
- Pressure gradient effect on mixing length for equilibrium turbulent boundary layers, calculating eddy viscosity [AIAA PAPER 72-213] 05 p0651 A72-16855
- Solar wind speed variations, examining velocity structure recurrence at various rotations, time interval of steady state flow and temporal velocity effects 06 p0872 A72-17442
- Equilibrium turbulent flow of incompressible fluid in plane diffusers, taking into account channel cross section including viscous sublayer 06 p0801 A72-18144
- Incompressible fluid near equilibrium turbulent flow velocity distribution through plane diffuser, taking into account upstream conditions 07 p0972 A72-20115
- Equations of motion for discrete structure fluid, discussing equilibrium pressure and fluid-wall interaction effects 09 p1296 A72-23691
- German monograph on flow calculation in axial thermal turbomachines covering boundary conditions and field computation for steady state inviscid flow 10 p1415 A72-23772
- Equilibrium state dynamics of Burger turbulence model with two velocity components, using Fourier amplitude representation 11 p1615 A72-25553
- Linear impulsive spin down from rigid body rotational equilibrium of radiation penetrated opaque compressible fluid in circular cylinder 11 p1680 A72-25555
- Eddies memory in turbulent shear flow from experiments on plane turbulent wakes undergoing equilibrium transition under impulsive pressure gradient effect 18 p2680 A72-36476
- A study of the asymptotic behaviour of the external fringes of compressible, laminar boundary layers of a dissociating gas 18 p2683 A72-36937
- Development of the AEDC-VKF tunnel J - A real gas high density, true velocity, hypersonic, aerodynamic test facility. 21 p3040 A72-41579
- A study of loss of radial equilibrium solution in axial-flow blade row design calculations. 24 p3393 A72-45358
- EQUILIBRIUM METHODS**
- Force system axial equilibrium conditions for reference coordinates to eliminate inadmissible axes, deriving theorem for applicability limits 02 p0260 A72-12439
- Finite element displacement field with internal equilibrium application to nine degrees of freedom triangular bending element stiffness matrix calculation 14 p2168 A72-30930
- EQUINOXES**
- Lunisolar precession and equinox motion, discussing determination methods based on proper motions referred to fundamental systems 04 p0575 A72-15026
- Astronomical coordinate system, examining equinox proper motion and precession corrections 04 p0575 A72-15029
- Lunisolar precession and equinox motion from Cepheids proper motion, using recently determined distance values 04 p0576 A72-15038
- Ephemeris time, lunar orbital elements and FK4 equinox correction from the observations of the moon by the method of equal altitudes. 17 p2603 A72-34274
- Equinoctial orbit elements position and velocity vectors partial derivatives matrices for two body problem, discussing application to general and special perturbations 17 p2609 A72-35104
- Equinoctial orbit elements - Application to artificial satellite orbits. 21 p3112 A72-41575
- [AIAA PAPER 72-937] Accuracy of the determination of the zero points of a fundamental catalog from observations of major and minor planets 24 p3447 A72-45676
- EQUIPMENT SPECIFICATIONS**
- ECG telemetry systems parameters, discussing manufacturers specifications and standardized laboratory performance test data 02 p0169 A72-12139
- Pioneer F and G space probe EMC specification limits, comparing computer analysis prediction and system test data 03 p0329 A72-14048
- Proposed ASME procurement standards for gas turbines and generators, with compilation and definitions of specification terms [ASME PAPER 71-WA/GT-2] 05 p0703 A72-15895
- Reliability data collection methods, considering equipment initial design, breadboard models, prototype, production, acceptance, qualification, field installation and operation 10 p1443 A72-23975
- Mathematical model as basis for equipment design-sensitive maintainability prediction technique, using information theory concepts of design interpretation 10 p1503 A72-23979
- Spacecraft electronic equipment design criteria for maintainability and installation, discussing mockup zero g demonstration tests of new packaging concepts [AIAA PAPER 72-235] 10 p1487 A72-24445
- General aviation equipment standards in light of air traffic system safety needs, emphasizing Technical Standard Order system 11 p1748 A72-25571
- MOS specifications and application to shift registers, considering maximum ratings, clock pulse level and width and pulse rate 11 p1611 A72-26387
- Specification requirements for quality assurance of automated data processing systems based on hardware development procedures 11 p1602 A72-26791
- Instrument landing systems specifications for civil and military aviation, suggesting replacement type development based on existing configurations 12 p1842 A72-27110
- Complete aircraft systems reliability and maintainability, discussing extraordinary variances causes, faulty data inferences and operational testing for equipment specifications validation 13 p1896 A72-28358
- Quantified design criteria for vibration and shock test fixtures to insure test repeatability, proposing chart inclusion in military test standards 15 p2215 A72-32619
- Attitude instruments, pitch and roll. I - Minimum performance standard for equipment. 18 p2692 A72-36534
- [SAE AS 1162] Reliable component procurement for Symphonie satellite, discussing parts list, specifications and subcontract monitoring and inspection 18 p2670 A72-37124
- Electronic primary flight control system requirements and equipment characteristics, discussing USAF and NASA fly by wire R and D programs [AIAA PAPER 72-882] 20 p2887 A72-39118
- Analog and digital data recording systems, discussing accuracy, versatility and cost factor tradeoffs in selecting equipment for given applications 22 p3155 A72-42707
- Electrohydraulic stand for vibration strength testing, discussing system design, specifications, frequency-amplitude characteristics and applications 23 p3278 A72-43760
- IR detector specifications, construction and applications to industry science and military 23 p3291 A72-44393
- Time ratio models of equipment availability for using and procuring agencies, considering performance effectiveness criterion and suboptimization risk 24 p3467 A72-44659
- EQUIPOTENTIALS**
- Best fitting triaxial ellipsoid representation of seleno-equipotential surface at Apollo 12 landing site based on observed local gravity and moon angular velocity 15 p2308 A72-31922
- EQUIVALENCE**
- Inertial and gravitational mass equivalence principle verified for aluminum and platinum, using torsional pendulum with large relaxation time 03 p0388 A72-13076
- Gravitational wave detection, discussing equivalence principle and force measurement 03 p0389 A72-13272
- Equivalence of integral equation form and infinite system of linear equations with eigenvalue localization, applying to linear ordinary differential equations. 09 p1342 A72-23367
- Equivalence conditions for optimal control problems for stochastic and deterministic plants in cases of nonrandomized strategies 10 p1457 A72-24637
- German book on gravitation theory and equivalence principle, covering Lorentz invariance in Riemann space, relativity and Einstein effects 10 p1512 A72-24752
- Inertial and gravitational mass equivalence principle verified for Al and Pt, using torsional pendulum with large relaxation time 13 p2004 A72-29426
- Equivalent baseband and passband delay line and transversal equalizers derivation for linear modulation systems, obtaining relationship between tap coefficients 15 p2211 A72-31844
- Minimum norm and gradient projection constrained optimization techniques for iterative solution of trajectory optimization problems, presenting mathematical relations to prove equivalence 17 p2576 A72-35232
- Classical physics treatment combined with constitutive equations for local relativistic equivalence and material indifference principles 21 p3085 A72-41201
- Equivalence conditions for classes of linear and non-linear distributed parameter systems. 23 p3277 A72-44369
- EQUIVALENT CIRCUITS**
- Large-signal IC equivalent circuit model for DC, linear and nonlinear transient time circuit analysis of lateral p-n-p transistors, including isolation junction interactions 01 p0044 A72-10126
- Equivalent current system from measured geomagnetic disturbance vectors, solving Biot-Savart formula

derived nonlinear equations by Newton-Raphson iterative method

01 p0055 A72-10430

Gunn diode microwave oscillator postcoupling to waveguide, deriving theory based on equivalent circuit for load impedance assessment

01 p0037 A72-10640

Equivalent circuit model for electroacoustic surface microwave transducer, discussing radiation properties determination from excitation fields distribution

01 p0041 A72-10704

Equivalent circuits and characteristics of multiwire and small active transistorized antennas including unipoles, loops, Franklin arrays and mast antennas

02 p0191 A72-11685

Antenna If impedance measurements of lower terrestrial plasma wave characteristics, using equivalent impedance probe circuit

02 p0172 A72-11946

TWT small parameters measurement for gain calculation, using equivalent transmission line model

02 p0193 A72-12229

MOS transistor frequency and transient response characteristics for equivalent circuit synthesis, using Bessel functions in differential equation solution

02 p0196 A72-12761

Equivalent circuit models in semiconductor transport for thermal, optical, Auger-impact and tunneling recombination-generation-trapping processes

[AD-740495] Self oscillating dc-dc converter analysis and optimal design, modeling by single loop nonlinear feedback system

03 p0401 A72-13585

Radiative coupling of fed and unfed adjacent antennas in navigation systems rotating beam circular arrays, deriving equivalent circuit via quadrupole theory

05 p0635 A72-16300

N-channel Si MOS microwave transistor, discussing fabrication, design, power gain, stability, noise figure, equivalent circuit and applications

05 p0636 A72-16361

Microwave frequency multiplier construction by hybrid circuits based on quasi-lumped components, calculating characteristics from equivalent circuit

06 p0785 A72-18313

Operational and equivalent circuit characteristics of low noise hf and shf transistors in wideband amplifiers

08 p1139 A72-21052

Two dimensional dynamic model for background noise generation in bipolar transistors, using equivalent circuit

09 p1286 A72-23105

Alternative TEM and waveguide type equivalent circuits for rectangular resonator loaded by lumped capacitance

09 p1289 A72-23365

Interdigital acoustic surface wave transducer immittance characteristics calculation from equivalent circuit, demonstrating effectiveness on delay lines

[AD-743552] 09 p1316 A72-23421

Junction transistor equivalent circuit small signal parameters determination at VHF and UHF

10 p1450 A72-24324

T equivalent circuit magnetic modulator system with split excitation windings on four separate cores magnetized by HF source, noting null drift due to hysteresis

11 p1603 A72-25281

Pump and unloading valve hydraulic system model with waves processes allowance in connecting pipe, discussing liquid mass and leakage effects on stability

11 p1578 A72-25770

Microwave resonators excited in coupled and E sub zero modes, determining equivalent circuit and Sommerfeld resonator Q factor and guide wavelength

11 p1605 A72-26369

Equivalent network for symmetric inductive irises, investigating simultaneous effect of finite thickness and higher order mode interaction by variational approach

11 p1607 A72-26993

Static and impedance characteristics and equivalent circuit of p-n-p-n inductance diode, using ambipolar diffusion length

12 p1790 A72-27499

Channel formation in insulated gate FET, obtaining equivalent circuit

12 p1791 A72-27548

Slow wave structures attenuation effect on dispersion characteristics from equivalent circuit representation at two terminal pair networks

13 p1926 A72-28376

Antenna I.F impedance measurements of lower terrestrial plasma wave characteristics, using equivalent impedance probe circuit

13 p1920 A72-29258

Noise control by Helmholtz resonators, considering equivalent circuits via feedback schemes

13 p2005 A72-29567

Hysteretic motor in steady synchronous operation with nonsinusoidal supply voltage, computing stator winding current based on superposition with two linear equivalent circuits

13 p1900 A72-29975

Equivalent circuit characterization of waveguide-mounted IMPATT diode oscillators and associated circuit parasitics at millimeter wave frequencies

15 p2205 A72-31315

Nodal equations derivation for lumped circuit representation of Gunn diode with steadily propagating domain under steady state and transient conditions

15 p2205 A72-31317

Simplified equivalent circuit analysis for Gunn diode coupling to rectangular waveguide by inductive post, using perturbation approximation

15 p2205 A72-31353

Transistorized microwave amplifiers with dissipative equalizing networks, describing transistor equivalent circuit

15 p2206 A72-31659

Pulsed IMPATT diode oscillators RF oscillations growth rate and frequency shift behavior during build-up period, comparing equivalent circuit derived electrical properties with measurements

15 p2208 A72-32472

A simulation method permitting the direct construction of an integrated fluidic circuit with predetermined frequency response curve

17 p2494 A72-34197

Pulsed Impatt diode oscillator circuit design and operation frequency prediction for high Q coaxial structures from equivalent circuit

17 p2526 A72-34466

Three-dimensional small-signal analysis of bipolar transistors.

17 p2530 A72-35099

Design of nonlinear networks with a prescribed small-signal behavior.

17 p2533 A72-35199

Development of a continuous linear model of a d-c to d-c flyback converter.

18 p2643 A72-36073

Equivalent circuits and oriented graphs for network analysis and synthesis of nonlinear transducers used in control systems

19 p2777 A72-37316

French monograph - Contribution to the study of the behavior of bipolar transistors during high frequency dynamic operation

19 p2772 A72-37485

German monograph - A theoretical and experimental contribution to the equivalent circuits of electrofluidic transducers operating on the nozzle/deflecting plate principle

19 p2754 A72-37653

An analytical equivalent circuit representation for waveguide-mounted Gunn oscillators.

19 p2773 A72-38291

Eigenfrequencies of monolithic filters.

19 p2774 A72-38608

A large-signal theory for current-driven frequency multipliers.

19 p2775 A72-38609

Theory of spontaneous mode locking in lasers using a circuit model.

19 p2813 A72-38690

MOS transistor frequency and transient response characteristics for equivalent circuit synthesis, using Bessel functions in differential equation solution

20 p2907 A72-39067

Temperature-time characteristics of pulse-loaded temperature-measuring resistors

20 p2926 A72-39571

Digital filters with cyclically variable coefficients

21 p3025 A72-40221

Communication receivers interference modeling - Nonlinear transfer functions from circuit analysis - Mild excitations.

21 p3019 A72-40890

Avalanche transistor circuit with controlled S shaped I-V characteristics, discussing equivalent circuits and operating points stability

21 p3034 A72-41119

Quantitative derivation of large signal equivalent circuit of Gunn element in domain mode based on current and space charge characteristics

21 p3034 A72-41401

The distribution of gate-channel capacitance between source and drain in the equivalent circuit of a MOS transistor

21 p3035 A72-41490

General transport theory of noise in pn junction-like devices. I Three-dimensional Green's function formulation.

22 p3160 A72-43083

A solid-state 'flux-drive' control circuit for latching-ferrite-phaser applications.

23 p3275 A72-43574

Excitation of oscillations in transistor oscillators

23 p3271 A72-43840

MOS logic circuit design simplification by replacing series and parallel transistor networks by equivalent single transistor inverter circuit

23 p3271 A72-43843

A single-tuned oscillator circuit for Gunn diode characterizations.

23 p3272 A72-44194

ERBIUM

High resolution atmospheric transmission measurement of wavelength dependence of absorption losses in carbon dioxide of solid state Er laser radiation

02 p0238 A72-12201

Yb and Er cations dominant sites examination in zinc selenide from fluorescence emission spectra

03 p0404 A72-14265

Photoluminescence of Er cations in CdS, observing group I co-dopants sensitizing behavior and broadband emission spectra

04 p0563 A72-15472

Coherent emission lines in visible spectrum from triply ionized Er in barium yttrium fluoride, discussing energy level transitions associated with various lines

16 p2401 A72-33387

ERBIUM ALLOYS

Phase diagrams of Hf-Ce and Hf-Er alloys, plotting hardness and electroconductivity curves

15 p2289 A72-31188

Phase diagram of the neodymium-erbium system

19 p2846 A72-38473

ERBIUM COMPOUNDS

Phase diagrams of yttrium, erbium and ytterbium oxides at 1500-2400 C, using annealing and quenching method with differential thermal analysis

07 p1047 A72-18858

ERECTON

U CONSTRUCTION

ERGODIC PROCESS

Quasi-ergodicity condition of dynamic electromagnetic scattering diagram of flying object in terms of amplitude or phase elements

02 p0183 A72-12765

Fixed level intersection by two stationary ergodic independent random processes in observation time for dynamic control sampling and reliability estimation

05 p0641 A72-16316

Upper bound on rate distortion function for discrete ergodic sources with memory, applying to pictorial data processing

06 p0776 A72-18390

Reliability tests improvement by ergodic processes failure prediction and data storage for high reliability products manufactured in small numbers

08 p1180 A72-22067

Wiener generalized harmonic analysis relationship to steady random functions, emphasizing higher order properties and ergodic process conditions

10 p1504 A72-24063

Fixed level intersection by two stationary ergodic independent random processes in observation time for dynamic control sampling and reliability estimation

11 p1610 A72-25799

Ergodic boundary in initial conditions space for turbulent two dimensional flow, explaining phenomenon in terms of negative temperatures for point vortex model

12 p1797 A72-27183

Ergodic theorems for operators generated by Markov transients, examining asymptotic properties of stochastic learning model

12 p1787 A72-27924

Nonlinear resonating correlator with orthogonal filters, considering cut-off frequency of ergodic random process with constant power spectral density

14 p2090 A72-31125

Automated problem solving in continuous stochastic processes, using nonergodic representation of Gaussian process with continuous spectral density

15 p2204 A72-32588

Nonlinear vibration damper system subject to forced vibrations considered as stochastic processes in form of white noise and stationary and ergodic processes

16 p2467 A72-33144

Atmospheric turbulence statistical theory, discussing random flow field characterization by property expressed in ergodic theorem

17 p2537 A72-34273

Generalized random systems with complete connections

17 p2573 A72-34276

Fatigue life gages use in combination with strain multipliers in field applications with random ergodic cyclic strains

17 p2554 A72-34822

Central probability limit theorems and asymptotic normality in fluid mechanics for random stationary processes with uniform ergodicity and strong mixing

18 p2677 A72-36003

Reliability of simulations of asymptotically steady and strictly ergodic stochastic processes

18 p2704 A72-36467

Negative temperatures in two dimensional vortex motion.

18 p2681 A72-36669

Dynamic electromagnetic scattering pattern of flying object, constructing quasi-ergodicity condition to compute standard statistical descriptions for recognition

20 p2903 A72-39071

On the ergodic coefficients concerning generalized random systems with complete bonds

22 p3199 A72-42637

ERGOMETERS

Maximum oxygen intake during exercise on treadmill compared with bicycle ergometer, analyzing circulatory dynamic factors and cardiac output relation to oxygen transport capacity

07 p0922 A72-20251

Bicycle ergometer measurements of thermoregulation input and output under wide range of work load and climatic conditions, deriving correlation equation

11 p1579 A72-25874

Physical work capacity comparison during bicycle ergometry and treadmill walking tests, measuring oxygen uptake, ventilatory parameters and excess carbon dioxide production

11 p1579 A72-26095

Maximal oxygen uptake and heart rate during ladder climbing, inclined treadmill running and cycling ergometer tests

11 p1586 A72-26612

Correlation between ergometry, ballistocardiography and coronary angiography in 267 patients.

18 p2649 A72-36034

Self-paced ergometer performance - Effects of pedal resistance, motivational contingency and inspired oxygen concentration.

18 p2653 A72-36911

ERGONOMICS

U HUMAN FACTORS ENGINEERING

EROSION

NT WIND EROSION

Ductile metal surface erosion by hard abrasive grains striking at grazing angles

03 p0373 A72-13650

Mechanical and thermochemical erosion during ablation of silicophenolic material

04 p0597 A72-15554

Erosion of materials under drip impact loads, determining wear rate dependence on drop size, impact velocity and material properties

05 p0734 A72-15981

Explosive erosion in Al, Cu, W and Pb electrodes during high current spark discharges, using time resolved photography

05 p0692 A72-16032

Cathode temperature measurement in erosion and heat transport reduction by cesium seeding of Ar plasma arc

06 p0862 A72-18334

Cavitation erosion of Al in liquid oxygen as function of static pressure and ultrasound frequency

07 p1034 A72-18921

Cavitation phenomena role in liquid drop impact erosion of steam turbine blades leading edges

07 p0967 A72-19262

Phase composition changes, crater formation and metal ejection during erosion by pulsed laser beam

07 p1009 A72-20610

Dimensional metal working by material erosion involving stereomechanical energy transmission to surface of nonrigid mechanical body

08 p1173 A72-21027

Electrical erosion efficiency of metal working under increased pressure in discharge gap in air and water

08 p1174 A72-21029

Automatic control of electroerosion machining by process computer, using pulse-voltage-metal removal relation

08 p1174 A72-21030

Electroerosion machining with optimal control of electrical parameters, number of passes and electrode wear, using nonlinear programming and critical path method

08 p1174 A72-21032

Optimization for maximum productivity of electric spark machining with vibrating electrode, noting erosion product removal difficulties

08 p1174 A72-21033

German monograph on model concept for erosion mechanism involved in crystalline material surface bombardment covering particle elastic deformation during impact

09 p1397 A72-22324

Solid teflon pulsed plasma thruster quasi-steady and short pulse discharge operations, discussing propulsion system performance and erosion behavior

[AIAA PAPER 72-459]

11 p1709 A72-26195

Lifetime limitations of ion extraction systems for electron bombardment ion thrusters due to sputter erosion of electrode by ion beam

[AIAA PAPER 72-477]

12 p1860 A72-27421

Relaxation hypothesis of cavitation erosion based on small perturbations, eliminating theory-experiment contradictions

13 p1941 A72-28776

Air dust erosive damage to helicopter gas turbine engine parts, discussing inertial rotorless filtering systems

13 p2026 A72-28786

Mars surface particulate matter eroded by atmospheric winds, noting erosive and settling velocities and yellow clouds distribution

13 p2036 A72-28794

Cavitation erosion of Al in liquid oxygen as function of static pressure and ultrasound frequency

13 p1942 A72-29207

Surface phase transformation during cavitation erosion in Co and Fe alloys, suggesting stacking fault energy effect on erosion resistance

14 p2119 A72-30603

Thermomechanical erosion prediction for ablative, composite material, reentry nosetip applications and model development for heating, pressure and shear forces

[AIAA PAPER 72-299]

14 p2171 A72-30827

Lunar surface microerosion relationship to interplanetary dust particle flux distributions, investigating sputter erosion and lunar rocks lifetimes

15 p2310 A72-31988

Atmospheric organic vapor effects on electric contact erosion, deriving showering arc duration, gap breakdown, arc number and energy

18 p2665 A72-36118

Mechanism for relaxation of cavitation erosion based on small perturbations, eliminating theory-experiment contradictions

21 p3044 A72-40271

Erosion effects on gas turbine engine compressor blades due to dust ingestion, discussing means for alleviating performance and service life losses

[ICAS PAPER 72-02]

21 p3099 A72-41127

Erosion of materials under drip impact loads, determining wear rate dependence on drop size, impact velocity and material properties

24 p3460 A72-45723

ERROR ANALYSIS

Analog computer simulation of automatic control systems containing time delay element in feedback loop, evaluating errors

01 p0044 A72-10152

Error probability distributions in navigational statistics involving single or identical and diverse instruments or operators

01 p0096 A72-10176

Wideband FSK receiver for space telemetry, calculating error probability in multipath signal fading due to planetary surface reflections

01 p0025 A72-10329

Bit error rate estimation for narrow band digital communication in presence of atmospheric radio noise bursts

01 p0025 A72-10334

Accuracy of spacecraft trajectory determination by complex expressions in multidimensional geometric representation

01 p0127 A72-10353

Precision photogrammetric techniques coordinated with classical geodetic surveys for moderate cost control surveys, discussing error sources

01 p0065 A72-10455

Error fluctuation component spectral density determination in closed automatic nonlinear system for controlling random vibration spectrum

01 p0045 A72-10505

Algorithms for object apparent velocity calculation from linear acceleration and angular velocity integrators readings, estimating errors

01 p0135 A72-10507

Invariant imbedding theory of aerosols multiple scattering induced telephotometric errors, determining scattering coefficients relative to optical thickness by Monte Carlo method

[AIAA PAPER 71-1062]

01 p0066 A72-10531

Stellar intensity effect on angular navigation sighting accuracy attainable between star and lunar limb using Apollo T2 sextant

01 p0097 A72-10566

Primary component corrections for global cosmic ray variations from latitudinal expeditions, discussing adaptation to computer

01 p0118 A72-10584

Smith method for radio wave propagation time lag calculation, assessing maximum error by comparing calculated with measured distance/frequency characteristics

01 p0028 A72-10617

Atmospheric radio refractive index computation errors derived from monthly averages of pressure, dry bulb temperature and vapor pressure

01 p0095 A72-10835

Terminal aerodrome forecasts usefulness and accuracy assessment

01 p0095 A72-10864

Cloud temperature determination from satellite IR images, presenting error corrections for various U.S.S.R. locations

01 p0095 A72-10956

Spacecraft attitude determination with single-axis sensor and single natural radiation source with relative mutual motion, deriving error equations

01 p0032 A72-11224

Second order Markov process statistical model for gravity anomalies in local region, applying to error analysis in inertial navigation system computerized simulation

02 p0207 A72-11596

Asymptotic methods application to differential equations in nonlinear solar convection theory at high Rayleigh number, noting discrepancy from numerical integration

02 p0276 A72-11644

Optimal stochastic /Kalman/ filters application to integrated air and submarine navigation systems, discussing measurement errors modeling as bias and colored noise

02 p0256 A72-12050

Bias and spread in extreme value theory performance tests of communications systems, comparing with bit error rate tests

02 p0173 A72-12129

Coherent demodulation of continuous phase binary FSK signals in additive white noise, determining error probability

02 p0174 A72-12135

Steerable receiving antennas L/S band solar calibration error statistical analysis, obtaining 0.5 db uncertainty by monitoring antenna gain-to-noise temperature ratio

02 p0192 A72-12159

Phase error in 136 MHz interferometer due to galactic nucleus passage, obtaining lower bound

02 p0175 A72-12160

Steerable vhf/uhf receiving antennas stellar calibration error analysis, obtaining worst-case uncertainty of 0.4 db by monitoring antenna gain-to-noise temperature ratio

02 p0175 A72-12161

Feedback control dynamic system described by linear differential equation with random coefficients, calculating parameters distribution effect on behavior precision

02 p0197 A72-12339

Extremal system with second control loop for search signal frequency regulation to optimize primary loop operation, determining system dynamic errors under random drift

02 p0197 A72-12340

Low angle monopulse radar tracking errors due to multipath, considering amplitude variation across antenna aperture and reduction by target-image resolution

02 p0178 A72-12391

Distance effects on radio interferometric measurement accuracy, discussing single error source influence on total error

02 p0182 A72-12708

Aircraft trajectory optimization for maximum profit as decisional problem under risk conditions, determining probabilities by Monte Carlo method

02 p0257 A72-12747

Numerical weather prediction, discussing automatic forecasting, error sources, models and four-day validity in Northern Hemisphere

02 p0254 A72-12781

Radar accuracy for precipitation measurements, discussing error sources

02 p0254 A72-12784

Kalman filter divergence due to errors, applying to orbital navigation

02 p0198 A72-12805

Birefringent filter theory and optical properties, discussing transmission profile and error sources

03 p0352 A72-12947

Target motion simulator with photographic recording of image velocity and motion compensation in cameras, discussing errors

03 p0356 A72-13226

Dynamic structural analysis by finite element method, describing error bounds for eigenvalue analysis by elimination of variables

03 p0442 A72-13401

Computer calculation for atmospheric total mass and seasonal redistribution from pressure and temperature field data, discussing error sources

03 p0348 A72-13480

Imperfect thermal modeling of spacecraft based on error states representation in multidimensional Euclidean space, evaluating approximate total error effect

03 p0441 A72-13635

Synchros as electromechanical function generators and receivers for analog computers, examining errors in standard resolvers operation

03 p0328 A72-13841

Mean value, repetition and discontinuity errors of spectral transposition method involving memory storage and compressed signal processing

03 p0338 A72-13892

Linear scheme to calculate errors of incorrectable inertial systems

03 p0387 A72-13911

Soviet book on gyroscopic systems and inertial guidance instruments, emphasizing system motion under various dynamic conditions and systematic errors

03 p0362 A72-14167

Planar phased array antennas with uniform current amplitudes, calculating beam-pointing error dependence on array geometry, phase errors and scan angle

03 p0325 A72-14179

Code performance evaluation over real digital channels, characterizing channel error process by multigap statistics

03 p0325 A72-14183

- Multidimensional Gaussian distribution integrals evaluation for correlator analysis, discussing fix error probability and variance 03 p0387 A72-14189
- PCM/NRZ signal band limiting effect on bit error probability, presenting SNR degradation as function of bandwidth-bit duration product and bit patterns 03 p0325 A72-14192
- Past meteorological data assimilation in dynamical analysis, computing initial condition with time sequential data for error reduction 04 p0541 A72-14455
- Near optimum limiting and blanking levels /error probability/ selection for binary signal matched filter reception in Gaussian and impulse noise, discussing performance simulation 04 p0486 A72-14485
- Iteration method error estimates for thin elastic shell basic stressed state and simple fringe effect relation to boundary stressed state 04 p0586 A72-15012
- Modified quasi-linearization algorithm for solving nonlinear two-point boundary value problems based on performance index and cumulative error in differential equations 04 p0539 A72-15045
- Linear feedback control systems with time lag, calculating integrated squared error by Liapunov function 04 p0506 A72-15110
- Jimsonde high resolution temperature "nsor for FPS-16 Radar/Jimsphere wind system, analyzing rms errors 04 p0522 A72-15157
- Stellar radial velocities observation with photoelectric spectrometer, discussing catalog errors 04 p0577 A72-15280
- Error distribution computation for combined Rayleigh-Gaussian statistics data, applying to antenna radiation beam-pointing example 04 p0500 A72-15303
- Statistical calculation of wear rate in friction pair with linear contact, analyzing errors 04 p0528 A72-15711
- Error bounds on elastic-plastic strain wave measurements, considering one dimensional wave propagation in semiinfinite bar [ASME PAPER 71-MET-W] 05 p0731 A72-15789
- Distributed parameter state regulator system, investigating order of spatial discretization error in finite difference approximation to optimal response, control and performance cost 05 p0639 A72-15805
- Wilt-type quadrature formulas with preassigned nodes, featuring existence of error bound without derivatives 05 p0632 A72-15816
- Pulse and Doppler microwave radars comparison with respect to accuracy of moving targets velocity measurements and power characteristics 05 p0661 A72-16034
- Elastic boundary value problems static and geometric field parameters pointwise upper and lower bounds, determining solution coefficients by error energy minimization 05 p0735 A72-16062
- Artificial earth satellites orbit plane determination accuracy in terms of local vertical sensor errors and gyroscope drift 05 p0717 A72-16441
- Interplanetary spacecraft trajectory error analysis by closed form approximation to state transition matrix, enabling rapid estimation with computer program 05 p0718 A72-16443
- Coefficient rounding effect in digital filters using floating point arithmetic 05 p0633 A72-16576
- Error covariance matrix square root calculation in orbit determination from ground based observations 05 p0720 A72-16752
- Dynamic system observation accuracy in spacecraft trajectory measurement, deriving processing algorithm based on state-estimate error correlation matrix analysis with maximum likelihood procedure 05 p0721 A72-16760
- Polynomial class random process realization based on statistical methods of processing spacecraft orbital measurement data, considering random and systematic errors 05 p0683 A72-16763
- Methodical errors in spacecraft local vertical determination due to variability of physical effects, considering planet oblateness, atmospheric refraction, incident radiation fluctuations, etc 05 p0721 A72-16764
- Group velocity and numerical error propagation in partial differential and finite difference equations of gas dynamics [AIAA PAPER 72-153] 05 p0652 A72-16952
- Decision error estimates applied to detection problem with digital radar, computing upper and lower bounds for error probability 05 p0632 A72-17093
- Binary differentially coherent phase shift keyed system, evaluating error probability performance in presence of thermal noise and intersymbol interference 06 p0772 A72-17408
- Linear system digital simulation by matrix exponentiation with generalized hold order algorithm for accuracy improvement at less computer time 06 p0839 A72-17630
- Reconstruction errors, quantization noise and channel bandwidth in high order digital to analog conversion 06 p0779 A72-17783
- Critical review on data accuracy of maximum principal elastic stresses and deflections of thin initially-flat square isotropic plates under uniform normal pressure 06 p0894 A72-17796
- Hollow rubber impact absorber stiffness and deformation characteristics derivation by classical elasticity theory, noting accuracy 06 p0895 A72-17797
- Book on mechanization and error analysis of inertial navigation systems, stressing terrestrial applications 06 p0845 A72-17944
- Lunar photometric studies, discussing surface light scattering properties, data reduction and relative and systematic errors in brightness 06 p0817 A72-18224
- Longitudinally magnetized fully filled square waveguide reciprocal ferrite phase shifter, predicting frequency characteristics by rotational error analysis 06 p0786 A72-18370
- Block orthogonal M-ary communication over fading dispersive channel with intermittent on-off noiseless feedback, calculating upper and lower bounds on error probability 06 p0776 A72-18389
- Variable length codes using Fano metric for minimum error probability sequential decoding 06 p0776 A72-18393
- Nonlinear self oscillation solution for systems with two degrees of freedom, comparing with harmonic linearization method for error of small parameter method 06 p0851 A72-18721
- Gyroscopic error analysis, solving nonlinear equations by continuous Markov processes theory 06 p0819 A72-18724
- Error analysis of finite element solutions for elastic-plastic sandwich plates 07 p1086 A72-18779
- Coefficient matrix for estimation of numerical solution error bounds for finite element models 07 p1025 A72-18786
- Round-off error analysis in numerical solutions of finite element equations in dynamic models 07 p1025 A72-18796
- Mean square error and bound on relative error for Reissner plate theory, including shear deformation effect 07 p1087 A72-18812
- Complex systems calibration based on computer derived transfer function, discussing theory, Fortran calibration program, error analysis and applications 07 p0949 A72-18818
- Small parameter method application to quasi-linear problems solution in nonstationary heat conduction with substantial nonlinearities and weak perturbation, analyzing error 07 p1098 A72-18937
- Differential equation initial value problem solution error bounds construction by interval arithmetic to guarantee exact solution inclusion 07 p1026 A72-18968
- Aircraft engine test data processing by polynomial relations, assuming normal measurement error distribution 07 p0994 A72-18978
- Influence coefficients method accuracy for design and adjustment of gas turbines, engines and parts 07 p1054 A72-18998
- Signal design for coherent M-ary communication systems by stochastic gradient algorithm for minimizing error rate 07 p0959 A72-19285
- Hyperstable algorithm for multiinput and output systems identification through equation error method, representing scheme as equivalent time varying nonlinear feedback system 07 p1027 A72-19290
- Concatenated coded command system for low error probabilities at moderate SNR, emphasizing spaceborne portions implementation 07 p0949 A72-19299
- Target azimuth and elevation estimation by four beam cluster, analyzing angle estimation accuracy as function of SNR by computerized Monte Carlo simulation 07 p0941 A72-19304
- Radio direction finding with discrete antenna scanning and multilevel beacon signal quantization, investigating accuracy 07 p0943 A72-19523
- Isotope radiometric density measurement errors for thin material sections, presenting mathematical analysis for measurement procedures optimization 07 p0995 A72-19651
- K and Ka bands standard electromagnetic horn gain measurement and error analysis at different wavelengths by two-antenna method 07 p0957 A72-19784
- Disturbing gravity potential and vertical deflection calculation error reduction based on pure gravity anomalies in geodesy 07 p0977 A72-19819
- Spurious physical effects in penetrating cosmic ray showers resulting from momentum measurement errors 07 p1060 A72-19853
- Analog/hybrid simulation of noise effect on adaptive delta modulation system consisting of transmitter, receiver and error simulator 07 p0951 A72-20339
- Statistical analysis of system component error propagation by digital simulation using Continuous System Modeling program, considering strapped down inertial guidance computer 07 p1033 A72-20347
- Stability and local error of difference formulas derived from characteristic polynomial for first order ordinary differential equation solution 07 p1028 A72-20472
- Quantization errors effect on recursive filter design for strapdown inertial navigation systems, developing suboptimal linear minimum variance 08 p1144 A72-20848
- Numerically exact nonlinear filter synthesis, describing confidence intervals for error performance statistical inferences 08 p1144 A72-20850
- Biased estimator as alternative to linear unbiased estimator for dynamic system model states and parameters optimization and regulation, noting squared errors sum 08 p1144 A72-20852
- Jeans escape rate prediction validity for hydrogen atoms in upper atmosphere and error sources in physical models 08 p1159 A72-21401
- Local level and space stable inertial navigation systems, comparing position error propagation 08 p1204 A72-21410
- Sidewall reflection induced borelight error in anechoic chamber used for missile test or simulation 08 p1141 A72-21421
- Feedback control dynamic system described by linear differential equation with random coefficients, calculating parameters distribution effect on behavior precision 08 p1146 A72-21554
- Extremal system with second control loop for search signal frequency regulation to optimize primary loop operation, determining system dynamic errors under random drift 08 p1146 A72-21555
- Vibrotactile warning device effectiveness under auditory and visual loadings, investigating reaction time and errors number 08 p1126 A72-21569
- Systematic errors in scan-and-measure devices for tracking cameras photographs analysis, discussing correction during measurements 08 p1209 A72-21913
- Conjugate gradient method for computerized antenna radiation pattern synthesis using error functional minimization and iterative procedure 08 p1143 A72-21988
- Intense precipitation contour zone distinguishing methods error estimation in seeding experiments on frontal clouds 08 p1201 A72-21994
- Meteorological radar signal reflectivity probability and quantization error dependence on incoherent storage device parameters from computer simulation 08 p1201 A72-21995
- Deviation accumulation conditions and maximum dynamic error of linear automatic control system under perturbation, including theorem for Bellman equation 08 p1146 A72-22177
- Component evaluation of linearity error of measuring instruments 09 p1284 A72-22241
- Lateral refraction dependence on earth rotation and correction formula for angle measurement errors in class I triangulation 09 p1299 A72-22946
- Terrestrial altitude differences effects on photogrammetric data accuracy in two step compensation with models 09 p1311 A72-22966
- Rectification process for transformation of single photograph orientation into setting value, noting reduced accidental residual errors 09 p1311 A72-22967
- Axial thermal stresses in beams, investigating error in elementary calculations 09 p1405 A72-22999

Lunar limb charts comparison, computing corrections to orbital elements and systematic and random errors
09 p1388 A72-23056

Disk diameter errors due to wire thickness in reduction of visual planetary observations
09 p1311 A72-23062

Power series solutions to transition and matrix covariance differential equations, obtaining truncation error bounds and polynomial approximations
09 p1341 A72-23093

Air velocity calculation from hot-wire anemometer measurements in variable density flow, discussing correction factors checking method and application to internal combustion engine
09 p1315 A72-23390

Stationary Kalman-Bucy filter synthesis from filter coefficients and correlation matrix of filtration errors, discussing random process estimation application
09 p1289 A72-23434

Data reduction for photographic catalog of AGK2-AGK3 stars in terms of random and systematic errors in plate constants
09 p1392 A72-23543

Functional analytical formulation of steady creep processes, using error estimations in solution of equations with monotonic potential operators in Banach spaces
09 p1409 A72-23567

Wind and temperature fields periodic updating, considering error reduction as function of time intervals between updates
09 p1348 A72-23659

Measured quantity distribution effect on measurement errors, noting application in mass production process control
09 p1316 A72-23662

Optimum bounding filter design based on error covariance for Kalman-Bucy and Wiener filters with inexactly known parameters, obtaining performance figure of merit
10 p1454 A72-23785

Remotely sensed imagery data photointerpretation by gray tone texture context feature extraction, noting identification accuracy
10 p1442 A72-23812

Software reliability engineering, emphasizing looping, deadlocks and difficulties due to imperfect logic, and error causes
10 p1486 A72-24020

Stereoscopic acuity for photometrically matched background wavelengths at scotopic and photopic levels, plotting variable depth error as function of retinal illuminance
10 p1425 A72-24269

Multichannel integral commutators with MOSFET as switching elements, calculating transmission errors
10 p1449 A72-24288

Electromagnetic wave scattering on inhomogeneities by Born approximation, estimating maximum error for small correlation radius
10 p1436 A72-24503

Error probability and reception stability in synchronous detection of phase manipulated signals with additive Gaussian noise at multiplied carrier frequency
10 p1436 A72-24587

Binary split phase FSK signal noncoherent detection by multiple predetection filtering, noting probability of error per bit
10 p1437 A72-24686

Observation errors effects on satellite attitude best least squares estimate based on direction measurements, using Monte Carlo method computer simulation
10 p1438 A72-24692

Amplitude comparison direction finding systems, calculating error due to clutter from incident signal and noise angular distribution relationship to measured arrival angle
10 p1439 A72-24803

Finite element method for approximate solution of elliptic partial differential equations on unbounded domains, proving error bounds
11 p1675 A72-25271

Predictor-corrector method for stiff linear differential equations, considering truncation error estimation and system stability
11 p1675 A72-25272

Receivers for PPM optical communication and pulsed signal detection in background light, evaluating upper bounds on error probability based on photoelectron Poisson statistics
11 p1591 A72-25311

Russian papers on cybernetic systems accuracy and reliability covering error correction schemes, statistical analysis and computer design
11 p1599 A72-25426

Cybernetic equipment reliability and precision analysis from algorithmic, conversion and instrumental errors, surveying digital, analog and hybrid computers and converters
11 p1608 A72-25427

Computer approximate computation of multidimensional normal distribution, examining error measure, random processes and correlation coefficient
11 p1676 A72-25429

Probabilistic analysis of technological systems precision, estimating distribution functions of random output parameters
11 p1609 A72-25430

Servo systems precision analysis with coefficients of output signal error caused by response inertia
11 p1609 A72-25431

Lower bound estimates of error distributions for analog computer solutions of linear algebraic equations
11 p1600 A72-25433

Accuracy and reliability in engineering design of discrete automata without memory /logic circuits/, using Boolean algebra for mathematical models
11 p1600 A72-25434

Error correlation technique to ensure reliability of discrete automatically controlled digital systems inputs, noting lower redundancy requirement
11 p1600 A72-25438

Narrow pulse optical communication digital systems with PPM and on-off keying, investigating timing error effects on bit error probabilities
11 p1592 A72-25885

Deterministic methods to calculate quantization error in digital control system
11 p1610 A72-25976

Weather stations data analysis with unequally spaced observations, considering errors and variance transfer functions
11 p1680 A72-26076

Satellite orbit tracking data accuracy estimation by partial differentiation, using Doppler and interferometer methods
11 p1593 A72-26097

Computer calculation for atmospheric total mass and seasonal redistribution from pressure and temperature field data, discussing error sources
11 p1623 A72-26250

Error analysis of measurement-type servo systems with constant product /or quotient/ of dependent and independent variables applying to phase loop AFC operation
11 p1595 A72-26301

Statistical analysis of errors in altitude readings of phase comparison AM radio altimeters
11 p1633 A72-26303

Statistical error analysis of phase comparison FM radio altimeter during signal processing, investigating range finding strength distribution of echo reflectance
11 p1633 A72-26305

Digital analog converter output voltage variation coefficient derivation, obtaining operational error statistical characteristics estimates and elements parameter
11 p1602 A72-26447

Trajectory correction problem optimal measurement set, showing solution by linear programming simplex algorithm method
11 p1684 A72-26901

Error bounds for finite element methods and approximation with piecewise polynomials for elliptical differential equations solution
11 p1679 A72-26956

Error bounds relationship to norm in approximate numerical solutions of initial value problems for ordinary differential equations
11 p1679 A72-26957

Probability minimization and detection of errors in computerized analysis of civil engineering frameworks, noting graphical output advantages
12 p1786 A72-27190

Equation difference minimization techniques for ordinary nonlinear differential equations approximate periodic solution generation, noting error bounding procedure validity
12 p1836 A72-27240

Test conduct inaccuracies effect estimation for statistical spread of experimental creep rate and long term strength values
12 p1813 A72-27456

Research measurement error determination for two frequency Doppler measurement of artificial satellites
12 p1782 A72-27532

Active notch filter circuits for extending accelerometers frequency response to near resonance, presenting error analysis of mismatching components
12 p1808 A72-27639

Numerical accuracy of electromagnetic field spherical wave expansions, considering horn antenna radiation pattern
12 p1791 A72-27670

Boundary layer analysis of wide capillary tube, deriving approximate error estimates
12 p1798 A72-27714

Radial bearing placed on journal of Cardan suspension, investigating ball dimension errors effect on gyro drift rate
13 p1962 A72-28385

Computer program analysis of errors in mutual orientation elements on aerial photographs with dif-

ferent lengthwise overlaps, discussing error minimization
13 p1955 A72-28497

Antenna synthesis and inverse problems solution by regularization methods, considering radiation patterns and random error effects
13 p1928 A72-28529

Satellite altimetry based on ocean backscattering, analyzing received signal model and altitude errors
13 p1955 A72-28533

Thermodynamic limiting relations between physical measurement accuracy and measurement performance energy dissipation, considering equilibrium and nonequilibrium dynamic models
13 p2003 A72-28761

Error probabilities estimates for communication systems using orthogonal multiposition signals in information transmission, noting techniques applicability to diversity reception systems with self selection
13 p1918 A72-28893

Ultrasonic inspection effectiveness and equipment errors relationship to a priori acceptability of products
13 p1963 A72-28925

Critique of paper on error distributions in air navigation, noting inappropriateness of Gaussian distribution
13 p1996 A72-29015

Analysis of errors generated by Kotelnikov series representation of finite signals during quantization by delta functions, finite duration sampling and constant amplitude sampling
13 p1919 A72-29044

Overestimation in optimization problems calculated by regressive equation, comparing with actual effect in static process
13 p1936 A72-29158

Optimal multistep sampling procedures for production quality control, discussing methods for minimization of error probabilities and total sampling volume
13 p1965 A72-29167

Noise resistance techniques for calculating linear signal interpolation errors in adaptive quantizers
13 p1931 A72-29268

Error analysis of ionospheric parameter measurement by satellite transmitted or reflected multiple frequency pulsed radiation signal, using perturbation method
13 p1920 A72-29276

Digital computer estimates of random processes spectral density by statistical correlation method, calculating errors in numerical integration techniques
13 p1937 A72-29495

VLF long distance radio propagation in earth-ionosphere waveguide, considering earth magnetic field effects in mode conversion and refraction error calculation
13 p1922 A72-29655

Digital FM signal receiver with postdetector integration, determining error probability as function of input SNR and noise stability
14 p2084 A72-30332

Error sources in numerical integration of spacecraft equations of motion in solar and planetary gravitational fields, suggesting methods for improving accuracy
14 p2151 A72-30453

Holomorphic rational functions involving error bounds without derivatives solution by numerical differentiation procedure
14 p2126 A72-30709

Hemoglobin determination in whole blood with Specol-Zeiss spectrophotometry, comparing accuracy to cyanmethemoglobin measurements
14 p2080 A72-30787

Galerkin method for subharmonic solutions of Duffing differential equation, noting error estimation
14 p2126 A72-31102

Temperature measurement error due to solid body and temperature sensor specific heat differences for unsteady heat transfer
14 p2106 A72-31160

Upper boundary layer conditions effects on atmospheric temperature profile reconstruction, by integro-differential equation substitution for Fredholm equation
15 p2265 A72-31399

Error corrections for UV photometric measurements with light filters involving Bouguer formula
15 p2233 A72-31400

Linear control systems optimal synthesis using AI.GOI, program for digital computers minimizing error square integral
15 p2210 A72-31687

Finite element analysis of circular and elliptical plates with curved boundaries, discussing high precision triangular plate bending element modification for accuracy improvement
15 p2326 A72-31715

Mixed triangular finite element model for plate bending problems including shear deformation effects, discussing error analysis and convergence
15 p2326 A72-31716

Orbit determination strategy, detailing optimization criterion correlation with measurement errors
15 p2307 A72-31817

Computerized Monte Carlo techniques for nonlinear error analysis of system behavior, using random number generators for input distribution simulation 15 p2264 A72-32184

Error analysis for digital avionics system involving Doppler navigation by intermittent scanning of single beam multimode radar, noting optimum statistical data processing 15 p2271 A72-32204

Incoherent receiver noise stability in multichannel system with channel frequency separation, deriving formula for receiver error probability 15 p2209 A72-32668

Mean value, repetition and discontinuity errors of spectral-transposition method involving memory storage and compressed signal processing 15 p2212 A72-32703

Photoelectric measurement of solar photosphere pole-equator temperature differences, analyzing statistical and systematic errors [AD-745809] 15 p2317 A72-32770

Shift register implemented binary transversal filter type digital pulse waveform generators truncation and approximation error spectrum analysis via inverse Fourier transform 16 p2362 A72-32854

Geomagnetic and meteorological elements lunar daily variation calculation by modified Chapman-Miller method, estimating confidence limits for parameters reliability 16 p2384 A72-32972

Angular measurement error for group and repetition techniques as function of observation time, deriving formulas for comparison in terms of economy and efficiency 16 p2389 A72-33030

Carrier synchronization and polyphase signal detection in digital communication network for high speed data transmission, deriving reconstructed noisy signal error probability 16 p2363 A72-33218

Error probability distribution of digital data magnetic recording in computer drum memory 16 p2367 A72-33262

Critique on experiment to measure gravitational constant differences between two elements, discussing errors in statistical analysis 16 p2426 A72-33769

Error analysis of East European triangulation network photographic observations of Echo and Pageos satellites from ground stations 16 p2387 A72-33798

Nomographic correction method for quantization error limited data systems, modifying root-summed-squared error analysis for non-Gaussian distribution 16 p2367 A72-33863

Fixed point computer mean square errors in multiplication as function of number of digital order 16 p2367 A72-33959

Error analysis of dynamic yield point measurements based on residual deformation from impact tests of Al alloy and steel specimens 16 p2472 A72-34016

Error probabilities in digital communication systems subject to mixture of man made or natural impulsive and Gaussian noise 16 p2365 A72-34106

Recursive filtering techniques in space navigation, describing initialization procedure to account for state vector errors correlation 17 p2532 A72-34214

The approximate solution of parabolic initial boundary value problems by weighted least-squares methods. 17 p2573 A72-34217

Statistical analysis of position-fixing general theory for systems with Gaussian errors. 17 p2578 A72-34294

Instrument for Hall and Gauss effects measurement in semiconductors and metals, noting instrument error analysis 17 p2529 A72-34758

An algorithm in arithmetic with a floating point to increase the accuracy of a sum 17 p2575 A72-34906

Gradient methods of parameter estimation during the mathematical treatment of measurements 17 p2522 A72-35038

The fitting, calibration, and validation of simulation models. 17 p2523 A72-35226

Smooth empirical Bayes estimation of observation error variances in linear systems. 17 p2576 A72-35248

Dynamic system observation accuracy in spacecraft trajectory measurement, deriving processing algorithm based on state-estimate error correlation matrix analysis with maximum likelihood procedure 17 p2610 A72-35263

Polynomial class random process realization based on statistical methods of processing spacecraft orbital measurement data, considering random and systematic errors 17 p2576 A72-35266

Methodical errors in spacecraft local vertical determination due to variability of physical effects, considering planet oblateness, atmospheric refraction, incident radiation fluctuations, etc 17 p2610 A72-35267

Correlation functions and reconstruction error for quantized Gaussian signals transmitted over discrete memoryless channels. 17 p2516 A72-35333

Error rate of phase-shift keying in the presence of discrete multipath interference. 17 p2516 A72-35334

Russian book on pyrometry principles covering high temperature measurement, error analysis, heat transfer and brightness temperature 17 p2556 A72-35447

Disturbing gravity potential and vertical deflection calculation error reduction based on pure gravity anomalies in geodesy 17 p2550 A72-35744

Low order model and error rates for two dimensional turbulent motion prediction in atmosphere spectrum 18 p2677 A72-36009

State feedback control law for linear multipoint multioutput time-invariant dynamic system under disturbance to obtain output with zero steady state error 18 p2672 A72-36054

Functional relationships between the conventional steady-state error characteristics and the weighting matrices in the quadratic performance index. 18 p2672 A72-36058

Two sided error estimates for electrodynamic impedance, admittance and scattering matrices in diffraction theory 18 p2657 A72-36104

Octal Reed-Solomon code to obtain decoding error probability approximation improvement over minimum distance bound 18 p2658 A72-36266

Finite word length effects on digital filter implementation. 18 p2663 A72-36303

Error investigation for the location of the sources of atmospheric by radio direction finding. 18 p2706 A72-36429

A basic theorem in the computation of ellipsoidal error bounds. 18 p2705 A72-36602

Error bounds for the Galerkin method applied to singular and nonsingular boundary value problems. 18 p2705 A72-36604

Spatial variations in atmospheric predictability. 18 p2706 A72-36627

Theory of optimum M-ary laser detection. 18 p2661 A72-36683

Calculation of coefficients and error estimation for the interpolation quadrature formulas of simplest Cauchy-type integrals and singular open-contour integrals 18 p2705 A72-36808

Optimal control laws for stochastic problems involving intentional errors, caution and probing 18 p2674 A72-36825

Error arising from experimenter influence on subject behavior and performance, discussing expectancy effects on stimulus presentation and IQ and success-failure judgments 18 p2653 A72-36907

Elastically supported dry two degrees of freedom tuned gyroscopes, analyzing open-loop transfer function for characteristic errors 19 p2794 A72-37280

Errors due to gimbaling system asymmetries and rotor angular offsets effects in multigimbal elastically supported tuned gyroscope, deriving gyro translational transfer function 19 p2794 A72-37281

A method for generalized statistical studies of discrete information transmission systems 19 p2764 A72-37301

Error of the statistical method for determining the dependence of the combustion characteristics of particles upon particle size 19 p2879 A72-37363

A posteriori error bounds for approximate solutions of linear second-order ordinary differential equations. 19 p2824 A72-37372

Numerical methods of solving weather forecasting problems 19 p2828 A72-37386

Error reduction in digitally generated holographic memories via parity sequence interlacing with true data sequence for spectrum shaping 19 p2796 A72-37581

Large object holographic image accuracy tests determining experimental sources of error 19 p2797 A72-37589

Accuracy of outer-planet ephemerides. 19 p2857 A72-37683

Gage-length errors in the resolution of dispersive stress waves. 19 p2800 A72-37729

Evaluation of the coefficients of influence of initial-information and model errors on optimization results 19 p2779 A72-37996

Stationary Kalman-Bucy filter synthesis from filter coefficients and correlation matrix of filtration errors, discussing random process estimation application 19 p2782 A72-38517

Differentially coherent detection scheme with error-correcting capability by means of decision patterns. 19 p2766 A72-38605

An approximate method for inverse Laplace transformation 19 p2828 A72-38853

Cup anemometer response to fluctuating wind speeds. 20 p2920 A72-38966

Interference performance degradation to digital systems. 20 p2901 A72-38984

Double-ended, folded-path and double-reflecting transmissometers operation principles, and measurement error sources consideration for relative merits and disadvantages 20 p2923 A72-39054

Critical frequency computation for partially filled elliptical waveguide with dielectric rod 20 p2902 A72-39058

Error analyses of Euler angle transformations arising in design of precision pointing systems, guidance sensors and instruments with gimbals [AIAA PAPER 72-851] 20 p2949 A72-39078

Error analysis of hybrid aircraft inertial navigation systems. [AIAA PAPER 72-848] 20 p2950 A72-39081

A versatile Kalman technique for aircraft or missile state estimation and error analysis using radar tracking data. [AIAA PAPER 72-838] 20 p2950 A72-39089

Enlarging the region of convergence of Kalman filters that encounter nonlinear elongation of measured range. [AIAA PAPER 72-879] 20 p2907 A72-39121

The observability of unforced physical systems by linear non-sequential estimators in the validation of linear error analysis. [AIAA PAPER 72-876] 20 p2910 A72-39123

Marcum Q function parameters approximations for error probabilities computation in multilevel frequency shift keying and differentially coherent phase shift keying systems 20 p2903 A72-39426

Richardson and effective work functions measurements for thermionic emission from alkali and extended red-sensitive trialkali photocathodes, discussing error minimization 20 p2890 A72-39646

Effects of finite register length in digital filtering and the fast Fourier transform. 20 p2904 A72-39780

Effects of errors in the direction of incidence on the performance of an adaptive array. 20 p2904 A72-39786

Microelectronic component reliability prediction technique with near Wiebull method accuracy in absence of detailed sampling life test results 20 p2930 A72-39857

Errors in static pressure measurements due to protruding pressure taps. 21 p3050 A72-40117

Radiometry error analysis for diffraction at radiation beam limiting screens, calculating corrections for circular source and detector 21 p3050 A72-40149

Assessment of the errors of a version of the hybrid quasi-analog system due to errors in quantization in time in the solution of systems of ordinary differential equations 21 p3024 A72-40158

Dynamic error of storing voltages at capacitors in the storage channel of an integrator of variable structure 21 p3024 A72-40165

Quantization error of the coefficients in digital filters with N shift sequences 21 p3025 A72-40223

Measurement and transformation of two-port S parameters in terms of three-port parameters for a more general characterization of transistors - Errors. 21 p3025 A72-40224

Application of the transmission-line-matrix method to homogeneous waveguides of arbitrary cross-section. 21 p3032 A72-40629

The behaviour of the solutions of the equations of motion of a mechanical system, with a parameter occurring as a coefficient of each derivative. 21 p3084 A72-40812

Diffraction of plane waves by a strip - Exact and asymptotic solutions. 21 p3016 A72-40839

Error probability for multilevel PAM transmission with intersymbol interference, Gaussian and impulsive noise. 21 p3019 A72-40888

ERROR BAND

Statistical analysis of influence coefficients and unbalance forces measurement errors in balancing of rotors 21 p2996 A72-41229

Gaussian elimination with floating point arithmetic, discussing algorithm for least squares scaling of matrices with less error than row and column norms equilibration 21 p3076 A72-41317

Regularized linear problem with perturbed equation as solution, presenting error overestimate 21 p3076 A72-41336

Reissner nonlinear equations for stability analysis of shallow shells of revolution, noting critical loads range and error analysis 22 p3232 A72-41856

Influence of dispersion on the accuracy of estimating the fatigue life from the results of accelerated investigations by the prefracture method. 22 p3232 A72-41928

Binary symmetric channel error effects on PCM color image transmission. 22 p3153 A72-41977

Error incidence probability for system control reliability determination, assuming Markov process 22 p3162 A72-42183

Radiogoniometer error analysis for receiver internal noise and external interference sources, noting sources angular distribution effect on instrument error 22 p3158 A72-42233

Evaluation of flight instrumentation for the identification of stability and control derivatives. [AIAA PAPER 72-963] 22 p3136 A72-42346

Error sensitivity of statistical models with pattern rearrangement for analysis of interplanetary scintillation in ecliptic plane 22 p3218 A72-42402

Prediction error growth computation by test-field model for inertial range atmospheric turbulent flows in three and two dimensions 22 p3167 A72-42501

Adjustment of the wind field to geopotential data in a primitive equations model. 22 p3200 A72-42502

Improved Curtis-Godson approximation in a non-homogeneous atmosphere. 22 p3201 A72-42511

Some effects of cognitive similarity on proactive and retroactive interference in short-term memory. 22 p3142 A72-42548

Error analysis of astronomical-geodetic network compensation methods, noting distortions minimization in polygon nodes by large blocks compensation with computers aid 22 p3173 A72-42721

An approximation to midcourse correction direction errors. 22 p3203 A72-42870

On the drift velocity of electrons in a gas. 22 p3212 A72-42996

The efficiency of the method of the least squares for adjusting observations with non-normal distributions 22 p3199 A72-42998

German monograph - Internal-analytic methods in systems of linear equations with interval coefficients and relations to error analysis. 22 p3200 A72-43061

The effect of geometry on area navigation system errors. 22 p3203 A72-43132

Optimal random disturbance intensity control of dynamic systems, minimizing error with respect to observed and controlled plant coordinates 23 p3274 A72-43221

Ballistic deviations of a gyroscopic navigation system 23 p3311 A72-43417

Spin stabilized ballistic air-to-ground or ground-to-ground rocket, discussing dynamic stability-impact error relationship [SAWE PAPER 928] 23 p3342 A72-43468

Rotating aerospace vehicles dynamic balance error terms due to despun masses misalignment and aerodynamic effects [SAWE PAPER 930] 23 p3342 A72-43470

Stochastic models for block triangulation by bundle approach, comparing theoretical accuracies obtained from different block adjustment methods 23 p3284 A72-43631

Error analysis of linear and nonlinear elements in hydraulic control circuits of flight vehicles, calculating accuracy of frequency response determination 23 p3252 A72-43671

Pointwise displacement errors in linear shell theory resulting from errors in the stress-strain relations. 23 p3347 A72-43720

Effect of fluorescence observation geometry on lifetime measurement, including the development of an approximation to the detector collection efficiency integral. 23 p3288 A72-43884

Study of target edge response viewed through atmospheric turbulence over water. 23 p3289 A72-43896

Potsdam correction from the satellite determined geopotential. 23 p3285 A72-43944

Approximate harmonic linearization method of stability analysis of nonlinear periodic systems, identifying fictitious oscillations due to computation errors 23 p3277 A72-44007

Absolute accuracy of the pulse-echo overlap method and the pulse-superposition method for ultrasonic velocity. 23 p3313 A72-44114

Forward-error correction with decision feedback. 23 p3268 A72-44175

Reciprocal mean-square error and signal-to-noise ratio as distinct performance measures in below-threshold communication. 23 p3265 A72-44177

Performance characterization for L-orthogonal signal transmission and detection, discussing tradeoffs between error probability, SNR and bandwidth by numerical evaluation 23 p3265 A72-44180

Problem of error estimation during solution of internal boundary value problems in microwave electrodynamics 23 p3265 A72-44201

Coronal lines photometry systematic error dependence on aureola spectral intensity, line half width, gradation curve slope, and neutral filter transmission coefficient 23 p3340 A72-44240

Fundamentals of multivariate analysis - Linear regression. 23 p3310 A72-44394

Behavior of the spatial distribution function of shower particles near the axis of a cascade shower 23 p3331 A72-44432

Radiation influences on a white-coated thermistor temperature sensor in a radiosonde. 24 p3401 A72-44620

The application of error control techniques in the design of an advanced augmented inertial surveying system. 24 p3421 A72-44641

Pressure and magnetic field probe measurements in transverse shock waves in ionizing hydromagnetic regimes, investigating bow shock effects on accuracy 24 p3390 A72-44708

Observation error in time determination of solar limb contact with optical instrument hair, noting effect on accuracy of time and longitude measurement 24 p3438 A72-44859

Human observation error effect on astronomical refraction calculation from time determination of solar limbs passages across optical instrument reticle 24 p3438 A72-44863

On an augmentation of the error made by numerical treatment of second-order conservative point transformations 24 p3419 A72-45071

The estimation of accuracy of short-term atmosphere density prediction. 24 p3398 A72-45173

Analysing vibration and shock data. I - Data acquisition and pre-processing. 24 p3382 A72-45287

High order explicit Runge-Kutta methods construction conditions, discussing error bounds and expansions 24 p3419 A72-45299

A general theory of convergence for numerical methods. 24 p3419 A72-45300

Optimal linear inertia-free processing of meter readouts with allowance for control-equipment signals 24 p3403 A72-45316

Pulse transient response function for gyroscopic course indicator with gyrocompass error filtered out and nondistorted directional gyroscope error 24 p3403 A72-45320

Accuracy of the determination of the zero points of a fundamental catalog from observations of major and minor planets 24 p3447 A72-45676

ERROR BAND

U ACCURACY

ERROR CORRECTING DEVICES

Reliable data transmission block coding techniques including burst error, fire, Reed-Solomon and product codes and majority decoding algorithm 01 p0025 A72-10335

Optimal burst correcting codes for bursty channels, comparing with automatic repeat-request 01 p0025 A72-10337

Forward error correction code performance on hf troposcatter and satellite channels, considering adaptive and nonadaptive convolutional and cyclic coding 01 p0026 A72-10338

Nonsystematic quick-look-in convolutional codes for sequential decoding in deep space channels 01 p0026 A72-10339

Digital computer program high speed algorithm for high resolution images geometric correction,

discussing application to ERTS return beam vidicon images 01 p0065 A72-10454

Inspiration time correction factor for pulmonary diffusing capacity measurement by single breath method 01 p0015 A72-11259

Separate and nonseparate arithmetic error detecting and correcting codes for digital computer design, considering cost and effectiveness tradeoffs 02 p0184 A72-11483

Distributed fault-tolerant aerospace digital computer design with duplicated central multiprocessor, triplicated memory and conventional redundancy local processors for error detection and correction 02 p0185 A72-11489

Kinetic energy correction in capillary viscometry, observing pressure drops and mass flow rates 02 p0202 A72-11724

ERTS-A satellite geometric and radiometric received image errors, presenting detection and correction with digital algorithms 02 p0171 A72-11847

One-way error correcting system with 1/3 rate interleaved block code, testing code performance over 1300 km vhf ionosscatter path and 1500 km hf path 02 p0175 A72-12153

Thermal zero signal instabilities and error reduction in devices using reluctance sensors 02 p0231 A72-12562

Gyro drift random error dispersion reduction in compensated closed loop multirotor gyroscopic systems by cross couplings 02 p0231 A72-12566

Correction factors for Aerodynamic Research Institute Goettingen transonic wind tunnel, comparing calculated values with AGARD calibration models test results [DFVLR-SONDDR-167] 03 p0308 A72-13610

Heat transfer coefficients to both sides of finite one dimensional slab subject to phase-change coating technique boundary conditions, deriving thin wing correction factors 03 p0457 A72-13956

Precession from proper motions of stars with respect to galaxies, discussing correction for systematic errors 04 p0575 A72-15027

Divergence prevention in decision directed adaptive recursive estimators in relation to error covariance 06 p0792 A72-17307

Spherical reflector antenna phase aberration correction by planar array feeds, discussing synthesis procedure for mean square error minimization 06 p0781 A72-17344

FSK transmission experiments on uhf satellite link, noting threshold convolutional decoding contribution to SNR 06 p0773 A72-17599

Gravity data free air and Bouguer correction/elevation correction/ by nomographic alignment chart 06 p0809 A72-18148

Aircraft turboalternator governing theory for frequency error detection, comparing performance of mechanical- and electro-hydraulic governors 06 p0868 A72-18249

Measuring device for holographic virtual image reconstruction deformations due to relative orientation errors between reference beam and holographic plate 06 p0818 A72-18329

Weighted acoustic surface wave dispersive microwave filter apodized interdigital array design modification for phase error correction to reduce distortion 06 p0787 A72-18380

Source permutation code optimum encoding for long block length, comparing performance with rate distortion function bound and various quantization schemes 06 p0776 A72-18391

Rate 1/n binary convolutional code free distance upper bound derivation and largest input sequence determination for equal weight 06 p0776 A72-18392

Variable length codes using Fano metric for minimum error probability sequential decoding 06 p0776 A72-18393

TDMA satellite communication system with convolutional encoding and Viterbi decoding, evaluating data buffering and control configurations 07 p0941 A72-19297

Error correcting data decoder assembly for mission independent sequential decoding at all stations in deep space tracking network, discussing design and performance 07 p0949 A72-19298

Concatenated coded command system for low error probabilities at moderate SNR, emphasizing spaceborne portions implementation 07 p0949 A72-19299

Truncation error correction based on Richardson extrapolation in finite difference approximation of nonlinear partial differential operators 07 p1101 A72-20328

Error coding techniques application to communication satellite links, discussing computer simulation results

07 p0948 A72-20495

Error correction in adders with systematic subcodes, preserving AN binary code error control properties

08 p1138 A72-21551

Systematic errors in scan-and-measure devices for tracking cameras photographs analysis, discussing correction during measurements

08 p1209 A72-21913

Paired Gill propeller anemometer response function in generalized wind vector sensor application, proposing algorithm for magnitude and direction errors reduction in output analyses

09 p1307 A72-22434

Interplanetary spacecraft midcourse guidance stochastic control, deriving algorithm for computing optimum velocity correction and execution time with allowance for correction-dependent errors

10 p1508 A72-23778

Random access memory with single error correction circuitry, predicting failure, card and module removal rates by computer simulation

10 p1443 A72-23980

Two-laser optical distance measuring instrument with atmospheric refractivity correction, noting accuracy

11 p1646 A72-25305

Correction to nonlinear refractivity calculation for cubic lattice crystal with allowance for higher induced multipoles

12 p1855 A72-27620

Secondary standard solar cells calibration method based on solar spectral response comparison with primary standard, discussing error correction method

12 p1759 A72-28043

Optimal quantization parameters for pseudonoise signals at radio receiver output, estimating static error in correlation function measurement

13 p1919 A72-29048

Self adaptive two channel iteration servosystems for input reconstruction by successive approximations, determining signal and noise error operators

13 p1936 A72-29155

Cascade section parameters calculation for multisection amplifiers with composite transistors and correction elements

13 p1934 A72-29978

Analog to digital converter for sinusoidal voltage amplitude pickup and subsequent digital coding with correction for conversion characteristic nonlinearity

13 p1934 A72-30020

Correcting electronic transducer for rapidly changing temperature measurement, discussing design peculiarities for superior metrological characteristics

13 p1961 A72-30024

Probability functional formulas for quasi-determinate signal on unsteady normal noise background for use in false alarm and correct detection

15 p2195 A72-31664

Pulsed solid state lasers with large area Si photodiode for output measurement in feedback control system to compensate flash lamp aging

15 p2247 A72-32027

High speed and resolution laser scanning by optomechanical methods, discussing theoretical bandwidth, resolution limits, position error correction measures and performance optimization

15 p2248 A72-32037

Two dimensional acousto-optical light beam deflection system for laser recorder error correction

15 p2248 A72-32038

Single closed loop discontinuous control system, determining discrete correcting element parameters from linear inequalities

15 p2212 A72-32175

Transfer function estimates in random vibration test control, using digital techniques for rapid reduction of statistical errors

15 p2215 A72-32626

Stress-strain curve correction for triaxial stress state and strain rate at arbitrary temperatures, describing instrument for continuous test specimen profile measurement

16 p2469 A72-33232

Random multiple access data transmission systems with feedback for message confirmation and retransmission in event of errors, evaluating channel capacity

16 p2372 A72-33794

Nomographic correction method for quantization error limited data systems, modifying root-sum-squared error analysis for non-Gaussian distribution

16 p2367 A72-33863

Meridian direction determination with angular accelerometer, noting reduction in effects of component imperfections on accuracy

16 p2421 A72-33962

A suboptimal error reduction scheme for a long-term self-contained inertial navigation system

17 p2578 A72-35560

Dynamic errors of a metering system with successive correction of the sensor's time constant for certain types of aperiodic input

17 p2557 A72-35787

Refraction correction of rocket tracking radar inputs in near real time

18 p2661 A72-36636

Error correction in redundant logic circuits without application of majority elements

19 p2769 A72-37758

Differentially coherent detection scheme with error-correcting capability by means of decision patterns

19 p2766 A72-38605

Effectiveness of error-correcting codes during reception on the whole in the presence of additive normal white noise

21 p3014 A72-40310

Correcting effects of corrugated boundaries on coaxial radiators asymmetry and sidelobes, investigating waveguide hybrid modes induced transverse fields

21 p3029 A72-40516

Error correcting codes applied to satellite channels

21 p3018 A72-40874

Correction of diffraction errors in acoustic-surface-wave pulse-compression filters

21 p3034 A72-41464

Q-ary output data transmission channel with burst errors, discussing burst-b distance measure and binary block code decoding algorithm for error correction

22 p3153 A72-41979

Code correcting asymmetric-error bursts during information exchange between computers

22 p3156 A72-42189

Mathematical model for lattice-type error distribution of parallel channels communication system, noting metric for algebraic signal coding method

22 p3154 A72-42234

An attitude reference system with discrete-correction capability

22 p3203 A72-42864

Automatic transmission and application of sky wave corrections with differential OMEGA navigation, discussing test equipment, procedures and results

22 p3203 A72-42948

Closed loop pulsed automatic control system, determining discrete correcting element parameters from linear equalities

22 p3163 A72-43009

Forward-error correction with decision feedback

23 p3268 A72-44175

A method for synthesizing feasible correcting devices with a minimum number of constraints on the optimized transient pulse response function

24 p3386 A72-45318

Application of external information about the linear velocity of an object for correcting inertial navigation systems

24 p3423 A72-45319

Semaphore channel signaling reliability, presenting error protection and correction system

24 p3381 A72-45770

ERROR DETECTION CODES

Reliable data transmission block coding techniques including burst error, fire, Reed-Solomon and product codes and majority decoding algorithm

01 p0025 A72-10335

Convolutional coding and decoding techniques in communication systems, discussing distance properties, optimal decoder in memoryless channel, error probabilities and bit synchronization

01 p0025 A72-10336

Optimal burst correcting codes for bursty channels; comparing with automatic repeat-request

01 p0025 A72-10337

Forward error correction code performance on hf troposcatter and satellite channels, considering adaptive and nonadaptive convolutional and cyclic coding

01 p0026 A72-10338

Nonsystematic quick-look-in convolutional codes for sequential decoding in deep space channels

01 p0026 A72-10339

Optimal metric programmable high speed sequential decoder for convolutional code deep space channels

01 p0026 A72-10340

High speed decision sequential decoder design and tests for digital errors, white noise and real channels

01 p0026 A72-10341

Convolutional coding, Viterbi decoding and binary phase shift keyed modulation for reliable communication on power limited satellite and space channels

01 p0026 A72-10342

Orthogonal convolutional coding with on-off signaling and Viterbi decoding for synchronous multiple access communication with bound bit error rate

01 p0026 A72-10343

Error correction techniques of convolutional coding with Viterbi maximum likelihood decoding for communications systems design, using computer simulation

01 p0026 A72-10344

Time division multiple access systems transmitting and receiving end synchronization control criteria derivation, discussing code pattern selection for reliable detection

01 p0033 A72-11304

Fail-safe sequential machines realization using k-out-of-n code for state assignment and onset and off-set methods for excitation circuit construction

02 p0184 A72-11477

Separate and nonseparate arithmetic error detecting and correcting codes for digital computer design, considering cost and effectiveness tradeoffs

02 p0184 A72-11483

One-way error correcting system with 1/3 rate interleaved block code, testing code performance over 1300 km vhf ionoscatter path and 1500 km hf path

02 p0175 A72-12153

Source permutation code optimum encoding for long block length, comparing performance with rate distortion function bound and various quantization schemes

06 p0776 A72-18391

Rate 1/n binary convolutional code free distance upper bound derivation and largest input sequence determination for equal weight

06 p0776 A72-18392

Variable length codes using Fano metric for minimum error probability sequential decoding

06 p0776 A72-18393

TDMA satellite communication system with convolutional encoding and Viterbi decoding, evaluating data buffering and control configurations

07 p0941 A72-19297

Concatenated coded command system for low error probabilities at moderate SNR, emphasizing spaceborne portions implementation

07 p0949 A72-19299

Error coding techniques application to communication satellite links, discussing computer simulation results

07 p0948 A72-20495

Sequential testing of actual and calculated error covariances consistency in recursive nonlinear estimators, noting method application to linear filters

08 p1197 A72-20857

Error correction in adders with systematic subcodes, preserving AN binary code error control properties

08 p1138 A72-21551

Optimal answer-back communications systems using feedback channel for error checking

09 p1277 A72-22568

Noise threshold improvement of PCM signals for satellite transmission, using quality detector and error detecting codes

10 p1441 A72-23102

Probability minimization and detection of errors in computerized analysis of civil engineering frameworks, noting graphical output advantages

12 p1786 A72-27190

Communication systems design with error control, applying algebraic codes to biphase and multiphase modulation systems

12 p1782 A72-27488

Q-ary output data transmission channel with burst errors, discussing burst-b distance measure and binary block code decoding algorithm for error correction

22 p3153 A72-41979

Code correcting asymmetric-error bursts during information exchange between computers

22 p3156 A72-42189

Mathematical model for lattice-type error distribution of parallel channels communication system, noting metric for algebraic signal coding method

22 p3154 A72-42234

Forward-error correction with decision feedback

23 p3268 A72-44175

ERROR FUNCTIONS

Computerized error function method of wreckage trajectory analysis in aircraft accident investigation, using fundamental equations of motion

03 p0309 A72-13250

Discrete time systems unknown parameter identification, considering unified error function minimization approach

04 p0506 A72-15106

Error covariance matrix evaluation at end of orbit extrapolation in terms of state vectors at measurement, discussing computation and interpretation

05 p0720 A72-16753

Ordinary differential equations convergent solutions growth estimates, computing error function asymptotic growth rate

05 p0683 A72-17000

German monograph on models for automatic radar tracking methods covering error probabilities, reliability and false information reception

09 p1348 A72-22321

Error probability estimates in two channel diversity reception systems with allowance for fading correlation and incomplete signal separation

09 p1278 A72-22572

Electronic filters realization by error function minimization, discussing parameter space algorithmic search and complex plane optimization methods

11 p1606 A72-26550

Algorithm for meteor velocity calculation from radio observation data, noting symmetrical error distribution function of velocities

13 p1924 A72-29014

Table of indefinite and definite integrals of products of error functions with transcendental and special functions

15 p2262 A72-31589

Optimal segment boundaries with composite error function in piecewise approximation chosen by dynamic program in scalar state variable, noting uniqueness properties

15 p2262 A72-31634

A bivariate normal theory maximum-likelihood technique when certain variances are known.

21 p3075 A72-40826

Error probability estimates in two channel diversity reception systems of digital data transmission with allowance for fading correlation and incomplete signal separation

24 p3379 A72-44751

Parametric optimization of the equivalent transfer function of a system with the aid of the error integral

24 p3387 A72-45700

ERROR SIGNALS

Model reference adaptive control system synthesis in presence of random perturbations, considering error signal derivative use to form parameter adjustment algorithm

05 p0640 A72-16208

Average time between successive false target indications in surveillance binary signal detector with variable storage capacity

11 p1595 A72-26295

Saturating nonlinear feedback systems stability under bounded input excitation, discussing error signals magnitude and duration

15 p2212 A72-32246

Frequency stabilization of pure neon laser.

23 p3296 A72-43951

ERRORS

NT INSTRUMENT ERRORS

NT PHASE ERROR

NT PILOT ERROR

NT POSITION ERRORS

NT RANDOM ERRORS

NT RANGE ERRORS

NT ROOT-MEAN-SQUARE ERRORS

NT TRUNCATION ERRORS

NT VELOCITY ERRORS

ERTS

U EARTH RESOURCES TECHNOLOGY SATELLITES

ERYTHROCYTES

NT RETICULOCYTES

Hypophysectomy in rats, resulting in prolonged red blood cell survival due to oxygen consumption decrease and altered erythrocyte enzymatic processes

01 p0010 A72-10075

Anaerobic glycolysis and specific gravity of red blood cells in rats exposed to pure oxygen at 600 torr

01 p0015 A72-11297

Normal and germ free rat antibody response to sheep erythrocyte inoculation in He-O atmosphere, analyzing microagglutinin and hemolysis titres

[AD-736324] 04 p0471 A72-14861

Prolonged muscular work effects on erythrocyte 2,3-DPG generation relation to oxyhemoglobin affinity

04 p0472 A72-14898

Holographic measurement of red blood cell rotation in orifice flow, transforming orientation into form distribution data

04 p0479 A72-15140

Physiological effects of transfusing 2,3-diphosphoglycerate (DPG)/depleted red cells with high oxygen affinity in anemic hypoxic patients

04 p0473 A72-15211

Active Na-K transport and passive permeability temperature adaptation in ground squirrel erythrocytes

04 p0475 A72-15546

Sublethal X radiation effects on rat erythropoietic system during altitude hypoxia acclimatization

04 p0476 A72-15721

Light scattering time dependence, erythrocyte aggregation rates and hydrodynamic characteristics in ox. pig and horse blood stream

05 p0621 A72-16230

Human urine regenerated water in various dilutions effect on fish and rat erythropoiesis

05 p0622 A72-16651

Erythrocytes catalase activity and number content relationship in human and albino rats blood, discussing compensatory effects

06 p0764 A72-18060

Hyperoxia effect on kidney blood flow erythropoietic properties in rabbits, noting inhibiting effect on erythroblast cells mitotic activity in bone marrow culture

06 p0765 A72-18061

Plasma erythropoietin concentration in men and mice during altitude acclimatization

07 p0917 A72-19440

Microcirculation study of intravascular erythrocyte aggregation/blood sludge/ in rats

07 p0920 A72-19686

Chinchilla and guinea pig tolerances to hypoxia and hyperoxia in pressure chamber tests, suggesting relation to red blood cell size and number

09 p1265 A72-22647

Erythrocyte hemolysate cataphoresis studies of human hemoglobin changes during stepwise adaptation to high mountain conditions

09 p1266 A72-22880

Picoscale blood diagnostic device for red and white cell count, noting piston principle electronic operation

09 p1272 A72-23257

Erythrocyte life span in mice under normal atmospheric pressure and various degrees of hypoxia acclimatization, using radioactive labeled diisopropyl phosphorofluoridate

11 p1579 A72-26608

Red cell mass plasma volume decrease in Apollo mission crews, indicating erythropoiesis inhibition

12 p1765 A72-28266

Suppression effects of hyperoxic breathing gases on red blood cell and erythropoietin hormone production following blood loss

12 p1766 A72-28298

Supercellular regulators of triggering mechanism of regenerative reaction in sternum erythropoietic bone marrow tissue

13 p1901 A72-28636

Red blood cell reserve mobilization in healthy and chronically irradiated dogs after treadmill exercise

14 p2074 A72-30379

Stepwise altitude acclimatization and subsequent reanimation after blood loss caused clinical death effects on dog peripheral blood erythrocytes, reticulocytes, hemoglobin and hematocrit

14 p2076 A72-30671

Whole blood flow dependence on optical density from light transmission measurement, showing photometric effects of red cell aggregation, deformation and orientation

15 p2185 A72-31639

Light transmission measurements of blood flow to quantify red cell aggregation and dispersion

15 p2185 A72-31640

Red blood cell metabolite 1,3 diphosphoglycerate determination method by rapid deproteinization, concentration by precipitation and enzymatic reaction

15 p2190 A72-32488

Exchange diffusion process contribution to human red blood cell transmembrane cation movement from sodium tracer influx studies

15 p2187 A72-32746

Astronauts red cell mass changes associated with space flight due to space and earth environment differences

16 p2356 A72-33564

Effects of in vivo inhalation of 100% oxygen at reduced pressure on serum and red cell lipids.

[AD-746090] 17 p2508 A72-34553

The effect of chronic erythrocytic polycythemia and high altitude upon plasma and blood volumes.

19 p2757 A72-38028

motion.

20 p2891 A72-38935

Nervous and humoral stimulation and hypoxia effects on erythropoiesis control, studying human blood serum additions to bone marrow cultures

21 p3001 A72-40762

Experimental studies of the production of erythropoietin in relation to the intensity and duration of hypoxia

21 p3002 A72-41189

Studies of renal and extrarenal production of erythropoietin in male and female rats

21 p3002 A72-41190

Influence of intracellular convection on the oxygen release by human erythrocytes.

21 p3003 A72-41625

Control of the circulating blood mass in the case of a functional detachment of various amounts of pulmonary tissue

21 p3012 A72-41825

Modulating effect of limbic brain formations on the blood system

22 p3142 A72-42282

ESAKI DIODES

U TUNNEL DIODES

ESCAPE

Galactic tidal field and multiple encounters role in stellar escape from star clusters, noting escape rates and kinetic energy involved

12 p1873 A72-27898

ESCAPE CAPSULES

Preventive and remedial space flight safety engineering, discussing escape capsules and onboard and earth-launched rescue systems

17 p2620 A72-34427

Spacecrews rescue requirements, considering escape capsules earth-based and orbit-based rescue systems and flight hazards

17 p2620 A72-34438

Development of an inflatable fabric structure for the early stabilization of the B-1 crew escape capsule.

[AIAA PAPER 72-801] 20 p2888 A72-40053

ESCAPE SYSTEMS

Parachute designs and applications to escape systems, paratrooping, supply dropping, aircraft braking, weapons systems stabilization, flight testing aids and sport

01 p0003 A72-10302

Dynamic response index /DRI/ minimization for personnel aircraft emergency catapult escape systems to reduce injury probability

08 p1112 A72-21576

Emergency systems for helicopter crew and passenger survivability improvement, discussing use of ejection seats, extraction systems parachute bail-out and shaped explosive charges

08 p1109 A72-21581

Emergency Life Saving Instant Exit system in aircraft fuselage for use after crash landing, discussing design and ground testing

08 p1109 A72-21583

Manned space flight escape, rescue and survival systems based on onboard, prepositioned aid and earth launched concepts, considering earth orbit, lunar and interplanetary missions

09 p1395 A72-23152

Escape systems evolution for manned space flight, considering X-15, Mercury, Gemini and Apollo programs and future space stations and planetary missions

09 p1395 A72-23153

Lunar landing mission escape and rescue concepts, considering emergencies during earth orbit, translunar, lunar orbit, surface and rendezvous, transearth and earth reentry phases

09 p1396 A72-23157

Chemically strengthened glass for eject-through frangible canopy design in aircraft emergency escape systems, noting protection against ejection injuries

12 p1813 A72-27016

Emergency escape from high performance military aircraft in flight and on ground, using explosive cord for transparent canopy material breakup

12 p1753 A72-27017

Lockheed ADP SR-1 ejection seat system for safe aircrew recovery under zero-zero, high Mach and altitude conditions, describing escape experiences with SR-71 aircraft

13 p1896 A72-28701

Aircraft emergency evacuation systems, discussing door designs, inflatable escape slide and slide/lifeboat combination

22 p3138 A72-42520

Design features of Soyuz life support and launch escape systems and Vostok rocket booster stage

23 p3343 A72-44335

Spacecraft rescue/recovery capabilities, discussing in-flight escape, ground egress and descent systems, performance and technical and human factors

24 p3450 A72-45147

ESCAPE VELOCITY

Particle escape within Newtonian gravitational system of three point masses, discussing necessary conditions

01 p0122 A72-10007

Optimal control algorithm for spacecraft descent in atmosphere at speed near escape velocity, using game theory

01 p0135 A72-10298

Fragment velocity for bursting gas containers in vacuum

02 p0295 A72-12473

Analytic solution for optimal control circular orbit escape with constant thrust rocket, using Euler-Lagrange equations and perturbation technique

03 p0437 A72-13839

Jeans escape rate prediction validity for hydrogen atoms in upper atmosphere and error sources in physical models

08 p1159 A72-21401

Electrostatic ion thruster ESKA 28 for interplanetary missions, calculating earth escape and optimal transfer orbits

11 p1707 A72-26177

Spacecraft motion control algorithm for reentry at escape velocity based on object motion model

11 p1684 A72-26900

Nuclear electric propulsion systems performance evaluation for various escape missions

17 p2606 A72-34577

Analysis of the possibility of planetary escape by means of the solar sail

22 p3230 A72-43072

Relativistic test particle escape from circular orbit around central mass due to mass loss, considering orbiting body corrections due to general relativity

23 p3335 A72-43265

Saturn-Jupiter rebound - A method of high-speed spacecraft ejection from the solar system.

23 p3340 A72-44323

ESCHERICHIA

Intestinal disbacteriosis and autoinfection occurrence in guinea pigs and rats under magnetic field effect, noting Escherichia population changes

05 p0622 A72-16647

Isolation of a polyvalent bacteriophage for *Escherichia coli*, *Klebsiella pneumoniae*, and *Aerobacter aerogenes*.

19 p2755 A72-37650

SG (GYROSCOPES)

U ELECTROSTATIC GYROSCOPES

ESRO SATELLITES

NT AZUR SATELLITE

NT COS-B SATELLITE

NT HEOS B SATELLITE

NT HEOS SATELLITES

ESRO polar orbiting meteorological satellite, discussing design features and operational instruments

01 p0126 A72-10186

Industrial challenge of European space R and D programs, discussing ELDO Europa 1 launcher vehicle and ESRO-HEOS satellite technological problems

01 p0146 A72-10948

European Space Research and Technology Center satellite project control system, describing critical path network analysis, work package cost control and project planning

02 p0304 A72-12035

ESRO satellite power supply solar paddles deployment mechanism, describing simulated zero gravity tests

02 p0286 A72-12713

Organizational structure and functions of ESTEC /ESRO branch/ concerned with scientific research and application satellites development

02 p0305 A72-12724

Celestial gamma rays arrival direction and energy spectra measurement and spectrum analysis using ESRO satellite COS-B data

03 p0408 A72-13029

Gimbaled telescope/UV spectrophotometer combination with star tracking facilities for use on ESRO TD-1 A satellite

03 p0355 A72-13061

ESRO program in imaging detector development for UV and soft X ray space missions, presenting image storage target details

08 p1171 A72-21971

Solar cells array design and assembly techniques, discussing tests for Esro satellites aerospace environments

12 p1758 A72-28033

ESRO satellites solar array performance under orbital environmental conditions, discussing radiation damage and earth albedo effects

12 p1759 A72-28047

Auroral spectra recorded at 2000-3000 A with fast Ebert Fastie scanning spectrometer aboard ESRO rockets

14 p2098 A72-30139

ESRO IA satellite observations of trapped and precipitated proton energy spectrum as function of invariant latitude on 8 March 1970

14 p2146 A72-30141

UV stellar spectra observation with orbiting stellar spectrophotometer aboard ESRO TDI A satellite, noting Mg II lines

15 p2308 A72-31927

Geomagnetic field aligned electron anisotropies at high latitudes for energies 1 and 6 keV observed by ESRO satellite, noting two regions of maximum occurrence frequency

15 p2226 A72-31928

ESRO report to COSPAR on satellites in orbit and under development and on 1971 sounding rocket program

15 p2338 A72-32016

Minimisation of the solar array generated electrical interference on the GEOS satellite.

20 p2889 A72-38990

ESRO 1 SATELLITE

ESRO 1 satellite residual gas outgassing rate and composition measurements during thermal heat balance tests, using mass spectrometer

09 p2163 A72-23260

Esro 1 /Aurorae/ satellite electron intensity measurements, explaining disparities between different experiments by detectors low-energy thresholds difference

22 p3173 A72-42648

ESRO 2 SATELLITE

Solar proton flux and energy spectra from 1968-1969 ESRO 2 satellite measurements, detailing 18 November 1968 event

02 p0273 A72-12073

ESSA SATELLITES

Snow lines determination from ESSA-APT weather satellite pictures, comparing with ground data

09 p1303 A72-23295

ESTERS

NT CARBAMATES [TRADENAME]

NT CELLULOSE NITRATE

NT GLUTAMATES

NT LACTATES

NT MALEATES

NT NITRATE ESTERS

NT NITROGLYCERIN

NT PHTHALATES

NT POLYCARBONATES

NT POLYESTERS

NT POLYETHYLENE TEREPHTHALATE

NT TRIACETIN

NT URETHANES

Organophosphorus antiwear additives in neopentyl polyol ester lubricants on 440C stainless steel surfaces, using four ball wear test machine

[AD-740055] 02 p0250 A72-12849

Mass spectrometric studies of solvent extractable acid methyl esters of oil shale from Colorado Green River Formation

03 p0320 A72-13742

Esters and amides participation in prebiotic polymers, discussing ribosome bonds and messenger RNA

04 p0468 A72-14767

Cholesterol esters polymorphic and mesomorphic behavior, using differential scanning calorimetry, X ray powder diffractometry and positron annihilation techniques

04 p0484 A72-15262

Synthetic fire resistant hydraulic fluids, comparing chlorinated hydrocarbons and phosphate esters chemical properties with water based products

08 p1197 A72-22160

Capillary gas chromatography with two moderately high temperature phases, testing esters and hydrocarbons resolution ability

12 p1778 A72-27225

Allyl esters of phosphoric acid preparation and application as substitutes for heavy metal sulfides and silver compounds in single operation photographic process

16 p2392 A72-33363

ESTIMATES

NT COST ESTIMATES

Estimation and control relations separation for discrete time stochastic systems, considering assumptions on linearity, criteria, information pattern, constraints and noise distributions

01 p0047 A72-11306

Fading medium transfer function estimation via homomorphic and Kalman filtering, considering multiplicative noise

03 p0326 A72-14195

Extended iterative weighted least squares estimation of coefficients for linearly independent component signals in linear model

04 p0539 A72-14913

Quantitative and qualitative reliability estimates for electronic and mechanical products, obtaining conditional probabilities of flawless operation

08 p1179 A72-22052

Reliability estimates for continuously inspected recoverable systems, determining readiness factor for periodic checkout

08 p1180 A72-22054

Probability estimates of aircraft encounters with hail, discussing variations with locality, hailstone size and height and supersonic transport experience

09 p1346 A72-23423

Optimal estimates for nonlinear dynamic systems with time delay, using calculus of variations

10 p1454 A72-23784

Brightness estimates of Markarian galaxies on photographic plates, measuring light variation amplitude

10 p1546 A72-24831

Numerical algorithm for guaranteed minimax /max-min/ estimates for multistep decision making processes, using ALGOL 60

13 p1924 A72-28708

Minimum phase systems application for linear estimation of steady random sequences of signals, obtaining transfer function for optimal frequency filter

13 p1937 A72-29999

Bayesian estimation for nonlinear filtration of nonstationary non-Gaussian radio signals, deriving second central moments and parameter estimate errors

15 p2195 A72-31656

Asymptotically optimal procedures for certain types of moments of cutoff and terminal decisions in sequential estimation

17 p2576 A72-35419

A priori estimates and nonlinear parabolic equations of arbitrary order.

17 p2577 A72-35796

Condition for the equivalence of two important adaptation algorithms and its relationship to effective estimates of probability-distribution parameters

19 p2825 A72-37439

Weight estimation methods.

19 p2871 A72-37451

French monograph - Linear estimation of the parameters of multidimensional dynamic systems and statistical validation of the model - Applications to process identification

19 p2778 A72-37486

Parameter identification of a class of multiple input/multiple output linear discrete-time systems.

19 p2826 A72-38269

Mean value of noisy signal quantized by analog/digital converter, noting input noise level relation to estimate accuracy

20 p2904 A72-39785

Limiting value of the lower indicator, and lower bounds for integral functions with positive zeros

20 p2947 A72-39863

Best-fit estimate of relativistic effects in time-delay experiments.

20 p2972 A72-39871

An estimation algorithm with learning feature for an adaptive bit synchronizer.

21 p3021 A72-40908

Techniques for power spectrum moment estimation.

21 p3021 A72-40911

Statistical estimation of the signal-to-noise ratio beyond a linear detector

21 p3022 A72-41073

Regularized linear problem with perturbed equation as solution, presenting error overestimate

21 p3076 A72-41336

Location estimation for spacecraft landed on Mars surface via statistical techniques application to earth based radio tracking data, taking into account ephemeris biases

21 p3082 A72-41554

A comparison of the effects of small nonlinearities on several estimation schemes.

21 p3076 A72-41555

Investigation of the stability and vibrations of beams of variable rigidity by the method of bilateral estimates

22 p3234 A72-42147

Estimation and prediction of Gumbel and Frechet distribution parameters, noting statistical decision in tests, sequential analysis and graphical procedures

22 p3199 A72-42968

The application of Monte Carlo methods to the nonlinear filtering problem.

23 p3274 A72-43541

Estimates of unknown parameter from quantized observations given as sequence of evenly distributed random values, noting optimal grouping equations for general distribution function

23 p3266 A72-44218

Boundary value problems for multidimensional hyperbolic equations with degeneration

23 p3310 A72-44487

A priori estimates at the boundary for solving second-order elliptic integrodifferential equations

24 p3420 A72-45648

ESTIMATING

NT ORBITAL POSITION ESTIMATION

Estimation method for surface pressure distribution on cascade airfoil in retarded flow, applying to axial flow turbomachines design with suction performance and efficiency

01 p0001 A72-10396

Learning-identification of unknown nonlinear discrete systems, using local estimation results for global function learning

01 p0046 A72-11199

Point estimate calculation of underlying distribution function for probability plot, developing confidence coefficient for Weibull model

02 p0252 A72-11557

Computerized estimation of deformation parameters for Sellars-Tegart equation relating stress, strain rate and temperature in creep and hot torsion testing of metals

07 p1090 A72-19736

Nonlinear estimation theory and applications - Conference, San Diego, September 1971

08 p1143 A72-20843

Recursive and nonrecursive real time spline methods for nonlinear estimation of independent trajectory parameters for vehicle entering earth atmosphere

08 p1197 A72-20862

Algorithms for spatially varying parameters estimation in nonlinear partial differential equations from noisy observations, noting diffusivity in heat equation

10 p1506 A72-24457

Asymptotic solutions to dynamic problems of thermoelectricity estimation under homogeneous boundary conditions

13 p2062 A72-30067

Computational difficulties reduction in optimal control and estimation problems, discussing controllability and observability

17 p2574 A72-34417

Role of recursive estimation in statistical image enhancement.

18 p2658 A72-36260

Two dimensional recursive filter for Bayesian estimate of pictorial data represented by dynamic model of random field with exponential autocorrelation

18 p2658 A72-36261

Book - Fundamentals of pattern recognition.

20 p2905 A72-39575

Linear estimation stochastic filtering and deterministic linear optimal regulation duality concept extension to problems with inequality constraints

21 p3074 A72-40228

A recursive least-squares approach to the on-line adaptive control problem.

21 p3037 A72-40640

A design procedure for intermediate-order observer-estimators for linear discrete-time dynamical systems

22 p3161 A72-41994

Parameter estimation of reflected signal in multichannel communication system with discrete readings, considering receiver with optimal signal processing under low noise level

22 p3154 A72-42239

Control and estimation separation in stochastic optimization, discussing Wonham observer matrix reversibility and replacement in closed and closed-open loop systems

22 p3163 A72-42740

Aerospace vehicle passive thermal protection systems heat shield and bulk insulation estimation by weight prediction in conceptual phases of design

[SAWE PAPER 934] 23 p3356 A72-43474

An estimate of expected critical-path length in PERT networks.

23 p3308 A72-43806

Reliability estimation in life testing in the presence of an outlier observation.

23 p3309 A72-43807

ESTIMATORS

System natural frequency standard deviation estimator, using Monte Carlo method

[ASME PAPER 71-WA/APM-8] 05 p0734 A72-15972

Divergence prevention in decision directed adaptive recursive estimators in relation to error covariance

06 p0792 A72-17307

Sequential testing of actual and calculated error covariances consistency in recursive nonlinear estimators, noting method application to linear filters

08 p1197 A72-20857

Discrete-time nonlinear estimators digital implementations by computerized Monte Carlo method, comparing with alternative techniques

08 p1145 A72-20864

Failure rate function nonparametric estimators comparison on basis of asymptotic and Monte Carlo mean square errors

13 p1985 A72-28364

Smooth empirical Bayes estimation of observation error variances in linear systems.

17 p2576 A72-35248

Radar cross section fluctuation statistics description by generalized chi-square distribution, discussing target detection probabilities maximum likelihood estimates

19 p2763 A72-37293

State-feedback-controllers and state-estimators design for roll-pitch-horizontal motions of helicopter near hover, using rotor dynamics model

[AIAA PAPER 72-778] 19 p2752 A72-38137

Receiver processing for direct-detection optical communication systems.

21 p3017 A72-40859

Extended Kalman filter application to delayed systems for state and time delay estimation, discussing two nonlinear estimators

[AIAA PAPER 72-902] 21 p3039 A72-41553

Optimal, on-line linear filtering with noisy, time-delayed observations.

23 p3276 A72-43855

ESTUARIES

Chesapeake Bay aquatic ecosystems observations, using satellite remote sensing multispectral photography and imagery

02 p0215 A72-11885

ETCHANTS

Chemical etchants and etching procedure for decorating areas of residual tensile elastic surface stresses in ultrahigh strength steels without aging

22 p3183 A72-43045

ETCHING

Electron microscope examination of freeze-etched air-filled lung alveoli extracellular lining layer, discussing sample preparation techniques

05 p0623 A72-16787

Etch pit technique for titanium and zirconium crystal orientation determination, discussing etch pit locations and polycrystalline specimen goniomicroscopic observation

05 p0679 A72-17124

Chemically etched notches effect on Al-Mg alloy mechanical properties

07 p1018 A72-20139

Gas etching of Ge and Si semiconductors with vapors of chemical elements, emphasizing hydrogen chloride

11 p1700 A72-25776

Semiconductor materials etching and surface coating with protective silicon dioxide film in low temperature oxygen plasma

11 p1700 A72-25777

Metal surface layer and microetching process along grain boundaries during electrochemical precision processing, verifying steel microcrack depths with mathematical model

11 p1640 A72-26260

Ordered growth and etching of uranium and zirconium oxide-tungsten fiber refractory composites, using X ray diffraction and scanning electron microscopy

11 p1668 A72-26943

Nitride phase microstructure in ferrochromium nitrided in liquid state, comparing electrolytic etching and film coloration methods

12 p1829 A72-27454

Fatigue crack growth rate in precracked steel samples observed at 100 C by etching technique, noting flow stress and yield in plastic zone

14 p2119 A72-30608

Freeze etching techniques in electron microscopic investigations of biological cells molecular structure

18 p2653 A72-36829

Regeneration metering methods and equipment for acidic and alkaline etching of normal plated circuit boards.

20 p2929 A72-39491

A study of the vestigial records of cosmic rays in lunar rocks using a thick section technique.

23 p3341 A72-44459

Chemically etched notches effect on Al-Mg alloy mechanical properties

24 p3417 A72-45764

ETHERS

NT ANISOLE

NT DIETHYL ETHER

Electron impact induced fragmentations of o-, m- and p-hydroxyalkylphenones and trimethylsilyl/TMS/ether derivatives, using high resolution mass spectrometry, metastable defocusing and deuterium labeling

07 p0936 A72-19499

ETHYL ALCOHOL

Dry spot formation in nonboiling ethanol thin film on horizontal surface heated from below

04 p0595 A72-14597

Transient gain measurements on laser dyes of flashlamp pumped rhodamine 6G-ethanol solutions with air and nitrogen

07 p1002 A72-19208

Surface active medium effect on free surface energy and strength of pyrographite in ethyl alcohol solution, using crack kinetics experiment

08 p1197 A72-22182

Hydrodynamics of turbulent free convection boundary layer on vertical flat plate and ethyl alcohol film

11 p1743 A72-25258

Ethanol liquid fuel counterflow diffusion flame stabilization and thermal structure determination by interferometry

13 p1913 A72-29306

Aluminum oxide chromatography for ethanol-amine acetyl derivatives detection and separation in animal tissue extracts, using water-butanol solution as solvent

14 p2077 A72-30972

Effects of different alcohol dosages and display illumination on tracking performance during vestibular stimulation.

17 p2508 A72-34554

ETHYL COMPOUNDS

Gaseous diethyl peroxide spontaneous ignition during decomposition in cylindrical vessel, investigating diluents and temperature effects on self heating

02 p0301 A72-12027

Dinitroxydiethyl nitramine burning, describing experimental facilities used to determine temperature profile of combustion front

09 p1411 A72-22884

Anodic oxide films separation from Al alloy surface using ethyl bromide at temperatures below 40 C

16 p2397 A72-33274

ETHYLENE

Noble and molecular gases addition in reactions induced in ethylene by carbon dioxide-nitrogen-helium laser

07 p1009 A72-20693

Ethylene-vinyl acetate-asphalt thermoplastic material properties, filler effects, application methods and commercial uses

12 p1835 A72-28094

Carbon dioxide power laser effects on IR spectra of HCl-ethylene and sulfur dioxide-ethylene mixtures, focusing with Ge lens

13 p1971 A72-29870

Hydrogen atom exchange in ion-molecule reactions of methane and ethylene determined from reaction products distribution, using ion cyclotron resonance techniques

14 p2084 A72-30522

ETHYLENE COMPOUNDS

Free and dissolved water contents determination in light petroleum products by modified Karl Fischer method using ethylene glycol solvent mixture

05 p0702 A72-16669

Methyl alcohol-ethylene glycol self mixing antifreeze solution for precipitation gages

11 p1682 A72-26088

ETIOLOGY

Age related diminutions in ballistocardiographic and electrocardiographic amplitudes, observing relation to heart position lateralization and size reduction

03 p0314 A72-13144

ETR [REACTORS]

U ENGINEERING TEST REACTORS

ETTINGSHAUSEN COOLERS

U THERMOELECTRIC COOLING

EUCLEIDEAN GEOMETRY

NT ANGLES [GEOMETRY]

NT BRAGG ANGLE

NT BREWSTER ANGLE

NT CARTESIAN COORDINATES

NT CHORDS [GEOMETRY]

NT CIRCLES [GEOMETRY]

NT CONICS

NT ELLIPSES

NT EPICYCLOIDS

NT GREAT CIRCLES

NT HYPERBOLAS

NT LINES [GEOMETRY]

NT LOCI

NT MERCATOR PROJECTION

NT OBLATE SPHEROIDS

NT PARALLELEPIPEDS

NT PARALLELOGRAMS

NT POINTS [MATHEMATICS]

NT POLYHEDRONS

NT PROJECTIVE GEOMETRY

NT PROLATE SPHEROIDS

NT QUADRANTS

NT RECTANGLES

NT RHOMBOHEDRONS

NT SPHEROIDS

NT SQUARES [MATHEMATICS]

NT TANGENTS

NT TETRAONS

NT TETRAHEDRONS

NT TORUSES

NT TRAPEZOIDS

NT TRIANGLES

Cauchy problem for nonlinear biharmonic equation in Euclidean n-space, deriving a priori inequality estimate by logarithmic convexity of functional F

04 p0539 A72-15044

Optimality conditions for safe time in linear pursuit problems within n-dimensional Euclidean space

05 p0683 A72-16584

Markov type isotropic random Gaussian field analysis in n-dimensional Euclidean space

08 p1198 A72-20999

Theorem of pursuit game with curvature constraints during two points motion in Euclidean space

11 p1675 A72-25320

Criteria for nonlinear systems controllability in terms of state variable analytic function and derivatives, implying strong accessibility for manifolds including Euclidean spaces

18 p2673 A72-36616

Convergence of Rothe's method in the construction of bounded almost periodic and periodic solutions to a parabolic boundary value problem

19 p2824 A72-37433

Optimality conditions for safe time in linear pursuit problems within n-dimensional Euclidean space

19 p2825 A72-37555

Existence theorems in multidimensional problems of optimization with distributed and boundary controls.

21 p3074 A72-40548

EUGLENA

Euglena cell division timing control by endogenous circadian rhythm, showing direct entrainment by low frequency dark-light cycles

07 p0919 A72-19539

EULER BUCKLING

Random temperature variations effect on life of Euler column with sandwich cross section under constant axial compressive load, using Norton nonlinear creep law

15 p2324 A72-31494

Euler method limitations in static stability analysis, noting criterion for follow-type problem of buckling

16 p2466 A72-33016

EULER EQUATIONS OF MOTION

Energy release and accelerating inner stream effects on flow field near fuel injection in gas core reactor, basing Euler equations energy diffusion term on radial radiative transport

01 p0100 A72-11351

Spacecraft trajectories optimization by gradient method combination with Euler equations in calculus of variations

04 p0571 A72-14631

Angular velocity vector active damping during spin-up of electrically supported gyro with mass-unbalance readout, using Euler equations of motion

07 p0986 A72-19691

Motion of heavy solid body about fixed point for Hess conditions, analyzing Euler-Poisson equations solution properties

08 p1207 A72-21345

Distribution theory application to fixed end point problem in variational calculus for extremal containing corners, obtaining Euler equation

12 p1885 A72-27849

Gradient method and Euler equations application to low thrust earth-to-Mars spacecraft orbital transfer trajectory optimization

13 p2034 A72-28438

Delaney case of Kovalevskaja gyroscope motion, analyzing Euler equations time dependence

13 p1956 A72-28722

Shock wave propagation in gas with discrete velocity distribution, comparing solutions based on Euler, exact and Navier-Stokes equations respectively 16 p2375 A72-32861

Delauney case of Kovalevskaya gyroscope motion, analyzing Euler equations time dependence 22 p3176 A72-42098

Inverse problems of the dynamics of a ponderous solid with one fixed point 23 p3312 A72-43219

Hydrodynamic equations for incompressible fluid in steady relativistic state extended to nonrelativistic velocities case, noting transition from Euler to Predvoditelev equations 23 p3279 A72-43686

EULER-LAGRANGE EQUATION

Variational perturbation problem solution in power series form for elliptic functional description of elastic continuous medium state by Euler-Lagrange equations 02 p0259 A72-12233

Elastic continuous media nonlinear models approximation, obtaining Euler-Lagrange functions 02 p0259 A72-12234

Variational solutions of nonlinear free boundary integrodifferential Euler equations for rotating star models 02 p0252 A72-12540

Optimal trajectory in phase space, deriving differential motion equations with Euler-Lagrange method 02 p0199 A72-12880

Analytic solution for optimal control circular orbit escape with constant thrust rocket, using Euler-Lagrange equations and perturbation technique 03 p0437 A72-13839

Linear nongyroscopic conservative system stability from modified Lagrange equations of motion, using pseudo degree of freedom concepts and vibration method 03 p0362 A72-14394

Euler-Lagrange equation construction to obtain phenomenological description of quasi-equilibrium systems in metrics, noting solution coincidence with Onsager equations 07 p1102 A72-20665

Beecham-Kryloff-Bogoliubov approximation method application to a degree of freedom nonlinear systems, using averaged kinetic energy and virtual work terms in Lagrange equation 09 p1342 A72-23454

Virtual displacement application to nonholonomic systems with arbitrary constraints to derive Lagrange and Appell equations of motion 10 p1513 A72-24995

Multiple index Lagrange equations of motion of second kind, proving analogy between mechanical and stereomechanical effects 12 p1844 A72-27318

Averaging variational Euler-Lagrange equation for nonlinear waves with dispersion in nonconservative system 13 p2003 A72-28774

Lagrange equations of second kind for rigid systems, using balances of linear and angular momenta for mass point or rigid body 16 p2466 A72-33021

Variational principles application to nonlinear heat transfer problems, using Euler-Lagrange equation 16 p2478 A72-33435

Invariance problems in terms of Lagrangian domain of definition and Euler-Lagrange mapping intrinsic geometric characterization, reviewing theory of fiber bundles 20 p2954 A72-40006

Russian book - Introduction to the theory of gyroscopes. 21 p3052 A72-40349

Explicit series solutions for the frequencies of motion around the Lagrangean points in the restricted problem of three bodies. 24 p3440 A72-45136

EUROPA

Photometric radii of Io and Europa. 17 p2619 A72-35946

EUROPA LAUNCH VEHICLES

Guiana Space Center launch complexes for Diamant B and Europa satellite launchers and rocket probes, discussing trajectory, telemetry and safety measures 03 p0339 A72-12912

Small power nuclear propulsion engines for Europa launching systems, discussing heat exchange reactor using hydrogen propellant 15 p2273 A72-31812

Integrated systems design procedures as exemplified by Europa 1, 2 and 3 rockets and Symphonie communication satellite development 19 p2869 A72-38302

EUROPA 1 LAUNCH VEHICLE

Industrial challenge of European space R and D programs, discussing ELDO Europa 1 launcher vehicle and ESRO-HEOS satellite technological problems 01 p0146 A72-10948

EUROPA 2 LAUNCH VEHICLE

Europa 2 launcher F 11 flight test review concerning countdown, flight plan and trajectory and organizational details 02 p0286 A72-12034

Dynamic test facility and methods for Europa 2 launch vehicle inertial guidance system 05 p0643 A72-16433

Europa 2 launch vehicle standardized PCM/FM and FM/PM telemetry system compared with Europa 1 05 p0630 A72-16751

Launch center for solid-liquid propellant rocket probes, Diamant and Europa 2, describing payload preparation hall [DGLR PAPER 72-0137] 13 p1939 A72-28962

EUROPA 3 LAUNCH VEHICLE

Europa 3 candidate propulsion modules system analysis, considering payload, mission flexibility, orbital injection precision, synchronous satellite design influence, satellite-booster interfaces and costs 02 p0287 A72-12731

Europa 3 booster rocket development for future European space programs, discussing performance characteristics, project management and international cooperation aspects 05 p0724 A72-16310

Europa III preparatory phase. 17 p2621 A72-34899

Viking 2 rocket engines for Europa 3 first stage propulsion, describing engine components design and functions and performance test results 22 p3216 A72-42649

On the utilization of thermonuclear propulsion for an upper stage of the Europa III launcher 24 p3424 A72-45227

EUROPEAN AIRBUS

European A300B airbus flying control hydraulic system and landing gear design for safety and reliability, fatigue life, weight and maintenance 01 p0005 A72-10724

European A300B airbus flap and slat systems and tailplane actuator for longitudinal pitch trim control 01 p0006 A72-10725

A-300B European Airbus cantilever wing design and manufacture, discussing skin forming, skin-stringer and torsion-box assembly, automatic riveting and root-end profile machining procedures 03 p0365 A72-14301

European passenger aircraft Airbus program, discussing various configurations performance, economic factors and technical support 12 p1753 A72-27108

European Airbus program, noting international cooperation juridical sources, content and organization, aircraft performance, financing, project chronology and Franco-German agreement 13 p2067 A72-28795

Airlines requirements for European airbus, discussing design of aircraft structure, control, pressurized cabin and propulsion system 21 p2994 A72-40174

EUROPEAN SPACE PROGRAMS

Frequency planning for Symphonie German-French telecommunication satellite microwave equipment 01 p0030 A72-10710

Organization, management, contract placement and financing of CECLIS/ELDO European multinational program for launcher development 01 p0146 A72-10947

Industrial challenge of European space R and D programs, discussing ELDO Europa 1 launcher vehicle and ESRO-HEOS satellite technological problems 01 p0146 A72-10948

Organizational structure and functions of ESTEC /ESRO branch/ concerned with scientific research and application satellites development [DGLR PAPER 71-048] 02 p0305 A72-12724

German ground operation system for satellites and space probes, discussing telemetric data processing, handling and flow [DGLR PAPER 71-123] 02 p0201 A72-12742

Faust project history, scientific objectives and present status, discussing stars, nebulae, quasars point sources and galactic photometry 04 p0583 A72-15691

Europa 3 booster rocket development for future European space programs, discussing performance characteristics, project management and international cooperation aspects 05 p0724 A72-16310

Automatic control of ESRO drag-free deep space probe for measuring Robertson matrix beta and gamma constants [ONERA, TP NO. 952] 05 p0727 A72-16468

European Space Research and Technology Center /ESTEC/ results in cosmic rays, ionospheric physics and surface physics 05 p0644 A72-16754

European space organization with scientific and technological research objectives, noting jurisdictional status 07 p1105 A72-19474

Satellite communication activities on French national level, European multinational level /Symphonie/ and worldwide level /Intelsat/ 08 p1132 A72-21202

ESRO program in imaging detector development for UV and soft X ray space missions, presenting image storage target details 08 p1171 A72-21971

European Special Space Tug electronic subsystem requirements, considering strapdown inertial measuring unit, remote sensors, computer and fail-safe backup system 09 p1396 A72-23258

European Special Space Tug structural and configurational layouts and problems 09 p1396 A72-23259

German-French DIAL aeronomy satellite project, describing geocoronal radiation, electron density and equatorial electrojet measurements 10 p1535 A72-24029

DIAL aeronomy satellite design and operational features, describing in-flight behavior 10 p1551 A72-24030

ESRO sounding rockets program survey, discussing launchings in terms of number, vehicle types and sites, member participation, payload integration policy and success rate 10 p1551 A72-24197

ESRO electric propulsion systems R and D, discussing various concepts in terms of weight, cost, thrust level, efficiency, simplicity, exhaust velocity and development potential [AIAA PAPER 72-478] 11 p1710 A72-26207

Meteorological satellite information and communication aspects, stressing METEOSAT European project for permanent cloud cover observation in visible and IR bands [AIAA PAPER 72-547] 12 p1839 A72-27370

British defense and civil communications satellite program, discussing Skynet, INTELSAT, ESRO and New Space Technology Program activities [AIAA PAPER 72-548] 12 p1781 A72-27371

Franco-German Symphonie project of point to point communication and TV distribution by satellite, describing spacecraft and ground station characteristics [AIAA PAPER 72-549] 12 p1794 A72-27372

Dynamical motion simulation facility for Symphonie satellite, using sensors, attitude control electronics and analog computer in closed loop system [DFVLR-SONDDR-201] 12 p1795 A72-27659

ESRO findings on optimal resistance welding of solar cell interconnections for silver coated metals and pure silver 12 p1814 A72-28030

European programs on space stations, tugs, shuttles, propulsion and avionics and consideration for participation in NASA programs for 1970s and 1980s 14 p1715 A72-31137

European space project priority in terms of technological competition, budget limitation and participation in NASA post-Apollo program 14 p1715 A72-31138

European space program for remote sensing techniques application, noting earth resources survey satellites 15 p2220 A72-31229

International programs for simultaneous ecological study via remote sensing techniques, discussing European and Italian space programs 15 p2220 A72-31230

Economic analysis of satellite network construction program, suggesting Italian national center formation for space exploration 15 p2319 A72-31231

European synchronous meteorological satellite system Meteostat, discussing mission, control and data acquisition 15 p2265 A72-31345

Second generation European multi-mission launcher system for scientific and application satellites, using high energy propulsion modular design 15 p2320 A72-31804

Report to COSPAR on Polish space program covering artificial satellites tracking, aerospace medicine, meteorology and bioastronautics 15 p2337 A72-32004

Report to COSPAR on UK ground based, rocket and satellite-borne space research experiments and 1971-1972 programs 15 p2337 A72-32005

Report to COSPAR on Swedish space research, discussing activities of astronomical, ionosphere and geophysical observatories and space technology, physics and cosmic ray groups 15 p2338 A72-32008

Norwegian report to COSPAR on space scientific activities and application program, including satellite geodesy and earth resources research 15 p2338 A72-32009

Report to COSPAR on Netherlands space research covering solar and stellar radiation, cosmic gamma and X rays, photometry and satellite geodesy 15 p2338 A72-32010

Report to COSPAR on East German space program covering ionosphere, geomagnetic phenomena and solar physics

15 p2338 A72-32013

Report to COSPAR on West German space program covering meteorology, aeronomy, ionospheric physics, magnetosphere, solar wind and radiation, solar system and life sciences

15 p2338 A72-32014

ESRO report to COSPAR on satellites in orbit and under development and on 1971 sounding rocket program

15 p2338 A72-32016

Europa III preparatory phase.

17 p2621 A72-34899

Present state of development and extension plans of the German satellite earth station at Raisting.

17 p2536 A72-35431

Controversy surrounding Sirio satellite project related to microwave atmospheric propagation above 10 GHz with possible application in earth-to-space communication systems

17 p2623 A72-35918

Incore thermionic reactor application to meet European TV broadcasting satellite and submarine and underwater laboratory power requirements

18 p2644 A72-36166

TD-1A - Europe's largest and most advanced satellite.

18 p2731 A72-37011

European co-ordination activities with particular reference to the Space Components Co-ordination Committee.

18 p2743 A72-37130

CNET Reliability Center and its activities in the field of aerospace devices

18 p2676 A72-37135

Heos-A2 satellite polar orbit mission to study electron, proton and alpha particle population outside magnetosphere and in neutral point region

19 p2857 A72-37783

Observations of the solar wind with the European satellite Heos-1

19 p2850 A72-37785

ESOC-Darmstadt - ESRO's European center of operations for space exploration

20 p2988 A72-39415

European participation in space shuttle and space tug programs, discussing funding and technical aspects

21 p3103 A72-40456

Mission model for European communication satellite system based on estimated future traffic requirements

21 p3017 A72-40853

Space shuttle mission and orbiter element description, discussing European participation

23 p3343 A72-44366

HEOS-2 in orbit - Its technical performance.

24 p3449 A72-45108

Government, military safety, police permission and insurance regulations for European rocket activities

24 p3467 A72-45124

Design and operation objectives and constraints for German scientific spacecrafts, discussing orbital performance and reliability and quality control requirements

24 p3451 A72-45205

The Franco-German telecommunications satellite Symphonie

24 p3451 A72-45230

EUROPEAN SPACE RESEARCH ORGANIZATION

SAT

NT AZUR SATELLITE

NT COS-B SATELLITE

EUROPIUM

Lunar basalt Eu abundance anomaly in Apollo 11 and 12 samples, considering partial melting with or without plagioclase

10 p1537 A72-24162

Eu and Sr distribution between coexisting feldspars in acidic rocks, using mass spectroscopic isotope dilution method

10 p1472 A72-24166

Sm and Eu binary alloys, investigating physicochemical interactions and phase diagrams

15 p2289 A72-31187

Eu, La and Sm in sunspot spectra.

20 p2973 A72-39884

EUTECTIC ALLOYS

Ductility enhancement in directionally solidified Ni base Mar-M200 alloy by Hf additions increasing gamma-gamma prime eutectic

01 p0089 A72-11104

Eutectic Ni-Cr alloy temperature effects on deformation rate on plasticity, noting superplasticity point

02 p0244 A72-12243

Visual investigation of semibounded axisymmetric MHD flow of liquid eutectic K-Na alloy under strong magnetic field effect

03 p0399 A72-14014

Al-AiCu intermetallic unidirectionally solidified eutectic composite structure and heat treatment effects on room temperature tensile properties

05 p0676 A72-17104

Ni-NiNb intermetallic unidirectional eutectic alloy crystal structure and high temperature behavior, considering mechanical twinning relationship to strain hardening and ductility

05 p0677 A72-17108

Directionally solidified Al-AlNi intermetallic eutectic composites creep tests, identifying time dependent fracture mechanism

05 p0678 A72-17114

Directionally solidified Al-AlNi intermetallic eutectic alloy microstructural characteristics and effects on creep fracture

05 p0678 A72-17115

Impurities effect on microstructure alignment in unidirectionally solidified Al-AlNi eutectic intermetallic, noting fiberless region defects

05 p0679 A72-17123

Interfacial dislocations and failure in tension of directionally solidified Al-Cu-Mg eutectic

07 p1016 A72-19937

Microstructure and high temperature mechanical properties of unidirectionally solidified pseudobinary Fe-Cr-Nb eutectic alloy

07 p1016 A72-19938

Al and Al-Si alloy thermal expansion at low temperatures, noting near-eutectic crystalline composition

07 p1019 A72-20156

Nonferrous metals melting, discussing solid and gaseous impurities removal, halide function and grain and Al-Si eutectic refinement method

07 p0999 A72-20570

Cr-Tb alloys monotectic, eutectic and eutectoidal phase transformations study with differential thermal, metallographic, X ray structural and durometric analysis

08 p1187 A72-21781

Ti-Ce-S alloys phase equilibria with isothermal cross section, discussing eutectic alloys anomalous structure and cerium monosulfide preparation method

08 p1187 A72-21784

Microstructure and mechanical behavior of unidirectionally solidified magnesium-magnesium nickelide eutectic composite over range of solidification rates

09 p1330 A72-23376

Micrograin superplasticity in eutectoid steel, discussing effect of transformation to austenite

09 p1330 A72-23380

Micrographic observation of Al and Al-Cu intermetallic dendrites shape at birth in liquid of nearly eutectic composition

10 p1496 A72-24239

Fracture energy and deformation of unidirectionally and randomly oriented lamellar Al-Cu eutectics from surface microstructure studies

10 p1499 A72-24893

Austenitizing condition effect on lower bainite transformation in eutectoid carbon steel

11 p1656 A72-25515

Temperature and strain rate effects on superplasticity of Ni-Cr eutectic alloy

11 p1659 A72-26129

Slip and mechanical twinning in nickel-nickel nitride directionally solidified eutectic alloy, showing variation with temperature of stress-strain curves

11 p1667 A72-26935

Low cycle fatigue deformation of lamellar eutectic and cast Ni-Sr alloys, noting microstructure and chemical composition effects on fracture energy

11 p1668 A72-26939

Two phase structure solidification of monovariant eutectic Co-Cr-C alloys near pseudobinary cut

13 p1976 A72-28674

Carbon distribution effect on cast Mo and alloys fracture studied by electron microscopy, microdiffraction and X ray analysis, noting annealing from eutectic temperature

15 p2255 A72-31575

Isotropic fiber coarsening in unidirectionally solidified eutectic alloys, showing effect on alloy microstructure

16 p2409 A72-33802

Ultrasonic velocity measurement of elastic constants of Al-Al3Ni unidirectionally solidified eutectic.

18 p2701 A72-36591

Fracture behavior of stainless steel fibers in Sn-Pb alloy matrix.

19 p2820 A72-38373

Unidirectionally oriented pseudobinary eutectic solidification in ternary systems, investigating crystallographic and mechanical characteristics of ZrCuSi fibers embedded in Cu matrix

20 p2940 A72-39441

Crystallization and structure of hypereutectic iron-carbon-chromium alloys

21 p3071 A72-41788

Contact interaction between high-melting compounds and liquid metals. I - Interaction between subgroup IVA metals and metals of the iron family

23 p3299 A72-43287

Desulfurization of cobalt, nickel, and their eutectic carbon alloys during noncrucible zone melting in vacuum

23 p3300 A72-43647

EUTECTIC DIAGRAMS

U PHASE DIAGRAMS

EUTECTICS

NT EUTECTIC ALLOYS

Experimental hybrid rocket engine combustion chamber with solid oxidizer lining of ammonium nitrate and perchlorate eutectic mixture

05 p0702 A72-17249

Modified Al-Si eutectic solidification behavior and microstructure, investigating LF mechanical vibration effects

14 p2120 A72-30617

Phase diagrams of Ni-C and Co-C systems with metastable equilibrium lines, investigating microstructure and microhardness of carbide eutectic

14 p2123 A72-30990

EVACUATING [TRANSPORTATION]

General aviation patient transportation, investigating military helicopter airlift performance

01 p0139 A72-10778

Psychiatric preventive intervention in emotional crisis situations during patients aeromedical evacuation and transportation, discussing personnel shortage

10 p1429 A72-23743

Helicopter search, rescue and transportation of wounded and ill persons in Denmark, discussing accidental hypothermia treatment

19 p2759 A72-38714

EVACUATING [VACUUM]

Space shuttle cryogenic tanks self evacuating multilayer insulation, evaluating thermal and dynamic performance

01 p0139 A72-10778

Hydrogen evacuation with He condensation pump in ultrahigh vacuum region

06 p0795 A72-17698

Analytical prediction of pressure-time relationship during evacuation of multilayer insulation thermal protection systems, taking into account outgassing effects

14 p2172 A72-30925

Study of the solidification of cryogenic fluids by means of evacuation

19 p2881 A72-38039

EVAPORATION

NT PROPELLANT EVAPORATION

NT TRANSPIRATION

Radiative, segregation and evaporation processes of ice particles surrounding early type stars of Orion association, justifying ice particle model for dust grains

01 p0129 A72-10794

Heat transfer during liquid film evaporation in centrifugal vaporizer, noting agreement between theory and experiment

03 p0458 A72-14158

Heat pipe evaporation zone length based on desiccation length calculations for various capillary cross sections and thermal loads

05 p0743 A72-15853

Biological phosphate origin through atmosphere-hydrosphere interrelations, discussing concentrative processes, dehydration mechanics and evaporation

05 p0617 A72-16129

Thermodynamic analysis of heat of evaporation of sweat, considering ambient temperature and humidity effects, body heat storage and presence of solutes

11 p1586 A72-26610

Weight loss due to respiratory tract evaporative water loss during exercise, from humidity change, ventilatory exchange and oxygen uptake data

11 p1586 A72-26613

Three dimensional heat propagation problem of copper electrode destruction under concentrated heat flux with allowance for metal evaporation

12 p1890 A72-28175

Mass spectroscopic determination of vapor composition during GaAs and GaP single crystals exposure to ruby laser radiation

14 p2109 A72-30316

Mass transfer effect on heat transfer to evaporating droplet, considering mass efflux shielding effect and forced convection flow field

14 p2172 A72-31051

Liquid drop evaporation in stagnant environment at high temperature and pressure, noting gas phase nonideal behavior effects

14 p2173 A72-31066

Velocity distributions of molecular beams evaporating into vacuum from polycrystalline hexachlorobenzene and sulfur surfaces

16 p2429 A72-33058

H I region molecular formation on interstellar dust grains, discussing nonequilibrium evaporation mechanism for adsorbed particles

16 p2452 A72-33128

Effect of evaporation of the volatile component on the electrical properties of CdSb

19 p2845 A72-38402

The film vaporization combustor and its physical principles. I - The vaporizer section of the combustor. II - The reaction chamber and the combustion [DFVLR-SONDDR-194]

20 p2963 A72-39074

Sensitivity enhancement of atom absorption measurements by the method of pulse vaporization from the microprobe into the flame

22 p3176 A72-42174

- Radiation, evaporation and the maintenance of turbulence under stable conditions in the lower atmosphere. 22 p3201 A72-42597
- Spacecraft functional properties degradation due to surface contamination with outgassing vapors, discussing contaminant materials transport and sorption characteristics 23 p3254 A72-43619
- Evaporation of metallic targets by intense optical radiation 23 p3297 A72-44485
- Pulsating conditions in the evaporation of optical materials under the influence of CO2 laser radiation. 24 p3411 A72-45610
- EVAPORATION RATE**
- Heat transfer for water at pressures near atmospheric in wicks formed of stainless steel screen layers, obtaining steady and maximum evaporation rates [ASME PAPER 71-WA/HT-12] 05 p0744 A72-15872
- Evaporation and combustion of liquids injected into high temperature supersonic flow, considering interrelation with pressure variations 08 p1253 A72-21454
- Two mechanism model for anomalous field ion microscope images in W, noting end form difference in high and low evaporation rates 09 p1370 A72-22803
- Exospheric temperatures in hydrogen dominated planetary atmospheres for evaporative loss rates estimation, noting two component diffusive equilibrium model 09 p1393 A72-23661
- Stefan problem of metal evaporation duration after intense heat flux termination as function of thermophysical properties 15 p2334 A72-31504
- Impulse liquid jet pressure reduction in closed vessel under adiabatic conditions and evaporation intensity dependence on jet velocity 16 p2476 A72-33259
- Lifetime nomogram for evaporating drop at vapor combustion, applying thermomechanical and aerodynamic decay to jet engine combustion chamber [DFVLR-SONDDR-203] 16 p2477 A72-33422
- Experimental investigation of the influence of acoustic oscillations on the evaporation intensity of liquid droplets 20 p2987 A72-40037
- Electron beam evaporator with multiple source suitable for use in ultrahigh vacuum, noting control of evaporation rate 21 p3051 A72-40205
- EVAPORATIVE COOLING**
- NT FILM COOLING
- NT SWEAT COOLING
- Capillary evaporation cooling system with water as working medium, measuring effectiveness in terms of heat flux density vs water consumption [DFVLR-SONDDR-112] 10 p1561 A72-24023
- Gasdynamic investigation of a turbine with evaporative air cooling of the nozzle guide vanes 23 p3325 A72-43662
- EVAPORATORS**
- Water heat pipes transient thermal impedance, monitoring evaporator, vapor space and condenser temperature [ASME PAPER 71-WA/HT-9] 05 p0743 A72-15869
- Heat pipe operating conditions and evaporator, condenser and adiabatic parts, discussing fluid capillary transport for heat pipe calculation 05 p0750 A72-17047
- Development of a laboratory prototype spraying flash evaporator. [ASME PAPER 72-ENAV-28] 20 p2894 A72-39149
- Electron beam evaporator with multiple source suitable for use in ultrahigh vacuum, noting control of evaporation rate 21 p3051 A72-40205
- EVAPOROGRAPHY**
- IR absorbent effects on evaporographic image contrast performance based on photometric study, presenting color photographs 15 p2188 A72-31615
- EVASIVE ACTIONS**
- Optimal thrust reversing in pursuit evasion games between two aircraft in horizontal plane, considering cost functions and termination criteria 07 p0912 A72-19282
- Position differential games of extremal stable evasion strategies for swerving motions with absorption in time 13 p2004 A72-29470
- EVECTION**
- U LUNAR ORBITS
- U ORBIT PERTURBATION
- U SOFAR GRAVITATION
- EVENTS**
- NT CONSECUTIVE EVENTS
- EVOLUTION**
- Solutions for multivalued evolution equations, considering monotonic maximal operator on finite dimensional Hilbert space 10 p1504 A72-24061
- EVOLUTION [DEVELOPMENT]**
- NT ABIOTIC GENESIS
- NT BIOLOGICAL EVOLUTION
- NT GALACTIC EVOLUTION
- NT LUNAR EVOLUTION
- NT PLANETARY EVOLUTION
- NT STELLAR EVOLUTION
- Secondary periodic solution for Navier-Stokes type evolution problems, observing stabilities [ONERA, TP NO. 1035] 03 p0389 A72-13786
- Minicomputers evolution, considering price reduction, performance improvement, operation simplification, and applications for data collection and transmission 06 p0780 A72-18179
- Meteorite genesis and formation processes from composition characteristics, discussing age determination methods and mineralogical classifications 07 p1082 A72-20302
- Astrophysical study of cosmological evolution, discussing evidence from radio source counts and quasar spatial distribution 07 p1084 A72-20471
- Chemical composition features of basalts from British Tertiary Volcanic Province, discussing possible evolution 10 p1472 A72-23915
- Generalized thermodynamic potentials and universal criteria for direction of evolution of irreversible processes from Gibbs function stability analysis 10 p1562 A72-24250
- Low cost meteorological sounding rocket evolution, including Arcas, Lokidart and Viper Dart systems for various altitude ranges 10 p1552 A72-25090
- On the ability of the luminosity-volume test to reveal the statistical evolution of the luminosity of quasi-stellar sources. 19 p2854 A72-37226
- Polyphosphate and trimetaphosphate formation under potentially prebiotic conditions. 23 p3261 A72-43566
- Studies in prebiotic synthesis. VII - Solid-state synthesis of purine nucleosides. 23 p3262 A72-43567
- EVOLUTION [LIBERATION]**
- NT GAS EVOLUTION
- EXACTNESS**
- U PRECISION
- EXAMINATION**
- NT EYE EXAMINATIONS
- EXCHANGING**
- NT CHARGE EXCHANGE
- NT GAS EXCHANGE
- NT ION EXCHANGING
- NT RESONANCE CHARGE EXCHANGE
- NT SPIN EXCHANGE
- EXCITATION**
- NT ACOUSTIC EXCITATION
- NT ATOMIC EXCITATIONS
- NT HARMONIC EXCITATION
- NT MOLECULAR EXCITATION
- NT SELF EXCITATION
- NT WAVE EXCITATION
- Dynamic systems stability under periodic impulsive parametric excitation, deriving simple closed-form analytic stability criteria for special cases from general theory [ASME PAPER 71-WA/APM-19] 05 p0733 A72-15961
- Optical hyperfine structure of Ne 2I excited states and quadrupole moment obtained by laser induced line narrowing techniques 10 p1515 A72-24601
- Oscillations excitation, proposing models for percussive rotational action machines operation and dog tooth clutches processes 13 p1954 A72-28386
- Stability conditions for damped single degree of freedom oscillator system under stationary narrow-band random excitation, obtaining approximate solution by perturbation method 14 p2131 A72-30718
- Dynamic stability of elastic systems under broadband random excitation, presenting solution for straight rod under axial pulsating forces via perturbation method 15 p2274 A72-31460
- Multidegree of freedom linear systems mean-square response to nonstationary random vibratory excitation, using staircase approximation to continuous intensity functions 15 p2331 A72-32552
- Structural system response to white noise excitation, deriving integral equation for first passage time-density function via Markov process model [ASME PAPER 72-APM-11] 17 p2629 A72-34805
- State vector moments of nonlinear mechanical systems under stochastic excitation, using Fokker-Planck equation for transition probability and differential equations derivation 21 p3084 A72-40679
- Vibration measurements of an airplane fuselage structure. I - Turbulent boundary layer excitation. II - Jet noise excitation. 22 p3139 A72-42912
- German monograph - Stability conditions for a linear homogeneous ordinary differential equation of second order with stochastic parameter excitation. 22 p3199 A72-43055
- EXCITED STATES**
- U EXCITATION
- EXCITONS**
- Internal Q switching in CdS laser activated by exciton recombination, observing lag in emission onset after input pulses delivery 04 p0528 A72-14575
- Coupled coherent and incoherent excitons motion effect on optical absorption line shape, deriving diffusion equation from density matrix equation of motion 07 p1035 A72-19672
- Light modulation by exciton electric absorption in thin high impedance recrystallized CdTe films within strong electric fields, showing spectral distribution curves 09 p1366 A72-22419
- Photoemission from tetracene organic semiconductors due to electron capture defect ionization by excitons 11 p1700 A72-25785
- Boundary conditions in the exciton absorption region. 21 p3096 A72-40139
- Exciton condensation in a momentum space under the action of optical pumping 22 p3185 A72-42161
- EXCRETION**
- Ground and flying activity endurance training effect on urinary excretion of noradrenaline and adrenaline 04 p0478 A72-14868
- Immobilization hypercalciuria, discussing treatment by diet-induced extracellular volume depletion and possible pathophysiologic mechanism of intercompartmental fluid and electrolyte shift 04 p0479 A72-14871
- Isolation stress effect on excretory products in unrestrained chimpanzee, suggesting Ca to P excretion ratio as physiological stress indicator [AD-739467] 07 p0921 A72-20179
- Food deprivation stress effects on urinary excretion values in unrestrained chimpanzees 10 p1426 A72-24822
- Calcium and phosphorus excretion relation to bone density changes in immobilized Macaca nemestrina monkeys 12 p1760 A72-27473
- Sleep deprivation effects on diurnal urine potassium excretion, showing individual circadian rhythm variations 13 p1904 A72-29320
- Weightlessness effects on calcium and electrolyte metabolism from measurements during Gemini 7 flight, using dietary control and excreta collection techniques 16 p2355 A72-33552
- Interrelation of interoceptors and exteroceptors in the process of urination and defecation reflex act maturation in ontogeny 17 p2504 A72-35022
- Nitrogen excretion as a measure of protein metabolism in man under different conditions of renal function. 21 p3003 A72-41523
- Capillary circulation as a regulator of sodium reabsorption and excretion. 23 p3257 A72-43995
- EXECUTIVE AIRCRAFT**
- U GENERAL AVIATION AIRCRAFT
- U PASSENGER AIRCRAFT
- EXERCISE [PHYSIOLOGY]**
- Human exercise capacity assessment from maximal oxygen intake estimates and Harvard step test 01 p0016 A72-10116
- Human patients with chest pain and normal ECG, examining diagnostic value of graded exercise test, history and lipid levels with coronary arteriography data 01 p0010 A72-10146
- Human cardiocirculatory responses to submaximal physiologically paced bicycle ergometry, recording prejection period, isovolumic contraction, left ventricular ejection and pulse transmission time 01 p0010 A72-10147
- Exercise and denervation effects on intrafusal muscle fibers morphology, noting 25-33 percent cross-sectional area atrophy in nuclear bag and chain fibers 04 p0472 A72-14895
- Exercise ECG multichannel radio telemetry equipment, discussing sources of malfunction and unreliability and remedial procedures 05 p0621 A72-16610
- Human temperature regulation during upright and supine exercise, showing nonlinear relationships between perspiration and skin and core temperatures 07 p0922 A72-20275
- Endurance exercise effect on respiratory capacity in white, red and intermediate muscles in rats, relating fiber type to oxidative capacity 08 p1115 A72-21083

Physiological and subjective responses of physically fit young men to combined exercise-carbon dioxide stress tests

12 p1767 A72-28311

ECG amplifier and cardiographometer for exercise studies, using digital algorithm for heart rate computation and ECG signal preprocessing for R wave detection

14 p2080 A72-30707

Human plasma free fatty acids relation to lactic acid concentration and maximum aerobic power, noting carbohydrate availability as exercise capacity limiter

21 p3003 A72-41520

EXERTION

U PHYSICAL WORK

EXHAUST DIFFUSERS

Curved-wall annular exhaust diffusers for hot engine parts IR shielding, evaluating performance tests for swirl flow and ejector secondary flow effects on pressure recovery

[ASME PAPER 71-WA/FE-35] 05 p0646 A72-15922

Small radial inflow turbines for space applications, considering blade-shroud clearance, blade loading and exit diffuser design

[ASME PAPER 72-GT-42] 11 p1704 A72-25636

EXHAUST FLOW SIMULATION

NT ATMOSPHERIC ENTRY SIMULATION

NT FLIGHT SIMULATION

Simulated testing of turbojet engine ingestion of missile exhaust, determining design criteria for aircraft engine inlets from altitude chamber test data

07 p1052 A72-18758

High pressure annular combustor with continuous analytical and sampling system for simulated gas turbine engines emission measurements

[ASME PAPER 72-GT-88] 11 p1705 A72-25663

Simulation model test for effects of cooling air exhaust into gas flow area on turbine blading efficiency, obtaining dimensionless expression for experimental data generalization

12 p1862 A72-28148

The use of an expansion tube with cold gas to determine rocket engine starting transient pressures during silo launch

[AIAA PAPER 72-997] 21 p3040 A72-41583

The simulation of high pressure hydrogen/oxygen rocket engines

[AIAA PAPER 72-1027] 21 p3042 A72-41606

EXHAUST GASES

Aircraft gas turbine engine emission reduction, showing nitrogen oxide control with water injection

[ASME PAPER 71-WA/GT-9] 05 p0704 A72-15902

Diffusion and fallout of polluting particulates emitted by aircraft engines, discussing effect of wing-tip vortices, plume visibility and monitoring, simulation and modeling

[ASME PAPER 71-WA/AV-2] 05 p0704 A72-15950

Diffuser for altitude simulation in rocket motor operation, featuring film cooling with water inflow by motor exhaust gas ejector action

05 p0704 A72-16004

Rocket plume contamination effect on transmitting and reflecting materials optical properties, noting predominant absorption and scattering effects

[AIAA PAPER 72-56] 05 p0750 A72-16967

Aircraft gas turbine engines smoke emission sampling by stained filter technique, comparing Navy specifications AS 1833 with SAE method ARP 1179

07 p1053 A72-18770

Space and atmosphere contamination by industrial wastes, aircraft and spacecraft exhaust and radioactive waste disposal, considering legal safeguards

07 p1104 A72-19466

Nitrogen oxide emission control in gas turbine combustion by lowering flame temperature

[ASME PAPER 72-GT-22] 11 p1744 A72-25620

Gas turbine engines emission data correlation based on combustor theoretical model, proposing correction factors for data reduction to standard test conditions

[ASME PAPER 72-GT-60] 11 p1704 A72-25651

Propulsion system design for military VTOL aircraft, emphasizing subsonic cruise to maximum thrust ratio and exhaust downwash characteristics

[ASME PAPER 72-GT-73] 11 p1704 A72-25655

Aircraft gas turbine engines exhaust emission characteristics identification, considering ambient temperature and humidity effects

[ASME PAPER 72-GT-75] 11 p1705 A72-25657

High pressure annular combustor with continuous analytical and sampling system for simulated gas turbine engines emission measurements

[ASME PAPER 72-GT-88] 11 p1705 A72-25663

Combustion research for reducing jet aircraft pollutant emissions, discussing fuel atomization improvement, smoke reduction and combustor design techniques

11 p1705 A72-26037

Exhaust composition and smoke emission reduction from aircraft with gas turbine power plants

12 p1860 A72-27270

Estimated peak regional concentration of SST exhaust in stratosphere from expected flight operation levels

13 p1991 A72-28837

Future projections of commercial jet aircraft fuel demands, estimating engine exhaust effects on air quality

13 p1897 A72-28879

Aromatic hydrocarbons and fuels, investigating engine parameters effects on combustion and exhaust gases temperatures

13 p2025 A72-29074

Climatic changes due to stratospheric perturbation by propulsion effluents of high altitude aircraft flights

[AIAA PAPER 72-658] 16 p2388 A72-34076

SST contrails stratospheric dispersion by aircraft wake, atmospheric turbulence and exhaust gases temperature induced buoyancy

[AIAA PAPER 72-650] 16 p2388 A72-34084

Stratospheric pollution by SST exhaust gases, discussing water vapor and nitrogen oxides effects on ozone concentration

17 p2597 A72-35327

Atmospheric composition to 40 km altitude from balloon-borne particle impacted electron microscope screens, discussing pollution effects from high flying aircraft exhaust gases

17 p2551 A72-35935

Procedure for the continuous sampling and measurement of gaseous emissions from aircraft turbine engines

[SAE ARP 1256] 18 p2721 A72-36532

Numerical prediction of the diffusion of exhaust products of supersonic aircraft in the stratosphere

19 p2748 A72-37824

Influence of cooling-air exhaust into the air-gas flow area on the flow-rate characteristics of cooled profiles

20 p2963 A72-39923

Backscattering of desorbed gas molecules from spacecraft

23 p3284 A72-43618

Aircraft gas turbine engines environmental effects, considering thermal radiation, acoustic emissions and exhaust gases in relation to propulsion system design parameters

23 p3328 A72-44296

Linear theory of a solid propellant rocket motor with modulated exhaust

24 p3433 A72-45116

EXHAUST JETS

U EXHAUST GASES

EXHAUST NOZZLES

NT CONVERGENT-DIVERGENT NOZZLES

NT PLUG NOZZLES

NT TURBINE EXHAUST NOZZLES

Capacitive electret pressure sensors calibration for interior measurements in turbine engines, jets and exhaust nozzles

[ONERA, TP NO. 982] 09 p1310 A72-22815

Turbojet simulator for supersonic wind tunnel models, simulating inlet mass flow ratio and exhaust nozzle pressure ratio

[ASME PAPER 72-GT-89] 11 p1705 A72-25664

Solid propellant rocket engine thrust vector control by four movable exhaust nozzles, nozzle exit cone secondary injection and flexible bearing nozzle

13 p2026 A72-28928

Three dimensional supersonic nozzle exhaust flow field numerical analysis based on reference plane characteristics, deriving difference equations for three coordinate systems

[AIAA PAPER 72-704] 16 p2344 A72-34040

Effect on supersonic jet noise of nozzle plenum pressure fluctuations

17 p2597 A72-35243

Servo pump nozzle area controls for gas turbines

18 p2694 A72-36048

Nonlinear equations solutions for interior ballistics parameters of solid rocket propellants combustion during rocket engine nozzle opening

19 p2878 A72-37352

Erosion combustion effect on unsteady solid rocket propellant burning stability during engine nozzle opening, noting combustion velocity and surface temperature

19 p2879 A72-37353

Thrust stand for evaluation of thrust vectoring nozzle performance

[AIAA PAPER 72-1029] 24 p3389 A72-45406

EXHAUST SYSTEMS

Concorde engine performance, reviewing control, reheat and exhaust systems

[SAE PAPER 710775] 01 p0116 A72-10267

Shock wave propagation from channel in free space for various Mach numbers, using method of characteristics

02 p0202 A72-11590

Electrical analog simulation of internal combustion engines intake and exhaust systems nonstationary gas flow, considering cylinder, turbine and supercharger operation

13 p2027 A72-29136

EXHAUST VELOCITY

Fluorine-ammonia as high energy liquid bipropellant for rocket engines, presenting ground test results regarding velocity and specific impulse characteristics as functions of mixture ratio

01 p0114 A72-11220

Hydrogen resistojet design and testing with Re heat exchanges, noting appropriate power efficiency and exhaust velocity for synchronous communication satellites orbital transfer

[AIAA PAPER 72-449] 11 p1708 A72-26186

Electrothermal thruster supersonic convergent-divergent nozzle performance with lithium vapor propellant, predicting exhaust velocity by isentropic flow equations

[AIAA PAPER 72-453] 11 p1708 A72-26189

Capillary fed annular colloid thruster operating characteristics, considering I-V relationship, thrust and exhaust velocities and propulsive efficiency

[AIAA PAPER 72-490] 11 p1710 A72-26215

EXHAUSTION

Human performance and exhaustion predictive model from responses to exercise and environmental stresses, considering circulation, thermal regulation, work load and oxygen pressure effects

07 p0934 A72-20358

Sweating relation to body temperature after exhaustive exercise for various oxygen uptakes and ambient temperatures

14 p2079 A72-30702

EXISTENCE

One dimensional conductive and radiative heat transfer through gray medium bounded by two diffuse surfaces, noting solutions existence and uniqueness

09 p1412 A72-23586

EXISTENCE THEOREMS

Soviet book on theory of differential equations with deviating argument covering step methods, existence and uniqueness theorems, solutions stability, approximations, etc

02 p0252 A72-12124

Periodic solution existence for second order differential equation

03 p0382 A72-14250

Mass service process differential equations with losses, annihilation and multiplication processes, demonstrating unique solution existence

04 p0538 A72-14627

Distributed parameter control system optimal control problems, formulating existence with minimum norm technique

04 p0505 A72-14667

Isolated fixed points existence in area preserving mappings considered with normal form for periodic Hamiltonians in celestial mechanics

04 p0576 A72-15041

Shooting method and contraction mapping application to existence-uniqueness theorem derivation for numerical solution of second order delay differential equations boundary value problems

04 p0539 A72-15042

Implicit equations in nonlinear network analysis, deriving conditions for existence of unique solutions

04 p0540 A72-15695

Time optimal control of system with distributed moments, deriving conditions for existence of fast response solution

05 p0683 A72-17134

Incompressible micropolar fluid flow equations, deducing stable periodic solutions existence by energy method

06 p0799 A72-17917

Lens antennas for amplitude and phase transformations, examining existence of solutions and bounds in terms of parameters

07 p0985 A72-19404

Sufficient conditions definition for existence of solution for heat conduction equation coupling to telegrapher equation

07 p1028 A72-19897

Optimal strategies for decision chain with controllable connections and finite number of states and decisions, deriving existence theorem

07 p1028 A72-19904

Time independent incompressible micropolar fluid flow existence

07 p0970 A72-20082

Theorems for averaging of first order linear hyperbolic system with time lag, proving existence and uniqueness of solution to Cauchy problem

07 p1028 A72-20214

Radial gas bearing air lubrication theory, proving existence and uniqueness theorems for Reynolds equation periodic solution

07 p0998 A72-20473

Liapunov theorem for polynomial solution existence for first order inhomogeneous system of linear partial differential equations

08 p1205 A72-20958

Solutions existence for nonlinear invariant relation to integrodifferential equations of motion of solid body about fixed point

08 p1207 A72-21347

Solutions existence and uniqueness for linear invariant relation to gyrostat motion under nonholonomic constraint

08 p1208 A72-21362

Nonflat central configuration N point masses existence for any integer greater than four, disproving Wintner conjecture of finite number of integers

08 p1236 A72-21639

Boundary value problem for degenerate quasi-linear parabolic differential equation, showing solution existence and smoothness dependence on region width
09 p1342 A72-23485

Existence and uniqueness theorem for weak solution of clamped elastic plate equilibrium problem, using micropolar flat plate bending theory
10 p1555 A72-24202

Small cross section steady vortex rings existence in inviscid uniformly dense ideal fluid, deriving asymptotic formulas for rings shape and properties
10 p1467 A72-24333

Kinetic equations solution for homogeneous multiatomic gas relaxation, proving solution existence and uniqueness
10 p1516 A72-24629

Dynamic logic control systems theory based on axiomatic concepts of models, deriving conditions for existence and uniqueness of solution for differential logic equations
10 p1457 A72-24636

Universal mathematical model of n-complete atomic theory, obtaining existence criterion for prehomogeneous relation in relation age
10 p1506 A72-24851

Function space linear bounded phase coordinate control problems under regularity and normality conditions discussing solution existence and uniqueness conditions
11 p1608 A72-25322

Nonlinear differential equations cycle properties and frequency, using Leray-Schauder theorem for cycle existence proof
11 p1675 A72-25325

Sufficient conditions for existence, uniqueness and finite-dimensional approximation of solution to first order infinite-dimensional vector differential equation
11 p1676 A72-25357

Geometric interpretation of solution existence for nonlinear ordinary differential equations with linear and nonlinear boundary conditions, analyzing funnel of solutions
11 p1676 A72-25503

Boundary value problems in boundary layer theory, discussing Falkner-Skan equation similar solutions existence theorems
11 p1677 A72-25525

McShane belated stochastic integral existence theorem with quasi-martingale process for sample continuity assumption
11 p1678 A72-26156

Oscillation criteria for fourth order differential equation conjugate point location relationship in terms of existence of solution with two double zeros
11 p1678 A72-26159

Existence and uniqueness of general solutions of initial value problem for nonlinear Maxwell-Boltzmann equation with finite time interval
12 p1836 A72-27122

Two heat conducting phases free boundary problem with temperature distribution within phases, proving existence and uniqueness theorems
12 p1836 A72-27124

Variational problems in automatic control theory, presenting existence theorems for solution of boundary value problems for nonlinear differential equations with deviating argument
12 p1837 A72-27995

Uniqueness and existence theorems for nonideal thermal contact between three dimensional solid parts in heat conduction theory, noting case of two dimensional body
12 p1889 A72-27996

Regularizing time transformation for conservative systems reduction to normal coordinates, studying normal configurations existence in terms of Hamiltonian structural properties
13 p2002 A72-28714

Boundary value problem solution uniqueness relation to existence for nonlinear differential equations of arbitrary order satisfying solution compactness condition
15 p2263 A72-31753

Regge calculus representation existence for solutions of initial value problem for spaces with axial symmetry
16 p2422 A72-32879

Solution existence for singular boundary value problem involving swirling flow, corresponding to problem of axisymmetric flow above rotating disk
16 p2377 A72-33186

Heat equation kernel functions existence proof based on Harnack selection principle and inequality
16 p2476 A72-33187

Existence and uniqueness theorems for Cauchy problem solution for linear singular integrodifferential operator equation
16 p2417 A72-34010

Existence of multiple solutions for nonlinear elliptic boundary value problems.
17 p2575 A72-34936

Boundary value problems for second order, ordinary differential equations involving a parameter.
18 p2705 A72-36619

Existence theorems for dynamical systems admissible controls for avoidance of given set of state spaces, considering control process governed by ordinary differential equations
19 p2778 A72-37723

Investigation of the solution of a two-dimensional nonlinear Volterra integral equation
19 p2825 A72-38203

Approximate integration of a nonlinear system of differential equations with time lag
19 p2827 A72-38468

Three body problem second kind periodic orbit existence proof based on Weinstein theorem
19 p2867 A72-38553

Proof of existence theorems for the principal dynamic problems of thermoelasticity
20 p2978 A72-39317

Existence theorems in multidimensional problems of optimization with distributed and boundary controls.
21 p3074 A72-40548

Propagation rate and the existence range of turbulent flame
21 p3131 A72-41660

Differential equation solution existence in complete locally convex topological Hausdorff vector space defined by saturated seminorms
21 p3076 A72-41783

Navier-Stokes evolution inequality bounded solution existence and uniqueness theorems for two dimensional space
22 p3200 A72-43201

Existence and uniqueness theorems of elliptic equations with eigenfunction exponential decrease at infinity and 2m order self adjoint differential operator in n-dimensional Euclidean space
23 p3307 A72-43223

Sufficient condition formulation for Lure type nonlinear continuous control system exponential absolute stability
23 p3309 A72-43854

Nonlinear nonautonomous dynamic systems practical stability conditions for specified settling time, verifying constant matrix Hurwitz property
23 p3309 A72-43858

Linear inequalities and P matrices, with applications to stability of nonlinear systems.
23 p3309 A72-43859

A priori bounds and upper and lower solutions for nonlinear second-order boundary-value problems.
23 p3309 A72-43980

Multistage rocket optimal control, deriving conditions for existence of minimum of performance index function of mass, position and velocity initial and final values
23 p3343 A72-44264

Necessary conditions for steady state in radiation - Matter interaction and the role of entropy.
24 p3461 A72-44806

EXOBIOLOGY

Industrial and biological processing possibilities under weightless condition, considering crystal growth, metal processing, vaccine production and electrophoresis in space manufacturing
02 p0278 A72-11961

Life origin in space from point of hydrocarbons, cyanides, abiogenetic organic synthesis and probiotics evolution
04 p0467 A72-14752

Comet collisions in planetary nebulae as source of organic compounds in universe in preplanetary era, noting nucleic acid bases in carbonaceous meteorites
04 p0471 A72-14802

Extraterrestrial life on Mars and Venus and Jupiter atmospheres, discussing abiogenesis failures on life-supportable planets
04 p0471 A72-14805

Extraterrestrial life origin and evolution, estimating possibilities on Mars, Venus and Jupiter
04 p0471 A72-14806

Papers on exobiology theory and experiments, considering extraterrestrial organic compound detection, Jupiter atmosphere, porphyrins, radiation production of life molecules, etc
05 p0617 A72-16126

Porphyrin exobiology, discussing organic and random biosynthesis and extraterrestrial existence based on interstellar spectral evidence
05 p0617 A72-16130

Apollo 11 lunar samples carbon compound geochemical analysis, using sequential scheme with minimum handling of solids and extracts
05 p0714 A72-16131

Exobiology research objectives, discussing planetary exploration data on origin, nature and distribution of life, spacecraft contamination, manned and unmanned missions and specific mission targets
05 p0714 A72-16133

Papers on exobiology covering abiogenesis, extraterrestrial life, primordial organic chemistry, biochemical evolution electronic factors, membranes origin, molecular chirality, protein and cellular evolution, etc
08 p1119 A72-22001

Cosmic sources of organic compounds from chemical evolution viewpoint, discussing comets, interstellar space, prestellar nebulae and cool stellar atmospheres
08 p1120 A72-22014

Terrestrial life origin understanding by investigating life possibilities in nonterrestrial environments
08 p1120 A72-22015

Review of NASA Ames Research Center 1971 conference on interstellar molecules and origin of life
09 p1265 A72-22645

Mars biology likelihood from long winter model, suggesting north polar cap summer remnant vaporization as atmosphere, liquid water and greenhouse effect source
10 p1424 A72-23717

Biological experiments of Viking Mars lander 1975 mission regarding Oparin-Haldane evolution hypothesis
10 p1430 A72-24384

Biological experiments on plants, animals and bacteria aboard Zond 5, 6 and 7 space probes, noting flight conditions effect on physiological functions and hereditary structures
11 p1579 A72-25941

Environmental chamber simulation to show terrestrial microorganisms survival under Jovian atmospheric conditions
15 p2183 A72-31293

Spacecraft bacteria population resistance to simulated Jovian trapped radiation belt electrons and solar wind protons, noting dependence on isolate, dose and electron energy
15 p2186 A72-31993

Report to COSPAR on French space program covering ionospheric and magnetospheric physics, meteorology, earth resources and exobiology
15 p2337 A72-32003

Complex organic molecules in interstellar space, discussing molecular identification reliability, prebiological organic synthesis, interstellar and planetary biology and UV natural selection
18 p2657 A72-36620

Survival of common terrestrial microorganisms under simulated Jovian conditions.
19 p2755 A72-37721

Scientific problem resolution during Jupiter missions, discussing Pioneer probes, trapped particle belts, Red Spot, atmosphere, biological activity, internal heat sources and radio emission
19 p2864 A72-38381

Russian book - Problems of the stability of biological system.
20 p2891 A72-38957

Adaptability limits on protein-nuclein-water life under exobiological extremal conditions, considering macromolecules, extraterrestrial life search and origin
20 p2891 A72-38958

Thermodynamic properties and mathematical modeling of complex biological systems, considering energy and mass exchange in photosynthesizing organisms for exobiological life support
20 p2891 A72-38960

Life sciences and space research X; Proceedings of the Fourteenth Plenary Meeting, Seattle, Wash., June 21-July 2, 1971.
23 p3253 A72-43381

Development of planetary quarantine in the United States.
23 p3259 A72-43382

Biological instrumentation for the Viking 1975 mission to Mars.
23 p3259 A72-43396

An integrated multi-purpose biology instrument utilizing a single detector, the mass spectrometer.
23 p3287 A72-43397

Viking Mars exploration project, discussing orbiter and lander design and operational features and scientific experiments relevant to existence of life
24 p3440 A72-45123

Biological aspects of communications with extraterrestrial intelligence, discussing life existence possibility on wandering planets
24 p3372 A72-45127

EXOSPHERE

Positive H, HE and O ions in exosphere from mass spectrometers mounted on Elektron 4 satellite
01 p0053 A72-10368

Rotating and nonuniform planetary exosphere model, examining density profiles
04 p0579 A72-15333

Diffusion model applicability to lateral transport in terrestrial and lunar exospheres, using kinetic theory
07 p1056 A72-18902

Exosphere geocoronal hydrogen density, vertical structure and diurnal variability from Lyman spectra observational data, discussing polar wind origins
07 p0978 A72-20041

High energy charged particles angular distribution measurements in equatorial region cosmic radiation above atmosphere by Proton 2 satellite
08 p1226 A72-20799

Exospheric temperatures in hydrogen dominated planetary atmospheres for evaporative loss rates esti-

mation, noting two component diffusive equilibrium model

09 p1393 A72-23661

Thermosphere and lower exosphere density and temperature variations from satellite decay

11 p1621 A72-25843

Non-Maxwellian collisionless transport properties of neutral gas constituents in planetary exospheres, discussing ballistic particle and heat transport and escape fluxes

11 p1716 A72-25846

Semiannual exospheric temperature and density variations from satellite observation and ionosonde measurements

11 p1626 A72-26420

ATS F/G radio beacon experiments for study of exosphere and ionosphere integrated electron content, spatial structure and time dependent behavior

12 p1782 A72-27526

Number density, particle, momentum and energy fluxes in model ion-exosphere with open magnetic field and asymmetric Maxwellian velocity distribution

13 p1948 A72-29115

Satellite measurements of exospheric density variations during June 1968-December 1970 at 1070 and 900 km, discussing solar activity effect

13 p1952 A72-29803

Explorer 19 satellite drag evidence for neutral exosphere He concentration asymmetry between Northern and Southern Hemispheres over entire solar activity cycle

15 p2228 A72-31977

Exobase atomic hydrogen densities for zero ballistic net flux as function of temperature distribution, noting support of McAfee hypothesis by OGO-4 polar UV observations

16 p2384 A72-32979

A calculated hydrogen distribution in the exosphere.

22 p3168 A72-42004

EXOTHERMIC REACTIONS

Blast wave techniques for exothermic processes in relation to propulsion systems, using shock or detonation tubes, point explosions, reflected shocks and implosion vessels

[AD-737415] 01 p0117 A72-10939

Supersonic oxygen molecules nozzle beam reactive scattering on barium atoms, detailing exothermic reaction energy in barium oxide formation

02 p0170 A72-11912

Thermal theory of criticality for spontaneous explosion of exothermic reactant mass in bodies of arbitrary shape

03 p0457 A72-13972

Heat transfer from burning gas mixture flow to receiver wall, taking into account exothermal reactions due to catalytic effects

03 p0458 A72-14166

Plane symmetrical exothermic reaction center dynamic behavior, deriving system nonlinear transfer function-pressure pulse and unit mass heat release relationships

[AIAA PAPER 72-67] 05 p0750 A72-16934

Differential equations describing dynamic behavior of unsteady plane exothermic reaction front in gasless system

06 p0903 A72-18204

Bounds estimation for thermal explosion critical parameters for exothermic reaction, using geometric transformation

07 p1098 A72-19364

Exothermic capture processes with ionization during nonelastic ion atom collisions, discussing cross sections of He ion collisions with Ar, Kr and Xe atoms

08 p1210 A72-20837

Population inversion in exothermal decomposition reactions of multiatomic molecules for chemical and collision laser systems

13 p1912 A72-28778

Potential energy curves for exothermic reaction between oxygen cations and nitrogen molecules to form nitric oxide and atomic nitrogen

16 p2360 A72-32921

Intense emission from high pressure pulsed carbon dioxide chemical transfer laser by flash photolysis initiated deuterium-fluorine exothermic chain reactions

16 p2401 A72-33392

Energy distribution among reaction products. VI - F + H₂, D₂.

19 p2763 A72-38804

Induction period, particle size distribution and medium temperature effects on thermal ignition of metal particles under exothermal oxidation reaction on surface

20 p2987 A72-40040

Propagation of the front of an exothermic reaction in condensed mixtures whose components interact through a high-melting layer

22 p3245 A72-43177

A kinetic-theory description of a chemically reacting gas.

23 p3357 A72-44272

Propagation of blast waves in a combustible gas.

24 p3462 A72-45034

Periodicity in exothermic hypersonic flows about blunt projectiles.

24 p3463 A72-45035

EXPANDABLE STRUCTURES

NT BALLOONS

NT BEACON SATELLITES

NT BELLOWS

NT GAS BAGS

NT HIGH ALTITUDE BALLOONS

NT INFLATABLE STRUCTURES

NT METEOROLOGICAL BALLOONS

NT TETHERED BALLOONS

EXPANSION

NT GAS EXPANSION

NT KARHUNEN-LOEVE EXPANSION

NT PRANDTL-MEYER EXPANSION

NT THERMAL EXPANSION

Expansion formulas for Kampe de Fariet and radial wave functions application to heat conduction and quantum mechanics problems

15 p2336 A72-32398

Shear-layer flow regimes and wave instabilities and reattachment lengths downstream of an abrupt circular channel expansion.

[ASME PAPER 72-APM-2] 17 p2538 A72-34811

Simple analyses for the non-symmetric dynamic expansion of cylindrical cavities.

22 p3240 A72-42893

EXPANSION WAVES

U ELASTIC WAVES

EXPECTANCY HYPOTHESIS

Analog and digital computers for automatic statistical analysis of unsteady random process recorded data, calculating correlation functions and expectancy

13 p1925 A72-29165

Mathematical models for passenger aircraft market forecast, discussing stock measurement and life expectancies

13 p2067 A72-30125

Allowance for correlation in the prediction of reliability parameters for radio equipment

23 p3270 A72-43767

EXPECTATION

Cyclic phenomena periodicity by expected mean square deviation statistical analysis of observational data samples, using null hypothesis and unequally spaced sample intervals

04 p0574 A72-14908

Upper and lower bounds for expected value and variance of minimum material weight necessary for random resistance structure able to support assigned loads

04 p0593 A72-15648

Conditional expectation and integral of random closed convexity in probability space

06 p0839 A72-17555

Safety factor distribution function for plastic collapse of structure with random resistance members, discussing variance-expected value ratio

09 p1406 A72-23075

Expected value of two dimensional Gaussian random array gain, assuming two dimensional isotropic noise field of single frequency

11 p1604 A72-26040

Analysis of discrete automatic control systems with variable parameters by the method of orthogonal expansions. I, II

19 p2778 A72-37438

EXPERIMENTAL DESIGN

NT FACTORIAL DESIGN

High speed tensile impact test for polymers at large loading rate, describing equipment design and test technique

01 p0048 A72-10782

Laser satellite range measurement at Ondrejov astronomical observatory, describing radar system and experiment design

03 p0326 A72-14332

ALSEP passive seismic experiment design, discussing instrument operation and performance parameters

04 p0508 A72-15095

ALSEP active seismic experiment design, investigating lunar subsurface geologic structure

04 p0508 A72-15096

Submodel similarity relations in single indirect experiment design

08 p1257 A72-22176

ALSEP heat flow experiment design and calibration, presenting independent vertical temperature gradient and thermal conductivity measurements in regolith

12 p1869 A72-27331

Viking mission gas exchange experiment for life detection in Martian soil, covering design of experiment

14 p2084 A72-30876

Notch toughness criteria of metals with S shape transition temperature curve, considering experimental design and impact test model

16 p2406 A72-33322

Acoustic emission experiments design based on piezoelectric transducer, discussing signal detection and data acquisition methods

20 p2924 A72-39278

Optimal planning of an experiment in a study of the properties of Ti-V-Al alloys

20 p2942 A72-39825

Variation analysis and design of experiments as an aid to design quality assurance.

20 p2930 A72-39856

Kullback-Leibler information function and the sequential selection of experiments to discriminate among several linear models.

21 p3075 A72-41187

Experiment design - An organized approach to data collection.

22 p3245 A72-41935

Experimental design algorithm based on information quantity optimization, noting measuring instrumentation synthesis adaptable to operational conditions

23 p3292 A72-44463

Lifetime estimation, optimal experimental design and stress level severity prediction in parametric and nonparametric accelerated life tests

24 p3406 A72-44671

New space processing experiments for the Skylab missions.

24 p3407 A72-45125

Skylab project participation by students to stimulate interest in science and technology, giving winning experiment proposals

24 p3467 A72-45158

Mariner Mars 1971 adaptive mission planning for scientific objectives flexibility based on planetary features observed, discussing plan change implementation

24 p3444 A72-45439

Unmanned OAO spacecraft series and experiment packages, discussing space astronomy scientific achievements, mission plans and space shuttle role

24 p3453 A72-45535

HEAO satellite to carry instruments required in high energy astrophysics missions, discussing observational objectives, configuration and experiments

24 p3453 A72-45538

EXPIRATION

Plethysmographic and laryngoscopic investigation of glottis opening and airway resistance relation to lung volume during panting and continuous slow expiration

11 p1586 A72-26611

Inspiration, expiration and hand muscle control comparison in psychophysical category production method for human voluntary breathing regulation investigation

12 p1763 A72-27843

EXPIRED AIR

Gaseous nitrogen production in humans under steady-state conditions, relating expired nitrogen minute volume increase after protein consumption to possible gastrointestinal and metabolic effects

08 p1122 A72-20882

Four-parallel-compartment lung model for emptying pattern study, using expired nitrogen concentration data to calculate alveolar dilution ratio and emptying rate

14 p2079 A72-37003

Myth of nitrogen equality in respiration - Its history and implications.

19 p2758 A72-38708

Expired air as a source of spacecraft environment carbon monoxide contamination

24 p3375 A72-45120

EXPLODING CONDUCTOR CIRCUITS

U CIRCUITS

U EXPLODING WIRES

EXPLODING CONDUCTORS

U EXPLODING WIRES

EXPLODING WIRES

Exploding wire restriking mechanisms, discussing shock generation for arc channels

02 p0260 A72-12362

Emission spectra of exploding copper wires in air and vacuum in IR, UV, visible and vacuum UV regions

05 p0691 A72-16991

Hot wire ignitor modeling including measured H value and heat generation by explosive chemical reaction

08 p1219 A72-20754

Emergency escape from high performance military aircraft in flight and on ground, using explosive cord for transparent canopy material breakup

12 p1753 A72-27017

Emission spectra of exploding copper wires in air and vacuum in IR, UV, visible and vacuum UV regions

12 p1843 A72-27134

Supersonic dense low temperature plasma jet generation by pulse mode accelerator based on dielectric erosion and electrically exploded conductor

13 p2011 A72-29007

Helium use to minimize deflection of modulated laser beam in measurement of free surface motion of expanding annular cylinder loaded by exploding wire

13 p1960 A72-29765

- Hot wire and exploding bridgewire detonators, design characteristics, handling safety and hazard situations 16 p2442 A72-33358
- German monograph - Behavior of an electric arc produced by an exploding wire in a granular medium 19 p2834 A72-37483
- Neutron production in exploding-wire discharges. 21 p3089 A72-40338
- An arrangement for the holographic study of electrical explosions of wires 21 p3058 A72-41742

EXPLORATION

- NT LUNAR EXPLORATION
- NT OIL EXPLORATION
- NT SPACE EXPLORATION
- Type of equations for the solution of some gravitational prospecting problems from the anomalies on a complex relief, using a correlation model 23 p3285 A72-43847

EXPLORER SATELLITES

- NT RADIO ASTRONOMY EXPLORER SATELLITE

Earth bow shock nonuniform structure observation correlation with interplanetary field orientation, using Explorer 33 and 35 data 11 p1722 A72-26395

Explorer satellites and Pioneer space probes development program, discussing launching rockets, reentry tests, payloads, radio communication, Van Allen belts discovery, etc 23 p3358 A72-44353

Analysis of the Radio Astronomy Explorer lunar orbit mission. [AIAA PAPER 72-940] 24 p3444 A72-45437

EXPLORER 28 SATELLITE

Ephemeris of a highly eccentric orbit - Explorer 28. 20 p2968 A72-39194

EXPLORER 34 SATELLITE

Internal neutral sheet in geomagnetic tail from Explorer 34 magnetic field experiment, noting quasi-periodic structure and magnetic loop formation 06 p0803 A72-17450

Explorer 34 satellite orbit perturbation, noting earth gravitational tesseral harmonic effect on perigee passage time 24 p3399 A72-45557

EXPLORER 35 SATELLITE

Explorer 35 observations of solar wind electron density and temperature, noting anisotropy direction correlation with magnetic field vector alignment 11 p1713 A72-26392

EXPLORER 38 SATELLITE

RAE-1 measurements of lf radio phenomena in magnetosphere, solar corona and Galaxy, discussing design, calibration and performance 08 p1137 A72-21984

EXPLOSIONS

- NT AERIAL EXPLOSIONS
- NT CHEMICAL EXPLOSIONS
- NT GAS EXPLOSIONS
- NT NUCLEAR EXPLOSIONS
- NT THERMONUCLEAR EXPLOSIONS
- NT UNDERGROUND EXPLOSIONS

Explosion induced plane shock wave propagation in gas medium with exponential density distribution, determining gas flow behavior by difference approximation method 02 p0201 A72-11578

Thermal theory of criticality for spontaneous explosion of exothermic reactant mass in bodies of arbitrary shape 03 p0457 A72-13972

Repeated explosions mechanism in nuclei of galaxies and quasars due to instability in twisted magnetic fields, noting clouds and relativistic plasma ejection 05 p0717 A72-16379

High speed photography and radiography applications to high explosives research, discussing shock wave visualization, illumination techniques for rapid processes time resolution, etc 06 p0813 A72-17436

High intensity laser beams for solid surface material removal by vaporization and explosion, noting surface and subsurface temperature relations 07 p1002 A72-19210

Bounds estimation for thermal explosion critical parameters for exothermic reaction, using geometric transformation 07 p1098 A72-19364

Aerodynamic characteristics of hypersonic velocity meteor traveling in earth atmosphere and shock wave propagation generated by explosion in air and on ground 07 p1081 A72-20094

Pyrotechnic hazard classification for property and personnel protection in event of accidental explosion 08 p1220 A72-20768

Developing cumulus clouds annihilation, considering ascending and descending spontaneous convective streams initiated by explosions 12 p1841 A72-27989

Siberian Popigay river basin hollow as meteoritic explosion crater, discussing pseudovolcanic properties 13 p1947 A72-28754

Shock wave propagation produced by explosive detonation in contact with inert solid, considering spallation occurrence and prevention 16 p2469 A72-33356

Instrumentation for space-time correlated measurement of explosion induced dynamic effects, discussing framing cameras, flash X-ray systems, pin switches and piezoresistive gages 16 p2392 A72-33360

Critical conditions of thermal explosion in the presence of chemical and mechanical heat sources 19 p2879 A72-37357

Determination of the parameters of a fluid in the neighborhood of the junction of wavefronts by the Legras method 22 p3165 A72-41927

Simple analyses for the non-symmetric dynamic expansion of cylindrical cavities. 22 p3240 A72-42893

Developing cumulus clouds annihilation, considering ascending and descending spontaneous convective streams initiated by explosions 22 p3202 A72-43003

Small disturbances propagation effect on self similar flow due to point explosion in medium with density varying according to distance from center 24 p3390 A72-44786

Electrical discharge-produced explosions aboard supertankers during cleaning operation and electrostatic charging of supersonic aircraft during passage through heavy rain, noting water drop disintegration 24 p3368 A72-44979

International Colloquium on Gasdynamics of Explosions and Reactive Systems, 3rd, Marseille, France, September 12-17, 1971, Proceedings. 24 p3461 A72-45016

Gas dynamics of the flight and explosion of meteorites. 24 p3439 A72-45020

EXPLOSIVE DECOMPRESSION

Medical and physiological hazards for SST passengers and crews, discussing cumulative cosmic radiation and high altitude decompression risks 11 p1583 A72-25816

Case report of rapid decompression in supersonic trainer aircraft pressurized cabin, discussing physical and blast effects, pressurization safety, decompression sickness and hypoxia 11 p1584 A72-26020

Influence of prolonged starvation on the frequency of occurrence of decompression-induced pulmonary hemorrhage. 17 p2508 A72-34545

Explosive instability temporal development, noting linear damping role in nonlinear wave interaction under conservation laws of energy and momentum 23 p3282 A72-44318

EXPLOSIVE DEVICES

- NT BOOSTERS [EXPLOSIVES]
- NT DETONATORS
- NT INITIATORS [EXPLOSIVES]
- NT PRIMERS [EXPLOSIVES]
- NT SHAPED CHARGES
- Lunar seismic profiling experiment, describing explosives package, electronics and SAFE/ARM assembly 04 p0509 A72-15104

Computerized numerical nodal analysis of heat transfer away from bridgewire of electroexplosive device to meet all- and no-fire requirements 08 p1219 A72-20761

Long life aerospace explosive components, examining material degradation mechanisms and effects of pressure, temperature, moisture, chemical reactions and impurities 08 p1219 A72-20761

Fast rise high current constant trigger circuit for electroexplosive devices, using flat two-conductor transmission line to minimize inherent inductance 08 p1219 A72-20761

Aerospace type electroexplosive devices gross sensitivity to short damped rf energy burst 08 p1220 A72-20765

Missile destruct systems explosive transmission line manifolds, discussing designs for high reliability under severe environmental conditions 08 p1221 A72-20782

Blast and detonation wave phenomena applications in war and peace, discussing hypervelocity launchers, shock tubes and explosive weapons 08 p1146 A72-21014

Electroexplosive devices firing energy parameters determination by capacitor discharge system providing exponential pulses terminated at adjustable width 14 p2143 A72-30200

Low-explosive actuated mechanical devices to actuate switches and valves, sever cables or bolts, dispensing fluids, inflating bags or starting engines 16 p2442 A72-33359

Aerospace vehicle explosive components initiation, separation and destruct systems 16 p2443 A72-33361

EXPLOSIVE FORMING

High energy rate compacting methods in powder metallurgy, considering use of high explosives in water or air and impulse pressing of metal powders 02 p0233 A72-11438

Explosive loading effect on Cr-Ni stainless steel structure with electron microscope study of gamma, alpha and epsilon phases 08 p1187 A72-21780

Explosive compaction of metal powders by direct method with emphasis on W 11 p1643 A72-26833

Testing method for materials exposed to explosive forming, noting applications in study of formability, heat treatment effects and crack initiation 16 p2391 A72-33235

Liquid and solid explosives detonation, initiation and shock interaction with inert materials for precision work 16 p2476 A72-33352

Technical and economic aspects of explosive metal fabrication, considering requirements for close tolerances, nonsymmetrical shapes, large size workpieces and unusual material properties 16 p2398 A72-33354

Explosive charge design to drive metal by detonation in terms of impulse, acceleration and final velocity, using Gurney model 16 p2398 A72-33355

Material thinout in deformed metal sheet specimens under explosive forming, using air cell effect 16 p2399 A72-33775

Al powder bonding during compaction by explosively driven plates, measuring shock wave amplitudes, pressure drop, layer separation and critical pressures in spall plane 22 p3184 A72-43183

Electron diffusion across a shock wavefront in metals 22 p3208 A72-43184

Non-steady shock waves in metals with phase transitions and hardening by explosion. 24 p3414 A72-45025

EXPLOSIVE WELDING

Bond zone wave formation in explosion cladding, predicting critical collision velocity and angle with fluid flow model 01 p0077 A72-11031

Electrical resistance and thermal joint conductance measurements at perfect contact interfaces from electroplating, soldering and explosive bonding [AIAA PAPER 72-19] 05 p0666 A72-16859

Bond zones morphology and composition in Invar-based explosive welds, using metallographic and electron microprobe techniques 06 p0820 A72-17707

Metals toughness under impact loading from explosive welding process, using optical metallographic techniques 06 p0822 A72-18214

Explosive welding of heat exchanger tubes and detonation produced compressive joining of cables as applications of explosive metalworking procedures 07 p0994 A72-18931

Al alloys welding with Pb sheathed linear ribbon RDX explosives by parallel plate process, achieving high weld strength 08 p1173 A72-20779

Thermal behavior of explosively welded metals, describing test facility for temperature measurements of joints 09 p1319 A72-22891

Magnetic-explosive welding /magneweld/ process using capacitor discharge through wire coil, noting sintered Al powder and Zircaloy 2 applications 09 p1321 A72-23638

Bonding conditions effects on wave mode formed at explosive bonded interfaces from experiments with bullets fired at thin metal targets 09 p1321 A72-23642

Mechanical properties and residual stresses in and adjacent to interface of explosively welded Al-Zn-Mg alloy with steel, noting microcracks effect on weld strength 15 p2257 A72-32111

Slurry explosives for metal cladding, discussing applications to pipe joints, bearing sleeves, recoil rods, gun barrels and cylinder liners 16 p2398 A72-33357

Thermal effects in the seam area during impact welding 19 p2809 A72-38461

Fabricating aluminum matrix composites. I - A survey of aluminum matrix composites. 22 p3182 A72-41996

EXPLOSIVES

- NT CELLULOSE NITRATE
- NT RDX
- NT TETRYL
- NT TRINITROTOLUENE

- Active ingredient oxidizing potential and pressure effects on burning rate of explosive substances
02 p0302 A72-12292
- Confined small diameter PETN, RDX and tetryl columns longitudinal detonations, using focused Q switched ruby laser
03 p0367 A72-13604
- Cumulative jet formation in elliptical cavity, investigating effect on liquid explosives ignition
06 p0799 A72-17909
- Explosives and pyrotechnics - Conference, Philadelphia, September 1971
08 p1218 A72-20751
- Loading current density effect on normal lead stypnate ignition in primary explosive hot wire initiation, using capacitor discharge and constant current activation signals
08 p1218 A72-20752
- Hot wire ignitor modeling including measured H value and heat generation by explosive chemical reaction
08 p1219 A72-20754
- Explosive/pyrotechnics performance monitoring for acceptance, lot qualification, comparison testing and system design guidelines
08 p1219 A72-20760
- Aerospace explosive components accelerated storage life and stability tests, basing method on Arrhenius reaction rate equation modification
08 p1220 A72-20762
- High neutron absorption doping material selection for enhancing explosive mixtures neutron radiographic image without interference with chemical reaction
08 p1220 A72-20769
- Direct detonation of insensitive PETN, RDX and tetryl explosives with Q switched ruby laser radiation
08 p1220 A72-20771
- Explosives injection molding into stainless steel, aluminum, plastic and rubber tubes, considering applications to fuse and detonation transfer trains and small warheads
08 p1221 A72-20781
- Simple composite propellant modelled by ammonium perchlorate-wax mixtures, noting stoichiometric composition effects on explosive properties
09 p1373 A72-23142
- Active ingredient oxidizing potential and pressure effects on burning rate of explosive substances
10 p1561 A72-23767
- One dimensional blast wave theory for trajectory analysis of shocks driven by solid explosives in linear shock tubes
14 p2093 A72-30179
- Rocket propellants, propulsive charges and explosives lifetime - Conference, Karlsruhe, Germany, September-October 1971
14 p2143 A72-30751
- Explosives life limitation due to aging phenomena, discussing chemical and physical processes and environmental effects
14 p2143 A72-30752
- Polyester bonded explosives mechanical and thermal properties, noting need for desensitizing against shock and friction effects
14 p2145 A72-30768
- Explosives in engineering design - Conference, University of New Mexico, Albuquerque, March 1972
16 p2398 A72-33351
- Liquid and solid explosives detonation, initiation and shock interaction with inert materials for precision work
16 p2476 A72-33352
- Initiation mechanisms for explosive materials and experiments for hazard evaluation, discussing subdetonation reactions and mathematical models of explosive processes
16 p2442 A72-33353
- A computation method for the determination of thermodynamic values and performance data of rocket propellants, propellant charges for cannons, and ignition mixtures
17 p2596 A72-35418
- Ignition, unsteady burning and flame collapse of a unitary fuel particle
19 p2882 A72-38453
- Burning rates of organic perchlorates of aliphatic, aromatic and heterocyclic amines and amidines with explosive compounds containing nitrogen dioxide group as oxidizer
22 p3153 A72-43181
- Condensed liquid explosive detonation pressure from free surface velocity measurement, noting pressure curve dependence on charge diameter and wall thickness
24 p3463 A72-45036
- Crack growth dependence on applied high stress level cycle number, showing fatigue life inversely proportional to stress exponential function
05 p0673 A72-16304
- Exponential conduction increase of semiconductors in strong magnetic fields, determining three dimensional random network resistance with percolation theory
07 p1047 A72-18918
- Integrodifferential equation exponential solutions for body motion about fixed point
08 p1208 A72-21353
- Orthonormalized exponential functions use in hydrometeorology
08 p1202 A72-22119
- Exponential signal reconstruction sampling rate restriction derivation based on pole-zero cancellations in Z transform
16 p2365 A72-33756
- Automatic computation of exponentials, logarithms, ratios and square roots.
18 p2705 A72-37021
- Exponential conduction increase of semiconductors in strong magnetic fields, determining three dimensional random network resistance with percolation theory
20 p2960 A72-39384
- Existence and uniqueness theorems of elliptic equations with eigenfunction exponential decrease at infinity and 2m order self adjoint differential operator in n-dimensional Euclidean space
23 p3307 A72-43223
- Exponential type equation for carbon steel stretched sample necking profile curve
23 p3348 A72-43753
- Regulator vector selection algorithm for largest estimate of exponential absolute control stability region based on Popov frequency condition reformulation
23 p3276 A72-43853
- Sufficient condition formulation for Lure type non-linear continuous control system exponential absolute stability
23 p3309 A72-43854
- The automatic computation of exponentials, logarithms, ratios, and square roots.
24 p3383 A72-45668
- EXPORTS**
U INTERNATIONAL TRADE
- EXPLOSURE**
Aircrews tolerance to cold water and life raft exposure, discussing prediction model based on thermal insulation effectiveness, assumed metabolism and body surface area and mass
10 p1428 A72-23734
- Exposure conditions and film processing parameters effects on sensitivity, diffraction efficiency and SNR of holograms recorded with continuous and pulsed radiation sources
11 p1637 A72-26796
- Holographic recording systems stabilization with intermittent exposure control for interference patterns fidelity
12 p1806 A72-27263
- Optical feedback exposure control mechanism of high resolution CRT film recorder intended for tactical military usage
12 p1810 A72-27932
- Aerial survey camera with automatic exposure control, discussing film emulsions sensitivity characteristics, object light intensity range and measuring methods
14 p2105 A72-30839
- EXPRESSIONS [MATHEMATICS]**
U FORMULAS [MATHEMATICS]
- EXPULSION BLADDERS**
Life prediction of expulsion bladders through fatigue test and fold strain analysis.
24 p3455 A72-44672
- EXTARS**
X ray stars atmospheric ionization effects by vlf phase tracking relative to Omega navigation accuracy, diurnal shift variations and astrophysical data
04 p0486 A72-14877
- Cyg X-1 type X ray sources evolution, discussing white dwarf and supernovae stages, parent mass and angular momentum
04 p0568 A72-15508
- X ray pulsations mechanism in Cyg X-1 related to high magnetic fields produced by flare-like events
06 p0873 A72-17636
- X ray pulsar observed near Crab Nebula by balloon-borne telescope, discussing identification with NP 0527 or NP 0532
07 p1070 A72-19122
- GX3 plus 1 identification by sounding rocket during lunar occultations, discussing magnitude
07 p1070 A72-19123
- Cen X-3 model with X ray emission from atmosphere heated by shock waves generated by surface pulsations of white dwarf
10 p1544 A72-24668
- High density models for ambient gas of eta Carinae star from X ray observations
10 p1530 A72-24947
- Bright stars X Per and HD 77581 as candidates for X ray sources 2U 0352plus30 and 2U 0900minus40 respectively
13 p2041 A72-29413
- White dwarf background radiation and optical emission variations due to thermal bremsstrahlung from stellar coronae
14 p2147 A72-30554
- X ray emitting component Centaurus X-3 mass limit in close eclipsing binary system with regard to Roche lobe principle
14 p2156 A72-30569
- Low mass neutron star source of pulsed X radiation in binary Centaurus X-3 ejected during low energy supernova explosion
14 p2156 A72-30570
- Variable circular polarization of X ray star SCO X-1 optical radiation due to Thomson scattering in magnetoeactive plasma shell
15 p2304 A72-31328
- Emission line star WRA 795 as optical counterpart of Cen X-3 occulting binary system
16 p2456 A72-33474
- Uhuru satellite data on periodic pulsating X ray source in Hercules, interpreting intensity variations as occulting binary star system effect
16 p2446 A72-33475
- Stellar X ray emission flux calculation for UV Ceti flares, using similarities between solar and stellar flares
16 p2450 A72-34161
- X ray flux anomalous minima observations in Cen X-3 with rocket-borne argon-methane proportional counter
16 p2461 A72-34162
- Pulsating X ray sources with 1 sec periods as stars with central densities between neutron stars and white dwarfs
17 p2599 A72-35074
- Soft X-rays from Cygnus X-2 and from Cygnus X-1 /in eclipse/.
17 p2600 A72-35297
- Radio detection of Cygnus X-3.
17 p2612 A72-35366
- Radio observations of Cygnus X-3.
17 p2612 A72-35367
- X ray spectrum analysis of Sco X-1 type sources, showing plasma sheath with high electron temperature
17 p2617 A72-35727
- Observation of a hard X-ray flare in Cyg X-1.
18 p2721 A72-36649
- The primary spectrum of the eclipsing binary LR Centauri.
19 p2856 A72-37505
- On the optical search for Centaurus X-3.
19 p2856 A72-37506
- The association of X-ray sources with bright stars.
19 p2856 A72-37507
- Eclipsing and spectroscopic binary beta Persei radio star, suggesting X ray source nature
19 p2851 A72-37889
- Interferometer detection of radio sources near pulsating extar Hercules X-1 during low X ray luminosity period
20 p2963 A72-38918
- Search for high frequency optical variability in X-ray sources.
21 p3100 A72-40685
- Accretion disc models for compact X-ray sources.
24 p3435 A72-44828
- A further high-resolution search for Fe XXV line emission from Scorpius X-1.
24 p3438 A72-44838
- Transfer effects on X-ray lines in optically thick celestial sources.
24 p3435 A72-44843
- Centaurus X-3 - Possible reactivation of an old neutron star by mass exchange in a close binary.
24 p3439 A72-44976
- EXTENSOMETERS**
Eddy current extensometer for monitoring long term creep in diameter of pressurized tubular stainless steel specimens
11 p1613 A72-25821
- Continuous volume-temperature dilatometer measurement of small liquid samples in biological application
13 p1959 A72-29752
- A ten-inch extensometer measuring small low-frequency strains.
21 p3052 A72-40234
- EXTERNAL STORES**
Weapon firing and external store separation tests by flight test methods for determining safe weapon release envelope
06 p0759 A72-18499
- Simulator for physical forces experienced by carrier aircraft during catapult launches and arrested landings, considering external stores safe suspension
15 p2215 A72-32620
- Aerodynamic interference between aircraft components - Illustration of the possibility for prediction. [ICAS PAPER 72-49]
21 p2992 A72-41174

The application of non-planar lifting surface theory to the calculation of external-store loads. [AIAA PAPER 72-971] 22 p3135 A72-42340

EXTINCTION

NT INTERSTELLAR EXTINCTION

Double 45 degree z cut KD P electro-optic Q switch simulation with programmable desk top computer, deriving extinction ratio dependence plot graphs 02 p0224 A72-11746

Spherical scatterers extinction efficiency effect on photometer optical systems transmittances, using Mie equation and numerical methods 07 p0987 A72-19831

EXTINGUISHERS

U FIRE EXTINGUISHERS

EXTINGUISHING

Flame quenching limits in narrow channels, considering effect of gas expansion during combustion on flame arresters use possibility 07 p1099 A72-19369

EXTRACTION

NT ION EXTRACTION

NT SOLVENT EXTRACTION

Slag powdery material moisture content determination by absolute pyridine adsorption method of moisture extraction 12 p1813 A72-27450

Heat resistant alloys conjugate phases extraction, separation and chemical analysis, discussing control of minor phases as precipitation products 13 p1978 A72-29443

EXTRAGALACTIC LIGHT

U EXTRATERRESTRIAL RADIATION

U LIGHT [VISIBLE RADIATION]

EXTRAGALACTIC MEDIA

U INTERGALACTIC MEDIA

EXTRAGALACTIC RADIO SOURCES

NT RADIO GALAXIES

Flux density variations incidence among extragalactic sources found by 3.8 cm sky survey 13 p2048 A72-29830

Electromagnetic emission in universe, discussing background radiation spectrum, extragalactic source brightness, intergalactic gas and energy density 14 p2152 A72-30479

Radio maps of extragalactic sources at 2.7 and 5.0 GHz presented with physical data for various components 16 p2458 A72-33718

Compact extragalactic nonthermal sources. 17 p2604 A72-34519

Decametric radio identification of an extragalactic X-ray source. 17 p2604 A72-34520

Interpretation of rotation measures of radio sources. 17 p2606 A72-34573

Extragalactic radio source 3C 1202 microwave flux density variations suggesting superrelativistic expansion 17 p2611 A72-35295

Cosmological models interpretation of extragalactic radio source counts 17 p2612 A72-35350

Flux densities, positions, and structures for a complete sample of intense radio sources at 1400 MHz. 21 p3105 A72-40575

Statistical studies of the evolution of extra-galactic radio sources. I, II, & III. 21 p3105 A72-41026

Extragalactic object categorization according to IR luminosities, considering radiation mechanism models and IR spectra relation to radio spectrum 22 p3228 A72-42571

Interpretation of rotation measures of radio sources. II. 23 p3337 A72-43828

Energy sources for extragalactic explosive phenomena in galactic nuclei and quasars, considering gravitation and double radio sources 24 p3439 A72-45018

Observation of M 82 in the near infrared 24 p3446 A72-45487

EXTRAPOLATION

Larson-Miller parameter application to N6 base alloys creep rupture data, discussing extrapolation method limitations 01 p0084 A72-10748

Survey and bibliography of extrapolation processes in numerical analysis based on polynomial or rational functions 02 p0252 A72-11546

Geomagnetic field extrapolated spherical data for years 1600 to 1800 from declination and inclination analysis, giving Gaussian coefficients and errors 02 p0218 A72-11953

Creep rupture test program for Al alloys, circumventing parametric methods limitations by extrapolation procedure with graphical extension of isostress curves 03 p0378 A72-14174

Ni alloy stress rupture data correlation and extrapolation from computerized evaluations of time-temperature parameters relative abilities [ASME PAPER 71-WA/MET-4] 05 p0670 A72-15905

Error covariance matrix evaluation at end of orbit extrapolation in terms of state vectors at measurement, discussing computation and interpretation 05 p0720 A72-16753

Wide angle lenses off-axis modulation transfer function measurement, explaining extrapolation method with MTF and conversion diagrams 06 p0813 A72-17439

Optimal control of lumped and distributed parameter systems with time lag, considering approach with extrapolator insertion and suboptimal solution based on system dynamic equation 07 p0962 A72-19718

Filtration and extrapolation of multivariable random processes described by linear differential equations system, examining adaptive filter synthesis 09 p1283 A72-23436

Individual melts stress rupture strength extrapolation based on limited number of tests, comparing results with parametric method 12 p1831 A72-28231

Geomagnetic field extrapolated spherical data for years 1600 to 1800 from declination and inclination analysis, giving Gaussian coefficients and errors 13 p1949 A72-29265

Filtration and extrapolation of multidimensional random processes described by linear differential equations system, examining adaptive filter synthesis 19 p2770 A72-38519

Prediction displays based on the extrapolation method. 21 p3010 A72-41409

Heat resistant steels long time strength determination by graph-analytical time-temperature extrapolation 23 p3301 A72-43739

EXTRASENSORY PERCEPTION

Exploratory test of extrasensory perception to identify random order of symbols in space during Apollo 14 flight with four subjects on earth 04 p0565 A72-14888

EXTRASOLAR PLANETS

Extraterrestrial life and civilization possibility in other planetary systems in universe, suggesting communication by hydrogen line frequency low harmonics 02 p0276 A72-11642

Extrasolar planets UVB color indices calculation, noting relative reflectivity and primary star color 04 p0570 A72-14507

Pulsar planetary systems observation from perturbation of pulse arrival time 05 p0712 A72-15771

Distant stellar satellites existence possibility based on maximum distance estimation for material particle motion stability with respect to sun or another star 08 p1231 A72-21133

EXTRATERRESTRIAL ENVIRONMENTS

NT CHROMOSPHERE

NT CISLUNAR SPACE

NT DEEP SPACE

NT INTERPLANETARY SPACE

NT INTERSTELLAR SPACE

NT JUPITER ATMOSPHERE

NT LUNAR ATMOSPHERES

NT LUNAR ENVIRONMENT

NT MARS ATMOSPHERE

NT MARS ENVIRONMENT

NT PLANETARY ATMOSPHERES

NT PLANETARY ENVIRONMENTS

NT SOLAR ATMOSPHERE

NT STELLAR ATMOSPHERES

Porphyin exobiology, discussing organic and random biosynthesis and extraterrestrial existence based on interstellar spectral evidence 05 p0617 A72-16130

Extraterrestrial environment utilization, describing space power plants, manufacturing operations in earth orbit and planetary mineral resources 12 p1871 A72-27625

Space technological advance effects on human extraterrestrial, scientific, economic and sociological progresses 19 p2867 A72-38545

EXTRATERRESTRIAL LIFE

Molecular processes in interstellar space and life origin, discussing radio astronomy observations, catalytic action and hydroxyl radicals in galaxies 01 p0128 A72-10398

Terrestrial biosphere back contamination from outer space organisms, discussing microbiologic control and prevention requirements 01 p0020 A72-10825

Mariner 1969 Mars mission, emphasizing planetary encounter, surface and atmospheric data and search for extraterrestrial life 01 p0130 A72-10930

Extraterrestrial life and civilization possibility in other planetary systems in universe, suggesting communication by hydrogen line frequency low harmonics 02 p0276 A72-11642

Extraterrestrial life on Mars and Venus and Jupiter atmospheres, discussing abiogenesis failures on life-supportable planets 04 p0471 A72-14805

Extraterrestrial life origin and evolution, estimating possibilities on Mars, Venus and Jupiter 04 p0471 A72-14806

Astrogenic and planetogenic environments characteristics examination for stellar spectral classes effect on intelligent life evolutionary pace and existence probability 04 p0573 A72-14887

Ti leaching from granitic rocks by Penicillium, simplicissimum, discussing extraterrestrial life detection 05 p0616 A72-15809

Papers on exobiology theory and experiments, considering extraterrestrial organic compound detection, Jupiter atmosphere, porphyrins, radiation production of life molecules, etc 05 p0617 A72-16126

Papers on exobiology covering abiogenesis, extraterrestrial life, primordial organic chemistry, biochemical evolution electronic factors, membranes origin, molecular chirality, protein and cellular evolution, etc 08 p1119 A72-22001

Extraterrestrial life origin and development possibilities from earth chemical and biological evolution description, noting external conditions requirements 08 p1119 A72-22002

Terrestrial life origin understanding by investigating life possibilities in nonterrestrial environments 08 p1120 A72-22015

Life beyond solar system, discussing planetary formation and prebiological organic chemistry developments and interstellar communication 08 p1120 A72-22016

Extraterrestrial abiogenic organic hollow spheres of Orgueil meteorite evaluated according to intrinsic and extrinsic criteria 09 p1385 A72-22640

Book on astronomy and cosmology covering big bang, steady state and oscillating universe theories, radio sources, galaxies, interstellar meteor relativity and extraterrestrial life 09 p1389 A72-23248

Life detection on earth from satellite 100 meter resolution photographs, discussing potential false positives and implications for Mars probes 10 p1471 A72-23718

Viking Mars 1975 mission with spacecraft orbiters and landers, describing experiments with emphasis on life detection 10 p1539 A72-24376

Biological experiments of Viking Mars lander 1975 mission regarding Oparin-Haldane evolution hypothesis 10 p1430 A72-24384

Viking Lander carbon 14 assimilation experiment for life detection in Martian soils 10 p1540 A72-24385

Viking Lander detection of metabolically produced radioactive labeled gas in Mars surface samples 10 p1540 A72-24386

Viking Lander light scattering experiment to detect microbial growth from aqueous turbidity changes in contact with Martian soil 10 p1430 A72-24387

Antarctica dry valley microbiology investigation for Martian life model 12 p1802 A72-27258

Life on Mars, investigating ground based and probe observations of atmospheric composition and pressure, surface temperature and features and UV radiation 12 p1761 A72-27624

Mars 1975 Viking mission profile, describing soft landing/orbiter probes and life detection experiments 12 p1877 A72-27687

Viking orbiter/lander spacecraft instrumentation for Mars soil biological life experiments, discussing pyrolytic and labeled release, light scattering and gas exchange techniques 13 p1956 A72-29024

Extraterrestrial life search, noting radio contact with civilizations, bioastronautics, Martian conditions and physicochemical parameters 14 p2076 A72-30694

Viking mission gas exchange experiment for life detection in Martian soil, covering design of experiment 14 p2084 A72-30876

Extrasolar civilization search via possibly used electromagnetic signal types, discussing frequency and time domains 15 p2302 A72-31292

Environmental chamber simulation to show terrestrial microorganisms survival under Jovian atmospheric conditions 15 p2183 A72-31293

Book on stellar astronomy covering H-R diagram, solar system, nuclear energy sources, Milky Way Galaxy, quasars, cosmology, planetology, etc 16 p2453 A72-33275

Soviet book on extraterrestrial civilizations and problems of interstellar communication 19 p2868 A72-38674

- Adaptability limits on protein-nuclein-water life under exobiological extremal conditions, considering macromolecules, extraterrestrial life search and origin 20 p2891 A72-38958
- Thermodynamic properties and mathematical modeling of complex biological systems, considering energy and mass exchange in photosynthesizing organisms for exobiological life support 20 p2891 A72-38960
- An integrated multi-purpose biology instrument utilizing a single detector, the mass spectrometer. 23 p3287 A72-43397
- Biological aspects of communications with extraterrestrial intelligence, discussing life existence possibility on wandering planets 24 p3372 A72-45127
- State of the art in the detection of intelligent extraterrestrial signals. 24 p3441 A72-45190
- Linguistic message decoding algorithms for communication with extraterrestrial intelligences, considering unified procedure and key problems solutions 24 p3382 A72-45226
- EXTRATERRESTRIAL MATTER**
- NT COSMIC GASES
- NT COSMIC PLASMA
- NT INTERPLANETARY GAS
- NT INTERSTELLAR GAS
- Organic cosmochemistry evolution, discussing radio astronomical observations, lunar soil samples, meteorite analysis and interstellar gas cloud molecules 03 p3320 A72-13171
- Extraterrestrial magnetic spheroid concentrations observed in October 1967 and 1969 proposing relationship to rainfall frequency 08 p1226 A72-21109
- Daily mean amount of cosmic matter falling on earth 09 p1389 A72-23195
- Orgueil meteorite examination by mass spectroscopy and gas chromatography, identifying amino acids of extraterrestrial origin 09 p1393 A72-23549
- Mesospheric clouds composed of molecular complexes of extraterrestrial origin, considering chemical reactions, hydroxyl luminescence, thermospheric water vapor and auroras 09 p1347 A72-23590
- EXTRATERRESTRIAL RADIATION**
- NT EXTRATERRESTRIAL RADIO WAVES
- NT GALACTIC RADIATION
- NT GALACTIC RADIO WAVES
- NT GEGENSCHNEID
- NT INTERSTELLAR RADIATION
- NT LUNAR RADIATION
- NT PLANETARY RADIATION
- NT PRIMARY COSMIC RAYS
- NT RADIO BURSTS
- NT SOLAR CORPUSCULAR RADIATION
- NT SOLAR COSMIC RAYS
- NT SOLAR PROTONS
- NT SOLAR RADIATION
- NT SOLAR RADIO BURSTS
- NT SOLAR RADIO EMISSION
- NT SOLAR WIND
- NT SOLAR X-RAYS
- NT STELLAR RADIATION
- NT STELLAR WINDS
- NT SUNLIGHT
- NT ZODIACAL LIGHT
- Extraterrestrial gamma ray flux contribution to total 0.7-4.5 MeV radiation at various latitudes by balloon sounding 01 p0120 A72-11007
- Protection against accelerator and space radiation Conference, Geneva, April 1971, Volume 1, Health physics [CERN-71-16] 02 p0160 A72-12051
- Gamma ray astronomy, discussing energy spectrum, diffuse background flux, extragalactic origin and Crab Nebula emission 03 p0408 A72-13027
- Nuclear and space radiation effects - Conference, University of New Hampshire, Durham, July 1971 03 p0402 A72-14076
- French Lyman alpha photometer experiment on OGO 5 satellite, describing geocoronal observations, extraterrestrial emission and Bennett and Encke comets hydrogen envelopes 04 p0582 A72-15684
- Intergalactic matter and radiation relation to origin and evolution of universe 05 p0717 A72-16385
- Metagalactic gamma rays from relativistic electron bremsstrahlung interactions under assumption of single power law source 05 p0710 A72-16712
- High energy gamma rays from Cygnus region, using balloon flight measurements with spark chamber telescope 06 p0873 A72-17891
- Energetic gamma quantum flux recording from extragalactic source 3C 120 by Cosmos 251 and 264 satellites 07 p1076 A72-19803
- Extragalactic origin of diffuse low energy cosmic gamma rays, using balloon-borne detector system 07 p1063 A72-20392
- Intercosmos 3 satellite vlf radiation and natural signals recording with circular antenna, whistler recorders, sonograms and spectroanalyzers 08 p1157 A72-21146
- Spectrum studies of extragalactic diffuse background radiation fields consisting of X ray and thermal or microwave background 10 p1529 A72-23914
- Coincidence effects of subionspheric extraterrestrial radiation focusing on ionospheric changes and stratospheric warmings 12 p1804 A72-27804
- Relict radio fluctuation observations, investigating adiabatic density perturbations related to formation of galaxies and galactic clusters 14 p2159 A72-30788
- Extraterrestrial He I 584 A background radiation suggested from rocket and satellite observations, noting interstellar medium temperature determination from isophotes 15 p2309 A72-31945
- Interplanetary radiation types in terms of possible space flight hazards, discussing electromagnetic and corpuscular radiation, cosmic rays and radiation belts 16 p2446 A72-33553
- A new model for estimating space proton dose to body organs. 17 p2508 A72-35354
- Extragalactic origin of the transient X-ray sources. 19 p2856 A72-37502
- Intercosmos 3 satellite VLF radiation and natural signals recording with circular antenna, whistler recorders, sonograms and spectroanalyzers 20 p2903 A72-39251
- A balloon search for extraterrestrial high energy gamma-rays in the northern hemisphere. 20 p2965 A72-39876
- Gamma radiation of Magellanic Clouds and metagalactic origin of cosmic rays. 23 p3328 A72-43264
- Summary of latent effects in long term survivors of whole body irradiations in primates. 23 p3254 A72-43393
- Origin of 200-keV interplanetary electrons. 23 p3333 A72-44547
- Extraterrestrial electromagnetic radiation and particle flux characteristics of low and medium energy, considering onboard spacecraft measuring instruments and data processing systems 24 p3404 A72-45398
- EXTRATERRESTRIAL RADIO WAVES**
- NT GALACTIC RADIO WAVES
- NT RADIO BURSTS
- NT SOLAR RADIO BURSTS
- NT SOLAR RADIO EMISSION
- Solar wind electron density variations, discussing radio source interplanetary scintillation and angular distribution measurements at various distances from sun 02 p0277 A72-11902
- Extragalactic astronomy observational paradoxes, discussing quasar red shifts and clumpings in directions of bright galaxies 04 p0568 A72-14414
- Radio telescope for cosmic radio emission reception at 50-2 cm wavelengths, describing parabolic and auxiliary reflectors 07 p0965 A72-20299
- F 2 layer diffuse reflections and critical frequencies increase on ionogram recordings during Northern Hemisphere nighttime magnetic storm of 2 December 1967, noting cosmic radio emission decrease 08 p1154 A72-20738
- Plasma inhomogeneities effect on radio wave absorption in interstellar clouds of ionized hydrogen, analyzing cosmic radio emission spectrum 08 p1231 A72-21120
- Magnetic fluctuations in elf and vlf waves in space, discussing whistler phenomena and applications to magnetospheric probes 08 p1158 A72-21189
- Spectral indices of extragalactic radio sources at 1.4 GHz independent on flux density 10 p1545 A72-24807
- Optical and physical properties and energy content of extragalactic radio sources, discussing radio galaxies and quasars 10 p1547 A72-24941
- F 2 layer spread reflections and critical frequencies increase on ionogram recordings during Northern Hemisphere nighttime magnetic storm of 2 December 1967, noting cosmic radio emission decrease 19 p2791 A72-38366
- EXTRATERRESTRIAL RESOURCES**
- Lunar mineral resources from analyses of moon samples, discussing solar cell and vacuum process manufacturing 05 p0722 A72-17099
- United Nations proposals concerning legal principles for use of natural resources of celestial bodies and ocean floor 07 p1103 A72-19464
- Extraterrestrial environment utilization, describing space power plants, manufacturing operations in earth orbit and planetary mineral resources 12 p1871 A72-27625
- Implications of new transport vehicles and cost analysis of supplying and maintaining a manned lunar laboratory. 24 p3441 A72-45209
- EXTRATERRESTRIAL ROVING VEHICLES**
- U ROVING VEHICLES
- EXTRAVEHICULAR ACTIVITY**
- Apollo 15 mission report, discussing lunar module powered descent, surface exploration with LRV, scientific instrument module, extravehicular activity, etc 08 p1230 A72-21007
- Extravehicular life support systems for shuttle, space station, lunar base and Mars missions, considering thermal control, carbon dioxide control and oxygen supply subsystems 10 p1430 A72-24441
- [AIAA PAPER 72-231]
- Electrostatic adhesive devices for zero-g intra/extravehicular activities, noting applications to astronaut and cargo maneuvering, worksite restraint, tool and equipment tiedown, etc 10 p1431 A72-24650
- Calculation procedures for some parameters of space suit gas medium supply systems 21 p3006 A72-40449
- EXTREMA**
- U RANGE [EXTREMES]
- EXTREMELY HIGH FREQUENCIES**
- Phase stable locked local oscillators for K band radiometers for long baseline interferometric measurements, emphasizing construction technique 01 p0044 A72-11307
- Millimeter wave and laser space-to-space communication links comparison, considering ehf system based on size, weight, power consumption and communication parameters calculations 04 p0493 A72-15609
- K band Gunn oscillator with high frequency stability, discussing construction, performance, output power and frequency saturation effect 06 p0786 A72-18375
- GaAs IMPATT diodes technology and performance at C, X and K band frequencies 06 p0788 A72-18466
- K beta emission spectrum of metallic Cr, discussing structural X ray analysis revealed cubic structure 14 p2116 A72-30414
- Focusing properties and efficiency of EHF waveguide lens with Al honeycomb as guiding medium, noting design considerations and performance test results 17 p2525 A72-34368
- K-band high power single-tuned IMPATT oscillator stabilized by hybrid-coupled cavities. 19 p2771 A72-37263
- EXTREMELY LOW FREQUENCIES**
- Magnetic storm strength ELF electromagnetic field effects on rabbits, dogs and bacteria, discussing changes in EEG, ECG and blood characteristics 12 p1763 A72-28214
- ELF and VLF waves propagation, deriving ionospheric field stable solutions by modified matrix multiplication technique for vertical geomagnetic field and large local refractivity 13 p1921 A72-29337
- Characteristic features of ELF-noise spectra during the excitation of the earth-ionosphere resonator by cosmic sources 18 p2662 A72-36861
- EXTREMELY LOW RADIO FREQUENCIES**
- Sudden enhancement and decrease of elf atmospherics, investigating diurnal variations for frequencies 03 p0321 A72-13090
- Magnetic field effect on elf radio wave attenuation during propagation under six ionospheres, showing dependence of minimum on propagation path geomagnetic latitude 08 p1131 A72-21103
- OGO 4 satellite observed band limited ELF hiss characteristics explanation by model based on generation at large wave normal angle in equatorial region 09 p1279 A72-23008
- Laboratory simulation of VLF/ELF radio waves transpolar ionospheric propagation, taking into account polar cap absorption 09 p1279 A72-23016
- ELF wideband noise receiver for atmospherics waveshape magnetic tape recording, computer processing and system simulation 12 p1791 A72-27637
- ELF wave propagation velocities in earth-ionosphere waveguide, studying fast and slow modes 12 p1784 A72-27789
- Quasi-static and full wave calculation of VLF/ELF input impedance of arbitrarily oriented loop antenna in cold collisionless multicomponent magnetoplasma 13 p2009 A72-28542
- Worldwide thunderstorm activity model selection from Schumann resonance observations, using ELF

noise measurements in lowest earth-ionosphere cavity modes

13 p1988 A72-28600

Low energy auroral electron precipitation associated ELF noise band observation by polar-orbiting satellite INJUN 5

17 p2517 A72-35593

Numerical solution to the problem of propagation of ELF electromagnetic waves in the lower ionosphere

19 p2767 A72-38651

A satellite survey of vector electric fields in the ionosphere at frequencies of 10 to 500 hertz. II - The electric component of ELF hiss.

19 p2768 A72-38743

A satellite survey of vector electric fields in the ionosphere at frequencies of 10 to 500 hertz. III - Low-frequency equatorial emissions and their relationship to ionospheric turbulence.

19 p2768 A72-38744

A small ELF electric field probe.

20 p2921 A72-38994

Polar ionosphere ELF/VLF noise distribution from Alouette 2 electric dipole observations

20 p2903 A72-39538

Worldwide thunderstorm activity model selection from Schumann resonance observations, using ELF noise measurements in lowest earth-ionosphere cavity modes

24 p3380 A72-45100

EXTREMUM VALUES

NT LIMITS (MATHEMATICS)

NT MINIMA

French monograph on extremum values of function with two variables and nonlinear feedback control systems stability, using associate recurrence solutions properties

01 p0044 A72-10164

Bias and spread in extreme value theory performance tests of communications systems, comparing with bit error rate tests

02 p0173 A72-12129

Extremal problems of natural vibration spectrum optimal control in mechanical systems with constraints, using mathematical programming methods

04 p0586 A72-15004

Extremum of satellite orbit perigee or apogee height in Hohmann transfer

05 p0713 A72-16006

Run length encoding for removing redundancy from video signals, determining upper bound on compression ratio based on first order Markov model

06 p0773 A72-17488

Extremal field properties in optimal control problem applied to aircraft flight over assigned distance with minimum fuel consumption

06 p0758 A72-17727

Upper bound on rate distortion function for discrete ergodic sources with memory, applying to pictorial data processing

06 p0776 A72-18390

Rate 1/n binary convolutional code free distance upper bound derivation and largest input sequence determination for equal weight

06 p0776 A72-18392

Coefficient matrix for estimation of numerical solution error bounds for finite element models

07 p1025 A72-18786

Differential equation initial value problem solution error bounds construction by interval arithmetic to guarantee exact solution inclusion

07 p1026 A72-18968

Multichannel communication system in adaptive system based on random parameter extremum criterion, deriving average usage time of extremal channel

07 p0938 A72-19008

One- and two-conductor transmission lines electromagnetically coupled to rocket, deriving current bounds in load impedances under incident plane monochromatic wave

07 p0956 A72-19556

Heat exchange extremum boundary value problems for flow direction reversal, considering thermal treatment of porous materials

08 p1253 A72-21457

Variational solutions to linear integral equations and extremal functions in physical gas dynamics problems, using stepwise constant trial functions

08 p1150 A72-21620

Extremal mechanical properties directions in orthotropic glass fiber reinforced plastics symmetry planes

08 p1196 A72-21866

Asymptotic analysis of activation energy limit for radiant ignition of reactive solid with in-depth absorption

08 p1255 A72-22044

Multidimensional function extremum for sectioned resonator type gyroamplifier efficiency optimization

08 p1172 A72-22050

German monograph on optimum principle for numerical representation of surfaces, discussing association with elasticity theory extremal requirements

09 p1340 A72-22319

Optimal temperature gradients determination over thickness of shell of revolution under axisymmetric heating, formulating variational problem for conditional extremum of elastic energy functional

09 p1399 A72-22706

Algorithms for optimal adaptive control of steady motions of single channel discrete extremal systems with independent search, studying quality functional behavior

09 p1291 A72-23437

Rayleigh-Ritz method supplement for optimal evaluation of eigenvalue bounds for semibounded self adjoint operators

09 p1353 A72-23484

Numerical computation of bilateral bounds for arbitrary vectorial and tensorial field quantities of elastic bodies eigenvibration states, applying to thin rectangular plate

09 p1409 A72-23566

Pressure jumps lower bounds across supersonic transports induced shock waves in homogeneous atmosphere, using Whitham function in terms of Riemann integral

10 p1420 A72-24846

Extremal field properties in optimal control problem applied to aircraft flight over assigned distance with minimum fuel consumption

11 p1574 A72-25329

Error bounds for finite element methods and approximation with piecewise polynomials for elliptical differential equations solution

11 p1679 A72-26956

Error bounds relationship to norm in approximate numerical solutions of initial value problems for ordinary differential equations

11 p1679 A72-26957

Lowest natural vibration frequencies of conical shell for various boundary conditions, using finite difference scheme

12 p1878 A72-27081

Maximum transmission delay in microwave TWT delay lines as function of electron beam size, current, shape and velocity distribution

12 p1782 A72-27436

Distribution theory application to fixed end point problem in variational calculus for extremal containing corners, obtaining Euler equation

12 p1885 A72-27849

Extremum search algorithm in multicompartment mixture optimization problem, using gradient method adaptation

13 p1924 A72-28460

Differential games extremal strategies with player control action subject to integral constraints

13 p2002 A72-28712

Statistical superoptimal search strategies of self optimizing systems, applying to one dimensional step type and multiextremal problems

13 p1936 A72-29160

Extremal correlation algorithm for automatic control of two image congruent superposition, using digital simulation and statistical trial techniques

13 p1924 A72-29161

Signal discretization frequency upper bounds determination to satisfy prescribed level of mean square error in continuous signal restoration

13 p1925 A72-30021

Green operator first invariant upper bound for free oscillations eigenvalue upper limit, exemplifying for quadratic plate with two free and two clamped edges

15 p2274 A72-31459

Dual extremum principles in functional analysis, including applications in nonlinear programming, networks, optimization, control theory, fluid mechanics, etc

15 p2262 A72-31630

Modified Rayleigh-Ritz method to obtain lower bounds of eigenvalues, applying to uniform cantilever column buckling

15 p2275 A72-31710

Electron impact low energy cross sections for transitions between highly excited states, obtaining upper bound via quantal impact parameter theory

15 p2315 A72-32715

Upper and lower bounds of effective thermal conductivity for statistically homogeneous composite materials, using variational principles

17 p2638 A72-35285

The bounding theory of turbulence and its physical significance in the case of turbulent Couette flow.

18 p2677 A72-36006

A basic theorem in the computation of ellipsoidal error bounds.

18 p2705 A72-36602

Error bounds for the Galerkin method applied to singular and nonsingular boundary value problems.

18 p2705 A72-36604

Extremal problems arising in the substantiation of heuristic procedures

19 p2824 A72-37381

Necessary and sufficient conditions for differentiable non-scalar-valued functions to attain extrema.

19 p2824 A72-38244

Algorithms for optimal adaptive control of steady motions of single channel discrete extremal systems with independent search, studying quality functional behavior

19 p2782 A72-38520

A statistical information theory for extremum search of a function

19 p2827 A72-38576

Simple algorithm for a search of the global extremum of a function of several variables and its application to the functional approximation problem

19 p2828 A72-38582

An advanced concept of the Woehler diagram and a new calculating procedure for the application of the extreme-value method to experimental data in the calculation of fatigue strength

20 p2926 A72-39572

Differential games extremal strategies with player control action subject to integral constraints

22 p3198 A72-42090

The branch and boundary method as a regular method of solving irregular problems of mathematical programming. I

22 p3198 A72-42188

Extremum principles for a class of dynamic rigid-plastic problems.

22 p3235 A72-42522

Impulsive loading in structural plasticity, obtaining displacement bounds via deformation theory based on extremum paths

22 p3237 A72-42759

Widely convergent method for finding multiple solutions of simultaneous nonlinear equations.

23 p3308 A72-43400

Lower and upper bounds for the lowest characteristic value of the elastically supported membrane

23 p3347 A72-43717

Extreme value analysis of flight load measurements.

24 p3367 A72-44737

On an augmentation of the error made by numerical treatment of second-order conservative point transformations

24 p3419 A72-45071

Dual extremum variational principles relevant to nonlinear heat transfer, applying to temperature distribution on thin walled spherical spacecraft surface

24 p3465 A72-45474

EXTROVERSION

Noise effects on human attention and work efficiency in extroverted and introverted individuals

08 p1128 A72-22137

Circadian rhythm effects on introverts and extroverts biochemistry, physiology and performance, suggesting arousal mechanism differences

11 p1581 A72-26693

Extraversion, neuroticism, and color preferences.

18 p2653 A72-36903

EXTRUDING

Coextruded Be fiber-Ti alloy matrix composite sheets for light weight structures, describing ultrasonic inspection and mechanical properties

01 p0084 A72-10734

Metallurgical defects in hot extruded aluminum alloys, describing investigation methods and remedies

01 p0077 A72-11041

Extruded anodized AlMgSi alloy matrix precipitate surface defects, noting wood grain effect, segregated bands, microstructural stains and heterogeneous zones

01 p0077 A72-11042

Two component flow and optimal strength ratios between core and shell materials during extrusion of composite bimetallic specimens into circular tubes

01 p0077 A72-11078

Ti powder technology, discussing pressed and sintered parts, forging and extrusion preforms and composites

02 p0233 A72-11437

Coextrusion of metal powder and ceramic dispersions clad alloyed Al as function of cartridge density and reactor core length

02 p0233 A72-11456

Transition metal oxides hot extrusion sintering, discussing temperature and pressure effects on compacting density

02 p0244 A72-12349

Tubular and rod extruded age hardenable Al alloys, determining mechanical anisotropic properties from yield loci and r values

03 p0369 A72-12957

Slip line field for plane strain extrusion of strain hardening material, calculating shear stress

03 p0363 A72-13708

Large length-to-diameter ratio two layer blank bimetallic hard alloy product manufacture by extrusion die method, noting mechanical properties

05 p0666 A72-16098

Hot pressing/extrusion/ of rods from metal-ceramic Ti, using pure and cermet powders with tungsten carbide

06 p0822 A72-18426

Nonheat treated extruded Mo alloy under tension and vacuum conditions at various temperatures, in-

- vestigating cylindrical samples size effects on mechanical properties 06 p0833 A72-18635
- Extruded superalloy powder structural shapes preparation by filled billet technique for improved chemical and mechanical properties 07 p0994 A72-19483
- Explosives injection molding into stainless steel, aluminum, plastic and rubber tubes, considering applications to fuse and detonation transfer trains and small warheads 08 p1221 A72-20781
- Thermal diffusivity and conductivity and specific heat of hard electrode graphite intermediate medium in hydraulic hot extrusion of metals 08 p1181 A72-22072
- Viscoplasticity techniques application to deforming portion strain and strain rate fields of axisymmetric Al alloy extrusion with various flow patterns 08 p1250 A72-22194
- High strength Ni alloy hot working properties evaluation from extrusion simulation by torsion testing, considering stress-strain-time relations, microstructure, recrystallization and ductility 08 p1190 A72-22199
- Pultrusion process for carbon fiber reinforced plastic, compared with wet lay up technique, noting mechanical properties [PI PAPER 10] 09 p1318 A72-22545
- Al alloys degree of deformation dependence on pulse energy during extrusion by pulsed magnetic field, showing hardening effect 09 p1319 A72-22865
- Flow rate limits increase and near homogeneous stress concentration in active hot extrusion of Al alloys 12 p1814 A72-27644
- Microfiber extrusion of plasticized mixtures based on titanium and silicon carbides, showing optimum extrusion rate dependent on deformation and strengthening 13 p1967 A72-30102
- Pressed and sintered preforms of Ti and alloys for forge and extrusion operations, noting processing time reduction and smooth surface 13 p1982 A72-30120
- Commercial and laboratory Mg alloys for die and sand casting, high strength and extruding applications 14 p2113 A72-30269
- Electron-microscopic investigation of the development of a cellular structure in molybdenum during hydroextrusion 17 p2569 A72-35524
- Metallurgical aspects in the development of AlMgSi alloys with a low sensitivity to quenching 18 p2699 A72-36224
- Precipitation caused surface defects on Al-Mg-Si alloy extrusions, considering segregation streaks, cooling induced microstructural stains and cold working-annealing produced heterogeneous zones 18 p2699 A72-36225
- Influence of hydraulic extrusion on the composition and properties of the Nb3Sn compound 23 p3323 A72-43597
- EYE [ANATOMY]**
- NT CHOROID MEMBRANES
- NT CORNEA
- NT FOVEA
- NT NYSTAGMUS
- NT OCULOMOTOR NERVES
- NT PUPILS
- NT RETINA
- Cerenkov radiation detection by human eye, discussing relativistic muons passage through vitreous humor and retina 02 p0272 A72-11754
- Anatomical-physiological, optical and behavioral-vision similarities of nonhuman and human primates 03 p0313 A72-13069
- Spectral response and vision thresholds of human eye for light detection and color sensation 08 p1125 A72-21332
- Biological hazards of high intensity light sources, considering physiological factors involved in threshold eye damage values determination 08 p1125 A72-21333
- Destructive changes in rabbit brain and eyes under pulsed laser beam irradiation 13 p1910 A72-29333
- Succinic dehydrogenase activity in rabbit eye ciliary epithelium during electric stimulation of hypothalamus, using histochemical techniques 14 p2078 A72-31099
- Fagle eye retinal image quality determination by ophthalmoscopic method, comparing to human visual acuity 15 p2186 A72-31724
- The distribution of the long wave photoreceptors in the compound eye of the honey bee as revealed by selective osmic staining. 17 p2500 A72-34877
- Light induced alterations in growth pattern of the avian eye. 17 p2500 A72-34880
- Sperry neuronal specificity hypothesis for nerve cell connections formation between eye and brain during embryonic development, proposing systems matching theory 17 p2504 A72-35070
- Intraocular noise - Origin and characteristics. 18 p2651 A72-36605
- Fly colour vision. 18 p2651 A72-36609
- The neurophysiology of binocular vision. 19 p2758 A72-37250
- An automatic measuring and recording system for clinical electro-oculography. 19 p2759 A72-37400
- Receptive fields of units in the visual cortex of the cat in the presence and absence of bodily tilt. 19 p2758 A72-38646
- Quantitative determination of fluorescence within the eye without disrupting the integrity of the eyeball 20 p2893 A72-38941
- Continuous objective measurement of the accommodation of the human eye 21 p3007 A72-40730
- Crystalline lens optical structure in human eye, representing on and off axis imaging characteristics by mathematical model 21 p3007 A72-40737
- Effect of spherical spectacle lenses on the monochromatic aberration of the eye 21 p3007 A72-40746
- Lysosomal enzymes of eye tissues during the action of hydrocortisone 22 p3141 A72-42279
- Ocular and induced visual effects of systemic and topical drugs in terms of eye neuroanatomy and pharmacology, stressing glaucoma therapy 22 p3150 A72-42499
- EYE DISEASES**
- NT ASTIGMATISM
- NT CATARACTS
- NT GLAUCOMA
- Optic disk drusen and Marcus Gunn pupillary phenomenon relation to visual field defects, discussing need for calibrated perimetry and binocular field testing [AD-737860] 07 p0933 A72-20190
- Keratoconus /noninflammatory conic protrusion of cornea/ diagnosis and rehabilitation in USAF flying personnel 12 p1768 A72-28331
- Color discrimination threshold determination for spectral sensitivity in subjects with congenital color vision disorders 13 p1903 A72-28763
- Sight impairment-caused flight personnel disqualification analysis, establishing eye disease structure, sight damage preconditions and ophthalmological practice inadequacies 14 p2080 A72-30748
- Pupil reflex loss /pupillotomy/ diagnosis in pilots, testing sensitivity to methacholine chloride [AD-744368] 14 p2082 A72-31096
- Keratoconus incidence in USAF flying personnel, discussing diagnosis, etiology and therapy 24 p3378 A72-45663
- EYE DOMINANCE**
- Interhemispheric effects on choice reaction times to single and multiple letter displays, analyzing cerebral dominance and visual information transmission compared with verbal response 12 p1768 A72-27075
- Quantitative decision criteria for identification of visual evoked responses obtained during binocular rivalry. 18 p2652 A72-36312
- Hering's law of equal innervation and the position of the binocular. 19 p2756 A72-37828
- Apparent movement and change in perceived location of a stimulus produced by a change in accommodative vergence. 21 p3002 A72-41024
- EYE EXAMINATIONS**
- Camera slit lamp apparatus design for anterior eye diagnosis in two dimensional and stereoscopic photography and ophthalmic application 04 p0478 A72-14725
- Retina visual acuity testing by zero and first order moire fringes, using square-wave amplitude gratings 12 p1772 A72-27953
- Landolt ring radioactive plague night vision tester comparison with electroretinography and Goldmann-Weekers dark adaptometry apparatus from special tests of night blind patients 12 p1777 A72-28332
- Considerations in the design of an automatic visual field tester. 18 p2654 A72-37013
- Visual Field Analyzer presentation of single and multiple stimuli for differential threshold levels investigation, discussing eccentricity, spatial orientation and supraliminal stimuli effects 19 p2756 A72-37831
- Ophthalmoscopic, photocalbrometric and ophthalmodynamometric examinations of test subjects visual acuity during bed rest in hypokinetic antiorthostatic position 23 p3255 A72-43916
- Information aspects in visual perimetry, obtaining memory requirement for control computer in automated perimetry 23 p3261 A72-44378
- EYE MOVEMENTS**
- NT NYSTAGMUS
- Position constancy and motion perception tests of head movement feedback calibration of perceived direction of optical motions 01 p0013 A72-10719
- Human centrifuge tests for gravito-inertial force effect on ocular counterrolling in normal and deaf subjects 02 p0159 A72-11956
- Head mounted monkey eye orientation measuring system for performance of brightness discrimination tasks 03 p0318 A72-13073
- Lateral geniculate body neurons activity during nystagmic eye movements in cats after vestibular stimulation related to visuo-motor mechanisms counteracting illusory shifts 03 p0315 A72-13623
- Eye movement control device for electronystagmography, describing construction, line drawing and basic circuits 03 p0319 A72-13724
- Alcohol ingestion effects on tracking performance during angular acceleration, observing nystagmic eye movements and eye-hand coordination 04 p0477 A72-14474
- Human vestibulo-ocular responses to oscillatory rotational stimulation during various sleep and arousal stages, discussing Sugie-Jones reflex system mathematical model 04 p0474 A72-15249
- Blink reflexes in man during sleep and wakefulness, discussing electromyographically recorded orbicularis oculi mono- and polysynaptic responses to electrical stimuli 04 p0474 A72-15250
- Saccadic eye movements significance for jet pilots, noting saccade rate diurnal fluctuations and alcohol and tranquilizer negative effects 05 p0616 A72-15800
- Involuntary eye movements effects on visual images, emphasizing drift and tremor effects on spatial frequency distortion 05 p0623 A72-16674
- Head movement adaptation to horizontal and vertical field displacements, discussing eye movement direction learning 06 p0765 A72-17410
- Eye mark recorder system for eyeball movement studies, describing operational principle and various optical systems 06 p0813 A72-17433
- Horizontal and vertical eye motions temporal relations in tracking light spot, discussing saccadic system orthogonal interaction mechanism 06 p0761 A72-17601
- Suppression of visual evoked responses to low intensity light flashes and shifting stripe patterns during saccadic eye movements 07 p0926 A72-19025
- Extraretinal inflow eye position information awareness from experimental load application to eyes in total darkness 07 p0926 A72-19026
- Dynamic visual acuity and eye movement data for moving targets, deriving retinal target image position and velocity errors during ocular pursuit 07 p0926 A72-19030
- Afterimage apparent motion preceding smooth eye movement association with target tracking, noting unequal impairment occurrence over entire visual field 07 p0927 A72-19034
- Computer graphics system simulation of saccadic eye movement made for time optimal control behavior study, incorporating eye muscle characteristics 07 p0928 A72-19309
- Human binocular visual system fusional information processing, evaluating compensatory eye movements role in overcoming retinal image disparity 07 p0929 A72-19314
- Field and intracellular potentials in cat trochlear nucleus following vestibular nerve and nuclei stimulation for synaptic organization study of vestibulo-ocular reflex 07 p0923 A72-20501
- Stochastic model for eye movements during fixation on stationary target 10 p1429 A72-23795
- Stimulus complexity effect on amplitude of human cyclofusional response, evaluating relative roles of compensatory eye movements and central responses 10 p1427 A72-25180

Image visual recognition during voluntary saccadic eye movements, noting stimuli visible luminance change effect

12 p1760 A72-27310

Computer analysis of helicopter pilots eye movement patterns dependence on visual task skill and performance time

12 p1770 A72-27475

Human electrophysiological changes during perceptual isolation from EEG, EMG, vertical eye movements and electrodermal measurements

12 p1771 A72-27484

Nystagmus eye movements relationship to ocularly induced illusion from test involving vestibular stimulation and visual stimuli velocity estimates

12 p1776 A72-28304

Foveal and nonfoveal afterimages effects on saccadic behavior of eye movement

13 p1907 A72-29971

Eye movements and dynamic visual acuity as function of tracking velocity, analyzing pursuit and saccadic component by electrooculography

13 p1912 A72-30043

Voluntary saccade length dependence on visual field nontarget stimuli number, locus and distance from target

14 p2077 A72-30966

Voluntary eye movement and convergence effects on relation between binocularly perceived and physical distance ratios

16 p2358 A72-33647

The effect of target contrast variation on dynamic visual acuity and eye movements.

17 p2508 A72-34876

Eye movement pattern monitoring to investigate retinal afterimage role in release of pursuit movements

17 p2508 A72-34886

Russian book - Eye movements as the basis of spatial vision and as a model of behavior

17 p2509 A72-35459

REM period functional maintenance of coordinated eye movement facilitation and binocular depth perception accuracy following sleep

17 p2509 A72-35462

Optokinetic thresholds in the normal monkey.

18 p2651 A72-36610

Vergence eye movements to pairs of disparity stimuli with shape selection cues.

18 p2651 A72-36612

Personality correlates of lateral eye movement and handedness.

18 p2653 A72-36905

Hering's law of equal innervation and the position of the binoculus.

19 p2756 A72-37828

Parallel swing with affixed luminous disks test for induced vestibular stimulation effects on moon illusion, noting eye movement factors

20 p2893 A72-38900

Fixation eye movements and the processing of visual information.

21 p3007 A72-40740

Parametric adjustment to a shifting target alternating with saccades to a stationary reference point.

21 p3009 A72-41250

Role of eye movements in the perception of apparent motion.

23 p3259 A72-43804

Involuntary eye movements during the performance of mental tasks

23 p3260 A72-44077

Conjugate and disjunctive optokinetic eye movements in the rabbit, evoked by rotatory and transitory motion.

23 p3257 A72-44243

Visual sensitivity measurement in retinal areas with stepwise change from one monochromatic light to another, discussing eye movements effects and perception thresholds

23 p3258 A72-44385

Eye movements evoked by collicular stimulation in the alert monkey.

24 p3371 A72-44906

Perception smear suppression during saccadic eye movements in terms of metacontrast determined by post-saccadic accumulated luminance relation to stimuli masking

24 p3373 A72-45377

EYE PROTECTION

Automatic laser tracking and ranging system for cooperative retroreflective aircraft targets, discussing design, performance, eyesafe distance and atmospheric attenuation [CLEA PAPER 9.3]

07 p0942 A72-19385

Industrial safety rules recommendations for lasers based on radiation biological effects and eye optical and physiological properties

12 p1771 A72-27615

Visual acuity restoration improvement after flash blindness by monocular shielding and ingestion of vitamin complexes containing ATP with pyridoxal, considering twilight vision

21 p3012 A72-41748

EYEPIECES

Oculomotor accommodation and convergence as distance perception cues, showing size perception change relation to glasses adaptation

06 p0765 A72-17411

Oculomotor cue-based distance perception, discussing glasses adaptation-caused accommodation and convergence changes in stereoscopic depth perception

06 p0765 A72-17414

F

F CENTERS

U COLOR CENTERS

F DISPLAYS

U F REGION

F REGION

Topside electron density profile from empirical relation between ionospheric slab thickness and mean gradient temperature in F region, using Saint Santin scatter data

01 p0052 A72-10085

Ionospheric horizontal drifts during large vertical convection of mid dip-latitude postmidnight F region, using spaced antenna measurements

01 p0052 A72-10087

Lindauer electron density profile for maximum F layer over sunspot cycle using frequency dependent radio ground echo in satellite ionograms

01 p0054 A72-10421

Ionogram observations of F layer electron rarefaction wake disturbance during small rocket ascent

01 p0054 A72-10423

Neutral gas wind effect on Doppler shifts in frequency spectrum of atmospheric gravity waves in F region with resultant phase altitude dependence alteration

01 p0054 A72-10426

Log normal random fluctuations of ionospheric electron concentration in F region from vertical sounding and incoherent scatter data

01 p0059 A72-10609

Sizes, shapes and temporal characteristics of small scale inhomogeneities in F region, using vertical sounding, space diversity reception and radio astronomy

01 p0059 A72-10610

Daytime and nighttime sporadic F layer regularities correlation with other ionospheric phenomena based on vertical sounding data

01 p0059 A72-10611

Daytime bottomside polar F layer latitudinal cross section construction from ionograms recorded in aircraft [AD-738278]

01 p0061 A72-10900

Ionospheric F region heating by hf transmitter, obtaining electron temperature maps and heating/cooling time constants

01 p0062 A72-10910

F region neutral thermosphere temperature perturbation and circulation pattern due to global wind with anomalies of ionization calculated from two dimensional dynamic model

01 p0096 A72-11283

Long range satellite signal Faraday fading rate revealing electron density profile near F layer peak

04 p0486 A72-14883

Electronic collision frequency relationship with radio frequency in F region, investigating height, diurnal and seasonal variations

04 p0516 A72-14933

Electrojet effects on critical frequencies in equatorial F region during magnetically quiet and disturbed days

04 p0516 A72-14936

Statistical analysis of low latitude F 2 layer disturbances associated with sudden commencement type geomagnetic storms, investigating critical frequencies

04 p0516 A72-14937

Small scale F region irregularities at Varanasi, plotting horizontal drift velocities and directions, axial ratios and orientations and rms random velocity values histograms

04 p0517 A72-14954

Diurnal and seasonal variations of F region irregularities drift and anisotropy parameters during IQSY from aerial fading records, noting magnetic activity effect

04 p0517 A72-14955

Molecular nitrogen dayglow emission in F region, noting volume emission rates, integrated overhead intensities and solar activity effects

04 p0518 A72-14959

Van Rhijn height and intensity variations of 5577 A emission in night E layer airglow

04 p0518 A72-14960

Intensity-height profiles for molecular oxygen first and second negative bands in F region, using equilibrium velocity distribution of photoelectrons

04 p0518 A72-14963

Oxygen ions vertical flux altitude distribution in F layer from incoherent scatter radar measurements, noting existence in protonosphere during daytime [AD-737929]

05 p0629 A72-16616

Latitudinal, diurnal, seasonal and solar cycle variations in vhf-uhf scintillation producing irregularities in F layer electron density

05 p0630 A72-16617

Lf instability mode in partly ionized plasma due to electron temperature gradient aligned perpendicular to magnetic field, applying to E and F regions [AD-737931]

06 p0804 A72-17460

Sunspot cycles effect on F region drifts and irregularities from observations at Ibadan during 1966/67, noting seasonal and diurnal variations

06 p0806 A72-17643

Midlatitude F region wavelike disturbances detection by hf radio echo techniques, discussing correlation with jet stream associated tropopause wind patterns

07 p0974 A72-18885

Quantum efficiency at 6300 and 6364 A of recombination mechanism in nighttime F layer, obtaining ionospheric electron density profiles

07 p0974 A72-18893

F region electron density variation above North America during geomagnetic disturbance on 28 May 1970 [AD-739792]

07 p0976 A72-19162

Ionospheric F region storms model accounting for global electron density changes due to abundance ratio of atomic oxygen to molecular oxygen or nitrogen

07 p0979 A72-20047

Radio wave alternating electric field heating of ionospheric plasma electrons with density increase below 200 km and decrease at F layer maximum

08 p1152 A72-20703

Ring current growth effects on midlatitude F region electron density change during large magnetic disturbances

08 p1152 A72-20706

F region ionization anomalous evening enhancement, discussing seasonal variations, solar activity and geomagnetic coordinates maximum in Yakutsk

08 p1153 A72-20707

F region electron-ion gas dynamic model with stability dependence on periodic solutions convergence of continuity equations

08 p1153 A72-20725

Quarter thickness variation and particle temperature dependence on height and frequency in summer daytime F region

08 p1155 A72-20815

Horizontal neutral winds meridional component from incoherent scatter measurements of F region ionization drifts, noting diurnal variations

08 p1156 A72-21098

Polar orbiting satellite ESRO-1A 1-13 keV electron measurements compared to bottomside ionosonde measurements for auroral particle precipitation and F region electron density

08 p1226 A72-21099

F region irregularity contours from correlation analysis of satellite amplitude scintillations, showing axially symmetric field-aligned and north-south elongated planes

08 p1156 A72-21105

Auroral F region electron density enhancement relation to sporadic F2 and red oxygen emission

08 p1226 A72-21111

F region disturbances, explaining critical frequency changes on basis of neutral winds, electrodynamic drift and temperature and chemical composition variation

08 p1158 A72-21222

Nocturnal F region electrodynamic drift at conjugate point sunrise time, discussing dynamo electrostatic field normal component change as cause of ionosphere vertical movement

09 p1297 A72-22576

Rocket sounding of auroral zone F region low energy electron precipitation and excitation and ionization processes

09 p1298 A72-22585

E and F region apparent and true drifts over magnetic equator correlated to solar activity, comparing electron density sensitivity to geomagnetic range

11 p1623 A72-26104

Anomalous F region ionization in darkened high latitudes during solar activity growth and abatement

11 p1623 A72-26270

F region critical frequencies deviation from median due to solar cycle phase, latitude and time, discussing short waves radio communications reliability

11 p1593 A72-26271

F region N/h/ profiles and parameters deviations during ionospheric and magnetic storms, discussing perturbation index

11 p1594 A72-26275

Noontime N/h/ profiles forecasts and annual variation in F region, relating solar activity levels to vertical distribution of electron concentration

11 p1594 A72-26277

Time and space characteristics of F scattering, investigating maximum appearance probability, intensity and seasonal and diurnal variations

11 p1595 A72-26280

Magnetic field line connection between F region irregularities causing scintillation and ionospheric conditions inducing spread E

11 p1625 A72-26405

Ionosonde observations and Faraday rotation measurements of E and F region total electron content during two solar eclipses

12 p1801 A72-27154

F region parameters relationship to night sky optical emission, considering electron distribution produced by dissociative recombination

12 p1802 A72-27308

F region mean electron density profile seasonal and solar cycle dependence, using Chapman function for nighttime F layer description

12 p1803 A72-27775

Ion velocity height profiles, ion temperature and electron density measurement with Thomson scatter facility during F region traveling ionospheric disturbance/gravity waves/

12 p1803 A72-27777

Subauroral zone F region disturbances latitudinal variations catalogs from vertical sounding data, taking into account ionospheric states

13 p1946 A72-28598

Virtual height dependence of ionospheric F region parameters including angular divergence of reflected radio waves, heterogeneity coefficient and random and drift motions velocity

13 p1948 A72-29038

Equatorial F region photoionization and chemical loss rates for electrons from simultaneous observations of vertical drift velocity and electron concentration, deriving plasma transport

13 p1949 A72-29336

E and F regions plasma horizontal drift measurements by oblique incidence incoherent scatter radar system, suggesting solar semidiurnal tidal oscillation dynamo action

13 p2031 A72-29386

Gravity wave observation in nighttime F region by measuring phase path length changes of stable CW signal reflected obliquely from ionosphere

13 p1953 A72-29814

Vertical distribution of atomic nitrogen ions in F region produced by dissociative photoionization and charge transfer, suggesting undiscovered source at 300 km altitude

13 p1954 A72-29815

Daytime F region inverse relationship between electron density and temperature, determining energy input profile and thermal flux

14 p2097 A72-30127

Seasonal features of nocturnal 6300 Å emission variation and decay coefficient in nightglow related to recombination coefficient for F layer ionization

14 p2097 A72-30132

Global electron concentration disturbances in low and middle latitude F2 during magnetic storm

14 p2100 A72-30635

Dipolar coordinate system for geomagnetic field dipole approximation in studies of diffusion and heat conduction in F region and outer ionosphere

14 p2102 A72-30652

Atmospheric gravity waves effects in ionosphere, discussing F region traveling ionospheric disturbances, sporadic E layer and D region radar scattering

15 p2222 A72-31285

Ion chemistry and heating of daytime ionosphere E and lower F regions, calculating neutral atmosphere densities, ion production rates and solar EUV radiation absorption

15 p2192 A72-32253

Nighttime F region vertical velocity estimation, using electron density profiles vs true height

15 p2231 A72-32267

F region plasma one dimensional nonisothermal diffusion for positive ions with allowance for ionization and recombinations and gravitational forces

15 p2232 A72-32731

Semidiurnal variation in O I 5577 Å nightglow due to lunar tidal dynamics effect in E and F regions

16 p2383 A72-32971

F region crossed field instability nonlinear theory based on energy transfer by mode coupling and absorption by linear damping with application to equatorial electrojet

16 p2384 A72-32976

Geomagnetic effect on the neutral temperature of the F region during the magnetic storm of September 1969,

17 p2549 A72-35603

Atomic oxygen green line emission in nightglow from OGO-F photometer observations, calculating tropical F region electron density spatial distribution

17 p2549 A72-35604

Calculations of electron-profile disturbances in the F region during the passage of a neutral wave

17 p2551 A72-35861

Certain characteristics of ionospheric disturbances in the F region during type A red colored polar auroras

17 p2551 A72-35866

Occurrence frequency of F2 layer sporadic ionization in auroral zone, noting solar activity effect

17 p2551 A72-35867

Models for F region and topside ionospheric storms morphology, discussing electric current disturbance at polar region

18 p2685 A72-35994

Radio wave alternating electric field heating of ionospheric plasma electrons with density increase below 200 km and decrease at F layer maximum

19 p2790 A72-38331

Ring current growth effects on midlatitude F region electron density change during large magnetic disturbances

19 p2794 A72-38334

F region ionization anomalous evening enhancement, discussing seasonal variations, solar activity effects and maximum value dependence on geomagnetic latitude and longitude

19 p2790 A72-38335

F region electron-ion gas dynamic model with stability dependence on continuity equations periodic solutions convergence

19 p2791 A72-38353

Nightglow observations and ionospheric soundings for red oxygen line intensity relation to F region parameters

19 p2792 A72-38638

Comparison between observed and numerically calculated atmospheric gravity waves in the F-region.

19 p2794 A72-38864

Diurnally varying neutral wind effects on lower F region ionization distribution, noting Appleton anomaly disappearance time

19 p2794 A72-38865

Seasonal, diurnal and magnetic dependence of ionospheric scintillation at 64 deg invariant latitude.

20 p2916 A72-39226

Simultaneous F-region conjugate point dawn effects at two mid-latitude stations.

20 p2916 A72-39234

High latitude variations of F-region electron temperature.

20 p2918 A72-39535

Horizontal and vertical electron drifts in the F-region at Thumba.

21 p3049 A72-41324

Aspect-sensitive reflections from ionization irregularities in the F-region.

22 p3154 A72-42364

Theoretical calculations of the F-region tropical ultraviolet airglow intensity.

22 p3171 A72-42418

Geomagnetic storm and seasonal effects on spread of monthly distribution and average behavior of midlatitude F region electron peak density and slab thickness

22 p3172 A72-42434

Source and identification of heavy ions in the equatorial F layer.

23 p3286 A72-44516

Subauroral zone F region disturbances latitudinal variations catalogs from vertical sounding data, taking into account ionospheric states

24 p3398 A72-45098

Computer simulation of the F-region seasonal anomaly.

24 p3400 A72-45586

Phenomena associated with very high power, high frequency F-region modification below the critical frequency.

24 p3400 A72-45596

F 1 REGION

F 1 layer appearance and critical frequencies average daily variations at Tsumeb, Southwest Africa, as function of sunspot cycle phase

01 p0055 A72-10428

F1 region ion structure during ionospheric magnetic disturbances by numerical simulation of quiet and disturbed conditions based on electron concentration profiles

05 p0656 A72-16247

Atmospheric composition and temperature effects on F1 region ion concentration structure from 140 to 220 km for low solar activity conditions

05 p0657 A72-16261

F1 layer diurnal and seasonal model for medium to high latitudes, comparing calculated and observed electron density diurnal variations

06 p0804 A72-17458

Beamed radio waves interaction in E and F1 regions propagation, noting beam width and field amplitude changes caused by defocusing

13 p1945 A72-28579

Variations of F1 layer thickness and maximum ionization height for high and low solar activity periods obtained from vertical ionospheric sounding

13 p1946 A72-28595

Beamed radio waves interaction in E and F1 regions propagation, noting beam width and field amplitude changes caused by defocusing

24 p3397 A72-45079

Variations of F1 layer thickness and maximum ionization height for high and low solar activity periods obtained from vertical ionospheric sounding

24 p3398 A72-45095

F 2 REGION

Magnetic declination effect on elevation control of F2 layer maximum, considering east component of geomagnetic field from Capetown and Canberra observations

01 p0054 A72-10427

Magnetoinic component with fluctuating elliptical polarization during wave reflection from F2 layer, discussing suppression mechanism

01 p0028 A72-10593

Cross correlation characteristics of deviations in critical frequencies of F2 region

01 p0059 A72-10594

F2 layer critical frequency variations relation to solar radio flux intensity, using mathematical approximations

01 p0059 A72-10613

Time between noontime and evening maxima in F2 layer critical frequency compared with evening maximum period, showing dependence on noontime solar zenith angle

01 p0059 A72-10615

F2 region maximum electron density level height and molecular temperature diurnal variations at equatorial latitudes from Ibadan station data

02 p0218 A72-11941

Vertical motions of midlatitude F2 layer during magnetospheric substorms, investigating electric field distribution

03 p0349 A72-13519

Thermospheric neutral-air wind effects on ionospheric F2 layer from atmospheric model

04 p0514 A72-14876

F2 layer anomalies association with equatorial electrojet, investigating midday critical frequencies of sporadic E layer

04 p0515 A72-14932

F2 layer 6300 Å night airglow emission photometric data on 31 January 1968, showing large electron content and movements

04 p0517 A72-14958

Elliptical polarization and depolarization coefficients for monochromatic radio waves reflected from F2 ionosphere using Stokes parameters

05 p0656 A72-16241

Latitudinal distribution of electron temperature in F2 layer during summer daytime period of low solar activity from electron density profile geometrical parameters

05 p0656 A72-16248

Magnetic storm disturbing effect on integral electron density in F2 layer and in topside ionosphere

05 p0657 A72-16262

F2 region electron density spatial and temporal distribution, investigating plasma vertical drift effects

05 p0657 A72-16263

F2 layer critical frequency deviations and negative disturbance zones during solar eclipse of 22 September 1968

05 p0657 A72-16264

Ionospheric storms features based on F2 critical frequency data, investigating magnetosphere during geomagnetic storms

06 p0810 A72-18280

F2 ionization distribution diurnal variations from airborne ionosonde measurements during June-July 1966 over Tamanrasset meridian, correlating magnetic activity with wind variations

06 p0810 A72-18731

Lower F2 region positive oxygen ion distribution with allowance for vertical motions, production and recombination processes, using atmospheric models

08 p1152 A72-20705

Unified coordinate system for earth planetary distribution of F2 and sporadic E layer transmission parameters, suggesting geomagnetic longitude and modified magnetic inclination

08 p1153 A72-20726

F2 layer diffuse reflections and critical frequencies increase on ionogram recordings during Northern Hemisphere nighttime magnetic storm of 2 December 1967, noting cosmic radio emission decrease

08 p1154 A72-20738

F2 region magnetic disturbances conjugacy mechanisms, considering vertical ionization profiles

08 p1155 A72-20801

Perturbation effects on F2 layer and outer ionosphere electron density profiles during successive magnetic storms from Alouette 1 satellite data

08 p1157 A72-21145

Ionization movement of charged and neutral particles in F2 region coupled to air movement by collision drag forces

11 p1621 A72-25839

Ionospheric disturbances and prediction dependence on solar and geophysical activities, discussing SID, pca, auroral absorption and F2 region

11 p1623 A72-26267

Ionospheric disturbances relation to interplanetary positive ion and proton fluxes intensity and velocity

- from Mariner 2, Venus 3 and Vela 2 observations, discussing F 2 region
11 p1713 A72-26268
- F 2 region critical radio frequencies forecasts from solar cycles, ionospheric disturbances data, latitude and annual and diurnal variations
11 p1594 A72-26272
- Diurnal variations of F 2 region critical frequencies and quiet and perturbed ionosphere N/h profiles during solar cycle, estimating signal reflection altitudes
11 p1594 A72-26274
- F 2 layer midlatitude local centers of anomalous nighttime ionization during winter and summer solstices
11 p1623 A72-26283
- Predawn effect on hot and cold electrons at magnetoconjugate point in F 2 layer, discussing electron shock wave speed and thermal collisionless wave energy dissipation
11 p1628 A72-26916
- Seasonal atmospheric composition changes relation to midlatitude F 2 layer seasonal anomaly during high solar activity
12 p1803 A72-27776
- Electric field nature required for DP current system development in disturbed high latitude ionosphere, discussing F 2 region ionization drift
13 p1946 A72-28596
- F 2 layer parameter forecasting by computer based on series coefficients dependence on Wolf number
13 p1946 A72-28597
- F 2 region maximum electron density level height and molecular temperature diurnal variations at equatorial latitudes from Ibadan station data
13 p1949 A72-29253
- Magnetic apex coordinate system for plasma density organization in low and middle latitude F 2 region
13 p1951 A72-29395
- F 2 layer electron concentration and maximum height variation with interplanetary magnetic field direction
15 p2226 A72-31920
- Ionized and neutral atmospheres coupled ionospheric continuity and motion equations, discussing nonlinear force effects on F 2 height and electron density
15 p2230 A72-32257
- Real height variations of the ionospheric F2-layer above some pairs of geomagnetically conjugate stations.
17 p2545 A72-34689
- Time delay measurements in the Athens/Greece/Roma /Lesotho/ VHF trans-equatorial propagation circuit.
17 p2515 A72-34693
- Atmospheric model synthesis of observed electron temperatures and concentrations in tropical ionosphere during 8 March 1970 magnetic storm, noting F 2 region features
18 p2686 A72-36296
- Lower F 2 region positive oxygen ion distribution with allowance for vertical motions, production and recombination processes, using atmospheric models
19 p2790 A72-38333
- Unified coordinate system for global distribution of F 2 and sporadic E layer transmission parameters, suggesting geomagnetic longitude and modified magnetic inclination
19 p2791 A72-38354
- F 2 layer spread reflections and critical frequencies increase on ionogram recordings during Northern Hemisphere nighttime magnetic storm of 2 December 1967, noting cosmic radio emission decrease
19 p2791 A72-38366
- Quasi-periodic variation in F 2 layer reflected signal field strength, noting predominance during periods with type 4 bursts, auroras and geomagnetic disturbances
19 p2792 A72-38639
- Perturbation effects on F 2 layer and outer ionosphere electron density profiles during successive magnetic storms from Alouette 1 satellite data
20 p2916 A72-39250
- The anomaly of the neutral wind at a height of approximately 200 km at high latitudes.
20 p2918 A72-39536
- Magnetospheric interactions with topside ionosphere in terms of polar wind ion flows and density related to plasma temperature, F 2 region and cusp observations
20 p2918 A72-39537
- Oxygen ion anticorrelation to molecular ion concentrations fromOGO 6 observations in F 2 region
22 p3169 A72-42016
- A method for determining the electron density distribution about the F2 peak of the ionosphere.
22 p3174 A72-42992
- Geometrical dimensions and effective number of large scale ionospheric inhomogeneities by F 2 critical frequency variability analysis
23 p3283 A72-43360
- Variations of the planetary values of the F2 layer thickness and the parameters of the neutral atmosphere
23 p3284 A72-43375
- Solar control over the evolution of F2-layer after sunrise.
24 p3395 A72-44822
- Electric field nature for DP current system development in disturbed high latitude ionosphere, discussing F 2 region ionization drift
24 p3398 A72-45096
- F 2 layer parameter forecasting by computer based on series coefficients dependence on Wolf number
24 p3398 A72-45097
- F-4 AIRCRAFT**
Buccaneer Mk 2 and F-4K Phantom takeoff and landing performance improvement due to boundary layer control by leading and trailing edge blowing
09 p1262 A72-22973
- Pilot and back-seat man physiological responses during high-g aerial combat maneuvers in F-4E aircraft, discussing ECG, respiratory rate and minute volume
12 p1767 A72-28317
- Electromechanical redundant activating mechanism for F-4 aircraft dual tandem hydraulic power servo, noting application to fly by wire control
14 p2072 A72-30422
- Synthesis and analysis of a fly-by-wire flight control system for an F-4 aircraft.
[AIAA PAPER 72-880] 20 p2887 A72-39119
- F-5 AIRCRAFT**
Graphite fiber-epoxy composite systems development for F-5 aircraft landing gear door, speed brake, leading and trailing edge flaps and horizontal stabilizer
12 p1835 A72-28097
- F-8 AIRCRAFT**
NF-8D aircraft variable stability system ground/in-flight calibration for determination of flight control system dynamics effects on flying qualities
05 p0611 A72-16660
- Design and flight experience with a digital fly-by-wire control system using Apollo guidance system hardware on an F-8 aircraft.
[AIAA PAPER 72-881] 20 p2889 A72-40060
- F-14 AIRCRAFT**
F-14A fighter accelerated flight test program with 18-month saving and 3600 flight time hours before 1973 operability
04 p0464 A72-14591
- Automated telemetry system providing real time analytical capability and reduction of flight test time for F-14
04 p0486 A72-14592
- F-14 Tomcat test program for hydraulic systems, spinning, low speed performance, stalling, afterburning turbofan engines, in-flight refueling and automatic telemetry equipment
06 p0758 A72-17582
- F-14 naval fighter aircraft flight test programs, discussing instrumentation and low-speed test results
08 p1108 A72-21005
- F-100 and F-401 turbofan engine design and development for F-15 and F-14, discussing impingement cooling, Ti alloys, powder metallurgy and metal composites, etc
17 p2597 A72-34390
- Real time flight flutter testing via Z-transform analysis technique.
[AIAA PAPER 72-784] 19 p2749 A72-38101
- Direct lift control feasibility for integration into F-14A automatic carrier landing system /ACLS/, using moving-base six-degree-of-freedom simulation
[AIAA PAPER 72-873] 20 p2951 A72-39127
- F-15 AIRCRAFT**
F-100 and F-401 turbofan engine design and development for F-15 and F-14, discussing impingement cooling, Ti alloys, powder metallurgy and metal composites, etc
17 p2597 A72-34390
- F-28 TRANSPORT AIRCRAFT**
Dynamic aspects of Fokker F-28 aircraft design.
22 p3138 A72-42831
- Fatigue testing of the F.28 Fellowship.
24 p3366 A72-44729
- F-104 AIRCRAFT**
Human, technical and environmental factors in accidents of naval F-104 squadron, considering temporal distribution of accidents and pilot physical condition
12 p1772 A72-27820
- F-111 AIRCRAFT**
Relative cost comparisons of composite applications with conventional material components selected from F-111A supersonic fighter bomber
03 p0310 A72-14234
- F-111 aircraft landing gear and speedbrake hydraulic system control by single dual-function valve, describing design features and performance characteristics
08 p1111 A72-21024
- Composite F-111 fuselage design, analysis and testing, considering graphite, boron and glass-epoxy and boron-aluminum systems
11 p1575 A72-25453
- Low temperature environmental chamber for F-111 proof load testing, describing components of cold air forced convection recirculation system with liquid nitrogen injection
15 p2214 A72-32612
- F-111 stall inhibitor system with angle of attack limitation, describing interface with stability augmentation system
17 p2493 A72-35577
- F-111A inlet nozzle dynamic distortion diagnostics for airframe-propulsion integration based on flight and transonic wind tunnel tests
[ICAS PAPER 72-18] 21 p2991 A72-41143
- FAB [PROGRAMMING LANGUAGE]**
U FORTRAN
- FABRICATION**
NT SPACE MANUFACTURING
CW and pulsed InP transferred electron microwave oscillators, discussing fabrication techniques and electrical properties
01 p0036 A72-10633
- Metal matrix fabrication processes, considering plasma sprayed and diffusion bonded tapes and consolidated sheet material
01 p0074 A72-10733
- Fe, Ni and Co based high temperature thin gauge sheet alloys, discussing chemical and mechanical properties, fabrication and availability
01 p0084 A72-10742
- Graphite filament reinforced plastics strength, performance properties, fabrication processes and tooling concepts
[SME PAPER EM 71-205] 01 p0076 A72-10968
- Space vehicles development and fabrication cost estimation, deriving statistical-analytical formulas with allowance for technical complexity and learning factor
01 p0147 A72-11219
- Low cost metal matrix composition fabrication techniques, considering plasma spraying and continuous casting
03 p0364 A72-14236
- Asbestos fiber reinforced plastics composites fabrication techniques, discussing possible applications
04 p0537 A72-15086
- Si monolithic multispectral image photosensor array for satellite application, presenting fabrication and spectral response data
04 p0500 A72-15304
- Bulk type variable resistors with properties controlled by composition during fabrication, evaluating inorganic binders with optimal properties
05 p0701 A72-15754
- Si planar unijunction transistor fabrication, operation principles, parameter measurements and applications
05 p0635 A72-16196
- N-channel Si MOS microwave transistor, discussing fabrication, design, power gain, stability, noise figure, equivalent circuit and applications
05 p0636 A72-16361
- Refractory metal multilevel interconnection systems, comparing materials fabrication, yield and circuit performance with diffused Si planar runs and polycrystalline Si films
05 p0636 A72-16362
- Vapor-grown GaAs transfer electron microwave oscillator, discussing design, fabrication and CW power conversion efficiency
05 p0637 A72-16366
- Refractory materials fabrication characteristics for aerospace technology, presenting listing of synergic agents for use with inhibitors
05 p0681 A72-16774
- Microwires and microstrips fabrication from high strength deformation resistant aluminum alloys
05 p0680 A72-17207
- High temperature GaAs bipolar transistor n-p-n junction fabrication by vapor phase growth technique, considering I-V characteristics dependence on procedure
06 p0783 A72-17607
- Circuit boards contact assembly by special type rivets, discussing technical and economic advantages for prototype or small series fabrication of printed circuit devices
06 p0784 A72-18192
- GaAs IMPATT diodes performance improvement, describing fabrication methods to achieve 6.7 watts output at 15 percent efficiency
06 p0789 A72-18474
- Thin film materials and fabrication methods, discussing substrate requirements, surface properties, chemical stability, thermal conductivity and preparation of various resistors and capacitors
06 p0790 A72-18572
- Porous materials fabrication from chromium carbide powders, considering compaction procedures involving sinusoidal and pulsating vibrations
07 p1017 A72-19968
- Electron microscope interfaced computer for generating, registering and fabricating microelectronic device and circuit patterns
10 p1459 A72-23955
- Computer controlled electron beam machine for microcircuit fabrication, using digital technique capable of working on complex patterns
10 p1459 A72-23956
- Corrosion resistant fabrication methods in jumbo jetliners components to reduce maintenance and

repair downtime, discussing clad wing and fuselage skins 10 p1487 A72-24025

Homogeneous computing media, examining microelectronic fabrication, interconnection and control problems for MOSFET, bipolar transistors and IC structures 10 p1448 A72-24277

Magnetic integrated circuits design and fabrication problems involving branched and logic circuits and solid state structures controlled domains 10 p1448 A72-24279

Integrated circuits fabrication and design, describing internal physical processes, input and output signal values, functional operations and topological features 10 p1448 A72-24283

Schottky barrier crystal microwave video diodes design and fabrication to maximize burnout resistance and dynamic range for given detection sensitivity 10 p1450 A72-24553

High strength steel strip reinforced aluminum, discussing fabrication techniques and mechanical properties 10 p1498 A72-24839

Thermal diode heat pipe for advanced thermal control flight experiment, discussing engineering model analysis, design, fabrication and test [AIAA PAPER 72-260] 11 p1739 A72-25205

Constituents, processing, fabrication and structure effects on artificial graphic materials ablation performance in sublimation regime from high temperature tests 11 p1742 A72-25235

Multichannel photomultiplier matrix anode design for various tube types fabrication 11 p1631 A72-25687

Microwires and microstrips fabrication from high strength deformation resistant Al alloys 11 p1660 A72-26142

P-n junction diodes fabricated by ion implantation doping, calculating I-V characteristics for comparison with measured breakdown voltages 12 p1789 A72-27312

Fast response thermal compensation system for gas laser resonator length and frequency stabilization, discussing fabrication and design calculation 12 p1822 A72-27607

Solid state array camera based on diffused junction phototransistors, discussing sensor technology and fabrication 12 p1810 A72-27931

Cadmium sulfide solar cells stress analysis in relation to degradation caused by fabrication technology, discussing barrier layer formation process 12 p1757 A72-28020

Silicon solar cell fabrication technology developments for long mission life performance reliability over wide temperature and radiation intensity ranges 12 p1757 A72-28029

Plywrap process for low cost automated fabrication of fiber reinforced plastic composites, noting applications from missile interstages to modular housing 12 p1815 A72-28081

Composite materials fabrication, emphasizing high strength/stiffness to weight ratio as critical performance requirements 12 p1815 A72-28082

Fabrication, and physical, mechanical and ablation properties of three dimensional carbon-carbon cylinder composite materials 12 p1834 A72-28086

Addition type polyimide-graphite fiber composites fabrication from monomeric reactant solutions to improve mechanical properties and thermal stability 12 p1834 A72-28091

Resin bonded B-Al composites, discussing fabrication techniques and mechanical properties 12 p1815 A72-28098

DC 10 aircraft wing stringers fabrication and processing, discussing stress relieving and stretch form contouring techniques, aging and tempering processes and flaw detection [ASM PAPER W 72-31.3] 12 p1817 A72-28161

Chalcogenide semiconductor monostable threshold and bistable memory switching devices, discussing fabrication and performance 13 p1934 A72-30090

Back surface electric field Si cell characteristics and fabrication using alloyed-through contact process 15 p2182 A72-32130

Thermoplastic photoconductor media for holographic recording, discussing structure fabrication techniques and performance 15 p2239 A72-32359

Screen printed large thick film multilayer interconnection board assemblies for electronic packaging, discussing fabrication and feasibility 16 p2368 A72-33194

Plastic composite container cylindrical wall fabrication by two stage procedure combining radial and cross winding of glass fiber rovings 16 p2398 A72-33305

Silicon solar energy conversion for electrical power generation on spacecraft 17 p2494 A72-34186

Fabrication of refractory metals.

Design features, fabrication technology and in-pile testing of thermionic reactor fuel elements 17 p2559 A72-34187

Fabrication and testing of tungsten heat pipes for heat pipe cooled reactors. 17 p2636 A72-34596

Cylindrical diode characteristics with sublimed electrode surfaces. 17 p2527 A72-34607

An investigation of amorphous semiconductor memory devices utilizing thick film fabrication techniques. 17 p2527 A72-34682

NAND gate logic transistor circuit design, layout, fabrication and electrical parameters, noting base and resistors diffusion welding 17 p2530 A72-35069

Refractory materials fabrication characteristics for aerospace technology, presenting listing of synergic agents for use with halogenous inhibitors 17 p2571 A72-35277

Fabrication of boron/aluminum tubes, I-beams, and other structural shapes from tape materials. 17 p2560 A72-35664

Multicell thermionic fuel element fabrication technology. 18 p2708 A72-36152

Organization of fabrication to obtain high-reliability hybrid circuits 18 p2669 A72-37118

Industrial production of high-quality active semiconductor components 18 p2670 A72-37123

Fabrication of Hastelloy B sheet by powder metallurgy using blends of elemental powders and homogenization/deformation processing. 19 p2815 A72-37596

Boron and carbon fibers fabrication and properties for composite materials reinforcing elements, noting strength and stiffness dependence on stress orientation 20 p2944 A72-39437

Fiber arrangements for one, two and three dimensional ideal composite materials, discussing fabrication processes 20 p2940 A72-39446

Burn-in technique cost effectiveness in semiconductor and IC reliability enhancement, noting failure rate relationship to operating time 20 p2909 A72-39770

Processing of carbon/carbon composites - An overview. 21 p3072 A72-40552

Fabrication studies of Nb3Al superconductors. 21 p3097 A72-41182

Masking techniques for thin film and semiconductor devices and ICs fabrication, discussing conventional and computerized optical and electron beam systems 22 p3159 A72-42634

Fabrication and properties of graphite fiber reinforced magnesium. 22 p3193 A72-43035

German monograph - A contribution to the fabrication of thin-film transistors. 22 p3160 A72-43069

Automation of high reliability multilayer printed circuit board fabrication. 22 p3184 A72-43173

FABRICS

NT PARACHUTE FABRICS

Static and dynamic load measurements for stress-strain behavior and load-time characteristics of aerodynamic decelerator canopy fabrics, using metal foil strain gages 02 p0287 A72-11507

Orthotropic glass fabric laminate creep under combined torsion and tension, describing test facility 02 p0250 A72-12677

Heat transfer through fabrics by convection, conduction, radiation and vaporization related to skin temperature and thermal injury 03 p0319 A72-13700

Stress-strain characteristics of nylon-polyurethane coated fabric under biaxial tension and shear forces 05 p0736 A72-16108

Fire resistant fibrous materials for potential military and transportation applications, considering aromatic polyamide polybenzimidazole, fluorocarbon resin polymer, phenolic and glass fibers and fabrics 08 p1191 A72-21586

Manufacturing process for glass fiber chopped strand mats, discussing physical and electrical properties and applications to filament winding 16 p2414 A72-33303

Tridimensional textiles for composites. 17 p2571 A72-34935

Bending vibration test of glass-textolites, noting temperature effect on vibration damping properties 21 p3073 A72-41357

Asbestos-textolite coating required thickness calculation with allowance for aerodynamic heating, discussing softening mechanisms 21 p3074 A72-41709

FABRY-PEROT INTERFEROMETERS

Fabry-Perot interferometer application as filter with transmission windows at regular intervals in wave numbers to detect Raman scattered radiation from atmospheric gases 01 p0067 A72-10537

Fabry-Perot interferometer for studying spatial distribution of plasma electron concentration, discussing resolution using solid state gas laser light source 02 p0223 A72-11403

Fabry-Perot interferometer employing gas laser for plasma bursts electron concentrations measurements at 3.39 micron wavelength 02 p0223 A72-11404

Solid state Q switched laser emission frequency drift from Fabry-Perot rings interferograms 02 p0237 A72-12108

Fabry-Perot interferometers as narrow band optical filters, discussing transmission and construction for various wavelengths 03 p0355 A72-13059

Scanning Fabry-Perot interferometer for He-Ne laser spectral composition, discussing transmission coefficient, resolution, resonator dissipative losses, active medium saturation and light field spatial nonuniformity 03 p0356 A72-13190

Ruby ring laser single mode operation with Fabry-Perot etalons for selective feedback, discussing laser emission spectrograms 03 p0366 A72-13194

Pressure scanning Fabry-Perot magnetometer using KDP crystal and Glan-Thompson prism with echelle interferometer spectrograph for polarized Zeeman components 03 p0356 A72-13283

Asymmetrical profile calculation of spherical multiple wave interference patterns at finite distance with nonparallel mirror Fabry-Perot interferometer 05 p0662 A72-16193

Unmodulated He-Ne laser output frequency stabilization, using quartz Fabry-Perot etalon 05 p0669 A72-16670

Holographic information storage with reference wave modulation by Fabry-Perot interferometer, using two coherent sources 07 p0985 A72-19417

Wavelength tunable dye laser pumped by dual pulse lamps with Fabry-Perot interferometer in resonator 07 p1009 A72-20614

Defocused confocal Fabry-Perot spherical interferometer for analysis of Q switched visible and near IR lasers longitudinal mode outputs 10 p1481 A72-24564

Twilight and nighttime ionospheric temperatures from oxygen 6300 and 5577 A spectral line profiles obtained with Fabry-Perot interferometers 11 p1625 A72-26406

Magnetic field direction measurement in Tokamak toroidal plasma by laser light scattering, using Fabry-Perot interferometer 11 p1697 A72-26583

Dual resonant cavity absorption cell composed of Fabry-Perot interferometers excited by microwave sources, observing spectroscopic double resonance effects 12 p1806 A72-27264

Astronomical spectroscopy using ultraviolet resolution single Fabry-Perot interferometer in tandem with echelle Hilger monochromator 12 p1811 A72-27942

GaAs laser array Fabry-Perot structure to produce uniform TE polarization in emitted light 12 p1827 A72-28223

Fabry-Perot interferometer for line structure of helical TEA-carbon dioxide laser, noting variable frequency single mode emission 13 p1968 A72-28687

Methane absorption stabilized 30 meter laser strain meter with Fabry-Perot geometry for earth tide, nuclear explosion and free earth oscillation observation 14 p2109 A72-30323

Diffraction analysis of Fabry-Perot interferometer with metal mirror gratings for oblique incident polarized plane electromagnetic wave reception 15 p2233 A72-31413

Plasma electron density measurements using flat plate and semicircular millimeter wave Fabry-Perot interferometers [AIAA PAPER 72-672] 16 p2440 A72-34067

Fabry-Perot interferometer measurements of Brillouin scattering from He-Ne laser excited low temperature condensed gases 21 p3051 A72-40151

Compensation of Fabry-Perot surface defects. II - Silicon oxide compensating layers. 21 p3053 A72-40608

Use of air bearings in the construction of a scanning Fabry-Perot interferometer. 21 p3054 A72-40621

Space applications of Fabry-Perot modulator as alternative to mechanical devices, presenting optical

and electrical performance data for different temperatures
21 p3055 A72-40824

The effect of an interferometer selector on the spectrum of the characteristic frequencies of a dispersion resonator
22 p3176 A72-42245

Flat optical surfaces production methods for Fabry-Perot interferometers, describing Otte polishing process and quality test methods
22 p3177 A72-42446

Investigation of several nebulae in Cassiopeia with a Fabry-Perot interferometer.
23 p3333 A72-43233

Digitally pressure-scanned Fabry-Perot interferometer for studying weak spectral lines.
23 p3289 A72-43891

A differential laser Doppler velocity meter employing a Fabry-Perot interferometer
23 p3292 A72-44472

On the use of a Fabry-Perot interferometer for the study of Raman spectra of gases under high resolution.
24 p3426 A72-44904

Rhodamine laser emission spectral band control by plane parallel plates and polarizing prisms, noting band widening by resonator loss modulation with Fabry-Perot interferometer
24 p3410 A72-45418

FABRY-PEROT LASERS
U LASERS

FABRY-PEROT SPECTROMETERS
Precision frequency calibrator for Raman spectrometers, using Fabry-Perot etalon
07 p0983 A72-19318

Fabry-Perot spectrometer/premonochromator assembly integral transmissivity as function of spectral tuning noting selectivity by amplitude modulation
08 p1172 A72-22035

Spectral transmittance enhancement in Fabry-Perot narrow band light filter by wavelength shifted dielectric mirror technique
15 p2233 A72-31414

Fabry-Perot spectrometer adjustment for the compensation of Doppler shift from rapidly rotating and rapidly flowing sources.
21 p3053 A72-40607

Pressure-scanned echelle grating plus Fabry-Perot stellar spectrophotometer.
21 p3053 A72-40609

FACE [ANATOMY]
NT CHIN
NT NOSE [ANATOMY]
Post-synaptic potentials of motor neurons of the facial nerve nucleus evoked by afferent and corticofugal pulse stimulation
23 p3257 A72-44091

FACE CENTERED CUBIC LATTICES
Carbon atoms thermodynamic properties in bcc and fcc Fe-Si-C solid solutions from equilibrium measurements with hydrogen-methane gas mixtures as function of temperature and carburizing gas composition
01 p0083 A72-10207

Binary alloys ground state energy and superstructures, examining bcc and fcc Ising model systems with first and second neighbor interactions
01 p0083 A72-10210

Magnetic transformation effect on creep behavior of fcc nickel-cobalt alloy compared with self diffusion data in Curie temperature vicinity
01 p0083 A72-10391

Cobalt and lanthanum with face and body centered lattices, studying plastic deformation during allotropic transformations under sliding friction and gripping
01 p0074 A72-10579

Ultrasonic bond formation between soft fcc metals, observing dislocation processes
04 p0526 A72-14837

Quaternary Mo-Zr-Cr-C system, investigating fcc phase ligation from phase diagram by chemical, metallographic and X ray analyses
05 p0666 A72-16099

Vacancy effects on residual electrical resistance of binary ordering fcc lattice alloys as function of composition and annealing temperature
06 p0832 A72-18422

Jerky flow /serrated yielding/ in Co-Ni-Cr-C fcc alloys during tensile testing, noting no correlation to dislocation-precipitate interactions
07 p1016 A72-19940

Ni-Cr-Ti alloy hardening during intermetallic phases precipitation, discussing atom segregations, Guinier-Preston zones and fcc and hcp lattices
07 p1019 A72-20152

Isotope effect calculation hydrogen and deuterium solubility in fcc metals, analyzing elastic vibrational spectrum of crystal with impurity atom in internode
10 p1498 A72-24873

Dislocation bands in electrolytically hydrogen charged fcc Ni-Co alloy, describing band structure in terms of band axis and planes and Burgers vector
11 p1669 A72-26947

Ordering in fcc lattice ternary alloys with allowance for atoms interactions, noting phase transformation critical temperature and superlattices existence
13 p1976 A72-28691

Fcc lattice ferronickel alloys para-process susceptibility anomalous increase explanation by phase transition thermodynamic theory
13 p1977 A72-28911

Microscopic substructure in high temperature fatigued fcc austenitic steel and aluminum, studying cross slip lines and crack initiation
13 p1979 A72-29448

Binary ordering alloys with fcc lattice, studying volume effects on solubility of impurity atoms in interstices
13 p2023 A72-29907

Electron microscope study of precipitated fines of austenitic steel containing V and N, noting heat treatment effect on fcc crystal structure
15 p2254 A72-31523

Fcc metal defect structure due to ultrasonic fatigue observation via transmission electron microscopy for dislocations
15 p2256 A72-31836

Face centered solid crystal cell spatial distribution effect on body surface-reflected molecular beam intensity distribution
16 p2430 A72-33046

Fcc in thin films and bcc in thick vacuum condensates deposited from Nb molecular beams obtained by evaporation and condensation in mass spectrometer
16 p2407 A72-33528

Crystal lattice disarrangement by melting In-Tl alloy, noting fcc and bcc metastable phases formation during rapid crystallization
16 p2441 A72-33536

Geometric/chemical model of lattice dimensions of Laves phases of binary alloy bcc and fcc structures
16 p2409 A72-33801

Tensile deformation of Co single crystal in high temperature fcc phase, noting dislocations effect on work hardening
16 p2410 A72-33819

Effects of disorientation of grains on the viscoplastic behavior of fcc polycrystals
17 p2634 A72-35407

Viscoplasticity of face-centered-cubic metals
18 p2703 A72-37017

Microscopic substructure in face centered cubic metals fatigued at elevated temperatures.
20 p2935 A72-38880

Antiferromagnetic dispersion, absorption and light scattering in NiO and other face centered cubic crystals.
20 p2960 A72-39458

A study of the effect of grain orientation misfit on the viscoplastic behavior of polycrystalline metals /fcc system/
24 p3414 A72-45251

FACETS
U FLAT SURFACES

FACSIMILE COMMUNICATION
Molnaya-Orbit communication satellite system, discussing operational quality, maintenance, television transmission facsimile, sound broadcast and multichannel telephony
01 p0023 A72-10046

Facsimile bandwidth compression by picture elements reduction with contrast preservation, discussing analog processing algorithm and application to weather satellite photographs
06 p0772 A72-17406

High speed facsimile transmission system based on LR70 laser scanner, presenting typical system output image
15 p2248 A72-32041

Intraframe coding for picture transmission.
18 p2657 A72-36252

FACSIMILE TRANSMISSION
U FACSIMILE COMMUNICATION

FACTOR ANALYSIS
Statistical methods application to parachute materials evaluation, using factorial experiments for multiple variables simultaneous effects analysis
01 p0005 A72-10317

Factor analysis of frontal and occipital brain regions EEG indices interzonal variability, relating autocorrelation function parameters to neuron ensembles force level
06 p0764 A72-18057

Application of factorial analysis of correspondences to the compression of image signals
17 p2517 A72-35671

Dual amplitude construction possibility from general field theory couplings and propagators, considering factorization on multiperipheral configuration in translational and rotational modes
18 p2713 A72-36516

FACTORIAL DESIGN
Factorial design model of materials fatigue failure under narrow band random vibrations
01 p0140 A72-10942

Welded machine component service history effects on residual fatigue life from statistical evaluation of factor experiment
14 p2107 A72-30278

FACTORIES
U INDUSTRIAL PLANTS

FACULAE

Brightness correlation and mapping of weak photospheric magnetic fields and faculae using CN 3883-A spectroheliograms
03 p0414 A72-12927

High resolution magnetographic and spectrographic observations of plage fields and photospheric effects in weakly active regions
03 p0429 A72-13308

Plage magnetic fields associated with downward velocities from magnetograph filtergrams of opposite circular polarizations in CA I absorption line
03 p0429 A72-13312

Solar magnetic field sector boundaries, discussing photospheric field direction, activity regions, flares, coronal enhancements, faculae and geomagnetic response [AD-734627]
03 p0433 A72-13359

Solar photospheric facula blue light limb photographs, determining spatial variation in contrast levels
03 p0434 A72-13494

Solar activity asymmetry on two hemispheres in 1959-1969, considering spots, faculae, prominences and corona
05 p0718 A72-16511

Photospheric network, magnetic fields, Ca emission and continuum faculae from multichannel magnetograph observations
13 p2045 A72-29705

Solar video magnetographic observations of magnetic and H alpha plage correspondence on 21 March 1971
13 p2045 A72-29707

Sunspot energy deficit relation to model depth, deriving facular model with two dimensional radiative transfer analysis
13 p2045 A72-29712

Alfven wave transmission in sunspot umbral magnetic flux tube, noting standing progressive waves and energy dissipation in facular regions
13 p2049 A72-29937

Eleven year period solar photospheric magnetic field evolution, comparing latitudinal variation with sunspots, faculae and prominences distribution and green-line corona intensity
15 p2317 A72-32778

Sunspot area east-west asymmetry dependence on location in chromospheric facula or plage, considering solar atmosphere optical and geometric depth changes
15 p2318 A72-32787

Doppler shift of solar photospheric spectral lines related to downward motions over plages
17 p2617 A72-35705

Photospheric faculae brightness influence on solar gravitational oblateness determination, considering criticism of Dicke-Goldenberg argument on Mercury excess perihelion motion
19 p2855 A72-37239

Faculae and the solar oblateness.
19 p2855 A72-37240

Behavior of carbon monoxide in the upper photosphere
21 p3114 A72-41777

FAHRENHEIT TEMPERATURE SCALE
U TEMPERATURE SCALES

FAIL-SAFE SYSTEMS
Fail-operational automatic landing system for Boeing 747 aircraft, noting reduction in allowable minimum weather conditions in U.S. and UK
01 p0098 A72-10961

Fail-safe sequential machines realization using k-out-of-n code for state assignment and onset and off-set methods for excitation circuit construction
02 p0184 A72-11477

Fault-tolerant digital computer logic design for dynamic and interactive recovery with data integrity after error, discussing hardware and software functions requirements
02 p0184 A72-11480

Mathematical reliability modeling for fault tolerant digital computers, summarizing error masking and standby sparing reliability equations
02 p0184 A72-11481

STAR self testing and repairing fault tolerant digital computer for outerplanet exploration spacecraft, discussing architecture, reliability analysis, software and peripheral system automatic maintenance
02 p0184 A72-11482

Soviet progress and bibliography on fault tolerant digital computers design, emphasizing redundancy application to achieve high reliability
02 p0184 A72-11484

Ultrareliable fault-tolerant digital computer design with protective standby replacement and hybrid redundancy, presenting mathematical models for system reliability evaluation
02 p0185 A72-11487

Three-failure-tolerant digital computer system design using adaptive majority voting in hardware and software for real time control application
02 p0185 A72-11488

Distributed fault-tolerant aerospace digital computer design with duplicated central multiprocessor,

- triplicated memory and conventional redundancy local processors for error detection and correction 02 p0185 A72-11489
- Hardware and software parallel digital computer system described by flow table model, calculating output hazard for unbounded line delay effects 02 p0185 A72-11490
- Government role in widebody aircraft introduction to air carrier service, discussing aircraft maintenance, design and fail-safe structural configurations 07 p0911 A72-18831
- Engine out flight training safety, recommending certification requirements or training procedures changes 07 p0911 A72-18834
- Lunar landing mission escape and rescue concepts, considering emergencies during earth orbit, translunar, lunar orbit, surface and rendezvous, transearth and earth reentry phases 09 p1396 A72-23157
- European Special Space Tug electronic subsystem requirements, considering strapdown inertial measuring unit, remote sensors, computer and fail-safe backup system 09 p1396 A72-23258
- N fail-safe logics for circuit fault restoration, comparing with failure probability of majority voting scheme and quadded logic 09 p1283 A72-23420
- DC 10 aircraft automatic flight guidance system, noting dual-dual fail-passive autoland 09 p1349 A72-23448
- Executive job handling program for operation with fault tolerant multiprocessor in real time control environment 10 p1442 A72-23816
- Fault tolerant redundancy for manned spacecraft computers considered as long term desirable solution from cost analysis 10 p1443 A72-23819
- Steering algorithm for fail-safe guidance of continuously thrusting interplanetary spacecraft to maintain ballistic intercept target objective 15 p2271 A72-32195
- Aerospace vehicle explosive components initiation, separation and destruct systems 16 p2443 A72-33361
- Random multiple access data transmission systems with feedback for message confirmation and retransmission in event of errors, evaluating channel capacity 16 p2372 A72-33794
- Achieving fail safe design in rotors. [AHS PREPRINT 673] 17 p2491 A72-34513
- Analysis of a partially cracked panel. 18 p2735 A72-36771
- Quadruple-redundancy management for fly-by-wire control system reliability, discussing analog circuit and digital computer voter/monitor techniques [AIAA PAPER 72-884] 20 p2910 A72-39117
- Failsafe hydraulic actuator flight control for jet aircraft. 20 p2890 A72-39351
- Reliability prediction of a two-unit standby redundant system with standby failure. 20 p2929 A72-39855
- Concorde electrically signalled fly by wire control system with mechanical linkages for standby fail-safe redundancy 21 p2994 A72-41068
- The fatigue and fail-safe program for the certification of the Lockheed Model 286 rigid rotor helicopter. 24 p3366 A72-44733
- The importance of service inspection in aircraft fatigue. 24 p3367 A72-44740
- Fault-tolerance experiments with the JPL STAR computer. 24 p3383 A72-45671
- A prognosis on fault-tolerant digital control systems. 24 p3383 A72-45672
- FAILURE**
- NT ENGINE FAILURE
- NT FAILURE ANALYSIS
- NT STRUCTURAL FAILURE
- NT SYSTEM FAILURES
- FAILURE ANALYSIS**
- Nylon parachute materials failure mechanics, considering friction, light, chemical and thermal effects 01 p0005 A72-10316
- Irredundant multiple output combinational logic network fault detection and diagnosis theorems derivation from structural models in labeled direct graph form 02 p0184 A72-11478
- Signal flow graph theory based computer diagnosis using blocking gate approach, constructing algorithm for gates optimal locations determination for maximum faults distinguishability 02 p0184 A72-11479
- Minimum length fault tests design for irredundant combinational logic circuits containing single faults based on Boolean difference function 02 p0185 A72-11485
- Random and algorithmic procedures employing three-valued logic system for sequential circuits fault detection test sequence generation 02 p0185 A72-11486
- Reliable combinational logic networks, deriving conditions for fault locatability from directed graph formal model 02 p0185 A72-11491
- Stress and failure analysis of glass-epoxy composite plate with circular hole under uniaxial tension by finite element method [SESA PAPER 1942] 02 p0248 A72-11517
- NASA quality assurance program, discussing management planning, assessment, failure prevention and cost effectiveness 02 p0304 A72-11554
- Redundancy with repair for system mean time to first failure, presenting differential equation coefficients for Markov process 02 p0236 A72-11556
- Single malfunction diagnosis models in systems failures, describing fixed and sequential testing schedules 02 p0186 A72-11689
- Reliability behavior of complex systems with standby redundancy under different failure and repair echelons 02 p0194 A72-12446
- Optimal smoothing application to testing of inertial navigation systems, gyros and component failure detection during mission 02 p0258 A72-12810
- Polycrystalline materials wedge crack growth enhancement by vacancy diffusion under creep failure conditions, considering grain boundary sliding mechanism 03 p0442 A72-12998
- Voltage contrast mode scanning electron microscopy application to defect and failure analysis of semiconductor memories 03 p0336 A72-14288
- Microcircuit failures due to electrical overstress, covering current density, thermally induced burn-out, junction shorts and second breakdown with nonuniform heat flow 03 p0336 A72-14290
- Oxygen hazards, mishaps and safety programs in NASA operations, considering material, design, cleaning and procedural deficiencies and failures 04 p0564 A72-14436
- Logically stable failures of discrete combination devices by practical behavior in response to given input vectors, using alpha state Boolean algebras 04 p0496 A72-14994
- German monograph on thermionic power supply equipment converter network reliability covering I-V characteristics and failure probability calculation 04 p0466 A72-15696
- Distortional energy theory for predicting failure of orthotropic materials exposed to three dimensional stress state [ASME PAPER 71-WA/DE-13] 05 p0732 A72-15942
- Composite materials durability and strength estimations, using reliability theory for failure rate characteristic 05 p0680 A72-15991
- Combinational tree networks of AND and OR gates without internal fan-out, proposing test generation strategy for maximizing detected multifault sets size 05 p0640 A72-16163
- Fatigue failure tests of soldered joint in solar cell interconnector designs under extended temperature cycling 05 p0615 A72-16552
- Bayesian analysis of onboard computer controlled aircraft avionics subsystem built-in test for failure detection 05 p0638 A72-16574
- Time to failure statistics for communications satellites redundant systems with spares and negative exponential reliability function, discussing perfect and imperfect switching 05 p0731 A72-17250
- Failure analysis of plastic materials susceptible to cyclic strain hardening under thermal load, considering residual stress concentration 06 p0898 A72-18547
- Fiberglass reinforced plastics under constant strain rate, deriving failure models as random process for microscopic crack propagation 06 p0898 A72-18548
- Gas turbine blades fatigue crack development and failure analysis under thermal cycling tests, considering chemical processes and thermal and mechanical stresses 06 p0898 A72-18550
- Diffused failure model as basis for plotting delayed fracture curves in space of principal stresses 06 p0898 A72-18552
- Low cyclic failure resistance at elevated temperatures and static defects calculation based on fatigue and empirical endurance curves 06 p0898 A72-18555
- Fibrous composite materials experimental failure studies at high temperatures and cyclic loading 06 p0838 A72-18654
- Spacecraft incipient failure detection, stressing acoustic energy release techniques 07 p0964 A72-18829
- Complex sampling with cascaded triple input majority logic redundant systems, deriving failure probability 07 p0949 A72-19173
- Failure analysis probability for structures excited by randomly varying dynamic loads, comparing Gaussian and filtered Poisson processes 07 p1093 A72-19948
- DC-10 aircraft automatic landing performance and failure assessment monitor system 08 p1204 A72-21003
- Quantitative and qualitative reliability estimates for electronic and mechanical products, obtaining conditional probabilities of flawless operation 08 p1179 A72-22052
- Reliability of redundant schemes with quorum element, noting optimal parameters for known failure damages 08 p1180 A72-22059
- Reliability theory distribution function construction for failure analysis in physical processes, considering mechanical system service life and living organisms life span 08 p1180 A72-22062
- Reliability tests improvement by ergodic processes failure prediction and data storage for high reliability products manufactured in small numbers 08 p1180 A72-22067
- Radio system failure prediction based on parameter variation a priori or a posteriori data, determining reliability and optimal preventive maintenance intervals 08 p1143 A72-22070
- Crystalline ceramics compressive fracture strength and microhardness tests at room temperature, suggesting microplasticity role in failure mechanisms 09 p1334 A72-22388
- Creep test for microfailures of glass reinforced epoxy and polyester laminates immersed in water at ultimate flexural stress 09 p1336 A72-22537
- Fatigue failure mechanism in short fiber reinforced plastics, determining crack growth rates under cyclic loading [PI PAPER 2] 09 p1336 A72-22539
- Nonlinear creep characteristics of variably thick rotating disks under nonuniform heating conditions, determining critical rpm and temperature field and time to failure 09 p1402 A72-22731
- Time and cycles to failure diagrams for strain rate and hold periods effects on high temperature metal creep fatigue in design analysis 09 p1407 A72-23199
- N fail-safe logics for circuit fault restoration, comparing with failure probability of majority voting scheme and quadded logic 09 p1283 A72-23420
- Failure modes, effects and criticality analysis method for evaluating spacecraft reliability characteristics 10 p1485 A72-23974
- Bayesian analysis application to reliability and life parameter estimation for Weibull failure model, using Monte Carlo simulation 10 p1503 A72-23978
- Random access memory with single error correction circuitry, predicting failure, card and module removal rates by computer simulation 10 p1443 A72-23980
- Computer reliability in terms of design criteria to minimize faults incidence, discussing failures detection and correction, fault diagnosis and system maintenance 10 p1444 A72-23985
- Reliability and time to failure prediction for degradation-prone systems via Markov processes theory 10 p1504 A72-23988
- Dormant aerospace electronic system sedentary or nonoperating failure rate analysis by prediction technique 10 p1447 A72-24008
- Reliability prediction for MOS/LSI devices based on chip circuit configurations evaluation, extrapolating bipolar IC failure rate model 10 p1447 A72-24009
- Complex system represented by fault-free with independent components, calculating confidence interval for failure probability by moment method 10 p1444 A72-24018
- System reliability improvement technique for identification and prevention of failures, using Experience Storage Program for design problem documentation collecting, storage and retrieval 10 p1486 A72-24021
- System diagnosis based on ordered statistical samples, discussing Kolmogoroff-Smirnoff detector use for on-line computers in testing noisy systems 10 p1482 A72-24597

Approximate stress intensity factor for corner flaw emanating from quarter infinite solid edge, based on Smith solution for semicircular flaw

10 p1559 A72-24898

Russian book on aircraft engine reliability covering defects, fractures and failure analysis, service life prediction, production deficiencies and operational conditions

11 p1706 A72-26068

Theoretical fatigue test procedure for reliability analysis of machine parts, calculating fatigue probability in load carrying components

11 p1640 A72-26244

Automatic search for Huffman sequential logic circuit breakdown detection sequence, using VEGA program through matrices and graphs utilization

11 p1612 A72-26549

Onboard localization of aircraft electrical equipment failures, using list checkout, automatic indication and dynamic programming method

11 p1578 A72-26895

Fatigue failure information in structural design, considering low cycle, cumulative damage and time dependent conditions

12 p1884 A72-27641

Reliability lower confidence limit estimation for serial systems with failure in any subsystems resulting in overall failure

13 p1962 A72-28362

Failure rate function nonparametric estimators comparison on basis of asymptotic and Monte Carlo mean square errors

13 p1985 A72-28364

Mathematical models for complex system debugging in initial life period, noting maximum likelihood estimates for failure rate functions

13 p1962 A72-28365

Finite time element method for failure probability prediction in multiple load-path system with random loads, noting flow chart for suggested computer program

13 p2052 A72-28369

High temperature low cycle fatigue of alloys as process of crack nucleation and growth to ultimate failure

13 p2058 A72-29445

Failure phenomena relationship to kinetic equation for defect buildup from brittle fracture analysis of composite glass plastic in uniaxial eccentric tension

14 p2164 A72-30426

Stress relieving heat treatment for service failure prevention of stressed austenitic stainless steel components of high temperatures, noting cracking regulation by oxidation mechanism

14 p2117 A72-30538

Solid rocket propellants storage life analysis and prediction by mathematical modeling of physical-chemical failure generating processes

14 p2145 A72-30762

Product reliability prediction from failure mode analysis, examining component design, quality control, engineering analysis configuration selection and product testing

[ASME PAPER 72-DE-17]

14 p2108 A72-30863

IC reliability assessment based on defects and failure mechanisms analysis instead of MTBF estimations

14 p2091 A72-31166

FRAM /failure rate appraisal machine/ concept and application for modular electronic and electromechanical assemblies environmental cycling tests, noting technical and economical effectiveness

14 p2093 A72-31169

Time to failure under axial tension determined for gallium selenide single crystals at constant temperatures, noting tensile strength dependence

15 p2290 A72-31387

Soft gyro and accelerometer failure detection for redundant gimbaled inertial measurement units by skew sensors

15 p2270 A72-32187

Optimal algorithm for failure detection and identification in redundant gyro-accelerator sensor systems, including Monte Carlo simulation

15 p2270 A72-32188

Failure detection techniques for Space Shuttle redundant multiple gimbaled inertial measurement units, using simulated boost and entry trajectories

15 p2270 A72-32189

Particulate composite model deformation and failure behavior under plane uniaxial compressive stress, using finite element method

15 p2258 A72-32556

Mathematical model for reliability analysis of modularly redundant electronic systems with unequal failure rates for operating and standby units

16 p2398 A72-33344

Weibull distribution parameters estimation for general device class from limited failure data through regression models, using least squares method

16 p2398 A72-33349

Russian book on metal fatigue and inelasticity covering structural inhomogeneities, static and dynamic loading, failure mechanisms, deformation, temperature effects and test methods

17 p2566 A72-34649

Development of electronic part failure rates for long-duration space missions.

17 p2527 A72-34684

Weibull life tests of Kemet solid tantalum chip capacitors at high accelerated voltages.

17 p2527 A72-34685

Techniques for control of long-term reliability of complex integrated circuits. II - A technique for the prediction of failure rates for MSI and LSI devices.

17 p2528 A72-34687

Failure analysis of plastic and ceramic packaged IC, describing plastic encapsulants chemical removal and radiographic failure detection procedures

17 p2528 A72-34707

On the measurement of mechanical tension in plastic encapsulated devices by means of piezo-resistance.

18 p2669 A72-37112

Production and test facilities availability effect on costs involved in obtaining item at required quality level, examining component rejects and defectives

18 p2670 A72-37133

A model of a nonlinear viscoelastic medium allowing for the effects of cumulative damage

19 p2871 A72-37528

Regularities in the deformation and failure of commercial iron in a complex stress state under low-temperature conditions

19 p2818 A72-38005

Interpreting electron fractographs of stress corrosion in aluminum alloys.

19 p2821 A72-38387

Maximum likelihood failure detection for redundant inertial instruments.

[AIAA PAPER 72-864]

20 p2923 A72-39133

Creep-fatigue interaction interpretation for austenitic stainless steels from crack growth viewpoint, investigating time and cycle dependent failure at elevated temperature

20 p2937 A72-39213

The broad range detection of incipient failure using the acoustic emission phenomena.

20 p2925 A72-39286

Probability model and causal approach to failure mechanisms and reliability of control systems applied to IC

21 p3024 A72-40711

Failure diagnostics in mathematical models of automatic control systems

21 p3038 A72-40712

Miniaturized IC semiconductor device fabrication and failure under electrical load, using scanning electron microscope

21 p3035 A72-41492

Investigation of fatigue-failure mechanisms and inelastic deformation of metals in torsion

21 p3071 A72-41703

Signal classification through quasi-singular detection with applications in mechanical fault diagnosis.

22 p3158 A72-41976

Computer-operated data acquisition and control system for automatic diagnostic monitoring of propulsion research instrument

22 p3216 A72-42684

Fracture analysis for linear elastic material in antiplane strain, discussing fast moving cracks propagation, flint knapping and equations of motion

22 p3237 A72-42801

Transport aircraft wing compression panel failure in bending test due to stringer interruptions, analyzing structural deficiency via column and beam bending theories

22 p3183 A72-42827

Dangerous structural failure characteristics due to idealized design optimization, discussing shell buckling instabilities

22 p3240 A72-42895

Statistical method of failure analysis for redundancy forms selection, noting aircraft safety and reliability

22 p3139 A72-42973

Prediction of thermal-shock resistance during heating at very high rates.

22 p3241 A72-43000

Man serviced spacecraft systems reliability and maintainability optimization methodology, developing parametric data based on failure modes analysis, components MTBF, duty cycles, redundancy and costs [SAWE PAPER 943]

23 p3343 A72-43483

Fracture mechanics of composites.

23 p3345 A72-43509

Asymptotic reliability estimates of monotonically structured complex logic systems with low and high component failure rates equivalent with exponential or Weibull distributions

23 p3267 A72-44004

Electron fractography of fatigue failure and macrocrack propagation in dual phase Ti alloy during cyclic loading at minus 140 to plus 150 C

23 p3303 A72-44097

Charts for confidence limits and tests for failure rates.

23 p3294 A72-44395

Logical groupings of preventive maintenance and replacement policies for stochastically failing items to reduce cost under continuous surveillance

24 p3406 A72-44653

An interactive approach for the generation and verification of test sequences in a logic system

24 p3382 A72-44662

Robert Bruce's spider problem extended - Reliability of adaptive experimental systems.

24 p3406 A72-44666

The problems of reliability growth and demonstration with military electronics.

24 p3384 A72-44670

Reliability analysis based on time to the first failure.

24 p3455 A72-44727

Automatic software diagnostic package for airborne computer, using testing computer for decision making based on received data

24 p3383 A72-45669

Fault-tolerance experiments with the JPL STAR computer.

24 p3383 A72-45671

Composite materials durability and strength estimations, using reliability theory for failure rate characteristic

24 p3418 A72-45733

Mechanical properties of heat treated hardened high strength steel, investigating microstructure relationship to failure characteristics

24 p3416 A72-45734

Graphites fracture under thermal stresses, considering stress-strain relations calculation method for annular samples

24 p3418 A72-45762

FAILURE MODES

Failure modes of IC containing MOS devices, considering threshold voltage variations, oxide and silicon defects and leakage

02 p0194 A72-12443

High intensity ionizing gamma ray pulsed radiation effects on Gunn diode microwave oscillator failure modes

03 p0334 A72-14089

Anodized aluminum metallization for reducing electromigration induced failure modes in silicon wafers

03 p0365 A72-14286

Thermal deformation effects on metal bond fatigue failure modes in small signal transistors, micro and LSI circuits

03 p0365 A72-14291

Bonding mechanisms and failure modes in thermocompression bonds of Au plated leads to Ti-Au metallized substrates, discussing Cu lead frames plated with Ni and Au

03 p0365 A72-14292

Anodic layer thickness effect on fatigue crack initiation and fracture mode in mono and polycrystalline aluminum

05 p0672 A72-16015

MOS IC reliability based on p-channel enhancement mode transistors, discussing failure modes and mechanisms

08 p1142 A72-21588

Laser radiation effects on optical glass volume and surface, discussing failure characteristics

08 p1182 A72-21655

Reliability analysis of redundant and nonredundant systems with different component failures, using probability theory

08 p1180 A72-22053

Functional readiness of periodically inspected recoverable systems with different failure causes

08 p1180 A72-22055

Helically bound wire reinforced sprayed Al tubes and rings, investigating failure mechanism dependence on fracture modes from tensile and bending tests

09 p1330 A72-23174

Failure modes, effects and criticality analysis method for evaluating spacecraft reliability characteristics

10 p1485 A72-23974

Failure mode control in plastic packaged IC for screening and quality assurance

10 p1447 A72-24010

Fatigue failure modes of composite materials, considering fiber breakage, delamination, matrix cracking, interface debonding and void growth

11 p1670 A72-25461

Failure modes effect on compressive strength of boron-epoxy composites tested on coupons, honeycomb sandwich columns and beams

11 p1671 A72-25466

Mathematical model for digital systems reliability, determining probability of success and of various failure modes

13 p1923 A72-28356

Axisymmetric ductile rotating shaft failure modes, considering fatigue, buckling and impact stress factors [ASME PAPER 72-DE-40]

14 p2167 A72-30873

Mechanical properties of composite materials, discussing elastic deformation and failure modes

15 p2260 A72-31442

Local buckling analysis for triangular-corrugated core sandwich panels in compression, noting buckling mode nodal line features

15 p2326 A72-31709

Electronic circuit reliability prediction model with statistical dependence for detailed failure modes

16 p2371 A72-33345

- Stress and parametric change analysis for failure mode identification and reliability screen tests of LSI circuits, noting MOS inverter operation and RAM mechanization
17 p2528 A72-34706
- Observations of failure modes in carbon composite materials.
17 p2571 A72-35288
- Reliability analysis of an intermittently used system with N types of failure.
18 p2693 A72-36024
- Composite materials crack propagation and failure modes leading to fracture instability, discussing maximum strength conditions and fatigue
18 p2703 A72-36394
- Reliability assurance of space equipment components, discussing drift and failure modes, computerized simulation and thermal maps
18 p2743 A72-37127
- Test structures - Powerful technique for quality evaluation and reliability assessment of MSI and LSI /medium and large scale integrated circuits/
18 p2671 A72-37143
- The grain-size-dependences of the failure mode and ductility transition temperatures of melted chromium and tungsten.
20 p2935 A72-39139
- Designing to avoid stress-corrosion and/or fatigue failures.
[AICHE PAPER 15C] 21 p3116 A72-40125
- Cyclic stress-strain induced buckling and fatigue failure in cold-rolled steel and tabulating and diagramming mechanical properties
21 p3065 A72-40233
- Low carbon steel S-N diagram for stresses ranging to fatigue limit, noting cyclic creep, macroplastic cyclic stress and fatigue failure
21 p3122 A72-41353
- Non-linear rotor bearing behavior.
21 p3061 A72-41518
- Ti based beta alloy strain hardening and failure characteristics, emphasizing initial deformation phase and microdefect onset and development
21 p3071 A72-41716
- Thermoplastics fatigue life dependence on stress with allowance for heating laws, noting heat accumulation effect on thermal failure
22 p3196 A72-42164
- Boundary value problems for concentrated forces acting inside semiinfinite anisotropic plate under plane stress, investigating failure modes of unidirectional composites
23 p3344 A72-43495
- Aluminum matrix composites fracture mechanism dependence on static loading conditions and reinforcing filament type, investigating failure modes in tension and compression tests
23 p3299 A72-43497
- Elastomers fracture strength and failure modes under tension, tearing, ozone cracking, fatigue and abrasive wear associated with viscous resistance energy losses
23 p3305 A72-43506
- Mechanics of failure of fibrous composites.
23 p3345 A72-43508
- Accelerated life testing of thick film resistors.
24 p3384 A72-44668
- Cumulative damage stochastic models and distributions of strength of steels and graphite.
24 p3412 A72-44673
- FAIRCHILD MILITARY AIRCRAFT**
U MILITARY AIRCRAFT
- FAIRINGS**
Motion equations of constrained split fairing for avoiding contamination of sounding rocket payload environment by uncontained explosive actuation device
05 p0724 A72-16102
- FALKNER-SKAN EQUATION**
Reversed flow solutions of Falkner-Skan equation in boundary layer theory
11 p1676 A72-25361
- Boundary value problems in boundary layer theory, discussing Falkner-Skan equation similar solutions existence theorems
11 p1677 A72-25525
- Falkner-Skan problem extension to MHD flow past nonconducting body by imposing magnetic field with lines of force parallel to undisturbed streamlines
15 p2287 A72-32405
- Numerical check on boundary layer equations asymptotic expansion solutions for Falkner-Skan reverse flow and unit Prandtl number compressible boundary layer with blowing
15 p2219 A72-32589
- Unsteady Falkner-Skan flow solution by finite difference method for pressure gradient effect on transient response of laminar boundary layer
16 p2376 A72-33015
- Falkner-Skan flows with slip.
23 p3281 A72-44068
- FALLING SPHERES**
Extraterrestrial magnetic spheroid concentrations observed in October 1967 and 1969 proposing relationship to rainfall frequency
08 p1226 A72-21109
- Nonstable oscillating motions positive measure set in dynamic system with noncompact phase space, considering elastically rebounded falling sphere on horizontal plate
08 p1210 A72-22188
- Atmospheric density variations from meteorological rocket soundings, discussing data reduction methods and error sources for bead thermistor and inflatable falling sphere instruments
11 p1626 A72-26473
- FAN IN WING AIRCRAFT**
Fan-in-wing model noise due to cross flow generated in- and outflow distortions and unsteady rotor blade forces
[ASME PAPER 72-GT-92] 11 p1571 A72-25666
- Flow distortion and performance measurements on a 12-inch fan-in-wing model for a range of forward speeds and angle of attack settings.
22 p3134 A72-42323
- FANLIFT DEVICES**
U LIFT FANS
- FANS**
Fan noise estimation from equation involving delivery volume and pressure to correct ratings to generated sound power levels
16 p2377 A72-33323
- Investigations on the stability of the characteristic of radial flow fans.
24 p3363 A72-45356
- Application of cascade and actuator disc theories to computer aided design of fans.
24 p3363 A72-45359
- An approximate method for the calculation of the characteristics of axial-flow fans.
24 p3363 A72-45369
- FAR FIELDS**
Far field patterns of hourglass reflector phased array for electronic despin of communications antenna on spin stabilized satellite
01 p0029 A72-10666
- Corrugated conical horn antennas with arbitrary groove depth, considering far field radiation patterns
01 p0040 A72-10680
- Far field diffraction due to annular apertures of plane wave light rendered partially coherent by atmospheric turbulence
01 p0103 A72-11166
- Spherical aberration effect on far field Fraunhofer diffraction for circular aperture illuminated by quasihomochromatic partially phase coherent light
01 p0103 A72-11188
- Fraunhofer hologram for recording square of modulus of far field radiation pattern due to mixture of known and unknown source distributions
02 p0224 A72-11548
- Gas dynamic laser analysis based on phase cancellation model, showing flow induced phase nonuniformity minimization for far field intensity improvement
[AIAA PAPER 72-217] 05 p0669 A72-16857
- Subsonic wind tunnel investigation of aircraft wake far field structure, measuring trailing vortex decay by yawhead pressure probe
[AIAA PAPER 72-40] 05 p0607 A72-16902
- E-plane dielectric slabs symmetrical loading effects on horn aperture efficiency enhancement from far field calculation
[AD-738714] 06 p0781 A72-17347
- Radio waves arrival angles distribution function in Fraunhofer diffraction zone upon plane wave normal incidence on inhomogeneous scattering layer
07 p0938 A72-19017
- Displacement and profile diffractographic measurement using changes in far field diffraction patterns of slit aperture between test and reference object
[CLEA PAPER 11.5] 07 p0984 A72-19390
- Antenna optimal radiation patterns, discussing antenna synthesis based on desired far field characteristics
08 p1138 A72-20743
- Gain function for planar phased array far field pattern, deriving calculation method for excitation pattern for prescribed radiated beam behavior
08 p1132 A72-21328
- Far field radiation pattern from magnetic line source covered with moving uniaxial or isotropic nondispersive dielectric or cold plasma sheaths
08 p1137 A72-21985
- Atmospheric refraction effects on IR far field irradiance distribution based on model of nonlinear interaction including absorption, transverse flow and vibrational relaxation effects
09 p1350 A72-22607
- Monograph on slotted circular waveguide analysis covering boundary value problem solution by Wiener-Hopf and Galerkin procedures and application to far field determination
09 p1279 A72-22925
- Electromagnetic wave scattering by arbitrarily oriented circular ice cylinders, deriving far field intensities for linearly polarized incident waves
09 p1280 A72-23341
- Hypersonic vehicle far field behavior for sonic boom strength, position and positive phase duration
11 p1617 A72-26002
- Far field diffraction of Gaussian light beam passing through ultrasonic cylindrical standing waves
11 p1687 A72-26052
- Radiation resistance of baffled beam modes from far field acoustic power intensity
11 p1687 A72-26058
- Radiation resistance for natural modes of rectangular panel from far field acoustic radiation energy distribution
11 p1687 A72-26059
- Diffraction coefficients of scalar field for higher order edges and vertices, noting far field behavior of boundary layer expansion
11 p1617 A72-26158
- Near and far field energy and power density distributions of multi-transverse mode double discharge TEA laser beam
[AD-743823] 11 p1651 A72-26671
- Microwave antenna radiation patterns from far field measurements by radio holograms with probe
11 p1598 A72-26718
- Radiation patterns of circular loop antenna in isotropic compressible plasma, discussing far fields for electromagnetic and electron plasma waves
12 p1790 A72-27491
- Torsional waves far-field structure in infinite elastic rod of elliptical cross section, using perturbation method
13 p2057 A72-29004
- Beam divergence prediction for multiple transverse laser modes, proposing tables and graphs to determine angular spread in far field
15 p2247 A72-32031
- Plane electromagnetic wave diffraction on periodic arbitrary profile array, presenting near and far field asymptotic characteristics
15 p2202 A72-32660
- Far field sonic boom approach effects, describing Whitham theory extension for ultimate N wave deviations for body configurations with continuous or discontinuous tangent
16 p2347 A72-33010
- Radiation from a magnetic line source covered with an anisotropic warm plasma slab.
17 p2587 A72-34386
- Theoretical analyses on Apollo lunar surface electrical properties experiment transmitter antenna.
17 p2515 A72-34423
- Focused irradiance fluctuations beyond a layer of turbulent atmosphere.
17 p2518 A72-35754
- Transient acoustic point source disturbance transmission in two dimensional idealized jet, noting velocity profile effects on noise radiated to far field
18 p2679 A72-36406
- Diffraction by an aperture between two wedges.
18 p2712 A72-36938
- A theoretical calculation of edge smear in far-field holography.
19 p2797 A72-37610
- Plane TE polarized electromagnetic wave diffraction on infinite conducting cylinder in nonhomogeneous medium, calculating far field diffraction patterns
19 p2768 A72-38656
- Integral equation and optics methods for far field radiation characteristics calculation of plane antennas with arbitrary reflector-source configurations
21 p3029 A72-40522
- Eigenvalues associated with balanced hybrid modes expressed in closed form to derive conical scalar horn antenna far field radiation patterns
21 p3032 A72-40630
- Single transverse mode operation of a pulsed volume excited atmospheric pressure CO₂ laser using an unstable resonator.
21 p3064 A72-41197
- Diffraction by an infinite corner reflector transversely loaded by concentric dielectric slabs.
22 p3159 A72-42301
- Machine code for finite difference solution of wake vortex governing equations and far flow field prediction in trailing vortices, developing turbulent energy model
[AIAA PAPER 72-989] 22 p3134 A72-42326
- Master oscillator/power amplifier laser systems output beam divergence and far field brightness, comparing to Gaussian plane waves
23 p3296 A72-43901
- Time variations in the far-field diffraction patterns of spatial modes from electron-beam-pumped semiconductor lasers.
24 p3409 A72-44712
- FAR INFRARED RADIATION**
Far IR Fourier spectrometer with built-in real time digital computer for routine physical and chemical spectroscopy
04 p0520 A72-14523

Gallium-doped Ge bolometers and triglycine sulfate pyroelectric far IR detector, testing performance as functions of frequency and temperature
04 p0525 A72-15601

Photoconductive detection and generation of far IR radiation in high purity epitaxial GaAs
04 p0563 A72-15605

Far IR molecular laser variable interference filter for optimization of output coupling conditions and maximum power output
04 p0532 A72-15616

Ruling defects of echelette diffraction gratings for far IR high luminosity spectrometers
05 p0689 A72-16192

CW gas laser operating in far IR, discussing water vapor excitation by dc discharges
07 p0946 A72-19961

Transmission and passband properties of polyethylene echelette gratings and combined filters for long wave IR spectrum
08 p1210 A72-22038

Michelson interferometer application for continuous gas analysis in far IR
10 p1480 A72-24174

Ground based IR astronomical telescope detectors, relating F number and optical requirements to near, far, and intermediate IR observation
10 p1481 A72-24249

Spherical specularly reflecting nonresonant cavities for use as absorption cells in far IR spectroscopy, predicting performance
11 p1629 A72-25301

Far IR filters for rocket-borne radiometer, discussing UH theory and characteristic impedance determination
11 p1629 A72-25310

Upper atmosphere mm emission spectrum from aircraft observation, comparing with rocket and ground based data
13 p1923 A72-29963

Cooperative enhanced scattering cross section of far IR laser radiation from nonthermal theta pinch plasmas in weak magnetic field
15 p2288 A72-32417

Hydrogen to helium mixing ratio in giant planets from far IR spectroscopy for atmospheric thermal models and greenhouse effect calculations
15 p2315 A72-32727

Variable output coupling device for far infrared laser.
17 p2562 A72-34643

Low temperature interference filter design for atmospheric windows far IR photometers based on selective reststrahlen reflection of crystals
19 p2796 A72-37586

Far-infrared and uvby photometry of V 1057 Cygni.
20 p2973 A72-39887

Pure and compensated Ge and Si far IR spectral properties at liquid He temperatures for bolometer detector application
21 p3013 A72-40822

Optical properties of transmission echelette high-pass filters.
21 p3055 A72-40823

Absolute measurement of the solar brightness in the spectral region between 100 and 500 microns.
22 p3225 A72-42389

Directional far IR emission from sunlit lunar surface, determining brightness temperature as function of observer and sun elevation angles and surface parameters
22 p3226 A72-42537

FAR ULTRAVIOLET RADIATION

NT LYMAN ALPHA RADIATION

NT LYMAN BETA RADIATION

Photometric calibration of long wavelength vacuum UV standards by synchrotron and plasma black body radiation
01 p0073 A72-11399

Stabilized hydrogen plasma arc spectral radiation as light source for vacuum UV radiometry, comparing output with W strip and carbon sources
01 p0073 A72-11400

Solar flares far UV radiation time structure correlation with hard X rays
02 p0272 A72-11773

EUV and soft X ray images of sun from sounding rocket experiments
03 p0415 A72-12934

Solar flare EUV flashes from sudden ionospheric frequency deviation observations
03 p0407 A72-12946

High spatial resolution solar X-ray and far UV instruments, employing glancing incidence optics
03 p0353 A72-13045

Far UV astronomical studies with moderate spectral and spatial resolution instruments, discussing Lyman alpha line background
03 p0417 A72-13049

Integral image tube optical systems for far UV narrow band and broad bandpass photography from spacecraft outside atmosphere
03 p0355 A72-13063

Vacuum UV spectra of free plasma column in microwave field at high pressures for discharge in helium-deuterium mixture
03 p0394 A72-13084

Extreme UV observations of solar chromosphere-corona transition region, evaluating various theoretical and empirical models
03 p0422 A72-13205

Solar far UV spectrum observations for chromospheric coronal structure determination, reviewing ionization balance, relative abundances and limb/disk ratios
03 p0423 A72-13216

Late twilight airglow vacuum UV spectra from sounding rocket observation, noting conjugate-point electron excitation role in O I emissions
03 p0350 A72-13525

Oso-3 satellite observation of solar flare associated EUV bursts, comparing with microwave radio bursts [AD-739641]
03 p0413 A72-13529

Formaldehyde photoionization and absorption spectrum measurements in vacuum UV region, using single configuration self consistent field procedure for Rydberg states and model
03 p0321 A72-13856

Vacuum UV irradiation of silicon dioxide, discussing positive charging for photon energies above threshold for electron-hole pair creation
03 p0403 A72-14080

Early type supergiant far UV spectrum observations, showing broad absorption feature near 1720 Å
04 p0578 A72-15315

Extreme UV observations of flare surge at solar limb
05 p0710 A72-16520

Interstellar extinction curves for stellar far UV radiation, discussing required multicomponent interstellar dust model
05 p0720 A72-16717

Neutral B I vacuum UV spectra from hollow cathode light source, remeasuring electron transitions to higher accuracy
06 p0852 A72-17896

Carbon like spectra and ground energy levels of Sc, Ti and V ions in 16-22 Å range, using vacuum spark source
07 p1037 A72-19833

Far UV Al line spectra from laser produced plasma in 35-50 Å range
07 p1038 A72-19835

Thermal plasma origin of solar X-ray emission and far UV flash observation during 28 August 1966 proton flare
07 p1060 A72-20013

Far UV view of Orion from Aerobee rocket-borne monochromatic camera photographs of Orion-Monoceros-Canis Major region
08 p1164 A72-20994

Atomic, ion and electron transition pulsed gas discharge lasers, considering power efficiency factors, vacuum UV region and gas density
08 p1182 A72-21644

Extreme UV absorption cross sections ratios for atomic oxygen in upper atmosphere, observing solar radiation attenuation with satellite instruments
09 p1297 A72-22578

Molecular gases absorption coefficients measurement in extreme UV, analyzing photoionization curves in energy range far beyond threshold
09 p1356 A72-22829

Absorption by Nd laser generated ionized Al plasma of extreme UV radiation due to inverse bremsstrahlung and photoionization
09 p1360 A72-22831

Vacuum UV excitation cross sections measurement by electron impact on nitric oxide, tabulating threshold energies and transition probabilities
09 p1357 A72-22857

EUV resonance radiation from He atoms and ions in geocorona, comparing model calculation based on solar radiation resonance scattering with rocket experiments
09 p1378 A72-23010

Early phase time development of far UV line radiation from plasma production by focusing Q switched ruby laser onto solid Mg target
09 p1325 A72-23232

Double beam scanning vacuum UV spectrometer and logarithmic radiometer for reflectivity and transmission measurements on solids, liquids and gases [AD-745497]
09 p1313 A72-23329

Relative intensity of solar XUV emission lines of Li isoelectronic sequence ions, taking into account transitional collision strengths
09 p1391 A72-23532

Electron impact excitation of nitric oxide in vacuum UV, measuring absolute cross sections for emission features [AD-742536]
10 p1515 A72-24341

Programmed electro-optical systems of multichannel solar spectrometer for ground observations of X ray and EUV emission regions
11 p1630 A72-25680

Fluorescence and absorption spectra from oxygen sulfur dichloride photodissociation in vacuum UV, discussing So formation
11 p1590 A72-26012

Auroral spectrum analysis in 1200-4000 Å band, obtaining photon emission rates
11 p1624 A72-26402

Stimulated laser emission in vacuum UV by liquid Xe excitation with electron beam, determining threshold current density, radiation divergence and line half width
12 p1820 A72-27582

Extreme UV solar images televised in flight with rocket-borne SEC vidicon system, noting pictures reconstruction enhancement
12 p1810 A72-27930

Vacuum UV spectra of free plasma column in microwave high pressure discharge in helium-deuterium mixture
13 p2015 A72-29434

Aerobee rocket far UV flash spectrum observations of chromosphere and corona during 7 March 1970 solar eclipse
13 p2042 A72-29539

Wavelength, intensity and spatial distribution identification of far UV solar coronal forbidden lines observed during 7 March 1970 solar eclipse
13 p2043 A72-29540

E region ionosonde observations to reconstruct ionizing X ray and far UV radiation source distribution over solar disk during March 1970 total solar eclipse
13 p2044 A72-29552

Flare related impulsive EUV solar emission lines enhancement in chromosphere-corona transition region
13 p2032 A72-29720

Solar transition zone and corona EUV lines formation heights measurement from OSO-4 spectroheliograms
13 p2050 A72-29939

Bond dissociation energy calculation for carbon disulfide in vacuum UV from fluorescence threshold energy of incident photons, measuring absorption coefficient at 1200-1400 Å
13 p1914 A72-30060

Spectral line identifications and classifications of Li like spectra of elements K through Mn in extreme UV region, detailing extrapolation procedures
14 p2133 A72-30563

K-2 astrophysical rocket observatory for far UV and X ray solar radiation recording, discussing trajectory, orientation and stabilization, electric and spectrophotographic instrumentation
14 p2163 A72-30970

EUV open channel photomultipliers satellite-borne long term performance degradation, attributing sensitivity loss to grating contamination
15 p2235 A72-31645

Geocorona and interplanetary He glow EUV emission altitude distribution measured by exospheric sounding rocket-borne thin film photon counters
15 p2231 A72-32327

Solar O VI, Ne VIII and Mg X spectral lines intensity ratios from XUV rocket measurements, comparing data with Jordan-Allen-Dupree ionization equilibrium calculations [AD-745811]
15 p2318 A72-32783

Solar white light flares relationship to EUV emission based on sudden frequency deviations observations, noting coincidence with H alpha flare areas
15 p2302 A72-32789

Solar vacuum UV flux measurement by photon ion chambers aboard WRESAT I satellite, obtaining 4600 K brightness temperature
16 p2452 A72-33040

K2 III star Arcturus far UV chromospheric emission line spectrum observation with rocket-borne spectrometer, identifying hydrogen L alpha and O I
16 p2453 A72-33136

OSO 1 observation of 300 second oscillation in solar transition region and coronal extreme UV emission line intensity
16 p2453 A72-33137

Dissociative excitation of vacuum ultraviolet emission features by electron impact on molecular gases. III - CO2
17 p2585 A72-34734

Photoionization of a gas by far ultraviolet radiation of a laser-created plasma
17 p2588 A72-34872

Solar chromosphere-corona transition region structure and energy balance calculation by static planar model compared with XUV resonance line observations
17 p2608 A72-35083

Attachment for studying optical properties of highly cooled crystals in the vacuum ultraviolet region
17 p2555 A72-35309

EUV observations of solar quiet region with OSO 6 spectroheliometer, noting chromospheric network structure
17 p2616 A72-35703

Solar flares in the extreme ultraviolet. I - The observations.
17 p2602 A72-35710

- Solar flares in the extreme ultraviolet. II - Comparisons with other observations. 17 p2602 A72-35711
- Rocket observation of Ar XII-XVI, Ca XIV-XVIII, and Fe XIV, XV, XXIV in the extreme-ultraviolet spectrum of a solar flare. 20 p2963 A72-38913
- Properties of metal interference filters for 1200-3000 Å, of dichroic mirrors for 1700-3000 Å and of multi-electric narrow passband interference filters for 2000-3000 Å. 20 p2923 A72-39051
- Apollo 16 far-ultraviolet camera/spectrograph - Earth observations. 21 p3105 A72-40600
- Absorption spectra in the far ultraviolet of Be, B, C, N, Mg, Al, and Si. 21 p3013 A72-40818
- OSO-4 observations of coronal EUV hole, considering association with regions of diverging magnetic fields. 21 p3106 A72-41042
- Photometric analysis of X-ray photographs of sun obtained with rocket-borne zone plate camera in XUV region. 21 p3108 A72-41289
- Atomic, ion and electron transition pulsed gas discharge lasers, considering power efficiency factors, vacuum UV region and gas density. 21 p3064 A72-41301
- Far UV radiating hot dense microplasma production by laser heating for measuring by resonant absorption small quantities of gaseous element. 21 p3093 A72-41341
- Theoretical calculations of the F-region tropical ultraviolet airglow intensity. 22 p3171 A72-42418
- Vacuum ultraviolet absorption measurements on ionized species. 23 p3316 A72-44330
- Excitation of vacuum ultraviolet radiation by electron impact on carbon monoxide - Some unresolved questions near threshold. 24 p3379 A72-45313
- FARADAY EFFECT**
- Ionspheric total electron content measurement with geostationary ATS 3 satellite during solar eclipse of 7 March 1970, plotting Faraday rotation as function of time. 01 p0059 A72-10838
- Electron density measurements for traveling ionospheric disturbances by Thomson scatter technique using Faraday rotation. 01 p0031 A72-10922
- Pulsar PSR 0833-45 linear polarization measurements at 300 and 1420 MHz, showing frequency invariance with interstellar scattering and Faraday rotation allowance. 01 p0133 A72-11119
- ATS Faraday rotation measurement data on total electron content during geomagnetic storms, giving first midlatitude ionosphere average storm patterns and seasonal influence analysis. 02 p0216 A72-11900
- Manual reduction of Faraday rotation observations of ionospheric electron density at low latitudes, comparing with computer ray trace analysis. 02 p0221 A72-12462
- Faraday rotation as perturbation for analytic solution of system of differential equations for line formation in inhomogeneous magnetic fields. 03 p0427 A72-13295
- Low birefringent orthoferrites for optical devices, considering improvement in Faraday rotation detection of magnetic domains in single crystal platelets [IEEE PAPER 10,10]. 03 p0360 A72-13760
- Long range satellite signal Faraday fading rate revealing electron density profile near F layer peak. 04 p0486 A72-14883
- Interstellar electron density and magnetic field fluctuations effects on Faraday rotation and signal dispersion measure in radio band. 04 p0487 A72-14901
- Radio propagation from transmitter moving through irregular stationary ionospheric plasma, obtaining fluctuation dispersions for Faraday rotation angle and rate, phase, Doppler shift and refractions. 04 p0489 A72-15395
- Weak magnetic moments measurement under pressure and over wide temperature range by Faraday method, discussing magnetometer and cryogenic equipment modifications [AD-740076]. 04 p0522 A72-15478
- Anisotropic effects use in passive semiconductor magnetoplasma for submillimeter isolators and circulators development, describing transmission devices based on Faraday rotation. 04 p0563 A72-15600
- Ionspheric electron content from Faraday rotation observed on satellite radio signals at various frequencies. 05 p0659 A72-17095
- Ionspheric electron content diurnal and latitudinal variations from differential Faraday effect, discussing solar elevation and geophysical mechanisms. 06 p0805 A72-17640
- Electron density distribution inhomogeneities from vhf Faraday rotation measurements, noting diurnal, seasonal, sunspot cycle and geomagnetic activity effects. 06 p0806 A72-17642
- Faraday rotators acting as optical isolators for high power giant pulse lasers used for plasma production. 07 p1008 A72-20368
- Ionspheric electron content determination at different latitudes from geostationary satellite signal Faraday rotation. 10 p1475 A72-24955
- Equatorial Faraday rotation measurements for night ionospheric electron density peak structures during equinoctial months, using ATS-C geostationary satellite radiation. 10 p1476 A72-24958
- Transmittance and Faraday effect characteristics of Te doped InSb samples with free carriers measured at 10.6 microns. 11 p1648 A72-26338
- Interferometer investigations of Cassiopeia linear polarization at centimeter wavelengths, explaining results by source model incorporating Faraday depolarization. 12 p1865 A72-27094
- Ionosonde observations and Faraday rotation measurements of E and F region total electron content during two solar eclipses. 12 p1801 A72-27154
- Polarization modes of anisotropic optical traveling wave resonator using half wave plate and Faraday rotation cell. 12 p1824 A72-27870
- Metagalactic magnetic field contributions to observed Faraday rotation measurements for distant extragalactic radio sources. 13 p2039 A72-29088
- Nonequilibrium Faraday MHD generator performance examined by double diaphragm shock tube within ionization region. 13 p2013 A72-29357
- Linear polarization and depolarization observation of quasar red shift explained as Faraday dispersion in or near source. 15 p2313 A72-32365
- Crystallographic structure, phase transformations, Curie temperature and Faraday rotation of Ti-substituted MnBi films. 15 p2294 A72-32522
- Faraday ring currents induction by radial magnetic field in low pressure plasma supersonic ring channel flow driven by inductive hydrodynamic shock tube. 16 p2437 A72-33749
- Polarization modes and phase shifts of normal oscillation modes in anisotropic optical traveling wave resonator with Brewster winders half wave plate and Faraday rotation cell. 16 p2403 A72-33979
- Magnetic materials. 17 p2595 A72-34571
- Interpretation of rotation measures of radio sources. 17 p2606 A72-34573
- Satellite beacons observations from 1964 to 1970. 17 p2547 A72-35125
- Faraday rotation in connection with Hoyle theory of intergalactic magnetic field existence in steady state cosmology, considering cosmological model with cosmic magnetic field. 17 p2614 A72-35504
- Observation of linear polarization of solar microwave bursts. 18 p2722 A72-36997
- Nature of losses introduced into a ring resonator by a nonreciprocal phase-shifting device that employs the Faraday effect. 19 p2814 A72-38788
- D-region electron densities and collision frequencies from Faraday rotation and differential absorption measurements. 19 p2793 A72-38858
- Faraday rotation by cosmic magnetic field in cosmology based on scalar-tensor theory of gravitation. 20 p2969 A72-39264
- Faraday rotation dual-mode ferrite reciprocal phaser with performance and cost advantages over toroidal type for microwave phased array applications. 20 p2909 A72-39733
- Polarization follower tracking linear vector transmitted by satellite with high precision, noting spacecraft attitude control and Faraday rotation measurements applications. 21 p3021 A72-40907
- Faraday rotation of linearly polarized radio waves from the Crab Nebula by the solar corona. 21 p3109 A72-41327
- Magneto-microwave free-carrier absorption in germanium in the Faraday configuration. 21 p3097 A72-41379
- Faraday depolarization of extragalactic radio sources. 23 p3335 A72-43268
- Faraday effect of incoherently scattered radar signals. 23 p3263 A72-43365
- Influence of the imperfection of resonator elements on the characteristics of a triangular ring laser with a 90-degree Faraday rotator. 24 p3408 A72-44622
- FARADAY ROTATION**
- UT FARADAY EFFECT**
- FARM CROPS**
- Crop discrimination with manual and automatic computerized side-looking radar imagery analysis for microtexture pattern recognition. 01 p0065 A72-10451
- Crop classification by airborne multispectral observations, suggesting sample regions selection method for spectral signatures identification based on statistical similarities. 11 p1628 A72-26985
- Crop surface albedo measurements, taking into account cloudiness, zenith angle and day period effects. 20 p2915 A72-38970
- FAST NEUTRONS**
- Fast neutron radiation damage to glass ceramics and amorphous semiconductors electrical properties. 09 p1336 A72-22405
- EPR for point defects produced in Si by fast neutron irradiation, emphasizing damage cluster model. 12 p1858 A72-28060
- Effect of fast-neutron irradiation on ceramics and ceramic-metal seals. 17 p2559 A72-34591
- Radiation damage to refractory metals as related to thermionic applications. 17 p2566 A72-34595
- Breeder reactor testing of fast neutron irradiation effect on alumina and yttria cylinders for thermionic fuel rod designs. 18 p2708 A72-36161
- Fast-neutron-compensated n-germanium as a model of amorphous semiconductors. 20 p2961 A72-39853
- Polyacrylonitrile based carbon fiber strengthening by fast neutron irradiation at high temperatures. 22 p3196 A72-41965
- Effect of voids on angular correlation of positron annihilation photons in molybdenum. 22 p3187 A72-41967
- FASTENERS**
- NT BOLTS**
- NT RIVETS**
- NT SCREWS**
- Space shuttle mechanical fastener design, discussing drives, threads, manufacturing and refractory alloys. 01 p0075 A72-10751
- Aerospace vehicle high tensile strength fasteners stress corrosion cracking and hydrogen embrittlement [AIAA PAPER 72-385]. 11 p1653 A72-25407
- Crack initiation detecting and recording instrument with optical strain gages for double shear fatigue tests of aircraft fasteners. 11 p1632 A72-25823
- Inertia welded bimetallic fasteners for aerospace industrial applications, noting cost advantages [ASM PAPER W 72-32,5]. 12 p1817 A72-28166
- Hi-Shear and Hi-Lok fastening systems for aircraft manufacture, comparing strength and weight with conventional rivets and bolts [SAWE PAPER 901]. 23 p3293 A72-43451
- FATIGUE [BIOLOGY]**
- NT FLIGHT FATIGUE**
- NT MUSCULAR FATIGUE**
- Environmental noise induced human fatigue, considering physiological and psychological effects. 01 p0016 A72-10050
- Extracardiac chronotropic effects on cardiac rhythm variations during fatigue, using variational pulsometry and autocorrelation and spectral analysis. 02 p0164 A72-12513
- Fatigue factors in aircrew related to shift working and technological advances, considering implications for industry and work-rest cycles. 10 p1432 A72-24988
- IR pupillography for screening narcotics and fatigue prone individuals from driver and pilot training applicants. 12 p1777 A72-28323
- Work capacity evaluation from fatigue, biological rhythm, tissue respiration and oxygen consumption studies, discussing pharmacological stimulation effects. 14 p2078 A72-30376
- The role of inhibition in the fatigue phenomenon. 17 p2503 A72-35015
- Changes of the catecholamine content in the brain of albino rats under overstrain caused by running in a rotating drum. 19 p2757 A72-38034
- FATIGUE [MATERIALS]**
- NT BENDING FATIGUE**
- NT METAL FATIGUE**
- NT THERMAL FATIGUE**
- Boeing 707 rapid decompression at 25,000 feet, noting rivet hole fatigue damage. 02 p0167 A72-11715

Structural inhomogeneities effect on fatigue phenomenon in rolling motion, discussing stress cycles preceding active surface degradation
04 p0526 A72-14473

Rotating shaft fatigue under variable stress cycles, determining safety, bending and torque coefficients
04 p0594 A72-15750

Subcritical crack extension in elastoplastic or viscoelastic-plastic matrix, showing similar mathematical representations for fatigue crack propagation and creep rupture under sustained loads
05 p0737 A72-16302

Fiberglass reinforced plastics fatigue failure prediction based on test demonstrated correlation between static and cyclic strainability
08 p1195 A72-21856

Static fatigue of borosilicate glass, fused silica and polycrystalline alumina, presenting log stress vs log failure time plots
09 p1335 A72-22398

Energy balance criterion application to crack growth under cyclic fatigue loading, considering stress-strain behavior of plastic deformation energy
09 p1404 A72-22911

Papers on design for high temperature environments covering structural fatigue, creep interaction and ratcheting deformation and inelastic stress analysis
09 p1406 A72-23196

Metallic coatings effect on high-strength steels fatigue properties, noting beneficial effect of shot peening
10 p1494 A72-24024

Fatigue crack propagation in epoxy resin matrix reinforced with discontinuous metal fibers
10 p1501 A72-24261

Material testing by holographic interferometry, discussing application to early detection of delayed cracking, fatigue damage and bond imperfections
10 p1482 A72-24575

Inspectability criteria for airframes with fatigue fail safe design requirements for small airplane certification
11 p1575 A72-25574

Fatigue certification of general aviation aircraft in Australia, describing ground taxi load spectra and endurance and radiographic inspection of laminated spar caps
11 p1734 A72-25575

Turbine blade alloys vibrational fatigue and creep properties under high and low frequency axisymmetric loads at room and elevated temperatures
11 p1662 A72-26798

Cooling efficiency and load endurance of aircraft turbine engine blades as function of ambient temperature and air flow rates
11 p1712 A72-26892

Boron and carbon reinforced fiberglass plastics tensile strength characteristics, presenting static fatigue curves vs Poisson coefficient and elastic modulus for various fiber contents
13 p1982 A72-28552

Stress levels and fatigue in aircraft structures subjected to jet noise, noting stress calculation for skin panels and control surfaces
13 p1898 A72-29579

Macroparametric, microstructural and general rationales methods for fatigue resistant materials, noting crack propagation and fracture mechanics
14 p2120 A72-30612

Axisymmetric ductile rotating shaft failure modes, considering fatigue, buckling and impact stress factors [ASME PAPER 72-DE-40]
14 p2167 A72-30873

Load cycle frequency and time characteristic effects on plastics fatigue behavior, considering relaxation, retardation and internal damping induced heating effects
16 p2416 A72-34145

Shape factors for nozzle corner cracks evaluated from epoxy-model pressure vessels.
17 p2630 A72-34814

Composite materials crack propagation and failure modes leading to fracture instability, discussing maximum strength conditions and fatigue
18 p2703 A72-36394

An advanced concept of the Woehler diagram and a new calculating procedure for the application of the extreme-value method to experimental data in the calculation of fatigue strength
20 p2926 A72-39572

Elastic wave energy absorption in structures under dynamic loads, noting fatigue fracturing decrease with energy transfer into damping medium
21 p3126 A72-41540

Reliability analysis in the estimation of transport-type aircraft fatigue performance.
22 p3241 A72-42971

Optimal fleet reliability under fatigue and chance overload in service.
24 p3365 A72-44656

Aircraft fatigue: Design, operational and economic aspects.
24 p3366 A72-44726

Reliability analysis based on time to the first failure.
24 p3455 A72-44727

Optimum design of joints - The stress severity factor concept.
24 p3455 A72-44728

The importance of service inspection in aircraft fatigue.
24 p3367 A72-44740

Structural fatigue cost penalties in airline operations, considering inspection, maintenance and carrying capacity reduction
24 p3367 A72-44743

Structural fatigue cost in aircraft maintenance and repair, considering inspections, defect rectification, preventive modifications, replacements and NDT
24 p3367 A72-44744

Observations on designing to combat fatigue and its effects on the economics of civil transport aircraft.
24 p3368 A72-44745

Evaluation of the danger of damage to mechanical systems exposed to random vibrations
24 p3459 A72-45449

FATIGUE DIAGRAMS
U - S-N DIAGRAMS
FATIGUE LIFE
European A300B airbus flying control hydraulic system and landing gear design for safety and reliability, fatigue life, weight and maintenance
01 p0005 A72-10724

Al-Mg alloy under reverse bending fatigue in aqueous sodium chloride with constant load and potentiostatic control, determining anodic polarization effect on fatigue life
01 p0087 A72-11033

Precipitation hardened Al-Cu alloy microstructure relation to fatigue and tensile properties, emphasizing particle size and distribution, moving dislocations and grain boundary effects
01 p0088 A72-11044

Fatigue crack initiation and growth in sharply notched mild steel, showing specimen size, geometry and loading effects on fatigue life
01 p0142 A72-11098

Misalignment effect on load distribution and fatigue life of tapered roller bearings
02 p0234 A72-11532

Rolling element fatigue lives of through hardened bearing materials, noting alloying percentage effect [ASME PAPER 71-LUB-13]
02 p0235 A72-11535

Asymmetrically loaded cylindrical roller bearings, describing hollow ended design for fatigue life improvement [ASME PAPER 71-LUB-14]
02 p0235 A72-11536

Heat resistant alloys thermal microstresses effect on creep and fatigue life under thermal cycling conditions
02 p0242 A72-11633

Heat treated carbonized, cyanided, nitrided and boronized steel fatigue strength dependence on static strength, residual stress, brittleness and stress concentration from test data
02 p0244 A72-12242

Metal fatigue time and cycle dependent deformation and fracture mechanisms in creep range from cumulative damage law standpoint for lifetime prediction
02 p0295 A72-12497

Metal fatigue damage avoidance, control and repair, considering design, metallurgical and service factors
02 p0296 A72-12500

Al-Mg-Si alloy fatigue, vibration creep and creep strength tests at room temperature, determining mean stress effects on fatigue strength and cumulative damage
02 p0297 A72-12536

Cumulative damage in metal fatigue, suggesting unified theory applicable to stress or strain controlled conditions
03 p0442 A72-12922

Austenitic steel under combined bending and torsion, showing fatigue strength dependence on temperature, load cycle asymmetry and stress concentration
03 p0371 A72-13469

Fatigue failure under cyclic stress, analyzing surface and temperature effects
03 p0372 A72-13588

Secondary fatigue curves for determining service life of metal specimens under unsteady loads
03 p0445 A72-13592

Ti alloys for aircraft structures, emphasizing weldability, tensile fatigue and residual strengths, shear-carrying qualities and fuselage shell design
03 p0373 A72-13616

Steels fatigue life tests as function of stress level, confirming Woehler curves mathematical model
03 p0373 A72-13673

Cu single crystal fatigue life explanation by work hardening using statistical theory of slip
03 p0379 A72-14258

Polymethyl methacrylate fatigue strength at elevated temperatures, discussing sample preparation, test equipment and procedures
04 p0537 A72-14750

Mean stress and overload effects on mild steel service life, using fatigue damage summation method
04 p0592 A72-15475

Anodizing effect on corrosion fatigue strength of sheet duralumin under low and high bending stress
04 p0535 A72-15662

Titanium alloy microstructure effect on fatigue strength under symmetric bending load cycles in air and NaCl solution
04 p0535 A72-15663

Fatigue strength optimization of bonded double strap metal joints, attributing stress concentration to plastic relaxation
05 p0731 A72-15791

Crack growth dependence on applied high stress level cycle number, showing fatigue life inversely proportional to stress exponential function
05 p0673 A72-16304

Fatigue limit amplitude diagram schemes and formulas
05 p0740 A72-16625

Mo- and Ta-base refractory alloys creep tests, determining interactions between creep strength, fatigue life and strain aging by fatigue vibration application
05 p0677 A72-17111

Dynamic overstressing and annealing effects on fatigue life of convoluted metal bellows, using dynamic model and strain gage measurements
05 p0742 A72-17245

Hardened and tempered Ni-Cr-Mo steel, testing rest periods caused fatigue life increase in terms of cycles to failure
06 p0895 A72-17802

Fatigue damage factor and failure probabilities in structural design for multilevel repetitive cyclic stresses
06 p0896 A72-17965

Fatigue life and creep tests of refractory materials under programmed thermal cycling for different stress levels
06 p0831 A72-18351

Nb and Nb-Zr alloy tubular and sheet samples cyclic loading tests, determining heat treatment effects on notch sensitivity and fatigue strength
06 p0834 A72-18646

Milling, band grinding, final manual polishing and tumbling polishing effects on fatigue life and surface finish of steel compressor blades
06 p0824 A72-18651

Plastic deformation fatigue theory extended to tests at stresses below elastic limit, explaining cyclic loading frequency effect on fatigue life
06 p0899 A72-18652

Aircraft performance parameters in terms of effect on lifting system service and fatigue life and on design
07 p0912 A72-19111

Static and fatigue strength in tension of welded joints composed of low carbon and austenitic steel
07 p0996 A72-19767

Stress variation effect on strength values obtained by low cycle fatigue tests involving bending with rotation
07 p1014 A72-19847

Fatigue life gages to determine cumulative fatigue damage due to variable cyclic strain history on unmatched materials
08 p1163 A72-20915

Fatigue life gages planning and application to airplane cyclic fatigue test, describing automatic data acquisition system
08 p1163 A72-20916

Fatigue strength and life estimation method for thick walled cylinders under pulsating internal pressure, using fracture mechanics crack propagation law [ASME PAPER 71-PVP-15]
08 p1244 A72-21482

Mechanical surface strengthening effect on small cycle fatigue life of Ti alloy weakened by stress raiser
08 p1186 A72-21725

Turbine blade root attachment service life determination from fatigue tests with T shaped models
09 p1373 A72-22300

Unidirectional and orthogonally cross-ply carbon fiber reinforced plastics laminates, determining interlaminar shear strength and fatigue life [PI PAPER 8]
09 p1337 A72-22543

Fatigue strength of heat resistant materials under thermal cyclic loads leading to sign variable plasticity and creep
09 p1402 A72-22732

Metal creep fatigue analysis and life prediction by inelastic strain ranges partitioning into reversed tensile and compressive plasticity and creep components
09 p1406 A72-23198

Fatigue fracture of polymethyl methacrylate at room temperature under uniaxial failure cyclic loading
09 p1339 A72-23244

Cumulative fatigue damage in Al-Zn-Mg alloy fillet welded joints, analyzing constant amplitude and programmed load fatigue test results
09 p1332 A72-23618

Data scatter reduction in Al-Zu-Mg welded specimens cumulative fatigue damage testing, noting fatigue life improvement by shot peening and static or dynamic prestressing
09 p1332 A72-23619

Carbon steel fatigue crack propagation rate dependence on strength and stress history, discussing conditions for crack nonpropagation

10 p1499 A72-24889

Fatigue strength characteristics of boron-epoxy reinforced Al stringers for helicopter airframe [AIAA PAPER 72-392]

11 p1574 A72-25413

Locati and Prot methods for metal fatigue limits evaluated by axial and rotating bending tests on steel specimens

11 p1657 A72-25824

Polycrystalline Mo fatigue behavior under cyclic stresses, discussing grain size effect on fatigue life and relationship between cycle dependent yield and French damage line

11 p1658 A72-25830

Fatigue life cumulative damage prediction procedure for engineering metals subjected to complicated stress-strain histories, noting errors in average mean stress method

11 p1658 A72-25831

Heat treated carbonized, cyanided, nitrided and boronized steels fatigue limit dependence on static strength, residual stress, brittleness and stress concentration

11 p1659 A72-26128

Statistical analysis of strain criteria and stochastic relations for Al alloy fatigue life and minimum creep rate at 175-250 C

11 p1663 A72-26800

Tungsten alloy wires strength, creep properties and fatigue limit, investigating fracture characteristics

11 p1663 A72-26807

Diamond burnishing effect on surface quality and fatigue strength of steel, noting work hardening increase and compressive residual stresses buildup in surface layer

11 p1642 A72-26811

Fatigue failure information in structural design, considering low cycle, cumulative damage and time dependent conditions

12 p1884 A72-27641

Ball bearings lubricated with oils and fire-resistant fluids, testing fatigue life relationship to steel quality, fluid film thickness and viscosity

12 p1816 A72-28108

Electroslag and vacuum remelted maraging steel rolling contact, investigating fatigue life as function of lubricant film thickness/surface roughness ratio

12 p1816 A72-28109

Deep groove ball bearing endurance tests to determine running conditions and lubricant film thickness/surface roughness ratio effects on fatigue life

12 p1816 A72-28112

Heat resistant blade alloy test temperature effects on fatigue life, tensile strength, hardness and chemical composition

12 p1831 A72-28230

Gas turbine engine compressor blade and materials fatigue strength dependence on pressure under contact friction corrosion

12 p1831 A72-28244

Metal fatigue strength testing under programmed temperature regimes, using HF induction generator

12 p1796 A72-28247

Material fatigue failure criterion during cyclic loading, noting energy dissipation and resonant frequency roles

12 p1888 A72-28250

Fatigue strength and cumulative damage in fiberglass-epoxy composite specimens under unsteady elastic bending loads, determining loading spectrum effect on service life

13 p1983 A72-28562

Steels shafts fatigue failure under cyclic loading and fretting corrosion, indicating fatigue strength increase through surface layer wear resistance augmentation

13 p1979 A72-29476

Chromium stainless steel fatigue life reduction due to embrittlement in gaseous hydrogen atmosphere at room temperature, noting alleviating effect of atmosphere contaminants

13 p1979 A72-29484

Fatigue limit and Woehler curve determined from notch tests, noting relation between fatigue damage and residual stresses in notched parts

[ONFRA, TP NO. 1083] 13 p1980 A72-29673

Airframe and wing fatigue life testing, discussing results recomputation for changed operating conditions

14 p2092 A72-30276

Welded steel airframe residual fatigue life tests by nonstationary random loading, applying to jet trainer aircraft landing gear

14 p2107 A72-30277

Welded machine component service history effects on residual fatigue life from statistical evaluation of factor experiment

14 p2107 A72-30278

Aircraft engine components fatigue life assessment under small cycle temperature conditions, including temperature field and stress-strain determination in critical spot

14 p2145 A72-30279

Fatigue life tests of structural sandwich plates with honeycomb layer, considering temperature effects, material scattering and defects inside honeycomb by nondestructive methods

14 p2164 A72-30280

Computer algorithms and programs contribution to aircraft structure operational reliability and fatigue life calculation

14 p2164 A72-30288

Refractory material blade alloys fatigue life up to 950 C under nonstationary loading, noting log-normal law distribution

14 p2116 A72-30428

Ni-Cr-Ti steel aircraft structural element fatigue life calculation based on failure mechanism involving crack propagation

14 p2164 A72-30429

High modulus composites structural design applications, considering fatigue performance vs cost [ASME PAPER 72-DE-24]

14 p2167 A72-30866

Adhesive bonding of L-1011 body shell panels for improved fatigue strength and corrosion resistance

15 p2245 A72-32429

Aircraft gas turbine engine Ni base alloy disks and shafts thermomechanical treatment, considering yield strength and high and low cycle fatigue resistance

16 p2406 A72-33299

Cumulative damage probability in dynamic or static fatigue failure of brittle graphite materials as function of stress

16 p2414 A72-33321

Incoloy low cycle fatigue tests at high temperatures and different strain rates, discussing fatigue life at 10 and 60 min hold times

16 p2410 A72-33820

Welded Al joints fatigue resistance from iterative nonlinear regression analysis with multiparameter endurance curves

16 p2412 A72-34141

Definition of the fatigue limit on the basis of the distribution of the resistance over the set of elementary volumes of which the sample is composed

17 p2565 A72-34196

Fretting corrosion fatigue prevention by barrier approach, discussing test program and application to helicopter part fatigue life increase

[AHS PREPRINT 672] 17 p2626 A72-34512

The use of airborne magnetic tape recorders for fatigue life monitoring.

17 p2553 A72-34812

Fatigue life gages use in combination with strain multipliers in field applications with random ergodic cyclic strains

17 p2554 A72-34822

Fatigue crack initiation and propagation in welded structures, considering low and high cyclic stresses, microstructure and environment effects

17 p2635 A72-35919

Creep damage role in governing elevated temperature strain cycling fatigue lives of heat resistant stainless steel and cobalt alloy

19 p2817 A72-37712

Stress calculations for lifetime prediction in turbine blades. [ONERA, TP NO. 1097]

19 p2875 A72-37770

Fatigue limits of cylindrical test pieces in rotative bending and in tension-compression, investigating strain gradient effect

19 p2875 A72-37788

Static and dynamic fatigue behavior of glass filament-wound pressure vessels at ambient and cryogenic temperatures.

19 p2823 A72-38832

Relation between the reliability and allowable stress amplitude in fatigue design.

20 p2977 A72-38879

Fatigue strength of welded aluminum-connections - Investigation with the aid of multiparameter life length lines

20 p2930 A72-39941

Designing to avoid stress-corrosion and/or fatigue failures. [AICHE PAPER 15C]

21 p3116 A72-40125

Fatigue behavior of glass filament-wound epoxy composites in water.

21 p3072 A72-40246

Fatigue damage of aluminum alloy at high temperature.

21 p3066 A72-40716

Temperature and strain rate dependences of low cycle fatigue life at high temperatures of austenitic stainless steel, examining crack behavior and stress-strain relations

21 p3069 A72-41010

Fatigue strength of overloaded stiffeners in cracked panels, evaluating stress intensity factor and overload coefficients for fatigue crack propagation via finite element method [ICAS PAPER 72-40]

21 p3120 A72-41165

The influence of grain and twin boundaries in fatigue cracking.

21 p3069 A72-41350

Creep test diagrams plotted to estimate heat resistance for turbine blades design, predicting fatigue life with allowance for loading cycle form and duration

21 p3123 A72-41366

Resonant frequency, fatigue and energy dissipation relations for endurance limit determination in Al alloy specimens under vibrational loads

21 p3070 A72-41368

Investigation of fatigue-failure mechanisms and inelastic deformation of metals in torsion

21 p3071 A72-41703

Influence of dispersion on the accuracy of estimating the fatigue life from the results of accelerated investigations by the prefracture method.

22 p2322 A72-41928

Thermoplastics fatigue life dependence on stress with allowance for heating laws, noting heat accumulation effect on thermal failure

22 p3196 A72-42164

An advanced strain level counter for monitoring aircraft fatigue.

22 p3179 A72-42688

Strain multiplier with S-N fatigue life gages, discussing design and performance

22 p3179 A72-42708

Fatigue strength and fail-safe aspects of lug joint in aircraft structures, considering tension-compression load, fretting corrosion, prestress and residual stress

22 p3239 A72-42851

Testing procedures for the design and life estimation of fatigue-sensitive structures.

22 p3241 A72-42974

German monograph - Contribution to the investigation of the fatigue strength of sintered iron.

22 p3194 A72-43066

Book - Effect of notches on low-cycle fatigue: A literature survey.

22 p3242 A72-43145

Gas turbine blade models of heat resistant Zr56K alloy under operational temperature variations, observing fatigue strength

23 p3347 A72-43735

Heat treatment effect on tensile and bending fatigue strength of Al alloy thin sheet

23 p3301 A72-43743

Fatigue strength of two phase Ti alloys, considering work hardening, electrochemical finishing, electropolishing and protective media

23 p3301 A72-43757

Fatigue fracture and crack propagation in aluminum alloys. II.

23 p3302 A72-43973

Bonded joints - Squeeze-out /flash/ effect on fatigue strength.

23 p3353 A72-44248

Low cycle fatigue under biaxial strain controlled conditions.

23 p3354 A72-44259

A comparison of the axial and reversed-torsional strain cycling low-cycle fatigue strength of several structural materials.

23 p3304 A72-44397

The fatigue strength under varying mean stress.

24 p3455 A72-44629

Development of a push-pull fatigue testing machine under high pressure, and the results of preliminary fatigue tests.

24 p3401 A72-44630

Life prediction of expulsion bladders through fatigue test and fold strain analysis.

24 p3455 A72-44672

The New Zealand light aircraft fatigue meter program.

24 p3401 A72-44735

Aircraft structures fatigue life expectancy under random acoustic excitation, describing testing methods and equipment

24 p3367 A72-44739

Fatigue design and test program for the American SST.

24 p3367 A72-44741

Design against fatigue failure in thermoplastics.

24 p3457 A72-44816

Ultrasonic detection of fatigue damage.

24 p3457 A72-44820

Austenitic steel under combined bending and torsion, showing fatigue strength dependence on temperature, load cycle asymmetry and stress concentration

24 p3414 A72-44944

Fatigue life and creep tests of refractory materials under programmed thermal cycling for different stress levels

24 p3416 A72-45738

Hydraulic sand blasting and annealing effects on Ti alloy sheet bending fatigue strength

24 p3416 A72-45744

FATIGUE TESTING MACHINES

Fatigue test machine for alternating cantilever bend and torsion testings at 50 Hz and 1.5-300 K

01 p0049 A72-11381

Combined bending/torque fatigue test machines design, operation, calibration and results, developing probabilistic S-N diagram from cycles-to-failure data statistical analysis

02 p0199 A72-11514

Automatic device for thermal and thermomechanical fatigue tests of steel specimens, noting crack

02 p0199 A72-11514

- nucleation and growth by hardening due to lattice defects
02 p0200 A72-11996
- Resonance type rotating bending fatigue testing machine using specimens with attached inertial mass, presenting test results with carbon steel specimens
02 p0201 A72-12823
- Cyclic deformation and fatigue testing equipment and techniques for biaxial stress, stress concentration and pure bending
03 p0339 A72-14168
- Fatigue testing machine for material behavior under elastoplastic bending loads with constant or smoothly varying programmed vibration frequency and amplitude
12 p1795 A72-27463
- Mathematical model for hydraulic fatigue testing machine, analyzing nonlinear control stability of vibratory loading process
12 p1796 A72-27978
- Design and operation of experimental facility for thermal fatigue testing of heat resistant materials
13 p1939 A72-29145
- Testing machine for creep resistance of foam plastics under simultaneous static and vibration loads
14 p2092 A72-30591
- Equipment for low cycle fatigue bending, torsion and tension-compression tests, considering design and performance
16 p2394 A72-33846
- The use of airborne magnetic tape recorders for fatigue life monitoring.
17 p2553 A72-34812
- Fatigue life gages use in combination with strain multipliers in field applications with random ergodic cyclic strains
17 p2554 A72-34822
- Device for fatigue testing of fiberglass-reinforced plastic samples in a symmetrical tension-compression regime at acoustic oscillation frequencies
20 p2920 A72-38944
- Quadrisectional facility for studying creep and fatigue strength under deep freezing conditions
21 p3057 A72-41719
- Fatigue test equipment for 293-233 K and 50-100 ton static or 25-50 ton cyclic loads, using Freon 22 as coolant
23 p3278 A72-43759
- Machine with programmed load control for studying the fatigue and inelasticity of metals at room and elevated temperatures
23 p3278 A72-43969
- Development of a push-pull fatigue testing machine under high pressure, and the results of preliminary fatigue tests.
24 p3401 A72-44630
- Self oscillating system resonant vibrations excitation for fatigue tests, determining frequency and amplitude relationship
24 p3458 A72-44931
- FATIGUE TESTS**
- Nondestructive radioactive gas penetrant tests for porosity and fatigue damage in jet engine castings
01 p0069 A72-10813
- Factorial design model of materials fatigue failure under narrow band random vibrations
01 p0140 A72-10942
- Cast high temperature Ni base alloy Udimet 500 low cycle fatigue, determining total stress and strain range vs fatigue life at elevated temperatures
01 p0087 A72-11030
- Ti-Al-V alloy under vacuum fatigue tests, examining temperature and chemical environment effects on fatigue crack growth
01 p0087 A72-11034
- Graphite-epoxy conductive polymers as fatigue damage indicators of structures under cyclic strain [SESA PAPER 1915]
02 p0287 A72-11509
- Temperature-time dependent torsional strength and fracture failure of Cr-Ni steel microalloyed with La and Ce as function of grain boundaries
02 p0243 A72-12010
- Heat treated carbonized, cyanided, nitrided and boronized steel fatigue strength dependence on static strength, residual stress, brittleness and stress concentration from test data
02 p0244 A72-12242
- Tension-compression cycling effects on fatigue crack growth in high strength alloys
02 p0294 A72-12469
- Papers on metal fatigue damage covering basic mechanisms, detection, field practices for repair, avoidance and control
02 p0295 A72-12495
- Metal fatigue damage nondestructive detection, discussing inspection methods, equipment, advantages, limitations and test results
02 p0296 A72-12498
- Al-Mg-Si alloy fatigue, vibration creep and creep strength tests at room temperature, determining mean stress effects on fatigue strength and cumulative damage
02 p0297 A72-12536
- Self oscillating system resonant vibrations excitation for fatigue tests, determining frequency and amplitude relationship
03 p0443 A72-13456
- Temperature dependence of low temperature endurance of Cr-Ni steels in bending fatigue tests
03 p0371 A72-13463
- Endurance tests of D16AMO alloy sheets under high intensity acoustic, harmonic and electrodynamic vibrator loading
03 p0371 A72-13470
- Cyclic deformation and energy dissipation during fatigue breakdown in steels under tension-compression and torsion
03 p0372 A72-13590
- Crack propagation rates during bending fatigue tests on flat hardened steel as function of stress intensity and plasticity area
03 p0445 A72-13593
- Fatigue crack onset and propagation from bending behavior of revolving flat specimens
03 p0445 A72-13594
- High temperature fatigue crack growth studies by compliance calibration test method, evaluating temperature and cycle rates effects
03 p0339 A72-14169
- Approximate S-N fatigue testing/digital computer method for quasi-static boundary value problems in plasticity theory, applying to continuum models
03 p0453 A72-14210
- Impact fatigue testing apparatus, presenting results for stainless steel
04 p0524 A72-15549
- Fatigue crack growth rate testing in gaseous environments at nonambient pressure and temperature in test chamber
05 p0643 A72-16186
- Silicate glasses fatigue in dynamic and static tests, discussing fracture stress dependence on time of loading
05 p0681 A72-16422
- INCO 713C and IN 100 cast Ni base alloy gas turbine blades under thermal fatigue tests
05 p0675 A72-16497
- Fatigue failure tests of soldered joint in solar cell interconnector designs under extended temperature cycling
05 p0615 A72-16552
- Test conditions, specimen batch and method effects on accuracy of rapid fatigue limit tests with increasing stress amplitude
05 p0741 A72-17085
- Fatigue test curves of notched Al alloys under bending with rotation
05 p0676 A72-17086
- Concorde airframe testing for thermal effects on structural strength and fatigue life, discussing facilities for flight conditions simulation
05 p0614 A72-17197
- Accelerated fatigue limits for Al and Mg alloys from transverse bend test data
06 p0827 A72-17398
- High purity polycrystalline Al hf low strain fatigue measurements by piezoelectrically driven exponential horn, estimating critical point defect concentration
06 p0893 A72-17420
- Fatigue crack formation speed relationship to stress intensity factor, investigating crack propagation by fracture mechanics methods
06 p0895 A72-17810
- Fatigue behavior of notched or cracked aircraft structure parts, examining service life prediction problem
06 p0895 A72-17811
- Al and Ti alloy fatigue after temperature reduction to 253, 77 and 4 K as function of surface purity after machining
06 p0831 A72-18356
- Airloads and structural integrity flight testing /U.S. Air Force/, noting dynamic response, fatigue tests and temperature data acquisition
06 p0759 A72-18490
- Gas turbine blades thermal fatigue test and analysis, investigating static tensile loading effects on heat resistance under thermal cycling
06 p0899 A72-18556
- High temperature fatigue test assembly for symmetric tension compression cycles at 10 kHz with specimen heating in resistance furnace
06 p0797 A72-18568
- Plastic deformation fatigue theory extended to tests at stresses below elastic limit, explaining cyclic loading frequency effect on fatigue life
06 p0899 A72-18652
- Fatigue testing machines for axial and torsional loadings at low temperatures in vacuum
06 p0797 A72-18667
- Sheet metal fatigue test method for transverse 100-1000 Hz bending at normal and high temperatures, applying to 1.5 mm Ti alloy sheet
06 p0900 A72-18671
- Stress variation effect on strength values obtained by low cycle fatigue tests involving bending with rotation
07 p1014 A72-19847
- Stepwise fatigue testing of high temperature alloy, noting strain hardening phenomena in prestressed samples
07 p1017 A72-20129
- Ni based superrefractory alloy high temperature fatigue tests, studying creep as function of stress load and frequency and temperature
07 p1022 A72-20487
- Fatigue life gages planning and application to airplane cyclic fatigue test, describing automatic data acquisition system
08 p1163 A72-20916
- Wilga 3 aircraft structure service life from structural fatigue theory and tests, emphasizing operational load distribution measurement
08 p1110 A72-21634
- Epoxy and polyester resin fatigue fracture tests for cyclic stress and moisture effects
08 p1192 A72-21680
- Setup to determine sonic creep and acoustic fatigue in polymers under symmetrical and asymmetrical load cycles at sonic and ultrasonic oscillation frequencies
08 p1147 A72-21763
- German monograph on computerized statistical analysis of Al alloy fatigue test data, considering welded samples and thin plates
08 p1188 A72-21848
- Metric swaged pipe coupling design and development for aircraft hydraulic systems, presenting fatigue test results
08 p1179 A72-21940
- Turbine blade root attachment service life determination from fatigue tests with T shaped models
09 p1373 A72-22300
- Fatigue failure mechanism in short fiber reinforced plastics, determining crack growth rates under cyclic loading
09 p1336 A72-22539
- Propagating crack properties characterization during fatigue cycling, using ultrasonic flaw detection and acoustic emission
09 p1310 A72-22922
- Quenched and tempered Ni carbon steel retained austenite transformation and crack observation by X ray diffraction under low cycle fatigue testing
09 p1329 A72-23149
- Ni carbon steel microstructure changes in retained austenite phase and crack observation during low cycle fatigue testing
09 p1330 A72-23150
- DC-10 aircraft structural design, flight handling characteristics and fatigue tests
09 p1262 A72-23446
- Welded high strength maraging steels fatigue performance, stressing nondestructive testing technique
09 p1332 A72-23617
- Cumulative fatigue damage in Al-Zn-Mg alloy fillet welded joints, analyzing constant amplitude and programmed load fatigue test results
09 p1332 A72-23618
- Data scatter reduction in Al-Zu-Mg welded specimens cumulative fatigue damage testing, noting fatigue life improvement by shot peening and static or dynamic prestressing
09 p1332 A72-23619
- Tensile and fatigue tests of dissimilar metal joints made by friction pressure welding
09 p1321 A72-23640
- Power transistor thermal cycling ratings and fatigue testing under operating conditions
10 p1447 A72-24011
- Crack toughness tests of fiber composite laminates, using linear elastic fracture mechanics
10 p1500 A72-24258
- Tensile, plane strain fracture toughness and fatigue tests of high strength Al alloy cylinders, discussing unstable crack growth conditions
10 p1498 A72-24887
- Calibration procedure for crack length determination based on in test crack opening displacement monitoring
10 p1559 A72-24900
- Statistical evaluation of welded airframe component fatigue damage increment during cyclic loading with constant force amplitude
10 p1559 A72-24922
- Cumulative shock loading fatigue in solids, describing experimental setup and fracture morphologies
10 p1560 A72-25124
- Fatigue failure modes of composite materials, considering fiber breakage, delamination, matrix cracking, interface debonding and void growth
11 p1670 A72-25461
- Two stress level cumulative fatigue damage prediction for glass fiber-epoxy laminates
11 p1670 A72-25462
- Soviet papers on high temperature metallography techniques and equipment covering test assemblies for fatigue and microhardness measurements
11 p1654 A72-25489
- Aircraft wing structure fatigue life estimates based on flight load time histories from counter accelerometers
11 p1733 A72-25569

Crack initiation detecting and recording instrument with optical strain gages for double shear fatigue tests of aircraft fasteners

11 p1632 A72-25823

Locati and Prot methods for metal fatigue limits evaluated by axial and rotating bending tests on steel specimens

11 p1657 A72-25824

Heat treated carbonized, cyanided, nitrided and boronized steels fatigue limit dependence on static strength, residual stress, brittleness and stress concentration

11 p1659 A72-26128

Theoretical fatigue test procedure for reliability analysis of machine parts, calculating fatigue probability in load carrying components

11 p1640 A72-26244

Udimet 500 alloy dislocation substructure and fracture surface topography during deformation to failure in low cycle fatigue at high temperatures

11 p1667 A72-26938

Fatigue failure criteria under combined stress conditions, considering complex form, thin and thick welded cylinders as test specimens

12 p1828 A72-27317

Fatigue failure tests of low carbon Mn steel, analyzing structural damage under cyclic loads in relation to temperature curve

12 p1829 A72-27458

Fatigue testing of blade materials at high temperatures with periodic spray moistening by liquid corrosive medium

12 p1829 A72-27459

Metal fatigue strength testing under programmed temperature regimes, using HF induction generator

12 p1796 A72-28247

Accelerated reliability, life, fatigue and performance tests of automatic systems components, noting mathematical models for minimum time techniques

13 p1965 A72-29172

Unsteady loading effects in high temperature fatigue tests of refractory alloys for turbine blades, noting steady and programmed notch tests

13 p1980 A72-29494

Literature survey of fatigue behavior of Al alloy welded joints, discussing testing and analysis methods

14 p2113 A72-30250

Airframe and wing fatigue life testing, discussing results recomputation for changed operating conditions

14 p2092 A72-30276

Resonance type facility using dynamic hysteresis loop method to test metal fatigue and anelasticity in torsion at room and high temperatures

14 p2092 A72-30443

Fatigue crack growth rate in precracked steel samples observed at 100 C by etching technique, noting flow stress and yield in plastic zone

14 p2119 A72-30608

Mill annealed Ti alloy fatigue at 600 F and room temperature, noting critical local stress for slip bands formation and cracking

14 p2120 A72-30611

Metal fatigue tests at various frequencies to observe surface structure, dislocations in crack vicinity, plastic deformation and ultrasonic resonance techniques

15 p2257 A72-31839

Rotating bending fatigue limit correlation with non-propagating crack for steel specimens with hole

15 p2329 A72-32140

Cost-saving techniques in helicopter structural test methods, suggesting system simulation, component replacement time calculation and computer techniques

16 p2373 A72-33221

Crack depth measuring instrument for fatigue crack propagation study in notch tests, noting application at high temperatures

16 p2391 A72-33234

Nondestructive vibration tests of fatigue crack damage in composite structures, investigating glass reinforced epoxy and polyester laminates

16 p2414 A72-33318

Cyclic compressive fatigue cracking tests of prenotched fiber reinforced epoxy materials at low stress

16 p2414 A72-33319

Incoloy low cycle fatigue tests at high temperatures and different strain rates, discussing fatigue life at 10 and 60 min hold times

16 p2410 A72-33820

Deformation substructures in stainless steels under low cycle high strain fatigue tests evaluation for application as fuel cladding for fast breeder reactors

16 p2411 A72-33825

Automatic recording instrument for crack initiation time and breakdown curve for low carbon and stainless steel corrosion-fatigue tests under bending and tensile loads

16 p2394 A72-33849

Results of preliminary studies of a bearingless helicopter rotor concept.

[AHS PREPRINT 600]

Full scale airframe fatigue testing of the CH-46.

[AHS PREPRINT 671]

17 p2489 A72-34490

17 p2491 A72-34511

Fretting corrosion fatigue prevention by barrier approach, discussing test program and application to helicopter part fatigue life increase

[AHS PREPRINT 672]

Use of special gauges for determining crack growth rate in fatigue in the AU4G1 aluminum alloy

17 p2626 A72-34512

Static and tension fatigue and free edge delamination damage induced by uniaxial tensile loads in flat graphite/epoxy laminate coupons

17 p2567 A72-34890

An approach to the analysis of the nonlinear deformation and fatigue response of components subjected to complex service load histories.

18 p2733 A72-36355

The effect of high vacuum on the low cycle fatigue law.

18 p2700 A72-36582

Comparison of experimental and theoretical thermal fatigue lives for five nickel-base alloys.

19 p2815 A72-37639

Evaluation of the tendency to brittle fracture of turbine rotors made from steels of medium strength

19 p2876 A72-38001

Heat resistant alloys stress-rupture strength tests for operating temperatures based on equivalent high temperatures damageability

19 p2818 A72-38008

Effect of the loading frequency on the fatigue strength of metals

19 p2818 A72-38012

Influence of the structure of VTZ-1 and VT-18 alloys on the fatigue strength for an asymmetrical loading cycle

19 p2819 A72-38017

On a method of analysis of the strain energy changes taking place during the rotary bending fatigue test of carbon steels and an effect of the pearlite patches to these changes.

20 p2935 A72-38881

On the fatigue crack propagation in polymeric materials.

20 p2943 A72-38886

On the cumulative fatigue damage of glass fiber reinforced plastics subjected to repeated tensile impact load.

20 p2943 A72-38888

Environmental acceleration of fatigue-crack growth in a high-strength steel.

20 p2935 A72-39140

The octahedral shear strain theory and its relation to biaxial cumulative fatigue damage.

20 p2978 A72-39202

The matrix fatigue behaviour of fibre composites subjected to repeated tensile loads - Application to B/Al 6061 composites.

20 p2936 A72-39208

Effect of thickness and orientation on fatigue crack growth rate in 4340 steel.

20 p2937 A72-39294

Fatigue tests at low cyclic loads of smooth and notched Ti alloy specimens, noting surface hardening effect on service life

20 p2941 A72-39580

Thermal fatigue resistance of KhN70VMuT boronized alloy

20 p2941 A72-39585

Possibility of determining the fracture toughness of materials on the basis of the form of static bend test fracture samples.

20 p2941 A72-39714

Review - Fatigue-crack propagation in metallic and polymeric materials.

20 p2980 A72-39793

Fatigue strength of welded aluminum-connections - Investigation with the aid of multiparameter life length lines

20 p2930 A72-39941

Fatigue-crack propagation characteristics of aluminum alloys in thick sections.

20 p2942 A72-39951

Criteria for valid plane strain fracture toughness testing dealing with straightness of fatigue crack front of metal specimens

20 p2981 A72-39958

Effect of notch root radius on the initiation and propagation of fatigue cracks.

20 p2981 A72-39960

Study of fatigue crack initiation from flaws using fracture mechanics theory.

20 p2981 A72-39961

Crack arrest and crack initiation in a titanium alloy.

20 p2942 A72-39962

Cyclic stress-strain induced buckling and fatigue failure in cold-rolled steel and tabulating and diagramming mechanical properties

21 p3065 A72-40233

Fatigue damage of aluminum alloy at high temperature.

21 p3066 A72-40716

Isothermal deformation behavior of structural metals in laboratory creep, relaxation and low cycle fatigue tests at high temperatures

21 p3119 A72-41009

Non-destructive examination of fibre reinforced polymers with special reference to continuous carbon fibre reinforcement.

[ICAS PAPER 72-44]

Influence of the cycling frequency and directional anisotropy on the fatigue strength of AMg6BM aluminum-alloy sheet

21 p3073 A72-41169

Facility for measuring and recording the electrical resistance of metallic samples during mechanical tests

21 p3043 A72-41718

Fatigue properties of 18-8 stainless steel at cryogenic temperatures.

21 p3071 A72-41845

The accumulation of damage in a glass-reinforced plastic under tensile and fatigue loading.

22 p3196 A72-42456

Testing procedures for the design and life estimation of fatigue-sensitive structures.

22 p3241 A72-42974

Effect of cyclic stress wave form on corrosion fatigue crack propagation in Al-Zn-Mg alloys.

22 p3194 A72-43043

Book - Effect of notches on low-cycle fatigue: A literature survey.

22 p3242 A72-43145

Influence of the cycling frequency on the fatigue and corrosion fatigue of steel samples with bushings

22 p3242 A72-43155

Investigation of the kinetics of low-cycle fatigue of steels in a hydrogen atmosphere and in vacuum

22 p3195 A72-43161

Heat treatment effectiveness criteria for thermomechanically strengthened steels, using creep rupture, fatigue, bending and tensile tests

23 p3300 A72-43643

Utilization of computers in mechanical strength studies

23 p3345 A72-43644

Some preliminary observations on the extension of cracks under static loadings at elevated temperatures.

23 p3301 A72-43712

Gas turbine blades of cast ZrSiO₂ heat resistant alloy, investigating structural strength from fatigue test data

23 p3347 A72-43734

Failure and crack formation in gas turbine engine compressor disks under variable stresses from fatigue tests, considering safety factors

23 p3347 A72-43736

Energy dissipation in metals during high-frequency fatigue tests. I

23 p3302 A72-43963

Energy dissipation in metals during high-frequency fatigue tests. II

23 p3302 A72-43964

High-frequency fatigue testing facility, U-20P, with programmed control of the sample's vibration amplitude

23 p3278 A72-43970

Electron fractography of fatigue failure and macrocrack propagation in dual phase Ti alloy during cyclic loading at minus 140 to plus 150 C

23 p3303 A72-44097

Fatigue behavior of a titanium 8Al-1Mo-1V alloy in a dry argon environment.

23 p3304 A72-44261

The difference in the plastic deformation of the surface and bulk layers of polycrystalline iron under fatigue loading

23 p3304 A72-44490

The stress-strain relation in the low-cycle fatigue of metallic materials under rotating-beam bending.

24 p3454 A72-44626

Mean stress effects on fatigue crack propagation rate from tests at various temperatures, assuming initial, tensile and shear modes and final propagation stages

24 p3454 A72-44627

The cyclic plastic strain and cumulative fatigue damage - Fatigue damage caused by the stress below the fatigue limit.

24 p3454 A72-44628

The fatigue strength under varying mean stress.

24 p3455 A72-44629

Polymer fatigue failure mechanism examination on constant deflection type testing machine, investigating applied stress and temperature effects on crack propagation rate

24 p3455 A72-44631

Life prediction of expulsion bladders through fatigue test and fold strain analysis.

24 p3455 A72-44672

Fatigue testing of the F.28 Fellowship.

24 p3366 A72-44729

Fan jet Falcon design and certification tests.

24 p3366 A72-44731

The fatigue and fail-safe program for the certification of the Lockheed Model 286 rigid rotor helicopter.

24 p3366 A72-44733

Aircraft structures fatigue life expectancy under random acoustic excitation, describing testing methods and equipment

24 p3367 A72-44739

Economic and operational aspects of fatigue - Figures of a Swiss ground attack/fighter aircraft. 24 p3367 A72-44742

Plane-stress fracture toughness testing using a crack-line-loaded specimen. 24 p3456 A72-44810

Fatigue crack closure at positive stresses. 24 p3457 A72-44819

Ultrasonic detection of fatigue damage. 24 p3457 A72-44820

Temperature dependence of low temperature endurance of Cr-Ni steels in bending fatigue tests. 24 p3413 A72-44938

Endurance tests of D16AMO alloy sheets under high intensity acoustic, harmonic and electrodynamic vibrator loading. 24 p3414 A72-44945

Al and Ti alloy fatigue after temperature reduction to 253, 77 and 4 K as function of surface purity after machining. 24 p3416 A72-45743

Stepwise fatigue testing of high temperature alloy, noting strain hardening phenomena in prestressed samples. 24 p3416 A72-45755

FATTY ACIDS

NT OLEIC ACID

Tobacco tissue cultures with Apollo 12 lunar material, determining endogenous sterols and fatty acids concentrations by gas chromatography and mass spectrometry. 07 p0920 A72-19850

Glucose and fatty acid metabolic response during impending myocardial infarction in animals. 07 p0921 A72-20175

Dose dependent hyperglycemia and hypolipemia response to pentobarbital sodium injection in rats from plasma glucose and fatty acid analysis. 08 p1116 A72-21187

Myocardial infarction stress effect on serum cortisol, plasma free fatty acid and urinary catecholamine levels. 11 p1582 A72-26787

Induction of ventricular arrhythmias by elevation of arterial free fatty acids in experimental myocardial infarction. 17 p2502 A72-34997

Dietary regulation of fatty acid synthesis in rat liver and hepatic autotransplants. 19 p2757 A72-38147

Human plasma free fatty acids relation to lactic acid concentration and maximum aerobic power, noting carbohydrate availability as exercise capacity limiter. 21 p3003 A72-41520

FAULT MECHANICS

U FRACTURE MECHANICS

FAULTS

Nondestructive testing of electroexplosive devices, considering bridgewire-explosive interface and faults-abnormalities interrelationship. 08 p1220 A72-20764

FAYALITE

Activity-composition relations in the fayalite-forsterite solid solution between 900 and 1300 C at low pressures. 20 p2915 A72-39178

FBFM [MODULATION]

U FEEDBACK FREQUENCY MODULATION

FCC LATTICES

U FACE CENTERED CUBIC LATTICES

FEAR

Hypothalamic stimulation conditioned negative fear reflex in cats before/after neocortex isolation. 07 p0920 A72-19859

FEASIBILITY

Radial inflow compressor feasibility, discussing blade loadings for various pressure ratios and efficiency of rotor and diffuser. 11 p1570 A72-25644

FEDERAL REPUBLIC OF GERMANY

U GERMANY

FEED SYSTEMS

Tunnel diode quartz oscillator frequency stability improvement and dc power requirement reduction using nonlinear feed circuits. 03 p0331 A72-13555

Satellite electrical power, discussing energy converters, satellite feeder subsystem and voltage requirements. 03 p0311 A72-13639

Design and performance characteristics of ion thruster feed system components including high voltage isolator, liquid Hg flowmeter and W vaporiser. 11 p1710 A72-26213

Miniaturized electronic system for controlling methanol concentration in aqueous electrolyte during fuel cell operation. 12 p1755 A72-27723

Investigation of the dynamic characteristics of the speed governor of a hydropneumatic feed drive. 23 p3253 A72-44022

FEEDBACK

NT NEGATIVE FEEDBACK

NT NONLINEAR FEEDBACK

NT POSITIVE FEEDBACK

NT SENSORY FEEDBACK

Motivation in vigilance, studying effects of subject self evaluation and experimenter /knowledge of results/ controlled feedback. 06 p0766 A72-17711

Hollow dielectric waveguide for distributed feedback lasers. 17 p2564 A72-35346

On a feedback communication system having iteration control in the forward channel. 21 p3039 A72-41826

FEEDBACK AMPLIFIERS

Balanced negative feedback circuits for reducing nonlinear distortions in distributed gain power amplifiers. 02 p0193 A72-12223

Superregenerative linear mode amplification in Q switched He-Xe laser as function of resonator phase, length and signal angle. 04 p0531 A72-15147

IMPATT diode avalanche region microwave self oscillation mechanism explanation by cavity resonator and feedback theories. 06 p0787 A72-18383

LF noise generator with Rice variable amplitude probability distribution law, using shielded vacuum tube superregenerative amplifier. 09 p1285 A72-22345

Noise characteristics of regenerative amplifier with direct coupling to load. 13 p1929 A72-28897

Selectivity evaluation for regenerative amplifiers of complex design. 13 p1929 A72-28898

Forward loop signal attenuation and phase shift diagrams for design of feedback amplifier and compensation network for dc flyback converter. 13 p1899 A72-29110

Forced oscillations in RC amplifier with negative feedback through nonlinear bandpass filter with varicaps. 13 p1931 A72-29266

Feedback ac compensating amplifier design for automatic AM signal envelope conversion, noting truncated equivalent transfer function expandability. 13 p1933 A72-29972

Theoretical model for computer calculation of transients in oscillator consisting of nonlinear amplifier with feedback through sequence of matched LC circuits. 16 p2371 A72-33280

High precision electrostatic feedback transducer for very low differential pressure measurement in gas media, suggesting low pressure standard role. 16 p2394 A72-33638

Optimal number of parallel transistor connections in feedback amplifier to improve SNR. 18 p2665 A72-36108

Regenerative nonlinear RC amplifier oscillations due to series opposed varicap diode capacitance. 18 p2783 A72-36109

Design considerations of a 3.1-3.5 GHz GaAs FET feedback amplifier. 19 p2771 A72-37269

Optimal delay control circuit adjustment by approximate calculation with quadratic error integral and ITAE criterion dependence on loop amplification. 19 p2783 A72-38643

Calculation of two- and three-stage broadband amplifiers with parallel correction from the standpoint of a maximum quality factor with an optimally flat amplitude characteristic. 21 p3027 A72-40477

Amplification cascade designs for harmonic and pulsed signals with a high frequency emitter correction. 21 p3033 A72-40946

SNR improvement by negative feedback and deterioration by positive feedback in amplifiers, discussing input circuit thermal noise. 21 p3034 A72-41123

FEEDBACK CIRCUITS

Motional feedback systems comparison for ultrasonic transducers operated as resonant emitters, describing circuitry for self excitation. 01 p0070 A72-11019

Coding for analog and digital data transmission over channels with noiseless and noisy feedback links. 02 p0197 A72-11680

Ruby ring laser single mode operation with Fabry-Perot etalons for selective feedback, discussing laser emission spectrograms. 03 p0366 A72-13194

Self oscillating dc-dc converter analysis and optimal design, modeling by single loop nonlinear feedback system. 04 p0465 A72-14571

Human neuromuscular coordination control optimization, discussing preprogrammed open-loop control with feedback monitoring loop. 04 p0477 A72-14705

M-ary orthogonal signal phase noncoherent detection in sequential decision feedback, comparing performance with optimal coherent reception. 06 p0773 A72-17596

Block orthogonal M-ary communication over fading dispersive channel with intermittent on-off noiseless feedback, calculating upper and lower bounds on error probability. 06 p0776 A72-18389

Frequency discriminator like two-channel device with greater sensitivity by crossed feedback, calculating variable frequency emf effect on operation. 07 p0938 A72-18853

Trajectory properties of roots of characteristic equations with complex coefficients for two dimensional systems with feedforward and feedback cross couplings. 08 p1200 A72-21768

Optimal answer-back communications systems using feedback channel for error checking. 09 p1277 A72-22568

Thermal and electric fields interaction in LF integrated circuits design, applying thermal feedback loops to bandpass filter, delay circuit and Schmidt-trigger oscillator. 10 p1448 A72-24280

Sequential machine realization with trigger or flip-flop elements and Boolean function feedback. 10 p1445 A72-24401

Capture range and acquisition time analysis of phase locked loop with active filter. 10 p1458 A72-24934

Wide dynamic range analog multiplier with variable transconductance divider in operational transistor amplifier feedback path. 11 p1603 A72-25742

Feedback and feedforward circuits to double operational amplifier output voltage swing with increased slew rate. 11 p1604 A72-25746

Transistorized measuring amplifiers optimal initial regimes calculation with generalized junction voltage method, noting circuits analysis and internal feedback loops. 11 p1605 A72-26467

Noise control by Helmholtz resonators, considering equivalent circuits via feedback schemes. 13 p2005 A72-29567

Nonlinear microwave circuit feedback model analysis by describing function in control theory, applying to oscillator phase locking problem. 15 p2210 A72-31355

Feedback averaging procedure application to M-ary polarization modulated laser communication system, obtaining error rate improvement over systems without feedback. 16 p2362 A72-33215

Noise stability of frequency-time adaptive transmission systems for discrete information, using resolving feedback circuits. 16 p2363 A72-33266

Random multiple access data transmission systems with feedback for message confirmation and retransmission in event of errors, evaluating channel capacity. 16 p2372 A72-33794

Data transmission systems with decision feedback in presence of burst noise, calculating statistical relations among received sequences as function of duration and spacing. 16 p2372 A72-33795

Linear negative feedback dc current magnetic transducers for telemetry input signals, discussing operation principles and design. 16 p2370 A72-33862

Ac voltage squaring with semiconductor power amplifier based on electronic servo principle and feedback circuit. 16 p2370 A72-33958

Transmission line with feedback, deriving Nyquist stability from Michailov criterion with application to liquid fuel rocket model. 17 p2621 A72-35100

One path ultrasonic flowmeter using electroacoustic feedback. 17 p2556 A72-35427

Development of a continuous linear model of a d-c to d-c flyback converter. 18 p2643 A72-36073

Digital simulation for radio frequency interference and specular multipath effects on FM spread spectrum demodulation with feedback and phase lock loops. 18 p2659 A72-36317

Feedback circuitry for dc amplifiers voltage drift compensation, discussing performance criteria in terms of residual offset voltage, system stability, correction and measurement time. 18 p2671 A72-37150

Effect of nonlinearity in the feedback circuit of a recirculation-type comb filter. 20 p2906 A72-38893

Feedback quantization noise effects on differential PCM systems, showing SNR relation to noise optimized prediction. 21 p3017 A72-40860

Phase locked feedback circuit for FM demodulation, discussing all digital circuit design and voltage controlled oscillator algorithm to avoid analog implementation problems. 21 p3018 A72-40873

- SNR improvement by negative feedback and deterioration by positive feedback in amplifiers, discussing input circuit thermal noise 21 p3034 A72-41123
- Effect of feedback and protective circuits on the reliability of electronic equipment 22 p3158 A72-42118
- Influence of a nonlinearity in a coherent accumulator of pulse signals on the gain in the signal-to-noise ratio 23 p3264 A72-43762
- Optimum reception algorithms in communication systems with decision feedback in presence of noise in forward and return channel 24 p3379 A72-44747

FEEDBACK CONTROL

- NT CASCADE CONTROL
- Analog computer simulation of automatic control systems containing time delay element in feedback loop, evaluating errors 01 p0044 A72-10152
- French monograph on extremum values of function with two variables and nonlinear feedback control systems stability, using associate recurrence solutions properties 01 p0044 A72-10164
- Information feedback application to AM laser communication system, predicting multiplicative error, background shot noise and photon arrival fluctuation effects on continuous parameter transmission [AD-736731] 01 p0025 A72-10326
- Frequency conditions of absolute stability for closed automatic control system with nonlinear unsteady units 01 p0045 A72-10499
- Plasma column equilibrium position feedback control based on combination principle, analyzing system stability 01 p0109 A72-10502
- Error fluctuation component spectral density determination in closed automatic nonlinear system for controlling random vibration spectrum 01 p0045 A72-10505
- Scientific satellite with simple inertial system, deriving discrete feedback reentry guidance algorithms based on closed-form equations solvable by onboard computer 01 p0098 A72-10944
- Human short term thermoregulation feedback-feedforward control mechanism, using hypothalamic temperature as set point 02 p0168 A72-12036
- Feedback control dynamic system described by linear differential equation with random coefficients, calculating parameters distribution effect on behavior precision 02 p0197 A72-12339
- Extremal system with second control loop for search signal frequency regulation to optimize primary loop operation, determining system dynamic errors under random drift 02 p0197 A72-12340
- Human operator dynamic characteristics measurement, using pseudorandom binary signals and mathematical models in closed loop control system 02 p0169 A72-12660
- Stochastic linear-quadratic-Gaussian problem role in optimal closed loop control system design, emphasizing philosophy, modeling and problem formulation [AD-738763] 02 p0198 A72-12801
- Optimal limited state variable feedback controllers design for static and dynamic linear systems [AD-738770] 02 p0198 A72-12809
- Linear multivariable interacting feedback control system optimal design by heuristic approach to determine input-output pairing and controller settings for satisfactory disturbance attenuation 03 p0337 A72-12905
- Neighboring optimal feedback control for multi-input nonlinear dynamical systems with discontinuous control, applying to minimum time satellite attitude acquisition problem solution 03 p0338 A72-13407
- Dc feedback controlled constant voltage transformer, comparing with ferroresonant regulator [IEEE PAPER 17.2] 03 p0311 A72-13771
- Double shunt feedback controlled ferroresonant voltage regulator using magnetic component with simulated core saturation [IEEE PAPER 17.3] 03 p0311 A72-13772
- Numerical method and computerized design for feedback controller pulse transfer function in overall error criterion minimization, comparing results with sampled error method 03 p0329 A72-14355
- Closed-loop temperature distribution optimal control by heater-sensor spatial configuration design for highest steady state temperature stiffness under heat flux disturbance 04 p0504 A72-14661
- Closed-loop nonlinear sampled-data systems with sampler and finite Hankel transformable distributed elements, deriving frequency domain stability criteria 04 p0504 A72-14662

- Nonlinear stochastic systems stability conditions description by Volterra integral equation, applying to distributed parameter feedback control system with nonlinear amplifier of random gain 04 p0504 A72-14663
- Dual variational principles application to distributed parameter system suboptimal control strategy evaluation, considering control variable and feedback gain as piecewise function of time 04 p0505 A72-14665
- Time-varying systems with observer for feedback control, investigating stability 04 p0506 A72-15108
- Minimal order precompensator with state feedback for decoupling linear time-invariant multivariable control system, discussing design parameters determination from linear equations 04 p0506 A72-15109
- Linear feedback control systems with time lag, calculating integrated squared error by Liapunov function 04 p0506 A72-15110
- Large linear time invariant dynamic control system optimum simplified model based on performance index connecting feedback errors 04 p0506 A72-15113
- Integrated PFM feedback control system, investigating stable periodic oscillation based on nonlinear discrete equivalence 04 p0506 A72-15114
- Multiple-input multiple-output linear time invariant feedback systems stability, investigating continuous-time case 04 p0507 A72-15694
- Analytical inversion of quasi-orthogonal matrix for Simpson method of state feedback gains calculation in multiloop linear mode control systems 05 p0639 A72-15807
- Linear single and multiloop control system synthesis for sensitivity reduction by introducing signals proportional to sensitivity functions with analyzer 05 p0640 A72-16207
- Optimal closed loop control of stochastic nonlinear systems by expanded cost function applied to reduced terminal error atmospheric entry problem 05 p0685 A72-16462
- Closed loop fluidic bidirectional jet flap airfoil lift control system, considering application to helicopter rotor blades 05 p0603 A72-16659
- Conventional open and closed loop servo analysis methods applied to Naval aircraft approach power compensator systems, using pilot model concepts [AIAA PAPER 72-124] 05 p0612 A72-16922
- Low density plasma flute oscillations stabilization by feedback system with potential sensors and electrodes, deriving dispersion equation 05 p0697 A72-16983
- Linear time-varying control systems with one feedback nonlinearity, determining combined time-frequency condition for stability 05 p0642 A72-17090
- Adaptive control for linear discrete time stochastic systems with unknown gain parameters, considering open loop feedback optimal control using quadratic performance index [AD-739126] 06 p0791 A72-17305
- Parameter adaptive self organizing control of linear discrete time systems, presenting stochastic approximation algorithms for feedback systems identification 06 p0791 A72-17306
- Optimally sensitive closed loop control synthesis for systems containing uncertain time varying parameters, applying to stochastic systems 06 p0792 A72-17309
- Third order nonlinear systems phase plane analysis, noting applicability to unity feedback closed-loop systems with linear memory 06 p0792 A72-17313
- Suboptimal feedback control for nonlinear dynamic processes, presenting control algorithm based on linear plant optimal solution 06 p0792 A72-17314
- On-off control system stability with feedback proportional to square of velocity, determining system frequency response 06 p0793 A72-17316
- Q-machine plasma column drift instability passive feedback control, regulating feedback drive current phase and amplitude by varying resonance circuit characteristics 06 p0857 A72-17532
- Second variational algorithm for iterative solution of unconstrained optimal control problems, examining linearized feedback control 06 p0839 A72-17592
- Optimal final value control systems in phase-variable canonical form, discussing feedback gain singularity structure for single and multiple input systems 06 p0793 A72-17954
- Noise, delay and interruption caused communication degradation effects on feedback control system performance, considering air navigation and computer aided command and control on battlefield 06 p0794 A72-18242

- German book on time variable multiparameter control systems covering reduction, canonical forms, decoupling, feedback stabilization, observers, inversion and multiloop synthesis 06 p0794 A72-18517
- Adaptive control system synthesis by steepest descent method, obtaining algorithms for parameters self adjustment loop construction 06 p0795 A72-18661
- Motion dynamics of aircraft-autopilot closed loop system under influence of atmospheric turbulence and electric circuitry thermal noise 07 p0911 A72-18990
- Phase lock loop receiving system digital simulation for estimating mean time to indicate lock and probability distribution function for wide SNR range 07 p0939 A72-19065
- Hybrid carrier and modulation tracking loops exploiting sideband coherency for phase coherent tracking, telemetry and command system performance improvements 07 p0939 A72-19066
- Real time near optimal closed loop control solution to fixed time nonlinear differential game by periodically updating to two point boundary value problem 07 p1027 A72-19278
- Aircraft optimal terminal guidance nonlinear feedback control law, deriving maximum principle by digital computer program 07 p1033 A72-19287
- Ultrasonic measurement technique for low microwave susceptibility on ferrite samples featuring feedback scheme for signal klystron locking 07 p0955 A72-19320
- Model-following algorithm and equicontrollability in multivariable feedback control systems, considering application to decoupling problem 07 p0960 A72-19698
- Linear multivariable systems feedback invariant structure of controllable matrix pair under rich transformation group including regular linear coordinate and state-feedback transformations 07 p0960 A72-19700
- Frequency response design for interactive multivariable feedback control systems, using characteristic transfer functions 07 p0960 A72-19704
- Linear time-invariant controllable plant, determining semiclosed loop nominally equivalent control realization for reduced sensitivity to plant parameter perturbations 07 p0961 A72-19705
- Linear multivariable system design based on relationship between performance index parameters and optimal response in frequency domain, exemplifying gas turbine feedback controller design 07 p0961 A72-19710
- Eigenvalue sensitivity in optimal feedback control systems with state estimation 07 p0962 A72-19716
- Linear multivariable feedback control system design techniques 07 p0963 A72-19723
- Absolute stability region of linear portion of single loop automatic control system with one nonlinear element determined by frequency criteria 07 p0963 A72-19723
- Control system stability with nonlinear feedback in steady equilibrium state 07 p0963 A72-20321
- Interactive graphics technique for design of single input linear feedback systems described by state equations or cascaded transfer functions 07 p0963 A72-20391
- Aircraft altitude two-loop feedback control system designed by compensation parameter variation technique, determining correlation between system sensitivity computations and observations 07 p0963 A72-20592
- Zero velocity lag servomechanism transient response sensitivity from intuitive approach to convolution problem, noting feedback compensation advantages in sensitivity reduction 07 p0964 A72-20593
- Time optimal closed loop control system synthesis by phase space technique verifying results by state variable approach 07 p0964 A72-20595
- Closed loop covariances prediction in reentry vehicle tracking and data compression, presenting simulation results 08 p1144 A72-20846
- Self excited oscillations and transient responses of spacecraft stabilization relay system with delayed feedback, analyzing time delay effects in actuator circuit 08 p1241 A72-21170
- Algorithm to compute inertial navigation system altitude and vertical velocity by closed feedback loop with accelerometer output mixed with pressure altitude reference 08 p1204 A72-21411
- Feedback control dynamic system described by linear differential equation with random coefficients,

calculating parameters distribution effect on behavior precision

08 p1146 A72-21554

Extremal system with second control loop for search signal frequency regulation to optimize primary loop operation, determining system dynamic errors under random drift

08 p1146 A72-21555

Adaptive statistical system with feedback loop for weather analysis and forecasting, examining learning process features

08 p1202 A72-22113

Hydraulic actuator servomechanism performance dependence on asymmetrical spool valve lap and closed loop system stability

08 p1113 A72-22153

Nonlinear closed loop system reduction of differential trajectory sensitivity to continuous variations or external disturbance

09 p1340 A72-22245

Linear multivariable system stabilization by output feedback technique based on gradient approach

09 p1290 A72-23097

High power Ar laser frequency stabilization technique using multiple feedback loop with optical cavity discriminator stabilized against iodine vapor absorption line

09 p1325 A72-23337

Stability degree analysis of linear feedback control systems with dead time, presenting proportional and integral compensation diagrams produced with digital computer program

09 p1291 A72-23370

Digital computer prepared optimal controls setting diagrams for single loop, linear and concentrated parameter control circuit design

09 p1291 A72-23372

Homogeneous plasma internal feedback mechanism and structure, discussing instabilities control by external feedback

09 p1365 A72-23474

Quadratic performance index generation for optimal design of completely controllable, scalar linear system with state feedback

10 p1454 A72-23783

Computer aided design of linear time-invariant multivariable feedback control systems, given specifications in frequency domain in stability margin form

10 p1455 A72-23789

Nonlinear programming and parameter optimization algorithms for constrained feedback control system design

10 p1441 A72-23790

Near optimal closed loop control laws for fixed time pursuit-evasion differential game between two aircraft in vertical plane, using dynamic modeling

10 p1421 A72-23805

Minimax feedback control of uncertain discrete time dynamic systems with set description, using dynamic programming

10 p1456 A72-23806

Optimal closed loop control of discrete stochastic nonlinear systems, considering guidance and navigation for space and terrestrial vehicles

10 p1456 A72-23811

Sensitivity comparison of equivalent open and closed loop optimal control systems, extending performance index formulas to instantaneous and isoperimetric constraints

10 p1456 A72-24456

Optimal closed loop control of discrete stochastic nonlinear systems, obtaining solution by cost function in power series around deterministic trajectory

10 p1457 A72-24499

YIG tuned Gunn oscillator phase locking and shifting over 3 GHz range in X band, using feedback control

10 p1451 A72-24596

Steady state operation of automatic control system to stabilize random vibration spectra, noting maximum control accuracy at optimum loop gain

10 p1457 A72-24635

Closed and open loop transfer function coefficients relationship for steady state linear system with proportional elements in feedback and parallel paths

10 p1457 A72-24724

Optimal control of linear stochastic feedback systems described by functional differential equations

10 p1458 A72-25145

Discrete time systems with periodic feedback gain, deriving stability conditions and Nyquist plot from linear operator spectral theory

11 p1608 A72-25318

Stationary weighting pattern synthesis by linear time varying dynamic system, noting feedback system input-output mapping properly

11 p1608 A72-25321

Input-output stability of linear time invariant multivariable closed loop control systems

11 p1608 A72-25327

Extremal feedback control system operation with integral PFM in extremum drift mode, determining equations of motion and steady state regime

11 p1610 A72-25449

Asymptotic stability of astatic pulse frequency modulated feedback control systems with discrete correction, obtaining sufficient conditions in closed form with Liapunov method

11 p1610 A72-25450

Suboptimal feedback control law synthesis for nonlinear systems, using second order approximation to optimal control

11 p1610 A72-25872

Computer aided iterative design of nonlinear single loop control system with sinusoidal describing function and time response display capability

11 p1601 A72-26042

Extremal feedback control system for IR and sub-millimeter range laser emission frequency stabilization

11 p1650 A72-26358

Closed loop system stability, considering small gain and passivity theorems interrelationship and scattering matrix

11 p1612 A72-26470

Hydraulic feedback servomechanism for dynamic response characteristics control, discussing design parameters and fluid properties influence on system performance

11 p1578 A72-26981

Low density plasma flute oscillations stabilization by feedback system with potential sensors and electrodes, deriving dispersion equation

12 p1850 A72-27127

Hydrofluidic stability augmentation system /HYSAS/ development for military helicopters, discussing test program and technical feasibility

12 p1754 A72-27407

Flight tests of stability augmentation system for light airplane improving pilot control during IFR encounter

12 p1754 A72-27513

Optical feedback exposure control mechanism of high resolution CRT film recorder intended for tactical military usage

12 p1810 A72-27932

Spurious oscillations in external excitation oscillators due to internal feedback in transistor, investigating frequency dependence of stability coefficient in cascade with common emitter

13 p1929 A72-28896

Random vibration statistics of lifting rotors with feedback controls, solving response variance matrix by random inputs shaping filters

13 p2057 A72-29096

Computerized synthesis technique for nonlinear feedback control systems, incorporating circle and Popov criteria

13 p1936 A72-29107

Ionization stabilization in MHD generators by sensing electron density perturbation with linear feedback into nonequilibrium plasma

13 p2014 A72-29369

Nonsingular feedback control system phase-amplitude frequency response graphical analysis using real circle diagram

13 p1937 A72-29974

Russian book on high precision servo systems synthesis covering combined feedback and open loop controls, accuracy improvement and root-mean-square errors minimization

15 p2210 A72-31273

Book on phase locked and frequency feedback systems covering FM and multiple loop principles, limiter-discriminator operation, phase detection techniques, etc

15 p2210 A72-31500

Optimal feedback controller design based on cooperative game described by quadratic cost functional under linear differential equation constraints, applying to satellite terminal rendezvous

15 p2267 A72-31789

Optimal thrust direction for planetary escape at residual speed, using approximate explicit closed loop guidance scheme

15 p2268 A72-31821

Suboptimal feedback control for aircraft gust alleviation design, using indirect perturbation information through normal acceleration factor measurement

15 p2181 A72-32025

Pulsed solid state lasers with large area Si photodiode for output measurement in feedback control system to compensate flash lamp aging

15 p2247 A72-32027

Single closed loop discontinuous control system, determining discrete correcting element parameters from linear inequalities

15 p2212 A72-32175

Infinite dimensional system optimal discrete-time feedback controller calculation by n-dimensional system approximation using recurrence relations with functional analysis

15 p2212 A72-32245

Flexible launch vehicle optimal and constrained-optimal control for performance index minimization, using sensors and constant feedback gains

15 p2321 A72-32585

Flexible space vehicle multiple closed loop attitude control system design, discussing stability, structure interaction and performance by analog simulation

15 p2321 A72-32587

Digital computer studies of control loop parameters and configurations effects on performance of synchronous turbogenerator with two field windings

15 p2183 A72-32793

Limit cycle stability of third and higher order feedback systems predicted from negative slope of describing function

15 p2213 A72-32796

Limit set configuration of optimal nonlinear feedback control scheme in n-dimensional state space

15 p2213 A72-32797

Discrete system feedback design based on complex number plane mapping, determining gain

15 p2213 A72-32800

Flutter instability control in continuous elastic system via feedback

16 p2463 A72-32843

Automatic systems design for monitoring dynamic control systems, noting feedback control system performance prediction based on subsystems characteristics

16 p2371 A72-33085

Hydrofluidic three-axis stability augmentation system to improve UH-1B helicopter damping and handling qualities during high speed gunfiring missions

16 p2350 A72-33650

Extremal feedback control system for IR and sub-millimeter range laser emission frequency stabilization

16 p2403 A72-33711

State dependent state variable feedback method to control multiple input multiple output nonlinear and/or time varying systems

17 p2532 A72-34420

Stabilization of magnetohydrodynamic flows by a distributed feedback system

17 p2587 A72-34459

Hingeless rotor - Experimental frequency response and dynamic characteristics with hub moment feedback controls.

17 p2489 A72-34494

[AHS PREPRINT 612] Constant voltage and constant emitter-temperature control schemes dynamics in thermionic reactor, showing closed loop responses to load changes, converter failures and reactivity perturbations

17 p2494 A72-34581

Modularized digital controller for closed loop systems using MOS, MSI and LSI components

17 p2521 A72-34703

Hydrofluidic stability augmentation system for U.S. Army helicopters, emphasizing reliability, maintainability and reduced cost

17 p2492 A72-34928

Controllability, observability and optimal feedback control of affine hereditary differential systems.

17 p2533 A72-34950

Equivalent predictions of the circle criterion and an optimum quadratic form for a second-order system.

17 p2577 A72-35534

Stability of linear time-invariant distributed parameter single-loop feedback systems.

17 p2534 A72-35535

Design of simple control loops in the time domain by simulation of the hybrid mode

17 p2534 A72-35756

State feedback control law for linear multiinput multioutput time-invariant dynamic system under disturbance to obtain output with zero steady state error

18 p2672 A72-36054

Nonlinear dynamic feedback control systems modeling by parameter estimation scheme with polynomial representation for state variables

18 p2672 A72-36057

Functional relationships between the conventional steady-state error characteristics and the weighting matrices in the quadratic performance index.

18 p2672 A72-36058

Feedback controller synthesis from nonlinear system modeling by linear equations, proving theorem relating stability properties

18 p2672 A72-36060

Closed loop dynamics of in-core thermionic reactor systems.

18 p2644 A72-36173

Feedback synthesis of an incore thermionic reactor control system for space.

18 p2645 A72-36186

Optimal signal design for digital center of gravity feedback communications over white noise channels, using energy ratio functions

18 p2659 A72-36316

Digital controller for high pressure rocket engine.

18 p2721 A72-36335

Second order differential guidance game, formulating strategy for optimal feedback control

18 p2673 A72-36660

Optimal control of plants whose transfer functions contain zeros.

18 p2673 A72-36724

Feedback influence coefficient on amplifier gain, using recurrent difference concept

19 p2777 A72-37314

Choice of parameters for measuring devices in a closed-loop linear control system

19 p2777 A72-37319

A fluidic sensor for closed loop engine acceleration control.

19 p2849 A72-38049

State-feedback-controllers and state-estimators design for roll-pitch-horizontal motions of helicopter near hover, using rotor dynamics model

[AIAA PAPER 72-778] 19 p2752 A72-38137

Digital programming techniques for maximum utility and flexibility in filament winding.

19 p2808 A72-38170

Optimal selection of stability augmentation parameters for excellent pilot acceptance.

19 p2752 A72-38227

The output control of linear time-invariant multivariable systems with unmeasurable arbitrary disturbances.

19 p2779 A72-38231

Algorithm for linear multivariable systems synthesis via combined dynamic feedforward compensation and linear state variable feedback

19 p2779 A72-38232

A circle criterion for nonlinear stochastic feedback systems.

19 p2779 A72-38235

Invariant poles feedback control of flexible, highly variable spacecraft.

19 p2869 A72-38240

Control theory stability criteria applied to discrete time feedback systems, investigating numerical integration methods for initial value problems solution

19 p2826 A72-38250

Recent results concerning a graphical test for checking the stability of a linear time-invariant system.

19 p2826 A72-38251

On-line identification of multivariable stochastic feedback systems.

19 p2781 A72-38270

Decoupling and synthesis of certain nonlinear systems.

19 p2827 A72-38275

The dynamic modeling technique for obtaining closed-loop control laws for aircraft/aircraft pursuit-evasion problems.

19 p2753 A72-38276

Feedback loop equations and discrete measuring point methods for synthesis of optimal control systems with location dependent controlled variables

19 p2782 A72-38311

Decoupling of linear discrete time systems by state variable feedback.

19 p2827 A72-38563

Study of the stability of a polar coordinate compensator

19 p2783 A72-38581

Problems and solutions related to the design of a control augmentation system for a longitudinally unstable supersonic transport.

[AIAA PAPER 72-871] 20 p2887 A72-39128

Synthesis of feedback systems with large plant ignorance for prescribed time-domain tolerances.

21 p3037 A72-40643

Bounded-input bounded-output stability of nonlinear discrete systems by a method of comparison.

21 p3037 A72-40645

Linear distributed parameter systems modal analysis and design for low sensitivity optimal feedback control, using linear differential operators

21 p3037 A72-40646

Certain features of the use of controllable-gain transistors

21 p3033 A72-40944

Linear analog to pulsewidth converter insertion into control loop in dc/dc regulators for space applications to permit high sampling frequencies

21 p2997 A72-41081

Effect of single-bit digitization in adaptive array control loops.

21 p3034 A72-41085

Lectures on theory of manual-vehicle control.

21 p3011 A72-41418

Some contributions to the theory of linear models describing the control behaviour of the human operation.

21 p3011 A72-41419

A method for the development and optimization of controller-models for man-machine systems.

21 p3011 A72-41420

Automatic measurement of microwave-cavity parameters using stable sampled control loops.

21 p3034 A72-41465

Investigation of the stability of a hydraulic servo motor with rigid feedback

22 p3139 A72-41858

Stabilities and settling times of nonlinear and time-varying feedback systems.

22 p3161 A72-41937

Compatible controllers for time-varying linear plants.

22 p3161 A72-41939

Development and optimization of a nonlinear multiparameter human operator model.

22 p3149 A72-41949

Construction of Liapunov functions for time-dependent systems containing inertialess nonlinearities

22 p3205 A72-42176

Liapunov function method in control problems of distributed parameter systems [Survey]

22 p3205 A72-42180

Low frequency measurement of mechanical impedance and frequency response.

22 p3164 A72-42700

Synthesis of linear stationary systems with the aid of proportional elements

22 p3162 A72-42738

Limitations on the synthesis of control systems in the case of incompletely accessible state variables

22 p3162 A72-42739

Choice of loop gain for a hydraulic servo system

22 p3140 A72-42921

Closed loop pulsed automatic control system, determining discrete correcting element parameters from linear equalities

22 p3163 A72-43009

Infinite-time reachability of state-space regions by using feedback control.

23 p3274 A72-43538

Extension of analytical design techniques to multivariable feedback control systems.

23 p3274 A72-43539

An improved general algorithm for arbitrary pole assignment.

23 p3275 A72-43546

Output-feedback control law for randomly distributed multivariable system.

23 p3275 A72-43608

Design of controllers for open-loop unstable multivariable system using inverse Nyquist array.

23 p3275 A72-43609

Decoupling and diagonalization conditions determination for nonlinear multivariable time-varying differential equations system by state feedback, giving illustrative examples

23 p3275 A72-43611

Optimally sensitive control for distributed parameter systems.

23 p3275 A72-43612

A direct method for computing optimal feedback control for linear systems.

23 p3275 A72-43613

Molecular-beam-stabilized argon laser.

23 p3296 A72-43817

Recent results in convolution feedback systems.

23 p3276 A72-43861

Digital filter design using observers.

23 p3276 A72-43864

An inertially balanced servo.

23 p3311 A72-43866

Forward-error correction with decision feedback.

23 p3268 A72-44175

A method for synthesizing feasible correcting devices with a minimum number of constraints on the optimized transient pulse response function

24 p3386 A72-45318

Algorithmic description of the generalized operational characteristic of a human operator

24 p3376 A72-45515

Estimate of the operational efficiency of a human operator in the follow-up mode of a closed-loop control system

24 p3376 A72-45516

Experimental determination of the distribution rule for the time of failure-free operator action in the tracking mode /with pursuit/

24 p3377 A72-45521

Allowable regions for stability multiplier characteristics.

24 p3420 A72-45787

FEEDBACK FREQUENCY MODULATION

Wideband modulation feedback technique for IMPATT diode oscillator AM-FM noise suppression

01 p0037 A72-10647

Signal frequency distortions in frequency-modulated oscillators with feedback delay

23 p3266 A72-44209

FEEDFORWARD CONTROL

Human short term thermoregulation feedback-feedforward control mechanism, using hypothalamic temperature as set point

02 p0168 A72-12036

Conventional open and closed loop servo analysis methods applied to Naval aircraft approach power compensator systems, using pilot model concepts

[AIAA PAPER 72-124] 05 p0612 A72-16922

Feedback and feedforward circuits to double operational amplifier output voltage swing with increased slew rate

11 p1604 A72-25746

Algorithm for linear multivariable systems synthesis via combined dynamic feedforward compensation and linear state variable feedback

19 p2779 A72-38232

Multiloop piloting aspects of longitudinal approach path control.

[ICAS PAPER 72-46] 21 p2995 A72-41171

FEEDING [SUPPLYING]

Feeder for the supply of powder materials to spraying setups

23 p3278 A72-43293

FEEDING DEVICES

U ANTENNA FEEDS

FEEL

U SENSORY FEEDBACK

FELDSPARS

Excess Xe 131 in lunar Ba feldspar rocks, discussing results of reactor irradiation experiments with fast and epithermal neutrons

03 p0414 A72-12901

Fossil track densities and thermoluminescence measurements of Luna 16 feldspar crystal samples compared to Apollo 12 samples

09 p1381 A72-22270

Lunik 16 samples trace element concentration, suggesting feldspar excess and local regolith derivation

09 p1381 A72-22272

Eu and Sr distribution between coexisting feldspars in acidic rocks, using mass spectroscopic isotope dilution method

10 p1472 A72-24166

Crystallization experiments on Apollo 11 magmas of K and Rb-rich basalt, discussing plagioclase characteristics

11 p1723 A72-26523

Brief review of thermoluminescence studies in lunar samples.

20 p2970 A72-39402

Phase transformations and exsolution in lunar and terrestrial calcic plagioclases.

20 p2970 A72-39480

A re-examination of relationships among pyroxene-plagioclase achondrites.

20 p2900 A72-39840

Minerals discovered in meteorites, tabulating formula and occurrence and plagioclase composition

23 p3262 A72-44132

Quartz and feldspar glasses produced by natural and experimental shock.

23 p3285 A72-44136

FELSITE

U IGNEOUS ROCKS

FEMUR

Stress distribution analysis of femoral neck, using three dimensional photoelastic model

03 p0318 A72-12952

Local and cardiac complications of selective percutaneous transfemoral coronary arteriography, noting hemorrhages thromboses, embolisms, myocardial infarction, bradyarrhythmia and ventricular fibrillation

09 p1267 A72-23325

FENCES [BARRIERS]

Scale model tests of high thrust engine blast deflection fence combinations for protection of adjacent roadway traffic

16 p2374 A72-33698

FERMENTATION

Carbohydrate metabolism, glycolytic ferment activities and leukocyte size under ionizing radiation, showing compensatory bone marrow cell formation with leukopenia

04 p0467 A72-14609

FERMI STATISTICS

U QUANTUM STATISTICS

FERMI SURFACES

Noninteracting Fermi gas in finite square-well potential, obtaining quantum mechanical solution of Schroedinger equation

02 p0262 A72-11671

Quantum oscillations of minority Fermi surface carriers as function of magnetic field in Hall effect and thermoelectric power in pressure-annealed pyrolytic graphite

02 p0268 A72-11673

Positive and negative deviations of linear electrical resistance of d-transition metals at high temperatures as function of Debye temperature and Fermi level

02 p0242 A72-12006

Local level filling and Fermi distribution in metal semiconductor contact as function of voltage and level location

09 p1372 A72-23355

Fermi level and scattering phase function nomograms for semiconductors with parabolic and isotropic energy bands, noting charge transfer effects

11 p1700 A72-25781

Rare earth metals and alloys technology assessment and utilization covering quantum mechanics concepts application to Fermi surface

15 p2289 A72-31184

Transition metals thermal conductivity periodic variations relation to free Fermi surfaces and valence electrons localization variations

21 p3070 A72-41646

FERMI-DIRAC STATISTICS

U QUANTUM STATISTICS

FERMIONS

NT BARYONS

NT FAST NEUTRONS

NT LEPTONS

NT NEUTRONS

NT PROTONS

NT RECOIL PROTONS
NT SOLAR PROTONS
NT THERMAL NEUTRONS
Correlation energy calculation for system of fermions by means of variational method
05 p0702 A72-16785
Neutron star properties, formation theories, crust composition and internal structure, examining interior neutron behavior, fermion systems superfluidity, magnetic field effects and stellar dynamics
10 p1533 A72-23890

FERRIC IONS
Ferric ion traces evidenced in lunar and meteoritic titanates by charge transfer bands observations during heating, interpreting origin as caused by cosmic radiation
14 p2154 A72-30515

FERRITES
High chromium ferritic stainless steels weldability and mechanical properties, showing C, N, Ti and residuals effects on recrystallization, toughness, tensile behavior and corrosion resistance
01 p0083 A72-10283
Nonreciprocal microwave ferrite device design, out-lining loss-free, cyclic symmetrical, multiport junction circulator theory
01 p0041 A72-10695
Ferrite microwave devices design, covering non-reciprocal circuit and electrical tuner
01 p0041 A72-10696
Ferrite-loaded waveguide Y-junction field mode identification by eigenvalue phase-frequency characteristics measurement, applying to millimeter wave circulator synthesis
01 p0041 A72-10697
Hot-rolled low-carbon Mn-Mo-Nb acicular ferrite steels with high strength, toughness and impact resistance
02 p0246 A72-12559
Ferrite rod antennas calibration for radio frequency measurements up to 1 MHz
02 p0195 A72-12606
Ferrite core memory for space flight devices, comparing 1 bit storage capacity power consumption with MOS cell
02 p0196 A72-12734
Garnet crystal structure type microwave ferrites with V and In ions, investigating ferromagnetic resonance linewidth reduction effect
03 p0400 A72-12971
Self consistent junction circulator theory, considering lossless ferrite loaded symmetric n-port junction and numerical design procedures
03 p0330 A72-13232
Low birefringent orthoferrites for optical devices, considering improvement in Faraday rotation detection of magnetic domains in single crystal platelets
03 p0360 A72-13760
Computerized design algorithm for ferrite core memory system, considering cross-temperature effect under worst driving conditions
03 p0327 A72-13766
Functional speed measurements of propagating devices based on cylindrical domains in orthoferrites and garnets, noting storage capability
03 p0333 A72-13783
Sigma phase formation in chromous ferrite, investigating vacuum diffusion, hot and cold working, welding and additives effects
03 p0375 A72-13940
Ferritic steel nil-ductility transition temperature data analysis correlating irradiation results with activation fluences and temperature
04 p0547 A72-14430
Low cost ferrite remanence microwave phase shifter design using periodic loading structures
04 p0497 A72-14716
Bandwidth widening of waveguide H-plane Y-circulator with cylindrical ferrite post coated by dielectric sleeve
04 p0499 A72-15244
Mathematical model for reciprocal and nonreciprocal magneto-optical effects in magnetized ferrite-filled microstrip transmission lines
04 p0502 A72-15434
Fe-Cr-Al and Fe-Cr-Si type ferritic steels, investigating additives effects on ductile-brittle transition temperature
05 p0672 A72-16012
Solidification, microsegregation and homogenization of austenitic stainless steels containing delta ferrite
05 p0672 A72-16142
Hardening of Fe-Mn-Ti ferritic and martensitic alloys, investigating microstructure and mechanical properties
05 p0672 A72-16144
Electromagnetic wave propagation in rectangular waveguide with periodic ferrite structure, presenting computer graphics for stop bandwidth vs magnetic field strength
05 p0627 A72-16342
Ferritic stainless steel roping /buckling/ morphology and texture explanation by anisotropic plastic flow
05 p0677 A72-17105

Dissipative magnetic parameters measurement in ferrite and insertion loss measurement in waveguide Y-circulators below microwave resonance
06 p0786 A72-18367
Longitudinally magnetized fully filled square waveguide reciprocal ferrite phase shifter, predicting frequency characteristics by rotational error analysis
06 p0786 A72-18370
Rectangular and orthogonal circular waveguides hybrid junction with magnetized ferrite resonators along axes, discussing design and applications
07 p0952 A72-18844
Welding thermal energy effect on residual ferrite of austenitic chrome-nickel steel deposits
07 p1010 A72-18971
Ultrasensitive measurement technique for low microwave susceptibility on ferrite samples featuring feedback scheme for signal klystron locking
07 p0955 A72-19320
High Cr ferritic steels intergranular and stress corrosion properties and resistance to sea water, organic and inorganic acids and acid mixtures
07 p0995 A72-19572
Austenite-martensitic steel with 25 percent delta ferrite, examining microstructural changes due to aging at 550 C by thin slide electron microscopy
07 p1021 A72-20484
Magnetic spectra measurement of powdered hexagonal ferrites in millimeter wavelength range during grinding and after heat treatment
08 p2128 A72-21875
Ferrites electrical conductivity variations with time caused by cations distribution modification after cooling
10 p1525 A72-24121
X band high power ferrite phase shifter design and performance
10 p1451 A72-24595
Transitional ferrite phase formation in Fe-Cr-Ni alloy evidenced on electron micrographs and diffraction patterns
11 p1657 A72-25760
Ferrite core memory for storage of Helios probe perisolar space data before transmission to telemetry system
11 p1601 A72-25806
Optimal flexible ferrite keeper for ferromagnetic thin film memories performance improvement, noting requirements for high permeability, low loss factor and dielectric constant, etc
11 p1601 A72-25899
Ferritic stainless weld metal ductility, investigating yield and fracture stresses after heat treatment
11 p1661 A72-26494
Austenite formation kinetics in Fe-C ferritic-pearlitic structure at 855 C, comparing experimental data with theoretical calculations
11 p1662 A72-26744
Decoupled formulation of vector wave equation in orthogonal curvilinear coordinates, applying to ferrite-filled and curved waveguide of general cross section
11 p1607 A72-26995
Ferrite loaded X band waveguide Y junctions eigenvalue frequency dependence measurement to identify modal resonance and arrange displacement for circulator operation
12 p1790 A72-27508
Ferrite microwave limiter-filters and circulators using resonant rotation of polarization plane
13 p1927 A72-28409
X ray and Mossbauer spectral analyses of thermomagnetically treated nickel ferrite samples containing Co, investigating ordering mechanism
13 p2020 A72-28490
Mossbauer and X ray structural analysis of nickel ferrite-chromite magnetic moments, comparing with theoretical data
14 p2141 A72-30171
Ferrite powder relative density as function of temperature, sintering time and pressure during hot pressing, noting creep activation energy and vacancy motion
14 p2107 A72-30775
Ferrite materials for microwave applications, discussing frequency and temperature limit extension, power level increase and loss reduction
14 p2088 A72-30833
Ferrite and dielectric element waveguide phase shifters with rectangular hysteresis loop, deriving differential phase and attenuation constants for wave propagation
15 p2202 A72-32662
Bilateral tunnel-diode amplifiers using ferrite transformers.
18 p2665 A72-36306
Slotted-line measurement of insertion loss in three-port ferrite junction circulator.
19 p2775 A72-38636
Faraday rotation dual-mode ferrite reciprocal phaser with performance and cost advantages over toroidal type for microwave phased array applications
20 p2909 A72-39733
Spectral analysis of microwave pulses by a ferrite transducer
22 p3158 A72-42119

Recent advances in diode and ferrite phaser technology for phased-array radars. I.
23 p3270 A72-43572
A solid-state 'flux-drive' control circuit for latching-ferrite-phaser applications.
23 p3275 A72-43574
Ferrite component for waveguide commutator used as microwave switching element and modulator, noting application in navigation instruments and avionics
23 p3270 A72-43768

FERRITIC STAINLESS STEELS
Stress corrosion cracking of 18% Cr ferritic stainless steels.
19 p2820 A72-38300
Correlation of irradiation data using activation fluences and irradiation temperature.
21 p3083 A72-40763
Decarburization kinetics of low alloy ferritic steels in sodium.
22 p3194 A72-43042
Differentiating stress corrosion cracking from hydrogen cracking of ferritic 18-8 stainless steels.
22 p3195 A72-43127

FERROCENES
Polymerization characteristics of 4-ferrocenyl-1, 3-pentadiene monomer, discussing synthesis on molar scale
17 p2512 A72-35934

FERROELECTRICITY
Electrical control of fixation and erasure of holographic patterns in ferroelectric materials
07 p0981 A72-18880
Strain biased transparent ferroelectric electro-optic ceramics for coherent transducers /page composers/ for holographic memories and optical data processing [CLEA PAPER 18,6]
07 p0950 A72-19401
Ferroelectrics with strong hydrogen bonds, deriving self consistent optical phonon frequency and coupled proton-phonon vibration spectrum
09 p1366 A72-22221
Stimulated emission and spectroscopic properties of activated ferroelectric crystal laser, noting Stark effect
09 p1323 A72-22981
Recording holographic networks in polycrystalline transparent ferroelectric ceramics of lead and lanthanum titanate-zirconate system
10 p1480 A72-24111
Sintered prepolarized perovskite type ferroelectric ceramics adiabatic depolarization and energy conversion under shock wave action
10 p1422 A72-24128
Polarization characteristics of ferroelectric barium strontium titanates in solid solution at 4-100 K
10 p1527 A72-24984
Photovoltaic effects in CdS films evaporated onto barium titanate single crystal and ceramic ferroelectric substrates
12 p1856 A72-28014
Ferroresonant circuit with inductor, resistor, nonlinear ferrocapacitor and voltage source, deriving oscillation stability condition
14 p2090 A72-31119
Ferroelectric nature of superficial layer on barium titanate crystals from scanning electron microscope and optical observations
15 p2291 A72-31681
Optically induced variation of birefringence in ferroelectric materials.
20 p2959 A72-39045
Raman scattering techniques applied to problems in solid state physics.
21 p3096 A72-40602
Stress induced birefringence in an isolated and a shortcircuited KH₂PO₄ crystal.
23 p3324 A72-44322

FERROMAGNETIC FILMS
Data holder made of three thin ferromagnetic coupled films for magneto-optic computer memory
01 p0035 A72-11317
Superferromagnetism in thin polycrystalline Gd and Gd-Au films having Curie points near room temperature
03 p0401 A72-13583
Magnetostatic interactions of cylindrical magnetic domain propagation circuits in ferromagnetic overlay without in-plane fields
03 p0331 A72-13752
Ferroelectric thin film magnetometers operation and performance characteristics for magnetic field measurement
09 p1308 A72-22467

FERROMAGNETIC MATERIALS
NT FERROMAGNETIC FILMS
NT MAGNETITE
NT PERMALLOYS [TRADEMARK]
Gravitational convection by magnetocaloric effect in incompressible nonconducting ferromagnetic fluid
03 p0457 A72-13993
Wind tunnel six component magnetic balance system, describing ferromagnetic body forces and moments relationship to applied magnet fields and gradients
05 p0645 A72-16829
[AIAA PAPER 72-164]

Quantum coherent spin wave interactions in ferromagnetics, showing retained electric field
07 p1007 A72-20125

Transition metal superconductors transition temperatures survey, considering d-band solid solution alloys and intermetallics and ferromagnetic element compounds
09 p1367 A72-22552

Dislocation structure analysis in ferromagnetic materials by magnetic techniques, discussing methods based on magnetization curve static properties and magnetic relaxation phenomena
10 p1487 A72-24574

Magnetovariometers design, operation and applications, discussing ferromagnetic materials properties effect on performance characteristics
12 p1792 A72-27739

Modulation oscillations in ferromagnetic core-based LF signal generators and frequency doublers, deriving differential equations for converter operation and formulas for static characteristics
13 p1930 A72-29049

Normal mode formulation of spin wave-helicon wave interactions in ferromagnetic semiconductors.
18 p2718 A72-36452

Special features of the operation of ferroprobes with low-permeability core moulds at small excitation fields.
19 p2804 A72-38760

Electron-electron collision induced anomalous Hall effect in ferromagnetic d metals at low temperatures
20 p2959 A72-39309

Ferromagnetic tau phase structure of Mn-Ac alloy with powder anisotropy related to platelet formation and twinning orientation
21 p3068 A72-40965

Spontaneous magnetization of Ni foils in high pressure H gas, noting Hall voltage measurement in ferromagnetic foils and thin plates
23 p3324 A72-44140

Approaches to verification and solution of magnetic particle inspection problems.
24 p3407 A72-44903

FERROMAGNETIC RESONANCE

Garnet crystal structure type microwave ferrites with V and In ions, investigating ferromagnetic resonance linewidth reduction effect
03 p0400 A72-12971

Variable flux reset ferroresonator voltage regulator with adjustable terminal characteristics using magnetic and thyristor circuits
03 p0311 A72-13770

Double shunt feedback controlled ferroresonant voltage regulator using magnetic component with simulated core saturation
03 p0311 A72-13772

Mathematical model for mechanical and electrical hysteresis, noting application to nonlinear ferromagnetic resonant circuit with saturable inductor
14 p2132 A72-31105

Oscillations in ferromagnetic resonant circuit of parametric amplifier with constant capacitance and periodically variable inductance modulated by input signal
14 p2089 A72-31107

Variable saturation of series LC circuit, discussing current response, ferroresonant jump, symmetry and subharmonic oscillations
14 p2090 A72-31116

Ferromagnetic and paramagnetic resonance spectra of lunar material - Apollo 12.
18 p2724 A72-36276

FERROMAGNETISM

Flow characteristics, wave propagation and thermal stability of ferrofluids within uniform magnetic field
01 p0050 A72-10235

Heisenberg ferromagnet thermodynamic properties in external magnetic field near Curie temperature, studying magnetization, susceptibility, entropy and magnetocaloric effect
08 p1217 A72-21520

Synthetic diamond single crystals, investigating impurities and inclusions effects on ferromagnetic properties and heat resistance
12 p1833 A72-27768

Landau orbital ferromagnetism appearance likelihood in white dwarf stars, noting temperature requirements of noninteracting electron gas
19 p2859 A72-37891

Self-excited parametric oscillations at the second harmonic in a parametric system with a triple-post ferromagnetic core
19 p2774 A72-38586

Direct fitting of spin wave energies to interatomic exchange parameters in the ferromagnetic rare earth metals.
21 p3097 A72-40625

Slow electromagnetic waves in antiferromagnetics near the point of transition to the ferromagnetic phase
21 p3098 A72-41685

FERROUS METALS

Plate microcracking of ferrous martensites containing Mn, Cr and Ni, discussing austenite grain size variations
05 p0678 A72-17119

Contact interaction between high-melting compounds and liquid metals. I - Interaction between subgroup IVA metals and metals of the iron family
23 p3299 A72-43287

FET (TRANSISTORS)

U FIELD EFFECT TRANSISTORS

FETUSES

Tentorium cerebelli microstructure and leaflets strength in study of chronic and acute hypoxia injury to fetus during pregnancy and labor
09 p1266 A72-23193

Irreversibility mechanism in postpartum ductus arteriosus closure in guinea pigs, studying vessel cellular changes and smooth muscle response to oxygen pressure
12 p1762 A72-27826

Intravascular injection and histology studies of human embryonic and fetal choroidal vasculature development
19 p2755 A72-37398

FIBER OPTICS

Southern radio sources optical identification by photography using fiber optics image tube
02 p0285 A72-12795

Kitt Peak 40 channel magnetograph using fiber optic probe for spectral and spatial resolution in weak photospheric field detection
03 p0356 A72-13282

Mie scattering by spherical particles in low loss glasses for fiber optic waveguides, discussing angular dependence
03 p0359 A72-13445

Optical communication technique based on fiber optic light pipes and time, space or wavelength division multiplexing
03 p0325 A72-14050

High resolution electrons image intensifier for particle spectrographs, using channel plate, scintillator and fiber optics
04 p0524 A72-15536

Emitting-absorbing flames diagnostics, measuring spectrally resolved radiant energy with fiber optic probe data
05 p0661 A72-15915

Fiber optics system for H beta line shape measurement in transient high temperature plasma, using narrow slits at spectrograph exit plane
05 p0663 A72-16816

Optical data transmission system with dielectric single-mode glass fiber waveguide, PCM semiconductor laser diode transmitter and avalanche photodiode receiver
06 p0774 A72-17770

Wave propagation in single mode clad glass fiber light waveguide, discussing fiber core minimum diameter and various loss mechanisms
06 p0825 A72-17773

Optical image transfer functions characteristics and modulation in isolated retinas and retinal receptors, noting similarity to optical fiber bundles
07 p0916 A72-19027

Picosecond pulse distortion under multimode conditions in optical fiber communication systems
07 p0940 A72-19231

Linear and circular birefringence of low loss single mode glass fiber dielectric optical waveguide as function of length
07 p0940 A72-19232

German monograph on sky scanner for short term sky spectral density distribution using glass fiber bundles for spectral components simultaneous measurement
07 p0983 A72-19266

Remote ignition with noncoherent light from pyrotechnic, electric and explosive sources through fiber optics
08 p1219 A72-20757

Laser pulse propagation measurements on multimode glass fibers to evaluate communication potential
09 p1323 A72-22868

Material dispersion contribution to signal envelope delay distortion in weakly guiding dielectric optical fiber waveguides
09 p1314 A72-23340

Power transfer in optical fiber with nonuniform refractivity in mode propagation direction, using coupled mode theory
12 p1779 A72-27164

Light power coupling efficiency from GaAs injection laser into single- and multimode fibers
12 p1820 A72-27507

Surface wave propagation mechanism on dielectric bodies noting compatibility with physical properties involved with optical cables for commercial transmission systems
12 p1782 A72-27556

Multimode millimeter waveguides and optical fibers, deriving signal transmission distortion from transfer function and corresponding impulse response statistics
15 p2193 A72-31351

Multimode optical fiber waveguide theoretical model to predict pulse propagation dispersion for comparison with measurements
15 p2194 A72-31546

Multimode fiber optics data transmission through high electrical noise environments for send-receive communication links
15 p2198 A72-32059

Night photography at 10,000 feet.
17 p2557 A72-35556

German monograph - Wave propagation in glass-fiber light waveguides
18 p2697 A72-36249

Free vibration mode shapes mapping of spherical and paraboloidal plastic shells under acoustic excitation via noncontact fiber optics instrumentation
18 p2690 A72-36372

Series solution for electromagnetic wave propagation in radially and axially nonuniform media - Geometrical-optics approximation.
18 p2712 A72-37024

Monocular and biocular magnifiers for night vision equipment.
20 p2921 A72-39030

Solid state laser sources, light modulators and silicon avalanche photodiode detectors for fiber optical communication, discussing performance and limitations from system design viewpoint
21 p3018 A72-40866

Hybrid digital transmission systems based on optical fiber waveguides and analog repeaters, noting YAG laser light modulation by phase shift keyed sub-carrier
21 p3018 A72-40868

Ground, satellite, terrestrial glass fiber channel and waveguide radiation systems for laser communications
21 p3023 A72-41398

Image intensifier systems and their applications to astronomy.
22 p3181 A72-42989

Fiber optics development and physical foundations, discussing reflection, optical waveguides, vibrational modes during light transmission and fabrication from inhomogeneous glass and mixed monomers
24 p3425 A72-44782

Transmission losses in glass and plastic single mode and liquid core optical fibers for long distance data links and image transmission
24 p3380 A72-45252

FIBER STRENGTH

Test equipment for glass and polymer fibers strength and lifetime in vacuum and inert bases under static loads
01 p0093 A72-11382

Surface damage effect on strength of c-axis sapphire filaments, assessing impact on sapphire reinforced metal technology
02 p0249 A72-11992

Potential energy principle in equilibrium stability problems for flexible extendable thread, using Liapunov method
03 p0390 A72-14208

Fiber flexural stiffness determination from bending moment and deflection relation, using bend test
03 p0365 A72-14300

Fiber pull-out from elastic matrix, calculating shear stress and load distribution dependence on elastic properties and fiber length
06 p0897 A72-18152

Alumoborosilicate glass fibers vacuum tensile strength tests, noting fiber strength increase with vacuum and exposure time
07 p1023 A72-19778

Mechanical strength and microstructural characterization of sapphire ribbons and continuous filaments for composite materials
07 p1023 A72-19929

Heat stretching-induced changes effect on strength, sorption and structural properties of polyformaldehyde fibers, noting structural orientation enhancement and porosity growth
08 p1194 A72-21757

Test procedures and apparatus for short and long term creep of polymer monofilaments under radial compression
08 p1194 A72-21758

Repeated stretching effect on triaxial fibers thermal destruction in vacuum after hot air or steam thermosetting
08 p1194 A72-21759

Morphology and physicochemical properties of carbonized polyacrylonitrile fibers by scanning electron microscopy, discussing macro and microdefects effects on strength characteristics
08 p1195 A72-21762

Fiber thermoplastics matrix breakdown and mechanical properties enhancement, examining lateral and longitudinal strain during uniaxial tensile creep and recovery
09 p1337 A72-22541

Aligned fibrous composites microstructural parameters, showing fiber thickness effect on fracture, fabrication, matrix cracking, creep resistance and fatigue
09 p1338 A72-23163

Stress concentration in elastic composite reinforced by two dimensional continuous parallel fiber array with one broken fiber
09 p1339 A72-23172

Torsion of embedded infinite elastic circular cylindrical fiber with penny shaped crack, investigating breaking behavior from Fredholm integral equation iterative solution
10 p1553 A72-24094

Molded carbon technique-produced carbon fiber/carbon composites, discussing flexural strength, toughness, crack resistance and rocket nozzle application
10 p1500 A72-24200

Fiber toughening mechanisms in continuous filament unidirectionally reinforced composites with elastoplastic matrices, discussing tensile energy storage in debonded region
11 p1671 A72-25463

Boron fibers tensile and transverse strengths, relating severe anisotropy to residual stress pattern from preexistent flaws
11 p1672 A72-25484

Layered anisotropic fiber composite (Tetra-Core) for sandwich construction and aircraft applications, discussing design, fabrication and strength characteristics [SAE PAPER 720343]
11 p1638 A72-25599

High temperature metal fiber reinforced ceramic matrix composites for turbine vanes, showing strength toughness and crack depths dependence on interfacial bond [ASME PAPER 72-GT-51]
11 p1704 A72-25643

Graphite fiber with high tensile strength and modulus and good elongation at low cost for aerospace applications
12 p1834 A72-28084

Chemical vapor deposition of boron on carbon monofilament substrate to eliminate fracture and boron damage and achieve good strength
12 p1834 A72-28085

Flexural strength of Pyco-bond polyacrylonitrile/PAN/ precursor carbon fiber substrates for carbon-carbon composite fabrication
12 p1835 A72-28092

Chemical interaction effects on single crystal sapphire filament strength in Ni and Ni alloy matrices during heat treatment in inert atmosphere
13 p1974 A72-28661

Brittle continuous and crazed anodic oxide coatings effect on Al filament stiffness, comparing with Dow analysis
13 p1974 A72-28663

High porosity nichrome fiber materials sintering at 1000-1350 C, considering size, electric conductivity, shear strength, interfibrillar contact and briquet quality
13 p1967 A72-30105

Steady state creep measurements of lead-phosphor bronze discontinuous fiber composites under nonuniform deformation, comparing to fiber and matrix alone
15 p2261 A72-32299

Steady state creep theory for discontinuous fiber composites, considering rigid and creeping fibers and sliding interface
15 p2261 A72-32300

Griffith equation applicability to graphite fiber fracture strength by measurement of work to break and critical flaw
16 p2413 A72-32871

Failure mechanism for carbon fibers in epoxy novolac matrices under tensile loads
17 p2633 A72-35286

Fracture of boron filaments in an aluminum matrix
17 p2571 A72-35655

High strength-high modulus boron vapor deposited on a carbon monofilament substrate
17 p2572 A72-35657

Sapphire filament mechanical property considerations of importance to Al₂O₃ reinforced metals
17 p2572 A72-35658

High performance graphite ribbon - An advanced reinforcement material
17 p2572 A72-35659

Carbon fiber structure at graphitization temperatures to 3100 C in terms of surface energy and internal stress accounting for low shear strength
17 p2572 A72-35660

Contractile and muscle-like fibers and autopolusation systems for polymer engine and spring action studies
19 p2760 A72-38200

Strength properties of highly porous materials made of metallic fibers
19 p2820 A72-38288

Fracture behavior of stainless steel fibers in Sn-Pb alloy matrix
19 p2820 A72-38373

Influence of technological factors upon the mechanical reliability of composite-material structures
20 p2943 A72-38945

High modulus fiber composites development from viewpoint of reinforcement patterns and material properties
20 p2943 A72-38946

Strength factors of fiber reinforced composites under tension, compression, shear, bending and plane stress
20 p2944 A72-38947

Longitudinal tensile failure of unidirectional fibrous composites.
20 p2944 A72-39789

An interpretation of radiation effects on mechanical properties of carbon fibres based on a 'sheath' and 'core' model of fibre structure.
20 p2944 A72-39794

Probabilistic model for tensile strength of brittle fibers, discussing clamping effects at various gage lengths and Weibull flaw structure
23 p3305 A72-43490

Mechanics of failure of fibrous composites.
23 p3345 A72-43508

Book - A review of the science of fibre reinforced plastics.
24 p3417 A72-44674

The fracture toughness of fibre composites.
24 p3417 A72-44899

Fiber and filament reinforcement of plastic and brittle matrix materials
24 p3414 A72-45276

FIBER GLASS

U GLASS FIBERS

FIBERS

- NT CARBON FIBERS
- NT GLASS FIBERS
- NT HAIR
- NT MICROFIBERS
- NT NYLON [TRADEMARK]
- NT REINFORCING FIBERS
- NT SYNTHETIC FIBERS

Thermally stable organic polymer fiber production methods and performance evaluation in high temperature environments, discussing structure types, flammability and tensile properties
02 p0248 A72-11771

Flame resistance requirements of high temperature resistant and highly chlorinated fibers [PI PAPER 11]
03 p0380 A72-13245

Fibrous structure of precipitates produced at bottom of trace due to friction in work hardened Al-Cu alloy solid solution
03 p0376 A72-13970

Trimethylchlorosilane film boiling for silicon carbide deposit on vertical heated tungsten filaments, investigating mass transport rate
04 p0595 A72-14600

Elastic deformations of porous Cu, Mo and W fiber materials after pressing and sintering due to residual stress relaxation
14 p2106 A72-30151

Wave propagation in a viscoelastic fiber subjected to transverse impact.
17 p2570 A72-34791

Physicomechanical properties of fiber carbides
23 p3299 A72-43291

Scattering of obliquely incident waves by inhomogeneous fibers.
24 p3379 A72-44710

FIBERS [MATHEMATICS]

Invariance problems in terms of Lagrangian domain of definition and Euler-Lagrange mapping intrinsic geometric characterization, reviewing theory of fiber bundles
20 p2954 A72-40006

Equivariant integrality theorems for differentiable manifolds.
22 p3199 A72-42310

Trajectory bundles in metric space for objects motion study in dynamic pursuit games, noting Pontryagin and Pshenichnii methods for differential games solution
23 p3308 A72-43415

FIBRILLATION

Electrode system for ventricular defibrillation, noting current density role and rounded edge effectiveness
11 p1588 A72-26628

FIBRIN

Dietary lipid effect on platelet adhesion and aggregation, blood coagulation and fibrinolysis and relation to atherosclerosis and thrombosis
08 p1117 A72-21543

Hypocapnic hypoxia effects on blood coagulation and fibrinolysis
19 p2756 A72-37880

FIBROBLASTS

NT COLLAGENS

FIBROSIS

Lungs fibrosis and cancer caused by asbestos fibers inhalation, noting environment control for protection against workers health hazards
11 p1583 A72-25548

FIBROUS MATERIALS

U FIBERS

FIELD EFFECT TRANSISTORS

Low driving power resistive gate MOSFET microwave switch with performance approaching P-I-N diode
01 p0038 A72-10658

Lateral photoelectric effect in junction FET under homogeneous illumination, detailing current-voltage characteristics
01 p0114 A72-10859

Dual gate GaAs microwave FET, measuring second gate voltage effects on power gain and noise
02 p0191 A72-11893

X band gallium arsenide field effect transistor, noting applications for radar receivers, microwave communication links and electronic countermeasures
02 p0193 A72-12184

Czech FET properties in low temperature region, measuring static characteristics, electrical parameters and noise levels at 4.2-296 K
02 p0195 A72-12670

Book on field effect electronics covering junction and insulated gate transistors and allied devices, monolithic and film IC and design techniques
03 p0333 A72-13846

Matched Si junction FET under neutron burst and pulsed gamma radiation, investigating device parameters degradation
03 p0335 A72-14093

Charged transfer devices and IGFT bucket brigade structures, discussing design measures and fabrication procedures for increased reliability
03 p0336 A72-14280

Two section model of junction-gate field effect transistor with short channel length
04 p0498 A72-15134

Carrier mobility field dependence effects on validity of gradual channel approximation in insulated-gate field effect transistors, discussing velocity field relationship
04 p0498 A72-15135

N-channel MOS FET, measuring X ray irradiation effects on drain current and transfer characteristics at room temperature
05 p0634 A72-16033

Direct coupled circuits in memory cell prototype with normally-off GaAs MESFET at 4.2 K
05 p0638 A72-17096

FET devices stacking faults induced leakage currents, pinpointing critical processing steps by diagnostic X ray charts
06 p0782 A72-17364

Si MOSFET substrate resistivity effect on surface state noise spectra
06 p0783 A72-17609

Moderate power GaAs FET switching experiment, obtaining rise and fall times
07 p0952 A72-18826

Low noise GaAs Schottky barrier FET for X and Ku bands applications
07 p0955 A72-19257

Normally off Si MESFET for simple dc coupled circuits, computing threshold voltage with two dimensional device model
08 p1141 A72-21426

Junction and MOS FETs noise sources interaction with small signal model parameters and signal source admittance parameters, investigating amplifier If performance
08 p1141 A72-21428

Multichannel junction gate FET /Gridistor/ for microwave power amplifier, discussing design, fabrication and performance
08 p1141 A72-21429

Acoustic wave detection in strain transducer consisting of silicon insulated gate field effect transistor with piezoelectric film incorporated in insulator region
08 p1168 A72-21556

Low level current operation in insulated gate FET, obtaining analytical expression for voltage
08 p1142 A72-21744

Junction FET drain source capacitance theory based on two-region physical model, taking into account carrier drift velocity saturation effect
08 p1142 A72-21745

Background noise in FETs with junction gate, formulating hypothesis of warm carriers for transistor channel
09 p1287 A72-23110

Excess, shot and channel thermal noises performance-limiting effects on junction FETs in high input impedance applications, considering minimization method
09 p1287 A72-23111

Ion implantation doping of MOSFET and IC for wafer production, using automatic vacuum pumpdown and cycle control
10 p1447 A72-23950

Homogeneous computing media, examining microelectronic fabrication, interconnection and control problems for MOSFET, bipolar transistors and IC structures
10 p1448 A72-24277

Multichannel integral commutators with MOSFET as switching elements, calculating transmission errors
10 p1449 A72-24288

MOSFET for input impedance measuring amplifier, discussing input stage temperature drift and protection from overvoltage
10 p1482 A72-24599

German book on HF semiconductor electronics covering planar and field effect transistors, varactors, n-p, p-i-n, avalanche and Schottky barrier diodes, Gunn devices, etc
10 p1452 A72-24699

Bipolar insulated gate FET IC buffer driver, discussing input and output interface capacitance and impedance characteristics and application to transistor-transistor logic

11 p1603 A72-25269

Schottky barrier gate FET design, device packaging and low noise characteristics

12 p1788 A72-27294

Spatial and time dependence of electron velocity in short channel microwave FET, using Monte Carlo method

12 p1790 A72-27434

Semiinsulated gate GaAs FET fabrication by proton bombardment

12 p1790 A72-27438

Noise behavior of GaAs Schottky barrier FET with short gate length, showing channel thickness effect on intervalley scattering noise

12 p1790 A72-27439

Channel formation in insulated gate FET, obtaining equivalent circuit

12 p1791 A72-27548

Integrated metal-nitride-oxide-silicon /MNOS/ semiconductor storage units characteristics, design and operation in FETs

12 p1791 A72-27574

Ge field effect dependence on surface roughness and finishing, noting relief elements dimensions ratio and orientation to current flow direction

12 p1855 A72-27859

Fetron high voltage hybrid junction field effect (J-FET) devices for direct replacement of vacuum tubes in unchanged circuits

13 p1928 A72-28431

Computer model study of FET with submicrometer gates, noting gain-bandwidth product increase with decreasing gate length

15 p2205 A72-31544

Junction field-effect transistor circuits for prescribed output functions.

18 p2665 A72-36307

The effects of electron bombardment on the noise properties of field effect transistors.

18 p2666 A72-36322

FET noise at high temperatures.

18 p2666 A72-36324

Thermal effects in JFET and MOSFET devices at cryogenic temperatures.

18 p2666 A72-36453

Temperature dependence of low-frequency excess noise in junction-gate FET's.

18 p2666 A72-36454

Si MOSFET elementary channel resistances before saturation onset from one dimensional theory, investigating current noise

18 p2668 A72-37037

Low noise high power bipolar and field effect transistors monolithic integration potentials for microwave applications

19 p2771 A72-37261

Design considerations of a 3.1-3.5 GHz GaAs FET feedback amplifier.

19 p2771 A72-37269

Single and dual gate GaAs FET integrated amplifiers in C band.

19 p2771 A72-37270

Self excited LC and RC oscillator networks based on FETs, discussing frequency tuning and FM methods

20 p2906 A72-38899

Measurements of the field-effect and effective mobilities in MOS transistors.

20 p2907 A72-39272

Control of high-field domain in GaAs by the field effect and its application to functional devices.

20 p2960 A72-39706

Differential negative resistance /DNR/ in n-channel MOSFETs of silicon.

20 p2961 A72-39711

Some results of testing M.O.S. transistors at elevated temperatures.

20 p2909 A72-39774

Hybrid monostable delay circuit based on bipolar and low threshold voltage MOSFET transistor

20 p2910 A72-39788

Voltage controlled miniaturized n-type negative resistance circuit based on junction transistor and FET without internal bias

21 p3038 A72-40998

Measurement of substrate impurity profile of MIS field-effect transistors.

21 p3035 A72-41488

Frequency dependent deep level trap admittance and field effect transparency of p-n junctions calculated by truncated space charge approximation

22 p3161 A72-43086

Cross-modulation dynamic range of amplifiers used in the input stages of receiver equipment

23 p3271 A72-43839

The field-effect modified transistor - A high-responsivity photosensor.

23 p3273 A72-44455

Circuit analysis and operation of analog multipliers with MOSFET, applying to industrial automatic control systems and measuring instruments

24 p3384 A72-44896

Shielded silicon gate complementary MOS integrated circuit.

24 p3385 A72-44972

Characteristics of P-channel MOS field effect transistors with ion-implanted channels.

24 p3385 A72-44981

FIELD EMISSION

CdS single crystal field emission spectral characteristics at room and cryogenic temperatures, discussing intrinsic and impurity levels

02 p0269 A72-12888

Two mechanism model for anomalous field ion microscope images in W, noting end form difference in high and low evaporation rates

09 p1370 A72-22803

High electric field effects on I-V characteristics of Te-As-Ge-Si type chalcogenide thin film, noting Poole-Frenkel emission and electron tunneling roles

15 p2291 A72-31641

Optical field emission effects on photoelectron emission nonlinearity from metal cathode using ultrashort mode locked laser pulses

15 p2250 A72-32303

Triode electron gun design for narrow electron beam under highly convergent lens action, using field emission source

19 p2775 A72-38611

Image point formation in field ion microscopy of metal surfaces, using atom probe detection of noble gas apex adsorption

21 p3050 A72-40086

Field emission from carbon fibres - A new electron source.

22 p3208 A72-41966

FIELD INTENSITY METERS

Field mill measurement of atmospheric electric space charge density, discussing effects of snow melting and artificial charge sources

13 p1952 A72-29666

Airplane-borne cylindrical field mill type instrument to record atmospheric electric field

13 p1961 A72-30085

FIELD IONIZATION SOURCES

U BRUSHES

FIELD MODE THEORY

Ion electromagnetic cyclotron modes growth rates in multicomponent magnetospheric plasmas, discussing instabilities enhancement

01 p0062 A72-10906

FIELD STRENGTH

NT ELECTRIC FIELD STRENGTH

NT MAGNETIC FLUX

Electromagnetic wave propagation anomalies over sea, comparing calculated and measured field strengths based on simultaneous refractivity vertical distribution measurement

01 p0026 A72-10405

Nighttime hf radio wave field intensity measurement and absorption observation by narrow band receiver

02 p0184 A72-12874

Hf circularly polarized field strength and plasma density self consistent stationary distribution in weakly inhomogeneous constant magnetic field

04 p0558 A72-15175

Self induced electron beam collapse prevention by external magnetic field, determining required field strength by scaling law based on simple orbit model

06 p0854 A72-17418

Geomagnetic micropulsations on ground and magnetic field fluctuations in tail, noting field strength changes

06 p0804 A72-17455

UHF band satellite TV broadcasting system with FM, calculating required field strength and transmitter power

10 p1435 A72-24033

Parametric instability of magnetoactive plasma relative to nonpotential oscillations excitation, deriving threshold value of HF field strength

13 p2016 A72-29601

VLF and LF electromagnetic waves amplitude and phase velocity in spherical earth-ionosphere waveguide, discussing wave hop method

13 p1923 A72-29661

Solar coronal magnetic field structure and energy content from synoptic data analysis, noting differential rotation effects

13 p2050 A72-29938

Radio waves field strength measurement and recording for D region behavior during partial solar eclipse of 25 February 1971

13 p1961 A72-30050

Single point thunderstorm ranging method based on two radio frequencies field intensity spectral components ratio

14 p2129 A72-30639

Ionospheric electron density changes caused by strong radio waves induced plasma heating

14 p2102 A72-30657

Short period geomagnetic pulsations with gradual amplitude increase and abatement, noting latitudinal variation

14 p2103 A72-30665

Electromagnetic waves penetration through conducting gasket used to protect sensitive devices in aircraft, investigating field strength variation with distance from gasket

15 p2202 A72-32571

Multiphoton ionization of atomic hydrogen in the presence of an intense electromagnetic field.

17 p2586 A72-35827

Anomalous motion of radiating particles in strong fields.

18 p2713 A72-36712

Observational evidence for strength and structure of intergalactic magnetic fields, discussing primordial fields effects on galaxy formations and early universe evolution

18 p2726 A72-36728

Quasi-periodic variation in F 2 layer reflected signal field strength, noting predominance during periods with type 4 bursts, auroras and geomagnetic disturbances

19 p2792 A72-38639

Parametric instability of magnetoactive plasma relative to nonpotential oscillations excitation, deriving threshold value of HF field strength

21 p3091 A72-40655

Detection of whistler mode signals from VLF transmitter in Australia.

21 p3023 A72-41386

A comparison of field-strengths of 164 kHz radio waves transmitted from Tashkent and received at Ahmedabad with flare-time solar X-ray emissions measured in satellites.

23 p3262 A72-43275

FIELD THEORY [ALGEBRA]

NT QUADRATIC EQUATIONS

Linear interpolation for homogeneous isotropic random field observed on denumerable system of spheres, deriving explicit formula analogous to Kotelnikov-Shannon

01 p0094 A72-11266

Compensating fields of homomorphic imaging problems in space symmetry, discussing quasi-tensors, covariant derivatives and Poincare group

23 p3312 A72-43336

FIELD THEORY [PHYSICS]

Stepped reflector image region fields at plane wave incidence angle to reflector axis, determining field components as Fourier series

01 p0035 A72-10115

Aligned fields in MHD shock polar equation, obtaining magnetic induction polar variables

01 p0106 A72-10135

Optimal flight of material point in central field of forces subject to controlled small thrust

01 p0127 A72-10356

Limited scan microwave antenna design, discussing angular coverage, feed motion and focal field distribution

01 p0039 A72-10670

Large aperture antenna feed design, calculating focused and unfocused amplitude and phase field distributions in front of circular aperture

01 p0029 A72-10674

Electric field induced splitting of drift shells composed of trapped particles, taking into account non-dipole field components to lowest order

01 p0062 A72-10905

Soviet book on electromagnetic fields and waves covering propagation in anisotropic media, waveguides and cavity resonators, diffraction interactions, etc

01 p0031 A72-11200

Materials science historical development from ancient theories of structure of matter to modern atomic and field theories leading to general theory of elastic continuum

02 p0297 A72-12611

General theory of relativity, examining differences between singularities in stationary and nonstationary fields from gravitational equations solutions

02 p0261 A72-12675

Transverse fields effects on electron dynamics and energy conversion in O-type linear beam devices of traveling wave amplifiers

03 p0330 A72-13231

Homogeneous isotropic elastic medium free vibration in unbounded space, obtaining relativistic relations in wave field from mathematical model

03 p0389 A72-13425

Dc flow through p-n junction by modified Melehy force field method, discussing space charge variation in depletion layer

03 p0338 A72-13866

Oxygen and oxygen-nitrogen mixtures dc and hf discharges, evaluating traveling low field domains in positive column

03 p0400 A72-14350

Rotationally symmetric force free magnetic field boundary value problem, using linear elliptic differential equation

03 p0400 A72-14352

General relativistic generalized field equations for scalar dependent tetrad, noting identity with Brans-Dicke theory

04 p0549 A72-15021

- Gyroresonance devices efficiency increase, discussing magnetostatic field distribution optimization in interaction space 04 p0502 A72-15575
- Elastic boundary value problems static and geometric field parameters pointwise upper and lower bounds, determining solution coefficients by error energy minimization 05 p0735 A72-16062
- Periodic model of time evolving universe, examining stability of Einstein static solution to field equations 05 p0723 A72-17180
- Variational principles in general relativity, deriving Einstein field equations and equations of motion for charged and uncharged self gravitating fluids 06 p0847 A72-17254
- General theory of relativity for symmetric field, discussing DE Donder incompressible fluid model and Tolman-Schwarzschild metrics 06 p0847 A72-17682
- Unsolved fluid dynamic problems, considering viscous fluids, epihydrodynamics, magnetohydrodynamics, relativistic field dynamics and interstellar gas dynamics 06 p0800 A72-18112
- Field-dynamic equilibrium of macroparticle motion in central field, comparing with Schroedinger equation 06 p0890 A72-18418
- Elementary particle theory and field equations in cosmological spaces, using four dimensional conformal imbeddings 06 p0891 A72-18421
- Neutral rotating mass shell surrounding concentric stationary electrically charged insulation, calculating induced dipole-like magnetic field from coupled linearized general relativity field equations 06 p0853 A72-18423
- Parametric solution of Brans-Dicke cosmological equations for flat Friedmann type expanding universe for time, density, expansion parameter and scalar field 07 p1074 A72-19525
- Field approach to gravitation accounting for energy release and nonthermal radiation occurrence in pulsars and quasars 07 p1075 A72-19576
- Modified Riemann geometry for scalar-tensor theory of gravitation, emphasizing scalar field role relation to vector length change during point-to-point transport 07 p1036 A72-20196
- Wightman field theory generalization for application to gravitational field quantization, describing curved space-time by strongly geodesically complete manifolds 07 p1036 A72-20198
- Atom interactions with rf field, using quantum mechanical interpretation in terms of photons 07 p1038 A72-20433
- Markov type isotropic random Gaussian field analysis in n-dimensional Euclidean space 08 p1198 A72-20999
- Variational principle of Hamiltonian type for classical field theory, noting application to nonlinear heat transfer and fluid flow in Eulerian description 08 p1252 A72-21287
- Stationary motions stability of four rotor vertical gyroscopic system on satellite in circular orbit in Newtonian central force field 08 p1205 A72-21804
- Toroidal gravitational waves in general relativity, considering analog to imploding-exploding cylindrical waves, linear field equations and symmetric metric 08 p1210 A72-21922
- Mass-zero spin-two particle field theory of gravitational interaction with covariance under full conformal group 09 p1355 A72-22684
- Star catalogs comparison and stellar positional differences and motion studies using random field theory 09 p1388 A72-23052
- Einstein field equation representing static fluids in general relativity, obtaining all solutions with degenerate Weyl tensor 10 p1511 A72-24349
- Collective self fields generated from intense electron beams for high energy positive particle acceleration and Astron hot plasma confinement for fusion control 10 p1523 A72-24788
- Field and geodesic line equations for light rays in open and closed isotropic radiative universe model 10 p1549 A72-25059
- Baroclinic wave field distributions and balances in rotating annulus with free surface in atmospheric circulation study, noting Ekman layer features 11 p1680 A72-25765
- Steady state plasma interactions with electromagnetic force field in plasma accelerators, showing shock wave formation [AIAA PAPER 72-413] 11 p1706 A72-26163
- Geomagnetic invariant coordinates and related field line parameters calculation via field model and fast numerical method 12 p1803 A72-27771
- Noncovariant gravitation theory field equations based on preferred reference frame applied to homogeneous isotropic cosmological model, finding conservation law for total energy 12 p1875 A72-28154
- Radiative properties of charged particles moving in attractive Coulomb fields related to repulsive fields by symmetry relationships 12 p1848 A72-28155
- Numerical analysis methods for solution stability of reduced field equations describing perturbed motion of body under nonconservative loads 13 p2001 A72-28485
- Mobility-field characteristics of GaAs below Gunn threshold with magnetoresistance technique, relating to device performance and other material parameters 13 p2021 A72-28573
- Convection instability in viscous incompressible liquid layer with free boundaries under modulated external force field 13 p2064 A72-28723
- Eigenstate field parameter bounds in elastomechanics natural vibration problems 13 p2059 A72-29598
- Microinhomogeneous solid bodies elastic fields and effective moduli calculation method within framework of random field theory, using singular approximation 13 p2062 A72-29884
- Lunar gravitational field expansion coefficients C20 and C22 calculation, using Cassini equator inclination and radial bulk density distribution 14 p2149 A72-30213
- Distortion corrections in geophysically traced gravitational, magnetic and geoelectric field maps, discussing automation 14 p2101 A72-30642
- Kinematic equations derivation for traveling displacements field in Cosserat continuum by Lagrange formalism, noting analogy with Maxwell equations 15 p2274 A72-31474
- Thermodynamic perturbation and scaling theory for multidimensional spherical models of lattice structure in terms of field of critical phenomena 15 p2293 A72-32219
- Angular force models with electron-ion interaction applied to bcc and fcc metals, calculating phonon dispersion curves for V, Nb and Ta 15 p2258 A72-32226
- Mechanical models in thermoelasticity associated with boundary problems of classical physical fields with postulated laws of variation and periodicity 15 p2330 A72-32288
- Wave packet theory application to multimode laser cavity electromagnetic/optical field analysis 15 p2251 A72-32649
- Constrained-impedance eigenfunctions, using projection method for field expansion in diffraction problems 15 p2202 A72-32661
- Lorentz-covariant procedure for equations of structure and motion of particles represented by singularities in Einstein relativistic field theory 16 p2422 A72-32880
- Field distribution and absorption coefficient calculations for normal incidence of extraordinary electromagnetic wave on linear plasma layer in hybrid resonance region 16 p2363 A72-33480
- Study of the stability of certain relative equilibria of a symmetrical satellite 17 p2620 A72-34282
- Laplace equation to generate stationary electromagnetic vacuum fields, generalizing from Papapetrou-Majumdar class of static fields 17 p2580 A72-34425
- Physical determination of fields of displacements and their derivatives in continuous media. [ASME PAPER 72-APM-15] 17 p2629 A72-34801
- Field variations of perfect fluid in axisymmetric stationary universe within general relativity theory concept, noting energy extremal properties for rotating stars 17 p2607 A72-34921
- On the stability of axisymmetric systems to axisymmetric perturbations in general relativity. I - The equations governing nonstationary, stationary, and perturbed systems. 17 p2611 A72-35315
- Intermediate-range gravity - A generally covariant model. 17 p2581 A72-35380
- Nonspherical perturbations of relativistic gravitational collapse. I - Scalar and gravitational perturbations. II - Integer-spin, zero-rest-mass fields. 17 p2612 A72-35390
- Hamiltonian formulation of spherically symmetric gravitational fields. 17 p2582 A72-35393
- Gravitational radiation from relativistic systems. 17 p2582 A72-35394
- Vortex concept and related vector analysis in fluid dynamics, crystal dislocations, superconductors and superfluid He 18 p2711 A72-36489
- Hulthen and Schwarzschild potentials in the Klein-Gordon equation. 18 p2711 A72-36515
- Dual amplitude construction possibility from general field theory couplings and propagators, considering factorization on multiperipheral configuration in translational and rotational modes 18 p2713 A72-36516
- Gravitation theory in terms of scalar and tensor field, noting Lyra general reference system transformations and scale invariance 18 p2711 A72-36713
- Hypo-elastic dielectrics. I - Constitutive equations. II - Birefringence in simple shear. 18 p2720 A72-37043
- Locally Lorentz covariant gravitational field theory of Pauli-Fierz type with massless symmetric spin-2 field having source term as matter stress-energy tensor 18 p2712 A72-37161
- Note on the 'alpha'-constant stiffness method for the analysis of non-linear problems. 18 p2739 A72-37172
- Finite range gravitation theory extension to generally covariant massive two-tensor field gravitation theory containing eight dynamically independent degrees of freedom 20 p2953 A72-39342
- Heuristic description for harmonic oscillator as quantized model of anharmonicity applied to excitation fields involving particle clusters and multibody configuration 20 p2953 A72-39398
- Maxwell electromagnetic field theory review, emphasizing relationship between integral forms of Faraday and Ampere laws in conventional space and time concepts 20 p2904 A72-39778
- Einstein theories of special and general relativity, taking into account physical concepts relation to mathematical formalism, equivalence principle, field equations and gravitational waves 20 p2954 A72-40002
- Electrical modeling of nonlinear problems of thermal engineering 21 p3128 A72-40182
- Perturbation theory for field moments in inhomogeneous media 21 p3016 A72-40780
- Gravitational theory strong discontinuity conditions, using fundamental variational equation for field and media bulk construction in general relativity theory 22 p3204 A72-42089
- Convection instability in viscous incompressible fluid layer with free boundaries under modulated external force field 22 p3243 A72-42099
- Metric gravitation theories classified according to field type and interaction mode, constructing post-Newtonian limit 22 p3206 A72-42567
- A simple coupling between the electromagnetic and gravitational fields. 22 p3207 A72-42855
- Book - Gravitation and cosmology: principles and applications of the general theory of relativity. 22 p3208 A72-43080
- Lunar gravitational field expansion coefficients C20 and C22 calculation, using Cassini equator inclination and radial bulk density distribution 23 p3334 A72-43243
- Representation of solenoidal vector fields in bounded domains by poloidal and toroidal scalar potentials, discussing applications in fluid mechanics, elastic vibrations and electromagnetic theory 23 p3313 A72-43716
- Motion of a solid with a nonholonomic constraint around a fixed point in a conservative force field 23 p3313 A72-43800
- Field dependence of gaseous-ion mobility - Theoretical tests of approximate formulas. 23 p3316 A72-43871
- Non-Abelian gauge fields with two masses 23 p3314 A72-44155
- On mechanical response of a non-uniform piezoelectric transducer under the influence of a body-force. 23 p3291 A72-44316
- Book - The effects of the turbulent atmosphere on wave propagation. 24 p3379 A72-44650

FIGHTER AIRCRAFT
NT HARRIER AIRCRAFT
NT JAGUAR AIRCRAFT

- Trainer-combat turbojet or turbofan aircraft characteristics, comparing flight, weight, size, maintenance and development costs 05 p0611 A72-16178
- Combat aircraft lateral aiming performance optimization and evaluation based on criterion of bullet stream response to pilot roll commands 05 p0611 A72-16657

- Fighter pilots training by simulators, determining learning effectiveness by mathematical model based on renewal theory
[AIAA PAPER 72-161] 05 p0644 A72-16827
- Fighter/attack aircraft turbojet and turbofan engines testing with/without afterburners 06 p0868 A72-18495
- Airstart flight testing for single engine fighter/attack aircraft, including flight conditions, windmilling, fuel flows, gas temperature, ignition and acceleration 06 p0868 A72-18496
- VAK 191 B V/STOL reconnaissance fighter prototype test program, describing simulations, bench, ground, static, hovering and flight tests 07 p0912 A72-19249
- V/STOL weapon system VJ-101, describing He-231 design development from tailsitter concept to canard configuration with tilting wing-tip engines 07 p0912 A72-19251
- Interactive computer graphics with three dimensional real time CRT display of air combat maneuvers for fighter pilot training 11 p1613 A72-26291
- Fighter aircraft maneuverability, range and armament requirements, discussing canard vs delta configurations 11 p1577 A72-26657
- German VAK 191B V/STOL fighter aircraft design, development and flight tests, noting redundant control systems 12 p1753 A72-27166
- General Dynamics model 401 air superiority single engine fighter design stressing light weight structure and maneuverability at high speeds and angles of attack 13 p1896 A72-28575
- Large amplitude flight simulator for fighter design refinement, noting extensive computer commitment 13 p1938 A72-28757
- Optimum low noise engine selection for transport and combat aircraft relative to range or payload performance, considering CTOL, VTOL, SST and fighter aircraft 15 p2297 A72-32127
- Multimode flight control for precision weapon delivery. 17 p2493 A72-35561
- Pilot-fighter aircraft system mathematical model relating pilot performance to air to ground weapon delivery accuracy 17 p2493 A72-35564
- Development of the Saab-Scania Viggen. 19 p2748 A72-37749
- The VAK 191 B VTOL fighter and reconnaissance aircraft 19 p2748 A72-37825
- Design for air combat. 19 p2751 A72-38124
- Naval air test center participation in development of air-to-air combat simulation. 19 p2783 A72-38130
- [AIAA PAPER 72-765] 19 p2783 A72-38130
- Optimum turns to a specified track for a supersonic aircraft. 19 p2753 A72-38277
- Advanced fighter controls flight simulator for all-systems compatibility testing. 20 p2911 A72-39090
- [AIAA PAPER 72-837] 20 p2911 A72-39090
- Maneuver load control and relaxed static stability applied to a contemporary fighter aircraft. 20 p2887 A72-39129
- [AIAA PAPER 72-870] 20 p2887 A72-39129
- Development of design criteria for predicting departure characteristics and spin susceptibility of fighter-type aircraft. 22 p3136 A72-42330
- [AIAA PAPER 72-984] 22 p3136 A72-42330
- Development and evaluation of an energy-oriented guidance logic for air combat models. 22 p3137 A72-42354
- [AIAA PAPER 72-949] 22 p3137 A72-42354
- Game theoretical modeling of fighter aircraft turning tactics competition in pursuit combat, using minimax technique 22 p3138 A72-42359
- [AIAA PAPER 72-950] 22 p3138 A72-42359
- Life estimation and prediction of fighter aircraft. 22 p3139 A72-42972
- Control requirements for control configured vehicles. 24 p3368 A72-45349
- Control configured fighter and bomber aircraft based on flight control technology, discussing development programs 24 p3369 A72-45386
- Military aircraft construction, design and economic requirements, discussing fighter payloads, armament efficiency and fire control systems 24 p3369 A72-45450
- FIGURE OF MERIT**
- Optical distortion induced by heated windows in high power laser systems, deriving figures of merit for window materials 02 p0237 A72-11470
- Optimum bounding filter design based on error covariance for Kalman-Bucy and Wiener filters with inexact known parameters, obtaining performance figure of merit 10 p1454 A72-23785
- Bayes analysis application to Weibull distribution parameters estimation, using entropy concept for figure of merit to assess reliability analysis 10 p1444 A72-23987
- Communication satellite systems reliability assessment using figure of merit method 10 p1435 A72-23991
- Thermoelectric cooling devices materials figure of merit upper limits above room temperature, using semiconductor parameters experimental values 12 p1755 A72-27722
- Magneto-optics materials for use in data storage, discussing quality evaluation based on figure of merit reflecting heat sensitivity and readout requirements 15 p2203 A72-32352
- Helicopter design figure of merit weight ratios definition in terms of rotor thrust coefficient, substituting pure airframe structure weight for conventionally used empty weight [SAWE PAPER 916] 23 p3250 A72-43463
- FILAMENT WINDING**
- Yield-fracture criterion for angle ply laminate cylinders wound with filament in biaxial tension 01 p0090 A72-10521
- Fiber reinforced filament wound composites for pressure vessel applications, investigating mechanical properties 01 p0090 A72-10741
- Acoustic emission evaluation of damage of filament wound composite materials under tensile loading applied to spherical test shapes 01 p0069 A72-10804
- Torsional stiffness /shear modulus/ of glass fiber reinforced plastic tubes as function of filament winding angle 01 p0141 A72-10999
- Material design for filament wound graphite-graphite fiber/matrix composite heat shields for improved performance during reentry 08 p1245 A72-21597
- Composite filament wound boron-epoxy rocket motor combustion chamber design, fabrication and hydrostatic tests 08 p1177 A72-21692
- Uniaxial, biaxial and shear loading tests on filament wound carbon-carbon composite tubes and rings 11 p1670 A72-25458
- Heating rate effects on residual stresses in thick walled cylinders produced by winding heated binder impregnated fiberglass tape on cold spool 13 p1982 A72-28553
- Manufacturing process for glass fiber chopped strand mats, discussing physical and electrical properties and applications to filament winding 16 p2414 A72-33303
- Plastic composite container cylindrical wall fabrication by two stage procedure combining radial and cross winding of glass fiber rovings 16 p2398 A72-33305
- Mechanical properties of carbon filament wound carbon matrix composite from tensile tests, noting reinforcement efficiency 17 p2573 A72-35669
- Calculation of residual stresses in wound materials produced by a layer-on-layer solidification process 19 p2872 A72-37532
- Model filament wound epoxy composites. 19 p2808 A72-38164
- Filament winding techniques for rotor blade applications. 19 p2808 A72-38165
- Filament wound cylindrical pressure vessel design and development for operation under cyclic-loaded high hydraulic pressure in underwater environment 19 p2877 A72-38166
- Inflatable mandrels use to manufacture filament wound casings examined in terms of suitable mandrel materials and required mechanical properties 19 p2808 A72-38167
- Mandrel design for the filament winding process. 19 p2808 A72-38168
- Digital programming techniques for maximum utility and flexibility in filament winding. 19 p2808 A72-38170
- Investigations into the impregnating behaviour of various reinforcing materials in the filament winding process. 19 p2808 A72-38171
- Static and dynamic fatigue behavior of glass filament-wound pressure vessels at ambient and cryogenic temperatures. 19 p2823 A72-38832
- Influence of technological factors upon the mechanical reliability of composite-material structures 20 p2943 A72-38945
- High modulus fiber composites development from viewpoint of reinforcement patterns and material properties 20 p2943 A72-38946
- Fatigue behavior of glass filament-wound epoxy composites in water. 21 p3072 A72-40246
- Boron polyimide composite development. 21 p3072 A72-40553
- Filament wound pressure vessel isotensoid theory, considering composite material as macroscopically homogeneous anisotropic continuum 22 p3238 A72-42838
- Stress-strain state in tension of orthogonally stiffened fiberglass-reinforced plastic with cracks in transversely stiffened layers 24 p3460 A72-45754
- FILAMENT WOUND CONSTRUCTION**
- U FILAMENT WINDING**
- FILAMENTS**
- Reduction of governing equation for thin non-stretching vortex filament in incompressible inviscid fluid to nonlinear Schrodinger equation describing helical motion propagation 10 p1466 A72-24293
- Solar activity correlation with filaments disintegration during transit across solar disk, analyzing statistical data 15 p2318 A72-32782
- Finite core infinite extent helical vortex filament stability to small sinusoidal displacements of centerline 21 p3045 A72-40649
- Errors caused by hot-wire filament vibration. 24 p3402 A72-44949
- FILLERS**
- Refractory alloy weldability and brazing, discussing manual and automatic tungsten arc and electron beam processes and fillers 01 p0075 A72-10752
- Three layer plates stability with light fillers, noting filler thickness effect on approximate solutions accuracy 03 p0454 A72-14377
- Polyfluoroethylene-based composite materials mechanical properties, discussing strengthening mechanism of filler additions 05 p0682 A72-15989
- Electron beam welding with filler metal, describing spot and butt welding applications 06 p0819 A72-17498
- Filler metal compositions and procedures for Al alloys vacuum brazing, describing experimental vacuum furnace apparatus 07 p0997 A72-20000
- Filler metal paste application effect on Hastelloy sheet brazing quality, describing results in terms of mechanical properties and microstructural characteristics 11 p1637 A72-25342
- Filler wires development for inert gas welding of stainless maraging steel 11 p1660 A72-26488
- Particulate fillers bulk effects on epoxy resin compositions flexural, compressive and tensile strengths and moduli 12 p1834 A72-28089
- Ethylene-vinyl acetate-asphalt thermoplastic material properties, filler effects, application methods and commercial uses 12 p1835 A72-28094
- Stability of transversely isotropic cylindrical shell with elastic filler under axial compression, deriving approximate equations for transverse shear stress effect 13 p2055 A72-28556
- Filler influence on critical load and buckling zone size in circular elastic three layer ring under uniformly distributed vertical load in rigid cavity 15 p3238 A72-31745
- Fillers effect on polytetrafluoroethylene friction properties, electroconductivity and thermal conductivity, noting friction coefficient reduction by laminar filler structures 16 p2413 A72-33269
- Filler wire composition effects on solidification cracking resistance in weldable Al-Zn-Mg alloy 18 p2699 A72-36426
- Electron microscope investigation of the effect of fillers on the formation of supramolecular structures and on the type of breakdown in amorphous and crystalline polymers 21 p3072 A72-40084
- Numerical analysis of wave processes in a three-layer strip with rigid filler 22 p3232 A72-41872
- Filler quantity and type effects on mechanical energy losses in polymers, discussing molecular interaction and chemical bond influences 23 p3306 A72-43731
- Polyfluoroethylene-based composite materials mechanical properties, discussing strengthening mechanism of filler additions 24 p3417 A72-45731
- FILLETS**
- Disk fillets stressed state, determining concentration coefficient and bearing capacity effect 23 p3347 A72-43747
- FILM BOILING**
- Vapor bubble growth on heated surface with random temperature distribution and liquid microfilm for water and boiling potassium 02 p0303 A72-12862

- Heat transfer during liquid film evaporation in centrifugal vaporizer, noting agreement between theory and experiment 03 p0458 A72-14158
- Trimethylchlorosilane film boiling for silicon carbide deposit on vertical heated tungsten filaments, investigating mass transport rate 04 p0595 A72-14600
- Dry areas occurrence on heating surface in pool boiling near burnout heat flux, discussing nucleate and film boiling stability and hysteresis 07 p1099 A72-19621
- Boundary layer model for laminar transient forced convection film boiling on isothermal flat plate, noting one dimensional conduction, intermediate and steady state regions [AIAA PAPER 72-289] 11 p1741 A72-25227
- Heat transfer during film and transition boiling on vertical surfaces, taking into account time dependence 11 p1746 A72-26537
- Momentum and energy equations for pool film boiling heat transfer from horizontal cylinder to saturated liquids, using integral boundary layer analysis 14 p2173 A72-31067
- German monograph on heat transfer and stability limits for boiling and nonboiling falling films covering surface and bubble boiling conditions 15 p2334 A72-31503
- Investigation of heat exchange during film boiling of underheated liquid under conditions of forced flow in channels 19 p2881 A72-38036
- Unconstrained liquid mass /Leidenfrost phenomenon/ pool and forced convective film boiling at cryogenic temperature 19 p2883 A72-38841
- A review of physical models and heat-transfer correlations for free-convection film boiling. 19 p2883 A72-38842
- The film vaporization combustor and its physical principles. I - The vaporizer section of the combustor. II - The reaction chamber and the combustion [DFVLR-SONDDR-194] 20 p2963 A72-39074
- Film boiling correlations for stable natural convection heat transfer for various heater substances and pressures 20 p2983 A72-39487
- Saturated liquid film boiling on vertical surface, calculating local heat transfer rates as function of height and superheat from turbulent vapor flow model [ASME PAPER 72-HT-38] 20 p2986 A72-39668
- Wall temperature, thermal conductivity and acoustic vibration frequency as function of critical heat flux density for unstable water film boiling conditions 21 p3130 A72-41063
- Diffusive and radiative effects on vaporization times of drops in film boiling. 21 p3130 A72-41185
- FILM CONDENSATION**
- Pitting and film deposits with organic fluid by electrolysis and fluid flow, discussing electrokinetically produced corrosion [ECS PAPER 84] 07 p1010 A72-18802
- Two phase boundary layer flow for laminar two dimensional steady forced film condensation with pressure gradients for fluids of small Prandtl numbers [ASME PAPER 71-HT-Y] 08 p1251 A72-20878
- Perturbation analysis for forced flow past semi-infinite flat plate parallel to uniform mainstream, calculating two dimensional laminar film condensation by boundary layer theory 10 p1469 A72-24563
- Noncondensable gas and forced convection effects on laminar film condensation for two phase flows 11 p1743 A72-25261
- An integral analysis of condensing annular-mist flow. 18 p2682 A72-36720
- Condensation on a downward-facing horizontal rippled surface. [ASME PAPER 72-HT-33] 20 p2983 A72-39485
- Theory of laminar film condensation of flowing vapor. 21 p3128 A72-40950
- FILM COOLING**
- Diffuser for altitude simulation in rocket motor operation, featuring film cooling with water inflow by motor exhaust gas ejector action 05 p0704 A72-16004
- Film and convection cooling interaction and effect on wall cooling efficiency for gas turbine applications [AIAA PAPER 72-8] 05 p0748 A72-16873
- Film cooled turbine vanes external heat transfer distribution in turbulent gas stream, measuring heat transfer coefficients with and without blowing [AIAA PAPER 72-9] 05 p0707 A72-16877
- Air injection from wall slot into turbulent boundary layer of high temperature gas channel flow, calculating film cooling effectiveness in flat plate 08 p1252 A72-21316
- Thin liquid surface water film cooling tests for mass loss under simulated reentry heating and shear conditions 10 p1563 A72-24648
- Double slot laminar film cooling, considering tangential gas injection velocities into laminar boundary layer and heat transfer to wall [AIAA PAPER 72-290] 11 p1741 A72-25228
- Parabolic boundary layer finite difference model for predicting film cooling and heat transfer near flush injection slots in gas turbine combustors [AIAA PAPER 72-291] 11 p1614 A72-25229
- Film cooling effectiveness for air-gas flow section of gas turbine engine under actual operating conditions 12 p1890 A72-28170
- Heat transfer measurement during flat plate cooling by air film, using electrical calorimetric technique 12 p1890 A72-28176
- Boundary layer theory for convective heat transfer of two dimensional film cooling systems in turbulent regime, noting momentum, enthalpy and concentration equations 13 p2063 A72-28630
- Thermal protection by liquid-gas laminar flow near critical point with coolant film liquid oxygen injection incident on blunt body 16 p2343 A72-33156
- A study of film-cooling effectiveness of some gas-turbine stator surfaces. 17 p2597 A72-34468
- Air film cooling in a nonadiabatic wall conical nozzle. 17 p2638 A72-35493
- Supplemental internal gaseous film cooling combined with external cooling of combustion chamber walls, analyzing effectiveness via nonadiabatic model [AICHE PREPRINT 3] 18 p2741 A72-36550
- A review of physical models and heat-transfer correlations for free-convection film boiling. 19 p2883 A72-38842
- Film cooling effect on surface heat transfer in laminarizing mainstream turbulent boundary layer for injection through flush angled two dimensional slots [ASME PAPER 72-HT-11] 20 p2986 A72-39682
- Arbitrary length thin liquid film cooling mass transfer data correlation, accounting for film roughness and entrainment effects 22 p3243 A72-41960
- An experimental study of film cooling through a rearward-facing slot. 23 p3356 A72-43971
- An experimental study of heat transfer downstream of a rearward-facing step with small coolant injection. 23 p3357 A72-44271
- FILM THICKNESS**
- Microwave emission characteristics of oil slicks, showing dependence on oil type, film thickness and sea state [AIAA PAPER 71-1071] 01 p0057 A72-10533
- Nb alloy silicide coating thickness data correlation by thermoelectric, metallographic and pointed micrometer techniques, discussing state of art in thickness control, penalties and substrate independence 01 p0075 A72-10750
- NbN film superconducting properties measured as function of thickness, discussing transition temperature, critical current and magnetic field 04 p0562 A72-15294
- Isothermal elastohydrodynamic theory for full range of pressure-viscosity coefficient, considering film thickness effect 06 p0821 A72-17805
- Hydrodynamic lubricating films with viscosity variations perpendicular to direction of motion, evaluating friction coefficient changes for constant film thickness and load carrying capacity [ASME PAPER 72-LUB-E] 06 p0821 A72-17806
- Thin film resistors and capacitors design, considering stability, power, size, film thickness, parasitic inductance capacitance and resistance and dielectric loss properties 06 p0790 A72-18573
- Resin bonded solid lubricant film thickness optimization from statistical analysis of bench and machine element test data 06 p0823 A72-18591
- Self lubricating polytetrafluoroethylene and polyimide composites transfer film formation tests, studying film thickness and uniformity 06 p0824 A72-18596
- Random vibrations and antitorque moments of rigid shaft with precision bearings, considering effects of geometrical fabrication defects and nonuniform film thickness 06 p0824 A72-18722
- Short time film stability followed by dry spot formation in thin heated draining liquid films on vertical walls, discussing minimum thickness 07 p1098 A72-18842
- Photometric monitoring of film thickness of stacked structures for high strength and laser flux resistance 07 p1049 A72-20126
- Quartz crystal oscillator device for continuous monitoring and controlling thin film thickness in optical and electronic applications, noting temperature effects on crystal oscillating frequency 07 p0990 A72-20284
- Thin films thickness control by piezoelectric quartz crystal, discussing electrically excited oscillations wavelength and damping characteristics 07 p0990 A72-20285
- Thin films thickness and refraction index calculation from curves of specularly reflected X ray intensity vs grazing angle, obtaining surface roughness variance 07 p1050 A72-20405
- Elastohydrodynamic lubrication of soft elastic-deformed contact surfaces, determining lubricant film thickness as function of inlet and outlet parameters 07 p0998 A72-20530
- Ball bearing rolling contact lubricating oil film thickness theoretical prediction compared with experiment 09 p1318 A72-22850
- Capacitance depth gage for thin liquid films thickness measurement, noting application to interface waves amplitude and frequency measurements 09 p1316 A72-23410
- Magnetic domains in cobalt and cementite observed by electron microscopy, investigating thin film thickness effect on temperature 10 p1496 A72-24088
- Velocity slip effect on squeeze film between porous rectangular plates, calculating pressure, load carrying capacity, film thickness and response time 10 p1488 A72-24820
- Metallic foils effects on thermal joint resistance of interface between lathe turned and optically flat surfaces, noting optimal thickness 11 p1685 A72-25223
- Ball bearings lubricated with oils and fire-resistant fluids, testing fatigue life relationship to steel quality, fluid film thickness and viscosity 12 p1816 A72-28108
- Electroslog and vacuum remelted maraging steel rolling contact, investigating fatigue life as function of lubricant film thickness/surface roughness ratio 12 p1816 A72-28109
- Deep groove ball bearing endurance tests to determine running conditions and lubricant film thickness/surface roughness ratio effects on fatigue life 12 p1816 A72-28112
- Contact potential difference effects on lubricant film thickness in electronic equipment joints, noting molecules orientation in electric field 13 p1930 A72-29052
- Equations of motion for incompressible viscous fluid thin layer on cylinder outer side under gravity, calculating wave number, phase velocity and film thickness 14 p2094 A72-30699
- Dynamic in situ thin film thickness monitoring during vacuum deposition by holographic interferometry, noting independence from high quality optical components 15 p2240 A72-32381
- Contribution to the study of creep in thin permalloy films. 17 p2596 A72-35759
- Structure and properties of transition layers formed in the epitaxy process. 18 p2718 A72-36340
- An integral analysis of condensing annular-mist flow. 18 p2682 A72-36720
- Thickness dependence of the electrical transport properties of germanium films. 19 p2844 A72-37685
- Dependence of critical supercurrent on normal layer thickness in S-N-S structures. 19 p2846 A72-38631
- Condensation on a downward-facing horizontal rippled surface. [ASME PAPER 72-HT-33] 20 p2983 A72-39485
- Transparent film thickness, refractivity and birefringence measurements by white light interferometric gage, noting performance insensitivity to chemical composition, film temperature and haze level 21 p3053 A72-40601
- Optimization of the structural parameters of galvanic laminar heat-flux sensors 21 p3056 A72-41058
- Asbestos-textolite coating required thickness calculation with allowance for aerodynamic heating, discussing softening mechanisms 21 p3074 A72-41709
- The direct study of crack formation in metals in a high-voltage electron microscope 24 p3401 A72-44717
- FILMS**
- Automatic device using tetragonal conducting film sheets to feed graphic information into computer 02 p0187 A72-12279
- Automatic device using tetragonal conducting film sheets to feed graphic information into computer 11 p1601 A72-25704
- Hemispherical elastic nonexpandable weightless film fastened along equator to inner wall of closed cylindrical vessel under hydrostatic pressure, determining film axisymmetric equilibrium shapes 13 p1940 A72-28392

Blackness degree calculation for semitransparent film on nontransparent substrate with layer temperature gradients, allowing for polarization emission and multiple reflections 14 p2130 A72-30296

Minimum ion source temperatures for glow discharge ion flux deposition of films and coatings on metallic and nonmetallic substrates 15 p2244 A72-31573

FILTERING

U FILTRATION

FILTERS

Porous stainless steels as filter medium, describing manufacturing techniques, properties and applications 02 p0233 A72-11449

Automatic switched Shuman filter for shock waves numerical computation, noting third and fourth order accurate finite difference schemes 11 p1619 A72-26668

FILTRATION

NT SPATIAL FILTERING

Solute rejection in hyperfiltration of sodium chloride and urea with porous glass ion exchange membrane as function of pressure, temperature and concentration 07 p0937 A72-20601

Nucleic acid hybridization with RNA immobilized on filter paper. 24 p3379 A72-45773

FIN STABILIZERS

U FINIS

U STABILIZERS [FLUID DYNAMICS]

FINANCE

National and international legal aspects relative to levying user fees for flight safety services in Germany 11 p1748 A72-26560

Swiss franc revaluation effect on Warsaw Treaty liability limits, discussing legal problems 11 p1749 A72-26562

FINANCIAL MANAGEMENT

Mathematical model for research payoff estimation by internal rate of return method used by large corporations for project evaluation 02 p0305 A72-12695

Airport financing, discussing funds, long term planning, commercial principles, finance enterprise, loans and revenue 05 p0753 A72-16698

Interflug national economic control system, discussing objectives, costs, labor, science and technology, material and price management plans 05 p0753 A72-16778

Military systems cost reduction via civil avionics procurement techniques, discussing cost-reliability design criteria 15 p2338 A72-32215

Financial methods employed in creating Brazilian aircraft industry via mixed public-private ownership 16 p2481 A72-33375

Economics of a new regional airport. 18 p2743 A72-36779

FINE STRUCTURE

Multichannel hf spectrograph for decimeter wave solar burst spectrum fine structure analysis, noting operation at any desired frequency and channel separation 01 p0065 A72-10416

Shielding and semitransparent sporadic E layer fine structure characteristics from summer observations data analysis 02 p0222 A72-12523

H alpha spectra and combined filtergram observations of chromospheric fine structure, using Becker model 03 p0414 A72-12929

Solar chromosphere fine structure at limb, measuring spicules and bright mottles lifetime 03 p0415 A72-12930

Prominent Zeeman multiplets in photosphere, penumbra, umbra and sunspot spectra, presenting ratios for temperature sensitivity measurements 03 p0415 A72-12933

Gyroresonance plasma wave absorption in corona, investigating solar radio bursts fine structure 03 p0415 A72-12935

Turbulent flow internal intermittency and fine structure distribution as function of Reynolds number, using hot-wire anemometer for velocity field measurements 03 p0340 A72-13156

Sunspot and active region magnetic fields and thermodynamic structure from umbral and penumbral models, discussing magnetic fine structure 03 p0427 A72-13296

Fine structure of magnetic field distribution in umbra and penumbra of sunspots 03 p0428 A72-13299

Magnetic field fine structure in undisturbed photosphere for high latitude solar regions, constructing model to explain magnetograph response 03 p0428 A72-13306

Solar magnetic field measurement with 10,830 A He I line photoelectric spectroheliograms, observing filamentary fine structure in active regions 03 p0429 A72-13310

Solar magnetic field fine structure from filter magnetograms, tabulating magnetic elements frequency distributions 03 p0429 A72-13315

Fine structure features of sunspot magnetic fields and umbral dots, showing magnetic and thermal or mechanical forces interaction 03 p0430 A72-13334

Solar magnetic field origin in fine structure elements of photosphere and sunspots 03 p0431 A72-13340

Solar polar and general magnetic field fine structure and statistical nature, discussing time fluctuations and interplanetary field 03 p0432 A72-13353

Linear polarization of pulsar PSR 22 18 plus 47 radio emission pulses, attributing periodic fine structure of spectrum to rotation of polarization plane in interstellar medium 03 p0436 A72-13824

Fine structure of Mo-Re alloys single crystals in solid solution region as function of Re content 03 p0377 A72-14019

Transverse shock waves fine structure and saturation of ion-acoustic turbulence in collisionless plasma, using magnetic field probe and MHD equations 03 p0399 A72-14068

Statistical investigations of solar burst time dependent fine structure, giving data for multichannel spectrograph and recording system design 05 p0708 A72-15767

Fine H alpha fibrils in middle chromosphere, discussing optical thickness and absorption features 05 p0718 A72-16506

H alpha fine structure, investigating chromospheric magnetic field distribution 05 p0718 A72-16507

Solar chromospheric fine structure at active region, magnetic polarity boundaries from high resolution H-alpha filtergrams 05 p0718 A72-16508

Solid bodies crack development theory, emphasizing crack tip fine and hyperfine structures concepts and time dependent effects 06 p0898 A72-18554

Fine structure elements of chromosphere, discussing spicules, fibrils and thermal effects 07 p1077 A72-19808

Hardening mechanisms during plastic deformation of pure bcc metals, discussing stresses relation to fine structure and crystal dislocation paths 07 p1018 A72-20142

Radio sources fine structure survey at 81.5 MHz, finding angular diameters by interplanetary scintillation technique 07 p1081 A72-20231

Fine structure of Pseudomonas saccharophila at early and late log phase of growth, using electron microscopy and various culture techniques 07 p0922 A72-20238

Solar cosmic rays propagation between shock front and solar flare hot plasma, examining fine structure from Explorer 34 and Venera 6 data 07 p1063 A72-20628

Fine structure of energy distribution function for electron beam interacting with plasma 08 p1215 A72-21722

X ray study of martensite fine structure produced by plastic deformation in Fe-Ni alloy 08 p1188 A72-21788

Solar general magnetic field nature, origin, fine structure and temporal variations, evaluating sunspots and active plage areas as field sources 09 p1387 A72-22752

Ta and W X ray spectra fine structure measurement, providing electron states density in unoccupied regions of energy bands of solids 09 p1370 A72-22842

Defects high temperature diffusion effect on Mossbauer spectral lines width and positions in crystals with quantum transfer between multiplet sublevels in fine structure 09 p1372 A72-23038

Positive ions excitation cross sections calculated for proton impact induced transitions among fine structure states 10 p1543 A72-24619

Fine structure and IR transmission functions of carbon dioxide absorption bands at high pressure and temperature, calculating transition lines strength and position 11 p1620 A72-25275

Near-ground daytime temperature and humidity fine structure relation to heat flux, net radiation and temperature and wind gradients 12 p1841 A72-27711

Slit spectrogram and direct photograph observation of inner corona fine structure during 7 March 1970 solar eclipse, describing line and continuum intensities 13 p2042 A72-29533

Solar magnetic field fine structure from chromospheric morphology, using high resolution H alpha filtergram and magnetogram 13 p2046 A72-29731

Spectroheliograph study of fine structure of Evershed effect, determining radial velocity in penumbra along dark filaments and interfilamentary space 13 p2047 A72-29739

Time varying magnetospheric electric field spatial distribution effect on plasmasphere temporal evolution, considering fine structure due to periodic gusts in convection electric field 13 p1953 A72-29804

Methane spectral band tetrahedral fine structure analysis, using vibration-rotation Hamiltonian 14 p2084 A72-30523

Quiescent solar prominences internal motions from fine structure wavelength shift observations in Ca II K line spectra 15 p2318 A72-32780

Atmospheric transmittance calculation from 0.76-micron oxygen band fine structure parameters 16 p2417 A72-33289

Balloon flight observation of charge composition fine details and gross features of isotopic abundance in near relativistic cosmic rays 16 p2447 A72-33729

Deformed Cu-Au single crystal surface slip bands fine structure, determining separation distance between individual slip lines 16 p2408 A72-33774

Fine structure similarities between solar flares and current sheath in laboratory hot plasma coaxial accelerator, noting X ray and high energy particles production mechanism 16 p2438 A72-33919

Microphotometric chemiluminescence measurement for analysis of turbulent flame fine structure for homogeneous air-fuel mixtures at high Reynolds numbers 16 p2479 A72-34005

Ultrastructure and geologic relations of some two-aeon old Nostocacean algae from northeastern Minnesota. 17 p2544 A72-34336

Solar mottles characteristics as seen on large scale H alpha filtergrams 17 p2616 A72-35700

Periodic intensity oscillations in center of H alpha supergranulation network, in rosette centers and in plage granules 17 p2616 A72-35701

Frequency separation in structure of solar continuum radio bursts. 17 p2602 A72-35713

Fine structure elements of chromosphere, discussing spicules, fibrils and thermal effects 17 p2617 A72-35733

Some measurements of the fine structure of large Reynolds number turbulence. 18 p2678 A72-36020

Satellite measurements of the moon's magnetic field - A preliminary report. 18 p2724 A72-36287

On the reflection of whistler mode waves from model lower ionospheres. 18 p2660 A72-36430

Physical parameters and structure of microwave power transistors, noting scanning electron microscope analysis of fine structure 18 p2671 A72-37144

Complex vortex core fine structure around propeller tip observed via smoke and stroboscopic lighting, presenting photographs 19 p2786 A72-37747

L-S coupling interpretation of high-resolution LMM Auger spectra of Cu and Zn. 19 p2846 A72-38597

Fine structure in quenched Fe-Al-C steels. 20 p2938 A72-39300

Flux densities, positions, and structures for a complete sample of intense radio sources at 1400 MHz. 21 p3105 A72-40575

H II region fine structure from 11 and 3.7 cm observations, deducing physical parameters from continuum spectra 21 p3105 A72-41031

Gravitational wave detector design based on fine components of scattered light spectrum 21 p3086 A72-41696

Frequency correlation measurement of pulsar spectral fine structure due to radio emission scattering by interstellar plasma 21 p3101 A72-41752

Observation procedures in high resolution spectrophotometry of solar chromospheric spectral fine structures 22 p3221 A72-42031

Some aspects of flare properties versus magnetic boundary morphology. 22 p3217 A72-42038

Ionization structure and coarse and fine analyses in planetary nebulae spatial spectroscopic diagnostics based on line profile monochromatic intensity integral equation inversion 23 p3339 A72-44236

Method of measuring the fine structure of detonation fronts in solid explosives. 24 p3463 A72-45039

Solar atmosphere fine structure observation limitations in terms of solar telescope angular resolution 24 p3404 A72-45529

FINENESS RATIO

Aerodynamic characteristics of bodies of revolution with large fineness ratios at Mach numbers ranging from 0.2 to 6.0 22 p3134 A72-42286

Correlation of Magnus force data for slender spinning cylinders. [AIAA PAPER 72-966] 22 p3135 A72-42344

FINES

Dunitite-norite olivine-rich microbreccia in Apollo 14 lunar fines sample 14002.8, discussing origin and chemical composition 01 p0126 A72-10106

Apollo 11 lunar fines behavior and gas evolution characteristics from high vacuum differential thermal analysis and mass spectroscopy 04 p0569 A72-14504

Lunar regolith top surface polarimetric properties of sunlight-exposed rocks and fines compared to terrestrial rocks and meteorites 06 p0887 A72-18225

Carbon chemistry of Apollo 14 size-fractionated fines, noting solar wind activity effect 07 p1082 A72-20290

Simulation study of lunar carbon chemistry, noting hydrocarbon production by solar wind interaction with fines 07 p1082 A72-20291

Igneous and microbreccia lithic fragments, glasses and chondrules from Luna 16 fines, confirming lunar surface melting and igneous differentiation 09 p1379 A72-22253

Rare gas concentrations in Luna 16 fines, using stepwise heating technique 09 p1380 A72-22266

Apollo lunar fine samples total emittance as function of temperature, using spectral emittance measurement technique 09 p1388 A72-23028

Thermoluminescent and luminescent properties of Apollo 12 lunar fines, core tube samples and rock chips 10 p1537 A72-24163

Apollo 12 lunar rocks and fines sulfur concentrations and isotope ratios measurement 10 p1538 A72-24168

Apollo 12 fines thermal conductivity in vacuum at 200-400 K, using least squares technique for curve fit 14 p2154 A72-30509

Rock size, mineralogy and fines size distribution in lunar regolith 17 p2615 A72-35683

The distribution of carbon in lunar samples from Apollo 11, 12 and 14. 17 p2615 A72-35685

Analysis of vegetable seedlings grown in contact with Apollo 14 lunar surface fines. 17 p2505 A72-35925

Ferromagnetic and paramagnetic resonance spectra of lunar material - Apollo 12. 18 p2724 A72-36276

Measurements of radon emanation from Apollo 11, 12, and 14 fines. 18 p2728 A72-36970

Spectral emittance of Apollo-12 lunar fines. 20 p2970 A72-39486

The carbon chemistry of the moon. 23 p3339 A72-44149

FINGER LAKES

U LAKES

FINGERS

Choice reaction task times for responses to signals by middle, little and index fingers 10 p1432 A72-24985

FINISHES

NT GLAZES

NT LACQUERS

Deposition of finishes and dyes in materials dried using microwave heating. 22 p3183 A72-42480

FINITE DIFFERENCE THEORY

Two dimensional transient inviscid flow field from secondary injection in missile control, describing distribution with artificial viscosity finite difference method 01 p0097 A72-10940

Finite difference technique for heat transfer rate in laminar flow in tube with step change in cross section, discussing velocity profiles 02 p0301 A72-11723

Circular cone in supersonic flow, obtaining self similar solution for effect of angle of attack on laminar boundary layer by finite difference method 02 p0150 A72-12095

Laminar flow between stationary and rotating disk with mass flow through concentric circular opening by finite difference method 02 p0203 A72-12098

Two dimensional underexpanded jet plumes flow distribution determination using time dependent finite difference method 02 p0301 A72-12257

Improved finite difference solutions for stress in thin cylindrical shells, using Donnell assumptions [ASME PAPER 71-PVP-24] 02 p0295 A72-12475

Finite difference schemes for grid and planetary boundary layer solutions using grid spacings proportional to mixing length and eddy viscosity 03 p0386 A72-14337

Finite difference scheme for collision of two axially symmetric liquid jets with free boundary in cylindrical coordinate system 03 p0344 A72-14370

Internal atmospheric gravity waves transient two-dimensional finite difference model, including nonlinear, viscosity and thermal conduction terms 04 p0544 A72-15119

Distributed parameter state regulator system, investigating order of spatial discretization error in finite difference approximation to optimal response, control and performance cost [AD-738401] 05 p0639 A72-15805

General MHD duct flow problems solution using machine transformation and finite difference technique supplemented by successive overrelaxation [ASME PAPER 71-WA/APM-15] 05 p0694 A72-15965

Stability characteristics of finite difference schemes based on lumped-parameter model and numerical integrator for wave propagation in continuous media 05 p0735 A72-16081

Laplace equation under Robin boundary conditions over unit square, discussing numerical solution by difference approximation and iterative procedure 05 p0682 A72-16100

Similarity and finite difference solutions of parabolic differential equations, exemplifying by heat conduction and boundary layer equations [ASME PAPER 71-WA/APM-6] 05 p0682 A72-16151

Discrete elasticity theory constitutive and motion equations, considering finite difference and partial differential equations 05 p0737 A72-16297

Finite difference calculations for two dimensional unsteady inviscid expanding flow of perfect gas through nozzle, obtaining flow field patterns 05 p0603 A72-16539

Hyperbolic boundary layer displacement interaction and surface curvature effects, employing implicit finite difference methods [AIAA PAPER 72-76] 05 p0603 A72-16803

Finite difference integration based on theoretical model analysis of three dimensional turbulent boundary layer on sharp cone at angle of attack in supersonic flow [AIAA PAPER 72-187] 05 p0650 A72-16842

Numerical analysis of three dimensional inviscid supersonic flow field about complex vehicle geometry, using finite difference technique and Rankine-Hugoniot relations [AIAA PAPER 72-192] 05 p0606 A72-16847

Space shuttle flow field fluid dynamic hyperbolic equations numerical solution by noncentered finite difference schemes, noting advantages in programming logic simplicity and multidimensional generalizations [AIAA PAPER 72-193] 05 p0729 A72-16848

Explicit finite difference procedure to solve time averaged equations of motion for unstalled turbulent duct flows in coordinate system approximating real flow streamlines [AIAA PAPER 72-43] 05 p0651 A72-16878

Transient compressible heat and mass transfer in porous media, solving coupled nonlinear partial differential equations in finite difference form by iterative technique [AIAA PAPER 72-23] 05 p0749 A72-16914

Nonlinear effects of inviscid supersonic flow field surrounding bodies in coning motion, using shock capturing finite difference technique [AIAA PAPER 72-27] 05 p0607 A72-16918

Multidimensional time dependent flow field analysis by split finite difference operator technique, using star mesh of quadrilateral cells [AIAA PAPER 72-154] 05 p0609 A72-16950

Finite difference model application to supersonic planar viscous near wake, determining parameter range by physical and numerical restraints [AIAA PAPER 72-115] 05 p0609 A72-16971

Finite difference method for transonic airfoil design for wide range of angles of attack and Mach numbers 06 p0755 A72-17629

Large deflection of rectangular thin elastic plates with unsupported edges, using finite difference technique based on dynamic relaxation methods 06 p0895 A72-17799

Numerical solution of supersonic flow past blunt bodies with large mass injection, deriving finite difference equations 06 p0756 A72-18114

Finite difference schemes with splitting operator for mixed type differential equations systems, considering solutions stability and convergence properties 06 p0839 A72-18117

Lax finite difference scheme application to transonic two dimensional Laval nozzle and supersonic blunt body flow with detached shock wave, considering inviscid thermally nonconducting 06 p0756 A72-18126

Convergent finite difference schemes for Navier-Stokes equations initial boundary value problems, using Temam systems approximation method 06 p0840 A72-18132

Hollow waveguide performance numerical solution review covering finite difference and element methods, polynomial approximation, point matching, integral equations and conformal transformation 06 p0784 A72-18237

Finite element and finite difference formulations for solid continua by variational principles, including potential energy, complementary energy and Reissner principles 07 p1087 A72-18792

Hollow and dielectric loaded waveguide modes solution, comparing finite element and finite difference methods based on coefficient matrices and computing time considerations 07 p0952 A72-18793

Quasi-static stability of sandwich plates hinged over edge in finite difference formulation 07 p1094 A72-20213

Truncation error correction based on Richardson extrapolation in finite difference approximation of nonlinear partial differential operators 07 p1101 A72-20328

First boundary value problem solution of nonlinear Poisson equation in rectangular region by finite difference equations approximation 08 p1198 A72-20902

Convergence and stability criteria of monotonic difference schemes for linear parabolic differential equations with interface boundary conditions 08 p1199 A72-21286

Conductive heat transfer equation solved by finite difference scheme with uniform rapid convergence 08 p1253 A72-21458

Finite difference method explicit solution of Cauchy problem for system of heat conduction differential equations 08 p1254 A72-21464

Sound refraction by sinusoidal point source in subsonic jet flow, obtaining solution by finite difference method for comparison with ray tracing results 08 p1152 A72-21894

Laplace operator eigenvalue computation for simply connected region with homogeneous Dirichlet and Neumann boundary conditions and finite difference problem 09 p1340 A72-22296

Filtered-equation pressure coordinate numerical weather prediction model in finite difference formulation, discussing various initialization procedures and boundary value specifications 09 p1343 A72-22427

Two point boundary value problems solved by finite difference method using optimal sequence of nodes 09 p1341 A72-22464

Axisymmetric grid plate bending and torsion under normal forces and moment vectors loads, determining stress-strain state from finite difference equations 09 p1398 A72-22692

Finite difference analysis of dynamic deformation of thin elastoplastic shells of revolution under intense heating 09 p1401 A72-22728

Confined three dimensional boundary layers prediction, describing finite difference methods for flow equations solution 10 p1464 A72-23871

Rigidly connected rectangular plates stress-strain calculation with finite difference method 11 p1733 A72-25538

Finite difference method application to axial flow compressors rotating stall nonlinear analysis, taking into account blade row characteristics [ASME PAPER 72-GT-3] 11 p1568 A72-25606

Characteristic finite difference method for solution of two dimensional wave equation represented by one parameter differential systems 11 p1677 A72-25863

Finite difference method for free vibration of axisymmetric shells, using inertia force terms in shell bending theory equilibrium equations 11 p1737 A72-26429

Finite difference approximation of eigenvalues of singular differential operators in Hilbert space 11 p1678 A72-26556

Automatic switched Shuman filter for shock waves numerical computation, noting third and fourth order accurate finite difference schemes 11 p1619 A72-26668

Finite difference method for bending stresses calculation in rotating disks subjected to irregularly dis-

tributed temperature, deriving digital computer program algorithm 11 p1712 A72-26976

Finite difference equations for plate and shell calculations with various boundary conditions 12 p1878 A72-27089

Finite difference equations of motion for conservative and nonconservative dynamic systems with finite degrees of freedom, obtaining numerical solution by Hamilton principle 12 p1844 A72-27193

Finite difference calculations for structure of finite amplitude thermal convection within self gravitating fluid sphere with uniform heat release 12 p1889 A72-27715

Finite difference approximation and Fourier analysis to determine mechanical system eigenfrequency, studying string and membrane vibration 13 p2000 A72-28417

Numerical methods for inverse solution to turbulent swirling boundary layer combustion flow problem 13 p2063 A72-28420

Atmospheric motion equations numerical integration, presenting conservative finite difference approximation for quasi-uniform spherical grids derived from regular polyhedrons 13 p1985 A72-28445

Nonuniform inlet velocity profile effect on laminar flow development between parallel plates, solving equations by finite difference method 13 p1941 A72-28706

Homogeneous difference schemes stability for ordinary differential equation of arbitrary order with discontinuous coefficients, analyzing positive definite operators class 13 p1986 A72-29076

Coefficient stability of homogeneous difference schemes using irregular networks for fourth order differential equation with discontinuous coefficients 13 p1986 A72-29081

Difference scheme application to Laplace operator eigenvalues determination for regions composed of rectangles, using summary representation formulas 13 p1986 A72-29082

Orr-Sommerfeld equation solution by variable mesh finite difference method, applying to plane Poiseuille flow 13 p1986 A72-29112

Eigenvalues examination for self adjoint singular differential operators in Hilbert space by finite difference methods 14 p2126 A72-30619

Classical and finite difference methods for diffusion and heat conduction problems 15 p2334 A72-31298

Finite difference solution to Navier-Stokes equations for axisymmetric flow of incompressible viscous fluid 15 p2216 A72-31446

Two dimensional incompressible turbulent boundary layer in arbitrary pressure gradient, obtaining mathematical model for solution by implicit finite difference method 15 p2217 A72-31718

Converging plane-walled channels, calculating laminar flow development and heat transfer by finite difference method 15 p2336 A72-32481

Sharp flat plate laminar, transitional and turbulent skin friction via finite difference integration of compressible boundary layer equations 15 p2180 A72-32596

Time dependent finite difference /fluid-in-cell/ method for supersonic aerodynamic problems concerning inviscid compressible flow with contact surface and shock discontinuities 16 p2342 A72-32884

Unsteady Falkner-Skan flow solution by finite difference method for pressure gradient effect on transient response of laminar boundary layer 16 p2376 A72-33015

Differential boundary value problem solution by FORTRAN program using finite difference method 16 p2416 A72-33524

Numerical finite difference prediction of inert turbulent boundary layer swirling jet flow, using nonisotropic energy-length model [AIAA PAPER 72-699] 16 p2380 A72-34044

Transonic airfoil section design to given surface pressure distribution, applying finite difference procedures to transonic small disturbance equations [AIAA PAPER 72-679] 16 p2346 A72-34062

Describing equations derivation by implicit finite difference scheme for chemically nonreactive two dimensional symmetric and axisymmetric jet and wake problem 16 p2381 A72-34170

Use of fast Fourier transforms for solving partial differential equations in physics 17 p2575 A72-34645

Self-adjusting hybrid schemes for shock computations 17 p2575 A72-34648

Study of circular arc airfoils with asymptotic critical Mach number. II 17 p2484 A72-34745

Constitutive equations to characterize rubberlike nonlinear viscoelastic materials under finite deformation stress, obtaining numerical solutions via finite difference technique 17 p2633 A72-35401

Relationship between finite differences and quadratures of a Green's function for a second-order ordinary differential operator 17 p2577 A72-35803

Recent extensions to Eulerian methods for numerical fluid dynamics. 18 p2682 A72-36803

Calculus of variations and finite difference method for combined free and forced convective heat transfer through vertical noncircular ducts, calculating Nusselt number 18 p2741 A72-36926

Hopscotch algorithm for numerical integration of nonlinear hyperbolic partial differential equation systems based on finite difference method 18 p2705 A72-37020

Convergence and accuracy of three finite difference schemes for a two-dimensional conduction and convection problem. 18 p2741 A72-37170

Steady state heat transfer in one dimensional flow involving simultaneous convective and diffusive transport via finite difference formulation 18 p2741 A72-37171

Solution of the equations of the compressible boundary layer (laminar, transition, turbulent) by an implicit finite difference technique. 19 p2785 A72-37521

A technique for numerical solution of boundary value problems in the plane theory of elasticity by the finite-difference method 19 p2878 A72-38204

Fractional steps method of difference schemes for approximate numerical solution of parabolic and elliptic initial boundary value problems 20 p2945 A72-39327

Simplified conservation laws for finite-difference computations. 20 p2946 A72-39637

Finite difference boundary value method for solving one-dimensional eigenvalue equations. 21 p3074 A72-40107

Finite difference calculus development of method to express thermodynamic limit of statistical-mechanical average as power series in number density, noting advantages and applicability 21 p3087 A72-40562

The effects of frictional drag on missile vibrations - A finite difference solution. 21 p3118 A72-40929

A calculation procedure for heat, mass and momentum transfer in three-dimensional parabolic flows. 22 p3243 A72-41954

Finite difference theory for Lamé equations of elastic waves propagation in two dimensional body under mixed boundary conditions 22 p3234 A72-42144

On the comparison of phase and multi-layer techniques for numerical solution of the scattering problems. 22 p3154 A72-42305

Machine code for finite difference solution of wake vortex governing equations and far flow field prediction in trailing vortices, developing turbulent energy model [AIAA PAPER 72-989] 22 p3134 A72-42326

Finite difference and extended Newton methods application to transient and steady state creep deformation in shells of revolution under high temperature and high stress 22 p3235 A72-42482

Large deflections of flat arbitrary membranes. 22 p3235 A72-42604

Nonlinear buckling of cylindrical shells. 22 p3236 A72-42607

On the efficient reduction of truncation error in numerical weather prediction models. 23 p3311 A72-43675

Stress state of arbitrary contour body of revolution under torsion using finite difference method 23 p3347 A72-43744

Integration scheme for two-dimensional impulsive waves in a linear acoustic medium. 23 p3314 A72-44250

Dynamic blast loads on preheated and prestressed thin plates. 24 p3454 A72-44607

Stability and oscillation characteristics of finite-element, finite-difference, and method of weighted residuals for transient two-dimensional heat conduction in structures. 24 p3461 A72-44608

One-level fine-mesh limited-area grid numerical weather prediction atmospheric model, evaluating various finite difference schemes, boundary conditions and initialization methods 24 p3420 A72-44619

Use of characteristics for boundaries in time dependent finite difference analysis of multidimensional gas dynamics. 24 p3359 A72-44879

Some experiences with the solution of potential flow in the plane cascade on the computer. 24 p3393 A72-45365

A finite-difference method for boundary layers with reverse flow. 24 p3395 A72-45789

FINITE ELEMENT METHOD

Airport apron surface pavement strain measurements under field loading conditions, considering static and dynamic loads with finite element method 01 p0047 A72-10192

Finite element method for determining transient response of box-type structure to traveling sonic pressure wave 01 p0136 A72-10219

Curved beam finite elements comparison for structural vibration problems, obtaining ring natural frequencies 01 p0136 A72-10222

Finite element analysis of creep due to stress and strain in double edge notched plates and round bars 01 p0138 A72-10519

Trapezoidal isoparametric and triangular singularity elements for crack tip elastic stress intensity factor for mesh having small number of degrees of freedom 01 p0140 A72-10992

Two-layered plane strain elastic cylinder with cracked inner bore under internal pressure loading, obtaining stress intensity factors by finite element method 01 p0141 A72-10994

Finite element method extension using computer program for solving problems of elastic bodies in contact with stiffness method advantages 01 p0141 A72-11047

Clearance, friction and load effects on turbine blade root fastening stress distribution, comparing finite element method with photoelastic experimental results 01 p0141 A72-11048

Stress concentration factors for fiber and matrix in axially loaded unidirectional composite with discontinuous fiber, using linearly elastic finite element analysis 02 p0292 A72-11987

Finite element technique for stress analysis of rotating bodies under axially symmetric stresses 02 p0293 A72-12343

Vertical thin circular cylindrical shells partially or completely filled with stationary liquid, determining free vibration characteristics with finite element theory 02 p0293 A72-12371

Shells finite element analysis, discussing inplane and normal displacements interpolation schemes and convergence rates [AD-739747] 02 p0296 A72-12532

Finite element formulation for nonlinear large deflection elastic analysis of displacements and stresses in thin plate structures 02 p0298 A72-12657

Finite element discrete model for large aspect ratio wing transverse vibrations, using inhomogeneous elements with various stiffness-length relations 03 p0442 A72-13189

Dynamic structural analysis by finite element method, describing error bounds for eigenvalue analysis by elimination of variables 03 p0442 A72-13401

Elastic-plastic stress-strain analysis of beams with uniform cross section under combined loadings by finite element method 03 p0449 A72-13975

Dynamic analysis of shallow shells with doubly-curved triangular finite element, investigating natural frequencies, mode shapes and convergence 04 p0585 A72-14844

Computational efficiency of minimization algorithm for solving eigenvalue problem arising from dynamic structural analysis by finite element method 04 p0585 A72-14845

Conforming rectangular and triangular finite elements for plate free vibrations analysis in bending 04 p0585 A72-14846

Ring finite elements use in analysis of shells of revolution under axisymmetric loads [ASME PAPER 71-WA/HT-22] 05 p0732 A72-15880

Nonlinear transient coupled thermoviscoelasticity problems solution by finite element method and iterative solution for integrodifferential equation 05 p0736 A72-16085

Vibration mode shapes and frequencies determination by finite element method using consistent and lumped masses formulations in differential equation solution, considering convergence rate [AD-739820] 05 p0736 A72-16086

Finite element micromechanical analysis of porous and filled ceramic composites for internal stresses and deformations 05 p0738 A72-16423

Bounds on condition number for irregular meshes of finite elements expressed in terms of extremal eigenvalues of element matrices
[AD-739416] 05 p0682 A72-16540

Triangular /KLI/ and quadrilateral /KQT/ thin shallow shell elements with 20 degrees of freedom, basing bending behavior on discrete Kirchhoff formulation
05 p0739 A72-16549

Finite element algorithm derived for partial differential equation system governing laminar three dimensional boundary layer flow of multicomponent compressible fluid
[AIAA PAPER 72-108] 05 p0604 A72-16817

Finite element analysis of hydroelastic properties of Saturn 5 full scale S-2 LOX tank, comparing with water tests
[AIAA PAPER 72-173] 05 p0740 A72-16833

Column axial load carrying capacity optimization vs structural weight, using finite element displacement method for buckling load, mode shape and strain energy density
[AIAA PAPER 72-141] 05 p0740 A72-16894

Axissymmetric stress analysis in various weld configurations of stub end high pressure pipe connections, using finite element method
06 p0820 A72-17709

Hollow waveguide performance numerical solution review covering finite difference and element methods, polynomial approximation, point matching, integral equations and conformal transformation
06 p0784 A72-18237

Porous cooling unsteady state problem approximation based on elementary thermal balance concept, solving differential equations by computerized Euler method
06 p0904 A72-18513

Error analysis of finite element solutions for elastic-plastic sandwich plates
07 p1086 A72-18779

Dual stress, strain and displacement formulations of linear finite element elasticity, showing Finzi stress function applicability
07 p1087 A72-18780

Large elastic deformation problems analysis by incremental finite element technique, using variational principles
07 p1087 A72-18782

Algorithm selection for optimization solutions by finite, ad hoc, conjugate, Newton and restricted step methods
07 p1025 A72-18783

Coefficient matrix for estimation of numerical solution error bounds for finite element models
07 p1025 A72-18786

Finite element and finite difference formulations for solid continua by variational principles, including potential energy, complementary energy and Reissner principles
07 p1087 A72-18792

Hollow and dielectric loaded waveguide modes solution, comparing finite element and finite difference methods based on coefficient matrices and computing time considerations
07 p0952 A72-18793

Finite element solution for Boussinesq approximation of two dimensional viscous fluid dynamic problems, using variational principle
07 p0965 A72-18794

Numerical methods for parabolic, hyperbolic and elliptic flows in fluid mechanics and heat transfer, considering finite element method
07 p1097 A72-18795

Round-off error analysis in numerical solutions of finite element equations in dynamic models
07 p1025 A72-18796

Finite element solutions for buckling of columns and beams, investigating restraints and cross section partial plasticity effects
07 p1088 A72-19117

Finite element method application to fracture mechanics problems of stress concentration and intensity factors and elastoplastic response to cyclic loading
07 p1088 A72-19130

Finite element method for elastic plastic sandwich plates analysis, presenting Lagrange multipliers interpretation
07 p1093 A72-19951

Axially nonuniform thin cylindrical shells dynamic analysis, obtaining free flexural vibration characteristics by hybrid of finite element and classical shell theories
07 p1097 A72-20531

NASTRAN /NASA structural analysis/ program for computer stress analysis based on finite element method, noting vibration, acoustics, transient motion and random response applications
08 p1138 A72-21325

Nonlinear modal response analysis of plate structures under random acoustic excitation, using finite element method and perturbation technique
08 p1245 A72-21607

Nonlinear large amplitude vibration of beams for various support conditions, using finite element matrix displacement method
08 p1245 A72-21626

Consistent finite element method to analyze random response of complex structures based on standard modal approach
08 p1248 A72-21823

Optimal gradient minimization scheme for finite element eigenvalue and eigenvector problems, including effect of round-off errors and termination criterion
08 p1200 A72-22140

Quadrilateral four node nonconforming plate bending finite elements for structural vibration and stability analysis
08 p1250 A72-22142

Plastic deformation friction fracturing, stress concentration, free surface changes and load displacement analysis with upper bound, slip line and finite element methods
08 p1250 A72-22197

German monograph on finite element method for elastic impact at half space, analyzing elasticity and inertia effects on energy absorption and contact time
09 p1397 A72-22338

Algorithm for automatic construction of finite element approximation to Laplace equation, noting convergence
10 p1502 A72-23719

Gradient iterative techniques application to finite element vibration and stability analysis of skew plates
10 p1558 A72-24878

Solid body elastic deformation potential energy and structure calculation on computer by finite element method and calculus of variations
10 p1559 A72-24924

Plate and thin and thick walled shells treated as three dimensional solids, noting finite element method limitation
10 p1559 A72-24925

Finite element generalization of plate displacement functions to shell analysis, using strain energy tensor concept
10 p1560 A72-25187

Finite element method for boundary value radiative and convective heat transfer problems
[AIAA PAPER 72-274] 11 p1740 A72-25214

Finite element method for approximate solution of elliptic partial differential equations on unbounded domains, proving error bounds
11 p1675 A72-25271

Computerized structural design of aerospace vehicle, stressing automated routines for finite element models generation
[AIAA PAPER 72-332] 11 p1727 A72-25367

Finite element structural analysis for local buckling stresses in flat plates, panels and thin walled columns, deriving elastic and geometric stiffness matrices
[AIAA PAPER 72-354] 11 p1729 A72-25383

Elastic finite element analysis for stress distribution in gripped thin walled tubular anisotropic three dimensional composite specimens
11 p1731 A72-25457

Anisotropic graphite composite laminates cutouts stress analysis by finite element method, predicting structural reinforcement behavior
11 p1672 A72-25475

Two dimensional elastoplastic finite element analysis of structural members under cyclic thermal-mechanical loadings
[ASME PAPER 72-GT-1] 11 p1734 A72-25604

Finite element method application to hydromagnetic plasma stability analysis, considering cylindrical plasma immersed in axial magnetic field and bounded by conducting shell
11 p1695 A72-25794

Curved cylindrical shell finite element with reduced stiffness matrix, noting convergence for symmetrical and unsymmetrical loading
11 p1735 A72-25896

Finite element method for buckling coefficients of isotropic rectangular plate subject to linearly varying axial compression, using general linear geometric matrix
11 p1736 A72-25999

Error bounds for finite element methods and approximation with piecewise polynomials for elliptical differential equations solution
11 p1679 A72-26956

Representational method for evolution type partial differential equations numerical solution, noting relationship to finite element method
11 p1679 A72-26961

Finite element method application to variable thickness circular and annular plates free transverse vibration
12 p1879 A72-27191

Convergence of plate bending eigenvalue solutions from conforming displacement finite elements based on thick plate free vibration conversion to isoperimetric variational problem
12 p1879 A72-27194

Mixed variational formulation and finite element method for axisymmetric cylindrical, conical, spherical and ellipsoidal shells
12 p1879 A72-27195

Finite element equations for hybrid coordinate dynamic analysis of interconnected rigid bodies with elastic flexible appendages for use in spacecraft simulation
12 p1876 A72-27257

Book on finite element method application to boundary value problems, nonlinear continuum thermodynamics and thermoviscoelasticity
12 p1882 A72-27325

Hybrid cylindrical shell finite element, determining natural frequencies from equilibrium equations, stress functions stress-strain relationships and boundary force transfer matrices
12 p1882 A72-27339

Nonlinear fracture toughness determination via three point bending test simulation by elastic-plastic finite element computer program
12 p1830 A72-27731

Structural system dynamic instability regions determination by finite element and conjugate gradient methods
12 p1884 A72-27847

Finite time element method for failure probability prediction in multiple load-path system with random loads, noting flow chart for suggested computer program
13 p2052 A72-28369

Finite element method for calculating vibrations of thin rectangular plate with four degrees of freedom
13 p2000 A72-28466

Lagrange multiplier method derivation of variational functional for finite element method and applications to plate and shell problems
13 p2055 A72-28623

Finite element method for in-plane free vibrations of shear wall type structures, noting rectangular plate elements with six degrees of freedom per node
13 p2057 A72-29092

Axissymmetric geometry and load finite element structural analysis of isotropic elastic materials for parametric and optimization studies
13 p2062 A72-29875

Modified finite element method application to plane elastic area elementary triangles strained and stressed state description by polynomial algebraic expressions and harmonic functions
14 p2163 A72-30188

Variational problem solution for solid strained body with nonlinear stress-strain relation, applying finite element method
14 p2130 A72-30189

Finite element method application to dynamic stability of thin plates and shells, noting nuclear reactor structural analysis
[SMRT PAPER M 2/1] 14 p2166 A72-30723

Finite element method for nonlinear analysis of nuclear reactor structures, noting elasticity, viscoelasticity and elastoplasticity problems
[SMRT PAPER M 2/2] 14 p2166 A72-30724

Finite element method with compliance equations determining energy release rates and stress intensity factors for complex crack configurations and loadings
14 p2168 A72-30908

Sandwich beams structural optimization for given deflection by iterative finite element procedure
14 p2168 A72-30927

Gaseous species diffusion in carrier gas under various geometries and flow conditions, using finite element method
14 p2095 A72-30928

Finite element displacement field with internal equilibrium application to nine degrees of freedom triangular bending element stiffness matrix calculation
14 p2168 A72-30930

Structural systems stability and natural frequency analysis eigenvalue problems solution by Sturm sequence method, using finite element technique
14 p2168 A72-30931

Matrices and permutation rules for tetrahedral polynomial finite elements for Helmholtz equation, commenting on computer time and convergence rate
14 p2126 A72-30932

Thin elastic plates finite displacement flexure behavior, using piecewise linear finite element incremental stiffness technique
14 p2168 A72-30933

Honeycomb sandwich beams dynamic analysis by finite element method with three degrees of freedom per discrete element, obtaining flexural, in-plane and shearing modes
14 p2169 A72-31146

Variational principle based Pian hybrid finite element procedure for static cylindrical shell analysis extended to plate and shell vibration
14 p2169 A72-31149

Cylindrical shell rectangular finite element from generalized independent strain functions and corresponding displacement functions
14 p2169 A72-31174

Rectangular, elliptical and parabolic waveguides TM and TE modes relation and cutoff wavelength analysis by finite element method, suggesting mode classifying system

15 p2205 A72-31354

Approximate values for elastic body stresses and displacements based on finite element method and virtual displacements and minimum potential energy principles equivalence

15 p2323 A72-31477

Shape functions for finite element analysis in n-dimensional space, examining completeness of polynomial interpolation and computational efficiency

15 p2326 A72-31713

Finite element analysis of circular and elliptical plates with curved boundaries, discussing high precision triangular plate bending element modification for accuracy improvement

15 p2326 A72-31715

Mixed triangular finite element model for plate bending problems including shear deformation effects, discussing error analysis and convergence

15 p2326 A72-31716

Numerical integration of equations of motion in finite element methods, investigating explicit methods stability

15 p2326 A72-31717

Isentropic perfect gas steady compressible flow finite element analysis through nonlinear equations linearization based on perturbation theory

15 p2217 A72-31719

Finite element method application to thin plate bending problem to illustrate efficiency of sector elements for sectorial and annular plates

15 p2326 A72-31720

Finite element method for discrete models of composite materials, discussing nonlinear dynamic problems

15 p2330 A72-32296

Unsymmetrical coupled columns stability under nonconservative lateral and end loading, using finite element method

15 p2331 A72-32557

Structural averaging of stresses in finite element method hybrid stress model, using additional equilibrium equations

15 p2332 A72-32597

Finite element method application to nonlinear dynamic problems exemplified by study of plastic deformation behavior of cylindrical billet under impact of heavy rigid body

16 p2466 A72-33019

Finite element method matrices in least squares approximation and elliptic partial differential equations, discussing numerical stability properties

17 p2573 A72-34219

Buekner formulation combined with finite element method for arbitrary shaped cracked bodies stress intensity factors in framework of linear fracture mechanics

17 p2623 A72-34253

Book - Approximation of elliptic boundary-value problems

17 p2574 A72-34622

Free vibrations analysis of linear aerodynamic conservative structures in elastic range by finite element method, applying to transient or random forced responses calculation

17 p2626 A72-34742

Elastic-plastic medium with doubly periodic square array of circular cylindrical voids, obtaining finite element solution for uniaxial deformation by variational principle

[ASME PAPER 72-APM-36] 17 p2628 A72-34784

Finite element analysis of elastoplastic structures with temperature dependent mechanical properties

17 p2631 A72-34947

A comparison of numerical methods for determining stress intensity factors.

17 p2631 A72-34973

Stress analysis of axisymmetric solids with asymmetric properties.

17 p2632 A72-35227

Fracture mechanics approach to adhesive joints.

17 p2633 A72-35282

The transverse Poisson's ratio of composites.

17 p2571 A72-35289

Finite element solutions for laminated thick plates.

17 p2633 A72-35292

Finite element analysis of the axisymmetric vibrations of cylinders.

17 p2634 A72-35409

Monograph - The finite-element method in plate bending analysis

17 p2634 A72-35547

Monograph - The elastic flexural-torsional buckling of beam-columns by discrete element techniques

17 p2634 A72-35548

Steady state response of nonlinear beam under periodic loading, using finite element techniques for nonlinear differential equation

18 p2732 A72-36078

Variational principle of linear differential equations.

18 p2705 A72-36717

On the numerical solution of a class of nonlinear problems in dynamic coupled thermoelasticity.

18 p2738 A72-37078

A finite element approach to optimal design of plastic structures in plane stress.

18 p2739 A72-37165

Combined finite element-weighted residuals method for linearized BGK Boltzmann kinetic theory equation, considering cylindrical Couette flow

18 p2684 A72-37168

Finite element models with rigid displacement for nonrigid structure analysis, noting curved beam and shells

18 p2739 A72-37173

Bounds on the extremal eigenvalues of the finite element stiffness and mass matrices and their spectral condition number.

18 p2705 A72-37202

Timoshenko finite element beam theory application to flexural vibration problems, considering shear deformation and rotary inertia effects

18 p2740 A72-37206

German monograph - Finite elements according to a theory of the second order on the basis of an extended variational principle with an application to the stability and stress computation of simple symmetrical I-beams under consideration of the deformation of the cross-section

19 p2871 A72-37479

Computerized finite element three dimensional stress analysis, taking into account mechanical and thermal stresses

19 p2878 A72-38649

Application of the finite element method to torsional flutter analysis on an analog computer

20 p2980 A72-39907

Finite element large deflection analysis of elastic-plastic shells of revolution subjected to axisymmetric loading.

20 p2982 A72-40064

Three-dimensional photoelastic and finite-element analysis of a propellant grain.

21 p3052 A72-40237

Free vibrations of finite element plates subjected to complex middle-plane force systems.

21 p3116 A72-40330

Geometrical non-linear analysis of structures by finite elements.

21 p3120 A72-41204

Study on an incremental variational principle and its applications to finite element method and incremental thin shell theory.

21 p3121 A72-41240

Mixed finite element analysis of elasto-plastic plates in bending.

21 p3124 A72-41502

On the application of the mixed finite element methods to the stress concentration problems of cylindrical shells with a circular cutout or a crack.

22 p2322 A72-41942

The use of simple three-dimensional acoustic finite elements for determining the natural modes and frequencies of complex shaped enclosures.

22 p3206 A72-42464

Continuum and finite element branching studies of the circular plate.

22 p3235 A72-42603

Symmetrical bending of circular plates using finite elements.

22 p3236 A72-42605

On the effect of the form of the strain energy function on the solution of a boundary-value problem in finite elasticity.

22 p3236 A72-42606

Wing flutter prevention in SST structural design, using finite element model and lifting surface aerodynamic theory

22 p3237 A72-42760

The application of the finite element displacement method to problems of elastoplastic deformation.

22 p3238 A72-42832

Steady state equations of motion, equilibrium shape and stability derivatives of elastic airplanes evaluated with finite element methods.

22 p3138 A72-42845

Rigid-body motions and strain-displacement equations of curved shell finite elements.

22 p3240 A72-42892

Finite element method optimization of orthotropic layered shells of revolution under mechanical and thermal loadings, considering stress-strain relationships

[SAWE PAPER 939] 23 p3344 A72-43479

Structural mass properties mathematical modeling for dynamic structural analysis, describing matrix notation for finite element methods application

[SAWE PAPER 944] 23 p3344 A72-43484

Combined mode crack extension in adhesive joints.

23 p3305 A72-43493

A finite element stress analysis of a crack in a bi-material plate.

23 p3346 A72-43707

Triangular element for multilayer sandwich plates.

23 p3351 A72-44108

Three-dimensional finite element analysis for fracture mechanics.

23 p3353 A72-44235

Vibration characteristics of cylindrical shells with several axially equispaced constraints.

23 p3355 A72-44371

Laminated thick plate and shell analysis by the assumed stress hybrid model.

24 p3453 A72-44601

Stability and oscillation characteristics of finite-element, finite-difference, and method of weighted residuals for transient two-dimensional heat conduction in structures.

24 p3461 A72-44608

Mixed-displacement finite-element analysis with particular application using plane-stress triangles.

24 p3455 A72-44789

Triangular facet finite element application in thin cylindrical shell analysis by displacement method

24 p3456 A72-44792

Computation of post-yield behaviour in notch-bend and tension testpieces.

24 p3456 A72-44796

Linear fracture mechanics in orthotropic materials.

24 p3457 A72-44818

A finite element model for shells based on the discrete Kirchhoff hypothesis.

24 p3457 A72-44876

Dual analysis for heat conduction problems by finite elements.

24 p3461 A72-44877

Multi-node elements model of isoparametric thin shell vibration for turbine blade application

24 p3457 A72-44881

Wave propagation in a thin hollow cone by a finite element method.

24 p3458 A72-44886

Best finite elements distribution around a singularity.

24 p3420 A72-45786

FINITE-STATE MACHINES U TURING MACHINES

FINNED BODIES

Hot versus shielded aerodynamic surfaces trade study for space shuttle booster wings and fins design, considering materials, structural weight and cost estimates

[AIAA PAPER 72-390] 11 p1726 A72-25411

Wind-tunnel Magnus testing of a canted fin or self-rotating configuration.

17 p2486 A72-35254

Aerodynamic characteristics of the slotted fin.

21 p2992 A72-41262

Finned missiles nonlinear rolling motion characteristics at large angles of attack, solving differential equation of motion by global nonlinear least squares method

[AIAA PAPER 72-980] 22 p3134 A72-42333

FINS

NT COOLING FINS

Shape factors of heat conduction for fin arrangements with isothermal boundaries, using conformal mapping

09 p1412 A72-23688

Unsteady-state temperature distribution in a connecting fin of constant area.

18 p2741 A72-36935

FIRE CONTROL

Tethered flying rotor platform for reconnaissance, fire control and radio transmission assignments in naval missions, discussing system characteristics

04 p0465 A72-15652

Combat aircraft lateral aiming performance optimization and evaluation based on criterion of bullet stream response to pilot roll commands

05 p0611 A72-16657

Low level light TV camera with Si intensifier target tube for fire control system to improve AH-1G Cobra helicopter night reconnaissance and attack capabilities

17 p2557 A72-35555

FIRE EXTINGUISHERS

Biomedical effects on air crews of chemical fire suppression agent Halon 1301/bromotrifluoromethane/ during simulated aircraft cabin fires

12 p1776 A72-28308

Destructive effect of combustion and pyrolysis products in intake air on fire extinguishers foam production

14 p2084 A72-30339

Tetrafluorodibromoethane - A new fire extinguishing agent in civil aviation

17 p2512 A72-35793

Investigation of Freon fire-extinguishing systems with a nucleonic gage.

18 p2648 A72-36674

Evaluation of film forming foams for the suppression of fuel fires in aircraft hangars.

[WSC1 PAPER 72-16] 20 p2982 A72-38974

FIRE FIGHTING

Flame resistant materials for aircraft fire fighter protective clothing from systems approach tests

08 p1126 A72-21585

Inert gas-oxygen mixtures fire retardant properties under atmospheric and hypobaric pressures, measuring effectiveness by standard fabric burning rate
12 p1890 A72-28309

FAA implemented airport certification legislation covering minimum safety standards, operation manual, emergency plan, fire and rescue service and pavement requirements
18 p2675 A72-36785

Apollo/Saturn 5 spacecraft liquid propellants safety procedures in event of fire on explosion in operations building at Kennedy Space Center
23 p3343 A72-43552

FIRE PREVENTION
Additives and reactive retardants flame inhibiting properties for polymers, discussing various testing techniques
01 p0090 A72-10286

Aircraft interior materials selection relative to fire hazards and smoke emission properties
[PI PAPER 18] 03 p0380 A72-13249

UV sensitive fire detector in manned space vehicle, discussing simulation in aircraft flying zero gravity parabolas
06 p0814 A72-17584

Antimisting kerosene fuels for aircraft crash fires reduction
07 p1050 A72-18837

Antimony-halogen synergistic reactions in fire retardants, noting antimony oxychloride role
07 p0935 A72-19056

Aircraft fuel system gunfire vulnerability and fire and explosion protection techniques
08 p1112 A72-21579

Jet engine fuel fire hazard evaluation by controlled laboratory tests, analyzing ignition characteristics under simulated survivable aircraft crash accidents
[SAE PAPER 720324] 11 p1702 A72-25587

Jet engine fuel modification to decrease fire hazard in survivable aircraft crashes
[ASME PAPER 72-GT-25] 11 p1702 A72-25621

Crash safe turbine fuel to reduce fire probability and severity during aircraft ground crash, investigating physical and chemical properties
[ASME PAPER 72-GT-28] 11 p1702 A72-25624

Procedure for the calibration of photoelectronic components in the IR spectral range
18 p2693 A72-37005

Static electricity in fueling of superjets.
21 p3040 A72-41375

FIREBALLS
Liquid propellant rocket abort fireball model, specifying heat flux as function of time
03 p0457 A72-13953

He plasma generation by transversely excited carbon dioxide laser, determining density and temperature profiles of luminous fireball
04 p0558 A72-15345

Shock front radius of subsonic radiation front driven by plasma fireball during final stages of decaying laser spark
20 p2934 A72-39844

Multifireball theory of particle production in inelastic high energy interactions, using elastic scattering amplitude for inelastic processes model
23 p3316 A72-44412

Study of high-energy hadron interactions by the nuclear photoemulsion method
23 p3330 A72-44416

FIREPROOFING
Flame resistance requirements of high temperature resistant and highly chlorinated fibers
[PI PAPER 11] 03 p0380 A72-13245

Fire retardant capabilities of bromine and chlorine compounds in polymers
[PI PAPER 13] 03 p0380 A72-13247

Aircraft crash fire protection, using passenger compartment heat shield of fire-retardant polyisocyanurate foam and intumescent paint
03 p0310 A72-13484

Flame resistant materials for aircraft fire fighter protective clothing from systems approach tests
08 p1126 A72-21585

Fire resistant fibrous materials for potential military and transportation applications, considering aromatic polyamide polybenzimidazole, fluorocarbon resin polymer, phenolic and glass fibers and fabrics
08 p1191 A72-21586

Chlorendic acid based Hetrion 92C fire retardant chemical resistant polyester for fiberglass reinforced structure applications
08 p1192 A72-21677

Synthetic fire resistant hydraulic fluids, comparing chlorinated hydrocarbons and phosphate esters chemical properties with water based products
08 p1197 A72-22160

Polyglycol aqueous solutions selection as fire resistant hydraulic fluid from hydraulic bench tests performed with various type pumps
08 p1197 A72-22161

Refractory materials fabrication characteristics for aerospace technology, presenting listing of synergic agents for use with halogenous inhibitors
17 p2571 A72-35277

FIREWORKS
U PYROTECHNICS
FIRING [IGNITING]
NT ROCKET FIRING
Weapon firing and external store separation tests by flight test methods for determining safe weapon release envelope
06 p0759 A72-18499

Secondary explosive spark detonators design and performance, determining ambient pressure variations effects on firing characteristics
08 p1219 A72-20758

Firing characteristics of insensitive electroexplosive devices under impulsive waveforms, discussing theory, design and application of waveform generators
08 p1220 A72-20763

Electroexplosive devices firing energy parameters determination by capacitor discharge system providing exponential pulses terminated at adjustable width
14 p2143 A72-30200

FIRING TIME
U BURNING TIME
FISH
U FISHES
FISHES
Fish electroreceptor system morphology, physiology and evolution, considering electric current action, peripheral coding activity and central subsystems
02 p0157 A72-11545

FISHTAILING
U YAW
FISSILE MATERIALS
U FISSIONABLE MATERIALS
FISSION
Fission origin of cosmic ray fossil tracks in augite achondrite high-uranium-concentration meteorite Angra dos Reis
05 p0714 A72-16078

FISSION PRODUCTS
Pu-244 fission Xe isotopic composition parameters in achondrite meteorites, using lunar spallation systematics
01 p0124 A72-10058

Space crew radiation dosage calculation from Mars mission high impulse gas core nuclear rocket engine exhaust plume fission fragments
01 p0022 A72-11353

High altitude thermonuclear explosion fission fragments localization mechanism, considering magnetogravitational trap as potential well for heavy charged fragments
11 p1713 A72-25950

Release of fission products from high temperature fuel materials
18 p2707 A72-36137

Xenon isotope fission component due to extinct Pu-244 in lunar breccia, noting storage details in terms of crustal material dating
20 p2967 A72-39182

FISSIONABLE MATERIALS
Ballistic piston fissioning plasma production involving compression of uranium hexafluoride
01 p0111 A72-11333

FITNESS
NT FLIGHT FITNESS
NT PHYSICAL FITNESS
FITTING
Flight helmet optimal fitting technique, using automatic recording audiometer and noise source for acoustic leakage detection
04 p0479 A72-14873

FITTINGS
Stainless steel circular tubes size and fittings effects on pneumatic pulse wave distortion and attenuation in fluidic pulse generation system
08 p1111 A72-20928

FITZGERALD-LORENTZ CONTRACTION
U LORENTZ CONTRACTION
FIXED POINTS [MATHEMATICS]
Isolated fixed points existence in area preserving mappings considered with normal form for periodic Hamiltonians in celestial mechanics
04 p0576 A72-15041

Computational mean square error due to roundoff in digital filters implemented on fixed point computers
07 p1033 A72-20346

Fixed point smoothing of sequentially correlated processes by extending filtering technique to simultaneous estimation of state and process noise contribution
11 p1610 A72-25871

Small change sensitivity of autonomous neutral functional differential equations in neighborhood of equilibrium point
15 p2263 A72-31752

Fixed point computer mean square errors in multiplication as function of number of digital order
16 p2367 A72-33959

Square root least squares and filtering solutions for fixed point and interval smoothing problems, comparing computational stability and precision and computer requirements
[AIAA PAPER 72-877] 20 p2910 A72-39122

FIXED WINGS
Wing-fuselage combination aerodynamic coefficients, comparing experimental data with subsonic linear and nonlinear theoretical results
[DGLR PAPER 71-115] 02 p0153 A72-12723

An aerodynamics model applicable to the synthesis of conventional fixed-wing aircraft.
[SAWE PAPER 908] 23 p3250 A72-43455

FIXED-WING AIRCRAFT
U AIRCRAFT CONFIGURATIONS
U FIXED WINGS
FIZEAU EFFECT
Interferometric testing of optical systems, discussing test plates, Fizeau, Lloyd moire, transmission, Twyman-Green, shearing, Ronchi, scatter fringe, grazing and holographic methods
10 p1482 A72-24567

FLAGELLATA
Metabolic control of temperature compensation in circadian rhythm of *Euglena gracilis* strain
07 p0919 A72-19538

FLAKING
Iron content and stress level effect on flaking corrosion of Al alloy sheets, describing experimental technique
13 p1980 A72-29826

FLAME FRONTS
U FLAME PROPAGATION
FLAME INTERACTION
U CHEMICAL REACTIONS
U FLAME PROPAGATION
FLAME IONIZATION
Additive and natural ionization in combustion reactions, discussing flame chemistry, ionic species and measurements
05 p0751 A72-17224

Recombination coefficient, ionization rates and average lifetime of ions in rarefied carbon-air flames, investigating pressure and additives effects
06 p0904 A72-18213

Experimental investigation of the effect of an electric field on a laminar flame
22 p3243 A72-41889

Ionization mechanism and condensed and gas phase kinetics of oxidizer burning during ammonium perchlorate combustion
22 p3215 A72-43140

Ionization zone formation and condensed and gaseous phase kinetics during ammonium perchlorate burning in nitrogen atmosphere
22 p3215 A72-43179

FLAME PROBES
Measurement techniques for electrically heated temperature probes in flames, considering wire sensor diameter and radiative transfer
03 p0456 A72-13925

Emitting-absorbing flames diagnostics, measuring spectrally resolved radiant energy with fiber optic probe data
[ASME PAPER 71-WA/FU-1] 05 p0661 A72-15915

Single and double probe measurements of electron temperatures in flames, discussing difficulties in obtaining reliable I-V characteristics
08 p1129 A72-22043

Heatable chamber burners design to increase sensitivity of flame spectrophotometry, separating solvent from aerosols
13 p1958 A72-29525

Flame probe sampling process effects on gas composition concentration gradient for two dimensional cylindrical and rectangular probes
16 p2361 A72-34004

I-V characteristics of electric noise generated by flame between double probe electrodes during coke particle burning in air flow
19 p2882 A72-38458

Nozzle beam-mass spectrometer system for studying one-atmosphere flames.
[WSCI PAPER 72-9] 20 p2921 A72-38975

Sensitivity enhancement of atom absorption measurements by the method of pulse vaporization from the microprobe into the flame
22 p3176 A72-42174

FLAME PROPAGATION
Flame spread rate over combustible polymer fuel specimens as function of surface, sample, composition, pressure and oxygen mole fraction
02 p0301 A72-11965

Flame propagation and overdense heating in laser beam created plasma, calculating density and temperature profiles by one dimensional continuum hydrodynamic theory
02 p0238 A72-12363

Dichlorodifluoromethane-fluorine flame structure, taking samples by molecular beam sampling system for analysis by mass spectrometry
02 p0303 A72-12483

Laminar flame front surface area determination, presenting graphical constructions from generatrix of arbitrary segment number
03 p0455 A72-13099

Angular momentum conservation law compliance of generalized triple configuration model for spin-detona-

tion nucleus, assuming transverse Chapman-Jouguet wave

03 p0342 A72-13734

Flames vibratory propagation appearance conditions at constant volume, considering expansion and compression waves amplitude

03 p0456 A72-13794

Combustible fuel-air mixture laminar and turbulent flame propagation mathematical model, with reference to detonation and prevention

03 p0456 A72-13876

Three dimensional transverse wave structure effect on detonation wave and Chapman-Jouguet gross properties, using planar model

04 p0510 A72-14410

Monograph on head-on collision of combustion wave with shock wave and rarefaction wave covering gas dynamics, interactions, reflection process, etc

05 p0746 A72-16046

Turbulent diffusion flame model in Couette flow, including wall effect

[AIAA PAPER 72-214]

05 p0748 A72-16856

Nonuniform potential and dissipation flow structure of turbulent diffusion flame front at high Reynolds numbers

06 p0902 A72-18104

Photorecorder for burning rate measurements, consisting of electric motor driven film carrying rotating drum in slitted housing and flame front imaging optical system

06 p0817 A72-18215

Pulsating flame spread on liquid alcohol surface over range of liquid temperatures, using shadow streak photography

07 p1099 A72-19375

Detonation propagation through tubes coated with thin liquid fuel films, considering boundary layer displacement effect on propagation speed, pressure ratio and reaction zone length

07 p1100 A72-19728

Boundary value solutions and computer programs for one dimensional laminar flame propagation equations

08 p1129 A72-22040

Bromine additions effect on normal laminar flame propagation velocity of methane-air mixture at high pressures

09 p1411 A72-22889

Oscillatory gas combustion mechanism and stability boundary characteristics, determining burning time from flame height and flow rate

11 p1745 A72-25753

Oscillatory relaxation combustion regions determination in high pressure gas injection tubes, noting flame propagation rate relationship with mixing concentration

11 p1745 A72-25754

One dimensional pulsating detonations calculation with induction zone kinetics, obtaining Chapman-Jouguet steady solution profiles

11 p1745 A72-25983

Solid combustibles flame spread rates in compressed atmospheres, noting dependence on oxygen concentration

14 p2170 A72-30340

Pressure increase induced by heat release for laminar flame sheet in hypersonic stream, considering fuel injection through semiinfinite porous flat plate

15 p2337 A72-32590

Aerogel combustion kinetics and continuous flame formation on coal, Mg, Al and Al alloy powders, using track method

16 p2476 A72-33252

Microphotometric chemiluminescence measurement for analysis of turbulent flame fine structure for homogeneous air-fuel mixtures at high Reynolds numbers

16 p2479 A72-34005

Flat flame deflagration tube measurements of laminar flame velocities for propane-ammonia-air mixtures in fuel rich region

16 p2480 A72-34006

Combustion of solid-propellant layer in contact with a solid-oxidizer layer

18 p2720 A72-36239

Acceleration of burning by a shock wave interacting with the flame

18 p2740 A72-36240

Influence of an electrical discharge in a flame on the propagation of the flame

18 p2740 A72-36244

Combustion propagation in cylindrical aluminum alloy specimens and some peculiarities of the aluminum combustion mechanism

19 p2847 A72-37362

Luminance profiles photometry for axisymmetrical propagation in propane-air turbulent flow combustion with turbulence level control in jet core

19 p2879 A72-37366

Hydrodynamic stability of periodic burning front for ideally conducting incompressible fluids in longitudinal or transverse magnetic field

19 p2882 A72-38457

Influence of water vapor on the normal flame velocity of a methane-air mixture at high pressures

19 p2882 A72-38459

Burke-Shumann-Zeldovich model for aerodynamic characteristics of straight jet laminar diffusion flames, considering free, semibounded and slipstream types

19 p2882 A72-38460

Measurements of burning velocity in a flat flame front

19 p2883 A72-38872

Laser power and pulse duration requirements for hot plasma production by flame propagation in solid DT targets for controlled thermonuclear fusion

20 p2931 A72-39354

Optical measurements in a pulsating flame. [ASME PAPER 72-HT-8]

20 p2926 A72-39679

Aerodynamic structure analysis of steady flame of homogeneous gas mixtures, noting streamlines, isotherms, isobars and flame front curves

21 p3129 A72-40979

Determination of the concentration range of flame propagation at elevated temperatures

21 p3129 A72-40984

Problem of oscillation self-excitation due to the dependence of the normal velocity of a flame on the thermodynamic parameters of a gas

21 p3129 A72-40985

Propagation rate and the existence range of turbulent flame

21 p3131 A72-41660

German monograph - The transfer behavior of premixed flames.

22 p3244 A72-43076

Propagation of the front of an exothermic reaction in condensed mixtures whose components interact through a high-melting layer

22 p3245 A72-43177

Two-dimensional supersonic flow with flame sheets.

24 p3360 A72-44988

Shock wave velocity, combustion front and pressure measurements of unstable detonations in propane-oxygen-nitrogen mixtures, comparing with double discontinuity theory

24 p3462 A72-45030

Chapman-Jouguet surface characteristics in flow field behind steady gaseous detonation wave, using schlieren photography

24 p3462 A72-45031

Determination of the detonation velocity of isoatomic mixtures

24 p3462 A72-45032

One dimensional theory of electric discharge detonation effects in flame propagation within square duct with combustible gas mixture, applying to electrochemical pulse jet engine

24 p3464 A72-45064

The shock-combustion /expansion-combustion/ polar with allowance for variation of the specific heat ratio of a gas passing through a flame front

24 p3465 A72-45446

FLAME QUENCHING

U EXTINGUISHING

U QUENCHING [COOLING]

FLAME SPRAYING

Electrical properties of thick-film barium titanate dielectrics produced by flame spraying.

19 p2846 A72-38616

Structural features of plasma and gas-flame deposited aluminum oxide coatings

19 p2810 A72-38680

Chemical composition, refractivity and temperature dependence of blackness levels of aluminum oxide-chromium oxide-phosphorus oxide ceramic coatings flame sprayed on steel

21 p3072 A72-40384

Particle temperature and flight velocity during gas-powder buildup

22 p3182 A72-42194

FLAME STABILIZATION

Flame autostabilization mechanism during gaseous oxygen-liquid ammonia mixture combustion in liquid fuel rocket engine chamber, measuring mean burnout time

08 p1224 A72-22091

Flame structure studies of stabilizing region of near stoichiometric laminar burner methane-air flame

09 p1411 A72-23147

Hydrogen chloride addition effect on hydrocarbon flammability under reduced pressure, studying flame stability limits of methane, ethylene, acetylene and n-butane in oxygen

10 p1562 A72-24236

Flow phenomena, mixing and stability of high speed enclosed multijet turbulent diffusion flames fed by propane and air

10 p1563 A72-25139

Ammonia-air opposed reacting jet /ORJ/ for flame stabilization, solving partial differential equations for flow field

10 p1564 A72-25141

Soviet papers on vibrational combustion systems covering flames relaxation in annular combustion chambers

11 p1745 A72-25751

Open-air jet engine test stand for flame stabilization, jet and compressor noise studies, noting provisions for rapid installation changes

12 p1795 A72-27416

Optical anemometers for mean and fluctuating velocities in premixed flame of town gas-air combustion system, noting velocity probability density distribution

13 p1955 A72-28546

Ethanol liquid fuel counterflow diffusion flame stabilization and thermal structure determination by interferometry

13 p1913 A72-29306

Ultrasonic wave excitation in potassium seeded flame, showing amplitude proportional to harmonic perturbation frequency imposed on plasma

14 p2170 A72-30417

Rotating flow introduction effects on jet noise levels, combustion and turbulent mixing processes and flame stability

[AIAA PAPER 72-645]

16 p2480 A72-34087

Flame autostabilization mechanism during gaseous oxygen-liquid ammonia mixture combustion in liquid fuel rocket engine chamber, measuring mean burnout time

17 p2597 A72-34662

Ignition, unsteady burning and flame collapse of a unitary fuel particle

19 p2882 A72-38453

Book - Combustion aerodynamics.

19 p2882 A72-38722

FLAME TEMPERATURE

Measurement techniques for electrically heated temperature probes in flames, considering wire sensor diameter and radiative transfer

03 p0456 A72-13925

Self absorption and temperature gradient effects on fluorine-hydrogen flame spectroscopic temperature determination, comparing calculated and theoretical Lorentz intensity profile

04 p0596 A72-14890

Flame temperatures, composition profiles and burning rates in liquid n-heptane droplet and sphere combustion

07 p1051 A72-19362

Analog simulation of normal thermal explosions and cool flames, observing oscillations limits, time dependence of parameters and effect of changes in activation energy or initial temperature

07 p1098 A72-19366

Nitrogen oxide emission control in gas turbine combustion by lowering flame temperature

11 p1744 A72-25620

Collisional ionization cross sections measurement for gaseous metal atoms in hydrogen-oxygen flames at 2000-2800 K

11 p1591 A72-26659

A mathematical model of cold propane flames

18 p2741 A72-37016

Discussion of the thermal state of an open air premixed methane-oxygen flame.

19 p2883 A72-38871

Electron attachment and compound formation in flames. V - Negative ion formation in flames containing chromium and potassium.

22 p3244 A72-42717

Measurement of the temperature of flames containing scattering particles on the basis of IR radiation

23 p3356 A72-43678

FLAMES

NT DIFFUSION FLAMES

NT PREMIXED FLAMES

Heat transfer from augmented flames and plasma jets based on magnetically rotated arcs, measuring transfer rate as function of electromagnetic torque

02 p0301 A72-12031

Solid propellant flame spectral and temporal details during unstable and stable combustion, using middle infrared spectrometer

[AIAA PAPER 72-32]

05 p0703 A72-16896

Wall thermal radiation influence on solid propellants burning rate in electrically heated tube furnace, noting correlation with laminar flame theory

[AIAA PAPER 72-35]

05 p0703 A72-16938

Vibrational laser Raman scattering from flame gases for nitrogen, oxygen and water vapor

09 p1276 A72-22978

Recirculation criteria for confined jet flames in cylindrical combustion chamber, using Thring-Newby number

09 p1411 A72-23144

Flame photometric detection of small concentrations of sulfur compounds in ambient air, describing spectrum scanning detector, rotating interference filter and correlation detector

10 p1480 A72-24101

Quasi-steady state combustion theories compared with observations of hydrocarbon fuel droplet and flame zone diameters, noting underestimation of burning rate

13 p2063 A72-28545

Competition criteria for chemical reactions selection in nonequilibrium computer calculations on combustion systems properties, noting seeded flames and rocket exhausts

13 p1912 A72-28548

Determination of the excess air coefficient with the aid of electrical properties in the case of laminar flames of gaseous fuels

17 p2636 A72-34931

Mean emissivity of a luminous flame - Spray combustion of liquid fuel.

18 p2740 A72-36148

The physically defined flame and its representation in the water model

18 p2656 A72-36242

Comparison of theoretical and experimental limits of detection in atomic absorption spectrometry using air-acetylene and nitrous oxide-acetylene flames.

19 p2762 A72-37725

Velocity distribution in turbulent mixing of compressible reacting gases, noting flame length measurement of submerged H jet

21 p3129 A72-40981

FLAMMABILITY

Additives and reactive retardants flame inhibiting properties for polymers, discussing various testing techniques

01 p0090 A72-10286

Flammability tests for polymer materials used in computers and business machines, evaluating procedures in terms of reproducibility, difficulty and equipment requirements

01 p0145 A72-10287

Polyethylene and polypropylene combustion, investigating additives and surrounding gaseous composition effects on flammability and volatile products during thermal degradation

02 p0248 A72-11767

Flammability smoke hazards and combustion product toxicity tests of plastics

03 p0379 A72-13243

Flame retardant mechanism in hydrocarbon polymer combustion, discussing halogen adverse effect on thermal stability

03 p0380 A72-13244

Plasticized PVC compounds, investigating chlorine based fire retardants role in increasing flame resistance

03 p0380 A72-13248

Polybenzimidazole fabric treatment for flammability reduction in oxygen atmospheres

07 p1023 A72-19055

Furan resins and chemically resistant furan-fiberglass composites flame resistance, heat distortion and physical properties at high temperatures

08 p1192 A72-21678

Hydrogen chloride addition effect on hydrocarbon flammability under reduced pressure, studying flame stability limits of methane, ethylene, acetylene and n-butane in oxygen

10 p1562 A72-24236

Polymers flammability tests for research, safety and acceptance purposes, noting ignition limits, decomposition and testing procedures

11 p1746 A72-26044

Glass reinforced thermoplastic resins flammability resistance, discussing test methods and flame retardant additives

16 p2415 A72-33419

Flame retardant glass reinforced thermoplastic polyester Celanex processing and performance, considering flammability, and electrical/mechanical properties

16 p2415 A72-33420

Combustible materials ignition temperature, time lag and burning rate in oxygen enriched atmosphere, deriving activation energy for fire resistance estimates

17 p2571 A72-35276

Studies on flame-resistant epoxy resin - Pyrolysis of tetra-brominated epoxy resin and flame-resistant mechanism.

18 p2704 A72-36519

Structure-property relationships in flame retardant systems - Relative effects of alkyl phosphates, phosphonates and phosphites on cellulose flammability.

20 p2987 A72-39698

Comparative evaluation of zinc borate 2:3:3.5 with antimony oxide using various fire testing methods.

20 p2898 A72-39699

FLAMMABLE GASES

NT PYROGEN

FLANGES

Circumferential undulations of flanges from theory of nonsymmetrical bending of circular plates

04 p0584 A72-14472

Secondary normal stresses in fixed flange zone of thin walled nonlinearly elastic pipe under bending moment and torsion

08 p1249 A72-22096

Numerical description of electromagnetic radiation from open-ended flanged waveguides, giving truncation corrected expressions for field behavior in aperture perimeter vicinity

13 p1915 A72-28520

FLAP CONTROL

U AIRCRAFT CONTROL

U FLAPS [CONTROL SURFACES]

FLAPPING

Articulated rotor blade flapping at 0-0.24 advance ratios and constant lift, discussing effects of shaft tilt and collective pitch variations

07 p0910 A72-20205

Hingeless blades flap-lag oscillations linear stability characteristics in hovering flight, examining precone, elastic and pitch-lag coupling and induced inflow aerodynamic effects

14 p2072 A72-30289

Hingeless elastic helicopter blades coupled flap-lag motion under quasi-steady aerodynamic loads, reducing equations of motion to coupled nonlinear differential equations

15 p2180 A72-31211

Parametric studies of instabilities associated with large, flexible rotor propellers.

[AHS PREPRINT 615] 17 p2490 A72-34496

Unsteady wake effects on progressing/regressing forced rotor flapping modes.

[AIAA PAPER 72-957] 22 p3137 A72-42350

Helicopter rotor blade flapping motion stability, applying perturbation technique to linear equations of motion for different advance ratios and Lock numbers

[AIAA PAPER 72-955] 22 p3137 A72-42351

FLAPPING HINGES

Flap-lag induced nonlinear oscillations in torsionally rigid helicopter blade, solving nonlinear equations of motion by multiple time scales asymptotic expansion

[AIAA PAPER 72-956] 22 p3137 A72-42356

FLAPS [CONTROL SURFACES]

NT JET FLAPS

NT LEADING EDGE SLATS

NT SPLIT FLAPS

NT TRAILING-EDGE FLAPS

NT WING FLAPS

European A300B airbus flap and slat systems and tailplane actuator for longitudinal pitch trim control

01 p0006 A72-10725

Externally blown flaps for STOL characteristics in medium and heavy jet transport aircraft, demonstrating aerodynamic and flight mechanical feasibility

02 p0155 A72-12502

Large scale high aspect ratio multielement suppressor nozzle arrays testing for augmentor wings and internally blown flaps

[AIAA PAPER 72-131] 05 p0612 A72-16888

Jet peak velocity decay in single and multielement nozzles for STOL aircraft externally blown flaps, noting noise reduction due to flow mixing

[AIAA PAPER 72-48] 05 p0608 A72-16927

Aerodynamic characteristics of STOL aircraft with externally blown jet augmented flaps, predicting interference between lifting surfaces and turbofan engines

[AIAA PAPER 72-63] 05 p0609 A72-16953

Environmental tests on carbon fiber Vulcan air-brake flap, including thermal cycling, sustained loading, immersion, corrosion and lightning strike tests

05 p0681 A72-16998

Book of aircraft design illustrations covering three view and perspective form low drag airfoil, aspect ratio, plain split, slotted and multiple flaps

14 p2167 A72-30776

FLARED BODIES

Dynamic behavior of M-4S rocket devices for strap-on booster separation and nose cone and flare deployment

22 p3232 A72-43143

FLARES

Flare spectra of AD Leo during strong burst, comparing Balmer discontinuity and line widths with UV Cet stars

06 p0883 A72-18020

Laser flare luminosity front displacements and atom density at surfaces of transparent dielectrics as function of pulse intensities

07 p1007 A72-20123

Dynamics of flare formation by pulsed laser beam at surface of alkali halide crystals

07 p1007 A72-20124

Simultaneous observations of radio flares from beta Persei on 25-25 January 1972 at 2.8, 3.7 and 11.1 cm, noting spectral characteristics difference from quasi-steady component

10 p1547 A72-24945

Flare spectra of AD Leonis during strong burst, comparing Balmer discontinuity and line widths with UV Cet stars

11 p1718 A72-25956

Pleiades slow flareup in photosphere, comparing with Orion flare stars

15 p2304 A72-31329

Flare mechanism of pulsar radiation near magnetic poles of rotating neutron stars

15 p2298 A72-31627

Observation of a hard X-ray flare in Cyg X-1.

18 p2721 A72-36649

Energy variation curves for direct flare radiation and reflection from eruptive star atmosphere, discussing color variations

19 p2858 A72-37808

Non-thermal bremsstrahlung of fast electrons and flare of stars.

20 p2974 A72-39894

FLASH

Optimal flash rate and duty cycle for flashing visual indicators, testing observer ability to determine indicator state

01 p0018 A72-10565

Fragmentation and closure in afterimages of bright flash stimuli

03 p0317 A72-13938

Scintillator crystal system with monitoring streak camera for flash X ray burst time measurements

04 p0523 A72-15482

Human dark adaptometric visual threshold recovery and electroretinograms in response to double light flashes, using Fourier analysis of oscillatory potentials

07 p0916 A72-19024

Flicker and flash threshold experiments, discussing flicker cut-off frequency and flash duration relations and visual sensitivity

07 p0926 A72-19028

Occipital electroencephalographic response to slowly repeated aperiodic light flashes, discussing alpha wave and rhythmic afteractivity amplitude changes

07 p0916 A72-19041

Rod-cone interaction in human scotopic vision, presenting test flash threshold as function of conditioning flash interval

08 p1116 A72-21460

Average evoked potentials correlates of two flash perceptual discrimination in cats, discussing parallel changes as function of interflash intervals and peripheral level

10 p1427 A72-25178

Visible light flash emission due to strong shock wave of laser spark, investigating strong external magnetic field effect and time variation of luminous intensity

13 p1972 A72-29983

Light flashes observed by astronauts on exposure to primary cosmic radiation during transatlantic flights, investigating effect upon retina in man and animal

15 p2189 A72-31917

Analytical model of the flash produced in aluminum-aluminum hypervelocity impacts.

22 p3207 A72-42867

FLASH BLINDNESS

Flash blindness effects during flight simulation, investigating recovery time

[AD-742863] 01 p0022 A72-11296

Physiological effects of intense anticollision flash light backscatter pulses on instrument rated pilots

12 p1775 A72-28303

Visual acuity restoration improvement after flash blindness by monocular shielding and ingestion of vitamin complexes containing ATP with pyridoxal, considering twilight vision

21 p3012 A72-41748

The suppression-recovery effect in relation to stimulus repetition and rapid light adaptation.

24 p3372 A72-44909

FLASH LAMPS

High stability electrodeless discharge lamps with less than 0.1 percent intensity variation, discussing construction and quality control procedures

04 p0509 A72-15485

Flashlamp pumped dye-doped polymethyl methacrylate laser thermal and photochemical effects decrease and peak power output increase by light converter

07 p1002 A72-19206

Fast coaxial flash lamp pumped liquid dye laser (LDL) for photolysis and biophysical and biochemical applications

09 p1326 A72-23406

Superradiant laser emission from organic dyes rhodamine 6G and B with coaxial flashlamp pumping source, relating input threshold energy to dye concentration

13 p1971 A72-29864

Xenon filled coaxial pulse tube for pumping organic dye solutions, obtaining intensive light flashes

13 p1971 A72-29923

Pulsed solid state lasers with large area Si photodiode for output measurement in feedback control system to compensate flash lamp aging

15 p2247 A72-32027

Flashlamp pumped cryptocyanine Q switched high peak power ruby lasers, noting UV radiation responsible for methanolic solution photochemical decomposition

15 p2249 A72-32156

Short flash characteristics of spiral pumping lamp for dye laser

16 p2400 A72-33079

Flash lamp optimal operating parameters determination by impedance matching to driving circuit and spectral matching to material of optically pumped solid state pulsed lasers

21 p3061 A72-40204

Flashlamp-pumped dye lasers for investigations of the upper atmosphere.

24 p3409 A72-44948

FLASH TUBES

U FLASH LAMPS

FLASH WELDING

German monograph - Improvement of the ductility characteristics of flash butt welding joints involving carbon steels by pulse normal annealing and hot heading in the welding machine

19 p2807 A72-37659

FLAT CONDUCTORS

Computed performance of ILS glide slope transmitting arrays sited over flat ground planes of one dimensional perfectly conducting strips in free space

05 p0686 A72-16559

Reliable interconnections for U.S. Army avionics, determining best technique for terminating flat conductor cables with electrical connectors

10 p1447 A72-24012

FLAT PLATES

Alternating directional implicit numerical solution for three dimensional steady low density hypersonic flow over finite width flat plate

[AD-736572] 01 p0049 A72-10230

MHD boundary layer calculation for conducting fluid along semiinfinite flat plate with transverse magnetic field, deriving momentum and kinetic energy integral equations

01 p0113 A72-11383

Unsteady compressible free convection near infinite vertical flat plate with temperature and velocity variations in boundary layer

01 p0146 A72-11392

Sonic line neighborhood of uniform axisymmetric supersonic air jet impinging on perpendicular flat plate, measuring shock shapes and surface pressures

01 p0002 A72-11398

Nozzle boundary layers effect on reattachment position of two dimensional jet to adjacent flat plate, noting Reynolds number influence

02 p0150 A72-11729

Dynamic and plastic behavior of mild steel and Al wide beams and rectangular flat plates

02 p0291 A72-11964

Flat plate incompressible smooth surface boundary layer examination emphasizing turbulence production near wall, using hydrogen-bubble and hot-wire measurements with dye visualization

02 p0203 A72-11975

Aeroelastic stability of flat anisotropic sandwich plates in supersonic compressible fluid flow

02 p0297 A72-12614

Unsteady flow in laminar boundary layers along infinite porous flat plate with time dependent suction

02 p0206 A72-12620

Heat transfer and temperature profiles in separated flow generated by transverse rectangular notch in flat plate

02 p0303 A72-12700

Time dependent unsteady flows visualization around circular cylinders and flat plates decelerated from steady speed

02 p0206 A72-12773

Laminar two dimensional hypersonic flow over stepwise accelerated flat plate at zero angle of attack, obtaining time dependent velocity and temperature profiles by linearized flow equations

03 p0442 A72-13236

Transition on plane plate in presence of vortices detached from cylinder in free flow

03 p0342 A72-13788

Flat plate in turbulent shear flow polymer solution, predicting maximum drag reduction with interactive layer concept

03 p0343 A72-14322

Velocity and shear stress in laminar boundary layer flow on flat plate with narrow suction slot

04 p0461 A72-14461

Optimum variable thickness reinforcement around circular hole in flat elastic sheet under radial tension

04 p0583 A72-14463

Forced and free transverse vibrations of flat rectangular plates with attached concentrated masses

04 p0584 A72-14521

Laminar viscous flow past finite flat plate at high Reynolds numbers, solving Navier-Stokes equations

04 p0511 A72-14859

Flat plate wing autorotation experiments about spanwise axis in low speed wind tunnel

04 p0462 A72-15117

Turbulence intensities and shear stress measurements in wake of thin flat plate by rotating single hot-wire anemometer

04 p0524 A72-15498

Holographic interferometer for heat transfer measurement, studying free convection thermal boundary layer on heated isothermal vertical flat plate

04 p0524 A72-15531

Flat plate, sphere and circular cylinder drag and lift coefficients in free molecular flow

04 p0463 A72-15645

Turbulent flow and heat transfer characteristics of non-Newtonian fluids on flat plate, measuring velocity and temperature distributions

05 p0648 A72-16003

Load or compression eccentricity effect on buckling and postbuckling behavior of flat plates, presenting stress distribution curves

05 p0737 A72-16116

Thin circular flat plate simply supported at three points on circumference, obtaining vibration mode shapes and eigenvalues

05 p0738 A72-16532

Jet interaction induced supersonic turbulent boundary layer separation, obtaining flat plate pressure measurements and jet plume shadowgraphs

05 p0602 A72-16537

Free convection flow along infinite vertical flat plate under periodically varying suction and with fluctuating plate temperature, analyzing mean velocity and temperature profiles

05 p0747 A72-16668

Turbulent boundary layer on yawed flat plate, measuring velocity profiles and flow directions

[DFVLR-SONDDR-177] 05 p0603 A72-16703

Concentration profile equations for finite length flat vertical plate moving in viscous incompressible fluid

05 p0650 A72-16783

Current collection characteristics of flush mounted electrostatic probes on sharp flat plate in ionized hypersonic flows

[AIAA PAPER 72-104] 05 p0696 A72-16814

Numerical solution method for laminar, time dependent and three dimensional boundary layer equations, applying to rotating flat plate in forward flight

[AIAA PAPER 72-109] 05 p0652 A72-16944

Environment acoustic resonant frequencies effect on flat steel plate vibration under direct and air flow vortex shedding excitations

06 p0894 A72-17768

Two dimensional flow attachment to flat plates, investigating Coanda effect

06 p0798 A72-17776

Critical review on data accuracy of maximum principal elastic stresses and deflections of thin initially-flat square isotropic plates under uniform normal pressure

06 p0894 A72-17796

Supersonic flow patterns near yawed obstacles around flat plate sharp leading edge with high pressure regions in reversed separated flow zone

06 p0756 A72-18122

Difference method for numerical integration of Navier-Stokes equations for two dimensional incompressible steady flow along flat thin plate

07 p0908 A72-19170

Flexure analysis of isotropic Reissner flat plates bonded by adhesive layer, deriving stress distribution equations in general tensor form

[AIAA PAPER 71-148] 07 p0189 A72-19688

Buckling under uniaxial compressive load of structural sections and stiffened flat plates reinforced with laminated composites

07 p0190 A72-19732

Thermal conductivity and thermal diffusion coefficients determination for plane plate heated unilaterally from above under fourth kind boundary conditions

08 p1252 A72-21313

Air injection from wall slot into turbulent boundary layer of high temperature gas channel flow, calculating film cooling effectiveness in flat plate

08 p1252 A72-21316

Molecular beam continuum model for calculation of hypersonic flow past flat plate at zero incidence angle

[AD-746387] 08 p1254 A72-21609

Laminar thermal boundary layer analysis, comparing heat transfer characteristics of continuous surface and semiinfinite plate

08 p1254 A72-21613

Flat plate boundary layer transition equations for supersonic wind tunnels, taking into account free stream turbulence

08 p1150 A72-21616

Boundary condition for plane or axisymmetric stagnation point flow of micropolar fluid over flat plate, giving numerical solutions for turbulent characteristics

09 p1293 A72-22621

Static pressure tube calibration for surface pressure measurements in flow over flat plate and airfoil

09 p1261 A72-22937

Parametric instability of flat rectangular plates under periodic or shear sinusoidal in-plane boundary loads

09 p1408 A72-23463

Forced convection heat transfer for turbulent flow over flat surface with attached protrusion for varying Reynolds number and boundary layer thickness

10 p1561 A72-23882

Existence and uniqueness theorem for weak solution of clamped elastic plate equilibrium problem, using micropolar flat plate bending theory

10 p1555 A72-24202

Rectilinear impulsive motion of compressible boundary layer on infinite plate, deriving integration method for differential equations of motion under energy dissipation neglect

10 p1465 A72-24203

Unsteady laminar boundary layer on semiinfinite flat plate induced by small free stream velocity fluctuations, showing far downstream double layer structure via asymptotic and numerical solutions

[AD-745486] 10 p1467 A72-24334

Uniform flow past semiinfinite flat plate for large Reynolds numbers and strong blowing, noting injected

fluid region separation from free stream by shear boundary layer

10 p1467 A72-24369

Thermal radiation effects on natural convection boundary layer adjacent to vertical flat surface with uniform heat flux input

10 p1562 A72-24466

Heat transfer process in boundary layer of transparent gas flowing past plane emitting plate with prescribed surface heat flux

10 p1418 A72-24540

Perturbation analysis for forced flow past semiinfinite flat plate parallel to uniform mainstream, calculating two dimensional laminar film condensation by boundary layer theory

10 p1469 A72-24563

Boundary layer model for laminar transient forced convection film boiling on isothermal flat plate, noting one dimensional conduction, intermediate and steady state regions

[AIAA PAPER 72-289] 11 p1741 A72-25227

Hydrodynamics of turbulent free convection boundary layer on vertical flat plate and ethyl alcohol film

11 p1743 A72-25258

Viscous liquid impulsive flow past semiinfinite plate, showing leading edge effects and boundary layer singularity existence

11 p1614 A72-25351

Finite element structural analysis for local buckling stresses in flat plates, panels and thin walled columns, deriving elastic and geometric stiffness matrices

[AIAA PAPER 72-354] 11 p1729 A72-25383

Linearized method of characteristics application to supersonic flow past oscillating flat plate cascades with supersonic leading edge locus

[AIAA PAPER 72-377] 11 p1730 A72-25401

Laminar viscous flow past semiinfinite flat plate at zero incidence, using Oseen approximation in matching leading edge and potential flow regions

11 p1615 A72-25522

High strength steel flat plates brake formability from bend tests on sheared edges specimens, noting Hutchinson method sensitivity for different crack propagation propensities materials

11 p1657 A72-25819

Single spiral vortex cavity termination model for second order solution of flat plate hydrofoil cavitation flow

11 p1616 A72-25879

Viscous effects on turbulent diffusion shear flow past semiinfinite flat plate, using Wiener-Hopf equations

[DFVLR-SONDDR-171] 11 p1617 A72-26370

Double passed Michelson interferometer with polarizing beam splitter, quarter wave plates and cube corner reflectors to obtain immunity to mirror misalignment

11 p1635 A72-26500

Rayleigh problem in presence of magnetic field, discussing transpiration effects on MHD flow near oscillating flat plate

11 p1696 A72-26542

Unsteady aerodynamic forces on flat plate in locally perturbed incompressible potential flow, investigating angle of attack frequency response to periodic local perturbations

11 p1573 A72-26579

Dynamic and thermal laminar compressible boundary layers on flat plate, noting interaction of two quasi-steady flows

[ONERA, TP NO. 1068] 12 p1797 A72-27167

Mean velocity distribution and Reynolds stresses in turbulent wake behind flat plate in uniform incompressible flow

12 p1798 A72-27718

Nonstationary interaction flow field between subsonic and composite jet on flat plate with vortex formation and reverse currents, using finite difference technique

12 p1799 A72-28168

Vorticity and energy transfer equations for subsonic jet impingement on flat plate, noting turbulent jet effect on friction factor

12 p1799 A72-28171

Heat transfer measurement during flat plate cooling by air film, using electrical calorimetric technique

12 p1890 A72-28176

Turbulent mixing length velocity, temperature pulsations and viscous sublayer thickness in steady incompressible fluid flow past infinite plate

12 p1799 A72-28179

Combined radiation-convection interaction for slow speed gas flow over flat plate, comparing with two dimensional and axisymmetric stagnation point geometries

13 p2064 A72-28631

Infinite plane plates sound radiation due to bending waves interactions with density and stiffness fluctuations in material

13 p2004 A72-29094

Hall currents effect on unsteady MHD flow of electrically conducting fluid past flat plate imbedded in uniform external transverse magnetic field

13 p2012 A72-29225

Wind tunnel investigation of supersonic air flow behavior on rotatable right dihedral formed by two plane plates with sharp edges

13 p1894 A72-29636

Numerical integration of boundary layer equations through region of reverse flow past parallel flat plate with negative surface velocity

13 p1944 A72-30033

French monograph on velocity profile in laminar boundary layer on semiinfinite flat plate in harmonic oscillation of uniform incompressible flow

14 p2095 A72-30949

Laminar to turbulent boundary layer transition in supersonic flow over flat plate investigated in supersonic wind tunnels, noting unit Reynolds number effect

14 p2069 A72-31004

Liquid film condensation of low pressure metal vapors on isothermal vertical flat plates, obtaining equations for heat transfer rate prediction

14 p2173 A72-31059

Heat transfer in MHD boundary layer flow of conducting incompressible fluid with aligned magnetic field on flat plate at high Prandtl number

14 p2141 A72-31068

Two dimensional viscous flow past semiinfinite flat plate and smooth obstacle, using Navier-Stokes equations for lift force relationship investigation

15 p2216 A72-31312

Navier-Stokes equation for unsteady asymptotic suction flow over flat plate, plotting velocity distribution profiles

15 p2178 A72-31406

Blade characteristics of axial flow fan with orifice fan guide investigation by theoretical model with flat plate parallel to wing tip surface

15 p2179 A72-32142

Holographic determination of local convective mass transfer coefficients over flat plate normally impinged with laminar air jet, using swollen polymer transparent coating

15 p2239 A72-32349

Thermal force exerted on spherical particle between two flat plates in stagnant monatomic rarefied gas, using moment solution to Boltzmann equation

15 p2336 A72-32403

Singularity method treatment of vortex distribution induced velocity perturbations on flat plate at angle of attack, noting results similarity to lifting surface theory

15 p2180 A72-32466

Streaming MHD flow past semiinfinite flat plate in presence of perpendicular uniform magnetic field, obtaining velocity field at large distances

15 p2288 A72-32480

Sharp flat plate laminar, transitional and turbulent skin friction via finite difference integration of compressible boundary layer equations

15 p2180 A72-32596

Simultaneous hypersonic skin friction and heat transfer measurements on sharp-edged flat plate, using thin-skin heat transfer gages and boundary layer pitot rake

15 p2219 A72-32598

Power law fluids impulsively started flow over plate, presenting analytical expressions for velocity distribution, shear stress and boundary layer thickness

16 p2375 A72-32833

Blowing and suction effects on free convection boundary layer on semiinfinite vertical flat plate, taking into account temperature difference between plate and fluid

16 p2477 A72-33429

Wall and ambient temperature distribution effects on free convection heat transfer from nonisothermal vertical flat plate in temperature stratified medium for Prandtl number range

16 p2477 A72-33434

Pohlhausen type integral method for dissociative binary mixture nonequilibrium laminar boundary layer on flat plate, using Crocco relationship between enthalpy and velocity profile

16 p2378 A72-33436

Temperature field in flat plate with selective radiation absorption coefficient, using asymptotic representations for internal heat flux radiation component

16 p2479 A72-33858

Flat plate leading edge blunting and wall cooling effects on supersonic laminar flow ramp-induced separation

[AIAA PAPER 72-716] 16 p2344 A72-34032

Perturbation methods for density stratified viscous flow past flat plate, using boundary layer and low Reynolds number approximations

[AIAA PAPER 72-646] 16 p2381 A72-34086

Effects of yielding and size upon fracture of plates and pressure cylinders.

17 p2565 A72-34251

Certain motions of micropolar fluids

17 p2538 A72-34771

Contact pressure between an elastic spherical shell and a rigid plate.

[ASME PAPER 72-APM-31] 17 p2628 A72-34788

Asymptotic character of turbulent boundary layer longitudinal velocity distribution along flat plate at low Reynolds number, using Hirsch theory for potential flow

17 p2539 A72-34908

Flow near an accelerated porous flat plate.

17 p2540 A72-35054

Downstream effects of discontinuous injection of foreign gases in inert laminar boundary layer flows.

17 p2542 A72-35632

Viscous hypersonic flow over a flat plate at angle of attack with leeside boundary layer separation.

[AD-744593] 17 p2486 A72-35634

Turbulent boundary layer with discontinuity in wall temperature and concentration

17 p2638 A72-35746

Flat plate withdrawal at high speed from quiescent liquid baths, calculating velocity profile via boundary condition transformation and eigenfunction expansion method

18 p2678 A72-36122

Strain measure determined plastic stress concentrations around discontinuities in flat plates compared with incremental theory

18 p2733 A72-36359

Drag of a flat plate with transition in the absence of pressure gradient.

18 p2641 A72-36775

Response of heat transfer from a moving flat plate in a parabolic flow.

18 p2741 A72-36798

Transition to a turbulent flow mode in the boundary layer of a plane plate with various turbulence scales in the incident flow

18 p2682 A72-36889

Clamped flat skew plates stability under inplane stresses in terms of oblique components, calculating elastic buckling coefficients via energy method

18 p2736 A72-36931

The forces on a flat plate in a Couette flow.

18 p2683 A72-36996

Drag of a finite flat plate set parallel to a uniform flow.

18 p2683 A72-37045

Alternate singular perturbation theory of high Reynolds number flow over flat plate to eliminate asymptotic matching and composite solution for accuracy improvement

18 p2684 A72-37083

Bending waves diffraction and scattering by mass impedance loadings of infinite plane plate, considering point load and semiinfinite rib arrays

18 p2739 A72-37203

Flow equations for flat plate turbulent boundary layer with Reynolds, continuity and energy components, deriving semiempirical differential equation for turbulence scale

19 p2785 A72-37471

Experimental investigation of nonstationary heat exchange for flow around a flat plate

19 p2880 A72-37665

Creep-buckling of flat rectangular plates when the creep exponent ranges from 3 to 7.

19 p2875 A72-37717

The enhancement of heat transfer by waves in stratified gas-liquid flow.

19 p2787 A72-38398

Hypersonic unsteady compressible boundary layer dependence on Prandtl number.

19 p2787 A72-38429

Compressible laminar wake behind a thin flat plate.

19 p2747 A72-38798

The prediction of compressible turbulent boundary-layer flows with mass addition.

[ASME PAPER 72-HT-58] 20 p2914 A72-39658

An analytical solution of wall-temperature distribution for transpiration and local mass injection over a flat plate.

[ASME PAPER 72-HT-57] 20 p2985 A72-39659

Theory of laminar film condensation of flowing vapor.

21 p3128 A72-40950

Laminar and turbulent boundary-layer studies at hypersonic speeds.

[ICAS PAPER 72-09] 21 p2990 A72-41134

The motion of a viscous fluid past an impulsively started semi-infinite flat plate.

21 p3046 A72-41316

Steady radiating gas flow past a semi-infinite flat plate at a constant temperature for an optically thick case.

21 p3131 A72-41497

Flat compressible turbulent boundary layers of air, predicting foreign gas injection effects on mass and heat transfer Stanton numbers and skin friction

22 p3165 A72-41958

Variational formulation and computer solution for thermal boundary layer flow over flat plate in entrance region, assuming temperature dependent thermal conductivity and viscosity

22 p3156 A72-41959

Bending waves propagation through flat plate forming rigid sound bridge between two parallel plates, calculating energy transfer at LF oscillations

22 p3234 A72-42128

Large deflections of flat arbitrary membranes.

22 p3235 A72-42604

Acoustic shock wave diffraction at moving or stationary flat plate immersed in ideal gas

22 p3206 A72-42732

Supersonic flow past a suddenly set plate

22 p3136 A72-42906

German monograph - Cooling of geometrically simple bodies /flat plate, cylinder, sphere/ by convection and radiation.

22 p3244 A72-43062

Free flexural vibrations of an elliptical plate with simply supported edge.

23 p3352 A72-44121

An experimental study of heat transfer downstream of a rearward-facing step with small coolant injection.

23 p3357 A72-44271

Laminated thick plate and shell analysis by the assumed stress hybrid model.

24 p3453 A72-44601

Dynamic blast loads on preheated and prestressed thin plates.

24 p3454 A72-44607

Post-buckling of axially compressed plates.

24 p3455 A72-44632

A numerical experiment on two-dimensional turbulent separation.

24 p3389 A72-44687

Measurement of the velocity distribution in the boundary layer over a flat plate with a diffusion flame.

24 p3464 A72-45062

Stability of the laminar flow of a 'power-law' non-Newtonian fluid in the boundary layer on a flat plate

24 p3393 A72-45255

Study of a turbine type flowmeter with helical blades.

24 p3404 A72-45354

FLAT SURFACES

Previous loading effect on contact area and prints number and size distribution and thermal conductance for two nominally flat surfaces in contact

[ASME PAPER 71-LUB-M] 02 p0234 A72-11528

Velocity, enthalpy and turbulent energy distributions calculation for plane wake behind flat body by asymptotic solution based on turbulence theory

23 p3249 A72-44083

FLATTENING

Jupiter equatorial radius and oblateness at atmospheric level from timings of 13-14 May 1971 occultations of beta Scorpi

04 p0571 A72-14615

FLAW DETECTION

U NONDESTRUCTIVE TESTS

FLEET BALLISTIC MISSILES

NT POSEIDON MISSILES

FLEXIBILITY

Potential energy principle in equilibrium stability problems for flexible extendable thread, using Liapunov method

03 p0390 A72-14208

Vibrational characteristics dependence on structural flexibility in gimbal bearings and supporting structure of two axis free gyroscopes and single axis rate gyroscopes

08 p1173 A72-22129

Short fiber reinforced thermoset composite materials for engineering construction, tabulating flexural properties and Charpy impact strengths

09 p1338 A72-23165

FLEXIBLE BODIES

Dynamic response of infinitely wide perfectly flexible foil bearings to small sinusoidal tensile variations

[ASME PAPER 71-LUB-20] 02 p0235 A72-11540

Flexible surface effects on shear stress fluctuations beneath turbulent boundary layer, using fiber optic displacement probe

03 p0343 A72-14324

Relay systems stability in orientation control of flexible satellites

05 p0725 A72-16439

Flexible elastic plate nonlinear vibration response and noise transmission from turbulent boundary layer by Monte Carlo technique, discussing subsonic and supersonic flow regions

[AIAA PAPER 72-199] 05 p0651 A72-16850

Liapunov direct method based approaches to hybrid dynamical systems stability, applying to attitude stability of flexible earth pointing satellite

[AIAA PAPER 72-18] 05 p0729 A72-16867

Rotational perturbation of three bodies in space tied by flexible elastic ropes, relating physical parameters to stable motion regions boundaries

08 p1240 A72-21141

Aerodynamic and gravitational effects on relative motion of two orbiting point masses connected by flexible nonexpandable thread

08 p1240 A72-21143

Equations of motion for structural flexibility influence on dual spin spacecraft dynamic response, noting elastic deformations and rotation rates coupling

[AIAA PAPER 72-348] 11 p1725 A72-25377

Unsteady aerodynamic loadings of flexible aircraft with nonplanar wings and wing-tail surfaces in supersonic flow

[AIAA PAPER 72-378] 11 p1574 A72-25402

British thin Si solar cells for large flexible lightweight arrays, considering radiation resistance, specific mass, area, contact material and antireflection coatings 12 p1756 A72-28004

American and European solar generator technology development review, discussing roll-up arrays, flexible panels, and stowage and deployment system components 12 p1756 A72-28005

Flexible solar cell array module design technique, discussing electric welding procedure and equipment parameters effects on breaking strength and reliability 12 p1758 A72-28036

Flexible space vehicle multiple closed loop attitude control system design, discussing stability, structure interaction and performance by analog simulation 15 p2321 A72-32587

Survey regarding present views, directives and standards, and the customary approaches for balancing flexible rotors 18 p2731 A72-36065

Orthogonal functions application to flexible rotors balance, expressing deflections vs angular velocity as sum of eigenvectors 18 p2731 A72-36066

Comparison of the balancing of a flexible rotor following the methods Federn-Kellenberger and Moore. 18 p2731 A72-36067

Flexible rotors balancing theory based on Fredholm integral equations, considering two- and three-bearing supported shafts with arbitrary mass distribution 18 p2731 A72-36068

Flexible rotor balancing over operational rotational speeds, deriving matrix equation for general conditions based on distributed and concentrated unbalance concept 18 p2732 A72-36071

Balancing of a flexible rotor by means of mode separation. 18 p2732 A72-36072

Flexible cable in uniform flow field, calculating coupling between longitudinal and transverse modes to obtain centripetal acceleration effects on tension 18 p2734 A72-36418

Astroelasticity in design and analysis of flexible space vehicles, presenting dynamics and control considerations 18 p2738 A72-37082

Convergence of a simple iteration scheme in equilibrium problems of flexible plates 19 p2877 A72-38201

Invariant poles feedback control of flexible, highly variable spacecraft. 19 p2869 A72-38240

Attitude dynamics of a three-axis stabilized satellite with a large flexible solar array. 20 p2976 A72-39137 [AIAA PAPER 72-857]

Rotational perturbation of three bodies in space tied by flexible elastic ropes, relating physical parameters to stable motion regions boundaries 20 p2977 A72-39246

Aerodynamic and gravitational effects on relative motion of two orbiting point masses connected by flexible nonexpandable thread 20 p2977 A72-39248

Determination of flexural-vibration deflections of structural elements with allowance for internal friction damping 20 p2981 A72-39921

A form of the translational dynamical equations for relative motion in systems of many non-rigid bodies. 22 p3205 A72-42113

A simple algorithmic method for the simulation of a spacecraft with flexible appendages. 23 p3343 A72-44552

Dynamics of spin-stabilized satellites having flexible appendages. 24 p3449 A72-45140

FLEXIBLE WINGS NT PARAWINGS

Inclined wind tunnel test section for free gliding investigation and aerodynamic design of flexible wing two body system 15 p2213 A72-31403

Flexible wing applications to passenger and cargo transport, discussing gliding and soaring sport, emergency use, powered flight, rocket payload recovery, etc 16 p2347 A72-33182

FLEXING

Composite materials testing with four point loading method, studying environmental and creep effects in flexure 04 p0537 A72-15091

Postbuckling behavior of cantilever columns with variable flexural rigidity, basing solution method on buckling mode assumption and principle of minimum total potential 04 p0591 A72-15278

Aircraft ejection simulation by human thoraco-lumbar spine flexion dynamic model, using strength of materials theory and shear effects for curved elastic beam [ASME PAPER 71-WA/BHF-7] 05 p0620 A72-15947

Flexure of micropolar elastic beams. 17 p2631 A72-35056

Torsion and flexure of curved, thin-walled beams or tubes. 19 p2874 A72-37696

Reduction of the effect of mount deformation on the flexure of the telescope mirror 19 p2801 A72-37967

FLICKER

Darkness enhancement measurement in intermittent light as function of flicker frequency, describing experimental assembly 06 p0762 A72-17605

Light variation threshold amounts for flicker and flickering pattern detection as function of variation frequency 09 p1269 A72-22615

Transistor I.F. flicker background noise generation mechanism in terms of bulk effect due to temperature fluctuation or phonon electron interactions 09 p1286 A72-23107

MOS transistor low level background flicker noise equivalent voltage relationship to gate voltage and input capacitance and interface state density 09 p1286 A72-23108

I.F. excess flicker noise in metal semiconductor Schottky barrier diodes due to barrier height fluctuation 09 p1287 A72-23114

Flicker adaptation, discussing intermittent lights effect on apparent brightness 10 p1427 A72-25181

Hue shifts accompany phase induced modulation enhancement of sinusoidally flickering lights. 18 p2651 A72-36613

Error search reading tasks to investigate practical applicability of blinking display coding techniques, noting reading speed reduction compared to steady display 21 p3008 A72-41018

FLICKER FUSION FREQUENCY U CRITICAL FLICKER FUSION

Aerial triangulation for optimum photogrammetric project parameters, discussing flight altitude, bridging distance and control points for computerized optimization 01 p0066 A72-10462

Minimum safety flight altitudes for aircraft landing systems and lateral deviations for correction maneuver 12 p1842 A72-27269

Low flight altitude atmospheric parameters spatial and temporal variability effects on aircraft flyover noise measurement 13 p1991 A72-28841

High cruise altitude operational advantages for commercial transport aircraft utilizing technological innovations in structures, propulsion, controls, avionics and aerodynamics 13 p1996 A72-28875

Low-altitude flight imposed psychophysiological stresses due to air turbulence discomfort, instrument dial vibration and ground-based navigational objects recognition difficulty 14 p2080 A72-30747

Aircraft geodetic coordinates computation from radar range measurements and flight altitude over earth ellipsoid 15 p2224 A72-31601

Analytical assessment of the accuracy of autonomous space navigation from measurements of the flight altitude and zenithal distance of one reference star 22 p3202 A72-42222

Aircraft longitudinal stability under conditions of varying atmospheric density, thrust force and velocity, determining critical altitude for vanishing oscillations [AIAA PAPER 72-951] 22 p3138 A72-42358

FLIGHT CHARACTERISTICS

Externally blown flaps for STOL characteristics in medium and heavy jet transport aircraft, demonstrating aerodynamic and flight mechanical feasibility 02 p0155 A72-12502

Soviet book on in-flight studies of aircraft stability and controllability covering dynamic characteristics, measurements, balancing curves, aerodynamic forces and limiting and special flight regimes 02 p0155 A72-12542

Control technique and flight quality for crew workload reduction to improve military and civil aircraft flight safety 03 p0310 A72-13640

Pilot evaluation of Boeing 747 handling, directional stability, stall, rudder feel forces, landing, inertial navigation and reliability 05 p0614 A72-16992

Aeromechanical analysis of flight conditions for conventional aircraft, including kinematics of curvilinear motions with constant speed 07 p0913 A72-20372

Dassault Falcon 10 turboprop powered executive aircraft, attributing safe stall characteristics to wing design optimization 08 p1108 A72-21274

Mystere business jet aircraft flight instruments, acceleration, control and stall characteristics 08 p1110 A72-21900

DC-10 aircraft structural design, flight handling characteristics and fatigue tests 09 p1262 A72-23446

Combat jet helicopter maneuverability, considering aircraft flying characteristics, pilot capability, flight configuration, altitude and load factor 10 p1421 A72-24923

Aft center of gravity travel effects on aircraft longitudinal control response characteristics [SAE PAPER 720318] 11 p1575 A72-25581

Fighter aircraft maneuverability, range and armament requirements, discussing canard vs delta configurations 11 p1577 A72-26657

L-1011 flight test program, discussing aircraft design, flight station, controls, flying qualities, etc 12 p1754 A72-27519

Aircraft flight characteristics for landing approach by spoiler-elevator deflection coupling, considering pitch, flight path angle and speed 16 p2343 A72-33423

Integrated airborne-ground based instrumentation system for variable stability X-22A aircraft flying qualities research, discussing telemetry, mobile van, landing aids and airplane design 16 p2348 A72-33628

Relationship between static pressure error /position error/ and measurable flight parameters for different aircraft weights and configurations 16 p2393 A72-33637

Flight test instrumentation system for measurement of aircraft performance, stability and control characteristics during nonsteady flight 16 p2349 A72-33639

Aircraft instrumentation system accuracy relation to aerodynamic derivatives evaluated from flight data, proposing input and transient response measurement system 16 p2394 A72-33640

Russian book on flight dynamics covering horizontal flight, takeoff, climb and landing characteristics, meteorological conditions, helicopters, trajectory problems, stability and controllability analysis, etc 16 p2349 A72-33874

Sailplane performance measured in flight. 17 p2487 A72-34215

The flight mechanics of STOL aircraft. 17 p2488 A72-34241

An integrated system of airborne and ground-based instrumentation for flying qualities research with the X-22A airplane. 17 p2536 A72-34486 [AHS PREPRINT 654]

Critical review of Mil-F-83300 V/STOL flying qualities specifications as applied to helicopter design and missions, suggesting inappropriateness for Navy helicopters [AHS PREPRINT 643] 17 p2490 A72-34503

Structural mode vibration control system design for B-1 aircraft to improve ride during atmospheric turbulence and terrain following 17 p2493 A72-35563

The fly-by-wire systems approach to aircraft flying qualities. 17 p2493 A72-35575

The Dassault Mystere 20. 19 p2748 A72-37900

Flight test report on L-1011 aerodynamic characteristics, discussing high and low speed performance, stability and control, stall behavior, etc 19 p2748 A72-38030

Aerodynamic design and development of the Lockheed S-3A Viking. 19 p2751 A72-38122 [AIAA PAPER 72-746]

An exploratory study of flying qualities of very large subsonic transport aircraft in landing approach. [ICAS PAPER 72-07] 21 p2995 A72-41132

Low-drag artillery projectile aerodynamic characteristics and dynamic flight behavior from wind tunnel, spark range and instrumented flight tests, describing mathematical trajectory simulation [AIAA PAPER 72-979] 22 p3134 A72-42334

Delta wing separation can dominate shuttle dynamics. [AIAA PAPER 72-976] 22 p3230 A72-42336

Analysis of the fundamental parameters and flight properties of aerobatic aircraft in a statistical framework 23 p3252 A72-44336

Effects of variations in lift and drag response to longitudinal control on the ease and quality of landing. 24 p3368 A72-45333

FLIGHT CLOTHING

Flight helmet optimal fitting technique, using automatic recording audiometer and noise source for acoustic leakage detection 04 p0479 A72-14873

FLIGHT CONDITIONS

Storm effects on SST operations, discussing wave initiation at storm top and tropospheric propagation 04 p0542 A72-14683

CAT inducing atmospheric conditions effects on SST flight, discussing turbulence in convective clouds and kinetic energy spectra of atmospheric motions

04 p0543 A72-14693

Interstellar flight conditions in photon vehicle

05 p0713 A72-15979

Aviation weather forecasting improvements due to radar, computer, satellites and high speed communications contributions

07 p1029 A72-18838

Head-up display flying under IMC and VMC flight conditions, considering takeoff, landing and navigation modes

08 p1204 A72-21004

Interdiction bombing mission effectiveness model for bad and good weather aircraft type selection depending on weather conditions at target site

13 p1896 A72-28400

Aircraft flight conditions effect on low altitude critical air turbulence in terms of gust velocity components for CAT prediction

13 p1993 A72-28861

Magnetic compass use in instrument flight conditions, suggesting emergency procedures during aircraft system failures

15 p2238 A72-32212

Aerodynamic analysis of various flight conditions of conventional aircraft. III - Mechanical fundamentals /Dynamics of a point mass/

17 p2492 A72-35440

Russian book on aircraft design covering flight conditions, structure and control characteristics, production and stress analysis

17 p2492 A72-35448

Flight-mechanical analysis of various flight conditions of conventional aircraft. V - Mechanical foundations /Dynamics of the rigid body/

21 p2994 A72-40175

Russian book - Aviation meteorology.

22 p3200 A72-42024

Aircraft longitudinal stability under conditions of varying atmospheric density, thrust force and velocity, determining critical altitude for vanishing oscillations

[AIAA PAPER 72-951] 22 p3138 A72-42358

Minimum operational costs of passenger and cargo transport aircraft, considering effects of flight distance, wind conditions and optimum speed and altitude

23 p3252 A72-44338

Raindrop breakup in the shock layer of a high-speed vehicle.

24 p3395 A72-45780

FLIGHT CONTROL

NT AUTOMATIC FLIGHT CONTROL

NT AUTOMATIC LANDING CONTROL

NT FLY BY WIRE CONTROL

NT POINTING CONTROL SYSTEMS

NT THRUST VECTOR CONTROL

Hybrid computer simulation program used in development and software design validation of digital flight control system for Titan 3C space booster

02 p0186 A72-11655

Scientific balloon data management system, discussing airborne and ground station equipment for telemetry, command and flight control

03 p0327 A72-13725

Feedback gains for STOL aircraft display pilot interactive flight director design, using computerized approach-touchdown simulation and optimal control theory

[ASME PAPER 71-WA/AUT-9] 05 p0684 A72-15956

Optimization algorithms for jet transport aircraft inertially based flight trajectory control in turbulent atmosphere, comparing with ILS

05 p0685 A72-16472

NF-8D aircraft variable stability system ground/in-flight calibration for determination of flight control system dynamics effects on flying qualities

05 p0611 A72-16660

Aircraft flight control system MTBF field operational and MIL-STD-781 testing, establishing data baseline for reliability predictions

05 p0638 A72-16662

Flight test evaluation of A-7D/E emergency backup flight control system, describing hydraulic power control systems design and function

05 p0687 A72-16664

Unmanned systems flight testing by test bed vehicle conversion to man operated mode, discussing T-33A jet trainer conversion to drone operation

05 p0623 A72-16665

Flight control systems development, discussing on-board computers use in subsystems functional integration, stabilization and landing systems, inertial navigation and flight simulation

05 p0687 A72-16736

Adaptive model following control systems design by hyperstability approach for flight control and simulation

[AIAA PAPER 72-95] 05 p0613 A72-16956

S-3A Viking land based antisubmarine warfare maritime and reconnaissance aircraft, describing flight

controls, structural design, underslung podded engines and operational equipment

06 p0758 A72-17583

Aircraft optimal control for case of continuous data flow on time variable flight conditions

07 p1032 A72-18979

Apollo manned mission real time ground support computer simulation for NASA flight controller training to maximize flight crew safety

07 p0933 A72-20329

Hybrid computer simulation for telemetry data collected during missile flight control system model post-flight verification and hardware performance analysis

07 p1085 A72-20332

Space shuttle flight crew/computer interface display and control functional requirements optimization by real time digital simulation

[AIAA PAPER 72-226] 10 p1460 A72-24437

Stochastic control theory application to flight problem, discussing aircraft identification and adaptive control over wide environmental range

10 p1458 A72-25146

Flight tests of combination flight director displayed and attitude command control system effect on and attitude command control system effect on general aviation aircraft handling qualities during ILS approach

[SAE PAPER 720316] 11 p1575 A72-25580

Terminology definitions for redundant flight control systems

11 p1684 A72-26031

German VAK 191B V/STOL fighter aircraft design, development and flight tests, noting redundant control systems

12 p1753 A72-27166

Semiconductor strain gage design and environmental performance for flight control systems

12 p1812 A72-27962

Shoran systems with onboard computers for aircraft position and trajectory parameters, noting coordinate plotting for flight path recovery maneuvers

13 p1996 A72-28785

Jaguar powered flight controls, discussing wing spoilers, slab tailplane, rudder, autostabilization system and integrated packaging of actuators

16 p2353 A72-34144

V/STOL flight control - Trend and requirements.

17 p2487 A72-34240

Ballistic-damage-tolerant composite flight control components.

[AHS PREPRINT 674] 17 p2626 A72-34514

Flight vehicle, control system and perturbations models synthesis from variational problem solution via control functions improvement

17 p2621 A72-35037

Multimode flight control for precision weapon delivery.

17 p2493 A72-35561

Hybrid mechanical-electrical mechanizing techniques for aircraft flight control systems

17 p2493 A72-35576

Dynamic verification of a digital flight control system.

18 p2673 A72-36336

Integrity of flight control system design.

18 p2643 A72-37032

Survivable flight control system compatibility test program.

[AIAA PAPER 72-761] 19 p2752 A72-38143

Optimal selection of stability augmentation parameters for excellent pilot acceptance.

19 p2752 A72-38227

An optimal model-following flight control system for manual control.

19 p2753 A72-38228

A simulation technique used in the development of a flight control system for an aerodynamically controlled missile.

[AIAA PAPER 72-858] 20 p2976 A72-39136

Failsafe hydraulic actuator flight control for jet aircraft.

20 p2890 A72-39351

High subsonic transport aircraft design development based on supercritical aerodynamic configuration and advanced structural, flight control and propulsion system technologies

[AIAA PAPER 72-756] 20 p2889 A72-40056

Real-time launch vehicle steering program selection.

[AIAA PAPER 72-830] 20 p2977 A72-40058

Unique features of the B-1 flight control systems.

[AIAA PAPER 72-872] 20 p2889 A72-40062

Design, operation and testing of integrated STOL flight control system, noting approach accuracy and passenger comfort improvement

21 p3080 A72-40292

High performance jet aircraft variable feel flight control systems for simulation of aerodynamic reaction forces proportional to dynamic pressure

21 p3039 A72-41069

Application of the head-up display /HUD/ to a commercial jet transport.

21 p3060 A72-41256

Problems arising in the transfer of training from simulated to real control systems.

21 p3010 A72-41412

Equations of motion appropriate to the analysis of control configured vehicles.

[AIAA PAPER 72-952] 22 p3137 A72-42353

A sight simulation technique using TV-screen perspective correction for restricted maneuver flight missions

24 p3388 A72-45298

Control configured fighter and bomber aircraft based on flight control technology, discussing development programs

24 p3369 A72-45386

FLIGHT CREWS

Spacecraft and aircraft crew survival after emergency landing in adverse environments, discussing water and food requirements, survival supplies and medical and first aid equipment

05 p0621 A72-16629

Transmeridian flight psychological effects on aircrews, discussing anxiety, stress, circadian rhythm disruption and sleep loss effects on performance deterioration

06 p0766 A72-17816

Crew members handling of emotionally disturbed aircraft passengers

07 p0926 A72-18836

Sleep pattern relation to duty hours of aircrew operating worldwide east-west routes

07 p0932 A72-20178

Physiological evaluation of crew piloting qualities, considering nervous/emotional stress, ECG, arterial pressure and breathing frequency recorded on simulator

07 p0934 A72-20375

Asthmatics evolution and treatments in armed forces aircrews, noting acetylcholine test

08 p1125 A72-21270

Hyperuricemia, gout and lithiasis among operating aircrews, discussing diagnosis and relation to arteriosclerosis

08 p1125 A72-21271

Dazzle glare effects and acuity recuperation among aircrew, noting civil and military aircraft accidents during daytime and nighttime flights

08 p1125 A72-21272

Permanent flight unfitness attributable to air service, noting orthopedic traumatic sequelae, cardiovascular illnesses, psychological and ophthalmological causes

08 p1125 A72-21273

Custom fit oxygen mask for life support of crew members

08 p1126 A72-21567

Aircrews tolerance to cold water and life raft exposure, discussing prediction model based on thermal insulation effectiveness, assumed metabolism and body surface area and mass

[AD-740276] 10 p1428 A72-23734

Work-rest schedules endocrine and metabolic effects on aircrews during 50 hour flight missions in C-141 aircraft, using urinary test techniques

[AD-740992] 10 p1428 A72-23737

Fatigue factors in aircrew related to shift working and technological advances, considering implications for industry and work-rest cycles

10 p1432 A72-24988

Hemodynamic criteria for physical fitness in airmen, discussing age dependent variations in heart beat, arterial pressure and body temperature

11 p1590 A72-26987

Flight crew training programs cost and quality, emphasizing safety and flight simulator application

11 p1590 A72-26998

Life support equipment and pressure suit operational requirements from viewpoint of flight crews and test pilots

12 p1771 A72-27516

Pilot selection criterion for replacement air group /RAG/, using scored maneuver item correlations for flight crew and pilot training

12 p1774 A72-28262

Multivariate algorithms of optimum content and form for cardiovascular risk assessment in pilots and air transport personnel

12 p1764 A72-28264

Biomedical effects on air crews of chemical fire suppression agent Halon 1301 /bromotrifluoromethane/ during simulated aircraft cabin fires

12 p1776 A72-28308

USAF aircraft accidents/incidents involving aircrewmembers with medical waiver on various visual, cardiopulmonary and other chronic pathological and psychiatric conditions

12 p1776 A72-28315

Place of tropical pathology in medical assessment of aircrew

19 p2757 A72-37882

Hemodynamic indices in flight crew personnel during hypertonic sickness and atherosclerosis of coronary arteries

20 p2892 A72-39391

The Macruz index and its clinical evaluation in electrocardiography with regard to the selection and control of air crews

21 p3009 A72-41193

FLIGHT FATIGUE

- Heuristic procedure solution for least cost commercial airline crew scheduling, emphasizing combinatorial space size reduction 24 p3466 A72-44584
- FLIGHT FATIGUE**
- Prolonged jet flight effect on passenger interstitial and intracellular fluid volumes from plasma, extracellular and total body water measurements, noting dehydration and foot swelling 06 p0767 A72-17866
- Psychological principles of active rest during long space flights 21 p3006 A72-40446
- FLIGHT FITNESS**
- Student naval aviator selection by multiple correlation technique using noncognitive college and flight background questionnaire to reduce attrition rate 02 p0166 A72-11704
- Psychological tests of airmen with performance error histories, considering psychic characteristics for limited assignment readjustment 03 p0316 A72-13723
- Pilot in-flight incapacitation probability from airline reports, career termination studies and questionnaire responses 04 p0479 A72-14870
- Physiological evaluation of crew piloting qualities, considering nervous/emotional stress, ECG, arterial pressure and breathing frequency recorded on simulator 07 p0934 A72-20375
- Flight personnel statistical survey of clinical, physical and psychic causes of temporary and permanent flight service unfitness 07 p0923 A72-20447
- Permanent flight unfitness attributable to air service, noting orthopedic traumatic sequelae, cardiovascular illnesses, psychological and ophthalmological causes 08 p1125 A72-21273
- ECG diagnostics for arrhythmia assessment in flying personnel flight fitness examination 12 p1775 A72-28294
- Sight impairment-caused flight personnel disqualification analysis, establishing eye disease structure, sight damage preconditions and ophthalmological practice inadequacies 14 p2080 A72-30748
- Medical factors in air racing accidents, investigating drug, fatigue and gastrointestinal symptoms effects on pilot reaction to emergency 14 p2081 A72-31089
- Active leisure effect on pilot work efficiency, health maintenance and job longevity 19 p2760 A72-38148
- Professional capabilities activation of flying personnel, discussing psychological training for flight fitness 21 p3004 A72-40172
- The prediction of the condition of man during a space flight 22 p3149 A72-42067
- FLIGHT HAZARDS**
- NT METEOROID HAZARDS**
- Effective dose change after repeated radiation exposures as function of time intervals between fractions, evaluating space flight radiation hazards [CERN-71-16] 02 p0161 A72-12059
- CAT, cloud cover and icing forecasting for aviation in terms of numerical model and real atmosphere 04 p0542 A72-14689
- Medical and physiological hazards for SST passengers and crews, discussing cumulative cosmic radiation and high altitude decompression risks 11 p1583 A72-25816
- Aviation hazards due to stably stratified shear and turbulence zones, discussing meteorological analysis of 747 jumbo jet turbulence incident 13 p1994 A72-28865
- Stapedectomy postoperative complications as flying hazard, discussing pilot reaction to middle ear pressure changes 14 p2082 A72-31094
- Long range planning for the development of space flight emergency systems 17 p2620 A72-34428
- Spacecrews rescue requirements, considering escape capsules earth-based and orbit-based rescue systems and flight hazards 17 p2620 A72-34438
- Airline management and flight crew role in prevention, detection and dealing with airline pilot incapacitation in flight, noting physiological and psychological factor recognition 17 p2508 A72-34555
- Head-up display performance in Falcon fan-jet aircraft during taxiing, takeoff, cruise, descent and landing approach, noting low-visibility hazards reduction during landing phase 20 p2952 A72-39744
- Electrostatic charge on an aircraft and lightning striking the aircraft 21 p2994 A72-40171

FLIGHT INSTRUMENTS

A-690

- NT FLIGHT TEST INSTRUMENTS**
- NT GYRO HORIZONS**
- NT HORIZON SCANNERS**
- NT RADIO ALTIMETERS**
- Space shuttle orbiter flight instrumentation, data handling and communication requirements, discussing data gathering methods, crew displays, computer processing, recording and digital data bus telemetry 02 p0179 A72-12406
- Flight display systems current state and future developments, discussing dual attitude indicators and automatic chart systems CRTs, engine displays and malfunction warning systems 03 p0357 A72-13423
- Airline crew familiarization with DC-10 Computerized Flight Guidance System to calculate steering signal from raw data to follow flight path 19 p2831 A72-37899
- Area navigation and its affect on aircraft operation and systems design 19 p2831 A72-38125
- [AIAA PAPER 72-754] The evolution of head-up displays 20 p2925 A72-39333
- Variometer system for sailplanes sinking or climbing rates direct readout, describing pressure difference measuring concept based on reservoir-capillary system 21 p3051 A72-40225
- Aircraft instrument panel redesign to alleviate crew task, proposing integral displays and controls for flight information 21 p3080 A72-40291
- A new concept of flight displays compatible with digital airborne computers 21 p3012 A72-41426
- Evaluation of flight instrumentation for the identification of stability and control derivatives 22 p3136 A72-42346
- [AIAA PAPER 72-963] Variometer system for sailplanes sinking or climbing rates direct readout, describing pressure difference measuring concept based on reservoir-capillary system 23 p3292 A72-44451
- FLIGHT LOAD RECORDERS**
- Extreme value analysis of flight load measurements 24 p3367 A72-44737
- FLIGHT MECHANICS**
- Approximations and bifurcations in flight dynamic system, investigating singular point motion over trajectory during partition process 05 p0611 A72-16582
- Flight mechanics derivative transformations by matrix methods for changing coordinate or independent variable systems [DFVLR-SONDDR-175] 05 p0612 A72-16706
- Optimal design of dynamic system with universality for series of maneuvers with various degrees of informativeness, considering flight mechanics of limited power engine system 06 p0848 A72-18299
- Book on dynamics of atmospheric flight covering unsteady motion, small disturbance theory, aerodynamic characteristics, aircraft stability and control, handling qualities, etc 08 p1109 A72-21491
- Nonlinear dynamics of flight vehicle - Conference, University of Technology, Loughborough, England, March 1972 09 p1407 A72-23451
- Nonlinear dynamic motion response analysis of flight vehicles typified by continuously changing vibration damping and frequency 09 p1262 A72-23452
- Approximate method for nonlinear differential equations of motion solution in flight dynamics, applying to control surface buzz and slender wing oscillations 09 p1262 A72-23453
- Flight mechanics of point with limited power propulsion system and energy storage unit, investigating variational maximum payload problem with singular control optimization 11 p1727 A72-25932
- Lie group theory application to linear differential equations of motion with variable parameters, considering flight vehicle example 12 p1847 A72-28127
- Optimal design of dynamic system with universality for series of maneuvers with various degrees of informativeness, considering flight mechanics of limited power engine system 13 p2052 A72-29439
- Control function improvement method for flight dynamics variational problems solution, discussing dynamic programming, trajectories with uncontrolled elements and coordinate transformation 17 p2607 A72-35036
- Conventional aircraft flight mechanics, reviewing vector analytical treatment of rigid body statics 17 p2493 A72-35794
- Approximations and bifurcations in flight dynamic system, investigating singular point motion over trajectory during partition process 19 p2748 A72-37553

Flight-mechanical analysis of various flight conditions of conventional aircraft. V - Mechanical foundations /Dynamics of the rigid body/ 21 p2994 A72-40175

Flight mechanics of spin stabilized rotating disks for special ordnance delivery, considering aerodynamic parameters relation to dynamic stability and orientation [AIAA PAPER 72-982] 22 p3134 A72-42332

Flight mechanics analysis of various flight conditions for conventional aircraft. V - Mechanical foundations /Dynamics of rigid bodies/ 23 p3251 A72-43641

Flight mechanics aspects in space transportation system for international rescue, analyzing potential crises situations requiring emergency action 24 p3451 A72-45217

Atmospheric Flight Mechanics Conference, 2nd, Palo Alto and Moffett Field, Calif., September 11-13, 1972, Informal Papers. 24 p3361 A72-45326

Perturbation methods in atmospheric flight mechanics. 24 p3368 A72-45350

FLIGHT OPTIMIZATION

- Minimum flight time routes model at SST altitudes, taking into account temperature, meteorological and wind factors 04 p0542 A72-14678
- Time optimal trajectory graphical construction procedure from energy state approximation as basis of computational algorithm for real time onboard flight optimization [AIAA PAPER 72-123] 05 p0688 A72-16968
- Extremal field properties in optimal control problem applied to aircraft flight over assigned distance with minimum fuel consumption 06 p0758 A72-17727
- Aircraft performance and flight path optimization algorithms for minimum fuel-fuel range, using calculus of variations 07 p0912 A72-19091
- Extremal field properties in optimal control problem applied to aircraft flight over assigned distance with minimum fuel consumption 11 p1574 A72-25329
- Jet lift VTOL flight path optimization for minimum landing transition distance, evaluating deceleration as function of incidence and thrust vector angles 15 p2272 A72-32323
- Optimum turns to a specified track for a supersonic aircraft. 19 p2753 A72-38277
- Optimization of the wing parameters of a glider hovercraft 20 p2888 A72-39902
- Supersonic aircraft energy turns. 23 p3252 A72-44196
- Energy management during the space shuttle transition. 24 p3452 A72-45347
- Maximum principle and penalty function technique for flight optimization, noting optimal control for climbing flight 24 p3369 A72-45444

FLIGHT PATHS

- NT GLIDE PATHS**
- Soviet book on course-indicating systems and automatic navigation aids for civil aviation aircraft covering design, operation principles, error analysis and reliability 02 p0256 A72-12298
- Minimum flight time routes model at SST altitudes, taking into account temperature, meteorological and wind factors 04 p0542 A72-14678
- Pilot perception tests on estimating flight path inclination, ground image and touchdown time under poor visibility 05 p0684 A72-16180
- Sign behavior of switching function defined for plane fuel-optimal flight on elliptical coast trajectories 05 p0728 A72-16705
- Automated ATC guidance technique for aircraft curved flight trajectories, describing flight profiles synthesizing algorithms and computerized simulation technique [AIAA PAPER 72-121] 06 p0845 A72-17922
- Cockpit instrumentation for jet transport aircraft flight path management, emphasizing dependability, safety and economy 08 p1168 A72-21524
- Hypersonic vehicles lateral dynamics during great circle flight, using linearized equations of motion and Newtonian theory for stability derivatives estimation 08 p1110 A72-21603
- Shoran systems with onboard computers for aircraft position and trajectory parameters, noting coordinate plotting for flight path recovery maneuvers 13 p1996 A72-28785
- Thunderstorm encounter probability at SST altitudes for selected cross country routes, using radar observation data 13 p1992 A72-28853

Air Force Global Weather Central computer simulation of specific aircraft flight plans, using update weather information for specified route profile
13 p1924 A72-28873

Head-up display for aircraft three dimensional sky path observation during navigation and landing, discussing computer units, CRT and image generating subsystems
15 p2268 A72-32042

Great circle intermediate waypoint computation method for inertial navigation equipped aircraft
15 p2271 A72-32205

Jet lift VTOL flight path optimization for minimum landing transition distance, evaluating deceleration as function of incidence and thrust vector angles
15 p2272 A72-32323

Theoretical and experimental studies of the focus of sonic booms.
18 p2642 A72-36506

Optimum turns to a specified track for a supersonic aircraft.
19 p2753 A72-38277

Test of direct lift control in the case of the experimental aircraft DFVLR-HFB 320
20 p2888 A72-39934

VTOL aircraft noise reduction through design methods and flight path management in terminal area, evaluating acoustical annoyance to surrounding community
[ICAS PAPER 72-34] 21 p2995 A72-41159

Multioop piloting aspects of longitudinal approach path control.
[ICAS PAPER 72-46] 21 p2995 A72-41171

The effect of geometry on area navigation system errors.
22 p3203 A72-43132

Optoelectronic flight path tracking systems
24 p3380 A72-45274

Lateral flight path control during aircraft landing in gusty cross-winds by lateral thrust deflection, discussing design optimization
24 p3368 A72-45330

An investigation of parameters and factors governing manual control of STOL aircraft in landing approach.
[AIAA PAPER 72-987] 24 p3369 A72-45415

Lifting entry optimization equations for fixed angle of attack with path control for roll modulation of lift, considering space shuttle orbiter configuration
[AIAA PAPER 72-933] 24 p3443 A72-45435

FLIGHT PERFORMANCE
U FLIGHT CHARACTERISTICS
FLIGHT PLANS

Europa 2 launcher F 11 flight test review concerning countdown, flight plan and trajectory and organizational details
02 p0286 A72-12034

Flight planning by ATC, discussing problems due to runway feeding from several converging airways
03 p0386 A72-13415

MARS digital simulation model in GPSS for determining scheduled flight operations and maintenance resources effects on aircraft availability and usage rates
06 p0779 A72-17976

Automation in planning and execution of flights, considering navigation, communication, flight instruments monitoring, control/stabilization and warning systems
09 p1269 A72-22780

Military weather forecasting requirements by 1980, discussing decision making, data processing, satellite data, mission and terminal forecasts, display and computer flight planning
10 p1508 A72-25096

Air Force Global Weather Central computer simulation of specific aircraft flight plans, using update weather information for specified route profile
13 p1924 A72-28873

The Gander automated air traffic system.
19 p2830 A72-37748

Cost effective algorithm for optimal route aircraft scheduling for airlines by mixed integer multi-commodity flow technique and Dantzig-Wolfe decomposition
24 p3466 A72-44582

FLIGHT RECORDERS
Magnetic tape recorded flight data analysis by FORTRAN program
01 p0017 A72-10215

STRADA landing trajectory recording system for real time flight path restitution during approach and landing, using computer and lidar techniques
16 p2420 A72-32895

FLIGHT RULES
NT INSTRUMENT FLIGHT RULES
NT VISUAL FLIGHT RULES

German Federal Republic territorial air traffic regulations covering general, VFR and IFR rules, equipment and personnel examination and certification, safety, takeoff and landing, accidents, etc
02 p0305 A72-12621

Flight safety from general aviation viewpoint in West Germany, discussing ATC and flight rules relative to airspace use
[DGLR PAPER 72-036] 24 p3467 A72-44615

FLIGHT SAFETY
Control technique and flight quality for crew workload reduction to improve military and civil aircraft flight safety
03 p0310 A72-13640

Aircraft integrated data systems application to flight safety analysis, engine performance monitoring, crew proficiency, autoland evaluation, operations and logistics
04 p0495 A72-14726

Cockpit information for pilot and flight crew as key to transport aircraft accident prevention, discussing cockpit layout and displays in terms of flight safety requirements
04 p0464 A72-14813

Pilot in-flight incapacitation probability from airline reports, career termination studies and questionnaire responses
04 p0479 A72-14870

Flight safety and ATC planning in German Federal Republic and on international level, discussing regional control stations, radio frequencies, navigation systems, automation, etc
05 p0687 A72-16738

Tranquilizers effect on pilot in-flight performance, discussing flight safety, alcohol potentiating effect, student pilot stress reactions and airsickness treatment
06 p0768 A72-18158

Engine out flight training safety, recommending certification requirements or training procedures changes
07 p0911 A72-18834

Hypnotic drug use effect on pilot performance and flight safety, using glutethimide, flurazepam and placebo in double blind study
07 p0933 A72-20188

Disorientation in naval aircraft accidents from psychophysiological and environmental factors, suggesting flight scheduling and training improvements
08 p1126 A72-21574

Spectrometric oil analysis program (SOAP) method for turbojet and helicopter transmissions damage monitoring and flight safety
09 p1319 A72-22933

National and international legal aspects relative to levying user fees for flight safety services in Germany
11 p1748 A72-26560

Book on air transportation, covering history, government agencies roles in economic and safety regulation of air carriers, accounting, financial and legal aspects, etc
12 p1891 A72-28205

Aircraft copilot assistance to pilot in flight phases, emphasizing takeoff and landing and man machine system reliability
14 p2072 A72-30815

Avionics equipment for signal processing onboard civil aircraft to improve flight safety, discussing uses of OMEGA navigation system and digital computers
15 p2193 A72-31178

Civil aviation safety - Conference, Beirut, Lebanon, November-December 1971
16 p2481 A72-33326

FAA policy in issuing civil airport operating certificates and establishing minimum safety standards
16 p2373 A72-33330

Preventive and remedial space flight safety engineering, discussing escape capsules and onboard and earth-launched rescue systems
17 p2620 A72-34427

Functional equipment active and standby redundancy for flight safety and air traffic punctuality improvement, noting Boeing 747 aircraft redundant systems
17 p2492 A72-35476

The onboard authority of the aircraft commanding officer as provided by the 1963 Tokyo Convention
17 p2639 A72-35763

Resumption of flight after retinal surgery
19 p2670 A72-37879

Future aspects of business aviation, discussing pilot training and aircraft reliability and maintenance in context of flight safety
20 p2988 A72-39741

Flight safety research, discussing NASA aviation hazards R and D programs involving fire, lightning and static, steep approaches, aircraft wakes, fog and visibility
20 p2888 A72-39742

Trends in the control of air-traffic flows in the air space
23 p3311 A72-43640

Flight safety from general aviation viewpoint in West Germany, discussing ATC and flight rules relative to airspace use
[DGLR PAPER 72-036] 24 p3467 A72-44615

Air traffic, collision risks, defense zones, airspace structure and central planning agency for flight safety problems reform
[DGLR PAPER 72-038] 24 p3467 A72-44617

Airline operational problems from traffic volume increase, discussing flight safety, passenger comfort, schedule adherence and economy aspects
[DGLR PAPER 72-037] 24 p3467 A72-44618

Government, military safety, police permission and insurance regulations for European rocket activities
24 p3467 A72-45124

Nuclear safety in nuclear power and propulsion devices for space.
24 p3424 A72-45180

Human organism and space flight stress endurance limits and manned space mission rescue capabilities requirements, considering cabin decompression, anoxia, radiation, onboard illness, etc
24 p3376 A72-45218

FLIGHT SIMULATION
Flash blindness effects during flight simulation, investigating recovery time
[AD-742863] 01 p0022 A72-11296

Three-axis flight table with dc torque motors, discussing servo loops design and mechanical oscillations frequencies
02 p0257 A72-12541

Dynamic test facility for Symphony satellite attitude control, discussing sun and earth sensors and analog computer for motion simulator
05 p0643 A72-16432

Electrofluid-dynamic wind tunnel velocity augmentation by enthalpy addition during expansion at constant static pressure and temperature for aerospace vehicles flight conditions simulation
[AIAA PAPER 72-166] 05 p0645 A72-16831

Adaptive model following control systems design by hyperstability approach for flight control and simulation
[AIAA PAPER 72-95] 05 p0613 A72-16956

Boeing 347 helicopter program, discussing simulation, wind tunnel, whirl tower, bench testing, flight test development and demonstration
05 p0614 A72-16993

Fast time simulation application to ATC systems, discussing control action exercise within strategic/tactical spectrum
05 p0645 A72-16994

Lightning simulation laboratory for aircraft strike testing, using high energy generators
07 p0964 A72-18774

Digital simulation model of N helicopter formation flight characterized by close aircraft spacing, parallel flight vector and low bandwidth external forcing functions
07 p0913 A72-20354

Space shuttle phase B design studies regarding configurational alternatives, propulsion systems, displays and controls, simulations and flight test programs
08 p1240 A72-21009

Pilot glide slope and localizer tracking performance during successive in-flight simulated ILS approaches
12 p1773 A72-28260

Pilot pursuit tracking performance under acceleration stress, simulating high performance aircraft dynamics via human centrifuge equipped with simulated head-up predictive gunsight
12 p1776 A72-28320

Time perception distortion level in simulated and real flight due to task complexity-related pilot emotional stress
14 p2078 A72-30392

Cost-saving techniques in helicopter structural test methods, suggesting system simulation, component replacement time calculation and computer techniques
16 p2373 A72-33221

A new approach to a cruise navigator evaluation using sparse reference data.
[AIAA PAPER 72-835] 20 p2950 A72-39092

Aircraft radar for weather data, ground mapping, avoidance modes and independent landing monitor function, presenting straight and slant approach simulation data
21 p3080 A72-40290

The airborne visual simulation as an electronic display.
21 p3010 A72-41410

FLIGHT SIMULATORS
NT COCKPIT SIMULATORS
Flight training simulator programming, noting operation under real time executive
02 p0199 A72-11653

Toulouse-Bretigny link involving ATC and flight simulators with Concorde cockpit replica
04 p0545 A72-15072

Spherical air bearing supported test facility for satellite attitude control system performance testing, discussing motion simulator and automatic balancing system
05 p0643 A72-16435

Flight simulator for aircraft design, emphasizing compromise between performance and control requirements to avoid excess weight and drag
06 p0796 A72-18245

Aircraft safety enhancement by computer controlled flight simulator training of air crews, discussing Boeing 747 program
07 p0926 A72-18839

Night Carrier Landing Trainer flight and carrier environment simulator for A-7 aircraft pilot training, discussing performance predictions from computer data analysis

07 p0927 A72-19137

Hypoxia effect on aircraft pilot performance during altitude and flight simulation, testing instrument landing approaches

[AMRL-TR-71-97]

07 p0933 A72-20186

Flight crew training programs cost and quality, emphasizing safety and flight simulator application

11 p1590 A72-26998

Large amplitude flight simulator for fighter design refinement, noting extensive computer commitment

13 p1938 A72-28757

Aircraft and other vehicle simulators for training crews, discussing evolution of needs, digital techniques, and visual and physiological experiences

14 p2092 A72-30844

Low cost flight simulator for general aviation pilot training, containing IFB instrumentation and turbulence injection device

15 p2214 A72-32211

Flight training simulator criteria and design considerations, noting avionics, model aircraft, control console and teaching aspects

16 p2374 A72-33501

Digital computer controlled flight simulators for undergraduate pilot, electronic warfare, air-to-air combat and helicopter training

17 p2535 A72-34393

Simulated blind approach trainer for general aviation aircraft pilot training, discussing design concept and instrumentation with emphasis on components simplicity and economy

17 p2536 A72-35325

How United trains DC-10 pilots.

19 p2760 A72-37898

Use of the flight simulator in the design of a STOL research aircraft.

[AIAA PAPER 72-762]

19 p2751 A72-38129

Naval air test center participation in development of air-to-air combat simulation.

[AIAA PAPER 72-765]

19 p2783 A72-38130

Survivable flight control system compatibility test program.

[AIAA PAPER 72-761]

19 p2752 A72-38143

Advanced fighter controls flight simulator for all-systems compatibility testing.

[AIAA PAPER 72-837]

20 p2911 A72-39090

Studies in pilot training - The anatomy of transfer.

20 p2897 A72-39718

Use of fixed and moving base flight simulators for the aerodynamic design and development of the S-3A airplane.

[AIAA PAPER 72-764]

20 p2888 A72-40052

FLIGHT STABILITY TESTS

Direct side force control by rudder deflection and asymmetrical drag utilization to cancel yawing moment, discussing variable stability T-33 flight tests

[AIAA PAPER 72-94]

05 p0613 A72-16946

Flight test instrumentation system for measurement of aircraft performance, stability and control characteristics during nonsteady flight

16 p2349 A72-33639

Flight test evaluation of a fluidically actuated monopropellant hydrazine roll control system.

[AIAA PAPER 72-975]

24 p3452 A72-45410

FLIGHT STRESS

Transmeridian flight psychological effects on aircrews, discussing anxiety, stress, circadian rhythm disruption and sleep loss effects on performance deterioration

06 p0766 A72-17816

Changes in the functional state of analysts in flying personnel during long flights

21 p3006 A72-40445

FLIGHT STRESS (BIOLOGY)

NT SPACE FLIGHT STRESS

Ground and flying activity endurance training effect on urinary excretion of noradrenaline and adrenaline

04 p0478 A72-14868

Tranquilizers effect on pilot in-flight performance, discussing flight safety, alcohol potentiating effect, student pilot stress reactions and airsickness treatment

06 p0768 A72-18158

Work-rest schedules endocrine and metabolic effects on aircrews during 50 hour flight missions in C-141 aircraft, using urinary test techniques

[AD-740992]

10 p1428 A72-23737

Case report of fighter pilot disorientation episode during night flying exercise, suggesting psychological stress factor

11 p1584 A72-26019

Flight stress and performance of training in general aviation simulator compared with actual flight

12 p1774 A72-28261

Anxiety relation to success or failure in naval flight training program

12 p1774 A72-28263

Mathematical expression for pilot incapacitation applied to data from high stress/short duration encounters with environmental problems

12 p1775 A72-28284

Time perception distortion level in simulated and real flight due to task complexity-related pilot emotional stress

14 p2078 A72-30392

Low-altitude flight imposed psychophysiological stresses due to air turbulence discomfort, instrumental vibration and ground-based navigational objects recognition difficulty

14 p2080 A72-30747

Russian book - Theory and practice of aviation medicine

19 p2760 A72-37447

Professional capabilities activation of flying personnel, discussing psychological training for flight fitness

21 p3004 A72-40172

FLIGHT TEST INSTRUMENTS

DAMIEN III digital magnetic tape recording system for aircraft flight test data acquisition, discussing components

16 p2393 A72-33629

Flight test instrumentation system for measurement of aircraft performance, stability and control characteristics during nonsteady flight

16 p2349 A72-33639

Serial PCM system for flight test data acquisition and reduction compared with Harrier system

16 p2364 A72-33644

Engine compressor face rake for flight test instrumentation F-14A/TF-30.

22 p3216 A72-42686

FLIGHT TEST VEHICLES

B-52 test vehicle flight demonstration program for control configured vehicles (CCV) technology concepts validation, noting gross weight reduction

[AIAA PAPER 72-747]

19 p2751 A72-38123

FLIGHT TESTS

NT FLIGHT STABILITY TESTS

TriStar commercial jet transport aircraft development, discussing design and flight tests for operating efficiency, reliability and safety

[SAE PAPER 710755]

01 p0003 A72-10252

Concorde airworthiness certification, discussing ground and flight test programs for performance, flying qualities and structures fatigue properties evaluation

[SAE PAPER 710756]

01 p0003 A72-10253

Flight test procedures for subsonic transport aircraft pilot static pressure system, recommending trailing cone calibration method

[SAE ARP 921]

01 p0064 A72-10389

Microwave hologram CW radar system, discussing theory and flight test imagery, optical processors and alignment procedures

02 p0171 A72-11819

Europa 2 launcher F 11 flight test review concerning countdown, flight plan and trajectory and organizational details

02 p0286 A72-12034

Army data analysis system for fixed and rotary wing aircraft flight testing, including airborne and computer controlled ground stations equipment

02 p0179 A72-12408

Flight vibration testing methods for ascertaining flutter stability of high speed aircraft

[DGLR PAPER 71-083]

02 p0155 A72-12725

Dynamic damping coefficient extraction from reentry vehicle flight test telemetered lateral rate data

03 p0441 A72-13951

F-14A fighter accelerated flight test program with 18-month saving and 3600 flight time hours before 1973 operability

04 p0464 A72-14591

Automated telemetry system providing real time analytical capability and reduction of flight test time for F-14

04 p0486 A72-14592

Meteorological information assistance for Concorde aircraft flight tests, discussing high tropospheric turbulence and lower stratospheric temperature predictions and instruments

04 p0542 A72-14680

Lifting reentry vehicle Bumerang design and development, discussing experimental verification of theoretical design concepts by aircraft launched unmanned flying model

05 p0724 A72-16312

U.S. Navy automatic carrier landing system (ACLS), discussing shore and ship based test techniques and problem areas

05 p0686 A72-16654

A-7 D/E navigation/weapon delivery system flight testing, using photogrammetric technique

05 p0663 A72-16656

Flight testing of Army helicopters terrain following and/or avoidance systems concepts for operational capability, performance and cost evaluation

05 p0686 A72-16658

NF-8D aircraft variable stability system ground/in-flight calibration for determination of flight control system dynamics effects on flying qualities

05 p0611 A72-16660

Navy hovering vehicle versatile automatic control system for V/STOL flight test program, using airborne

digital computer for navigation/guidance computations

05 p0687 A72-16661

Aircraft flight control system MTBF field operational and MIL-STD-781 testing, establishing data baseline for reliability predictions

05 p0638 A72-16662

BQM-34A and E/F target drone aircraft versatile automatic flight control system flight test program and results for basic and advanced flight modes

05 p0687 A72-16663

Flight test evaluation of A-7D/E emergency backup flight control system, describing hydraulic power control systems design and function

05 p0687 A72-16664

Unmanned systems flight testing by test bed vehicle conversion to man operated mode, discussing T-33A jet trainer conversion to drone operation

05 p0623 A72-16665

Model following variable stability system for X-14B VTOL aircraft, discussing hardware design and flight evaluation

05 p0613 A72-16978

Boeing 347 helicopter program, discussing simulation, wind tunnel, whirl tower, bench testing, flight test development and demonstration

05 p0614 A72-16993

F-14 Tomcat test program for hydraulic systems, spinning, low speed performance, stalling, afterburning turbofan engines, in-flight refueling and automatic telemetry equipment

06 p0758 A72-17582

Papers on critical and exploratory flight testing covering rotary wings, lifting bodies and jet engine airstart

06 p0758 A72-18487

Procedures followed by test pilot on first flight of new aircraft design

06 p0758 A72-18488

Structural demonstration flight testing /U.S. Navy/ of new aircraft, presenting maneuver checklist

06 p0759 A72-18489

Airloads and structural integrity flight testing /U.S. Air Force/, noting dynamic response, fatigue tests and temperature data acquisition

06 p0759 A72-18490

Flight flutter boundary testing, describing steps to minimize risk

06 p0759 A72-18491

Flight initial spin testing, discussing aircraft autorotation due to stalled angle of attack and sideslip

06 p0759 A72-18492

Rotary wing aircraft first flight and envelope expansion at design gross weight

06 p0759 A72-18493

Rocket powered air launched lifting body reentry vehicles testing, stressing performance, handling qualities and crew preparation

06 p0892 A72-18494

Airstart flight testing for single engine fighter/attack aircraft, including flight conditions, windmilling, fuel flows, gas temperature, ignition and acceleration

06 p0868 A72-18496

Weapon firing and external store separation tests by flight test methods for determining safe weapon release envelope

06 p0759 A72-18499

Thunderstorm flight testing for evaluation of rain, ice, lightning and turbulence effects on aircraft, engine and systems operating characteristics

06 p0760 A72-18500

Federal Air Regulations procedures for civil transport aircraft flight testing under natural and/or simulated icing conditions

06 p0760 A72-18501

Crashproof rotorcraft STOL aircraft for rescue operation, discussing orthodox rigid and special rotary wings design, air tunnel experiment and flight tests

06 p0760 A72-18582

VAK 191 B V/STOL reconnaissance fighter prototype test program, describing simulations, bench, ground, static, hovering and flight tests

07 p0912 A72-19249

Tactical missile controlled test vehicle flight test analysis by six-degree-of-freedom digital simulation

07 p1086 A72-20351

F-14 naval fighter aircraft flight test programs, discussing instrumentation and low-speed test results

08 p1108 A72-21005

Test pilot role in attack aircraft avionics systems integration consisting of head-up display, projected map, digital computer, inertial platform, radar and Doppler systems, etc

08 p1165 A72-21012

Inflight validation of laboratory scaled-down simulation experiments on optimal hierarchy of colors for markers and signals

[AD-737901]

Olympus engine flight testing for relighting and anti-icing, engine control and noise and vibration assessments in support of Concorde aircraft development

08 p1224 A72-21898

Airfoil ram-wing air-water hybrid vehicle X-113 AM design and operational principles based on

aerodynamic ground effect, discussing flight tested performance characteristics

09 p1262 A72-22971

Flight testing of automated modular area navigation system for L-1011, describing computer, data storage and control-display units and electronic automatic chart system

10 p1509 A72-24271

Thermal diode heat pipe for advanced thermal control flight experiment, discussing engineering model analysis, design, fabrication and test

[AIAA PAPER 72-260]

11 p1739 A72-25205

Control surface dynamic hinge moment coefficients estimation based on system state measurements from flight tests, using least squares criterion

[AIAA PAPER 72-379]

11 p1730 A72-25403

Aircraft wing structure fatigue life estimates based on flight load time histories from counter accelerometers

[SAE PAPER 720305]

11 p1733 A72-25569

Flight tests of combination flight director displayed and attitude command control system effect on and attitude command control system effect on general aviation aircraft handling qualities during ILS approach

[SAE PAPER 720316]

11 p1575 A72-25580

Supercritical thick wing for structural weight reduction and increased cruise speeds flight tested on Navy T2-C aircraft

[SAE PAPER 720320]

11 p1576 A72-25583

Cessna 210 aircraft electrically driven hydraulic power pack for landing gear system, noting engine and flight tests

[SAE PAPER 720327]

11 p1577 A72-25589

Boron/epoxy and graphite/epoxy composites application to aircraft structural design, discussing flight test and developmental programs

11 p1577 A72-26234

German VAK 191B V/STOL fighter aircraft design, development and flight tests, noting redundant control systems

12 p1753 A72-27166

Parachute based recovery system for experimental lifting body LB-21 developed and flight tested

12 p1877 A72-27411

Flight tests of stability augmentation system for light airplane improving pilot control during IFR encounter

12 p1754 A72-27513

Man computer weapons effectiveness and system test environment /WESTE/ instrumentation system with Decca navigation for simulated combat environmental flight tests

12 p1754 A72-27515

Project pilot criteria for preparation and execution of flight test specifications

12 p1754 A72-27517

L-1011 flight test program, discussing aircraft design, flight station, controls, flying qualities, etc

12 p1754 A72-27519

Flight test of direct side force control by rudder deflection and asymmetrical drag on T-33 airplane, noting use in dive bombing

12 p1754 A72-27520

Weapon systems reliability assessment based on limited prototype flight test results

13 p1962 A72-28359

Concorde dynamic behavior from flight tests, discussing integrated design effects, wing, fin and elevator flutter, gust and runway response and engine surge effects

[AIAA PAPER 72-381]

13 p1897 A72-28958

Airborne OMEGA navigation system performance, discussing transmission facilities, three frequency receiver, flight tests and optimization of receiving antenna

13 p1998 A72-29191

Preproduction OMEGA aircraft receivers and antennas development and flight testing, noting signal loss problems in high noise or precipitation static environments

13 p1998 A72-29198

OMEGA receiver integration into Navy P-3C airborne computerized navigation system, describing flight test, maintainability and laboratory simulation programs

13 p1999 A72-29202

Test flights into weather at midlatitudes and tropical systems with airborne OMEGA navigation system, discussing E field and H field antennas

13 p1999 A72-29203

VFW 614 twin jet transport aircraft flight test program, detailing general task plan, test equipment installations and test schedule

14 p2072 A72-30679

Inclined wind tunnel test section for free gliding investigation and aerodynamic design of flexible wing two body system

15 p2213 A72-31403

Flight experiments to determine horizontal visual restriction effects on T-33 aircraft front cockpit during approaches and landings

15 p2180 A72-31697

Cassiopeia attitude control apparatus flight tests on Tacite rocket, describing aiming accuracy, target acquisition and gas consumption

15 p2321 A72-31824

Dynamic input to cargo in turbojet aircraft studied during C141 and CSA flights, discussing instrumentation, test procedures, data reduction processes and results

15 p2181 A72-32625

Bumerang lifting body design for reentry vehicles, discussing optimal configurations and experimental flight testing

16 p2462 A72-33050

Autoland system flight testing in Trident 3B and British Civil Aviation Authority approval for ICAO Cat 3a weather

16 p2420 A72-33539

Airborne flight test data acquisition system modular design to provide digital readings from monitoring transducers analog signal

16 p2364 A72-33645

SECANT collision avoidance system, describing operational principles and flight test results

16 p2421 A72-34137

Helicopter testing of inertial navigation systems. [AHS PREPRINT 634]

17 p2578 A72-34478

S-67 flight test program. [AHS PREPRINT 653]

17 p2488 A72-34479

Flight investigation of design features of the S-67 winged helicopter. [AHS PREPRINT 601]

17 p2488 A72-34485

Helicopter stability derivative extraction and data processing using Kalman filtering techniques. [AHS PREPRINT 641]

17 p2490 A72-34501

A pilot's opinion - VTOL control design requirements for the instrument approach task. [AHS PREPRINT 644]

17 p2490 A72-34504

The world speed records of the SA 341 - Gazelle. [AHS PREPRINT 651]

17 p2491 A72-34506

Flight tests correlation with mathematical models to predict electro-optical viewing systems capability for military missions

17 p2557 A72-35553

Configuration and flight test of the only operational Air Force area navigation system.

17 p2578 A72-35557

USAF development of electrostatic gyros for inertial air navigation, noting flight tests and associated airborne digital computer

17 p2578 A72-35558

Aircraft flight test facilities deficiencies and modernization impediments, recommending integrated facility research program establishment

19 p2783 A72-37676

A time-frequency high performance collision avoidance system. [ONERA, TP NO. 1091]

19 p2830 A72-37764

Flight test report on L-1011 aerodynamic characteristics, discussing high and low speed performance, stability and control, stall behavior, etc

19 p2748 A72-38030

VJ-101 V/STOL aircraft design, development and flight testing, discussing takeoff and landing, hovering and transition flight and associated control problems

19 p2749 A72-38032

Real time flight flutter testing via Z-transform analysis technique. [AIAA PAPER 72-784]

19 p2749 A72-38101

The development of dynamic flight test techniques for the extraction of aircraft performance. [AIAA PAPER 72-785]

19 p2749 A72-38102

Flyover noise testing of commercial jet airplanes. [AIAA PAPER 72-786]

19 p2749 A72-38103

Status of U.S. Navy stall/post-stall/spin flight testing. [AIAA PAPER 72-787]

19 p2749 A72-38104

A-X Air Force flight evaluation. [AIAA PAPER 72-770]

19 p2751 A72-38131

Generating high Reynolds-number flows. [AIAA PAPER 72-770]

19 p2787 A72-38222

A generalized method for the identification of aircraft stability and control derivatives from flight test data.

19 p2753 A72-38260

Flight-test experience in digital control of a remotely piloted vehicle. [AIAA PAPER 72-883]

20 p2889 A72-40059

Design and flight experience with a digital fly-by-wire control system using Apollo guidance system hardware on an F-8 aircraft. [AIAA PAPER 72-881]

20 p2889 A72-40060

F-111A inlet nozzle dynamic distortion diagnostics for airframe-propulsion integration based on flight and transonic wind tunnel tests [ICAS PAPER 72-18]

21 p2991 A72-41143

Improved qualitative flight data rating scales. [AIAA PAPER 72-883]

21 p2996 A72-41257

Ground and flight tests of the Ramzes rocket sonde. [AIAA PAPER 72-883]

21 p3115 A72-41499

Flying experience with the SC1 research aircraft and the PI127 prototype at the Royal Aircraft Establishment, Bedford, England.

22 p3136 A72-42324

Flight test studies of the formation of trailing vortices and a method to accelerate vortex dissipation. [AIAA PAPER 72-988]

22 p3134 A72-42327

Applications of a technique for estimating aircraft states from recorded flight test data. [AIAA PAPER 72-965]

22 p3138 A72-42360

Ka-26 helicopter operational flight testing in high mountain environment, discussing takeoff, landing and climb performance as function of altitude dependent engine characteristics

23 p3251 A72-43638

Influence of wing deformations measured during flight tests upon the flight performance of a glider made of synthetic materials. I

23 p3252 A72-44452

The fatigue and fail-safe program for the certification of the Lockheed Model 286 rigid rotor helicopter. [AIAA PAPER 72-965]

24 p3366 A72-44733

Flight test investigation of the aerodynamic behavior of various-sized stabilizers on a small helicopter.

24 p3362 A72-45328

Determination of aerodynamic drag from radar data. [AIAA PAPER 72-1008]

24 p3362 A72-45337

SAM-D control test vehicle trajectory planning and flight test analysis.

24 p3451 A72-45338

Transonic wall interference effects on bodies of revolution. [AIAA PAPER 72-1008]

24 p3389 A72-45404

FLIGHT TIME Minimum flight time routes model at SST altitudes, taking into account temperature, meteorological and wind factors

04 p0542 A72-14678

Aircraft on-time operation and air traffic problems, considering solution requirement formulation and funding suggestions

15 p2339 A72-32462

FLIGHT TRAINING NT SPACE FLIGHT TRAINING

Instrument flying skills retention, discussing initial training, discrete procedural and tracking responses

01 p0018 A72-10564

Flight training simulator programming, noting operation under real time executive

02 p0199 A72-11653

Student naval aviator selection by multiple correlation technique using noncognitive college and flight background questionnaire to reduce attrition rate

02 p0166 A72-11704

Ground and flying activity endurance training effect on urinary excretion of noradrenaline and adrenaline

04 p0478 A72-14868

Engine out flight training safety, recommending certification requirements or training procedures changes

07 p0911 A72-18834

Aircraft safety enhancement by computer controlled flight simulator training of air crews, discussing Boeing 747 program

07 p0926 A72-18839

Instructor station design for automated flight training systems, considering human factors and informational requirements

07 p0928 A72-19277

Flight crew training programs cost and quality, emphasizing safety and flight simulator application

11 p1590 A72-26998

Factor analysis of grades for successful performance skill identification during undergraduate and graduate jet pilot training

12 p1769 A72-27472

Flight stress and performance of training in general aviation simulator compared with actual flight

12 p1774 A72-28261

Anxiety relation to success or failure in naval flight training program

12 p1774 A72-28263

Pilot landing performance prediction criteria based on day and night carrier qualification trials and flight training

14 p2081 A72-31084

ECG heart rate recording of helicopter instructor pilots during flight training tasks, administrative work, automobile driving and eating

14 p2082 A72-31097

Military aviation navigator training, discussing objectives, methods, instructors and equipment

15 p2272 A72-32207

Canadian Armed Forces air navigation training program, noting emphasis on training flights

15 p2272 A72-32209

USAF Academy air navigation training program, discussing systems development course and descriptive and applied astronomy

15 p2272 A72-32210

Flight training simulator criteria and design considerations, noting avionics, model aircraft, control console and teaching aspects

16 p2374 A72-33501

Effects of instructions on measures of state and trait anxiety in flight students.

17 p2507 A72-34464

Professional capabilities activation of flying personnel, discussing psychological training for flight fitness 21 p3004 A72-40172

Problems arising in the transfer of training from simulated to real control systems. 21 p3010 A72-41412

FLIGHT VEHICLES

Air law concept as totality of legal regulations related to atmosphere use by flying devices, discussing relation to international environmental protection 01 p0147 A72-11107

Airborne computer programmed adaptive optimal control for subsonic vehicle automatic landing with aerodynamic performance 05 p0685 A72-16430

Nonlinear control systems of vehicles angular orientation, investigating dynamic properties by method of harmonic linearization 05 p0727 A72-16474

Air jet propelled flight vehicles optimal design parameters for constant altitude flight at given speed 07 p0911 A72-18991

On-line digital computer maximum likelihood estimate of Earth atmosphere profile ahead of flight vehicle using discrete measurements of density, temperature and pressure [AD-739472] 08 p1156 A72-20853

Towed cable flight vehicle system motion in uniform flow field, calculating equilibrium configuration during coordinated turn from two point boundary value problem numerical solution 08 p1110 A72-21604

Tube flight vehicle system thrust and power requirements prediction by aerodynamic analysis with division of near and far flow fields 08 p1107 A72-21608

Flying machine using reaction forces on body moving in compressible fluids within piston device equivalent to air pressure pump 08 p1108 A72-21798

Soviet book on control system technology for flight vehicles covering production of mechanical, hydraulic, pneumatic, electric and electronic elements 08 p1179 A72-22024

Nonlinear dynamics of flight vehicle - Conference, University of Technology, Loughborough, England, March 1972 09 p1407 A72-23451

Nonlinear dynamic motion response analysis of flight vehicles typified by continuously changing vibration damping and frequency 09 p1262 A72-23452

Flight vehicle angular velocity measurement by accelerometers, deriving equations of motion 10 p1481 A72-24497

Flight vehicle structures optimum design for random vibration environment, presenting formulation as nonlinear programming problem 11 p1736 A72-26003

Complete and simplified equations of motion for rate gyro installed in flight vehicle, taking into account bearing torques [DFVLR-SONDDR-190] 11 p1635 A72-26580

Flight vehicle motion described by linear differential equations with variable parameters, discussing programmed optimal control solution by functional analysis 12 p1755 A72-28128

Axisymmetric flight vehicles motion stability and transient behavior via Liapunov method, taking into account nonlinear characteristics 15 p2318 A72-31203

Flight vehicle, control system and perturbations models synthesis from variational problem solution via control functions improvement 17 p2621 A72-35037

Russian book - Calculation and analysis of flight-vehicle motion: Engineering handbook 17 p2492 A72-35451

Russian book - Assembly and testing of hydraulic and pneumatic systems of flight vehicles 19 p2753 A72-37300

Experimental results regarding drag in supersonic flow without lift in the case of flight bodies with three in front pointed bodies [DFVLR-SONDDR-215] 19 p2747 A72-38686

Despun conical flight vehicles eccentric insulation mass properties history, deriving preflight and in-flight equations for weight, center of gravity coordinates and moments and products of inertia [SAWE PAPER 938] 23 p3342 A72-43478

Stochastically optimal terminal control system synthesis for loss function dependence on finite phase coordinates of dynamic system, considering soft landing of flight vehicle 23 p3275 A72-43781

FLIP-FLOPS

Contacting-both-wall switching transients of bistable fluidic amplifiers with low setbacks, including unsteady effects in jet and attachment zone [ASME PAPER 71-WA/FLCS-6] 05 p0615 A72-15917

Optimization algorithm for minimum margin efficiency of electronic circuits, applying to IC TTL gate and transistorized bistable multivibrator /flip-flop/ 07 p0944 A72-19568

Sequential machine realization with trigger or flip-flop elements and Boolean function feedback 10 p1445 A72-24401

Fluid amplification principles, discussing bistable and proportional amplification, signal transmission and transduction to and from fluid signals [ASME PAPER 72-DE-20] 14 p2073 A72-30864

Fluidic digital logic devices vs electrochemical-electronic equivalents, describing Coanda effect application to bistable jet amplifiers /flip-flops/ as switching or memory devices 15 p2182 A72-31218

Optimization algorithm for minimum margin efficiency of electronic circuits, applying to IC TTL gate and transistorized bistable multivibrator /flip-flop/ 22 p3158 A72-42086

FLOATING

Interface stability of floating liquid zones of water/ethanol solutions in simulated zero gravity 07 p1036 A72-20561

Flow equations for floating body flowmeters, discussing density and viscosity effect, instrument characteristics and computer algorithms 14 p2104 A72-30484

Floating forces contribution to heat flux during turbulent mixing of upper atmosphere 16 p2417 A72-33292

FLOATING POINT ARITHMETIC

Floating point cellular logic multiplier with variable dynamic range suitable for scientific satellites, missiles, desk calculators and cellular computers 04 p0499 A72-15208

Coefficient rounding effect in digital filters using floating point arithmetic 05 p0633 A72-16576

Digital control system instability caused by introduction of floating point arithmetic in controller 09 p1341 A72-23096

Floating point arithmetic operators with variable dynamic range and multiple precision, noting word method for numerical data processing in computation and process control 12 p1787 A72-27666

An algorithm in arithmetic with a floating point to increase the accuracy of a sum 17 p2575 A72-34906

Gaussian elimination with floating point arithmetic, discussing algorithm for least squares scaling of matrices with less error than row and column norms equilibration 21 p3076 A72-41317

FLOATS

Parachute systems and flotation gear used to recover sounding rocket payloads and components after water landings 15 p2320 A72-31691

FLOOD PREDICTIONS

Rain induced flood mathematical model, optimizing parameters and applying to hydrological forecasts 07 p1029 A72-18862

Hydrologic data collection via ATS 1 satellite for river and flood forecast of National Weather Service, planning geostationary operational environmental satellites /GOES/ 09 p1296 A72-22315

FLOODS

NT FLOOD PREDICTIONS

FLOORS

Thin airfoil and bridge deck flutter derivative from transient oscillatory states in test procedure 02 p0298 A72-12665

FLORA

U PLANTS (BOTANY)

FLORIDA

Southeast Florida 13 year urban and agricultural development recorded by high altitude color and color-IR photographs, demonstrating capability for detail and macroscale patterns 02 p0230 A72-12199

FLOTATION SYSTEMS

U FLOATS

FLOW CHARACTERISTICS

NT BOUNDARY LAYER STABILITY

NT FLAME STABILITY

NT FLOW DISTRIBUTION

NT FLOW STABILITY

NT FLOW VELOCITY

NT MAGNETOHYDRODYNAMIC STABILITY Fluid flow numerical solution by contour dynamics methodology with flow features resolution advantage 01 p0049 A72-10227

Flow in turbulent trailing vortex, considering circulation profiles and Reynolds stress distribution [AD-740436] 01 p0049 A72-10232

Flow characteristics, wave propagation and thermal stability of ferrofluids within uniform magnetic field 01 p0050 A72-10235

Parachutes flow characteristics in low speed free descent, discussing glide angle effect on total drag and water channel flow pattern studies 01 p0004 A72-10309

Chapman-Korst model for prediction of flow characteristics within plume induced boundary layer separation in rocket propelled vehicles during power-on maneuvers 01 p0050 A72-10376

Flow momentum losses during gas mixture chemically nonequilibrium expansion in nozzle 01 p0145 A72-10487

Boundary conditions for monatomic gas flow in constant cross section channel with heat supply and ionization 01 p0111 A72-11211

Flow characteristics of colloid core reactor rocket engine, studying two component vortex flows with solid to gas mass density ratios over 100 [AD-735527] 01 p0100 A72-11359

Axisymmetric inviscid compressible transonic flow of electrically conducting, heat nonconducting gas in Laval nozzle in presence of meridional magnetic field, deriving equations for magnetic effects on dynamic flow characteristics 02 p0149 A72-11576

Explosion induced plane shock wave propagation in gas medium with exponential density distribution, determining gas flow behavior by difference approximation method 02 p0201 A72-11578

Cross flow through in-line tube bank, investigating surface roughness effects on behavior by pressure drop, static pressure and skin friction distributions measurements 02 p0203 A72-12102

Flow characteristics of pin type nozzles in constant pressure carburetors of Otto cycle engines 02 p0206 A72-12853

German monograph on gas type and nozzle flow conditions effect on condensed molecular jets properties 03 p0391 A72-13275

Chaplygin compressibility law in calculation of flow characteristics around compressor blading of axial turbomachines 03 p0308 A72-13544

Dynamic and electromagnetic characteristics of MHD flow in square tube with walls differing in electroconductivity within oblique transverse magnetic field 03 p0398 A72-14007

Flow development in gas nozzles with depressive networks, describing geometric and functional characteristics 04 p0510 A72-14467

Kinetic rate theory extended to time dependent flow behavior of viscoelastic materials /polymers/ under constant stress and shear 04 p0512 A72-15263

Non-Newtonian real fluids flow characteristics, determining stress-deformation relationship by tensor analysis, with application to lubrication theory 04 p0528 A72-15742

Hypersonic boundary layer displacement interaction and surface curvature effects, employing implicit finite difference methods 05 p0603 A72-16803

Trajectory and flow properties of submerged heated effluents discharging into moving waterway [AIAA PAPER 72-79] 05 p0659 A72-16912

Internal compressible spatially nonuniform ducted flow performance, defining diffuser efficiency, loss coefficient and static pressure rise coefficient [AIAA PAPER 72-85] 05 p0652 A72-16960

Marginally unstable plane parallel flow nonlinear response to two dimensional disturbance, noting localized burst relationship to Landau constant 06 p0801 A72-18163

Blading, flow and characteristic line calculations for machine with axial turbulent flow, using plane cascade measurements 06 p0757 A72-18690

Thermally induced convection flow characteristics in separated or wake formation regions over heated cylindrical surface submerged in water 07 p1100 A72-19630

Wall stabilized dc arc channel for plasma viscosity and flow characteristics studies, using pressure probe 07 p1043 A72-19877

Hydraulic servomechanism spool type control valve orifice flow characteristics, measuring mass flow for various spool determined port shapes 07 p0915 A72-20533

Nonisentropic flow behavior behind propagating self similar blast wave [AD-745485] 08 p1252 A72-21260

Steady axisymmetric twisted gas flow parameters in channels with geometries similar to turbojet engine units 08 p1149 A72-21310

Flow characteristics of liquid layers adjacent to vapor bubble, visualizing flow via particle motion 08 p1151 A72-21670

Flow analysis and dimensioning data for parallel walled radial diffusers, stating flow separation criterion 09 p1260 A72-22629

Pseudoviscous method application to computation of supersonic flow of inviscid ideal gas through two dimensional or annular axisymmetric ducts
10 p1417 A72-23876

Two and three dimensional pistons motion in stationary gas, calculating potential flow characteristics near weak discontinuities as function of piston geometry and acceleration
10 p1468 A72-24431

Axisymmetric plane transonic flow past convex corner point, obtaining characteristics by mapping into hodograph plane
10 p1468 A72-24435

Slender body theory for flow calculation past low aspect ratio delta wing with straight trailing edge, noting lifting vortices distribution
10 p1420 A72-25131

Flow phenomena, mixing and stability of high speed enclosed multijet turbulent diffusion flames fed by propane and air
10 p1563 A72-25139

Axial pressure variations in incompressible laminar tube flow with uniform suction, noting application to heat pipes
[AIAA PAPER 72-257] 11 p1614 A72-25202

Four stage gas turbine, measuring blade surface roughness and profile changes effects on flow characteristics and efficiency
[ASME PAPER 72-GT-34] 11 p1704 A72-25630

Two dimensional transonic turbine blade cascade downstream flow losses determination
[ASME PAPER 72-GT-43] 11 p1570 A72-25637

Two dimensional flow losses of turbine blade cascade with incompressible boundary layer injection
[ASME PAPER 72-GT-46] 11 p1570 A72-25638

Supersonic turbine cascade flow properties and pressure distributions on blades, comparing calculated results with experimental data
[ASME PAPER 72-GT-47] 11 p1570 A72-25639

Near field megawatt single shot exhaust flow and propulsion characteristics of pulsed MPD arc thruster
[AIAA PAPER 72-500] 11 p1711 A72-26223

Mathematical model of gas turbine parameters scatter and geometrical fabrication tolerances of flow through section
11 p1712 A72-26974

Steady bifurcating time periodic solutions stability for flows in bounded domain with complex conjugate simple eigenvalues at critical Reynolds number
12 p1837 A72-27712

Flow characteristics in air injection through porous surface of blunt bodies, noting blowing parameter effect on boundary layer flow
12 p1752 A72-28143

Computer program for gas turbine characteristics and influence coefficients calculation, allowing for cascade loss distribution during flow choking
12 p1862 A72-28151

Swirling flow in round pipe with sudden expansion, discussing separation and reversal characteristics
13 p1942 A72-29640

Hypersonic turbulent boundary layer flow parameters and heat exchange during blowing of coolant air and He through slot
13 p1895 A72-29901

Inhomogeneous two phase flow past sphere comparing structural and hydrodynamic characteristics on basis of X ray photographs
13 p2066 A72-30003

Small transport aircraft horizontal tail surfaces flow characteristics determination for stress calculation during flight in turbulent atmosphere
14 p2071 A72-30284

Numerical analysis of inviscid hypersonic flow characteristics in shock layer between bow shock and cone at angles of attack, taking into account laminar separated flow
14 p2069 A72-30328

Turbulent Ekman boundary layer characteristics in laboratory rotating apparatus compared with atmospheric field observation data and theories, noting similarity relation validity
14 p2094 A72-30418

Concentration stress convection in slow gas mixture flow due to density gradients, noting similarity to thermal stress convection
14 p2096 A72-31015

Longitudinal and circumferential boundary layer characteristics for concave and convex axisymmetric bodies at small angles of attack, using Cooke equivalent radius concept
15 p2177 A72-31205

Frictionless, Helmholtz and flat jet incompressible flows from slot in thick plane wall, comparing characteristics with free jet vicinity
15 p2216 A72-31464

Turbulent viscous flow near wall, deriving characteristics from equations of motion for comparison with hot wire anemometer measurement
15 p2216 A72-31469

Characteristic parameters of stationary supersonic plasma flow in magnetic de Laval nozzle calculated for collisional and collisionless cases, measuring ion saturation currents
15 p2285 A72-32268

Blunt nose cone flow field characteristics microwave measurement at stagnation point during atmospheric reentry, using plasma diagnostic sensors with antennas and electrostatic probes
[AIAA PAPER 72-693] 16 p2345 A72-34049

Hydrodynamic characteristics of a cambered hydrofoil with a jet flap.
[ASME PAPER 71-APMW-17] 17 p2537 A72-34303

Boundary layer velocity profiles on a helicopter rotor blade in hovering and forward flight.
[AHS PREPRINT 622] 17 p2484 A72-34482

Wall stabilized dc arc channel for plasma viscosity and flow characteristics studies, using pressure probe.
17 p2590 A72-35127

An experimental investigation of an asymmetrical turbulent wake.
17 p2485 A72-35187

Rarefied hypersonic flow characteristics of delta wings and trailing edge spoilers.
17 p2485 A72-35229

Incident thermal flux parameters and wall temperature effects on flow characteristics in prepreparation zone of laminar boundary layer and separation point location
17 p2487 A72-35927

Closed system of differential equations derived for kinematic characteristics of nonstationary turbulent flow in pressurized smooth pipe
19 p2785 A72-37473

The motion of a vortex pair in a stratified atmosphere.
19 p2785 A72-37571

Complex vortex core fine structure around propeller tip observed via smoke and stroboscopic lighting, presenting photographs
19 p2786 A72-37747

Temperature probes for flows at high enthalpy
[ONERA, TP NO. 1074] 19 p2800 A72-37767

On a method of computing the plane steady flow around a profile situated between straight parallel lines.
19 p2786 A72-38098

Forced convection heat transfer from cylinders to water in cross flow, quantifying method of accounting for fluid property variation
19 p2881 A72-38397

Martin-Ludford gas expansion into vacuum, investigating rarefaction wave penetration and flow characteristics
19 p2788 A72-38715

Turbulence theory generalization for flow near wall with various surface roughness modes, presenting velocity profiles
20 p2912 A72-39359

Turbulent diffusion in Laval nozzle, studying mixing of weakly heated jet coaxial with main flow in subsonic flow region
20 p2913 A72-39368

Mixing in initial portion of coflowing jets of incompressible gases of different densities, defining mixing zone widths relationship to velocity and density ratios
20 p2913 A72-39369

Flow calculation for polytropic process with friction and heat transfer
20 p2913 A72-39371

Decay of a diamond shock pattern.
20 p2913 A72-39606

Influence of cooling-air exhaust into the air-gas flow area on the flow-rate characteristics of cooled profiles.
20 p2963 A72-39923

Comparison of the experimental characteristics of disk-type and rotodynamic centrifugal pumps
20 p2930 A72-39924

Stability of a liquid film in a lateral gas flow and the size of droplets during the breaking of the film
20 p2987 A72-39925

An inverse problem in boundary-layer flows - Numerical determination of pressure gradient for a given wall shear.
21 p3043 A72-40108

A flow induced by thermal stress in rarefied gas.
21 p2989 A72-40193

Experimental study of flows in supersonic compressors
[ICAS PAPER 72-11] 21 p2990 A72-41136

Asymptotic behavior of the flow created by a shock wave incident on a wedge-shaped cavity
21 p3047 A72-41668

Characteristics of gas flows in diffusers at transonic velocities
21 p2994 A72-41698

New results concerning the numerical calculation of the sonic flow around a given airfoil section
22 p3135 A72-42639

Inhomogeneous two phase flow past sphere, comparing structural and hydrodynamic characteristics on basis of X ray photographs
22 p3167 A72-42726

Study of the flow kinetics of metal melt spread over hard surfaces
23 p3293 A72-43284

Flow parameters and geometric factors effect on wake structure behind nozzle cascades with cooling air ejection through blade trailing edges, evaluating energy losses due to flow mixing process
23 p3248 A72-43665

Investigation of the interaction between a circular wing and a flow of ideal liquid
23 p3348 A72-43796

Experimental investigation of the structure of turbulent jets expelled from a rectangular nozzle and nozzles with a limited head
23 p3280 A72-44020

An experimental study of flows in planar nozzles.
[ASME PAPER 72-FLCS-2] 23 p3249 A72-44066

An investigation of confined vortex flow phenomena
[ASME PAPER 72-FLCS-3] 23 p3281 A72-44067

Small disturbances propagation effect on self similar flow due to point explosion in medium with density varying according to distance from center
24 p3390 A72-44786

The structure of turbulent flows adjacent to walls.
24 p3390 A72-45001

Pressure and temperature change on the wall surface in strong shock wave diffraction.
24 p3391 A72-45047

Performance and flow properties change through a rocket turbine by presence of solid particles.
24 p3361 A72-45206

Investigation of the characteristics of turbulent air flow in a channel with elastic walls
24 p3393 A72-45257

Optimal modes of operation of a centrifugal-compressor wheel with preswirling of the flow
24 p3364 A72-45622

FLOW CHARTS

Chain and branched type electrical and mechanical systems, establishing algorithms with linear flow graphs
04 p0504 A72-14516

DELTA flow chart and network method for R and D projects planning and scheduling
04 p0598 A72-15456

Modal synthesis techniques for large structures dynamic analysis, presenting flow charts for computer programming
05 p0736 A72-16083

Computerized PCM data presentation and real-time monitoring system, presenting functional flow diagrams for computer program
05 p0633 A72-16677

Finite time element method for failure probability prediction in multiple load-path system with random loads, noting flow chart for suggested computer program
13 p2052 A72-28369

Flow and circulation diagrams formed by events involved in optimum aircraft design configuration and structural weight selection, outlining calculation methods
19 p2748 A72-37452

Energy flow diagrams.
24 p3369 A72-44686

FLOW COEFFICIENTS

NT DISCHARGE COEFFICIENT

Flow parameters behind shock waves propagating in carbon dioxide-nitrogen mixtures at Mach numbers from 5 to 10
07 p0966 A72-18936

Turbulent flow time averaged description by Navier-Stokes equations, determining Reynolds number dependent stress tensor coefficients
11 p1615 A72-25722

FLOW DEFLECTION

Ionized argon recombination rate constant determination as function of temperature, using dual frequency laser interferometry measurement of corner expansion flow
01 p0050 A72-10851

Velocity field of sonic flow about aircraft wing profile, solving mixed Cauchy problem
01 p0001 A72-11178

Two dimensional wedge shaped body base heat transfer to separated nonreattaching flow region in subsonic wind tunnel
[ASME PAPER 71-HT-D] 02 p0152 A72-12314

Plane cavity flow past symmetric ogival obstacles, applying variational principle to fixed point theorem
02 p0206 A72-12625

Time dependent unsteady flows visualization around circular cylinders and flat plates decelerated from steady speed
02 p0206 A72-12773

Viscous fluid flow at small Reynolds numbers past porous permeable sphere, obtaining drag formula
04 p0511 A72-14858

Laminar viscous flow past finite flat plate at high Reynolds numbers, solving Navier-Stokes equations
04 p0511 A72-14859

Slow motion in shear flow of doublet of two spheres in contact, using Stokes equations solution
04 p0511 A72-14860

Axisymmetric deflected turbulent jet flow, analyzing physical features and trajectories
04 p0462 A72-15177

Nonlinear calculation of three dimensional flow of perfect incompressible fluid around wing of finite span with arbitrary form
04 p0463 A72-15558

Two dimensional unsteady flow of incompressible fluid around passing turbomachine blades, determining instantaneous pressure, forces and moments as function of time

04 p0463 A72-15559

Two dimensional flow of gas jet around dihedral obstacle, investigating screen proximity and fluid compressibility effects

06 p0799 A72-17912

Cavitation flow around plate in transverse gravitational field, investigating boundary condition approximation on free boundary

06 p0799 A72-17913

Numerical solution of supersonic flow past blunt bodies with large mass injection, deriving finite difference equations

06 p0756 A72-18114

Ideal gas flow past blunt body in supersonic stream, discussing sonic lines, characteristics and Mach number

06 p0756 A72-18119

Fluidic devices electrostatic modulation, verifying jet deflection analytical model by experimental results

07 p0913 A72-18819

Unsteady flow of viscous incompressible electrically conducting fluid past infinite nonconducting plate within uniform transverse magnetic field

08 p1212 A72-21079

Shock layer emission associated with hypersonic air flow past spherical segment, solving flow equations by iteration technique

10 p1418 A72-24539

Steady rarefied gas flow around sphere with radial reflection of particles along normals, calculating gas dynamics variables of conservation equation

10 p1419 A72-24628

Unsteady flow evolution at sphere and elliptical cylinder obtained by flow visualization techniques, showing streamline sequence dependence on angle of attack

12 p1797 A72-27469

Convective heat transfer for fluid flow on plate with internal heat sources in boundary layer, solving laminar-turbulent transition equations by difference method

12 p1889 A72-28138

Numerical solution of algebraic equation encountered in aerodynamics of hypersonic boundary layer interacting with external flow on thin solids of revolution

13 p1895 A72-29848

Inhomogeneous two phase flow past sphere comparing structural and hydrodynamic characteristics on basis of X ray photographs

13 p2066 A72-30003

Three dimensional structure of transverse uniform flow around motionless circular cylinder for Reynolds number 45,000, investigating correlations of velocities on parallels to generatrices

15 p2179 A72-31684

Falkner-Skan problem extension to MHD flow past nonconducting body by imposing magnetic field with lines of force parallel to undisturbed streamlines

15 p2287 A72-32405

Numerical calculation of the supersonic flow of a viscous fluid about a parabolic obstacle

17 p2484 A72-34887

Contributions to the study of the steady-state regime of fluidic amplifiers with jet deflection

17 p2497 A72-35122

Axisymmetric rotating flow past a circular disk

17 p2540 A72-35190

Transonic viscous flow around lifting two-dimensional airfoils

[AIAA PAPER 72-678]

17 p2486 A72-35479

Cavitation zone structure behind circular cylinder model in plane flow investigated by high speed motion picture photography and with short exposure time flash

17 p2544 A72-35897

Numerical tests of resolution of detached flows on thick bodies

18 p2684 A72-37198

French monograph - An asymptotic theory of the Boltzmann equation and its application to the study of near continuum flows

19 p2785 A72-37489

On a method of computing the plane steady flow around a profile situated between straight parallel lines.

19 p2786 A72-38098

Steady flow past body fixed in uniform flow of dusty gas, obtaining velocity distribution

21 p2989 A72-40195

Behavior of a laminar boundary layer in the presence of a positive pressure gradient

[ICAS PAPER 72-17]

21 p3045 A72-41142

An experimental investigation of the formation of vortices behind the isosceles triangular cross-sectional obstacles protruding from the plane wall.

21 p2992 A72-41246

Karman vortex street in a uniform shear flow.

21 p2992 A72-41247

Inhomogeneous two phase flow past sphere, comparing structural and hydrodynamic characteristics on basis of X ray photographs

22 p3167 A72-42726

Three dimensional supersonic flow past bodies with a smooth generatrix

23 p3248 A72-43651

Turbulent supersonic boundary layer flow in the neighborhood of a 90 deg corner.

24 p3361 A72-45204

Longitudinal curvature and displacement speed effects on incompressible laminar boundary layers.

24 p3393 A72-45249

FLOW DIRECTION INDICATORS

NT WIND VANES

Sensors and circuit design for flow angle and shear stress measurements using heated film and wires

[ASME PAPER 71-WA/FE-17]

05 p0661 A72-15930

Eruptive center location and flow direction measurements for andesite and quartz latite lava flows in Mogollon Mountains

15 p2223 A72-31579

Gas flow direction measurement using flow to electric pulse converter

16 p2395 A72-33957

FLOW DISTORTION

Free stream and shock layer disturbances effect on hypersonic boundary layer transition in wind tunnels from hot wire measurements

02 p0230 A72-12274

Unsteady supersonic flow disturbance by slender bodies in strong contact discontinuities in shock tube studies

04 p0462 A72-15507

Cross flow effect on lifting fan noise at subsonic blade tip speeds, analyzing radiation pattern change due to inlet flow distortion

[AIAA PAPER 72-128]

05 p0608 A72-16921

Cylindrically symmetrical low viscosity fluid distortion and homogeneous spiral flow stability under rotational self excitation

06 p0799 A72-17981

Numerical solutions to gas dynamic problems with large deformations by particle in cell method

06 p0800 A72-18102

Circumferential inlet pressure distortion index derivation for high hub-tip ratio multistage axial flow compressor from one dimensional isentropic flow expressions

07 p1053 A72-18762

Aortic flow disturbances in vivo study by hot-film anemometer, considering peak flow velocity and pulse rate effects

07 p0934 A72-20537

Flat face cylinders in rarefied supersonic gas flow, investigating perturbed region evolution based on pitot tube method

10 p1415 A72-23751

Two and three dimensional pistons motion in stationary gas, calculating potential flow characteristics near weak discontinuities as function of piston geometry and acceleration

10 p1468 A72-24431

Columnar disturbance strengths upstream of obstacle in uniformly stratified or rotating flows relative to validity of Long hypothesis

10 p1470 A72-25063

Unsteady lift on airfoils in moving cascades with inlet axial flow disturbances, estimating lift on reference blade between blade channels

[ASME PAPER 72-GT-5]

11 p1568 A72-25608

Fan-in-wing model noise due to cross flow generated in- and outflow distortions and unsteady rotor blade forces

[ASME PAPER 72-GT-92]

11 p1571 A72-25666

Skin friction response to angle and perturbation in flow past axisymmetric body with unsteady main stream

13 p1941 A72-28887

Localized point centered initial disturbances effects on marginally unstable plane parallel flow, presenting differential equations solution for nonlinear response

14 p2094 A72-30366

Grid-generated turbulence distortion approaching two dimensional bluff body stagnation region

16 p2344 A72-33569

Finite amplitude disturbances in the flow 8019 of inviscid rotating and stratified fluids over obstacles.

18 p2679 A72-36383

Engine inlet total pressure distortion effects on multistage axial compressor and turbojet/turbofan engine performance and stability, considering inlet-engine compatibility

[ICAS PAPER 72-19]

21 p2991 A72-41144

The development of inlet flow distortions in multistage axial compressors of high hub-tip ratio.

[ICAS PAPER 72-20]

21 p3099 A72-41145

Installation caused flow distortion and its effect on noise from a fan designed for turbofan engines.

[AIAA PAPER 72-1006]

21 p2993 A72-41590

Wind tunnel data correction for interference due to flow boundary constraints /wall effects/, acoustic and model support effects

21 p3043 A72-41640

Theory of a boundary layer with abruptly varying boundary conditions

22 p3166 A72-42259

Flow distortion and performance measurements on a 12-inch fan-in-wing model for a range of forward speeds and angle of attack settings.

22 p3134 A72-42323

Spin induced boundary layer distortion on rotating cone at supersonic speeds via spark shadowgraphs, correlating Magnus and normal force measurements with boundary layer configurations

[AIAA PAPER 72-967]

22 p3135 A72-42343

High response two-transducer pressure measurement for evaluating nonuniform and unsteady inlet air-flow distortion effects on supersonic jet engine stability and performance

22 p3216 A72-42683

Iterative method for calculating the deformations of an induced flow

22 p3136 A72-42919

Analytical method for combining the interaction of inlet distortion and turbulence.

23 p3247 A72-43330

Experimental study of the plane deformation of a homogeneous turbulence

23 p3280 A72-43822

Response of convectively controlled burning to nonlinear disturbances.

24 p3464 A72-45055

FLOW DISTRIBUTION

Momentum jet and electric discharge from same hole in plane wall bounding viscous incompressible conducting fluid, investigating flow field with similarity solutions

01 p0107 A72-10139

Weather map numerical analysis for Northern Hemisphere, describing program with flow field for geopotential value checking

01 p0094 A72-10196

Statistical analysis of atmospheric average arrival time distribution, using simultaneous data from Berlin and equatorial latitude positioned research ship Meteor

01 p0056 A72-10443

Two dimensional transient inviscid flow field from secondary injection in missile control, describing distribution with artificial viscosity finite difference method

01 p0097 A72-10940

Nonhomogeneous fluid geostrophic flow, establishing relationship between velocity and density fields

01 p0051 A72-11230

Energy release and accelerating inner stream effects on flow field near fuel injection in gas core reactor, basing Euler equations energy diffusion term on radial radiative transport

01 p0100 A72-11351

Hypersonic source flow past wedges and cones, calculating flow nonuniformities effects on shock shape, velocity, pressure and density by perturbation analysis

01 p0033 A72-11394

Supersonic and hypersonic flows with attached shock waves over delta wing at angle of attack, deriving unified theory for flow field

02 p0150 A72-12030

Two dimensional diffusers flow patterns with laminar boundary layer entry, investigating wall shape and vanes effects with water table test facility

02 p0204 A72-12231

Two dimensional underexpanded jet plumes flow distribution determination using time dependent finite difference method

02 p0301 A72-12257

Classical optical measurement and holographic methods of flow field visualization, discussing operating principles, measurement sensitivity, three dimensional and depth-focusing properties

02 p0230 A72-12300

Turbulence intensity effects on mass transfer from cylinders in cross flow at various Reynolds numbers

[ASME PAPER 70-WA/HT-3]

02 p0205 A72-12312

Turbulent supersonic separated flow field analysis and pressure measurements for two dimensional and axisymmetric internal and external flow models

[DGLR PAPER 71-076]

02 p0152 A72-12710

Analog circuit method for slender profile flow field shock front boundary value problem for simple profile variation, using known mapping plane solutions

[DGLR PAPER 71-069]

02 p0153 A72-12743

Solar streamline flow patterns analysis test on terrestrial wind data

03 p0414 A72-12928

Integral conservation laws derivation for geostrophic zonal flow field disturbance, applying to flow stabilization

03 p0348 A72-13478

Vortex flow structure in axial gas turbines near inlet and outlet of blade row

03 p0307 A72-13538

Uniqueness of turbomachinery flow calculations using streamline curvature and matrix through-flow methods

03 p0308 A72-13648

Hydrodynamic field around sphere moving along Poiseuille flow axis determined by least squares method, formulating flow resistance

04 p0511 A72-14968

Spatial structure coherence in sublayer of turbulent boundary layer, using spanwise flow hot-wire anemometer measurements

04 p0462 A72-15116

Laminar shear flow over impulsively started wedges, describing flow field by Goldstein-Rosenhead method of approximate series expansion

04 p0590 A72-15190

Radiative cooling effects on flow field and heat transfer behind reflected shock wave

[AD-737423] 04 p0597 A72-15338

Flow distribution behind shock wave with intense laser radiation absorption and laser-triggered thermonuclear reactions

[AD-736299] 04 p0559 A72-15351

Approximate numerical method for calculating flow profiles in arteries from local pressure measurements, taking into account Navier-Stokes equations nonlinear terms

[ASME PAPER 71-WA/BHF-3] 05 p0621 A72-15948

Conservation equations for blast waves one dimensional nonsteady flow field, considering Eulerian space and time profiles

[ASME PAPER 71-WA/APM-1] 05 p0745 A72-15974

Aerodynamic interference between parallel bodies for estimating aerodynamic characteristics of rocket engine with auxiliary boosters, obtaining flow field by slender body theory

05 p0600 A72-16005

Fluid properties for mechanically similar flow fields, discussing dissociating and thermally radiating gas flow

[DFVLR-SONDDR-172] 05 p0648 A72-16064

Flow field due to diffraction of shock wave at wedge moving at supersonic speed

05 p0600 A72-16212

Radiative transfer and chemical nonequilibrium phenomena for radiating flow field predictions behind high altitude hypervelocity normal shock waves

05 p0603 A72-16545

Turbulent boundary layer on yawed flat plate, measuring velocity profiles and flow directions

[DFVLR-SONDDR-177] 05 p0603 A72-16703

Vortex production of intense localized heating to leeward regions of bodies in hypersonic flows, proposing flow field models

[AIAA PAPER 72-77] 05 p0604 A72-16804

Laminar incompressible flow over yawed spinning bodies of revolution by Navier-Stokes solutions, discussing flow fields and corresponding force coefficients

05 p0605 A72-16820

Difference equations and relaxation method for three dimensional transonic flow field about wings in terms of velocity potential

[AIAA PAPER 72-189] 05 p0605 A72-16843

Numerical analysis of three dimensional inviscid supersonic flow field about complex vehicle geometry, using finite difference technique and Rankine-Hugoniot relations

[AIAA PAPER 72-192] 05 p0606 A72-16847

Space shuttle flow field fluid dynamic hyperbolic equations numerical solution by noncentered finite difference schemes, noting advantages in programming logic simplicity and multidimensional generalizations

[AIAA PAPER 72-193] 05 p0729 A72-16848

Mean velocity and turbulent fluctuation distributions for sub- and supersonic jets in convergent nozzles, obtaining sound power spectra

[AIAA PAPER 72-157] 05 p0651 A72-16872

Subsonic and transonic compressible potential flow over nonlifting hovering helicopter rotor blades, calculating flow field by three-dimensional nonlinear relaxation scheme

[AIAA PAPER 72-39] 05 p0607 A72-16901

Nonlinear effects of inviscid supersonic flow field surrounding bodies in coning motion, using shock capturing finite difference technique

[AIAA PAPER 72-27] 05 p0607 A72-16918

Wind tunnel measurements for near flow field velocity distribution in rectangular wing wake turbulence, comparing with flight measurements

[AIAA PAPER 72-41] 05 p0609 A72-16948

Multidimensional time dependent flow field analysis by split finite difference operator technique, using star mesh of quadrilateral cells

[AIAA PAPER 72-154] 05 p0609 A72-16950

Combined viscous-inviscid analytical procedure for predicting boundary layer effects on supersonic inlet flow field

[AIAA PAPER 72-44] 05 p0609 A72-16975

Vector analysis of three dimensional nonequilibrium dissociative gas flow quantity variations along stream lines

05 p0652 A72-17001

Rotating homogeneous incompressible fluid flow field over step with interior geostrophic regions, horizontal surfaces Ekman layers and vertical shear layers

05 p0653 A72-17008

Turbulent flow field velocity fluctuations errors by hot-wire anemometer filaments vibrations from fluctuating aerodynamic loads in Karman vortex street

05 p0664 A72-17013

Curved shocks discontinuities in nonequilibrium dissociative gas flows, investigating flow gradient variables

05 p0653 A72-17080

Poloidal Hall current calculation in hydrodynamic approximation for stationary weakly interacting and conducting cylindrical plasma flow with uniform transverse flow parameter distribution

05 p0701 A72-17240

Circular vortex rings with nonsimilar vorticity distributions submerged in inviscid stream, considering motion and decay by inner and outer asymptotic expansions matching

[AD-741267] 06 p0798 A72-17781

Flow field quantities for nearly free axisymmetric steady molecular gas flow through circular orifice from high pressure region into vacuum

06 p0800 A72-18118

Supersonic flow patterns near yawed obstacles around flat plate sharp leading edge with high pressure regions in reversed separated flow zone

06 p0756 A72-18122

V-shaped wings supersonic characteristics at 0-15 deg angles of attack, investigating flow structure between wings by pitot tube rake

06 p0757 A72-18129

Incipient wing stall detection by unsteady pressure monitoring via flush-mounted microphones, discussing flow patterns on models

07 p0908 A72-19093

Flow field induced by electric current jet in incompressible viscous conducting fluid, solving nonlinear momentum equation by series expansion procedure

07 p0967 A72-19504

Two dimensional and axisymmetric flow with heat addition, deriving flow field by inverse methods

07 p0909 A72-20062

Flow structure between bow shock wave and blunted cone surface, studying interior shock waves by numerical solution via finite difference methods

07 p0910 A72-20108

Boundary conditions for unsteady flow fields bounded by incompressible elastic thick plane wall fixed to rigid surface

07 p0972 A72-20113

Flow field model of convective heat transfer along reattachment surface in planar supersonic turbulent flow

[ASME PAPER 71-HT-W] 08 p1251 A72-20876

Stream functions for steady two dimensional flow field of viscous liquid near circular whirl

08 p1148 A72-20937

Rectangular channel mixed boundary layer flow patterns dependence on inlet edge configurations, channel geometry and hydrodynamic flow core parameters

08 p1150 A72-21317

Towed cable flight vehicle system motion in uniform flow field, calculating equilibrium configuration during coordinated turn from two point boundary value problem numerical solution

08 p1110 A72-21604

Tube flight vehicle system thrust and power requirements prediction by aerodynamic analysis with division of near and far flow fields

08 p1107 A72-21608

Instabilities development in flow field generated by shock wave propagation in exothermic gas mixture

08 p1255 A72-22042

Viscoplasticity techniques application to deforming portion strain and strain rate fields of axisymmetric Al alloy extrusion with various flow patterns

08 p1250 A72-22194

Comet gas production and interaction with solar wind, discussing visible plasma tail within flow pattern

09 p1387 A72-22755

Self similar flow patterns due to cylindrical ionizing symmetrical strong shock and detonation wave propagation outwards into gas at rest

09 p1295 A72-23564

German monograph on flow calculation in axial thermal turbomachines covering boundary conditions and field computation for steady state inviscid flow

10 p1415 A72-23772

Experimentally produced vortex ring structure and stability, using dye and hydrogen bubble techniques for flow field, ring velocity and growth rate observations

10 p1466 A72-24327

Cavity flow driven by buoyancy and shear, obtaining flow and temperature fields from Navier-Stokes equation numerical solution

10 p1467 A72-24366

Prolate and oblate spheroids flow field generated by axial translatory oscillations in still incompressible viscous fluid from Stokes linearized equations, deriving formulas for drag

10 p1418 A72-24462

Hydrodynamic field generated by sphere motion along viscous fluid filled cylinder axis beyond Stokes regime

10 p1470 A72-24852

Ammonia-air opposed reacting jet /ORJ/ for flame stabilization, solving partial differential equations for flow field

10 p1564 A72-25141

Rarefied flow fields and heating rates for space shuttle orbiter reentry at high angles of attack, using Monte Carlo simulation technique

[AIAA PAPER 72-314] 11 p1567 A72-25248

Color schlieren technique for simultaneous photographic recording of flow fields and heat transfer patterns in aerodynamic heating, noting application to shock-boundary layer interactions

11 p1629 A72-25257

Digital computer calculation of complex electric networks described by mathematical models, calculating flow distribution

11 p1577 A72-25282

Flow fields and inviscid core of two dimensional diffuser with fluid extraction on diverging walls, describing streamline patterns, stagnation region and stall conditions

[ASME PAPER 72-GT-2] 11 p1568 A72-25605

Jet turbine engine front fans with and without snubbers, estimating flow field by streamline curvature technique

[ASME PAPER 72-GT-4] 11 p1568 A72-25607

Hodograph method involving conformal mapping for turbomachine blade subsonic flow profile calculation

[ASME PAPER 72-GT-41] 11 p1570 A72-25635

Two dimensional cascades supersonic exit flow field, using Oswatitsch method of characteristics and conservation laws

[ASME PAPER 72-GT-49] 11 p1570 A72-25641

Constant density solutions for flow fields behind concave shock waves, noting approximation for transonic free stream Mach numbers

11 p1572 A72-25919

Critique of general momentum theory of propeller actuator disk model, showing flow field determination from nonlinear elliptic differential equation solution

11 p1572 A72-25998

Transverse outflow effects on flow field characteristics of hypersonic finite span separated flows with turbulent boundary layer

11 p1572 A72-26004

Integral conservation laws derivation for geostrophic zonal flow field disturbance, applying to flow stabilization

11 p1623 A72-26248

Nonlinear integral equations solution for heavily loaded actuator disk induced flow field, taking into account blade tip vortices and thrust coefficient effects

11 p1573 A72-26577

Self similar blast waves propagation, studying flow field in terms of shock front velocity and ambient atmospheric density variation ahead of front

[AD-745816] 12 p1889 A72-27832

Shadowgraph photography method for supersonic air flow pattern around porous cone in uniform injection, noting pressure distribution dependence

12 p1752 A72-27986

Incompressible potential flow model of porous parachute canopy flow field, using Stokes stream function for axisymmetric vortex sheet in uniform steady stream

12 p1755 A72-28123

Nonstationary interaction flow field between subsonic and composite jet on flat plate with vortex formation and reverse currents, using finite difference technique

12 p1799 A72-28168

Path arrangement optimization method for fluid distribution network with separable and concave cost function, using simplex method in nonlinear programming

13 p2053 A72-28423

Apollo 14 experiments to demonstrate flow patterns of convection and heat transfer in gases and liquids under weightlessness

13 p2035 A72-28614

Slender profile in nonuniform flow, deriving lift, normal force distribution and moment from vortex and source distribution induced flow field

13 p1894 A72-29005

Mathematical model for flow field inside raindrop under aerodynamic transient stresses before impingement at stagnation point of blunt body in supersonic flight

13 p1942 A72-29224

Nonequilibrium dissociating inviscid nitrogen flow pattern over spheres and circular cylinders, obtaining temperature, pressure and density fields

13 p1895 A72-30032

Passive scalar dispersion in turbulent incompressible flow characterized by inhomogeneous and nonstationary statistics, expanding velocity and scalar concentration fields in Wiener-Hermite functions

14 p2128 A72-30348

Initial dihedral wing-body interaction for supersonic leading edges, determining expansion of velocity potential on root chord

14 p2069 A72-30365

Two dimensional two phase steady supersonic wedge flow patterns analysis based on equations for flow between wedge surface and shock wave

14 p2070 A72-31011

Turbulent boundary layer separation zone subsonic flow before two dimensional rectangular step, examining flow pattern and static pressure distribution

14 p2096 A72-31020

Regional stratigraphy and fabric distribution of volcanic ash flow sheets in northwestern Mogollon Plateau by flow direction technique

15 p2223 A72-31578

High acceleration effects on gas flow patterns in rocket nozzles, detailing stagnation condition in combustion chamber and gas velocity and pressure at exit

15 p2297 A72-31813

Molecular flux distribution in cylindrical vacuum chambers with various inlet and pumping configurations under assumption of Knudsen law validity, describing computer program

15 p2183 A72-32382

Thermal radiation effects on semiinfinite planar blunt leading edged body hypersonic flow field, using Lax and Rusanov artificial viscosity methods

15 p2337 A72-32593

Supersonic interaction effects on boundary layer flow structure in intersecting wedge corner at high Reynolds numbers from surface pressure measurements and oil flow visualization

16 p2341 A72-32830

Monte Carlo simulation method for flow field around two dimensional or axisymmetric body immersed in hypersonic rarefied gas flow

16 p2342 A72-32882

Flow distribution, vibration, wear and rupturing of rods in vertical pipe for various inlet flows investigated with high speed cameras, photography and transducers

16 p2376 A72-32996

Imploding spherical and cylindrical shocks, considering rear flow field with nonadiabatic isothermal flow and zero temperature gradient

16 p2376 A72-33009

Stability analysis of ideal incompressible liquid steady flow for given distribution, discussing velocity distribution effect on longitudinal cylindrical flow instability

16 p2376 A72-33093

Airborne electrostatic probe for cloud droplet size measurement, calculating flow distribution and particle trajectories

16 p2390 A72-33150

Coordinate perturbation and multiple scale techniques application to supersonic flow field around two dimensional wing and oscillations in closed tube

16 p2379 A72-33576

Negative pressure gradients effects on turbulent viscosity profiles for gas flow through tubes, comparing dependence on transverse coordinates to incompressible flow case

16 p2380 A72-33860

Analytical model for crosshatch ablation patterns geometric features and stability characteristics prediction based on viscoelastic melt layer interaction with gas boundary layer

[AIAA PAPER 72-718]

16 p2480 A72-34030

Shock wave interactions with nozzle wall turbulent boundary layer, discussing shock strength variation to produce unseparated, incipient and fully separated flow fields

[AIAA PAPER 72-715]

16 p2380 A72-34033

Flow area computerized prediction for multicomponent series-parallel spacecraft venting satisfying pressure differential requirements

[AIAA PAPER 72-707]

16 p2462 A72-34038

Three dimensional supersonic nozzle exhaust flow field numerical analysis based on reference plane characteristics, deriving difference equations for three coordinate systems

[AIAA PAPER 72-704]

16 p2344 A72-34040

Finite difference method computation of multi-shocked three dimensional wing-body supersonic flow fields with real gas effects, applying to delta winged space shuttle

[AIAA PAPER 72-702]

16 p2345 A72-34042

Steady state magnetically balanced cross flow arc, calculating flow and temperature fields and boundary shape under assumption of two independent variables

[AIAA PAPER 72-687]

16 p2439 A72-34055

Sonic boom alleviation by flow field alteration near supersonic aircraft, considering finite rise times, reduced overpressures and shock pressure rises

[AIAA PAPER 72-653]

16 p2349 A72-34081

Sonic boom induced flow field at supersonic/hypersonic speeds, using shock expansion method and hypersonic equivalence principle for sharp and blunt nosed bodies

[AIAA PAPER 72-652]

16 p2349 A72-34082

Flow distribution for inviscid nonconducting uniform supersonic stream past unyawed semiinfinite circular cone with attached shock wave

17 p2483 A72-34325

Circulating toroidal vortex pattern in initial region of turbulent coaxial jet stream mixing obtained with hot-

wire anemometer, static pressure probes and shadowgraphy

[ASME PAPER 72-APM-30]

17 p2538 A72-34789

Computation of transonic flow about finite lifting wings.

17 p2486 A72-35258

The inviscid flowfield of an unsteady airfoil.

[AIAA PAPER 72-681]

17 p2486 A72-35481

Analytical solutions for straight oblique shock waves in radiating gases.

17 p2542 A72-35616

Computer aided study of nondiffusive plane convection mixing of scalar field by isotropic turbulence of single velocity modes

18 p2678 A72-36017

Near flow field and aerodynamic loading in subsonic and supersonic flow over body-wing configuration, surveying numerical, kernel function and image methods

18 p2641 A72-36390

Prediction of electron concentration reductions in re-entry flow fields due to electrophilic liquid and water injection.

[AIAA PAPER 72-670]

18 p2730 A72-36537

Transient mode of a flow in the plane wake of a thin plate or cylinder

18 p2642 A72-36899

Viscosity effect on hypersonic flow field near slender body, discussing eigenvalue solutions for two and three dimensional flow around triangular plate

19 p2745 A72-37393

Ultimate configuration of the self-similar separated flow of an ideal fluid

19 p2785 A72-37396

A method for increasing thrust reverser utilization on STOL aircraft.

[AIAA PAPER 72-782]

19 p2752 A72-38141

Temperature distribution in hot wires in high-enthalpy low-density flows

[DFVLR-SONDDR-216]

19 p2804 A72-38685

Analytical prediction of vortex-ring boundaries for helicopters in steep descents.

20 p2886 A72-38949

Effect of vertical flow structures on the cloud cover in the intratropical convergence zone

20 p2949 A72-39950

High Reynolds number turbulence and vortices in journal bearings, discussing validity of flow field models based on mixing length and pipe flow theory

20 p2930 A72-39972

Steady flow past body fixed in uniform flow of dusty gas, obtaining velocity distribution

21 p2989 A72-40195

Asymptotic theory of an optically thick radiating gas flow past a smooth boundary at moderate radiation strength.

21 p2989 A72-40196

Rotating fluids density stratification effect on characteristic features of homogeneous Taylor column, noting flow patterns

21 p2989 A72-40652

Experimental CW chemical laser studies.

[AIAA PAPER 72-712]

21 p3063 A72-40920

Ultrasonic sound beam measurement of flow circulation variations in circular cylinder wake, evaluating probability distribution of beam phase fluctuations

21 p2990 A72-40947

Microstructure of turbulent flow in the stabilized flow region in a channel

21 p3045 A72-41054

An experimental investigation of the formation of vortices behind the isosceles triangular cross-sectional obstacles protruding from the plane wall.

21 p2992 A72-41246

Wall porosity and angle of attack effects on jet stretcher flow field for supersonic engine inlet testing, using three dimensional method of characteristics

[AIAA PAPER 72-1025]

21 p3042 A72-41603

Transverse mass flow past a sphere at small Reynolds numbers

21 p3047 A72-41664

Machine code for finite difference solution of vortex governing equations and far field prediction in trailing vortices, developing turbulent energy model

[AIAA PAPER 72-989]

22 p3134 A72-42326

Singular points in conical flow streamline patterns, considering rotational and irrotational flows

22 p3135 A72-42580

Laser Doppler velocimeter operating in forward- and back-scatter modes for supplementing wind tunnel flow field measurements in subsonic, transonic and supersonic regimes

22 p3179 A72-42678

German monograph - The transfer behavior of premixed flames.

22 p3244 A72-43076

Turbulent interaction of air jets issuing from perforated surfaces into free space, determining three dimensional flow field via Reichardt free turbulence theory

23 p3248 A72-43625

Flow and energy loss distribution in annular sector nozzle cascades with cylindrical blade profiles of different twist, measuring flow exit angle along blade span

23 p3248 A72-43664

Unsteady flow field near wall and Reynolds stress measurement in turbulent boundary layer, using conditional sampling technique with digital computer

23 p3282 A72-44304

Two-dimensional supersonic flow with flame sheets.

24 p3360 A72-44988

Chapman-Jouguet surface characteristics in flow field behind steady gaseous detonation wave, using schlieren photography

24 p3462 A72-45031

Response of convectively controlled burning to nonlinear disturbances.

24 p3464 A72-45055

Jet pumps for compressible fluids at supersonic velocities.

24 p3393 A72-45362

Electron-beam flow visualization - Applications in the definition of configuration aerothermal characteristics.

[AIAA PAPER 72-1016]

24 p3404 A72-45405

Jet impingement under VTOL aircraft.

24 p3364 A72-45779

A finite-difference method for boundary layers with reverse flow.

24 p3395 A72-45789

FLOW EQUATIONS

NT VON KARMAN EQUATION

NT VORTICITY EQUATIONS

Equivalence laws and approximate equations for incompressible and compressible viscous flows in pipes with variable cross sections

01 p0051 A72-11256

Two phase flow equations model application to fluidized beds and foams, predicting bed stability to small perturbations for comparison with experiment

01 p0093 A72-11272

Inertia effects in fully developed axisymmetric laminar flow between two parallel rotating walls, solving Navier-Stokes equation in nonlinear form

[ASME PAPER 71-LUB-J]

02 p0234 A72-11529

Three dimensional boundary layer gas flow in large pressure gradient region, using two dimensional boundary layer equations

02 p0201 A72-11580

Incompressible nonsimilar turbulent and transitional flows numerical analysis in wakes, jets and boundary layers, using turbulent viscosity equations

02 p0202 A72-11587

Self similar solutions for three dimensional laminar boundary layer equations under arbitrary surface conditions by quasi-linearization method

02 p0203 A72-11739

Passive scalar field diffusion in homogeneous turbulence, solving Fourier transformed flow equations by iterative procedure

02 p0204 A72-12174

Wall jet flow displacement on curved surface, deriving two dimensional solution for second-order boundary layer equations

03 p0307 A72-13159

Generalized equation for incompressible unsteady laminar boundary layer in external flow with arbitrary time dependent velocity distribution, discussing expanding cylindrical body

03 p0343 A72-14315

Slow motion in shear flow of doublet of two spheres in contact, using Stokes equations solution

04 p0511 A72-14860

Unsteady radial flow between fixed and oscillating walls, obtaining flow equations and air bearings stability conditions

04 p0511 A72-14970

Unsteady nonisothermal gas flow through semi-infinite porous medium, using linearized flow equations for small pressure variation

04 p0512 A72-15200

Hydrodynamic resistance reduction for bodies moving under water, analyzing dynamic equations of viscous incompressible fluid

04 p0514 A72-15703

High velocity unsteady flow calculations in metal pipes by numerical methods for boundary conditions, including turbomachinery, column separation and gas accumulator

[ASME PAPER 71-WA/FE-13]

05 p0646 A72-15931

Concentration profile equations for finite length flat vertical plate moving in viscous incompressible fluid

05 p0650 A72-16783

Statistical equations for turbulent fluctuations of energy, concentration and rotation in compressible flows

06 p0797 A72-17557

Incompressible micropolar fluid flow equations, deducing stable periodic solutions existence by energy method

06 p0799 A72-17917

Two dimensional transonic and hypersonic shock structures, discussing flow equations, mathematical properties and similarity rules

[AD-742561]

06 p0799 A72-17960

Numerical methods for parabolic, hyperbolic and elliptic flows in fluid mechanics and heat transfer, considering finite element method

07 p1097 A72-18795

Inviscid relaxing gas flow through tube with variable cross sectional area, deriving governing equation for weak discontinuity amplitude evolution

07 p0970 A72-20073

Iterative solution of differential equations for steady plane flow with heat and mass transfer at high Reynolds numbers

07 p0971 A72-20098

Perfect fluid two dimensional steady flow equation solution for viscous flow with specified boundary conditions, considering vortex flow

07 p0971 A72-20099

Invariant free boundary problems of Navier-Stokes equations with nonzero vector of volume forces, investigating liquid layer flow on vertical cylinder surface

07 p0972 A72-20105

Plane irrotational flow of fluid with arbitrary thermodynamic properties in throat of Laval nozzle, solving flow equations

07 p0972 A72-20111

Linearized two level model for atmospheric motion equations systems, using Psi-balanced system for 24 hour forecast

08 p1156 A72-20995

Unsteady gas flow in thrust bearing with spiral grooves, presenting Navier-Stokes and discontinuity equation

08 p1176 A72-21167

Viscous incompressible flow past circular cylinder at Reynolds numbers 100-1000, obtaining oscillatory drag, lift and torque by governing equations numerical solution

08 p1107 A72-21251

Accuracy tests of Wang method for calculating three dimensional laminar compressible boundary layer flow equations

08 p1150 A72-21625

MGD equations for ideal plasma steady plane adiabatic flow in magnetic field, considering analogy to Chaplygin equations

08 p1214 A72-21645

Turbulent flow model based on two equations for kinetic energy distribution and vorticity fluctuations, comparing flow and heat transfer prediction with experimental data

08 p1152 A72-22169

Numerical integration of viscous and inviscid fluid flow equations, comparing various methods with exact solution

09 p1293 A72-22463

Numerical solution of thermal shock equations for incompressible fluid with free convection and of motion equations in gravitational force field

09 p1410 A72-22882

Viscous boundary layer equations for MHD flow near rear stagnation point at small Reynolds number

09 p1296 A72-23674

Turbulence models application to internal flow prediction, using two-, three- and five-equation models and shear stress hypothesis

10 p1463 A72-23854

Confined three dimensional boundary layers prediction, describing finite difference methods for flow equations solution

10 p1464 A72-23871

Equation of isovolumetric fluid pulsed and potential flow in convergent duct solved by perturbation method

10 p1465 A72-24118

Velocity and magnetic field expressed by six scalar potentials from MHD equations system, noting compressible fluids flow

10 p1520 A72-24219

MHD sheet pinch model time dependent nonequilibrium stability determined by equations of incompressible viscous resistive magnetofluid

10 p1523 A72-24751

Response equation for hot-wire anemometry over wide velocity range using modified King law

11 p1629 A72-25265

Time dependent viscous flow past impulsively started sphere using numerical solutions for governing equations based on Legendre series expansion of stream and vorticity functions

11 p1615 A72-25551

Boundary value problems to initial value problems transformation method extended by physical parameters invariant properties, noting fluid mechanics nonlinear equations

11 p1616 A72-25878

Relativistic fluids dynamic equations, using Banach type Lagrangians

11 p1689 A72-26503

Limiting form of equations for perfect gas steady two dimensional flow under gravity effects

12 p1797 A72-27177

Plane unsteady potential isentropic gas flow equations solution interpreted as shallow water motion over horizontal bottom

13 p1893 A72-28717

Iterative solution of coupled nonlinear differential equations under boundary conditions for flow and heat transfer of Rivlin-Ericksen fluid between rotating parallel disks

13 p1986 A72-28881

Orr-Sommerfeld equation solution by variable mesh finite difference method, applying to plane Poiseuille flow

13 p1986 A72-29112

Numerical integration of boundary layer equations through region of reverse flow past parallel flat plate with negative surface velocity

13 p1944 A72-30033

Flow equations for floating body flowmeters, discussing density and viscosity effect, instrument characteristics and computer algorithms

14 p2104 A72-30484

Third order extension of perturbation method to solve Oseen equations for two dimensional steady viscous flow past cylindrical body at low Reynolds number

14 p2095 A72-30722

Local subsonic flow region in transonic free flow past airfoil profile, transforming flow differential equations into linear Beltrami equations system via Chaplygin transformation

15 p2178 A72-31473

Perfect gas steady flow under gravity action, analyzing limiting equations

15 p2178 A72-31682

Numerical check on boundary layer equations asymptotic expansion solutions for Falkner-Skan reverse flow and unit Prandtl number compressible boundary layer with blowing

15 p2219 A72-32589

Three dimensional compressible turbulent boundary layer growth prediction, deriving entrainment equations from two dimensional incompressible flow relations

16 p2375 A72-32835

Pseudo-one dimensional dissociative nonequilibrium nozzle flow, presenting governing equations transformation via similarity parameter for oxygen

16 p2375 A72-32906

Unsteady boundary layer flow equations for arbitrarily smooth bodies moving relatively slowly through rotating liquid

16 p2376 A72-33007

Ideal fluids isentropic flow equations solution via Riemann invariants method, describing nonlinear waves linear interactions

16 p2376 A72-33110

Flow equations for corner boundary layer with favorable pressure gradients, indicating separation type main velocity profile

16 p2378 A72-33406

Energy balance equation of free turbulent boundary layer in incompressible fluid, deriving semiempirical formulas for turbulent viscosity coefficient

16 p2380 A72-34022

Compressible boundary layer with normal pressure gradients, investigating quasi-similar, nonlinear integro-differential equations properties at wall and sharp and blunt leading edges

16 p2345 A72-34048

Elliptic-hyperbolic relaxation algorithm for solution to three dimensional nonlinear transonic small disturbance potential equation for flow about swept wings

16 p2346 A72-34063

A method of solving partial differential equations for boundary layers

17 p2537 A72-34195

Subsonic, transonic, and supersonic nozzle flow by the inverse technique.

17 p2483 A72-34206

Symmetries of the boundary-layer equations under groups of linear transformations.

17 p2541 A72-35241

On the stability of axisymmetric systems to axisymmetric perturbations in general relativity. I - The equations governing nonstationary, stationary, and perturbed systems.

17 p2611 A72-35315

Theoretical models for cavity and wake flows, outlining numerical methods for solving functional equations

18 p2679 A72-36387

Asymptotic estimate of steady state solution to Euler equations for ideal incompressible fluid flow with free boundaries

18 p2682 A72-36805

Time dependent solution to motion and energy equations for unsteady laminar spherical Couette flow of incompressible constant viscosity fluid

18 p2684 A72-37055

A kinematic theory of large magnetic Reynolds number dynamos.

19 p2833 A72-37248

Prandtl equations solution nonuniqueness for outside boundary layer flow tangential velocity inversely proportional to power of abscissa measured distance

19 p2784 A72-37394

General solutions of the heat equation in finite regions.

19 p2880 A72-37411

Flow equations for flat plate turbulent boundary layer with Reynolds, continuity and energy components, deriving semiempirical differential equation for turbulence scale

19 p2785 A72-37471

The motion of a vortex pair in a stratified atmosphere.

19 p2785 A72-37571

Numerical integration of nonlinear convective flow equations for arbitrary atmospheric temperature and wind profiles, discussing cloud streets formation

19 p2828 A72-37998

A theoretical solution of the Lockhart and Martinelli flow model for calculating two-phase flow pressure drop and hold-up.

19 p2787 A72-38392

Numerical analysis of three dimensional steady laminar free convection boundary layer due to heated ellipsoid, solving flow equations

19 p2881 A72-38394

Three-dimensional wings in hypersonic flow.

19 p2747 A72-38797

Compressible boundary-layer equations solved by the method of parametric differentiation.

20 p2914 A72-39614

Simplified conservation laws for finite-difference computations.

20 p2946 A72-39637

Non-isothermal laminar flow of gases through cooled tubes.

20 p2985 A72-39665

[ASME PAPER 72-HT-45] The solution of sharp-cone boundary-layer equations in the plane of symmetry.

21 p2989 A72-40650

Convergence of the successive approximation method in the problem of flows past bodies with strong injection

21 p2990 A72-41096

Behavior of a laminar boundary layer in the presence of a positive pressure gradient

21 p3045 A72-41142

Three-dimensional supersonic flows at large distances from a body of finite volume

21 p2994 A72-41661

Asymptotic behavior of the flow created by a shock wave incident on a wedge-shaped cavity

21 p3047 A72-41668

A system of linear equations with partial derivatives

21 p3077 A72-41822

Plane unsteady potential isentropic gas flow equations solution interpreted as shallow water motion over horizontal bottom

22 p3165 A72-42094

Numerical integration of three dimensional flow equations for supersonic jets of ideal gas exhausted from elliptical and rectangular nozzles

22 p3133 A72-42264

Flow equations for axisymmetric compressible conical flow in Busemann nozzle, noting numerical method for integral lines construction for given Mach number

22 p3134 A72-42288

A steady vortex ring close to Hill's spherical vortex.

22 p3166 A72-42312

On the solution of non-linear simultaneous equations with particular reference to fluid-dynamics.

22 p3199 A72-42325

Calculation of laminar boundary layers by means of a differential-difference method.

22 p3167 A72-42578

German monograph - Three-dimensional boundary layers at curved walls.

22 p3167 A72-43051

German monograph - Solution of the boundary layer equations for chemically reacting gases by a collocation method.

22 p3167 A72-43071

Boundary layer flow on a circular cylinder moving in a fluid at rest.

23 p3248 A72-43715

Second order boundary layer solutions on a curved surface.

23 p3280 A72-44063

[ASME PAPER 72-FE-21] Falkner-Skan flows with slip.

23 p3281 A72-44068

Averaged equations of laser heating of plasma in a focus-type system taking into account the heat of nuclear fusion.

23 p3322 A72-44223

Transonic flow past a wavy wall with compression shocks

24 p3360 A72-44999

Approximate equations of the flow behind a detonation with lateral confinement

24 p3463 A72-45041

Longitudinal curvature and displacement speed effects on incompressible laminar boundary layers.

24 p3393 A72-45249

Explicit numerical solution of the three-dimensional incompressible turbulent boundary-layer equations.

24 p3395 A72-45781

FLOW FIELDS

U FLOW DISTRIBUTION

FLOW GEOMETRY

Flow passage geometry optimization in compressor rotor design treated as boundary value problem with variational calculus solution

02 p0151 A72-12179

Aircraft engine exhaust geometry effects on smoke plume visibility, describing carbon particles light absorption characteristics by Beer-Lambert law [ASME PAPER 71-WA/GT-10] 05 p0704 A72-15903

Steady inviscid diabatic complex lamellar gas flow geometric properties, correlating stream and vortex lines via Beltrami surfaces in Euclidean space 05 p0747 A72-16667

Multistage axial flow compressor adjustment by flow geometrical dimension changes obtaining influence coefficient from linearized mathematical model 05 p0708 A72-17064

Multistage gas turbine flow area dimension change influence coefficient calculation from discrete nonlinear mathematical model through equation linearization 05 p0708 A72-17065

Blood flow mathematical formulation, considering tissues constitutive equations, geometrical configurations, arterial wave propagation, etc 06 p0768 A72-17959

Turbulent velocity field calculation for rectilinear duct with noncircular cross section, using integral transformation and dimensionless velocity ratio 06 p0800 A72-18110

Geometrical characterization of steady noncompressible fluid flow described by first order partial differential equations system 09 p1295 A72-23366

Wide angle conical diffuser performance improvement by conical splitter vanes, considering static pressure recovery 10 p1416 A72-23860

Vortex fluid amplifier design with asymmetrical flow fields, discussing effects of geometrical parameters variations on performance characteristics 10 p1423 A72-25053

Discharge coefficients of centrifugal screw-type swirl injector with helical channel, calculating drag and surface geometry effects 11 p1712 A72-26970

Gaseous species diffusion in carrier gas under various geometries and flow conditions, using finite element method 14 p2095 A72-30928

Analytical model for crosshatch ablation patterns geometric features and stability characteristics prediction based on viscoelastic melt layer interaction with gas boundary layer [AIAA PAPER 72-718] 16 p2480 A72-34030

Water table study of monostable fluidic amplifiers with allowance for geometrical similarity and Reynolds number for air operated models 16 p2353 A72-34139

Vortex growth in two-dimensional coalescing jets, 17 p2539 A72-34970

Electrostatic generator nonlinear internal resistance determination as function of flow parameters and model geometry via boundary conditions formulation 18 p2643 A72-35998

Random geometric problems suggested by turbulence, 18 p2678 A72-36016

Extendible variable profile nozzle for various flow regimes operation, developing numerical design algorithm 18 p2641 A72-36661

Effect of the slope and curvature of meridional current lines on the long-blade twist in axial turbomachines 20 p2979 A72-39588

Nonaxisymmetrical disturbances effect on stability of cylindrical fluid flow with exponential density variation in radial direction and axial and azimuthal velocities 21 p3045 A72-40682

Performance and limitations of shock tubes with imploding detonation drivers, 21 p3128 A72-40767

Researches on the two-dimensional retarded cascade. I, II, 22 p3133 A72-41944

Characteristics of the propagation of swirling jets of variable density 22 p3166 A72-42255

Iterative method for calculating the deformations of an induced flow 22 p3136 A72-42919

Perturbation of the shape of the cavity during motion in a ponderable liquid 23 p3280 A72-43797

Experimental investigation of the structure of turbulent jets expelled from a rectangular nozzle and nozzles with a limited head 23 p3280 A72-44020

Streamline and fieldline geometry with applications to MHD flow kinematic properties, discussing field

and momentum relations decomposition in terms of sound velocity 23 p3322 A72-44270

Temperature freezing in spherical or cylindrical expansion into a vacuum, 23 p3357 A72-44498

Suction side velocity distribution parameter characteristic relationship to profile geometrical parameters in turbine blade cascade system 24 p3394 A72-45366

FLOW GRAPHS

Aerodynamic profiles lift coefficient determination by empirical formula based on potential flow lines obtained by conformal mapping 13 p1894 A72-29132

FLOW MEASUREMENT

Fluidic sensors for flow velocity and fluid pressure, temperature and density measurements, emphasizing analog transducers with output signal FM and AM 01 p0006 A72-10151

Gas turbine nozzles aerodynamic throat area air flow measurement, describing accuracy, standards, reference nozzles and mounting flanges [SAE ARP 1195] 01 p0065 A72-10390

Open cycle gas core nuclear rocket engine flow studies to obtain maximum system reactivity at low uranium/coolant gas loss ratio 01 p0100 A72-11349

Laser flow anemometer technology, discussing velocity and spatial resolution, chromatic and temporal coherence, signal processing, frequency discrimination, spectrum analyzer and tracking filter 02 p0224 A72-11743

He-Ne traversing laser velocimeter for instantaneous axial fluid velocity measurement, describing signal analyzing system, construction and calibration 02 p0224 A72-11744

Fluidic sensors methods for position, angular velocity, fluid level, flow rate and temperature measurement 02 p0155 A72-11998

Cross flow through in-line tube bank, investigating surface roughness effects on behavior by pressure drop, static pressure and skin friction distributions measurements 02 p0203 A72-12102

Ballistocardiographic measurement of net cranial blood inflow during cardiac ejection 03 p0314 A72-13145

Myocardial blood flow measurement value in ischemic heart disease assessment, discussing Xenon 133 injection into coronary arteries 03 p0315 A72-13179

Xenon 133 method for coronary blood flow measurement during exercise, noting unsuitability for patients with coronary disease 03 p0319 A72-13180

Xenon 133 myocardial clearance method accuracy and reliability in determining high and low left coronary artery blood flow under different hemodynamic conditions 03 p0319 A72-13181

Myocardial blood flow measurement by Xe 133 clearance method after direct application of isotope into subendocardial and subepicardial layers of left ventricle 03 p0315 A72-13182

Coronary blood flow measurement in various hemodynamic conditions by argon technique, determining oxygen consumption and coronary vascular resistance 03 p0315 A72-13183

Spatial structure coherence in sublayer of turbulent boundary layer, using spanwise flow hot-wire anemometer measurements 04 p0462 A72-15116

Disk pump driven fluid layer device for density stratified water channel flow measurements, using hydrogen bubble technique 04 p0509 A72-15118

Combination flow-pressure measuring instrument based on rotating Flosdorf manometer with switching relay system 04 p0525 A72-15665

Sensors and circuit design for flow angle and shear stress measurements using heated film and wires [ASME PAPER 71-WA/FE-17] 05 p0661 A72-15930

Axial flow multistage compressor design, discussing high speed flow measurements and Reynolds number and blade airfoil shape effect on aerodynamic performance 05 p0601 A72-16483

High resolution mean flow and turbulence measurements in turbulent boundary layer on cooled hypersonic wind tunnel side wall at Mach 9.37 [AIAA PAPER 72-73] 05 p0650 A72-16802

Hot-wire anemometers signals resolution into velocity-temperature fluctuations correlations in compressible flow with shear turbulence wakes [AIAA PAPER 72-117] 05 p0664 A72-16822

Reciprocal temperature changes in dogs during constant thermodilation for coronary sinus blood flow measurement 06 p0769 A72-18197

Muscle blood flow relation to oxygen consumption from measurements during bicycle ergometer exercises, using Xe 133 clearance method 08 p1123 A72-20888

Turbulence measurements in liquids - Conference, Rolla, Missouri, September 1969 09 p1292 A72-22301

Electrochemical techniques for time averaged turbulent velocity gradient and components of fluctuating velocity gradient at solid surface 09 p1306 A72-22305

Turbulence measurements in shear flow systems including pipe, tank and multijet reactor configurations 09 p1292 A72-22306

German monograph on shaft and wall effect in aerodynamic measurements with three orifice pressure probes in wind tunnels 09 p1259 A72-22320

Small scale atmospheric turbulence measurement with airborne hot-wire anemometer, discussing optimal choice of experimental parameters 09 p1307 A72-22435

Multihole flow probe measurement data evaluation by multidimensional approximation of calibration curves and surfaces 09 p1260 A72-22631

Secondary flow types and measurement in axial flow compressor cascades, discussing energy losses 09 p1260 A72-22633

Electromagnetic velocity and flow measurements techniques application to cardiovascular patients, discussing utilization problems 09 p1272 A72-23275

Alternative heating local heat clearance probes for human muscle blood flow measurement 09 p1273 A72-23442

Turbulent boundary layer growth measurement on annular diffuser containing free vortex swirl 10 p1416 A72-23857

Living being inhalation flow rate measurement, discussing performance and characteristics of respiratory flowmeter 10 p1479 A72-23971

Ultrasonic Doppler flowmeter for instantaneous measurement of blood vessel flow velocity by averaging frequency shift over received signal power density spectrum 10 p1430 A72-24373

Axisymmetric turbulent jets local entrainment rate as function of axial distance from nozzle exit, using Ricou-Spalding porous wall technique 10 p1481 A72-24425

Assessment of regional myocardial temperature changes effect on blood flow measurements by heated cross-thermocouples in dogs 10 p1432 A72-25071

Two phase axisymmetrical air jet turbulence intensity determination from heat distribution parameters in wake of wire heated by electric current 10 p1471 A72-25172

Separation flow field measurements for space shuttle cylindrical configurations in hypersonic streams, using pressure heat transfer and visualization techniques [AIAA PAPER 72-294] 11 p1567 A72-25232

Non-Newtonian pipe flow turbulence measurements by laser anemometer, describing optical system and signal processing instrumentation [AD-742872] 11 p1646 A72-25554

Secondary flow measurements in rotating ducts, obtaining pressure distributions and cross-flow velocities [ASME PAPER 72-GT-17] 11 p1569 A72-25616

Flow measurement instrumentation for turbomachine rotors, noting telemetry type data transmission system with strain gage pressure transducers for turbocompressor [ASME PAPER 72-GT-55] 11 p1630 A72-25646

Measurement techniques for separated gas flows mean and fluctuating aerodynamic properties, discussing improved optical geometry for laser Doppler anemometer 13 p1956 A72-28632

Velocimeter design for MHD boundary layer flow velocity measurement, using Doppler frequency shift of laser light scattered from added macroscopic particles 13 p1957 A72-29360

Hydraulic fluids flow measurement in pipes by ultrasonic waves convection method, discussing transducers performance and mounting [ONERA, TP NO. 1078] 13 p1959 A72-29668

Aircraft atmospheric flow measurements of horizontal and vertical motions on mesoscales, using inertial reference system 14 p2127 A72-30300

Lagrange interpolation formula to determine flow elements shape in pneumatic sensor head with extended measurement range 14 p2104 A72-30372

Turbulent friction values diminished by reading errors in pitot tube flow measurement of solid particles suspensions and polymer solutions caused by viscoelastic associations 14 p2106 A72-31007

Eruptive center location and flow direction measurements for andesite and quartz latite lava flows in Mogollon Mountains

15 p2223 A72-31579

Laser Doppler velocimetry system design for optical measurement of intrablade flow velocity in turbomachinery

15 p2237 A72-32045

Turbulent mixing layers analytical and experimental mean velocity profiles, discussing Goetler eddy viscosity theory

16 p2374 A72-32832

Spanwise correlation measurement of vortex shedding behind circular cylinder in subcritical Reynolds number region

16 p2379 A72-33658

Gas flow direction measurement using flow to electric pulse converter

16 p2395 A72-33957

Optical method for measuring the velocity of particles entrained in a flow

17 p2554 A72-34892

Simple two-dimensional laser velocimeter optics.

17 p2558 A72-35845

Experiments using the birefringence of fluids in motion

18 p2679 A72-36367

Free convection similarity and measurements in flows with and without shear.

18 p2706 A72-36634

Investigation of Freon fire-extinguishing systems with a nucleonic gage.

18 p2648 A72-36674

Coronary flow determination in experimental conditions with the use of radioactive xenon.

19 p2755 A72-37475

Secondary flows in ducts of square cross-section.

19 p2789 A72-38795

Re-developing turbulent boundary layers behind yawed separation bubbles.

19 p2747 A72-38812

An investigation of the flow around rectangular cylinders.

19 p2747 A72-38813

Techniques for determining average density and related parameters in two-phase cryogenic flow systems.

19 p2805 A72-38835

Theoretical considerations of significance to the design of optical anemometers.

[ASME PAPER 72-HT-7] 20 p2926 A72-39678

Sting-free measurements of sphere drag in laminar flow.

21 p2989 A72-40110

Motion due to a moving internal heat source.

21 p3044 A72-40115

Hot wire data corrections in low and in high turbulence intensity flows.

21 p3051 A72-40220

Optical method for measuring the concentrations of axisymmetric gas jets

21 p3055 A72-40990

Peclet number, length/diameter ratio, Grashof number, Knudsen number, overheat ratio and yaw angle interaction effects in cylindrical hot-wire and hot-film probes cooling

21 p3057 A72-41620

Investigation of the operation of a vane anemometer in vacuum with the aid of an optical transducer for the rotational frequency

21 p3059 A72-41820

Pressure transmitter for flow parameter measurements of aerodynamic nozzles and static pressure taps rotating on turbine rotor blades

22 p3176 A72-42250

The characteristics of a cylindrical probe at high subsonic speeds. I - The case of zero inclination angle.

22 p3135 A72-42484

Carotid rete role in brain protection against extreme elevations of systemic blood pressure, presenting goat cerebral blood flow measurement procedure

22 p3144 A72-42671

Measurements of magnetotail plasma flow made with Vela 4B.

23 p3342 A72-44514

Measurement of the velocity distribution in the boundary layer over a flat plate with a diffusion flame.

24 p3464 A72-45062

Status of hotshot wind tunnels for hypersonic aerodynamic studies.

24 p3388 A72-45203

Jet impingement under VTOL aircraft.

24 p3364 A72-45779

FLOW PATTERNS

U FLOW DISTRIBUTION

FLOW RATE

U FLOW VELOCITY

FLOW REGULATORS

Distributed impedance controller synthesis for stabilization of plane fluid flows, investigating Rayleigh-Taylor instability

01 p0050 A72-10504

Flow control circuits design based on unvented bistable fluid amplifiers

10 p1422 A72-23970

FLOW RESISTANCE

NT AERODYNAMIC DRAG

NT FRICTION DRAG

NT SUPERSONIC DRAG

NT VISCOUS DRAG

Local skin friction evaluation in compressible flow, using incompressible Clauser charts and sublayer methods for adiabatic and nonadiabatic situations

03 p0341 A72-13614

Hydrodynamic field around sphere moving along Poiseuille flow axis determined by least squares method, formulating flow resistance

04 p0511 A72-14968

Respiratory flow resistance measurements in man, comparing esophageal catheter, plethysmographic, forced pressure oscillations and airway interrupter methods

04 p0481 A72-15222

Hydrodynamic resistance reduction for bodies moving under water, analyzing dynamic equations of viscous incompressible fluid

04 p0514 A72-15703

Rectangular channel flow of two immiscible viscoelastic Maxwell fluids with transient pressure gradient, deriving interface velocity, flow rate and wall resistance components

04 p0514 A72-15705

Gas turbine blade cooling channel hydraulic resistance calculation based on energy and continuity equations

05 p0707 A72-17061

Nonadiabatic real gas nozzle flow with friction and heat transfer to wall, obtaining solution by Runge-Kutta method

05 p0610 A72-17066

Heat transfer and hydraulic resistance of lamellar type heat exchangers with water/air working media, testing efficiency for various duct cross sections and Reynolds numbers

06 p0904 A72-18510

Viscous fluid steady nonaxisymmetric flow past rotating sphere, obtaining antitorque moment expressions and resisting force projections

10 p1469 A72-24547

Plethysmographic and laryngoscopic investigation of glottis opening and airway resistance relation to lung volume during panting and continuous slow expiration

11 p1586 A72-26611

Hyperoxia effect on human airways resistance during high pressure oxygen breathing

11 p1586 A72-26614

Heat transfer and hydraulic resistance for cooled air forced flows in narrow rectangular channels as function of pressure and Reynolds number

14 p2093 A72-30291

Turbulent friction relation to averaged velocity profile of liquid flow in pipes and channels

14 p2096 A72-31019

Estimation of the conductance of channels for rarefied gas flow by means of an optical analogue.

19 p2795 A72-37466

Heat transfer and resistance in a laminar gas flow with variable properties in an annular channel

19 p2786 A72-38040

Intensification of heat transfer in channels with turbulent gas flows

21 p3127 A72-40127

Influence of blowing on the resistance of a sphere in laminar viscous fluid flow

21 p3047 A72-41665

Heat transfer, adiabatic enthalpy (temperature) of the wall, and hydrodynamic resistance in the presence of turbulent and laminar flow of a compressible fluid in a round tube

22 p3164 A72-41883

Flow-stress recovery of nickel-aluminum alloys.

23 p3299 A72-43563

Baroclinic effects on the resistance law for the planetary boundary layer of the atmosphere.

24 p3397 A72-44956

Resistance in potential flows with no wakes and with steady closed wake, calculating normal and tangential thrusts contributions for sphere and circular cylinder

24 p3390 A72-44986

Heat release and resistance of the cylindrical heat exchangers of blades with a dual flow cooling system

24 p3434 A72-45625

FLOW SEPARATION

U BOUNDARY LAYER SEPARATION

U SEPARATED FLOW

FLOW STABILITY

NT BOUNDARY LAYER STABILITY

NT FLAME STABILITY

NT MAGNETOHYDRODYNAMIC STABILITY

MHD instabilities of plasma with current, using two fluid model in crossed magnetic-electric fields

01 p0109 A72-10486

Momentum exchange coefficient for surface layer neutrally stable flow after surface roughness change, noting error possibility in flow estimates for heterogeneous terrain

01 p0094 A72-10827

Two phase flow equations model application to fluidized beds and foams, predicting bed stability to small perturbations for comparison with experiment

01 p0093 A72-11272

Laminar liquid flow stability in vertical slots under natural convection, showing critical layer level for nonstationary perturbations

02 p0202 A72-11591

Hydrodynamic convective stability in catalytic chemical reaction with thermal and concentration coupling dependent on Lewis number

02 p0301 A72-12092

One dimensional plane magnetocoustic wave stability from synchronous flow in narrow flow gap MHD induction machine

02 p0265 A72-12263

Nonlinear development of instability wave in turbulent wake behind thin body based on integrals of mean flow momentum and kinetic energy equations

02 p0152 A72-12351

Incompressible two dimensional plane jet spatial stability analysis, presenting disturbance vorticity, Reynolds stress and energetics distribution in cross stream direction

02 p0152 A72-12352

Thin liquid layer linear hydrodynamic stability in vertical rotating tube with core gas flow

02 p0303 A72-12353

Rotation effects on three dimensional infinitesimal wave stability in Blasius boundary layer

02 p0205 A72-12354

Low density monatomic gas supersonic physical source flow, presenting departure from translational equilibrium

02 p0205 A72-12359

Book on thermodynamic theory of structure, flow stability and fluctuations covering equilibrium and nonequilibrium states, nonlinear situations and space-time behavior

02 p0261 A72-12624

Axial flow effect on vortex filaments stability by slender body analysis of force balance between Kutta-Joukowski lift and momentum flux inside filament

03 p0307 A72-13157

Integral conservation laws derivation for geostrophic zonal flow field disturbance, applying to flow stabilization

03 p0348 A72-13478

Rigid and compliant walls longitudinal curvature and compliance effects on incompressible laminar boundary layer hydrodynamic stability

03 p0342 A72-13854

Barotropic stability of stratified shear flow to non-geostrophic disturbances by linear analysis

04 p0541 A72-14453

Linear stability of nearly parallel steady plane viscous flows, using method of multiple scales

[ONERA, TP NO. 1044] 04 p0511 A72-14969

German monograph on two dimensional unsteady boundary layer calculation with unstable effects, using Navier-Stokes equations

04 p0512 A72-15245

Nonlinear disturbances of viscous flow in pipes and between rotating cylinders, considering Couette and Poiseuille flows

05 p0648 A72-16027

Unsteady axisymmetric incompressible pipe flow stability near piston, using Navier-Stokes equations solution with finite difference forms

05 p0653 A72-17006

Plane Poiseuille flow stability from Orr-Sommerfeld equation solution by Chebyshev polynomials expansion and QR matrix eigenvalue algorithm

05 p0653 A72-17009

Hartmann number for velocity pulsation free transition from turbulent MHD flow to laminar, noting difference relative to linear stability theory

06 p0860 A72-17679

Linearized hydrodynamic stability of viscoelastic fluid Couette flow in gravity field

06 p0798 A72-17778

Cylindrically symmetrical low viscosity fluid distortion and homogeneous spiral flow stability under rotational self excitation

06 p0799 A72-17981

Wall curvature and flexibility effect on incompressible laminar boundary layer hydrodynamic stability, considering Tollmein-Schlichting transverse wave disturbances

06 p0801 A72-18134

Marginally unstable plane parallel flow nonlinear response to two dimensional disturbance, noting localized burst relationship to Landau constant

06 p0801 A72-18163

Polar night jet idealized model with zero tropospheric and constant vertical stratospheric shear, considering instability due to small wave disturbances

07 p0130 A72-19103

Homogeneous laminar combustion in semiclosed cylindrical tube, relating stability to hydrodynamic and thermodynamic flow parameters longitudinal high frequency disturbances

07 p1101 A72-19988

Hydrodynamic stability problems with reference to Navier-Stokes equation solutions, discussing linearization principle application 07 p0969 A72-20066

Hydrodynamic stability small perturbation theory, considering potential flow in contact with flexible membrane 07 p0969 A72-20067

Flow stability of viscous fluid in annular space between rotating inner and axially oscillating coaxial outer cylinder, using perturbation method 07 p0971 A72-20089

Nonlinear stability theory for laminar flow of viscous incompressible liquids, noting application to Couette-Taylor flow between two concentric rotating cylinders 07 p0971 A72-20091

Rayleigh method convergence in ideal fluids axisymmetric flow stability with free boundaries and perturbations without mass forces 08 p1148 A72-20909

Critical Reynolds numbers estimation for flows having velocity profile with point of inflection, discussing plane parallel flows stability energetic analysis 08 p1151 A72-21660

Free convection effect on plane crystallization front instability under conditions of phase transition, using method of small perturbations 08 p1151 A72-21661

Instabilities development in flow field generated by shock wave propagation in exothermic gas mixture 08 p1255 A72-22042

Hydrodynamic stability of electrically conducting hot viscous fluid surrounded by perfectly conducting rigid boundary in presence of magnetic field 09 p1359 A72-22825

Motion equations approximate solution for viscous fluid Couette flow instability caused by spiral symmetry vortices 09 p1295 A72-23073

Turbulent gas flow induced by laser heating, emphasizing Rayleigh number as stability criterion 09 p1295 A72-23492

Initial disturbance level effects on laminar viscous jet stability from calculation of maximum amplification rate as function of physical parameters 10 p1465 A72-24149

Spiral flow stability between rotating and sliding cylinders, using modified energy theory based on assumption of disturbance invariance along preferred spiral direction 10 p1466 A72-24298

Experimentally produced vortex ring structure and stability, using dye and hydrogen bubble techniques for flow field, ring velocity and growth rate observations 10 p1466 A72-24327

Inviscid parallel stratified shear flow stability to two dimensional disturbances, solving Taylor-Goldstein stability equation for eigenvalues by computerized numerical integration 10 p1466 A72-24329

Aerodynamic noise generation mechanism of ideally expanded supersonic jet based on large scale flow instabilities, deriving mathematical model 10 p1418 A72-24331

Antisymmetric turbulences linear stability in incompressible plane Poiseuille flow between flexible walls solved by variational boundary value problem formulation 10 p1468 A72-24372

Finite amplitude disturbances effect on plane Poiseuille flow hydrodynamic stability, presenting numerical method for solving parabolic partial differential equations derived from Navier-Stokes equation 10 p1468 A72-24422

Transverse shear flow stability analysis based on disturbance energy balance determination, applying to ducted and jet stream boundary layer flows 10 p1469 A72-24531

Joule dissipation effect on convective instability of current carrying fluid in magnetic field 10 p1522 A72-24533

Laminar and turbulent boundary layer flow stability with forward separation areas 10 p1418 A72-24535

Laminar boundary layer instability to longitudinal vortices onset due to homogeneous suction from slightly concave permeable wall, determining Goertler parameter and wavenumber critical values 10 p1470 A72-25064

Second order fluids plane Poiseuille flow instability to finite amplitude disturbances, noting implications to Toms friction pressure reduction phenomenon in pipe flow 10 p1470 A72-25065

Drazin method application to thermal stratification effects on unbounded jets and shear layers stability characteristics 11 p1615 A72-25552

Small gap approximation for axial magnetic field effects on stability of nonrotationally symmetric

disturbances in inviscid flow between concentric rotating cylinders 11 p1694 A72-25773

Russian monograph on self oscillatory noise generation during gas jet ejection covering single, parallel, supersonic, flat and cylindrical jets stability 11 p1617 A72-26066

Integral conservation laws derivation for geostrophic zonal flow field disturbance, applying to flow stabilization 11 p1623 A72-26248

Stability of free shear layer in wind tunnel two layered temperature differentiated air flow against small periodic disturbances, noting critical Richardson number 11 p1619 A72-26638

Low carbon ultrafine grain steel tensile behavior, noting critical grain size for stable/unstable plastic flow transition 11 p1661 A72-26651

Barotropic instability and vorticity equation of zonal flow with superposed Rossby waves limiting predictability of real atmosphere 12 p1838 A72-27021

Incompressible viscoelastic isotropic fluid stability in Couette flow, discussing physical parameters effect on critical Reynolds number and cells shape of secondary flow 12 p1797 A72-27169

Viscous flow stability between two rotating nonconcentric cylinders, obtaining approximate solution to eigenvalue problem by perturbation method 12 p1799 A72-27846

Plane potential flow stability with respect to bounded and free hollow vortices, using conformal mapping method 13 p1941 A72-28716

Convection instability in viscous incompressible liquid layer with free boundaries under modulated external force field 13 p2064 A72-28723

Laminar channel flow stability loss dependence on Reynolds number and wave number, discussing conditions for separated flow self oscillations 13 p1941 A72-28765

CAT forecasting based on fluid mechanics experimental studies of stratified shear flows stability and meteorological analyses of aircraft CAT encounters 13 p1994 A72-28866

Prandtl number effect on stratified free shear layer stability, comparing critical Richardson number to linear inviscid theory result 13 p1942 A72-29111

Natural instabilities development in laminar boundary layer of incompressible flow, considering AM spectrum and abscissa-ordinate development compared to Orr-Sommerfeld equation solution 13 p1943 A72-29784

Inviscid plane Couette flow infinitesimal instability as initial value problem, using distribution-theoretic approach 14 p1216 A72-30230

Hydromagnetic channel flow stability computation via energy method, solving eigenvalue problem by direct forward numerical integration 15 p2283 A72-31212

Uniform rotation and magnetic field effects on gravitational stability of interface between two semi-infinite homogeneous streams 15 p2284 A72-31593

Thin liquid films on rotating horizontal disk, measuring flow, thickness and stability with asymptotic-expansion solution 15 p2334 A72-31616

Velocity gradient induced by local wall deformation, investigating effect on unstable natural frequencies amplification in laminar boundary layer 15 p2217 A72-31683

Attachment length as stability criterion for bluff-body stabilized electrodeless arc, showing linear dependence on flow velocity ratio to power density 15 p2336 A72-32406

Nonlinear stability theory for plane Poiseuille flow under finite amplitude perturbations, solving Orr-Sommerfeld boundary value problem via finite difference method 15 p2218 A72-32469

Nonrotating Hadley cells turbulence from steady one dimensional flow instabilities in thin nonrotating differentially heated atmosphere or ocean 15 p2219 A72-32722

Three dimensional ideal incompressible fluid flows under small velocity perturbation, using linearized Euler equations with respect to steady flow 16 p2375 A72-32932

Nonlinear instability of two dimensional unbounded incompressible viscous fluid flows under periodic small perturbation 16 p2376 A72-32933

Stability analysis of ideal incompressible liquid steady flow for given distribution, discussing velocity distribution effect on longitudinal cylindrical flow instability 16 p2376 A72-33093

Linearization and perturbation procedures to calculate nonlinear effects in fluid stability problems with application to nonlinear critical layer 16 p2377 A72-33338

Plane Poiseuille flow stability of incompressible second order fluids, noting destabilizing influence of viscoelasticity 16 p2379 A72-33829

Stabilization of magnetohydrodynamic flows by a distributed feedback system 17 p2587 A72-34459

Theorem for instability of rectilinear vortices in two dimensional steady flow of ideal liquid with or without submerged obstacle 17 p2539 A72-34910

Stability of spiral flow and of the flow in a curved channel. 17 p2540 A72-35051

Mechanism by which a two-dimensional roughness element induces boundary-layer transition. 17 p2542 A72-35611

The stability of Poiseuille flow in a pipe of circular cross-section. 18 p2681 A72-36480

Poiseuille flow linear spatial stability in rigid pipe under infinitesimal disturbances, obtaining propagation modes eigenvalues 18 p2681 A72-36481

Convective cells formation in fluid unsteady flow between two horizontal rigid boundaries with time periodic temperature distribution 18 p2681 A72-36483

Instability of a moving plane-parallel layer 18 p2682 A72-36883

Nonlinear development of capillary waves in a fluid jet 18 p2682 A72-36885

The influence of geostrophic force on the stability of an heterogeneous conducting fluid with a radial gravitational force. 18 p2683 A72-36933

Perturbations development in laminar flow and transition to turbulent flow based on nonlinear theory of hydrodynamic stability 19 p2785 A72-37468

Finite amplitude neutrally stable two dimensional disturbances in parallel flows for large Reynolds numbers, investigating phase shift across critical layer 19 p2786 A72-37572

Stability of the Couette rotatory motion of two-phase media 19 p2787 A72-38209

Spectral theory of Taylor vortices. I - Structure of unstable modes. 19 p2788 A72-38550

Coriolis force influence on convective stability in viscoelastic fluid layer heated from below, contrasting with rotation effects on ordinary viscous fluid 20 p2982 A72-39326

Instability of hypersonic viscous shock layer with finite rate chemistry. 20 p2886 A72-39635

The linear stability of flow in a circular pipe in the presence of a strong transverse magnetic field. 20 p2958 A72-40018

Non-local effects in the stability of flow between eccentric rotating cylinders. 21 p3043 A72-40111

Large-scale instabilities of turbulent wakes. 21 p3044 A72-40116

Stability loss in Poiseuille flow within two dimensional channel during Reynolds number passage through critical value 21 p3044 A72-40265

Finite core infinite extent helical vortex filament stability to small sinusoidal displacements of centerline 21 p3045 A72-40649

Nonaxisymmetrical disturbances effect on stability of cylindrical fluid flow with exponential density variation in radial direction and axial and azimuthal velocities 21 p3045 A72-40682

Microstructure of turbulent flow in the stabilized flow region in a channel 21 p3045 A72-41054

Flow quality improvements in a blowdown wind tunnel using a multiple shock entrance diffuser. [AIAA PAPER 72-1002] 21 p3041 A72-41587

Investigation of the self-oscillations of a continuous medium arising at a stability loss in operation steadiness 22 p3164 A72-41907

Time-periodic solutions of boundary layer equation systems 22 p3164 A72-41908

Plane potential flow stability with respect to small perturbation flow of bounded and free hollow vortices, using conformal mapping method 22 p3165 A72-42093

Convection instability in viscous incompressible fluid layer with free boundaries under modulated external force field 22 p3243 A72-42099

Flow stability of ideal compressible and incompressible fluids, solving Navier-Stokes equation for rotating liquid with free boundary in gravitational field 22 p3165 A72-42151

Convective instability of a fluid in hydrodynamically connected vertical channels 22 p3166 A72-42260

Mars - The effects of topography on baroclinic instability. 22 p3225 A72-42504

Incompressible free shear layers instability, considering Reynolds number, velocity profile, disturbances and compressibility effects 22 p3167 A72-42579

Explosive instability temporal development, noting linear damping role in nonlinear wave interaction under conservation laws of energy and momentum 23 p3282 A72-44318

Experiment of supersonic air intake buzz. 23 p3249 A72-44496

Instabilities in the reaction zones of detonation waves. 24 p3462 A72-45029

Stability of the laminar flow of a 'power-law' non-Newtonian fluid in the boundary layer on a flat plate 24 p3393 A72-45255

Investigation of the stability of the tip vortex generated by hovering propellers and rotors. 24 p3361 A72-45327

Stability of coaxial rotating jet and vortex of different densities. 24 p3394 A72-45562

FLOW THEORY

NT MIXING LENGTH FLOW THEORY

Subsonic linearized theory for symmetrical cranked wings at zero incidence, presenting corrected formulas for streamwise and spanwise perturbation velocity components due to wing thickness 01 p0001 A72-11154

High speed jet noise source physical properties interpretation by theory and scale-model experiments for supersonic transport aircraft noise suppression problem 02 p0154 A72-11973

Nonlinearity effects on two dimensional steady supersonic dissipative flow governed by Navier-Stokes equations, obtaining expressions for flows past thin airfoil and wedge 02 p0203 A72-11976

Supersonic and hypersonic flows with attached shock waves over delta wing at angle of attack, deriving unified theory for flow field 02 p0150 A72-12030

Compressible viscous flow between concentric fixed and rotating disks, comparing analog computer calculation with experiment on radial flow 02 p0203 A72-12099

Turbulent flow development in concentric annuli from modified Reichart integral equation model for eddy diffusivity of momentum 02 p0203 A72-12103

Incompressible boundary layer theory development to include second order curvature effects, determining suction velocity to maintain constant displacement thickness on sphere 02 p0204 A72-12104

Book on mathematical fluid dynamics covering viscous and ideal fluid motion, boundary theory, constitutive equations, hydrodynamics and kinematics 02 p0206 A72-12623

Plane cavity flow past symmetric ogival obstacles, applying variational principle to fixed point theorem 02 p0206 A72-12625

Intermittency factor of diffuser flow boundary layer with positive pressure gradient, using hot wire anemometers and multichannel analyzer 04 p0461 A72-14411

Unsteady approach to nonisothermal flow theory for Couette flow, making general assumptions concerning rheological law and temperature dependence of fluidity 04 p0512 A72-14985

Book on fluid dynamics covering theories of perfect, viscous and compressible fluids, infinite and finite span wings, boundary layer flow, etc 04 p0462 A72-15357

German book on turbulent flow theory and applications covering isotropic and homogeneous nonisotropic fields, shear flows, pipe flows, free turbulence, boundary layers, etc 05 p0649 A72-16286

Explicit finite difference procedure to solve time averaged equations of motion for unstalled turbulent duct flows in coordinate system approximating real flow streamlines [AIAA PAPER 72-43] 05 p0651 A72-16878

Circular crown theorems with aerodynamics applications 06 p0756 A72-18109

Fluctuating and steady model for turbulent reactive and nonreactive flow, solving for turbulent kinetic energy and density by averaging procedure [AIAA PAPER 72-68] 07 p0966 A72-18948

German book on nonlinear free boundary value problems of two dimensional hydrodynamics covering gravity, capillary and irrotational waves, liquid flow in channel, etc 07 p0967 A72-19183

Axial flow turbomachines three dimensional flow theory, using orthogonal curved coordinate system 07 p0910 A72-20104

Solid cylinder stress-strain state under thermal and mechanical loads, obtaining analytical solutions via flow theory based on Von Mises yield condition 09 p1401 A72-22723

Analog simulation of hyperbolic differential equations with split boundary conditions, comparing to digital solutions to nonlinear flow 10 p1445 A72-24454

Computerization of panel flutter boundary calculations with aerodynamic forces derived from linear three dimensional unsteady potential flow theory [AIAA PAPER 72-403] 11 p1731 A72-25424

Sheet flow theory for pulmonary alveolar blood flow, discussing blood pressure effects, membrane tension, blood volume and transit time distribution 11 p1589 A72-26702

Tacky adhesive tearing between two flexible strips, solving Newtonian viscous fluid slow flow problem by iterative numerical scheme 12 p1798 A72-27831

Rotating airfoil experimental test program for verification of Himmelskamp and Dwyer-McCroskey theoretical analysis, presenting graphs of lift coefficient vs angle of attack 12 p1752 A72-28124

Velocity distribution downstream of nonuniform single and multiple smoothing screens, presenting theory based on energy losses and flow direction changes 13 p1940 A72-30100

Free stream turbulence and pressure gradient effects on boundary layer transition, correlating theoretical prediction methods and experimental results 14 p2093 A72-30253

Linear theory based analysis of compressible electroconductive fluid flow satisfying perfect gas equation in presence of thin profiles within quasi-aligned magnetic field 14 p2095 A72-30824

Classical flow problem solution by fixed point approach, using quasi-Lipschitz conditions for Newtonian potential gradients 15 p2216 A72-31468

Flow theory improvement for laminar radial flow between parallel plates, considering inertial effects 15 p2219 A72-32479

Russian book on magnetogasdynamics flow theory and calculations covering plasma flows and energy conversion in MHD channels of dc generator 16 p2438 A72-33873

Book on mathematical methods for viscoelasticity problems covering shear stress, viscometric flow, stress analysis, Fourier and Laplace transforms, momentum, equilibrium and constitutive equations, etc 16 p2427 A72-33975

Subsonic, transonic, and supersonic nozzle flow by the inverse technique. 17 p2483 A72-34206

Atmospheric turbulence statistical theory, discussing random flow field characterization by property expressed in ergodic theorem 17 p2537 A72-34273

A comparison of flow and deformation theories in a radially stressed annular plate. [ASME PAPER 72-APM-44] 17 p2627 A72-34781

A new theoretical model for representing jet penetration into a subsonic stream 17 p2538 A72-34888

Unsteady flow at the junction of a branched duct. 17 p2539 A72-34971

Mathematical models for flow ejection and aorta pressures based on displacement ballistocardiography and time dependent incompressible flow theories respectively 18 p2649 A72-36035

Expansion solution for subsonic compressible flow. 18 p2679 A72-36124

One-dimensional theory of flows with combustion 18 p2740 A72-36246

Flow problems solutions estimation by variational principles application, exemplifying by plane Couette and Poiseuille and axisymmetric pipe flow 18 p2679 A72-36391

A new method of analysis in laminar-flow theory. 18 p2681 A72-36551

Alternate singular perturbation theory of high Reynolds number flow over flat plate to eliminate asymptotic matching and composite solution for accuracy improvement 18 p2684 A72-37083

The Poincare Lighthill perturbation technique and its generalizations. 19 p2827 A72-38383

High Reynolds number turbulence and vortices in journal bearings, discussing validity of flow field models based on mixing length and pipe flow theory 20 p2930 A72-39972

Two-dimensional subsonic linearized theory of the unsteady flow through a blade-row with small steady pitch and camber angle. [ICAS PAPER 72-12] 21 p2990 A72-41137

Turbulent flow experimental and theoretical investigation, discussing Reynolds stress transport equations, shear layers and turbulence models in context of digital prediction methods 21 p3047 A72-41639

Calculation of potential flow about aerofoils using approximation by splines. 22 p3135 A72-42849

A simple theory for the two-dimensional compressible turbulent boundary layer. [ASME PAPER 72-FE-15] 23 p3280 A72-44062

Streamline and fieldline geometry with applications to MHD flow kinematic properties, discussing field and momentum relations decomposition in terms of sound velocity 23 p3322 A72-44270

FLOW VELOCITY

Space-time correlations of convection turbulent velocities in smooth circular duct with longitudinal separations 01 p0049 A72-10038

Velocity field of sonic flow about aircraft wing profile, solving mixed Cauchy problem 01 p0001 A72-11178

Turbulent flow velocity measurement pulsed wire technique 01 p0072 A72-11229

Slow viscous flow shear stress and velocity field analysis, using photoviscosity and bubble technique [SESA PAPER 1902] 02 p0201 A72-11508

Compressible boundary layer flow problems, using weighted residuals method with exponentials in velocity and enthalpy approximations 02 p0204 A72-12258

High temperature and pressure detonation gas expansion as shock wave from cylindrical volume, calculating flow velocity, pressure and density 02 p0302 A72-12285

German book on liquids flow rate measurement techniques covering physical principles of flow measurement including pressure, magnetic or inductive and ultrasonic methods 02 p0230 A72-12299

Turbulent boundary layer fluid dynamic behavior under transpiration and acceleration effects, presenting mean velocity profile data, skin friction and mixing length model [ASME PAPER 71-HT-F] 02 p0205 A72-12315

Concentric spherical heat exchanger, showing heat transfer coefficient decrease with coolant flow rate increase 02 p0303 A72-12320

Approximate solution in gas kinetic theory, considering temperature jump, velocity and viscous slip problems 02 p0205 A72-12356

Self magnetic coaxial plasma accelerator integral output data, presenting mass velocities and thrust measurement [DGLR PAPER 71-103] 02 p0266 A72-12736

Upstream influence on MHD flow velocity by Rankine body moving parallel to uniform magnetic field in conducting fluid 03 p0394 A72-13153

Cold plasma flow rate determination from emission inhomogeneities, using time of flight method and high speed streak photography for instantaneous velocity measurements 03 p0396 A72-13663

Turbulent shear flow mean velocity profiles, calculating eddy diffusivity for momentum and Reynolds stress 03 p0343 A72-14323

Photomultiplier signal for water axial velocity in glass pipe, providing turbulent liquid flow information and laser Doppler velocimeter evaluation 04 p0520 A72-14438

Velocity and shear stress in laminar boundary layer flow on flat plate with narrow suction slot 04 p0461 A72-14461

Comparative velocities of high energy gas jets of Ne, oxygen and carbon dioxide from outlet pipes, using Voitenko compressors 04 p0510 A72-14537

Pressure distribution and compressible gas critical flow rate in constant cross section circular pipe with impermeable adiabatic wall from Frossel equations 04 p0511 A72-14640

MHD approximation to solve natural convection problem in vertical channel under external inhomogeneous magnetic field, noting fluid flow rate 04 p0555 A72-14646

Linearized constant temperature hot-wire anemometer calibration for shock tube unsteady flow velocity measurements with low strength wave propagation 04 p0521 A72-14920

Turbulent flow from rotating disk, calculating mean velocities, turbulent intensities and Reynolds stress component 04 p0513 A72-15332

Viscoelastic fluid flow past infinite plane porous wall with time dependent suction, investigating mean velocity profile and wall shear stress 04 p0514 A72-15704

Rectangular channel flow of two immiscible viscoelastic Maxwell fluids with transient pressure gradient, deriving interface velocity, flow rate and wall resistance components 04 p0514 A72-15705

Plasma velocity, gas pressure, wall heat flux and shock heated region extent measured in electrical discharge shock tube, discussing ionization relaxation process 05 p0693 A72-15849

Cylindrical positive probe behavior in high speed collisionless mesothermal plasma flow [ONERA, TP NO. 1000] 05 p0660 A72-15860

Mathematical analysis of Vuilleumier refrigerator, calculating internal pressures, temperatures and gas flow rates via computer program [ASME PAPER 71-WA/HT-33] 05 p0745 A72-15886

Average stagnation pressure measurement in low velocity ducted gas flow with nonuniform velocity profiles, discussing mathematical technique and computer program [ASME PAPER 71-WA/PUR-1] 05 p0645 A72-15910

Turbulent flow in smooth and rough pipes at Reynolds numbers 30,000-480,000, presenting velocity mean and fluctuating components rms and cross correlation values [ASME PAPER 71-WA/FE-7] 05 p0647 A72-15935

Superposable and self-superposable MGD flows from nonlinear differential equations, considering entropy, flow velocity and magnetic field strength 05 p0694 A72-16030

High Reynolds number flow between two infinite rotating disks, investigating viscosity effects on flow velocity distribution type from analytic approximation 05 p0649 A72-16611

High speed boundary layer flow three dimensional disturbances interaction with thermal and ablative response in adjacent surface material, considering laminar and turbulent compressible flows [AIAA PAPER 72-93] 05 p0748 A72-16811

Internal axisymmetrical steady inviscid rotational flow velocity profiles simulation by means of shaped wire gauze screens [AIAA PAPER 72-165] 05 p0650 A72-16830

Turbine blade row coolant flow velocity, injection location and temperature effects on kinetic energy output [AIAA PAPER 72-12] 05 p0707 A72-16866

Jet peak velocity decay in single and multielement nozzles for STOL aircraft externally blown flaps, noting noise reduction due to flow mixing [AIAA PAPER 72-48] 05 p0608 A72-16927

Velocity and exit angle determination for flow behind turbine blade cascade with cooling air exhaust through blade trailing edges from continuity equations 05 p0707 A72-17063

Uniformly curved fluid conveying tube free vibration and stability, showing flow velocity, fluid pressure and Coriolis force effects on natural frequency 06 p0821 A72-17853

Anticavitation properties improvement of volute centrifugal pumps during low flow rate operation by reducing back currents with truncated cone 07 p0914 A72-18984

Hydrodynamic flow parameters in laminar incompressible water boundary layer on heated plate, noting plate surface heating effect on velocity profile 07 p0968 A72-19766

Axisymmetric flow of ideal incompressible liquid with free boundary and variable velocity, taking into account external mass forces effect 07 p0968 A72-19899

Steady viscous incompressible fluid flow in circular disk with prescribed velocity components at low Reynolds numbers, considering computer tested numerical method 07 p0972 A72-20102

Incompressible fluid near equilibrium turbulent flow velocity distribution through plane diffuser, taking into account upstream conditions 07 p0972 A72-20115

Aortic flow disturbances in vivo study by hot-film anemometer, considering peak flow velocity and pulse rate effects 07 p0934 A72-20537

Pneumatic fluid power valve flow rate derivation in terms of flow passage effective area and critical pressure ratio 08 p1113 A72-22158

Electrochemical techniques for time averaged turbulent velocity gradient and components of fluctuating velocity gradient at solid surface 09 p1306 A72-22305

Turbulence generated by moving obstacle in tank of stably stratified fluid, measuring velocity and concentration fluctuations with hot-film and electrode conductivity probes 09 p1293 A72-22308

Spatial plastic flow in arbitrary incompressible continuous medium with instantaneously inextensible family of planes, deriving velocity field formulas 09 p1403 A72-22758

Convective heat transfer between jets produced by plasmotrons and heated substrate, showing independence of plasma flow rate 09 p1319 A72-23189

Air velocity calculation from hot-wire anemometer measurements in variable density flow, discussing correction factors checking method and application to internal combustion engine 09 p1315 A72-23390

Interstellar gas streaming velocity due to galactic spiral density waves, deriving mathematical expressions for Oort constant and differential galactic rotation nodes from Lin theory 09 p1391 A72-23538

High temperature and pressure detonation gas expansion as shock wave from cylindrical volume, calculating flow velocity, pressure and density 10 p1561 A72-23759

Anemometer probe with thermistors for low velocities of liquids derived from pulsed thermal conductivity gage 10 p1479 A72-24066

Argon plasma jet mean flow velocity radial distribution measurement method 10 p1520 A72-24205

Wind tunnel inlet effect on pulsed flow, relating velocity and pressure pulses 10 p1417 A72-24216

Velocity and magnetic field expressed by six scalar potentials from MHD equations system, noting compressible fluids flow 10 p1520 A72-24219

Shock wave patterns near sonic line in accelerating or decelerating nonhomotropic flows, extending Busemann homotropic flow description 10 p1419 A72-24841

Equilibrium state dynamics of Burger turbulence model with two velocity components, using Fourier amplitude representation 11 p1615 A72-25553

T-tube plasma flow velocity measurement via shock wave attenuation recording technique 11 p1693 A72-25561

Gas-particle flow trajectories, velocities and pressure distribution in axial flow turbine stage, using cascade tunnel and high speed photographic techniques [ASME PAPER 72-GT-57] 11 p1571 A72-25648

Oscillatory gas combustion mechanism and stability boundary characteristics, determining burning time from flame height and flow rate 11 p1745 A72-25753

Current sheet velocity limitation in magnetically driven shock tube with plasma electrodes, examining wall ablation and friction and Hall current effects [AIAA PAPER 72-409] 11 p1695 A72-26160

Porous-tungsten mercury vaporizers design and tests for flow rate, liquid intrusion pressure level and mechanical strength [AIAA PAPER 72-484] 11 p1710 A72-26210

Anodic dissolution of metals during electrochemical precision processing, studying electrolyte composition and flow and mixing rates 11 p1640 A72-26255

Electromagnetic wave interaction with irrotational moving fluid based on Maxwell equations and Minkowski constitutive relation, noting flow velocity effects on scattering 11 p1689 A72-26471

Instantaneous and continuous blood flow velocity measurement by Doppler ultrasonic flowmeter using transcutaneous and implanted probes 11 p1589 A72-26778

Hot-wire measurement of vector velocity modulus and sign in one dimensional unsteady gas flow 12 p1806 A72-27178

Radiation distribution and power output characteristics of Nd in phosphorus oxychloride solution circulating liquid pulsed laser for various flow velocities 12 p1821 A72-27599

Flow rate limits increase and near homogeneous stress concentration in active hot extrusion of Al alloys 12 p1814 A72-27644

Tracer particle motion behavior in laser anemometry for turbulent flow, comparing liquids with gases for accuracy 12 p1809 A72-27763

Viscoplastic media flow rate in noncircular tube from Newtonian fluid velocity profile, using Green formula 12 p1799 A72-27981

Gas turbine engine combustion chamber, investigating swirl vane air flow rate effects on circumferential nonuniformity of gas temperature field at outlet 12 p1861 A72-28132

Flow velocity fluctuation intensity relationship to turbulent energy dissipation based on Kolmogoroff similarity hypothesis 12 p1799 A72-28133

Parametric approximation of unsteady laminar boundary layer in incompressible fluid in terms of flow velocity and friction characteristics 12 p1799 A72-28177

Shock wave propagation and damping in system of constant density gas bubble suspension in liquid flow with uniform velocity 13 p1940 A72-28436

Uniform suction effect at stationary plate on longitudinal and transverse velocities of plane Couette flow between parallel plates 13 p1941 A72-28884

Constant pressure gradient valves static characteristics, describing approximate procedures for flow rate determination without allowance for hydrodynamic effects 13 p1899 A72-29134

Coaxial source accelerating circuit resistance, capacitance and inductance effect on velocity imparted to plasma jet 13 p2015 A72-29453

Undisturbed and active solar photospheric turbulent velocity determination by comparing half widths of observed weak Fraunhofer line profiles with model calculation 13 p2049 A72-29929

Velocity calculation from pitot tube pressure measurements in compressible two phase flow, taking into account droplet momentum loss 14 p2104 A72-30252

Differential turbulent shear flow equation reduction to deduce similarity criteria for velocity pulsations, using Karman transformation 14 p2094 A72-30292

Velocity perturbation functions in linear theory for bounded stream flow past slender profile 14 p2070 A72-31018

Plasma velocity, gas pressure, wall heat flux and shock heated region length measured in electrical discharge shock tube without diaphragms, discussing ionization relaxation process 15 p2283 A72-31268

Navier-Stokes equation for unsteady asymptotic suction flow over flat plate, plotting velocity distribution profiles 15 p2178 A72-31406

Velocity gradient induced by local wall deformation, investigating effect on unstable natural frequencies amplification in laminar boundary layer 15 p2217 A72-31683

Velocity distributions for slow steady rotational motion of non-Newtonian inelastic viscous fluid contained between two concentric spheres, using successive approximations 15 p2217 A72-31689

Contracting or diverging stream flow mean velocity change effects on airfoil pressure distribution, circulation and lift, deriving vortex distribution expression 15 p2179 A72-32023

Attachment length as stability criterion for bluff-body stabilized electrodeless arc, showing linear dependence on flow velocity ratio to power density 15 p2336 A72-32406

Streaming MHD flow past semiinfinite flat plate in presence of perpendicular uniform magnetic field, obtaining velocity field at large distances 15 p2288 A72-32480

Three dimensional flow of steady neutral horizontally inhomogeneous planetary boundary layer, studying hodograph, velocity, vorticity, energetics and eddy coefficients 15 p2266 A72-32723

Subsonic wind tunnel for pulsed flows with speed modulation as periodic function of time 16 p2372 A72-32898

Spatial flow velocity fields of incompressible continuous media with family of instantaneously inextensible planes, applying plastic flow theory 16 p2423 A72-33107

Flow equations for corner boundary layer with favorable pressure gradients, indicating separation type main velocity profile 16 p2378 A72-33406

Transonic plane flow past wavy wall during choked wind tunnel operation, calculating flow velocity from Mach-Zehnder interferometer measured density distribution 16 p2378 A72-33508

Hydrodynamic equations for low speed steady external rarefied gas flows past circular cylinder, noting drag and heat transfer coefficients 16 p2344 A72-33568

Monitor and regulator for automatic speed control and flow velocity measurement in wind tunnel 16 p2392 A72-33609

Vapor pressure and velocity distributions in rarefied gas flows through narrow slits under vacuum conditions with ice sublimation 16 p2380 A72-33854

Supersonic vortex boundary layer flow velocity profiles behind flat plate indentation for Mach numbers 1.7-3.0 and Reynolds numbers to 40,000,000 16 p2380 A72-33857

Resonant diffusion in strongly turbulent plasmas, deriving equations for evolution of macroscopic properties including temperature and flow speed
16 p2439 A72-33934

Operation and calibration of three blade rotating vane anemometer for rarefied gas flow velocity measurement
16 p2395 A72-33966

Three dimensional small perturbation effects on laminar and turbulent low and high speed boundary layer flows
[AIAA PAPER 72-713] 16 p2344 A72-34034

Nitrogen plasma jet flow, attributing discrepancies in electrical conductivity and velocity to shock effects on probe measurements
[AIAA PAPER 72-671] 16 p2440 A72-34069

Scattering of electromagnetic waves from an inhomogeneous magnetoplasma column moving in the axial direction.
17 p2587 A72-34359

Memories of longitudinal fluctuations of velocity in a smooth circular duct
17 p2539 A72-34907

Velocity and flux dependence of the solar-wind helium abundance.
17 p2602 A72-35607

Hydrogen and helium velocities in the solar wind.
17 p2602 A72-35716

Turbulent micro and macromotion velocities in solar photosphere from CN molecule vibrational band line contours
17 p2617 A72-35735

Simple two-dimensional laser velocimeter optics.
17 p2558 A72-35845

Expansion solution for subsonic compressible flow.
18 p2679 A72-36124

Flow of a viscous liquid round a cylinder for Reynolds numbers 60 and 80.
18 p2679 A72-36233

Experiments using the birefringence of fluids in motion
18 p2679 A72-36367

Fluid transition through critical value, considering self oscillation onset mode frequency
18 p2681 A72-36663

Turbulence characteristics of flows with large velocity gradients in rectangular MHD channel with copper walls
18 p2715 A72-36813

The unsteady boundary layer flow in a convergent channel.
18 p2683 A72-36930

Study by phase detection of the velocity of a molecular jet
18 p2714 A72-37200

Prandtl equations solution nonuniqueness for outside boundary layer flow tangential velocity inversely proportional to power of abscissa measured distance
19 p2784 A72-37394

Magnetohydrodynamic channel flow with an arbitrary inlet velocity profile.
19 p2842 A72-38446

Thermoanemometer measurements of turbulence degree in wake behind square mesh grids in water flow within low speed wind tunnel
20 p2912 A72-39364

Direct measurement of the velocity gradient in a fluid flow.
20 p2926 A72-39633

Uniformly exact solution of the problem of the flow past a slender profile
20 p2886 A72-39904

Flow of a non-Newtonian fluid in a tube with sinusoidal deformation.
21 p3044 A72-40192

Nonaxisymmetrical disturbances effect on stability of cylindrical fluid flow with exponential density variation in radial direction and axial and azimuthal velocities
21 p3045 A72-40682

Iterative solution to aerodynamic design of axial flow compressors used in turbojet engines, calculating meridional velocity distribution
21 p3099 A72-40930

Optimum design of MHD generator combustion chamber, noting effects of heating temperature, oxygen enrichment degree and flow velocities
21 p2997 A72-41065

Water film formation and breakdown during motion over solid surfaces, predicting flow rate difference due to contact angle hysteresis
21 p3085 A72-41178

Critical flow rate and pressure ratio for nitrogen flowing through convergent-divergent nozzle at stagnation conditions, emphasizing thermodynamic critical region
21 p3046 A72-41180

Combined buoyancy and flow direction effects on saturated boiling critical heat flux in liquid nitrogen.
21 p3130 A72-41184

Measurement of flow speed by the correlation method
21 p3056 A72-41252

Transverse mass flow past a sphere at small Reynolds numbers
21 p3047 A72-41664

Throttle characteristics and mixing chamber geometry effects on low pressure gas ejector operation, noting air flow and pressure rates in air ejectors
22 p3133 A72-41859

Constant coefficients for linearized flow rate equation of hydraulic throttle servodrive in closed circuit stability solution by Liapunov theorem
22 p3139 A72-41873

Unsteady laminar flow in a tube with arbitrary variation of the flow rate in time
22 p3164 A72-41892

Velocity distribution of quasi-steady and steady flow of ideal incompressible fluids with congruent streamlines, investigating conditions for vortex and irrotational flow
22 p3164 A72-41906

Fluidic flow-mode amplifiers physical dimensions and operating pressures restrictions, presenting design and performance evaluation theory and velocity profiles
22 p3139 A72-42048

Reverse flow sensing hot wire anemometer.
22 p3177 A72-42392

New results concerning the numerical calculation of the sonic flow around a given airfoil section
22 p3135 A72-42639

Analysis of the structure of the flow downstream of a sudden widening
22 p3167 A72-42643

Aircraft clamp-on flowmeter using IR heat source in thermistor bridge to monitor flow rate in hydraulic lines
22 p3180 A72-42715

Metallic corrosion testing in high velocity liquids
22 p3183 A72-42858

Iterative method for calculating the deformations of an induced flow
22 p3136 A72-42919

German monograph - Contribution to the experimental investigation of the heat transfer in a turbulent wall boundary layer in the region of a strong pressure rise.
22 p3167 A72-43064

Calculation of a profile or of a cascade of profiles for a velocity distribution given as a function of potential
22 p3136 A72-43096

Flow direction and velocity effects on metal burning rates of low carbon and Ni-Cr steels in pure oxygen, using diffusion model
22 p3245 A72-43185

Influence of tangential fluid injection on the performance of two-dimensional diffusers.
[ASME PAPER 72-FE-16] 23 p3280 A72-44064

Effects of transport velocity of wake vortex on aerofoil oscillations.
23 p3249 A72-44494

Boundary layer on bodies of revolution in longitudinal flows
24 p3390 A72-44723

Application of the method of hydrodynamic singularities to the calculation of the velocity distribution in doubly-periodic infinite blade cascade systems
24 p3390 A72-44874

Effect of the ratio of the axial-flow velocities in front of and behind the cascade on the aerodynamic coefficients of a plane compressor cascade
24 p3360 A72-44995

Velocity profiles of plane turbulent flow of incompressible fluid on porous surface in presence of suction
24 p3390 A72-45007

Statistical analysis of the turbulence near a wall by conditional sampling
24 p3392 A72-45066

Intermittent character of the viscous sublayer and interpretation of probability density measurements
24 p3392 A72-45072

Hydraulic duct transfer function determination for prediction of liquid-fuel engine space launcher LF vibrations, investigating incompressible flow rate modulation by deformable walls
24 p3392 A72-45117

Turbulent flow of drag reducing fluids between concentric rotating cylinders.
[CSME PAPER 71-52] 24 p3393 A72-45254

A means of measuring the rms value of velocity fluctuations in unsteady turbulent flow
24 p3403 A72-45259

Velocity profile of near-wall turbulent boundary layer with adverse pressure gradient, noting skin friction
24 p3393 A72-45357

Contributions to the study of turbulent flow in the vicinity of a flat wall
24 p3394 A72-45443

FLOW VISUALIZATION

NT NUMERICAL FLOW VISUALIZATION

Gas flow visualization technique using fluorescent plate with UV irradiated ozone tracer, noting application to wall attachment fluidic elements
01 p0072 A72-11198

Harmonium reed self excited oscillation mechanism, describing flow visualization, jet instability potential flow and aerodynamic forces
01 p0002 A72-11232

Hypersonic projectiles wake visualization with holography, using single mode ruby laser and reflected diffuse light techniques
02 p0224 A72-11742

Flat plate incompressible smooth surface boundary layer examination emphasizing turbulence production near wall, using hydrogen-bubble and hot-wire measurements with dye visualization
02 p0203 A72-11975

Classical optical measurement and holographic methods of flow field visualization, discussing operating principles, measurement sensitivity, three dimensional and depth-focusing properties
02 p0230 A72-12300

Optical visualization and probe measurements on combustion characteristics of liquid fuel in compression-ignition engine swirl chamber
02 p0271 A72-12436

Time dependent unsteady flows visualization around circular cylinders and flat plates decelerated from steady speed
02 p0206 A72-12773

Solid particle influence on underexpanded gas jet shock structures, using schlieren photographs
03 p0342 A72-13840

Visual investigation of semibounded axisymmetric MHD flow of liquid eutectic K-Na alloy under strong magnetic field effect
03 p0399 A72-14014

Bistable fluidic amplifiers switching dynamics, developing analytic performance prediction method from flow visualization studies
[ASME PAPER 71-WA/FLCS-8] 05 p0615 A72-15916

Supersonic interaction in streamwise corner of intersecting wedges, including pitot traverse, surface pressure and oil flow visualization measurements
[AIAA PAPER 72-6] 05 p0606 A72-16862

Recirculating cells in laminar coaxial jets investigated by smoke introduction into flow field and hot-wire techniques
[AIAA PAPER 72-150] 05 p0651 A72-16880

HF tracer gas detection in inert and combusting flows, using IR absorption technique for gaseous flow visualization
[AIAA PAPER 72-70] 05 p0651 A72-16904

Supersonic turbulent boundary layer interaction with compression corner, noting static pressure distributions, flow visualization and schlieren photographs
[AIAA PAPER 72-114] 05 p0610 A72-16976

Flow visualization in supersonic axial compressor by short exposure schlieren photography of shock wave patterns in rotating annular cascade of compressor blades
[ONERA, TP NO. 1026] 05 p0708 A72-17192

Laminar to turbulent flow transition spectral evolution and catastrophic transition, discussing visual experiments and analytical methods
06 p0800 A72-18121

Towing tank for flow visualization studies of trailing vortices formation and breakdown
07 p0909 A72-20088

Direct simulation Monte Carlo method for rarefied gas dynamics, discussing computer display units use for flow visualization
07 p0973 A72-20344

Flow characteristics of liquid layers adjacent to vapor bubble, visualizing flow via particle motion
08 p1151 A72-21670

Boundary layer stability and turbulence observation by flow visualization using dense Al flake suspension
09 p1292 A72-22304

Visual observations of wall in turbulent pipe flow, using suspending solid MgO particles
09 p1306 A72-22310

Supersonic and subsonic jet flows coexistence in constant section duct, analyzing pressure on walls and in fluid and schlieren visualization
[ONERA, TP NO. 976] 09 p1294 A72-22813

Reynolds number and cylindrical spacing effect on Karman vortex street formation from smoke visualizations of single and tandem cylinder wakes
09 p1261 A72-22939

Holographic interferometry application to weak inhomogeneities visualization in gas flows, using photographic emulsion nonlinear properties
09 p1311 A72-22965

Schlieren optics for visualization and differentiation of density gradients with color and brightness distinctions, applying to supersonic flow through tandem grid
09 p1316 A72-23669

Experimentally produced vortex ring structure and stability, using dye and hydrogen bubble techniques for flow field, ring velocity and growth rate observations
10 p1466 A72-24327

Hydraulic tank application to internal flow visualization in turbomachinery, describing test equipment and methods used for axial flow model
10 p1419 A72-24654

Color schlieren technique for simultaneous photographic recording of flow fields and heat transfer patterns in aerodynamic heating, noting application to shock-boundary layer interactions

11 p1629 A72-25257

Real time hologram-moire interferometry for visualization of turbulence phenomena in liquid flow through cylindrical pipe

11 p1629 A72-25317

Flow separation reduction by transverse jet blowing, illustrating flow patterns by water tunnel visualization on cylinders, perpendicular flat plates, contoured walls, steps, wings, etc [ONERA, TP NO. 1070]

11 p1572 A72-25814

Smoke generator for fluid flow visualization, presenting photographs of turbulent rotating air flow in cylindrical enclosure

[AD-746416]

11 p1613 A72-26540

Unsteady flow evolution at sphere and elliptical cylinder obtained by flow visualization techniques, showing streamline sequence dependence on angle of attack

12 p1797 A72-27469

Holographic interferometry of Mach wave field generation by supersonic turbulent jet, noting visible conical wave front from core edge

13 p1898 A72-29580

Point density measurement in gas jets by flow visualization based on Raman spectrum lines proportionality

[ONERA, TP NO. 1080]

13 p1959 A72-29670

Pressure distribution and heat transfer in flow separation zone of cone tipped cylindrical body, using shadowgraph photography for flow visualization

14 p2070 A72-31005

Fuel injection, mixing and combustion processes investigated in model cylindrical swirl chamber, describing flow visualization method for turbulence observation

15 p2297 A72-32297

Photographic flow visualization of steady recirculating wakes behind sphere and oblate spheroids for low Reynolds numbers

15 p2180 A72-32419

Holographic interferometry application to weak inhomogeneities visualization in gas flows, using photographic emulsion nonlinear properties

17 p2558 A72-35893

Cavitation study of pump with semiopen impeller, obtaining hydraulic performance, flow photographs and noise level

17 p2561 A72-35899

The physically defined flame and its representation in the water model

18 p2656 A72-36242

In-line holography of reacting liquid sprays

19 p2798 A72-37619

Three dimensional flow field visualization, data acquisition and reduction via holography, noting applications in schlieren and interferometric techniques

19 p2798 A72-37620

Single pulse holographic flow visualization

19 p2798 A72-37622

Book - Combustion aerodynamics

19 p2882 A72-38722

Visualization study of flow near the trailing edge of an oscillating airfoil

20 p2886 A72-40067

Hydrodynamic test tunnel for unsteady pressure and force measurements and hydrogen bubble flow visualization data acquisition

[AIAA PAPER 72-999]

21 p3041 A72-41585

Electron beam visualization in hypersonic air flows

[AIAA PAPER 72-1017]

21 p3042 A72-41596

Three-dimensional disturbances in the boundary layer along a concave wall

22 p3165 A72-42111

Method of characteristics for ideal gas flow in annular space of axisymmetric plug nozzle, noting flow visualization by schlieren photography

22 p3166 A72-42263

Effects of rifling and N-vanes on the Magnus characteristics of bodies of revolution

[AIAA PAPER 72-970]

22 p3135 A72-42341

A time-interval amplitude analyzer for turbulent flow processes and its application for the control of a chronophotographic measurement installation

22 p3177 A72-42393

Laser interferometer for studying boundary layers in liquids

22 p3178 A72-42473

Smoke-trail method for obtaining wind profiles

22 p3202 A72-43144

The vortex street in the wake of a vibrating cylinder

23 p3281 A72-44302

Smoked foil observation technique for transient behavior produced by perturbing equilibrium configuration detonation waves

24 p3462 A72-45033

Electron-beam flow visualization - Applications in the definition of configuration aerothermal characteristics

[AIAA PAPER 72-1016]

24 p3404 A72-45405

Fraunhofer single beam holography application to gas/liquid mixture high velocity flow cross section determination, observing liquid component effects on droplet dispersion composition

24 p3405 A72-45624

FLOWMETERS

NT HOT-WIRE FLOWMETERS

NT RHEOMETERS

Fluidic sensors for flow velocity and fluid pressure, temperature and density measurements, emphasizing analog transducers with output signal FM and AM

01 p0006 A72-10151

German book on liquids flow rate measurement techniques covering physical principles of flow measurement including pressure, magnetic or inductive and ultrasonic methods

02 p0230 A72-12299

Combination flow-pressure measuring instrument based on rotating Flosdorf manometer with switching relay system

04 p0525 A72-15665

Flow rate metering by multiple Venturi systems, discussing internal fluid mechanics for design optimization

[ASME PAPER 71-WA/FE-27]

05 p0661 A72-15926

Ultrasonic Doppler flowmeter for instantaneous measurement of blood vessel flow velocity by averaging frequency shift over received signal power density spectrum

10 p1430 A72-24373

Design and performance characteristics of ion thruster feed system components including high voltage isolator, liquid Hg flowmeter and W vaporiser

[AIAA PAPER 72-487]

11 p1710 A72-26213

Instantaneous and continuous blood flow velocity measurement by Doppler ultrasonic flowmeter using transcutaneous and implanted probes

11 p1589 A72-26778

Flow equations for floating body flowmeters, discussing density and viscosity effect, instrument characteristics and computer algorithms

14 p2104 A72-30484

One path ultrasonic flowmeter using electroacoustic feedback

17 p2556 A72-35427

Optimal invariant conversion of information from a turbine flow meter and a capacitive fuel gauge

21 p3058 A72-41801

Aircraft clamp-on flowmeter using IR heat source in thermistor bridge to monitor flow rate in hydraulic lines

22 p3180 A72-42715

Analysis of a nuclear magnetic resonance blood flowmeter for pulsatile flow

24 p3401 A72-44574

Study of a turbine type flowmeter with helical blades

24 p3404 A72-45354

FLOX

Polyethylene-FLOX hybrid stage optimum combustion chamber pressure, representing pressure dependent factors by simple analytical models

01 p0117 A72-11221

FLUCTUATION THEORY

Asymptotic intensity fluctuations of plane light wave propagating in turbulent medium, using parabolic equation and Markov model

01 p0050 A72-10348

Fluctuation theory for single mode laser detuning effect on photon intensity and spectral line width

03 p0368 A72-13671

Two mode lasers with photon intensity coupling near threshold treated by fluctuation theory detailing intensity, correlations and line widths

05 p0667 A72-16017

Finite amplitude fluctuations evolution in extended self-gravitating media for initial disturbances, taking into account pressure effects

06 p0880 A72-17888

Fluctuating and steady model for turbulent reactive and nonreactive flow, solving for turbulent kinetic energy and density by averaging procedure

[AIAA PAPER 72-68]

07 p0966 A72-18948

Long wave fluctuations in nonequilibrium gas with pair collisions, using Bogoliubov equations for simultaneous correlation functions

15 p2282 A72-32450

Thin film superconductors conductivity evaluation above transition temperature through renormalization of impurity-scattering vertex by pair fluctuation effect inclusion

15 p2295 A72-32540

Fluctuation renormalized transport coefficients in corrected nonlinear transport equations derivation from generalized Fokker-Planck equation

15 p2337 A72-32653

Overall detection probability for fluctuating and nonfluctuating target models

19 p2763 A72-37294

Spectral characteristics of surface-layer turbulence

19 p2829 A72-38559

Weakly divergent beam propagation of electromagnetic waves in statistically inhomogeneous nonlinear

medium with dielectric constant dependence, using small perturbation method

23 p3263 A72-43426

Fluctuation mechanism of ultrashort pulse generation by laser with saturable absorber

23 p3297 A72-44184

Inertial effects in motion driven by hydrodynamic fluctuations

24 p3430 A72-45560

FLUENCE

Portable X ray calorimeter for simultaneous fluence and front surface dose measurement in Ta from pulsed electron accelerations

15 p2241 A72-32440

FLUERICIS

Matched acoustic generator for sweep frequency testing of power gain of flueric amplifiers

[ASME PAPER 71-WA/FLCS-2]

10 p1423 A72-25051

FLUID AMPLIFICATION

U FLUID AMPLIFIERS

FLUID AMPLIFIERS

NT JET AMPLIFIERS

Bistable fluidic amplifiers switching dynamics, developing analytic performance prediction method from flow visualization studies

[ASME PAPER 71-WA/FLCS-8]

05 p0615 A72-15916

Hydraulic amplification of electric step motor torque, discussing system dynamic characteristics

09 p1263 A72-22689

Monostable three output fluid amplifier models with curved walls in turbulent jet flow, comparing wall design in dynamic and static tests

09 p1263 A72-22931

Flow control circuits design based on unvented bistable fluid amplifiers

10 p1422 A72-23970

Matched acoustic generator for sweep frequency testing of power gain of flueric amplifiers

[ASME PAPER 71-WA/FLCS-2]

10 p1423 A72-25051

Vortex fluid amplifier design with asymmetrical flow fields, discussing effects of geometrical parameters variations on performance characteristics

10 p1423 A72-25053

Fluidic proportional and digital amplifiers environmental effects on sensitivity of gain, noise and null shift based on dependence on Reynolds number

[ASME PAPER 72-GT-84]

11 p1577 A72-25660

Hydraulic vortex amplifiers with and without diffusers, discussing supply pressure and liquid viscosity effects on system performance

11 p1578 A72-26980

Fluid amplification principles, discussing bistable and proportional amplification, signal transmission and transduction to and from fluid signals

[ASME PAPER 72-DE-20]

14 p2073 A72-30864

Jet turbulence interaction and velocity effects on noise level of proportional fluid amplifiers

16 p2350 A72-33177

Water table study of monostable fluidic amplifiers with allowance for geometrical similarity and Reynolds number for air operated models

16 p2353 A72-34139

Contributions to the study of the steady-state regime of fluidic amplifiers with jet deflection

17 p2497 A72-35122

Fluidic flow-mode amplifiers physical dimensions and operating pressures restrictions, presenting design and performance evaluation theory and velocity profiles

22 p3139 A72-42048

FLUID BOUNDARIES

NT GAS-SOLID INTERFACES

NT JET BOUNDARIES

NT LIQUID-LIQUID INTERFACES

NT LIQUID-SOLID INTERFACES

NT LIQUID-VAPOR INTERFACES

Dynamic stabilization of Rayleigh-Taylor instability at interface between two heavy fluids by viscosity and interfacial tension

01 p0108 A72-10231

Invariant characteristics of hydrodynamic systems with stationary boundaries, 3 degrees of freedom and second order nonlinear motion of Liouville type

06 p0801 A72-18136

Entrainment interface evolution in turbulent flow, examining surface slope discontinuities and curvature and overall speed of advance

10 p1467 A72-24332

Isochoric heat capacity peaks of water and argon near boundary in two phase region at critical state

11 p1747 A72-26964

French monograph on turbulent free flow boundaries covering two dimensional plane jet mixing zone characteristics from thermal signal measurements

14 p2095 A72-30948

Natural convection initiation in fluid confined above and below by rigid conducting surfaces and laterally by rigid insulating vertical walls

14 p2172 A72-31054

Uniform rotation and magnetic field effects on gravitational stability of interface between two semi-infinite homogeneous streams

15 p2284 A72-31593

Microwave acoustic surface waves attenuation at solid and monatomic gas boundary, detailing frequency, molecular weight, pressure and temperature effects

15 p2278 A72-32505

Asymptotic estimate of steady state solution to Euler equations for ideal incompressible fluid flow with free boundaries

18 p2682 A72-36805

Interaction between two streams of incompressible fluids in flat duct, using Chaplygin method of singular points

20 p2913 A72-39370

Effect of wall conduction on the stability of a fluid in a rectangular region heated from below.

[ASME PAPER 72-HT-G] 20 p2985 A72-39655

Two phase flow types defined as flow problems of two-phase matter mixtures /solid, liquid, gas or plasma/ and interface interaction

20 p2915 A72-39971

Determination of the parameters of a fluid in the neighborhood of the junction of wavefronts by the Legras method

22 p3165 A72-41927

The equilibrium configuration of a slowly rotating mass of liquid in the presence of a poloidal magnetic field.

23 p3322 A72-44306

FLUID DYNAMICS

NT AERODYNAMICS
NT AEROTHERMODYNAMICS
NT ELASTOHYDRODYNAMICS
NT ELECTROHYDRODYNAMICS
NT GAS DYNAMICS
NT HYDRODYNAMICS
NT HYPERSONICS
NT MAGNETOHYDRODYNAMICS
NT RAREFIED GAS DYNAMICS
NT ROTOR AERODYNAMICS
NT SUPERSONICS

Modified implicit continuous fluid Eulerian technique for numerical solution of time dependent fluid flow for Mach numbers from zero to infinity

01 p0049 A72-10226

Fluid flow numerical solution by contour dynamics methodology with flow features resolution advantage

01 p0049 A72-10227

Fluid dynamical study of accretion process with gravitating point source motion through adiabatic gas, applying to galaxies

01 p0126 A72-10289

Turbulent boundary layer fluid dynamic behavior under transpiration and acceleration effects, presenting mean velocity profile data, skin friction and mixing length model

[ASME PAPER 71-HT-F] 02 p0205 A72-12315

Book on mathematical fluid dynamics covering viscous and ideal fluid motion, boundary theory, constitutive equations, hydrodynamics and kinematics

02 p0206 A72-12623

Relativistic cosmological model, showing relation to fluid dynamics in Newtonian theory and space-time dependence on causality condition

03 p0426 A72-13267

Soviet book on hydraulics, hydraulic machines and hydraulic drives covering fluid dynamics, pipe flows, jet pumps, turbines, bladed transmissions, etc

04 p0466 A72-15247

Book on fluid dynamics covering theories of perfect, viscous and compressible fluids, infinite and finite span wings, boundary layer flow, etc

04 p0462 A72-15357

Airplane hydraulic control systems digital simulation, using method of characteristics for distributed parameter analysis of transmission line dynamics

[ASME PAPER 71-WA/FE-21] 05 p0615 A72-15928

Fluid motion model with gas bubbles, noting energy dependence on temperature and density

05 p0649 A72-16224

Circle moving under fluid dynamic and gravitational forces in viscous incompressible flow, describing dynamic interaction by numerical method

[AIAA PAPER 72-111] 05 p0604 A72-16819

Space shuttle flow field fluid dynamic hyperbolic equations numerical solution by noncentered finite difference schemes, noting advantages in programming logic simplicity and multidimensional generalizations

[AIAA PAPER 72-193] 05 p0729 A72-16848

Equations of motion for oscillating heavy symmetrical gyroscope with cylindrical cavity partially filled with inviscid incompressible liquid

05 p0664 A72-17145

Relativistic fluid dynamics - Conference, Bressanone, Italy, June 1970

06 p0846 A72-17251

Electromagnetic wave propagation and thermal spread in uniform magnetoplasma at electron-cyclotron resonance frequencies, discussing kinetic and multifluid theory

06 p0854 A72-17489

Unsolved fluid dynamic problems, considering viscous fluids, epihydrodynamics, magnetohydrodynamics, relativistic field dynamics and interstellar gas dynamics

06 p0800 A72-18112

Finite element solution for Boussinesq approximation of two dimensional viscous fluid dynamic problems, using variational principle

07 p0965 A72-18794

Hf diffusion type chemical laser fluid dynamic and optical properties, discussing computerized numerical analysis

[AIAA PAPER 72-146] 07 p1001 A72-19063

Book on compressible fluid dynamics covering steady flow, shock waves and self similar motions

07 p0967 A72-19448

Bilaterally symmetric vortex rings dynamic behavior, computing pointwise induced velocity via Biot-Savart law for hydrodynamic and Rankine vortex models

[AD-739139] 07 p0967 A72-19501

Dynamo action of magnetohydrodynamic fluid motions with two dimensional periodicity

07 p1042 A72-19611

Flow characteristics of liquid layers adjacent to vapor bubble, visualizing flow via particle motion

08 p1151 A72-21670

Flying machine using reaction forces on body moving in compressible fluids within piston device equivalent to air pressure pump

08 p1108 A72-21798

Book on ideal and real compressible fluid dynamics covering supersonic flow past airfoils and shock wave interaction with laminar boundary layer

09 p1295 A72-23045

Equations of motion for discrete structure fluid, discussing equilibrium pressure and fluid-wall interaction effects

09 p1296 A72-23691

Axisymmetric three component flow of viscous incompressible fluid, finding exact solutions to second problem of dynamics

10 p1471 A72-25133

Fluid dynamics stability of double radio sources in intergalactic medium, discussing evolution, ram pressure mechanism and Rayleigh-Taylor and Kelvin-Helmholtz effects

10 p1550 A72-25196

Fluid dynamics layer-type singular perturbation problems, constructing inner and outer asymptotic approximations with overlapping domains of validity

11 p1615 A72-25502

Relativistic fluids dynamic equations, using Banach type Lagrangians

11 p1689 A72-26503

Finite difference calculations for structure of finite amplitude thermal convection within self gravitating fluid sphere with uniform heat release

12 p1889 A72-27715

Fluid discharge rate relationship to space fraction for fluidized layers in reactor

13 p1943 A72-29786

Relaxation oscillations in dynamic systems describing turbulence in fluid, rigid body and particle motions

15 p2263 A72-31755

Mathematical problems in geophysical sciences - Conference, Rensselaer Polytechnic Institute, Troy, New York, July 1970

16 p2384 A72-33335

Geophysical fluid dynamics approach to dynamical processes in ocean and atmospheric motions, discussing equations of motion, vorticity, geostrophism, Ekman layer, Rossby waves, etc

16 p2377 A72-33336

Nonlocal fluid dynamics continuum theory with equilibrium and constitutive equations derived by generalizing Stokes Laws, noting steady channel and shear flow

16 p2379 A72-33832

Convective clouds fluid dynamic numerical modeling, considering plumes, thermals and vortex rings formation

[AIAA PAPER 72-651] 16 p2419 A72-34083

Certain motions of micropolar fluids

17 p2538 A72-34771

An application of the generalized Langevin equation to the study of correlations in simple, classical fluids.

17 p2581 A72-35154

Shock tube investigation of low-density heated fluid element dynamic reaction to reflected shock wave passage, noting similarity to atmospheric thermals

17 p2542 A72-35615

Fluid dynamics problems self similar solutions as descriptions of intermediate asymptotic behavior of solutions for initial, boundary and mixed problems

18 p2709 A72-36388

Theoretical investigation of the interfacial stability of inviscid fluids in motion, considering surface tension.

18 p2681 A72-36482

Recent extensions to Eulerian methods for numerical fluid dynamics.

18 p2682 A72-36803

Time dependent solution to motion and energy equations for unsteady laminar spherical Couette flow of incompressible constant viscosity fluid

18 p2684 A72-37055

On the intrinsic representation of flows with Lamb surfaces.

18 p2684 A72-37085

Buildup of thermal equilibrium in a fluid near the critical point

22 p3242 A72-41882

Extension of the Curie principle and constitutive relations for fluids with antisymmetric stress.

22 p3166 A72-42311

On the solution of non-linear simultaneous equations with particular reference to fluid-dynamics.

22 p3199 A72-42325

Fluid sphere of uniform density and vanishing pressure at periphery, expressing internal motion in terms of Schwarzschild mass and radius and central pressure

22 p3205 A72-42451

Boundary value problems of viscous fluid dynamic system generated by Navier-Stokes equations, using Hopf theory

22 p3208 A72-43137

The dynamics and control of Eulerian turbomachines.

[ASME PAPER 72-AUT-S] 23 p3279 A72-43633

Lumped parameter model description of distributed parameter fluid dynamic systems by bond graph techniques

[ASME PAPER 72-AUT-J] 23 p3279 A72-43634

Fluid dynamic forces exerted by Newtonian fluid axisymmetric creeping flow on accelerating body of arbitrary shape, calculating pressure gradient via Navier-Stokes equation

23 p3347 A72-43726

FLUID FILMS

Velocity slip effect on porous walled squeeze fluid films, obtaining film load carrying capacity and thickness-time relation

[ASME PAPER 71-LUB-4] 02 p0234 A72-11526

Series hybrid fluid film-rolling element bearing analytical and test evaluation for high speed thrust load turbine applications

[ASME PAPER 71-LUB-15] 02 p0235 A72-11537

Thin liquid layer linear hydrodynamic stability in vertical rotating tube with core gas flow

02 p0303 A72-12353

Heat transfer during liquid film evaporation in centrifugal vaporizer, noting agreement between theory and experiment

03 p0458 A72-14158

Lubrication and friction problems regrouping in thin viscous fluid films mechanics

03 p0364 A72-14271

Carbon fiber reinforced material porosity source, applying equilibrium configurations of liquid films on parallel uniform cylindrical rod hexagonal and cubic arrays

04 p0537 A72-15087

MHD squeeze film lubrication between electrically conducting parallel plates, showing graphically approach time under magnetic field in free space

05 p0665 A72-16031

Hydrodynamic lubricating films with viscosity variations perpendicular to direction of motion, evaluating friction coefficient changes for constant film thickness and load carrying capacity

[ASME PAPER 72-LUB-E] 06 p0821 A72-17806

MHD convection in rotating electrically conducting viscous fluid layer within magnetic field, investigating linear stability

06 p0861 A72-18069

Nonlinear motion stability of finite amplitude wave solution in thin viscous incompressible liquid film

06 p0801 A72-18142

Molybdenum disulfide lubricating film and wear-in study by scanning electron microscopy and testing machine

06 p0836 A72-18586

Short time film stability followed by dry spot formation in thin heated draining liquid films on vertical walls, discussing minimum thickness

07 p1098 A72-18842

Conical gas film between rotating and vibrating conical rotor and nonmoving bearing, determining gas film stiffness and optimum angle

07 p0971 A72-20093

Squeeze-film bearings nonlinear vibration performance in aircraft gas turbine engines, emphasizing lubricant viscosity importance

07 p0999 A72-20532

Spatial-temporal temperature distribution on CW laser irradiated materials, noting application to water film

08 p1252 A72-21289

Fluid sealing theory based on surface tension effects at roughness asperities within seal film

08 p1177 A72-21928

Dynamics of rigid rotor supported on squeeze oil film bearings

08 p1225 A72-22134

Gas flow effect on undulating flow of viscous fluid film down vertical wall, using Fourier series

10 p1469 A72-24532

Thin liquid surface water film cooling tests for mass loss under simulated reentry heating and shear conditions

10 p1563 A72-24648

Hydrodynamics of turbulent free convection boundary layer on vertical flat plate and ethyl alcohol film

11 p1743 A72-25258

Liquid film transpiration cooling concept application to space shuttle leading edge heating and shock heating

[AIAA PAPER 72-389] 11 p1744 A72-25410

Ball bearings lubricated with oils and fire-resistant fluids, testing fatigue life relationship to steel quality, fluid film thickness and viscosity

12 p1816 A72-28108

Liquid film condensation of low pressure metal vapors on isothermal vertical flat plates, obtaining equations for heat transfer rate prediction

14 p2173 A72-31059

Thin liquid films on rotating horizontal disk, measuring flow, thickness and stability with asymptotic-expansion solution

15 p2334 A72-31616

Danckwert liquid film surface layer renewal concept as refinement of Reynolds theory of correlation between convective heat transfer and momentum transfer

17 p2637 A72-35050

Damping characteristics of a liquid squeeze film.

18 p2683 A72-37053

Stability considerations for a gas-lubricated tilting pad bearing. II - Analytical refinements and stability data.

[ASME PAPER 72-LUB-G] 19 p2807 A72-37697

Heat transfer with the helium II superfluid film.

19 p2883 A72-38839

Mathematical model for surface tension induced thermocapillary fluid flow influence on conductive heat transfer through condensate film broken by non-wetting strips

[ASME PAPER 72-HT-H] 20 p2985 A72-39654

Stability of a liquid film in a lateral gas flow and the size of droplets during the breaking of the film

20 p2987 A72-39925

Water film formation and breakdown during motion over solid surfaces, predicting flow rate difference due to contact angle hysteresis

21 p3085 A72-41178

Arbitrary length thin liquid film cooling mass transfer data correlation, accounting for film roughness and entrainment effects

22 p3243 A72-41960

Study of the flow kinetics of metal melt spread over hard surfaces

23 p3293 A72-43284

FLUID FILTERS

NT AIR FILTERS

Water disinfection by Ag coated filters obtained by silver nitrate reduction with ascorbic acid, hydroquinone, formaldehyde and sodium tartrate activated carbon and ion exchange resin surfaces

05 p0622 A72-16637

Lubrication system filtration effects on rolling element bearing life and extended mean time to failure of gas turbine engines

07 p1052 A72-18754

Continuous NDT of coalescers /jet fuel filters/ by liquid crystals, detecting split seams, cap leaks, cracks, material imperfections and epoxy filled voids

[ASME PAPER 72-DE-25] 14 p2108 A72-30867

Combined centrifugal oil filter, pump and deaerator for gas turbine engine lubrication systems, noting heat transfer effectiveness increase

18 p2694 A72-36050

FLUID FLOW

NT ADIABATIC FLOW

NT AIR CURRENTS

NT AIR FLOW

NT AIR JETS

NT ANNULAR FLOW

NT AXIAL FLOW

NT AXISYMMETRIC FLOW

NT BAROTROPIC FLOW

NT BASE FLOW

NT BELTRAMI FLOW

NT BLASIUS FLOW

NT BLOOD FLOW

NT BOUNDARY LAYER FLOW

NT BOUNDARY LAYER SEPARATION

NT CAPILLARY FLOW

NT CASCADE FLOW

NT CAVITATION FLOW

NT CHANNEL FLOW

NT COAXIAL FLOW

NT COMBUSTIBLE FLOW

NT COMPRESSIBLE FLOW

NT CONICAL FLOW

NT CONTINUUM FLOW

NT CONVECTIVE FLOW

NT CORE FLOW

NT COUETTE FLOW

NT COUNTERFLOW

NT CRITICAL FLOW

NT CROSS FLOW

NT DUCTED FLOW

NT EQUILIBRIUM FLOW

NT FREE FLOW

NT FREE MOLECULAR FLOW

NT FROZEN EQUILIBRIUM FLOW

NT FUEL FLOW

NT GAS FLOW

NT HARTMANN FLOW

NT HEAD FLOW

NT HELICAL FLOW

NT HYPERSONIC FLOW

NT HYPERVELOCITY FLOW

NT INCOMPRESSIBLE FLOW

NT INLET FLOW

NT INVISCID FLOW

NT ISOTHERMAL FLOW

NT JET FLOW

NT JET MIXING FLOW

NT JET STREAMS [METEOROLOGY]

NT KNUDSEN FLOW

NT LAMINAR FLOW

NT LIQUID FLOW

NT MAGNETOHYDRODYNAMIC FLOW

NT MASS FLOW

NT MERIDIONAL FLOW

NT MOLECULAR FLOW

NT MULTIPHASE FLOW

NT NONEQUILIBRIUM FLOW

NT NONNEWTONIAN FLOW

NT NONUNIFORM FLOW

NT NOZZLE FLOW

NT ONE DIMENSIONAL FLOW

NT ORIFICE FLOW

NT OSCILLATING FLOW

NT PIPE FLOW

NT PLASTIC FLOW

NT POTENTIAL FLOW

NT PROPELLANT TRANSFER

NT RADIAL FLOW

NT REATTACHED FLOW

NT RECIRCULATIVE FLUID FLOW

NT REVERSED FLOW

NT SECONDARY FLOW

NT SEPARATED FLOW

NT SHEAR FLOW

NT SINGLE-PHASE FLOW

NT SLIP FLOW

NT SMALL PERTURBATION FLOW

NT SOLIDS FLOW

NT STAGNATION FLOW

NT STEADY FLOW

NT STEAM FLOW

NT STOKES FLOW

NT STRATIFIED FLOW

NT SUBCRITICAL FLOW

NT SUBSONIC FLOW

NT SUPERCAVITATING FLOW

NT SUPERCRITICAL FLOW

NT SUPERSONIC FLOW

NT SUPERSONIC JET FLOW

NT THREE DIMENSIONAL FLOW

NT TRANSITION FLOW

NT TRANSONIC FLOW

NT TRESKA FLOW

NT TURBULENT FLOW

NT TWO DIMENSIONAL FLOW

NT TWO PHASE FLOW

NT UNIFORM FLOW

NT UNSTEADY FLOW

NT VERTICAL AIR CURRENTS

NT VISCOUS FLOW

NT WALL FLOW

NT WATER FLOW

NT WEDGE FLOW

Modified implicit continuous fluid Eulerian technique for numerical solution of time dependent fluid flow for Mach numbers from zero to infinity

01 p0049 A72-10226

Fluid flow numerical solution by contour dynamics methodology with flow features resolution advantage

01 p0049 A72-10227

Electrostatic charging mechanisms leading to streaming current generation in moving fluids, considering initial discharge, electrode change and mobility charging current

02 p0261 A72-12553

Directional selector valves with proportional flow control under varying load conditions, discussing hydraulic spool valves design

03 p0312 A72-13963

Decelerating MHD effect on rotational funnel flow excited by vortex line or radial converging currents

03 p0397 A72-13994

Zhukovskii potentials for ideal fluid motion in spherical or cylindrical cavity with arbitrary radial partitions

05 p0648 A72-16218

Thermal signal propagation in flowing fluid, plane, line and point sources of varying heat, calculating temperature distribution with conduction and convection heat transfer equation

05 p0746 A72-16295

Velocity distribution in mixing layer between fluid at rest and in uniform stream by solving Blasius equation with boundary points

05 p0653 A72-17078

Pitting and film deposits with organic fluid by electrolysis and fluid flow, discussing electrokinetically produced corrosion

[ECS PAPER 84] 07 p1010 A72-18802

Rotational flow computation, using iteration methods for irrotational and solenoidal vector field components

07 p0966 A72-18811

Similarity theory for turbulently stratified fluid with horizontal and vertical dimensionalities analysis, discussing Karman constant dependence

07 p1031 A72-20698

Variational principle of Hamiltonian type for classical field theory, noting application to nonlinear heat transfer and fluid flow in Eulerian description

08 p1252 A72-21287

Fluid motion near wave front junction point, expanding unknown functions and independent variables into series of parameters characterizing shock wave and angular distances

08 p1152 A72-21945

Soviet book on heat and mass transfer and friction in gradient fluid flows in variable cross sectioned ducts and at surface of bodies

08 p1152 A72-22022

Frequency response of hot-film wedge probe in turbulent flow of viscoelastic fluid

09 p1293 A72-22309

Geometrical characterization of steady nondissipative compressible fluid flow described by first order partial differential equations system

09 p1295 A72-23366

Internal flows - Conference, Salford, England, April 1971

10 p1415 A72-23853

Optimal control computation for nonlinear hyperbolic partial differential system by gradient and quasilinearization techniques, noting MHD, fluid flow and electromagnetic wave propagation

10 p1456 A72-24453

German book on flow technology and fluid flow machines covering hydrodynamics, gas dynamics, aerodynamics, airfoils, wind tunnels, propellers, helicopters, turbomachines, blade cascades, etc

10 p1471 A72-25122

Fluid flow and heat transfer in tube bank with two cylinders in cross flow, determining static pressure, Nusselt number and drag coefficients

11 p1743 A72-25259

Electromagnetic wave interaction with irrotational moving fluid based on Maxwell equations and Minkowski constitutive relation, noting flow velocity effects on scattering

11 p1689 A72-26471

Convective heat transfer for fluid flow on plate with internal heat sources in boundary layer, solving laminar-turbulent transition equations by difference method

12 p1889 A72-28138

Mathematical model of reactive fluid flows during postignition transients in hybrid propellant rocket system

13 p2025 A72-28416

Liquid droplets behavior in high velocity gas jets, deriving fluid flow model solutions near symmetry axis and for liquid-gas boundary layer

[DFVLR-SONDDR-200] 13 p1941 A72-29003

Sound generation by fluid flow interaction with sharp-edged vibrator, predicting sound radiation pressure by quasi-steady analysis based on reed velocity

13 p2005 A72-29562

Concentration profile derivation for fluid flow near rotating disk with chemical reactions, considering concentration gradient and barodiffusion effects

13 p1944 A72-30049

German book on heat transfer and fluid flow, covering heat conduction and temperature distribution in bodies of simple and complex geometries, fluid mechanics, etc

14 p2171 A72-30902

Optical acoustic field recordings application to turbulent characteristics measurement for transparent media of fluid flows

15 p2232 A72-31267

Flow induction by cylinder performing transverse periodic vibrations in viscous fluid, noting jet flow with large streaming Reynolds number

15 p2217 A72-31617

Rotating flow introduction effects on jet noise levels, combustion and turbulent mixing processes and flame stability

[AIAA PAPER 72-645] 16 p2480 A72-34087

Perturbation method for two point boundary value problem for fluid flow applied to optimal reentry control problem

16 p2462 A72-34166

Sudden freeze approximation for fluid flow systems relaxation time at constant enthalpy and pressure

17 p2542 A72-35633

Invariant solutions of the Navier-Stokes equations describing motions with a free boundary

18 p2679 A72-36234

Experiments using the birefringence of fluids in motion

18 p2679 A72-36367

- On motions with a history of constant deformation
18 p2680 A72-36463
- A note on the effects of pressure gradients on fluid flow with atmospheric applications.
18 p2706 A72-36644
- Fluid transition through critical value, considering self oscillation onset mode frequency
18 p2681 A72-36663
- Solution of the general heat transfer problem by the integral Tolubinskii method for a longitudinal flow past cylindrical bodies
18 p2742 A72-37182
- Thermal stress induced flow around constant temperature solid sphere in rarefied gas with uniform temperature gradient, using asymptotic theory
19 p2788 A72-38433
- Blade passage measurement with the aid of a graphite pin probe in the case of fluid flow engines
19 p2804 A72-38724
- Similarity theory for turbulence in stratified fluid from horizontal and vertical dimensional analysis approach, discussing Karman constant dependence
20 p2948 A72-39013
- Fluid flow across balance surface moving at constant velocity relative to coordinate system, calculating energy balance of turbojet engine
21 p3099 A72-40814
- The construction of invariant transformations in plane rotational gasdynamics.
22 p3199 A72-42399
- Descriptive model of the turbulent motion of an isovolumetric fluid
23 p3279 A72-43699
- FLUID INJECTION**
NT GAS INJECTION
NT LIQUID INJECTION
NT WATER INJECTION
Two dimensional transient inviscid flow field from secondary injection in missile control, describing distribution with artificial viscosity finite difference method
01 p0097 A72-10940
- Two dimensional unsteady incompressible boundary layer near forward stagnation point of infinite plane wall with uniform suction or injection, obtaining iterative solution
01 p0050 A72-11106
- Injection geometry and inlet flow conditions application to open cycle gas nuclear reactor engine, evaluating fuel containment from cylindrical and spherical chambers experiments
01 p0100 A72-11350
- Velocity profiles of turbulent boundary layers with injection or suction through porous walls as function of momentum thickness by Truelsenbrodt method
02 p2002 A72-11663
- Turbine blade row coolant flow velocity, injection location and temperature effects on kinetic energy output
[AIAA PAPER 72-12] 05 p0707 A72-16866
- Laminar MHD boundary layer lateral velocity component profile for conducting fluid injection at oblique incidence, considering drag force and pressure gradient effects
08 p1214 A72-21647
- Mixing length model for turbulent boundary layer in incompressible flow with fluid injection at wall, extending solution to compressible case
[ONERA, TP NO. 986] 09 p1294 A72-22818
- Trailing vortex core decay with axial injection as function of momentum flux parameter
09 p1261 A72-23623
- Uniform flow past semiinfinite flat plate for large Reynolds numbers and strong blowing, noting injected fluid region separation from free stream by shear boundary layer
10 p1467 A72-24369
- Parabolic boundary layer finite difference model for predicting film cooling and heat transfer near flush injection slots in gas turbine combustors
[AIAA PAPER 72-291] 11 p1614 A72-25229
- Thermodynamic coupling effects on temperature distribution, Nusselt number and cooling requirements in laminar nonisothermal pipe flow with coolant injection
11 p1745 A72-25734
- Turbulent pipe flow laminarization by fluid injection, measuring axial turbulence intensity field and streamwise velocity distribution by hot-film anemometer
11 p1619 A72-26636
- Viscous incompressible flow between two coaxial rotating circular cylinders with small uniform injection at inner cylinder, obtaining solution of Navier-Stokes equations
13 p1941 A72-28883
- Flow over infinite wedge with mass transfer by boundary suction or injection, solving nonlinear boundary layer equations by parametric differentiation method
17 p2485 A72-35230
- Self-similar separation flows in a laminar magneto-hydrodynamic boundary layer during injection and suction
18 p2716 A72-36886
- Heat transfer during uniform injection on a vertical surface under conditions of combined free and forced convection
20 p2982 A72-39225
- Film cooling effect on surface heat transfer in laminarizing mainstream turbulent boundary layer for injection through flush angled two dimensional slots
[ASME PAPER 72-HT-11] 20 p2986 A72-39682
- Fundamental studies of turbulent boundary layers with injection or suction through porous wall. III - Investigations on the separation of turbulent boundary layers in strong adverse pressure gradients with injection through porous flat plate.
22 p3165 A72-41945
- Influence of wall injection on the turbulent tensions in the exterior regions of a boundary layer
23 p3279 A72-43698
- An experimental study of film cooling through a rearward-facing slot.
23 p3356 A72-43971
- Influence of tangential fluid injection on the performance of two-dimensional diffusers.
[ASME PAPER 72-FE-16] 23 p3280 A72-44064
- An experimental study of heat transfer downstream of a rearward-facing step with small coolant injection.
23 p3357 A72-44271
- Three dimensional shock wave configurations in front of cylindrical body on supersonic wing or of fluid jet injected into main supersonic flow, examining high pressure gradient regions
24 p3361 A72-45113
- FLUID JET AMPLIFIERS**
U FLUID AMPLIFIERS
U JET AMPLIFIERS
- FLUID JETS**
NT AIR JETS
NT FREE JETS
NT GAS JETS
NT HYDRAULIC JETS
Viscoelastic effect on cylindrical liquid jets capillary breakup after ejection into inviscid atmosphere
05 p0654 A72-17246
- Fluidic devices electrostatic modulation, verifying jet deflection analytical model by experimental results
07 p0913 A72-18819
- Parameter calculation for laminar incompressible fluid jet expanding in gradient slipstream along moving surface, determining velocity distribution in jet axis
08 p1149 A72-21309
- Plane laminar semibounded incompressible fluid jet propagation into slipstream along moving plate, solving boundary layer equations
10 p1471 A72-25136
- Fluid jets formation in collisions between metal plates for large angles at subsonic velocities
13 p1963 A72-28771
- Shear stress and dimensionless velocity profiles of plane incompressible fluid wall jet propagation along curved surface
16 p2380 A72-33856
- A new theoretical model for representing jet penetration into a subsonic stream
17 p2538 A72-34888
- Flow pattern of two impinging circular jets.
17 p2540 A72-35233
- Fluid jets and droplets deformation in transverse supersonic two phase gas flow
17 p2544 A72-35932
- Fluid jets formation region in subsonic collisions between metal plates at large angles
21 p3059 A72-40262
- Propagation of viscous fluid jets in a medium with a density discontinuity
21 p3047 A72-41666
- FLUID LOGIC**
Modular fluidic elements in pneumatic logic system based on Coanda effect
02 p0156 A72-11999
- Fluidic threshold logic application to fluidic control systems, comparing with AND-OR logic for number of elements and weight
[ASME PAPER 71-WA/FLCS-5] 05 p0615 A72-15918
- Hydraulic ball valve elements and logic gates for applications requiring short switching times under large flow and high pressure conditions
08 p1114 A72-22159
- Pneumatic fluidic logic elements design based on Coanda effect to realize conjunction, equivalence, nonequivalence, alternative and implication functions.
10 p1423 A72-25112
- Hybrid low power consumption magnetic/fluidic pulse shortener for fluid logic control circuits consisting of short cylindrical chamber with input and output port
16 p2350 A72-33179
- Perturbation extremum controller with simple coincidence logic, discussing fluidic implementation and performance in simulated plant control
16 p2350 A72-33193
- Multivariable static /combination/ switching characteristics of TRIMELOG pneumatic logic elements
19 p2754 A72-38644
- The mathematical synthesis and analysis of fluid logic networks.
22 p3161 A72-42049
- FLUID MECHANICS**
NT AERODYNAMICS
NT AEROTHERMODYNAMICS
NT ELASTOHYDRODYNAMICS
NT ELECTROHYDRODYNAMICS
NT FLUID DYNAMICS
NT GAS DYNAMICS
NT HYDRODYNAMICS
NT HYDROMECHANICS
NT HYDROSTATICS
NT HYPERSONICS
NT MAGNETOHYDRODYNAMICS
NT MAGNETOHYDROSTATICS
NT RAREFIED GAS DYNAMICS
NT ROTOR AERODYNAMICS
NT SUPERSONICS
German Research and Test Institute for Aero- and Astronautics 1970 report covering flow mechanics, power conversion, aerospace medicine, atmospheric physics, etc
01 p0048 A72-11151
- Cauchy-Poisson problem of infinitely deep fluid wave motion resulting from initial particle velocities and horizontal equilibrium surface change
04 p0511 A72-14648
- Flow rate metering by multiple Venturi systems, discussing internal fluid mechanics for design optimization
[ASME PAPER 71-WA/FE-27] 05 p0661 A72-15926
- Fluid properties for mechanically similar flow fields, discussing dissociating and thermally radiating gas flow
[DFVLR-SONDDR-172] 05 p0648 A72-16064
- Through flow analysis of low speed axial flow compressor, deriving blades deviations and losses
05 p0600 A72-16114
- Plane two dimensional wall jet, investigating flow dynamic structure
06 p0901 A72-17562
- Fluid mechanics - Conference, Kazimierz, Poland, September 1969, Parts 1 and 2
06 p0800 A72-18101
- Numerical methods for parabolic, hyperbolic and elliptic flows in fluid mechanics and heat transfer, considering finite element method
07 p1097 A72-18795
- Fluid mechanics - Conference, Rynia, Poland, September 1971
07 p0969 A72-20060
- Geometrical methods in fluid mechanics, solving quasi-linear nonelliptic systems by method of characteristics
07 p0969 A72-20063
- Fluid mechanics of blood pulsatile flow in microcirculation, considering plasma layer nature and transcapillary mass transfer
07 p0931 A72-20087
- Wave mechanics theory of turbulence based on Schroedinger equation, discussing resonance and flutter aspects
07 p0971 A72-20095
- Nonlinear system of differential equations for gravity perturbation on geometrical form of thin axisymmetric cavity in heavy fluid
08 p1151 A72-21705
- Similarity analysis group theory methods application to dimensional analysis, discussing incompressible fluid mechanics case
10 p1503 A72-23917
- Cochlea enclosed two dimensional cavity potential flow model for fluid mechanical theory of hearing
10 p1430 A72-24295
- Fluid mechanics of left ventricle model with mitral and aortic valves, showing ring vortex relation to diastole and closure
11 p1589 A72-26775
- German book on heat transfer and fluid flow, covering heat conduction and temperature distribution in bodies of simple and complex geometries, fluid mechanics, etc
14 p2171 A72-30902
- Landau-Placzek autocorrelation functions analysis method application to fluids transport coefficients LF characteristics
15 p2279 A72-32648
- Book - The method of weighted residuals and variational principles: With application in fluid mechanics, heat and mass transfer
17 p2573 A72-34250
- Supplement to the asymptotic theory of steady turbulent flows with bubbles
17 p2537 A72-34278
- Book - Nonlinear partial differential equations in engineering, Volume 2
17 p2576 A72-35449
- Heat Transfer and Fluid Mechanics Institute, 23rd, San Fernando Valley State College, Northridge, Calif., June 14-16, 1972, Proceedings.
17 p2542 A72-35631

- Central probability limit theorems and asymptotic normality in fluid mechanics for random stationary processes with uniform ergodicity and strong mixing
18 p2677 A72-36003
- Book - Annual review of fluid mechanics, Volume 4
18 p2679 A72-36382
- Muller entropy principle-imposed restrictions on thermodynamic and thermodynamic constitutive relations for fluids in electromagnetic fields
19 p2834 A72-37843
- Fluid mechanics anemometry based on laser light frequency modulation/Doppler effect, describing measurement of extensions of vortices and oscillations in flow boundary layers
19 p2801 A72-37934
- Book - Progress in aerospace sciences. Volume 12.
22 p3135 A72-42576
- Polish book - Fluid mechanics. Volume 2 - Gasdynamics.
22 p3168 A72-43199
- FLUID POWER**
- Fluid power - Conference, London, September 1970
03 p0312 A72-13960
- Laboratory evaluation of engine oils, transmission lubricants and hydraulic fluids utilization in hydraulic power transmission systems
08 p1192 A72-21635
- Fluid power - Conference, University of Surrey, England, January 1971
08 p1113 A72-22151
- Pneumatic fluid power valve flow rate derivation in terms of flow passage effective area and critical pressure ratio
08 p1113 A72-22158
- Conference on Fluid Machinery, 4th, Budapest, Hungary, September 11-16, 1972, Proceedings.
24 p3393 A72-45351
- FLUID ROTOR GYROSCOPES**
- Motion of a rotationally symmetrical gyro with an arbitrary number of vessels containing liquid
24 p3395 A72-45578
- FLUID SWITCHING ELEMENTS**
- Modular fluidic elements in pneumatic logic system based on Coanda effect
02 p0156 A72-11999
- Contacting-both-wall switching transients of bistable fluidic amplifiers with low setbacks, including unsteady effects in jet and attachment zone
[ASME PAPER 71-WA/FLCS-6]
05 p0615 A72-15917
- Hydraulic ball valve elements and logic gates for applications requiring short switching times under large flow and high pressure conditions
08 p1114 A72-22159
- Multivariable static/combination/switching characteristics of TRIMELOG pneumatic logic elements
19 p2754 A72-38644
- FLUID TRANSMISSION LINES**
- Logic networks with hydraulic elements, considering dynamic qualities of hydraulic transmission system
03 p0312 A72-13965
- Soviet book on hydraulics, hydraulic machines and hydraulic drives covering fluid dynamics, pipe flows, jet pumps, turbines, bladed transmissions, etc.
04 p0466 A72-15247
- Seminfinite circular fluid transmission line transient response to step function
[ASME PAPER 71-WA/FE-10]
05 p0646 A72-15932
- Modeling techniques for fluid line transients, considering heat transfer and viscous dissipation
[ASME PAPER 71-WA/FE-9]
05 p0646 A72-15933
- Temperature, flow, end conditions and branching on small signal sinusoidal amplitude frequency response of pneumatic lines, investigating transfer functions
[ASME PAPER 71-WA/AUT-5 (FLCS)]
05 p0615 A72-15958
- Viscoelastic fluid lines dynamic behavior, considering viscosity, stress-strain relaxation times and compressibility effects in transfer functions derivation for pressure-velocity relations
18 p2684 A72-37077
- FLUID TRANSPIRATION**
- U TRANSPIRATION**
- FLUIDIC CIRCUITS**
- NT FLIP-FLOPS
- Fluidic threshold logic application to fluidic control systems, comparing with AND-OR logic for number of elements and weight
[ASME PAPER 71-WA/FLCS-5]
05 p0615 A72-15918
- Dynamic response predictions of fluidically controlled pulsatile hydraulic flow and pressure generator for biomedical systems
07 p0914 A72-18820
- Hybrid low power consumption magnetic/fluidic pulse shortener for fluid logic control circuits consisting of short cylindrical chamber with input and output port
16 p2350 A72-33179
- German monograph - A theoretical and experimental contribution to the equivalent circuits of electrofluidic transducers operating on the nozzle/deflecting plate principle
19 p2754 A72-37653
- Fluidics - A potential technology for aircraft engine control.
19 p2849 A72-38047
- Use of fluidic elements for jet engine controllers
23 p3327 A72-44290
- FLUIDICS**
- NT FLUERICs
- Fluidic sensors for flow velocity and fluid pressure, temperature and density measurements, emphasizing analog transducers with output signal FM and AM
01 p0006 A72-10151
- Fluidic device for measuring angular velocities based on pressure output proportional to shaft revolutions per unit time, discussing equivalent circuit
01 p0064 A72-10171
- Gas flow visualization technique using fluorescent plate with UV irradiated ozone tracer, noting application to wall attachment fluidic elements
01 p0072 A72-11198
- German book on fluidics covering pneumatic logic elements and systems with and without moving parts and applications in sensors, transducers, power amplifiers, analog-to-digital converters, decoders, etc.
01 p0072 A72-11276
- Fluidic sensors methods for position, angular velocity, fluid level, flow rate and temperature measurement
02 p0155 A72-11998
- Aerodynamic compensation for ambient medium temperature effect on fluidic standard components and timing devices
04 p0466 A72-14993
- Bistable fluidic amplifiers switching dynamics, developing analytic performance prediction method from flow visualization studies
[ASME PAPER 71-WA/FLCS-8]
05 p0615 A72-15916
- Logical synthesis of hybrid off-on control systems with proportional and binary variables, presenting example of fluid power, electronic and fluidic implementation
[ASME PAPER 71-WA/FLCS-1]
05 p0640 A72-15919
- Closed loop fluidic bidirectional jet flap airfoil lift control system, considering application to helicopter rotor blades
05 p0603 A72-16659
- Fluidic sensors for temperature measurement at gas turbine inlet, noting long life and fast dynamic response
[SAE PAPER 720158]
06 p0811 A72-17320
- Fluidic devices electrostatic modulation, verifying jet deflection analytical model by experimental results
07 p0913 A72-18819
- Fluid oscillator temperature sensor, noting fast dynamic response and application in high temperature environments
08 p1164 A72-20926
- Analog fluidics systems status, exemplifying attitude reaction control for solar observation rocket and air gauging in textile industry
08 p1111 A72-20927
- Fluidic wind sensor measurements from low threshold to high velocities, noting wind angle resolution from output differential pressure signal
10 p1484 A72-25083
- Fluidic digital logic devices vs electromechanical equivalents, describing Coanda effect application to bistable jet amplifiers/flip-flops/ as switching or memory devices
15 p2182 A72-31218
- Fluidics - Conference, Prague, June-July 1971
16 p2350 A72-33176
- Perturbation extremum controller with simple coincidence logic, discussing fluidic implementation and performance in simulated plant control
16 p2350 A72-33193
- Hydrofluidic three-axis stability augmentation system to improve UH-1B helicopter damping and handling qualities during high speed gunfiring missions
16 p2350 A72-33650
- A simulation method permitting the direct construction of an integrated fluidic circuit with predetermined frequency response curve
17 p2494 A72-34197
- Gas bearing gyroscope for fluidic guidance and control system, satisfying missile and recoverable booster requirements
18 p2648 A72-36557
- Transmission of a fluidic signal at intermediate distances.
19 p2754 A72-38046
- Fluidics - A potential technology for aircraft engine control.
19 p2849 A72-38047
- A fluidic sensor for closed loop engine acceleration control.
19 p2849 A72-38049
- Fluidics control technology applications to thrust reversal, turbine engine speed, pressure valves, nozzle and fuel flow, discussing life and reliability
19 p2849 A72-38050
- Fluidic implementation of a perturbation extremum controller.
22 p3139 A72-42050
- Fluidic heat sensors for measuring fuel temperature in jet engines
23 p3326 A72-44280
- FLUIDIZED BED PROCESSORS**
- Two phase flow equations model application to fluidized beds and foams, predicting bed stability to small perturbations for comparison with experiment
01 p0093 A72-11272
- Heat transfer coefficient, maximum Nusselt number and particle thermal conductivity effect for gas fluidized beds, using surface renewal-penetration theory
[ASME PAPER 71-HT-Z]
08 p1251 A72-20879
- Two phase propellant flow rate through simulated rotating liquid core nuclear rocket fuel bed under high centrifugal acceleration
14 p2129 A72-30923
- Local vertical porosity and heat transfer coefficient relation to diluted fluidized bed relative height
16 p2479 A72-33851
- Pressure effects on heat transfer from heated surface to fluidized bed at 150-1000 C, noting carrier gas heat conductivity effects
16 p2479 A72-33852
- High-speed carburizing with natural gas in a fluidized bed
20 p2929 A72-39582
- Study of the process of niobium carbide production in a fluidized bed
23 p3293 A72-43294
- FLUIDS**
- Flexural vibrating free edge plate transducer with stepped thickness for high directional ultrasonic radiation generation in fluids
11 p1687 A72-26060
- Vibration of an infinite thin plate coupled with a fluid
18 p2736 A72-37002
- FLUORESCENCE**
- NT PHOSPHORESCENCE
- NT X RAY FLUORESCENCE
- Laser fluorosensor for remote environmental probing, considering applications to oil slick mapping, locating lignin sulphate pollution sources and hydrologic monitoring of tracer dye dispersal
[AIAA PAPER 71-1121]
01 p0080 A72-10559
- Excited IR fluorescence in gas compounds with negligible absorption, using CW carbon dioxide laser
03 p0367 A72-13554
- Fluorescence polarization and intensities of nitric oxide vibrational bands from Cd line and continuum excitation for spectrometer calibration
04 p0552 A72-14893
- Rate constant for quenching of B⁺/super 2Sigma-plus state of CN radical as function of quenching collision relative velocity and total pressure in fluorescence cell
04 p0553 A72-15635
- Laser pulse induced stimulated Raman scattering /SRS/ in linearly dispersionless medium measuring delay between laser and Stokes pulse maxima by photon absorption fluorescence technique
05 p0693 A72-17170
- Remote sensing of oil pollution on water by laser induced fluorescence, using airborne spectroscopy
[AIAA PAPER 71-1076]
07 p0981 A72-18822
- Abiogenic formation and fluorescence spectra of porphyrin, chlorin and bacteriochlorin during chemical evolution, using pyrrol-formaldehyde model
08 p1122 A72-22185
- Biological cell sorting by differential fluorescence generated electric signals via laser beam illuminated liquid stream
09 p1273 A72-23403
- Statistical equilibrium analysis of fluorescent Fe I emission in long period variables
10 p1542 A72-24610
- Electron beam fluorescence method for normal shock wave velocity distribution in Ar-He mixtures
11 p1615 A72-25556
- Fluorescence and absorption spectra from oxygen sulfur dichloride photodissociation in vacuum UV, discussing So formation
11 p1590 A72-26012
- Evanescent photons absorption and emission in light excited molecules fluorescence
11 p1691 A72-26745
- Nonlinear radiation absorption and resonance molecular fluorescence of saturated diatomic Rb vapors excited by Q switched ruby laser
14 p2109 A72-30353
- Supernovae produced fluorescence pulses search in upper atmosphere by automatic coincident light receivers
15 p2313 A72-32233
- Oil spills remote sensing in marine environment, using laser excited fluorescence for detection, identification and quantification
15 p2251 A72-32623
- Heavily doped ruby optical properties review, discussing N-lines, absorption and fluorescence spectra, interactions with phonon and photon fields and ionic reactions
16 p2441 A72-33522

Atomic, molecular and ionic species detection in upper atmosphere by measurement of resonance fluorescence radiation excited by tunable laser radiation
[AIAA PAPER 72-661] 16 p2388 A72-34073
HF vibrational relaxation measurements using the combined shock tube-laser-induced fluorescence technique.

17 p2511 A72-34735
Photon trapping in photosystem II of photosynthesis - The fluorescence rise curve in the presence of 3-/3,4-dichlorophenyl/-1,1-dimethylurea.

17 p2505 A72-35761
Evaluation of rotational temperature at high vibrational temperature in electron beam fluorescence technique.

19 p2803 A72-38434
Fluorescence of anthracene single crystals whose surface is disturbed by an impurity

19 p2847 A72-38781
Quenching of fluorescence and the photoeffect in anthracene crystals

19 p2847 A72-38782
Quantitative determination of fluorescence within the eye without disrupting the integrity of the eyeball
20 p2893 A72-38941

Frequency-tunable stimulated IR parametric fluorescence produced by barium sodium niobate crystal pumped with picosecond pulses from frequency-doubled mode locked Nd-glass laser

20 p2933 A72-39560
Electron beam visualization in hypersonic air flows.
[AIAA PAPER 72-1017] 21 p3042 A72-41596

Effect of fluorescence observation geometry on lifetime measurement, including the development of an approximation to the detector collection efficiency integral.

23 p3288 A72-43884
Diffusion of a filament of gas injected into a super-sonic free jet.

23 p3280 A72-43947

FLUORESCENT EMISSION

U FLUORESCENCE

FLUORIDES

NT ALUMINUM FLUORIDES
NT BARIUM FLUORIDES
NT BORON FLUORIDES
NT CALCIUM FLUORIDES
NT CHLORINE FLUORIDES
NT HYDROFLUORIC ACID
NT LANTHANUM FLUORIDES
NT LITHIUM FLUORIDES
NT MAGNESIUM FLUORIDES
NT NITROGEN FLUORIDES
NT OXYFLUORIDES
NT SODIUM FLUORIDES
NT SULFUR FLUORIDES
NT TUNGSTEN FLUORIDES
NT URANIUM FLUORIDES

Niobium trifluoride synthesis, noting semiconductor and paramagnetic properties

02 p0243 A72-12170
Thin sintered fluoride films bonding with monoa-luminum phosphate, investigating friction and wear behavior

06 p0821 A72-17804
Graphite fluoride as solid lubricant, investigating friction coefficient and wear resistance

06 p0837 A72-18598
Chemical vapor deposition of W and Mo by hydrogen reduction of hexafluorides, noting crystal structure and microporosity

11 p1644 A72-26837
Hydrated iron silicon fluoride internal motion pressure dependence examined by wideline and NMR techniques, noting corrections of second moments for bulk paramagnetic effects

13 p1914 A72-30061
Uranyl fluoride crystals luminescence spectrum study, calculating anion normal vibration frequencies

20 p2960 A72-39413

FLUORINE

Fluorine-ammonia as high energy liquid bipropellant for rocket engines, presenting ground test results regarding velocity and specific impulse characteristics as functions of mixture ratio

01 p0114 A72-11220
Time dependent progress of vibrational-rotational transitions in hydrogen-fluorine chemical laser investigated by oscillography with IKM-1 monochromator

08 p1183 A72-21715
Chemical bond effect on K emission spectrum of oxygen and fluorine

09 p1275 A72-22522
Trajectory dynamics for fluorine atoms reaction with H molecules, predicting total available energy from energy release on potential energy surface

10 p1434 A72-24343
Energy distribution among reaction products. VI - F + H₂, D₂.

19 p2763 A72-38804

Development of a rocket propulsion system with 500 kgf vacuum thrust for liquid hydrogen/liquid fluorine

23 p3325 A72-43620

Quasi-equilibrium analysis of the reaction of atomic and molecular fluorine with tungsten.
23 p3262 A72-44050

FLUORINE COMPOUNDS

NT ALUMINUM FLUORIDES
NT BARIUM FLUORIDES
NT BORON FLUORIDES
NT CALCIUM FLUORIDES
NT CARBON TETRAFLUORIDE
NT CHLORINE FLUORIDES
NT DIFLUORO COMPOUNDS
NT FLUORIDES
NT FLUORITE
NT FLUORO COMPOUNDS
NT FLUOROCARBONS
NT FLUOROHYDROCARBONS
NT FLUOROSILICATES
NT HYDROFLUORIC ACID
NT LANTHANUM FLUORIDES
NT LITHIUM FLUORIDES
NT MAGNESIUM FLUORIDES
NT NITROGEN FLUORIDES
NT OXYFLUORIDES
NT POLYTETRAFLUOROETHYLENE
NT SODIUM FLUORIDES
NT SULFUR FLUORIDES
NT TUNGSTEN FLUORIDES
NT URANIUM FLUORIDES

Pulsed chemical laser started by transverse electrical discharge, observing output energy dependence on fluorine compound used

04 p0530 A72-14974
Ho doped YLF and YAG laser threshold and slope characteristics at room temperature, considering Q-switched operation lifetime

07 p1004 A72-19233
Formation of fluorine-containing solid solutions based on barium titanate

19 p2845 A72-38407
Book on liquid rocket propellants development, history and ignition problem covering nitrogen tetroxide, hydrogen peroxide, fluorine compounds, boranes and monopropellants

19 p2884 A72-38675

FLUORINE ORGANIC COMPOUNDS

NT CARBON TETRAFLUORIDE
NT FLUOROCARBONS
NT FLUOROHYDROCARBONS

FLUORINE-LIQUID OXYGEN

U FLOX

FLUORITE

Recording holographic interferograms in a lanthanum-doped fluorite crystal

21 p3053 A72-40476

FLURO COMPOUNDS

NT CARBON TETRAFLUORIDE
NT DIFLUORO COMPOUNDS
NT FLUOROCARBONS
NT FLUOROHYDROCARBONS
NT POLYTETRAFLUOROETHYLENE

Tetrafluorodibromomethane - A new fire extinguishing agent in civil aviation

17 p2512 A72-35793

FLUOROCARBONS

Kinetic model and analysis of elementary characteristics of carbon trifluoriodide photodissociation laser

03 p0366 A72-13078
Electric pulse initiated pyrogen jet squid igniter consisting of magnesium-fluorocarbon coated bridgewire and pellet enclosed in Mk 1 or 2 gilding metal cup

08 p1221 A72-20774
Kinetic model and analysis of time characteristics of trifluoriodomethane photodissociation laser

13 p1968 A72-29428

FLUROHYDROCARBONS

NT CARBON TETRAFLUORIDE
Kinetics of shock wave pyrolysis of pen-tafluoroethane dilute mixture in Ar at 1180-1470 K

02 p0170 A72-11520
Biomedical effects on air crews of chemical fire suppression agent Halon 1301 /bromotrifluoromethane/ during simulated aircraft cabin fires

12 p1776 A72-28308

FLUOROMICA

U FLUOROSILICATES

U MICA

FLUOROSILICATES

Proton and fluorine nuclear magnetic spin-lattice relaxations due to internal rotations in magnesium fluorosilicate hexahydrate

04 p0564 A72-15636
Nuclear magnetic resonance of Al 27 in topaz /aluminum fluorosilicate/, determining nuclear quadrupolar coupling constant and asymmetry parameter

04 p0564 A72-15638

FLUSHING

Reliability design for airborne ecological system for jumbo jets, discussing toilet flushing and multiple server queueing model

10 p1429 A72-23999

FLUTING

U GROOVING

FLUTTER

NT PANEL FLUTTER
NT SUBSONIC FLUTTER
NT SUPERSONIC FLUTTER
NT TRANSONIC FLUTTER

Thermoelastic effect on flutter and vibration of built up delta wings with solid, stiffened and honeycomb/corrugated sandwich skins

[AIAA PAPER 72-174] 05 p0740 A72-16834
Autoparametric excitation in relation to divergence and flutter of autonomous mechanical cantilever systems under nonpotential circulatory forces

06 p0851 A72-18726

FLUTTER ANALYSIS

Flutter equation approximate true damping or rate-of-decay solution by determinant iteration

01 p0142 A72-11133
Self adjustment for time optimal nonstationary system control, developing algorithm for flutter

02 p0196 A72-11675
Thin airfoil and bridge deck flutter derivative from transient oscillatory states in test procedure

02 p0298 A72-12665
Aeroelastic models construction for flutter analysis of aircraft design, noting error risk reduction

[DGLR PAPER 71-082] 02 p0299 A72-12722
Flight vibration testing methods for ascertaining flutter stability of high speed aircraft

[DGLR PAPER 71-083] 02 p0155 A72-12725
Flutter problem wing-air flow energy exchange at instability limit, obtaining vibration mode shapes from homogeneous boundary value problem analog model

03 p0442 A72-13191
Chordwise bending vibrations and flutter of thin isotropic rectangular plates, considering static and dynamic responses

03 p0443 A72-13404
Hydroelastic behavior of heavily loaded lifting surfaces, investigating flutter and divergence

04 p0592 A72-15562
Flutter of thin homogeneous isotropic cylindrical panels from analog computer study

04 p0593 A72-15646
Navier-Stokes equations solution for unsteady viscous flow around oscillating elliptic airfoil in turbomachinery flutter analysis, obtaining pressure and shear stress distributions

05 p0600 A72-16002
Finite pitch airfoil theory relations for turbomachine moving blade rows interference effect on cascade flutter

05 p0738 A72-16488
Minimum weight panel designs subject to super-sonic flutter constraint, approximating governing differential equations by difference equations

[AIAA PAPER 72-170] 05 p0741 A72-16908
Flutter of thin elastic circular cylindrical fluid filled shells, presenting potential flow theory for coupled hydrodynamic forces

06 p0894 A72-17763
Flight flutter boundary testing, describing steps to minimize risk

06 p0759 A72-18491
Vibration analysis of shaft supported low aspect ratio control surfaces on guided rockets, using Rayleigh-Ritz method

07 p1097 A72-20602
Natural inertia moment effect of balance weight at wing tip on critical flutter rate

08 p1242 A72-21092
Orthotropic point-supported rectangular panel vibration and flutter analysis for natural frequencies and flutter boundaries, applying to space shuttle design

[AIAA PAPER 72-350] 11 p1728 A72-25379
Dynamic model of high bypass ratio turbofan engines for L-1011 wind tunnel flutter test program

[AIAA PAPER 72-376] 11 p1703 A72-25400
Linearized method of characteristics application to supersonic flow past oscillating flat plate cascades with supersonic leading edge locus

[AIAA PAPER 72-377] 11 p1730 A72-25401
Unsteady airfoil stall and stall flutter analysis, discussing application to space shuttle configuration

[AIAA PAPER 72-380] 11 p1730 A72-25404
Flutter analysis of propeller whirl flutter, twin boom aircraft, T tail configuration, servo tabs and all-moving tail, discussing structural variations effects on service life

[SAE PAPER 720309] 11 p1575 A72-25573
Wind tunnel tests for flutter characteristics of rectangular block model oscillating freely in uniform flow, discussing galloping and vortex excitation

11 p1572 A72-26373
Simultaneous iteration for eigenvalue problem numerical solution by mutually orthogonal trial vectors

close to required eigenvectors, applying to flutter analysis and Markov chains 11 p1679 A72-26959

Concorde dynamic behavior from flight tests, discussing integrated design effects, wing, fin and elevator flutter, gust and runway response and engine surge effects 13 p1897 A72-28958

[AIAA PAPER 72-381] 13 p1897 A72-28958

Wind tunnel testing of Dassault-Breguet-Dornier Alpha Jet twin engine trainer, emphasizing tests for wing-empennage flutter and jet induced interference effects 13 p1940 A72-30077

Aeroelasticity, discussing gust and maneuver load alleviation, flutter suppression, aircraft stability, computerized aeroelastic analysis, aeroelastic optimization, composite structures, etc 15 p2322 A72-31202

Probstein-Gold viscoelastic model of supersonic flow induced surface cross-hatching assessment against Dowell studies on plates and shells flutter 16 p2463 A72-32838

Flutter instability control in continuous elastic system via feedback 16 p2463 A72-32843

Influence of airfoils on stall flutter boundaries of articulated helicopter rotors. 17 p2484 A72-34489

[AHS PREPRINT 621] 17 p2484 A72-34489

The elastic stability of two-parameter nonconservative systems. 17 p2627 A72-34782

[ASME PAPER 72-APM-43] 17 p2627 A72-34782

On the flutter of thin cylindrical shells conveying fluid. 17 p2634 A72-35415

Some properties pertaining to the stability of circulatory systems. 18 p2737 A72-37060

Real time flight flutter testing via Z-transform analysis technique. 19 p2749 A72-38101

[AIAA PAPER 72-784] 19 p2749 A72-38101

A flutter optimization program for aircraft structural design. 19 p2876 A72-38111

[AIAA PAPER 72-795] 19 p2876 A72-38111

Application of the finite element method to torsional flutter analysis on an analog computer 20 p2980 A72-39907

Unsteady rotor aerodynamics at low inflow and its effect on flutter. 22 p3135 A72-42349

[AIAA PAPER 72-959] 22 p3135 A72-42349

Wing flutter prevention in SST structural design, using finite element model and lifting surface aerodynamic theory 22 p3237 A72-42760

Treatment of the flutter equation by functional analysis, using the Newton method 22 p3240 A72-42907

Flutter analysis and unsteady pressure fields induced by pitching motions of wall mounted sweptback wing, verifying experimentally lifting surface theory in high subsonic range 22 p3241 A72-43094

Blade torsional tuning to manage rotor stall flutter. 24 p3369 A72-45412

[AIAA PAPER 72-958] 24 p3369 A72-45412

Supersonic flutter of plane, rectangular, anisotropic, heterogeneous structures 24 p3459 A72-45440

FLUX [RATE PER UNIT AREA]

U FLUX DENSITY

FLUX [RATE]

NT HEAT FLUX

NT MAGNETIC FLUX

NT SOLAR FLUX

Ion production rates during electron-flux-atmosphere interactions based on atmospheric models with different energy and angular distributions 01 p0059 A72-10597

Rocket-observed energetic electron flux association with ground recorded plasmasphere whistler in terms of gyroresonant wave-particle interaction 15 p2198 A72-31948

FLUX DENSITY

NT CURRENT DENSITY

NT ELECTRON FLUX DENSITY

NT ILLUMINANCE

NT IRRADIANCE

NT LUMINANCE

NT LUMINOUS INTENSITY

NT NEUTRON FLUX DENSITY

NT PARTICLE FLUX DENSITY

NT PHOTON DENSITY

NT PROTON FLUX DENSITY

NT RADIANCE

NT RADIANT FLUX DENSITY

NT SOLAR CONSTANT

NT SOLAR FLUX DENSITY

NT SOUND INTENSITY

Steady heat conduction plane problem solution for infinitely long cylinder with constant surface thermal flux density and temperature 04 p0595 A72-14644

Flux lines interaction with dislocations in twisted superconducting niobium single crystals, measuring flux gradient and dislocation arrangement 06 p0830 A72-18055

Crab Nebula and Vela pulsar constant elastic energy density contours, discussing micro and macroquakes 06 p0886 A72-18095

Light beam time stationary multifocal structure in medium with Kerr type nonlinearity, relating maximum energy density and absorption coefficients 07 p0944 A72-19635

Statistical analysis of magnetic energy-density antenna performance in mobile communication, comparing two-crossed-slot design to three element unit 07 p0957 A72-19801

Output power calculation of gas lasers with active elements of varying lengths, using extreme emission fluxes equations 08 p1184 A72-22031

Heat transfer through glass plate in solar radiation flux, discussing temperature distribution and thermal flux meter design 10 p1562 A72-24318

Turbulent plasma electric field energy density spectrum from statistical mechanics investigation based on canonical formalism for electron plasma 12 p1851 A72-27387

Joule heating power density in NbZr superconductor hollow cylinder, estimating temperature changes and instability locations 13 p2023 A72-29855

Seasonal changes in magnetospheric directional fluxes at synchronous altitudes due to solar wind induced field line knee effect and drift shell asymmetry 14 p2097 A72-30131

Flux densities, electron energies and brightness temperature determination from radio telescope observations of galactic sources and nonthermal radiation 14 p2155 A72-30553

Attachment length as stability criterion for bluff-body stabilized electrodeless arc, showing linear dependence on flow velocity ratio to power density 15 p2336 A72-32406

Rechargeable high energy density battery with Al and Cl electrodes and molten aluminum chloride-alkali chloride eutectic electrolyte 16 p2352 A72-33896

Observations of some small-diameter radio sources at 408 MHz. 17 p2603 A72-34440

German monograph - Investigation of electron beam welding with particular consideration of the mean power density and the radial power density distribution in the beam cross section 19 p2807 A72-37658

Investigation of the critical heat flux density in heat transfer with and without turbulization of the flow at the inlet of an annular channel 21 p3129 A72-41057

Wall temperature, thermal conductivity and acoustic vibration frequency as function of critical heat flux density for unstable water film boiling conditions 21 p3130 A72-41063

Cosmological model radiation pressure and density calculation by red shift-stellar magnitude ratios from galactic observations 21 p3109 A72-41441

Forced-convective-flow carbon monoxide laser. 22 p3184 A72-41968

Plasma sheet characteristics of geomagnetic tail at 60 earth radii, inferring spatial distribution of magnetic field magnitude and plasma energy density 22 p3211 A72-42407

Upper limit on the gravitational flux reaching the earth from the Crab pulsar. 23 p3337 A72-43874

Light beam time stationary multifocal structure in medium with Kerr type nonlinearity, relating maximum energy density and absorption coefficients 24 p3408 A72-44567

Increase in the ratio of the energy of ultrashort laser pulses to the energy of the background radiation. 24 p3411 A72-45613

FLUX MAPPING

U FLUX DENSITY

U MAPPING

FLUX QUANTIZATION

Radio variable sources PKS 0727-11 and 1514-24 observation at 2295 MHz, presenting flux measurements and drift curves 01 p0134 A72-11161

Flux quantization in superconductors demonstrated by magnetometer probe measurement of magnetic field trapped in thin In film holes 16 p2441 A72-33225

FLUXMETERS

U MAGNETIC MEASUREMENT

U MEASURING INSTRUMENTS

FLY BY WIRE CONTROL

Multiplex electrohydraulic system for aircraft fly by wire actuators with majority voting and pressure logic, discussing frequency response and environmental tests 08 p1113 A72-22152

Electromechanical redundant activating mechanism for F-4 aircraft dual tandem hydraulic power servo, noting application to fly by wire control 14 p2072 A72-30422

The fly-by-wire systems approach to aircraft flying qualities. 17 p2493 A72-35575

Quadruple-redundancy management for fly-by-wire control system reliability, discussing analog circuit and digital computer voter/monitor techniques 20 p2910 A72-39117

[AIAA PAPER 72-884] 20 p2910 A72-39117

Electronic primary flight control system requirements and equipment characteristics, discussing USAF and NASA fly by wire R and D programs 20 p2887 A72-39118

[AIAA PAPER 72-882] 20 p2887 A72-39118

Synthesis and analysis of a fly-by-wire flight control system for an F-4 aircraft. 20 p2887 A72-39119

[AIAA PAPER 72-880] 20 p2887 A72-39119

Design and flight experience with a digital fly-by-wire control system using Apollo guidance system hardware on an F-8 aircraft. 20 p2889 A72-40060

[AIAA PAPER 72-881] 20 p2889 A72-40060

Concorde electrically signalled fly by wire control system with mechanical linkages for standby fail-safe redundancy 21 p2994 A72-41068

FLYBY MISSIONS

NT GRAND TOURS

Minimum velocity change noncoplanar two and three impulse orbital transfer from regressing oblate earth assembly parking ellipse into flyby trans-Martian asymptotic velocity vector 03 p0434 A72-13634

Mariner Venus/Mercury 1973 flyby mission imaging experiment, discussing mission constraints, objectives and use of real time transmission vidicon camera and high resolution UV photography 04 p0568 A72-14494

Trajectory characteristics for multiple asteroid flyby missions to determine physical properties of minor planets 05 p0721 A72-16928

Mission analysis of Helios spacecraft swingby past Venus to acquire extraecliptic trajectory 05 p0721 A72-16951

[AIAA PAPER 72-50] 05 p0721 A72-16951

Future deep space missions, discussing exploration of interplanetary conditions outside ecliptic plane and solar system Grand Tour with outer planets flyby 07 p1068 A72-19059

German monograph on optimal planetary atmosphere effects for increasing hyperbolic velocity at flyby for Venus and Earth 09 p1383 A72-22322

Planetary swingby optimum transfer between hyperbolic asymptotes with less than maximum natural turn angle 10 p1552 A72-24487

Encounter sequences determination techniques for multitarget flyby and rendezvous missions to asteroids and comets by spacecraft using solar electric propulsion 13 p2037 A72-28940

[AIAA PAPER 72-429] 13 p2037 A72-28940

Trajectory analysis for swingby technique using Jovian gravitational field for leaving ecliptic plane along heliocentric orbit and for solar flyby at specified distance 14 p2150 A72-30452

Spacecraft and missions for Jupiter exploration, discussing launch vehicle requirements, solar electric propulsion for midcourse correction, Pioneer flyby and orbiter missions, TOPS mission, etc 21 p3103 A72-40457

Approximate analytic solution method for trajectory problem of planetary flyby or impact case of restricted three body problem 21 p3111 A72-41558

[AIAA PAPER 72-911] 21 p3111 A72-41558

Flyby missions to comets, asteroids and meteors for obtaining solar system geological information, considering space dynamics feasibility 23 p3340 A72-44351

Mission strategy for combined comet-asteroid flybys. 24 p3444 A72-45436

[AIAA PAPER 72-939] 24 p3444 A72-45436

Mariner spacecraft Jupiter-Saturn 1977 gravity assisted flyby, discussing mission objectives and trajectory options 24 p3444 A72-45438

[AIAA PAPER 72-943] 24 p3444 A72-45438

FLYING BEDSTEAD AIRCRAFT

U FLYING PLATFORMS

FLYING PERSONNEL

NT AIRCRAFT PILOTS

NT ASTRONAUTS

NT COSMONAUTS

NT FLIGHT CREWS

NT ORBITAL WORKERS

NT PILOTS [PERSONNEL]

NT SPACECREWS

NT TEST PILOTS

CO hemoglobin concentration measurement in blood of smokers, nonsmokers and deceased crewmembers of crashed aircraft 01 p0010 A72-10211

Control technique and flight quality for crew workload reduction to improve military and civil aircraft flight safety

03 p0310 A72-13640

Fainting prevention in flying personnel, discussing constitutional susceptibility, health irregularities, alcohol, heavy smoking, lack of sleep, emotions and medical histories

03 p0316 A72-13722

Psychological tests of airmen with performance error histories, considering psychic characteristics for limited assignment readjustment

03 p0316 A72-13723

Isoniazid tuberculosis chemoprophylaxis safety in aviation personnel, discussing renal function, serum transaminase activity, hematology, electrocardiograms and neurological examinations

04 p0479 A72-14872

Early diagnostics of cerebral arteriosclerosis in flying personnel, investigating hypertension, neurocirculatory dystonia and myocarditic cardiosclerosis effects on flight performance

06 p0765 A72-18198

Aging effect on visual acuity variations relation to refraction variations in flight deck personnel, noting eye functional value diminution

07 p0927 A72-19244

Flight personnel statistical survey of clinical, physical and psychic causes of temporary and permanent flight service unfitness

07 p0923 A72-20447

Hyperlipidemia progressive increase among flying personnel, showing Clofibrate treatment effect on lowering rate

08 p1117 A72-21545

Brief vestibular disorientation test technique for assessment of potential nonpilot airborne specialists or naval flight officers

12 p1773 A72-28256

Statistical survey of barosinusitis incidence in U.S. Navy flying personnel during altitude chamber training, discussing diagnostic methods and clinical management

12 p1765 A72-28274

Frontal sinus hematoma incidence in flying personnel and scuba divers, discussing diagnosis and clinical treatment

12 p1765 A72-28275

Change in Naval Flight Officer operational role due to modern equipment design in weapons systems, sensors and navigational aids

12 p1775 A72-28291

Serum cholesterol, phospholipid and lipoprotein levels relation to atherosclerotic heart disease occurrence in USAF personnel

12 p1766 A72-28292

Clofibrate treatment for atherosclerotic cardiovascular disease prevention among Sabena flying personnel

12 p1766 A72-28293

ECG diagnostics for arrhythmia assessment in flying personnel flight fitness examination

12 p1775 A72-28294

Review of aeromedical records for grounding USAF flying personnel during 1956-1970, noting increased age factor effect

12 p1776 A72-28316

Keratoconus /noninflammatory conic protrusion of cornea/ diagnosis and rehabilitation in USAF flying personnel

12 p1768 A72-28331

Sight impairment-caused flight personnel disqualification analysis, establishing eye disease structure, sight damage preconditions and ophthalmological practice inadequacies

14 p2080 A72-30748

Psychological criteria for flying personnel selection in civil aviation, noting performance prediction based on maximum likelihood estimates

14 p2080 A72-30816

Low pressure chamber as aerospace medical diagnostics tool for flying personnel examinations regarding oxygen deficiency, low air pressure and air pressure fluctuations tolerance

14 p2080 A72-30819

The legal position of civil air personnel

17 p2639 A72-35762

Renal polycystoma - Incidence among flight personnel

19 p2756 A72-37877

Description of an easy and simplified test for electromyographic diagnosis of latent spasmodia in flight personnel

19 p2760 A72-37878

Resumption of flight after retinal surgery

19 p2760 A72-37879

Systematic detection of myocardial infarction in the course of medical screening of flight personnel

19 p2757 A72-37881

A model corporate pilot physical program

20 p2897 A72-39746

Professional capabilities activation of flying personnel, discussing psychological training for flight fitness

21 p3004 A72-40172

Changes in the functional state of analysors in flying personnel during long flights

21 p3006 A72-40445

Flying personnel auditory defects caused by environmental conditions, discussing aircraft noise, vibrations and atmospheric pressure effects

21 p3002 A72-40924

Potassium chloride test for electrocardiogram evaluation in flight personnel medical appraisal

21 p3012 A72-41747

Hazard rate of recurrence in germinal cell tumors of the testis.

22 p3150 A72-42498

A special vitamin complex for prophylaxis of atherosclerosis in aviation personnel

23 p3261 A72-44153

Hodgkins disease post-surgery recurrence hazard rate in flying personnel, developing statistical base for decision regarding return to military flying duty

24 p3377 A72-45661

Keratoconus incidence in USAF flying personnel, discussing diagnosis, etiology and therapy

24 p3378 A72-45663

Paranasal sinus barotrauma in military flying personnel, discussing radiographic diagnostic methods and hypobaric test procedures for flight status restoration time determination

24 p3378 A72-45664

FLYING PLATFORM STABILITY

U AERODYNAMIC STABILITY

U FLYING PLATFORMS

FLYING PLATFORMS

Circumpolar region object position autonomous determination from arbitrarily zenith-oriented moving horizontal platform position coordinates

04 p0545 A72-15002

Tethered flying rotor platform for reconnaissance, fire control and radio transmission assignments in naval missions, discussing system characteristics

04 p0465 A72-15652

Combined hydrostatic suspension Hg cushion effects on gyrocompass response precision during irregular roll of platform

13 p1961 A72-30022

Tethered autostabilized rotor platform for military surveillance, target location and communication, discussing flight vehicle, tethering cable, ground station and guidance-control system

13 p1898 A72-30078

FLYING QUALITIES

U FLIGHT CHARACTERISTICS

FLYING SPOT SCANNERS

Operation and performance characteristics of flying spot scanning X ray imaging systems for rapid film safe parcel inspection

18 p2692 A72-36671

FLYWHEELS

Torsional vibrations of shaft with multiple flywheels, presenting computer generated graphs for vibration modes

04 p0584 A72-14517

FM/PM [MODULATION]

Computer search for optimum narrow band FM and PM systems bandpass filters, noting low index angle modulated signals

06 p0783 A72-17484

Phase coherent frequency synthesizer as modulation source for multiple feature communication system, noting noise resistance, navigation capability, Doppler correction and transmitter to receiver ranging

06 p0777 A72-18619

FOAMS

Liquid-base foam sound absorbing properties for jet aircraft noise reduction

01 p0115 A72-10160

Sound propagation and absorption mechanism in liquid-base foams explored by bubble pulsation and coupling mathematical model and distributed parameter mechanical analog

01 p0115 A72-10161

Two phase flow equations model application to fluidized beds and foams, predicting bed stability to small perturbations for comparison with experiment

01 p0093 A72-11272

Sea foam emission and reflection characteristics at microwave frequencies from radiometric measurements, correlating data as functions of frequency and angle

10 p1475 A72-24749

Destructive effect of combustion and pyrolysis products in intake air on fire extinguishers foam production

14 p2084 A72-30339

Foam content effect on fiberglass reinforced thermoplastic foam tensile and impact strength, thermal distortion and mold shrinkage properties

16 p2415 A72-33418

Experimental determination of ultrasonic wave velocities in plastics, elastomers, and syntactic foam as a function of temperature.

18 p2703 A72-36415

Evaluation of film forming foams for the suppression of fuel fires in aircraft hangars.

[WSCIPAPER 72-16] 20 p2982 A72-38974

FOCI

Prime focus paraboloid antenna performance with cylindrical hybrid mode feeds, detailing radiation patterns and distribution

02 p0173 A72-12110

Abastumani Observatory 70 cm meniscus telescope, determining performance from primary focus field data

03 p0359 A72-13498

Three element einzel and asymmetric voltage lenses for electron optics, calculating focal lengths and spherical aberrations based on potential distribution inside equidiameter coaxial cylinders

07 p0992 A72-20585

Focal length determination for on-axis parabolic mirrors by He-Ne laser reflection

09 p1315 A72-23352

Centers and foci composition of united trajectories of two autonomous scalar second order differential equations

15 p2262 A72-31551

FOCUSING

NT DEFOCUSING

NT SELF FOCUSING

Large aperture antenna feed design, calculating focused and unfocused amplitude and phase field distributions in front of circular aperture

01 p0029 A72-10674

Periodic magnetic field effects at gun cathode on electron beam focusing stability under nonoptimal conditions

02 p0190 A72-11572

Focused image holographic interferometer for reduced blur in deep object image reconstruction with white light source

02 p0224 A72-11747

Ionic focusing of electron beam in transverse gas flow, using air, argon and helium

02 p0261 A72-12764

Focused image holography in multimode He-Ne laser radiation, using diffusely scattered reference wave and lens for high quality reconstruction

03 p0357 A72-13370

Flange angle effects on sectional horn antenna E-plane radiation patterns and beam focusing and broadening

04 p0497 A72-14511

Gravitational radiation focusing by interior gravitational fields of diffuse static spherically symmetric matter distribution

04 p0549 A72-15024

Gathering power, geometrical factor and directional response of single and multielement particle telescopes

06 p0811 A72-17317

Electrostatic focusing field inhomogeneity /gradients/ effects on high frequency electron-wave interaction processes in linear beam backward wave oscillator tube

07 p0952 A72-18845

Transverse mode effects on gain and dispersion focusing in high gain Xe laser

07 p1005 A72-19409

Constant period discrete holograms features, investigating laser visualization, recording, reconstruction and image focusing

08 p1163 A72-20747

Incoherently light radiating object and background light focusing on photosensitive mosaic, observing linear restoration by comparison of mean square error with Wiener filter theory

09 p1350 A72-22611

Fresnel diffraction integrals for irradiance and power distribution calculations of Gaussian beams focused through annular apertures

09 p1352 A72-23334

Electron beam welding focus effect on fusion zone penetration in thick austenitic stainless steel

09 p1321 A72-23643

Broadband electrostatically focused klystron for airborne radar application, discussing focusing cell design, amplification and efficiency

10 p1446 A72-23821

Plasma equilibrium configurations, considering magnetically contained focus in external magnetic field

11 p1694 A72-25788

Heat conduction heating of plasma by high power ultrashort laser pulse incident on solid target, noting focusing and energy absorption role

12 p1852 A72-27622

Charged particle beams focusing in combined dual spiral system with homogeneous magnetic field along axis

13 p1932 A72-29292

Atmospheric turbulence from illuminance and intensity fluctuation measurements at focused light beam

16 p2364 A72-33488

Modulation measurement applied to the focusing of aerial cameras.

17 p2558 A72-35948

Theoretical and experimental studies of the focus of sonic booms.

18 p2642 A72-36506

Properties of the electrostatic field of a system of annular electrets and possibilities of its application for focusing in molecular generators

19 p2804 A72-38538
A design method for the electron beams of TWT's.

19 p2775 A72-38610
Electron beam focusing by ions in transverse gas flows, considering air, argon and helium residuals

20 p2952 A72-39070
Thermal emissivity and directivity for V groove and rectangular cavities, optimizing geometry and surface properties for maximum focusing of emitted energy [ASME PAPER 72-HT-L]

20 p2984 A72-39651
Single-cycle electron acceleration in focused laser fields.

20 p2934 A72-39720
On diffraction and focusing in anisotropic crystals.

20 p2961 A72-39779
Double-dipole exciter for the primary focus of the 100-m radio telescope Effelsberg

21 p3029 A72-40518
Focus field and horn exciter regarding parabolic antennas with small f/D-relation

21 p3029 A72-40523
Spherical focusing transducers with Gaussian surface velocity distribution.

21 p3057 A72-41477
Experimental determination of some optical characteristics of a double magnetic prism-electrostatic mirror system

22 p3180 A72-42937
German monograph - Contributions to the study of the astigmatic image.

22 p3207 A72-43067
Supersonic aircraft focused sonic boom suppression by slowing down during turning flight, obtaining conditions for focus cut-off at ground by atmospheric refraction

23 p3251 A72-44125
Averaged equations of laser heating of plasma in a focus-type system taking into account the heat of nuclear fusion.

23 p3322 A72-44223
Averaged equations of laser heating of two-temperature plasma in a focus-type system taking into account the heat of nuclear fusion.

23 p3322 A72-44224
Measurement of the modulation transfer functions of focusing screens.

24 p3425 A72-44770
Optical system chromatic aberration correction relationship to focus plane position in white light based on Strehl and Hopkin criteria

24 p3425 A72-44772
Focusing characteristics of CO₂ laser beam.

24 p3409 A72-44776
Remotely controlled astronomical observatory telescope Cassegrain focus, evaluating computerized automated electronic system advantage over conventional instrument

24 p3405 A72-45543
Focusing properties of converging-beam holograms.

24 p3405 A72-45602

FOETUSES

U FETUSES

FOG

Visibility relationships to atmospheric liquid water content in fog derived from fog drop size distribution model

01 p0096 A72-11281

Scattering media visibility improvement analysis, using theoretical evaluations and experimental electro-optical measurement techniques in fog and underwater

02 p0253 A72-12644

Algorithm design for objective high altitude fog prognosis, considering geostrophic vorticity, thermal advection, wind direction and dew point difference

02 p0254 A72-12782

Economic evaluation of airport fog dispersal methods in the U.S., including crushed dry ice and liquid propane

04 p0542 A72-14677

Airport cold fog attenuation by propane atomization technique, discussing application at Orly

04 p0508 A72-14686

Warm fog dissipation by helicopter downwash mixing, heat, hygroscopic particle and polyelectrolytes seeding

04 p0543 A72-14694

Fog modification at all temperatures with physicochemical techniques, discussing blowing hygroscopic salts and use of alginates of sodium and marine algae extracts

04 p0543 A72-14696

Supercooled and warm fog dispersion technology, considering air heating, helicopter downwash and seeding methods

04 p0543 A72-14812

Light field in cloud and fog plane layers from stationary collimated point source propagation

06 p0848 A72-17937

Airport fog dispersion methods review, noting seeding and hot air injection techniques

08 p1201 A72-21920

Runway fog dispersal system based on underground installed flight-discarded turbojet engines, discussing system efficiency and economics

09 p1292 A72-22910

Fog and cloud microstructure and density distributions from directional light scattering coefficient /halo indicatrix/

11 p1683 A72-26883

Light beams propagation in clouds and fog, discussing scattering and attenuation coefficients

13 p1988 A72-28517

Coastal and inland fog microphysical features, discussing visibility, liquid water content, drop size distributions and haze droplet concentration

13 p1991 A72-28842

FAA airport fog dispersal program, discussing techniques effectiveness evaluation vs defined goals

13 p1992 A72-28843

Mathematical model for numerical simulation of warm fog modification by seeding hygroscopic particles, taking into account turbulent diffusion and horizontal wind advection

13 p1992 A72-28844

Slant range visibility measurements by lidar for aircraft landing operations under low clouds and fog at coastal region

13 p1992 A72-28847

Airport runway fog dispersal in UK, discussing cost projection for chemical seeding system combined with lidar remote sensing

16 p2418 A72-33500

Light field in cloud and fog plane layers from stationary collimated point source propagation

16 p2426 A72-33778

Laser IR radiation attenuation in natural and artificial fogs, noting dependence on particle size distribution

18 p2697 A72-36102

Atmospheric transmittance measurements time and spatial representativeness optimization by allowing for fog element caused discontinuities

20 p2947 A72-38971

Fog and cloud microstructure and particle size distributions from directional light scattering coefficient /halo indicatrix/

20 p2948 A72-39570

Light transmission, reflection and environment problems of hydrophilic coatings for fog and frost protection in aviation instrument window design

22 p3196 A72-42519

Visibility variations at Schiphol-Airport, Amsterdam.

22 p3202 A72-42886

FOIL BEARINGS

Dynamic characteristics of turborotor simulator supported on gas lubricated foil bearings of reduced length with starting and stopping unaided by external pressurization

[ASME PAPER 71-LUB-16] 02 p0235 A72-11538

Dynamic response of infinitely wide perfectly flexible foil bearings to small sinusoidal tensile variations

[ASME PAPER 71-LUB-20] 02 p0235 A72-11540

FOILS (MATERIALS)

NT METAL FOILS

Beam-foil-gas spectroscopy and relative cross section measurements for studying steady state nonequilibrium processes

10 p1434 A72-24325

Joining plastic foils with the aid of high-frequency welding

20 p2930 A72-39942

FOKKER AIRCRAFT

VFW 614 twin jet transport aircraft flight test program, detailing general task plan, test equipment installations and test schedule

14 p2072 A72-30679

Fokker VTOL transport aircraft designs, considering payload, range, runway conditions, noise, military capabilities and operational costs

16 p2347 A72-33048

New VTOL transport aircraft designs by VFW Fokker. II

17 p2492 A72-35477

FOKKER BOND TESTERS

U ADHESION TESTS

FOKKER-PLANCK EQUATION

Isotropic turbulence energy transport approximation by local differential equation analogous to Fokker-Planck equation, noting Kolmogoroff distribution for infinite Reynolds number

02 p0205 A72-12449

Dust grain orientation parameter from Fokker-Planck equation, considering magnetic relaxation time, nearly spherical grains and oblate spheroids

02 p0283 A72-12627

Shock wave structure in monatomic gases, using Fokker-Planck model for particle collisions and Mott-Smith distribution for shock front

04 p0512 A72-15162

Ray statistics of electromagnetic wave scattering in homogeneous isotropic turbulent medium with ellipsoidal inhomogeneities of refractive index, using Fokker-Planck equation

05 p0626 A72-16243

Fokker-Planck equations for charged particle dynamics rederived for random fields, finding pitch angle scattering

08 p1227 A72-21385

Nonlinear vibrations under random excitation, discussing equivalent linearization and small parameter perturbation methods and Fokker-Planck equation

09 p1353 A72-23604

Nonlinearity effects on random vibration displacement and frequency characteristics of one degree of freedom system, using Fokker-Planck equation

09 p1353 A72-23605

Multivariable probability density determination of random vibration systems with n degrees of freedom by Fokker-Planck equation

09 p1353 A72-23609

Superradiant laser stationary behavior and photon statistics, solving Fokker-Planck equation for quantum mechanical distribution function in Hilbert space of atomic system

10 p1514 A72-24247

Random walk models replacing Fokker-Planck equation for many particle systems with Coulomb interactions

10 p1513 A72-25041

Collisional distributions in mirror plasmas, using successive approximation technique for Fokker-Planck equation lowest eigenvalue and eigenmode

11 p1694 A72-25792

Whistler waves amplification in magnetosphere, obtaining particles pitch angle and energy diffusion coefficients and one dimensional Fokker-Planck equation

15 p2194 A72-31427

Fluctuation renormalized transport coefficients in corrected nonlinear transport equations derivation from generalized Fokker-Planck equation

15 p2337 A72-32653

Soft collision plasma scattering function, conductivity and particle energy loss from simplified Fokker-Planck collision model

17 p2592 A72-35621

State vector moments of nonlinear mechanical systems under stochastic excitation, using Fokker-Planck equation for transition probability and differential equations derivation

21 p3084 A72-40679

FOLDING

Uniaxially stressed elastic /soft/ shells with fold formation during compressive strain, formulating equilibrium and boundary conditions for uniaxial region

08 p1247 A72-21812

FOLDING STRUCTURES

NT SAILWINGS

Flexible rolled-up solar array /FRUSA/ operational performance from spaceborne accelerometers, strain gages and temperature sensors telemetered data, noting damage-free extension-retraction exercises

[AIAA PAPER 72-510] 13 p2051 A72-28952

FOLIAGE

Ponderosa pine foliage visible and near IR spectra, investigating soil copper contents effect on foliage spectral reflectance

02 p0209 A72-11790

FOOD INTAKE

Chronic centrifugation effects on rat deep body temperature by implant biotelemetry, comparing with body mass and food consumption changes

02 p0163 A72-12089

Spacecraft and aircraft crew survival after emergency landing in adverse environments, discussing water and food requirements, survival supplies and medical and first aid equipment

05 p0621 A72-16629

Food ration effect on metabolite elimination rate in humans wearing isolation garment at rest or performing physical labor

05 p0622 A72-16644

Food deprivation stress effects on urinary excretion values in unrestrained chimpanzees

10 p1426 A72-24822

High gravity, cold and starvation space stress effects on oxidative metabolism of ethylmorphine, aniline and p-nitroanisole in male rat liver

15 p2185 A72-31700

Myocardial lipid and carbohydrate metabolism in fasting men during prolonged exercise.

17 p2499 A72-34347

Influence of prolonged starvation on the frequency of occurrence of decompression-induced pulmonary hemorrhage.

17 p2508 A72-34545

Influence of thermal, osmotic, and chemical stimulations on food and water intake

17 p2504 A72-35016

Effect of fasting on tolerance to moderate hypoxia.

22 p3150 A72-42487

Spinal cord heating and cooling effects on body temperature, respiratory and heart rates and arterial blood pressure, investigating feeding and drinking behaviors

22 p3150 A72-42672

FORBIDDEN BANDS

Forbidden O I and molecular nitrogen ions emission lines ratio variation with height in aurora

03 p0352 A72-14382

Solar silicon abundance from low excitation forbidden Si I lines

04 p0579 A72-15326

Atomic hydrogen 6300 Å forbidden line emission altitude and intensity during predawn enhancement, using rotating photometer

06 p0806 A72-17644

Galactic nucleus IR measurements in terms of forbidden NE II emission line at 12.8 microns

07 p1081 A72-20229

Forbidden band thermal deformation effect on homogeneous steady state stability of semiconductor

09 p1367 A72-22492

Radiation induced extrinsic photoconductivity in Li doped Si, examining localized energy levels in forbidden gap

09 p1372 A72-23238

Photoelectric Fabry-Perot measurements of M8 and M42 nebulae H alpha and forbidden N II emission lines profiles, determining temperatures and turbulent motions

09 p1390 A72-23528

Forbidden O I lines brightness and shadow bands properties during 7 March 1970 solar eclipse, comparing with rocket measurements

12 p1800 A72-27143

Planetary nebula classification based on forbidden line ratios and morphology, discussing galactic plane distribution, radial velocities and evolution

12 p1867 A72-27209

Laplace transform method in unsteady radiation field theory, discussing generalization from steady luminescence to inhomogeneous media and forbidden band frequency radiative transport

13 p2001 A72-28506

Molecular adsorption on semiconducting surfaces, discussing conditions for formation of local surface levels in forbidden gap

15 p2296 A72-32760

Forbidden band thermal deformation effect on homogeneous steady state stability of semiconductor

17 p2595 A72-34656

Galactic nebulae electron temperature and density from forbidden line emissions interpreted in terms of transition probabilities and collision strengths

18 p2723 A72-36090

Forbidden line intensities in cesium plasmas

19 p2840 A72-37776

Cooling associated with minority carriers exclusion effect in semiconductors, discussing influence of electroconductivity and forbidden bandwidth

21 p3097 A72-40788

FORBIDDEN TRANSITIONS

Solar UV line spectrum identification and intensity analysis, emphasizing electron spectra in soft X ray region and forbidden transitions

03 p0420 A72-13124

Diatom molecules forbidden transitions moments, Franck-Condon factors and lifetimes, calculating CO Cameron system intensity by perturbation theory

05 p0692 A72-16750

Wavelength, intensity and spatial distribution identification of far UV solar coronal forbidden lines observed during 7 March 1970 solar eclipse

13 p2043 A72-29540

High power carbon dioxide laser produced dense He plasma, comparing experimental and theoretical Stark profile of forbidden and allowed transitions

15 p2285 A72-32223

Particle excitation processes in solar corona, ionosphere and astrophysics, discussing electron affinities, ion-molecule reactions, forbidden atomic transitions and Fe II problem

16 p2432 A72-34150

Measurements of the limb darkening in the forbidden Mg I line at 4571.1 Å

17 p2608 A72-35078

Various ground configuration level intervals from gaseous nebulae and solar coronal forbidden transitions observations and laboratory investigations of resonance lines

21 p3108 A72-41286

FORBUSH DECREASES

Jupiter decametric radio emission relation to solar wind, geomagnetic activity and shock waves causing Forbush decreases

03 p0436 A72-13820

Forbush decreases in galactic cosmic ray flux and associated vlf nighttime ionospheric propagation phenomena

07 p1056 A72-18900

Forbush decreases in cosmic radiation, discussing cosmic ray flow pattern deduction from anisotropies, modulation dependence on rigidity and theoretical models

07 p1058 A72-19355

Transient North-South anisotropies in cosmic radiation intensity, noting occurrence during Forbush decreases

15 p2298 A72-31432

Solar flare producing regions statistical correlation to SC/SI events accounting for geomagnetic storms and Forbush decreases in terms of interplanetary streams

16 p2445 A72-33376

Interplanetary magnetic field irregularities and shock effects associated with cosmic ray Forbush decreases

16 p2449 A72-33939

Change in the eleven-year modulation at the time of the June 8, 1969, Forbush decrease.

22 p3172 A72-42424

Statistical analysis of Forbush decreases and the preceding increases in cosmic-ray intensity

23 p3328 A72-43354

Nature of the long-term and short-term modulations of cosmic-ray intensity.

23 p3332 A72-44521

Diffusion processes of cosmic rays with energies between 2 and 20 GV during Forbush decreases - The diurnal effect.

24 p3434 A72-44785

FORBUSH EFFECT

U FORBUSH DECREASES

FORCE DISTRIBUTION

Griffith crack stress intensity factor and crack face displacement in elastic solid, detailing symmetrical, antisymmetrical and point body force distributions

01 p0136 A72-10185

Polycrystalline bodies thermoelastic behavior under random external forces, determining thermal microstress distribution parameters by statistical boundary value formulation

02 p0290 A72-11632

Force system axial equilibrium conditions for reference coordinates to eliminate inadmissible axes, deriving theorem for applicability limits

02 p0260 A72-12439

Prismatic shells membrane and bending fields induced by concentrated forces, applying Fourier analysis to semiinfinite plates geometry

02 p0296 A72-12527

Force and pressure distribution measurements on delta wing-body combination in compressible flow, investigating Reynolds number effect

02 p0152 A72-12707

Gravitational wave detection, discussing equivalence principle and force measurement

03 p0389 A72-13272

Double forces distribution over elastic body surface from Lamé equation describing static defects, discussing Kupradse potential and sources corresponding to plane dislocations and cracks

03 p0444 A72-13501

Stress-strain state of shallow shells of positive Gaussian curvature loaded by arbitrary concentrated force

03 p0450 A72-14106

Closed quasi-linear cubic theory of viscoelasticity for bodies with force and moment physical nonlinearity

03 p0454 A72-14218

Disturbances in infinite plate of viscoelastic material due to impulsive radial forces and twist on inner surface of circular hole, using Laplace transformation

04 p0594 A72-15709

Castigliano theorem in energy method, considering global static constraints and restriction for generalized force variables reduction through integration

05 p0732 A72-15803

Nearby spherical planet with two irrotational force fields, comparing identical frequency along latitude and meridian circles

05 p0656 A72-16185

Stress intensity factors for pair of coplanar Griffith cracks subject to asymmetrical surface tractions

05 p0737 A72-16320

Formulas derived for forces on receptor formation of vestibular apparatus from mathematical analysis of natural human head movements, discussing otoliths and semicircular canals

05 p0622 A72-16641

Axisymmetric flow of ideal incompressible liquid with free boundary and variable velocity, taking into account external mass forces effect

07 p0968 A72-19899

Side force and shock wave induced by obstacle on rocket engine nozzle wall, investigating pressure distribution

07 p1055 A72-20250

Mellin transforms application to two dimensional elasticity problem for anisotropic wedge with continuous mechanical characteristics under concentrated force

08 p1243 A72-21238

Projective geometry method for elastic curve shape of equilibrium-state thin rod subject to end forces

08 p1209 A72-21365

Metal cold working mechanics, discussing model based on equality of internal and external forces needed for plastic deformation

08 p1176 A72-21439

Nonlinear plane bending of thin elastic rectilinear bar guide elements under concentrated force and torque

09 p1397 A72-22350

Stress analysis of isotropic linearly elastic square plate of constant thickness loaded by concentrated forces at edges

09 p1399 A72-22698

Thermal buckling of parallelogram shaped plate under stationary temperature field and uniformly distributed forces, deriving critical load

09 p1402 A72-22733

Pinning force of vortex lines and microstructural inhomogeneities in superconductors, using magnetization and critical current measurements

09 p1369 A72-22796

Higher order forces effect on shock absorbing systems of masses interconnected by elastic and damping members of aircraft landing gears

09 p1318 A72-22861

Electromagnetic field interaction with nonconducting polarizable and magnetizable continuum from theory based on total impulse energy tensor, deriving force density from relativistic balance approximation

10 p3510 A72-24124

Ritz method application to transformations and complementations of polygenic force problems of mechanics

10 p1512 A72-24521

Pulsar radiation mechanism study from magnetosphere structure model, taking into account neutron star evaporated gas accumulation in gravitation-centrifugal force balance region

10 p1544 A72-24672

Normal and tangential force factors in casing shaping by bend roll method

11 p1642 A72-26817

Resonant frequency and vibration modes of variable cross section bar in elastic medium under transversal force, noting dynamic programming combined with optimization principle

12 p1845 A72-27538

Stokes flow about slender particle with nonuniform cross section under distributed force, obtaining solution to integral equation for twisted particle by perturbation scheme

12 p1798 A72-27834

Force distribution in refractory Ti alloy cutting with circular self turning blades, noting effects of feeding speed, cut area and cutter angle

13 p1966 A72-29467

Tangential force distribution at fiber surface in composite material under tensile stress without displacement at fiber axis

15 p2260 A72-31743

Decomposition of the force function of two homogeneous spheroids with noncoinciding symmetry planes

21 p3114 A72-41771

Cylindrical shells vibration under external forces with allowance for internal and external friction, obtaining harmonic influence functions in series form

22 p3233 A72-42056

Fibers-matrix force interaction effects in metal composites, analyzing stress-strain state of reinforced plate

23 p3306 A72-43728

Orthotropic photoelasticity methods application to concentrated force on half plane edge and to stress distribution on elliptical hole boundary in tensile strip

24 p3455 A72-44790

Plastic design of regular orthotropic grids with two adjacent edges fixed, free, or hinged.

24 p3456 A72-44794

Analogy between body force and inelastic strain gradient in all crystal systems.

24 p3459 A72-45247

FORCE FIELDS

U FIELD THEORY [PHYSICS]

FORCE-FREE MAGNETIC FIELDS

Force-free magnetic fields effects on plasma column stability

06 p0860 A72-17744

Numerical method for force-free magnetic field structures in solar active regions, discussing rotation effects

16 p2455 A72-33462

Alpha force-free magnetic field representation for solution of boundary value problem for chromosphere and lower corona magnetic fields

22 p3222 A72-42037

FORCED CONVECTION

Forced convective heat transfer of laminar flow in curved channel with square cross section at constant wall heat flux

04 p0510 A72-14595

Supercritical pressure turbulent forced fluid heat transfer mechanism hypothesis, explaining anomalous transfer improvements and deteriorations

04 p0511 A72-14641

Forced convective heat transfer for laminar flow of Newtonian fluid inside noncircular duct, taking into account viscous dissipation and work compression

07 p1100 A72-19628

Correlation for Prandtl number effect on laminar forced convective heat transfer with secondary flow

07 p1100 A72-19629

Axial arc column interaction with shock waves and high velocity gas flow effects in forced convection, proposing heat transfer theory

07 p1047 A72-20548

- Forced convection heat transfer for turbulent flow over flat surface with attached protrusion for varying Reynolds number and boundary layer thickness
10 p1561 A72-23882
- Boundary layer model for laminar transient forced convection film boiling on isothermal flat plate, noting one dimensional conduction, intermediate and steady state regions
[AIAA PAPER 72-289] 11 p1741 A72-25227
- Noncondensable gas and forced convection effects on laminar film condensation for two phase flows
11 p1743 A72-25261
- Forced heat convection from sphere immersed in inviscid fluid stream at small Peclet number, using matched asymptotic expansions
11 p1747 A72-26669
- Three dimensional hydrodynamic and thermal boundary layers and heat transfer for forced convection flow in rotating cylinder system
12 p1890 A72-28167
- Carbon dioxide turbulent flow heat exchange in single phase near critical region under forced and free convection
13 p2066 A72-29900
- Unsteady laminar natural and forced convection at transparent medium boundary layer radiating surface, noting turbulence effects on heat exchange
13 p2066 A72-29902
- Mass transfer effect on heat transfer to evaporating droplet, considering mass efflux shielding effect and forced convection flow field
14 p2172 A72-31051
- Forced convection and thermal boundary condition in parallel and tapered passages, discussing Nusselt numbers for exponentially decreasing wall heat fluxes
14 p2173 A72-31062
- Microelectronic devices liquid cooling by free and forced convection, investigating component size effects on heat transfer by boundary layer analysis and experiment
14 p2091 A72-31172
- Heat transfer to two dimensional laminar flow, calculating axial conduction and fluid preheating effects on adiabatic forced convection at low Peclet number
15 p2336 A72-32478
- Computer aided thermal design of LSI module packs for forced convection air cooling, using modal conductance matrix method
16 p2368 A72-33195
- Computer-aided thermal design of LSI packages.
17 p2527 A72-34681
- Effects of vorticity, displacement speed and curvature on heat transfer with dissipation.
17 p2638 A72-35747
- Heat transfer from a slowly rotating sphere.
18 p2741 A72-36934
- Forced convection heat transfer from cylinders to water in cross flow, quantifying method of accounting for fluid property variation
19 p2881 A72-38397
- Unconstrained liquid mass /Leidenfrost phenomenon/ pool and forced convective film boiling at cryogenic temperature
19 p2883 A72-38841
- Unsteady heat transfer and temperature for Stokesian flow about a sphere.
[ASME PAPER 72-HT-C] 20 p2983 A72-39482
- Forced-convective-flow carbon monoxide laser.
22 p3184 A72-41968
- A method of calculating meteorological elements for mesoscale processes
24 p3420 A72-44633
- FORCED OSCILLATION**
U FORCED VIBRATION
FORCED VIBRATION
- Matrix calculation of forced atmospheric oscillations for Hall, Coriolis and Pedersen regions
01 p0053 A72-10090
- Nonautonomous systems periodic solutions through Liapunov functions construction, considering application to nth-order dynamic systems forced oscillations
02 p0251 A72-11498
- Digital computer programmed numerical calculation based on admittance method for torsional forced vibration spectra of masses and stress distribution in transmission system
02 p0271 A72-12435
- Forced and free transverse vibrations of flat rectangular plates with attached concentrated masses
04 p0584 A72-14521
- Forced vibrations of elastic plate with infinite series of identical circular holes, discussing elastic wave diffraction and stresses at/near holes
04 p0587 A72-15017
- Circular disks, rings and perforated plates steady state field components, evolving forced and free vibration natural frequency equations
04 p0592 A72-15505
- Hydroelastic vibrations of incompressible inviscid liquid with free surface in uniformly rotating infinitely long circular cylindrical container, investigating response to cylinder walls forced excitations
05 p0735 A72-16065
- Forced vibration and mechanical impedance of damped circular and annular membranes under central mass loads
05 p0739 A72-16615
- Electrostatic waves perturbed distribution function behavior in presence of forced oscillations, considering Maxwellian ion and electron plasma waves excited by dipole
06 p0855 A72-17508
- Forced transverse vibration damping of end loaded elastic cantilever beam, determining hysteresis loop contour from resonance curves
06 p0900 A72-18673
- Stationary small elastoplastic longitudinal forced vibrations of rods with internal resonance obtaining asymptotic solution of nonlinear partial differential equations
06 p0900 A72-18676
- Rigid shaft rotating in hinged and elastic supports with nonlinear characteristics of restoring force, determining free and forced vibration characteristics
06 p0900 A72-18696
- Forced nonlinear oscillations of finite plate in plane supersonic gas flow, considering elastic forces and resonant characteristics deformation
06 p0901 A72-18708
- Forced vibrations and stability of one degree of freedom system with damping proportional to velocity, determining amplitude and phase resonance curves
06 p0901 A72-18710
- Steel/teflon sliding friction in high vacuum at stepwise controlled oscillation frequencies, sliding rates and loads
07 p0964 A72-18863
- Periodically supported beams acoustically induced vibration response based on equivalent structural wavelength definition
07 p1089 A72-19330
- Coupled motions of rotating free solid body and elastic rod torsional bending vibrations with precession and forced vibrations from energy exchange
08 p1205 A72-20959
- Oscillographic transient analysis of electric spark machining processes with electrode natural or forced vibrations
08 p1174 A72-21037
- Frictional stick-slip autooscillations suppression by resonance effect during forced vibration in normal direction
08 p1181 A72-22181
- Forced vibrations of two-mass system with damping through inelastic collisions, determining periodic motions stability regions with allowance for elastic coupling and friction
09 p1352 A72-23179
- Confocal spherical laser resonator deformation analysis based on perturbation method, investigating forced oscillation
10 p1493 A72-25150
- Nonlinear dynamic response of single elastic cables with low initial tension, examining free and forced vibrations with incremental deformations theory
10 p1560 A72-25185
- Periodic solutions of forced oscillatory system with hysteresis damping
12 p1844 A72-27246
- Stability and oscillation in linear and nonlinear systems, examining existence of T-periodic solutions /harmonic forced vibrations/
13 p2000 A72-28484
- Averaging technique for nonlinear viscoelastic dynamic problems, considering forced oscillations of oscillator with weakly nonlinear hereditary elastic characteristics
13 p2054 A72-28551
- Forced oscillations in RC amplifier with negative feedback through nonlinear bandpass filter with varicaps
13 p1931 A72-29266
- Superposed forced oscillations of liquid and of elastically mounted bulkhead with translational harmonic displacements of cavity, noting damping increase
13 p1942 A72-29498
- Free and forced vibrations of circular plates with associated rigidities and masses, obtaining orthogonality condition for natural vibration modes
13 p2059 A72-29501
- Nonlinear autooscillatory systems forced vibration under random perturbations, calculating dynamic processes by statistical linearization
14 p2132 A72-31114
- Dynamic response of thin circular arches to in-plane forced excitation under cyclic symmetric and unsymmetric support movement
14 p2169 A72-31175
- Free and forced vibrations of two dimensional grids with simple and bridge-type boundary conditions, presenting closed form solutions for nodal deflections and moments
15 p2332 A72-32561
- Radial vibrations and plane wave propagation in elastic deforming sphere with superimposed time dependent displacement field
16 p2467 A72-33117
- Nonlinear vibration damper system subject to forced vibrations considered as stochastic processes in form of white noise and stationary and ergodic processes
16 p2467 A72-33144
- Forced vibrations of thick homogeneous anisotropic elastic sphere, studying dynamic response to uniformly distributed internal and external pressure
16 p2424 A72-33147
- Kinematically forced vibration damping in mechanical systems, discussing amplitude reduction by inertial compensation
16 p2424 A72-33149
- Theoretical study of electromagnetic coupling in the forced oscillatory regime of two one-dimensional laminar flows of a viscous and electroconducting liquid in the presence of a transverse uniform magnetic field
17 p2587 A72-34281
- Asymptotic solutions of inhomogeneous initial boundary value problems for weakly nonlinear partial differential equations.
17 p2574 A72-34342
- Free vibrations analysis of linear aerodynamic conservative structures in elastic range by finite element method, applying to transient or random forced responses calculation
17 p2626 A72-34742
- Forced oscillations in a circuit with a nonlinear p-n junction capacitance
17 p2533 A72-34756
- Transverse vibration of a viscoelastic beam carrying an arbitrary number of mass bodies.
17 p2631 A72-35053
- Frictional stick-slip autooscillations suppression by resonance effect during forced vibration in normal direction
18 p2695 A72-36238
- Periodic vortex formation and shedding in flows past bluff bodies, considering cylinder forced and self excited vibrations and interaction with wake
18 p2679 A72-36389
- On the dynamic response of an infinite Bernoulli-Euler beam.
18 p2735 A72-36758
- The effect of an elastic edge restraint on the forced vibration of a rectangular plate.
18 p2737 A72-37066
- Nonsymmetric oscillations in certain symmetric nonautonomous systems
19 p2777 A72-37436
- Small forced oscillations produced by infinite plate vibrations in stratified and rotating viscous fluids, investigating resonance effects on propagation
20 p2912 A72-39330
- Free and forced trapped oscillation properties in inviscid rotating fluid, considering modifications for viscosity
21 p3049 A72-40654
- Analysis of impact vibrations by delta-function method - Case of one degree-of-freedom system. I - Perfectly elastic collision.
21 p3121 A72-41238
- Forced vibration solution and wind tunnel investigation of shallow cylindrical shells under moving pulsating pressure discontinuities, noting compression shock effects
21 p3122 A72-41352
- Hysteresis curve equation for calculation of elastoplastic deformations caused by forced vibrations, taking into account medium compressibility and inertial forces
21 p3123 A72-41359
- Unsteady wake effects on progressing/regressing forced rotor flapping modes.
[AIAA PAPER 72-957] 22 p3137 A72-42350
- Liapunov method extension to dynamically loaded elastically end-restrained columns stability and frames forced vibration boundedness problems
[ASCE PREPRINT 1639] 23 p3352 A72-44110
- Forced harmonic and random vibrations of concentric cylindrical shells immersed in acoustic fluids.
23 p3352 A72-44117
- Forced vibration analysis of sandwich beams with viscoelastic core.
23 p3354 A72-44253
- Errors caused by hot-wire filament vibration.
24 p3402 A72-44949
- Forced and free vibrations of shallow cylindrical shell in rectangular duct filled with ideal fluid
24 p3459 A72-45004
- The influence of static stresses on the dissipation of energy due to forced oscillations.
24 p3461 A72-45767
- FORCED VIBRATORY MOTION EQUATIONS**
U FORCED VIBRATION
FOREARM
- Forearm skin and muscle blood flow change measurements during whole body heating, using

plethysmography, isotopic labeling and blood sampling techniques

11 p1587 A72-26617

Water filled volume and strain gage phethysmography for forearm blood flow measurement during isometric exercise

11 p1587 A72-26622

FOREBODIES

NT ABLATIVE NOSE CONES

NT NOSE CONES

NT NOSES [FOREBODIES]

NT ROCKET NOSE CONES

Aerodynamic design of atmospheric reentry vehicles forebody, considering maximum drag for hyper-sonic bodies

02 p0149 A72-11726

FORECASTING

NT LONG RANGE WEATHER FORECASTING

NT NUMERICAL WEATHER FORECASTING

NT PERFORMANCE PREDICTION

NT PREDICTION ANALYSIS TECHNIQUES

NT STATISTICAL WEATHER FORECASTING

NT TECHNOLOGICAL FORECASTING

NT WEATHER FORECASTING

Solar proton flares forecasting methods in connection with active region developments for spacecraft radiation shielding

07 p1061 A72-20017

Subjective iterative group (SIG) methodology in forecasting involving computer and computer related technology

14 p2174 A72-30450

Aircraft accident statistical projections from human error review, analyzing situational circumstance limitations

14 p2081 A72-31086

Individual regions and nationwide air traffic demands forecasting for airport planning

16 p2481 A72-33311

Major civil airport planning, discussing information gathering and processing for aviation demand, aircraft movements revenue and cost forecasts and pricing policy evaluation

16 p2481 A72-33327

Major civil airport development plan, discussing traffic forecasts, runways, noise, airspace capacity, access systems, freight installations, maintenance facilities, navigation aids, buildings, etc

16 p2373 A72-33328

Statistical forecasting models for USAF CONUS outbound cargo airlift requirements by averaging and exponential smoothing models

24 p3466 A72-44578

Mean square invariant forecasters for the Weibull distribution.

24 p3418 A72-44664

FORECASTS

U FORECASTING

FOREIGN POLICY

NT INTERNATIONAL COOPERATION

FORENSIC SCIENCES

U LAW [JURISPRUDENCE]

FOREST FIRE DETECTION

Aerial IR line scanner systems for forest fire detection, considering escalation from aircraft to space platform

15 p2221 A72-31250

The accuracy of the intermittent photographic film advance in the camera of an airborne thermal scanner.

18 p2692 A72-36697

FORESTS

Forestry and agricultural applications of multiband photography, considering photointerpretation of black and white, color and IR photographs

01 p0057 A72-10459

Forest vegetation distributional and statistical parameters ecological analysis by multiband remote sensing in areas devoid of ground control

02 p0212 A72-11815

Multiband color aerial photography interpretation for forest appraisal in U.S.S.R.

09 p1302 A72-23285

Color aerial photographs interpretation for forest tree type composition determination, comparing to IR sensitive black and white films

09 p1302 A72-23286

Multiband photointerpretation of forested land units, using aerial black and white photographs and film-filter combinations

09 p1302 A72-23288

Color aerial photograph evaluation for forest damage demarkation, using film-filter combinations

09 p1302 A72-23289

False color aerial photographs for road quality classification in forests

09 p1302 A72-23290

Aerial photointerpretation in forest administration, discussing electronic data processing methods

09 p1302 A72-23291

FORGING

Ti powder technology, discussing pressed and sintered parts, forging and extrusion preforms and composites

02 p0233 A72-11437

Forged Inconel alloy 718 metal powder preforms for dense aircraft engine compressor rotor blades

02 p0233 A72-11441

Forging techniques and applications for YF-12A aircraft Ti alloy bulkhead production, considering diffusion bonding and die shimming

04 p0527 A72-14914

Statistical evaluation for forged jet engine parts tensile tests cost reduction, using regression analysis

07 p0995 A72-19484

Press forged ceramic crystals deformation, recrystallization, strength and fracture properties, comparing sapphires, rubies and spinels

08 p1196 A72-21917

Heat treatment and machining for distortion control of large Al alloy forgings for DC 10 aircraft

09 p1317 A72-22476

Metal forming techniques for gas turbine engines, considering isothermal, radial and powder metallurgy preform forgings, contoured cross and form rolling, and squeeze casting

11 p1638 A72-25649

Al alloys hand forgings fracture strength and stress corrosion characteristics from precracked specimens bending tests in air and sea water

11 p1658 A72-25833

Iron base powders material requirements and forging processes, discussing powder composition, inclusions effect and preform densification

11 p1639 A72-26241

Chemical composition, physical properties, microstructure and production of 1300 kg powder metallurgy forged billets

11 p1644 A72-26845

Heat treated Al alloy forgings stress relief by cold deformation between quench and age, examining effect on tensile properties and residual stresses

12 p1817 A72-28165

Pressed and sintered preforms of Ti and alloys for forge and extrusion operations, noting processing time reduction and smooth surface

13 p1982 A72-30120

High temperature forging apparatus for refractory metals under vacuum or inert atmosphere

15 p2241 A72-32443

Al-Zn-Mg-Cu forgings fracture toughness increase with Fe content reduction, discussing overload fracture following grain and stringers

16 p2405 A72-33000

Cold rotatory forging and subsequent heating effects on microstructure, texture and mechanical properties of dispersion hardened Ni specimens obtained by hot extrusion

16 p2407 A72-33530

Hot forging of sintered stainless steel.

19 p2815 A72-37592

Deformation, densification and material fracture characteristics for powder preform design for hot forging

19 p2806 A72-37593

Precision forging technology for Al sintered powder metal preforms for prototype fabrication

19 p2806 A72-37594

Flow and fracture criteria for powder forging.

19 p2815 A72-37597

Ti fabrication advances in forging, diffusion bonding, hot forming, chemical milling and laser cutting

21 p3061 A72-41335

Precision forged turbine and compressor blades.

22 p3183 A72-42518

Investigation of the drop forging process applied to magnesium alloys

22 p3183 A72-42816

FORM FACTORS

Analysis of pion-helium scattering for the pion charge form factor.

19 p2837 A72-37922

Possibilities of determining complex form factors from experiments with polarized particles

21 p3086 A72-40100

Improved calculation of resonant frequencies of Helmholtz resonators.

23 p3315 A72-44372

FORM PERCEPTION

U SPACE PERCEPTION

FORMALDEHYDE

Interstellar formaldehyde and ammonia molecules effects on prebiological amino acids evolution

02 p0165 A72-12846

Formaldehyde photoionization and absorption spectrum measurements in vacuum UV region, using single configuration self consistent field procedure for Rydberg states and model

03 p0321 A72-13856

Methanol and formaldehyde photoionization by UV irradiation, determining ion yields as function of wavelength by mass spectrometric analysis

07 p1038 A72-20498

Sunlight irradiated atmosphere formaldehyde photolysis as hydrogen atom source, estimating photodecomposition rates from extinction rates and photochemical results

08 p1230 A72-20981

Formaldehyde concentration into cloud formation compared to atomic hydrogen from analysis of molecular lines near galactic center

08 p1235 A72-21386

Allende carbonaceous chondrite composition analysis, suggesting formaldehyde presence and significance about possible origins

10 p1549 A72-25022

Interstellar anomalous 6 centimeter formaldehyde absorption in diffuse dark nebulae, discussing quantum mechanics of collisional pumping process

11 p1720 A72-26112

C-13 and C-12 formaldehyde absorption near Sgr A and Sgr B2, noting optical depths and abundance ratio

15 p2315 A72-32712

Beam maser spectrometric measurements of normal, C-13 and O-18 formaldehyde transitions, determining coupling constants for all rotational transitions hyperfine structure

16 p2431 A72-33132

Aqueous formaldehyde effects on *Bacillus subtilis* spores, showing sporostasis due to germination inhibition and sporocide due to temperature dependent inactivation

16 p2357 A72-33772

Absolute rate constant for the reaction H + H₂CO

17 p2511 A72-34739

FORMAT

Format logic design for airborne memory controlled PCM telemetry multiplex digital and analog data system

02 p0187 A72-12130

FORMATION HEAT

U HEAT OF FORMATION

FORMING TECHNIQUES

NT AUSFORMING

NT CASTING

NT COINING

NT COLD ROLLING

NT COLD WORKING

NT ELECTROHYDRAULIC FORMING

NT EXPLOSIVE FORMING

NT EXTRUDING

NT FORGING

NT HOT WORKING

NT INVESTMENT CASTING

NT MAGNETIC FORMING

NT METAL DRAWING

NT PRESSING [FORMING]

NT ROLL FORMING

NT SLIP CASTING

NT STAMPING

Ductile plastics solid phase forming, discussing forging, extrusion deep drawing and rubber cushion forming techniques

04 p0538 A72-15451

Forming of 7075-T6 Al in high pressure environments, predicting fracture occurrence via finite element stress analysis computer programs and pressure dependent model

[ASM PAPER 71-WA/PT-11] 05 p0671 A72-15912

Adherent solid lubricant films electrochemical deposition, noting method application to metal forming techniques

06 p0824 A72-18606

Metal forming - AIME Conference, Cleveland, October 1970

08 p1250 A72-22193

Refractory glass-ceramics forming systems characteristics and production, discussing crystallization factors

10 p1501 A72-24728

Hot isostatic pressing techniques for thin wall Be tubes manufacture

11 p1643 A72-26831

Shotpeen contouring of Boeing 747 wing skins combined with incremental chip forming, noting principles and manufacturing process

[ASM PAPER W 72-31,4] 12 p1817 A72-28160

Electrohydraulic and electromagnetic metal forming, using capacitor stored energy conversion into hydraulic shock waves or magnetic pressure to deform sheet metal components, pipes, etc

15 p2243 A72-31323

Technical and economic aspects of explosive metal fabrication, considering requirements for close tolerances, nonsymmetrical shapes, large size workpieces and unusual material properties

16 p2398 A72-33354

Forming techniques and heat treatment effects on recrystallization characteristics of heat resistant Cr alloy, noting high temperature influence on crystal structure

16 p2407 A72-33531

Fabrication of boron/aluminum tubes, I-beams, and other structural shapes from tape materials.

17 p2560 A72-35664

Testing the impact accuracy of the NEK-8 HERF machine

18 p2695 A72-36274

Causes for the formation of internal discontinuities of the metal in forged blanks of turbine blades prepared from E1893 alloy

22 p3216 A72-42249

FORMULAS [MATHEMATICS]

Wilf-type quadrature formulas with preassigned nodes, featuring existence of error bound without derivatives
05 p0632 A72-15816

Backward differentiation formulas application to differential algebraic equations, obtaining efficient algorithm as compared to Gear-Nordieck method
06 p0779 A72-17479

Algorithm and formulas for lunar limb absolute heights determination in selenodetic reference points system from lunar photographs
09 p1388 A72-23057

Many-term formulas for parabolic differential equations solution in boundary layer theory, using linearized second order ordinary differential equations
15 p2216 A72-31467

Elementary formulas for scalar and matrix valued functions gradient calculation, including continuum mechanics application
15 p2262 A72-31587

Characteristic curve formulas of cosmic objects and stellar focal images for photometric measurement processing on computer
23 p3267 A72-44030

FORSTERITE

Activity-composition relations in the fayalite-forsterite solid solution between 900 and 1300 C at low pressures.
20 p2915 A72-39178

FORTAN

Magnetic tape recorded flight data analysis by FORTRAN program
01 p0017 A72-10215

FORTAN programs for calculating principal stresses, strains and directions from rosette readings
06 p0781 A72-18324

FORTAN digital simulation of ATC radar beacon system making possible computer generated movie display
07 p0950 A72-19301

FORTAN IV program for small structure analysis with maximum 10 deg of indeterminacy
15 p2328 A72-31772

Differential boundary value problem solution by FORTRAN program using finite difference method
16 p2416 A72-33524

Computer programming languages, discussing system dependent and problem-oriented languages, ALGOL, FORTRAN and applicability ranges
17 p2523 A72-35444

An estimate of expected critical-path length in PERT networks.
23 p3308 A72-43806

Precompiler to simplify programming of celestial mechanics problems in TRIGMAN formula manipulation system, introducing data tube SERIES into FORTRAN program
24 p3442 A72-45242

FORWARD SCATTERING

Tropospheric forward electromagnetic scatter propagation path loss prediction by modified Yeh method with empirically derived correction function
03 p0323 A72-14031

Spatial structure of sinusoidally modulated light beam propagating in medium with forward extended scattering characteristics
08 p1136 A72-21742

Geometric optics approximation for rf wave forward and backscatter characteristics by spherical overdense clouds for several electron density distributions
[AD-739797] 08 p1136 A72-21980

Transequatorial off-path propagation outside of great circle at decametric waves associated with forward scattering by field aligned irregularities in equatorial ionosphere
14 p2084 A72-30129

Forward scattering of laser coherent light by acoustic or turbulent wave pressure variations, noting phase fluctuation spectrum
23 p3313 A72-44113

FOSSIL METEORITE CRATERS

U FOSSILS

U METEORITE CRATERS

FOSSILS

Artificial microfossil permineralization of blue green algae in silica, simulating Precambrian geochemical preservation
04 p0514 A72-14415

Molecular paleontology of fossil organic remnants in Molluscan shell proteins
04 p0467 A72-14753

Monograph on Jurassic and Cretaceous Hagiastriidae from Blake-Bahama Basin and Great Valley Sequence in California
04 p0519 A72-15255

Northeast Bank, Southern California Borderland volcanic petrology and geologic history, investigating basaltic rocks, hyaloclastites and fossil fragments
04 p0520 A72-15589

Paleomicrobiological analysis of northwest Scotland Stoer Formation black shale pre-Paleozoic spheroidal

unicellular fossils as probable form of marine phytoplankton
05 p0655 A72-16042

Fission origin of cosmic ray fossil tracks in augite achondrite high-uranium-concentration meteorite Angra dos Reis
05 p0714 A72-16078

Book on origin of life by natural causes covering physical geology, astronomy, biopoiesis and evolution of life stages, orogenetic cycle, fossils, and primeval atmosphere
07 p0917 A72-19185

Precambrian paleobiological history from fossil records, discussing heterotrophic living systems and eucaryote emergence in evolutionary organization development
08 p1162 A72-22003

Fossil track densities and thermoluminescence measurements of Luna 16 feldspar crystal samples compared to Apollo 12 samples
09 p1381 A72-22270

Ultrastructure and geologic relations of some two-aeon old Nostocacean algae from northeastern Minnesota.
17 p2544 A72-34336

Prokaryotic algae associated with Australian proterozoic stromatolites.
22 p3174 A72-42981

A study of the vestigial records of cosmic rays in lunar rocks using a thick section technique.
23 p3341 A72-44459

FOUNDATIONS

Parametric and adaptive non-parametric system identification procedures in boundary value problem of string on elastic foundation, considering various approximation methods
07 p1096 A72-20349

Asymptotic dynamic response of infinite beam on elastic foundation to randomly moving load
11 p1727 A72-25292

Large amplitude deflections and induced stresses in uniformly pressure loaded circular plate on elastic foundation, using von Karman coupled nonlinear partial differential equations
15 p2331 A72-32558

Sudden heating-induced deflection of rectangular plate fitted into equal sized excavation in elastic foundation with relatively very low thermal conductivity
16 p2475 A72-33148

Beams on bilinear elastic foundations.
20 p2980 A72-39692

Machine vibration diagnostics and damping, emphasizing filter lattice foundation structures, probability analysis and Bayes formula application
22 p3182 A72-42127

Thermoelastic contact problem of an elastic layer resting on an elastic foundation.
23 p3354 A72-44269

FOUR BODY PROBLEM

Generalization of the sphere of interaction for the restricted four-body problem
20 p2975 A72-40073

FOURIER ANALYSIS

NT FOURIER SERIES

NT HARMONIC GENERATIONS

Spaceborne Fourier interference spectrometer for environmental pollutant sensor, discussing IR detection systems, instrument servo, data reduction and handling systems and optical tolerance
[AIAA PAPER 71-1108] 01 p0067 A72-10552

Remote sensing of atmospheric pollutants and trace contaminants, presenting high speed high resolution, Fourier interferometer breadboard model
[AIAA PAPER 71-1109] 01 p0068 A72-10553

Sea waves energy spectra from optical Fourier analysis of ocean photographs under particular skylight irradiance
02 p0211 A72-11809

Prismatic shells membrane and bending fields induced by concentrated forces, applying Fourier analysis to seminfinite plates geometry
02 p0296 A72-12527

Jones matrix representation of optical instruments applied to Fourier interferometers/spectrometers and spectropolarimeters/
03 p0358 A72-13434

Mercury radar scattering properties, producing Fourier power spectrum from echo signals
06 p0880 A72-17864

Human dark adaptometric visual threshold recovery and electroretinograms in response to double light flashes, using Fourier analysis of oscillatory potentials
07 p0916 A72-19024

Automatic recognition of aircraft by Fourier harmonics of slope densities of silhouettes
07 p0949 A72-19053

Laser pulse description by Fourier analysis, showing broadened spectral line widths relationship to cavity modes
09 p1324 A72-23078

Paris Observatory Danjon astrolabe observation of latitude variations, obtaining periodograms by Fourier analysis
12 p1868 A72-27217

Finite difference approximation and Fourier analysis to determine mechanical system eigenfrequency, studying string and membrane vibration
13 p2000 A72-28417

Compressor directivity determination at discrete frequencies by tone power separation from noise background, using Fourier analysis of sound pressure autocorrelation
13 p2028 A72-29572

Fourier analysis for geopotential resonance effect on satellite orbits, calculating 13th harmonic influence on GEOS 2 and BE-C mean longitude
15 p2309 A72-31939

Signal analyzer for LF real time measurement of mechanical impedance by Fourier integral analysis
15 p2215 A72-32628

Fourier analysis of Pluto light curve in terms of geometrical model consisting of bright and dark areas
16 p2452 A72-33131

Grid modulation information encoding technique for image features extraction with simple Fourier filtering to replace heuristic method
16 p2365 A72-33752

Investigation of a solution to an almost everywhere multidimensional mixed problem of a class of second-order hyperbolic equations with a nonlinear operator-containing right side
17 p2577 A72-35841

Investigation of a strongly generalized solution to a multidimensional mixed problem of a class of second-order hyperbolic equations with a nonlinear operator-containing right side
17 p2577 A72-35843

Anisotropic rectangular plate free flexural vibration improved solution via Fourier analysis
18 p2734 A72-36419

Fourier series analysis of multielement circular loop antenna with arbitrary circumference for current distribution and self and mutual admittances
19 p2775 A72-38615

Application of holographic Fourier spectroscopy to the analysis of the microwave radiation spectrum
21 p3058 A72-41733

Investigation with the aid of a Fourier method of the classical solution of a multidimensional composite problem for a class of hyperbolic equations of the second order with a nonlinear operator right-hand part
22 p3198 A72-41897

Light beam modulated by uniformly spaced circular apertures, calculating Fourier power spectrum for homogeneous and bivariate normal intensity distributions
23 p3289 A72-43900

FOURIER LAW

Relativistic heat propagation models, considering hyperbolic system of partial differential equations, momentum-energy tensor for ideal fluid and classical Fourier law
06 p0847 A72-17256

FOURIER SERIES

Fourier series terms number effect on sandwich plate critical shear stress calculation accuracy
02 p0294 A72-12438

Summability and absolute convergence of Fourier series in large, proving theorems on boundedness of trigonometric polynomials integral norms sequence
03 p0382 A72-13947

Lf spectrum analysis instrumentation, describing stored data signals Fourier series parameters analog computation techniques
04 p0523 A72-15487

Computerized simulation of two dimensional turbulent flow in Fourier space with random initial conditions on coefficients, discussing velocity, pressure and vorticity fields
07 p0971 A72-20084

Resonant frequencies of rectangular plate with two sides subject to mixed boundary conditions, expressing vibration modes in terms of Fourier series
08 p1249 A72-21946

Approximation for mechanical system equilibrium perturbation anharmonic analysis based on Fourier series with real multiplication factors of fundamental pulsation
12 p1845 A72-27542

Continuous signal representations in time and frequency domains by Fourier series
12 p1783 A72-27628

Real time interferential spectrum analysis of deterministic signals in form of partially summed Fourier series
13 p1919 A72-29041

Periodic waveform expression in truncated Fourier series, determining polynomial coefficients relationship to amplitude density function
13 p1920 A72-29108

One-wavelength MHD induction generator operated on NaK flow system with various excitation conditions, calculating magnetic flux density and power by Fourier series
13 p1900 A72-29364

Special boundary value problems solution method for Mathieu differential equation, transforming

- Mathieu equation to Hill differential equation via Fourier series expansion 15 p2264 A72-32468
- Stress analysis in circular disk loaded along circumference, noting results identity for stress presentation by Fourier series, Poisson integral and Green function 16 p2470 A72-33593
- Linear normed space subsets approximation by sums based on Fourier-Laplace series 16 p2417 A72-34009
- Difference frequency signal from two sinusoidal voltages linear detection, estimating amplitude modulation envelope representation accuracy by Fourier series 17 p2518 A72-35781
- Pattern synthesis of linear arrays using Fourier coefficient matching. 18 p2659 A72-36298
- Approximation of partial sums of multiple conjugate Fourier series of functions whose measure of continuity is given in the mean by Poisson integrals 20 p2945 A72-39394
- Maximum deflection and bending moments of simply supported anisotropic rectangular plate under uniform transverse load, using double Fourier series 20 p2981 A72-39973
- Approximation of continuous periodic functions by Faward sums 24 p3419 A72-45547
- Evaluation of the norm of a function in terms of its Fourier coefficients, convenient in problems of approximation theory 24 p3419 A72-45549
- Approximation of a continuous function of two variables by particular sums of a Fourier-Laguerre series 24 p3419 A72-45647
- FOURIER TRANSFORMATION**
- Passive scalar field diffusion in homogeneous turbulence, solving Fourier transformed flow equations by iterative procedure 02 p0204 A72-12174
- Radar signal and data processing with digital techniques, using pipeline fast Fourier transform methods 02 p0188 A72-12397
- Fast Fourier transforms for digital matched filters in wideband radars, using computer simulation for word size and dynamic range relationship determination 02 p0188 A72-12398
- Coarsely stabilized spacecraft-borne Michelson interferometer, obtaining high resolution by computerized spectrum reconstruction with fast Fourier transform 03 p0354 A72-13055
- Fourier transform lens design in coherent optical filtering systems 03 p0358 A72-13439
- Far IR Fourier spectrometer with built-in real time digital computer for routine physical and chemical spectroscopy 04 p0520 A72-14523
- Photomaterial nonlinear effects on contour distortion in holographic recording of Fourier image slit for graphic memory use 04 p0522 A72-15150
- On-line digital spectrum analysis based on fast Fourier transform algorithm, exemplifying by plasma density fluctuations correlation 04 p0496 A72-15488
- Asymmetric micropolar elasticity plane problem, solving equilibrium equations with Fourier transformation for displacements, rotation and stresses 05 p0737 A72-16296
- Electromagnetic wave scattering from curved rough surfaces and transmission through turbulent medium, obtaining solution by spatial Fourier transform of three transfer functions product 06 p0771 A72-17340
- Fourier, Hadamard and Karhunen-Loeve transformations for digital speech processing, comparing bit rate requirements 06 p0772 A72-17405
- Acquisition and processing of plasma fluctuation data using fast Fourier transform analog-digital spectral analysis technique 06 p0859 A72-17548
- Stratified anisotropic multilayer plasma wave propagation from transverse field equations, using Green function and Fourier transform method 06 p0773 A72-17597
- Computing techniques for finite Fourier transform, applying to Poisson equation, interpolation and quadrature and data smoothing 07 p1025 A72-18784
- Multidimensional Fourier transforms application to theoretical physics partial differential equations, using singular delta function for homogeneous equations general integral 07 p1027 A72-19436
- Source distribution estimate in radar mapping, comparing prolate spherical wave functions inverse versus truncated Fourier transform methods 07 p0946 A72-19792
- Reduced data storage requirement of synthetic aperture radar for target classification by fast Fourier transform 08 p1134 A72-21422
- Inverse integral Fourier transforms to solve steady periodic motions of wing close to solid surface, deriving equations of lift and principal moment 08 p1108 A72-21701
- Two dimensional optical signals Fourier transform properties and local frequency filtering methods 09 p1351 A72-22982
- Fourier transform plane irradiance distribution for random phase data masks in holographic data recording, discussing phase quantization level change effects 09 p1314 A72-23335
- Standard deviation in ghost lines size due to random sampling position errors of monochromatic spectral line in Fourier transform spectroscopy 09 p1314 A72-23344
- High resolution NMR spectrometer conversion from continuous wave to Fourier transform operation, permitting computer systems and pulse amplifiers use 09 p1316 A72-23408
- Fourier transform and angular distribution of light diffusion by plasma with strong correlations 10 p1519 A72-24129
- Radiographic image enhancement based on mathematical concepts of image convolution, Fourier transformation and spatial frequency filtering, discussing hardware and computer needs [LA-DC-72-57] 10 p1481 A72-24322
- Data window for digital spectrum estimation of random data by fast Fourier transform techniques, noting bandwidth increase by various data smoothing sequences 10 p1439 A72-24804
- Digital signal analyzer design based on fast Fourier transform algorithm shift register coupled with single flow-through arithmetic unit 10 p1446 A72-25062
- Spacecraft structural dynamics, design and testing, using Fourier transform and analog vibration simulation [AIAA PAPER 72-349] 11 p1728 A72-25378
- PCM and FDM/FM systems noise and signal distortion analysis by digital simulation with FORTRAN language based on fast Fourier transform 11 p1601 A72-26043
- Fourier phase angle models of intermittent atmospheric turbulence 12 p1838 A72-27025
- Fourier transform approximate inversion solution for transient pulse propagation from spherical cavity with surface under impulsive pressure in viscoelastic medium 12 p1844 A72-27196
- Lens MTF calculation in presence of diffraction patterns via image mathematical model construction yielding Fourier transform 12 p1810 A72-27937
- Off center sampled interferograms correction by change of origin in Fourier transform, noting overlapping aliases effect 12 p1811 A72-27941
- Generalized Fourier transformation method for mixed boundary value problems of second order parabolic differential equation in unbounded region, noting singular differential operator 12 p1837 A72-27998
- Fourier transform solution for fields from current dipole element radiating in free space 13 p1916 A72-28540
- Fourier transforms for linear systems transient time and frequency characteristics, using discrete functional values for initial information 13 p1985 A72-28675
- Dispersion method for real time spectral analysis of signals by Fourier transform for class of integrable functions with finite energy 13 p1919 A72-29042
- Digital computer synthesis of transparent object holograms, noting image discretization, two dimension Fourier transformations spectrum and digital data correlation with optical parameters 13 p1958 A72-29617
- Fourier transformations for convolution integral calculation in image distortion correction by ground visual observations of solar intensity distribution, noting successive approximations method 13 p2046 A72-29726
- Sound transmission loss and diffraction measurements by combined correlation and Fourier techniques 13 p2006 A72-29768
- Fourier transformation for natural abundance C 13 free induction decays of cyclic antibiotic valinomycin and K ion complex, noting chemical shift differences 13 p1913 A72-29862
- Solar photospheric fluctuations, applying fast Fourier transform to power coherence and phase spectra calculations 13 p2049 A72-29928
- Three dimensional elasticity boundary value problems solution via multidimensional Fourier transforms, applying to semiinfinite solid and hollow cones 15 p2324 A72-31481
- Integral Laplace-Fourier transform stability during transient response functions reconstruction from frequency characteristics in linear circuits 15 p2264 A72-31879
- Data storage and retrieval by holographic techniques, noting parallel recording of complex function at Fourier transform plane 15 p2236 A72-32040
- Off-axis phase holograms of photographic transparencies recording, comparing Fresnel, Fraunhofer and lensless Fourier transform holograms 15 p2239 A72-32358
- Shift register implemented binary transversal filter type digital pulse waveform generators truncation and approximation error spectrum analysis via inverse Fourier transform 16 p2362 A72-32854
- Fourier transform /subtractive/ holographic imaging technique for microwave antenna apertures 16 p2368 A72-33072
- Displacements, rotations and stresses equilibrium equations solution for plane micropolar elastic half space, using exponential Fourier transforms 16 p2466 A72-33105
- Performance criteria for transform data coding schemes evaluation under computational constraints, presenting numerical examples for Fourier, Walsh, Haar and Karhunen-Loeve transforms 16 p2366 A72-33214
- Image enhancement by computer programs, discussing digital filtering, fast Fourier transform algorithm, data management and large matrix handling 17 p2520 A72-34404
- Use of fast Fourier transforms for solving partial differential equations in physics. 17 p2575 A72-34645
- Fourier transform of two-dimensional signals. II 17 p2516 A72-35185
- Computational algorithms compared for spatial frequency image filtering, considering tradeoffs between direct convolution and fast Fourier transform under equal point-spread functions assumption 18 p2658 A72-36263
- Vibration of an infinite thin plate coupled with a fluid 18 p2736 A72-37002
- An application of correlation to radar systems. 19 p2764 A72-37927
- Solution of the problem of a fast Fourier transform in a homogeneous associative parallel processor 19 p2779 A72-37993
- Fourier transform C-13 nmr analysis of some free and potassium-ion complexed antibiotics. 20 p2898 A72-39399
- Temperature distribution control in n-dimensional space via quasi-inversion method with Fourier transformation for Cauchy problem solution of heat conductivity equation 20 p2983 A72-39466
- Fourier transformation relating autocorrelation to spectral density of power bounded and energy bounded functions, discussing unsteady stochastic processes 20 p2953 A72-39552
- Lowest order two particle correlation function solution to BBGKY hierarchy obtained via Green function with Fourier transform satisfying analyticity requirements for causality 20 p2956 A72-39725
- Effects of finite register length in digital filtering and the fast Fourier transform. 20 p2904 A72-39780
- A variable spacing modulation collimator for X-ray astronomy. 20 p2928 A72-39891
- Digital computer synthesis of Fourier holograms of transparencies, noting significance to digital filtering method development for optical signal processing 21 p3054 A72-40670
- Determination of optical transfer functions by Fourier transformation in spatially incoherent light 22 p3205 A72-42296
- Comparison of theoretical and experimental results concerning spatial filtering in coherent optics 23 p3288 A72-43724
- Fast Fourier transform algorithm for astronomical line spectra resolution enhancement, estimating central line intensity, line width parameter and line shape 24 p3438 A72-44841
- FOURIER-BESSEL TRANSFORMATIONS**
- Triple and quadruple integral equations solution in analogy to Fourier-Bessel series with mixed boundary values, using Erdelyi, Kober, Sneddon and Srivastav operators 16 p2416 A72-33663
- FOVEA**
- Simultaneous brightness contrast under scotopic conditions, investigating fovea rod and cone systems interaction in subjects with normal color vision 03 p0317 A72-13937
- Foveal luminosity magnitude estimations validity, measuring relative effects of preadaptation and contrast 10 p1427 A72-25179

Foveal and nonfoveal afterimages effects on saccadic behavior of eye movement

13 p1907 A72-29971

Heat chamber treadmill work-induced thermal stress effects on reaction time to foveally and peripherally presented visual stimuli

14 p2078 A72-31154

Foveal light pulse duration effects on reaction time, showing stimulus intensity-time reciprocity

15 p2188 A72-31509

Colorimetric photometric matching tests, showing subject differences in parafoveal spectral sensitivity indicated by photopic curve peaks

17 p2508 A72-34882

Effect of selective adaptation on detection of simple and compound parafoveal stimuli.

18 p2651 A72-36607

Threshold detection model for foveal viewing by human observers using naked eye

21 p3007 A72-40733

Discrimination sensitivity and black light density in the mesopic range

21 p3007 A72-40735

The effect of size, retinal locus, and orientation on the visibility of a single afterimage.

21 p3003 A72-41253

Photopic and scotopic contributions to the human visually evoked cortical potential.

23 p3261 A72-44380

Small field tritanopia of central fovea in terms of dichromatic area color response mechanism and adaptation speed

23 p3259 A72-44390

FR-1 SATELLITE

VLF waves propagation dependence on ionospheric horizontal electron density gradients associated with midlatitude depression from FR-1 satellite observation

10 p1472 A72-24060

FRACTIONATION

Xe and Kr mass fractionation and isotopic anomalies in ordinary chondrites, analyzing meteorite samples by mass spectrometry

07 p1084 A72-20497

German monograph on liquid air fractionation during flight of recoverable spacecraft carrier propelled by air breathing propulsion systems

09 p1374 A72-23160

Gas rich meteorites and lunar materials solar rare gases component observed and predicted relative abundance agreement indicating absence of fractionation in solar nebula formation

11 p1721 A72-26118

Microprobe analysis of Murchison and Vigarano meteorites, noting fractionation processes for Ca distribution in olivines

13 p2036 A72-28752

Metal/silicate fractionation in the solar system.

20 p2967 A72-39177

Ordinary chondrite chemical and mineralogical properties establishment during solar system formation, noting fractionation events

20 p2969 A72-39334

Results of a study of heat and mass transfer during the purification of helium from nitrogen by the condensation method

21 p3127 A72-40130

Evidence for vapor fractionation in the origin of chondrules.

23 p3339 A72-44134

FRACTIONS

Truncation error bounds for continued fractions, considering application to Gauss hypergeometric functions

[AD-738403]

04 p0538 A72-14728

FRACTOGRAPHY

Metallographic and fractographic analyses of cracking in T53-L13 gas turbine engine compressor disks

01 p0085 A72-10816

Breakdown surfaces of thin Ti alloy specimens under tension as function of composition and heat treatment temperature

01 p0088 A72-11079

Microfractographic fatigue fracture analysis of steels, aluminum, brass, nickel and molybdenum by scanning electron microscope

03 p0372 A72-13543

Grain orientation effect on fatigue crack propagation in notched test specimens cut from cold rolled prestressed annealed brass plate

03 p0375 A72-13934

Automatic recording of crack length in slow fracture tests of flat high strength steel in water

05 p0741 A72-17087

Fractographic analysis of failure kinetics and crack formation in Al alloys, showing microfatigue intrusions and extrusions for various initial stress levels

06 p0834 A72-18653

Fractography of high boron ceramics under ballistic impact, suggesting macroscopic and microscopic textures relationship to stress states and microstructure

09 p1334 A72-22391

Electron fractographic investigation of fracture properties via removal of metal oxide film accumulated on crack surface during service life of steel structures

09 p1309 A72-22639

Hexagonal metals stress corrosion cracking fractographs interpretation, noting striations as prominent feature of transgranular fractures

11 p1652 A72-25288

Fractographic study of stress corrosion fractures of low carbon steels with electron microscope

11 p1666 A72-26924

High temperature microporosity in W wire at 3000-3350 C, using electron microscopy and fractography

13 p1973 A72-28651

Fractography of fiber reinforced metal composites.

17 p2560 A72-35654

Fractographic lines in maraging steel - A link to fracture toughness.

18 p2700 A72-36584

Factors governing radiographic crack detectability in steel weld specimens.

18 p2695 A72-36673

A new morphological element on the viscous breakdown microsurface of hypoeutectoid steels

19 p2817 A72-37737

Interpreting electron fractographs of stress corrosion in aluminum alloys.

19 p2821 A72-38387

Electron fractography of fatigue failure and macrocrack propagation in dual phase Ti alloy during cyclic loading at minus 140 to plus 150 C

23 p3303 A72-44097

Approaches to verification and solution of magnetic particle inspection problems.

24 p3407 A72-44903

FRACTURE MECHANICS

Monograph on stress corrosion failure, covering threshold stresses, fracture mechanics, electrochemical processes, hydrogen embrittlement, corrosion, various steels and alloys, environmental effects, etc

01 p0082 A72-10166

Griffith crack stress intensity factor and crack face displacement in elastic solid, detailing symmetrical, antisymmetrical and point body force distributions

01 p0136 A72-10185

Upset steel cylinders under axial compression loads, determining localized surface stress and strain critical values at fracture

01 p0141 A72-11032

Fracture analysis of two dimensional thermal loaded solid propellant rocket grain models under cooldown [SESA PAPER 1927A]

02 p0270 A72-11513

Macroscopic fracture mechanics of composite laminates, discussing flawed specimen static strength prediction

02 p0249 A72-11983

Hardened steel inhibited crack propagation mechanism, observing striation in microstructure on fracture surface

02 p0243 A72-12212

Springs fracture and vibration in injection pumps by analog model

02 p0236 A72-12437

Fracture toughness values from engineering tests related to fracture mechanics analytical capability by interpretive diagram systems

02 p0245 A72-12509

Metal ductile facies fracture study of cups formation from cracks by cleavage, noting roles of dislocations and inclusions

02 p0246 A72-12600

Elastoplastic material crack propagation behavior under arbitrary loading, introducing plastic zone, intensity and retardation factor concepts

[DGLR PAPER 71-111]

02 p0300 A72-12726

Soviet conference papers on fatigue of metals, alloys and composite materials covering breakdown mechanisms, failure kinetics, cyclic strength and hardening

03 p0372 A72-13587

Fracture mechanics of interfacial cracks between two bonded dissimilar anisotropic elastic half spaces, presenting two dimensional analysis of stress fields

03 p0446 A72-13707

Crack growth criteria, formulating nonlinear fracture mechanics theory

03 p0446 A72-13709

Crack development in thin viscoelastic polymer plate, using two phase fracture model without Volterra principle

03 p0448 A72-13901

Elastoplastic bodies with crack at tip, determining limiting loads and crack propagation from variational relations

03 p0451 A72-14117

Ductility and fracture of metallic thin walled tubular samples under complex stress of internal pressure and axial tension

03 p0454 A72-14215

Generalized epicyclic properties application to fracture mechanics, considering stress fields of constrained plastic zones around cracks in thin elastic plate

03 p0455 A72-14388

Double cantilevered specimen crack growth, computing fracture surface energies from dynamical cleavage analysis

05 p0735 A72-16019

Fracture theory application to rotating cylinder velocity field determination, emphasizing plastic equilibrium and flow behavior

05 p0738 A72-16424

Fatigue crack formation speed relationship to stress intensity factor, investigating crack propagation by fracture mechanics methods

06 p0895 A72-17810

Semibrittle tears and fractures by progressive cracking in metallic structures, discussing metal fatigue and environmental stress

06 p0897 A72-18297

Deformation stresses and strains in quasi-static low cycle fracture of stabilizing, softening and strain hardening materials

06 p0831 A72-18352

Diffused failure model as basis for plotting delayed fracture curves in space of principal stresses

06 p0898 A72-18552

Solid bodies crack development theory, emphasizing crack tip fine and hyperfine structures concepts and time dependent effects

06 p0898 A72-18554

Plastic strain and fracture of metals by specific internal energy change method, investigating mechanical work and heat release

06 p0900 A72-18691

Finite element method application to fracture mechanics problems of stress concentration and intensity factors and elastoplastic response to cyclic loading

07 p1088 A72-19130

Stress redistribution in statically indeterminate structures under creep, discussing effects on time to brittle fracture and service life determinations

07 p1088 A72-19259

Recrystallized and unrecrystallized deformed semifinished wrought Al alloy under cyclic and static loads, investigating macrofracture kinetics

07 p1014 A72-19840

Book on materials low temperature mechanical properties covering metals, polymers, ceramics and composites, temperature effects on deformation processes, fracture mechanics, test methods, etc

07 p1015 A72-19909

Fatigue strength and life estimation method for thick walled cylinders under pulsating internal pressure, using fracture mechanics crack propagation law [ASME PAPER 71-PVP-15]

08 p1244 A72-21482

Transparent and opaque materials fracture mechanism analogies under laser beam action, determining dislocation structure

08 p1185 A72-22093

Plastic deformation friction fracturing, stress concentration, free surface changes and load displacement analysis with upper bound, slip line and finite element methods

08 p1250 A72-22197

Workability tests from material deformation stress determination and fracture strain rate relation for forging, extrusion and rolling limits predictions

08 p1190 A72-22198

Fracture mechanical analysis for stability criteria and propagation behavior of thermal stress cracks in brittle ceramics in severe thermal environments

09 p1333 A72-22382

Brittle fracture dynamics, deriving motion equations and stability conditions of surface cracks under stress waves from energy balance and angular momentum conservation law

09 p1404 A72-22916

Single and multiple fractures in brittle matrix fibrous composites, discussing fracture energetics, stress-strain curves and hysteresis effects

09 p1338 A72-23164

Fatigue fracture of polymethyl methacrylate at room temperature under uniaxial failure cycled loading

09 p1339 A72-23244

Tensile plastic flow and fracture behavior of PdSi based alloys in glassy microcrystalline and crystalline states, noting shear deformation bands

09 p1339 A72-23382

Fracture mechanics application to welded structures fatigue, using crack propagation law

09 p1409 A72-23616

Crack toughness tests of fiber composite laminates, using linear elastic fracture mechanics

10 p1500 A72-24258

Interaction diagram for mixed crack extension modes in unidirectional graphite-epoxy laminates from critical load test data

10 p1501 A72-24265

Statistical bounding approach to fracture analysis of fiber reinforced composite materials tensile strength

10 p1502 A72-24883

Notched bend test crack opening displacement gage for continuous measurement of apparent rotation axis and true displacement location at crack tip

10 p1483 A72-24885

- Crack arrest in transversely loaded elastic plates from fracture mechanics combined with stress intensity factor for tensile and compression loads
10 p1499 A72-24890
- Fracture energy and deformation of unidirectionally and randomly oriented lamellar Al-Cu eutectics from surface microstructure studies
10 p1499 A72-24893
- Approximate stress intensity factor for corner flow emanating from quarter infinite solid edge, based on Smith solution for semicircular flaw
10 p1559 A72-24898
- Linear elastic fracture mechanics extension to fiber reinforced plastic composite laminates, noting dependence on homogeneous model validity
[AIAA PAPER 72-384]
11 p1730 A72-25406
- Acoustic emission analysis of deformation and fracture modes under straining of fiber glass-epoxy composite structures, including NOL rings and vessels
11 p1671 A72-25469
- Hardened steel inhibited crack propagation mechanism, observing striation in microstructure on fracture surface
11 p1656 A72-25710
- Fracture surface energy and acoustic emission of boron fiber-epoxy resin composite, using linear elastic fracture mechanics and compliance variation methods
11 p1674 A72-25858
- Glass textolites and high strength oriented plastics fracture mechanism in tension and bending, noting equalizing effect through proper cohesion characteristics between layers
11 p1674 A72-26804
- Carbon-graphite fracture mechanics dependence on graphite crystallite structure, discussing crystal size effects on strength
11 p1674 A72-26812
- Characteristic friction curves (Mohr circle envelopes) to describe stressed state region with various stresses produced by slide friction in steel due to indentation
12 p1819 A72-28198
- Axisymmetric temperature problem with arbitrary load duration for disk-shaped crack fracture mechanics, using Fredholm equation with symmetrical kernel for temperature field determination
13 p2055 A72-28720
- Temperature and strain rate dependence of austenitic stainless steel fracture by low cycle fatigue at high temperatures, studying striations with scanning electron microscopes
13 p1979 A72-29449
- Mohr formulas construction for composite structures including frames and cylindrical and conical shells
13 p2058 A72-29460
- Stress wave propagation and fracture in composites, discussing micromechanical and homogeneous-continuum theories
13 p2060 A72-29692
- Model for metal fatigue fracturing, noting crack initiation and two stages of propagation, emphasizing experimental fractographic/electron microscopy/research
13 p2061 A72-29773
- Ti alloys hot salt stress corrosion cracking mechanism, discussing cold deformation and heat treatment effects, tensile tests, hydrogen analysis and microscope investigation
14 p2117 A72-30535
- Macroparametric, microstructural and general rationales methods for fatigue resistant materials, noting crack propagation and fracture mechanics
14 p2120 A72-30612
- Steady creep and delayed fracture dependence on metal structure and composition, considering strain hardening at small strain rate and elevated temperature
15 p2254 A72-31559
- Elastic properties of media with cracks, discussing elastic anisotropy and crack distribution
15 p2327 A72-31733
- Ultrahigh tensile strength steel pressure chamber fracture behavior in high stress concentration fields
15 p2330 A72-32345
- Al-Zn-Mg-Cu forgings fracture toughness increase with Fe content reduction, discussing overload fracture following grain and stringers
16 p2405 A72-33000
- Metal fracture by electron pulse generated stress waves, noting intergranular fracture mechanism
16 p2472 A72-33845
- Effects of yielding and size upon fracture of plates and pressure cylinders
17 p2565 A72-34251
- Buekner formulation combined with finite element method for arbitrary shaped cracked bodies stress intensity factors in framework of linear fracture mechanics
17 p2623 A72-34253
- Transparent and opaque crystal surface fracture mechanism analogies under laser beam action, determining dislocation structure
17 p2562 A72-34664
- The fracture energy of a glass fibre composite.
17 p2570 A72-34670
- Shape factors for nozzle corner cracks evaluated from epoxy-model pressure vessels.
17 p2630 A72-34814
- A fracture mechanics analysis of adhesive failure in a single lap shear joint.
[SESA PAPER 1990A]
17 p2630 A72-34815
- Fracture mechanics approach to adhesive joints.
17 p2633 A72-35282
- Failure mechanism for carbon fibers in epoxy novolac matrices under tensile loads
17 p2633 A72-35286
- Fracture mechanics of a fiber composite.
17 p2633 A72-35293
- Composite materials crack propagation and failure modes leading to fracture instability, discussing maximum strength conditions and fatigue
18 p2703 A72-36394
- An atomistic study of cracks in diamond-structure crystals.
18 p2718 A72-36509
- Surface energy and cleavage plane observation of brittle fracture for W single crystal in tension as function of orientation and temperature
18 p2702 A72-36750
- Asymmetric collinear internal cracks interaction evaluation by measuring diameter variation and shape distortion of caustic surface impinged upon by retarded laser radiation
19 p2870 A72-37224
- Deformation, densification and material fracture characteristics for powder preform design for hot forging
19 p2806 A72-37593
- Flow and fracture criteria for powder forging.
19 p2815 A72-37597
- Book - Advances in creep design
19 p2874 A72-37701
- Creep rupture under stress concentration.
19 p2874 A72-37702
- Creep rupture theory covering viscous and brittle scattered fractures and major crack growth
19 p2874 A72-37703
- Creep fracture theory investigating ratio of ultimate creep rupture time to latent failure under multiaxial states of stress
19 p2874 A72-37704
- Investigation of the effect of some surface-active media on the variations in strength characteristics of steel U8 in a high strength state
19 p2817 A72-37738
- Thermo-hypo-elasticity and derived fracture and yield conditions.
19 p2875 A72-37841
- Crack toughness - Physical and technological significance
19 p2875 A72-37854
- Evaluation of the tendency to brittle fracture of turbine rotors made from steels of medium strength
19 p2876 A72-38001
- Fracture behavior of stainless steel fibers in Sn-Pb alloy matrix.
19 p2820 A72-38373
- The fracture energy and some mechanical properties of a polyurethane elastomer.
19 p2823 A72-38450
- Quasi-static impact of hard hemisphere against brittle half space, investigating fracture mechanics
20 p2981 A72-39952
- Metal fatigue crack propagation under cyclic loads, assuming specific energy dissipation as material constant
20 p2981 A72-39953
- Criteria for delayed fracture in solids and their experimental verification.
20 p2981 A72-39954
- Elastic analysis for a radial crack in a circular ring.
20 p2981 A72-39959
- Study of fatigue crack initiation from flaws using fracture mechanics theory.
20 p2981 A72-39961
- Crack tip vicinity stress generated by plane transient tension-stress wave diffraction, examining ductility effects on fracture modes
21 p3117 A72-40672
- Simple structures behavior under constant loads, considering low stress levels and creep rupture mechanism with internal damage affecting strain rate
21 p3117 A72-40673
- Stress-corrosion cracking of high strength steels and titanium alloys.
21 p3067 A72-40849
- Analytical fracture mechanics application to stress corrosion cracking test methods for examining crack growth kinetics and time-to-failure
21 p3067 A72-40913
- Bursting of wire reinforced composite tubes under biaxial tension stresses.
21 p3121 A72-41209
- Bent plates and shells equations and rupture modes, characterizing cracks and stress intensity
21 p3122 A72-41338
- The stress gradient as a cause for the manifestation of the scale effect in brittle fracture of materials
21 p3123 A72-41364
- Axisymmetric temperature problem with arbitrary load duration for disk-shaped crack fracture mechanics, using Fredholm equation with symmetrical kernel for temperature field determination
22 p2333 A72-42097
- A general program for computer plotting of Mohr's circle.
22 p3156 A72-42608
- Some recent experimental investigations in stress-wave propagation and fracture.
22 p2337 A72-42768
- Fracture analysis for linear elastic material in antiplane strain, discussing fast moving cracks propagation, flint knapping and equations of motion
22 p2337 A72-42801
- Brittle fracture under dynamic loading conditions.
22 p2339 A72-42848
- Criteria of fracture initiation from the view of fracture mechanics
22 p2339 A72-42857
- Aluminum matrix composites fracture mechanism dependence on static loading conditions and reinforcing filament type, investigating failure modes in tension and compression tests
23 p3299 A72-43497
- Book - Fracture: An advanced treatise. Volume 7 - Fracture of nonmetals and composites.
23 p3345 A72-43501
- Glass fracture mechanics, discussing microcrack stress concentration, Griffith theory, statistical failure theories, static fatigue and strength measurements
23 p3305 A72-43502
- Microscopic aspects of fracture in ceramics.
23 p3305 A72-43504
- Molecular mechanical aspects of the isothermal rupture of elastomers.
23 p3305 A72-43507
- Mechanics of failure of fibrous composites.
23 p3345 A72-43508
- Fracture mechanics of composites.
23 p3345 A72-43509
- Microstructural aspects of the fracture of two-phase alloys.
23 p3299 A72-43510
- Theoretical approach to the fracture of two-phase glass-crystal composites.
23 p3306 A72-43560
- A practical method for determining Dugdale model solutions for cracked bodies of arbitrary shape.
23 p3346 A72-43701
- Computer simulation of fracture spreading in a visco-elastic solid.
23 p3267 A72-43702
- Fracture mechanics and cumulative damage of simulated solid propellant under dynamic loads, obtaining low cycle fatigue curve
23 p3325 A72-43706
- Stress distribution at defects in the form of rigid sharply-angled inclusions
23 p3349 A72-43952
- Experimental and theoretical study of the fracture of sheet materials in the presence of cracks
23 p3349 A72-43958
- The surface flaw in aircraft structures and related fracture mechanics analysis problems.
23 p3352 A72-44228
- Surface flaws measurement devices and quasi-static fracture tests, discussing cyclic crack growth, elastic compliance derivative method and stress intensity equations
23 p3353 A72-44229
- Experimental characterization of yield induced by surface flaws.
23 p3353 A72-44230
- Stress intensity factors for embedded elliptical crack in semiinfinite solid and for semielliptical surface crack in plate under tension and/or bending
23 p3353 A72-44231
- The elastic analysis of the part-circular surface flaw problem by the alternating method.
23 p3353 A72-44232
- Three-dimensional finite element analysis for fracture mechanics.
23 p3353 A72-44235
- Dynamic fracture criteria for ductile and brittle metals.
23 p3354 A72-44260
- Determination of the optical thickness of polymer fracture surface layers from interference phenomena.
23 p3307 A72-44317
- Fracture mechanics development from Griffith to crack opening displacement /COD/ concept, discussing crack initiation and propagation, stress-strain characteristics and yield point
24 p3456 A72-44814
- Fracture of WC-Co from a continuum viewpoint.
24 p3413 A72-44815
- Design against fatigue failure in thermoplastics
24 p3457 A72-44816
- Linear fracture mechanics in orthotropic materials.
24 p3457 A72-44818

Deformation stresses and strains in quasi-static low cycle fracture of stabilizing, softening and strain hardening materials 24 p3460 A72-45739

FRACTURE RESISTANCE U FRACTURE STRENGTH FRACTURE STRENGTH

Yield-fracture criterion for angle ply laminate cylinders wound with filament in biaxial tension 01 p0090 A72-10521

Ductile tensile cracking macroscopic simulation with perforated pure Al specimens, determining fracture energy as function of hole size and pattern 01 p0086 A72-10987

Crack angle effect on high strength metals fracture toughness, using Al alloys and tool steel ASTM-type single edge notch tension specimens 01 p0086 A72-10988

Nonlinear effects due to crack front plastic yield and slow crack extension in energy release rate and fracture toughness calculations 01 p0140 A72-10993

Crack stability dependence on energy demand or release characteristics, discussing application to fracture tests analysis 01 p0141 A72-10996

Ni maraging steel microstructure effects on strength and fracture toughness 01 p0087 A72-11024

Crack opening displacement concept for fracture toughness testing, presenting elastic and plastic notch tip stress and deformation relationships in plane strain 02 p0292 A72-12005

Fracture toughness values from engineering tests related to fracture mechanics analytical capability by interpretive diagram systems 02 p0245 A72-12509

Fracture extension resistance features of aluminum alloys 02 p0245 A72-12510

Metal ductility and toughness - Conference, Kyoto, October 1971 02 p0246 A72-12557

Heat treatable high strength steels fracture toughness dependence on temperature, examining surfaces with electron scanning microscope 03 p0369 A72-12959

Crack notched three point loaded bend specimens plain strain fracture toughness determination, showing relation between elastic work and stress intensity factor 03 p0442 A72-12960

Plane strain fracture toughness of notched high strength Al and Ti alloys at low temperatures 03 p0371 A72-13464

High alloy chromium and manganese steels brittle fracture susceptibility, showing notch effects 03 p0371 A72-13466

Optimal cyclic fatigue strength of low C steel from critical deformation rate during thermomechanical treatment 03 p0372 A72-13597

Shock precompression effect on dynamic fracture strength of steel and Al alloy, investigating crack initiation and growth 04 p0533 A72-14541

Cyclic loading effects on resistance to brittle fracture of low carbon structural steels, using crack with criterion 06 p0831 A72-18353

Plasticity onset and brittle fracture of annealed steel as function of preceding strains 06 p0831 A72-18354

Low temperature slip discontinuity and strength of pure Al crystals as function of strain rate 06 p0831 A72-18355

Maximum temperature-holding time effects on plastic deformation and fracture of steel under thermal cyclic loads 06 p0831 A72-18359

High pressure hydrogen effects on austenitic stainless steel embrittlement, determining yield, tensile and fracture strength 07 p1011 A72-19479

Residual stresses effect on technical cohesive strength of welded cylindrical shell with surface defects, presenting plane strain fracture toughness determination method 07 p0997 A72-20131

Test facility for graphite fracture under thermal stresses, considering stress-strain relations calculation method for annular samples 07 p1024 A72-20137

Glass fiber reinforced plastic composites fracture characteristics, considering fiber content, fiber-matrix bond strength, yarn geometry, orientation and ply stacking sequence effects 08 p1192 A72-21679

Epoxy and polyester resin fatigue fracture tests for cyclic stress and moisture effects 08 p1192 A72-21680

Chopped fiber glass reinforced high density thermoplastic polyethylene composite, determining critical fiber length, interfacial adhesion and fracture toughness 08 p1193 A72-21684

Press forged ceramic crystals deformation, recrystallization, strength and fracture properties, comparing sapphires, rubies and spinels 08 p1196 A72-21917

German monograph on fracture formation and behavior in Ni maraging steel under repeated stress alternations, considering Al and Ti effects on steel strength 08 p1190 A72-22172

High strength solids compositional, heat treatment and chemical environmental effects on fracture strength, considering alumina as example 09 p1334 A72-22387

Crystalline ceramics compressive fracture strength and microhardness tests at room temperature, suggesting microplasticity role in failure mechanisms 09 p1334 A72-22388

Carbon fiber reinforced epoxy resin composites, testing fracture behavior in flexural and shear modes under static, fatigue and creep loading 09 p1334 A72-22389

Carbon fiber reinforced epoxy resin composites fracture toughness dependence on fiber strength, diameter, volume fraction, modulus, fiber/matrix interface strength and temperature [PI PAPER 9] 09 p1337 A72-22544

Fracture toughness tests on Al-Cu alloy plate, noting insensitivity to strain rate 09 p1328 A72-22913

Aligned fibrous composites microstructural parameters, showing fiber thickness effect on fracture, fabrication, matrix cracking, creep resistance and fatigue 09 p1338 A72-23163

Core and tube duplex fiber reinforced composites with fracture toughness capable of high stress level operation 09 p1338 A72-23166

Carbon fiber reinforced plastic toughness from strain concentration and plastic flow observation near crack tip by moire technique 09 p1339 A72-23170

Strength and fracture energies and toughness in fibre reinforced ceramics 09 p1339 A72-23171

Helically bound wire reinforced sprayed Al tubes and rings, investigating failure mechanism dependence on fracture modes from tensile and bending tests 09 p1330 A72-23174

Metastable austenitic steel fiber to increase Al matrix strength to density ratio and fracture toughness 09 p1331 A72-23385

Fracture toughness expressions including nonlinear effects due to crack front plastic yield and possible crack extension prior to fracture instability [SMRT PAPER L 1/4] 10 p1497 A72-24396

Mean stress effect on fatigue crack propagation rate in half inch thick Al alloy specimens of high and low fracture toughness 10 p1498 A72-24884

Al alloy notch-bend and compact-tension specimens thickness and crack length effects on plane-strain fracture toughness test results 10 p1498 A72-24886

Tensile, plane strain fracture toughness and fatigue tests of high strength Al alloy cylinders, discussing unstable crack growth conditions 10 p1498 A72-24887

Ti alloys fracture strength in air and sea water obtained by bending tests of notched specimens, noting stress corrosion resistance enhancement by Mo addition 10 p1499 A72-24891

Fracture strength relation to austenite stability in steels with plastic deformation caused by strain induced austenite-martensite transformation 10 p1499 A72-24894

Two dimensionally reinforced quartz-phenolic composite material dynamic fracture behavior under stress wave loading in uniaxial strain, noting spallation threshold time dependence 11 p1669 A72-25291

Fracture toughness of anisotropic heterogeneous filamentary boron/aluminum composites, correlating test results with acoustic emissions from filament breakage 11 p1672 A72-25470

Fiberglass-graphite reinforcement of unidirectional epoxy laminates, examining longitudinal composite fracture stress and strain and tensile and compressive stiffness 11 p1672 A72-25485

Specimen preparation effects on fracture strength measurements, noting critical stress intensity factor for single edge notch and compact tension high strength steel samples 11 p1657 A72-25825

Al alloys hand forgings fracture strength and stress corrosion characteristics from precracked specimens bending tests in air and sea water 11 p1658 A72-25833

Fracture toughness anisotropy and crack sensitivity of Al alloys extruded bars notched cylindrical samples 11 p1659 A72-26130

Statistical estimation method for brittle metals fracture strength, taking into account stress nonuniformities due to dislocation defects 11 p1738 A72-26803

Filament reinforced boron-aluminum composites multiple fracture behavior dependence on cross section geometry from tensile test 11 p1668 A72-26944

Fracture toughness of high strength alloys, discussing rocket motor cases, nondestructive test standards and subcritical crack growth 12 p1829 A72-27656

Fiber composites plastic flow and fracture, using plane strain model for analysis 12 p1884 A72-27730

Nonlinear fracture toughness determination via three point bending test simulation by elastic-plastic finite element computer program 12 p1830 A72-27731

Al-Zn-Mg alloy tear resistance relationship to stress corrosion cracking from tear, tensile and corrosion tests 12 p1830 A72-27750

Al alloy plate material microstructural variations and specimen orientation effects on tensile and fracture toughness properties 12 p1830 A72-28080

Chemical vapor deposition of boron on carbon monofilament substrate to eliminate fracture and boron damage and achieve good strength 12 p1834 A72-28085

Impact fracture resistance of Cr-Mn-Si steel, investigating alloying effects on crack initiation and propagation 12 p1831 A72-28238

Precracked Charpy specimens for fracture toughness impact and slow bend tests of Ti alloys, using energy values 13 p1974 A72-28656

Increased volume fraction effect on transverse rupture strength and fracture toughness of hot pressed and annealed composites of polycrystalline magnesium oxide 13 p1980 A72-29828

Failure phenomena relationship to kinetic equation for defect buildup from brittle fracture analysis of composite glass plastic in uniaxial eccentric tension 14 p2164 A72-30426

Temperature effects on critical crack opening as fracture toughness criterion for medium strength steel, taking into account local plasticity and propagation resistance 14 p2118 A72-30590

Ti alloy fracture strength determination by crack propagation observation in specimen center, noting load-displacement curve construction from cyclic loading test 15 p2259 A72-32804

Griffith equation applicability to graphite fiber fracture strength by measurement of work to break and critical flaw 16 p2413 A72-32871

Al-Zn-Mg-Cu forgings fracture toughness increase with Fe content reduction, discussing overload fracture following grain and stringers 16 p2405 A72-33000

Fracture toughness measurements of polyester composites reinforced with chopped steel wires compared with Cooper theory 16 p2413 A72-33203

Safe stress range for metal fatigue deformation preceding fracture under combined cyclic and steady push-pull loads 16 p2468 A72-33228

Plane strain fracture toughness tests of compact thick maraging steel specimens at various yield strength levels as function of aging 16 p2406 A72-33317

Fracture-surface energy model for Cu-W fiber metal matrix composites, using plastic flow analysis 16 p2470 A72-33613

Notch sensitivity of sintered stainless steel powder as function of density from application of sharp crack fracture mechanics methods to plane strain fracture toughness 16 p2408 A72-33700

Ti comparison with Al for effects on Fe alloy deformation and fracture, discussing intergranular failure suppression 16 p2411 A72-33823

Composite cylinder of helically wound fiber laminates, calculating torsional fracture strength with allowance for plastic deformation due to matrix distortion 16 p2472 A72-33949

Composite cylinders of helically wound fiber laminates, predicting burst fracture strength under internal pressure for comparison with experiment on epoxy-glass cylinders 16 p2472 A72-33950

Note on dynamic fracture toughness measurement. 17 p2566 A72-34257

Model with lamellae and tie molecules disordered alignments to explain relation between stress-strain behavior and bond fracture in highly oriented polymer fibers

Fracture of cylindrical and spherical shells containing a crack.

Fracture of boron filaments in an aluminum matrix.

Fractographic lines in maraging steel - A link to fracture toughness.

Effects of combined high and low temperature deformation processing of beta III titanium.

Optimal composition equation with austenite retention index for high strength maraging stainless steel development for improved toughness.

Strength of titania and aluminum silicate under combined stresses.

Plasticity and rupture of heat-resistant materials subjected to a small number of cycles of simultaneous variation of temperature and load

Heat resistant alloys stress-rupture strength tests for operating temperatures based on equivalent high temperatures damageability

Estimation of the cleavage strength of polycrystalline metals from the internal energy

Resistance to brittle fracture of high-strength steels in various structural states

Strength properties of highly porous materials made of metallic fibers

Relations between mechanical properties and microstructures in TiC-Mo2C-Ni alloy.

Prediction of deformability and fracture processes for polymer materials

Crack growth behavior correlation to acoustic emission signal amplitude distribution in high strength steel heat treated to different fracture toughness values

Possibility of determining the fracture toughness of materials on the basis of the form of static bend test fracture samples.

Criteria for valid plane strain fracture toughness testing dealing with straightness of fatigue crack front of metal specimens

The use of pre-cracked Charpy specimens to determine dynamic fracture toughness.

Fracture toughness of the heat-affected zone in 14CrMoV69 steel and 18Ni maraging steel.

Bursting strength and toughness of wire reinforced composite tubes under uniaxial/hoop stress.

Comparison of the resistance to fracture of the K1c of the AK4-1T1, V95T1, and D16T aluminum alloys and VT8 and VT9 titanium alloys under static and cyclic loading

Yielding and fracture of D16T alloy at low temperatures under conditions of complex stress-strain state

Influence of the test temperature on the fracture energy of graphite

Stress-strain diagrams and fracture characteristics of fiber-reinforced aluminum alloys

Influence of hydrogen on the fracture structure of OT4 titanium alloy

Combined mode crack extension in adhesive joints.

Temperature-time effects on fracture failure mode and strength of polymeric glasses in terms of Ludwik brittle-ductile transition hypothesis and Griffith theory

Polycrystalline aluminum and magnesium oxide ceramics fracture strength, considering plastic deformation and twinning role in crack nucleation

Elastomers fracture strength and failure modes under tension, tearing, ozone cracking, fatigue and abrasive wear associated with viscous resistance energy losses

Mechanics of failure of fibrous composites.

Work of fracture of fibre-reinforced polymers.

Tendency toward brittle failure of a simulated weld-seam region in Ti-Al-V system alloys

Plane elastostatic analysis of V grooved rectangular plates notch angle and specimen geometry effects on stress intensity factors and fracture toughness measurements

Crack opening displacement relationship to notch root contraction from fracture toughness tests, describing plastic deformation mechanism at notch tip

Cast heterophase Mo and alloys fracture strength and plastic characteristics, investigating crystal growth texture, orientation and substructure

Creep and fracture of OT-4 titanium alloy in the temperature range from 400 to 550 C

Cold shortness of 14Kh2NZMA steel

Measuring fracture toughness - A simplified approach using controlled crack propagation.

Plane-stress fracture toughness testing using a crack-line-loaded specimen.

Crack growth resistance in plane-stress fracture testing.

The fracture toughness of fibre composites.

Plane strain fracture toughness of notched high strength Al and Ti alloys at low temperatures

High alloy chromium and manganese steels brittle fracture susceptibility, showing notch effects

Influence of oxygen and hydrogen on the strength of titanium alloys

The mechanism of void formation, void growth, and tensile fracture in an alloy consisting of two ductile phases.

Cyclic loading effects on resistance to brittle fracture of low carbon structural steels, using crack width criterion

Plasticity onset and brittle fracture of annealed steel as function of preceding strains

Low temperature slip discontinuity and strength of pure Al crystals as function of strain rate

Maximum temperature-holding time effects on plastic deformation and fracture of steel under thermal cyclic loads

Residual stresses effect on technical cohesive strength of welded cylindrical shell with surface defects, presenting plane strain fracture toughness determination method

Graphites fracture under thermal stresses, considering stress-strain relations calculation method for annular samples

FRACTURE TOUGHNESS

U FRACTURE STRENGTH

FRACTURES [MATERIALS]

VT3-1 Ti alloy with Al, Mo, Cr and Fe additives, investigating ductile type fracture after heat treatment by electron microscopy and tensile tests

Microfractographic fatigue fracture analysis of steels, aluminum, brass, nickel and molybdenum by scanning electron microscope

Forming of 7075-T6 Al in high pressure environments, predicting fracture occurrence via finite element stress analysis computer programs and pressure dependent model

Unstable propagation and brittle fracture arrest in steels from double cantilever beam test under compression

Directionally solidified Al-AlNi intermetallic eutectic alloy microstructural characteristics and effects on creep fracture

Ductility and fracture of heat resistant steels at high temperatures and unsteady loading, estimating loading cycle effect on plastic strain buildup to failure

Electron fractographic investigation of fracture properties via removal of metal oxide film accumulated on crack surface during service life of steel structures

Ductile type fracture after heat treatment of VT3-1 Ti alloy with Al, Mo, Cr and Fe additives investigated by electron microscopy and tensile tests

Ductile fracture development in steel due to microcracks and pores formation

Laser induced transparent dielectrics surface fracture mechanism determination based on electron microscopic photograph analysis and disturbed specular reflection under predischage conditions study

Fractographic study of stress corrosion fractures of low carbon steels with electron microscope

Mechanical properties, microstructural characteristics and fracture behavior of beta Ti-V-Cr-Al alloy

Transmission and scanning electron microscope observations of Nb-Hf alloys fracture morphology, noting precipitate free zone

Udimet 500 alloy dislocation substructure and fracture surface topography during deformation to failure in low cycle fatigue at high temperatures

Fracture micromechanism in liquid-phase sintered W-Fe-Ni powder composites, using scanning electron microscopy

Neutronically generated He irradiation effects on high temperature fracture of fcc, bcc and hcp structural metals and alloys

High strength fine grain structural steels fracture characteristics from notch-bar impact and tensile tests, determining inclusions effect on mechanical properties

Deformation and fracture of dispersion-strengthened nickel charged with hydrogen.

Ductility and fracture of heat resistant steels at high temperatures and unsteady loading, estimating loading cycle effect on plastic strain buildup to failure

FRACTURING

Zircaloy plastic properties and fatigue fracture modes under strain controlled push-pull cyclic loads, noting plastic anisotropy changes for warm cross rolled and recrystallized materials

Snapping process dynamics of shallow elastic hinged cylindrical panel of rectangular platform under gaseous, liquid and solid loads

Lunar glass particle micrometeorite crater morphology, showing radial fracture and spallation zone relationships

Model for metal fatigue fracturing, noting crack initiation and two stages of propagation, emphasizing experimental fractographic /electron microscopy/ research

Elastic wave energy absorption in structures under dynamic loads, noting fatigue fracturing decrease with energy transfer into damping medium

FRAGMENTATION

Bevatron nuclear fragmentation of N 14 nuclei, discussing isotopic fragments identification

Fragmentation and closure in afterimages of bright flash stimuli

Small meteor bodies fragmentation, using radar diffraction patterns

Asteroids origin, discussing Phaethon model, masses, distribution, fragmentation and disintegration

Electron impact induced fragmentations of o-, m- and p-hydroxyalkylphenones and trimethylsilyl/TMS/ ether derivatives, using high resolution mass spectrometry, metastable defocusing and deuterium labeling

Electron impact induced fragmentation of alkyl-N-1-phenylethyl-/carbamates of primary, secondary and tertiary alcohols, using deuterium labeling and high resolution mass spectrometry

Hydrogen gas cloud gravitational contraction and fragmentation in expanding universe, noting cooling and massive stars formation

Inclusive isotope spectra of secondary nuclei produced by Bevatron heavy ion fragmentation in carbon and polyethylene targets, noting partial differential cross sections

Breakup of accelerating liquid drops in gas dynamic flow, presenting unified theory for acceleration and aerodynamic effects

Lognormal fragment mass distribution of Lowicz meteorite shower 1935

Low temperature shock effects on lunar glass spherules from two beam interferometry, discussing mechanical and thermal causes of fragmentation 14 p2149 A72-30266

FRAGMENTS

Fragment velocity for bursting gas containers in vacuum [ASME PAPER 71-PVP-14] 02 p0295 A72-12473
Frost rule for meteoroid spatial sorting as basis for Allende meteorite shower strewn field examination of fragment mass and position 08 p1237 A72-21651

Ar-39/Ar-38 cosmic ray exposure age calculation from Sikhote-Alin meteorite fall fragment content of Ar-39, Ar-38, Ne-21 and He-3 14 p2157 A72-30584

FRAME PHOTOGRAPHY

Two beam high speed frame holographic recording of dynamic processes, using passive shutter ruby laser with diaphragmed resonator 15 p2233 A72-31417

High speed frame photography application in spectroscopic studies of plasma jet in cylindrical pulsed accelerator with dielectric 15 p2283 A72-31418

Solar chromospheric flare details motion differences from spectrum analysis and H alpha line frame photography, noting radial velocities difference 19 p2851 A72-37816

Experimental observations of the instability of stellar images from a bichromatic two-channel television system 19 p2860 A72-37956

Study of target edge response viewed through atmospheric turbulence over water. 23 p3289 A72-43896

FRAMES

NT AIRFRAMES
NT CHASSIS
NT UNDERCARRIAGES

Minimum weight beams and frames calculation for random loads taking into account material carrying capacity 02 p0291 A72-11727

Straight beams and rectangular frames stress-strain calculation under pulsed loading, taking into account shock waves finite propagation velocity and internal damping 02 p0300 A72-12855

Disk shaped frame corner stress under external load, using complex variables and conformal mapping 03 p0448 A72-13886

Automatic plastic minimum weight design of structural frames comparing with linear programming techniques 05 p0737 A72-16117

Dynamic matrix analysis of vibrating three dimensional frame structures, comparing discrete and continuous mass systems 06 p0897 A72-17971

Optimality criterion for beams and frames with segmentwise constant cross sections and alternative loading exceeding plastic load carrying capacity 07 p1088 A72-19119

Torsional bending vibrations mode shapes of space frame with variable elastic and mass characteristics, determining eigenvalue error limits 08 p1205 A72-20957

Probability minimization and detection of errors in computerized analysis of civil engineering frameworks, noting graphical output advantages 12 p1786 A72-27190

Mohr formulas construction for composite structures including frames and cylindrical and conical shells 13 p2058 A72-29460

Minimum weight reliable beams and frames calculation for random loads, using one degree of freedom system to obtain closed form solution 14 p2164 A72-30237

Optimal plastic design of doubly symmetric closed ring and frame structures of idealized sandwich section under uniform internal pressure 15 p2322 A72-31346

The carrying capacity of frames under the influence of concentrated forces 20 p2981 A72-39919

FRAMING CAMERAS

High speed frame photography application in spectroscopic studies of plasma jet in cylindrical pulsed accelerator with dielectric 15 p2283 A72-31418

FRANCK-CONDON PRINCIPLE

Diatomic molecules forbidden transitions moments, Franck-Condon factors and lifetimes, calculating CO Cameron system intensity by perturbation theory 05 p0692 A72-16750

Hydrogen protons and atoms interaction with hydrogen and nitrogen molecules, showing electron transfers agreement with Franck-Condon principle 08 p1210 A72-20835

Franck-Condon phonon displacement effects on mobility edge and energy gap in disordered materials 09 p1357 A72-22986

SiO transitions radiative lifetimes and absolute oscillator strengths from RKR Franck-Condon factors 13 p2008 A72-30054

RKR Franck-Condon factors for blue and UV transitions of metal oxides, hydrides and halides, discussing interstellar abundances 14 p2160 A72-30898

Oscillator strength for sulfur monoxide transition band systems calculated from radiative lifetime with Franck-Condon factors 20 p2966 A72-38916

FRAUNHOFER LINES

Spherical aberration effect on far field Fraunhofer diffraction for circular aperture illuminated by quasi-monochromatic partially space coherent light 01 p0103 A72-11188

Transfer equation system solution for nonscattering medium with stationary homogeneous magnetic field, considering boundary value problem in Fraunhofer line theory 05 p0690 A72-16513

Solar Fraunhofer line profiles determination by digital data recording double-pass spectrophotometer, presenting observed atomic Ni and Fe lines intensity distributions 06 p0884 A72-18028

Solar Fraunhofer line profiles determination by digital data recording double-pass spectrophotometer, presenting observed atomic Ni and Fe lines intensity distributions 11 p1719 A72-25964

Undisturbed and active solar photospheric turbulent velocity determination by comparing half widths of observed weak Fraunhofer line profiles with model calculation 13 p2049 A72-29929

Photoelectric observations of Fraunhofer ionized metal lines in sunspot spectrum relating to umbral dots 16 p2458 A72-33687

Fraunhofer lines emergent intensity fluctuation caused by temperature and pressure perturbation in solar atmosphere 17 p2608 A72-35080

A first order analysis of variations of the limb darkening and the shapes for solar Fraunhofer lines. 17 p2616 A72-35694

On the choice of boundary conditions for integration of transfer equations. 17 p2577 A72-35695

Theoretical explanation of the solar limb effect. 17 p2618 A72-35895

Effect of photographic factors on the line intensities in the Fraunhofer spectrum of the sun 19 p2860 A72-37960

Magneto-optic effects in Fraunhofer lines with Zeeman splitting 19 p2835 A72-38495

Investigation of physical conditions in the solar photosphere by a curve of growth technique 21 p3102 A72-40097

The solar abundance of calcium and collision broadening of Ca I- and Ca II-Fraunhofer lines by hydrogen. 22 p3221 A72-42027

FRAUNHOFER REGION

U FAR FIELDS

FREDHOLM EQUATIONS

Static load transfer to discontinuous elastic filament in fiber reinforced composite, determining fiber force longitudinal distribution by approximation to Fredholm integral equation 03 p0455 A72-14384

Dirichlet problem reduction to boundary value problem via invariant imbedding techniques and Fredholm integral equation method 04 p0540 A72-15632

Operator approach solution to boundary value problems with infinite defect for differential equations with deviating argument, considering Fredholm alternative validity and compressed mappings application 08 p1199 A72-21465

Mixed boundary value problem for infinite parallel cracks row solved by reduction to Fredholm integral equation 09 p1398 A72-22534

Stress distribution determination for long isotropic elastic cylinder with strip crack on diametral plane by complex variable technique and Fredholm equation solution 09 p1409 A72-23574

Torsion of embedded infinite elastic circular cylindrical fiber with penny shaped crack, investigating breaking behavior from Fredholm integral equation iterative solution 10 p1553 A72-24094

Finite range Fredholm integral equations with band limited displacement kernels in terms of prolate spheroidal wave functions 10 p1506 A72-24460

Variational methods for approximate solutions to Fredholm integral equations describing stress intensity factors and plastic regions of Dugdale cracks [AD-744365] 10 p1558 A72-24892

Mellin transforms for finite elastic disk radial crack stress intensity factor and energy formulae in terms of Fredholm equation solution, considering constant loading case 11 p1738 A72-26724

Random Fredholm and Volterra integral equations applied to stochastic systems, investigating absolute stability concept 11 p1679 A72-26780

Neuronal network numerical and analytic studies, using invariant imbedding and matrix Fredholm integral equation 13 p1986 A72-29400

Upper boundary layer conditions effects on atmospheric temperature profile reconstruction, by integro-differential equation substitution for Fredholm equation 15 p2265 A72-31399

Vectorial differential equations in potential theory, discussing Fredholm alternative in normalized spaces, generalized harmonic vector fields, Poisson equation and Robins-Praeger problem 15 p2261 A72-31452

Numerical calculation of stresses and displacements in variable radius bodies of revolution under axially symmetric torsional load, using Fredholm type integral equation 15 p2324 A72-31480

Internal waves in sheeted thermocline with finite discontinuities in density profile formulating eigenvalue problem as homogeneous Fredholm integral equation 16 p2386 A72-33573

Flexible rotors balancing theory based on Fredholm integral equations, considering two- and three-bearing supported shafts with arbitrary mass distribution 18 p2731 A72-36068

The numerical solution of Fredholm integral equations of the second kind with singular kernels. 18 p2705 A72-36603

A certain property of standard Fredholm-type nonlinear integro-differential equations 19 p2825 A72-38178

The Galerkin method for the numerical solution of Fredholm integral equations of the second kind. 19 p2827 A72-38384

The equivalence of several initial value methods for solving integral equations. 20 p2945 A72-39346

Initial-value methods in the theory of Fredholm integral equations. II. 21 p3075 A72-40550

Approximate optimal control solution to boundary value problem for one dimensional heat conduction equation, using Fredholm linear integral and degenerate kernels 23 p3274 A72-43526

On the solution of plane, orthotropic elasticity problems by an integral method. [ASME PAPER 72-APM-BB] 23 p3350 A72-44056

Thermoelastic contact problem of an elastic layer resting on an elastic foundation. 23 p3354 A72-44269

FREDHOLM OPERATORS

U FREDHOLM EQUATIONS

U OPERATORS [MATHEMATICS]

FREE ATMOSPHERE

Free atmosphere vertical temperature structure at mesoscale, using continuous recording sonde [AD-739147] 04 p0519 A72-15158

Ionospheric potential and thunderstorm activity annual variations during 1959-70 solar cycle from radiosonde measurements in free atmosphere 09 p1301 A72-23265

FREE BOUNDARIES

Variational solutions of nonlinear free boundary integro-differential Euler equations for rotating star models 02 p0252 A72-12540

Geomagnetic tail natural oscillations, applying model of plasma cylinder with free boundary immersed in interplanetary medium 05 p0659 A72-17044

Capillary forces effects on free surface liquid behavior in partial or total weightlessness, reviewing sloshing problem mathematical treatments 06 p0802 A72-18717

German book on nonlinear free boundary value problems of two dimensional hydrodynamics covering gravity, capillary and irrotational waves, liquid flow in channel, etc 07 p0967 A72-19183

Axisymmetric flow of ideal incompressible liquid with free boundary and variable velocity, taking into account external mass forces effect 07 p0968 A72-19899

Gas motion behind plane detonation wave orthogonal to free surface, solving Goursat problem for perturbed region 07 p0969 A72-19979

Invariant free boundary problems of Navier-Stokes equations with nonzero vector of volume forces, investigating liquid layer flow on vertical cylinder surface 07 p0972 A72-20105

- Rayleigh method convergence in ideal fluids axisymmetric flow stability with free boundaries and perturbations without mass forces 08 p1148 A72-20909
- Two heat conducting phases free boundary problem with temperature distribution within phases, proving existence and uniqueness theorems 12 p1836 A72-27124
- Convection instability in viscous incompressible liquid layer with free boundaries under modulated external force field 13 p2064 A72-28723
- French monograph on hot-wire anemometry techniques covering support aerodynamic perturbations, crossed wire probes and turbulent flow free boundary 14 p2106 A72-30946
- Initial value techniques in free-surface hydrodynamics. 17 p2538 A72-34644
- Invariant solutions of the Navier-Stokes equations describing motions with a free boundary. 18 p2679 A72-36234
- Asymptotic estimate of steady state solution to Euler equations for ideal incompressible fluid flow with free boundaries 18 p2682 A72-36805
- Gas motion behind plane detonation wave orthogonal to free surface, solving Goursat problem for perturbed region 20 p2915 A72-40035
- Draining of a fluid from a rotating cylindrical tank. 21 p3046 A72-41307
- Two-dimensional stationary problem with a free boundary for the Navier-Stokes equations 21 p3047 A72-41663
- Comet tail wave motion explanation via consideration as plasma cylinder with free boundary tangential discontinuity surface immersed in interplanetary plasma 22 p3221 A72-42011
- Convection instability in viscous incompressible fluid layer with free boundaries under modulated external force field 22 p3243 A72-42099
- Convective interaction in a partially-liquid-filled vertical vessel with heat influxes in its lateral and free surfaces and bottom 22 p3244 A72-42261
- Axisymmetric and two-dimensional flow with attached shock waves. 24 p3361 A72-45161
- FREE CONVECTION**
- Unsteady compressible free convection near infinite vertical flat plate with temperature and velocity variations in boundary layer 01 p0146 A72-11392
- Laminar liquid flow stability in vertical slots under natural convection, showing critical layer level for nonstationary perturbations 02 p0202 A72-11591
- Laminar free convection from vertical nonisothermal rigid circular cone with boundary layer control by injection or suction, investigating heat transfer by perturbation method 02 p0204 A72-12232
- Free convective motion of conducting fluid past vertical plate in uniform transverse magnetic field, determining optimum dimensions of heat exchangers 03 p0399 A72-14011
- MHD approximation to solve natural convection problem in vertical channel under external inhomogeneous magnetic field, noting fluid flow rate 04 p0555 A72-14646
- Uniform normal magnetic field effect upon MHD free convection from vertical wall with instantaneous heat source, considering shear stress 04 p0556 A72-14856
- Newtonian fluid laminar free convection over curved wall with arbitrary temperature variation, investigating similarity solutions existence by method of free parameters 04 p0596 A72-15193
- Holographic interferometer for heat transfer measurement, studying free convection thermal boundary layer on heated isothermal vertical flat plate 04 p0524 A72-15531
- Free convection flow along infinite vertical flat plate under periodically varying suction and with fluctuating plate temperature, analyzing mean velocity and temperature profiles 05 p0747 A72-16668
- Transient three dimensional natural convective modes in porous media as function of Rayleigh number 07 p1099 A72-19623
- Thermally induced convection flow characteristics in separated or wake formation regions over heated cylindrical surface submerged in water 07 p1100 A72-19630
- Atmospheric free convection turbulence and diffusion, proposing statistical characteristics and formulas with horizontal thermal flux vertical and transverse velocity components 07 p1031 A72-20697
- Laminar natural convection heat transfer from leading edge of isothermal plate under nonuniform gravity [ASME PAPER 71-HT-CC] 08 p1250 A72-20875
- Free convection velocity fields measurements and stagnation point location around horizontal torus in air, using fine particle trajectories [ASME PAPER 71-HT-X] 08 p1163 A72-20877
- Free convection effect on plane crystallization front instability under conditions of phase transition, using method of small perturbations 08 p1151 A72-21661
- Free convection and hydrodynamics of inclined liquid layers in laminar flow and in stepwise change of heat exchange surfaces temperature 08 p1151 A72-21663
- Heat and mass exchange in laminar boundary layer in air-carbon dioxide binary mixture under free convection on porous heated vertical surface 08 p1255 A72-21664
- Free convective heat transfer measurement from solid copper inner cylinder to cylindrical casing 09 p1410 A72-22351
- Numerical solution of thermal shock equations for incompressible fluid with free convection and of motion equations in gravitational force field 09 p1410 A72-22882
- Statistical solution of steady natural turbulent convection at large Grashof numbers 10 p1465 A72-24103
- Conducting fluid laminar free convective flow over heated rotating horizontal plate in presence of strong magnetic field aligned with rotation vector 10 p1522 A72-24465
- Thermal radiation effects on natural convection boundary layer adjacent to vertical flat surface with uniform heat flux input 10 p1562 A72-24466
- Free convection-radiative heat transfer interaction of real gases in laminar boundary layer on vertical plate, using exponential wideband model for total band absorbance 11 p1740 A72-25218
- Gas role in radiative transfer and free convection between concentric spheres, noting gray gas assumption validity [AIAA PAPER 72-278] 11 p1740 A72-25218
- Hydrodynamics of turbulent free convection boundary layer on vertical flat plate and ethyl alcohol film 11 p1743 A72-25258
- Laminar free convection about isothermal horizontal cylinders with constant heat flux, calculating velocity and temperature profiles 11 p1743 A72-25263
- Laminar transition and turbulent natural convection mass transfer measurements on inclined and vertical surfaces by electromechanical method 11 p1635 A72-26536
- Three dimensional free convection boundary layer equations solution at two dimensional isothermal stagnation point with various Prandtl numbers 11 p1747 A72-26662
- Streak photography for three dimensional structure of thermal convection in rotating fluid under horizontal temperature gradient, noting time variations of baroclinic waves 12 p1809 A72-27701
- Free convection excitation and maintenance method, discussing occurrence around high power laser beam 13 p2063 A72-28628
- Isothermal vertical plate turbulent thermal boundary layer during free convection, noting temperature pulsations dispersion 13 p2066 A72-29899
- Carbon dioxide turbulent flow heat exchange in single phase near critical region under forced and free convection 13 p2066 A72-29900
- Unsteady laminar natural and forced convection at transparent medium boundary layer radiating surface, noting turbulence effects on heat exchange 13 p2066 A72-29902
- Natural convection initiation in fluid confined above and below by rigid conducting surfaces and laterally by rigid insulating vertical walls 14 p2172 A72-31054
- Free convection effect on vertical porous insulation layer thermal conductivity in high pressure gas environment 14 p2172 A72-31057
- Experimental setup and flow patterns for natural convective heat transfer from plate with arbitrary inclination 14 p2173 A72-31060
- Steady asymptotic suction profiles in free convection laminar boundary layer flows on heated vertical circular cylinder 14 p2096 A72-31070
- Microelectronic devices liquid cooling by free and forced convection, investigating component size effects on heat transfer by boundary layer analysis and experiment 14 p2091 A72-31172
- Thermal drift of floated spherical gyroscope calculation based on two dimensional free convection analysis of supporting fluid 15 p2235 A72-31727
- Time behavior of two dimensional laminar free convection flow between heated vertical parallel plates, calculating temperature and velocity distributions as function of Grashof number 16 p2477 A72-33426
- Blowing and suction effects on free convection boundary layer on semiinfinite vertical flat plate, taking into account temperature difference between plate and fluid 16 p2477 A72-33429
- Wall and ambient temperature distribution effects on free convection heat transfer from nonisothermal vertical flat plate in temperature stratified medium for Prandtl number range 16 p2477 A72-33434
- Heat transfer by free convection from a longitudinally vibrating vertical plate. 17 p2637 A72-35045
- Radiation with free convection in an absorbing, emitting and scattering medium. 17 p2637 A72-35046
- Viscous dissipation effects on unsteady free convective flow past an infinite, vertical porous plate with constant suction. 17 p2637 A72-35047
- Transient turbulent free convection in a closed container with heating at the sides only. 17 p2638 A72-35642
- Free convection similarity and measurements in flows with and without shear. 18 p2706 A72-36634
- Numerical analysis of three dimensional steady laminar free convection boundary layer due to heated ellipsoid, solving flow equations 19 p2881 A72-38394
- A review of physical models and heat-transfer correlations for free-convection film boiling. 19 p2883 A72-38842
- Atmospheric free convection turbulence and diffusion, proposing statistical formulas for components of horizontal thermal flux, vertical and transverse velocity and free diffusion tensor 20 p2948 A72-39012
- Heat emission from the lower faces of plane surfaces in the presence of a steady thermal flux under conditions of natural convection 20 p2982 A72-39322
- Film boiling correlations for stable natural convection heat transfer for various heater substances and pressures 20 p2983 A72-39487
- Heat transfer by laminar natural convection in low aspect ratio cavities. [ASME PAPER 72-HT-52] 20 p2985 A72-39661
- Laminar free convection from a rotating radial plate. [ASME PAPER 72-HT-46] 20 p2985 A72-39664
- Transient laminar free convection in closed spherical containers. [ASME PAPER 72-HT-37] 20 p2986 A72-39669
- Magnetic field and suction effects on unsteady MHD free convection flow of conductive fluid around nonconductive porous flat plate 21 p3095 A72-41787
- Interferometric investigation of natural convection in rectangular air cavities of different orientation 22 p3244 A72-42262
- Numerical analysis of the natural convection in a porous medium between two concentric cylinders 22 p3244 A72-42640
- Dynamo theory for lunar magnetic field based on hypothetical thermal convection in rotating moon core analogous to earth 23 p3341 A72-44448
- FREE ELECTRONS**
- Free electron density, electron temperature and gas ionization during shock wave propagation in Ar-filled shock tube from microwave radiation measurements 02 p0263 A72-12020
- Tunneling current calculation for free electrons subject to arbitrary one-electron potential, using Keldysh perturbation theory 03 p0404 A72-14266
- Optical properties changes of Al alloys containing impurities, noting band structure modification and tendency toward free electron response 08 p1186 A72-21593
- One dimensional time independent solution to Vlasov-Poisson system of nonlinear electrostatic plasma waves, noting Maxwell distributions for free and trapped particles 11 p1697 A72-26596
- Predawn effect on hot and cold electrons at magnetoconjugate point in F 2 layer, discussing electron shock wave speed and thermal collisionless wave energy dissipation 11 p1628 A72-26916
- Gunn diode active region thickness, free electron mobility/concentration, structure and contacts, including treatment of GaAs 13 p1934 A72-30036

- Free electron waves interaction with coherent laser light in crystalline medium, discussing quantum mechanical treatment and path integral approach
14 p2110 A72-30725
- Free electrons in condensed matter under high pressure, calculating number with Thomas-Fermi statistical model
15 p2305 A72-31338
- Free electrons-laser interaction induced electron forward drift and dc current generation, deriving drift velocity by nonrelativistic classical and quantum mechanical theories
16 p2402 A72-33397
- Coupling of free electron and nitrogen vibrational temperature nonequilibrium in weakly ionized nozzle expansions of shock heated nitrogen
[AIAA PAPER 72-683] 16 p2380 A72-34059
- Distribution function for free electrons in a molecular-nitrogen plasma
17 p2593 A72-35891
- Effect of atomic polarizability on low-energy free-free radiative transitions
19 p2837 A72-37839
- Chou-Tien nonplane-parallel solution to transfer equation for radiation scattering by free electrons in stellar spherical atmosphere by regional averaging procedure
21 p3109 A72-41434
- A comparison of the observed twilight with the vertical scatter distribution
22 p3170 A72-42373
- Free electrons and holes concentration calculated for quadratic dispersion law in doped semiconductors without degeneration, noting additive atoms effect
23 p3324 A72-43849
- Measurement of the rate coefficient for the recombination of He⁺ with electrons
23 p3315 A72-43869
- Radiation from a free electron interacting with a circularly polarized laser pulse
23 p3296 A72-43875
- Electron bremsstrahlung from hot plasma in the presence of strong magnetic field
24 p3431 A72-45627
- FREE ENERGY**
NT GIBBS FREE ENERGY
- Rare earth metals microadditions influence on Ni grain boundaries free energy and compounds formation
07 p1012 A72-19676
- Electromechanical machining metal removal mechanism based on configurational localization model, relating wear processes to electron exchange and free energy margin decrease
07 p0996 A72-19989
- Wien intravascular effect on plasma carbon dioxide gradients near pulmonary capillary wall, discussing free energy requirements
08 p1114 A72-20890
- Surface active medium effect on free surface energy and strength of pyrographite in ethyl alcohol solution, using crack kinetics experiment
08 p1197 A72-22182
- Temperature anisotropy quasi-linear relaxation thermodynamics in collisionless plasma, analyzing system free energy
11 p1698 A72-26599
- Constitutive equations for multipolar solid with memory, deriving boundary conditions and free energy equation from first and second thermodynamics laws respectively
15 p2273 A72-31363
- Molecular and atomic interaction forces as interfacial free energy sources, discussing molecular attachment kinetics and surface configuration models
18 p2718 A72-36393
- Cluster variation method for boundary free energy solution in lattice model applied to Ising phase and gas-liquid interface and longer range interaction
18 p2711 A72-36565
- Free energy changes and boundary segregation of tin and antimony in CrV steels
21 p3070 A72-41648
- Changes in the grain-boundary free energy and the segregation of tin and antimony at grain boundaries in CrV steels
24 p3415 A72-45394
- FREE FALL**
- Absolute gravity acceleration determination using free-falling laser interferometer apparatus with rotation-insensitive mirror at different sites
02 p0207 A72-11597
- Heart and respiration rates response to free fall parachuting, using FM/FM telemetry
02 p0167 A72-11709
- Human and animal controlled self rotating maneuvers during free fall, comparing theoretical motion analysis with photographs of falling cats
04 p0478 A72-14709
- Hydrodynamic characteristics of freely falling water droplets in air, establishing relationships among Reynolds, Laplace and Bond criteria
07 p1030 A72-19854

- Supercooled cloud water droplets in free fall shattered by shock waves measuring ice crystal formation probability
09 p1345 A72-22446
- Neutral gas velocity distribution, transverse drift velocity, particle and energy densities in column under free fall conditions, considering wastage by ionization processes
11 p1698 A72-26645
- Spacecraft free fall trajectory calculation, using numerical optimization procedure based on Hamilton principle for two point boundary value problems
16 p2460 A72-34021
- The geometry of free fall and light propagation
20 p2954 A72-40005
- Experimental determination of fall rate of 'N5' chaff on the heights 50-90 km
21 p3049 A72-41498

FREE FLIGHT

- Inclined wind tunnel test section for free gliding investigation and aerodynamic design of flexible wing two body system
15 p2213 A72-31403

FREE FLIGHT TEST APPARATUS

- Free flight simulation tests for V/STOL aircraft nonlinear attitude control system adaptation to helicopter pitch and roll control
[DGLR PAPER 71-060] 02 p0155 A72-12714
- High speed photographic pyrometer for surface temperature measurements on aerodynamic models during free flight in aeroballistic range
15 p2237 A72-32050
- Free flight follower support system with data reduction for V/STOL or helicopter models, recording flight path and attitude angles
16 p2372 A72-32886
- Bi-planar wind tunnel free flight test and instrumentation for difference between nonplanar and planar dynamic stability of blunt and sharp half cones, providing angular documentation
[AIAA PAPER 72-983] 22 p3163 A72-42331
- Free-flight projectiles aerodynamic characteristics and trajectories from yawsonde and radar track data, obtaining best fit coefficients by equations of motion numerical integration
[AIAA PAPER 72-978] 22 p3134 A72-42335
- Telemetry acquisition of aerodynamic heat rates to conical, free-flight models at Mach 6 in an aeroballistic range
22 p3155 A72-42703

FREE FLOW

- Shock wave propagation from channel in free space for various Mach numbers, using method of characteristics
02 p0202 A72-11590
- Free stream and shock layer disturbances effect on hypersonic boundary layer transition in wind tunnels from hot wire measurements
02 p0230 A72-12274
- Transition on plane plate in presence of vortices detached from cylinder in free flow
03 p0342 A72-13788
- Initial boundary layer effect on turbulent free shear layer velocity profiles, deriving procedure applicable at any streamwise station
05 p0645 A72-15795
- Flat plate boundary layer transition equations for supersonic wind tunnels, taking into account free stream turbulence
08 p1150 A72-21616
- Numerical analysis of capture area ratio effect on shock wave propagation from free stream into moving flowing duct
08 p1150 A72-21619
- Laminar free convective flow of viscoelastic fluid past infinite porous plate
08 p1151 A72-21748
- Unsteady laminar boundary layer on semiinfinite flat plate induced by small free stream velocity fluctuations, showing far downstream double layer structure via asymptotic and numerical solutions
[AD-745486] 10 p1467 A72-24334
- Uniform flow past semiinfinite flat plate for large Reynolds numbers and strong blowing, noting injected fluid region separation from free stream by shear boundary layer
10 p1467 A72-24369
- Fast and slow ion acoustic free streaming wave propagation in drifting plasma, showing phase velocity and damping in agreement with Maxwellian distribution
11 p1692 A72-25518
- Constant density solutions for flow fields behind concave shock waves, noting approximation for transonic free stream Mach numbers
11 p1572 A72-25919
- Turbulent free shear flow intermittency factor determination by electronic circuit, discussing calibration and errors
11 p1617 A72-25997
- Noise generated by free flow turbulence incident on rotor or stator in axial flow fans and compressors, noting sound spectrum dependence
13 p2028 A72-29575

- French monograph on turbulent free flow boundaries covering two dimensional plane jet mixing zone characteristics from thermal signal measurements
14 p2095 A72-30948
- Nonlinear instability of two dimensional unbounded incompressible viscous fluid flows under periodic small perturbation
16 p2376 A72-32933
- Simplified conservation laws for finite-difference computations
20 p2946 A72-39637
- An approximate method for solving problems involving separated flows past bodies
21 p2990 A72-41088

FREE JETS

- Laminar free jets characteristics, investigating transition to turbulence
02 p0150 A72-11730
- Induction heated low density supersonic free plasma jet diagnosis, determining velocities and heavy particle temperatures
02 p0265 A72-12361
- Acoustical oscillations effect on free jet flow stability and boundary layer structure, using inviscid Orr-Sommerfeld equation for flow disturbances frequency, wavelength and velocity
03 p0340 A72-12913
- Method of characteristics calculations of inviscid free jet flow with low specific heat ratios for perfect gas at 1.10 Mach number
03 p0309 A72-13926
- Finite difference scheme for collision of two axially symmetric liquid jets with free boundary in cylindrical coordinate system
03 p0344 A72-14370
- Interaction produced by diametrically opposed plane turbulent wall jet collision in still air, discussing resultant free jet
[AIAA PAPER 72-211] 05 p0606 A72-16854
- Axial structure of free air jet in rarefied atmosphere, measuring pressure and density
06 p0797 A72-17561
- Supersonic plasma flow in narrow rectangular channel and free incompressible inviscid conducting liquid jet motion within pulsating transverse magnetic field
08 p1214 A72-21652
- Free turbulent jet heat and mass exchange and axial flow characteristics
09 p1292 A72-22235
- Wear resistance of steel and Ti alloys in free abrasive gas jet, noting surface microhardness increase effect
09 p1319 A72-23188
- Drazin method application to thermal stratification effects on unbounded jets and shear layers stability characteristics
11 p1615 A72-25552
- Intermolecular collisions distribution on centerline of freely expanding axisymmetrical jet, using ellipsoidal statistical model and simplified transport equations
11 p1615 A72-25557
- Molecular scattering in free jet expansion, using spherical source and two component background gas mathematical models
11 p1615 A72-25558
- Anomalous excitation of nitrogen positive bands in seeded Ar free plasma jet, measuring oscillator strengths of atoms
14 p2140 A72-30899
- Frictionless, Helmholtz and flat jet incompressible flows from slot in thick plane wall, comparing characteristics with free jet vicinity
15 p2216 A72-31464
- Potassium atomic beam aerodynamic acceleration by He-Ar free jet, determining beam intensity as function of nozzle-skimmer distance, carrier gas pressure and nozzle temperature
16 p2429 A72-33056
- Free jet reenergization efficiency, mixing distance and similarity analysis for boundary layer control at sharp trailing edges and cusps
[AIAA PAPER 72-700] 16 p2345 A72-34043
- Interaction between free oil jets and plates of various profiles
17 p2539 A72-34915
- Combustion driven resonance tubes
17 p2597 A72-34974
- Heat mass and momentum transport in free turbulent mixing
17 p2543 A72-35638
- The turbulence diffusion in free jets and flames
18 p2740 A72-36245
- Free hot jet turbulence space-time correlation function measurement based on IR detection
18 p2680 A72-36468
- Free gas jets turbulent mixing flow, considering development of submerged air jet with action of mechanical turbulence generator ahead of nozzle
20 p2913 A72-39367
- Study of the flow of a heavy fluid with free surface from a symmetrical tank
20 p2913 A72-39417

Two dimensional underexpanded free jet flow into static medium, presenting wind tunnel nozzle experimental data and graphic solutions from method of characteristics
20 p2885 A72-39619

The lift coefficient of a supercavitating jet-flapped foil in a free jet.
21 p2992 A72-41236

Simulation of the interaction of high altitude plumes and a high-speed free-stream flow.
[AIAA PAPER 72-1019] 21 p3042 A72-41598
Diffusion of a filament of gas injected into a supersonic free jet.
23 p3280 A72-43947

FREE MOLECULAR FLOW

Magnetosphere deformation by solar wind, comparing accuracy of free molecular flow and double dipole models
02 p0218 A72-11948

Impulsive spatial interaction model between monoenergetic molecular beam and rough isotropic rigid metal surface in free molecule flow
03 p0392 A72-14058

Gas-metal surface interactions effect on aerodynamic lift and drag coefficients in free molecular flow
03 p0342 A72-14059

Nearly free molecular slit flow of gas from reservoir at finite pressure and temperature ratios
04 p0512 A72-15120

Flat plate, sphere and circular cylinder drag and lift coefficients in free molecular flow
04 p0463 A72-15645

Free molecular flow heat transfer to rough surface, discussing surface/molecule interaction model for digital simulation
[ASME PAPER 71-WA/HT-8] 05 p0743 A72-15868

Heat transfer, drag and lift coefficients for free molecular flow over concave surfaces, describing Monte Carlo simulation technique
[ASME PAPER 71-WA/HT-17] 05 p0744 A72-15876

Flow field quantities for nearly free axisymmetric steady molecular gas flow through circular orifice from high pressure region into vacuum
06 p0800 A72-18118

High altitude rocket plume rarefaction effects, predicting inviscid, merged, transition, first collision and free molecular flow regimes
08 p1128 A72-21610

Pitot tube pressure measurements in supersonic gas flow, calculating free molecular conditions limits
10 p1419 A72-24548

Thermosphere temperature measurement by high velocity probe, admitting atmospheric sample via free molecular flow inlet
12 p1806 A72-27044

Magnetosphere deformation by solar wind, comparing accuracy of free molecular flow and double dipole models
13 p1949 A72-29260

Kinetic freezing effects of supersonic gas flow with solid particles into vacuum, analyzing continuous to collisionless transition flow for Maxwell molecules
14 p2094 A72-30295

Mesospheric air density and temperature measurements from rocket-borne resistance thermometers based on free molecular flow
15 p2225 A72-31911

Optimum nonslender bodies of revolution minimum drag in free molecular flow under integral constraints
15 p2180 A72-32395

Free molecular flow over rotating sphere satellite, deriving aerodynamic forces on differential surface to determine drag and lift coefficients
16 p2341 A72-32844

A semiempirical method for the evaluation of aerothermodynamic properties in the intermediate hypersonic flow regimes.
[ICAS PAPER 72-03] 21 p2990 A72-41128

Rarefied gas flow through a slit.
24 p3395 A72-45572

FREE OSCILLATIONS

U FREE VIBRATION

FREE RADICALS

Mesospheric OH volume density profile measurements by rocket-borne high resolution polarized Ebert-Fastie spectrometer
01 p0062 A72-10912

Free radicals participation in cell membrane biopotential generation mechanism, comparing properties of protein molecules with semiconductors
02 p0169 A72-12348

Free atoms and radicals elementary reactions, passing parent molecules through electrodeless rf or microwave discharge at various pressures and temperatures
03 p0320 A72-13392

Carbon monoxide oxidation by hydroxyl radicals at high and low temperatures from transition state theory, confirming flame and shock tube results
[WSCI PAPER 71-36] 04 p0482 A72-14584

Free radicals formation during elastomers mechanical degradation by grinding below and above glass

transition point at liquid nitrogen and room temperatures
04 p0484 A72-15264

Rate constant for quenching of B /super 2/Sigma-plus state of CN radical as function of quenching collision relative velocity and total pressure in fluorescence cell
04 p0553 A72-15635

Ethyl radicals reactions in shock tube produced pyrolysis of azoethane, using time of flight mass spectrometer
07 p0935 A72-19433

Interstellar free radicals and molecules spectra, noting catalyzers, temperature and abundances role
11 p1722 A72-26434

UV light production of free radicals in proteins and model compounds in vacuum and low temperatures, using EPR techniques
12 p1778 A72-27223

Stellar OH radical emission amplification by maser effect raising low energy molecules to high energy by pumping
14 p2110 A72-30578

Existence, structure and thermodynamic and kinetic stability of CIOO radical in Venus atmosphere, using quantum statistics methods for unimolecular decomposition rate
18 p2726 A72-36647

Molecular orbital calculation of the isotropic hyperfine interactions in triatomic nitrogen radicals.
21 p3013 A72-40564

Biology and molecular biophysics progress review, discussing synthetic semibiological systems, molecular pathology, free radicals and longevity
22 p3142 A72-42474

A shock tube determination of the electronic transition moment of the CN red band system.
23 p3316 A72-44329

Quantitative evaluation of the kinetics of free-radical processes in animal organs under hypoxic conditions
24 p3371 A72-44596

The structure and formation of comets.
24 p3445 A72-45464

FREE STREAM EFFECTS

U FREE FLOW

FREE STREAMS

U FREE FLOW

FREE VIBRATION

Flexural vibrations of arbitrary ring with axial symmetric cross section, noting validity for natural frequencies prediction
01 p0138 A72-10395

Lateral vibration of thin conical bar with clamped base and free tip, calculating characteristic modes and frequencies
01 p0138 A72-10509

Static loads effect on natural vibrations of thin truncated conical shells by shallow shell theory, determining resonant frequency spectrum due to prestressing
01 p0142 A72-11362

Natural vibrations of closed crosswise reinforced orthotropic circular cylindrical shells, using digital computer solution
01 p0142 A72-11363

Barrel shaped cylindrical shell stability and free vibrations under torque, evaluating distortion influence by small parameter method
01 p0142 A72-11364

Natural vibrations and resonant stresses of turbomachine blade rings and elastic bodies with cyclic symmetry, noting paradoxical frequency decrease
01 p0143 A72-11369

Natural bending-torsional vibrations of turbine blades connected by ring junctions, using dynamic pliability principle
01 p0143 A72-11370

Moving load effect on circular cylindrical shell in acoustic medium, discussing free axisymmetric vibration mode, shape and frequencies
02 p0290 A72-11627

Vertical thin circular cylindrical shells partially or completely filled with stationary liquid, determining free vibration characteristics with finite element theory
02 p0293 A72-12371

Homogeneous isotropic elastic medium free vibration in unbounded space, obtaining relativistic relations in wave field from mathematical model
03 p0389 A72-13425

Symplectic structure of continuous system, constructing relativistic free vibrating cord without linearization
03 p0389 A72-13792

Free vibration and buckling of orthotropic skew plates with different edge conditions, using Ritz variational method
04 p0584 A72-14508

Forced and free transverse vibrations of flat rectangular plates with attached concentrated masses
04 p0584 A72-14521

Three dimensional analysis for free vibrations of simply supported viscoelastic rectangular plates
04 p0585 A72-14841

Conforming rectangular and triangular finite elements for plate free vibrations analysis in bending
04 p0585 A72-14846

Linearized equilibrium equations for thin spherical shell with internal pressure, obtaining free vibration modes
04 p0587 A72-15018

Lunar surface gravimeter experiment to search for gravitational radiation from cosmic sources exciting moon if free oscillations
04 p0509 A72-15105

Concentrated inertias effects on cantilever beams and shafts free vibrations by Laplace transform technique
04 p0591 A72-15276

Wave harmonics method application to problems of free oscillations in longitudinally regular screened waveguides partially filled with homogeneous isotropic media
04 p0488 A72-15379

Circular disks, rings and perforated plates steady state field components, evolving forced and free vibration natural frequency equations
04 p0592 A72-15505

Free oscillations of liquid masses contained in tanks, analyzing variational and Ritz methods
04 p0513 A72-15557

Large deflection microstructure continuum model for composite beam flexural wave propagation and free vibration, deriving equations of motion
[AIAA PAPER 72-140] 05 p0741 A72-16937

Uniformly curved fluid conveying tube free vibration and stability, showing flow velocity, fluid pressure and Coriolis force effects on natural frequency
06 p0821 A72-17853

Spectral properties of differential displacement equations system describing natural vibrations of shell of revolution with m waves along parallel
06 p0897 A72-17990

Autonomous two body system described by nonlinear differential equations of motion, obtaining free relative vibration solution in terms of elliptic functions
06 p0849 A72-18694

Rigid shaft rotating in hinged and elastic supports with nonlinear characteristics of restoring force, determining free and forced vibration characteristics
06 p0900 A72-18696

Free vibration determination method for thin rectangular plate with arbitrary boundary conditions and thickness variations
07 p1092 A72-19857

Trapped modes structure of rotating fluid in thin spherical shell, noting constitution of free oscillation periods
07 p0973 A72-20455

Axially nonuniform thin cylindrical shells dynamic analysis, obtaining free flexural vibration characteristics by hybrid of finite element and classical shell theories
07 p1097 A72-20531

Oscillographic transient analysis of electric spark machining processes with electrode natural or forced vibrations
08 p1174 A72-21037

Free oscillations frequencies and mode shapes determination of two parallel elastically coupled rods of variable cross section, applying Bubnov-Galerkin iterative method
08 p1243 A72-21231

Numerical solution of disintegration and surface stability of gas bubbles under nonspherical free oscillation
08 p1149 A72-21295

Linear inverse problem of coefficient matrix eigenvectors, implying surface waves and free oscillations for earth structure
08 p1159 A72-21495

Electron beam interaction with bounded homogeneous plasma layer natural oscillations, using collisionless kinetic equation
08 p1215 A72-21720

Thin viscoelastic beam free oscillations and material properties description by Volterra type nonlinear integral equation
08 p1249 A72-21869

Soviet book on longitudinal vibrations of rocket with liquid propellant engine covering rocket element dynamic characteristics and free vibration mode shape and frequency calculations
08 p1241 A72-22025

Nonlinear programming analysis of free vibration of simply supported beam
08 p1249 A72-22136

Mechanical system with inertial vibration skewer and nonlinear spring, obtaining global asymptotic stability of zero solution of differential equations describing natural vibration
09 p1399 A72-22697

Perturbation analysis of nonlinear free flexural vibrations of circular cylindrical shell, using Donnell equations
09 p1405 A72-22998

Resonant frequencies of viscous liquid in rectangular tank calculated from stream functions, assuming two dimensional oscillations and laminar flow

09 p1295 A72-23074

Circular plates free flexural vibrations with and without damping, calculating resonant frequencies from corresponding Bessel functions

10 p1555 A72-24194

Natural axisymmetric vibration of thin elastic shell of revolution, deriving eigenvalues convergence to spectrum lower bound by asymptotic method

10 p1557 A72-24429

Free flexural vibration of truncated conical shells, using Galerkin method and Donnell type basic equation

10 p1559 A72-25024

Nonlinear dynamic response of single elastic cables with low initial tension, examining free and forced vibrations with incremental deformations theory

10 p1560 A72-25185

Free in-plane vibrations of hinged and fixed uniform circular arches, discussing natural frequencies and flexural and extensional vibration modes

10 p1560 A72-25186

Optimal parameters selection for natural vibrations maximum damping rate, applying method to two mass electromechanical system

11 p1686 A72-25533

Shrouded propellers and rotor blades free vibrations determination by variational method, showing Coriolis effect on critical flutter speed

11 p1732 A72-25536

Cylindrical panel natural vibrations, describing motion of base with dynamic elasticity equations

11 p1733 A72-25539

Plasma layer effect on natural oscillations of magnetosphere tail, using infinite plasma cylinder model immersed in interplanetary plasma

11 p1622 A72-25944

Finite difference method for free vibration of axisymmetric shells, using inertia force terms in shell bending theory equilibrium equations

11 p1737 A72-26429

Lowest natural vibration frequencies of conical shell for various boundary conditions, using finite difference scheme

12 p1878 A72-27081

Finite element method application to variable thickness circular and annular plates free transverse vibration

12 p1879 A72-27191

Convergence of plate bending eigenvalue solutions from conforming displacement finite elements based on thick plate free vibration conversion to isoperimetric variational problem

12 p1879 A72-27194

Natural vibration modes of coupled spring-mass nonlinear system with two degrees of freedom from stability analysis

12 p1844 A72-27245

High power pulse generation by ruby laser under free oscillation, using resonator with dielectric mirrors

12 p1821 A72-27597

Emission characteristics of single mode ring ruby laser under free oscillation conditions, discussing mode selection difficulties

12 p1821 A72-27598

Thin circular plate free vibrations with mixed boundary conditions from differential equations for vibration modes of circular isotropic plate in dimensionless polar coordinates

13 p2053 A72-28395

Numerical analytical determination of natural vibration frequencies for membrane elastically clamped along portion of contour, using method of summary representations

13 p2004 A72-29078

Finite element method for in-plane free vibrations of shear wall type structures, noting rectangular plate elements with six degrees of freedom per node

13 p2057 A72-29092

Free and forced vibrations of circular plates with associated rigidities and masses, obtaining orthogonality condition for natural vibration modes

13 p2059 A72-29501

Eigenstate field parameter bounds in elastomechanics natural vibration problems

13 p2059 A72-29598

Spectral properties of differential displacement equations system describing natural vibrations of shell of revolution with m waves along parallel

14 p2163 A72-30217

Equations of motion and free vibration for trusswork structures under nonperiodic dynamic loads, calculating longitudinal and transverse end forces

15 p2322 A72-31360

Nonlinear analysis of helicopter rotor blade free transverse vibration under air and centrifugal loadings during forward flight, using matrix method

15 p2323 A72-31407

Properties of natural waves excited in Fabry-Perot resonator by external laser beams, noting stability dependence on wave type

15 p2245 A72-31420

Green operator first invariant upper bound for free oscillations eigenvalue upper limit, exemplifying for quadratic plate with two free and two clamped edges

15 p2274 A72-31459

Large deflection vibrations of free circular plate of lenticular section with constant temperature gradient through thickness, noting thermal stresses effect

15 p2325 A72-31552

Variable cross section rod free longitudinal and torsional vibration frequencies and mode shapes determined by slowly varying parameters approximation method

15 p2327 A72-31740

Elastic shell initial stress effects on dynamic response in all free vibration modes, considering transverse shear and normal strains

15 p2328 A72-32021

Cantilever beam tapered linearly in horizontal and vertical planes, obtaining computer solution for free transverse vibration fundamental frequency and harmonics

15 p2328 A72-32022

Quantitative measure for sensitivities of natural frequencies to perturbations leaving modes invariant

15 p2278 A72-32279

Preloaded thin walled open section elastic column dynamic stability under free longitudinal vibrations, deriving criterion for flexural and torsional vibrations nonlinear coupling

15 p2332 A72-32560

Free and forced vibrations of two dimensional grids with simple and bridge-type boundary conditions, presenting closed form solutions for nodal deflections and moments

15 p2332 A72-32561

Atmospheric motions prediction with numerical model based on discrete stratified fluid free oscillations

15 p2266 A72-32720

Free small steady oscillations of liquid in solid tanks, considering HF modes

16 p2375 A72-32931

Natural vibration frequency spectra of circular cylindrical and spherical shells of revolution, using Bessel function

16 p2465 A72-32936

Natural frequency of free beam-like vibration of coupled fluid/structural system of cylindrical rod submerged in ideal fluid enclosed by cylindrical shell

16 p2465 A72-32985

Singular perturbation methods for deflections, frequencies and eigenmodes of statically loaded or freely vibrating circular or annular membrane

16 p2467 A72-33106

Natural frequencies and vibration modes of free glider, using symmetrical matrix to replace three dimensional structure by approximate model

16 p2348 A72-33409

Coupled thermoelastic theory for thin plates, using perturbation method to find free vibration frequencies of plates under various boundary conditions

16 p2471 A72-33785

Matrix progression method analysis of free vibration problem for cantilever thin circular cylindrical elastic shells, using Flugge equations

16 p2475 A72-34173

Free vibrations of elastic plate with random properties - The eigenvalue problem.

17 p2623 A72-34228

Stability analysis of a pinned-end beam undergoing non-linear free vibration.

17 p2623 A72-34236

Large amplitude vibration of a circular plate with concentric rigid mass.

[ASME PAPER 71-APMW-11] 17 p2625 A72-34319

Finite length inhomogeneous elastic rod free vibration, deriving asymptotic expressions for eigenvalues and eigenfunctions

17 p2625 A72-34320

Free vibrations analysis of linear aerodynamic conservative structures in elastic range by finite element method, applying to transient or random forced responses calculation

17 p2626 A72-34742

Transverse vibration of a viscoelastic beam carrying an arbitrary number of mass bodies.

17 p2631 A72-35053

Finite element analysis of the axisymmetric vibrations of cylinders.

17 p2634 A72-35409

The effects of damping on a non-linear system with two degrees of freedom.

18 p2709 A72-36080

Free vibration mode shapes mapping of spherical and paraboloidal plastic shells under acoustic excitation via noncontact fiber optics instrumentation

18 p2690 A72-36372

Anisotropic rectangular plate free flexural vibration improved solution via Fourier analysis

18 p2734 A72-36419

Shell of revolution natural vibration spectrum, investigating moment and momentless type systems of differential equations

18 p2735 A72-36665

Elastic momentless shell completely filled with ideal incompressible liquid, detailing small steady free vibrations

18 p2681 A72-36667

Free vibrations of a spherically isotropic hollow sphere.

18 p2736 A72-37004

Free vibrations of multilayer sandwich plates in the presence of in-plane loads.

19 p2876 A72-38020

Free vibrations of finite element plates subjected to complex middle-plane force systems.

21 p3116 A72-40330

Free and forced trapped oscillation properties in inviscid rotating fluid, considering modifications for viscosity

21 p3049 A72-40654

Application of methods in perturbation theory to the calculation of the natural vibrations of rod systems

21 p3119 A72-41097

A new method of calculating the natural vibrations of a free airplane.

21 p3120 A72-41130

Free vibrations of a system with a generalized piecewise-continuous characteristic

21 p3122 A72-41349

Free oscillations of a liquid rotating in a cylindrical vessel under conditions of weightlessness

22 p3165 A72-42251

The use of simple three-dimensional acoustic finite elements for determining the natural modes and frequencies of complex shaped enclosures.

22 p3206 A72-42464

Free oscillations of the sun and their possible stimulation by solar flares.

22 p3219 A72-42570

Nonlinear natural vibrations of rectangular plates and cylindrical panels

22 p3242 A72-43134

Nonaxisymmetric vibrations of arbitrarily thick circular cylindrical shells

23 p3345 A72-43624

Bearing supports elasticity effect on pendulum vibration of rigid rotating shaft with disk, noting vibrational frequencies relation to resonant frequencies

23 p3293 A72-43668

Spline transformation of independent variable for free transverse vibration of elastic bars with piecewise constant rigidity, calculating resonant frequencies

23 p3348 A72-43793

On free vibrations at temperature-dependent material properties and transient temperature fields.

[ASME PAPER 72-APM-J] 23 p3350 A72-44053

Free vibrations of an arbitrary structure in terms of component modes.

[ASME PAPER 72-APM-T] 23 p3350 A72-44054

Equivalent linear solution for transient free vibration of beams with strain dependent, frequency independent stress-strain hysteresis loop with sharp corners

23 p3352 A72-44120

Free flexural vibrations of an elliptical plate with simply supported edge.

23 p3352 A72-44121

The coupled transverse vibrations of a spinning membrane disk with a central hub.

23 p3355 A72-44367

Vibration characteristics of cylindrical shells with several axially equipaced constraints.

23 p3355 A72-44371

Non-linear free vibration of a beam with time-dependent material properties.

23 p3355 A72-44374

Non-linear flexural vibration of orthotropic skew plates.

23 p3355 A72-44375

Free-transverse vibrations of an axially moving mass.

23 p3355 A72-44457

Free vibration frequencies and critical buckling loads for thin walled shells of revolution constructed out of layered or heterogeneous anisotropic materials

24 p3455 A72-44676

Free vibrations of thick, layered cylinders having finite length with various boundary conditions.

24 p3425 A72-44884

Preliminary design of a sailplane wing for dynamic gust loads

24 p3368 A72-44992

Numerical analysis of natural frequency spectrum of plastic plate free vibrations in compressible inviscid fluid

24 p3459 A72-45003

Forced and free vibrations of shallow cylindrical shell in rectangular duct filled with ideal fluid

24 p3459 A72-45004

Limitations in the acquisition of nonlinear aerodynamic coefficients from free-oscillation data by means of the Chapman-Kirk technique.

24 p3362 A72-45336

A method of determining the eigenfrequencies of closed circular conical plates in the Vlasov-Mustari hypothesis

24 p3459 A72-45441

FREEZING
 NT VIBRATIONAL FREEZING
 NT ZONE MELTING
 Freezing of hot fluid flowing onto flat cold wall, solving nonlinear integrodifferential equation for temperature distribution by iteration method
 04 p0595 A72-14650
 Acoustic measurement of solid-liquid interface motion and solidification during freezing of Hg and paraffins
 10 p1563 A72-25044
 Thermodynamic freezing theory of small solution droplets containing insoluble particles, considering ammonium sulfate concentration for ice formation in clouds
 16 p2476 A72-33380
 Freeze etching techniques in electron microscopic investigations of biological cells molecular structure
 18 p2653 A72-36829
 Three-phase heat transfer - Transient condensing and freezing from a pure vapor onto a cold horizontal plate - Analysis and experiment.
 22 p3243 A72-41957

FREEZING POINTS
 U MELTING POINTS

FREIGHT COSTS
 Air cargo growth potential, marketing and profitability, considering need for improvements in ground handling, rate structure, container standardization, documentation, etc
 13 p1896 A72-28452

FREIGHTERS
 Transoceanic helium cooled thermal reactor powered air cushion freighter of gross weight 4500 metric tons, discussing design and performance characteristics
 04 p0464 A72-14431
 Potential effects of air cushion vehicle (ACV)/ multithousand ton freighter on city development
 05 p0752 A72-15776

FRENCH SATELLITE
 NT EOLE SATELLITES

FRENCH SPACE PROGRAMS
 Frequency planning for Symphonie German-French telecommunication satellite microwave equipment
 01 p0030 A72-10710
 Soviet-French Project Omega for near space disturbance studies, using ground and balloon measurements at conjugate points
 01 p0063 A72-11075
 Diamant B launcher first stage Valois rocket motor combustion if, acoustic mode and if instabilities
 [ONERA, TP NO. 1027] 03 p0406 A72-13641
 Symphonie communication satellite technology application to subsequent satellites, discussing three axes stabilization, use of microwave frequencies, components and subsystems reliability
 04 p0494 A72-15681
 French Lyman alpha photometer experiment on OGO 5 satellite, describing geocoronal observations, extraterrestrial emission and Bennett and Encke comets hydrogen envelopes
 04 p0582 A72-15684
 D-2A satellite antisolar mission, examining Lyman alpha emission from geocorona and interstellar hydrogen wind
 04 p0582 A72-15688
 D-2B satellite mission, describing attitude, orbit and experiments on zodiacal light, stellar radiation and antisolar data
 04 p0583 A72-15689
 Geodetic satellite systems applications, describing trajectory beacons, telecontrol and telemetry stations and computing and operations center of French Geole system
 06 p0809 A72-18258
 French space applications program for telecommunications, meteorology, natural resources survey and air/sea traffic control
 08 p1256 A72-21201
 Satellite communication activities on French national level, European multinational level/Symphonie/and worldwide level/Intelsat/
 08 p1132 A72-21202
 French Geole satellite system for geodetic survey, discussing frequency selection, antenna problems, distance measuring equipment and instrument errors
 08 p1158 A72-21206
 French R and D work on ion propulsion systems for communication satellite stabilization, discussing principal characteristics, mathematical modeling, design and economic problems
 [AIAA PAPER 72-437] 11 p1727 A72-26179
 Report to COSPAR on French space program covering ionospheric and magnetospheric physics, meteorology, earth resources and exobiology
 15 p2337 A72-32003
 French aerospace industry difficulties in procuring parts, suggesting purchasing centralization or setting up of parts stocks
 17 p2639 A72-35951
 Development and production of French high-reliability components: The Concerto Program - The CNES-Concerto certificate
 18 p2744 A72-37136

SRET-1 'solar cells'
 French space program management planning, discussing orientation, operation and control of activities
 19 p2869 A72-37822

FRENKEL DEFECTS
 German monograph on Frenkel defect structures in thin gold wire at high electron irradiation dose, using electrical resistance measurements
 19 p2884 A72-38566

FREON
 Clinical and laboratory examinations of workers exposed to trichlorofluoroethane vapor for long range health effects study
 10 p1431 A72-24590
 Freon 30 bidistillate as washing liquid for flight vehicle hydraulic systems, discussing industrial methylene chloride purification
 11 p1675 A72-26818
 Boundary conditions influence on heat and mass transfer in low temperature heat pipes with freon as working fluid
 16 p2479 A72-33853
 Investigation of Freon fire-extinguishing systems with a nucleonic gage.
 18 p2648 A72-36674
 Thermal control design for research applications module (RAM) shuttle compatible payload carriers, using Freon 21-water system
 [ASME PAPER 72-ENAV-31] 20 p2894 A72-39146

FREQUENCIES
 NT AUDIO FREQUENCIES
 NT BEAT FREQUENCIES
 NT BROADBAND
 NT C BAND
 NT CARRIER FREQUENCIES
 NT CRITICAL FREQUENCIES
 NT CYCLOTRON FREQUENCY
 NT EXTREMELY HIGH FREQUENCIES
 NT EXTREMELY LOW FREQUENCIES
 NT EXTREMELY LOW RADIO FREQUENCIES
 NT HIGH FREQUENCIES
 NT INFRASONIC FREQUENCIES
 NT INTERMEDIATE FREQUENCIES
 NT IONIZATION FREQUENCIES
 NT LOW FREQUENCIES
 NT LOW FREQUENCY BANDS
 NT MAXIMUM USABLE FREQUENCY
 NT MICROWAVE FREQUENCIES
 NT PLASMA FREQUENCIES
 NT RADIO FREQUENCIES
 NT RESONANT FREQUENCIES
 NT SUPERHIGH FREQUENCIES
 NT SWEEP FREQUENCY
 NT ULTRAHIGH FREQUENCIES
 NT VERY HIGH FREQUENCIES
 NT VERY LOW FREQUENCIES

FREQUENCY AMPLIFIERS
 U AMPLIFIERS

FREQUENCY ANALYZERS
 Multichannel frequency spectrum analyzer for single radio pulse component frequency measurement
 07 p0988 A72-19960
 Dynamic verification of a digital flight control system.
 18 p2673 A72-36336
 Frequency detection with digital resonators without damping
 19 p2773 A72-37939
 Electronic analyzer of structural vibration frequency characteristics and mutual spectra, considering bandpass filter and automatic frequency spectra recorder
 22 p3176 A72-42134

FREQUENCY ASSIGNMENT
 Spacecraft-ground communications system, discussing electromagnetic wave propagation and frequency bands
 01 p0027 A72-10445
 Frequency planning for Symphonie German-French telecommunication satellite microwave equipment
 01 p0030 A72-10710
 International frequency allocation table revision by World Administrative Radio Conference for Space Telecommunications
 02 p0177 A72-12385
 Frequency allocation for space research, radio astronomy, time signal and earth resources exploration, reviewing allowable power flux density and emitter power
 02 p0177 A72-12386
 Frequency sharing criteria for terrestrial and space services, showing improved radio spectrum utilization and permissible interference
 02 p0178 A72-12388
 EMC criteria for sharing frequency bands between communication satellite and terrestrial microwave radio relay systems
 03 p0324 A72-14045
 Graphical and tubular methods for frequency assignment to avoid intermodulation interference in channelized bands
 03 p0325 A72-14046

Optimum manned spacecraft electrical power distribution voltage and frequency selection, discussing corona, radiation and safety
 03 p0313 A72-14187

Communication satellites rf assignment by ITU for prevention of jamming, discussing radio communication conferences regulatory actions
 07 p1104 A72-19469

International cooperation in space law problems, considering space communication systems, geostationary orbits use, frequency band allocation, world weather watch and earth resources survey programs
 07 p1105 A72-19475

Frequency allocation effectiveness and mutual interference calculation for adjacent geostationary communication satellites
 07 p0943 A72-19563

Direct broadcasting communication satellites, discussing frequency allocation, modulation and data processing systems
 07 p0948 A72-20266

Geostationary communication satellites and terrestrial radio relays frequency sharing, controlling interference by flux density and transmitter power limitation
 07 p0948 A72-20490

French Geole satellite system for geodetic survey, discussing frequency selection, antenna problems, distance measuring equipment and instrument errors
 08 p1158 A72-21206

Inexpensive solid state microwave sources development and applications considering spectrum allocations, health hazards and reliability problems
 09 p1285 A72-22595

Satellite technology for TV broadcasting service to Canadian remote areas, considering new frequency band allocation
 [AIAA PAPER 72-553] 12 p1781 A72-27373

Communication aspects of aeronautical satellite system, considering aircraft equipment, ground stations, ATC, type of access and frequency assignment
 12 p1783 A72-27658

Tactical satellite communication system and ground terminal design options for efficiency improvement, considering power sharing, priority system frequency allocation and system control concepts
 12 p1785 A72-27844

Linear radio receiver circuit synthesis for output signal structure and rational selection, using reduction algorithm
 15 p2202 A72-32705

Feasibility of collocating a radio relay station with a sharing earth station.
 17 p2512 A72-34268

Electromagnetic compatibility and interference problems of radar altimeters, collision avoidance systems and air and marine mobile satellite communication equipment in 1600 MHz region
 20 p2901 A72-38977

Frequency sharing between broadcast satellites and tropospheric scatter systems.
 20 p2901 A72-38978

Frequency assignment for collocated transmitters using the branch-and-bound technique.
 20 p2901 A72-38986

Book - Eleventh report by the International Telecommunication Union on telecommunication and the peaceful uses of outer space.
 20 p2988 A72-39025

Multiple-frequency operation of the Culgoora radioheliograph.
 21 p3053 A72-40397

Utilization of frequency bands allocated to satellite broadcasting for regional or domestic systems.
 21 p3018 A72-40875

Orbital and frequency sharing between the broadcasting-satellite service and the fixed-satellite service.
 21 p3018 A72-40877

Commercial satellite communication system development, considering external constraints, orbital geometry, frequency allocations, multiple access transmission techniques, and satellite and earth station designs
 21 p3021 A72-40921

Frequency allocation effectiveness and mutual interference calculation for adjacent geostationary communication satellites
 22 p3153 A72-42081

FREQUENCY CONTROL
 NT AUTOMATIC FREQUENCY CONTROL.
 Axial mode locking and equidistant frequency generation in solid state lasers due to active medium saturation, using self consistent equations with broadened amplification line
 01 p0079 A72-10347
 Extremal system with second control loop for search signal frequency regulation to optimize primary loop operation, determining system dynamic errors under random drift
 02 p0197 A72-12340
 Optimal synthesis of pulse repetition frequency control and filtering circuits of radar range finder in Gaussian approximation
 02 p0183 A72-12759

Traveling wave Ar laser with only fundamental TEM modes, examining mode self locking and composition and intensity as functions of frequency misalignment
03 p0366 A72-13366

Narrow band electrically controlled interferential polarization filter with fine tuning capability for solar physical research, discussing design and operation
03 p0357 A72-13369

Stability and perturbation of oscillator system with frequency fixed by all pass ring transmission function with delayed amplitude regulation
03 p0331 A72-13410

Passively mode locked Rhodamine 6G dye laser, obtaining frequency tuning with intracavity Fabry-Perot filter and transform limited duration picosecond pulses
03 p0368 A72-13605

Three terminal voltage-tunable Gunn effect microwave oscillator, discussing depletion depth and electric field control modes for frequency
04 p0496 A72-14479

Aircraft turbo-alternator speed control for constant frequency power supply, presenting theoretical relationships for electrohydraulic or mechanohydraulic control loops
04 p0466 A72-15462

Dye laser monochromatic coherent light wavelength tuning with minimized optical cavity degradation and without external optics
04 p0531 A72-15502

Tunable coherent IR signal generation and propagation by mixing carbon dioxide laser and millimeter wave klystron output in GaAs loaded waveguide
04 p0532 A72-15614

Frequency characteristics effect to determine voltage and current smoothing coefficients and resistances of transistor ripple filter with emitter circuit load
05 p0634 A72-16168

Tunable lasers using improved Littrow-mounted diffraction grating technique with mirror for spectral characteristics control
07 p1000 A72-19037

Rhodamine 6G dye laser tuning by variable birefringence filter using lead lanthanum zirconate titanate electrooptic ceramics for wavelength selection
07 p1002 A72-19203

Magnetic-transistor master oscillator with digital analog converter as programmer for needed output voltage frequency shifts
07 p0946 A72-19959

Wavelength tunable dye laser pumped by dual pulse lamps with Fabry-Perot interferometer in resonator
07 p1009 A72-20614

Extremal system with second control loop for search signal frequency regulation to optimize primary loop operation, determining system dynamic errors under random drift
08 p1146 A72-21555

Smooth variation of He-Ne laser spectral line width in single to multifrequency mode transition, passing laser beam through coated quartz plate
10 p1490 A72-24051

Four-photon parametric frequency selection within broad stimulated emission lines during coherent light interaction, considering dye solution laser pumping
11 p1648 A72-26335

Frequency agile radar techniques for improving detection and range resolution and reducing interference and sea and ground clutter
13 p1917 A72-28696

Destabilizing factors effect on parameters of transistorized single circuit phase modulator with varicap control
13 p1932 A72-29455

Precise time and frequency dissemination via Loran C navigation system, discussing user techniques, economics and radio propagation mode and terrain effects on accuracy
15 p2268 A72-32067

Time/frequency technology application to reliable aircraft collision avoidance system, discussing precision time-ordered techniques, frequency control and synchronization and flying clocks
15 p2268 A72-32072

YIG filter banks for FCM and communications.
19 p2772 A72-37523

Some tuning characteristics and oscillation conditions of a waveguide-mounted transferred-electron diode oscillator.
19 p2772 A72-37569

Nonautonomous phase system of equations with a small parameter, containing invariant tori and rough homoclinic curves
19 p2828 A72-38579

Stabilization of relaxation oscillators with components having an S-shaped current-voltage characteristic
20 p2906 A72-38891

Optimal synthesis of pulse repetition frequency control and filtering circuits of radar range finder in Gaussian approximation
20 p2902 A72-39065

Spectral characteristics of a single-frequency argon laser with an absorbing film.
20 p2932 A72-39509

Continuously tunable dye laser to obtain output wavelength variation by changing pump laser beam incidence angle on prism lateral face
20 p2933 A72-39563

Preliminary frequency selection during matched signal filtering
21 p3021 A72-40941

The effect of an interferometer selector on the spectrum of the characteristic frequencies of a dispersion resonator
22 p3176 A72-42245

Calculation of the electronic readjustment of a tunnel-diode oscillator by a varactor
22 p3159 A72-42246

High gain He-Ne laser with forbidden cavity configuration, discussing elimination of unwanted lasing mode by temperature detuning with mirrors
23 p3296 A72-43903

Frequency-variable semiconductor-oscillator in the microwave region.
23 p3272 A72-43948

Magnitude of the attenuation troughs of a two-branch filter with multiple-frequency quartz resonators
23 p3272 A72-44170

A single-tuned oscillator circuit for Gunn diode characterizations.
23 p3272 A72-44194

Signal frequency distortions in frequency-modulated oscillators with feedback delay
23 p3266 A72-44209

Wideband parametric up-conversion of infrared waves into visible region using tunable dye laser pumping.
24 p3410 A72-45286

FREQUENCY CONVERSION

U. FREQUENCY CONVERTERS

FREQUENCY CONVERTERS

NT DOWN-CONVERTERS

NT FREQUENCY DIVIDERS

NT FREQUENCY MULTIPLIERS

NT FREQUENCY SYNTHESIZERS

NT PARAMETRIC FREQUENCY CONVERTERS

Homodyne frequency converter design using microwave oscillator with bitonal frequency modulation
02 p0223 A72-11415

Josephson junction as 100 GHz oscillator-mixer for heterodyne frequency conversion in millimeter and submillimeter regions, observing I-V characteristics
04 p0503 A72-15604

Single pulse Nd laser with KDP cascade multipliers and tunable frequency converter using organic dye solution
06 p0825 A72-17841

Conversion coefficients of optical heterodyne receiver mixer for various amplitude-phase distributions of interfering signal
07 p1000 A72-19012

Millimeter and submillimeter band frequency conversion in nonlinear bulk n-InSb semiconductor at liquid helium temperature
08 p1140 A72-21060

Steady state plane wave theory of intracavity coupled parametric oscillator upconverter, obtaining efficiency, pump power transmission and optimum output coupling
09 p1325 A72-23086

Double balanced frequency converter design for selective microwave generation by combination of CW or swept signal with local oscillator source
10 p1448 A72-24038

Near field characteristics of solid state laser frequency converters emission, determining medium transluence during single pulse excitation of organic phosphors
10 p1490 A72-24052

FM measurement system with linear resistance-to-frequency converter realized in RC oscillator form, discussing design problems
10 p1482 A72-24598

I.F. modulation suppression at frequency converters output
11 p1603 A72-25276

Solid state RC network for single sideband frequency converter using phase difference carrier suppression
11 p1598 A72-26731

Conversion losses as function of signal power and circuit impedance in narrow band triode frequency converter under large amplitude operating conditions
11 p1598 A72-26733

Phase matched nonlinear frequency conversion of laser light in tetragonal mercury thiocyanate complex crystals
12 p1854 A72-27549

Linear and nonlinear continuous self adaptive frequency converter filters with minimum error under SNR change
13 p1936 A72-29156

Frequency converter dynamics, considering transverse vibrations of mechanical system composed of spring with centrally lumped mass
13 p1932 A72-29457

Frequency stabilized self-oscillating microwave up-converter with transferred electron diodes, noting maximum power output and bandwidth
16 p2369 A72-33764

Nonlinear characteristics of semiconductor diode multiplier circuits for frequency converters
16 p2370 A72-33951

Development of a continuous linear model of a d-c to d-c flyback converter.
18 p2643 A72-36073

Mixing process at the emitter-base junction of a high-frequency transistor.
18 p2667 A72-36948

Russian book - Methods of measurement-information conversion and separation from harmonic signals
19 p2764 A72-37449

German monograph - Investigations concerning a new frequency changer with 'forced' commutation for supplying power to one- or multiple phase consumers
19 p2753 A72-37482

French monograph - Ultrahigh-performance frequency generators
19 p2772 A72-37488

Schottky diode frequency converter characteristics, considering series resistance, housing reactance, barrier layer capacitance, noise sources and noise temperature
19 p2773 A72-37937

Parametric amplification and frequency conversion in a dual section TWT
19 p2774 A72-38411

Mechanism and controlling factors of infrared-to-visible conversion process in Er³⁺/+ and Yb³⁺/+ doped phosphors.
21 p3096 A72-40186

Stable current-to-frequency converter with continuous integration of analog input signal providing digital output suitable for input to scaler
21 p2996 A72-40207

The effect of pump coherence on frequency conversion and parametric amplification.
21 p3014 A72-40238

Experimental investigation of a millimeter-wavelength n-InSb frequency converter at 4.2 K
21 p3016 A72-40786

Low noise compact down converter for 12 GHz to UHF based on waveguide mounting microwave ICs, measuring conversion loss for GaAs Schottky diode
21 p3033 A72-40885

Inductive frequency converter with a characteristic having enhanced linearity
21 p3058 A72-41802

Transient response of threshold lowering circuit with frequency converter for single contour IF amplifier with resonant frequency equal to carrier frequency
22 p3153 A72-42121

Frequency conversion and limiter action for an angle-modulated wave with amplitude fluctuation in a half-wave linear mixer.
23 p3265 A72-44179

FREQUENCY DISTRIBUTION

Atomic models of velocity noncorrelated radiation line scattering with frequency redistribution at large distance from atmosphere
01 p0104 A72-10094

Sporadic E layer occurrence frequency distribution during 1958-1960, investigating characteristics over equatorial, temperate and auroral zones
01 p0059 A72-10596

Pulsar PSR 0833-45 linear polarization measurements at 300 and 1420 MHz, showing frequency invariance with interstellar scattering and Faraday rotation allowance
01 p0133 A72-11119

Thick orthotropic off-axis laminated plates vibration equations solution, presenting natural frequencies spectra and modal functions
02 p0249 A72-11988

Solar flare EUV flashes from sudden ionospheric frequency deviation observations
03 p0407 A72-12946

Solar microwave bursts impulsive and gradual rise and fall type comparison, noting frequency response and distribution
05 p0713 A72-16022

Pressure source model of sound radiated by sonic jet, deriving frequency spectra ratio and jet pressure
05 p0600 A72-16105

Traveling ionospheric perturbations investigation by vertical sounding with interference method, presenting group path difference measurements as function of frequency and time
05 p0657 A72-16269

Multifrequency plane, spherical and beam waves propagation, calculating temporal frequency spectra in turbulent atmosphere
06 p0771 A72-17339

- Radio galaxy spectra determination from measurements over various frequencies, noting correlation with physical parameters 06 p0879 A72-17859
- Ionospheric movements measured by frequency spectra of signals incoherently scattered by ionospheric electrons [AD-738717] 06 p0808 A72-18085
- Dynamic properties of turbine wheels under bending vibrations, classifying resonant frequencies on basis of vibration modes 06 p0899 A72-18644
- Second order mode locked GaAs junction laser, observing mode frequencies and phases configurations during self pulsing 07 p1001 A72-19200
- Frequency analysis of tapered rectangular orthotropic plates, determining bounds 07 p1092 A72-19945
- Solar radio emission, considering sources of slowly varying waves, brightness temperature distribution, frequency spectra and fluctuations 08 p1228 A72-20827
- Electromagnetic potentials excited by dipole oscillator moving in homogeneous uniformly drifting medium, analyzing frequency spectrum and finite dimensions effect on higher harmonics 08 p1135 A72-21736
- Velocity measurement by Doppler light scattering due to particle finite residence time, estimating ambiguity and noise effects on turbulent spectra of frequency fluctuation 09 p1305 A72-22302
- German monograph on narrow band mechanical filter design, using resonant circuit and coupled four terminal network analogy 09 p1284 A72-22326
- Frequency and angular correlation function relationship for signal scattering cross section of extensive bodies 10 p1436 A72-24586
- Frequency distribution of ionospheric horizontal winds vertical shear, noting altitude independence, turbulence and viscous energy dissipation 10 p1477 A72-25157
- Multifrequency ultrasonic pulse echo interference effect applying to flaw detection in metals 11 p1687 A72-26051
- Sporadic E layer frequency variations from space-diversity sounding data from three ionospheric stations 13 p1946 A72-28599
- Frequency distribution changes of energy deposited in short pathlengths as function of energy degradation of primary proton beam 13 p2004 A72-29425
- Cosmic objects and phenomena frequency distribution functions monotone decrease with respect to importance, considering star clusters, binaries, lunar craters, solar activity, etc 14 p2160 A72-30912
- Van der Pol oscillator periodic pulling behavior under weak perturbation near natural frequency, analyzing Fourier frequency spectrum 14 p2132 A72-31122
- Metal fatigue tests at various frequencies to observe surface structure, dislocations in crack vicinity, plastic deformation and ultrasonic resonance techniques 15 p2257 A72-31839
- Integral Laplace-Fourier transform stability during transient response functions reconstruction from frequency characteristics in linear circuits 15 p2264 A72-31879
- Time/frequency techniques in land, sea and air transportation environments, discussing characteristics and electronic traffic control systems applications 15 p2338 A72-32073
- Nonstationary fluctuation signal analysis into predetermined frequency band by passing digitized information through resonant LCR filter mathematical analog 16 p2362 A72-32855
- Ionospheric gravity waves spectral frequency distribution from ATS 3 electron concentration measurements, using numerical filters for statistical frequency analysis 16 p2382 A72-32891
- Slowly varying component spectrum of the solar radio emission at millimetre wavelengths. 17 p2617 A72-35708
- Microwave generation with high energy electrons in magnetic undulator with transverse electromagnetic field, calculating frequency distribution of undulator radiation 23 p3265 A72-44158
- Bounds to bending frequencies of a rotating beam. 23 p3354 A72-44249
- Lossless multiplication of images and their spatial frequency spectra with the aid of Fresnel holograms 23 p3292 A72-44470
- Extreme value analysis of flight load measurements. 24 p3367 A72-44737
- Numerical analysis of natural frequency spectrum of plastic plate free vibrations in compressible inviscid fluid 24 p3459 A72-45003
- Sporadic E layer frequency variations from space-diversity sounding data from three ionospheric stations 24 p3398 A72-45099
- FREQUENCY DIVIDERS**
- Frequency splitting by diffraction at resonator mirrors of gas ring laser, deriving opposed waves lasing equations 10 p1490 A72-24045
- Tunnel diode harmonic relaxation frequency divider, obtaining large division factors and wide synchronization bands with sinusoidal output signal 15 p2206 A72-31666
- Fluctuation analysis of parametric frequency multipliers and dividers, discussing short time instabilities caused by system noise 15 p2212 A72-32736
- Subharmonic frequency division for neon discharge plasma oscillations under resonance due to nonuniform electric field 18 p2714 A72-36111
- FREQUENCY DIVISION MULTIPLEXING**
- Microwave communication via satellites, discussing FDMA and TDMA transponders design 01 p0029 A72-10709
- Intermodulation noise in multichannel frequency division multiplex telemetry systems due to nonlinearities in transmitter-receiver links and tape recorder 02 p0175 A72-12145
- Optical communication technique based on fiber optic light pipes and time, space or wavelength division multiplexing 03 p0325 A72-14050
- Intermodulation noise distortion due to multipath transmission over FM/FDM microwave links, deriving distortion probability distribution for Nakagami-Rice randomly distributed signal reception 04 p0493 A72-15517
- PCM and FDM/FM systems noise and signal distortion analysis by digital simulation with FORTRAN language based on fast Fourier transform 11 p1601 A72-26043
- Optical communications with FDM digital data channels, examining signal optimal reception and noise stability 14 p2084 A72-30331
- Data transmission developments, considering computer improvements, networks, routes and frequency multiplexed PCM system 15 p2195 A72-31619
- Optical PCM communication system with megabits/sec information rate based on dye laser with combined frequency-time division multiplexing 15 p2198 A72-32060
- TDM and FDM digital communication systems performance comparison, noting equivalence in theoretical efficiency and generated waveforms 16 p2363 A72-33216
- Intelsat satellite SPADE demand-assignment multiple access system design for increased communication flexibility and efficiency 17 p2512 A72-34269
- Aircraft FDM and TDM systems, considering signal processing, cable requirements and applications to aircraft weapon systems and telemetry [SAE AIR 1207] 18 p2692 A72-36529
- Variants of conventional FM demodulation having the aim of improving poor signal-to-noise ratios. 18 p2661 A72-36843
- YIG filter banks for ECM and communications. 19 p2772 A72-37523
- Satellite adjacent-channel interference due to multicarrier transponder operation. 21 p3020 A72-40892
- Convolution noise and distortion in FDM/FM systems. 21 p3020 A72-40893
- Intermodulation distortion of FDM-FM in injection locked oscillator. 21 p3020 A72-40899
- Subharmonic generation in plane-parallel plate for light wave propagation perpendicularly to plate, noting frequency division near multiplicative resonance 23 p3295 A72-43408
- FREQUENCY MEASUREMENT**
- Power conditioners operating frequencies determination by series resonant circuits, noting frequency stability and reliability 01 p0008 A72-11061
- Seasonal effects and propagation fluctuations in time-frequency comparison measurements with vlf waves, noting optimal RC filter 06 p0818 A72-18289
- High temperature fatigue test assembly for symmetric tension compression cycles at 10 kHz with specimen heating in resistance furnace 06 p0797 A72-18568
- OH ground state transition frequency measurement, using beam maser spectrometer 07 p1006 A72-19423
- Pulsar distance determination from electron density distribution in line of sight estimated from frequency dispersion measures 07 p1080 A72-20054
- Free oscillations frequencies and mode shapes determination of two parallel elastically coupled rods of variable cross section, applying Bubnov-Galerkin iterative method 08 p1243 A72-21231
- Eros and ATA /Air Transport Association/ time-frequency collision avoidance systems, discussing synchronization methods, back-up mode operation, threat computation and displays 09 p1349 A72-22823
- Frequency measurements of square wave signal with unknown amplitude by two mismatched channels, comparing rms error with effective estimate variance 10 p1436 A72-24509
- Spectral density of frequency deviating process for performance predictions from oscillator testing and frequency noise calibration, discussing sample averages convergence to statistical values 11 p1593 A72-25892
- Laser apparatus for resonant frequencies and oscillation amplitudes measurement of semiconductor devices structural elements 11 p1649 A72-26348
- Research measurement error determination for two frequency Doppler measurement of artificial satellites 12 p1782 A72-27532
- Precise time and frequency dissemination via Loran C navigation system, discussing user techniques, economics and radio propagation mode and terrain effects on accuracy 15 p2268 A72-32067
- Radio navigation satellite systems for ship and aircraft location determination, using time-frequency measurements 15 p2199 A72-32071
- Frequency marker measurement of nuclear quadrupole resonance /NQR/ signal in pulsed radio spectrometer compared with zero beat method 16 p2390 A72-33078
- Laser apparatus for natural resonant frequencies and oscillation amplitudes measurement of semiconductor devices structural elements 16 p2402 A72-33701
- Digital methods of frequency measurement - A comparison. 17 p2530 A72-35363
- Methods for measuring the HF oscillation frequency in ultrasound pulses of equipment for diagnostic ultrasonography. 19 p2759 A72-37399
- Frequency instability due to discrete noise in frequency synthesizers. 19 p2775 A72-38618
- High resolution Michelson interferometer for spectral investigations of lasers. 21 p3062 A72-40610
- Automatic measurement of microwave-cavity parameters using stable sampled control loops. 21 p3034 A72-41465
- Elimination of an ambiguity in the reading of digital computational devices 21 p3035 A72-41810
- Improved calculation of resonant frequencies of Helmholtz resonators. 23 p3315 A72-44372
- Laser frequency measurement by comparison with stable molecular oscillator Doppler shift produced by reflection of UHF modulated coherent optical signal 24 p3411 A72-45425
- FREQUENCY MODULATION**
- NT FEEDBACK FREQUENCY MODULATION
- NT FM/PM [MODULATION]
- NT FREQUENCY SHIFT KEYING
- NT PULSE FREQUENCY MODULATION
- NT PULSE FREQUENCY MODULATION TELEMETRY
- Microwave Gunn oscillator frequency modulation in quenched domain mode, calculating signal admittance as function of bias voltage and amplitude 01 p0035 A72-10224
- FM communication system multifilter phase lock loop state equations derivation from phase model, predicting noise improvement characteristics by analog and digital simulation 01 p0044 A72-10328
- FM radio link superposed parabolic antenna systems adjustment for space diversity reception for scatter propagation and broadband multichannel transmission in 1.9 GHz range 01 p0027 A72-10410
- FM/CW laser radar technique for smoke plume opacity remote measurement, discussing eye safety [AIAA PAPER 71-1081] 01 p0080 A72-10539
- AM and FM noise reduction of cavity and injection stabilized microwave Gunn and avalanche diode oscillators 01 p0037 A72-10644
- FM homodyne phase meter with klystron oscillator for measuring plasma electron concentration, presenting block diagrams of meter, detector and oscillator 02 p0223 A72-11414

Homodyne frequency converter design using microwave oscillator with bitonal frequency modulation

02 p0223 A72-11415

Parachuting and aerial towing physiological and force data FM telemetry for biomedical response assessment leading to human engineered equipment improvement and midair retrieval system development

02 p0168 A72-12138

Notch noise loading tests on predetection tape recording of FM carriers, showing noise power ratio dependence on record level and bias levels and output equalization

02 p0175 A72-12146

Multiplex FM recording system parameters effect on system design, considering SNR, deviation ratio, wow and flutter, tape speed errors, crosstalk and FM filters

02 p0230 A72-12409

Fm of gas laser emission during sinusoidal modulation of relative excitation, evaluating collision parameters determination method

02 p0180 A72-12581

Nonlinear distortion coefficient measurement in broadband FM signal generator

03 p0333 A72-13898

CW avalanche diode microwave oscillator frequency modulation, using injected rf signal

03 p0334 A72-14075

Angle modulation distortions and measurements in broadband FM microwave links

04 p0485 A72-14466

All digital IC FM discriminator design, computing output SNR above threshold

04 p0486 A72-14489

Self mode locked dual polarization carbon dioxide laser, obtaining simultaneous active stabilization and frequency modulation

04 p0529 A72-14604

Gas lasers mode locking, describing use of amplitude and frequency modulation and moving mirrors

04 p0530 A72-14738

Intermodulation noise distortion due to multipath transmission over FM/FDM microwave links, deriving distortion probability distribution for Nakagami-Rice randomly distributed signal reception

04 p0493 A72-15517

Combined FM CW radar and radiometer at millimeter wavelengths, investigating objects signatures measurement

04 p0494 A72-15611

Frequency domain representation of Doppler invariant FM signal defining matched pulse compression filter

04 p0507 A72-15693

Distortion measuring equipment for determining FM signal transmission errors due to amplitude and group delay frequency response deficiencies and AM/PM conversion

05 p0626 A72-16299

Computational model of post mixer spectra of periodic FM altimeters with area target returns, using radar scattering coefficient

05 p0637 A72-16568

Wideband electro-optic FM of laser light for optical communication, discussing modulator design, construction and testing

05 p0631 A72-16961

Low deviation FM wave spectral density estimation as infinite series by low pass Gaussian random process

06 p0772 A72-17407

Ground and atmospheric scattered radiation discrimination by ground modulation based on chopper signal frequency analysis, considering feasibility from airborne tests results

06 p0814 A72-17587

Sensitivity calibration of dual beam vertically pointing FM-CW radar, presenting antenna main lobe radiation patterns

06 p0776 A72-18443

FM/CW varactor Gunn diode oscillator powered subminiature IC radar altimeter design on homodyne principle for ultralight reliable minimum chance detection

06 p0819 A72-18473

Low noise Ku band klystron oscillators for Doppler radar, discussing FM noise induced frequency deviation, spurious modulation and countermeasures

07 p0954 A72-19049

FM mf equipment for 2700-channel Hertzian beam, considering thermal noise, intermodulation and equivalent distortion of amplifiers, discriminator, limiter, etc

07 p0954 A72-19190

FM-CW radar range measurement by carbon dioxide laser, considering laser output nonlinear variation due to frequency pulling/pushing and refractivity changes

07 p0940 A72-19205

Parametric converter mixers with FM and AM signal and pump oscillator, investigating SNR behavior

07 p0956 A72-19658

Adjacent channel interference effects in multicarrier telephony FM communications system

07 p0948 A72-20493

Respiration rate transmitter with miniature pressure transducer for measuring pneumograph variations in animals over FM-FM telemetry system

08 p1124 A72-20898

Statistical noise characteristics and conditional signal distribution function measurements at output of standard FM demodulator

09 p1277 A72-22570

FM mode locked Nd-YAG pulsed laser controlled bistable phase position operation, using modulator cut as Brewster angle prism

[AD-741511] 09 p1325 A72-23089

Random frequency FM noise model for microwave Gunn effect oscillators

09 p1288 A72-23122

Double beam single detector wavelength modulation spectrometer for background elimination from observed spectra, noting application to semiconductors band structure determination

09 p1315 A72-23402

UHF band satellite TV broadcasting system with FM, calculating required field strength and transmitter power

10 p1435 A72-24033

Intraresonator modulation of ruby laser with frequency near neighboring axial oscillations frequency difference, describing Q switch based on transverse electro-optical effect in KDP crystal

10 p1490 A72-24047

Nonlinear conductivity of plasma with FM electromagnetic wave propagation, proposing electronic current density calculation method

10 p1519 A72-24130

FM electromagnetic wave propagation in Lorentzian plasma, taking into account harmonic generations effect

10 p1520 A72-24209

FM measurement system with linear resistance-to-frequency converter realized in RC oscillator form, discussing design problems

10 p1482 A72-24598

Noise measurements of AM and FM microwave generators and amplifiers in nonlinear regime

10 p1452 A72-24643

Spectral distribution of signal power in AM, FM and PM PCM systems with time division multiplexing

10 p1439 A72-24909

LF modulation suppression at frequency converters output

11 p1603 A72-25276

Si Pd-n-p-plus/ transit time diode microwave oscillator, discussing fabrication, FM noise spectrum and bias current fluctuation

11 p1604 A72-25748

Canonical equations for frequency demodulator using feedback, calculating harmonic distortion for sinusoidal modulating signal

11 p1593 A72-25891

PCM and FDM/FM systems noise and signal distortion analysis by digital simulation with FORTRAN language based on fast Fourier transform

11 p1601 A72-26043

Frequency modulation of CW GaAs laser emission by injection current, noting temperature effects

11 p1648 A72-26337

Frequency modulation demodulation technique for turbulence velocity measurements by laser Doppler velocimeter

[AD-744534] 12 p1809 A72-27836

Frequency modulation and transient effects in resonant propagation of coherent light pulses

12 p1826 A72-27939

FM distortion in injection phase locked oscillator amplifiers from generalized Alder equation

12 p1793 A72-27965

Local FM radio pulse scattering by cylinder and linear cylinder array in Kirchhoff approximation

13 p1914 A72-28407

Optimal reception system synthesized for FM signal with phase fluctuation masked by narrow band AM and white noise

13 p1914 A72-28414

Frequency discriminator use for range measurements with FM radar systems, deriving reflecting target distance relationship to output voltage

13 p1918 A72-28892

Spectrum analysis of PCM/AM-FM and PCM/FM-FM telemetry signals, using approximation technique to Fourier transform time signal to frequency domain

13 p1919 A72-29025

Microwave amplifier with internal negative feedback, using IF output for frequency modulation of mixer oscillator signal

13 p1930 A72-29057

Microwave pulse frequency shift and frequency modulation in YIG bar magnetostatic delay line with adiabatically varying parameters

13 p1923 A72-30095

Planetary distance and velocity measurement with radar signal frequency modulation, describing Venus observations

14 p2148 A72-32029

Digital FM signal receiver with postdetector integration, determining error probability as function of input SNR and noise stability

14 p2084 A72-30332

Noiselike FM signals shaping by numerical periodic sequences, analyzing FSK signals

14 p2085 A72-30337

Nonlinear AM and FM due to bonded nature of quasi-monochromatic whistler packets in magnetosphere

14 p2085 A72-30448

Book on phase locked and frequency feedback systems covering FM and multiple loop principles, limiter-discriminator operation, phase detection techniques, etc

15 p2210 A72-31500

Filtering and hard-limiting effects on digital FM signals power spectra, using Postl direct method

15 p2194 A72-31543

Signal spectrum sidebands asymmetry of LF waves in plasma with electric current and ion stream, suggesting amplitude and frequency modulation

15 p2284 A72-31650

Discrete frequency modulated signals with frequency shifted identical envelope pulses, discussing transmission, construction and correlation functions

15 p2197 A72-31878

Frequency modulated laser radiation detection, studying photomultiplier current harmonics, phase/amplitude detector nonlinearities and noise-resonator coupling effects

15 p2246 A72-31882

Multidimensional asynchronous FM pulse systems stability, considering continuous linear part transmission matrix poles located on imaginary axis

15 p2212 A72-32172

Dye-induced saturated frequency sweeping effects on mode-locked laser pulse broadening and substructures

15 p2250 A72-32523

Nonlinear distortion coefficient measurement in broadband FM signal generator

15 p2210 A72-32709

FM/FM multiplex receiver with carrier and subcarrier demodulators, deriving average click rate, output noise spectrum and SNR from Rice model

16 p2362 A72-33212

Digital phase locked loop realization for near-optimum demodulation of continuous-time FM signal using stochastic estimation theory

16 p2362 A72-33213

Nonlinear and phase delay distortion of FM modulation in tuned and detuned injection phase-locked oscillator-amplifiers

16 p2369 A72-33760

Baseband distortion caused by intermodulation in multicarrier FM systems

17 p2512 A72-34266

A method of phase detection of the beat signal in FM-CW radar

17 p2514 A72-34383

Superconductivity

17 p2594 A72-34565

Stability of injection-locked oscillators

18 p2665 A72-36265

Digital simulation for radio frequency interference and specular multipath effects on FM spread spectrum demodulation with feedback and phase lock loops

18 p2659 A72-36317

Frequency-modulation sensitivity and frequency-pushing factor of a Pd-n-p/+/- punchthrough microwave diode

18 p2667 A72-36686

Variants of conventional FM demodulation having the aim of improving poor signal-to-noise ratios

18 p2661 A72-36843

Earth station receivers for global and domestic FM systems

18 p2662 A72-36848

Synchronization and noise performance of mutually coupled oscillators

18 p2668 A72-37036

Thermal modulation and FM noise of Gunn oscillators

18 p2668 A72-37038

Improved injection locking of microwave FM-oscillators

19 p2771 A72-37262

Construction, analysis, and design of FM digital devices for controlling and measuring rapidly varying quantities

19 p2776 A72-37303

Cross-ambiguity function for a linear FM pulse compression radar

19 p2764 A72-37868

An application of correlation to radar systems

19 p2764 A72-37927

Fluid mechanics anemometry based on laser light frequency modulation /Doppler effect/, describing measurement of extensions of vortices and oscillations in flow boundary layers

19 p2801 A72-37934

Transmission of two partially time coincident linearly frequency modulated signals through limiter-filter system, noting distortion and satellite signals generation

19 p2766 A72-38419

Correlation and indeterminate functions of signals with discrete frequency-time structure, noting linear frequency modulation of signal element
19 p2768 A72-38669

Additive fluctuation noise rejection during the quasi-coherent reception of phase-manipulated signals
20 p2900 A72-38896

Self excited LC and RC oscillator networks based on FETs, discussing frequency tuning and FM methods
20 p2906 A72-38899

VHF-FM radio transmitting antenna for waves of circular, elliptical, and horizontally, vertically, or obliquely linear polarization
21 p3031 A72-40543

Horizontally polarized polydirectional or beam antenna, which is slightly out of round and consists of beam units, for television and FM radio
21 p3031 A72-40544

Frequency distortions of signals in frequency-modulated self-excited oscillators
21 p3032 A72-40782

Frequency deviation equations for FM gas laser with modulation achieved by resonator optical length variations
21 p3063 A72-40798

Susceptibility measurements on PCM-FM and four phase differential PSK digital receivers simulated on analog computer
21 p3016 A72-40852

Phase locked feedback circuit for FM demodulation, discussing all digital circuit design and voltage controlled oscillator algorithm to avoid analog implementation problems
21 p3018 A72-40873

Satellite adjacent-channel interference due to multicarrier transponder operation.
21 p3020 A72-40892

Convolution noise and distortion in FDM/FM systems.
21 p3020 A72-40893

Impulse noise in FM receivers in the presence of adjacent channel interference and thermal noise.
21 p3020 A72-40894

Intermodulation distortion of FDM-FM in injection locked oscillator.
21 p3020 A72-40899

FM signal distortion during passage through two-element antenna array to determine usable bandwidth from transmission characteristics viewpoint
21 p3022 A72-41265

Variable-bandwidth frequency-modulation chirp pulse compression using a longitudinal acoustic-wave convolver at 1.3 GHz.
21 p3023 A72-41468

Multidimensional asynchronous FM sampled data systems stability, considering continuous linear part transfer matrix poles located on imaginary axis
22 p3162 A72-42080

Investigation of the threshold properties of a phase-lock AFC detecting a sinusoidally frequency modulated signal against a noise background
22 p3154 A72-42231

Threshold noise of an FM receiver at small signal-to-noise ratios
22 p3154 A72-42236

Influence of fluctuations on the synchronization of frequency-modulated oscillators
22 p3159 A72-42658

FM receiver noise figure measurement - A simplified method.
22 p3155 A72-42704

Planetary distance and velocity measurement with radar signal frequency modulation, describing Venus observations
23 p3333 A72-43239

Optical considerations for an acoustooptic deflector.
23 p3288 A72-43885

Reciprocal mean-square error and signal-to-noise ratio as distinct performance measures in below-threshold communication.
23 p3265 A72-44177

Statistical noise characteristics and conditional signal distribution function measurements at output of standard FM demodulator
24 p3379 A72-44749

Analysis of a single-loop parametric amplifier by the phase plane method
24 p3384 A72-44893

Amplitude dependence of frequency in oscillators.
24 p3385 A72-44964

Measurement of best time-delay resolution obtainable along east-west and north-south ionospheric paths.
24 p3381 A72-45637

FREQUENCY MULTIPLIERS

Quasi-optical 30-60 GHz varactor doubler circuit filters, waveguide tuners and mounts for frequency multipliers
04 p0507 A72-15617

Single pulse Nd laser with KDP cascade multipliers and tunable frequency converter using organic dye solution
06 p0825 A72-17841

Microwave frequency multiplier construction by hybrid circuits based on quasi-lumped components, calculating characteristics from equivalent circuit
06 p0785 A72-18313

Phase locking loop synchronized quartz oscillator for integral frequency multiplication in wideband carrier frequency systems
07 p0954 A72-19174

High power UV light pulse generation using Nd-YAG laser with frequency doubling
07 p1002 A72-19202

Flow graph analysis of optimal operation of frequency multipliers with idler circuits using non-linear n-p junction capacitance
08 p1140 A72-21061

Uniform plane wave theory of internal upconversion and frequency doubling in optical parametric oscillators
09 p1324 A72-23079

Modulation oscillations in ferromagnetic core-based LF signal generators and frequency doublers, deriving differential equations for converter operation and formulas for static characteristics
13 p1930 A72-29049

Mechanical oscillator model for experimental investigation of multistage electrical frequency multipliers subharmonic transient oscillations, considering energy flow under constant and/or phase modulated excitation
14 p2131 A72-30719

Millimeter wave third harmonic generation and frequency multiplication in n-type InSb at 77 K
14 p2142 A72-30799

Magnetron crossed field amplifier multistage frequency multiplier HF field properties, obtaining numerical solutions for nonlinear governing equations
15 p2209 A72-32669

Fluctuation analysis of parametric frequency multipliers and dividers, discussing short time instabilities caused by system noise
15 p2212 A72-32736

Millimeter-wavelength frequency multipliers employing gallium arsenide diodes
17 p2529 A72-34851

Gallium arsenide varactors
18 p2671 A72-37145

Calculation of the transmission factor of a parametric microwave transistor multiplier
19 p2774 A72-38423

A large-signal theory for current-driven frequency multipliers.
19 p2775 A72-38609

A regenerative high multiplicity tunnel-diode frequency multiplier
21 p3034 A72-41122

Parallel-type varactor frequency multipliers. I - Spectral analysis of the voltage at a partially forward-biased varactor
23 p3270 A72-43764

Optimal parallel-type varactor frequency multiplier calculation for reverse-biased conditions in terms of nonlinear conductance loss and diffusion capacitance Q factor
23 p3270 A72-43774

The efficient generation of coherent radiation continuously tunable from 2500 A to 3250 A.
24 p3409 A72-44803

Frequency multiplication with a traveling-wave tube. I - Computation of the current harmonics in a traveling-wave tube by the large-signal theory.
24 p3386 A72-45284

Frequency multiplication with a traveling-wave tube. II - Numerical analysis of a traveling-wave frequency multiplier by the large-signal theory.
24 p3386 A72-45285

Continuous He-He laser radiation intensity correlation function measurement, using Michelson interferometer and frequency doubler
24 p3412 A72-45704

FREQUENCY RANGES

NT RADIO RANGE

Frequency characteristics of selectively reflecting screens in multichannel parabolic mirror antennas and determination of Fresnel coefficients dependence on polarized plane wave incidence angle
04 p0499 A72-15241

TV programs direct broadcasting by satellites, discussing frequency range, amplitude vs frequency modulation, satellite stabilization and economic aspects
04 p0494 A72-15678

Type 3 bursts mean polarization level at 20-200 MHz, considering vertical spacing of radio waves emission levels
07 p1077 A72-19813

Earth and interplanetary magnetic fields spectral power density characteristics at 0.0001-1 Hz
08 p1153 A72-20718

Frequency bands for space-earth links in broadcasting satellite service, stressing application to educational television
10 p1435 A72-24032

Experimental earth station for wave propagation studies in satellite communications using frequency range above 10 GHz
12 p1785 A72-27801

Integrated inductorless quadratic bandpass filters for constant bandwidth wide frequency range, using IC analog multipliers network
13 p1927 A72-28403

Silicone based elastomers acoustic excitation damping properties at 213-423 K, discussing testing technique and results at 200-1000 Hz
13 p1957 A72-29090

Ferrite materials for microwave applications, discussing frequency and temperature limit extension, power level increase and loss reduction
14 p2088 A72-30833

Precision frequency standards practical utility under field operating conditions, discussing propagation effects due to atmospheric and frequency parameters
15 p2199 A72-32066

Monochromatic radio wave propagation in interplanetary plasma, deriving frequency spectrum and phase and amplitude fluctuations
15 p2202 A72-32656

Passive Q switching extension of carbon dioxide laser output frequency range using dichloro-difluoro methane as saturable absorber
17 p2564 A72-35347

Type 3 bursts mean polarization level at 20-200 MHz, considering vertical spacing of radio waves emission levels
17 p2618 A72-35738

Earth and interplanetary magnetic fields spectral power density characteristics at 0.0001-1 Hz, noting ambiguities due to variable investigation conditions
19 p2791 A72-38346

**FREQUENCY REGULATION
U FREQUENCY CONTROL
FREQUENCY RESPONSE**

Atmospheric wave propagation mode parameters frequency dependence analysis from duct model, calculating received signal time behavior by waveguide transfer function
01 p0027 A72-10408

Equatorial E region short wave oblique incidence propagation experiment showing transmitted impulse delay increase with frequency decrease
01 p0056 A72-10437

Lateral vibration of thin conical bar with clamped base and free tip, calculating characteristic modes and frequencies
01 p0138 A72-10509

Electron density profile determination in D region based on frequency dependence of radio waves absorption, discussing lower ionosphere anomalous ionization
01 p0059 A72-10595

Liquid phase epitaxial GaAs transferred electron microwave oscillators with high dc to rf conversion efficiencies dependent on frequencies
01 p0036 A72-10631

Doping profile effects on reflection-type IMPATT diode microwave amplifiers, presenting power-gain vs frequency curves
01 p0037 A72-10643

Optimal frequency domain design of two dimensional low pass finite impulse response digital filters by linear programming
01 p0046 A72-10868

H I radio recombination line observation in H II region NGC 2024 microwave spectrum, detailing radiation frequency dependence
01 p0133 A72-11143

Acoustic impedance of body surface at thorax and at abdomen, showing dependence on frequency and body pressure and position
01 p0021 A72-11195

Respiratory system frequency response analysis for chemical regulation of breathing, using time domain method and step functions
02 p0168 A72-12040

Laser pumped organic dye laser frequency-time characteristics, noting noncoincidence of amplification and photon density maxima
02 p0238 A72-12118

Weak dipole magnetic field effect on oscillation frequencies of conducting gaseous polytrope stars, using variational equation
02 p0260 A72-12310

Nomogram determination of frequency characteristics of closed loop linear automatic control systems
02 p0197 A72-12563

MOS transistor frequency and transient response characteristics for equivalent circuit synthesis, using Bessel functions in differential equation solution
02 p0196 A72-12761

Solar decameter and hectometer wavelength radio burst generation, examining dynamic spectra and source position as function of frequency and time
03 p0424 A72-13221

Frequency criteria for stability of nonlinear multivariable RLC networks with bounded solutions approaching equilibrium
03 p0338 A72-13411

Limiting approximation theorems for synthesis of linear circuits and signals in time-frequency domains 03 p0338 A72-13896

Ultrasonic resonance thickness gage sensitivity and accuracy, noting damper, piezoelectric plate, protector and frequency band influence 03 p0361 A72-13986

Absorption effects on circular polarization in synchrotron radiation, discussing frequency and magnetic field dependence 04 p0570 A72-14550

Closed-loop nonlinear sampled-data systems with sampler and finite Hankel transformable distributed elements, deriving frequency domain stability criteria 04 p0504 A72-14662

Reciprocal dual mode millimeter wavelength phase shifter design for use in phased array antennas, calculating phase shift and insertion loss vs frequency 04 p0498 A72-14719

Ring loaded corrugated waveguide for improved frequency broadbanding and transformer matching in horn antenna systems for satellite communication ground stations 04 p0498 A72-14721

Impulse noise reproduction for temporary threshold shift and impulse noise measurements, considering rise time, frequency response and limitations of tape recorders 04 p0521 A72-14847

Density waves propagation and amplification in p-InSb electron-hole plasmas, investigating dependence on frequency and injection level 04 p0561 A72-14851

Frequency response and I-V characteristics of metal/chalcogenide glass/metal diode structures 04 p0498 A72-15079

High and low pass filtered clicks lateralization tests, suggesting lateral position discrimination dependence on lf content and cochlear partition apical end 04 p0550 A72-15297

High purity epitaxial GaAs frequency response, determining heterodyne detection in millimeter and submillimeter regimes 04 p0563 A72-15613

Frequency response of passive dipole antennas fed by transistor circuit, investigating power gain, bandwidth and voltage SWR 04 p0503 A72-15670

Frequency domain representation of Doppler invariant FM signal defining matched pulse compression filter 04 p0507 A72-15693

Temperature, flow, end conditions and branching on small signal sinusoidal amplitude frequency response of pneumatic lines, investigating transfer functions [ASME PAPER 71-WA/AUT-5 (FLCS)] 05 p0615 A72-15958

Solar microwave bursts impulsive and gradual rise and fall type comparison, noting frequency response and distribution 05 p0713 A72-16022

Frequency-contrast characteristics of optical system producing image of distant object in turbulent boundary layer of atmosphere, determining refractive index fluctuation intensities 05 p0689 A72-16172

Distortion measuring equipment for determining FM signal transmission errors due to amplitude and group delay frequency response deficiencies and AM/PM conversion 05 p0626 A72-16299

N/h/ electron concentration profile in ionospheric D layer by exponent of frequency dependence of radio wave absorption 05 p0627 A72-16401

Amplitude, time and frequency domain analysis of random signals, measuring probability density, cross correlation and cross spectral density functions 05 p0629 A72-16598

Dissipative loss effects on frequency response and miniaturization limits for minimum loss conditions in microwave filters with Chebyshev characteristics 05 p0638 A72-17188

On-off control system stability with feedback proportional to square of velocity, determining system frequency response 06 p0793 A72-17316

Mf/hf/vhf scattering from sea, deriving received power and spectral energy density dependence on grazing angle, frequency, range and surface impedance 06 p0770 A72-17338

Condenser microphones sensitivity and frequency response characteristics measurement at normal and elevated atmospheric pressures in hyperbaric chamber air and He-air environments 06 p0766 A72-17808

Longitudinally magnetized fully filled square waveguide reciprocal ferrite phase shifter, predicting frequency characteristics by rotational error analysis 06 p0786 A72-18370

Resonant systems frequency characteristics measurement by sinusoidal input signal, determining op-

timal law of change in frequency scanning rate for minimal scan time 06 p0795 A72-18663

Polymers mechanical losses temperature-frequency dependence, using nonlinear viscoelastic theory 06 p0838 A72-18678

Lightly damped nonlinear mechanical oscillators under random excitation, calculating stationary response frequency and autocorrelation by heuristic procedures 06 p0849 A72-18693

Frequency discriminator like two-channel device with greater sensitivity by crossed feedback, calculating variable frequency emf effect on operation 07 p0938 A72-18853

Gigahertz reflection amplifiers with low cost avalanche transit time diodes, measuring characteristics of amplification by synchronization at center frequency 07 p0955 A72-19191

Cadmium mercury telluride photovoltaic cell features, noting gigahertz range frequency response, heterodyne sensitivity, operating temperature and nonstoichiometric p-n junction preparation 07 p1003 A72-19224

Frequency and power characteristics of transistorized generators of harmonic oscillations 07 p0956 A72-19569

Frequency response design for interactive multivariable feedback control systems, using characteristic transfer functions 07 p0960 A72-19704

Linear multivariable system design based on relationship between performance index parameters and optimal response in frequency domain, exemplifying gas turbine feedback controller design 07 p0961 A72-19710

Synchrotron emission source identification from spectral index dependence on frequency 07 p1059 A72-19807

Symmetrical amplitude-frequency characteristics of microwave reflection amplifiers with active resonators connected in series by nonhalf wave transmission line 08 p1138 A72-20791

Quarter thickness variation and particle temperature dependence on height and frequency in summer daytime F region 08 p1155 A72-20815

Two mode coupling and frequency pulling in He-Ne laser without absorbing medium in resonator 08 p1183 A72-21728

Frequency dependent condensation method for vibration problems in structural dynamics, presenting results for spring-mass system with six degrees of freedom 08 p1250 A72-22143

Multiplex electrohydraulic system for aircraft fly by wire actuators with majority voting and pressure logic, discussing frequency response and environmental tests 08 p1113 A72-22152

Frequency response of spectral noise amplitude in chalcogenide glass switches 09 p1366 A72-22215

Frequency response of hot-film wedge probe in turbulent flow of viscoelastic fluid 09 p1293 A72-22309

Phase angle measurements of frequency-oxygen atom lifetime relationship in pulsating auroras 09 p1298 A72-22589

Optical properties of Gd polycrystals in IR, explaining frequency dependence of complex permittivity 09 p1372 A72-23040

LF noise spectral density measurements in avalanche diodes as function of frequency, considering mean square voltage drift 09 p1287 A72-23118

VLF atmospherics count comparability in broad- and narrow-band operation, presenting amplitude frequency response 09 p1301 A72-23268

Nonlinearity effects on random vibration displacement and frequency characteristics of one degree of freedom system, using Fokker-Planck equation 09 p1353 A72-23605

Sound field measurement in circular and rectangular air duct with sound-absorbing walls/mufflers/, deriving empirical formula for attenuation frequency characteristics 09 p1354 A72-23683

Computer aided design of linear time-invariant multivariable feedback control systems, given specifications in frequency domain in stability margin form 10 p1455 A72-23789

Compensator improvement for relative stability and frequency response of large space vehicle, using nonlinear programming 10 p1442 A72-23791

Frequency characteristics of traveling wave deflection system for wideband CRT deflector, improving sensitivity by low beam accelerating voltage 10 p1446 A72-23939

GaAs abrupt junction IMPATT diode large signal operation analysis, noting oscillation efficiency HF fall-off characteristics 10 p1450 A72-24557

Electro-optical Fabry-Perot modulator with KDP and ADP crystals as optical resonators, determining modulation and frequency response characteristics 10 p1492 A72-24583

Wideband microwave device with diode and single component correction circuits Q factors measurement from frequency dependence of input traveling wave coefficients 10 p1453 A72-24918

Topography of swath around Venus equator from wavelength dependence of radar cross section 10 p1548 A72-24972

Spatial frequency specificity of edge continent color aftereffects 10 p1427 A72-25182

Nonlinear elastic suspension system with two spring pairs in parallel, measuring nondimensional load versus deflection curve and frequency response 11 p1736 A72-26007

Aircraft pilot seating protection from dynamic environment by active vibration isolation, discussing human frequency response characteristics 11 p1585 A72-26391

Ideal low pass filter with fastest monotonic step response to permit no signal transmission outside prescribed frequency band 11 p1605 A72-26469

Method of characteristics for solution of quasilinear hyperbolic partial differential equations, analyzing frequency response 11 p1678 A72-26551

Unsteady aerodynamic forces on flat plate in locally perturbed incompressible potential flow, investigating angle of attack frequency response to periodic local perturbations 11 p1573 A72-26579

IC lateral p-n-p multijunction transistor frequency characteristics analysis, noting parasitic effects, cutoff frequencies and power gain 12 p1788 A72-27311

Auditory flutter fusion frequency changes in humans during prolonged visual deprivation 12 p1769 A72-27418

First order systems steady state frequency response to general harmonic amplitude modulated input, noting signal attenuation and absence of distortion 12 p1845 A72-27540

Continuous signal representations in time and frequency domains by Fourier series 12 p1783 A72-27628

Active notch filter circuits for extending accelerometers frequency response to near resonance, presenting error analysis of mismatching components 12 p1808 A72-27639

Nonequilibrium carrier distribution in drift junction transistor, considering base region hindering field effect on transit time, current gain cut-off and frequency response 13 p1926 A72-28371

Active transistorized low pass RC filter providing fourth-order transfer function and uniform frequency response 13 p1927 A72-28381

Fourier transforms for linear systems transient time and frequency characteristics, using discrete functional values for initial information 13 p1985 A72-28675

Pulse-pulse frequency agility influence on radar detection in sea and rain clutter with decorrelation, eliminating multiple-time-around echoes 13 p1917 A72-28695

Spurious oscillations in external excitation oscillators due to internal feedback in transistor, investigating frequency dependence of stability coefficient in cascade with common emitter 13 p1929 A72-28896

Frequency response data identification technique using adaptive hybrid computer to improve quality and acquisition time 13 p1935 A72-29103

Binaural frequency discrimination in masking level difference /MLD/ noise under homophasic and antiphase conditions 13 p2006 A72-29771

Nonsingular feedback control system phase-amplitude frequency response graphical analysis using real circle diagram 13 p1937 A72-29974

Microwave device phase and amplitude frequency response measuring equipment with wide range test pulse generation, discussing design and performance 13 p1934 A72-30091

Hollow elliptical waveguide numerical analysis by polygon approximation with computer program to obtain cutoff wavelength without Mathieu functions 14 p2087 A72-30943

Two-variable resonant ladder network synthesis for prescribed amplitude response with closed-form solution, illustrating with waveguide bandstop filter 14 p2091 A72-30945

Amplitude and frequency characteristics of avalanche diode microwave oscillator loaded with resonant circuits, noting Q value effect on self oscillations
14 p2089 A72-31109

Rectangular, elliptical and parabolic waveguides TM and TE modes relation and cutoff wavelength analysis by finite element method, suggesting mode classifying system
15 p2205 A72-31354

GaAs Gunn diode LSA operation mode in multiloop circuit to extend high frequency limit
15 p2207 A72-31888

Limiting approximation theorems for synthesis of linear circuits and signals in time-frequency domains
15 p2212 A72-32707

Phase and gain response of wideband coaxial X band microwave avalanche diode amplifiers
16 p2368 A72-33073

Rolling tire frequency response for angular oscillations about vertical axis through axle in wheel plane, using point contact theory
16 p2426 A72-33696

Periodic perturbation effect on oscillatory system behavior at frequencies approaching resonance
16 p2426 A72-33789

A simulation method permitting the direct construction of an integrated fluidic circuit with predetermined frequency response curve
17 p2494 A72-34197

Pulse length evaluation from frequency domain phase function, applying to mode locked laser theory
17 p2562 A72-34292

Calculations showing the reduction in the frequency dependence of a two-element array antenna fed by microwave transistors.
17 p2514 A72-34369

Frequency domain design of two-dimensional finite impulse response digital filters.
17 p2532 A72-34406

Hingeless rotor - Experimental frequency response and dynamic characteristics with hub moment feedback controls.
17 p2489 A72-34494

[AHS PREPRINT 612]
Linear-nonlinear-linear transition as a function of frequency in the retinal response to light.
17 p2508 A72-34885

Synchrotron emission source identification from spectral index dependence on frequency
17 p2602 A72-35731

Frequency dependent loss in self-pulsing ring laser.
18 p2697 A72-36337

The behaviour of a Gunn oscillator in the domain-delayed mode.
18 p2667 A72-36945

Mixing process at the emitter-base junction of a high-frequency transistor.
18 p2667 A72-36948

Effect of electrode thickness on the frequency response of a piezoelectric transducer
18 p2693 A72-37218

Computerized design of electric filters with given frequency response, discussing attenuation characteristic approximation by Chebyshev method
19 p2776 A72-37307

Frequency response optimization of electric filters, modulators and impedance matching circuits using minimax criterion, noting nonlinear programming sequence
19 p2771 A72-37310

Admissible changes in the parameters of a matching four-terminal network
19 p2772 A72-37315

Synthesis of a resin-metal damper whose characteristic shows minimum deviation from a constant-frequency response
19 p2806 A72-37429

Experimentally observed admittance properties of the semiconductor-insulator-semiconductor /SIS/ diode.
19 p2772 A72-37568

Frequency-selective networks suitable for microelectronic realization. II.
19 p2773 A72-37874

Frequency response studies of human and avian respiratory regulation.
19 p2761 A72-38229

RC gyrator filters frequency characteristics stability analysis, noting elements sensitivity as function of frequency and Q value
19 p2774 A72-38421

Calculating the perceived level of light and sound.
19 p2761 A72-38567

Dissipative loss effects on frequency response and miniaturization limits for minimum loss conditions in microwave filters with Chebyshev characteristics
19 p2775 A72-38624

An improved design and measurement of attenuation characteristics of RF suppressors.
20 p2902 A72-38997

MOS transistor frequency and transient response characteristics for equivalent circuit synthesis, using Bessel functions in differential equation solution
20 p2907 A72-39067

A frequency transformation chart for RC-active band-pass filters.
20 p2907 A72-39432

Response of linear periodically time varying systems to random excitation.
20 p2946 A72-39636

Small-signal admittance of the insulator-n type-gallium-arsenide interface region.
20 p2909 A72-39775

Influence of a protective coating on the frequency characteristics of hot-film anemometer sensors
21 p3050 A72-40131

A method of calculating the parameters of a linearized transistor model
21 p3027 A72-40475

Calculation of two- and three-stage broadband amplifiers with parallel correction from the standpoint of a maximum quality factor with an optimally flat amplitude characteristic
21 p3027 A72-40477

Synthesis of feedback systems with large plant ignorance for prescribed time-domain tolerances.
21 p3037 A72-40643

Analysis of large-signal noise in Read oscillators.
21 p3032 A72-40698

Comparative analysis of frequency response determination methods for searchless adaptive systems
21 p3038 A72-40709

Ground and torque relation to swivel angle and lateral displacement of wheel rim plane, using string model for tire
21 p2996 A72-41260

Design and frequency characteristics of cylindrical waveguide diode for microwave range, noting semiconductor junction effect on device efficiency
21 p3036 A72-41837

Frequency and power characteristics of transistorized generators of harmonic oscillations
22 p3158 A72-42087

Network analysis and frequency response of LF filter with distributed RC structure and voltage converter
22 p3158 A72-42120

Electronic analyzer of structural vibration frequency characteristics and mutual spectra, considering bandpass filter and automatic frequency spectra recorder
22 p3176 A72-42134

Diffraction by an infinite corner reflector transversely loaded by concentric dielectric slabs.
22 p3159 A72-42301

Spectrally shaped transient forcing functions for frequency response testing.
22 p3206 A72-42463

Use of rotated electrodes for amplitude weighting in interdigital surface-wave transducers.
22 p3178 A72-42619

Low capacitance high speed lead tin telluride photodiodes via liquid phase epitaxial growth, discussing frequency response to Nd-YAG and carbon dioxide lasers
22 p3159 A72-42620

Low frequency measurement of mechanical impedance and frequency response.
22 p3164 A72-42700

Frequency dependent deep level trap admittance and field effect transcapacitance of p-n junctions calculated by truncated space charge approximation
22 p3161 A72-43086

Computation of optimal parameter domains of components in the design of electronic circuits
23 p3268 A72-43440

Frequency dependent antenna impedance characteristics in ionospheric plasma, discussing anisotropic and isotropic electron plasmas, loop antennas, resonance rectification and ion effects
23 p3319 A72-43512

Error analysis of linear and nonlinear elements in hydraulic control circuits of flight vehicles, calculating accuracy of frequency response determination
23 p3252 A72-43671

Frequency response of ducts in the shape of a truncated cone
23 p3279 A72-43697

Electrohydraulic stand for vibration strength testing, discussing system design, specifications, frequency-amplitude characteristics and applications
23 p3278 A72-43760

Relationship between the dissipative properties of a vibrational system and its amplitude-phase-frequency characteristics
23 p3313 A72-43785

Amplitude-phase-frequency characteristics of a high-rpm centrifugal pump
23 p3294 A72-44021

Sound absorption in atmosphere at 20 C, predicting relaxation times and strengths in 100 Hz to 1 MHz as functions of relative humidity
23 p3285 A72-44112

Useful range of a mechanical impedance technique for measurement of dynamic properties of materials.
23 p3294 A72-44126

GaAs light emitting diodes intensity fluctuations measurements at .025-20 kHz
23 p3297 A72-44190

A wide-band Gunn-effect CW waveguide amplifier.
23 p3272 A72-44193

Frequency dependence of axially oscillated nozzles admittance real and imaginary parts for different Mach numbers, convergence angles and curvature radii, comparing theory and experiment
24 p3433 A72-45144

Operational dynamics of inductive and capacitive differential circuits of small-displacement transducers
24 p3403 A72-45314

The transient electromagnetic response of a spherical shell of arbitrary thickness.
24 p3381 A72-45638

FREQUENCY SCANNING
Bragg crystal spectrometer for Sco X-1 spectrum scanning, using Aerobee 170 rocket
[AD-736552]
03 p3353 A72-13039

Resonant systems frequency characteristics measurement by sinusoidal input signal, determining optimal law of change in frequency scanning rate for minimal scan time
06 p0795 A72-18663

Frequency-scanned X-band waveguide array
17 p2525 A72-34374

FREQUENCY SHIFT
Pitch shift of pure tone by masking tones and band limited noise
01 p0101 A72-10159

Turbomachine blade frequency disalignment effects on resonant vibrations and stress distribution, using wheel model and computer solution
01 p0143 A72-11367

Orbital elements and onboard transmitter frequency drift of active satellite from Doppler and angle data recorded at single receiving station
02 p0171 A72-11664

Geomagnetic PDP pulsations oscillation frequency drift, considering proton motion characteristics in magnetospheric equatorial plane
02 p0217 A72-11931

Solid state Q switched laser emission frequency drift from Fabry-Perot rings interferograms
02 p0237 A72-12108

Differential line shifts in spectrum of supergiant beta Ori attributed to radial spreading of stellar atmosphere
03 p0436 A72-13810

He-Ne laser controlled frequency shift in wideband optical heterodyne communications systems with Currie low reflection mirror
05 p0668 A72-16346

Radiation transfer by resonant scattering in expanding nebula with applications to quasars having blueward absorption wings
05 p0716 A72-16374

Magnetic-transistor master oscillator with digital analog converter as programmer for needed output voltage frequency shifts
07 p0946 A72-19959

Multicarrier communications satellite signal power, center frequency and rms deviation computer controlled monitoring system with frequency shift radiometer principle
07 p0948 A72-20491

Shf resonator small resonant frequency shift and Q factor changes measurement based on FM signal envelope shape analysis
07 p1046 A72-20508

Minimum frequency separation between avionics receivers and transmitters for acceptable interference level
08 p1131 A72-20929

Local and integral ionospheric electron concentrations and horizontal gradients effects on reduced Doppler frequency shift difference along satellite orbit
08 p1132 A72-21144

Positive pressure cooling of cryogenic baths of liquid nitrogen by helium gas addition for frequency shift of ruby laser
09 p1326 A72-23411

Narrow band frequency drifts of polarized Jovian L bursts from simultaneous radio observations
10 p1532 A72-23713

Rb 87 line shift produced by rare buffer gases and molecular nitrogen measured from applied magnetic field magnitude and hyperfine structure of D lines
10 p1490 A72-24040

Reflected short wave signal frequency shift due to reflecting ionospheric layer movement and electron concentration changes, considering oblique incidence on isotropic and anisotropic layers
10 p1436 A72-24576

Nonlinear interaction between circular coherent light and modulating electromagnetic waves in presence of quadratic electrooptical effect, noting frequency shift
10 p1493 A72-24912

Uncertainty functions side maxima for phase manipulated signals with low sidelobe levels in autocorrelation functions, noting Doppler frequency shift effect
10 p1440 A72-24916

Trapped particle induced frequency shift in response of electrostatic wave to adiabatic and sudden

excitations, obtaining distribution functions and non-linear dispersion relation [AD-741547] 11 p1693 A72-25566

Pulse width relationship to frequency broadening during self phase modulation of propagating short laser pulse 11 p1647 A72-26151

Short term frequency instability in mm wave reflex klystrons, obtaining rms frequency drift 11 p1605 A72-26319

Plane monochromatic electromagnetic wave scattering by rotating metallic cylinder, noting frequency shift dependence on cylinder translational motion velocity 13 p1914 A72-28370

Geomagnetic PDP pulsations oscillation frequency drift, considering proton motion characteristics in magnetospheric equatorial plane 13 p1949 A72-29243

Microwave pulse frequency shift and frequency modulation in YIG bar magnetostatic delay line with adiabatically varying parameters 13 p1923 A72-30095

Buffer gas mixture and pumping light effects on shifts from ground state hyperfine frequency in Rb-85 maser frequency standard 14 p2109 A72-30196

Phononless lines shift and broadening and electron phonon interaction in lanthanum trifluoride-Nd crystal, obtaining temperature dependence of non-radiative transition probability 14 p2142 A72-30359

Doppler carrier frequency shift measurement accuracy, finding relationships in errors for coherent and noncoherent pulse trains 15 p2195 A72-31657

Discrete frequency modulated signals with frequency shifted identical envelope pulses, discussing transmission, construction and correlation functions 15 p2197 A72-31878

Electro-optical media for initial light radiation frequency shift maximum, analyzing circular light/modulating wave interactions 15 p2197 A72-31880

Pulsed IMPATT diode oscillators RF oscillations growth rate and frequency shift behavior during build-up period, comparing equivalent circuit derived electrical properties with measurements 15 p2208 A72-32472

Quiescent solar prominences internal motions from fine structure wavelength shift observations in Ca II K line spectra 15 p2318 A72-32780

Solar white light flares relationship to EUV emission based on sudden frequency deviations observations, noting coincidence with H alpha flare areas 15 p2302 A72-32789

Magnetic field effect on polarization plane rotation and emission frequency shift of He-Ne ring laser at 3.39 micron wavelength 16 p2402 A72-33485

Generalized radar equations derivation to obtain Doppler frequency shift and variance in Fresnel zone due to target movement 16 p2365 A72-33765

Alouette 2 plasma resonances observation near ionospheric electron cyclotron frequency harmonics, interpreting frequency shift as wave dispersion effects 17 p2546 A72-34692

A stability mechanism for the ion-acoustic waves. 17 p2592 A72-35625

Frequency separation in structure of solar continuous radio bursts. 17 p2602 A72-35713

Observability of hyperfine structure and Lamb, nuclear-volume shifts in $1s_{n1}-1s_{n1}'$ transitions of helium-like ions. 19 p2837 A72-37544

Local and integral ionospheric electron concentrations and horizontal gradients effects on reduced Doppler frequency shift difference along satellite orbit 20 p2903 A72-39249

Filaments formation behind nonlinear focus and frequency shift in transient self focusing of light beam in medium with given time dependent permittivity 20 p2953 A72-39502

Broadening and shift of magnesium lines by van der Waals interaction with argon atoms and by microfields. 22 p3208 A72-42388

Uniform moving source radiated sound field from equivalent stationary source distribution via transformation based on retarded-time position and Doppler frequency shift 22 p3205 A72-42461

The role of time/frequency in Navy navigation satellites. 22 p3202 A72-42749

Light spectral width and constant frequency shift during spontaneous diffusion in ideal gas for fixed photon wave 23 p3315 A72-44479

FREQUENCY SHIFT KEYING

Wideband FSK receiver for space telemetry, calculating error probability in multipath signal fading due to planetary surface reflections 01 p0025 A72-10329

Coded multiple FSK in presence of random variable phase, predicting optimum reception performance relationship to phase distribution and SNR 01 p0025 A72-10330

Coherent demodulation of continuous phase binary FSK signals in additive white noise, determining error probability 02 p0174 A72-12135

Fast frequency switching for shift keying pulse code modulation with two cavity modes for Gunn oscillator frequency states 05 p0631 A72-17072

FSK transmission experiments on uhf satellite link, noting threshold convolutional decoding contribution to SNR 06 p0773 A72-17599

Digital frequency shift keying modulation of Gunn microwave oscillator by cavity placed between output and transmission line 08 p1141 A72-21432

Binary split phase FSK signal noncoherent detection by multiple predetection filtering, noting probability of error per bit 10 p1437 A72-24686

Noise immunity and code sequence rejection probability in real multifrequency communications systems with multipositional frequency shift keying 11 p1598 A72-26729

Noiselike FM signals shaping by numerical periodic sequences, analyzing FSK signals 14 p2085 A72-30337

Marcum Q function parameters approximations for error probabilities computation in multilevel frequency shift keying and differentially coherent phase shift keying systems 20 p2903 A72-39426

Spectra of a frequency-shift-keyed signal amplitude-modulated by a sinusoidal wave. 20 p2904 A72-39771

Effects of bandlimiting on the coherent detection of PSK, ASK and FSK signals. 24 p3380 A72-44900

FREQUENCY STABILITY

Random background noise effect on nonlinear self oscillation envelope passage time moments, discussing relationship between amplitude and frequency stabilities 01 p0035 A72-10032

CW X-band Gunn oscillator in coaxial cavities, investigating frequency variation with ambient temperature 01 p0037 A72-10641

Dispersion characteristics and frequency stabilization of 0.63 micron laser in magnetic field 02 p0180 A72-12583

Frequency fluctuations in nonlinear self oscillating system in presence of periodic nonstationary random noise effects 02 p0195 A72-12586

Tunnel diode quartz oscillator frequency stability improvement and dc power requirement reduction using nonlinear feed circuits 03 p0331 A72-13555

Enhanced He-Ne laser frequency and output power stabilities obtained by constructing mirror and gas discharge tube as integral unit 04 p0529 A72-14603

Self mode locked dual polarization carbon dioxide laser, obtaining simultaneous active stabilization and frequency modulation 04 p0529 A72-14604

Unmodulated He-Ne laser output frequency stabilization, using quartz Fabry-Perot etalon 05 p0669 A72-16670

K band Gunn oscillator with high frequency stability, discussing construction, performance, output power and frequency saturation effect 06 p0786 A72-18375

High power GaAs LSA transmitter oscillator refinements, noting pulsed development to change load and thermal environment frequency stability 06 p0789 A72-18482

Single frequency oscillations in nonlinear mechanical systems described by one dimensional mixed boundary value problems, using asymptotic methods 06 p0850 A72-18715

Quartz oscillator short term frequency instability lower limit estimation by calculating Q values and nonlinearity and resonator parameter fluctuation effects 07 p0953 A72-19009

Amplitron stability in optimal frequency regime, relating cut-off voltage and plate current as function of magnetic field, input power and geometrical parameters 07 p0953 A72-19014

Millimeter wave techniques for laser stabilization to frequency standards, using phase locked HCN laser and high resolution IR spectrometer [CLEA PAPER 6,7] 07 p1004 A72-19383

Optical coupling effects in frequency stabilized He-Ne lasers, finding instabilities for interferometric length measurement 07 p1005 A72-19414

RF excitation produced plasma instability, considering density fluctuation and drive frequency introduction by amplitude modulation 07 p1045 A72-20041

Frequency stability of free running methane stabilized He-Ne lasers with dc excitation, comparing to rf excitation 07 p1008 A72-20562

IMPATT diode microwave oscillator stabilized by two external resonant circuits, investigating self oscillation characteristics 08 p1138 A72-20745

Stationary statistical model for microwave oscillator flicker frequency noise, leading to power spectral density and time domain frequency instability [ONERA, TP NO. 1085] 08 p1141 A72-21431

High power Ar laser frequency stabilization technique using multiple feedback loop with optical cavity discriminator stabilized against iodine vapor absorption line 09 p1325 A72-23337

Short and long term frequency stability improvement in X band klystron oscillator stabilized by high Q superconducting cavity 10 p1449 A72-24303

CW X band Gunn microwave oscillators, measuring frequency variation relationship to ambient temperature 10 p1450 A72-24555

Frequency stabilization of He-Ne two mode laser with internal mirror plasma tube 11 p1646 A72-25303

Stable single frequency Ar laser radiation with coupled transitions emission 11 p1650 A72-26356

Extremal feedback control system for IR and sub-millimeter range laser emission frequency stabilization 11 p1650 A72-26358

Power resonance and frequency stabilization of gas laser with nonlinear absorption cell, considering He-Ne laser with Fabry-Perot resonator 12 p1820 A72-27584

Gas laser with strong absorption saturation to obtain high peak power and frequency self stabilization by generation of quasi-traveling wave in resonator 12 p1820 A72-27585

Fast response thermal compensation system for gas laser resonator length and frequency stabilization, discussing fabrication and design calculation 12 p1822 A72-27607

Gas laser oscillation frequency stabilization by comparing mode separation with RF standard 12 p1822 A72-27608

Laser resonator transverse and longitudinal mode selection techniques, considering single frequency stabilization, gain saturation theory and applications 12 p1826 A72-27964

Short term instability of frequency standard using AFC of quartz crystal oscillator by phase locking to optically pumped Rb 87 vapor clock 13 p1968 A72-29296

Stable single frequency operation of molecular laser using carbon dioxide-helium mixture, ensuring vibrational-rotational transition by special selection of active element parameters 13 p1970 A72-29682

High power monopulse Nd laser, obtaining single longitudinal frequency stabilized mode with anisotropic spar or quartz plates 13 p1971 A72-29922

Base resistance coupled transistorized multivibrator design characterized by superior frequency stability regardless of wide voltage fluctuation 13 p1934 A72-30017

Flashlamp pumped tunable narrowband traveling wave dye ring laser, stabilizing emission frequency by intracavity Fabry-Perot etalon 14 p2110 A72-30675

Correlation measurements of LF current noise and frequency fluctuations in Gunn oscillators, emphasizing generation-recombination noise component 14 p2088 A72-30916

Two cavity self exciting SHF microwave oscillator with resistance coupling through low Q-factor resonant diaphragm, noting frequency stability 14 p2090 A72-31121

Giant pulse radiation in Q factor modulated Nd glass laser frequency stabilization by molecular Cs vapor 15 p2245 A72-31411

Fluctuation analysis of parametric frequency multipliers and dividers, discussing short time instabilities caused by system noise 15 p2212 A72-32736

Carbon dioxide waveguide gas laser performance characteristics, noting mode pattern stability and insensitivity to resonator disturbances 16 p2402 A72-33396

Parametric amplifiers for satellite microwave communication systems, discussing frequency stability, noise temperature and gain relationships 16 p2369 A72-33520

Single frequency and mode carbon dioxide laser frequency and power stabilization by phase control with electronic servosystem 16 p2402 A72-33621

Stable single frequency Ar laser radiation with coupled transitions emission 16 p2403 A72-33709

Extremal feedback control system for IR and sub-millimeter range laser emission frequency stabilization 16 p2403 A72-33711

Frequency stabilized self-oscillating microwave up-converter with transferred electron diodes, noting maximum power output and bandwidth 16 p2369 A72-33764

Noise-to-carrier ratio and rms frequency deviation evaluation for X band Gunn and Si and GaAs avalanche diode oscillators 16 p2370 A72-34177

Hybrid injection locking of higher power CO₂ lasers. 17 p2564 A72-35343

Superconducting-cavity-stabilized oscillator of high stability. 17 p2530 A72-35386

Stability of injection-locked oscillators. 18 p2665 A72-36265

Frequency/temperature characteristics of Gunn devices. 18 p2667 A72-36684

Study of unsteady processes in the ionosphere and outer space by using quantum frequency stabilizers 18 p2687 A72-36853

French monograph - Ultrahigh-performance frequency generators 19 p2772 A72-37488

Active Q switching technique for producing high laser power in a single longitudinal mode. 19 p2811 A72-37845

Using ring lasers as rate sensors. 19 p2812 A72-38223

Frequency instability due to discrete noise in frequency synthesizers. 19 p2775 A72-38618

Certain results of a study of the emission-frequency stability of gas lasers at 0.63, 1.5, 3.39, and 9.6 micron wavelengths 19 p2814 A72-38786

Frequency stabilization of a gas laser using mode-interaction effects. 19 p2814 A72-38822

Unstable resonator theory with geometrical optics and diffraction approximation, applying to laser mode selection and beam divergence reduction 20 p2932 A72-39501

Absolute instability of nonlinear pulse-amplitude modulated control systems - Frequency criteria 21 p3038 A72-40707

Temperature effects on modulation sensitivity and vibrational spectra in Gunn diode oscillators, suggesting frequency stability improvement method 21 p3032 A72-40792

A stable neodymium-glass laser harmonic generator 21 p3064 A72-41739

Nonlinear molecular absorption cell for frequency stabilization of carbon dioxide laser radiation, discussing stability limit dependence on amplification, absorptivity and Q value 22 p3184 A72-42102

Nonpeaked emission of a ruby laser with frequency tuning and selection 22 p3184 A72-42103

Frequency stability criterion for variable-structure automatic control systems 22 p3162 A72-42185

Stability bounds for nonlinear systems designed via frequency domain stability criteria. 23 p3275 A72-43636

Hysteresis in a gas laser when passing from a single-frequency emission mode to a two-frequency mode 23 p3295 A72-43680

Molecular-beam-stabilized argon laser. 23 p3296 A72-43817

Fluctuations in a quantum frequency standard 23 p3271 A72-43842

Pure Ne laser and its fundamental characteristics. 23 p3296 A72-43946

Frequency stabilization of pure neon laser. 23 p3296 A72-43951

The effect of a harmonic-oscillator velocity distribution on an ideal solid-state laser. 24 p3409 A72-44953

Frequency stability of Gunn oscillators with variation of ambient temperature. 24 p3385 A72-44980

FREQUENCY STANDARDS

Accurately stabilized lasers application to frequency standards, reporting inverted Lamb dip experiments data 06 p0827 A72-18461

Gaussian rf noise effect on optical detection signal fluctuations in optically pumped frequency standards 07 p0938 A72-19013

Precision frequency calibrator for Raman spectrometers, using Fabry-Perot etalon 07 p0983 A72-19318

Millimeter wave techniques for laser stabilization to frequency standards, using phase locked HCN laser and high resolution IR spectrometer [CLEA PAPER 6,7] 07 p1004 A72-19383

Time metrology achievements review, discussing time unit development, atomic and molecular frequency standards, atomic clocks, time scales and time signal broadcasting 10 p1481 A72-24399

Two axial modes competition in He-Ne laser with uniform line broadening, noting application for high stability frequency standards 11 p1649 A72-26349

Calorimeter calibration for laser energy and power measurements in terms of electrical energy based on voltage, resistance and frequency standards 11 p1652 A72-26781

Single mode gas laser with internal absorption cell, emphasizing frequency standard application 12 p1819 A72-27285

Gas laser oscillation frequency stabilization by comparing mode separation with RF standard 12 p1822 A72-27608

Microwave and optical quantum electronic sources for frequency standards, noting primary Cs reference and multimode laser-RF oscillator beat technique 12 p1824 A72-27867

Short term instability of frequency standard using AFC of quartz crystal oscillator by phase locking to optically pumped Rb 87 vapor clock 13 p1968 A72-29296

Buffer gas mixture and pumping light effects on shifts from ground state hyperfine frequency in Rb-85 maser frequency standard 14 p2109 A72-30196

Time data dissemination techniques, discussing astronomical and atomic time scales, frequency standards, broadcasting and TV, navigation and satellite systems 14 p2085 A72-30364

Time-frequency dissemination system design, discussing radio propagation, time signals, noise effects, synchronous satellite transponders and TV use, accuracy, geographical coverage and costs 15 p2198 A72-32065

Precision frequency standards practical utility under field operating conditions, discussing propagation effects due to atmospheric and frequency parameters 15 p2199 A72-32066

Navy navigation satellite system, discussing time and frequency role, TIMATION satellite time standard and application for user equipment clock signal comparison 15 p2268 A72-32070

Long baseline radio interferometry with independent frequency standards for geodetic and astrometric applications 15 p2199 A72-32074

Two axial modes competition in He-Ne laser with uniform line broadening, noting application for high stability frequency standards 16 p2402 A72-33702

Microwave and optical quantum electronic sources for frequency standards, noting primary Cs reference and multimode laser-RF oscillator beat technique 16 p2403 A72-33976

Italian national time scale design and operation, discussing frequency standards, comparisons with national and international laboratories and time keeping 20 p2925 A72-39430

Fluctuations in a quantum frequency standard 23 p3271 A72-43842

Laser frequency measurement by comparison with stable molecular oscillator Doppler shift produced by reflection of UHF modulated coherent optical signal 24 p3411 A72-45425

FREQUENCY SYNCHRONIZATION

Solid state oscillator phase and frequency synchronization by injection of stable sinusoidal uhf signal modulated by 0-180 deg phase jump 02 p0194 A72-12569

Propagation delays for clock synchronization from synchronous satellite tracking by range measurements 05 p0628 A72-16563

Multicircuit hf filters tuning drive with mechanical synchronization correction 06 p0774 A72-17749

Gigahertz reflection amplifiers with low cost avalanche transit time diodes, measuring characteristics of amplification by synchronization at center frequency 07 p0955 A72-19191

Power-combining methods for synchronous detuned solid state microwave oscillators with stable large signal locking characteristics, noting feasibility 10 p1449 A72-24306

Solid state laser with slow relaxation bleachable filter, calculating modes self synchronization probability statistics relationship to relaxation time 10 p1492 A72-24512

Radio pulse synchronous detection with wideband preamplifier, evaluating frequency mismatch effects on signal distortion by transient response analysis 12 p1783 A72-27631

Time/frequency technology application to reliable aircraft collision avoidance system, discussing precision time-ordered techniques, frequency control and synchronization and flying clocks 15 p2268 A72-32072

Determination of the locking range from the reactive power balance of the oscillator. 17 p2530 A72-35430

Capture of a signal with a linearly varying frequency in an astatic phase autotuning system 19 p2766 A72-38420

FREQUENCY SYNTHESIZERS

Phase coherent frequency synthesizer as modulation source for multiple feature communication system, noting noise resistance, navigation capability, Doppler correction and transmitter to receiver ranging 06 p0777 A72-18619

Digital precision frequency synthesizers constructed on IC logic modules without using LC filters, analyzing restrictive factors 13 p1930 A72-29050

FREQUENCY TRANSLATION

FREQUENCY CONVERTERS

FRESNEL DIFFRACTION

Fresnel diffraction on opaque half plane screens with statistically rough surfaces, using Kirchhoff approximation 02 p0183 A72-12755

Real time coherent optical processor of pulse Doppler radar signals with Fresnel diffraction masks for PCW target range rate determination 03 p0322 A72-13437

Kirchhoff diffraction theory of scalar and electromagnetic waves application to elastic media, discussing Huygens principle, elastic waves tensor potential and Fresnel and Fraunhofer diffraction 04 p0548 A72-14740

Nonrelativistic charged particle resonating with circularly polarized transverse electromagnetic wave in nonuniform magnetic field, showing Fresnel diffraction pattern-like motion 04 p0557 A72-14951

Frequency characteristics of selectively reflecting screens in multichannel parabolic mirror antennas and determination of Fresnel coefficients dependence on polarized plane wave incidence angle 04 p0499 A72-15241

Laser beam diffraction effects on self induced thermal distortion in crosswind, noting dependence on Fresnel number [CLEA PAPER 2,4] 07 p0942 A72-19379

Earth location effect in Fresnel diffraction zone on comparator performance, measuring phase difference fluctuations in turbulent atmospheric boundary layer radio waves 09 p1284 A72-22232

Fresnel diffraction integrals for irradiance and power distribution calculations of Gaussian beams focused through annular apertures 09 p1352 A72-23334

Fresnel diffraction on opaque absorbing screen half planes with small rough surfaces, deriving field attenuation factor and structure/correlation functions 10 p1435 A72-24502

Kirchhoff-Fresnel diffraction field fluctuation at plane screen aperture in turbulent atmosphere 16 p2425 A72-33487

Ultrasonic velocity measurement by small power He-Ne laser visualization of standing waves in Fresnel diffraction region 18 p2697 A72-36416

Fresnel diffraction on opaque half plane screens with statistically rough surfaces, using Kirchhoff approximation 20 p2902 A72-39061

The efficiency of near-field Cassegrainian antennas. 21 p3027 A72-40367

Lensless multiplication of images and their spatial frequency spectra with the aid of Fresnel holograms 23 p3292 A72-44470

FRESNEL REFLECTORS

Fock reflecting formulae expansion to moving interfaces from Fresnel laws, interpreting solution in terms of geometrical optics 04 p0491 A72-15422

FRESNEL REGION

Scattering diagram for mutual cross coupling between antennas in Fresnel zone 02 p0196 A72-12757

Apodized Fresnel zone plate construction for solar X-ray image formation 03 p0354 A72-13047

Axial sound sources number, strengths and phases in jets, using experimental measurements of audio pressure in near field [AIAA PAPER 72-159] 05 p0652 A72-16910

Complex filter properties of Fresnel hologram with converging beam for optical filtration of three dimensional objects in Fourier or image planes 06 p0817 A72-18013

Radiation pattern determination parabolic Cassegrain radio telescope reflector antennas from Fresnel zone emission source, using holographic technique 10 p1482 A72-24783

Radiation pattern reconstruction of radio telescope parabolic Cassegrain reflector antennas from Fresnel zone emission source, using holography and optical processing 14 p2103 A72-30221

Optical modeling of antenna radiation patterns from radio hologram of Fresnel region field 15 p2209 A72-32664

Generalized radar equations derivation to obtain Doppler frequency shift and variance in Fresnel zone due to target movement 16 p2365 A72-33765

Scattering diagram for mutual cross coupling between antennas in Fresnel zone 20 p2907 A72-39063

Reflector optimization of backfire antennas with the aid of the theory of the Fresnel zones 21 p3031 A72-40541

Computer aided directivity measurements of large antennas in Fresnel zone 23 p3274 A72-44491

FRETTING CORROSION

Steels shafts fatigue failure under cyclic loading and fretting corrosion, indicating fatigue strength increase through surface layer wear resistance augmentation 13 p1979 A72-29476

Fretting corrosion fatigue prevention by barrier approach, discussing test program and application to helicopter part fatigue life increase [AHS PREPRINT 672] 17 p2626 A72-34512

FRICITION

NT AERODYNAMIC DRAG

NT DRY FRICTION

NT FLOW RESISTANCE

NT FRICTION DRAG

NT INTERNAL FRICTION

NT KINETIC FRICTION

NT SKIN FRICTION

NT SLIDING FRICTION

NT STATIC FRICTION

NT SUPERSONIC DRAG

NT VISCOUS DRAG

Frictional electrification from supersonic particle impact, determining particle charge and concentration, body intercepting area and velocity variations with speed 02 p0261 A72-12555

Pneumatic machine for microfriction stud welding of dissimilar metals 09 p1320 A72-23631

Surface reaction mechanisms analysis in adhesion, friction, wear and lubrication, using electron diffraction, Auger spectroscopy and ellipsometry techniques 12 p1813 A72-27036

Possible regimes and solutions for adiabatic one dimensional compressible gas flow in convergent and divergent ducts with friction 12 p1797 A72-27348

Russian papers on solid bodies friction mechanism and properties covering adhesion, lubricants effects, wear in presence of aircraft fuels and temperature effects 12 p1817 A72-28180

Solids deformation resistance increased by active lubricants effects on coupled friction surfaces, noting damage localization to thin surface layers 12 p1817 A72-28181

Statistical methods for friction and wear processes, noting Rayleigh distribution of wear particles, surface dispersion velocity, energy dissipation and friction force 12 p1818 A72-28186

Thin surface film lamination in antifriction carbon-graphite materials under critical specific pressure, discussing crystalline phase in wear products 12 p1818 A72-28192

Molecular-mechanical theory of external friction, taking into account surface roughness, time and temperature dependent mechanical properties and chemical processes 12 p1818 A72-28195

Plane-strain compression of rigid plastic material between flat platens, approximating frictional boundary conditions by entrapped viscous fluid lubricant 16 p2428 A72-34171

Russian book - Mathematical theory of friction 19 p2806 A72-37350

FRICITION COEFFICIENT

U COEFFICIENT OF FRICTION

FRICITION DRAG

NT AERODYNAMIC DRAG

NT SUPERSONIC DRAG

NT VISCOUS DRAG

Global angular momentum balance, considering atmospheric frictional torques and fluxes, ocean water mass exchanges and seasonal variations effects 03 p0384 A72-14142

Friction drag coefficient determination for cylindrical bodies in laminar and turbulent incompressible fluid flow 10 p1420 A72-25135

Tornado model from atmospheric thermodynamics nonlinear equations, examining air flow from lower boundary layer and ground friction 11 p1682 A72-26880

Polarization and dynamical friction drags on star in uniform infinite media and flat rotation sheet 12 p1872 A72-27892

High temperature skin friction meter design for drag measurements, using motor-transducer air core assembly 12 p1812 A72-27959

Friction drag and heat transfer on long blunt-nosed cylinder in supersonic flow, determining location of transition zone as function of Mach number 13 p1895 A72-29642

Hydrodynamic pivoting-pad vane tips for high-speed vane pumps. 18 p2694 A72-36046

Friction term formulation and convective instability in a shallow atmosphere. 18 p2706 A72-36633

Drag of a flat plate with transition in the absence of pressure gradient. 18 p2641 A72-36775

Influence of a trailing vortex on friction pulsations in the near-wall region of the leading stagnation point of a cylinder in transverse flow 19 p2786 A72-38041

The friction drag factor for an unsteady motion in tubes 20 p2913 A72-39392

The effects of frictional drag on missile vibrations - A finite difference solution. 21 p3118 A72-40929

FRICITION FACTOR

Wall friction effect on current sheet speed of magnetically driven shock tube, establishing steady state existence 01 p0105 A72-10027

Shock isolator model, using passive elements and variable Coulomb friction force to minimize transmitted shock and relative displacement 01 p0047 A72-10218

Physical inconsistencies of mechanico-mathematical concepts of metal deformation, considering friction forces, lubricant action and plastic tensors and deviators 01 p0102 A72-11077

Luna 16 lunar soil sample tests, comparing friction coefficients and microhardness with terrestrial analogs 02 p0280 A72-12286

Solid phase friction welding, discussing metallurgy and engineering applications 03 p0362 A72-12990

Fibrous structure of precipitates produced at bottom of trace due to friction in work hardened Al-Cu alloy solid solution 03 p0376 A72-13970

Long wave radiation and surface friction effects on midlatitude cyclone development in eight-level primitive equation orographic model 03 p0385 A72-14229

Lubrication and friction problems regrouping in thin viscous fluid films mechanics 03 p0364 A72-14271

Turbulent mixing length formulation and velocity profiles for non-Newtonian power law fluids, determining friction factor for pipe flow at high Reynolds numbers 03 p0343 A72-14318

Plasma shock wave oscillation profile dependence on ion and electron friction and viscosity 04 p0555 A72-14620

Hydrodynamic equations for non-Lagrangian statistical mechanical particle systems with three degrees of freedom under frictional and velocity dependent forces 04 p0512 A72-15202

Dynamic analysis of straight shaft with constant noncircular section and internal friction forces, delineating trajectories for shaft center of symmetry 04 p0593 A72-15707

Statistical calculation of wear rate in friction pair with linear contact, analyzing errors 04 p0528 A72-15711

Thin sintered fluoride films bonding with monoaluminum phosphate, investigating friction and wear behavior 06 p0821 A72-17804

Friction and wear characteristics at high temperature of plain bearing embedded with pellets of graphite, sodium fluoride and tungsten disulfide lubricating mixture 06 p0823 A72-18584

Lubrication with thin molybdenum disulfide solid film under various temperatures and atmospheric pressures, examining friction and lifetime 06 p0823 A72-18587

Filler particles orientation effects on plastic bearing materials friction and wear properties, discussing experimental testing methods 06 p0836 A72-18595

Geostrophic drag coefficient for heterogeneous terrain as function of effective roughness length, considering surface friction effects in large scale atmospheric models 07 p1030 A72-19108

Approximate stress calculation in friction pulley shells of multipulley hoisting machines, using method of initial parameters 07 p1094 A72-20134

Soviet monograph on solid inorganic compounds as high temperature lubricants covering powder lubricants mechanism under different friction conditions, gas media, temperature effects, etc 08 p1191 A72-20913

Friction and bending effect on unidirectional glass fiber reinforced plastic ring deformation distribution 08 p1191 A72-21504

Soviet book on heat and mass transfer and friction in gradient fluid flows in variable cross sectioned ducts and at surface of bodies 08 p1152 A72-22022

Negative slip reversal effect formation mechanism during friction, discussing elimination via oleic acid 08 p1181 A72-22092

Plastic flow properties and stress measurement for metal working conditions with flat ring compression specimens and interfacial friction consideration 08 p1250 A72-22196

Plastic deformation friction fracturing, stress concentration, free surface changes and load displacement analysis with upper bound, slip line and finite element methods 08 p1250 A72-22197

German monograph on tire rubber friction on dry and wet rough surfaces, taking into account loading, velocity and temperature effects 09 p1332 A72-22323

Frictioned force modification of lower thermosphere vertical neutral gas velocities with resulting atomic oxygen and molecular nitrogen density-height distribution deviation from barometric law 09 p1298 A72-22582

Aerodynamics of vortex chambers with symmetrical air injection, discussing core and end boundary layer flows interaction and momentum loss from end surfaces friction 09 p1260 A72-22676

Slip contact joint frictional damping of vibration of beam on elastic support 09 p1408 A72-23464

Self lubricating materials for maintenance-free clocks antifriction bearings, discussing friction and wear behavior 09 p1319 A72-23562

Long period pulsations of finite amplitude baroclinic wave, noting stable limit cycle for small friction effect 09 p1347 A72-23653

Luna 16 lunar soil sample tests, comparing friction coefficients and microhardness with terrestrial analogs 10 p1532 A72-23755

Surface textures in rolled Al sheets, investigating friction and reduction 11 p1638 A72-25509

Current sheet velocity limitation in magnetically driven shock tube with plasma electrodes, examining wall ablation and friction and Hall current effects [AIAA PAPER 72-409] 11 p1695 A72-26160

Metal powder mixing, examining friction effects and optimal particle sizes, shapes and amounts 11 p1642 A72-26828

Parametric approximation of unsteady laminar boundary layer in incompressible fluid in terms of flow velocity and friction characteristics 12 p1799 A72-28177

Physicochemical processes in metal surface layers subjected to contact friction with aircraft fuels presence, noting secondary compounds and thermal oxidation acceleration 12 p1817 A72-28183

Friction characteristics of high melting point metal chalcogenides as function of load and temperature, noting friction coefficient variations 12 p1817 A72-28185

Temperature effects on crystalline solids adhesion, noting friction rise above seizure point 12 p1818 A72-28187

Oxide thin films effects on surface layers deformation and wear resistance of coated metals under friction, noting electrical resistance changes in annealing 12 p1818 A72-28189

Metal surface layers structural changes under external friction, noting hardening, softening and phase transformations of active layer material 12 p1818 A72-28190

Cumulative damage and structural changes in friction contact areas of steel plates under cyclic pulsed loads, noting microhardness distribution and surface layers microstructure 12 p1818 A72-28191

Surface roughness effects on seizure and friction of contacting metal plates under atmospheric pressure and vacuum 12 p1819 A72-28197

Tribochemical effects during friction of non-lubricated amorphous and crystalline polymer surfaces under mild and hard contacting conditions 12 p1835 A72-28200

Gas turbine engine compressor blade and materials fatigue strength dependence on pressure under contact friction corrosion

12 p1831 A72-28244

Friction force electron component for superconductor dynamic dislocation at various temperatures and propagation rates

13 p2021 A72-28901

Chemical reactions between solids during boundary friction, presenting literature review on mechanochemical or tribo-chemical reactions between solid lubricants and metal surfaces
[ASLE PREPRINT 72AM 1]

13 p1964 A72-28969

Metallic, ceramic, polymeric, composite and solid film lubricant friction and wear properties and testing
[ASME PAPER 72-DE-28]

14 p2108 A72-30869

Friction and adhesive and abrasive wear of ceramics, discussing effect of environmental water and hydrocarbons

15 p2260 A72-32129

PTFE thin films interspersal with lumps and streaks from transfer to smooth surface during low speed sliding, discussing friction coefficient under various conditions

16 p2396 A72-32870

Friction and wear properties of carbon fiber reinforced polymers sliding against metals in pure and sea water and aqueous solutions

16 p2396 A72-33123

Supramolecular scale microscopic dynamic model for solid body macroscopic friction and wear effects

16 p2398 A72-33367

Negative slip reversal effect formation mechanism during friction, discussing elimination via oleic acid as lubricant additive

17 p2559 A72-34663

Effect of rotation on laminar compressible fluid flow in a vertical cylinder.

17 p2539 A72-34972

Friction and wear of electroplated hard gold deposits for connectors

18 p2693 A72-35981

Mathematical model and simulation for contact problems involving elastic half spaces and viscoelastic and friction effects

18 p2734 A72-36371

Independent moving vibrational /acoustic/ source-induced wave losses during friction of two elastic bodies

18 p2696 A72-36966

Vacuum-friction temperature resistance and durability of a molybdenum-disulfide coating deposited on steel by the detonation method

19 p2809 A72-38290

The temperature dependence of the friction stress for basal dislocations in beryllium in the range 300-500 K.

20 p2935 A72-39191

Flow calculation for polytropic process with friction and heat transfer

20 p2913 A72-39371

Heat flux and friction force minimization problems equivalence in optimal control of incompressible boundary layer on isothermal plate

20 p2914 A72-39918

Magnetic field effects on turbulent shear flow of electrically conducting fluid, discussing turbulence level, friction stress and heat exchange

21 p3089 A72-40260

Internal energy and conductive and frictional dissipation, mass, momentum and energy production as functions of density, entropy and geometric state variables

21 p3130 A72-41228

Frictional effects with neutrals and the gravitational instability of a plasma.

21 p3093 A72-41332

Experimental friction factors for turbulent flow with suction in a porous tube.

21 p3047 A72-41618

Cylindrical shells vibration under external forces with allowance for internal and external friction, obtaining harmonic influence functions in series form

22 p3233 A72-42056

Bending evaluation of test section in tensile tests with axial loads and resistance strain gages, noting friction moment role

24 p3456 A72-44791

FRICION LOSS COEFFICIENT

U. FRICION FACTOR

FRICION MEASUREMENT

Skin friction measurement in nonisobaric subsonic flow with pressure gradient over airfoil section by surface impact probes

02 p0151 A72-12275

Vacuum chamber and instrumentation for friction and wear tests at temperatures to 1800 C in vacuum and inert media

04 p0510 A72-15659

Solid lubricant antifriction properties test methods and measuring apparatus design for wide temperature range

05 p0665 A72-16096

Al alloy and brass deformation compression tests inadequacy for friction determination and boundary agents, EP additives and hydrodynamic and solid lubricants evaluation

08 p1181 A72-22195

Heated thin film gages calibration for skin friction measurements in laminar and turbulent flows, discussing wall temperature distribution and turbulence effects

15 p2241 A72-32577

Day-to-day operational airplane-airport relationship, discussing runway grooving impact and friction coefficient measurement
[AIAA PAPER 72-813]

19 p2750 A72-38118

Measurements of skin friction on the wall of a hypersonic nozzle.

24 p3365 A72-45792

FRICION PRESSURE DROP

U. SKIN FRICION

FRICION REDUCTION

Plasma jet technique for self lubricating antifriction Ni, Sn or Cu coatings for MoS2 particle oxidation protection

04 p0527 A72-15664

Solid lubricant antifriction properties test methods and measuring apparatus design for wide temperature range

05 p0665 A72-16096

Frictional stick-slip autooscillations suppression by resonance effect during forced vibration in normal direction

08 p1181 A72-22181

Second order fluids plane Poiseuille flow instability to finite amplitude disturbances, noting implications to Toms friction pressure reduction phenomenon in pipe flow

10 p1470 A72-25065

Metal rolling speed effect on force and friction reduction by ultrasonic vibrations imposed on rollers, noting coefficient of friction dependence on deformation

12 p1814 A72-27645

Frictional stick-slip autooscillations suppression by resonance effect during forced vibration in normal direction

18 p2695 A72-36238

Industrial pyroceramic materials usable under friction without lubrication

21 p3061 A72-41374

Thermal stability of sulphides of some metals in iron-base cermets

23 p3298 A72-43285

FRINGE PATTERNS

U. DIFFRACTION PATTERNS

FROGS

Frog Rana temporaria striated muscle tension response recording during sudden fiber length alteration, suggesting force generation mechanism

01 p0009 A72-10017

Glycogen content and distribution determination in frog retina by histochemical analysis with intravascular injection of mixture preventing decomposition

06 p0764 A72-17987

FRONTAL AREAS [METEOROLOGY]

U. FRONTS [METEOROLOGY]

FRONTS [METEOROLOGY]

Numerical two layer model of frontal motions development in atmosphere

06 p0840 A72-17384

Vertical air motion three dimensional field measurement near mobile fronts by high precision tracking of air-dropped radar reflectors, noting quantitative rainfall prediction

07 p1029 A72-19098

Intense precipitation contour zone distinguishing methods error estimation in seeding experiments on frontal clouds

08 p1201 A72-21994

Numerical solutions of linear and nonlinear hydrostatic primitive equations for frontogenesis forced by nondivergent horizontal wind, noting discontinuities prediction

09 p1347 A72-23651

Frontogenesis models based on horizontal deformation field, noting uniform and nonuniform potential vorticity

09 p1347 A72-23652

Persistent intense CAT in upper level frontal zone, discussing synoptic features, vertical wind shears, radar echoes and turbulence intensity

13 p1995 A72-29622

Non-Boussinesq effects and further development in a model of upper tropospheric frontogenesis.

19 p2829 A72-38558

Computer program for numerical analysis of atmospheric fronts in lower troposphere based on models for spatial distribution of hydrothermal characteristic in air mass

19 p2829 A72-38771

Direct observation of a complete unit of meridian circulation from the equatorial belt up to the polar front - Synthesis of concepts of the pseudofront, of the equatorial mesosystem, and of the subsidence well

21 p3078 A72-41344

Atmospheric frontal motion stability via two-layer homogeneous incompressible fluid model, solving eigenvalue problem by small perturbation method

22 p3201 A72-42505

FROST

Light transmission, reflection and environment problems of hydrophilic coatings for fog and frost protection in aviation instrument window design

22 p3196 A72-42519

FROZEN EQUILIBRIUM FLOW

Laminar boundary layers on heated plane wall behind shock wave in dissociating oxygen for thermodynamic and frozen flow

03 p0344 A72-14342

Nonlinear acoustic propagation in chemically reacting media, discussing quasi-frozen and quasi-equilibrium flow processes behind shock fronts

07 p0969 A72-19974

Intrinsically transonic /almost equal frozen and equilibrium sound velocities/ flows of chemically active gas mixture, developing nonlinear perturbation theory

19 p2745 A72-37390

Nonlinear acoustic propagation in chemically reacting media, discussing quasi-frozen and quasi-equilibrium flow processes behind shock fronts

20 p2955 A72-40031

FROZEN LAKES

U. LAKES

FRUSTUMS

Ring stiffened truncated cone shells vibration mode tests, describing air and electrodynamic shakers and mobile noncontacting displacement sensitive sensor system

12 p1882 A72-27340

FUEL CAPSULES

Cylindrical nuclear fueled capsules heat transfer gaps, determining dimensional changes with neutron radiographs

04 p0546 A72-14428

FUEL CELL CATALYSTS

U. ELECTROCATALYSTS

FUEL CELLS

NT. HYDROGEN OXYGEN FUEL CELLS

Power supply and converters for satellite and spacecraft, discussing fuel cells, radioisotopes, nuclear reactors, etc

05 p0615 A72-16745

Proportional-integral control of reactants supply for hydrazine-oxygen fuel cells with pulse controlled solenoids

06 p0867 A72-18290

High temperature and ZrO2 ceramic electrolyte effects on ionic partial conductivity and fuel cells longevity

06 p0760 A72-18337

Monograph on fuel cells covering thermodynamics, electrode polarization principles, electrocatalysis, system requirements, operational principles and applications

10 p1423 A72-24700

Miniaturized electronic system for controlling methanol concentration in aqueous electrolyte during fuel cell operation

12 p1755 A72-27723

Electrocatalysis and fuel cells - Conference, Seattle, December 1970

16 p2351 A72-33876

Electrochemical oxidation and classification of fuel cells according to electrolyte, electrode, fuel, catalyst and temperature

16 p2351 A72-33877

Hydrocarbon oxidation and catalysis on Pt fuel cell electrodes, using electrochemical methods with isotopic exchange and gas chromatography

16 p2361 A72-33878

Raney Pd-Ag catalysts for methanol oxidation in alkaline electrolyte in fuel cells

16 p2361 A72-33879

Alloying component effect on Pt catalytic activity in anodic oxidation of methanol for fuel cells

16 p2361 A72-33881

Sintered WC effects on fuel cell electrochemical oxidation in acid electrolytes, analyzing hydrogen, hydrazine, formaldehyde, acetaldehyde, formic acid and carbon monoxide fuels

16 p2351 A72-33882

Electrodes converting hydrogen, methanol or oxygen for use in fuel cells with alkaline electrolyte, using Ag-Pd, Ni, Si and C catalysts

16 p2351 A72-33885

Hydrazine fuel cell development, electrochemical problems and applications, noting batteries with air oxidant

16 p2351 A72-33886

Alkaline fuel cell development and trends, noting carbon dioxide removal technique and applications ranging from portable batteries to automobile power

16 p2351 A72-33887

Hydrocarbon electrochemical oxidation kinetics for fuel cells at low temperature, considering adsorption and bond cleavage

16 p2361 A72-33891

- Diffusion limitation avoidance at high current densities by fuel cell preparation via Pt thin film sputtering on porous vycor substrates 16 p2352 A72-33893
- Cubic stabilized zirconia utilization as solid electrolyte in high temperature fuel cell system for efficient and economical energy conversion 16 p2352 A72-33894
- Composition of initial mixtures for production of the gaseous C-H-O fuel for fuel cells with molten alkaline carbonates. 19 p2754 A72-37778
- Developmental status of thermionic materials. [GULF-GA-A12128] 19 p2833 A72-38575
- ### FUEL COMBUSTION
- Laser light scattering by fuel droplets in flame combustion zone, measuring intensity distribution with contactless optical probe 01 p0066 A72-10495
- Polyethylene and polypropylene combustion, investigating additives and surrounding gaseous composition effects on flammability and volatile products during thermal degradation 02 p0248 A72-11767
- Flame spread rate over combustible polymer fuel specimens as function of surface, sample, composition, pressure and oxygen mole fraction 02 p0301 A72-11965
- Optical visualization and probe measurements on combustion characteristics of liquid fuel in compression-ignition engine swirl chamber 02 p0271 A72-12436
- Chemical efficiency improvement of aluminum combustion with nitric acid in organic solid fuel 03 p0405 A72-13540
- Heat transfer to liquid fuel burning from sandfilled pan burner, measuring burning rate, wick temperature distribution and flame radiation heat flux distribution as function of time 03 p0458 A72-14221
- Bipropellant fuel droplets combustion in oxidizing atmospheres from spherico-symmetrical nonconvective quasi-steady state model, discussing supercritical pressures and forced convection probability 04 p0596 A72-15273
- Reactive solid or fuel combustion, deriving equations for movement and deformation of reaction front during oxidant diffusion through ash mantle 06 p0902 A72-18155
- Critical conditions for self ignition of solid fuel particles suspended in gas 06 p0903 A72-18203
- Detonation propagation through tubes coated with thin liquid fuel films, considering boundary layer displacement effect on propagation speed, pressure ratio and reaction zone length 07 p1100 A72-19728
- Small perturbation stability of discontinuous solution of equations of motion for solid fuel combustion processes 08 p1253 A72-21463
- Flame autostabilization mechanism during gaseous oxygen-liquid ammonia mixture combustion in liquid fuel rocket engine chamber, measuring mean burnout time 08 p1224 A72-22091
- Emissivity calculation for radiant heat flux from isothermal gas mixture of hydrocarbon fuel combustion products 10 p1561 A72-23839
- Carbohydrate based gelling agent for gas turbine fuel, describing development and chemical and physical properties [ASME PAPER 72-GT-9] 11 p1702 A72-25612
- Wall effects on deflagration, combustion rate, and self and hot-point ignition temperature and delay 11 p1747 A72-26789
- Aromatic hydrocarbons and fuels, investigating engine parameters effects on combustion and exhaust gases temperatures 13 p2025 A72-29074
- Ethanol liquid fuel counterflow diffusion flame stabilization and thermal structure determination by interferometry 13 p1913 A72-29306
- Nonequilibrium ionization phenomena effects on electric conductivity of combustion gas-particle plasma generated by aluminized fuel seeded with potassium nitrate 13 p2013 A72-29363
- Thermal nozzle combustion effects on supersonic flow of chemically reacting gas in thermodynamic equilibrium 15 p2334 A72-31265
- Formation mechanism of sodium sulfate from gas turbine fuel combustion, discussing thermodynamic equilibria and reaction kinetics 15 p2297 A72-31294
- Chain reaction mechanisms of fuel combustion in presence of metal oxides for ores reduction application 15 p2335 A72-31850
- Fuel injection, mixing and combustion processes investigation in model cylindrical swirl chamber, describing flow visualization method for turbulence observation 15 p2297 A72-32297
- Flat flame deflagration tube measurements of laminar flame velocities for propane-ammonia-air mixtures in fuel rich region 16 p2480 A72-34006
- Flame autostabilization mechanism during gaseous oxygen-liquid ammonia mixture combustion in liquid fuel rocket engine chamber, measuring mean burnout time 17 p2597 A72-34662
- Mathematical model of nitric oxide formation by fuel droplet burning above fuel critical pressure, applying to diesel engine operations 17 p2511 A72-34901
- Liquid fuel droplet transient combustion in supercritical hot stagnant oxidizing environment, solving conservation equations 17 p2636 A72-34903
- Mean emissivity of a luminous flame - Spray combustion of liquid fuel. 18 p2740 A72-36148
- Detonation shock wave study of liquid fuel droplets in gaseous oxidizing agent flow, using schlieren and scanning photography 20 p2962 A72-40044
- Device for measuring the kinetic characteristics of particle combustion 20 p2928 A72-40050
- Unsteady burning of reacting mixture of air and condensed-phase combustion products in closed variable volume, noting mathematical model for parameters calculation 21 p3128 A72-40977
- Radiation intensity of a steady flame above a burning fluid 22 p3243 A72-42166
- Experimental facility and diffusion technique for measuring turbulence characteristics during hydrocarbon fuels burning in air streams 23 p3287 A72-43658
- Self ignition behaviour of some liquid fuels in an adiabatic compression machine. 23 p3325 A72-44252
- Supersonic jet engine fuels production by gasoline vapor pyrolysis, discussing physico-chemical characteristics and combustion properties 24 p3432 A72-44625
- A laser interferometer for combustion, aerodynamics and heat transfer studies. 24 p3402 A72-44950
- Reacting and nonreacting swirl recirculation bubble gasdynamic structure in fuel combustion systems, noting anisotropic turbulence from hot-wire anemometer measurements 24 p3461 A72-45024
- Chemical aspects in the shock initiation of fuel droplets. 24 p3433 A72-45051
- Theoretical analysis of a rotating two-phase detonation in liquid rocket motors. 24 p3433 A72-45053
- Measurement of the velocity distribution in the boundary layer over a flat plate with a diffusion flame. 24 p3464 A72-45062
- ### FUEL CONSUMPTION
- Small three spool, reverse and mixed flow turbofan engine for business jets, discussing fuel consumption reduction, thermodynamic performance, efficiency and maintainability [SAE PAPER 710776] 01 p0116 A72-10268
- Pulse shaped small parameter variation effects on performance index of minimum fuel control systems with initial and final manifolds 03 p0337 A72-12906
- Missile trajectory stochastic optimal control systems with fuel constraint by mean path deviation optimization 05 p0725 A72-16452
- Nonlinear multivariable and linear systems optimal control in aerospace field, discussing use of performance indexes for fuel consumption, process evolution time or combination 05 p0725 A72-16453
- KS-transformation based regularization technique modification for minimal fuel consumption rocket trajectory control during space maneuver 05 p0726 A72-16454
- Iterative method for approximate determination of local minima in fuel optimal finite thrust orbit transfer 05 p0719 A72-16541
- Sign behavior of switching function defined for plane fuel-optimal flight on elliptical coast trajectories 05 p0728 A72-16705
- Altitude-velocity dependence of turboprop engine equivalent horse power, propeller output and specific fuel consumption, discussing performance characteristics relation to ambient air temperature 05 p0708 A72-17100
- Gas jet control for spinning satellites attitude correction, deriving relations between satellite and control system parameters, response time and fuel consumption 05 p0731 A72-17196
- Dither adaptive control technique application to constant fuel rate problem, illustrating with analog computer solution 06 p0792 A72-17308
- Extremal field properties in optimal control problem applied to aircraft flight over assigned distance with minimum fuel consumption 06 p0758 A72-17727
- Aircraft performance and flight path optimization algorithms for minimum fuel-fixed range, using calculus of variations 07 p0912 A72-19091
- Nonlinear multivariable system optimal control with respect to time and fuel consumption, discussing Gauss-Newton and Davidson methods and application to geostationary satellite 07 p0962 A72-19719
- Nonoptimality of Lawden spiral for minimum fuel transfer orbits in space navigation 07 p1033 A72-20246
- High turbine entry temperature effects on gas turbine engine specific power and fuel consumption, noting thrust/weight ratio increase in turbojet and turbofan engines 07 p1055 A72-20311
- Soviet civil gas turbine engines construction and performance, noting relatively high specific fuel consumption 08 p1223 A72-21275
- Extremal field properties in optimal control problem applied to aircraft flight over assigned distance with minimum fuel consumption 11 p1574 A72-25329
- Liquid metal regenerator design and test evaluation for gas turbine engine fuel consumption improvement. [ASME PAPER 72-GT-33] 11 p1704 A72-25629
- Propulsion system flexibility in V/STOL aircraft with one lift-cruise engine, discussing takeoff thrust requirements and cruise fuel consumption efficiency [ASME PAPER 72-GT-105] 11 p1576 A72-25670
- Spacecraft interplanetary guidance trajectory correction, deriving algorithm for optimal accuracy and minimum fuel expenditure 11 p1718 A72-25931
- Stratospheric meteorological characteristics effects on Concorde supersonic flight performance, fuel consumption, dynamic behavior and passenger comfort 13 p1994 A72-28876
- Future projections of commercial jet aircraft fuel demands, estimating engine exhaust effects on air quality 13 p1897 A72-28879
- Elliptical orbiting spacecraft minimum fuel consumption rendezvous maneuver, formulating variational extremum problem with constraints 14 p2150 A72-30329
- Orbital correction problems for vehicle around spherical planet, considering velocity, fuel consumption and trajectory optimization 15 p2308 A72-31819
- Low thrust spacecraft navigation requirements for minimum propellant guidance, using neighboring extremal law 15 p2270 A72-32194
- Analytical guidance in the neighborhood of optimal multi-impulse trajectories. 17 p2609 A72-35102
- Limit-cycle bounds of a satellite attitude-control system. 17 p2622 A72-35529
- Reachable sets and singular arcs for minimum fuel problems based on norm-invariant systems. 17 p2534 A72-35533
- Thermionic fuel element development status summary. 18 p2708 A72-36151
- Parabolic switching boundaries method for optimal fuel consumption control of manned orbital space vehicles 18 p2672 A72-36325
- Specific fuel consumption and specific thrust optimization methods in turbofan cycles, noting optimum fan pressure ratio increase with turbine inlet temperature 19 p2848 A72-37746
- Considerations regarding the choice of the number of stages in long-range or high-altitude rockets 20 p2977 A72-39596
- N-burn analytic solution for propellant-optimal transfer trajectories in vacuum, taking into account gravitational effects [AIAA PAPER 72-929] 21 p3112 A72-41569
- Thermodynamic cycle parameter effects on bypass turbofan jet engine fuel consumption and performance under various flight conditions and engine ratings 23 p3326 A72-44281
- Contribution to the discussion of mixed-mode propulsion and reusable one-stage-to-orbit vehicles. 24 p3450 A72-45191
- ### FUEL CONTAMINATION
- Surface active agent detection by device using ultrasonic vibrating mechanism to emulsify water with fuel, determining water retention or turbidity by photoelectric cell 04 p0564 A72-14419

Proposed gas turbine procurement standards for gaseous and liquid fuel specifications emphasizing fuel contaminants
[ASME PAPER 71-WA/GT-3] 05 p0703 A72-15896
Purity requirements of aircraft gas turbine fuels, considering mechanical impurities, water, microorganisms, and surface active, corrosive, resinlike and paraffin substances 07 p1052 A72-20373

FUEL CONTROL

Minimum propellant impulsive optimal spacecraft guidance and trajectory problem, developing deterministic theory in discrete linear quadratic form with second order perturbation analysis 01 p0130 A72-10929

Open cycle gas core nuclear rocket engine, determining scaling laws for buoyancy force effect on fuel containment at various flow parameters 01 p0099 A72-11348

Injection geometry and inlet flow conditions application to open cycle gas nuclear reactor engine, evaluating fuel containment from cylindrical and spherical chambers experiments 01 p0100 A72-11350

Nonlinear programming iteration scheme for fuel-time optimization of satellite orbital rendezvous terminal phase 03 p0437 A72-13838

Time optimal and fuel optimal control of spin stabilized space vehicle for body-fixed and gimbaled jets, using maximum principle 05 p0728 A72-16476

Algorithm for iterative computation of time and fuel optimal control functions for linear systems, presenting flow chart 07 p0962 A72-19714

Minimum fuel continuous low thrust orbit transfer problem of optimal control, solving boundary value problem with Multiple Substitution Polynomials and Marquardt method 10 p1552 A72-24486

Miniaturized electronic system for controlling methanol concentration in aqueous electrolyte during fuel cell operation 12 p1755 A72-27723

Turboprop engines dynamic parameters experimental determination by rpm transient response to instantaneous fuel supply changes 13 p2027 A72-29137

Minimum fuel control of second order system in n-dimensional Euclidean space, examining Pontryagin maximum principle applicability 18 p2673 A72-36696

Fluidic heat sensors for measuring fuel temperature in jet engines 23 p3326 A72-44280

A digital model of jet engine hydraulic fuel controller 23 p3327 A72-44291

FUEL CORROSION

JP-5 fuel sulfur content effect on aircraft engine turbine blades hot corrosion under marine environmental conditions 07 p1010 A72-18752

Purity requirements of aircraft gas turbine fuels, considering mechanical impurities, water, microorganisms, and surface active, corrosive, resinlike and paraffin substances 07 p1052 A72-20373

Hot corrosion effects on Inconel-700 and Inconel-X gas turbine rotor blades during burning of high sulfur concentration residual oil fuels
[ASME PAPER 72-GT-87] 11 p1656 A72-25662

Interaction between vanadium in gas turbine fuels and sulfidation attack. 19 p2817 A72-37766

Effect of fuel on gas corrosion in jet engine combustion chambers 19 p2849 A72-38091

FUEL ELEMENTS [NUCLEAR REACTORS]

U NUCLEAR FUEL ELEMENTS

FUEL FLOW

NT PROPELLANT TRANSFER

Prediction of tank pressure history in a blowdown propellant feed system. 17 p2537 A72-34211

FUEL GAGES

Optimal invariant conversion of information from a turbine flow meter and a capacitive fuel gauge 21 p0308 A72-41801

FUEL INJECTION

Energy release and accelerating inner stream effects on flow field near fuel injection in gas core reactor, basing Euler equations energy diffusion term on radial radiative transport 01 p0100 A72-11351

Fuel vaporizer for gas turbine engine, investigating heat transfer coefficient 05 p0747 A72-16492

Steady two dimensional laminar compressible boundary layer of reacting gas mixture with surface vaporization and fuel injection, using integral method 07 p0967 A72-19129

Fuel injection, mixing and combustion processes investigation in model cylindrical swirl chamber, describing flow visualization method for turbulence observation 15 p2297 A72-32297

Pressure increase induced by heat release for laminar flame sheet in hypersonic stream, considering fuel injection through semifinite porous flat plate 15 p2337 A72-32590

Experimental performance of coaxial injectors in thrust-variable LO2/GH2-rocket engines. 24 p3434 A72-45181

Swirling base injection for supersonic combustion ramjets. 24 p3434 A72-45785

FUEL OILS

Buffalo photographic aircraft for oil slick remote sensing, using aerial cameras and thermal IR scanner 05 p0658 A72-16600

Improvement of the anticorrosion properties of water-containing hydropurified diesel fuels with the aid of saltless additions 17 p2596 A72-35177

FUEL PUMPS

Fuel lubricity effects on aircraft engine fuel pump wear, discussing remedial use of corrosion inhibitors and change to noncorroding pump construction materials 08 p1222 A72-21450

Automatic control for selective precision joint assembly of fuel pump equipment, reducing unfinished product volume 16 p2397 A72-33261

Military jet engines centrifugal fuel pumps power requirements for throttled operation, noting pressure stability improvement at low flow rates 18 p2694 A72-36041

Inlet throttle centrifugal fuel pumps for jet engine augmentation, discussing design features, performance, noise, life and reliability characteristics 18 p2694 A72-36044

Aircraft gas turbine engine fuel pump design, discussing sizing for given mass flow and pressure requirements with procedure for temperature rise calculations 18 p2694 A72-36049

Deterioration of shaft bearings of electromotor driving aircraft centrifugal fuel pump, determining lateral force acting on impeller 23 p3252 A72-43663

Aircraft gas turbine engine controllers and fuel pump testing under extreme fuel temperatures, noting cavitation characteristics 23 p3327 A72-44287

FUEL SPRAYS

Mean emissivity of a luminous flame - Spray combustion of liquid fuel. 18 p2740 A72-36148

The track method and its application in studies of atomized-fuel combustion kinetics 18 p2720 A72-36243

Two-phase detonations with bimodal drop distributions. 24 p3463 A72-45052

Low speed steady one dimensional flow models for monodisperse spray deflagration, considering homogeneous, heterogeneous and premixed combustion 24 p3464 A72-45054

FUEL SYSTEMS

NT AIRCRAFT FUEL SYSTEMS

Pulsed electric microthruster with solid fuel feed system, noting electrode geometry effects on performance and ablation patterns
[AIAA PAPER 72-210] 05 p0705 A72-16799

Electrically heated thermal decomposition hydrazine thrusters, discussing propellant supply pressures compatibility and thrust levels
[AIAA PAPER 72-451] 11 p1708 A72-26188

Pressurized air assisted gas turbine fuel system, describing single stage centrifugal turbocompressor and rotary-lobe compressor designs and performance characteristics 18 p2694 A72-36043

Principles of modelling studies of fuel systems and hydraulic systems by electronic analog computers 22 p3157 A72-42922

FUEL TANK PRESSURIZATION

Prediction of tank pressure history in a blowdown propellant feed system. 17 p2537 A72-34211

FUEL TANKS

NT WING TANKS

Discretely oriented thread reinforced polyurethane cryogenic foam insulation systems for liquid hydrogen fuel tanks
[MDAC-WD-1756] 01 p0092 A72-10981

Mars 3 spacecraft structure and experiments, noting central hypergolic fuel tanks, S-band directional antenna and solar panels 06 p0892 A72-17400

Aircraft hydrocarbon fuel tank lightning protection in airframes, using adhesive bonding, high strength materials and high modulus fiber structures 07 p1086 A72-18767

Graphite reinforced epoxy stiffeners for variable geometry fuel tank to meet light weight requirement, discussing billet fabrication, assembly and installation 08 p1176 A72-21688

Low cost 300 gallon fiber reinforced plastic aircraft wing fuel tank manufacturing technology 08 p1177 A72-21693

Utilization of wing and empennage volume for aircraft fuel tankage, presenting equations and charts for quick determination of available volume 11 p1576 A72-25811

The long fluid storage bag - A contact problem for a closed membrane. 20 p2980 A72-39691

Radiation intensity of a steady flame above a burning fluid 22 p3243 A72-42166

FUEL TESTS

Viscosity and additive effects on jet engine fuel antiwear properties improvement 02 p0270 A72-11968

Surface active agent detection by device using ultrasonic vibrating mechanism to emulsify water with fuel, determining water retention or turbidity by photoelectric cell 04 p0564 A72-14419

Purity requirements of aircraft gas turbine fuels, considering mechanical impurities, water, microorganisms, and surface active, corrosive, resinlike and paraffin substances 07 p1052 A72-20373

Jet engine fuel fire hazard evaluation by controlled laboratory tests, analyzing ignition characteristics under simulated survivable aircraft crash accidents
[SAE PAPER 720324] 11 p1702 A72-25587

Out-of-core evaluations of a nonfueled and a UO2-fueled cylindrical thermionic converter. 17 p2497 A72-36408

Evaluations of uranium-nitride fueled converters. 17 p2497 A72-36409

In-core thermionic converter emitters irradiation tests to determine fuel, fission gas venting system and emission layer performances 18 p2708 A72-36158

FUEL-AIR RATIO

Supersonic diffusion flame in duct configuration to study mixing with combustion of two parallel methane and air flows 03 p0405 A72-13545

Combustible fuel-air mixture laminar and turbulent flame propagation mathematical model, with reference to detonation and prevention 03 p0456 A72-13876

NO formation in spherical diffusion flames around hydrocarbon fuel drops burning in air
[WSCI PAPER 71-29] 04 p0482 A72-14582

Boron containing solid propellant combustion efficiency and fuel-air ratio determination from particle laden plume nonequilibrium effects in ducted subsonic flow
[AIAA PAPER 72-36] 05 p0750 A72-16972

Nitric oxide formation rate in combustion products of propane-air and hydrogen-air diluent flames 07 p0935 A72-19361

Onboard turbogenerator igniter operating conditions determination from fuel-air ratio obtained from nomogram 12 p1861 A72-28145

Determination of the concentration range of flame propagation at elevated temperatures 21 p3129 A72-40984

FUELING

U REFUELING

FUELS

NT AEROZINE

NT AIRCRAFT FUELS

NT CERAMIC NUCLEAR FUELS

NT CHEMICAL FUELS

NT CRYOGENIC ROCKET PROPELLANTS

NT DOUBLE BASE ROCKET PROPELLANTS

NT FUEL OILS

NT GASOLINE

NT HYDROCARBON FUELS

NT HYDROGEN FUELS

NT HYPERGOLIC ROCKET PROPELLANTS

NT JET ENGINE FUELS

NT LIQUID ROCKET PROPELLANTS

NT METAL PROPELLANTS

NT MONOPROPELLANTS

NT NUCLEAR FUELS

NT SOLID ROCKET PROPELLANTS

Russian book on combustion products thermodynamic and thermophysical properties covering fuels and propellants characteristics, equilibrium fuel compositions, gas phase transfer and expansion processes, etc 12 p1890 A72-28336

FULL SCALE FATIGUE TESTS

U FATIGUE TESTS

FUNCTION GENERATORS

Aerodynamic multivariable function generation in real time simulation of high performance missile 02 p0186 A72-11656

- Synchros as electromechanical function generators and receivers for analog computers, examining errors in standard resolvers operation 03 p0328 A72-13841
- Generating function procedure of combinatorial identities for sums of composition coefficients applied to graph theory 03 p0383 A72-14374
- Liapunov functions generation, using auxiliary functional differential equations table for invariance determination 06 p0838 A72-17378
- Algorithm for asymptotic power series for Poisson process residence time function generation in band with delaying screen 08 p1198 A72-20998
- Solid state ac square law function generator based on fixed elements and operating on electrical servo system principle 13 p1933 A72-29973
- German monograph - A theoretical and experimental contribution to the equivalent circuits of electrofluidic transducers operating on the nozzle/deflecting plate principle 19 p2754 A72-37653
- FUNCTION SPACE**
 NT BANACH SPACE
 NT HILBERT SPACE
- Positive additive functionals of homogeneous processes with independent increments in phase space, considering continuity condition for process distribution Laplace transform 01 p0094 A72-11264
- Walsh functions, sequency and Gray codes computations on finite binary n-tuple domain 03 p0326 A72-14248
- Variational theory for optimal relaxed control systems with time lag described by bounded uniformly continuous function defined on bounded closed sets 04 p0506 A72-15199
- Topology of convergence precompact on locally convex space, defining p-infratunnelled spaces by Banach-Dieudonne theorem 10 p1505 A72-24113
- Sobolov-Orlicz anisotropic spaces application to calculus of variations equations with strongly nonlinear coefficients 10 p1505 A72-24215
- Function space linear bounded phase coordinate control problems under regularity and normality conditions discussing solution existence and uniqueness conditions 11 p1608 A72-25322
- Inferential structure of variational statements for equations of motion and constitutive relations, noting function space choice 11 p1690 A72-26554
- Russian book on random processes theory covering random sequences and functions and probability measures in functional spaces, limit theorems, etc 12 p1837 A72-28339
- Linear normed space subsets approximation by sums based on Fourier-Laplace series 16 p2417 A72-34009
- Intermediate space concept extension to Sobolev-Orlicz spaces defined over subset with Lebesgue measure, generalizing trace theorems 18 p2704 A72-36460
- Banach space order and compactness properties extension to general case of arbitrary regular space, discussing system topologies 18 p2704 A72-36461
- Necessary and sufficient conditions for space linear operator factorization, noting summation operators theory 18 p2704 A72-36462
- Some problems concerning stability in the presence of small random disturbances 19 p2833 A72-37324
- Temperature distribution control in n-dimensional space via quasi-inversion method with Fourier transformation for Cauchy problem solution of heat conductivity equation 20 p2983 A72-39466
- Methods of solving boundary value problems of linear conjugation for functions that are holomorphic in bicylindrical domains 21 p3074 A72-40254
- Motion concept formulation by linear algebra of n dimensional spaces, emphasizing tensor character of velocity and acceleration 21 p3084 A72-40816
- Book on nonhomogeneous boundary value problems covering Hilbert theory for trace and interpolation spaces, elliptic operators and variational equations 21 p3076 A72-41526
- Compensating fields of homomorphic imaging problems in space symmetry, discussing quasi-tensors, covariant derivatives and Poincare group 23 p3312 A72-43336
- Reduction to diagonal form of some triangular matrix classes in spaces of functions that are analytic in multicircular regions 23 p3308 A72-43581
- Schauder bases in certain spaces of holomorphic functions 24 p3418 A72-44826
- FUNCTIONAL ANALYSIS**
 NT BANACH SPACE
 NT CONVOLUTION INTEGRALS
 NT FOURIER TRANSFORMATION
 NT FREDHOLM EQUATIONS
 NT HARMONIC ANALYSIS
 NT HILBERT SPACE
 NT HILBERT TRANSFORMATION
 NT INTEGRAL EQUATIONS
 NT INTEGRAL TRANSFORMATIONS
 NT LAPLACE TRANSFORMATION
 NT SINGULAR INTEGRAL EQUATIONS
 NT TESSERAL HARMONICS
 NT VOLTERRA EQUATIONS
 NT WIENER HOPF EQUATIONS
 NT ZONAL HARMONICS
- High order optimality conditions of singular controls, considering Pontryagin maximum principle, Bellman dynamic programming and functional analysis 01 p0044 A72-10297
- Positive additive functionals of homogeneous processes with independent increments in phase space, considering continuity condition for process distribution Laplace transform 01 p0094 A72-11264
- Thin shell creep and plasticity analyses reduced to linear programming problem by functionals and finite difference equations 02 p0290 A72-11622
- Nonlinear viscoelasticity theory, considering simplified stress-strain functional relationships with respect to time based on isotropy postulate 02 p0290 A72-11624
- Prolate spheroidal functions application to optical system performance characteristics, discussing laser modes, signals maximal concentration, image data extrapolation, etc 04 p0548 A72-14741
- Shooting and imbedding methods for theoretical analysis and approximate numerical solution of two-point boundary value problems involving n-vector-valued functions [AD-743615] 04 p0539 A72-15043
- Cauchy problem for nonlinear biharmonic equation in Euclidean n-space, deriving a priori inequality estimate by logarithmic convexity of functional F 04 p0539 A72-15044
- Weakly interacting waves Langevin equation in fluid, using characteristic functionals and time asymptotic methods 04 p0549 A72-15289
- R-function theory application for solution of boundary value problems in electrodynamics, considering field behavior at infinity 04 p0488 A72-15377
- Minimal-time control of linear systems with energy constraints on input components, obtaining functional analysis solution by iterative method for nonlinear problem 05 p0639 A72-15802
- Static perturbation technique functional form for postbuckling equilibrium path analysis by asymptotic approximation, noting relationship to Koiter method 05 p0742 A72-17244
- Liapunov functions generation, using auxiliary functional differential equations table for invariance determination 06 p0838 A72-17378
- Signal detection in stationary, Markov and other noise background, discussing functional method of statistical and probabilistic representation 07 p0943 A72-19520
- Smoothed randomized functionals and algorithms in adaptation and learning theory, accounting for constraints by generalized penalty function method 07 p0960 A72-19653
- Stationary functionals for introducing eigenfunctions in diffraction theory of electrodynamic systems 08 p1133 A72-21372
- Stable equilibrium conditions for linear elastic body, using Reissner functional 08 p1248 A72-21819
- Conjugate gradient method for computerized antenna radiation pattern synthesis using error functional minimization and iterative procedure 08 p1143 A72-21988
- Ordinary differential and functional equations - Conference, Kyoto, Japan, September 1971 09 p1341 A72-23251
- Functional analysis techniques for existence of holonomic solutions to linear differential equation systems with singular points 09 p1342 A72-23254
- Optimal control synthesis for linear passive stationary plants with symmetrical coefficient matrices of minimized functional 09 p1291 A72-23431
- Liapunov functional stability analysis in structural dynamics problems including wave equations with nonlinear damping 09 p1407 A72-23457
- Darlington method in dissipative systems studies, representing R-functions as fractionally linear transforms with coefficients matrix function 10 p1512 A72-24780
- Optimal control of linear stochastic feedback systems described by functional differential equations 10 p1458 A72-25145
- Russian papers on functional analysis covering approximate solution of linear integral equations, averaging principle for partial differential equations and boundary value problems 12 p1837 A72-27994
- Flight vehicle motion described by linear differential equations with variable parameters, discussing programmed optimal control solution by functional analysis 12 p1755 A72-28128
- Liapunov direct stability method extension to partial differential equations, using functional analysis and wave equation example 13 p1985 A72-28483
- Lagrange multiplier method derivation of variational functional for finite element method and applications to plate and shell problems 13 p2055 A72-28623
- Optimizing functional for combined control of dynamic control plant, synthesizing stabilization system for maximal transient damping 13 p1935 A72-28713
- Linear functional equations with constant coefficients for generalized partial derivative operators introduced in certain spaces of functions of many complex variables 13 p1987 A72-30083
- Higher order differential equations solutions for viscoelastic stress-strain functional relationships, recommending Runge-Kutta integration technique 14 p2168 A72-30929
- Elementary formulas for scalar and matrix valued functions gradient calculation, including continuum mechanics application 15 p2262 A72-31587
- Dual extremum principles in functional analysis, including applications in nonlinear programming, networks, optimization, control theory, fluid mechanics, etc 15 p2262 A72-31630
- Optimal segment boundaries with composite error function in piecewise approximation chosen by dynamic program in scalar state variable, noting uniqueness properties 15 p2262 A72-31634
- Shape functions for finite element analysis in n-dimensional space, examining completeness of polynomial interpolation and computational efficiency 15 p2326 A72-31713
- Small change sensitivity of autonomous neutral functional differential equations in neighborhood of equilibrium point 15 p2262 A72-31752
- Infinite dimensional system optimal discrete-time feedback controller calculation by n-dimensional system approximation using recurrence relations with functional analysis 15 p2212 A72-32245
- Turbulent dynamo theory based on functional analysis, noting equation with variational derivatives of characteristic functional 16 p2427 A72-34155
- Dissipative periodic process theory for application to elasticity and distributed parameter and hereditary systems defined by partial and functional differential equations 17 p2575 A72-34867
- Functional equations for optimal spacecraft or rocket interception by similar vehicle within limits of dense atmosphere 17 p2621 A72-35121
- Nonlinear functional homogeneous chaos expansions for stationary stochastic processes in turbulence theory 18 p2678 A72-36011
- Computer adapted for Boolean functions analysis and synthesis, describing structure and method of design 18 p2664 A72-36792
- Simple algorithm for a search of the global extremum of a function of several variables and its application to the functional approximation problem 19 p2828 A72-38582
- A boundary value problem for a mixed-type equation with two perpendicular parabolic-degeneration lines 19 p2828 A72-38630
- Book - Functional analysis and approximation theory in numerical analysis. 20 p2946 A72-39729
- Quasi-regularity of infinite systems in problems of two-dimensional elasticity theory for doubly connected domains 22 p3233 A72-42063
- Treatment of the flutter equation by functional analysis, using the Newton method 22 p3240 A72-42907

- Functional method investigations of imbedding theorems for random weight spaces of high order irregular elliptic equations with uniform boundary conditions 23 p3307 A72-43222
- FUNCTIONAL INTEGRATION**
Step width for gradient projection method in Hilbert space for optimal linear control problems with quadratic functional 01 p0047 A72-11386
Aircraft and spacecraft integrated avionics systems design with emphasis on telemetry, discussing space shuttle subsystems integration 02 p0179 A72-12403
Asymmetric three layer beam design for elastic impact, proposing functional equation integration by computer method 11 p1732 A72-25531
Degree of approximation of functions by integral operators in an infinite domain as related to the Hausdorff metric 23 p3310 A72-44163
- FUNCTIONALS**
Dissipative systems of ordinary differential equations concepts extension to functional and partial differential equations 15 p2263 A72-31754
Optimal control synthesis for linear passive stationary plants with symmetrical coefficient matrices of minimized functional 19 p2782 A72-38514
Optimizing functional for combined control of dynamic control plant, synthesizing stabilization system for maximal transient damping 22 p3162 A72-42091
A 'length and area principle' type inequality for images in which certain integral functionals remain bounded in an n-dimensional space 24 p3419 A72-45261
Duality in problems of the calculus of variations and optimal control 24 p3419 A72-45390
Formation of an optimizing functional in control systems 24 p3386 A72-45511
Selection of an optimizing functional in control system synthesis 24 p3387 A72-45512
- FUNCTIONS [MATHEMATICS]**
NT ABEL FUNCTION
NT ANALYTIC FUNCTIONS
NT APERIODIC FUNCTIONS
NT ASYMPTOTES
NT BOOLEAN FUNCTIONS
NT CONFORMAL MAPPING
NT COORDINATE TRANSFORMATIONS
NT DELTA FUNCTION
NT DISCRETE FUNCTIONS
NT DISTRIBUTION FUNCTIONS
NT DISTURBING FUNCTIONS
NT ELLIPTIC FUNCTIONS
NT ENTIRE FUNCTIONS
NT ERROR FUNCTIONS
NT EXPONENTIAL FUNCTIONS
NT FOURIER TRANSFORMATION
NT FOURIER-BESSEL TRANSFORMATIONS
NT GAMMA FUNCTION
NT GREEN FUNCTION
NT HAMILTONIAN FUNCTIONS
NT HANKEL FUNCTIONS
NT HARMONIC FUNCTIONS
NT HYPERBOLIC FUNCTIONS
NT HYPERGEOMETRIC FUNCTIONS
NT KERNEL FUNCTIONS
NT LAGUERRE FUNCTIONS
NT LAME FUNCTIONS
NT LAPLACE TRANSFORMATION
NT LEGENDRE FUNCTIONS
NT LIAPUNOV FUNCTIONS
NT LINEAR TRANSFORMATIONS
NT LOGARITHMS
NT LORENTZ TRANSFORMATIONS
NT MATHIEU FUNCTION
NT MAXWELL-BOLTZMANN FUNCTION
NT MELLIN TRANSFORMS
NT MEROMORPHIC FUNCTIONS
NT MONOTONE FUNCTIONS
NT NORMAL DENSITY FUNCTIONS
NT ORTHOGONAL FUNCTIONS
NT ORTHONORMAL FUNCTIONS
NT PEARSON DISTRIBUTIONS
NT PERIODIC FUNCTIONS
NT POISSON DENSITY FUNCTIONS
NT PROBABILITY DENSITY FUNCTIONS
NT PROBABILITY DISTRIBUTION FUNCTIONS
NT RATIONAL FUNCTIONS
NT RAYLEIGH DISTRIBUTION
NT RECURSIVE FUNCTIONS
NT SPACE-TIME FUNCTIONS
NT SPHERICAL HARMONICS
NT SPLINE FUNCTIONS
NT STEP FUNCTIONS
NT STRESS FUNCTIONS

- NT TANGENTS
NT TIME FUNCTIONS
NT TRANSCENDENTAL FUNCTIONS
NT TRANSFER FUNCTIONS
NT TRIGONOMETRIC FUNCTIONS
NT WALSH FUNCTION
NT WEIBULL DENSITY FUNCTIONS
NT WEIGHTING FUNCTIONS
NT WHITTAKER FUNCTIONS
French monograph on extremum values of function with two variables and nonlinear feedback control systems stability, using associate recurrence solutions properties 01 p0044 A72-10164
Trajectory optimization problems solution with terminal state constraints using combined parallel tangents/penalty function approach 02 p0280 A72-12264
Complex geometry inhomogeneous sandwich plate, calculating temperature field with R functions 03 p0456 A72-13738
Approximation of functions with diophantine conditions by polynomials with integral coefficients 03 p0382 A72-13948
Convex figures in mathematical geodesy, applying function h for ellipse and ellipsoid of revolution 03 p0351 A72-14328
Vibration theory calculations using parametric matrix function method and associated operators 04 p0550 A72-15543
Continuous linear probability functions characterization, applying to p-radonizing operators 06 p0838 A72-17554
Passive radio interference filtration analysis, obtaining SNR maximization by ambiguity function partial volume minimization 07 p0937 A72-18848
Tangent methods for nonlinear equations iterative solution using alternate tangent and derivative values 07 p1026 A72-19039
Best approximation estimates for function of many variables by sums of two functions of smaller number of variables 08 p1199 A72-21299
Fatou theorem at Martin boundary derived from Dynkin theory on excessive functions and exit space of Markov process 10 p1504 A72-24062
Separation of real zeros of certain classes of functions related to hypersurface and curve intersection 10 p1506 A72-25119
Inverse contour problem of approximating functions for compacta of positive logarithmic capacity in complex plane 12 p1836 A72-27070
Random retrieval algorithms in finite set of preset movement directions, considering quadratic function minimization 13 p1924 A72-28610
Masking functions for intensity discrimination of pulsed sinusoids with and without noise masker 13 p2006 A72-29772
Coordinate functions in Kantorovich variational method, noting application to stationary heat conduction boundary value problems 14 p2170 A72-30592
Two fluid cosmological model in conformal and conformally flat forms, deriving solutions in elementary functions 15 p2307 A72-31796
Numerical construction of the Hill functions. 17 p2573 A72-34216
Hybrid processing of empirical functions in mechanics 18 p2710 A72-36423
A statistical information theory for extremum search of a function 19 p2827 A72-38576
Variable metric algorithms - Necessary and sufficient conditions for identical behavior of nonquadratic functions. 21 p3074 A72-40227
- FUNGI**
NT GIBBERELLINS
NT SPORES
NT YEAST
- FUNGICIDES**
NT GUANINES
NT URIC ACID
NT XANTHINES
- FUNNELS**
Decelerating MHD effect on rotational funnel flow excited by vortex line or radial converging currents 03 p0397 A72-13994
- FURAN RESINS**
NT POLYAMIDE RESINS
Furan resins and chemically resistant furan-fiberglass composites flame resistance, heat distortion and physical properties at high temperatures 08 p1192 A72-21678
- FURNACES**
NT SOLAR FURNACES
NT VACUUM FURNACES
Furnace technology review, stressing need for higher sintering temperatures, better automatic at-

- mosphere controls and faster preforms transfer to forging operation 11 p1640 A72-26242
- FUSELAGE MOUNTING**
U AIRCRAFT PRODUCTION
FUSELAGES
Acoustic power radiated by jet aircraft fuselage structure exposed to turbulent boundary layer pressure field, evaluating noise reduction treatments 01 p0002 A72-10216
Wing-fuselage combination aerodynamic coefficients, comparing experimental data with subsonic linear and nonlinear theoretical results [DGLR PAPER 71-115] 02 p0153 A72-12723
Shear and direct stresses on fuselage model cross section due to concentrated radial loads on frame comparing measurement with prediction by matrix force analysis 06 p0898 A72-18322
Emergency Life Saving Instant Exit system in aircraft fuselage for use after crash landing, discussing design and ground testing 08 p1109 A72-21583
Transport aircraft fuselage computerized design, determining optimal structural distribution for strength and displacement constraints [AIAA PAPER 72-330] 11 p1727 A72-25366
Composite F-111 fuselage design, analysis and testing, considering graphite, boron and glass-epoxy and boron-aluminum systems 11 p1575 A72-25453
Subsonic and supersonic flow around nonaxisymmetric fuselages, deriving streamlines differential equations based on camber line distribution of source, dipole and quadrupole singularities [DFVLR-SONDDR-189] 11 p1573 A72-26578
Aircraft fuselage acrylic glazing design, covering passenger cabin window, cockpit windscreen and various surface coatings 12 p1753 A72-27008
Fiberglass reinforced plastic fuselage production for AN-2m aircraft, noting plastic-plastic and metal-plastic joints 13 p1897 A72-29462
- FUSES [ORDNANCE]**
Detonating cut-off pyrotechnic chain of explosive devices for stage separation involving primers, relays and fuses 08 p1221 A72-20777
Explosives injection molding into stainless steel, aluminum, plastic and rubber tubes, considering applications to fuse and detonation transfer trains and small warheads 08 p1221 A72-20781
- FUSIFORM SHAPES**
U CONES
FUSION [MELTING]
Oxygen determination in Nb with reduction fusion, determining metallic bath temperature, nature and composition effects on extraction efficiency 03 p0374 A72-13674
Thermally activated crystal microcrack initiation by fusion of leading and following dislocations 06 p0898 A72-18551
Electron beam welding focus effect on fusion zone penetration in thick austenitic stainless steel 09 p1321 A72-23643
Fusion cast zirconia-alumina-silica refractories manufacturing process, phase diagrams, chemical and physical properties and industrial applications 10 p1502 A72-24734
Vanadium enthalpy and heat of fusion measurement using massive copper calorimeter with isothermal jacket 14 p2113 A72-30222
Sintering and melting preparation effects on mechanical properties of refractory W-Re alloys, considering sigma phase in solid alpha solution 14 p2116 A72-30530
Ablation rate growth phenomenon in fusible material with diminished thermal flux, discussing quartz glass characteristics 22 p3244 A72-42728
- FUSION WELDING**
NT ARC WELDING
NT BRAZING
NT ELECTRON BEAM WELDING
NT GAS TUNGSTEN ARC WELDING
NT GAS WELDING
NT PLASMA ARC WELDING
Mathematical model of porosity gas transport test for automated fusion welding operation using mass spectrometer 01 p0076 A72-10815
Laser beam welding by solid state pulsed lasers, discussing heat conduction relation to power density utilization 06 p0822 A72-18254
Permanent electric connections by alloy and solid phase bonding and fusion welding, considering surface contamination, interface contact, activation energy and connection stability 06 p0822 A72-18581

Vanadium enthalpy and heat of fusion measurement with massive copper calorimeter

10 p1497 A72-24784

Fusion welding of Ti-W and Ti-graphite composites, determining weldability and effect of weld thermal energy on fiber matrix reactions

13 p1966 A72-29423

Ta alloys fusion weld ductility, discussing welding parameters, alloy components, interstitial impurities and weldment microstructure effects

15 p2244 A72-31775

Welding with a CW YAG laser beam

17 p2563 A72-35181

High strength bimetallic rivets produced by inertia welding Al-Ti alloy shank with pure Ti tail, noting weight and cost reduction for aerospace vehicle production

23 p3293 A72-43452

Welding airframe structures in titanium using tensile loading to overcome distortion.

24 p3407 A72-45000

G

G FORCE

U ACCELERATION (PHYSICS)

G-222 AIRCRAFT

G-222 aircraft design and operation, examining marketing problems

03 p0309 A72-13098

GADOLINIUM

Superferromagnetism in thin polycrystalline Gd and Gd-Au films having Curie points near room temperature

03 p0401 A72-13583

Gd and Sm isotopic composition measurement in Luna 16 soil with largest low energy neutron fluence

09 p1380 A72-22265

Optical properties of Gd polycrystals in IR, explaining frequency dependence of complex permittivity

09 p1372 A72-23040

Neutron capture effects on Gd isotopic composition and irradiation histories of lunar rocks from Apollo sites, using mass spectroscopic measurements

10 p1536 A72-24154

Calorimetric measurement of dissolution heat and partial enthalpy limit of Ga in Sn at 969 K

10 p1526 A72-24237

Isolation and sintering techniques and thermochemical properties of lanthanum, yttrium and gadolinium borides

11 p1645 A72-26858

High refractory gadolinium oxide-strontium oxide system phase diagram and transition temperature by X ray and differential thermal analyses

13 p1984 A72-30109

In and Gd substitution effect in calcium-vanadium garnets as potential microwave materials, discussing magnetic properties, resonance linewidth and temperature stability

15 p2293 A72-32243

Gd and Sm isotope composition in Apollo 15 soils and drill stem samples, discussing lunar sedimentary processes dating from neutron capture dependence on depth

18 p2729 A72-36974

GAGES

U MEASURING INSTRUMENTS

GAIN [AMPLIFICATION]

U AMPLIFICATION

GALACTIC CLUSTERS

Japanese cosmological studies covering evolutionary cosmology, astrophysics, relativity, nuclear physics and metagalactic phenomena

13 p2038 A72-29083

Cosmic X ray background intensity and spectrum interpretation in terms of metagalactic origin within evolutionary cosmology framework

13 p2030 A72-29087

Metagalactic magnetic field contributions to observed Faraday rotation measurements for distant extragalactic radio sources

13 p2039 A72-29088

High X ray luminosity associated with richest galaxy clusters, finding inverse Compton effect by relativistic electrons and bremsstrahlung from hot gas

13 p2040 A72-29412

Two body model for three body problem of uniformly distributed and isotropically expanding gravitational matter of Einstein-Sitter universe, noting metagalaxy cooling rate

14 p2149 A72-30211

Relict radio fluctuation observations, investigating adiabatic density perturbations related to formation of galaxies and galactic clusters

14 p2159 A72-30788

Double radio extensions in galactic cluster members, rejecting interacting galaxy hypothesis in favor of independent nonoptical radio galaxies in cluster intergalactic media

16 p2451 A72-32989

Radio source concentration mapping near NGC 7331 and Stephan quintet group

16 p2455 A72-33469

Red shift observations for galactic studies, discussing Stephan Quintet in Pegasus, spiral galaxy expulsion evolutionary hypothesis and Andromeda velocity patterns

16 p2456 A72-33541

Radio sources reidentification in field of Coma Cluster of galaxies by Schmidt telescope

16 p2458 A72-33719

Intergalactic ionized gas and member galaxies mass relationship in local group and nearby galactic clusters, considering gravitational potential

17 p2604 A72-34475

Decametric radio identification of an extragalactic X-ray source.

17 p2604 A72-34520

X ray sources associated with galactic clusters resulting from relativistic electrons Compton scattering on microwave background radiation

17 p2599 A72-35072

Vortex model of galactic clusters evolution, estimating velocity dispersion and rotation and chaotic velocity contributions to kinetic energy

17 p2617 A72-35729

X ray observation inadequacy in detection of background radiation surface brightness fluctuations due to irregular distribution within galactic cluster sources

18 p2729 A72-37006

The correlation of redshift with magnitude and morphology in the coma cluster.

19 p2854 A72-37228

The structure of the Coma cluster of galaxies.

19 p2854 A72-37229

Relationship between X-ray luminosity and velocity dispersion in clusters of galaxies.

19 p2856 A72-37501

Problem of n bodies with a variable gravitational constant, and some dynamic characteristics of large-scale cosmic systems

19 p2863 A72-38077

On the infall of matter into clusters of galaxies and some effects on their evolution.

20 p2965 A72-38901

Absolute magnitudes of E and S0 galaxies in the Virgo and Coma clusters as a function of U-B color.

20 p2965 A72-38902

X-ray emission from intergalactic gas in the neighbourhood of galaxies.

20 p2964 A72-39240

Quasar 3C 323.1 in rich compact galactic cluster Zw Cl 1545.1+2104, considering red shift, energy distribution and luminosity

21 p3107 A72-41268

Formation of clusters of galaxies - Photocluster fragmentation and intergalactic gas heating.

22 p3224 A72-42377

The estimation of masses of individual galaxies in clusters of galaxies.

22 p3227 A72-42551

Approximate solutions of the relativistic gravitational field equations to describe clusters of galaxies.

22 p3229 A72-42993

Two body model for three body problem of uniformly distributed and isotropically expanding gravitational matter of Einstein-Sitter universe, noting metagalaxy cooling rate

23 p3334 A72-43241

Galaxies and galactic cluster distance determination from Palomar chart angular diameters related to Holmberg-Vaucouleurs photometric systems

23 p3338 A72-44034

GALACTIC EVOLUTION

Fluid dynamical study of accretion process with gravitating point source motion through adiabatic gas, applying to galaxies

01 p0126 A72-10289

Galactic rotation origin, discussing tidal, vortex and spinning core theories

01 p0127 A72-10290

Galactic clusters red shifts and absolute spectral energy distributions, inferring evolutionary effects by comparison with giant elliptical galaxies light energy distribution

02 p0279 A72-12185

Galactic wind formation in elliptical galaxies by stellar ejected gas heating by supernovae, discussing thermally unsteady cores

02 p0279 A72-12189

Magellanic Clouds early evolutionary state importance in extragalactic studies

03 p0426 A72-13264

Galactic formation theories, discussing hot big bang and Friedmann models, primordial fireball and Hubble diagram

03 p0426 A72-13271

Stability of plane rotating galaxies in magnetic field parallel to axis of rotation, showing linearized MHD equations self conjugate for radial disturbance case

03 p0435 A72-13806

One zone model formulation and mathematical behavior for evolution of galaxies, discussing stellar birth rate and end states

04 p0570 A72-14551

Energy equipartition among unequal masses in galactic nuclei and gravitating systems, discussing time scale for dynamical evolution

04 p0570 A72-14552

Expanding source model for quasars and Seyfert galaxy nuclei radio outbursts from extension of radio galaxy evolution models

04 p0573 A72-14874

Galactic evolution and cosmology implications of primordial solar D/H ratio, discussing deuterium production mechanisms

04 p0574 A72-14980

Galactic cluster lifetimes compared with star cluster model evaporation times, discussing general galactic and interstellar clouds tidal fields effects

05 p0713 A72-16051

Vlasov equation phase space boundary integration for evolution of one dimensional self gravitating collisionless stellar systems with constant density

05 p0714 A72-16056

Collective relaxation of two phase space density collisionless one dimensional self gravitating stellar systems, following boundary curve motion

05 p0714 A72-16057

Cosmological evolution theories, discussing big bang theory, galactic evolution, quasars, pulsars, gravitational collapse, stellar evolution, supernovae, black holes, etc

05 p0716 A72-16311

Virgo cluster galaxies evolutionary sequence in radial velocity-nuclear magnitude diagram in terms of morphology, radial color variations, nuclear size and radio emission

05 p0717 A72-16382

Four phase space density collisionless one dimensional stellar system evolution in time by following motion of boundary curves

06 p0876 A72-17577

Galactic star clusters dynamic evolution, using King type equilibrium and stellar mass distribution models

06 p0879 A72-17860

Numerical experiments in collisionless stellar systems evolution by gravitational n-body calculations using computers

06 p0885 A72-18076

Isolated rotating disks of stars galactic evolution model for gravitational field studies, noting dynamic instabilities and final exponential mass distribution

06 p0885 A72-18077

Monte Carlo scheme for dynamic evolution of spherical stellar systems

06 p0885 A72-18080

Computer models for simulating self consistent collisionless stellar systems evolution under gravitational field

06 p0885 A72-18081

Galactic evolution model, tracing stellar and supernova nucleosynthesis influence on interstellar gas composition

06 p0886 A72-18082

Hadron era evolution, discussing equation of state, ultimate temperature, galactic formation and adiabatic exponent application to Friedman universes

06 p0886 A72-18096

Cosmological red shift and galactic evolution effects on line features in X ray background due to young pulsars in supernova remnants

06 p0891 A72-18509

Galactic nucleus explosive events and mass expulsion evidence from high velocity hydrogen survey with 20 ft horn reflector

07 p1070 A72-19086

Stellar dynamical and density wave theories for spiral pattern persistence in Galaxy with differential rotation

07 p1074 A72-19430

Dynamic model of galactic clusters in terms of cosmological turbulence, estimating velocity dispersion and rotation and chaotic velocity contributions to kinetic energy

07 p1076 A72-19805

Elemental nucleosynthesis, considering cosmological, stellar, galactic and solar system evolution and atomic nuclei energetic levels

07 p1083 A72-20466

Population II stars age determination by main sequence turnover luminosity and other methods, noting cosmological and galactic evolution implications

07 p1083 A72-20468

Structure and evolution of radio galaxies and quasars, considering luminosity-sustaining energy source, emission mechanism, variability and mean activity time

07 p1083 A72-20469

Big bang theory for age determination of galaxies, considering formation through gravitational instability and primeval gas velocity distribution fluctuations

07 p1084 A72-20470

Cosmological model with negative and positive mass particles, discussing cosmological term, gravita-

tion shielding, red shift and interacting Vorontsov Veliaminov galaxies

Initially stationary axisymmetric disk of stars evolution calculated by gravitational potential solver for various values of velocity dispersion

Intergalactic matter infall in galaxies, discussing quasar absorption spectra, hydrogen clouds, accretion rate and relations to spiral structure

Liapunov theory solutions stability for oscillations along galactic axis of symmetry

Galactic nuclei origins, evolution, observational evidence and activity relation to cosmological problems, examining Milky Way, spiral and radio galaxies and quasars

Galactic nuclei evolution and stellar content models from nearby stars spectral synthesis

Seyfert, N-type, compact and radio galaxies spectroscopic properties, noting two dwarf emission line galaxies as possible young galactic nuclei

Galactic nucleus evolutionary processes, considering mass ejection from newly formed massive stars, gas concentration toward center, kinetic energy exchange and stellar collisions

Bright black holes from quasars condensation toward Schwarzschild radius, investigating primeval galaxies angular momentum increase and core concentration due to frictional effects

Galaxy and globular cluster ages in relation to Hubble constant, deceleration parameter and Friedmann expansion time

Nonlinear hydrodynamic effects in dynamic motions of metagalactic turbulence in pre-Friedmann universe

Spiral galaxy density wave maintenance mechanism from rotating disk star-gas system model description of stellar birth and disintegration effects

Galaxy formation process in expanding universe from study of hydrodynamic equations for rotating gaseous ellipsoid with uniform density

Newtonian hydrodynamic equations derived from scalar-tensor theory field equations for cosmic fluid nonlinear effects during galaxy formation

Fowler quasars and exploding galaxies model tested by hydrodynamic equations numerical solution for premain sequence contraction and relativistic collapse of nonrotating supermassive star

Vertex deviation of stellar samples in terms of reflection and galactic potential perturbation

Galactic disk systems relaxation time due to particle encounters, discussing validity of Boltzmann-Vlasov equation

Small perturbations in collisionless stellar dynamics, discussing linear modes for flat axisymmetric galaxy and effects introduced by nonlinear theory of spiral structure

Instabilities initiation in spiral arm formation and stellar cluster evolution, noting analogy to hose-pipe instability in plasma physics

Numerical experimentation in collisionless systems for Jeans instability, static self consistent models and spiral patterns

Computer model for evolution of isolated rotating disks of stars, noting gravitational two stream dynamic instability for infinite double periodic stellar systems

Spiral density wave structure persistence conditions determined from computer simulations of galaxies evolution, noting gravitational azimuthal and radial forces effects

Expanding hot universe evolution from astrophysical cosmology point of view, emphasizing galaxy formation relation to state of matter and radiation in early universe

Gravitational instability and galaxy formation in expanding universe, considering primordial turbulence and density perturbations

Galactic formation initiation mechanism with thermal instability in expanding universe, noting Compton scattering energy exchange ensuring gravitational instability dominance

Quasars interpreted as active stage in galactic evolution with successive explosions in nucleus condensations

Parker dynamo theory failure in explanation for galactic magnetic field origin and form, noting reasons

Galactic astronomy - Conference, State University of New York, Stony Brook, June-July 1968, covering Galactic structure, spiral shape theories, star migration, etc

Stellar radiation and gravitational effects on neutral atoms and dust grains at large distances for various spectral type stars in schematic evolutionary galaxy

Relict radio fluctuation observations, investigating adiabatic density perturbations related to formation of galaxies and galactic clusters

Galactic tidal interactions, computing mass loss for hyperbolic collisions and giant system formation from density distribution models

Book on astronomy covering optical and radio telescopes properties and atmospheres of inner and outer planets, stellar lifetimes and evolution, galaxies, cosmology, etc

Red shift observations for galactic studies, discussing Stephan Quintet in Pegasus, spiral galaxy expulsion evolutionary hypothesis and Andromeda velocity patterns

Spiral structure generation by outward angular momentum transfer, considering gravitational stress tensor, star-spiral wave momentum transfer and galactic secular evolution

Supernova explosion mechanism and quantitative game for galactic chemical evolution, discussing relationship to cosmic rays

Galactic magnetic field origin and large scale instability associated with Galactic field and cosmic rays, discussing thermal instability in interstellar gas

Heavy element enrichment of protogalactic primordial gas by quasars matter ejection into intergalactic medium

Random gravitational encounters and the evolution of spherical systems. IV - Isolated systems of identical stars.

The equilibria and oscillations of a family of uniformly rotating stellar disks.

On galaxy formation from primeval universal turbulence.

Vortex model of galactic clusters evolution, estimating velocity dispersion and rotation and chaotic velocity contributions to kinetic energy

Galactic spiral structure temporal decay based on density waves hypothesis

Observational evidence for strength and structure of intergalactic magnetic fields, discussing primordial fields effects on galaxy formations and early universe evolution

Polarization and velocity field in the galaxy M 82.

Mixing processes of newly made elements in Galaxy, taking into account thermodynamics, galactic structure and nucleosynthesis parameters

Central galactic plane, interstellar medium and spiral arm conditions for star formation in Milky Way

Relationship between X-ray luminosity and velocity dispersion in clusters of galaxies.

Gas ejections in NGC 4486 and activity problems of galactic nuclei

Single body and stellar cluster models of quasars and galactic nuclei stability, noting neutron and collapsing star lifetimes

Decay of pregalactic vortex motions

Direction of trailing in spiral galaxies

Rotatory perturbations in anisotropic cosmology

Generation of the large-scale magnetic field of the galaxy. II

Astronomical models for matter sources leading to galaxy formation, considering source nature and origin

Galactic structure at galactic longitudes from 230 to 355 deg on the basis of photoelectric UBV H beta photometry of 55 southern open star clusters

On the infall of matter into clusters of galaxies and some effects on their evolution.

Differentially rotating magnetoid model for quasar and radio galaxies matter ejection and luminosity mechanisms in terms of magnetic field evolution and current sheet generation

Gas density as function of galactic radius according to Jeans unstable criterion for star formation from known galaxy rotation curve and gas sound speed

Galaxy formation in generic dust filled anisotropic cosmology, analyzing density perturbations growth rate

The origin and form of the galactic magnetic field. II.

Studies of heavy-element synthesis in the galaxy. I - Separation of r- and s-process abundances.

Unsteady phenomena in the world of stars and galaxies

Galactic evolution - Program and initial results.

Collapse of massless nonrotating gas particle nonuniform spheroidal shell contracting around gravitating massive point nucleus, interpreting galactic evolution

Observation of M 82 in the near infrared

GALACTIC MAGNETIC FIELDS

U INTERSTELLAR MAGNETIC FIELDS

NT GALACTIC RADIO WAVES

Book on solar and galactic cosmic rays covering collisions with matter, propagation through geomagnetic field and atmosphere and origin

Long term galactic cosmic ray intensity modulation correlation to 5303 A coronal intensity during rising part of solar activity cycle

Spiral galaxies radio continuum emission origin, discussing supernovae and relativistic electrons effects

NGC 5128 nucleus radio emission flux density measurement, noting angular size

Centaurus A NGC 5128 nucleus IR radiation measurement, suggesting small nonstellar core superposed on extended reddened stellar component

Extragalactic cosmic ray hypothesis plausibility from viewpoints of energy supply, acceleration process efficiency, galactic nucleus activity and intergalactic space

Galaxy source of ultrahigh energy cosmic rays, interpreting energy spectrum kinks as galactic to metagalactic radiation transition

Galactic IR astronomy, discussing findings on emission from H II regions of Orion Nebula and late and early type stars

Ultrahigh energy cosmic ray models indication of galactic origin and composition, based on energy spectrum flattening data

Galactic cosmic ray-solar wind nonlinear interaction effects on solar wind geometry near and far from sun

Correlation coefficients for galactic cosmic rays relation to solar activity indices in interplanetary space

Galactic cosmic ray self trapping, discussing hydromagnetic wave velocity of ray propagation from sources

Magellanic Clouds X ray sources from Uhuru satellite observations, discussing time variability

Emission nebulae in Magellanic Clouds observed at 408 MHz, calculating electron density and total mass

Galactic disk component of diffuse X radiation from unresolved red dwarf flare stars

Diffuse galactic light absolute intensity interpretation, showing interstellar dust discrete cloud structure effect on grain properties determination

Low energy gamma ray telescope with active honeycomb collimator and anticoincidence detector, describing directivity techniques for galactic sources

Galactic structure at galactic longitudes from 230 to 355 deg on the basis of photoelectric UBV H beta photometry of 55 southern open star clusters

On the infall of matter into clusters of galaxies and some effects on their evolution.

Differentially rotating magnetoid model for quasar and radio galaxies matter ejection and luminosity mechanisms in terms of magnetic field evolution and current sheet generation

Gas density as function of galactic radius according to Jeans unstable criterion for star formation from known galaxy rotation curve and gas sound speed

Galaxy formation in generic dust filled anisotropic cosmology, analyzing density perturbations growth rate

The origin and form of the galactic magnetic field. II.

Studies of heavy-element synthesis in the galaxy. I - Separation of r- and s-process abundances.

Unsteady phenomena in the world of stars and galaxies

Galactic evolution - Program and initial results.

Collapse of massless nonrotating gas particle nonuniform spheroidal shell contracting around gravitating massive point nucleus, interpreting galactic evolution

Observation of M 82 in the near infrared

GALACTIC MAGNETIC FIELDS

U INTERSTELLAR MAGNETIC FIELDS

NT GALACTIC RADIO WAVES

Book on solar and galactic cosmic rays covering collisions with matter, propagation through geomagnetic field and atmosphere and origin

Long term galactic cosmic ray intensity modulation correlation to 5303 A coronal intensity during rising part of solar activity cycle

Spiral galaxies radio continuum emission origin, discussing supernovae and relativistic electrons effects

NGC 5128 nucleus radio emission flux density measurement, noting angular size

Centaurus A NGC 5128 nucleus IR radiation measurement, suggesting small nonstellar core superposed on extended reddened stellar component

Extragalactic cosmic ray hypothesis plausibility from viewpoints of energy supply, acceleration process efficiency, galactic nucleus activity and intergalactic space

Galaxy source of ultrahigh energy cosmic rays, interpreting energy spectrum kinks as galactic to metagalactic radiation transition

Galactic IR astronomy, discussing findings on emission from H II regions of Orion Nebula and late and early type stars

Ultrahigh energy cosmic ray models indication of galactic origin and composition, based on energy spectrum flattening data

Galactic cosmic ray-solar wind nonlinear interaction effects on solar wind geometry near and far from sun

Correlation coefficients for galactic cosmic rays relation to solar activity indices in interplanetary space

Galactic cosmic ray self trapping, discussing hydromagnetic wave velocity of ray propagation from sources

Magellanic Clouds X ray sources from Uhuru satellite observations, discussing time variability

Emission nebulae in Magellanic Clouds observed at 408 MHz, calculating electron density and total mass

Galactic disk component of diffuse X radiation from unresolved red dwarf flare stars

Diffuse galactic light absolute intensity interpretation, showing interstellar dust discrete cloud structure effect on grain properties determination

Low energy gamma ray telescope with active honeycomb collimator and anticoincidence detector, describing directivity techniques for galactic sources

Galactic structure at galactic longitudes from 230 to 355 deg on the basis of photoelectric UBV H beta photometry of 55 southern open star clusters

On the infall of matter into clusters of galaxies and some effects on their evolution.

Differentially rotating magnetoid model for quasar and radio galaxies matter ejection and luminosity mechanisms in terms of magnetic field evolution and current sheet generation

Gas density as function of galactic radius according to Jeans unstable criterion for star formation from known galaxy rotation curve and gas sound speed

Galaxy formation in generic dust filled anisotropic cosmology, analyzing density perturbations growth rate

The origin and form of the galactic magnetic field. II.

Balloon-borne galactic X ray detection unit, obtaining high directivity with honeycomb collimator and angular resolution with solar sensor

03 p0353 A72-13043

He production from H to maintain Galactic luminosity, discussing interstellar gas enrichment

03 p0419 A72-13116

Heavier-than-helium cosmic ray nuclei composition inferring galactic confinement of particles, path lengths and transit times

03 p0409 A72-13137

Radiation exposure during high altitude flights, considering normal radiation levels due to galactic radiation and short term increases due to solar flares

03 p0315 A72-13234

Synchrotron and thermal H II region radio emission in Magellanic Clouds

03 p0425 A72-13259

Inner solar system particle propagation model solved for radial gradient of galactic protons, comparing to Mariner 4 measurements

03 p0412 A72-13527

X ray background model based on photons bremsstrahlung emission by subcosmic metalgalactic electrons or protons

03 p0413 A72-13804

Solar flare, galactic and magnetically trapped (Van Allen) nuclear particle radiation environments calculation for three outer planet Grand Tour missions

03 p0413 A72-14095

Universal steady X ray background theory, examining superposition of radiation from pulsars in various galaxies

04 p0566 A72-14909

Quasar red shift origin in terms of cosmological, gravitational and Doppler hypothesis, comparing with Seyfert galaxies

04 p0577 A72-15165

Markarian galaxies photometric observations, presenting emission line intensities and UVB magnitudes

04 p0578 A72-15309

Interstellar sodium lines intensities and widths as discriminants for two component models of galactic H I cloud regions

04 p0578 A72-15310

Galactic center region, Virgo and Crab Nebula gamma ray observations, measuring intensity and energy spectra

04 p0578 A72-15312

Interstellar propagation of 2-8 Z galactic cosmic ray nuclei at 10-1000 MeV/nucleon, analyzing differential kinetic energy spectra

04 p0567 A72-15323

Heavy nuclei enrichment in solar accelerated particles, discussing differential energy spectra, photospheric and coronal abundances, satellite observation and agreement with galactic cosmic rays

04 p0568 A72-15366

Li, Be and B production rate in interstellar gas by galactic cosmic rays from diffusion model of fast particles, accounting for He component

05 p0708 A72-15760

Galactic high energy electron differential spectrum, estimating spatial distribution and random magnetic field intensity

05 p0709 A72-16237

Radio emission from compact extragalactic objects, including quasars and nuclei of compact, Seyfert and N type galaxies

05 p0716 A72-16376

Active solar regions effects on galactic cosmic ray intensity

05 p0710 A72-16526

Venus, M17 and M82 observation on ground through 345 micron atmospheric window, discussing IR fluxes

05 p0710 A72-16709

Altitude effects on high energy neutrons and galactic gamma rays flux and spectrum variations from balloon flight studies

06 p0873 A72-17639

Radio emitting giant loops in the Galaxy, considering supernova radiation induced nebulae model to explain spectral and polarization properties

06 p0876 A72-17649

Compact galaxies photometry, determining historical variability from photographic plates obtained by large aperture cameras

06 p0880 A72-17886

Red shift determination for two galaxies near PSK 2251 plus 11 quasar from Ca II H and K absorption line measurements

06 p0881 A72-17898

Galactic nuclei and quasars as IR source, noting critical accretion of gas at neutron stars

06 p0883 A72-18015

Extragalactic radio sources, discussing galactic radiation, quasars, nonthermal emissions, energy dissipation and spectrum analysis

06 p0886 A72-18172

Interstellar heterocyclic carbon ring molecules furan and imidazole search from upper limits in galactic sources brightness temperature

06 p0891 A72-18502

Nighttime ionospheric dynamo current modulation due to galactic X ray ionization, observing diurnal sidereal time variation in geomagnetic field

07 p1056 A72-18898

Forbush decreases in galactic cosmic ray flux and associated vlf nighttime ionospheric propagation phenomena

07 p1056 A72-18900

Spiral galaxies hypothesis for higher mass-luminosity ratio of outer parts from undetected cold neutral hydrogen, using model of NGC 300

07 p1068 A72-19071

Solar modulated galactic cosmic rays radial gradient idealized model for comparable deceleration and convection effects

07 p1057 A72-19138

Monte Carlo calculations of lunar photon albedo from galactic and solar proton bombardment for lunar soil composition information

07 p1070 A72-19139

Radionuclides formation rate as function of depth in moon for bombardments by galactic cosmic ray particles and by solar protons

07 p1057 A72-19140

Low energy gamma radiation spectrum from galactic center region, using balloon altitude observation

07 p1059 A72-19420

Galactic cosmic ray modulation by interplanetary medium, including solar wind boundary problem

07 p1061 A72-20021

Low energy solar cosmic ray measurements in interplanetary space with Zond space probes, comparing to galactic cosmic rays

07 p1061 A72-20022

Galactic nucleus IR measurements in terms of forbidden NE II emission line at 12.8 microns

07 p1081 A72-20229

Galactic cosmic ray particle intensity decrease relationship to low energy proton flux increase based on interplanetary Zond 3 and Venera probes measurements

07 p1063 A72-20626

Galactic cosmic ray modulation region evaluation from meteoroid orbit, velocity and radioactive dating data

07 p1065 A72-20644

Solar active regions effects on galactic cosmic ray distribution and interplanetary magnetic field structure

07 p1065 A72-20646

Diffusion and stochastic variations of galactic cosmic rays in solar wind

07 p1066 A72-20648

Solar wind propagation limitations by galactic magnetic field and cosmic rays and solar system motion relative to interstellar gas

08 p1225 A72-20701

Solar modulation process for galactic cosmic ray particle time variation, discussing interplanetary magnetic fields and plasma, energy losses from solar wind deceleration, etc

08 p1227 A72-21188

High energy gamma radiation intensity from galactic plane in Cygnus-Cassiopeia region, using balloon-borne telescope

08 p1227 A72-21215

Spectroscopic observations and classification of luminous galactic nuclei with broad emission lines, discussing gas density, velocity and outflow and electron scattering

08 p1234 A72-21279

NGC 3031 spiral galaxy photometry and large scale structure determination by UBVR integral equidensity curves method

08 p1234 A72-21280

Quasars and Seyfert galaxies radiation, discussing dust clouds, synchrotron and unstable plasma models

08 p1234 A72-21383

Formaldehyde concentration into cloud formation compared to atomic hydrogen from analysis of molecular lines near galactic center

08 p1235 A72-21386

Models of galactic diffuse sources of soft cosmic X rays, estimating spectrum and intensity

08 p1228 A72-21650

RAE-1 measurements of If radio phenomena in magnetosphere, solar corona and Galaxy, discussing design, calibration and performance

08 p1137 A72-21984

Seyfert galactic nuclei structure, discussing thermal X rays indication of significant random motions and difficulty of energy source determination

09 p1386 A72-22686

Intense IR radiation from galaxies central regions, comparing power levels with galactic nuclei optical and radio emission

10 p1534 A72-23899

Nonthermal emission and ejection of matter from galactic nuclei, discussing radio, optical and IR synchrotron sources and background radiation

10 p1535 A72-23906

X ray background radiation from discrete sources, considering inverse Compton mechanism in galaxies and intergalactic space and soft component origin

10 p1529 A72-23913

Radio continuum survey of spiral galaxies M51 and NGC 5195 for study of galactic magnetic field and cosmic rays origin and distribution

10 p1543 A72-24623

Outer space and earth surface galactic cosmic ray intensity data correlation analysis for studying interplanetary magnetic field structure

11 p1713 A72-25936

Galactic nuclei and quasars as IR sources, noting critical accretion of gas at neutron stars

11 p1718 A72-25951

Diffuse galactic light observation, suggesting emanation from discrete sources

11 p1720 A72-26113

Elliptical radio galaxies and quasars intrinsic emitted radio power correlation to spectral indices interpreted as evolutionary track in terms of model

12 p1867 A72-27210

Heavily obscured galaxy IC 10 21-cm line observation with radio telescope and neutral hydrogen diameter measurement for distance estimation

12 p1868 A72-27215

Soft X ray emission from supernova remnants, considering maximum linear diameter dependence on remnant distance from galactic plane

12 p1863 A72-27222

High energy solar and galactic cosmic ray chemical composition, considering electron chemical abundances and beryllium-boron ratio

12 p1863 A72-27426

Black hole concept in general relativity and gravitational collapse, considering deviations from spherical symmetry and gravitational wave emanation from Galactic center

12 p1871 A72-27690

Solar wind distortion of stellar anisotropy of galactic cosmic rays, associating annual particle density variation with earth revolution about sun

13 p2029 A72-28590

Galactic cosmic ray-solar wind nonlinear interaction effects on solar wind geometry near and far from sun

13 p2030 A72-29229

Correlation coefficients for galactic cosmic rays relationship to solar activity indices in interplanetary space

13 p2030 A72-29249

Velocity field measurements from M82 /NGC 3034/ galaxy H alpha, forbidden N II and S II emission lines, suggesting expanding ejecta cloud rotating about axis normal to galactic plane

13 p2040 A72-29401

Self consistent model for cosmic ray propagation from sources in Galaxy toward earth, using H and He isotope interstellar spectra

13 p2031 A72-29409

Galactic cosmic ray anisotropy due to radial and diffusive streaming in direction of interplanetary magnetic field, using neutron monitor data

13 p1033 A72-29747

Galactic cosmic rays density distribution normal to solar equatorial plane and resultant semidiurnal anisotropy, comparing different methods results with experimental observations

13 p1033 A72-29807

Spectral variability of radio sources in cm excess category, including quasi-stellar, Seyfert galaxy, optical variable and compact sources

13 p2050 A72-29964

Astrophysical equipment for Cerenkov radiation measurement from atmospheric showers, discussing source of high energy gamma rays in galactic equator direction

14 p2146 A72-30201

Solar cyclic intensity variation of excessive radiation with respect to galactic radiation background at low altitudes from satellite data analysis

14 p2146 A72-30475

Flux densities, electron energies and brightness temperature determination from radio telescope observations of galactic sources and nonthermal radiation

14 p2155 A72-30553

Galactic spiral arm hypothesis for positive velocity neutral hydrogen clouds above galactic plane, surveying distribution

14 p2158 A72-30732

List of galaxies with UV continuum, noting emission lines, Seyferts, quasars and spectral energy distribution

15 p2304 A72-31326

Cosmic ray chemical composition from particle sampling by rockets and satellites, comparing galactic rays, solar rays and sun

15 p2299 A72-31648

Galactic background continuous radiation observation at 15 GHz, determining brightness temperature and thermal radiation component

15 p2313 A72-32348

Galactic X and gamma ray astronomical observations from balloons, rockets and satellites, discussing radiation counters

16 p2445 A72-33075

Diffuse X ray emission from galaxy interarm region, suggesting population of unresolvable low luminosity sources as emission model

16 p2445 A72-33138

Uhuru observed galactic X ray sources related to binary systems or supernova remnants, noting galaxy clusters

16 p2454 A72-33362

Galactic X ray sources from June 1969 rocket flight in Brazil, comparing spectra to bremsstrahlung, black body and power law models

16 p2446 A72-33457

Weak H beta emission at 26 deg galactic latitude, noting derived electron density agreement with pulsar data

16 p2455 A72-33460

Diffuse galactic light polarization characteristics from OSO-5 observations, discussing model of starlight scattering by interstellar dust

16 p2446 A72-33468

Magnitude redshift relation in flat Brans-Dicke cosmology, discussing gravitational constant effects on stellar evolution and galactic luminosity

16 p2455 A72-33471

Optical circular polarization search in quasars, Seyfert galaxies nuclei, BL Lac and OJ 287

16 p2456 A72-33472

Radiation hazards in space with respect to galactic radiation shielding, solar flare prediction and conventional terrestrial safety standards

16 p2358 A72-33556

HEAO experiment proposal for Be to Sn flux and energy spectra and Be to Fe isotopic composition of galactic primary cosmic rays

16 p2447 A72-33733

Li, Be and B spallation reactions in galactic cosmic rays from observations of cross sections of energetic protons incident on C and O targets

16 p2447 A72-33734

Li, Be and B nuclei production via nuclear spallation reactions generated by Galactic cosmic ray bombardment of interstellar gas

16 p2448 A72-33737

Be isotopic ratio in galactic cosmic rays, noting mean interstellar hydrogen density and rays age

16 p2448 A72-33738

Nitrogen existence in galactic cosmic ray sources, considering formation from CNO cycle hydrogen and He burning and ejection from normal stars

16 p2448 A72-33739

Diffusion propagation and source distribution effects on cosmic ray charge composition and anisotropy in galactic disk, considering nuclear fragmentation

16 p2448 A72-33742

Neutron star acceleration of He, Fe and supernova debris into cosmic ray flux throughout Galaxy, discussing magnetic and superfluidity effects

16 p2448 A72-33745

Galactic ridge of discrete diffuse X ray sources, calculating intensity in terms of scale height and radial gradient

17 p2598 A72-34523

Slope-gradient diagram of galaxies and quasars

17 p2607 A72-34919

Galactic cosmic rays anisotropy prediction as function of energy for various assumed source distributions and magnetic field configurations

17 p2599 A72-34924

X ray sources associated with galactic clusters resulting from relativistic electrons Compton scattering on microwave background radiation

17 p2599 A72-35072

Disk-shaped diffusion model with inhomogeneous distribution of gas and heavy relativistic nuclei sources for galactic cosmic rays chemical composition

17 p2600 A72-35206

Brief survey of the problems of space radiobiology and radiation safety in space flights

17 p2509 A72-35376

Radio galaxies monochromatic luminosity-spectral index relationship from 3CR spectra studied at 10 MHz to 10,700 MHz

18 p2726 A72-36621

Galactic and metagalactic background radiation

18 p2722 A72-36723

Galactic center emitted gravitational wave discrepancy with astrophysics explained by self focusing and trapping concepts

18 p2729 A72-36985

Galactic gamma-radiation between 200 MeV and 10 GeV

18 p2722 A72-37008

Soft X-ray emission from intergalactic gas in the neighbourhood of the Galaxy

19 p2855 A72-37345

Galactic X rays investigation with X ray telescope on Lunokhod 1, noting observed singularities connection with statistical distribution of quasars and radio galaxies

19 p2802 A72-38090

Solar wind propagation limitations by galactic magnetic field and cosmic ray pressure and solar system motion relative to interstellar gas

19 p2851 A72-38329

Radiobiological problems caused by supersonic transport /With a survey of the first results established by tests performed on board the Concorde prototype/

19 p2762 A72-38713

Observations of the radial gradient of galactic cosmic radiation over a solar cycle

20 p2964 A72-39337

Recent developments in the history of the nucleosynthesis of the solar system

20 p2971 A72-39837

On a galactic origin for the soft X-ray background

21 p3100 A72-41029

High resolution observations of 3C390.3 at 2.7 and 5 GHz

21 p3111 A72-41471

Stratospheric balloons role in galactic cosmic radiation research with detection techniques for study of rate and heavy elements abundances and isotopic composition analysis

21 p3101 A72-41615

Convection and diffusion transport equation of galactic cosmic ray electrons with energy loss and absorption allowance for supernova compressed halo models

22 p3217 A72-42210

A photoelectric study of Messier 81

22 p3229 A72-42975

Astrophysical equipment for Cerenkov radiation measurement from atmospheric showers, discussing source of high energy gamma rays in galactic equator direction

23 p3328 A72-43226

The emission-line spectrum of Cygnus A

23 p3334 A72-43251

Calculation of stellar and diffuse radiation for a plane-parallel semiinfinite model of the Galaxy

23 p3338 A72-44027

Low energy X-ray survey from the Crab Nebula to Cygnus

24 p3435 A72-44842

An H I velocity-longitude diagram for the Southern Milky Way

24 p3438 A72-44845

Solar wind distortion of stellar anisotropy of galactic cosmic rays, associating annual particle density variation with earth revolution about sun

24 p3435 A72-45090

Observation of M 82 in the near infrared

24 p3446 A72-45487

GALACTIC RADIO WAVES

Phase error in 136 MHz interferometer due to galactic nucleus passage, obtaining lower bound

02 p0175 A72-12160

Galactic H II regions with radio emission at 1400 MHz, using National Radio Astronomy Observatory 300 ft telescope

11 p1724 A72-26785

Radio observation of neutral hydrogen near galactic center, noting expanding and rotating ring of gas from kinematic model

12 p1867 A72-27211

Galactic structure, ionized gas distribution and radio source diameter studies from interstellar scattering at 81.5 MHz, comparing with pulsars

13 p2050 A72-29962

Galactic radio feature Loop III extension south of galactic plane from Jodrell Bank Mk I radio telescope observations at 38 MHz

16 p2458 A72-33690

Galactic radio emission spectrum analysis via horn antennas with wavelength proportional apertures, calculating full beam antenna temperatures for selected radio frequencies

19 p2852 A72-38484

A study of galactic supernova remnants. II - Supernova rate, galactic radio emission and pulsars

23 p3337 A72-43829

Galactic submillimeter background radiation energy density limit, taking into account recalibrated gamma ray flux measurements agreement with cosmic ray-interstellar matter interactions

23 p3329 A72-43942

Linear polarization survey for galactic background radiation at 1415 MHz in North Polar Spur, Cetus Arc and Loop III, noting continuous maxima shift

24 p3438 A72-44835

GALAXIES

NT ANDROMEDA GALAXIES

NT GALACTIC CLUSTERS

NT MAGELLANIC CLOUDS

NT MILKY WAY GALAXY

NT RADIO GALAXIES

NT SPIRAL GALAXIES

Galaxy clusters stability, obtaining mass distribution function from combined virial theorem and mass to light ratios

01 p0131 A72-11003

Astronomical research, discussing Venus exploration, stellar evolution quasar structure, Maffei galaxies, black holes, dwarfs and neutron star model

01 p0133 A72-11099

Galactic clusters red shifts and absolute spectral energy distributions, inferring evolutionary effects by comparison with giant elliptical galaxies light energy distribution

02 p0279 A72-12185

Bright galaxies and quasars associations based on spatial distribution and red shift considerations, discussing probability analysis

02 p0279 A72-12188

Polycyclic hydrocarbon molecules formation in cool stars atmospheres and gases ejected by supernovae and Seyfert galaxies, discussing Planck particles origin

02 p0284 A72-12634

Emission nebulae in Magellanic Clouds observed at 408 MHz, calculating electron density and total mass

02 p0285 A72-12796

Einstein light deflection by galaxy cluster gravitational field effect on extragalactic observations, explaining uniform background inhomogeneities

02 p0286 A72-12892

Six color photometry of F-G giants in Large Magellanic Cloud, noting color similarity with galactic stars

03 p0416 A72-13019

Galactic superclusters and matter distribution in universe, considering systematic catalog errors and uncertainty of statistical tests

03 p0421 A72-13172

Magellanic Clouds kinematics, composition and other properties, discussing radio sources, atomic abundances, stellar luminosity limits, regional magnetic fields and polarization

03 p0424 A72-13252

Magellanic Clouds hot supergiants color-magnitude arrays from spectroscopic and photometric measurements

03 p0424 A72-13253

Magellanic Clouds star clusters spatial distribution, color-magnitude diagrams, structures, dynamics and origins

03 p0425 A72-13254

Cepheid variables compared for Milky Way and Small and Large Magellanic Clouds, discussing amplitudes, period-luminosity relations and light curves

03 p0425 A72-13255

Magellanic Clouds neutral hydrogen distribution, concentrations and velocity structure, noting H II correlation with supergiant stars

03 p0425 A72-13256

Magellanic Clouds bright star intermediate band photometry, discussing interstellar extinction and luminous supergiants

03 p0425 A72-13257

Small Magellanic Cloud NGC 371 region photometric studies for cepheids period-luminosity relations, noting domination by young supergiant stars

03 p0425 A72-13258

Synchrotron and thermal H II region radio emission in Magellanic Clouds

03 p0425 A72-13259

Magellanic Clouds supergiant stars intrinsic colors, observing in five spectral bands to separate from Galactic foreground stars

03 p0425 A72-13260

Magellanic Clouds cepheid variables compared to Milky Way cepheids, discussing evolution tracks

03 p0425 A72-13261

Magellanic Clouds and Galactic nucleosynthesis from chemical composition

03 p0426 A72-13263

Magellanic Clouds early evolutionary state importance in extragalactic studies

03 p0426 A72-13264

Gas heating by If radiation due to Compton scattering near quasars, Seyfert galaxies nuclei and pulsars

03 p0435 A72-13801

Statistical investigation of 1500 galaxies in MCG catalog with weak surface brightness, noting sculpture type spheroidal galaxies in Virgo cluster

03 p0435 A72-13807

Extragalactic astronomy observational paradoxes, discussing quasar red shifts and clumpings in directions of bright galaxies

04 p0568 A72-14414

Precession from proper motions of stars with respect to galaxies, discussing correction for systematic errors

04 p0575 A72-15027

N galaxies and quasars properties comparison, suggesting continuous distribution and luminosity function

04 p0578 A72-15285

Gas cloud motions in Seyfert galaxy NGC 7469 center from image tube spectra, discussing size, mass and radial velocities

04 p0580 A72-15370

Optical object identified with radio source 3C 455 as quasar, noting relationship to SO galaxy NGC 7413

04 p0580 A72-15371

NGC 5128 X ray spectrum from sounding rocket and balloon observations, presenting inverse Compton models

04 p0568 A72-15372

Red shift data for galaxies in clusters, groups and pairs, discussing type, magnitude, diameter, color and inclination

05 p0714 A72-16077

External galaxies and quasars - IAU Conference, University of Uppsala, Sweden, August 1970

05 p0716 A72-16369

Stellar populations in galaxies as function of luminosity, investigating spectroscopic and photometric properties

05 p0716 A72-16370

Neutral hydrogen distribution in spiral and irregular galaxies, discussing H II regions

05 p0716 A72-16371

Spectral energy distributions of peculiar galaxies and quasars by photoelectric spectrometry, observing emission lines strength

05 p0716 A72-16373

Repeated explosions mechanism in nuclei of galaxies and quasars due to instability in twisted magnetic fields, noting clouds and relativistic plasma ejection

05 p0717 A72-16379

Hubble parameter derivation for regions beyond local anisotropy, discussing cluster galaxies magnitude-red shift diagram

05 p0717 A72-16380

Extragalactic distance scales, discussing brightest galactic cluster member utilization as distance indicators

05 p0717 A72-16381

Peculiar interacting extragalactic system NGC 6438, noting same red shift velocity of irregular and SO components

05 p0720 A72-16715

Compact galaxies photometry, determining historical variability from photographic plates obtained by large aperture cameras

06 p0880 A72-17886

Double and multiple galaxies relative number and space distribution with respect to single galaxies number from sky survey map analysis

06 p0882 A72-18005

Radial velocity effects on diameter and luminosity functions of dwarf galaxies

06 p0883 A72-18019

Stellar motion in asymmetric galaxies with three degrees of freedom, using four dimensional surface of section mapping and stochastic measurement

07 p1034 A72-19072

UBV photometry for stars near quasars and N and Seyfert galaxies, noting suitability as secondary photoelectric standards or photographic sequences for monitoring programs

07 p1071 A72-19336

Inherent uncertainties in virial mass determinations of bound and unstable groups of galaxies, computing evolution tracks for different mass loss mechanisms and rates

07 p1072 A72-19341

Seyfert galaxy hypothesis with galactic center containing hot gas region with density decreasing toward boundary, discussing nucleus brightness variability

07 p1075 A72-19560

Dynamic model of galactic clusters in terms of cosmological turbulence, estimating velocity dispersion and rotation and chaotic velocity contributions to kinetic energy

07 p1076 A72-19805

Isophote equidensity role in astronomical photometric investigation of solar corona, galactic nebulas, comets and extragalactic stellar systems

07 p1082 A72-20301

Statistical treatment of galaxy clusters shape, using flattening measurement data

08 p1229 A72-20842

Quasars and Seyfert and N-galaxies compact nuclei radiation polarization from polarimetric and photometric observations

08 p1234 A72-21281

Galactic clusters size determination from known red shift relation, discussing distribution inhomogeneities, evolution, universe expansion and Hubble constant correction

08 p1234 A72-21282

Quasars and optical quasi-stellar galaxies comparisons for red shifts and luminosities distributions

08 p1234 A72-21283

Redshifted I. alpha flux upper limit restricting hot ionized gas models for gravitational binding of Coma galactic cluster

09 p1383 A72-22292

Seyfert galactic nuclei structure, discussing thermal X rays indication of significant random motions and difficulty of energy source determination

09 p1386 A72-22686

Astronomical models for gas kinematics near galactic center, discussing gas jets origin and kinetic energy

09 p1386 A72-22687

Book on astronomy and cosmology covering big bang, steady state and oscillating universe theories, radio sources, galaxies, interstellar meteor relativity and extraterrestrial life

09 p1389 A72-23248

Galaxy NGC 253 mass and distance from neutral hydrogen spectral line observations with radio telescope

09 p1391 A72-23533

Large Magellanic Cloud star membership, comparing Sanduleak catalog based on objective-prism spectroscopy with Fehrenbach-Duflo catalog based on radial velocities

09 p1392 A72-23547

Galactic nuclei origins, evolution, observational evidence and activity relation to cosmological problems, examining Milky Way, spiral and radio galaxies and quasars

10 p1532 A72-23884

Seyfert galaxies emission, absorption, IR and optical spectral characteristics, suggesting model with sharp forbidden and Balmer line outer region and broad wing core

10 p1532 A72-23885

Galactic nuclei - Conference, Vatican City, April 1970

10 p1533 A72-23894

Seyfert, N-type, compact and radio galaxies spectroscopic properties, noting two dwarf emission line galaxies as possible young galactic nuclei

10 p1534 A72-23896

Quasar and galactic nuclei emission line spectral data corrected for interstellar extinction

10 p1534 A72-23898

Compact radio sources in galactic nuclei, discussing similarity to quasars in repetitive generation of relativistic particles

10 p1534 A72-23900

Optical properties of nuclei of normal, Seyfert and N-type galaxies and quasars from spectrographic and photometric observations

10 p1534 A72-23902

Velocity dispersions and discrepant red shifts in groups of galaxies, using virial theorem for galaxy mass calculations

10 p1534 A72-23903

Massive rotating objects with magnetic fields in galactic nuclei, considering similarities between Crab Nebula and quasars

10 p1535 A72-23908

Relative orientation of major axes of double radio sources, comparing with Brown ordering of galaxies on megaparsec scale

10 p1541 A72-24472

Quasars as cosmological and local objects, considering red shift origin and optical and radio luminosities comparison with galaxies

10 p1541 A72-24522

Coma galaxy cluster X ray and radio source region magnetic field origin as primordial metagalactic flux or strong radio source remnant

10 p1542 A72-24617

Radio telescope observation of galaxy NGC 5253 in 21 cm line, noting centrally condensed emission complex of ionized gas

10 p1543 A72-24620

Intergalactic medium presence in clusters of galaxies from investigation of separation and size-separation ratio of double radio sources located inside and outside clusters

10 p1544 A72-24670

Zero-pressure universe model parameters from red shift and apparent magnitude data for clusters of galaxies

10 p1545 A72-24809

Brightness estimates of Markarian galaxies on photographic plates, measuring light variation amplitude

10 p1546 A72-24831

Galaxies clusters classification on basis of relative contrast between brightest member and typical bright galaxy population of cluster

10 p1548 A72-24964

Radial velocities of galaxies derived from spectrograms, describing reduction procedure

10 p1548 A72-24965

Extragalactic eclipsing binaries parallax determination by Gaposchkin method, noting application to distance determination of nearby galaxies

10 p1549 A72-25057

Critique of Rees theory of primordial gravitational radiation concerning galaxy clusters interaction with very long wavelength universal gravitational waves

10 p1550 A72-25200

Large grazing incidence X ray telescope mirrors for HEAO-C mission observations, noting single stars resolution in clusters and galaxies study

11 p1630 A72-25682

Compact galaxies morphology and related properties from blue and red prints of Palomar Sky Survey, correlating to color and apparent magnitude

11 p1717 A72-25902

Radial velocity effects on diameter and luminosity functions of dwarf galaxies

11 p1718 A72-25955

Inclination and absorption effects on galaxies apparent diameters, optical luminosities and neutral atomic hydrogen radiation

11 p1724 A72-26725

Radio source and radio quiet quasars identifications for statistical correlation with bright galaxies positions

12 p1871 A72-27742

Intergalactic extinction relationship to large galactic clusters from statistical analysis of fourth and fifth Zwicky catalogs

12 p1872 A72-27759

Velocity field measurements from M82/NGC 3034/galaxy H alpha, forbidden N II and S II emission lines,

suggesting expanding ejecta cloud rotating about axis normal to galactic plane

13 p2040 A72-29401

Circular polarization disputed for Seyfert galaxy NGC 1068, quasar 3C 273 and X ray source Sco X-1

13 p2041 A72-29414

Universe evolution, discussing constituents, matter and antimatter, quasars and radio stars in various galaxies

14 p2157 A72-30623

Photometric, photographic and spectroscopic observations of Seyfert galaxies NGC 1068 and 1566, noting nuclear luminosity and surface brightness

15 p2315 A72-32713

Stellar velocity dispersion in elliptical galaxy NGC 7332 from coude spectrum obtained by SEC vidicon TV camera and telescope

16 p2454 A72-33453

Red shift observations for galactic studies, discussing Stephan Quintet in Pegasus, spiral galaxy expulsion evolutionary hypothesis and Andromeda velocity patterns

16 p2456 A72-33541

A comparison between the emission-line galaxies NGC 5253 and NGC 5408.

17 p2611 A72-35310

Internal kinematics of two compact galaxies from spectroscopic observations, noting velocity dispersion, luminosity function and mass/light ratio

17 p2611 A72-35311

The tidal interaction of galaxies

17 p2613 A72-35473

Optical observations of the supernova in NGC 5253.

18 p2726 A72-36648

Physical associations between quasi-stellar objects and galaxies.

19 p2854 A72-37227

Computational models of gravitationally interacting galaxies.

19 p2855 A72-37344

Turbulent plasma 'caldrons' in galactic nuclei

21 p3114 A72-41772

Nonvelocity origin of excess red shift in companion galaxies from observation of H and K absorption lines of Ca II

22 p3220 A72-41962

Propagation of radiative shock waves in an inhomogeneous cosmic medium.

22 p3225 A72-42452

21 cm observations of NGC45.

22 p3229 A72-42995

Quasars as images of Seyfert nuclei.

23 p3336 A72-43559

Russian book - Problems of the physics of nebulas and unsteady stars.

23 p3338 A72-44026

Numerical models of elliptical galaxy based on rotational speed and integral equations for mass distribution

23 p3338 A72-44033

Galaxies and galactic cluster distance determination from Palomar chart angular diameters related to Holmberg-Vaucouleurs photometric systems

23 p3338 A72-44034

GALERKIN METHOD

Overdetermined collocation method change into Ritz-Galerkin method for applications to boundary value problems with eigenvalues

01 p0093 A72-10122

Pretwisted tapered cantilever beam torsional vibration natural frequencies determination by Galerkin method for solution of differential equation of motion

02 p0297 A72-12533

Additive type composite oscillations in nonlinear damped vibratory system with two degrees of freedom, presenting modified Galerkin method

03 p0382 A72-13628

Distributed systems modeled by partial differential equations, identifying unknown parameters by Galerkin method using steepest descent method and nonlinear filter

04 p0505 A72-14674

Planetary wave spectrum calculation by Galerkin method, discussing angular velocity of longest Rossby waves distortable by zonal flow

05 p0655 A72-16170

Numerical algorithm for Galerkin solutions of nonlinear ordinary differential equations in dynamic system applications

07 p1025 A72-18785

Galerkin method application to nonconservative nonself-adjoint aerelasticity problems based on interpretation as mathematical formulation of virtual work principle

07 p1025 A72-18788

Convergence conditions for Galerkin method, applying to boundary value problems of structural stability and critical buckling loads

07 p1025 A72-18798

Complex transmission coefficient of waveguide with two arbitrarily spaced infinitely thin plane parallel inhomogeneities, using Galerkin method for single-parameter approximation of electrodynamic problem

07 p0938 A72-19002

- Digital simulation of two dimensional or marginally turbulent three dimensional flows by discretization and numerical integration, noting Galerkin method efficiency in avoiding errors 07 p0951 A72-20355
- Ritz-Galerkin process applied to coupled differential equations of motion of pretwisted tapered cantilever turbine blade vibrating in flexure 08 p1244 A72-21483
- Numerical simulation of two dimensional and marginal three dimensional turbulent flows, discussing variable eddy viscosity model, discretization, numerical integration and Galerkin methods 08 p1200 A72-21492
- Galerkin method for numerical simulation of incompressible boundary flows in box geometries with periodic and free slip conditions, noting Taylor-Green vortex decay 09 p1294 A72-22941
- Ritz-Galerkin procedure used for nonlinear boundary value problems solution, noting convergence of perturbed Galerkin method 09 p1343 A72-23561
- Free flexural vibration of truncated conical shells, using Galerkin method and Donnell type basic equation 10 p1559 A72-25024
- Bubnov-Galerkin method for dynamic stability of closed thin walled orthotropic cylindrical shell loaded by variable external pressure 11 p1739 A72-26977
- Galerkin boundary method as variational approach to low Peclet number heat transfer in laminar flow 13 p2063 A72-28418
- Inverse variants of Galerkin-Krylov method, discussing convergence patterns of approximate solutions to boundary value problems 13 p1986 A72-29063
- Planetary wave spectrum calculation by Galerkin method, discussing discrete modes of longest Rossby waves distortable by zonal flow 14 p2099 A72-30239
- Galerkin method for subharmonic solutions of Duffing differential equation, noting error estimation 14 p2126 A72-31102
- Large amplitude vibration of a circular plate with concentric rigid mass. [ASME PAPER 71-APMW-11] 17 p2625 A72-34319
- Error bounds for the Galerkin method applied to singular and nonsingular boundary value problems. 18 p2705 A72-36604
- Application of the Bubnov-Galerkin method to the approximate integration of a Timoshenko-type equation 19 p2877 A72-38188
- The Galerkin method for the numerical solution of Fredholm integral equations of the second kind. 19 p2827 A72-38384
- The utility of the Galerkin method for the acoustic transmission in an attenuating duct. 21 p3083 A72-40332
- On the sufficiency of the energy criterion for the stability of certain nonconservative systems of the follower-load type. [ASME PAPER 72-APM-1] 23 p3350 A72-44052
- Stability and oscillation characteristics of finite-element, finite-difference, and method of weighted residuals for transient two-dimensional heat conduction in structures. 24 p3461 A72-44608
- GALL**
- Roentgenologic studies of the effects of rapid decompression and hypoxia on the gall bladder in cats. 19 p2758 A72-38705
- GALLIUM**
- NT GALLIUM ISOTOPES**
- Thermal conductivity measurements of liquid InSb and Ga at 250-550 C 07 p1036 A72-20566
- Tensile properties from high temperature and room temperature tests of Ti alloys containing Ga correlated with creep resistance at 1000 F, noting activation energy 14 p2120 A72-30614
- Determination of Ni, Ga, and Ge in iron meteorites by X-ray fluorescence analysis. 23 p3262 A72-44128
- GALLIUM ALLOYS**
- Ga alloying effect on Al single crystals work hardening, noting Portevin-Chatelier effect at higher Ga contents 11 p1662 A72-26739
- Phase diagram study of Cr-Ga alloys, investigating intermetallic compounds presence and polymorphic transformation and temperature effects 20 p2942 A72-39987
- Thermoelectric properties of alloys of the gallium-nickel system under standard conditions 22 p3215 A72-43191
- GALLIUM ANTIMONIDES**
- Epitaxial layer preparation on GaSb single crystal by liquid phase method, discussing crystal orientation effects 03 p0402 A72-13859
- Electron tunneling into amorphous InSb and GaSb films, discussing effects of temperature, voltage, coevaporation doping and Cu and Au diffusion 10 p1527 A72-24874
- Dielectric and optical constants of p-type GaSb single crystals, interpreting singularities by energy bands diagram 11 p1689 A72-26485
- Radiation effects in InSb, GaSb and GaAs, stressing orientation dependence of damage production at electron energies near threshold and recovery data 12 p1858 A72-28066
- Phase diagrams of AlSb-GaSb and InAs-GaAs systems, noting mixing energy for liquid and solid phases 19 p2845 A72-38207
- Variations as a function of the temperature of the moduli of elasticity of monocrystalline P-type GaSb 19 p2846 A72-38542
- GALLIUM ARSENIDE LASERS**
- Mode guiding improvement in p-n junction of symmetrical AlGaAs-GaAs heterojunction laser diode with narrow active region, obtaining low room temperature threshold current 01 p0080 A72-10788
- Current dependent intensity of spontaneous emission of GaAs injection laser operated at 300 K 02 p0238 A72-12204
- Tactical optical ground communication systems, discussing use of GaAs and carbon dioxide lasers and ultrawideband data links 04 p0485 A72-14482
- Wavelength tuning effect on lasing threshold in electron beam pumped GaAs lasers as function of current density and voltage 04 p0528 A72-14545
- GaAs junction laser, determining second order dispersion in mode locking and self pulsing from output field amplitude correlation measurement 07 p1001 A72-19198
- Second order mode locked GaAs junction laser, observing mode frequencies and phases configurations during self pulsing 07 p1001 A72-19200
- Carbon dioxide lasers and GaAs electro-optical crystals 110-MHz bandwidth with coupling modulation technique 07 p1005 A72-19413
- GaAs, injection lasers with homojunctions and single and double heterostructures, observing energy dependence of internal optical losses due to band-to-band absorption 07 p1006 A72-19823
- Uncooled GaAs injection laser with high pulse repetition rate, discussing structural features and current-power characteristics 08 p1181 A72-20748
- Pulse rate and pumping power effects on emission spectra and I-V characteristics of multielement GaAs injection lasers 08 p1181 A72-20796
- Pulsed GaAs injection laser active region anisotropy and radiation polarization under spontaneous and coherent emission conditions 08 p1183 A72-21772
- GaAs semiconductor injection lasers, discussing time characteristics of current carriers, population inversion and resonator Q factor modulation 08 p1184 A72-22032
- German monograph on luminous intensity amplification by means of solid state lasers covering experiments with GaAs and ruby lasers and traveling wave amplifiers 09 p1322 A72-22331
- Modal behavior and temperature tuning of pulsed room temperature GaAs laser, using hyperfine energy level separation 09 p1323 A72-22768
- Gold-Weisberg phonon kick and extended Longini field-inhibited diffusion degradation mechanisms for GaAs double heterostructure injection lasers, discussing experimental tests 09 p1325 A72-23088
- GaAs lidar reflectance of fair weather cumulus clouds at 0.903 micron from aircraft observation 09 p1280 A72-23349
- Internal Q switching and long time delay emission in electron beam excited p-type and n-type GaAs lasers, indicating optical absorption traps 10 p1489 A72-23947
- GaAs injection laser optical link assembly with silicon photodiode and optical transistor, noting applicability to optical data processing 11 p1648 A72-26328
- Frequency modulation of CW GaAs laser emission by injection current, noting temperature effects 11 p1648 A72-26337
- Light power coupling efficiency from GaAs injection laser into single- and multimode fibers 12 p1820 A72-27507
- Te-doped GaAs injection laser, investigating crystal growth dislocations effects on output radiation-injection current characteristics 12 p1822 A72-27617
- Multielement electron beam pumped semiconductor laser using emitting GaAs disks with vapor deposited dielectric mirror coatings 12 p1824 A72-27876
- GaAs laser array Fabry-Perot structure to produce uniform TE polarization in emitted light 12 p1827 A72-28223
- Lightly doped InP and vapor epitaxial GaAs laser, observing long wavelength shift in photoemission spectra peak 14 p2108 A72-30182
- Moderate power GaAs single heterojunction injection laser diodes fabrication and operation characteristics in pulsed mode at 250-400 K 15 p2247 A72-32033
- Spacecraft onboard compact low-power coherent optical data processing system, using GaAs laser and paraboloid mirror segments 15 p2248 A72-32052
- Dynamic particle field in-line holographic recordings using IR film and p-n junction GaAs lasers 15 p2337 A72-32056
- GaAs laser properties determination by gallium arsenide-aluminum gallium arsenide double heterostructure junction diode laser, noting gain and loss at room temperature 15 p2250 A72-32519
- Coherent CW radiation by tunable GaAs injection laser in external dispersive cavity at 77 K, discussing monochromatic output spectral analysis by Fabry-Perot interferometer 16 p2401 A72-33393
- Multielement electron beam pumped semiconductor laser using emitting GaAs disks with vapor deposited dielectric mirror coatings 16 p2404 A72-33985
- Cs vapor photoionization by sequential method via thermally tunable Ga-As laser and arc-lamp monochromator radiation 17 p2585 A72-34614
- High-radiance room-temperature GaAs laser with controlled radiation in a single transverse mode. 17 p2563 A72-35342
- Behavior of spontaneous emission across threshold in GaAs junction lasers. 19 p2811 A72-37865
- Generation of controllable light pulses in an electron-beam-pumped laser. 20 p2933 A72-39514
- Time characteristics of heterojunction injection lasers. 20 p2933 A72-39516
- Reading of holograms by a semiconductor injection laser. 20 p2933 A72-39518
- Effect of uniaxial pressure on the threshold current of double-heterostructure GaAs lasers. 20 p2933 A72-39559
- An arrangement for studying the time characteristics of injection lasers 21 p3064 A72-41738
- Pulsed GaAs injection laser heating application to thermal conductivity coefficient measurement in thin films, discussing lasing spectra kinetics 21 p3064 A72-41740
- Absorption coefficient and gain of a GaAs injection laser 22 p3184 A72-42104
- Effect of increasing beam voltage on the internal quantum efficiency of spontaneous emission in electron-beam-excited p-type GaAs. 22 p3185 A72-42308
- Pulsed room temperature laser action of Si-doped double heterostructure GaAs p type diodes within 9100-9500 A wavelengths, discussing threshold current densities and power efficiency 22 p3186 A72-42621
- Interferometric measurement of the elongation of a pulsed diode laser. 23 p3297 A72-44185
- Experimental studies of injection lasers - Spontaneous spectrum at room temperature. 24 p3409 A72-44713
- GaAs semiconductor injection laser and amplifier-absorber emission and light pulse transmission characteristics determination, noting nonlinear absorptivity, bleaching threshold and pulse compression factor 24 p3412 A72-45619
- GALLIUM ARSENIDES**
- High power Q-band pulsed Gunn diode microwave oscillator constructed from thin GaAs sandwich layers grown by vapor phase epitaxy 01 p0036 A72-10630
- Liquid phase epitaxial GaAs transferred electron microwave oscillators with high dc to rf conversion efficiencies dependent on frequencies 01 p0036 A72-10631
- GaAs, Si and alumina performance as substrates in integrated microwave circuits 01 p0046 A72-10700
- High peak power I.S.A epitaxial GaAs diode relaxation oscillator breakdown under neutron irradiation 01 p0044 A72-11309

Dual gate GaAs microwave FET, measuring second gate voltage effects on power gain and noise

02 p0191 A72-11893

X band gallium arsenide field effect transistor, noting applications for radar receivers, microwave communication links and electronic countermeasures

02 p0193 A72-12184

High efficiency GaAs transferred electron device operation and microwave oscillator design by simple static I-V characteristics description for time domain computer simulation

02 p0193 A72-12230

Transverse photoconductivity and dark I-V characteristics of n-GaAs compensated with Cr in high electric field at room temperature

03 p0401 A72-13586

Narrow band medium power X, Ku and C band solid state amplifiers, demonstrating TWT replacement with GaAs and avalanche diodes

03 p0334 A72-14072

GaAs Schottky barrier and germanium backward diodes in microwave integrated circuit applications, describing design and performance as frequency changers and low level detectors

03 p0334 A72-14073

Se and Zn doped n and p type gallium arsenide point defects, considering thermal conductivity, relaxation time and phonon scattering cross section effects

03 p0404 A72-14239

Light wave electric field Franz-Keldysh effect on GaAs absorption edge, using electroabsorption, electroluminescence and photoconductivity spectrum and internal photoeffect analysis

04 p0561 A72-14621

Transit time and LSA oscillations at millimeter and submillimeter wavelengths in n-type GaAs

04 p0563 A72-15593

Photoconductive detection and generation of far IR radiation in high purity epitaxial GaAs

04 p0563 A72-15605

High purity epitaxial GaAs frequency response, determining heterodyne detection in millimeter and submillimeter regimes

04 p0563 A72-15613

Tunable coherent IR signal generation and propagation by mixing carbon dioxide laser and millimeter wave klystron output in GaAs loaded waveguide

04 p0532 A72-15614

Microstrip configuration for microwave GaAs IMPATT diode oscillators and power amplifiers

05 p0633 A72-15782

Vapor-grown GaAs transfer electron microwave oscillator, discussing design, fabrication and CW power conversion efficiency

05 p0637 A72-16366

GaAs Schottky barrier diodes design, manufacture and characteristics, discussing radar receiver and communication equipment applications

05 p0638 A72-16595

Direct coupled circuits in memory cell prototype with normally-off GaAs MESFET at 4.2 K

05 p0638 A72-17096

High temperature GaAs bipolar transistor n-p-n junction fabrication by vapor phase growth technique, considering I-V characteristics dependence on procedure

06 p0783 A72-17607

Piezoresonance modulation of IR amplitude in GaAs crystal by electric field at single, doubled and quadrupled frequencies

06 p0866 A72-17843

GaAs IMPATT diode with plated heat sink for microstrip circuit applications, exemplifying X band oscillator experiment

06 p0787 A72-18385

Transferred electron effect in GaAs, presenting three level solid state microwave oscillator advantages

06 p0866 A72-18454

GaAs IMPATT diodes technology and performance at C, X and K band frequencies

06 p0788 A72-18466

Millimeter wave GaAs avalanche diode oscillator processing on plated Cu heat sinking block resulting in epitaxially grown p-n junctions

06 p0788 A72-18467

Neutron irradiation induced material degradation and circuit failure in high power GaAs Gunn diode oscillator operating in LSA relaxation mode

06 p0788 A72-18472

GaAs IMPATT diodes performance improvement, describing fabrication methods to achieve 6.7 watts output at 15 percent efficiency

06 p0789 A72-18474

High power efficiency CW Gunn devices design and fabrication, discussing GaAs preparation techniques and device physics

06 p0789 A72-18478

High power GaAs LSA transmitter oscillator refinements, noting pulsed development to change load and thermal environment frequency stability

06 p0789 A72-18482

GaAs and Si millimeter wave Schottky barrier mixer diodes fabrication, noting low noise broadband mixer/preamp

06 p0790 A72-18486

Moderate power GaAs FET switching experiment, obtaining rise and fall times

07 p0952 A72-18826

Optically pumped indium-gallium-arsenides laser coherent emission at room temperature, measuring total power conversion efficiency [AD-737941]

07 p0999 A72-18882

Carrier wave growth during propagation through negative differential mobility n-type GaAs under nonuniform dc bias conditions

07 p1047 A72-19044

Low noise GaAs Schottky barrier FET for X and Ku bands applications

07 p0955 A72-19257

High power negative resistance amplifiers, calculating relationship among output, gain, gain compression and efficiency for comparison with GaAs avalanche diode amplifier experiment

07 p0958 A72-19920

Thermostimulated autophotocurrent emission from Cr-alloyed p-type GaAs electrode, determining spectral distribution and light and electric field effects on current

08 p1216 A72-21071

Noise in optical output of small area electroluminescent GaAs diffused junction diodes, comparing with theoretical shot noise limit

09 p1286 A72-23087

Background noise in amplification and oscillation in Si and GaAs avalanche diodes

09 p1287 A72-23119

Noise of high electric field biased gallium arsenide diodes, calculating LF power spectrum

09 p1288 A72-23123

Be and Mg ion generation and p-type layer electrical properties production by implantation in GaAs substrates

09 p1372 A72-23245

Millimeter wave pumped X band balanced diode type parametric amplifier using GaAs Schottky barrier varactors for operation at room temperature

09 p1289 A72-23417

Supercritical CW GaAs transferred electron broadband reflection amplifier power gain and noise figure at 34 GHz

10 p1449 A72-24301

Gunn domain oscillations suppression by dielectric surface loading of transversely thin GaAs diodes

10 p1526 A72-24305

Electric field profile in n-type GaAs layer biased above transferred electron threshold for small signal amplifier operation

10 p1450 A72-24554

Liquid phase epitaxy GaAs growth in rotary reactors from Ga solution, noting thickness, doping uniformity, reproducibility and surface morphology

10 p1526 A72-24556

GaAs abrupt junction IMPATT diode large signal operation analysis, noting oscillation efficiency HF fall-off characteristics

10 p1450 A72-24557

Temperature dependence of internal quantum efficiency of spontaneous emission as function of beam voltage in electron beam excited p-type GaAs

10 p1526 A72-24559

High conversion efficiency microwave second harmonic generator using negative resistance nonlinearity of n-type GaAs

11 p1591 A72-25741

GaAs solar batteries for spacecraft power supplies, comparing effectiveness with Si cells for optimum utilization

11 p1578 A72-25940

Heterojunction p-GaAs-n-ZnSe diodes electrical and photovoltaic properties, showing space charge limited current effects

11 p1606 A72-26624

High quality GaAs varactor diodes for double diode low noise wideband parametric amplifiers at idler frequencies up to 43 GHz without refrigeration

12 p1788 A72-27174

Seminsulated gate GaAs FET fabrication by proton bombardment

12 p1790 A72-27438

Noise behavior of GaAs Schottky barrier FET with short gate length, showing channel thickness effect on intervalley scattering noise

12 p1790 A72-27439

Many element GaAs and CdS semiconductor laser achieving high power output by electron beam pumping

12 p1822 A72-27616

Microwave time of flight method for measuring electron drift velocity in GaAs semiconductors

12 p1855 A72-27667

Pulse generation in planar Gunn devices of epitaxially grown GaAs layers, measuring current reduction by domain nucleation

12 p1791 A72-27671

GaAs semiconductor devices role in microwave communications, discussing physical properties and potential applications

12 p1792 A72-27736

C and X band CW GaAs Schottky barrier IMPATT oscillators with nichrome as barrier metal, noting high power efficiency and low noise performance

12 p1793 A72-27966

Radiation effects in InSb, GaSb and GaAs, stressing orientation dependence of damage production at electron energies near threshold and recovery data

12 p1858 A72-28066

Electron irradiation of n-type Si or Te doped GaAs, determining carrier removal rate, mobility changes and annealing characteristics

12 p1858 A72-28067

Annealing behavior of electrical properties and photoluminescence spectra in electron irradiated n-type GaAs semiconductors

12 p1859 A72-28068

IR absorption bands in mechanically and chemically polished GaAs single crystals irradiated with varying neutron and electron doses

12 p1859 A72-28069

Lattice damage measurement of Cd ion implanted GaAs semiconductors by optical reflection and scanning electron microscope

12 p1859 A72-28075

Surface damage equations for heavy ion irradiated Si and GaAs single crystals in terms of incident fluence

13 p2020 A72-28430

Mobility-field characteristics of GaAs below Gunn threshold with magnetoresistance technique, relating to device performance and other material parameters

13 p2021 A72-28573

Electrical characterization of GaAs by Hall and magnetoresistance measurements, analyzing temperature dependence of carrier concentration

13 p2024 A72-30034

Epitaxial GaAs carrier concentration profile, deep traps detection and properties determination, using Schottky barrier on semiconductors

13 p2024 A72-30035

Gunn diode active region thickness, free electron mobility/concentration, structure and contacts, including treatment of GaAs

13 p1934 A72-30036

Au film optical refractivity, absorptivity and transmittance in visible and UV ranges of Au-GaAs and Au-GaP photoelectric converters

14 p2141 A72-30224

Solar photosensitive elements prepared p-type GaAs liquid epitaxy on n-type GaAs substrate, measuring dark and light I-V characteristics and spectral response

14 p2142 A72-30225

Mass spectroscopic determination of vapor composition during GaAs and GaP single crystals exposure to ruby laser radiation

14 p2109 A72-30316

GaAs varactor diode design optimization based on calculation of cut-off frequency vs carrier concentration with consideration of skin effect

14 p2088 A72-30588

Carrier wave behavior in n-type GaAs slab under crossed dc electric and magnetic fields, investigating traveling space charge amplifier magnetic control

14 p2143 A72-30941

Gallium aluminum arsenide light emitting diode thin structures grown on GaP substrates by liquid phase epitaxial method

15 p2290 A72-31381

Difference-frequency mixing of pulsed carbon dioxide lasers with non-phase-matched GaAs for submillimeter wave generation

15 p2290 A72-31384

I-V characteristics of polarized and nonpolarized memory effects in GaAs thin films evaporated on tungsten substrates

15 p2292 A72-31869

Transverse magnetic field effects on n-type GaAs Gunn diodes microwave power, coherence and dynamic I-V characteristics

[ONERA, TP NO. 1051]

15 p2207 A72-31884

GaAs Gunn diode LSA operation mode in multiloop circuit to extend high frequency limit

15 p2207 A72-31888

Room temperature GaAlAs single-heterojunction diode lasers structure, fabrication, threshold current density and quantum efficiency dependence on wavelength and temperature

15 p2247 A72-32032

Gallium arsenide-aluminum gallium arsenide double heterostructure wafer fabrication, describing reproducible liquid phase epitaxial growth

15 p2250 A72-32518

Photoconductivity in depleted surface layer of quasi-monopolar semiconductors with arbitrary diffusion to Debye lengths ratio, noting n-type low resistance gallium arsenide

15 p2296 A72-32694

Surface defects evaluation on GaAs and Si wafers by metallographic and electrochemical techniques

15 p2296 A72-32758

Boltzmann-Matano analysis of substitutional interstitial diffusion profiles of Zn in GaAs by radio tracer techniques

16 p2441 A72-33209

N-type GaAs absorption spectra construction from transmission spectra, considering effects of irradiation by fast protons, electrons, neutrons and alpha particles 16 p2441 A72-33368

Transient 10 MeV electron radiation effects on RF power and recovery time of GaAs Schottky barrier IMPATT diodes 16 p2370 A72-33766

Gunn effect - Bulk instabilities. 17 p2594 A72-34562

Millimeter-wavelength frequency multipliers employing gallium arsenide diodes 17 p2529 A72-34851

Gallium arsenide varactors 18 p2671 A72-37145

High burnout gallium arsenide Schottky barrier diodes. 19 p2770 A72-37259

A C-band all ferrite integrated wideband high power GaAs avalanche diode amplifier. 19 p2771 A72-37264

Design considerations of a 3.1-3.5 GHz GaAs FET feedback amplifier. 19 p2771 A72-37269

Single and dual gate GaAs FET integrated amplifiers in C band. 19 p2771 A72-37270

Electrical and thermoelectrical effects in GaAs-InAs solid solutions 19 p2844 A72-37752

Quantum efficiency and radiative lifetime of the band-to-band recombination in heavily doped n-type GaAs. 19 p2844 A72-37947

Phase diagrams of AlSb-GaSb and InAs-GaAs systems, noting mixing energy for liquid and solid phases 19 p2845 A72-38207

Low-temperature photoluminescence of GaAs under conditions of strong interaction of the non-equilibrium carriers. 19 p2847 A72-38821

Air cooled CW 30 W carbon dioxide laser construction for technological applications, using radiation energy extraction through GeAs or GaAs plate 20 p2932 A72-39507

Effects of magnetic field on electron transport properties in gallium arsenide. 20 p2960 A72-39704

Control of high-field domain in GaAs by the field effect and its application to functional devices. 20 p2960 A72-39706

Small-signal admittance of the insulator-n type-gallium-arsenide interface region. 20 p2909 A72-39775

Influence of a surface space charge on certain photoelectric properties of p-type gallium arsenide 21 p3098 A72-41684

Theory of microwave amplification with electron transfer 23 p3269 A72-43550

GaAs light emitting diodes intensity fluctuations measurements at .025-20 kHz 23 p3297 A72-44190

Utilization of a composite resonator for improving the monochromaticity of a semiconductor laser with electron-beam excitation 23 p3297 A72-44468

Reflection amplification in thin layers of n-GaAs. 24 p3385 A72-44971

GALLIUM COMPOUNDS
 NT GALLIUM ANTIMONIDES
 NT GALLIUM ARSENIDES
 NT GALLIUM PHOSPHIDES
 NT GALLIUM SELENIDES
 Hopping electroconductivity of n-type GaS single crystals, observing frequency dependence 06 p0866 A72-18181

Temperature and stress dependence of steady state creep rate for dispersion strengthened Ag-gallium oxide alloys, noting grain size effect on activation energy 16 p2411 A72-34094

GALLIUM ISOTOPES
 The isotopic composition and elemental abundance of gallium in meteorites and in terrestrial samples. 18 p2723 A72-36061

GALLIUM PHOSPHIDES
 Localized vibration modes of light impurities in gallium phosphide crystals from absorption spectrum analysis 06 p0866 A72-18182

Neutron damage effects on red and green output of GaP light emitting diodes at 300 K 07 p1047 A72-19043

Thin GaP film composition and structure determination by laser Raman scattering 09 p1314 A72-23345

Electroreflectance study of mixed gallium and indium phosphides 10 p1525 A72-24228

Minority carrier diffusion length in liquid epitaxial GaP, noting dependence on dominant impurity and

substrate growth orientation from Schottky diode photocurrent technique 10 p1526 A72-24551

Enhanced indirect optical absorption measurement in AlAs and GaP with energy denominator variation for direct band gap evaluation 13 p2022 A72-29627

Au film optical refractivity, absorptivity and transmittance in visible and UV ranges of Au-GaAs and Au-GaP photoelectric converters 14 p2141 A72-30224

Mass spectroscopic determination of vapor composition during GaAs and GaP single crystals exposure to ruby laser radiation 14 p2109 A72-30316

Photomultiplier negative electron affinity emitter materials photosensitivity performance, considering Cs-activated GaP and applications for low light level detection 15 p2291 A72-31531

Near junction doping characteristics of p-n GaP red emitting diodes by scanning electron microscope correlated with electrical and electroluminescent measurements 15 p2208 A72-32521

Coherent orange emission and bright electroluminescence from indium gallium phosphides vapor grown p-n junction laser diodes 15 p2251 A72-32532

Average energy to form electron-hole pairs in GaP diodes with alpha particles. 20 p2908 A72-39564

GaP /Zn-O/ diodes light emission efficiency increase by forward bias, relating to precipitation in n and p layers 22 p3159 A72-42613

GALLIUM SELENIDES
 IR luminescence and photoconductivity in p-type GaSe single crystals alloyed with Sn and Ge impurities 08 p1216 A72-21069

Time to failure under axial tension determined for gallium selenide single crystals at constant temperatures, noting tensile strength dependence 15 p2290 A72-31387

GALVANIC CELLS
 U ELECTROLYTIC CELLS
GALVANIC SKIN RESPONSE
 Physiological response to affective visual stimuli, observing signal value change effect on forehead pulse amplitude and galvanic skin response 01 p0014 A72-10854

Spatio-temporal scalp mapping localization of human visual evoked responses to full field light adapted stimulation, comparing to half-field situation 01 p0015 A72-11185

Human trace responses generation and storage under light stimulus reinforcement of sound conditioning from galvanic skin reactions observation 04 p0475 A72-15581

Short-time memory and electrographic effective and trace processes relationship from visual and Rolandian cortical regions activity and Tarkhanov galvanocutaneous reaction 06 p0764 A72-17993

Galvanic skin response techniques for palmar and dorsal sweat detection during motion sickness by vestibular stimulation, comparing arousal and thermal sweat response 07 p0933 A72-20185

Human electrophysiological changes during perceptual isolation from EEG, EMG, vertical eye movements and electrodermal measurements 12 p1771 A72-27484

GALVANIZING
 U ZINC COATINGS
GALVANOMAGNETIC EFFECTS
 NT NERNST-ETTINGSHAUSEN EFFECT
 Galvanomagnetic properties of well-oriented graphite in relation to the structural imperfections. 21 p3073 A72-40691

GALVANOMAGNETISM
 U GALVANOMAGNETIC EFFECTS
GAME THEORY
 NT MINIMAX TECHNIQUE
 NT SADDLE POINTS [GAME THEORY]
 Impulse motion convergence in game theory, considering control problems of pursuit involving escape and capture 05 p0690 A72-16583

Discrete stochastic differential games with quadratic payoff function, deriving deterministic, randomized and game optimal control strategies 06 p0793 A72-17956

Suboptimal security solution of linear quadratic pursuit evasion game with state dependent, control dependent and additive noises, deriving equations for state estimation 06 p0794 A72-18151

Suboptimal stochastic control strategies class based on game theory and optimin principle, investigating completeness in closed discrete-time systems 06 p0794 A72-18167

Game theory application to time optimal control strategy for independent operations set 06 p0794 A72-18168

Real time near optimal closed loop control solution to fixed time nonlinear differential game by periodically updating to two point boundary value problem 07 p1027 A72-19278

Singular surfaces for time optimal control in zero sum differential games between two aircraft in three dimensional space, assuming spherical acceleration vectogram 07 p1027 A72-19279

Optimal thrust reversing in pursuit evasion games between two aircraft in horizontal plane, considering cost functions and termination criteria 07 p0912 A72-19282

Minimax terminal state estimator existence and structure for linear discrete system, applying to stochastic pursuit evasion games of LQG variety 07 p1027 A72-19283

Optimal control of linear multivariable plants with one or more quality criteria, considering control channels and game theory 07 p0962 A72-19720

Optimal strategies conditions for game problems in conflictingly controlled system, discussing minimax technique and Bellman equation solution 07 p1028 A72-19971

Epsilon technique for optimal control computation in pursuit and evasion problems, reducing dynamic to nondynamic optimization problem 09 p1342 A72-23253

Near optimal closed loop control laws for fixed time pursuit-evasion differential game between two aircraft in vertical plane, using dynamic modeling 10 p1421 A72-23805

Differential games with deviation from encounter, considering strategies for continuous, programmed and discontinuous controlled motion onto given set 10 p1511 A72-24426

Theorem of pursuit game with curvature constraints during two points motion in Euclidean space 11 p1675 A72-25320

Antagonistic pursuit games of prescribed duration in abstract topological space with defined distance function 11 p1676 A72-25326

Multistage pursuit-evasion game on circle, constructing player optimal strategies via measure theory 12 p1836 A72-27511

Russian papers on adaptive control systems covering automata and game theory, learning models, Markov processes and probability theory 12 p1787 A72-27921

Differential games extremal strategies with player control action subject to integral constraints 13 p2002 A72-28712

Position differential games of extremal stable evasion strategies for swerving motions with absorption in time 13 p2004 A72-29470

Optimal feedback controller design based on cooperative game described by quadratic cost functional under linear differential equation constraints, applying to satellite terminal rendezvous 15 p2267 A72-31789

Game problem of impulse controlled soft rendezvous of two material particles under attractive forces 16 p2422 A72-32928

Supernova explosion mechanism and quantitative game for galactic chemical evolution, discussing relationship to cosmic rays 16 p2459 A72-33744

On behavior strategy solutions in two-person zero-sum finite extended games with imperfect information. I - A method for determination of minimally complex behavior strategy solutions. 17 p2574 A72-34343

Second order differential guidance game, formulating strategy for optimal feedback control 18 p2673 A72-36660

Optimal terminal rendezvous as a stochastic differential game problem. 19 p2869 A72-37284

The problem of encounter avoidance in linear differential games 19 p2824 A72-37377

Application of a learning recognition system for classification of game situations 19 p2769 A72-37422

Impulse motion encounter in game theory, considering control problems of pursuit involving escape and capture 19 p2825 A72-37554

Optimality conditions for safe time in linear pursuit problems within n-dimensional Euclidean space 19 p2825 A72-37555

The dynamic modeling technique for obtaining closed-loop control laws for aircraft/aircraft pursuit-evasion problems. 19 p2753 A72-38276

Programmed minimax target acquisition in rendezvous game between conflict controlled motion and given set of vectors 20 p2947 A72-40026

- Optimal strategies conditions for game problems in conflict controlled system, discussing minimax technique and Bellman equation solution
20 p2947 A72-40028
- Trajectory deviation conditions in second order linear differential escape game, using Pontryagin principle
22 p3204 A72-41903
- Differential games extremal strategies with player control action subject to integral constraints
22 p3198 A72-42090
- Game theoretical modeling of fighter aircraft turning tactics competition in pursuit combat, using minimax technique
[AIAA PAPER 72-950]
22 p3138 A72-42359
- Linear vector formulation of pursuit problems with pursuer discrimination, using Mishchenko-Pontryagin curvature conditions
23 p3307 A72-43220
- Trajectory bundles in metric space for objects motion study in dynamic pursuit games, noting Pontryagin and Pshenichnii methods for differential games solution
23 p3308 A72-43415
- Differential pursuit games with nonlinear evading player and linear pursuer, considering determination of initial states
23 p3277 A72-44001
- Methodical aspects of studies of ergatic differential-game systems
24 p3376 A72-45517
- Differential games problem of pursuit tracking solved by invariants theory, noting explicit laws of pursuer activity control
24 p3387 A72-45518
- Man in a control circuit during an information game synthesis
24 p3377 A72-45520
- Aircraft interception avoidance problem solved by differential game theory, discussing human operator decision making for random pursuit tracking
24 p3377 A72-45523
- GAMMA FUNCTION**
Wiener Hopf integral equation for problem of smooth stamp impression into elastic wedge face, solving by gamma and hypergeometric functions
13 p2059 A72-29500
- Torsion problem of solid rod with wing profile shaped cross section solved by conformal mapping and gamma function derivative, calculating maximum stresses and rigidities
15 p2327 A72-31741
- An approximate method for inverse Laplace transformation
19 p2828 A72-38853
- GAMMA RADIATION**
U GAMMA RAYS
GAMMA RAY BEAMS
Comparative study of two direct methods of bone mineral measurement.
17 p2508 A72-34552
- Investigation of Freon fire-extinguishing systems with a nucleonic gage.
18 p2648 A72-36674
- GAMMA RAYS**
Cosmic gamma rays at 0.3-3.7 MeV measured by NaI/Tl crystal detector 64-channel spectrometer on-board Cosmos 135 and 163
01 p0118 A72-10153
- Average energy electron capture coefficient dependence on air density, temperature and altitude under gamma radiation
01 p0059 A72-10599
- Extraterrestrial gamma ray flux contribution to total 0.7-4.5 MeV radiation at various latitudes by balloon sounding
01 p0120 A72-11007
- Antimatter existence on cosmological scale in universe, comparing calculated annihilation gamma ray spectrum with background observations
02 p0278 A72-11967
- Gamma ray astronomy, discussing energy spectrum, diffuse background flux, extragalactic origin and Crab Nebula emission
03 p0408 A72-13027
- Gamma ray detection system using scintillation counter and active anticoincidence shield
03 p0352 A72-13028
- Celestial gamma rays arrival direction and energy spectra measurement and spectrum analysis using ESR0 satellite COS-B data
03 p0408 A72-13029
- Low energy gamma ray telescope with active honeycomb collimator and anticoincidence detector, describing directivity techniques for galactic sources
03 p0408 A72-13030
- Stilbene scintillator detector for gamma ray spectrometry in energy range 0.5-5 MeV, separating gamma rays from neutrons by pulse shape discrimination technique
03 p0408 A72-13031
- Major sources of background counts for collimation gamma ray detector, measuring radiation direction and energy spectrum from balloon altitudes
03 p0352 A72-13032

- High energy gamma ray telescope based on absorption induced Cerenkov radiation in low density gas, using parabolic mirror for focusing on photomultiplier tubes
03 p0352 A72-13033
- Gas-Cerenkov detector for 10-100 MeV gamma rays based on conversion and Compton scattering in plastic scintillator
03 p0352 A72-13034
- Optical multiplate spark chamber in balloon-borne gamma ray telescope, describing triggering signal from plastic scintillator directional Cerenkov counter and photographic recording system
03 p0353 A72-13035
- Air ionization, secondary electron emission and Compton currents at W-Be interfaces under Co 60 gamma radiation
03 p0403 A72-14083
- High intensity ionizing gamma ray pulsed radiation effects on Gunn diode microwave oscillator failure modes
03 p0334 A72-14089
- Gamma and neutron radiation effects on bipolar transistor current gain response predicted from multiple linear regression analysis
03 p0335 A72-14091
- Matched Si junction FET under neutron burst and pulsed gamma radiation, investigating device parameters degradation
03 p0335 A72-14093
- Nucleosynthesis model for gamma ray astronomy, covering explosive events
03 p0413 A72-14275
- Heavy elements gamma heating, using LiF thermoluminescent dosimeters and computer programmed photon transport calculations
04 p0546 A72-14427
- Airborne gamma ray spectrometer investigation circle, considering altitude, air density, source density and gamma ray attenuation coefficient effects
04 p0520 A72-14564
- Proliferative blood forming tissue activity under chronic gamma ray irradiation in guinea pigs by quantitative methods, showing myeloid and reticular disturbances of bone marrow
04 p0467 A72-14607
- Gamma ray and neutron emissions from sun, considering acceleration of charged particles in solar atmosphere
04 p0566 A72-14724
- Galactic center region, Virgo and Crab Nebula gamma ray observations, measuring intensity and energy spectra
04 p0578 A72-15312
- Cosmic ray induced radioactivity effects on diffuse gamma ray background measurement from 600 MeV proton irradiation experiment
04 p0567 A72-15324
- Blue green algae *Anacystis nidulans* photorecovery after Co 60 gamma radiation exposures, using white and red light
04 p0475 A72-15516
- X ray and gamma astronomy, discussing old and blue stars, supernova remnants, radio galaxies, quasars and pulsars
04 p0582 A72-15687
- TD-1, HEOS-B and COS-B satellite-borne experiments, discussing X ray and gamma astronomy
04 p0582 A72-15690
- X ray and gamma astronomy, discussing satellite-borne experiments for electromagnetic and nuclear reaction rates and antimatter existence in cosmic radiation
04 p0582 A72-15692
- High energy X ray and gamma ray astronomy for galactic and extragalactic observations, noting SAS satellite and HEAO program
05 p0712 A72-15773
- Cosmic gamma radiation theoretical and experimental investigations, discussing sources, interactions with interstellar and intergalactic media, atmospheric backgrounds, balloon and satellite measurements, etc
05 p0709 A72-16328
- ATP injection protection against Co 60 or Cs 137 gamma radiation in albino mice, guinea pigs and dogs
05 p0621 A72-16636
- Illumination effect on proton and gamma irradiated cabbage plant growth, height and foliage, indicating radiation protective effect for certain light intensities
05 p0622 A72-16649
- Metagalactic gamma rays from relativistic electron bremsstrahlung interactions under assumption of single power law source
05 p0710 A72-16712
- Background phonon X ray and gamma quanta intensities dependence on solar activity from Geiger counter recordings in deep space
05 p0711 A72-17046
- Gamma ray absorption near Crab Nebula pulsar NP 0532 within beam model, discussing pair production in photon field
05 p0711 A72-17161
- Multilayer X ray chamber for gamma quanta energy spectrum determination by primary photon impact and absorber calorimetric methods
06 p0869 A72-17266

- Altitude effects on high energy neutrons and galactic gamma rays flux and spectrum variations from balloon flight studies
06 p0873 A72-17639
- Biological damage inflicted to rats by protons, X rays and gamma rays
06 p0762 A72-17675
- Visual discrimination task-trained monkeys performance and physiology after pulsed mixed gamma-neutron irradiation, noting blood pressure and respiratory and heart rate changes
06 p0763 A72-17873
- High energy gamma rays from Cygnus region, using balloon flight measurements with spark chamber telescope
06 p0873 A72-17891
- Low energy gamma radiation spectrum from galactic center region, using balloon altitude observation
07 p1059 A72-19420
- Balloon measurement of low energy cosmic gamma ray flux, obtaining energy spectrum
07 p1059 A72-19585
- Energetic gamma quantum flux recording from extragalactic source 3C 120 by Cosmos 251 and 264 satellites
07 p1076 A72-19803
- Pulsed gamma ray emission measurement above 50 MeV from Crab Nebula pulsar with balloon-borne spark chamber
07 p1063 A72-20235
- Extragalactic origin of diffuse low energy cosmic gamma rays, using balloon-borne detector system
07 p1063 A72-20392
- High energy gamma quanta point sources from extensive air showers Cerenkov flares records, finding flux limits of radio galaxy and pulsars
07 p1064 A72-20635
- Cosmos satellite measurements of high energy gamma quanta from Crab Nebula region, indicating excess flux association with Taurus constellation point source
07 p1064 A72-20636
- High energy electrons and gamma quantum flux in upper atmospheric layers from high altitude balloon measurements
07 p1065 A72-20639
- Primary cosmic ray high energy gamma quanta flux measurements on Cosmos 208 satellite-borne instruments
08 p1225 A72-20798
- Gamma irradiation effects on temperature of reversible solid-to-liquid phase transformation in Al
08 p1185 A72-21075
- High energy gamma radiation intensity from galactic plane in Cygnus-Cassiopeia region, using balloon-borne telescope
08 p1227 A72-21215
- Balloon observations of low energy Scorpius X-1 gamma ray spectrum
08 p1227 A72-21395
- Gamma ray spectrometer with antiCompton shield for OSO-7 spacecraft
08 p1167 A72-21515
- Optimal pulse height analyzer with quadratic transfer function for gamma ray spectrometer on OSO-H
08 p1167 A72-21516
- Mossbauer gamma radiation diffraction by Y-Fe garnet crystals with Mossbauer nuclei in magnetic and electric field nodes
08 p1217 A72-21767
- Gamma radiation source energy and activity determination for radiometric flaw detection in steel
08 p1177 A72-21775
- Gamma radiation effect on cracking and tensile strength of polycapromide / capron/ film
08 p1196 A72-21870
- Electric field voltage effect on dispersion of electrostatically atomized liquids and hydrocarbon fuels with and without gamma irradiation
09 p1350 A72-22546
- Resonance occurrence in generation-recombination noise spectrum of Co 60 gamma irradiated Ge single crystals, investigating Hall effect
09 p1372 A72-23112
- Radical concentrations in gamma irradiated poly(ethylene 2,6-naphthalene dicarboxylate) by ESR spectrum analysis
10 p1433 A72-23847
- Spacecraft-based observations of gamma and X radiation resulting from planetary surface and atmosphere processes to obtain source medium chemical composition
10 p1530 A72-25060
- Gamma ray radiation effects on epoxy resin electric properties, studying electric insulation and arc resistances and dielectric breakdown strength
10 p1502 A72-25149
- X and gamma ray astronomy with multiple pinhole cameras and a posteriori image synthesis, obtaining SNR gain
11 p1629 A72-25313
- Recombination parameters in low resistivity gamma irradiated n-type Ge, obtaining energy levels and tem-

- perature dependence of electron and hole capture probabilities 12 p1857 A72-28056
- Annealing effects on gamma ray irradiated Li compensated p-type B doped Si semiconductor 12 p1858 A72-28065
- Adhesives polymerization and rapid ambient temperature curing, using Co 60 gamma rays and electron beams 12 p1833 A72-28079
- Russian book on penetrating radiation effect on radio components covering resistors and capacitors electrophysical characteristics and parameters changes under gamma and neutron radiation 12 p1793 A72-28342
- Efficiency response of covered Si detectors to monoenergetic gamma rays, considering Lucite, Al, Cu and Pb absorbers 13 p1954 A72-28429
- Permanent operational characteristics changes of Si and Ge transistors bombarded by gamma and neutron radiation 13 p1928 A72-28700
- Three year varied dose and acute exposure gamma irradiation of dogs, noting radiobiological effects from hematological, cytological and physiological examinations 13 p1903 A72-29307
- Gamma irradiation effects on epoxy-diane resin creep and stress relaxation properties indicated by loaded specimens birefringence patterns 13 p1984 A72-29481
- Temporal, energetic and spectral properties of stimulated emission from Cr doped ruby laser irradiated by Co 60 gamma rays 13 p1969 A72-29613
- Adiabatic effect of slow rotational molecular diffusion on perturbed angular correlations of gamma radiation for radioactive studies in viscous media 13 p2008 A72-29863
- Co 60 gamma radiation effect on stimulated ruby laser emission delay time, pulse duration, energy curve and intensity 13 p1972 A72-30005
- Radiation defectoscopy methods based on calculating perturbations in gamma radiation field due to inhomogeneities 14 p2106 A72-30150
- Astrophysical equipment for Cerenkov radiation measurement from atmospheric showers, discussing source of high energy gamma rays in galactic equator direction 14 p2146 A72-30201
- Amitravite /biological protectant/ effect on natural immunity state of dogs exposed to chronic gamma irradiation simulating space flight environment 14 p2074 A72-30380
- Semiconductor gamma ray detectors development, using cadmium dichlorides, dibromides, diiodides and difluorides as doping agents in CdTe crystal growth 14 p2142 A72-30549
- Celestial sources investigation for high energy cosmic gamma rays with particular attention to Crab Nebula 14 p2147 A72-30560
- Trillion electron volt pulsed gamma rays from Crab Nebula pulsar NP 0532 14 p2156 A72-30566
- Organ cell lysosomes polymorphic properties and formation by Golgi complex, discussing role in neurocyte structure restitution following gamma irradiation 14 p2075 A72-30594
- Geomagnetic field perturbation by gamma quanta pulsating source, studying accompanying radio emission behavior 14 p2101 A72-30645
- Gamma radiation effects on composite propellants stability, investigating polyurethane, polybutadiene, silicone and polyisoprene binders mechanical properties 14 p2144 A72-30760
- Radioisotope camera based on electron avalanche in liquid Xe, noting spatial and energy resolution advantages over existing gamma ray cameras 15 p2234 A72-31537
- Semiconductor devices application to gamma ray, X ray and nuclear radiations detection and analysis 15 p2235 A72-31644
- Diffuse cosmic gamma ray flux density and energy spectrum observation at equatorial balloon altitude, discussing photon count, flux and spectra 15 p2299 A72-31924
- Mossbauer spectroscopy theory and application to steel technology, discussing spectral characteristics of various iron phases and corrosion and stress effects 16 p2405 A72-32824
- Galactic X and gamma ray astronomical observations from balloons, rockets and satellites, discussing radiation counters 16 p2445 A72-33075
- Dosimetric characteristics of CdS semiconductor detectors and photoresistors for gamma rays recording 16 p2390 A72-33076
- Primary cosmic rays extragalactic origin, considering high energy electrons, background X and gamma rays and cosmic protons 16 p2445 A72-33126
- Computer simulation of airborne gamma ray spectrometer with prescribed photopeak windows from flight over surfaces with arbitrary-dimension radiation sources 16 p2392 A72-33617
- Pulsars radiation mechanism relationship to magnetospheric conditions, considering optical, X ray and gamma radiation 16 p2460 A72-33928
- Observation of the diffuse cosmic gamma radiation in the 30-50-MeV region. 17 p2598 A72-34522
- A search for high energy gamma-rays from solar active regions. 17 p2599 A72-35092
- Electrons and photons interaction with relic radiation, establishing high energy gamma rays energy and intensity attenuation length 17 p2600 A72-35145
- Effect of lunar ground on radiation damage in mice 17 p2504 A72-35214
- Energetic gamma quantum flux recording from radio galaxy 3C 120 by Cosmos 251 and 264 satellites 17 p2617 A72-35726
- Theoretical studies of the flux and energy spectrum of gamma radiation from the sun. 18 p2721 A72-35993
- Gamma radiation production through interaction between high energy particles emitted by pulsar originating in supernova core and gas in supernova envelope 18 p2721 A72-36088
- Optimal temperature control for microbial inactivation by composite environment of heat and gamma radiation, using quadratic technique 18 p2649 A72-36313
- High energy gamma radiation from the galactic centre region. 18 p2722 A72-36998
- Galactic gamma-radiation between 200 MeV and 10 GeV. 18 p2722 A72-37008
- The use of a scintillation counter to measure diagnostic X-ray tube kilovoltage, radiation exposure rates and contamination by low energy gamma emitters. 18 p2655 A72-37197
- Detection of high-energy gamma rays from the Crab Nebula. 19 p2850 A72-37503
- NASA-Lewis experiences with multigroup cross sections and shielding calculations. 19 p2833 A72-37633
- High energy gamma ray sources search by Cerenkov radiation recording from extensive air showers, noting atmospheric transparency effects 19 p2850 A72-37805
- Yields of gamma rays emitted following capture of negative muons by Si28 and Mg24. 19 p2837 A72-38026
- Properties of stimulated neodymium laser emission under the action of Co 60 gamma emission 19 p2812 A72-38214
- Relation between diffusion and defect formation rates in silicon detectors exposed to gamma radiation 20 p2959 A72-38956
- Radiation models and explanations for absence of ground level gamma ray background periodic fluctuations 20 p2964 A72-39386
- Electron spin resonance of gamma-irradiated poly(ethylene 2,6-naphthalene dicarboxylate). 20 p2898 A72-39400
- Neutron activation and neutron-capture gamma ray analyses of igneous rock trace elements, discussing Tyrone Igneous Series granites 20 p2899 A72-39831
- Numerical integration of gamma ray photopeak digital data from nondestructive activation analysis 20 p2899 A72-39834
- A balloon search for extraterrestrial high energy gamma-rays in the northern hemisphere. 20 p2965 A72-39876
- The gamma-ray-irradiation method applied to three-dimensional thermal photoelasticity. 21 p3051 A72-40230
- Gamma quanta recording efficiency and energy determination by gamma telescopes, calculating root-mean-square error of real gamma spectra 21 p3026 A72-40323
- Effect of prolonged gamma irradiation on the functional capacity of leukocytes 21 p3103 A72-40438
- Temporal, energy and spectral properties of Cr laser output, considering ruby absorption before/after Co 60 gamma irradiation and radiation density distribution during pumping flashes 21 p3063 A72-40666
- Effects of impurities on gamma-irradiated silicon crystal examined by photovoltaic effect of p-n junction diode. 21 p3097 A72-40693
- Balloon-borne telescope search for solar neutrons and gamma rays during enhanced solar activity periods 21 p3101 A72-41298
- Investigation of the influence of cobalt on the redistribution of the atoms of the alloying elements in iron-base alloys by the NGR method 22 p3188 A72-42162
- Rapid determination of total carbon content in titanium carbide 22 p3176 A72-42200
- Co 60 gamma radiation effect on stimulated ruby laser emission delay time, pulse duration, energy curve and intensity 22 p3186 A72-42731
- Gamma ray scattering asymmetries of Fe 57 nucleus, discussing hyperfine structure and conjugate spin transition 22 p3209 A72-42924
- Astrophysical equipment for Cerenkov radiation measurement from atmospheric showers, discussing source of high energy gamma rays in galactic equator direction 23 p3328 A72-43226
- Gamma radiation of Magellanic Clouds and metagalactic origin of cosmic rays. 23 p3328 A72-43264
- Influence of Cosmos 368 space flight conditions on radiation effects in yeasts, hydrogen bacteria and seeds of lettuce and pea. 23 p3254 A72-43390
- Physiological and hematological effects of chronic irradiation. 23 p3254 A72-43392
- Analysis of survival and cause of death statistics for mice under single and duration-of-life gamma irradiation. 23 p3254 A72-43394
- High energy gamma ray point sources in Cassiopeia and Cygnus regions, using extensive air shower Cerenkov flashes detection technique 23 p3329 A72-43941
- Galactic submillimeter background radiation energy density limit, taking into account recalibrated gamma ray flux measurements agreement with cosmic ray-interstellar matter interactions 23 p3329 A72-43942
- Ultrahigh energy gamma quanta families detection by airborne emulsion chamber at 500-2500 m altitude, calculating energy distribution distortion by Monte Carlo method 23 p3329 A72-44403
- Natural aging and radiation-induced life shortening in Drosophila melanogaster. 24 p3373 A72-45279
- Gamma-neutrino angular correlations in muon capture. 24 p3427 A72-45774

- GANGLIA**
NT NERVES
NT NEURONS
- Bainbridge reflex mechanism, showing sinus ganglion role in tachycardia onset 02 p0165 A72-12514
 - Stellate ganglion stimulation and hypoxia effects on hemodynamics and coronary circulation in dogs, discussing myocardial oxygen consumption, sympathetic nerve vasoconstrictor effect and vasodilatory response 05 p0617 A72-16153
 - Synaptic contacts in vertebrate retinas, reviewing bipolar terminals, ganglion cells and amacrine responses from electron microscopy 06 p0762 A72-17719
 - Retinal ganglion cell spikes (timing in mammalian retina, using electroretinography and computer analysis 06 p0762 A72-17721
 - Stimulation transmission tracts, synaptic mechanisms and tonic activity of cat sympathetic ganglia 07 p0924 A72-20617
 - Cat retina ganglion cell threshold and latent responses to separate stimulation of receptive field center and periphery 08 p1117 A72-21474
 - Linear systems theory for mathematical model of retinal image and ganglion cell excitation, calculating receptor layer luminance distributions for several stimulus patterns 15 p2184 A72-31367
 - Monkey retinal ganglion and lateral geniculate nucleus cell maintained discharge rate indication of receptive field organization for various light stimulus intensities 15 p2184 A72-31370
 - Differential effects of refractive errors and receptive field organization of central and peripheral ganglion cells. 19 p2756 A72-37826
 - Threshold excitation, temporal summation, and impulse response function in the retina of the cat - Temporal receptive fields of retinal ganglion cells 19 p2758 A72-38648

Supraspinal effects in the activity of preganglionic sympathetic neurons delivering axons to the cervical sympathetic nerve

21 p3000 A72-40599

Changes produced in the nerve structures of the stellate ganglion by total X-ray irradiation

22 p3140 A72-41925

Cerebral auditory system acoustic information processing, discussing ganglia and cochlea neurophysiological functions in response to afferent stimulations

22 p3146 A72-42786

Functional organization of the periphery effect in retinal ganglion cells.

24 p3371 A72-44908

GAPS

NT SPARK GAPS

GARNETS

NT YTTRIUM-ALUMINUM GARNET

NT YTTRIUM-IRON GARNET

Garnet crystal structure type microwave ferrites with V and In ions, investigating ferromagnetic resonance linewidth reduction effect

03 p0400 A72-12971

Functional speed measurements of propagating devices based on cylindrical domains in orthoferrites and garnets, noting storage capability

[IEEE PAPER 28,2] 03 p0333 A72-13783

Hugoniot equation of state measurements on iron-silicate garnet, showing shock induced transition to high pressure phase

11 p1627 A72-26524

In and Gd substitution effect in calcium-vanadium garnets as potential microwave materials, discussing magnetic properties, resonance linewidth and temperature stability

15 p2293 A72-32243

Olivine-garnet reaction in peridotites from Tanzania.

17 p2551 A72-35937

Bubble and strip magnetic domains creation, annihilation and manipulation in epitaxial magnetic garnet films by laser beam thermal absorption induced local heating

22 p3185 A72-42612

GARP

U GLOBAL ATMOSPHERIC RESEARCH PROGRAM

GAS ANALYSIS

NT OZONOMETRY

Toxicological control and chemical analysis of outgassing products from nonmetals in high temperature oxygen atmosphere, investigating use within LM crew compartment

01 p0019 A72-10771

Apollo 12 lunar soil samples solar wind noble gas analysis of KREEP fragments, estimating Surveyor Crater age

03 p0414 A72-12902

High temperature creep of niobium alloy, obtaining creep limit, microhardness and gas analysis data

06 p0833 A72-18637

Gas content determination in metals by melting and vaporizing measured microvolumes using laser microprobe and magnetic mass spectrometer

07 p1006 A72-19549

CO contamination of cabin and hazard to pilots, discussing concentrations, avoidance, control and analysis

07 p0933 A72-20267

German monograph on electron beam focusing in partial pressure analyzer with two compartment ion source, eliminating residual gas-filament interaction

09 p1306 A72-22318

Airborne gas chromatograph for real time diffusion analyses, describing flight test results with sulfur hexafluoride plumes

09 p1307 A72-22451

Respiration function testing device using spirometers and gas analyzers

09 p1272 A72-23256

Michelson interferometer application for continuous gas analysis in far IR

10 p1480 A72-24174

Contaminant analysis in gaseous oxygen generated by chlorate candle combustion, using Draeger tubes

12 p1779 A72-28254

Procedure for the continuous sampling and measurement of gaseous emissions from aircraft turbine engines.

[SAE ARP 1256] 18 p2721 A72-36532

GAS BAGS

Deceleration attenuation effectiveness of airbag restraint systems compared with seat belt-shoulder harness for aircraft occupants crash protection

15 p2191 A72-32605

GAS BEARINGS

Pneumatic hammer /self oscillation/ in gas lubricated externally pressurized annular thrust bearing, presenting stability maps

[ASME PAPER 71-LUB-U] 02 p0234 A72-11527

Load capacity, attitude angle and power loss of herringbone grooved gas lubricated journal bearings operating in air at 60,000 rpm

[ASME PAPER 71-LUB-B] 02 p0234 A72-11530

Narrow groove theory for spiral groove viscous pump gas bearings generalized to include rarefied gas and turbulence effects

[ASME PAPER 71-LUB-1] 02 p0234 A72-11531

Unbalance response of rotor supported in hydrodynamic gas lubricated journal bearings

[ASME PAPER 71-LUB-10] 02 p0235 A72-11534

Dynamic characteristics of turborotor simulator supported on gas lubricated foil bearings of reduced length with starting and stopping unaided by external pressurization

[ASME PAPER 71-LUB-16] 02 p0235 A72-11538

Static properties of circular hydrostatic thrust gas bearings with curved surfaces, comparing theory with measurements

[ASME PAPER 71-LUB-22] 02 p0236 A72-11542

Spiral grooves gas bearing theory, taking into account sliding and gas compressibility effects on load carrying capacity

02 p0236 A72-11585

Unsteady flow theory for radial gas lubricated bearing, deriving velocity and pressure distribution expressions

03 p0363 A72-13577

Herringbone grooved gas bearing load carrying capacity optimization, considering lubricant film thickness, groove width and length ratios and angle

04 p0527 A72-14915

Unsteady radial flow between fixed and oscillating walls, obtaining flow equations and air bearings stability conditions

04 p0511 A72-14970

Hydrodynamic journal gas bearing with herringbone grooved portion for self generating air supply pump hydrostatic starting and stopping

[ASME PAPER 71-WA/DE-7] 05 p0664 A72-15944

Spherical air bearing supported test facility for satellite attitude control system performance testing, discussing motion simulator and automatic balancing system

05 p0643 A72-16435

Narrow groove theory of spiral grooved gas bearings, obtaining pressure distribution and small perturbation stiffness performance

06 p0821 A72-17807

Flow in gas lubricated conical bearings, considering analytical and numerical solutions for axisymmetric flow model with temperature dependent viscosity and dissipation coefficients

06 p0801 A72-18124

Aerodynamic radial bearing analysis based on Reynolds equation, emphasizing gas bearing nonlinear oscillation stability

06 p0824 A72-18702

Conical gas film between rotating and vibrating conical rotor and nonmoving bearing, determining gas film stiffness and optimum angle

07 p0971 A72-20093

Switching sequence analysis of gas bearing gyros for low cost inertial sensors in short risetime navigation devices

07 p0989 A72-20281

Radial gas bearing air lubrication theory, proving existence and uniqueness theorems for Reynolds equation periodic solution

07 p0998 A72-20473

German monograph on optimal design of gyroscope using spherical static gas bearing

08 p1173 A72-22174

Vibration measurements of gyromotors with aerodynamic spherical and ball bearings

09 p1263 A72-22347

Air lubricated bearings for high performance aircraft gas turbines, studying design and performance in turboshaft engine

[ASME PAPER 72-GT-38] 11 p1638 A72-25632

Thin lubricant film angular inertia effect on externally pressurized MGD bearings load carrying capacity, solving nonlinear differential equation by Runge-Kutta method

13 p1963 A72-28747

Nonuniform gas pressure distribution near circular multiple inlet of inherently compensated thrust bearing, considering inward-outward radial flow resistance differential

13 p1963 A72-28748

Gas bearing gyroscope for fluidic guidance and control system, satisfying missile and recoverable booster requirements

18 p2648 A72-36557

Stability considerations for a gas-lubricated tilting pad bearing. II - Analytical refinements and stability data.

[ASME PAPER 72-LUB-G] 19 p2807 A72-37697

Optimization of self-acting step thrust bearings for load capacity and stiffness.

19 p2807 A72-37895

Characteristics of a closed-type aerostatic slider bearing

19 p2809 A72-38565

Book - Advances in cryogenic engineering, Volume 17

19 p2883 A72-38826

Theoretical analysis of a cryogenic gas bearing with a flexible damped support.

19 p2810 A72-38837

Use of air bearings in the construction of a scanning Fabry-Perot interferometer.

21 p3054 A72-40621

Use of a linear air bearing sled for dynamic calibration of velocity transducers.

22 p3179 A72-42693

GAS CHROMATOGRAPHY

Organic materials detection on planetary surfaces with in situ gas chromatography and mass spectrometry

04 p0573 A72-14808

Cyclohexylamine determination in aqueous solutions of sodium cyclamate by electron capture gas chromatography

07 p0935 A72-19488

Polyethylene oxidative degradation study with gas chromatographic techniques, obtaining aliphatic and organic compounds at 75-200 C in varying oxygen concentrations

08 p1128 A72-21425

Airborne gas chromatograph for real time diffusion analyses, describing flight test results with sulfur hexafluoride plumes

09 p1307 A72-22451

Chromatographic analysis of reaction products of HCl-accelerated neopentene pyrolysis, showing tert-butyl chloride formation

10 p1434 A72-24235

Capillary gas chromatography with two moderately high temperature phases, testing esters and hydrocarbons resolution ability

12 p1778 A72-27225

The steric analysis of aliphatic amines with two asymmetric centres by gas-liquid chromatography of diastereoisomeric amides.

17 p2510 A72-34337

Study of the surface reactivity of carbon fibers by gas chromatography

17 p2570 A72-34891

Geochemistry of amino acid enantiomers - Gas chromatography of their diastereomeric derivatives.

19 p2762 A72-38224

Transmission efficiency of gas chromatography algorithmic data compression and coding for spacecraft atmosphere studies

21 p3053 A72-40549

The carbon chemistry of the moon.

23 p3339 A72-44149

A portable self-contained gas chromatograph.

23 p3292 A72-44544

GAS COMPOSITION

NT CARBON DIOXIDE CONCENTRATION

Ionospheric composition of ions and neutral gases during magnetic storm, using coupled differential equations

01 p0054 A72-10425

Niobium-oxygen-nitrogen system solid solution, noting gas composition effects on hardness and electrical resistivity

03 p0369 A72-12958

ESRO 1 satellite residual gas outgassing rate and composition measurements during thermal heat balance tests, using mass spectrometer

09 p1263 A72-23260

Gaseous air pollutant detection and measurement by chemiluminescence method for continuous monitoring of given pollutant concentration

10 p1434 A72-24099

Hypersonic base heating investigation on Mars atmosphere entry blunt bodies, taking into account gas composition and angle of attack effects

[AIAA PAPER 72-317] 11 p1568 A72-25251

Atmospheric abundance ratios of gas inclusions in Muong Nong and Libyan Desert glass tektites by mass spectrometric analysis, indicating terrestrial origin

12 p1866 A72-27117

Exhaust composition and smoke emission reduction from aircraft with gas turbine power plants

12 p1860 A72-27270

Air composition and thermodynamic properties at 12,000-25,000 K and 0.1-100 atm with allowance for Coulomb interaction effect on pressure and for ionization potential decrease

13 p2018 A72-29878

Atmospheric sound absorption prediction based four-gases composition and energy transfer mechanisms, comparing results with experiments at different humidities

15 p2277 A72-32020

Velocity independent fast response hot-wire probe for binary gas mixtures composition measurement, describing design and operational principle based on dimensional analysis

16 p2389 A72-32829

Interstellar cosmic ray electron component and isotopic composition relations from positron observations

16 p2448 A72-33741

Flame probe sampling process effects on gas composition concentration gradient for two dimensional cylindrical and rectangular probes

16 p2361 A72-34004

Gas retention chronology of Petersburg and other meteorites.

18 p2723 A72-36062

Thermodynamic properties of Cs-vapors.
18 p2713 A72-36210

Effect of concentration gradient on composition of sampled gas. II - Experimental verification.
19 p2805 A72-38870

GAS COOLED REACTORS
NT HIGH TEMPERATURE NUCLEAR REACTORS

Transoceanic helium cooled thermal reactor powered air cushion freighter of gross weight 4500 metric tons, discussing design and performance characteristics
04 p0464 A72-14431

Conductive heat transfer from rib roughened surfaces in gas cooled reactor fuel elements
04 p0595 A72-14596

GAS COOLING

Gas quenching technique for vacuum brazing of Al, Ti and ferrous alloys, evaluating mechanical properties, surface contamination and He leak tightness
07 p0997 A72-19997

Al, Ti and ferrous alloys suitability for vacuum brazing-gas quenching processing for He leak-tight joints, using photomicrography
07 p0997 A72-19999

Metallographic properties of vacuum brazed, heat treated and gas quenched Al alloys, low alloy steels and corrosion resistant steel alloys
07 p1017 A72-20001

Thermal radiation shielding of porous surface on heated plate by absorbing gas transpiration, suggesting carbon dioxide, metal vapors and particulate mixture [AIAA PAPER 72-277]
11 p1740 A72-25217

Hypersonic turbulent boundary layer flow parameters and heat exchange during blowing of coolant air and He through slot
13 p1895 A72-29901

Laser emission from pulsed transverse electric discharge in supersonic nozzle downstream region gas dynamic cooled mixture
15 p2245 A72-31385

Supplemental internal gaseous film cooling combined with external cooling of combustion chamber walls, analyzing effectiveness via nonadiabatic model [AICHE PREPRINT 3]
18 p2741 A72-36550

Effect of a cooling gas layer on the geometrical dimensions of an induction plasma
20 p2957 A72-39219

The cooling problem in the case of laminar boundary layers of real gases
21 p3131 A72-41619

GAS DENSITY

Liquid containment in gas driven vortex with air-water mixture densities above 100 times gas flow, discussing applicability to colloidal core nuclear reactor performance estimation
01 p0100 A72-11360

Low density monatomic gas supersonic spherical source flow, presenting departure from translational equilibrium
02 p0205 A72-12359

Hydrogen shock waves density profiles measurement, noting uncoupled translational and rotational relaxation processes
02 p0263 A72-12360

Neutral interstellar hydrogen atoms mean volume density from Lyman alpha absorption and radio measurements in solar region
06 p0886 A72-18098

Cs and Hg vapors compressibility factor in supercritical range as function of density, considering charged particles and atoms polarization interactions in ionized metal vapors
07 p1040 A72-18943

Gas density distributions in argon and carbon dioxide supersonic jets with low angular divergence in vacuum, using Laval supersonic nozzle
07 p0973 A72-20512

Atomic, ion and electron transition pulsed gas discharge lasers, considering power efficiency factors, vacuum UV region and gas density
08 p1182 A72-21644

Thirteen moment closed system of approximate integral equations for rarefied gases density, velocity, temperature, stress tensor and thermal flux vector
09 p1259 A72-22425

Snow-plough model of plasma acceleration for determining time dependence, gas density distribution and energy transfer
09 p1359 A72-22819

Thermodynamic properties of high temperature and density hydrogen, using Rowlinson equation of state
09 p1412 A72-23234

Air velocity calculation from hot-wire anemometer measurements in variable density flow, discussing correction factors checking method and application to internal combustion engine
09 p1315 A72-23390

Mathematical model for compressed gas convection into lower atmosphere with substantial density changes
10 p1563 A72-24778

Galaxy formation process in expanding universe from study of hydrodynamic equations for rotating gaseous ellipsoid with uniform density
11 p1717 A72-25865

Constant density solutions for flow fields behind concave shock waves, noting approximation for transonic free stream Mach numbers
11 p1572 A72-25919

Neutral gases density and flux distribution in lunar atmosphere, using kinetic theory of gases
11 p1722 A72-26394

Charge carrier density, neutral gas density, electric potential and electron temperature profiles in cylindrical diffusion column, considering electron pressure
11 p1698 A72-26646

Two dimensional Lagrangian hydrodynamic code for stability of shock acceleration perturbed interface between two gases of different density
13 p1942 A72-29114

Point density measurement in gas jets by flow visualization based on Raman spectrum lines proportionality [ONERA, TP NO. 1080]
13 p1959 A72-29670

Mathematical model for compressed gas thermal convection into lower atmosphere with substantial density changes
14 p2170 A72-30215

Limiting ratio between ideal gas densities before and behind vertical shock wave in elastic thermal insulators
15 p2334 A72-31475

Numerical solution to Percus-Yevick equation and thermodynamic functions of dense gas in supercritical temperature range with Lenard-Jones potential
16 p2476 A72-33160

Viscous boundary layer generated weak shock wave effects on gas dynamic laser medium density homogeneity [AIAA PAPER 72-709]
16 p2380 A72-34037

The equilibrium configuration of the gaseous component of the Galaxy.
17 p2611 A72-35312

On the role of density gradients in the continuum theory of mixtures.
18 p2712 A72-37076

Molecular equilibrium abundances in interstellar H I gas clouds, noting formation dependence on gas density and degree of interstellar radiation extinction
19 p2854 A72-37230

Strong shock propagation through decreasing density.
19 p2789 A72-38796

Gas density as function of galactic radius according to Jeans unstable criterion for star formation from known galaxy rotation curve and gas sound speed
20 p2966 A72-38917

Dimensionless pressure method to account for air density variations in gas turbine cooling system design.
21 p3099 A72-41059

Atomic, ion and electron transition pulsed gas discharge lasers, considering power efficiency factors, vacuum UV region and gas density
21 p3064 A72-41301

The density of H₂ molecules in dark interstellar clouds.
22 p3224 A72-42385

Thermospheric atomic oxygen and molecular nitrogen densities fromOGO 6 neutral atmospheric composition experiment, comparing with prediction by Jacchia models
22 p3172 A72-42431

Effects of externally imposed mechanical resistance on breathing dense gas at exercise - Mechanics of breathing.
22 p3150 A72-42489

GAS DETECTORS

Trace gas pollutant monitoring by microwave rotational absorption spectroscopy, discussing test results with Gunn diode cavity spectrometer [AIAA PAPER 71-1048]
01 p0023 A72-10524

Absorption cell heterodyne method for nondestructive IR detection of trace gases with molecular vibrational-rotational spectrum [AIAA PAPER 71-1064]
01 p0023 A72-10532

Gaseous pollutants remote detection by IR heterodyne radiometer with tunable lasers [AIAA PAPER 71-1079]
01 p0080 A72-10538

Gas-Cerenkov detector for 10-100 MeV gamma rays based on conversion and Compton scattering in plastic scintillator
03 p0352 A72-13034

Gaseous air pollutant detection and measurement by chemiluminescence method for continuous monitoring of given pollutant concentration
10 p1434 A72-24099

Aviator breathing oxygen contaminant detector using gas chromatography and portable IR analyzer
12 p1773 A72-28253

GAS DISCHARGE COUNTERS

U COUNTERS
U GAS DISCHARGE TUBES

GAS DISCHARGE TUBES

Pulsed hf discharge in hydrogen based on laser light scattering on plasma electrons, noting position of satellites in spectra
02 p0237 A72-11406

Enhanced He-Ne laser frequency and output power stabilities obtained by constructing mirror and gas discharge tube as integral unit
04 p0529 A72-14603

High voltage axially pulsed carbon dioxide laser performance test, determining output energy dependence on tube parameters
07 p1001 A72-19197

PIG discharge system with plasma feed from duoplasmatron ion source for steady state operation with ion energies 1.5-5 keV
08 p1214 A72-21435

High power Ar ion laser with plasma tube using current conducting graphite bore for stable long life operation
10 p1489 A72-23944

Radial small-signal gain profile measurement in carbon dioxide laser discharge tube explained by axial gas temperature increase with discharge current
11 p1647 A72-26145

Ar laser levels population inversion dependence on current density, discharge tube pressure and magnetic flux
11 p1649 A72-26350

Radiation efficiency of electric power-energy conversion during pulsed discharge in Xe tube
11 p1651 A72-26364

Moving striations in tapered gaseous discharge tube, noting frequency dependence on tube radius
11 p1698 A72-26644

Helium-neon laser with Hg cathode in gas discharge tube, providing 250 mW output at 6328 Å
13 p1969 A72-29518

Discharge tube geometry effects on sensitivity of plasma electron density measurement by cylindrical cavity resonators
13 p2018 A72-29822

Electron-ion collision frequency and conductivity of non-Debye plasma formed in high pressure discharge from Ar, Kr and Xe tubes
13 p2018 A72-29891

Intensity and energy spectrum calculation of albedo electrons recorded in cosmic particle showers by gas discharge counters
14 p2105 A72-30629

Relaxation oscillations in He gas discharge tubes with cold Mo cathode as function of pressure and discharge length
15 p2245 A72-31408

Cs plasma electron density radial distributions from resonance absorption in discharge tube
15 p2286 A72-32302

Weakly ionized nonequilibrium plasma flow from gas discharge tube positive column, obtaining electron temperature axial decay rate from energy equation
16 p2437 A72-33655

Ar laser levels population inversion dependence on current density, discharge tube pressure and magnetic flux
16 p2402 A72-33703

Radiation efficiency of electric power-energy conversion during pulsed discharge in Xe tube
16 p2403 A72-33716

Results of a computer simulation of an arc plasma in a curved discharge tube.
19 p2841 A72-38085

GAS DISCHARGES

NT RING DISCHARGE
NT TOROIDAL DISCHARGE

Carbon dioxide laser electrical plasma properties from probe and techniques, discussing effects of electron energy distributions, dissociation and N, He and Xe additions
01 p0079 A72-10514

Mass spectroscopic analysis of addition effects of Xe, hydrogen and oxygen on CO-He laser discharge
01 p0079 A72-10517

Nonlinear skin effects in gas discharge and semiconductor plasmas during electromagnetic wave propagation and dissipation, obtaining wave amplitude and carrier temperature dependence on reflection parameters
01 p0102 A72-10974

Microwave measurements of plasma parameters in medium pressure gas discharges in absence of constant magnetic field and in weak electromagnetic field
01 p0072 A72-11215

Time of flight mass spectrometers for plasmoids generated by theta pinch and discharge over organic glass, showing ion and electron currents oscillograms
02 p0223 A72-11420

Pulsed current changes in positive column of He and Ne discharges, observing gradient and electron concentration transient behavior
03 p0399 A72-14348

Low pressure glow cathode triodes gas discharges, determining electron energy distribution function in double layer by probe measurements
03 p0400 A72-14349

Oxygen and oxygen-nitrogen mixtures dc and hf discharges, evaluating traveling low field domains in positive column

03 p0400 A72-14350

Uniform discharges in flowing carbon dioxide laser mixtures at atmospheric pressure, observing fluorescence intensity variation with discharge power density

03 p0369 A72-14400

CW CO laser by discharging premixed carbon disulfide-oxygen flame, suggesting chemical pumping mechanism and flame laser possibility

04 p0529 A72-14589

Pulsed Ar ion laser quantitative level population mechanism in gas discharges, discussing radiation trapping effects on 4s doublet based on spontaneous emission line data

04 p0529 A72-14602

Ar gas dc discharge plasma characteristics in crossed electric and magnetic fields, examining equivalent pressure concept

04 p0556 A72-14945

Electromagnetic radiation modulators in millimeter and submillimeter wave range using gas-discharge plasma magneto-optical effects in alternating magnetic field

05 p0625 A72-15826

Quasi-stationary pulsed discharge characteristics of nitrogen plasma as function of current density and pressure

05 p0693 A72-15839

Mean and fluctuating temperature dependence of gas discharging from orifice to atmosphere on pressure vessel wall heat transfer [ASME PAPER 71-WA/HT-32]

05 p0745 A72-15884

Neutral atoms pressure distribution along capillary and pressure compensating channel during discharge in argon ion laser

05 p0670 A72-16990

Ion-acoustic waves and ionization waves instabilities in gas discharge plasmas

05 p0699 A72-17222

Pulsed cylindrical converging shock wave generation in decreasing density medium by axial explosion-implosion discharge

05 p0700 A72-17233

Equilibrium hf gas discharge theory for waveguides and gas flow without restrictions on penetration depth and skin effect magnitude of field

07 p1040 A72-18917

Stepwise ionization effects on ionic wave propagation and oscillation stability in inert gas dc discharges

07 p1046 A72-20503

He-Ne laser discharge gap oscillation modes observation, noting applied magnetic field, gas parameters and cathode type effects on stimulated emission

07 p1008 A72-20510

Microwave radiation intensity and spectral frequencies of Knudsen discharge in cesium plasma

07 p1046 A72-20515

Optical and electrical characteristics of gas discharge plasma in pulsed radiation sources as function of power dissipation

07 p1047 A72-20611

Gas discharge plasma detection characteristics, examining electron and ion densities and collision rates dependence on electromagnetic field frequency and amplitude

09 p1361 A72-22956

Hollow cylindrical cathode discharge sustaining potential reduction and recombination probability increase from transverse magnetic field and rising pressure and plasma density

09 p1361 A72-22957

Electron energy distribution and losses existence limit at Langmuir paradox pressures in gas discharge, hypothesizing wall mechanism of electron collisions

09 p1361 A72-22958

Microwave, X ray and corpuscular emission by gas discharges in coaxial plasma gun, measuring pressure and current distribution

09 p1362 A72-23212

Excitation and relaxation of upper laser state in carbon dioxide discharge from Q spoiled pulse-produced fluorescence measurements

09 p1326 A72-23577

Nonequilibrium ionization theories for high pressure discharge in inert gas-alkali metal vapor

10 p1515 A72-24414

Electrically excited carbon dioxide-nitrogen laser using high repetition rate discharge pulses from pin electrode array transverse to supersonic flow

11 p1647 A72-26147

Vortex discharge in Ar as optical pumping source for YAG-Nd crystal CW lasers, comparing efficiency with YAG-Nd crystal pumping

11 p1648 A72-26331

Molecular energy levels population inversions calculated from vibrational temperatures in carbon dioxide laser discharge plasma

11 p1649 A72-26339

Discharge current effect on refractive index in carbon dioxide laser

11 p1650 A72-26361

Neutral atoms pressure distribution along capillary and pressure compensating channel during discharge in argon ion laser

12 p1819 A72-27133

Electron beam velocity distribution function fine structure for plasma-beam discharge in hydrogen within longitudinal magnetic field

12 p1850 A72-27261

Double discharge transversely excited atmospheric pressure TEA/ carbon dioxide laser construction, operation and output energy

12 p1819 A72-27266

Triplasmatron using crossed field hydrogen discharge between cold cathode and disk anode, noting pulse modulation applications

13 p1927 A72-28380

Vacuum UV spectra of free plasma column in microwave high pressure discharge in helium-deuterium mixture

13 p2015 A72-29434

Transverse magnetic field effect on electron temperature and energy distribution and spectral lines of gas discharge plasma

13 p2017 A72-29635

Dispersion characteristics of ion-acoustic waves in positive gas discharge plasma column

13 p2019 A72-29912

Charged particle inertial-electrostatic containment in spherical diode gas discharge gap, measuring flux radial and energy distributions

13 p1933 A72-29915

Detonation wave generation in gas discharge plasma by pulsed electrical discharge

14 p2137 A72-30313

Plasma containment by superposed fields/sustained field/ technique application to theta pinch, studying hydrogen and helium discharge behavior

14 p2138 A72-30400

Multiply charged ions motion velocity measurement for pulsed discharge plasma in nitrogen, krypton and xenon

14 p2139 A72-30777

Comparative electron density measurements in positive low pressure He discharge column with Langmuir probes and microwave interferometer and cavity

14 p2105 A72-30808

Hollow dielectric waveguide used for carbon dioxide laser gas discharge, noting increased gain, volumetric output and saturation parameters

15 p2245 A72-31386

Time-of-flight measurements of molecular and atomic beams produced by cooled microwave discharge source, using hydrogen, helium, argon and nitrogen

16 p2430 A72-33061

Photographic-oscillographic study of discharges in atmospheric pressure helium-carbon dioxide mixtures, discussing discharge paths nonuniformity and energy input maximization

16 p2435 A72-33391

Continuously burning optical discharge in Ar and Xe at atmospheric pressures, evaluating laser beam energy absorption, electron density and plasma temperature

16 p2402 A72-33691

Refractive index in carbon dioxide laser effect on discharge current

16 p2403 A72-33714

Low pressure He and Ne discharge generated positive plasma column potential, determining electron concentration from electron energy distribution functions

16 p2437 A72-33746

Hot probe determination of space potential in low pressure He and Ne discharge plasmas via probe characteristics second derivative

16 p2437 A72-33748

Probe temperature, shape and size effects on electron energy distribution measurements for positive plasma column of low pressure He and Ne discharges

16 p2437 A72-33750

CW argon ion laser characteristics at high steady discharge currents, discussing output limitation by low inversion utilization efficiency due to cavity mirrors optical degradation

[AIAA PAPER 72-711]

16 p2404 A72-34035

Possible mechanism for CO₂-discharge current variation under the influence of laser radiation

17 p2562 A72-34840

Theory of a coaxial gas-discharge generator loaded by a spiral line

17 p2529 A72-34841

Initial-boundary-value problem of the formation of an electrical discharge in a flow

17 p2592 A72-35627

Gas discharge plasma detection characteristics, examining electron and ion densities and collision rates dependence on electromagnetic field frequency and amplitude

17 p2593 A72-35885

Transverse magnetic field effects on cylindrical hollow cathode discharge voltage-current characteristics, noting sustaining potential and recombination probability changes

17 p2593 A72-35886

Electron energy distribution and losses existence limit at Langmuir paradox pressures in gas discharge, hypothesizing wall mechanism of electron collisions randomization

17 p2593 A72-35887

Strong shock wave acceleration during passage through decreasing density region observed in experiments with gas discharges and Ar-H mixture explosions

17 p2544 A72-35890

Subharmonic frequency division for neon discharge plasma oscillations under resonance due to nonuniform electric field

18 p2714 A72-36111

The vapor deposition of high work function materials in a gas discharge

18 p2656 A72-36149

Secondary ionization coefficients in a low-pressure discharge in mercury vapour

19 p2836 A72-37459

Equilibrium HF gas discharge theory for waveguides and gas flow without restrictions on penetration depth and skin effect magnitude of field

20 p2957 A72-39383

Isotropically and anisotropically polarized He-Ne lasers output dependence on longitudinal magnetic fields, noting electron density radial redistribution in gas discharge plasma

20 p2932 A72-39411

Observation of superheat instability in a fully ionized current-carrying plasma

20 p2958 A72-39854

Output power saturation with increasing discharge current in powerful argon CW lasers

21 p3062 A72-40404

A new method of exciting uniform discharges for high pressure lasers

21 p3062 A72-40568

Uniform low temperature gas discharge plasma diagnostics in shielded volume, noting application of stable plasma generation effect for isotope analysis

22 p3210 A72-42152

Measurement of the electronic density in a hollow cathode discharge working with argon

22 p3181 A72-43098

Pulse discharge plasma in Ar with gas ionization level near unity, noting plasma cylinder parameters, electron temperature and I-V characteristics

22 p3212 A72-43103

Detonation wave generation in gas discharge plasma by pulsed electrical discharge

23 p3318 A72-43215

Self-ignited impulsive optical discharge in a laser erosion plasma

23 p3295 A72-43308

Effect of capacitance on gain in a transversely pulsed CO₂ discharge

23 p3298 A72-44534

Excitation mechanisms in the argon-ion spectrum at near laser conditions and temperatures and densities in a hollow cathode argon-arc discharge

24 p3428 A72-44807

Nonlinear effects in the dynamic behavior of the positive column from a low-voltage low-pressure discharge

24 p3428 A72-44965

GAS DISSOCIATION

Heat transfer in turbulent flow of equilibrium dissociating nitrogen tetroxide within round tube, considering pressure, temperature and mass flow rate effects

01 p0145 A72-10490

Uncondensed components effects on heat transfer in condensation of nitrogen tetroxide partly in second dissociation stage, deriving heat of vaporization

01 p0145 A72-10494

Interstellar OH formation through inverse predissociation from continuum to vibrational level of repulsive molecular state originating from asymptotic atomic ground state

01 p0133 A72-11414

Sound wave propagation velocity in partially dissociated and ionized gas, discussing attenuation coefficient, chemical process relaxation time and high temperature oxygen and nitrogen calculations

01 p0051 A72-11212

Thermal conductivity measurement of dissociating nitrogen dioxide over 548-792 K and 1-30 atm

02 p0170 A72-12091

Intracavity radiation induced air breakdown in TEA carbon dioxide laser for application in plasma heating

02 p0238 A72-12205

Heat transfer of nonequilibrium dissociating nitrogen dioxide in round tube, allowing for finite reaction velocity

02 p0303 A72-12861

Sequential dielectric breakdown of air by focused radiation from mode locked pulsed carbon dioxide TEA laser

03 p0366 A72-12966

Photochemical models of aeronomical formation and dissociation of hydrogen and ozone in mesosphere and stratosphere

03 p0346 A72-13377

- Molecular oxygen photodissociation in Schumann-Runge bands, discussing determination of solar radiation penetration depth into chemosphere 03 p0412 A72-13386
- Laminar boundary layers on heated plane wall behind shock wave in dissociating oxygen for thermodynamic and frozen flow 03 p0344 A72-14342
- Airglow considered as faint light emission during atomic and molecular dissociations in atmosphere, yielding clues to physical and chemical processes from spectrum 04 p0520 A72-15642
- Sodium heat pipes sonic limit, describing vapor dissociation-recombination and homogeneous vapor condensation phenomena [ASME PAPER 71-WA/HT-11] 05 p0743 A72-15871
- Laser induced gas breakdown in chemical reactions and explosions during plasma creation, using time resolved spectroscopy and titanium oxide probes 05 p0624 A72-16666
- Vector analysis of three dimensional nonequilibrium dissociative gas flow quantity variations along stream lines 05 p0652 A72-17001
- Curved shocks discontinuities in nonequilibrium dissociative gas flows, investigating flow gradient variables 05 p0653 A72-17080
- Nonequilibrium dissociating gases high speed laminar mixing layers, comparing approximate closed form solution with numerical solution [VPI-E-71-22] 05 p0653 A72-17150
- Dissociative excitation of CO and metastable fragments by electron impact on carbon dioxide, investigating cross sections 06 p0803 A72-17447
- Molecular oxygen dissociation rate constant determination during interaction with He atoms in cylindrical shock tube 06 p0852 A72-17686
- Gas breakdown in front of metal targets laser flare from UV radiation ionizing action, using pulsed holographic technique 06 p0818 A72-18412
- Electron beam induced dissociative excitation of vacuum UV emission from atomic nitrogen multiplets, using normal incidence monochromator and pulse counting techniques [AD-736008] 07 p1036 A72-18925
- Scattering cross section for excited oxygen atoms production by electron impact dissociation of molecular oxygen 07 p1037 A72-18964
- Metastable argon-carbon dioxide dissociation and electronic excitation of carbon monoxide or oxygen 07 p1037 A72-19496
- Methane pyrolysis in glow discharges /cold plasmas/, discussing chemical reactions initiated by high energy electrons inelastic collisions with gas molecules 07 p0937 A72-20286
- Nitrogen dioxide photodissociation by pulsed ruby laser at 6943 Å, noting single photon energy relationship to dissociation energy 07 p0937 A72-20676
- Cometary carbon dioxide molecules annihilation by recharging and dissociative charge exchange with solar protons 08 p1229 A72-20830
- Chemical reactions in shock waves, discussing diatomic molecules dissociation and combustion processes 08 p1148 A72-21016
- Molecular hydrogen dissociation by He, observing molecule initial quantum states effect on temperature dependent reaction cross section 09 p1357 A72-22855
- Magnetic field effect on threshold pressure reduction for He and Ar gas breakdown by carbon dioxide laser radiation, taking into account inhibition of radial electron diffusion [AD-741539] 09 p1365 A72-23493
- Simple waves in one dimensional unsteady nonequilibrium dissociative gas dynamics, discussing internal, chemical bond and dissociation energies 11 p1616 A72-25982
- Spontaneous radiative dissociation in molecular hydrogen vibrational levels as function of emission wavelength, discussing fluorescent spectra, radiation lifetimes and centrifugal distortion 13 p2008 A72-30058
- Photoelectron precipitation induced dissociation of atmospheric nitrogen molecules during moderate solar activity 14 p2102 A72-30659
- Cross sections for dissociative excitation of hydrogen ions by electrons determined by coincident detection of protons and H atoms 14 p2134 A72-30804
- Diatomic molecular vibrational excitation and dissociation effects on imploding shock waves, comparing shock tube data to prediction 15 p2192 A72-32148
- Metastable /2S/ atoms production by electron impact induced dissociative excitation of molecular deuterium, measuring total cross section via Lyman alpha flux 15 p2282 A72-32645
- Solar radiation induced molecular oxygen photodissociation rate as function of column density and temperature in mesosphere and lower thermosphere 16 p2383 A72-32967
- Pohlhausen type integral method for dissociative binary mixture nonequilibrium laminar boundary layer on flat plate, using Crocco relationship between enthalpy and velocity profile 16 p2378 A72-33436
- Lifetime and quenching of metastable CO produced by dissociative recombination of positive carbon dioxide ions in He afterglow 16 p2432 A72-33771
- Catalytic dissociation, hydrogen embrittlement, and stress corrosion cracking. 17 p2566 A72-34256
- Dissociative excitation of vacuum ultraviolet emission features by electron impact on molecular gases. III - CO₂. 17 p2585 A72-34734
- Gas breakdown in front of metal targets laser flare from UV radiation ionizing action, using pulsed holographic technique 17 p2554 A72-34860
- Density distribution in a high-pressure gas jet measured by laser-induced gas breakdown. 17 p2486 A72-35630
- Continuous arc generation in Ar via focused CW carbon dioxide TEA laser, inducing gas breakdown by focal volume preionization with single pulse 18 p2697 A72-36082
- A study of the asymptotic behaviour of the external fringes of compressible, laminar boundary layers of a dissociating gas. 18 p2683 A72-36937
- Linear momentum transfer effects in molecular dissociation produced by electron impact. 21 p3087 A72-40557
- Cardiac output, arterial and mixed-venous O₂ saturation, and blood O₂ dissociation curve in growing rats adapted to a simulated altitude of 3500 m. 21 p3003 A72-41623
- Questions in the theory of monomolecular decay of a one-component gas and the dissociation constant of CO₂ at high temperatures 21 p3088 A72-41657
- Diatomic molecular dissociation in pure gas and mixtures with inert diluent, expressing as set of coupled quadratically nonlinear differential equations [AICHE PAPER 68] 22 p3208 A72-42400
- Limit Mach number in a gas undergoing partial dissociation and single ionization 22 p3244 A72-42624
- Laminar high speed mixing of nonequilibrium dissociating gases. 24 p3392 A72-45056
- Dissociative attachment in carbon dioxide. 24 p3427 A72-45303
- Dissociation of carbon monoxide in the discharge of a continuous-flow CO laser 24 p3411 A72-45499
- Effect of plasma mirror in the breakdown of air in a CO₂ laser cavity. 24 p3412 A72-45775
- GAS DYNAMICS**
- NT AERODYNAMICS
- NT AEROTHERMODYNAMICS
- NT HYPERSONICS
- NT RAREFIED GAS DYNAMICS
- NT ROTOR AERODYNAMICS
- NT SUPERSONICS
- Altitude dependent superrotation of earth upper atmosphere, using nonlinear continuity, momentum conservation and state equations of gas dynamics 01 p0052 A72-10076
- Rankine vortex conducting gas rotating about cylinder axis, investigating magnetic field effects on transverse waves 01 p0106 A72-10132
- Brownian motion kinetic equation from Boltzmann equation for two component neutral gas by simultaneous expansion in density and mass ratios 01 p0050 A72-10233
- Kinetic equation for gases with rotational degrees of freedom under equality of probabilities of direct and inverse transitions and stereoisomerism of molecules. 01 p0050 A72-10350
- High speed interstellar gas dynamic resonant hydromagnetic wave interaction with cosmic ray shocks 01 p0121 A72-11140
- Applied MHD and high temperature gas dynamics - Conference, Gdansk, Poland, May 1970 01 p0110 A72-11201
- Detonation waves collision in vibrating gas medium with plane, cylindrical or spherical obstruction, determining gas parameters behind reflected shock wave 02 p0201 A72-11579
- Approximate solution in gas kinetic theory, considering temperature jump, velocity and viscous slip problems 02 p0205 A72-12356
- Milky Way Galaxy spiral structure determination, presenting arms anatomy, gas and star kinetics and radio astronomy data 03 p0417 A72-13104
- Kinetic theory application to initially nonuniform gas relaxation to equilibrium, obtaining macroscopic velocity, density and temperature solutions by multi-time scale perturbation methods 03 p0340 A72-13155
- Shocks structure and kinetic theory of gases, discussing density profiles, velocity and temperature measurement techniques 03 p0341 A72-13686
- Maxwell boundary conditions method application in kinetic theory of gases, investigating linearized plane Couette flow 04 p0510 A72-14594
- Nonlinear heat conduction equation explicit solution in combustion theory with allowance for gas dynamics model equation and resulting Cauchy problem solution 04 p0595 A72-14643
- Nonisothermal gas layer IR radiation in multiautomolecular vibrational-rotational band range, determining lowest level energy for wide line spectrum 04 p0547 A72-14657
- Initial viscous heat conducting gas dynamic state one dimensional decay problem solution, using kinetic theory with Boltzmann equation 04 p0512 A72-14982
- Carbon dioxide gas dynamic laser mixture at high pressure, investigating gain and vibrational kinetics 04 p0531 A72-15336
- Gas cloud motions in Seyfert galaxy NGC 7469 center from image tube spectra, discussing size, mass and radial velocities 04 p0580 A72-15370
- Solar prominences, considering heavy gas suspension in magnetic arches with grooved tops 05 p0708 A72-15976
- Monograph on head-on collision of combustion wave with shock wave and rarefaction wave covering gas dynamics, interactions, reflection process, etc 05 p0746 A72-16046
- Nighttime polar atmospheric structure and temperature variations due to gas kinetic and electron energy changes 05 p0656 A72-16240
- Telemetry system on board beryllium sphere reentry vehicle for hypersonic gas dynamics and wake chemistry experiments, using flush mounted antennas with isotropic radiation pattern [AIAA PAPER 72-176] 05 p0631 A72-16836
- Group velocity and numerical error propagation in partial differential and finite difference equations of gas dynamics [AIAA PAPER 72-153] 05 p0652 A72-16952
- Lattice gas critical point and nonanalytical three dimensional models comparison with experimental data 05 p0691 A72-17062
- General relativistic kinetic theory of gases, discussing microscopic model, space-time, self-consistent Einstein-Maxwell-Liouville equations and irreversible processes 06 p0847 A72-17255
- State of gas parameters measurement apparatus at high temperatures and pressures involving constant volume piezometer with internal heating 06 p0814 A72-17616
- Infinite homogeneous self gravitating compressed gas media nonlinear condensations, describing finite amplitude motion with asymptotic expansions 06 p0880 A72-17889
- Numerical solutions to gas dynamic problems with large deformations by particle in cell method 06 p0800 A72-18102
- Statistical-hydrodynamic description of nonequilibrium gas dynamics of single component and binary mixtures and systems with chemical reactions 07 p0968 A72-19886
- Gas motion behind plane detonation wave orthogonal to free surface, solving Goursat problem for perturbed region 07 p0969 A72-19979
- Nonlinear difference schemes for quasi-linear transfer equation in gas dynamics and shock wave computations 07 p0971 A72-20085
- Gas dynamics K-wave interaction in nonlinear media described by nonlinear partial differential equations 07 p0972 A72-20103
- One dimensional nonlinear waves propagation in dissipative gas, obtaining exact solutions by method of separation of variables 07 p0973 A72-20500
- Iterative solution to gas dynamics equations for hypersonic flow past slender three dimensional body, applying to Cauchy problem 08 p1107 A72-20971

Averaged Bogoliubov-derived chains of kinetic theory gas dynamics equations with strong statistical correlation for macroprocess description

08 p1149 A72-21175

Hydrodynamic analogy for astrophysical effects of general relativity theory, analyzing Chaplygin gas motion in three dimensional curvilinear coordinate system

08 p1209 A72-21876

Self-similar adiabatic expansion of gas behind shock wave front sustained by radiation, describing gas pressure, density and velocity profiles

08 p1152 A72-22049

Astronomical models for gas kinematics near galactic center, discussing gas jets origin and kinetic energy

09 p1386 A72-22687

Laser beam induced thermal blooming in absorbing gases from combined fluid dynamics and eikonal geometric optics theory, considering wind effects

09 p1352 A72-23333

Eigenmodes growth rate in convectively unstable self gravitating gas sphere, using spherical harmonic series expansion and Laplace transforms

09 p1392 A72-23545

German monograph on gas dynamic properties of turbulent subsonic compressible flow of ideal gas at insulator walls in MHD generator

10 p1517 A72-23771

Transport coefficients calculation in gas kinetic theory by relativistic generalization of Enskog-Chapman method

10 p1510 A72-24106

Second order Cowley-Imai analogy application to transcribe gas dynamic perturbation solutions into magnetogasdynamic solutions for perfect gas axisymmetric super-Alfvénic flows

10 p1521 A72-24464

Phase plane method for one dimensional stationary problem solution in radiative gas dynamics, calculating temperature behind shock wave front

10 p1469 A72-24544

Kinetic equations solution for homogeneous multiatomic gas relaxation, proving solution existence and uniqueness

10 p1516 A72-24629

German book on flow technology and fluid flow machines covering hydrodynamics, gas dynamics, aerodynamics, airfoils, wind tunnels, propellers, helicopters, turbomachines, blade cascades, etc

10 p1471 A72-25122

Simple waves in one dimensional unsteady nonequilibrium dissociative gas dynamics, discussing internal, chemical bond and dissociation energies

11 p1616 A72-25982

Modified gas dynamic functions of total momentum of plane boundary layer for arbitrarily oriented control surfaces and for stratified flows with potential layer

11 p1574 A72-26973

Unsteady state of ideal quiescent heat conducting gas in half space, deriving asymptotic solutions to mass, temperature, pressure and density dynamic behavior expressions

13 p2064 A72-28678

Linearized steady motion of gas with mass sources and sinks, determining resonance onset conditions

13 p1893 A72-28731

Interstellar gas motions and density and temperature variations, discussing galactic structure, radiation fields and cosmic ray effects

13 p2038 A72-29009

Sonic boom magnitude and location in stratified atmosphere calculated from gas dynamical equations for lifting body of revolution

13 p1898 A72-29585

Energy flux intensity in selectively radiating gas nonisothermal layer from radiant transfer equation and mathematical model

13 p2066 A72-29898

Strong shock wave formation and propagation in interplanetary space after chromospheric flares calculated by gas dynamic approximation, determining magnetic field configuration

13 p2050 A72-29955

Gas dynamics of steady rotating azimuthally dependent solar wind under magnetic field influence, calculating azimuthal distribution of radial velocity near earth orbit

13 p2034 A72-29960

Shock waves internal structure in gas of elastic spheres, solving nonlinear Boltzmann equation

13 p1944 A72-30029

Protoplanet cloud model of solar system as flat gas-dust disk, discussing density profile, gravitational stability and mass loss

14 p2148 A72-30206

Laminar mixing zone calculated for two homogeneous compressible gas flows with pressure gradient, noting coincidence of velocity distribution for identical gas dynamic parameters

14 p2070 A72-31009

Spectral stability characteristics of difference schemes for hyperbolic differential equations in gas dynamics involving triangular and tetragonal bases

15 p2178 A72-31444

Computerized determination of cryogenic gas behavior near vapor region, obtaining state equation coefficients from curve fitting program

15 p2334 A72-31580

Counterflow diffusion flame gas dynamic structure analysis in porous cylinder forward stagnation region, using surface and boundary layer approximations

15 p2336 A72-32310

Long wave fluctuations in nonequilibrium gas with pair collisions, using Bogoliubov equations for simultaneous correlation functions

15 p2282 A72-32450

Numerical results of carbon dioxide-nitrogen-water gas dynamic laser comparison with arc-driven supersonic laser in gas dynamic mode

15 p2250 A72-32517

Vorticity jump across stationary MHD discontinuity generalization from gas dynamics problem, noting results validity for shock and detonation waves

16 p2435 A72-33011

Self similar breakdown problem of two dimensional shock discontinuity in gas dynamics

16 p2377 A72-33154

Mathematical model for nonequilibrium gas composed of hard spherical nonattracting molecules, deriving gas dynamics theory in terms of multiple integrals

17 p2538 A72-34424

On the kinematic distribution of galactic neutral hydrogen.

17 p2606 A72-34572

Nonlinear system consisting of gas filled tube with pressure sensitive heat source, noting oscillation evolution due to equilibrium perturbation

[ASME PAPER 72-APM-21] 17 p2580 A72-34796

Statistical-hydrodynamic description of nonequilibrium gas dynamics of single component and binary mixtures and systems with chemical reactions

17 p2540 A72-35134

The one-dimensional N-body problem and rectilinear gas motion

17 p2584 A72-35909

Chemical reactions effects on gas dynamics, considering relaxation phenomena in fluid flow

18 p2679 A72-36384

Gas dynamics and chemistry of lightning-produced shock waves/thunder/ in postulated primordial reducing atmosphere, noting amino acid production

18 p2650 A72-36443

A contribution to the gas dynamics of oblique shocks with change of total enthalpy.

18 p2682 A72-36725

Conservative difference schemes for linear and nonlinear problems of mathematical physics, discussing gas dynamics and magnetogasdynamics problems requirements

19 p2833 A72-37383

Large particle method differential approximations in difference equation schemes for gas dynamics problems, discussing viscous effects and solution stability

19 p2745 A72-37385

Bright nebulae near concentrations of high-velocity gas.

19 p2856 A72-37504

Interferometric holography of laser-produced gas breakdown.

19 p2798 A72-37623

CW gasdynamic thermally excited and selectively pumped CO₂-N₂ mixing laser.

19 p2811 A72-38097

Numerical gas dynamic calculations by difference method with two moving curve families, noting water mass impact on plane solid wall

19 p2789 A72-38851

Solution of the equations of consumption in gasdynamic problems

20 p2914 A72-39927

Gas motion behind plane detonation wave orthogonal to free surface, solving Goursat problem for perturbed region

20 p2915 A72-40035

Interaction between weak gravitational waves and a gas

21 p3084 A72-40402

Problem of oscillation self-excitation due to the dependence of the normal velocity of a flame on the thermodynamic parameters of a gas

21 p3129 A72-40985

Three-dimensional supersonic flows at large distances from a body of finite volume

21 p2994 A72-41661

The construction of invariant transformations in plane rotational gasdynamics.

22 p3199 A72-42399

Multisectional CW gas dynamic laser output radiation density distribution control via transmitting mirror with variable reflection coefficient

22 p3186 A72-42632

A study of the electronic and gasdynamic parameters of a hypersonic wake behind models moving in argon

22 p3168 A72-43111

Application of gasdynamic flows in laser technology

22 p3187 A72-43176

Polish book - Fluid mechanics. Volume 2 - Gasdynamics.

22 p3168 A72-43199

Protoplanet cloud model of solar system as flat gas-dust disk, discussing density profile, gravitational stability and mass loss

23 p3333 A72-43236

Physical and chemical properties and stratification of neutral matter in comet atmospheres, discussing neutral gas dynamics and surface brightness distribution in comet images

23 p3335 A72-43299

Use of characteristics for boundaries in time dependent finite difference analysis of multidimensional gas dynamics.

24 p3359 A72-44879

Study of dynamic and thermal processes during steady motion of a viscous gas

24 p3390 A72-44996

International Colloquium on Gasdynamics of Explosions and Reactive Systems, 3rd, Marseille, France, September 12-17, 1971, Proceedings.

24 p3461 A72-45016

Shock waves role in coronal heating, solar wind and energy and material transfer to earth and in solar system

24 p3439 A72-45019

Radiation gasdynamics of planetary entry - Concepts and recent advances.

24 p3361 A72-45188

Gas dynamics problems of oblique shock waves around aerodynamic bodies, noting exact quasi-explicit and approximate explicit solutions

24 p3394 A72-45445

A gasdynamical view on the motion, heating and accretion of solid bodies in the solar system.

24 p3444 A72-45456

Gas dynamics and shock wave physics of supersonic flow in two phase media, noting evaporation, condensation and phase transformations

24 p3364 A72-45525

GAS EVACUATING

U EVACUATING [VACUUM]

GAS EVOLUTION

Apollo 11 lunar fines behavior and gas evolution characteristics from high vacuum differential thermal analysis and mass spectroscopy

04 p0569 A72-14504

Partial pressure gage to measure water vapor-produced hydrogen content in metal samples, using reference gas evolution curves

12 p1807 A72-27451

GAS EXCHANGE

Acute, short and long term and life long high altitude hypoxia exposure effects on pulmonary gas exchange control and efficiency during physical exercise

01 p0014 A72-10848

Air exchange between stratosphere and troposphere from cosmic ray produced radionuclides and fallout comparison with weather development

03 p0351 A72-14359

Digital computer simulation of circulatory and respiratory systems interaction model for oxygen and carbon dioxide gas exchange between pulmonary blood and alveolar air

09 p1268 A72-22456

Aerobic work capacity indices of gas exchange pulse rate, pulmonary ventilation and acid base balance in runners, determining maximum oxygen utilization

09 p1268 A72-23596

Blood flow stratification effect on alveolar gas exchange in liquid filled lungs in dogs from Xe 133 concentration measurements

10 p1425 A72-24481

Diurnal changes in gas exchange and metabolic rate under normal and inverted day-night schedule conditions, studying human adaptation to shifted schedule

13 p1904 A72-29318

Man, chlorella and wheat plant in life-supporting biological system, showing compatibility relative to gas and water exchange

15 p2189 A72-31826

Pulmonary gas exchange in Andean natives at high altitude.

18 p2650 A72-36570

A model of fluctuating alveolar gas exchange during the respiratory cycle.

18 p2650 A72-36571

Influence of intracellular convection on the oxygen release by human erythrocytes.

21 p3003 A72-41625

Cardiac output, hemodynamic and gas exchange variations as function of basal metabolism during bed rest in hypokinetic recumbent or antihypostatic position

23 p3255 A72-43915

Gas exchange mechanism in lung alveolar and capillaries, discussing cell metabolism for oxygen uptake and carbon dioxide formation

24 p3371 A72-44599

GAS EXPANSION

Flow momentum losses during gas mixture chemically nonequilibrated expansion in nozzle

01 p0145 A72-10487

Ionized argon recombination rate constant determination as function of temperature, using dual frequency laser interferometry measurement of corner expansion flow

01 p0050 A72-10851

Optical emission spectrum of Ba and CuO combustion products during nozzle expansion into vacuum

01 p0146 A72-11312

High temperature and pressure detonation gas expansion as shock wave from cylindrical volume, calculating flow velocity, pressure and density

02 p0302 A72-12285

Seigel state equation validity limit application to isentropic hydrogen and nitrogen steady and unsteady flow expansions at high pressure

02 p0206 A72-12597

Solid particle influence on underexpanded gas jet shock structures, using schlieren photographs

03 p0342 A72-13840

Navier-Stokes equation analysis of three dimensional steady radial expansion of viscous heat-conducting compressible fluid from spherical sonic source into vacuum

03 p0343 A72-14247

Carbon dioxide-nitrogen-water or He mixtures expansion through supersonic nozzles, showing population inversion of vibrational energy levels

04 p0513 A72-15337

Rapid expansion nozzles for gas dynamic laser working gas vibrational energy freezing to obtain population inversion, considering size and shape effects on performance

[AIAA PAPER 72-148]

05 p0669 A72-16965

Flame quenching limits in narrow channels, considering effect of gas expansion during combustion on flame arresters use possibility

07 p1099 A72-19369

One dimensional expansion of hot vapor and gases remaining behind meteor body

08 p1238 A72-21884

Self-similar adiabatic expansion of gas behind shock wave front sustained by radiation, describing gas pressure, density and velocity profiles

08 p1152 A72-22049

Pressure, temperature and nozzle size effects on molecular cluster formation in expanding supersonic jets of rare gases, nitrogen and carbon dioxide

09 p1294 A72-22853

High temperature and pressure detonation gas expansion as shock wave from cylindrical volume, calculating flow velocity, pressure and density

10 p1561 A72-23759

Ionization equilibrium description by quantum statistical fugacity expansion of pressure for partially ionized plasmas

10 p1524 A72-24929

Intermolecular collisions distribution on centerline of freely expanding axisymmetrical jet, using ellipsoidal statistical model and simplified transport equations

11 p1615 A72-25557

Molecular scattering in free jet expansion, using spherical source and two component background gas mathematical models

11 p1615 A72-25558

Radio observation of neutral hydrogen near galactic center, noting expanding and rotating ring of gas from kinematic model

12 p1867 A72-27211

Source gas expansion flow into vacuum, solving spherical coordinates representation of BGK kinetic equation by numerical method

13 p1942 A72-29116

Artificial barium ion cloud spatial-temporal growth in ionosphere, solving ion diffusion equation by numerical methods

13 p1950 A72-29387

Model of solar wind expansion beyond heliosphere, taking into account effect of relative motion between cool interstellar atomic hydrogen and solar wind protons

13 p1033 A72-29801

Radiative transfer in freely expanding gaseous Ba clouds, deriving atomic states level populations ratio

15 p2223 A72-31428

German monograph on wave expansion in gases with thermodynamic relaxation covering steady dispersed compression wave development in piston barrel for two component mixtures

[DFVLR-SONDDR-184]

15 p2218 A72-31768

Core axial density distribution in gas jets freely expanding into vacuum from double concentric orifices, using electron beam fluorescence technique

15 p2218 A72-32150

Spherical source jet flow expansion of single monatomic gas into vacuum on basis of BGK kinetic equation

16 p2375 A72-32887

Coupling of free electron and nitrogen vibrational temperature nonequilibrium in weakly ionized nozzle expansions of shock heated nitrogen

[AIAA PAPER 72-683]

16 p2380 A72-34059

Experimental evidence for stationary population inversions of atomic levels in an expanding hydrogen plasma

[DFVLR-SONDDR-213]

17 p2589 A72-34898

Martin-Ludford gas expansion into vacuum, investigating rarefaction wave penetration and flow characteristics

19 p2788 A72-38715

The behavior of two-phase systems during adiabatic expansion

20 p2953 A72-39595

Two dimensional underexpanded free jet flow into static medium, presenting wind tunnel nozzle experimental data and graphic solutions from method of characteristics

20 p2885 A72-39619

Boundary-layer effects on pressure variations in Ludwig tubes.

20 p2914 A72-39620

Transfer of resonance-line radiation in differentially expanding atmospheres. II - Analytic solution for the case of coherence in the frame of the fluid.

21 p3106 A72-41038

The study of gaseous jet exhausting into vacuum.

21 p3046 A72-41161

Averaged equations of simultaneous hydrodynamic expansion and thermal heating of two-temperature plasma, taking the recovery of thermonuclear fusion into account. I - The plane problem. II - The spherical problem.

21 p3093 A72-41476

Simulation of the interaction of high altitude plumes and a high-speed free-stream flow.

[AIAA PAPER 72-1019]

21 p3042 A72-41598

Averaged equations for joint treatment of hydrodynamic expansion and conduction-type heating of plasma, the energy of nuclear fusion being taken into consideration. II - Spherical problem.

22 p3211 A72-42630

Ion acceleration during expansion of a rarefied plasma

23 p3322 A72-44482

Temperature freezing in spherical or cylindrical expansion into a vacuum.

23 p3357 A72-44498

GAS EXPLOSIONS

Fragment velocity for bursting gas containers in vacuum

[ASME PAPER 71-PVP-14]

02 p0295 A72-12473

Cylindrical blast wave propagation in MGD, deriving closed-form solutions for line explosion in medium with constant pressure, density and axial magnetic field

03 p0400 A72-14391

Laser induced gas breakdown in chemical reactions and explosions during plasma creation, using time resolved spectroscopy and titanium oxide probes

05 p0624 A72-16666

Strong shock wave acceleration during passage through decreasing density region observed in experiments with gas discharges and Ar-H mixture explosions

17 p2544 A72-35890

Equimolar oxyhydrogen detonation wave behavior near pressure limit, considering unsteadiness caused by tube length

22 p3244 A72-42485

Initiation of a detonation by a laser beam focused in a gaseous medium

24 p3410 A72-45026

Combustion product gas dynamic motion effects on detonation front propagation, discussing reacting blast wave and finite kinetic rate models and asymptotic results

24 p3391 A72-45027

Mach stem generation by colliding spherical pressure waves in spark ignited combustible gas, noting simultaneous deflagration wave characteristics

24 p3462 A72-45028

GAS FLOW

NT AIR CURRENTS

NT AIR FLOW

NT CONTINUUM FLOW

NT EQUILIBRIUM FLOW

NT FREE MOLECULAR FLOW

NT FROZEN EQUILIBRIUM FLOW

NT JET STREAMS [METEOROLOGY]

NT KNUDSEN FLOW

NT MERIDIONAL FLOW

NT MOLECULAR FLOW

NT NONEQUILIBRIUM FLOW

NT SLIP FLOW

NT TRANSITION FLOW

NT VERTICAL AIR CURRENTS

Fluid droplet collapse in two phase gas flows, noting time dependence

01 p0145 A72-10573

Gas flow visualization technique using fluorescent plate with UV irradiated ozone tracer, noting application to wall attachment fluidic elements

01 p0072 A72-11198

Boundary conditions for monatomic gas flow in constant cross section channel with heat supply and ionization

01 p0111 A72-11211

Open cycle gas core nuclear rocket engine flow studies to obtain maximum system reactivity at low uranium/coolant gas loss ratio

01 p0100 A72-11349

Axisymmetric inviscid compressible transonic flow of electrically conducting, heat nonconducting gas in Laval nozzle in presence of meridional magnetic field, deriving equations for magnetic effects on dynamic flow characteristics

02 p0149 A72-11576

Radiative heat transfer between gas flow and axisymmetric ablating body near stagnation point, considering ablation products effects under boundary layer chemical equilibrium conditions

02 p0300 A72-11577

Three dimensional boundary layer gas flow in large pressure gradient region, using two dimensional boundary layer equations

02 p0201 A72-11580

Numerical solution for swirling ideal gas flow in Laval nozzle, determining swirling effects on nozzle performance

02 p0149 A72-11583

Difference schemes for continuous computation of supersonic steady gas flows with internal compression shock waves

02 p0150 A72-11737

Compressible gas subsonic or transonic flow in front of obstacle, determining stagnation pressure with thermal relaxation time by numerical and wind tunnel methods

02 p0151 A72-12097

Optically thin radiation effects on local heat transfer in gas flow narrow duct thermal entrance region, presenting Nusselt number variations terms for uniform and parabolic velocity profiles

02 p0303 A72-12321

Thin liquid layer linear hydrodynamic stability in vertical rotating tube with core gas flow

02 p0303 A72-12353

Rarefied gases pressure flow and self diffusion through cylindrical tubes, presenting kinetic model with velocity independent mean free path

02 p0205 A72-12357

Low density monatomic gas supersonic spherical source flow, presenting departure from translational equilibrium

02 p0205 A72-12359

Seigel state equation validity limit application to isentropic hydrogen and nitrogen steady and unsteady flow expansions at high pressure

02 p0206 A72-12597

Ionic focusing of electron beam in transverse gas flow, using air, argon and helium

02 p0261 A72-12764

Heat transfer of nonequilibrium dissociating nitrogen dioxide in round tube, allowing for finite reaction velocity

02 p0303 A72-12861

Heat transfer in rarefied Couette gas flow, obtaining reduced distribution function, macroscopic temperature profile and heat flux

03 p0456 A72-13242

German monograph on gas type and nozzle flow conditions effect on condensed molecular jets properties

03 p0391 A72-13275

Acoustic, turbulent and thermal fluctuating motions interdependence in gas flow, considering application to aerodynamic noise theory

03 p0341 A72-13405

French papers on shock waves in fluids and solids covering gas flows in thermodynamic equilibrium and across conic shocks of revolution

03 p0341 A72-13683

Transformation of differential equations describing interaction between electric arc and gas flow by taking temperature as independent variable, considering Laval nozzle example

03 p0344 A72-14392

Flow development in gas nozzles with depressive networks, describing geometric and functional characteristics

04 p0510 A72-14467

Orthotropicity orientation effect on supersonic flutter of infinite-length thin heterogeneous circular cylindrical structures in axisymmetric gas flow

04 p0584 A72-14520

Plane shock wave and blunt body interaction in supersonic gas flow in two-diaphragm shock tube

04 p0461 A72-14639

Pressure distribution and compressible gas critical flow rate in constant cross section circular pipe with impermeable adiabatic wall from Frossel equations

04 p0511 A72-14640

Gas flow fluctuations near stagnation point on hot wall, taking into account laminar boundary layer compressibility effects

[ASME PAPER 71-APM-RR]

04 p0462 A72-15178

Unsteady nonisothermal gas flow through seminfinitesimal porous medium, using linearized flow equations for small pressure variation

04 p0512 A72-15200

Weakly ionized turbulent gas flow in pipe, comparing neutral and plasma fluctuations with laser beam scintillations 04 p0558 A72-15331

Underexpanded nitrogen jet from sonic orifice, investigating axial rotational temperature distribution 04 p0597 A72-15335

Small pressure difference measurement in gas flow, using transducer based on liquid electrical conductivity measurement 04 p0523 A72-15483

Book on similarity laws and modeling covering dimensional analysis, transformations, differential equations, gas flows and nonequilibrium processes 04 p0513 A72-15675

Thermal nozzle combustion effects on supersonic flow of chemically reacting gas in thermodynamic equilibrium 05 p0599 A72-15846

Similar unsteady one dimensional motion of viscous heat conducting gas due to sudden energy release at surface [ASME PAPER 71-WA/HT-3] 05 p0743 A72-15864

Navier-Stokes equations solution by finite difference methods for steady incompressible laminar vapor flow in symmetrical and unsymmetrical heat pipes, calculating pressure losses [ASME PAPER 71-WA/HT-15] 05 p0744 A72-15874

Mathematical analysis of Vuilleumier refrigerator, calculating internal pressures, temperatures and gas flow rates via computer program [ASME PAPER 71-WA/HT-33] 05 p0745 A72-15886

Average stagnation pressure measurement in low velocity ducted gas flow with nonuniform velocity profiles, discussing mathematical technique and computer program [ASME PAPER 71-WA/PUR-1] 05 p0645 A72-15910

Dutch monograph on heat transfer of gas with vibrational relaxation at shock tube end wall covering mathematical model, induced velocity effect on pressure, etc 05 p0648 A72-16045

Fluid properties for mechanically similar flow fields, discussing dissociating and thermally radiating gas flow [DFVLR-SONDDR-172] 05 p0648 A72-16064

Suspended compression shock construction near supersonic point in plane nonuniform ideal gas flow by hodograph technique 05 p0600 A72-16213

Cascade nozzle gas particle flow properties, discussing flow pressure experiments and theory at different streamlines 05 p0602 A72-16490

Steady inviscid diabatic complex lamellar gas flow geometric properties, correlating stream and vortex lines via Beltrami surfaces in Euclidean space 05 p0747 A72-16667

Noncoagulating polydisperse aerosol deposition from two dimensional turbulent boundary layer and fully developed turbulent pipe flows [AIAA PAPER 72-81] 05 p0650 A72-16806

Gas dynamic laser analysis based on phase cancellation model, showing flow induced phase nonuniformity minimization for far field intensity improvement [AIAA PAPER 72-217] 05 p0669 A72-16857

Film cooled turbine vanes external heat transfer distribution in turbulent gas stream, measuring heat transfer coefficients with and without blowing [AIAA PAPER 72-9] 05 p0707 A72-16877

HF tracer gas detection in inert and combustions flows, using IR absorption technique for gaseous flow visualization [AIAA PAPER 72-70] 05 p0651 A72-16904

Ultrahigh enthalpy gas generation by steady multicomponent flow process with kinetic energy transfer from low molecular weight gas to higher weight working medium [AIAA PAPER 72-167] 05 p0750 A72-16979

Nonadiabatic real gas nozzle flow with friction and heat transfer to wall, obtaining solution by Runge-Kutta method 05 p0610 A72-17066

Optimal airfoil profile for minimum drag in supersonic linearized gas flow with allowance for random fabrication errors and surface melting and sublimation at high temperatures 05 p0610 A72-17136

Nonequilibrium dissociating gases high speed laminar mixing layers, comparing approximate closed form solution with numerical solution [VPI-E-71-22] 05 p0653 A72-17150

Chapman-Enskog method modification for gas flow Prandtl boundary layer zero approximation distribution function construction, applying Mises transform to Boltzmann equation 05 p0653 A72-17209

Electron-ion recombination rate measurements in flowing afterglow, using sampling mass spectrometer and floating double probe 06 p0851 A72-17318

Critical streamline length in axisymmetric and plane ideal gas flows past conical bodies as function of Mach number and form parameter 06 p0755 A72-17677

Population inversion of carbon dioxide molecules in gas flow expanding from nozzle 06 p0852 A72-17904

Two dimensional flow of gas jet around dihedral obstacle, investigating screen proximity and fluid compressibility effects 06 p0799 A72-17912

Flow field quantities for nearly free axisymmetric steady molecular gas flow through circular orifice from high pressure region into vacuum 06 p0800 A72-18118

Ideal gas flow past blunt body in supersonic stream, discussing sonic lines, characteristics and Mach number 06 p0756 A72-18119

Steady subsonic potential gas flow in multiply connected regions, determining velocity field via boundary value problem solution for quasi-linear elliptic equations set 06 p0801 A72-18123

Nonequilibrium thermodynamics description of rarified gas relaxation phenomena for very fast flow processes with translational temperatures 06 p0902 A72-18137

Self regenerating molten seed electrodes for open cycle MHD power generators longevity, regulating combustion chamber and gas flow seeding 06 p0862 A72-18336

Cascading turbomachine blades vibration measurement in subsonic and sonic high temperature gas flows, describing test facility 06 p0797 A72-18689

Forced nonlinear oscillations of finite plate in plane supersonic gas flow, considering elastic forces and resonant characteristics deformation 06 p0901 A72-18708

Equilibrium hf gas discharge theory for waveguides and gas flow without restrictions on penetration depth and skin effect magnitude of field 07 p1040 A72-18917

Hypersonic gas flow around asymmetric triangular metal plate with blunt leading edges, using two layer model 07 p0909 A72-19985

Inviscid relaxing gas flow through tube with variable cross sectional area, deriving governing equation for weak discontinuity amplitude evolution 07 p0970 A72-20073

Shape and structure of shock wave moving along plane wall in gas, comparing experimental results with De Boer theory 07 p0971 A72-20096

Plane oblique shock wave diffraction on wedge moving in homogeneous gas flow at supersonic speed, reducing boundary value problem to Hilbert problem 07 p0910 A72-20317

Secondary gas flow effect on energy transfer distributions from plasma torches, obtaining radial distributions of current and energy flux 07 p1046 A72-20546

Axial arc column interaction with shock waves and high velocity gas flow effects in forced convection, proposing heat transfer theory 07 p1047 A72-20548

Parabolic differential equation system for boundary layer behavior of steady plane gas flow 08 p1107 A72-20911

Unsteady gas flow in thrust bearing with spiral grooves, presenting Navier-Stokes and discontinuity equation 08 p1176 A72-21167

Steady axisymmetrical twisted gas flow parameters in channels with geometries similar to turbojet engine units 08 p1149 A72-21310

Surface friction coefficient dependence on Mach number and velocity gradients in adiabatic compressible laminar gas flow 08 p1107 A72-21311

Dust content effect on heat transfer in hypervelocity wind tunnels, discussing gas flow pattern distortion due to interaction with particles 08 p1253 A72-21453

IR emission at 2.7 microns from carbon dioxide-molecular nitrogen mixture flow, noting energy redistribution 09 p1357 A72-22854

Holographic interferometry application to weak inhomogeneities visualization in gas flows, using photographic emulsion nonlinear properties 09 p1311 A72-22965

German monograph on pulsed laser induced spherical unsteady blast waves in stationary and flowing gases 09 p1325 A72-23161

Turbulent gas flow induced by laser heating, emphasizing Rayleigh number as stability criterion 09 p1295 A72-23492

Taylor series truncation method for steady supersonic inviscid gas flow past nonaxisymmetric conical bodies 09 p1295 A72-23498

Flat face cylinders in rarefied supersonic gas flow, investigating perturbed region evolution based on pitot tube method 10 p1415 A72-23751

Pseudoviscous method application to computation of supersonic flow of inviscid ideal gas through two dimensional or annular axisymmetric ducts 10 p1417 A72-23876

Two and three dimensional pistons motion in stationary gas, calculating potential flow characteristics near weak discontinuities as function of piston geometry and acceleration 10 p1468 A72-24431

Plane transonic gas flows through Laval nozzle and symmetrical wedge-shaped profile, solving boundary value problem by reduction to singular integral equation 10 p1418 A72-24433

Gas flow effect on undulating flow of viscous fluid film down vertical wall, using Fourier series 10 p1469 A72-24532

Heat transfer process in boundary layer of transparent gas flowing past plane emitting plate with prescribed surface heat flux 10 p1418 A72-24540

Steady two dimensional flow of monatomic rarefied gas past semiinfinite beam 10 p1418 A72-24543

Pitot tube pressure measurements in supersonic gas flow, calculating free molecular conditions limits 10 p1419 A72-24548

Modular carbon dioxide laser design and operational features, reporting measured data on plasma tube current, pressure and gas mixture flow rate effects on power output 10 p1492 A72-24565

Temperature dependence of gas flow coefficients at low pressures, determining isothermal permeability and heats of transport of He, Ne and Ar capillary flow 10 p1469 A72-24600

Steady rarefied gas flow around sphere with radial reflection of particles along normals, calculating gas dynamics variables of conservation equation 10 p1419 A72-24628

Energy transfer in thermally developing laminar gas flows with radiative interaction, using total band absorptance model [AD-745475] 10 p1563 A72-25043

Noncondensable gas and forced convection effects on laminar film condensation for two phase flows 11 p1743 A72-25261

Chapman-Enskog method modification for gas flow Prandtl boundary layer zero approximation distribution function construction, applying Mises transform to Boltzmann equation 11 p1614 A72-25332

Gas-particle flow trajectories, velocities and pressure distribution in axial flow turbine stage, using cascade tunnel and high speed photographic techniques [ASME PAPER 72-GT-57] 11 p1571 A72-25648

Boundary layer turbulence development by gas flow interaction with arc plasma in supersonic nozzle, causing light emission fluctuations [AIAA PAPER 72-415] 11 p1617 A72-26165

Neutral gases density and flux distribution in lunar atmosphere, using kinetic theory of gases 11 p1722 A72-26394

Breakup of accelerating liquid drops in gas dynamic flow, presenting unified theory for acceleration and aerodynamic effects 11 p1619 A72-26641

Discharge and pressure recovery coefficients of blocked gas flow in curvilinear channel with guide vanes, minimizing losses and separation at convex wall 11 p1574 A72-26971

Hot-wire measurement of vector velocity modulus and sign in one dimensional unsteady gas flow 12 p1806 A72-27178

Possible regimes and solutions for adiabatic one dimensional compressible gas flow in convergent and divergent ducts with friction 12 p1797 A72-27348

Cubic SiC film growth rate on Si substrate by methyltrichlorosilane decomposition in hydrogen flow, noting dependence on mixture flow rate and temperature 12 p1860 A72-28114

High temperature gaseous disperse flow radiation spectra photoelectric recording by DFS-8 spectrograph 12 p1812 A72-28116

Viscous incompressible gas turbulent flow in axisymmetric channel under preliminary twist conditions at inlet, using computer numerical solution 12 p1752 A72-28126

Turbulent gas flow mass transfer coefficient derived from Lapin relation between vertical velocity and concentration distributions in turbulent boundary layer near semipermeable surface 12 p1889 A72-28136

Simulation model test for effects of cooling air exhaust into gas flow area on turbine blading efficiency, obtaining dimensionless expression for experimental data generalization 12 p1862 A72-28148

Film cooling effectiveness for air-gas flow section of gas turbine engine under actual operating conditions 12 p1890 A72-28170

Turbulence microcharacteristics of rarefied suspension gas flow, using Topler schlieren-diffusion technique

12 p1752 A72-28172

Two dimensional Prandtl-Meyer flow anisotropy of ideal gas expanding into vacuum, using free path probe-molecule technique

12 p1799 A72-28178

Heat transfer to surfaces in turbulent compressible gas flows with various boundary conditions

13 p2063 A72-28627

Combined radiation-convection interaction for slow speed gas flow over flat plate, comparing with two dimensional and axisymmetric stagnation point geometries

13 p2064 A72-28631

Measurement techniques for separated gas flows mean and fluctuating aerodynamic properties, discussing improved optical geometry for laser Doppler anemometer

13 p1956 A72-28632

Plane unsteady potential isentropic gas flow equations solution interpreted as shallow water motion over horizontal bottom

13 p1893 A72-28717

Profile losses at turbine rotor blade in unsteady gas flow from experimental data analysis, noting effect of turbulence caused by trailing edge wakes

13 p1893 A72-28783

Source gas expansion flow into vacuum, solving spherical coordinates representation of BGK kinetic equation by numerical method

13 p1942 A72-29116

Internal rarefied gas flow, taking into account molecular backscattering due to wall surface roughness

13 p1942 A72-29117

Electrical analog simulation of internal combustion engines intake and exhaust systems nonstationary gas flow, considering cylinder, turbine and supercharger operation

13 p2027 A72-29136

Probe gas flow modulation in leak search device tested in vacuum system

13 p2007 A72-29921

Stream surfaces of three dimensional sub and supersonic irrotational gas flows in variable cross section channels and nozzles

13 p1895 A72-30004

Viscosity, velocity gradient and wall effects on pitot tube measurement of gas flow velocity measurement in turbulent boundary sublayer

14 p2094 A72-30294

Molecular band model for inhomogeneous radiating gases nonuniform transfer paths based on single collision broadened spectral line growth

14 p2135 A72-30891

Approximate analytical solution for spherical particle acceleration in uniform gas flow, examining nozzle geometry and particle size effects

14 p2095 A72-30924

Gaseous species diffusion in carrier gas under various geometries and flow conditions, using finite element method

14 p2095 A72-30928

Laminar mixing zone calculated for two homogeneous compressible gas flows with pressure gradient, noting coincidence of velocity distribution for identical gas dynamic parameters

14 p2070 A72-31009

Concentration stress convection in slow gas mixture flow due to density gradients, noting similarity to thermal stress convection

14 p2096 A72-31015

Supersonic ideal gas flow in corner formed by intersecting plates, using direct computation method for nonequilibrium flows with detached shock waves

14 p2071 A72-31021

Convective heat transfer of sphere in rarefied gas subsonic flow, comparing calculation with measurement

14 p2071 A72-31023

Thermal nozzle combustion effects on supersonic flow of chemically reacting gas in thermodynamic equilibrium

15 p2334 A72-31265

N-dimensional traveling waves in nonviscous polytropic gas with prescribed flow variable boundary conditions on arbitrarily shaped hypersurface, discussing application to radial flow

15 p2216 A72-31310

Heat conductivity equation solution for laminar gas flow in tubes, calculating temperature field and heat removal for molecular lasers with gas pumping

15 p2245 A72-31421

Ideal gas supersonic axial flow past circular cylinder, solving Navier-Stokes equations by Van Dyke matched asymptotic expansions method

15 p2178 A72-31463

Isoenergetic and irrotational planar supersonic cascade ideal gas flow computation by analytic method of characteristics

15 p2178 A72-31466

Perfect gas steady flow under gravity action, analyzing limiting equations [ONERA, TP NO. 1087]

15 p2178 A72-31682

Isentropic perfect gas steady compressible flow finite element analysis through nonlinear equations linearization based on perturbation theory

15 p2217 A72-31719

High acceleration effects on gas flow patterns in rocket nozzles, detailing stagnation condition in combustion chamber and gas velocity and pressure at exit

15 p2297 A72-31813

Perfect gas unsteady compressible homentropic flow with zero spatial pressure gradient, deriving characteristic equations

15 p2218 A72-32324

Linearized stability analysis of collapsing uniform nonrotating oblate gaseous spheroid, noting subcondensation growth rate dependence on shape and size

15 p2313 A72-32364

Shock wave propagation in gas with discrete velocity distribution, comparing solutions based on Euler, exact and Navier-Stokes equations respectively

16 p2375 A72-32861

Spherical source jet flow expansion of single monatomic gas into vacuum on basis of BGK kinetic equation

16 p2375 A72-32887

Energy and momentum losses of high temperature gas flow through externally cooled tube, solving laminar flow differential equations numerically on digital computer

16 p2378 A72-33430

Diatom gas flow behind blast wave, discussing vibrational nonequilibrium effects and solution of governing equations via characteristics method

16 p2378 A72-33440

Hydrodynamic equations for low speed steady external rarefied gas flows past circular cylinder, noting drag and heat transfer coefficients

16 p2344 A72-33568

Gas flow direction measurement using flow to electric pulse converter

16 p2395 A72-33957

Flow of a real gas in annular channels with curvilinear walls at large MHD-interaction parameters

17 p2587 A72-34457

Experimental study of the aerodynamic characteristics of burning gas-air jets in the transient flow region of natural gas

17 p2637 A72-35169

Measurement of the error of temperature sensors in flowing gases.

17 p2555 A72-35247

Kinetic and kinematic equations for inviscid unsteady gas flow, noting pseudostationary vortex geometry

17 p2541 A72-35436

Book - Introduction to the kinetic theory of gas flows

17 p2541 A72-35450

Initial-boundary-value problem of the formation of an electrical discharge in a flow.

17 p2592 A72-35627

A hypersonic flow about a body of revolution with fanned jet injection

17 p2487 A72-35805

Laminar gas flow in narrow channels of constant and variable cross sections in the presence of heat transfer

17 p2543 A72-35807

Holographic interferometry application to weak inhomogeneities visualization in gas flows, using photographic emulsion nonlinear properties

17 p2558 A72-35893

Method of characteristics application to supersonic jet and nozzle gas flow with allowance for equilibrium and nonequilibrium condensation

17 p2544 A72-35929

Fluid jets and droplets deformation in transverse supersonic two phase gas flow

17 p2544 A72-35932

Electrodynamic generator nonlinear internal resistance determination as function of flow parameters and model geometry via boundary conditions formulation

18 p2643 A72-35998

A contribution to the gas dynamics of oblique shocks with change of total enthalpy.

18 p2682 A72-36725

Numerical study of a viscous gas flow in the wake of a plane body

18 p2642 A72-36804

A through-type counting method for two-dimensional and spatial supersonic flows. II

18 p2642 A72-36810

Self-similar motions of a viscous heat conducting gas during an abrupt energy release

18 p2683 A72-36894

Carbon and graphite sublimation in inert gas flow at 2800-3000 K, determining rate dependence on temperature under kinetic and diffusive conditions

18 p2704 A72-37186

Solid rocket propellant erosion burning in turbulent gas flow, discussing burning velocity dependence on Pobodonostsev criterion

19 p2878 A72-37351

Pressure rise during combustion in semiclosed volume with reduced gas flow cross section in condensed system channel

19 p2879 A72-37354

Luminance profiles photometry for axisymmetrical propagation in propane-air turbulent flow combustion with turbulence level control in jet core

19 p2879 A72-37366

Interplanetary-gas motion induced by a solar flare

19 p2855 A72-37391

Experimental investigation of the flow past a cylinder with a flat nose

19 p2745 A72-37397

Linearized problem of one-dimensional periodic gas flow in a pipe

19 p2786 A72-37666

Mechanism and characteristics of condensed system ignition by a dispersed flow

19 p2882 A72-38451

Burning of carbon particles in a supersonic chemically active gas flow

19 p2882 A72-38454

Pressure propagation rate relation to local sound speed in unsteady anisotropic gas flow with particle-varying specific entropy

19 p2788 A72-38564

Electron beam focusing by ions in transverse gas flows, considering air, argon and helium residuals

20 p2952 A72-39070

Equilibrium HF gas discharge theory for waveguides and gas flow without restrictions on penetration depth and skin effect magnitude of field

20 p2957 A72-39383

Solution of some boundary value problems in the theory of potential gas flows and weak shock wave propagation

20 p2913 A72-39404

Non-isothermal laminar flow of gases through cooled tubes.

20 p2985 A72-39665

[ASME PAPER 72-HT-45] Stability of a liquid film in a lateral gas flow and the size of droplets during the breaking of the film

20 p2987 A72-39925

One dimensional stationary gas flow across normal shock wave, taking into account nonequilibrium factors and momentum, mass and energy transport

20 p2914 A72-39970

Two phase flow types defined as flow problems of two-phase matter mixtures /solid, liquid, gas or plasma/ and interface interaction

20 p2915 A72-39971

Determination of the characteristics of the averaged motion of the carrier medium in turbulent gas flow with suspended particles

21 p3044 A72-40126

Steady flow past body fixed in uniform flow of dusty gas, obtaining velocity distribution

21 p2989 A72-40195

Asymptotic theory of an optically thick radiating gas flow past a smooth boundary at moderate radiation strength.

21 p2989 A72-40196

Design modeling of external and internal cooling systems for bodies exposed to high temperature gas flow, discussing operation similarity conditions

21 p3129 A72-41052

Convergence of the successive approximation method in the problem of flows past bodies with strong injection

21 p2990 A72-41096

Computation of three-dimensional non-equilibrium supersonic flows.

21 p2992 A72-41162

[ICAS PAPER 72-37] Critical mass flow and nonequilibrium nozzle flow of vibrationally relaxing, ideal dissociating diatomic and singly ionizing monatomic gases, using steepest descent method

21 p3046 A72-41249

On the conditions for the appearance of the Mach effect in the reflection of an oblique shock wave in supersonic flow

21 p3046 A72-41339

Steady radiating gas flow past a semi-infinite flat plate at a constant temperature for an optically thick case.

21 p3131 A72-41497

Peclet number, length/diameter ratio, Grashof number, Knudsen number, overhear ratio and yaw angle interaction effects in cylindrical hot-wire and hot-film probes cooling

21 p3057 A72-41620

Multicomponent diffusion and heat transfer in flows of a chemically balanced ionized gas past bodies

21 p3047 A72-41658

Thermal state of selectively absorbing plane gas layer blown from porous plate into stabilized turbulent high temperature gas flow, considering radiative and convective heat transfer

21 p3131 A72-41672

Characteristics of gas flows in diffusers at transonic velocities

21 p2994 A72-41698

Experimental determination of the vibrational temperature of a supersonic gas flow

22 p3242 A72-41879

- Hot wire anemometer calibration for measurements of small gas velocities. 22 p3175 A72-41953
- Plane unsteady potential isotropic gas flow equations solution interpreted as shallow water motion over horizontal bottom 22 p3165 A72-42094
- Gas permeability of high-porosity nickel cermet 22 p3188 A72-42196
- Numerical solution to the Navier-Stokes equations in the problem of a gas flow past a rectangle 22 p3166 A72-42252
- Laminar boundary layer at critical point of blunt body in molecular oxygen flow, noting wall influence on condensation 22 p3243 A72-42257
- Method of characteristics for ideal gas flow in annular space of axisymmetric plug nozzle, noting flow visualization by schlieren photography 22 p3166 A72-42263
- Numerical integration of three dimensional flow equations for supersonic jets of ideal gas exhausted from elliptical and rectangular nozzles 22 p3133 A72-42264
- Blowing of a foreign gas in a hypersonic viscous shock layer 22 p3133 A72-42265
- Entropy and simple waves in multidimensional gas flow. 22 p3166 A72-42314
- Influence of the intermodal exchange on the wall heat flow in a gas possessing internal energy 22 p3244 A72-42641
- Stream surfaces of three dimensional sub and supersonic irrotational gas flows in variable cross section channels and nozzles 22 p3135 A72-42727
- Variational solution of a nonlinear boundary value problem for unsteady flow of gas. 22 p3199 A72-42854
- German monograph - Solution of the boundary layer equations for chemically reacting gases by a collocation method. 22 p3167 A72-43071
- Polish book - Fluid mechanics, Volume 2 - Gasdynamics. 22 p3168 A72-43199
- Chaplygin gas flow equation for analogy between hydrodynamic and electrodynamic equations, noting special theory of relativity 22 p3312 A72-43404
- Approximation for boundary value problem of homogeneous stationary combustion in laminar gas flow through cylindrical tube 22 p3356 A72-43798
- Velocity distribution in the turbulent boundary layer of a supersonic gas flow 22 p3249 A72-44084
- One dimensional steady conducting gas flow in nonaccelerating coordinate system under magnetic field, calculating pressure, density and temperature variations with boundary shock wave 22 p3281 A72-44265
- A kinetic-theory description of a chemically reacting gas. 22 p3357 A72-44272
- Experimental study of heat transfer during cooling of a high-temperature gas flow in a pipe. 22 p3357 A72-44539
- Boundary layer on bodies of revolution in longitudinal flows 22 p3390 A72-44723
- Various efficiencies of fluid flows and application to the hypersonic ramjet 22 p3360 A72-44993
- Propagation of blast waves in a combustible gas. 22 p3462 A72-45034
- Approximate equations of the flow behind a detonation with lateral confinement 22 p3463 A72-45041
- Weak shock wave propagation in a relaxing gas. 22 p3391 A72-45042
- The breakup of liquid droplet columns by shock waves. 22 p3391 A72-45048
- Hypersonic flow around plane and axisymmetric bodies of arbitrary shape with inviscid radiating gas. 22 p3360 A72-45110
- Performance and flow properties change through a rocket turbine by presence of solid particles. 22 p3361 A72-45206
- The shock-combustion /expansion-combustion/polar with allowance for variation of the specific heat ratio of a gas passing through a flame front 22 p3465 A72-45446
- GAS GENERATOR ENGINES**
U GAS GENERATORS
GAS GENERATORS
Proposed ASME procurement standards for gas turbines and generators, with compilation and definitions of specification terms [ASME PAPER 71-WA/GT-2] 05 p0703 A72-15895
- Gas generator performance shifts involving military trim level variations by TF-30 engines in high relative humidity environment caused by condensation in inlet duct 07 p1052 A72-18759
- Solid propellant gas generators, discussing propellant processing, grain, ignition, insulation and restrictions 09 p1263 A72-23600
- Ionization turbulence effect on nonequilibrium plasma MHD generator performance, using I-V characteristics equation 13 p1900 A72-29354
- Thermocatalytic pyrolysis for hydrogen generation from liquid hydrocarbon fuels with absolute cracking reaction efficiency 16 p2361 A72-33890
- Temperature dependent aluminum-water reaction generation of free hydrogen and aluminum hydroxide 16 p2362 A72-34159
- GAS GUNS**
NT LIGHT GAS GUNS
SLINGSHOT pilot aerodynamic test facility for very high acceleration, using encapsulated gas slug over fixed model [AIAA PAPER 72-168] 05 p0645 A72-16962
- GAS HEATING**
Gaseous diethyl peroxide spontaneous ignition during decomposition in cylindrical vessel, investigating diluents and temperature effects on self heating 02 p0301 A72-12027
- Galactic wind formation in elliptical galaxies by stellar ejected gas heating by supernovae, discussing thermally unsteady cores 02 p0279 A72-12189
- Interelectrode gap position control of discharge in coaxial gas heater with arc rotated by magnetic field 02 p0201 A72-12865
- Gas heating by If radiation due to Compton scattering near quasars, Seyfert galaxies nuclei and pulsars 03 p0435 A72-13801
- Pulsed combustion heated gas dynamic carbon dioxide laser, comparing with continuous version 07 p1003 A72-19219
- High performance shock tube using electromagnetically compressed and heated driver gas 07 p0965 A72-20559
- Conductive heat flux propagation rate in gases as function of absolute temperature 08 p1253 A72-21447
- Charpy impact tests of neutron irradiated nuclear reactor component steels to determine ductile/brittle transition temperature, describing setup and gas heating and cooling procedures 16 p2373 A72-33222
- Low pressure gas heating expediency for stagnation temperature increase in gas flow of shock tube 16 p2480 A72-34168
- Cosmic-ray heating of low-density interstellar H II regions. 17 p2600 A72-35296
- Ionisation equilibrium and line intensities for an X-ray heated H I gas. 19 p2852 A72-38509
- Stability of convective heat transfer through horizontal air layer heated from below and constrained internally by thin walled honeycomb panels [ASME PAPER 72-HT-60] 20 p2985 A72-39656
- Formation of clusters of galaxies - Photocenter fragmentation and intergalactic gas heating. 22 p3224 A72-42377
- Effect of capacitance on gain in a transversely pulsed CO2 discharge. 23 p3298 A72-44534
- Formation of a jet of shock-heated gas outflowing into evacuated space. 24 p3391 A72-45046
- GAS INJECTION**
Flow characteristics of colloid core reactor rocket engine, studying two component vortex flows with solid to gas mass density ratios over 100 [AD-735527] 01 p0100 A72-11359
- Interaction forces of gas jet injected into supersonic stream, examining data from thrust vector control gas injection tests 03 p0342 A72-13958
- Plasma density profiles by microwave interferometry technique in Sirius stellarator diverter for two magnetic field configurations and injection methods 04 p0555 A72-14619
- Water vapor injection into stratosphere by thunderstorms from IR radiometric inference measurements on NASA jet laboratory 04 p0544 A72-15358
- Nonequilibrium stagnation heat transfer mathematical models for injecting He, Ar or H into ionizing air laminar viscous layers at low Reynolds numbers [ASME PAPER 71-WA/HT-18] 05 p0744 A72-15877
- Low Reynolds number nonequilibrium stagnation heat transfer with helium, argon and hydrogen injection into air boundary and thin viscous shock layers [ASME PAPER 71-WA/HT-19] 05 p0744 A72-15878
- Diffuser for altitude simulation in rocket motor operation, featuring film cooling with water inflow by motor exhaust gas ejector action 05 p0704 A72-16004
- Mass addition distribution and gas injectant effects on heat transfer rates, transition locations and surface pressures of sharp cone 05 p0748 A72-16838
- [AIAA PAPER 72-183]
- Surface heat transfer and pressure measurements for downstream effects of transpiration cooled nose tip, using nitrogen as injectant fluid 05 p0605 A72-16840
- [AIAA PAPER 72-185]
- Air injection from wall slot into turbulent boundary layer of high temperature gas channel flow, calculating film cooling effectiveness in flat plate 08 p1252 A72-21316
- Approximation method for gas ejection calculation, assuming zero mixer flow velocity and ejection coefficient and suction side optimum operation for uniform pressure distribution 08 p1107 A72-21320
- Aerodynamics of vortex chambers with symmetrical air injection, discussing core and end boundary layer flows interaction and momentum loss from end surfaces friction 09 p1260 A72-22676
- Double slot laminar film cooling, considering tangential gas injection velocities into laminar boundary layer and heat transfer to wall 11 p1741 A72-25228
- [AIAA PAPER 72-290]
- Oscillatory relaxation combustion regions determination in high pressure gas injection tubes, noting flame propagation rate relationship with mixing concentration 11 p1745 A72-25754
- Heat transfer during gas injection through mesh packet porous wall, using gradient method 11 p1748 A72-26972
- Shadowgraph photography method for supersonic air flow pattern around porous cone in uniform injection, noting pressure distribution dependence 12 p1752 A72-27986
- Flow characteristics in air injection through porous surface of blunt bodies, noting blowing parameter effect on boundary layer flow 12 p1752 A72-28143
- Surface temperature distribution for porous plate in supersonic flow with gas injection into turbulent boundary layer 13 p1893 A72-28917
- Wind tunnel investigation of pressure perturbations on plane surface due to gas jet injected from surface into subsonic air drift flow 13 p1894 A72-29637
- Cold flow tests of mixing and atomization characteristics of gas/liquid circular coaxial injector elements in pressurized facilities [AIAA PAPER 71-672] 14 p2146 A72-30920
- Air and carbon dioxide intensive injection effects on turbulent boundary layer of subsonic channel air flow 14 p2097 A72-31159
- Thermodynamic properties of axisymmetric and planar stagnation flows of air with gas injection, taking into account mass transfer effects on heat transfer rate 16 p2477 A72-33428
- Foreign gas injection into three-dimensional stagnation point flows. 17 p2483 A72-34205
- Linear air mass flow injection at helicopter rotor blade tips, considering effects on trailing vortex circulation strength [AHS PREPRINT 624] 17 p2484 A72-34498
- Binary diffusion of a jet embedded in a boundary layer. 17 p2541 A72-35238
- Downstream effects of discontinuous injection of foreign gases in inert laminar boundary layer flows. 17 p2542 A72-35632
- Inert and reactive gas injection in near wake behind blunt bodies in supersonic flow, considering influence on base pressure and temperature 17 p2487 A72-35930
- Experimental study of the structure of a turbulent boundary layer on a plate with helium injection 18 p2682 A72-36888
- Inversion of a laminar boundary layer during the injection of CO2 through a vertical porous surface under natural convection conditions 19 p2881 A72-38191
- Turbulent boundary layer static pressure and heat exchange dependence on gas injection through porous surface 20 p2912 A72-39363
- Convergence of the successive approximation method in the problem of flows past bodies with strong injection 21 p2990 A72-41096
- Flat compressible turbulent boundary layers of air, predicting foreign gas injection effects on mass and heat transfer Stanton numbers and skin friction 22 p3165 A72-41958
- Velocity distribution in turbulent air flow over perforated plates with gas injection in turbulent boundary layer 22 p3166 A72-42256
- Blowing of a foreign gas in a hypersonic viscous shock layer 22 p3133 A72-42265

- Effect of air injection on the torque produced by a trailing vortex. 23 p3247 A72-43333
- Pressure at the trailing edge and losses in turbine bladings with air injection into the blade wake 23 p3248 A72-43661
- Gasdynamic investigation of a turbine with evaporative air cooling of the nozzle guide vanes 23 p3325 A72-43662
- Diffusion of a filament of gas injected into a supersonic free jet. 23 p3280 A72-43947
- Interferograms of turbulent boundary layer separation in critical blowing of gas through porous plate, noting velocity and concentration profiles of blowing parameters 23 p3281 A72-44082

GAS IONIZATION

- NT ATMOSPHERIC IONIZATION
- NT AURORAL IONIZATION
- NT FLAME IONIZATION
- Strong ionizing shock waves production in hydrogen and deuterium gases, measuring plasma electron temperature, axial electric field and density and magnetic field compression [AD-734469] 01 p0108 A72-10237
- Interstellar medium physical properties and distribution, discussing ionization heating by starlight, cosmic X rays and subcosmic rays 01 p0128 A72-10413
- Sound wave propagation velocity in partially dissociated and ionized gas, discussing attenuation coefficient, chemical process relaxation time and high temperature oxygen and nitrogen calculations 01 p0051 A72-11212
- Carbon dioxide laser pumping with nuclear reactions, indicating improved laser performance due to additional ionization by energetic charged particles 01 p0082 A72-11331
- Free electron density, electron temperature and gas ionization during shock wave propagation in Ar-filled shock tube from microwave radiation measurements 02 p0263 A72-12020
- Lf drift-type and ion-acoustic oscillations in weakly ionized currentless plasma at low gas pressures in longitudinal magnetic field 02 p0265 A72-12291
- Helium shock wave two step collisional ionization model comparison to observed profile data from laser Fabry-Perot interferometer 02 p0266 A72-12368
- Nonequilibrium effects on ionization growth in molecular hydrogen, tabulating experimental data for comparison with Monte Carlo computation 02 p0267 A72-12793
- Atomic oxygen coupled electron excitation and ionization by electron-atom and atom-atom collisions in nonequilibrium relaxation zone behind shock wave 02 p0207 A72-12896
- Penetration depth of hf electromagnetic waves in weakly ionized plasma, considering nonlinearity effect on ionization balance 03 p0394 A72-13085
- Power and gas consumption for inductive plasma formed in Ar atmosphere, measuring radial distribution of magnetic field axial component 03 p0395 A72-13652
- Multiphotonic ionization of atomic cesium jet by Q switched ruby laser beam 03 p0392 A72-14061
- Air ionization, secondary electron emission and Compton currents at W-Be interfaces under Co 60 gamma radiation 03 p0403 A72-14083
- Nonlinear ionization wave equation, calculating nonlinear response of unstable positive plasma column to weak pulse disturbance 03 p0399 A72-14346
- Atmospheric pressure pulsed carbon dioxide laser using preionization by injected high energy electrons from surrounding glow discharge, obtaining highest output from gas mixture [AD-746376] 04 p0529 A72-14586
- One dimensional continuous electrode shock tube driven MHD accelerator, analyzing unsteady flow behind ionizing shock wave by method of characteristics [AIAA PAPER 72-102] 05 p0697 A72-16973
- Molecular Cs role in multiphoton ionization process during interaction with low intensity Q switched Nd-glass laser radiation 05 p0670 A72-17082
- Ar core polarizability effect on photoionization cross section calculation for ground state configuration 05 p0693 A72-17173
- Shock wave deceleration and boundary layer mass loss effects on electron density and ionization levels of air in shock tube 05 p0700 A72-17225
- Plane supersonic ionizing shock wave in magnetic field under small wave plane perturbation from equilibrium position, calculating stability from linearized equations 06 p0798 A72-17678

- Voltage breakdown of microwave antennas, discussing ionization rates in hot air and breakdown suppression by electron flow 06 p0783 A72-17739
- Ionization mechanism for low voltage neon plasma arcs, determining non-Maxwellian energy distribution effects and excited atoms collisions role 06 p0862 A72-18333
- Transverse ionizing shock waves in gaseous hydrogen at speeds to 4000 km/sec, presenting magnetic shock structure and magnetic field jump measurements [AD-738620] 06 p0863 A72-18531
- Fast ionization fronts ahead of laser produced plasma expansion into low density gas, noting Langmuir probe and microwave diagnostics indication of photoionization density augmentation 06 p0864 A72-18532
- Electric field induced ionizing potential waves in dense gas, describing avalanching electron gas breakdown into filaments by fluid dynamic and Maxwell field equations 06 p0864 A72-18534
- Ionization wave propagation in inert gas due to microwave resonance quanta diffusion, explaining plasmaguide phenomena 07 p1040 A72-18916
- Ionization change induced striation instability of low temperature plasma with ambipolar diffusion in transverse magnetic field 07 p1043 A72-19878
- Stepwise ionization effects on ionic wave propagation and oscillation stability in inert gas dc discharges 07 p1046 A72-20503
- Langmuir electron oscillation excitation by ion beam at velocity exceeding average electron thermal velocity in plasma formed by residual gas ionization 07 p1046 A72-20505
- Ionization loss effects on cosmic ray lifetime in galactic interstellar medium, noting dependence on particle energy 07 p1064 A72-20637
- Interstellar gas role in cosmic ray yearly variations determined from solar short wave radiation induced gas ionization 07 p1065 A72-20640
- Gas mixture properties at high temperatures, pressures and densities, applying to thermal ionization of adiabatically compressed air 08 p1210 A72-20942
- He ionization and excitation in optically thick solar prominences, considering recombination excitation for observed triplet-level populations at 5000-10,000 K electron temperature 08 p1231 A72-21123
- Electromagnetic plasma accelerator with electron drift and diffusion towards anodes, neutral gas ionization and extended ion acceleration zone 09 p1361 A72-22955
- Magnetic mirror system to study Lorentz ionization of highly excited hydrogen atoms with quantum numbers 6-7 in strong magnetic fields 09 p1363 A72-23222
- Transit tube manometric system with fast particle beam ionization of residual gas molecules for vacuum measurements 09 p1364 A72-23226
- Self similar flow patterns due to cylindrical ionizing symmetrical strong shock and detonation wave propagation outwards into gas at rest 09 p1295 A72-23564
- I.F drift-type and ion-acoustic oscillations in weakly ionized currentless plasma at low gas pressures in longitudinal magnetic field 10 p1517 A72-23765
- Electron bombardment SERT II ion thruster operation using Xe, Kr, Ar, Ne, He, nitrogen and carbon dioxide 10 p1528 A72-23964
- Observation and ionization relaxation times of Ar plasma produced in shock tube at Mach 10-13, describing experimental arrangement 10 p1519 A72-24056
- Collisional cyclotron instability nature in ionized gases in presence of Ramsauer effect 10 p1520 A72-24224
- Ionization kinetics influence on light absorption zone behind plane stationary shock wave in hydrogen 10 p1467 A72-24358
- Nonequilibrium ionization theories for high pressure discharge in inert gas-alkali metal vapor 10 p1515 A72-24414
- Plane ionizing shock wave stability in MHD channel within magnetic field 10 p1522 A72-24542
- Interaction solutions of steady crossed field MHD channel flows for perfect, singly ionizing monatomic and thermodynamically unspecified gases 10 p1523 A72-24789
- Cylindrical tube geometry and electrode separation effects on normal ionizing shock waves, showing speed proportional to azimuthal drive and axial magnetic fields 10 p1470 A72-24794

- Ionization equilibrium description by quantum statistical fugacity expansion of pressure for partially ionized plasmas 10 p1524 A72-24929
- Performance characteristics of various types of PIG sources for multiply charged heavy ions production 10 p1516 A72-25027
- Normal ionizing shock waves characteristics in He under varying conditions of magnetic field strength, discharge current and gas pressure 11 p1694 A72-25789
- Critical shock wave velocity for ionization front propagation with photoionization of hydrogen by radiation, using pinch discharge tube measurements [AIAA PAPER 72-410] 11 p1706 A72-26161
- Electrostatic ion thruster theoretical model, deriving ionization rate density as function of discharge current 11 p1707 A72-26175
- Chemical ionizing mass spectrometry with electron bombardment of reactant gas, discussing plasma chromatography 11 p1590 A72-26389
- Skew magnetic structure of ionizing shock waves with ohmic dissipation as dominant diffusion mechanism 11 p1618 A72-26605
- Magnetic structure of ionizing oblique shock waves with transverse and normal components in zero magnetic Prandtl number limit 11 p1618 A72-26606
- Magnetic structure of normal ionizing shock waves with zero transverse energetic component 11 p1618 A72-26607
- Neutral gas velocity distribution, transverse drift velocity, particle and energy densities in column under free fall conditions, considering wastage by ionization processes 11 p1698 A72-26645
- Merging beams study of positive ion ionization by electron impact for atomic He, N and O 11 p1692 A72-26658
- High pressure electroionization carbon dioxide and nitrogen filled carbon dioxide lasers 11 p1652 A72-26793
- Chemical and ionizational equilibrium equations of heterogeneous gas mixture composition with allowance for condensed phase ionization 11 p1747 A72-26965
- Boltzmann distribution of nitrogen ions according to rotational energy levels in nitrogen ionization by slow electrons impact 12 p1847 A72-27050
- Cascade ionization of air by RF electric fields and intense laser pulses, solving Boltzmann equation for electron distribution 12 p1848 A72-27390
- Plasma ionization traveling disturbances velocity and spatial structure in strong electromagnetic waves field 13 p1915 A72-28469
- Nonequilibrium Faraday MHD generator performance examined by double diaphragm shock tube within ionization region 13 p2013 A72-29357
- Nonequilibrium ionization phenomena effects on electric conductivity of combustion gas-particle plasma generated by aluminized fuel seeded with potassium nitrate 13 p2013 A72-29363
- MHD laser discharge characteristics under generator conditions, emphasizing interaction of gas ionization instabilities and lasing radiation field 13 p2014 A72-29367
- Cs seeded nonequilibrium MHD Ar plasma stability in fully ionized seed regime 13 p2014 A72-29368
- Ca and Na ionization equilibrium ratio in dust filled interstellar clouds, considering cosmic ray and charge transfer influence 13 p2040 A72-29405
- Penetration depth of HF electromagnetic waves in weakly ionized plasma, considering nonlinearity effect on ionization balance 13 p2015 A72-29435
- Massive red supergiants radial pulsations from adiabatic theory application to convective envelope models based on mixing length theory and H-He ionization zones 14 p2159 A72-30743
- Interferometric investigation of impurities effects on electron density distribution in ionization-relaxation zone behind shock waves in monatomic gas 15 p2215 A72-31213
- Electron production cross section during He atom ionization by proton impact, noting peak existence for electrons near incident proton velocities 15 p2281 A72-32220
- Solar wind and planetary atmosphere interaction observation by simulation of ionization mechanism in comet, using gun produced plasma stream and gas cloud 15 p2301 A72-32341

Precursor photoionization production of ionization onset point equivalent electron number densities, calculating phenomenon occurrence Mach number

15 p2281 A72-32407

Boundary layer ionization on flat plate and cylindrical plasma probes in high speed flow, considering ionized continuum flow and collisionless plasma

16 p2374 A72-32831

Gas ionization buildup behind hypersonic shock waves, calculating onset point properties from plasma conservation and electron energy equations

16 p2434 A72-32902

Precursor ionization upstream from shock wave due to shock emitted radiation absorption by easily ionizable impurity species

16 p2379 A72-33512

Random ionization waves convective instability in glow discharge positive column, calculating fluctuations spectrum as function of position along column for localized white noise source

16 p2437 A72-33747

Solar wind expansion analysis with allowance for interaction with neutral interstellar matter, discussing kinetic energy loss due to EUV ionization of interstellar gas

16 p2449 A72-33910

Photoionization models for the emission-line regions of quasi-stellar and related objects.

17 p2605 A72-34527

Photoionization of a gas by far ultraviolet radiation of a laser-created plasma

17 p2588 A72-34872

Ionization kinetics influence on light absorption zone behind plane stationary shock wave in hydrogen

17 p2539 A72-34957

Ionization change induced striation instability of low temperature plasma with ambipolar diffusion in transverse magnetic field

17 p2590 A72-35128

Hydrogen plasma ionization equilibrium and thermodynamic stability existence condition based on Saha equation

17 p2590 A72-35137

High temperature turbulent jet facility for studying ionic species produced by high temperature air and ablation products interaction with cool ambient air [AIAA PAPER 72-676]

17 p2536 A72-35480

Breakdown in argon and nitrogen under the influence of a 0.35-micron picosecond laser pulse.

17 p2564 A72-35508

Lunar local surface magnetic fields production mechanism, considering convection currents due to ionization of volcanic-ash particle flow by electrodynamic model

17 p2614 A72-35586

Ionization mechanisms for quiescent prominence He II 4686 line emission under coronal UV radiation and high temperature conditions

17 p2618 A72-35737

Multiphoton ionization of atomic hydrogen in the presence of an intense electromagnetic field.

17 p2586 A72-35827

Electromagnetic plasma accelerator with electron drift and diffusion towards anodes, neutral gas ionization and extended ion acceleration zone

17 p2593 A72-35884

Ionization of mercury vapor and cesium vapor in a nuclear reactor.

18 p2713 A72-36208

Short cesium plasma discharge diode as physical model for thermionic converter, studying ionization, recombination and microwave radiation

18 p2714 A72-36212

Excitation and ionization processes in a low-voltage arc discharge

18 p2714 A72-36213

Excitation transfer and Penning ionization reactions between helium metastables and carbon monoxide.

18 p2713 A72-36563

The measurement of partial pressure in vacuum technology and vacuum physics

18 p2692 A72-36836

On the influence of excited ions and crossed electric and magnetic fields on ionisation cross-sections.

18 p2714 A72-36956

Time-dependent ionization equilibrium and line radiation under flarelike conditions.

19 p2849 A72-37241

Collisional excitation and impact ionization coefficients of hydrogen

19 p2837 A72-37807

A preliminary model for the shell ionisation of the nova RS Ophiuchi.

19 p2866 A72-38504

Low energy cosmic particle and soft X ray photon produced nonthermal electrons effect on interstellar gas ionization and thermal energy equilibrium

19 p2867 A72-38508

Ionisation equilibrium and line intensities for an X-ray heated H I gas.

19 p2852 A72-38509

Radio-frequency preionization in a supersonic transverse electrical discharge laser.

19 p2813 A72-38694

Propagation of ionization wave in rarefied noble gases due to microwave resonance quanta diffusion, explaining plasmaguide phenomena

20 p2957 A72-39382

Gas breakdown in the laser as the limitation of pulsed high-pressure CO₂ lasers.

20 p2934 A72-39565

Inverse bremsstrahlung caused fast cascade of electrons with Boltzmann energy distribution to explain laser induced gas breakdown via plasma heating

20 p2934 A72-39645

Nonlinear interaction of p and s ionization waves in neon.

21 p3090 A72-40487

Free fall column theory allowing for 'neutral gas reduction' by ionization processes, and application of this theory to noble gas ion lasers

21 p3090 A72-40488

Pressure jump across normal ionizing shock waves.

21 p3045 A72-40566

One-to-one telescope with pressurized Ar gas for nanosecond and picosecond laser output pulse sensitive detection via gas breakdown and energy absorption

21 p3062 A72-40618

Influence of the lowering of the ionization energy on the continuous radiation of an argon plasma

21 p3093 A72-41343

The interaction of Sco X-1 with its environment.

22 p3218 A72-42387

Propagation of radiative shock waves in an inhomogeneous cosmic medium.

22 p3225 A72-42452

Limit Mach number in a gas undergoing partial dissociation and single ionization

22 p3244 A72-42624

German monograph - Ionization of nitrogen-oxygen gas mixtures by shock waves.

22 p3209 A72-43073

Pulse discharge plasma in Ar with gas ionization level near unity, noting plasma cylinder parameters, electron temperature and I-V characteristics

22 p3212 A72-43103

Disequilibria created by an electric field in a nitrogen plasma

23 p3321 A72-43695

Electron impact ionization of ions trapped in a hollow electron beam.

23 p3316 A72-44343

Electromagnetic instabilities produced by neutral-particle ionization in interplanetary space.

23 p3332 A72-44506

Influence of atom-atom collisions on the collisional-radiative ionization and recombination coefficients of helium plasmas.

24 p3428 A72-44798

The critical velocity of gas-plasma interaction and its possible heterogenic relevance.

24 p3429 A72-45468

Microwave observations of a partially ionized interstellar cloud.

24 p3447 A72-45551

Boltzmann distribution of nitrogen ions according to rotational energy levels in nitrogen ionization by slow electrons impact

24 p3427 A72-45703

GAS JETS

Solid particle influence on underexpanded gas jet shock structures, using schlieren photographs

03 p0342 A72-13840

Circular jet discharging perpendicular to solid surface into transverse flow, discussing effects on infinitely thin circular wing aerodynamic characteristics

03 p0309 A72-13915

Interaction forces of gas jet injected into supersonic stream, examining data from thrust vector control gas injection tests

03 p0342 A72-13958

Plane mixing boundary layer flow of high temperature turbulent gas jet in longitudinal magnetic field

03 p0397 A72-13998

Comparative velocities of high energy gas jets of Ne, oxygen and carbon dioxide from outlet pipes, using Voitenko compressors

04 p0510 A72-14537

Gas jet attitude control systems for spacecraft, discussing accuracy and time of active operation

05 p0728 A72-16479

Gas jet control for spinning satellites attitude correction, deriving relations between satellite and control system parameters, response time and fuel consumption

05 p0731 A72-17196

Electric arc in submerged gas jet, investigating laminar combustion zone extent, thermal layer radius and electric field strength

06 p0861 A72-17903

Approximation method for gas ejection calculation, assuming zero mixer flow velocity and ejection coefficient and suction side optimum operation for uniform pressure distribution

08 p1107 A72-21320

Gas jet combination with laser for cutting operations, discussing laser characteristics, beam guiding

mirror, lens, nozzle, nozzle gas and workpiece materials

09 p1320 A72-23629

Oxygen jet-carbon dioxide laser beam cutting in mild and stainless steels, noting speed and material thickness limitations

09 p1321 A72-23639

Supersonic Ar, He and molecular nitrogen jets, determining electron temperature and concentration and atomic state population in shock waves region by spectroscopic measurement

10 p1517 A72-23837

Aerodynamic noise produced by gas jet flow around airfoil, discussing sound reduction

10 p1417 A72-24107

Russian monograph on self oscillatory noise generation during gas jet ejection covering single, parallel, supersonic, flat and cylindrical jets stability

11 p1617 A72-26066

High pressure injector optimum design and performance for gas jet boosters, using one dimensional theory with friction allowance

12 p1861 A72-27535

Liquid droplets behavior in high velocity gas jets, deriving fluid flow model solutions near symmetry axis and for liquid-gas boundary layer [DFVLR-SONDDR-200]

13 p1941 A72-29003

Optimization of high temperature supersonic gas jets for metal powders production by melts atomization, discussing excess air ratio effect on gas parameters

13 p2025 A72-29133

Point density measurement in gas jets by flow visualization based on Raman spectrum lines proportionality

13 p1959 A72-29670

Core axial density distribution in gas jets freely expanding into vacuum from double concentric orifices, using electron beam fluorescence technique

15 p2218 A72-32150

Combustion process in mixing gas jets of different density, using argon and nitrogen for internal flow and air for external jet

16 p2381 A72-34169

Experimental study of the aerodynamic characteristics of burning gas-air jets in the transient flow region of natural gas

17 p2637 A72-35169

Binary diffusion of a jet embedded in a boundary layer.

17 p2541 A72-35238

Density distribution in a high-pressure gas jet measured by laser-induced gas breakdown.

17 p2486 A72-35630

A hypersonic flow about a body of revolution with fanned jet injection

17 p2487 A72-35805

Turbulent gas jets formed in cryogenic substance discharge into gas at supercritical pressure and gas into gas of different molecular weight and temperature

20 p2912 A72-39366

Mixing in initial portion of coflowing jets of incompressible gases of different densities, defining mixing zone widths relationship to velocity and density ratios

20 p2913 A72-39369

Velocity distribution in turbulent mixing of compressible reacting gases, noting flame length measurement of submerged H jet

21 p3129 A72-40981

Optical method for measuring the concentrations of axisymmetric gas jets

21 p3055 A72-40990

The study of gaseous jet exhausting into vacuum. [ICAS PAPER 72-36]

21 p3046 A72-41161

Particle temperature and flight velocity during gas-powder buildup

22 p3182 A72-42194

Light scattering by the medium created by a spacecraft. I - Luminescence of the gas jets of the spacecraft microthrusters

22 p3230 A72-42216

Formation of a jet of shock-heated gas outflowing into evacuated space.

24 p3391 A72-45046

GAS LASERS

NT CARBON DIOXIDE LASERS

NT CARBON MONOXIDE LASERS

NT HCN LASERS

NT HELIUM-NEON LASERS

Laser power transmission, examining heat transformation into coherent radiation by closed cycle gas dynamic laser system

01 p0080 A72-10925

Gas dynamic lasers theory based on two fluid model of optically active medium, investigating medium velocity effect on lasing mechanism

01 p0081 A72-11210

Fabry-Perot interferometer employing gas laser for plasma bursts electron concentrations measurements at 3.39 micron wavelength

02 p0223 A72-11404

Pulsed laser emission in carbon monoxide, calculating molecular excited state populations

02 p0237 A72-11471

- Laser generator research, discussing metallic vapor, heterojunction semiconductor, liquid, neodymium and organic colorant types 02 p0237 A72-11696
- Fm of gas laser emission during sinusoidal modulation of relative excitation, evaluating collision parameters determination method 02 p0180 A72-12581
- Cross-excited carbon-dioxide-nitrogen laser with pulse sharpening effect due to self-Q-switching, finding optimal nitrogen mixing ratio for peak power 02 p0239 A72-12827
- Electrically excited tunable IR molecular gas lasers with rotational lines overlapping due to high pressure broadening 03 p0366 A72-12965
- Kinetic model and analysis of elementary characteristics of carbon trifluoriodide photodissociation laser 03 p0366 A72-13078
- Gas laser longitudinal mode locking during single sideband modulation with nonuniform broadening in mode intensity distribution 03 p0366 A72-13365
- HCN laser amplifier gain measurement at IR wavelengths in gas mixtures by recording with pyroelectric receiver 03 p0368 A72-13667
- Water vapor laser pumping by upper lasing level excitation through direct electron impact, explaining mechanism by model 04 p0529 A72-14587
- Pulsed nitrous oxide molecular laser upper energy level relaxation time measurement by afterglow pulse-gain technique 04 p0529 A72-14601
- High power CW gas dynamic laser mode-control experiment with unstable resonator at high Fresnel number, obtaining near and far field intensity distribution 04 p0529 A72-14605
- Book on optics covering gas lasers, power output vs frequency, picosecond laser pulses, Q switching principles, mode locking, optical propagation through turbulent atmosphere, etc 04 p0548 A72-14733
- Gas lasers application to precise length measurements via absorbing medium resonance determined wavelength 04 p0530 A72-14734
- Gas lasers mode locking, describing use of amplitude and frequency modulation and moving mirrors 04 p0530 A72-14738
- Superregenerative linear mode amplification in Q switched He-Xe laser as function of resonator phase, length and signal angle 04 p0531 A72-15147
- Amplitude characteristics of Q switched He-Xe laser at 3.5 microns, using rotating reflection prism and velocity equations 04 p0531 A72-15149
- Nitrogen to carbon dioxide vibrational energy transfer time measurement in gas dynamic laser 04 p0531 A72-15352
- Submillimeter wave sulfur dioxide molecular laser, investigating lasing lines, plasma decay and relaxation, line interactions and signal temporal behavior 04 p0532 A72-15595
- Submillimeter wavelength HCN laser stabilization, describing AFC and phase locking 04 p0532 A72-15596
- Monograph on semiclassical gas laser theory covering electromagnetic fields, atomic polarization, multimode theory, traveling- and standing-wave laser principles, collision effects, etc 05 p0668 A72-16398
- High pressure gas lasers excitation, determining energy introduction and space charge stability 05 p0668 A72-16415
- Flash photolysis HF chemical laser pulse delay measurements, showing pressure, flash lamp intensity and optical cavity loss dependence 05 p0668 A72-16606
- Gas dynamic laser analysis based on phase cancellation model, showing flow induced phase nonuniformity minimization for far field intensity improvement [AIAA PAPER 72-217] 05 p0669 A72-16857
- Gas dynamic laser technology advances, discussing water content, temperature and Na effects and nozzle design [AIAA PAPER 72-143] 05 p0669 A72-16895
- Rapid expansion nozzles for gas dynamic laser working gas vibrational energy freezing to obtain population inversion, considering size and shape effects on performance 05 p0669 A72-16965
- [AIAA PAPER 72-148] 05 p0669 A72-16965
- High power tunable IR gas lasers based on anharmonic molecules vibrational-rotational transitions excitation at gas pressures of 10 atm 06 p0825 A72-17786
- Handbook on lasers and optical technology covering gas, dye, liquid, injection and insulating crystal lasers, materials, sources, transmission, hazards and holographic recording 06 p0826 A72-17945
- Output power dependence on pressure and magnetic field strength in Kr ion laser for green, yellow and red lines 06 p0826 A72-18010
- Population inversion production in sulfur dioxide molecular laser 06 p0827 A72-18459
- Gas laser emission fluctuations of total radiation energy, polarized field components and line widths in longitudinal magnetic field 07 p0999 A72-18911
- Time behavior and spectra of relaxation oscillations in high gain IR xenon laser 07 p1001 A72-19199
- High gain xenon laser spectral narrowing dependence on line-broadening mechanism including saturation and distributed loss effects 07 p1001 A72-19201
- High repetition rate pulsed IR xenon laser using transversely excited discharge 07 p1003 A72-19221
- Transverse mode effects on gain and dispersion focusing in high gain Xe laser [AD-739448] 07 p1005 A72-19409
- Optically pumped gas lasers with electron transitions to molecular excited state and resonant absorption lines 07 p1006 A72-19634
- CW gas laser operating in far IR, discussing water vapor excitation by dc discharges 07 p0946 A72-19961
- Laser applications in industrial machining and welding, describing theory and operation of optically pumped ruby, glass-Nd, YAG-Nd, Ar and carbon dioxide lasers 07 p1007 A72-20224
- Nb-Nb point-contact Josephson junctions response to submillimeter radiation from HCN and DCN lasers 07 p0992 A72-20551
- Nonlinear mode relationship of gas ring laser due to light scattering at inhomogeneities in active medium 07 p1009 A72-20612
- High power visible output gas dynamic lasers, discussing supersonic flow generation 08 p1182 A72-21337
- Spectral density curves for intensity fluctuations of stimulated emission from low and ultralow frequency gas lasers as function of thermal oscillation, mode interference and beat effects 08 p1182 A72-21379
- Atomic, ion and electron transition pulsed gas discharge lasers, considering power efficiency factors, vacuum UV region and gas density 08 p1182 A72-21644
- Population inversion development and breakdown in active medium produced by plasma generation during pulsed discharge in molecular nitrogen laser 08 p1183 A72-21716
- Output power calculation of gas lasers with active elements of varying lengths, using extreme emission fluxes equations 08 p1184 A72-22031
- Gas, solid state and semiconductor lasers review, discussing applications 09 p1322 A72-22594
- High power electron beam pumped nitrogen super-radiant laser with 60 kW output 09 p1323 A72-22624
- Subnanosecond light pulse generation by Ne laser at 5401 Å by amplified spontaneous emission 09 p1323 A72-22869
- Hologram diffraction efficiency for bleached high resolution photoemulsions for blue line of He-Cd laser 09 p1311 A72-22964
- Chemistry and performance characteristics of flash photolysis and microwave discharge initiated CW carbon disulfide/oxygen lasers 09 p1325 A72-23236
- Lasing length, power and efficiency of cw HF chemical laser with nitrogen or He diluent [AD-742962] 09 p1325 A72-23241
- High power Ar ion laser with plasma tube using current conducting graphite bore for stable long life operation 10 p1489 A72-23944
- Gas laser excitation by relativistic electron beam pulse axial propagation through optical cavity, studying mechanism through timing and pressure dependence measurements 10 p1489 A72-23946
- Nuclear reaction-produced high energy ion beams for gas laser pumping and output enhancement 10 p1489 A72-23948
- Frequency splitting by diffraction at resonator mirrors of gas ring laser, deriving opposed waves lasing equations 10 p1490 A72-24045
- Molecular diffusion laser gain determination from interaction kinetics between diatomic and cold working gases, examining annihilation processes 10 p1491 A72-24360
- Pressure dependence of gas laser intensity, taking into account velocity changing collisions with foreign gas atoms [AD-740403] 10 p1492 A72-24604
- Rb87 vapor laser with optical pumping, measuring nitrogen or nitrogen argon mixture buffer gas partial pressure effect on power output 10 p1493 A72-24911
- Electron densities and drift velocities dependence on macroscopic discharge parameters in positive column of He-Cd laser 10 p1493 A72-25048
- Time resolved gain in water and water-gas mixtures as function of composition and excitation current, considering relaxation rate in pulsed water vapor laser 11 p1691 A72-25302
- Rhesus monkey retinal image diameter estimation during exposure to Ar and He-Ne laser irradiation, using microphotometer scans 11 p1582 A72-25314
- Chemical laser with deuterium and nitrogen fluorides mixture, examining excited molecules emission spectra 11 p1649 A72-26351
- Populations modulation and spatial harmonics influence on gas and solid state laser radiation characteristics, discussing uniform and nonuniform line broadening 11 p1650 A72-26353
- Total emitted power calculated for transversely pumped pulsed molecular nitrogen laser at 3371 Å 11 p1651 A72-26504
- Rare gas ion laser excited by electrodeless microwave discharges, noting external magnetic field effects on output 11 p1651 A72-26571
- Single mode gas laser with internal absorption cell, emphasizing frequency standard application 12 p1819 A72-27285
- Gas laser with strong absorption saturation to obtain high peak power and frequency self stabilization by generation of quasi-traveling wave in resonator 12 p1820 A72-27585
- Fast response thermal compensation system for gas laser resonator length and frequency stabilization, discussing fabrication and design calculation 12 p1822 A72-27607
- Gas laser oscillation frequency stabilization by comparing mode separation with RF standard 12 p1822 A72-27608
- Carbon dioxide-helium-nitrogen mixture laser, comparing GaAs, CdSe, CdS and CdTe electro-optical crystals suitability for radiation modulation at 20.6 microns 12 p1822 A72-27610
- Coaxial integrated pulse generator and gas laser with double transmission line for energy storage, noting design parameters selection 12 p1823 A72-27700
- Spectral output of pulsed discharge initiated hydrogen fluoride chemical laser as function of pressure and gas composition 12 p1823 A72-27839
- Gas and solid state lasers amplitude and phase fluctuations calculated from Langevin equations, noting spectral line width and collision waves 12 p1826 A72-28050
- Gas dynamic lasers and combustion driven devices design, operation, performance and industrial applications 13 p1965 A72-29420
- Kinetic model and analysis of time characteristics of trifluoriodomethane photodissociation laser 13 p1968 A72-29428
- Standing wave and colliding wave lasing and synchronization region in ring laser using active gas isotope mixture 13 p1968 A72-29511
- Light polarization modes in gas ring laser with optically active isotopic cell, showing dependence on circular field coupling coefficient 13 p1968 A72-29512
- Nonlinear light amplification in molecular nitrogen amplifier as function of input pulse delay relative to excitation start 13 p1969 A72-29522
- Opposing wave generation in gas ring laser with allowance for diffraction by finite apertures of cavity mirrors 13 p1970 A72-29678
- Interference method for gas laser phase front measurements based on comparison with radiation shifted in mirror plane 13 p1970 A72-29681
- Polarimetric determination of angle between polarization planes of emission and external radiation field in three level gas laser, noting resonator anisotropy properties 13 p1970 A72-29687
- He-Cd laser emission wavelength determination at Lamb dip center for development of interferometer operation in violet spectral region 13 p1970 A72-29688
- Pulsed chemical high pressure laser efficiency and output energy increase due to carbon dioxide introduction into deuterium-fluorine mixture 13 p1970 A72-29698

Wide tuning range organic dye laser design, using nitrogen laser line as transverse pumping source
13 p1971 A72-29869

Methane absorption stabilized 30 meter laser strain meter with Fabry-Perot geometry for earth tide, nuclear explosion and free earth oscillation observation
14 p2109 A72-30323

Lamb dip for 119 micron line of CW gas laser, noting decay constants due to pressure
14 p2110 A72-30424

Small parameter method for analysis of encounter waves nonlinear self oscillations in ring gas laser, noting periodic energy transfer
14 p2111 A72-31104

Heat conductivity equation solution for laminar gas flow in tubes, calculating temperature field and heat removal for molecular lasers with gas pumping
15 p2245 A72-31421

Gas laser asynchronous coupling modulation, examining dependence on lasing threshold, optical spectrum and transition line shape
15 p2246 A72-31660

Molecular nitrogen pulsed laser wavelength measurements, observing IR bands, stimulated emission lines and population inversion mechanisms
15 p2249 A72-32151

High gain CW He-Xe laser transitions due to Xe 5d level long-lived decaying emission
15 p2250 A72-32301

Optically pumped pulsed hydrogen fluoride gas laser, observing anisotropic ultrahigh gain emission in rotational transitions
15 p2251 A72-32531

Stimulated emission in molecular iodine vapor phase laser optically pumped by Q switched Nd-YAG laser second harmonics
15 p2251 A72-32538

Mathematical model for fast transverse glow discharges for pumping high pressure gas lasers, noting short rise time of applied voltage pulse
16 p2399 A72-33012

Room temperature vibrational relaxation measurements in gases subsequent to laser pumping by picosecond pulse generated transient stimulated Raman scattering
16 p2401 A72-33389

Chemical laser with deuterium and nitrogen fluorides mixture, examining excited molecules emission spectra
16 p2402 A72-33704

Populations modulation and spatial harmonics influence on gas and solid state laser radiation characteristics, discussing uniform and nonuniform line broadening
16 p2402 A72-33706

Transverse modes competition in high power homogeneously broadened gas laser with confocal geometry, noting corresponding longitudinal mode in atomic excitation
16 p2403 A72-33841

Viscous boundary layer generated weak shock wave effects on gas dynamic laser medium density homogeneity
16 p2380 A72-34037

Effect of nozzle throat radius of curvature on gasdynamic laser gain
17 p2561 A72-34210

UV laser parameters calculation for operation on I₂ man transition between H atom resonant excited state and ground state
17 p2562 A72-34349

Design of an inexpensive, 30 cm diameter, long path difference interferometer.
17 p2553 A72-34640

Molecular diffusion laser gain determination from interaction kinetics between diatomic and cold working gases, examining annihilation processes
17 p2563 A72-34959

Quantum Boltzmann equation for a laser.
17 p2563 A72-35160

Simple technique for sequential Q-switching of molecular lasers.
17 p2563 A72-35193

Influence of molecular laser parameters on the pulse shape in Q-switched operation
17 p2563 A72-35301

Mode stability in a gas laser with nonlinear selection losses
17 p2563 A72-35304

A gas laser with external mirrors generating non-polarized radiation
17 p2563 A72-35308

Hollow dielectric waveguide for distributed feed-back lasers.
17 p2564 A72-35346

Excitation modes and operating characteristics of electric discharge convection lasers
17 p2565 A72-35962

Optical polarization effects in a gas laser.
18 p2697 A72-36487

Importance of nozzle geometry to high-pressure gas-dynamic lasers.
19 p2811 A72-37867

Using ring lasers as rate sensors.

19 p2812 A72-38223

Pulse nitrogen laser at high repetition rate.
19 p2813 A72-38696

Certain results of a study of the emission-frequency stability of gas lasers at 0.63, 1.5, 3.39, and 9.6 micron wavelengths
19 p2814 A72-38786

Gas laser emission fluctuations of total radiation energy, polarized field components and line widths in longitudinal magnetic field
20 p2931 A72-39377

Polarization effect of attenuation of opposed-wave competition in ring lasers
20 p2932 A72-39412

He-Cd lasers using recirculation geometry.
21 p3061 A72-40239

Laser action on unclassified xenon transitions in a highly ionized plasma.
21 p3089 A72-40242

The beam-plasma discharge laser
21 p3062 A72-40406

Free fall column theory allowing for 'neutral gas reduction' by ionization processes, and application of this theory to noble gas ion lasers
21 p3090 A72-40488

Frequency deviation equations for FM gas laser with modulation achieved by resonator optical length variations
21 p3063 A72-40798

Atomic, ion and electron transition pulsed gas discharge lasers, considering power efficiency factors, vacuum UV region and gas density
21 p3064 A72-41301

The phase difference between coupled laser oscillations
22 p3184 A72-42109

Spontaneous self mode locking in transversely excited nitrogen laser operation in first positive system
22 p3186 A72-42618

Superradiant laser excitation at 3371 Å in molecular nitrogen second positive band system by high energy electron beam, noting 6 nsec pulse outputs to 24 MW
22 p3186 A72-42623

Approximate theory of the CW gasdynamic laser with an unstable resonator.
22 p3186 A72-42631

Multisectional CW gas dynamic laser output radiation density distribution control via transmitting mirror with variable reflection coefficient
22 p3186 A72-42632

The photochemical iodine laser - A high-power laser
22 p3186 A72-42940

Application of gasdynamic flows in laser technology
22 p3187 A72-43176

Pure Ne laser and its fundamental characteristics.
23 p3296 A72-43946

Frequency stabilization of pure neon laser.
23 p3296 A72-43951

A new method of measuring temperature, inversion ratio, and pressure-broadened linewidth in a CW molecular laser.
23 p3297 A72-44188

Elements of a theory of CW gasdynamic quantum generators.
23 p3297 A72-44225

Influence of weak disturbances on the operation of a gas laser with a homogeneous working-transition line
23 p3297 A72-44467

Reconstruction of phase holograms by means of a helium-cadmium laser
23 p3292 A72-44469

Optically pumped gas lasers with electron transitions to molecular excited state and resonant absorption lines
24 p3408 A72-44566

GAS LIQUEFACTION

U CONDENSING

GAS LUBRICANTS

Radial gas bearing air lubrication theory, proving existence and uniqueness theorems for Reynolds equation periodic solution
07 p0998 A72-20473

Thin lubricant film angular inertia effect on externally pressurized MGD bearings load carrying capacity, solving nonlinear differential equation by Runge-Kutta method
13 p1963 A72-28747

GAS LUBRICATED BEARINGS

U GAS BEARINGS

GAS MASERS

Oscillation transient in molecular Q switched ammonia beam maser following Stark voltage pulse in resonant cavity
01 p0081 A72-11186

Ammonia beam maser with electret focuser providing semipermanent molecular separation under high vacuum for use in relaxation studies
01 p0081 A72-11187

Apparent-actual size relation in astronomical masers for internal physical conditions of homogeneous spherical and tubular OH or water maser clouds
16 p2455 A72-33456

Fluctuations in a quantum frequency standard

23 p3271 A72-43842

GAS MIXTURES

NT AIR

NT DETONABLE GAS MIXTURES

Flow momentum losses during gas mixture chemically nonequilibrium expansion in nozzle
01 p0145 A72-10487

Temperature, concentration and heat conductivity profiles of chemically reacting gas mixtures with thermal gradient, using classical transfer equations
01 p0023 A72-10489

Numerical analysis of nonequilibrium gas mixture flow through nozzle
02 p0149 A72-1589

Carbon dioxide and hydrogen mixtures in shock tube, noting rotational- and translational-vibrational energy transfer role from relaxation time measurement
02 p0203 A72-12028

Hypersonic two component gas mixture nozzle flow with condensation or evaporation discontinuity, determining Pitot pressure limits
02 p0230 A72-12255

Monatomic He-Ar binary gas mixtures heat transfer to cylinders in low Reynolds number flow, considering internal energy effects
02 p0303 A72-12358

Jupiter atmospheric hydrogen-helium mixing ratio from binary star beta Sco occultation by planet in May 1971
03 p0416 A72-13009

Combustible fuel-air mixture laminar and turbulent flame propagation mathematical model, with reference to detonation and prevention
03 p0456 A72-13876

Heat transfer from burning gas mixture flow to receiver wall, taking into account exothermal reactions due to catalytic effects
03 p0458 A72-14166

Oxygen and oxygen-nitrogen mixtures dc and hf discharges, evaluating traveling low field domains in positive column
03 p0400 A72-14350

Macroscopic integrodifferential transport equations for gas mixture with internal degrees of freedom and chemical reactions from model kinetic equation
04 p0552 A72-14633

Adenine, guanine, cytosine and other nitrogen compounds synthesis from carbon monoxide, hydrogen and ammonia mixtures by Fischer-Tropsch-like process
04 p0483 A72-14765

Velocity /viscous/ slip coefficient and diffusion slip velocity in multicomponent gas mixtures by linearized Boltzmann equation
04 p0513 A72-15334

Carbon dioxide gas dynamic laser mixture at high pressure, investigating gain and vibrational kinetics
04 p0531 A72-15336

Carbon dioxide-nitrogen-water or He mixtures expansion through supersonic nozzles, showing population inversion of vibrational energy levels
04 p0513 A72-15337

Steady normal shock wave analysis in binary inert monatomic gas mixtures using kinetic theory moment method
04 p0513 A72-15340

Slush, boiling methane and methane mixture characteristics, noting advantages as potential rocket, aircraft and motor vehicle fuels
04 p0564 A72-15542

Performance similarity of supersonic axial compressors with gas mixtures of different thermodynamic properties, verifying validity of critical Mach number of rotation
04 p0463 A72-15556

Statistical group theory of two component associated gas mixtures, noting erroneous virial coefficient
05 p0692 A72-16356

Transport processes theory in mixtures of chemically active gases using Boltzmann equation and Sonin polynomials expansion
06 p0852 A72-17989

Surface catalytic properties effect on multicomponent gas hypersonic boundary layer with simultaneous vibrational-dissociative relaxation, considering plate and blunt body laminar boundary layer
06 p0757 A72-18130

Flow parameters behind shock waves propagating in carbon dioxide-nitrogen mixtures at Mach numbers from 5 to 10
07 p0966 A72-18936

Laser action in carbon monoxide vibrational-rotational bands produced by electrical excitation of carbon monoxide-nitrogen-oxygen-helium mixtures following expansion in supersonic nozzle
07 p1001 A72-19047

Steady two dimensional laminar compressible boundary layer of reacting gas mixture with surface vaporization and fuel injection, using integral method
07 p0967 A72-19129

- Thermal conductivities of gaseous binary mixtures of methyl nitrate with helium, neon, argon and nitrogen
07 p1051 A72-19365
- Rate controlled partial thermodynamic equilibrium method for treating reacting gas mixtures, applying to freezing reactions in internal combustion engine
07 p1099 A72-19371
- Hot-wire measurement of binary gaseous mixtures in unsteady concentration fields, investigating heat loss
07 p0993 A72-20587
- Binary gas mixtures calculation for Schmidt, Prandtl and Lewis number dependence on pressure, temperature and chemical composition
07 p1101 A72-20600
- Third harmonic radiation generation in phase matched mixture of Rb vapor and Xe, observing nonlinear susceptibility
[AD-739764] 08 p1211 A72-21197
- Nonlinear vibrational relaxation equations for expanding carbon dioxide-helium-nitrogen laser gas mixture, obtaining mode temperatures and gain coefficients by Runge-Kutta technique
08 p1149 A72-21261
- Circuits for pulse rise time discrimination in proportional counters with different gas mixtures
08 p1167 A72-21511
- Time dependent progress of vibrational-rotational transitions in hydrogen-fluorine chemical laser investigated by oscillography with IKM-1 monochromator
08 p1183 A72-21715
- Carbon dioxide-air-helium molecular systems population excitation rates with current, gas composition and partial pressures dependence
08 p1183 A72-22028
- Burning velocity inhibitors effect on hydrocarbon-oxygen-nitrogen mixtures ignition by hot wires
[AD-744624] 08 p1129 A72-22039
- Instabilities development in flow field generated by shock wave propagation in exothermic gas mixture
08 p1255 A72-22042
- Burning velocity measurement techniques for methane-air mixtures
08 p1255 A72-22047
- Respiration in altered gas environment for spontaneous breathing and voluntarily maintained pulmonary ventilation level conditions
08 p1120 A72-22077
- Hypoxic and normoxic gas mixture breathing during intense muscular activity, relating oxygen consumption and carbon dioxide elimination magnitudes and motor performance
08 p1121 A72-22081
- IR emission at 2.7 microns from carbon dioxide-molecular nitrogen mixture flow, noting energy redistribution
09 p1357 A72-22854
- Visual and motion picture studies of ignition and burning characteristics of Mg particle clusters in flames of gas mixtures
09 p1411 A72-22886
- Bromine additions effect on normal laminar flame propagation velocity of methane-air mixture at high pressures
09 p1411 A72-22889
- Strong shock wave acceleration during passage through decreasing density region observed in experiments with explosions in Ar-H mixture
09 p1295 A72-22961
- Thermal conductivity measurement for gases and gas mixtures with water vapor, describing methods and results
09 p1413 A72-23689
- Emissivity calculation for radiant heat flux from isothermal gas mixture of hydrocarbon fuel combustion products
10 p1561 A72-23839
- Momentum transfer theory for ion drift velocity in multicomponent gas mixture at arbitrary electric field strengths
10 p1519 A72-24096
- Mass spectrometric analysis of positive ions in carbon dioxide laser systems with nitrogen-helium mixture
10 p1492 A72-24411
- Rb87 vapor laser with optical pumping, measuring nitrogen or nitrogen argon mixture buffer gas partial pressure effect on power output
10 p1493 A72-24911
- Electron beam fluorescence method for normal shock wave velocity distribution in Ar-He mixtures
11 p1615 A72-25556
- Heat and momentum transfer of binary gas mixture flow in parallel plate channel with mass injection from porous wall, calculating velocity, pressure and temperature distributions
11 p1746 A72-26538
- Chemical and ionizational equilibrium equations of heterogeneous gas mixture composition with allowance for condensed phase ionization
11 p1747 A72-26965
- Pressure effects on resonance fluorescence lifetimes in sulfur hexafluoride-air mixtures exposed to carbon dioxide laser radiation
12 p1826 A72-27929
- Inert gas-oxygen mixtures fire retardant properties under atmospheric and hypobaric pressures, measuring effectiveness by standard fabric burning rate
12 p1890 A72-28309
- Cardiorespiratory response to breathing dense sulfur fluoride-oxygen mixture under physical exercise conditions
12 p1767 A72-28314
- Spatially resolved gain measurements in carbon dioxide laser amplifier, considering gas mixture, flow rate, temperature, pressure and current effects
13 p1967 A72-28448
- Hydrocarbon-air mixtures reaction in incident shock waves of pressure greater than 25 atmospheres, correlating with shock tube results
13 p2063 A72-28549
- Active gas mixture pressure relationship to excitation during single to multifrequency operation transition in He-Ne laser
13 p1969 A72-29614
- Carbon dioxide power laser effects on IR spectra of HCl-ethylene and sulfur dioxide-ethylene mixtures, focusing with Ge lens
13 p1971 A72-29870
- Buffer gas mixture and pumping light effects on shifts from ground state hyperfine frequency in Rb-85 maser frequency standard
14 p2109 A72-30196
- Transport processes theory in chemically active gases mixtures using Boltzmann equation and Sonin polynomials expansion
14 p2133 A72-30216
- Diatom-monomeric molecular gas mixtures oscillation and rotation energies relaxation equations, taking into account transport and chemical reaction processes
[DFVLR-SONDDR-198] 14 p2083 A72-30327
- Gaseous species diffusion in carrier gas under various geometries and flow conditions, using finite element method
14 p2095 A72-30928
- Binary gas mixture slipping rate determination from joined solution of Hamel kinetic model linearized equations, and Navier-Stokes and Boltzmann equations
14 p2096 A72-31013
- Concentration stress convection in slow gas mixture flow due to density gradients, noting similarity to thermal stress convection
14 p2096 A72-31015
- Stationary heat conduction between stagnant binary gas mixture and two constant temperature plane parallel walls for arbitrary Knudsen numbers
15 p2334 A72-31462
- Carbon dioxide TEA high output pulsed laser, testing wide range of carbon dioxide-nitrogen-helium mixtures at various pressures
15 p2246 A72-31638
- Rising temperature reactor technique to evaluate catalysts for initiating hydrogen-oxygen reaction in gas mixtures at 78 K
15 p2193 A72-32550
- Velocity independent fast response hot-wire probe for binary gas mixtures composition measurement, describing design and operational principle based on dimensional analysis
16 p2389 A72-32829
- Binary gas mixture density correlation functions from initial value problem based on linearized Boltzmann equation for analysis of Rayleigh-Brillouin scattering
16 p2428 A72-32942
- Rayleigh-Brillouin light scattering in He-Xe gas mixtures, noting thermal fluctuations effect
16 p2422 A72-32943
- Gas mixtures separation in Kantrowitz-Grey underexpanded molecular jet background as function of rarefaction degree, using electron beam fluorescence technique for concentration measurements
16 p2429 A72-33054
- Potassium atomic beam aerodynamic acceleration by He-Ar free jet, determining beam intensity as function of nozzle-skimmer distance, carrier gas pressure and nozzle temperature
16 p2429 A72-33056
- Photographic-oscillographic study of discharges in atmospheric pressure helium-carbon dioxide mixtures, discussing discharge paths nonuniformity and energy input maximization
16 p2435 A72-33391
- Nonequilibrium steady quasi-one dimensional expanding nozzle flow of chemically reacting gas mixture, using time dependent finite difference technique
[AIAA PAPER 72-684] 16 p2480 A72-34058
- Radiative and convective heat transfer for stagnation point flow of emitting carbon dioxide and nitrogen gas mixture, assuming thermodynamic equilibrium in shock layer
17 p2636 A72-34470
- Applications of an improved formalism for the analysis of transport phenomena in gaseous mixtures and plasmas.
17 p2587 A72-34615
- Viscosity and thermal conductivity of moderately dense gas mixtures.
17 p2636 A72-34737
- High temperature oxidation of ammonia.
17 p2511 A72-34904
- Comments upon shock-initiated oxidations by nitrous oxide.
17 p2511 A72-34905
- Chemical reactions in inhomogeneous mixtures - The effect of the scale of turbulent mixing.
17 p2543 A72-35640
- Equilibrium distribution of chemical species in a reacting gas mixture
17 p2512 A72-35808
- Strong shock wave acceleration during passage through decreasing density region observed in experiments with gas discharges and Ar-H mixture explosions
17 p2544 A72-35890
- Thermionic converter I-V performance improvement via oxygen addition, examining feasibility of cesium oxide-cesium solution as source
18 p2647 A72-36204
- Blood oxygenating ability of helium- and argon-oxygen environments relative to air, using alveolar gas equation to predict arterial oxygen pressure
18 p2649 A72-36438
- Nonequilibrium transport equations for chemically reacting inhomogeneous gas mixtures, using Hermite tensor polynomials of molecular velocities
18 p2713 A72-36895
- On the role of density gradients in the continuum theory of mixtures.
18 p2712 A72-37076
- Heterogeneously combusting binary gas mixture ignition time as function of initial state and thermokinetic properties, noting heat conduction equations for fuel and oxidizer
19 p2879 A72-37358
- Intrinsically transonic /almost equal frozen and equilibrium sound velocities/ flows of chemically active gas mixture, developing nonlinear perturbation theory
19 p2745 A72-37390
- Experimental technique for oxygen negative ions destruction by associative detachment reaction with hydrogen in oxygen-hydrogen mixtures, calculating transport and ionization coefficients
19 p2836 A72-37458
- Composition of initial mixtures for production of the gaseous C-H-O fuel for fuel cells with molten alkaline carbonates.
19 p2754 A72-37778
- Relaxation of a reacting gas described by the Boltzmann kinetic equation
19 p2838 A72-38856
- Effect of concentration gradient on composition of sampled gas. II - Experimental verification.
19 p2805 A72-38870
- Experimental investigation of the detonation properties of hydrogen-oxygen and hydrogen-nitric oxide mixtures at initial pressures up to 40 atmospheres.
19 p2883 A72-38875
- Comparison of homogeneous gas-phase reaction kinetics for complete segregation and complete micromixing.
20 p2982 A72-38972
- [WSCJ PAPER 72-6] 20 p2982 A72-38972
- Ionization behind shock waves in nitrogen-oxygen mixtures.
20 p2958 A72-39601
- Shock tube boundary layers in ionized argon-helium mixtures.
20 p2914 A72-39639
- The mass spectrographic measurement of gas separation with the aid of ambipolar effusion in neon-krypton mixtures
21 p3053 A72-40486
- Active gas mixture pressure relationship to excitation during single to multifrequency operation transition in He-Ne laser
21 p3063 A72-40667
- Unsteady burning of reacting mixture of air and condensed-phase combustion products in closed variable volume, noting mathematical model for parameters calculation
21 p3128 A72-40977
- Aerodynamic structure analysis of steady flame of homogeneous gas mixtures, noting streamlines, isotherms, isobars and flame front curves
21 p3129 A72-40979
- Critical description of combustion stability in a turbulent flow of a homogeneous mixture
21 p3129 A72-40980
- Equation of state of a mixture of nonideal chemically reacting gases
22 p3152 A72-41881
- Energy exchange processes in a low temperature N2-CO transfer laser.
22 p3184 A72-41993

- Blowing of a foreign gas in a hypersonic viscous shock layer
22 p3133 A72-42265
- Kinetic equations of chemically reacting gas mixtures
22 p3152 A72-42267
- German monograph - Ionization of nitrogen-oxygen gas mixtures by shock waves.
22 p3209 A72-43073
- Application of gasdynamic flows in laser technology
22 p3187 A72-43176
- Microwave spectrum of compressed O₂-foreign gas mixtures in the 48-81 GHz region.
24 p3378 A72-44871
- Flame structure and flame reaction kinetics. VI - Structure, mechanism and properties of rich hydrogen + nitrogen + oxygen flames.
24 p3461 A72-44919
- Flame structure and flame reaction kinetics. VII - Reactions of traces of heavy water, deuterium and carbon dioxide added to rich hydrogen + nitrogen + oxygen flames.
24 p3378 A72-44920
- Shock wave velocity, combustion front and pressure measurements of unstable detonations in propane-oxygen-nitrogen mixtures, comparing with double discontinuity theory
24 p3462 A72-45030
- Supersonic combustion photochemical initiation feasibility, measuring quantum yields and induction times in hydrogen, oxygen and chlorine mixtures
24 p3464 A72-45058
- Electronic energy transfer phenomena in rare gases.
24 p3429 A72-45310
- Dissociation of carbon monoxide in the discharge of a continuous-flow CO laser
24 p3411 A72-45499
- GAS PHASES**
U VAPOR PHASES
GAS POCKETS
Dynamics of dissolution of gas bubbles or pockets in tissues.
18 p2655 A72-37027
- GAS PRESSURE**
High pressure gaseous hydrogen effect on space shuttle main engine components alloys under static loads, using surface flawed flat plate PTC samples
01 p0085 A72-10774
- Atmospheric ozone pressure variations in high altitude cyclones, anticyclones, troughs and crests at low pressure levels
02 p0207 A72-11734
- Rarefied gases pressure flow and self diffusion through cylindrical tubes, presenting kinetic model with velocity independent mean free path
02 p0205 A72-12357
- Cavity resonator thermal stabilization, using gas pressure controlled membrane
02 p0196 A72-12698
- Argon plasma electromagnetic wave transformation and absorption measurements under various gas pressures
03 p0395 A72-13571
- Ionization waves linear theory for low pressure noble gas strong current column, showing self excitation limit and temperature dependence of energy loss rate
03 p0400 A72-14351
- Small pressure difference measurement in gas flow, using transducer based on liquid electrical conductivity measurement
04 p0523 A72-15483
- Single and double channel laser triggered 1-3 MV switches design in high pressure gas, noting low jitter and built-in voltage isolation
04 p0532 A72-15532
- Plasma velocity, gas pressure, wall heat flux and shock heated region extent measured in electrical discharge shock tube, discussing ionization relaxation process
05 p0693 A72-15849
- Anisotropic plasma rotational discontinuity theory, considering parallel and perpendicular components of plasma pressure and magnetic induction
05 p0695 A72-16074
- High pressure gas lasers excitation, determining energy introduction and space charge stability
05 p0668 A72-16415
- Teflon diffusion membrane for in vivo blood and intramycocardial tissue gas tension measurement by mass spectroscopy without chemically bonded heparin surface
08 p1124 A72-20901
- Rotating stellar system with stars and interstellar gas within magnetic field, discussing gravitational and magnetic effects on gas pressure
09 p1384 A72-22511
- Ionization equilibrium description by quantum statistical fugacity expansion of pressure for partially ionized plasmas
10 p1524 A72-24929
- Normal ionizing shock waves characteristics in He under varying conditions of magnetic field strength, discharge current and gas pressure
11 p1694 A72-25789
- Resistance wires and wire thermocouple junctions temperature response in low pressure gases, taking into account wire mounting temperature effect
11 p1632 A72-26000
- Hot wire cell measurement of specific heat in low pressure gases, determining thermal conductivity and accommodation coefficient
11 p1634 A72-26367
- High pressure injector optimum design and performance for gas jet boosters, using one dimensional theory with friction allowance
12 p1861 A72-27535
- Gaseous buffering for oxygen fugacity control in high temperature gas systems at one atmosphere
12 p1778 A72-28104
- Analog simulation of direct acting gas pressure regulators in terms of spring, flow and friction forces
13 p1956 A72-28703
- Thin lubricant film angular inertia effect on externally pressurized MGD bearings load carrying capacity, solving nonlinear differential equation by Runge-Kutta method
13 p1963 A72-28747
- Nonuniform gas pressure distribution near circular multiple inlet of inherently compensated thrust bearing, considering inward-outward radial flow resistance differential
13 p1963 A72-28748
- Active gas mixture pressure relationship to excitation during single to multifrequency operation transition in He-Ne laser
13 p1969 A72-29614
- Analytical prediction of pressure-time relationship during evacuation of multilayer insulation thermal protection systems, taking into account outgassing effects
14 p2172 A72-30925
- Plasma velocity, gas pressure, wall heat flux and shock heated region length measured in electrical discharge shock tube without diaphragms, discussing ionization relaxation process
15 p2283 A72-31268
- Entropy waves effect on gas pressure oscillations during powder combustion in semiclosed volume, noting resonant frequencies equation
16 p2475 A72-33096
- Pressure measuring instruments design, considering fluid, piston, spring, electrical and ultrasonic manometers
16 p2391 A72-33240
- High precision electrostatic feedback transducer for very low differential pressure measurement in gas media, suggesting low pressure standard role [RAE-TR-71022]
16 p2394 A72-33638
- Transversely excited high pressure carbon dioxide laser cavity dumping with reproducible time delay between current excitation and gain-switched laser pulses
16 p2403 A72-33844
- Measuring instruments for gas pressure determination in vacuum systems, noting application of thermal conductivity or ionization characteristics of gas molecules
18 p2692 A72-36835
- Pressure rise during combustion in semiclosed volume with reduced gas flow cross section in condensed system channel
19 p2879 A72-37354
- Pressure propagation rate relation to local sound speed in unsteady anisotropic gas flow with particle-varying specific entropy
19 p2788 A72-38564
- Gas breakdown in the laser as the limitation of pulsed high-pressure CO₂ lasers.
20 p2934 A72-39565
- Active gas mixture pressure relationship to excitation during single to multifrequency operation transition in He-Ne laser
21 p3063 A72-40667
- Molecular abundances and gas-to-electron pressure ratios as function of temperatures and pressures in solar composition gaseous mixture of late type stellar atmospheres
21 p3110 A72-41446
- Throttle characteristics and mixing chamber geometry effects on low pressure gas ejector operation, noting air flow and pressure rates in air ejectors
22 p3133 A72-41859
- Determination of the mechanical properties of steels by short-time rupture in hydrogen at high temperatures and pressures
22 p3195 A72-43160
- Steady-state lasing spectrum of a CO₂ laser at reduced working-mixture pressures
23 p295 A72-43681
- Digitally pressure-scanned Fabry-Perot interferometer for studying weak spectral lines.
23 p289 A72-43891
- Temperature of a free plasma filament in a high-frequency field at high pressures
23 p3322 A72-44464
- Effect of capacitance on gain in a transversely pulsed CO₂ discharge.
23 p3298 A72-44534
- Pressure, temperature, current density, and potential difference fluctuations in subsonic flow of combustion products plasma, noting steadiness, ergodicity and distribution functions
24 p3429 A72-45502
- GAS REACTORS**
Fission and fusion propulsion for deep space missions, discussing gas and colloid core reactors, controlled fusion, MHD and laser plasma systems
24 p3423 A72-45168
- GAS SPECTROSCOPY**
Trace gas pollutant monitoring by microwave rotational absorption spectroscopy, discussing test results with Gunn diode cavity spectrometer
01 p0023 A72-10524
- Raman scattering cross sections and depolarization ratios of atmospheric gaseous pollutants as function of incident photon energy
01 p0104 A72-10543
- Spontaneous emission from driven Doppler broadened gas of two level atoms radiating into free space, predicting power spectrum
07 p0940 A72-19194
- High resolution Raman spectroscopy of low pressure gases, using single mode Ar laser
09 p1323 A72-22613
- Excitation accompanying photoionization in atoms and molecules and relationship to electron correlation observed from rare gases inner and valence shell satellite lines measurements
09 p1356 A72-22835
- Vibrational laser Raman scattering from flame gases for nitrogen, oxygen and water vapor
09 p1276 A72-22978
- Raman band rotational structure computer simulation, noting application to gaseous chlorine spectrum analysis
09 p1358 A72-23050
- Tunable dye laser system with narrow band filter for Raman spectroscopy of gases
09 p1326 A72-23351
- Beam-foil-gas spectroscopy and relative cross section measurements for studying steady state nonequilibrium processes
10 p1434 A72-24325
- High temperature gaseous disperse flow radiation spectra photoelectric recording by DFS-8 spectrograph
12 p1812 A72-28116
- Ion-molecule collision frequencies in gases by phase coherent pulsed ion cyclotron resonance spectrometry [ONERA, TP NO. 1071]
14 p2133 A72-30524
- Electrons angular distribution effect on photoionization branching ratio measurement by photoelectron spectroscopy
17 p2552 A72-34288
- Fringe shift and slope analysis of interferometric spectrogram formed by NO-gamma system spectral band
17 p2586 A72-35833
- Spectroscopic determination of the rotational temperature in a rarefied supersonic flow in glowing-discharge excited nitrogen.
17 p2544 A72-35928
- A simple combination mass spectrometer inlet and oxygen electrode chamber for sampling gases dissolved in liquids.
19 p2762 A72-38146
- Lunar volcanic gas release rate estimation from orbiting Apollo spacecraft-borne mass spectrometer detection, noting atmospheric perturbation
19 p2868 A72-38736
- Laser-source spectroscopy. II - Experimental study of line broadening for the 00 1-1/10 0, 02 0/ transition of CO₂ disturbed by N₂: Application of the theory of Anderson, Tsao, and Cornutte to the calculation of pure and N₂-disturbed CO₂ linewidths
23 p3298 A72-44535
- On the use of a Fabry-Perot interferometer for the study of Raman spectra of gases under high resolution.
24 p3426 A72-44904
- Some infrared diagnostic techniques in high temperature gasdynamics.
24 p3402 A72-45043
- GAS STREAMS**
Hot corrosion of thorium dispersed nickel and thorium dispersed Ni-Cr alloy in high velocity gas stream of jet fuel combustion products
07 p1010 A72-18753
- Body drag measurement in low density supersonic gas stream in various Knudsen number ranges
08 p1166 A72-21409
- Local emission coefficients fields for ionized gas in arbitrary and rectangular cross section streams
13 p2008 A72-29894
- Uniform rotation and magnetic field effects on gravitational stability of interface between two semi-infinite homogeneous streams
15 p2284 A72-31593
- Satellite instrument to observe atmospheric composition by energy analysis of incoming gas stream, using velocity mass spectrometer for neutral particles measurement
15 p2236 A72-31966
- Atomization of liquid droplets in a convective gas stream.
17 p2540 A72-35044

Gas ejections in NGC 4486 and activity problems of galactic nuclei 19 p2862 A72-38051

Photometric elements of corpuscular unstable AH Vir eclipsing binary at 4400 and 5600 Å, comparing stellar gas stream and solar chromosphere densities 23 p3338 A72-44028

GAS TEMPERATURE

Shock tube gas temperature measuring equipment using spectrum line reversal method 01 p0072 A72-11217

Temperature dependent gas internal diatomic laminar heat transfer, investigating continuity, energy, momentum for two dimensional flow between heated parallel plates [ASME PAPER 71-HT-N] 02 p0302 A72-12317

Approximate solution in gas kinetic theory, considering temperature jump, velocity and viscous slip problems 02 p0205 A72-12356

Aeros satellite mass spectrometer, retarding potential analyzer and neutral gas thermograph onboard experiments, noting measurements and data transmission triggering by flight direction sensor [DGLR PAPER 71-093] 02 p0284 A72-12727

Second virial coefficient, temperature derivatives and additive components for /12-7/ potential of charged particle interaction in gas 05 p0692 A72-15841

Radial heat propagation in cylindrical rarefied gas column from impulsive axial line source input, obtaining perturbed gas temperature by summation procedure [ASME PAPER 71-WA/HT-7] 05 p0743 A72-15867

Mean and fluctuating temperature dependence of gas discharging from orifice to atmosphere on pressure vessel wall heat transfer [ASME PAPER 71-WA/HT-32] 05 p0745 A72-15884

Macroscopic boundary conditions of gas-solid interface interaction as function of gas temperature and transport coefficients variation in shock reflection problems 06 p0902 A72-18107

Gas kinetic cooling by absorption of carbon dioxide laser radiation, explaining by vibrational energy transfer and relaxation rates 07 p1000 A72-19046

Gas temperature variation effects on powder burning stability in rocket combustion chamber from unsteady powder burning theory 08 p1255 A72-21659

Steady state and temperature relaxation of rarefied gas between two plane parallel plates 08 p1211 A72-21871

Thirteen moment closed system of approximate integral equations for rarefied gases density, velocity, temperature, stress tensor and thermal flux vector 09 p1259 A72-22425

Two spool gas turbine engine characteristics with speed reduction, determining time dependence of turbocompressor rpm, gas temperature and engine power 09 p1374 A72-23185

Chemical lasers diatomic and multiatomic molecules dissociation in nonequilibrium conditions, discussing vibrational energy exceeding gas temperature 11 p1646 A72-25713

Resistance wires and wire thermocouple junctions temperature response in low pressure gases, taking into account wire mounting temperature effect 11 p1632 A72-26000

Turbine inlet gas temperature limiting systems design and operation in turboprop engines, describing blocking mechanism, delaying element and altitude compensation 12 p1861 A72-27863

Aromatic hydrocarbons and fuels, investigating engine parameters effects on combustion and exhaust gases temperatures 13 p2025 A72-29074

Time constant of aircraft gas turbine engines gas temperature regulating system, using two thermocouples with different rise times 13 p2028 A72-29138

Combustion products thermodynamic parameters for natural gas burning in oxygen atmosphere, plotting gas temperature and flow rates against pressure and excess oxidant ratio 13 p2065 A72-29451

Temperature-slip problem in rarefied gases, obtaining exact solution by generalized BGK scattering model and Wiener Hopf technique 14 p2095 A72-30882

Second virial coefficient, temperature derivatives and additive components for /12-7/ potential of charged particle interaction in gas 15 p2280 A72-31260

Gas temperature from Raman rotational line intensities generated by lidar techniques applied to inelastic Raman scattering 15 p2232 A72-31373

Rotatory gas temperature determination in carbon dioxide laser discharge plasma, plotting dependence on discharge current 15 p2245 A72-31419

Critical analysis of Senftleben modified hot-wire method for gas heat conductivity measurement 16 p2479 A72-33861

H-He ions solar wind expansion absence for case of equal gas temperature, noting mass flux relationship to He ion temperature 16 p2449 A72-33911

Measurement of the error of temperature sensors in flowing gases. 17 p2555 A72-35247

Inert and reactive gas injection in near wake behind blunt bodies in supersonic flow, considering influence on base pressure and temperature 17 p2487 A72-35930

Turbine engine sensors for high temperature applications. 19 p2802 A72-38048

Low energy cosmic particle and soft X ray photon produced nonthermal electrons effect on interstellar gas ionization and thermal energy equilibrium 19 p2867 A72-38508

An experimental study in the application of the Raman scattering technique as a remote sensor of gas temperature and number density in hypersonic CF4 flow. [AIAA PAPER 72-1018] 21 p3057 A72-41597

Nitrogen temperature determination in arc tunnel air flows. [AIAA PAPER 72-1022] 21 p3042 A72-41600

Experimental determination of the vibrational temperature of a supersonic gas flow 22 p3242 A72-41879

Nonstationary method for measuring the heat conductivity of liquids and gases under high pressures 22 p3243 A72-41886

Determination of the mechanical properties of steels by short-time rupture in hydrogen at high temperatures and pressures 22 p3195 A72-43160

Temperature freezing in spherical or cylindrical expansion into a vacuum. 23 p3357 A72-44498

Some features of the behavior of an intense light beam in a nonideal gas. 24 p3411 A72-45609

GAS TRANSPORT

Pulmonary functional inhomogeneities effects on steady state oxygen and CO diffusing capacity estimates in gas transfer resistances terms 01 p0014 A72-10847

Transport coefficients of relativistic gas by method of moments, assuming constant differential cross section of particle interactions in center of mass system 04 p0547 A72-14630

Nearly free molecular slit flow of gas from reservoir at finite pressure and temperature ratios 04 p0512 A72-15120

Kinetic theory and nonequilibrium distribution functions of reacting gases with simultaneous reactions 07 p1035 A72-20114

High mass transfer rate effect of foreign gas on transport coefficients in fully developed turbulent flow [AIAA PAPER 72-293] 11 p1614 A72-25231

Low voltage transversely excited gas transport CW carbon dioxide laser, discussing construction and power output, gain and efficiency 11 p1646 A72-25304

Non-Maxwellian collisionless transport properties of neutral gas constituents in planetary exospheres, discussing ballistic particle and heat transport and escape fluxes 11 p1716 A72-25846

Pulmonary oxygen transport dynamic model representing lung gas-side airway and alveolar regions and blood-side capillary bed 13 p1909 A72-28996

Laser coupling through nonlinear gas filled absorber cell, discussing molecules mean free path 15 p2246 A72-31883

Perturbation method in inelastic interaction model for transport processes in reacting gases described by Boltzmann kinetic equation 18 p2713 A72-36807

GAS TUBES

High temperature deuterium plasma production by laser heating of gas filled cylindrical tube, optimizing pulse duration and configuration 12 p1849 A72-27059

Gain and line width in stimulated Brillouin scattering in gases. 24 p3412 A72-45616

GAS TUNGSTEN ARC WELDING

Refractory alloy weldability and brazing, discussing manual and automatic tungsten arc and electron beam processes and fillers 01 p0075 A72-10752

Dye penetrant surface defect indications on 2014-T6 Al gas metal arc weldments heat affected zone, considering minimization by arc stabilization and caustic etch time reduction 02 p0236 A72-12775

Al content caused defect in gas tungsten arc welded Hastelloy, using electron microprobe analysis 06 p0820 A72-17708

Electrode vertex angle effect on fused weld bead geometry related to plate thickness in tungsten inert gas /TIG/ welding 09 p1320 A72-23634

Pulse shaping, arc plasma jets and torch movement indexing for high precision pulsed tungsten inert gas /TIG/ welding 09 p1321 A72-23635

Nucleation mechanism for weld solidification in electron beam and tungsten-inert gas welding processes 09 p1332 A72-23641

A preliminary investigation of joining methods for aluminum-graphite composites. 17 p2561 A72-35665

GAS TURBINE ENGINES

NT JET ENGINES

NT PULSEJET ENGINES

NT RAMJET ENGINES

NT SUPERSONIC COMBUSTION RAMJET ENGINES

NT TURBOFAN ENGINES

NT TURBOJET ENGINES

NT TURBOPROP ENGINES

Gas turbine nozzles aerodynamic throat area air flow measurement, describing accuracy, standards, reference nozzles and mounting flanges [SAE ARP 1195] 01 p0065 A72-10390

Thermal shock fatigue tests on aircraft gas turbine engine inlet nozzles, showing cracks as function of material 01 p0143 A72-11373

Aircraft gas turbine rotating disks thermal and mechanical stresses under variable thermal conditions, describing test assembly 02 p0199 A72-11637

PT6 and JT15D gas turbine aircraft engines development and service experience 02 p0271 A72-11699

Differential nonstationary heat equations numerical solution for bladed gas turbine air cooled disk, taking into account cascade vertical temperature variation and coolant heating 02 p0301 A72-12251

Soviet book on gas turbine engines control systems design based on similarity theory, determining optimal controller formula from engine parameters 02 p0271 A72-12543

USAF small gas turbine test complex, discussing machinery, equipment, simulated testing, altitude chambers and instrumentation [ASME PAPER 71-WA/GT-7] 05 p0642 A72-15900

Aircraft gas turbine engine emission reduction, showing nitrogen oxide control with water injection [ASME PAPER 71-WA/GT-9] 05 p0704 A72-15902

Soot oxidation rate from diffusion flame measurements extrapolated for gas turbine combustion chambers 05 p0747 A72-16368

Fuel vaporizer for gas turbine engine, investigating heat transfer coefficient 05 p0747 A72-16492

Aircraft gas turbine engine and components post-war development in Japan 05 p0705 A72-16499

Gas turbine blade temperature measurement by radiation pyrometer, discussing thermal radiation sensing and fiber optics transmission, signal processing and real time temperature characteristic display [SAE PAPER 720159] 06 p0812 A72-17321

Turbine inlet temperature sensor for gas turbine engines, using noble metal thermoelements with high signal level [SAE PAPER 720160] 06 p0812 A72-17322

Lubrication system filtration effects on rolling element bearing life and extended mean time to failure of gas turbine engines 07 p1052 A72-18754

Gas turbine engine inlet solid particle separator designed as integral engine part, discussing semireverse flow superiority 07 p1052 A72-18755

Aircraft gas turbine engine monitoring for failure prevention, evaluating condition through spectrum analysis and real time correlation techniques 07 p1053 A72-18766

Aircraft gas turbine engines smoke emission sampling by stained filter technique, comparing Navy specifications AS 1833 with SAE method ARP 1179 07 p1053 A72-18770

Army aircraft gas turbine engines pollution potential evaluation program, considering smoke emission, noise and invisible pollutants 07 p1053 A72-18772

National Environmental Policy Act /PL 91-190/ impact on Army aircraft turbine engine development in terms of performance, additional cost and time 07 p1053 A72-18773

Influence coefficients method accuracy for design and adjustment of gas turbines, engines and parts 07 p1054 A72-18998

Diffusion welding of cast and wrought Udimet 700 superalloy gas turbine engine components, discussing interfacial grain boundary migration and microstructural homogeneity effects on weld joint quality
07 p0997 A72-19998

High turbine entry temperature effects on gas turbine engine specific power and fuel consumption, noting thrust/weight ratio increase in turbojet and turbofan engines
07 p1055 A72-20311

Squeeze-film bearings nonlinear vibration performance in aircraft gas turbine engines, emphasizing lubricant viscosity importance
07 p0999 A72-20532

Soviet civil gas turbine engines construction and performance, noting relatively high specific fuel consumption
08 p1223 A72-21275

Optimal control of two shaft gas turbine engine in helicopter, using cybernetic equipment
09 p1374 A72-22862

Two spool gas turbine engine characteristics with speed reduction, determining time dependence of turbocompressor rpm, gas temperature and engine power
09 p1374 A72-23185

Aerodynamic efficiency of plane slotted blade cascades of adjustable nozzle diaphragms in transport aircraft axial flow gas turbine engines
09 p1374 A72-23186

Intercomponent complex annular ducts design for gas turbine engines
10 p1416 A72-23872

Hydrothermodynamic foundations of hydrofoil engines employing gas-water mixtures and gas turbine generators, analyzing thrust coefficient and power efficiency
10 p1528 A72-25128

Low conductivity insulating coating/graded thermal barrier/ to cool gas turbine engine with high pressure ratio and inlet temperature
[AIAA PAPER 72-361] 11 p1669 A72-25389

Gas turbine engine icing, discussing atmospheric conditions, damage due to ice ingestion and anticice systems
[ASME PAPER 72-GT-6] 11 p1703 A72-25609

Recrystallized silicon carbide and reaction bonded silicon nitride as construction materials for gas turbine engine components, describing thermal and mechanical properties
[ASME PAPER 72-GT-20] 11 p1673 A72-25619

Liquid metal regenerator design and test evaluation for gas turbine engine fuel consumption improvement
[ASME PAPER 72-GT-33] 11 p1704 A72-25629

Air lubricated bearings for high performance aircraft gas turbines, studying design and performance in turboshaft engine
[ASME PAPER 72-GT-38] 11 p1638 A72-25632

Metal forming techniques for gas turbine engines, considering isothermal, radial and powder metallurgy preform forgings, contoured cross and form rolling, and squeeze casting
[ASME PAPER 72-GT-58] 11 p1638 A72-25649

Gas turbine engines emission data correlation based on combustor theoretical model, proposing correction factors for data reduction to standard test conditions
[ASME PAPER 72-GT-60] 11 p1704 A72-25651

Solid state joining in gas turbine engines, discussing diffusion bonding, friction welding and coextrusion metal bonding
[ASME PAPER 72-GT-74] 11 p1639 A72-25656

Aircraft gas turbine engines exhaust emission characteristics identification, considering ambient temperature and humidity effects
[ASME PAPER 72-GT-75] 11 p1705 A72-25657

Hot corrosion effects on Inconel-700 and Inconel-X gas turbine rotor blades during burning of high sulfur concentration residual oil fuels
[ASME PAPER 72-GT-87] 11 p1656 A72-25662

High pressure annular combustor with continuous analytical and sampling system for simulated gas turbine engines emission measurements
[ASME PAPER 72-GT-88] 11 p1705 A72-25663

Constraining U-shaped frames for blade edges protection during hydrojet shot blasting of compressor blades for gas turbine engines
11 p1642 A72-26819

Exhaust composition and smoke emission reduction from aircraft with gas turbine power plants
12 p1860 A72-27270

Composite materials application to gas turbine fan guide vane fabrication, noting economic factors and prototypes performance in engine tests
12 p1815 A72-28100

Heat generation sources in high speed cylindrical roller bearings for gas turbine oil cooler design
12 p1816 A72-28111

Turbulent intensity induced by wakes near secondary air jet inlet to gas turbine engine flame tube
12 p1861 A72-28131

Gas turbine engine combustion chamber, investigating swirl vane air flow rate effects on circumferential nonuniformity of gas temperature field at outlet
12 p1861 A72-28132

Gas turbine units with constant pressure cycle, discussing design and optimization method
12 p1862 A72-28149

Film cooling effectiveness for air-gas flow section of gas turbine engine under actual operating conditions
12 p1890 A72-28170

Gas turbine engine hot part equivalent tests duration determination by analytical method based on Larson-Miller parametric description of stress rupture strength
12 p1887 A72-28243

Gas turbine engine compressor blade and materials fatigue strength dependence on pressure under contact friction corrosion
12 p1831 A72-28244

Air dust erosive damage to helicopter gas turbine engine parts, discussing inertial rotorless filtering systems
13 p2026 A72-28786

Time constant of aircraft gas turbine engines gas temperature regulating system, using two thermocouples with different rise times
13 p2028 A72-29138

Mathematical model for gas turbine engine inlet noise caused by shock wave impingement, noting dynamic wave system with overpressure and distortion
13 p2028 A72-29576

Radiographic measurement of gas turbine components during response to thrust changes, using linear accelerator for X ray generation
14 p2092 A72-30620

RB 211 three-shaft turbofan engine for L-1011 airliner, describing design for noise reduction
15 p2298 A72-32428

Aircraft gas turbine engine Ni base alloy disks and shafts thermomechanical treatment, considering yield strength and high and low cycle fatigue resistance
16 p2406 A72-33299

Jet aircraft gas turbine engine technology impact on safety, reliability, airline profitability and international trade
16 p2443 A72-33315

A study of film-cooling effectiveness of some gas-turbine stator surfaces.
17 p2597 A72-34468

The starting of turbine engines in helicopters.
[AHS PREPRINT 662] 17 p2597 A72-34509

Lynx helicopter RS 360 turboshaft engine, describing modular design for maintainability
17 p2597 A72-34927

Developments in vacuum braze coating of aero-engine nozzle guide vanes.
17 p2559 A72-34937

Pressurized air assisted gas turbine fuel system, describing single stage centrifugal turbocompressor and rotary-lobe compressor designs and performance characteristics
18 p2694 A72-36043

Servo pump nozzle area controls for gas turbines.
18 p2694 A72-36048

Aircraft gas turbine engine fuel pump design, discussing sizing for given mass flow and pressure requirements with procedure for temperature rise calculations
18 p2694 A72-36049

Combined centrifugal oil filter, pump and deaerator for gas turbine engine lubrication systems, noting heat transfer effectiveness increase
18 p2694 A72-36050

Performance of low pressure ratio ejectors for engine nacelle cooling.
[SAE AIR 1191] 18 p2721 A72-36530

Turbine engine sensors for high temperature applications.
19 p2802 A72-38048

Calculation of the tightness of threshold joints of gas turbine engine rotor bearings
20 p2979 A72-39589

Influence of the structural format on the range of critical rotational speeds of rotors in aircraft engines
20 p2963 A72-39801

Steady combustion limits in afterburner gas turbine engine chambers
20 p2987 A72-39922

Erosion effects on gas turbine engine compressor blades due to dust ingestion, discussing means for alleviating performance and service life losses
[ICAS PAPER 72-02] 21 p3099 A72-41127

Elements of the theory of gas-turbine-unit designs
21 p3100 A72-41700

Digital computer controlled testing equipment for separately driven coaxial gas turbine low and high pressure compressors, emphasizing reliability and flexibility in system design
22 p3157 A72-42682

Gas turbine engine performance measurement via parameters averaging method, noting integration time determination for given error limits
23 p3325 A72-43669

Basic dimensionless geometrical relations for the combustion chambers of aircraft gas turbine engines
23 p3325 A72-43674

Gas turbine blades of cast ZhS6K heat resistant alloy, investigating structural strength from fatigue test data
23 p3347 A72-43734

Gas turbine blade models of heat resistant ZhS6K alloy under operational temperature variations, observing fatigue strength
23 p3347 A72-43735

Failure and crack formation in gas turbine engine compressor disks under variable stresses from fatigue tests, considering safety factors
23 p3347 A72-43736

Developing a synthetic turbine oil.
23 p3306 A72-43810

Contribution to the determination of the characteristics of a gas turbine engine for a helicopter and to the choice of the throttling law
23 p3326 A72-44277

Optimal control of the speed of a two-shaft helicopter turbine
23 p3326 A72-44278

Use of modeling and simulation methods in the design of gas turbine engine control systems
23 p3326 A72-44283

Aircraft gas turbine engine controllers and fuel pump testing under extreme fuel temperatures, noting cavitation characteristics
23 p3327 A72-44287

Synthesis of the control systems of a two-shaft helicopter gas turbine engine
23 p3327 A72-44289

Determination of the operational transfer functions of a gas turbine engine on a digital computer
23 p3327 A72-44292

Analog model of gas turbine engine control systems, using statistical estimates and flow rate, heat conduction and dynamic equations
23 p3327 A72-44293

Nonlinear digital modeling of gas turbine propulsion units
23 p3327 A72-44294

Aircraft gas turbine engines environmental effects, considering thermal radiation, acoustic emissions and exhaust gases in relation to propulsion system design parameters
23 p3328 A72-44296

GAS TURBINES

Gas turbine rotor disk and blade vibrations piezoelectric measurement, describing capacitive transmitter system devoid of rotor mounted power supplies
[DGLR PAPER 71-113] 02 p0232 A72-12735

Vortex flow structure in axial gas turbines near inlet and outlet of blade row
03 p0307 A72-13538

Soviet book on thermal and gas dynamic design of gas turbines in aircraft and liquid propellant rocket engines, covering three dimensional flows, temperature distribution, component cooling, etc
04 p0565 A72-15246

Gas turbine procurement standard rating and performance indicators, noting dependence on ambient conditions
[ASME PAPER 71-WA/GT-1] 05 p0703 A72-15894

Proposed ASME procurement standards for gas turbines and generators, with compilation and definitions of specification terms
[ASME PAPER 71-WA/GT-2] 05 p0703 A72-15895

Proposed gas turbine procurement standards for gaseous and liquid fuel specifications emphasizing fuel contaminants
[ASME PAPER 71-WA/GT-3] 05 p0703 A72-15896

Proposed gas turbine procurement standards for shipment and installation preparation
[ASME PAPER 71-WA/GT-4] 05 p0703 A72-15897

Gas turbine combustors performance model, using reaction rate equation from elementary mass balance equation
[ASME PAPER 71-WA/GT-5] 05 p0704 A72-15898

Environmental effects on superalloy high temperature corrosion in gas turbines, noting blade surface temperature as critical factor
[ASME PAPER 71-WA/CD-1] 05 p0704 A72-15945

Gas turbine wheel design analysis, presenting procedures for estimating revolution rates, blade numbers and component configurations effects on wheel weight for prescribed stresses
05 p0735 A72-15995

Gas turbines - Conference, Tokyo, October 1971
05 p0601 A72-16480

Transonic compressor design for minimum number of stages and hub/tip ratio and maximum inlet axial velocity, assuming axisymmetric flow
05 p0601 A72-16482

Radial inflow gas turbine rotating blades aerodynamic characteristics, noting exducer shape effect on turbine performance
05 p0601 A72-16484

High intensity combustion chamber design for gas turbine of jet engine, considering primary, secondary and dilution zones
05 p0705 A72-16491

Air stream from air entry holes of aeronautical gas turbine combustor, investigating jets maximum penetration, flow path, and mixing
05 p0705 A72-16493

Heat and corrosion resisting alloys development for gas turbine combustion liner, presenting microstructure of specimens after thermal shock test
05 p0675 A72-16494

INCO 713C and IN 100 cast Ni base alloy gas turbine blades under thermal fatigue tests
05 p0675 A72-16497

Bleed air type gas turbine compressor development, presenting reliability improvement program
05 p0705 A72-16500

Heat transfer rate prediction in cooling system design for gas turbines
[AIAA PAPER 72-10] 05 p0707 A72-16865

Film and convection cooling interaction and effect on wall cooling efficiency for gas turbine applications
[AIAA PAPER 72-8] 05 p0748 A72-16873

Gas turbine blade cooling channel hydraulic resistance calculation based on energy and continuity equations
05 p0707 A72-17061

Multistage gas turbine flow area dimension change influence coefficient calculation from discrete non-linear mathematical model through equation linearization
05 p0708 A72-17065

Fluidic sensors for temperature measurement at gas turbine inlet, noting long life and fast dynamic response
[SAE PAPER 7201-58] 06 p0811 A72-17320

Gas turbine superalloys high temperature oxidation resistance by fiber strengthening, rare earth alloying, precipitation hardening and intermetallic compounds
06 p0828 A72-17611

Algorithm for gas turbine labyrinth seals design, presenting flow chart for seal leakage analysis
[ASME PAPER 72-LUB-C] 06 p0821 A72-17803

Gas turbine blades fatigue crack development and failure analysis under thermal cycling tests, considering chemical processes and thermal and mechanical stresses
06 p0898 A72-18550

Stress and temperature fields in cooled gas turbine blades with allowance for elasticity, plasticity and creep
06 p0899 A72-18628

Gas turbine blades dynamics characteristics determination, investigating vibrational stresses, thermal cycles, alloy physicomechanical properties and coatings effects
06 p0900 A72-18683

Linear multivariable system design based on relationship between performance index parameters and optimal response in frequency domain, exemplifying gas turbine feedback controller design
07 p0961 A72-19710

Closed type gas turbines heated with nuclear energy, calculating heat transmitter dynamic behavior with computer program
07 p1055 A72-20598

Soviet papers on heat transfer in gas turbines covering heat conduction and boundary conditions for rotors and blades
08 p1222 A72-20943

Boundary conditions in steady and unsteady heat conduction for gas turbine rotors, using blade-disk temperature relation
08 p1222 A72-20944

Gas flow analysis of heat transfer coefficient in turbine blade cascades of active and reactive profiles
08 p1222 A72-20946

Dimensionless functions for heat transfer coefficients on blade cascade rotor surfaces of axial flow gas turbine for arbitrary ambient air temperature
08 p1223 A72-20947

Steady heat conduction of cooled gas turbine hollow nozzle blades with gas temperature variation along cascade
08 p1223 A72-20948

Steady heat conduction solution for gas turbine shrouded blade and disk of hyperbolic profile with central hole
08 p1223 A72-20949

Numerical integration of unsteady heat conduction equations for gas turbine rotor with shrouded blades, using grid method
08 p1223 A72-20950

Profile thickness effect on air cooling of gas turbine disks in central and peripheral sections
08 p1223 A72-20952

Temperature measurements of axial gas turbine rotor for start-up heating and cooling tests
08 p1223 A72-20953

Gas turbine nozzle guide vane trailing edge protection by air films cooling, measuring gas temperatures with chromel-alumel thermocouples
08 p1224 A72-21318

Vibration of reciprocating engine crankshafts and steam turbine, alternator and gas turbine rotor shafts supported on hydrodynamic sleeve bearings
08 p1225 A72-22133

Ceramic fiber reinforced Ni base alloy for gas turbine blades, improving creep resistance at high temperatures
09 p1335 A72-22396

Heat transfer research review, discussing gas turbines, aeronautics, astronautics, nuclear power, thermal pollution and controlled fusion challenges
09 p1412 A72-23684

Parabolic boundary layer finite difference model for predicting film cooling and heat transfer near flush injection slots in gas turbine combustors
[AIAA PAPER 72-291] 11 p1614 A72-25229

Heat transfer rates of impingement cooling in gas turbine airfoils, noting leading edge sharpness effects for slot and circular jet configurations
[ASME PAPER 72-GT-7] 11 p1703 A72-25610

Carbohydrate based gelling agent for gas turbine fuel, describing development and chemical and physical properties
[ASME PAPER 72-GT-9] 11 p1702 A72-25612

Hot pressed silicon nitride with high strength and good oxidation and thermal shock resistance for gas turbine applications
[ASME PAPER 72-GT-19] 11 p1673 A72-25618

Nitrogen oxide emission control in gas turbine combustion by lowering flame temperature
[ASME PAPER 72-GT-22] 11 p1744 A72-25620

Gas turbine recuperator technology, discussing use of compact efficient heat transfer surfaces developed for aerospace heat exchangers
[ASME PAPER 72-GT-32] 11 p1703 A72-25628

Four stage gas turbine, measuring blade surface roughness and profile changes effects on flow characteristics and efficiency
[ASME PAPER 72-GT-34] 11 p1704 A72-25630

Dense silicon nitride and carbide ceramics for gas turbines, discussing critical properties for thermal stress calculation
[ASME PAPER 72-GT-56] 11 p1674 A72-25647

Local heat transfer coefficient distribution in multiple air jet cooled cavity, noting application to gas turbine blade leading edge cooling
[ASME PAPER 72-GT-59] 11 p1745 A72-25650

Mathematical model of combustion region of steam boilers or gas turbines based on turbulent flow and transport equations
11 p1747 A72-26592

Computerized numerical model of mixed subsonic and supersonic gas flow with sonic transition in turbine curvilinear channel
11 p1574 A72-26967

Mathematical model of gas turbine parameters scatter and geometrical fabrication tolerances of flow through section
11 p1712 A72-26974

Gas side, coolant side and interstitial heat transfer in gas turbines transpiration air cooling
12 p1860 A72-27350

Computer program for gas turbine characteristics and influence coefficients calculation, allowing for cascade loss distribution during flow choking
12 p1862 A72-28151

Russian papers on cooled high temperature gas turbines covering engine theory and design, power plants development, heat transfer and air cooling systems
13 p2029 A72-29925

Linear mathematical model for twin shaft gas turbine with isolated turbocompressor, calculating dynamic constants as function of operational modes
14 p2146 A72-30581

Formation mechanism of sodium sulfate from gas turbine fuel combustion, discussing thermodynamic equilibria and reaction kinetics
15 p2297 A72-31294

Dispersion hardening Ni base alloys for gas turbine blades, considering composition, structure, gamma phase and embrittlement avoidance
15 p2255 A72-31568

Mechanical properties of high temperature steels and alloys for gas turbine rotors, disks and blades
15 p2256 A72-31703

Gas turbine pumps; Proceedings of the Joint Conference, San Francisco, Calif., March 26, 27, 1972.
18 p2693 A72-36040

Liquid or solid propellant hot gas turbines as power source for hydraulic and electrical energy
18 p2648 A72-36558

Russian book - Optimization of thermal circuits of complex gas-turbine power plants
19 p2848 A72-37450

Ceramic coatings measure the complex stresses in gas-turbine blades.
19 p2875 A72-37732

Interaction between vanadium in gas turbine fuels and sulfidation attack.
19 p2817 A72-37766

Temperature field of a gas turbine rotor blade externally cooled by an air-liquid mixture
19 p2849 A72-38043

Heat transfer in a channel with a porous wall for turbine cooling application.
[ASME PAPER 72-HT-39] 20 p2986 A72-39667

Formulation of boundary conditions in the statement of thermal problems for bladed rotors of gas turbines
20 p2987 A72-39926

Dimensionless pressure method to account for air density variations in gas turbine cooling system design
21 p3099 A72-41059

Nonstationary processes in the intervane apertures of turbomachines
22 p3133 A72-42247

Vortex and source lattices in a variable layer of an incompressible fluid
22 p3133 A72-42248

Causes for the formation of internal discontinuities of the metal in forged blanks of turbine blades prepared from EI893 alloy
22 p3216 A72-42249

Electrical components in gas turbine control systems.
22 p3216 A72-42521

Gasdynamic investigation of a turbine with evaporative air cooling of the nozzle guide vanes
23 p3325 A72-43662

Infrared spectroscopy for chemical composition of inorganic and organic products formed on friction surfaces of gas turbine parts immersed in hydrocarbon fuels
23 p3325 A72-43974

Application of the method of hydrodynamic singularities to the calculation of the velocity distribution in doubly-periodic infinite blade cascade systems
24 p3390 A72-44874

Various efficiencies of fluid flows and application to the hypersonic ramjet
24 p3360 A72-44993

Gas turbine wheel design analysis, presenting procedures for estimating revolution rates, blade numbers and component configurations effects on wheel weight for prescribed stresses
24 p3460 A72-45737

GAS VALVES
Aircraft high pressure oxygen cylinder system filler valve optimum standards, discussing automatic fill rate and pressure sensitive closing control, design, construction and performance
[SAE AS 1225] 01 p0006 A72-10385

In-line high vacuum conductance valve with attached diffusion pump for shock tube evacuation
13 p1959 A72-29758

GAS VISCOSITY
Continuum gas viscoseals performance, comparing two seal groove aspect ratio geometries
02 p0237 A72-12850

Velocity /viscous/ slip coefficient and diffusion slip velocity in multicomponent gas mixtures by linearized Boltzmann equation
04 p0513 A72-15334

Atomic and molecular hydrogen mixture viscosity measurement, considering mutual diffusion coefficient, collision cross sections and interaction potentials
04 p0553 A72-15637

Magnetic field influence on shear viscosity of polyatomic gases, measuring rectangular cross section capillary flow resistance for different field orientations
07 p1038 A72-20398

Atomic hydrogen viscosity and thermal conductivity coefficients for 1-100,000 K, using quantum theory for low temperatures and classical mechanics for high temperatures
13 p2065 A72-29299

Negative pressure gradients effects on turbulent viscosity profiles for gas flow through tubes, comparing dependence on transverse coordinates to incompressible flow case
16 p2380 A72-33860

Influence of viscosity on the characteristics of compressor bladings for supersonic flow conditions
20 p2963 A72-39912

GAS WELDING
Metal inert gas /MIG/ welding of thin sheets, using Si controlled rectifier power source
09 p1320 A72-23627

Metal inert gas /MIG/ spot welding process effects on weld dimensions, shape and strength
09 p1320 A72-23630

Plasma arc and MIG /metal inert gas/ welding combination with filler wire, obtaining high melting rates and penetration control
09 p1322 A72-23645

Filler wires development for inert gas welding of stainless maraging steel
11 p1660 A72-26488

GAS-GAS INTERACTIONS
German monograph on heat transfer in chemically reacting gases covering laminar and turbulent tube flows for dissociated dinitrogen tetroxide
09 p1274 A72-22339

Foreign gas collisional broadening of nitrous oxide absorption lines, obtaining optical collision cross sections
09 p1276 A72-23332

Free convection-radiative heat transfer interaction of real gases in laminar boundary layer on vertical plate, using exponential wideband model for total band absorbance
[AIAA PAPER 72-278] 11 p1740 A72-25218

Differential collision cross sections for argon pairs with neon, methane and ethane at angular region of two crossed nozzle molecular beams
16 p2431 A72-33070

Rotating plasma-neutral gas collision interaction studies, determining particle energy and velocity in partially ionized plasmas

16 p2438 A72-33916

Rotational excitation of rigid rotor in argon-nitrogen system, measuring energy transfer moments by particle-body and perturbation technique

17 p2585 A72-34740

Atomic oxygen-ozone gas phase reaction rate constant direct measurement in steady state flow system at 269-409 K under excess ozone conditions

19 p2762 A72-38221

Simulation of the interaction of high altitude plumes and a high-speed free-stream flow.

[AIAA PAPER 72-1019]

21 p3042 A72-41598

Modeling the rise and combustion of a cloud of light gas in the atmosphere

23 p3357 A72-44493

GAS-ION INTERACTIONS

Associative attachment and gas-to-particle conversion mechanisms in positive and negative ion formation up to 50 km

03 p0347 A72-13390

Ionospheric ion-molecule and ion-electron reaction rate constants determination from nighttime flight of rocket-borne ion mass spectrometer data least square fitting

03 p0347 A72-13396

Effective cross sections of ion collisions with gaseous target and argon atoms collision with argon target by molecular beam intensity attenuation method

03 p0392 A72-14060

Nonuniform sinusoidal electric field anomalous influence on ion motion in gas with allowance for ion-atom collisions

04 p0547 A72-14622

Lateral diffusion measurement for mass identified positive ions in oxygen, noting spiralling, charge exchange and collisions effects on ion-molecule system

15 p2281 A72-32224

Ion-ion correlation effects on electron-nucleus neutrino bremsstrahlung.

18 p2723 A72-36089

Charge states and charge-changing cross sections of fast heavy ions penetrating through gaseous and solid media.

19 p2837 A72-37849

Effect of ionic viscosity on the stability of a finite-pressure plasma

19 p2842 A72-38529

Influence of a variable electric field on the diffusion of ions in a gas

21 p3086 A72-41676

Field dependence of gaseous-ion mobility - Theoretical tests of approximate formulas.

23 p3316 A72-43871

GAS-LIQUID INTERACTIONS

NT AIR WATER INTERACTIONS

Differential pressure effects of gas-liquid configuration on porous electrode activity in oxygen cathodes

03 p0311 A72-12923

Nitrogen interaction with Ni-based melts at 1600 C, noting absorption rate dependence on nitrogen diffusion rates and melt viscosities

07 p1011 A72-19546

Nitrogen interaction with liquid binary Ni alloys, investigating solubility as function of temperature and pressure and titanium nitrides existence conditions

07 p1011 A72-19547

Cluster variation method for boundary free energy solution in lattice model applied to Ising phase and gas-liquid interface and longer range interaction

18 p2711 A72-36565

Model for shock wave propagation through gas-liquid drop medium based on liquid phase atomization by boundary layer stripping

24 p3391 A72-45049

GAS-METAL INTERACTIONS

Stress induced oxygen diffusion in alpha Zr, attributing temperature dependent internal friction peak to oxygen-titanium interactions

02 p0247 A72-12818

Cold pressed powdered boron nitride, Mo, W, Nb disulfides and diselenides, investigating thermal dissociation in He by X ray analysis

03 p0380 A72-13551

Iron aluminides and borides diffusion layers morphology on alpha iron surface by metal surface/gas phase interaction, observing preferential orientation

03 p0376 A72-13971

Spatial distribution of gaseous nitrogen molecules scattered from metal surface, estimating beam capture coefficient

03 p0392 A72-14056

Digital computer simulation of rarefied gas molecular beam-rough metal surface interaction

03 p0392 A72-14057

Impulsive spatial interaction model between monoenergetic molecular beam and rough isotropic rigid metal surface in free molecule flow

03 p0392 A72-14058

Gas-metal surface interactions effect on aerodynamic lift and drag coefficients in free molecular flow

03 p0342 A72-14059

Windowless ultrahigh vacuum photoelectron spectrometer for high resolution studies of gas-metal surface reactions, measuring electron energy levels

04 p0523 A72-15489

Trapping probability in gas-surface interactions from empirical accommodation coefficients, using simple model based on assumed attractive square well and impulsive-repulsive potential

05 p0624 A72-16394

Environmental analysis of gas particle/probe aeroshell interaction in rarefied flow of high altitude Jupiter entry

[AIAA PAPER 72-203]

05 p0721 A72-16844

Steady state high temperature niobium creep in torsion under rarefied oxygen infiltration conditions, discussing surface interactions kinetics

07 p1012 A72-19679

Gas saturation of Ti alloy in air and vacuum at 750-1050 C for 1-6 hr, discussing surface layer microstructure change after heat treatment

07 p1013 A72-19742

Gas-solid surface interaction semicontinuous model, predicting accommodation coefficient as function of gas atoms initial energy on tungsten

07 p0970 A72-20081

Gas-surface interaction parameters and atmospheric density determination from satellite drag induced orbital decay measurements

07 p0910 A72-20116

Exoelectronic emission method for examining deformation induced structural changes and interactions with ambient medium of metals and alloys surfaces

07 p0989 A72-20157

Pressure effects on molten metals reactions with ambient atmosphere during purification by distillation, obtaining impurities concentration ratio via Langmuir relative volatility rule

07 p0997 A72-20287

Nitrogen adsorption kinetics on bulk W targets investigated by ultrahigh vacuum, molecular beam, reflexion detector method

09 p1276 A72-22806

Internal friction peak in fresh tempered martensite from Fe-Ni-C alloy cooled to 77 K, suggesting hypothetical carbon atoms interactions with mobile dislocations

10 p1496 A72-24232

Gas etching of Ge and Si semiconductors with vapors of chemical elements, emphasizing hydrogen chloride

11 p1700 A72-25776

Low energy electron diffraction structures due to CO and oxygen adsorption on clean Re surfaces produced by Ar ion bombardment at 20 to 920 C

13 p2020 A72-28522

Statistical adsorption kinetics model with electron desorption of oxygen on polycrystalline W, noting sticking coefficients

13 p1912 A72-28523

Sulfur dioxide and carbon dioxide interaction with clean silver surface at ultrahigh vacuum, using Auger electron spectroscopy and work function measurement

13 p1912 A72-28684

Rarefied gas flows effect on metals creep properties, examining molecular flow density distribution as function of specimen surface distance from nozzle

13 p1979 A72-29483

Effect on physical and mechanical properties of hard metals due to gas sorption by metallic films spray-coated on surfaces, describing vacuum apparatus

13 p1939 A72-29488

Hydrogen gas solubility measurement in solid Mo at atmospheric pressure and 905-1521 C, noting quasi-regular linearity of Arrhenius plot

14 p2113 A72-30246

Oxygen chemisorption effect on rare gas beams reflection from refractory metals polycrystalline surfaces, interpreting experimental results by simple correlation model

16 p2431 A72-33068

Oxygen and nitrogen atoms effect on defects recovery in cold rolled Nb during annealing

16 p2406 A72-33208

Internal nitridation zones and growth kinetics for Cr and Cr-Ti alloys at 1000-1400 C, using Maak analysis

16 p2409 A72-33807

Contact contamination - Formation of carbonaceous deposits on electrical contacts.

18 p2665 A72-36119

Thermodynamics and phase relations in refractory metal solid solutions containing carbon, nitrogen, and oxygen.

18 p2699 A72-36576

Effect of low-pressure oxygen on the creep properties of W-25 pct Re.

18 p2700 A72-36581

Hydrogen and nitrogen desorption phenomena associated with a stainless steel 304 low energy electron diffraction /LEED/ and molecular beam assembly.

19 p2762 A72-38023

Creep of porous nickel in oxidizing and neutral media

19 p2819 A72-38287

Gaseous hydrogen-induced cracking of Ti-5Al-2.5Sn.

20 p2937 A72-39292

The effect of oxygen on tantalum-sodium compatibility.

20 p2938 A72-39297

Hydrogen gas effects on cleavage cracking in Ti-Al-Mo-V samples under static and cyclic loading

20 p2939 A72-39308

High-speed carburizing with natural gas in a fluidized bed

20 p2929 A72-39582

Vapor phase formation during high temperature oxidation.

21 p3066 A72-40551

Gas adsorption by refractory metal single crystals.

22 p3187 A72-41940

Chemisorption of CO on tungsten /100/ - Combined flash desorption and electron stimulated desorption study. I.

22 p3152 A72-42297

Influence of hydrogen on the fracture structure of OT4 titanium alloy

22 p3196 A72-43162

Inflammation and burning of powdered aluminum in high-temperature gaseous media and in heterogeneous condensed systems

22 p3245 A72-43178

Flow direction and velocity effects on metal burning rates of low carbon and Ni-Cr steels in pure oxygen, using diffusion model

22 p3245 A72-43185

Adsorbed oxygen inhibition of reactions of hydrogen with tungsten.

23 p3298 A72-43270

Effect of oxygen on the scale resistance of titanium alloys

23 p3300 A72-43592

Influence of the sintering medium on the quality of metalceramic hard alloys containing zirconium and hafnium carbides

23 p3303 A72-44017

Quasi-equilibrium analysis of the reaction of atomic and molecular fluorine with tungsten.

23 p3262 A72-44050

GAS-SOLID INTERFACES

Thermal conductivity, electrical conductivity, viscosity and diffusivity of ionized gas-solid suspension in electric field, using transport equations and particle interaction potentials

01 p0111 A72-11332

Electric or magnetic field tangential components at ground-air interface, discussing secondary electromagnetic sources

04 p0492 A72-15438

Windowless ultrahigh vacuum photoelectron spectrometer for high resolution studies of gas-metal surface reactions, measuring electron energy levels

04 p0523 A72-15489

Trapping probability in gas-surface interactions from empirical accommodation coefficients, using simple model based on assumed attractive square well and impulsive-repulsive potential

05 p0624 A72-16394

Macroscopic boundary conditions of gas-solid interface interaction as function of gas temperature and transport coefficients variation in shock reflection problems

06 p0902 A72-18107

Surface catalytic properties effect on multicomponent gas hypersonic boundary layer with simultaneous vibrational-dissociative relaxation, considering plate and blunt body laminar boundary layer

06 p0757 A72-18130

Solid thermal motion influence on atom colliding with solid surface linear semiinfinite atomic chain, preventing accommodation coefficient calculation method

06 p0853 A72-18140

Solid propellant reaction kinetics at gaseous fuel and catalyst-containing ammonium perchlorate interface, studying ignition and deflagration

07 p1051 A72-19367

Thermodynamic models of gas-solid equilibria in cosmochemical systems containing H, O, Si, Mg, S, C, Cl and F

07 p1075 A72-19587

Neutral monatomic rarefied gas-surface interaction at energy levels 0.1-10 eV, using Boltzmann equation

07 p0969 A72-20061

Monatomic gas atoms scattering by solid surfaces, using classical three dimensional lattice model

07 p0969 A72-20064

Neutral unexcited gas atoms or molecules scattering at solid surfaces, interpreting molecular beam experimental results in terms of classical dynamics

07 p0969 A72-20065

Gas-surface interactions study by molecular beam technique, discussing measurement and target surface conditions control methods 07 p0969 A72-20069

Gas-solid surface interaction semicontinuous model, predicting accommodation coefficient as function of gas atoms initial energy on tungsten 07 p0970 A72-20081

Heat and mass exchange in laminar boundary layer in air-carbon dioxide binary mixture under free convection on porous heated vertical surface 08 p1255 A72-21664

Vibrating membrane generated acoustic pressure wave propagation in rarefied gas, applying to solid surface-gas interaction models 09 p1294 A72-22762

Combustion surface acoustic admittance model of blended solid propellant with allowance for foam zone inertia and solid/gas interface reactions 12 p1889 A72-27980

Gas surface interactions models, computing scattering kernels by reduction to boundary value problem 14 p2134 A72-30880

Surface phonon appearance criteria associated with crystal surface gas adsorption, discussing entropy variation and colliding particle-crystal energy exchange 15 p2280 A72-31858

Spatical distribution of nitrogen molecular beam scattering from solid nitrogen surface as function of beam energy and incidence angle 16 p2430 A72-33063

Ionized gas-solid suspension thermal physical properties verification by micro-sized MgO dispersion in AR plasma [AIAA PAPER 72-688] 16 p2439 A72-34054

Radiant interchange among suspended particles and its effect on thermal relaxation in gas-particle mixtures. [DFVLR-SONDDR-210] 17 p2638 A72-35643

High-sensitivity resonant-quartz scales operating in high vacuum at very low temperature - Application to the study of gas-solid interactions 19 p2800 A72-37834

Recombination of hydrogen atoms on the surfaces of solid bodies 19 p2838 A72-38199

A technique for determining the transient heat flux at a solid interface using the measured transient interfacial temperature. [ASME PAPER 72-HT-18] 20 p2987 A72-39687

Investigation of the influence of the gas medium on the phase composition and certain properties of refractory materials containing zirconium 23 p3306 A72-43690

Study of a reactive nozzle flow associated with solid gas-phase interaction. 24 p3433 A72-45063

GASEOUS CAVITATION
U CAVITATION FLOW
U GAS FLOW

GASEOUS DIFFUSION
Nondestructive radioactive gas penetrant tests for porosity and fatigue damage in jet engine castings 01 p0069 A72-10813

Pulmonary functional inhomogeneities effects on steady state oxygen and CO diffusing capacity estimates in gas transfer resistances terms 01 p0014 A72-10847

Hydrogen diffusion kinetics in Nb under various temperatures during gas-metal absorption experiments, observing room temperature hardness profile 01 p0087 A72-11026

Hydrogen diffusion, electron transfer and density distribution in Ta as function of temperature and field strength 02 p0242 A72-12009

Rarefied gases pressure flow and self diffusion through cylindrical tubes, presenting kinetic model with velocity independent mean free path 02 p0205 A72-12357

Iron aluminides and borides diffusion layers morphology on alpha iron surface by metal surface/gas phase interaction, observing preferential orientation 03 p0376 A72-13971

Free oxygen content and diffusion coefficient in adrenalectomized rat skeletal muscles after physical strain 03 p0317 A72-13991

Alloying and heat treatment ordering effect on hydrogen diffusion coefficients, penetrability and solubility in Pd-Ag alloys 03 p0376 A72-14016

Hydrogen diffusivity in Fe with cavities at room temperature calculated by mathematical model and numerical methods 03 p0378 A72-14256

Diffusion and thermal equilibrium models of stationary Tokamak, analyzing differences 04 p0558 A72-15173

Velocity /viscous/ slip coefficient and diffusion slip velocity in multicomponent gas mixtures by linearized Boltzmann equation 04 p0513 A72-15334

Atomic and molecular hydrogen mixture viscosity measurement, considering mutual diffusion coefficient, collision cross sections and interaction potentials 04 p0553 A72-15637

Angular momentum and Li diffusive transport induced by mild thermally driven turbulence associated with Goldreich-Schubert-Fricke instability, discussing solar rotation slowdown 05 p0720 A72-16718

Single breath method for pulmonary diffusing capacity measurement with respect to total lung capacity and inspiration time 05 p0620 A72-17174

CW diffusion type chemical HF laser and two-vibrational level HF molecular models, analyzing laser performance [AIAA PAPER 72-145] 07 p1000 A72-18955

Surface processes effect on hydrogen penetration and diffusion into thick Mo membranes 07 p1014 A72-19772

Airborne gas chromatograph for real time diffusion analyses, describing flight test results with sulfur hexafluoride plumes 09 p1307 A72-22451

High altitude acclimatization effects on human lung diffusing capacity for carbon monoxide at different oxygen tensions 10 p1425 A72-24476

Gaseous species diffusion in carrier gas under various geometries and flow conditions, using finite element method 14 p2095 A72-30928

Teflon-bonded hydrophobic gas diffusion electrode performance prediction by mathematical treatment of flooded catalyst agglomerate model 16 p2352 A72-33892

Effects of diffusion impairment on O2 and CO2 time courses in pulmonary capillaries. 17 p2506 A72-35967

Singularities of nonstationary solutions to the equation of diffusion in a gravitational field. I, II 18 p2687 A72-36655

New measurement and evaluation method for the determination of the diffusion coefficient of hydrogen in solid metals 18 p2692 A72-36841

Hypoxic theory for atherosclerosis formation, noting blood plasma protein concentration effects on oxygen diffusion 18 p2651 A72-37030

He-Cd lasers using recirculation geometry. 21 p3061 A72-40239

The mass spectrographic measurement of gas separation with the aid of ambipolar effusion in neon-krypton mixtures 21 p3053 A72-40486

Experimental CW chemical laser studies. [AIAA PAPER 72-712] 21 p3063 A72-40920

Variance reduction in Monte Carlo analysis of rarefied gas diffusion. 21 p3046 A72-41183

Hypoxic pulmonary steady-state diffusing capacity for CO and alveolar-arterial O2 pressure differences in growing rats after adaptation to a simulated altitude of 3500 m. 21 p3003 A72-41622

Cardiac hypertrophy, capillary and muscle fiber density, muscle fiber diameter, capillary radius and diffusion distance in the myocardium of growing rats adapted to a simulated altitude of 3500 m. 21 p3003 A72-41624

Multicomponent diffusion and heat transfer in flows of a chemically balanced ionized gas past bodies 21 p3047 A72-41658

A possible problem in measuring hydrogen diffusivity at low temperatures by the Gorsky effect. 22 p3190 A72-42443

Gaseous and particulate iodine in the marine atmosphere. 22 p3173 A72-42469

Gaseous and particulate bromine in the marine atmosphere. 22 p3173 A72-42470

Diffusion of a filament of gas injected into a supersonic free jet. 23 p3280 A72-43947

An experimental study of turbulent diffusion of helium jets issued upwards into the air at rest. 23 p3281 A72-44273

Determination of the diffusional capability of lungs by the method of delayed respiration 24 p3374 A72-44598

GASEOUS FISSION REACTORS
High temperature gaseous U fission plasma core reactor engine concepts for space propulsion 01 p0099 A72-11327

Radiant heat attenuation of W seeded hydrogen aerosol at high pressure and temperature for gas core nuclear rocket propellant application 01 p0112 A72-11340

Shock tube technique for opacity measurement at high pressures in seeded hydrogen for gas core nuclear rockets 01 p0099 A72-11342

Open cycle gas core nuclear rocket engine, determining scaling laws for buoyancy force effect on fuel containment at various flow parameters 01 p0099 A72-11348

Open cycle gas core nuclear rocket engine flow studies to obtain maximum system reactivity at low uranium/coolant gas loss ratio 01 p0100 A72-11349

Injection geometry and inlet flow conditions application to open cycle gas nuclear reactor engine, evaluating fuel containment from cylindrical and spherical chambers experiments 01 p0100 A72-11350

Energy release and accelerating inner stream effects on flow field near fuel injection in gas core reactor, basing Euler equations energy diffusion term on radial radiative transport 01 p0100 A72-11351

Coaxial flow gaseous core nuclear reactor system dynamic analysis, developing mathematical model and equations solution by computer program 01 p0100 A72-11352

Space crew radiation dosage calculation from Mars mission high impulse gas core nuclear rocket engine exhaust plume fission fragments 01 p0022 A72-11353

Minicavity reactor rocket engine combining high specific impulse of central gaseous fueled cavity and low weight NERVA type fuel elements in driver region external to moderator-reflector zone 01 p0100 A72-11358

Uranium hexafluoride pulsed plasma core reactor with artificial neutron source for spark plug and enclosed by cylinder and piston analogous to internal combustion engine 01 p0100 A72-11361

Mini-cavity gas core reactor concept for low thrust high impulse probe propulsion, using U 233 or 235 fuel 04 p0546 A72-14422

Gas core nuclear rocket reactor program for 60 day Mars, shuttle and Skylab applications 05 p0688 A72-15778

Critical spherical symmetry benchmark experiment on gas core nuclear reactor using uranium hexafluoride 05 p0688 A72-16387

Release of fission products from high temperature fuel materials 18 p2707 A72-36137

GASEOUS ROCKET PROPELLANTS
Simulation of nuclear light bulb engine propellant radiative heating, using argon seeded with micronized carbon particles and 500 kw dc arc as radiant energy source 01 p0099 A72-11344

Design of 6000 Mw open cycle gas core nuclear rocket engine with hydrogen as propellant, considering critical U 235 mass, major reactor components and specific impulse 01 p0099 A72-11347

Two constituent gaseous propellant micropropulsion engines for satellite orbit correction and attitude control, discussing thermodynamic and reaction kinetics problems 02 p0271 A72-12711

Electrothermal thruster supersonic convergent-divergent nozzle performance with lithium vapor propellant, predicting exhaust velocity by isentropic flow equations [AIAA PAPER 72-453] 11 p1708 A72-26189

Boron reaction characteristics in ducted rockets under varying primary chamber conditions detailing various gaseous propellants effects 15 p2296 A72-32311

GASES
NT AIR
NT ARGON
NT ARGON ISOTOPES
NT CARBON DIOXIDE
NT CARBON MONOXIDE
NT COLD GAS
NT COMPRESSED GAS
NT COSMIC GASES
NT DETONABLE GAS MIXTURES
NT DEUTERIUM
NT DEUTERIUM PLASMA
NT DIATOMIC GASES
NT EXHAUST GASES
NT GAS MIXTURES
NT GAS STREAMS
NT GRAY GAS
NT HELIUM
NT HELIUM ATOMS
NT HELIUM FILM
NT HELIUM ISOTOPES
NT HIGH TEMPERATURE AIR
NT HIGH TEMPERATURE GASES
NT HYDROGEN
NT HYDROGEN ATOMS
NT HYDROGEN IONS
NT HYDROGEN ISOTOPES
NT HYDROGEN PLASMA
NT IDEAL GAS
NT INTERPLANETARY GAS
NT INTERSTELLAR GAS

- NT IONIZED GASES
 NT LIQUEFIED GASES
 NT LIQUID AMMONIA
 NT LIQUID HELIUM
 NT LIQUID HYDROGEN
 NT LIQUID NITROGEN
 NT LIQUID OXYGEN
 NT LORENTZ GAS
 NT MOLECULAR GASES
 NT MONATOMIC GASES
 NT NATURAL GAS
 NT NEON
 NT NEON ISOTOPES
 NT NITROGEN
 NT NONGRAY GAS
 NT OXYGEN
 NT OXYGEN PLASMA
 NT POLYATOMIC GASES
 NT PYROGEN
 NT RADON
 NT RADON ISOTOPES
 NT RARE GASES
 NT RAREFIED GASES
 NT REAL GASES
 NT RESIDUAL GAS
 NT SOLIDIFIED GASES
 NT TRITIUM
 NT XENON
 NT XENON ISOTOPES
 Total line intensities interpretation from optically thin gases, considering matter partitioning bivariate distribution function and chemical composition
 13 p2008 A72-29930
- GASKETS**
 Stress-deformation effects on gasket joint of metal seals at high pressures
 08 p1178 A72-21933
- GASOLINE**
 Turbulent hot gas stream self ignition in oxidizer flow for hydrogen-air and gasoline-air mixtures
 14 p2170 A72-30293
 Thermionic converter heated by gasoline flame or heat pipe, describing materials protection against corrosion and furnace design and operation
 18 p2644 A72-36165
- GASTROINTESTINAL SYSTEM**
 NT INTESTINES
 Parenterally introduced protein hydrolyzates and aminopeptides influence on human pancreas enzyme secretion activity
 09 p1268 A72-23595
 Age-induced long-term memory changes in animals
 23 p3257 A72-44079
- GATES [CIRCUITS]**
 NT THRESHOLD GATES
 Low driving power resistive gate MOSFET microwave switch with performance approaching P-I-N diode
 01 p0038 A72-10658
 Signal flow graph theory based computer diagnosis using blocking gate approach, constructing algorithm for gates optimal locations determination for maximum faults distinguishability
 02 p0184 A72-11479
 Dual gate GaAs microwave FET, measuring second gate voltage effects on power gain and noise
 02 p0191 A72-11893
 Dual-gate MOS transistor structure, operational principles and electrical characteristics, noting suitable properties for use in low noise microwave amplifier
 03 p0330 A72-12969
 Logic functions for magnetic bubble devices based on interaction of circular magnetic domains in rare earth iron oxides, considering gates for dynamic memory
 [IEEE PAPER 2.3] 03 p0327 A72-13753
 Book on field effect electronics covering junction and insulated gate transistors and allied devices, monolithic and film IC and design techniques
 03 p0333 A72-13846
 Al, Mo and Cr radiation resistance as gate electrodes and corresponding MOS devices, discussing radiation behavior model revision
 03 p0403 A72-14079
 P-channel MOS devices radiation hardening by thermal silicon dioxide gate insulator optimization, applying to circuit fabrication
 03 p0403 A72-14082
 MNOS transistors charge storage properties at high electric field strengths and current densities near gate insulator breakdown, determining reliable operating limits
 03 p0336 A72-14277
 MOS Si-gate arrays for static, dynamic and programmable read-only memories, investigating information storage reliability
 03 p0336 A72-14282
 Two section model of junction-gate field effect transistor with short channel length
 04 p0498 A72-15134
 Combinational tree networks of AND and OR gates without internal fan-out, proposing test generation strategy for maximizing detected multifault sets size
 05 p0640 A72-16163

- Logic circuit binary signal autocorrelation determination as function of 0 and 1 signals duration distribution considering AND and OR gates
 05 p0632 A72-17094
 Binary detector with dual gating function between first and second quantization processes, estimating false alarm and rejection probabilities
 07 p0937 A72-18851
 Algorithm for asynchronous multilevel sequential circuits design, stressing NOR networks
 07 p0963 A72-20387
 Low level current operation in insulated gate FET, obtaining analytical expression for voltage
 08 p1142 A72-21744
 Hydraulic ball valve elements and logic gates for applications requiring short switching times under large flow and high pressure conditions
 08 p1114 A72-22159
 Fluxgate magnetometry, discussing weak field sensors, low power devices and various applications
 09 p1308 A72-22469
 Gating duration influence in reception channel on singular signal detection in normal noise
 09 p1278 A72-22571
 Background noise in FETs with junction gate, formulating hypothesis of warm carriers for transistor channel
 09 p1287 A72-23110
 Bipolar insulated gate FET IC buffer driver, discussing input and output interface capacitance and impedance characteristics and application to transistor-transistor logic
 11 p1603 A72-25269
 Schottky barrier gate FET design, device packaging and low noise characteristics
 12 p1788 A72-27294
 Semiinsulated gate GaAs FET fabrication by proton bombardment
 12 p1790 A72-27438
 Noise behavior of GaAs Schottky barrier FET with short gate length, showing channel thickness effect on intervalley scattering noise
 12 p1790 A72-27439
 Channel formation in insulated gate FET, obtaining equivalent circuit
 12 p1791 A72-27548
 Sense coil geometry and drive waveform effects on low level flux gate magnetometers sensor noise
 15 p2233 A72-31507
 Computer model study of FET with submicrometer gates, noting gain-bandwidth product increase with decreasing gate length
 15 p2205 A72-31544
 NAND gate logic transistor circuit design, layout, fabrication and electrical parameters, noting base and resistors diffusion welding
 17 p2530 A72-35069
 Charge injection into the gate dielectric of MOS transistors during junction avalanche
 18 p2668 A72-37104
 Single and dual gate GaAs FET integrated amplifiers in C band
 19 p2771 A72-37270
 Forward and reverse characteristics of self-aligned double-diffused M.O.S. transistors
 22 p3160 A72-42754
 Gating duration influence in reception channel on singular signal detection in normal noise
 24 p3379 A72-44750
- GAUGE INVARIANCE**
 Inhomogeneous cosmological models in terms of impulse energy tensor, discussing coupled Einstein equations, gauge invariance and Lorentz gauge
 21 p3110 A72-41442
 Non-Abelian gauge fields with two masses
 23 p3314 A72-44155
- GAUSS EQUATION**
 Optimality and strategy efficiency in Gaussian elimination on sparse matrix, using graphical method
 11 p1678 A72-26496
- GAUSS FUNCTION**
 U GAUSS EQUATION
GAUSSIAN DISTRIBUTIONS
 U NORMAL DENSITY FUNCTIONS
GAUSSIAN NOISE
 U RANDOM NOISE
GAUSSMETERS
 U MAGNETOMETERS
GCR [REACTORS]
 U GAS COOLED REACTORS
- GEAR TEETH**
 Point contact realization between helical transmission wheels teeth
 05 p0667 A72-17058
 Discrete model of dynamic forces between teeth of single stage transmission with parallel gear axes
 09 p1404 A72-22772
 Real time holographic contouring and coherent light interferometry of gear tooth surfaces
 19 p2797 A72-37606
 Experimental procedure for determining the strength losses in the individual elements of wave-type toothed gears
 22 p3182 A72-41866

GEARS

- Gear transmission systems statistical characteristics under dynamic loads, noting normal Gaussian curve for operating conditions
 04 p0585 A72-14614
 Carbon fiber reinforced thermoplastics tested for gears and bearings applications, including wear, static, dynamic, surface tension, stereoscan and microscopy effects
 04 p0537 A72-14748
 Astafan turbopfan engine with variable pitch fan rotor blades for thrust variation, discussing gearbox and core engine design
 07 p1055 A72-20459
 Mandelshtam couplings theory for subdividing discrete mechanical system of three degrees of freedom gear transmission
 09 p1409 A72-23614
 German monograph on losses in gear pumps, discussing leakage, mechanical and hydraulic losses, measurement techniques and equipment, etc
 10 p1422 A72-23774
 Use of digital computer graphics in gear design
 17 p2520 A72-34338
 Reduction of noise and acoustic-frequency vibrations in aircraft transmissions.
 [AHS PREPRINT 661] 17 p2491 A72-34508
 Properties of internally lubricated glass-fortified thermoplastics for gears and bearings.
 19 p2822 A72-37896
 Optoelectronic speed control for replacing mechanical gear drives for precisely variable shaft speed ratios
 21 p2997 A72-40259
 Machine elements vibration parameters from dynamic model of planetary gears, noting energy spectrum, correlation and amplitude distribution functions
 22 p3182 A72-42132
- GEGENSCHEIN**
 Satellite photometric observation of diffuse celestial sources such as Milky Way, zodiacal light and gegenschein
 10 p1546 A72-24863
- GELATINS**
 Thick phase holograms in dichromated gelatin, discussing physical properties requirements and reliable processing procedures
 15 p2239 A72-32355
- GELATION**
 Metals and metal oxides powders mixture formation by mixed metal halides gelation in alcohol solution
 02 p0233 A72-11455
 Linear polyethylene irradiation, investigating chain scission processes importance, critical conditions for gelation and sol/gel partitioning
 04 p0484 A72-15258
 Irradiation effects on linear polyethylene molecular weight fractions in molten and crystalline states, determining sol-gel partitioning to establish critical conditions for gelation
 09 p1337 A72-22550
 Acrylamide polymerization - New method for determining the oxygen content in blood.
 24 p3376 A72-45376
- GELLED PROPELLANTS**
 Carbohydrate based gelling agent for gas turbine fuel, describing development and chemical and physical properties
 [ASME PAPER 72-GT-9] 11 p1702 A72-25612
- GELS**
 NT DOUBLE BASE ROCKET PROPELLANTS
 Antioxidant additives effect on chemical stability and rheological properties of silica gel lubricants with SU type mineral oil dispersion medium
 16 p2413 A72-33173
 Aerogel combustion kinetics and continuous flame formation on coal, Mg, Al and Al alloy powders, using track method
 16 p2476 A72-33252
- GEMINID METEOROIDS**
 Geomagnetic field effect on radar echoes from meteor trains during Geminid shower
 03 p0345 A72-12982
- GENERAL AVIATION AIRCRAFT**
 Electromechanical nose wheel steering system for general aviation aircraft ground maneuverability improvement, describing design
 01 p0006 A72-10963
 General aviation patient transportation, investigating military helicopter airlift performance
 01 p0022 A72-11298
 General and commercial aircraft service needs in air transportation, considering FAA and CAB roles and policies
 02 p0304 A72-11716
 Air traffic control long range planning for airlines and general aviation, discussing use of IFR, RNAV and IPC equipment
 04 p0545 A72-14818
 Airborne collision avoidance system equipment for general aviation aircraft, discussing logic functions, transmission modes, data handling tradeoffs and ATC procedure interactions
 04 p0545 A72-14830

General aviation type light airplanes pilot workload during steep landing approach, comparing flight tested control response parameters with handling qualities criteria
[AIAA PAPER 72-125] 05 p0613 A72-16941

Dassault Falcon 10 turboprop powered executive aircraft, attributing safe stall characteristics to wing design optimization
08 p1108 A72-21274

Eight-place turboprop powered business jet aircraft design, discussing structure, fuel system, engines crew station and safety features
08 p1109 A72-21572

Mystere business jet aircraft flight instruments, acceleration, control and stall characteristics
08 p1110 A72-21900

Book on general aviation safety covering statistical accident records, accident analysis, crashworthiness, preventive measures, etc
10 p1420 A72-23750

Flight airworthiness requirements development for supersonic transports, V/STOL and transport and general aviation aircraft, exploring critical control and stability parameters
[SAE PAPER 720306] 11 p1575 A72-25570

General aviation equipment standards in light of air traffic system safety needs, emphasizing Technical Standard Order system
[SAE PAPER 720307] 11 p1748 A72-25571

General aviation aircraft structural safety studied with 1547 accident histories, noting IFR and turbulent weather conditions predominance
[SAE PAPER 720308] 11 p1575 A72-25572

Fatigue certification of general aviation aircraft in Australia, describing ground taxi load spectra and endurance and radiographic inspection of laminated spar caps
[SAE PAPER 720311] 11 p1734 A72-25575

Flight tests of combination flight director displayed and attitude command control system effect on and attitude command control system effect on general aviation aircraft handling qualities during ILS approach
[SAE PAPER 720316] 11 p1575 A72-25580

Dynamic deceleration anthropomorphic dummy tests of general aviation occupant lap belt/shoulder harness restraint systems
[SAE PAPER 720325] 11 p1583 A72-25588

Stall warning system for general aviation aircraft, using signal discriminator for rough or gusting air
[SAE PAPER 720331] 11 p1630 A72-25592

Business V/STOL aircraft economic viability based on cost benefit analysis and comparison with turbine powered aircraft
[SAE PAPER 720334] 11 p1576 A72-25594

Transport aircraft aerodynamic design technology application to general aviation propeller driven twin engine aircraft, discussing wing loading and aspect ratio optimization
[SAE PAPER 720337] 11 p1576 A72-25595

Flight stress and performance of training in general aviation simulator compared with actual flight
12 p1774 A72-28261

FAA program for revision of aviation aircraft maximum allowable control forces specifications, taking into account female pilots capabilities
12 p1777 A72-28325

General aviation crashworthy personnel restraint systems, discussing strap take-up devices, comfort, fit and ease of use
13 p1908 A72-28726

Winds aloft forecast use to predict southwestern mountain lee wave behavior for general aviation cross country flights
13 p1993 A72-28863

Cost effectiveness model for evaluating general aviation weather dissemination techniques, stressing design variables and time periods
13 p1994 A72-28871

Low cost flight simulator for general aviation pilot training, containing IFB instrumentation and turbulence injection device
15 p2214 A72-32211

The future of general aviation in Europe.
18 p2743 A72-37093

Private aircraft ownership and use for family travel and pleasure, discussing costs, maintenance and operational problems
[AIAA PAPER 72-812] 19 p2750 A72-38119

Annual Corporate Aircraft Safety Seminar, 17th, Washington, D.C., April 17, 18, 1972, Proceedings.
20 p2887 A72-39740

Future aspects of business aviation, discussing pilot training and aircraft reliability and maintenance in context of flight safety
20 p2988 A72-39741

Corporate business aviation performance record in light of aircraft accident statistics, noting high percentage of approach-landing accidents and means for improvement
20 p2888 A72-39743

Aircraft accidents during nonprecision approaches under adverse weather conditions, discussing landing aids use for corporate jet aircraft
20 p2952 A72-39745

Flight safety from general aviation viewpoint in West Germany, discussing ATC and flight rules relative to airspace use
[DGLR PAPER 72-036] 24 p3467 A72-44615

International and regional scheduled air traffic terminals and general aviation airports characteristic objectives and operational aspects, discussing ATC, safety and noise problems
[DGLR PAPER 72-033] 24 p3387 A72-44616

Design and certification for executive type aircraft.
24 p3366 A72-44730

An assessment of repeated loads on general aviation and transport aircraft.
24 p3366 A72-44736

Intoxicating liquor and the general aviation pilot in 1971.
24 p3377 A72-45662

GENERAL DYNAMICS MILITARY AIRCRAFT
U MILITARY AIRCRAFT
GENETIC CODE
Molecular evolutionary changes in amino acids of proteins due to mutant random fixation, comparing human and fish hemoglobin chains
02 p0158 A72-11761

Amino acid code comparisons of polypeptide chains of globins due to mutations during vertebrate evolution from ancestral gene
02 p0159 A72-11764

Site binding model of nucleic acid-protein interactions for chemical evolution and genetic code studies
02 p0159 A72-11765

Nucleic acid, protein and cell primordial sequence, ribosomes and genetic code for life origin, discussing experiments on homopolyamine acids reaction with mononucleotides
04 p0468 A72-17775

Genetic code numerical structure association with logarithmic optimization rule for hierarchy of structures from molecular biology experiments
04 p0470 A72-14794

Enzymically synthesized homopolynucleotide and lysine-rich proteinoid microparticles effect on aminoacyl adenylate condensation as basis for genetic code origin
06 p0770 A72-17724

Empirical support for a stochastic model of evolution.
23 p3254 A72-43565

Amino acid substitution correlation with genetic code in human, bovine, ovine, porcine and salmon calcitonins, suggesting mutation occurrence time during evolution
23 p3254 A72-43568

Recently published protein sequences. I.
23 p3254 A72-43570

GENETICS
NT GENETIC CODE
NT MUTATIONS
Retinomotor light/darkness responses phylogenetic variations, discussing retinal elements structural and functional development in fishes and amphibians
02 p0164 A72-12484

Genetic organization emergence, considering pretranslational evolution in nontranslational protein synthesis, nucleic acid evolution and gene origin
08 p1119 A72-22010

Evolutionary significance of primary amino acid or nucleotide base sequences of DNAs within various phylogenetic groups
12 p1759 A72-27160

Genetic aspects of the blunted chemoreflex ventilatory response to hypoxia in high altitude adaptation.
22 p3144 A72-42591

GENITOURINARY SYSTEM
NT BLADDER
NT TESTES
GEOASTROPHYSICS
U ASTROPHYSICS
U GEOPHYSICS
GEOCENTRIC COORDINATES
Earth triaxiality from satellite data, obtaining non-zero values for harmonic coefficients
03 p0351 A72-14327

Venus and Mars visible geocentric declinations from daytime observations with Wanschaff vertical circle compared to nighttime results
09 p1388 A72-23065

Radar observation of meteor geocentric velocity dependence on radiant elongation angle
13 p2038 A72-29035

Geodetic latitude and altitude from geocentric coordinates.
17 p2547 A72-35103

Geocentric coordinates transformation from system related to mean pole and mean equator into instantaneous pole and instantaneous equator system, noting Cartesian coordinates
17 p2548 A72-35359

Prime geocentric meridian longitudes and UT, discussing position in terrestrial rectangular coordinates in relation to earth pole motion
17 p2549 A72-35741

Accurate positions of the planet Pluto in the years 1969-1970.
21 p3105 A72-40576

GEOCHEMISTRY
NT BIOGEOCHEMISTRY
Japanese lava geochemical analysis, determining K, Rb, Sr, Ba and rare earth concentrations with mass spectrometric stable isotope dilution
01 p0051 A72-10059

Siderophilic element content relation to oxidation state of ordinary chondrites, using Ir/Ni concentrations from neutron activation analysis
02 p0277 A72-11896

Carbon chemistry of moon based on lunar samples analysis
04 p0573 A72-14807

Southern Great Basin upper Cenozoic high Sr87/Sr86 and Sr/Rb ratio basalt initial composition, showing mantle material derivation
05 p0655 A72-16043

Volcanic basalt geochemistry in Afar Triple Junction, suggesting relation to crustal thinning and melting zone shallowing under rift
05 p0658 A72-16722

Classification of mass spectra on computers /COM-SOC/ for compound characterization of complex mixtures with geochemical and environmental applications
07 p0980 A72-20393

Geochemistry of lunar opaque minerals in Apollo 14 crystalline rocks, including Fe/Ni metal, ilmenite, spinels, schreibersite, baddeleyite, fayalite and tranquillityite
10 p1538 A72-24164

Eu and Sr distribution between coexisting feldspars in acidic rocks, using mass spectroscopic isotope dilution method
10 p1472 A72-24166

Electron spectroscopy for chemical analysis /ESCA/ technique for nondestructive elemental analysis of lunar and terrestrial minerals
16 p2454 A72-33447

Lunar surface mapping for Mg, Al and Si along ground tracks swept out by orbiting Apollo 16 spacecraft, noting geochemical X ray fluorescent analysis
18 p2726 A72-36556

Apollo and terrestrial geochemical samples examination for indigenous amino acids distribution and optical configuration, stressing close monitoring of contamination sources
19 p2762 A72-37648

Geochemistry of amino acid enantiomers - Gas chromatography of their diastereomeric derivatives.
19 p2762 A72-38224

Activation analysis in geochemistry and cosmochemistry; Proceedings of the Advanced Study Institute, Kjeller, Norway, September 7-12, 1970.
20 p2898 A72-39826

Rocks and meteorites analysis techniques evaluation, using Apollo 11 fines results to evaluate activation analysis for geochemistry and cosmochemistry applications
20 p2899 A72-39827

In-situ geochemical analysis of Martian and lunar composition via alpha particle activation technique, discussing Surveyor instrument performance
20 p2899 A72-39828

Multielement neutron activation analysis of geological and lunar material using chemical group separations and high resolution gamma spectrometry.
20 p2899 A72-39830

Neutron activation and neutron-capture gamma ray analyses of igneous rock trace elements, discussing Tyrone Igneous Series granites
20 p2899 A72-39831

Neutron activation techniques for nondestructive analysis of meteorites and lunar rocks, noting types of nuclear reactions for geochemical application
20 p2899 A72-39832

Neutron activation and mass spectrometry methods for geochemical analysis of rare earth elements in meteoritic, lunar and terrestrial materials
20 p2899 A72-39835

Coincidence counting applied to the activation analysis of meteorites and rocks.
20 p2900 A72-39841

Chemical and structural classification of Apollo 11 lunar rocks, showing lunar surface material temperature history and meteoritic component presence
20 p2900 A72-39842

Neutron activation analysis of tin in geochemical and cosmochemical material, using 40 minute Sn-123.
20 p2900 A72-39843

Shmidt cosmological hypothesis impact on geophysics, geochemistry and geology, discussing planetary evolution, initial earth temperature and gravitational differentiation
22 p3230 A72-43154

Trace element geochemistry of Apollo 16 soil 68501.
23 p3337 A72-43939

GEOCHRONOLOGY
Cosmic ray exposure age of australites and far-east tektites, using C14 content as indication of terrestrial age
06 p0878 A72-17761

- Chemical, geochronological and petrogenetic analyses of Apollo 15 lunar mare basalt rock from Hadley Rille, comparing with Apollo 12 and 14 basalts
06 p0888 A72-18264
- Fractional crystallization and crustal contamination roles in origin of quaternary basaltic magmas from Black Rock Desert Region in Utah
06 p0810 A72-18515
- Meteorite genesis and formation processes from composition characteristics, discussing age determination methods and mineralogical classifications
07 p1082 A72-20302
- Martian crater abundance correlation with surface albedo, discussing relative age of light and dark terrains
08 p1230 A72-20983
- Stopfenheim Kuppel area as part of meteorite crating event forming Reis Kessel and Steinheim Basin from quartz grain shock feature analysis
10 p1537 A72-24159
- Geological setting, petrography and history of Apollo 15 anorthosite sample, tracing fragmentation and thermal metamorphic events
11 p1722 A72-26239
- Sr isotope data indication of Glass Mountain rhyolite lava as part of parent silicic magma
11 p1623 A72-26240
- Apollo 14 Rb-Sr isotope rock sample date, relating isochron age to igneous crystallization time
17 p2607 A72-35073
- Gas retention chronology of Petersburg and other meteorites.
18 p2723 A72-36062

GECORONAL EMISSIONS

- French Lyman alpha photometer experiment on OGO 5 satellite, describing geocoronal observations, extraterrestrial emission and Bennett and Encke comets hydrogen envelopes
04 p0582 A72-15684
- D-2A satellite antisolar mission, examining Lyman alpha emission from geocorona and interstellar hydrogen wind
04 p0582 A72-15688
- Ionospheric geocoronal L alpha emission intensity related to solar activity level from Cosmos 215 satellite data
05 p0659 A72-17038
- Exosphere geocoronal hydrogen density, vertical structure and diurnal variability from Lyman spectra observational data, discussing polar wind origins
07 p0978 A72-20041
- Geocoronal hydrogen Lyman alpha glow intensity and zenith angle dependence from observations by rocket-borne extreme UV photometers
09 p1298 A72-22593
- EUV resonance radiation from He atoms and ions in geocorona, comparing model calculation based on solar radiation resonance scattering with rocket experiments
09 p1378 A72-23010
- Geocorona and interplanetary He glow EUV emission altitude distribution measured by exospheric sounding rocket-borne thin film photon counters
15 p2231 A72-32327
- Solar and geocoronal hydrogen Lyman alpha radiation detector, discussing ion chamber with magnesium difluoride window and nitric oxide gas
15 p2239 A72-32336
- Neutral hydrogen Lyman-alpha measurements in outer geocorona and in interplanetary space by two channel photometer on OGO 5
16 p2450 A72-32955

GEODESY

- NT CELESTIAL GEODESY**
- Geodetic applications of earth-moon laser ranging, discussing methods, accuracy, equipment, experiments and station characteristics
02 p0207 A72-11698
- Astronomical method of satellite photograph reduction in geodesy using photogrammetric technique
02 p0231 A72-12602
- Grazing lunar occultation method application to geodetic measurement of geographical longitude differences, noting advantage over equal-limb-line method
03 p0420 A72-13128
- Earth compartmentalization by meridians and parallels, discussing structuralization and latitude-longitude dissymmetry
03 p0350 A72-13800
- Rotating earth oblateness and equator ellipticity influence on near-equatorial synchronous satellite behavior, using nonlinear mechanics asymptotic method
03 p0436 A72-13835
- Convex figures in mathematical geodesy, applying function h for ellipse and ellipsoid of revolution
03 p0351 A72-14328
- Spatial transformation in geodesy, considering point in space as position function for orthogonal and curvilinear coordinates
03 p0351 A72-14329

Europe-Africa geodetic link in spatial triangulation of passive Pageos satellite, discussing laser telemetry operation
04 p0520 A72-15725

Iterative process convergence in least squares and maximum likelihood methods of processing measurements in spacecraft trajectory control, space navigation and geodesy systems
05 p0633 A72-16761

Soviet book on geometrical space geodesy covering satellite observation, Keplerian laws, two body problem and orbit element determination
06 p0879 A72-17817

Disturbing gravity potential and vertical deflection calculation error reduction based on pure gravity anomalies in geodesy
07 p0977 A72-19819

Laser applications in metrology and geodesy, discussing use of beam directionality for alignment purposes, interference patterns and interferometry, modulated light methods, optical Doppler methods, etc
07 p1007 A72-20222

Design and operation of hand control of automatic camera for astrogodesy used for measuring artificial earth satellites orbits
08 p1165 A72-21021

Geodetic optical distance measuring instruments with electro-optical polarization modulators, comparing characteristics of four possible configurations
09 p1314 A72-23336

Simultaneous determination of chord length and direction by artificial earth satellite geodetic observations in Arctic and Antarctic regions
13 p1945 A72-28493

Norwegian report to COSPAR on space scientific activities and application program, including satellite geodesy and earth resources research
15 p2338 A72-32009

Long baseline radio interferometry with independent frequency standards for geodetic and astrometric applications
15 p2199 A72-32074

Helmert solution for least squares method application to mean scale factor, orientation and positioning of free geodetic net
16 p2384 A72-33028

Iterative process convergence in least squares and maximum likelihood methods of processing measurements in spacecraft trajectory control, space navigation and geodesy systems
17 p2523 A72-35264

Disturbing gravity potential and vertical deflection calculation error reduction based on pure gravity anomalies in geodesy
17 p2550 A72-35744

WKB approximation and oscillatory behaviour of null geodesics in general relativity.
17 p2583 A72-35795

Comparison of two methods of astrogodetic geoid determination based on least squares prediction and collocation.
21 p3048 A72-40469

Fundamental geodetic parameters of the earth's figure and the structure of the earth's gravity field derived from satellite data.
21 p3048 A72-40494

Russian book - Space research 1970: Investigation of the gravitational fields and shapes of the earth, other planets, and the moon on the basis of spacecraft observations.
24 p3443 A72-45399

GEODETIC COORDINATES

- Lunar laser tracking determination of geodetic coordinates relative to earth gravity center
05 p0659 A72-16726
- Combined solution for station coordinates determination by geometric and dynamic satellite geodesy
07 p0974 A72-18887
- Prime geocentric meridian longitudes and UT, discussing position in terrestrial rectangular coordinates in relation to earth pole motion
07 p0976 A72-19816
- Loxodrome and geodetic line azimuths relationship on ellipsoid of revolution
08 p1158 A72-21159
- Geodetic azimuth determination by multiple observations of bright stars near meridian
09 p1297 A72-22485
- Aerial stereopair photograph orientation for geodetic coordinate adjustment in terms of collinearity, coplanarity and scaling
09 p1308 A72-22486
- Molodenski integral equation for gravitational field calculation at point M on earth surface as function of neighboring region astronomical geodetic measurements
09 p1299 A72-22675
- Stepwise adjustment of astronomic-geodetic grid, complying with exact solution
09 p1299 A72-22945
- Aircraft geodetic coordinates computation from radar range measurements and flight altitude over earth ellipsoid
15 p2224 A72-31601

Topographic mapping from airborne radar geodetic measurements, evaluating photogrammetric accuracy
15 p2224 A72-31603

Mathematical adjustment model for lunar laser ranging, noting accuracy improvement of points coordinates and orientation parameters
15 p2310 A72-31971

Geodetic latitude and altitude from geocentric coordinates.
17 p2547 A72-35103

Means of obtaining versions of orthogonal cartographic projections
17 p2548 A72-35361

Prime geocentric meridian longitudes and UT, discussing position in terrestrial rectangular coordinates in relation to earth pole motion
17 p2549 A72-35741

Great circle navigation for inertial equipped aircraft, describing procedure for determining waypoint coordinates with reference to VORTAC stations
22 p3203 A72-42949

GEODETIC SATELLITES

- NT PAGEOS SATELLITE**
- International Satellite Geodesy Experiment based on laser telemetry technique, discussing ground stations network and tracking cameras
04 p0520 A72-15726
- Geodetic satellite systems applications, describing trajectory beacons, telecontrol and telemetry stations and computing and operations center of French Geole system
06 p0809 A72-18258
- Geodetic and oceanographic applications of radar equipped satellites in polar orbits for measuring heights along geoid
06 p0809 A72-18259
- International Satellite Geodetic Experiment /ISAGEX/, using laser telemetry techniques for accurate measurement of earth gravitational field
06 p0888 A72-18261
- Report to COSPAR on Netherlands space research covering solar and stellar radiation, cosmic gamma and X rays, photometry and satellite geodesy
15 p2338 A72-32010
- NASA global tracking network clock time synchronization to microseconds accuracy via GEOS-11 satellite
15 p2199 A72-32079
- Satellite orbit computations using gravity anomalies.
21 p3104 A72-40493
- Numerical analysis of global satellite triangulation grid projects
24 p3397 A72-44868
- Exact localization of isolated points on earth surface with Geole system satellite observation, noting applications in geodetic survey, geodynamics and geophysics
24 p3398 A72-45228

GEODETIC SURVEYS

- Precision photogrammetric techniques coordinated with classical geodetic surveys for moderate cost control surveys, discussing error sources
01 p0065 A72-10455
- Geodetic determination of geoid shape by computerized laser-effect space telemetry ground stations
04 p0495 A72-15724
- European local geodetic datum centering by Doppler measurements of navigation and geodetic satellites [DFVLR-SONDDR-139]
07 p1033 A72-20273
- French Geole satellite system for geodetic survey, discussing frequency selection, antenna problems, distance measuring equipment and instrument errors
08 p1158 A72-21206
- High accuracy position determination from hyperbolic radio navigation time differences based on Sodano inverse solution of geodesics
11 p1684 A72-26498
- Vertical deflections estimation with inertial navigation system, geodetic position and velocity reference and optimal data smoother, noting applicability to surveys from moving vehicles
12 p1843 A72-27634
- Cosmological geodetic survey network construction via spacecraft tracking and laser beams, calculating power required for balloon satellite photography
13 p1922 A72-29631
- Large scale mapping by photogrammetric method based on contour points of outdated small scale aerial survey photographs, noting root-mean-square errors
13 p1959 A72-29633
- Ground station-observed balloon-borne radio beacon method for Finnish stellar triangulation network measurement
15 p2226 A72-31929
- Mathematical adjustment model for lunar laser ranging, noting accuracy improvement of points coordinates and orientation parameters
15 p2310 A72-31971
- Timing requirements in geodetic measurements with optical and electronic equipment, considering lunar laser ranging technique for high accuracy
15 p2229 A72-32075
- Three dimensional transformation for continental scale geodetic grids photogrammetry by satellite

method, noting scale alteration and Euler angles determination

16 p2387 A72-33799

Astro-azimuth comparative studies with Wild T3, Wild T4, and Kern DKM3 theodolites.
[AIAA PAPER 72-842]

20 p2923 A72-39087

Aerotriangulation by simultaneous adjustment of photogrammetric and geodetic observations /SAPGO/ incorporating geodetic distances, horizontal angles, Laplace azimuths, longitudes, latitudes and elevation differences

20 p2927 A72-39738

Russian book - Stereophotogrammetric processing methods for photographs made from a mobile basis.

22 p3175 A72-42025

The application of error control techniques in the design of an advanced augmented inertial surveying system.

24 p3421 A72-44641

Determination of the mutual position of points on the earth's surface from synchronous laser observations of artificial earth satellites

24 p3397 A72-44860

Numerical analysis of global satellite triangulation grid projects

24 p3397 A72-44868

Exact localization of isolated points on earth surface with Geole system satellite observation, noting applications in geodetic survey, geodynamics and geophysics

24 p3398 A72-45228

GEODIMETERS

Mathematical adjustment model for lunar laser ranging, noting accuracy improvement of points coordinates and orientation parameters

15 p2310 A72-31971

GROELECTRICITY

NT TELLURIC CURRENTS

Geoelectric field strengths deduction from mid-frequency slopes on diurnal incidence plot of pc 1 hydromagnetic whistlers

07 p0974 A72-18904

Distortion corrections in geophysically traced gravitational, magnetic and geoelectric field maps, discussing automation

14 p2101 A72-30642

GEOFRACTURES

U GEOLOGICAL FAULTS

GEOGRAPHY

NT OROGRAPHY

Mars surface features Schiaparelli nomenclature from Mediterranean Sea area classical geography

04 p0569 A72-14500

High-orbital satellite global photographs and TV pictures, discussing planetary geographical and topographical data interpretation

15 p2225 A72-31807

Radar imaging systems application to cartography, geology, hydrology, biogeography, oceanography and geography, emphasizing remote sensing in cloudy environments

16 p2364 A72-33634

GEOIDS

Geodetic determination of geoid shape by computerized laser-effect space telemetry ground stations

04 p0495 A72-15724

Geoid isostasy, protrusions and hollows, discussing attenuations and intensifications of gravity

17 p2548 A72-35425

Self-consistent statistical models for the gravity anomaly, vertical deflections, and undulation of the geoid.

18 p2723 A72-36028

Comparison of two methods of astrogeodetic geoid determination based on least squares prediction and collocation.

21 p3048 A72-40469

GEOLOGICAL FAULTS

Remote sensor viewing angle effect on detectability of geological faults in side-looking airborne radar image data by optical spatial frequency analysis

02 p0209 A72-11791

GEOLOGY

NT GEOCHRONOLOGY

NT GEOMORPHOLOGY

NT LITHOLOGY

NT LUNAR GEOLOGY

NT OROGRAPHY

NT PETROGRAPHY

NT PETROLOGY

NT PHOTOGEOLOGY

NT TECTONICS

NT VOLCANOLOGY

Remote sensing of environment - Conference, University of Michigan, May 1971

02 p0207 A72-11776

Regional geological surveying by satellite-borne TV, discussing image interpretation methodology

02 p0208 A72-11780

Northern Alps geology, hydrology, lithology and tectonic survey, using aircraft-borne thermal IR scanner remote sensor

02 p0209 A72-11795

Crop, soil and geological mapping from digitized multispectral satellite photography, discussing data processing requirements and surface features distinguishable from satellite altitudes

02 p0214 A72-11876

Thermal modeling for IR images geologic interpretation, discussing physical parameters role in materials natural environmental diurnal temperature behavior

02 p0214 A72-11877

Automatic geologic mapping with calibrated narrow band visible and near IR rock reflectivity data and computer processing

02 p0215 A72-11878

Hyperaltitude photography evaluation for geological mapping, comparing Gemini 4 and aerial photographs

02 p0216 A72-11891

Satellite communication regional and domestic applications, discussing educational, earth resources, geological survey, environmental and maritime uses

04 p0487 A72-15073

Q values contradiction between lunar and earth rocks, discussing internal friction

04 p0580 A72-15450

Northeast Bank, Southern California Borderland volcanic petrology and geologic history, investigating basaltic rocks, hyaloclastites and fossil fragments

04 p0520 A72-15589

Meteoritic cosmic catastrophe, interpreting flat depression in northern Siberian plateau Khatanga river basin

05 p0713 A72-15977

Remote sensing methods in geology, discussing air/satellite-borne black and white, color and multispectral photographic, TV, multispectral scanning, IR and radar techniques

06 p0809 A72-18228

Meteorological satellites and Gemini and Apollo earth photographs, showing annual and diurnal oceanographic, hydrologic and geologic dynamic features

06 p0810 A72-18614

Origin of life as chemical evolution product, tracing juvenile carbon history through planetary and geological phases

08 p1162 A72-22004

Regional geologic features of Alaska and Western Canada from Nimbus 4 satellite image dissection camera system /IDCS/ photographs

10 p1477 A72-25109

Geological verification in search for origin of vagabond tektites, commenting on Caribbean label bediasite find

15 p2303 A72-31307

Radar imaging systems application to cartography, geology, hydrology, biogeography, oceanography and geography, emphasizing remote sensing in cloudy environments

16 p2364 A72-33634

Microwave emission from geological materials - Observations of interference effects.

20 p2917 A72-39477

Schmidt cosmological hypothesis impact on geophysics, geochemistry and geology, discussing planetary evolution, initial earth temperature and gravitational differentiation

22 p3230 A72-43154

GEOLOGICAL ANOMALIES

U MAGNETIC ANOMALIES

GEOLOGICAL CROTCHETS

U SUDDEN IONOSPHERIC DISTURBANCES

U MAGNETIC EFFECTS

GEOLOGICAL EQUATOR

U MAGNETIC EQUATOR

GEOLOGICAL FIELD

U GEOMAGNETISM

GEOLOGICAL LATITUDE

Primary component corrections for global cosmic ray variations from latitudinal expeditions, discussing adaptation to computer

01 p0118 A72-10584

Nighttime ionospheric radio wave propagation, determining geomagnetic latitude variations effects on absorption and reflection

02 p0218 A72-11944

Magnetic latitude effect on wave dispersion in drifts and random movements of ionization irregularities in E region, suggesting charged particle precipitation role

04 p0518 A72-14964

Auroral absorption prediction during disturbed conditions in communications as function of frequencies and radio ranges at different geomagnetic time and coordinates

05 p0626 A72-16009

Latitudinal distribution of electron temperature in F 2 layer during summer daytime period of low solar activity from electron density profile geometrical parameters

05 p0656 A72-16248

Latitudinal, diurnal, seasonal and solar cycle variations in vhf-uhf scintillation producing irregularities in F layer electron density

05 p0630 A72-16617

GEOMAGNETIC MICROPULSATIONS

Imp 5 magnetic field measurements at high geomagnetic latitudes in outer magnetosphere near noon meridian, noting depressed field region centered on polar cusp

07 p0975 A72-19146

F region ionization anomalous evening enhancement, discussing seasonal variations, solar activity and geomagnetic coordinates maximum in Yakutsk

08 p1153 A72-20707

Geomagnetic Pc3 pulsations amplitude distribution patterns along meridional profile, determining source from maximum near 60 N

08 p1155 A72-20741

Magnetic field effect on elf radio wave attenuation during propagation under six ionospheres, showing dependence of minimum on propagation path geomagnetic latitude

08 p1131 A72-21103

Nighttime ionospheric radio wave propagation, determining geomagnetic latitude variations effects on absorption and reflection

13 p1949 A72-29256

Short period geomagnetic pulsations with gradual amplitude increase and abatement, noting latitudinal variation

14 p2103 A72-30665

Latitudinal energy distribution of geomagnetic disturbances

18 p2688 A72-36868

Latitudinal rotation direction daytime characteristics of pc 5 pulsation polarization based on global magnetic observations

18 p2689 A72-36870

F region ionization anomalous evening enhancement, discussing seasonal variations, solar activity effects and maximum value dependence on geomagnetic latitude and longitude

19 p2790 A72-38335

Geomagnetic Pc 3 pulsations amplitude distribution patterns along meridional profile, determining source from maximum near 60 N

19 p2791 A72-38369

Cosmic ray muon sea level momentum spectra and charge ratios geomagnetic latitude dependence measurements by spark chamber technique

19 p2853 A72-38754

East-west asymmetry of cosmic rays at the sea level in the range of geomagnetic latitudes from 50 N to 20 S

23 p3328 A72-43355

GEOMAGNETIC MICROPULSATIONS

Decreasing period micropulsations during elementary magnetospheric substorms, discussing relation to ring current asymmetry development

01 p0059 A72-10602

Spectrum analysis of synchronous recordings of Pi 1 irregular pulsations and auroral brightness at Sogra for ionospheric electric fields

02 p0216 A72-11923

Broadband geomagnetic micropulsations relations to magnetospheric, interplanetary and solar phenomena

02 p0222 A72-12869

Coastline effect on electric field strength of geomagnetic micropulsations

03 p0344 A72-12977

Nighttime plasmopause and thermal ion plasma structures relationship to micropulsations, considering excitation in post storm recovery and diurnal plasma bulge regions

06 p0804 A72-17453

Geomagnetic storm associated quasi-sinusoidal magnetic field micropulsations due to Alfvén/drift instability or enhanced storm-time ring current

06 p0804 A72-17454

Geomagnetic micropulsations on ground and magnetic field fluctuations in tail, noting field strength changes

06 p0804 A72-17455

Midlatitude geomagnetic micropulsations polarization and spectral characteristics, explaining behavior in terms of MHD wave propagation theories

07 p0975 A72-19152

Midlatitude and equatorial geomagnetic micropulsations during 13-14 January 1967 world-wide magnetic storm from ground and satellite observations

08 p1157 A72-21107

OGO-E plasmopause crossing correlation with ground observations of Pi geomagnetic micropulsations

08 p1159 A72-21223

Polarization characteristics measurement for PC 1 geomagnetic micropulsations propagated through ionospheric ducts, noting hydromagnetic emissions and whistlers relation to high latitude source region

09 p1299 A72-22989

Spectrum analysis of synchronous recordings of Pi 1 irregular pulsations and auroral brightness at Sogra for ionospheric electric fields

13 p1948 A72-29235

Polarization and spatial and frequency characteristics of ground signal resulting from finite source Pc 1 micropulsation disturbance

13 p1922 A72-29391

Plasmapause and geomagnetic micropulsations correlation from universal magnetospheric instability model, noting drift waves conversion to sound or Alfvén waves

16 p2387 A72-33906

Association between quasi-periodic VLF emission and micropulsation.

17 p2516 A72-35065

Day to day variation of Schumann resonance frequency and occurrence of Pc 1 in view of solar activity.

17 p2548 A72-35464

Ground recorded Pc 1 micropulsations occurrence frequency relationship to ionospheric spread F based on long term ionosonde recordings

18 p2685 A72-35987

Latitudinal rotation direction daytime characteristics of pc 5 pulsation polarization based on global magnetic observations

18 p2689 A72-36870

Elliptically polarized ionospheric source generation of short period geomagnetic disturbances at earth surface

19 p2791 A72-38347

Geomagnetic Pc 3 pulsations amplitude distribution patterns along meridional profile, determining source from maximum near 60 N

19 p2791 A72-38369

Nonlinear theory of particle motion in monochromatic Alfvén wave field application to Pc-1 geomagnetic pulsations evolution

20 p2917 A72-39408

Propagation of HM-waves with periods corresponding to periods of Pci micropulsations through the lower ionosphere.

21 p3015 A72-40497

Pc 1 hydromagnetic whistlers and emissions polarization characteristics measured in plane of earth surface

22 p3169 A72-42019

Occurrence of Pc 4, 5 micropulsation activity at the polar cusp.

22 p3171 A72-42411

Investigation of interaction between Pc 1 and 2 and Pc 5 micropulsations at the synchronous orbit during magnetic storms.

22 p3171 A72-42412

Statistical characteristics of storm-associated Pc 5 micropulsations observed at the synchronous equatorial orbit.

22 p3171 A72-42413

Some results of an analysis of Pc4-type steady geomagnetic pulsations at a network of stations

23 p3283 A72-43372

Diurnal variation of the correlation of Pc 3 and Pc 4 micropulsation characteristics with magnetic activity.

23 p3286 A72-44524

Micropulsations and VLF emissions during substorms.

24 p3396 A72-44855

GEOMAGNETIC PULSATIONS

NT GEOMAGNETIC MICROPULSATIONS

Plasma electron and proton motion in equatorial plane of magnetosphere under geomagnetic disturbance generated electric field

01 p0058 A72-10586

Geomagnetic PDP pulsations oscillation frequency drift, considering proton motion characteristics in magnetospheric equatorial plane

02 p0217 A72-11931

Long period geomagnetic pulsation generation at boundary of magnetosphere and incoming solar wind, considering possibility from idealized model

02 p0218 A72-11950

Damped geomagnetic pulsations associated with geomagnetic storms interpreted as interaction between hydromagnetic oscillations and solar wind induced magnetospheric motions, discussing modified mathematical model

02 p0222 A72-12872

Geomagnetic micropulsation activity relationship to magnetospheric processes and interplanetary magnetic field, investigating time dependence of telluric current

04 p0515 A72-14927

Solar effects contradictory relationships with earth atmosphere, discussing geomagnetic disturbance, annual variations, stratospheric transport and high energy particles

05 p0656 A72-16233

Arctic polar region geomagnetic perturbations during IQSY, noting diurnal variations

05 p0658 A72-16278

Geomagnetic pulsations correlation with h type ionospheric sporadic echoes, considering effects on electromagnetic disturbances transmission

05 p0659 A72-16725

Geomagnetic disturbances morphology, considering development and decay of magnetic storms and appearance of geomagnetic pulsations

06 p0802 A72-17367

Solar wind discontinuities and shock waves in interplanetary medium at magnetospheric boundary related to geomagnetic impulses

07 p1061 A72-20024

Elliptically polarized ionospheric source generation of short period geomagnetic disturbances at earth surface

08 p1153 A72-20719

Geomagnetic Pc3 pulsations amplitude distribution patterns along meridional profile, determining source from maximum near 60 N

08 p1155 A72-20741

Geophysical data analysis for high latitude negative geomagnetic disturbances revealing geomagnetic pulsations during auroral arcs passage

08 p1155 A72-20809

Geomagnetic activity annual variations from daily international magnetic character figures analysis by time series numerical filter method, discussing sunspot cycle effect

09 p1298 A72-22584

Solar activity effects in magnetosphere and ionosphere relation to geomagnetic activity and biospheric development, noting 11 year geomagnetic perturbation cycles

12 p1805 A72-28209

Geomagnetic field perturbation biological effects, studying geomagnetic storm field energy levels and magnetic flux variables relation to human sensitivity thresholds

12 p1773 A72-28210

Pc 5 type geomagnetic pulsations correlation with nighttime magnetosphere auroral magnetic disturbances from magnetograms obtained at Murmansk, College /Alaska/ and Tiksi

13 p1947 A72-28606

Geomagnetic PDP pulsations oscillation frequency drift, considering proton motion characteristics in magnetospheric equatorial plane

13 p1949 A72-29243

Long period geomagnetic pulsation generation at boundary of magnetosphere and incoming solar wind, considering possibility from idealized model

13 p1949 A72-29262

Impulsive pulsations /Pi 2/ identification as geomagnetic field distension coincident with oscillatory component from high resolution Rb vapor magnetometer recordings

13 p1951 A72-29656

Geomagnetic field perturbation by gamma quanta pulsating source, studying accompanying radio emission behavior

14 p2101 A72-30645

Harmonic analysis of solar wind geometry and geomagnetic activity levels during even and odd cycles based on cosmic ray intensity variations for 1900-1969 period

14 p2147 A72-30651

Short period geomagnetic pulsations with gradual amplitude increase and abatement, noting latitudinal variation

14 p2103 A72-30665

Earth electrical conductivity radial distribution effect on solar quiet day geomagnetic field variations

14 p2103 A72-30666

Earth core hydromagnetic oscillations with respect to geomagnetic secular variation time scales and role in dynamo process-produced geomagnetic field

15 p2222 A72-31279

Geomagnetic pulsations long term statistical forecast, obtaining averaged yearly pearls activity

15 p2222 A72-31426

Indices of geomagnetic pulsations.

17 p2545 A72-34628

High speed spectrum analyzer /hissa/ and its application to the study of geomagnetic pulsations. I - S-type hissa.

17 p2554 A72-35061

Daytime irregular geomagnetic pulsation, P_{id}, and its relation to magnetospheric substorm.

17 p2546 A72-35062

Auroral substorm and proton auroras during moderate geomagnetic disturbances

17 p2550 A72-35857

Earth magnetosphere pinch effect related to geomagnetic field pulsations and polar aurora luminosity fluctuations

17 p2688 A72-36867

Earth surface magnetic field intensity variations in terms of magnetospheric resonator excitation, assuming three dimensional Alfvén waves

18 p2688 A72-36869

Secular variation of the geomagnetic field in epoch 1965 to 1970 according to observatory and satellite data

18 p2689 A72-36871

Geomagnetic field fluctuations during storms, considering Alfvén waves generation and propagation in solar wind and magnetosphere

19 p2791 A72-38345

DP-2 mode daily magnetic variation in polar cap based on magnetic and auroral records, noting relationship to magnetospheric substorms

22 p3168 A72-42005

Nature of polar-aurora light intensity pulsations associated with Pi2-type geomagnetic pulsations

23 p3282 A72-43359

Earth collisionless plasma bow shock oblique structure assessment by pulsation index Ip devised from empirical results

23 p3341 A72-44511

Pc 5 type geomagnetic pulsations correlation with nighttime magnetosphere auroral magnetic disturbances from magnetograms obtained at Murmansk, College /Alaska/ and Tiksi

24 p3398 A72-45106

GEOMAGNETIC STORMS

U MAGNETIC STORMS

GEOMAGNETIC TAIL

Auroral absorption and DR currents development during magnetic storms, discussing corpuscular fluxes arrival from magnetospheric tail into lower ionosphere

01 p0059 A72-10619

High latitude magnetotail highly directed nearly monoenergetic positive ions population observation during geomagnetic storms, using Vela satellites electrostatic analyzers

01 p0060 A72-10887

Magnetic field and plasma sheet variations observation by IMP 3 satellite in distant magnetotail during magnetospheric substorms

01 p0060 A72-10888

Magnetosphere and adjacent regions magnetic surveys by OGO 1 and 3 satellites, discussing magnetopause, bow shock, magnetosheath, geomagnetic tail, ring current and polar substorms

02 p0220 A72-12084

Magnetosphere model for low energy cosmic ray proton propagation mode to synchronous orbit satellite, calculating geomagnetic cutoffs and penetration regions

02 p0274 A72-12453

Solar proton entry observations over polar caps in relation to magnetosphere, magnetotail and magnetopause models

02 p0275 A72-12463

Plasma sheet thinning in substorms correlated to auroral oval poleward expansion and associated phenomena in magnetotail

03 p0348 A72-13514

Geomagnetic tail natural oscillations, applying model of plasma cylinder with free boundary immersed in interplanetary medium

05 p0659 A72-17044

Internal neutral sheet in geomagnetic tail from Explorer 34 magnetic field experiment, noting quasi-periodic structure and magnetic loop formation

06 p0803 A72-17450

Geomagnetic micropulsations on ground and magnetic field fluctuations in tail, noting field strength changes

06 p0804 A72-17455

Magnetic flux determination in magnetosphere tail during substorm from auroral oval boundary and center location observation

06 p0807 A72-17985

Neutral current sheath formation from plane dipole magnetic field extension by plasma flow, discussing solar corona streamers and geomagnetic tail

07 p1039 A72-18914

Solar electrons and protons measurements in interplanetary space and in magnetotail, noting access to north polar cap

07 p1058 A72-19156

Solar wind and geomagnetic tail interaction with moon, discussing lunar Mach cone evidence for anisotropic wave propagation in magnetized collisionless warm plasma

07 p1061 A72-20025

Spherical harmonic representations of geomagnetic field including magnetosphere and tail regions based on ground based and low altitude spacecraft measurements within several earth radii

07 p0977 A72-20026

Magnetospheric and polar substorms model for auroral particles acceleration and geomagnetic tail current diversion to auroral oval night side

07 p0977 A72-20029

Plasma sheet distribution in magnetosphere from low energy particle observations in equatorial region of magnetotail

07 p0977 A72-20031

Geomagnetic tail role in magnetospheric substorms, discussing solar wind energy storage, magnetic merging process and plasma sheet origin

07 p0977 A72-20032

Shock wave excitation by moving solar wind discontinuity in geomagnetic tail as cause of active phase of magnetospheric substorm

08 p1153 A72-20716

Atmospheric model for plasma motion along surface of geomagnetic tail under action of interplanetary, magnetic lines of forces

08 p1153 A72-20722

Plasma layer effect on natural oscillations of magnetosphere tail, using infinite plasma cylinder model immersed in interplanetary plasma

11 p1622 A72-25944

Average plasma sheet configuration in geomagnetic tail at lunar orbit, presenting seasonal dependence and variations with geomagnetic activity

11 p1624 A72-26396

- Geomagnetic tail model with plasma cylinder immersed into solar wind, obtaining dispersion equation for oscillations 11 p1627 A72-26532
- Geomagnetic tail and substorm activity structure from IMP-3 magnetic data, discussing plasma sheet thickness changes and magnetic flux distribution 11 p1627 A72-26533
- Theory of magnetotail elongation based on magnetosphere neutral layer drift notion due to electric current from trapped charge carriers inside surrounding plasma sheath 12 p1802 A72-27770
- Russian book on geomagnetic field cosmic rays covering charged particle motion theory, extraionosphere currents, magnetosphere tail and solar wind effects, etc 12 p1864 A72-28345
- Two dimensional equilibrium solution of plasma sheet, applying to tail magnetosphere problem 13 p1954 A72-29959
- Anomalies detected in Mars 3 solar wind recordings interpreted as possibly caused by geomagnetic tail crossed by interplanetary probe 13 p2034 A72-30010
- Magnetosphere tail internal plasma boundary layer dynamics during substorms based on aurora data 14 p2103 A72-30663
- Model for magnetospheric substorm growth phase, noting dayside magnetopause convection onset, geomagnetic tail configurational changes and breakup with auroral electrojet development 16 p2387 A72-33903
- Conducting fluid flow near neutral sheet in magnetic field, assuming cold polar wind plasma geomagnetic tail 16 p2438 A72-33930
- Consequences of an isotropic static plasma sheet in models of the geomagnetic tail. 17 p2545 A72-34636
- Entry of high-energy solar protons into the distant geomagnetic tail. 17 p2601 A72-35588
- Flaring-tail model explanation for geomagnetic tail configuration changes during magnetospheric substorm growth phase 17 p2548 A72-35589
- Shock wave excitation by moving solar wind discontinuity in geomagnetic tail as cause of active phase of magnetospheric substorm 19 p2791 A72-38344
- Atmospherical model for plasma motion along surface of geomagnetic tail under action of interplanetary magnetic lines of force 19 p2791 A72-38350
- Reconnection of the geomagnetic tail deduced from solar-particle observations. 19 p2792 A72-38730
- Explorer 35 observation of geomagnetic tail low energy electrons, noting plasma sheet extension to lunar distance and correlation with solar wind 19 p2853 A72-38737
- Persistent particle anisotropies and magnetospheric models. 20 p2916 A72-39233
- Neutral current sheath formation from plane dipole magnetic field extension by plasma flow, discussing solar corona streamers and geomagnetic tail. 20 p2957 A72-39380
- Magnetospheric shapes, flows and substorms in terms of magnetotail flux, solar wind pressure, dipole moment and plasma sheet interaction 20 p2919 A72-39546
- Magnetic neutral sheet model in terms of self-consistency between current and tail field in reversal region 20 p2919 A72-39548
- Auroral space-time regularities relationship to magnetospheric variations, precipitating electron fluxes, magnetic tail formation and substorms 20 p2920 A72-39977
- Sudden impulses in the geomagnetotail and the vicinity. 22 p3168 A72-42002
- Resonant interaction of an electrostatic wave with electrons in a current sheet. 22 p3169 A72-42008
- Simultaneous solar-wind plasma and magnetic-field measurements in the expected region of the extended geomagnetic tail. 22 p3170 A72-42405
- Plasma sheet characteristics of geomagnetic tail at 60 earth radii, inferring spatial distribution of magnetic field magnitude and plasma energy density 22 p3211 A72-42407
- Magnetic tension induced stress balance in plasma sheet, considering pressure gradient along geomagnetic tail axis, plasma flow kinetic energy and pressure anisotropy 22 p3211 A72-42408
- Coordinated observations of the magnetosphere - The development of a substorm. 22 p3171 A72-42410
- Self-consistent description of the magnetotail current system. 22 p3172 A72-42429
- Solar-wind parameter variation, magnetic activity, and electrons in the magnetospheric tail and outer radiation belt 23 p3283 A72-43367
- A current instability in the neutral layer of the tail of the earth's magnetosphere 23 p3283 A72-43368
- Outer magnetosphere near midnight at quiet and disturbed times. 23 p3341 A72-44513
- Measurements of magnetotail plasma flow made with Vela 4B. 23 p3342 A72-44514
- Detection of earthward flow of keV protons in the geomagnetic tail at lunar distances. 23 p3333 A72-44532
- Ionospheric current relation to magnetospheric field-aligned and ring currents, noting effect of magnetospheric tail electric field on polar magnetic substorms 24 p3396 A72-44852
- Magnetic field fluctuations during substorms. 24 p3396 A72-44853
- Substorm related changes in the geomagnetic tail - The growth phase. 24 p3397 A72-44856
- Geomagnetic tail magnetic and electric fields ULF, VLF and ELF fluctuations, considering relationship to substorm processes 24 p3397 A72-44857
- GEOMAGNETICALLY TRAPPED PARTICLES**
- U RADIATION BELTS**
- GEOMAGNETISM**
- Plasma sheet structures, dynamics and role in magnetospheric substorm onset as function of near earth and distant merging regions 01 p0052 A72-10082
- Skylark rocket observations of sporadic E layer magnetic fields, winds and ionization indicating ion divergence region 01 p0052 A72-10086
- Geomagnetic storm field recovery near synchronous satellite ATS 1 in terms of ring current belt and plasma sheet variations 01 p0053 A72-10088
- Geomagnetism, discussing world field distribution, secular variation, paleomagnetism, archaeomagnetism, origin, magnetic anomaly and earth electromagnetic induction 01 p0053 A72-10168
- Equivalent current system from measured geomagnetic disturbance vectors, solving Biot-Savart formula derived nonlinear equations by Newton-Raphson iterative method 01 p0055 A72-10430
- Optical aurora relationship to radio counterpart, showing backscattered signal peak amplitude close correlation to magnetic bay peaks 01 p0056 A72-10440
- Hall effect and magnetic field characteristics in lower ionosphere by vertical magnetospheric currents, using gyrotropic model 01 p0059 A72-10590
- Earth magnetosphere boundary position, bow shock wave, transition region thickness and magnetopause currents magnetic fields during geomagnetic storms 01 p0059 A72-10605
- Magnetospheric magnetic field distortions under quiet and slightly disturbed conditions, obtaining scalar intensity withOGO 3 and 5 rubidium vapor magnetometer 01 p0060 A72-10886
- Lower ionospheric nighttime absorption as ionization processes indicator, discussing relationship to geomagnetic activity 02 p0216 A72-11921
- Geomagnetic field and AU/AL index variations with UT during international quiet days at high latitudes interpreted as electrojet diurnal redistribution 02 p0217 A72-11930
- Dynamo theory MHD equations numerical solution, showing rapid variation of electromagnetic field, hydrodynamic velocities and earth core magnetic moment 02 p0217 A72-11933
- Geomagnetic field extrapolated spherical data for years 1600 to 1800 from declination and inclination analysis, giving Gaussian coefficients and errors 02 p0218 A72-11953
- Idealized model for small scale internal structure of magnetopause separating distorted geomagnetic field in magnetosphere from solar plasma flow in magnetosheath 02 p0218 A72-11977
- Ionospheric effects related to production, maintenance and control of geomagnetically aligned Birke-land current system 02 p0219 A72-11978
- Papers on world geomagnetic survey 1957-1969 covering land, sea, airplane and polar-orbiting geophysical observatory satellite observations, magnetic anomalies and reference field 02 p0219 A72-12080
- Geomagnetic dynamo theory postulating magnetic field by self excitation due to electric currents within earth core 02 p0220 A72-12086
- Conducting fluid convective motion in earth core estimated from geomagnetic field and time derivative data at earth surface 02 p0220 A72-12087
- Geomagnetism theory of dynamos in homogeneous fluid masses, considering Rikitake self reversing, kinematic and hydromagnetic dynamo problems 02 p0220 A72-12088
- Meteor trail forms diversity explanation from magnetic pressure and Reynolds number and plasma diffusion in magnetic fields, discussing geomagnetic effect on trail shape 02 p0282 A72-12336
- Equatorial ionospheric drift measurements and relation to electrojet from H component geomagnetic field variations 02 p0221 A72-12459
- Cosmos 65 global ozone contour data similarity with geomagnetic L shells configuration, discussing South Pacific region depletion area 02 p0221 A72-12466
- Chapman uniform electrical conductivity core model for geomagnetic disturbance daily variations due to solar wind, noting error in analysis 02 p0222 A72-12794
- Plasmasphere size changes from K indices of geomagnetic activity, comparing with Binsack formula 03 p0344 A72-12909
- Geomagnetic field effect on radar echoes from meteor trains during Geminid shower 03 p0345 A72-12982
- Sporadic E disappearance due to temporary reversal of equatorial electrojet current, observing horizontal geomagnetic field component 03 p0345 A72-12999
- Geomagnetic field and interplanetary plasma parameters daily variations correlation, taking into account corrections for storm time effects 03 p0348 A72-13511
- Meridian and local vertical gyro errors effects on geomagnetic field elements determination accuracy 03 p0359 A72-13559
- Jupiter decametric radio emission relation to solar wind, geomagnetic activity and shock waves causing Forbush decreases 03 p0436 A72-13820
- Earth triaxiality from satellite data, obtaining non-zero values for harmonic coefficients 03 p0351 A72-14327
- Quiet day diurnal variability of equatorial geomagnetic field H component related to ionospheric dynamics 04 p0515 A72-14878
- Electrojet effects on critical frequencies in equatorial F region during magnetically quiet and disturbed days 04 p0516 A72-14936
- Geomagnetic effects on lower ionosphere at lower midlatitude station, discussing long wave propagation 04 p0516 A72-14939
- Planetary magnetic activity effects on hf cosmic noise absorption measurements at low and temperature latitudes 04 p0516 A72-14941
- Radio stars wave amplitude scintillation during passage through ionosphere observed by interferometer, noting association with geomagnetic field fluctuation 04 p0567 A72-14953
- Five component electromagnetic field station to record geomagnetic field magnetic and electric components variations 05 p0643 A72-16253
- Noncircular ionospheric current conversion into longitudinal currents in magnetosphere along lines of force of geomagnetic field 05 p0657 A72-16259
- Electrical conduction in orthogonal coordinates from nondipole geomagnetic field effect on conductivity tensor of ionospheric dynamo region 05 p0657 A72-16260
- Lower ionospheric currents fields, determining Hall conductivity and geomagnetic lines of force slope effects 05 p0657 A72-16266
- Magnetospheric current effects on geomagnetic field structure, noting electron and proton precipitation into auroral zone 05 p0657 A72-16275
- Nonlinear propagation effects of monochromatic circularly polarized vlf waves /whistlers, heli cons/ along field lines in magnetosphere 05 p0658 A72-16603
- Geomagnetic field-hf sky wave orthogonality conditions, discussing ray tracing for signals reflected in ionosphere 05 p0630 A72-16619
- Proton measurements in ring current byOGO-3 satellite compared with geomagnetic field data at low and high latitudes 05 p0711 A72-17034

Worldwide magnetic storm due to solar wind interaction with geomagnetic field, discussing field deformation 06 p0803 A72-17368

Statistical criteria of geomagnetic activity, considering solar corpuscular radiation effect 06 p0803 A72-17369

Geomagnetic field measurement, discussing variometers and magnetographs theory 06 p0812 A72-17370

Geomagnetic field vector components measurement methods, considering data processing problems 06 p0812 A72-17371

Aeromagnetic surveying with airborne fluxgate magnetometer, discussing field data compilation and interpretation 06 p0812 A72-17373

Sounding rocket observations of magnetic field aligned electron pitch angle distributions coincident with auroral precipitation band northern boundary 06 p0804 A72-17457

Geomagnetic dipole field kinematic reversals due to cyclonic convective cell distribution fluctuations in earth core 06 p0807 A72-17895

Misalignment angle of Azur satellite orientation axis relative to geomagnetic field vector 06 p0892 A72-18145

Geomagnetic field intensity fluctuations due to events in atmosphere, ionosphere, magnetosphere and in interplanetary space connected with solar activity 06 p0809 A72-18276

Low latitude surface horizontal magnetic field intensity depression due to quiet time ring current in magnetosphere as function of solar wind velocity 07 p1055 A72-18884

Magnetospheric field model from magnetosphere surface approximation by paraboloid of revolution 07 p0974 A72-18903

Pitch angle distributions of energetic protons for different geomagnetic activity levels as function of invariant latitude and magnetic local time from ESO IB satellite measurements 07 p1057 A72-19141

Earth bow shock magnetic field data correlation with Ogo 5 flux gate magnetometer, using Tidman-Northrop theory 07 p0975 A72-19145

Trapped particle motion response to collapsing dipole moment in secularly varying geomagnetic field 07 p1058 A72-19158

Secular geomagnetic dipole moment decrease effect on inner proton belt proton energy distribution, comparing with radial diffusion influences 07 p1058 A72-19159

High time resolution of low latitude asymmetric disturbances in geomagnetic field by Fourier analysis for substorm activity studies 07 p0976 A72-19165

Spherical harmonic representations of geomagnetic field including magnetosphere and tail regions based on ground based and low altitude spacecraft measurements within several earth radii 07 p0977 A72-20026

Particle motions in earth magnetospheric tail and core, estimating maximum rate of magnetic field annihilation and magnetic drift shell 07 p1062 A72-20027

Magnetic disturbance singularities searched for in horizontal intensity, showing field depressions around September 5 07 p0980 A72-20406

Geomagnetic phenomena associated with auroras and magnetic storms, investigating analog modeling experiment by stationary electrical discharges under laboratory conditions 07 p0980 A72-20457

Geomagnetic field optimal model with expansion of spherical harmonic series by least squares method 07 p0980 A72-20657

Earth and interplanetary magnetic fields spectral power density characteristics at 0.0001-1 Hz 08 p1153 A72-20718

Unified coordinate system for earth planetary distribution of F2 and sporadic E layer transmission parameters, suggesting geomagnetic longitude and modified magnetic inclination 08 p1153 A72-20726

Solar unipolar magnetic regions relation to geomagnetic disturbances variability, discussing 11 year cycle 08 p1155 A72-20808

Digital computer numerical procedure to solve dynamo theory MHD equations for earth nucleus, using combination of Fourier and finite difference methods for integration 08 p1155 A72-20810

Solar wind flux velocity diurnal variations relation to magnetic activity index based on Mariner 2 and 4, Pioneer 6 and Vela satellites data 08 p1226 A72-20821

Comet brightness variations correlation with geomagnetic field and solar corpuscular flux variations in interplanetary space 08 p1231 A72-21132

Solar energetic particle access characteristics to magnetosphere from PCA riometer and satellite measurements, determining relationship between earth dipole field and interplanetary field 08 p1228 A72-21497

Auroral zone neutral wind velocity and atmospheric temperature correlations with geomagnetic activity, considering ion-neutral particle drag as accelerating mechanism during magnetic storms 08 p1161 A72-21535

Spectral distribution characteristics of geomagnetic field mean intensity variations, relating longitudinal specific resistance and integral conductivity of top rock layer 09 p1296 A72-22236

Geomagnetic field effects on initially spherically symmetric ion cloud diffusive motion in earth upper atmosphere 09 p1297 A72-22577

Solar particles latitudes dayside profiles as function of geomagnetic activity, suggesting closed field lines limit location 09 p1378 A72-23002

Geomagnetic field short term variations as function of solar activity from solar radiation data harmonic analysis, relating large amplitude fluctuation to seasonal variations 09 p1304 A72-23503

Geomagnetic field inflation during magnetic storm main phase, considering energy sources and injected proton plasma radial velocity 10 p1472 A72-24274

Earth precession as origin of geomagnetic field, discussing dynamo theory and core electroconductivity 10 p1472 A72-24254

Topside ionosphere characteristics, discussing particle mean free path and geomagnetic field effects on conductivity, plasma anisotropies and latitudinal variations 10 p1473 A72-24704

Equatorial sporadic E sudden disappearance associated with magnetic field depressions, noting irregularities and electron velocities role 10 p1475 A72-24956

Semiannual and annual modulation of geomagnetic field horizontal intensity, suggesting two component model of generating mechanism 10 p1476 A72-24960

Apollo 14 charged particle lunar environment experiment data analysis, noting earth plasma sheet absence at lunar distance during geomagnetically quiet times 10 p1476 A72-24961

Book on earth environment covering atmospheric structure, terrestrial magnetic field, solar radiation, micrometeorites, ionosphere and van Allen belts 10 p1478 A72-25173

Geomagnetic field and magnetosphere variations due to solar wind interactions, using rocket, satellite and indirect measurements 11 p1621 A72-25841

Interplanetary and magnetospheric magnetic force lines reconnection and effects on geomagnetic activity 11 p1718 A72-25933

Declinational component of geomagnetic lunar tide diurnal variations, noting effects of electric currents induced in oceans 11 p1622 A72-26103

Changes in total magnetic energy stored outside earth core accompanying earth dipole field decrease over 60 years period from paleomagnetic measurement 11 p1623 A72-26108

Low latitude geomagnetic field diurnal variations caused by solar wind associated component, noting evening side depression 11 p1713 A72-26109

Lunar variations of Peruvian electrojet, analyzing E region electron drift and geomagnetic field H component data 11 p1626 A72-26415

Geomagnetic Sq current electric field mapping into lower atmosphere, calculating equipotential surfaces 11 p1626 A72-26416

Geomagnetic activity index response time to fluctuations in interplanetary electric field azimuthal component, relating to magnetosphere average energy content 11 p1627 A72-26670

Magnetospheric midday boundary width dependence on geomagnetic dipole axis orientation, discussing different positions for magnetosphere boundary 11 p1628 A72-26914

Nonadiabatic and atmosphere induced energy losses as causes of proton capture in geomagnetic field 11 p1715 A72-26915

Geomagnetic invariant coordinates and related field line parameters calculation via field model and fast numerical method 12 p1803 A72-27771

Analytic models of large scale electric fields in atmosphere, considering geomagnetic Sq current in lower atmosphere and inner magnetosphere 12 p1804 A72-27790

Russian book on geomagnetic field cosmic rays covering charged particle motion theory, extraionosphere currents, magnetosphere tail and solar wind effects, etc 12 p1864 A72-28345

Relations between normal mode radio propagation parameters and properties of earth-lower ionosphere isotropic waveguide, allowing for geomagnetic field 13 p1945 A72-28583

Abridged version of 1970 Soviet conference on constant geomagnetic field and paleomagnetism, reviewing secular variation data 13 p1946 A72-28588

Autocorrelation functions of anomalous magnetic field and earth crust structure of central portion of Arctic Ocean, using sliding energy spectrum method 13 p1946 A72-28589

West German-United States Barium Ion Cloud Project meteorological support at Wallops Station, discussing magnetospheric magnetic and electric fields 13 p1947 A72-28802

Meteor trail forms diversity explanation from magnetic pressure and Reynolds number and plasma diffusion in magnetic fields, discussing geomagnetic effect on trail shape 13 p2039 A72-29220

Lower ionospheric nighttime absorption as ionization processes indicator, discussing relationship to geomagnetic activity 13 p1948 A72-29233

AU and AL indices variations effect on geomagnetic field during international quiet days at high latitudes interpreted as electrojet diurnal redistribution 13 p1948 A72-29242

Dynamo theory MHD equations numerical solution, showing rapid variation of electromagnetic field, hydrodynamic velocities and earth core magnetic moment 13 p1949 A72-29245

Geomagnetic field extrapolated spherical data for years 1600 to 1800 from declination and inclination analysis, giving Gaussian coefficients and errors 13 p1949 A72-29265

Geomagnetic data testing by including monopole term in spherical harmonic reduction 13 p1951 A72-29394

Magnetic apex coordinate system for plasma density organization in low and middle latitude F2 region 13 p1951 A72-29395

VLF long distance radio propagation in earth-ionosphere waveguide, considering earth magnetic field effects in mode conversion and refraction error calculation 13 p1922 A72-29655

Magnetospheric ring current relation to polar magnetic substorm from charged particle measurements by satellites and magnetic field measurements at ground 13 p1952 A72-29658

Radio aurora ion-acoustic wave propagation direction divergence due to magnetic field distortion by large ionospheric horizontal sheet current [AD-746367] 13 p1923 A72-29662

Range and frequency spread F diurnal and seasonal variations at magnetic equatorial station Thumba, noting geomagnetic activity effect 14 p2097 A72-30130

Nonoriented astronomical satellite attitude determination from onboard measurements of geomagnetic field and stellar luminosity 14 p2151 A72-30460

Solar cosmic rays spectrum and geomagnetic cut-off rigidity determination from ion production rates in lower ionosphere 14 p2147 A72-30627

Molniya 1 satellite slow neutron monitor with photomultiplier scanned scintillator, noting limiting effect of geomagnetic perturbations 14 p2105 A72-30628

Distortion corrections in geophysically traced gravitational, magnetic and geoelectric field maps, discussing automation 14 p2101 A72-30642

DR ring current belt formation due to electron and proton gradient drift in inhomogeneous geomagnetic field, calculating charged particles trajectories 14 p2101 A72-30646

Magnetospheric quasi-stationary pinch effect and filamentary structure due to electron streams parallel to geomagnetic field lines 14 p2103 A72-30664

Eccentric geomagnetic dipole drift field as function of time dependent parameters, calculating potential components in spherical coordinates 14 p2103 A72-30667

Weber experiment gravitational signals correlation to solar and geomagnetic activity and cosmic ray intensity 14 p2160 A72-30886

- Geomagnetic field multipoles effects on radiation belt particle motion for analysis of true anomalies 15 p2222 A72-31280
- Midlatitude nighttime sporadic E layer relationship to geomagnetic field, considering wind shear theory 15 p2224 A72-31798
- Geomagnetic field aligned electron anisotropies at high latitudes for energies 1 and 6 keV observed by ESRO satellite, noting two regions of maximum occurrence frequency 15 p2226 A72-31928
- Report to COSPAR on East German space program covering ionosphere, geomagnetic phenomena and solar physics 15 p2338 A72-32013
- Geomagnetic activity index Ap correlation with daily magnetic variations during quiet sun year 1964 15 p2230 A72-32260
- Spin effects on satellite-borne cylindrical probe electron density measurements, considering satellite wake and geomagnetic field effects 16 p2389 A72-32962
- Geomagnetic field line tracing by plasma clouds produced by Ba vapor release, noting different ion drift rates and directions 16 p2384 A72-32977
- Precessional torque of conducting fluid as source of geodynamo action, noting oblate spheroidal experiment 16 p2385 A72-33341
- Planetary waves in terms of geomagnetic secular variation due to earth core fluid oscillation under MHD forces, using thick shell model 16 p2385 A72-33342
- Cosmic ray isotopic data extraction via geomagnetic field, discussing magnetic effects on particle flux and finite resolution limitations of counters 16 p2447 A72-33728
- Geomagnetic attitude control of an axisymmetric spinning satellite. 17 p2619 A72-34201
- The perturbation of alternating geomagnetic fields by three-dimensional conductivity inhomogeneities. 17 p2545 A72-34350
- Real height variations of the ionospheric F2-layer above some pairs of geomagnetically conjugate stations. 17 p2545 A72-34689
- Lunar semidiurnal variations of the geomagnetic field determined from the 2.5-min data scalings. 17 p2545 A72-34691
- The magnetic control of the lower ionospheric absorption at lower latitudes. 17 p2546 A72-34697
- Theory of magnetically conjugate transport of cold plasma in the outer low-latitude ionosphere 17 p2548 A72-35218
- On the state of the geomagnetic field and its reversals. 17 p2548 A72-35323
- Geomagnetically trapped alpha particles. I - Off-equator particles in the outer zone. 17 p2548 A72-35595
- Geomagnetic activity annual variation investigation, showing 12-month wave existence 17 p2549 A72-35605
- Magnetosphere resonant oscillations space-time characteristics for arbitrary azimuthal number, noting frequency dependence on geomagnetic shell 17 p2551 A72-35859
- Comprehensive investigation of individual geomagnetic storms. 18 p2686 A72-36226
- Geomagnetic activity and the solar situation in the neighbourhood of proton effects. 18 p2686 A72-36227
- Sudden commencements of geomagnetic storms at the turn of two solar cycles. 18 p2686 A72-36228
- Dependence of sporadic ionization in the high-latitude ionospheric E-region on magnetic activity 18 p2688 A72-36860
- Drift characteristics of the main eccentric geomagnetic dipole 18 p2689 A72-36872
- Possibility of determining the secular variation of geomagnetic field components from the distribution of total-vector modulus variation 18 p2689 A72-36873
- Spherical analyses of the principal geomagnetic field for the years 1550 through 1800 18 p2689 A72-36874
- Permanent rotations of an equatorial satellite in the geomagnetic field 19 p2869 A72-37437
- Some problems of electromagnetic induction in the equatorial electrojet region. II - The analysis of magnetic and telluric variations at Zaria, Nigeria. 19 p2789 A72-37772
- Magnetospheric and ionospheric conjugate point phenomena as solar events manifestations via solar wind shock wave interaction with geomagnetic field 19 p2790 A72-37858
- Earth and interplanetary magnetic fields spectral power density characteristics at 0.0001-1 Hz, noting ambiguities due to variable investigation conditions 19 p2791 A72-38346
- Unified coordinate system for global distribution of F 2 and sporadic E layer transmission parameters, suggesting geomagnetic longitude and modified magnetic inclination 19 p2791 A72-38354
- Geomagnetic cutoffs for cosmic-ray protons for seven energy intervals between 1.2 and 39 Mev. 19 p2852 A72-38728
- Geomagnetic activity index Ap variation spectral data analysis, noting correlation to sunspot number variation 19 p2793 A72-38747
- The interpretation of surface equatorial magnetic daily variations on disturbed days. 20 p2916 A72-39238
- Identification of short polarity events by transforming marine magnetic profiles to the pole. 20 p2917 A72-39476
- Morphologic maps of pulsating aurora for late afternoon and evening geomagnetic sector near Tromso during 1967-1969 20 p2918 A72-39540
- Midday auroras and polar cap auroras. 20 p2920 A72-39978
- Mathematical model of earth liquid core dynamo mechanism for magnetic field maintenance based on simple motions with spherical harmonic form 21 p3048 A72-40400
- A contribution to the numerical treatment of the electromagnetic field /H-polarization/ in horizontally non-homogeneous models of the earth. 21 p3048 A72-40498
- On the diffusion of the perturbing toroidal magnetic field from the core to the mantle. 21 p3048 A72-40501
- Influence of the terrestrial magnetic field on the motion of a satellite around its center of gravity 21 p3106 A72-41048
- Rarefaction wave generation by solar wind shock wave interaction with magnetosphere, noting geomagnetic field weakening during magnetic storm 22 p3217 A72-41894
- Activity of the secular behavior of the geomagnetic field 22 p3168 A72-41924
- Geomagnetic DP-2 variation base level from E region electron drift velocity measurements in equatorial electrojets 22 p3169 A72-42013
- Height structure of tidal winds as inferred from incoherent scatter observations. 22 p3169 A72-42014
- Auroral photometric observations at geomagnetically conjugate points. 22 p3169 A72-42020
- Spatial distribution of excess-radiation intensity at low altitudes 22 p3218 A72-42212
- Nonadiabatic condition effects on ultrarelativistic electron energy losses in geomagnetic trap in remote magnetosphere regions 22 p3218 A72-42224
- Daily variation of electron and proton geomagnetic cutoffs calculated for Fort Churchill, Canada. 22 p3170 A72-42401
- Spatial and temporal variations of thermal plasma ion and electron densities as function of L at 3000-5700 km from polar orbiting OV 3-1 satellite observation 22 p3211 A72-42414
- Short period geomagnetic variations, discussing origin by different solar activity mechanisms 22 p3173 A72-42544
- ULF wave observation by satellite, considering geomagnetic activity control of magnetospheric wave occurrence 22 p3174 A72-42902
- Magnetic storm classification from geomagnetic field H and Z components behavior, associating with solar corpuscular flux 22 p3174 A72-42952
- Earth main magnetic field description by cartography and analytic methods based on dipole or spherical harmonic series representations 23 p3283 A72-43366
- Different conductivities effect in ionospheric E layer of polar cap regions, noting electric current along high latitude magnetic field force lines 23 p3283 A72-43370
- Families of geomagnetic storms, direction of the interplanetary magnetic field, and solar activity 23 p3283 A72-43371
- The Z sub e field, some of its properties, and its geophysical informativeness 23 p3283 A72-43373
- Generation threshold of anomalous resistance for longitudinal currents in the magnetosphere 23 p3284 A72-43379
- Magnetic anomalies in New Guinea-New Zealand region from geomagnetic measurements with proton magnetometer, noting effects of andesite-basalt volcanic processes and nuclear precession signal 23 p3284 A72-43380
- Electromagnetic induction in a half-space with a cylindrical inhomogeneity. 23 p3284 A72-43423
- The effect of change in the geomagnetic dipole moment on the rate of the earth's rotation. 23 p3285 A72-43819
- Relation between satellite radio signal scintillations and magnetic activity 23 p3264 A72-43850
- Electron polar cap and the boundary of open geomagnetic field lines. 23 p3286 A72-44522
- Weak electrostatic turbulence observation in earth bow shock magnetic field gradient, suggesting cyclotron drift instability role 23 p3342 A72-44523
- Relations between normal mode radio propagation parameters and properties of earth-lower ionosphere isotropic waveguides, taking into account geomagnetic field 24 p3397 A72-45083
- Abridged version of 1970 Soviet conference on constant geomagnetic field and paleomagnetism, reviewing secular variation data 24 p3397 A72-45088
- Autocorrelation functions of anomalous magnetic field and earth crust structure of central portion of Arctic Ocean, using sliding energy spectrum method 24 p3397 A72-45089
- GEOMETRICAL HYDROMAGNETICS**
U MAGNETOHYDRODYNAMICS
- GEOMETRICAL OPTICS**
U OPTICS
- GEOMETRODYNAMICS**
U RELATIVITY
- GEOMETRY**
NT ANGLES [GEOMETRY]
NT BRAGG ANGLE
NT BREWSTER ANGLE
NT CARTESIAN COORDINATES
NT CHORDS [GEOMETRY]
NT CIRCLES [GEOMETRY]
NT COLLINEARITY
NT CONICS
NT CURVATURE
NT CURVES [GEOMETRY]
NT DIFFERENTIAL GEOMETRY
NT ELLIPSES
NT EPICYCLOIDS
NT EUCLIDEAN GEOMETRY
NT FIXED POINTS [MATHEMATICS]
NT FLOW GEOMETRY
NT GREAT CIRCLES
NT HYPERBOLAS
NT IMBEDDINGS [MATHEMATICS]
NT INVARIANT IMBEDDINGS
NT LIE GROUPS
NT LINES [GEOMETRY]
NT LOCI
NT MERCATOR PROJECTION
NT METRIC SPACE
NT NOZZLE GEOMETRY
NT OBLATE SPHEROIDS
NT PARALLELEPIPEDS
NT PARALLELOGRAMS
NT POINTS [MATHEMATICS]
NT POLYhedRONS
NT PROJECTIVE GEOMETRY
NT PROLATE SPHEROIDS
NT QUADRANTS
NT RECTANGLES
NT RHOMBOhedRONS
NT RIEMANN MANIFOLD
NT SPHEROIDS
NT SPINOR GROUPS
NT SQUARES [MATHEMATICS]
NT TANGENTS
NT TANK GEOMETRY
NT TENSOR ANALYSIS
NT TETRAGONS
NT TETRAhedRONS
NT TOPOLOGY
NT TORUSES
NT TRAPEZOIDs
NT TRIANGLES
NT VECTOR ANALYSIS
NT VORTICITY
- Visual space geometry and perception experiments, demonstrating size-distance relations for various visual cues 07 p0926 A72-19031
- Bounds estimation for thermal explosion critical parameters for exothermic reaction, using geometric transformation 07 p1098 A72-19364
- Geometric interpretation of solution existence for nonlinear ordinary differential equations with linear and nonlinear boundary conditions, analyzing funnel of solutions 11 p1676 A72-25503

Analysis of geometry effects in the detection of Cerenkov light from extensive air showers.

17 p2599 A72-35141

Microwave junction transistor geometric design factors effect on reliability and performance, comparing overlay, interdigitated, mesh and inverse overlay structures

18 p2666 A72-36553

The geometry of free fall and light propagation.

20 p2954 A72-40005

GEOMORPHOLOGY

Elevation-relief ratio, hypsometric integral and geomorphic area-altitude analysis, discussing calculation time

05 p0654 A72-16039

Small lunar maria craters morphological maturity as function of age and dimensions

05 p0722 A72-17041

Geomorphic evidence for basalt lava tubes and channels in Lunar Marius Hills, comparing with terrestrial analogs

07 p1067 A72-18870

Geomorphological and thermographic reconnaissance of Central Sahara, using orbital photographs

09 p1303 A72-23297

Gosses Bluff impact structure in Central Australia, discussing geologic, seismic, gravity, and magnetic surveys and lunar crater analog

09 p1304 A72-23494

Orbiter 4 photographs to update System of Lunar Craters [1966], cataloging positions, diameters and morphological data

13 p2037 A72-28991

Mars craters degradation and density regional variations from Mariner 6 and 7 imagery, using numerical scoring method

14 p2149 A72-30318

Observations of the auroral oval by the Alaskan meridian chain of stations.

17 p2548 A72-35594

Prokaryotic algae associated with Australian proterozoic stromatolites.

22 p3174 A72-42981

GEON [TRADEMARK]

U POLYVINYL CHLORIDE

GEOPHYSICAL OBSERVATORIES

NT OGO

NT OGO-A

NT OGO-B

NT OGO-D

NT OGO-E

NT OSO-G

Upper atmosphere observatory, noting application to long distance radio communication, long range weather prediction and international cooperation in research and education

13 p1947 A72-28613

GEOPHYSICAL SATELLITES

NT INTERCOSMOS SATELLITES

NT OGO

NT OGO-A

NT OGO-B

NT OGO-D

NT OGO-E

NT OSO-G

Geophysical satellites high resolution imaging systems data redundancy reduction, using Apollo 9 photographs for computerized statistical analysis of picture structure

02 p0226 A72-11837

Papers on world geomagnetic survey 1957-1969 covering land, sea, airplane and polar-orbiting geophysical observatory satellite observations, magnetic anomalies and reference field

02 p0219 A72-12080

Geomagnetic storms and anomaly observation by Satellite 1964 83C telemetry data transmission to ground stations network

02 p0219 A72-12083

Exact localization of isolated points on earth surface with Geole system satellite observation, noting applications in geodetic survey, geodynamics and geophysics

24 p3398 A72-45228

GEOPHYSICS

Thermal IR remote sensing of surface geothermal heat flow, presenting nighttime heat budget equation based on solar and geothermal energy

02 p0208 A72-11786

Geophysical and gravimetric measurement time recording techniques, describing satellite tracking photochronograph and electronic printing chronographs

04 p0525 A72-15571

Earth gravity field, movement and temporal form variation determination by satellite tracking, long base interferometry or lunar observation

04 p0520 A72-15723

Long base radio interferometry at centimeter wavelength for angular measurement accuracy improvement in astronomy and geophysics

04 p0495 A72-15728

Atmospheric optics and geophysics problems modeling arrangement reproducing radiation field within light scattering medium

05 p0658 A72-16293

Papers on geophysics covering magnetic measurements and natural vlf phenomena

06 p0802 A72-17366

Ionospheric electron content diurnal and latitudinal variations from differential Faraday effect, discussing solar elevation and geophysical mechanisms

06 p0805 A72-17640

Book on origin of life by natural causes covering physical geology, astronomy, biopoiesis and evolution of life stages, orogenic cycle, fossils, and primeval atmosphere

07 p0917 A72-19185

Transportable lunar ranging with neodymium glass laser and Coude optical system, noting geophysical applications

[CLEA PAPER 9,6]

Geoscience electronics - IEEE Conference, Washington, D.C., August 1971

09 p1306 A72-22311

Papers on electromagnetic probing in geophysics covering ground wave propagation, rough surface effects, geocrustal electric properties, HF radio backscatter from sea, etc

10 p1438 A72-24736

Rough surface effects on EM reflection for electromagnetic probing in geophysics, using Rayleigh and Kirchhoff methods

10 p1512 A72-24738

Laboratory electromagnetic scale modelling for studying geophysical and propagation boundary value problems

10 p1512 A72-24741

Solar activity relation to geophysical phenomena, discussing atmospheric circulation and climatic variation cyclicity and sunspot corpuscular fluxes

12 p1842 A72-28207

Nightglow ground based spectrophotometric observations of hydroxyl emission intensity and rotational temperature variations related with solar and geophysical activity

14 p2098 A72-30144

Distortion corrections in geophysically traced gravitational, magnetic and geoelectric field maps, discussing automation

14 p2101 A72-30642

Lunar orbital photography of astronomical and geophysical phenomena during Apollo 15 flight, noting solar corona and Milky Way

15 p2236 A72-31974

Mathematical problems in geophysical sciences - Conference, Rensselaer Polytechnic Institute, Troy, New York, July 1970

16 p2384 A72-33335

Geophysical fluid dynamics approach to dynamical processes in ocean and atmospheric motions, discussing equations of motion, vorticity, geostrophism, Ekman layer, Rossby waves, etc

16 p2377 A72-33336

Independent random test values effective sample numbers for mean and variance distributions in meteorological and geophysical statistical tests

16 p2385 A72-33382

Bandpass-filtered geophysical and meteorological time series data statistical evaluation by comparison with filtered test series with same variance and autocorrelation function

16 p2363 A72-33383

Relationship between auroral radio echoes and other geophysical phenomena

17 p2519 A72-35876

Laboratory model information relating to modeled geophysical phenomena, noting magnetosphere study from plasma physics experiments

17 p2551 A72-35904

Geophysical signal statistical model parameter evaluation by selection of operators in form of dimensionless quantile ratios

19 p2765 A72-38352

Easterly and westerly polar electrojets intensity diurnal variations with respect to universal time and geo- and heliophysical phenomena

19 p2791 A72-38368

Solar activity effects on sun-earth space physical processes, considering galactic cosmic rays, comets, ionospheric disturbances, and noctilucent clouds

19 p2867 A72-38629

Sunrise and sunset period of helio-geophysical processes in terms of optical, X ray, corpuscular and radio characteristics of solar activity

19 p2868 A72-38637

Deformation of the earth by surface loads.

20 p2916 A72-39335

Russian book - Hydrodynamic evolution model of the earth.

21 p3103 A72-40461

Fragments of terra rock in the Apollo 12 soil samples and a structural model of the moon.

21 p3110 A72-41452

Earth geophysical effects due to tidal capture of moon from direct orbit, discussing volcanism, at-

mosphere and hydrosphere origins and biological evolution

22 p3226 A72-42539

August solar activity and its geophysical effects.

22 p3174 A72-42982

Shmidt cosmological hypothesis impact on geophysics, geochemistry and geology, discussing planetary evolution, initial earth temperature and gravitational differentiation

22 p3230 A72-43154

Statistical analysis of Forbush decreases and the preceding increases in cosmic-ray intensity

23 p3328 A72-43354

The Z sub e field, some of its properties, and its geophysical informativeness

23 p3283 A72-43373

Type of equations for the solution of some gravitational prospecting problems from the anomalies on a complex relief, using a correlation model

23 p3285 A72-43847

GEOPOTENTIAL

NT GEOPOTENTIAL HEIGHT

Recurrence relation derived for general normalized satellite inclination function with three parameters in series expansion for geogravitational potential

01 p0123 A72-10012

Weather map numerical analysis for Northern Hemisphere, describing program with flow field for geopotential value checking

01 p0094 A72-10196

Tropospheric processes effects on Northern Hemisphere stratospheric meridional transformations in geopotential field and air circulation

02 p0253 A72-11732

Earth gravity field representation by simple layer potential from Doppler tracking of satellites

04 p0514 A72-14565

Earth gravitational potential, including surface density, crystal thickness, potential coefficients, contour maps and spherical harmonic expansion

06 p0877 A72-17657

Geopotential and longitudinal and transverse wind components correlation coefficients in nonhomogeneous nonisotropic atmosphere

06 p0843 A72-18444

Secular perturbations of artificial earth satellites Keplerian orbital elements from arbitrary-order zonal harmonics in geopotential series expansion

07 p1078 A72-19982

Longitude dependent perturbation inducing portion of geopotential as function of artificial earth satellite orbital elements

08 p1158 A72-21160

High order harmonic equations in gravitational potential from Transit 1B orbit inclination, comparing with Ariel 3

08 p1158 A72-21216

Isobaric correlation coefficient functions for wind and geopotential, describing relationship by two differential equations derived from geostrophic wind equations

09 p1344 A72-22432

Three parameter prognosis model for geopotential vertical profile in troposphere and stratosphere, describing vortex and heat influx in quasi-geostrophic and adiabatic approximations

09 p1297 A72-22549

Earth gravity anomalies sources depth, testing hypothesis of density variations origin

10 p1472 A72-24523

Atmospheric electricity problems, considering air pollution effects on ion concentration and air conductivity and solar activity effects on ionosphere-earth potential difference

10 p1473 A72-24528

Time dependent geopotential as function of position weighted atmospheric density from Poisson equation, noting satellite orbit perturbations due to mass shifts in planetary atmospheres

12 p1838 A72-27022

Upper atmosphere electric fields derived from ionosphere-earth electric potential measurements following solar flare activity

12 p1804 A72-27805

Solar event-related ionospheric horizontal electric fields derived from balloon measurement of mid-European and equatorial ionosphere potentials

15 p2223 A72-31556

Geopotential induced secular perturbations, using second approximation to achieve analytic accuracy

15 p2309 A72-31934

Fourier analysis for geopotential resonance effect on satellite orbits, calculating 13th harmonic influence on GEOS 2 and BE-C mean longitude

15 p2309 A72-31939

Geopotential harmonics of fifteenth order obtained from decaying satellite orbits analysis

15 p2311 A72-32001

Atmospheric energy spectra from two dimensional synoptic scales applicable to pressure or geopotential surface variables

15 p2266 A72-32721

Earth surface layer potential density from gravity anomalies combined with satellite Doppler observations

16 p2382 A72-32888

Variations of the earth's gravity field due to the free nutation.

17 p2544 A72-34272

Longitude dependent perturbation inducing portion of geopotential as function of artificial earth satellite orbital elements

17 p2545 A72-34451

A geopotential model /APL 5.0-1967/ determined from satellite Doppler data at seven inclinations.

18 p2685 A72-36029

Evaluation of 15th-order harmonics in the geopotential.

18 p2729 A72-36986

The determination of zonal harmonic coefficients of the terrestrial potential

19 p2790 A72-38173

Dynamic adjustment of initial model fields by using complete equations of hydrothermodynamics

20 p2949 A72-39943

Measurements of gradients of gravity in mines.

21 p3048 A72-40500

The equilibrium potential of a magnetospheric satellite in an eclipse situation.

22 p3168 A72-42003

Equations for 15th-order geopotential coefficients from the orbit of Transit 1B.

22 p3169 A72-42009

Adjustment of the wind field to geopotential data in a primitive equations model.

22 p3200 A72-42502

Potsdam correction from the satellite determined geopotential.

23 p3285 A72-43944

A method for balancing geopotential and wind fields

24 p3420 A72-44765

Experimental determination of the vertical gradient of the gravity force from a known geopotential

24 p3397 A72-44862

GEOPOTENTIAL HEIGHT

Stratosphere geopotential height and temperature data observed at Northern Hemisphere radiosonde stations comparison with objectively analyzed data

11 p1682 A72-26474

Scale analysis of large scale tropical disturbances in conditionally unstable atmosphere, estimating geopotential height dependence on stream function via heat balance equation

14 p2128 A72-30345

Stratospheric general circulation patterns from geographical, vertical and annual distribution for Northern Hemisphere temperatures, geopotential heights and winds

21 p3078 A72-41611

GEOS 1 SATELLITE

GEOS satellite orbit determination and prediction errors from optical tracking systems and gravity models, estimating resonant coefficients

06 p0877 A72-17653

GEOS 2 SATELLITE

Geos B satellite laser range experiment, discussing ruby oscillator and amplifier as transmitter and optical Schmidt system as receiver

03 p0365 A72-12950

GEOS satellite orbit determination and prediction errors from optical tracking systems and gravity models, estimating resonant coefficients

06 p0877 A72-17653

Fourier analysis for geopotential resonance effect on satellite orbits, calculating 13th harmonic influence on GEOS 2 and BE-C mean longitude

15 p2309 A72-31939

GEOSTATIONARY SATELLITES

U SYNCHRONOUS SATELLITES

GEOSTROPHIC WIND

Nonhomogeneous fluid geostrophic flow, establishing relationship between velocity and density fields

01 p0051 A72-11230

Integral conservation laws derivation for geostrophic zonal flow field disturbance, applying to flow stabilization

03 p0348 A72-13478

Ultralong wave baroclinic instability, obtaining linearized perturbation equations from layered geostrophic hydrostatic adiabatic model

04 p0541 A72-14451

Steady state geostrophic wind vector variation hodographs in planetary baroclinic boundary layer, considering thermal influence linear superposition on internal friction effects

06 p0841 A72-17667

Geostrophic drag coefficient for heterogeneous terrain as function of effective roughness length, considering surface friction effects in large scale atmospheric models

07 p1030 A72-19108

Isobaric correlation coefficient functions for wind and geopotential, describing relationship by two differential equations derived from geostrophic wind equations

09 p1344 A72-22432

Jet stream types derived from vector conditions for surface with maximum geostrophic wind velocity

10 p1507 A72-25002

Integral conservation laws derivation for geostrophic zonal flow field disturbance, applying to flow stabilization

11 p1623 A72-26248

Upper troposphere-lower stratosphere geostrophic wind deviation from rawinsonde and pressure-height data in El Paso-White Sands area, using finite difference method

13 p1988 A72-28447

Equilibrium diabatic Ekman layer geostrophic drag, heat and mass transfer coefficients, presenting velocity and temperature profiles

14 p2100 A72-30346

Mixing length theory derivation of barotropic planetary boundary layer profiles for geostrophic wind deviations, Reynolds stress, eddy viscosity and turbulent kinetic energy dissipation

15 p2224 A72-31675

Temporal behavior of hemispherically averaged geostrophic zonal and meridional flow from dynamic climatology studies of Northern Hemisphere large scale circulation

21 p3077 A72-40251

Adjustment of the wind field to geopotential data in a primitive equations model.

22 p3200 A72-42502

Wind velocity components determination in Cartesian coordinates based on rectilinear uniform air particle motion, noting difference with respect to geostrophic approximation

23 p3310 A72-43532

Scale analysis of atmospheric large-scale motions in low latitudes.

23 p3311 A72-44241

Baroclinic effects on the resistance law for the planetary boundary layer of the atmosphere.

24 p3397 A72-44956

GEOTROPISM

Gravity effects on plant organ orientation with respect to force direction from Chara rhizoid cell statoliths

15 p2189 A72-31932

GEP TELESCOPES

U PARTICLE TELESCOPES

GERDIEN ARC HEATERS

U ARC HEATING

U HEATING EQUIPMENT

GERMANIUM

Resistometric investigation of Ge addition effect on Al-Zn alloy clustering kinetics, determining Ge atom-vacancy binding energy

02 p0247 A72-12821

High resolution electron microscope observation of voids in amorphous Ge films, noting density dependence on substrate temperature

04 p0562 A72-15152

Low temperature Ga doped Ge bolometer for IR detection, improving sensitivity by load resistance noise elimination

05 p0662 A72-16195

Parallel and perpendicular magnetic field effects on optically injected electron-hole plasma diffusion in Ge from density measurement by infrared beam absorption technique

05 p0702 A72-17167

Third harmonic generation in Ge induced by conduction nonlinearity during bulk heating of charge carriers by microwave fields

07 p1047 A72-19023

Electron and hole recombination at deep impurity centers during nonequilibrium current carriers excitation by Nd-glass laser light in p- and n-type germanium

09 p1322 A72-22214

Noncrystalline Ge film preparation by rf sputtering onto substrate with explosive crystallization triggered by localized transient energy pulse at room temperature

09 p1369 A72-22625

Anisotropic electrical properties and void structure of amorphous Ge, discussing low- and high-field resistivity measurement in planar and transverse directions

09 p1371 A72-22873

Resonance occurrence in generation-recombination noise spectrum of Co 60 gamma irradiated Ge single crystals, investigating Hall effect

09 p1372 A72-23112

Temperature dependence of Ge solubility in CdSb single crystals from microstructural observations and measurements of microhardness and electrical properties

09 p1372 A72-23480

Ge field effect dependence on surface roughness and finishing, noting relief elements dimensions ratio and orientation to current flow direction

12 p1855 A72-27859

Point defects investigation in Si and Ge by diffusion techniques, precipitation from supersaturated solid solutions, quenching from high temperatures and plastic deformation

12 p1856 A72-28053

Low temperature irradiation and annealing effects in germanium, calculating charge states for donor and acceptor centers

12 p1857 A72-28054

Recombination parameters in low resistivity gamma irradiated n-type Ge, obtaining energy levels and temperature dependence of electron and hole capture probabilities

12 p1857 A72-28056

Phonon scattering and induced energy levels in electron irradiated Sb doped Ge in n to p-type conversion region, measuring thermal conductivity and Hall effect

12 p1857 A72-28057

Permanent operational characteristics changes of Si and Ge transistors bombarded by gamma and neutron radiation

13 p1928 A72-28700

Clean Ge crystal surface oxidation process investigation by LEED and conductivity measurements

15 p2292 A72-31868

Theory of photon-induced hopping on acceptors in p-type germanium.

17 p2595 A72-34750

Device for ac induction measurements in air, using the Gauss effect in germanium semiconductor diodes

17 p2529 A72-34767

Thickness dependence of the electrical transport properties of germanium films.

19 p2844 A72-37685

New efficient method for calculating hot electron effects applied to n-Ge.

19 p2844 A72-37686

Anisotropic electrical properties of amorphous germanium.

20 p2960 A72-39457

Fast-neutron-compensated n-germanium as a model of amorphous semiconductors.

20 p2961 A72-39853

Pure and compensated Ge and Si far IR spectral properties at liquid He temperatures for bolometer detector application

21 p3013 A72-40822

Magneto-microwave free-carrier absorption in germanium in the Faraday configuration.

21 p3097 A72-41379

Theory of Poole-Frenkel conduction in low-mobility semiconductors.

22 p3214 A72-42317

Physicochemical problems in silicon and germanium heat treatment, covering solubility and solid solutions stability and saturation variation with temperature

23 p3324 A72-43687

Effect of substrate temperature on electrical properties of amorphous germanium films.

23 p3324 A72-44069

Determination of Ni, Ga, and Ge in iron meteorites by X-ray fluorescence analysis.

23 p3262 A72-44128

The chemical classification of iron meteorites. VI - A reinvestigation of irons with Ge concentrations lower than 1 ppm.

24 p3436 A72-44697

Determination of electron and hole capture rates in nickel-doped germanium using photomagnetolectric and photoconductive methods.

24 p3432 A72-45388

GERMANIUM ALLOYS

Yield stress of solid solution iron and Fe-Ge alloys with bcc structure, obtaining interaction energy between solute atoms and screw dislocation

03 p0402 A72-13974

Sb 124 dopant redistribution in Ge semiconductor during diffusion alloying with In at 750-850 C

05 p0701 A72-15751

Zn, Ge and P based semiconductor alloy specimens chemical composition determination via x polarograms

12 p1854 A72-27443

Metastable phases in very rapidly solidified aluminum-germanium alloys

21 p3070 A72-41644

GERMANIUM ANTIMONIDES

Optical weak absorption measurements in amorphous semiconductors AsS, GeAs and GeSbSe, showing dependence on band gap localized states

13 p2022 A72-29629

GERMANIUM COMPOUNDS

NT GERMANIUM ANTIMONIDES

Germanium nitride thermolysis, discussing allotropic alpha and beta phases stability and activation energies

01 p0023 A72-10191

Chemical and spectroscopic activity of germanium tetrahydride in Jovian atmosphere in 4.7 micron window

15 p2312 A72-32094

Twinning faults in epitaxial films of germanium telluride and GeTe-SnTe alloys.

19 p2844 A72-37688

GERMANIUM DIODES

GaAs Schottky barrier and germanium backward diodes in microwave integrated circuit applications,

- describing design and performance as frequency changers and low level detectors 03 p0334 A72-14073
- Transient behaviour of laser generated carrier mobility in n-Ge. 18 p2697 A72-36351
- GERMANIUM RECTIFIERS**
U GERMANIUM DIODES
GERMANY
 German Federal Republic territorial air traffic regulations covering general, VFR and IFR rules, equipment and personnel examination and certification, safety, takeoff and landing, accidents, etc 02 p0305 A72-12621
- German book on air traffic law covering norms relative to vehicles and air space, international air law, organizations, etc 02 p0305 A72-12622
- Meteorites fall in Germany, discussing composition, size and color classification, frequency and locations 07 p1070 A72-19124
- GERMINATION**
 Chromosome aberrations and germination speedup in Soyuz 5 carried oat seeds, noting stimulating effect by preflight ethylenimine treatment 05 p0623 A72-16777
- Relative biological effectiveness of high X ray doses given to radish seeds, studying irradiation rate effect on germination probability 09 p1265 A72-22524
- Chromosome aberrations and germination speedup in Soyuz 5 carried barley seeds, noting stimulating effect by preflight ethylenimine treatment 17 p2505 A72-35280
- GERT**
 Graphical analysis of accelerated life test data on insulating fluids, capacitors, bearings and electronic devices, using inverse power law model 08 p1176 A72-21587
- GETTERS**
 Physicochemical properties of rare earth metals for alloying Al, Mg, Cu and Ti, noting getter and permanent magnet materials 22 p3191 A72-42806
- GHOSTS**
 Effect of environmental changes on the ghosting of distant objects in twin-glazed windows. 21 p3084 A72-40616
- GIANT STARS**
 G and K giants atmospheric parameters determination by photoelectric indices, considering effective temperature, chemical composition and surface gravity 01 p0132 A72-11013
- IR radiation variability from circumstellar grains around carbon-rich supergiant R Coronae Borealis, noting spectrum similarity to black bodies 01 p0121 A72-11093
- IR point source Becklin star spectrum consistent with highly reddened early-type supergiant with weak absorption masked by low resolution 01 p0133 A72-11094
- Helium production within supermassive stars and disks and little bangs, discussing conversion from hydrogen 03 p0419 A72-13117
- Massive star evolution, discussing stellar structure theory uncertainties, young clusters, helium burning and evolutionary tracks 03 p0425 A72-13262
- Differential line shifts in spectrum of supergiant beta Ori attributed to radial spreading of stellar atmosphere 03 p0436 A72-13810
- Giant M stars atmospheres absorption coefficient calculation from vibrational and pure rotational bands of H₂O, CO and OH 05 p0715 A72-16167
- UV spectrophotometry of late-type giant star (Arc-turus) from Aerobee rocket, identifying Mg II doublet resonance line for stellar chromosphere 06 p0881 A72-17893
- Fe I and Ti I excitation temperatures and ionization potentials of late G and K giant stellar atmospheres, comparing with model predictions 07 p1069 A72-19077
- Orbital elements from radial velocity measurements for single line K giant binary star 4 Ursae Minoris 07 p1071 A72-19337
- Astrophysical helium production by massive pulsationally unstable pure hydrogen stars evolving inhomogeneously with mass loss 07 p1084 A72-20691
- Main sequence, red giant and white dwarf stars convective envelopes evolution, discussing mixing length theory inadequacy 10 p1545 A72-24826
- Evolution of extreme population I massive stars from main sequence to He exhaustion phase, discussing various development phases in H-R diagram 14 p2158 A72-30727
- Fundamental data for massive stars compared with theoretical models. 17 p2611 A72-35317

- Clustering properties of the luminosity function in galactic globular clusters. 18 p2723 A72-36091
- Absolute magnitudes and color indexes of red giant concentration centers on a color-luminosity diagram 19 p2863 A72-38069
- Hydrodynamic model calculations for dynamically unstable supermassive stars. 19 p2866 A72-38490
- H and K emission intensity and line width dependence on stars age and luminosity, discussing dwarf stars and giants 19 p2866 A72-38503
- An estimate of stellar wind mass loss during the red giant phase of evolution. 20 p2967 A72-39187
- Relaxation oscillations in the envelopes of luminous red giants. 21 p3105 A72-41034
- Bright red giants of the globular clusters M 3, M 5, and M 13 21 p3113 A72-41756
- Model atmosphere analysis of the A 31a-O supergiant HD 33579 in the Large Magellanic Cloud. 22 p3225 A72-42386
- Giant stars iron abundance from narrow band spectrophotometric analysis and model atmospheres, isolating super metal rich stars below H-R diagram subgiant branch 23 p3334 A72-43256
- Iterative solution for adiabatic radial pulsation in massive main sequence star, noting transition to non-linearity via Eddington stability integral extension 24 p3438 A72-44833
- GIBBERELLINS**
 Gibberellic acid effects on Chlorella algae growth rates, using algal suspension optical density as measuring technique 03 p0313 A72-12975
- GIBBS EQUATIONS**
 Generalized thermodynamic potentials and universal criteria for direction of evolution of irreversible processes from Gibbs function stability analysis 10 p1562 A72-24250
- Nonlocal elasticity theory from global equilibrium and second thermodynamics laws, deriving constitutive equations from Clausius-Duhem inequality and Gibbs thermodynamics 11 p1738 A72-26721
- GIBBS FREE ENERGY**
 Dislocation velocity-stress relationship in plastically deformed Al at room temperature, noting entropy term in Gibbs free energy equation 11 p1661 A72-26652
- GIBBS-HELMHOLTZ EQUATIONS**
 Reversible thermodynamic cycle of chemical to electric energy conversion with electron gas as working body, discussing Gibbs-Helmholtz equations 16 p2350 A72-32994
- GIMBALS**
 Gimbaled control moment gyro for Skylab telescope mount stringent pointing requirements, investigating normal and clamped operation modes and dynamic response of attitude control 01 p0097 A72-10382
- Equivalent harmonic solutions for systematic drift of astatic gyroscope about outer gimbal axis with base under random angular vibrations 02 p0231 A72-12564
- Gimbaled telescope/UV spectrophotometer combination with star tracking facilities for use on ESRO TD-1 A satellite 03 p0355 A72-13061
- Stationary motions, stability of satellite with rotary gyroscope and gimbals in circular orbit and central Newtonian force field 08 p1241 A72-21801
- Vibrational characteristics dependence on structural flexibility in gimbal bearings and supporting structure of two axis free gyroscopes and single axis rate gyroscopes 08 p1173 A72-22129
- Fourth order normal modes and resonances of nonlinear vibrations, applying to gyro horizon compass sensitive element gimbal motion 13 p2000 A72-28382
- Elastic deformation and rigidity of rectangular, circular and elliptic gimbals for gyroscope suspension 13 p1957 A72-29272
- Soft gyro and accelerometer failure detection for redundant gimbaled inertial measurement units by skew sensors 15 p2270 A72-32187
- Failure detection techniques for Space Shuttle redundant multiple gimbaled inertial measurement units, using simulated boost and entry trajectories 15 p2270 A72-32189
- Error analyses of Euler angle transformations arising in design of precision pointing systems, guidance sensors and instruments with gimbals [AIAA PAPER 72-851] 20 p2949 A72-39078
- Russian book - Introduction to the theory of gyroscopes. 21 p3052 A72-40349

- Reduction principle application to solution stability of system of differential equations in critical cases, noting instability of free gyroscope in gimbal suspension 23 p3287 A72-43416
- Compass effect of a gyroscope with forced rotation of the Cardan suspension 24 p3403 A72-45321
- GIRDERS**
 Coupled flexural longitudinal vibrations of circular arc girder with symmetrical cross section, discussing optimal design 15 p2324 A72-31487
- GLACIERS**
 Holographic Ice Survey System for down looking radar probing and measurement of sea ice and glaciers, discussing ice electrical properties and system design 06 p0814 A72-17590
- GLANDS [ANATOMY]**
 NT ADRENAL GLAND
 NT ENDOCRINE GLANDS
 NT GONADS
 NT PANCREAS
 NT PARATHYROID GLAND
 NT PITUITARY GLAND
 NT TESTES
 NT THYROID GLAND
 Myoepithelial mechanism of high frequencies pulsatile discharge of human sweat glands 07 p0930 A72-19444
- GLARE**
 Dazzle glare effects and acuity recuperation among aircrew, noting civil and military aircraft accidents during daytime and nighttime flights 08 p1125 A72-21272
- GLASS**
 NT BOROSILICATE GLASS
 NT GLASS FIBERS
 NT PYROCERAM [TRADEMARK]
 NT S GLASS
 NT SILICA GLASS
 Glass compositions in Apollo 14 soil, discussing correspondence to Fra Mauro basalts, mare basalts and soils, and gabbroic anorthosite and potash granite 01 p0123 A72-10054
- Absorption and exposure characteristics of silver halide photochromic glasses for hologram recording 01 p0068 A72-10622
- High performance aerospace vehicles transparent materials, discussing glasses, plastics and optical coatings, solar properties, refractive index, UV transmittance and radiation damage susceptibility 01 p0091 A72-10765
- Stress and failure analysis of glass-epoxy composite plate with circular hole under uniaxial tension by finite element method [SESA PAPER 1942] 02 p0248 A72-11517
- Nonlinear deflections and radial surface stresses in thin elastic circular glass plates with coaxial rings 02 p0249 A72-12418
- Mie scattering by spherical particles in low loss glasses for fiber optic waveguides, discussing angular dependence 03 p0359 A72-13445
- Defective IC device glass surface passivation effects on scanning electron microscope analysis 03 p0365 A72-14287
- Glass variables effect on polypropylene, polystyrene and Nylon-6 glass filled thermoplastic composites mechanical properties, discussing silane coupling agents and injection moulding machine conditions 04 p0537 A72-15085
- Holographic measurements of dioptric powers and glass defects in thin transparent sheet under vertical or oblique parallel and divergent light 05 p0662 A72-16190
- Spectral heterogeneous lasing media with asymmetric luminescence bands, considering neodymium phosphate and germanate glass 06 p0824 A72-17392
- Temporal characteristics of emission line broadening in lasers with dispersive resonators for Nd ion activated phosphate glasses and disordered crystals 06 p0826 A72-18011
- Cer-Vit glass mirror replacement for AFCRL lunar laser observatory inverted Dall-Kirkham Cassegrain telescope, noting one arc sec resolution from wire and null optics tests 07 p0985 A72-19410
- Solute rejection in hyperfiltration of sodium chloride and urea with porous glass ion exchange membrane as function of pressure, temperature and concentration 07 p0937 A72-20601
- End holes effects on dielectric constant measurement of long glass tubes by cylindrical microwave resonant cavity 08 p1164 A72-20940
- Laser radiation effects on optical glass volume and surface, discussing failure characteristics 08 p1182 A72-21655

- Graphite fiber reinforcement of glass composite structure for increased cost effectiveness as compared to laminates and sandwich structures
08 p1193 A72-21694
- Frequency response of spectral noise amplitude in chalcogenide glass switches
09 p1366 A72-22215
- Microscopic and electron microprobe analyses of silicate melt inclusions and glasses in lunar soil fragments from Lunik 16 core sample
09 p1379 A72-22255
- High energy particle and ionizing radiation effects on glasses in aerospace environment
09 p1336 A72-22402
- Fast neutron radiation damage to glass ceramics and amorphous semiconductors electrical properties
09 p1336 A72-22405
- Anisotropy and nonuniformity of bonded glass mat thermoelastic properties, investigating thermal buckling origin
09 p1337 A72-22703
- Glass ceramics mechanical properties as function of temperature during bending, taking into account scale factor
09 p1337 A72-22742
- Heat transfer through glass plate in solar radiation flux, discussing temperature distribution and thermal flux meter design
10 p1562 A72-24318
- Papers on high temperature oxides covering refractory glasses, glass-ceramics, mullite, oxide spinels, glass networks theory and physical chemistry principles application
10 p1501 A72-24726
- Refractory glass-ceramics forming systems characteristics and production, discussing crystallization factors
10 p1501 A72-24728
- Glass network physical properties model, using physical chemistry description of crystal structure without regularly repeating lattice
10 p1502 A72-24735
- Glass styrene acrylonitrile bead filled composites tensile behavior, discussing relationship between yield stress, filler content, strain rate and temperature
11 p1673 A72-25487
- Impact glass-like objects as evidence of meteoritic origin of Loner Crater (India), discussing physical, chemical and optical properties
11 p1723 A72-26521
- Vaporization and condensation effects on Apollo 11 glass spherules from microbreccia samples, suggesting concentration gradients as result of impact event
11 p1723 A72-26522
- Aircraft windscreen design, discussing high impact strength glass, electroconductive film, transparency service life and weight reduction
12 p1753 A72-27006
- Glass sample mechanical strength testing, considering abrasion process, concentric ring stress calculation and laser light scattering techniques
12 p1832 A72-27007
- Chemically strengthened glass for eject-through frangible canopy design in aircraft emergency escape systems, noting protection against ejection injuries
12 p1813 A72-27016
- Atmospheric abundance ratios of gas inclusions in Muong Nong and Libyan Desert glass tektites by mass spectrometric analysis, indicating terrestrial origin
12 p1866 A72-27117
- Epitaxial and textured Pb films on mica and glasses, using reflection electron diffraction, etching and optical microscopy for structure study
12 p1854 A72-27289
- Optical Kerr constant measurement in liquid phosphoryl chloride and toluene and glasses, noting nonlinear refractivity
12 p1823 A72-27756
- I-V characteristics of metal-semiconductor-metal structures based on oxide glasses, noting temperature dependence and current limitation
13 p2021 A72-28688
- Lunar glass particle micrometeorite crater morphology, showing radial fracture and spallation zone relationships
13 p2036 A72-28755
- Stimulated luminescence in activated Nd glass by pulsed laser radiation at 1060 nm wavelength
13 p1969 A72-29519
- Ablation rate growth phenomenon in melttable material with increasing thermal flux, discussing quartz glass characteristics
13 p2066 A72-30007
- Low temperature shock effects on lunar glass spherules from two beam interferometry, discussing mechanical and thermal causes of fragmentation
14 p2149 A72-30266
- Failure phenomena relationship to kinetic equation for defect buildup from brittle fracture analysis of composite glass plastic in uniaxial eccentric tension
14 p2164 A72-30426
- Glazed rock fragments and glass splatter origin in bottom of small lunar craters from Apollo 15 observation
15 p2306 A72-31577
- Thermal history, heterogeneity, refraction and transition phenomena of lunar glassy fragments and spherules, using electron microprobe analysis
15 p2306 A72-31586
- Glass silvered Dewar for liquid helium without auxiliary shielding cryogenics, using surrounding annular space for radiation shielding
15 p2214 A72-32431
- Compressive strength and stiffness improvement for crystalline thermoplastic polymers via solid glass sphere reinforcement
16 p2414 A72-33370
- Laser irradiation induced refractive index change in evaporated chalcogenide glass films of As-S-Ge system
16 p2401 A72-33395
- Lithology of Apollo 14 lunar clastic rocks from Fra Mauro region, noting different makeups of glassy matrix and particles, plagioclase, pyroxene and lithic clasts
16 p2457 A72-33675
- Glass choice for two lens uncemented objectives, calculating surface and aberration coefficients
16 p2395 A72-33965
- Carbon fibre composites with ceramic and glass matrices. II - Continuous fibres.
17 p2570 A72-34669
- Structure, electrical conductivity and electron transport mechanisms in chalcogenide glasses
17 p2596 A72-35750
- Interdependence of the combination and memorization effects and the thermal behavior in a series of chalcogenide glasses
18 p2718 A72-36344
- Reliability of nichrome film resistors deposited in vacuum by sublimation on a glass substrate
18 p2669 A72-37117
- Electrical changes in the surface region of chalcogenide glasses.
19 p2822 A72-37454
- Quantum yield variations of Nd ion activated glass as function of electron beam energy and intensity, noting nuclear particles effect on laser radiation
19 p2823 A72-38205
- Analogy in the evolution of surface and bulk damage features produced by laser radiation in transparent glasses
19 p2812 A72-38541
- Anatomy and thermal history of laser self-focusing damage tracks in glass.
21 p3062 A72-40245
- Highly aluminous glasses in lunar soils and the nature of the lunar highlands.
21 p3104 A72-40490
- Changes in the phase composition of metal-glass materials depending on the sintering temperature
21 p3073 A72-41370
- Interpretation of the preswetting behaviour of chalcogenide-glass switches in terms of a space-charge-injection mechanism.
21 p3034 A72-41466
- Ablation rate growth phenomenon in fusible material with diminished thermal flux, discussing quartz glass characteristics
22 p3244 A72-42728
- Glassy materials rheological behavior description in terms of stress function, discussing molecular processes transformation range thermodynamics
22 p3196 A72-42791
- Isotope effect measurements application to determination of sodium diffusion mechanism and rate in sodium silicate glass
22 p3196 A72-42794
- Structons /close-neighbor arrangements/ stability and characteristics in anhydrous borate crystals and glasses containing bridging and nonbridging or tribonded oxygens
22 p3197 A72-42795
- Glass fracture mechanics, discussing microcrack stress concentration, Griffith theory, statistical failure theories, static fatigue and strength measurements
23 p3305 A72-43502
- Temperature-time effects on fracture failure mode and strength of polymeric glasses in terms of Ludwik brittle-ductile transition hypothesis and Griffith theory
23 p3305 A72-43503
- Change in the sign of the thermal lens of glass laser rods during variation of the thermo-optical constant of glass
23 p3296 A72-43926
- Major element composition of glasses in three Apollo 15 soils.
23 p3339 A72-44137
- Lunar ultramafic glasses, chondrules and rocks.
23 p3340 A72-44340
- Laser spin melting experiments for glass production in space from high melting metal and rare earth oxide ceramics
24 p3417 A72-45156
- GLASS COATINGS**
Dynamic characteristics of hot-wire anemometers with glass-coated thermistors
21 p3050 A72-40132
- GLASS FIBERS**
Fiberglass overwrapped Al alloy for space shuttle cryogenic hydrogen and oxygen tanks, noting weight reduction and impeding effect on cyclic loading induced crack growth rate
01 p0139 A72-10738
- Cryogenically formed prestressed stainless steel glass fiber reinforced vessels, demonstrating structural performance for space shuttle life support oxygen/nitrogen high pressure gas tanks
01 p0139 A72-10770
- Unidirectional glass/graphite fiber-epoxy resin composite, discussing fabrication and performance tests for mechanical properties
01 p0092 A72-10971
- Torsional stiffness /shear modulus/ of glass fiber reinforced plastic tubes as function of filament winding angle
01 p0141 A72-10999
- Glass fiber surfaces of revolution under axisymmetric pressure loads combined with centrifugal forces
01 p0143 A72-11365
- Test equipment for glass and polymer fibers strength and lifetime in vacuum and inert bases under static loads
01 p0093 A72-11382
- Nonlinear creep of glass fabric-plastic composite under loading in uniaxial stressed state
02 p0250 A72-12676
- Orthotropic glass fabric laminate creep under combined torsion and tension, describing test facility
02 p0250 A72-12677
- Temperature effects on strength and deformability of randomly reinforced fiberglass polyamides
02 p0250 A72-12678
- Mechanical breakdown prediction of loaded fiberglass reinforced plastic by seismoacoustic technique, investigating load effects on seismoacoustic emission
02 p0250 A72-12679
- Reinforcing fibers length effect on cross breaking strength and rupture area size at surface for silicoorganic glass reinforced plastic
02 p0250 A72-12681
- Fiberglass reinforced plastics heat conductivity as function of porosity, reinforcement factor and density
02 p0250 A72-12686
- Glass fabric reinforced composite materials stress distribution under longitudinal loading, using finite element method with two dimensional model
03 p0381 A72-13720
- Glass fiber reinforced plastic composites design, strain limitation and creep fatigue properties for large structures
04 p0537 A72-14749
- S-glass fiber bundles and composites under quasi-static loads, investigating strength characteristics and failure mechanism
04 p0592 A72-15474
- Heat resistant reinforced plastics from glass and pyrolytic carbon fibers by silicoorganic polymer treatment
06 p0835 A72-17735
- Wave propagation in single node clad glass fiber light waveguide, discussing fiber core minimum diameter and various loss mechanisms
06 p0825 A72-17773
- Soviet book on nonmetallic material strength during nonuniform heating covering, load endurance, bending phenomena and thermal stability of fiberglass, pyroceramics and reinforced plastics
06 p0796 A72-18521
- Fiberglass reinforced plastics under constant strain rate, deriving failure models as random process for microscopic crack propagation
06 p0898 A72-18548
- Stimulated Raman emission in glass fiber optical waveguides with low threshold broadband gain, permitting construction of wideband amplifiers and oscillators
07 p0953 A72-18876
- Linear and circular birefringence of low loss single mode glass fiber dielectric optical waveguide as function of length
07 p0940 A72-19232
- German monograph on sky scanner for short term sky spectral density distribution using glass fiber bundles for spectral components simultaneous measurement
07 p0983 A72-19266
- Alumoboronisilicate glass fibers vacuum tensile strength tests, noting fiber strength increase with vacuum and exposure time
07 p1023 A72-19778
- Stress-strain state in tension of orthogonally stiffened fiberglass-reinforced plastic with cracks in transversely stiffened layers
07 p1094 A72-20128
- Elastic properties of bonded orthotropic layer plates, finding good agreement with fiberglass reinforced plastic laminates
07 p1097 A72-20596

Stress concentration and elastoheredity values at curvilinear hole in fiberglass reinforced plastic plate under bending moment

08 p1243 A72-21237

Fiberglass heat transfer mathematical model, noting scattering effect and thermal conductivity

08 p1191 A72-21452

Glass fiber reinforced plastics irreversible cumulative damage under axial cyclic tension compression loads with heat production

08 p1191 A72-21500

Friction and bending effect on unidirectional glass fiber reinforced plastic ring deformation distribution

08 p1191 A72-21504

Fire resistant fibrous materials for potential military and transportation applications, considering aromatic polyamide polybenzimidazole, fluorocarbon resin polymer, phenolic and glass fibers and fabrics

08 p1191 A72-21586

Prestressed glass reinforced composites mechanical behavior, taking into account manufacture induced residual stress concentrations

08 p1192 A72-21674

Chlorendic acid based Hetrion 92C fire retardant chemical resistant polyester for fiberglass reinforced structure applications

08 p1192 A72-21677

Furan resins and chemically resistant furan-fiberglass composites flame resistance, heat distortion and physical properties at high temperatures

08 p1192 A72-21678

Glass fiber reinforced plastic composites fracture characteristics, considering fiber content, fiber-matrix bond strength, yarn geometry, orientation and ply stacking sequence effects

08 p1192 A72-21679

Thermal and mechanical properties of randomly reinforced fiber/resin composites including boron/epoxy, Thorne/epoxy and S glass/epoxy materials

08 p1192 A72-21682

Chopped fiber glass reinforced high density thermoplastic polyethylene composite, determining critical fiber length, interfacial adhesion and fracture toughness

08 p1193 A72-21684

Boron-epoxy structure repair technology based on titanium plugs and fiberglass, discussing equipment, graphical design and nondestructive tests

08 p1193 A72-21691

Adverse environmental effects on epoxy composites resin-glass interface properties, investigating epoxy-compatible silanes contribution to composite performance

08 p1194 A72-21696

Oriented glass fiber reinforced plastics fatigue strength and creep under interlayer shear and compression

08 p1194 A72-21752

Glass fiber reinforced polymer composite model for tensile stress distribution in matrix and fibers and at bond interface

08 p1194 A72-21753

Deformability and carrying capacity of glass fiber-polymer composite thick walled rings under internal or external pressure

08 p1195 A72-21764

Climatic load effects on carrying capacity of thick walled glass reinforced polymer rings with residual stresses

08 p1195 A72-21765

Nondestructive determination of glass reinforced plastics normal elastic and shear moduli and strength characteristics by vibrational, pulsed and acoustic methods

08 p1195 A72-21773

Heat absorption and liberation by glass fabric laminates under uniaxial tension, determining thermal effects dependence on strain rate and test temperature by calorimetric measurements

08 p1195 A72-21853

Additional vibrational loading effect on thin tubular glass fabric reinforced plastic samples creep under shear in reinforcement plane at 20-50°C

08 p1195 A72-21854

Fiberglass reinforced plastics creep characteristics under high strain rate loading-unloading conditions

08 p1195 A72-21855

Fiberglass reinforced plastics fatigue failure prediction based on test demonstrated correlation between static and cyclic strainability

08 p1195 A72-21856

Material properties nonuniformities effect on wound fiber glass reinforced plastic rings and cylinders thermoelastic residual stresses

08 p1196 A72-21858

Radial and axial residual stress components in glass fiber reinforced polyethylene, comparing with adhesion strength obtained by shear method

08 p1196 A72-21862

Extremal mechanical properties directions in orthotropic glass fiber reinforced plastics symmetry planes

08 p1196 A72-21866

Creep characteristics of unidirectional plastics reinforced by hollow glass fibers with insignificant capillary effect

08 p1196 A72-21868

Deposition of Ni-B coatings with specified electrical resistance onto fiberglass cloth reinforced plastics

09 p1318 A72-22528

Temperature induced stresses and displacements in fiberglass reinforced plastic cylindrical shell

09 p1399 A72-22704

Laser pulse propagation measurements on multimode glass fibers to evaluate communication potential

09 p1323 A72-22868

Tensile strength of notched carbon and glass fiber reinforced epoxy resin composites as function of crack size

10 p1500 A72-24253

Glass content and temperature effects on fabric reinforced plastic laminates static behavior, analyzing tensile and bending strength and elastic moduli

10 p1501 A72-24660

Low thermal flux glass fiber composite over-wrapped tubing with metallic liners for leak free cryogenic propulsion plumbing systems

11 p1637 A72-25364

Two stress level cumulative fatigue damage prediction for glass fiber-epoxy laminates

11 p1670 A72-25462

Acoustic emission analysis of deformation and fracture modes under straining of fiber glass-epoxy composite structures, including NOL rings and vessels

11 p1671 A72-25469

Elastic glass and Thorne fiber/epoxy matrix composite material creep tests, determining creep rate dependence on specimen geometry and stress state

11 p1672 A72-25481

Fiberglass-graphite reinforcement of unidirectional epoxy laminates, examining longitudinal composite fracture stress and strain and tensile and compressive stiffness

11 p1672 A72-25485

Experimental weave pattern for three dimensional continuously woven fiber glass reinforced composite fabric impregnated with epoxy resin

11 p1673 A72-25597

Chemical surface treatment effects on mechanically gripped fiberglass rods tensile strength

11 p1674 A72-25827

Glass textolites and high strength oriented plastics fracture mechanism in tension and bending, noting equalizing effect through proper cohesion characteristics between layers

11 p1674 A72-26804

Water damage in glass fiber-polyester resin composites, discussing fiber debonding, crack propagation and water resistance

11 p1675 A72-26950

Thin cylindrical shells prepared from fiberglass reinforced plastics under long term compression, investigating strain buildup nature during creep process

12 p1878 A72-27078

Fiberglass reinforced thermoplastics and thermosets for corrosive environments, noting composites performance increase by constituents change

12 p1833 A72-27404

Glass fiber reinforced thermoplastic resins chemical and hydrolytic resistance, noting composites and polymers long term performance prediction in aggressive environments

12 p1833 A72-27405

Fiberglass replacement by organic fiber for L-1011 interior sandwich panels and laminates, considering Nomex fiber in woven fabric

12 p1835 A72-28099

Boron and carbon reinforced fiberglass plastics tensile strength characteristics, presenting static fatigue curves vs Poisson coefficient and elastic modulus for various fiber contents

13 p1982 A72-28552

Heating rate effects on residual stresses in thick walled cylinders produced by winding heated binder impregnated fiberglass tape on cold spool

13 p1982 A72-28553

Stress-strain concentrations near circular holes in fiberglass reinforced plastic plates under various types of load as function of hole diameter/plate width ratio, anisotropy and load

13 p1983 A72-28560

Fatigue strength and cumulative damage in fiberglass-epoxy composite specimens under unsteady elastic bending loads, determining loading spectrum effect on service life

13 p1983 A72-28562

Tensile strength of fiber glass reinforced plastic elements joined by cover plates and nonlinearly elastic adhesives

13 p1962 A72-28737

Glass and carbon fiber reinforced plastic beam specimens dynamic moduli and loss factors determination from vibration frequency and decay rate measurements

13 p1984 A72-29095

Fiberglass reinforced plastic fuselage production for AN-2m aircraft, noting plastic-plastic and metal-plastic joints

13 p1897 A72-29462

Fiber glass reinforced plastic structure design based on anisotropy, calculating optimum angle between reinforcement and horizontal axis

13 p2058 A72-29463

Fiberglass performance as duct liner in presence of spinning modes from free field measurements, noting ineffectiveness for plane wave attenuation

13 p2028 A72-29573

Ribbon glass effect on thermal expansion of reinforced thermoplastic composites, comparing with fiber reinforced materials

15 p2259 A72-31255

Porosity effect on mechanical properties, airtightness, corrosion resistance and moisture absorption of glass fiber reinforced plastics

16 p2414 A72-33270

Physical and chemical surface characteristics investigation methods for fiberglass rovings to consider suitability as reinforcement for synthetic resins

16 p2414 A72-33302

Manufacturing process for glass fiber chopped strand mats, discussing physical and electrical properties and applications to filament winding

16 p2414 A72-33303

Foam content effect on fiberglass reinforced thermoplastic foam tensile and impact strength, thermal distortion and mold shrinkage properties

16 p2415 A72-33418

Glass reinforced thermoplastic resins flammability resistance, discussing test methods and flame retardant additives

16 p2415 A72-33419

Flame retardant glass reinforced thermoplastic polyester Celanex processing and performance, considering flammability, and electrical/mechanical properties

16 p2415 A72-33420

Ballistic-damage-tolerant composite flight control components

[AHS PREPRINT 674] 17 p2626 A72-34514

The fracture energy of a glass fiber composite.

17 p2570 A72-34670

German monograph - Wave propagation in glass-fiber light waveguides

18 p2697 A72-36249

Coupled glass-fiber/polypropylene composite - An initial evaluation.

18 p2703 A72-36269

Improving the impact resistance of glass-fibre composites.

18 p2703 A72-36270

Nonlinear physical dependence of reticular polymers and glass fiber reinforced plastics under conditions of diminishing creep

19 p2822 A72-37527

Calculation of residual stresses in wound materials produced by a layer-on-layer solidification process

19 p2872 A72-37532

Behavior of glass fiber reinforced plastic cylindrical shells under the action of external pressure pulses

19 p2872 A72-37538

Dynamic stability of axisymmetrically heated glass fiber reinforced cylindrical plastic shells which are coupled with elastic cylinders

19 p2872 A72-37539

Temperature-time superposition applied to the relaxation properties of a glass fiber reinforced plastic and its binder

19 p2822 A72-37543

Properties of internally lubricated glass-fortified thermoplastics for gears and bearings.

19 p2822 A72-37896

Model filament wound epoxy composites.

19 p2808 A72-38164

Variation of the coordination number of boron during heat treatment of alumborasilicate fiberglass

19 p2823 A72-38681

The study on dynamical behavior of fiberglass reinforced plastics (FRP) by dynamical mechanical model

20 p2943 A72-38887

On the cumulative fatigue damage of glass fiber reinforced plastics subjected to repeated tensile impact load.

20 p2943 A72-38888

Fiberglass reinforced plastics tensile test specimens aspect ratio effect on tensile properties, considering deformation of orthotropic rectangular plate with uniform forced displacement

20 p2943 A72-38889

Device for fatigue testing of fiberglass-reinforced plastic samples in a symmetrical tension-compression regime at acoustic oscillation frequencies

20 p2920 A72-38944

Fatigue behavior of glass filament-wound epoxy composites in water.

21 p3072 A72-40246

Strength of S-glass fiber.

21 p3072 A72-40554

On the stress-strain curve of polyethylene filled with randomly oriented glass fibers.

21 p3073 A72-40721

Random function theory method for estimation of tensile, compressive and shear strength and elastic constants of monodirectional fiberglass reinforced plastics 21 p3073 A72-41708

Thermal expansion coefficients of some fiberglass-reinforced plastics and their components under conditions of low and high temperatures 21 p3074 A72-41715

Influence of elastic constants on the stability margins and weight characteristics of fiberglass-reinforced shells 22 p3196 A72-41864

Heat transfer by radiation in a glass fiber insulator 22 p3243 A72-41891

Fiber glass reinforced plastics elastoplastic behavior due to microcrack propagating across matrix, using elastic index of work done 22 p3232 A72-41943

The accumulation of damage in a glass-reinforced plastic under tensile and fatigue loading. 22 p3196 A72-42456

Strength and deformation characteristics of fiberglass under torsional and compressive shear loads, investigating temperature effects on elastic modulus 23 p3306 A72-43730

Fiber optics development and physical foundations, discussing reflection, optical waveguides, vibrational modes during light transmission and fabrication from inhomogeneous glass and mixed monomers 24 p3425 A72-44782

Transmission losses in glass and plastic single mode and liquid core optical fibers for long distance data links and image transmission 24 p3380 A72-45252

Stress-strain state in tension of orthogonally stiffened fiberglass-reinforced plastic with cracks in transversely stiffened layers 24 p3460 A72-45754

GLAUCOMA

Ocular and induced visual effects of systemic and topical drugs in terms of eye neuroanatomy and pharmacology, stressing glaucoma therapy 22 p3150 A72-42499

GLAUERT COEFFICIENT

U AERODYNAMIC FORCES
U MACH NUMBER

GLAZES

Transparent aircraft polycarbonate glazing systems shielding properties for projectile and bird impacts 12 p1832 A72-27015

GLIDE ANGLES

U GLIDE PATHS

GLIDE LANDINGS

Pilot glide slope and localizer tracking performance during successive in-flight simulated ILS approaches 12 p1773 A72-28260

Tactical approach landing radar tests for low lift drag ratio aircraft in unpowered flight, using F-104D as test aircraft 15 p2267 A72-31694

GLIDE PATHS

Parachutes flow characteristics in low speed free descent, discussing glide angle effect on total drag and water channel flow pattern studies 01 p0004 A72-10309

Computed performance of ILS glide slope transmitting arrays sited over flat ground planes of one dimensional perfectly conducting strips in free space 05 p0686 A72-16559

Optimal angle selection of commercial aircraft glide path, taking into account vertical velocity, propulsion units operation and landing procedure 14 p2072 A72-30814

Microwave scale model of ILS glide path, considering interference and aircraft taxiing effects 14 p2129 A72-30944

Energy management during the space shuttle transition. 24 p3452 A72-45347

GLIDE SLOPES

U GLIDE PATHS

GLIDERS

NT FLEXIBLE WINGS
NT PARAWINGS

Laminar flow airfoils for gliders, optimizing profiles for favorable velocity and pressure distribution 05 p0610 A72-17194

All-moving tail plane parameters influence on glider static and dynamic characteristics, discussing lateral and longitudinal stability, maneuverability and pilot induced oscillations 08 p1110 A72-21632

Sailplane computer displaying rate of climb simultaneously with airspeed for pilot determination of best strategy for local upcurrent-downcurrent conditions 09 p1316 A72-23550

Natural frequencies and vibration modes of free glider, using symmetrical matrix to replace three dimensional structure by approximate model 16 p2348 A72-33409

Sailplane performance measured in flight. 17 p2487 A72-34215

Optimization of the wing parameters of a glider hovercraft 20 p2888 A72-39902

Variometer system for sailplanes sinking or climbing rates direct readout, describing pressure difference measuring concept based on reservoir-capillary system 21 p3051 A72-40225

A new method of calculating the natural vibrations of a free aeroplane. [ICAS PAPER 72-05] 21 p3120 A72-41130

Procedures for simple resonance testing of sailplanes 22 p3139 A72-42920

Variometer system for sailplanes sinking or climbing rates direct readout, describing pressure difference measuring concept based on reservoir-capillary system 23 p3292 A72-44451

Influence of wing deformations measured during flight tests upon the flight performance of a glider made of synthetic materials. I 23 p3252 A72-44452

GLIDING

Gliding flight atmospheric energy utilization through aerology, discussing value of weather forecasts to glider pilots 04 p0542 A72-14684

Inclined wind tunnel test section for free gliding investigation and aerodynamic design of flexible wing two body system 15 p2213 A72-31403

GLOBAL ATMOSPHERIC RESEARCH PROGRAM

Global horizontal sounding technique balloon flights, determining Southern Hemisphere temperate latitude circulation climatology 13 p1988 A72-28443

Investigation of the mesoscale convective processes during the forthcoming GARP implementation. 20 p2948 A72-39800

GLOBAL TRACKING NETWORK

Apollo centralized ground support and communication system, describing network support team, mission control center, instrumentation support team and manned space flight network 13 p1940 A72-29860

NASA global tracking network clock time synchronization to microseconds accuracy via GEOS-11 satellite 15 p2199 A72-32079

GLOBULAR CLUSTERS

Spatial distribution of galactic globular clusters stars from Palomar sky survey 18 p2724 A72-36092

Stellar evaporation in globular clusters passing through galactic plane, considering gravitational perturbation increase of total energy within system 21 p3107 A72-41269

Photometry of RR Lyrae variables in the globular cluster NGC 6981. 21 p3111 A72-41475

Red variables in globular clusters, in the galactic centre and in the solar neighbourhood. 22 p3222 A72-42135

A survey for RR Lyrae stars at high galactic latitude. 22 p3222 A72-42137

Extended horizontal branch loci. 23 p3337 A72-43830

Upper limits on the atomic hydrogen abundance in 12 globular clusters. 23 p3340 A72-44246

GLOBULES

Lunar dumbbell shaped glass globules formation due to rotation and surface tension effects of ejecta from meteoric impacts 15 p2306 A72-31628

GLOBULINS

Thyroglobulin content and variations in the proteolytic activity of the thyroid gland tissue in animals under hypoxic conditions 20 p2893 A72-39727

Effects of the space flight environment on man's immune system. I - Serum proteins and immunoglobulins. 22 p3150 A72-42493

Quantitation of serum proteins on whole blood-electroimmunodiffusion technique applicable to capillary blood. 22 p3150 A72-42495

GLOMERULUS

Aortic constriction and release effects on kidney glomerulotubular balance in saline- and water-loaded dogs, studying sodium reabsorption changes 08 p1115 A72-21084

GLOTRAC (TRACKING NETWORK)

U GLOBAL TRACKING NETWORK

GLOTTIS

Air flow and acoustic characteristics of speech sounds produced with turbulence noise at glottal constriction, using flow equations 01 p0101 A72-10162 [AD-744389]

Plethysmographic and laryngoscopic investigation of glottis opening and airway resistance relation to

lung volume during panting and continuous slow expiration 11 p1586 A72-26611

GLOW DISCHARGES

Low pressure glow cathode triodes gas discharges, determining electron energy distribution function in double layer by probe measurements 03 p0400 A72-14349

Methane pyrolysis in glow discharges /cold plasmas/, discussing chemical reactions initiated by high energy electrons inelastic collisions with gas molecules 07 p0937 A72-20286

Thermodynamics of Mo silicidation reactions from gas phase in silicon chloride and hydrogen media, discussing glow discharge maximum yield 07 p0937 A72-20417

Transient lunar phenomena theories, investigating surface features obscuration, lunar material melting, ejected gas glow dischargeluminescence processes 08 p1233 A72-21212

Minimum ion source temperatures for glow discharge ion flux deposition of films and coatings on metallic and nonmetallic substrates 15 p2244 A72-31573

Glow mode electron plasma source for space chamber, measuring electron density and temperature for comparison with back diffusion sources 15 p2286 A72-32339

Mathematical model for fast transverse glow discharges for pumping high pressure gas lasers, noting short rise time of applied voltage pulse 16 p2399 A72-33012

Random ionization waves convective instability in glow discharge positive column, calculating fluctuations spectrum as function of position along column for localized white noise source 16 p2437 A72-33747

Flowing air glow discharge near IR emission spectrum as function of pressure, noting atomic lines 16 p2427 A72-34097

Inertial plasma effect in a glow discharge - A new principle of oscillation measurement 19 p2800 A72-37756

Nonlinear interaction of p and s ionization waves in neon. 21 p3090 A72-40487

Pulsed atmospheric-pressure carbon-dioxide laser initiated by a cold-cathode glow-discharge electron gun. 22 p3186 A72-42753

Glow discharge in rare-gas and metal vapour mixture. I - Distribution functions and kinetic coefficients in He-Cd mixture discharge. 23 p3322 A72-44320

GLUCOSE

Short term response of insulin, glucose, growth hormone and corticosterone to acute vibration stress in rats 01 p0015 A72-11289

Hypoxia, hypercapnia and hyperoxia effects on active glucose transport in rat small intestines 05 p0618 A72-16633

Glucose and fatty acid metabolic response during impending myocardial infarction in animals 07 p0921 A72-20175

Dose dependent hyperglycemia and hypopolemia response to pentobarbital sodium injection in rats from plasma glucose and fatty acid analysis 08 p1116 A72-21187

GLUES

Impact effect on strength of glued metal joints mounted in groove cut in baseplate and pressed by yokes 01 p0144 A72-11380

GLUTAMATES

Acute and chronic hypercapnia effect on lactate, pyruvate, alpha-ketoglutarate, glutamate and phosphocreatine contents of rat brain 03 p0316 A72-13677

GLUTATHIONE

Succinate and glutathione as protective agents against chronic effects of hyperbaric oxygen toxicity in rats 14 p2082 A72-31091

GLYCOGENS

Daily prolonged exercises effects on human muscle glycogen utilization, noting reduced lactate accumulation and increased free fatty acid levels 04 p0480 A72-15213

Glycogen content and distribution determination in frog retina by histochemical analysis with intravascular injection of mixture preventing decomposition 06 p0764 A72-17987

Biochemical analysis of cat brain regions for gamma-aminobutyric, aspartic and glutamic acids, glycogen and phosphatidopeptide concentrations during paradoxical sleep deprivation 16 p2356 A72-33559

Muscle metabolism of ATP, CP, glycogen and lactates at rest and during submaximal and maximal exercise 21 p3005 A72-40421

Localization and dynamic changes of glycogen in frog retina adapted to darkness or light, I, II.
23 p3258 A72-44377

GLYCOLS

Free and dissolved water contents determination in light petroleum products by modified Karl Fischer method using ethylene glycol solvent mixture
05 p0702 A72-16669

Polyglycol aqueous solutions selection as fire resistant hydraulic fluid from hydraulic bench tests performed with various type pumps
08 p1197 A72-22161

Methyl alcohol-ethylene glycol self mixing antifreeze solution for precipitation gages
11 p1682 A72-26088

GLYCOLYSIS

Anaerobic glycolysis and specific gravity of red blood cells in rats exposed to pure oxygen at 600 torr
01 p0015 A72-11297

Preglycolytic energy metabolism in biochemical evolution, concerning anaerobic oxidation of pyruvate and acetaldehyde to acetate and ATP
04 p0471 A72-14799

Yeast glycolytic pathway oscillations relation to concentration of diphosphopyridine nucleotide and other metabolites, noting analogy to behavioral and physiological rhythms
07 p0920 A72-19541

Substrate utilization and glycolysis in the heart.
17 p2501 A72-34977

Muscle metabolism during isometric exercise performed at constant force.
21 p3005 A72-40425

GODDARD EXPERIMENT PACKAGE TELESCOPE

U PARTICLE TELESCOPES

GOLD

Au thin film effective optical constant calculation from measured reflection and transmission coefficients and thickness by approximate formulas
03 p0401 A72-13363

Emission energy of positrons thermalized in moderators and coated with Au, suggesting Au negative work function existence
08 p1217 A72-21339

German monograph on Frenkel defect structures in thin gold wire at high electron irradiation dose, using electrical resistance measurements
09 p1354 A72-22325

High light transmission electrically conducting Hyviz and gold film laminates for aircraft windshields and window heating applications
13 p1898 A72-30038

The solar abundance of gold.
17 p2607 A72-35077

Platinum and gold in chondritic meteorites.
17 p2610 A72-35149

Tribological properties of gold for electric contacts.
18 p2693 A72-35980

Friction and wear of electroplated hard gold deposits for connectors
18 p2693 A72-35981

Evaluation of gold electrodeposits for use in dry circuit applications.
18 p2664 A72-35983

Evaluation of testing methods for gold plated or gold clad contacts.
18 p2664 A72-35984

Changes of electrical and structural properties of Au thin films obtained by sputtering during the annealing process.
18 p2720 A72-36955

Thermally-stimulated current from the gold acceptor trapping level in silicon.
21 p3097 A72-40996

Measurement of the stacking-fault energy of gold using the weak-beam technique of electron microscopy.
22 p3177 A72-42320

GOLD ALLOYS

Superferromagnetism in thin polycrystalline Gd and Gd-Au films having Curie points near room temperature
03 p0401 A72-13583

Au-Al wire bond, discussing intermetallic phase formation under elevated temperature treatments and reliability design limitations
03 p0364 A72-14284

Ordered Cu-Au alloy atomic order parameters, using field ion microscopy
04 p0560 A72-14548

Au alloys metallization system as alternative to aluminum for junction transistor reliability improvement, considering metal migration, microcracking and current leakage
18 p2666 A72-36554

GOLD COATINGS

Bonding mechanisms and failure modes in thermocompression bonds of Au plated leads to Ti-Au metallized substrates, discussing Cu lead frames plated with Ni and Au
03 p0365 A72-14292

Au film optical refractivity, absorptivity and transmittance in visible and UV ranges of Au-GaAs and Au-GaP photoelectric converters
14 p2141 A72-30224

On the radiation of discontinuous gold films by electric current transmission.
18 p2718 A72-36349

Auger spectroscopic observation of Si-Au mixed-phase formation at low temperatures.
22 p3178 A72-42616

GOLD PLATE

U GOLD COATINGS

GOLD 198

Au distribution parameters in Si semiconductor devices, using radioactive isotope diagnostic methods
03 p0400 A72-12970

GONADS

Human male gonadotropin secretion relation to sleep stages, using electrophysiologic recordings and radioimmunoassay techniques
05 p0620 A72-17128

Changes in the pituitary-thyroid and in the pituitary-gonad systems under conditions of functional loading and of physiological immobilization.
24 p3371 A72-44823

GONDOLAS

Two gyro three axis stabilizer with gyrocompass effect for gravimeter or magnetometer sensor stabilization in towed gondola
13 p1957 A72-29271

GONIOMETERS

NT RADIOGONIOMETERS

Digital lightning goniometry for flash locations at great distances by atmospheric and whistlers analysis
09 p1304 A72-23471

GOSS (SUPPORT SYSTEM)

U GROUND OPERATIONAL SUPPORT SYSTEM

GOVERNMENT PROCUREMENT

Parametric cost estimating aids DOD in systems acquisition decisions.
17 p2639 A72-34461

Cost-to-produce estimation consideration as design parameter in defense material contractual arrangement
17 p2639 A72-34462

Defense system procurement evaluation before documentation release to industry, discussing improved specifications, competition, planning and data requirements
17 p2639 A72-34463

Competitive prototype strategy to reduce weapon system development risks and uncertainties with emphasis on simplified management and procurement
18 p2742 A72-36074

Successful engineering design teams characteristics in development of complex defense systems, discussing organization size, experience, documentation and procurement practices
21 p1312 A72-40972

GOVERNMENT/INDUSTRY RELATIONS

FAA activity in collision avoidance system and pilot warning instrument areas
02 p0256 A72-12379

Configuration management on small production contracts for U.S. Government, including identification, control and accounting
03 p0460 A72-14204

Price and technical quality effectiveness in winning government R and D contracts
06 p0905 A72-17397

Government role in widebody aircraft introduction to air carrier service, discussing aircraft maintenance, design and fail-safe structural configurations
07 p0911 A72-18831

Federal regulation of airline mergers from viewpoint of history and current evaluating procedures in U.S.
07 p1106 A72-20675

Profit policy for defense contract negotiations relating to capital employed for cost reduction
09 p1413 A72-22237

Collaborating parties cooperation with outsiders, examining relationship with government organizations, airworthiness authorities, financial institutions and marketing agencies
10 p1565 A72-24882

Book on world airlines economic regulation, analyzing multilateral international agreements, national aviation interests and competitive situation
11 p1748 A72-25923

Book on air transportation, covering history, government agencies roles in economic and safety regulation of air carriers, accounting, financial and legal aspects, etc
12 p1891 A72-28205

Developing countries civil aviation airlines evolution, considering government fund allocation, international money credibility, skilled manpower, equipment, fare and tourism expansion
16 p2481 A72-33332

Government regulations effects on local service airlines cost performance and growth strategies
16 p2481 A72-33374

Financial methods employed in creating Brazilian aircraft industry via mixed public-private ownership
16 p2481 A72-33375

Defense system procurement evaluation before documentation release to industry, discussing im-

proved specifications, competition, planning and data requirements
17 p2639 A72-34463

Canadian industrial participation in domestic, U.S. and overseas space projects, emphasizing technology advancement as national objective
18 p2742 A72-36544

Federal legislation impact on airport and airway system planning, considering budget and schedule requirements
18 p2743 A72-36777

Polaris submarine-weapon system autonomous organization and management technique based on team combining Navy and civilian contractors in close working relationship
23 p3358 A72-44358

Reliability, safety, maintainability and system effectiveness disciplines acquisition, processing, dissemination and exchange via Government-Industry Data Exchange Program and Failure Rate Data Program
24 p3467 A72-44660

GOVERNMENTS

International and domestic governmental interests in aircraft hijacking, discussing deterrents, enforcement and accepted action
05 p0752 A72-15835

GOVERNORS

U SPEED REGULATORS

GRABENS

U GEOLOGICAL FAULTS

GRADIENTS

NT ELECTRON DENSITY PROFILES

NT POTENTIAL GRADIENTS

NT PRESSURE GRADIENTS

NT TEMPERATURE GRADIENTS

NT THERMOCLINES

Gradient catastrophe /solution derivative discontinuity/ occurrence time for quasi-linear hyperbolic differential equations describing elastic string oscillations
14 p2130 A72-30194

Elementary formulas for scalar and matrix valued functions gradient calculation, including continuum mechanics application
15 p2262 A72-31587

Flame probe sampling process effects on gas composition concentration gradient for two dimensional cylindrical and rectangular probes
16 p2361 A72-34004

Rate of convergence of several conjugate gradient algorithms.
17 p2573 A72-34218

Gradient methods of parameter estimation during the mathematical treatment of measurements
17 p2522 A72-35038

An automated gradient projection algorithm for optimal control problems.
17 p2576 A72-35244

Certain algorithms for obtaining an approximate solution of incorrect problems on a set of monotonic functions
19 p2828 A72-38846

Polak-Ribiere conjugate gradient algorithm modifications to eliminate minimization at each iteration for efficient implementation with convergence
22 p3198 A72-41931

A gradient method of expanding a group data handling method to new plants not studied by experiments
22 p3162 A72-42242

GRADIOMETERS

U MAGNETOMETERS

GRAFTING

Histologic analysis of hypoxia exposure effects on mouse skin homograft reaction due to lymphatic organ function changes
22 p3144 A72-42675

GRAIN BOUNDARIES

Interstitial impurities and grain size effects on cold brittleness in W melts in deformed and recrystallized states
01 p0088 A72-11082

Grain boundary migration measurements in bicrystalline Al under intense electric field, using optical microscope
01 p0089 A72-11182

Hydropressed sintered U-700 superalloy powder, noting weakened particle grain boundary conditions from mechanical properties and fracture studies
02 p0240 A72-11444

Matrix hardening in dispersion strengthened powder products, discussing dispersion, grain boundary and solid solution hardening
02 p0241 A72-11457

Gamma prime precipitate hardened Ni base alloys, attributing strengthening mechanism to coherency strains and precipitates antiphase boundary energy
02 p0247 A72-12817

Fan shaped precipitate formation during supersaturated Al-Zr solid solution decomposition, discussing interpretation as grain boundary migration
02 p0247 A72-12820

Polycrystalline materials wedge crack growth enhancement by vacancy diffusion under creep failure

conditions, considering grain boundary sliding mechanism

03 p0442 A72-12998

Grain size effect on age hardened Mg-Zn alloy yield and flow stress, using tensile test and electron and optical microscopy at various temperatures

03 p0374 A72-13716

Aluminum intergranular entropy estimation, neglecting coupling between atomic vibrations

03 p0376 A72-13969

Boundary segregate concentration during grain growth annealing of ultrapure Al as function of migration rate and distance

03 p0379 A72-14259

Al-Zn-Mg alloy intergranular corrosion in un-stressed condition, detecting anodic paths at grain boundaries by potentiostatic technique

04 p0535 A72-15731

Grain boundary region constituents corrosion behavior and solution chemistry within stress corrosion cracks in Al alloys observed from pH changes

04 p0535 A72-15733

Preferential concentration of impurities and alloying elements at grain boundaries, noting role of equilibrium type interfacial segregation in intergranular corrosion

04 p0535 A72-15734

Neutron irradiation effect on grain boundary relaxation in Al and Al-Li alloy by internal friction investigation

06 p0830 A72-18292

Rutile creep resistant substructure recovery at 1000-1040 C, discussing stress relaxation mechanism due to dislocation walls or subgrain boundaries migration

07 p1023 A72-18800

Rare earth metals microadditions influence on Ni grain boundaries free energy and compounds formation

07 p1012 A72-19676

Hf addition effects on grain boundary structure of cast Ni-base superalloys

07 p1015 A72-19931

Diffusion creep influence on grain boundary-adjacent precipitate free zone formation in Ni-Cr alloys subjected to high temperature tensile and creep tests

07 p1021 A72-20437

Bcc solid solutions formation in Cr-W binary alloys, investigating interface reaction and two phase grain boundary diffusion by X ray diffraction and microscopy

08 p1185 A72-21246

Ceramic materials stress-strain behavior dependence on microstructural factors, discussing point defects, pore size and grain boundaries

09 p1334 A72-22392

Surface defects absence after intergranular creep from Al bicrystals grain boundaries observation by transmission electron microscopy

10 p1495 A72-24084

Stress corrosion crack paths in Al-Zn-Mg alloys, showing normal coincidence with grain boundaries

11 p1652 A72-25289

Aluminum nitride amount and particle size measurement at austenitic grain coarsening temperatures in low carbon steels

11 p1656 A72-25755

Crystal grain size effect on fracture initiation in mild steel under triaxial stress, using notch tests at low temperatures

11 p1657 A72-25756

Grain size and carbon content effects on recrystallized Mo wire ductility at room and low temperatures

11 p1657 A72-25758

Light figure microscope construction for crystal grain orientation determination in metal specimens

11 p1632 A72-25759

Metallographic examination of stainless steel specimens exposed to long term creep rupture tests, noting carbides precipitation and stress induced grain boundary migration

11 p1658 A72-25832

Metal surface layer and microetching process along grain boundaries during electrochemical precision processing, verifying steel microcrack depths with mathematical model

11 p1640 A72-26260

Impurity atoms effects on grain boundary motion velocity, considering interactions with metal lattice vacancies

11 p1662 A72-26655

Stress corrosion cracking mechanism of low carbon steels to explain transcrystalline brittle mechanical cracks development along grain boundaries

11 p1666 A72-26923

Grain boundary network of allotropic phase change for ductility enhancement in Fe-Ta alloys

11 p1668 A72-26941

CdS thin film conductivity reactions to grain boundary and stacking faults, correlating grain size to mobility

12 p1856 A72-28012

Electron microprobe analysis of solute segregation near grain boundaries in Al-Zn-Mg alloy after quenching and aging heat treatment

13 p1973 A72-28652

Strain rate controlling mechanisms of superplastic deformation at various stresses and temperatures, considering vacancy and dislocation creep and grain boundary sliding

13 p1974 A72-28657

Ultrafine grained microstructures and mechanical properties of alloy steels developed by cold working followed by annealing

13 p1974 A72-28662

Reversed creep deformation behavior of metals, observing acceleration at high temperatures due to grain boundary sliding enhancement

13 p1978 A72-29444

Chemical and mechanical properties relationship to stress corrosion in high strength Al-Cu and Al-Zn-Mg alloys, emphasizing grain boundaries cleavage energy

14 p2117 A72-30536

Heat resistant Ni alloys grain boundaries constituents as function of composition and heat treatment, noting effects on mechanical properties

14 p2118 A72-30589

Mn, Zr and Cr alloying effects on grain size and solid solution decomposition of cast Al-Zn-Mg alloy bars

14 p2125 A72-31039

Micropores pinning effect on grain boundaries mobility during drawn tungsten wire recrystallization, determining pores induced repulsive force

15 p2257 A72-32116

Electron microscopic investigation of slip processes during plastic deformation of WC-Co based cermets, observing WC grain boundary sliding and Co phase crystal lattice transformations

15 p2257 A72-32117

Orientation and elongation effects on grain boundary correction term in foil surface energy measurement by zero creep, using virtual work method

15 p2258 A72-32637

Ti comparison with Al for effects on Fe alloy deformation and fracture, discussing intergranular failure suppression

16 p2411 A72-33823

Metal fracture by electron pulse generated stress waves, noting intergranular fracture mechanism

16 p2472 A72-33845

Grain-size dependence of Snoek peaks in niobium.

17 p2566 A72-34671

Study of the diffusion of iron and cobalt along the grain boundaries of tungsten

17 p2569 A72-35522

Studies of the influence of CVD tungsten depositing conditions on the formulation of pores resulting from interdiffusion in the emitters of thermionic converters.

18 p2698 A72-36145

Grain-boundary relaxations in an Fe-Ni-Cr alloy.

18 p2700 A72-36588

Physical and metallurgical factors causing embrittlement and creep rupture life reduction determined by tests, discussing crystal and grain boundary deformation and notch effects

19 p2874 A72-37711

Grain size distribution in recrystallized alpha-titanium.

19 p2820 A72-38297

The interaction of lattice defects and grain boundaries.

20 p2962 A72-39996

The influence of grain and twin boundaries in fatigue cracking.

21 p3069 A72-41350

Free energy changes and boundary segregation of tin and antimony in CrV steels.

21 p3070 A72-41648

Grain size and temperature effects on Cr and Al diffusion coefficients and mobility in Ni-20Cr and thoriated dispersed NiCr alloys from measurement at 1038-1200 C

22 p3193 A72-43028

Recrystallization and grain growth in titanium. I - Characterization of the structure.

22 p3193 A72-43032

Effect of grain size on the thermal diffusion of copper in aluminum.

22 p3193 A72-43036

Chemistry of grain boundaries and its relation to intergranular corrosion of austenitic stainless steel.

22 p3195 A72-43126

Increasing the boundary strength of electron-beam-melted cast molybdenum by vanadium microadditions

23 p3302 A72-43967

Electron-microscope study on the recrystallization in technically pure aluminum.

24 p3412 A72-44719

Changes in the grain-boundary free energy and the segregation of tin and antimony at grain boundaries in CrV steels

24 p3415 A72-45394

GRAINS

Objects optical granularity in diffuse coherent light, noting similarity to image formation in diffuse incoherent light

01 p0073 A72-11313

Interstellar circular polarization.

23 p3336 A72-43556

GRAMMARS

Terminal context in context-sensitive grammars.

17 p2524 A72-35924

GRAND TOURS

Outer planet low thrust orbiter missions, comparing three body numerical results with two methods of patching together two body solutions

01 p0128 A72-10379

Solar flare, galactic and magnetically trapped /Van Allen/ nuclear particle radiation environments calculation for three outer planet Grand Tour missions

03 p0413 A72-14095

Adaptive variable length coding for efficient compression of spacecraft TV data of Grand Tour missions

06 p0771 A72-17401

Outer planets Grand Tour trajectory correction requirements, examining combined radio/onboard navigation system and delta V estimates [AIAA PAPER 72-54]

07 p1068 A72-18947

Future deep space missions, discussing exploration of interplanetary conditions outside ecliptic plane and solar system Grand Tour with outer planets flyby

07 p1068 A72-19059

Programming systems for onboard unmanned deep space probe computers, describing Mariner and outer planet Grand Tour Programs

07 p0949 A72-19295

Outer Planet Grand Tours Missions radio science experiments for planetary and satellite atmospheres and surfaces, celestial mechanics, relativity, interplanetary medium and solar corona

12 p1870 A72-27347

Image tube /TV/ and scanning photometer sensor comparison for outer planet mission onboard navigation

15 p2270 A72-32192

Thermionic reactor electric propulsion system requirements.

18 p2720 A72-36167

Minimum energy trajectory and propellant consumption considerations for launch windows to Mars and Venus planets with Grand Tour mission possibilities

23 p3336 A72-43553

Maneuver strategies for multi-planet missions. [AIAA PAPER 72-914]

24 p3443 A72-45431

GRANITE

Ti leaching from granitic rocks by Penicillium, simplicissimum, discussing extraterrestrial life detection

05 p0616 A72-15809

GRANULAR MATERIALS

Single domain grain distribution deduction method obtained from Neel theory, applying to Apollo 11 lunar dust iron grains

01 p0125 A72-10071

Dc and ac Josephson effects in bulk granular superconductor, presenting junction I-V characteristics

02 p0268 A72-11472

Equilibrium temperatures of interstellar grains around early stars, discussing dependency on grain size and stellar distance

06 p0875 A72-17297

Lunar granular materials thermophysical properties, emphasizing thermal conductivity data and heat transfer mechanisms

12 p1869 A72-27333

Crowded photographic emulsions, predicting granularity of multilayer sandwich as function of layers number

12 p1808 A72-27676

Grain heating model of H II region to explain 100 micron emission predominance in IR sources

12 p1871 A72-27693

German monograph - Behavior of an electric arc produced by an exploding wire in a granular medium

19 p2834 A72-37483

The effect of a thermal and ultrahigh vacuum environment on the strength of precompressed granular materials.

22 p3173 A72-42528

Jet stream formation from uniform distribution of grains in similar elliptical orbits, discussing models with numerical simulation

24 p3445 A72-45461

Photoelastic verification of a mechanical model for the flow of a granular material.

24 p3460 A72-45697

GRAPHIC EVALUATION AND REVIEW

TECHNIQUES

U GERT

GRAPHITE

NT PYROLYTIC GRAPHITE

Characterization of graphite/polyimide composites for space shuttle applications

01 p0092 A72-10784

Radiographic detection of small flaws in bulk graphite and carbon/carbon composites, improving image quality and sensitivity by contrasting liquid impregnation

01 p0069 A72-10808

High modulus high strength graphite composites for aerospace structures, noting materials, machining properties and applications [SME PAPER EM 71-191]

01 p0092 A72-10965

Minority carriers similarity in graphite natural single crystals and pyrolytic samples

01 p0114 A72-11035

Graphite surface temperature and ablation rate for various stagnation pressures, radiative heat fluxes, stagnation enthalpies, heat transfer coefficients and test gas compositions

02 p0249 A72-12021

Graphite, Mo, Ta and W thermal radiation total emittance measurement in 1200-2400 K range, evaluating recorded data by computer program

02 p0243 A72-12101

Ultralow sliding friction during bombardment of polypropylene, molybdenum disulfide and graphite surfaces with charged helium atoms at room temperature in vacuum chamber

02 p0249 A72-12282

Epoxy- and polyimide-graphite composites electrical dissipation factor and capacitance measurements as guide to molding quality, describing equipment

02 p0250 A72-12609

Graphite and molybdenum disulfide surface and lubricating properties, examining basal plane proportion relationship with edge sites

02 p0236 A72-12847

Ni-based metal graphite materials, investigating sintering process control variables effects on structure and phase composition responses

05 p0665 A72-16090

Graphite ablation in combined convective and radiative heating, considering mass and energy transfer effects

[AIAA PAPER 72-88]

05 p0750 A72-16954

Spherical ice and graphite particles absorption, scattering and radiation pressure coefficients and albedo, noting application to interstellar extinction

06 p0875 A72-17296

Structural and strength characteristics of carbon graphite materials, considering composites preparation and applications

06 p0836 A72-18361

Friction and wear characteristics at high temperature of plain bearing embedded with pellets of graphite, sodium fluoride and tungsten disulfide lubricating mixture

06 p0823 A72-18584

Graphite fluoride as solid lubricant, investigating friction coefficient and wear resistance

06 p0837 A72-18598

Basal plane and edge surface areas measurement in graphitized molybdenum disulfide powders

06 p0837 A72-18601

Graphite and molybdenum disulfide, investigating temperature effect, thermal stability and oxidation effect on weight by TGA and DTA

06 p0837 A72-18602

Graphite and molybdenum disulfide powders lubricating properties relation to surface crystalline orientation

06 p0824 A72-18608

Test facility for graphites fracture under thermal stresses, considering stress-strain relations calculation method for annular samples

07 p1024 A72-20137

Optimal selection of flawless nose cones from graphite billets, obtaining mathematical model based on ultrasonic reflection test data

07 p1086 A72-20350

High temperature black body model based on induction heating of graphite crucible, noting application to stellar energy spectral distribution determination

07 p0991 A72-20404

Material design for filament wound graphite-graphite fiber/matrix composite heat shields for improved performance during reentry

08 p1245 A72-21597

Random filament misalignment effects on rigidity and tensile strength of unidirectional graphite composites under shear loading

08 p1192 A72-21681

Graphite reinforced epoxy stiffeners for variable geometry fuel tank to meet light weight requirement, discussing billet fabrication, assembly and installation

08 p1176 A72-21688

Graphite fiber reinforced composites with high mechanical strength and modulus at low weights, fatigue resistance, vibration damping and tailorable thermal expansion coefficient

08 p1193 A72-21689

Graphite fibers surface treatment and interfacial adhesive bonding, considering resin composites shear strength enhancement by sulfuric acid and sodium chlorate oxidation

08 p1194 A72-21697

Thermal diffusivity and conductivity and specific heat of hard electrode graphite intermediate medium in hydraulic hot extrusion of metals

08 p1181 A72-22072

High temperature tests of graphite composites in air, determining material loss time dependence and correlation with observed strength data after oxidation

09 p1333 A72-22381

Yttria stabilized hafnia based graphite and tungsten composites, investigating factors affecting thermal shock resistance

09 p1327 A72-22385

Neutron irradiation effect on submicroporosity formation and redistribution in structural graphite

09 p1340 A72-23482

Graphite morphology in metallic materials from scanning electron micrographs, discussing sulfur contents effect in tempered cast iron

10 p1500 A72-23825

Interaction diagram for mixed crack extension modes in unidirectional graphite-epoxy laminates from critical load test data

10 p1501 A72-24265

Statistical multiple regression equations for identification of artificial graphite properties effect on ablation performance

[AIAA PAPER 72-295]

11 p1669 A72-25233

Constituents, processing, fabrication and structure effects on artificial graphitic materials ablation performance in sublimation regime from high temperature tests

[AIAA PAPER 72-298]

11 p1742 A72-25235

Thermal expansion measurements on graphite reinforced plastics, using Leitz dilatometer

11 p1670 A72-25460

Anisotropic graphite composite laminates cutouts stress analysis by finite element method, predicting structural reinforcement behavior

11 p1672 A72-25475

Fiberglass-graphite reinforcement of unidirectional epoxy laminates, examining longitudinal composite fracture stress and strain and tensile and compressive stiffness

11 p1672 A72-25485

Ultralow sliding friction during bombardment of polypropylene, molybdenum disulfide and graphite surfaces with charged helium atoms at room temperature in vacuum chamber

11 p1639 A72-25707

Al alloy-graphite composites brazing and welding feasibility, tabulating spot welding parameters

11 p1641 A72-26491

Carbon-graphite fracture mechanics dependence on graphite crystallite structure, discussing crystal size effects on strength

11 p1674 A72-26812

Carbon monoxide and hydrogen adsorption on graphite, measuring sticking probabilities

12 p1777 A72-27039

Graphite fiber with high tensile strength and modulus and good elongation at low cost for aerospace applications

12 p1834 A72-28084

Addition type polyimide-graphite fiber composites fabrication from monomeric reactant solutions to improve mechanical properties and thermal stability

12 p1834 A72-28091

Graphite fiber-epoxy composite systems development for F-5 aircraft landing gear door, speed brake, leading and trailing edge flaps and horizontal stabilizer

12 p1835 A72-28097

Thin surface film lamination in antifriction carbon-graphite materials under critical specific pressure, discussing crystalline phase in wear products

12 p1818 A72-28192

Phase composition and lattice constants of carbide films from vaporized Zr interaction on graphite surface at 1700 C

13 p1912 A72-28566

A-4 Skyhawk horizontal stabilizer experimental graphite-epoxy composite construction, describing design, manufacturing and testing techniques

[AIAA PAPER 72-358]

13 p2056 A72-28954

Carboids effects on pyrolytic coke structure and graphite product properties

13 p1984 A72-29072

Antifriction phase structure of friction formed thin surface layer of sulfurized iron-graphite metal-ceramic materials, using transmission microscopy

13 p1967 A72-30108

Mass entrainment products effect on radiative and convective heat transfer during decomposition of graphite blunt body in steady hypersonic flow of radiating air

14 p2174 A72-31158

Graphite wetting with liquid V, Nb and Mo as function of metal melting point and sample temperature

15 p2243 A72-31223

Dispersed particle shape effect on elastic behavior of magnesium oxide composites at low graphite concentrations

15 p2260 A72-31585

Graphite band structure investigated by secondary electron emission, observing electron transitions to higher excited states

15 p2260 A72-31856

Carbon and graphite fiber reinforced composites elastic constants derived from ultrasonic immersion technique

15 p2261 A72-32503

Graphite ablation rate inhibition and surface temperature depression by chlorine gas in supersonic high temperature air environment

16 p2475 A72-32842

Griffith equation applicability to graphite fiber fracture strength by measurement of work to break and critical flaw

16 p2413 A72-32871

Cumulative damage probability in dynamic or static fatigue failure of brittle graphite materials as function of stress

16 p2414 A72-33321

C concentration and temperature dependence of graphite wetting by liquid Ni and Co and melts of Ni-C and Co-C alloys, noting nonequilibrium effect

16 p2415 A72-33537

Low recession graphite nosetip design for ballistic reentry, considering blunt and sharp configurations in terms of thermally induced tensile strain survival

[AIAA PAPER 72-705]

16 p2472 A72-34039

A graphite crystal polarimeter for stellar X-ray astronomy.

17 p2553 A72-34637

Tailoring the interface in graphite-reinforced polycarbonate.

17 p2570 A72-34713

The development of high strength three dimensionally reinforced graphite composites.

17 p2573 A72-35670

High temperature cesium vapor sources based on a cesium-graphite system for thermionic converters

18 p2646 A72-36201

A non-linear integral-type theory of inelasticity for transversely isotropic materials.

18 p2738 A72-37075

Viscoelastic analysis of graphite under neutron irradiation and temperature distribution.

18 p2704 A72-37186

Carbon and graphite sublimation in inert gas flow at 2800-3000 K, determining rate dependence on temperature under kinetic and diffusive conditions

18 p2704 A72-37186

A graphite calorimeter

18 p2693 A72-37192

Lubrication with solids.

19 p2807 A72-37771

Investigation of the lubricant properties of molybdenum disulfide, graphite, and phthalocyanine

19 p2823 A72-38094

Role of an electric field in the diffusion mechanism of the graphite-to-diamond phase transformation

19 p2823 A72-38405

Galvanomagnetic properties of well-oriented graphite in relation to the structural imperfections.

21 p3073 A72-40691

Physical, mechanical and thermal characteristics of reimpregnated pyrolyzed carbon-carbon and graphite-graphite composites

[ICAS PAPER 72-29]

21 p3073 A72-41154

Graphite content effect on vibration damping properties of Al-Sn and Al-Zn alloys

21 p3070 A72-41358

Influence of the test temperature on the fracture energy of graphite

21 p3074 A72-41714

Usability of a graphite dish for atom absorption analyses of laser collected samples

22 p3176 A72-42175

Influence of the protective medium during sintering on the properties of iron-base cermets

23 p3299 A72-43289

Study of the process of niobium carbide production in a fluidized bed

23 p3293 A72-43294

Thermal and mechanical stresses concentration near peripheral notches on ring-shaped graphite, noting notch sensitivity relationship to tip curvature and graphite grain size

23 p3306 A72-43755

Some strength characteristics of graphite/zirconium carbide composites

23 p3307 A72-44013

Influence of the oxidation of finely dispersed graphite powders on their compactability

23 p3307 A72-44018

Cumulative damage stochastic models and distributions of strength of steels and graphite.

24 p3412 A72-44673

Structural and strength characteristics of carbon materials, considering composites preparation and applications

24 p3418 A72-45748

Graphites fracture under thermal stresses, considering stress-strain relations calculation method for annular samples

24 p3418 A72-45762

GRAPHITIZATION

Graphitization kinetics of amorphous thin carbon films under light impulses, discussing crystallite sizes, optical and electrical properties and two-stage character

12 p1833 A72-27857

Carbon fiber structure at graphitization temperatures to 3100 C in terms of surface energy and internal stress accounting for low shear strength

17 p2572 A72-35660

Successive graphitization of amorphous carbon

19 p2823 A72-38676

GRAPHS [CHARTS]

NT PATTERSON MAP

Bond graph methods for assembling structural dynamic models from component models, using EN-PORT programs for simulation or analysis

[SAE PAPER 710781]

01 p0137 A72-10273

- Double 45 degree z cut KD P electro-optic Q switch simulation with programmable desk top computer, deriving extinction ratio dependence plot graphs
02 p0224 A72-11746
- DT Cyg and T Vul cepheid variables light curves and periodic variations from photoelectric observations
03 p0416 A72-13018
- Laminar flame front surface area determination, presenting graphical constructions from generatrix of arbitrary segment number
03 p0455 A72-13099
- Plane and conical shock waves, presenting graphs and tables for numerical applications
03 p0341 A72-13684
- Creep rupture test program for Al alloys, circumventing parametric methods limitations by extrapolation procedure with graphical extension of isostress curves
03 p0378 A72-14174
- Time optimal trajectory graphical construction procedure from energy state approximation as basis of computational algorithm for real time onboard flight optimization
[AIAA PAPER 72-123] 05 p0688 A72-16968
- Deschamps graphical method application to multiport waveguide junction scattering coefficient measurement with averaging and least square fitting for error reduction
06 p0787 A72-18379
- Graphic determination of reflecting points location on active curve of given point meteor radiant based on stereographic projection and radio transmission properties
08 p1239 A72-21892
- Digital computer prepared optimal controls setting diagrams for single loop, linear and concentrated parameter control circuit design
09 p1291 A72-23372
- Nonsingular feedback control system phase-amplitude frequency response graphical analysis using real circle diagram
13 p1937 A72-29974
- Operator identities unification and classification, presenting reformulation as algebraic closure properties of graphs
14 p2125 A72-30229
- Graphical design technique based on Nyquist plane construction using circle criterion for nonlinear systems controller synthesis
14 p2091 A72-30375
- Distributed lumped active network configuration and design chart for realizing all-pass voltage transfer function
15 p2210 A72-31508
- Graph-analytic technique to plot Cr steel stress relaxation curve from primary and isochronous creep diagrams
16 p2472 A72-33848
- Satellite beacons observations from 1964 to 1970.
17 p2547 A72-35125
- Temperature distribution in solids under laser irradiation.
17 p2564 A72-35355
- Admissible changes in the parameters of a matching four-terminal network
19 p2772 A72-37315
- Recent results concerning a graphical test for checking the stability of a linear time-invariant system.
19 p2826 A72-38251
- Angular distribution of interstellar atomic hydrogen.
23 p3315 A72-43834
- RC, RL and RLC networks associated tunnel diode circuits normalized graphs, design method and stability consideration
23 p3272 A72-43988
- Charts for confidence limits and tests for failure rates.
23 p3294 A72-44395
- Unique charts for space missions.
24 p3422 A72-44644
- GRASHOF NUMBER**
Statistical solution of steady natural turbulent convection at large Grashof numbers
10 p1465 A72-24103
- Time behavior of two dimensional laminar free convection flow between heated vertical parallel plates, calculating temperature and velocity distributions as function of Grashof number
16 p2477 A72-33426
- GRASSES**
Grasslands mapping for ecosystem analysis, determining spectroradiance/reflectance characteristics by aerial and satellite-borne multispectral scanner imagery, aerial and ground photography and spectrometry
02 p0208 A72-11783
- GRASSMANN ALGEBRA**
U VECTOR SPACES
- GRATINGS**
Neural effects on human visual resolution of horizontal and vertical gratings resulting from early abnormal visual inputs due to astigmatism
10 p1430 A72-24348
- GRATINGS (SPECTRA)**
NT ECHELETTE GRATINGS
- Apollo 12 liquid oxygen cloud spectrum observations, describing spectrograph with off axis zone plate for transmission grating and sieve plate collimator
01 p0071 A72-11172
- Solid body surface strain field optical determination, using diffraction gratings
[SESA PAPER 1751] 02 p0199 A72-11512
- Iterative truncation error estimates in solution for plane wave diffraction by grating
02 p0171 A72-11738
- Spectrophotometer and tristimulus mask calorimeter using double grating mirror dispersion system
03 p0358 A72-13427
- Plane wave diffraction by infinite strip grating, providing closed form solution by boundary value problem reduction to singular integral equation
04 p0490 A72-15411
- Electrodynamical theory of artificial dielectrics based on rigorous solution for diffraction on system scattering elements consisting of periodical gratings formed by thin metallic strips
04 p0490 A72-15412
- Diffraction anamoly from infinitely extended strip grating solution by successive approximation technique combination with singular integral equation
04 p0491 A72-15418
- Ultrasonic diffraction grating for noninterference sampling of high power carbon dioxide laser beam, discussing diffraction profiles obtained from lasers operating in Gaussian and donut modes
05 p0669 A72-16608
- Transient plane wave reflection and scattering by periodic grating of thin conducting cylinders
06 p0777 A72-18736
- Tunable lasers using improved Littrow-mounted diffraction grating technique with mirror for spectral characteristics control
07 p1000 A72-19037
- Real time hologram photosensitive materials, determining power requirements and resolution for diffraction gratings in saturable absorbers and absorbing liquids
[CLEA PAPER 15,4] 07 p0984 A72-19397
- Spectrometers with electrostatic analyzers alternating with shielding and suppressing gratings for low energy electron flux measurement
07 p0988 A72-19955
- Passive optical shutter implementation for unidirectional emission from traveling wave ruby laser, using diffraction grating
08 p1184 A72-22037
- Delphinus Nova positions determination from plates obtained with photographic telescope with/without diffraction gratings
09 p1389 A72-23067
- Vibration measurement based on moire pattern fringes motion due to line gratings respective displacement, noting high accuracy and resolution
09 p1315 A72-23388
- Ultrahigh strain rate measurement via diffraction gratings directly impressed into test material surface, recording outputs by high speed cameras or photoelectric techniques
10 p1487 A72-24573
- Spectroscopy by synthesis of two or more fixed or moving diffraction gratings, obtaining transfer functions for total information increase
12 p1811 A72-27943
- Opaque scatterers disadvantages in interferometric images recording of transparent objects obtained by double exposure holography, noting phase type diffraction gratings
13 p1958 A72-29616
- UV solar spectrum recorded by rocket-borne spectrograph with diffraction grating echelle in Czerny-Turner arrangement
13 p2044 A72-29703
- Holographic diffraction grating production by impressing interference fringes with photographic procedure, using two laser beams
14 p2105 A72-30579
- Diffraction analysis of Fabry-Perot interferometer with metal mirror gratings for oblique incident polarized plane electromagnetic wave reception
15 p2233 A72-31413
- Visual evaluation of concave diffraction gratings with high ruling frequency, noting Foucault knife edge test limitations due to image faults
15 p2238 A72-32155
- Spectral image formation and aberration by spherical concave grating for point light source, using geometric optics method
15 p2278 A72-32337
- Ar plasma radiation dispersion by plane grating, measuring ionic spectral lines and continuous spectrum intensity time variation
15 p2286 A72-32340
- Mode locked lasers, investigating effect of grating-induced phase and spatial modulations by multiple transverse modes on pulse compression across beam cross section
16 p2403 A72-33840
- A compact grating spectroheliograph for the MgII resonance lines.
17 p2554 A72-35079
- Efficiency of holographic gratings in nonpolarized light under vacuum in the ultraviolet
19 p2799 A72-37670
- Scattering resonances of electromagnetic wave by an infinite plane grating with reflector.
19 p2767 A72-38612
- Plane electromagnetic wave diffraction on thin ribbons grating, discussing scattered field singularities for E polarized waves
19 p2769 A72-38850
- Grid polarisers for use in the near infrared.
20 p2922 A72-39046
- A method for directly determining surface strain fields using diffraction gratings.
21 p3052 A72-40236
- Dielectric coating effects on millimeter wave diffraction pattern of gratings, noting sharp anomalous dips in transmission intensity for P and S polarizations
21 p3031 A72-40604
- Exit slit mirror system in rocket-borne scanning Ebert grating spectrometer, discussing imaging properties and required adjustments
21 p3053 A72-40606
- Opaque scatterers disadvantages in interferometric images recording of transparent objects obtained by double exposure holography, noting phase type diffraction gratings
21 p3054 A72-40669
- Dark field method for phase diffraction grating visualization by microwave holography, using radio lens for object microwave spectrum formation
21 p3055 A72-40795
- Diffraction of a plane wave by a ribbon grating in the case of short wavelengths
23 p3264 A72-43527
- Laser beam periodic coupler design based on radiation property reciprocity theorem, suggesting use of reflecting layers and long wavelength gratings
23 p3288 A72-43888
- Spectrometer for absolute stellar spectrometry
23 p3290 A72-44039
- Reconstruction of phase holograms by means of a helium-cadmium laser
23 p3292 A72-44469
- GRAVEL DEPOSITS**
U GRAVELS
GRAVELS
Microwave emission from geological materials - Observations of interference effects.
20 p2917 A72-39477
- GRAVIMETERS**
Lunar surface gravimeter experiment to search for gravitational radiation from cosmic sources exciting moon if free oscillations
04 p0509 A72-15105
- Absolute gravity meter based on gradiometer system with additional mass, discussing working principle and calibration procedure
06 p0817 A72-18149
- Semiautomatic self leveling transverse gravimeter for gravity measurement along Lunar Rover Vehicle route on lunar surface
09 p1306 A72-22316
- Vibrating string accelerometer sea gravity meter with electronics for digital readout, discussing performance tests
11 p1635 A72-26499
- Two gyro three axis stabilizer with gyrocompass effect for gravimeter or magnetometer sensor stabilization in towed gondola
13 p1957 A72-29271
- Absolute and relative gravity measurement and instrumentation, using gradiometer array and modified gravity meter
14 p2150 A72-30320
- Some results of calibrating CG-2 gravimeters /Sharpe/ by the tilt method.
21 p3053 A72-40499
- GRAVIMETRY**
Apollo 14 landing site gravity determination from accelerometer data
02 p0285 A72-12844
- Geophysical and gravimetric measurement time recording techniques, describing satellite tracking photochronograph and electronic printing chronographs
04 p0525 A72-15571
- Lunar gravity measurements via Apollo 14 Doppler radio tracking over 100 kilometer band during low periapsis altitude orbits, relating to surface features
05 p0722 A72-17126
- Vertical gravity gradient measurements for areal density contrast exploration in gravity surveys and prospecting applications
06 p0809 A72-18147
- Gravity data free air and Bouguer correction /elevation correction/ by nomographic alignment chart
06 p0809 A72-18148
- Absolute gravity measurement methods and instruments, noting portable laser interferometer and formula derived from satellite observations
07 p1034 A72-19595

- Disturbing gravity potential and vertical deflection calculation error reduction based on pure gravity anomalies in geodesy 07 p0977 A72-19819
- Vertical deflections estimation with inertial navigation system, geodetic position and velocity reference and optimal data smoother, noting applicability to surveys from moving vehicles 12 p1843 A72-27634
- Absolute and relative gravity measurement and instrumentation, using gradiometer array and modified gravity meter 14 p2150 A72-30320
- Lunar orbiting dumbbell gravity gradiometer for measurement and mapping of lunar gravity field anomalies 14 p2104 A72-30511
- Correlation function measurements of optical gravity center roaming of spatially limited light beams in turbulent atmosphere 16 p2364 A72-33486
- Disturbing gravity potential and vertical deflection calculation error reduction based on pure gravity anomalies in geodesy 17 p2550 A72-35744
- Gravimetric and polarographic determination of W in binary W-Mo alloys, noting methods accuracy 18 p2655 A72-36098
- Type of equations for the solution of some gravitational prospecting problems from the anomalies on a complex relief, using a correlation model 23 p3285 A72-43847
- Solution of the inverse problem of gravimetry on the basis of harmonic moments of the gravitational field 23 p3285 A72-43928
- Potsdam correction from the satellite determined geopotential. 23 p3285 A72-43944
- Experimental determination of the vertical gradient of the gravity force from a known geopotential 24 p3397 A72-44862
- GRAVIRECEPTORS**
- NT OTOLITH ORGANS
- Soviet book on gravitation receptor covering evolution of structural, cytochemical and functional organization in invertebrates /statocyst/ and vertebrates /vestibular apparatus/ 03 p0316 A72-13850
- Vestibular system functional relationship to postural reflex mechanism involving labyrinth and gravireceptors responses 22 p3147 A72-42788
- OFO A orbital flight recording of bullfrog vestibular gravity sensor nerve fiber pulses for assessing necessity of artificial gravity during prolonged weightlessness 23 p3254 A72-43391
- GRAVITATION**
- NT ARTIFICIAL GRAVITY
- NT GRAVITY ANOMALIES
- NT LUNAR GRAVITATION
- NT LUNAR GRAVITATIONAL EFFECTS
- NT PLANETARY GRAVITATION
- NT REDUCED GRAVITY
- NT SOLAR GRAVITATION
- Differential equations systems formulation and numerical integration in gravitational problem of stellar n-bodies, discussing close approaches 05 p0713 A72-16052
- GRAVITATION THEORY**
- Inertial-gravitational mass ratio in classical and quantum case, proving equivalence principle non-validity for Brans-Dicke gravitation theory compared to Einstein theory 01 p0102 A72-10861
- Spatially homogeneous rotating and expanding universe models, deriving Lagrangian function from Einstein field equations 01 p0103 A72-11260
- Relativistic nonlinear gravitational instability theory for hydrodynamical system of equations applicable to early cosmic expansion, deriving density perturbations associated with rotational and gravitational waves 02 p0275 A72-11524
- Einstein gravitational field equations plane-front parallel ray wave exact solutions generalization to f-g gravity theory equations exact solutions 02 p0260 A72-12375
- Gravity model for spacecraft orbit prediction with gravitational anomalies, discussing gravity dipoles and disturbing acceleration tangential component [AAS PAPER 71-375] 02 p0283 A72-12424
- General theory of relativity, examining differences between singularities in stationary and nonstationary fields from gravitational equations solutions 02 p0261 A72-12675
- Cosmological gravity fourth-order equation system yielding geodesic lines, considering cylindrical and spherical universes 03 p0435 A72-13726
- Tensor-tensor theory of gravitation, introducing first effect of Mach principle 04 p0573 A72-14905
- Guided gravitational wave possibility from analogy to Maxwell electromagnetic equations 04 p0574 A72-14979
- Solar gravitational field precision measurements for gravitation theory validity verification 05 p0713 A72-16050
- Tachyon generation of gravitational radiation analogous to Cerenkov emission of electromagnetic radiation 05 p0711 A72-17160
- GEOS satellite orbit determination and prediction errors from optical tracking systems and gravity models, estimating resonant coefficients 06 p0877 A72-17653
- Gravitational intensification due to focusing of massive rotating gravitational wave emitting oblate object in galactic center 06 p0880 A72-17887
- Energy complex in general relativity in form of tetrahedral gravitational theory, including solutions to Einstein equations 06 p0849 A72-18419
- Field approach to gravitation accounting for energy release and nonthermal radiation occurrence in pulsars and quasars 07 p1075 A72-19576
- Redundancy of Hamiltonian constraints in classical and Dirac quantum theories of gravitation, suggesting replacement by single integral-form condition 07 p1035 A72-20195
- Modified Riemann geometry for scalar-tensor theory of gravitation, emphasizing scalar field role relation to vector length change during point-to-point transport 07 p1036 A72-20196
- Quantum and classical gravitation theory Mercury perihelion motion dependence on fourth order potential in scalar and Dirac fields 07 p1084 A72-20689
- Quantum gravitation theory and Mercury perihelion motion, calculating three body potentials from treatment of celestial bodies as nucleon assemblies 07 p1084 A72-20690
- Soviet monograph on universal gravitation covering prerelativistic theories, inverse square law, relativistic effects, celestial mechanics, stellar structures and evolution, etc 08 p1231 A72-21025
- Cosmological model with negative and positive mass particles, discussing cosmological term, gravitation shielding, red shift and interacting Vorontsov Veliainov galaxies 09 p1379 A72-22202
- Mass-zero spin-two particle field theory of gravitational interaction with covariance under full conformal group 09 p1355 A72-22684
- Linear theories of gravitational fields, discussing Lorentz invariant approximation use to obtain Einstein equations approximation 09 p1352 A72-23386
- Nonlinear analysis of gravitational stability perturbation based on Maxwellian velocity distribution 10 p1538 A72-24214
- Gravitational field angular momentum transfer analogy with Einstein gravitational energy transfer in general relativity 10 p1511 A72-24246
- Equations of motion with gravitational radiation reaction terms for gravitating system as source of asymptotically flat space 10 p1511 A72-24416
- Friedmann cosmological models in terms of conformally invariant gravitation theory, noting two physically connected universe halves 10 p1541 A72-24474
- Cosmological models with astrophysical and geophysical properties by introducing particles mass field and dimensionless coupling constant in conformally invariant gravitational theory 10 p1541 A72-24475
- German book on gravitation theory and equivalence principle, covering Lorentz invariance in Riemann space, relativity and Einstein effects 10 p1512 A72-24752
- Gravitational quadrupole radiation derivation from Einstein equations integration by successive approximation and variable separation procedures 10 p1513 A72-25167
- Nonlinear theory of gravitational instability in expanding universe, discussing density and velocity perturbations amplification at intermediate stage 11 p1715 A72-25527
- Second order gravitational waves in Einstein-Riemann four dimensional space-time, using method of characteristics 11 p1685 A72-25529
- Gravitational collapse in Brans-Dicke and Einstein theories of gravity 11 p1716 A72-25530
- Potential or gravitational energy in Newtonian physics based on Maxwell definition, noting energy transfer 12 p1843 A72-27187
- Conservation laws and symmetry properties of scalar tensor gravitational theories in terms of Einstein, von Freud, Moller and Komar extensions 12 p1847 A72-28153
- Noncovariant gravitation theory field equations based on preferred reference frame applied to homogeneous isotropic cosmological model, finding conservation law for total energy 12 p1875 A72-28154
- Structural and integral parameters for rotating stellar configurations within Newton gravitation theory, giving equations for gravitational potential, outer surface geometry and multipole moments 13 p2035 A72-28677
- Gravitational theory strong discontinuity conditions, using basis variational equation for field and media model construction in general relativity theory 13 p2002 A72-28711
- Invariant mechanics principles for two body system dynamic properties, analyzing mass center motion, system energy and gravitational theory role 14 p2152 A72-30481
- Radiation pressure on quasar outer envelope material as cause of mass outflow for masses less than gravitational force-determined critical value 14 p2155 A72-30552
- Uniqueness principle application to construction of gravitational field generated by complex of elastic bodies for mass tensor 16 p2424 A72-33366
- Nonlocal linear theory of gravitation without zero divergence assumption, deriving field equations by variational means 16 p2426 A72-33622
- A study of the upward continuation of gravity data from a plane surface. 17 p2544 A72-34271
- Relativistic hydrodynamics and gravitational instability. 17 p2581 A72-35380
- Intermediate-range gravity - A generally covariant model. 17 p2582 A72-35393
- Russian book - Theory of gravitation and the evolution of stars 17 p2613 A72-35452
- Thermal and gravitational instability in universe, obtaining equation for growth rate of density contrast 17 p2618 A72-35910
- Stochastic electrodynamics based on zero electromagnetic field motion, deriving Schrodinger equation and electromagnetic model of gravitation 17 p2584 A72-35912
- Gravitation theory in terms of scalar and tensor field, noting Lyra general reference system transformations and scale invariance 18 p2711 A72-36713
- Locally Lorentz covariant gravitational field theory of Pauli-Fierz type with massless symmetric spin-2 field having source term as matter stress-energy tensor 18 p2712 A72-37161
- The influence of local conditions in the interstellar medium upon star formation. 19 p2868 A72-38699
- Hamiltonian approach to the dynamics of expanding homogeneous universes in the Brans-Dicke cosmology. 19 p2869 A72-38807
- Faraday rotation by cosmic magnetic field in cosmology based on scalar-tensor theory of gravitation 20 p2969 A72-39264
- Finite range gravitation theory extension to generally covariant massive two-tensor field gravitation theory containing eight dynamically independent degrees of freedom 20 p2953 A72-39342
- Harmonic frames of reference in Einstein's theory of gravitation 20 p2953 A72-39406
- Cosmological electrodynamics and gravitation theory, considering singularity, constraint, Mach, Olbers, arrow-of-time and tail problems 20 p2974 A72-40004
- Stationary motions of a triaxial body and their stabilities. 21 p3109 A72-41334
- Gravitational theory strong discontinuity conditions, using fundamental variational equation for field and media model construction in general relativity theory 22 p3204 A72-42089
- Metric gravitation theories classified according to field type and interaction mode, constructing post-Newtonian limit 22 p3206 A72-42567
- A simple coupling between the electromagnetic and gravitational fields. 22 p3207 A72-42855

- Solar neutrino flux dependence on gravitational effects, discussing Brans-Dicke gravitation theory and general relativity equations
22 p3229 A72-42957
- Book - Gravitation and cosmology: principles and applications of the general theory of relativity.
22 p3208 A72-43080
- Generalization of the Taub-Kazner cosmological metric in the scalar-tensor gravitation theory.
23 p3313 A72-43500
- Natural rotation of bodies in Einstein's theory of gravitation
23 p3313 A72-44038
- Theoretical framework for testing gravitation and general relativity theories, considering completeness, self consistency and agreement with Newtonian physics
23 p3314 A72-44262
- Solar neutrino and dilaton theory of non-Newtonian gravity.
23 p3329 A72-44315
- Gravitational emission in the scalar-tensor theory of gravitation
23 p3315 A72-44476
- Lorentz-covariant reference-tetrad theories of gravitation
24 p3425 A72-44913
- Dynamic behavior of three point mass system with variable body mass ratios and constant total system mass, applying results to stellar systems
24 p3442 A72-45240
- On the gauge groups of linear conservative gravitational theories.
24 p3447 A72-45630
- GRAVITATIONAL COLLAPSE**
NT BLACK HOLES [ASTRONOMY]
Planetary mass distribution in solar system from gravitational contraction of nebula formed by accretion of ring shaped particle cloud
02 p0282 A72-12311
- Halos around black holes, showing luminosities caused by synchrotron radiation of magnetized plasma
03 p0435 A72-13803
- Electromagnetic fields produced by quasi-stationary gravitational collapse of uniformly rotating current carrying relativistic thin disk
04 p0579 A72-15321
- Cosmological evolution theories, discussing big bang theory, galactic evolution, quasars, pulsars, gravitational collapse, stellar evolution, supernovae, black holes, etc
05 p0716 A72-16311
- Black hole prediction in gravitational collapse of star and universe in terms of quantum principle, chemical mechanics and superspace dynamics
05 p0690 A72-16528
- Particle creation by strong rapidly changing gravitational fields in gravitational collapse of heavy star and in initial singularity
07 p1068 A72-19000
- Particle production and vacuum polarization, in anisotropic gravitational field, discussing energy momentum tensor values and collapse behavior
07 p1034 A72-19632
- Transcendence of baryon number conservation law, discussing static black hole properties as final massive star collapse state
07 p1076 A72-19667
- Neutron star evolution theories, emphasizing neutrino emission processes and stellar collapse
07 p1080 A72-20056
- Synchro-Compton theory for variable compact components in extragalactic radio sources, suggesting stellar mass object collapse as energy source
08 p1233 A72-21181
- Pulsar and quasar energy sources, discussing Crab nebula, rotating neutron stars and gravitational collapse role
08 p1233 A72-21208
- General relativistic gravitational waves analogy with electromagnetic radiation, examining relation to collapsed astronomical objects from black hole properties
10 p1533 A72-23893
- Gravitational collapse /black holes/ search in universe, noting application of optical astronomy and radiation detectors on satellites and rockets
10 p1541 A72-24407
- Cosmic ray ionization rate for hydrogen calculated for ambipolar diffusion efficiency in decoupling magnetic flux from gas during cloud collapse with angular momentum
10 p1544 A72-24664
- Hydrogen gas cloud gravitational contraction and fragmentation in expanding universe, noting cooling and massive stars formation
10 p1547 A72-24870
- Gravitational collapse in Brans-Dicke and Einstein theories of gravity
11 p1716 A72-25530
- Electron gas in superstrong magnetic fields of gravitationally collapsed objects outer region, noting Wigner transition to ordered structure
11 p1699 A72-26704
- Fowler quasars and exploding galaxies model tested by hydrodynamic equations numerical solution for premain sequence contraction and relativistic collapse of nonrotating supermassive star
12 p1866 A72-27202
- Black hole concept in general relativity and gravitational collapse, considering deviations from spherical symmetry and gravitational wave emanation from Galactic center
12 p1871 A72-27690
- Stellar gravitational collapse to neutron stars and black holes, discussing gravitational wave emission from Galactic center
12 p1875 A72-27958
- Relativistic and Newtonian theory compared for orbiting satellite matter release criteria and subreleasing change effects during gravitational collapse of central dense core
13 p2040 A72-29407
- Black holes due to gravitational collapses, including radiation emission/absorption, pulsars and binary stars
14 p2151 A72-30478
- Near-solar mass star secular stability during gravitational contraction and main sequence phases, considering static and quasi-static models
14 p2158 A72-30734
- Shell formation during star collapse due to rotational instability, discussing relativistic effects
15 p2305 A72-31337
- Linearized stability analysis of collapsing uniform nonrotating oblate gaseous spheroid, noting subcondensation growth rate dependence on shape and size
15 p2313 A72-32364
- Coordinate system valid for Oppenheimer-Snyder spherical dust cloud collapse into black hole
16 p2452 A72-33046
- Numerical calculation for axisymmetric gas cloud rotation effects on collapse, noting implications for star formation and fragmentation
16 p2458 A72-33722
- Collapse calculations for 0.25-10 solar mass spherical protostars, discussing stellar core evolution and temperature distribution in infalling cloud
17 p2606 A72-34674
- Nonspherical perturbations of relativistic gravitational collapse. I - Scalar and gravitational perturbations. II - Integer-spin, zero-rest-mass fields.
17 p2612 A72-35390
- Negative index polytropic sphere gravitational collapse structure, noting application to interstellar gas clouds thermal equilibrium
19 p2857 A72-37794
- Protostars formation through interstellar atomic hydrogen clouds gravitational collapse, deriving critical mass, surface temperatures and luminosities
19 p2865 A72-38478
- On the infall of matter into clusters of galaxies and some effects on their evolution.
20 p2965 A72-38901
- Kinetic equations for ultradense matter neutronization, noting stellar configuration of given mass with variable volume
21 p3086 A72-40096
- Slowly rotating axisymmetric star gravitational collapse derivation from general relativistic hydrodynamic and gravitational field equations formulated under Bondi-Sachs coordinate condition
23 p3335 A72-43488
- Gravitational emission in the scalar-tensor theory of gravitation
23 p3315 A72-44476
- Particle production and vacuum polarization in anisotropic gravitational field, discussing energy momentum tensor values and collapse behavior
24 p3424 A72-44564
- Collapse of massless nonrotating gas particle nonuniform spheroidal shell contracting around gravitating massive point nucleus, interpreting galactic evolution
24 p3438 A72-44844
- Stellar implosion, gas cloud collapse into white dwarf or neutron star and atomic hydrogen cloud collapse, considering effects of cosmic bodies at high velocities
24 p3439 A72-45017
- GRAVITATIONAL CONSTANT**
Absolute gravity acceleration determination using free-falling laser interferometer apparatus with rotation-insensitive mirror at different sites
02 p0207 A72-11597
- Gravitational constant determination by resonance method, describing experimental setup and procedure
10 p1510 A72-24127
- Curved space cosmological bounds on time variation of gravitational constant in terms of Brans-Dicke theory for Friedmann expanding cosmologies
16 p2450 A72-32864
- Magnitude redshift relation in flat Brans-Dicke cosmology, discussing gravitational constant effects on stellar evolution and galactic luminosity
16 p2455 A72-33471
- Critique on experiment to measure gravitational constant differences between two elements, discussing errors in statistical analysis
16 p2426 A72-33769
- A study of the upward continuation of gravity data from a plane surface.
17 p2544 A72-34271
- Many-body forces and the effect of the matter distribution in the universe to the gravitational constant.
18 p2728 A72-36800
- Problem of n bodies with a variable gravitational constant, and some dynamic characteristics of large-scale cosmic systems
19 p2863 A72-38077
- Theory of an experiment in an orbiting space laboratory to determine the gravitational constant.
20 p2968 A72-39200
- Gravitational constant time variations measurement by high flying laser tracked satellite, considering non-conservative forces effects on orbital perturbations
22 p3174 A72-42925
- Potsdam correction from the satellite determined geopotential.
23 p3285 A72-43944
- Inconsistency of gravitational constant variability in inverse proportion to time from viewpoint of stellar and solar system age, life development and physical three dimensional space
23 p3338 A72-44037
- Solar neutrino and dilaton theory of non-Newtonian gravity.
23 p3329 A72-44315
- GRAVITATIONAL EFFECTS**
NT LAGRANGIAN EQUILIBRIUM POINTS
NT LUNAR GRAVITATIONAL EFFECTS
NT STELLAR GRAVITATION
Particle escape within Newtonian gravitational system of three point masses, discussing necessary conditions
01 p0122 A72-10007
- Dynamical behavior classification for three bodies moving in plane under mutual gravitational influence
01 p0123 A72-10015
- Mice tolerance to long term accelerations or supergravities, detailing physiological consequences
01 p0014 A72-10934
- Human centrifuge tests for gravito-inertial force effect on ocular counterrolling in normal and deaf subjects
02 p0159 A72-11956
- Industrial and biological processing possibilities under weightless condition, considering crystal growth, metal processing, vaccine production and electrophoresis in space manufacturing
02 p0278 A72-11961
- Gravitational biology theory problems, discussing possibility of applying relativistic phenomena to living organisms in inertial or inertialess systems
02 p0160 A72-12016
- Hydromagnetic cylindrical blast wave propagation in self gravitating polytropic gas, obtaining graphs for velocity, pressure, density and magnetic field distributions
02 p0264 A72-12181
- Einstein light deflection by galaxy cluster gravitational field effect on extragalactic observations, explaining uniform background inhomogeneities
02 p0286 A72-12892
- Gravitational lens effect in black holes detection, computing light curves
03 p0416 A72-13011
- Inertial and gravitational mass equivalence principle verified for aluminum and platinum, using torsional pendulum with large relaxation time
03 p0388 A72-13076
- Gravitational convection by magnetocaloric effect in incompressible nonconducting ferromagnetic fluid
03 p0457 A72-13993
- Gravity effects of infinite homogeneous elliptical cylinder segment
03 p0351 A72-14330
- Energy equipartition among unequal masses in galactic nuclei and gravitating systems, discussing time scale for dynamical evolution
04 p0570 A72-14552
- Acceleration force simulation for altered weight effect on animal tolerance to restraint, discussing body mass loss, reduced lymphocyte count and disorientation
04 p0472 A72-14866
- Gravitational and inertial masses equivalence principle verification by pendulum torsional oscillation experiment with laser beam
04 p0519 A72-15070
- Encounterless one-dimensional constant density self gravitating system stability for symmetric disturbances, using analytic treatment and computer experiments
05 p0713 A72-16054
- Maxwell equation spinor formulation for Schwarzschild gravitational field effects on spherical electromagnetic waves propagation
05 p0689 A72-16165
- Circle moving under fluid dynamic and gravitational forces in viscous incompressible flow, describing dynamic interaction by numerical method
05 p0604 A72-16819
- Center of mass motion of spacecraft in central gravitational field, analyzing programming of size and

position of elements in mass geometry leading to arbitrarily large displacements 05 p0731 A72-17032

Soviet book on gravitational effects on animal evolution covering land and aqueous conditions adaptation and weightlessness in space 06 p0763 A72-17818

Finite amplitude fluctuations evolution in extended self-gravitating media for initial disturbances, taking into account pressure effects 06 p0880 A72-17888

Statistical mechanics of N-body self-gravitating system one dimensional model, using canonical and microcanonical ensembles 06 p0885 A72-18075

Numerical experiments in collisionless stellar systems evolution by gravitational n-body calculations using computers 06 p0885 A72-18076

N-body gravitational problem direct integration techniques, discussing fourth order polynomial method, computer algorithm and regularization procedure for two body encounters and close binaries 06 p0885 A72-18078

Computer models for simulating self consistent collisionless stellar systems evolution under gravitational field 06 p0885 A72-18081

Optimization problems in gravitational attraction, considering homogeneous ellipsoids interaction and free particle simple harmonic motion 06 p0851 A72-18740

Particle creation by strong rapidly changing gravitational fields in gravitational collapse of heavy star and in initial singularity 07 p1068 A72-19000

Statistical and probabilistic analyses of comet groups existence with similar orbital elements, considering gravitational capture by trans-Neptunian planets 07 p1075 A72-19559

Particle production and vacuum polarization, in anisotropic gravitational field, discussing energy momentum tensor values and collapse behavior 07 p1034 A72-19632

Branching theory application to convection and axisymmetric flow formation in internally heated self-gravitating liquid filled sphere 07 p0968 A72-19973

Short period comets orbital evolution and major planets gravitational effects, discussing cometary cloud formation, diffusion, motion and discovery 07 p1078 A72-19981

Big bang theory for age determination of galaxies, considering formation through gravitational instability and primeval gas velocity distribution fluctuations 07 p1084 A72-20470

Laminar natural convection heat transfer from leading edge of isothermal plate under nonuniform gravity [ASME PAPER 71-HT-CC] 08 p1250 A72-20875

Ideal liquid small oscillations natural frequencies and mode shapes in shell of revolution under weak gravitational field 08 p1148 A72-20956

Gravitational system dynamics, discussing massive-light star mixtures with collisions and systems with equal mass objects 08 p1231 A72-21121

Saturn ring motion stability factors for atomized material resistance to gravitational field, discussing ring thickness, density and other parameters 08 p1231 A72-21128

Aerodynamic and gravitational effects on relative motion of two orbiting point masses connected by flexible nonexpandable thread 08 p1240 A72-21143

Motion equations of gyrost with nonholonomic constraint under gravitational force 08 p1208 A72-21359

Nonlinear system of differential equations for gravity perturbation on geometrical form of thin axisymmetric cavity in heavy fluid 08 p1151 A72-21705

Earth-moon system gravitational effect on Venera automatic interplanetary stations motion away from earth 08 p1239 A72-22086

Redshifted I. alpha flux upper limit restricting hot ionized gas models for gravitational binding of Coma galactic cluster 09 p1383 A72-22292

Model stability of globular star cluster with nonzero rotational moment, discussing gravitational effects 09 p1383 A72-22494

Rotating stellar system with stars and interstellar gas within magnetic field, discussing gravitational and magnetic effects on gas pressure 09 p1384 A72-22511

Landau instability effect on density waves propagation in self-gravitating disk of differentially rotating and nonrotating stars populations, noting radial flow of matter 09 p1384 A72-22518

Physical optics approximation study of gravitational waves effect on electromagnetic propagation, noting unobservability of local scintillation effect 09 p1351 A72-22683

Gravity darkening effects on rapidly rotating B stars He I and Mg II spectral lines 09 p1391 A72-23530

Eigenmodes growth rate in convectively unstable self-gravitating gas sphere, using spherical harmonic series expansion and Laplace transforms 09 p1392 A72-23545

Gravitational red shift due to three body effect as relativity test 10 p1532 A72-23850

Schwarzschild solution to Vlasov equation for velocity distribution function of self-gravitating stellar system 10 p1535 A72-24112

Linear analysis of gravitational perturbations in strongly collisional initially homogeneous and Maxwellian medium 10 p1536 A72-24138

Short period comets origin and orbital evolution, discussing Jupiter perturbations and statistical study 10 p1536 A72-24143

Stopfenheim Kuppel area as part of meteorite cratering event forming Reis Kessel and Steinheim Basin from quartz grain shock feature analysis 10 p1537 A72-24159

Steady state exact solutions of MHD equations for perfectly conducting self-gravitating incompressible fluid, showing solutions existence for rotating planetary ellipsoid free liquid surface 10 p1539 A72-24328

Solar gravitational red shift measurement from solar and laboratory potassium absorption line comparison, using atomic beam resonance scattering technique 10 p1541 A72-24415

Atmospheric models of vertical structure of semidiurnal atmospheric gravitational tides, taking into account Coriolis force and vertical acceleration components 10 p1473 A72-24530

Binary stars convective zones reaction to periodic gravitational fluctuations due to stellar revolutions asynchronism, using incompressible fluid plane layer model 10 p1543 A72-24631

Magnetic simulation of gravity for wind tunnel investigations of aircraft jettison processes, considering Froude number and relationships between model and full scale aircraft 10 p1462 A72-24775

Galactic plane distance effect on interstellar reddening in north galactic polar cap, discussing line blanketing and surface gravity role 10 p1546 A72-24834

Blast wave propagation in uniform or gravitationally stratified media, using Brinkley-Kirkwood shock propagation theory 10 p1471 A72-25069

Tunnel wick heat pipe artery with priming in gravity environment by temperature induced pressure differences, using ammonia as working fluid [AIAA PAPER 72-273] 11 p1740 A72-25213

Aft center of gravity travel effects on aircraft longitudinal control response characteristics [SAE PAPER 720318] 11 p1575 A72-25581

Plasma interchange instability and convection in gravitational field, showing viscosity and resistivity stabilization and critical Reynolds number 11 p1697 A72-26584

Limiting form of equations for perfect gas steady two dimensional flow under gravity effects [ONERA, TP NO. 1087] 12 p1797 A72-27177

Potential or gravitational energy in Newtonian physics based on Maxwell definition, noting energy transfer 12 p1843 A72-27187

Variable white dwarf radial pulsation periods explained by nonradial oscillations and gravity modes, considering atmospheric mixing with degenerate core 12 p1868 A72-27260

Simulated gravity environment tests of vertical jump features, recording work performed, body center of gravity upward velocity, potential and kinetic energy changes 12 p1770 A72-27479

Finite difference calculations for structure of finite amplitude thermal convection within self-gravitating fluid sphere with uniform heat release 12 p1889 A72-27715

Gravitational n body problem - IAU Conference, Cambridge, England, August 1970 12 p1872 A72-27890

Probability and collisional relaxation in stellar systems, discussing gravitational polarization, collective interactions and spatial inhomogeneity 12 p1872 A72-27891

Galactic tidal field and multiple encounters role in stellar escape from star clusters, noting escape rates and kinetic energy involved 12 p1873 A72-27898

Gravitational many body problem differential equation system formulation and numerical integration 12 p1874 A72-27902

Integrals utilization in numerical integration of n body gravitational systems, discussing accuracy and reduced computation time 12 p1874 A72-27903

Stability of encounterless self-gravitating constant density system from computer experiment, using Fourier series expansions and Bessel functions 12 p1874 A72-27906

Statistical mechanics of one dimensional model for many body self-gravitating system with canonical and microcanonical ensembles, noting isothermal solution of Vlasov equation 12 p1846 A72-27907

Spiral density wave structure persistence conditions determined from computer simulations of galaxies evolution, noting gravitational azimuthal and radial forces effects 12 p1874 A72-27910

One and two boundary curves systems for Vlasov equation of one dimensional collisionless self-gravitating stellar systems evolution with constant phase space density 12 p1874 A72-27912

Boundary curves for collective relaxation in one dimensional collisionless two phase space density self-gravitating stellar system evolution, noting velocity dispersions dependence 12 p1875 A72-27913

Stability properties for collisionless plasma and encounterless self-gravitating stellar gas described by Vlasov equations 12 p1875 A72-27916

Close approaches in numerical integration of gravitational many body problem, discussing smoothing and regularization 12 p1875 A72-27918

Ear oximeter design for human subject blood oxygen saturation estimation during increased g-loads 12 p1774 A72-28278

Tilt table test for gravitational stress effects on human pulmonary capillary blood flow 12 p1765 A72-28286

General relativity equation of motion for spherically symmetric surface layer of ideal gas under central gravitational field 13 p2035 A72-28646

Galactic formation initiation mechanism with thermal instability in expanding universe, noting Compton scattering energy exchange ensuring gravitational instability dominance 13 p2039 A72-29086

Thromboelastographic and coagulographic studies of gravitational effects on blood coagulation in cats under acceleration stress 13 p1904 A72-29309

Star escape and accumulation in halo from stellar random gravitational encounters in spherical system dense central core 13 p2040 A72-29402

Two phase flow model of cloud and star formation by galactic shocks in quasi-steady interstellar gas flow in spiral gravitational field 13 p2040 A72-29404

Relativistic and Newtonian theory compared for orbiting satellite matter release criteria and subreleasing change effects during gravitational collapse of central dense core 13 p2040 A72-29407

Luminosity variation of star in circular orbit around extreme Kerr black hole due to Doppler effects and gravitational field light focusing 13 p2041 A72-29416

Inertial and gravitational mass equivalence principle verified for Al and Pt, using torsional pendulum with large relaxation time 13 p2044 A72-29426

Hypergravity effects on bats spatial orientation, noting resistance to head-pelvis and pelvis-head accelerations 13 p1907 A72-30015

Tangential MHD discontinuity stability for ideally conducting compressible fluid in magnetic and gravitational fields 13 p2020 A72-30068

Two body model for three body problem of uniformly distributed and isotropically expanding gravitational matter of Einstein-Sitter universe, noting metagalaxy cooling rate 14 p2149 A72-30211

Equations of motion for incompressible viscous fluid thin layer on cylinder outer side under gravity, calculating wave number, phase velocity and film thickness 14 p2094 A72-30699

Stellar radiation and gravitational effects on neutral atoms and dust grains at large distances for various spectral type stars in schematic evolutionary galaxy 14 p2158 A72-30735

Dynamic behavior of three masses moving under mutual gravitational attraction examined by numerical 14 p2158 A72-30735

experiments for binary star formation via third star hyperbolic escape

14 p2160 A72-30877

Galactic tidal interactions, computing mass loss for hyperbolic collisions and giant system formation from density distribution models

14 p2161 A72-31043

Stability analysis of satellite motions in Newton planetary field by Liapunov method, considering ellipsoid of revolution under gravitation of sphere

14 p2162 A72-31081

Uniform rotation and magnetic field effects on gravitational stability of interface between two semi-infinite homogeneous streams

15 p2284 A72-31593

Perfect gas steady flow under gravity action, analyzing limiting equations [ONERA, TP NO. 1087]

15 p2178 A72-31682

Gravity effects on plant organ orientation with respect to force direction from Chara rhizoid cell statoliths

15 p2189 A72-31932

Heavy body mass distribution gravitational effects in nonlocal linear theory, noting refractive index, rosette motion and perihelion advance

15 p2278 A72-32484

Stability analysis of gyrostat satellites possible equilibria under gravitational torques, considering inertia, equilibrium and angular momentum parameters

15 p2321 A72-32586

F region plasma one dimensional nonisothermal diffusion for positive ions with allowance for ionization and recombinations and gravitational forces

15 p2232 A72-32731

Initial value problem for compressible viscous heat-conducting fluid flows with basic rotation and density stratification in gravitational field

16 p2377 A72-33337

Critique of papers on quasars covering theory of gravitational lens intensified bright compact objects

16 p2454 A72-33452

The gravitational acceleration perpendicular to the galactic plane.

17 p2603 A72-34441

Effects of combined O-G simulation and hypergravity on eggs of the nematode, *Ascaris suum*. [DFVLR-SONDDR-225]

17 p2499 A72-34547

Vestibular behavior of fish during diminished g-force and weightlessness.

17 p2499 A72-34549

Earth-moon system gravitational effect on Venera automatic interplanetary stations motion away from earth

17 p2606 A72-34655

Model stability of globular star cluster with nonzero angular momentum, discussing gravitational effects

17 p2606 A72-34658

Analytical guidance in the neighborhood of optimal multi-impulse trajectories.

17 p2609 A72-35102

Slipping stream instability of a self-gravitating hydromagnetic gas cloud.

17 p2613 A72-35501

Spiral galaxies self gravitating cold disk model, considering equilibrium state, instability, oscillation modes, bending motions, pressure effects and angular momentum distribution

18 p2725 A72-36386

The influence of clinostat rotation on the fertilized amphibian egg.

18 p2649 A72-36435

On the effects of gravitational absorption on orbits of artificial earth satellites.

18 p2728 A72-36761

Linear pulsations and stability of differentially rotating stellar models. I - Newtonian analysis. II - General relativistic analysis.

19 p2855 A72-37247

Computational models of gravitationally interacting galaxies.

19 p2855 A72-37344

Gravitational spin interaction.

19 p2835 A72-38425

Inviscid non-monatomic interstellar gas radial flow, considering gravitational and heat conducting effects in stellar winds

20 p2967 A72-39193

Aerodynamic and gravitational effects on relative motion of two orbiting point masses connected by flexible nonexpandable thread

20 p2977 A72-39248

Structure of spherically symmetrical clusters in the relaxation phase

20 p2974 A72-40022

Branching theory application to convection and axisymmetric fluid formation in internally heated self gravitating liquid filled sphere

20 p2915 A72-40030

An upper limit on the neutrino rest mass.

21 p3088 A72-40830

Gravitational radiation interaction with background fluid of collisionless particles with zero rest mass in homogeneous isotropic Friedmann universe

21 p3105 A72-41028

Gravitational perturbations as source for solar oblateness fluctuations, considering density in upper convective zone

21 p3106 A72-41039

Stellar evaporation in globular clusters passing through galactic plane, considering gravitational perturbation increase of total energy within system

21 p3107 A72-41269

Finite radial oscillations of uniformly rotating gravitating magnetized fluid cylinder model of star formation dynamics

21 p3109 A72-41331

Frictional effects with neutrals and the gravitational instability of a plasma.

21 p3093 A72-41332

N-burn analytic solution for propellant-optimal transfer trajectories in vacuum, taking into account gravitational effects

[AIAA PAPER 72-929]

21 p3112 A72-41569

Quasi-periodic orbits about the transplanar libration point.

[AIAA PAPER 72-935]

21 p3112 A72-41573

Self similar procedure derived for gas fall to solid surface in constant gravitational field, applying to initial phase of neutron star matter accretion

21 p3113 A72-41753

Decomposition of the force function of two homogeneous spheroids with noncoinciding symmetry planes

21 p3114 A72-41771

Cometary parent bodies transfer to short period orbits by Jupiter caused gravitational disturbances, noting qualitative analysis of orbits evolution

22 p3219 A72-41913

Gravitational deflection of light by radially and cylindrically symmetric masses, considering effect on apparent luminosity of distant object

22 p3204 A72-42000

Martian light sources generated by suspended crystals producing parhelic halo in atmosphere, noting randomly oriented and gravitationally arranged suspensions

22 p3223 A72-42142

Hypothermia and resistance of mice to lethal exposures to high gravitational forces.

22 p3142 A72-42494

Homogeneous stellar system with purely gravitational interactions, predicting oscillatory relaxation time

22 p3207 A72-42853

Solar neutrino flux dependence on gravitational effects, discussing Brans-Dicke gravitation theory and general relativity equations

22 p3229 A72-42957

Shmidt cosmological hypothesis impact on geophysics, geochemistry and geology, discussing planetary evolution, initial earth temperature and gravitational differentiation

22 p3230 A72-43154

Two body model for three body problem of uniformly distributed and isotropically expanding gravitational matter of Einstein-Sitter universe, noting metagalaxy cooling rate

23 p3334 A72-43241

Lunar and solar gravitational effects on earth atmosphere, describing latitudinal distribution of cyclone centers by momentum distribution of horizontal tide-generating forces

23 p3310 A72-43249

Solar system thin disk form planet formation in equatorial plane from nebula dust component, discussing gravitational effects and mass increase rate

23 p3335 A72-43261

Quasars as images of Seyfert nuclei.

23 p3336 A72-43559

The equilibrium configuration of a slowly rotating mass of liquid in the presence of a poloidal magnetic field.

23 p3322 A72-44306

Saturn-Jupiter rebound - A method of high-speed spacecraft ejection from the solar system.

23 p3340 A72-44323

Particle production and vacuum polarization in anisotropic gravitational field, discussing energy momentum tensor values and collapse behavior

24 p3424 A72-44564

Rotating black holes - Separable wave equations for gravitational and electromagnetic perturbations.

24 p3439 A72-45014

Energy sources for extragalactic explosive phenomena in galactic nuclei and quasars, considering gravitation and double radio sources

24 p3439 A72-45018

Explorer 34 satellite orbit perturbation, noting earth gravitational tesseral harmonic effect on perigee passage time

24 p3399 A72-45557

GRAVITATIONAL FIELDS

NT STELLAR GRAVITATION

Integrability of rotating satellite differential equation of motion in axially symmetric gravitational field

01 p0122 A72-10008

Gravitational potential tensor and equations of motion of relativistic mechanics for isolated system of masses

01 p0127 A72-10345

Optimal control of material point motion in thin spherical layer of central gravitational field, solving by approximation

01 p0127 A72-10355

Anomalous magnetic and gravitational fields energy spectra model, examining autocorrelation functions changes

02 p0217 A72-11932

Gyroscope precession in earth gravitational field, considering impulse energy vector and angular momentum tensor

02 p0229 A72-11970

Collision kinetics of jet streams of inelastic grains in neighboring orbits around central gravitating body

02 p0281 A72-12304

Einstein gravitational field equations plane-front parallel ray wave exact solutions generalization to f-g gravity theory equations exact solutions

02 p0260 A72-12375

Diffuse gravitational background radiation in universe, assuming gravitational field fluctuations macroscopic nature and Einstein equations applicability

03 p0417 A72-13095

Lorentz transformation between fixed and inertial reference frame in uniform gravitational field, discussing application to clock paradox problem

03 p0388 A72-13228

General relativity and cosmology of quasi-stellar objects, covering distances, red shifts and gravitational fields

03 p0426 A72-13270

Relative stellar orbit determination in clusters NGC 5460, 5617, 6067, 6405 and 6494, presenting gravitational potential, orbital elements and anomalous period

03 p0434 A72-13495

Stellar orbits in galactic symmetry plane, using gravitational potential theories

03 p0434 A72-13496

Mascon free lunar gravitational potential calculations, showing hydrostatic equilibrium in early evolution

03 p0434 A72-13552

German book on gyroscope theory and applications, covering artificial satellites motion in gravitational field

03 p0360 A72-13675

Gravitational fields of giant planets in hydrostatic equilibrium, solving equations for linear and quadratic density distributions

03 p0436 A72-13818

Lunar gravitational potential determination from Stokes and selenocentric constant

03 p0440 A72-14326

Gravitational field of bounded and isolated material in empty four-dimensional locally Minkowskian space-time, emphasizing radiation zone and gravitational waves

04 p0570 A72-14556

Earth gravity field representation by simple layer potential from Doppler tracking of satellites

04 p0514 A72-14565

Magnetic and gravitational energy release by resistive MHD instabilities responsible for solar flares

04 p0571 A72-14578

Gravitational radiation focusing by interior gravitational fields of diffuse static spherically symmetric matter distribution

04 p0549 A72-15024

Earth planetary structure from gravitational information, discussing crust, mantle, gravity anomalies, satellite and ground observation methods and improved earth model

04 p0519 A72-15075

Numerical instability of gravitational n-body problem considering differences between computed systems and exact solutions to differential equations

04 p0581 A72-15629

Partial iterative refinements of parameters by reduced Newton-Raphson process based on generalized inversion, noting method use in gravitational n-body equation

04 p0581 A72-15630

Earth gravity field, movement and temporal form variation determination by satellite tracking, long base interferometry or lunar observation

04 p0520 A72-15723

Galactic cluster lifetimes compared with star cluster model evaporation times, discussing general galactic and interstellar clouds tidal fields effects

05 p0713 A72-16051

Maxwell equation spinor formulation for Schwarzschild gravitational field effects on spherical electromagnetic waves propagation

05 p0689 A72-16165

Relative motion of active interceptor spacecraft approaching passive craft in central gravitational field, using dimensionless differential equations similarity coefficients method

05 p0728 A72-16592

Rocket orbit in mass point gravitational field, studying KS variables separability, elliptic functions and equivalent problems 06 p0877 A72-17656

Earth gravitational potential, including surface density, crystal thickness, potential coefficients, contour maps and spherical harmonic expansion 06 p0877 A72-17657

Linearized hydrodynamic stability of viscoelastic fluid Couette flow in gravity field 06 p0798 A72-17778

Infinite homogeneous self gravitating compressed gas media nonlinear condensations, describing finite amplitude motion with asymptotic expansions 06 p0880 A72-17889

Cavitation flow around plate in transverse gravitational field, investigating boundary condition approximation on free boundary 06 p0799 A72-17913

Close binary system average gravity and effective temperature at Roche limit for 90 deg phase and both conjunctions, taking into account mass ratios and orbital inclination 06 p0882 A72-18002

Isolated rotating disks of stars galactic evolution model for gravitational field studies, noting dynamic instabilities and final exponential mass distribution 06 p0885 A72-18077

N-body gravitational problem numerical integration treatment of close approaches, using transformations for eliminating differential equations of motion singularities 06 p0885 A72-18079

Absolute gravity meter based on gradiometer system with additional mass, discussing working principle and calibration procedure 06 p0817 A72-18149

International Satellite Geodetic Experiment (ISAGEX), using laser telemetry techniques for accurate measurement of earth gravitational field 06 p0888 A72-18261

Mariner 9 radio tracking measurements of Mars gravity field and pole direction, comparing to moon and earth 06 p0890 A72-18346

Rocket motion in general central force field, obtaining primer vector integration for optimal coasting arc during orbital transfer [AD-741964] 06 p0890 A72-18386

Tensor analysis of electromagnetic energy localization in space, generating gravitational field and space curvature via equation to Einstein tensor 07 p1035 A72-19685

Earth gravitational field determination based on long periodic perturbations in orbital motion of satellites, estimating tesseral coefficients errors 07 p0976 A72-19817

Wightman field theory generalization for application to gravitational field quantization, describing curved space-time by strongly geodesically complete manifolds 07 p1036 A72-20198

Spectral distribution of electromagnetic radiation emitted by charge moving in gravitational field of spherically symmetric black holes 07 p1081 A72-20226

Gravitational field simulation by centrifugal force for structural stability and self weight buckling studies 07 p1096 A72-20428

High order harmonic equations in gravitational potential from Transit 1B orbit inclination, comparing with Ariel 3 08 p1158 A72-21216

Gravitational field potential energy-momentum pseudotensor component determination in general relativity theory 08 p1207 A72-21301

Solid body motion with fixed point in central Newtonian force field, classifying angular velocity vector hodograph as function of dimensionless parameters 08 p1208 A72-21363

Particle motion in conformal spaces in general relativity, deriving gravitational potential and proper energy of mass point 08 p1209 A72-21369

Stationary motions, stability of satellite with rotary gyroscope and gimbals in circular orbit and central Newtonian force field 08 p1241 A72-21801

Stationary motions stability of four rotor vertical gyroscopic system on satellite in circular orbit in Newtonian central force field 08 p1205 A72-21804

Liapunov stability of circular equatorial motions of light bodies in Kerr gravitational field of massive rotating body, using geodesic lines equations 08 p1210 A72-22071

Initially stationary axisymmetric disk of stars evolution calculated by gravitational potential solver for various values of velocity dispersion 09 p1383 A72-22460

Coordinate mapping for solutions of Einstein initial value problem for vacuum gravitational fields 09 p1350 A72-22471

Molodenski integral equation for gravitational field calculation at point M on earth surface as function of neighboring region astronomical geodetic measurements 09 p1299 A72-22675

Numerical solution of thermal shock equations for incompressible fluid with free convection and of motion equations in gravitational force field 09 p1410 A72-22882

Minimum time duration rocket interception, calculating trajectory parameters and target orbits in Earth gravitational field 09 p1393 A72-23573

Gravitational field angular momentum transfer analogy with Einstein gravitational energy transfer in general relativity 10 p1511 A72-24246

Earth gravity anomalies sources depth, testing hypothesis of density variations origin 10 p1472 A72-24523

Diffuse gravitational background radiation in universe, assuming gravitational field fluctuations macroscopic nature and Einstein equations applicability 11 p1716 A72-25703

Time optimal transfer trajectory in central Newtonian force field between two arbitrary points under jet acceleration 11 p1718 A72-25942

Vertical gravitational gradiometer capable of separating in space gravitational field elements and mechanical motion translational acceleration 11 p1635 A72-26463

Spacelike hypersurface conformally invariant three-geometry role in unconstrained dynamical degrees of freedom of gravitational field 11 p1691 A72-26706

Body of revolution /saucer/ with nongeodesic internal stresses under gravitational field in terms of general relativity theory 12 p1843 A72-27048

Time-space nonholonomic characteristics of curvature tensor for three dimensional physical space in gravitational and inertial fields 12 p1843 A72-27049

Computer models for collisionless stellar systems equations of motion, obtaining force from smoothed gravitational field 12 p1875 A72-27920

Stages optimum selection for step rocket moving in plane gravitational field 13 p2051 A72-28384

Covariant statistical mechanics equations system for distribution function of relativistic particles in steady external gravitational field, noting Vlasov equation as limiting case 13 p2035 A72-28465

Transstructural topographic and gravity profiles of three Mauritanian meteorite craters, showing residual negative gravity anomalies 13 p1947 A72-28756

Gravitational instability and galaxy formation in expanding universe, considering primordial turbulence and density perturbations 13 p2038 A72-29085

Anomalous magnetic and gravitational fields energy spectra model, examining autocorrelation functions changes 13 p1949 A72-29244

Natural oscillation frequencies of cavity-contained liquid in weak gravitational field, using variational principles 13 p1943 A72-29791

Lunar orbiting dumbbell gravity gradiometer for measurement and mapping of lunar gravity field anomalies 14 p2104 A72-30511

Distortion corrections in geophysically traced gravitational, magnetic and geoelectric field maps, discussing automation 14 p2101 A72-30642

Anomalous magnetic and gravitational field models autocorrelation function behavior dependence on circular cylindrical sources depth and spacing 14 p2101 A72-30647

Lunar origin and evolution, considering gravitational energy, radioactive isotopes and tidal deformations as heat sources 14 p2161 A72-30997

Dynamic system motion stability estimation with Liapunov function in quadratic form, applying to circular satellite orbit stability in axisymmetric gravitational field 14 p2161 A72-31079

Charge and mass densities relation for stationary charged dust distribution in general relativity, investigating Einstein-Maxwell equations for stationary gravitational field 15 p2275 A72-31591

Quasar electromagnetic radiation emission in terms of general relativistic coupling between gravitational field and charged particle radiation field 15 p2306 A72-31592

Body of revolution motion in fixed center Newtonian field, investigating plane trajectories of center of inertia 15 p2307 A72-31677

Capture resonance of asteroid 1685 Toro by earth due to gravitational interaction at close encounters 15 p2307 A72-31721

Nonsymmetric gyrosteady motions analysis in axisymmetric gravity field based on Routh-Liapunov theorem, calculating stability conditions 15 p2320 A72-31728

Secular and long term periodic perturbation effects of third body upon particle motion in three body problem, discussing mass motion in Jovian gravitational field 15 p2312 A72-32120

Early B stars with normal helium abundances and small rotational velocities, deducing gravity from H lines and ESW stark broadening 15 p2316 A72-32751

Nonlocal linear theory of gravitation without zero divergence assumption, deriving field equations by variational means 16 p2426 A72-33622

A study of the upward continuation of gravity data from a plane surface. 17 p2544 A72-34271

Variations of the earth's gravity field due to the free nutation. 17 p2544 A72-34272

Intergalactic ionized gas and member galaxies mass relationship in local group and nearby galactic clusters, considering gravitational potential 17 p2604 A72-34475

Time evolution of a rotating black hole immersed in a static scalar field. 17 p2605 A72-34536

Gravitational field potential energy-momentum pseudotensor component determination in general relativity theory 17 p2580 A72-34659

Propagation of spherical waves in a weak static gravitational field 17 p2581 A72-35170

The stability of a self-gravitating, nonrotating gas layer with stellar, magnetic, and cosmic-ray components. I. 17 p2611 A72-35313

Hamiltonian formulation of spherically symmetric gravitational fields. 17 p2582 A72-35393

Earth gravitational field determination based on long periodic perturbations in orbital motion of synchronous satellites, estimating tesseral coefficients errors 17 p2550 A72-35742

Motion of a gyrosteady with respect to its center of mass in a central field 17 p2622 A72-35804

Structural analysis of gravitational field in asymptotic limit at spatial infinity, introducing three dimensional spacelike surface carrying initial data for space-time 17 p2583 A72-35824

Magnetized deformable media in general relativity. 17 p2584 A72-35911

Hulthen and Schwarzschild potentials in the Klein-Gordon equation. 18 p2711 A72-36515

Singularities of nonstationary solutions to the equation of diffusion in a gravitational field. I, II 18 p2687 A72-36655

General relativistic planetary structures comparison with Newton gravitational theory, deriving field equations for spherically symmetric planets with explicit pressure and density distributions 18 p2728 A72-36751

Book on classical relativity theory covering relativistic kinematics and mechanics, tensor calculus, electrodynamics, gravitational fields and effects, elastic continua mechanics, thermomechanics and cosmology 18 p2712 A72-36850

The influence of geostrophic force on the stability of an heterogeneous conducting fluid with a radial gravitational force. 18 p2683 A72-36933

Polarization effects during electron scattering in the gravitational field of a rotating source 18 p2712 A72-36967

The Rayleigh-Taylor problem with a vertical magnetic field, including the effects of Hall current and resistivity. 19 p2839 A72-37339

Relative motion of active interceptor spacecraft approaching passive craft in central gravitational field, using dimensionless differential equations similarity coefficients method 19 p2869 A72-37564

Gravitational fields of Jupiter and Saturn 19 p2857 A72-37734

The impact of gradiometer techniques on the performance of inertial navigation systems. [AIAA PAPER 72-850] 20 p2949 A72-39079

- High energy particle and photon orbital and vortical motions in Kerr metric outside equatorial plane in gravitational field 20 p2953 A72-39341
- Plane-symmetric similarity solutions for self-gravitating fluids. 20 p2955 A72-40009
- Gravitational field of arbitrarily thick steadily rotating shell in general relativity, using successive approximation method 20 p2955 A72-40010
- The Robertson-Walker cosmology and the Friedmann cosmology 20 p2975 A72-40071
- Fundamental geodetic parameters of the earth's figure and the structure of the earth's gravity field derived from satellite data. 21 p3048 A72-40494
- Measurements of gradients of gravity in mines. 21 p3048 A72-40500
- Flow stability of ideal compressible and incompressible fluids, solving Navier-Stokes equation for rotating liquid with free boundary in gravitational field 22 p3165 A72-42151
- Hydrostatic pressure effects on atomic configuration based on principle of equivalence related to Einstein gravitational equations 22 p3205 A72-42459
- A simple coupling between the electromagnetic and gravitational fields. 22 p3207 A72-42855
- Approximate solutions of the relativistic gravitational field equations to describe clusters of galaxies. 22 p3229 A72-42993
- Slowly rotating axisymmetric star gravitational collapse derivation from general relativistic hydrodynamic and gravitational field equations formulated under Bondi-Sachs coordinate condition 23 p3335 A72-43488
- Type of equations for the solution of some gravitational prospecting problems from the anomalies on a complex relief, using a correlation model 23 p3285 A72-43847
- Solution of the inverse problem of gravimetry on the basis of harmonic moments of the gravitational field 23 p3285 A72-43928
- Potsdam correction from the satellite determined geopotential. 23 p3285 A72-43944
- Gravitational instability of perturbed and unperturbed matter distribution in form of density and velocity fluctuations associated with continuity relationship between wavelength and rotation direction 23 p3338 A72-44036
- Experimental determination of the vertical gradient of the gravity force from a known geopotential 24 p3397 A72-44862
- Lorentz-covariant reference-tetrad theories of gravitation 24 p3425 A72-44913
- Russian book - Space research 1970: Investigation of the gravitational fields and shapes of the earth, other planets, and the moon on the basis of spacecraft observations. 24 p3443 A72-45399
- Body of revolution /saucer/ with nongeodesic internal stresses under gravitational field in terms of general relativity theory 24 p3425 A72-45701
- Time-space nonholonomic characteristics of curvature tensor for three dimensional physical space in gravitational and inertial fields 24 p3425 A72-45702
- GRAVITATIONAL POTENTIAL**
U GRAVITATIONAL FIELDS
GRAVITATIONAL RADIATION
U GRAVITATIONAL FIELDS
GRAVITATIONAL WAVES
- Diffuse gravitational background radiation in universe, assuming gravitational field fluctuations macroscopic nature and Einstein equations applicability 03 p0417 A72-13095
- Guided gravitational wave possibility from analogy to Maxwell electromagnetic equations 04 p0574 A72-14979
- Gravitational waves proposed origin, considering black holes, star collapse, white dwarf and neutron star formation and galaxy center neutron star clustering 04 p0576 A72-15074
- Lunar surface gravimeter experiment to search for gravitational radiation from cosmic sources exciting moon if free oscillations 04 p0509 A72-15105
- Gravitational radiation short bursts detector, treating SNR by fluctuations method 05 p0715 A72-16183
- Tachyon generation of gravitational radiation analogous to Cerenkov emission of electromagnetic radiation 05 p0711 A72-17160
- Dumbbell and Weber cylindrical gravitational wave detectors sensitivity comparison 06 p0848 A72-17828
- Emission characteristics of relativistic charge in rectilinear motion within gravitational wave field 08 p1206 A72-21072
- Mathematical model of gravitational wave zone for ring emanated smooth axisymmetric toroidal pulse 08 p1158 A72-21177
- Toroidal gravitational waves in general relativity, considering analog to imploding-exploding cylindrical waves, linear field equations and symmetric metric 08 p1210 A72-21922
- Black hole vibrations explained as gravitational waves in spiral orbits 09 p1383 A72-22291
- Random gravitational plane wave metric effect on electromagnetic wave mean value, noting light dispersion and attenuation 09 p1351 A72-22682
- Gravitational radiation from isolated material source in terms of van der Burg solution to Einstein field equations 09 p1352 A72-23359
- Gravitational radiation spectrum and energy computation from point test particle falling radially into Schwarzschild black hole 09 p1393 A72-23646
- Long wave trains of gravitational waves from vibrating black hole, stressing hole dynamical entity 09 p1394 A72-23697
- General relativistic gravitational waves analogy with electromagnetic radiation, examining relation to collapsed astronomical objects from black hole properties 10 p1533 A72-23893
- Equations of motion with gravitational radiation reaction terms for gravitating system as source of asymptotically flat space 10 p1511 A72-24416
- Post-Newtonian approximation for calculation of energy and angular momentum radiated in form of gravitational waves by two point particles system, noting masses in hyperbolic Kepler orbit 10 p1547 A72-24933
- Gravitational quadrupole radiation derivation from Einstein equations integration by successive approximation and variable separation procedures 10 p1513 A72-25167
- Wave equation derivation for electromagnetic and gravitational radiations in Schwarzschild field, obtaining third order corrections for scalar waves 10 p1514 A72-25168
- Critique of Rees theory of primordial gravitational radiation concerning galaxy clusters interaction with very long wavelength universal gravitational waves 10 p1550 A72-25200
- Second order gravitational waves in Einstein-Riemann four dimensional space-time, using method of characteristics 11 p1685 A72-25529
- Diffuse gravitational background radiation in universe, assuming gravitational field fluctuations macroscopic nature and Einstein equations applicability 11 p1716 A72-25703
- Gravitational wave antenna response to linear, mixed and randomly polarized sources, discussing Weber signals galactic nucleus source 11 p1717 A72-25882
- Gravitational wave observation interpretations, discussing Weber theory of galactic nucleus isotropic radiation and synchrotron radiation sources in terms of black hole existence 11 p1717 A72-25883
- General relativity equations solution for interaction of gravitational radiation and conducting fluids in magnetic field, noting energy absorption in specified depth surface layer 11 p1720 A72-26116
- Constraint on astrophysical sources of gravitational waves, using microwave radiometers 11 p1721 A72-26124
- Colliding plane gravitational waves equations for linear polarization 12 p1845 A72-27409
- Black hole concept in general relativity and gravitational collapse, considering deviations from spherical symmetry and gravitational wave emanation from Galactic center 12 p1871 A72-27690
- Stellar gravitational collapse to neutron stars and black holes, discussing gravitational wave emission from Galactic center 12 p1875 A72-27958
- X ray flux associated with gravitational radiation pulses, determining upper limit with balloon-borne apparatus 13 p2007 A72-30121
- Relativistic analysis for synchrotron gravitational radiation emitted by particle in circular orbit around Schwarzschild black hole, noting astrophysical implications 13 p2007 A72-30123
- Gravitational wave diffraction by liquid on surface of vertical cylindrical shells, determining velocity potentials 14 p2093 A72-30192
- Electromagnetic and gravitational waves emission by superlight sources in vacuum, considering multi-particle and form factor cut-off effect 14 p2130 A72-30625
- Fourth order linear filter function suggested for pulse signal detection from gravitational antennas, noting parameters optimization 14 p2086 A72-30800
- Weber experiment gravitational signals correlation to solar and geomagnetic activity and cosmic ray intensity 14 p2160 A72-30886
- Relativistic theory gravitational analogue to electromagnetic radiation, suggesting black hole collision as galactic center flux mechanism 15 p2273 A72-31286
- Gravitational radiation generation and detection, discussing Weber detector, interaction with electric and magnetic fields and gravitational astronomy 15 p2273 A72-31287
- Gravitational absorption investigation from lunisolar attraction observed by tracking high flying satellite in eccentric polar orbit 16 p2382 A72-32892
- Time domain analysis of long thin bar antenna response to gravitational signals, estimating sensitivity limit via noise background analysis 16 p2423 A72-33013
- Gravitational radiation from relativistic systems. 17 p2582 A72-35394
- Synchrotron radiation-like angular distribution of gravitational synchrotron radiation produced by ultrarelativistic geodesic particle orbits in Schwarzschild geometry 17 p2583 A72-35820
- Elastic cylindrical antenna detection relationship to gravitational radiation sources 17 p2584 A72-35914
- Pulses of gravitational radiation of a particle falling radially into a Schwarzschild black hole. 18 p2711 A72-36714
- Galactic center emitted gravitational wave discrepancy with astrophysics explained by self focusing and trapping concepts 18 p2729 A72-36985
- Weber coincidence experiments in terms of cosmological gravitational waves, noting inconsistency in radiated pulse energy estimate 19 p2866 A72-38491
- Stability of nonradial vibrational modes of relativistic neutron stars. 20 p2972 A72-39869
- Einstein theories of special and general relativity, taking into account physical concepts relation to mathematical formalism, equivalence principle, field equations and gravitational waves 20 p2954 A72-40002
- Minkowski space-times for impulsive gravitational waves, considering idealized plane fronted wave form and limiting case of Robinson-Trautman null spherically fronted wave 20 p2955 A72-40007
- The detection of gravitational waves by electromagnetic oscillators. 20 p2974 A72-40024
- Interaction between weak gravitational waves and a gas 21 p3084 A72-40402
- Gravitational radiation interaction with background fluid of collisionless particles with zero rest mass in homogeneous isotropic Friedmann universe 21 p3105 A72-41028
- Polarization characteristics of Schwarzschild black hole gravitational synchrotron radiation in terms of Stokes parameters 21 p3107 A72-41215
- Very-high-frequency gravitational radiation from neutron stars. 21 p3111 A72-41484
- Construction and operation of a Weber-type gravitational-wave detector and of a divided-bar prototype. 21 p3057 A72-41486
- Gravitational wave detector design based on fine components of scattered light spectrum 21 p3086 A72-41696
- Book - Gravitation and cosmology: principles and applications of the general theory of relativity. 22 p3208 A72-43080
- Gravitational radiation from charged black holes. 23 p3336 A72-43499
- Upper limit on the gravitational flux reaching the earth from the Crab pulsar. 23 p3337 A72-43874
- A positive signature for the recognition of gravitational radiation. 23 p3337 A72-43943
- Gravitational emission in the scalar-tensor theory of gravitation 23 p3315 A72-44476
- GRAVITONS**
Solar neutrino and dilaton theory of non-Newtonian gravity. 23 p3329 A72-44315

GRAVITY ANOMALIES

Gravity and magnetic anomalies interpretation in terms of buried spherical bodies, calculating bodies size and depth of burial

01 p0064 A72-11101

Second order Markov process statistical model for gravity anomalies in local region, applying to error analysis in inertial navigation system computerized simulation

02 p0207 A72-11596

Gravity model for spacecraft orbit prediction with gravitational anomalies, discussing gravity dipoles and disturbing acceleration tangential component

[AAS PAPER 71-375] 02 p0283 A72-12424

Earth planetary structure from gravitational information, discussing crust, mantle, gravity anomalies, satellite and ground observation methods and improved earth model

04 p0519 A72-15075

Lunar gravitational anomalies and plumb deviations mapping, reflecting global structure of Lorell JPL-3 model

07 p0976 A72-19818

Disturbing gravity potential and vertical deflection calculation error reduction based on pure gravity anomalies in geodesy

07 p0977 A72-19819

Earth gravity anomalies sources depth, testing hypothesis of density variations origin

10 p1472 A72-24523

Transstructural topographic and gravity profiles of three Mauritanian meteorite craters, showing residual negative gravity anomalies

13 p1947 A72-28756

Lunar orbiting dumbbell gravity gradiometer for measurement and mapping of lunar gravity field anomalies

14 p2104 A72-30511

Anomalous magnetic and gravitational field models autocorrelation function behavior dependence on circular cylindrical sources depth and spacing

14 p2101 A72-30647

Gravity anomalies interpretation by iterative data processing, discussing convergence improvement

15 p2231 A72-32347

Earth surface layer potential density from gravity anomalies combined with satellite Doppler observations

16 p2382 A72-32888

Geoid isostasy, protrusions and hollows, discussing attenuations and intensifications of gravity

17 p2548 A72-35425

Lunar gravitational anomalies and plumb deviations mapping, reflecting global structure of Lorell JPL-3 model

17 p2618 A72-35743

Disturbing gravity potential and vertical deflection calculation error reduction based on pure gravity anomalies in geodesy

17 p2550 A72-35744

Self-consistent statistical models for the gravity anomaly, vertical deflections, and undulation of the geoid.

18 p2723 A72-36028

Lunar gravitational field, relief and internal structure, suggesting two layer model and crust thickness change relation to field characteristics

18 p2730 A72-37151

Moon model - An offset core.

20 p2969 A72-39374

Satellite orbit computations using gravity anomalies.

21 p3104 A72-40493

Stokes series for perturbing potential determination from gravity anomalies expressed as sum of two convergent series

24 p3418 A72-44858

GRAVITY GRADIENT SATELLITES

NT APPLICATIONS TECHNOLOGY SATELLITES

Solar radiation effects on planar librational motion and attitude of gravity oriented satellites at high altitudes

03 p0434 A72-13613

Magnetic damper for gravity gradient stabilized satellite rotational and librational motions, deriving formula for calculating damping coefficients

05 p0726 A72-16463

Time optimal control for pitch damping of gravity gradient stabilized satellite by mass distribution variation

05 p0727 A72-16465

Orbiting space vehicle life extension by momentum management using gravity gradient torques

05 p0727 A72-16467

Attitude control of satellite with protruding stabilizing booms from analysis of gravity gradient stabilization systems dynamics, discussing rotation about mass center

05 p0727 A72-16469

Flexible antennas effect on three dimensional motion stability of gravity gradient satellite, using coupled rigid-elastic analysis

05 p0727 A72-16470

Direct earth radiation, albedo and shadow effects on attitude dynamics of gravity orientated satellites

05 p0730 A72-16995

Solar radiation pressure effects on gravity oriented satellites librational dynamics, using digital computer aided numerical analysis and analog simulation

07 p1067 A72-18789

Environmental forces effects on gravity oriented satellites attitude dynamics, considering earth atmosphere aerodynamic and solar radiation forces effects

07 p1085 A72-19060

Laser tracking of magnetically and gravity gradient stabilized satellites, noting latitude effect on efficiency

07 p0947 A72-20263

Coupled librational motion of gravity oriented satellite in circular orbit under aerodynamic forces, discussing limiting stability and periodic solutions

11 p1726 A72-25914

Gravitational stabilization systems parameters determination for minimum amplitude of satellite eccentric vibrations

14 p2162 A72-30457

Pulsed motion of gravity gradient vehicle in central gravity field, presenting expressions of optimized attitude control

14 p2162 A72-30473

Gravitational stabilization of a satellite in a fixed inertial orientation.

17 p2622 A72-35487

Optimal aerodynamic attitude stabilization of near-earth satellites.

17 p2622 A72-35488

Periodic libration solutions in attitude control stability study of slowly spinning satellites under gravity gradient torques, using Floquet theory

20 p2968 A72-39195

Theory of an experiment in an orbiting space laboratory to determine the gravitational constant.

20 p2968 A72-39200

Small oscillations of gravity gradient satellite in circular near-equatorial orbit, discussing operational efficiency of magnetic damping systems

22 p3230 A72-42223

GRAVITY GRADIOMETERS

Vertical gravity gradient measurements for areal density contrast exploration in gravity surveys and prospecting applications

06 p0809 A72-18147

Absolute and relative gravity measurement and instrumentation, using gradiometer array and modified gravity meter

14 p2150 A72-30320

Lunar orbiting dumbbell gravity gradiometer for measurement and mapping of lunar gravity field anomalies

14 p2104 A72-30511

GRAVITY WAVES

NT BAROCLINIC WAVES

Small harmonic oscillations of isothermal atmosphere due to acoustic-gravity wave downward reflection caused by kinematic viscosity increase with altitude

01 p0102 A72-10229

Neutral gas wind effect on Doppler shifts in frequency spectrum of atmospheric gravity waves in F region with resultant phase altitude dependence alteration

01 p0054 A72-10426

Relativistic nonlinear gravitational instability theory for hydrodynamical system of equations applicable to early cosmic expansion, deriving density perturbations associated with rotational and gravitational waves

02 p0275 A72-11524

Detection of atmospheric gravity waves produced by focusing of shock front generated by supersonic aircraft, calculating flight trajectories

03 p0345 A72-12984

Cylindrical gravitational waves propagation modes in hot plasma subject to axial magnetic field, investigating instability conditions

03 p0388 A72-13025

Rotating relativistic stellar models, covering coordinate systems injection energy, convection, red shift, external gravitational waves and black holes

03 p0426 A72-13269

Gravitational wave detection, discussing equivalence principle and force measurement

03 p0389 A72-13272

Internal gravity waves and tidal oscillations excitation mechanism in upper atmosphere

03 p0346 A72-13383

Gravitational field of bounded and isolated material in empty four-dimensional locally Minkowskian space-time, emphasizing radiation zone and gravitational waves

04 p0570 A72-14556

Ionospheric hydromagnetic and acoustic gravity wave interactions, examining stratified nonisothermal atmospheric model

04 p0516 A72-14934

Gravitational radiation focusing by interior gravitational fields of diffuse static spherically symmetric matter distribution

04 p0549 A72-15024

Internal atmospheric gravity waves transient two-dimensional finite difference model, including nonlinear, viscosity and thermal conduction terms

04 p0544 A72-15119

Dispersion equation derived for acoustic-gravity type natural modes in solar atmosphere

05 p0712 A72-15769

Power spectra of ionospheric electron content fluctuations from 6 year continuous records, noting gravity wave and seasonal daily variations

05 p0655 A72-16066

Internal gravity wave interaction with median wind in upper atmosphere from solution of system of linearized hydrothermodynamic equations

05 p0656 A72-16175

Gravitational radiation detector angular dependence, obtaining directivity pattern

05 p0656 A72-16184

Tesseral equilibrium shapes of rotating neutron stars emitting gravitational radiation pulses

05 p0719 A72-16602

Sporadic E ionization during 1955 partial solar eclipse, considering gravity waves effect due to fast moving shadow region cooling spot

06 p0805 A72-17466

Gravitational intensification due to focusing of massive rotating gravitational wave emitting oblate object in galactic center

06 p0880 A72-17887

German book on nonlinear free boundary value problems of two dimensional hydrodynamics covering gravity, capillary and irrotational waves, liquid flow in channel, etc

07 p0967 A72-19183

Acoustic and gravity waves nonlinear propagation and structural deformation in isothermal and incompressible atmospheres with traveling wave induction

07 p0981 A72-20696

Internal atmospheric gravity wave effects on ionospheric parameters obtained by vertical sounding, considering electron concentration isoline pattern

08 p1154 A72-20735

Thermospheric wind directional filtering of gravity waves traveling ionospheric disturbances over Australia

08 p1158 A72-21217

Energy transfer from radiative heat source near summer pole to radiative heat sink near winter pole, investigating large scale eddies and gravity waves

08 p1161 A72-21536

Inferred perturbation effects of Arceibo large nighttime gravity wave on neutral atmosphere velocity and temperature

09 p1300 A72-23021

Internal Alfvén gravity waves propagation in rotating Boussinesq inviscid adiabatic conducting fluid shear flow within transverse magnetic field, considering electromagnetic and Coriolis forces effects

10 p1511 A72-24470

Plane wave solutions to atmospheric gravity waves, including effects of nonlinearity, instability, molecular dissipation, temperature, wind and diurnal tides

10 p1473 A72-24705

HF radio wave backscatter from sea surface to obtain gravity wave structure information

10 p1438 A72-24739

Regular tidal winds and irregular gravity waves domination of E region transport processes

10 p1477 A72-25161

Internal gravity waves effects on energy budgets and vertical angular momentum transport over mountainous terrain in southwestern U.S. from handheld camera pictures on Apollo 9

11 p1682 A72-26472

Numerical model of global scale propagating waves in equatorial stratosphere generated by tropospheric heat sources for Kelvin and Rossby-gravity modes

12 p1839 A72-27029

Temperature oscillations associated with surface gravity waves at two fluid model compressible vapor-incompressible superfluid interface

12 p1845 A72-27386

High level Canberra flight for three dimensional picture of wind and temperature fields, showing CAT, gravity waves and smooth flight characteristics

12 p1841 A72-27709

Ion velocity height profiles, ion temperature and electron density measurement with Thomson scatter facility during F region traveling ionospheric disturbance /gravity waves/

12 p1803 A72-27777

Daily difference analysis of magnitude, vertical and latitudinal structure of irregular mesospheric wind variations due to gravity waves

13 p1948 A72-28832

Gravity wave propagation in realistic thermospheric model, considering temperature, wind, Coriolis force, viscosity, thermal conduction and ion drag effects

13 p1951 A72-29652

- Gravity wave observation in nighttime F region by measuring phase path length changes of stable CW signal reflected obliquely from ionosphere
13 p1953 A72-29814
- Internal gravity wave interaction with median wind in upper atmosphere from solution of system of linearized hydrothermodynamic equations
14 p2099 A72-30244
- Gravity waves on leeward side of Continental Divide in Colorado, noting generation by winds and storms
14 p2128 A72-30343
- Laminar Ekman boundary layer instability for incompressible fluid over rigid boundary with fixed vertical temperature gradient, investigating internal gravity waves generation
14 p2100 A72-30347
- Internal gravity waves and convective instability caused by liquid layer nonuniform vertical density distribution, noting error in thermal conductivity measurement near critical point
14 p2095 A72-31008
- Gravity waves parametric generation on liquid surface, presenting threshold values for space distribution of amplitudes and phases
14 p2097 A72-31111
- Oceanic and atmospheric flow geostrophic adjustment by means of gravity-inertial wave propagation from initially imbalanced regions
15 p2222 A72-31278
- Atmospheric gravity waves effects in ionosphere, discussing F region traveling ionospheric disturbances, sporadic E layer and D region radar scattering
15 p2222 A72-31285
- Ionospheric gravity waves spectral frequency distribution from ATS 3 electron concentration measurements, using numerical filters for statistical frequency analysis
16 p2382 A72-32891
- Plane acoustic-gravity wave reflection, refraction and amplification at interface separating two fluids in relative motion, noting shear flow speed effect
16 p2383 A72-32968
- Dispersive motions in the ionosphere.
17 p2546 A72-34696
- WKB approximation to suggest vertical phase velocity measurement at turning points of acoustic-gravity wave propagation in thermosphere
18 p2686 A72-36411
- Mathematical model for internal atmospheric gravity waves breaking process modification by momentum exchange between wave and mean flow
18 p2687 A72-36630
- Internal atmospheric gravity wave effects on ionospheric parameters obtained by vertical sounding, considering electron concentration soline pattern
19 p2791 A72-38363
- Propagation of internal acoustic-gravity waves around a spherical earth.
19 p2793 A72-38748
- Propagation of Alfvén-gravitational waves in a stratified perfectly conducting flow with transverse magnetic field.
19 p2843 A72-38791
- Momentum transport by gravity waves in a perfectly conducting shear flow.
19 p2788 A72-38792
- Comparison between observed and numerically calculated atmospheric gravity waves in the F-region.
19 p2794 A72-38864
- Acoustic and gravity waves nonlinear propagation and structural deformation in isothermal and incompressible atmospheres with traveling wave induction
20 p2915 A72-39011
- Internal wave instability in stratified jet streams
20 p2949 A72-39944
- Steady capillary-gravitational waves of finite amplitude generated by pressure periodically distributed along the flow surface of a fluid of finite depth.
21 p3044 A72-40261
- Resonant growing standing internal gravity waves, considering transient behavior, numerical results, break due to local gravitational instability, maximum amplitude and secondary flow generation
21 p3048 A72-40648
- Instability of rotational and gravitational modes of oscillation.
21 p3078 A72-40773
- Atmospheric model for numerical simulation of five minute oscillation field properties of solar granular convection-excited gravity waves
21 p3107 A72-41277
- Evanescent and internal gravity wave propagation effects on atmospheric dynamics, considering momentum transfer, energy dissipation and turbulence
22 p3168 A72-41964
- Quasi-static loading of the earth by propagating air waves.
22 p3172 A72-42468
- An updated theory for the quasi-biennial cycle of the tropical stratosphere.
22 p3201 A72-42503
- GRAY GAS**
Radiative transfer in gray medium with prescribed spatial temperature distribution in rectangular enclosures with nonisothermal walls, deriving exact solutions by radiation transport theory
[AIAA PAPER 72-21] 05 p0748 A72-16869
- Non-LTE effects on mechanical heating in gray atmosphere applied to nonradiative energy input estimates for solar chromosphere from negative hydrogen ion emission
08 p2355 A72-21391
- Book on stellar atmospheric physics covering gray and nongray atmospheres, radiation emission and absorption, transfer equation, Eddington approximation, spectral lines formation, etc
10 p1532 A72-23725
- Gas role in radiative transfer and free convection between concentric spheres, noting gray gas assumption validity
[AIAA PAPER 72-280] 11 p1740 A72-25220
- Radiative energy transfer through gray gas layer between black concentric spheres at different temperatures
13 p2066 A72-30055
- Asymptotic theory of an optically thick radiating gas flow past a smooth boundary at moderate radiation strength.
21 p2989 A72-40196
- Radiative transfer in a gray isothermal spherical layer.
24 p3461 A72-44805
- GREASES**
Engine lubrication under cold weather conditions, discussing polymer thickened and synthetic oils, automotive and industrial gear oils, hydraulic oils and lubricating greases
03 p0363 A72-13450
- Rust inhibited chemically inert perfluorinated polymer greases for liquid fueled rocket engines, discussing lubricating and nonreactive properties under high pressure operating conditions
06 p0837 A72-18604
- Molybdenum disulfide addition effect on compounded model greases lubricating performance, determining oxidation stability, rust preventive behavior and consistency
12 p1832 A72-27047
- Properties of lithium greases as a function of the saturation level of commercial 12-oxytetrastearic acid
19 p2823 A72-38093
- GREAT CIRCLES**
Spread F effects on transequatorial ionospheric short wave oblique incidence path great circle deviations
01 p0056 A72-10438
- VLF signals Antarctic ice cap attenuation determined at Byrd station from relative phase and amplitude observations over short and long great circle paths
09 p1281 A72-23511
- Great circle intermediate waypoint computation method for inertial navigation equipped aircraft
15 p2271 A72-32205
- Investigation of the screw turn magnitude of a contact micrometer attached to the Toepfer meridian circle on the basis of observed right ascensions of stars
19 p2802 A72-37975
- Great circle navigation for inertial equipped aircraft, describing procedure for determining waypoint coordinates with reference to VORTAC stations
22 p3203 A72-42949
- GREAT POLAR CAPS**
U POLAR CAPS
GREEN FUNCTION
First order admittance of coaxially driven infinite monopole antenna, obtaining Green function expansion
01 p0043 A72-11247
- Contact problem of rigid sphere intrusion into viscoelastic half space, obtaining solution by Green function construction and integral-operator equation formulation
02 p0289 A72-11615
- Hollow waveguide problem considering numerical solution with scalar field approximation, Green function and conformal transformation
02 p0191 A72-11692
- Periodic lattice one-electron Green function calculation based on pseudopotential matrix element, applying to impurity levels in semiconductors
03 p0404 A72-14268
- Green vector function smoothness in elliptic boundary value problem with pseudodifferential conditions
03 p0383 A72-14372
- Nonlinear nonlaminar 3D electron motion calculation through output cavity of klystron amplifier by Green function
04 p0497 A72-14697
- Stratified anisotropic multilayer plasma wave propagation from transverse field equations, using Green function and Fourier transform method
06 p0773 A72-17597
- Electromagnetic radiation in uniformly moving homogeneous medium obtained by transformation and four dimensional Green function method
06 p0847 A72-17712
- Selective summation techniques for coherent Green function in random isotropic turbulent media, comparing Dyson, Keller and renormalization methods
06 p0777 A72-18735
- Boundary value problems in supporting surfaces vibrations theory, constructing Green function from part of differential operator
07 p1093 A72-19984
- Nonlocal elliptical boundary value problem solvability in terms of smooth functions, deriving Green formula and homeomorphism theorems
08 p1199 A72-21300
- Green functions in heat conduction solutions for hollow cylinder with mixed boundary conditions
08 p1253 A72-21448
- Background medium anisotropy effect on electromagnetic waves scattering from ionospheric irregularities, calculating scattered power by Green function
09 p1282 A72-23519
- Green function for stress components in circumferentially loaded circular disk, noting conformal mapping for arbitrary shape
10 p1557 A72-24717
- Green function for stress components in straight edge loaded half plane disk, noting conformal mapping for arbitrary shape
10 p1558 A72-24718
- Dyadic Green functions for cylindrical circular or rectangular waveguides with moving isotropic homogeneous media
10 p1440 A72-25046
- Nonthermal ultrarelativistic plasmas covariant analysis with quantum electrodynamics and Green function theory of nonequilibrium statistical mechanics, discussing electron-positron pair production and annihilation
10 p1525 A72-25100
- Eigenfunction transform investigation of wedge diffraction of scalar pulse wave in three space dimensions, analyzing Green function
11 p1591 A72-25359
- Short wave oscillations point source problem near convex curve, deriving asymptotic expression for Green function
11 p1678 A72-26379
- Waveguide point source field, analyzing short wave asymptotic properties of Helmholtz equation Green function in inhomogeneous medium
11 p1689 A72-26382
- Green function for stress distribution in plane shaped disk with edge loaded circular hole, noting conformal mapping for arbitrary shape
12 p1883 A72-27391
- Metallic chromium band structure determination by Green functions method, explaining transition metals X ray emission lines by single electron approach
13 p1972 A72-28489
- Statistical physics multiple wave scattering-phenomenological radiation transfer equation relations, using Green function
13 p2002 A72-28512
- Green function solution for electric field intensity in space due to electric dipole at another point under boundary conditions on surface of revolution
13 p1921 A72-29341
- Green operator first invariant upper bound for free oscillations eigenvalue upper limit, exemplifying for quadratic plate with two free and two clamped edges
15 p2274 A72-31459
- Paramagnetic phase induced moment system containing substitutional impurities, calculating mode energies by Green function method in random phase approximation
15 p2295 A72-32546
- Stress analysis in circular disk loaded along circumference, noting results identity for stress presentation by Fourier series, Poisson integral and Green function
16 p2470 A72-33593
- Relationship between finite differences and quadratures of a Green's function for a second-order ordinary differential operator
17 p2577 A72-35803
- Use of the Sturmian function for the calculation of the third harmonic generation coefficient of the hydrogen atom.
17 p2586 A72-35830
- Spheroids with surface vibration at specified normal velocity distributions, calculating acoustic radiation by Green function approach
18 p2710 A72-36412
- Green function for temporal electromagnetic plasma wave echoes oblique to external magnetic field, calculating current density and damping term
19 p2839 A72-37333
- Formal extension of the possibilities of the method of integral transforms in the study of linear distributed systems with constant parameters
19 p2834 A72-37432
- Complex resonant frequencies calculation in external diffraction problems for arbitrary shaped bodies,

noting Green function poles correspondence to eigenvalue zeros of integral equation

19 p2767 A72-38652

Transverse isotropy effects on beams static behavior, considering Green functions, deflection under distributed loads and beam-column deflection

20 p2980 A72-39613

Lowest order two particle correlation function solution to BBGKY hierarchy obtained via Green function with Fourier transform satisfying analyticity requirements for causality

20 p2956 A72-39725

Calculation of electronic Green functions using nonorthogonal basis functions - Application to crystals.

20 p2961 A72-39810

General transport theory of noise in pn junction-like devices. I Three-dimensional Green's function formulation.

22 p3160 A72-43083

A new variational principle for finite elastic displacements.

23 p3350 A72-44047

Column buckling under random initial deformations influence, determining mean square nonstationary deflection by Green function technique

23 p3351 A72-44106

GREEN THEOREM

U GREEN FUNCTION

GREENHOUSE EFFECT

Venus lower atmosphere from Venera 4, 5 and 6 and Mariner 5 data, evaluating greenhouse effect by microwave absorption and by nongray radiative model

01 p0129 A72-10795

Mars biology likelihood from long winter model, suggesting north polar cap summer remnant vaporization as atmosphere, liquid water and greenhouse effect source

10 p1424 A72-23717

Jupiter atmospheric greenhouse effect modeled by two layer emission, deriving temperatures from non-gray step function approximation of IR absorption

15 p2312 A72-32096

Numerical experiment of radiative-convective equilibrium of the Martian atmosphere.

21 p3105 A72-40772

GRIDS

Noncoherent moire contour-surf contour-difference and vibration analysis of three dimensional objects using grid projection and offset camera

03 p0358 A72-13438

Plane discrete elastic lattice plates buckling, presenting plane and bending state of force equations

03 p0444 A72-13502

Dished accelerator grids design, fabrication and operation in electron bombardment ion thruster, studying ion extraction capability and discharge chamber performance

[AIAA PAPER 72-486]

11 p1710 A72-26212

Atmospheric motion equations numerical integration, presenting conservative finite difference approximation for quasi-uniform spherical grids derived from regular polyhedrons

13 p1985 A72-28445

Free and forced vibrations of two dimensional grids with simple and bridge-type boundary conditions, presenting closed form solutions for nodal deflections and moments

15 p2332 A72-32561

Grid modulation information encoding technique for image features extraction with simple Fourier filtering to replace heuristic method

16 p2365 A72-33752

Properties of a nonisosceles triangular grid planar phased array.

17 p2524 A72-34352

Averaged boundary conditions for a grid consisting of nonparallel and nonrectilinear conductors positioned on a nonplanar surface

17 p2529 A72-34830

Decay of isotropic turbulence generated by a mechanically agitated grid.

19 p2787 A72-38426

Statistically dilute antenna groups with enhanced minimum distance between elements

21 p3028 A72-40504

One-level fine-mesh limited-area grid numerical weather prediction atmospheric model, evaluating various finite difference schemes, boundary conditions and initialization methods

24 p3420 A72-44619

Plastic design of regular orthotropical grids with two adjacent edges fixed, free, or hinged.

24 p3456 A72-44794

GRIFFITH CRACK

Griffith crack stress intensity factor and crack face displacement in elastic solid, detailing symmetrical, antisymmetrical and point body force distributions

01 p0136 A72-10185

Griffith crack propagation in polymethyl methacrylate, examining stress changes by photoelastic method

03 p0380 A72-13719

Griffith fracture theory application to thermal crack propagation, computing stress-strain field and critical temperature

[ASME PAPER 71-MET-N]

05 p0731 A72-15790

Stress intensity factors for pair of coplanar Griffith cracks subject to asymmetrical surface tractions

05 p0737 A72-16320

Stress intensity factor of Griffith crack in elastic solid opened by thin symmetric wedge, using triple integral equations

12 p1883 A72-27558

Griffith equation applicability to graphite fiber fracture strength by measurement of work to break and critical flaw

16 p2413 A72-32871

Antiplane shear wave diffraction by two coplanar Griffith cracks in infinite isotropic homogeneous elastic medium

16 p2464 A72-32919

Effects of yielding and size upon fracture of plates and pressure cylinders.

17 p2565 A72-34251

Griffith crack propagation through viscoelastic solid at under subcritical stresses, measuring growth rate for comparison with theory

18 p2733 A72-36366

A note on the low frequency diffraction of elastic waves by a Griffith crack.

19 p2870 A72-37414

Glass fracture mechanics, discussing microcrack stress concentration, Griffith theory, statistical failure theories, static fatigue and strength measurements

23 p3305 A72-43502

Theoretical approach to the fracture of two-phase glass-crystal composites.

23 p3306 A72-43560

A note on the twisting deformation of a non-homogeneous shaft containing a circular crack.

23 p3346 A72-43708

Fracture mechanics development from Griffith to crack opening displacement /COD/ concept, discussing crack initiation and propagation, stress-strain characteristics and yield point

24 p3456 A72-44814

GRINDING [COMMUNITION]

Magnetic spectra measurement of powdered hexagonal ferrites in millimeter wavelength range during grinding and after heat treatment

08 p1218 A72-21875

Device for comparing powders friability to ascertain quality of compacts fabricated on automatic sintering presses, noting applications in ceramic, chemical and pharmaceutical industry

12 p1795 A72-27468

GRINDING [MATERIAL REMOVAL]

NT METAL GRINDING

Milling, band grinding, final manual polishing and tumbler polishing effects on fatigue life and surface finish of steel compressor blades

06 p0824 A72-18651

Photoelectric temperature measurements in contact zone during grinding of aluminum oxide ceramic materials by synthetic diamond disks

07 p0997 A72-20252

Wear resistance of artificial and natural diamond grindstones in ruby cutting, noting tests for grain geometry and fabrication technique effects

12 p1814 A72-27765

Thermal flux on contact area and temperature distribution on specimen surface during diamond grinding

12 p1814 A72-27767

Thermophysical aspects of abrasive belt grinding, determining maximum contact temperatures and heat balance

13 p1963 A72-28745

Material removal nature during focused laser radiation action on substances with different thermal diffusivity coefficients

13 p1968 A72-29508

Large astronomical telescopes construction, discussing aspherical surfaces control, grinding, polishing and optical testing procedures

15 p2334 A72-31612

The use of an electrical induction method for determining the physical condition of a ground steel surface.

19 p2805 A72-38762

Wide-band abrasive grinding of complex surfaces with flexible contact wire elements

23 p3293 A72-43672

GRINDING MILLS

Optimum dispersion time and size particle determination for zirconium diboride powder grinding in vibrating mill, using gas flow ratio method

13 p1967 A72-30101

GROOVES

Narrow groove theory for spiral groove viscous pump gas bearings generalized to include rarefied gas and turbulence effects

[ASME PAPER 71-LUB-1]

02 p0234 A72-11531

Spiral grooves gas bearing theory, taking into account sliding and gas compressibility effects on load carrying capacity

02 p0236 A72-11585

Cylindrical shafts with deep circumferential grooves, determining effective stress concentration under axial tension or bending

03 p0451 A72-14125

Cylindrical shaft with circumferential groove, obtaining approximate solution for stress concentration at groove contour under torsion

03 p0452 A72-14130

Spiral groove shaft vacuum seals, presenting mathematical ballpark performance model

[ASME PAPER 71-WA/PID-5]

05 p0664 A72-15914

Narrow groove theory of spiral grooved gas bearings, obtaining pressure distribution and small perturbation stiffness performance

06 p0821 A72-17807

Corrugated conical horn antenna groove electromagnetic field analysis for design of scalar feed radiation pattern

07 p0945 A72-19661

Sealing pressure and optimal groove form for concentric running screw viscosity seals in laminar flow

08 p1178 A72-21931

Surface waves in the corrugated conical horn.

17 p2517 A72-35387

Effect of polarization on the apparent emittance of rectangular groove cavities.

20 p2954 A72-39629

GROOVING

Load capacity, attitude angle and power loss of heringbone grooved gas lubricated journal bearings operating in air at 60,000 rpm

[ASME PAPER 71-LUB-B]

02 p0234 A72-11530

Effects of rifling and N-vanes on the Magnus characteristics of bodies of revolution.

[AIAA PAPER 72-970]

22 p3135 A72-42341

Spin response of symmetric ablating vehicle at zero angle of attack, noting spin-up by ablation-induced grooving and spin-down by crosshatching effects

24 p3362 A72-45339

GROUND BASED CONTROL

NT AIR TRAFFIC CONTROL

NT RADAR APPROACH CONTROL

Orbiting multispectral scanner with independent land and oceanographic spectrometers for ground controlled dual mode operation

02 p0226 A72-11823

Airfield surface radar detection equipment to control aircraft and ground vehicles under reduced visibility and darkness

02 p0173 A72-12105

Real time ground control optimization of data acquisition of solar spectra scans from OSO 6

03 p0417 A72-13060

Ground based satellite control center data processing for Azur satellite, using automatic guidance

05 p0632 A72-16138

Computed performance of ILS glide slope transmitting arrays installed over flat ground planes of one dimensional perfectly conducting strips in free space

05 p0686 A72-16559

Ground based Doppler navigation system for wide range elevation and azimuth aircraft approach guidance, using linear directive antenna array for conical surface definition

06 p0845 A72-18183

Solid state modular ground based distance measuring equipment /DME/ receiver for en route aircraft navigation and landing

16 p2420 A72-33521

Global network of ground based facilities /infrastructure/ including spacecraft launching, tracking, communication and readout sites for international space operations

[AIAA PAPER 72-739]

18 p2742 A72-36545

Flight-tested experience in digital control of a remotely piloted vehicle.

[AIAA PAPER 72-883]

20 p2889 A72-40059

Earth-based navigation capabilities for outer planet missions.

[AIAA PAPER 72-925]

24 p3423 A72-45430

GROUND CREWS

Ground and flight crews coordinated effort in Apollo mission operations, noting experts on ground and spacecrew spot judgments capability

[ASME PAPER 72-236]

11 p1586 A72-26557

Rotary wing and VTOI aircraft induced downwash effects on ground personnel, considering injuries, body heat loss, work capability impairment and sound pressure effects

14 p2072 A72-30425

The legal position of civil air personnel

17 p2639 A72-35762

GROUND EFFECT

Sky wave propagation over multisectionally homogeneous plane ground, calculating ground loss profile along path by compensation theorem

02 p0181 A72-12604

Conducting ground half space effects on dipole antenna input impedance computed by current distribution Fourier transform

06 p0781 A72-17353

Ground and atmospheric scattered radiation discrimination by ground modulation based on chopper

signal frequency analysis, considering feasibility from airborne tests results

06 p0814 A72-17587

Input resistance derivation for finite horizontal loops with uniform current distribution located above lossy half-space ground

06 p0777 A72-18737

Ground focus line location of sonic bang propagating in stratified atmosphere with wind for transonically accelerating aircraft

07 p0912 A72-19645

Electromagnetic scattering of square pulse from lossy dielectric slab mounted on perfectly conducting planar ground surface

07 p0945 A72-19660

Ground plane absorption coefficient effects on admittance of slot antenna radiating into warm lossy plasma

07 p0957 A72-19797

Sonic boom effects on structures, discussing ground motion, direct excitation by shock waves and damages

09 p1304 A72-23318

Backscattering properties of ground observed with HF high resolution oblique sounding equipment

09 p1281 A72-23512

Lift and induced drag characteristics of jet flapped finite span wings in close proximity to ground, using method of matched asymptotic expansions

16 p2341 A72-32827

Calculation of the recirculation flow of VTOL lift engines.

21 p3099 A72-41167

[ICAS PAPER 72-42] German monograph - Studies of the ground effect on the noise levels and their frequency distribution in the near field of an engine jet directed vertically against the ground.

22 p3217 A72-43060

GROUND EFFECT MACHINES

NT HOVERCRAFT GROUND EFFECT MACHINES

Transoceanic helium cooled thermal reactor powered air cushion freighter of gross weight 4500 metric tons, discussing design and performance characteristics

04 p0464 A72-14431

Potential effects of air cushion vehicle /ACV/ multithousand ton freighter on city development

05 p0752 A72-15776

Nuclear energy for power and transportation, discussing ship, submarine, air cushion vehicle, aircraft and rocket propulsion applications

05 p0688 A72-15777

Composite propeller blades with carbon fiber reinforced plastics spar for hovercraft, presenting mechanical properties test data for different composite configurations

07 p0912 A72-19062

Hovercraft noise and vibration source and reduction for improved crew and passenger comfort

07 p0912 A72-19648

Nonlinear computerized simulation of air cushion vehicle dynamics, using bond graph techniques

07 p0913 A72-20343

Physical principles, design and operation of air cushion vehicles for passenger transportation over water

07 p0913 A72-20371

Hovercraft internal and external aerodynamic forces, discussing control, suspension, yawing moments, directional and roll stability and random surface performances

09 p1260 A72-22824

Airfoil ram-wing air-water hybrid vehicle X-113 Am design and operational principles based on aerodynamic ground effect, discussing flight tested performance characteristics

09 p1262 A72-22971

Ground effect wing vehicles stability in forward motion, deriving characteristic equations by linear analysis

10 p1421 A72-24844

Analog dynamic model of tracked air cushion vehicle for high speed ground transportation systems

13 p1896 A72-28704

Air cushion aircraft landing systems advantages and suitability for arctic transportation applications

13 p1897 A72-28793

Hovercraft state of development and utilization potential, comparing performance to other transportation modes

14 p2073 A72-30818

Arctic environment surface effect vehicle design, considering structures, drag, lift, propulsive power and range

15 p2181 A72-32125

Air cushion landing system application for civil air transportation, discussing operation, braking and parking

16 p2348 A72-33184

On the prediction of acceleration response of air cushion vehicles to random seaways and the distortion effects of the cushion inherent in scale models.

[AIAA PAPER 72-598] 18 p2642 A72-36538

Optimization of the wing parameters of a glider hovercraft

20 p2888 A72-39902

GROUND HANDLING

Air cargo intermodal and interline containers handling in warehouse storage, transportation and distribution, considering total pack and interlock requirements

16 p2372 A72-33174

Simulation of an air cargo handling system

17 p2536 A72-34472

Terminal airspace navigation and aircraft ground handling control, discussing air traffic controllers and pilots functions in context of workload and automation

21 p3081 A72-40546

Air freight ground handling and distribution terminal facilities and methods, discussing future technical and organizational developments for efficient handling of increased traffic volume

23 p3358 A72-43246

Frankfurt/Main international airport central terminal facilities, describing efficiency oriented layout for large volume passenger and baggage handling and links to rail and road nets

23 p3278 A72-43247

GROUND OPERATIONAL SUPPORT SYSTEM

A method of solving the operational planning problem for an engineering aircraft base

21 p3039 A72-40178

Operational support of space shuttle transportation and payload systems with modular checkout and test equipment, noting service life and economy of operations

24 p3388 A72-45111

GROUND RESONANCE

U GROUND EFFECT

U RESONANCE

GROUND RUN-UP

U ENGINE TESTS

U GROUND TESTS

GROUND SQUIRRELS

RNA content changes in ground squirrel brain during active and hibernation states

06 p0764 A72-18058

GROUND STATE

Binary alloys ground state energy and superstructures, examining bcc and fcc Ising model systems with first and second neighbor interactions

01 p0083 A72-10210

Hydrogen molecular ion g tensor calculation, determining approximate ground state wave functions

03 p0391 A72-13152

Ground state energy of interacting electrons for entire density range from two-point Padé approximation

04 p0549 A72-15229

Fe group transition metal impurities in semiconductors, calculating ground state wave functions and photoionization cross section dependence on wavelength

04 p0563 A72-15473

Ar core polarizability effect on photoionization cross section calculation for ground state configuration

05 p0693 A72-17173

OH ground state transition frequency measurement, using beam maser spectrometer

07 p1006 A72-19423

Ground state He long range interaction with triplet metastable He, discussing gerade and ungerade states

07 p1037 A72-19495

Carbon like spectra and ground energy levels of Sc, Ti and V ions in 16-22 A range, using vacuum spark source

07 p1037 A72-19833

Zero temperature relativistic plasma ground state energy calculation using Fermi momentum and Green function

11 p1694 A72-25715

Ground state and metastable atoms and ions optical pumping, presenting critical survey on pumping and relaxation mechanisms, light propagation and spin exchange

14 p2109 A72-30325

Hydrogen atom ground state ionization probability derivation as function of electric field strength and distance to metal surface

15 p2279 A72-32699

Oxygen molecule electron affinity role in ion chemistry of lower ionosphere, noting binding energy of ground state

17 p2585 A72-34260

UV laser parameters calculation for operation on Lyman transition between H atom resonant excited state and ground state

17 p2562 A72-34349

Wave function and resonance parameters for autoionization and ground states of helium and hydrogen

17 p2586 A72-35774

A simple, radially correlated ground state wavefunction for two electron atoms.

17 p2586 A72-35828

The exact evaluation of certain partial sums of the second order energies of atoms. I - The ground and the singly excited states.

17 p2586 A72-35829

Ground and low-lying excited electronic states of FeH.

21 p3096 A72-40563

Various ground configuration level intervals from gaseous nebulae and solar coronal forbidden transitions observations and laboratory investigations of resonance lines

21 p3108 A72-41286

Dipole moment derivative of triatomic hydrogen ion electronic ground state, considering fundamental spectrum observation in hydrogen gas in local thermodynamic equilibrium

22 p3209 A72-42720

GROUND STATIONS

NT SPACE DETECTION AND TRACKING SYSTEM

Direct readout ground system /DRGS/ for receiving, recording and displaying visible and IR imagery collected by Itos and synchronous meteorological satellite radiometers

01 p0047 A72-10452

Aerial multispectral scanners and ground data stations for water quality measurements and pollution abatement

[AIAA PAPER 71-1096]

01 p0067 A72-10545

Magnetospheric diagnostics from ground stations data, considering dimensions, cusp, ring current, tail flux, electric fields, radiation zone, solar wind and interplanetary field

01 p0132 A72-11072

Laser station coordinate determination by geometrical method and satellite observations

02 p0219 A72-12046

Army data analysis system for fixed and rotary wing aircraft flight testing, including airborne and computer controlled ground stations equipment

02 p0179 A72-12408

Economics in electromagnetic field measurement surveys for siting of earth stations operating in shared frequency bands at 4 and 6 GHz, considering interference detection

03 p0324 A72-14044

Microstrip double down-converter receiver in civil satellite earth stations for reduced interface problems, increased reliability and minimum initial cost

03 p0334 A72-14074

ATS F and G ground station mobile terminal, discussing system flexibility, utility and reliability features and parabolic antenna design

04 p0485 A72-14478

Geodetic determination of geoid shape by computerized laser-effect space telemetry ground stations

04 p0495 A72-15724

Atomic clocks application to spacecraft position determination, discussing ground stations synchronization and accuracy improvement by lasers

05 p0660 A72-15858

Azur satellite ground station network with polar stations for telemetry reception

05 p0643 A72-16140

Ultralow noise microwave parametric amplifiers in communication satellite earth terminals, discussing technology basis of millimeter wave paramps

06 p0784 A72-17741

Earth resources technology satellite program, discussing mission requirements, payload, orbital characteristics, earth stations, data processing, system design and international features

06 p0892 A72-18230

Combined solution for station coordinates determination by geometric and dynamic satellite geodesy

07 p0974 A72-18887

Single-channel-per-voice-carrier transmission system application to data communication and small earth station operation, discussing modular design and performance

07 p0948 A72-20494

Classification of automatic meteorological ground stations networks in populated areas, discussing required equipment, data transmission, real time operation and costs

10 p1507 A72-25021

VOR and Doppler VOR ground station equipment based on reliable solid state radio transmitters and signal generating devices for aircraft navigation

12 p1779 A72-27104

Aircraft distance measuring equipment with VOR radio receivers and ground station transponder for pulse interrogation

12 p1842 A72-27105

AMSAT-OSCAR-B series of radio communication satellite for worldwide use with low cost terminals in amateur and education services

12 p1779 A72-27351

Earth station parabolic antenna gain-noise temperature ratio measurement using radio star and Applications Technology Satellite technique

12 p1779 A72-27354

[AIAA PAPER 72-528]

12 p1779 A72-27354

Intelsat V satellite system with large telephone channels capacity and full earth station network connectivity, discussing system concepts and technology [AIAA PAPER 72-556] 12 p1780 A72-27359

Satellite supplement to domestic communication systems, discussing network management, system reliability, broadband capacity, earth station flexibility and market proposals [AIAA PAPER 72-554] 12 p1781 A72-27374

Communication aspects of aeronautical satellite system, considering aircraft equipment, ground stations, ATC, type of access and frequency assignment 12 p1783 A72-27658

Satellite and ground station observed ionospheric plasma parameters comparison, considering electron density and temperature and ion temperature and composition 12 p1804 A72-27785

Global ground stations for lower VLF atmospheric arrival directions and spectral parameters observation 12 p1804 A72-27792

Experimental earth station for wave propagation studies in satellite communications using frequency range above 10 GHz 12 p1785 A72-27801

Tactical satellite communication system and ground terminal design options for efficiency improvement, considering power sharing, priority system frequency allocation and system control concepts 12 p1785 A72-27844

Sporadic E layer frequency variations from space-diversity sounding data from three ionospheric stations 13 p1946 A72-28599

Ground terminals spatial diversity for earth satellite mm wave communication systems to avoid attenuations by rainfall 13 p1989 A72-28810

Ground satellite control station network, including tracking stations for measuring Doppler effect with IRIS receivers [DGLR PAPER 72-009] 13 p1938 A72-28960

Helios solar probe project command station design, discussing equipment details and command transmission operation sequence [DGLR PAPER 72-018] 13 p1939 A72-28963

Ground station with control, communication and information processing centers, discussing automation, data transfer, system control and emergencies [DGLR PAPER 72-007] 13 p1939 A72-28965

International telephone hierarchical earth network organization for satellite communication extension, considering guidelines and constitution 15 p2193 A72-31179

Report to COSPAR on UK ground based, rocket and satellite-borne space research experiments and 1971-1972 programs 15 p2337 A72-32005

Report to COSPAR on Indian space program covering organizations, ground station facilities, atmosphere and astronomy studies and international collaborations 15 p2338 A72-32012

Error analysis of East European triangulation network photographic observations of Echo and Pagedos satellites from ground stations 16 p2387 A72-33798

Feasibility of collocating a radio relay station with a sharing earth station. 17 p2512 A72-34268

Space tracking stations in Spain. I - The Madrid space station and its activities 17 p2536 A72-34945

Present state of development and extension plans of the German satellite earth station at Raisting. 17 p2536 A72-35431

Intelsat 4 multichannel communication network earth station equipment components and characteristics experimental system (SPADE) study to realize demand assignment 18 p2659 A72-36272

Satellite communications and the Pleumeur-Bodou centre. 18 p2659 A72-36273

Global network of ground based facilities /infrastructure/ including spacecraft launching, tracking, communication and readout sites for international space operations [AIAA PAPER 72-739] 18 p2742 A72-36545

Earth station receivers for global and domestic FM systems. 18 p2662 A72-36848

Receiver terminals for satellite television systems. 18 p2662 A72-36849

18 GHz paramps with both liquid helium and room temperature operations and with triple-tuned gain characteristics. 19 p2770 A72-37254

Ground based optical astronomy developments, emphasizing faint objects positional observation, trigonometric parallaxes, data analysis and measuring techniques 19 p2865 A72-38477

Satellite communications in Japan. 19 p2766 A72-38603

A time-frequency localization system applied to acoustic certification of aircraft. 20 p2950 A72-39091 [AIAA PAPER 72-836]

Investigation of moisture content in the atmosphere by the method of ground radar thermal measurements 20 p2949 A72-39945

Near-field Cassegrain antennas of high surface efficiency for satellite communication links 21 p3029 A72-40520

Television transmission performance of an experimental small aperture earth station. 21 p3018 A72-40878

Multiple beam fixed reflector antenna configuration selection for reliable satellite communication earth stations, considering tradeoffs between gain, transmitter power and receiver noise temperature 21 p3032 A72-40879

Commercial satellite communication system development, considering external constraints, orbital geometry, frequency allocations, multiple access transmission techniques, and satellite and earth station designs 21 p3021 A72-40921

Economic considerations for low-traffic satellite earth stations. 21 p3022 A72-41320

Implementation status of the Omega Navigation System. 22 p3203 A72-42945

Great circle navigation for inertial equipped aircraft, describing procedure for determining waypoint coordinates with reference to VORTAC stations 22 p3203 A72-42949

The effect of geometry on area navigation system errors. 22 p3203 A72-43132

Some results of an analysis of Pc4-type steady geomagnetic pulsations at a network of stations 23 p3283 A72-43372

Ground-based sensing of temperature profiles from angular and multi-spectral microwave emission measurements. 23 p3285 A72-44147

Determination of the mutual position of points on the earth's surface from synchronous laser observations of artificial earth satellites 24 p3397 A72-44860

Point-to-point national data communication geostationary satellite system associated with computers, describing organization, earth station equipment and technical and economical feasibility 24 p3380 A72-44975

Sporadic E layer frequency variations from space-diversity sounding data from three ionospheric stations 24 p3398 A72-45099

GROUND SUPPORT EQUIPMENT

NT GROUND OPERATIONAL SUPPORT SYSTEM

German vhf ground telemetry satellite tracking system radio interferometer, discussing specifications and performance [DGLR PAPER 71-124] 02 p0182 A72-12732

Airborne traffic display system using beacon and radar surveillance network and ground computer processing 06 p0844 A72-17329

Telemetry equipment of network tracking stations for CNES Symphonie satellites at 136-138 and 148 MHz [DGLR PAPER 72-015] 13 p1939 A72-28966

Mobile launching facility for high altitude sounding rockets, describing telemetry data recording, radar and optical tracking, range safety and payload recovery equipment [DGLR PAPER 72-012] 16 p2374 A72-33499

Integrated airborne-ground based instrumentation system for variable stability X-22A aircraft flying qualities research, discussing telemetry, mobile van, landing aids and airplane design 16 p2348 A72-33628

Integrated civil/military ATC system for upper airspace control /UAC/ center at Karlsruhe 16 p2421 A72-34108

Mediator plan for joint civil/military ATC organization at London center, discussing sectorization, control and radar facilities, flight plan processing and communications 16 p2421 A72-34109

GROUND SUPPORT SYSTEMS

German ground operation system for satellites and space probes, discussing telemetric data processing, handling and flow [DGLR PAPER 71-123] 02 p0201 A72-12742

Ground station systems of operational control and data processing for satellites and space probes projects Aeros, Symphonie and Helios 03 p0326 A72-14309

Military aircraft operations and logistics computerized simulation for support and maintenance cost estimates 06 p0758 A72-17974

Geodetic satellite systems applications, describing trajectory beacon, telecontrol and telemetry sta-

tions and computing and operations center of French Geole system 06 p0809 A72-18258

Apollo centralized ground support and communication system, describing network support team, mission control center, instrumentation support team and manned space flight network 13 p1940 A72-29860

Aircraft industry product support role in time delays minimization for aircraft operators, discussing malfunction report, minimum equipment decision and fault diagnosis 15 p2339 A72-32456

Airborne equipment electric power supply standards to provide characteristics limits for compatibility with ground support systems [SAE AS 1212] 18 p2648 A72-36535

GROUND TESTS

NT COLD FLOW TESTS NT PRELAUNCH TESTS

Concorde airworthiness certification, discussing ground and flight test programs for performance, flying qualities and structures fatigue properties evaluation [SAE PAPER 710756] 01 p0003 A72-10253

Ground test determination of design data for low supersonic high density air deployable deceleration systems, considering high strain rate effects on parachute materials 01 p0005 A72-10313

Computer simulation techniques in aerospace ground equipment design for maintenance testing of avionic systems 03 p0329 A72-14196

Three-axis attitude control and stabilization system for sounding rocket payload, discussing performance from simulation and ground test results 05 p0728 A72-16478

NF-8D aircraft variable stability system ground/in-flight calibration for determination of flight control system dynamics effects on flying qualities 05 p0611 A72-16660

Emergency Life Saving Instant Exit system in aircraft fuselage for use after crash landing, discussing design and ground testing 08 p1109 A72-21583

Statistical correlation techniques applied to jet aircraft autoland system dynamic ground tests with simulated engine and aerodynamic characteristics 16 p2420 A72-33641

Ground and flight tests of the Ramzes rocket sonde. 21 p3115 A72-41499

Development of the AEDC-VKF tunnel J - A real gas high density, true velocity, hypersonic, aerodynamic test facility. [AIAA PAPER 72-993] 21 p3040 A72-41579

GROUND TRUTH

Forest vegetation distributional and statistical parameters ecological analysis by multiband remote sensing in areas devoid of ground control 02 p0212 A72-11815

Multispectral scanner data training sets size effect on correlation between soil reflectance and organic matter content obtained from ground truth 02 p0227 A72-11845

Ocean wave height measurements with nanosecond radar, using ground truths to relate radar measurements to actual sea conditions 02 p0172 A72-11869

Remote sensing possibilities by aerial photographic methods based on scanning, scatterometer, radiometer and vidicon systems, discussing ground resolution, data automation and satellite observation [DGLR PAPER 71-128] 06 p0818 A72-18234

Earth resources survey systems, discussing benefits, ground truth problem, data analysis, experimental satellites, operational system, and developing countries needs and activities 14 p2175 A72-31142

Computer controlled ground truth station for environmental agricultural aerial photographic remote sensors data processing, discussing system components, printout format and computer program 15 p2213 A72-31249

GROUND WATER

Reclaimed surface, ground and sewage water oxidizability measurement, studying oxidation kinetics of potassium bichromate distilled urine condensate admixtures 13 p1910 A72-29313

GROUND WAVE PROPAGATION

Sky wave propagation over multisectionally homogeneous plane ground, calculating ground loss profile along path by compensation theorem 02 p0181 A72-12604

Soviet book on ground wave radio propagation at medium and long wavelengths covering field strength calculations over plane and spherical earth, soil conductivity, etc 03 p0323 A72-13950

Analytical optimization of point to point communication above spherical ground, obtaining frequency minimizing transmission losses 03 p0325 A72-14193

Full wave solution for vertically polarized radio wave propagation over rough variable impedance surface by Fourier transform 04 p0492 A72-15437

Electromagnetic scattering by ungrounded conducting sphere above ground plane, calculating if ground wave backscatter 09 p1279 A72-22905

Earth electrical parameters measurement by radio wave methods involving electromagnetic propagation along or reflection from surface, considering penetration depth, earth stratification and surface inhomogeneities 10 p1474 A72-24737

Ground wave propagation over spherical earth, considering land-sea and homogeneous paths 10 p1438 A72-24740

Electromagnetic theory of HF radio ground wave backscattering from gently rippled sea surfaces, discussing approximations for separated transmitting and receiving antennas case 10 p1438 A72-24742

VLF and LF electromagnetic ground wave propagation between points on smooth curved lunar surface surrounded by free space or cold isotropic plasma 12 p1783 A72-27635

Millimeter to meter waves propagation conditions prediction in horizontally inhomogeneous coastal foreground by meteorological parameters, considering wind effects on refractivity 12 p1784 A72-27798

Ground reflections effect on satellite transmission link fading characteristics, computing transmitter field intensity fluctuations as function of terrain profile elevation angle 12 p1785 A72-27800

Simplified method of calculating microwave diffraction loss over spherical earth. 18 p2660 A72-36517

Ground, satellite, terrestrial glass fiber channel and waveguide radiation systems for laser communications 21 p3023 A72-41398

GROUND WIND

Airport meteorological instrumentation, discussing ground wind, visibility, cloud height, air temperature and humidity detectors and radar equipment 10 p1484 A72-25093

Conditional instability of second kind /CISK/ model of surface cyclonic vorticity dependence on vertical distribution of latent heat release 12 p1838 A72-27019

Low level vertical wind shear effect on aircraft control, considering runway selection with respect to surface wind conditions 13 p1993 A72-28862

Effect of ground wind shear on aircraft trailing vortices. 20 p2886 A72-39630

Low-altitude atmospheric turbulence around an airport. 24 p3421 A72-45334

GROUND-AIR-GROUND COMMUNICATIONS

Spacecraft-ground communications system, discussing electromagnetic wave propagation and frequency bands 01 p0027 A72-10445

Airline air/ground radio communications and data link service implementation for San Francisco-Hawaii center 06 p0770 A72-17337

Earth-space path attenuation statistics and fade duration at 15.3 GHz, using ATS 5 satellite transmission and radiometric sun/sky techniques 07 p0948 A72-20496

Real time pilot reports via digital ground-air-ground data link, discussing encoding and processing equipment, meteorological codes and automatic real time weather forecasts 10 p1440 A72-25079

Space communications period forecasting algorithm for limited power ground based transmitters and spacecraft in earth orbit 11 p1598 A72-26735

Air/ground digital communications in airline operations. 18 p2660 A72-36561

Automatic position reporting, ATC communication, weather information and message identification via digital ground-air-ground data link, discussing operational and maintenance requirements 21 p3080 A72-40286

Meteorological and takeoff and landing information transmission by proposed automated meteorological and information service, discussing air-ground data link 21 p3080 A72-40287

Ground-based Doppler navigation waveguide slot antenna design for optimal directional multilobe reception from aircraft 21 p3028 A72-40509

Discrete address beacon system /DABS/ development for surveillance and ground-air communications in support of ATC automation 22 p3204 A72-43151

GROUND-TO-AIR MISSILES

U SURFACE TO AIR MISSILES

GROUP BEHAVIOR

U GROUP DYNAMICS

GROUP DYNAMICS

Group composition and n-dominance personality trait effects on decision and communication task efficiency in laboratory triads 08 p1125 A72-21200

Ideas of individual on group members majority behavior in various situations, noting norm concept confirmation from psychological tests on reference groups 13 p1903 A72-28796

Subjective iterative group /SIG/ methodology in forecasting involving computer and computer related technology 14 p2174 A72-30450

Social and emotional crises with respect to isolation, confinement and group dynamics of astronaut crews during long duration space flight 16 p2354 A72-33545

Psychic adaptation of man to a long-duration stay in space 22 p3149 A72-41988

GROUP THEORY

NT HOMOMORPHISMS

NT SUBGROUPS

Group matrix representation theory application to elastic spacecraft stabilization 01 p0135 A72-10497

Electron scattering off atoms, diatomic and polyatomic molecules in impact spectroscopy, applying simple group theory 02 p0262 A72-11913

Tensor description of laser beam second harmonic generation in dc magnetic field, using group theory derivation of nonzero element relations for all crystallographical classes 03 p0365 A72-12963

Mixtures, periods and factors of tau-regular probability laws in topological group or half group 05 p0682 A72-16121

Statistical group theory of two component associated gas mixtures, noting erroneous virial coefficient 05 p0692 A72-16356

Subgroup structure of symmetry group g of stress tensor for stored energy function in hyperelasticity 06 p0893 A72-17302

Self similar invariant group solutions to Bellman nonlinear partial differential equation for optimal correction problems of control systems motion with random disturbances 07 p0963 A72-20322

Elimination of spherical cavity resonators natural frequencies degeneration through symmetry disrupting disturbance, using group theory for fields and frequencies calculations 08 p1209 A72-21737

Group and symmetry theory application to degenerate mode splitting in magnetron cavity systems with electromagnetic fields disturbances 08 p1142 A72-21740

Differential geometry of reductive homogeneous spaces with invariant affine connections, identifying geodesic lines with subgroup trajectories of space motions 09 p1340 A72-22295

Long distance communications multimode waveguides and probability distributions on symplectic group in extension of mathematical model with random inhomogeneities 09 p1277 A72-22474

Similarity analysis group theory methods application to dimensional analysis, discussing incompressible fluid mechanics case 10 p1503 A72-23917

Dimensional analysis pi-theorem local generalization by Lie transformation group investigation, constructing local canonical coordinate systems to obtain factoring properties of certain functions 10 p1503 A72-23921

Ubiquitous convex groups of real vectorial space of infinite dimension, obtaining characterization via decomposition family concept 13 p1987 A72-29777

Nonlinear systems normal mode vibrations analysis by group theory using symmetry properties 15 p2275 A72-31732

Exponential representation of isotropy groups of simple solids, noting conditions for conjugation of unimodular to orthogonal group subgroups 16 p2423 A72-33111

Formula for the product of semigroups which is determined by the method of bilinear forms, and the application of the formula to the Schroedinger equation 19 p2825 A72-37735

Optimal strategies for control of a semi-Markovian process by a set of observers 19 p2770 A72-38584

Group properties of ordinary linear second-order differential equations 20 p2946 A72-39471

A charged particle in the field of a transverse electromagnetic plane wave - A group-theoretical analysis. 21 p3084 A72-40722

Group properties and invariant solutions of electric-field equations in the case of nonlinear Ohm's laws 21 p3086 A72-41654

An application of the theory of Lie groups in the optimal control problem for linear dynamic systems with time-variable coefficients 22 p3162 A72-42181

Group theory for spontaneous coherent radiation of multilevel sources, noting angular distribution of photon echo effects 23 p3295 A72-43306

Book - Dimensional analysis and group theory in astrophysics. 23 p3341 A72-44500

GROUP VELOCITY

Frequency variations from uniformly moving source in homogeneous and inhomogeneous isotropic plasmas, calculating source-to-transmitted-wave group velocity ratio from Doppler curves slopes 02 p0264 A72-12120

Conduction velocity groups in cat optic nerve from antidromic responses recorded in peripheral retina and area centralis 03 p0315 A72-13621

Optic nerve axon diameters in central and peripheral cat retina related to conduction velocity groups 03 p0315 A72-13622

Radio signal group trajectory in ionosphere expressed as series expansion in terms of increasing power of beam reflection height 05 p0626 A72-16250

Traveling ionospheric perturbations investigation by vertical sounding with interference method, presenting group path difference measurements as function of frequency and time 05 p0657 A72-16269

Distortion measuring equipment for determining FM signal transmission errors due to amplitude and group delay frequency response deficiencies and AM/PM conversion 05 p0626 A72-16299

Group velocity and numerical error propagation in partial differential and finite difference equations of gas dynamics 05 p0652 A72-16952

[ALAA PAPER 72-153]

Phase and group velocity of electromagnetic waves in drifting uniaxial magnetoplasma, obtaining dispersion relation from Maxwell and plasma equations 06 p0853 A72-17349

Linear network sensitivity and group delay evaluation without topology or component restraints, using computer technique 06 p0793 A72-17594

Hydromagnetic waves propagation and horizontal group velocity westward from dawn terminator to dark hemisphere, inferring magnetospheric properties 11 p1625 A72-26414

Cylindrical waveguide proper modes instability regions boundary calculation, determining dispersion characteristics and waves phase and group velocities 12 p1791 A72-27537

Wave packet group velocity concept interpretation and application, considering propagation in dissipative media 12 p1783 A72-27719

First mode calculations for VLF atmospheric parameters of group delay time and spectral amplitude ratio based on Wait-Walters model 16 p2362 A72-32890

UHF radio signals refraction angles and group delay times for biexponential model of ionospheric electron density profile 18 p2657 A72-36101

Similarity solutions to nonlinear equations of motion of n dislocations group in slip plane under stress 18 p2719 A72-36745

Quasi-static loading of the earth by propagating air waves. 22 p3172 A72-42468

The concepts of mean force, mean velocity, and ensemble velocity for a particle ensemble 24 p3425 A72-45070

GROUP 1A COMPOUNDS

U ALKALI METAL COMPOUNDS

GROUP 7A COMPOUNDS

U HALOGEN COMPOUNDS

GROWTH

NT CROP GROWTH

NT CRYSTAL GROWTH

NT CZOCHRALSKI METHOD

NT EPITAXY

Chlorella growth rate model, presenting specific photosynthetic and urea and carbon dioxide utilization rates 02 p0160 A72-12038

Gibberellic acid effects on Chlorella algae growth rates, using algal suspension optical density as measuring technique 03 p0313 A72-12975

Cardiorespiratory functions in child swimmers and nonathletes during growth, relating training to oxygen transport system dimensions

08 p1123 A72-20894

Biological similarity theory for numerical relationships of morphometric and physiometric organization in mammals, using allometric growth equations and body weight correlations

10 p1432 A72-25098

Light induced alterations in growth pattern of the avian eye.

17 p2500 A72-34880

Interrelation of interoceptors and exteroceptors in the process of urination and defecation reflex act maturation in ontogeny

17 p2504 A72-35022

Functional development of the altitude convulsion mechanism in mice and rabbits [Research note].

18 p2650 A72-36445

Cardiac hypertrophy, capillary and muscle fiber density, muscle fiber diameter, capillary radius and diffusion distance in the myocardium of growing rats adapted to a simulated altitude of 3500 m.

21 p3003 A72-41624

GRUMMAN MILITARY AIRCRAFT

U MILITARY AIRCRAFT

GUANIDINES

Formation of urea and guanidine by irradiation of ammonium cyanide.

23 p3262 A72-43569

GUANINES

Adenine, guanine, cytosine and other nitrogen compounds synthesis from carbon monoxide, hydrogen and ammonia mixtures by Fischer-Tropsch-like process

04 p0483 A72-14765

GUIDANCE [MOTION]

NT AIRCRAFT GUIDANCE

NT COMMAND GUIDANCE

NT INERTIAL GUIDANCE

NT INJECTION GUIDANCE

NT MIDCOURSE GUIDANCE

NT REENTRY GUIDANCE

NT SATELLITE GUIDANCE

NT SPACECRAFT GUIDANCE

NT STRAPDOWN INERTIAL GUIDANCE

NT TERMINAL GUIDANCE

Visual guidance of locomotion, discussing expansion information and target drift theories

03 p0319 A72-13879

Unified single rf channel tracking, telemetry and command control systems for guidance of unmanned vehicles, including pilotless aircraft and satellites

05 p0685 A72-16556

Optimal allocation and guidance for linear time varying interception and rendezvous problems of dynamic deterministic or stochastic systems

05 p0686 A72-16558

Optimal control design for digital guidance system, conducting efficiency and reliability analyses

11 p1600 A72-25437

Gas bearing gyroscope for fluidic guidance and control system, satisfying missile and recoverable booster requirements

18 p2648 A72-36557

GUIDANCE SENSORS

Pulsed relay control system for stabilizing spacecraft orientation in flight, allowing for changes in characteristics of guidance sensor systems and slave mechanisms

05 p0731 A72-17031

Strapdown inertial guidance and navigation systems state of art, discussing recent developments in computers, sensors and systems technology

08 p1204 A72-21089

Multichannel area stellar photometer using photosensitive cell array for individual photoelectron counting, applying to autoguidance

11 p1631 A72-25690

Aeronautical navigation/guidance standardization in conjunction with OMEGA, covering sensor and computer equipment life cycles

13 p1999 A72-29199

Doppler navigation system suitability for area navigation, discussing routes versatility, accuracy and continuous velocity vector sensor

15 p2271 A72-32203

Error analyses of Euler angle transformations arising in design of precision pointing systems, guidance sensors and instruments with gimbals

[AIAA PAPER 72-851]

20 p2949 A72-39078

Real time homing guidance geometry and interceptor/sensor tradeoff studies based on reachable sets of target states analysis

[AIAA PAPER 72-825]

20 p2951 A72-39101

EOSS - A dynamic six degree-of-freedom environmental simulator for evaluation of electro-optical guidance systems.

[AIAA PAPER 72-862]

20 p2911 A72-39135

Alignment of the figure axis of a spin-stabilized spacecraft perpendicular to sun and earth

23 p3343 A72-43621

GUIDANCE STABILITY

U CONTROL STABILITY

U GUIDANCE [MOTION]

GUIDE VANES

NT JET VANES

Leaning vanes for fan noise reduction, discussing rotor-stator plane fluctuating pressure amplitude decrease and radial distribution modification

[AIAA PAPER 72-126] 05 p0706 A72-16823

Aircraft engines high pressure turbine guide vanes air cooling by internal insert, analyzing thermal stresses

[AIAA PAPER 72-7] 05 p0707 A72-16864

Gas turbine nozzle guide vane trailing edge protection by air films cooling, measuring gas temperatures with chromel-alumel thermocouples

08 p1224 A72-21318

Discharge and pressure recovery coefficients of blocked gas flow in curvilinear channel with guide vanes, minimizing losses and separation at convex wall

11 p1574 A72-26971

Composite materials application to gas turbine fan guide vane fabrication, noting economic factors and prototypes performance in engine tests

12 p1815 A72-28100

Energy dissipation for turbulent flow in turbine blades guide vanes calculated with allowance for effects of Reynolds number and turbulence intensity

12 p1752 A72-28137

Developments in vacuum braze coating of aero-engine nozzle guide vanes.

17 p2559 A72-34937

Effects of rifling and N-vanes on the Magnus characteristics of bodies of revolution.

[AIAA PAPER 72-970] 22 p3135 A72-42341

Investigation of a partial admission double-vane-ring stage with bypass of the second ring

24 p3364 A72-45621

GUIDED MISSILES

U MISSILES

GULF STREAM

Gulf Stream surface front structure, temperature and salinity observation from ship, aircraft and satellite

11 p1620 A72-25348

GUMBEL THEORY

U RANGE [EXTREMES]

GUN PROPELLANTS

Burning gunpowder surface reactions relative to temperature, chemical enthalpy and acoustic waves of pressure, velocity and density

05 p0511 A72-17211

Gunpowder burning stability in pressurized volume from automatic control theory methods application to temperature and pressure dynamics

06 p0903 A72-18205

Burning gunpowder surface reactions relative to temperature, chemical enthalpy and acoustic waves of pressure, velocity and density

11 p1744 A72-25337

Acoustic admittance measurement for burning surface of nitroglycerin gunpowders, using combustion product velocity and wave pressure ratio

16 p2391 A72-33257

GUNFIRE

Combat aircraft lateral aiming performance optimization and evaluation based on criterion of bullet stream response to pilot roll commands

05 p0611 A72-16657

Aircraft fuel system gunfire vulnerability and fire and explosion protection techniques

08 p1112 A72-21579

GUNN EFFECT

Microwave Gunn oscillator frequency modulation in quenched domain mode, calculating signal admittance as function of bias voltage and amplitude

01 p0035 A72-10224

Trace gas pollutant monitoring by microwave rotational absorption spectroscopy, discussing test results with Gunn diode cavity spectrometer

[AIAA PAPER 71-1048] 01 p0023 A72-10524

Planar Gunn effect devices for microwave oscillators, discussing impedance matching and diode conductivity profile effect on output power

01 p0028 A72-10628

High power Q-band pulsed Gunn diode microwave oscillator constructed from thin GaAs sandwich layers grown by vapor phase epitaxy

01 p0036 A72-10630

L-band Gunn oscillator using nonsinusoidal device voltage /switching mode/, comparing efficiency and output power with sinusoidal mode

01 p0036 A72-10635

Electronic tuning of transverse Gunn effect microwave oscillators by varying voltage on third electrode incorporated between cathode and anode

01 p0036 A72-10637

Output power, efficiency and fundamental frequency resistance of Gunn microwave self oscillator in single and multiresonant mode

01 p0037 A72-10638

Lf noise spectrum of Gunn oscillators due to direct modulation of rf admittance for constant voltage bias source

01 p0037 A72-10639

Gunn diode microwave oscillator postcoupling to waveguide, deriving theory based on equivalent circuit for load impedance assessment

01 p0037 A72-10640

CW X-band Gunn oscillator in coaxial cavities, investigating frequency variation with ambient temperature

01 p0037 A72-10641

Microwave oscillator detector Gunn diode as inexpensive alarm device for Doppler radar application

01 p0028 A72-10642

AM and FM noise reduction of cavity and injection stabilized microwave Gunn and avalanche diode oscillators

01 p0037 A72-10644

Large signal nonlinear modeling and digital simulation of microwave transistor power amplifier and GaAs Gunn relaxation oscillator

01 p0041 A72-10691

Integrated receiver module for satellite transponders, including tunnel diode amplifier, Schottky barrier mixer, Gunn oscillator and low pass filter

01 p0041 A72-10701

Gunn and IMPATT diodes applications for microwave power oscillators and amplifiers in radio link equipment

01 p0042 A72-10711

Magnetic field effect on Gunn diode oscillator frequency and output power, discussing strong field domain

02 p0196 A72-12885

Gunn effect and associated phenomena, covering semiconductor domain formation and movement, space charge waves and thin samples with dielectric coatings

02 p0270 A72-12889

Abnormal rf hysteresis and bias voltage effect in resonant cavity Gunn devices

03 p0331 A72-13646

Book on microwave semiconductor devices, considering point contact crystal, varactor, Schottky-barrier, tunnel, backward and p-i-n diodes, transistors, Gunn effect devices and integrated circuits

03 p0333 A72-13845

High intensity ionizing gamma ray pulsed radiation effects on Gunn diode microwave oscillator failure modes

03 p0334 A72-14089

Ionizing radiation effects in cavities of microwave Gunn oscillators, noting large dose rate effects on circuit performance

03 p0335 A72-14094

Three terminal voltage-tunable Gunn effect microwave oscillator, discussing depletion depth and electric field control modes for frequency

04 p0496 A72-14479

Gunn diode large signal admittance dependence on bias and frequency, discussing computer simulation and broadband oscillator and amplifier design

04 p0497 A72-14712

Gunn diode microwave oscillator with moving reflector as self-excited mixer and load variation detector, analyzing performance by I-V characteristics model

04 p0497 A72-14713

Closed solution to Gunn effect field domain formation and propagation, using approximate I-V curve and method of characteristics

04 p0563 A72-15503

Computer simulation in optimized 5-GHz Gunn diode oscillator design

05 p0633 A72-16360

Fast frequency switching for shift keying pulse code modulation with two cavity modes for Gunn oscillator frequency states

05 p0631 A72-17072

Noise effect in IMPATT and Gunn diode oscillators on phase/frequency fluctuation using series/parallel connected multiple active devices

06 p0783 A72-17483

Analytical model of Gunn diode oscillating in resonant mode with domain quenching, determining current harmonics

06 p0783 A72-17573

Microwave IC oscillators design for broadband high performance receivers, exemplifying thin film Gunn effect, step- and varactor-tuned transistor oscillators

06 p0786 A72-18373

K band Gunn oscillator with high frequency stability, discussing construction, performance, output power and frequency saturation effect

06 p0786 A72-18375

System potential of microwave solid state generation and amplification, comparing IMPATT, TRAPATT, Gunn, LSA, transistor and transistor-multiplier devices

06 p0787 A72-18456

X band IMPATT and Gunn oscillator, calculating injection lock time, modulation bandwidth, noise and FM suppression and dynamic response

06 p0788 A72-18471

Neutron irradiation induced material degradation and circuit failure in high power GaAs Gunn diode oscillator operating in LSA relaxation mode

06 p0788 A72-18472

- FM/CW varactor Gunn diode oscillator powered subminiature IC radar altimeter design on homodyne principle for ultralight reliable minimum chance detection 06 p0819 A72-18473
- S band module with Gunn diode oscillators in series connection used as phased array radar 250 W power sources with efficient heat sink 06 p0789 A72-18476
- High power efficiency CW Gunn devices design and fabrication, discussing GaAs preparation techniques and device physics 06 p0789 A72-18478
- Varactor tuned high performance Gunn oscillators, emphasizing specifications for level power output with frequency, tuning linearity and rate 06 p0789 A72-18479
- Solid state Ku-band local Gunn oscillator for airborne radar applications, discussing design and batch process fabrication 06 p0789 A72-18480
- Low frequency modulation noise generation due to conductance fluctuations in Gunn oscillators, measuring noise spectra temperature dependence 07 p0954 A72-19050
- Resonator second harmonic influence on Gunn oscillator parameters for transit and hybrid modes, discussing bias voltage, harmonic amplitudes, phase difference, doping level and frequency 07 p0955 A72-19254
- YIG tuning of X band Gunn effect stripline oscillator circuit, noting application to microwave ICs 07 p0955 A72-19357
- Waveguide cavity Gunn microwave power amplifiers, predicting maximum small signal gain and FM and AM noise performance 07 p0958 A72-19921
- Gunn diode microwave oscillator thermal resistance reduction for increased output power and efficiency 07 p0958 A72-20685
- Digital frequency shift keying modulation of Gunn microwave oscillator by cavity placed between output and transmission line 08 p1141 A72-21432
- Cavity resonator frequency detuning effects on FM and AM noise in cavity stabilized Gunn microwave oscillator 09 p1285 A72-22651
- If originated background noise in Gunn oscillators, developing evolution equation for oscillator weakly perturbed by noise 09 p1288 A72-23121
- Random frequency FM noise model for microwave Gunn effect oscillators 09 p1288 A72-23122
- Gunn domain oscillations suppression by dielectric surface loading of transversely thin GaAs diodes 10 p1526 A72-24305
- CW X band Gunn microwave oscillators, measuring frequency variation relationship to ambient temperature 10 p1450 A72-24555
- YIG tuned Gunn oscillator phase locking and shifting over 3 GHz range in X band, using feedback control 10 p1451 A72-24596
- German book on HF semiconductor electronics covering planar and field effect transistors, varactors, n-p, p-i-n, avalanche and Schottky barrier diodes, Gunn devices, etc 10 p1452 A72-24699
- Bulk negative resistance devices equivalent noise temperature derivation via diffusion-impedance field noise formula, obtaining Gunn oscillators SNR approximate value 10 p1454 A72-25106
- IMPATT diode and transferred electron Gunn devices for systems applications, comparing thermal noise and physical properties 12 p1788 A72-27295
- Encapsulation influence on Gunn effect devices from circuit analysis of wideband tunable transferred electron microwave oscillators 12 p1790 A72-27440
- Pulse generation in planar Gunn devices of epitaxially grown GaAs layers, measuring current reduction by domain nucleation 12 p1791 A72-27671
- Transit time, retarded domain and suppressed domain mode simulation of Gunn oscillator, using LF analog 13 p1927 A72-28405
- Mobility-field characteristics of GaAs below Gunn threshold with magnetoresistance technique, relating to device performance and other material parameters 13 p2021 A72-28573
- CW Gunn oscillator cavity loading and bias voltage effects on external negative differential conductance 13 p1933 A72-29825
- Conversion efficiency and polarization behavior of Gunn diodes in resonant cavities, using I-V characteristics 13 p1937 A72-29866
- Gunn diode active region thickness, free electron mobility/concentration, structure and contacts, including treatment of GaAs 13 p1934 A72-30036
- Correlation measurements of LF current noise and frequency fluctuations in Gunn oscillators, emphasizing generation-recombination noise component 14 p2088 A72-30916
- Nodal equations derivation for lumped circuit representation of Gunn diode with steadily propagating domain under steady state and transient conditions 15 p2205 A72-31317
- Simplified equivalent circuit analysis for Gunn diode coupling to rectangular waveguide by inductive post, using perturbation approximation 15 p2205 A72-31353
- High efficiency X band pulse operation of transferred electron oscillator in hybrid mode, noting high material quality and optimum impedance match 15 p2206 A72-31548
- Transverse magnetic field effects on n-type GaAs Gunn diodes microwave power, coherence and dynamic I-V characteristics [ONERA, TP NO. 1051] 15 p2207 A72-31884
- GaAs Gunn diode LSA operation mode in multiloop circuit to extend high frequency limit 15 p2207 A72-31888
- Gunn diode elements design, operation, performance, efficiency, heat dissipation, lifetime and applications as microwave oscillators 15 p2208 A72-32500
- Noise-to-carrier ratio and rms frequency deviation evaluation for X band Gunn and Si and GaAs avalanche diode oscillators 16 p2370 A72-34177
- Simple Doppler radar using the CL8630 Gunn effect oscillator for the observation of small rotating objects. 17 p2524 A72-34245
- BARITT, IMPATT, TRAPATT and Gunn diodes, discussing power, noise and thermal dissipation problems 17 p2526 A72-34465
- Gunn effect - Bulk instabilities. 17 p2594 A72-34562
- New measurement method of Gunn-diode impedance. 17 p2529 A72-35000
- Characteristics of Gunn elements CGY 11 to 14 and their application as microwave oscillators. II 17 p2530 A72-35150
- Superconducting-cavity-stabilised oscillator of high stability. 17 p2530 A72-35386
- Frequency/temperature characteristics of Gunn devices. 18 p2667 A72-36684
- The behaviour of a Gunn oscillator in the domain-delayed mode. 18 p2667 A72-36945
- Synchronization and noise performance of mutually coupled oscillators. 18 p2668 A72-37036
- Thermal modulation and FM noise of Gunn oscillators. 18 p2668 A72-37038
- Microwave and optoelectronic devices performance and component reliability, considering varactors, p-i-n, avalanche and Gunn diodes, ICs, FETs, light emitters and liquid crystals 18 p2720 A72-37137
- Electronic and optical phenomena in semiconductors. 19 p2844 A72-37445
- Some tuning characteristics and oscillation conditions of a waveguide-mounted transferred-electron diode oscillator. 19 p2772 A72-37569
- An analytical equivalent circuit representation for waveguide-mounted Gunn oscillators. 19 p2773 A72-38291
- Binary information storage with bipolar transistors, tunnel diodes, MIS and glass semiconductors, considering Gunn effect devices application 20 p2905 A72-39425
- Gunn effect threshold and domain formation in transverse magnetic fields in indium antimonide. 20 p2960 A72-39566
- Acousto-optic modulation with coupled Gunn oscillator-piezoelectric structure. 20 p2960 A72-39702
- A general analysis of noise in Gunn oscillators. 20 p2909 A72-39782
- Temperature effects on modulation sensitivity and vibrational spectra in Gunn diode oscillators, suggesting frequency stability improvement method 21 p3032 A72-40792
- Quantitative derivation of large signal equivalent circuit of Gunn element in domain mode based on current and space charge characteristics 21 p3034 A72-41401
- Thermal resistance of Gunn diodes - Analysis and measurement. 21 p3035 A72-41491
- Low temperature characteristics of the Gunn diode. 22 p3159 A72-42307
- A CW Gunn diode bistable switching element. 22 p3159 A72-42610
- Theory of microwave amplification with electron transfer 23 p3269 A72-43550
- A wide-band Gunn-effect CW waveguide amplifier. 23 p3272 A72-44193
- A single-tuned oscillator circuit for Gunn diode characterizations. 23 p3272 A72-44194
- Noise properties of the injection-limited Gunn diode. 24 p3385 A72-44962
- Frequency stability of Gunn oscillators with variation of ambient temperature. 24 p3385 A72-44980
- GUNPOWDER**
U GUN PROPELLANTS
GUNS [ORDNANCE]
NT ARTILLERY
GUST ALLEVIATORS
- Atmospheric turbulence effects on aircraft flight and design, covering accidents and costs, turbulence generation, prediction, measurements and load alleviation devices [AIAA PAPER 72-219] 05 p0684 A72-16885
- Aeroelasticity, discussing gust and maneuver load alleviation, flutter suppression, aircraft stability, computerized aeroelastic analysis, aeroelastic optimization, composite structures, etc 15 p2322 A72-31202
- Suboptimal feedback control for aircraft gust alleviation design, using indirect perturbation information through normal acceleration factor measurement 15 p2181 A72-32025
- GUST LOADS**
High speed helicopter elastic rotor blade suboptimal motion controller decreasing flapping motion and bending loads despite small control angles and vertical gusts 04 p0465 A72-15504
- Semimomentless theory of closed cylindrical plastic shells subject to random gust loads, obtaining normal circumferential force, shear, transverse bending moment and shell thickness 07 p1092 A72-19851
- Lift and pressure fluctuations of cambered airfoil under periodic longitudinal and transverse gusts, applying to axial flow turbomachines [ASME PAPER 72-GT-30] 11 p1569 A72-25626
- Aerodynamic lag effects on wing bending dynamic response at supersonic speeds, noting application to stress estimation under gust loads 11 p1572 A72-25922
- Concorde dynamic behavior from flight tests, discussing integrated design effects, wing, fin and elevator flutter, gust and runway response and engine surge effects [AIAA PAPER 72-381] 13 p1897 A72-28958
- Low altitude gust load spectra above Czechoslovak territory interpreted in terms of equivalent velocity cumulative frequencies for light aircraft 14 p2071 A72-30282
- Bending and torsional mode deformations of two dimensional elastic wing under sinusoidal and random gust 16 p2469 A72-33229
- Rigid aircraft longitudinal dynamic response to random atmospheric turbulence, defining spectral gust alleviation factors in terms of mass scale and damping ratio parameters 21 p2996 A72-41641
- Aircraft structural design loads definition by mission analysis criteria, taking into account gust loads via power spectral density method 22 p3138 A72-42828
- Optimal fleet reliability under fatigue and chance overload in service. 24 p3365 A72-44656
- Preliminary design of a sailplane wing for dynamic gust loads 24 p3368 A72-44992
- GUSTATORY PERCEPTION**
U TASTE
GUSTS
- Airplane sideslip and yaw rate perturbations by continuous random vertical and side gusts, using low pass filtered white noise representation for mathematical modeling 12 p1755 A72-28125
- Aircraft flight conditions effect on low altitude critical air turbulence in terms of gust velocity components for CAT prediction 13 p1993 A72-28861
- GYMNASTICS**
U EXERCISE [PHYSIOLOGY]
GYRATION
- NT AUTOROTATION
NT EARTH ROTATION
NT I.ARMOR PRECESSION
NT MOLECULAR ROTATION
NT PRECESSION
NT PROTON PRECESSION
NT ROTATION
NT SATELLITE ROTATION
NT SOLAR ROTATION

- NT STELLAR ROTATION
Quasi-linear theory of relativistic particle acceleration by hydromagnetic turbulence for small gyration radius expansion, using Vlasov equation
02 p0265 A72-12301
- Lunar shadowing of charged particles with arbitrary gyroradii and steady drift transverse to magnetic field applied to detector in low lunar orbit
21 p3104 A72-40482
- Kepler second law based moment of gyration concept application to spacecraft and missiles mechanics and kinematics, proposing Skylab weightless environment experiment for validation [SAWE PAPER 931]
23 p3342 A72-43471
- GYRATORS**
NT MICROWAVE FILTERS
Lumped capacitors, inductors, resistors and gyrators for use at microwave frequencies, discussing design and applications up to X band
04 p0497 A72-14717
- Antoniou bridge type gyrator circuit stability, showing sensitivity to resistors ratio variations
12 p1792 A72-27698
- RC gyrator filters frequency characteristics stability analysis, noting elements sensitivity as function of frequency and Q value
19 p2774 A72-38421
- GYRO HORIZONS**
Small motions of two rotor gyro horizon compass sensitive element with linear azimuthal correction of housing
07 p0986 A72-19758
- Reduction principle validity in perturbed motion stability theory for near-critical systems with gyro horizon application
07 p1035 A72-19972
- Fourth order normal modes and resonances of nonlinear vibrations, applying to gyro horizon compass sensitive element gimbal motion
13 p2000 A72-28382
- Motion stability of inertial navigation gyroscopic system with gyro horizon compass, noting constant and time dependent coefficients of motion equations
19 p2830 A72-37320
- Reduction principle validity in perturbed motion stability theory for near-critical systems with gyro horizon application
20 p2955 A72-40029
- Theory of a gyrohorizon compass with an azimuthally free casing of the sensitive element
23 p3287 A72-43585
- GYROCOMPASSES**
Military aircraft inertial navigation system design, discussing gyroscope, gyro compassing alignment, accuracy and performance
04 p0545 A72-15666
- Angular and linear vibrations effect on dynamic errors of two stage gyrocompass, obtaining nonlinear equations of motion approximate solutions
07 p0981 A72-18928
- Small motions of two rotor gyro horizon compass sensitive element with linear azimuthal correction of housing
07 p0986 A72-19758
- Optimal nomographic determination of surface gyrocompass parameters ensuring minimum period of undamped precession oscillations
09 p1307 A72-22346
- Accelerated aperiodic actuation of pendulous mass surface gyrocompass to meridian direction, using inertial moment from rotor start-up
10 p1481 A72-24496
- Fourth order normal modes and resonances of nonlinear vibrations, applying to gyro horizon compass sensitive element gimbal motion
13 p2000 A72-28382
- Two gyro three axis stabilizer with gyrocompass effect for gravimeter or magnetometer sensor stabilization in towed gondola
13 p1957 A72-29271
- Combined hydrostatic suspension Hg cushion effects on gyrocompass response precision during irregular roll of platform
13 p1961 A72-30022
- Coordinate and speed error dependence on instrumental errors of inertial navigation system using gyrohorizoncompass
16 p2420 A72-33960
- Motion stability of inertial navigation gyroscopic system with gyro horizon compass, noting constant and time dependent coefficients of motion equations
19 p2830 A72-37320
- Behavioral features of a composite hydrostatic suspension of a gyrocompass under conditions of vibration
21 p3058 A72-41807
- Ballistic deviations of a gyroscopic navigation system
23 p3311 A72-43417
- Theory of a gyrohorizon compass with an azimuthally free casing of the sensitive element
23 p3287 A72-43585
- Pulse transient response function for gyroscopic course indicator with gyrocompass error filtered out and nondistorted directional gyroscope error
24 p3403 A72-45320
- Compass effect of a gyroscope with forced rotation of the Cardan suspension
24 p3403 A72-45321
- GYROFREQUENCY**
Magnetoplasma with skin current characterized by current and electron temperature nonuniformity, analyzing instabilities for perturbations above ion gyrofrequency
03 p0396 A72-13713
- Gyroresonance devices efficiency increase, discussing magnetostatic field distribution optimization in interaction space
04 p0502 A72-15575
- Quasi-linear theory of magnetosphere gyroresonant wave-particle interactions, discussing particle distribution function anisotropy, wave packet effects, whistler mode, energy and pitch angle distributions, etc
07 p0978 A72-20034
- Rocket-observed energetic electron flux association with ground recorded plasmasphere whistler in terms of gyroresonant wave-particle interaction
15 p2198 A72-31948
- Magnetoactive plasma transverse waves propagation near electron gyrofrequency harmonics, taking into account electron collisions and relativistic effects
15 p2289 A72-32734
- Plasma accumulation in electrostatic potential well produced by electron space charges, determining diocotron instability as function of electron plasma and gyrofrequency ratio
16 p2434 A72-32819
- Plasma frequency, hybrid frequency and harmonic gyrofrequency electron resonances due to electrostatic waves in ionosphere observed with topside sounders aboard rockets and satellites
23 p3263 A72-43513
- Optimal gyroresonator control in electric oscillating field by HF magnetic Lorentz force in terms of relativistic electron trajectory drifts
23 p3290 A72-44200
- GYROINTERACTION**
U MAGNETIC RIGIDITY
GYROMAGNETISM
NT GYROFREQUENCY
Microwave propagation through laminated metallic media with gyromagnetic effects, applying dc magnetizing field normal to film plate [IEEE PAPER 31.6]
03 p0323 A72-13784
- Gyrosynchrotron radiation fields from mildly relativistic electrons in magnetoactive plasma, studying radiative transfer problem
14 p2138 A72-30556
- Solar stationary type 4 radio bursts caused by gyromagnetic radiation of bunched electrons
16 p2449 A72-33920
- Heat conduction as mechanism for solar microwave bursts attenuation, noting effect of gyromagnetic absorption layers
19 p2852 A72-38497
- GYROPLANES**
U HELICOPTERS
GYROS
U GYROSCOPES
GYROSCOPE FLUIDS
Thermal drift of floated spherical gyroscope calculation based on two dimensional free convection analysis of supporting fluid
15 p2235 A72-31727
- GYROSCOPES**
NT CONTROL MOMENT GYROSCOPES
NT ELECTROSTATIC GYROSCOPES
NT FLUID ROTOR GYROSCOPES
NT GYRO HORIZONS
NT GYROCOMPASSES
NT GYROSCOPIC PENDULUMS
NT GYROSTABILIZERS
NT OPTICAL GYROSCOPES
NT ROTARY GYROSCOPES
Passenger aircraft onboard automated inertial navigation devices, emphasizing accelerometer and gyroscope design and construction
01 p0096 A72-10070
- Gyroscope precession in earth gravitational field, considering impulse energy vector and angular momentum tensor
02 p0229 A72-11970
- Optimal smoothing application to testing of inertial navigation systems, gyros and component failure detection during mission
02 p0258 A72-12810
- Howe gyroscope mounted on fixed base, deriving equations of motion with Laplace method
03 p0359 A72-13558
- Meridian and local vertical gyro errors effects on geomagnetic field elements determination accuracy
03 p0359 A72-13559
- Axial and radial displacements determination in rotor center of gravity for gyroscope with elastic suspension
03 p0360 A72-13560
- German book on gyroscope theory and applications, covering artificial satellites motion in gravitational field
03 p0360 A72-13675

Soviet book on gyroscopic systems and inertial guidance instruments, emphasizing system motion under various dynamic conditions and systematic errors
03 p0362 A72-14167

Human centrifuge tests for semicircular canal gyroscopic stimulation during sensory deprivation, discussing angular acceleration detection thresholds
04 p0478 A72-14865

Gyroscope precession equations over infinite time interval from conditions based on solutions to differential equations with small parameters at derivatives
04 p0521 A72-15001

Military aircraft inertial navigation system design, discussing gyroscope, gyro compassing alignment, accuracy and performance
04 p0545 A72-15666

Zero crossing photoelectric autoreflector pickoffs for readout gyro systems with suspended spherical rotors, classifying systems according to modulation type
05 p0661 A72-16036

Gyrostal translational rotational motion equations in canonical form without trigonometric expressions in Hamiltonian
05 p0724 A72-16164

Equations of motion for oscillating heavy symmetrical gyroscope with cylindrical cavity partially filled with inviscid incompressible liquid
05 p0664 A72-17145

Gyroscopic error analysis, solving nonlinear equations by continuous Markov processes theory
06 p0819 A72-18724

Time behavior of single axis gyro platforms, considering linear and nonlinear-suboptimal control
07 p0983 A72-19169

Gyro technology - Conference, Kiel, Germany, May 1971
07 p0989 A72-20276

Stability requirement of gyro systems in generalized Thomson-Tait theory
07 p0989 A72-20277

Nonlinear controls for single axis gyro platforms, using time optimal Luenberger observers
07 p0989 A72-20278

Time optimal self alignment of inertial platforms using gyros and accelerometers with Kalman-Bucy filter
07 p0989 A72-20279

Switching sequence analysis of gas bearing gyros for low cost inertial sensors in short risetime navigation devices
07 p0989 A72-20281

Analog simulation of dual-spin satellite dynamics and control, emphasizing Hughes gyrostal spacecraft
07 p1086 A72-20352

Motion of body similar to Lagrange gyroscope, using Kolmogoroff theorem
08 p1207 A72-21343

Periodic motion of gyroscope, using geometrical method of analysis
08 p1207 A72-21348

Kharlamov kinematic equations application to gyrostal motion problem, deriving angular velocity hodograph
08 p1207 A72-21350

Goriachev-Chaplygin solution to gyroscopic motion of body around fixed point for periodic motion
08 p1208 A72-21355

Sretenskii-Chaplygin integral in polynomial form for solution to gyrostal motion problem
08 p1208 A72-21356

Motion equations of gyrostal with nonholonomic constraint under gravitational force
08 p1208 A72-21359

Gyrostal inertial motion under nonholonomic constraint of mass center coincidence with fixed point
08 p1208 A72-21360

Linear invariant solution to gyrostal motion under nonholonomic constraint
08 p1208 A72-21361

Solutions existence and uniqueness for linear invariant relation to gyrostal motion under nonholonomic constraint
08 p1208 A72-21362

Vibrational characteristics dependence on structural flexibility in gimbal bearings and supporting structure of two axis free gyroscopes and single axis rate gyroscopes
08 p1173 A72-22129

German monograph on optimal design of gyroscope using spherical static gas bearing
08 p1173 A72-22174

Nonstationary nonlinear multidegree-of-freedom systems resonant response analysis by asymptotic method, investigating gyroscopic system for combination differential resonances [AIAA PAPER 72-401]
11 p1629 A72-25422

Complete and simplified equations of motion for rate gyro installed in flight vehicle, taking into account bearing torques [DFVLR-SONDDR-190]
11 p1635 A72-26580

Limiting stability cases of vehicle with linear attitude control and pointed at star by two power gyroscopes in conical suspensions

13 p2051 A72-28383

Delauney case of Kovalevskaja gyroscope motion, analyzing Euler equations time dependence

13 p1956 A72-28722

Elastic deformation and rigidity of rectangular, circular and elliptic gimbals for gyroscope suspension

13 p1957 A72-29272

Equations of motion for contactless suspension gyroscope in force field

15 p2235 A72-31726

Thermal drift of floated spherical gyroscope calculation based on two dimensional free convection analysis of supporting fluid

15 p2235 A72-31727

Nonsymmetric gyrostad steady motions analysis in axisymmetric gravity field based on Routh-Liapunov theorem, calculating stability conditions

15 p2320 A72-31728

Soft gyro and accelerometer failure detection for redundant gimbal inertial measurement units by skew sensors

15 p2270 A72-32187

Optimal algorithm for failure detection and identification in redundant gyro-accelerator sensor systems, including Monte Carlo simulation

15 p2270 A72-32188

Gyro drift detection and isolation for redundant inertial measuring unit configuration of Carousel V system

15 p2270 A72-32190

Gyroscope drive systems, discussing various ac and dc electric motor types and switching and control circuits

16 p2396 A72-34135

Motion of a gyrostad with respect to its center of mass in a central field

17 p2622 A72-35804

Motion integrals conservation under Hamiltonian function variations, examining gyroscope equations of motion with parameter disturbances

18 p2711 A72-36666

Elastically supported dry two degrees of freedom tuned gyroscopes, analyzing open-loop transfer function for characteristic errors

19 p2794 A72-37280

Errors due to gimballing system asymmetries and rotor angular offsets effects in multigimbal elastically supported tuned gyroscope, deriving gyro translational transfer function

19 p2794 A72-37281

Mathematical model of ideal incompressible gyroscope fluid with internal angular momentum using kinematic equations

19 p2835 A72-37929

Three dimensional seismic monitoring system developed from inertial guidance gyroscopes and accelerometers, noting pole shift observation, tilting during earth tides and earthquakes forecasting

20 p2923 A72-39088

Russian book - Introduction to the theory of gyroscopes.

21 p3052 A72-40349

Delauney case of Kovalevskaja gyroscope motion, analyzing Euler equations time dependence

22 p3176 A72-42098

Dynamic characteristics, stability and steady state accuracy for orbital gyroscope with digital control, noting bit density requirements of onboard computer

22 p3202 A72-42207

Method of equivalent turns in the kinematics of inertial systems

23 p3311 A72-43583

Pulse transient response function for gyroscopic course indicator with gyrocompass error filtered out and nondistorted directional gyroscope error

24 p3403 A72-45320

GYROSCOPIC COUPLING

Nonlinear differential second order equation system development for gyroscopic coupling of forced nonlinear oscillators

03 p0389 A72-13631

Gyroscopic effects on elastically supported high speed rotors, examining critical velocity and disturbance behavior via equations of motion

11 p1686 A72-25723

GYROSCOPIC DRIFT

U GYROSCOPES

U GYROSCOPIC STABILITY

GYROSCOPIC PENDULUMS

Gyro-pendulum accelerometers, calculating moving base oscillation effect on performance by random function representation through canonical expansions

06 p0819 A72-18723

Systematic deviation of flat gyroscopic pendulum during irregular motions of ridden vehicle, comparing with physical pendulum

13 p1957 A72-29273

GYROSCOPIC STABILITY

Optimal stabilization of permanent rotation of solid body with arbitrary mass distribution by controlled gyroscope

02 p0230 A72-12337

Optimal stabilization law for ensuring gyroscope equilibrium position asymptotic stability in rms error, aperiodicity and system transient response time

02 p0230 A72-12338

Equivalent harmonic solutions for systematic drift of astatic gyroscope about outer gimbal axis with base under random angular vibrations

02 p0231 A72-12564

Elastic strain effects in ball bearing supports on motion of gyroscope Cardan suspension

02 p0231 A72-12565

Gyro drift random error dispersion reduction in compensated closed loop multirotor gyroscopic systems by cross couplings

02 p0231 A72-12566

Self oscillations and drift motion of gyroscopic integrator of linear accelerations under hf vibrations, assuming ideal relay gimbal compensation

02 p0231 A72-12567

Artificial earth satellites orbit plane determination accuracy in terms of local vertical sensor errors and gyroscope drift

05 p0717 A72-16441

Equations of motion for stable member of three axis gyro stabilized platform for inertial navigation, including friction, inertia and torque motor effects

05 p0662 A72-16557

Optimal alignment and calibration of gyro stabilized platforms, using Kalman filter and minimal weighted squared errors

07 p0989 A72-20280

Optimal stabilization of permanent rotation of solid body with arbitrary mass distribution by controlled gyroscope

08 p1168 A72-21552

Optimal stabilization law for ensuring gyroscope equilibrium position asymptotic stability in rms error, aperiodicity and system transient response time

08 p1168 A72-21553

Liquid filled spinning projectiles and satellites flight stability based on Stewartson gyroscope analysis method

08 p1168 A72-21600

Stationary motions stability of four rotor vertical gyroscopic system on satellite in circular orbit in Newtonian central force field

08 p1205 A72-21804

Twin spool jet engine system, predicting shaft speed effects on whirling frequencies due to gyroscopic action with computer model

08 p1224 A72-22130

Angular rigidity of support shaft elastic suspension of dynamically adjustable gyroscope

09 p1307 A72-22348

Earth pointing rotating satellites attitude control system based on two-degree of freedom gyroscope, determining conditions for rotor spin axis fixation in inertial space

10 p1509 A72-24646

Electric propulsion spacecraft design for ion thruster systems testing with circular solar cells array as gyroscopic stable platform

11 p1578 A72-26200

Radial bearing placed on journal of Cardan suspension, investigating ball dimension errors effect on gyro drift rate

13 p1962 A72-28385

Systematic deviation of flat gyroscopic pendulum during irregular motions of ridden vehicle, comparing with physical pendulum

13 p1957 A72-29273

Hove gyroscope on base uniformly rotating about axis perpendicular to drive axis, considering forced motion elimination possibility

13 p1961 A72-30023

Monograph on rotor-bearing stability and sliding bearing calculation covering rigid and flexible supports, gyroscopic effects, cavitation, load capacity, etc

15 p2243 A72-31349

Nonsymmetric gyrostad steady motions analysis in axisymmetric gravity field based on Routh-Liapunov theorem, calculating stability conditions

15 p2320 A72-31728

Precession theory for transient response of gyroscope to rotation by Hook sphere using supplementary rotor

15 p2235 A72-31897

Variable rigidity effects of ball bearings on axial loading stability and failure of gyromotor supports

15 p2235 A72-31898

Gyro drift detection and isolation for redundant inertial measuring unit configuration of Carousel V system

15 p2270 A72-32190

Stability analysis of gyrostad satellites possible equilibria under gravitational torques, considering inertia, equilibrium and angular momentum parameters

15 p2321 A72-32586

Uniaxial gyro stabilizer dynamic control system based on degenerate equations neglecting small time constant terms

16 p2421 A72-33961

Rotating body linear dynamic control by complex transfer function approach with application to stability conditions for controlled gyro and homing missiles

17 p2583 A72-35528

Optimum aiding of inertial navigation systems using air data.

[AIAA PAPER 72-847] 20 p2950 A72-39082

Relativity gyroscope experiment at arbitrary orbit inclinations.

20 p2972 A72-39870

Russian book - Introduction to the theory of gyroscopes.

21 p3052 A72-40349

The stability of a uniaxial gyro stabilizer under conditions of dry friction in the stabilization and precession axes

21 p3059 A72-41813

Dynamic characteristics, stability and steady state accuracy for orbital gyroscope with digital control, noting bit density requirements of onboard computer

22 p3202 A72-42207

Reduction principle application to solution stability of system of differential equations in critical cases, noting instability of free gyroscope in gimbal suspension

23 p3287 A72-43416

Kalman filter design considerations for space-stable inertial navigation systems.

24 p3421 A72-44640

Relative equilibrium positions and their stability for a general gyrostad-satellite in a circular orbit.

24 p3449 A72-45142

Motion of a rotationally symmetrical gyro with an arbitrary number of vessels containing liquid

24 p3395 A72-45578

GYROSTABILIZERS

Differential equations of motion for stable member of three-axis gyro stabilized platform

03 p0387 A72-14190

Gyroscopic device for compensating displacement of sextants or binoculars optical axis due to spontaneous hand movements

07 p0988 A72-19894

Aiming stabilization by gyroscopic system, discussing mechanical mirror-gyroscope links, mirrors lightening and prism or lens anamorphosers

07 p0990 A72-20403

Intelsat 4 nutation dynamics and gyrostad stabilization technique for precision pointing in international telecommunication, discussing damper and fuel sloshing

12 p1780 A72-27360

Two gyro three axis stabilizer with gyrocompass effect for gravimeter or magnetometer sensor stabilization in towed gondola

13 p1957 A72-29271

Uniaxial gyro stabilizer dynamic control system based on degenerate equations neglecting small time constant terms

16 p2421 A72-33961

Attitude instruments, pitch and roll. I - Minimum performance standard for equipment.

18 p2692 A72-36534

Black Arrow satellite launch vehicle attitude control as part of inertial guidance system, describing four-gimbal gyroscopically stabilized platform and associated electronics

21 p3115 A72-40121

Vertical flight direction determination by gyro stabilizers with integral compensation, noting variable platform orientation and vibration damping correction

21 p3059 A72-41812

The stability of a uniaxial gyro stabilizer under conditions of dry friction in the stabilization and precession axes

21 p3059 A72-41813

GYROSTATS

U GYROSCOPES

GYROTROPISM

Solar magnetic field generation by gyrotropic turbulence, noting inadequacy of Steenbeck explanation for quantitative estimates of solar cycle parameters

03 p0436 A72-13825

Thermal equilibrium fluctuations and Rayleigh light scattering in isotropic gyrotropic continuous medium with internal rotational degrees of freedom

07 p1034 A72-18909

Wave propagation in thin film optical waveguides with gyrotropic and anisotropic substrates, deriving TE and TM mode conversion conditions

07 p0940 A72-19230

Geomagnetic variations propagation theory for If electromagnetic and Alfvén waves diffraction at stratified earth in thin gyrotropic ionosphere

08 p1130 A72-20711

Magnetic field generation in presence of turbulent velocity distribution, considering gyrotropy parameter equation and nonlinearity

11 p1686 A72-25716

Geomagnetic variations propagation theory for LF electromagnetic and Alfvén waves diffraction at stratified earth in thin gyrotropic ionosphere

19 p2765 A72-38339

H

H ALPHA LINE

Red interference filter design for high performance prominence telescope for H alpha line observation

01 p0064 A72-10203

H alpha spectra and combined filtergram observations of chromospheric fine structure, using Becker model

03 p0414 A72-12929

Topological features of force free magnetic field near bipolar sunspots, considering chromospheric fibrils and filaments in H alpha lines

03 p0415 A72-12932

Solar magnetic field structure determination in active regions from H alpha morphology obtained with chromospheric magnetograph, discussing emerging flux region role

03 p0428 A72-13304

Solar magnetic field observations with birefringent filter for 5324 Å Fe I line, showing H alpha fine structure

03 p0430 A72-13316

H alpha solar flare association with photospheric magnetic field patterns, discussing flare insertion and relation to magnetic structure evolution

03 p0410 A72-13320

Magnetic-channel solar flare volume characteristics based on proton flare H alpha pictures, using Petschek model

03 p0411 A72-13331

Mercury isophotometric measurements in white and H alpha light during transit across sun on 9 May 1970

04 p0573 A72-14904

Fine H alpha fibrils in middle chromosphere, discussing optical thickness and absorption features

05 p0718 A72-16506

H alpha fine structure, investigating chromospheric magnetic field distribution

05 p0718 A72-16507

High dispersion spectroscopic study of H alpha and K lines profile and velocity structure in quiescent prominences

05 p0719 A72-16516

Upper atmosphere atomic hydrogen H alpha emission, correlating intensity and hydroxyl vibration temperature

05 p0659 A72-17036

Potential gradient and air-earth current increases during period of increasing solar activity, discussing H alpha flare effects

09 p1378 A72-23264

Photoelectric Fabry-Perot measurements of M8 and M42 nebulae H alpha and forbidden N II emission lines profiles, determining temperatures and turbulent motions

09 p1390 A72-23528

Ring current and polar electrojet effects on proton auroras oval during magnetic disturbances from H alpha line observation

13 p1952 A72-29659

Solar video magnetographic observations of magnetic and H alpha plage correspondence on 21 March 1971

13 p2045 A72-29707

Brightenings and surgelike spikes associated with low amplitude soft solar X-ray background flux in H alpha above limb, assessing energy budget

13 p2032 A72-29718

Solar magnetic field fine structure from chromospheric morphology, using high resolution H alpha filtergram and magnetogram

13 p2046 A72-29731

Comparative spectroheliograms of He 10830 Å and H alpha lines in chromosphere

13 p2047 A72-29733

Solar H alpha profile formation from non-LTE radiative transfer solutions through model atmosphere by integro-differential equation technique

13 p2049 A72-29931

Spicular field morphology near solar limb from photographs taken with H alpha filter

15 p2305 A72-31512

Expanding loops of H alpha filaments in peculiar galaxy M 82 investigated by microwave radio map, suggesting thermal and nonthermal radiation sources

15 p2317 A72-32757

Solar white light flares relationship to EUV emission based on sudden frequency deviations observations, noting coincidence with H alpha flare areas

15 p2302 A72-32789

Photoelectric observation of H alpha, sodium deuteride and He solar umbral line profiles, using pressure scanning spectrometer

17 p2608 A72-35082

Helium and H alpha emission relationship observation in 11 February 1970 solar flare from photometric reduction of filtergrams

17 p2599 A72-35117

Arch prominence outside west limb on 24 April 1971, noting H alpha monochromatic image, internal motion of matter and radio emission

17 p2614 A72-35503

Solar mottles characteristics as seen on large scale H alpha filtergrams

17 p2616 A72-35700

Periodic intensity oscillations in center of H alpha supergranulation network, in rosette centers and in plage granules

17 p2616 A72-35701

Photographic magnetograms comparison with H alpha filtergrams, investigating chromospheric features relationship to photospheric magnetic fields

17 p2616 A72-35702

H alpha loops incompatibility with stable filaments /prominences/ noting magnetic loops existence between regions of opposite polarity

17 p2617 A72-35704

Polarization and velocity field in the galaxy M 82.

18 p2727 A72-36729

Solar radio burst time profiles comparison with H alpha line emission curves for corresponding flares, noting neutral hydrogen emission relation to electrons acceleration

19 p2850 A72-37802

Tabulation of physical conditions in proton and non-proton solar flares from observations and H alpha line width measurements

19 p2851 A72-37815

Solar chromospheric flare details motion differences from spectrum analysis and H alpha line frame photography, noting radial velocities difference

19 p2851 A72-37816

Study of a faint nebula identified as the HB-21 radio source

19 p2862 A72-38054

Atmospheric pressure, density and scale height calculated from H Lyman-alpha absorption allowing for the variation in cross-section with wavelength.

19 p2793 A72-38859

Solar magnetic fields derived from hydrogen alpha filtergrams.

20 p2969 A72-39338

Photometric study of the NGC 3587 planetary nebula /the Owl/ observed in H sub alpha light - Structure of hydrogen in the nebula

20 p2973 A72-39890

He-D3 spectroheliogram absorption features correlation with magnetic field regions and H alpha structures

21 p3108 A72-41279

Measurement of the electron temperature of small 3-cm radio bursts /Research note/.

21 p3100 A72-41291

H 157 alpha recombination line from H I region before NGC 2024 radio source, considering average electron concentration and line origin

21 p3102 A72-41776

Simultaneous measurements of H alpha and H beta Balmer lines and He D3 line in faint prominences, showing emission intensity ratios dependence on layer total optical thickness

22 p3221 A72-42034

Some aspects of flare properties versus magnetic boundary morphology.

22 p3217 A72-42038

A longitude survey of radio recombination lines from the diffuse interstellar medium.

22 p3227 A72-42552

H BETA LINE

H beta satellites observation in presence of oscillating electric field associated with plasma turbulence [AD-741085]

04 p0555 A72-14576

Fiber optics system for H beta line shape measurement in transient high temperature plasma, using narrow slits at spectrograph exit plane [AIAA PAPER 72-106]

05 p0663 A72-16816

OB star distribution in Puppis from UVB and H beta photometry, noting correlation with hydrogen concentration

10 p1542 A72-24615

Planetary nebulae RF observations comparison with optically determined H-beta intensity for extinction coefficients

15 p2307 A72-31797

Weak H beta emission at 26 deg galactic latitude, noting derived electron density agreement with pulsar data

16 p2455 A72-33460

OI 6300 and 5577 Å, NI 5200 Å and H beta 4861 Å emission line measurement during 8-9 March 1970 auroral arc event

22 p3169 A72-42018

Simultaneous measurements of H alpha and H beta Balmer lines and He D3 line in faint prominences, showing emission intensity ratios dependence on layer total optical thickness

22 p3221 A72-42034

H GAMMA LINE

Early star absolute magnitude from equivalent H gamma and delta line widths and Balmer hydrogen series line

19 p2859 A72-37908

H LINES

NT H ALPHA LINE

NT H BETA LINE

NT H GAMMA LINE

NT K LINES

NT LYMAN SPECTRA
NT PASCHEN SERIES
NT RYDBERG SERIES
NT TELLURIC LINES

Extraterrestrial life and civilization possibility in other planetary systems in universe, suggesting communication by hydrogen line frequency low harmonics

02 p0276 A72-11642

Single electron approximation of Stark broadening of hydrogen spectral lines without constraints of collision and quasi-static theories

03 p0391 A72-13079

Rf diagnostic technique for carbon and hydrogen /H I/ cloud recombination lines in cool interstellar medium

04 p0570 A72-14525

Stark contours of hydrogen spectral lines in turbulent plasma with high noise level due to hf Langmuir oscillations

04 p0557 A72-14986

Photometric standard star 29 Piscium abundance analysis with flux constant hydrogen line blanketed model atmospheres

04 p0578 A72-15317

Book on auroras, discussing primary particle-atmosphere interactions, H line emission, geometry, intensity, height and atmospheric temperature determination from auroral spectra

04 p0519 A72-15356

Astrophysics of interstellar medium, discussing direct and indirect observations including 21 cm H lines and starlight extinction and polarization

04 p0581 A72-15622

Interstellar Ca II, H and K optical absorption lines of bright O and early B stars in Orion region

05 p0723 A72-17200

Red shift determination for two galaxies near PSK 2251 plus 11 quasar from Ca II H and K absorption line measurements

06 p0881 A72-17898

Maffei 2 galaxy radio maps and H line studies, discussing distances, intrinsic luminosity, flux density and apparent size

06 p0886 A72-18097

Hydrogen line broadening in plasma theory with limitations of Stark component intensity distribution by quasi-static and impact approximations

09 p1358 A72-22493

H Balmer lines H alpha/H beta ratios as electron temperature indicators in nonequilibrium plasmas

09 p1359 A72-22666

Hydrogen atom emission spectrum calculation in uniform rotating electric field, applying to charged particles collisions and Stark broadening of plasma H lines

10 p1514 A72-24039

Radio recombination lines broadening in hydrogen by electron collisions, using Baranger impact theory

10 p1435 A72-24142

HD 4180 shell H lines width variations comparison with Be stars, noting thirty year period emission decrease followed by outer shell absorption

12 p1867 A72-27213

Single electron approximation of Stark broadening of hydrogen spectral lines without constraints of collision and quasi-static theories

13 p2007 A72-29429

Adiabatic characteristics of impact to quasi-static transition during electron induced Stark hydrogen line broadening in plasmas

13 p2016 A72-29516

Early B stars with normal helium abundances and small rotational velocities, deducing gravity from H lines and ESW stark broadening

15 p2316 A72-32751

Hydrogen line broadening in plasma theory with limitations of Stark component intensity distribution by quasi-static and impact approximations

17 p2588 A72-34657

Spectral line contours in the solar chromosphere, hydrogen line. IV - Contours in the chromosphere on the disk

19 p2859 A72-37905

H and K emission intensity and line width dependence on stars age and luminosity, discussing dwarf stars and giants

19 p2866 A72-38503

Hot star with broad H lines with weak variable central emission, noting Ca II and He I

20 p2966 A72-38920

Gross properties of five Scd galaxies as determined from 21-centimeter observations.

21 p3105 A72-41027

Intensity ratios of He I and H lines in a prominence and the chromosphere.

21 p3109 A72-41329

Nonvelocity origin of excess red shift in companion galaxies from observation of H and K absorption lines of Ca II

22 p3220 A72-41962

High resolution spectroscopy of the disk chromosphere. II - Time sequence observations of Ca II H and K emissions.

22 p3221 A72-42032

Investigation of several nebulae in Cassiopeia with a Fabry-Perot interferometer. 23 p3333 A72-43233

Determination of magnetic fields in plasmas from hydrogen spectral line profiles 23 p3318 A72-43313

Radial velocity periodic variability determination from shell star 88 Herculis hydrogen lines, obtaining hypothetical spectroscopic binary elements 23 p3340 A72-44237

Upper limits on the atomic hydrogen abundance in 12 globular clusters. 23 p3340 A72-44246

An H I velocity-longitude diagram for the Southern Milky Way. 24 p3438 A72-44845

H WAVES

Electromagnetic wave transmission and reflection by semiinfinite moving anisotropic plasma with parallel static magnetic field, considering incident H wave 05 p0696 A72-16623

H-53 HELICOPTER

HH-53 rescue helicopter automatic approach and hover coupler for automatic transition from forward flight at constant deceleration and rate of descent 05 p0686 A72-16653

The application of Ti-6Al-4V titanium to helicopter fatigue loaded components. 24 p3366 A72-44732

HABITABILITY

Future spacecraft habitable compartment layout from psychophysiological viewpoint, considering human visual and motor field parameters and crew members social needs 13 p1910 A72-29321

Habitability factors in a rotating space station. 18 p2652 A72-36436

HABITUATION [LEARNING]

Monotonous auditory stimulation frequency effects on human orienting reaction habituation and sleep onset 02 p0169 A72-12494

Heat acclimatization, work habituation and exercise effects on body thermoregulation, measuring tympanic temperature, sweat rate and oxygen intake 04 p0472 A72-14896

Visual cortex repetitive stimulation effect on primary response habituation in young normal rabbits and adults with septum pellucidum lesion 14 p2076 A72-30596

HADRONS

NT BARYONS

NT MESONS

Hadrons in extensive air showers, predicting arrival time spectra from fireball and isobar-p ionization models for high energy interactions 03 p0409 A72-13147

Cosmological density fluctuations in hadron stage, examining relativistic free particle and high temperature hadron gas models 03 p0426 A72-13273

Cosmic ray hadrons inelastic collision cross sections and partial K-neutral pion inelasticity factor in ionization calorimeter 06 p0868 A72-17262

Energy transfer to electron-photon component during hadron interaction in lead, using ionization calorimeter 06 p0869 A72-17268

Inelastic ionization cross section of cosmic ray hadrons with carbon nuclei at energies of 100 to 300 GeV 06 p0869 A72-17271

Cosmic radiation high energy hadron component relation to extensive electron-photon showers, comparing sampling events based on multicore structure and total energy 06 p0870 A72-17282

K-neutral pion energy fractions and inelasticity coefficients at primary energies of 100-1500 GeV during hadron-target interaction 06 p0872 A72-17295

Hadron era evolution, discussing equation of state, ultimate temperature, galactic formation and adiabatic exponent application to Friedman universes 06 p0886 A72-18096

High energy hadrons time structure in extensive air showers, considering production of nucleon-antinucleon pairs in particle interactions 07 p1067 A72-20687

High energy cosmic ray hadrons energy measurement using glass scintillator ionization spectrometer 09 p1309 A72-22523

Equations of state for ultrahigh densities, obtaining relativistic statistical thermodynamics description of hadronic interactions 10 p1533 A72-23891

Inelasticity fluctuations effect on cosmic ray showers development, proposing criteria for lateral electron distribution and relative abundance of hadrons and muons 10 p1529 A72-24213

Study of high energy /25-10,000 GeV/ interactions with a multiplate cloud chamber using Monte Carlo simulations for energy calibration. 17 p2585 A72-34922

Test of hadronic scaling at cosmic-ray energies. 21 p3100 A72-40831

Investigation of hadron interactions with atomic nuclei at energies greater than 100 GeV 23 p3329 A72-44404

Ionization calorimeter for neutral pion production investigation in high energy hadrons interaction, noting energy transfer identity for nucleon and pion interactions 23 p3330 A72-44409

Effective cross section of the inelastic interaction of hadrons with lead-atom nuclei at energies from 3 to 30 TeV 23 p3330 A72-44410

Study of high-energy hadron interactions by the nuclear photoemulsion method 23 p3330 A72-44416

HAFNIUM

Electron microscopic investigation of niobium-oxygen alloys with Zr and Hf additions, measuring oxygen solubility 08 p1187 A72-21787

Exploratory investigation of Y, La, and Hf coatings for nitridation protection of chromium alloys. 20 p2944 A72-39290

HAFNIUM ALLOYS

Ductility enhancement in directionally solidified Ni base Mar-M200 alloy by Hf additions increasing gamma-gamma prime eutectic 01 p0089 A72-11104

Hf-B system alloys phase diagram and impurities effect, discussing synthesis and heat treatment regime 07 p1010 A72-18857

Hf addition effects on grain boundary structure of cast Ni-base superalloys 07 p1015 A72-19931

Hf-Co-Al system phase equilibria determination by partial microstructural and X ray analysis 07 p1017 A72-19991

Precipitates dispersion and fluxoid pinning /critical current density/ in superconducting Nb-Hf alloy during aging, using transmission electron microscopy 07 p1020 A72-20409

Mo-Hf alloys high temperature mechanical properties improvement by internal diffusion nitriding, noting precipitates effects 11 p1644 A72-26843

Transmission and scanning electron microscope observations of Nb-Hf alloys fracture morphology, noting precipitate free zone 11 p1667 A72-26934

Phase composition of Nb-O-Hf and Nb-O-Zr ternary alloys, noting O solubility decrease 14 p2122 A72-30980

Phase diagrams of Hf-Ce and Hf-Er alloys, plotting hardness and electroconductivity curves 15 p2289 A72-31188

Dispersion hardening of Nb-Zr-O and Nb-Hf-O alloys, discussing composition and heat treatment effects on aging, recrystallization temperature and grain growth 15 p2255 A72-31567

Boron concentrations in Mo-Hf alloy samples from neutron activation analysis, measuring Li beta radiation with plastic scintillation detector 16 p2391 A72-33238

HAFNIUM CARBIDES

Structure of the energy bands of titanium, hafnium, and tantalum monocarbides 20 p2939 A72-39311

Influence of the sintering medium on the quality of metalceramic hard alloys containing zirconium and hafnium carbides 23 p3303 A72-44017

HAFNIUM COMPOUNDS

NT HAFNIUM CARBIDES

NT HAFNIUM OXIDES

Sputtering sources fabrication by plasma spraying for nitride films deposition with Ta-Hf mixtures 04 p0527 A72-15494

Tungsten dispersion strengthening by hafnium nitride covapor deposition, discussing effects of matrix microstructure and dispersoids number, size and spacing variations 07 p1019 A72-20366

Hf binary systems phase diagrams, noting components effect on melting point, polymorphous transformations and mutual solubility 14 p2122 A72-30979

HfB2 and ZrN alloys 19 p2845 A72-38409

Niobium and molybdenum alloys containing borides and carbides of the IV-a group metals 22 p3191 A72-42814

HAFNIUM OXIDES

Yttria stabilized hafnia based graphite and tungsten composites, investigating factors affecting thermal shock resistance 09 p1327 A72-22385

Contribution to the study of some HfO2-MO systems 23 p3302 A72-43999

Influence of the nature of the particle distribution of the hardening phase in powders on the thermal stability of dispersion-strengthened nickel 23 p3302 A72-44011

HAIL

Hailstone impact simulator for prediction of hail damage to aircraft structures, presenting data on damage to flat metal sheets and spherical caps [AIAA PAPER 72-163] 05 p0645 A72-16957

Al alloy plates and D-nosed specimens indentation and penetration under hail impact test 07 p1086 A72-18764

Supercell, multicell and sheared severe hailstorms structure and motion observation by radar echoes, noting propagation characteristics 09 p1345 A72-22447

Visual and radar echo location of organized updraft on thunderstorms and hailstorms 09 p1346 A72-22452

Probability estimates of aircraft encounters with hail, discussing variations with locality, hailstone size and height and supersonic transport experience 09 p1346 A72-23423

Hail damage to aircraft, predicting metal surfaces dent depth and deformation shape with computer program [AIAA PAPER 72-335] 11 p1574 A72-25370

Hailstone size estimation to design exposed equipment for irreversible impact damage prevention 13 p1993 A72-28854

Hailstone impact simulator for aircraft damage prediction in testing prospective structural designs 13 p1938 A72-28855

Hail size distribution and concentration in thunderstorm updraft regions from aircraft and S band radar observations 16 p2419 A72-33946

Time dependent one dimensional numerical model of hail-bearing cumulus cloud, using microphysical process parameterization and exponential raindrop and hailstone size distributions 22 p3201 A72-42513

Hail formation model based on injection of finite embryo size classes into horizontally homogeneous steady nondivergent updraft, considering growth and accumulation zones 22 p3201 A72-42514

HAILSTONES

U HAIL

HAIR

Hair hygrometer for FM radiosonde in-flight air humidity measurements, discussing design, operation and accuracy test in extreme weather conditions 10 p1483 A72-25005

HALF CONES

Ablative nose shape change effects on re-entry vehicle aerodynamic performance. [AIAA PAPER 72-974] 22 p3230 A72-42337

HALF PLANES

Contact stress between half plane and elastic cover plate, reducing problem to Prandtl type integrodifferential equation with Hilbert kernel 02 p0294 A72-12433

Fresnel diffraction on opaque half plane screens with statistically rough surfaces, using Kirchhoff approximation 02 p0183 A72-12755

Acoustical field from streamlined body of revolution moving in homogeneous gaseous medium past semiinfinite rigid screen, using Wiener-Hopf method for diffraction radiation 03 p0340 A72-12916

Stress distribution at contour of connected region in plane elasticity solved for half plane and circle 03 p0449 A72-13909

Trigonometric series solution of Tricomi problem for Chaplygin-type equation in half plane 04 p0461 A72-14628

Elastic stiffener bonded to elastic half plane with different mechanical properties, reducing governing integral equation to infinite system of linear algebraic equations [ASME PAPER 71-APM-TT] 04 p0589 A72-15182

Plane harmonic electromagnetic wave diffraction by conducting parallel half planes in uniaxially anisotropic media 04 p0492 A72-15447

Maximum stress concentration in two dimensional elasticity theory for half plane and circle as function of contour distribution, using Cauchy-Buniakovskii inequality in Banach space 07 p1095 A72-20325

Elastic unbounded homogeneous layer separation from half plane under normal load pressures, determining contact area with base for elastic moduli relationships 08 p1243 A72-21233

Plastic slip in notched half plane undergoing antiplane deformation, using screw dislocation continuous distribution theory 09 p1403 A72-22747

Aerodynamic noise generation in turbulent fluid at low Mach number due to source near half plane by applying Kutta-Joukowski condition

10 p1415 A72-23724

Two dimensional low Mach number sound field from line vortex passage around rigid half plane edge, calculating space-time variation by perturbation methods

10 p1468 A72-24370

Fresnel diffraction on opaque absorbing screen half planes with small rough surfaces, deriving field attenuation factor and structure/correlation functions

10 p1435 A72-24502

Emission of density modulated electron flux passing over diffraction structures formed by half planes and combs with oblique teeth, discussing optimum emitted power conditions

12 p1793 A72-27858

Contact problems for elastic semiplane reinforced with symmetric and asymmetric loaded elastic stiffeners

15 p2329 A72-32281

Wave propagation in half plane consisting of two joined elastic quarter planes under in-plane disturbances normal to free surface, obtaining stresses at interface

18 p2738 A72-37069

Strain distribution in and around strain gauges.

19 p2870 A72-37225

Fresnel diffraction on opaque half plane screens with statistically rough surfaces, using Kirchhoff approximation

20 p2902 A72-39061

Singular stress concentration at sharp edge of wedge in contact with half plane in elastostatics

21 p3119 A72-41104

Stresses in bonded materials with a crack perpendicular to the interface.

21 p3124 A72-41396

Stress-strain state of an isotropic half-plane with an elliptic hole, deformed by concentrated loads

22 p3233 A72-42057

Orthotropic photoelasticity methods application to concentrated force on half plane edge and to stress distribution on elliptical hole boundary in tensile strip

24 p3455 A72-44790

HALF SPACES

Subsurface electromagnetic fields of current carrying cable line source on flat earth conducting half space, considering mine rescue operations

01 p0060 A72-10840

Hertzian dipole radiation with impulsive currents in nondispersive dielectric half space

01 p0030 A72-10841

Multipole methods for electromagnetic scattering from conducting cylinder over dielectric half space, noting application to radar cross sections

01 p0030 A72-10842

Conducting half space electric dipole model of radio propagation through earth at 1-10 MHz

01 p0033 A72-11254

Three dimensional elasticity mixed boundary value problems associated with Laplace equation in half space, including slotted regions and stamp contact solutions

02 p0289 A72-11610

Contact problem of rigid sphere intrusion into viscoelastic half space, obtaining solution by Green function construction and integral-operator equation formulation

02 p0289 A72-11615

One dimensional elastoplastic wave propagation symposia review emphasizing elastoviscoplastic media, jet penetration into half space and polymer tests by transverse impact

02 p0290 A72-11628

Beams and plates resting on elastic base with loads moving along line or strip, calculating wave processes based on half space dynamic model

02 p0290 A72-11629

Micropolar elastic theory axial symmetric problems, deriving differential equations for elastic potential and half space

02 p0260 A72-12239

Principal boundary value problems solution for Helmholtz equation in half space with spherical cavities, reducing problems to infinite systems of algebraic equations

03 p0387 A72-12915

Fracture mechanics of interfacial cracks between two bonded dissimilar anisotropic elastic half spaces, presenting two dimensional analysis of stress fields

03 p0446 A72-13707

Axisymmetric contact problem for circular flat stamp on laminated half space, using matrix calculus and Hankel transforms

03 p0448 A72-13903

Tangential stress pulse effects on transversally isotropic half space surface wave motion under torsion

03 p0452 A72-14128

Dynamic boundary value problem for elastic half space with rotational concentrated moment of variable magnitude, using Fourier and Laplace transforms

04 p0591 A72-15198

Half wavelength antenna radiation admittance into warm lossy two layer plasma half space, using effects of slot width and electron collision frequency

06 p0781 A72-17348

Conducting ground half space effects on dipole antenna input impedance computed by current distribution Fourier transform

06 p0781 A72-17353

Input resistance derivation for finite horizontal loops with uniform current distribution located above lossy half-space ground

06 p0777 A72-18737

Limiting equilibrium of elastic half space with randomly oriented crack

07 p1092 A72-19780

Moving isotropic plasma half space effect on magnetic or electric line source radiation patterns

07 p1044 A72-20192

Critical compressive stresses leading to instability of layer fastened to elastic half space

08 p1244 A72-21368

Contact problem of semiinfinite plate deflection on linearly deformed half space with depth dependent elasticity modulus

08 p1247 A72-21808

Normal axial impact of thin liquid filled elastic cylindrical shell with rigid bottom on compressible fluid half space surface

09 p1350 A72-22207

German monograph on finite element method for elastic impact at half space, analyzing elasticity and inertia effects on energy absorption and contact time

09 p1397 A72-22338

Penny shaped interface crack between elastic layer and half space, calculating stress intensity factors and strain energy release rate for aluminum-epoxy combination

09 p1398 A72-22530

Tensionless contact area between beam and elastic half space determined by approximate technique

09 p1398 A72-22623

Thermoelastic disturbance wave front propagation in elastic half space after thermal shock at surface

09 p1399 A72-22705

Plane and antiplane elasticity boundary value problems reduced to integral equations by dislocation layers, noting closed form solutions for half and whole space

10 p1557 A72-24561

Variational minimum principle for two elastic bodies frictionless contact, discussing Hertzian and non-Hertzian normal half space problems

11 p1690 A72-26667

Bending of unbounded plate coupled to elastic isotropic half space with vertical and horizontal springs, calculating contact stresses by double Fourier transforms

12 p1878 A72-27082

Elastic fields of dislocation loop in two phase material consisting of isotropic elastic half spaces

12 p1884 A72-27567

Variational solution to axisymmetric problem of rigid stamp quasi-static impression into elastoplastic half space

13 p2053 A72-28387

Unsteady state of ideal quiescent heat conducting gas in half space, deriving asymptotic solutions to mass, temperature, pressure and density dynamic behavior expressions

13 p2064 A72-28678

Plane longitudinal displacement wave reflection from fixed surface in micropolar elastic half space, presenting reflection laws and amplitude ratios for specific cases

13 p2056 A72-29001

Boussinesq problem for homogeneous viscoelastic half space governed by deformation law of typical body under concentrated or sinusoidal loads

13 p2062 A72-30092

Kinetic model for electromagnetic field fluctuations in bounded isotropic plasma half space with specular reflection of electrons at boundary

14 p2135 A72-30170

Wire antenna half-space problem analysis by Sommerfeld integral approach and plane wave reflection coefficient approximation

14 p2085 A72-30338

Elastic body stress concentration problem formulation as singular integral operator eigenvalue problem for half space

15 p2323 A72-31478

Thermal stress and temperature distribution in rigidly bounded elastic half-space, taking into account coupling effects

15 p2325 A72-31637

Thin wire parallel to interface between two homogeneous half spaces, deriving transmission current wave propagation constant from boundary value problem solution

15 p2200 A72-32108

Surface stress solution for elastic half space weakened by spherical cut under internal pressure

15 p2333 A72-32681

Displacements, rotations and stresses equilibrium equations solution for plane micropolar elastic half space, using exponential Fourier transforms

16 p2466 A72-33105

Electromagnetic transient coupling between ungrounded loops for two layer conducting half space approximation of earth

16 p2388 A72-34007

Ultrarelativistic electrons beam steady injection into plasma filled half space, using weak turbulence theory for assumed beam excited oscillations interaction

16 p2440 A72-34156

The perturbation of alternating geomagnetic fields by three-dimensional conductivity inhomogeneities.

17 p2545 A72-34350

Determining electrical ground constants from the mutual impedance of small coplanar loops.

17 p2514 A72-34371

Mathematical model and simulation for contact problems involving elastic half spaces and viscoelastic and friction effects

18 p2734 A72-36371

Scattering of elastic waves by moving objects.

18 p2709 A72-36403

Transmission and reflection of an electromagnetic wave incident normally on a plasma half-space.

19 p2840 A72-37726

Fourier-Bessel superposition and Laplace transformation methods for surface displacement produced by time dependent dipole in elastic half space, noting buried dipole case

19 p2876 A72-37887

Mixed boundary value problem in the theory of elasticity for a half-space with circular lines of separation between boundary conditions

19 p2876 A72-38152

Solution of a problem with a skew derivative in a half-space for certain elliptical equations

20 p2945 A72-39393

Rayleigh wave effects in an elastic half-space.

20 p2980 A72-39615

Quasi-static impact of hard hemisphere against brittle half space, investigating fracture mechanics

20 p2981 A72-39952

Stress concentration around circular crack on interface between two bonded dissimilar isotropic elastic half spaces

20 p2982 A72-40020

Partial derivatives of dispersion curves for higher modes of Love waves in a single-layered medium.

21 p3084 A72-40496

Integral equation for pressure distribution by rigid punch contact with elastic half space, solving by Mathieu function expansion in Fourier series

21 p3126 A72-41541

Electromagnetic induction in a half-space with a cylindrical inhomogeneity.

23 p3284 A72-43423

Reflection of pulses at the interface between an elastic rod and an elastic half-space.

23 p3314 A72-44119

The effect of shear on a penny-shaped crack at the interface of an elastic half-space and a rigid foundation.

24 p3459 A72-45250

Plane thermoelastic one-dimensional waves in an inhomogeneous medium with allowance for connectedness

24 p3459 A72-45266

HALIDES

NT ALKALI HALIDES
NT ALUMINUM FLUORIDES
NT AMMONIUM CHLORIDES
NT BARIUM FLUORIDES
NT BORON FLUORIDES
NT CALCIUM FLUORIDES
NT CESIUM IODIDES
NT CHLORIDES
NT CHLORINE FLUORIDES
NT DICHLORIDES
NT FLUORIDES
NT HYDROCHLORIC ACID
NT HYDROFLUORIC ACID
NT HYDROGEN CHLORIDES
NT IRON CHLORIDES
NT LANTHANUM FLUORIDES
NT LITHIUM CHLORIDES
NT LITHIUM FLUORIDES
NT MAGNESIUM FLUORIDES
NT METAL HALIDES
NT NITROGEN FLUORIDES
NT OXYFLUORIDES
NT POTASSIUM CHLORIDES
NT SILVER BROMIDES
NT SILVER HALIDES
NT SODIUM CHLORIDES
NT SODIUM FLUORIDES
NT SODIUM IODIDES
NT SULFUR CHLORIDES
NT SULFUR FLUORIDES
NT TUNGSTEN FLUORIDES
NT URANIUM FLUORIDES

Laser action in pulsed transverse discharge initiated chemical reactions forming hydrogen and deuterium halides, noting production of previously unobserved transitions
07 p0999 A72-18879

Hydrogen halide rotational relaxation to thermal distribution without intermediate quantum number peak, discussing IR chemiluminescence data correction method
07 p0936 A72-19673

Nonferrous metals melting, discussing solid and gaseous impurities removal, halide function and grain and Al-Si eutectic refinement method
07 p0999 A72-20570

Repulsive potential determination for alkali cations, halide anions and anisotropic molecules from scattering experiments and bond energy data
21 p3087 A72-40555

Bond energy electrostatic potential calculation and equilibrium and rate constants prediction for alkali and halide ions association with neutrals
21 p3087 A72-40556

Study of the variation of the intensity of vibration-rotation spectra of hydrogen halide molecules under the action of compressed foreign gases
22 p3209 A72-43047

HALL ACCELERATORS

Russian book on electrodynamic plasma acceleration covering charged particles motion in electromagnetic field and pulsed, MHD, steady and Hall accelerators
12 p1853 A72-28341

HALL COEFFICIENT

U HALL EFFECT

HALL CURRENTS

U ELECTRIC CURRENT

U HALL EFFECT

HALL EFFECT

Dember-Hall voltage ratio for low magnetoconcentration in intrinsic semiconductor
01 p0113 A72-10044

Matrix calculation of forced atmospheric oscillations for Hall, Coriolis and Pedersen regions
01 p0053 A72-10090

Hall effect and magnetic field characteristics in lower ionosphere by vertical magnetospheric currents, using gyrotopic model
01 p0059 A72-10590

MHD channels magnetoacoustic and ionization instabilities effect on mean current density and electric field strength, determining effective electroconductivity and Hall parameter
01 p0110 A72-11208

Quantum oscillations of minority Fermi surface carriers as function of magnetic field in Hall effect and thermoelectric power in pressure-annealed pyrolytic graphite
02 p0268 A72-11673

Cascade connected electrode scheme for MHD applications, noting potential and current distributions and Hall voltage buildup
02 p0265 A72-12276

Hall effect and conductivity dependence on applied electric field in multivalley semiconductor for power dependent intervalley scattering time
02 p0269 A72-12887

Hall effect mobility dependence on dispersion law in degenerate electron gas on semiconductor surface
02 p0270 A72-12890

Electroacoustic magnetic and Hall effects in semiconductors in strong electric field involving phonon production by supersonic electron drift
03 p0401 A72-13088

Plasma flow under inhomogeneous axially symmetric magnetic field, investigating axial component of poloidal Hall induction current
03 p0395 A72-13570

Immersion-type electroconductivity probe for anisotropic plasmas, calculating Hall coefficient
03 p0397 A72-13922

Computer controlled automatic system for measuring electroconductivity and Hall effect in semiconductors, noting data acquisition instrumentation
04 p0496 A72-15534

Lower ionospheric currents fields, determining Hall conductivity and geomagnetic lines of force slope effects
05 p0657 A72-16266

MHD shock waves stability, showing Hall term effect on number of shock boundary conditions
05 p0699 A72-17025

Screened impurity scattering determination in heavily doped covalent semiconductors from Hall mobility and thermoelectric power measurements
05 p0702 A72-17073

Hall fields effect on interaction of MHD waves in inhomogeneous plasma, considering MHD wave dispersion
05 p0701 A72-17237

Poloidal Hall current calculation in hydrodynamic approximation for stationary weakly interacting and conducting cylindrical plasma flow with uniform transverse flow parameter distribution
05 p0701 A72-17240

Stationary plasma flow interaction with axisymmetric spatially periodic magnetic field in presence of Hall effect, determining electric currents structure
05 p0701 A72-17241

Electrical resistance, Hall coefficient and magnetic susceptibility of transition metal nitrides at low and room temperatures
06 p0827 A72-17386

Book on electronic processes in noncrystalline materials covering liquid metals, semimetals and semiconductors, Hall effect, phonons and polarons, thermoelectricity, photoconductivity, etc
06 p0866 A72-18516

Anomalous Hall effect of polarized electrons spin-orbit interactions in semiconductors, involving emf appearance in electric field and polarized light
07 p1048 A72-19642

Electric field in flow of medium with tensor conductivity due to Hall effect, studying eddy currents structure in magnetic field variation region
07 p1044 A72-20316

Hall effect influence on magnetospheric boundary magnetic field generation by solar wind perturbation, using beam-magnetic field interface model
07 p0980 A72-20407

Anisotropic conducting fluid flow in presence of traveling magnetic field, determining Hall effect via solution to electromagnetic field distribution boundary value problem
08 p1214 A72-21648

Resonance occurrence in generation-recombination noise spectrum of Co 60 gamma irradiated Ge single crystals, investigating Hall effect
09 p1372 A72-23112

Temperature dependence of emf coefficient Hall constant and conductivity in solid and liquid phases of InSe semiconductor during melting
10 p1526 A72-24267

Ohmic law generalization in electrodynamics for electrically conductive fluid medium in turbulent motion, taking into account Hall effect
10 p1524 A72-24931

Current sheet velocity limitation in magnetically driven shock tube with plasma electrodes, examining wall ablation and friction and Hall current effects [AIAA PAPER 72-409]
11 p1695 A72-26160

Larmor frequency influence on Rayleigh-Taylor instability of viscous Hall plasma with magnetic field
11 p1698 A72-26604

Plasma flow under inhomogeneous axially symmetric magnetic field, investigating axial component of poloidal Hall induction current
11 p1699 A72-26757

Electron irradiation of Li doped Ge at low temperatures, measuring Hall effect and minority carriers diffusion length
12 p1857 A72-28055

Te single crystal electrical resistivity and Hall coefficient effects of electron irradiation, suggesting point defects and dislocations interaction
12 p1859 A72-28073

Ni-Co alloys Nerst-Ettingshausen and Hall effects anomalous constants relationship determination from emf and electrical conductivity measurements
13 p1977 A72-28910

Hall currents effect on unsteady MHD flow of electrically conducting fluid past flat plate imbedded in uniform external transverse magnetic field
13 p2012 A72-29225

Electroacoustomagnetic and Hall effects in semiconductors within strong electric field involving phonon production by supersonic electron drift
13 p2022 A72-29437

Steady barotropic inviscid flows of rarefied gas plasmas as free jet and within cylindrical channel in axisymmetric external magnetic field with Hall effect
13 p2018 A72-29823

Electrical characterization of GaAs by Hall and magnetoresistance measurements, analyzing temperature dependence of carrier concentration
13 p2024 A72-30034

Electrical conductivity, reluctance and Hall effect of n-type semiconductors determined at extremely low temperatures
15 p2291 A72-31389

Tensor analysis for planar magnetoresistivity and Hall effect in Ni single crystal thin films, noting anisotropy effects in ferromagnetic crystals
15 p2294 A72-32386

Two band model explanation of Hall effect in dirty type-II transition metal superconductors near upper critical field, noting interband impurity scattering role
15 p2295 A72-32542

Skin friction effects due to Hall currents in conducting unsteady slip flow over porous flat plate under transverse magnetic field
16 p2435 A72-33108

Instrument for Hall and Gauss effects measurement in semiconductors and metals, noting instrument error analysis
17 p2529 A72-34758

A physical mechanism for the production of solar flares
17 p2608 A72-35088

Transient behaviour of laser generated carrier mobility in n-Ge
18 p2697 A72-36351

Combined Rayleigh and Kelvin instability of a Hall plasma with a vertical magnetic field
18 p2715 A72-36502

Hall phenomena in a plasma flow situated in a traveling magnetic field
18 p2716 A72-36816

Electric fields in MHD channels in the case of anisotropic and nonuniform conductivity
18 p2716 A72-36817

Measurement of Hall mobility of current carriers in inhomogeneous semiconductor samples
18 p2720 A72-36964

Boundary conditions in the presence of Hall current or finite ion Larmor radius effects
19 p2839 A72-37338

The Rayleigh-Taylor problem with a vertical magnetic field, including the effects of Hall current and resistivity
19 p2839 A72-37339

Hall and resistance measurements on single crystal HgTe-InTe alloy systems for high pressure phases in terms of conduction state, band structure and impurity effects
19 p2844 A72-37464

Electroconductivity, thermal emf and Hall coefficient for single crystals of Bi-Sb alloys with Cd, In and Sn additions
19 p2847 A72-38683

Hall field occurrence conditions in small semiconductor plates, discussing Hall generator design and layer temperature as function of time
19 p2776 A72-38725

Electron-electron collision induced anomalous Hall effect in ferromagnetic d metals at low temperatures
20 p2959 A72-39309

LF circularly polarized electromagnetic waves /helicons/ resonance crystal plates, deriving magneto-resistivity and Hall coefficient
21 p3066 A72-40624

Galvanomagnetic properties of well-oriented graphite in relation to the structural imperfections
21 p3073 A72-40691

Electrodynamic mathematical model for electroconductivity of nonuniform plasma with Hall effect, calculating current distribution from Riemann problem solution
22 p3210 A72-41888

Longitudinal magnetospheric currents contribution to auroral electrojet from satellite observation data, noting magnetosphere electric field excitation of meridional Pedersen and Hall currents
22 p3169 A72-42225

Spontaneous magnetization of Ni foils in high pressure H₂ gas, noting Hall voltage measurement in ferromagnetic foils and thin plates
23 p3324 A72-44140

Anomalous Hall effect of polarized electrons spin-orbit interactions in semiconductors, involving emf appearance in electric field and polarized light
24 p3431 A72-44573

Approaches to verification and solution of magnetic particle inspection problems
24 p3407 A72-44903

Application of a strongly doped semiconductor model to the study of thermodynamic and conductivity properties
24 p3432 A72-45068

An apparatus for measuring the Hall effect of high-resistivity materials in alternating electric and magnetic fields
24 p3405 A72-45698

HALL GENERATORS

Mercury Hall ion engine principles and design, discussing plasma ion acceleration, mercury evaporation and ionization and acceleration channel electrical and thermal insulation
20 p2963 A72-39937

Hall generator operation characteristics under load, power, temperature and nuclear radiation conditions
24 p3385 A72-45270

HALO ORBIT SPACE STATION

Lunar exploration integrated program for 1980s, discussing halo orbit lunar far side data relay satellite advantages vs lunar orbit space station
15 p2321 A72-32318

HALO PARACHUTING

U PARACHUTE DESCENT

HALOGEN COMPOUNDS

- NT ALKALI HALIDES
- NT ALUMINUM FLUORIDES
- NT AMMONIUM CHLORIDES
- NT AMMONIUM PERCHLORATES
- NT BARIUM FLUORIDES
- NT BORON FLUORIDES
- NT BROMINE COMPOUNDS
- NT CALCIUM FLUORIDES
- NT CARBON TETRAFLUORIDE
- NT CESIUM IODIDES
- NT CHLORATES
- NT CHLORIDES
- NT CHLORINE COMPOUNDS
- NT CHLORINE FLUORIDES

- NT CHLOROSILANES
 NT DICHLORIDES
 NT DIFLUORO COMPOUNDS
 NT FLUORITE
 NT FLUORO COMPOUNDS
 NT FLUOROCARBONS
 NT FLUOROHYDROCARBONS
 NT HALIDES
 NT HYDROCHLORIC ACID
 NT HYDROFLUORIC ACID
 NT HYDROGEN CHLORIDES
 NT IODATES
 NT IODIDES
 NT IODINE COMPOUNDS
 NT IRON CHLORIDES
 NT LANTHANUM FLUORIDES
 NT LITHIUM CHLORIDES
 NT LITHIUM FLUORIDES
 NT MAGNESIUM FLUORIDES
 NT METAL HALIDES
 NT NITROGEN FLUORIDES
 NT OXYFLUORIDES
 NT PERCHLORATES
 NT POLYTETRAFLUOROETHYLENE
 NT POTASSIUM CHLORIDES
 NT POTASSIUM PERCHLORATES
 NT SILVER BROMIDES
 NT SILVER HALIDES
 NT SODIUM CHLORIDES
 NT SODIUM FLUORIDES
 NT SODIUM IODIDES
 NT SULFUR CHLORIDES
 NT SULFUR FLUORIDES
 NT TUNGSTEN FLUORIDES
 NT URANIUM FLUORIDES
 Ti anodic behavior in anhydrous liquid ammonia, noting oxidation by halogen intermediary
 04 p0484 A72-14976
 Antimony-halogen synergistic reactions in fire retardants, noting antimony oxychloride role
 07 p0935 A72-19056

HALOGENATION

- NT BROMINATION
 Refractory materials fabrication characteristics for aerospace technology, presenting listing of synergic agents for use with halogenous inhibitors
 17 p2571 A72-35277

HALOGENS

- NT BROMINE
 NT CHLORINE
 NT FLUORINE
 NT IODINE
 NT IODINE ISOTOPES
 Flame retardant mechanism in hydrocarbon polymer combustion, discussing halogen adverse effect on thermal stability
 03 p0380 A72-13244
 Dispersion strengthened nickel-chromium-thoria alloy production methods, noting halogen gas phase diffusion process
 11 p1645 A72-26850
 Current-voltage and specific power-energy relationships for high temperature electrochemical cells with alkali metal anodes and chalcogen or halogen cathodes
 16 p2352 A72-33900

HALOPHILES

- Effect of salt on activity, stability and allosteric properties of catabolic threonine deaminase from extremely halophilic bacteria
 09 p1275 A72-22535
 Isolation of extremely halophilic carbohydrate-utilizing bacteria, using acid formation from various sugars as carbohydrate metabolism index
 15 p2187 A72-32729

HALOS

- Icy halo influence on photometric continuum of comet Burnham within cometary head model
 01 p0125 A72-10080
 Cometary head model for photometric profiles of carbon molecular emission in comet Burnham assuming icy grain halo
 01 p0125 A72-10081
 Halos around black holes, showing luminosities caused by synchrotron radiation of magnetized plasma
 03 p0435 A72-13803
 Fog and cloud microstructure and density distributions from directional light scattering coefficient /halo indicatrix/
 11 p1683 A72-26883
 Photometric search for Venus halo effect during 1970 inferior conjunction in relation to brightness maximum and ice in cloud tops
 15 p2312 A72-32089
 Fog and cloud microstructure and particle size distributions from directional light scattering coefficient /halo indicatrix/
 20 p2948 A72-39570
 Convection and diffusion transport equation of galactic cosmic ray electrons with energy loss and absorption allowance for supernova compressed halo models
 22 p3217 A72-42210

HAMILTON-JACOBI EQUATION

- Hamilton-Jacobi equation for bounded plane circular three body problem with construction of algebraic partial integrals and periodic orbits
 06 p0850 A72-18709
 Dynamic equations integration with constraint factors, discussing Hamilton-Jacobi method applicability conditions
 13 p2003 A72-28724
 Restricted three body problem in elliptical coordinate representation, solving Hamilton-Jacobi equation by separation of variables method
 15 p2274 A72-31455
 Dynamic equations integration with constraint factors, discussing Hamilton-Jacobi method applicability conditions
 22 p3205 A72-42100

HAMILTONIAN FUNCTIONS

- Autonomous Hamiltonian system with two degrees of freedom, investigating origin and periodic orbits stability with two time variable method
 01 p0123 A72-10030
 MHD wave modes nonlinear coupling by quantum field approach with Hamiltonian formulation, applying to solar coronal heating
 01 p0129 A72-10797
 Book on celestial mechanics covering Hamiltonian systems and equations of motion for three body problem
 02 p0285 A72-12857
 Jahn-Teller Hamiltonian for triplet electron state coupling to phonon vibrations in cubic symmetry
 03 p0404 A72-14264
 Conditionally periodic motions of particle in gravitational field of axisymmetric oblate planet, describing canonical transformations for Hamiltonian function reduction to normal form
 04 p0572 A72-14638
 Isolated fixed points existence in area preserving mappings considered with normal form for periodic Hamiltonians in celestial mechanics
 04 p0576 A72-15041
 Computer aided Foldy-Wouthuysen canonical transformation on Dirac Hamiltonian with electromagnetic potentials included
 04 p0496 A72-15627
 Hamiltonian algorithms based on Lie transforms and von Zeipel method, discussing application to non-Hamiltonian system perturbation solution
 06 p0839 A72-17660
 Time independent or periodic Hamiltonian conservative differential equations, studying open, oscillating, limited and abnormal trajectories
 [ONERA, TP NO. 1046]
 06 p0877 A72-17661
 Triaxial space station orbit around oblate earth, presenting equations of motion, Hamiltonian and integration methods
 06 p0878 A72-17663
 Quasi-periodic n-degrees of freedom solutions to Hamiltonian systems with 2n plus 2 variables, noting applicability to planar three body problem
 06 p0839 A72-17882
 Third-order resonance during oscillations of Hamiltonian system of nonlinearly coupled oscillators, obtaining equations of motion and phase portraits
 07 p1035 A72-19978
 Redundancy of Hamiltonian constraints in classical and Dirac quantum theories of gravitation, suggesting replacement by single integral-form condition
 07 p1035 A72-20195
 Variational principle of Hamiltonian type for classical field theory, noting application to nonlinear heat transfer and fluid flow in Eulerian description
 08 p1252 A72-21287
 Atomic variational scattering calculation by method of models, using modified Hamiltonian form to avoid difficulties due to inexact target wave functions
 09 p1355 A72-22787
 Hamiltonian used as Liapunov function in stability evaluation of one dimensional continuous system loaded with polygenic forces
 09 p1406 A72-23077
 Hall-Weaire tight binding Hamiltonian solution in cycle free approximation for band structures and delta functions of amorphous semiconductors
 11 p1700 A72-25725
 Finite difference equations of motion for conservative and nonconservative dynamic systems with finite degrees of freedom, obtaining numerical solution by Hamilton principle
 12 p1844 A72-27193
 Regularizing time transformation for conservative systems reduction to normal coordinates, studying normal configurations existence in terms of Hamiltonian structural properties
 13 p2002 A72-28714
 Asymptotic expansion method for nonsinusoidal wave processes described by Lagrange-type partial differential equations, using averaged form of generalized Hamiltonian variational principle
 13 p2003 A72-28718
 Periodic two-parameter solution families of dynamical systems having first integral, showing stability and

bifurcation existence criteria relationships to dimensionality and Hamiltonian systems
 15 p2261 A72-31309

- Generalized differential system for Hamiltonian, Hermitian and corresponding symmetric nonreal linear matrix differential equations systems
 15 p2263 A72-31756
 Variational calculus methods for periodic solutions of autonomously perturbed Hamiltonian systems of differential equations
 15 p2263 A72-31759
 Direct periodic orbits in planar restricted barycentric three body problem, using Poincare variables and Hamiltonian function
 15 p2307 A72-31763
 Orbiting electron magnetic susceptibility derivation from many band Hamiltonian using Bloch representation to avoid decoupling transformation ambiguity
 15 p2282 A72-32547
 Hamiltonian for first order wave function in charge exchange perturbation theory
 17 p2584 A72-34259
 Discrete and continuous systems spurious solutions avoidance through Hamilton principle reciprocal form derivation of geometric compatibility conditions
 [ASME PAPER 72-APM-54]
 17 p2627 A72-34777
 Hamiltonian system evolutionary stability via area preserving mapping, using Bartlett eigenvector method
 17 p2547 A72-35108
 Hamiltonian formulation of spherically symmetric gravitational fields.
 17 p2582 A72-35393
 A simple, radially correlated ground state wavefunction for two electron atoms.
 17 p2586 A72-35828
 Motion integrals conservation under Hamiltonian function variations, examining gyroscopic equations of motion with parameter disturbances
 18 p2711 A72-36666
 Optimal control with partially specified input functions.
 18 p2673 A72-36821
 Hamiltonian approach to the dynamics of expanding homogeneous universes in the Brans-Dicke cosmology.
 19 p2869 A72-38807
 On the choice of a reference state in the application of Hamilton's principle in elastodynamics.
 20 p2979 A72-39420
 Third-order resonance during oscillations of Hamiltonian system of nonlinearly coupled oscillators, obtaining equations of motion and phase portraits
 20 p2956 A72-40034
 Asymptotic expansion method for nonsinusoidal wave processes described by Lagrange-type partial differential equations, using averaged form of generalized Hamiltonian variational principle
 22 p3204 A72-42095
 Celestial mechanics ideal resonance problem global solution via Bohlin-von Zeipel perturbation technique, modifying Hamiltonian expansion point and separatrix and libration region singularities suppression method
 24 p3440 A72-45138

HAND [ANATOMY]

- Eye-hand coordination modifiable parameters under optical distortion conditions, deriving quadratic equation for hand response adaptation
 02 p0167 A72-11897
 Hand steadiness during unrestricted linear arm movements and eye-hand coordination tasks, showing tremor occurrence in up-down plane
 10 p1432 A72-25113
 Human hand-arm system vibration characteristics, describing mechanical impedance measurements for mathematical modeling
 13 p1910 A72-29559
 Hand tremor measurement methods, discussing pickup system selection for given tasks
 21 p3012 A72-41521

HANDBOOKS

- Book - Aluminum brazing handbook
 19 p2810 A72-38720

HANDEDNESS

- Personality correlates of lateral eye movement and handedness.
 18 p2653 A72-36905

HANDLES

- Optimum cylindrical handle size determination by muscle electromyography, considering gripping task, routine performance and fatigue test
 01 p0017 A72-10119

HANDLING

U MATERIALS HANDLING

HANDLING EQUIPMENT

NT CRANES

- Vacuum handling system for lunar materials thermophysical properties measurements under contamination preventive conditions
 04 p0509 A72-15496
 Air cargo intermodal and interline containers handling in warehouse storage, transportation and distribution, considering total pack and interlock requirements
 16 p2372 A72-33174

Terminal handling environment and air cargo requirements for noncontainerized freight 16 p2372 A72-33175

HANDLING QUALITIES
U CONTROLLABILITY
HANGARS
Evaluation of film forming foams for the suppression of fuel fires in aircraft hangars. [WSCI PAPER 72-16] 20 p2982 A72-38974

HANKEL FUNCTIONS
Sampling theorem application to time varying systems, considering Hankel transform as example 11 p1675 A72-25293

HARDENING [MATERIALS]
NT CARBURIZING
NT HOT PRESSING
NT MARAGING
NT NITRIDING
NT PRECIPITATION HARDENING
NT PULSE HEATING
NT SHOT PEENING
NT SILICONIZING
NT STRAIN HARDENING
NT WORK HARDENING
Hardened steel inhibited crack propagation mechanism, observing striation in microstructure on fracture surface 02 p0243 A72-12212
Ti-Al-Mo alloys thermomechanical treatment, investigating alloy composition effects on hardening 02 p0244 A72-12246
Metal fatigue mechanisms in subcreep temperature range, discussing response to cyclic loading including hardening, softening and inhomogeneous plastic strain development 02 p0295 A72-12496
Ta and Nb addition effects on W solid solution strengthening, determining W-Nb-Ta alloys phase diagram and melting point 03 p0375 A72-13943
Mechanical properties of heat treated hardened high strength steel, investigating microstructure relationship to breakdown characteristics 05 p0671 A72-15992
Hardening of Fe-Mn-Ti ferritic and martensitic alloys, investigating microstructure and mechanical properties 05 p0672 A72-16144
Nb-O and Nb-N alloys, investigating oxygen and nitrogen solute-hardening effects on room temperature flow stress 05 p0675 A72-16729
Hardened and tempered Ni-Cr-Mo steel, testing rest periods caused fatigue life increase in terms of cycles to failure 06 p0895 A72-17802
Hardening phases effect on plastic deformation resistance of Ti and Ti alloys 06 p0835 A72-18746
Hardenability and pearlite stage isothermal transformation properties of direct-quenching low Cr case-hardening steels, discussing Mn, Mo and Ni alloying effects on machinability 07 p0995 A72-19571
Tempering temperature effect on hydrogen penetration level and brittleness of hardened carbon steel 07 p1014 A72-19773
Hardening mechanisms during plastic deformation of pure bcc metals, discussing stresses relation to fine structure and crystal dislocation paths 07 p1018 A72-20142
Ni-Cr-Ti alloy hardening during intermetallic phases precipitation, discussing atom segregations, Guinier-Preston zones and fcc and hcp lattices 07 p1019 A72-20152
Heat treatment of martensitically aging steels with Co, Ni and Mo, considering hardening effects and optimal conditions for high mechanical properties 07 p1020 A72-20414
Heat treatment, water quenching and aging effects on Ti-V alloys hardening and structural properties, discussing omega phase formation 07 p1023 A72-20667
Machine parts surface hardening and smoothing by vibrating hard alloy sphere impact at ultrasonic frequency 08 p1176 A72-21050
Intermetallics and carbide forming additions of Cr, Ti, Ce, V and Nb for hardening of cold worked Mn rich steel from crystal dislocations growth 09 p1327 A72-22230
German monograph on deep drawing of pre-hardened and partially annealed Al and Al alloys, noting anisotropy effect of bottom zone of plate samples 09 p1317 A72-22329
Al alloys degree of deformation dependence on pulse energy during extrusion by pulsed magnetic field, showing hardening effect 09 p1319 A72-22865
Iron emission spectrum in phase transformations and recrystallization study of austenitic and carbon steels under high temperature hardening 11 p1655 A72-25496
Co, Al and Mn additions effect on secondary hardening during aging in Fe-Mo-C martensite 11 p1655 A72-25511

Hardened steel inhibited crack propagation mechanism, observing striation in microstructure on fracture surface 11 p1656 A72-25710
Numerical calculation of temperature distribution and tempering depth for inductive hardening process with automatic material feed, taking into account temperature dependent material properties 11 p1639 A72-25898
Ti-Al-Mo alloys thermomechanical treatment, investigating alloying effects on hardening 11 p1660 A72-26132
Critical resolved shear stress and solute atom concentrations relationship in solid solution hardening of metal crystals 12 p1853 A72-27101
Mathematical model to describe complete creep process in metal from hardening and brittle failure theories 12 p1828 A72-27322
Metal surface layers structural changes under external friction, noting hardening, softening and phase transformations of active layer material 12 p1818 A72-28190
Laplace equation iterative solution for boundary value problems in structural hardening and heat resistance formulation, noting convergence 12 p1887 A72-28226
Hardened coarse-grained steels recrystallization during fast heating, investigating martensite phase macro- and microstructural changes by X ray analysis 13 p1977 A72-28908
Heat treatment hardening effect on stress corrosion resistance of ultrapur maraging and stainless steels, emphasizing hydrogen embrittlement 14 p2117 A72-30540
Elastoplastic equilibrium theorems for solid subjected to variable external effects, considering perfectly plastic and arbitrary hardening materials 14 p2165 A72-30574
Mo, W, Nb, Ti, V and N complex alloying to harden cast heat resistant austenitic steel, discussing phase composition and stress-rupture strength 15 p2254 A72-31563
Structural decomposition and hardening of super-saturated Al-Cu, Al-Cu-Ag, Al-Zn, Cu-Sn and Cu-Ni-Co solid solutions 15 p2255 A72-31565
Creep theory with anisotropic hardening compared to curves obtained from verification experiments with loading and unloading in steps 15 p2256 A72-31707
Complex Ca lubricants strength, colloidal and mechanical stability and thermal hardening relationship to dispersion medium viscosity 16 p2413 A72-33172
Physics of strengthening mechanisms in crystalline solids. 19 p2843 A72-37444
Effect of residual elements on radiation strengthening in iron alloys, pressure vessel steels, and welds. 20 p2937 A72-39289
Fatigue tests at low cyclic loads of smooth and notched Ti alloy specimens, noting surface hardening effect on service life 20 p2941 A72-39580
The effect of Si, Zr, Al and Mo on the structure and strength of Ti martensite. 20 p2941 A72-39792
Interactions between dislocations or flux lines moving through hardened crystal, discussing distribution functions method applications to diffuse and localized obstacles 20 p2962 A72-39994
Influence of dislocations in subgrains on the substructural hardening of aluminum 21 p3068 A72-40961
Alpha stabilizing Al and Sn suppression effect on beta-omega transformation during Ti alloy hardening 22 p3189 A72-42278
Cold shortness of 14Kh2NZMA steel 23 p3303 A72-44023
Non-steady shock waves in metals with phase transitions and hardening by explosion. 24 p3414 A72-45025
A study of the hardening of the subspinoidal alloy Fe-Ni-Al 24 p3415 A72-45395
Mechanical properties of heat treated hardened high strength steel, investigating microstructure relationship to failure characteristics 24 p3416 A72-45734

HARDNESS
NT MICROHARDNESS
Hydrogen diffusion kinetics in Nb under various temperatures during gas-metal absorption experiments, observing room temperature hardness profile 01 p0087 A72-11026
Hot formed Cr-Ni-Mo and Ni-Mo prealloyed steel powders fatigue and toughness properties, determining hardness effects by varying draw temperature from 400 to 1000 F 02 p0240 A72-11435

Pure metals creep or self diffusion activation energy from hot-hardness data, noting temperature and elastic modulus effects 03 p0375 A72-13931
High temperature tests of short time strength, hardness and moduli of elasticity of W-Mo alloys subject to plastic deformation and annealing 06 p0833 A72-18633
Austenitizing conditions effects on hardness and microstructure of tempered steel, emphasizing martensite structure and grain size changes produced by controlled heat treatment 07 p0995 A72-19486
Mo-Zr solid solutions internal boring, discussing diffusion controlled process and hardness dependence on Zr 10 p1494 A72-23833
Cold rolled Zircaloy 2 sheet microstructure, microstrains and hardness by X ray diffraction and electron microscopy 11 p1657 A72-25757
Underbead hardness determination in carbon and low alloy steels, noting weld tests/theory correlation 11 p1641 A72-26493
Cold working effect on Cu-Ni-Si-Mg and Cu-Ni-Si-Cr alloys age hardening behavior, presenting hardness and tensile strength vs aging time at 350 and 400 C 11 p1662 A72-26743
Heat treatment effects on martensitic bainitic steel hardness, tensile strength and impact endurance, examining carbide and alpha phases 11 p1666 A72-26922
Carbon and low alloy steels resistance to abrasive wear as function of hardness, heat treatment and composition 12 p1829 A72-27455
Heat resistant blade alloy test temperature effects on fatigue life, tensile strength, hardness and chemical composition 12 p1831 A72-28230
Russian book on hard alloys strength covering WC-Co and WC-TiC-Co alloys microstructure, thermal stresses and fracture mechanism 12 p1831 A72-28348
Ti-Mo-Ni system polythermal section microstructure, hardness, resistivity and thermal expansion characteristics 14 p2112 A72-30153
Ni-Mo-W alloys hardness rating and corrosion resistance to sulfuric and hydrochloric acids, discussing dispersion hardening, quenching and aging treatments 14 p2114 A72-30272
Mo-Ni-Al system phase equilibria at 600 C from X ray and microstructural analysis, noting hardness dependence on composition 14 p2123 A72-30985
Yttrium alloys isoperiodic lines, solidus isotherms, equal hardness lines and resistivity presented diagrammatically 15 p2289 A72-31185
Phase diagrams of Hf-Ce and Hf-Er alloys, plotting hardness and electroconductivity curves 15 p2289 A72-31188
Relations between mechanical properties and microstructures in TiC-Mo2C-Ni alloy. 19 p2821 A72-38375
Prospects of using carbonitrides as the hard component of cermet hard alloys 22 p3188 A72-42195

HARDNESS TESTS
Ti-Cr alloys omega phase formation by measurements of hardness, Young modulus and internal friction 02 p0246 A72-12672
Stress distribution during plastic deformation of steel turbine disk from hardness measurements 06 p0900 A72-18670
Magnetic properties, electrical resistivity and hardness of vacuum melted Ni-Fe-Ta alloys 11 p1655 A72-25512
Austenite deformation effect on thermal stability and hardness of Ni steels at various C and Ni concentrations 13 p1977 A72-29019
Tensile, creep and creep rupture strength hot hardness tests for metallic and nonmetallic materials 13 p1958 A72-29442
Elastic effects in metal hardness testing with blunt indenter, considering indentation in rigid plastic manner 14 p2113 A72-30268
Cr-N alloy phase diagram from thermal and X ray analysis, metallographic observation and hardness tests, noting melts crystallization 14 p2123 A72-30987
Ultrasonic tests for incipient fatigue, hardness and elastic constants-tensile strength relationship in metals 18 p2690 A72-36125
Russian book - Determination of stresses in the plastic region from the hardness distribution 18 p2732 A72-36300
A simple method for determination of the elongation before reduction of area using a 100-degree cone indentation 18 p2676 A72-37098

- Tempered hardness and tensile strength of ausforming Mn-Cr-B spring steels at low temperatures in austenite stable phase by electron microscopy 21 p3066 A72-40718
- Influence of alloying elements on ordering in alloys of the nickel-molybdenum system 22 p3192 A72-43016
- The limiting strength of worn metal surfaces. 22 p3194 A72-43039
- Determination of the stressed state in a welded joint in plastic deformation 23 p3293 A72-44019

HARDWARE

- Computer storage hierarchy hardware influence on data base management systems software technology [IEEE PAPER 13.5] 04 p0598 A72-15712
- Hardware software firmware tradeoffs - IEEE Conference, Boston, September 1971 10 p1442 A72-23815
- Hardware monitor and associated analysis programs to evaluate real time satellite command and control digital computer system performance 10 p1442 A72-23817
- Specification requirements for quality assurance of automated data processing systems based on hardware development procedures 11 p1602 A72-26791

HARDWOOD FORESTS

U FORESTS

HARMONIC ANALYSIS

- NT TESSERAL HARMONICS
- NT ZONAL HARMONICS
- Space potential determination in plasma diagnostics, comparing second harmonic analysis with experimental results 02 p0268 A72-12868
- Single mode solid state laser periodic Q switching effects on spike pulse shape and synchronization by harmonic analysis with convergent series 03 p0366 A72-13371
- Biharmonic problem of displacements in plane theory of elasticity, analyzing stress-strain state by iterative solution in series form 03 p0454 A72-14312
- Earth triaxiality from satellite data, obtaining nonzero values for harmonic coefficients 03 p0351 A72-14327
- Second and third degree harmonic interpolation formulas for given point in bounded simply connected n-dimensional region, indicating approximate solution of Dirichlet problem 04 p0538 A72-14727
- Wave harmonics method application to problems of free oscillations in longitudinally regular screened waveguides partially filled with homogeneous isotropic media 04 p0488 A72-15379
- Turbofan multiple pure tone noise analysis, discussing rotor geometry, relative Mach number and incidence angle effect on sound emission [AIAA PAPER 72-127] 05 p0706 A72-16824
- High order harmonic equations in gravitational potential from Transit 1B orbit inclination, comparing with Ariel 3 08 p1158 A72-21216
- RR Lyrae variables period-luminosity relations explained by linearized pulsation calculations for quenching of first harmonic 08 p1235 A72-21388
- Harmonic analysis of E layer drift measurements by closely spaced receiver method combined with on-line analog computer 08 p1160 A72-21529
- Radio meteor observations of upper atmosphere long period wind variations, determining oscillation spectra peaks by harmonic analysis 08 p1161 A72-21537
- Interplanetary space three dimensional cosmic ray anisotropy from harmonic components of diurnal variations 09 p1377 A72-22926
- Single degree of freedom systems with nonlinear spring characteristics of skew symmetric form, discussing 1/2 subharmonic oscillation analysis by harmonic balance method 09 p1342 A72-23455
- Geomagnetic field short term variations as function of solar activity from solar radiation data harmonic analysis, relating large amplitude fluctuation to seasonal variations 09 p1304 A72-23503
- Wiener generalized harmonic analysis relationship to steady random functions, emphasizing higher order properties and ergodic process conditions 10 p1504 A72-24063
- Least squares method algorithm for estimating unsteady harmonic signal parameter in presence of normally distributed additive noise 13 p1915 A72-28435
- Nonlinear harmonic analysis of reflex klystrons with high electron conductance, using average method in second approximation 13 p1931 A72-29290

- Linearization method to determine changes in principal harmonic resulting from nonlinear device characteristic deformation due to HF components 13 p1937 A72-30019
- Mars upper cover temperature, representing diurnal variations at different areographic latitudes as harmonic series 14 p2148 A72-30207
- Control theory of second order linear hyperbolic partial differential equations, discussing relation to harmonic and spectral analysis 15 p2263 A72-31757
- Cantilever beam tapered linearly in horizontal and vertical planes, obtaining computer solution for free transverse vibration fundamental frequency and harmonics 15 p2328 A72-32022
- Discrete frequencies search in time series via anharmonic frequency analysis, using integral transform 17 p2574 A72-34450
- Identification of periodicities in the structure of natural stochastic processes 17 p2534 A72-35783
- Fundamental, harmonic and combination frequency components amplitude analysis via dual input describing function for nonlinear element response under two incommensurate frequency sinusoidal signals 18 p2671 A72-36051
- Evaluation of 15th-order harmonics in the geopotential. 18 p2729 A72-36986
- Lunar magnetic variations at Trelew /Argentina/. 19 p2794 A72-38860
- The effects of transmitter source and load impedance on harmonic output spectrum - A new measurement method. 20 p2921 A72-38996
- Higher harmonics and transport coefficients of plasmas in circularly polarized magnetic fields and additional electromagnetic fields. 21 p3091 A72-40489
- Nonlinear differential equation periodic solution approximation by pseudo-linear representation of nonlinear terms effects on single harmonic, using describing function matrix method 21 p3076 A72-41314
- Mars upper cover temperature, representing diurnal variations at different areographic latitudes as harmonic series 23 p3333 A72-43237
- Approximate harmonic linearization method of stability analysis of nonlinear periodic systems, identifying fictitious oscillations due to computation errors 23 p3277 A72-44007
- The accuracy of Donnell's theory for very high harmonic loading on closed cylinders. 23 p3350 A72-44059
- Frequency multiplication with a traveling-wave tube. I - Computation of the current harmonics in a traveling-wave tube by the large-signal theory. 24 p3386 A72-45284
- Frequency multiplication with a traveling-wave tube. II - Numerical analysis of a traveling-wave frequency multiplier by the large-signal theory. 24 p3386 A72-45285
- HARMONIC EXCITATION**
- Ruby and Nd lasers fundamental emission effects on excitation of stimulated Raman scattering in liquid and crystalline media by second harmonics 03 p0366 A72-13364
- Solution stability of linear differential equations systems with harmonic coefficients, using Jordan canonical forms and perturbation method 03 p0382 A72-13918
- Subharmonic oscillations excited by horizontal vibrations of mathematical pendulum suspension 07 p1036 A72-20323
- Static loading and monoharmonic excitation influence on transverse vibrations of eccentrically prestressed metallic beam 11 p1732 A72-25535
- Third harmonic current density excitation by HF electric field in Lorentz plasma, calculating electron distribution function with unnormalized spherical harmonics and Fourier series 11 p1697 A72-26553
- Complex elastic systems natural frequencies computation from measured dynamic response to harmonic excitation, applying to helicopter and transport aircraft 14 p2164 A72-30326
- Nonlinear coupled cyclotron oscillators excitation by external sine wave force, analyzing amplitude/phase variation and negative absorption 14 p2132 A72-31115
- Rotating shaft bending vibrations under harmonically varying transverse load and periodic parametrically exciting axial force, using linearized theory of small displacements 16 p2463 A72-32877
- Train synchronism of second harmonic excitation/pumping/ by periodic sequence of ultrashort light pulses 16 p2402 A72-33493

Wavelength tunable UV dye laser pumped by the fourth harmonic of Nd:YAG laser. 19 p2810 A72-37407

The locking effect in an autooscillatory system with two degrees of freedom 19 p2783 A72-38580

HARMONIC FUNCTIONS

- Static thermoelasticity problems solutions using harmonic functions applied to contact problem of hot stamps 03 p0448 A72-13902
- Computer aided iterative design of nonlinear single loop control system with sinusoidal describing function and time response display capability 11 p1601 A72-26042
- Harmonic equation for antipane shear deformation of elastic composite materials with multiple circular inclusions 12 p1883 A72-27562
- Harmonic functions system for resonant vibrations of liquid in elastic circular cylindrical tank, calculating shells surface pressure from equations of motion 13 p1940 A72-28394
- Harmonic functions skew derivative problem reduction to study of integrodifferential equation by constraints imposition on boundary condition coefficients 13 p1987 A72-29469
- Modified finite element method application to plane elastic area elementary triangles strained and stressed state description by polynomial algebraic expressions and harmonic functions 14 p2163 A72-30188
- Instrumental errors estimation in photomultipliers and photodiodes during measurement of short time phase fluctuations in quasi-harmonic signals 15 p2246 A72-31424
- Completeness proof for linear elasticity theory set of three harmonic functions based on theory of linear differential equations with constant coefficients 16 p2466 A72-33018
- Cylindrical shells vibration under external forces with allowance for internal and external friction, obtaining harmonic influence functions in series form 22 p3233 A72-42056
- HARMONIC GENERATIONS**
- Electron cyclotron harmonics emission as function of electron plasma frequency in He reflex discharge, measuring electron densities 01 p0105 A72-10026
- Second harmonic emission from plasma hybrid resonance region during electromagnetic wave normal incidence on nonhomogeneous magnetoactive plasma layer 02 p0180 A72-12578
- Stimulated Raman scattering effect on two quantum absorption during RF radiation first and third harmonics interaction 02 p0180 A72-12582
- Tensor description of laser beam second harmonic generation in dc magnetic field, using group theory derivation of nonzero element relations for all crystallographical classes 03 p0365 A72-12963
- Laser pumping pulse shape effects on second harmonic emission waveform during nonlinear crystal excitation by ultrashort light pulse 03 p0366 A72-13368
- Two photon method of measuring ultrashort pulses and nonlinear optical effectiveness of lasers in synchronized mode 03 p0369 A72-14063
- Second harmonic generation, coherence lengths and second order susceptibilities near band edge in InSb as function of magnetic field 03 p0404 A72-14269
- Harmonic power extraction from series-stacked high efficiency avalanche diodes at superhigh frequencies on simple microstrip circuits 06 p0788 A72-18468
- Third harmonic generation in Ge induced by conduction nonlinearity during bulk heating of charge carriers by microwave fields 07 p1047 A72-19023
- Third harmonic radiation generation in phase matched mixture of Rb vapor and Xe, observing nonlinear susceptibility [AD-739764] 08 p1211 A72-21197
- Pulse duration reduction with power gain during second harmonic generation by nonlinear crystal in Q switched buildup resonator 08 p1183 A72-21729
- Thermal self disturbance effect on second harmonic generation in crystals and CW and pulsed lasers 08 p1184 A72-22034
- FM electromagnetic wave propagation in Lorentzian plasma, taking into account harmonic generations effect 10 p1520 A72-24209
- Ternary chalcopyrite semiconductors refractivity measurement over range of wavelengths and optical nonlinear coefficient for second harmonic generation from carbon dioxide laser 11 p1701 A72-26148

- Lithium niobate crystal refractive index inhomogeneity influence on second harmonic generation from He-Ne laser 11 p1650 A72-26360
- High order optical harmonic generation and many-quantum processes efficiency in multimode laser radiation field 12 p1821 A72-27593
- Second, third and fourth optical harmonics generation of Nd-doped YAG laser radiation under Q switching fast repetition pulse conditions 12 p1821 A72-27594
- Nd laser second harmonic generation by organic crystalline powders, noting suitability of benzophenon, xanthon, benzimidazol and resorcin 12 p1823 A72-27854
- Second harmonic conversion of CW YAG-Nd laser radiation on lithium metaniobate crystals, discussing conversion coefficient optimization 12 p1825 A72-27886
- Picosecond pulse efficient second harmonic generation by crystals inside high power dye mode locked Nd-glass laser folded cavity 12 p1826 A72-28220
- Microwave source four hundredth order harmonic mixing with laser radiation, using Josephson junction and maser 12 p1827 A72-28221
- Angular spectrum of second harmonic generation during two frequency interactions in KDP laser 13 p1969 A72-29524
- Kinetics of monopulse development in cavity with nonlinear element converting generated radiation into second harmonic, considering energy and time characteristics 13 p1970 A72-29683
- Ruby laser emission second harmonic generation effectiveness in organic polycrystals from comparison to lithium niobate 13 p1970 A72-29689
- Quasi-monochromatic wave interaction with second harmonic in weakly nonlinear medium, obtaining exact nonstationary solutions 13 p1971 A72-29911
- Millimeter wave third harmonic generation and frequency multiplication in n-type InSb at 77 K 14 p2142 A72-30799
- Collisions role in nonlinear mode coupling and harmonic generation associated with electromagnetic wave in plasma, describing plasma electron distribution function by kinetic equation 15 p2195 A72-31679
- Lithium niobate crystal refractive index inhomogeneity influence on second harmonic generation from He-Ne laser 16 p2403 A72-33713
- Frequency tuning and intracavity high efficiency extraction of second harmonic radiation from prism type Nd laser 16 p2404 A72-33994
- Second harmonic conversion of CW YAG-Nd laser radiation on lithium metaniobate crystals, discussing conversion coefficient optimization 16 p2404 A72-33995
- Optical second harmonic generation and parametric oscillation. 17 p2594 A72-34566
- Use of the Sturmian function for the calculation of the third harmonic generation coefficient of the hydrogen atom. 17 p2586 A72-35830
- Use of generalized theory of optical diffraction for the study of second harmonic generation. 19 p2811 A72-37673
- Subharmonic generation in plane-parallel plate for light wave propagation perpendicularly to plate, noting frequency division near multiplicative resonance 23 p3295 A72-43408
- Influence of a linear inhomogeneity of the refractive index of nonlinear crystals on second-harmonic generation. 24 p3411 A72-45604
- Temperature and angular widths of the phase-matching curve of a lithium niobate crystal. 24 p3432 A72-45615
- HARMONIC GENERATORS**
- Resonator second harmonic influence on Gunn oscillator parameters for transit and hybrid modes, discussing bias voltage, harmonic amplitudes, phase difference, doping level and frequency 07 p0955 A72-19254
- Frequency and power characteristics of transistorized generators of harmonic oscillations 07 p0956 A72-19569
- Dielectrics breakdown under ultrashort neodymium laser pulses at fundamental and second harmonic frequencies 11 p1647 A72-25719
- High conversion efficiency microwave second harmonic generator using negative resistance nonlinearity of n-type GaAs 11 p1591 A72-25741
- EHF double-drift IMPATT oscillator small and large signal behavior analysis with computer program, noting second harmonic tuning and single frequency operation possibilities 15 p2204 A72-31314
- A stable neodymium-glass laser harmonic generator 21 p3064 A72-41739
- Frequency and power characteristics of transistorized generators of harmonic oscillations 22 p3158 A72-42087
- HARMONIC MOTION**
- NT SIMPLE HARMONIC MOTION**
- Two dimensional airfoil unsteady stall in incompressible flow, comparing calculated loading during transient and sinusoidal pitching motions with measured values [AIAA PAPER 72-37] 05 p0607 A72-16899
- Superposed forced oscillations of liquid and of elastically mounted bulkhead with translational harmonic displacements of cavity, noting damping increase 13 p1942 A72-29498
- Determination of the motion of a model, possessing a mass and a viscoelastic element, for a given harmonic law of motion of the vibrating support 19 p2871 A72-37427
- Generalized subharmonic response of a missile with slight configurational asymmetries. [AIAA PAPER 72-972] 22 p3134 A72-42339
- Infinite rectangular elastic bar surface mass distribution effects on harmonic wave propagation modes, obtaining approximate solution by expanding displacement as power series 23 p3352 A72-44123
- HARMONIC OSCILLATION**
- Higher order cyclotron harmonic resonance of electrons with electromagnetic wave propagation through collisionless magnetoplasma, deriving energy oscillation time period 01 p0105 A72-10023
- Duffing type quasi-linear differential equation system, obtaining ultrasubharmonic resonance by small parameter and harmonic balance methods for comparison with analog computer solutions 01 p0101 A72-10034
- Small harmonic oscillations of isothermal atmosphere due to acoustic-gravity wave downward reflection caused by kinematic viscosity increase with altitude 01 p0102 A72-10229
- Anharmonic thickness shear oscillations in hf quartz resonators with round coaxial electrodes, using Mindlin approximation to wave equation 02 p0191 A72-12032
- Low subsonic region unsteady interference effects on harmonically oscillating wing-tailplane model with variable sweep wing [DGLR PAPER 71-081] 02 p0152 A72-12709
- Unsteady pressure distribution on harmonically oscillating circular cylindrical fuselage body with conical nose and delta wing with straight, cubic or sinusoidal leading edges 02 p0153 A72-12730
- Self oscillating system stability under parametric excitation and harmonic force for large and small natural frequency mismatch 04 p0549 A72-15046
- Wave harmonics method application to problems of free oscillations in longitudinally regular screened waveguides partially filled with homogeneous isotropic media 04 p0488 A72-15379
- Thin wing harmonic oscillation in subsonic flow, developing analytical form of kernel function in generalized Possio integral equation 05 p0603 A72-16707
- Incompressible fluid unsteady kinetic energy equation periodic solution for harmonic oscillation viscous dissipation influence on temperature field, considering Couette steady flow solution 05 p0750 A72-17007
- Aerospace structures harmonic vibration tests, discussing structures natural frequency spectrum, mode isolation, eigenmodes and inertial characteristics 06 p0896 A72-17948
- Dynamic response and functional state of human operator subjected to harmonic and random vibrational excitations, discussing biodynamic nonlinear oscillatory system model construction 06 p0770 A72-18728
- Harmonic oscillations sum conversion by two terminal pair network with complex nonlinearity 07 p0956 A72-19565
- Frequency and power characteristics of transistorized generators of harmonic oscillations 07 p0956 A72-19569
- Subharmonic oscillations excited by horizontal vibrations of mathematical pendulum suspension 07 p1036 A72-20323
- Nonlinear ion acoustic instability in plasma for subharmonic and harmonic forcing oscillations similar to Van der Pol effect 07 p1046 A72-20541
- Quasi-harmonic vibrations of dynamic system with arbitrary number of degrees of freedom and finite number of discrete nonlinearities, using Van der Pol method 09 p1352 A72-23178
- Single degree of freedom systems with nonlinear spring characteristics of skew symmetric form, discussing 1/2 subharmonic oscillation analysis by harmonic balance method 09 p1342 A72-23455
- General structure steady state response under harmonic forcing in internal resonance relation, noting inertial nonlinearity effects on autoparametric interactions and energy flow 09 p1408 A72-23462
- Nonlinear dispersive medium characteristics determination from higher harmonic oscillations and beats analysis based on traveling waves concept 09 p1353 A72-23486
- Analog computers application to resonance phenomena analysis in oscillating systems, describing programming of variable frequency harmonic oscillations 10 p1445 A72-24492
- Higher harmonics intensities dependence on fundamental of electron oscillation in beam generated plasma 10 p1524 A72-24920
- Dynamic calibration of inclined and crossed hot-wire flowmeters for absolute turbulence intensity measurements, using known sinusoidal oscillations in steady flow 11 p1636 A72-26637
- Harmonically oscillating rectangular wing in unsteady transonic flow, obtaining two part boundary value problem for linear potential equation 12 p1751 A72-27545
- Stability and oscillation in linear and nonlinear systems, examining existence of T-periodic solutions /harmonic forced vibrations/ 13 p2000 A72-28484
- Mechanical oscillator model for experimental investigation of multistage electrical frequency multipliers subharmonic transient oscillations, considering energy flow under constant and/or phase modulated excitation 14 p2131 A72-30719
- French monograph on velocity profile in laminar boundary layer on seminfinit flat plate in harmonic oscillation of uniform incompressible flow 14 p2095 A72-30949
- Steady state combination oscillations stability, examining geometrical properties of amplitude surfaces 14 p2133 A72-31128
- First mode ultraharmonics in nonlinear beam vibration with various boundary conditions and structural properties 16 p2463 A72-32845
- Linearized supersonic flow past harmonically vibrating cylindrical body, solving boundary value problem by cylindrical integral transformation 16 p2342 A72-32878
- WKB large frequency expansion solution for elastic waves propagating into inhomogeneous elastic medium with harmonic periodicity, using perturbation method [ASME PAPER 72-APM-3] 17 p2630 A72-34810
- Heat transfer by free convection from a longitudinally vibrating vertical plate. 17 p2637 A72-35045
- Evaluation of Reissner's correction for finite span aerodynamic effects. 18 p2736 A72-36774
- Amplitude and harmonic oscillation characteristics of quaternary RC parametron using tunnel diodes 19 p2773 A72-38211
- Self-excited parametric oscillations at the second harmonic in a parametric system with a triple-post ferromagnetic core 19 p2774 A72-38586
- Harmonic oscillation characteristics of avalanche Si diode with nonlinear and negative resistance characteristics 20 p2908 A72-39705
- Complex amplitude four-pole network nonlinear conversion of sum of sinusoidal oscillations 22 p3158 A72-42083
- Frequency and power characteristics of transistorized generators of harmonic oscillations 22 p3158 A72-42087
- Nonaxisymmetric vibrations of arbitrarily thick circular cylindrical shells 23 p3345 A72-43624
- The effects of magnetic field oscillations on the boundary layer flow past a magnetized plate. 23 p3321 A72-43725
- Modified Hellinger-Reissner variational method applicable to harmonic waves moving normal to fiber reinforced layered elastic composite, tabulating eigenfrequencies 23 p3351 A72-44061
- Forced harmonic and random vibrations of concentric cylindrical shells immersed in acoustic fluids. 23 p3352 A72-44117

HARMONIC OSCILLATORS

Stochastic differential equations vector solution by two-time method, applying to random harmonic oscillators and wave propagation in random media [AD-733125] 01 p0093 A72-10510

Orthogonal 2-port network impedance transforming properties and applications to harmonic oscillators and filters 04 p0502 A72-15521

Weakly damped harmonic oscillator, using perturbation methods for approximate solution to boundary value problem differential equation 07 p1034 A72-18816

German monograph on multielement linear mechanical oscillator analysis covering behavior of harmonically excited bar chains of arbitrary structure 09 p1350 A72-22337

Network synthesis for various second and third order sinusoidal oscillators consisting of linear passive or active RC circuits and amplifier 10 p1452 A72-24802

Oscillation modes and stability region of harmonic oscillators with homogeneous nonlinear rheological differential equations of motion 10 p1513 A72-24998

Mathematical model of weak coupling influence on damped harmonic oscillators with different eigenfrequencies applied to bounded plasma oscillations 11 p1698 A72-26600

Tunnel diode harmonic relaxation frequency divider, obtaining large division factors and wide synchronization bands with sinusoidal output signal 15 p2206 A72-31666

Diatomic molecules partition functions derivation by classical and quantum mechanical theories for simple harmonic oscillator and square-well potential 15 p2280 A72-31693

Harmonic oscillators with negative resistance elements, discussing simplified mathematical calculation for I-V characteristics nonlinearity and applications to various diodes and transistors 16 p2368 A72-32858

ADP or KDP crystal induced second harmonic emission from Ar laser resonator, noting crystal temperature effects on primary/secondary radiation phase synchronism 16 p2400 A72-33281

Amplitude-controlled harmonic oscillator transient response time reduction by sampling techniques in control loop without introducing distortion 16 p2369 A72-33763

A one-dimensional harmonic oscillator in quantum mechanics with a nonnegative distribution function in the phase space 17 p2579 A72-34198

Stability of injection-locked oscillators 18 p2665 A72-36265

Heuristic description for harmonic oscillator as quantized model of anharmonicity applied to excitation fields involving particle clusters and multibody configuration 20 p2953 A72-39398

Influence of a magnetic field on the operation of an oscillator employing a two-base diode 21 p3032 A72-40791

Local-oscillator-circuit optimisation for minimum distortion in double-balanced modulators 23 p3270 A72-43603

The effect of a harmonic-oscillator velocity distribution on an ideal solid-state laser 24 p3409 A72-44953

HARMONIC RADIATION

NT HARMONIC GENERATIONS

Acoustic radiation pressure of small radius spherical obstacle in high level harmonic plane field for application to microphone calibration [ONERA, TP NO. 1008] 05 p0661 A72-16023

Ion acoustic and cyclotron harmonic plasma waves parametric excitation by hf electric field, measuring thresholds and growth rates agreeable with theory 06 p0861 A72-17827

Third harmonic radiation generation in phase matched mixture of Rb vapor and Xe, observing nonlinear susceptibility [AD-739764] 08 p1211 A72-21197

Frequency tuning and intracavity high efficiency extraction of second harmonic radiation from prism type Nd laser 12 p1825 A72-27885

Harmonic elastic wave propagation in composites with periodic structures by variational methods developed from crystal lattice studies 13 p2060 A72-29696

Harmonic waves propagation in infinite transversely isotropic cylinder with elliptic cross section, obtaining solution in terms of Mathieu functions 14 p2163 A72-30190

Electrostatic cyclotron harmonic waves propagation in inhomogeneous electron plasma slab, deriving RF electric field 14 p2138 A72-30397

Experimental investigation of electrostatic cyclotron harmonic waves excited in inhomogeneous

plasma column with axial magnetic field by RF capacitor field 14 p2138 A72-30398

Signal level fluctuations line spectra energy characteristics comparison for oblique and oblique-backscatter sounding, noting changes in harmonics intensity and period 14 p2085 A72-30638

Laminated plate continuum theory with microstructure, studying one dimensional harmonic wave propagation in infinite laminate 14 p2169 A72-31147

CO overtone band and vibrational transitions in CW carbon disulfide-oxygen chemical laser, discussing pressure effects 15 p2250 A72-32525

Radio spectrographic measurements of type 4 solar radio bursts harmonic and pulsation structures 16 p2459 A72-33921

Frequency tuning and intracavity high efficiency extraction of second harmonic radiation from prism type Nd laser 16 p2404 A72-33994

Alouette 2 plasma resonances observation near ionospheric electron cyclotron frequency harmonics, interpreting frequency shift as wave dispersion effects 17 p2546 A72-34692

Turbulence of electrostatic electron cyclotron harmonic waves observed by Ogo 5 17 p2549 A72-35599

Instability of electromagnetic cyclotron harmonic waves in plasmas 17 p2592 A72-35775

Propagation and attenuation of harmonic waves in a viscoelastic circular cylinder 18 p2738 A72-37070

Variational theorems for harmonic waves in elastic composites with periodic structures, considering wave propagation in layered and in fiber reinforced composites 21 p3119 A72-41101

HARMONICS

NT HARMONIC EXCITATION

NT HARMONIC GENERATIONS

NT HARMONIC OSCILLATION

NT SIMPLE HARMONIC MOTION

NT SPHERICAL HARMONICS

NT SUPERHARMONICS

NT TESSERAL HARMONICS

NT ZONAL HARMONICS

Linear nonadiabatic pulsation constants for fundamental mode and first two harmonics of stellar models including Cepheids, observing mass scattering 04 p0579 A72-15319

Higher harmonics in lunar transfer functions for surface magnetic field tangential components, discussing lunar electrical conductivity models 06 p0875 A72-17448

Abrupt junction Si IMPATT diodes large signal analysis, discussing subharmonic modes and second harmonics effects 07 p0956 A72-19591

Longitudinal plasma oscillations nonlinear instability due to energy transformation into harmonics and subharmonics 11 p1695 A72-25795

Populations modulation and spatial harmonics influence on gas and solid state laser radiation characteristics, discussing uniform and nonuniform line broadening 11 p1650 A72-26353

Monograph on perceptual analysis of sound covering peripheral auditory system functions, subjective pitch perception, periodic pulse and white noise harmonic audibility, masking behavior, etc 15 p2188 A72-31514

Fourier analysis for geopotential resonance effect on satellite orbits, calculating 13th harmonic influence on GEOS 2 and BE-C mean longitude 15 p2309 A72-31939

Heliograph and interferometer observations of type 3 bursts, plotting relative positions of fundamental and second harmonic radiation sources 16 p2445 A72-33043

Populations modulation and spatial harmonics influence on gas and solid state laser radiation characteristics, discussing uniform and nonuniform line broadening 16 p2402 A72-33706

Generalised method of harmonic reduction in a.c.-d.c. converters by harmonic current injection 18 p2648 A72-37209

Russian book - Methods of measurement-information conversion and separation from harmonic signals 19 p2764 A72-37449

Inductive post influence in perfectly conducting waveguides, calculating shunt impedance with allowance for spatial harmonics effect 19 p2766 A72-38413

Quantum impulse autocorrelation function of one dimensional harmonic crystal lattice, noting periodic time dependence at high and low temperatures 23 p3312 A72-43405

Solution of the inverse problem of gravimetry on the basis of harmonic moments of the gravitational field 23 p3285 A72-43928

HARNESSES

Dynamic deceleration anthropomorphic dummy tests of general aviation occupant lap belt/shoulder harness restraint systems [SAE PAPER 720325] 11 p1583 A72-25588

Impact tests on anthropomorphic dummies for protection effectiveness evaluation of lap belt, Air Force shoulder harness-lap belt and airbag-lap belt restraints [AD-741530] 12 p1769 A72-27471

General aviation crashworthy personnel restraint systems, discussing strap take-up devices, comfort, fit and ease of use 13 p1908 A72-28726

Deceleration attenuation effectiveness of airbag restraint systems compared with seat belt-shoulder harness for aircraft occupants crash protection 15 p2191 A72-32605

HARRIER AIRCRAFT

The INAS device of Ferranti as integrated weapon system for the HS Harrier 21 p3083 A72-41846

Harrier two seat aircraft design, performance, weapon systems, thrust vectoring and combat characteristics comparison with GR.1 23 p3252 A72-44391

HARTMANN FLOW

Viscous electroconducting liquid two unidimensional Hartmann flows electromagnetic coupling under transverse magnetic field induction 03 p0396 A72-13790

Hydrodynamic stability of the gradient flow of a conducting fluid with a rheological power law in a transverse magnetic field 18 p2716 A72-36814

Linearized analysis of magnetohydrodynamic channel entrance flow 24 p3430 A72-45573

HARTMANN NUMBER

Nonuniform magnetic field effects in MHD slider bearing, showing inertia terms contribution dependence on Hartmann number [ASME PAPER 71-LUB-8] 02 p0235 A72-11533

MHD flow development in parallel plate channel entrance region, obtaining numerical solution for velocity distribution, pressure drop and length at different Hartmann numbers 02 p0266 A72-12493

Moderate Hartmann number MHD duct flow with applied transverse magnetic field, using numerical methods 06 p0859 A72-17619

Hartmann number for velocity pulsation free transition from turbulent MHD flow to laminar, noting difference relative to linear stability theory 06 p0860 A72-17679

Extremal bounds for mass flow rate of laminar MHD flow in circular and thin walled conducting pipes at high Hartmann number 22 p3210 A72-42315

MHD Couette flow between conducting walls with heat transfer 24 p3428 A72-44970

HARTREE APPROXIMATION

The exact evaluation of certain partial sums of the second order energies of atoms. I - The ground and the singly excited states 17 p2586 A72-35829

Ground and low-lying excited electronic states of FeH 21 p3096 A72-40563

HARTREE-APPLETON APPROXIMATION

U HARTREE APPROXIMATION

HARTREE-FOCK APPROXIMATION

U HARTREE APPROXIMATION

HASTELLOY [TRADEMARK]

Al content caused defect in gas tungsten arc welded Hastelloy, using electron microprobe analysis 06 p0820 A72-17708

Cyclic oxidation kinetics of Hastelloy X sheet and wire specimens for high temperature alloy evaluation in transpiration cooled engine components manufacture 09 p1331 A72-23476

Filler metal paste application effect on Hastelloy sheet brazing quality, describing results in terms of mechanical properties and microstructural characteristics 11 p1637 A72-25342

Fabrication of Hastelloy B sheet by powder metallurgy using blends of elemental powders and homogenization/deformation processing 19 p2815 A72-37596

Elevated temperature ductility minimum in Hastelloy alloy X 20 p2938 A72-39304

HAWAII

Gaseous or solid particle Hg from fumaroles, suggesting natural and industrial sources of Hawaiian air pollution 09 p1305 A72-23648

HAWKER SIDDELEY AIRCRAFT

NT BUCCANEER AIRCRAFT

NT HARRIER AIRCRAFT
HAZARDS
 NT AIRCRAFT HAZARDS
 NT FLIGHT HAZARDS
 NT METEOROID HAZARDS
 NT OPERATIONAL HAZARDS
 NT RADIATION HAZARDS
 NT TOXIC HAZARDS
 Pyrotechnic hazard classification for property and personnel protection in event of accidental explosion
 08 p1220 A72-20768
 Therapeutic electromedical equipment hazards due to electromagnetic interaction, considering implantation and simulation of human body
 15 p2191 A72-32572
 Initiation mechanisms for explosive materials and experiments for hazard evaluation, discussing subdetonation reactions and mathematical models of explosive processes
 16 p2442 A72-33353
HAZE
 Lidar measurements of atmospheric aerosol distributions over large areas including urban haze, scattering layers, trade wind inversion and Sahara dust stream in Caribbean
 [AIAA PAPER 71-1055]
 01 p0057 A72-10526
 Airborne ruby lidar application to cirrus and haze layers measurements, deriving optical parameters
 06 p0777 A72-18448
HCN LASERS
 Visual observation of continuous hydrocyanic acid laser modes and beam energy distribution, using cholesteric liquid crystal image converter
 14 p2111 A72-30851
 Variable output coupling device for far infrared laser.
 17 p2562 A72-34643
 Gain and visualization of the modes of a thermally stabilized HCN laser.
 19 p2810 A72-37455
 High power pulsed HCN laser.
 19 p2811 A72-37583
 HCN laser mechanical, pressure, temperature and voltage environmental factors effects on output power stability
 20 p2934 A72-39967
 Laser magnetic resonance of the O₂ molecule using the 337-micron HCN laser.
 22 p3209 A72-42896
HD-1 GROUND EFFECT MACHINES
 U HOVERCRAFT GROUND EFFECT
 MACHINES
HEAD [ANATOMY]
 NT CRANIUM
 NT INTRACRANIAL CAVITY
 NT OCCIPITAL LOBES
 EEG discharges between vertical dipolar sources computation, using mathematical model with homogeneous spherical conductive medium to simulate human head
 06 p0769 A72-18201
 Ear site body temperature measurement relation to radiant heating of scalp and upper face
 12 p1768 A72-28333
 Water cooled suits efficiency and effectiveness for heat removal, noting importance of head area
 14 p2081 A72-31085
 Analytical model for nonpenetrating impact caused head injuries, evaluating protective device effectiveness via energy absorption characteristics
 15 p2191 A72-32602
HEAD [PRESSURE]
 U PRESSURE HEADS
HEAD FLOW
 Influence of viscosity on the characteristics of compressor bladings for supersonic flow conditions
 20 p2963 A72-39912
HEAD MOVEMENT
 Position constancy and motion perception tests of head movement feedback calibration of perceived direction of optical motions
 01 p0013 A72-10719
 Human vestibular stability under frontal and sagittal head tilts in rotating chairs, discussing motion sickness onset
 05 p0622 A72-16640
 Formulas derived for forces on receptor formation of vestibular apparatus from mathematical analysis of natural human head movements, discussing otoliths and semicircular canals
 05 p0622 A72-16641
 Head movement adaptation to horizontal and vertical field displacements, discussing eye movement direction learning
 06 p0765 A72-17410
 Involuntary head movement and helmet motion displacements during human centrifuge runs to 6 Gz from photographic recordings
 12 p1766 A72-28288
 Hypergravity effects on bats spatial orientation, noting resistance to head-pelvis and pelvis-head accelerations
 13 p1907 A72-30015
 Experimental motion sickness studies in slow rotation room simulating rotating spacecraft conditions,

noting relation between subject susceptibility and number of head motions
 16 p2354 A72-33542
 Fixation eye movements and the processing of visual information.
 21 p3007 A72-40740
 Target distance and adaptation in distance perception in the constancy of visual direction.
 21 p3008 A72-41022
 Visual stimuli distance estimation with head stationary or moving, discussing performance after monocular motion parallax training
 24 p3374 A72-44557
HEAD-UP DISPLAYS
 Head-up display flying under IMC and VMC flight conditions, considering takeoff, landing and navigation modes
 08 p1204 A72-21004
 Pilot pursuit tracking performance under acceleration stress, simulating high performance aircraft dynamics via human centrifuge equipped with simulated head-up predictive gunsight
 12 p1776 A72-28320
 Head-up omnidirectional two dimensional auditory display device for visual detection facilitation in aircraft collision avoidance systems
 12 p1777 A72-28327
 Electronic head-up displays for aircraft instrument indication in symbolic form at pilot eye level
 15 p2188 A72-31513
 The evolution of head-up displays.
 20 p2925 A72-39333
 Head-up display performance in Falcon fan-jet aircraft during taxiing, takeoff, cruise, descent and landing approach, noting low-visibility hazards reduction during landing phase
 20 p2952 A72-39744
 Application of the head-up display /HUD/ to a commercial jet transport.
 21 p3060 A72-41256
 Evolution of the electronic head-up display.
 22 p3176 A72-42295
HEADACHE
 Vascular headache of acute mountain sickness.
 22 p3150 A72-42491
HEALING
 Human and animal central nervous system repair processes for brain damage caused motor function disturbances
 14 p2078 A72-31100
HEALTH
 NT HEALTH PHYSICS
 NT MENTAL HEALTH
 Protection against accelerator and space radiation Conference, Geneva, April 1971, Volume 1, Health physics
 [CERN-71-16]
 02 p0160 A72-12051
 Fainting prevention in flying personnel, discussing constitutional susceptibility, health irregularities, alcohol, heavy smoking, lack of sleep, emotions and medical histories
 03 p0316 A72-13722
 Collaboration of World Health Organization and various international astronomical organizations for space technology applications to man-environment relationships and medical and communication sciences
 07 p0933 A72-20300
 Functional diagnostics of teeth condition as pilot health factor in stomatological aviation medicine, discussing caries, parodontosis and aerodontalgia
 07 p0922 A72-20374
 Active leisure effect on pilot work efficiency, health maintenance and job longevity
 19 p2760 A72-38148
 Methods for measurement of the state of health
 21 p3005 A72-40395
HEALTH PHYSICS
 Environmental, medical and acoustic investigations with underwater laboratory, discussing cabin atmosphere control, depressurization, health conditions and sonar operation
 20 p2898 A72-39938
HEAO
 High energy X ray and gamma ray astronomy for galactic and extragalactic observations, noting SAS satellite and HEAO program
 05 p0712 A72-15773
 Large grazing incidence X ray telescope mirrors for HEAO-C mission observations, noting single stars resolution in clusters and galaxies study
 11 p1630 A72-25682
 HEAO experiment proposal for Be to Sn flux and energy spectra and Be to Fe isotopic composition of galactic primary cosmic rays
 16 p2447 A72-33733
 Precision X-ray telescopes on HEAO-C.
 24 p3403 A72-45202
 Radiation pressure supported stars, degenerate dwarfs, neutron stars and black holes high energy observations from space platforms
 24 p3446 A72-45536
 HEAO satellite to carry instruments required in high energy astrophysics missions, discussing observational objectives, configuration and experiments
 24 p3453 A72-45538

NASA X ray satellite UHURU and HEAO-C instruments and observational data on supernova remnants, pulsars, extars quasars, radio galaxies and galactic clusters
 24 p3446 A72-45539
 Charged and neutral cosmic rays radioactive isotope and momentum distribution measuring techniques in high energy particle astronomy observatories /HEAO/
 24 p3404 A72-45540
HEARING
 NT ACOUSTIC FATIGUE
 NT BINAURAL HEARING
 Neurophysiological hearing mechanisms of inner ear in peripheral auditory pattern recognition
 01 p0012 A72-10481
 Cochlea enclosed two dimensional cavity potential flow model for fluid mechanical theory of hearing
 10 p1430 A72-24295
 The physiology of hearing. I - The middle and the inner ear
 22 p3146 A72-42785
 Cerebral auditory system acoustic information processing, discussing ganglia and cochlea neurophysiological functions in response to afferent stimulations
 22 p3146 A72-42786
HEARING LOSS
 U AUDITORY DEFECTS
HEART
 NT CARDIAC AURICLES
 NT CARDIAC VENTRICLES
 NT EPICARDIUM
 NT MYOCARDIUM
 Chin-sternum-heart syndrome from partial parachute failure, with close reference to atrial endocardial and myocardial lacerations
 02 p0167 A72-11711
 Artificial heart-lungs model with contractile polymer membrane as synthetic muscles to react with gases and liquids, discussing design features
 10 p1431 A72-24640
 The effects of acute hypoxia on lipid synthesis in the rat heart.
 17 p2501 A72-34979
 Changes in energy stores in the hypoxic heart.
 17 p2501 A72-34985
 Helium effect on cardiac mitochondria of mice.
 19 p2759 A72-38712
 Hypoxic acclimation effects on rats heart, liver and kidney mitochondria, measuring cytochrome oxidase and succinic dehydrogenase activities
 22 p3144 A72-42673
HEART DISEASES
 Human patients with chest pain and normal ECG, examining diagnostic value of graded exercise test, history and lipid levels with coronary arteriography data
 01 p0010 A72-10146
 Paroxysmal supraventricular tachycardia initiated by sinus beats in patient, observing A-V nodal conduction delay by ECG and electrophysiological methods
 02 p0156 A72-11423
 Ventricular ectopic arrhythmias from treadmill exercise in patients observed during ECG monitoring
 02 p0156 A72-11424
 Incidence rates of myocardial infarction and sudden death from coronary heart disease for adult black and white populations in Nashville
 02 p0156 A72-11425
 Arrhythmias relation to coronary artery disease, discussing conduction defects, sudden death prodromata and prevention and digitalis as antiarrhythmic agent
 02 p0157 A72-11476
 Coronary heart disease - Conference, Frankfurt am Main, West Germany, January 1970
 03 p0314 A72-13176
 Coronary angiography findings in 263 patients of different age groups compared with history of angina pectoris, risk factors and ECG at rest
 03 p0314 A72-13177
 Exercise ECG correlation to morphological patterns of selective cinecoronary arteriography and ventriculography, revealing significant information on occlusion and stenosis
 03 p0314 A72-13178
 Myocardial blood flow measurement value in ischemic heart disease assessment, discussing Xenon 133 injection into coronary arteries
 03 p0315 A72-13179
 Clinical assessment of degree of obstruction from coronary arteriograms of ischemic and rheumatic heart patients
 03 p0316 A72-13847
 Ballistocardiographic and angiographic correlations of ventricular function in patients with idiopathic hypertrophic subaortic stenosis
 04 p0466 A72-14442
 Familial cardiomyopathy detection by electrocardiography noting arrhythmias, ventricular hypertrophy, abnormal Q waves and intraventricular conduction defects
 04 p0466 A72-14443

Human epicardial arterial circulation platelet aggregates role in sudden coronary death, discussing relation to atherosclerotic stenosis and acute thrombosis 05 p0616 A72-16013

Doppler cardiometry determination of human cardiovascular velocities in patients with heart diseases, discussing impaired left ventricular function detection 05 p0617 A72-16155

Asymmetrical hypertrophic cardiomyopathy symptoms simulating mitral stenosis, suggesting electrocardiography, chest X ray and hemodynamic studies as diagnostic procedures 06 p0761 A72-17380

Sudden death in myocardial infarction, discussing heart electrical stability, neural control, arrhythmias and cardiac conduction disturbances 06 p0761 A72-17381

Electrocardiographic age trends in adult healthy populations, discussing diagnostic implications and overweight, exercise and latent coronary artery disease influence 06 p0761 A72-17425

Cardiac murmur level dependence on blood stream Reynolds number, tracing cardiac noise origin to blood turbulence 06 p0762 A72-17676

Airline pilot postexercise electrocardiograms, showing S-T segment depression correlation to subsequent coronary heart disease 06 p0768 A72-17881

Clinical response to nitroglycerin therapy correlation with coronary angiography as diagnostic test for coronary artery disease in patients with chest pain 07 p0920 A72-19993

Coronary artery disease and vessel involvement severity predictions from electrocardiographic and vectorcardiographic patterns of anterior wall myocardial infarction 07 p0931 A72-19994

ECG evidence of myocardial ischemia in patients without arteriographic evidence of coronary artery disease, studying myocardial oxygen supply 07 p0920 A72-19995

Idiopathic subvalvular aortic stenosis characterized by muscular or membrane obstruction in left ventricular infundibulum, discussing diagnostic importance for pilots 07 p0933 A72-20189

Abnormal ECG in healthy man due to former disease, subclinical disease, congenital anomalies, hereditary disease or functional aberrations 07 p0924 A72-20574

Myocardial infarction effects on drug tolerance and hemodynamic changes due to digitalis doses, discussing toxic arrhythmias 08 p1115 A72-21082

Atheromatosis, chest angina and arrhythmia - Conference, Brussels, October 1970 08 p1117 A72-21541

Hypertension and blood sugar and lipid level increase as ischemic heart disease risk factors 08 p1117 A72-21542

Vectorcardiographic and ECG diagnosis of left anterior hemiblock combined with complete right bundle branch block, discussing coexisting myocardial infarction influence 08 p1127 A72-21850

Ventricular and supraventricular arrhythmias incidence during maximal treadmill exercise in normal man, noting age factor and cardiovascular disease presence effects 09 p1266 A72-23272

Intraventricular conduction defects incidence and mortality in acute myocardial infarction, noting left anterior hemiblock dominance 09 p1266 A72-23273

Clinical reliability and normal variations of Frank ECG computer analysis by Smith-Hyde program for healthy and cardiac patients 09 p1272 A72-23274

Local and cardiac complications of selective percutaneous transluminal coronary arteriography, noting hemorrhages thromboses, embolisms, myocardial infarction, bradyarrhythmia and ventricular fibrillation 09 p1267 A72-23325

Serum petidase activity determination as enzymatic diagnostic test for myocardial infarction 11 p1579 A72-25851

Triglyceridemia relation to age, relative weight and ischemic cardiopathy probability from ECG, anthropometry and lipid and glucid metabolism studies 12 p1759 A72-27238

High altitude hypoxia preadaptation effects on left ventricle myocardium noradrenaline concentration in rats with experimental vitium cordis 12 p1761 A72-27648

Hemodynamic effects of angiographic contrast medium in patients with and without heart disease, discussing myocardial performance during first ten beats 12 p1762 A72-27732

Clinical diagnosis of ST/T depression in resting ECG, noting coronary heart disease and left ventricular hypertrophy 12 p1772 A72-27733

Two stage description of middle germ layer chronic polyarthritis, noting heart muscle and vascular wall tissues necrosis 12 p1772 A72-27822

Multivariate algorithms of optimum content and form for cardiovascular risk assessment in pilots and air transport personnel 12 p1764 A72-28264

Potential coronary heart disease susceptibility indicators in ATC population, using Framingham age/obesity parameters 12 p1764 A72-28265

Stress vectorcardiography quantitative analysis of ECG response to treadmill exercise test to establish diagnosis criteria for coronary heart disease 12 p1775 A72-28282

Serum cholesterol, phospholipid and lipoprotein levels relation to atherosclerotic heart disease occurrence in USAF personnel 12 p1766 A72-28292

Clofibrate treatment for atherosclerotic cardiovascular disease prevention among Sabena flying personnel 12 p1766 A72-28293

Quantitative angiocardiology of abnormal left ventricular function and contractile spectrum in ischemic heart disease patients 14 p2077 A72-30968

Coronary heart disease discriminatory factors from comparison with healthy controls, noting diastolic hypertension significance 15 p2183 A72-31282

Platelet electrophoretic mobility response to adenosine diphosphate/ADP/ in patients with coronary artery disease 15 p2183 A72-31283

Platelet aggregates role in intramyocardial vessel circulation impedance in patients dying suddenly of coronary artery disease 15 p2186 A72-31770

Serial ECG change detection and description in myocardial infarction survivors, using computer analysis to find best diagnostic discriminants from multiple criteria 16 p2357 A72-34008

Exchangeable potassium in heart disease - Long-term effects of potassium supplements and amiloride 17 p2500 A72-34932

Myocardial ultrastructure in acute and chronic hypoxia 17 p2502 A72-34988

Morphological alterations in the ischemic heart 17 p2502 A72-34995

Acquired complete right bundle branch block without overt cardiac disease - Clinical and hemodynamic study of 37 patients 17 p2505 A72-35821

Work capacity and physiological responses to maximum exercise in 54 year old men in relation to heart disease and cardiovascular hazard studies 17 p2505 A72-35822

Correlation between ergometry, ballistocardiography and coronary angiography in 267 patients 18 p2649 A72-36034

Changes of the mitral echocardiogram with ageing and the influence of atherosclerotic risk factors 18 p2652 A72-37031

Echocardiography in the diagnosis of congenital mitral stenosis and in evaluation of the results of mitral valvotomy 19 p2755 A72-37499

The incidence of hypertension and associated factors - The Israel ischemic heart disease study 19 p2756 A72-37870

Prognostic value of an electrocardiographic sign in acute myocardial infarction 19 p2756 A72-37871

Interrelationship of hemodynamic alterations of valvular heart disease and renal function - Influences on renal sodium reabsorption 19 p2756 A72-37872

Influence of inotropic alteration on the severity of myocardial ischemia after experimental coronary occlusion 19 p2758 A72-38552

Hemodynamic indices in flight crew personnel during hypertonic sickness and atherosclerosis of coronary arteries 20 p2892 A72-39391

The mitral apparatus - Functional anatomy of mitral regurgitation 20 p2892 A72-39460

Relationship of pulmonary artery to left ventricular diastolic pressures in acute myocardial infarction 20 p2892 A72-39461

An indirect method for evaluation of left ventricular function in acute myocardial infarction 20 p2892 A72-39462

Vectorcardiographic and electrocardiographic differentiation between cor pulmonale and anterior wall myocardial infarction 21 p3001 A72-40769

The standard 12-lead scalar electrocardiogram - An assessment of left ventricular performance 23 p3255 A72-43812

Continuous recording of His bundle electrogram during selective coronary cineangiography in man. 23 p3255 A72-43813

Analysis of intracavitary electrocardiograms through a saline bridge in the diagnosis of cardiac arrhythmias. 24 p3370 A72-44559

The scoliosis of congenital heart disease. 24 p3370 A72-44560

Clinicoarteriographic correlations in angina pectoris with and without myocardial infarction. 24 p3372 A72-45010

Longevity and cardiovascular mortality among former college athletes. 24 p3374 A72-45689

H-V intervals in left bundle-branch block - Clinical and electrocardiographic correlations. 24 p3374 A72-45690

Clinical and anatomic implications of intraventricular conduction blocks in acute myocardial infarction. 24 p3374 A72-45691

HEART FUNCTION

NT HEART MINUTE VOLUME

Extrasystolic potentiation of ventricular contraction effect on dog mitral valve function, using roentgen videodensitometry 01 p0015 A72-11036

Computer aided biplane roentgen videometry system for dynamic circulatory structure studies including blood flow and heart volume determination 01 p0020 A72-11040

Cardiac output and autonomic nervous system role in antidiuretic response to acute thoracic superior vena cava constriction 02 p0157 A72-11661

Physical exercise effect on ECG atrial recovery wave duration and magnitude in humans with A-V blocks 02 p0166 A72-12891

Idiopathic hypertrophic subaortic stenosis ballistocardiography, measuring ventricular function by angiography 03 p0314 A72-13142

Regular sinus rhythm bundle branch block effect on ballistocardiogram dynamics 03 p0314 A72-13143

Quotient of arrhythmia relation to physical work load, noting heart rate amplitude and frequency variations 04 p0472 A72-14899

Physical conditioning effect on central and peripheral circulatory responses to arm work, measuring cardiac output at 80 percent maximum aerobic power 04 p0473 A72-14900

Regional myocardial contraction mechanics during transient ischemia and reoxygenation in anesthetized dogs 04 p0476 A72-15719

In vivo investigation of dogs natural mitral valve flow dynamics, developing cardiohemodynamic system physical model for data analysis and electrical analog simulation [ASME PAPER 71-WA/BHF-2] 05 p0621 A72-15949

Hydrodynamic model of human systemic arterial circulation to test artificial heart pumps [ASME PAPER 71-WA/AUT-13] 05 p0621 A72-15954

Myorelaxant 3,5-dimethyl-4-bromopyrazol injection effect on rabbit and dog heart during direct extracardiac nerve stimulation 05 p0618 A72-16358

Electrocardiography telemetry system for intense radiation environment, describing electrode and transmitter implantation in monkey and heart signal transmission and reception 05 p0623 A72-16678

Heart pacemaker activity during muscular exertion, developing mathematical model based on system dynamics transient processes analysis 06 p0764 A72-18059

Maximum oxygen intake during exercise on treadmill compared with bicycle ergometer, analyzing circulatory dynamic factors and cardiac output relation to oxygen transport capacity 07 p0922 A72-20251

Stretch activation of myogenic oscillation of isolated contractile structures of heart muscle in ATP salt solution 07 p0923 A72-20427

Atypical ECG of sportsmen, considering repolarization disorders due to ischemia, lesion, excitability and conduction signs 07 p0924 A72-20575

Cardiographic interpretation of computerized apexo-carotid diagram, using heart-motor pump comparison 07 p0934 A72-20607

Myocardium catecholamine level reduction by heart hyperfunction from aortic coarctation during moderate thyroidin doses 07 p0924 A72-20622

- CO hypoxia effect on oxygen transport during exercise, discussing changes in cardiac and respiratory functions and work capacity
08 p1114 A72-20893
- Cardiorespiratory functions in child swimmers and nonathletes during growth, relating training to oxygen transport system dimensions
08 p1123 A72-20894
- Cardiovascular analog computing circuits with outputs for left ventricular pressure maximum rise rate, cardiac stroke volume and atrioventricular conduction time
08 p1124 A72-20899
- Dynamic orthosympathetic control of cardiovascular system, studying efferent element link between autonomic vasomotor and cardiac centers and effector cells
08 p1118 A72-21548
- Ventricular myocardium contractile function disorder diagnosis by phase coordinate method with intracardiac hemodynamics application
08 p1122 A72-22186
- Myocardium excitation-contraction mechanism in heart regulation, discussing surface membrane structure and cell action potential
09 p1264 A72-22222
- Cardiovascular system model for demonstration of biological system analog simulation and computation, describing components for heart pumping action and systemic circulation
09 p1268 A72-22454
- Cardiac cycle intervals measurement with multibeam cathode oscilloscope synchronized with multichannel polycardiographic automatic recording machine
09 p1272 A72-23192
- Mathematical, physical and engineering aspects of electro- and magnetocardiography, noting heart field nonbipolar properties and heart vector determination difficulties
09 p1273 A72-23414
- Clinical effects on atrio-ventricular pacing system of electromagnetic weapon detector systems used for air passenger screening at airports in air hijacking prevention efforts
10 p1428 A72-23740
- Human left ventricle measurements, modeling, control and simulation for heart monitoring purposes, describing muscle performance mathematical model and stress effect prediction control system
10 p1429 A72-23924
- On-line analog display system for cardiovascular functions and beat-by-beat cardiac output derived from single aortic blood flow measurement
10 p1430 A72-24375
- Ear densitograph for noninvasive cardiac performance measurements during physical activities, exercise tests, flight conditions and for critical patients long-term monitoring
11 p1582 A72-25500
- Electronic and hematocrit devices to investigate cardiovascular system functions including blood coagulation process, pressure and flow
11 p1585 A72-26464
- TV microscopic system for on-line measurement of cat omentum microvessels diameter relative to heart action
11 p1587 A72-26621
- Physical training effect on rat cardiac function and metabolic response to hypoxia
11 p1581 A72-26701
- Heart and circulatory system functional diagnostics, discussing ECG, blood pressure, X ray, phonocardiographical and pulmonary examinations
12 p1760 A72-27271
- Human cardiovascular function change as indication of hypoxic circulatory stress, using noninvasive cardiographic measurements of cardiac electromechanical time intervals
12 p1769 A72-27470
- Acute hypoxia effects on dog coronary blood flow and cardiac function from cardiac beta-adrenergic and hemodynamics study
12 p1760 A72-27482
- Case report of pilot near-syncope episode with bradycardia due to hyperactive right carotid sinus reflex
12 p1771 A72-27487
- Cat and rat cardiac and cardiovascular reflexes response to electric pulse stimulation of sensorimotor cerebral cortex
12 p1761 A72-27647
- Renal clearance studies of left atrial distention effect in dog, indicating antidiuretic hormone inhibition mechanism of diuresis
12 p1763 A72-27828
- Autonomic nervous system role in controlling coronary and cardiac responses to hypoxic hypoxia, measuring blood flow with Doppler ultrasonic flow transducer
12 p1767 A72-28313
- Cardiorespiratory response to breathing dense sulfur fluoride-oxygen mixture under physical exercise conditions
12 p1767 A72-28314
- Heart enzyme activity under experimental myocardial ischemia in rabbits determined for blood, left and right ventricles and atrium
13 p1901 A72-28463
- Coronary system autoregulation patterns and mechanisms from coronary flow shift measurements during circumflex artery perfusion experiments in dogs
13 p1901 A72-28637
- Contractile responses of guinea pig, rat and human isolated ventricular myocardium to increased stimulation frequency
13 p1907 A72-30044
- Cardiac stroke volume measurements during supine bicycle exercise and recovery period, using indicator-dilution technique
14 p2079 A72-30701
- Quantitative angiocardiology of abnormal left ventricular function and contractile spectrum in ischemic heart disease patients
14 p2077 A72-30968
- Cardiac output and body temperature response to prolonged intermittent exercise
15 p2185 A72-31448
- Human heart physiopathology from cardiac performance analysis, treating heart as pump and muscle
15 p2187 A72-32493
- Apexocardiograms and carotid pulse measurements as indicators of cardiac function and myocardial contractility
15 p2190 A72-32494
- Indicator dilution methods for ventricular volume measurements from washout curves, discussing intraventricular blood mixing uniformity
15 p2190 A72-32496
- Baboon heart endocardial structure dynamic behavior, comparing left ventricle septum and epicardium contractile force and intramyocardial pressure changes
15 p2187 A72-32748
- Unconditioned/muscular load stimulus/ and conditioned/metronome stimulus/ cardiac reflexes in hypnotic and alert states
16 p2353 A72-32991
- Computerized angiographic heart geometry analysis for three dimensional ventricle models of man and dog, using Ta markers
16 p2354 A72-33424
- Non-invasive assessment of prosthetic mitral paravalvular and intravalvular regurgitation.
17 p2498 A72-34221
- Hemodynamic changes in man during immersion with the head above water.
17 p2507 A72-34543
- Influence of hyperosmolality on left ventricular stiffness.
17 p2499 A72-34727
- Metabolism of the hypoxic and ischaemic heart; Proceedings of the Symposium, Geneva, Switzerland, June 14-17, 1971. Part 1.
17 p2501 A72-34976
- Substrate utilization and glycolysis in the heart.
17 p2501 A72-34977
- The influence of exogenous ATP on cardiac metabolism in acute hypoxia.
17 p2501 A72-34987
- Cardiac performance and the coronary circulation of man in chronic hypoxia.
17 p2502 A72-34992
- Effect of chronic hypoxia on the kinetics of energy transformation in heart mitochondria.
17 p2502 A72-34993
- Effects of hypoxia and ischemia on myocardial contraction - Alterations in the time course of force and ischemia-dependent inhomogeneity of contractility.
17 p2502 A72-34996
- Trophic support of cardiac activity
17 p2504 A72-35020
- Mathematical models for flow ejection and aorta pressures based on displacement ballistocardiography and time dependent incompressible flow theories respectively
18 p2649 A72-36035
- Some preliminary observations on the correlation of the high frequency /acceleration/ direct-body ballistocardiogram with the apex cardiogram, carotid pulse and their derivatives.
18 p2649 A72-36036
- Computerized simulation of ballistocardiograph subjective evaluation and objective manual measurements, correlating heart beat with ideal pattern
18 p2652 A72-36037
- Thermoregulation during positive and negative work at different environmental temperatures.
18 p2650 A72-36559
- Analysis of left ventricular wall motion by reflected ultrasound - Application to assessment of myocardial function.
19 p2755 A72-37497
- Evaluation of left ventricular function by echocardiography.
19 p2755 A72-37498
- Determination of systolic time intervals using the apex cardiogram and its first derivative.
19 p2759 A72-38817
- Echocardiographic determination of left ventricular dimensions, volumes and performance.
19 p2762 A72-38819
- The mitral apparatus - Functional anatomy of mitral regurgitation.
20 p2892 A72-39460
- An indirect method for evaluation of left ventricular function in acute myocardial infarction.
20 p2892 A72-39462
- A modified acetylene method for the determination of cardiac output during muscular exercise.
20 p2898 A72-39807
- Evaluation of cardiopulmonary function and work performance in man during caloric restriction.
21 p3005 A72-40423
- Cortico-visceral studies of spinal cord reticular formation stimulation and destruction effects on electroencephalogram, cardiac activity and interoceptive glycemic reflexes
21 p3000 A72-40757
- Cardiac output, arterial and mixed-venous O₂ saturation, and blood O₂ dissociation curve in growing rats adapted to a simulated altitude of 3500 m.
21 p3003 A72-41623
- Localization and structural-functional organization of the system of vagus nerve nuclei constituting the 'cardiac center' of the medulla oblongata
21 p3004 A72-41673
- Myocardium automatism, excitability, conductivity and contractility under cooling, noting complete inhibition at 9-3 deg C
22 p3141 A72-42072
- Heart function and pulmonary circulation in humans suffering from chronic mountain sickness
22 p3143 A72-42587
- Specific ATP action on metabolism of isolated heart - Influence of pH, divalent cation concentration and stability of complexes.
22 p3147 A72-42986
- A rapid assay of dipolar and extrapolar content in the human electrocardiogram.
23 p3259 A72-43811
- The standard 12-lead scalar electrocardiogram - An assessment of left ventricular performance.
23 p3255 A72-43812
- Excitation contraction correlates in true ischemia.
23 p3255 A72-43814
- Cardiac output, hemodynamic and gas exchange variations as function of basal metabolism during bed rest in hypokinetic recumbent or antihorosthatic position
23 p3255 A72-43915
- Evaluation of the pulse-contour method of determining stroke volume in man.
23 p3256 A72-43934
- Collagen in human myocardium as a function of age.
23 p3256 A72-43935
- A critical assessment of an open circuit technique for measuring oxygen consumption.
23 p3260 A72-43937
- Carotid displacement pulse first time derivative recording as noninvasive technique for heart function assessment
24 p3370 A72-44561
- Animal studies of effect of chronic exercise on the heart and atherosclerosis - A review.
24 p3370 A72-44563
- General index for the assessment of cardiac function.
24 p3372 A72-45011
- HEART MINUTE VOLUME**
Cardiovascular analog computing circuits with outputs for left ventricular pressure maximum rise rate, cardiac stroke volume and atrioventricular conduction time
08 p1124 A72-20899
- Electrically sensed changes in chest and abdomen diameter for tidal volume, respiratory frequency and minute ventilation measurements
21 p3006 A72-40428
- Factors limiting the increase in stroke volume obtainable by positive inotropism - Investigations regarding the sufficient heart in the case of continued postextrasystolic potentiation
22 p3145 A72-42748
- HEART RATE**
NT ARRRHYTHMIA
NT BRADYCARDIA
NT SYSTOLE
NT TACHYCARDIA
Right heart ventricle intracardiac phonocardiograms, recording pulmonary early diastolic click simultaneous with artery pressure curve dirotic wave
01 p0010 A72-10121
- Respiration effects on human heart rate deceleration and biphasic cardiac response in aversive shock conditioning situation
01 p0010 A72-10195
- Age and physique effects on human continuous work capacity, monitoring heart rates during task performance
01 p0018 A72-10568
- Heart and respiration rates response to free fall parachuting, using FM/FM telemetry
02 p0167 A72-11709

Extracardiac chronotropic effects on cardiac rhythm variations during fatigue, using variational pulsometry and autocorrelation and spectral analysis
02 p0164 A72-12513

Bainbridge reflex mechanism, showing sinus ganglion role in tachycardia onset
02 p0165 A72-12514

Hippocampus electric activity and cardiac rhythms variations responses to various intensity electric stimulation of central gray matter
02 p0165 A72-12881

Physical exercise effect on ECG atrial recovery wave duration and magnitude in humans with A-V blocks
02 p0166 A72-12891

Physical training effect on subjective rating of perceived exertion, investigating correlation with heart rate and blood lactate concentration
03 p0319 A72-13678

Maximal oxygen intake prediction in acute moderate hypoxia during exercise, showing heart rate linearity with work load
07 p0916 A72-18966

Phase relations between alpha waves in EEG and automated rhythmic motoric activity as function of subject behavioral activity and thalamic pacemaker zones
07 p0916 A72-19109

Cardiac acceleration by voluntary muscle contractions of minimal duration in men due to vagal tone inhibition
07 p0929 A72-19442

Aortic flow disturbances in vivo study by hot-film anemometer, considering peak flow velocity and pulse rate effects
07 p0934 A72-20537

Oxygen intake and cardiac output measurements during various treadmill and bicycle ergometer exercises, relating exercise type to heart rate and arteriovenous oxygen differences
08 p1123 A72-20885

Time series analysis of physiological and work study data in ATC tasks, using heart rate as strain indicator
09 p1271 A72-23137

Aerobic work capacity indices of gas exchange pulse rate, pulmonary ventilation and acid base balance in runners, determining maximum oxygen utilization
09 p1268 A72-23596

Human tilt tolerance relation to aerobic capacity, weight, height and physical fitness, determining correlation coefficient between heart rate and orthostatic response
10 p1428 A72-23733

Positive acceleration effects on human cardiovascular system during centrifuge tests, studying ECG changes in terms of cardiac rhythm, heart rate and wave parameters
11 p1584 A72-26015

Maximal oxygen uptake and heart rate during ladder climbing, inclined treadmill running and cycling ergometer tests
11 p1586 A72-26612

Computer assisted monitoring of ECG waveforms and heart sounds frequency spectra to detect bubble laden blood during decompression sickness
11 p1587 A72-26626

Nose installed thermistor device for in-flight monitoring of pilot respiration and pulse rate
12 p1769 A72-27417

Parachutist biomedical responses in aerial tow at 110-175 knots, determining heart and respiration rates and urinary catecholamines
12 p1774 A72-28272

Physiological evaluation of diastole mechanism in rat hypertrophied myocardium as function of heart rate, Ca ion concentrations and temperature
13 p1901 A72-28521

Pulse rate studies of human adaptation to 16 hour work-rest cycle, showing persistence of 24 hour cycle
13 p1904 A72-29316

Heart rate change regularities during inverted work-rest cycle of isolated man, noting relation to circadian rhythm
13 p1904 A72-29317

Medical monitoring system for enclosed men, using ultrasonic Doppler-cardiography for heart rate determination
14 p2078 A72-30384

Heart rate diurnal rhythm adaptation to work-rest cycle change, using recumbent and sitting position data parameters
14 p2075 A72-30391

ECG amplifier and cardiographometer for exercise studies, using digital algorithm for heart rate computation and ECG signal preprocessing for R wave detection
14 p2080 A72-30707

Exercise cardiographometer with heart rate display on beat to beat basis, R wave recognition circuit and noise linear filtering efficiency
14 p2082 A72-31092

ECG heart rate recording of helicopter instructor pilots during flight training tasks, administrative work, automobile driving and eating
14 p2082 A72-31097

Apexocardiograms and carotid pulse measurements as indicators of cardiac function and myocardial contractility
15 p2190 A72-32494

Cardiac cycle length /RR interval/ and QT interval mathematical relationship from ECG obtained during exercise and recovery periods
15 p2187 A72-32747

Heat, noise and vibration stress combined effects on skin and rectal temperature, heart rate, weight loss and biochemical urinalysis
17 p2508 A72-34551

[AD-746083] Reproducibility of indirect /CO2/ Fick method for calculation of cardiac output.
17 p2506 A72-35971

Synchronous and asynchronous BASH /body acceleration synchronous with heart beat/ effects on hemodynamics and ventilation in dogs and humans
18 p2648 A72-36033

Some preliminary observations on the correlation of the high frequency /acceleration/ direct-body ballistocardiogram with the apex cardiogram, carotid pulse and their derivatives.
18 p2649 A72-36036

Tilt table tests for orthostatic tolerance, measuring heart rate, blood pressure and responses of fainers and nonfainers
21 p3008 A72-41020

Reflexive cardiac rhythm changes and arterial tension during hypoxia, noting differences due to animals, controlled respiration and pharmacological effects
22 p3141 A72-41984

Heat strain in hot and humid environments.
22 p3150 A72-42492

Spinal cord heating and cooling effects on body temperature, respiratory and heart rates and arterial blood pressure, investigating feeding and drinking behaviors
22 p3150 A72-42672

Control parameters of the blood-pressure regulatory system. I - Heart-rate sensitivity.
22 p3145 A72-42771

Control parameters of the blood-pressure regulatory system. II - Open-loop gain, reference pressure and basal heart rate.
22 p3145 A72-42772

Yield of ischaemic exercise electrocardiograms in relation to exercise intensity in a normal population.
22 p3151 A72-42900

Echocardiographic investigation of heart rate, sex and normal aging effects on mitral valve leaflet movement in healthy subjects
22 p3148 A72-43021

The effect of hypoxia on the coronary blood flow in reserpinized dogs.
24 p3370 A72-44562

HEART VALVES

In vivo investigation of dogs natural mitral valve flow dynamics, developing radiohemodynamic system physical model for data analysis and electrical analog simulation
05 p0621 A72-15949

[ASME PAPER 71-WA/BHF-2] Single linear measure of systolic pressure gradient for calculation of aortic valve area in stenosis severity assessment
12 p1762 A72-27734

Aortic regurgitation variation with respiratory sinus arrhythmia and respiratory cycle in dogs during tachycardia and bradycardia
22 p3151 A72-42674

Echocardiographic investigation of heart rate, sex and normal aging effects on mitral valve leaflet movement in healthy subjects
22 p3148 A72-43021

HEAT ACCLIMATIZATION

U ACCLIMATIZATION

U HEAT TOLERANCE

HEAT BALANCE

Annual heat balance in Martian northern polar cap, considering atmospheric, ground and solar heat flux absorbed by snow
03 p0436 A72-13817

Equilibrium temperature formula derived for surface subjected to aerodynamic heating by gas from heat balance between convective and radiative heat flow
04 p0595 A72-14651

High temperature thermal properties of solid and liquid metals and rocks and minerals, discussing earth heat balance and measurement methods for heat capacity and conductivity
04 p0596 A72-14653

Porous cooling unsteady state problem approximation based on elementary thermal balance concept, solving differential equations by computerized Euler method
06 p0904 A72-18513

Solar coronal plasma radiative capacity and temperature structure from cooling function in thermal balance equation
08 p1231 A72-21124

Integral contact temperatures and heat balance calculation for heat transfer between contacting bodies with rotational motions
08 p1252 A72-21444

ESRO 1 satellite residual gas outgassing rate and composition measurements during thermal heat balance tests, using mass spectrometer
09 p1263 A72-23260

Thermophysical aspects of abrasive belt grinding, determining maximum contact temperatures and heat balance
13 p1963 A72-28745

Scale analysis of large scale tropical disturbances in conditionally unstable atmosphere, estimating geopotential height dependence on stream function via heat balance equation
14 p2128 A72-30345

Lateral heat exchange in a thermocouple
17 p2498 A72-35513

Contribution to the theoretical study of the distribution of the emittance along the walls of an antiradiating cell
18 p2742 A72-37199

Low energy cosmic particle and soft X ray photon produced nonthermal electrons effect on interstellar gas ionization and thermal energy equilibrium
19 p2867 A72-38508

Thermal balance in man during 24 hours in a controlled environment
22 p3145 A72-42747

Energy flow diagrams.
24 p3369 A72-44686

HEAT BUDGET

NT ATMOSPHERIC HEAT BUDGET

HEAT CAPACITY

U SPECIFIC HEAT

HEAT CONDUCTION

U CONDUCTIVE HEAT TRANSFER

HEAT CONTENT

U ENTHALPY

HEAT DISSIPATION

U COOLING

HEAT DISSIPATION CHILLING

U COOLING

HEAT EFFECTS

U TEMPERATURE EFFECTS

HEAT EQUATIONS

U THERMODYNAMICS

HEAT EXCHANGERS

NT TUBE HEAT EXCHANGERS

Concentric spherical heat exchanger, showing heat transfer coefficient decrease with coolant flow rate increase
02 p0303 A72-12320

Free convective motion of conducting fluid past vertical plate in uniform transverse magnetic field, determining optimum dimensions of heat exchangers
03 p0399 A72-14011

Ti-Ni-Cu and Ti-Zr-Be alloys for brazing Ti heat exchangers, discussing flow characteristics and corrosion resistance
06 p0820 A72-17703

Heat transfer and hydraulic resistance of lamellar type heat exchangers with water/air working media, testing efficiency for various duct cross sections and Reynolds numbers
06 p0904 A72-18510

Explosive welding of heat exchanger tubes and detonation produced compressive joining of cables as applications of explosive metalworking procedures
07 p0994 A72-18931

Transient processes in heat exchanger, allowing for coolant variable density
09 p1410 A72-22413

Gas turbine recuperator technology, discussing use of compact efficient heat transfer surfaces developed for aerospace heat exchangers
11 p1703 A72-25628

[ASME PAPER 72-GT-32] Hydrogen resistojet design and testing with Re heat exchangers, noting appropriate power efficiency and exhaust velocity for synchronous communication satellites orbital transfer
11 p1708 A72-26186

[AIAA PAPER 72-449] Jet compression role in high temperature mechanical energy conversion heat exchanger based on ejector principle
12 p1755 A72-27724

Book on extended surface thermal transfer covering heat exchanger design, convective transfer, radiation and computer programs
14 p2172 A72-30975

Steady state lumped linear formulation of heat transfer in multichannel parallel-and-mixed-flow heat exchangers
14 p2173 A72-31065

German monograph on pressure loss and heat transfer in heat exchangers, taking into account hydrodynamic and thermal inflow velocity and temperature distribution
16 p2478 A72-33504

The apparent heat transfer coefficient of plate heat exchangers
20 p2984 A72-39649

Heat transfer ratios in multifluid regenerative systems
20 p2984 A72-39650

- A general method for the analysis of compact multi-fluid heat exchangers.
[ASME PAPER 72-HT-14] 20 p2986 A72-39684
 - Mathematical models for temperature profiles and heat transfer rates in two-stream and multistream cross flow heat exchanger
21 p3128 A72-40931
 - Application of the elementary-balance method to the calculation of the nonstationary temperature fields and aerodynamic characteristics of several versions of a surface-type heat exchanger
21 p3130 A72-41064
 - Temperature distribution in a perforated stiffener
23 p3356 A72-43684
 - Heat release and resistance of the cylindrical heat exchangers of blades with a dual flow cooling system
24 p3434 A72-45625
- HEAT FLOW**
U HEAT TRANSMISSION
HEAT FLUX
- Plasma source with arc stabilized by supersonic air stream, measuring enthalpy, heat flux and potential distribution
01 p0048 A72-10491
 - Higher moment Vlasov equations of collisionless fully ionized plasma for studying solar wind proton thermal anisotropy, heat flux and distribution function
01 p0119 A72-10880
 - Hydraulic analogy application to heat conduction problems, considering seepage and network pipe flow models for complex heat flux phenomena representation
01 p0145 A72-11174
 - Finite difference technique for heat transfer rate in laminar flow in tube with step change in cross section, discussing velocity profiles
02 p0301 A72-11723
 - Anode heat flux for cascade atmospheric Ar arc of Maecquer type, checking anode heat transfer model validity
02 p0302 A72-12266
 - Thermal flux model of lithium plasma source at various temperatures and pressures, using arc channel model with conducting cross section
02 p0268 A72-12859
 - Liquid propellant rocket abort fireball model, specifying heat flux as function of time
03 p0457 A72-13953
 - Elastic plate with two collinear thermally insulated cracks, calculating steady temperature field and stresses for uniform heat flux at infinity
03 p0450 A72-14112
 - Heat transfer in rectangular annular channel during external heating under supercritical pressure, discussing thermal flux, mass flow rates and enthalpy
03 p0457 A72-14152
 - Critical thermal loads during external and internal heating of annular channels, discussing curvature effect on density level in thermal flux during forced fluid motion
03 p0458 A72-14157
 - Tube wall temperature and acoustic noise spectra dependence on thermal flux density in bubble coalescence
03 p0458 A72-14162
 - Thermal flux sensors high temperature calibration, using vacuum chamber technique
03 p0362 A72-14163
 - Unsteady thermal conductivity inverse problems, obtaining heated body surface temperature and heat flux from temperature measurement in interior
03 p0458 A72-14164
 - Heat transfer to liquid fuel burning from sandfilled pan burner, measuring burning rate, wick temperature distribution and flame radiation heat flux distribution as function of time
03 p0458 A72-14221
 - Steady heat conduction plane problem solution for infinitely long cylinder with constant surface thermal flux density and temperature
04 p0595 A72-14644
 - Magnetospheric heat flux effect on height variation of electron and ion temperatures and ion composition in topside ionosphere
04 p0515 A72-14929
 - Plasma velocity, gas pressure, wall heat flux and shock heated region extent measured in electrical discharge shock tube, discussing ionization relaxation process
05 p0693 A72-15849
 - Heat flux calculation in laminar turbulent boundary layer transition zone using Schlichting model of turbulent spot formation
05 p0649 A72-16222
 - Heat transfer rate prediction in cooling system design for gas turbines
[AIAA PAPER 72-10] 05 p0707 A72-16865
 - Hg vapor condensation on cooled vertical steel cylinder at 70-185 C, considering heat flux relation to saturated vapor/cooling surface temperature difference
06 p0903 A72-18190
 - Heat transfer and drag during air laminar flow in circular pipe with constant heat flux density at wall
07 p0966 A72-18938
 - Atmospheric eddy flux spatial variations in constant flux layer, noting heat and momentum flux variability of less than 10 percent
07 p1030 A72-19107
 - Dry areas occurrence on heating surface in pool boiling near burnout heat flux, discussing nucleate and film boiling stability and hysteresis
07 p1099 A72-19621
 - Pulse energy and heat distribution in dielectric and metal during electroerosive machining
08 p1174 A72-21035
 - Calibration technique for conductive thermal flux sensors operating at low temperatures
08 p1166 A72-21315
 - Conductive heat flux propagation rate in gases as function of absolute temperature
08 p1253 A72-21447
 - Biot variational principle for phase change problem with constant heat flux boundary condition and without melt removal, noting linear temperature profile choice
08 p1254 A72-21611
 - Calorimetric gage for convective and radiative wall heat flux measurements in Ar arc plasma
08 p1254 A72-21628
 - Convective plumes model with heat flux, layer depth and surface turbulence intensity as parameters
[AD-745511] 09 p1347 A72-23655
 - Emissivity calculation for radiant heat flux from isothermal gas mixture of hydrocarbon fuel combustion products
10 p1561 A72-23839
 - Radiant heat flux measurement during pulsed processes from surface in high temperature emitting gas, using thin film sensor with small time constant
10 p1561 A72-23843
 - Capillary evaporation cooling system with water as working medium, measuring effectiveness in terms of heat flux density vs water consumption
[DFVLR-SONDDR-112] 10 p1561 A72-24023
 - Thermal radiation effects on natural convection boundary layer adjacent to vertical flat surface with uniform heat flux input
10 p1562 A72-24466
 - Laminar free convection about isothermal horizontal cylinders with constant heat flux, calculating velocity and temperature profiles
11 p1743 A72-25263
 - Low thermal flux glass fiber composite over-wrapped tubing with metallic liners for leak free cryogenic propulsion plumbing systems
[ALAA PAPER 72-328] 11 p1637 A72-25364
 - Heat transfer characteristics of liquid metal filled closed thermophosphors for hot wall boundary conditions of constant temperature and uniform heat flux
[ASME PAPER 72-GT-36] 11 p1745 A72-25631
 - Nucleate pool boiling three component heat flux theory, taking into account latent heat transport, molecular heat conduction and turbulent convection
11 p1746 A72-26539
 - Energy capacity margin of heat absorbing liquid /water/ in cooling system, considering specific heat and maximum critical heat flux
11 p1747 A72-26969
 - Near-ground daytime temperature and humidity fine structure relation to heat flux, net radiation and temperature and wind gradients
12 p1841 A72-27711
 - Thermal flux on contact area and temperature distribution on specimen surface during diamond grinding
12 p1814 A72-27767
 - Three dimensional heat propagation problem of copper electrode destruction under concentrated heat flux with allowance for metal evaporation
12 p1890 A72-28175
 - Underwater tests of instrument system for combined skin temperature and direct heat flow measurement in thermally stressful environments
12 p1768 A72-28334
 - Semiempirical determination of local thermal fluxes and heat transfer coefficients for turbine blades based on thin film thermocouples
13 p2025 A72-28730
 - Time history model of transient ignition to self sustained propellant burning, taking into account pressure effects and igniter heat flux
13 p2065 A72-29305
 - Thermal flux distribution in sectioned plasmatron channel with supersonic Ar plasma injection, discussing energy dissipation
13 p2017 A72-29634
 - Ablation rate growth phenomenon in melttable material with increasing thermal flux, discussing quartz glass characteristics
13 p2066 A72-30007
 - Daytime F region inverse relationship between electron density and temperature, determining energy input profile and thermal flux
14 p2097 A72-30127
 - Temperature distribution of structural element with heat shield and metallic layer, determining ablation process for thermal flux at surface
14 p2170 A72-30593
 - Ionospheric electrons and neutral particles temperature and concentration profiles explained by electron gas cooling due to atomic hydrogen excitation, calculating heat flow
14 p2101 A72-30641
 - Steady state thermal transfer during ablation and radiation of single scattering albedo with constant heat flux at boundary
14 p2171 A72-30892
 - Boundary layer temperature profile for ablating asbestos-plastic composite samples measured under combined convection and radiant heat fluxes
14 p2172 A72-31003
 - Thermal flux transmitted from hot surface to boiling fluid near nucleation site measured simultaneously with bubble growth rate
14 p2172 A72-31056
 - Forced convection and thermal boundary condition in parallel and tapered passages, discussing Nusselt numbers for exponentially decreasing wall heat fluxes
14 p2173 A72-31062
 - Shear stress distribution and local heat flux at surface of axisymmetric bodies for laminar and turbulent boundary layer flows
14 p2071 A72-31163
 - Plasma velocity, gas pressure, wall heat flux and shock heated region length measured in electrical discharge shock tube without diaphragms, discussing ionization relaxation process
15 p2283 A72-31268
 - Heat flux nondestructive inspection methods for laminate and sandwich structures and electronic components
15 p2232 A72-31322
 - Unsteady heat flux sensor types and characteristics, considering flux level, measurement time and frequency response
15 p2233 A72-31374
 - Stefan problem of metal evaporation duration after intense heat flux termination as function of thermophysical properties
15 p2334 A72-31504
 - Blunt planetary entry vehicles thermal flux prediction, taking into account viscosity, conduction, dissociation, ionization, nongray radiation, surface emissivity and ablation effects
15 p2335 A72-31816
 - Floating forces contribution to heat flux during turbulent mixing of upper atmosphere
16 p2417 A72-33292
 - Steady state temperature field and heat flux at wall for metallic coolant flow in thin walled axisymmetric pipe with nonhomogeneous Neumann boundary condition
16 p2477 A72-33413
 - Subcooling and acceleration effects on nucleate boiling heat flux, comparing heat transfer prediction models with experimental measurements
16 p2477 A72-33433
 - Stress and heat flux constitutive equations dependence on observer reference frame, considering fluid equation for temperature of gas at rest
16 p2478 A72-33526
 - Temperature field in flat plate with selective radiation absorption coefficient, using asymptotic representations for internal heat flux radiation component
16 p2479 A72-33858
 - Solar wind heat flux measurements comparison with collision dominated heat transfer theory in ionized medium, noting deviations from Maxwellian velocity distribution
16 p2449 A72-33908
 - A modified Navier-Stokes equation, and its consequences on sound dispersion.
17 p2540 A72-35146
 - Russian monograph on heat measurement covering methods and instruments for heat flux determination, radiometers, thermal conductivity gages and electrical calorimeters
17 p2556 A72-35495
 - Incident thermal flux parameters and wall temperature effects on flow characteristics in pre-separation zone of laminar boundary layer and separation point location
17 p2487 A72-35927
 - The Apollo 15 lunar heat-flow measurement.
18 p2724 A72-36285
 - Calculation of thermal fluxes and temperatures on the surfaces of a plate in the presence of heat exchange between fluids incident on the surfaces
18 p2742 A72-37183
 - Similarity predictions for shear stress and heat flux cospectral behavior in atmospheric turbulent boundary layer
19 p2829 A72-38560
 - The indirect determination of stability, heat and momentum fluxes in the atmospheric boundary layer from simple scalar variables during dry unstable conditions.
20 p2947 A72-38964
 - Heat emission from the lower faces of plane surfaces in the presence of a steady thermal flux under conditions of natural convection
20 p2982 A72-39322

- Straight fins with periodic base temperature variation, calculating design parameters effects on heat transfer rates, temperature distributions and efficiencies [ASME PAPER 72-HT-E] 20 p2983 A72-39484
- Thermohydrodynamic conditions at the peak flux of horizontal heaters in superfluid liquid helium II at zero net mass flow. 20 p2984 A72-39647
- Heat transfer measurements with a Wollaston prism schlieren interferometer. [ASME PAPER 72-HT-9] 20 p2927 A72-39680
- A technique for determining the transient heat flux at a solid interface using the measured transient interfacial temperature. [ASME PAPER 72-HT-18] 20 p2987 A72-39687
- Heat flux and friction force minimization problems equivalence in optimal control of incompressible boundary layer on isothermal plate 20 p2914 A72-39918
- Investigation of the critical heat flux density in heat transfer with and without turbulization of the flow at the inlet of an annular channel 21 p3129 A72-41057
- Optimization of the structural parameters of galvanic laminar heat-flux sensors 21 p3056 A72-41058
- Wall temperature, thermal conductivity and acoustic vibration frequency as function of critical heat flux density for unstable water film boiling conditions 21 p3130 A72-41063
- Theoretical and experimental study of the pressure and heat-flux distributions on a control surface in the presence of a thick hypersonic turbulent boundary layer [ICAS PAPER 72-23] 21 p2991 A72-41148
- Combined buoyancy and flow direction effects on saturated boiling critical heat flux in liquid nitrogen. 21 p3130 A72-41184
- Heat transfer performance of stationary two phase closed thermosiphon with water and Freon as working fluids, discussing effects of operating pressure and heat flux 21 p3131 A72-41621
- Buoyancy effects on laminar heat transfer in the thermal entrance region of horizontal rectangular channels with uniform wall heat flux for large Prandtl number fluid. 22 p3243 A72-41956
- Temperature distribution and heat flux in infinite length rectangular and finite length cylindrical fins, examining validity of one dimensional approximation 22 p3243 A72-41961
- Recent progress regarding the measurement techniques in the hypersonic area [ONERA, TP NO. 1055] 22 p3178 A72-42581
- Influence of the intermodal exchange on the wall heat flow in a gas possessing internal energy 22 p3244 A72-42641
- Ablation rate growth phenomenon in fusible material with diminished thermal flux, discussing quartz glass characteristics 22 p3244 A72-42728
- Some characteristics of an electron-beam induced discharge in a vacuum 22 p3208 A72-43123
- ## HEAT GAIN
- ### U HEATING
- ## HEAT GENERATION
- Temperature fluctuation structure in turbulent wake behind heated circular cylinder, investigating thermal convection, production and diffusion [AD-740540] 04 p0596 A72-15330
- Gegenbauer/ultraspherical/polynomials and Meijer G-functions for solution of heat production and diffusion in cylinder with internal sources leading to axisymmetric temperature distribution 05 p0747 A72-16791
- Temperature distribution in composite media with internal heat generation, solving diffusion equation via Voldicka type orthogonality relationship 07 p1100 A72-19626
- Hot wire ignitor modeling including measured H value and heat generation by explosive chemical reaction 08 p1219 A72-20754
- Heat absorption and liberation by glass fabric laminates under uniaxial tension, determining thermal effects dependence on strain rate and test temperature by calorimetric measurements 08 p1195 A72-21853
- Laser heating of plasma based on heat conduction mechanism of spherical thermal wave, taking into account nuclear fusion heat generation 09 p1365 A72-23551
- Linearized thermal viscoelasticity theory for stability, large strain and wave propagation problems, taking into account heat generating effects 12 p1880 A72-27233
- Nitrate ester propellants self ignition hazard and ballistics stability, describing heat generation test at various temperatures for long term storage 14 p2144 A72-30754
- Heat generation in oscillating torsional spring modeled by viscoelastic hollow cylinder subjected to sinusoidal shear stresses, calculating stress and temperature distribution and displacement 17 p2635 A72-34232
- Heat production effects in general linearized thermoviscoelasticity theory, deriving equations of motion, state and energy and boundary conditions for intensely strained objects 19 p2871 A72-37526
- Numerical analysis of microwave heat generation in disc-shaped Luneberg lenses. 21 p3032 A72-40627
- Thermomechanical coupling effects in the longitudinal oscillations of a viscoelastic cylinder. 23 p3352 A72-44122
- ## HEAT MEASUREMENT
- Calorimetric and radiometric methods for thermal radiation properties of solids, considering reflectance, absorptance, transmittance and spectral emittance 02 p0223 A72-11499
- Quasi-static measurement and electron phonon interpretation of specific heat of metals at low temperature 03 p0456 A72-13843
- High temperature properties of composite contact stack composed of alternating thermal flux sensors and heaters, determining heat conductivity and energy dissipation 03 p0458 A72-14160
- High temperature thermal properties of solid and liquid metals and rocks and minerals, discussing earth heat balance and measurement methods for heat capacity and conductivity 04 p0596 A72-14653
- Heat flow resistance measurement in avalanche diodes, noting junction temperature effect 04 p0498 A72-15133
- Holographic interferometer for heat transfer measurement, studying free convection thermal boundary layer on heated isothermal vertical flat plate 04 p0524 A72-15531
- Surface heat transfer and pressure measurements for downstream effects of transpiration cooled nose tip, using nitrogen as injectant fluid [AIAA PAPER 72-185] 05 p0605 A72-16840
- Thermal contact resistance measurement in double contact thermocouple specimens at 250-650 C in Ar and air-vacuum 07 p1098 A72-18987
- Thermal diffusivity and heat capacity measurement by temperature vs time curve shape by laser pulse absorption, using thermocouple 07 p1101 A72-19890
- Calorimetric measurements of human body temperature and of hot saline solution drinking effects on sweating rate 09 p1267 A72-23440
- Calorimetric study of sweating man response to drinking hot saline solution as function of temperature, volume and salinity of ingested liquid 09 p1267 A72-23441
- Radiant heat flux measurement during pulsed processes from surface in high temperature emitting gas, using thin film sensor with small time constant 10 p1561 A72-23843
- Local and macroscopic thermal transport in turbulent air stream, discussing measurement from calorimeter instrumented sphere 10 p1417 A72-24148
- Calorimetric measurement of dissolution heat and partial enthalpy limit of Ga in Sn at 969 K 10 p1526 A72-24237
- Levitation calorimetry for solid and liquid Mo enthalpy measurement, calculating specific heat and heat of fusion 10 p1496 A72-24243
- Human body calorimetry with water cooled garment for dynamic and continuous recording of heat dissipation from surface over extended time 10 p1431 A72-24485
- Multilayer insulation apparent thermal conductivity measurement at low compressive loads, describing test calorimeter and experimental technique [AIAA PAPER 72-367] 11 p1670 A72-25392
- Thermodynamics of human body metabolism, discussing energy conversion calorimetric measurements, body size, food intake, age, sex, endocrine and nervous effects 11 p1584 A72-26072
- Hot wire cell measurement of specific heat in low pressure gases, determining thermal conductivity and accommodation coefficient 11 p1634 A72-26367
- Internal gravity waves and convective instability caused by liquid layer nonuniform vertical density distribution, noting error in thermal conductivity measurement near critical point 14 p2095 A72-31008
- Unsteady heat flux sensor types and characteristics, considering flux level, measurement time and frequency response 15 p2233 A72-31374
- Microcalorimetric investigation of energy transfer from atomic and molecular hydrogen beams to various surfaces at liquid helium temperatures and ultrahigh vacuum conditions 15 p2281 A72-31863
- Solar wind heat flux measurements comparison with collision dominated heat transfer theory in ionized medium, noting deviations from Maxwellian velocity distribution 16 p2449 A72-33908
- Thermodynamic properties of liquid Co and Pd metals by levitation calorimetry, including specific heat, heats of fusion and surface emissivities 16 p2480 A72-34025
- Thermal conductivity and heat capacity measurement by temperature vs time curve shape by laser pulse absorption, using thermocouple 17 p2637 A72-35138
- Russian monograph on heat measurement covering methods and instruments for heat flux determination, radiometers, thermal conductivity gages and electrical calorimeters 17 p2556 A72-35495
- A graphite calorimeter 18 p2693 A72-37192
- Heat transfer measurements with a Wollaston prism schlieren interferometer. [ASME PAPER 72-HT-9] 20 p2927 A72-39680
- Calorimetric investigation of atom ordering effects in a NiCr alloy 21 p3068 A72-40958
- Nonstationary method for measuring the heat conductivity of liquids and gases under high pressures 22 p3243 A72-41886
- Apparatus for measurement of specific heats between 0.3 and 3 K in the oscillating thermal region 22 p3180 A72-42936
- Thermal anomalies in stressed Teflon. 24 p3417 A72-44766
- A thermal mapping technique for shock tunnels and a practical data reduction procedure. [AIAA PAPER 72-1031] 24 p3389 A72-45408
- ## HEAT OF COMBUSTION
- Combusting polymers gasification effective heat values determination from correlation of surface regression rate and oxygen impingement rate data [AIAA PAPER 72-34] 05 p0749 A72-16898
- ## HEAT OF FORMATION
- Gaseous boron dioxide and oxyfluoride heat of formation determination by mass spectroscopy and molecular effusion technique [AD-740421] 07 p0936 A72-19682
- Zinc oxide effect on alumina dispersion, energy of formation, nucleation and particle size reduction, calculating critical nucleus radii 16 p2476 A72-33255
- ## HEAT OF SOLUTION
- Calorimetric measurement of dissolution heat and partial enthalpy limit of Ga in Sn at 969 K 10 p1526 A72-24237
- ## HEAT OF VAPORIZATION
- Uncondensed components effects on heat transfer in condensation of nitrogen tetroxide partly in second dissociation stage, deriving heat of vaporization 01 p0145 A72-10494
- Cathode and anode temperatures effect on effective heat of condensation of electrons at anode for particular current density and different cesium vapor pressures 02 p0156 A72-12858
- Vaporization heat transfer characteristics for heat pipe wick samples of felted metal and sintered metal powder [AIAA PAPER 72-256] 11 p1739 A72-25201
- Vaporization characteristics of carbon heat shields under radiative heating, presenting estimates of vaporization heat from energy balance [AIAA PAPER 72-296] 11 p1741 A72-25234
- Thermodynamic analysis of heat of evaporation of sweat, considering ambient temperature and humidity effects, body heat storage and presence of solutes 11 p1586 A72-26610
- Lunar rock and mineral shock melting and vaporization from hypervelocity meteoroid impacts, calculating entropy, phase changes and thermal equilibrium 14 p2155 A72-30520
- ## HEAT PIPES
- Split core heat pipe nuclear reactor dynamics, describing shutdown mechanisms, ramp reactivity inputs fuel melting temperature and wall heat flux 04 p0546 A72-14421
- Split-core heat pipe reactor for out-of-core thermionic power systems, using center gap for fuel reactivity control 04 p0546 A72-14425
- High temperature thermal conductivity measurements of solids at 800-1500 C using heat pipe technique 04 p0547 A72-14544
- Variable conductance heat pipe technology for overcoming thermal resistance barrier in electronic package design 04 p0596 A72-15227

- Heat pipe evaporation zone length based on desiccation length calculations for various capillary cross sections and thermal loads 05 p0743 A72-15853
- Water heat pipes transient thermal impedance, monitoring evaporator, vapor space and condenser temperature [ASME PAPER 71-WA/HT-9] 05 p0743 A72-15869
- Alkali liquid metal heat pipes, showing heat transport rate for boiling initiation [ASME PAPER 71-WA/HT-10] 05 p0743 A72-15870
- Sodium heat pipes sonic limit, describing vapor dissociation-recombination and homogeneous vapor condensation phenomena [ASME PAPER 71-WA/HT-11] 05 p0743 A72-15871
- Pressure drop of homogeneous and annular wick heat pipes using hydrogen, nitrogen and oxygen working fluids, discussing heat transfer capacity [ASME PAPER 71-WA/HT-13] 05 p0744 A72-15873
- Navier-Stokes equations solution by finite difference methods for steady incompressible laminar vapor flow in symmetrical and unsymmetrical heat pipes, calculating pressure losses [ASME PAPER 71-WA/HT-15] 05 p0744 A72-15874
- Heat pipe radiator with 50 kW heat rejection capability for potassium working fluid of Rankine cycle space power system, discussing design, fabrication and testing [ASME PAPER 71-WA/HT-16] 05 p0744 A72-15875
- High thermal power density ammonia heat pipe with porous grooved wick concept [ASME PAPER 71-WA/HT-20] 05 p0744 A72-15879
- Nitrogen heat pipe axial temperature distribution and vapor pressure measurement, noting effective thermal conductivity variation with power load and inclination angle [ASME PAPER 71-WA/HT-28] 05 p0744 A72-15881
- Heat and mass transfer along axially conducting gas controlled heat pipes, discussing wall temperature profiles and condenser characteristics [ASME PAPER 71-WA/HT-29] 05 p0745 A72-15882
- Steady state operational characteristics of two component heat pipes, applying mass and energy conservation laws and thermodynamic phase equilibrium relations [ASME PAPER 71-WA/HT-30] 05 p0745 A72-15883
- Arterial and grooved wick cryogenic nitrogen heat pipe performance tests, comparing elevation sensitivity, priming and heat transfer characteristics [ASME PAPER 71-WA/HT-42] 05 p0745 A72-15889
- Heat pipe temperature gradient initial conditions for ideal gas model, introducing two phase Mach number for choking phenomena analysis [AIAA PAPER 72-22] 05 p0749 A72-16913
- Heat pipe operating conditions and evaporator, condenser and adiabatic parts, discussing fluid capillary transport for heat pipe calculation 05 p0750 A72-17047
- Vaporization heat transfer characteristics for heat pipe wick samples of felted metal and sintered metal powder [AIAA PAPER 72-256] 11 p1739 A72-25201
- Axial pressure variations in incompressible laminar tube flow with uniform suction, noting application to heat pipes [AIAA PAPER 72-257] 11 p1614 A72-25202
- Self priming high capacity spiral artery heat pipe with ammonia as working fluid for flight on OAO 3, discussing development models analysis, design and testing [AIAA PAPER 72-258] 11 p1725 A72-25203
- Sounding rocket heat pipe experiment in zero gravity, testing spiral and pedestal arteries and plain groove designs [AIAA PAPER 72-259] 11 p1739 A72-25204
- Thermal diode heat pipe for advanced thermal control flight experiment, discussing engineering model analysis, design, fabrication and test [AIAA PAPER 72-260] 11 p1739 A72-25205
- Experimental cold pads provided with heat pipes for thermal control of electronic equipment [AIAA PAPER 72-269] 11 p1740 A72-25210
- Precision temperature control system for spacecraft equipment thermal loads rejection by space radiator, using acetone variable conductance heat pipes [AIAA PAPER 72-270] 11 p1740 A72-25211
- Heat pipe applications for waste heat rejection, cooling and temperature control in space shuttle, discussing design and performance [AIAA PAPER 72-272] 11 p1725 A72-25212
- Tunnel wick heat pipe artery with priming in gravity environment by temperature induced pressure differences, using ammonia as working fluid [AIAA PAPER 72-273] 11 p1740 A72-25213
- Arc cast vacuum melted Mo base alloy properties, production and applications to heat pipes, aerospace structures and pressure vessels 11 p1644 A72-26844
- Apollo 16 lunar surface magnetometer cooling system variable conductance heat pipe/radiator design and thermal performance [AIAA PAPER 72-271] 14 p2171 A72-30828
- High reliability long life heat pipe thermal control system for space station application [AIAA PAPER 72-261] 14 p2171 A72-30835
- Satellite sensor cooling systems, considering cryogenic heat pipes, sublimation, radiation cones and surface treatment 15 p2319 A72-31240
- Optimization of heat pipe with wick and annulus liquid flow, investigating effect of pressure loss and recovery in vapor passage [ASME PAPER 71-HT-V] 15 p2335 A72-31767
- Chemically vapor deposited W heat pipe fabrication and evaluation for application to high temperature nuclear reactors 15 p2244 A72-32126
- Boundary conditions influence on heat and mass transfer in low temperature heat pipes with freon as working fluid 16 p2479 A72-33853
- Fabrication and testing of tungsten heat pipes for heat pipe cooled reactors. 17 p2636 A72-34596
- Thermionic converter heated by gasoline flame or heat pipe, describing materials protection against corrosion and furnace design and operation 18 p2644 A72-36165
- The development of a 150,000 watt-inch variable conductance heat pipe for space vehicle thermal control. [ASME PAPER 72-ENAV-14] 20 p2896 A72-39163
- Heat-pipe plasma oven for microwave and spectroscopic measurements. 20 p2912 A72-39433
- Simple conduction model for theoretical steady-state heat pipe performance. 20 p2984 A72-39607
- Nb heat pipe design with Na coolant for high temperature operation, discussing slopes effect on transmitted power 21 p3129 A72-41051
- Application of the elementary-balance method to the calculation of the nonstationary temperature fields and aerodynamic characteristics of several versions of a surface-type heat exchanger 21 p3130 A72-41064
- HEAT PUMPS**
- Semiconductor air-air heat pumps with solar cell feed current, determining hot air flow temperature effects and energy conversion efficiency 10 p1423 A72-24319
- Thermal control concept evaluation for a ten-year life modular space station. [ASME PAPER 72-ENAV-30] 20 p2894 A72-39147
- HEAT RADIATORS**
- NT SPACECRAFT RADIATORS
- Thermal conductivity and boundary conditions for unsteady thermal fields in thin anisotropic plates with heat emission 02 p0291 A72-11635
- Optimal radiative capacity of star shaped radiator with mirror reflecting surfaces for vacuum cooling of elongated finned bodies 02 p0304 A72-12867
- Radiative heat transfer characteristics of optimal geometry radiating stainless steel fin 07 p1098 A72-18997
- Apollo 16 lunar surface magnetometer cooling system variable conductance heat pipe/radiator design and thermal performance [AIAA PAPER 72-271] 14 p2171 A72-30828
- Modular heat rejection system to accommodate widely varying thermal loads in space shuttles and future spacecraft, emphasizing commonality design philosophy for cost reduction [ASME PAPER 72-ENAV-34] 20 p2976 A72-39144
- HEAT REGULATION**
- U TEMPERATURE CONTROL
- HEAT REJECTION DEVICES**
- U HEAT RADIATORS
- HEAT RESISTANCE**
- U THERMAL RESISTANCE
- HEAT RESISTANT ALLOYS**
- NT MOLYBDENUM ALLOYS
- NT NIMONIC ALLOYS
- NT NIOBIUM ALLOYS
- NT REFRACTORY METAL ALLOYS
- NT RHENIUM ALLOYS
- NT TANTALUM ALLOYS
- NT TUNGSTEN ALLOYS
- NT UDIMET ALLOYS
- NT WASPALOY
- Fe, Ni and Co based high temperature thin gauge sheet alloys, discussing chemical and mechanical properties, fabrication and availability 01 p0084 A72-10742
- Titanium alloys and superalloys selection for elevated temperature use on space shuttle 01 p0084 A72-10743
- Dispersion strengthened Ni-Cr alloys processing technique and mill products development, noting increased strength at elevated temperatures 01 p0075 A72-10744
- High temperature high strength Ni alloys with Ti, Nb and Hf additions, using modified Hastelloy N 01 p0084 A72-10746
- Continuous seam diffusion bonding application to Ti and superalloys lap, butt and T joints production [SME PAPER AD 71-264] 01 p0076 A72-10970
- Plasma arc testing of space shuttle Nb and Co alloys thermal protection materials, using IR radiometric and photographic techniques 01 p0048 A72-10977
- Diffusion aluminide protective coating formation mechanisms on Ni-base superalloys observed from microstructures and compositions in Ni-Al intermetallics 01 p0089 A72-11165
- Creep strength analysis of heat resistant alloys under repeated unsteady loads 01 p0144 A72-11376
- Ni base superalloy powder with refractory oxide particle dispersion, presenting high temperature creep, stress rupture, microstructure activation energy and processing history 02 p0240 A72-11442
- Powder metallurgy advantages for Ni-based superalloys, presenting thermomechanical process results 02 p0240 A72-11443
- Aluminum oxide dispersion hardened ferritic heat resisting Cr steel, describing liquid phase sintering effects on high temperature tensile strength 02 p0241 A72-11448
- Heat resistant alloys thermal microstresses effect on creep and fatigue life under thermal cycling conditions 02 p0242 A72-11633
- Refractory materials strength testing equipment and techniques at high temperatures, covering creep, hardness, fatigue, ultrasonic, energy dissipation and loading tests 02 p0291 A72-11636
- Temperature-time dependent torsional strength and fracture failure of Cr-Ni steel microalloyed with La and Ce as function of grain boundaries 02 p0243 A72-12010
- Microstructure and mechanical properties of iron base superalloys, examining precipitation hardening by gamma prime and secondary intermetallic compounds formation 02 p0245 A72-12505
- Wrought superalloys microstructure and mechanical properties control by precipitating phases 02 p0245 A72-12506
- Fabricable high strength Inconel 706 precipitation hardening superalloy, noting savings in Ni, Nb and Mo content 02 p0245 A72-12507
- Titanium and aluminum variations effects on eta and gamma prime solvus temperatures and on mechanical properties of iron-nickel superalloy 02 p0245 A72-12508
- Superalloys ductility and workability improvements without sacrificing elevated temperature strength for aircraft engine applications 02 p0246 A72-12561
- Superalloy compositions prealloyed powders strengthening by secondary gamma phase precipitation, noting high temperature strength without ductility loss after thermomechanical treatment and aging 02 p0247 A72-12856
- Structural features of heat resistant Ni-Cr alloy from electron diffraction microscopy, observing coherent lattice bond and plastic deformation 03 p0376 A72-14015
- Ni-Cr-Al-Si and Fe-Cr-Al-Y oxidation resistant claddings for superalloys, comparing to commercial aluminide coatings by cyclic furnace and high velocity burner rig tests 04 p0533 A72-14700
- Environmental effects on superalloy high temperature corrosion in gas turbines, noting blade surface temperature as critical factor [ASME PAPER 71-WA/CD-1] 05 p0704 A72-15945
- Al and Al-Zr coating effects on heat resistant alloy turbine blades high temperature fatigue resistance under bending-torsion cyclic loads 05 p0671 A72-15990
- High temperature brazing of heat resistant alloys, determining tensile strengths 05 p0666 A72-16189
- Heat and corrosion resisting alloys development for gas turbine combustion liner, presenting microstructure of specimens after thermal shock test 05 p0671 A72-16494
- Superalloys for gas turbine rotor and stator blades, testing long term heating effects on microstructure and mechanical and thermal fatigue properties 05 p0675 A72-16495
- Prolonged heatings effect on heat resistant magnesium alloys microstructure and mechanical properties 05 p0680 A72-17208
- Superplasticity relation to heat resistance in metal systems Ni-Cr, Ni-Cr-W-Ti-Al and Ti-Si 05 p0680 A72-17212
- Gas turbine superalloys high temperature oxidation resistance by fiber strengthening, rare earth alloying, precipitation hardening and intermetallic compounds 06 p0828 A72-17611
- Microstructure properties of heat resistant alloy for gas turbine blades as function of operational time 06 p0832 A72-18360

Thermal resistance estimation for machine parts of heat resistant alloys under real working conditions

06 p0833 A72-18559
Damping characteristics of Ni base heat resistant alloys at high temperatures, showing increase with cyclic strain amplitude

06 p0833 A72-18630
Semifinished product production technology influence on heat resistant alloys mechanical properties, considering forging, rolling, casting, melting, diffusion welding and powder metallurgy

06 p0834 A72-18647
Stress-strain diagrams of heat resistant alloys at high temperatures, describing test facility

06 p0834 A72-18684
Thermostable and heat resistant steels and alloys vibration loading frequency effects on fatigues at high temperatures

06 p0834 A72-18688
Extruded superalloy powder structural shapes preparation by filled billet technique for improved chemical and mechanical properties

07 p0994 A72-19483
Boron addition effects on scaling resistance of Ni-Cr steel at high temperatures

07 p1012 A72-19738
Mechanical properties of fiber reinforced heat resistant alloys

07 p1013 A72-19743
Tungsten alloy filaments as reinforcing agent of heat resistant composite chromium alloy, investigating long term high temperature effects

07 p1013 A72-19745
Heat resistant Nichrome composite alloy with tungsten filament reinforcement, discussing manufacture and mechanical properties at 1100°C

07 p1013 A72-19747
Aluminized layer phase and chemical composition on heat resistant iron and nickel alloys

07 p1013 A72-19748
Heat resistant weldable precipitation hardened Ni base alloy, discussing intermetallic phase hardening

07 p1014 A72-19842
Hf addition effects on grain boundary structure of cast Ni-base superalloys

07 p1015 A72-19931
Ductility and fracture of heat resistant steels at high temperatures and unsteady loading, estimating loading cycle effect on plastic strain buildup to failure

07 p1017 A72-20127
Stepwise fatigue testing of high temperature alloy, noting strain hardening phenomena in prestressed samples

07 p1017 A72-20129
Fe addition effects on structural and mechanical properties of heat resistant Ni-Cr alloys

07 p1020 A72-20416
High temperature alloy deformation superplasticity and formability relation with microstructure, fine structure and load requirements for hot working with high strain rate

08 p1250 A72-22200
Mechanical properties anisotropy in heat resistant Ni alloys due to strengthening phase nonmetallic inclusions distribution, suggesting purification by vacuum melting

09 p1327 A72-22231
High temperature Co-base alloy for nuclear, chemical and reentry vehicle applications

09 p1327 A72-22478
Creep properties in turbine disks of heat resistant alloy under plastic deformation due to nonstationary thermal conditions

09 p1401 A72-22730
Thermomechanical strengthening of gamma prime precipitation hardened nickel base superalloy, emphasizing working operation and dislocation substructure

09 p1330 A72-23377
Cyclic oxidation kinetics of Hastelloy X sheet and wire specimens for high temperature alloy evaluation in transpiration cooled engine components manufacture

09 p1331 A72-23476
Hot-stage optical microscopes for microhardness measurements at elevated temperatures, describing techniques to determine heat resistant alloys mechanical and physical properties temperature dependence

10 p1478 A72-23827
Physicochemical principles of inorganic materials production, considering heat resistant alloys, oxygen free and oxide cermets, glasses, glass ceramics and protective coatings

10 p1501 A72-24408
Superplasticity relation to heat resistance in metal systems Ni-Cr, Ni-Cr-W-Ti-Al and Ti-Si

11 p1727 A72-25338
Space shuttle heat shield metallic refractory, superalloy and composite materials joining, discussing vacuum furnace brazing of Al/B matrix structures [AIAA PAPER 72-387]

11 p1638 A72-25408
High temperature metallographic methods in microstructure study of austenitic heat resistant steel under plastic deformation and heat treatment

11 p1654 A72-25495

Prolonged heating effect on heat resistant Mg alloys microstructure and mechanical properties

11 p1660 A72-26143
Superalloys and refractory materials high temperature protective coatings, noting lack of uniformity in testing methods

11 p1674 A72-26286
NDT of diffusion formed coatings on refractory alloys and superalloys, stressing eddy current technique

11 p1641 A72-26287
Hydroplasma metal removal for surface cleaning of heat resistant alloys, using electric contact plasma arc machine

11 p1641 A72-26673
Ultrasonic oscillations effects on alloy castings grain size and heat resistance, suggesting waveguide direction for oriented solidification

11 p1642 A72-26822
Oxygen, carbon and boron effect on liquid phase sintering behavior and mechanical properties of Ni base superalloys

11 p1645 A72-26848
High melting point alloy and metal powder production by vacuum atomization, using rotary vane and electron beam melting techniques

11 p1645 A72-26860
Powder metallurgy versus melting and casting of high temperature alloys, tool steels and specialty alloys

11 p1646 A72-26869
Superalloy powder metallurgy process based on inert gas atomization of molten metal to low interstitial content powders and densification by extrusion

11 p1665 A72-26870
Ordered crystallization casting of Ni superalloys for turbine blades, using power down and high rate solidification processes

11 p1646 A72-26894
High temperature Ni base alloys microstructure via transmission electron microscopy and electron diffraction contrast theory, predicting yield and creep strength

11 p1667 A72-26931
Electron microscope study of commercial Ni superalloys, discussing intermetallic compound and carbide precipitation hardening

12 p1827 A72-27137
Electrochemical conditions for separation of gamma prime phase from heat resistant Ni alloys by electrolysis

12 p1828 A72-27446
Russian book on work hardening of surface components of heat resistant and Ti alloys for high temperature operation

12 p1816 A72-28156
Heat resistant blade alloy test temperature effects on fatigue life, tensile strength, hardness and chemical composition

12 p1831 A72-28230
Cyclic nonisothermal plastic deformation of ductile disk, verifying experimentally with turbine disk of heat resistant alloys

13 p2053 A72-28398
Haynes high strength heat resistant Ni-Cr-W alloy metallurgical and structural relationship, mechanical and physical properties, oxidation and corrosion behavior and fabrication processes

13 p1973 A72-28649
Mo influence on gamma prime phase precipitate in wrought Ni-base superalloys, considering solvus temperature, weight fraction and lattice parameters

13 p1975 A72-28669
Vacuum induction melting process for high temperature steels and superalloys fabrication, emphasizing control over temperature, pressure, beneficial trace elements and harmful impurities

13 p1964 A72-29100
Cu surface contamination effect on hot crack susceptibility and weldability of Co based superalloys

13 p1965 A72-29419
Heat resistant alloys conjugate phases extraction, separation and chemical analysis, discussing control of minor phases as precipitation products

13 p1978 A72-29443
Precipitated carbide role in Cr-Ni stainless steels high temperature properties and creep rupture strength

13 p1979 A72-29447
Microstructure and mechanical properties of heat resistant Fe-Mn-Al alloys at 650-1150°C

13 p1981 A72-30093
Cobalt-base superalloys powder-metallurgical fabrication techniques and related effects on physical and mechanical properties

13 p1982 A72-30126
Thin oxidation resistant alloy claddings for superalloys, comparing performance with aluminide coatings by cyclic furnace and high velocity burner rig tests

14 p2113 A72-30271
Sn alloying effect on heat resistant Ni-Cr alloys plastic strain resistance and strength at room and high temperatures

14 p2114 A72-30274

Superalloys properties and utilization at high temperatures, discussing chemical resistance, diffusion treatment, B and Zr action and grain size

14 p2116 A72-30527
Heat resistant Ni alloys grain boundaries precipitates as function of composition and heat treatment, noting effects on mechanical properties

14 p2118 A72-30589
Russian papers on alloying and properties of heat resistant alloys covering creep, solid solution and dispersion hardening, chemical interactions and protective coatings

15 p2254 A72-31557
Steady creep and delayed fracture dependence on metal structure and composition, considering strain hardening at small strain rate and elevated temperature

15 p2254 A72-31559
Heat resistance improvement by interface dissociation, dispersion hardening and reinforcement of Mo, Fe, Ni and Al metals and alloys

15 p2254 A72-31560
Mo, W, Nb, Ti, V and N complex alloying to harden cast heat resistant austenitic steel, discussing phase composition and stress-rupture strength

15 p2254 A72-31563
Alloying characteristics of heat resistant Ni base Ni-Cr-Al-Ti-Nb-Mo disk alloy

15 p2255 A72-31566
Refractory steels heat resistance improvement by surface saturation with Be and subsequent oxidation in air at 900-1000°C, comparing with aluminized steels

15 p2255 A72-31574
Chemical inhomogeneity of high melting metals and alloys of Ti, Zr, Nb and Cr from radio isotopic and nuclear emission studies

15 p2255 A72-31576
Mechanical properties of high temperature steels and alloys for gas turbine rotors, disks and blades

15 p2256 A72-31703
Forming techniques and heat treatment effects on recrystallization characteristics of heat resistant Cr alloy, noting high temperature influence on crystal structure

16 p2407 A72-33531
Ternary Ni-Cr-Al superalloys oxidation at 800-1300°C as function of composition, temperature, oxygen pressure and reaction time

16 p2410 A72-33811
Electric spark activated hot pressing application for sintered composite structures, noting process parameters optimization for superalloy powders

16 p2411 A72-34093
Phase stability and mechanical properties of carbide and boride strengthened chromium-base alloys

18 p2700 A72-36579
The effects of environment on the elevated temperature fatigue behavior of nickel-base superalloy single crystals

18 p2700 A72-36587
Hot corrosion of experimental aluminum-coated cobalt-base alloys

18 p2702 A72-36797
New developments in the study of fiber superalloys obtained by directional solidification

18 p2702 A72-37015
Phenomenology and engineering significance of creep recovery in heat resistant steels, stressing ductility and microstructural effects

19 p2816 A72-37707
Plasticity and rupture of heat-resistant materials subjected to a small number of cycles of simultaneous variation of temperature and load

19 p2818 A72-38006
Heat resistant alloys stress-rupture strength tests for operating temperatures based on equivalent high temperatures damageability

19 p2818 A72-38008
Inconel alloy 617 - A new high-temperature alloy

19 p2821 A72-38388
Quench-ageing behaviour of 40Co-38Ni-17Cr-5Ti alloy

20 p2935 A72-39141
Super-alpha Ti alloy development, measuring physical and mechanical properties

20 p2936 A72-39205
A review of the science, technology, and applications of dispersion strengthened Ni-Cr- and Co-Cr-base alloys

20 p2936 A72-39209
Elevated temperature ductility minimum in Hastelloy alloy X

20 p2938 A72-39304
A comparison of the effect of inward and outward diffusion aluminide coatings on the fatigue behavior of nickel-base superalloys

21 p3067 A72-40916
The properties and structures of a heat resistant 1Cr-Mo-V steel and alloy A-286 after long time exposures at elev. temps.

21 p3069 A72-41012
The effect of alloying elements on creep rupture strength and microstructure of 12 percent chromium heat resisting steel

21 p3069 A72-41014

Causes for the formation of internal discontinuities of the metal in forged blanks of turbine blades prepared from EI893 alloy 22 p3216 A72-42249

Heat-resistant copper-base alloys containing rare-earth and high-melting metals, characterized by high electrical conductivity 22 p3192 A72-42819

Mechanical and thermophysical properties of heat resistant Nb alloys, noting application for thermionic cathodes 22 p3192 A72-42821

Carbide phases in nickel-based heat-resistant alloys 22 p3192 A72-43018

Composite Al- and Ni-base alloys strengthened by B and W/Mo fibers respectively for reduced weight wing spars and high temperature applications 22 p3197 A72-43139

Gas turbine blades of cast ZhS6K heat resistant alloy, investigating structural strength from fatigue test data 23 p3347 A72-43734

Gas turbine blade models of heat resistant ZhS6K alloy under operational temperature variations, observing fatigue strength 23 p3347 A72-43735

Heat resistant steels long time strength determination by graph-analytical time-temperature extrapolation 23 p3301 A72-43739

Heat resistant Ni-base composite stiffened with W wires, investigating interaction between alloy and fibers from metallographic and X ray diffraction microscopy data 23 p3301 A72-43740

Heat resistant ZhS6K alloy precision and ground cast specimens, determining short and long term strength and fatigue 23 p3301 A72-43761

Investigation of the state of the structure of turbine-disk materials after operation 23 p3302 A72-43965

Phase extraction and analysis in superalloys - Summary of investigations by ASTM Committee E-4 Task Group I. 23 p3304 A72-44257

Al and Al-Zr coating effects on heat resistant alloy turbine blades high temperature fatigue resistance under bending-torsion cyclic loads 24 p3415 A72-45732

Microstructure properties of heat resistant alloy for gas turbine blades as function of operational time 24 p3416 A72-45747

Ductility and fracture of heat resistant steels at high temperatures and unsteady loading, estimating loading cycle effect on plastic strain buildup to failure 24 p3416 A72-45753

Stepwise fatigue testing of high temperature alloy, noting strain hardening phenomena in prestressed samples 24 p3416 A72-45755

HEAT SHIELDING

NT REENTRY SHIELDING

Nondestructive tests of Nb alloy radiative thermal protection heat shield design for space shuttle requirements 01 p0048 A72-10980

Aircraft crash fire protection, using passenger compartment heat shield of fire-retardant polyisocyanurate foam and intumescent paint 03 p0310 A72-13484

Ablation performance of dielectric heat shields for planetary entry, testing diffuse reflectance by convective and radiative heating 05 p0747 A72-16809

Heat and mass transfer blowing correction correlations for graphite and charring ablator reentry nosetip and heat shield applications 05 p0748 A72-16810

Multilayer heat reflective coating optical thickness effect on temperature distributions, taking into account interlayer contact resistance and thermal radiation volume absorption 06 p0904 A72-18511

Thermal shielding and reduced resistance determination of flat thermoelectric battery in sandwich solar cell assembly 10 p1422 A72-24313

Vaporization characteristics of carbon heat shields under radiative heating, presenting estimates of vaporization heat from energy balance 11 p1741 A72-25234

Space shuttle heat shield metallic refractory, superalloy and composite materials joining, discussing vacuum furnace brazing of Al/B matrix structures [AIAA PAPER 72-387] 11 p1638 A72-25408

Hot versus shielded aerodynamic surfaces trade study for space shuttle booster wings and fins design, considering materials, structural weight and cost estimates [AIAA PAPER 72-390] 11 p1726 A72-25411

Thin Ta sheet spiral configuration for high efficiency high temperature vacuum heat shield 12 p1888 A72-27035

Elastomeric silicone ablator heat shields thermal characteristics from NASA Planetary Atmosphere Experiments Test vehicle earth atmosphere entry measurements [AIAA PAPER 72-326] 13 p2064 A72-28953

Temperature distribution of structural element with heat shield and metallic layer, determining ablation process for thermal flux at surface 14 p2170 A72-30593

Carbon-carbon composites for space shuttle reentry thermal protection. 17 p2572 A72-35667

The manufacture of mullite reusable surface insulation materials for space shuttle. [SME PAPER EM 72-714] 18 p2695 A72-36527

Simplified theory for optimizing the design of a heat shield in an isochorically operated toroidal dewar. 19 p2805 A72-38843

Shadow shields for minimizing radiant heat transfer into cryogenic propellant tanks on interplanetary missions, predicting performance for comparison with scale model experiment 21 p3130 A72-41181

Calculation of heat shield with local mass injection in hypersonic flow. 21 p3131 A72-41235

Mechanical tests of laminated plastics in solar installations 22 p3197 A72-43192

Aerospace vehicle passive thermal protection systems heat shield and bulk insulation estimation by weight prediction in conceptual phases of design [SAWE PAPER 934] 23 p3356 A72-43474

Diffusion bonded columbium panels for the shuttle heat shield. 24 p3406 A72-44889

HEAT SINKS

Double heat sinking high power CW TRAPATT diode oscillators using integral metallic heat spreaders 06 p0784 A72-17788

Inhomogeneous sink distribution effect on vacancy annealing kinetics and activation energy in metals 10 p1499 A72-24983

Heat pipe applications for waste heat rejection, cooling and temperature control in space shuttle, discussing design and performance [AIAA PAPER 72-272] 11 p1725 A72-25212

Space shuttle booster and orbiter thermal protection systems, examining heat sink, metallic radiative, reusable surface insulation and surface cooled designs [AIAA PAPER 72-391] 11 p1726 A72-25412

Temperature and electric field profiles in two TRAPATT diode structures in nonoscillatory state under dc bias, comparing geometrical limitations on diamond heat sinks 15 p2205 A72-31316

HEAT SOURCES

Infinite slab, cylindrical or spherical shells with nonuniform heat generation sources and equal surface temperatures, obtaining maximum internal temperature from error bounds 01 p0145 A72-10511

Isotopic heat source unit multiple elliptical orbit reentry unperturbed by solar-lunar gravitational forces, deriving analytical model of grazing trajectories, aerodynamic heating and thermochemical ablation 03 p0457 A72-13959

Uniform normal magnetic field effect upon MHD free convection from vertical wall with instantaneous heat source, considering shear stress 04 p0556 A72-14856

Thermal conductivity cell for dielectric materials powdered samples and thermal diffusivity and conductivity measurements, using line heat source principle 04 p0523 A72-15493

Radial heat propagation in cylindrical rarefied gas column from impulsive axial line source input, obtaining perturbed gas temperature by summation procedure [ASME PAPER 71-WA/HT-7] 05 p0743 A72-15867

Thermal signal propagation in flowing fluid, plane, line and point sources of varying heat, calculating temperature distribution with conduction and convection heat transfer equation 05 p0746 A72-16295

Gegenbauer/ultraspherical/ polynomials and Meijer G-functions for solution of heat production and diffusion in cylinder with internal sources leading to axisymmetric temperature distribution 05 p0747 A72-16791

Temperature distribution in infinite slab during and after heat generation by plane source of finite duration 07 p1100 A72-19627

Conjugate solution for Poisson equation of heat transfer in laminar flow with developed velocity profile in flat channel with internal constant heat sources 08 p1252 A72-21314

Spatial layer cooling during surface emission according to Stefan-Boltzmann law, assuming heat source inside body 08 p1253 A72-21445

Thin plates heated by heat sources, solving two dimensional problem in thermoelasticity via Fourier and Laplace transformations with allowance for heat propagation rate 09 p1400 A72-22718

Nonstationary temperature field of semitransparent shell with nonuniformly distributed heat sources 09 p1412 A72-23184

Thermoelastic waves propagation in homogeneous isotropic medium under external generic forces and with distributed heat sources 11 p1734 A72-25676

Thermoelastic stress and displacement in thin finite rod due to distributed time dependent heat sources 11 p1736 A72-25991

Pulsating heat source model for physical processes in metal surface layer under fatigue limit stress level, calculating critical volume to limit energy buildup 11 p1738 A72-26801

Lunar interior thermal history discussing mathematical models for radioactive heat source, initial conditions, temperature distribution and time dependent fractionation 12 p1870 A72-27336

Heat generation sources in high speed cylindrical roller bearings for gas turbine oil cooler design 12 p1816 A72-28111

Convective heat transfer for fluid flow on plate with internal heat sources in boundary layer, solving laminar-turbulent transition equations by difference method 12 p1889 A72-28138

Temperature distribution in rotating cylinder with moving surface source, allowing for heat transfer to ambient medium 13 p2064 A72-28916

Three dimensional steady temperature field calculation for solid bodies under concentrated heat source, using flow kinetic heat conduction method 13 p2065 A72-29151

Thermospheric parameters seasonal and latitudinal variations calculation based on atmospheric model with components ionization and molecular oxygen dissociation as main heat sources 14 p2128 A72-30463

Ionosphere heating effects produced by transverse electric field, discussing strong nighttime source 14 p2100 A72-30631

Thermosphere kinetic temperature diurnal variation from heat conduction equation periodic solution, determining heat sources from solar radiation atmospheric absorption 14 p2101 A72-30640

Point heat source induced thermal stresses in elliptic plate with circular holes, determining stress-strain field by two dimensional elasticity theory 14 p2166 A72-30689

Lunar origin and evolution, considering gravitational energy, radioactive isotopes and tidal deformations as heat sources 14 p2161 A72-30997

Quasi-static thermal stresses in circular disk due to rotating point heat source on surface 16 p2470 A72-33594

Magnetothermoelastic temperature distribution effects due to linear heat source in infinite circular cylinder acted upon by magnetic field 16 p2425 A72-33595

Nonlinear system consisting of gas filled tube with pressure sensitive heat source, noting oscillation evolution due to equilibrium perturbation [ASME PAPER 72-APM-21] 17 p2580 A72-34796

Distortion of the semi-infinite solid due to transient surface heating. 17 p2635 A72-35974

Equatorial tropospheric waves induced by diabatic heat sources. 18 p2687 A72-36628

Thermo-elastic interactions in an infinite elastic solid due to a concentrated transient heat source. 18 p2735 A72-36754

Thermal displacements and stresses in cylindrical shells due to instantaneous line heat sources. 19 p2870 A72-37272

Critical conditions of thermal explosion in the presence of chemical and mechanical heat sources 19 p2879 A72-37357

Calculation of a plane stationary temperature field in the presence of a heat source 20 p2987 A72-39915

Motion due to a moving internal heat source. 21 p3044 A72-40115

Application of the Monte-Carlo method to the calculations of the configuration of a heat source whose material is subjected to the action of electron beams 21 p3127 A72-40135

Equatorial stratospheric waves induced by diabatic heat sources. 22 p3201 A72-42508

Stress function for thermal shock in plate with cylindrical heat source, noting thermal stress concentration in optical materials under electromagnetic radiation 23 p3348 A72-43792

Focusing characteristics of CO2 laser beam. 24 p3409 A72-44776

HEAT STORAGE

Unsteady temperature field and conductive heat accumulating properties of bodies with dihedral and polyhedral angles

08 p1251 A72-20954

Thermal storage type resistojets design for satellite attitude control, discussing heat loss minimization

13 p2026 A72-28927

HEAT TESTS

U HIGH TEMPERATURE TESTS

HEAT TOLERANCE

Heat exposure effect on Sidman avoidance performance in rats, discussing organism thermoregulatory capacity disruption and shock and body temperature regulation

02 p0169 A72-12525

Heat acclimatization, work habituation and exercise effects on body thermoregulation, measuring tympanic temperature, sweat rate and oxygen intake

04 p0472 A72-14896

Dry heat resistance of bacillus spores on spacecraft metal surfaces for different pressures, atmospheres and materials

04 p0475 A72-15261

Body thermal stress, local heating and arterial occlusion effects on sweat electrolyte content

07 p0929 A72-19437

Heat and cold acclimatization in hamsters, relating thermoregulatory response to helium-cold hypothermia induction

08 p1115 A72-21085

Safe exposure times for men working in high temperature environments, showing hyperbolic heat collapse relationship to environmental severity

10 p1432 A72-24990

Natural acclimatization to work in severe heat.

17 p2508 A72-34550

Hemodynamic thermoregulatory and sympathoadrenal responses to heat acclimatization in man during supine and upright position exercise

17 p2506 A72-35963

Skin temperatures in warm environments and the control of sweat evaporation.

17 p2506 A72-35969

Sweat depression during controlled hyperthermia in man - Effects on the sweat rate and sweat electrolytes

20 p2892 A72-35991

Comparison of physical, biophysical and physiological methods of evaluating the thermal stress associated with wearing protective clothing.

20 p2898 A72-39808

Influence of high temperature on the onset of motion sickness

21 p3004 A72-41749

Heat strain in hot and humid environments.

22 p3150 A72-42492

Heat acclimatization by exercise-induced elevation of body temperature.

22 p3151 A72-42741

HEAT TRANSFER

NT AERODYNAMIC HEAT TRANSFER

NT CONDUCTIVE HEAT TRANSFER

NT CONVECTIVE HEAT TRANSFER

NT HYPERSONIC HEAT TRANSFER

NT LAMINAR HEAT TRANSFER

NT RADIATIVE HEAT TRANSFER

NT SUPERSONIC HEAT TRANSFER

NT TURBULENT HEAT TRANSFER

Heat transfer in turbulent flow of equilibrium dissociating nitrogen tetroxide within round tube, considering pressure, temperature and mass flow rate effects

01 p0145 A72-10490

Uncondensed components effects on heat transfer in condensation of nitrogen tetroxide partly in second dissociation stage, deriving heat of vaporization

01 p0145 A72-10494

Linear heat transfer boundary value problem series solution in Cartesian and cylindrical coordinate systems

01 p0145 A72-10575

Laser power transmission, examining heat transformation into coherent radiation by closed cycle gas dynamic laser system

01 p0080 A72-10925

Wall conduction effect on heat transfer to laminar boundary layer, obtaining temperature distributions at plate surface by energy transport equation

02 p0202 A72-11670

Heat transfer in low Reynolds number flow - ASME Conference, Washington, D.C., November 1971

02 p0301 A72-11722

Laminar free convection from vertical nonisothermal right circular cone with boundary layer control by injection or suction, investigating heat transfer by perturbation method

02 p0204 A72-12232

Anode heat flux for cascade atmospheric Ar arc of Maecr type, checking anode heat transfer model validity

02 p0302 A72-12266

Locally nonsimilar solutions for thermal boundary layer, presenting surface heat transfer and temperature distribution

[ASME PAPER 71-HT-1.] 02 p0302 A72-12313

Two dimensional wedge shaped body base heat transfer to separated nonreattaching flow region in subsonic wind tunnel

[ASME PAPER 71-HT-D] 02 p0152 A72-12314

Monatomic He-Ar binary gas mixtures heat transfer to cylinders in low Reynolds number flow, considering internal energy effects

02 p0303 A72-12358

Heat transfer and temperature profiles in separated flow generated by transverse rectangular notch in flat plate

02 p0303 A72-12700

Heat transfer of nonequilibrium dissociating nitrogen dioxide in round tube, allowing for finite reaction velocity

02 p0303 A72-12861

Lateral surface heat transfer effect on thermophysical characteristics in thin layer coatings, discussing temperature gradients in corundum and zirconium oxide on copper

02 p0304 A72-12864

Heat transfer in rarefied Couette gas flow, obtaining reduced distribution function, macroscopic temperature profile and heat flux

03 p0456 A72-13242

Current lines and temperature fields in square cavity with one movable wall and viscous flow and heat transfer, solving equations numerically

03 p0456 A72-13629

Diffusion saturation effects on thermal stress concentration in plate with circular hole under edge heating and lateral surface heat transfer

03 p0451 A72-14124

Heat transfer in rectangular annular channel during external heating under supercritical pressure, discussing thermal flux, mass flow rates and enthalpy

03 p0457 A72-14152

Heat and mass transfer equations for unsteady transpiration cooling, taking into account temperature gradient between coolant and surface

03 p0457 A72-14154

Heat transfer during liquid film evaporation in centrifugal vaporizer, noting agreement between theory and experiment

03 p0458 A72-14158

Heat and mass transfer processes in systems of bodies with variable phase boundaries, proposing difference scheme

03 p0458 A72-14159

Heat transfer from burning gas mixture flow to receiver wall, taking into account exothermal reactions due to catalytic effects

03 p0458 A72-14166

Heat transfer to liquid fuel burning from sandfilled pan burner, measuring burning rate, wick temperature distribution and flame radiation heat flux distribution as function of time

03 p0458 A72-14221

Buoyancy effect on shear stress and heat transfer in horizontal boundary layer, considering Boussinesq approximation

03 p0343 A72-14320

Cylindrical nuclear fueled capsules heat transfer gaps, determining dimensional changes with neutron radiographs

04 p0546 A72-14428

Drill hole heat transfer upon hot liquid injection into productive layer, enhancing oil extraction process effectiveness

04 p0594 A72-14515

Rarefied gas heat transfer problem between two parallel plates of different temperatures, evaluating nonlinear Boltzmann equation with Monte Carlo techniques

04 p0595 A72-14599

Supercritical pressure turbulent forced fluid heat transfer mechanism hypothesis, explaining anomalous transfer improvements and deteriorations

04 p0511 A72-14641

Heat transfer from nitrogen plasma jet mixed with cold gas to cooled reactor channel walls at various channel expansion degree values

04 p0555 A72-14645

Heat transfer from gas to air-cooled turbine blade, obtaining solution by brute force technique

04 p0595 A72-14649

Nonsteady high-rate heat transfer control in boundary layer by conjugate problem treatment and reduction to Volterra equation, considering limiting-regime and stability

04 p0596 A72-14666

Biological tissue heat transport dimensionless parameters for steady state and transient analysis of homeotherm thermoregulation

04 p0472 A72-14864

Holographic interferometer for heat transfer measurement, studying free convection thermal boundary layer on heated isothermal vertical flat plate

04 p0524 A72-15531

Quasi-linear parabolic equations loaded system first boundary value problem for heat and mass transfer equations inverse problems

04 p0540 A72-15545

Magnetic field effect on heat transfer in steady plane laminar conducting incompressible viscoelastic liquid flow in channel with nonconducting walls

04 p0560 A72-15580

Heat losses in oil wells hot liquid injections, modifying Oroveanu approximation method for exact solution

04 p0597 A72-15743

Asymptotic integration method solution of heat transfer equation with constant wall temperature for low speed slip flow regime

[ASME PAPER 71-WA/HT-5] 05 p0599 A72-15866

Free molecular flow heat transfer to rough surface, discussing surface/molecule interaction model for digital simulation

[ASME PAPER 71-WA/HT-8] 05 p0743 A72-15868

Heat transfer for water at pressures near atmospheric in wicks formed of stainless steel screen layers, obtaining steady and maximum evaporation rates

[ASME PAPER 71-WA/HT-12] 05 p0744 A72-15872

Nonequilibrium stagnation heat transfer mathematical models for injecting He, Ar or H into ionizing air laminar viscous layers at low Reynolds numbers

[ASME PAPER 71-WA/HT-18] 05 p0744 A72-15877

Low Reynolds number nonequilibrium stagnation heat transfer with helium, argon and hydrogen injection into air boundary and thin viscous shock layers

[ASME PAPER 71-WA/HT-19] 05 p0744 A72-15878

Heat and mass transfer along axially conducting gas controlled heat pipes, discussing wall temperature profiles and condenser characteristics

[ASME PAPER 71-WA/HT-29] 05 p0745 A72-15882

Mean and fluctuating temperature dependence of gas discharging from orifice to atmosphere on pressure vessel wall heat transfer

[ASME PAPER 71-WA/HT-32] 05 p0745 A72-15884

Steady state heat transfer problem solutions in living tissue modeled as cylindrical shells, discussing blood flow and temperature distributions in extremities

[ASME PAPER 71-WA/HT-34] 05 p0745 A72-15885

Analytical model for living biological tissue transient heat transfer, taking into account conduction, storage, generation, convection and blood flow effects

[ASME PAPER 71-WA/HT-36] 05 p0620 A72-15887

Thermal modeling of space shuttle cryogenic turbopump, considering heat transfer for two-phase cryogen and gas impingement on turbine blades and rotating disks

[ASME PAPER 71-WA/HT-43] 05 p0664 A72-15890

Modeling techniques for fluid line transients, considering heat transfer and viscous dissipation

[ASME PAPER 71-WA/FE-9] 05 p0646 A72-15933

Turbulent flow and heat transfer characteristics of non-Newtonian fluids on flat plate, measuring velocity and temperature distributions

05 p0648 A72-16003

Intense noise measurement device for heat flow environments, discussing applications to jet engines, nozzle exits, turbine exhausts and volcanic craters

[ONERA, TP NO. 1010] 05 p0661 A72-16025

Dutch monograph on heat transfer of gas with vibrational relaxation at shock tube end wall covering mathematical model, induced velocity effect on pressure, etc

05 p0648 A72-16045

German monograph on analog model of thermoregulation in human body at rest and at work, describing heat transfer

05 p0621 A72-16047

Nonstationary oncoming flow temperature effect on heat transfer in thermal boundary layer at forward stagnation point

05 p0746 A72-16217

Jet mixing flow from slotted source into longitudinal cross flow showing analogous to heat expansion in plane jets

05 p0648 A72-16220

Heat transfer in kinetic burning in turbulent boundary layer on porous surface for carbon dioxide blown in air stream with dissociated oxygen

05 p0746 A72-16223

Theoretical and experimental heat transfer at plate in longitudinal jet flow with strong transverse inhomogeneity

05 p0649 A72-16228

Book on heat and mass transfer, covering research results over 1953-1969 on supersonic aircraft and missiles cooling problems, rarefied gas dynamics boundary layer flow, etc

05 p0747 A72-16399

Two dimensional cascade test of air-cooled turbine nozzle, describing aerodynamic characteristics and heat transfer properties

05 p0602 A72-16489

Shock interference heating in hypersonic flows, measuring pressure and heat transfer in wind tunnels

[AIAA PAPER 72-78] 05 p0604 A72-16805

Heat and mass transfer blowing correction correlations for graphite and charring ablator reentry nosetip and heat shield applications

[AIAA PAPER 72-91] 05 p0748 A72-16810

Surface heat transfer and pressure measurements for downstream effects of transpiration cooled nose tip, using nitrogen as injectant fluid
[AIAA PAPER 72-185] 05 p0605 A72-16840

Film cooled turbine vanes external heat transfer distribution in turbulent gas stream, measuring heat transfer coefficients with and without blowing
[AIAA PAPER 72-9] 05 p0707 A72-16877

Transient compressible heat and mass transfer in porous media, solving coupled nonlinear partial differential equations in finite difference form by iterative technique
[AIAA PAPER 72-23] 05 p0749 A72-16914

Two phase heat transfer in porous metal transpiration cooling system, comparing measured with calculated temperature distribution
[AIAA PAPER 72-25] 05 p0749 A72-16916

Two dimensional turbulent boundary layer before rectangular step, investigating heat exchange in separation regions
05 p0751 A72-17048

Nonadiabatic real gas nozzle flow with friction and heat transfer to wall, obtaining solution by Runge-Kutta method
05 p0610 A72-17066

Relativistic heat propagation models, considering hyperbolic system of partial differential equations, momentum-energy tensor for ideal fluid and classical Fourier law
06 p0847 A72-17256

Simultaneous solutions for turbulent boundary layers in compressible flow with pressure gradient and heat transfer at wall, obtaining velocity and enthalpy profiles
06 p0798 A72-17845

Two dimensional stability of condensed systems combustion, evaluating effects of heat transfer from combustion region
06 p0902 A72-17906

Solid thermal motion influence on atom colliding with solid surface linear semiinfinite atomic chain, presenting accommodation coefficient calculation method
06 p0853 A72-18140

Coolant flow and heat transfer in rotating circular cylindrical enclosure, solving Navier-Stokes and energy equations by finite difference formulation
06 p0802 A72-18189

Thermal behavior of electron and ion gases in ionosphere, analyzing heat gain, transfer, loss and conductivity terms of energy equation
06 p0809 A72-18278

Heat transfer and hydraulic resistance of lamellar type heat exchangers with water/air working media, testing efficiency for various duct cross sections and Reynolds numbers
06 p0904 A72-18510

Two dimensional dynamic thermal stresses in Al plate, allowing for Newtonian surface heat transfer
06 p0899 A72-18642

Numerical methods for parabolic, hyperbolic and elliptic flows in fluid mechanics and heat transfer, considering finite element method
07 p1097 A72-18795

Meteorological elements vertical profiles under cloud cover condition by solving heat and humidity transfer equations based on satellite data
07 p1029 A72-18860

Rectangular capacitor overheating calculation with allowance for heat transfer from all surfaces, discussing chassis heat removing action computation during natural cooling
07 p0953 A72-18930

Heat transfer and drag during air laminar flow in circular pipe with constant heat flux density at wall
07 p0966 A72-18938

Tropical disturbances effect on general atmospheric circulation, considering Hadley cell rising branch and cumulonimbus clouds heat release
07 p1029 A72-19096

Heat transfer in thermal entrance region with turbulent flow between parallel plates, solving energy equation by difference methods
07 p1099 A72-19622

Second order effects in incompressible boundary layer flow with heat transfer, deriving numerical solutions for skin friction
07 p0968 A72-19625

Heat and mass transfer in initial section of circular pipe under stabilized laminar flow, using modified Leveque method
07 p0968 A72-19883

Unsteady thermal conductivity and heat transfer in solid bodies heated by radiation, using cascade linearization method
07 p1100 A72-19884

Heat transfer steady state and transient response problems nodal formulation and numerical solution on digital computer
07 p1101 A72-19918

Two dimensional and axisymmetric flow with heat addition, deriving flow field by inverse methods
07 p0909 A72-20062

Iterative solution of differential equations for steady plane flow with heat and mass transfer at high Reynolds numbers
07 p0971 A72-20098

Compressible boundary layer flow past swept wavy wall with heat transfer and ablation, measuring pressure and temperature disturbances
07 p1101 A72-20247

Temperature fields and mass and heat transfer at surface of solid spherical particle in laminar viscous fluid flow
07 p0973 A72-20318

Storm available potential energy generation and boundary layer frictional dissipation estimation in heat transfer from ocean to atmosphere within east coast cyclone
07 p0980 A72-20451

Computerized numerical nodal analysis of heat transfer away from bridgwire of electroexplosive device to meet all- and no-fire requirements
08 p1219 A72-20753

Soviet papers on heat transfer in gas turbines covering heat conduction and boundary conditions for rotors and blades
08 p1222 A72-20943

Heat transfer in laminar and turbulent Newtonian fluid flow in narrow channels with allowance for temperature dependence of viscosity and energy dissipation
08 p1148 A72-20955

Heat exchange effects in thermal diffusivity measurements in dielectrics by plane temperature wave method, applying to rock and mineral studies
08 p1251 A72-21095

Heat transfer effect on Poiseuille flow in channel, using modified Orr-Sommerfeld equation with additional viscosity gradient terms
08 p1252 A72-21253

Variational principle of Hamiltonian type for classical field theory, noting application to nonlinear heat transfer and fluid flow in Eulerian description
08 p1252 A72-21287

Temperature gradients and dynamics of transient heating and cooling processes in metallic thermistors connected in series to power supplies
08 p1252 A72-21307

Conjugate solution for Poisson equation of heat transfer in laminar flow with developed velocity profile in flat channel with internal constant heat sources
08 p1252 A72-21314

Matsevityi nonlinear resistances method for contact heat exchange boundary value problems of fourth kind
08 p1252 A72-21319

Transcendent Si power rectifier with high current and power dissipation capacity, discussing design, fabrication and performance tests
08 p1111 A72-21413

Integral contact temperatures and heat balance calculation for heat transfer between contacting bodies with rotational motions
08 p1252 A72-21444

Fiberglass heat transfer mathematical model, noting scattering effect and thermal conductivity
08 p1191 A72-21452

Dust content effect on heat transfer in hypervelocity wind tunnels, discussing gas flow pattern distortion due to interaction with particles
08 p1253 A72-21453

Poisson heat transfer equation for complex boundary three dimensional region, solving by constant sign functions with aid of R conjunctions
08 p1253 A72-21456

Heat exchange extremum boundary value problems for flow direction reversal, considering thermal treatment of porous materials
08 p1253 A72-21457

Laminar thermal boundary layer analysis, comparing heat transfer characteristics of continuous surface and semiinfinite plate
08 p1254 A72-21613

Steady flow of dual temperature plasma into vacuum from widening nozzle, taking into account electron thermal conductivity and heat exchange between components
08 p1214 A72-21653

Soviet book on heat and mass transfer and friction in gradient fluid flows in variable cross sectioned ducts and at surface of bodies
08 p1152 A72-22022

Tropical storms generated midlatitudinal cloud bands relation to autumnal large scale circulation, analyzing heat and moisture injection effects
09 p1344 A72-22429

Burning process of low boiling Mg particle moving in relation to gaseous oxidizer, assuming heat and mass transfer occurrence by diffusion-conduction mechanism
09 p1411 A72-22888

Heat transfer research review, discussing gas turbines, aeronautics, astronautics, nuclear power, thermal pollution and controlled fusion challenges
09 p1412 A72-23684

Newton cooling law applicability to unsteady heat and mass transfer approximate calculation for ion exchange process
09 p1412 A72-23685

Steady turbulent flow and heat transfer downstream of circular pipe sudden enlargement, computing streamline and temperature profiles and wall fluxes
09 p1412 A72-23687

Book on heat and mass transfer analysis covering conduction, boundary layer and channel flow convection, thermal radiation, rarefied gas mechanics, thermophysical properties, etc
10 p1561 A72-23748

Heat transfer through glass plate in solar radiation flux, discussing temperature distribution and thermal flux meter design
10 p1562 A72-24318

Heat transfer between alternating hot and cold parallel plates of constant temperature situated in low density gas
10 p1562 A72-24537

Heat transfer process in boundary layer of transparent gas flowing past plane emitting plate with prescribed surface heat flux
10 p1418 A72-24540

Vaporization heat transfer characteristics for heat pipe wick samples of felted metal and sintered metal powder
11 p1739 A72-25201

Double slot laminar film cooling, considering tangential gas injection velocities into laminar boundary layer and heat transfer to wall
11 p1741 A72-25228

Parabolic boundary layer finite difference model for predicting film cooling and heat transfer near flush injection slots in gas turbine combustors
11 p1614 A72-25229

Color schlieren technique for simultaneous photographic recording of flow fields and heat transfer patterns in aerodynamic heating, noting application to shock-boundary layer interactions
11 p1629 A72-25257

Fluid flow and heat transfer in tube bank with two cylinders in cross flow, determining static pressure, Nusselt number and drag coefficients
11 p1743 A72-25259

Heat transfer and laminarization prediction by two equation turbulence model for accelerated boundary layer flows at low Reynolds number
11 p1743 A72-25260

Flow and heat transfer model for turbulent cylindrical wall jets based on Prandtl mixing length theory
11 p1744 A72-25268

Reusable external insulation materials for space shuttle thermal protection, evaluating local heat transfer at interface areas in plasma arc test facility
11 p1744 A72-25409

Kinetic model for polyatomic gas heat transfer between parallel plates, considering boundary value problem with arbitrary accommodation coefficients
11 p1744 A72-25559

Heat transfer characteristics of liquid metal filled closed thermosiphons for hot wall boundary conditions of constant temperature and uniform heat flux
[ASME PAPER 72-GT-36] 11 p1745 A72-25631

Upper atmosphere /thermosphere/ physical variations, discussing diffusive equilibrium, energy absorption and heat transfer
11 p1621 A72-25842

Resistance wires and wire thermocouple junctions temperature response in low pressure gases, taking into account wire mounting temperature effect
11 p1632 A72-26000

Noncoincidence of maximum velocity and zero shear stress due to asymmetric turbulent velocity profiles, considering effect on momentum, heat and mass transfer in noncircular channels
11 p1618 A72-26534

Heat transfer during film and transition boiling on vertical surfaces, taking into account time dependence
11 p1746 A72-26537

Heat and momentum transfer of binary gas mixture flow in parallel plate channel with mass injection from porous wall, calculating velocity, pressure and temperature distributions
11 p1746 A72-26538

Heat transfer during gas injection through mesh packet porous wall, using gradient method
11 p1748 A72-26972

Conditional instability of second kind /CISK/ model of surface cyclonic vorticity dependence on vertical distribution of latent heat release
12 p1838 A72-27019

Stress-strain state and temperature distribution in transversely isotropic layer under mixed heat transfer conditions
12 p1878 A72-27085

Chernikov approximation for general relativistic thermodynamics nonstationary equations of heat transfer, thermal and viscous stresses and entropy balance
12 p1844 A72-27188

Lunar granular materials thermophysical properties, emphasizing thermal conductivity data and heat transfer mechanisms

12 p1869 A72-27333

Gas side, coolant side and interstitial heat transfer in gas turbines transpiration air cooling

12 p1860 A72-27350

Localized magnetic field for wind tunnel wall-plasma heat transfer minimization, preserving flow characteristics

12 p1852 A72-27684

Heat and momentum transfer properties and storm propagation speed under steady convective overturning in shear, considering cumulonimbus convection scale of atmospheric motion

12 p1840 A72-27704

Heat transfer to casing in axial clearance space between nozzle diaphragm and turbine wheel

12 p1861 A72-28134

Dimensionless heat transfer equations of reacting media in chemical equilibrium, using Lewis-Semenov criterion

12 p1889 A72-28140

Three dimensional hydrodynamic and thermal boundary layers and heat transfer for forced convection flow in rotating cylinder system

12 p1890 A72-28167

Three dimensional heat propagation problem of copper electrode destruction under concentrated heat flux with allowance for metal evaporation

12 p1890 A72-28175

Heat transfer measurement during flat plate cooling by air film, using electrical calorimetric technique

12 p1890 A72-28176

Galerkin boundary method as variational approach to low Peclet number heat transfer in laminar flow

13 p2063 A72-28418

Apollo 14 experiments to demonstrate flow patterns of convection and heat transfer in gases and liquids under weightlessness

13 p2035 A72-28614

Papers on heat and mass transfer covering physicochemical conversions, transonic gas flow in closed channels, drying theory, turbulent flows, liquid evaporation, electrorheology, etc

13 p2063 A72-28626

Heat transfer to surfaces in turbulent compressible gas flows with various boundary conditions

13 p2063 A72-28627

Iterative solution of coupled nonlinear differential equations under boundary conditions for flow and heat transfer of Rivlin-Ericksen fluid between rotating parallel disks

13 p1986 A72-28881

Temperature distribution in rotating cylinder with moving surface source, allowing for heat transfer to ambient medium

13 p2064 A72-28916

Mechanical seals for high temperature heat transfer fluids, noting configuration and construction materials [ASLE PREPRINT 72AM 30]

13 p1964 A72-28976

Heat transfer dynamics during cooling of thin vertical plates, observing boundary layer formation and motion

13 p2065 A72-29454

Friction drag and heat transfer on long blunt-nosed cylinder in supersonic flow, determining location of transition zone as function of Mach number

13 p1895 A72-29642

Quasi-static thermoviscoelasticity problem for infinite plate with circular hole, investigating plate surface heat transfer and material viscosity effect on temperature stresses

13 p2061 A72-29796

Carbon dioxide turbulent flow heat exchange in single phase near critical region under forced and free convection

13 p2066 A72-29900

Hypersonic turbulent boundary layer flow parameters and heat exchange during blowing of coolant air and He through slot

13 p1895 A72-29901

Russian papers on cooled high temperature gas turbines covering engine theory and design, power plants development, heat transfer and air cooling systems

13 p2029 A72-29925

Interferometric investigation of temperature fields and heat transfer in air layers between vertical, inclined and horizontal parallel walls

14 p2170 A72-30251

Heat transfer and hydraulic resistance for cooled air forced flows in narrow rectangular channels as function of pressure and Reynolds number

14 p2093 A72-30291

Relaxation method for thermal computation programs to solve nonlinear heat exchange equations for steady state temperature distribution, discussing numerical instability due to linearization

14 p2170 A72-30684

Steady state thermal transfer during ablation and radiation of single scattering albedo with constant heat flux at boundary

14 p2171 A72-30892

Book on extended surface thermal transfer covering heat exchanger design, convective transfer, radiation and computer programs

14 p2172 A72-30975

Pressure distribution and heat transfer in flow separation zone of cone tipped cylindrical body, using shadowgraph photography for flow visualization

14 p2070 A72-31005

Mass transfer effect on heat transfer to evaporating droplet, considering mass efflux shielding effect and forced convection flow field

14 p2172 A72-31051

Integral method application to convective flows with axial diffusion, obtaining heat and mass transfer characteristics

14 p2096 A72-31058

Heat and mass transfer in steady viscous flow through curved circular tubes, investigating velocity and temperature profiles

14 p2173 A72-31064

Steady state lumped linear formulation of heat transfer in multichannel parallel-and-mixed-flow heat exchangers

14 p2173 A72-31065

Momentum and energy equations for pool film boiling heat transfer from horizontal cylinder to saturated liquids, using integral boundary layer analysis

14 p2173 A72-31067

Heat transfer in MHD boundary layer flow of conducting incompressible fluid with aligned magnetic field on flat plate at high Prandtl number

14 p2141 A72-31068

Heat transfer distribution in supersonic arc plasma constrictor of variable cross sectional area ducts, including pressure and compression shock front effects

14 p2141 A72-31071

Temperature measurement error due to solid body and temperature sensor specific heat differences for unsteady heat transfer

14 p2106 A72-31160

German monograph on heat transfer and stability limits for boiling and nonboiling falling films covering surface and bubble boiling conditions

15 p2334 A72-31503

Monograph on hot environments stress covering heat exchange at skin surface, clothing effect, body temperature regulation and sweating control

15 p2185 A72-31515

Heat transfer and longitudinal temperature distribution at Hartmann-Sprenger tube inlet calculated approximately on basis of boundary layer data in steady compressible flow

15 p2217 A72-31685

Radiation effect on isothermal discontinuity amplitude for stationary shock wave structure with heat transfer and dissipation

15 p2335 A72-32099

Pressure increase induced by heat release for laminar flame sheet in hypersonic stream, considering fuel injection through semiinfinite porous flat plate

15 p2337 A72-32590

Exact boundary layer calculations for heat and mass transfer on cones at angle of attack, considering Mach number, enthalpy ratio and cross flow effects

15 p2337 A72-32591

Metal melting heat relationship to diffusion activation energy with vacancy mechanism equal numerically to crystal internal energy maximum change

15 p2259 A72-32691

Internal aerodynamic problem solution by kinetic equation for Couette and Poiseuille flows and heat transfer between plane plates

16 p2343 A72-33153

Heat transfer through laminar boundary layer with allowance for streamline pressure gradient effect on velocity field, using Lighthill method

16 p2477 A72-33427

Thermodynamic properties of axisymmetric and planar stagnation flows of air with gas injection, taking into account mass transfer effects on heat transfer rate

16 p2477 A72-33428

Blowing and suction effects on heat transfer and friction coefficients of transpired turbulent boundary layer, presenting theoretical models and experimental results

16 p2378 A72-33431

Subcooling and acceleration effects on nucleate boiling heat flux, comparing heat transfer prediction models with experimental measurements

16 p2477 A72-33433

Variational principles application to nonlinear heat transfer problems, using Euler-Lagrange equation

16 p2478 A72-33435

German monograph on pressure loss and heat transfer in heat exchangers, taking into account hydrodynamic and thermal inflow velocity and temperature distribution

16 p2478 A72-33504

German monograph on surface roughness effects on pressure loss and heat transfer in high temperature turbulent flow, deriving universal laws

16 p2478 A72-33506

Pressure effects on heat transfer from heated surface to fluidized bed at 150-1000 C, noting carrier gas heat conductivity effects

16 p2479 A72-33852

Boundary conditions influence on heat and mass transfer in low temperature heat pipes with freon as working fluid

16 p2479 A72-33853

Critical analysis of Senftleben modified hot-wire method for gas heat conductivity measurement

16 p2479 A72-33861

Solar wind heat flux measurements comparison with collision dominated heat transfer theory in ionized medium, noting deviations from Maxwellian velocity distribution

16 p2449 A72-33908

Solar wind structure from observations and mathematical models, discussing effects of relativistic protons, heat transfer from electrons to protons and magnetic fields

16 p2449 A72-33909

Digital equilibrium temperature model for diurnal surface thermal and energy transfer simulation based on Myrup analog solution

16 p2419 A72-33942

Reattachment heat transfer for laminar or turbulent separated shear layers, comparing predictions with measurements for cavities, ramps, spiked-nose bodies and forward facing step

[AIAA PAPER 72-717]

16 p2344 A72-34031

Magnetogasdynamic heat transfer to hemispherical body in supersonic low density plasma, noting magnetic field effects on heat flux

[AIAA PAPER 72-686]

16 p2346 A72-34056

Book - The method of weighted residuals and variational principles: With application in fluid mechanics, heat and mass transfer

17 p2573 A72-34250

A first initial boundary value problem for a semilinear heat equation.

17 p2573 A72-34339

Applications of an improved formalism for the analysis of transport phenomena in gaseous mixtures and plasmas.

17 p2587 A72-34615

A study of the heat flow and thermal instabilities in high power hybrid integrated circuits.

17 p2527 A72-34678

The effect of ionization on heat transfer to wires immersed in a highly thermally-ionized plasma.

17 p2637 A72-34998

Measurement of the parameters and the structure of a wet vapor flow with interphase heat and mass transfer in the relaxation zone behind the front of a shock wave.

17 p2637 A72-35130

Heat and mass transfer in initial section of circular pipe under stabilized laminar flow, using modified Leveque method

17 p2637 A72-35131

Unsteady thermal conductivity and heat transfer in solid bodies heated by radiation, using cascade linearization method

17 p2637 A72-35132

Russian book on pyrometry principles covering high temperature measurement, error analysis, heat transfer and brightness temperature

17 p2556 A72-35447

Experimental determination of the aeroacoustic environmental about a slender cone.

[AIAA PAPER 72-706]

17 p2486 A72-35482

Heat Transfer and Fluid Mechanics Institute, 23rd, San Fernando Valley State College, Northridge, Calif., June 14-16, 1972, Proceedings.

17 p2542 A72-35631

Heat mass and momentum transport in free turbulent mixing.

17 p2543 A72-35638

Variables influencing the characteristics of plasma-sprayed coatings.

17 p2561 A72-35920

Book - Investigation of nonstationary heat and mass transfer processes by the net-point method

18 p2740 A72-36248

Book - Annual review of fluid mechanics, Volume 4

18 p2679 A72-36382

Solution of heat transfer problems with the aid of Laplace transforms. I - Development of analytical solutions for two specific boundary value problems

18 p2740 A72-36422

Elementary plane waves in a Signorini-Cattaneo's thermoelastic solid.

18 p2735 A72-36512

Equatorial tropospheric waves induced by diabatic heat sources.

18 p2687 A72-36628

Calculation of airflow over an arbitrary ridge including diabatic heating and cooling.

18 p2706 A72-36629

Response of heat transfer from a moving flat plate in a parabolic flow.

18 p2741 A72-36798

Optimality conditions in a problem of heat transfer process control

18 p2741 A72-36809

Solution of the general heat transfer problem by the integral Tolubinskii method for a longitudinal flow past cylindrical bodies

18 p2742 A72-37182

Calculation of thermal fluxes and temperatures on the surfaces of a plate in the presence of heat exchange between fluids incident on the surfaces

18 p2742 A72-37183

Calculation of the temperature field of a heated zone of complex form consisting of a chassis and built-in components

18 p2742 A72-37187

General solutions of the heat equation in finite regions.

19 p2880 A72-37411

Experimental investigation of nonstationary heat exchange for flow around a flat plate

19 p2880 A72-37665

Linearized problem of one-dimensional periodic gas flow in a pipe

19 p2786 A72-37666

Pressure loss and heat transmission in cylindrical ducts

[ONERA, TP NO. 1057] 19 p2880 A72-37768

Investigation of heat exchange during film boiling of underheated liquid under conditions of forced flow in channels

19 p2881 A72-38036

Heat transfer and resistance in a laminar gas flow with variable properties in an annular channel

19 p2786 A72-38040

The enhancement of heat transfer by waves in stratified gas-liquid flow.

19 p2787 A72-38398

Two state system analytic modelling as nonlinear heat transfer problem

19 p2882 A72-38445

Heat transfer with the helium II superfluid film.

19 p2883 A72-38839

A review of physical models and heat-transfer correlations for free-convection film boiling.

19 p2883 A72-38842

A thermal stratification model of a cryogenic tank at supercritical pressures.

19 p2883 A72-38845

Heat transfer in water droplets and its role in the calculation of highly stressed injection coolers

[DFVLR-SONDDR-196] 20 p2911 A72-39075

Turbulent boundary layer static pressure and heat exchange dependence on gas injection through porous surface

20 p2912 A72-39363

Flow calculation for polytropic process with friction and heat transfer

20 p2913 A72-39371

Straight fins with periodic base temperature variation, calculating design parameters effects on heat transfer rates, temperature distributions and efficiencies

[ASME PAPER 72-HT-E] 20 p2983 A72-39484

Heat transfer ratios in multifluid regenerative systems

20 p2984 A72-39650

An analysis of heat transfer in turbulent pipe flow with variable properties.

[ASME PAPER 72-HT-59] 20 p2985 A72-39657

Theory of heat transfer in a two-dimensional porous cooled medium and application to an eccentric annular region.

[ASME PAPER 72-HT-47] 20 p2985 A72-39663

Stagnation-point heat transfer - The effect of the first Damkohler similarity parameter.

[ASME PAPER 72-HT-44] 20 p2985 A72-39666

Heat transfer in a channel with a porous wall for turbine cooling application.

[ASME PAPER 72-HT-39] 20 p2986 A72-39667

A parametric study of the transient ablation of Teflon.

[ASME PAPER 72-HT-32] 20 p2986 A72-39671

Heat and mass transfer in the initial mixing region of confined coaxial laminar jets.

[ASME PAPER 72-HT-22] 20 p2986 A72-39674

Film cooling effect on surface heat transfer in laminarizing mainstream turbulent boundary layer for injection through flush angled two dimensional slots

[ASME PAPER 72-HT-11] 20 p2986 A72-39682

A general method for the analysis of compact multifluid heat exchangers.

[ASME PAPER 72-HT-14] 20 p2986 A72-39684

A two-equation model of turbulence applied to the prediction of heat and mass transfer in wall boundary layers.

[ASME PAPER 72-HT-15] 20 p2986 A72-39685

A technique for determining the transient heat flux at a solid interface using the measured transient interfacial temperature.

[ASME PAPER 72-HT-18] 20 p2987 A72-39687

Characteristics of turbulent transfer in jets of variable density

20 p2914 A72-39910

Heat and mass transfer in Venturi tubes

20 p2928 A72-40048

Bounds for heat transport in a porous layer.

21 p3127 A72-40119

Intensification of heat transfer in channels with turbulent gas flows

21 p3127 A72-40127

Results of a study of heat and mass transfer during the purification of helium from nitrogen by the condensation method

21 p3127 A72-40130

Magnetic field effects on turbulent shear flow of electrically conducting fluid, discussing turbulence level, friction stress and heat exchange

21 p3089 A72-40260

Radiation effects on isothermal discontinuity amplitude for stationary shock wave structure with heat transfer and dissipation

21 p3128 A72-40266

Russian book - Heat and mass transfer: A reference book.

21 p3128 A72-40350

Synthesis of Tolubinskii's integral method and the perturbation method in nonstationary transport problems with nonlinear boundary conditions

21 p3129 A72-41053

Investigation of the critical heat flux density in heat transfer with and without turbulization of the flow at the inlet of an annular channel

21 p3129 A72-41057

Influence of baffle geometry on heat transfer in the cooling channel of air-cooled blades

21 p3099 A72-41062

Solution of the Stefan problem by the collocation method

21 p3130 A72-41089

Transition in compressible free shear layers.

21 p2993 A72-41310

Heat exchange with external medium along boundary of region bounded by smooth contours with heat insulated lateral surfaces, noting thermoelastic confocal elliptic ring

21 p3126 A72-41544

The cooling problem in the case of laminar boundary layers of real gases

[DFVLR-SONDDR-223] 21 p3131 A72-41619

Peclet number, length/diameter ratio, Grashof number, Knudsen number, overhear ratio and yaw angle interaction effects in cylindrical hot-wire and hot-film probes cooling

21 p3057 A72-41620

Heat transfer performance of stationary two phase closed thermosiphon with water and Freon as working fluids, discussing effects of operating pressure and heat flux

21 p3131 A72-41621

Direct acquisition and processing of data in thermal tests with the aid of a programmable desk computer system

21 p3043 A72-41850

Heat transfer, adiabatic enthalpy /temperature/ of the wall, and hydrodynamic resistance in the presence of turbulent and laminar flow of a compressible fluid in a round tube

22 p3164 A72-41883

Predvoditelev critical revision of hydrodynamic and heat transfer theory based on Navier-Stokes and Boltzmann equations, developing statistical system of molecular interactions

22 p3165 A72-41951

Anode heat transfer for a flowing argon plasma at elevated electron temperature.

22 p3210 A72-41952

Hot wire anemometer calibration for measurements of small gas velocities.

22 p3175 A72-41953

A calculation procedure for heat, mass and momentum transfer in three-dimensional parabolic flows.

22 p3243 A72-41954

Three-phase heat transfer - Transient condensing and freezing from a pure vapor onto a cold horizontal plate - Analysis and experiment.

22 p3243 A72-41957

Flat compressible turbulent boundary layers of air, predicting foreign gas injection effects on mass and heat transfer Stanton numbers and skin friction

22 p3165 A72-41958

Differential equations for heat transfer in turbulent boundary layer flow of incompressible fluid with constant thermophysical characteristics

22 p3166 A72-42253

Convective interaction in a partially-liquid-filled vertical vessel with heat influxes in its lateral and free surfaces and bottom

22 p3244 A72-42261

Calculation of two-dimensional flows in hydrodynamics and the heat-transfer of a viscous fluid

22 p3166 A72-42287

Heat transfer effects on reentry vehicle surfaces boundary layer stability and aerodynamic characteristics, noting stall angle reduction and drag increase from wind tunnel tests

[AIAA PAPER 72-960] 22 p3137 A72-42357

German monograph - Heat transfer at a vapor bubble growing on a heated wall during boiling.

22 p3244 A72-43059

German monograph - Contribution to the experimental investigation of the heat transfer in a turbulent

HEAT TRANSFER COEFFICIENTS

wall boundary layer in the region of a strong pressure rise.

22 p3167 A72-43064

Three dimensional temperature distribution of internally cooled hollow airfoil section turbine blades, deriving heat transfer equations for digital computation

23 p3325 A72-43667

Descriptive model of the turbulent motion of an isovolumetric fluid

23 p3279 A72-43699

Transfer equations for stellar systems

23 p3338 A72-44035

Application of the 'vanishing viscosity' method to improve stability conditions for higher-accuracy difference schemes used with the heat-conduction equation

23 p3356 A72-44046

Heat conduction with allowance for the temperature dependence of the coefficient of thermal conductivity. II - Correctness of the variational formalism

23 p3357 A72-44085

Determination of the stationary temperature field in a plate with a crack in the presence of heat release from the lateral surfaces

23 p3357 A72-44086

Viscous interaction over concave and convex surfaces at hypersonic speeds.

23 p3249 A72-44308

Experimental study of heat transfer during cooling of a high-temperature gas flow in a pipe.

23 p3357 A72-44539

A laser interferometer for combustion, aerodynamics and heat transfer studies.

23 p3402 A72-44950

MHD Couette flow between conducting walls with heat transfer.

24 p3428 A72-44970

Flow model for the determination of the heat transfer on the base of vehicles with clustered H2-O2 rocket engines.

24 p3434 A72-45201

Developing turbulent flow and heat transfer in concentric annuli.

[CSME PAPER 71-39] 24 p3465 A72-45253

Calculation of the temperature field in a ventilated cassette-type radio electronic device

24 p3386 A72-45324

Dual extremum variational principles relevant to nonlinear heat transfer, applying to temperature distribution on thin walled spherical spacecraft surface

24 p3465 A72-45474

Heat release and resistance of the cylindrical heat exchangers of blades with a dual flow cooling system

24 p3434 A72-45625

Methods for determining thermal properties of anisotropic systems.

24 p3465 A72-45633

HEAT TRANSFER COEFFICIENTS

Pyrolytic graphite heat conductivity coefficients in direction perpendicular to deposition surface at high temperatures

01 p0090 A72-10488

Split-film anemometer probe determination of convective heat transfer coefficient azimuthal dependence in low Reynolds number flow over cylinders, discussing axial heat losses

02 p0224 A72-11725

Heat transfer from augmented flames and plasma jets based on magnetically rotated arcs, measuring transfer rate as function of electromagnetic torque

02 p0301 A72-12031

Heat transfer coefficients to both sides of finite one dimensional slab subject to phase-change coating technique boundary conditions, deriving thin wing correction factors

03 p0457 A72-13956

Alkali liquid metal heat pipes, showing heat transport rate for boiling initiation

[ASME PAPER 71-WA/HT-10] 05 p0743 A72-15870

Heat transfer, drag and lift coefficients for free molecular flow over concave surfaces, describing Monte Carlo simulation technique

[ASME PAPER 71-WA/HT-17] 05 p0744 A72-15876

Fuel vaporizer for gas turbine engine, investigating heat transfer coefficient

05 p0747 A72-16492

Turbine blade local heat transfer coefficient calculation with digital computer program and naphthalene blade mass transfer in cascade flow

05 p0747 A72-16498

Mass addition distribution and gas injectant effects on heat transfer rates, transition locations and surface pressures of sharp cone

[AIAA PAPER 72-183] 05 p0748 A72-16838

Local or radiative-convective heat transfer coefficient determinatin at porous surface in presence of two dimensional temperature field, using temperature gradient method

05 p0751 A72-17070

Temperature stress distribution in infinite plate with time varying heat transfer coefficient

06 p0899 A72-18565

Convective heat transfer coefficient for particles of arbitrary shape in flow at low Reynolds number, using equivalent radius method

07 p1098 A72-18985

Viscous interaction effects on pressure distributions and heat transfer rate on two dimensional surface under high altitude hypersonic flight conditions

07 p0910 A72-20110

Heat transfer coefficient, maximum Nusselt number and particle thermal conductivity effect for gas fluidized beds, using surface renewal-penetration theory

[ASME PAPER 71-HT-Z] 08 p1251 A72-20879

Heat transfer characteristics of transpired and accelerated turbulent boundary layer on porous plate, comparing with prediction techniques

[ASME PAPER 71-HT-BB] 08 p1251 A72-20880

Hot gas heat transfer measurements in separation, reattachment and redevelopment regions downstream of abrupt circular channel expansion

[ASME PAPER 71-HT-DD] 08 p1251 A72-20881

Gas flow analysis of heat transfer coefficient in turbine blade cascades of active and reactive profiles

08 p1222 A72-20946

Dimensionless functions for heat transfer coefficients on blade cascade rotor surfaces of axial flow gas turbine for arbitrary ambient air temperature

08 p1223 A72-20947

Nonuniform temperature distribution effect on heat conduction coefficient of hot-wire cell, using computerized net point method

08 p1166 A72-21449

Thermal stresses in anisotropic annular, circular and perforated plates with temperature dependent coefficients for lateral surfaces heat removal

08 p1245 A72-21505

Heat and mass transfer analogy based on coefficients ratio and boundary layer theory

09 p1412 A72-23686

Evaluation of Collis-Williams and Davies-Fisher heat transfer formulas for flow past fine wires based on Nusselt vs Reynolds number relationship

10 p1562 A72-24294

Spacecraft cabin atmosphere thermal scale modeling based on radiative-convective-convective heat transfer, obtaining adequate thermal similitude through mass flux and heat transfer coefficient preservation

[AIAA PAPER 72-288] 11 p1741 A72-25226

Heat transfer rates of impingement cooling in gas turbine airfoils, noting leading edge sharpness effects for slot and circular jet configurations

[ASME PAPER 72-GT-7] 11 p1703 A72-25610

Local heat transfer coefficient distribution in multiple air jet cooled cavity, noting application to gas turbine blade leading edge cooling

[ASME PAPER 72-GT-59] 11 p1745 A72-25650

Thermal stress distribution in orthotropic plates with variable heat transfer coefficient, using Fourier and Laplace transforms

12 p1878 A72-27084

Semiempirical determination of local thermal fluxes and heat transfer coefficients for turbine blades based on thin film thermocouples

13 p2025 A72-28730

Equilibrium diabatic Ekman layer geostrophic drag, heat and mass transfer coefficients, presenting velocity and temperature profiles

14 p2100 A72-30346

Steady flow of compressible heat conducting fluid, discussing effect of small transfer coefficient on isentropic sonic singularity in Laval nozzle

14 p2171 A72-30713

Hypersonic limit for equilibrium laminar constant pressure boundary layer equations of planetary entry, obtaining skin friction and heat transfer parameters

14 p2071 A72-31052

Liquid film condensation of low pressure metal vapors on isothermal vertical flat plates, obtaining equations for heat transfer rate prediction

14 p2173 A72-31059

Temperature distribution and heat transfer coefficients in turbulent separated flow region downstream of rearward step in subsonic wind tunnel, using Mach-Zehnder interferometer

15 p2333 A72-31204

Heat transfer and friction coefficients for turbulent flow in rough tubes as function of Reynolds and Prandtl number, using von Karman method

16 p2478 A72-33513

Pure metal unidirectional solidification as function of liquid superheat, metal/mold heat transfer coefficient and mold material

16 p2399 A72-33804

Local vertical porosity and heat transfer coefficient relation to diluted fluidized bed relative height

16 p2479 A72-33851

Onset of convection near a suddenly heated horizontal wire

17 p2637 A72-35048

Lateral heat exchange in a thermocouple

17 p2498 A72-35513

Experimental study of conditions for heat transfer deterioration in a turbulent carbon dioxide flow under supercritical pressure

18 p2742 A72-37185

Correctness of boundary conditions in the method of measuring the heat exchange coefficient by the rate of the thermal deformation of samples

19 p2881 A72-38038

Determination of the temperature dependence of the thermophysical characteristics of solid materials by the method of successive approximations

19 p2881 A72-38044

An experimental study of the sensitivity to free-stream turbulence of heat transfer in wakes of cylinders in crossflow

19 p2787 A72-38396

The effect of changing CO₂ concentration on radiative heating rates - Further comments

20 p2947 A72-38969

Bulk viscosity coefficient and the second heat conduction coefficient near the critical condensation point

20 p2983 A72-39396

Heat transfer coefficient measurement and thermal network analysis computer program for improving performance and reliability of microelectronic package/board and chip/substrate systems

20 p2908 A72-39497

The apparent heat transfer coefficient of plate heat exchangers

20 p2984 A72-39649

Saturated liquid film boiling on vertical surface, calculating local heat transfer rates as function of height and superheat from turbulent vapor flow model

[ASME PAPER 72-HT-38] 20 p2986 A72-39668

The effect of entrance configuration on local heat transfer coefficients in subsonic diffusers

[ASME PAPER 72-HT-34] 20 p2986 A72-39670

A differential interferometer and its application to heat and mass transfer measurements

[ASME PAPER 72-HT-12] 20 p2927 A72-39683

Prediction of turbulent boundary layer heat transfer with pressure gradient and mass transfer

[ASME PAPER 72-HT-16] 20 p2987 A72-39686

Influence of thermal instability on the convective heat transfer coefficient for flows past slender bodies of arbitrary configuration

20 p2987 A72-39914

Mathematical models for temperature profiles and heat transfer rates in two-stream and multistream cross flow heat exchanger

21 p3128 A72-40931

Laplace transformation for unsteady convective heat transfer with nonlinear and time dependent heat transfer coefficients, obtaining nonlinear integral equation solution

21 p3130 A72-41066

Heat transfer in separated regions in supersonic and hypersonic flows

[ICAS PAPER 72-14] 21 p2991 A72-41139

Investigation of heat transfer at high temperature heads in the case of cooling by a dispersed flow of liquid nitrogen

23 p3356 A72-43683

Influence of wall temperature on heat transfer in a compressible three-dimensional turbulent boundary layer

23 p3248 A72-43694

Similarity problems of a non-isothermal boundary layer of an incompressible non-linear viscous medium with regard for dissipation

24 p3395 A72-45634

HEAT TRANSMISSION

NT AERODYNAMIC HEAT TRANSFER

NT CONDUCTIVE HEAT TRANSFER

NT CONVECTIVE HEAT TRANSFER

NT HEAT TRANSFER

NT HYPERSONIC HEAT TRANSFER

NT LAMINAR HEAT TRANSFER

NT RADIATIVE HEAT TRANSFER

NT SUPERSONIC HEAT TRANSFER

NT TURBULENT HEAT TRANSFER

Forced air cooling of cylindrical body with distributed thermal input, calculating temperature distribution and optimum mechanical dimensions for temperature rise minimization

02 p0189 A72-11560

Thermal IR remote sensing of surface geothermal heat flow, presenting nighttime heat budget equation based on solar and geothermal energy

02 p0208 A72-11786

Ritz approximation to two dimensional strain elasticity and heat flow boundary value problems, considering piecewise linear and cubic functions for complete triangulation

03 p0381 A72-13620

ALSEP lunar heat flow experiment, describing instrument for temperature and thermal conductivity measurements in lunar subsurface

04 p0577 A72-15098

Heat flow resistance measurement in avalanche diodes, noting junction temperature effect

04 p0498 A72-15133

Radial heat propagation in cylindrical rarefied gas column from impulsive axial line source input, obtaining

ing perturbed gas temperature by summation procedure

[ASME PAPER 71-WA/HT-7] 05 p0743 A72-15867

Human skin thermal radiation properties, presenting data on reflection, emission, transmission and complex refraction

[ASME PAPER 71-WA/HT-37] 05 p0620 A72-15888

Closed type gas turbines heated with nuclear energy, calculating heat transmitter dynamic behavior with computer program

07 p1055 A72-20598

Thermal and electric flow analogy application to heat transfer determination on basis of three dimensional model

09 p1410 A72-22628

Impulse-energy tensor for heat flow-crossed continuum subjected to electromagnetic field, using energy balance and quantity of movement equations

09 p1351 A72-22673

Thin plates heated by heat sources, solving two dimensional problem in thermoelasticity via Fourier and Laplace transformations with allowance for heat propagation rate

09 p1400 A72-22718

ALSEP heat flow experiment design and calibration, presenting independent vertical temperature gradient and thermal conductivity measurements in regolith

12 p1869 A72-27331

Apollo 15 lunar heat flow experiment, discussing temperature data from probes and long lived radioisotopes decay effects

12 p1869 A72-27332

The Apollo 15 lunar heat-flow measurement

18 p2774 A72-36285

Thermoviscoelastic problem for seminfinitesimal plate, determining temperature field and stresses permitting heat propagation

23 p3347 A72-43749

Modification of the Rankine-Hugoniot relations for shocks in space

23 p3341 A72-44510

Dual analysis for heat conduction problems by finite elements

24 p3461 A72-44877

HEAT TREATMENT

NT ANNEALING

NT MARAGING

NT NITRIDING

NT PULSE HEATING

NT STRESS RELIEVING

NT TEMPERING

Book on vacuum brazing covering dissimilar metals joining, stress cracking, corrosion resistance, joint design, heat treatment and production engineering problems

01 p0073 A72-10165

Plastic deformation, heat treatment and grinding of set blank W casts for strip and foil production

01 p0088 A72-11085

Flattening, heat treatment and machining of narrow rectangular vacuum melt Mo strips for microwave devices

01 p0078 A72-11087

Thermal treatment for delayed and reduced crystal grain growth during sintering of oxides, metals and alloys

02 p0232 A72-11431

Thorium oxide dispersion strengthened Ni powder metallurgy alloys, noting thermomechanical processing effects on tensile strength

02 p0241 A72-11447

Sintering and heat treatment effects on mechanical properties of atomized and mixed powders of Ni-Mo steel

02 p0234 A72-11462

Heat treated carbonized, cyanided, nitrided and boronized steel fatigue strength dependence on static strength, residual stress, brittleness and stress concentration from test data

02 p0244 A72-12242

Ti-Nd and Ti-Nd-Al alloys heat treatment effects on tensile and bending strengths

02 p0244 A72-12245

Ti-Al-Mo alloys thermomechanical treatment, investigating alloy composition effects on hardening

02 p0244 A72-12246

VT22 high strength Ti alloy beta phase decomposition kinetics studies under heat treatment, noting omega and alpha phases role for low plasticity

02 p0244 A72-12247

Heat treatment, quenching and aging caused metastable and stable alpha and beta structures effects on nitrogen diffusion rate in Ti alloy during nitriding

02 p0244 A72-12248

VT3-1 Ti alloy with Al, Mo, Cr and Fe additives, investigating ductile type fracture after heat treatment by electron microscopy and tensile tests

02 p0244 A72-12249

Dielectric properties of high purity polycrystalline barium titanate, observing temperature effects as function of heat treatment

[AD-737022] 02 p0269 A72-12417

Heat treatable high strength steels fracture toughness dependence on temperature, examining surfaces with electron scanning microscope

03 p0369 A72-12959

Beta structure effect on cyclic fatigue strength in Ti alloy under various heat treatments

03 p0372 A72-13595

Heat treated microstructures relation to equilibrium diagram in beta and alpha Ti alloys

03 p0374 A72-13715

Alloying and heat treatment ordering effect on hydrogen diffusion coefficients, penetrability and solubility in Pd-Ag alloys

03 p0376 A72-14016

Alloying elements effects on aging response of austenitic-ferritic alloys in Fe-Cr-Mn-Ni base, determining mechanical properties dependence on processing and heat treatment

03 p0377 A72-14170

Alloy additions and heat treatment effects on mechanical properties and weldability of quenched and aged high strength Ni steels

03 p0378 A72-14173

Heat treatable Al alloys tensile and compressive moduli of elasticities data from USAF programs, comparing to long-accepted typical values

03 p0378 A72-14175

Strain hardening for steel strength increase to 300 kg/sq mm by sequentially combined mechanical and thermal processing, involving plastic deformation, quenching and aging

04 p0527 A72-15454

Alloying, thermal and mechanical treatment effects on Mg alloys damping properties under elastic vibrations, showing test results consistency with materials microdeformation theory

05 p0671 A72-15987

Mechanical properties of heat treated hardened high strength steel, investigating microstructure relationship to breakdown characteristics

05 p0671 A72-15992

Electron microscopic examination of molybdenum alloy thin plates aging at 700 C observing nucleation and precipitated phase

05 p0673 A72-16147

Superalloys for gas turbine rotor and stator blades, testing long term heating effects on microstructure and mechanical and thermal fatigue properties

05 p0675 A72-16495

Heating effect on potassium bichromate-saturated anodic aluminum oxide electrical characteristics, discussing surface conductivity and capacity and solution pH

05 p0667 A72-17052

Al-AlCu intermetallic unidirectionally solidified eutectic composite structure and heat treatment effects on room temperature tensile properties

05 p0676 A72-17104

High strength Al-Zn-Mg-Cu alloys, testing heat treatment and Ag addition effects on tensile strength

05 p0677 A72-17112

Ti-Zr-O ternary alloys radiocrystallographic analysis, relating microstructure to composition and thermal treatment

06 p0827 A72-17569

Internal friction spectrum peaks in Fe-Ni alloy at 20-1100 C upon heating and cooling, explaining by grain boundary relaxation and martensitic transformations

06 p0830 A72-18293

Nb and Nb-Zr alloy tubular and sheet samples cyclic loading tests, determining heat treatment effects on notch sensitivity and fatigue strength

06 p0834 A72-18646

Thermocycling treatment influence on structural changes and strength in coarse grain Ni under creep tests

06 p0834 A72-18686

Hf-B system alloys phase diagram and impurities effect, discussing synthesis and heat treatment regime

07 p1010 A72-18857

Economical methods for cast maraging steel production, describing composition, heat treatment and mechanical properties

07 p1010 A72-18970

Increased microplastic deformation resistance, relaxation stability and aging of beryllium by cyclic heat treatment

07 p1013 A72-19740

Cast and wrought Ti alloys Ar arc weldments microstructural and mechanical properties after different heat treatment sequences

07 p1013 A72-19750

Heat treatment effects on strength differential of high strength martensitic stainless and Ni maraging steels

07 p1015 A72-19926

Corrosion resistance decrease and embrittlement in Ni-Mo cermet alloys after heat treatment from electrical resistance measurement

07 p1017 A72-19965

Metallographic properties of vacuum brazed, heat treated and gas quenched Al alloys, low alloy steels and corrosion resistant steel alloys

07 p1017 A72-20001

Nb and Nb alloys mechanical properties during plastic deformation and heat treatment, discussing grain size, dislocation structure and substructural changes effects

07 p1018 A72-20144

Critical temperature dependence of Nb-Al-Ge superconducting alloys on composition and heat treatment, discussing phase boundaries and electron state densities

07 p1049 A72-20154

Heat treatment of martensitically aging steels with Co, Ni and Mo, considering hardening effects and optimal conditions for high mechanical properties

07 p1020 A72-20414

Heat treatment effect on elastic properties of steel clad material for devices in sulfuric acid, discussing structural changes and optimal conditions

07 p1020 A72-20415

Austenite stabilization in maraging steel by cumulative heat cycling, using dilatometric and X ray analysis techniques

07 p0998 A72-20483

Resistivity, thermoelectric power and magnetoresistance of carbon fibers derived from heat treated polyacrylonitrile

07 p1024 A72-20550

Heat treatment, water quenching and aging effects on Ti-V alloys hardening and structural properties, discussing omega phase formation

07 p1023 A72-20667

Cr-Ti-V-B alloys rod specimens grain size and brittleness-viscosity transition temperature after heat treatment, cooling and bending tests

07 p1023 A72-20668

Cast Nb-C alloys carbon solubilities of 1.4 and 0.25 percent at 2100 and 1200 C, showing molten microstructure and measuring procedures

07 p1023 A72-20669

Heat exchange extremum boundary value problems for flow direction reversal, considering thermal treatment of porous materials

08 p1253 A72-21457

Critical supercurrents in heat treated and cold worked Nb-Ti wires, proposing pinning model based on enhancement of Ginzburg-Landau parameter in cell walls

08 p1186 A72-21594

Residual temperature stresses and deformations during thermal treatment of thick walled glass fiber reinforced plastic wound cylinders and rings

08 p1194 A72-21755

Heat stretching-induced changes effect on strength, sorption and structural properties of polyformaldehyde fibers, noting structural orientation enhancement and porosity growth

08 p1194 A72-21757

Magnetic spectra measurement of powdered hexagonal ferrites in millimeter wavelength range during grinding and after heat treatment

08 p1218 A72-21875

Work hardening after ausforming and heat treatment effects on mechanical properties of metastable austenitic Ni-Cr steel

08 p1190 A72-22165

Cast Nb alloys plasticity enhancement by heat treatment, discussing solid solution decay kinetics and carbides composition of Nb-Mo-Zr-C system

09 p1327 A72-22229

High strength solids compositional, heat treatment and chemical environmental effects on fracture strength, considering alumina as example

09 p1334 A72-22387

Thermomechanical treatment effects on microstructure and mechanical properties of Al alloy

09 p1327 A72-22470

Heat treatment and machining for distortion control of large Al alloy forgings for DC 10 aircraft

09 p1317 A72-22476

X ray diffraction and chemical phase analysis of Nb alloys in cast and heat treated state, considering hardening mechanism

09 p1327 A72-22636

Maximum internal friction onset temperature and magnitude in Co as function of thermomechanical treatment and crystal lattice defects

09 p1329 A72-23035

Thermomechanical strengthening of gamma prime precipitation hardened nickel base superalloy, emphasizing working operation and dislocation substructure

09 p1330 A72-23377

Beta-III Ti alloy mechanical properties dependence on heat treatment and elevated temperature exposure, illustrating associated microstructures

09 p1331 A72-23384

Electron microscopic, area diffraction and spectral analyses of carbide precipitates in Cr-Mo steels with different heat treatments and microstructures

10 p1494 A72-23828

Ellipsometric characterization of oxide films obtained by heat treatment of Al in air and vacuum, noting interface disruption due to gamma crystal penetration into coated metal

10 p1495 A72-24078

Fe-Ni-C alloy mixed austeno-martensitic microstructure embrittlement, investigating mechanical properties after thermomechanical treatment

10 p1495 A72-24087

High temperature sintering induced dislocations in refractory materials, studying material and diffusion transport processes

10 p1496 A72-24244

Low temperature resistant stainless steels mechanical properties, microstructure and weldability, discussing compositions and heat treatments

10 p1498 A72-24838

Acoustic emission monitoring of postweld heat treatment cracking in Rene 41 weldments, correlating relative crack susceptibility of different microstructures

11 p1653 A72-25345

Pendulum impact resistance of tungsten fiber-metal matrix composites, noting heat treatment and test temperature effects

11 p1653 A72-25473

B-Al composite mechanical properties improvement through heat treatment and steel addition

11 p1653 A72-25478

Fe-Cr-Mn alloys structural changes during high temperature oxidation, noting subscale layer thickening and alpha phase detection after heat treatment

11 p1655 A72-25498

Heat treated carbonized, cyanided, nitrided and boronized steels fatigue limit dependence on static strength, residual stress, brittleness and stress concentration

11 p1659 A72-26128

Ti-Nb and Ti-Nb-Al alloys heat treatment effects on tensile and bending strengths

11 p1659 A72-26131

Ti-Al-Mo alloys thermomechanical treatment, investigating alloying effects on hardening

11 p1660 A72-26132

VT22 high strength Ti alloy beta phase decomposition kinetics under heat treatment, noting omega and alpha phases formation effect on ductility

11 p1660 A72-26133

Heat treatment produced metastable and stable alpha and beta structures effects on nitrogen diffusion rate in Ti alloy during nitriding

11 p1660 A72-26134

Ductile type fracture after heat treatment of VT3-1 Ti alloy with Al, Mo, Cr and Fe additives investigated by electron microscopy and tensile tests

11 p1660 A72-26135

Microstructure and mechanical properties of heat treated friction welds at high temperatures

11 p1641 A72-26489

Microstructure and mechanical properties of dispersion strengthened Co alloys, investigating heat treatment effects

11 p1664 A72-26851

Heat treatment effects on martensitic bainitic steel hardness, tensile strength and impact endurance, examining carbide and alpha phases

11 p1666 A72-26922

High strength hypereutectoid steel with low carbon needle-like martensite matrix obtained by conventional heat treatment

12 p1827 A72-27100

Plane titanium and niobium carbide precipitation in microalloyed steels during heat treatment above 1300 C, noting eutectic sulfide effect

12 p1827 A72-27102

Carbon and low alloy steels resistance to abrasive wear as function of hardness, heat treatment and composition

12 p1829 A72-27455

Tensile plastic deformation effect on structural evolution of Ti-Ni alloy under anisothermal heat treatment

12 p1830 A72-27738

Postdip heat treatment effects on thin film copper sulfide-cadmium sulfide junction solar cells spectral response, diode parameters and resistance

12 p1855 A72-28010

Heat treatment and electron irradiation tests for spatial reliability of CdS and CdTe thin film solar cells, noting photovoltaic properties

12 p1756 A72-28019

Austenite grain growth characteristics of heat treated Ni maraging steel

13 p1976 A72-28673

Plastic properties of locally heated refractory metals in hot pressing calculated from temperature distribution

13 p1966 A72-29465

High stress state mechanical properties of steels with different carbon contents and heat treatments

13 p1979 A72-29478

Combined thermal, vibrational and dimensional treatments effect on WC-Co alloy physical and mechanical properties, noting tensile and impact strength increase

13 p1979 A72-29480

Ti-Ni alloy strengthening by titanium nickelide intermetallic epsilon phase formation control via heat treatment

13 p1981 A72-29829

Chemical composition, powder particle size, porosity and heat treatment effects on sulfurized iron graphite cermets durability

13 p1984 A72-30118

Stress relieving heat treatment for service failure prevention of stressed austenitic stainless steel components of high temperatures, noting cracking regulation by oxidation mechanism

14 p2117 A72-30538

Heat treatment and grain size effects on stress corrosion resistance and life duration of maraging steels, investigating crack initiation and propagation

14 p2117 A72-30539

Heat treatment hardening effect on stress corrosion resistance of ultrapure maraging and stainless steels, emphasizing hydrogen embrittlement

14 p2117 A72-30540

Heat treated light alloy bar deformation, temperature and time factor effects macrostructure and mechanical properties

14 p2124 A72-31038

Combined heat treatment and machining effects on Mg-Nd alloys structure and mechanical properties, noting strain hardening mechanism

14 p2125 A72-31042

Crack propagation in biaxially stressed and heat treated cylindrical pressure vessel observed by strain gage displacement measurement, noting effects of initial surface cracks

14 p2169 A72-31176

Electron microscope study of precipitated fines of austenitic steel containing V and N, noting heat treatment effect on FCC crystal structure

15 p2254 A72-31523

Plastic deformations accumulation and breakdown initiation in notched steel specimens, discussing effects of mechanical properties, geometry and heat treatment

15 p2256 A72-31607

Time-temperature correlated phase transformations in zirconia nucleated magnesium-aluminum-silicon oxide glass ceramics for isothermal heat treatment

16 p2413 A72-33205

Testing method for materials exposed to explosive forming, noting applications in study of formability, heat treatment effects and crack initiation

16 p2391 A72-33235

Aircraft gas turbine engine Ni base alloy disks and shafts thermomechanical treatment, considering yield strength and high and low cycle fatigue resistance

16 p2406 A72-33299

Forming techniques and heat treatment effects on recrystallization characteristics of heat resistant Cr alloy, noting high temperature influence on crystal structure

16 p2407 A72-33531

Transformation induced plasticity (TRIP) Ni-C steel strengthening by thermal cycling between martensite and reverted austenite

16 p2399 A72-33815

The effect of firing temperature on properties of natural sialite and pyrophyllite.

17 p2569 A72-34666

Tailoring the interface in graphite-reinforced polycarbonate.

17 p2570 A72-34713

Carbon-carbon composite process and fabrication techniques, discussing heat treatment effects and physical properties correlation to material structure

17 p2561 A72-35666

Aluminum alloys electron beam weldability, considering precleaning, welding speed, voltage, pre- and post-weld heat treatments effects

17 p2561 A72-35799

Nondestructive test for measuring the state of heat treatment in closure welds.

18 p2695 A72-36672

Techniques to curb static austenite recrystallization rate in martensitic sheet steel during high temperature thermomechanical treatment through minute Ti or Zr additions

18 p2701 A72-36702

Secondary recrystallization of nickel 270 work-hardened by tension

18 p2702 A72-36704

An investigation of impurities segregation to the (001) nickel surface during thermal treatment - Work function changes and Auger electron spectroscopy using the LEED camera.

18 p2720 A72-37022

Influence of heat treatment on the properties of Cr-SiO cermet thin films

19 p2844 A72-37948

Optimization of thermo-mechanical deformation parameters for Ti-6Al-4V.

19 p2821 A72-38385

Variation of the coordination number of boron during heat treatment of aluminoborosilicate fiberglass

19 p2823 A72-38681

Factors affecting acoustic emission response from materials.

20 p2924 A72-39279

Precipitation of aluminum nitride in low-alloy steel

21 p3068 A72-40956

Brazing furnaces and heat treatment under vacuum

22 p3163 A72-42635

Technological aspects concerning the structural elements in the development of resistance furnaces under vacuum

22 p3163 A72-42636

Enhanced strengthening of a spinodal Fe-Ni-Cu alloy by martensitic transformation.

22 p3194 A72-43040

Thermomechanical manipulation of precipitate shape in a titanium-base alloy.

22 p3194 A72-43044

Electrical resistivity changes in nichrome films sintering of various thickness with different heat treatment conditions, noting heat stability and thermal shock tests

23 p3292 A72-43280

Characteristics of the state of particles of titanium and vanadium mononitrides after nitriding and heat treatment

23 p3298 A72-43282

High strength boron and boric fiber reinforced aluminum composites.

23 p3299 A72-43491

Mechanical properties of titanium alloys with isomorphous beta-stabilizing elements

23 p3300 A72-43590

Magnetostriction of stainless steels as a function of heat treatment

23 p3300 A72-43596

Heat treatment effectiveness criteria for thermomechanically strengthened steels, using creep rupture, fatigue, bending and tensile tests

23 p3300 A72-43643

Physicochemical problems in silicon and germanium heat treatment, covering solubility and solid solutions stability and saturation variation with temperature

23 p3324 A72-43687

Heat treatment effect on tensile and bending fatigue strength of Al alloy thin sheet

23 p3301 A72-43743

Effect of overheating on the creep resistance of metastable alloys

23 p3301 A72-43927

Cold shortness of 14Kh2NZMA steel

23 p3303 A72-44023

Heat treatment effects in multipass weldments of a high-strength steel.

23 p3304 A72-44310

Mechanical properties of heat treated hardened high strength steel, investigating microstructure relationship to failure characteristics

24 p3416 A72-45734

HEATERS

High temperature properties of composite contact stack composed of alternating thermal flux sensors and heaters, determining heat conductivity and energy dissipation

03 p0458 A72-14160

Closed-loop temperature distribution optimal control by heater-sensor spatial configuration design for highest steady state temperature stiffness under heat flux disturbance

04 p0504 A72-14661

Geometry comparisons for weight and safety of multiwatt radioisotope heaters.

17 p2579 A72-35352

HEATING

NT AERODYNAMIC HEATING

NT ARC HEATING

NT ATMOSPHERIC HEATING

NT BASE HEATING

NT GAS HEATING

NT INDUCTION HEATING

NT IONOSPHERIC HEATING

NT KINETIC HEATING

NT LASER HEATING

NT PLASMA HEATING

NT PULSE HEATING

NT RADIANT HEATING

NT RADIO FREQUENCY HEATING

NT RESISTANCE HEATING

NT SHOCK HEATING

NT SOLAR HEATING

NT SUPERHEATING

NT TRANSIENT HEATING

One dimensional heat insulated structure under dynamic loads, showing thermoviscoelastic effects on spontaneous heating and stress-strain state

03 p0444 A72-13460

Rare gas concentrations in Luna 16 fines, using stepwise heating technique

09 p1380 A72-22266

Periodic liquid heating through infinite plate, taking into account temperature induced variation in heat capacity and conductivity

12 p1888 A72-27227

Effects of heat addition in divergent nozzles with application to MPD thrusters.

17 p2635 A72-34213

Study of reliability of Al-Au thermocompressions by measurement of resistance

18 p2668 A72-37105

Thermoplastics fatigue life dependence on stress with allowance for heating laws, noting heat accumulation effect on thermal failure

22 p3196 A72-42164

One dimensional heat insulated structure under dynamic loads, showing thermoviscoelastic effects on spontaneous heating and stress-strain state

24 p3458 A72-44935

HEATING EQUIPMENT

NT BOILERS

NT EVAPORATORS

NT FURNACES

NT SOLAR FURNACES

NT VACUUM FURNACES

NT VAPORIZERS

Cartridge system for substrate heating to 500 C in vacuum chamber during metals or semiconductor vapor deposition, describing carbon block-high intensity quartz lamp assembly

07 p0984 A72-19325

Zirconia ceramics for high performance storage heaters, discussing operating conditions, optimal properties for heater design, engineering evaluation tests and in-service performance

[AD-737021] 09 p1333 A72-22383

Aircraft cockpit electrical heating system, converting three phase ac energy from alternator with economy and safety

[SAE PAPER 720329] 11 p1577 A72-25591

High temperature biowaste resistojects with electrically conducting ceramic heaters, discussing lifetime and space station power systems adaptability

[AIAA PAPER 72-454] 11 p1708 A72-26190

Heatable chamber burners design to increase sensitivity of flame spectrophotometry, separating solvent from aerosols

13 p1958 A72-29525

Sound attenuation in lined air ducts, describing experimental determination of lining materials acoustical properties for central air heating systems

13 p2005 A72-29577

A high-accuracy temperature stabilizing and control device also operating in the cryogenic range

19 p2804 A72-38645

HEAVING

Hovercraft heaving response to regular head or following seas, determining dependency on craft natural frequency and damping, wave frequency and cushion planform

14 p2071 A72-30254

HEAVY COSMIC RAY PRIMARIES

U HEAVY NUCLEI

U PRIMARY COSMIC RAYS

HEAVY ELEMENTS

NT PLUTONIUM ISOTOPES

NT TRANSURANIUM ELEMENTS

Heavy elements gamma heating, using LiF thermoluminescent dosimeters and computer programmed photon transport calculations

04 p0546 A72-14427

Spectrographic analysis of K-type supergiant epsilon Pegasi for effective temperature, surface gravity and heavy and light element abundances

10 p1543 A72-24621

Enhanced abundances of low energy heavy elements in solar cosmic rays due to preferential acceleration within flare region

10 p1530 A72-24673

Laser pulse heating of plasma, predicting efficiency enhancement by addition of heavy element impurities or deuterides to solid target surface

12 p1852 A72-27621

Heavy element enrichment of protogalactic primordial gas by quasars matter ejection into intergalactic medium

17 p2604 A72-34526

Stratospheric balloons role in galactic cosmic radiation research with detection techniques for study of rate and heavy elements abundances and isotopic composition analysis

21 p3101 A72-41615

Studies of heavy-element synthesis in the galaxy. I - Separation of r- and s-process abundances.

22 p3228 A72-42563

HEAVY IONS

Depth ionization properties and biological effects of bevarion produced heavy ion beams, discussing utilization in tumor therapy, space biology and radiobiology

03 p0316 A72-13693

He and heavy ions properties and behavior in solar wind from expanding solar corona theoretical models

06 p0874 A72-18065

Relativistic heavy ion in plasma, calculating energy loss based on electron scattering and momentum transfers

10 p1515 A72-24344

Multiply charged heavy ion sources and accelerating systems - Conference, Gatlinburg, Tennessee, October 1971

10 p1516 A72-25026

Performance characteristics of various types of PIG sources for multiply charged heavy ions production

10 p1516 A72-25027

Multiply charged ion plasmas production in heavy ion accelerator by laser beam interaction with vaporized target material

10 p1516 A72-25033

Heavy ion acceleration from strong electron beam in metallic plasma obtained with ruby laser and positive voltage pulses

10 p1524 A72-25034

Magnetic mirrors for highly stripped heavy ions production in hot electron plasmas by low voltage high current electron beam

10 p1524 A72-25035

Fast iodine ions charge exchange in dense carbon dioxide supersonic jet, determining electron capture cross sections by least squares method

10 p1516 A72-25036

Inclusive isotope spectra of secondary nuclei produced by Bevatron heavy ion fragmentation in carbon and polyethylene targets, noting partial differential cross sections

10 p1517 A72-25144

High altitude thermonuclear explosion fission fragments localization mechanism, considering magnetogravitational trap as potential well for heavy charged fragments

11 p1713 A72-25950

Heavy ions from interplanetary dust, estimating contribution to solar wind flux

11 p1713 A72-26393

Surface damage equations for heavy ion irradiated Si and GaAs single crystals in terms of incident fluence

13 p2020 A72-28430

Simplified expressions for the calculation of the contribution of the heavy components to the transport coefficients of partially ionized gases.

17 p2589 A72-34896

Charge states and charge-changing cross sections of fast heavy ions penetrating through gaseous and solid media.

19 p2837 A72-37849

Book - Excitation in heavy particle collisions.

21 p3088 A72-41525

Evidence for radiative electron capture by fast, highly stripped heavy ions.

23 p3316 A72-44073

Source and identification of heavy ions in the equatorial F layer.

23 p3286 A72-44516

HEAVY NUCLEI

Nuclear emulsion and solid track threshold dosimetry for ion spectrum division of heavy relativistic particles in primary cosmic rays

[CERN-71-16] 02 p0162 A72-12065

Thin-down intensities for heavy primaries at SST flight levels, using plastic stacks measurements

[CERN-71-16] 02 p0274 A72-12077

Heavy nuclei enrichment in solar accelerated particles, discussing differential energy spectra, photo-spheric and coronal abundances, satellite observation and agreement with galactic cosmic rays

04 p0568 A72-15366

Inelastic ionization cross section of cosmic ray hadrons with carbon nuclei at energies of 100 to 300 GeV

06 p0869 A72-17271

Heavy nonrelativistic single charge particle recording in cosmic rays at sea level, using scintillation and anticoincidence Cerenkov counters

06 p0870 A72-17276

Cosmic ray heavy nuclear component during solar activity minimum, using Cerenkov counters onboard Elektron satellites

07 p1060 A72-19872

Mathematical model for superheavy cosmic ray production by spallation on interstellar hydrogen, assuming single source for particle injection with given charge spectrum

07 p1062 A72-20197

Solar cosmic ray heavy nuclei acceleration independence from solar activity phenomena, based on Elektron 4 satellite observation

07 p1064 A72-20632

Solar cosmic ray diffusion in interplanetary medium, describing solar flare proton and heavy nuclei propagation in terms of time of arrival measurements

08 p1227 A72-21157

Particle detector assembly for low energy heavy mass cosmic ray nuclei identification

08 p1167 A72-21508

Pion generation during collective interactions between nucleons of heavy cosmic ray nuclei, using Proton 4 satellite data

08 p1228 A72-22179

Symmetric fission of superheavy nuclei, observing overabundance of rare earth elements

10 p1515 A72-24526

Time variable energy losses effects on cosmic ray nuclei composition, discussing fragmentation processes during heavy nuclei propagation through interstellar matter

12 p1864 A72-27692

Random matrix spectra of eigenvalues in terms of Wigner set for statistical description of heavy nuclei energy levels

15 p2282 A72-32449

Ionization energy loss of relativistic heavy nuclei for close collisions as function of charge, computing

Born approximation corrections via Mott exact cross section

15 p2282 A72-32647

Heavy cosmic ray nuclei tracks in etched plastic sheets flown in satellites and balloons, discussing detector response as function of velocity

16 p2447 A72-33730

Disk-shaped diffusion model with inhomogeneous distribution of gas and heavy relativistic nuclei sources for galactic cosmic rays chemical composition

17 p2600 A72-35206

Pion generation during collective interactions between nucleons in heavy cosmic ray nuclei, using Proton 4 satellite data

18 p2721 A72-36235

Solar flare composition and energy spectra of heavy nuclei from 1971 rocket observations comparing to cosmic ray abundances

19 p2850 A72-37509

Solar cosmic ray diffusion in interplanetary medium, describing solar flare proton and heavy nuclei propagation in terms of time of arrival measurements

20 p2964 A72-39262

Composition of cosmic-ray nuclei at high energies.

20 p2965 A72-39716

Solar wind noble gases and solar flare emitted Fe group nuclei energetic tracks in chondrite Weston, considering galactic cosmic ray generated tracks

22 p3228 A72-42863

Collective interactions of the nucleons of heavy nuclei in high-energy cosmic rays

23 p3330 A72-44408

HEAVY WATER

Laser effect in solution of neodymium oxide in mixture of phosphorus oxychloride and heavy water, presenting preparation procedure

15 p2246 A72-31680

Flame structure and flame reaction kinetics. VII - Reactions of traces of heavy water, deuterium and carbon dioxide added to rich hydrogen-nitrogen+oxygen flames.

24 p3378 A72-44920

HEIGHT

Approximate height formula for radio ray propagating through spherically stratified smoothly varying troposphere, evaluating exponential model atmosphere

01 p0032 A72-11253

Pulse radar equipment for meteor height measurement from nonsaturated trails by phase difference method

13 p1929 A72-29028

HEISENBERG THEORY

Energy spectrum equations for steady state turbulent convection model based on Heisenberg statistical theory, noting application to convection in planetary and stellar atmospheres

01 p0146 A72-11311

Heisenberg ferromagnet thermodynamic properties in external magnetic field near Curie temperature, studying magnetization, susceptibility, entropy and magnetocaloric effect

08 p1217 A72-21520

HELICAL ANTENNAS

Yagi-Uda helical antenna array with moderate gain and compact mechanical design, determining electrical characteristics

19 p2773 A72-37941

Wave propagation on helical antennas.

21 p3015 A72-40352

HELICAL FLOW

Rotary self excitation of helical flows in incompressible liquids, using Navier-Stokes equation

06 p0798 A72-17730

Vaneless diffuser air flow calculation based on helical flow model with back currents in boundary layer

09 p1259 A72-22299

Turbulent boundary layer characteristics of rotating helical blade in annulus contained fluid, calculating boundary layer growth and streamline angles via momentum integral equations

10 p1466 A72-24296

Spiral flow stability between rotating and sliding cylinders, using modified energy theory based on assumption of disturbance invariance along preferred spiral direction

10 p1466 A72-24298

Inhomogeneous plasma effect on helical slow wave systems approximated by anisotropically conducting plane

10 p1522 A72-24518

Helical turbulent flow through concentric annulus with rotating inner cylinder, examining axial and tangential velocity distribution and shear stresses

10 p1471 A72-25190

Rotary self excitation of helical flows in incompressible liquids, using Navier-Stokes equation

11 p1614 A72-25333

The motion of a vortex filament with axial flow.

19 p2786 A72-37598

Nonlinear evolution of a quasi-monochromatic packet of spiral waves in a plasma

23 p3318 A72-43324

HELICAL WINDINGS

Helically bound wire reinforced sprayed Al tubes and rings, investigating failure mechanism dependence on fracture modes from tensile and bending tests

09 p1330 A72-23174

Magnetic configuration for plasma confinement in toratron with helical windings and no toroidal field coils

16 p2433 A72-32816

Composite cylinder of helically wound fiber laminates, calculating torsional fracture strength with allowance for plastic deformation due to matrix distortion

16 p2472 A72-33949

Composite cylinders of helically wound fiber laminates, predicting burst fracture strength under internal pressure for comparison with experiment on epoxy-glass cylinders

16 p2472 A72-33950

Magnetic field stability in Tornado-2 trap as function of helical currents on concentric spheres

17 p2588 A72-34856

Separatrix shape, presence and position and electron lifetime and space charge in helical Tornado trap magnetic field

17 p2588 A72-34857

Temperature distribution in a helically heated tube

20 p2984 A72-39648

Helical field experiments on a three-meter theta pinch.

21 p3094 A72-41636

HELICOPTER ATTITUDE INDICATORS

U ATTITUDE INDICATORS

U HELICOPTERS

HELICOPTER CONTROL

Free flight simulation tests for V/STOL aircraft nonlinear attitude control system adaptation to helicopter pitch and roll control [DGLR PAPER 71-060]

02 p0155 A72-12714

High speed helicopter elastic rotor blade suboptimal motion controller decreasing flapping motion and bending loads despite small control angles and vertical gusts

04 p0465 A72-15504

HH-53 rescue helicopter automatic approach and hover coupler for automatic transition from forward flight at constant deceleration and rate of descent

05 p0686 A72-16653

Digital simulation model of N helicopter formation flight characterized by close aircraft spacing, parallel flight vector and low bandwidth external forcing functions

07 p0913 A72-20354

Spectrometric oil analysis program /SOAP/ method for turbojet and helicopter transmissions damage monitoring and flight safety

09 p1319 A72-22933

Helicopter automatic flight control approach/hover coupler systems, hands off stability and handling qualities

12 p1843 A72-27522

Hydrofluidic three-axis stability augmentation system to improve UH-1B helicopter damping and handling qualities during high speed gunfiring missions

16 p2350 A72-33650

The controllable twist rotor performance and blade dynamics [AHS PREPRINT 614]

17 p2488 A72-34483

Stability and control dynamics of helicopter hovering with heavy sling load, analyzing maneuvers for minimal excitation of pendulous motion

17 p2489 A72-34488

Hydrofluidic stability augmentation system for U.S. Army helicopters, emphasizing reliability, maintainability and reduced cost

17 p2492 A72-34928

Analytical prediction of vortex-ring boundaries for helicopters in steep descents.

20 p2886 A72-38949

Helicopter development, discussing articulated, rigid, tilt and stowed rotors, compound helicopters, rotor drives, flight control and avionics systems

24 p3369 A72-45558

HELICOPTER DESIGN

Matrix method calculation for aerodynamic loads, transverse forces, bending moments, torques and twist of hinged main rotor blades in helicopter during forward flight

02 p0294 A72-12440

Rotary wing aircraft design features and performance, discussing military and civilian helicopters and future developments

05 p0612 A72-16734

Hingeless rotor helicopter blade steady state response with nonuniform inflow and elastic blade bending [AIAA PAPER 72-65]

05 p0741 A72-16933

Boeing 347 helicopter program, discussing simulation, wind tunnel, whirl tower, bench testing, flight test development and demonstration

05 p0614 A72-16993

Carbon fiber laminates for helicopter components weight reduction

05 p0681 A72-16999

Rotary wing aircraft first flight and envelope expansion at design gross weight 06 p0759 A72-18493

Emergency systems for helicopter crew and passenger survivability improvement, discussing use of ejection seats, extraction systems parachute bail-out and shaped explosive charges 08 p1109 A72-21581

Marchetti SV-20-A twin engine winged commercial utility helicopter, describing design details, on-board systems and payload accommodations 09 p1262 A72-22907

Fatigue strength characteristics of boron-epoxy reinforced Al stringers for helicopter airframe [AIAA PAPER 72-392] 11 p1574 A72-25413

Bolkow 105C 5-place helicopter with twin turbine engine driven rigid glass-reinforced plastic rotor blades, emphasizing design philosophy of easy maintainability 13 p1898 A72-29871

German Bo 105 five/six seat light utility helicopter with rigid glass-fiber reinforced plastic rotor blades, presenting design and performance 14 p2072 A72-30678

Civil helicopter electronic display requirements contrasted with fixed wing aircraft 15 p2182 A72-32633

Design requirements for a quiet helicopter. [AHS PREPRINT 604] 17 p2488 A72-34484

Flight investigation of design features of the S-67 winged helicopter. [AHS PREPRINT 601] 17 p2488 A72-34485

Critical review of Mil-F-83300 V/STOL flying qualities specifications as applied to helicopter design and missions, suggesting inappropriateness for Navy helicopters [AHS PREPRINT 643] 17 p2490 A72-34503

Ballistic-damage-tolerant composite flight control components. [AHS PREPRINT 674] 17 p2626 A72-34514

State-feedback-controllers and state-estimators design for roll-pitch-horizontal motions of helicopter near hover, using rotor dynamics model [AIAA PAPER 72-778] 19 p2752 A72-38137

Rotary wing head weight estimation for helicopter preliminary design and parametric studies, deriving semiempirical trend formula [SAWE PAPER 914] 23 p3344 A72-43461

PRD-49, a new composite material - Its characteristics and its application to the BO-105 helicopter. [SAWE PAPER 915] 23 p3305 A72-43462

Helicopter design figure of merit weight ratios definition in terms of rotor thrust coefficient, substituting pure airframe structure weight for conventionally used empty weight [SAWE PAPER 916] 23 p3250 A72-43463

Helicopter development, discussing articulated, rigid, tilt and stowed rotors, compound helicopters, rotor drives, flight control and avionics systems 24 p3369 A72-45558

HELICOPTER ENGINES

Optimal control of two shaft gas turbine engine in helicopter, using cybernetic equipment 09 p1374 A72-28262

T63/250 engine program current status, covering turboshaft helicopter engine and fixed wing aircraft powerplant models and applications [SAE PAPER 720350] 11 p1703 A72-25601

Air dust erosive damage to helicopter gas turbine engine parts, discussing inertial rotorless filtering systems 13 p2026 A72-28786

The starting of turbine engines in helicopters. [AHS PREPRINT 662] 17 p2597 A72-34509

Lynx helicopter RS 360 turboshaft engine, describing modular design for maintainability 17 p2597 A72-34927

Ka-26 helicopter operational flight testing in high mountain environment, discussing takeoff, landing and climb performance as function of altitude dependent engine characteristics 23 p3251 A72-43638

Contribution to the determination of the characteristics of a gas turbine engine for a helicopter and to the choice of the throttling law 23 p3326 A72-44277

Optimal control of the speed of a two-shaft helicopter turbine 23 p3326 A72-44278

Synthesis of the control systems of a two-shaft helicopter gas turbine engine 23 p3327 A72-44289

Nonlinear digital modeling of gas turbine propulsion units 23 p3327 A72-44294

HELICOPTER PERFORMANCE

Rotary wing aircraft design features and performance, discussing military and civilian helicopters and future developments 05 p0612 A72-16734

Helicopter rotor blade response to random loads treated by theory of linear dynamic systems with time-varying coefficients [AIAA PAPER 72-169] 05 p0613 A72-16940

Helicopter noise and vibration testing and cabin soundproofing for improved comfort 08 p1128 A72-22141

Critical lift and flow separation on helicopter rotor under dynamic loading as function of flow and blade characteristics 11 p1568 A72-25285

Flow separation effects on critical lift of helicopter rotor, using blade angle of attack criterion 11 p1573 A72-26893

Hughes 500 and OH-6 helicopter tail rotor cambered blades, comparing thrust and stall characteristics with symmetrical blades 14 p2072 A72-30290

German Bo 105 five/six seat light utility helicopter with rigid glass-fiber reinforced plastic rotor blades, presenting design and performance 14 p2072 A72-30678

Free flight follower support system with data reduction for V/STOL or helicopter models, recording flight path and attitude angles 16 p2372 A72-32886

American Helicopter Society Noise Subcommittee report on physical characteristics and major controlling parameters of rotor induced aerodynamic noise [AHS PREPRINT 625] 17 p2483 A72-34476

Boundary layer velocity profiles on a helicopter rotor blade in hovering and forward flight. [AHS PREPRINT 622] 17 p2484 A72-34482

The controllable twist rotor performance and blade dynamics. [AHS PREPRINT 614] 17 p2488 A72-34483

Flight investigation of design features of the S-67 winged helicopter. [AHS PREPRINT 601] 17 p2488 A72-34485

Helicopter maneuverability factors, discussing flight direction change ability, acceleration limitations and rotor thrust requirements [AHS PREPRINT 640] 17 p2490 A72-34500

Helicopter stability derivative extraction and data processing using Kalman filtering techniques. [AHS PREPRINT 641] 17 p2490 A72-34501

Low level light TV camera with Si intensifier target tube for fire control system to improve AH-IG Cobra helicopter night reconnaissance and attack capabilities 17 p2557 A72-35555

Analytical investigation of the effects of blade flexibility, unsteady aerodynamics, and variable inflow on helicopter rotor stall characteristics. 20 p2887 A72-38950

Ka-26 helicopter operational flight testing in high mountain environment, discussing takeoff, landing and climb performance as function of altitude dependent engine characteristics 23 p3251 A72-43638

The heavy lift helicopter - An operations research/technology/performance blend. 24 p3466 A72-44581

Blade torsional tuning to manage rotor stall flutter. [AIAA PAPER 72-958] 24 p3369 A72-45412

HELICOPTER PROPELLER DRIVE

New hubs for multi-bladed tail rotors. [AHS PREPRINT 602] 17 p2489 A72-34491

Hydraulic systems for driving helicopter tail rotors. II 18 p2642 A72-36524

HELICOPTER ROTORS

U ROTARY WINGS

HELICOPTER WAKES

Warm fog dissipation by helicopter downwash mixing, heat, hygroscopic particle and polyelectrolytes seeding 04 p0543 A72-14694

The wake geometry of a hovering helicopter rotor and its influence on rotor performance. [AHS PREPRINT 620] 17 p2484 A72-34497

Analytical prediction of vortex-ring boundaries for helicopters in steep descents. 20 p2886 A72-38949

Main results of nonlinear rotor theory 23 p2427 A72-43419

HELICOPTERS

NT COMPOUND HELICOPTERS

NT MILITARY HELICOPTERS

NT RIGID ROTOR HELICOPTERS

Helicopter antenna placement, using scale models for three dimensional radiation pattern semiautomatic recording under free space conditions 01 p0024 A72-10149

Helicopter elastomeric bearing rotors, discussing downtime and cost reduction, maintenance, endurance and inspection 01 p0073 A72-10150

Helicopter rotor tip drag relief estimate based on two dimensional drag divergence with Mach number, airfoil parameters and flight conditions 02 p0154 A72-12882

Hybrid computing techniques in helicopter simulation, taking into account complex dynamic systems nonlinear effects 09 p1283 A72-22936

Helicopter landing on ships, discussing wind, visibility limitations and flight deck motions vs aircraft stability and handling characteristics 12 p1754 A72-27413

Pilots seating active and passive isolation from LF vibrations in helicopters and jet aircrafts, discussing human factors and dynamic environment 13 p1910 A72-29558

Integral equation for calculation of unsteady aerodynamic forces on helicopter lifting rotor blades, taking into account air compressibility [ONERA, TPNO. 1081] 13 p1895 A72-29671

Structural design and electrical drive mechanism of helicopter hoist for rescue operations 13 p1912 A72-30097

Twin-turboprop transport aircraft, helicopter and all-terrain ground vehicle simulators, discussing control load, visual attachment, cabin motion and sound subsystems 14 p2092 A72-30845

Nonlinear analysis of helicopter rotor blade free transverse vibration under air and centrifugal loadings during forward flight, using matrix method 15 p2323 A72-31407

Hierarchical system of helicopter service terminals, calculating passenger lots for single and multiloop arrangements under given stochastic input conditions 15 p2337 A72-31498

Cost-saving techniques in helicopter structural test methods, suggesting system simulation, component replacement time calculation and computer techniques 16 p2373 A72-33221

Russian book on flight dynamics covering horizontal flight, takeoff, climb and landing characteristics, meteorological conditions, helicopters, trajectory problems, stability and controllability analysis, etc 16 p2349 A72-33874

Helicopter testing of inertial navigation systems. [AHS PREPRINT 634] 17 p2578 A72-34478

Low level night operations of Army aircraft. [AHS PREPRINT 631] 17 p2488 A72-34481

Helicopters vibration reduction through fuselage nodalization, discussing analysis method and dynamic scale model and full scale flight test results [AHS PREPRINT 611] 17 p2489 A72-34487

Exploration of aeroelastic stability boundaries with a soft-in-plane hingeless-rotor model. [AHS PREPRINT 610] 17 p2489 A72-34493

The wake geometry of a hovering helicopter rotor and its influence on rotor performance. [AHS PREPRINT 620] 17 p2484 A72-34497

The world speed records of the SA 341 - Gazelle. [AHS PREPRINT 651] 17 p2491 A72-34506

Helicopters technical and marketing projections for 1980s, emphasizing reliability, maintainability and maneuverability in design philosophy 17 p2491 A72-34926

Helicopters and turboprops as space conserving alternatives for automobile urban transportation, emphasizing comfort and convenience 17 p2639 A72-35505

Performance measurement in helicopter training and operations. [PP-10-72] 17 p2509 A72-35550

Russian book - Experimental studies of helicopter aerodynamics. 20 p2887 A72-39598

Flying crane helicopters utilization in construction industry for materials transport and structural erection work, discussing technical and economic aspects 23 p3251 A72-43637

HELIOCENTRIC ORBITS

U SOLAR ORBITS

HELIOGRAPHS

U SPECTROHELIOGRAPHS

HELIOGRAPHY

U SPECTROHELIOGRAPHS

HELIOMAGNETISM

U SOLAR MAGNETIC FIELD

HELIOMETERS

NT PYROHELIOMETERS

Solar coronal MHD disturbance off eastern limb correlation with complex radio event observed simultaneously with white light coronameter and Culgoora radioheliograph 02 p0276 A72-11647

Type 4 solar radio burst multiple magnetic loop structure and polarization observation by 80 MHz heliography 02 p0272 A72-11648

Circumsolar radiation measurement discrepancy explanation based on comparison with results obtained by international pyrheliometer scale 15 p2238 A72-32169

HELIOMETRY

U HELIOMETERS

U PYROHELIOMETERS

HELIOS PROJECT

Helios solar probe mission, describing project management, data reception system, trajectory monitoring and international cooperation [DGLR PAPER 71-052] 02 p0284 A72-12720

- German-American interplanetary solar probes Helios A and B mission characteristics and ground operations system, discussing planning phase [DGLR PAPER 71-122] 02 p0285 A72-12741
- Mission analysis of Helios spacecraft swingby past Venus to acquire extraelectric trajectory [AIAA PAPER 72-50] 05 p0721 A72-16951
- Heated lithium ion system /HELIOS/ facility for quiescent steady state plasma studies, noting MHD instabilities minimization 06 p0854 A72-17502
- Helios solar probe project command station design, discussing equipment details and command transmission operation sequence [DGLR PAPER 72-018] 13 p1939 A72-28963
- Paraboloid and elliptical mirrors in 100 m radio telescope for Helios space probe signals reception, noting device compatibility for data exchange with NASA [DGLR PAPER 72-019] 13 p1939 A72-28964
- Investigation of the optical and pyrometric behavior of surface coatings for the Helios probe 19 p2880 A72-37493
- Structural problems of the helios solar probe. 24 p3449 A72-45122
- Helios solar probe development, discussing scientific experiments, structural, thermal and engineering models and systems tests 24 p3451 A72-45214
- HELIPORTS**
- Design of V/STOL ports. 18 p2675 A72-36783
- HELIUM**
- NT HELIUM ATOMS
- NT HELIUM FILM
- NT HELIUM IONS
- NT HELIUM ISOTOPES
- NT LIQUID HELIUM
- Voice quality improvement in He atmospheres by on-line segment dilation 01 p0101 A72-10158
- Balloon measurements for differential energy spectra of cosmic ray protons and He over half solar cycle 1965-1969, using Geiger tube hodoscope [AD-745870] 01 p0119 A72-10876
- He emission line star G61-29, discussing spectral features and proper motion limits on maximum distance 01 p0133 A72-11095
- Spectroscopic He abundance in population II stars from viewpoint of big-bang cosmology, taking into account neutrino emission according to photon-neutrino coupling theory 02 p0281 A72-12303
- Helium shock wave two step collisional ionization model comparison to observed profile data from laser Fabry-Perot interferometer 02 p0266 A72-12368
- Isotopic composition of trapped helium, neon and argon in carbonaceous chondrites, observing covariance based on mass-dependent fractionation 03 p0414 A72-12904
- Absorption profiles of neutral helium lines lambda 4471 and lambda 4026 for BoV star tau Sco, observing flux near peak of forbidden component 03 p0417 A72-13022
- Series summations for perturbation theory of multiple photon ionization probabilities of atoms applied to hydrogen and helium 03 p0391 A72-13080
- He abundances in universe, discussing stellar structure and evolution, He production, variable stars and globular clusters H-R diagrams shape 03 p0418 A72-13112
- He abundance in population I and II stellar atmospheres 03 p0418 A72-13113
- Helium abundance in stellar interiors, considering mass-luminosity relations of Hyades 03 p0419 A72-13114
- He abundances in gaseous nebulae by optical and radio observation, discussing hydrogen and helium recombination spectra interpretation 03 p0419 A72-13115
- He production from H to maintain Galactic luminosity, discussing interstellar gas enrichment 03 p0419 A72-13116
- Helium production within supermassive stars and disks and little bangs, discussing conversion from hydrogen 03 p0419 A72-13117
- Helium production in different cosmological models based on solar system, stars and nebulae observations and stellar evolution calculations 03 p0419 A72-13118
- Solar magnetic field measurement with 10,830 A He I line photoelectric spectroheliograms, observing filamentary fine structure in active regions 03 p0429 A72-13310
- Spectroscopic characteristics of continuous wave neutral argon laser using helium and chlorine for power enhancement 03 p0367 A72-13432
- Pulsed current changes in positive column of He and Ne discharges, observing gradient and electron concentration transient behavior 03 p0399 A72-14348
- Heuristic theory of positron-helium elastic scattering phase shifts and cross sections 03 p0393 A72-14399
- Solar radio recombination lines observation at hydrogen and helium frequencies 04 p0568 A72-15328
- Helium-cold hypothermia induction and maintenance effect on hamster myocardia, with ventricle analysis of hypoxic damage, glycogen and catecholamines 04 p0476 A72-15720
- Quasar primordial He content prediction from primordial temperature fluctuations necessary for galaxy formation 05 p0717 A72-16384
- Ground state He long range interaction with triplet metastable He, discussing gerade and ungerade states 07 p1037 A72-19495
- Hydrogen-helium stars evolution, noting high surface temperature 07 p1075 A72-19581
- Stellar structure calculation by real gas equation of state, considering He abundances and solar lines of ionizable metal atoms 07 p1078 A72-19925
- Differential and integral scattering cross sections for helium excitation by electron impact from ground state to 2/super 1/S state 07 p1038 A72-20679
- Astrophysical helium production by massive pulsationally unstable pure hydrogen stars evolving inhomogeneously with mass loss 07 p1084 A72-20691
- Coalescence /collapse/ of overlapping spectral lines due to nonadiabatic broadening for Stark structure of hydrogen and helium lines in discharge plasma 08 p1211 A72-21717
- Spectroscopic measurements of light emission from carbon dioxide positive ions and carbon monoxide in metastable He interaction with carbon dioxide 09 p1354 A72-22667
- Molecular hydrogen dissociation by He, observing molecule initial quantum states effect on temperature dependent reaction cross section 09 p1357 A72-22855
- Equipment and techniques for He sorption by condensed gas layers at 0.1 picotorr 09 p1364 A72-23227
- Lasing length, power and efficiency of cw HF chemical laser with nitrogen or He diluent [AD-742962] 09 p1325 A72-23241
- Magnetic field effect on threshold pressure reduction for He and Ar gas breakdown by carbon dioxide laser radiation, taking into account inhibition of radial electron diffusion [AD-741539] 09 p1365 A72-23493
- Low energy elastic scattering cross section measurements for helium-nitrogen system, using two collimated aerodynamically intensified crossed molecular beams 10 p1515 A72-24338
- Normal ionizing shock waves characteristics in He under varying conditions of magnetic field strength, discharge current and gas pressure 11 p1694 A72-25789
- Molecular and eddy diffusion transport velocities for helium and hydrogen distributions in upper atmosphere 11 p1622 A72-25845
- He-like lines in solar X-ray spectrum observed by Bragg crystal spectrometer, noting absolute wavelengths determination with shaft encoder for angle readout 11 p1714 A72-26572
- Mechanical seal for airborne Stirling cycle cryogenic refrigerator, noting He cross leaks and sealing faces galling and blistering [ASLE PREPRINT 72AM 16] 13 p1964 A72-28973
- Perturbation theory of hydrogen and helium atoms multiphoton ionization probabilities, proposing series summation method 13 p2007 A72-29430
- Comparative spectroheliograms of He 10830 A and H alpha lines in chromosphere 13 p2047 A72-29733
- Helium use to minimize deflection of modulated laser beam in measurement of free surface motion of expanding annular cylinder loaded by exploding wire 13 p1960 A72-29765
- Hydrogen and hydrogen-helium isothermal radiative intensity at various temperatures, density ratios and path lengths, accounting for reabsorption due to overlapping lines 13 p2008 A72-30056
- Evolution of extreme population I massive stars from main sequence to He exhaustion phase, discussing various development phases in H-R diagram 14 p2158 A72-30727
- Soft X ray emission for plasma temperature determination in laser induced gas breakdown for air and He 14 p2139 A72-30805
- Pressure effects of Ar and He mixtures on Cs atomic line shapes calculated assuming additivity of perturber interactions 14 p2134 A72-30838
- Out-of-plane density distribution and in-plane velocity distribution measurements for low energy helium scattering inelastically from 550 K silver 15 p2276 A72-31861
- Extraterrestrial He I 584 A background radiation suggested from rocket and satellite observations, noting interstellar medium temperature determination from isophotes 15 p2309 A72-31945
- Explorer 19 satellite drag evidence for neutral exosphere He concentration asymmetry between Northern and Southern Hemispheres over entire solar activity cycle 15 p2228 A72-31977
- Steady state electron mean energy variation between parallel plates in Ar and He calculated by Monte Carlo simulation for comparison 15 p2285 A72-32222
- Neutronically generated He irradiation effects on high temperature fracture of fcc, bcc and hcp structural metals and alloys 15 p2258 A72-32487
- Hydrogen to helium mixing ratio in giant planets from far IR spectroscopy for atmospheric thermal models and greenhouse effect calculations 15 p2315 A72-32727
- Solar wind He enrichment origin in solar flares connection with type 2 radio emission from analysis of Vela 3 spectra 15 p2302 A72-32791
- Sounding rocket observations of quasar 3C 273 X ray spectrum for upper limits to absolute abundance of He in intergalactic medium 16 p2446 A72-33451
- Helium stars linear and nonlinear pulsation and evolutionary computations, establishing instability strip with two solar mass models 16 p2458 A72-33720
- Photoelectric observation of H alpha, sodium deuteride and He solar umbral line profiles, using pressure scanning spectrometer 17 p2608 A72-35082
- Helium and H alpha emission relationship observation in 11 February 1970 solar flare from photometric reduction of filtergrams 17 p2599 A72-35117
- Velocity and flux dependence of the solar-wind helium abundance. 17 p2602 A72-35607
- Theoretical He-triplet line strengths compared with astronomical observations of planetary nebulae and H II regions 17 p2614 A72-35646
- On the temperature of the helium emission regions in the solar atmosphere. 17 p2616 A72-35699
- Hydrogen and helium velocities in the solar wind. 17 p2602 A72-35716
- Brueckner-Goldstone many-body perturbation calculation of helium photoionization. 17 p2586 A72-35773
- Wave function and resonance parameters for autoionization and ground states of helium and hydrogen 17 p2586 A72-35774
- Nd-glass laser interaction with singly stimulated two-photon emission and anti-Stokes Raman scattering from metastable state He, calculating cross sections 17 p2565 A72-35831
- The helium abundance in thirty-three main sequence B stars. 18 p2726 A72-36726
- Experimental study of the structure of a turbulent boundary layer on a plate with helium injection 18 p2682 A72-36888
- The use of known helium line cross sections for investigation of unknown transition in neon. 18 p2713 A72-36954
- Gas-liquid hydrogen mixture and helium adiabatic model of Jupiter temperature and pressure distribution, estimating planet center temperature 19 p2863 A72-38074
- Coude spectra, abundance ratios and radial and rotational velocities of He rich stars, using microphotometer equivalent width tracings 19 p2866 A72-38502
- Helium effect on cardiac mitochondria of mice. 19 p2759 A72-38712
- He abundance relationship to solar wind bulk speed and temperature from Explorers 34 and 43 observations, noting dependence on sunspot number 19 p2853 A72-38749
- Shock tube boundary layers in ionized argon-helium mixtures. 20 p2914 A72-39639

- Examples of multiple solutions for equilibrium stars with helium cores. 20 p2973 A72-39878
- Results of a study of heat and mass transfer during the purification of helium from nitrogen by the condensation method 21 p3127 A72-40130
- He-Cd lasers using recirculation geometry. 21 p3061 A72-40239
- The abundance of helium in the cosmos. I. 21 p3103 A72-40379
- Some features of instantaneous point source diffusion within a turbulent boundary layer. 21 p3078 A72-40467
- Statistical mechanics of light elements at high pressure. II - Hydrogen and helium alloys. 21 p3106 A72-41044
- He-D3 spectroheliogram absorption features correlation with magnetic field regions and H alpha structures 21 p3108 A72-41279
- Energy and angular distributions of secondary electrons resulting from ionizing collisions of electrons with helium and krypton. 21 p3088 A72-41493
- Simultaneous measurements of H alpha and H beta Balmer lines and He D3 line in faint prominences, showing emission intensity ratios dependence on layer total optical thickness 22 p3221 A72-42034
- Nucleosynthesis theory for advanced thermonuclear evolution models of massive stars from helium burning through final hydrodynamic stages 22 p3227 A72-42561
- Helium absorption into nitrogen tetroxide (NTO) and aerazine-50 (A-50). 22 p3215 A72-42869
- Numerical models for He stars structural evolution, considering main sequence models of 1-8 solar masses and different carbon enrichments 23 p3334 A72-43258
- An experimental study of turbulent diffusion of helium jets issued upwards into the air at rest. 23 p3281 A72-44273
- Spectroscopic measurements for atmospheric nitrogen and helium arcs. 23 p3322 A72-44326
- Calculation of photoabsorption processes in helium. 24 p3426 A72-45012
- Distribution of hydrogen and helium in the upper atmosphere. 24 p3400 A72-45593
- Unconjugated urinary corticosterone excretion in laboratory rats exposed to high pressure helium-oxygen environments. 24 p3374 A72-45656
- ### HELIUM AFTERGLOW
- Circularly polarized electromagnetic wave propagation through afterglow helium slab plasma near electron cyclotron frequency 02 p0266 A72-12653
- Collisional radiative recombination applicability to time dependent electron density decay in helium afterglow before reaching quasi-steady state 04 p0555 A72-14579
- Ionization mechanisms of quiescent prominence of He II 4686 line luminescence under coronal UV radiation at high temperatures 07 p1077 A72-19812
- Geocorona and interplanetary He glow EUV emission altitude distribution measured by exospheric sounding rocket-borne thin film photon counters 15 p2231 A72-32327
- Lifetime and quenching of metastable CO produced by dissociative recombination of positive carbon dioxide ions in He afterglow 16 p2432 A72-33771
- ### HELIUM ATOMS
- Ultralow sliding friction during bombardment of polypropylene, molybdenum disulfide and graphite surfaces with charged helium atoms at room temperature in vacuum chamber 02 p0249 A72-12282
- Orion and planetary gaseous nebula helium atoms metastable triplet states population calculations 04 p0578 A72-15314
- Metastable He atoms concentration in plasma from absorption characteristics at temperatures 4-300 K and pressures 1-70 mm Hg 05 p0696 A72-16612
- Molecular oxygen dissociation rate constant determination during interaction with He atoms in cylindrical shock tube 06 p0852 A72-17686
- Repeatable hermetic seal quality determination by He bombardment technique based on measured leak rate decay with time 08 p1220 A72-20766
- EUV resonance radiation from He atoms and ions in geocorona, comparing model calculation based on solar radiation resonance scattering with rocket experiments 09 p1378 A72-23010
- Ultralow sliding friction during bombardment of polypropylene, molybdenum disulfide and graphite surfaces with charged helium atoms at room temperature in vacuum chamber 11 p1639 A72-25707
- Elastic and one-phonon inelastic scattering of monoenergetic He atoms from cleaved LiF crystal surface 15 p2281 A72-31862
- Electron production cross section during He atom ionization by proton impact, noting peak existence for electrons near incident proton velocities 15 p2281 A72-32220
- Na-He atomic collisions induced D lines broadening, fine structure transitions cross sections and multipole polarization resonance levels relaxation 15 p2283 A72-32651
- Excitation transfer and Penning ionization reactions between helium metastables and carbon monoxide. 18 p2713 A72-36563
- Emission and absorption RF recombination lines of interstellar neutral atomic H and He, discussing electron transition processes in nebula 20 p2975 A72-40070
- Intensity ratios of He I and H lines in a prominence and the chromosphere. 21 p3109 A72-41329
- Angular distribution of electrons autodetached from H- in slow collisions with He. 23 p3316 A72-44074
- The influence of ultraviolet line blanketing on the neutral helium triplet lines in B-type stars. 24 p3438 A72-44834
- ### HELIUM FILM
- He film two fluid model consistency with equilibrium between film and vapor 03 p0390 A72-14375
- Quartz microbalance studies of an adsorbed helium film. 18 p2719 A72-36675
- ### HELIUM IONS
- Positive H, He and O ions in exosphere from mass spectrometers mounted on Elektron 4 satellite 01 p0053 A72-10368
- Low energy He ion bombardment effects on Ni alloy single crystal surface, observing defect structure with stacking faults, tangled dislocations and carbide precipitation 04 p0533 A72-15159
- He and heavy ions properties and behavior in solar wind from expanding solar corona theoretical models 06 p0874 A72-18065
- Exothermic capture processes with ionization during nonelastic ion atom collisions, discussing cross sections of He ion collisions with Ar, Kr and Xe atoms 08 p1210 A72-20837
- He ionization and excitation in optically thick solar prominences, considering recombination excitation for observed triplet-level populations at 5000-10,000 K electron temperature 08 p1231 A72-21123
- Elastic singlet p wave phase shift calculation for electron scattering by H atom and He cation, using time dependent Hartree-Fock perturbation theory 09 p1355 A72-22786
- EUV resonance radiation from He atoms and ions in geocorona, comparing model calculation based on solar radiation resonance scattering with rocket experiments 09 p1378 A72-23010
- Cosmic ray proton and He nuclei differential energy spectra measurements by balloon-borne ionization spectrometer 11 p1712 A72-25881
- Radial profiles of ionized He flux and protons in magnetosphere, taking into account charge exchange processes and fluctuating electrostatic fields 11 p1624 A72-26397
- Quasi-projection operators for calculating electron resonances in multitrail scattering tested on He ion autoionization system 12 p1847 A72-27385
- He ions motion normal to magnetic field under induced electric field, analyzing resonance mechanism 13 p2016 A72-29606
- Solar plasmas intensity ratios of He-like ion line emission, showing dependence on atomic number and electron temperature 13 p2018 A72-29737
- Annual variations of singly charged positive He ion density distribution in solar wind from Vela 3 observations 15 p2299 A72-31944
- H-He ions solar wind expansion absence for case of equal gas temperature, noting mass flux relationship to He ion temperature 16 p2449 A72-33911
- The solar wind H and He/+ content. 17 p2598 A72-34627
- Ionization mechanisms for quiescent prominence He II 4686 line emission under coronal UV radiation and high temperature conditions 17 p2618 A72-35737
- Improved Stark-profile calculations for the He II lines at 256, 304, 1085, 1216, 1640, 3203, and 4686 Å. 17 p2585 A72-35768
- He ions motion normal to magnetic field under induced electric field, analyzing resonance mechanism 21 p3091 A72-40660
- He II line emission in cold regions of solar prominences and chromosphere, noting hydrogen, metal and He I emissions 21 p3108 A72-41281
- Measurement of the rate coefficient for the recombination of He+ with electrons. 23 p3315 A72-43869
- Annual variation of the interplanetary He+ velocity distribution at 1 AU. 23 p3332 A72-44505
- ### HELIUM ISOTOPES
- High conductivity superfluid region in cryogenic liquid helium 4 bath with temperature gradient in equilibrium with saturating vapor 01 p0101 A72-10040
- L-chondrite Assam, determining He, Ne and Ar concentrations and isotopic compositions and galactic and solar flare irradiation track densities 01 p0124 A72-10060
- Cosmic and solar wind abundance analysis for He and He-3 in protosolar gas, noting chemical equilibrium reaction role in D enrichment 12 p1868 A72-27216
- Torsional crystal measurements of viscosity for He 4 and He 3-He 4 mixture at lambda points 12 p1888 A72-27388
- Self consistent model for cosmic ray propagation from sources in Galaxy toward earth, using H and He isotope interstellar spectra 13 p2031 A72-29409
- Ar-39/Ar-38 cosmic ray exposure age calculation from Sikhote-Alin meteorite fall fragment content of Ar-39, Ar-38, Ne-21 and He-3 14 p2157 A72-30584
- Spallation origin of anomalous He 3/He 4 ratio in 3 Centauri A, considering thermonuclear processes model 14 p2158 A72-30731
- Low energy cosmic ray deuteron and He 3 source spectra observation implications for adiabatic deceleration in solar cavity, discussing interstellar propagation 16 p2448 A72-33743
- Analysis of pion-helium scattering for the pion charge form factor. 19 p2837 A72-37922
- Universe evolution study from contemporary chemical composition of cosmic matter, noting concentration changes of protons, neutrons and He 4 22 p3222 A72-42140
- ### HELIUM PLASMA
- Electron cyclotron harmonics emission as function of electron plasma frequency in He reflex discharge, measuring electron densities 01 p0105 A72-10026
- High resolution apparatus to record time dependent light flux variations at 380-700 nm, discussing He plasma decay investigation 01 p0064 A72-10375
- Electron density microwave measurements in helium-neon laser plasma, discussing population inversion during glow discharge 01 p0081 A72-11216
- Circularly polarized electromagnetic wave propagation through afterglow helium slab plasma near electron cyclotron frequency 02 p0266 A72-12653
- Electron-ion recombination and ambipolar diffusion disruption of electron density in cryogenic helium plasma, using cavity resonator measurements 03 p0399 A72-14067
- He plasma generation by transversely excited carbon dioxide laser, determining density and temperature profiles of luminous fireball 04 p0558 A72-15345
- Collisional radiative model of population densities of metastable electron levels of orthohelium in low pressure rf helium plasma 05 p0694 A72-15998
- Acoustic waves generation in afterglow of weakly ionized low pressure He plasma, using electrostatic probe 05 p0699 A72-17083
- Nonequilibrium plasma production by induced electric field in helium and argon streams in magnetic field 05 p0700 A72-17229
- Quiescent large volume collisionless He and Ar plasma generation via hf electric fields, noting low cost 06 p0854 A72-17504
- Magnetic multipole confinement of magnetic field-free He and Ar plasmas in vacuum chamber, observing decay 06 p0854 A72-17505
- Vibration modes and stability of nonequilibrium low density He-Cs plasma in magnetic field 07 p1043 A72-19876

Thermodynamic properties of atomic hydrogen-helium plasma for postulated conditions present in stagnation shock layer of spacecraft entering Jupiter atmosphere

08 p1254 A72-21598

Ar/He plasma acoustic wave properties, expressing phase velocity and damping as function of ion-electron temperature ratio and relative species densities

10 p1520 A72-24300

Electron-neutral collisions effects on wavelength and damping of electrostatic waves propagation in Ar and He plasmas

10 p1525 A72-25143

He and Ar plasma transport by magnetic fields after expulsion from pulsed linear discharge

14 p2135 A72-30167

Comparative electron density measurements in positive low pressure He discharge column with Langmuir probes and microwave interferometer and cavity

14 p2105 A72-30808

Absorption coefficient of H-He plasma measured in temperature and electron density range of inverse bremsstrahlung and photoionization absorption

15 p2284 A72-31522

High power carbon dioxide laser produced dense He plasma, comparing experimental and theoretical Stark profile of forbidden and allowed transitions

15 p2285 A72-32223

Magnetic probe measurement of random fluctuations in transverse magnetic field caused by He plasma produced in arc discharge

15 p2287 A72-32408

Dense helium theta pinch plasma heating by TEA carbon dioxide laser, studying temperature and density with high speed photography and spectroscopy

15 p2251 A72-32530

Singly and doubly ionized He plasma recombination and ionization coefficients due to electronic collisions and radiative absorption

19 p2841 A72-38083

Glow discharge in rare-gas and metal vapour mixture. I - Distribution functions and kinetic coefficients in He-Cd mixture discharge.

23 p3322 A72-44320

Influence of atom-atom collisions on the collisional-radiative ionization and recombination coefficients of helium plasmas.

24 p3428 A72-44798

Electron-ion recombination in a helium plasma produced by laser.

24 p3428 A72-44799

HELIUM 2 U HELIUM ISOTOPES U LIQUID HELIUM

HELIUM 3 U HELIUM ISOTOPES

HELIUM 4 U HELIUM ISOTOPES

HELIUM-NEON LASERS

Radiation spectral properties in mode locking region of He-Ne 20 laser at 0.63 microns, generating three axial modes

01 p0078 A72-10154

Unlocked multimode He-Ne lasers If noise, discussing different modes intensity fluctuations mutual correlations

01 p0080 A72-10850

Electron density microwave measurements in helium-neon laser plasma, discussing population inversion during glow discharge

01 p0081 A72-12116

Acousto-optical extraction of energy stored in pulsed He-Ne laser cavity, using modulator with piezoelectric transducer at light-ultrasound interaction region

01 p0081 A72-13122

Mode locked He-Ne laser for optical communication, investigating steady state pulse behavior from injection locking theory

02 p0237 A72-11559

Laser sources for space research, considering He-Ne, carbon dioxide, Nd-YAG and argon lasers performance

02 p0237 A72-11695

He-Ne traversing laser velocimeter for instantaneous axial fluid velocity measurement, describing signal analyzing system, construction and calibration

02 p0224 A72-11744

He-Ne laser velocimeter for roller bearing elements rotational speed measurements, discussing instrument construction and spatial resolution

02 p0224 A72-11745

Precision alignment device using He-Ne laser with small beam divergence

02 p0238 A72-12115

Soviet book on gas lasers covering operation, population inversion, helium-neon, argon and carbon dioxide lasers and atomic frequency standards

02 p0238 A72-12121

He-Ne laser active medium excitation and resonator geometry effects on TEM wave field

02 p0239 A72-12520

Directly heated cathode effect on He-Ne laser power output and relaxation oscillations in discharge gap

02 p0239 A72-12763

Scanning Fabry-Perot interferometer for He-Ne laser spectral composition, discussing transmission coefficient, resolution, resonator dissipative losses, active medium saturation and light field spatial nonuniformity

03 p0356 A72-13190

Focused image holography in multimode He-Ne laser radiation, using diffusely scattered reference wave and lens for high quality reconstruction

03 p0357 A72-13370

Spectrum of low modulation frequencies of He-Ne laser radiation produced by motion of external reflector of matched and unmatched three-mirror resonators

03 p0368 A72-13666

Enhanced He-Ne laser frequency and output power stabilities obtained by constructing mirror and gas discharge tube as integral unit

04 p0529 A72-14603

Plasma diagnostic technique using three-mirror He-Ne laser interferometer for electron concentration measurement

04 p0555 A72-14654

Multimode Ne-He laser in strong magnetic field, discussing plasma-optical effects, emission cut-off magnetic field strength for various discharge levels and single-mode construction

04 p0530 A72-14656

He-Ne laser controlled frequency shift in wideband optical heterodyne communications systems with Currie low reflection mirror

05 p0668 A72-16346

He-Ne laser amplitude fluctuations with hot and cold cathode discharge tube operation, determining emission spectral line width

05 p0669 A72-16613

Unmodulated He-Ne laser output frequency stabilization, using quartz Fabry-Perot etalon

05 p0669 A72-16670

Two-photon time distribution in mixture of light from He-Ne laser and Gaussian source of same central frequency

05 p0669 A72-16691

Automatic frequency adjustment of pair of He-Ne lasers with different oscillation frequency fluctuations under various heating conditions

06 p0825 A72-17840

Polarizer circuit for reduction of output power fluctuations in He-Ne laser

06 p0825 A72-17842

Rough surfaces with orthogonal parallel V grooves, studying shadowing, interreflection and masking effects on bidirectional reflectance from He-Ne laser illumination

06 p0848 A72-17924

Optical sweep generator using single frequency He-Ne lasers with Michelson interferometer for mode selection to provide smooth tuning throughout Doppler width

07 p1000 A72-19010

Single isotope He-Ne laser gyro comparison with multiisotope system, noting strong mode competition in ring laser

07 p1005 A72-19402

Optical coupling effects in frequency stabilized He-Ne lasers, finding instabilities for interferometric length measurement

07 p1005 A72-19414

Optical losses, reflectivity and transmissivity measurements of He-Ne laser Fabry-Perot resonator elements, using laser output power dependence on element losses

07 p1006 A72-19905

He-Ne laser discharge gap oscillation modes observation, noting applied magnetic field, gas parameters and cathode type effects on stimulated emission

07 p1008 A72-20510

Frequency stability of free running methane stabilized He-Ne lasers with dc excitation, comparing to rf excitation

07 p1008 A72-20562

Internal asynchronous modulation of multifrequency He-Ne laser with Doppler broadened transition line

08 p1181 A72-20793

He-Ne laser resonator misalignment effect on output power, determining mirror arrangement precision tolerance for set fluctuation levels

08 p1181 A72-21163

Sealed-off He-Ne laser construction and performance, comparing with He-Cd, He-Zn and He-Ne lasers

08 p1182 A72-21437

Two mode coupling and frequency pulling in He-Ne laser without absorbing medium in resonator

08 p1183 A72-21728

Reduced air pressure effect on He-Ne laser output power via self heating

08 p1184 A72-22033

Single mode He-Ne laser output, predicting intensity correlation function form and decay time near threshold

09 p1324 A72-23081

Focal length determination for on-axis parabolic mirrors by He-Ne laser reflection

09 p1315 A72-23352

Methane absorption line profile, intensity and width studied with magnetically tuned He-Ne laser

10 p1490 A72-24041

He-Ne laser output dependence on transverse magnetic field, ascribing magneto-optical effects to IR radiation decrease

10 p1490 A72-24046

Smooth variation of He-Ne laser spectral line width in single to multifrequency mode transition, passing laser beam through coated quartz plate

10 p1490 A72-24051

Frequency stabilization of He-Ne two mode laser with internal mirror plasma tube

11 p1646 A72-25303

He-Ne laser with absorption cell, investigating high contrast power resonances due to Lamb dip at nonuniformly broadened absorption line center

11 p1649 A72-26340

Two axial modes competition in He-Ne laser with uniform line broadening, noting application for high stability frequency standards

11 p1649 A72-26349

Lithium niobate crystal refractive index inhomogeneity influence on second harmonic generation from He-Ne laser

11 p1650 A72-26360

Continuous He-Ne laser radiation power interferometry using Michelson interferometer with frequency doubler

12 p1819 A72-27051

Power resonance and frequency stabilization of gas laser with nonlinear absorption cell, considering He-Ne laser with Fabry-Perot resonator

12 p1820 A72-27584

Helium-neon laser with Hg cathode in gas discharge tube, providing 250 mW output at 6328 Å

13 p1969 A72-29518

Active gas mixture pressure relationship to excitation during single to multifrequency operation transition in He-Ne laser

13 p1969 A72-29614

He-Ne laser light modulation with lithium niobate crystals, noting lower light power and modulator volume requirements, better mechanical properties and lower thermal sensitivity

13 p1969 A72-29632

Relaxation oscillations in He gas discharge tubes with cold Mo cathode as function of pressure and discharge length

15 p2245 A72-31408

Construction, tuning and characteristics of high resolution spectrometers with scanning interferometers for He-Ne laser radiation analysis

16 p2400 A72-33080

Magnetic field effect on polarization plane rotation and emission frequency shift of He-Ne ring laser at 3.39 micron wavelength

16 p2402 A72-33485

Two axial modes competition in He-Ne laser with uniform line broadening, noting application for high stability frequency standards

16 p2402 A72-33702

Lithium niobate crystal refractive index inhomogeneity influence on second harmonic generation from He-Ne laser

16 p2403 A72-33713

He-Ne laser resonator misalignment effect on output power, determining mirror arrangement precision tolerance for set fluctuation levels

17 p2562 A72-34454

Holographic image reconstruction using He-Ne laser as coherent light source and black-white and color photographic emulsions

17 p2554 A72-34930

He-Ne laser radiation modulator at 1.5 GHz using X and Z cut lithium niobate crystals in toroidal microwave cavity

18 p2697 A72-36113

The influence of a nonuniform transversal magnetic field on the power output of a gas laser.

18 p2715 A72-36338

Variation of the longitudinal electric field by the internally modulated beam in a He-Ne laser.

19 p2810 A72-37408

Pressure shift of the magnetic resonance line of neon in a He-Ne laser.

19 p2811 A72-37930

Coherent optical signal superregenerative amplification in Q switched gas laser, calculating sensitivity of He-Ne laser light amplifier

19 p2813 A72-38663

The effect of cross relaxation on the behavior of gas laser oscillators.

19 p2813 A72-38691

Optimum generation conditions for a neon-helium laser operating in the axial TEM/sub 00/ mode

19 p2814 A72-38784

A helium-neon laser active element with a metallic inner wall surface

19 p2814 A72-38785

Investigation of the 0.63-micron line shift in an He-Ne/20/ laser with an absorbing cell

19 p2814 A72-38787

- Frequency stabilization of a gas laser using mode-interaction effects. 19 p2814 A72-38822
- Intracavity modulation of high-gain gas laser with traveling light waves nonuniform amplitude distribution, considering lithium niobate crystal resonator equipped He-Ne laser 20 p2931 A72-39068
- Directly heated cathode effect on He-Ne laser power output and relaxation oscillations in discharge gap 20 p2931 A72-39069
- Isotropically and anisotropically polarized He-Ne lasers output dependence on longitudinal magnetic fields, noting electron density radial redistribution in gas discharge plasma 20 p2932 A72-39411
- Determination of the angular divergence of laser radiation by a transforming system of prisms. 20 p2933 A72-39523
- Optical measurements in a pulsating flame. [ASME PAPER 72-HT-8] 20 p2926 A72-39679
- Relaxation oscillations induced in semi-insulating CdS with helium neon laser irradiation. 20 p2934 A72-39817
- Investigations on spectroscopy by nonlinear Zeeman-resonances of a multimode laser. 20 p2934 A72-39845
- Influence of polarization of laser fields on nonlinear interference effects 21 p3062 A72-40405
- Active gas mixture pressure relationship to excitation during single to multifrequency operation transition in He-Ne laser 21 p3063 A72-40667
- Resonance absorption of laser emission by methane behind the shock front 21 p3063 A72-40986
- Pulse modulation of a laser during the tuning of an auxiliary passive resonator with the aid of ultrasound 22 p3186 A72-42666
- Hysteresis in a gas laser when passing from a single-frequency emission mode to a two-frequency mode 23 p3295 A72-43680
- High gain He-Ne laser with forbidden cavity configuration, discussing elimination of unwanted lasing mode by temperature detuning with mirrors 23 p3296 A72-43903
- The influence of the atmosphere on the wavelength of the He-Ne laser and the solution of corrections of the laser interferometer. 24 p3409 A72-44771
- A laser interferometer for combustion, aerodynamics and heat transfer studies. 24 p3402 A72-44950
- Temperature and angular widths of the phase-matching curve of a lithium niobate crystal. 24 p3432 A72-45615
- Continuous He-He laser radiation intensity correlation function measurement, using Michelson interferometer and frequency doubler 24 p3412 A72-45704
- HELIX TUBES**
- U TRAVELING WAVE TUBES
- HELIXES**
- U CURVES [GEOMETRY]
- HELMETS**
- Flight helmet optimal fitting technique, using automatic recording audiometer and noise source for acoustic leakage detection 04 p0479 A72-14873
- Helmet systems for head protection from concussion and deformation, discussing design and testing 08 p1126 A72-21568
- Vertical drop rig test equipment for measuring shock attenuation of crash helmets, discussing shock absorption criteria for impact protection 11 p1584 A72-26016
- Involuntary head movement and helmet motion displacements during human centrifuge runs to 6 Gz from photographic recordings 12 p1766 A72-28288
- Positive acceleration force-produced displacements of helmet-attached reticle in front of left eye 12 p1777 A72-28330
- Crash helmet performance prediction through maximum strain criteria, using brain injury biodynamic model 15 p2192 A72-32607
- HELMHOLTZ EQUATIONS**
- Principal boundary value problems solution for Helmholtz equation in half space with spherical cavities, reducing problems to infinite systems of algebraic equations 03 p0387 A72-12915
- Helmholtz equation numerical solution for potential field problems with arbitrary boundary conditions of wave propagation, diffusion and thermal conduction in mathematical physics 12 p1846 A72-27553
- Algorithms for eigenvalue spectrum determination in Dirichlet and Neumann problems for Helmholtz equation in configuration domains 12 p1847 A72-27985
- Matrices and permutation rules for tetrahedral polynomial finite elements for Helmholtz equation, commenting on computer time and convergence rate 14 p2126 A72-30932
- Poisson equations solution in orthogonal curvilinear coordinate systems to allow Laplace and Helmholtz equations separability, applying to hydrodynamic, electrostatic, electromagnetic and MHD problems 15 p2278 A72-32249
- Electromagnetic field in MHD generator active zone approximated by cruciform plate, calculating secondary fields from Helmholtz equation 16 p2435 A72-33283
- The Helmholtz equation in a waveguide / Factorization of the boundary condition from infinity/ 19 p2768 A72-38848
- Approximate calculation of a cavity resonator for n given initial natural frequencies 23 p3269 A72-43449
- HEMATITE**
- On the magnon interaction in haematite. I - Magnon energy of optical mode. 17 p2595 A72-35358
- HEMATOCRIT**
- Electronic and hematocrit devices to investigate cardiovascular system functions including blood coagulation process, pressure and flow 11 p1585 A72-26464
- Plasma protein concentration, volume and hematocrit changes during exercise, bed rest and high forward acceleration 12 p1766 A72-28296
- Stepwise altitude acclimatization and subsequent reanimation after blood loss caused clinical death effects on dog peripheral blood erythrocytes, reticulocytes, hemoglobin and hematocrit 14 p2076 A72-30671
- Disproportional changes in hematocrit, plasma volume, and proteins during exercise and bed rest. 17 p2506 A72-35966
- HEMATOLOGY**
- Astronauts red cell mass changes associated with space flight due to space and earth environment differences 16 p2356 A72-33564
- Hematologic responses to hypobaric hyperoxia. 20 p2892 A72-39345
- Hematological modifications due to acute exposure to heat 21 p3002 A72-41191
- Ionizing radiation effects on mitosis and nucleic acid synthesis, noting protective chemical agents and hematological evaluation of radiation damage and marrow regeneration 22 p3141 A72-41986
- Physiological and hematological effects of chronic irradiation. 23 p3254 A72-43392
- Human blood monocytes - Stimulators of granulocyte and mononuclear colony formation in vitro. 24 p3373 A72-45374
- HEMATOPOIESIS**
- Human urine regenerated water in various dilutions effect on fish and rat erythropoiesis 05 p0622 A72-16651
- Plasma erythropoietin concentration in men and mice during altitude acclimatization 07 p0917 A72-19440
- Suppression effects of hyperoxic breathing gases on red blood cell and erythropoietin hormone production following blood loss 12 p1766 A72-28298
- Hemopoiesis in the pig-tailed monkey *Macaca nemestrina* during chronic altitude exposure. 20 p2892 A72-39344
- Experimental studies of the production of erythropoietin in relation to the intensity and duration of hypoxia 21 p3002 A72-41189
- Studies of renal and extrarenal production of erythropoietin in male and female rats 21 p3002 A72-41190
- Pyrogenal injection test for hematopoietic tissue function in dogs, describing response as transient leukopenia followed by pronounced leukocytosis due to bone marrow granulocyte ejection 23 p3255 A72-43911
- HEMATOPOIETIC SYSTEM**
- Proliferative blood forming tissue activity under chronic gamma ray irradiation in guinea pigs by quantitative methods, showing myeloid and reticular disturbances of bone marrow 04 p0467 A72-14607
- Sublethal X radiation effects on rat erythropoietic system during altitude hypoxia acclimatization 04 p0476 A72-15721
- Hypoxia effect on diurnal mitotic activity rhythm of marrow erythropoiesis system of guinea pigs in pressure chamber 05 p0618 A72-16631
- Mathematical model for blood leucocyte population changes after radiation exposure within Blair model leucocytes hemopoietic to cardiovascular systems transport 05 p0618 A72-16635
- Nervous and humoral stimulation and hypoxia effects on erythropoiesis control, studying human blood serum additions to bone marrow cultures 21 p3001 A72-40762
- HEMISPHERES**
- Unsteady boundary layer on hemisphere embedded on infinite plane during normal liquid impingement, using inner and outer expansions method to study separation time 05 p0653 A72-17003
- Magnetogasdynamics heat transfer to hemispherical body in supersonic low density plasma, noting magnetic field effects on heat flux [AIAA PAPER 72-686] 16 p2346 A72-34056
- Electromagnetic radiation and scattering from loaded bodies of revolution of arbitrary shape, calculating plane wave scattering from apertures in cylinders and hemispheres 18 p2662 A72-36927
- HEMISPHERICAL SHELLS**
- Rocket-borne inflatable sphere for radar signal backscatter calibrations at reentry altitudes and for simultaneous atmospheric density determination 13 p1918 A72-28819
- HEMODYNAMIC RESPONSES**
- Extrastolic potentiation of ventricular contraction effect on dog mitral valve function, using roentgen videodensitometry 01 p0015 A72-11036
- Hemodynamics, pulmonary gas exchange and circulatory responses to high altitude in subjects with previous history of high altitude pulmonary edema 02 p0156 A72-11422
- Cardiac output and autonomic nervous system role in antidiuretic response to acute thoracic superior vena cava constriction 02 p0157 A72-11661
- Beta-adrenergic and vagal blockage altered autonomous control effects on left ventricular function in conscious dogs, noting heart rate, stroke volume and end-diastolic and end-systolic diameters 02 p0163 A72-12090
- Spinal mesenteric vascular reflexes of vasoconstriction effect of pressure drop in coeliac artery relation to Rein nutritional hepatic reflex 04 p0473 A72-15125
- Hemodynamic and blood oxygen parameter changes comparison in dogs during hypoxia at rest and muscle activity in various oxygen concentrations 04 p0474 A72-15232
- Hemodynamic response to hypoxia in dogs with experimental myocardial infarction, discussing changes in cardiac output, stroke volume, left ventricular pressure and systemic vascular resistance 05 p0617 A72-16152
- Stellate ganglion stimulation and hypoxia effects on hemodynamics and coronary circulation in dogs, discussing myocardial oxygen consumption, sympathetic nerve vasoconstrictor effect and vasodilatory response 05 p0617 A72-16153
- Hemodynamic response to running exercise stress for aeronautics personnel selection, determining systolic ejection variation measurement and cardiac frequency increase 07 p0927 A72-19242
- Carotid sinus counterpressure as baroreceptor stimulus in intact dog, recording arterial pressure response in closed loop gain [AD-739805] 07 p0917 A72-19439
- Nonurgical ultrasonic technique to measure wall displacement and pulsatile changes in thoracic aorta [AD-739809] 07 p0930 A72-19447
- Maximum oxygen intake during exercise on treadmill compared with bicycle ergometer, analyzing circulatory dynamic factors and cardiac output relation to oxygen transport capacity 07 p0922 A72-20251
- Stretch activation of myogenic oscillation of isolated contractile structures of heart muscle in ATP salt solution 07 p0923 A72-20427
- Hyperbaric chamber tests for hemodynamic response to oxygen inhalation at 1 and 2 atm pressure for myocardial infarction treatment assessment 08 p1114 A72-20891
- Myocardial infarction effects on drug tolerance and hemodynamic changes due to digitalis doses, discussing toxic arrhythmias 08 p1115 A72-21082
- Tachycardia role in coronary vascular bed hemodynamic response to severe exercise in dogs 10 p1426 A72-24483
- Beta-adrenergic blocking effect on canine coronary and systemic hemodynamic adaptation during treadmill exercise 11 p1579 A72-25802
- Hemodynamic criteria for physical fitness in air-men, discussing age dependent variations in heart beat, arterial pressure and body temperature 11 p1590 A72-26987
- Physiological index changes in parachutists of various ages, considering plasma recalcification, blood prothrombin, heparin time, fibrinolytic activity, pressure and heart beat 11 p1590 A72-26988

Hemodynamic effects of angiographic contrast medium in patients with and without heart disease, discussing myocardial performance during first ten beats 12 p1762 A72-27732

Hemodynamic response to physical exercise stress in dogs with angiotensin-induced acute arterial hypertension 12 p1764 A72-28216

Autonomic nervous system role in controlling coronary and cardiac responses to hypoxic hypoxia, measuring blood flow with Doppler ultrasonic flow transducer 12 p1767 A72-28313

Noninvasive polygraphic technique to assess cardiovascular responses to intravenous glucagon injection 13 p1901 A72-28570

Cardiovascular system functional state elevation during controlled cooling, studying hemodynamic changes 14 p2075 A72-30386

Cardiac output and body temperature response to prolonged intermittent exercise 15 p2185 A72-31448

Hemodynamic changes in man during immersion with the head above water. 17 p2507 A72-34543

Hemodynamic thermoregulatory and sympathoadrenal responses to heat acclimatization in man during supine and upright position exercise 17 p2506 A72-35963

Bradycardia diving reflex to apneic face immersion related to physical exercise 17 p2506 A72-35964

Venous responses to stimulation of carotid chemoreceptors by hypoxia and hypercapnia. 18 p2648 A72-36025

Synchronous and asynchronous BASH/body acceleration synchronous with heart beat/ effects on hemodynamics and ventilation in dogs and humans 18 p2648 A72-36033

Left ventricular dynamics during handgrip. 19 p2755 A72-37243

Systemic haemodynamics in borderline arterial hypertension - Responses to static exercise before and under the influence of propranolol. 19 p2756 A72-37773

Influence of inotropic alteration on the severity of myocardial ischemia after experimental coronary occlusion. 19 p2758 A72-38552

Relation of the electrocardiogram to hemodynamic alterations in pulmonary embolism. 19 p2759 A72-38816

Study of hemodynamics during the action of decompression and accelerations 21 p3006 A72-40444

Hemodynamic reflexes during acceleration stresses, considering vessel walls, cardiac rhythm, blood distribution and sinus carotis receptors 22 p3141 A72-41983

Reflexive cardiac rhythm changes and arterial tension during hypoxia, noting differences due to animals, controlled respiration and pharmacological effects 22 p3141 A72-41984

Prediction of vegetative reactions in the case of stress and extreme effects upon the organism 22 p3149 A72-42069

Cardiovascular system venous part responsiveness to central nervous and humoral influences 22 p3148 A72-43167

Effects of coronary arteriography on myocardial blood flow. 23 p3256 A72-43933

Changes in certain hemodynamic indices during muscular strain in people with differing capacity to perform work 24 p3370 A72-44591

Induction of hemodynamic deterioration by the hypogravic state - An evaluation of mechanisms and prevention. 24 p3373 A72-45199

HEMODYNAMICS

Antinatriuretic effect of acute thoracic and abdominal inferior vena cava constriction on arterial pressure, renal hemodynamics and electrolyte excretion 02 p0157 A72-11660

Exercise effects on pulmonary circulation in dogs, measuring pulsatile arterial flow and pressure and vascular input impedance, resistance and hydraulic power 04 p0475 A72-15464

In vivo investigation of dogs natural mitral valve flow dynamics, developing cardiohemic system physical model for data analysis and electrical analog simulation [ASME PAPER 71-WA/BHF-2] 05 p0621 A72-15949

Nonlinear model for computer simulation of human arterial system, using finite difference technique for pressure and flow calculations 07 p0934 A72-20357

Ventricular myocardium contractile function disorder diagnosis by phase coordinate method with intracardial hemodynamics application 08 p1122 A72-22186

QRS wave detectors for arrhythmia and hemodynamic data analysis, using standardized FM magnetic tape containing various artifacts for evaluation 11 p1582 A72-25499

Hemodynamic variables relation to coronary blood flow and myocardial oxygen consumption during upright bicycle exercise 11 p1587 A72-26618

Left ventricular dynamic function in terms of internal diameter, pressure and flow in dogs at rest and during isoproterenol and metaraminol infusions 11 p1582 A72-26773

Hemodynamic assessment of arterial blood flow from radiograph measurements of aorta branching points 11 p1582 A72-26774

Acute hypoxia effects on dog coronary blood flow and cardiac function from cardiac beta-adrenergic and hemodynamics study 12 p1760 A72-27482

Calibrated L.F acceleration vibrocardiography to examine hemodynamics indices relation to main wave amplitudes 15 p2188 A72-31313

Human cerebral hemodynamic changes during arousal and orienting reactions to auditory stimuli 16 p2353 A72-32993

Acquired complete right bundle branch block without overt cardiac disease - Clinical and hemodynamic study of 37 patients. 17 p2505 A72-35821

Interrelationship of hemodynamic alterations of valvular heart disease and renal function - Influences on renal sodium reabsorption. 19 p2756 A72-37872

Temporal relation of the second heart sound to aortic flow in various conditions. 19 p2759 A72-38818

motion. 20 p2891 A72-38935

Hemodynamic indices in flight crew personnel during hypertonic sickness and atherosclerosis of coronary arteries 20 p2892 A72-39391

Control of the circulating blood mass in the case of a functional detachment of various amounts of pulmonary tissue 21 p3012 A72-41825

Aortic regurgitation variation with respiratory sinus arrhythmia and respiratory cycle in dogs during tachycardia and bradycardia 22 p3151 A72-42674

Cardiac output, hemodynamic and gas exchange variations as function of basal metabolism during bed rest in hypokinetic recumbent or antiothostatic position 23 p3255 A72-43915

Cerebral blood filling reduction and blood vessel tone deterioration during 120 day clinostatic hypokinesia of healthy male subjects 23 p3256 A72-43922

Comparative study of regional hemodynamics during tilt test and lower body negative pressure exposure. 24 p3373 A72-45131

HEMOGLOBIN

NT CARBOXYHEMOGLOBIN

NT OXYHEMOGLOBIN

CO hemoglobin concentration measurement in blood of smokers, nonsmokers and deceased crewmembers of crashed aircraft 01 p0010 A72-10211

Molecular evolutionary changes in amino acids of proteins due to mutant random fixation, comparing human and fish hemoglobin chains 02 p0158 A72-11761

Evolutionary rate of cistrons in vertebrates, discussing hemoglobin and cytochrome c changes involving amino acid mutant substitution 02 p0158 A72-11762

Amino acid code comparisons of polypeptide chains of globins due to mutations during vertebrate evolution from ancestral gene 02 p0159 A72-11764

Volumetric analysis of blood oxygen and CO, showing combination with hemoglobin without significant molecular volume increase 05 p0619 A72-16786

Erythrocyte hemolysate cataphoresis studies of human hemoglobin changes during stepwise adaptation to high mountain conditions 09 p1266 A72-22880

Light absorption and scattering factors in whole blood related to hemoglobin concentration, discussing oxygen saturation, cardiac output and pathological conditions 11 p1588 A72-26630

Stepwise altitude acclimatization and subsequent reanimation after blood loss caused clinical death effects

on dog peripheral blood erythrocytes, reticulocytes, hemoglobin and hematocrit 14 p2076 A72-30671

Hemoglobin determination in whole blood with Specol-Zeiss spectrophotometry, comparing accuracy to cyanmethemoglobin measurements 14 p2080 A72-30787

Hemoglobin-facilitated diffusion of oxygen - Interfacial and thickness effects. 18 p2650 A72-36569

Lack of effect of high altitude on hemoglobin oxygen affinity. 21 p3006 A72-40430

Comparative studies of the respiratory functions of mammalian blood. 21 p3002 A72-40919

HEMOLYSIS

Case report on compensated hemolytic anemia associated with Gilbert syndrome, discussing implication in aviation 01 p0022 A72-11299

Erythrocyte hemolysate cataphoresis studies of human hemoglobin changes during stepwise adaptation to high mountain conditions 09 p1266 A72-22880

In vivo hemolysis due to hyperoxia - Role of H2O2 accumulation. 24 p3374 A72-45651

HEMORRHAGES

Sudden pilot incapacitation and death due to subarachnoid hemorrhage secondary to ruptured intracranial aneurysm 10 p1429 A72-23742

Influence of prolonged starvation on the frequency of occurrence of decompression-induced pulmonary hemorrhage. 17 p2508 A72-34545

Effects of vagotomy and increased blood pressure on the incidence of decompression-induced pulmonary hemorrhage. 18 p2650 A72-36446

HEMOSTASIS

U

HEMOSTATICS

Hyperbaric environment decompression effects on human blood and urine chemistry and hemostatic system, showing physiological parameter alteration in presence and absence of bends symptoms 14 p2081 A72-31087

HEOS B SATELLITE

TD-1, HEOS-B and COS-B satellite-borne experiments, discussing X ray and gamma astronomy 04 p0582 A72-15690

HEOS-2 in orbit - Its technical performance. 24 p3449 A72-45108

HEOS SATELLITES

NT

HEOS B SATELLITE

Industrial challenge of European space R and D programs, discussing ELDO Europa 1 launcher vehicle and ESRO-HEOS satellite technological problems 01 p0146 A72-10948

Anomalous earth bow shock locations during 1969 from plasma and magnetic observations aboard European satellite Heos-1 02 p0274 A72-12461

Satellite projects Azur, Dial and Heos - Conference, Bremen, West Germany, April 1971 05 p0714 A72-16134

Heos 1 data on interplanetary magnetic field, solar wind and proton characteristics, noting barium cloud experiment 19 p2850 A72-37492

Heos-A2 satellite polar orbit mission to study electron, proton and alpha particle population outside magnetosphere and in neutral point region 19 p2857 A72-37783

Observations of the solar wind with the European satellite Heos-1 19 p2850 A72-37785

HEPTANES

Flame temperatures, composition profiles and burning rates in liquid n-heptane droplet and sphere combustion 07 p1051 A72-19362

HEREDITY

Biological experiments on plants, animals and bacteria aboard Zond 5, 6 and 7 space probes, noting flight conditions effect on physiological functions and hereditary structures 11 p1579 A72-25941

Cytoplasmic heredity theory linking mitochondria origin to bacteria 19 p2758 A72-38549

HERMETIC SEALS

Spiral groove shaft vacuum seals, presenting mathematical ballpark performance model [ASME PAPER 71-WA/PIB-5] 05 p0664 A72-15914

Hf and microwave hybrid circuits encapsulation, discussing hermetic seals formation 05 p0634 A72-16182

Repeatable hermetic seal quality determination by He bombardment technique based on measured leak rate decay with time 08 p1220 A72-20766

- Fully redundant hermetically sealed cable cutter for application to electroexplosive devices in space
08 p1221 A72-20775
- Test method and apparatus to pressurize hermetically sealed components with Kr 85, comparing obtained leak rates with He mass spectrometric values
12 p1854 A72-27550
- Long life leak-proof hermetic compression seals for alkaline batteries, describing design, fabrication and accelerated thermal cycle test method
[ECS PAPER 72] 13 p1899 A72-28434
- Design and manufacturing considerations in hermetic microcircuit enclosures.
20 p2908 A72-39495
- Automatic hermetic-sealing systems for semiconductor devices prepared by electron-beam welding
22 p3158 A72-42124
- A survey of the costs of hermetic packaging and testing microcircuits.
22 p3161 A72-43175
- HERMITIAN POLYNOMIAL**
Orthogonal expansion of estimators and estimands in Hermite series for Monte Carlo computation
04 p0540 A72-15631
- Poised and nonpoised Hermite-Birkhoff interpolation problems application to quadratic formulas and expansions and completely convex functions
11 p1732 A72-25504
- HERTZSPRUNG-RUSSELL DIAGRAM**
Helium abundance in stellar interiors, considering mass-luminosity relations of Hyades
03 p0419 A72-13114
- Magellanic Clouds hot supergiants color-magnitude arrays from spectroscopic and photometric measurements
03 p0424 A72-13253
- Magellanic Clouds star clusters spatial distribution, color-magnitude diagrams, structures, dynamics and origins
03 p0425 A72-13254
- Book on stellar astronomy covering H-R diagram, solar system, nuclear energy sources, Milky Way Galaxy, quasars, cosmology, planetology, etc
16 p2453 A72-33275
- Giant stars iron abundance from narrow band spectrophotometric analysis and model atmospheres, isolating super metal rich stars below H-R diagram subgiant branch
23 p3334 A72-43256
- HERZBERG BANDS**
Oxygen Herzberg bands excitation in nightglow, obtaining quenching reaction rate coefficients
07 p0976 A72-19579
- HETEROCYCLIC COMPOUNDS**
NT ACETAZOLAMIDE
NT ADENINES
NT ADENOSINE DIPHOSPHATE [ADP]
NT ADENOSINE TRIPHOSPHATE [ATP]
NT ADENOSINES
NT ANISOLE
NT ASCORBIC ACID
NT AZOLES
NT AZULENE
NT GUANINES
NT INDOLES
NT MORPHINE
NT NICOTINE
NT NICOTINIC ACID
NT PHTHALOCYANIN
NT PYRIDOXINE
NT PYRROLES
NT RDX
NT RESERFINE
NT THYMIDINE
NT TOCOPHEROL
NT TRYPTOPHAN
NT URIC ACID
NT XANTHINES
Interstellar heterocyclic carbon ring molecules furan and imidazole search from upper limits in galactic sources brightness temperature
06 p0891 A72-18502
- Cyclohexylamine determination in aqueous solutions of sodium cyclamate by electron capture gas chromatography
07 p0935 A72-19488
- Vibrational analysis of electronic absorption spectra of 3-methyldiazirine and 3-methyl-d3-diazirine in vapor phase
18 p2657 A72-36566
- HETERODYNING**
NT OPTICAL HETERODYNING
Pyroelectric detector noise equivalent power limitation factors, discussing heterodyne systems and pulsed submillimeter lasers detection
04 p0551 A72-15602
- Pyroelectric IR detectors hf performance in direct and heterodyne modes, including thermal expansion effects
04 p0563 A72-15603
- Josephson junction as 100 GHz oscillator-mixer for heterodyne frequency conversion in millimeter and submillimeter regions, observing I-V characteristics
04 p0503 A72-15604

- High purity epitaxial GaAs frequency response, determining heterodyne detection in millimeter and submillimeter regimes
04 p0563 A72-15613
- HEURISTIC METHODS**
Linear multivariable interacting feedback control system optimal design by heuristic approach to determine input-output pairing and controller settings for satisfactory disturbance attenuation
03 p0337 A72-12905
- Heuristic theory of positron-helium elastic scattering phase shifts and cross sections
03 p0393 A72-14399
- Monograph on nonequilibrium relativistic kinetic theory covering heuristic approach, Boltzmann equation, H theorem, equilibrium distributions, relativistic thermodynamics, phenomenological transport theory, heat conduction coefficients, etc
05 p0689 A72-16289
- Lightly damped nonlinear mechanical oscillators under random excitation, calculating stationary response frequency and autocorrelation by heuristic procedures
06 p0849 A72-18693
- Artificial intelligence application to mass spectra interpretation, discussing heuristic Dendritic Algorithm based computer program to generate structural isomers
07 p0950 A72-19608
- Automatic classification algorithms using heuristic, partitioning and variational techniques
09 p1283 A72-23429
- Probability density functions shape estimation by deterministic heuristic and entropy maximization algorithms
10 p1442 A72-23798
- Self learning estimator for tracking, using heuristic technique for time-varying estimates sequence determination
10 p1457 A72-24500
- Heuristic recognition algorithms with learning for homogeneous irreducible stationary Markov chain sequence of recognized objects
12 p1837 A72-27824
- Digital image enhancement heuristic, superresolution and positive restoration techniques, providing bibliography
18 p2658 A72-36264
- Extremal problems arising in the substantiation of heuristic procedures
19 p2824 A72-37381
- Heuristic description for harmonic oscillator as quantized model of anharmonicity applied to excitation fields involving particle clusters and multibody configuration
20 p2953 A72-39398
- Heuristic procedure solution for least cost commercial airline crew scheduling, emphasizing combinatorial space size reduction
24 p3466 A72-44584
- Problems of complex object modeling based on heuristic self-organization
24 p3376 A72-45509
- Invariant transformation of the control laws in ergatic systems
24 p3376 A72-45510
- HEXAGONAL CELLS**
Hexagonal close packed Ti-Al alloys, determining stacking fault probability with X ray powder diffraction line profiles and Fourier analysis
01 p0087 A72-11029
- CdTe condensed films hexagonal modification and twinning boundaries birefringence reflection, using electron microscope and diffraction analysis
07 p1047 A72-18856
- Refractivity measurement of pure hexagonal structure 2H SiC over visible range, determining birefringence from curve fitting of data to Cauchy dispersion equation
09 p1309 A72-22603
- Hexagonal metals stress corrosion cracking fractographs interpretation, noting striations as prominent feature of transgranular fractures
11 p1652 A72-25288
- W addition effect on Co-Nb alloys, noting phase structure transformation from cubic to hexagonal due to mean electron density increase
12 p1829 A72-27642
- Quenching produced martensitic transformations from equilibrium beta phase region for Ti alloys with Ta
16 p2408 A72-33618
- Phase diagram, isomorphism and temperature dependence of hexagonal, monoclinic and triclinic modifications of Sr-Ba polycrystalline aluminosilicates
21 p3072 A72-40382
- Phonon dispersion relations and Debye characteristic temperature for Ti, Hf and Y hcp lattices
24 p3415 A72-45629
- HIBERNATION**
Book on hibernation and hypothalamus covering central nervous system regulating mechanisms,

- biologic rhythmicity, migration, thermoregulation, torpor, human implications, etc
01 p0010 A72-10169
- RNA content changes in ground squirrel brain during active and hibernation states
06 p0764 A72-18058
- Satellite system for telemetering environmental and physiological data from winter den of hibernating black bear, discussing instrumentation and equipment performance
07 p0931 A72-19913
- Thermoregulation in deeply hibernating rodents during separate chilling and steady hibernation temperature maintenance of skin and brain
12 p1762 A72-27827
- Seasonal rhythms of endocrine system in hibernating mammals, discussing central and peripheral biological clocks in relation to hypothalamus and pancreas/thyroid gland
16 p2353 A72-33100
- HIERARCHIES**
NT BBGKY HIERARCHY
NT DICHOTOMIES
Genetic code numerical structure association with logarithmic optimization rule for hierarchy of structures from molecular biology experiments
04 p0470 A72-14794
- Closure approximation in hierarchy stochastic differential operator equations in statistical mechanics
04 p0540 A72-15257
- Hierarchically structured man machine control systems synthesis, outlining iterative procedure for optimizing functional
05 p0727 A72-16471
- Hierarchical control structures aggregation and construction for class of complex systems
09 p1292 A72-23489
- Hierarchical system of helicopter service terminals, calculating passenger lots for single and multiloop arrangements under given stochastic input conditions
15 p2337 A72-31498
- Multilevel hierarchical structural design optimization, proposing component by component ascent method of dynamic programming
17 p2533 A72-35171
- Three point distribution function related to lower order functions for closure of hierarchy of equations for turbulent probability distribution functions
18 p2677 A72-36005
- Certain problems of the theory of hierarchical control systems
19 p2824 A72-37379
- Digital computer hierarchical structure based on tree model using request/service resources as nodes, examining parallel multiple-stream organizations effectiveness
20 p2906 A72-39735
- Automatic complex control systems with digital computer application for optimal control of production systems, selecting optimality criterion from hierarchically distributed local criteria
24 p3387 A72-45513
- HIGH ACCELERATION**
Plasma protein concentration, volume and hematocrit changes during exercise, bed rest and high forward acceleration
12 p1766 A72-28296
- High acceleration effects on gas flow patterns in rocket nozzles, detailing stagnation condition in combustion chamber and gas velocity and pressure at exit
15 p2297 A72-31813
- HIGH ALTITUDE**
Soviet book on civil aircraft high altitude equipment covering air conditioning systems, oxygen equipment and cabin pressurization
02 p0156 A72-12295
- Attitude reference platforms in ASTRID and DACHS control systems for high altitude research rockets
07 p0990 A72-20283
- Correction procedures for spherical surface transformation on plane for high altitude aerial photographs
09 p1310 A72-22948
- Pneumatically assisted parachute deployment at high altitudes with low accelerations
10 p1421 A72-24273
- Reference radiosondes for quality control of global high altitude temperature, pressure and humidity measurements, discussing dual soundings and synoptic comparison
10 p1484 A72-25077
- Cost analysis of high altitude meteorological network data with respect to research effectiveness and data reduction
13 p1990 A72-28820
- Observation of ultraviolet radiation from a rocket exhaust plume at high altitudes.
20 p2984 A72-39641
- Plume impingement force during tandem stage separation at high altitudes.
22 p3231 A72-42872
- The sweepback effect in the subsonic region in the lower atmosphere and in the hypersonic region at high altitudes
24 p3359 A72-44983

- Various efficiencies of fluid flows and application to the hypersonic ramjet 24 p3360 A72-44993
- HIGH ALTITUDE BALLOONS**
- French tetrahedral and spherical meteorological balloons, discussing projects Eole and Essov to sound Southern Hemisphere and stratosphere respectively 13 p1897 A72-28828
- Ground station-observed balloon-borne radio beacon method for Finnish stellar triangulation network measurement 15 p2226 A72-31929
- Balloon-nacelle for small scale photography and multispectral photometric ground measurements, describing automatic adjustment device for photographic lens diaphragm 16 p2349 A72-33633
- Stratospheric balloons role in galactic cosmic radiation research with detection techniques for study of rate and heavy elements abundances and isotopic composition analysis 21 p3101 A72-41615
- Absolute measurement of the solar brightness in the spectral region between 100 and 500 microns. 22 p3225 A72-42389
- Plastic balloons development for high altitude research, discussing construction technology, launch methods and scientific achievements 24 p3368 A72-45141
- Balloon nacelle for terrain photography from very high altitudes 24 p3403 A72-45229
- HIGH ALTITUDE BREATHING**
- Acute, short and long term and life long high altitude hypoxia exposure effects on pulmonary gas exchange control and efficiency during physical exercise 01 p0014 A72-10848
- Hemodynamics, pulmonary gas exchange and circulatory responses to high altitude in subjects with previous history of high altitude pulmonary edema 02 p0156 A72-11422
- Altitude hypoxia human pulmonary compliance relation between static transpulmonary pressure and inspired volume 02 p0159 A72-11958
- Unattenuated ventilatory hypoxic drive in ovine and bovine species native to high altitude 07 p0917 A72-19445
- Stepwise adaptation to high mountain conditions effect on brain and sural muscle oxidation processes in rats 08 p1121 A72-22085
- USAF custom fit oxygen mask program. 17 p2508 A72-34559
- HIGH ALTITUDE ENVIRONMENTS**
- Radiation exposure during high altitude flights, considering normal radiation levels due to galactic radiation and short term increases due to solar flares 03 p0315 A72-13234
- Solar radiation effects on planar librational motion and attitude of gravity oriented satellites at high altitudes 03 p0434 A72-13613
- Physiological and clinical effects of long distance flight in pressurized commercial planes with simulated altitudes over 15000 meters 12 p1771 A72-27486
- Native highlander and lowlander chemoreflex ventilatory response to transient carbon dioxide inhalation at low and high altitudes 12 p1762 A72-27728
- Concentrated and extended learning effects on formation rate and retention degree of conditioned reflex during mice adaptation to high altitude hypoxia 13 p1903 A72-28770
- Insecticide dichlorvos vapor toxicity in aircraft cabin atmosphere at 8000 ft, studying plasma cholinesterase activity, erythrocytes, dark adaptation and bronchiolar resistance 14 p2081 A72-31082
- High temperature and altitude combined effects on performance of tracking, monitoring and mental arithmetic complex task 14 p2083 A72-31155
- Blood coagulation changes at high altitude predisposing to pulmonary hypertension. 17 p2498 A72-34222
- Silicon carbide rotating rectifier alternator with solid lubricated bearings for high altitude environments, noting applicability to supersonic aircraft 17 p2498 A72-35565
- Evaluating the light from the sun. 19 p2790 A72-37933
- High altitude physiology: Cardiac and respiratory aspects; Proceedings of the Symposium, London, England, February 17, 18, 1971. 22 p3143 A72-42583
- Adaptive processes responsible for natural acclimatization of human organism to low ambient pressures at high altitudes 22 p3143 A72-42584
- Morphometric evaluation of changes in lung structure due to high altitude. 22 p3143 A72-42585
- Transarterial leakage - A possible mechanism of high altitude pulmonary oedema. 22 p3143 A72-42588
- The carotid body in animals at high altitude. 22 p3143 A72-42589
- Suprapontine influences on hypoxic ventilatory control. 22 p3143 A72-42590
- Succinic and lactic dehydrogenases activities in homogenates from myocardial tissues of guinea pigs, rabbits and dogs in high altitude environments 22 p3144 A72-42592
- Coronary blood flow and myocardial metabolism in man at high altitude. 22 p3144 A72-42593
- Anatomy of the coronary circulation at high altitude. 22 p3144 A72-42594
- HIGH ALTITUDE FLIGHT**
- U HIGH ALTITUDE**
- HIGH ALTITUDE NUCLEAR DETECTION**
- High altitude thermonuclear explosion fission fragments localization mechanism, considering magnetogravitational trap as potential well for heavy charged fragments 11 p1713 A72-25950
- Seismic wave prediction from high altitude nuclear detonation, using ground reflected spherical shock parameters 11 p1627 A72-26519
- HIGH ALTITUDE PRESSURE**
- Atmospheric ozone pressure variations in high altitude cyclones, anticyclones, troughs and crests at low pressure levels 02 p0207 A72-11734
- Effects of simulated high altitude on renin-aldosterone and Na homeostasis in normal man. 21 p3005 A72-40422
- HIGH ALTITUDE TESTS**
- Human factors relation to pressurized cabin development, discussing aircraft safety, high altitude tests, pressure loss predictions and cabin altitude selection 04 p0479 A72-14869
- Urine and plasma protein and creatinine measurements in acclimatized and unacclimatized men before, during and after high altitude ascent 10 p1426 A72-24482
- Solar cells calibration by high altitude aircraft, using extrapolation method to zero air density 12 p1758 A72-28041
- Physiological effects on anesthetized and conscious dogs during exposure at 80,000 ft for different decompression rates, discussing cardiovascular, biochemical and pathological effects 12 p1768 A72-28322
- Rocket engines simulated high altitude testing, using multiple stage ejector augmented supersonic diffuser system 13 p1938 A72-28692
- Altitude effects on decision making performance of cognitive, psychomotor and complex card sorting tasks 16 p2357 A72-34096
- The effect of chronic erythrocytic polycythemia and high altitude upon plasma and blood volumes. 19 p2757 A72-38028
- HIGH ASPECT RATIO**
- Power law sealant effects on high aspect ratio viscoelastic performance under laminar isothermal conditions 02 p0237 A72-12851
- Large scale high aspect ratio multielement suppressor nozzle arrays testing for augmentor wings and internally blown flaps [AIAA PAPER 72-131] 05 p0612 A72-16888
- HIGH ASPECT RATIO WINGS**
- U SLENDER WINGS**
- HIGH CURRENT**
- Relativistic beam equilibria above 10,000 amps, considering axial, diffuse, sharp boundary and azimuthal current models 02 p0267 A72-12840
- Fast acting nonmechanical self healing mercury fuse for high current circuit protection 03 p0335 A72-14203
- Investigation of the structure of a high-current discharge in a lithium plasma 22 p3209 A72-41878
- HIGH ENERGY ASTRONOMY OBSERVATORIES**
- U HEAO**
- HIGH ENERGY ELECTRONS**
- Supernova Vela X and local remnants as origin of below 1000 GeV cosmic electrons, deducing existence at 10 to 15 GeV from muon poor showers 01 p0119 A72-10853
- Relativistic electron beams in plasma, considering electrostatic instability conditions and critical currents 01 p0109 A72-10975
- Thermonuclear microbomb ignition with intense relativistic electron beams for rocket propulsion, discussing achievable exhaust velocities and system optimization 01 p0117 A72-11222
- Strong linearly polarized electromagnetic wave propagation in overdense plasmas, considering relativistic electron velocities and nonlinear penetration effect [AD-736322] 01 p0111 A72-11226
- High energy electrons behavior and sunspot magnetic fields in solar flares, using hard X ray and microwave radio burst balloon observations 03 p0410 A72-13323
- Energy transfer rate from photoelectrons to thermal electrons, presenting function of three independent variables 03 p0413 A72-13532
- Nonthermal electron spectra hardness limit during flash phase of solar flares fromOGO-5 observation. 04 p0566 A72-14561
- Atmospheric pressure pulsed carbon dioxide laser using preionization by injected high energy electrons from surrounding glow discharge, obtaining highest output from gas mixture [AD-746376] 04 p0529 A72-14586
- Primary cosmic ray electrons energy spectrum measurements, using balloon-borne absorption spectrometer 04 p0568 A72-15509
- High energy cosmic ray electrons anisotropy, considering diffusion from discrete source model 04 p0568 A72-15510
- Energetic electrons absorption cross sections in weakly ionized atomic oxygen gas, showing energy losses through excitation 05 p0655 A72-16071
- Galactic high energy electron differential spectrum, estimating spatial distribution and random magnetic field intensity 05 p0709 A72-16237
- Additional high energy electrons flux detection in upper atmosphere after magnetic perturbations 05 p0710 A72-16525
- Metagalactic gamma rays from relativistic electron bremsstrahlung interactions under assumption of single power law source 05 p0710 A72-16712
- Relativistic electron pitch-angle diffusion driven by oblique If whistler-mode turbulence in collisionless plasma immersed in static magnetic field 05 p0699 A72-17024
- Fast charged particles measurement in inner radiation belt by Cerenkov counter mounted on Cosmos 137 satellite indicating presence of high energy electrons 05 p0711 A72-17035
- Vlf wave excitation during sudden storm commencement, causing magnetosphere trapped energetic electrons to diffuse and precipitate into lower ionosphere 06 p0803 A72-17451
- Reflection mode high energy electron diffraction study of titanium carbide single crystal surfaces in ultrahigh vacuum environment 07 p1019 A72-20408
- Hypotheses for excess background radiation at 200-500 km, suggesting single high energy electrons or electron clusters 07 p1064 A72-20638
- High energy electrons and gamma quantum flux in upper atmospheric layers from high altitude balloon measurements 07 p1065 A72-20639
- High energy electron precipitation events in auroral zone X rays, showing exponential daytime and flat nighttime energy spectra 08 p1226 A72-21110
- High resolution multiple particle spectrometer for measuring energetic protons, electrons and alpha particles during solar particle events 08 p1167 A72-21509
- Gas laser excitation by relativistic electron beam pulse axial propagation through optical cavity, studying mechanism through timing and pressure dependence measurements 10 p1489 A72-23946
- Gas rotation temperature measurement by means of high energy electron beam probe with allowance for secondary electrons [ONERA, TP NO. 1069] 10 p1480 A72-24222
- Dayside magnetosphere stably trapped radiation zone high latitude boundary determination from energetic electron intensity spatial distribution observation by Imp 3 satellite 11 p1713 A72-26106
- Strong pitch angle scattering of energetic electrons in presence of electrostatic waves due to ion cyclotron instability above midlatitude ionospheric trough region 11 p1714 A72-26398
- Magnetosphere fast electron precipitation investigated by simulation experiments with model created by plasma stream interaction with dipole magnetic field 11 p1714 A72-26531
- High current relativistic electron beam properties, noting application in thermonuclear synthesis and accelerators 12 p1788 A72-27250

Radiation damage in carbon doped silicon irradiated at low temperatures by 2 MeV electrons, noting isotope shifts

12 p1857 A72-28059

Diamond powder lattice parameter changes during fast electron irradiation at various temperatures, discussing crystal defect stability and neutron irradiation comparison

13 p1983 A72-28760

Energetic electron and proton trapping in lower solar atmosphere magnetic field, discussing particle injection, bremsstrahlung and gyro synchrotron radiation

13 p2046 A72-29719

High energy electron heating of solar flare plasma with X-ray emission due to thermal and nonthermal bremsstrahlung

13 p1033 A72-29745

Radio emission due to relativistic electrons spiral orbit motion in rotating pulsating neutron star

15 p2304 A72-31333

Energetic electrons generation and relaxation in narrow belt near 2.8 L measured with Cosmos 137 Cerenkov counter

15 p2299 A72-31909

Relativistic electron characteristics in interplanetary space from onboard satellite detector measurements beyond magnetospheric influence [IGPP-UCR-72-11]

15 p2300 A72-31998

Thermonuclear microexplosion ignition by bombarding dense target with intense relativistic electron beam, noting energy requirement reduction by self magnetic beam field

16 p2433 A72-32814

Primary cosmic rays extragalactic origin, considering high energy electrons, background X and gamma rays and cosmic protons

16 p2445 A72-33126

Electromagnetic wave propagation in uniform and nonuniform plasmas with enough strength to cause relativistic electron velocities, considering linear polarization and nonlinear penetration effects

16 p2438 A72-33926

Ultrarelativistic electrons beam steady injection into plasma filled half space, using weak turbulence theory for assumed beam excited oscillations interaction

16 p2440 A72-34156

Parametric emission of relativistic electron clusters in a waveguide with a layered dielectric filling

17 p2529 A72-34850

Emission of coherent microwave radiation from a relativistic electron beam propagating in a spatially modulated field

17 p2589 A72-34874

High latitude observation of precipitating electron spikes by polar orbiter OGO 4 satellite, noting population dependence on local trapping limit

17 p2601 A72-35591

Energetic electron intrusion into inner radiation zone during and after 2 September 1966 geomagnetic storm, noting radial diffusion role

17 p2601 A72-35596

Structure of the power-law spectra of relativistic electrons in a turbulent plasma

17 p2593 A72-35907

Electron and nuclear components and transformations of matter under extreme conditions of pressure and temperature exemplified in stellar/pulsar/evolution

18 p2725 A72-36520

Linear and circular polarization of synchro-Compton radiation scattered by optically thin power law distribution of gyrating ultrarelativistic electrons

20 p2965 A72-39893

High energy electrons monokinetic beam propagation in Cu and Al crystals, investigating critical voltage effect on contrast

21 p3069 A72-41342

Solar flare associated relativistic electron acceleration relationship to cosmic ray and type 4 radio burst production

22 p3217 A72-42010

Nonadiabatic condition effects on ultrarelativistic electron energy losses in geomagnetic trap in remote magnetosphere regions

22 p3218 A72-42224

Solar-wind and interplanetary electron measurements on the Apollo 15 subsatellite

22 p3218 A72-42403

High energy electron spatial distribution in plasma sheet from Ogo 5 magnetometer experiments

22 p3211 A72-42406

Equilibrium energy spectrum for the galactic cosmic electrons

23 p3328 A72-43831

Microwave generation with high energy electrons in magnetic undulator with transverse electromagnetic field, calculating frequency distribution of undulator radiation

23 p3265 A72-44158

Controlled secondary electron emission and some possibilities for its application in particle detectors

23 p3316 A72-44159

Energy spectrum and composition of primary cosmic radiation at energies from 50 to 5000 TeV

23 p3330 A72-44422

Mathematical model for secondary electron production fall-off, calculating ionization cross section from electron distribution

24 p3400 A72-45592

HIGH ENERGY INTERACTIONS

Book on nuclear reactions in stellar surfaces and relations with stellar evolution covering high energy L elements formation, Li-Be observations and thermonuclear and spallative theories

01 p0122 A72-10002

Spectral and polarization characteristics of type 4 bursts with respect to energetic particle emission and solar-terrestrial phenomena

03 p0407 A72-12938

NASA spacecraft instrumentation for high energy phenomena measurements, discussing collimated proportional counters, wire grid digitized spark chambers and modulation and slit collimators

03 p0353 A72-13038

Hadrons in extensive air showers, predicting arrival time spectra from fireball and isobar-p ionization models for high energy interactions

03 p0409 A72-13147

Dispersion energy relation for ultrahigh energy nuclear reactions in cosmic ray emulsion

03 p0410 A72-13148

High energy primary cosmic ray particle evidence from energetic air shower observation data analysis

03 p0413 A72-14097

Cosmic ray physics - Conference, Moscow, USSR, October-November 1970

06 p0868 A72-17257

Inelastic nuclear interactions between 200-GeV cosmic ray particles and polyethylene targets, correlating similarity property, angular momentum spectra and secondary particle pairs

06 p0868 A72-17258

Particle multiplicity and momentum spectra for high energy inelastic nuclear interactions in Wilson chamber with polyethylene target

06 p0868 A72-17261

Multiple production processes hydrodynamic-type models validated by high energy particle collision collective interactions

06 p0869 A72-17265

High energy cosmic ray pions and nucleons interactions with atomic nuclei, using ionization calorimeter and spark chambers system

06 p0869 A72-17267

Cosmic ray particle high energy inelastic interactions, discussing pion and nucleon interaction angular and energy characteristics and muon production mechanism

06 p0869 A72-17270

Inelastic ionization cross section of cosmic ray hadrons with carbon nuclei at energies of 100 to 300 GeV

06 p0869 A72-17271

Nuclear photoemulsions under bombardment by pion beam of 60 GeV/c momentum, investigating pion-nucleon interactions involving recoil protons

06 p0851 A72-17273

Pion-nucleon high energy interactions, determining inelasticity coefficient distribution

06 p0851 A72-17274

High energy cosmic ray interactions at one TeV, including X process, horizontal showers and muon poor showers

06 p0871 A72-17285

Muon densities in penetrating high energy particles, comparing with extensive atmospheric showers

06 p0871 A72-17289

K-neutral pion energy fractions and inelasticity coefficients at primary energies of 100-1500 GeV during hadron-target interaction

06 p0872 A72-17295

Papers on high energy cosmic ray and nuclear interactions covering extensive air showers, cloud chamber data, electron-photon cascades, solar activity effects, etc

07 p1060 A72-19863

Inelastic high energy multiple interactions between cosmic ray particles and atomic nucleus targets, using Wilson chamber and ionization calorimeter

07 p0988 A72-19864

High energy inelastic interactions in cosmic ray showers, using Wilson chamber

07 p1060 A72-19866

Extensive atmospheric showers and high energy transfer from interacting nucleons to electron photon cascades

07 p1060 A72-19867

Radiation measuring instruments assembly for extensive air showers and cosmic ray particle nuclear interactions at high energies

07 p0988 A72-19868

Quasi-nucleonic interactions of high energy protons in nuclear emulsion irradiated within pulsed magnetic field

07 p1038 A72-19869

High energy hadrons time structure in extensive air showers, considering production of nucleon-antinucleon pairs in particle interactions

07 p1067 A72-20687

Angular distributions of proton polarization during elastic scattering by V, Cr, Ni and Co nuclei in high energy region

08 p1211 A72-21093

Pion generation during collective interactions between nucleons of heavy cosmic ray nuclei, using Proton 4 satellite data

08 p1228 A72-22179

High energy particle and ionizing radiation effects on glasses in aerospace environment

09 p1336 A72-22402

High energy astrophysics - Conference, Erice, Italy, May-June 1971

10 p1532 A72-23883

Equations of state for ultrahigh densities, obtaining relativistic statistical thermodynamics description of hadronic interactions

10 p1533 A72-23891

Nucleonic cascade model analysis of underground vertical muon curve for primary cosmic ray nucleon spectrum below 40 TeV

10 p1529 A72-24417

Scaling of energy spectrum of particles emitted in high energy nucleon-nucleon collisions

10 p1529 A72-24527

Time structure of massive interacting particles with energies above 20 GeV near axes of cosmic ray showers of energy above 100 TeV

12 p1864 A72-27737

Microscopic processes within high energy ion acceleration in laser-produced plasmas, discussing transient electric field role

14 p2136 A72-30178

Resonant and semiweak process production cross sections for massive Lee-Wick spin-zero and spin-one bosons at high energies

15 p2280 A72-31290

Scintillation TlCl /I,Be/ crystal response to 8 GeV ionizing negative pions, noting pulse shape and resolution characteristics

15 p2291 A72-31535

Cerenkov counter for astronomical observatory high energy cosmic ray experiments, discussing UV-reflecting paint, radiator and photomultiplier positioning improvements

15 p2234 A72-31536

Russian book - Characteristics of radiation damage caused by high energy particles in semiconductors

17 p2595 A72-34700

Test of scale invariance in pion production at high energies using cosmic ray primary nucleon and sea level muon intensities

17 p2599 A72-34875

Study of high energy /25-10,000 GeV/ interactions with a multiplate cloud chamber using Monte Carlo simulations for energy calibration

17 p2585 A72-34922

Electrons and photons interaction with relic radiation, establishing high energy gamma rays energy and intensity attenuation length

17 p2600 A72-35145

Electron showers of high primary energy in lead

17 p2585 A72-35472

Gamma radiation production through interaction between high energy particles emitted by pulsar originating in supernova core and gas in supernova envelope

18 p2721 A72-36088

Pion generation during collective interactions between nucleons in heavy cosmic ray nuclei, using Proton 4 satellite data

18 p2721 A72-36235

Space and upper atmosphere environmental effects on spacecraft and instrument surfaces, considering high energy particle radiation, interstellar and lunar dust effects, etc

18 p2712 A72-36832

Pion exchange and the cosmic-ray nucleon cascade

19 p2851 A72-37923

Test of hadronic scaling at cosmic-ray energies

21 p3100 A72-40831

Evidence for radiative electron capture by fast, highly stripped heavy ions

23 p3316 A72-44073

Angular distribution of electrons autodetached from H- in slow collisions with He

23 p3316 A72-44074

High altitude cosmic ray pion and nucleon interaction characteristics at high energies, using spark chamber, Cerenkov absorption spectrometer and ionization calorimeter measurements

23 p3329 A72-44402

Ultrahigh energy gamma quanta families detection by airborne emulsion chamber at 500-2500 m altitude, calculating energy distribution distortion by Monte Carlo method

23 p3329 A72-44403

Investigation of hadron interactions with atomic nuclei at energies greater than 100 GeV

23 p3329 A72-44404

- Multiplicity of particles generated in inelastic interactions of nucleons with LiH nuclei at energies from 150 to 550 GeV
23 p3329 A72-44405
 - High energy inelastic interactions in cosmic ray showers from Wilson chamber and ionization calorimeter observations, noting secondary particles occurrence dependence on primary energy
23 p3330 A72-44406
 - Particle production in inelastic high energy interactions, noting correlation between particle pairs and groups
23 p3330 A72-44407
 - Collective interactions of the nucleons of heavy nuclei in high-energy cosmic rays
23 p3330 A72-44408
 - Ionization calorimeter for neutral pion production investigation in high energy hadrons interaction, noting energy transfer identity for nucleon and pion interactions
23 p3330 A72-44409
 - Effective cross section of the inelastic interaction of hadrons with lead-atom nuclei at energies from 3 to 30 TeV
23 p3330 A72-44410
 - Nuclear interactions in the atmosphere at energies greater than 100 TeV
23 p3330 A72-44411
 - Multifireball theory of particle production in inelastic high energy interactions, using elastic scattering amplitude for inelastic processes model
23 p3316 A72-44412
 - Multiple collisions and an optical model of the inelastic interaction between cosmic particles and nuclei
23 p3330 A72-44413
 - Approximation for Monte Carlo method modeling of pion-nucleon and nucleon-nucleon inelastic collisions at high energies
23 p3317 A72-44414
 - General characteristics of proton-nucleon and coherent interactions at an energy of 67 GeV
23 p3317 A72-44415
 - Study of high-energy hadron interactions by the nuclear photoemulsion method
23 p3330 A72-44416
 - High energy inelastic collisions of pions and protons with nuclear emulsion nucleons, noting pion pulse spectra
23 p3317 A72-44417
 - Angular distribution of extensive air showers in a range of large zenith angles
23 p3330 A72-44421
 - Energy dependence of muon-nucleon inelastic interaction, calculating photonuclear cross section for high energy interactions in iron
23 p3331 A72-44429
 - Characteristics of pion and nucleon interaction with carbon and aluminum nuclei over the energy range from 30 to 300 GeV
23 p3331 A72-44435
 - S-system motion effect on angular distribution of secondary high energy particle cluster in showers formed by primary and neutral particles, considering nucleon collision line
23 p3331 A72-44436
 - Recording high-energy particle interactions by the method of the controlled emulsion stack of large volume
23 p3291 A72-44438
 - Coherent cross section effects on primary particle energy in inelastic proton interaction with carbon nuclei at 20-600 GeV
23 p3332 A72-44439
 - Device for studying the photonuclear interaction of superhigh-energy muons
23 p3291 A72-44440
 - Study of the angular distribution of charged and neutral pions during inelastic interactions in the energy region above 1 TeV
23 p3291 A72-44443
 - Experimental investigation of electromagnetic cascades at an energy greater than 20 GeV
23 p3291 A72-44444
 - High energy nucleon inelastic collision characteristics dependence on secondary particle energy and meson velocity, using Wilson chamber measurement
23 p3291 A72-44445
 - Angular and impulse characteristics of negative-pion interactions at an energy of 60 GeV in the emulsion
23 p3292 A72-44446
 - Relationship between the energies of charged and neutral particles generated in the energy region above 100 GeV
23 p3332 A72-44447
 - Primary cosmic ray nucleon spectrum from sea-level muon spectrum and scaling hypothesis parameters
23 p3332 A72-44458
 - Classical calculations of H₂O rotational excitation in energetic atom-molecule collisions.
24 p3427 A72-45309
- HIGH ENERGY OXIDIZERS**
Ideal high energy liquid rocket propellants combinations for high propulsive efficiencies, considering hydrogen, hydrazine, diborane and ammonia and various oxidizers
23 p3358 A72-44355
- HIGH ENERGY PROPELLANTS**
Combustion chamber and nozzle materials for fluorine and/or metal burning high energy propellant rocket engines, considering cooled and uncooled nozzles and spoiler plates
01 p0117 A72-10941
- Fluorine-ammonia as high energy liquid bipropellant for rocket engines, presenting ground test results regarding velocity and specific impulse characteristics as functions of mixture ratio
01 p0114 A72-11220
- High energy chemical propellant combustion under adiabatic and nonadiabatic conditions, calculating product equilibrium state as functions of temperature and pressure with computer program
06 p0903 A72-18212
- Controllable high energy hydrogen-oxygen rocket propulsion systems performance and combustion characteristics, considering mixture ratio, pressure, chamber geometric characteristics, injection area and velocity ratios
11 p1703 A72-25298
- High energy rocket propellants for space probe propulsion systems, evaluating various propellant combinations in terms of specific impulse, toxicity, corrosiveness, cost and availability
11 p1702 A72-25299
- Ideal high energy liquid rocket propellants combinations for high propulsive efficiencies, considering hydrogen, hydrazine, diborane and ammonia and various oxidizers
23 p3358 A72-44355
- HIGH EXPLOSIVES**
U EXPLOSIVES
- HIGH FIELD MAGNETS**
Cu clad N8-Ti wire wound superconducting solenoids with large fields at 1.6-5.2 K
10 p1446 A72-23762
- HIGH FREQUENCIES**
Low loss high power hf coaxial, twin wire and surface waveguides for long distance transmission
02 p0190 A72-11677
- Nighttime hf radio wave field intensity measurement and absorption observation by narrow band receiver
02 p0184 A72-12874
- Penetration depth of hf electromagnetic waves in weakly ionized plasma, considering nonlinearity effect on ionization balance
03 p0394 A72-13085
- Hf electromagnetic field spectrum in one dimensional plasma cavity in pressure balance for arbitrary density
05 p0696 A72-16604
- Thin antenna hf time response from thin wire approximation and source gap model for integral equation solution
07 p0957 A72-19798
- HF radio waves induced incoherent scatter spectrum enhancement, noting parametric instabilities in ionosphere
09 p1279 A72-23014
- German book on HF semiconductor electronics covering planar and field effect transistors, varactors, n-p, p-i-n, avalanche and Schottky barrier diodes, Gunn devices, etc
10 p1452 A72-24699
- Travel time effects on electron motion in HF electromagnetic fields, reviewing phase focusing and achromatic electron lens development
10 p1513 A72-24976
- Penetration depth of HF electromagnetic waves in weakly ionized plasma, considering nonlinearity effect on ionization balance
13 p2015 A72-29435
- HF follower currents effect on dc arc I-V characteristics, indicating use of HF follower arc for quasi-steady arc power control
13 p2017 A72-29645
- Physical interpretation of electromagnetic waves attenuation function HF singularity during diffraction over spherical surface, applying to short wave diffraction in tropospheric model
15 p2195 A72-31651
- HF radiation in type 3 burst sources, discussing amplification by proton and electron streams
15 p2316 A72-32753
- A periodic laser in high-frequency Q-switched operation
17 p2563 A72-35305
- Quiescent large-volume collisionless HF discharge plasma generator with zero magnetic field, noting low noise level due to self-stabilizing feature
17 p2592 A72-35814
- Emitter-dip model of diffusion anomalies of n-p-n Si HF transistors doped with B and P
21 p3035 A72-41489
- A high-frequency transmitted power meter using a laser signal
21 p3064 A72-41730
- HIGH GAIN**
Broadband high gain large aperture Schwarzschild antenna systems design, considering compromises and tradeoffs in scan angle, F/D ratio and surface shapes
01 p0039 A72-10672
- High gain CW He-Xe laser transitions due to Xe 5d level long-lived decaying emission
15 p2250 A72-32301
- HIGH GRAVITY [ACCELERATION]**
U HIGH GRAVITY ENVIRONMENTS
- HIGH GRAVITY ENVIRONMENTS**
High gravity environment exposure effects on gravity preference in chronically centrifuged rats, showing dependence on reference level
08 p1122 A72-20787
- Pilot and back-seat man physiological responses during high-g aerial combat maneuvers in F-4E aircraft, discussing ECG, respiratory rate and minute volume
12 p1767 A72-28317
- HIGH IMPULSE**
German monograph on small variable-speed motors with high impulse performance, considering asynchronous cage type, dc shunt type and pneumatic motors
15 p2182 A72-31325
- HIGH LATITUDES**
U POLAR REGIONS
- HIGH LIFT DEVICES**
U LIFT DEVICES
- HIGH MELTING COMPOUNDS**
U REFRACTORY MATERIALS
- HIGH PASS FILTERS**
Computerized optimization procedure for microwave circuits without tuning elements, applying to high pass filter design
01 p0040 A72-10686
- Low and high pass, bandpass and bandstop active filters, tabulating cut-off frequencies, thermal stability, impedance, power dissipation and voltage specifications
07 p0955 A72-19248
- Optical properties of transmission echelette high-pass filters.
21 p3055 A72-40823
- HIGH PRESSURE**
High pressure gaseous hydrogen effect on space shuttle main engine components alloys under static loads, using surface flawed flat plate PTC samples
01 p0085 A72-10774
- High pressure gas lasers excitation, determining energy introduction and space charge stability
05 p0668 A72-16415
- State of gas parameters measurement apparatus at high temperatures and pressures involving constant volume piezometer with internal heating
06 p0814 A72-17616
- Rhenium carbide synthesis at high pressure and temperature, searching for superconducting properties
06 p0828 A72-17617
- Microwave absorption in high pressure hydrogen based on radio astronomical measurements of Uranus brightness temperature
08 p1239 A72-22088
- High pressure bulk modulus test rig for composite material specimen nondestructive test, discussing measurement method and errors
09 p1315 A72-23391
- High pressure CO and N plasmas production by uncoupling electron temperature from number density, measuring electron-ion recombination rates
10 p1518 A72-23962
- Oscillatory relaxation combustion regions determination in high pressure gas injection tubes, noting flame propagation rate relationship with mixing concentration
11 p1745 A72-25754
- High pressure electroionization carbon dioxide and nitrogen filled carbon dioxide lasers
11 p1652 A72-26793
- High pressure injector optimum design and performance for gas jet boosters, using one dimensional theory with friction allowance
12 p1861 A72-27535
- Papers on high pressure-high temperature research techniques covering laboratory procedures for control, calibration and measurement of solid-vapor and liquid-vapor equilibria
12 p1778 A72-28103
- Externally pressurized automatic barrier seals for high pressure applications in chemical industry, nuclear power plants and deep - submergence vessels, discussing theory, design and test results
13 p1964 A72-28974
- Liquid drop evaporation in stagnant environment at high temperature and pressure, noting gas phase nonideal behavior effects
14 p2173 A72-31066
- High pressure cryogenic hydraulically actuated valve for repeated sealing of liquid He-containing cell
15 p2183 A72-32436

Microwave absorption in high pressure hydrogen based on radio astronomical measurements of Uranus brightness temperature

17 p2606 A72-34651

Mathematical model of nitric oxide formation by fuel droplet burning above fuel critical pressure, applying to diesel engine operations

17 p2511 A72-34901

Electron and nuclear components and transformations of matter under extreme conditions of pressure and temperature exemplified in stellar/pulsar/evolution

18 p2725 A72-36520

Importance of nozzle geometry to high-pressure gas-dynamic lasers.

19 p2811 A72-37867

Influence of water vapor on the normal flame velocity of a methane-air mixture at high pressures

19 p2882 A72-38459

X-ray diffraction studies on liquids at very high pressures along the melting curve. I, II.

21 p3084 A72-40558

An apparatus to investigate plasmas at very high pressure.

21 p3056 A72-41004

Refinements in high-Reynolds-number shock-tunnel technology.

[AIAA PAPER 72-996] 21 p3040 A72-41582

Nonstationary method for measuring the heat conductivity of liquids and gases under high pressures

22 p3243 A72-41886

Development of a push-pull fatigue testing machine under high pressure, and the results of preliminary fatigue tests.

24 p3401 A72-44630

HIGH PRESSURE OXYGEN

Aircraft high pressure oxygen cylinder system filler valve optimum standards, discussing automatic fill rate and pressure sensitive closing control, design, construction and performance

[SAE AS 1225] 01 p0006 A72-10385

Anaerobic glycolysis and specific gravity of red blood cells in rats exposed to pure oxygen at 600 torr

01 p0015 A72-11297

Hypoxia pretreatment for decreased pulmonary oxygen toxicity during high pressure oxygen breathing in rats

07 p0917 A72-19328

Rapid eye movement sleep deprivation and hyperbaric oxygenation influence on gamma-aminobutyric acid levels in mice brains, suggesting protective mechanism against nerve cell oxygen intoxication

07 p0922 A72-20191

Hyperbaric chamber tests for hemodynamic response to oxygen inhalation at 1 and 2 atm pressure for myocardial infarction treatment assessment

08 p1114 A72-20891

Cardiovascular responses to positive pressure oxygen breathing from blood pressure and heart and respiratory rate measurements

11 p1584 A72-26017

High pressure oxygen control for synthesis and vapor phase equilibria, discussing tensiometric measurements and cold seal pressure vessel techniques

12 p1778 A72-28105

Physiological and biochemical responses of Paramacium caudatum to hypo- and hyperbaric stresses, discussing protoplasmic inactivation by high oxygen pressure

12 p1766 A72-28299

Hydrogen peroxide formation relationship to lipid peroxidation and seizures in brain during high pressure oxygen exposure

12 p1766 A72-28300

Succinate and glutathione as protective agents against chronic effects of hyperbaric oxygen toxicity in rats

14 p2082 A72-31091

Unconjugated urinary corticosterone excretion in laboratory rats exposed to high pressure helium-oxygen environments.

24 p3374 A72-45656

HIGH Q

U Q FACTORS

HIGH RESOLUTION

Airborne high resolution multispectral TV camera system, describing special objective configuration for improved ground resolution

02 p0227 A72-11850

High spatial resolution solar X-ray and far UV instruments, employing glancing incidence optics

03 p0353 A72-13045

High spectral resolution UV space astronomy spectrographs with echelle gratings

03 p0354 A72-13052

Coarsely stabilized spacecraft-borne Michelson interferometer, obtaining high resolution by computerized spectrum reconstruction with fast Fourier transform

03 p0354 A72-13055

Martian surface relief observation from earth distance, showing telescope resolution requirements above dense atmospheric layers

03 p0438 A72-13983

High resolution Galactic center interferometric observations at 5 GHz, showing compact components in Sagittarius A

04 p0580 A72-15511

German monograph on vibration amplitudes interferometric measurement, discussing methods for resolution improvement and phase measurements, distortion and sonic field effects, etc

07 p0983 A72-19264

High resolution Raman spectroscopy of low pressure gases, using single mode Ar laser

09 p1323 A72-22613

Model solar atmosphere from mm and cm wavelength high resolution observations of chromosphere by lunar limb antenna tracking during 7 March 1970 eclipse

13 p2042 A72-29532

High speed and resolution laser scanning by optomechanical methods, discussing theoretical bandwidth, resolution limits, position error correction measures and performance optimization

15 p2248 A72-32037

High time resolution observations of photopheric velocity field, interpreting short period oscillations origin as result of combined image motion and Doppler velocity gradients

15 p2317 A72-32776

Construction, tuning and characteristics of high resolution spectrometers with scanning interferometers for He-Ne laser radiation analysis

16 p2400 A72-33080

High-resolution spectroscopy using magnetic-field-tuned semiconductor lasers.

20 p2933 A72-39561

High resolution Michelson interferometer for spectral investigations of lasers.

21 p3062 A72-40610

On the use of a Fabry-Perot interferometer for the study of Raman spectra of gases under high resolution.

24 p3426 A72-44904

High resolution multispectral camera system for ERTS A & B.

24 p3402 A72-45182

Precision X-ray telescopes on HEAO-C.

24 p3403 A72-45202

High resolution imagery with the large space telescope.

24 p3404 A72-45537

HIGH SENSITIVITY

U SENSITIVITY

HIGH SPEED

High speed and resolution laser scanning by optomechanical methods, discussing theoretical bandwidth, resolution limits, position error correction measures and performance optimization

15 p2248 A72-32037

The world speed records of the SA 341 - Gazelle.

[AHS PREPRINT 651] 17 p2491 A72-34506

High angular velocity device design problems, considering gyroscopes, ultracentrifuges, yarn-spinning textile machinery and dental drill

19 p2809 A72-38544

Computer control of the General Dynamics High Speed Wind Tunnel.

22 p3157 A72-42697

HIGH SPEED CAMERAS

NT FRAMING CAMERAS

High speed photographs of plasma emission spectra in UV and soft X radiation spectrum regions, discussing theory, design and operation of facilities

02 p0223 A72-11408

High speed streak cameras applicability to low density theta pinch studies, describing image converters design, operation and block diagrams

02 p0263 A72-11410

Velocity measurement of glass particles emerging from plasma flame by high speed cine-streak photography

03 p0361 A72-13992

Ultrarapid holographic camera for plasma diagnostics, noting exposure time and reconstructed image resolution

04 p0521 A72-14972

Ultrahigh speed holographic camera for three-dimensional photographs and interferograms, using ruby laser output

04 p0522 A72-15139

Blunt bodies-shock wave interaction in shock tubes, using interferometer with laser light source and high speed streak camera

05 p0601 A72-16225

Ultrahigh speed electro-optical cameras with exposure times of several picoseconds, using bipplanar image converter, electron multiplier and Kerr cell

06 p0812 A72-17415

High speed photography in high temperature short duration plasmas, using Kerr cell, image converter, framing and streak cameras

06 p0813 A72-17435

High speed photography and radiography applications to high explosives research, discussing shock wave visualization, illumination techniques for rapid processes time resolution, etc

06 p0813 A72-17436

Laser triggered avalanche transistor voltage generator for picosecond streak camera used in laser pulse diagnostics

07 p0999 A72-18881

High speed rotating mirror camera adapted to solid state laser radiation, noting continuous recording and simultaneous imaging

07 p0990 A72-20401

High speed rotating mirror camera, describing multiplier device for doubling beam scanning speed

07 p0990 A72-20402

Q switched laser system emitting light pulses for high speed cinematography synchronized illumination

11 p1649 A72-26343

High speed photographic analysis of spot welding galvanized steel, observing three stage process

13 p1958 A72-29421

Two beam high speed frame holographic recording of dynamic processes, using passive shutter ruby laser with diaphragmed resonator

15 p2233 A72-31417

High speed photography ultrafast shutter based on polymethylene cyanide dyes saturability for measuring mode locked ruby laser pulse duration

15 p2241 A72-32535

Flow distribution, vibration, wear and rupturing of rods in vertical pipe for various inlet flows investigated with high speed cameras, photography and transducers

16 p2376 A72-32996

The laser - A source of light in high speed photography

17 p2563 A72-35182

High-speed photography of a plasma focus.

18 p2716 A72-36946

An improved Cranz-Schardin high-speed camera for two-dimensional photomechanics.

19 p2795 A72-37516

Investigation of radiation field distribution in a ruby laser with a SFR high speed camera

20 p2931 A72-39318

A large viewfield laser photographic system for in-flight model contour measurements in an aeroballistic range.

22 p3179 A72-42679

HIGH SPEED FLIGHT

U HIGH SPEED

HIGH SPEED TRANSPORTATION

U RAPID TRANSIT SYSTEMS

HIGH STRENGTH

High strength solids compositional, heat treatment and chemical environmental effects on fracture strength, considering alumina as example

09 p1334 A72-22387

Hot pressed silicon nitride with high strength and good oxidation and thermal shock resistance for gas turbine applications

[ASME PAPER 72-GT-19] 11 p1673 A72-25618

Composite materials fabrication, emphasizing high strength/stiffness to weight ratio as critical performance requirements

12 p1815 A72-28082

The development of high strength three dimensionally reinforced graphite composites.

17 p2573 A72-35670

HIGH STRENGTH ALLOYS

NT HIGH STRENGTH STEELS

NT MARAGING STEELS

Electrochemical potential microstructure and stress intensity factor effect on aqueous stress corrosion crack propagation rate in high strength Ti alloy

01 p0085 A72-10776

High temperature carbide dispersion strengthened Nb alloys, using heat and thermomechanical treatments

01 p0085 A72-10863

High strength Ti alloy development, composition modifications, physical and mechanical properties, ingot, heat treatment and fatigue crack evaluation

01 p0088 A72-11100

Carbon content effect on phase relationships and mechanical properties of sintered Fe-WC alloys, noting high strength

02 p0241 A72-11452

VT22 high strength Ti alloy beta phase decomposition kinetics studies under heat treatment, noting omega and alpha phases role for low plasticity

02 p0244 A72-12247

Tension-compression cycling effects on fatigue crack growth in high strength alloys

[ASME PAPER 71-PVP-2] 02 p0294 A72-12469

Fabricable high strength Inconel 706 precipitation hardening superalloy, noting savings in Ni, Nb and Mo content

02 p0245 A72-12507

Plane strain fracture toughness of notched high strength Al and Ti alloys at low temperatures

03 p0371 A72-13464

High strength Ti alloys for aircraft accessories structural materials, comparing room temperature physical properties of ultrahigh tensile steels and other alloys

03 p0373 A72-13617

- High strength Al-Zn-Mg-Cu alloys, testing heat treatment and Ag addition effects on tensile strength 05 p0677 A72-17112
- Ag addition effects on high strength Al-Zn-Mg-Cu alloys tensile properties and resistance to stress corrosion cracking 05 p0677 A72-17113
- Microwires and microstrips fabrication from high strength deformation resistant aluminum alloys 05 p0680 A72-17207
- Structure, hardness, density and electrical resistance of binary alloys V-Ti, V-Cr, V-Al and V-Sn 07 p1013 A72-19741
- Metal working by plasma beam in turning machine, applying to high strength alloys 08 p1175 A72-21045
- High strength Ni alloy hot working properties evaluation from extrusion simulation by torsion testing, considering stress-strain-time relations, microstructure, recrystallization and ductility 08 p1190 A72-22199
- VT22 high strength Ti alloy beta phase decomposition kinetics under heat treatment, noting omega and alpha phases formation effect on ductility 11 p1660 A72-26133
- Microwires and microstrips fabrication from high strength deformation resistant Al alloys 11 p1660 A72-26142
- Microstructural effects on high strength Mg, Al and Ti alloys stress corrosion crack growth in aqueous environments, discussing correlations relative to composition and preferred orientation 11 p1668 A72-26946
- Fracture toughness of high strength alloys, discussing rocket motor cases, nondestructive test standards and subcritical crack growth 12 p1829 A72-27656
- Tungsten free Inconel high strength alloy for high temperature service, noting stress rupture strength and oxidation resistance [ASM PAPER W 72-51,4] 12 p1830 A72-28159
- Haynes high strength heat resistant Ni-Cr-W alloy metallurgical and structural relationship, mechanical and physical properties, oxidation and corrosion behavior and fabrication processes 13 p1973 A72-28649
- Quenched powder metallurgy of high strength-high conductivity wrought Cu-Zr and Cu-Zr-Cr alloys, using nitrogen atomization 13 p1974 A72-28659
- Commercial and laboratory Mg alloys for die and sand casting, high strength and extruding applications 14 p2113 A72-30269
- Chemical and mechanical properties relationship to stress corrosion in high strength Al-Cu and Al-Zn-Mg alloys, emphasizing grain boundaries cleavage energy 14 p2117 A72-30536
- Heat resistance improvement by interface dislocation, dispersion hardening and reinforcement of Mo, Fe, Ni and Al metals and alloys 15 p2254 A72-31560
- Temperature effect on fatigue crack growth in high strength annealed Ti-Al-V alloy in water, oxygen/hydrogen and vacuum environments 16 p2406 A72-33320
- Tensile and compressive stress coarsening effects on coherent gamma prime precipitate yield strength of Ni-base superalloy single crystals 20 p2938 A72-39299
- Fatigue cumulative damage in cases of rotating-bending and torsional multistep loading. 21 p3118 A72-40933
- Ti based beta alloy strain hardening and failure characteristics, emphasizing initial deformation phase and microdefect onset and development 21 p3071 A72-41716
- High strength bimetallic rivets produced by inertia welding Al-Ti alloy shank with pure Ti tail, noting weight and cost reduction for aerospace vehicle production [SAWE PAPER 902] 23 p3293 A72-43452
- Shear-strain-rate effects in a high-strength aluminum alloy. 23 p3302 A72-43983
- Plane strain fracture toughness of notched high strength Al and Ti alloys at low temperatures 24 p3413 A72-44939
- HIGH STRENGTH STEELS**
- NT MARAGING STEELS
- High temperature high strength Ni alloys with Ti, Nb and Hf additions, using modified Hastelloy N 01 p0084 A72-10746
- High strength steels stress corrosion crack propagation velocity relationship to crack tip stress intensity 02 p0295 A72-12482
- High strength low alloy type ferrite pearlite steel microstructural and compositional variations effect on work hardening, ductility and impact toughness 02 p0246 A72-12558
- Hot-rolled low-carbon Mn-Mo-Nb acicular ferrite steels with high strength, toughness and impact resistance 02 p0246 A72-12559
- Quenched and tempered high strength and maraging steels delayed failure properties from notched-tensile sustained-load tests in distilled water 02 p0246 A72-12560
- Heat treatable high strength steels fracture toughness dependence on temperature, examining surfaces with electron scanning microscope 03 p0369 A72-12959
- Tempered Fe-Cr-C-Co steels microstructural and mechanical properties, investigating martensite and bainite 03 p0375 A72-13929
- Alloy additions and heat treatment effects on mechanical properties and weldability of quenched and aged high strength Ni steels 03 p0378 A72-14173
- Strain hardening for steel strength increase to 300 kg/sq mm by sequentially combined mechanical and thermal processing, involving plastic deformation, quenching and aging 04 p0527 A72-15454
- Mechanical properties of heat treated hardened high strength steel, investigating microstructure relationship to breakdown characteristics 05 p0671 A72-15992
- Purity effect on fatigue crack growth in high strength steel at room temperature 05 p0674 A72-16325
- Automatic recording of crack length in slow fracture tests of flat high strength steel in water 05 p0741 A72-17087
- Cr and U contents effect on high strength Cr-Mo-Va alloy steel sheet hot cracking susceptibility, using Huxley test method 06 p0820 A72-17704
- Strength and plasticity characteristics of hardened multilayer structural steels, investigating layer thickness effect 07 p1013 A72-19746
- Hydrogen cracking of high strength steels during cathode polarization in acidic media, investigating time to cracking variation with current density 07 p1013 A72-19770
- Static hydrogen fatigue of high strength steels, deriving relationship between time to cracking and tensile stresses magnitude for cadmium-plated steel 07 p1014 A72-19774
- Prestressing effect on stress corrosion resistance of fatigue precracked high strength steels 07 p1016 A72-19941
- Intermetallics and carbide forming additions of Cr, Ti, Ce, V and Nb for hardening of cold worked Mn rich steel from crystal dislocations growth 09 p1327 A72-22230
- Soviet monograph on thermoplastic hardening of high strength martensitic steels and Ti alloys by ordering dislocation structure 09 p1327 A72-22520
- Welded high strength maraging steels fatigue performance, stressing nondestructive testing technique 09 p1332 A72-23617
- Metallic coatings effect on high-strength steels fatigue properties, noting beneficial effect of shot peening 10 p1494 A72-24024
- High strength steel strip reinforced aluminum, discussing fabrication techniques and mechanical properties 10 p1498 A72-24839
- High strength steel flat plates brake formability from bend tests on sheared edges specimens, noting Hutchinson method sensitivity for different crack propagation propensities materials 11 p1657 A72-25819
- Specimen preparation effects on fracture strength measurements, noting critical stress intensity factor for single edge notch and compact tension high strength steel samples 11 p1657 A72-25825
- High strength quenched steel with high ductility at cryogenic temperatures and negligible cooling rate effects on plasticity during welding 11 p1660 A72-26136
- High strength hypereutectoid steel with low carbon needle-like martensite matrix obtained by conventional heat treatment 12 p1827 A72-27100
- Protective coatings for corrosion prevention of high strength steels under environmental conditions of humidity, salt fog, tap and salt water immersion 12 p1835 A72-28157
- High strength low alloy steel and stainless steel recrystallization after hot working at plastic deformation temperature 13 p1973 A72-28654
- Cr and V additions effects on Mn steels mechanical properties and wear resistance, noting strength limit increase 13 p1977 A72-29021
- High stress state mechanical properties of steels with different carbon contents and heat treatments 13 p1979 A72-29478
- Ultrahigh tensile strength steel pressure chamber fracture behavior in high stress concentration fields 15 p2330 A72-32345
- High strength fine grain structural steels fracture characteristics from notch-bar impact and tensile tests, determining inclusions effect on mechanical properties 16 p2406 A72-33236
- Transformation induced plasticity /trip/ Ni-C steel strengthening by thermal cycling between martensite and reverted austenite 16 p2399 A72-33815
- Interstitial and substitutional dynamic strain aging of Fe-Nb alloy and Al-Nb bearing steel at 295-950 K 18 p2699 A72-36342
- German monograph - Significance of the manganese-carbon ratio in the brittle-fracture behavior and weldability of high-strength fine-grained structural steels 19 p2816 A72-37661
- Cathodic protection and hydrogen in stress corrosion cracking. 19 p2817 A72-37765
- Resistance to brittle fracture of high-strength steels in various structural states 19 p2819 A72-38014
- Crack growth behavior correlation to acoustic emission signal amplitude distribution in high strength steel heat treated to different fracture toughness values 20 p2924 A72-39282
- Stress-corrosion cracking of high strength steels and titanium alloys. 21 p3067 A72-40849
- Precipitation of aluminum nitride in low-alloy steel 21 p3068 A72-40956
- Strength of welded joints of high-strength stainless steels at cryogenic temperatures 21 p3061 A72-41365
- Antiscratch properties of nitrided layers of creep-resisting steels at high temperatures 22 p3187 A72-41868
- Chemical etchants and etching procedure for decorating areas of residual tensile elastic surface stresses in ultrahigh strength steels without aging 22 p3183 A72-43045
- The effect of some electrolytes on the stress corrosion cracking of AISI 4340 steel. 22 p3195 A72-43128
- Heat treatment effectiveness criteria for thermomechanically strengthened steels, using creep rupture, fatigue, bending and tensile tests 23 p3300 A72-43643
- Heat treatment effects in multipass weldments of a high-strength steel. 23 p3304 A72-44310
- Mechanical properties of heat treated hardened high strength steel, investigating microstructure relationship to failure characteristics 24 p3416 A72-45734
- HIGH TEMPERATURE**
- Positive and negative deviations of linear electrical resistance of d-transition metals at high temperatures as function of Debye temperature and Fermi level 02 p0242 A72-12006
- Rhenium carbide synthesis at high pressure and temperature, searching for superconducting properties 06 p0828 A72-17617
- High temperature mechanical properties - Conference, Clermont-Ferrand, France, October 1970 14 p2116 A72-30526
- Current-voltage and specific power-energy relationships for high temperature electrochemical cells with alkali metal anodes and chalcogen or halogen cathodes 16 p2352 A72-33900
- Electron and nuclear components and transformations of matter under extreme conditions of pressure and temperature exemplified in stellar /pulsar/ evolution 18 p2725 A72-36520
- Developments in the field of metallic diffusion protective layers employed against high-temperature corrosion 20 p2944 A72-39450
- HIGH TEMPERATURE AIR**
- Radiative heat transfer within nonisothermal air plasma, presenting centerline temperature data for various boundary pressures and temperatures [ASME PAPER 71-HT-G] 02 p0302 A72-12316
- Voltage breakdown of microwave antennas, discussing ionization rates in hot air and breakdown suppression by electron flow 06 p0783 A72-17739
- X band microwave attenuation measurements in high density air plasma layer at aperture antenna in rectangular shock tube 07 p0949 A72-20560
- Gas mixture properties at high temperatures, pressures and densities, applying to thermal ionization of adiabatically compressed air 08 p1210 A72-20942
- TiC high temperature oxidation and thermodynamic equilibria in air, using metallographic and X ray analyses 14 p2112 A72-30155
- Graphite ablation rate inhibition and surface temperature depression by chlorine gas in supersonic high temperature air environment 16 p2475 A72-32842

High temperature turbulent jet facility for studying ionic species produced by high temperature air and ablation products interaction with cool ambient air [AIAA PAPER 72-676] 17 p2536 A72-35480

HIGH TEMPERATURE ALLOYS

U HEAT RESISTANT ALLOYS

HIGH TEMPERATURE ENVIRONMENTS

Space shuttle mechanical fastener design, discussing drives, threads, manufacturing and refractory alloys 01 p0075 A72-10751

Toxicological control and chemical analysis of outgassing products from nonmetals in high temperature oxygen atmosphere, investigating use within LM crew compartment 01 p0019 A72-10771

Oxidation screening at 2200 F of Ni, Fe and Co wrought alloys for space shuttle thermal protection system, noting microstructural changes 01 p0085 A72-10781

Body cooling effect on human vigilance in hot environments, testing reaction time to visual stimuli and auditory signal detection rate 01 p0021 A72-11290

Screw connections high temperature behavior, discussing creep induced tension relaxation and cyclic loads long term tolerance 03 p0363 A72-13375

Microorganism life in extreme high temperature, PH and solute concentration environments, noting salt effect on enzyme activity 04 p0471 A72-14801

Refractory metal thermocouple research program, describing design and performance of ultrahigh vacuum high temperature furnace system 04 p0524 A72-15550

Environmental effects on superalloy high temperature corrosion in gas turbines, noting blade surface temperature as critical factor [ASME PAPER 71-WA/CD-1] 05 p0704 A72-15945

Intense noise measurement device for heat flow environments, discussing applications to jet engines, nozzle exits, turbine exhausts and volcanic craters [ONERA, TP NO. 1010] 05 p0661 A72-16025

High temperature brazing of heat resistant alloys, determining tensile strengths 05 p0666 A72-16189

Hot corrosion of thorium dispersed nickel and thorium dispersed Ni-Cr alloy in high velocity gas stream of jet fuel combustion products 07 p1010 A72-18753

Hot corrosion resistant Pt-Al coating for high temperature aircraft engine Ni alloy components, presenting cyclic sulfidation and thermal shock test results 07 p1012 A72-19573

Refractory alloys softening under stress relaxation conditions at high temperatures, noting plastic strain hardening effect absence 07 p1018 A72-20138

Fluid oscillator temperature sensor, noting fast dynamic response and application in high temperature environments 08 p1164 A72-20926

Stoichiometry effect on high temperature creep in oxides, relating impurities, point defects concentration and diffusion 09 p1335 A72-22397

Structural model application to construction material alternate stress description at elevated temperatures 09 p1401 A72-22727

Vibration string static strain gage for high temperature operation, proposing relations for measurement error calculation 09 p1310 A72-22741

Defects high temperature diffusion effect on Mossbauer spectral lines width and positions in crystals with quantum transfer between multiplet sublevels in fine structure 09 p1372 A72-23038

Papers on design for high temperature environments covering structural fatigue, creep interaction and ratcheting deformation and inelastic stress analysis 09 p1406 A72-23196

Creep ratcheting deformation and rupture damage from thermal transient stress cycle and constant membrane force under high temperature metal creep conditions 09 p1406 A72-23197

Time and cycles to failure diagrams for strain rate and hold periods effects on high temperature metal creep fatigue in design analysis 09 p1407 A72-23199

Mathematical model and inelastic stress analysis for metal creep-fatigue interaction and progressive deformation in breeder reactors operation 09 p1407 A72-23200

Thin Ta sheet spiral configuration for high efficiency high temperature vacuum heat shield 12 p1888 A72-27035

High temperature dislocation rearrangement in lightly cold deformed Nb as function of time and temperature, using etch pit technique for evaluation 12 p1827 A72-27136

High temperature skin friction meter design for drag measurements, using motor-transducer air core assembly 12 p1812 A72-27959

Composite turbofan blades for high temperature applications, discussing weight reduction and design procedure 12 p1816 A72-28102

Tungsten free Inconel high strength alloy for high temperature service, noting stress rupture strength and oxidation resistance [ASM PAPER W 72-51.4] 12 p1830 A72-28159

Parotid fluid 17-hydroxycorticosteroid level relation to hyperthermia stress at various heat levels during thermal environmental testing 12 p1768 A72-28335

High temperature environment effects on rat organ and muscle tissue respiration, discussing temperature homeostasis maintenance 13 p1905 A72-29331

High temperature low cycle fatigue of alloys as process of crack nucleation and growth to ultimate failure 13 p2058 A72-29445

Microscopic substructure in high temperature fatigued fcc austenitic steel and aluminum, studying cross slip lines and crack initiation 13 p1979 A72-29448

Air composition and thermodynamic properties at 12,000-25,000 K and 0.1-100 atm with allowance for Coulomb interaction effect on pressure and for ionization potential decrease 13 p2018 A72-29878

Reflectivity of metals at high temperatures based on Drude theory and electron-phonon scattering, detailing temperature dependence and optical constants 14 p2129 A72-30183

Human physiological function variations dependence on hyperthermia levels in high temperature environment 14 p2074 A72-30257

Stress relieving heat treatment for service failure prevention of stressed austenitic stainless steel components of high temperatures, noting cracking regulation by oxidation mechanism 14 p2117 A72-30538

Co-Cr alloy high temperature oxidation kinetics reduction by Y addition, presenting metallographic study 14 p2118 A72-30543

Ni additions effect on Fe-Cr alloys oxidation behavior at high temperatures during varied exposure time periods, noting dichromium trioxide scale formation 14 p2118 A72-30545

W and Nb effect on Ta base alloys high temperature oxidation behavior 14 p2118 A72-30547

Zirconium diboride oxidation processes at temperatures above 520 C, noting zirconium oxide formation 14 p2121 A72-30850

Liquid drop evaporation in stagnant environment at high temperature and pressure, noting gas phase nonideal behavior effects 14 p2173 A72-31066

High temperature and altitude combined effects on performance of tracking, monitoring and mental arithmetic complex task 14 p2083 A72-31155

Approximate solution of nonlinear boundary value problems in high temperature conductive heat transfer 14 p2174 A72-31161

Y and La action on oxidation rates of Cr and Mo at high temperature in air 15 p2252 A72-31191

Water loss replacement effect during rest and exercise in high temperature environment thermoregulation experiment 15 p2185 A72-31449

Monograph on hot environments stress covering heat exchange at skin surface, clothing effect, body temperature regulation and sweating control 15 p2185 A72-31515

Neutronically generated He irradiation effects on high temperature fracture of fcc, bcc and hcp structural metals and alloys 15 p2258 A72-32487

Laser ignition and combustion of boron particles, developing oxide coating and droplet burning models for low and high temperature stages respectively 15 p2296 A72-32582

Liquid fuel droplet transient combustion in supercritical hot stagnant oxidizing environment, solving conservation equations 17 p2636 A72-34903

High temperature oxidation of ammonia 17 p2511 A72-34904

Oxidizability of boron-carbon compounds at high temperatures, determining chemical composition effect on oxidation resistance 18 p2703 A72-36095

Oxidation resistance at high temperatures of refractory materials based on silicon nitride and carbide in

various concentrations, showing time and temperature dependence 18 p2703 A72-36096

Techniques to curb static austenite recrystallization rate in martensitic sheet steel during high temperature thermomechanical treatment through minute Ti or Zr additions 18 p2701 A72-36702

High-stability capacitance strain gauge for use at extreme temperatures. 18 p2693 A72-37210

High temperature and vacuum solar furnace processing of refractory metals in space or on moon 19 p2857 A72-37675

Creep damage role in governing elevated temperature strain cycling fatigue lives of heat resistant stainless steel and cobalt alloy 19 p2817 A72-37712

The effect of hydrostatic pressure on plastic deformation and creep of polycrystalline metals at elevated temperatures. 20 p2977 A72-38878

Dynamic recrystallization occurrence during deformation at elevated temperatures, examining subgrain structure role in austenitic stainless steels 20 p2942 A72-39990

Effects of scale porosity, second-phase oxides, and doping in the high-temperature oxidation of cobalt and dilute cobalt-chromium alloys. 21 p3067 A72-40845

Effect of cold work on the oxidation of nickel at high temperature. 21 p3067 A72-40846

Mechanism of high temperature creep of aluminum-magnesium solid solution alloys. 21 p3069 A72-41299

Finite difference and extended Newton methods application to transient and steady state creep deformation in shells of revolution under high temperature and high stress 22 p3235 A72-42482

German monograph - Gas-phase precipitation and high-temperature oxidation of titanium carbide. 22 p3194 A72-43053

Recovery of high temperature deformed Ni-Al alloys. 23 p3300 A72-43564

Refractory alloys softening under stress relaxation conditions at high temperatures, noting plastic strain hardening effect absence 24 p3416 A72-45763

HIGH TEMPERATURE FLUIDS

NT HIGH TEMPERATURE AIR

NT HIGH TEMPERATURE GASES

Freezing of hot fluid flowing onto flat cold wall, solving nonlinear integrodifferential equation for temperature distribution by iteration method 04 p0595 A72-14650

Evaporation and combustion of liquids injected into high temperature supersonic flow, considering interaction with pressure variations 08 p1253 A72-21454

Hydrodynamic stability of electrically conducting hot viscous fluid surrounded by perfectly conducting rigid boundary in presence of magnetic field 09 p1359 A72-22825

Mechanical seals for high temperature heat transfer fluids, noting configuration and construction materials [ASLE PREPRINT 72AM 30] 13 p1964 A72-28976

HIGH TEMPERATURE GASES

NT HIGH TEMPERATURE AIR

Applied MHD and high temperature gas dynamics - Conference, Gdansk, Poland, May 1970 01 p0110 A72-11201

Thermodynamic properties of gases at high temperatures, tabulating composition, enthalpy, entropy and thermal conductivity of combustion products with ion seeding 01 p0145 A72-11202

Cooled miniature pneumometric probes for high temperature gases dynamic or stagnation pressure and velocity measurement 01 p0072 A72-11213

Differential thermal radiation scattering coefficients of submicron W refractory particles in hydrogen and nitrogen at temperatures to 1080 K 01 p0112 A72-11341

High temperature and pressure detonation gas expansion as shock wave from cylindrical volume, calculating flow velocity, pressure and density 02 p0302 A72-12285

Externally water cooled conical nozzle throat wall thickness design for high pressure and temperature argon flow medium [DGLR PAPER 71-095] 02 p0299 A72-12702

Cosmological density fluctuations in hadron stage, examining relativistic free particle and high temperature hadron gas models 03 p0426 A72-13273

Plane mixing boundary layer flow of high temperature turbulent gas jet in longitudinal magnetic field 03 p0397 A72-13998

- Comparative velocities of high energy gas jets of Ne, oxygen and carbon dioxide from outlet pipes, using Voitenko compressors 04 p0510 A72-14537
- Equilibrium temperature formula derived for surface subjected to aerodynamic heating by gas from heat balance between convective and radiative heat flow 04 p0595 A72-14651
- Model intermolecular interaction potentials constants determination for extrapolating thermodynamic properties of gases at high temperatures and pressures 05 p0692 A72-15842
- State of gas parameters measurement apparatus at high temperatures and pressures involving constant volume piezometer with internal heating 06 p0814 A72-17616
- Shock tube experimental techniques for studying fast processes coupled to shock wave propagation in reactive gases, describing pressure, density and temperature measurement methods 06 p0800 A72-18120
- Cascading turbomachine blades vibration measurement in subsonic and sonic high temperature gas flows, describing test facility 06 p0797 A72-18689
- Seyfert galaxy hypothesis with galactic center containing hot gas region with density decreasing toward boundary, discussing nucleus brightness variability 07 p1075 A72-19560
- Heterogeneous composite solid propellants ignition behavior under exposure to hot oxidizing gas, using gas phase model with species and energy radial diffusion 07 p1051 A72-19726
- Shock wave properties in RR Lyra type star atmospheres, discussing high temperature region structure behind wave front and emission line profiles 08 p1229 A72-20841
- Hot gas heat transfer measurements in separation, reattachment and redevelopment regions downstream of abrupt circular channel expansion [ASME PAPER 71-HT-DD] 08 p1251 A72-20881
- Temperature and concentration fields of liquid solution droplets during unsteady vaporization process in high temperature gas media 08 p1252 A72-21308
- Air injection from wall slot into turbulent boundary layer of high temperature gas channel flow, calculating film cooling effectiveness in flat plate 08 p1252 A72-21316
- Slip cast fused silica ablation in high temperature hydrogen-oxygen environment, comparing analytical results with measured data from rocket motor exhaust experiments 08 p1191 A72-21601
- One dimensional expansion of hot vapor and gases remaining behind meteor body 08 p1238 A72-21884
- Air pollution monitoring with tunable lasers employing Raman scattering, resonantly excited or hot gases emission and resonant absorption 09 p1322 A72-22313
- Carburization kinetics of Nb in acetylene or methane at high temperatures and low pressure 09 p1319 A72-22985
- Thermodynamic properties of high temperature and density hydrogen, using Rowlinson equation of state 09 p1412 A72-23234
- High temperature and pressure detonation gas expansion as shock wave from cylindrical volume, calculating flow velocity, pressure and density 10 p1561 A72-23759
- Radiant heat flux measurement during pulsed processes from surface in high temperature emitting gas, using thin film sensor with small time constant 10 p1561 A72-23843
- Gaseous buffering for oxygen fugacity control in high temperature gas systems at one atmosphere 12 p1778 A72-28104
- Gas compressibility measurements at high pressure and temperature using externally heated pressure vessels 12 p1889 A72-28106
- High temperature gaseous disperse flow radiation spectra photoelectric recording by DFS-8 spectrograph 12 p1812 A72-28116
- Optimization of high temperature supersonic gas jets for metal powders production by melts atomization, discussing excess air ratio effect on gas parameters 13 p2025 A72-29133
- High X ray luminosity associated with richest galaxy clusters, noting inverse Compton effect by relativistic electrons and bremsstrahlung from hot gas 13 p2040 A72-29412
- Carbon dioxide arc plasma emissivity in visible range at atmospheric pressure and 6500-9500 K, discussing diatomic carbon concentration 13 p2016 A72-29520
- Microwave interferometry as plasma diagnostic technique to measure electron densities in partially ionized dense gases 14 p2103 A72-30177
- Model intermolecular interaction potentials constants determination for extrapolating thermodynamic properties of gases at high temperatures and pressures 15 p2280 A72-31261
- Distribution of high velocity hydrogen near Galactic center due to free-free emission from exploding hot gas or cosmic ray pressure 15 p2317 A72-32756
- Water vapor condensation in jet turbulent mixing zone of confluent high velocity high temperature gas streams for finite axisymmetric nozzle 16 p2377 A72-33260
- Energy and momentum losses of high temperature gas flow through externally cooled tube, solving laminar flow differential equations numerically on digital computer 16 p2378 A72-33430
- German monograph on surface roughness effects on pressure loss and heat transfer in high temperature turbulent flow, deriving universal laws 16 p2478 A72-33506
- Analytical solutions for straight oblique shock waves in radiating gases 17 p2542 A72-35616
- High temperature cesium vapor sources based on a cesium-graphite system for thermionic converters 18 p2646 A72-36201
- Liquid or solid propellant hot gas turbines as power source for hydraulic and electrical energy 18 p2648 A72-36558
- Study of cesium vapor pressure by the boiling point method 18 p2713 A72-37179
- Two chamber adiabatic test compression system design with controlled throttle for high temperature nitrogen and nitrous oxide-type gases with exothermal reactions 18 p2676 A72-37189
- Hot rarefied neutral gas existence in interstellar space on basis of data collected in 21 cm hydrogen line 19 p2865 A72-38480
- Design modeling of external and internal cooling systems for bodies exposed to high temperature gas flow, discussing operation similarity conditions 21 p3129 A72-41052
- Questions in the theory of monomolecular decay of a one-component gas and the dissociation constant of CO₂ at high temperatures 21 p3088 A72-41657
- Thermal state of selectively absorbing plane gas layer blown from porous plate into stabilized turbulent high temperature gas flow, considering radiative and convective heat transfer 21 p3131 A72-41672
- Russian book - Radiation characteristics of gases at high temperatures. 22 p3243 A72-42075
- Inflammation and burning of powdered aluminum in high-temperature gaseous media and in heterogeneous condensed systems 22 p3245 A72-43178
- Experimental study of heat transfer during cooling of a high-temperature gas flow in a pipe. 23 p3357 A72-44539
- Some infrared diagnostic techniques in high temperature gasdynamics. 24 p3402 A72-45043
- HIGH TEMPERATURE LUBRICANTS**
- Plasma jet technique for self lubricating antifriction Ni, Sn or Cu coatings for MoS₂ particle oxidation protection 04 p0527 A72-15664
- Oxidation resistant solid lubricants for high temperature air and gaseous environments applications, considering oxide and fluoride coatings with silicate additives for wear life improvement 06 p0837 A72-18600
- Soviet monograph on solid inorganic compounds as high temperature lubricants covering powder lubricants mechanism under different friction conditions, gas media, temperature effects, etc 08 p1191 A72-20913
- Aircraft gas turbine engines synthetic lubricants thermal stability characteristics, describing coke deposition test apparatus and results [ASLE PREPRINT 72AM 14] 13 p1983 A72-28971
- Lubrication with solids. 19 p2807 A72-37771
- HIGH TEMPERATURE MATERIALS**
- U REFRACTORY MATERIALS**
- HIGH TEMPERATURE NUCLEAR REACTORS**
- High temperature gaseous U fission plasma core reactor engine concepts for space propulsion 01 p0099 A72-11327
- Chemically vapor deposited W heat pipe fabrication and evaluation for application to high temperature nuclear reactors 15 p2244 A72-32126
- Design of high-temperature liquid-metal systems. [ASME PAPER 72-AERO-13] 22 p3204 A72-43149
- HIGH TEMPERATURE PLASMAS**
- High temperature nongray kernel functions application to radiative heat transfer for bounded hydrogen plasma 01 p0145 A72-10100
- Hot magnetoplasmas cyclotron radiation, investigating thermal particle motion effects 01 p0107 A72-10142
- Electrostatic potential fluctuations spectrum in turbulent hot ion plasma confined between magnetic mirrors, investigating mode coupling, energy cascading and electron concentration 01 p0108 A72-10242
- Nuclear pumped laser, noting electrically excited carbon dioxide laser experiment and high temperature multiple ionized plasma concepts 01 p0082 A72-11329
- High temperature U plasma generation at near gas core reactor conditions by sliding spark discharge into capillary channel lined with sintered uranium dioxide 01 p0112 A72-11338
- Millimeter and submillimeter microwave spectrometric studies of high temperature plasmas and noise emission, discussing instrumentation and absolute measurements 02 p0223 A72-11409
- Scintillation counter to determine neutrons number and distribution in time in pulses generated in hot plasma 02 p0263 A72-11419
- Coulomb logarithm for hot plasma viscosity coefficient in magnetic field by quantum mechanical unified theory 02 p0267 A72-12770
- Right handed circularly polarized electromagnetic wave propagation in hot inhomogeneous plasma, deriving local dispersion equation by WKB methods 03 p0393 A72-12949
- Cylindrical gravitational waves propagation modes in hot plasma subject to axial magnetic field, investigating instability conditions 03 p0388 A72-13025
- High temperature dense plasma formation by laser heating of gas target, noting fusion reaction in deuterium-tritium mixture 03 p0399 A72-14066
- Radiation intensity and losses in dense high temperature hydrogen plasma containing bare nuclei and hydrogen-, helium-, lithium- and beryllium-like ions as impurities 04 p0557 A72-15170
- Transient signal propagation in unbounded time-spatial dispersive hot plasmas, using convolution integral equations 04 p0490 A72-15402
- Spherical antenna covered by lossy hot plasma layer, calculating radiation fields by transmission line theory 04 p0493 A72-15525
- Fiber optics system for H beta line shape measurement in transient high temperature plasma, using narrow slits at spectrograph exit plane [AIAA PAPER 72-106] 05 p0663 A72-16816
- Hot plasma transverse and longitudinal wave parametric excitation by intense laser light near plasma frequency, noting instability role in resonant coupling mechanism 05 p0699 A72-17172
- Half wavelength antenna radiation admittance into warm lossy two layer plasma half space, using effects of slot width and electron collision frequency 06 p0781 A72-17348
- High speed photography in high temperature short duration plasmas, using Kerr cell, image converter, framing and streak cameras 06 p0813 A72-17435
- Magneto-viscous interactions in combustion plasma, measuring velocity distributions for ordinary hydrodynamic and MHD flow with transverse magnetic field 06 p0859 A72-17618
- Magnetic and electric field intensities measurement with charged particle beams in coaxial high temperature plasma sources 06 p0863 A72-18415
- X ray spectrum and D-D neutrons emission from high temperature plasma produced by two pulsed Nd-glass laser systems [CLEA PAPER 12,3] 07 p1041 A72-19394
- Electrostatic oscillations of multivelocity electron streams in hot inhomogeneous plasma 07 p1046 A72-20502
- Solar cosmic rays propagation between shock front and solar flare hot plasma, examining fine structure from Explorer 34 and Venera 6 data 07 p1063 A72-20628
- Velocity space instability in hot electron plasma created by adiabatic compression in pulsed magnetic mirror, observing radiation bursts below electron cyclotron frequency during compression [AD-740408] 08 p1213 A72-21257
- Laser systems for lunar ranging and high temperature plasma generation 08 p1182 A72-21336
- Electron temperature effects on radiation fields and resistance of short electric dipole antenna embedded in hot uniaxial plasma 08 p1215 A72-21991

Electrostatic longitudinal waves propagation and detection in isotropic collisionless hot electron plasma, calculating Landau dispersion curve and damping

09 p1359 A72-22794

Star stellarator model for hot electron plasma production by steady electron beam injection in closed magnetic traps

09 p1363 A72-23219

Spectrum of hot hydrogen plasma continuum radiation, discussing models for Scorpius X-1 source and inhomogeneous clouds

09 p1391 A72-23536

Monochromatic absorption coefficients determination for Ar heated in wall-stabilized arc at high temperatures and pressures

10 p1517 A72-23836

Superconducting levitron machine for trapped hot plasma stability and confinement studies in vacuum, discussing construction and coil performance

10 p1460 A72-24758

Quadrupole probe theory for hot collisionless isotropic plasma, noting impedance dependence on electron temperature at resonance and optimum dimension relationship to Debye length

10 p1523 A72-24798

Ion sources for high temperature operation based on electron bombardment and beam-plasma interactions

10 p1516 A72-25031

Ion and electron temperature ratios in hot plasma, discussing energy relaxation, heating and cooling effects and electrostatic confinement by ambipolar diffusion

10 p1524 A72-25032

Magnetic mirrors for highly stripped heavy ions production in hot electron plasmas by low voltage high current electron beam

10 p1524 A72-25035

High temperature deuterium plasma production by laser heating of gas filled cylindrical tube, optimizing pulse duration and configuration

12 p1849 A72-27059

Explicit numerical modeling method for dynamics of dense high temperature laser-produced plasmas, discussing time scale for energy transfer from electrons to ions

13 p2009 A72-28424

Input impedances and current distributions of cylindrical monopole antennas of various lengths in hot lossy plasma as function of plasma density

13 p2009 A72-28538

Computerized calculation of wave dispersion curves for hot Maxwellian electron magnetoplasma, applying to upper hybrid and cyclotron frequencies

13 p2013 A72-29340

Singly ionized Ca and Mg electron impact broadened resonance lines from rapid scanning Fabry-Perot spectrometer measurements in shock tube generated high temperature plasma

15 p2282 A72-32643

Galaxy M87 X ray source origin, suggesting hot plasma thermal emission or ejected relativistic electrons interacting with intergalactic magnetic or radiation fields

16 p2452 A72-33135

Fine structure similarities between solar flares and current sheath in laboratory hot plasma coaxial accelerator, noting X ray and high energy particles production mechanism

16 p2438 A72-33919

Laser pulse produced high temperature plasma engine propulsion system, noting thrust/power ratio and requirements for orbital applications

16 p2443 A72-34029

Gas breakdown in front of metal targets laser flare from UV radiation ionizing action, using pulsed holographic technique

17 p2554 A72-34860

Magnetic and electric field intensities measurement with charged particle beams in coaxial high temperature plasma sources

17 p2588 A72-34864

A review of the unified theory of relaxations in plasmas.

17 p2590 A72-35159

Kinetic theory of waves in hot, low density plasma.

17 p2591 A72-35161

Vlasov and Maxwell equations solution for surface waves dispersion in semiinfinite hot plasma

18 p2716 A72-36925

Spectral intensity measurements from high-pressure nitrogen plasmas.

19 p2840 A72-37836

The incoherent scattering of radiation from a high temperature plasma.

19 p2842 A72-38523

Radial penetration of a hot plasma associated with a large-scale electric field in the magnetosphere, and some related problems.

20 p2916 A72-39228

Laser power and pulse duration requirements for hot plasma production by flame propagation in solid DT targets for controlled thermonuclear fusion

20 p2931 A72-39354

Double-beam interferometry method for investigating axisymmetric configurations of dense plasma.

20 p2958 A72-39505

Far UV radiating hot dense microplasma production by laser heating for measuring by resonant absorption small quantities of gaseous element

21 p3093 A72-41341

Investigation of the structure of a high-current discharge in a lithium plasma

22 p3209 A72-41878

Magnetic-field-enhanced heating of plasmas with CO₂ lasers.

22 p3210 A72-41969

Kinetic equation for electron distribution in high temperature laser plasma, calculating nonequilibrium conditions for strong field and plasma parameters

23 p3318 A72-43323

Temperature of a free plasma filament in a high-frequency field at high pressures

23 p3322 A72-44464

Spectral composition and phase function of plane monochromatic light wave scattering by electrons in high temperature plasma

23 p3322 A72-44465

Steady-state distribution of the charged and neutral particle concentration in a bounded high-temperature turbulent plasma

24 p3429 A72-45493

Electron bremsstrahlung from hot plasma in the presence of strong magnetic field.

24 p3431 A72-45627

Effects of pseudosonic and electroacoustic waves on the radiation of a plasma-coated spherical antenna.

24 p3386 A72-45645

High temperature deuterium plasma production by laser heating of gas filled cylindrical tube, optimizing pulse duration and tube configuration

24 p3431 A72-45712

HIGH TEMPERATURE PROPELLANTS

High temperature biowaste resistojets with electrically conducting ceramic heaters, discussing lifetime and space station power systems adaptability

[AIAA PAPER 72-454] 11 p1708 A72-26190

HIGH TEMPERATURE RESEARCH

Kinetics of shock wave pyrolysis of pentafluoroethane dilute mixture in Ar at 1180-1470 K

02 p0170 A72-11520

Papers on high temperature physics and chemistry covering peaceful nuclear explosions, radiative transfer, hydrodynamics, stellar opacity and solar He abundance

07 p1078 A72-19922

Temperature effects on kinetics of methane decomposition on carbon fiber at high temperatures, showing characteristics relationship to carbon gasification reactions

10 p1433 A72-24086

Papers on high pressure-high temperature research techniques covering laboratory procedures for control, calibration and measurement of solid-vapor and liquid-vapor equilibria

12 p1778 A72-28103

HIGH TEMPERATURE TESTS

High temperature strength degradation of graphite and boron reinforced epoxy composites after room temperature aging

01 p0090 A72-10728

Thermal and environmental exposure effects on high temperature mechanical properties of graphite/polyimide composites

01 p0090 A72-10730

High temperature testing of metal matrix composites mechanical properties, noting aerospace structural applications

01 p0084 A72-10732

Bare and coated Nb alloy in high temperature vacuum conditions, discussing tensile and bend tests and mechanical properties

01 p0084 A72-10747

Plasma arc testing of space shuttle Nb and Co alloys thermal protection materials, using IR radiometric and photographic techniques

01 p0048 A72-10977

Cast high temperature Ni base alloy Udimet 500 low cycle fatigue, determining total stress and strain range vs fatigue life at elevated temperatures

01 p0087 A72-11030

High speed measurement techniques for thermophysical properties at temperatures above 2500 K, emphasizing subsecond duration methods for solid phase electrical conductors

02 p0223 A72-11500

Refractory materials strength testing equipment and techniques at high temperatures, covering creep, hardness, fatigue, ultrasonic, energy dissipation and loading tests

02 p0291 A72-11636

Thermally stable organic polymer fiber production methods and performance evaluation in high temperature environments, discussing structure types, flammability and tensile properties

02 p0248 A72-11771

Thermal conductivity measurement of dissociating nitrogen dioxide over 548-792 K and 1-30 atm

02 p0170 A72-12091

Electrical conductivity of pyrographite at high temperatures along and across deposition plane, using optical pyrometer measurements

02 p0251 A72-12860

Materials stability testing in high temperature propane-butane combustion product flow, selecting compact silicon carbide for structural use in redox medium

02 p0251 A72-12866

Al-Mo alloys under high temperature, determining phase equilibria and intermetallic phases

03 p0370 A72-12961

High temperature creep activation energies relationship to diffusion in TiC, ZrC and UC

03 p0371 A72-13461

High temperature fatigue crack growth studies by compliance calibration test method, evaluating temperature and cycle rates effects

03 p0339 A72-14169

Laminate materials, sockets and connectors for cost-effective high temperature accelerated life testing of IC

03 p0336 A72-14283

High temperature thermal conductivity measurements of solids at 800-1500 C using heat pipe technique

04 p0547 A72-14544

Ni-Cr-Al-Si and Fe-Cr-Al-Y oxidation resistant claddings for superalloys, comparing to commercial aluminide coatings by cyclic furnace and high velocity burner rig tests

04 p0533 A72-14700

Polymethyl methacrylate fatigue strength at elevated temperatures, discussing sample preparation, test equipment and procedures

04 p0537 A72-14750

High temperature CIF reaction kinetics in thermal decomposition shock tube study, using chlorine atom two-body emission

04 p0484 A72-15463

Vacuum chamber and instrumentation for friction and wear tests at temperatures to 1800 C in vacuum and inert media

04 p0510 A72-15659

German monograph on refractory materials elasticity modulus determination at elevated temperatures, describing device based on characteristic vibrations frequency relation to temperature

04 p0510 A72-15698

Zirconium carbide high temperature heat conductivity measurement by radial heat flux method combined with photographic technique

05 p0680 A72-15852

Dislocation splitting and stacking fault energy variation during plastic deformation of TaC at 2200 C, using bending tests and microscope observations

[ONERA, TP NO. 1005] 05 p0670 A72-15861

Waspalloy sheet creep rupture time dependent sensitivity to sharp-edged notches at 1000-1400 deg F, optimizing smooth and notched specimen yield strengths

[ASME PAPER 71-WA/MET-3] 05 p0670 A72-15906

Elastoplastic creep analysis for cylindrical pressure vessel structural response during cyclic thermal shock, internal pressure and extended high temperature loading

[ASME PAPER 71-WA/PVP-12] 05 p0732 A72-15911

Al and Al-Zr coating effects on heat resistant alloy turbine blades high temperature fatigue resistance under bending-torsion cyclic loads

05 p0671 A72-15990

Mono- and polycrystalline Ni high temperature creep kinetics, investigating substructural changes

05 p0671 A72-16000

High temperature low cycle fatigue of Cr-Mo-V steel, observing crack growth rate correlation with crack tip stress

05 p0673 A72-16321

Ta-W-Hf alloy ultrahigh vacuum high temperature creep tests, showing deoxidation effect on creep behavior and early test stage oxygen-associated dynamic strain aging

05 p0674 A72-16392

Nb alloy oxidation behavior dependence on temperature in 550-1316 C range

05 p0676 A72-16732

Homologous temperature method to compare mechanical properties of metals tested at different temperatures

06 p0827 A72-17399

Refractory metallic and nonmetallic materials thermal conductivity above 1500 K, noting unreliable white oxides lattice conductivity results

06 p0828 A72-17612

Oxidation and hot corrosion tests of coated Ta and Ta based alloys between 800 and 1500 C in still air and in oxidizing gas stream

06 p0828 A72-17614

Thermal conductivity of aluminum, beryllium and magnesium oxides lattices at high temperatures

06 p0828 A72-17615

Book on refractory metals creep rupture behavior to high temperatures covering test procedures and data analysis for W, Re, Ta, Mo and Nb alloys

06 p0828 A72-17725

- High temperature tests of creep rupture strength of W composite cast with heat resistant alloy coatings
06 p0829 A72-17947
- Thermal emittance measuring methods for solids at temperatures above 1500 K, discussing emittance dependence on surface characteristics
06 p0818 A72-18253
- Enthalpy measurements of niobium silicides at 1200-2200 K by mixing method, using isothermal calorimeter
06 p0833 A72-18431
- Low cyclic failure resistance at elevated temperatures and static defects calculation based on fatigue and empirical endurance curves
06 p0898 A72-18555
- High temperature fatigue test assembly for symmetric tension compression cycles at 10 kHz with specimen heating in resistance furnace
06 p0797 A72-18568
- High temperature testing assembly for reinforced plastics and binders in oxidizing and inert media under tension, compression, bending and cleavage loads
06 p0797 A72-18569
- Friction and wear characteristics at high temperature of plain bearing embedded with pellets of graphite, sodium fluoride and tungsten disulfide lubricating mixture
06 p0823 A72-18584
- Damping characteristics of Ni base heat resistant alloys at high temperatures, showing increase with cyclic strain amplitude
06 p0833 A72-18630
- High temperature tests of short time strength, hardness and moduli of elasticity of W-Mo alloys subject to plastic deformation and annealing
06 p0833 A72-18633
- Carbon effects on strength, ductility, brittle transition and plastic strains of tungsten at high temperatures
06 p0833 A72-18634
- High temperature creep of niobium alloy, obtaining creep limit, microhardness and gas analysis data
06 p0833 A72-18637
- Stress-strain diagrams of heat resistant alloys at high temperatures, describing test facility
06 p0834 A72-18684
- Rutile creep resistant substructure recovery at 1000-1040 C, discussing stress relaxation mechanism due to dislocation walls or subgrain boundaries migration
07 p1023 A72-18800
- Electroconductivity, thermal conductivity and diffusivity, specific heat and emissivities of Ti at 1000-1700 K
07 p1010 A72-18935
- Test facility for thermal diffusivity measurements in solids by method of plane temperature waves using periodic optical heating at 1500 K
07 p0982 A72-18942
- Printed circuit boards and RC elements soldered connections reliability under high temperature and excessive current conditions, discussing test procedure and evaluation criteria
07 p0994 A72-19247
- Ti, Fe, Co, Ni, Pt and steels phase transformation and thermal defect effects on high temperature thermal conductivity
07 p1012 A72-19548
- Thermal conductivity of argon, helium, hydrogen, nitrogen, carbon dioxide, methane and ethane gases at high temperature and pressure
07 p1099 A72-19620
- Nb-Mo alloys behavior in aggressive boron containing medium at high temperatures, relating boride phases growth rate to component percentages
07 p1012 A72-19680
- Tungsten alloy filaments as reinforcing agent of heat resistant composite chromium alloy, investigating long term high temperature effects
07 p1013 A72-19745
- Heat resistant Nichrome composite alloy with tungsten filament reinforcement, discussing manufacture and mechanical properties at 1100 C
07 p1013 A72-19747
- High temperature strengthening of vacuum melted W-Ti alloys with Mo and Zr additions
07 p1014 A72-19843
- Age hardening of Mo alloys with titanium and zirconium carbides at high temperatures after quenching
07 p1014 A72-19844
- Lattice and photon components of thermal conductivity of cerium dioxide at high temperatures
07 p1044 A72-19881
- Ductility and fracture of heat resistant steels at high temperatures and unsteady loading, estimating loading cycle effect on plastic strain buildup to failure
07 p1017 A72-20127
- High temperature tensile tests of Mo with helical and circular V grooves, discussing stress concentration sensitivity relations for grooved and smooth samples
07 p1018 A72-20141
- Ni based superrefractory alloy high temperature fatigue tests, studying creep as function of stress load and frequency and temperature
07 p1022 A72-20487
- High temperature strain measurement accuracy improvement by gage spot welding
08 p1163 A72-20920
- Al single crystals relationship between stress, strain and dislocation density ring elevated temperature creep by direct observation of etch pits
08 p1185 A72-20990
- Thermal shock transient test burner to test gas turbine ceramics under simulated operational environment conditions
08 p1147 A72-21434
- Furan resins and chemically resistant furan-fiberglass composites flame resistance, heat distortion and physical properties at high temperatures
08 p1192 A72-21678
- Metallic four-lip seal performance, discussing force cycle, mechanical spring-back, reusability at room and higher temperatures and thermal shock behavior
08 p1179 A72-21939
- High temperature testing of metals, discussing specimen preparation and oxidation behavior evaluation by gravimetric, volumetric and optical techniques
08 p1189 A72-22107
- High temperature radiographic techniques for measurements of molten ceramics density, melting point, phase transitions, surface tension and viscosity up to 3000 C
09 p1333 A72-22378
- High temperature tests of graphite composites in air, determining material loss time dependence and correlation with observed strength data after oxidation
09 p1333 A72-22381
- Compression creep mechanisms in ceramic materials at elevated temperatures by lattice dislocations, grain boundary sliding and stress directed diffusion
09 p1334 A72-22393
- Thermomechanical and plastic deformation behavior of polycrystalline alumina at elevated temperatures
09 p1335 A72-22394
- Extruded dispersion strengthened Mg-MgO alloys microstructure, discussing high temperature creep effect on dislocation structure changes
09 p1328 A72-22984
- Loading path effect on yield surfaces of pure Al at elevated temperatures under tension
09 p1328 A72-22993
- Tensile microstrain and cyclic loading behavior of carbon fiber reinforced plastic composites at elevated temperature
09 p1338 A72-23169
- Cyclic oxidation kinetics of Hastelloy X sheet and wire specimens for high temperature alloy evaluation in transcription cooled engine components manufacture
09 p1331 A72-23476
- Hot-stage optical microscopes for microhardness measurements at elevated temperatures, describing techniques to determine heat resistant alloys mechanical and physical properties temperature dependence
10 p1478 A72-23827
- High temperature creep behavior of sintered polycrystalline strontium zirconate as function of temperature, stress, grain size and strain level, using pure bending test method
10 p1497 A72-24275
- Constituents, processing, fabrication and structure effects on artificial graphitic materials ablation performance in sublimation regime from high temperature tests
[AIAA PAPER 72-298]
11 p1742 A72-25235
- High temperature gradients in pulsed heated Mo specimen under vacuum, using photomicrographic technique
11 p1629 A72-25267
- Soviet papers on high temperature metallography techniques and equipment covering test assemblies for fatigue and microhardness measurements
11 p1654 A72-25489
- Ni and Ni alloys microstructure under tensile stress, determining Cr and Ti effects on plastic deformation at high temperature
11 p1654 A72-25494
- High temperature metallographic methods in microstructure study of austenitic heat resistant steel under plastic deformation and heat treatment
11 p1654 A72-25495
- Ni fatigue crack propagation under low cyclic loads at high temperature in vacuum after annealing and mechanical treatment
11 p1655 A72-25497
- Superalloys and refractory materials high temperature protective coatings, noting lack of uniformity in testing methods
11 p1674 A72-26286
- Microstructure and mechanical properties of heat treated friction welds at high temperatures
11 p1641 A72-26489
- Collisional ionization cross sections measurement for gaseous metal atoms in hydrogen-oxygen flames at 2000-2800 K
11 p1591 A72-26659
- Mo-Hf alloys high temperature mechanical properties improvement by internal diffusion nitriding, noting precipitates effects
11 p1644 A72-26843
- High temperature effects on stability, corrosion behavior, structure and protective effectiveness of Al coatings on Ni and Co alloys
11 p1664 A72-26852
- Mg addition effect on high temperature mechanical properties of nickel-alumina alloy, studying particle coarsening mechanism changes
11 p1664 A72-26856
- High temperature creep properties of W-Re alloy under vacuum for thoria dispersion hardening from electron microscope and activation energy studies
11 p1665 A72-26863
- Transition metals silicides additions effect on sintering and oxidation resistance at high temperatures of Ti and Zr diborides
11 p1665 A72-26874
- Carbide precipitation effect on structure and high temperature strength of Co based alloys
11 p1667 A72-26932
- High temperature low pressure reaction kinetics of nitrogen sorption by titanium foil, using ultrahigh vacuum microbalance
12 p1777 A72-27045
- High temperature solubility and diffusion coefficient of nitrogen in rhenium
12 p1827 A72-27138
- Fatigue testing of blade materials at high temperatures with periodic spray moistening by liquid corrosive medium
12 p1829 A72-27459
- Electronic system for continuous automatic recording of internal friction and modulus of elasticity at high temperatures
12 p1807 A72-27462
- Long term high temperature test machine to record structural changes of materials
12 p1795 A72-27464
- Cyclic stress ratio effects on stainless steel fatigue crack propagation at 1000 F, using linear elastic fracture mechanics
12 p1829 A72-27663
- Stress rupture strength, short term strength, creep and heat resistance measurement arrangement for coated refractory materials at 1500-1700 C in air with radiative heating
12 p1796 A72-28248
- Electronic heating test arrangement for high temperature testing of metals and electrically conducting ceramics in vacuum, describing temperature control systems
12 p1796 A72-28249
- High temperature microporosity in W wire at 3000-3550 C, using electron microscopy and fractography
13 p1973 A72-28651
- Time-temperature-precipitation (TTP) diagrams and phase instabilities of high temperature exposed Mo containing austenitic stainless steels
13 p1974 A72-28658
- High temperature constant load creep tests on pure powder metallurgy W and tungsten-thoria alloy, discussing stress dependence
13 p1975 A72-28665
- High temperature steady state tensile creep behavior of Ni-W solid solutions, showing creep rate relation to stress and stacking fault energy
13 p1975 A72-28668
- High temperature contact creep tests in vacuum and in metal melts, noting adsorption effect on surfaces plastic deformation
13 p1963 A72-28768
- Polycrystalline microstructure changes of corundum during high temperature creep tests, using optical microscopy
13 p1983 A72-28775
- Thermostat for electrical measurements of high resistance materials in air up to 1200 C
13 p1957 A72-29274
- Reversed creep deformation behavior of metals, observing acceleration at high temperatures due to grain boundary sliding enhancement
13 p1978 A72-29444
- High temperature strength of low ductile refractory metals, describing test equipment
13 p1978 A72-29446
- Temperature and strain rate dependence of austenitic stainless steel fracture by low cycle fatigue at high temperatures, studying striations with scanning electron microscopes
13 p1979 A72-29449
- Unsteady loading effects in high temperature fatigue tests of refractory alloys for turbine blades, noting steady and programmed notch tests
13 p1980 A72-29494
- Thermal diffusivity measurements by laser flash technique for liquid metals at high temperatures
13 p1971 A72-29756
- Pyrometric obturation devices effect on sample temperature level during high temperature tests with radiant heating
13 p1960 A72-29903
- Activation energy of high temperature creep in Cr alloy with aluminum oxide, comparing with moving monovacancies in pure Cr
14 p2112 A72-30161

Tungsten and carbon combined solubility in solid niobium at 2000, 1700 and 1100 C

14 p2113 A72-30165

Refractory material blade alloys fatigue life up to 950 C under nonstationary loading, noting log-normal law distribution

14 p2116 A72-30428

Zirconium carbide creep characteristics and limit at 2450-2810 K, examining test conditions effects on parameters

14 p2116 A72-30435

Resonance type facility using dynamic hysteresis loop method to test metal fatigue and anelasticity in torsion at room and high temperatures

14 p2092 A72-30443

Superalloys properties and utilization at high temperatures, discussing chemical resistance, diffusion treatment, B and Zr action and grain size

14 p2116 A72-30527

Tensile properties from high temperature and room temperature tests of Ti alloys containing Ga correlated with creep resistance at 1000 F, noting activation energy

14 p2120 A72-30614

Creep velocity and rupture strength calculated for tensile stress, noting high temperature tests of austenitic steel

14 p2121 A72-30697

Double base solid propellants life determination from accelerated aging tests at elevated temperatures, discussing surface properties effect on weight loss and autocatalytic decomposition

14 p2144 A72-30757

High temperature oxidation resistance and mechanical properties of Fe-Al-Cr alloys with Ti and Mo additions

15 p2253 A72-31520

High temperature steady creep of Nb and niobium-aluminum oxide alloys at 850-1400 C

15 p2254 A72-31561

Steam-hydrogen treatment tests for high temperature stability of noble metal catalysts in hydrogen-oxygen reaction initiation

15 p2192 A72-32225

High temperature forging apparatus for refractory metals under vacuum or inert atmosphere

15 p2241 A72-32443

Thermal simulation tests for kinetic heating of aerospace structures and materials, describing facilities for supersonic flight and atmospheric reentry

16 p2475 A72-32897

Crack depth measuring instrument for fatigue crack propagation study in notch tests, noting application at high temperatures

16 p2391 A72-33234

High temperature strength and ductility study of hot working behavior of steels, using hot impact tension tests

16 p2406 A72-33316

Ternary Ni-Cr-Al superalloys oxidation at 800-1300 C as function of composition, temperature, oxygen pressure and reaction time

16 p2410 A72-33811

Incoloy low cycle fatigue tests at high temperatures and different strain rates, discussing fatigue life at 10 and 60 min hold times

16 p2410 A72-33820

Aluminum oxide high temperature equilibrium morphology in Ni matrix prepared via vapor deposition and internal oxidation methods

16 p2411 A72-33824

Cubic stabilized zirconia utilization as solid electrolyte in high temperature fuel cell system for efficient and economical energy conversion

16 p2352 A72-33894

Compatibility of buffered uranium carbides with tungsten.

17 p2579 A72-34620

High temperature solid-solubility limit and phase studies in the system tantalum-oxygen.

17 p2567 A72-34731

Physical property measurements at high temperatures.

17 p2554 A72-34934

Derivative graph method of thermal analysis for lubricating oils

17 p2571 A72-35180

Austenitic steel stress corrosion prevention at high temperatures and pressures, investigating inhibitor adsorption properties from capacitance measurements and polarization curves

17 p2568 A72-35474

Dislocation mechanisms in creep.

17 p2635 A72-35921

Creep of different molybdenum alloys at high temperature and under strong stresses

18 p2698 A72-36144

Pure and thoriated W compatibility with uranium carbide alloys at 1800 C, noting thermal gradient and thorium noneffects

18 p2699 A72-36163

FET noise at high temperatures.

18 p2666 A72-36324

Kinetics and annealing and mechanical properties of W chemical vapor deposition, discussing high temperature tests

18 p2656 A72-36398

Analysis of primary creep of molybdenum at high temperatures.

18 p2700 A72-36580

Directional dependence of the high-temperature thermal diffusivity of crystal-oriented pyrolytic graphite

18 p2704 A72-37180

Carbon and graphite sublimation in inert gas flow at 2800-3000 K, determining rate dependence on temperature under kinetic and diffusive conditions

18 p2704 A72-37186

New method for determining the integral radiative capacity of partially transparent materials at high temperatures

18 p2704 A72-37190

Enthalpy and heat capacity of boron carbide at temperatures ranging from 273 to 2600 K

18 p2704 A72-37191

German monograph - The effect of alloying elements on the dry high temperature oxidation of cobalt in the temperature range from 800 C to 1000 C in air and pure oxygen

19 p2816 A72-37656

German monograph - Studies of high-temperature corrosion of cobalt and cobalt alloys with radioactive isotopes

19 p2816 A72-37657

Stress criterion for creep rupture in tubes under combined axial load and internal pressure, deriving stress concentration from high temperature tests

19 p2874 A72-37715

Determination of the emission potential of cesium-coated surfaces at high temperatures with a plane-parallel cesium diode. I - Technology. II - Physical foundations and measurement results

19 p2754 A72-37779

Emissivity and electrical resistivity of tungsten-yttrium oxide cermets as function of composition at 1200-3200 K

19 p2819 A72-38286

Influence of impurities on the high-temperature electrical conductivity of CdTe crystals

19 p2847 A72-38677

Microscopic substructure in face centered cubic metals fatigued at elevated temperatures.

20 p2935 A72-38880

Creep-fatigue interaction interpretation for austenitic stainless steels from crack growth viewpoint, investigating time and cycle dependent failure at elevated temperature

20 p2937 A72-39213

Effect of twins produced by annealing on high-temperature failure of chromium-nickel-molybdenum steel

20 p2939 A72-39316

Measurement of melting point and electrical resistivity /above 3600 K/ of tungsten by a pulse heating method.

20 p2941 A72-39722

Autoclaves for the study of the effects of deformation on the high temperature aqueous corrosion of metals.

21 p3039 A72-40216

Application of holography in high-temperature displacement measurements.

21 p3052 A72-40235

Corundum polycrystalline microstructure changes during high temperature creep tests, using optical microscopy

21 p3072 A72-40269

Influence of the structure on the emissivity of aluminum-chromium-phosphate coatings at high temperatures

21 p3072 A72-40383

An experimental investigation of yield surfaces at elevated temperatures.

21 p3117 A72-40678

Fatigue damage of aluminum alloy at high temperature.

21 p3066 A72-40716

Extension Seminar on High Temperature Strength of Metals, Kyoto, Japan, August 21, 1971, Preprints.

21 p3068 A72-41007

A study on the correlation between thermal fatigue and low-cycle fatigue at elevated temperatures.

21 p3119 A72-41008

Isothermal deformation behavior of structural metals in laboratory creep, relaxation and low cycle fatigue tests at high temperatures

21 p3119 A72-41009

Temperature and strain rate dependences of low cycle fatigue life at high temperatures of austenitic stainless steel, examining crack behavior and stress-strain relations

21 p3069 A72-41010

On the growth kinetics of Laves phase precipitates in Fe-Ti alloys at elevated temperatures.

21 p3069 A72-41011

The properties and structures of a heat resistant 1Cr-Mo-V steel and alloy A-286 after long time exposures at elev. temps.

21 p3069 A72-41012

Stainless steels high temperature creep rupture strength relationship to carbide precipitation morphology

21 p3069 A72-41013

Nb heat pipe design with Na coolant for high temperature operation, discussing slopes effect on transmitted power

21 p3129 A72-41051

Strain curves of VT-6C and VT-14 titanium alloys in the temperature range between 20 and 400 C

21 p3070 A72-41362

Investigation of the strength and deformability of thin composite materials of magnetic recorder type. I. Strength and deformability at elevated temperatures

21 p3073 A72-41707

Rheological properties of molybdenum and platinum of bamboo structure under bending loads

21 p3071 A72-41712

Influence of the test temperature on the fracture energy of graphite

21 p3074 A72-41714

Facility for studying the failure of structural elements in a supersonic high-temperature flow containing a controlled number of abrasive particles

21 p3043 A72-41717

Antiscratch properties of nitrided layers of creep-resisting steels at high temperatures

22 p3187 A72-41868

Enthalpy and specific heat of tantalum carbide over the temperature range from 273 to 3600 K

22 p3187 A72-41890

Polyacrylonitrile based carbon fiber strengthening by fast neutron irradiation at high temperatures

22 p3196 A72-41965

Self-propagating high-temperature synthesis of refractory inorganic compounds

22 p3188 A72-42165

Alloys of thorium with certain transition metals. VI - The constitution of thorium-nickel alloys containing 50-96% nickel.

22 p3190 A72-42769

Oxidation rate anisotropy investigation on coupon specimen of Ta-Mo alloy at 950 C

22 p3190 A72-42770

Thermal control techniques used in space simulation laboratory testing.

22 p3164 A72-42997

High-temperature thermodynamic properties of the chromium carbides determined using the torsion-effusion technique.

22 p3193 A72-43029

Determination of the mechanical properties of steels by short-time rupture in hydrogen at high temperatures and pressures

22 p3195 A72-43160

Mechanical tests of laminated plastics in solar installations

22 p3197 A72-43192

Formation of defects in reflecting coatings under the action of high temperatures

22 p3197 A72-43193

Investigation of the influence of the gas medium on the phase composition and certain properties of refractory materials containing zirconium

23 p3306 A72-43690

Some preliminary observations on the extension of cracks under static loadings at elevated temperatures.

23 p3301 A72-43712

Elastic stiffness of AT-2 and AT-3 titanium alloys and their welds at high and low temperatures

23 p3302 A72-43966

Fatigue fracture and crack propagation in aluminum alloys. II.

23 p3302 A72-43973

High temperature interaction between W and ZrC constructing isothermal structure

23 p3303 A72-44151

High-temperature creep of polycrystalline chromium.

23 p3304 A72-44449

Materials creep behavior and elevated temperature design.

24 p3453 A72-44553

Estimates of creep-fatigue interaction in irradiated and unirradiated austenitic stainless steels.

24 p3412 A72-44554

Fatigue-crack growth in 20% cold-worked Type 316 stainless steel at elevated temperatures.

24 p3435 A72-44555

Stress-strain diagrams from high and low temperature tests of Y alloy rods, noting temperature effects on plastic deformation

24 p3413 A72-44724

Estimation of creep and fatigue behaviour under cyclic loading.

24 p3456 A72-44793

High temperature creep activation energies relationship to diffusion in TiC, ZrC and UC

24 p3413 A72-44936

- Oxidation of W/110. I - LEED study of the oxide formation at 1000 K. 24 p3378 A72-44952
- Al and Al-Zr coating effects on heat resistant alloy turbine blades high temperature fatigue resistance under bending-torsion cyclic loads 24 p3415 A72-45732
- Ductility and fracture of heat resistant steels at high temperatures and unsteady loading, estimating loading cycle effect on plastic strain buildup to failure 24 p3416 A72-45753
- High temperature tensile tests of Mo with helical and circular V grooves, discussing stress concentration sensitivity relations for grooved and smooth samples 24 p3417 A72-45766
- HIGH VACUUM**
- High vacuum and rarefied atmosphere creep apparatus. 17 p2536 A72-35846
- Book - Results of high-vacuum technology and the physics of thin films. Volume 2 18 p2712 A72-36826
- High vacuum technology applications in surface physics research, discussing atomic collisions and adsorption processes 18 p2712 A72-36827
- High and ultrahigh vacuum equipment and components selection, discussing gas-surface interactions, contamination and cleaning problems 19 p2835 A72-38391
- HIGH VOLTAGES**
- Multiphase, 2 kw, high voltage, regulated, conditioned power supply for space application, discussing efficiency, weight, design and performance 01 p0008 A72-11063
- High tension exciter output voltage measurement based on cathode ray oscilloscope and high voltage probe, stressing calibration procedure [SAE AIR 1092] 11 p1604 A72-26028
- High voltage electron microscope applications to materials reactions in gaseous environments, exemplifying by stress corrosion morphology in stainless steel, Al-Zn-Mg and Ti-Al 11 p1668 A72-26945
- High voltage solar array technology, studying power conditioning control system design and array-space plasma interactions [AIAA PAPER 72-443] 13 p1899 A72-28942
- Solar cells insulating dielectrics breakdown tests in dilute Ar plasma at positive bias voltages to 20 kV 14 p2140 A72-30926
- Electrical breakdown of hexane investigated by high voltage nanosecond pulses, noting electron avalanche and streamer processes in time lag 15 p2278 A72-32244
- High voltage dc arc interrupter for use in high power pulse generators and switching application in high voltage dc power transmission system 15 p2201 A72-32569
- High voltage single nanosecond pulse generator for variable load using commutator with shaping line charging circuit 16 p2368 A72-33077
- High voltage nanosecond pulse generator triggered by laser radiation from transmission stripline discharger for multichannel synchronous operation 16 p2400 A72-33083
- Electron microscopy at 3 million volts 17 p2535 A72-34199
- Losses in high-voltage transformers encapsulated by epoxy resins. 18 p2669 A72-37113
- A sealed, sectionalized million-V X-ray tube. 19 p2776 A72-38767
- HIGHLY ECCENTRIC ORBIT SATELLITES**
- U HEOS SATELLITES
- HIJACKING**
- U AIR PIRACY
- HILBERT SPACE**
- NT BANACH SPACE
- Step width for gradient projection method in Hilbert space for optimal linear control problems with quadratic functional 01 p0047 A72-11386
- Plane theory of elasticity for infinite triangular wedge with notched apex, reducing problem to non-homogeneous Hilbert problem 05 p0737 A72-16301
- Equilibrium conditions of closed elastic spherical shell under uniform nearly critical compression loads, determining shell deformation in Hilbert spaces 05 p0739 A72-16587
- Elastic equilibrium of infinite wedge with apical asymmetric notch, reducing to Hilbert problem for holomorphic vectors 07 p1093 A72-19976
- Multiple completeness characteristics of eigenvectors and adjoint vectors of polynomial operator packets in separable Hilbert space 08 p1198 A72-21096
- Hilbert space filling curves for solutions of sets of nonlinear equations 09 p1340 A72-22244
- Solutions for multivalued evolution equations, considering monotonic maximal operator on finite dimensional Hilbert space 10 p1504 A72-24061
- Spectral continuity conditions of linear operator, noting application to elliptical operators approximation in separable Hilbert spaces 10 p1505 A72-24070
- Collision operator behavior in linear Boltzmann equation model of molecular gas in Hilbert space 10 p1510 A72-24102
- Finite difference approximation of eigenvalues of singular differential operators in Hilbert space 11 p1678 A72-26556
- Uniform Markov processes properties in Hilbert space, examining operator subgroups 12 p1836 A72-27071
- Eigenvalues examination for self adjoint singular differential operators in Hilbert space by finite difference methods 14 p2126 A72-30619
- Structure, analysis and synthesis of time series models, discussing kernel Hilbert space, spectral estimation, moving averages, identification, etc 18 p2678 A72-36023
- Compact self adjoint differential operators in family of Hilbert interpolation spaces, applying perturbation theorem to boundary value problems 18 p2704 A72-36511
- Equilibrium conditions of closed elastic spherical shell under uniform nearly critical compression loads, determining shell deformation in Hilbert spaces 19 p2872 A72-37558
- Formula for the product of semigroups which is determined by the method of bilinear forms, and the application of the formula to the Schroedinger equation 19 p2825 A72-37735
- Stability of solutions to the Hill equation with an operator coefficient having a negative mean value 21 p3074 A72-40256
- Direct methods of qualitative spectral analysis for the singular Sturm-Liouville equation with an unrestricted operator potential 23 p3308 A72-43578
- Cauchy problem for abstract Love equations 23 p3309 A72-44042
- HILBERT TRANSFORMATION**
- Binary single sideband phase modulation with simultaneous AM by signal and Hilbert transformation 06 p0776 A72-18395
- Strong shock wave diffraction from wedge reduced to Hilbert problem, noting nonregular refraction theory nonexistence 08 p1151 A72-21662
- HILL CURVES**
- U HILL METHOD
- HILL DETERMINANT**
- Special boundary value problems solution method for Mathieu differential equation, transforming Mathieu equation to Hill differential equation via Fourier series expansion 15 p2264 A72-32468
- HILL LUNAR THEORY**
- Book on perturbation theory in celestial mechanics, covering absolute perturbation, Hill lunar theory and application to Jupiter satellites 09 p1389 A72-23247
- On the tidal effects in the motion of artificial satellites. 24 p3441 A72-45233
- HILL METHOD**
- Hill variable modification of Brouwer satellite theory algorithm for simplified orbital element and perturbation calculations and orbital eccentricity generalization 08 p1237 A72-21749
- A steady vortex ring close to Hill's spherical vortex. 22 p3166 A72-42312
- HILLER MILITARY AIRCRAFT**
- U MILITARY AIRCRAFT
- HIMALAYAS**
- Satellite photographs of Himalayan-Indian Ocean tectonic patterns, showing major left and right lateral shear belts as evidence of wrench movements 05 p0655 A72-16040
- HINDRANCE**
- U CONSTRAINTS
- HINGE MOMENTS**
- U TORQUE
- HINGED ROTOR BLADES**
- U HINGES
- U ROTARY WINGS
- HINGELESS ROTORS**
- U RIGID ROTORS
- HINGES**
- NT FLAPPING HINGES
- Motion of two symmetrical rigid bodies connected by frictionless spherical hinge positioned at dynamic symmetry axes intersection 08 p1206 A72-21168
- Control surface dynamic hinge moment coefficients estimation based on system state measurements from flight tests, using least squares criterion [AIAA PAPER 72-379] 11 p1730 A72-25403
- HIPPOCAMPUS**
- Hippocampus electric activity and cardiac rhythms variations responses to various intensity electric stimulation of central gray matter 02 p0165 A72-12881
- Hippocampus neuron reactions and memory function realization with incoming information and stored imprints comparison by brain 08 p1122 A72-22191
- Neuronal spike activity changes in rabbit visual and sensorimotor neocortex and hippocampus during EEG activation 13 p1902 A72-28643
- Electric stimulation of rabbit brain limbic formations /claustrum, amygdala, hippocampus/, showing effect on emotional response motor and vegetative components 14 p2076 A72-30668
- Hippocampus morphology and physiology in relationship to emotion and memory mechanisms, time links, visceral activity and motivations and endocrine control 16 p2353 A72-33099
- Changes in the overall electrical activity of the mesencephalic reticular formation, the hippocampus, and the cerebral cortex under the influence of hydrocortisone and DOCA 20 p2890 A72-38929
- HISS**
- Ionospheric propagation, reflection and absorption of vlf hiss in aurora from rocket observation during quiet and substorm conditions 02 p0221 A72-12458
- Electron lifetime in earth radiation belt due to resonant scattering with hiss vlf radiation 05 p0711 A72-17045
- Auroral zone vlf hiss and associated low energy electron precipitation in polar magnetosphere [AD-736327] 06 p0804 A72-17456
- Vlf auroral hiss comparison with low energy electron precipitation, using Ogo 4 data 07 p1058 A72-19149
- Visual aurora and Explorer 40 satellite simultaneous observations of VLF radio noise, noting hiss associated with light emissions and associated charged particle flux [AD-740047] 09 p1299 A72-23006
- Vlf hiss with lower hybrid resonance cut-off recorded by Alouette 1, emphasizing midlatitude events and electromagnetic energy transportation by multion duct in topside ionosphere 09 p1279 A72-23007
- OGO 4 satellite observed band limited ELF hiss characteristics explanation by model based on generation at large wave normal angle in equatorial region 09 p1279 A72-23008
- Ogo-5 observation of lower hybrid resonance noise, bursts, VLF hiss and whistlers near plasmopause during large magnetic storm 11 p1624 A72-26399
- VLF hiss intensity, polarization, incidence angle and arriving direction observation at Antarctica station during magnetic disturbances 18 p2660 A72-36431
- VLF-ELF hiss polarization and right/left component ratios recording at antarctic station, using sweep polarimeter 18 p2660 A72-36432
- An evaluation of the intensity of Cerenkov radiation from auroral electrons with energies down to 100 ev. 19 p2792 A72-38741
- A satellite survey of vector electric fields in the ionosphere at frequencies of 10 to 500 hertz. II - The electric component of ELF hiss. 19 p2768 A72-38743
- Magnetospheric propagation of auroral hiss with whistler mode dispersive properties, suggesting burst source locations and mechanisms 21 p3048 A72-40399
- HISTOGRAMS**
- Neuronal systems short-latency paired interactions detection method, obtaining histogram for action potentials 07 p0934 A72-20624
- HISTOLOGY**
- Electron microscope examination of freeze-etched air-filled lung alveoli extracellular lining layer, discussing sample preparation techniques 05 p0623 A72-16787
- Clinical death period and reanimation concepts, noting erroneous interpretations of irreversible histological alterations, revival attempt period and organism self reanimation potential 09 p1266 A72-22876
- Enzyme activity and ascorbic acid concentration as index of rat thyroid gland tissue functional activity during hyperthermia 14 p2077 A72-31098
- Succinic dehydrogenase activity in rabbit eye ciliary epithelium during electric stimulation of hypothalamus, using histochemical techniques 14 p2078 A72-31099
- The carotid body in animals at high altitude. 22 p3143 A72-42589

Histologic analysis of hypoxia exposure effects on mouse skin homograft reaction due to lymphatic organ function changes

22 p3144 A72-42675

Influence of X-ray irradiation in 25- and 250-r doses on the transplant immunity in mice differing by weak and strong histoincompatibility systems

23 p3255 A72-43910

Collagen in human myocardium as a function of age.

23 p3256 A72-43935

Localization and dynamic changes of glycogen in frog retina adapted to darkness or light. I, II.

23 p3258 A72-44377

HISTORIES

NT CASE HISTORIES

HMX

Thermal decomposition kinetics of tetramethylene tetranitramine beta HMX from differential thermal analysis and activation energy calculation

08 p1219 A72-20755

HODOGRAPHS

Steady state geostrophic wind vector variation hodographs in planetary baroclinic boundary layer, considering thermal influence linear superposition on internal friction effects

06 p0841 A72-17667

Kharlamov kinematic equations application to gyrost motion problem, deriving angular velocity hodograph

08 p1207 A72-21350

Solid body motion about fixed point, determining moving and fixed angular velocity hodographs

08 p1208 A72-21351

Hodograph geometrical analysis of heavy gyrost motion for center of mass and gyrostatic moment located on first and third principal axes of rotation

08 p1208 A72-21352

Moving hodograph of angular velocity vector in solution to problem of body motion about fixed point

08 p1208 A72-21354

Asymptotically uniform motions of heavy solid body with fixed point, assuming moving hodograph intersections with Staude cone

08 p1208 A72-21358

Solid body motion with fixed point in central Newtonian force field, classifying angular velocity vector hodograph as function of dimensionless parameters

08 p1208 A72-21363

Axisymmetric plane transonic flow past convex corner point, obtaining characteristics by mapping into hodograph plane

10 p1468 A72-24435

Hodograph method involving conformal mapping for turbomachine blade subsonic flow profile calculation

11 p1570 A72-25635

Hodographic equations solution containing critical point for compressible fluid two dimensional flow, noting calculation of wing profiles and turbine engine cascades

[ONERA, TP NO. 1048]

14 p2095 A72-30841

Three dimensional flow of steady neutral horizontally inhomogeneous planetary boundary layer, studying hodograph, velocity, vorticity, energetics and eddy coefficients

15 p2266 A72-32723

The hodograph transformation in plastic waves with discontinuous loading conditions.

[ASME PAPER 71-APMW-12]

17 p2624 A72-34308

Calculation of a profile or of a cascade of profiles for a velocity distribution given as a function of potential

22 p3136 A72-43096

HODOSCOPES

German monograph on experimental search for quarks in cosmic ultraradiation, describing hodoscope for particle ionization measurement

[PITHA-52]

09 p1378 A72-23100

HOHMANN TRAJECTORIES

U ELLIPTICAL ORBITS

U TRANSFER ORBITS

HOHMANN TRANSFER ORBITS

U ELLIPTICAL ORBITS

U TRANSFER ORBITS

HOLE DISTRIBUTION [ELECTRONICS]

Impurity concentration relationship to electrons and holes density and potential fluctuations in completely compensated crystalline semiconductors with randomly distributed donors and acceptors

13 p2024 A72-29993

High microwave voltage effects on p-n junction conductance under inverse dc bias, noting role of hole generation and accumulation by impact ionization

15 p2206 A72-31643

HOLE DISTRIBUTION [MECHANICS]

Holes dispersion hardening in sintered metal powder, discussing dispersed particle effects

02 p0233 A72-11446

Stress concentration at eccentric holes and effect on strength of full size rotating turbine disks

03 p0450 A72-14108

Inverse periodic plane deformation of isotropic elastoplastic surface with infinite series of curvilinear holes

05 p0741 A72-17146

Metal strip with circular hole under tension, calculating plastic strain and stress concentration coefficients

06 p0899 A72-18567

End holes effects on dielectric constant measurement of long glass tubes by cylindrical microwave resonant cavity

08 p1164 A72-20940

Stress distribution in circular cylindrical shell weakened by two identical holes on common generatrix

12 p1886 A72-27984

The bursting speed of a symmetrical conical disk with radial holes.

22 p3238 A72-42835

HOLE MOBILITY

Room temperature time of flight electron and hole mobility and trapping time measurements in zinc selenides as function of electric field

12 p1855 A72-27835

HOLES

Drill hole heat transfer upon hot liquid injection into productive layer, enhancing oil extraction process effectiveness

04 p0594 A72-14515

Determination of the time of hole formation in a metallic film under the action of single-pulse laser radiation

19 p2812 A72-38540

Stress concentration around holes in plates and shells.

22 p3238 A72-42834

HOLES [ELECTRON DEFICIENCIES]

Bulk recombination effects on nonstationary pinching and collapse of electron-hole plasma by magnetic field in crystal

03 p0401 A72-13581

Vacuum UV irradiation of silicon dioxide, discussing positive charging for photon energies above threshold for electron-hole pair creation

03 p0403 A72-14080

Electron tunneling probabilities through slowly varying potential energy barrier with potential holes evaluated by T scattering matrix interaction formalism

04 p0563 A72-15471

Parallel and perpendicular magnetic field effects on optically injected electron-hole plasma diffusion in Ge from density measurement by infrared beam absorption technique

05 p0702 A72-17167

Strong electric field recombinational domains in semiconductors with mobile holes and electrons during band-band illumination or double injection

07 p1048 A72-19638

Numerical solution of theta pinch in electron-hole plasma of Ge semiconductor under surface recombination as contactless method of current carrier injection

08 p1218 A72-22178

Effective current carrier electron and hole lifetime in amorphous photodiode semiconductor Se and As-Se films with randomly distributed capture levels

09 p1366 A72-22418

Model of dynodes system with random electron-hole pairs number, calculating equations for mean fluxes transport and correlated noise fluctuations

09 p1280 A72-23116

Vehicle components oxidation in thermal control coatings, investigating resistance to oxidation by UV photoproducted ZnO electronic holes

11 p1699 A72-25207

Carbon dioxide laser cross relaxation effects on hole burning process in Doppler broadened gain or absorption line

11 p1647 A72-26146

Be doped p-type Si piezoresistance and hole transport properties dependence on temperature, crystal orientation and doping concentration

16 p2442 A72-33834

Stimulated effects in the radiative recombination from electron-hole liquid in semiconductors.

19 p2844 A72-37932

Effect of the filling of the capture levels with increasing current on the formation of negative resistance under double injection conditions

19 p2846 A72-38574

Average energy to form electron-hole pairs in GaP diodes with alpha particles.

20 p2908 A72-39564

Pinch effect in a germanium electron-hole plasma

21 p3096 A72-40414

Free electrons and holes concentration calculated for quadratic dispersion law in doped semiconductors without degeneration, noting additive atoms effect

23 p3324 A72-43849

Strong electric field recombinational domains in semiconductors with mobile holes and electrons during band-band illumination or double injection

24 p3431 A72-44570

Determination of electron and hole capture rates in nickel-doped germanium using photomagnetolectric and photoconductive methods.

24 p3432 A72-45388

Investigation of radiation paramagnetic defects in alkaline-silicate glass subjected to the action of high quasi-hydrostatic pressures - Structure of hole defects

24 p3417 A72-45421

HOLLOW CATHODES

Hollow cathode neutralizer for electron bombardment ion thruster, discussing performance from SERT II flight

[AIAA PAPER 72-207]

05 p0706 A72-16853

Neutral B I vacuum UV spectra from hollow cathode light source, remeasuring electron transitions to higher accuracy

06 p0852 A72-17896

Hollow cylindrical cathode discharge sustaining potential reduction and recombination probability increase from transverse magnetic field and rising pressure and plasma density

09 p1361 A72-22957

Langmuir probe techniques for plasma measurement in ion thruster hollow cathode discharge configurations

[AIAA PAPER 72-416]

11 p1706 A72-26166

Magnetic field and polar region geometry effects on hollow cathode thruster performance of Kaufman electric engine

[AIAA PAPER 72-417]

11 p1706 A72-26167

Current flow across double layer plasma in SERT 2 type hollow cathode ion thruster, using Langmuir probes

[AIAA PAPER 72-418]

11 p1706 A72-26168

Hollow cathode discharge effects on throttled electron bombardment ion thruster performance, considering discharge region diameter and length and baffle aperture area

[AIAA PAPER 72-421]

11 p1706 A72-26169

Electron bombardment ion thruster performance characteristics with variable magnetic baffle and hollow cathode

[AIAA PAPER 72-489]

11 p1710 A72-26214

Model for mercury vapor electron bombardment ion thruster hollow cathodes operation and effects on thrust subsystem performance predictability

[AIAA PAPER 72-420]

13 p2026 A72-28936

Hg flow and hollow cathode temperature effects on ion thruster neutralizer stability and lifetime capability, using bell jar tests

[AIAA PAPER 72-422]

13 p2026 A72-28937

Hg fed hollow cathode ion thruster thermal and plasma heating characteristics, using Wiener-Kalman filtered temperature measurements

[AIAA PAPER 72-476]

13 p2027 A72-28947

Hollow cathode plasma discharge model, calculating variation of pressure upstream from active zone in terms of discharge current

15 p2286 A72-32275

Transverse magnetic field effects on cylindrical hollow cathode discharge voltage-current characteristics, noting sustaining potential and recombination probability changes

17 p2593 A72-35886

Measurement of the electronic density in a hollow cathode discharge working with argon

22 p3181 A72-43098

Excitation mechanisms in the argon-ion spectrum at near laser conditions and temperatures and densities in a hollow cathode argon-arc discharge.

24 p3428 A72-44807

HOLMIUM

Ho doped YLF and YAG laser threshold and slope characteristics at room temperature, considering Q-switched operation lifetime

07 p1004 A72-19233

Cooperative and sequential sensitization effect on He emissive states population in polycrystalline barium and yttrium fluorides with trivalent Yb

10 p1525 A72-24044

Phase diagram of the chromium-holmium system

19 p2821 A72-38474

HOLOGRAPHY

Absorption and exposure characteristics of silver halide photochromic glasses for hologram recording

01 p0068 A72-10622

Diffraction theory of microwave holography, presenting computer aided imaging approach for alleviating optically reconstructed image distortion

01 p0068 A72-10707

NDT holographic interference pattern technique to determine Advanced Test Reactor fuel element swage joint tightness

01 p0078 A72-11110

Microwave holographic interferometry with optical wave front reconstruction for visual mapping of large objects deformation

01 p0072 A72-11236

Optics for data processing, discussing magneto-optic and holographic memories in computer systems

01 p0035 A72-11315

Crimped films for object reconstruction and image storage, comparing performance to holographic films

01 p0073 A72-11318

Digital holographic memory with acousto-optical deflection random access and automatic inscription

01 p0073 A72-11319

Electronic deflection printer with holographic memory, using photosensitive device for textual recording

01 p0073 A72-11320

Air holography interferometry for acrylic model materials inspection and selection for optical flatness, comparing with photoelasticity
[SESA PAPER 1941]

02 p0224 A72-11516

Fraunhofer hologram for recording square of modulus of far field radiation pattern due to mixture of known and unknown source distributions

02 p0224 A72-11548

Hypersonic projectiles wake visualization with holography, using single mode ruby laser and reflected diffuse light techniques

02 p0224 A72-11742

Focused image holographic interferometer for reduced blur in deep object image reconstruction with white light source

02 p0224 A72-11747

Double reference beam holograms, evaluating interference effects of misalignment on image reconstruction

02 p0225 A72-11749

Pohlman cell for ultrasonic hologram production, describing construction, resolution and real time reconstruction

02 p0225 A72-11751

Microwave hologram CW radar system, discussing theory and flight test imagery, optical processors and alignment procedures

02 p0171 A72-11819

Diffusely illuminated objects holographic reconstruction with suppressed granularity by incoherent superposition of reconstruction waves longitudinal modes, describing experimental setup

02 p0229 A72-12116

Classical optical measurement and holographic methods of flow field visualization, discussing operating principles, measurement sensitivity, three dimensional and depth-focusing properties

02 p0230 A72-12300

Impending metal fatigue failure holographic detection by optical correlation of coherent light reflection from deformed surface structure as function of time

02 p0294 A72-12442

Projected interference fringes in holographic interferometry for large surface movements measurements

02 p0231 A72-12544

Wave front sampling points in spatial filtering of nonequidistant discrete holograms of flat objects

02 p0232 A72-12751

Holographic investigation of acoustical fields, describing shadowgraph recording apparatus for sound pressure amplitude distribution

03 p0352 A72-12918

Holographically produced zone plates for solar X ray imaging, using Ar laser produced interference figure

03 p0354 A72-13046

Focused image holography in multimode He-Ne laser radiation, using diffusely scattered reference wave and lens for high quality reconstruction

03 p0357 A72-13370

Nonperiodically moving object holographic interferometry by time-averaging method, considering single exposure technique advantage over multiple exposure in thermal deformation observation

03 p0357 A72-13373

Computer based analysis of holography using ray tracing and wave front matching aberrations

03 p0358 A72-13433

Domain configuration observation of magnetic holograms in oriented MnBi films

03 p0359 A72-13447

Three dimensional hologram synthesis from two dimensional pictures with parallax preservation
[AD-736057]

03 p0359 A72-13448

Surface phase holograms recorded on materials with depth removal effect on exposure, noting emulsion thickness effect on image quality

03 p0359 A72-13449

Holographic analysis of periodic microobjects at X ray wavelengths, obtaining high contrast

03 p0360 A72-13669

Magneto-optic storage density and read-write rate, discussing transducer cost, solid state injection lasers, holographic techniques and high activity data base applications
[IEEE PAPER 19,1]

03 p0361 A72-13774

Holographic optical techniques application to bulk magnetic storage for high information density and memory capacity and fast random access
[IEEE PAPER 19,4]

03 p0361 A72-13776

Thin amplitude dynamic holograms diffraction efficiency, showing dependence on interference pattern, modulation depth, radiation intensity and material properties

04 p0521 A72-14659

Ultrarapid holographic camera for plasma diagnostics, noting exposure time and reconstructed image resolution

04 p0521 A72-14972

Ultrahigh speed holographic camera for three-dimensional photographs and interferograms, using ruby laser output

04 p0522 A72-15139

Holographic measurement of red blood cell rotation in orifice flow, transforming orientation into form distribution data

04 p0479 A72-15140

Photomaterial nonlinear effects on contour distortion in holographic recording of Fourier image slit for graphic memory use

04 p0522 A72-15150

Book on holographic technology covering fundamentals of holography and classical optics, diffraction theory, Huygens principle, lasers, illumination sources, holographic interferometry, etc

04 p0522 A72-15271

Holographic interferometer for heat transfer measurement, studying free convection thermal boundary layer on heated isothermal vertical flat plate

04 p0524 A72-15531

Book on holography applications covering wave front reconstruction, wave sources, propagation, interference and coherence, single and split beam, color and polarization holography, etc

04 p0525 A72-15682

Optical image recording, transformation, readout, transmission and data processing techniques and instruments, discussing transfer function, cut-off frequency and information quantity concepts and holography

04 p0525 A72-15700

Holographic multicolor moving map display using photoresist recording and He-Cd laser

05 p0660 A72-15787

Holographic measurements of dioptric powers and glass defects in thin transparent sheet under vertical or oblique parallel and divergent light

05 p0662 A72-16190

Amplitude holograms diffraction effectiveness increase by conversion to phase holograms through photoemulsion bleaching, evaluating various bleaching agents effectiveness

05 p0663 A72-16614

Pinhole, fly-eye and holographic stereogram methods, examining resolution relationships, horizontal and vertical parallax and aberrations

05 p0663 A72-16673

Holographic measurement for optical transfer function of lenses, considering negative black and white photographic indicator emulsion effect

05 p0663 A72-16728

Ultrasonic acoustic holography for real time non-destructive testing of cracks, voids, nonbonds and other defects in metals, ceramics and plastics
[SAE PAPER 720173]

06 p0811 A72-17319

Pulsed ruby laser and photopolymer materials applications to holography, considering research programs for surmounting difficulties

06 p0813 A72-17427

Microwave holography using transmitting and receiving antenna for generation of synthetic aperture in angular direction

06 p0814 A72-17486

Holographic Ice Survey System for down looking radar probing and measurement of sea ice and glaciers, discussing ice electrical properties and system design

06 p0814 A72-17590

White light shadowgram production during holographically recorded distorted wavefront reconstruction, discussing illuminating slit performance, image producing diaphragm, lenses and collimator

06 p0815 A72-17790

Holographic methods of antenna radiation pattern measurement, noting applications to radio astronomy and radar

06 p0816 A72-17920

Holography utilization effectiveness in three dimensional image displays, information storage, image multiplication and recording, interferometry, coding, lens corrosion, pattern recognition, etc

06 p0816 A72-17951

Brownian particle sedimentation rate and diffusion coefficient determination by holographic double exposure interferometry

06 p0816 A72-17982

Hologram data treatment comparison to human brain function, discussing recognition signals, Pavlovian qualities and intelligence function

06 p0768 A72-17997

Holographic recording of focused images using reference laser beam reflected from object in direction of diffraction maxima

06 p0817 A72-18012

Complex filter properties of Fresnel hologram with converging beam for optical filtration of three dimensional objects in Fourier or image planes

06 p0817 A72-18013

Complete measurement in holography using complex coefficients of conversion matrix of interaction between coherent beam and recorded object

06 p0817 A72-18014

Measuring device for holographic virtual image reconstruction deformations due to relative orientation errors between reference beam and holographic plate

06 p0818 A72-18329

Interferometric holography application to photoelastic stress analysis of opaque anisotropic composite plates under static and dynamic transverse and in-plane loads

06 p0898 A72-18349

Gas breakdown in front of metal targets laser flare from UV radiation ionizing action, using pulsed holographic technique

06 p0818 A72-18412

Electrical control of fixation and erasure of holographic patterns in ferroelectric materials

07 p0981 A72-18880

Subtractive microwave holography application to plasma discharge diagnostics

07 p0981 A72-18889

Optical holographic storage in lithium niobate single crystals, noting erasability and rewritability

07 p0981 A72-18890

Acoustic /ultrasonic/ holography techniques for acoustic field recording and image reconstruction in coherent light, including applications

07 p0981 A72-18920

Random bias holographic technique for imaging three dimensional objects, using laser, one mirror, one diffuser and photographic plate
[AD-743777]

07 p0982 A72-19036

Schlieren cinematographic and holographic diagnostic of giant pulse ruby laser produced plasma in Xe
[CLEA PAPER 12,2]

07 p1040 A72-19393

Real time hologram photosensitive materials, determining power requirements and resolution for diffraction gratings in saturable absorbers and absorbing liquids

07 p0984 A72-19397

High resolution portable hologram microscope based on pulsed ruby laser to avoid vibration degrading effects

07 p0984 A72-19398

MnBi thin films as potential storage media within holographic optical memory system having write-in reference beam for readout
[CLEA PAPER 18,1]

07 p0950 A72-19399

Electro-optic materials and fixing techniques for holographic recording and storage performance improvements
[CLEA PAPER 18,2]

07 p0950 A72-19400

Strain biased transparent ferroelectric electro-optic ceramics for coherent transducers /page composers/ for holographic memories and optical data processing
[CLEA PAPER 18,6]

07 p0950 A72-19401

Holographic information storage with reference wave modulation by Fabry-Perot interferometer, using two coherent sources

07 p0985 A72-19417

Scanned reference beam holography techniques with limited exposure time, noting use of hypersensitized photographic plates

07 p0985 A72-19418

Hologram interference fringe relationship to non-linearity of simple oscillations

07 p0987 A72-19836

Displacement measuring instrument based on holographic interferometry using He-Ne laser with split beam for interference fringes on photographic plate

07 p0987 A72-19848

Papers on laser applications covering holography, metrology, geodesy, etc

07 p1007 A72-20220

Holography applications and processes, discussing holographic microscopy, particle analysis, high speed photography, data storage and retrieval, interferometry, nondestructive testing, etc

07 p0989 A72-20221

Holographic weak signal enhancement technique in presence of strong noise for seismic and oceanographic applications

07 p0992 A72-20563

Plateholder for on site wet processing of holograms in real time holographic interferometry, obtaining undistorted reconstructed image by liquid gate immersion

07 p0992 A72-20581

Constant period discrete holograms features, investigating laser visualization, recording, reconstruction and image focusing

08 p1163 A72-20747

Strain measurements by holographic interferometry, considering data input to computer by digitization of video signals

08 p1163 A72-20917

Holographic interferometry for nondestructive testing, discussing applicability to laminate structures

08 p1164 A72-20924

Laser holographic imagery of plane and three dimensional objects for supersonic field representation of standing wave in isotropic liquid

08 p1165 A72-21078

Physical analysis of photoelastic interferometry and holography, considering retardation, isochromac and isopachic fringe systems and model materials

08 p1166 A72-21330

Limiting resolution of reconstructed image of focused hologram in electron microscopes as function of aberration and spatial coherence

08 p1166 A72-21380

Three dimensional hologram recording and reconstruction, discussing image geometry, reference beam intensity, size finiteness, transition limits and photosensitive materials

08 p1166 A72-21399

Two point analysis of phase, coherence and emulsion response effects on holographic image resolution

08 p1168 A72-21698

Holographic image reconstruction for individual transverse laser modes radiation intensity distribution

08 p1169 A72-21915

Time dependent phase modulation for high effective reference to object beam intensity ratio, noting linear recording of holograms

09 p1310 A72-22649

Hologram diffraction efficiency for bleached high resolution photoemulsions for blue line of He-Cd laser

09 p1311 A72-22964

Holographic interferometry application to weak inhomogeneities visualization in gas flows, using photographic emulsion nonlinear properties

09 p1311 A72-22965

Phase and amplitude error effects on image reconstruction in conventional and weak signal enhancement holography

09 p1312 A72-23242

Fourier transform plane irradiance distribution for random phase data masks in holographic data recording, discussing phase quantization level change effects

09 p1314 A72-23335

Speckle reference beam holography for object motion compensation with reduced vibration isolation requirements, discussing CW and pulsed laser use

09 p1314 A72-23338

Interferometry in volume holograms with recording of wave fronts by double exposure technique and reconstruction by diffraction

09 p1315 A72-23350

Holographic technique development review, discussing current and future applications and unsolved problems

09 p1315 A72-23375

Holographic method for investigating piston type vibrations with phase modulated reference light beam

09 p1317 A72-23682

Holographic image structure spatial filtering resulting from nonlinear distortions in hologram recording

10 p1479 A72-24048

Holographic correction of reflecting refracting telescope objective mirror deformation aberrations, noting interferometric attachment

10 p1479 A72-24049

Recording holographic networks in polycrystalline transparent ferroelectric ceramics of lead and lanthanum titanate-zirconate system

10 p1480 A72-24111

Photopolymers formulations and processing for holography applications, discussing sensitivity, keeping and reciprocity properties

10 p1482 A72-24566

Interferometric testing of optical systems, discussing test plates, Fizeau, Lloyd moire, transmission, Twyman-Green, shearing, Ronchi, scatter fringe, grazing and holographic methods

10 p1482 A72-24567

Material testing by holographic interferometry, discussing application to early detection of delayed cracking, fatigue damage and bond imperfections

10 p1482 A72-24575

Radiation pattern determination parabolic Cassegrain radio telescope reflector antennas from Fresnel zone emission source, using holographic technique

10 p1482 A72-24783

Mathematical description of frequency difference hologram obtained by superposition of two holograms of same object produced with light of different frequencies

10 p1483 A72-24915

Reflecting surface roughness measurement by holographic interferometry, applying to lapped steel specimens

11 p1629 A72-25309

Linear optimization of holographic process, investigating application to three dimensional diffusive object

11 p1629 A72-25315

High efficiency low noise volume /Lippmann-Bragg/ holograms recorded on photographic plate, using bleaching-darkening procedure

11 p1629 A72-25316

Real time hologram-moire interferometry for visualization of turbulence phenomena in liquid flow through cylindrical pipe

11 p1629 A72-25317

Holograms image formation characteristics with extended reference beam source, presenting reconstructed image and noise field calculations

11 p1633 A72-26352

Algorithm for moving object hologram synthesis with digital computer

11 p1633 A72-26365

Long wave radio and acoustic holograms recording by complex scanning for transmission over communication channels

11 p1636 A72-26714

Microwave antenna radiation patterns from far field measurements by radio holograms with probe

11 p1598 A72-26718

Holographic method of correlation and spectral analysis of radio signals applied to stable oscillator, randomly inhomogeneous media fields and stereophonic transmission measurements

11 p1636 A72-26726

Probability density function of hologram exposure irradiation in terms of Bessel function, adding uniform beam coherently to random speckle pattern

11 p1636 A72-26749

Exposure conditions and film processing parameters effects on sensitivity, diffraction efficiency and SNR of holograms recorded with continuous and pulsed radiation sources

11 p1637 A72-26796

Spatial and temporal coherence effects on image formation by in-line Fraunhofer holography

12 p1806 A72-27121

Holographic Fourier spectroscopy for microwave radiation spectra of toroidal plasma with turbulent heating

12 p1850 A72-27135

Holographic recording systems stabilization with intermittent exposure control for interference patterns fidelity

12 p1806 A72-27263

Holographic memory devices for bulk information recording, discussing use of image converter for brightness amplification and lithium niobate electro-optical deflector for beam switching

12 p1807 A72-27588

Diffraction efficiency of phase holograms formed by surface deformation of light sensitive dichromated gelatin films

12 p1808 A72-27600

Multiple exposure hologram recording on photosensitive plate for extended reference-beam source

12 p1808 A72-27601

Photosensitive polymeric films for hologram recording with high diffraction efficiency, requiring low laser powers

12 p1808 A72-27602

Laser irradiance modulation effect on high error fringes brightness in time average hologram reconstruction, noting exposure time increase

12 p1809 A72-27682

Holographic interferometer and fringe analyzer with laser sources, discussing design and application to supersonic flow imaging in wind tunnel

12 p1809 A72-27760

Holographic interferometry for impact loaded object transient impulse response recording with double-pulse Q switched laser

12 p1809 A72-27761

Real time depth gated acoustic image holography, using scanning laser beam pulse echo technique

12 p1809 A72-27840

Spatial noise in holographic images of diffusely scattering objects with allowance for recording apparatus resolving capacity

12 p1810 A72-27871

Holograms with high diffraction efficiency, describing bleaching experiments and SNR measurements in reconstructed image

12 p1810 A72-27887

Analog computer for practical evaluation of hologram interference fringes, analyzing errors

12 p1811 A72-27940

Organic dye desensitization of bleached AgBr phase holograms against printout darkening by Ar ion laser light

12 p1811 A72-27949

Dispersive optical imaging systems for chromatic aberration correction, considering broadband holographic reconstruction and generation, optical information processing and diffraction pattern achromatization

12 p1811 A72-27950

Hologram generation, electric signal conversion and transmission and remote location simultaneous Lumatron reconstruction

12 p1811 A72-27951

Amplitude and phase local distribution analysis by filtering of spatial frequencies, examining holographic system by Hilbert and Fourier transformation

12 p1811 A72-27952

Holographic method of character recognition, describing transformation from real space Cartesian coordinates to characteristic space

12 p1846 A72-27955

Developers evaluation for processing of photoresist used in hologram recording

12 p1812 A72-27956

Transparent materials study by interferometric methods, emphasizing holographic bench advantages for stress analysis and aerodynamic flows observation [ONERA, TP NO. 1037]

12 p1812 A72-28048

Composite materials evaluation methods, discussing high quality photographs, radiography, laser holographic interferometry, thermographic fluorescent phosphors, liquid crystals and acoustic techniques

12 p1815 A72-28101

Holographic system stability tested by diffraction efficiency-exposure curves obtained in real time from probing holograms sequence, emphasizing temperature effects

13 p1956 A72-28685

Acoustic /ultrasonic/ holography techniques for acoustic field recording and image reconstruction in coherent light, including applications

13 p1957 A72-29206

Artificial compensation holograms for complex optical objective substitution, using interference fringe image technique

13 p1958 A72-29513

Sensitivity limits in moire picture application to holographic interferometry

13 p1958 A72-29514

Holographic interferometry of Mach wave field generation by supersonic turbulent jet, noting visible conical wave front from core edge

13 p1898 A72-29580

Acoustic holography Doppler effects due to sound source or receiver motion during recording process

13 p1958 A72-29615

Opaque scatterers disadvantages in interferometric images recording of transparent objects obtained by double exposure holography, noting phase type diffraction gratings

13 p1958 A72-29616

Digital computer synthesis of transparent object holograms, noting image discretization, two dimension Fourier transformations spectrum and digital data correlation with optical parameters

13 p1958 A72-29617

Quantization background noise during hologram approximation by step function, discussing effect on diffraction field forming reconstructed image

13 p1959 A72-29684

Photoemulsion diffraction efficiency from latent holographic image signal formed during beam incidence on one or both photoplate sides

13 p1959 A72-29685

Experimental development by holography of three dimensional moire fringes for very large deformations study

13 p1960 A72-29781

Radiation pattern reconstruction of radio telescope parabolic Cassegrain reflector antennas from Fresnel zone emission source, using holography and optical processing

14 p2103 A72-30221

Holographic diffraction grating production by impressing interference fringes with photographic procedure, using two laser beams

14 p2105 A72-30579

Holographic interferometry for strain measurements in bodies, obtaining frozen interference fringes for stressed plane mechanical component via double exposure

14 p2105 A72-30840

Composite materials stress analysis techniques, discussing strain gages, photoelastic coatings moire and holographic applications [ASME PAPER 72-DE-6]

14 p2167 A72-30861

Three dimensional medium recording of multicolor holographic interferometry, comparing scale factor, spatial frequency and optical distortions with two dimensional medium

15 p2233 A72-31412

Real time focused image holographic interferometry for deformation recording in diffusively reflecting plate under compression

15 p2233 A72-31415

Two beam high speed frame holographic recording of dynamic processes, using passive shutter ruby laser with diaphragmed resonator

15 p2233 A72-31417

Time-average holography with thin phase recording materials, obtaining characteristic function solution for sinusoidal vibration and constant velocity motion

15 p2235 A72-31614

Airborne microwave hologram radar system, discussing along- and cross-track direction resolution realization by synthetic aperture technique and phased receiving array respectively

15 p2196 A72-31788

Data storage and retrieval by holographic techniques, noting parallel recording of complex function at Fourier transform plane

15 p2236 A72-32040

Real time holographic quasi-dynamic 3-D image display, discussing computerized synthetic hologram generator concept and system block diagram

15 p2237 A72-32054

- Liquid crystal detector design for IR holography and interferometry with applications to NDT of semiconductors, plasma diagnostics and material research
15 p2237 A72-32055
- Dynamic particle field in-line holographic recordings using IR film and p-n junction GaAs lasers
15 p2237 A72-32056
- In-line holography, determining effects of limited information on reconstructed image characteristics
15 p2237 A72-32057
- Emulsion response and phase effects on two point resolution in coherent holographic imaging systems, using Rayleigh criterion
15 p2237 A72-32058
- Harmonics, intermodulation noise and small signal effects in discrete image points holographic recording on photopolymer material characterized by linear phase shift vs exposure
15 p2238 A72-32158
- Diffraction theory for large storage capacity holographic random access memory design, discussing geometric optimization of detector array and storage plate
15 p2238 A72-32159
- Holographic determination of local convective mass transfer coefficients over flat plate normally impinged with laminar air jet, using swollen polymer transparent coating
15 p2239 A72-32349
- Holographic information storage survey, discussing hologram classification, characteristics, physical recording processes, and capacity-limiting factors
15 p2239 A72-32351
- Undoped lithium niobate for holographic storage applications, reviewing physics and recording performance
15 p2239 A72-32353
- Transition metal doped lithium niobate for holographic storage, measuring recording sensitivity, maximum diffraction efficiency and erase behavior
15 p2239 A72-32354
- Thick phase holograms in dichromated gelatin, discussing physical properties requirements and reliable processing procedures
15 p2239 A72-32355
- Holographic prerecorded TV system, discussing coherent light noise elimination and redundancy effects on image quality
15 p2239 A72-32356
- Fraunhofer holograms wavelength dependent distortion reduction by system parameters optimization, applying to color holotape
15 p2239 A72-32357
- Off-axis phase holograms of photographic transparencies recording, comparing Fresnel, Fraunhofer and lensless Fourier transform holograms
15 p2239 A72-32358
- Thermoplastic photoconductor media for holographic recording, discussing structure fabrication techniques and performance
15 p2239 A72-32359
- Recyclable holographic recording media performance parameters comparison to develop tradeoffs for storage and imaging applications
15 p2239 A72-32360
- Dynamic in situ thin film thickness monitoring during vacuum deposition by holographic interferometry, noting independence from high quality optical components
15 p2240 A72-32381
- Optical modeling of antenna radiation patterns from radio hologram of Fresnel region field
15 p2209 A72-32664
- Minimum elements number on discrete two dimensional hologram with constant distance between emitters, considering reduction of matrix elements
15 p2242 A72-32665
- Computer technique to synthesize binary holograms for wave beams analysis in quasi-optical communication channels
15 p2242 A72-32674
- Microwave modulated incoherent light for large volume scenes holography, noting object image reconstruction by coherent light transillumination of hologram
15 p2242 A72-32675
- Holographic interferometric measurement of materials time dependent deformation responses to various environmental influences, discussing CW and pulsed laser techniques and holographic microscopy
16 p2388 A72-32820
- Speckle pattern method of laser holography for structural vibration and surface strain study, noting real time operation
16 p2388 A72-32821
- Holography application to photoelastic stress analysis, showing information content correspondence to angles of incidence for different model regions
16 p2389 A72-32905
- Fourier transform/subtractive/ holographic imaging technique for microwave antenna apertures
16 p2368 A72-33072
- Computer printing device for improved image recording of binary and half tone synthesized amplitude holograms
16 p2390 A72-33084
- Holograms on bismuth and paraffin thin films with pulsed high power TEA carbon dioxide IR laser, discussing photosensitivity and capability for interferometric measurement
16 p2392 A72-33390
- Holographic virtual image formation and magnification by classical geometrical optics laws application, deriving equivalent law of refraction
16 p2392 A72-33599
- Digital recording techniques for airborne data acquisition, emphasizing laser beam holographic recorders
16 p2394 A72-33642
- Holograms image formation characteristics with extended reference beam source, presenting reconstructed image and noise field calculations
16 p2394 A72-33705
- Algorithm for moving object hologram synthesis with digital computer
16 p2394 A72-33717
- Holographic developments during 1948-1971, discussing three dimensional object imaging, phase, diffused and three-color holograms, Soret lens, electron microscopy and interferometry, etc
16 p2394 A72-33751
- Spatial noise in holographic images of diffusely scattering objects with allowance for recording apparatus resolving capacity
16 p2395 A72-33980
- Holograms with high diffraction efficiency, describing bleaching experiments and SNR measurements in reconstructed image
16 p2395 A72-33996
- Laser systems.
17 p2562 A72-34567
- An improved method for obtaining the general-displacement field from a holographic interferogram.
17 p2553 A72-34721
- The surface plasmon resonance effect in holography.
17 p2553 A72-34723
- Quantization and other nonlinear distortions of the hologram transmittance.
17 p2553 A72-34724
- Differential stress-holo-interferometry.
17 p2554 A72-34816
- [SESA PAPER 1989A] Gas breakdown in front of metal targets laser flare from UV radiation ionizing action, using pulsed holographic technique
17 p2554 A72-34860
- Principle of control of aspherical surfaces by holography and moires
17 p2554 A72-34912
- Holographic image reconstruction using He-Ne laser as coherent light source and black-white and color photographic emulsions
17 p2554 A72-34930
- Holographic photogrammetry and cartography
17 p2555 A72-35184
- Holographic nondestructive testing with impact excitation.
17 p2555 A72-35197
- Stabilizing techniques for holographic recording.
17 p2556 A72-35416
- Holographic imaging of a point object in higher diffraction orders.
17 p2557 A72-35753
- Off-axis hologram recording on thin bismuth film with picosecond pulse train from mode-locked Nd-glass laser
17 p2558 A72-35817
- Holographic interferometry application to weak inhomogeneities visualization in gas flows, using photographic emulsion nonlinear properties
17 p2558 A72-35893
- Electronically restored holographic data recording process for analog shape visualization with random access computer storage, discussing system design and capabilities
18 p2659 A72-36271
- Generalized multi-dimensional sampling theory and applications in optical systems.
18 p2672 A72-36333
- Photoelasticity, holography, moire and strain gage methods in European experimental mechanics research
18 p2733 A72-36357
- Two-phase crystal structure microdeformation measurement by combined holographic interferometry and X ray diffraction
18 p2690 A72-36358
- Polarization offset angle effect on isochromatic fringe visibility of holographic photoelasticity recordings, noting reference beam ellipticity adjustment
18 p2733 A72-36360
- Real-time vibration analysis of rib-stiffened plates by holographic interferometry.
18 p2690 A72-36361
- Holographic interferometry analyzed from the point of view of moire patterns.
18 p2690 A72-36362
- Holographic interferometer employing spherical mirrors.
18 p2692 A72-36699
- Analysis of multiple hologram optical elements with low dispersion and low aberrations.
19 p2796 A72-37578
- Long range holography theory based on reference beam technique for removing distorting effects of atmosphere on imaging, discussing visible light use
19 p2796 A72-37579
- Double exposure holographic recording of rapidly changing object via mode locked ruby laser generated interference pattern
19 p2796 A72-37580
- Error reduction in digitally generated holographic memories via parity sequence interlacing with true data sequence for spectrum shaping
19 p2796 A72-37581
- Method of stationary phase for analysis of fringe functions in hologram interferometry.
19 p2796 A72-37582
- Synthetic aperture radar data processing via tilted plane optical system, explaining technique in terms of holographic analogy
19 p2796 A72-37584
- Large object holographic image accuracy tests determining experimental sources of error
19 p2797 A72-37589
- Engineering applications of holography; Proceedings of the Symposium, Los Angeles, Calif., February 16, 17, 1972.
19 p2797 A72-37601
- Microwave hologram radar imagery.
19 p2764 A72-37602
- Optical holography and holographic interferometry applications in solid mechanics, considering surface physics, bomb breakup, transverse wave propagation, nondestructive testing and vibration analysis
19 p2797 A72-37603
- Acoustical holography imaging methods and applications, reviewing liquid levitation, sampling holography, dynamic surface deformation and scanned pulse-echo holography
19 p2797 A72-37604
- Surface evaluation of airfoils via contouring.
19 p2806 A72-37605
- Real time holographic contouring and coherent light interferometry of gear tooth surfaces.
19 p2797 A72-37606
- Interferometric holography for bond inspection in aerospace composite materials and honeycomb structures
19 p2806 A72-37607
- Applications of holographic nondestructive testing techniques in engineering.
19 p2806 A72-37608
- Holography application in photogrammetric contour mapping, discussing topographic data acquisition, storage, retrieval and display problems
19 p2797 A72-37609
- A theoretical calculation of edge smear in far-field holography.
19 p2797 A72-37610
- Holographic strain analysis using spline functions.
19 p2797 A72-37611
- Quantitative data reduction with the use of fringe control techniques in conjunction with holographic interferometry.
19 p2797 A72-37612
- Displacement field analysis via holographic interferogram, measuring fringe pattern shift due to change of observation direction through double exposure hologram
19 p2797 A72-37613
- Determination of influence coefficients for composite structures by holographic interferometry.
19 p2873 A72-37614
- Holographic strain measurement on a tensile specimen.
19 p2798 A72-37615
- Holometric deformation measurement on carbon carbon biaxial test specimens.
19 p2822 A72-37616
- Applications of holography to vibrations of segmented shells.
19 p2873 A72-37617
- The non-stroboscopic visualisation of vibrational patterns by real-time/time averaged hologram interferometry.
19 p2873 A72-37618
- In-line holography of reacting liquid sprays.
19 p2798 A72-37619
- Three dimensional flow field visualization, data acquisition and reduction via holography, noting applications in schlieren and interferometric techniques
19 p2798 A72-37620
- Measurement of three-dimensional refractive-index fields by holographic interferometry.
19 p2798 A72-37621
- Single pulse holographic flow visualization.
19 p2798 A72-37622

Interferometric holography of laser-produced gas breakdown.

19 p2798 A72-37623

Microwave holographic imaging techniques for aircraft landing aids and airport security applications, discussing real time operation

19 p2798 A72-37625

Swept frequency resolution and optical processing in propellant grain flaw detection by microwave holography, using Vander Lugt filter imaging

19 p2798 A72-37626

A general theory of polarization holography and its application to photoelastic analysis.

19 p2799 A72-37627

Application of video techniques and speckle pattern interferometry to engineering measurement.

19 p2799 A72-37628

Three dimensional holographic interferometry program for study of fringes due to displacement or deformation

19 p2799 A72-37630

Efficiency of holographic gratings in nonpolarized light under vacuum in the ultraviolet

19 p2799 A72-37670

A holographic method for optical adjustment of pulsed laser beams

19 p2811 A72-37674

Holography for aerodynamics.

19 p2799 A72-37682

Historical review of holographic interferometry development, giving attention to contouring technique and image reconstruction

19 p2800 A72-37775

Influence of an optically nonhomogeneous medium on the coherence of laser radiation and the possibility of obtaining a holographic image

19 p2812 A72-38536

Pulsed and repetitively Q switched ruby and Nd laser design characteristics for optical applications and holography

20 p2930 A72-39027

The non-stroboscopic visualization of vibration patterns by the real time-time averaged hologram interferometry.

20 p2921 A72-39028

Scatterplate, artificial hologram, moire and null lens methods for aspheric mirror testing for space astronomy and laser communication

20 p2922 A72-39033

Optical information processing analysis for coherent optics and holography, discussing characteristic spectral bands, sampling and signal averaging

20 p2922 A72-39035

Computer aided analysis of hologram optical elements for aberration and dispersion reduction and recording on thick media

20 p2922 A72-39036

A holographic memory recording matrix permitting real-time data modification.

20 p2922 A72-39037

Electro-optical TV technique with laser source illumination to provide engineering metrology and NDT procedure resembling real time holographic interferometry

20 p2930 A72-39038

Optically induced variation of birefringence in ferroelectric materials.

20 p2959 A72-39045

Wave front sampling points in spatial filtering of nonequidistant discrete holograms of flat objects

20 p2923 A72-39057

Reading of holograms by a semiconductor injection laser.

20 p2933 A72-39518

Phase holograms wave front formation as replacement of optical elements with aspherical surfaces and multilens objectives

20 p2926 A72-39519

A unitized and portable holographic interferometer. [ASME PAPER 72-HT-10]

20 p2927 A72-39681

Two-frequency microwave holographic interferometry.

20 p2927 A72-39784

Determination of three orthogonal displacement components from one double exposure hologram.

20 p2927 A72-39847

The study of vibration patterns using real-time hologram interferometry.

20 p2927 A72-39848

Application of holography in high-temperature displacement measurements.

21 p3052 A72-40235

Russian book - Principles of holography and coherent optics.

21 p3052 A72-40388

Photographic material characteristics for adequate diffraction efficiency and contrast and noise levels and acceptable nonlinear distortions of holograms, noting optical transfer function optimization

21 p3052 A72-40389

Production of holograms developed on a film by white light

21 p3053 A72-40392

Recording holographic interferograms in a lanthanum-doped fluorite crystal

21 p3053 A72-40476

Experimental investigation of a holographic system that records front surface detail from a scene moving at high velocities.

21 p3053 A72-40612

Possibilities of optical elements design using phase holograms.

21 p3054 A72-40613

Photoanodic engraving process produced high bit density surface relief holograms on semiconductor crystals for data storage, retrieval and replication applications

21 p3054 A72-40614

Scatter plate and lens methods of holographic cinematography

21 p3054 A72-40615

Dry photopolymer holographic recording film with ability to form images in near real time by exposure without processing

21 p3054 A72-40620

Acoustic holography Doppler effects due to sound source or receiver motion during recording process

21 p3054 A72-40668

Opaque scatterers disadvantages in interferometric images recording of transparent objects obtained by double exposure holography, noting phase type diffraction gratings

21 p3054 A72-40669

Digital computer synthesis of Fourier holograms of transparencies, noting significance to digital filtering method development for optical signal processing

21 p3054 A72-40670

Image quality of binary and multigradation microwave holograms, noting HF components and background noise

21 p3055 A72-40794

Dark field method for phase diffraction grating visualization by microwave holography, using radio lens for object microwave spectrum formation

21 p3055 A72-40795

Holographic interference as a means for quality determination of adhesive bonded metal joints.

21 p3060 A72-41131

Holographic technique for investigation of critical phenomena in aniline-cyclohexane and triethylamine-water binary critical mixtures, noting phase transition visualization

21 p3056 A72-41219

Application of holographic Fourier spectroscopy to the analysis of the microwave radiation spectrum

21 p3058 A72-41733

An arrangement for the holographic study of electrical explosions of wires

21 p3058 A72-41742

Small-size phase holograms for binary data storage

21 p3058 A72-41744

Holographic interferometry with variable sensitivity

21 p3058 A72-41745

Holographic system resolving capacity increase by oblique illumination of object, analyzing plane monochromatic wave transmission through one dimensional semitransparent body

21 p3058 A72-41791

Double exposure holographic interferometry for distinguishing surface deformations by changing illuminating beam inclination in successive exposures

22 p3175 A72-41992

Investigation of optical inhomogeneities in large fields by holographic methods

22 p3176 A72-42106

Effect of radiation polarization on hologram quality

22 p3176 A72-42107

Analysis of static deflections by holographically recorded vibration modes.

22 p3177 A72-42397

Improved holographic matched filter systems for pattern recognition using a correlation method.

22 p3177 A72-42445

German monograph - A hologram interferometer for the determination of amplitude and phase of optical excitation in diffraction patterns.

22 p3181 A72-43056

Holograms of spark discharges excited by nanosecond electric pulses

22 p3181 A72-43112

Modeling a holographic process on a computer

23 p3287 A72-43531

Holographic techniques in high intensity acoustic fields analysis, applying to chemistry, medicine and engineering

23 p3287 A72-43549

Advanced optical storage techniques for computers.

23 p3288 A72-43876

Characteristics and measurements of an aperture-limited in-line hologram image.

23 p3288 A72-43886

Scanning electron microscope stereophotographic picture synthesis from sequential holographic recording of three dimensional objects

23 p3290 A72-43904

A cathode-ray tube with a semiconductor laser screen

23 p3272 A72-43925

A simple method of hologram transmission by using random phase reference - Principle and computer simulation.

23 p3290 A72-43949

Ultrasonic holography in large phase disturbance.

23 p3290 A72-43950

A neoteric interferometer for use in holographic photoelasticity.

23 p3290 A72-43985

Broad-band information transfer with the aid of laser-beam coupling fields

23 p3266 A72-44359

Reconstruction of phase holograms by means of a helium-cadmium laser

23 p3292 A72-44469

Lossless multiplication of images and their spatial frequency spectra with the aid of Fresnel holograms

23 p3292 A72-44470

Acoustical holography with a scanned linear array.

24 p3401 A72-44705

Projective properties of holographic imaging.

24 p3401 A72-44767

Studying hologram imagery by a ray-tracing method.

24 p3401 A72-44713

A new method for linear recording in holography retaining the reconstruction efficiency.

24 p3401 A72-44775

Simplified, low-noise processing technique for photographic phase holograms.

24 p3401 A72-44804

NDT techniques selection, economics and organization for aircraft industry, considering ultrasonic holographic and adhesion tests

24 p3408 A72-45292

Focusing properties of converging-beam holograms.

24 p3405 A72-45602

Fraunhofer single beam holography application to gas/liquid mixture high velocity flow cross section determination, observing liquid component effects on droplet dispersion composition

24 p3405 A72-45624

HOLOMORPHISM

U ANALYTIC FUNCTIONS

HOMEOSTASIS

Altitude hypoxia resistance and endurance in dogs of various ages, discussing homeostasis retention, altitude ceiling and survival time

04 p0474 A72-15234

Rhythmogenesis as fundamental life characteristic analogous to homeostasis, discussing human circadian rhythm and cycle desynchrony during air travel

07 p0923 A72-20445

High temperature environment effects on rat organ and muscle tissue respiration, discussing temperature homeostasis maintenance

13 p1905 A72-29331

Gas induced osmosis as factor in pulmonary homeostasis, showing differential water retention in lungs ventilated with normoxic nitrous oxide compared with air

17 p2506 A72-35970

Effects of simulated high altitude on renin-aldosterone and Na homeostasis in normal man.

21 p3005 A72-40422

Mathematical methods of man machine control system synthesis, using homeostasis and functional compatibility principle

22 p3162 A72-42243

HOMEOTHERMS

Biological tissue heat transport dimensionless parameters for steady state and transient analysis of homeotherm thermoregulation

04 p0472 A72-14864

Evidence for a metabolic limitation of survival in hypothermic hamsters.

23 p3258 A72-44364

HOMING DEVICES

Real time homing guidance geometry and interceptor/sensor tradeoff studies based on reachable sets of target states analysis

20 p2951 A72-39101

[ATAA PAPER 72-825]

HOMODYNE RECEPTION

FM homodyne phase meter with klystron oscillator for measuring plasma electron concentration, presenting block diagrams of meter, detector and oscillator

02 p0223 A72-11414

Homodyne frequency converter design using microwave oscillator with bitonal frequency modulation

02 p0223 A72-11415

Upper atmosphere temperature measurement by homodyne detection of excited atoms and molecules radiation, using photodiode beat frequencies produced by spectral line emission

08 p1154 A72-20739

Upper atmosphere temperature measurement by homodyne detection of excited atoms and molecules radiation, using photodiode beat frequencies produced by spectral line emission

19 p2791 A72-38367

HOMOGENEITY

Electromagnetic radiation in uniformly moving homogeneous medium obtained by transformation and four dimensional Green function method

06 p0847 A72-17712

Local deviation limits of universe from homogeneous isotropic model, considering velocity field perturbations and galaxy counts

General dimensional analysis as extension of conventional/restricted/ dimensional analysis of physical phenomena, using progressive homogeneity law and fundamental magnitudes

HOMOGENEOUS TURBULENCE

Passive scalar field diffusion in homogeneous turbulence, solving Fourier transformed flow equations by iterative procedure

Ray statistics of electromagnetic wave scattering in homogeneous isotropic turbulent medium with ellipsoidal inhomogeneities of refractive index, using Fokker-Planck equation

Numerical simulations of three dimensional homogeneous isotropic turbulence at wind tunnel Reynolds numbers, solving Navier-Stokes equations for incompressible flow

Homogeneous compressible turbulence field with large amplitude and density fluctuations generated in subsonic wind tunnel by rapid mixing of hot and cold air streams

Homogeneous turbulence with rotatory anisotropy, determining alternating tensor with moment equations

Relative atmospheric dispersion in enstrophy/half squared vorticity/- cascading inertial range of homogeneous two dimensional turbulence

Random number method for particle motion in homogeneous turbulence field, using Brownian motion Markov process for turbulence approximation

Random homogeneous turbulence generation of rms weak magnetic field fluctuation in infinite medium with short correlation time

Homogeneous turbulence with rotatory anisotropy, determining alternating tensor with moment equations

Weak homogeneous turbulence analysis by Bogoliubov statistical mechanics theory, deriving kinetic equations for nonlinear wave interaction

The Reynolds tensor in a homogeneous turbulence associated with a pure deformation

Nonlinear functional homogeneous chaos expansions for stationary stochastic processes in turbulence theory

Simple proof of fluid line growth in stationary homogeneous turbulence.

Statistical continuous random process theory of homogeneous and isotropic turbulence in terms of energy transfer in wave number space based on Kolmogoroff hypothesis

On a resolution of the equations governing the second order correlation functions for an isotropic hydromagnetic turbulence.

Kinetic equations solution approximation for two species isothermal reactions in homogeneous turbulent mixing

A theory of homogeneous, isotropic turbulence of incompressible fluids.

HOMOGENIZATION

U HOMOGENIZING

Solidification, microsegregation and homogenization of austenitic stainless steels containing delta ferrite

Lithium diffusion into silicon by evaporation and homogenization technique, discussing dislocations and oxygen effects from aging in Ar at 150°C

HOMOLOGY

Nonhomologous expansion in modified Friedmann cosmological model, neglecting particle collisions

HOMOMORPHISMS

NT SUBGROUPS

Nonlocal elliptical boundary value problem solvability in terms of smooth functions, deriving Green formula and homeomorphism theorems

Nonlinear resistive network analysis by piecewise linear mappings, studying Lipschitz condition and global homomorphism

Finite group homomorphic sequential systems generalization from linear system theory, developing

controllability, observability, minimality and realizability concepts

Compensating fields of homomorphic imaging problems in space symmetry, discussing quasi-tensors, covariant derivatives and Poincare group

HONEYCOMB CORES

Ti alloy honeycomb core sandwich panels fabricated by brazing or spot diffusion bonding, investigating elevated temperature effects on mechanical properties

Ti honeycomb brazing, discussing filler metals, furnace temperature and atmosphere control and use of protected graphite as furnace material

Elastic buckling of simply supported sandwich panels with fiber reinforced laminated face plates and honeycomb cores subjected to uniform end loading

Contribution to the theoretical calculation of sandwich structures with tube core

A crack stopper concept for filamentary composite laminates.

Zeta core for sandwich construction with rigidity-to-weight ratio comparable to honeycomb core, discussing elastic properties and cost

HONEYCOMB STRUCTURES

NT HONEYCOMB CORES

Metal-skin honeycomb composite structure design and manufacture for Concorde rudder, noting structural adhesive bonding in aircraft construction

Fatigue life tests of structural sandwich plates with honeycomb layer, considering temperature effects, material scattering and defects inside honeycomb by nondestructive methods

Honeycomb sandwich beams dynamic analysis by finite element method with three degrees of freedom per discrete element, obtaining flexural, in-plane and shearing modes

Exact analysis of a thick sandwich conical shell by forward integration.

Focusing properties and efficiency of EHF waveguide lens with Al honeycomb as guiding medium, noting design considerations and performance test results

Study of vacuum furnace atmospheres for brazing titanium honeycomb panels.

Interferometric holography for bond inspection in aerospace composite materials and honeycomb structures

Applications of holographic nondestructive testing techniques in engineering.

Stability of convective heat transfer through horizontal air layer heated from below and constrained internally by thin walled honeycomb panels

Thermal conductivity of honeycomb sandwich panels for space applications.

Bonded honeycomb structures. II - Bonded joints and non-destructive testing.

HOOKE'S LAW

Neo-Hookean material circular plate under finite axisymmetric stretching, showing approximately constant deformed thickness

Hookes law formulation by multindex sequences for stereomechanical multiple system optimization

Cross-ply laminates effective elastic moduli relations based on generalized Hookes law

Invariant solutions of the differential equations of the uniform motion of a Hooke medium

Mathematical model for plastic deformation of polycrystalline materials with Hookes law elastic strains

HORIZON

NT RADIO HORIZONS

Brightness profiles of earth daytime horizon from Soyuz spacecraft photographic photometry, deriving atmospheric scattering coefficient relation to optical thickness vertical distribution

Near horizon anomalies in astronomical refraction due to ground air layer effects on tropospheric processes

Slope angle determination with respect to photograph surface from visible horizon line configuration

HORIZON SCANNERS

Safety factors of aircraft flight instruments, discussing altimeter and artificial horizon reading errors and modifications

A horizon sensor with a bolometer and electrooptical modulators

An albedo horizon sensor using hybrid circuitry.

Slope angle determination with respect to photograph surface from visible horizon line configuration

HORIZON SCANNERS

Safety factors of aircraft flight instruments, discussing altimeter and artificial horizon reading errors and modifications

A horizon sensor with a bolometer and electrooptical modulators

An albedo horizon sensor using hybrid circuitry.

HORIZON SENSING

U HORIZON SCANNERS

HORIZONTAL FINS

U FINS

HORIZONTAL FLIGHT

Circumpolar region object position autonomous determination from arbitrarily zenith-oriented moving horizontal platform position coordinates

Passive detection radar system for bombers, calculating target distance during horizontal flight

HORIZONTAL STABILIZERS

U STABILIZERS [FLUID DYNAMICS]

HORIZONTAL TAIL SURFACES

European A300B Airbus flap and slat systems and tailplane actuator for longitudinal pitch trim control

Low subsonic region unsteady interference effects on harmonically oscillating wing-tailplane model with variable sweep wing

Lifting surface linearized potential theory for unsteady aerodynamic forces on wing and horizontal tail surfaces, using computer program

All-moving tail plane parameters influence on glider static and dynamic characteristics, discussing lateral and longitudinal stability, maneuverability and pilot induced oscillations

A-4 Skyhawk horizontal stabilizer experimental graphite-epoxy composite construction, describing design, manufacturing and testing techniques

Jaguar powered flight controls, discussing wing spoilers, slab tailplane, rudder, autostabilization system and integrated packaging of actuators

HORIZONTAL TAILS

U HORIZONTAL TAIL SURFACES

HORMONE METABOLISMS

Hypophysectomy in rats, resulting in prolonged red blood cell survival due to oxygen consumption decrease and altered erythrocyte enzymatic processes

Radioimmunoassay and gel filtration determination of molecular size and immunochemical reactivity of parathyroid hormone in gland extracts, peripheral circulation and parathyroid effluent blood

Ecdysone hormonal control of Drosophila circadian rhythms and synchronizing mechanisms, discussing light stimulation and neurohormone secretion

Thyroid and adrenocortical hormonal state effect on cell number and functional maturation of brain, discussing neurogenesis in infants

Bed rest and centrifuging effects on human plasma thyroid hormone level, discussing total protein, albumin and thyroxin binding globulin concentrations

Renal clearance studies of left atrial distention effect in dog, indicating antidiuretic hormone inhibition mechanism of diuresis

Metabolic and hormonal response adaptation to prolonged hypodynamics in water immersion/head out/, noting diurnal and nocturnal differences in circadian rhythms

Suppression effects of hyperoxic breathing gases on red blood cell and erythropoietin hormone production following blood loss

Noninvasive polygraphic technique to assess cardiovascular responses to intravenous glucagon injection

Vasopressin /antidiuretic hormone/ role in central vascular volume and fluid balance maintenance during continuous positive pressure breathing in dogs

Effects of simulated high altitude on renin-aldoosterone and Na homeostasis in normal man.

Prediction of vegetative reactions in the case of stress and extreme effects upon the organism

A-857

Exogenous modifications of circadian rhythms of adrenal hormones in man. 22 p3147 A72-42978

Human prolactin - 24-hour pattern with increased release during sleep. 23 p3316 A72-43977

Changes in the pituitary-thyroid and in the pituitary-gonad systems under conditions of functional loading and of physiological immobilization. 24 p3371 A72-44823

HORMONES

NT ALDOSTERONE

NT CORTICOSTEROIDS

NT CORTISONE

NT HYDROXYCORTICOSTEROID

NT PITUITARY HORMONES

NT THYROXINE

Short term response of insulin, glucose, growth hormone and corticosterone to acute vibration stress in rats 01 p0015 A72-11289

Hypokinesia effects on neurosecretory system of rat hypothalamus and hypophysis, noting increased antidiuretic hormone contents in blood 05 p0618 A72-16634

Low molecular active hormones isolation from cat blood, obtaining eluates with phosphate buffer by chromatography 14 p2077 A72-30971

Pancreas insular apparatus biosynthesis of neurohumoral mechanism compounds stimulating coronary ectasia hormones discharge from brain into blood in cats with alloxan diabetes 14 p2077 A72-30973

Role of the thyrotropic region of the hypothalamus in the adaptation activity of the organism 22 p3141 A72-42167

Limbico-neocortical, cardiovascular and hormonal system vegetative shifts associated with emotional behavior response, presenting neurogenic stress model for animals 22 p3148 A72-43166

HORN ANTENNAS

Corrugated horn antenna design, discussing difficulties associated with mode amplitude and phase control 01 p0040 A72-10679

Corrugated conical horn antennas with arbitrary groove depth, considering far field radiation patterns 01 p0040 A72-10680

Radiation patterns from rectangular guide horns with impedance walls, analyzing hybrid modes 01 p0040 A72-10681

Radiation pattern of corrugated conical horn with wide flare angle, deriving horn feed design criteria 01 p0040 A72-10682

Microwave half blinder for sidelobe reduction in large horn reflector antennas in E plane radiation for horizontal polarization 01 p0043 A72-11243

Narrow flare angle scalar antenna feed radiation pattern derivation, showing horn gain variation with respect to length 02 p0191 A72-11895

Flange angle effects on sectional horn antenna E-plane radiation patterns and beam focusing and broadening 04 p0497 A72-14511

Ring loaded corrugated waveguide for improved frequency broadbanding and transformer matching in horn antenna systems for satellite communication ground stations 04 p0498 A72-14721

Reflection from aperture of long E-plane sectoral horn antenna, determining electrical impedance by asymptotic diffraction theory 04 p0501 A72-15424

Broadband corrugated conical horn antennas with small flare angles, investigating radiation patterns and bandwidth 04 p0501 A72-15425

Horn lens antennas for millimeter wave radiometric applications, discussing medium gain polystyrene lens design to obtain low peak sidelobes 04 p0503 A72-15608

Reflection and transmission characteristics of circularly polarized horn antenna, discussing bandwidth properties, phase differences, polarization characteristics and voltage SWR 05 p0635 A72-16334

Long E-plane sectoral horn, deriving complex reflection coefficient from aperture by geometrical diffraction theory 06 p0781 A72-17346

E-plane dielectric slabs symmetrical loading effects on horn aperture efficiency enhancement from far field calculation [AD-738714] 06 p0781 A72-17347

Pyramidal horn antenna with mesh conducting surface comparing response with geometrically similar horn with continuous walls 06 p0783 A72-17600

Corrugated conical horn antenna groove electromagnetic field analysis for design of scalar feed radiation pattern 07 p0945 A72-19661

K and Ka bands standard electromagnetic horn gain measurement and error analysis at different wavelengths by two-antenna method 07 p0957 A72-19784

Wideband dual mode dielectric loaded horn antenna, discussing structure and radiation patterns 07 p0957 A72-19793

Polarization distortion of partially polarized wave emission and reception by two channel horn antennas, noting radio astronomy, radar and optics applications 08 p1138 A72-20788

Hoghorn parabolic antenna design, presenting relations for dimensions, aperture field and radiation patterns calculation by computer 09 p1284 A72-22242

Horn antenna synthesis for determining impedance boundary conditions at walls for aperture field distribution 09 p1285 A72-22574

Conical scalar horn for paraboloidal reflector illumination, discussing half flare angle calculation for prescribed sidelobe realization 10 p1435 A72-24302

Launching horn effect on radiation pattern of dielectric cone feeds, proposing wide angle sidelobe reduction via absorbent sheath 12 p1791 A72-27669

Numerical accuracy of electromagnetic field spherical wave expansions, considering horn antenna radiation pattern 12 p1791 A72-27670

Waveguides for primary and hybrid mode horns for secondary feeders of deep paraboloid reflector radio telescope in Effelsburg, West Germany 12 p1793 A72-27811

Microwave horn and lens antennas radiation spatial coherence characteristics, noting effect on picture contrast 13 p1928 A72-28475

Design of parabolic reflector antenna with pyramidal horn radiator closed by quadratic waveguide, calculating radiation pattern 13 p1929 A72-29039

Parabolic, Cassegrain, spherical and horn-parabolic axisymmetric mirror antennas, calculating primary radiating element orientation effects on radiation polarization characteristics 13 p1931 A72-29277

Cross coupling in a five horn monopulse tracking system. 17 p2513 A72-34356

Five-horn feed system design for improving large steerable antenna monopulse performance, discussing weight and cost reductions by focal length selection 17 p2526 A72-34467

Engineering approach to the design of tapered dielectric-rod and horn antennas. 17 p2530 A72-35362

Surface waves in the corrugated conical horn. 17 p2517 A72-35387

Correlation between two base-station antennas affected by local scatterers and directions of incoming mobile radio waves. 18 p2661 A72-36846

An artificial dielectric lens suitable for high power applications. 18 p2671 A72-37148

Galactic radio emission spectrum analysis via horn antennas with wavelength proportional apertures, calculating full beam antenna temperatures for selected radio frequencies 19 p2852 A72-38484

Focus field and horn exciter regarding parabolic antennas with small f/D-relation 21 p3029 A72-40523

Eigenvalues associated with balanced hybrid modes expressed in closed form to derive conical scalar horn antenna far field radiation patterns 21 p3032 A72-40630

Null placing in radiation patterns by shaping antenna edges. 21 p3034 A72-41467

Radiation patterns of wideband horn antenna loaded by dielectric belt, noting satellite and terrestrial radio relay applications 21 p3036 A72-41832

Optimisation of slope of difference-mode radiation pattern in sum-and-difference-comparison monopulse radar. 23 p3264 A72-43606

Radiation patterns and structural design of two mirror millimeter wave Cassegrain antennas with horn radiator 23 p3271 A72-43778

Synthesis of horn antenna with impedance boundary conditions on walls and specified aperture field distribution 24 p3384 A72-44753

HORSEPOWER

Altitude-velocity dependence of turboprop engine equivalent horse power, propeller output and specific fuel consumption, discussing performance characteristics relation to ambient air temperature 05 p0708 A72-17100

Noncontact rotating shaft horsepower measurement, using phase displacement technique [ASME PAPER 72-GT-29] 11 p1630 A72-25625

HOSES

Lightweight low pressure plastic hose assemblies in aircraft and missile petroleum base fuel and synthetic lubricating oil systems at 395-710 R and up to 200 psi [SAE ARP 1180] 01 p0006 A72-10388

HOSPITALS

Computerized EEG data acquisition and transmission system for large hospitals with multiple critical care patient monitoring units, noting telephone access from outside 07 p0928 A72-19307

HOT AIR

U HIGH TEMPERATURE AIR

HOT CATHODES

He-Ne laser amplitude fluctuations with hot and cold cathode discharge tube operation, determining emission spectral line width 05 p0669 A72-16613

Cathode temperature measurement in erosion and heat transport reduction by cesium seeding of Ar plasma arc 06 p0862 A72-18334

Ultrahigh vacuum measurement by Bayard-Alpert hot cathode ionization gages, showing ion current component influence on lower pressure limit 07 p0914 A72-19907

Some results of studies of cathode luminescence in cerium-activated glass 19 p2845 A72-38190

Electric field intensity distribution function for thermoelectronic emission from hot cathodes in low temperature plasma, using Richardson formula 21 p3094 A72-41656

HOT CYCLE PROPULSION SYSTEM

U TIP DRIVEN ROTORS

HOT ELECTRONS

Ion and electron temperature ratios in hot plasma, discussing energy relaxation, heating and cooling effects and electrostatic confinement by ambipolar diffusion 10 p1524 A72-25032

Magnetic mirrors for highly stripped heavy ions production in hot electron plasmas by low voltage high current electron beam 10 p1524 A72-25035

Gunn effect - Bulk instabilities. 17 p2594 A72-34562

New efficient method for calculating hot electron effects applied to n-Ge. 19 p2844 A72-37686

HOT EXTRUDING

U EXTRUDING

HOT FORMING

U HOT WORKING

HOT GAS SYSTEMS

U HIGH TEMPERATURE GASES

HOT GASES

U HIGH TEMPERATURE GASES

HOT JET EXHAUST

U HIGH TEMPERATURE GASES

U JET EXHAUST

HOT JETS

U JET FLOW

HOT PLASMAS

U HIGH TEMPERATURE PLASMAS

HOT PRESSING

Hot pressed Ti alloy powders, evaluating strength and toughness at cryogenic temperatures 02 p0240 A72-11439

Static thermoelasticity problems solutions using harmonic functions applied to contact problem of hot stamps 03 p0448 A72-13902

Metal powder hot compacting under vacuum and ultrasound action, considering porous body three dimensional viscous flow 05 p0665 A72-16091

Steady and unsteady creep stages in porous body sintering and hot compacting, using three dimensional viscous flow theory 05 p0665 A72-16092

Hot pressing /extrusion/ of rods from metal-ceramic Ti, using pure and cermet powders with tungsten carbide 06 p0822 A72-18426

Hot pressing of sintered refractory metal oxide powders of Ti, Zr, U, Nb and Cr, showing improved compacting by raising temperature 06 p0822 A72-18427

Hot pressed silicon nitride with high strength and good oxidation and thermal shock resistance for gas turbine applications [ASME PAPER 72-GT-19] 11 p1673 A72-25618

Hot isostatic pressing techniques for thin wall Be tubes manufacture 11 p1643 A72-26831

Continuous hot pressing of high density reactive ceramic and metal powder materials in alumina die 11 p1643 A72-26832

Plastic properties of locally heated refractory materials in hot pressing calculated from temperature distribution 13 p1966 A72-29465

Compacting kinetics of fiber reinforced sandwich composites during hot pressing controlled by plastic matrix sliding velocity 13 p1967 A72-30103

Shock wave reduction, microcracks and dislocation density of hot pressed titanium, zirconium and niobium carbide powders, using X ray crystal analysis 13 p1982 A72-30110

Aluminum-stainless steel and Ni-Mo composites prepared by dynamic hot pressing, determining bond strength between fibers and reinforced metal matrix 14 p2107 A72-30431

Ferrite powder relative density as function of temperature, sintering time and pressure during hot pressing, noting creep activation energy and vacancy motion 14 p2107 A72-30775

Electric spark activated hot pressing application for sintered composite structures, noting process parameters optimization for superalloy powders 16 p2411 A72-34093

Hot pressing of transition metal nitrides and their properties 19 p2808 A72-38281

Oxidation protection of tantalum and tantalum alloys at up to 1500 C 22 p3188 A72-41973

Study of the hot pressing kinetics for niobium-cemented tungsten and titanium carbide alloys 22 p3182 A72-42191

HOT STARS

NT A STARS

NT B STARS

NT O STARS

NT WHITE DWARF STARS

UBV photometric studies of eclipsing variable R Canis Majoris confirming primary component as F1V star, discussing ordinary semidetached system possibility 01 p0129 A72-10793

Magellanic Clouds hot supergiants color-magnitude arrays from spectroscopic and photometric measurements 03 p0424 A72-13253

Magellanic Clouds bright star intermediate band photometry, discussing interstellar extinction and luminous supergiants 03 p0425 A72-13257

Spectrographic observation of hot OB subdwarf HD 149382 03 p0435 A72-13799

Wolf-Rayet type stars emission line variations from outer convective zone opening and matter ejection 03 p0439 A72-14243

UV astronomy techniques and devices, discussing hot stars, stellar chemical composition and interstellar medium 04 p0582 A72-15686

Interstellar gas motion model of nebulae formation by Wolf-Rayet stars 06 p0883 A72-18016

Disk population F-type star photometric luminosities, motions and metal abundance indices, discussing ultrashort period cepheids 07 p1071 A72-19333

Galactic cluster M67 blue straggler stars in pseudohorizontal branch, determining stellar mass relative to turnoff point stars and zero-age main sequence 07 p1071 A72-19335

Zeta Orionis spectra at 922-1453 A from rocket spectroscopy, matching lines with stellar atmosphere models 07 p1072 A72-19346

WR hot stars CIII, NIV and OV emission spectra structure associated with excitation of 2pn and pd ion configurations 10 p1549 A72-25169

Interstellar gas motion model of nebulae formation by Wolf-Rayet stars 11 p1718 A72-25952

Model for hot stars mass outflow due to gas acceleration by radiation absorption in UV resonance lines 15 p2305 A72-31341

Spectral characteristics of hot stars with emission lines, discussing Ba, Of, P Cygni, Wolf-Rayet and B type supergiant stars 16 p2462 A72-34183

Stellar evolution and rotation data acquisition from photometric analysis of B-F main sequence stars, considering different models for rotating atmospheres 16 p2462 A72-34184

The metal-to-hydrogen ratio in F1-F5 stars, as determined by a model-atmosphere analysis of photoelectric observations of a group of weak metal lines. 18 p2727 A72-36737

Hot star with broad H lines with weak variable central emission, noting Ca II and He I 20 p2966 A72-38920

Photometric and power spectrum observation of peculiar blue variable star, showing low amplitude high frequency luminosity oscillations, hydrogen deficiency and degeneracy 20 p2966 A72-38921

Spectrophotometry of the Wolf-Rayet type stars HD 195765, HD 192163, and HD 192103 21 p3109 A72-41437

Infrared photometry of Northern Wolf-Rayet stars. 23 p3337 A72-43827

Extended horizontal branch loci. 23 p3337 A72-43830

Radial velocity periodic variability determination from shell star 88 Herculis hydrogen lines, obtaining hypothetical spectroscopic binary elements 23 p3340 A72-44237

HOT SURFACES

Refractory titanium oxide deposition by hot front method of chemical reaction in vapor phase 02 p0170 A72-12166

Gas flow fluctuations near stagnation point on hot wall, taking into account laminar boundary layer compressibility effects [ASME PAPER 71-APM-RR] 04 p0462 A72-15178

HOT WATER ROCKET ENGINES

Hot water rocket engine design and operation principles, discussing high pressure tank and nozzle characteristics 15 p2297 A72-31830

HOT WORKING

Thermomechanical conditions of plasticity-to-brittleness transition temperature for optimal rolling of cermet W strips 01 p0078 A72-11088

Hot formed Cr-Ni-Mo and Ni-Mo prealloyed steel powders fatigue and toughness properties, determining hardness effects by varying draw temperature from 400 to 1000 F 02 p0240 A72-11435

Empirical power law application to secondary creep, steady state hot working and high temperature tensile or compressive yielding, discussing activation parameters interrelations 02 p0247 A72-12814

Optimal cyclic fatigue strength of low C steel from critical deformation rate during thermomechanical treatment 03 p0372 A72-13597

Stepwise thermomechanical treatment effect on improved cyclic fatigue strength of Ni-Cr sheet steel with tension and rolling deformations 03 p0372 A72-13598

Cr and U contents effect on high strength Cr-Mo-Va alloy steel sheet hot cracking susceptibility, using Huxley test method 06 p0820 A72-17704

Austenitic stainless steel with improved corrosion resistance, yield strength and hot workability 07 p1011 A72-19487

Computerized estimation of deformation parameters for Sellars-Tegart equation relating stress, strain rate and temperature in creep and hot torsion testing of metals 07 p1090 A72-19736

High strength Ni alloy hot working properties evaluation from extrusion simulation by torsion testing, considering stress-strain-time relations, microstructure, recrystallization and ductility 08 p1190 A72-22199

High temperature alloy deformation superplasticity and formability relation with microstructure, fine structure and load requirements for hot working with high strain rate 08 p1250 A72-22200

Torsion testing machine for hot metal workability tests at constant strain rate 11 p1639 A72-25820

High strength low alloy steel and stainless steel recrystallization after hot working at plastic deformation temperature 13 p1973 A72-28654

Mo single crystal weakening after hot rolling and annealing, showing decreased dislocation density and hardness recovery by electron microscopy 14 p2112 A72-30160

Hot worked Al alloy machine elements mechanical properties scattering, discussing quality control procedures 14 p2114 A72-30275

High temperature strength and ductility study of hot working behavior of steels, using hot impact tension tests 16 p2406 A72-33316

Hot forging of sintered stainless steel. 19 p2815 A72-37592

Deformation, densification and material fracture characteristics for powder preform design for hot forging 19 p2806 A72-37593

Ti fabrication advances in forging, diffusion bonding, hot forming, chemical milling and laser cutting 21 p3061 A72-41335

Plastic flow and strain hardening theories for short time tensile creep in high temperature metal formation, applying to Al alloys 21 p3125 A72-41510

Investigation of the drop forging process applied to magnesium alloys 22 p3183 A72-42816

Thermomechanical manipulation of precipitate shape in a titanium-base alloy. 22 p3194 A72-43044

HOT-FILM ANEMOMETERS

Sensors and circuit design for flow angle and shear stress measurements using heated film and wires [ASME PAPER 71-WA/FE-17] 05 p0661 A72-15930

Aortic flow disturbances in vivo study by hot-film anemometer, considering peak flow velocity and pulse rate effects 07 p0934 A72-20537

Frequency response of hot-film wedge probe in turbulent flow of viscoelastic fluid 09 p1293 A72-22309

Arterial velocity profiles measurement in dogs thoracic aorta by hot-film probe, relating flow disturbances and turbulence to Reynolds number 10 p1431 A72-24468

Heated thin film gages calibration for skin friction measurements in laminar and turbulent flows, discussing wall temperature distribution and turbulence effects 15 p2241 A72-32577

Reynolds stress development in wall region of turbulent shear flow of oil investigated by hot film measurement technique and anemometer signal analysis 18 p2680 A72-36478

Influence of a protective coating on the frequency characteristics of hot-film anemometer sensors 21 p3050 A72-40131

Peclet number, length/diameter ratio, Grashof number, Knudsen number, overheat ratio and yaw angle interaction effects in cylindrical hot-wire and hot-film probes cooling 21 p3057 A72-41620

HOT-WIRE ANEMOMETERS

Pt coated W hot-wire anemometer sensitivities in supersonic turbulent flow at low Reynolds numbers [ONERA, TP NO. 1024] 01 p0064 A72-10037

Linearization errors and calibration functions for hot-wire anemometry taking into account higher order velocity fluctuations 01 p0071 A72-11170

Free stream and shock layer disturbances effect on hypersonic boundary layer transition in wind tunnels from hot wire measurements 02 p0230 A72-12274

Local stagnation temperature measurement in supersonic flow, using hot-wire anemometer 03 p0309 A72-13789

Linearized constant temperature hot-wire anemometer calibration for shock tube unsteady flow velocity measurements with low strength wave propagation 04 p0521 A72-14920

Turbulence intensities and shear stress measurements in wake of thin flat plate by rotating single hot-wire anemometer 04 p0524 A72-15498

Sensors and circuit design for flow angle and shear stress measurements using heated film and wires [ASME PAPER 71-WA/FE-17] 05 p0661 A72-15930

Hot-wire anemometers signals resolution into velocity-temperature fluctuations correlations in compressible flow with shear turbulence wakes [AIAA PAPER 72-117] 05 p0664 A72-16822

Turbulent flow field velocity fluctuations errors by hot-wire anemometer filaments vibrations from fluctuating aerodynamic loads in Karman vortex street 05 p0664 A72-17013

Temperature effects on hot-wire anemometer calibrations, plotting Nusselt number variation with Reynolds number 07 p0990 A72-20369

Hot-wire measurement of binary gaseous mixtures in unsteady concentration fields, investigating heat loss 07 p0993 A72-20587

Overheat resistance calibration of constant temperature hot-wire anemometers at low velocities in water with variable temperature [ASME PAPER 71-HT-9] 08 p1163 A72-20873

Constant temperature hot-wire anemometer compensation for thermal lag of wire or film resistance thermometer 09 p1306 A72-22307

Small scale atmospheric turbulence measurement with airborne hot-wire anemometer, discussing optimal choice of experimental parameters 09 p1307 A72-22435

Air velocity calculation from hot-wire anemometer measurements in variable density flow, discussing correction factors checking method and application to internal combustion engine 09 p1315 A72-23390

- Instantaneous velocity vector determination in two dimensional flow by hot-wire anemometer and on-line digital computer technique 10 p1478 A72-23877
- Kinematic and thermal turbulent fluctuations isolation by means of hot-wire anemometric probe 10 p1479 A72-24055
- Carbon dioxide concentration effect on calibration of linearized hot-wire anemometer in operation at constant temperature 10 p1480 A72-24217
- Hot thermistor and hot-wire anemometer principles for photocardigraphic transducer design, using theory of hydraulic amplification with high SNR 10 p1430 A72-24374
- Response equation for hot-wire anemometry over wide velocity range using modified King law 11 p1629 A72-25265
- Hot-wire measurement of vector velocity modulus and sign in one dimensional unsteady gas flow 12 p1806 A72-27178
- Doppler laser velocimeter and hot-wire anemometer readings in cylinder wake compared, describing instrument caused spectrum broadening effects neutralization method 13 p1960 A72-29889
- French monograph on hot-wire anemometry techniques covering support aerodynamic perturbations, crossed wire probes and turbulent flow free boundary 14 p2106 A72-30946
- Hot-wire anemometer output linearization by squaring and straight line sequence circuits combination, supplementing Bruun error estimates 16 p2392 A72-33606
- The aeroelastic behaviour of hot-wire anemometer filaments in an air stream 17 p2552 A72-34229
- Development of a hot-wire anemometer for hypersonic turbulent flows 19 p2795 A72-37517
- The effect of wire length and separation on X-array hot-wire anemometer measurements 19 p2801 A72-37903
- Direct measurement of the velocity gradient in a fluid flow 20 p2926 A72-39633
- Dynamic characteristics of hot-wire anemometers with glass-coated thermistors 21 p3050 A72-40132
- Hot wire data corrections in low and in high turbulence intensity flows 21 p3051 A72-40220
- Peclet number, length/diameter ratio, Grashof number, Knudsen number, overheat ratio and yaw angle interaction effects in cylindrical hot-wire and hot-film probes cooling 21 p3057 A72-41620
- Hot wire anemometer calibration for measurements of small gas velocities 22 p3175 A72-41953
- Reverse flow sensing hot wire anemometer 22 p3177 A72-42392
- A comparison of disturbance levels measured in hypersonic tunnels using a hot-wire anemometer and a pitot pressure probe 24 p3388 A72-45402
- HOT-WIRE FLOWMETERS**
- Turbulent flow velocity measurement pulsed wire technique 01 p0072 A72-11229
- Dynamic calibration by sound wave of hot wire operated by constant resistance method, using open resonance tube in homogeneous incompressible air flow 03 p0356 A72-13235
- Turbulence generation in hypersonic boundary layer from hot-wire correlation and disturbance convection velocity measurements on cone-ogive-cylinder in Mach 7.2 flow [AIAA PAPER 72-182] 05 p0650 A72-16837
- Recirculating cells in laminar coaxial jets investigated by smoke introduction into flow field and hot-wire techniques [AIAA PAPER 72-150] 05 p0651 A72-16880
- Jet noise intensity reduction by screen across nozzle exit, using acoustic and hot wire measurements 07 p0968 A72-19873
- Nonuniform temperature distribution effect on heat conduction coefficient of hot-wire cell, using computerized net point method 08 p1166 A72-21449
- Hot wire cell measurement of specific heat in low pressure gases, determining thermal conductivity and accommodation coefficient 11 p1634 A72-26367
- Dynamic calibration of inclined and crossed hot-wire flowmeters for absolute turbulence intensity measurements, using known sinusoidal oscillations in steady flow 11 p1636 A72-26637
- Hot-wire probes to measure turbulent three dimensional flows with allowance for transducer directional sensitivity 11 p1636 A72-26698
- Velocity independent fast response hot-wire probe for binary gas mixtures composition measurement, describing design and operational principle based on dimensional analysis 16 p2389 A72-32829
- Critical analysis of Senftleben modified hot-wire method for gas heat conductivity measurement 16 p2479 A72-33861
- Temperature distribution in hot wires in high-enthalpy low-density flows [DEVL-SONDDR-216] 19 p2804 A72-38685
- Simultaneous measurements of temperature and velocity in heated flows 23 p3292 A72-44541
- Errors caused by hot-wire filament vibration 24 p3402 A72-44949
- HOT-WIRE TURBULENCE METERS**
- U HOT-WIRE FLOWMETERS**
- U TURBULENCE METERS**
- HOTSHOT WIND TUNNELS**
- Status of hotshot wind tunnels for hypersonic aerodynamic studies 24 p3388 A72-45203
- HOURLASS VALLEYS**
- U VALLEYS**
- HOUSINGS**
- NT RADOMES**
- Rocket-borne photomultipliers housing, recommending fiber reinforced epoxy resin structure with metal flanges 03 p0440 A72-13062
- Compact photomultiplier housing with controlled cooling, discussing temperature control and measurement 12 p1806 A72-27265
- HOVERCRAFT**
- U GROUND EFFECT MACHINES**
- HOVERCRAFT GROUND EFFECT MACHINES**
- Hovercraft heaving response to regular head or following seas, determining dependency on craft natural frequency and damping, wave frequency and cushion planform 14 p2071 A72-30254
- Internal noise reduction in hovercraft 18 p2642 A72-36574
- Comparative analysis of the operative costs of large amphibious hovercraft 18 p2643 A72-37212
- HOVERING**
- HH-53 rescue helicopter automatic approach and hover coupler for automatic transition from forward flight at constant deceleration and rate of descent 05 p0686 A72-16653
- The wake geometry of a hovering helicopter rotor and its influence on rotor performance [AHS PREPRINT 620] 17 p2484 A72-34497
- Main results of nonlinear rotor theory 23 p3247 A72-43419
- HOVERING STABILITY**
- Optimal fixed point hovering rotor design for improved static performance by pulse theory 05 p0601 A72-16350
- Helicopter automatic flight control approach/hover coupler systems, hands off stability and handling qualities 12 p1843 A72-27522
- V/STOL weapon system VJ-101 design, discussing one axis rocking device, suspension structure and hovering flight thrust control 16 p2347 A72-33049
- Stability and control dynamics of helicopter hovering with heavy sling load, analyzing maneuvers for minimal excitation of pendulous motion [AHS PREPRINT 630] 17 p2489 A72-34488
- Optimization of the wing parameters of a glider hovercraft 20 p2888 A72-39902
- HP-115 AIRCRAFT**
- HP-115 slender wing research aircraft linear motion and undamped Dutch roll oscillations at high angles of attack [AIAA PAPER 72-62] 05 p0613 A72-16932
- HUBBLE DIAGRAM**
- Hubble diagram history, present status, extension and improvement, considering quasars, galactic red shifts and other extragalactic radio sources 07 p1068 A72-18999
- Hubble constant, Friedmann time and expanding universe limits from measurements of distances to furthest galaxies, considering quasar red shift cut-off 22 p3222 A72-42138
- HUBS**
- Hub and shroud boundary layer growth in centrifugal compressor vaneless diffusers, comparing predicted and measured performance at high pressure ratio per stage [ASME PAPER 72-GT-54] 11 p1570 A72-25645
- Disks with inclined face, investigating effects of joint between hub and disk face on stress-strain state 14 p2164 A72-30430
- New hubs for multi-bladed tail rotors [AHS PREPRINT 602] 17 p2489 A72-34491
- The development of inlet flow distortions in multi-stage axial compressors of high hub-tip ratio [ICAS PAPER 72-20] 21 p3099 A72-41145
- Rotary wing head weight estimation for helicopter preliminary design and parametric studies, deriving semiempirical trend formula [SAWE PAPER 914] 23 p3344 A72-43461
- The coupled transverse vibrations of a spinning membrane disk with a central hub 23 p3355 A72-44367
- Decay of swirl in a straight pipe flow /with hub at the entrance/ 24 p3394 A72-45367
- HUGHES AIRCRAFT**
- Hughes 500 and OH-6 helicopter tail rotor cambered blades, comparing thrust and stall characteristics with symmetrical blades 14 p2072 A72-30290
- HUGHES MILITARY AIRCRAFT**
- U HUGHES AIRCRAFT**
- U MILITARY AIRCRAFT**
- HUGONIOT ADIABAT**
- U HUGONIOT EQUATION OF STATE**
- HUGONIOT EQUATION OF STATE**
- Hugoniot analysis of shock disturbance propagation with steady velocity through composite material, deriving conservation equations 02 p0248 A72-11982
- Composites response to shock loading via Hugoniot synthesis based on theory of mixtures, expressing mass, momentum and energy balance 02 p0291 A72-11986
- Hugoniot equation of state for impact shock wave propagation along fiber direction in Al epoxy matrix composites 09 p1407 A72-23235
- Shock response of two constituent composites /Eikonites/, predicting Hugoniot states with allowance for thermal energy transfer 10 p1556 A72-24259
- Hugoniot equation of state measurements on iron-silicate garnet, showing shock induced transition to high pressure phase 11 p1627 A72-26524
- HUMAN BEHAVIOR**
- Operant conditioning for producing gross motor responses, discussing application to physical medicine and rehabilitation with mentally retarded Downs syndrome children 04 p0478 A72-14706
- Conditioned reflex as component of artificial conditioned-natural unconditioned reflex system controlling adaptive behavioral patterns, noting contribution to complex nervous activity understanding 04 p0476 A72-15582
- Rhythmogenesis as fundamental life characteristic analogous to homeostasis, discussing human circadian rhythm and cycle desynchronization during air travel 07 p0923 A72-20445
- Human behavior analysis based on nine component functional brain model, discussing information transmission mechanism via nerve path channels 07 p0923 A72-20460
- Behavioral inaction under stress conditions similar to survivable aircraft accident, tabulating hesitation statistics 08 p1109 A72-21570
- Soviet papers on human higher nervous activity physiology covering conditioned reflexes and adaptive behavior, neurotropic substance effects, mathematical and structural modeling, etc 08 p1118 A72-21834
- Human nervous system properties responsible for individual behavioral differences, discussing methodological problems in future research from biological criteria viewpoint 08 p1118 A72-21839
- Cortical synthesis and information handling properties of evoked potential in human normal and pathological behavior 08 p1119 A72-21840
- Human biodynamic and behavioral response to whole body vibration, discussing subjective judgment of vibration intensity and effects on performance 10 p1431 A72-24797
- EEG measurement of sleep behavior patterns, discussing sleep stages, temporal patterns, circadian rhythm, intrasleep process stability and age factor 11 p1580 A72-26679
- Integrated medical and behavioral laboratory for detection and measurement of space flight stresses, specific etiologies and human tolerances and adaptivity 12 p1796 A72-28279
- Passenger behavioral inaction in survivable aircraft accidents, suggesting maladaptive behavior counteraction by leadership and/or training 13 p1908 A72-28727
- Ideas of individual on group members majority behavior in various situations, noting norm concept confirmation from psychological tests on reference groups 13 p1903 A72-28796
- Russian book - Eye movements as the basis of spatial vision and as a model of behavior 17 p2509 A72-35459

Behavioral properties of somatosensory-motor interhemispheric transfer.

17 p2505 A72-35463

Error arising from experimenter influence on subject behavior and performance, discussing expectancy effects on stimulus presentation and IQ and success-failure judgments

18 p2653 A72-36907

Self-paced ergometer performance - Effects of pedal resistance, motivational contingency and inspired oxygen concentration.

18 p2653 A72-36911

Vicarious influence effect on eliciting pain in individuals subjected to previously reported nonpainful electric shocks

18 p2654 A72-36916

Historical development of right and left hand patterns in horsemanship, land vehicle, ship and aircraft control and navigation

18 p2707 A72-37050

Behavioural characteristics of men in the performance of some decision-making task components.

20 p2898 A72-39805

Two explanations of temporal changes in ability-skill relationships - A literature review and theoretical analysis.

21 p3008 A72-41015

Some contributions to the theory of linear models describing the control behaviour of the human operation.

21 p3011 A72-41419

The functional organisation of object directed human intended-movement and the forming of a mathematical model.

21 p3011 A72-41422

HUMAN BEINGS

Human biology, including evolution, organism structure, organizations of people, degeneracy, interactions with environment and philosophical concepts

06 p0765 A72-18315

Pigs role as ideal experimental animal in human biomedical research, discussing investigations to emphasize similarities

18 p2649 A72-36440

HUMAN BODY

Human body dynamics, discussing configuration, modeling techniques, kinematics, equations of motions and various limb motions examples

01 p0016 A72-10110

Anatomical-physiological, optical and behavioral-visual similarities of nonhuman and human primates

03 p0313 A72-13069

Human body movements basic kinematics, measuring static force, angle and tangential acceleration of horizontal arm swings

04 p0478 A72-14707

Human body kinematics numerical analysis, obtaining space-time resolution by photogrammetric restitution and electronic data processing of photographic recordings

04 p0478 A72-14710

Calorimetric measurements of human body temperature and of hot saline solution drinking effects on sweating rate

09 p1267 A72-23440

Calorimetric study of sweating man response to drinking hot saline solution as function of temperature, volume and salinity of ingested liquid

09 p1267 A72-23441

Skeletal bones ash content in man and primates, implying differences due to adaptive physiological function

10 p1424 A72-23736

Human body calorimetry with water cooled garment for dynamic and continuous recording of heat dissipation from surface over extended time

10 p1431 A72-24485

Human body efficiency in paced and unpaced performance as function of age

10 p1432 A72-24987

German papers on human body energy balance and temperature control covering energy conversion processes, chemical secretions, muscle activity, etc

11 p1584 A72-26071

Thermodynamics of human body metabolism, discussing energy conversion calorimetric measurements, body size, food intake, age, sex, endocrine and nervous effects

11 p1584 A72-26072

Human body thermoregulatory processes under varying environmental conditions and metabolic rates, discussing role of blood circulation, sweating, nervous stimuli, hormones, etc

11 p1584 A72-26073

Human body biochemical energy conversion processes during muscular activity, discussing nutrition, circulation and respiration roles

11 p1585 A72-26075

Geomagnetic field perturbation biological effects, studying geomagnetic storm field energy levels and magnetic flux variables relation to human sensitivity thresholds

12 p1773 A72-28210

Supine human body mechanical impedance under combined stress of vibration and sustained acceleration

12 p1765 A72-28270

Human torso surface mathematical model to determine equivalent heart dipole and quadrupole locations for ECG measurements

13 p1908 A72-28571

Human body or dummy mechanical impedance calculation by acceleration measurement at two point reference system with circular spring supporting mass

15 p2192 A72-32608

Two-mass system as human body dynamic model in ballistocardiography, outlining transfer function parameter computation procedure

18 p2652 A72-36039

Lipid peroxidation on the human skin surface following erythrogenic UV irradiation

19 p2757 A72-38087

Equal comfort contours for whole body vertical, pulsed sinusoidal vibration.

20 p2897 A72-39551

Man movements directed at reaching a preset goal

21 p3006 A72-40710

Thermal balance in man during 24 hours in a controlled environment

22 p3145 A72-42747

Mutual relations between different physiological functions in circadian rhythms in man.

22 p3147 A72-42979

HUMAN CENTRIFUGES

Human centrifuge tests for gravito-inertial force effect on ocular counterrolling in normal and deaf subjects

02 p0159 A72-11956

Human centrifuge tests for semicircular canal gyroscopic stimulation during sensory deprivation, discussing angular acceleration detection thresholds

04 p0478 A72-14865

Acceleration tolerance increase by static forearm muscular contraction exercise comparison to g-suit protection during human centrifuge tests

08 p1114 A72-20887

Positive acceleration effects on human cardiovascular system during centrifuge tests, studying ECG changes in terms of cardiac rhythm, heart rate and wave parameters

11 p1584 A72-26015

Human centrifuge studies of high positive acceleration effects on blood oxygenation and arterial oxygen and carbon dioxide tension

12 p1766 A72-28287

Involuntary head movement and helmet motion displacements during human centrifuge runs to 6 Gz from photographic recordings

12 p1766 A72-28288

Acceleration protection properties of modified partial pressure suit, determining tolerance limits by vision impairment criteria during centrifuge tests

12 p1776 A72-28319

Pilot pursuit tracking performance under acceleration stress, simulating high performance aircraft dynamics via human centrifuge equipped with simulated head-up predictive gunsight

12 p1776 A72-28320

Human physiological responses to high magnitude short duration positive accelerations, considering peripheral vision loss as function of time

24 p3377 A72-45660

HUMAN ENGINEERING

U HUMAN FACTORS ENGINEERING

HUMAN FACTORS ENGINEERING

Legibility of cold cathode, side illumination and straight projection electronic digital displays under varying ambient light and viewing positions

01 p0016 A72-10118

Optimum cylindrical handle size determination by muscle electromyography, considering gripping task, routine performance and fatigue test

01 p0017 A72-10119

General purpose electronic modular units for human factors research bioinstrumentation, considering digital and analog computers, logic modules and interface and auxiliary equipment

01 p0048 A72-10569

Human factors engineering of aircraft cockpit data entry keyboards on area navigation control and display units

01 p0020 A72-11138

Aircraft ride comfort problem in turbulent air, comparing free and fixed wing aircraft responses

02 p0154 A72-11720

Visual display systems for man-machine communications, discussing applications, data processing, hardware designs and human engineering

02 p0230 A72-12419

Book on human factors engineering covering systems design requirements and interface equipment for man machine interaction implementation

03 p0318 A72-13023

Human factors relation to pressurized cabin development, discussing aircraft safety, high altitude tests, pressure loss predictions and cabin altitude selection

04 p0479 A72-14869

ALSEP human engineering design criteria for crew interface, describing astronaut trainer

04 p0479 A72-15100

Fatal aviation accident human factors investigation by roentgenography, noting flight environment factors, injury pattern relation to aircraft design and victim identification

06 p0768 A72-17880

Maximum aerobic power response and oxygen consumption to training stimulus intensity, duration and frequency, using bicycle ergometer exercise

07 p0916 A72-18965

Man computer dialogue, considering human factors effects on interaction course

07 p0927 A72-19128

Instructor station design for automated flight training systems, considering human factors and informational requirements

07 p0928 A72-19277

Book on physiological approach to ergonomics covering muscular system, performance, work and fatigue, working efficiency and environment, man machine systems, etc

07 p0930 A72-19875

Helmet systems for head protection from concussion and deformation, discussing design and testing

08 p1126 A72-21568

Crashworthy upper torso restraint systems for general aviation, incorporating strap take-up devices

08 p1126 A72-21578

Man machine systems in navigation, discussing problems of integrating man with high speed and high capacity electromechanical systems with allowance for human weaknesses and abilities

09 p1269 A72-22777

Anthropotechnical aspects of V/STOL aircraft control, discussing instrument and control systems concepts based on development and flight tests of experimental Do-31 V/STOL aircraft

09 p1270 A72-22784

Space flight experience application to human factors engineering problems in air and maritime navigation, considering use of small digital computers, display and sensing devices

09 p1348 A72-22785

ATC tasks work load assessment - Conference, Darmstadt University of Technology, June 1971

09 p1270 A72-23126

Time analyses of ATC approach controller tasks, developing flow diagram for task component sequencing and quantifying

09 p1271 A72-23133

Multichannel automatic data acquisition and processing in ergonomic measurements of radar controller work from ECG, EOG, EMG and respiration

09 p1271 A72-23136

Ergonomic simulators for testing individual mental working capacity, using stress-strain and fatigue relation

09 p1272 A72-23140

Human operator role in space systems reliability, suggesting approaches to system design and program planning to exploit human potential

10 p1430 A72-24439

Space maintainability experiment aboard submersible during 30 day drift mission, noting application to Skylab manpower distribution

10 p1431 A72-24442

Fatigue factors in aircrew related to shift working and technological advances, considering implications for industry and work-rest cycles

10 p1432 A72-24988

Optimum performance typewriter keyboard design, discussing biomechanical improvements in finger positioning facilitation, operator postural muscular strain reduction, etc

10 p1433 A72-25114

Medical evaluation of manned space flight physiological effects, considering Mercury, Gemini and Apollo programs

11 p1585 A72-26100

Aircraft pilot seating protection from dynamic environment by active vibration isolation, discussing human frequency response characteristics

11 p1585 A72-26391

Weightlessness effects on human organism, discussing physiological changes, artificial gravity by spacecraft rotation and exercise to counter adverse reactions

11 p1589 A72-26891

Military R and D organization questionnaires data analysis to obtain relationship between job productivity, satisfaction, ability, age and salary

12 p1891 A72-27655

Human, technical and environmental factors in accidents of naval F-104 squadron, considering temporal distribution of accidents and pilot physical condition

12 p1772 A72-27820

Change in Naval Flight Officer operational role due to modern equipment design in weapons systems, sensors and navigational aids

12 p1775 A72-28291

FAA program for revision of aviation aircraft maximum allowable control forces specifications, taking into account female pilots capabilities

12 p1777 A72-28325

Future spacecraft habitable compartment layout from psychophysiological viewpoint, considering human visual and motor field parameters and crew members social needs

13 p1910 A72-29321

Pilots seating active and passive isolation from LF vibrations in helicopters and jet aircrafts, discussing human factors and dynamic environment

13 p1910 A72-29558

Computerized navigator training simulator for complete array of air navigation instruments, discussing design and human factors

15 p2214 A72-32208

Human factors engineering techniques in pilot-aircraft-environment adaptation to ease workload and in performance efficiency improvement

17 p2493 A72-35792

Meaningful shape coding for aircraft switch knobs.

17 p2510 A72-35944

Historical development of right and left hand patterns in horsemanship, land vehicle, ship and aircraft control and navigation

18 p2707 A72-37050

Area navigation and its affect on aircraft operation and systems design.

[AIAA PAPER 72-754]

19 p2831 A72-38125

Man machine systems operational effectiveness augmentation through human factors engineering to enhance human operator capability for parallel data processing and decision making

19 p2761 A72-38308

Visual information electronic display systems from human factors engineering viewpoint, discussing intelligibility optimization in terms of human vision physiological characteristics

19 p2803 A72-38309

A time-sharing computer program for defining human thermal comfort conditions in any atmosphere.

[ASME PAPER 72-ENAV-33]

20 p2905 A72-39142

The measurement of three-dimensional body movements by the use of photogrammetry.

20 p2898 A72-39806

Russian book - Space ergonomics.

21 p3004 A72-40300

USAF aerospace medical research on human capabilities as limiting factor in defense systems development, discussing environmental simulators and human test facilities

21 p3008 A72-40973

Design of vibration absorbers minimizing human discomfort.

21 p3009 A72-41231

Anthropotechnics/human engineering/ approach to man machine system optimization, discussing task allocation and adaptations of machine dynamics, displays and controls to human operator

21 p3009 A72-41403

Display device layout based on human operator manual control information requirements consideration, discussing functional categories, motion compatibility, indicators relation and integration

21 p3009 A72-41404

Display device design and human operator training based on visual and auditory sensation and perception principles, emphasizing fitting between man and information

21 p3010 A72-41407

Human operator decision making role in information presentation system determined by experiments using laboratory performance and test measures, field observation, electrical and biochemical measures

21 p3010 A72-41408

Man machine system input via human controller output transformation, illustrating with spacecraft lateral position manual control problem

21 p3010 A72-41411

Manual workload determination by control characteristics, control-display relationships, demands for dexterity and sensitivity and speed and accuracy requirements

21 p3010 A72-41414

Human engineering requirements in aircraft system development.

21 p3011 A72-41423

Applied research into the effects of vibration upon displays.

21 p3011 A72-41424

A new concept of flight displays compatible with digital airborne computers.

21 p3012 A72-41426

Influence of stick efficiency on tracking error applying two slightly different control elements.

21 p3012 A72-41429

A psychologist's laboratory approach to a human factors problem.

21 p3012 A72-41430

Spacecraft rescue/recovery capabilities, discussing in-flight escape, ground egress and descent systems, performance and technical and human factors

24 p3450 A72-45147

Human organism and space flight stress endurance limits and manned space mission rescue capabilities requirements, considering cabin decompression, anoxia, radiation, onboard illness, etc

24 p3376 A72-45218

Spacecraft food synthesis, using carbon dioxide and water from chemically regenerated human metabolic and waste products

24 p3376 A72-45277

Formation of an optimizing functional in control systems

24 p3386 A72-45511

Mathematical description of a human operator in ergatic control systems

24 p3376 A72-45514

Algorithmic description of the generalized operational characteristic of a human operator

24 p3376 A72-45515

Estimate of the operational efficiency of a human operator in the follow-up mode of a closed-loop control system

24 p3376 A72-45516

Methodical aspects of studies of ergatic differential-game systems

24 p3376 A72-45517

HUMAN FACTORS LABORATORIES

Computerized man machine systems human factors research simulator, discussing application to railroad train operations

06 p0795 A72-17434

Human annoyance reactions to sonic booms, discussing field and laboratory findings

09 p1273 A72-23321

HUMAN PATHOLOGY

Myokinase activity determination as diagnostic test for human myocardial infarction, comparing to creatine phosphokinase activity test

05 p0618 A72-16388

Book on experimental brain hypoxia covering changes in hemodynamics, energy metabolisms, electrolyte and water movement and cerebral and peripheral venous blood serum proteins

09 p1264 A72-22238

Vagus nerve regeneration in humans after stomach cancer surgery

13 p1903 A72-28779

Human heart physiopathology from cardiac performance analysis, treating heart as pump and muscle

15 p2187 A72-32493

Place of tropical pathology in medical assessment of aircrew

19 p2757 A72-37882

Pathology of the cardiovascular system in terms of the theory of cortico-visceral interrelations

21 p3000 A72-40756

Hazard rate of recurrence in germinal cell tumors of the testis.

22 p3150 A72-42498

Chronic altitude sickness pathology based on anatomical and histological findings in abnormal mountain inhabitants autopsies, comparing with cardiovascular system morphology in normal people

22 p3143 A72-42586

Time series analysis of meteoropathological disturbances of human regulation mechanisms, investigating annual variations of diurnal rhythms

22 p3147 A72-42977

HUMAN PERFORMANCE

NT ASTRONAUT PERFORMANCE

NT BLACKOUT PREVENTION

NT OPERATOR PERFORMANCE

NT PILOT PERFORMANCE

Human exercise capacity assessment from maximal oxygen intake estimates and Harvard step test

01 p0016 A72-10116

Optimal psychomotor performance in relation to thermal comfort conditions in man, using complex dual tests and subjective rating scales

01 p0016 A72-10117

Human touch deficiency in artificial pattern recognizers regarding handwriting, speech and pattern recognition involving nonevents

01 p0017 A72-10464

Sensory psychological invariance formation for perceptual functions in human visual system

01 p0011 A72-10468

Sensorimotor preconditions of single image impression in human binocular vision

01 p0018 A72-10477

Optimal flash rate and duty cycle for flashing visual indicators, testing observer ability to determine indicator state

01 p0018 A72-10565

Stellar intensity effect on angular navigation sighting accuracy attainable between star and lunar limb using Apollo T2 sextant

01 p0097 A72-10566

Age and physique effects on human continuous work capacity, monitoring heart rates during task performance

01 p0018 A72-10568

Psychological threshold for successiveness, tabulating probabilities for correct guesses of stimuli order

01 p0013 A72-10713

Methodological problems in unidimensional information transmission involving circular light identification tasks

01 p0013 A72-10718

Human pattern analysis by stabilized retinal image fragmentation as function of fade frequencies for angle and line stimuli in different orientations

01 p0014 A72-10721

Threshold stimulus for visual motion discrimination as function of velocity and luminance

01 p0014 A72-10722

Skill acquisition in performance of three phase code transformation task

01 p0021 A72-11193

Time sharing three phase code transformation multitask effects on sustained performance

01 p0021 A72-11194

Body cooling effect on human vigilance in hot environments, testing reaction time to visual stimuli and auditory signal detection rate

01 p0021 A72-11290

Human mental and psychomotor performance measurements in compressed oxygen-helium atmosphere pressure chamber for dive between 100 and 1500 feet

02 p0166 A72-11701

Aerospace vehicle acceleration effects on human performance, noting visual, motor and intellectual impairment levels relation to physiological tolerance limits

02 p0166 A72-11702

Human postural control system dynamic model, discussing stick man pitch axis dynamics digital simulation and difficulties in linearizing equations of motion

03 p0318 A72-13163

Human mental working capacity estimation relation to functional state, discussing brain performance tests

03 p0316 A72-13721

Psychological tests of airmen with performance error histories, considering psychic characteristics for limited assignment readjustment

03 p0316 A72-13723

Biomechanics - Conference, Eindhoven, Netherlands, August 1969

04 p0477 A72-14703

Human taste papillae sensitivity to chemical stimuli, showing stable quality and intensity response patterns

05 p0620 A72-17129

Human visual system selective adaptability to speed, size and orientation, suggesting motion analysis by visual cortex neural subsystems

06 p0761 A72-17603

Motivation in vigilance, studying effects of subject self evaluation and experimenter/knowledge of results/ controlled feedback

06 p0766 A72-17711

Human immediate memory adaptation to speed stress, discussing response time and performance accuracy relationship to stimuli complexity and input speed

06 p0766 A72-17716

Transmeridian flight psychological effects on aircrews, discussing anxiety, stress, circadian rhythm disruption and sleep loss effects on performance deterioration

06 p0766 A72-17816

Terminal area ATC specialists and trainees job attitude and motivation from questionnaire on challenge, tasks, salary, work schedule, etc

06 p0766 A72-17865

Color defective vision performance predictions during day and night tests of aviation color signal light discrimination

06 p0767 A72-17871

Bisensory performance in simultaneous auditory and visual verbal information recognition, demonstrating integrative action between hearing and vision

06 p0768 A72-17949

Book on sustained attention/vigilance/, discussing effects of signal frequency, magnitude and distribution, task complexity, noise, age, intelligence, etc

07 p0930 A72-19910

Eastbound and westbound transmeridian flights effect on body temperature and psychomotor and visual performance circadian rhythms, discussing readjustment times

[AMRL-TR-71-89]

07 p0921 A72-20176

Human performance and exhaustion predictive model from responses to exercise and environmental stresses, considering circulation, thermal regulation, work load and oxygen pressure effects

07 p0934 A72-20358

Acoustic tests of jet aircraft noise and sonic boom effects on sleep pattern and human performance, using EEG analysis

[ASA PAPER W 11]

08 p1125 A72-21487

Hypoxic and normoxic gas mixture breathing during intense muscular activity, relating oxygen consumption and carbon dioxide elimination magnitudes and motor performance

08 p1121 A72-22081

Noise effects on human attention and work efficiency in extroverted and introverted individuals

08 p1128 A72-22137

Loudness function correlations to illusory spiral aftereffect persistence, motion sickness susceptibility and auditory reaction time in individuals

08 p1128 A72-22138

Rest and activity patterns effect on space crews well-being and operational effectiveness during prolonged extraterrestrial missions, noting work load effect on long-haul transport aircrews

10 p1427 A72-23727
Prediction method for computing maintenance technician reliability as probability of equipment repair completion within given time

10 p1486 A72-24000
Stochastic models of human performance effectiveness functions reliability and correctability from error data generated by tracking and vigilance tasks

10 p1429 A72-24001
Human performance prediction dependence on task and equipment variables effects, using experimental data for performance classification system

10 p1429 A72-24003
Human biodynamic and behavioral response to whole body vibration, discussing subjective judgment of vibration intensity and effects on performance

10 p1431 A72-24797
Choice reaction task times for responses to signals by middle, little and index fingers

10 p1432 A72-24985
Human body efficiency in paced and unpaced performance as function of age

10 p1432 A72-24987
Anisotropic responses to dot and line visual stimuli, obtaining judgments on apparent straightness for various visual field locations and dot densities

10 p1427 A72-25183
Human performance under intense noise, measuring effects on muscle tension, metabolism, respiration rate, visual accommodation, saccadic eye movement and dark adaptation

11 p1583 A72-25728
Diurnal rhythm and loss of sleep effects on human efficiency - Conference, Strasbourg, July 1970

11 p1580 A72-26676
Human performance dependence on time of day, discussing circadian and physiological rhythms relation and environmental change effects

11 p1580 A72-26677
Sleep deprivation effects relation to work duration, time of day, circadian rhythm, memory function, task performance, environmental factors, drug use and age

11 p1580 A72-26678
Sleep loss effect on reaction and movement times during information processing in step tracking task

11 p1580 A72-26680
Time displacement effects on human physiological and psychological functions, discussing circadian rhythm phase shift and performance deficits

11 p1580 A72-26681
Mental performance tests in sleep deprived subjects for indication of recuperative function of slow wave and REM sleep stages

11 p1580 A72-26682
Cumulative partial sleep deprivation effects on human performance in auditory vigilance, routine addition and running digit span tests, observing circadian rhythms

11 p1581 A72-26683
Sleep, lack of sleep and circadian rhythm effects on psychometric test performance

11 p1581 A72-26684
Sleep interruption, sleep deprivation and continuous darkness effects on circadian rhythms in human performance

11 p1581 A72-26685
Sleep loss and work-rest cycle effects on combat efficiency, considering psychomotor reactivity, vigilance and decision making capacity

11 p1588 A72-26688
Cumulative sleep deficit, preceding sleep or wakefulness period duration and body temperature effects on reaction time in multiple choice visual task

11 p1581 A72-26690
Human functional level performance characteristics, noting relationship between spontaneous rhythm diurnal variations in psychic and physical performance

11 p1589 A72-26691
Sleep deprivation effect on circadian rhythms in human performance, psychological fatigue ratings, catecholamine excretion and urine flow

11 p1581 A72-26692
Circadian rhythm effects on introverts and extroverts biochemistry, physiology and performance, suggesting arousal mechanism differences

11 p1581 A72-26693
Project Pegasus vigilance tasks for mental performance aspects of time zone change effects on human circadian rhythms

11 p1589 A72-26695
Time zone transition induced circadian rhythm disturbance effect on military personnel mental and physiological performance

11 p1589 A72-26696
Auditory flutter fusion frequency changes in humans during prolonged visual deprivation

12 p1769 A72-27418

Jet aircraft noise effect on sleeping EEG and subsequent waking performance, showing presence of carry-over effects

12 p1770 A72-27474
Individuals with high information potential in informal communications networks of government R and D organizations, discussing personal characteristics

12 p1891 A72-27654
Detection probability for moving small targets embedded in random white noise on TV display, comparing machine processed pattern recognition techniques and human performances

12 p1843 A72-27933
Parachutist biomedical responses in aerial tow at 110-175 knots, determining heart and respiration rates and urinary catecholamines

12 p1774 A72-28272
Periodic, continuous and aperiodic white noise effects on human serial decoding performance, relating subjective and autonomic responses

12 p1775 A72-28289
Self estimated distractibility in subjects related to attention lapses during perceptual motor performance, indicating psychophysiological changes

12 p1776 A72-28307
EEG diurnal rhythms during 72 hour insomnia, considering adaptation to altered work-rest cycle in subjects with stable and unstable brain activity rhythms

13 p1904 A72-29319
Human flexible processing accomplishment in speeded recognition task with visual stimulus dimension relevancy contingent upon other dimension stimuli values

13 p1911 A72-29832
Statistical periodic analysis of cyclic activity in human perceptual-motor performance

13 p1911 A72-29845
Divided attention effect localization, using choice tracking task reaction times in sequential stage model for human information processing

13 p1911 A72-29852
Vigilance effects for noise or vibration stimuli duration judgment task performed with or without simultaneous mental arithmetic task

14 p2080 A72-30964
Noise and vibration stress combined effects on human mental performance as function of time of day, taking into account circadian rhythm factor

14 p2081 A72-31083
High temperature and altitude combined effects on performance of tracking, monitoring and mental arithmetic complex task

14 p2083 A72-31155
White background noise intensity effects on human visual target detection performance considering display difficulty levels, target location, detection time and error

14 p2083 A72-31156
Momentary velocity measurement of human walking in forward movement by frequency response of signal on magnetic tape

15 p2190 A72-32200
Hypokinesia and motor activity of humans in industrial societies, noting prolonged inactivity and posture maintaining effects

16 p2353 A72-33098
Predictive model for human operator performance in short term visual information processing based on psychological research to obtain decision accuracy and response time

16 p2359 A72-33865
Auditory display in dual-axis compensatory tracking task, discussing performance measures in terms of squared error integral and human operator describing functions

16 p2359 A72-33866
Altitude effects on decision making performance of cognitive, psychomotor and complex card sorting tasks

16 p2357 A72-34096
Possibilities and dangers during long working periods in space rescue.

17 p2507 A72-34436
Natural acclimatization to work in severe heat.

17 p2508 A72-34550
Effects of different alcohol dosages and display illumination on tracking performance during vestibular stimulation.

17 p2508 A72-34554
Error arising from experimenter influence on subject behavior and performance, discussing expectancy effects on stimulus presentation and IQ and success-failure judgments

18 p2653 A72-36907
Psychological tests to judge maximum and minimum nonphysical subjective attraction forces between two parallel bars

18 p2654 A72-36919
Theoretical models for speed-accuracy tradeoff during difficult visual discrimination tasks under time pressure

18 p2655 A72-37220

Psychological tests for diurnal variations of human visual discrimination threshold by varying test object illumination level

20 p2891 A72-38931
Psychophysical information content evaluation of aerial photographic images by human viewer for photointerpretation and search in reference library

20 p2894 A72-39042
Behavioural characteristics of men in the performance of some decision-making task components.

20 p2898 A72-39805
Evaluation of cardiopulmonary function and work performance in man during caloric restriction.

21 p3005 A72-40423
Threshold detection model for foveal viewing by human observers using naked eye

21 p3007 A72-40733
Night vision performance measure based on object recognition experiments with optical instruments, noting improvement with image intensifier

21 p3007 A72-40741
Noise and stimuli current time and spatial distribution effect on visual performance of eye with image intensifier

21 p3054 A72-40742
The minimum brightness gain required in viewers using image intensifiers.

21 p3055 A72-40744
The visibility range when observing an aircraft with and without field-glasses.

21 p3007 A72-40750
Vestibular and optical stimuli interaction in human orientation, testing via Barany chair on rotating platform surrounded by optokinetic drum

21 p3007 A72-40751
USAF aerospace medical research on human capabilities as limiting factor in defense systems development, discussing environmental simulators and human test facilities

21 p3008 A72-40973
Two explanations of temporal changes in ability-skill relationships - A literature review and theoretical analysis.

21 p3008 A72-41015
Team size and decision rule in the performance of simulated monitoring teams.

21 p3008 A72-41016
Error search reading tasks to investigate practical applicability of blinking display coding techniques, noting reading speed reduction compared to steady display

21 p3008 A72-41018
Body orientation under vertical sinusoidal vibration.

21 p3008 A72-41019
Manual workload determination by control characteristics, control-display relationships, demands for dexterity and sensitivity and speed and accuracy requirements

21 p3010 A72-41414
Human engineering requirements in aircraft system development.

21 p3011 A72-41423
Applied research into the effects of vibration upon displays.

21 p3011 A72-41424
The foot as input device for control operation.

21 p3012 A72-41428
The influence of a prediction display on the human transfer characteristics.

21 p3012 A72-41432
Changes in certain hemodynamic indices during muscular strain in people with differing capacity to perform work

24 p3370 A72-44591
Human observation error effect on astronomical refraction calculation from time determination of solar limbs passages across optical instrument reticle

24 p3438 A72-44863
Content and time aspects of short and long term memory operation theories, relating attention and memory spans

24 p3373 A72-45243

HUMAN REACTIONS

Environmental noise induced human fatigue, considering physiological and psychological effects

01 p0016 A72-10050
Human cardiocirculatory responses to submaximal physiologically paced bicycle ergometry, recording prejection period, isovolumic contraction, left ventricular ejection and pulse transmission time

01 p0010 A72-10147
Respiration effects on human heart rate deceleration and biphasic cardiac response in aversive shock conditioning situation

01 p0010 A72-10195
Vibration space analysis for human voice characteristics change during unintended speech under experimental psychological stresses and actual emergency situations

01 p0017 A72-10213
Long term bed rest effect on humans and primates, detailing cardiovascular metabolic and musculoskeletal physiological systems

[AD-737557]

01 p0014 A72-10932

Spatio-temporal scalp mapping localization of human visual evoked responses to full field light adapted stimulation, comparing to half-field stimulation
01 p0015 A72-11185

Hemodynamics, pulmonary gas exchange and circulatory responses to high altitude in subjects with previous history of high altitude pulmonary edema
02 p0156 A72-11422

Visual masking effect due to light offset, investigating human identification response to tachistoscopic test stimuli on lighted background with simultaneous shut-off
02 p0166 A72-11550

Physiological effects of localized ventilation, noting human comfort improvement association with reductions in average skin temperature and sweat rate
02 p0159 A72-11955

Skin and hypothalamic temperature effects on human thermoregulatory responses, developing control mechanism for peripheral effects on skin sensors
02 p0160 A72-12041

Alpha-L-fucosidase, beta- and alpha-D-galactosidases and alpha-D-mannosidase activity changes in human placenta at various embryogenesis phases
02 p0163 A72-12294

External respiration gas metabolism and energy consumption measurements for test pilots during parabolic trajectory flights in weightlessness simulation experiments
02 p0163 A72-12347

Monotonous auditory stimulation frequency effects on human orienting reaction habituation and sleep onset
02 p0169 A72-12494

Reactions choice limiting cueing signals effect on reaction time, considering dependence on time interval between cueing and start signals
02 p0165 A72-12852

Rating scale judgments of aircraft noise based on surveys around airport
03 p0309 A72-12956

Astronaut zero gravity adaptive responses in performance, locomotion, orientation, sleep and physiological and functional characteristics
03 p0319 A72-13867

Fast and slow human muscle fibers temporal response characteristics, using tensometric recording
03 p0317 A72-13989

Human muscular electrical activity in various body positions, noting potentials during natural and unaccustomed postures
03 p0317 A72-13990

Human neuromuscular coordination control optimization, discussing preprogrammed open-loop control with feedback monitoring loop
04 p0477 A72-14705

Daily prolonged exercises effects on human muscle glycogen utilization, noting reduced lactate accumulation and increased free fatty acid levels
04 p0480 A72-15213

Human vestibulo-ocular responses to oscillatory rotational stimulation during various sleep and arousal stages, discussing Sugie-Jones reflex system mathematical model
04 p0474 A72-15249

Blink reflexes in man during sleep and wakefulness, discussing electromyographically recorded orbicularis oculi mono- and polysynaptic responses to electrical stimuli
04 p0474 A72-15250

External biodynamic models for human mechanical response to various environmental forces, emphasizing injury mechanisms
04 p0481 A72-15266

Human trace responses generation and storage under light stimulus reinforcement of sound conditioning from galvanic skin reactions observation
04 p0475 A72-15581

Successive visual motion illusion during perception of rotating kymograph drum by human eye
04 p0476 A72-15588

Human reaction to inhalation of gas mixtures with 3-9 percent carbon dioxide, measuring respiration rates, minute breathing volume, heart rates, arterial pressures, etc
05 p0618 A72-16632

Airport surrounding communities survey on attitudes toward aircraft noise, noting daily activity disturbance, emotional reactions, economic effects, noise abatement awareness, etc
06 p0767 A72-17870

Crew members handling of emotionally disturbed aircraft passengers
07 p0926 A72-18836

Electromyogram study of antagonist muscles reactions to Achilles tendon percussion or whole body sudden motion via test stand jerking
07 p0915 A72-18864

Acid base balance in arterialized capillary blood in men after maximal short duration exercise
07 p0929 A72-19441

Weak If electric field influence on circadian rhythms of human rectal temperature and activity
07 p0918 A72-19531

Community response prediction to noise based on laboratory tests of individual acceptability judgments
07 p0932 A72-20172

Design criteria for transportation system noise regulation, considering ambient noise, hearing damage, speech interference and subjective reactions
07 p0932 A72-20173

Hypoxia effect on aircraft pilot performance during altitude and flight simulation, testing instrument landing approaches
07 p0933 A72-20186

Hypnotic drug use effect on pilot performance and flight safety, using glutethimide, flurazepam and placebo in double blind study
07 p0933 A72-20188

Human temperature regulation during upright and supine exercise, showing nonlinear relationships between perspiration and skin and core temperatures
07 p0932 A72-20275

Motoneuron pool fraction determination in human monosynaptic response of healthy and neuropathological subjects, comparing diagnostic methods
07 p0924 A72-20619

Human response to sonic booms, discussing supersonic commercial flights acceptability
08 p1127 A72-21910

Sonic boom exposure effect on humans based on visual performance and tracking tests
08 p1127 A72-21912

Three color response of human vision, noting relationships to color matching function and brightness
09 p1269 A72-22617

Human reactions to sonic boom acoustic stimuli, noting startle reflex responses
09 p1267 A72-23320

Human annoyance reactions to sonic booms, discussing field and laboratory findings
09 p1273 A72-23321

Summary of 1971 Stockholm workshop on sonic boom effects, discussing humans, animals and structure exposure and interdisciplinary aspects
09 p1273 A72-23324

Human tilt tolerance relation to aerobic capacity, weight, height and physical fitness, determining correlation coefficient between heart rate and orthostatic response
10 p1428 A72-23733

Sympathetic responses in human skin nerves with accompanying vasomotor reactions induced by emotional, thermal and respiratory stimuli
10 p1424 A72-24241

Stimulus complexity effect on amplitude of human cyclofusional response, evaluating relative roles of compensatory eye movements and central responses
10 p1427 A72-25180

Pilot warning systems for visual midair collision avoidance, noting reaction to imminent threats, scanning patterns and display sector size effects
11 p1583 A72-25576

Audiometric determination of human temporary threshold shifts due to steady state and impulsive noise
11 p1583 A72-25873

Ear oximeter design for human subject blood oxygen saturation estimation during increased g-loads
12 p1774 A72-28278

EEG recording and analysis by analog technique as means of studying human responses to hyperventilation
12 p1767 A72-28312

Human visual accommodation biorhythm and reactions under hard physical work and visual stress
13 p1909 A72-28749

Spatial and temporal summation characteristics and relationship in human peripheral retina investigated for stimuli viewed at eccentricity against luminous background
13 p1907 A72-29970

Human respiratory rate diurnal rhythm adjustments during inverted work-rest cycles in isolation chamber with controlled comfortable atmospheres
14 p2075 A72-30390

Heart rate diurnal rhythm adaptation to work-rest cycle change, using recumbent and sitting position data parameters
14 p2075 A72-30391

Medical factors in air racing accidents, investigating drug, fatigue and gastrointestinal symptoms effects on pilot reaction to emergency
14 p2081 A72-31089

Aircraft pilot reaction capability for switch activation in response to voice countdown, tone initiation and termination, noting standard deviation
15 p2188 A72-31787

Human cerebral hemodynamic changes during arousal and orienting reactions to auditory stimuli
16 p2353 A72-32993

Noise pollution measurements parameter selection based on human reactions and attitudes, discussing psychoacoustic experiments, ratings and acoustic instruments
16 p2390 A72-33165

Model to account for visual responses to light flashes of dark adapted eye, discussing perceived brightness variation with intensity
18 p2651 A72-36611

Repression-sensitization and duration of visual attention
18 p2654 A72-36917

Equal comfort contours for whole body vertical, pulsed sinusoidal vibration
20 p2897 A72-39551

Changes in the functional state of analysts in flying personnel during long flights
21 p3006 A72-40445

Blood serum enzymes activity changes in polytraumatized humans injured in automobile accidents
21 p3002 A72-41188

Prediction of vegetative reactions to extremal actions on the organism
22 p3141 A72-42168

Reaction time to the second of two shortly spaced auditory signals both varying in intensity
22 p3142 A72-42549

Pain perception anatomical and neurophysiological mechanism, discussing human response to mechanical, thermal and chemical pain inducing stimuli
22 p3146 A72-42780

Sonic boom effects on sleep - A field experiment on military and civilian populations
23 p3261 A72-44370

Ensemble characteristics of the human visual evoked response - Periodic and random stimulation
24 p3374 A72-44575

Sonic boom startle - A field study in Meppen, West Germany
24 p3374 A72-44916

HUMAN TOLERANCES

Reproducibility of acute mountain sickness severity and duration in individuals under high altitude simulation, noting relationship to hypoxia
01 p0021 A72-11287

Cosmic ray exposure thindown tracks in human tissue from solar minimum to maximum at SST flight level
02 p0163 A72-12079

Spacecraft and aircraft crew survival after emergency landing in adverse environments, discussing water and food requirements, survival supplies and medical and first aid equipment
05 p0621 A72-16629

Human vestibular stability under frontal and sagittal head tilts in rotating chairs, discussing motion sickness onset
05 p0622 A72-16640

Duration effect on judged acceptability of noise, discussing interpretation and meaning of laboratory determinations
06 p0766 A72-17765

Harmful influence of random vibrations on human organism, discussing Fokker-Planck analysis and amplitude and frequency variation effects
06 p0770 A72-18720

Dynamic response and functional state of human operator subjected to harmonic and random vibrational excitations, discussing biodynamic nonlinear oscillatory system model construction
06 p0770 A72-18728

Human external respiration characteristics changes during increasing hypercapnia, relating carbon dioxide concentration rate to compensatory mechanisms and endurance
08 p1121 A72-22084

Circadian adrenal periodicity of plasma corticosteroid levels in man under random living schedule
09 p1265 A72-22643

Safe exposure times for men working in high temperature environments, showing hyperbolic heat collapse relationship to environmental severity
10 p1432 A72-24990

Pathophysiology of exposure to UV, IR, coherent, microwave and RF radiations, discussing potential hazards, damage, human tolerance threshold, protection guides and safety standards
12 p1772 A72-27963

Integrated medical and behavioral laboratory for detection and measurement of space flight stresses, specific etiologies and human tolerances and adaptivity
12 p1796 A72-28279

Centrifugation tolerance reduction after 14 days bed rest with moderate exercise, determining rehydration effects
12 p1766 A72-28295

Physiological and subjective responses of physically fit young men to combined exercise-carbon dioxide stress tests
12 p1767 A72-28311

Pilot and back-seat man physiological responses during high-g aerial combat maneuvers in F-4E aircraft, discussing ECG, respiratory rate and minute volume
12 p1767 A72-28317

Valsalva and M-1 maneuvers acceleration tolerance protective effects during high-g centrifuging with and without anti-g suits
12 p1767 A72-28318

Human acceleration stress tolerance monitoring techniques for temporal, brachial and radial arterial blood flow and indirect systolic and diastolic blood pressure measurements

12 p1777 A72-28328

Miniature swine as human analog to investigate physiological response to high positive acceleration, comparing human and animal tolerances

12 p1768 A72-28329

Low pressure chamber as aerospace medical diagnostics tool for flying personnel examinations regarding oxygen deficiency, low air pressure and air pressure fluctuations tolerance

14 p2080 A72-30819

Crash energy absorption for prevention of fatal injuries, considering human deceleration tolerance with respect to required energy absorber force-deflection relationship

15 p2192 A72-32630

Individual functions and intersubject differences of noise annoyance susceptibility, noting relationship to Rorschach test

16 p2357 A72-32987

A new model for estimating space proton dose to body organs.

17 p2508 A72-35354

Hemodynamic thermoregulatory and sympathoadrenal responses to heat acclimatization in man during supine and upright position exercise

17 p2506 A72-35963

Respiratory frequency and alveolar oxygen and carbon dioxide tension relationship to hypercapnia in man

17 p2506 A72-35965

Skin temperatures in warm environments and the control of sweat evaporation.

17 p2506 A72-35969

Human tolerance to high, sustained +Gz acceleration.

19 p2758 A72-38702

Comparison of irregular vibrations of a limited frequency range with sinusoidal vibrations in regard to their effect on man

20 p2897 A72-39804

Acceleration tolerance of man after a lasting exposure to conditions of simulated weightlessness

21 p3006 A72-40442

Effect of psychotropic substances on human resistance to acceleration

21 p3006 A72-40443

Study of hemodynamics during the action of decompression and accelerations

21 p3006 A72-40444

Influence of high temperature on the onset of motion sickness

21 p3004 A72-41749

Influence of prolonged longitudinal accelerations on control habits

21 p3004 A72-41750

Effect of fasting on tolerance to moderate hypoxia.

22 p3150 A72-42487

Adaptive processes responsible for natural acclimatization of human organism to low ambient pressures at high altitudes

22 p3143 A72-42584

Human tolerance limitations related to aircraft crashworthiness.

22 p3151 A72-42765

Toxicity of rocket fuels

24 p3433 A72-44781

Biochemical and physiological evaluation of nourishment of subjects feeding on dehydrated products in test chamber with regenerative life support system, discussing metabolic data and hormone function

24 p3375 A72-45128

Human organism and space flight stress endurance limits and manned space mission rescue capabilities requirements, considering cabin decompression, anoxia, radiation, onboard illness, etc

24 p3376 A72-45218

Relationship of sodium deprivation to +Gz acceleration tolerance.

24 p3377 A72-45653

Human physiological responses to high magnitude short duration positive accelerations, considering peripheral vision loss as function of time

24 p3377 A72-45660

HUMAN WASTES

NT SWEAT

NT URINE

Food ration effect on metabolite elimination rate in humans wearing isolation garment at rest or performing physical labor

05 p0622 A72-16644

Catalytic oxidation of gaseous products formed during thermal treatment of human wastes, considering hopcalite, Cu-Cr, Cu-Co, Pt and Pd

05 p0622 A72-16646

Human waste management system evaluation in zero gravity flight tests, presenting design concept for collection by air flow technique

15 p2189 A72-31825

Space shuttle waste collection system development, discussing human-interface requirements, zero gravity effects and operational considerations

[ASME PAPER 72-ENAV-13] 20 p2896 A72-39164

Dry incineration of wastes for aerospace waste management systems.

[ASME PAPER 72-ENAV-2] 20 p2896 A72-39175

Some transport techniques for liquid human wastes and wash water under space flight conditions

21 p3006 A72-40436

HUMIDITY

Atmospheric vertical humidity profile from ground measurements of radio wave absorption at 1.35 cm water vapor line

08 p1158 A72-21192

Near-ground daytime temperature and humidity fine structure relation to heat flux, net radiation and temperature and wind gradients

12 p1841 A72-27711

Total precipitable water in atmosphere vertical column relation to surface humidity from measurements at desert, coastal and maritime sites

13 p1989 A72-28812

Atmospheric humidity, temperature, vibrational and static loads effects on composite and double base rocket propellants strength and safety characteristics

14 p2145 A72-30764

Atmospheric surface layer temperature, humidity and vertical wind velocity variances dependence on turbulent fluctuation inputs

16 p2419 A72-34148

Brittle lacquer of air-drying type, investigating coating ingredients and plasticizers effect on strain sensitivity for various temperature and humidity levels

20 p2920 A72-38890

Ground humidity and wind velocity effects on terrestrial scintillation, considering adiabatic temperature stratification factor

21 p3007 A72-40738

Heat strain in hot and humid environments.

22 p3150 A72-42492

HUMIDITY MEASUREMENT

Raman scattering from water vapor for Ar laser wavelengths in remote atmospheric humidity measurements

[AIAA PAPER 71-1085] 01 p0104 A72-10542

Atmospheric humid cover measurement with airborne/spaceborne microwave radiometric sounding, considering radiothermal radiation models

02 p0253 A72-11733

Airborne or satellite-mounted millimeter wave radiometer for atmospheric water vapor determination noting accuracy advantage over IR measurement

06 p0814 A72-17589

Refractometer design based on air dielectric constant dependence on humidity, comparing performance with Ly-alpha humidimeter

06 p0841 A72-17668

Atmospheric humidity forecasts from field evolution and transfer and specific humidity deficit description with equations system

07 p1031 A72-20699

Hair hygrometer for FM radiosonde in-flight air humidity measurements, discussing design, operation and accuracy test in extreme weather conditions

10 p1483 A72-25005

LiCl dew point hygrometer operation investigated by double ventilation psychrometers, noting measurement error dependence on relative humidity and temperature

10 p1483 A72-25015

Air hygrometer with heated electrolytic sensor for atmospheric humidity determination by automatic meteorological stations

10 p1483 A72-25016

Airport meteorological instrumentation, discussing ground wind, visibility, cloud height, air temperature and humidity detectors and radar equipment

10 p1484 A72-25093

Atmospheric humidity vertical profile determination by measuring microwave radiation from satellite

11 p1620 A72-25274

HURRICANES

Storm forecasts by meteorological satellites, describing TV monitoring of cyclones and hurricanes

05 p0683 A72-15978

Tropical hurricane model describing initial whirlwind and self exciting wind velocity development and dependence on ocean surface temperature

11 p1682 A72-26879

Elementary considerations of the fluid mechanics of tornadoes and hurricanes.

24 p3421 A72-45021

HUYGENS PRINCIPLE

Kirchhoff diffraction theory of scalar and electromagnetic waves application to elastic media, discussing Huygens principle, elastic waves tensor potential and Fresnel and Fraunhofer diffraction

04 p0548 A72-14740

First and second moment of an optical wave propagating in a random medium - Equivalence of the solution of the Dyson and Bethe-Salpeter equation to that obtained by the Huygens-Fresnel principle.

17 p2580 A72-34290

HYBRID COMBUSTION

U HYBRID PROPELLANT ROCKET ENGINES

HYBRID COMPUTERS

Hybrid computer simulation program used in development and software design validation of digital flight control system for Titan 3C space booster

02 p0186 A72-11655

Monte Carlo methods for hybrid computer solution of nonlinear parabolic partial differential equations with two spatial dimensions

02 p0186 A72-11657

Hybrid computer for solving complex problems in distributed parameter systems in terms of parabolic differential equations

02 p0188 A72-12655

Hyperbolic partial differential equations solution by hybrid computer, simulating wave propagation by track hold circuits

02 p0188 A72-12656

Hybrid computer simulation of spinning satellite dynamic behavior during flexible booms deployment and attitude control maneuvers, deriving equations of motion from Lagrange equations

02 p0286 A72-12658

Hybrid computer study of phenomenological biophysics, discussing regular information isolation from biological noise

02 p0169 A72-12662

Simulation language for digital static checks for hybrid and analog computers

04 p0495 A72-14417

Hsu-Howe iterative hybrid method for partial differential equations solution by time sharing analog components, using dynamic scaling and incremental formulations for reduced sensitivity

04 p0495 A72-14418

Time shared electronically patched hybrid computer for design automation, discussing remote terminal graphics capabilities and simulation language compiler

06 p0778 A72-17476

Hybrid computer aided design of thick electrostatic electron lenses by Laplace equation solution in terms of cylindrical harmonics, applying to CRT

06 p0779 A72-17481

Hybrid computer solution of partial differential equations by invariant imbedding application to serial method

06 p0839 A72-17631

Digital differential analyzers number comparison in realization of direction cosine, Euler angle and quaternion attitude algorithms

07 p0949 A72-19296

Hybrid computer simulation for telemetry data collected during missile flight control system model post-flight verification and hardware performance analysis

07 p1085 A72-20332

Hybrid computer and graphics terminals for real time dynamic man machine interaction, discussing AM communication system simulation

07 p0951 A72-20335

Hybrid computer synthesis and simulation algorithm for optimal discrete nonlinear filters, giving timing, accuracy and equipment requirement estimates

08 p1137 A72-20851

Hybrid computer simulation of cardiovascular system in biomedical engineering education

09 p1268 A72-22455

Hybrid computing techniques in helicopter simulation, taking into account complex dynamic systems nonlinear effects

09 p1283 A72-22936

Hybrid computer aided synthesis of thick electrostatic electron lenses by Laplace equation solution in terms of cylindrical harmonics with gradient used in trajectory integration

10 p1509 A72-23940

Analog and hybrid computers automated programming, setup and checking facilities for off and on-line program preparation and debugging

10 p1445 A72-24090

Hybrid computation interpolation procedure, using table of function values represented by two dimensional array stored in digital computer core memory

10 p1445 A72-24092

Heat conductivity differential equation solution by hydraulic model system, facilitating temperature values conversion into electrical quantities for hybrid computer

12 p1888 A72-27301

Hybrid computers application to digital communication systems design, using real time simulation

12 p1786 A72-27324

Hybrid computer Monte Carlo solution algorithm for parabolic partial differential equations with time varying boundary conditions, applying to ferromagnetic rod magnetization problem

12 p1787 A72-28119

Frequency response data identification technique using adaptive hybrid computer to improve quality and acquisition time

13 p1935 A72-29103

Pilot trainer transfer function identification for man-machine and on-line adaptive control system using analog/hybrid computer

14 p2091 A72-30721

- Programmable digital differential analyzer for connection to digital computer, discussing dynamical problem solution and real time systems simulation capability
15 p2204 A72-32387
- Hybrid computer simulation of cochlea mathematical model, noting nonlinear damping
16 p2359 A72-33971
- Laser computer technology - Today and tomorrow.
III
17 p2523 A72-35186
- Hybrid computer Monte Carlo solution algorithm for parabolic partial differential equations with time varying boundary conditions, applying to ferromagnetic rod magnetization problem
19 p2770 A72-38620
- A simulation technique used in the development of a flight control system for an aerodynamically controlled missile.
[AIAA PAPER 72-858]
20 p2976 A72-39136
- Assessment of the errors of a version of the hybrid quasi-analog system due to errors in quantization in time in the solution of systems of ordinary differential equations
21 p3024 A72-40158
- A hybrid quasi-analog system for solving boundary value problems
21 p3024 A72-40159
- The possibility of constructing an algorithmically universal hybrid computer
21 p3024 A72-40177
- Computer simulations of transport processes.
21 p3024 A72-40247
- Book - Computer simulation of dynamic systems.
22 p3157 A72-43081
- Respiratory control system benchmark simulation on hybrid computer for Cheyne-Stokes breathing, emphasizing equations for arterial and venous carbon dioxide and oxygen stores
23 p3268 A72-44551
- ### HYBRID NAVIGATION SYSTEMS
- A hybrid navigation concept using a spinning satellite-borne interferometer and self-contained equipment.
21 p3082 A72-41083
- ### HYBRID PROPELLANT ROCKET ENGINES
- Polyethylene-FLOX hybrid stage optimum combustion chamber pressure, representing pressure dependent factors by simple analytical models
01 p0117 A72-11221
- Experimental hybrid rocket engine combustion chamber with solid oxidizer lining of ammonium nitrate and perchlorate eutectic mixture
05 p0708 A72-17249
- Solid charge design for hybrid rocket engine with constant liquid propellant component consumption, deriving differential equation for perforated grain burning rate
07 p1053 A72-18994
- Hybrid rocket engine design, operation and performance, discussing optimum liquid and solid fuel combinations
07 p1055 A72-20303
- Mathematical model of reactive fluid flows during postignition transients in hybrid propellant rocket system
13 p2025 A72-28416
- Development of a solid fuel on a polyurethane basis for a hybrid rocket propulsion system with 98% nitric acid as oxidizer
20 p2962 A72-39416
- ### HYBRID PROPELLANTS
- The transient processes in hybrid solid propellant combustion chamber throttled by supersonic nozzle.
24 p3434 A72-45198
- ### HYBRID PROPULSION
- Mach 0.80 quiet intercity STOL transport design comparison for turbofan, prop-fan and turboprop systems
[SAE PAPER 710759]
01 p0003 A72-10256
- Space vehicle with solid-liquid propulsion system, determining optimal initial mixing ratio for cylindrical configuration
[DGLR PAPER 71-101]
02 p0271 A72-12706
- Wave energy exchanger for hybrid propulsion system.
[ICAS PAPER 72-47]
21 p3100 A72-41172
- ### HYBRID ROCKET ENGINES
- High efficiency hybrid rocket motor based on polyester fuel and RFNA oxidizer, determining correlation between burning rate, oxidizer and total flow rates
15 p2297 A72-31207
- ### HYDRATES
- Proton and fluorine nuclear magnetic spin-lattice relaxations due to internal rotations in magnesium fluorosilicate hexahydrate
04 p0564 A72-15636
- Hydrated iron silicon fluoride internal motion pressure dependence examined by wide-line and NMR techniques, noting corrections of second moments for bulk paramagnetic effects
13 p1914 A72-30061
- Phase transition between solid hydrate and saturated solution of lithium chloride electrically detected on a lithium chloride heated hygrometer.
21 p3054 A72-40689
- ### HYDRATION
- Centrifugation tolerance reduction after 14 days bed rest with moderate exercise, determining rehydration effects
12 p1766 A72-28295
- Biomembrane hydration mechanism of Na-K ion pump of living cell based on fractionation at air-sea interface
18 p2649 A72-36441
- ### HYDRAULIC ACTUATORS
- #### U ACTUATORS
- #### U HYDRAULIC EQUIPMENT
- ### HYDRAULIC ANALOGIES
- Hydraulic analogy application to heat conduction problems, considering seepage and network pipe flow models for complex heat flux phenomena representation
01 p0145 A72-11174
- Hydraulic transmission line equations for computer simulation of arterial circulatory systems
10 p1431 A72-24811
- Morning glory, showing squall formation by atmospheric hydraulic jump favored by slack pressure gradients, cloudless skies and low latitudes
11 p1681 A72-26080
- Reynolds analogy for twisted liquid flow in tube with swirl vanes
11 p1619 A72-26968
- Numerical shallow fluid model for air flow across orographic variable grid barrier, using idealized Andes Mountains range
12 p1838 A72-27023
- Heat conductivity differential equation solution by hydraulic model system, facilitating temperature values conversion into electrical quantities for hybrid computer
12 p1888 A72-27301
- Water table study of monostable fluidic amplifiers with allowance for geometrical similarity and Reynolds number for air operated models
16 p2353 A72-34139
- Analysis by hydraulic analogy of rotating separation in compressors
22 p3167 A72-43091
- ### HYDRAULIC CONTROL
- Concorde supersonic transport hydraulic control systems, describing design features with emphasis on reliability
03 p0312 A72-13962
- Directional selector valves with proportional flow control under varying load conditions, discussing hydraulic spool valves design
03 p0312 A72-13963
- Airplane hydraulic control systems digital simulation, using method of characteristics for distributed parameter analysis of transmission line dynamics
[ASME PAPER 71-WA/FE-21]
05 p0615 A72-15928
- Flight test evaluation of A-7D/E emergency backup flight control system, describing hydraulic power control systems design and function
05 p0687 A72-16664
- Aircraft turboalternator governing theory for frequency error detection, comparing performance of mechanical- and electro-hydraulic governors
06 p0868 A72-18249
- Dynamic response predictions of fluidically controlled pulsatile hydraulic flow and pressure generator for biomedical systems
07 p0914 A72-18820
- Hydraulic servomechanism spool type control valve orifice flow characteristics, measuring mass flow for various spool determined port shapes
07 p0915 A72-20533
- F-111 aircraft landing gear and speedbrake hydraulic system control by single dual-function valve, describing design features and performance characteristics
08 p1111 A72-21024
- Electrochemical machining with forward speed control via hydraulic means
08 p1175 A72-21043
- Three phase bidirectional pulsating flow hydraulic control system, discussing design, performance and applications
08 p1114 A72-22162
- Open capillaries control mechanism of pulmonary diffusion capacity, presenting mathematical interpretation of humoral and hydraulic blood pressure control
10 p1426 A72-24787
- Hydraulic feedback servomechanism for dynamic response characteristics control, discussing design parameters and fluid properties influence on system performance
11 p1578 A72-26981
- Hydrofluidic stability augmentation system /HYSAS/ development for military helicopters, discussing test program and technical feasibility
12 p1754 A72-27407
- Pressure recovery and control characteristics of turbulence amplifiers with jet of rectangular section, using large scale water model
16 p2350 A72-33178
- Hydrofluidic three-axis stability augmentation system to improve UH-1B helicopter damping and handling qualities during high speed gunfiring missions
16 p2350 A72-33650
- Hydrofluidic stability augmentation system for U.S. Army helicopters, emphasizing reliability, maintainability and reduced cost
17 p2492 A72-34928
- Constant coefficients for linearized flow rate equation of hydraulic throttle servodrive in closed circuit stability solution by Liapunov theorem
22 p3139 A72-41873
- Aircraft hydraulic control systems modular design for maintainability, emphasizing component removal with minimum hydraulic fluid loss and air entrainment
22 p3140 A72-42294
- Error analysis of linear and nonlinear elements in hydraulic control circuits of flight vehicles, calculating accuracy of frequency response determination
23 p2522 A72-43671
- Electrohydraulic stand for vibration strength testing, discussing system design, specifications, frequency-amplitude characteristics and applications
23 p3278 A72-43760
- Investigation of the dynamic characteristics of the speed governor of a hydropneumatic feed drive
23 p3253 A72-44022
- A digital model of jet engine hydraulic fuel controller
23 p3327 A72-44291
- ### HYDRAULIC EQUIPMENT
- #### NT AIRCRAFT HYDRAULIC SYSTEMS
- Hydraulic systems and components stationary operating conditions determination, discussing measuring apparatus, test equipment and interpretation methods
03 p0312 A72-13961
- Poppet valve design with flow force compensation for high pressure oil hydraulic systems, discussing dynamic stabilization
03 p0312 A72-13964
- Logic networks with hydraulic elements, considering dynamic qualities of hydraulic transmission system
03 p0312 A72-13965
- Soviet book on hydraulics, hydraulic machines and hydraulic drives covering fluid dynamics, pipe flows, jet pumps, turbines, bladed transmissions, etc
04 p0466 A72-15247
- Laboratory evaluation of engine oils, transmission lubricants and hydraulic fluids utilization in hydraulic power transmission systems
08 p1192 A72-21635
- Hydraulic actuator servomechanism performance dependence on asymmetrical spool valve lap and closed loop system stability
08 p1113 A72-22153
- Bistable hydraulic servomechanisms limit cycle stable oscillations from bang-bang control and cavitation effects, discussing valve driving gear hysteresis and time lag
08 p1113 A72-22155
- Mathematical models for hydraulic position servo, deriving time optimal controllers
08 p1113 A72-22156
- Hydraulic ball valve elements and logic gates for applications requiring short switching times under large flow and high pressure conditions
08 p1114 A72-22159
- Loaded hydraulic cylinder response to step inputs in on-off servos with three position valves, considering cavitation effect on system natural frequency
[ASME PAPER 72-AUT-A]
10 p1423 A72-25052
- Pump and unloading valve hydraulic system model with waves processes allowance in connecting pipe, discussing liquid mass and leakage effects on stability
11 p1578 A72-25770
- Mathematical model for hydraulic fatigue testing machine, analyzing nonlinear control stability of vibratory loading process
12 p1796 A72-27978
- Cavitation failure of aircraft hydraulic plunger pump elements from microscopic and metallographic analysis
13 p1899 A72-28732
- Hydraulic test facility for dynamic characteristics of potentiometric pressure sensors with connecting lines of various geometries, shaping pressure pulse signal by electromagnetic valve
13 p1957 A72-29133
- Hydraulic servosystem performance analysis, determining transfer function for time variant input-output relationship, gain levels and stability assurance
14 p2073 A72-30420
- Space shuttle umbilical systems for mating, connection and checkout of carrier assemblies and couplings for cryogenic, electrical, pneumatic and hydraulic services
15 p2213 A72-31695
- High pressure cryogenic hydraulically actuated valve for repeated sealing of liquid He-containing cell
15 p2183 A72-32436

Die-casting machine design trends, considering uses of elbow lever and hydraulic systems and programmed control 16 p2399 A72-34142

Hydraulic pump design for efficiency increase, weight reduction and service life and reliability improvement 18 p2694 A72-36045

Hydrodynamic pivoting-pad vane tips for high-speed vane pumps. 18 p2694 A72-36046

Hydraulic systems for driving helicopter tail rotors. II 18 p2642 A72-36524

Liquid or solid propellant hot gas turbines as power source for hydraulic and electrical energy 18 p2648 A72-36558

Dynamic models for hydraulic machine parts, discussing resonant properties of one degree of freedom system and dynamic characteristics of nonlinear parametric systems 20 p2953 A72-39421

Investigation of the stability of a hydraulic servo motor with rigid feedback 22 p3139 A72-41858

Choice of loop gain for a hydraulic servo system 22 p3140 A72-42921

Principles of modelling studies of fuel systems and hydraulic systems by electronic analog computers 22 p3157 A72-42922

The problem of the minimum frequency of natural pressure oscillations in pneumo-hydraulic systems 23 p3252 A72-43652

HYDRAULIC FLUIDS

Hydraulic fluids behavior under extreme temperature, pressure and filtration conditions, considering viscosity, wear and corrosion resistance 05 p0681 A72-17084

Laboratory evaluation of engine oils, transmission lubricants and hydraulic fluids utilization in hydraulic power transmission systems 08 p1192 A72-21635

Synthetic fire resistant hydraulic fluids, comparing chlorinated hydrocarbons and phosphate esters chemical properties with water based products 08 p1197 A72-22160

Polyglycol aqueous solutions selection as fire resistant hydraulic fluid from hydraulic bench tests performed with various type pumps 08 p1197 A72-22161

Hydraulic transmission for driving helicopter tail rotor, noting compensatory system for engine failure 12 p1755 A72-27862

Hydraulic fluids flow measurement in pipes by ultrasonic waves convection method, discussing transducers performance and mounting [ONERA, TP NO. 1078] 13 p1959 A72-29668

Fuels, lubricating oils and hydraulic fluids for supersonic aircraft, discussing chemical properties, propellant combustion efficiency and production 20 p2945 A72-39930

HYDRAULIC HEATING SOURCES

U HEAT SOURCES

U HYDRAULIC EQUIPMENT

HYDRAULIC JETS

High velocity water jet generation dynamics, deriving equations of motion for mathematical model with nozzle profiles and liquid compressibility approximations 14 p2093 A72-30180

HYDRAULIC PUMPS

U HYDRAULIC EQUIPMENT

U PUMPS

HYDRAULIC SHOCK

Hydraulic shock of incompressible heavy fluid in closed cylindrical tank under abrupt deceleration 15 p2219 A72-32685

HYDRAULIC SYSTEMS

U HYDRAULIC EQUIPMENT

HYDRAULIC TEST TUNNELS

Rotating homogeneous incompressible fluid flow over various bottom topographies, comparing numerical and analytical solutions with water tunnel experimental results 07 p0970 A72-20071

Hydraulic tank application to internal flow visualization in turbomachinery, describing test equipment and methods used for axial flow model 10 p1419 A72-24654

Flow separation reduction by transverse jet blowing, illustrating flow patterns by water tunnel visualization on cylinders, perpendicular flat plates, contoured walls, steps, wings, etc [ONERA, TP NO. 1070] 11 p1572 A72-25814

Laser Doppler anemometer for three dimensional liquid and gas flow velocity measurements in water tunnels 16 p2396 A72-34158

Hydrodynamic test tunnel for unsteady pressure and force measurements and hydrogen bubble flow visualization data acquisition [AIAA PAPER 72-999] 21 p3041 A72-41585

Water tunnel study of turbulent boundary layers structure in incompressible fluid with longitudinal

pressure gradient at inlet section of converging and diverging nozzles 24 p3390 A72-45006

Hydrodynamic weak-turbulence facility, equipment, and procedure for studying the stability of laminar boundary layers 24 p3388 A72-45258

HYDRAULIC VALVES

U HYDRAULIC EQUIPMENT

U VALVES

HYDRAZINE ENGINES

Proportional-integral control of reactants supply for hydrazine-oxygen fuel cells with pulse controlled solenoids 06 p0867 A72-18290

Hydrazine and ammonia resisto-jet systems for satellites orbit and attitude control, discussing component redundancy and mass requirements in terms of system optimization 07 p1054 A72-19603

Electrically heated thermal decomposition hydrazine thrusters, discussing propellant supply pressures compatibility and thrust levels [AIAA PAPER 72-451] 11 p1708 A72-26188

Electrostatic ion thruster and hydrazine monopropellant systems for communication satellites, noting weight savings 17 p2596 A72-34265

HYDRAZINES

NT CHLORPROMAZINE

NT DIMETHYLHYDRAZINES

Hydrazine fuel cell development, electrochemical problems and applications, noting batteries with air oxidant 16 p2351 A72-33886

Vacuum thermal decompositions of the nitrate salts of hydrazine. 19 p2848 A72-38876

Analysis of reaction products of nitrogen tetroxide with hydrazines under nonignition conditions. 20 p2898 A72-39610

Hydrazine thrusters for space application. 21 p3098 A72-40123

Popping phenomena with the hydrazine nitrogen-tetroxide propellant system. 22 p3215 A72-42866

Complex compounds of cobalt and nickel with hydrazine 23 p3262 A72-44165

HYDRIDES

NT BORANES

NT BORON HYDRIDES

NT CHLOROSILANES

NT LITHIUM HYDRIDES

NT METAL HYDRIDES

NT PHOSPHINES

NT SILANES

NT ZIRCONIUM HYDRIDES

Phosphorus hydride electron affinity determination by electron photodetachment cross section measurement, using ion cyclotron resonance spectrometer 07 p0935 A72-19432

HD absorption spectrum measurements in vacuum UV region for Rydberg states and ionization energy determination 16 p2431 A72-33583

Ground and low-lying excited electronic states of FeH. 21 p3096 A72-40563

HYDROACOUSTICS

U UNDERWATER ACOUSTICS

HYDROAEROMECHANICS

U AERODYNAMICS

HYDROCARBON COMBUSTION

Materials stability testing in high temperature propane-butane combustion product flow, selecting compact silicon carbide for structural use in redox medium 02 p0251 A72-12866

Flame retardant mechanism in hydrocarbon polymer combustion, discussing halogen adverse effect on thermal stability [PI PAPER 10] 03 p0380 A72-13244

Reaction kinetics of NO and CO formation in lean premixed hydrocarbon-air flames 04 p0594 A72-14409

NO formation in spherical diffusion flames around hydrocarbon fuel drops burning in air [WSCI PAPER 71-29] 04 p0482 A72-14582

Flame temperatures, composition profiles and burning rates in liquid n-heptane droplet and sphere combustion 07 p1051 A72-19362

Burning velocity inhibitors effect on hydrocarbon-oxygen-nitrogen mixtures ignition by hot wires [AD-744624] 08 p1129 A72-22039

Burning velocity measurement techniques for methane-air mixtures 08 p1255 A72-22047

Emissivity calculation for radiant heat flux from isothermal gas mixture of hydrocarbon fuel combustion products 10 p1561 A72-23839

Hydrogen chloride addition effect on hydrocarbon flammability under reduced pressure, studying flame stability limits of methane, ethylene, acetylene and n-butane in oxygen 10 p1562 A72-24236

Supersonic combustion of liquid fuels, hydrogen and propane, discussing initiation and stabilization in supersonic flow 12 p1889 A72-27686

Shock delayed methane-oxygen-argon mixtures ignition heat time from reaction kinetics calculations 12 p1778 A72-27852

Heterogeneous-homogeneous catalytic effects on combustion rate of hydrocarbons, ammonia and hydrogen mixtures 13 p1912 A72-28777

Aromatic hydrocarbons and fuels, investigating engine parameters effects on combustion and exhaust gases temperatures 13 p2025 A72-29074

Hydrocarbon electrochemical oxidation kinetics for fuel cells at low temperature, considering adsorption and bond cleavage 16 p2361 A72-33891

Autoignition behind reflected shock waves for hydrocarbon-oxygen mixtures, demonstrating two ignition modes via schlieren photographic records 16 p2479 A72-34002

Experimental study of the aerodynamic characteristics of burning gas-air jets in the transient flow region of natural gas 17 p2637 A72-35169

Aromatic hydrocarbons - Methane ignition inhibitors 19 p2879 A72-37364

Experimental investigation of the effect of an electric field on a laminar flame 22 p3243 A72-41889

Experimental facility and diffusion technique for measuring turbulence characteristics during hydrocarbon fuels burning in air streams 23 p3287 A72-43658

Self ignition behaviour of some liquid fuels in an adiabatic compression machine. 23 p3325 A72-44252

Two-phase detonations with bimodal drop distributions. 24 p3463 A72-45052

HYDROCARBON FUELS

NT GASOLINE

NT JET ENGINE FUELS

Jet fuels hydrocarbon composition effect on thermal stability, considering nonaromatic components influence on aromatic hydrocarbons oxidation products coagulation 02 p0271 A72-12800

Slush, boiling methane and methane mixture characteristics, noting advantages as potential rocket, aircraft and motor vehicle fuels 04 p0564 A72-15542

Fuels and lubricants development trends for subsonic and supersonic aircraft, discussing thermostable hydrocarbons, ramjet fuels, esters, oxidation inhibitors, metal deactivators, high pressure lubricant additives, etc 05 p0681 A72-16739

Additives effect on liquid hydrocarbon fuels ignition delay, testing peroxides, esters, polyethers and alcohols [AIAA PAPER 72-71] 05 p0703 A72-16958

Aircraft hydrocarbon fuel tank lightning protection in airframes, using adhesive bonding, high strength materials and high modulus fiber structures 07 p1086 A72-18767

Electric field voltage effect on dispersion of electrostatically atomized liquids and hydrocarbon fuels with and without gamma irradiation 09 p1350 A72-22546

Quasi-steady state combustion theories compared with observations of hydrocarbon fuel droplet and flame zone diameters, noting underestimation of burning rate 13 p2063 A72-28545

Jet fuel hydrocarbon group chemical composition effects on antiwear characteristics in sliding friction and rolling simulation experiments 13 p2024 A72-29073

Hydrocarbon oxidation and catalysis on Pt fuel cell electrodes, using electrochemical methods with isotopic exchange and gas chromatography 16 p2361 A72-33878

Thermocatalytic pyrolysis for hydrogen generation from liquid hydrocarbon fuels with absolute cracking reaction efficiency 16 p2361 A72-33890

Graph-analytical method of determining cetane numbers of light catalytic gas oil grades 17 p2571 A72-35178

Extractability of antioxidative additions from fuels by means of water and NaCl solutions 17 p2596 A72-35179

Composition of initial mixtures for production of the gaseous C-H-O fuel for fuel cells with molten alkaline carbonates. 19 p2754 A72-37778

Infrared spectroscopy for chemical composition of inorganic and organic products formed on friction surfaces of gas turbine parts immersed in hydrocarbon fuels

23 p3325 A72-43974

Chemical aspects in the shock initiation of fuel droplets.

24 p3433 A72-45051

HYDROCARBONS

NT ACETYLENE
NT ANTHRACENE
NT BENZENE
NT BUTANES
NT BUTENES
NT CETANE
NT CYCLIC HYDROCARBONS
NT CYCLOPROPANE
NT ETHYLENE
NT HEPTANES
NT METHANE
NT NAPHTHALENE
NT NATURAL GAS
NT NEOPENTANE
NT OCTANES
NT PARAFFINS
NT PROPANE
NT PROPYLENE
NT TOLUENE
NT XYLENE

Product of net branching factor and induction period in hydrocarbon oxidation at low temperatures, tabulating results

07 p1051 A72-19374

Organic origin of meteoritic hydrocarbons in early solar system related to Fischer-Tropsch reaction

07 p1076 A72-19590

Simulation study of lunar carbon chemistry, noting hydrocarbon production by solar wind interaction with fines

07 p1082 A72-20291

Synthetic fire resistant hydraulic fluids, comparing chlorinated hydrocarbons and phosphate esters chemical properties with water based products

08 p1197 A72-22160

Capillary gas chromatography with two moderately high temperature phases, testing esters and hydrocarbons resolution ability

12 p1778 A72-27225

Hydrocarbon-air mixtures reaction in incident shock waves of pressure greater than 25 atmospheres, correlating with shock tube results

13 p2063 A72-28549

Aliphatic hydrocarbons in phytopathogenic fungi spores, discussing similarity to higher plant alkanes, functional roles and species distribution and occurrence

13 p1906 A72-29834

Apiezone lubricants physicochemical properties comparison, noting aromatic hydrocarbons effect on thermo-oxidation stability and polyisoprene rubber type polymer additive effect on adhesiveness

16 p2413 A72-33171

Hydrogen and hydrocarbon diatomic molecules and cations rotational state upper limits determination, noting potential energy functions

16 p2432 A72-34098

The influence of molecular binding on the stopping power of alpha particles in hydrocarbons.

18 p2655 A72-37193

Synthesis of polymers with conjugate bonds on the basis of dilithium-derivative aromatic hydrocarbons

23 p3262 A72-43929

Variation in the hyperfine state of a hydrogen atom during its collision with unsaturated hydrocarbons in the gaseous phase

23 p3317 A72-44477

HYDROCHLORIC ACID

Gas filter correlation spectral analysis technique for measuring pollutant concentrations in presence of interfering gases, describing application to hydrochloric and hydrofluoric acids monitoring
[AIAA PAPER 71-1049]

01 p0066 A72-10525

Distillation experiments showing volatility-caused amino acid contamination of commercially available aqueous hydrochloric acid

05 p0624 A72-16079

Venus clouds composition from spectral and polarization data, considering hydrochloric acid particles model

08 p1230 A72-20980

Hydrogen chloride addition effect on hydrocarbon flammability under reduced pressure, studying flame stability limits of methane, ethylene, acetylene and n-butane in oxygen

10 p1562 A72-24236

Gas etching of Ge and Si semiconductors with vapors of chemical elements, emphasizing hydrogen chloride

11 p1700 A72-25776

Carbon dioxide power laser effects on IR spectra of HCl-ethylene and sulfur dioxide-ethylene mixtures, focusing with Ge lens

13 p1971 A72-29870

HCl and HF in carbon dioxide atmosphere, determining line intensities, halfwidths and shapes at room temperature

14 p2135 A72-30894

HYDROCYANIC ACID

U HYDROGEN CYANIDES HYDRODYNAMIC EQUATIONS

Hydrodynamic equations for non-Lagrangian statistical mechanical particle systems with three degrees of freedom under frictional and velocity dependent forces

04 p0512 A72-15202

Hydrodynamic model of human systemic arterial circulation to test artificial heart pumps
[ASME PAPER 71-WA/AUT-13]

05 p0621 A72-15954

Equilibrium diffusion of rotating plasma in toroidal systems, deriving two fluid hydrodynamic equations with allowance for ion temperature perturbation

05 p0701 A72-17242

Averaged Bogoliubov-derived chains of kinetic theory gas dynamics equations with strong statistical correlation for macroprocess description

08 p1149 A72-21175

Explicit difference schemes for hydrodynamic equations with no stability condition constraints on time step

09 p1295 A72-23491

Three component flow calculation at inlet of axial flow compressor stage, linearizing hydrodynamic equations of ideal incompressible fluid with velocity perturbations

10 p1420 A72-25132

Fowler quasars and exploding galaxies model tested by hydrodynamic equations numerical solution for premain sequence contraction and relativistic collapse of nonrotating supermassive star

12 p1866 A72-27202

Quasi-hydrodynamic equations for transverse waves in inhomogeneous plasma, using geometric optics approximation

13 p2019 A72-29986

Hydrodynamic theory of atmospheric action center formation due to pressure migration for Northern troposphere two level meteorological forecasting

14 p2127 A72-30261

Hydrodynamic and molecular velocity characteristics of rarefied gas motion between infinite plane parallel emitting and absorbing surfaces, using Boltzmann equation

14 p2096 A72-31025

Flow-plasma system described by hydrodynamic equations, comparing self oscillatory process features with other systems

14 p2141 A72-31129

Hydrodynamic equations for low speed steady external rarefied gas flows past circular cylinder, noting drag and heat transfer coefficients

16 p2344 A72-33568

Initial value techniques in free-surface hydrodynamics.

17 p2538 A72-34644

A modified Navier-Stokes equation, and its consequences on sound dispersion.

17 p2540 A72-35146

Studies of hydrodynamic events in stellar evolution. I - Method of computation.

17 p2611 A72-35316

The one-dimensional N-body problem and rectilinear gas motion

17 p2584 A72-35909

Rotatory motions of a body with a liquid-containing cavity

19 p2787 A72-38151

Collisionless solar wind protons - A comparison of kinetic and hydrodynamic descriptions.

19 p2853 A72-38732

Characteristics of turbulent transfer in jets of variable density

20 p2914 A72-39910

Dynamic adjustment of initial model fields by using complete equations of hydrothermodynamics

20 p2949 A72-39943

Russian book - Hydrodynamic evolution model of the earth.

21 p3103 A72-40461

Convective instability of a fluid in hydrodynamically connected vertical channels

22 p3166 A72-42260

Hydrodynamic and Wiener-Siegel hidden parameter models incapability for quantum mechanics reduction to classical mechanics, obtaining proofs to von Neumann theorem

23 p3312 A72-43298

Chaplygin gas flow equation for analogy between hydrodynamic and electrodynamic equations, noting special theory of relativity

23 p3312 A72-43404

Slowly rotating axisymmetric star gravitational collapse derivation from general relativistic hydrodynamic and gravitational field equations formulated under Bondi-Sachs coordinate condition

23 p3335 A72-43488

Nonlinear hydrothermodynamic model of steady atmospheric motion in equatorial latitudes with energy influx approximation

23 p3284 A72-43533

Hydrodynamic equations for incompressible fluid in steady relativistic state extended to nonrelativistic velocities case, noting transition from Euler to Predvoditelev equations

23 p3279 A72-43686

A kinetic-theory description of a chemically reacting gas.

23 p3357 A72-44272

Inertial effects in motion driven by hydrodynamic fluctuations.

24 p3430 A72-45560

HYDRODYNAMIC STABILITY

U FLOW STABILITY

HYDRODYNAMIC TUNNELS

U PLASMA JET WIND TUNNELS

HYDRODYNAMICS

NT ELASTOHYDRODYNAMICS

NT ELECTROHYDRODYNAMICS

NT MAGNETOHYDRODYNAMICS

Plasma hydrodynamic Buneman current instability under strong electric field, considering nonlinear stage in one dimensional case

01 p0105 A72-10024

Difference analog of nonlinear hydrodynamic boundary value problem from Navier-Stokes steady state theory

01 p0050 A72-10576

Combustion fronts in relativistic hydrodynamics, considering theorem of detonation and deflagration velocity distribution

01 p0145 A72-11179

Unbalance response of rotor supported in hydrodynamic gas lubricated journal bearings
[ASME PAPER 71-LUB-10]

02 p0235 A72-11534

Hydrodynamics of matter-antimatter system embedded in thermal radiation, observing coalescence effect

03 p0416 A72-13013

Stellar evolution in close binary systems, discussing post main sequence stage, hydrodynamical processes and dwarf binaries

03 p0437 A72-13868

Hydrodynamic field around sphere moving along Poiseuille flow axis determined by least squares method, formulating flow resistance

04 p0511 A72-14968

Hydrodynamic journal gas bearing with herringbone grooved portion for self generating air supply pump hydrostatic starting and stopping

05 p0664 A72-15944

Hydrodynamic asymptotic characteristics of autocorrelation function for molecule velocity in classical liquid, obtaining Lagrangian diffusion coefficient.

05 p0692 A72-16684

Relativistic hydrodynamics, considering Cauchy problem in fluid evolution, ideal isentropic fluids, electromagnetic field effect and viscous/heat conducting thermodynamic flow models

06 p0846 A72-17252

Magnetosonic, Alfvén, shock and infinitesimal waves and corresponding rays in relativistic hydrodynamics and magnetohydrodynamics, using tensor distributions

06 p0847 A72-17253

Multiple production processes hydrodynamic-type models validated by high energy particle collision collective interactions

06 p0869 A72-17265

Invariant characteristics of hydrodynamic systems with stationary boundaries, 3 degrees of freedom and second order nonlinear motion of Liouville type

06 p0801 A72-18136

Nonlinear oscillations of liquids in complex geometrically shaped moving vessels, using approximation methods for boundary value problem solution in Cartesian coordinate system

06 p0802 A72-18712

German book on nonlinear free boundary value problems of two dimensional hydrodynamics covering gravity, capillary and irrotational waves, liquid flow in channel, etc

07 p0967 A72-19183

Hydrodynamic flow parameters in laminar incompressible water boundary layer on heated plate, noting plate surface heating effect on velocity profile

07 p0968 A72-19766

Hydrodynamic characteristics of freely falling water droplets in air, establishing relationships among Reynolds, Laplace and Bond criteria

07 p1030 A72-19854

Statistical-hydrodynamic description of nonequilibrium gas dynamics of single component and binary mixtures and systems with chemical reactions.

07 p0968 A72-19886

High temperature radiative transfer and hydrodynamics, discussing radiant heat transfer dominant equation, diffusion descriptions, scattering kernel, dispersive media and heavy electron model of scattering

07 p1101 A72-19923

Atmospheric hydrodynamic simulation model for cascade energy transfer in turbulent flow, using Euler gyro equations

08 p1158 A72-21190

Rectangular channel mixed boundary layer flow patterns dependence on inlet edge configurations, channel geometry and hydrodynamic flow core parameters

08 p1150 A72-21317

Free convection and hydrodynamics of inclined liquid layers in laminar flow and in stepwise change of heat exchange surfaces temperature

08 p1151 A72-21663

Hydrodynamics of dispersed annular two phase flow in cylindrical channels characterized by concurrent motion of flow core and liquid film at wall

08 p1151 A72-21667

Hydrodynamic analogy for astrophysical effects of general relativity theory, analyzing Chaplygin gas motion in three dimensional curvilinear coordinate system

08 p1209 A72-21876

Nonlinear hydrodynamic effects in dynamic motions of metagalactic turbulence in pre-Friedmann universe

10 p1536 A72-24141

Two dimensional hydrodynamic flow analysis of pneumatic tire hydroplaning, taking into account tire deformation, viscous, inertial and turbulence effects

10 p1512 A72-24819

Interior and exterior hydrodynamics of spherical droplet submerged in unbounded arbitrary velocity field, including effects of surface active agents

10 p1470 A72-25042

German book on flow technology and fluid flow machines covering hydrodynamics, gas dynamics, aerodynamics, airfoils, wind tunnels, propellers, helicopters, turbomachines, blade cascades, etc

10 p1471 A72-25122

Hydrothermodynamic foundations of hydrofoil engines employing gas-water mixtures and gas turbine generators, analyzing thrust coefficient and power efficiency

10 p1528 A72-25128

Hydrodynamic forces in sinusoidal vibrations of disk in water channel with toroidal vorticity wake pattern, applying results to flapping wing mechanics

10 p1471 A72-25129

Hydrodynamics of turbulent free convection boundary layer on vertical flat plate and ethyl alcohol film

11 p1743 A72-25258

Axisymmetric shock wave propagation in continuous inhomogeneous medium, taking into account shock geometry orthogonality conditions and flow hydrodynamics behind shock

11 p1616 A72-25864

Galaxy formation process in expanding universe from study of hydrodynamic equations for rotating gaseous ellipsoid with uniform density

11 p1717 A72-25865

Newtonian hydrodynamic equations derived from scalar-tensor theory field equations for cosmic fluid nonlinear effects during galaxy formation

11 p1717 A72-25866

Spherical probe impedance characteristics in isotropic plasma predicted by hydrodynamic theory compared to experimental results

11 p1699 A72-26768

Nonregular oceanic level fluctuations dependence on atmospheric pressure and tangential wind stress, deriving fluctuation spectrum from linear hydrodynamic model

11 p1682 A72-26882

Constant pressure gradient valves static characteristics, describing approximate procedures for flow rate determination without allowance for hydrodynamic effects

13 p1899 A72-29134

High velocity water jet generation dynamics, deriving equations of motion for mathematical model with nozzle profiles and liquid compressibility approximations

14 p2093 A72-30180

Reversible instantaneous deformations and internal energy in viscoelastic incompressible fluids, using Oldroyd and De Witt hydrodynamic models

16 p2376 A72-32937

Hydrodynamic characteristics of a cambered hydrofoil with a jet flap.

[ASME PAPER 71-APMW-17] 17 p2537 A72-34303

Combustion fronts velocity comparison with light speed in relativistic hydrodynamics and MHD

17 p2589 A72-34911

Statistical-hydrodynamic description of nonequilibrium gas dynamics of single component and binary mixtures and systems with chemical reactions

17 p2540 A72-35134

Relativistic hydrodynamics and gravitational instability.

17 p2581 A72-35356

Fluid dynamics of convective stellar envelopes.

17 p2618 A72-35933

A new method of analysis in laminar-flow theory.

18 p2681 A72-36551

Studies of hydrodynamic events in stellar evolution. II - Dynamic instabilities in stellar envelopes.

19 p2854 A72-37234

Astronomical observations supporting stellar atmosphere microturbulence concept, noting Cepheid variables high dispersion spectra, supergiants irregular changes and microturbulence hydrodynamic effect

19 p2857 A72-37525

Hydrodynamic model of white dwarf envelope thermonuclear runaway evolution producing nova outburst, computed for various CNO nuclei initial abundances

20 p2966 A72-38908

Nonperiodic oceanic level fluctuations dependence on atmospheric pressure and tangential wind stress, deriving fluctuation spectrum from linear hydrodynamic model

20 p2948 A72-39569

Hydrodynamic forces acting on rigid disk and circular membrane vibrating in ideal incompressible fluid, noting dependence on phase shift between vibration modes

21 p3126 A72-41552

Predvoditelev critical revision of hydrodynamic and heat transfer theory based on Navier-Stokes and Boltzmann equations, developing statistical system of molecular interactions

22 p3165 A72-41951

Averaged equations for joint treatment of hydrodynamic expansion and conduction-type heating of plasma, the energy of nuclear fusion being taken into consideration. II - Spherical problem.

22 p3211 A72-42630

Hydrodynamic fluid pressure on a shell during hydraulic impact

23 p3280 A72-43788

Application of the method of hydrodynamic singularities to the calculation of the velocity distribution in doubly-periodic infinite blade cascade systems

24 p3390 A72-44874

Study of a turbine type flowmeter with helical blades.

24 p3404 A72-45354

HYDROELASTICITY

Hydroelastic behavior of heavily loaded lifting surfaces, investigating flutter and divergence

04 p0592 A72-15562

Hydroelastic vibrations of incompressible inviscid liquid with free surface in uniformly rotating infinitely long circular cylindrical container, investigating response to cylinder walls forced excitations

05 p0735 A72-16065

Finite element analysis of hydroelastic properties of Saturn 5 full scale S-2 LOX tank, comparing with water tests

05 p0740 A72-16833

HYDROFLUORIC ACID

Gas filter correlation spectral analysis technique for measuring pollutant concentrations in presence of interfering gases, describing application to hydrochloric and hydrofluoric acids monitoring

01 p0066 A72-10525

Flash photolysis HF chemical laser pulse delay measurements, showing pressure, flash lamp intensity and optical cavity loss dependence

05 p0668 A72-16606

HF tracer gas detection in inert and combustive flows, using IR absorption technique for gaseous flow visualization

05 p0651 A72-16904

HF and/or HF-carbon dioxide transfer laser potential power output and design criteria, considering deuterium and fluorine combustion, reaction product expansion and mixing rate

05 p0670 A72-16970

Self pulsed electrically initiated HF and DF chemical laser with high pulse repetition frequency gain switched operation

06 p0826 A72-18458

CW diffusion type chemical HF laser and two-vibrational level HF molecular models, analyzing laser performance

07 p1000 A72-18955

HF diffusion type chemical laser fluid dynamic and optical properties, discussing computerized numerical analysis

07 p1001 A72-19063

Lasing length, power and efficiency of cw HF chemical laser with nitrogen or He diluent

[AD-742962] 09 p1325 A72-23241

Spectral output of pulsed discharge initiated hydrogen fluoride chemical laser as function of pressure and gas composition

12 p1823 A72-27839

Computer simulation of pulsed hydrofluoric acid laser pumped by chain reaction, investigating cavity and chemical parameters effects on laser pulse

12 p1826 A72-27938

HCl and HF in carbon dioxide atmosphere, determining line intensities, halfwidths and shapes at room temperature

14 p2135 A72-30894

Optically pumped pulsed hydrogen fluoride gas laser, observing anisotropic ultrahigh gain emission in rotational transitions

15 p2251 A72-32531

Spectroscopy of pulsed HF chemical lasers using an infrared vidicon camera tube.

17 p2562 A72-34641

HF vibrational relaxation measurements using the combined shock tube-laser-induced fluorescence technique.

17 p2511 A72-34735

Gain and relaxation studies in transversely excited HF lasers.

17 p2564 A72-35344

HF chemical lasers pumped by atomic fluorine with molecular hydrogen, calculating intensity and efficiency by reaction kinetics analysis for comparison with computer solutions

21 p3062 A72-40617

Catalytic efficiencies of H₂O, D₂O, NO, and HCl in the vibrational relaxation of HF and DF.

24 p3378 A72-45306

HYDROFOILS

Viscous incompressible flow past longitudinally cambered small aspect ratio slender wing near solid interface

05 p0600 A72-16215

Hydrothermodynamic foundations of hydrofoil engines employing gas-water mixtures and gas turbine generators, analyzing thrust coefficient and power efficiency

10 p1528 A72-25128

Single spiral vortex cavity termination model for second order solution of flat plate hydrofoil cavitation flow

11 p1616 A72-25879

Hydrodynamic characteristics of a cambered hydrofoil with a jet flap.

[ASME PAPER 71-APMW-17] 17 p2537 A72-34303

HYDROGEN

NT DEUTERIUM

NT DEUTERIUM PLASMA

NT HYDROGEN ATOMS

NT HYDROGEN IONS

NT HYDROGEN ISOTOPES

NT HYDROGEN PLASMA

NT LIQUID HYDROGEN

NT METALLIC HYDROGEN

NT TRITIUM

Hydrogen partial molar volume in metal-hydrogen two component systems under externally applied uniform hydrostatic stress field, using thermodynamic analysis

01 p0083 A72-10205

Hydrogen chemical permeation through iron and steel as function of compressive and tensile stress

01 p0083 A72-10206

High pressure gaseous hydrogen effect on space shuttle main engine components alloys under static loads, using surface flawed flat plate PTC samples

01 p0085 A72-10774

Hydrogen diffusion kinetics in Nb under various temperatures during gas-metal absorption experiments, observing room temperature hardness profile

01 p0087 A72-11026

Hydrogen condensation on tungsten as function of temperature, coverage and population of binding states, noting initial sticking coefficients variations

01 p0089 A72-11113

Radiant heat attenuation of W seeded hydrogen aerosol at high pressure and temperature for gas core nuclear rocket propellant application

01 p0112 A72-11340

Differential thermal radiation scattering coefficients of submicron W refractory particles in hydrogen and nitrogen at temperatures to 1080 K.

01 p0112 A72-11341

Shock tube technique for opacity measurement at high pressures in seeded hydrogen for gas core nuclear rockets

01 p0099 A72-11342

Hydrogen diffusion, electron transfer and density distribution in Ta as function of temperature and field strength

02 p0242 A72-12009

Hydrogen shock waves density profiles measurement, noting uncoupled translational and rotational relaxation processes

02 p0263 A72-12360

Hydrogen density and proton flux in topside ionosphere over Arecibo from incoherent scatter observations

02 p0274 A72-12455

Hydrogen diffusivity and solubility in alpha-Ti alloys, considering absorption effect on stress corrosion cracking

02 p0244 A72-12481

Seigel state equation validity limit application to isentropic hydrogen and nitrogen steady and unsteady flow expansions at high pressure

02 p0206 A72-12597

Nonequilibrium effects on ionization growth in molecular hydrogen, tabulating experimental data for comparison with Monte Carlo computation

02 p0267 A72-12793

He abundances in gaseous nebulae by optical and radio observation, discussing hydrogen and helium recombination spectra interpretation

03 p0419 A72-13115

Magellanic Clouds neutral hydrogen distribution, concentrations and velocity structure, noting H II correlation with supergiant stars

03 p0425 A72-13256

Oxygen, hydrogen and nitrogen constituents in mesosphere, investigating ionization process in D region at midlatitudes

03 p0346 A72-13379

Hydrogen charging of iron-chrome-nickel austenitic stainless alloys, investigating crack initiation in Inconel 600

03 p0373 A72-13600

Hydrogen diffusivity in Fe with cavities at room temperature calculated by mathematical model and numerical methods

03 p0378 A72-14256

Hydrogen generation mechanism during cadmium plating of steel, describing porosity testing technique

04 p0527 A72-15548

D-2A satellite antisolar mission, examining Lyman alpha emission from geocorona and interstellar hydrogen wind

04 p0582 A72-15688

Low velocity neutral hydrogen spur coincidence with radio continuum Loop IV, discussing average excess surface density and total mass

05 p0711 A72-15765

Neutral hydrogen distribution in spiral and irregular galaxies, discussing H II regions

05 p0716 A72-16371

Surface oxide film effects on hydrogen liberation rate from Al and alloys in high vacuum at 20-450 C

05 p0675 A72-16627

Hydrogen environment effects on fatigue crack growth rates in Ti-Al-V weldments over low ambient temperature range

05 p0678 A72-17116

Hydrogen 2p and 2s states formation during 1-25 keV atomic collisions with rare gases from Lyman alpha radiation cross section measurement

05 p0693 A72-17168

Self ignition in hydrogen oxidation kinetics, considering convection, molecular diffusion, mixing and pressure

05 p0625 A72-17213

Hydrogen evacuation with He condensation pump in ultrahigh vacuum region

06 p0795 A72-17698

Transverse ionizing shock waves in gaseous hydrogen at speeds to 4000 km/sec, presenting magnetic shock structure and magnetic field jump measurements

06 p0863 A72-18531

Spiral galaxies hypothesis for higher mass-luminosity ratio of outer parts from undetected cold neutral hydrogen, using model of NGC 300

07 p1068 A72-19071

High radial velocity neutral hydrogen outside galactic plane, noting inability to correlate with radio spurs, absorption and emission regions

07 p1069 A72-19082

Surface and thermal effects on hydrogen oxidation, calculating explosion limits and slow reaction rates

07 p0935 A72-19370

High pressure hydrogen effects on austenitic stainless steel embrittlement, determining yield, tensile and fracture strength

07 p1011 A72-19479

Hydrogen cracking of high strength steels during cathode polarization in acidic media, investigating time to cracking variation with current density

07 p1013 A72-19770

Formation kinetics, phase composition and structure of oxide films in binary and ternary iron-base chromium aluminum alloys, studying hydrogen penetration characteristics

07 p1013 A72-19771

Surface processes effect on hydrogen penetration and diffusion into thick Mo membranes

07 p1014 A72-19772

Tempering temperature effect on hydrogen penetration level and brittleness of hardened carbon steel

07 p1014 A72-19773

Static hydrogen fatigue of high strength steels, deriving relationship between time to cracking and tensile stresses magnitude for cadmium-plated steel

07 p1014 A72-19774

Environmental hydrogen embrittlement of Ti-Al alloy as function of test displacement rate and microstructure variation

07 p1016 A72-19933

Exosphere geocoronal hydrogen density, vertical structure and diurnal variability from Lyman spectra observational data, discussing polar wind origins

07 p0978 A72-20041

Reversible hydrogen brittleness development conditions in metals, deriving equations for hydrogen content effect on plasticity dip

07 p1018 A72-20132

Hydrogen embrittlement of stable austenitic Ni-Cu steel, observing intergranular decohesion in fractured

specimens by microfractography, electron microscopy and X ray crystallography

07 p1021 A72-20485

Electron impact cross section and energy deposition in molecular hydrogen, using generalized oscillator strength in Born-Bethe approximation

07 p1038 A72-20567

Local interstellar hydrogen survey from OAO-2 observations of Lyman alpha absorption at 1216 A for B2 or earlier stars

08 p1235 A72-21392

Time dependent progress of vibrational-rotational transitions in hydrogen-fluorine chemical laser investigated by oscillography with IKM-1 monochromator

08 p1183 A72-21715

Coalescence /collapse/ of overlapping spectral lines due to nonadiabatic broadening for Stark structure of hydrogen and helium lines in discharge plasma

08 p1211 A72-21717

Microwave absorption in high pressure hydrogen based on radio astronomical measurements of Uranus brightness temperature

08 p1239 A72-22088

Start reaction effect on burning time sequence of hydrogen combustion in air

08 p1129 A72-22171

Quasi-stellar objects hydrogen L-alpha lines computation via cloud collapse and ionizing radiation field model, comparing computed distribution with PHL 957 and 4C 05.34 observations

09 p1382 A72-22280

D region negative ion reaction schemes, discussing reaction rates of nitrogen dioxide with hydrogen

09 p1275 A72-22592

Ti crystallographic and topographical features determination by hydrogen-ion microscopy, noting temperature effects on surface films and low index facets production

09 p1327 A72-22805

Methane, hydrogen and oxygen adsorption and displacement on crystal surface of W investigated by thermal desorption and work function changes

09 p1276 A72-22807

Parallel air and hydrogen flows confluence numerical examination to determine self ignition conditions in turbulent mixing layer, noting reaction zone

[ONERA, TP NO. 981]

09 p1410 A72-22814

Molecular hydrogen dissociation by He, observing molecule initial quantum states effect on temperature dependent reaction cross section

09 p1357 A72-22855

Thermodynamic properties of high temperature and density hydrogen, using Rowlinson equation of state

09 p1412 A72-23234

Ion and laser microprobes for concentration measurements of hot salt stress corrosion produced hydrogen on Ti alloy on microscopic scale

09 p1276 A72-23477

Galaxy NGC 253 mass and distance from neutral hydrogen spectral line observations with radio telescope

09 p1391 A72-23533

Steady state model for Venus atmosphere water vapor loss, noting hydrogen and oxygen escape due to dynamic outflow of constituents from upper region

09 p1393 A72-23657

Exospheric temperatures in hydrogen dominated planetary atmospheres for evaporative loss rates estimation, noting two component diffusive equilibrium model

09 p1393 A72-23661

Autoradiographic study of stress intensity factor influence on hydrogen distribution at crack tips in Ti-Al-V alloy, using tritium doped salt water as corrosive medium

[ONERA, TP NO. 1052]

10 p1496 A72-24234

Trajectory dynamics for fluorine atoms reaction with H molecules, predicting total available energy from energy release on potential energy surface

10 p1434 A72-24343

Ionization kinetics influence on light absorption zone behind plane stationary shock wave in hydrogen

10 p1467 A72-24358

Molecular and eddy diffusion transport velocities for helium and hydrogen distributions in upper atmosphere

11 p1622 A72-25845

Molecular process and pressure effects on hydrogen formation in methyl acetylene photolysis at 1236 A

11 p1590 A72-26011

Critical shock wave velocity for ionization front propagation with photoionization of hydrogen by radiation, using pinch discharge tube measurements

[ALAA PAPER 72-410]

11 p1706 A72-26161

Solar wind ion temperature association with influx of neutral hydrogen from heliosphere boundary

11 p1714 A72-26527

Carbon monoxide and hydrogen adsorption on graphite, measuring sticking probabilities

12 p1777 A72-27039

Low pressure hydrogen and titanium thin film reaction rate measurement, using flow technique

12 p1778 A72-27046

Radio observation of neutral hydrogen near galactic center, noting expanding and rotating ring of gas from kinematic model

12 p1867 A72-27211

Heavily obscured galaxy IC 10 21-cm line observation with radio telescope and neutral hydrogen diameter measurement for distance estimation

12 p1868 A72-27215

Partial pressure gage to measure water vapor-produced hydrogen content in metal samples, using reference gas evolution curves

12 p1807 A72-27451

TEA pulsed carbon dioxide laser with continuous shaped electrodes, investigating hydrogen addition effects on power output and gain

12 p1827 A72-28224

Trioplasmatron using crossed field hydrogen discharge between cold cathode and disk anode, noting pulse modulation applications

13 p1927 A72-28380

Heterogeneous-homogeneous catalytic effects on combustion rate of hydrocarbons, ammonia and hydrogen mixtures

13 p1912 A72-28777

Chromium stainless steel fatigue life reduction due to embrittlement in gaseous hydrogen atmosphere at room temperature, noting alleviating effect of atmosphere contaminants

13 p1979 A72-29484

Hydrogen and hydrogen-helium isothermal radiative intensity at various temperatures, density ratios and path lengths, accounting for reabsorption due to overlapping lines

13 p2008 A72-30056

Spontaneous radiative dissociation in molecular hydrogen vibrational levels as function of emission wavelength, discussing fluorescent spectra, radiation lifetimes and centrifugal distortion

13 p2008 A72-30058

Absolute cross sections for Werner band system excitation of molecular hydrogen by electron impact, discussing relative spectral response calibration

13 p2009 A72-30065

Interstellar medium physical conditions from 21 cm hydrogen emission line observations in direction of pulsars, using 25 meter Dwingeloo radiotelescope

14 p2159 A72-30744

Spoke and disk mode for rotating plasma production in hydrogen, using high speed photographic, electrical and magnetic diagnostic techniques

14 p2139 A72-30855

Hydrogen molecule highly excited electronic levels, developing transition probabilities estimation method

14 p2135 A72-30888

Ti alloy initial H content effect on resistance to hot salt stress corrosion embrittlement and cracking, discussing annealing treatment influence

15 p2253 A72-31296

Total energy distributions of field emitted electrons from tungsten as function of coverage by hydrogen and deuterium, observing elastic and inelastic spectrum

15 p2275 A72-31851

Hydrogen adsorption and absorption by niobium, investigating sticking probability and heat of solution

15 p2276 A72-31864

Hydrogen impregnated Ta superconducting to normal transition and M-H curves, discussing effect on impure surface layer superconducting properties

15 p2293 A72-32242

Solute quenching technique to determine hydrogen solubility in Ta to liquid He temperature, comparing with equilibrium measurements

15 p2259 A72-32640

Hydrogen to helium mixing ratio in giant planets from far IR spectroscopy for atmospheric thermal models and greenhouse effect calculations

15 p2315 A72-32727

Neutral hydrogen Lyman-alpha measurements in outer geocorona and in interplanetary space by two channel photometer onOGO 5

16 p2450 A72-32955

Hydrogen direct photoionization and photoexcited autoionization cross sections calculation for radiation in 600-800 A region

16 p2431 A72-33579

Molecular and atomic mechanisms for hydrogen-iodine exchange reaction dynamics, using classical trajectory analysis

16 p2360 A72-33581

Be isotopic ratio in galactic cosmic rays, noting mean interstellar hydrogen density and rays age

16 p2448 A72-33738

Hydrogen solubility in Zr-Nb-H systems as function of composition, temperature and hydrogen equilibrium pressure

16 p2410 A72-33816

Electrodes converting hydrogen, methanol or oxygen for use in fuel cells with alkaline electrolyte, using Ag-Pd, Ni, Si and C catalysts

16 p2351 A72-33885

Thermocatalytic pyrolysis for hydrogen generation from liquid hydrocarbon fuels with absolute cracking reaction efficiency

16 p2361 A72-33890

Hydrogen and hydrocarbon diatomic molecules and cations rotational state upper limits determination, noting potential energy functions

16 p2432 A72-34098

Temperature dependent aluminum-water reaction generation of free hydrogen and aluminum hydroxide

16 p2362 A72-34159

Interstellar molecular hydrogen formation on water, ice and solid CO, using laboratory adsorption energy measurements

16 p2461 A72-34160

Catalytic dissociation, hydrogen embrittlement, and stress corrosion cracking.

17 p2566 A72-34256

Calculation procedure involving wave function for vibrational correction to electron scattering cross section of hydrogen molecule in Born approximation

17 p2585 A72-34261

UV laser parameters calculation for operation on Lyman transition between H atom resonant excited state and ground state

17 p2562 A72-34349

Titan spectrum absorption features, estimating hydrogen abundances

17 p2606 A72-34540

On the kinematic distribution of galactic neutral hydrogen.

17 p2606 A72-34572

Microwave absorption in high pressure hydrogen based on radio astronomical measurements of Uranus brightness temperature

17 p2606 A72-34651

Ionization kinetics influence on light absorption zone behind plane stationary shock wave in hydrogen

17 p2539 A72-34957

Spectral analysis of highly inhomogeneous chromospheric flares.

17 p2617 A72-35709

Hydrogen and helium velocities in the solar wind.

17 p2602 A72-35716

Wave function and resonance parameters for autoionization and ground states of helium and hydrogen

17 p2586 A72-35774

Relation between hydrogen embrittlement and the formation of hydride in the group V transition metals.

18 p2700 A72-36578

New measurement and evaluation method for the determination of the diffusion coefficient of hydrogen in solid metals

18 p2692 A72-36841

Strain rate, stress concentration and temperature effects on hydrogen environment embrittlement of metals

19 p2816 A72-37640

Chain interaction during the inhibited burning of hydrogen

19 p2880 A72-37741

Cathodic protection and hydrogen in stress corrosion cracking.

19 p2817 A72-37765

Solar radio burst time profiles comparison with H alpha line emission curves for corresponding flares, noting neutral hydrogen emission relation to electrons acceleration

19 p2850 A72-37802

Strong shock propagation through decreasing density.

19 p2789 A72-38796

Energy distribution among reaction products. VI - F + H₂, D₂.

19 p2763 A72-38804

Relative safety afforded operator by various hydrogen pressure gage case designs, recommending specific features and mounting requirements

19 p2755 A72-38833

Formation of hydrogen from amine oxidation and pyrolysis.

19 p2883 A72-38874

Rayleigh and Raman scattering by H₂ in a planetary atmosphere.

20 p2966 A72-38914

Testing of hydrogen pressure or stress concentration induced crack propagation theory for steels based on decohesion mechanism

20 p2935 A72-39003

Deformation and fracture of dispersion-strengthened nickel charged with hydrogen.

20 p2935 A72-39004

Environmental acceleration of fatigue-crack growth in a high-strength steel.

20 p2935 A72-39140

Electronic and nuclear magnetic resonances of the oxygen and hydrogen labile negative molecular ions.

20 p2956 A72-39189

Jupiter atmosphere methane deuterium/hydrogen ratio estimate from exchange reaction and temperature studies

20 p2968 A72-39242

Gaseous hydrogen-induced cracking of Ti-5Al-2.5Sn.

20 p2937 A72-39292

Hydrogen gas effects on cleavage cracking in Ti-Al-Mo-V samples under static and cyclic loading

20 p2939 A72-39308

Pressure jump across normal ionizing shock waves.

21 p3045 A72-40566

Shapes and widths of ammonia lines collision-broadened by hydrogen.

21 p3013 A72-40817

Velocity distribution in turbulent mixing of compressible reacting gases, noting flame length measurement of submerged H jet

21 p3129 A72-40981

Hydrogen in intermetallic phases, taking into account as an example the system titanium-nickel-hydrogen

21 p3070 A72-41647

Chromium carbides synthesis by carburizing chromium hydroxide or oxalate in hydrogen-methane gas mixture at temperatures below 1000 C

22 p3188 A72-41974

A possible problem in measuring hydrogen diffusivity at low temperatures by the Gorsky effect.

22 p3190 A72-42443

Equimolar oxyhydrogen detonation wave behavior near pressure limit, considering unsteadiness caused by tube length

22 p3244 A72-42485

Coulomb approximation method for photoionization cross sections of hydrogen molecule singly excited states

22 p3208 A72-42718

German monograph - Determination of the diffusion coefficient of hydrogen in the binary iron-nickel system at 25 and 58 C.

22 p3194 A72-43057

Differentiating stress corrosion cracking from hydrogen cracking of ferritic 18-8 stainless steels.

22 p3195 A72-43127

Determination of the mechanical properties of steels by short-time rupture in hydrogen at high temperatures and pressures

22 p3195 A72-43160

Investigation of the kinetics of low-cycle fatigue of steels in a hydrogen atmosphere and in vacuum

22 p3195 A72-43161

Influence of hydrogen on the fracture structure of OT4 titanium alloy

22 p3196 A72-43162

Laser compression of matter to super-high densities - Thermonuclear/CTR/ applications.

23 p3294 A72-43262

Adsorbed oxygen inhibition of reactions of hydrogen with tungsten.

23 p3298 A72-43270

Standard Ti bars samples for spectral determination of H concentration and distribution in Ti alloys, using mathematical statistical method

23 p3287 A72-43676

Spontaneous magnetization of Ni foils in high pressure H gas, noting Hall voltage measurement in ferromagnetic foils and thin plates

23 p3324 A72-44140

Modeling the rise and combustion of a cloud of light gas in the atmosphere

23 p3357 A72-44493

Relationship between the electrical resistivity and solute concentration in the solid solution of tantalum-hydrogen system.

24 p3412 A72-44718

Influence of oxygen and hydrogen on the strength of titanium alloys

24 p3414 A72-45379

Multiphoton dissociation, predissociation, and autoionization of the hydrogen molecule.

24 p3427 A72-45476

Distribution of hydrogen and helium in the upper atmosphere.

24 p3400 A72-45593

Reversible hydrogen brittleness development conditions in metals, deriving equations for hydrogen content effect on plasticity dip

24 p3416 A72-45758

HYDROGEN ATOMS

Neutral H concentration in upper atmosphere during solar minimum, using ion thermal energies from rocket and satellite mass spectrometric, radio and proton whistler measurements

01 p0053 A72-10361

Series summations for perturbation theory of multiple photon ionization probabilities of atoms applied to hydrogen and helium

03 p0391 A72-13080

Oxygen and hydrogen atoms production in atmosphere by photodissociation, investigating terrestrial hydrogen escape efficiency

03 p0346 A72-13381

Atomic and molecular hydrogen mixture viscosity measurement, considering mutual diffusion coefficient, collision cross sections and interaction potentials

04 p0553 A72-15637

Upper atmosphere atomic hydrogen H alpha emission, correlating intensity and hydroxyl vibration temperature

05 p0659 A72-17036

Atomic hydrogen 6300 A forbidden line emission altitude and intensity during predawn enhancement, using rotating photometer

06 p0806 A72-17644

Neutral interstellar hydrogen atoms mean volume density from Lyman alpha absorption and radio measurements in solar region

06 p0886 A72-18098

Doppler broadening elimination in red Balmer line of atomic hydrogen at 6563 A by high resolution saturation spectroscopy

07 p1037 A72-19132

Lyman alpha radiation emission cross sections due to H/2p and H/2s formation in protons and hydrogen atoms collisions with hydrogen molecules

07 p1038 A72-20678

Sunlight irradiated atmosphere formaldehyde photolysis as hydrogen atom source, estimating photodecomposition rates from extinction rates and photochemical results

08 p1230 A72-20981

Formaldehyde concentration into cloud formation compared to atomic hydrogen from analysis of molecular lines near galactic center

08 p1235 A72-21386

Jeans escape rate prediction validity for hydrogen atoms in upper atmosphere and error sources in physical models

08 p1159 A72-21401

Elastic singlet p wave phase shift calculation for electron scattering by H atom and He cation, using time dependent Hartree-Fock perturbation theory

09 p1355 A72-22786

Polarization fraction calculation for Lyman alpha radiation from excited H atom collisions, using Glauber, Born and Vainshtein approximations

09 p1355 A72-22790

Semiquantal theory application to cross section calculation for excitation and ionization produced by impact between two H atoms

09 p1355 A72-22791

Magnetic mirror system to study Lorentz ionization of highly excited hydrogen atoms with quantum numbers 6-7 in strong magnetic fields

09 p1363 A72-23222

Hydrogen atom emission spectrum calculation in uniform rotating electric field, applying to charged particles collisions and Stark broadening of plasma H lines

10 p1514 A72-24039

Inclination and absorption effects on galaxies apparent diameters, optical luminosities and neutral atomic hydrogen radiation

11 p1724 A72-26725

Interstellar atomic hydrogen observations in radio nebula W 3 direction, noting 21-cm absorption line profile coincidence with Cn alpha recombination line in radial velocity

12 p1868 A72-27219

Atomic hydrogen viscosity and thermal conductivity coefficients for 1-100,000 K, using quantum theory for low temperatures and classical mechanics for high temperatures

13 p2065 A72-29299

Excitation cross section in dipole approximation of semiclassical impact parameter and Born approximation, using asymptotic expansion of hydrogen-like atoms oscillator strength

13 p2040 A72-29411

Perturbation theory of hydrogen and helium atoms multiphoton ionization probabilities, proposing series summation method

13 p2007 A72-29430

Model of solar wind expansion beyond heliosphere, taking into account effect of relative motion between cool interstellar atomic hydrogen and solar wind protons

13 p1033 A72-29801

Thermospheric atomic hydrogen concentration diurnal variations from time dependent continuity and diffusion equations, using Jacchia background atmosphere thermal and density structure formulas

13 p1953 A72-29806

Expanding elliptical H I ring with major and minor axes of 1300 and 560 pc from type III supernova in solar neighborhood

13 p2048 A72-29831

Hydrogen atom exchange in ion-molecule reactions of methane and ethylene determined from reaction products distribution, using ion cyclotron resonance techniques

14 p2084 A72-30522

Atomic hydrogen collisional and radiative transition rates, computing excitation and ionization cross sections

14 p2133 A72-30564

Ionospheric electrons and neutral particles temperature and concentration profiles explained by electron gas cooling due to atomic hydrogen excitation, calculating heat flow

14 p2101 A72-30641

Atomic hydrogen 3s state destruction by impact on nitrogen, argon and hydrogen molecules, considering collisional ionization and electron capture mechanisms

14 p2134 A72-30883

Microcalorimetric investigation of energy transfer from atomic and molecular hydrogen beams to various

surfaces at liquid helium temperatures and ultrahigh vacuum conditions

15 p2281 A72-31863

Eikonal distorted wave analysis of inelastic electron-atom collisions at intermediate energies application to electron impact induced atomic hydrogen 2s and 2p states excitation

15 p2282 A72-32646

Hydrogen atom ground state ionization probability derivation as function of electric field strength and distance to metal surface

15 p2279 A72-32699

Exobase atomic hydrogen densities for zero ballistic net flux as function of temperature distribution, noting support of McAfee hypothesis by OGO-4 polar UV observations

16 p2384 A72-32979

Fast metastable hydrogen atom beam production by proton beam-Cs vapor charge exchanges

16 p2429 A72-33057

Interstellar H I region strong polarization shock structure, obtaining charge separation field via beam continuum distribution and Mott-Smith approach

16 p2453 A72-33168

Model for low energy galactic cosmic ray effects on young and F star Li abundance and H I region heating

16 p2448 A72-33740

The solar wind H and He/+ content.

17 p2598 A72-34627

Absolute rate constant for the reaction $H + H_2CO$.

17 p2511 A72-34739

Multiphoton ionization of atomic hydrogen in the presence of an intense electromagnetic field.

17 p2586 A72-35827

Use of the Sturman function for the calculation of the third harmonic generation coefficient of the hydrogen atom.

17 p2586 A72-35830

Absolute detection and collisional destruction of 2.5-keV metastable hydrogen atoms produced by a charge-exchange process in cesium vapor.

19 p2837 A72-37547

Collisional excitation and impact ionization coefficients of hydrogen

19 p2837 A72-37807

Two quantum induced photon-plasmon transition probability for hydrogen atom in processes of nebulae and stellar chromospheres

19 p2837 A72-38058

Ionisation equilibrium and line intensities for an X-ray heated H I gas.

19 p2852 A72-38509

Intercloud atomic H gas density distribution from 21 cm line width variations with galactic longitude

19 p2867 A72-38512

Laser output power increase with plasma dynamic carbon dioxide laser configuration, noting steady population inversion in pure hydrogen atoms

20 p2934 A72-39932

Emission and absorption RF recombination lines of interstellar neutral atomic H and He, discussing electron transition processes in nebula

20 p2975 A72-40070

Electron loss in atom-molecule collisions.

21 p3087 A72-40473

Gross properties of five Scd galaxies as determined from 21-centimeter observations.

21 p3105 A72-41027

Correlation between the work function of transition metal carbides and the surface recombination of hydrogen atoms in the region of homogeneity

21 p3070 A72-41372

A calculated hydrogen distribution in the exosphere.

22 p3168 A72-42004

Hydrogen cold work peak measurements in Nb, showing hydrogen atoms-dislocations binding energy extent and temperature effects on internal friction

22 p3189 A72-42440

Equatorial UV airglow azimuthal variations from spinning rocket measurements, attributing origin to electron collision excited atomic hydrogen Lyman alpha emission

23 p3282 A72-43263

Charge state variation processes in hydrogen atom collisions with H₂ molecules

23 p3315 A72-43304

Angular distribution of interstellar atomic hydrogen.

23 p3315 A72-43834

Upper limits on the atomic hydrogen abundance in 12 globular clusters.

23 p3340 A72-44246

Variation in the hyperfine state of a hydrogen atom during its collision with unsaturated hydrocarbons in the gaseous phase

23 p3317 A72-44477

HYDROGEN CHLORIDES

NT HYDROCHLORIC ACID

The identification of the I-0 and 2-1 bands of HCl in the infrared sunspot spectrum.

17 p2611 A72-35299

HYDROGEN CLOUDS

Rf diagnostic technique for carbon and hydrogen /H I/ cloud recombination lines in cool interstellar medium

04 p0570 A72-14525

Interstellar sodium lines intensities and widths as discriminants for two component models of galactic H I cloud regions

04 p0578 A72-15310

Intergalactic matter infall in galaxies, discussing quasar absorption spectra, hydrogen clouds, accretion rate and relations to spiral structure

09 p1386 A72-22660

Hydrogen cloud structure of interstellar medium, assuming UV star Stromgren sphere radiation effects

09 p1390 A72-23526

Spectral indications of activity in galactic center, discussing radio source Sagittarius A and expanding hydrogen clouds

10 p1541 A72-24568

Hydrogen gas cloud gravitational contraction and fragmentation in expanding universe, noting cooling and massive stars formation

10 p1547 A72-24870

Gas and dust cloud evolution with allowance for dimensional finiteness and stellar evolution into red supergiant after hydrogen depletion

11 p1715 A72-25297

Galactic center region neutral hydrogen self absorbing cold cloud, discussing matter, spatial and radial velocity distributions and cloud temperature and density

12 p1867 A72-27208

Habing galactic model extension and confirmation from observations of high velocity neutral hydrogen clouds and outer spiral arm structure

13 p2048 A72-29817

Galactic spiral arm hypothesis for positive velocity neutral hydrogen clouds above galactic plane, surveying distribution

14 p2158 A72-30732

H II regions radial velocities in Carina arms from Fabry-Perot interferometric H alpha measurements, determining early stars distances from spectroscopic and photoelectric observations

14 p2159 A72-30740

Distribution of high velocity hydrogen near Galactic center due to free-free emission from exploding hot gas or cosmic ray pressure

15 p2317 A72-32756

H I region molecular formation on interstellar dust grains, discussing nonequilibrium evaporation mechanism for adsorbed particles

16 p2452 A72-33128

Numerical calculation for axisymmetric gas cloud rotation effects on collapse, noting implications for star formation and fragmentation

16 p2458 A72-33722

Theoretical He-triplet line strengths compared with astronomical observations of planetary nebulae and H II regions

17 p2614 A72-35646

Molecular equilibrium abundances in interstellar H I gas clouds, noting formation dependence on gas density and degree of interstellar radiation extinction

19 p2854 A72-37230

Formation of clouds in a cooling interstellar medium.

19 p2854 A72-37231

Protostars formation through interstellar atomic hydrogen clouds gravitational collapse, deriving critical mass, surface temperatures and luminosities

19 p2865 A72-38478

Interstellar molecules and dense clouds.

20 p2970 A72-39600

H II region fine structure from 11 and 3.7 cm observations, deducing physical parameters from continuum spectra

21 p3105 A72-41031

H 157 alpha recombination line from H I region before NGC 2024 radio source, considering average electron concentration and line origin

21 p3102 A72-41776

Dark dust nebulae and bright H II clouds, considering light molecules, stellar birth region, radio and IR astronomy

22 p3220 A72-41995

The density of H₂ molecules in dark interstellar clouds.

22 p3224 A72-42385

Gum nebula origin as ionized hydrogen cloud from prehistorical supernova explosion, discussing different ionization mechanisms

22 p3227 A72-42543

Stellar implosion, gas cloud collapse into white dwarf or neutron star and atomic hydrogen cloud collapse, considering effects of cosmic bodies at high velocities

24 p3439 A72-45017

HYDROGEN COMPOUNDS

NT BORANES

NT BORON HYDRIDES

NT CHLOROSILANES

NT DEUTERIDES

NT DEUTERIUM COMPOUNDS

NT HEAVY WATER

NT HYDRIDES

NT HYDROGEN CYANIDES

NT HYDROGEN PEROXIDE

NT HYDROGEN SULFIDE

NT LITHIUM HYDRIDES

NT METAL HYDRIDES

NT PHOSPHINES

NT SILANES

NT ZIRCONIUM HYDRIDES

Hydrogen iodide flash photolysis in presence of nitrous oxide, carbon dioxide and water investigated by kinetic spectroscopy, observing imidogen as intermediate reaction product

01 p0023 A72-11114

Meridional model of oxygen and hydrogen compounds reactions in mesosphere and lower thermosphere, determining diurnal variations and vertical profiles

03 p0346 A72-13378

IR chemiluminescence study of chlorine reaction with hydrogen iodide at enhanced collision energies, investigating energy conversion efficiency and forward scattering

06 p0770 A72-17300

Laser action in pulsed transverse discharge initiated chemical reactions forming hydrogen and deuterium halides, noting production of previously unobserved transitions

07 p0999 A72-18879

Hydrogen halide rotational relaxation to thermal distribution without intermediate quantum number peak, discussing IR chemiluminescence data correction method

07 p0936 A72-19673

Stratospheric ozone photochemistry through nitrogen oxides and hydrogen compounds reactions, noting controlling effect of water vapor

09 p1298 A72-22674

Neutron diffraction study of inorganic materials atomic structure, examining symmetry properties and group arrangements of hydrogen compounds

09 p1358 A72-23478

Intermolecular hydrogen bond study of hydroxyl group in caranol and caranonol compounds, listing IR absorption bands for valence oscillations

15 p2192 A72-32100

Russian book - Water in the universe

19 p2789 A72-37743

Study of the variation of the intensity of vibration-rotation spectra of hydrogen halide molecules under the action of compressed foreign gases

22 p3209 A72-43047

HYDROGEN CYANIDES

HCN laser amplifier gain measurement at IR wavelengths in gas mixtures by recording with pyroelectric receiver

03 p0368 A72-13667

Atmospheric model for proteins abiogenesis, considering heteropolypeptides formation from hydrogen cyanide and water

04 p0468 A72-14772

Catalytic action in organic catalyst predecessors of contemporary enzymes, discussing polymers of alpha-amino acids and hydrogen cyanide

05 p0624 A72-16128

Nb-Nb point-contact Josephson junctions response to submillimeter radiation from HCN and DCN lasers

07 p0992 A72-20551

Visual observation of continuous hydrocyanic acid laser modes and beam energy distribution, using cholesteric liquid crystal image converter

14 p2111 A72-30851

Interstellar nitrogen-15 and U169.3 - Possibly a new methanol line.

21 p3107 A72-41272

HYDROGEN DEUTERIUM OXIDE

U HEAVY WATER

HYDROGEN FLUORIDES

U HYDROFLUORIC ACID

HYDROGEN FUELS

Hydrogen fueled supersonic burning combustor testing, determining wall static pressure, hydrogen radial distribution, Pitot pressure and Mach number at combustor exit

05 p0704 A72-16107

Nitric oxide formation rate in combustion products of propane-air and hydrogen-air diluent flames

07 p0935 A72-19361

Future interstellar ramjet concepts, considering interstellar hydrogen fuel use for thermonuclear reactor and problems of fuel energy losses, plasma containment and structural limitations

09 p1374 A72-23250

Turbulent hot gas stream self ignition in oxidizer flow for hydrogen-air and gasoline-air mixtures

14 p2170 A72-30293

Energy supply calculation for two dimensional steady laminar compressible boundary layer flows with hypersonic hydrogen-air combustion

15 p2334 A72-31465

Toppler schlieren study of diffusion flame structure of plane laminar hydrogen-air jets in rectangular channel with vortex generators

19 p2879 A72-37365

Two component reaction kinetics model for numerical analysis of combustion during two- and three dimensional supersonic steady flow of hydrogen-air fuel mixtures

19 p2880 A72-37389

- Influence of pressure, mass flow rate, and nozzle angle on the chemical relaxation in nozzles
19 p2880 A72-37494
- Effect of the temperature on the burn-out of hydrogen diffusion flames in a supersonic flow in a closed channel
21 p3129 A72-40983
- Determination of the concentration range of flame propagation at elevated temperatures
21 p3129 A72-40984
- HYDROGEN IONS**
- Positive H, HE and O ions in exosphere from mass spectrometers mounted on Elektron 4 satellite
01 p0053 A72-10368
- Hydrogen ions concentration in daytime region of plasmasphere from OGO 5 satellite mass spectrometry, noting plasmopause position as function of magnetic activity
01 p0061 A72-10892
- Triatomic hydrogen positive ions dissociation at 410, 510 and 550 keV in molecular hydrogen gas, measuring atoms yield as function of target thickness
01 p0104 A72-11148
- Galactic IR astronomy, discussing findings on emission from H II regions of Orion Nebula and late and early type stars
02 p0276 A72-11643
- Eta Carinae model with IR spectrum details described by compact H II region photoionized by hot massive star radiation
02 p0277 A72-11668
- Hydrogen molecular ion g tensor calculation, determining approximate ground state wave functions
03 p0391 A72-13152
- Synchrotron and thermal H II region radio emission in Magellanic Clouds
03 p0425 A72-13259
- Venusian ionosphere thermal proton destruction, discussing helium and oxygen replacement candidates for principal ion components
03 p0434 A72-13537
- Distance estimation for supernova remnants and H II regions from H I absorption measurements
05 p0712 A72-15770
- Negative hydrogen ion production during charge exchange between protons in thick Li, Na, K and Mg vapor jets
06 p0863 A72-18410
- Plasma inhomogeneities effect on radio wave absorption in interstellar clouds of ionized hydrogen, analyzing cosmic radio emission spectrum
08 p1231 A72-21120
- Number of molecular hydrogen ion vibrational levels, using phase function method for scattering length and potential energy
08 p1211 A72-21293
- IR emission sources in NGC 2264, IC 2087 and M1-82 H II regions
08 p1236 A72-21397
- OH emission source and H II region bright knots coincidence in NGC 7538 nebula, suggesting physical model
09 p1392 A72-23548
- Duoplasmatron as negative hydrogen ion source to study geometrical and electrical parameters effects on beam and analyze composition, energy spectrum and emittance
10 p1518 A72-23963
- Galactic H II regions with radio emission at 1400 MHz, using National Radio Astronomy Observatory 300 ft telescope
11 p1724 A72-26785
- Grain heating model of H II region to explain 100 micron emission predominance in IR sources
12 p1871 A72-27693
- Proton accretion effect on circumstellar dust grains mass, noting impossibility of grain formation in H II region
13 p2048 A72-29790
- H II regions radial velocities in Carina arms from Fabry-Perot interferometric H alpha measurements, determining early stars distances from spectroscopic and photoelectric observations
14 p2159 A72-30740
- Cross section determination of proton production in collisions of electrons and hydrogen ions
14 p2134 A72-30801
- Cross sections for dissociative excitation of hydrogen ions by electrons determined by coincident detection of protons and H atoms
14 p2134 A72-30804
- Energy and angular distribution of hydrogen and rare gas ions backscattered from polycrystalline metal surfaces
15 p2276 A72-31852
- High resolution radio observation of H II region W 51, noting compact components with emission measures agreement with recombination line data non-LTE analysis
16 p2457 A72-33684
- H-He ions solar wind expansion absence for case of equal gas temperature, noting mass flux relationship to He ion temperature
16 p2449 A72-33911
- Cosmic-ray heating of low-density interstellar H II regions.
17 p2600 A72-35296
- Recombination of protons and negative hydrogen ions in slow collisions.
18 p2713 A72-36953
- Diurnal variation of the H+ flux between the ionosphere and the plasmasphere.
19 p2793 A72-38759
- Interpretation of experimental differential elastic scattering cross section for H+/+ Ne.
20 p2956 A72-39721
- H II region fine structure from 11 and 3.7 cm observations, deducing physical parameters from continuum spectra
21 p3105 A72-41031
- Dark dust nebulae and bright H II clouds, considering light molecules, stellar birth region, radio and IR astronomy
22 p3220 A72-41995
- Dipole moment derivative of triatomic hydrogen ion electronic ground state, considering fundamental spectrum observation in hydrogen gas in local thermodynamic equilibrium
22 p3209 A72-42720
- Angular distribution of electrons autodetached from H- in slow collisions with He.
23 p3316 A72-44074
- O/plus/ H/plus/ and He/plus/ ion distributions in a new polar wind model.
24 p3400 A72-45587
- HYDROGEN ISOTOPES**
- NT DEUTERIUM
- NT METALLIC HYDROGEN
- NT TRITIUM
- Oxygen and hydrogen stable isotopes utilization for studying water vapor in precipitations, constructing meteorological model
05 p0684 A72-16793
- Reduced mass and asymmetry differences effects on elastic collision integrals and thermal diffusion factors for isotopic hydrogen molecules
10 p1515 A72-24340
- Isotope effect calculation hydrogen and deuterium solubility in fcc metals, analyzing elastic vibrational spectrum of crystal with impurity atom in intermode
10 p1498 A72-24873
- Self consistent model for cosmic ray propagation from sources in Galaxy toward earth, using H and He isotope interstellar spectra
13 p2031 A72-29409
- HYDROGEN OXYGEN ENGINES**
- Controllable high energy hydrogen-oxygen rocket propulsion systems performance and combustion characteristics, considering mixture ratio, pressure, chamber geometric characteristics, injection area and velocity ratios
11 p1703 A72-25298
- Development of a GH2/GO2 pulsejet engine with 6.7 kN thrust for the attitude control system of the space shuttle
19 p2848 A72-37495
- The simulation of high pressure hydrogen/oxygen rocket engines.
21 p3042 A72-41606
- [AIAA PAPER 72-1027]
- Ideal high energy liquid rocket propellants combinations for high propulsive efficiencies, considering hydrogen, hydrazine, diborane and ammonia and various oxidizers
23 p3358 A72-44355
- Experimental performance of coaxial injectors in thrust-variable LO2/GH2-rocket engines.
24 p3434 A72-45181
- Flow model for the determination of the heat transfer on the base of vehicles with clustered H2-O2 rocket engines.
24 p3434 A72-45201
- HYDROGEN OXYGEN FUEL CELLS**
- Rechargeable oxygen electrode research program for hydrogen oxygen fuel cells and metal-oxygen batteries, discussing KOH solutions effects
04 p0466 A72-14675
- Metal catalyst theory for electrocatalysis in alkaline hydrogen oxygen fuel cells, using Tafel equation
16 p2351 A72-33880
- Hydrogen oxygen fuel cell development for spacecraft power supply systems, emphasizing service life and reliability under elevated temperature and high current density
19 p2754 A72-37643
- HYDROGEN PEROXIDE**
- Hydrogen peroxide formation relationship to lipid peroxidation and seizures in brain during high pressure oxygen exposure
12 p1766 A72-28300
- The reaction of hydrogen peroxide with nitrogen dioxide and nitric oxide.
17 p2511 A72-35466
- Book on liquid rocket propellants development, history and ignition problem covering nitrogen tetroxide, hydrogen peroxide, fluorine compounds, boranes and monopropellants
19 p2884 A72-38675
- In vivo hemolysis due to hyperoxia - Role of H2O2 accumulation.
24 p3374 A72-45651
- HYDROGEN PLASMA**
- NT DEUTERIUM PLASMA
- High temperature nongray kernel functions application to radiative heat transfer for bounded hydrogen plasma
01 p0145 A72-10100
- Spectral distribution of total continuous emission coefficient for LTE hydrogen plasma over 8000-16,000 K and 400-15,000 A ranges, observing Stark broadening
01 p0108 A72-10175
- Argon-hydrogen plasma seeded with submicron tungsten particles, measuring composition, temperature, radiant heat output and opacity
01 p0112 A72-11343
- Stabilized hydrogen plasma arc spectral radiation as light source for vacuum UV radiometry, comparing output with W strip and carbon sources
01 p0073 A72-11400
- Pulsed hf discharge in hydrogen based on laser light scattering on plasma electrons, noting position of satellites in spectra
02 p0237 A72-11406
- Single electron approximation of Stark broadening of hydrogen spectral lines without constraints of collision and quasi-static theories
03 p0391 A72-13079
- Radiation intensity and losses in dense high temperature hydrogen plasma containing bare nuclei and hydrogen-, helium-, lithium- and beryllium-like ions as impurities
04 p0557 A72-15170
- Hydrogen plasma absorption coefficients at laser frequencies over 0.3371-10.6 microns
05 p0694 A72-15997
- Thermodynamic equilibrium relations in optically thin plasma models for hydrogen and argon systems
06 p0699 A72-17218
- Spontaneous collisionless drift waves due to pressure gradient in hydrogen plasma column, studying magnetic field and reflecting conditions effects
06 p0857 A72-17534
- Supersonic hydrogen plasma flow in collapsing postsunset upper ionosphere, noting nonvanishing temperature gradient effect on critical point location
07 p0974 A72-18899
- Closed line magnetic confinement device filled with laser produced hydrogen plasma, discussing laser beam high speed numerical control for injected pellet interception
07 p1040 A72-19392
- [CLEA PAPER 12,1]
- Hydrogen plasma ionization equilibrium and thermodynamic stability existence condition based on Saha equation
07 p1044 A72-19889
- Hydrogen plasma generation by microwave field in magnetic-mirror device due to electron cyclotron resonance, measuring transverse diffusion coefficient dependence on magnetic field
07 p1046 A72-20506
- Artificial magnetosphere interaction with 8 keV electrons in hydrogen plasma beam simulating solar wind, noting penetration caused by boundary instability
08 p1156 A72-20823
- Thermodynamic properties of atomic hydrogen-helium plasma for postulated conditions present in stagnation shock layer of spacecraft entering Jupiter atmosphere
08 p1254 A72-21598
- Chemionization in oxyhydrogen plasma detonation waves
08 p1129 A72-22045
- Hydrogen line broadening in plasma theory with limitations of Stark component intensity distribution by quasi-static and impact approximations
09 p1358 A72-22493
- Short plasmoids production in hydrogen plasma jets by applying pulsed multipole magnetic field generated in linear quadrupole system
09 p1362 A72-23203
- Plasma production from hydrogen solid targets by pulsed carbon dioxide TEA laser, noting diagnostic methods
09 p1325 A72-23237
- Spectrum of hot hydrogen plasma continuum radiation, discussing models for Scorpius X-1 source and inhomogeneous clouds
09 p1391 A72-23536
- Geomagnetic field inflation during magnetic storm main phase, considering energy sources and injected proton plasma radial velocity
10 p1472 A72-24274
- Absorption spectra and plasma of laser spark in hydrogen, studying electron and atoms temperature and concentrations time variations
10 p1491 A72-24359
- Nonisothermal hydrogen plasma channel flow and radiative heat transfer combined with convective and conductive transfer between isothermal black parallel boundaries
[AIAA PAPER 72-279]
- 11 p1692 A72-25219

Dense hydrogen plasmoids injection with linear pinch gun into biconical cusp field, observing axial reciprocating motion

11 p1697 A72-26575

Hydroplasma metal removal for surface cleaning of heat resistant alloys, using electric contact plasma arc machine

11 p1641 A72-26673

Pulsed RF hydrogen plasma heating in mirror machine near ion cyclotron frequency and harmonics

11 p1699 A72-26703

High temperature deuterium plasma production by laser heating of gas filled cylindrical tube, optimizing pulse duration and configuration

12 p1849 A72-27059

Electron beam velocity distribution function fine structure for plasma-beam discharge in hydrogen within longitudinal magnetic field

12 p1850 A72-27261

Hydrogen plasma production, using linearly polarized microwaves with superimposed magnetic field

13 p2010 A72-28683

Single electron approximation of Stark broadening of hydrogen spectral lines without constraints of collision and quasi-static theories

13 p2007 A72-29429

Absorption coefficient of H-He plasma measured in temperature and electron density range of inverse bremsstrahlung and photoionization absorption

15 p2284 A72-31522

Hydrogen plasma ion density determination from atomic beam attenuation by resonant charge exchange with protons

15 p2284 A72-31582

Hydrogen line broadening in plasma theory with limitations of Stark component intensity distribution by quasi-static and impact approximations

17 p2588 A72-34657

Experimental evidence for stationary population inversions of atomic levels in an expanding hydrogen plasma

[DFVLR-SONDDR-213]

17 p2589 A72-34898

Absorption spectra and plasma of laser spark in hydrogen, studying electron and atoms temperature and concentrations time variations

17 p2562 A72-34958

Hydrogen plasma ionization equilibrium and thermodynamic stability existence condition based on Saha equation

17 p2590 A72-35137

Time-resolved diagnostic method for hydrogen plasmas

18 p2716 A72-36949

Dispersion curves of mixing mode between electrostatic and electromagnetic waves propagating perpendicularly to ambient magnetic field for hydrogen plasma with Maxwellian velocity profile

19 p2839 A72-37335

Purification of hydrogen plasmoids by the magnetic field of an injector-diverter device

19 p2843 A72-38539

Lyman alpha resonance line asymmetry calculation in dense hydrogen plasma, noting disagreement between theory and experiment

22 p3212 A72-42917

Determination of magnetic fields in plasmas from hydrogen spectral line profiles

23 p3318 A72-43313

Longitudinal magnetic field effect on the characteristics of a high frequency ion source

24 p3428 A72-45015

Influence of a temperature dependent spectral absorption coefficient on radiative flux

24 p3466 A72-45791

HYDROGEN RECOMBINATIONS

H I radio recombination line observation in H II region NGC 2024 microwave spectrum, detailing radiation frequency dependence

01 p0133 A72-11143

Solar radio recombination lines observation at hydrogen and helium frequencies

04 p0568 A72-15328

Hydrogen protons and atoms interaction with hydrogen and nitrogen molecules, showing electron transfers agreement with Franck-Condon principle

08 p1210 A72-20835

Radio recombination lines broadening in hydrogen by electron collisions, using Baranger impact theory

10 p1435 A72-24142

Extragalactic clouds supersonic collisions with galactic gases, discussing high velocity neutral hydrogen gas result of recombination following post-shock surplus energy radiation

10 p1538 A72-24248

Recombination of hydrogen atoms on the surfaces of solid bodies

19 p2838 A72-38199

HYDROGEN SULFIDE

Hydrogen sulfide detection in Galactic sources via observation of single line corresponding to rotational transition, comparing abundance to formaldehyde, CS, HCN and CO

21 p3107 A72-41271

HYDROGEN 2

U DEUTERIUM

HYDROGEN 3

U TRITIUM

HYDROGENATION

Porous Ti alloys production with Mo, Cr and Pd, considering optimum sintering temperatures and hydrogenation

13 p1981 A72-30106

Hydrogen gas solubility measurement in solid Mo at atmospheric pressure and 905-1521 C, noting quasi-regular linearity of Arrhenius plot

14 p2113 A72-30246

Properties of pyrolytic oil hydrogenated aromatic fraction, noting suitability for jet fuels applications

14 p2145 A72-31075

Microcracks observed in hydrogenated niobium foil

21 p3069 A72-41300

HYDROGENOMONAS

Kinetics of heat inactivation of phosphoglycerate kinase in soluble fraction from hydrogenomonas facilis

07 p0922 A72-20237

Influence of Cosmos 368 space flight conditions on radiation effects in yeasts, hydrogen bacteria and seeds of lettuce and pea

23 p3254 A72-43390

HYDROGRAPHY

On the hydrographic response to transient meteorological disturbances

21 p3077 A72-40465

HYDROKINETICS

U HYDROMECHANICS

HYDROLOGY

Northern Alps geology, hydrology, lithology and tectonic survey, using aircraft-borne thermal IR scanner remote sensor

02 p0209 A72-11795

Remote sensing with sounding rockets and balloons, discussing cost, mineralogical surveys, land use and hydrological assessments

05 p0654 A72-15756

Meteorological satellites and Gemini and Apollo earth photographs, showing annual and diurnal oceanographic, hydrologic and geologic dynamic features

06 p0810 A72-18614

Rain induced flood mathematical model, optimizing parameters and applying to hydrological forecasts

07 p1029 A72-18862

Hydrologic data collection via ATS 1 satellite for river and flood forecast of National Weather Service, planning geostationary operational environmental satellites /GOES/

09 p1296 A72-22315

Radar imaging systems application to cartography, geology, hydrology, biogeography, oceanography and geography, emphasizing remote sensing in cloudy environments

16 p2364 A72-33634

Streamflow forecasting project to assess feasibility of air and spaceborne remote sensed data acquisition application to watershed hydrological behavior prediction

24 p3398 A72-45215

HYDROLYSIS

Alpha amino acids proteinoids or thermal polymers enzyme activity, investigating hydrolytic activities and decarboxylation reactions

04 p0483 A72-14776

Glass fiber reinforced thermoplastic resins chemical and hydrolytic resistance, noting composites and polymers long term performance prediction in aggressive environments

12 p1833 A72-27405

Solar activity effects on bismuth chloride hydrolysis tests from statistical results following solar flares

12 p1773 A72-28212

Resin selection for manufacture of chemically resistant glass fiber reinforced polyesters, considering structural factors of chain for susceptibility to alkaline hydrolysis

16 p2414 A72-33304

HYDROMAGNETIC FLOW

U MAGNETOHYDRODYNAMIC FLOW

HYDROMAGNETIC STABILITY

U MAGNETOHYDRODYNAMIC STABILITY

HYDROMAGNETIC WAVES

U MAGNETOHYDRODYNAMIC WAVES

HYDROMAGNETICS

U MAGNETOHYDRODYNAMICS

HYDROMAGNETISM

U MAGNETOHYDRODYNAMICS

HYDROMECHANICS

NT ELASTOHYDRODYNAMICS

NT ELECTROHYDRODYNAMICS

NT HYDRODYNAMICS

NT HYDROSTATICS

NT MAGNETOHYDRODYNAMICS

NT MAGNETOHYDROSTATICS

Book on applied mechanics covering hydromechanics, biomechanics, transonic and hypersonic shock structures, random vibrations, plasticity, viscoplasticity, etc

06 p0896 A72-17958

Small scale flow and surface effects in multiphase media hydromechanics, obtaining entropy production

in mixture for interphase transformations characterization

10 p1468 A72-24430

HYDROMETALLURGY

Hydropressed sintered U-700 superalloy powder, noting weakened particle grain boundary conditions from mechanical properties and fracture studies

02 p0240 A72-11444

HYDROMETEOROLOGY

Hydrometeors linear depolarization ratios measurements by monostatic lidar, using different size water drops and ice crystal clouds

01 p0095 A72-10830

Cloud and precipitation elementary processes effects on reflected radar signal fluctuation spectrum during hydrometeor formation

08 p1201 A72-21997

Orthonormalized exponential functions use in hydrometeorology

08 p1202 A72-22119

Discriminatory analysis application in hydrometeorological forecasts, discussing use of bunch map analysis

08 p1203 A72-22122

Standardized automatic telemetering hydrometeorological station, discussing structure, operation, working principles and sensors

10 p1462 A72-25009

Automatic hydrometeorological stations standardized sensors, describing data converters for atmospheric pressure, precipitation, humidity and wind and water and soil temperature measurements

10 p1483 A72-25014

Wavelength choice for ground based operational weather radar systems as function of reflectivity dependence on scattering hydrometeors /raindrops, hailstones/

13 p1917 A72-28694

Hybrid forecast model for hydrometeors short range prediction based on meteorological satellites cloud pattern observations and quasi-Lagrangian advection analog

13 p1993 A72-28858

Fog, cloud, rain and snow detection by acoustic echo sounding, noting effects of energy scattered from atmospheric boundary layer velocity and temperature fluctuations

15 p2267 A72-32725

Measurement of unsteady hydrometeorological processes on inertial devices

19 p2830 A72-38774

Russian book - Long-term variations of atmospheric circulation and long-range hydrometeorological forecasts

22 p3200 A72-42078

HYDROPLANES [SURFACES]

Two dimensional hydrodynamic flow analysis of pneumatic tire hydroplaning, taking into account tire deformation, viscous, inertial and turbulence effects

10 p1512 A72-24819

HYDROSKIS

U HYDROPLANES [SURFACES]

HYDROSPHERE [EARTH]

U EARTH HYDROSPHERE

HYDROSTATIC PRESSURE

Hydrogen partial molar volume in metal-hydrogen two component systems under externally applied uniform hydrostatic stress field, using thermodynamic analysis

01 p0083 A72-10205

Hydrostatic pressure and temperature effects on growth of psychrophilic marine bacterium, emphasizing inhibited amino acid transport and respiration

01 p0011 A72-10322

Hydrostatic pressurized gas seals for rotating shafts under extreme operating conditions, discussing design requirements for small clearances and avoidance of pneumatic instabilities

02 p0236 A72-12425

Creep buckling of cylindrical finite two-layer shell under external hydrostatic pressure, considering rigidly clamped and hinged end conditions

03 p0444 A72-13574

Sheet metal biaxial creep testing, using edge clamped circular diaphragm deflected by lateral hydrostatic pressure

03 p0373 A72-13649

Hydrodynamic journal gas bearing with herringbone grooved portion for self generating air supply pump hydrostatic starting and stopping

05 p0664 A72-15944

[ASME PAPER 71-WA/DE-7] Hydrostatic pressure effects on I-V characteristics of amorphous semiconductor germanium telluride sulfide arsenide

06 p0865 A72-17493

Stress-strain state in elastic plane with small radial cracks and circular hole under hydrostatic tension

07 p1091 A72-19765

Imperfection influence on nonlinear stability of long circular cylindrical shells subject to critical hydrostatic pressure

09 p1403 A72-22763

Electrolyte hydrostatic pressure measurement in limited volume biological compartments by fluid filled glass micropipette used in microtransducer capacity 11 p1587 A72-26623

Boron doped n-type Si planar diode and n-p-n epitaxial planar Si transistor junctions investigating hydrostatic pressure effects on static characteristics and breakdown voltage 12 p1789 A72-27314

Hemispherical elastic nonexpandable weightless film fastened along equator to inner wall of closed cylindrical vessel under hydrostatic pressure, determining film axisymmetric equilibrium shapes 13 p1940 A72-28392

Hydrostatic pressure effect on tensile creep and creep rupture of polycrystalline metals at high temperatures 13 p2058 A72-29450

Nonlinear critical stability of truncated conical shell uniformly loaded by external hydrostatic pressure, using Bubnov-Galerkin method 16 p2470 A72-33412

Stable bifurcation mode prior to instability in thick walled cylindrical viscoplastic pressure vessel under internal hydrostatic pressure 16 p2474 A72-34129

The effect of hydrostatic pressure on plastic deformation and creep of polycrystalline metals at elevated temperatures. 20 p2977 A72-38878

Anisotropy and hydrostatic stress effects on yield criteria of nonwork-hardening plastic material under plane strain conditions 21 p3117 A72-40674

Hydrostatic pressure effects on atomic configuration based on principle of equivalence related to Einstein gravitational equations 22 p3205 A72-42459

Effects of hydrostatic stress on the yielding of cold rolled metals and fiber-reinforced composites. 23 p3299 A72-43496

Lower-body negative pressure as a method of preventing shifts associated with changes in the hydrostatic pressure of blood 23 p3256 A72-43919

Development of a push-pull fatigue testing machine under high pressure, and the results of preliminary fatigue tests. 24 p3401 A72-44630

HYDROSTATICS
NT MAGNETOHYDROSTATICS
 Static properties of circular hydrostatic thrust gas bearings with curved surfaces, comparing theory with measurements [ASME PAPER 71-LUB-22] 02 p0236 A72-11542
 Mascon free lunar gravitational potential calculations, showing hydrostatic equilibrium in early evolution 03 p0434 A72-13552
 Ultralong wave baroclinic instability, obtaining linearized perturbation equations from layered geostrophic hydrostatic adiabatic model 04 p0541 A72-14451
 Zeta Puppis visual line spectrum discrepancy from non-LTE stellar atmospheres models, necessitating hydrostatic equilibrium deviations consideration for temperature derivation 08 p1232 A72-21178
 Cold static superdense model for white dwarf and neutron stars, using relativity theory and variational principles for stellar structure in hydrostatic equilibrium 11 p1715 A72-25528
 Hydrostatic oxygen burning in stars. II. 19 p2854 A72-37236
 General relativity equations for hydrostatic equilibrium of spherical distribution of mass combined with equations of state for highly relativistic neutron star central regions 20 p2955 A72-40011
 Behavioral features of a composite hydrostatic suspension of a gyrocompass under conditions of vibration 21 p3058 A72-41807

HYDROX ENGINES
U HYDROGEN OXYGEN ENGINES
HYDROXIDES
NT POTASSIUM HYDROXIDES
 Interstellar OH formation through inverse predissociation from continuum to vibrational level of repulsive molecular state originating from asymptotic atomic ground state 01 p0133 A72-11141
 Carbon monoxide oxidation by hydroxyl radicals at high and low temperatures from transition state theory, confirming flame and shock tube results [WSCI PAPER 71-36] 04 p0482 A72-14584
 Lubricating mixtures of mineral oil with inorganic phosphates, hydroxides and sulfides, discussing lubrication mechanism and physical properties 06 p0837 A72-18603
 Chromium carbides synthesis by carburizing chromium hydroxide or oxalate in hydrogen-methane gas mixture at temperatures below 1000 C 22 p3188 A72-41974

HYDROXYCORTICOSTEROID
NT CORTISONE
 Parotid fluid 17-hydroxycortico steroid level relation to hyperthermia stress at various heat levels during thermal environmental testing 12 p1768 A72-28335

HYDROXYL COMPOUNDS
NT ALCOHOLS
NT BISPHENOLS
NT ETHYL ALCOHOL
NT GLYCOLS
NT METHYL ALCOHOLS
NT PHENOLS
 Hydroxyapatite isotropic and anisotropic elastic properties compared with experimentally observed anisotropic behavior of bone 01 p0018 A72-10625
 Mesospheric OH volume density profile measurements by rocket-borne high resolution polarized Ebert-Fastie spectrometer 01 p0062 A72-10912
 Temperature dependence of carbon monoxide reaction rate with hydroxyl, noting activation energy 07 p0935 A72-19376
 Electron impact induced fragmentations of o-, m- and p-hydroxyalkylphenones and trimethylsilyl/TMS/ether derivatives, using high resolution mass spectrometry, metastable defocusing and deuterium labeling 07 p0936 A72-19499
 Intermolecular hydrogen bond study of hydroxyl group in caranol and caranol-ol compounds, listing IR absorption bands for valence oscillations 15 p2192 A72-32100

HYDROXYL EMISSION
 Molecular processes in interstellar space and life origin, discussing radio astronomy observations, catalytic action and hydroxyl radicals in galaxies 01 p0128 A72-10398
 Interstellar OH and water maser regions, deriving density, diameter and temperature 01 p0133 A72-11142
 Quenching rate of vibrationally excited hydroxyl with molecular oxygen in fast flows for airglow studies in upper atmosphere 03 p0321 A72-13899
 Curve of line width correlation application to alpha Orionis OH lines, determining atmospheric turbulence and thermal velocities 04 p0571 A72-14558
 Lower ionosphere 5577 and 5893 A and hydroxyl band emissions interrelationships, observing atomic O and vertical eddy transport effects 04 p0518 A72-14961
 Upper atmosphere atomic hydrogen H alpha emission, correlating intensity and hydroxyl vibration temperature 05 p0659 A72-17036
 MHz IR/OH sources, discussing M type Mira variables or M supergiants photospheric temperature and dust shell structure 07 p1069 A72-19075
 Astronomical IR spectroscopy of Alpha Ori, discussing OH line formation, LTE, rms turbulence velocity and abundance 07 p1072 A72-19345
 OH ground state transition frequency measurement, using beam maser spectrometer 07 p1006 A72-19423
 Ignition time delay measurement between leading shock front and hydroxyl emission onset in two phase detonation of decane-oxygen 08 p1255 A72-22041
 Dynamic model of night time hydroxyl rotational temperature variations from airborne and ground measurements 09 p1298 A72-22587
 Airglow IR spectrum between 3 and 4 microns during morning and evening twilight, showing OH intensity drop 09 p1299 A72-22903
 OH emission source and H II region bright knots coincidence in NGC 7538 nebula, suggesting physical model 09 p1392 A72-23548
 Mesospheric clouds composed of molecular complexes of extraterrestrial origin, considering chemical reactions, hydroxyl luminescence, thermospheric water vapor and auroras 09 p1347 A72-23590
 OH emission characteristics of IR stars from model with asymmetrical expansion outward of circumstellar OH clouds 10 p1542 A72-24613
 Hydroxyl vibration levels excitation rates calculation from transition probabilities and band sequence nightglow intensity measurements 13 p1954 A72-29816
 Hydroxyl emission bands intensity, and vibrational and rotational temperatures sporadic and harmonic components in seasonal and diurnal variations 14 p2098 A72-30142
 Nightglow ground based spectrophotometric observations of hydroxyl emission intensity and rotational

temperature variations related with solar and geophysical activity 14 p2098 A72-30144

Stellar OH radical emission amplification by maser effect raising low energy molecules to high energy by pumping 14 p2110 A72-30578

OH and IR emission from NML Cygnus, discussing gas cloud model with flattening and gas expansion 14 p2157 A72-30681

Hydroxyl emission sources classification from observed main line polarization and satellite lines 15 p2315 A72-32710

IR photometry of IR-OH sources, showing IR colors correlation with velocity separation of OH emission peaks 15 p2315 A72-32711

Apparent-actual size relation in astronomical masers for internal physical conditions of homogeneous spherical and tubular OH or water maser clouds 16 p2455 A72-33456

Interstellar OH maser size determination, discussing scattering by inhomogeneities in electron distribution 16 p2456 A72-33473

Observation of the intensity ratio between 5,1/ and 9,4/ bands of OH emission in the night airglow. 17 p2546 A72-35059

Rates of interaction of vibrationally excited hydroxyl $v = 9/$ with diatomic and small polyatomic molecules. 17 p2511 A72-35648

Microwave celestial water-vapor sources. 18 p2729 A72-36990

OH airglow IR observation from high altitude sites with bandpass filter, noting average spatial and diurnal fluctuations 19 p2794 A72-38861

Interstellar medium hydroxyl radiation model, considering amplified spontaneous emission and hot spots 20 p2964 A72-38919

Hydroxyl and water radio sources scale and geometry constraints placed by interstellar maser gain saturation relation to emission solid angle 21 p3062 A72-40565

OH maser sources parametric down-conversion, deriving nonlinear current densities, electron cyclotron wave damping and parametric gain coefficient 21 p3064 A72-41030

Recoil effect on inverted molecules changing pumping conditions and gain for interstellar, OH maser intensity and radial velocity variations 21 p3102 A72-41773

Statistics of the radiation from astronomical masers. 23 p3337 A72-43872

HYGIENE
 Zero-g showers for long duration space flight crews hygiene, describing flexible mummy bag and truncated conical shell design 15 p2190 A72-32320

HYGROMETERS
NT PSYCHROMETERS
 Hair hygrometer for FM radiosonde in-flight air humidity measurements, discussing design, operation and accuracy test in extreme weather conditions 10 p1483 A72-25005
 LiCl dew point hygrometer operation investigated by double ventilation psychrometers, noting measurement error dependence on relative humidity and temperature 10 p1483 A72-25015
 Air hygrometer with heated electrolytic sensor for atmospheric humidity determination by automatic meteorological stations 10 p1483 A72-25016
 Calibration technique for meteorological superpressure balloon hygrometers designed for horizontal sounding of troposphere and stratosphere 10 p1484 A72-25087
 Phase transition between solid hydrate and saturated solution of lithium chloride electrically detected on a lithium chloride heated hygrometer. 21 p3054 A72-40689

HYGROSCOPICITY
 Fog modification at all temperatures with physicochemical techniques, discussing blowing hygroscopic salts and use of alginates of sodium and marine algae extracts 04 p0543 A72-14696
 Droplet growth on passivated hygroscopic condensation nuclei in device with controllable relative humidity 08 p1172 A72-22000
 Porosity effect on mechanical properties, airtightness, corrosion resistance and moisture absorption of glass fiber reinforced plastics 16 p2414 A72-33270
 Influence of hygroscopic substances on the transparency of aerosols from combustion products of condensed systems 20 p2987 A72-40043

HYPERBARIC CHAMBERS

Hyperbaric chamber tests for hemodynamic response to oxygen inhalation at 1 and 2 atm pressure for myocardial infarction treatment assessment

08 p1114 A72-20891

Decompression sickness treatment in USAF hyperbaric oxygen chambers

08 p1126 A72-21575

Physiological and biochemical responses of Paramaecium caudatum to hypo- and hyperbaric stresses, discussing protoplasmic inactivation by high oxygen pressure

12 p1766 A72-28299

HYPERBOLAS

Finite bending of a compressible anisotropic rectangular block into a hyperbolic shell.

17 p2634 A72-35438

HYPERBOLIC FUNCTIONS

Hyperbolic partial differential equations solution by hybrid computer, simulating wave propagation by track hold circuits

02 p0188 A72-12656

Hyperbolic and parabolic partial differential equations behavior comparison by studying point-to-point time optimal control for heat conduction and vibrating string motion

04 p0505 A72-14673

Lagrange method extended to method of characteristics for solving first order hyperbolic partial differential equations, applying to ionospheric ion density distribution

04 p0539 A72-14885

One dimensional nonhomogeneous wave equations solution for linear and hyperbolic moving boundary conditions applied to resonator fields

05 p0627 A72-16407

Space shuttle flow field fluid dynamic hyperbolic equations numerical solution by noncentered finite difference schemes, noting advantages in programming logic simplicity and multidimensional generalizations

05 p0729 A72-16848

Optimal averaging of control in distributed random parameter system described by hyperbolic partial differential equations, considering boundary values on characteristics as control functions

05 p0683 A72-17133

Optimal control of one dimensional physical system with delayed argument described by nonlinear first order hyperbolic partial differential equations, using maximum principle

05 p0691 A72-17138

Validity proof of asymptotic methods in oscillation theory of one dimensional nonlinear dynamic systems described by hyperbolic and parabolic differential equations

06 p0839 A72-17681

Wave diffusion related to phenomena governed by linear hyperbolic partial differential equations of second order, presenting Cauchy problem solution

07 p1035 A72-20090

Theorems for averaging of first order linear hyperbolic system with time lag, proving existence and uniqueness of solution to Cauchy problem

07 p1028 A72-20214

Perturbation method for asymptotic solutions of initial value problems for hyperbolic wave equations with small nonlinearities

11 p1676 A72-25355

Characteristic shocks propagation velocity, showing exceptionality of hyperbolic conservative system multiple waves

11 p1689 A72-26479

Method of characteristics for solution of quasi-linear hyperbolic partial differential equations, analyzing frequency response

11 p1678 A72-26551

Spectral stability characteristics of difference schemes for hyperbolic differential equations in gas dynamics involving triangular and tetragonal bases

15 p2178 A72-31444

Control theory of second order linear hyperbolic partial differential equations, discussing relation to harmonic and spectral analysis

15 p2263 A72-31757

Self-adjusting hybrid schemes for shock computations.

17 p2575 A72-34648

Investigation of a strongly generalized solution to a multidimensional mixed problem of a class of second-order hyperbolic equations with a nonlinear operator-containing right side

17 p2577 A72-35843

The first Cauchy-Goursat problem of a hyperbolic-type equation degenerating at the boundary and having singular coefficients at the degeneration line

17 p2577 A72-35844

Differential inequalities for semilinear hyperbolic operators with two independent variables.

18 p2705 A72-36618

A characteristic problem for a hyperbolic-type equation degenerating at the boundary

19 p2825 A72-38187

Investigation of a mixed boundary value problem for one class of second-order hyperbolic equations with a nonlinear operator-type right-hand side

19 p2827 A72-38447

A boundary value problem for a mixed-type equation with two perpendicular parabolic-degeneration lines

19 p2828 A72-38630

Difference schemes with a divergent operator for a general system of second-order hyperbolic equations

19 p2828 A72-38854

Problem of the analytical design of controllers for parabolic and hyperbolic equations

20 p2946 A72-39468

Investigation with the aid of a Fourier method of the classical solution of a multidimensional composite problem for a class of hyperbolic equations of the second order with a nonlinear operator right-hand part

22 p3198 A72-41897

Solution method for some boundary problems of nonlinear hyperbolic-type equations and propagation of weak shock waves

22 p3164 A72-41904

Time evaluation of discontinuity occurrence in solutions of boundary problems for second-order hyperbolic quasi-linear systems

22 p3198 A72-41912

Book - The method of fractional steps: The solution of problems of mathematical physics in several variables

22 p3208 A72-43200

A difference method for plane problems in magnetoelastodynamics.

[ASME PAPER 72-APM-A]

23 p3321 A72-44051

Hyperbolic two body problem in celestial mechanics, discussing E , r , α , β , summability procedure for analytic continuation

24 p3442 A72-45236

HYPERBOLIC NAVIGATION

NT DECCA NAVIGATION

NT LORAN

NT LORAN C

NT LORAN D

NT SHORAN

High accuracy position determination from hyperbolic radio navigation time differences based on Sodano inverse solution of geodesics

11 p1684 A72-26498

HYPERBOLIC REENTRY

Spacecraft trajectories for reentry at hyperbolic velocity, examining aerodynamic control loads and characteristics in atmospheric skip

11 p1718 A72-25929

Landing control algorithm using onboard digital computer for spacecraft hyperbolic velocity reentry, discussing simulation test results

11 p1684 A72-26898

Analytical evaluation of the spacecraft descent range for hyperbolic reentry trajectories

17 p2610 A72-35203

Investigation of the range of landing area distances for earth atmosphere reentries at hyperbolic velocities

17 p2622 A72-35204

HYPERBOLIC SYSTEMS

Fast hyperbolic MHD flow past point source, considering geometry and disturbances singularities of MHD Mach cones

02 p0266 A72-12369

Relativistic heat propagation models, considering hyperbolic system of partial differential equations, momentum-energy tensor for ideal fluid and classical Fourier law

06 p0847 A72-17256

Optimal control computation for nonlinear hyperbolic partial differential system by gradient and quasi-linearization techniques, noting MHD, fluid flow and electromagnetic wave propagation

10 p1456 A72-24453

Shock wave solutions of nonlinear hyperbolic system of conservation laws, considering case of zero viscosity

13 p1940 A72-28616

Direct and inverse problems of scattering theory for hyperbolic system of equations on plane, emphasizing unsteady approach and integral equation class with kernels

13 p2004 A72-29468

The numerical solution of hyperbolic systems using bicharacteristics.

17 p2574 A72-34449

Hopscotch algorithm for numerical integration of nonlinear hyperbolic partial differential equation systems based on finite difference method

18 p2705 A72-37020

Numerical solution of quasi-conservative hyperbolic systems - The cylindrical shock problem.

21 p3043 A72-40101

HYPERBOLIC TRAJECTORIES

German monograph on optimal planetary atmosphere effects for increasing hyperbolic velocity at flyby for Venus and Earth

09 p1383 A72-22322

Planetary swingby optimum transfer between hyperbolic asymptotes with less than maximum natural turn angle

10 p1552 A72-24487

Post-Newtonian approximation for calculation of gravity and angular momentum radiated in form of gravitational waves by two point particles system, noting masses in hyperbolic Kepler orbit

10 p1547 A72-24933

Energy optimal single impulse transfer from hyperbolic trajectory to circular orbit

11 p1718 A72-25926

First order asymptotic matching computational technique for calculation of perturbed moon-centered hyperbola parameters in earth-moon trajectory

11 p1720 A72-25996

Spacecraft optimal control after transfer from hyperbolic trajectory to planetary satellite orbit by atmospheric drag, minimizing engine thrust

14 p2129 A72-30470

Interplanetary spacecraft transfer maneuver for hyperbolic trajectory change into eccentric orbit, using aerodynamic drag to obtain nearly circular orbit

14 p2151 A72-30471

Improved criteria for hyperbolic-elliptic motion in the general three-body problem.

21 p3109 A72-41333

On required guidance for transfer from hyperbolic trajectory to the planetary satellite orbit by aerodynamic drag in atmosphere.

24 p3450 A72-45176

Application of the restricted hyperbolic three-body problem to a star-sun-comet system.

24 p3442 A72-45234

HYPERCAPNIA

Intracellular pH prime regulation in rat brain during acute and sustained hypercapnia, discussing cellular bicarbonate accumulation

01 p0012 A72-10623

Hypoxia, hyperoxia and hypercapnia short period effect on rat brain oxygen supply, measuring blood gas values, tissue oxygen partial pressure time variations, etc

02 p0159 A72-11957

Acute hypercapnia neurotropic effect in rabbits, describing carbon dioxide inhalation period, preanesthetic and narcotic stages and recovery phase

02 p0160 A72-12015

Acute and chronic hypercapnia effect on lactate, pyruvate, alpha-ketoglutarate, glutamate and phosphocreatine contents of rat brain

03 p0316 A72-13677

Human reaction to inhalation of gas mixtures with 3-9 percent carbon dioxide, measuring respiration rates, minute breathing volume, heart rates, arterial pressures, etc

05 p0618 A72-16632

Hypoxia, hypercapnia and hyperoxia effects on active glucose transport in rat small intestines

05 p0618 A72-16633

Confinement, physical deconditioning and hypercapnia effects on human musculoskeletal protein by chromatographic method for quantifying urinary peptides and free amino acids

[AD-736665]

06 p0767 A72-17869

Arterial chemoreceptor deafferentation influence on rat respiratory response to hypoxic and hypercapnic gas mixture breathing

08 p1120 A72-22078

Human external respiration characteristics changes during increasing hypercapnia, relating carbon dioxide concentration rate to compensatory mechanisms and endurance

08 p1121 A72-22084

Oxygen consumption and body temperature in anesthetized, paralyzed and artificially ventilated dogs cooled in water bath at 34 C, measuring hypercapnia and beta-adrenergic blockade effects

[AD-740991]

10 p1424 A72-23735

Chronic hypoxia adapted rat myocardial tissue sensitivity to increased carbon dioxide tension

11 p1579 A72-26616

Interaction of chronic hypoxia and hypercapnia upon blood gases and acid base status.

17 p2504 A72-35166

Respiratory frequency and alveolar oxygen and carbon dioxide tension relationship to hypercapnia in man

17 p2506 A72-35965

Venous responses to stimulation of carotid chemoreceptors by hypoxia and hypercapnia.

18 p2648 A72-36025

Hypercapnia with relief of hypoxia in normal individuals with increased work of breathing.

21 p3005 A72-40420

Comparison of three methods for quantitating respiratory response to hypoxia in man.

24 p3372 A72-44960

HYPERFINE STRUCTURE

Molecular ordering in smectic A liquid crystals, evaluating spectrum hyperfine splitting as function of orientation to spectrometer magnetic field

08 p1217 A72-21490

Optical hyperfine structure of Ne 21 excited states and quadrupole moment obtained by laser induced line narrowing techniques

10 p1515 A72-24601

Zeeman effects in hyperfine structure of atomic iodine photodissociation laser emission, noting magnetic fields effect on time behavior

11 p1692 A72-26558

Solar spectrum Mg I multiplet lines hyperfine structures, examining emission lines with Fabry-Perot and Fourier transform spectrometers

14 p2158 A72-30730

Temperature dependent Mg and Fe hyperfine doublets in lunar olivine, indicating slow cooling crystallization

15 p2303 A72-31302

Solar Mg abundance and hyperfine structure from oscillator strengths measurement by comparing absorption lines at furnace temperatures

15 p2317 A72-32774

Beam maser spectrometric measurements of normal, C-13 and O-18 formaldehyde transitions, determining coupling constants for all rotational transitions hyperfine structure

16 p2431 A72-33132

Observability of hyperfine structure and Lamb, nuclear-volume shifts in $1s_{n1}-1s_{n1}'$ transitions of helium-like ions.

19 p2837 A72-37544

Gamma ray scattering asymmetries of Fe 57 nucleus, discussing hyperfine structure and conjugate spin transition

22 p3209 A72-42924

Variation in the hyperfine state of a hydrogen atom during its collision with unsaturated hydrocarbons in the gaseous phase

23 p3317 A72-44477

Electron paramagnetic resonance hyperfine spectral observation of double quantum transitions of Ti positive ions in strontium chloride single cubic crystal host

24 p3378 A72-45311

HYPERGEOMETRIC FUNCTIONS

Truncation error bounds for continued fractions, considering application to Gauss hypergeometric functions

[AD-738403] 04 p0538 A72-14728

Shooting and imbedding methods for theoretical analysis and approximate numerical solution of two-point boundary value problems involving n-vector-valued functions

[AD-743615] 04 p0539 A72-15043

Boundary value problem related to iteration equation of generalized axisymmetrical potential theory, obtaining exact solution via Jacobi polynomials and difference scheme

07 p1036 A72-20219

Wiener Hopf integral equation for problem of smooth stamp impression into elastic wedge face, solving by gamma and hypergeometric functions

13 p2059 A72-29500

On the algebraic structure of a class of solvable quantum problems.

18 p2711 A72-36514

HYPERGEOMETRY

U HYPERSPACES

HYPERGLYCEMIA

Dose dependent hyperglycemia and hypolipemia response to pentobarbital sodium injection in rats from plasma glucose and fatty acid analysis

08 p1116 A72-21187

HYPERGOLIC ROCKET PROPELLANTS

Analysis of reaction products of nitrogen tetroxide with hydrazines under nonignition conditions.

20 p2898 A72-39610

HYPEROXIA

Anaerobic glycolysis and specific gravity of red blood cells in rats exposed to pure oxygen at 600 torr

01 p0015 A72-11297

Hypoxia, hyperoxia and hypercapnia short period effect on rat brain oxygen supply, measuring blood gas values, tissue oxygen partial pressure time variations, etc

02 p0159 A72-11957

Rat central nervous system oxygen toxicity seizure susceptibility relation to circadian rhythms

04 p0472 A72-14867

Hypoxia, hypercapnia and hyperoxia effects on active glucose transport in rat small intestines

05 p0618 A72-16633

Rat brain acetylated and unacetylated coenzyme A aberration in marginally hyperoxic space capsule environments

06 p0763 A72-17875

Hyperoxia effect on kidney blood flow erythropoietic properties in rabbits, noting inhibiting effect on erythroblast cells mitotic activity in bone marrow culture

06 p0765 A72-18061

Hypoxia pretreatment for decreased pulmonary oxygen toxicity during high pressure oxygen breathing in rats

07 p0917 A72-19328

Hyperbaric oxygen exposure effect on cardiovascular system in rats, discussing pulmonary edema relation to hypertensive left ventricular failure

07 p0921 A72-20182

Rapid eye movement sleep deprivation and hyperbaric oxygenation influence on gamma-aminobutyric acid levels in mice brains, suggesting protective mechanism against nerve cell oxygen intoxication

07 p0922 A72-20191

Respiration control during hyperoxia, discussing chemoreceptor significance in minute volume respiration rate reduction mechanism from Pamir mountain aborigines oxygen breathing reaction studies

08 p1120 A72-22076

Chinchilla and guinea pig tolerances to hypoxia and hyperoxia in pressure chamber tests, suggesting relation to red blood cell size and number

09 p1265 A72-22647

Hyperoxia effect on human airways resistance during high pressure oxygen breathing

11 p1586 A72-26614

Electron microscope study of hyperoxia-induced pathogenetic ultrastructural changes in rat lung

12 p1761 A72-27531

Suppression effects of hyperoxic breathing gases on red blood cell and erythropoietin hormone production following blood loss

12 p1766 A72-28298

Russian book on functional morphology under extremal space flight conditions covering overloads, hypoxia and hyperoxia effects on organism and cellular structure and metabolism

14 p2077 A72-30996

Succinate and glutathione as protective agents against chronic effects of hyperbaric oxygen toxicity in rats

14 p2082 A72-31091

Neurologic oxygen toxicity - Effects of switch of inert gas and change of pressure.

19 p2758 A72-38704

Hematologic responses to hypobaric hyperoxia.

20 p2892 A72-39345

Regional lung function during early acclimatization to 3,100 m altitude.

21 p3005 A72-40424

Effect of hyperoxic media on the stability of rats during acute carbon monoxide exposure

21 p2998 A72-40437

Changes in blood serum proteins under the effect of hyperoxia in intact rats with thyroid gland dysfunction

22 p3142 A72-42283

Influence of a high oxygen content on the rate of formation and elimination of gaseous wastes in albino rats

23 p3255 A72-43906

Influence of elevated partial oxygen pressure on the sympathetic-adrenal and acetylcholine systems

24 p3371 A72-44595

In vivo hemolysis due to hyperoxia - Role of H2O2 accumulation.

24 p3374 A72-45651

HYPERSONIC AIRCRAFT

Convective cooling system design for Mach 6 hypersonic transport Al alloy airframe, using water glycol loop network

[AIAA PAPER 72-334] 11 p1574 A72-25369

Hypersonic commercial aircraft operational problems, considering passenger physiology limits flight profile, sonic pollution, traffic demands, route structure, etc

14 p2073 A72-30830

Laminar and turbulent boundary-layer studies at hypersonic speeds.

[ICAS PAPER 72-09] 21 p2990 A72-41134

Hypersonic transports commercial applications, examining economic and noise and air pollution aspects

[ICAS PAPER 72-32] 21 p2995 A72-41157

HYPERSONIC BOUNDARY LAYER

Free stream and shock layer disturbances effect on hypersonic boundary layer transition in wind tunnels from hot wire measurements

02 p0230 A72-12274

Hypersonic boundary layer transition in presence of wind tunnel noise, indicating rms sound pressure relationship to transition Reynolds number

02 p0151 A72-12278

Laminar three dimensional boundary layer nonequilibrium effects at hypersonic wing swept leading edge with intensively cooled surface, considering sweep induced crossflow effect

[VPI-E-71-23] 02 p0152 A72-12422

High velocity boundary layer problems for space shuttle, investigating free interaction with detachment, shock wave, penetration, air bubbles in circulation and adherence conditions

03 p0308 A72-13699

Compressible turbulent boundary layer properties on porous cone at Mach 8, examining Crocco theory for flows with mass addition

05 p0602 A72-16536

Hypersonic boundary layer displacement interaction and surface curvature effects, employing implicit finite difference methods

[AIAA PAPER 72-76] 05 p0603 A72-16803

Wind tunnel disturbances effects on hypersonic boundary layer transition on sharp cones, comparing hot-wire anemometer and surface pressure measurements

[AIAA PAPER 72-181] 05 p0605 A72-16825

Turbulence generation in hypersonic boundary layer from hot-wire correlation and disturbance convection velocity measurements on cone-ogive-cylinder in Mach 7.2 flow

[AIAA PAPER 72-182] 05 p0650 A72-16837

Mass transfer effects on hypersonic turbulent boundary layer properties from profile measurements on porous cone

[AIAA PAPER 72-184] 05 p0650 A72-16839

Three dimensional hypersonic turbulent boundary layer under normal and longitudinal pressure gradients and cross flow along windward symmetry plane of body of revolution

[AIAA PAPER 72-186] 05 p0605 A72-16841

Laser schlieren measurement of density gradients in laminar hypersonic boundary layer interacting with corner expansion wave in shock tunnel

[AIAA PAPER 72-75] 05 p0606 A72-16879

Pressure gradient effects on hypersonic turbulent skin friction and boundary layer temperature, velocity and Mach number distributions and shape factors

[AIAA PAPER 72-215] 06 p0799 A72-17923

Surface catalytic properties effect on multicomponent gas hypersonic boundary layer with simultaneous vibrational-dissociative relaxation, considering plate and blunt body laminar boundary layer

06 p0757 A72-18130

Vorticity effect on shock wave-boundary layer interactions on blunt edged compression surfaces of hypersonic inlets

10 p1419 A72-24649

Axisymmetric hypersonic motion around thin solid of revolution, taking into account boundary layer interaction with inviscid external flow

13 p1895 A72-29847

Numerical solution of algebraic equation encountered in aerodynamics of hypersonic boundary layer interacting with external flow on thin solids of revolution

13 p1895 A72-29848

Hypersonic turbulent boundary layer flow parameters and heat exchange during blowing of coolant air and He through slot

13 p1895 A72-29901

Hypersonic blowdown tunnel investigation of turbulent shock-boundary layer interactions at two dimensional wedge compression corner

13 p1944 A72-30030

Hypersonic limit for equilibrium laminar constant pressure boundary layer equations of planetary entry, obtaining skin friction and heat transfer parameters

14 p2071 A72-31052

Hypersonic transition boundary layers, obtaining disturbance convection velocities as function of fluctuation scale and wall distance

15 p2219 A72-32581

Hypersonic boundary layer profiles upstream of transition point on cone surface from pitot surveys, heat transfer and wall pressure measurements and spark schlieren photographs

16 p2341 A72-32837

On the structure of hypersonic turbulent boundary layers.

17 p2540 A72-35188

Spreading of a turbulent disturbance.

17 p2541 A72-35249

A study of the asymptotic behaviour of the external fringes of compressible, laminar boundary layers of a dissociating gas.

18 p2683 A72-36937

Hypersonic unsteady compressible boundary layer dependence on Prandtl number.

19 p2787 A72-38429

Proper equations and similar approximations in the hypersonic merged layer.

20 p2885 A72-39621

The effect of angle of attack on boundary-layer transition on cones.

20 p2886 A72-39638

Theoretical and experimental study of the pressure and heat-flux distributions on a control surface in the presence of a thick hypersonic turbulent boundary layer

[ICAS PAPER 72-23] 21 p2991 A72-41148

Blowing of a foreign gas in a hypersonic viscous shock layer

22 p3133 A72-42265

German monograph - Solution of the boundary layer equations for chemically reacting gases by a collocation method.

22 p3167 A72-43071

Viscous interaction over concave and convex surfaces at hypersonic speeds.

23 p3249 A72-44308

HYPERSONIC COMBUSTION

Energy supply calculation for two dimensional steady laminar compressible boundary layer flows with hypersonic hydrogen-air combustion

15 p2334 A72-31465

Supersonic and hypersonic combustion processes three dimensional characteristics, comparing wind tunnel test data with boundary layer equations numerical integration results
[ICAS PAPER 72-21] 21 p3130 A72-41146

Various efficiencies of fluid flows and application to the hypersonic ramjet 24 p3360 A72-44993

HYPERSONIC FLIGHT

Three degrees of freedom motions of slender cones with slight compounded asymmetries in hypersonic flight wind tunnel stability tests
[AIAA PAPER 72-28] 05 p0608 A72-16939

Viscous interaction effects on pressure distributions and heat transfer rate on two dimensional surface under high altitude hypersonic flight conditions
07 p0910 A72-20110

Hypersonic missile trail conductivity measurement on ballistic test stand, calculating electron concentration decrease 14 p2069 A72-30312

Collection efficiency of conical and blunted axisymmetric power law bodies in hypersonic flight through dust clouds and of impact angle and velocity 15 p2180 A72-32580

Telemetry acquisition of aerodynamic heat rates to conical, free-flight models at Mach 6 in an aeroballistic range. 22 p3155 A72-42703

HYPERSONIC FLOW

Alternating directional implicit numerical solution for three dimensional steady low density hypersonic flow over finite width flat plate
[AD-736572] 01 p0049 A72-10230

Hypersonic source flow past wedges and cones, calculating flow nonuniformities effects on shock shape, velocity, pressure and density by perturbation analysis
01 p0033 A72-11394

Supersonic and hypersonic flows with attached shock waves over delta wing at angle of attack, deriving unified theory for flow field 02 p0150 A72-12030

Hypersonic two component gas mixture nozzle flow with condensation or evaporation discontinuity, determining Pitot pressure limits 02 p0230 A72-12255

Closed boundary layer separation regions in super- and hypersonic flow, deriving mathematical model for neutral stability curves calculation
[DGLR PAPER 71-065] 02 p0153 A72-12715

Laminar two dimensional hypersonic flow over stepwise accelerated flat plate at zero angle of attack, obtaining time dependent velocity and temperature profiles by linearized flow equations 03 p0442 A72-13236

Skimmer design optimization for maximum nozzle beam intensity yields in hypersonic flow 03 p0362 A72-14052

Hypersonic axially symmetric laminar boundary layer electrically conducting fluid flow in blunt body stagnation region in presence of radial magnetic field 05 p0600 A72-16063

Vortex production of intense localized heating to leeward regions of bodies in hypersonic flows, proposing flow field models
[AIAA PAPER 72-77] 05 p0604 A72-16804

Shock interference heating in hypersonic flows, measuring pressure and heat transfer in wind tunnels
[AIAA PAPER 72-78] 05 p0604 A72-16805

Current collection characteristics of flush mounted electrostatic probes on sharp flat plate in ionized hypersonic flows
[AIAA PAPER 72-104] 05 p0696 A72-16814

Forebody blowing induced dynamic instability effect on slender cones at hypersonic speeds, presenting theory based on unsteady imbedded Newtonian flow concepts
[AIAA PAPER 72-31] 05 p0607 A72-16919

Hypersonic flow past final thickness delta wing, presenting conical flow equations with boundary value solution 06 p0757 A72-18128

Attached and separated turbulent viscous regions resulting from shock wave-boundary layer interactions in hypersonic flow
[AIAA PAPER 72-74] 07 p0966 A72-18949

Boundary layer transition on slender cone in hypersonic flow as function of nose bluntness, free stream Reynolds number and angle of attack
[AIAA PAPER 72-216] 07 p0908 A72-18961

Hypersonic gas flow around asymmetric triangular metal plate with blunt leading edges, using two layer model 07 p0909 A72-19985

Matched asymptotic expansions method application to problems with two independent perturbation parameters, considering application to boundary layer and hypersonic flow theory
[ONERA, TP NO. 1007] 07 p0970 A72-20076

Iterative solution to gas dynamics equations for hypersonic flow past slender three dimensional body, applying to Cauchy problem 08 p1107 A72-20971

Molecular beam continuum model for calculation of hypersonic flow past flat plate at zero incidence angle
[AD-746387] 08 p1254 A72-21609

Shock layer emission associated with hypersonic air flow past spherical segment, solving flow equations by iteration technique 10 p1418 A72-24539

Separation flow field measurements for space shuttle cylindrical configurations in hypersonic streams, using pressure heat transfer and visualization techniques
[AIAA PAPER 72-294] 11 p1567 A72-25232

Transverse outflow effects on flow field characteristics of hypersonic finite span separated flows with turbulent boundary layer 11 p1572 A72-26004

Hypersonic polytropic transformation of ideal fluid under mechanical or geometrical conditions 11 p1572 A72-26092

Newton-Busemann pressure law derived for hypersonic rotationally symmetric flow from momentum theory considerations and plane flows 12 p1751 A72-27120

Predictor-corrector multiple iteration technique for three dimensional viscous flow problems applied to hypersonic leading edges and Burger equation
[PIBAL-72-19] 13 p1893 A72-28422

Hypersonic flow of nonequilibrium ionized monatomic inviscid radiating gas past axisymmetric blunt body with allowance for electron and ion temperatures difference 13 p1895 A72-29877

Hypersonic blowdown tunnel investigation of turbulent shock-boundary layer interactions at two dimensional wedge compression corner 13 p1944 A72-30030

Numerical analysis of inviscid hypersonic flow characteristics in shock layer between bow shock and cone at angles of attack, taking into account laminar separated flow 14 p2069 A72-30328

Mass entrainment products effect on radiative and convective heat transfer during decomposition of graphite blunt body in steady hypersonic flow of radiating air 14 p2174 A72-31158

Pressure increase induced by heat release for laminar flame sheet in hypersonic stream, considering fuel injection through semiinfinite porous flat plate 15 p2337 A72-32590

Thermal radiation effects on semiinfinite planar blunt leading edge body hypersonic flow field, using Lax and Rusanov artificial viscosity methods 15 p2337 A72-32593

Simultaneous hypersonic skin friction and heat transfer measurements on sharp-edged flat plate, using thin-skin heat transfer gages and boundary layer pitot rake 15 p2219 A72-32598

Monte Carlo simulation method for flow field around two dimensional or axisymmetric body immersed in hypersonic rarefied gas flow 16 p2342 A72-32882

Direct integral method to calculate subsonic and supersonic regions in planar and axisymmetric hypersonic flow, using stream function for velocity and density
[DFVLR-SONDDR-202] 16 p2343 A72-33421

Rarefied hypersonic flow characteristics of delta wings and trailing edge spoilers. 17 p2485 A72-35229

Unified area rule for hypersonic and supersonic wing-bodies. 17 p2485 A72-35251

Closed form solution to conical inviscid hypersonic flow over circular cone at zero angle of attack 17 p2486 A72-35433

Analytical solutions for straight oblique shock waves in radiating gases. 17 p2542 A72-35616

Viscous hypersonic flow over a flat plate at angle of attack with leeside boundary layer separation.
[AD-744593] 17 p2486 A72-35634

Turbulence model equations for calculation of supersonic and hypersonic flows, representing Reynolds stresses and turbulent heat flux vector in terms of eddy viscosity 17 p2543 A72-35639

A hypersonic flow about a body of revolution with fanned jet injection 17 p2487 A72-35805

Triangular and conical wings in hypersonic flow with Mach reflection of shock waves from leading edge with optimal L/D ratio 18 p2642 A72-36893

Viscosity effect on hypersonic flow field near slender body, discussing eigenvalue solutions for two and three dimensional flow around triangular plate 19 p2745 A72-37393

Development of a hot-wire anemometer for hypersonic turbulent flows. 19 p2795 A72-37517

Three-dimensional wings in hypersonic flow. 19 p2747 A72-38797

Effect of angle of incidence on the response of cylindrical electrostatic probes at supersonic speeds. 20 p2926 A72-39602

Hypersonic viscous, slip flow over insulated wedges. 20 p2885 A72-39612

Aerodynamics of a slender cone with asymmetric nose bluntness at Mach 14. 20 p2886 A72-39634

Investigations concerning reentry bodies in the hypersonic tunnels of Goettingen 20 p2886 A72-39933

A semiempirical method for the evaluation of aerothermodynamic properties in the intermediate hypersonic flow regimes.
[ICAS PAPER 72-03] 21 p2990 A72-41128

Heat transfer in separated regions in supersonic and hypersonic flows. 21 p2991 A72-41139

Behavior of a laminar boundary layer in the presence of a positive pressure gradient
[ICAS PAPER 72-17] 21 p3045 A72-41142

Calculation of heat shield with local mass injection in hypersonic flow. 21 p3131 A72-41235

Formation of a shock wave around a blunt conical body placed in a rarefied hypersonic flow 21 p2993 A72-41340

Electron beam visualization in hypersonic air flows.
[AIAA PAPER 72-1017] 21 p3042 A72-41596

An experimental study in the application of the Raman scattering technique as a remote sensor of gas temperature and number density in hypersonic CF₄ flow. 21 p3057 A72-41601

Evaluation of windward streamline effective cone boundary-layer analyses. 22 p3136 A72-42874

An experimental study of film cooling through a rearward-facing slot. 23 p3356 A72-43971

Determination of slender bodies of minimum total drag in hypersonic flow using Newton-Busemann pressure coefficient law. 23 p3249 A72-44267

Periodicity in exothermic hypersonic flows about blunt projectiles. 24 p3463 A72-45035

Hypersonic flow around plane and axisymmetric bodies of arbitrary shape with inviscid radiating gas. 24 p3360 A72-45110

Asymmetric nose bluntness effects on the aerodynamics of a slender cone at Mach 14. 24 p3363 A72-45342

Effects of upstream unsteadiness on hypersonic flow past a wedge. 24 p3364 A72-45565

Hypersonic leading edge problem - Wedges and cones. 24 p3364 A72-45778

HYPERSONIC FORCES

Hypersonic nonlinear aerodynamic loading effect on panel flutter, examining stability for various initial conditions
[AIAA PAPER 72-345] 11 p1728 A72-25374

HYPERSONIC HEAT TRANSFER

Aerothermochemical analysis of thermosetting hydrocarbon plastic ablation rate under heat transfer at reentry vehicle hypersonic stagnation point, describing pyrolysis by chemical kinetic equation 15 p2335 A72-32149

Simultaneous hypersonic skin friction and heat transfer measurements on sharp-edged flat plate, using thin-skin heat transfer gages and boundary layer pitot rake 15 p2219 A72-32598

Inviscid surface streamlines and laminar, transitional and turbulent heating of blunt nose shuttle configurations in hypersonic flow
[AIAA PAPER 72-703] 16 p2345 A72-34041

An experimental study of heat transfer downstream of a rearward-facing step with small coolant injection. 23 p3357 A72-44271

Heat addition to supersonic flow by shock induced combustion studied by spherical and conical projectiles shot into explosive gas mixtures 24 p3360 A72-45038

HYPERSONIC INLETS

Hypersonic air inlet of revolution with mixed supersonic compression, analyzing shock-boundary layer interaction process
[ONERA, TP NO. 977] 05 p0599 A72-15857

Vorticity effect on shock wave-boundary layer interactions on blunt edged compression surfaces of hypersonic inlets 10 p1419 A72-24649

HYPERSONIC NOZZLES

Measurements of skin friction on the wall of a hypersonic nozzle. 24 p3365 A72-45792

HYPERSONIC REENTRY

Aerodynamic design of atmospheric reentry vehicles forebody, considering maximum drag for hypersonic bodies
02 p0149 A72-11726

Telemetry system on board beryllium sphere reentry vehicle for hypersonic gas dynamics and wake chemistry experiments, using flush mounted antennas with isotropic radiation pattern
[AIAA PAPER 72-176] 05 p0631 A72-16836

Monatomic ionized radiating gas nonequilibrium flow in blunt body stagnation region behind shock wave during hypersonic atmospheric reentry
07 p0909 A72-20083

Delta wing configuration design with anhedral heat shield for high lift reentry in 6-20 Mach number range
[AIAA PAPER 72-132] 09 p1259 A72-22501

Ablation phase duration during spacecraft decelerated hypersonic reentry flight, using theoretical model based on quasi-steady assumptions
11 p1745 A72-25815

Minimum ballistic factor missile shapes.
19 p2746 A72-37522

Theoretical and experimental investigations on the problem of aerodynamic heating of re-entry vehicles.
[ICAS PAPER 72-39] 21 p3130 A72-41164

Correlations of peak heating in shock interference regions at hypersonic speeds.
21 p2992 A72-41309

Optimal guidance for the space shuttle transition.
24 p3422 A72-45186

HYPERSONIC SHOCK

Two dimensional transonic and hypersonic shock structures, discussing flow equations, mathematical properties and similarity rules
[AD-742561] 06 p0799 A72-17960

Mach 26 shock wave in nitrogen investigated by electron beam fluorescence technique, determining population distribution among rotational states
15 p2281 A72-32404

Gas ionization buildup behind hypersonic shock waves, calculating onset point properties from plasma conservation and electron energy equations
16 p2434 A72-32902

Instability of hypersonic viscous shock layer with finite rate chemistry.
20 p2886 A72-39635

Pressure and temperature change on the wall surface in strong shock wave diffraction.
24 p3391 A72-45047

HYPERSONIC SPEED

Hypersonic melting ablation waves simulation near stagnation region by frozen oil models
[AIAA PAPER 72-92] 05 p0750 A72-16977

Flow parameters behind shock waves propagating in carbon dioxide-nitrogen mixtures at Mach numbers from 5 to 10
07 p0966 A72-18936

Conical and spherical nose shapes effects on drag and static stability at Mach 10
07 p0908 A72-19695

Aerodynamic characteristics of hypersonic velocity meteor traveling in earth atmosphere and shock wave propagation generated by explosion in air and on ground
07 p1081 A72-20094

Optimal configuration of lifting bodies for hypersonic speeds, noting negligible effect of blunt leading edges
10 p1418 A72-24536

Base pressure distribution measurement for free flying sharp cone at hypersonic speeds and high angles of attack
[AIAA PAPER 72-316] 11 p1567 A72-25250

Sonic boom induced flow field at supersonic/hypersonic speeds, using shock expansion method and hypersonic equivalence principle for sharp and blunt nosed bodies
[AIAA PAPER 72-652] 16 p2349 A72-34082

Laminar and turbulent boundary-layer studies at hypersonic speeds.
[ICAS PAPER 72-09] 21 p2990 A72-41134

Average circumferential pressure on inclined bodies of revolution at hypersonic speed.
24 p3365 A72-45788

HYPERSONIC TEST APPARATUS

Status of hotshot wind tunnels for hypersonic aerodynamic studies.
24 p3388 A72-45203

A comparison of disturbance levels measured in hypersonic tunnels using a hot-wire anemometer and a pilot pressure probe.
[AIAA PAPER 72-1003] 24 p3388 A72-45402

HYPERSONIC VEHICLES

NT LIFTING REENTRY VEHICLES

Area rule for change in lift/drag ratio of hypersonic delta wing due to conical body addition on compression side
02 p0151 A72-12270

Hypersonic vehicles lateral dynamics during great circle flight, using linearized equations of motion and Newtonian theory for stability derivatives estimation
08 p1110 A72-21603

Hypersonic vehicle far field behavior for sonic boom strength, position and positive phase duration
11 p1617 A72-26002

Longitudinal dynamic stability of hypersonic shuttle vehicle designed for operation to planetary atmosphere rim
16 p2462 A72-34019

Exact solution for dynamic oscillations of re-entry bodies.
17 p2622 A72-35231

Minimum weight passive insulation requirements for hypersonic cruise vehicles.
17 p2638 A72-35256

Theoretical and experimental study of a dual-mode ramjet/flight range from Mach 3.5 to 7/
[ICAS PAPER 72-24] 21 p3099 A72-41149

Optimal three dimensional maneuvering of a rocket powered hypervelocity vehicle.
24 p3450 A72-45151

HYPERSONIC WAKES

Hypersonic projectiles wake visualization with holography, using single mode ruby laser and reflected diffuse light techniques
02 p0224 A72-11742

Wake analysis of asymmetric hypersonic flow past two dimensional profiles at small angles of attack, using perturbation techniques
06 p0757 A72-18143

Book on steady laminar supersonic and hypersonic wakes covering near and far region solutions, boundary layer separation, etc
09 p1261 A72-23029

Turbulent wake of slender cone at Mach 12.5, measuring density and temperature fluctuations simultaneously
[AIAA PAPER 72-118] 10 p1479 A72-24080

Ionized and neutral specie concentration in rarefied hypersonic wake flow behind cone, using electrostatic and electron density probes
15 p2177 A72-31209

Electron density fluctuation measurements in hypervelocity projectile hypersonic turbulent wakes, showing power spectra
15 p2242 A72-32584

Spin effects on satellite-borne cylindrical probe electron density measurements, considering satellite wake and geomagnetic field effects
16 p2389 A72-32962

High temperature turbulent jet facility for studying ionic species produced by high temperature air and ablation products interaction with cool ambient air
[AIAA PAPER 72-676] 17 p2536 A72-35480

Hypersonic wake aerodynamics at high Reynolds numbers.
[AIAA PAPER 72-701] 17 p2486 A72-35484

Turbulent base heating on a slender re-entry vehicle.
21 p2992 A72-41308

Determination of the velocity field of the wake of a hypersonic sphere with the aid of ion probe arrays
21 p3057 A72-41725

A study of the electronic and gasdynamic parameters of a hypersonic wake behind models moving in argon
22 p3168 A72-43111

Hypersonic missile trail conductivity measurement on ballistic test stand, calculating electron concentration decrease
23 p3247 A72-43214

HYPERSONIC WIND TUNNELS

U HYPERVELOCITY WIND TUNNELS

HYPERSONICS

Hypersonic sound attenuation and velocity dispersion in sulfur fluoride near critical point determined by light scattering measurement
16 p2422 A72-32946

HYPERSPACES

Second and third degree harmonic interpolation formulas for given point in bounded simply connected n-dimensional region, indicating approximate solution of Dirichlet problem
04 p0538 A72-14727

Multidimensional random hypersurfaces generation with given statistical properties on digital computer, using linear filter theory
04 p0540 A72-15628

Separation of real zeros of certain classes of functions related to hypersurface and curve intersection
10 p1506 A72-25119

Spacelike hypersurface conformally invariant three-geometry role in unconstrained dynamical degrees of freedom of gravitational field
11 p1691 A72-26706

Computer graphics for invariant torus behavior in four dimensional phase space, varying equation parameter over large intervals
15 p2263 A72-31758

WKB approximation and oscillatory behaviour of null geodesics in general relativity.
17 p2583 A72-35795

On the existence of an instantaneous rotation axis during the motion of a solid body with a constant point in Euclidian n-dimensional space.
19 p2835 A72-38635

HYPERTENSION

Long term prognosis of transient hypertension in young male adults, evaluating importance in pilot selection
01 p0022 A72-11295

Functional condition of rabbits cerebrum precortical arteries during hypertension produced by intravenous noradrenaline infusion, discussing hypo and hyperkinesia
06 p0762 A72-17674

Hyperbaric oxygen exposure effect on cardiovascular system in rats, discussing pulmonary edema relation to hypertensive left ventricular failure
07 p0921 A72-20182

Hypertension and blood sugar and lipid level increase as ischemic heart disease risk factors
08 p1117 A72-21542

Negative and positive emotional states influence on blood cholesterol and arterial pressure levels in dogs, suggesting common subcortical genesis of atherosclerosis and hypertension
09 p1264 A72-22498

Hemodynamic response to physical exercise stress in dogs with angiotensin-induced acute arterial hypertension
12 p1764 A72-28216

Coronary heart disease discriminatory factors from comparison with healthy controls, noting diastolic hypertension significance
15 p2183 A72-31282

Blood coagulation changes at high altitude predisposing to pulmonary hypertension.
17 p2498 A72-34222

Changes of intracellular myocardial electrolytes in experimental hypertension.
17 p2501 A72-34984

Systemic haemodynamics in borderline arterial hypertension - Responses to static exercise before and under the influence of propranolol.
19 p2756 A72-37773

The incidence of hypertension and associated factors - The Israel ischemic heart disease study.
19 p2756 A72-37870

Renin in differential diagnosis of hypertension.
19 p2757 A72-38144

Metabolism of angiotensin II in sodium depletion and hypertension in humans.
23 p3257 A72-43998

H-V intervals in left bundle-branch block - Clinical and electrocardiographic correlations.
24 p3374 A72-45690

HYPERTHERMIA

Central cooling and warming effects of preoptic/anterior hypothalamic region on thermoregulatory activity of neuroendocrine, cardiovascular and neuromuscular systems
03 p0313 A72-13070

Splanchnic vasoconstriction in hyperthermic man independent of falling blood pressure
04 p0480 A72-15217

Heat and cold acclimatization in hamsters, relating thermoregulatory response to helium-cold hypothermia induction
08 p1115 A72-21085

Parotid fluid 17-hydroxycorticoid steroid level relation to hyperthermia stress at various heat levels during thermal environmental testing
12 p1768 A72-28335

Human physiological function variations dependence on hyperthermia levels in high temperature environment
14 p2074 A72-30257

Cardiovascular and respiratory changes in dogs exposed to acute overheating, relating ECG changes to adrenergic and hypoxia effects
14 p2074 A72-30382

Enzyme activity and ascorbic acid concentration as index of rat thyroid gland tissue functional activity during hyperthermia
14 p2077 A72-31098

Sweat depression during controlled hyperthermia in man - Effects on the sweat rate and sweat electrolytes
20 p2892 A72-39591

Analysis of changes in thermal regulation after destruction of the medial preoptic area of the hypothalamus
24 p3371 A72-44593

HYPERTONIA

U OSMOSIS

HYPERVELOCITY ACCELERATORS

U HYPERVELOCITY GUNS

HYPERVELOCITY CRATERING

U HYPERVELOCITY PROJECTILES

U PROJECTILE CRATERING

HYPERVELOCITY FLOW

Radiative transfer and chemical nonequilibrium phenomena for radiating flow field predictions behind high altitude hypervelocity normal shock waves
05 p0603 A72-16545

HYPERVELOCITY GUNS

SLINGSHOT pilot aerodynamic test facility for very high acceleration, using encapsulated gas slug over fixed model
[AIAA PAPER 72-168] 05 p0645 A72-16962

HYPERVELOCITY IMPACT

- High velocity impact reduced temperature increase due to shock compression in metals, discussing pressure and charge effects
03 p0442 A72-13240
- Varying energy and gamma /quasi-steady/ models for point source blast waves from high speed solids impact, comparing 1100-0-aluminum shock decay data
05 p0736 A72-16101
- Hypervelocity impact parameters calculated from shock wave equations of motion, discussing viscosity effect on velocity and stress distributions
14 p2164 A72-30297
- Lunar rock and mineral shock melting and vaporization from hypervelocity meteoroid impacts, calculating entropy, phase changes and thermal equilibrium
14 p2155 A72-30520
- Glass lined microcraters on lunar rocks attributed to hypervelocity impact of extralunar particles
17 p2615 A72-35682
- Solution of the impact problem of an elastic body and a rigid obstacle by the source-sink method
18 p2736 A72-36811
- Photographic observations of W particle clusters high velocity impact against polystyrene, paraffin and W targets for energy dissipation in meteorite impact simulations
20 p2969 A72-39257
- Basalt plates craters produced by high velocity impact of steel spheres, noting profiles at normal and oblique angles
20 p2978 A72-39258
- Craters formed in mineral dust by hypervelocity microparticles.
20 p2970 A72-39474
- Metal barrier maximum puncturable thickness dependence on high velocity meteorite particle impact parameters
22 p3234 A72-42217
- Analytical model of the flash produced in aluminum-aluminum hypervelocity impacts.
22 p3207 A72-42867
- Gas dynamics of the flight and explosion of meteorites.
24 p3439 A72-45020
- HYPERSOUND LAUNCHERS**
Blast and detonation wave phenomena applications in war and peace, discussing hypervelocity launchers, shock tubes and explosive weapons
08 p1146 A72-21014
- HYPERSOUND PROJECTILES**
Dc X ray timing pulse generator for light gas gun triggering based on projectile interruption technique
15 p2241 A72-32441
- Electron density fluctuation measurements in hypervelocity projectile hypersonic turbulent wakes, showing power spectra
15 p2242 A72-32584
- Profile and depth of microcraters formed in glass.
18 p2736 A72-36972
- HYPERSOUND WIND TUNNELS**
NT CASCADE WIND TUNNELS
NT HOTSHOT WIND TUNNELS
NT PLASMA JET WIND TUNNELS
NT SHOCK TUNNELS
- High resolution mean flow and turbulence measurements in turbulent boundary layer on cooled hypersonic wind tunnel side wall at Mach 9.37
[AIAA PAPER 72-73]
05 p0650 A72-16802
- Dust content effect on heat transfer in hypervelocity wind tunnels, discussing gas flow pattern distortion due to interaction with particles
08 p1253 A72-21453
- Magnetic balance measurements of aerodynamic forces on spheres and slender cones in hypersonic low density wind tunnels, noting sting effect
10 p1462 A72-24771
- Hypersonic gun tunnel balance and pressure measurements on sharp leading edge delta wings, comparing experimental coefficients and shock angles with predicted values
11 p1571 A72-25735
- Pressure distribution over delta wing with blunted edges at small angles of attack in hypersonic wind tunnel tests
14 p2071 A72-31022
- Development of a hypervelocity wind tunnel.
18 p2676 A72-37095
- The S4MA hypersonic wind tunnel - Its use for tests of ramjet engines with supersonic combustion of hydrogen
19 p2783 A72-37823
- Investigations concerning reentry bodies in the hypersonic tunnels of Goettingen
20 p2886 A72-39933
- Development of the AEDC-VKF tunnel J - A real gas high density, true velocity, hypersonic, aerodynamic test facility.
[AIAA PAPER 72-993]
21 p3040 A72-41579
- Recent progress regarding the measurement techniques in the hypersonic area
[ONERA, TP NO. 1055]
22 p3178 A72-42581

- A comparison of disturbance levels measured in hypersonic tunnels using a hot-wire anemometer and a pitot pressure probe.
[AIAA PAPER 72-1003]
24 p3388 A72-45402
- HYPERVENTILATION**
Breathing control during speech, noting carbon dioxide response, hyperventilation and apnea
04 p0480 A72-15218
- Hyperventilation relationship with spasmophilia, noting psychoemotional cause and neuromuscular excitability
07 p0922 A72-20384
- EEG recording and analysis by analog technique as means of studying human responses to hyperventilation
12 p1767 A72-28312
- Physiologic effects of passive hyperventilation on oxygen delivery and consumption.
23 p3258 A72-44365
- HYPNOSIS**
Abdominal injected barbamyd somnifacient and toxic effect on mice subjected to hypokinesia and isolation
05 p0622 A72-16650
- Hypnotic drug use effect on pilot performance and flight safety, using glutethimide, flurazepam and placebo in double blind study
07 p0933 A72-20188
- Unconditioned /muscular load stimulus/ and conditioned /metronome stimulus/ cardiac reflexes in hypnotic and alert states
16 p2353 A72-32991
- HYPOBARIC ATMOSPHERES**
Physiological and biochemical responses of Paramoicum caudatum to hypo- and hyperbaric stresses, discussing protoplasmic inactivation by high oxygen pressure
12 p1766 A72-28299
- Effects of in vivo inhalation of 100% oxygen at reduced pressure on serum and red cell lipids.
[AD-746090]
17 p2508 A72-34553
- Hematologic responses to hypobaric hyperoxia.
20 p2892 A72-39345
- HYPOCAPNIA**
Hypocapnic hypoxia effects on blood coagulation and fibrinolysis
19 p2756 A72-37880
- HYPODYNAMIA**
Metabolic and hormonal response adaptation to prolonged hypodynamics in water immersion /head out/, noting diurnal and nocturnal differences in circadian rhythms
12 p1765 A72-28267
- Long term space flight weightlessness and hypodynamic effects on orthostatic and vestibular tolerances, infection susceptibility and drug reactivity
16 p2355 A72-33550
- Calcium metabolism conditions in calcified tissues of rats during a lasting hypodynamia and thyrocalcin administration
21 p2997 A72-40432
- Physical training as a prophylactic measure against the hypodynamic syndrome
23 p3260 A72-43920
- HYPOGLYCEMIA**
High carbohydrate diet-induced hypoglycemia as potential cause of pilot unconsciousness during flight acceleration
[AD-736564]
06 p0767 A72-17878
- HYPOKINESIA**
Hypokinesia effects on neurosecretory system of rat hypothalamus and hypophysis, noting increased antidiuretic hormone contents in blood
05 p0618 A72-16634
- Rat tissue autolysis rate during hypokinesia, discussing relation to free amino acid background changes
05 p0619 A72-16648
- Abdominal injected barbamyd somnifacient and toxic effect on mice subjected to hypokinesia and isolation
05 p0622 A72-16650
- Functional condition of rabbits cerebrum precortical arteries during hypertension produced by intravenous noradrenaline infusion, discussing hypo and hyperkinesia
06 p0762 A72-17674
- Radioprotectants /mexamine and cystamine/ effects on histo-hematic barrier permeability in rats under hypokinetic conditions
13 p1904 A72-29308
- Delayed growth of rats carcasses and skeletal muscles during prolonged hypokinesia, comparing effects on flexor muscles to ankle joint extensors
14 p2074 A72-30378
- Hypokinesia effect on fluid and electrolyte metabolism change patterns in rabbits from blood plasma studies
14 p2075 A72-30389
- Human organism readaptation after prolonged hypokinesia and weightlessness, discussing coordination disturbances, vegetative and vascular system instabilities, reduced orthostatic stability and asthenia
14 p2076 A72-30745

- Hypokinesia and motor activity of humans in industrial societies, noting prolonged inactivity and posture maintaining effects
16 p2353 A72-33098
- Effect of hypoxia on the condition of skeleton muscles in rats under hypokinesia
21 p2998 A72-40433
- The effect of space flight conditions and prolonged hypokinesia on the kidney function in man
22 p3149 A72-42068
- Functional insufficiency of the neuromuscular system caused by weightlessness and hypokinesia.
23 p3253 A72-43387
- Adrenal morphology changes in rats subjected to hypokinesia
23 p3255 A72-43905
- Influence of a preliminary exposure to carbon monoxide on the development of hypokinetic disturbances in albino rats
23 p3255 A72-43909
- Health condition changes in test subjects during strict bed rest in hypokinetic recumbent and antiorthostatic position subject to lower body negative pressure
23 p3259 A72-43913
- Cardiac output, hemodynamic and gas exchange variations as function of basal metabolism during bed rest in hypokinetic recumbent or antiorthostatic position
23 p3255 A72-43915
- Ophthalmoscopic, photocalorimetric and ophthalmodynamometric examinations of test subjects visual acuity during bed rest in hypokinetic antiorthostatic position
23 p3255 A72-43916
- Otorhinolaryngological organ response during hypokinetic antiorthostatic bed rest for control, exercising and muscular electric-stimulated groups
23 p3256 A72-43917
- Cerebral blood filling reduction and blood vessel tone deterioration during 120 day clinostatic hypokinesia of healthy male subjects
23 p3256 A72-43922
- HYPOTHALAMUS**
Book on hibernation and hypothalamus covering central nervous system regulating mechanisms, biological rhythmicity, migration, thermoregulation, torpor, human implications, etc
01 p0010 A72-10169
- Visual cortex neuron responses to light flashes under hypothalamic and reticular electric stimulation in rats
02 p0158 A72-11758
- Neurosecretory cell functional activity of supraoptic and paraventricular hypothalamic nuclei in rats after electrical stimulation of midbrain reticular formation
02 p0158 A72-11759
- Human short term thermoregulation feedback-feedforward control mechanism, using hypothalamic temperature as set point
02 p0168 A72-12036
- Skin and hypothalamic temperature effects on human thermoregulatory responses, developing control mechanism for peripheral effects on skin sensors
02 p0160 A72-12041
- Central cooling and warming effects of preoptic-anterior hypothalamic region on thermoregulatory activity of neuroendocrine, cardiovascular and neuromuscular systems
03 p0313 A72-13070
- Thermoregulatory hypothalamic and body sites for behavioral temperature regulation in squirrel monkey
03 p0314 A72-13072
- Cat mean renal nerve activity modification by hypothalamus stimulation and baroreceptor reflex interactions, discussing mean aortic pressure variation effects
04 p0477 A72-15722
- Hypokinesia effects on neurosecretory system of rat hypothalamus and hypophysis, noting increased antidiuretic hormone contents in blood
05 p0618 A72-16634
- Thermal stability variations in blood serum protein after electrical stimulation of rabbit hypothalamic structures
07 p0920 A72-19649
- Hypothalamic stimulation conditioned negative fear reflex in cats before/after neocortex isolation
07 p0920 A72-19859
- Hypothalamus increased noradrenaline turnover after adrenal glands demedullation in rats given disulfiram inhibitor
07 p0924 A72-20621
- Hypothalamic single neuron unit discharge pattern response to acoustic, light and somatosensory stimulation in cats
08 p1116 A72-21471
- Adrenocortical response to prolonged high altitude hypoxia in hypothalamic deafferented rats, showing rapid neural stimulation with delayed humoral activation
12 p1763 A72-27829
- Serotonin precursor 5-oxytryptophan effects on hypothalamic-hypophyseal-adrenal complex under

- complete deafferentation of medial-basal hypothalamus 13 p1907 A72-30016
 - Cat cerebellum cortex evoked response impulses in interaction during stimulation of hypothalamus and peripheral nerves 14 p2076 A72-30669
 - Succinic dehydrogenase activity in rabbit eye ciliary epithelium during electric stimulation of hypothalamus, using histochemical techniques 14 p2078 A72-31099
 - Thermal relationship between tympanic membrane and hypothalamus in conscious cat and monkey. 17 p2499 A72-34344
 - Effect of a magnetic field on experimental tumors /direct and via nervous system/ 17 p2503 A72-35011
 - Influence of thermal, osmotic, and chemical stimulations on food and water intake 17 p2504 A72-35016
 - Trophic support of cardiac activity 17 p2504 A72-35020
 - Influence of cooling of the sensorimotor region of the cerebral cortex on the neurons of the mesencephalic reticular formation 20 p2890 A72-38926
 - Effects of chloralose-urethan anesthesia on temperature regulation in dogs. 21 p2997 A72-40426
 - Hypothalamic control of the electrical activity of the spinal cord 21 p3000 A72-40598
 - Role of the hypothalamus and limbic system in the regulation of the motor and secretory functions of the digestive apparatus 21 p3000 A72-40754
 - Role of the thyrotropic region of the hypothalamus in the adaptation activity of the organism 22 p3141 A72-42167
 - Hypothalamic control of the systemic and lung circulation and functional significance of this control 22 p3148 A72-43168
 - Cat hypothalamus regions neurons background activity characterized by single nonrhythmic spikes with large interspike intervals, noting frequency of discharge bursts 24 p3370 A72-44588
 - Role of the dorso-medial area of the posterior hypothalamus in thermal regulation and its functional relationships with the anterior hypothalamus 24 p3371 A72-44592
 - Analysis of changes in thermal regulation after destruction of the medial preoptic area of the hypothalamus 24 p3371 A72-44593
 - Pulse activity of neurons in the thermal regulation center of the anterior hypothalamus during chill shivering 24 p3371 A72-44594
 - Temperature-sensitive neurons in the brain stem - Their responses to brain temperature at different ambient temperatures. 24 p3373 A72-45232
- HYPOTHERMIA**
- Hypothermia induced by hypoxia in rats, discussing colonic temperature during high altitude exposures and seasonal variations 01 p0011 A72-10214
 - Hypoxic hypothermia effects on endocrine organs phospholipid metabolism during chronic hypoxic hypoxia 02 p0165 A72-12516
 - Central cooling and warming effects of preoptic/anterior hypothalamic region on thermoregulatory activity of neuroendocrine, cardiovascular and neuromuscular systems 03 p0313 A72-13070
 - Helium-cold hypothermia induction and maintenance effect on hamster myocardia, with ventricle analysis of hypoxic damage, glycogen and catecholamines 04 p0476 A72-15720
 - Albino rats spinal cord capillaries ultrastructure upon hypothermy, noting endothelial cells sinking to lower levels from microscopic observation 12 p1760 A72-27304
 - Cardiovascular system functional state elevation during controlled cooling, studying hemodynamic changes 14 p2075 A72-30386
 - Hypothermia, asphyxia and ionizing radiation effects on rat immunological defense mechanisms against particulate antigens 16 p2355 A72-33555
 - Bioelectric activity of the medulla oblongata during hypothermia and bloodletting 17 p2504 A72-35024
 - Helicopter search, rescue and transportation of wounded and ill persons in Denmark, discussing accidental hypothermia treatment 19 p2759 A72-38714
 - RNA content in the cortex neurons in connection with the change in its function during the emergence of an animal from hypothermia 20 p2890 A72-38928
 - Hypothermia and resistance of mice to lethal exposures to high gravitational forces. 22 p3142 A72-42494
 - Evidence for a metabolic limitation of survival in hypothermic hamsters. 23 p3258 A72-44364
- HYPOTHESES**
- NT EXPECTANCY HYPOTHESIS
 - NT NULL HYPOTHESIS
 - NT VORTICITY TRANSPORT HYPOTHESIS
 - Bayesian estimate of signal parameters in random noise background under mutually exclusive hypotheses about statistical properties 07 p0943 A72-19515
- HYPOXEMIA**
- Nervous respiratory disorder in patients with diencephalic and vegetative vascular syndromes, discussing arterial hypoxemia development and resulting oxygen insufficiency 02 p0160 A72-12012
 - Arterial hypoxemia development during hypoxic ontogenesis early stages related to age in dogs 09 p1266 A72-22879
 - Cardiac performance and the coronary circulation of man in chronic hypoxia. 17 p2502 A72-34992
- HYPOXIA**
- Hypothermia induced by hypoxia in rats, discussing colonic temperature during high altitude exposures and seasonal variations 01 p0011 A72-10214
 - Acute, short and long term and life long high altitude hypoxia exposure effects on pulmonary gas exchange control and efficiency during physical exercise 01 p0014 A72-10848
 - Reproducibility of acute mountain sickness severity and duration in individuals under high altitude simulation, noting relationship to hypoxia 01 p0021 A72-11287
 - Hypoxia, hyperoxia and hypercapnia short period effect on rat brain oxygen supply, measuring blood gas values, tissue oxygen partial pressure time variations, etc 02 p0159 A72-11957
 - Altitude hypoxia human pulmonary compliance relation between static transpulmonary pressure and inspired volume 02 p0159 A72-11958
 - Hypoxic hypothermia effects on endocrine organs phospholipid metabolism during chronic hypoxic hypoxia 02 p0165 A72-12516
 - High altitude hypoxia effects on rat myocardium lactic dehydrogenase isozyme complement and anoxic tolerance 02 p0165 A72-12834
 - Posthypoxic thirst and relative dehydration of rats after return from hypoxia to normoxia, measuring body weight and water intake 02 p0165 A72-12835
 - Hypoxia tolerance among pupil pilots during aeromedical instruction in decompression chamber, obtaining EEG and cardiac rhythm recordings 04 p0466 A72-14567
 - Hemodynamic and blood oxygen parameter changes comparison in dogs during hypoxia at rest and muscle activity in various oxygen concentrations 04 p0474 A72-15232
 - Altitude hypoxia resistance and endurance in dogs of various ages, discussing homeostasis retention, altitude ceiling and survival time 04 p0474 A72-15234
 - Helium-cold hypothermia induction and maintenance effect on hamster myocardia, with ventricle analysis of hypoxic damage, glycogen and catecholamines 04 p0476 A72-15720
 - Sublethal X radiation effects on rat erythropoietic system during altitude hypoxia acclimatization 04 p0476 A72-15721
 - Hemodynamic response to hypoxia in dogs with experimental myocardial infarction, discussing changes in cardiac output, stroke volume, left ventricular pressure and systemic vascular resistance 05 p0617 A72-16152
 - Stellate ganglion stimulation and hypoxia effects on hemodynamics and coronary circulation in dogs, discussing myocardial oxygen consumption, sympathetic nerve vasoconstrictor effect and vasodilatory response 05 p0617 A72-16153
 - Potassium cyanide effect on phospholipid exchange in rat brain and liver during histotoxic hypoxia as function of body temperature 05 p0618 A72-16357
 - Hypoxia effect on diurnal mitotic activity rhythm of marrow erythropoiesis system of guinea pigs in pressure chamber 05 p0618 A72-16631
 - Hypoxia, hypercapnia and hyperoxia effects on active glucose transport in rat small intestines 05 p0618 A72-16633
 - Maximal oxygen intake prediction in acute moderate hypoxia during exercise, showing heart rate linearity with work load 07 p0916 A72-18966
 - Hypoxia pretreatment for decreased pulmonary oxygen toxicity during high pressure oxygen breathing in rats 07 p0917 A72-19328
 - Carbon monoxide induced hypoxia inhibition of reflex vasoconstriction in man in presence of normal arterial oxygen tension 07 p0929 A72-19438
 - Unattenuated ventilatory hypoxic drive in ovine and bovine species native to high altitude 07 p0917 A72-19445
 - Hypoxia effect on aircraft pilot performance during altitude and flight simulation, testing instrument landing approaches [AMRL-TR-71-97] 07 p0933 A72-20186
 - Thyroid glands iodine concentrations, blood proteins and morphological changes in rats with acute hypoxic hypoxia and pulmonary edema 07 p0924 A72-20620
 - CO hypoxia effect on oxygen transport during exercise, discussing changes in cardiac and respiratory functions and work capacity 08 p1114 A72-20893
 - Hypoxia incidents in Strategic Air Command due to cabin pressurization malfunction 08 p1126 A72-21566
 - Arterial chemoreceptor deafferentation influence on rat respiratory response to hypoxic and hypercapnic gas mixture breathing 08 p1120 A72-22078
 - Breathing regulation characteristics showing reflex control of respiratory functions in normal environment and brain tissue receptor control under hypoxia 08 p1121 A72-22079
 - Respiratory function control and physiological adaptation mechanisms evolution during changing earth atmosphere oxygen content, noting hypoxia sensitivity development 08 p1121 A72-22080
 - Hypoxic and normoxic gas mixture breathing during intense muscular activity, relating oxygen consumption and carbon dioxide elimination magnitudes and motor performance 08 p1121 A72-22081
 - Corticosterone content in blood plasma, cerebral cortex and skeletal muscles during hypoxia adaptation in rats 08 p1121 A72-22083
 - Book on experimental brain hypoxia covering changes in hemodynamics, energy metabolisms, electrolyte and water movement and cerebral and peripheral venous blood serum proteins 09 p1264 A72-22238
 - Chinchilla and guinea pig tolerances to hypoxia and hyperoxia in pressure chamber tests, suggesting relation to red blood cell size and number 09 p1265 A72-22647
 - Arterial hypoxemia development during hypoxic ontogenesis early stages related to age in dogs 09 p1266 A72-22879
 - Tentorium cerebelli microstructure and leaflets strength in study of chronic and acute hypoxia injury to fetus during pregnancy and labor 09 p1266 A72-23193
 - In vitro measurements of oxygen tension effect on teleost and amphibian retinal lactate dehydrogenase activity, discussing acetazolamide produced hypoxia effects 10 p1424 A72-23729
 - Erythrocyte life span in mice under normal atmospheric pressure and various degrees of hypoxia acclimatization, using radioactive labeled diisopropyl phosphorofluoridate 11 p1579 A72-26608
 - Chronic hypoxia adapted rat myocardial tissue sensitivity to increased carbon dioxide tension 11 p1579 A72-26616
 - Physical training effect on rat cardiac function and metabolic response to hypoxia 11 p1581 A72-26701
 - Human cardiovascular function change as indication of hypoxic circulatory stress, using noninvasive cardiographic measurements of cardiac electromechanical time intervals 12 p1769 A72-27470
 - Mountain sickness relation to ventilation response to hypoxia, noting response intensity dependence on peripheral chemoreceptor sensitivity 12 p1771 A72-27481
 - Acute hypoxia effects on dog coronary blood flow and cardiac function from cardiac beta-adrenergic and hemodynamics study 12 p1760 A72-27482
 - High altitude hypoxia preadaptation effects on left ventricle myocardium noradrenaline concentration in rats with experimental vitium cordis 12 p1761 A72-27648
 - Exercise role in ventilatory acclimatization to graded hypoxia in goats from carbon dioxide response curve measurements 12 p1762 A72-27727
 - Adrenocortical response to prolonged high altitude hypoxia in hypothalamic deafferented rats, showing rapid neural stimulation with delayed humoral activation 12 p1763 A72-27829

Ascorbic acid influence on blood coagulation and anticoagulation systems in dogs with acute hypoxia, discussing plasma recalcification time and heparin tolerance

12 p1764 A72-28217

Hypoxia effect on aircraft pilot performance, using Link GAT 1 trainer and controlled composition atmosphere under varied altitude conditions for simulated ILS landing approaches

12 p1776 A72-28310

Autonomic nervous system role in controlling coronary and cardiac responses to hypoxic hypoxia, measuring blood flow with Doppler ultrasonic flow transducer

12 p1767 A72-28313

Pressure chamber training effects on rats chain motor reflexes hypoxia adaptation, noting sinocarotid receptors importance in compensatory-adaptive reactions

13 p1902 A72-28641

Concentrated and extended learning effects on formation rate and retention degree of conditioned reflex during mice adaptation to high altitude hypoxia

13 p1903 A72-28770

Piloting aptitude evaluation from ECG during hypoxia, considering right intraventricular conduction and ventricular repolarization anomalies

13 p1906 A72-29857

High altitude natives cerebral arterial-venous oxygen difference measurement during ambient air and oxygen breathing, showing chronic hypoxia effect on cerebral blood flow

14 p2079 A72-30704

Low pressure chamber as aerospace medical diagnostics tool for flying personnel examinations regarding oxygen deficiency, low air pressure and air pressure fluctuations tolerance

14 p2080 A72-30819

Russian book on functional morphology under extremal space flight conditions covering overloads, hypoxia and hyperoxia effects on organism and cellular structure and metabolism

14 p2077 A72-30996

Mountain inhabitants cardiocirculatory adaptation to chronic hypoxia, studying coronary flow and myocardial oxygen consumption and efficiency

15 p2187 A72-32498

Hypoxia and peripheral visual stimulus position effects on response time during monitoring of centrally located stimulus light

16 p2357 A72-34095

Ventilatory peripheral chemoreflex response to hypoxia during physical exercise in native highlanders and altitude-acclimated lowlanders

17 p2499 A72-34345

Effect of Acetazolamide /Diamox/ at different dose levels on survival time of rats under acute hypoxia and on Na⁺/K⁺-ATPase activity of rat tissue microsomes.

17 p2499 A72-34546

Metabolism of the hypoxic and ischaemic heart; Proceedings of the Symposium, Geneva, Switzerland, June 14-17, 1971. Part 1.

17 p2501 A72-34976

Normal and hypoxic myocardium mitochondrial metabolism process, studying electron transport system

17 p2501 A72-34978

The effects of acute hypoxia on lipid synthesis in the rat heart.

17 p2501 A72-34979

Myocardial protein synthesis in acute myocardial hypoxia and ischemia.

17 p2501 A72-34980

Acute hypoxia of the myocardium - Ultrastructural changes.

17 p2501 A72-34982

Extracellular acid-base changes in the dog myocardium during hypoxia and local ischemia, measured by means of glass micro-electrodes.

17 p2501 A72-34983

Changes in energy stores in the hypoxic heart.

17 p2501 A72-34985

The intramyocardial oxygen pressure at normoxia and hypoxia.

17 p2501 A72-34986

The influence of exogenous ATP on cardiac metabolism in acute hypoxia.

17 p2501 A72-34987

Myocardial ultrastructure in acute and chronic hypoxia.

17 p2502 A72-34988

Myocardial metabolic changes in chronic hypoxia.

17 p2502 A72-34989

Role of the synthesis of nucleic acids and proteins in the adaptation of the organism to altitude hypoxia.

17 p2502 A72-34990

Anoxic tolerance of the heart muscle in different types of chronic hypoxia.

17 p2502 A72-34991

Cardiac performance and the coronary circulation of man in chronic hypoxia.

17 p2502 A72-34992

Effect of chronic hypoxia on the kinetics of energy transformation in heart mitochondria.

17 p2502 A72-34993

Effects of hypoxia and ischemia on myocardial contraction - Alterations in the time course of force and ischemia-dependent inhomogeneity of contractility.

17 p2502 A72-34996

Interaction of chronic hypoxia and hypercapnia upon blood gases and acid base status.

17 p2504 A72-35166

Venous responses to stimulation of carotid chemoreceptors by hypoxia and hypercapnia.

18 p2648 A72-36025

Functional development of the altitude convulsion mechanism in mice and rabbits /Research note/.

18 p2650 A72-36445

Role of the autonomic nervous system in the hypoxic response of the pulmonary vascular bed.

18 p2650 A72-36572

Hypoxic theory for atherosclerosis formation, noting blood plasma protein concentration effects on oxygen diffusion

18 p2651 A72-37030

Nucleic acid contents in cholinergic and adrenergic spinal cord neurons and in their glial satellite-cells during hypoxic hypoxia and a post-hypoxia period

19 p2756 A72-37742

Hypocapnic hypoxia effects on blood coagulation and fibrinolysis

19 p2756 A72-37880

Roentgenologic studies of the effects of rapid decompression and hypoxia on the gall bladder in cats.

19 p2758 A72-38705

Thyroglobulin content and variations in the proteolytic activity of the thyroid gland tissue in animals under hypoxic conditions

20 p2893 A72-39727

Hypercapnia with relief of hypoxia in normal individuals with increased work of breathing.

21 p3005 A72-40420

Regional lung function during early acclimatization to 3,100 m altitude.

21 p3005 A72-40424

Lack of effect of high altitude on hemoglobin oxygen affinity.

21 p3006 A72-40430

Effect of hypoxia on the condition of skeleton muscles in rats under hypokinesia

21 p2998 A72-40433

Morpho-functional changes in the endocrine system during oxygen starvation

21 p2998 A72-40447

Nervous and humoral stimulation and hypoxia effects on erythropoiesis control, studying human blood serum additions to bone marrow cultures

21 p3001 A72-40762

Experimental studies of the production of erythropoietin in relation to the intensity and duration of hypoxia

21 p3002 A72-41189

Effect of hypoxia and physical activity on plasma enzyme levels in man.

21 p3003 A72-41522

Hypoxic pulmonary steady-state diffusing capacity for CO and alveolar-arterial O₂ pressure differences in growing rats after adaptation to a simulated altitude of 3500 m.

21 p3003 A72-41622

Cardiac output, arterial and mixed-venous O₂ saturation, and blood O₂ dissociation curve in growing rats adapted to a simulated altitude of 3500 m.

21 p3003 A72-41623

Reflexive cardiac rhythm changes and arterial tension during hypoxia, noting differences due to animals, controlled respiration and pharmacological effects

22 p3141 A72-41984

Prediction of vegetative reactions to extremal actions on the organism

22 p3141 A72-42168

Effect of fasting on tolerance to moderate hypoxia.

22 p3150 A72-42487

Vascular headache of acute mountain sickness.

22 p3150 A72-42491

Transarterial leakage - A possible mechanism of high altitude pulmonary oedema.

22 p3143 A72-42588

The carotid body in animals at high altitude.

22 p3143 A72-42589

Suprapontine influences on hypoxic ventilatory control.

22 p3143 A72-42590

Genetic aspects of the blunted chemoreflex ventilatory response to hypoxia in high altitude adaptation.

22 p3144 A72-42591

Hypoxic acclimation effects on rats heart, liver and kidney mitochondria, measuring cytochrome oxidase and succinic dehydrogenase activities

22 p3144 A72-42673

Histologic analysis of hypoxia exposure effects on mouse skin homograft reaction due to lymphatic organ function changes

22 p3144 A72-42675

Cardiocirculatory adaptation to chronic hypoxia. II - Comparative study of myocardial metabolism of glucose, lactate, pyruvate and free fatty acids between sea level and high altitude residents.

22 p3148 A72-43022

Mechanism of adaptation to hypoxic hypoxia

23 p3255 A72-43907

Altitude limit as function of acclimatization time length for investigation of enhanced resistance to acute hypoxia in rats

23 p3255 A72-43908

The effect of hypoxia on the coronary blood flow in reserpinized dogs.

24 p3370 A72-44562

Quantitative evaluation of the kinetics of free-radical processes in animal organs under hypoxic conditions

24 p3371 A72-44596

Comparison of three methods for quantitating respiratory response to hypoxia in man.

24 p3372 A72-44960

HYPSONETERS

Elevation-relief ratio, hypsometric integral and geomorphic area-altitude analysis, discussing calculation time

05 p0654 A72-16039

Selenodetic catalog centers mutual positions determination from lunar near side hypsometric charts

11 p1724 A72-26911

HYSTERESIS

Oscillographically measured semiconductor element I-V characteristics plotting optimization by considering measuring instrument and sampling signal shape and frequency effects on hysteresis

03 p0330 A72-12968

Abnormal rf hysteresis and bias voltage effect in resonant cavity Gunn devices

03 p0331 A72-13646

Iterative hysteretic model for calculating magnetization distribution in thin magnetic layer for digital recording systems

03 p0328 A72-13769

Cobalt-rare earth single particles hysteresis loops interpretation, considering coercive force relationship to particle size

03 p0402 A72-13781

High precision strain gage dynamometers design and testing at ONERA Modane test center, discussing accuracy limitation due to hysteresis and creep effects [ONERA, TP NO. 995]

05 p0642 A72-15859

Hysteresis loops during breakdown in reverse bias segment of p-PbS point contact diodes I-V curves

05 p0638 A72-17177

Forced transverse vibration damping of end loaded elastic cantilever beam, determining hysteresis loop contour from resonance curves

06 p0900 A72-18673

Vibration simulation of elastohysteretic systems on analog computers using photocurrent-voltage relationship of polycrystalline photoresistors

06 p0900 A72-18674

Dry areas occurrence on heating surface in pool boiling near burnout heat flux, discussing nucleate and film boiling stability and hysteresis

07 p1099 A72-19621

Bistable hydraulic servomechanisms limit cycle stable oscillations from bang-bang control and cavitation effects, discussing valve driving gear hysteresis and time lag

08 p1113 A72-22155

Single and multiple fractures in brittle matrix fibrous composites, discussing fracture energetics, stress-strain curves and hysteresis effects

09 p1338 A72-23164

Iron rotational hysteresis effect in cold magnetic balance wind tunnel system for spinning aircraft configurations and subsonic flow regimes

10 p1462 A72-24776

Periodic solutions of forced oscillatory system with hysteresis damping

12 p1844 A72-27246

Structural energy loss mechanisms, considering hysteresis, edge damping of panels, acoustic losses, dry friction, multilayer sandwich damping, etc

12 p1882 A72-27342

Low carbon steel prior plastic deformation effects on mechanical hysteresis loop shape

12 p1887 A72-28234

Magnetization and temperature interrelationship in high constant magnetic field for Apollo 11, 12 and 14 rocks, obtaining magnetic hysteresis curves

14 p2155 A72-30517

Apollo 11 and 12 lunar surface rocks electrical conductivity at 300-1200 K in vacuum, Ar, He and He-hydrogen atmospheres, noting large hysteresis above 500 C

14 p2155 A72-30518

Energy losses due to hysteresis friction during oscillations of dislocations in elastic field of point defect in solids, discussing temperature and amplitude effects

14 p2121 A72-30955

Mathematical model for mechanical and electrical hysteresis, noting application to nonlinear ferromagnetic resonant circuit with saturable inductor

14 p2132 A72-31105

Nonlinear self excited oscillations with negative hysteresis in automatic control systems

14 p2091 A72-31127

- Ferrite and dielectric element waveguide phase shifters with rectangular hysteresis loop, deriving differential phase and attenuation constants for wave propagation 15 p2202 A72-32662
- Correlation technique for transient response of a hysteretically-damped dynamic system to stationary random excitation. 17 p2579 A72-34231
- Arc discharge transition from diffusion to arc mode, presenting theory on I-V characteristics negative resistance section and on hysteresis causes 18 p2714 A72-36207
- A certain generalization of the hysteresis loop contour equations to the case of an asymmetric cycle 19 p2876 A72-38003
- Water film formation and breakdown during motion over solid surfaces, predicting flow rate difference due to contact angle hysteresis 21 p3085 A72-41178
- Hysteresis curve equation for calculation of elastoplastic deformations caused by forced vibrations, taking into account medium compressibility and inertial forces 21 p3123 A72-41359
- Allowance for the hysteresis behavior of a continuous medium in a complex state of stress under conditions of simple cyclic loading 21 p3127 A72-41711
- Stress amplitude and hysteresis loop width changes in alpha Ti during cyclic work softening-work hardening with constant strain amplitude 22 p3189 A72-42438
- Rotational hysteresis in single crystals of powdered nickel 22 p3192 A72-43011
- Hysteresis in a gas laser when passing from a single-frequency emission mode to a two-frequency mode 23 p3295 A72-43680
- Relationship between the dissipative properties of a vibrational system and its amplitude-phase-frequency characteristics 23 p3313 A72-43785
- Equivalent linear solution for transient free vibration of beams with strain dependent, frequency independent stress-strain hysteresis loop with sharp corners 23 p3352 A72-44120

I

I BEAMS

- Critical loads for elastic buckling of monosymmetric beams and cantilevers 06 p0897 A72-17969
- Tapered I-beams elastic twisting and flexural-torsional buckling, considering critical loads as function of taper ratio 08 p1249 A72-21924
- Limiting load calculation for thin walled I-beam in oblique bending and torsion beyond elastic limit 13 p2055 A72-28734
- German monograph - Finite elements according to a theory of the second order on the basis of an extended variational principle with an application to the stability and stress computation of simple symmetrical I-beams under consideration of the deformation of the cross-section 19 p2871 A72-37479

IAPETUS

- Polarization observations of Saturnian satellite Iapetus leading and trailing hemispheres, showing albedo difference consistent with light curve amplitude 16 p2453 A72-33139

ICARUS ASTEROID

- Results of observations of the minor planet Icarus by the Maksutov meniscus astrograph in Chile 19 p2859 A72-37916
- Ephemerides and improved orbital elements of minor planets, noting general theory of relativity verification from astronomical observations of Icarus 24 p3437 A72-44758

ICBM (MISSILES)

- U INTERCONTINENTAL BALLISTIC MISSILES

ICE

- NT GLACIERS
- NT SEA ICE
- Radiative, segregation and evaporation processes of ice particles surrounding early type stars of Orion association, justifying ice particle model for dust grains 01 p0129 A72-10794
- Hydrometeors linear depolarization ratios measurements by monostatic lidar, using different size water drops and ice crystal clouds 01 p0095 A72-10830
- Mathematical model for radiative transfer properties of high albedo carbon dioxide and water cryodeposits on opaque substrate [AIAA PAPER 72-58] 05 p0749 A72-16929

- Spherical ice and graphite particles absorption, scattering and radiation pressure coefficients and albedo, noting application to interstellar extinction 06 p0875 A72-17296

- Electromagnetic wave scattering by arbitrarily oriented circular ice cylinders, deriving far field intensities for linearly polarized incident waves 09 p1280 A72-23341

- Radiational cooling and heating rates for ice and water clouds based on radiative divergence measurements with allowance for latent load 09 p1348 A72-23660

- Remote measurement of cloud ice and water content from Raman scattering of ground based laser signal 12 p1840 A72-27547

- Parhelia phenomenon origin, proposing flat hexagonal ice platelets descending in relatively quiet atmosphere 13 p1954 A72-30087

- Light intensity and linear polarization for single scattering by ice clouds in visible and IR, approximating crystals with long circular cylinders 14 p2128 A72-30349

- Antarctic ice sheet complex permittivity in VLF band from reduction of measurement data with buried dipole antenna under snow surface 15 p2200 A72-32104

- Spectroscopic sounding of clouds and snow and ice covers from below /earth surface/ and above /space or planet/ 16 p2417 A72-33288

- Mathematical models for radio attenuation in ice by electromagnetic absorption and reflection from interfaces, noting radar tracking 16 p2363 A72-33290

- Friction of rubber on ice. 17 p2560 A72-35225

ICE FORMATION

NT CLOUD GLACIATION

- Ice particles and frozen droplets formation on nuclei in supercooled cloud by shock waves under laboratory conditions 06 p0843 A72-18452

- Thunderstorm flight testing for evaluation of rain, ice, lightning and turbulence effects on aircraft, engine and systems operating characteristics 06 p0760 A72-18500

- Federal Air Regulations procedures for civil transport aircraft flight testing under natural and/or simulated icing conditions 06 p0760 A72-18501

- Supercooled water drops freezing by contact nucleation with AgI and silicate particles, determining effective temperature in updraft wind tunnel experiments 09 p1345 A72-22445

- Supercooled cloud water droplets in free fall shattered by shock waves measuring ice crystal formation probability 09 p1345 A72-22446

- Gas turbine engine icing, discussing atmospheric conditions, damage due to ice ingestion and anticice systems [ASME PAPER 72-GT-6] 11 p1703 A72-25609

- Ice formation on helicopter rotor blades, discussing atmospheric moisture and temperature conditions, blade surface temperature, centrifugal and aerodynamic forces and preventive measures 12 p1754 A72-27414

- Mathematical criteria for probable and potential aircraft icing occurrence, using radiosonde and empirical climatological data 13 p1993 A72-28856

- Ice adhesive shear strength to steel bearing surfaces coated with bonded solid lubricants, describing low temperature test apparatus and results [ASLE PREPRINT 72AM 4] 13 p1964 A72-28970

- Microwave /60 GHz/ radiometer for air temperature measurement outside aircraft during icing conditions 16 p2393 A72-33631

- Hail formation model based on injection of finite embryo size classes into horizontally homogeneous steady nondivergent updraft, considering growth and accumulation zones 22 p3201 A72-42514

- Liquid and solid precipitation on aircraft structure surfaces, discussing potential hazards to engine components and aircraft controls due to ice formation 23 p3252 A72-44339

ICE MAPPING

- Side-looking airborne radar imagery for sea ice drift size, shape and surface characteristics determination [AD-733605] 02 p0215 A72-11882

- Image enhancement techniques for sea-ice mapping from satellite IR data, discussing gray scale contrast augmentation scheme for visual quantitative information 06 p0807 A72-17825

ICE NUCLEI

- Icy halo influence on photometric continuum of comet Burnham within cometary head model 01 p0125 A72-10080

- Cometary head model for photometric profiles of carbon molecular emission in comet Burnham assuming icy grain halo 01 p0125 A72-10081

- Ice particles and frozen droplets formation on nuclei in supercooled cloud by shock waves under laboratory conditions 06 p0843 A72-18452

- Cumulus and stratocumulus ice crystal and nuclei concentrations, drop size distributions, glaciation differences and enhancement mechanisms 07 p1030 A72-19101

- One dimensional model for climatological evaluation of ice phase seeding for isolated cumulus cloud modification 09 p1345 A72-22448

- Comet core ice particle dust cover failure conditions, noting critical dust matrix thickness relation to sun proximity 14 p2160 A72-30831

- Mathematical formulation of ice crystal formation and propagation mechanism in seeded supercooled convective clouds 23 p3311 A72-43722

ICE OBSERVATION

U ICE REPORTING

ICE PACKS

U SEA ICE

ICE PREVENTION

- Aircraft engine anti-icing tests and evaluation describing ground and airborne techniques [AIAA PAPER 72-162] 05 p0706 A72-16828
- JT15D turbofan engine antiicing system development, discussing icing test program and results 07 p1053 A72-18765

- Gas turbine engine icing, discussing atmospheric conditions, damage due to ice ingestion and anticice systems [ASME PAPER 72-GT-6] 11 p1703 A72-25609

- Ice formation on helicopter rotor blades, discussing atmospheric moisture and temperature conditions, blade surface temperature, centrifugal and aerodynamic forces and preventive measures 12 p1754 A72-27414

- Calculation procedure for reaction thrust of semibounded turbulent jet in boundary layer blowing and blow type antiicing systems 13 p1897 A72-28728

ICE REPORTING

- Lake ice surveillance via airborne radar, presenting images of ice forms and land features 02 p0211 A72-11805

- CAT, cloud cover and icing forecasting for aviation in terms of numerical model and real atmosphere 04 p0452 A72-14689

- Holographic Ice Survey System for down looking radar probing and measurement of sea ice and glaciers, discussing ice electrical properties and system design 06 p0814 A72-17590

- Worldwide inventory and monitoring of ice and snow aggregations via satellite photography, discussing climatological aspects 09 p1303 A72-23302

- Melting snow and ice packs detection by multispectral /visible and near IR/ remote sensing from earth satellites 16 p2387 A72-33999

ICING

U ICE FORMATION

IDEAL FLUIDS

- Initial interaction phase between thin shallow conical shell vibrating axisymmetrically and ideal incompressible fluid, determining hydrodynamic pressure effects 01 p0050 A72-10574

- Variable volume spherical cavity motion in ideal liquid near plane surface 02 p0202 A72-11586

- Electrohydrodynamic ideal incompressible fluid flow in flat and circular channels, determining electric potential and field distribution 02 p0266 A72-12431

- Book on mathematical fluid dynamics covering viscous and ideal fluid motion, boundary theory, constitutive equations, hydrodynamics and kinematics 02 p0206 A72-12623

- Perturbation induced long waves boundary effects in ideal incompressible fluid in uniformly rotating basin with stepwise depth difference, using Schwarz symmetry principle 03 p0340 A72-13094

- Curved shock waves in steady flow of perfect fluid, confirming Hugoniot relations validity 03 p0341 A72-13685

- Book on fluid dynamics covering theories of perfect, viscous and compressible fluids, infinite and finite span wings, boundary layer flow, etc 04 p0462 A72-15357

- Nonlinear calculation of three dimensional flow of perfect incompressible fluid around wing of finite span with arbitrary form 04 p0463 A72-15558

Zhukovskii potentials for ideal fluid motion in spherical or cylindrical cavity with arbitrary radial partitions

05 p0648 A72-16218

Turbulent layer generation in ideal two dimensional fluid flow, determining vortices time evolution from initial velocity discontinuity by numerical methods

06 p0802 A72-18525

Plane stationary flow of ideal incompressible fluid past large camber profiles of arbitrary shape and thickness, using computerized Fourier expansion

07 p0908 A72-18976

Axisymmetric flow of ideal incompressible liquid with free boundary and variable velocity, taking into account external mass forces effect

07 p0968 A72-19899

Rayleigh method convergence in ideal fluids axisymmetric flow stability with free boundaries and perturbations without mass forces

08 p1148 A72-20909

Ideal liquid small oscillations natural frequencies and mode shapes in shell of revolution under weak gravitational field

08 p1148 A72-20956

Variable wall thickness influence on axisymmetric vibrations frequencies and reduced masses of cylindrical elastic shell filled with ideal incompressible fluid

08 p1247 A72-21815

Book on ideal and real compressible fluid dynamics covering supersonic flow past airfoils and shock wave interaction with laminar boundary layer

09 p1295 A72-23045

Small cross section steady vortex rings existence in inviscid uniformly dense ideal fluid, deriving asymptotic formulas for rings shape and properties

10 p1467 A72-24333

Plane irrotational motion of ideal incompressible fluid perturbed by profile movement and deformation, obtaining aerodynamic forces power

10 p1420 A72-24853

Three component flow calculation at inlet of axial flow compressor stage, linearizing hydrodynamic equations of ideal incompressible fluid with velocity perturbations

10 p1420 A72-25132

Stationary MHD aligned flows of ideal incompressible fluids with same streamline patterns in plane, axisymmetric and spatial flows

11 p1695 A72-25910

Hypersonic polytropic transformation of ideal fluid under mechanical or geometrical conditions

11 p1572 A72-26092

Unbounded wall effect on complex potential of two dimensional flow produced by arbitrary displacement of body within ideal incompressible fluid

12 p1797 A72-27119

Multiple scale asymptotic method for nonlinear theory of dispersive periodic waves with slowly varying parameters, noting equations for irrotational motion of perfect relativistic fluid

12 p1843 A72-27170

Velocity dominated singularities generalized to solutions of Einstein equations with irrotational perfect fluid sources within hydrodynamic cosmological models

12 p1870 A72-27410

Axial impact effect on thin elliptical layer of viscous/ideal fluid with allowance for inertial forces, analyzing spreading process stability

13 p1943 A72-29880

Ideal liquid theory application for unsteady separated flow calculation around arbitrary shape bodies, noting numerical solution for plane flow around circular cylinder

14 p2070 A72-31010

Particular and general exact solutions of Einstein equations for matter filled space under assumption of spherically symmetric distribution of perfect fluid

15 p2305 A72-31343

Three dimensional ideal incompressible fluid flows under small velocity perturbation, using linearized Euler equations with respect to steady flow

16 p2375 A72-32932

Natural frequency of free beam-like vibration of coupled fluid/structural system of cylindrical rod submerged in ideal fluid enclosed by cylindrical shell

16 p2465 A72-32985

Stability analysis of ideal incompressible liquid steady flow for given distribution, discussing velocity distribution effect on longitudinal cylindrical flow instability

16 p2376 A72-33093

Ideal fluids isentropic flow equations solution via Riemann invariants method, describing nonlinear waves linear interactions

16 p2376 A72-33110

Theorem for instability of rectilinear vortices in two dimensional steady flow of ideal liquid with or without submerged obstacle

17 p2539 A72-34910

Field variations of perfect fluid in axisymmetric stationary universe within general relativity theory concept, noting energy extremal properties for rotating stars

17 p2607 A72-34921

Elastic momentless shell completely filled with ideal incompressible liquid, detailing small steady free vibrations

18 p2681 A72-36667

Ultimate configuration of the self-similar separated flow of an ideal fluid

19 p2785 A72-37396

Mathematical model of ideal incompressible gyroscopic fluid with internal angular momentum using kinematic equations

19 p2835 A72-37929

Rotatory motions of a body with a liquid-containing cavity

19 p2787 A72-38151

Plane-symmetric similarity solutions for self-gravitating fluids.

20 p2955 A72-40009

Velocity distribution of quasi-steady and steady flow of ideal incompressible fluids with congruent streamlines, investigating conditions for vortex and irrotational flow

22 p3164 A72-41906

Conformal mapping for interaction of two dimensional flow of ideal fluid and injected counterflow with jet formation, calculating cavitation void dimensions

22 p3165 A72-42065

Flow stability of ideal compressible and incompressible fluids, solving Navier-Stokes equation for rotating liquid with free boundary in gravitational field

22 p3165 A72-42151

Stationary spherical vortices in a perfect fluid.

22 p3167 A72-42980

Investigation of the interaction between a circular wing and a flow of ideal liquid

23 p3348 A72-43796

Plane stationary flow of ideal incompressible fluid past large camber profiles of arbitrary shape and thickness, using computerized Fourier expansion

24 p3360 A72-45002

IDEAL GAS

Numerical solution for swirling ideal gas flow in Laval nozzle, determining swirling effects on nozzle performance

02 p0149 A72-11583

Thermodynamics of holonomic media applied to perfect gases

05 p0648 A72-16123

Finite difference calculations for two dimensional unsteady inviscid expanding flow of perfect gas through nozzle, obtaining flow field patterns

05 p0603 A72-16539

Heat pipe temperature gradient initial conditions for ideal gas model, introducing two phase Mach number for choking phenomena analysis

05 p0749 A72-16913

Critical streamline length in axisymmetric and plane ideal gas flows past conical bodies as function of Mach number and form parameter

06 p0755 A72-17677

Ideal gas flow past blunt body in supersonic stream, discussing sonic lines, characteristics and Mach number

06 p0756 A72-18119

Downwash behind lifting surface related to loading in ideal incompressible gas by equations of motion linearization

07 p0908 A72-19110

Equations of free particle motion, gas energy, distribution evolution and cosmic indeterminacy for Friedmann universe filled with uniform density and pressure ideal gas

07 p1074 A72-19429

Scattered light coherence in optically thin vapors and ideal gases in energy level crossing experiment formulated in terms of autocorrelation function

08 p1206 A72-21294

Ideal gas many particle distribution functions in microspace from solution of chain of integrodifferential equations

09 p1354 A72-22220

German monograph on gas dynamic properties of turbulent subsonic compressible flow of ideal gas at insulator walls in MHD generator

10 p1517 A72-23771

Pseudoviscous method application to computation of supersonic flow of inviscid ideal gas through two dimensional or annular axisymmetric ducts

10 p1417 A72-23876

Curvature and thickness corrective terms in Rankine-Hugoniot relation for shock wave propagation of ideal gases binary mixture

10 p1417 A72-24117

Second order Cowley-Imai analogy application to transcribe gas dynamic perturbation solutions into magnetogasdynamic solutions for perfect gas axisymmetric super-Alfvénic flows

10 p1521 A72-24464

Perturbation analysis of perfect gas unsteady transonic irrotational inviscid flow in two dimensional channel, presenting numerical computation of flow structure temporal change

11 p1618 A72-26635

Limiting form of equations for perfect gas steady two dimensional flow under gravity effects

12 p1797 A72-27177

Two dimensional Prandtl-Meyer flow anisotropy of ideal gas expanding into vacuum, using free path probe-molecule technique

12 p1799 A72-28178

General relativity equation of motion for spherically symmetric surface layer of ideal gas under central gravitational field

13 p2035 A72-28646

Unsteady state of ideal quiescent heat conducting gas in half space, deriving asymptotic solutions to mass, temperature, pressure and density dynamic behavior expressions

13 p2064 A72-28678

Acoustic shock wave diffraction at moving or static plate immersed in ideal gas

13 p1943 A72-30011

Ideal gas axisymmetric flow created in supersonic flow interaction with blunt body with strong blowing at surface, obtaining boundary layer approximate solution

14 p2070 A72-31012

Supersonic ideal gas flow in corner formed by intersecting plates, using direct computation method for nonequilibrium flows with detached shock waves

14 p2071 A72-31021

Ideal gas supersonic axial flow past circular cylinder, solving Navier-Stokes equations by Van Dyke matched asymptotic expansions method

15 p2178 A72-31463

Isoenergetic and irrotational planar supersonic cascade ideal gas flow computation by analytic method of characteristics

15 p2178 A72-31466

Limiting ratio between ideal gas densities before and behind vertical shock wave in elastic thermal insulators

15 p2334 A72-31475

Perfect gas steady flow under gravity action, analyzing limiting equations

15 p2178 A72-31682

Isentropic perfect gas steady compressible flow finite element analysis through nonlinear equations linearization based on perturbation theory

15 p2217 A72-31719

Perfect gas unsteady compressible homentropic flow with zero spatial pressure gradient, deriving characteristic equations

15 p2218 A72-32324

Mathematical model of atmospheric tides using Navier-Stokes equations for perfect gas in thermodynamic equilibrium

16 p2385 A72-33343

Sonic discontinuities in a radiative gas

17 p2582 A72-35435

Inviscid perfect gas supersonic steady irrotational flow past wedge, investigating analytical solution validity in downstream region behind shock

17 p2544 A72-35900

State equation for superdense stars treated as perfect degenerate tachyon gas, noting dynamic stability for arbitrarily large central densities

18 p2726 A72-36715

Classification of shock waves in a radiating gas

18 p2682 A72-36806

Fast magnetoacoustic wave interaction with shock wave propagating in ideal electrically conducting gas, showing magnetic field stabilizing effect

18 p2711 A72-36812

Calculation of spatial ideal gas flows without a symmetry plane

18 p2642 A72-36901

A study of the asymptotic behaviour of the external fringes of compressible, laminar boundary layers of a dissociating gas.

18 p2683 A72-36937

A method of straight-through calculation for two-dimensional and three-dimensional supersonic flows. I

19 p2747 A72-38852

Blowing of a foreign gas in a hypersonic viscous shock layer

22 p3133 A72-42265

Entropy and simple waves in multidimensional gas flow.

22 p3166 A72-42314

Acoustic shock wave diffraction at moving or stationary flat plate immersed in ideal gas

22 p3206 A72-42732

Three dimensional supersonic flow past bodies with a smooth generatrix

23 p3248 A72-43651

Light spectral width and constant frequency shift during spontaneous diffusion in ideal gas for fixed photon wave

23 p3315 A72-44479

IDENTIFYING

NT TIMBER IDENTIFICATION

Hyperstable algorithm for multinput and output systems identification through equation error method, representing scheme as equivalent time varying nonlinear feedback system

07 p1027 A72-19290

Stochastic control theory application to flight problem, discussing aircraft identification and adaptive control over wide environmental range

10 p1458 A72-25146

Uniqueness of the solution for identification of linear systems by the modulating function method 19 p2779 A72-38086

Air traffic density effect on secondary surveillance radar operation in ATC for aircraft identification and position determination, proposing selective address system 21 p3080 A72-40289

Algorithm for identification of unsteady dynamic objects described by linear differential equation, noting quasi-optimal system operation 22 p3205 A72-42290

Atmospheric density from spacecraft drag data by successive optimization of control laws, using quadratic programming 23 p3277 A72-44003

IDENTITIES

Integrability and identity relations for Newman-Penrose formalism equations in spinor description, assuming Einstein equations validity for vacuum 10 p1510 A72-24105

Operator identities unification and classification, presenting reformulation as algebraic closure properties of graphs 14 p2125 A72-30229

FR (RULES)

U INSTRUMENT FLIGHT RULES

GNEOUS ROCKS

NT ANORTHOSITE

NT BASALT

NT ECLOGITE

NT GRANITE

NT MOLDAVITE

NT PERIDOTITE

Lunar igneous activity and differentiation, discussing volcanic flows near Tycho, flow patterns in maria, sinuous rilles and crust lineaments 03 p0418 A72-13107

Lunar maria material igneous origin, relating surface features to various volcanic eruption types 06 p0887 A72-18220

Igneous and microbreccia lithic fragments, glasses and chondrules from Luna 16 fines, confirming lunar surface melting and igneous differentiation 09 p1379 A72-22253

Eu and Sr distribution between coexisting feldspars in acidic rocks, using mass spectroscopic isotope dilution method 10 p1472 A72-24166

Photogeologic evidence of differentiation and deposition of lunar highland volcanic rocks at Apollo 16 landing site 12 p1866 A72-27115

Neutron activation and neutron-capture gamma ray analyses of igneous rock trace elements, discussing Tyrone Igneous Series granites 20 p2899 A72-39831

On the applicability of lunar breccias for paleomagnetic interpretations. 22 p3226 A72-42532

Lunar interior composition constraints from chemical composition of igneous rocks on surface 22 p3226 A72-42533

Metastable growth patterns in some terrestrial and lunar rocks. 23 p3339 A72-44133

IGNIMBRITE

U IGNEOUS ROCKS

IGNITERS

NT BOOSTERS (EXPLOSIVES)

NT DETONATORS

NT INITIATORS (EXPLOSIVES)

NT PRIMERS (EXPLOSIVES)

Electric pulse initiated pyrogen jet squid igniter consisting of magnesium-fluorocarbon coated bridgewire and pellet enclosed in Mk 1 or 2 gilding metal cup 08 p1221 A72-20774

Onboard turbogenerator igniter operating conditions determination from fuel-air ratio obtained from nomogram 12 p1861 A72-28145

RF discharge gap in cascaded plasma limiters, using tritium igniter as reliable electron priming source 18 p2715 A72-36451

IGNITION

NT ELECTRIC IGNITION

NT SOLID PROPELLANT IGNITION

NT SPARK IGNITION

Boron ignition and combustion mechanisms based on high speed photographs of laser ignited boron particles [AIAA PAPER 72-72] 05 p0703 A72-16801

Additives effect on liquid hydrocarbon fuels ignition delay, testing peroxides, esters, polyethers and alcohols [AIAA PAPER 72-71] 05 p0703 A72-16958

Cumulative jet formation in elliptical cavity, investigating effect on liquid explosives ignition 06 p0799 A72-17909

Time characteristics preceding self-ignition of solid particle system suspended in gas, discussing quasi-steady state duration 06 p0903 A72-18202

Ignition conditions for pyroxylin and polyvinyl-nitrate in air flow containing spherical aluminosilicate and aluminum oxide particles 06 p0903 A72-18211

Burning velocity inhibitors effect on hydrocarbon-oxygen-nitrogen mixtures ignition by hot wires [AD-744624] 08 p1129 A72-22039

Ignition time delay measurement between leading shock front and hydroxyl emission onset in two phase detonation of decane-oxygen 08 p1255 A72-22041

Asymptotic analysis of activation energy limit for radiant ignition of reactive solid with in-depth absorption [AD-741533] 08 p1255 A72-22044

Parallel air and hydrogen flows confluence numerical calculation to determine self ignition conditions in turbulent mixing layer, noting reaction zone [ONERA, TP NO. 981] 09 p1410 A72-22814

Ignition delay time and combustion mechanism of Al-Mg alloys single particles in combustion products of oxidizer-fuel mixture 09 p1373 A72-22885

Visual and motion picture studies of ignition and burning characteristics of Mg particle clusters in flames of gas mixtures 09 p1411 A72-22886

Ignition and incendiarity of laser irradiated single micron size Mg particles suspended in stoichiometric methane air mixture 10 p1564 A72-25140

Jet engine fuel fire hazard evaluation by controlled laboratory tests, analyzing ignition characteristics under simulated survivable aircraft crash accidents [SAE PAPER 720324] 11 p1702 A72-25587

Supersonic combustion of liquid fuels, hydrogen and propane, discussing initiation and stabilization in supersonic flow 12 p1889 A72-27686

Shock heated methane-oxygen-argon mixtures ignition delay time from reaction kinetics calculations 12 p1778 A72-27852

Time history model of transient ignition to self sustained propellant burning, taking into account pressure effects and igniter heat flux 13 p2065 A72-29305

Laser ignition and combustion of boron particles, developing oxide coating and droplet burning models for low and high temperature stages respectively 15 p2296 A72-32582

Mg ignition in nitrous oxide at 600-800 C, determining induction period as function of particle mass and gas stream temperature 16 p2476 A72-33254

Autoignition behind reflected shock waves for hydrocarbon-oxygen mixtures, demonstrating two ignition modes via schlieren photographic records 16 p2479 A72-34002

Polymers ignition time measurement in cabinet with benzene flames and W filament lamps, noting black body radiation source absorbance and incident irradiance effects 17 p2636 A72-34719

Mechanism and characteristics of condensed system ignition by a dispersed flow 19 p2882 A72-38451

Characteristics of the development of steady burning rates during the ignition of gasless compositions by a hot surface 19 p2882 A72-38452

Ignition, unsteady burning and flame collapse of a unitary fuel particle 19 p2882 A72-38453

Book on liquid rocket propellants development, history and ignition problem covering nitrogen tetroxide, hydrogen peroxide, fluorine compounds, boranes and monopropellants 19 p2884 A72-38675

Self ignition behaviour of some liquid fuels in an adiabatic compression machine. 23 p3325 A72-44252

Chemical aspects in the shock initiation of fuel droplets. 24 p3433 A72-45051

Supersonic combustion photochemical initiation feasibility, measuring quantum yields and induction times in hydrogen, oxygen and chlorine mixtures 24 p3464 A72-45058

IGNITION LIMITS

Self ignition in hydrogen oxidation kinetics, considering convection, molecular diffusion, mixing and pressure 05 p0625 A72-17213

Safe aircraft fuels crashworthiness evaluation in terms of ignition susceptibility parameter, noting full scale crash environment simulation [ASME PAPER 72-GT-27] 11 p1702 A72-25623

Polymers flammability tests for research, safety and acceptance purposes, noting ignition limits, decomposition and testing procedures 11 p1746 A72-26044

Turbulent hot gas stream self ignition in oxidizer flow for hydrogen-air and gasoline-air mixtures 14 p2170 A72-30293

Aromatic hydrocarbons - Methane ignition inhibitors 19 p2879 A72-37364

Chain interaction during the inhibited burning of hydrogen 19 p2880 A72-37741

IGNITION SYSTEMS

Thermonuclear microbomb ignition with intense relativistic electron beams for rocket propulsion, discussing achievable exhaust velocities and system optimization 01 p0117 A72-11222

Loading current density effect on normal lead styphnate ignition in primary explosive hot wire initiation, using capacitor discharge and constant current activation signals 08 p1218 A72-20752

Hot wire ignitor modeling including measured H value and heat generation by explosive chemical reaction 08 p1219 A72-20754

Differential thermal and X ray analyses of ignition and preignition solid-solid reactions in Zr-Mo trioxide delay system over 440-475 C 08 p1219 A72-20756

Remote ignition with noncoherent light from pyrotechnic, electric and explosive sources through fiber optics 08 p1219 A72-20757

Engine ignition electronic system for triggering detonators in Aeros aeronomy satellite blastoff and release devices, discussing prototypes acceptance tests 11 p1610 A72-25803

Thermonuclear microexplosion ignition by bombarding dense target with intense relativistic electron beam, noting energy requirement reduction by self magnetic beam field 16 p2433 A72-32814

Man-made electromagnetic noise in southern California and southern Nevada. 19 p2764 A72-37869

Experiments on methods for improved fuel ignition in scramjet combustion systems. [ICAS PAPER 72-15] 21 p3099 A72-41140

IGNITION TEMPERATURE

Ambipolar diffusion influence on MHD generator electrical conductivity, discussing plasma radiation, electron escape generator geometry and efficiency and ignition temperature range 04 p0554 A72-14404

Combustible materials ignition temperature, time lag and burning rate in oxygen enriched atmosphere, deriving activation energy for fire resistance estimates 05 p0681 A72-16773

Wall effects on deflagration, combustion rate, and self and hot-point ignition temperature and delay 11 p1747 A72-26789

Multicomponent system combustion of Al suspensions in kerosene, determining ignition temperature as function of metal particle size and concentration 16 p2476 A72-33256

Combustible materials ignition temperature, time lag and burning rate in oxygen enriched atmosphere, deriving activation energy for fire resistance estimates 17 p2571 A72-35276

Inflammation and burning of powdered aluminum in high-temperature gaseous media and in heterogeneous condensed systems 22 p3245 A72-43178

IGY (GEOPHYSICAL YEAR)

U INTERNATIONAL GEOPHYSICAL YEAR

IL-62 AIRCRAFT

Technical experience in operating the equipment in the IL-62 aircraft 17 p2558 A72-35791

IL-62 aircraft propulsion system design and installation details, operational surveillance system and maintenance operations 23 p3325 A72-43639

ILLIAC 4 COMPUTER

Bulk storage applications in Illiac 4 system, discussing Unicon 690 mass memory for Advanced Research Projects Agency network of telephone lines and interface message processors [IEEE PAPER 23,4] 04 p0496 A72-15714

ILLUMINANCE

Laser radiation pressure applications to isotope and particle separation, optical levitation, high velocity acceleration and atomic beam analysis 06 p0826 A72-18176

Stability of motion at collinear libration centers in the restricted problem of three bodies with allowance for light pressure 24 p3437 A72-44762

ILLUMINATING

Moving display visibility effect on pilot tracking performance, discussing dependence on illumination intensity and color 04 p0477 A72-14445

Geometric optics method accuracy in design of dual-mirror antenna illumination system, noting diffraction effects and near field influence 04 p0499 A72-15242

ILLUMINATION

Lateral photoelectric effect in junction FET under homogeneous illumination, detailing current-voltage characteristics

01 p0114 A72-10859

Q switched laser system emitting light pulses for high speed cinematography synchronized illumination

11 p1649 A72-26343

Memory and photoconductivity in CdSe polycrystals at 77 and 300 K, plotting photocurrent vs illumination levels

13 p2024 A72-30012

Random parameters effect on divergence of focused light beams in turbulent atmosphere, noting light patch dependence on illumination source diameter

14 p2131 A72-30810

Shadowing function calculation as rough surface point illumination probability by point source radiation, assuming surface elevation as random process

18 p2710 A72-36407

Calculation of electrostatic potential distribution in semiconductor's contact region during passage of injecting into blocking contact due to illumination.

19 p2846 A72-38626

Distribution of illumination in a point image in the presence of birefringence in the optical system /case of axial symmetry/

19 p2836 A72-38789

Intermittent movement control theory for prediction of visual correction applied to target aiming during illumination loss

22 p3142 A72-42546

Cd Se polycrystal memory and photoconductivity at 77 and 300 K, plotting photocurrent vs illumination levels

22 p3214 A72-42734

ILLUMINATORS

Human vision sensitivity to covert IR illuminators for image intensification during night observation

15 p2189 A72-32046

Lightweight man-portable uncooled semiconductor laser illuminator design for field use in night vision applications

15 p2248 A72-32047

ILLUSIONS

NT MOON ILLUSION

NT OCULOGRAPHIC ILLUSIONS

Intervening discrete elements effects on filled duration illusion in auditory, tactual and visual presentation

01 p0014 A72-10720

Successive visual motion illusion during perception of rotating kymograph drum by human eye

04 p0476 A72-15588

Loudness function correlations to illusory spiral aftereffect persistence, motion sickness susceptibility and auditory reaction time in individuals

08 p1128 A72-22138

ILMENITE

Hyperfine interactions of Fe cations in ilmenite determined by Mossbauer spectroscopy, noting internal magnetic field and quadrupole coupling constant

09 p1367 A72-22457

ILS [LANDING SYSTEMS]

U INSTRUMENT LANDING SYSTEMS

ILYUSHIN AIRCRAFT

U.S.S.R. high-subsonic freight transport jet aircraft IL-76 for arctic areas, Siberia and Far East, noting independence of large airports availability

03 p0310 A72-13471

IMAGE CONTRAST

Contrast reversal or distance paradox in temperature perception aftereffect

01 p0013 A72-10716

Information content in simulated ERTS space photographs as function of various levels of image resolution

02 p0212 A72-11834

Frequency contrast characteristics derivation method with devices for determining transfer functions of objectives and film, using electron-optical bench

02 p0229 A72-12171

Solar photospheric facula blue light limb photographs, determining spatial variation in contrast levels

03 p0434 A72-13494

Contrast vision enhancement in Hermann grid with variable figure-ground ratio, using Baumgartner receptive field hypothesis

03 p0315 A72-13624

Holographic analysis of periodic microobjects at X ray wavelengths, obtaining high contrast

03 p0360 A72-13669

Simultaneous brightness contrast under scotopic conditions, investigating fovea rod and cone systems interaction in subjects with normal color vision

03 p0317 A72-13937

Photomaterial nonlinear effects on contour distortion in holographic recording of Fourier image slit for graphic memory use

04 p0522 A72-15150

Frequency-contrast characteristics of optical system producing image of distant object in turbulent

boundary layer of atmosphere, determining refractive index fluctuation intensities

05 p0689 A72-16172

Atmospheric contrast degradation and turbulence effects on photography from space with computerized optimization of ground resolution

06 p0813 A72-17431

Image enhancement techniques for sea-ice mapping from satellite IR data, discussing gray scale contrast augmentation scheme for visual quantitative information

06 p0807 A72-17825

SNR expressions for image transmission through turbid medium, showing quality dependence on energy transfer, contrast frequency and sensor phonon illumination level

06 p0774 A72-17936

Image resolutions for ERTS return beam vidicon TV, Skylab multispectral cameras and Gemini/Apollo photographs

06 p0818 A72-18328

Objects visual detection probability distribution as function of angular size, contrast and search time, comparing binocular and monocular searches effectiveness

07 p0931 A72-19919

Limiting resolution of reconstructed image of focused hologram in electron microscopes as function of aberration and spatial coherence

08 p1166 A72-21380

Two point analysis of phase, coherence and emulsion response effects on holographic image resolution

08 p1168 A72-21698

Computer calculation of spectral brightness coefficients on aerial photographs, determining contrast features density gradients

09 p1308 A72-22484

Partially coherent imaging in microdensitometer, investigating conditions for linear operation from difference between high and low contrast edge images

09 p1309 A72-22608

Psychological aspects in aerial photointerpretation, discussing importance of perception of image contrast, contours and areal distribution

09 p1272 A72-23299

Zeiss aerial photographic lens systems imaging quality characteristics in visible and near IR spectral ranges

09 p1313 A72-23311

Photoemission electron microscopy application to refractory metals and nonmetallic materials, discussing image formation and contrast enhancement problems

10 p1493 A72-23823

Visual and automatic stereometric image analysis, citing minimum measurable contrast thresholds for various devices

10 p1478 A72-23826

Oxygen adsorption effects on Mo orientation contrasts and emission image under electron microscope

10 p1513 A72-24875

Foveal luminosity magnitude estimations validity, measuring relative effects of preadaptation and contrast

10 p1427 A72-25179

Radiographs electronic image contrast enhancement by video signal generation with amplitude proportional to density rate of change, discussing system dynamic response and resolution

11 p1633 A72-26034

Contrast enhancement for switch-on and off modes of bar patterns, noting spatial transients due to primary image interaction with negative afterimage

12 p1808 A72-27679

Spatial characteristics of equal energy visual stimuli in metacontrast design for targets and masks of constant separation and varying width, deriving weighting functions

12 p1762 A72-27680

One stage approximation to color conversion model, predicting gain setting control dependence on achromatic contrast

12 p1809 A72-27681

Microwave horn and lens antennas radiation spatial coherence characteristics, noting effect on picture contrast

13 p1928 A72-28475

Experimental method to directly determine frequency-contrast and phase-frequency characteristics of optical objectives from boundary curve.

13 p2003 A72-28798

Modulation transfer functions of optical system producing image of distant object in turbulent boundary layer of atmosphere, determining refractive index fluctuation intensities

14 p2130 A72-30241

IR absorbent effects on evaporographic image contrast performance based on photometric study, presenting color photographs

15 p2188 A72-31615

High contrast and sensitivity thermal erase cathodochromic sodalite for storage and display applications, measuring contrast ratio versus electron beam flux

15 p2240 A72-32362

Computer printing device for improved image recording of binary and half tone synthesized amplitude holograms

16 p2390 A72-33084

SNR expressions for image transmission through turbid medium, showing quality dependence on energy transfer, contrast frequency and sensor phonon illumination level

16 p2426 A72-33777

Gain control and contrast sensitivity in the vertebrate retina.

17 p2507 A72-34418

The effect of target contrast variation on dynamic visual acuity and eye movements.

17 p2508 A72-34876

The influence of the modulation transfer function of the dioptic apparatus on the acuity and contrast of the retinal image in Rana esculenta.

17 p2508 A72-34883

Peripheral contrast thresholds for moving images.

17 p2509 A72-35688

The relative importance of contrast and motion in visual detection.

17 p2509 A72-35689

Lunar color boundaries and their relationship to topographic features - A preliminary survey.

18 p2724 A72-36281

Minimum perceivable stellar magnitudes in visual observations by naked eye and telescope, discussing image contrast and angular scale

19 p2860 A72-37961

Electron microscope double contrast images to identify Burgers vectors of close packed metal crystal dislocations

19 p2846 A72-38590

An application of atmospheric light scattering for contrast analysis in electro-optical detection systems.

20 p2923 A72-39056

Edge effect improved fringe definition on high contrast film by pseudo-solarization for polariscopes in photoelastic stress analysis

21 p3052 A72-40232

Photographic material characteristics for adequate diffraction efficiency and contrast and noise levels and acceptable nonlinear distortions of holograms, noting optical transfer function optimization

21 p3052 A72-40389

The effect exerted on pictorial-analytical measurements at the television microscope by subjective contrast enhancement with color filters

21 p3055 A72-40749

Complete assimilation of briefly presented lines.

23 p3261 A72-44150

Phase correlation between two sources formed on a diffusing surface - Application to the human retina

23 p3261 A72-44379

Line length detectors in the human visual system - Evidence from selective adaptation.

23 p3258 A72-44384

The effects of simultaneous and successive contrast on perceived brightness.

24 p3372 A72-44910

Perception smear suppression during saccadic eye movements in terms of metacontrast determined by post-saccadic accumulated luminance relation to stimuli masking

24 p3373 A72-45377

IMAGE CONVERTERS

NT CELESTOPES

NT IMAGE TUBES

High speed streak cameras applicability to low density theta pinch studies, describing image converters design, operation and block diagrams

02 p0263 A72-11410

Generalized quantum yield for sensitivity of photoelectric devices, considering multistage image converter and photomultiplier

02 p0223 A72-11411

Electroluminescent image converter with positive optical feedback, investigating steady state bistable operation mode stability

02 p0193 A72-12341

Photosensitive MOS devices array as converters performing optical image data analysis, considering sensor sensitivity regulation

02 p0193 A72-12342

Visible displays of millimeter and submillimeter wave images for all-weather ground surveillance, discussing image conversion

[AD-736578]

04 p0494 A72-15612

Ultrahigh speed electro-optical cameras with exposure times of several picoseconds, using biplanar image converter, electron multiplier and Kerr cell

06 p0812 A72-17415

High speed photography in high temperature short duration plasmas, using Kerr cell, image converter, framing and streak cameras

06 p0813 A72-17435

Electroluminescent image converter with positive optical feedback, investigating steady state bistable operation mode stability

08 p1143 A72-21947

Photosensitive MOS devices array as converters performing optical image data analysis, considering sensor sensitivity regulation

08 p1143 A72-21948

UV/visible image converter for use with TV camera tubes for astronomical photometry and spectroscopy from satellites and sounding rockets

08 p1169 A72-21955

Image-to-signal conversion by TV tube in automatic contactless measuring systems, producing mosaics of object by optical, X ray and ultrasonic techniques

11 p1634 A72-26460

Scanning photoelectric image conversion/photoanalyzing/ systems for data telemetry from remote optical sensors

11 p1634 A72-26461

Holographic memory devices for bulk information recording, discussing use of image converter for brightness amplification and lithium niobate electro-optical deflector for beam switching

12 p1807 A72-27588

Image conversion from 10.6 to 0.65 micron wavelength by nonlinear optical method in proustite crystal

12 p1821 A72-27604

Low energetic efficiency of semiconductor microwave scanning converters for radio images of fog obscured objects

13 p1932 A72-29297

Visual observation of continuous hydrocyanic acid laser modes and beam energy distribution, using cholesteric liquid crystal image converter

14 p2111 A72-30851

IR and visible parametric laser image upconversion experiments, demonstrating wavelength dependence on view field by black body radiometric measurements

15 p2249 A72-32152

Study of transient phenomena by a TEA CO₂ laser associated with a liquid-crystal deflector

17 p2562 A72-34285

Book on Soviet astronomical reflecting telescopes, paraboloid mirrors, computer control, microphotometers and image converters

17 p2553 A72-34623

Pump laser design for an infrared upconverter

20 p2934 A72-39873

IR night vision instruments range calculation, taking into account atmospheric optics and electro-optical image converter characteristics

21 p3059 A72-41816

Regenerative optical link assembly for weak image amplification and spectral conversion, using photoreceptor as light receiver

22 p3159 A72-42272

IMAGE CORRELATORS

Digital correlator for change detection in picture element processing with CDC 1700 computer to obtain spatial alignment accuracy

17 p2556 A72-35538

Digital technique for automatic change detection in aerial reconnaissance side-looking radar imagery, discussing image correlators

17 p2557 A72-35554

Epipolar scanning to convert image correlation from two dimensional to one dimensional task for application to photogrammetric automation

18 p2691 A72-36492

Nonholographic coherent optical correlation for automatic stereoperception

18 p2691 A72-36493

Two-frequency microwave holographic interferometry

20 p2927 A72-39784

IMAGE DISSECTOR TUBES

Nimbus satellite image dissector camera system for continuous meteorological scanning, noting special suitability for cloud and ice features discrimination from brightness changes

08 p1171 A72-21967

Star sensor with image dissector as pickup tube for Astronomical Netherlands Satellite attitude control system

08 p1171 A72-21974

Image dissector, silicon photodiode and vidicon behavior comparison for medium resolution star mappers design for three axis stabilized vehicles

08 p1172 A72-21975

Image dissector application to D2B astronomical satellite position field plotting in solar and stellar UV photometry

08 p1172 A72-21976

Image dissector system fabrication for two dimensional area scanning, applying to photograph digitization

11 p1631 A72-25688

Lick observatory image-dissector scanner for faint astronomical spectra, describing design and performance of system based on individual photon pulse counting and memory storage

11 p1631 A72-25691

IMAGE ENHANCEMENT

Operator interactive computer controlled electro-optical system for photographic image enhancement prior to target or pattern identification

01 p0070 A72-10869

Computer image processing for photoreconnaissance, enhancement and calibration applications

01 p0070 A72-10870

Focused image holographic interferometer for reduced blur in deep object image reconstruction with white light source

02 p0224 A72-11747

Computer enhancement of multispectral satellite- and air-photographs and imagery for earth resources

02 p0186 A72-11801

ERTS-A satellite geometric and radiometric received image errors, presenting detection and correction with digital algorithms

02 p0171 A72-11847

Digital picture processing techniques for increased detail resolution, applying equidensity film methods [DFVLR-SONDDR-170]

02 p0229 A72-12018

Diffusely illuminated objects holographic reconstruction with suppressed granularity by incoherent superposition of reconstruction waves longitudinal modes, describing experimental setup

02 p0229 A72-12116

High resolution UV stellar spectroscopy in star stabilized Skylark rocket vehicle, using Cassegrain echelle optics and image intensification

03 p0354 A72-13056

Bayes theorem based iterative method for image restoration by treating degraded images as probability-frequency functions, noting adaptability to computer processing

05 p0690 A72-16671

Image enhancement techniques for sea-ice mapping from satellite IR data, discussing gray scale contrast augmentation scheme for visual quantitative information

06 p0807 A72-17825

Image noise reduction by least squares polynomial filtering method, comparing with Wiener filtering

07 p0987 A72-19829

Commercial radiographic system with data enhancement based on monochromatic blue film, noting image quality and exposure range

07 p0991 A72-20425

Holographic weak signal enhancement technique in presence of strong noise for seismic and oceanographic applications

07 p0992 A72-20563

High neutron absorption doping material selection for enhancing explosive mixtures neutron radiographic image without interference with chemical reaction

08 p1220 A72-20769

Phase and amplitude error effects on image reconstruction in conventional and weak signal enhancement holography

09 p1312 A72-23242

Radiographic image enhancement based on mathematical concepts of image convolution, Fourier transformation and spatial frequency filtering, discussing hardware and computer needs

10 p1481 A72-24322

Rotating mirror image position sensor for high angular resolution optical tracking, discussing performance improvement by computer generated variable density spatial filter

11 p1591 A72-25312

Color enhanced black and white IR satellite images for oceanographic applications

11 p1620 A72-25346

Radiographic electronic image contrast enhancement by video signal generation with amplitude proportional to density rate of change, discussing system dynamic response and resolution

11 p1633 A72-26034

Contrast enhancement for switch-on and -off modes of bar patterns, noting spatial transients due to primary image interaction with negative afterimage

12 p1808 A72-27679

Fast computational techniques for generalized two dimensional Wiener filtering

17 p2532 A72-34402

Image enhancement by computer programs, discussing digital filtering, fast Fourier transform algorithm, data management and large matrix handling

17 p2520 A72-34404

Computerized photographic imagery analysis system with interactive operator controls for processing option selection in image enhancement prior to pattern identification

17 p2520 A72-34407

Computer processed image enhancement applications to spacecraft returned photoreconnaissance, discussing data transmission and resolution vs recognition and color quality

17 p2520 A72-34408

Bayesian recursive estimation by Kalman filtering for enhancement of image corrupted by additive random noise

17 p2557 A72-35539

Image processing by digital computer

18 p2663 A72-36247

Recent developments in digital image processing at the image processing laboratory at the Jet Propulsion Laboratory

18 p2658 A72-36255

Role of recursive estimation in statistical image enhancement

18 p2658 A72-36260

Two dimensional recursive filter for Bayesian estimate of pictorial data represented by dynamic model of random field with exponential autocorrelation

18 p2658 A72-36261

Data structures and computational organization in digital image enhancement

18 p2658 A72-36262

Digital image enhancement heuristic, superresolution and positive restoration techniques, providing bibliography

18 p2658 A72-36264

IMAGE FILTERS

Remote sensing photointerpretation tests, discussing film-filter combinations, image acquisition time, scale and detection accuracy

01 p0065 A72-10450

Dynamic model for estimating Bayesian recursive images by linear Kalman filtering

01 p0046 A72-10866

Birefringent filter theory and optical properties, discussing transmission profile and error sources

03 p0352 A72-12947

Solc-type tunable birefringent filter for near UV spectrum, discussing optical design and transmission characteristics

03 p0355 A72-13058

Solar magnetic field observations with birefringent filter for 5324 A Fe I line, showing H alpha fine structure

03 p0430 A72-13316

Radiation thermometry trends, considering photodetectors, optical pyrometers and filters [ASME PAPER 71-WA/TEMP-3]

05 p0661 A72-15909

Image noise reduction by least squares polynomial filtering method, comparing with Wiener filtering

07 p0987 A72-19829

Optical image filtering to simplify and facilitate automatic aerial photointerpretation processes

09 p1313 A72-23310

Blue filter polarimeter observations of Deimos and Phobos, discussing polarization-phase angle curve for Deimos dust surface layer

12 p1865 A72-27097

Grid modulation information encoding technique for image features extraction with simple Fourier filtering to replace heuristic method

16 p2365 A72-33752

Inverse filtering for linear shift-variant imaging systems

18 p2658 A72-36259

Two dimensional recursive filter for Bayesian estimate of pictorial data represented by dynamic model of random field with exponential autocorrelation

18 p2658 A72-36261

Computational algorithms compared for spatial frequency image filtering, considering tradeoffs between direct convolution and fast Fourier transform under equal point-spread functions assumption

18 p2658 A72-36263

Coherent optical terrain-relief determination using a matched filter

18 p2691 A72-36491

Determination of three orthogonal displacement components from one double exposure hologram

20 p2927 A72-39847

IMAGE INTENSIFIERS

NT IMAGE ORTHICONS

High resolution electrons image intensifier for particle spectrographs, using channel plate, scintillator and fiber optics

04 p0524 A72-15536

Image photon counting technique using digital accumulation of individual events registered by high gain image intensifier and TV camera and stored in on-line computer

08 p1170 A72-21960

Low light level small intensifier/vidicon camera tube using bombardment induced conductivity target, and planar photocathode, detailing design and performance

08 p1171 A72-21969

Channel electron multiplier arrays for double proximity focusing image intensifier design

08 p1171 A72-21973

Design and operation of digital image recorder based on single stage intensifier and silicon target intensifier television camera tube coupled to large memory

11 p1631 A72-25685

Image intensifier tube scanner replacement of slit and multiplier tube of spectrograph, discussing application to rockets

11 p1631 A72-25689

Astronomical reflector telescope design, describing thermal effects on Al mirror and image intensification

12 p1807 A72-27428

Intensified electron bombarded Si camera tube performance in low light level TV systems, predicting sensor resolution vs irradiance characteristics

12 p1810 A72-27934

Human vision sensitivity to covert IR illuminators for image intensification during night observation

15 p2189 A72-32046

- Low level light TV camera with Si intensifier target tube for fire control system to improve AH-IG Cobra helicopter night reconnaissance and attack capabilities
17 p2557 A72-35555
- Night photography at 10,000 feet.
17 p2557 A72-35556
- Monocular and biocular magnifiers for night vision equipment.
20 p2921 A72-39030
- The theory and measurement of the signal-to-noise ratio of second generation image intensifiers.
20 p2922 A72-39039
- Night vision performance measure based on object recognition experiments with optical instruments, noting improvement with image intensifier
21 p3007 A72-40741
- Noise and stimuli current time and spatial distribution effect on visual performance of eye with image intensifier
21 p3054 A72-40742
- The minimum brightness gain required in viewers using image intensifiers.
21 p3055 A72-40744
- Regenerative optical link assembly for weak image amplification and spectral conversion, using photoreceptor as light receiver
22 p3159 A72-42272
- Image intensifier systems and their applications to astronomy.
22 p3181 A72-42989
- IMAGE MOTION COMPENSATION**
- Aerial focal plane shuttered camera high velocity images mathematical model based on collinearity equations, incorporating translational and rotational camera motion during exposure for image motion compensation
01 p0066 A72-10461
- Target motion simulator with photographic recording of image velocity and motion compensation in cameras, discussing errors
03 p0356 A72-13226
- Survey camera design for continuous film advancement and prismatic image displacement compensation
07 p0987 A72-19860
- Speckle reference beam holography for object motion compensation with reduced vibration isolation requirements, discussing CW and pulsed laser use
09 p1314 A72-23338
- Moon radius from Lunar Orbiter 1 angular velocity data obtained from camera image motion compensator sensor /V/H sensor/
17 p2603 A72-34207
- Space-variant image motion degradation and restoration.
18 p2658 A72-36258
- Digital processing for motion compensation in high resolution airborne synthetic aperture radar imagery in presence of simultaneous longitudinal, lateral and vertical maneuvers
21 p3022 A72-41076
- Image motion in the Culgoora solar magnetograph - The role of vibration.
23 p3278 A72-43617
- IMAGE ORTHICONS**
- High resolution vidicons, image orthicons, esicons and ebicons design for space missions
08 p1171 A72-21972
- IMAGE TRANSDUCERS**
- Electrothermal NDT of metal structures by IR scanning camera or thermal image transducer
12 p1813 A72-27200
- Image pickup and display devices.
17 p2552 A72-34568
- A diffraction transducer for vibration analysis.
17 p2626 A72-34722
- Low light level optics for image forming photoemissive sensors, discussing refractive and catadioptric lenses and reflective systems with magnetic focusing
20 p2921 A72-39029
- Optical devices to produce transmitted image rotation about axis, comparing derotation systems and roll and high-speed prisms
20 p2927 A72-39849
- IMAGE TUBES**
- Southern radar sources optical identification by photography using fiber optics image tube
02 p0285 A72-12795
- Integral image tube optical systems for far UV narrow band and broad bandpass photography from spacecraft outside atmosphere
03 p0355 A72-13063
- Anastigmatic optical systems with two high aperture ratio mirrors for UV image tubes
08 p1169 A72-21952
- TV tube type image sensors to replace photographic film for space telescope, discussing design and performance
08 p1169 A72-21956
- TD-1 satellite mounted slow analysis camera with supervidicon image tube to observe cosmic ray tracks in spark chamber
08 p1170 A72-21961
- Image tube, film and mechanical scan camera imaging systems comparison for spacecraft-borne planetary photography based on maximum data return at acceptable cost
08 p1170 A72-21964
- IR image tube with electronic scanning and pyroelectric target for uncooled operation at ambient temperature, noting wideband spectral sensitivity
08 p1171 A72-21966
- ESRO program in imaging detector development for UV and soft X ray space missions, presenting image storage target details
08 p1171 A72-21971
- Image intensifier tube scanner replacement of slit and multiplier tube of spectrograph, discussing application to rockets
11 p1631 A72-25689
- Image tube scanner photon loss probability, considering effects of system gain, aperture time and sweep rate via computer simulation
11 p1631 A72-25694
- Image tube /TV/ and scanning photometer sensor comparison for outer planet mission onboard navigation
15 p2270 A72-32192
- The L14-120GJ, a new bistable image storage tube
18 p2667 A72-36677
- IMAGE VELOCITY SENSORS**
- Target motion simulator with photographic recording of image velocity and motion compensation in cameras, discussing errors
03 p0356 A72-13226
- Oscillating slot-and-bar and sinusoidal reticle scanners for measuring optical image velocity
03 p0326 A72-14202
- Moon radius from Lunar Orbiter 1 angular velocity data obtained from camera image motion compensator sensor /V/H sensor/
17 p2603 A72-34207
- IMAGERY**
- NT AERIAL PHOTOGRAPHY
NT ALL SKY PHOTOGRAPHY
NT ASTRONOMICAL PHOTOGRAPHY
NT BLACK AND WHITE PHOTOGRAPHY
NT CHRONOPHOTOGRAPHY
NT CINEMATOGRAPHY
NT CLOUD PHOTOGRAPHY
NT COLOR PHOTOGRAPHY
NT ELECTRO-OPTICAL PHOTOGRAPHY
NT HOLOGRAPHY
NT INFRARED IMAGERY
NT INFRARED PHOTOGRAPHY
NT LUNAR PHOTOGRAPHY
NT MICROWAVE IMAGERY
NT MICROWAVE PHOTOGRAPHY
NT PHOTOMICROGRAPHY
NT PHOTORECONNAISSANCE
NT RADAR IMAGERY
NT RADAR PHOTOGRAPHY
NT RADIOGRAPHY
NT ROCKET-BORNE PHOTOGRAPHY
NT SATELLITE-BORNE PHOTOGRAPHY
NT SCHLIEREN PHOTOGRAPHY
NT SHADOWGRAPH PHOTOGRAPHY
NT SPACEBORNE PHOTOGRAPHY
NT SPECTROHELIOGRAPHS
NT SPECTROPHOTOGRAPHY
NT STEREOGRAPHY
NT ULTRAVIOLET PHOTOMETRY
- First order imagery in neighborhood of base ray transversing arbitrary optical system, discussing relationships among anamorphic nature, astigmatism and image rotation
09 p1309 A72-22606
- Fourier transformations for convolution integral calculation in image distortion correction by ground visual observations of solar intensity distribution, noting successive approximations method
13 p2046 A72-29726
- A theoretical calculation of edge smear in far-field holography.
19 p2797 A72-37610
- Image forming mechanism in photographic silver halide emulsions due to incident optical signals, considering latent image amplification process efficiency
19 p2800 A72-37857
- Application of the optical transfer function to visual instruments.
20 p2922 A72-39043
- IMAGES**
- NT AFTERIMAGES
NT IMAGE VELOCITY SENSORS
NT RETINAL IMAGES
- Stepped reflector image region fields at plane wave incidence angle to reflector axis, determining field components as Fourier series
01 p0035 A72-10115
- Visual and acoustic image processing rates during letter sequencing tasks, suggesting implicit verbal control involvement
15 p2188 A72-32764
- Digital techniques for image data processing and analysis, discussing data sampling, conversion, computer implementation, image matching, etc
18 p2664 A72-36490
- IMAGING TECHNIQUES**
- NT IMAGE ENHANCEMENT

NT RADAR IMAGERY

- Remote sensing photointerpretation tests, discussing film-filter combinations, image acquisition time, scale and detection accuracy
01 p0065 A72-10450
- Digital computer program high speed algorithm for high resolution images geometric correction, discussing application to ERTS return beam vidicon images
01 p0065 A72-10454
- ERTS satellite image processing for multispectral scanning system, discussing distortion from geometrical properties
01 p0066 A72-10458
- EROS program thematic mapping system for binary graphic overlays of open water, snow and ice, reflective IR vegetation and human works
01 p0066 A72-10460
- Transfer function compensation technique for processing sampled imagery data prior to recording on hard copy to remove degrading effect for quality improvement
01 p0046 A72-10873
- Microwave holographic interferometry with optical wave front reconstruction for visual mapping of large objects deformation
01 p0072 A72-11236
- Double reference beam holograms, evaluating interference effects of misalignment on image reconstruction
02 p0225 A72-11749
- Regional geological surveying by satellite-borne TV, discussing image interpretation methodology
02 p0208 A72-11780
- IR remote scanning of natural resources, discussing thermal to optical image conversion on photographic film
02 p0208 A72-11781
- Environments susceptibility to low resolution imaging for land-use mapping, relating landscapes spatial frequency distributions to expected ERTS resolutions
02 p0210 A72-11796
- Natural resources multispectral remote sensing for national emergencies, discussing various imaging techniques
02 p0212 A72-11828
- Soviet monograph on variable stars observation covering photographic photometry, photoelectric observation, image processing devices and computer techniques
02 p0279 A72-12122
- Wave front sampling points in spatial filtering of nonequidistant discrete holograms of flat objects
02 p0232 A72-12751
- Holographically produced zone plates for solar X ray imaging, using Ar laser produced interference figure
03 p0354 A72-13046
- Apodized Fresnel zone plate construction for solar X-ray image formation
03 p0354 A72-13047
- Nonperiodically moving object holographic interferometry by time-averaging method, considering single exposure technique advantage over multiple exposure in thermal deformation observation
03 p0357 A72-13373
- Surface phase holograms recorded on materials with depth removal effect on exposure, noting emulsion thickness effect on image quality
03 p0359 A72-13449
- Symmetrical three component pancratic system with intermediate constant image plane and linear displacement of components
03 p0360 A72-13562
- Holographic analysis of periodic microobjects at X ray wavelengths, obtaining high contrast
03 p0360 A72-13669
- Microelectronic computer system with image data cross correlation generation for real time video pattern abstraction, discussing design and operating characteristics
03 p0329 A72-14178
- Visual film, TV and optical data systems unified classification for performance criteria based on equation similar to ideal imaging system description by Rose
03 p0329 A72-14188
- Mariner Venus/Mercury 1973 flyby mission imaging experiment, discussing mission constraints, objectives and use of real time transmission vidicon camera and high resolution UV photography
04 p0568 A72-14494
- Intermittent ion emission enhancement from tungsten surface in He-W field-ion microscope upon Ne addition to imaging gas
04 p0552 A72-14547
- Optical image recording, transformation, readout, transmission and data processing techniques and instruments, discussing transfer function, cut-off frequency and information quantity concepts and holography
04 p0525 A72-15700
- Ultrasonic acoustic holography for real time non-destructive testing of cracks, voids, nonbonds and other defects in metals, ceramics and plastics [SAE PAPER 720173]
06 p0811 A72-17319

Spatial digital transform coding of color images using three primary color data planes

06 p0772 A72-17403

Earth resources applications of multispectral remote sensing techniques for airborne and satellite-borne imaging systems, discussing microwave radiometer augmentation of visual and IR data

06 p0813 A72-17430

Stereoscopic projection screens for three-dimensional image display, discussing classification by diffusing properties, surface types and applications

06 p0814 A72-17440

Holography utilization effectiveness in three-dimensional image displays, information storage, image multiplication and recording, interferometry, coding, lens corrosion, pattern recognition, etc

06 p0816 A72-17951

Holographic recording of focused images using reference laser beam reflected from object in direction of diffraction maxima

06 p0817 A72-18012

Acoustic/ultrasonic/ holography techniques for acoustic field recording and image reconstruction in coherent light, including applications

07 p0981 A72-18920

Ventricular function determination by computer graphic techniques for increasing speed, accuracy, reliability and scope of angiocardio-graphic analyses determining human heart dimensions

07 p0928 A72-19308

Image processing of diagnostic echocardiogram by ultrahigh speed analog to digital converter interfacing digital computer

07 p0928 A72-19312

Fabry lens application in stellar photometry, describing technique of image construction on photomultiplier tube cathode

07 p0985 A72-19419

Electronic imaging devices in astronomy, describing TV readout image tubes

07 p0985 A72-19580

Borrmann X ray topographic examination of dislocation structures, discussing geometric effects on linear defects image width

07 p0989 A72-20158

Method of images solution for stress systems in rectangular plate under general self equilibrant edge tractions

07 p1095 A72-20244

Latent image formation in radiographic emulsion of AgBr crystals dispersed in gelatin layer, considering crystal structure and X and gamma rays energy recording

07 p0991 A72-20424

Constant period discrete holograms features, investigating laser visualization, recording, reconstruction and image focusing

08 p1163 A72-20747

Telescopic requirements posed by Venus near sun, discussing sky brightness in image plane, atmospheric dust and Rayleigh scattering

08 p1230 A72-20993

Laser holographic imagery of plane and three dimensional objects for supersonic fluid representation of standing wave in isotropic liquid

08 p1165 A72-21078

Three dimensional hologram recording and reconstruction, discussing image geometry, reference beam intensity, size finiteness, transition limits and photosensitive materials

08 p1166 A72-21399

Holographic image reconstruction for individual transverse laser modes radiation intensity distribution

08 p1169 A72-21915

TV tube type image sensors to replace photographic film for space telescope, discussing design and performance

08 p1169 A72-21956

Image photon counting technique using digital accumulation of individual events registered by high gain image intensifier and TV camera and stored in on-line computer

08 p1170 A72-21960

Image tube, film and mechanical scan camera imaging systems comparison for spacecraft-borne planetary photography based on maximum data return at acceptable cost

08 p1170 A72-21964

Si diode array vidicon for ground based and spaceborne planetary and stellar imaging, noting integration time, storage and slow scan capabilities extension through cooling

08 p1171 A72-21970

Digital image processing for TV camera noise suppression and photometric and geometric distortions calibration and rectification

08 p1172 A72-21977

Rock type discrimination from ratioed airborne thermal IR scanner images of Pisgah Crater/California

08 p1162 A72-22018

First order imagery in neighborhood of base ray transversing arbitrary optical system, discussing relationships among anamorphic nature, astigmatism and image rotation

09 p1309 A72-22606

Partially coherent imaging in microdensitometer, investigating conditions for linear operation from difference between high and low contrast edge images

09 p1309 A72-22608

Incoherently light radiating object and background light focusing on photosensitive mosaic, observing linear restoration by comparison of mean square error with Wiener filter theory

09 p1350 A72-22611

Two mechanism model for anomalous field ion microscope images in W, noting end form difference in high and low evaporation rates

09 p1370 A72-22803

Image scale selection for topographic map revision in orthophotograph production considering economics and suitability

09 p1311 A72-22968

Object reconstruction procedure in two- and multi-media photogrammetry involving image distortion by refraction on interfaces

09 p1311 A72-22970

Pulsed laser sensitizer using multiple imaging technique to retrieve average energy distribution from photographic plate optical density

09 p1325 A72-23346

Vibration measurement based on moire pattern fringes motion due to line gratings respective displacement, noting high accuracy and resolution

09 p1315 A72-23388

Remotely sensed imagery data photointerpretation by gray tone texture context feature extraction, noting identification accuracy

10 p1442 A72-23812

Laser recording real time imagery for use in tactical reconnaissance aircraft

10 p1488 A72-23928

Imagewise electrostatic charge buildup in electron beam recordings, determining trajectories by Runge-Kutta method

10 p1479 A72-23929

High speed material transfer recording equipment for alphanumeric printers, toned image graphic and microimage computer printer applications

10 p1489 A72-23934

Electron image projection system using converter tube technique for microcircuit lithography, discussing performance tests and design changes

10 p1447 A72-23957

Viking Mars Orbiter imaging experiment with high resolution contiguous coverage by vidicon cameras for landing sites selection and surface study

10 p1539 A72-24377

Viking Lander imaging experiments with stereoscopic camera system to study Martian surface and atmospheric morphology, composition and evolution

10 p1540 A72-24382

Electron-optical system with electro- and magneto-static lenses, ensuring large image reduction for producing printed microcircuits

10 p1482 A72-24589

X and gamma ray astronomy with multiple pinhole cameras and a posteriori image synthesis, obtaining SNR gain

11 p1629 A72-25313

Linear optimization of holographic process, investigating application to three dimensional diffusive object

11 p1629 A72-25315

Visual image indicator used beside and behind objects for neutron radiography quality determination and radiographs series grading

11 p1632 A72-25822

Holograms image formation characteristics with extended reference beam source, presenting reconstructed image and noise field calculations

11 p1633 A72-26352

Spatial and temporal coherence effects on image formation by in-line Fraunhofer holography

12 p1806 A72-27121

Electrothermal NDT of metal structures by IR scanning camera or thermal image transducer

12 p1813 A72-27200

Optical and electronic imaging systems optimization for solar system exploration, discussing effects on public support for national funding

12 p1807 A72-27346

Photosensor aperture shape and line scan spacing effect in reducing facsimile camera aliasing

12 p1807 A72-27408

Thermal and shot noise and distortion in charge-coupled semiconductor devices used for imaging applications

12 p1791 A72-27673

Ultrasonic imaging technique based on optical pulse compression, noting image forming and range discriminating capability

12 p1808 A72-27677

Holographic interferometer and fringe analyzer with laser sources, discussing design and application to supersonic flow imaging in wind tunnel

12 p1809 A72-27760

Image deformation sources correction in space photography, discussing stationary and moving cameras and panoramic and complex sensing systems

12 p1809 A72-27817

Real time depth gated acoustic image holography, using scanning laser beam pulse echo technique

12 p1809 A72-27840

Spatial noise in holographic images of diffusely scattering objects with allowance for recording apparatus resolving capacity

12 p1810 A72-27871

Dispersive optical imaging systems for chromatic aberration correction, considering broadband holographic reconstruction and generation, optical information processing and diffraction pattern achromatization

12 p1811 A72-27950

Computerized reconstruction of orthogonal representations from cylindrical and conical mapped projections with known parameters and base

13 p1956 A72-28738

Extremal correlation algorithm for automatic control of two image congruent superposition, using digital simulation and statistical trial techniques

13 p1924 A72-29161

Image discretization accuracy in recognition system, considering two dimensional object reconstruction on element network

13 p1925 A72-29163

Acoustic/ultrasonic/ holography techniques for acoustic field recording and image reconstruction in coherent light, including applications

13 p1957 A72-29206

Artificial compensation holograms for complex optical objective substitution, using interference fringe image technique

13 p1958 A72-29513

Opaque scatterers disadvantages in interferometric images recording of transparent objects obtained by double exposure holography, noting phase type diffraction gratings

13 p1958 A72-29616

Radiation measurements and thermal IR and photographic imaging techniques in meteorology and earth resources survey applications

15 p2221 A72-31241

Miniature high gain photomultiplier for pulse counting applications in close-packed arrays and mosaics for scintillation imaging and spectrum analyzing

15 p2234 A72-31534

IR absorbent effects on evaporographic image contrast performance based on photometric study, presenting color photographs

15 p2188 A72-31615

Optimum processing structure/likelihood functional/ determination for signal sequence detection given noisy common background image sets

15 p2196 A72-31783

Color band selection for Mars lander multispectral imaging system for surface constituent discrimination

15 p2307 A72-31809

Mariner 9 TV experiment image data display, processing and production for real time analysis, noting computer algorithms

15 p2236 A72-31982

High speed facsimile transmission system based on LR70 laser scanner, presenting typical system output image

15 p2248 A72-32041

Head-up display for aircraft three dimensional sky path observation during navigation and landing, discussing computer units, CRT and image generating subsystems

15 p2268 A72-32042

Real time holographic quasi-dynamic 3-D image display, discussing computerized synthetic hologram generator concept and system block diagram

15 p2237 A72-32054

In-line holography, determining effects of limited information on reconstructed image characteristics

15 p2237 A72-32057

Emulsion response and phase effects on two point resolution in coherent holographic imaging systems, using Rayleigh criterion

15 p2237 A72-32058

Transverse wind self-induced thermal lens effects on target image quality in laser beam tracking systems

15 p2249 A72-32164

Coherent light signal optoelectronic processing techniques application to engineering components displacement measurement and vibration amplitude real time imaging

15 p2238 A72-32168

Spectral image formation and aberration by spherical concave grating for point light source, using geometric optics method

15 p2278 A72-32337

Holographic prerecorded TV system, discussing coherent light noise elimination and redundancy effects on image quality

15 p2239 A72-32356

Thermoplastic photoconductor media for holographic recording, discussing structure fabrication techniques and performance

15 p2239 A72-32359

Recyclable holographic recording media performance parameters comparison to develop tradeoffs for storage and imaging applications

15 p2239 A72-32360

Aircraft electronic display for pilot precise control in complex tasks, discussing clarity, stability and readability of CRT images

15 p2181 A72-32632

Microwave modulated incoherent light for large volume scenes holography, noting object image reconstruction by coherent light transillumination of hologram

15 p2242 A72-32675

Fourier transform /subtractive/ holographic imaging technique for microwave antenna apertures

16 p2368 A72-33072

Field-ion microscopy as experimental metallurgical technique for metal surface atomic structure studies, discussing image formation, ionization and field evaporation

16 p2392 A72-33444

Comet Tago-Sato-Kosaka /1969g/ L alpha emission image recorded by f/2 objective-grating spectrograph aboard Aerobee rocket, discussing ice sublimation in nucleus

16 p2455 A72-33466

Holographic virtual image formation and magnification by classical geometrical optics laws application, deriving equivalent law of refraction

16 p2392 A72-33599

Holograms image formation characteristics with extended reference beam source, presenting reconstructed image and noise field calculations

16 p2394 A72-33705

Holographic developments during 1948-1971, discussing three dimensional object imaging, phase, diffused and three-color holograms, Soret lens, electron microscopy and interferometry, etc

16 p2394 A72-33751

Spatial noise in holographic images of diffusely scattering objects with allowance for recording apparatus resolving capacity

16 p2395 A72-33980

Image pickup and display devices.

17 p2552 A72-34568

An improved method for obtaining the general-displacement field from a holographic interferogram.

17 p2553 A72-34721

Quantization and other nonlinear distortions of the hologram transmittance.

17 p2553 A72-34724

Three dimensional model images information content increasing in coherent light interference shadow marking, noting automatic systems for distant objects recognition

17 p2529 A72-34844

Holographic image reconstruction using He-Ne laser as coherent light source and black-white and color photographic emulsions

17 p2554 A72-34930

A two-dimensional color schlieren technique.

17 p2554 A72-34933

Two dimensional images from remote sensors, discussing geometrical properties and imaging equations for aerial, IR and radar photographs

17 p2555 A72-35335

Texture synthesis by image processing equipment consisting of digital computer and input/output unit, noting image signatures of constant parameter areas

17 p2555 A72-35338

Stabilizing techniques for holographic recording.

17 p2556 A72-35416

Digital simulation for sampled electro-optical imaging system performance prediction and optimization

17 p2557 A72-35552

Flight tests correlation with mathematical models to predict electro-optical viewing systems capability for military missions

17 p2557 A72-35553

Image autocorrelation function models and power spectra, obtaining probability distribution, variance and correlation coefficients of image orthogonal transformations

17 p2518 A72-35672

Range coding application to TV and videophone images, stressing plug memory

17 p2518 A72-35675

Holographic imaging of a point object in higher diffraction orders.

17 p2557 A72-35753

Image processing in the context of a visual model.

18 p2658 A72-36256

Image restoration - The removal of spatially invariant degradations.

18 p2658 A72-36257

Inverse filtering for linear shift-variant imaging systems.

18 p2658 A72-36259

High-speed image scanning devices using acoustic surface waves and photodiode array.

18 p2658 A72-36267

Digital image processing and interpretation of photographic film data.

18 p2690 A72-36319

The imaging properties of the positron camera

18 p2652 A72-36424

Mathematical methods for improving the significance of scintigrams

18 p2652 A72-36425

Remotely sensed data processing by scanner/printer designed for photograph scanning, geometric correction and photographic printing of corrected image

18 p2691 A72-36495

The image-processing system for the Earth Resources Technology Satellite.

18 p2674 A72-36496

Stereoplotting instrument concept based on image data selection independence from object space model reconstruction

18 p2691 A72-36498

A digital portable line-drawing rectifier.

18 p2692 A72-36500

Operation and performance characteristics of flying spot scanning X ray imaging systems for rapid film safe parcel inspection

18 p2692 A72-36671

The L14-120GJ, a new bistable image storage tube

18 p2667 A72-36677

Large object holographic image accuracy tests determining experimental sources of error

19 p2797 A72-37589

Acoustical holography imaging methods and applications, reviewing liquid levitation, sampling holography, dynamic surface deformation and scanned pulse-echo holography

19 p2797 A72-37604

Ultrasonic imaging system based on side-looking synthetic aperture radar principles, using B-scan technique

19 p2798 A72-37624

Microwave holographic imaging techniques for aircraft landing aids and airport security applications, discussing real time operation

19 p2798 A72-37625

A holographic method for optical adjustment of pulsed laser beams

19 p2811 A72-37674

Historical review of holographic interferometry development, giving attention to contouring technique and image reconstruction

19 p2800 A72-37775

Experimental observations of the instability of stellar images from a bichromatic two-channel television system

19 p2860 A72-37956

Certain results of the statistical processing of a large series of large-scale television images of stars

19 p2860 A72-37957

Method for transforming three-dimensional images on maps, plans, and other documents with the aid of an electronic computer

19 p2802 A72-38082

Influence of an optically nonhomogeneous medium on the coherence of laser radiation and the possibility of obtaining a holographic image

19 p2812 A72-38536

Experimental investigation of direct quasi-optical radiovision of small objects

19 p2768 A72-38673

Distribution of illumination in a point image in the presence of birefringence in the optical system /case of axial symmetry/

19 p2836 A72-38789

Low light level optics for image forming photoemissive sensors, discussing refractive and catadioptric lenses and reflective systems with magnetic focusing

20 p2921 A72-39029

The theory and measurement of the signal-to-noise ratio of second generation image intensifiers.

20 p2922 A72-39039

Incoherent radiation imaging system analysis from detector-display characteristics, target response function and noise characteristics

20 p2922 A72-39044

Partially coherent light for image formation of objects with amplitude, phase and complex variations, discussing system concepts, coherence control, apodization and techniques

20 p2931 A72-39048

Visual aid-to-eye direct coupling, evaluating partial coherence effects on imagery optical performance by computer program

20 p2931 A72-39050

Wave front sampling points in spatial filtering of nonequidistant discrete holograms of flat objects

20 p2923 A72-39057

An iterative array which can represent the rotation and translation of objects.

20 p2905 A72-39422

Radio astronomical event visible image generation by electro-optical processing comparing SNR performance and electronic complexity with conventional technique

20 p2904 A72-39787

The study of vibration patterns using real-time hologram interferometry.

20 p2927 A72-39848

Optical devices to produce transmitted image rotation about axes, comparing derotation systems and roll and high-speed prisms

20 p2927 A72-39849

Image point formation in field ion microscopy of metal surfaces, using atom probe detection of noble gas apex adsorption

21 p3050 A72-40086

New technique of image multiplexing using random diffuser.

21 p3050 A72-40145

Experimental investigation of a holographic system that records front surface detail from a scene moving at high velocities.

21 p3053 A72-40612

Scatter plate and lens methods of holographic cinematography

21 p3054 A72-40615

Effect of environmental changes on the ghosting of distant objects in twin-glazed windows.

21 p3084 A72-40616

Dry photopolymer holographic recording film with ability to form images in near real time by exposure without processing

21 p3054 A72-40620

Opaque scatterers disadvantages in interferometric images recording of transparent objects obtained by double exposure holography, noting phase type diffraction gratings

21 p3054 A72-40669

Image quality of binary and multigraded microwave holograms, noting HF components and background noise

21 p3055 A72-40794

The airborne visual simulation as an electronic display.

21 p3010 A72-41410

An orthographic photomap of the South Pole of Mars from Mariner 7.

21 p3110 A72-41455

Holographic system resolving capacity increase by oblique illumination of object, analyzing plane monochromatic wave transmission through one dimensional semitransparent body

21 p3058 A72-41791

Double exposure holographic interferometry for distinguishing surface deformations by changing illuminating beam inclination in successive exposures

22 p3175 A72-41992

A large viewfield laser photographic system for in-flight model contour measurements in an aerobalistic range.

22 p3179 A72-42679

Experimental determination of some optical characteristics of a double magnetic prism-electrostatic mirror system

22 p3180 A72-42937

Sunspots and solar granulation recording and imaging with 64-element array of PbS IR detector for obtaining high SNR and resolution

23 p3288 A72-43883

Characteristics and measurements of an aperture-limited in-line hologram image.

23 p3288 A72-43886

A simple method of hologram transmission by using random phase reference - Principle and computer simulation.

23 p3290 A72-43949

A transmitting television tube for collecting information from streamer spark chambers

23 p3290 A72-44160

Photographic processing method for solar activity macrostructural distributions determination, suppressing minor and sporadic formations by defocusing technique

23 p3340 A72-44239

The precise simulation of image transfer systems with the aid of an optical convolution obtained with a rotating slit of prescribed form

23 p3261 A72-44361

Lensless multiplication of images and their spatial frequency spectra with the aid of Fresnel holograms

23 p3292 A72-44470

Acoustical holography with a scanned linear array.

24 p3401 A72-44705

Projective properties of holographic imaging.

24 p3401 A72-44767

Measurement of the modulation transfer functions of focusing screens.

24 p3425 A72-44770

Studying hologram imagery by a ray-tracing method.

24 p3401 A72-44773

Image formation using antenna properties of optical heterodyne receivers.

24 p3409 A72-44802

Remote sensing of earth resources by microwave radiometry.

24 p3402 A72-45107

High resolution multispectral camera system for ERTS A & B.

24 p3402 A72-45182

A sight simulation technique using TV-screen perspective correction for restricted maneuver flight missions

24 p3388 A72-45298

Electronic imaging devices for astronomy from a space platform.

24 p3404 A72-45542

IMBEDDINGS

Magnetic shielding effectiveness of metal cylinder tubes with periodically imbedded annular transverse Bloch walls of high permeability

16 p2369 A72-33669

IMBEDDINGS [MATHEMATICS]

NT INVARIANT IMBEDDINGS

Shooting and imbedding methods for theoretical analysis and approximate numerical solution of two-point boundary value problems involving n-vector-valued functions

[AD-743615] 04 p0539 A72-15043

Numerical integration solution of nonlinear equations and two point boundary value problems, using quasi-linearization and imbedding methods

06 p0839 A72-17957

Rectangular domain boundary value problem biharmonic equation and Cauchy system equivalence, noting semigroup properties analysis in terms of nonclassical imbedding variables

11 p1737 A72-26663

Functional method investigations of imbedding theorems for random weight spaces of high order irregular elliptic equations with uniform boundary conditions

23 p3307 A72-43222

A manifold imbedding algorithm for optimization problems.

23 p3268 A72-44197

IMIDES

NT SUCCINIMIDES

IMINES

Chromosome aberrations and germination speedup in Soyuz 5 carried barley seeds, noting stimulating effect by preflight ethylenimine treatment

17 p2505 A72-35280

IMMERSION

U SUBMERGING

IMMISCIBILITY

U SOLUBILITY

IMMITTANCE

U ELECTRICAL IMPEDANCE

IMMOBILIZATION

Immobilization hypercalciuria, discussing treatment by diet-induced extracellular volume depletion and possible pathophysiological mechanism of intercompartmental fluid and electrolyte shift

04 p0479 A72-14871

Inhibitive effect of immobilization on urinary catecholamine excretion and blood plasma thyroxine level in rats

09 p1265 A72-22648

Calcium and phosphorus excretion relation to bone density changes in immobilized Macaca nemestrina monkeys

12 p1760 A72-27473

Calcium metabolism under stress and in repose.

23 p3254 A72-43389

Changes in the pituitary-thyroid and in the pituitary-gonad systems under conditions of functional loading and of physiological immobilization.

24 p3371 A72-44823

IMMUNITY

Amitetravite /biological protectant/ effect on natural immunity state of dogs exposed to chronic gamma irradiation simulating space flight environment

14 p2074 A72-30380

Influence of X-ray irradiation in 25- and 250-r doses on the transplant immunity in mice differing by weak and strong histoincompatibility systems

23 p3255 A72-43910

IMMUNOLOGY

Radioimmunoassay and gel filtration determination of molecular size and immunochemical reactivity of parathyroid hormone in gland extracts, peripheral circulation and parathyroid effluent blood

04 p0473 A72-15228

Immunochemical properties of human oxymyoglobin comparison with complex of dog hemoglobin and human hemoglobin reactions in anti-hemoglobin serum

09 p1268 A72-23695

Human immunobiological status during prolonged maintenance in bioregenerative life support system, discussing possible allergic reaction to chlorella gaseous metabolites

13 p1910 A72-29312

Hypothermia, asphyxia and ionizing radiation effects on rat immunological defense mechanisms against particulate antigens

16 p2355 A72-33555

Acute myocardial anoxia - Anatomical changes and their possible relation to immunological processes.

17 p2501 A72-34981

The magnetic field, infection and immunity

17 p2503 A72-35009

The production and characterization of specific antibodies to aldosterone.

19 p2757 A72-38175

Effects of the space flight environment on man's immune system. I - Serum proteins and immunoglobulins.

22 p3150 A72-42493

Quantitation of serum proteins on whole blood-electroimmunodiffusion technique applicable to capillary blood.

22 p3150 A72-42495

Histologic analysis of hypoxia exposure effects on mouse skin homograft reaction due to lymphatic organ function changes

22 p3144 A72-42675

IMPACT

NT ELECTRON IMPACT

NT HYPERVELOCITY IMPACT

NT ION IMPACT

NT PROTON IMPACT

Kinematic impact theory for inertial motion of rigid bodies of revolution and energy flow through wire grid

10 p1512 A72-24520

IMPACT ACCELERATION

Chin-sternum-heart syndrome from partial parachute failure, with close reference to atrial endocardial and myocardial lacerations

02 p0167 A72-11711

Modified Van der Pol wave motion oscillator model for prediction of aortic dynamic response to negative g impact accelerations

12 p1765 A72-28271

Human tolerance limitations related to aircraft crashworthiness.

22 p3151 A72-42765

Utilization of the CACTUS microaccelerometer as a detector of micrometeorite impacts

22 p3181 A72-43097

IMPACT DAMAGE

NT METEORITIC DAMAGE

NT RAIN IMPACT DAMAGE

Human craniocerebral trauma dependence on impact conditions, giving case histories

05 p0619 A72-16643

Hailstone impact simulator for prediction of hail damage to aircraft structures, presenting data on damage to flat metal sheets and spherical caps

[AIAA PAPER 72-163] 05 p0645 A72-16957

Lunar far side crater Tsiolkovsky geology, indicating formation by meteoroid, asteroid or comet impact explosion

06 p0887 A72-18222

Cavitation phenomena role in liquid drop impact erosion of steam turbine blades leading edges

07 p0967 A72-19262

Gosses Bluff impact structure in Central Australia, discussing geologic, seismic, gravity, and magnetic surveys and lunar crater analog

09 p1304 A72-23494

Lunar and Mars crater genetic similarities, discussing scale dependent effects and post-impact geologic development

10 p1531 A72-23704

Hail damage to aircraft, predicting metal surfaces dent depth and deformation shape with computer program

[AIAA PAPER 72-335] 11 p1574 A72-25370

Craters produced by high speed hardened spherical particles, investigating depth and diameter relationship to impact speed

11 p1738 A72-26919

Hailstone size estimation to design exposed equipment for irreversible impact damage prevention

13 p1993 A72-28854

Hailstone impact simulator for aircraft damage prediction in testing prospective structural designs

13 p1938 A72-28855

Ion bombardment and partial discharges effects on polyethylene sheet, observing structural changes by IR spectroscopy

13 p1984 A72-29788

Shock heating caused material phase transformation effects on bumper shield performance, studying thin metal sheets response to like-material spheres impact

14 p2168 A72-30921

Surface damage induced by ion bombardment of monocrystalline W and Mo, determining degradation rate dependence on collisional energy transfer

15 p2276 A72-31853

Analytical model for nonpenetrating impact caused head injuries, evaluating protective device effectiveness via energy absorption characteristics

15 p2191 A72-32602

Probabilistic analysis of aircraft crash-caused structural damage to nuclear power plant, using Monte Carlo method and yield line theory for perforation and collapse modes

16 p2421 A72-33600

Impact crater formation at intermediate velocities. [ASME PAPER 72-MAT-C] 17 p2631 A72-34967

Displacements within impact craters.

17 p2549 A72-35686

Seismic data from lunar geophysical stations network, noting moonquakes and meteoroid impacts

18 p2724 A72-36283

Profile and depth of microcraters formed in glass.

18 p2736 A72-36972

Effects of projectile damage on critical helicopter components.

24 p3454 A72-44609

IMPACT DECELERATION

U DECELERATION

U IMPACT ACCELERATION

IMPACT LOADS

Parachute opening shock and filling time calculation based on aerodynamic drag, air mass and effective porosity time functions, using momentum and continuity equations

01 p0004 A72-10310

Transient response of Al cylindrical shells to longitudinal impact, indicating wave front propagation at plate velocity

[SESA PAPER 1885] 02 p0287 A72-11505

Rigid mass impact against viscoelastic bear of finite length, investigating longitudinal waves propagation and interaction

02 p0298 A72-12682

Secondary slip in impact loaded Al single crystal disks, interpreting face deformation bands

02 p0247 A72-12819

Plate under projectile impact, calculating motion response due to random initial velocity distribution over surface by stochastic model

03 p0447 A72-13852

Finite amplitude stress wave propagation behind shock in unidirectionally reinforced fiber matrix composites under impact loads

04 p0585 A72-14534

Anisotropic elasticity effects on plane shock wave propagation for arbitrary loading directions in plate impact experiments

04 p0585 A72-14538

Erosion of materials under drip impact loads, determining wear rate dependence on drop size, impact velocity and material properties

05 p0734 A72-15981

Approximate maximum shock stress analysis for curved bar bending vibration due to longitudinal impact by disregarding elements inertia with regard to axial motion

05 p0737 A72-16285

Crack propagation in presence of crack branching events in semiinfinite nonhomogeneous elastic brittle plate under edge impact loading

06 p0896 A72-17914

Metals toughness under impact loading from explosive welding process, using optical metallographic techniques

06 p0822 A72-18214

Combined stress wave propagation in thin walled prestressed tube under longitudinal and torsional impact loading

06 p0898 A72-18321

Similarity solution for nonlinear viscoplastic semiinfinite rod under constant velocity impact

07 p1088 A72-19115

Transient high speed deformations analysis of annealed Al under impact loads by three dimensional moire fringe techniques

07 p0983 A72-19131

Wave propagation in hollow elastic/viscoplastic sphere under impact load, assuming Mises condition, isotropic hardening and incompressibility

07 p1096 A72-20429

Heavy falling body elastic impact against circular plate center analyzed by Timoshenko type wave equation

08 p1247 A72-21814

Normal axial impact of thin liquid filled elastic cylindrical shell with rigid bottom on compressible fluid half space surface

09 p1350 A72-22207

German monograph on finite element method for elastic impact at half space, analyzing elasticity and inertia effects on energy absorption and contact time

09 p1397 A72-22338

Impact detonation mechanism in ammonium perchlorate mixtures with inflammable additions, determining critical detonation triggering stresses

09 p1373 A72-22890

Explosive strain hardening of hard metal-ceramic alloy, presenting photographs of carbide and cobalt phases structural changes after impact loading

09 p1337 A72-22892

Constitutive equations for materials with time dependent and time independent plasticity, applying to impact of identical bars

09 p1328 A72-22996

One dimensional nonviscous dynamic plasticity theory applicability to impacting rod problems tested experimentally using results from three dimensional and viscous similarity considerations

09 p1408 A72-23557

Lunar seismograms for LM and S-4B impacts in Apollo 12 experiment, indicating modulation mirage effect on signal distortion

10 p1536 A72-24153

Transient strain in axially impacted hollow nonhomogeneous cone with axially varying modulus of elasticity and density

10 p1555 A72-24195

Stress wave surfaces in graphite fiber-epoxy matrix anisotropic plates under transverse impact forces, using Mindlin approximation theory

10 p1555 A72-24255

Longitudinal vibrations of composite rod under concentrated impact forces at junctions between prismatic sections 10 p1557 A72-2627

Impact-produced deformations in nonlinear viscoelastic rod of finite length, studying pulse propagation as nonlinear boundary value problem 11 p1685 A72-25353

Asymmetric three layer beam design for elastic impact, proposing functional equation integration by computer method 11 p1732 A72-25531

Elastic body transverse impact against vibrating rectangular plate with allowance for rotatory inertia and shearing forces, using wave equation 11 p1732 A72-25532

Impact probe displacement effects in supersonic turbulent boundary layer in terms of Mach number profiles 11 p1572 A72-26005

Coupled nonlinear equations of motion of large deflections of impacted helical springs, comparing with streak photographs 11 p1688 A72-26061

Geometrically nonlinear structure elastic stress propagation, deformation and dynamic response under impact, using finite element matrix displacement method and computer programs 12 p1879 A72-27189

Longitudinal elastic impact wave propagation along branched thin rods, using Timoshenko theory 12 p1881 A72-27256

Holographic interferometry for impact loaded object transient impulse response recording with double-pulse Q switched laser 12 p1809 A72-27761

Impact fracture resistance of Cr-Mn-Si steel, investigating alloying effects on crack initiation and propagation 12 p1831 A72-28238

Microcuts as equivalent mechanical stress concentrators for breakdown energy estimation in flat polymethyl methacrylate glass specimens under impact bending loads 13 p1983 A72-28563

Moonquakes and meteorite and manmade impacts as sources of seismic signals detected by Apollo lunar seismic stations 13 p2037 A72-28988

Borated steels strength under static bending, cyclic flexure and torsion and impact loads, correlating fatigue strength, residual stresses and core properties 13 p1979 A72-29477

Axial impact effect on thin elliptical layer of viscous/ideal fluid with allowance for inertial forces, analyzing spreading process stability 13 p1943 A72-29880

Dynamic behavior of thin walled semiinfinite elastic cylindrical shell with liquid under axial impact loads 13 p1943 A72-30008

Aircraft landing gears structural systems design, taking into account different design criteria imposed by various national impact load norms 13 p1898 A72-30025

Average stress and strain across thickness of liquid filled cylindrical elastic thin walled shell with rigid bottom under axial impact loads 14 p2166 A72-30698

Axisymmetric ductile rotating shaft failure modes, considering fatigue, buckling and impact stress factors [ASME PAPER 72-DE-40] 14 p2167 A72-30873

Tapered elastic rod transient behavior under end impact due to mass striking, computing fixed end stress, struck end velocity and impact time duration 15 p2323 A72-31404

Spherical cap dynamic buckling under impulsive loading, comparing prediction by energy criterion with experiment using spray deposited explosive 15 p2323 A72-31405

Transverse impacts of hard cones on elastic membranes for various apex angles, using high speed photography 15 p2323 A72-31445

Impulse excited spatial systems of rigid bodies linked by pivot joints with arbitrary kinematics, applying Maxwell-Betti theorem 15 p2323 A72-31461

Dynamic analysis of transient impact response of finite crack opened by in-plane shear tractions 16 p2464 A72-32920

Finite element method application to nonlinear dynamic problems exemplified by study of plastic deformation behavior of cylindrical billet under impact of heavy rigid body 16 p2466 A72-33019

Axisymmetrical stability loss in elastic cylindrical shell under longitudinal and transverse impact waves, discussing buckling and similarity parameter for simulation 16 p2468 A72-33159

Axisymmetric jet impact on ground board for different nozzle configurations and heights in VTOL aircraft aerodynamic studies 16 p2377 A72-33404

Transient elastic wave propagation in circular cylinder during sudden torsional shear stress application to end surface, noting surface particle velocity and stress 16 p2426 A72-33660

Wave propagation in a viscoelastic fiber subjected to transverse impact. [ASME PAPER 72-APM-27] 17 p2570 A72-34791

Longitudinal impact of cylindrical shells with discontinuous cross-sectional area. [ASME PAPER 72-APM-24] 17 p2628 A72-34793

Determination of the unloading boundary in transverse impact of an elastic-plastic string. [ASME PAPER 72-APM-12] 17 p2629 A72-34804

Holographic nondestructive testing with impact excitation. 17 p2555 A72-35197

Testing the impact accuracy of the NEK-8 HERF machine 18 p2695 A72-36274

Reflection and refraction of elastic waves in edge-impacted rectangular plates. 18 p2737 A72-37065

A comparison of initial velocities for dynamic instability of a shallow arch. 18 p2738 A72-37080

Longitudinal impact on a thin cylindrical shell 19 p2870 A72-37321

Buckling of an elastic cylindrical shell during longitudinal impact against an obstacle 19 p2870 A72-37322

Elastic impact on a three-layer plate in the presence of concentrated masses and nonlinear restraints 19 p2877 A72-38159

On the cumulative fatigue damage of glass fiber reinforced plastics subjected to repeated tensile impact load. 20 p2943 A72-38888

Rayleigh wave effects in an elastic half-space. 20 p2980 A72-39615

Strongly coupled stress waves in heterogeneous plates. 20 p2980 A72-39616

Quasi-static impact of hard hemisphere against brittle half space, investigating fracture mechanics 20 p2981 A72-39952

Axisymmetric impact of compactible rods subjected to finite deformations. 21 p3117 A72-40455

Dutch monograph - Analysis of dynamic aircraft landing loads, and a proposal for rational design landing load requirements. 21 p2994 A72-40925

Modern landing impact load calculations and old-fashioned requirements. [ICAS PAPER 72-31] 21 p2995 A72-41156

Force-time investigations for the elastic impact between a rigid sphere and a thin layer. 21 p3121 A72-41212

Buckling of inelastic cylindrical shells under axial impact. 21 p3124 A72-41507

Surface effects during high-speed impact of metals 22 p3188 A72-42163

Wave propagation in a truncated conical shell. 22 p3235 A72-42524

Dynamic behavior of thin walled semiinfinite elastic cylindrical shell with compressible liquid under axial impact loads 22 p3167 A72-42736

Internal to total energy relation dependence on deformation time in impulsive loading of homogeneous free rod, noting energy conversion efficiency 23 p3344 A72-43338

Hydrodynamic fluid pressure on a shell during hydraulic impact 23 p3280 A72-43788

Experimental investigation of displacements and stresses in a rod during impact loading 23 p3348 A72-43795

Erosion of materials under drip impact loads, determining wear rate dependence on drop size, impact velocity and material properties 24 p3460 A72-45723

IMPACT PREDICTION

Hollow rubber impact absorber stiffness and deformation characteristics derivation by classical elasticity theory, noting accuracy 06 p0895 A72-17797

Impact interaction between free two body system with elastic spring coupling and fixed plane, considering mass ratio and velocity restitution coefficient 08 p1209 A72-21803

German monograph on model concept for erosion mechanism involved in crystalline material surface bombardment covering particle elastic deformation during impact 09 p1397 A72-22324

Lift variation effect on rolling reentry vehicle trajectory, calculating deviation from zero-lift impact point 10 p1552 A72-24651

Range correction computations for weapons dropped from aircraft. 19 p2747 A72-37286

Allowance for the striking angle of a meteoric body with penetration-depth and piezoelectric sensors in the evaluation of the spatial density of meteoric matter 22 p3234 A72-42219

IMPACT PRESSURES

U IMPACT LOADS

IMPACT RESISTANCE

Carbon fiber-resin laminates ballistic impact resistance, discussing damage and interlaminar shear strength 04 p0537 A72-15089

Hollow rubber impact absorber stiffness and deformation characteristics derivation by classical elasticity theory, noting accuracy 06 p0895 A72-17797

Micromechanical and impact test investigation of unidirectional fiber composites impact resistance properties, considering longitudinal, transverse and shear modes 11 p1672 A72-25472

Concord aircraft windshield panels bird impact resistance, noting effects of edge clamping width, ply thickness, composition and temperature 12 p1812 A72-27013

Aircraft windshield bird impact resistance, noting weight, speed, angle and window geometry effects 12 p1813 A72-27014

Transparent aircraft polycarbonate glazing systems shielding properties for projectile and bird impacts 12 p1832 A72-27015

Improving the impact resistance of glass-fibre composites. 18 p2703 A72-36270

A technique for position sensing and improved momentum evaluation of microparticle impacts in space. 19 p2795 A72-37518

IMPACT SENSITIVITY

U IMPACT RESISTANCE

IMPACT STRENGTH

Impact effect on strength of glued metal joints mounted in groove cut in baseplate and pressed by yokes 01 p0144 A72-11380

Hot-rolled low-carbon Mn-Mo-Nb acicular ferrite steels with high strength, toughness and impact resistance 02 p0246 A72-12559

Inconel 718 welding techniques, investigating microfissuring, impact strength, penetration and ductility 02 p0246 A72-12774

Al-Mg alloy with Ti, Zr, Mo and B additions under tensile and impact loads, investigating mechanical properties, strength and crack formation 07 p1014 A72-19839

Short fiber reinforced thermoset composite materials for engineering construction, tabulating flexural properties and Charpy impact strengths 09 p1338 A72-23165

Charpy impact strength data for unidirectional graphite, boron and glass-resin composites tested in fiber direction, noting tensile stress-strain characteristics importance 11 p1672 A72-25471

Pendulum impact resistance of tungsten fiber-metal matrix composites, noting heat treatment and test temperature effects 11 p1653 A72-25473

Low temperature mechanical properties of Ti-base alloys, examining notched samples impact strength as function of temperature and notch depth 11 p1663 A72-26806

Heat treatment effects on martensitic bainitic steel hardness, tensile strength and impact endurance, examining carbide and alpha phases 11 p1666 A72-26922

Aircraft windscreen design, discussing high impact strength glass, electroconductive film, transparency service life and weight reduction 12 p1753 A72-27006

Dynamic load tests for impact strength of ceramic composites with fiber reinforced alumina matrix, obtaining dynamic stress-strain curves 16 p2414 A72-33300

High temperature strength and ductility study of hot working behavior of steels, using hot impact tension tests 16 p2406 A72-33316

Foam content effect on fiberglass reinforced thermoplastic foam tensile and impact strength, thermal distortion and mold shrinkage properties 16 p2415 A72-33418

Ductility relationship to plasticity characteristics in cylindrical steel samples with short notch under tension 24 p3458 A72-44933

IMPACT TESTING MACHINES

Impact fatigue testing apparatus, presenting results for stainless steel 04 p0524 A72-15549

Shock testing machine based on free falling weight striking resilient block, describing design details and electrical circuitry 09 p1292 A72-23472

Vertical drop rig test equipment for measuring shock attenuation of crash helmets, discussing shock absorption criteria for impact protection
11 p1584 A72-26016

High strain rate and thermal instability torsional-impact machines for metal dynamic testing, using shear pin mode control
21 p3039 A72-40229

IMPACT TESTS

NT CHARPY IMPACT TEST

Impact sensitivity of space shuttle materials in liquid and gaseous oxygen at high pressures
01 p0102 A72-10772

High speed tensile impact test for polymers at large loading rate, describing equipment design and test technique
01 p0048 A72-10782

One dimensional elastoplastic wave propagation symposia review emphasizing elastoviscoplastic media, jet penetration into half space and polymer tests by transverse impact
02 p0290 A72-11628

Infinite elastic-plastic beam impact by semiinfinite elastic rod, computing strain-time profiles
04 p0583 A72-14447

Al and steel plate penetration, perforation and fragmentation under hard steel sphere impact at and above ballistic velocities, investigating velocity and strain histories
05 p0672 A72-16115

Split Hopkinson pressure bar for studying material plastic behavior under impact, discussing principles, equipment and test results
06 p0814 A72-17742

Bridge circuit to minimize parasitic electrical disturbances in resistance strain gage measurements of dynamic stresses in impact tests
06 p0819 A72-18672

Al alloy plates and D-nosed specimens indentation and penetration under ball impact test
07 p1086 A72-18764

Photographic observations of W particle clusters high velocity impact against polystyrene, paraffin and W targets for energy dissipation in meteorite impact simulations
08 p1232 A72-21152

Basalt plates craters produced by steel balls, noting profiles at normal and oblique impacts
08 p1232 A72-21153

Axial impact of semiinfinite elastic cylindrical shell filled with inviscid compressible fluid, obtaining equations of motion
08 p1149 A72-21166

Notch length effect on stress concentration in polymethyl methacrylate sample from tensile, impact and bending tests
08 p1196 A72-21867

Micromechanical and impact test investigation of unidirectional fiber composites impact resistance properties, considering longitudinal, transverse and shear modes
11 p1672 A72-25472

Impact tests on anthropomorphic dummies for protection effectiveness evaluation of lap belt, Air Force shoulder harness-lap belt and airbag-lap belt restraints [AD-741530]
12 p1769 A72-27471

Stress-service life relations for duralumin samples from impact and nonimpact tensile tests with cyclic axial loads, noting notch sensitivity
13 p1978 A72-29147

Stress distribution variations and wave propagation in viscoelastic rod of finite length under impact
14 p2163 A72-30191

Notch toughness criteria of metals with S shape transition temperature curve, considering experimental design and impact test model
16 p2406 A72-33322

Forces and strain rates measurement in elastic elements of dynamic systems under impact, discussing test equipment and strain gage transducers
16 p2395 A72-33964

Error analysis of dynamic yield point measurements based on residual deformation from impact tests of Al alloy and steel specimens
16 p2472 A72-34016

Stress pulse attenuation in cloth-laminate quartz phenolic.
17 p2571 A72-35284

Displacements within impact craters.
17 p2549 A72-35686

Energy absorbing characteristics of rigid urethane foams.
20 p2943 A72-38885

Photographic observations of W particle clusters high velocity impact against polystyrene, paraffin and W targets for energy dissipation in meteorite impact simulations
20 p2969 A72-39257

Basalt plates craters produced by high velocity impact of steel spheres, noting profiles at normal and oblique angles
20 p2978 A72-39258

Surface effects during high-speed impact of metals
22 p3188 A72-42163

Metal barrier maximum puncturable thickness dependence on high velocity meteorite particle impact parameters
22 p3234 A72-42217

Impact tests for aid in data interpretation of measured meteor particles impact on spacecraft structures, noting transducer response dependence on impact angle
22 p3234 A72-42218

A re-evaluation of material effects on microbial release from solids.
23 p3253 A72-43383

Mo alloy under impact tests, investigating notch sharpness effects on cold shortness threshold and strength
23 p3301 A72-43756

Cold shortness of 14Kh2NZMA steel
23 p3303 A72-44023

Method for applying a fatigue crack to impact test specimens made from tough materials.
24 p3417 A72-45765

IMPEDANCE

NT ACOUSTIC IMPEDANCE

NT CONTACT RESISTANCE

NT ELECTRICAL IMPEDANCE

NT ELECTRICAL RESISTANCE

NT LC CIRCUITS

NT MECHANICAL IMPEDANCE

NT REACTANCE

NT RESPIRATORY IMPEDANCE

NT SKIN RESISTANCE

Spectral characteristics of the scattering field of a uniformly traveling and rotating impedance cylinder
23 p3265 A72-44202

IMPEDANCE MATCHING

Planar Gunn effect devices for microwave oscillators, discussing impedance matching and diode conductivity profile effect on output power
01 p0028 A72-10628

Parallel longitudinal resonant slots in rectangular waveguide broad wall, determining mutual impedance from magnetic field reaction
02 p0173 A72-12109

Fast Fourier transforms for digital matched filters in wideband radars, using computer simulation for word size and dynamic range relationship determination
02 p0188 A72-12398

Ring loaded corrugated waveguide for improved frequency broadbanding and transformer matching in horn antenna systems for satellite communication ground stations
04 p0498 A72-14721

Waveguide radiators linear phased array impedance matching during E-plane wide angle scanning improved by reflection coefficient variation compensation
04 p0499 A72-15239

Wideband tunnel diode microwave amplifier design with coaxial line, considering band-edge stability and impedance matching
06 p0785 A72-18310

Low induction 500-kV 1-microsecond 5-kJ pulsed voltage generator, discussing design features
07 p0946 A72-19958

Impedance strip synthesis on symmetric cylindrical antenna excited by phased magnetic flux ring, determining radiation pattern for pure reactance conditions
08 p1131 A72-20932

Noise factor formula of antenna matched multiple loop radio receiver input network with series connected coupled stages
11 p1598 A72-26732

Matching two port network synthesis for prescribed damping poles and impedances
12 p1794 A72-27573

Iterative method for synthesis of reflector antenna array of dipole elements to provide given radiation pattern, obtaining impedance matching values
13 p1926 A72-28372

Quasi-static and full wave calculation of VLF/ELF input impedance of arbitrarily oriented loop antenna in cold collisionless multicomponent magnetoplasma
13 p2009 A72-28542

Conditions derived for reactive two-terminal-pair matching transformer networks operation at maximum power transfer efficiency
14 p2087 A72-30334

Lossless low pass ladder network synthesis in terms of reflection coefficient poles and zeros with application to bandpass matching problem
15 p2212 A72-32248

Input match conditions for broadband mixer conversion loss minimization, comparing optimization procedures
15 p2208 A72-32392

Log periodic dipole antenna input impedance and gain characteristics derivation via periodically loaded line theory and Poynting vector method, discussing separation angle effect
15 p2208 A72-32473

Theoretical model for computer calculation of transients in oscillator consisting of nonlinear amplifier with feedback through sequence of matched LC circuits
16 p2371 A72-33280

A broad-band wide-angle scan matching technique for large environmentally restricted phased arrays.
17 p2513 A72-34353

Computer aided impedance matching of an interleaved waveguide phased array.
17 p2525 A72-34373

End line matching for high gain traveling wave amplifier constructed from heterogeneous transmission line sections with negative resistance
18 p2665 A72-36110

Frequency response optimization of electric filters, modulators and impedance matching circuits using minimax criterion, noting nonlinear programming sequence
19 p2771 A72-37310

Admissible changes in the parameters of a matching four-terminal network
19 p2772 A72-37315

The effects of transmitter source and load impedance on harmonic output spectrum - A new measurement method.
20 p2921 A72-38996

Synthesis of passive matching two-ports with given apparent resistances. III
20 p2907 A72-39424

High speed logic circuit interconnecting transmission line matching by nonlinear resistance, recommending use of Schottky diodes
20 p2909 A72-39737

Flash lamp optimal operating parameters determination by impedance matching to driving circuit and spectral matching to material of optically pumped solid state pulsed lasers
21 p3061 A72-40204

Microstrip matching networks synthesis for microwave integrated circuits, calculating passband of configurations with lumped and distributed elements
23 p3269 A72-43445

Application of logarithmic characteristics to calculate wideband load matching of an oscillator
23 p3271 A72-43836

IMPEDANCE MEASUREMENTS

Acoustic impedance of body surface at thorax and at abdomen, showing dependence on frequency and body pressure and position
01 p0021 A72-11195

Antenna lf impedance measurements of lower terrestrial plasma wave characteristics, using equivalent impedance probe circuit
02 p0172 A72-11946

Impedance determination for symmetrical spherical probes and spacecraft housing with flat screen separation, using partial capacitance formula
05 p0662 A72-16268

Characteristic impedance formulas for rectangular waveguides with dielectric slab, discussing interference filter design application
05 p0627 A72-16343

Microwave lumped element impedance measurements from 1 to 12 GHz by resonant transmission line frequency and Q perturbation technique
05 p0637 A72-16419

Small array technique for active impedance amplitude and phase measurement of large phased arrays
06 p0782 A72-17361

Dipolar rf probe admittance measurements in simulated ionosphere for satellite plasma experiments
06 p0811 A72-18733

Electrochemical tests, noting electric potential, current and electrode impedance measurements for corrosion rate and oxidizing power evaluation
08 p1189 A72-22105

Horn antenna synthesis for determining impedance boundary conditions at walls for aperture field distribution
09 p1285 A72-22574

Two fluid MHD model for flat plasma condenser in crossed magnetic and alternating electric fields, calculating impedance and disturbed plasma parameters
09 p1360 A72-22953

MOSFET for input impedance measuring amplifier, discussing input stage temperature drift and protection from overvoltage
10 p1482 A72-24599

Flectra method of plasma diagnosis around reentry vehicle head, describing onboard antennas impedance measurements and use of triple Langmuir probe mounted on telescopic mast
10 p1552 A72-24659

Electromagnetic properties of semiconductor diffusion films, using impedance measurements
11 p1700 A72-25779

Quasi-linear approximation of input impedance of epitaxial n-type Si unijunction transistors for predominant drift conditions
13 p1927 A72-28406

Antenna LF impedance measurements of lower terrestrial plasma wave characteristics, using equivalent impedance probe circuit
13 p1920 A72-29258

Human hand-arm system vibration characteristics, describing mechanical impedance measurements for mathematical modeling
13 p1910 A72-29559

- Human body or dummy mechanical impedance calculation by acceleration measurement at two point reference system with circular spring supporting mass
15 p2192 A72-32608
- Signal analyzer for LF real time measurement of mechanical impedance by Fourier integral analysis
15 p2215 A72-32628
- Computer calculations of horizontal linear antenna impedance for multilayer plane stratified medium, using induced emf method
16 p2368 A72-33492
- Liquid propellant rocket engines three dimensional nozzle admittance determination by impedance tube method from pressure distribution measurement, taking into account nozzle geometry effect
[AIAA PAPER 72-666]
16 p2443 A72-34071
- New measurement method of Gunn-diode impedance.
17 p2529 A72-35000
- Two fluid MHD model for flat plasma condenser in crossed magnetic and alternating electric fields, calculating impedance and disturbed plasma parameters
17 p2593 A72-35882
- Novel and accurate methods for measuring small-signal and large-signal impedances of IMPATT diodes.
18 p2664 A72-35997
- Measurement of specific mechanical impedance of the skin - Effects of static force, site of stimulation, area of probe, and presence of a surround.
21 p3005 A72-40347
- Impedance of a partially ionized cesium plasma.
21 p3091 A72-40694
- Admittance measurements of a 36-m dipole antenna in the topside ionosphere.
22 p3153 A72-42007
- Linear system proper frequencies and vibration dampings obtained by mathematical smoothing of mechanical admittance measurements
22 p3241 A72-43093
- Frequency dependent antenna impedance characteristics in ionospheric plasma, discussing anisotropic and isotropic electron plasmas, loop antennas, resonance rectification and ion effects
23 p3319 A72-43512
- Useful range of a mechanical impedance technique for measurement of dynamic properties of materials.
23 p3294 A72-44126
- Synthesis of horn antenna with impedance boundary conditions on walls and specified aperture field distribution
24 p3384 A72-44753
- IMPEDANCE PROBES**
NT RADIO FREQUENCY IMPEDANCE PROBES
- IMPELLER BLADES**
U ROTOR BLADES [TURBOMACHINERY]
- IMPELLERS**
NT PUMP IMPELLERS
- Centrifugal compressor diagonal type impeller profiling through ruled surfaces delineated by rectilinear generatrices, calculating velocity field of rotating cascade
05 p0603 A72-16626
- Stress analysis of radial flow impeller disk due to centrifugal force in steady state of high speed rotation by matrix finite element method
05 p0741 A72-16996
- Centrifugal impeller slip factor prediction from three dimensional flow influences, discussing fluid passage guidance, flow separation, eddy and viscous effects
05 p0610 A72-17247
- Pressure measurement between compressor impeller blades during steady and transient operation, discussing system circuit diagram
13 p1957 A72-29139
- Cylindrical pitot tube displacement effects on stagnation point and static pressure angle in impeller nonuniform peripheral flow
14 p2094 A72-30720
- Investigations on the stability of the characteristic of radial flow fans.
24 p3363 A72-45356
- Prediction of velocity profiles for turbulent boundary layers on the blading of radial impellers.
24 p3393 A72-45360
- Study of a viscous flow in rotating centrifugal impellers.
24 p3363 A72-45368
- Flow analysis in the axial-flow compressor impeller with meridional stream acceleration.
24 p3394 A72-45371
- IMPERFECTIONS**
U DEFECTS
- IMPERMEABILITY**
U PERMEABILITY
- IMPINGEMENT**
NT JET IMPINGEMENT
- IMPLANTATION**
Electrocardiography telemetry system for intense radiation environment, describing electrode and transmitter implantation in monkey and heart signal transmission and reception
05 p0623 A72-16678

- Cerebro-spinal fluid pressure remote monitoring by intracranially implanted radio pressure transducers, describing receiver-detector-recorder system
07 p0930 A72-19911
- Electrode design and implantation method for chronic experiments, discussing information loss factor elimination
14 p2078 A72-30393
- Implantable blood pressure telemetry system.
19 p2762 A72-38824
- Use of implantable telemetry systems for study of cardiovascular phenomena.
23 p3260 A72-43996
- Experimental development of a method for long-term implantation of plastic catheters in different sections of the cardiovascular system
24 p3375 A72-45118

IMPLEMENTATION U PERFORMANCE IMPLSIONS

- Plasma layer implosion in theta pinch, deriving modified snow plov equations from MHD equations
04 p0556 A72-14855
- Combined plasma and magnetic field cumulation due to heavy conducting liner implosion, noting compression parameters for plane and cylindrical bodies
10 p1523 A72-24723
- Electromagnetic plane field cumulation by heavy conducting shells implosion with quasi-relativistic velocity, solving Maxwell equations by characteristics method
12 p1851 A72-27396
- Thermonuclear detonation and reimplosion of dense stellar cores, studying beta-processes effect on post-detonation evolution
13 p2044 A72-29625
- Diatomic molecular vibrational excitation and dissociation effects on imploding shock waves, comparing shock tube data to prediction
15 p2192 A72-32148
- Imploding spherical and cylindrical shocks, considering rear flow field with nonadiabatic isothermal flow and zero temperature gradient
16 p2376 A72-33009
- Performance and limitations of shock tubes with imploding detonation drivers.
21 p3128 A72-40767

IMPREGNATING

- Continuous woven fabric or roving filament reinforced thermoplastics production, discussing polymer binder systems, coupling agents, impregnation technique, processing parameters and equipment
12 p1815 A72-28083
- Investigations into the impregnating behaviour of various reinforcing materials in the filament winding process.
19 p2808 A72-38171
- Physical, mechanical and thermal characteristics of reimpregnated pyrolyzed carbon-carbon and graphite-graphite composites
[ICAS PAPER 72-29]
21 p3073 A72-41154
- IMPULSE NOISE**
U ELECTROMAGNETIC NOISE
- IMPULSE TRANSFER ORBITS**
U TRANSFER ORBITS
- IMPULSES**
Dynamic systems stability under periodic impulsive parametric excitation, deriving simple closed-form analytic stability criteria for special cases from general theory
[ASME PAPER 71-WA/APM-19]
05 p0733 A72-15961
- Impulse motion convergence in game theory, considering control problems of pursuit involving escape and capture
05 p0690 A72-16583
- Impulse and kinetic momentum equations for dynamics of variable mass solid using mechanical model
12 p1846 A72-2/543
- Approximate calculation of the magnitude of the momentum during the passage of a material particle past an elongated homogeneous biaxial ellipsoid
17 p2618 A72-35812
- Impulse motion encounter in game theory, considering control problems of pursuit involving escape and capture
19 p2825 A72-37554
- Internal to total energy relation dependence on deformation time in impulsive loading of homogeneous free rod, noting energy conversion efficiency
23 p3344 A72-43338

- IMPURITIES**
Impurity, surrounding gas and pressure effects on organic semiconducting material electrical conductivity, discussing carrier origin and number, and measurement techniques
01 p0113 A72-10125
- Impurity-related color centers and electron-hole traps in quartz by electron spin resonance and thermoluminescence observations
02 p0207 A72-11598

- Impurities effects on crack initiation and propagation in polymethyl methacrylate under laser pulsed radiation
02 p0250 A72-12689
- Impurity diffusion of Ag, Cd, In, Sn and Sb in magnesium single crystals, observing valence effect on activation energy
03 p0378 A72-14254
- Metal-insulator-metal tunneling junction, calculating effect of localized impurity states in barrier on tunneling current
03 p0404 A72-14267
- Periodic lattice one-electron Green function calculation based on pseudopotential matrix element, applying to impurity levels in semiconductors
03 p0404 A72-14268
- Deep seated substitutional acceptor impurity levels in semiconductors
04 p0561 A72-15076
- Radiation intensity and losses in semiconductor hydrogen plasma containing bare nuclei and hydrogen-, helium-, lithium- and beryllium-like ions as impurities
04 p0557 A72-15170
- Fe group transition metal impurities in semiconductors, calculating ground state wave functions and photoionization cross section dependence on wavelength
04 p0563 A72-15473
- Preferential concentration of impurities and alloying elements at grain boundaries, noting role of equilibrium type interfacial segregation in intergranular corrosion
04 p0535 A72-15734
- Ordinary and macroporous structured polycondensation oxidation-reduction polymers synthesis, discussing application to organic impurities removal from atmospheric moisture condensates
05 p0622 A72-16645
- Screened impurity scattering determination in heavily doped covalent semiconductors from Hall mobility and thermoelectric power measurements
05 p0702 A72-17073
- Localized vibration modes of light impurities in gallium phosphide crystals from absorption spectrum analysis
06 p0866 A72-18182
- Plastic deformation and elastic stiffness of refractory metals, discussing impurities, alloying, temperature, work hardening, strain rate and texture effects
06 p0822 A72-18519
- Impurity content, particle size and abrasion resistance role in abrasiveness of molybdenum disulfide
06 p0836 A72-18589
- Hf-B system alloys phase diagram and impurities effect, discussing synthesis and heat treatment regime
07 p1010 A72-18857
- Electrons and ionized impurities interaction in thin quantizing layers, discussing donor activation energy and kinetic characteristics
07 p1048 A72-19640
- Impurities and crystal lattice role in metal brittleness, discussing stress concentration and relaxation, crack initiation and plastic deformation
07 p1018 A72-20145
- Ultracure metals microimpurities determination from crystal lattice and atomic properties, comparing spectral analysis activation, mass spectrometric, thermophysical, recrystallization and kinetic methods
07 p1049 A72-20149
- Pressure effects on molten metals reactions with ambient atmosphere during purification by distillation, obtaining impurities concentration ratio via Langmuir relative volatility rule
07 p0997 A72-20287
- Purity requirements of aircraft gas turbine fuels, considering mechanical impurities, water, microorganisms, and surface active, corrosive, resinlike and paraffin substances
07 p1052 A72-20373
- Drift waves propagation in ionized plasma, considering drift rate, ion sound phase velocity and effect of impurities
07 p1045 A72-20444
- Temperature dependence of strain rate sensitivity in low temperature deformation processes, considering inherent lattice conditions and impurity atoms effects
07 p1022 A72-20573
- Reverse biased p-n diffused junction design with two impurities in nonhomogeneous semiconductors, calculating depleted space charge region thickness
08 p1140 A72-21062
- One dimensional model for drift transistor at low injection level with minority carrier mobility dependence on impurity concentration
08 p1140 A72-21063
- Multiphonon capture of charge carriers by deep impurity centers in homopolar semiconductors from generalized Lucovsky model
08 p1216 A72-21094
- Optical properties changes of Al alloys containing impurities, noting band structure modification and tendency toward free electron response
08 p1186 A72-21593

- Impurities and temperature effects on microdeformation of Mo single crystals under dynamic loads
08 p1188 A72-21789
- Small impurity amounts effect on packing defect density and deformation energy in Ni
08 p1188 A72-21791
- Electron and hole recombination at deep impurity centers during nonequilibrium current carriers excitation by Nd-glass laser light in p- and n-type germanium
09 p1322 A72-22214
- Cold shortness of W and related refractory metals, noting oxide phases and impurities effects on mechanical properties temperature dependence
09 p1326 A72-22226
- Impurities effect on Mo plastic properties and toughness, suggesting lower vacuum arc welding rates and increased electron beam zone refining runs
09 p1326 A72-22228
- Alumina microstructure, grain size and impurities effects on ballistic performance, discussing results in terms of microplasticity
09 p1334 A72-22390
- Spin excitation effects in superconductors, noting impurity concentration effects on transition temperature and thermodynamic properties
09 p1368 A72-22558
- Mossbauer lines diffusion broadening and weakening in crystals impurity atoms nuclear spectra
09 p1371 A72-23030
- Impurities effects on stress corrosion and work hardening induced dislocation structures in stainless steels, considering stacking fault energy relationship
10 p1496 A72-24231
- Impurities effect on level density of electron gas within strong magnetic field, discussing included self energy
11 p1693 A72-25526
- Impurity atoms effects on grain boundary motion velocity, considering interactions with metal lattice vacancies
11 p1662 A72-26655
- Nb-Ti alloy elasticity modulus temperature dependence, considering foreign atoms interactions with dislocations
11 p1662 A72-26737
- Impurity centers formation and development in AgBr/I photographic emulsion under ultrasonic irradiation
11 p1636 A72-26794
- Laser pulse heating of plasma, predicting efficiency enhancement by addition of heavy element impurities or deuterides to solid target surface
12 p1852 A72-27621
- Synthetic diamond single crystals, investigating impurities and inclusions effects on ferromagnetic properties and heat resistance
12 p1833 A72-27768
- Recombination luminescence in irradiated Si, investigating thermal annealing and Li impurity effects
12 p1858 A72-28062
- Varactor broken voltage-capacitance curve due to uncompensated impurities concentration change at p-n junction
13 p1926 A72-28379
- Impurities effect on platinum resistance thermometers temperature reading accuracy, presenting empirical formula for approximate error estimate as function of operational conditions
13 p1960 A72-29906
- Binary ordering alloys with fcc lattice, studying volume effects on solubility of impurity atoms in interstices
13 p2023 A72-29907
- Spectral analysis for Cu, Cl, Br and I impurity distribution in doped bismuth telluride crystals prepared by Bridgeman method
13 p2023 A72-29979
- Rare earth metals interactions with V, Nb and Mo alloys, describing procedures for interstitial impurities removal
15 p2252 A72-31190
- Interferometric investigation of impurities effects on electron density distribution in ionization-relaxation zone behind shock waves in monatomic gas
15 p2215 A72-31213
- Superconducting to normal transition field as function of temperature for Ta with thin surface layer variable density impurities
15 p2293 A72-32241
- Two band model explanation of Hall effect in dirty type-II transition metal superconductors near upper critical field, noting interband impurity scattering role
15 p2295 A72-32542
- Paramagnetic phase induced moment system containing substitutional impurities, calculating mode energies by Green function method in random phase approximation
15 p2295 A72-32546
- Precursor ionization upstream from shock wave due to shock emitted radiation absorption by easily ionizable impurity species
16 p2379 A72-33512
- Impurities and additives effects on electrode properties in Cs vapor thermionic converter, noting coadsorption model for Cs-W-O surface
17 p2496 A72-34598
- Impurity effects in carbon fibres.
17 p2569 A72-34667
- Comparison of infrared and activation analysis results in determining the oxygen and carbon content in silicon.
17 p2511 A72-35330
- Impurity controlled deformation mechanism for softening control of interstitial bcc alloys, discussing low temperature and composition effects
18 p2699 A72-36341
- Ways of reducing porosity in argon-arc welding of thin titanium sheets.
18 p2695 A72-36428
- Propagation of an impurity in a laminar flow in a circular tube
18 p2682 A72-36892
- An investigation of impurities segregation to the /001/ nickel surface during thermal treatment - Work function changes and Auger electron spectroscopy using the LEED camera.
18 p2720 A72-37022
- Concentration dependences and equilibrium values of the impurity distribution coefficients in bismuth telluride
19 p2845 A72-38177
- Influence of impurities on the high-temperature electrical conductivity of CdTe crystals
19 p2847 A72-38677
- Fluorescence of anthracene single crystals whose surface is disturbed by an impurity
19 p2847 A72-38781
- Boron p-type region impurity concentration calculation technique to establish anomalous base profile in n-p-n bipolar transistors
20 p2908 A72-39567
- Effects of impurities on gamma-irradiated silicon crystal examined by photovoltaic effect of p-n junction diode.
21 p3097 A72-40693
- Measurement of substrate impurity profile of MIS field-effect transistors.
21 p3035 A72-41488
- Electromechanical, photomechanical and concentration effects of impurities in semiconductors
21 p3098 A72-41677
- Alloying and impurity effects on mechanical and recrystallization properties of Ta obtained by arc, electron beam and zone melting
22 p3191 A72-42809
- Phase compositions, impurity effects, crystallization and production of plastic W and Mo alloys and heat resistant W-based alloys
22 p3192 A72-42815
- Thermal conductivity in the two-band model of superconducting transition metals containing nonmagnetic impurities.
23 p3323 A72-43274
- Model of degenerate semiconductor near semiconducting phase transformation, noting superconducting state at low temperatures with corresponding impurity concentrations
23 p3323 A72-43317
- Static and dynamic characteristics of double-injection currents in p⁺-n-n⁺ diode structures with deep impurities and nonideally injecting junctions
23 p3268 A72-43346
- IN-FLIGHT MONITORING**
In-flight warning meter for solar and cosmic radiation dose equivalent measurements for radiological protection in SST aircraft
[CERN-71-16]
02 p0274 A72-12078
- Shock hardened delayed transmission pulse code modulated system for artillery projectile instrumentation with in-barrel and in-flight monitoring capability
02 p0175 A72-12155
- Soviet book on in-flight studies of aircraft stability and controllability covering dynamic characteristics, measurements, balancing curves, aerodynamic forces and limiting and special flight regimes
02 p0155 A72-12542
- Aircraft in-flight monitoring instruments for meteorological service in U.S.
04 p0464 A72-14687
- Bayesian analysis of onboard computer controlled aircraft avionics subsystem built-in test for failure detection
05 p0638 A72-16574
- Incipient wing stall detection by unsteady pressure monitoring via flush-mounted microphones, discussing flow patterns on models
07 p0908 A72-19093
- DC-10 aircraft automatic landing performance and failure assessment monitor system
08 p1204 A72-21003
- Automation in planning and execution of flights, considering navigation, communication, flight instruments monitoring, control/stabilization and warning systems
09 p1269 A72-22780
- Pulse operated multichannel annunciator system for pilot warning of aircraft systems malfunctions, describing circuit design
[SAE PAPER 720333]
11 p1630 A72-25593
- Nose installed thermistor device for in-flight monitoring of pilot respiration and pulse rate
12 p1769 A72-27417
- Clear line-of-sight probabilities for atmosphere from whole sky photos, visual cloud cover, sunshine recorder traces, satellite and in-flight observations
13 p1989 A72-28809
- Space Shuttle Orbiter onboard ultrasonic system for structural integrity tests and assessment, noting limitation factors due to configuration and vehicle launch noise effects
15 p2256 A72-31698
- Avionics effects on airline operations timekeeping, considering gains due to all-weather capability and engine monitoring vs possible losses due to equipment failures
15 p2208 A72-32461
- The use of airborne magnetic tape recorders for fatigue life monitoring.
17 p2553 A72-34812
- Engine condition monitoring - The Pan Am approach: Phase II.
17 p2597 A72-35324
- Determination of the radiation characteristics of aircraft antennas in flight
21 p3030 A72-40534
- A large viewfield laser photographic system for in-flight model contour measurements in an aeroballistic range.
22 p3179 A72-42679
- In-flight and flight-line monitor system to detect foreign object damage in jet engines.
22 p3179 A72-42690
- Variable impedance transducer measuring instruments for in-flight aircraft performance tests under environmental thermal effects
22 p3180 A72-42711
- OFO A orbital flight recording of bullfrog vestibular gravity sensor nerve fiber pulses for assessing necessity of artificial gravity during prolonged weightlessness
23 p3254 A72-43391
- IN-FLIGHT THRUST MEASUREMENT**
U IN-FLIGHT MONITORING
U THRUST MEASUREMENT
- INACTIVATION**
U DEACTIVATION
- INCANDESCENCE**
Ignition of a mixture of ammonium perchlorate and starch by incandescent wires
19 p2847 A72-37367
- INCENTIVE TECHNIQUES**
Multiple performance parameters related to single incentive scale for contract management
04 p0598 A72-15225
- Incentive contracts with price differential acceptance test plans to motivate producer to product improvement, defining admissible strategies in terms of risk limitation
13 p2066 A72-28354
- Estimation, confidence intervals, and incentive plans for sequential three way decision procedures.
24 p3406 A72-44667
- INCIDENT RADIATION**
Reflector antennas with very high front-to-back ratio - Theory and experiments on models.
01 p0029 A72-10673
- Multiple scattering of incident coherent light wave propagating in turbulent medium, considering irradiance intensity fluctuations and spectral and correlation characteristics
01 p0103 A72-11167
- Radar target thin rectangular plate model backscattering from incident and reflected waves, noting front and trailing edge phenomena with emphasis on side edge contribution
01 p0032 A72-11250
- Diffraction of plane electromagnetic waves of arbitrary orientation and incidence on triangular grid of cylindrical conductors
02 p0183 A72-12753
- Radiation pattern and reflected field analysis for incident plane wave on phased arrays of thick wall rectangular waveguides
03 p0330 A72-13168
- Electrostatic field excitation in plasma layer by plane transverse electromagnetic wave as function of incident angle
06 p0862 A72-18339
- Electromagnetic field around thin linear receiving antenna by superposition of incident wave with antenna scattered field, deriving differential equations solution for field lines
08 p1132 A72-21327
- Radio signal attenuation by thin overdense plasma boundary layer on reentry body as function of incident power
08 p1135 A72-21624
- Scattering computations of albedo reflectance for model media as function of incidence angle
09 p1299 A72-22808

Electromagnetic wave scattering by arbitrarily oriented circular ice cylinders, deriving far field intensities for linearly polarized incident waves

09 p1280 A72-23341

Current distribution approximation for toroidal antennas of small cross section under incident electromagnetic excitation

10 p1453 A72-25104

Specular components of thermal reflectance as function of directional incident intensity variations

11 p1746 A72-25993

Field distribution and absorption coefficient calculations for normal incidence of extraordinary electromagnetic wave on linear plasma layer in hybrid resonance region

16 p2363 A72-33480

Plane electromagnetic waves diffraction at arbitrary orientation and incidence on triangular grid of cylindrical conductors

20 p2902 A72-39059

Reflection coefficient method of remote probing for inhomogeneous media, using plane wave incidence angle dependence

20 p2927 A72-39719

Absorption of an obliquely incident extraordinary wave in a weakly inhomogeneous plasma in the hybrid resonance region

21 p3095 A72-41694

The diffraction of light by progressive supersonic waves: Oblique incidence of light. I - Approximate solution of the Raman-Nath equations.

22 p3207 A72-42852

Calculation of the solar radiation incident on an inclined ribbed surface

22 p3140 A72-43194

Analytic ray trajectory model of radio wave lateral incidence on traveling large scale ionospheric inhomogeneities as function of location and azimuthal angle departure

23 p3263 A72-43377

Influence of the polarization of incident radiation on the distribution of the energy absorbed in a particle

24 p3424 A72-44621

INCINERATION

U INCINERATORS

INCINERATORS

Dry incineration of wastes for aerospace waste management systems.

[ASME PAPER 72-ENAV-2] 20 p2896 A72-39175

INCLINATION

Geomagnetic field extrapolated spherical data for years 1600 to 1800 from declination and inclination analysis, giving Gaussian coefficients and errors

02 p0218 A72-11953

Inner magnetosheath hydromagnetic disturbances, presenting magnetometer data in inclination-declination coordinate system

03 p0348 A72-13510

Geomagnetic field extrapolated spherical data for years 1600 to 1800 from declination and inclination analysis, giving Gaussian coefficients and errors

13 p1949 A72-29265

INCLUSIONS

Porosity and W inclusions effects on Al alloy weld strength, presenting radiographic and tensile test data

01 p0074 A72-10282

Finite stretching of isotropic incompressible annular plate with inner edge rigid inclusion, noting edge zone thickness variation due to transverse normal strain

02 p0296 A72-12528

Metal ductile facies fracture study of cups formation from cracks by cleavage, noting roles of dislocations and inclusions

02 p0246 A72-12600

Steel cleanliness conditions for formation and decantation of inclusions due to deoxidation during production up to solidification

03 p0371 A72-13198

Steel castings made in electric furnace with Al additive, observing magnesium and lime aluminates inclusions

03 p0371 A72-13199

Asymptotic methods for complex mixed problems of elasticity related to stress concentration in plates with cracks or inclusions

03 p0449 A72-14102

Martensite and solid Cr-containing inclusion effects on wear resistance of cermet steel during dry friction with R18 steel

05 p0665 A72-16095

Isotropic continuum model of elastic interaction of edge and screw dislocation with nearby inclusion

06 p0894 A72-17492

Fine oxide particle inclusions in mild steel weld metal deposited by carbon dioxide shielded metal arc process, using electron micrography and diffraction pattern photography

06 p0820 A72-17706

Fluid inclusions in quartz crystals from calcite in Precambrian metasedimentary rocks in South-West Africa

07 p0975 A72-18907

Micrographic evaluation of inclusions in austenitic stainless steel tubes ensuring surface quality control

07 p0994 A72-18972

Physicomechanical properties of steel with oxide, sulfide, silicon, phosphorus and mixed metal-non-metal inclusions

07 p1022 A72-20618

Mechanical properties anisotropy in heat resistant Ni alloys due to strengthening phase nonmetallic inclusions distribution, suggesting purification by vacuum melting

09 p1327 A72-22231

Stress intensity factor of crack near inclusion in infinite elastic plane, using numerical methods

09 p1398 A72-22531

Plane elastostatic problem of stress concentration near flat interface inclusion in bonded dissimilar materials

09 p1405 A72-22997

Iron base powders material requirements and forging processes, discussing powder composition, inclusions effect and preform densification

11 p1639 A72-26241

Carbon and other inclusions effects on cast W strength at elevated temperatures from microscopic observation

11 p1666 A72-26877

Harmonic equation for antipane shear deformation of elastic composite materials with multiple circular inclusions

12 p1883 A72-27562

Synthetic diamond single crystals, investigating impurities and inclusions effects on ferromagnetic properties and heat resistance

12 p1833 A72-27768

Xenolithic origin for silicate inclusions in anatase of Landes meteorite from West Virginia

13 p2036 A72-28753

Oxide inclusions induced reductions in Nabarro-Herring creep and sintering rates of metals, discussing effect of inclusions diffusional mobility in metal matrix

15 p2257 A72-32112

High strength fine grain structural steels fracture characteristics from notch-bar impact and tensile tests, determining inclusions effect on mechanical properties

16 p2406 A72-33236

Grain orientation and nonmetallic inclusion distribution and identification by color etching of single crystal and polycrystalline Mo

16 p2407 A72-33532

Rotating disk with eccentric elliptic insert determining elastic field in inclusion by complex variable technique

16 p2427 A72-33790

Photoelastic study of stress concentration in rectangular panels with inlets.

18 p2734 A72-36376

Stresses in a perforated, continuously loaded cantilever beam.

21 p3117 A72-40453

The effect of couple-stresses on stress concentration of a ring inclusion.

21 p3117 A72-40681

Study of the composition of inclusions in synthetic diamond crystals by the local analysis method

22 p3196 A72-42155

Stress distribution at defects in the form of rigid sharply-angled inclusions

23 p3349 A72-43952

The stress distribution near the tip of an array of screw dislocations piled-up against an inclusion.

24 p3460 A72-45694

INCOHERENCE

Incoherently light radiating object and background light focusing on photosensitive mosaic, observing linear restoration by comparison of mean square error with Wiener filter theory

09 p1350 A72-22611

Conditions for space invariance in optical data processors used with coherent or noncoherent light.

23 p3288 A72-43887

INCOHERENT SCATTERING

Log normal random fluctuations of ionospheric electron concentration in F region from vertical sounding and incoherent scatter data

01 p0059 A72-10609

Autocorrelation functions of topside incoherent scatter data, using computerized least square gradient search

02 p0220 A72-12454

Hydrogen density and proton flux in topside ionosphere over Arecibo from incoherent scatter observations

02 p0274 A72-12455

Boundary effects on light incoherent scattering by dispersing molecules, using quantum statistics

04 p0490 A72-15398

Oxygen ions vertical flux altitude distribution in F layer from incoherent scatter radar measurements, noting existence in protonosphere during daytime

[AD-737929] 05 p0629 A72-16616

Ionospheric movements measured by frequency spectra of signals incoherently scattered by ionospheric electrons

[AD-738717] 06 p0808 A72-18085

Photoelectron flux measurement of intensities of plasma lines in radar incoherent scatter spectrum by uhf radar

06 p0874 A72-18732

Horizontal neutral winds meridional component from incoherent scatter measurements of F region ionization drifts, noting diurnal variations

08 p1156 A72-21098

Antenna near field correction for backscatter gain in two-beam incoherent scatter radar measurements at Arecibo Observatory

08 p1137 A72-21983

E region ion density and composition determination by incoherent scatter radar measurement

[AD-742618] 09 p1375 A72-22365

D and E regions electron densities measurement by incoherent scattering technique, noting sporadic E layer and echoes

[AD-742616] 09 p1376 A72-22371

HF radio waves induced incoherent scatter spectrum enhancement, noting parametric instabilities in ionosphere

09 p1279 A72-23014

Simultaneous measurements of ionospheric electrons number vertical distribution by incoherent ground radio wave scattering and coherent signals from Intercosmos 2 and Cosmos 321 satellites

11 p1628 A72-26918

E and F regions plasma horizontal drift measurements by oblique incidence incoherent scatter radar system, suggesting solar semidiurnal tidal oscillation dynamo action

13 p2031 A72-29386

Atmospheric oxygen concentration latitudinal and diurnal variations from incoherent scatter and satellite drag data, noting compatibility with Jacchia model

13 p1951 A72-29389

Noncoherent isotropic scattering in plane parallel finite layer, considering Doppler line broadening

15 p2273 A72-31331

Monostatic radar measurement for incoherent scatter correlation function in lower ionosphere, using spaced short pulses transmission to obtain adequate height resolution

15 p2200 A72-32106

Ionospheric ion temperatures and velocities and electron and neutral densities from incoherent scatter observations during 11 February 1969 magnetic storm

15 p2229 A72-32254

Spread F association with ionospheric tilts due to total electron content drift, using incoherent scatter radar

15 p2230 A72-32261

Phenomenological model for incoherent microwave scatter attenuation from turbulent plasma, establishing relation between plasma parameters and attenuation coefficient

17 p2517 A72-35622

Chatanika, Alaska, auroral-zone incoherent-scatter facility.

18 p2674 A72-36297

Incoherent scatter observations at Arecibo using compressed pulses.

18 p2659 A72-36299

The incoherent scattering of radiation from a high temperature plasma.

19 p2842 A72-38523

Direct measurements of plasma drift velocities at high magnetic latitudes.

19 p2793 A72-38757

Incoherent radiation imaging system analysis from detector-display characteristics, target response function and noise characteristics

20 p2922 A72-39044

Backscatter from gated fluctuating regions - A Bremmer series approach.

21 p3015 A72-40361

Noncoherent scattering probabilistic formulation in terms of mean intensity averaged over absorption profile and mean scatterings number required for photon escape

22 p3206 A72-42559

Coherent/incoherent elastic/inelastic neutron scattering in amorphous solids, presenting neutron intensity and correlation functions

22 p3206 A72-42799

Faraday effect of incoherently scattered radar signals

23 p3263 A72-43365

Evaluation of the performance of an ionospheric sounder with incoherent scatter

24 p3381 A72-45768

INCOMPRESSIBILITY

Elastic incompressible isotropic transparent media, deriving photoelastic effect relationship to stress function

01 p0089 A72-10123

Variational principles for elasticity theory problem of three dimensional linearly elastic incompressible anisotropic body with highly elastic deformations

05 p0741 A72-17143

Large deformations of incompressible isotropic materials with parabolic stress-strain relations, deriving constitutive equation from strain energy function

06 p0848 A72-17919

- Strain hardening law for rigid incompressible material with plastic properties independent of mean normal stress 08 p1248 A72-21820
- Plane unstable deformation and stability loss of incompressible laminated composites under highly elastic strains 12 p1880 A72-27229
- Variational principles for linearized dynamic and static problems of elastic incompressible bodies for highly elastic initial deformations 13 p2059 A72-29499
- Strain energy method for finite deformation of solid and tubular cylinders of incompressible isotropic elastic material, noting torsional and tensile tests on natural rubber 16 p2468 A72-33198
- Incompressible continuous media three dimensional boundary problems solution by pure shear state analysis, discussing application to plasticity theory 23 p3314 A72-44222
- INCOMPRESSIBLE FLOW**
- NT. STOKES FLOW**
- Simplified Marker and Cell method extension for numerical solution of almost three dimensional incompressible flow and internal obstacle treatment 01 p0049 A72-10228
- Equivalence laws and approximate equations for incompressible and compressible viscous flows in pipes with variable cross sections 01 p0051 A72-11256
- Book on pressure probe methods for wind speed and direction covering incompressible and subsonic compressible flow pressures, temperature, etc 01 p0072 A72-11273
- Incompressible nonself similar turbulent and transitional flows numerical analysis in wakes, jets and boundary layers, using turbulent viscosity equations 02 p0202 A72-11587
- Flat plate incompressible smooth surface boundary layer examination emphasizing turbulence production near wall, using hydrogen-bubble and hot-wire measurements with dye visualization 02 p0203 A72-11975
- Incompressible boundary layer theory development to include second order curvature effects, determining suction velocity to maintain constant displacement thickness on sphere 02 p0204 A72-12104
- Electrohydrodynamic ideal incompressible fluid flow in flat and circular channels, determining electric potential and field distribution 02 p0266 A72-12431
- Incompressible two dimensional laminar/turbulent wall jet characteristics, obtaining Prandtl mixing theory from apparent kinematic viscosity 02 p0206 A72-12619
- Two and three dimensional turbulent boundary layer development in incompressible and compressible flows, obtaining boundary layer equations similarity solutions using mixing length model [DGLR PAPER 71-066] 02 p0206 A72-12719
- Blade cascades pressure distribution for plane incompressible flow with boundary layer separation near trailing edges, replacing blade profiles by vortex fields [DGLR PAPER 71-097] 02 p0153 A72-12728
- High subsonic velocity aerodynamics boundary problem, transforming compressible flow to incompressible 03 p0307 A72-13238
- Rigid and compliant walls longitudinal curvature and compliance effects on incompressible laminar boundary layer hydrodynamic stability 03 p0342 A72-13854
- Generalized equation for incompressible unsteady laminar boundary layer in external flow with arbitrary time dependent velocity distribution, discussing expanding cylindrical body 03 p0343 A72-14315
- Rotational symmetry solutions to differential equations of stationary barotropic or axisymmetric incompressible flow 03 p0344 A72-14345
- Incompressible power law pseudo-plastic material plane flow in converging channel and axially symmetric converging flow in circular cone 04 p0513 A72-15287
- Inviscid incompressible conducting fluid motion under line sink in uniform strong magnetic field [AD-740535] 04 p0550 A72-15343
- Incompressible laminar flow in conduit with arbitrary cross section, time varying pressure gradient and initial velocity, constructing finite series solution by orthonormalizing procedure [ASME PAPER 71-WA/FE-22] 05 p0646 A72-15927
- Stator-rotor induced annular incompressible rotating flow, allowing for blade loading generated vorticity within actuator disk theory [ASME PAPER 71-WA/FE-18] 05 p0599 A72-15929
- Velocity profiles of turbulent three-dimensional incompressible air jet flow from rectangular orifice tangent to and along curved wall surface [ASME PAPER 71-WA/FE-2] 05 p0647 A72-15938
- Incompressible turbulent flow in parallel-plate channel with one porous bounding wall, using velocity slip model [ASME PAPER 71-WA/FE-1] 05 p0647 A72-15939
- Viscous incompressible flow past longitudinally cambered small aspect ratio slender wing near solid interface 05 p0600 A72-16215
- Numerical simulations of three dimensional homogeneous isotropic turbulence at wind tunnel Reynolds numbers, solving Navier-Stokes equations for incompressible flow 05 p0649 A72-16685
- Navier-Stokes equations numerical solution for laminar incompressible flow past paraboloid of revolution at zero angle of attack [AIAA PAPER 72-110] 05 p0604 A72-16818
- Circle moving under fluid dynamic and gravitational forces in viscous incompressible flow, describing dynamic interaction by numerical method [AIAA PAPER 72-111] 05 p0604 A72-16819
- Laminar incompressible flow over yawed spinning bodies of revolution by Navier-Stokes solutions, discussing flow fields and corresponding force coefficients [AIAA PAPER 72-112] 05 p0605 A72-16820
- Two dimensional and axisymmetric body viscous drag in incompressible flows, using implicit finite difference boundary layer method 05 p0606 A72-16860
- Atmospheric turbulence incompressible two dimensional model, comparing Navier-Stokes equations numerical integration results with finite difference simulation [AIAA PAPER 72-152] 05 p0651 A72-16871
- Two dimensional airfoil unsteady stall in incompressible flow, comparing calculated loading during transient and sinusoidal pitching motions with measured values [AIAA PAPER 72-37] 05 p0607 A72-16899
- Viscous incompressible flow in straight duct, relating duct wall drag, axial pressure gradient, flux rate and cross sectional area 05 p0653 A72-17002
- Unsteady axisymmetric incompressible pipe flow stability near piston, using Navier-Stokes equations solution with finite difference forms 05 p0653 A72-17006
- Rotating homogeneous incompressible fluid flow field over step with interior geostrophic regions, horizontal surfaces Ekman layers and vertical shear layers 05 p0653 A72-17008
- Navier-Stokes equation solution for laminar incompressible flow past parabolic cylinder, investigating skin friction and pressure drag 06 p0798 A72-17782
- Incompressible micropolar fluid flow equations, deducing stable periodic solutions existence by energy method 06 p0799 A72-17917
- Incompressible microstretch fluid flow in rigidly bounded domain, deriving kinetic energy decay rate via linear model subject to entropy principle and boundary adherence condition 06 p0799 A72-17918
- Viscous incompressible flow past circular cylinder at Reynolds numbers 20-100 by finite difference methods, taking into account wake region behind body 06 p0756 A72-18125
- Small parameter method solution of two dimensional incompressible flow Navier-Stokes equations, exemplifying application to viscous incompressible flow past semiinfinite plate 06 p0801 A72-18127
- Wall curvature and flexibility effect on incompressible laminar boundary layer hydrodynamic stability, considering Tollmein-Schlichting transverse wave disturbances 06 p0801 A72-18134
- Wall blowing discontinuity effect on two dimensional incompressible turbulent boundary layers, discussing flow relaxation length separation by penetration point trajectory 07 p0966 A72-18841
- Vorticity transport and definition of equations for axisymmetric incompressible viscous vortex ring, solving coupled system numerically [AIAA PAPER 72-151] 07 p0907 A72-18956
- Difference method for numerical integration of Navier-Stokes equations for two dimensional incompressible steady flow along flat thin plate 07 p0908 A72-19170
- Second order effects in incompressible boundary layer flow with heat transfer, deriving numerical solutions for skin friction 07 p0968 A72-19625
- Hydrodynamic flow parameters in laminar incompressible water boundary layer on heated plate, noting plate surface heating effect on velocity profile 07 p0968 A72-19766
- Monograph on three dimensional turbulent boundary layers in unsteady incompressible flow covering flow equations, eddy viscosity and mixing length models, etc 07 p0968 A72-19953
- Rotating homogeneous incompressible fluid flow over various bottom topographies, comparing numerical and analytical solutions with water tunnel experimental results 07 p0970 A72-20071
- Time independent incompressible micropolar fluid flow existence 07 p0970 A72-20082
- Generalized Navier-Stokes equations for incompressible turbulent flow time mean values, using nonlinear phenomenological theory 07 p0972 A72-20109
- MHD dynamo model for incompressible real electrically conducting fluid unsteady flow 07 p1044 A72-20304
- Viscous incompressible flow past circular cylinder at Reynolds numbers 100-1000, obtaining oscillatory drag, lift and torque by governing equations numerical solution 08 p1107 A72-21251
- Unsteady incompressible laminar boundary layer theory on two dimensional body motion through fluid at rest at infinity, considering skin friction 08 p1151 A72-21794
- Mixing length model for turbulent boundary layer in incompressible flow with fluid injection at wall, extending solution to compressible case [ONERA, TP NO. 986] 09 p1294 A72-22818
- Galerkin method for numerical simulation of incompressible boundary flows in box geometries with periodic and free slip conditions, noting Taylor-Green vortex decay 09 p1294 A72-22941
- Navier-Stokes equations numerical solution for symmetric laminar incompressible flow past parabolic cylinder, presenting surface pressure, friction and pressure drag results 10 p1465 A72-24291
- Small turbulences growth in two dimensional incompressible wake, noting transverse oscillations of mean velocity profile [AD-742006] 10 p1467 A72-24367
- Antisymmetric turbulences linear stability in incompressible plane Poiseuille flow between flexible walls solved by variational boundary value problem formulation 10 p1468 A72-24372
- Laminar boundary layer velocity profiles in convergent nozzle incompressible swirling flow, considering boundary layer growth effects on free stream axial and tangential velocities 10 p1471 A72-25068
- Axial pressure variations in incompressible laminar tube flow with uniform suction, noting application to heat pipes [AIAA PAPER 72-257] 11 p1614 A72-25202
- Temperature distributions in constant viscosity incompressible Couette flow with additional pressure gradients 11 p1743 A72-25262
- Jet flaps for high turning compressor cascades in incompressible axial flow, calculating blade pressure and jet slope distributions [ASME PAPER 72-GT-16] 11 p1569 A72-25615
- Stationary MHD aligned flows of ideal incompressible fluids with same streamline patterns in plane, axisymmetric and spatial flows 11 p1695 A72-25910
- Nose bluntness effect on bodies of revolution pitching moment characteristics in incompressible flow at various angles of attack 11 p1573 A72-26576
- Unsteady aerodynamic forces on flat plate in locally perturbed incompressible potential flow, investigating angle of attack frequency response to periodic local perturbations 11 p1573 A72-26579
- Incompressible laminar subcritical flow with separated wake past symmetric two dimensional bluff body calculating upstream pressure distribution and separation point 12 p1751 A72-27172
- Mean velocity distribution and Reynolds stresses in turbulent wake behind flat plate in uniform incompressible flow 12 p1798 A72-27718
- Incompressible potential flow model of porous parachute canopy flow field, using Stokes stream function for axisymmetric vortex sheet in uniform steady stream 12 p1755 A72-28123
- Viscous incompressible gas turbulent flow in axisymmetric channel under preliminary twist conditions at inlet, using computer numerical solution 12 p1752 A72-28126
- Statistical theory of nonuniform turbulent incompressible fluid flow, presenting approximate formulas of nonisotropic two point correlation tensors 13 p1941 A72-28629

Inviscid incompressible flow past longitudinally curved small aspect ratio slender wing, investigating aerodynamic characteristics

13 p1893 A72-28729

Viscous incompressible flow between two coaxial rotating circular cylinders with small uniform injection at inner cylinder, obtaining solution of Navier-Stokes equations

13 p1941 A72-28883

Incompressible boundary layer velocity profile on swept wings, comparing critical Reynolds number to straight wing value

13 p1894 A72-29639

Round air jet turbulent mixing with incompressible transverse flow, examining interaction behavior as function of relative momentum

13 p1943 A72-29641

Natural instabilities development in laminar boundary layer of incompressible flow, considering AM spectrum and abscissa-ordinate development compared to Orr-Sommerfeld equation solution

13 p1943 A72-29784

Passive scalar dispersion in turbulent incompressible flow characterized by inhomogeneous and nonstationary statistics, expanding velocity and scalar concentration fields in Wiener-Hermite functions

14 p2128 A72-30348

Steady nonrotating axisymmetric viscous incompressible flows with zero and negative ring circulation flux, studying solutions in three dimensional phase space

14 p2094 A72-30708

French monograph on velocity profile in laminar boundary layer on semiinfinite flat plate in harmonic oscillation of uniform incompressible flow

14 p2095 A72-30949

Frictionless, Helmholtz and flat jet incompressible flows from slot in thin plane wall, comparing characteristics with free jet vicinity

15 p2216 A72-31464

Kinematic eddy viscosity for incompressible two dimensional turbulent flow, obtaining Navier-Stokes equations and conditions for equilibrium and nonequilibrium boundary layers

15 p2216 A72-31470

Two dimensional incompressible turbulent boundary layer in arbitrary pressure gradient, obtaining mathematical model for solution by implicit finite difference method

15 p2217 A72-31718

Aerodynamic properties prediction procedure for thin jet-flapped airfoil in incompressible inviscid flow bounded by different types of boundaries

15 p2179 A72-32147

Nonlinear instability of two dimensional unbounded incompressible viscous fluid flows under periodic small perturbation

16 p2376 A72-32933

Wind tunnel ventilation duct aerodynamic stability analysis for incompressible and slightly compressible flow

16 p2378 A72-33439

Incompressible flow drag caused by slot suction provided in bodies of revolution for preventing laminar boundary layer transition into turbulent state

16 p2344 A72-33678

Lateral pressure gradient and suction effects on laminar incompressible boundary layer separation on curved surfaces predicted by generalized tow-layer flow model

[AIAA PAPER 72-698] 16 p2380 A72-34045

Flows between stationary surfaces of revolution, having similarity solutions.

[ASME PAPER 72-APM-4] 17 p2537 A72-34304

Flow near an accelerated porous flat plate.

17 p2540 A72-35054

Vortex induced wing loads.

17 p2486 A72-35257

The inviscid flowfield of an unsteady airfoil.

[AIAA PAPER 72-681] 17 p2486 A72-35481

Shear stresses distribution in isothermal incompressible turbulent boundary layer with positive pressure gradient by diffusers in open jet wind tunnel

17 p2544 A72-35931

Non-analytic character of the shear-tensor distribution function in incompressible turbulence.

18 p2678 A72-36012

A new method of analysis in laminar-flow theory.

18 p2681 A72-36551

Incompressible potential flow solution for axisymmetric body-duct configurations.

18 p2683 A72-36940

Determination of the separation parameter of an incompressible magnetohydrodynamic boundary layer by applying the dimensionality theory

18 p2717 A72-37181

Numerical solution of the problem of the motion of a circular cylinder in a viscous fluid flow

19 p2784 A72-37395

Flow between eccentric rotating cylinders.

[ASME PAPER 72-LUB-J] 19 p2786 A72-37699

Prediction of the stalling of a wing section in incompressible flow

[ONERA, TP NO. 1088] 19 p2746 A72-37760

Pressure loss and heat transmission in cylindrical ducts

[ONERA, TP NO. 1057] 19 p2880 A72-37768

On a method of computing the plane steady flow around a profile situated between straight parallel lines.

19 p2786 A72-38098

Three-dimensional wall jet originating from a circular orifice.

19 p2747 A72-38811

Prediction of turbulent boundary layer heat transfer with pressure gradient and mass transfer.

[ASME PAPER 72-HT-16] 20 p2987 A72-39686

Uniformly exact solution of the problem of the flow past a slender profile

20 p2886 A72-39904

Steady capillary-gravitational waves of finite amplitude generated by pressure periodically distributed along the flow surface of a fluid of finite depth.

21 p3044 A72-40261

Incompressible free shear layers instability, considering Reynolds number, velocity profile, disturbances and compressibility effects

22 p3167 A72-42579

Calculation of separation points in incompressible turbulent flows.

23 p3279 A72-43328

An investigation of confined vortex flow phenomena.

[ASME PAPER 72-FLCS-3] 23 p3281 A72-44067

The boundary layer of higher order at the stagnation line of a yawed cylinder in the case of strong suction or injection

23 p3249 A72-44297

Hydraulic duct transfer function determination for prediction of liquid-fuel engine space launcher LF vibrations, investigating incompressible flow rate modulation by deformable walls

24 p3392 A72-45117

Longitudinal curvature and displacement speed effects on incompressible laminar boundary layers.

24 p3393 A72-45249

Similarity problems of a non-isothermal boundary layer of an incompressible non-linear viscous medium with regard for dissipation.

24 p3395 A72-45634

Explicit numerical solution of the three-dimensional incompressible turbulent boundary-layer equations.

24 p3395 A72-45781

INCOMPRESSIBLE FLUIDS

NT MICROPOLAR FLUIDS

Initial interaction phase between thin shallow conical shell vibrating axisymmetrically and ideal incompressible fluid, determining hydrodynamic pressure effects

01 p0050 A72-10574

Unsteady boundary layer flow of viscous incompressible fluid between two rotating coaxial parallel disks

02 p0205 A72-12538

Elastico-viscous incompressible fluid laminar boundary layer flow past infinite plane porous wall, deriving velocity and temperature distributions by two-sided Laplace transform technique

03 p0340 A72-13024

Perturbation induced long waves boundary effects in ideal incompressible fluid in uniformly rotating basin with stepwise depth difference, using Schwarz symmetry principle

03 p0340 A72-13094

Base pressure determination for subsonic isothermal central and peripheral jets of incompressible fluid discharging into subsonic slipstream

03 p0342 A72-13912

Gravitational convection by magnetocaloric effect in incompressible nonconducting ferromagnetic fluid

03 p0457 A72-13993

Steady flow of viscous incompressible conducting fluid in rectangular channel with sectional walls under longitudinal external magnetic field, deriving velocity distribution

03 p0398 A72-14009

Thermal boundary layer of incompressible fluid unsteady laminar flow, obtaining temperature field from energy equation for various wall temperature conditions

03 p0343 A72-14314

Start-up flow of viscous incompressible fluid under constant head in entrance region of circular tube

03 p0344 A72-14343

Asymptotic theory of heat transfer in two dimensional turbulent boundary layers of incompressible fluid at large Reynolds numbers

03 p0459 A72-14390

Boundary value problem for steady parallel axisymmetric irrotational flow of inviscid incompressible fluid past cylinder having common axis with tube

04 p0512 A72-15056

Conducting incompressible fluid in laminar pipe flow under traveling magnetic field, investigating friction coefficient and energy balance

04 p0558 A72-15341

Stationary viscous incompressible conducting fluid in conical flow, investigating diverging and converging electric current effects

[AD-740536] 04 p0558 A72-15342

Nonlinear calculation of three dimensional flow of perfect incompressible fluid around wing of finite span with arbitrary form

04 p0463 A72-15558

Two dimensional unsteady flow of incompressible fluid around passing turbomachine blades, determining instantaneous pressure, forces and moments as function of time

04 p0463 A72-15559

Hydrodynamic resistance reduction for bodies moving under water, analyzing dynamic equations of viscous incompressible fluid

04 p0514 A72-15701

Two dimensional axisymmetric surface waves motion in inviscid incompressible homogeneous electrically conducting fluid under uniform magnetic and electric fields, considering surface tension effects

04 p0560 A72-15744

Hydroelastic vibrations of incompressible inviscid liquid with free surface in uniformly rotating infinitely long circular cylindrical container, investigating response to cylinder walls forced excitations

05 p0735 A72-16065

Nonlinear unsteady potential flow of incompressible fluid past slender wing, using linearized vortex distribution method

05 p0600 A72-16214

Vortical flow of incompressible fluid in finite region bounded by potential flow and with Bernoulli constant jump at boundary

05 p0649 A72-16581

Concentration profile equations for finite length flat vertical plate moving in viscous incompressible fluid

05 p0650 A72-16783

Incompressible fluid unsteady kinetic energy equation periodic solution for harmonic oscillation viscous dissipation influence on temperature field, considering Couette steady flow solution

05 p0750 A72-17007

Equations of motion for oscillating heavy symmetrical gyroscope with cylindrical cavity partially filled with inviscid incompressible liquid

05 p0664 A72-17145

Two-dimensional asymptotic solutions to Navier-Stokes equations for weak vortex discontinuity flow with vanishing viscosity

06 p0798 A72-17680

General theory of relativity for symmetric field, discussing DE Donder incompressible fluid model and Tolman-Schwarzschild metrics

06 p0847 A72-17682

Rotary self excitation of helical flows in incompressible liquids, using Navier-Stokes equation

06 p0798 A72-17730

Plane Couette flow of incompressible non-Newtonian viscous fluid between parallel plates, using minimum entropy production variational principle

06 p0798 A72-17779

Asymptotic theory of turbulent boundary layer in incompressible liquid with positive pressure gradient and injection

06 p0799 A72-17910

Incompressible fluid turbulent flow variational principles, discussing Malkus principle for maximum dissipation rate and minimum entropy production principle for convective and dissipative systems

06 p0800 A72-18116

Dynamics of two dimensional body with cavity containing viscous incompressible fluid, noting obstacle interaction and free surface motion problems

06 p0801 A72-18133

Equilibrium turbulent flow of incompressible fluid in plane diffusers, taking into account channel cross section including viscous sublayer

06 p0801 A72-18144

Kubo type time correlation formulas for incompressible heat conducting fluids turbulent transport coefficients, establishing relation to cascade and closure-of-hierarchy methods

06 p0801 A72-18173

Navier-Stokes equations numerical solution for viscous incompressible fluid in circular cylinder with rotating top disk, computing secondary flow at Reynolds numbers to 400

06 p0802 A72-18526

Plane stationary flow of ideal incompressible fluid past large camber profiles of arbitrary shape and thickness, using computerized Fourier expansion

07 p0908 A72-18976

Downwash behind lifting surface related to loading in ideal incompressible gas by equations of motion linearization

07 p0908 A72-19110

Flow field induced by electric current jet in incompressible viscous conducting fluid, solving nonlinear momentum equation by series expansion procedure

07 p0967 A72-19504

Axisymmetric flow of ideal incompressible liquid with free boundary and variable velocity, taking into account external mass forces effect

07 p0968 A72-19999

- Nonlinear stability theory for laminar flow of viscous incompressible liquids, noting application to Couette-Taylor flow between two concentric rotating cylinders 07 p0971 A72-20091
- Steady viscous incompressible fluid flow in circular disk with prescribed velocity components at low Reynolds numbers, considering computer tested numerical method 07 p0972 A72-20102
- Incompressible fluid near equilibrium turbulent flow velocity distribution through plane diffuser, taking into account upstream conditions 07 p0972 A72-20115
- Unsteady laminar viscous incompressible electrically conducting flow between nonconducting parallel flat plates with applied constant magnetic field 07 p1044 A72-20245
- Viscosity measurement error estimates for Newtonian incompressible fluid flow through deformed capillary tube 07 p0991 A72-20535
- Unsteady flow of viscous incompressible electrically conducting fluid past infinite nonconducting plate within uniform transverse magnetic field 08 p1212 A72-21079
- Ideal incompressible fluid sloshing under centrifugal force in partially filled conical cavity rotating at constant angular velocity 08 p1149 A72-21244
- Parameter calculation for laminar incompressible fluid jet expanding in gradient slipstream along moving surface, determining velocity distribution in jet axis 08 p1149 A72-21309
- Descriptive geometric method for distribution of axes of uniform rotation of body containing ideal homogeneous incompressible fluid in uniform turbulent motion 08 p1209 A72-21364
- Unsteady uniform turbulent flow of incompressible liquid in circular pipe, verifying mathematical model with velocity distribution calculations 08 p1151 A72-21666
- German monograph on experimental investigations of annular channels with axial flow of incompressible fluids covering graphical and computational determination of flow volume 09 p1293 A72-22332
- Corrugated cylinder steady rotation in incompressible viscous fluid based on linear or Stokes approximation 09 p1293 A72-22411
- Spatial plastic flow in arbitrary incompressible continuous medium with instantaneously inextensible family of planes, deriving velocity field formulas 09 p1403 A72-22758
- Numerical solution of thermal shock equations for incompressible fluid with free convection and of motion equations in gravitational force field 09 p1410 A72-22882
- Perfectly conducting incompressible fluid motion past thin body in oblique field, discussing magnetic field influence on lift 09 p1365 A72-23559
- Similarity analysis group theory methods application to dimensional analysis, discussing incompressible fluid mechanics case 10 p1503 A72-23917
- Reduction of governing equation for thin nonstretching vortex filament in incompressible inviscid fluid to nonlinear Schroedinger equation describing helical motion propagation 10 p1466 A72-24293
- Steady state exact solutions of MHD equations for perfectly conducting self gravitating incompressible fluid, showing solutions existence for rotating planetary ellipsoid free liquid surface 10 p1539 A72-24328
- Magnetic diffusion into moving cylindrical incompressible plasma with radial divergence 10 p1521 A72-24413
- Prolate and oblate spheroids flow field generated by axial translatory oscillations in still incompressible viscous fluid from Stokes linearized equations, deriving formulas for drag 10 p1418 A72-24462
- Fully developed turbulence spectrum of incompressible viscoelastic fluids 10 p1469 A72-24534
- Incompressible fluid jet propagation beyond charged particle source exit section, investigating electrodynamical interaction parameter 10 p1522 A72-24549
- MHD sheet pinch model time dependent nonequilibria stability determined by equations of incompressible viscous resistive magnetofluid [AD-739661] 10 p1523 A72-24751
- Plane irrotational motion of ideal incompressible fluid perturbed by profile movement and deformation, obtaining aerodynamic forces power 10 p1420 A72-24853
- Ohmic and internal friction loss minimization in stationary rotating incompressible plasmas, assuming magnetic and velocity fields as Trkal fields 10 p1524 A72-24928
- Cylindrical shell vibrations in incompressible inviscid fluid near free interface, calculating natural frequencies with Fourier transforms 10 p1471 A72-25130
- Three component flow calculation at inlet of axial flow compressor stage, linearizing hydrodynamic equations of ideal incompressible fluid with velocity perturbations 10 p1420 A72-25132
- Axisymmetric three component flow of viscous incompressible fluid, finding exact solutions to second problem of dynamics 10 p1471 A72-25133
- Navier-Stokes equations system integration for axisymmetric vortex flow of viscous incompressible three component fluid 10 p1471 A72-25134
- Friction drag coefficient determination for cylindrical bodies in laminar and turbulent incompressible fluid flow 10 p1420 A72-25135
- Plane laminar semibounded incompressible fluid jet propagation into slipstream along moving plate, solving boundary layer equations 10 p1471 A72-25136
- Rotary self excitation of helical flows in incompressible liquids, using Navier-Stokes equation 11 p1614 A72-25333
- Unbounded wall effect on complex potential of two dimensional flow produced by arbitrary displacement of body within ideal incompressible fluid 12 p1797 A72-27119
- Incompressible viscoelastic isotropic fluid stability in Couette flow, discussing physical parameters effect on critical Reynolds number and cells shape of secondary flow 12 p1797 A72-27169
- Unsteady viscous incompressible electrically conducting fluid flow generated by porous disk rotation, investigating transverse magnetic field effect 12 p1851 A72-27305
- Temperature oscillations associated with surface gravity waves at two fluid model compressible vapor-incompressible superfluid interface 12 p1845 A72-27386
- Asymptotic behavior of velocity profiles in laminar boundary layers of steady incompressible fluid two dimensional flow past rigid wall 12 p1798 A72-27713
- Parametric approximation of unsteady laminar boundary layer in incompressible fluid in terms of flow velocity and friction characteristics 12 p1799 A72-28177
- Equations of motion for incompressible viscous fluid thin layer on cylinder outer side under gravity, calculating wave number, phase velocity and film thickness 14 p2094 A72-30699
- Arbitrary cascade profiles aerodynamic characteristics calculation via integral equation numerical solution for attached potential incompressible fluid problem 14 p2070 A72-31014
- Momentum transport in thermal incompressible turbulent boundary layers with constant wall temperature, using dimensional analysis and Stratford model 14 p2096 A72-31055
- Plane unsteady convective motion of viscous incompressible liquid in infinite horizontal vessel of rectangular cross section due to wall temperature fluctuations 14 p2174 A72-31157
- Finite difference solution to Navier-Stokes equations for axisymmetric flow of incompressible viscous fluid 15 p2216 A72-31446
- Turbulent flow between rotating disk and turbine engine body calculated from equations of axisymmetric viscous incompressible fluid flow 15 p2217 A72-31702
- Incompressible elastico-viscous liquid steady state laminar source flow between stationary infinite porous disks, noting Reynolds number effects 15 p2219 A72-32512
- Velocity and temperature distribution for viscous incompressible fluid unsteady flow between two parallel plates with pressure gradient linearly varying with time 15 p2219 A72-32599
- Hydraulic shock of incompressible heavy fluid in closed cylindrical tank under abrupt deceleration 15 p2219 A72-32685
- Reversible instantaneous deformations and internal energy in viscoelastic incompressible fluids, using Oldroyd and De Witt hydrodynamic models 16 p2376 A72-32937
- Stability analysis of ideal incompressible liquid steady flow for given distribution, discussing velocity distribution effect on longitudinal cylindrical flow instability 16 p2376 A72-33093
- Spatial flow velocity fields of incompressible continuous media with family of instantaneously inextensible planes, applying plastic flow theory 16 p2423 A72-33107
- Heat conduction in infinite incompressible fluid with turbulent velocity field, deriving physically impossible growth in time of long-wavelength modes of average temperature 16 p2424 A72-33127
- Turbulent flow of viscous incompressible liquid film falling down semiinfinite vertical plate under gravity influence 16 p2376 A72-33142
- Plane Poiseuille flow stability of incompressible second order fluids, noting destabilizing influence of viscoelasticity 16 p2379 A72-33829
- Plane vortex sheet in incompressible inviscid and finitely conducting fluids, investigating discontinuity in density and conductivity on hydromagnetic stability 16 p2438 A72-33842
- Shear stress and dimensionless velocity profiles of plane incompressible fluid wall jet propagation along curved surface 16 p2380 A72-33856
- Energy balance equation of free turbulent boundary layer in incompressible fluid, deriving semiempirical formulas for turbulent viscosity coefficient 16 p2380 A72-34022
- Certain motions of micropolar fluids 17 p2538 A72-34771
- The flow caused by the differential rotation of a right circular cylindrical depression in one of two rapidly rotating parallel planes. 17 p2540 A72-35189
- Unsteady temperature distribution for laminar flow in a porous straight channel. 17 p2541 A72-35434
- Motion of a gyrostat with respect to its center of mass in a central field 17 p2622 A72-35804
- Numerical simulations of three dimensional isotropic turbulence in incompressible fluid at low wind tunnel Reynolds numbers 18 p2677 A72-36007
- Combined Rayleigh and Kelvin instability of a Hall plasma with a vertical magnetic field. 18 p2715 A72-36502
- Solution of some mixed boundary value problems of conducting medium thermodynamics by the method of variable separation 18 p2715 A72-36802
- Asymptotic estimate of steady state solution to Euler equations for ideal incompressible fluid flow with free boundaries 18 p2682 A72-36805
- Rotational theory of laminar boundary layer separation of incompressible fluid from smooth surface under pressure gradients 18 p2682 A72-36887
- The influence of geostrophic force on the stability of an heterogeneous conducting fluid with a radial gravitational force. 18 p2683 A72-36933
- Heat transfer from a slowly rotating sphere. 18 p2741 A72-36934
- Numerical studies of flow between rotating coaxial disks. 19 p2784 A72-37374
- Statistical characteristics of surface pressure pulsations in turbulent boundary layer of incompressible fluid, discussing effects near smooth flat wall 19 p2785 A72-37472
- Vortical flow of incompressible fluid in finite region bounded by potential flow and with Bernoulli constant jump at boundary 19 p2785 A72-37552
- Mathematical model of ideal incompressible gyroscopic fluid with internal angular momentum using kinematic equations 19 p2835 A72-37929
- Hydrodynamic stability of periodic burning front for ideally conducting incompressible fluids in longitudinal or transverse magnetic field 19 p2882 A72-38457
- MHD instability of two dimensional laminar boundary layer in incompressible electrically conducting fluid along concave wall with periodic three dimensional disturbances 20 p2957 A72-39328
- Interaction between two streams of incompressible fluids in flat duct, using Chaplygin method of singular points 20 p2913 A72-39370
- An asymptotic solution for steady flow above an infinite rotating disc with suction. 20 p2886 A72-40015
- Linear and Alfven waves propagation in incompressible beam-plasma systems, deriving dispersion law 21 p3092 A72-40994
- Hydrodynamic forces acting on rigid disk and circular membrane vibrating in ideal incompressible fluid, noting dependence on phase shift between vibration modes 21 p3126 A72-41552
- A system of linear equations with partial derivatives 21 p3077 A72-41822

Velocity distribution of quasi-steady and steady flow of ideal incompressible fluids with congruent streamlines, investigating conditions for vortex and irrotational flow 22 p3164 A72-41906

Flow stability of ideal compressible and incompressible fluids, solving Navier-Stokes equation for rotating liquid with free boundary in gravitational field 22 p3165 A72-42151

Vortex and source lattices in a variable layer of an incompressible fluid 22 p3133 A72-42248

Differential equations for heat transfer in turbulent boundary layer flow of incompressible fluid with constant thermophysical characteristics 22 p3166 A72-42253

Lumped parameter model description of distributed parameter fluid dynamic systems by bond graph techniques [ASME PAPER 72-AUT-J] 23 p3279 A72-43634

Hydrodynamic equations for incompressible fluid in steady relativistic state extended to nonrelativistic velocities case, noting transition from Euler to Predvoditelev equations 23 p3279 A72-43686

Noncoaxial rotations of a disk and a fluid at infinity 23 p3248 A72-43824

Periodic solutions of a nonlinear mixed problem for the Navier-Stokes equations 24 p3418 A72-44780

Plane stationary flow of ideal incompressible fluid past large camber profiles of arbitrary shape and thickness, using computerized Fourier expansion 24 p3360 A72-45002

Water tunnel study of turbulent boundary layers structure in incompressible fluid with longitudinal pressure gradient at inlet section of converging and diverging nozzles 24 p3390 A72-45006

Tidal waves of a two-layer liquid in a cylindrical basin of revolution rotating about its axis 24 p3392 A72-45073

A theory of homogeneous, isotropic turbulence of incompressible fluids. 24 p3392 A72-45245

Contributions to the study of turbulent flow in the vicinity of a flat wall 24 p3394 A72-45443

INCONEL [TRADEMARK]

Inconel 718 surface integrity from various manufacturing processes, tabulating data on surface finish effects on fatigue, microhardness and metallurgical properties [SME PAPER IQ 71-239] 01 p0076 A72-10967

Forged Inconel alloy 718 metal powder preforms for dense aircraft engine compressor rotor blades 02 p0233 A72-11441

Fabricable high strength Inconel 706 precipitation hardening superalloy, noting savings in Ni, Nb and Mo content 02 p0245 A72-12507

Inconel 718 welding techniques, investigating microfissuring, impact strength, penetration and ductility 02 p0246 A72-12774

Hydrogen charging of iron-chrome-nickel austenitic stainless alloys, investigating crack initiation in Inconel 600 03 p0373 A72-13600

Optical and electron microscopic study of Inconel 625 precipitation and recrystallization behavior over temperature range under plastic deformation 10 p1494 A72-23829

Solidification mode of weld metal in Inconel 718, using optical and electron transmission microscopy, etch-pit technique and electron-microprobe analysis 11 p1653 A72-25344

Hot corrosion effects on Inconel-700 and Inconel-X gas turbine rotor blades during burning of high sulfur concentration residual oil fuels [ASME PAPER 72-GT-87] 11 p1656 A72-25662

Tungsten free Inconel high strength alloy for high temperature service, noting stress rupture strength and oxidation resistance [ASM PAPER W 72-51.4] 12 p1830 A72-28159

Inconel alloy 617 - A new high-temperature alloy. 19 p2821 A72-38388

INDENTATION

Characteristic friction curves /Mohr circle envelopes/ to describe stressed state region with various stresses produced by slide friction in steel due to indentation 12 p1819 A72-28198

Elastic effects in metal hardness testing with blunt indenter, considering indentation in rigid plastic manner 14 p2113 A72-30268

A simple method for determination of the elongation before reduction of area using a 100-deg cone indentation 18 p2676 A72-37098

INDEPENDENT VARIABLES

NT LATTICE PARAMETERS

Stability relative to part of variables of n-dimensional vector equation, considering applications to solid bodies with fluid filled cavities and gyrostabilized satellite optimal stabilization 02 p0251 A72-11494

Multiplication operator unidimensional perturbation by independent variable, considering spectral function density poles and branch points 03 p0382 A72-13728

Dual variational principles application to distributed parameter system suboptimal control strategy evaluation, considering control variable and feedback gain as piecewise function of time 04 p0505 A72-14665

Local theorem in strengthened form for independent integral-valued lattice random variables 04 p0539 A72-15256

Algorithms for optimal planning of trajectory measurement times during sampling several parameters 05 p0641 A72-16759

Intermolecular interaction potential parameters determination from gas compressibility data based on equation of state in kinetic theory 05 p0692 A72-17068

Optimal averaging of discontinuous processes with distributed parameters, taking into account random disturbances and measurement errors 05 p0683 A72-17130

Lemma for determining relatively prime relationship between two multivariable polynomials, considering singularities of second kind 06 p0783 A72-17485

Ordinary differential equations with highest derivatives multiplied by small parameters, discussing initial value problems and use of implicit function theorem methods 06 p0839 A72-17628

Elliptic restricted three body problem, using motion anomaly as independent variable 06 p0877 A72-17654

Interpolation of function of two variables by surface splines method, solving linear equations system by digital computer 07 p1026 A72-19095

Bayesian estimate of signal parameters in random noise background under mutually exclusive hypotheses about statistical properties 07 p0943 A72-19515

Optimal Bayesian system synthesis for simultaneous discrimination and parameter estimation of several signals in noise background 07 p0943 A72-19516

Dynamic control system parameters optimization for series of maneuvers under different degrees of informability 07 p0959 A72-19652

Linear multivariable discrete time cyclic system sensitivity model yielding sensitivity functions with respect to any system parameters and initial conditions 07 p0961 A72-19706

Matched asymptotic expansions method application to problems with two independent perturbation parameters, considering application to boundary layer and hypersonic flow theory [ONERA, TP NO. 1007] 07 p0970 A72-20076

Ordinary linear differential equation boundary value problem solution in form of asymptotic series in powers of small parameter 08 p1199 A72-21462

Pi-theorem alternative formulation, defining independent dimensionless products in terms of universal constants, governing equations and initially and additionally specified physical quantities 10 p1503 A72-23920

Probability model of statistical independence relationships among two events and environmental event, examining all combinations of definition statements for reliability analysis 10 p1504 A72-24015

Junction transistor equivalent circuit small signal parameters determination at VHF and UHF 10 p1450 A72-24324

Local limit theorems for sequence of nonidentically distributed independent integral-valued lattice random variables 11 p1676 A72-25356

Algorithms for optimal planning of trajectory measurement times during sampling several parameters 17 p2533 A72-35262

Differential inequalities for semilinear hyperbolic operators with two independent variables. 18 p2705 A72-36618

Suboptimal stochastic control of a class of linear distributed parameter regulators. 19 p2780 A72-38243

One fluid solar wind model prediction from corona base density and temperature for parameters at earth 19 p2853 A72-38733

Variability of solutions to higher-order time-lag linear differential equations 20 p2947 A72-39864

INDEXES [DOCUMENTATION]

Cumulative index of papers on radar systems published in IRE/IEEE journals since World War II 10 p1438 A72-24694

1972 seminar supplement to bibliography and abstracts on electrical contacts, circuit breakers and arc phenomena. 18 p2664 A72-35986

1970-1971 Holm Seminar supplement to bibliography and abstracts on electrical contacts, circuit breakers and arc phenomena. 18 p2665 A72-36120

INDEXES [RATIOS]

NT KP INDEX

NT MORPHOLOGICAL INDEXES

Screening test for physical fitness on bicycle ergometer, comparing endurance indices derived from heart rate, oxygen consumption, oxygen debt and work rate measurements 01 p0010 A72-10212

Pulse shaped small parameter variation effects on performance index of minimum fuel control systems with initial and final manifolds 03 p0337 A72-12906

Plasmasphere size changes from K indices of geomagnetic activity, comparing with Binsack formula 03 p0344 A72-12905

Quadratic performance index generation for optimal design of completely controllable, scalar linear system with state feedback 10 p1454 A72-23783

Multiple index Lagrange equations of motion of second kind, proving analogy between mechanical and stereomechanical effects 12 p1844 A72-27318

Indices of geomagnetic pulsations. 17 p2545 A72-34628

Geomagnetic activity index Ap variation spectral data analysis, noting correlation to sunspot number variation 19 p2793 A72-38747

Mathematical determination of decibel-loudness index, tables for various frequencies. 20 p2956 A72-40076

INDIAN OCEAN

Satellite photographs of Himalayan-Indian Ocean tectonic patterns, showing major left and right lateral shear belts as evidence of wrench movements 05 p0655 A72-16040

INDICATING INSTRUMENTS

NT ANEMOMETERS

NT APPROACH INDICATORS

NT ATTITUDE INDICATORS

NT CLOUD HEIGHT INDICATORS

NT FLOW DIRECTION INDICATORS

NT GYRO HORIZONS

NT GYROCOMPASSES

NT HOT-FILM ANEMOMETERS

NT HOT-WIRE ANEMOMETERS

NT MICROBALANCES

NT MICROWAVE SENSORS

NT PLAN POSITION INDICATORS

NT POSITION INDICATORS

NT RADIO DIRECTION FINDERS

NT SPACECRAFT POSITION INDICATORS

NT SPEED INDICATORS

NT TACHOMETERS

NT WEIGHT INDICATORS

NT WIND VANES

Airfield Vehicle Obstacle Indication Device short range high-definition radar system for aircraft navigation aid 02 p0173 A72-12042

Soviet book on course-indicating systems and automatic navigation aids for civil aviation aircraft covering design, operation principles, error analysis and reliability 02 p0256 A72-12298

Multibeam indicator with block diagram description for meteor ranging radar and photofilm based recording system 09 p1308 A72-22508

Visual image indicator used beside and behind objects for neutron radiography quality determination and radiographs series grading 11 p1632 A72-25822

Digital indicators design and logic circuits employing gas discharge tubes and illuminated and synthesizing indicators 11 p1605 A72-26458

Compressor blade vibration indicator measurement by positioning one inductive sensor by rotor blades and another by toothed gear on rotor shaft 13 p1956 A72-28784

Electronic head-up displays for aircraft instrument indication in symbolic form at pilot eye level 15 p2188 A72-31513

Semiconductor optoelectronic devices, discussing light emitting indicator diodes, data display systems, photosensitive arrays and optical data transmission links 17 p2594 A72-34332

- Spectrum transformation in differential amplitude indicators with commutation of the harmonic signals being compared
17 p2518 A72-35780
- Problem of improving the accuracy of differential meters with commutation of the compared harmonic signals
17 p2519 A72-35788
- Combined reliability and durability estimation for machines and devices under working conditions with the use of indicators of service life consumption
19 p2808 A72-38219
- Methods for monitoring the parameters of phased antenna arrays.
19 p2767 A72-38622
- INDIUM**
- Atmospheric neutron production by cosmic rays, calculating Cd-In ratio
05 p0662 A72-16258
- In and Gd substitution effect in calcium-vanadium garnets as potential microwave materials, discussing magnetic properties, resonance linewidth and temperature stability
15 p2293 A72-32243
- Flux quantization in superconductors demonstrated by magnetometer probe measurement of magnetic field trapped in thin In film holes
16 p2441 A72-33225
- INDIUM ALLOYS**
- Sb 124 dopant redistribution in Ge semiconductor during diffusion alloying with In at 750-850 C
05 p0701 A72-15751
- In-Tl alloys electron phonon interaction and superconductivity electron tunneling examined by sum rule and mass defect theory
15 p2295 A72-32543
- Crystal lattice disarrangement by melting In-Tl alloy, noting fcc and bcc metastable phases formation during rapid crystallization
16 p2441 A72-33536
- INDIUM ANTIMONIDES**
- Second harmonic generation, coherence lengths and second order susceptibilities near band edge in InSb as function of magnetic field
03 p0404 A72-14269
- Nonparabolic n-InSb semiconductors, presenting microwave conductivity dc field induced anisotropy
04 p0560 A72-14543
- Density waves propagation and amplification in p-InSb electron-hole plasmas, investigating dependence on frequency and injection level
04 p0561 A72-14851
- Microwave biased millimeter and submillimeter wave detector with n-type InSb, using down conversion process and free carrier absorption for detection
06 p0866 A72-18384
- Thermal conductivity measurements of liquid InSb and Ga at 250-550 C
07 p1036 A72-20566
- Millimeter and submillimeter band frequency conversion in nonlinear bulk n-InSb semiconductor at liquid helium temperature
08 p1140 A72-21060
- Temperature dependence of intrinsic light absorption band edge characteristics in p-type InSb
09 p1366 A72-22213
- Q factor over temperature range of microwave resonator coupled with drifting indium antimonide plasma
09 p1285 A72-22895
- Solid state sinusoidal signal generator based on current density oscillation effect in high resistivity p-type InSb with transmutation doping
09 p1288 A72-23191
- Tempering effects on weakly doped n-InSb electrical properties at 77 K, discussing diffusion and activation energies in reversible/irreversible defect change processes
10 p1526 A72-24242
- Electron tunneling into amorphous InSb and GaSb films, discussing effects of temperature, voltage, coevaporation doping and Cu and Au diffusion
10 p1527 A72-24874
- Thermal neutrons anomalous absorption by indium antimonide crystals, determining absorption coefficient by integral reflectivity measurements
10 p1527 A72-24980
- Transmittance and Faraday effect characteristics of Te doped InSb samples with free carriers measured at 10.6 microns
11 p1648 A72-26338
- Radiation effects in InSb, GaSb and GaAs, stressing orientation dependence of damage production at electron energies near threshold and recovery data
12 p1858 A72-28066
- Uniaxial compressive stress apparatus for InSb investigation at low temperatures in large magnetic fields
13 p1959 A72-29753
- Millimeter wave third harmonic generation and frequency multiplication in n-type InSb at 77 K
14 p2142 A72-30799
- Surface treatment effects on light and X ray irradiated surface photoconductivity of InSb semiconductor single crystals at liquid nitrogen temperature
15 p2292 A72-31866
- Tunable monochromatic IR laser based on magneto-Raman scattering from conduction electrons in n-type InSb, discussing physical processes and experimental techniques
15 p2250 A72-32393
- Plasma magnetoresistance in variable magnetic field measured on n-type InSb sample for SHF inertialless power sensor development
16 p2436 A72-33482
- Effect of magnetic field on the performance of millimeter-wave detectors using bulk InSb.
19 p2772 A72-37570
- The effect of contacts on microwave emission from InSb.
19 p2844 A72-37728
- Coherent radiation emission by indium antimonide in a transverse magnetic field
19 p2845 A72-38176
- Gunn effect threshold and domain formation in transverse magnetic fields in indium antimonide.
20 p2960 A72-39566
- Solid state physics experiment for conduction electrons effective mass determination in ultrapure n-type InSb by means of magnetophonon effect
21 p3096 A72-40203
- Experimental investigation of a millimeter-wavelength n-InSb frequency converter at 4.2 K
21 p3016 A72-40786
- Experimental investigation of the propagation of electromagnetic waves in a rectangular waveguide partially filled with n-InSb in the presence of a transverse magnetic field
21 p3016 A72-40796
- Plasma echo-type oscillations in n-type InSb semiconductor, noting conduction band nonparabolicity effects
21 p3098 A72-41687
- INDIUM ARSENIDES**
- Optically pumped indium-gallium-arsenides laser coherent emission at room temperature, measuring total power conversion efficiency
07 p0999 A72-18882
- Epitaxial InP diode for high efficiency circuit controlled microwave oscillator, discussing solution growth technique, layers electrical properties and I-V performance
12 p1854 A72-27162
- Decomposition mechanism of Cn, Ag and Au solid solutions in InAs single crystals, using isotopic radiography
14 p2143 A72-30961
- Angular distribution measurements of photoemitted electrons for InAs by means of magnetic field.
19 p2843 A72-37406
- Electrical and thermoelectrical effects in GaAs-InAs solid solutions
19 p2844 A72-37752
- Phase diagrams of AlSb-GaSb and InAs-GaAs systems, noting mixing energy for liquid and solid phases
19 p2845 A72-38207
- INDIUM COMPOUNDS**
- NT INDIUM ANTIMONIDES
NT INDIUM ARSENIDES
NT INDIUM PHOSPHIDES
NT INDIUM TELLURIDES
- Investigation of the fast recombination channel in InSe during excitation by neodymium laser light
23 p3295 A72-43339
- INDIUM PHOSPHIDES**
- Bulk InP three level transferred electron microwave oscillators, observing current-controlled instabilities and operation modes
01 p0036 A72-10632
- CW and pulsed InP transferred electron microwave oscillators, discussing fabrication techniques and electrical properties
01 p0036 A72-10633
- InP transferred electron microwave oscillators, observing higher efficiency than IMPATT and GaAs devices
06 p0784 A72-18063
- Electroreflectance study of mixed gallium and indium phosphides
10 p1525 A72-24228
- CW circuit stabilized InP microwave reflection amplifiers in Q band, determining power gain and noise figure
10 p1450 A72-24308
- High efficiency CW performance of InP transferred electron microwave oscillator with anomalous I-V characteristics temperature dependence
11 p1604 A72-25750
- Solid state InP sources for microwave transferred electron oscillators and amplifiers with improved conversion efficiencies, comparing with GaAs
13 p2020 A72-28432
- Negative photoconductivity effect in high resistance n-type indium phosphide single crystals, noting
- photocurrent spectral distribution and I-V characteristics
13 p2022 A72-29647
- High resistance n-type InP crystals electrical conductivity and photoconductivity characteristics at 80 K, discussing photosensitivity spectral distribution and temperature dependence
15 p2290 A72-31371
- Coherent orange emission and bright electroluminescence from indium gallium phosphides vapor grown p-n junction laser diodes
15 p2251 A72-32532
- Avalanche generation process interpretation for nontransit frequency oscillations association with current runaway in bulk InP microwave diode oscillators
16 p2369 A72-33755
- Electrical characteristics of bulk n-InP oscillators.
18 p2666 A72-36456
- INDIUM TELLURIDES**
- Hall and resistance measurements on single crystal HgTe-InTe alloy systems for high pressure phases in terms of conduction state, band structure and impurity effects
19 p2844 A72-37464
- INDOLES**
- NT TRYPTOPHAN
- Molecular complexes of methoxyindoles with 1,3,5-trinitrobenzene and tetracyanoethylene /Spectroscopy/association constants/NMR/.
17 p2512 A72-35649
- INDUCED FLUID FLOW**
- U FLUID FLOW
- INDUCERS**
- U INTAKE SYSTEMS
- INDUCTANCE**
- Continuous transducer measurement of left ventricular wall thickness in open chest dogs, adapting mutual inductance coil technique
08 p1124 A72-20897
- Transfer function sensitivity characteristics comparison of doubly terminated LC filters with active cascade and inductance simulation schemes
10 p1452 A72-24801
- Energy distribution in plasma jet as function of capacitance and energy of storage elements and storage circuit inductance
13 p2015 A72-29452
- Some problems of microwave electromagnetic oscillation phase control by using an inductance transistor
19 p2776 A72-38670
- Self-excitation of oscillations in a system consisting of a delay line, inductance, and tunnel diodes
24 p3384 A72-44895
- INDUCTION**
- Auditory induction of fainter by louder sounds as perceptual phenomenon cancelling masking effects
16 p2354 A72-33170
- The use of an electrical induction method for determining the physical condition of a ground steel surface.
19 p2805 A72-38762
- Electromagnetic induction in a half-space with a cylindrical inhomogeneity.
23 p3284 A72-43423
- INDUCTION HEATING**
- Induction plasma heating simulation of open cycle gas core nuclear rocket engine, describing plasma forming material feed, permeable walls and propellant seeding
01 p0112 A72-11346
- Thermal environment and fuel region simulation for nuclear light bulb engine, using rf induction heater and uranium and tungsten hexafluorides injection
01 p0113 A72-11355
- High temperature black body model based on induction heating of graphite crucible, noting application to stellar energy spectral distribution determination
07 p0991 A72-20404
- Numerical calculation of temperature distribution and tempering depth for inductive hardening process with automatic material feed, taking into account temperature dependent material properties
11 p1639 A72-25898
- Vacuum induction melting process for high temperature steels and superalloys fabrication, emphasizing control over temperature, pressure, beneficial trace elements and harmful impurities
13 p1964 A72-29100
- Shock induction melting and vaporization in metals, investigating initial porosity effect
14 p2113 A72-30185
- Thermal induction plasmas phase measurements, using dual magnetic probe system
15 p2289 A72-32511
- Effect of a cooling gas layer on the geometrical dimensions of an induction plasma
20 p2957 A72-39219
- INDUCTION SYSTEMS**
- U INTAKE SYSTEMS
- INDUCTORS**
- High Q oscillator with simulated inductor circuit consisting of negative immittance converter and RC elements
01 p0035 A72-10127

- Inductor design for minimum inductance at given dc level, using computer programs
[IEEE PAPER 8.6] 03 p0332 A72-13759
- Lumped capacitors, inductors, resistors and gyrators for use at microwave frequencies, discussing design and applications up to X band
04 p0497 A72-14717
- Monolithic Si IC design and fabrication including resistors, capacitors, diodes, n-p-n, p-n-p, p-n-p-n and field effect transistors and inductors
06 p0791 A72-18576
- Magnetosphere theory of pulsar electrodynamics, discussing unipolar inductor with iron sphere having uniform magnetization parallel to rotation axis
07 p1080 A72-20058
- Mathematical model for mechanical and electrical hysteresis, noting application to nonlinear ferromagnetic resonant circuit with saturable inductor
14 p2132 A72-31105
- INDUSTRIAL MANAGEMENT**
NT ENGINEERING MANAGEMENT
NT INVENTORY MANAGEMENT
NT PERSONNEL MANAGEMENT
- Soviet book on determinate, stationary, nonstationary and industrial random processes prediction, covering adaptive filters and algorithms
08 p1146 A72-21675
- Electron beam welding, discussing problem areas, equipment trends and industrial needs
10 p1485 A72-23966
- Optimization of diagnostic tests for monitoring industrial system efficiency, obtaining compromise between costs and utilization
11 p1611 A72-26441
- Industrial enterprise training expense planning in terms of staff productivity and work time
11 p1748 A72-26543
- Employee motivation programs as a means of cost reduction in aerospace industries.
24 p3468 A72-45221
- INDUSTRIAL PLANTS**
Multidimensional variable structure systems synthesis for automatic optimization of inertialess technological plants in presence of constraints
01 p0045 A72-10498
- Soviet papers on industrial plants automatic control systems organization, design and technological arrangement, covering information handling requirements and man machine interfaces
08 p1256 A72-22144
- Automated administrative control systems design, discussing man machine interactions in industrial and economic enterprises management
08 p1256 A72-22145
- Computer aided administrative control systems development for industrial enterprises management, covering product manufacture
08 p1256 A72-22146
- Selection, arrangement and use of computers and peripheral equipment in automated administrative control management system within industrial enterprise
08 p1256 A72-22147
- Data transmission system design in computerized administrative control system for industrial enterprise management
08 p1257 A72-22148
- Industrial enterprises preparation for computerized administrative control systems introduction
08 p1257 A72-22149
- Utility function construction for engineering plants quality criteria
09 p1413 A72-22216
- Noise and vibration control in industrial and aerospace environments, discussing materials and techniques for structural vibration damping
13 p2059 A72-29557
- Electronic control systems for industrial applications, discussing electrical and mechanical properties, circuit reliability and mechanical design features
19 p2782 A72-38314
- INDUSTRIAL SAFETY**
Lungs fibrosis and cancer caused by asbestos fibers inhalation, noting environment control for protection against workers health hazards
11 p1583 A72-25548
- Asbestos reinforced plastics safe handling and manipulation ensured by regulations provided precautions
11 p1583 A72-25549
- Russian book on powdered metals toxicity covering industrial dust, physiological effects, safety standards, electron configurations and crystalline structure
11 p1584 A72-26067
- Industrial safety rules recommendations for lasers based on radiation biological effects and eye optical and physiological properties
12 p1771 A72-27615
- Pathophysiology of exposure to UV, IR, coherent, microwave and RF radiations, discussing potential hazards, damage, human tolerance threshold, protection guides and safety standards
12 p1772 A72-27963

- U.S. federal regulation on occupational noise exposure control for hearing loss prevention, discussing noise measurement, reduction and periodic tests
16 p2358 A72-33324
- Clinical hygienic and experimental data on magnetic field effects under working conditions
17 p2503 A72-35012
- INDUSTRIES**
NT AEROSPACE INDUSTRY
NT AIRCRAFT INDUSTRY
NT DEFENSE INDUSTRY
- INELASTIC BODIES**
U RIGID STRUCTURES
- INELASTIC COLLISIONS**
Collision kinetics of jet streams of inelastic grains in neighboring orbits around central gravitating body
02 p0281 A72-12304
- Dynamic equations for nonequilibrium stationary state superconductors with electron-phonon and electron-electron inelastic collisions
03 p0401 A72-13089
- Cosmic ray particle high energy inelastic interactions, discussing pion and nucleon interaction angular and energy characteristics and muon production mechanism
06 p0869 A72-17270
- Inelastic ionization cross section of cosmic ray hadrons with carbon nuclei at energies of 100 to 300 GeV
06 p0869 A72-17271
- Pion-nucleon high energy interactions, determining inelasticity coefficient distribution
06 p0851 A72-17274
- K-neutral pion energy fractions and inelasticity coefficients at primary energies of 100-1500 GeV during hadron-target interaction
06 p0872 A72-17295
- Boltzmann integrals for inelastic collisions and radiative processes in stationary monatomic plasma, using Grad 8-moment approximation of particles momentum distribution functions
06 p0861 A72-18174
- Inelastic high energy multiple interactions between cosmic ray particles and atomic nucleus targets, using Wilson chamber and ionization calorimeter
07 p0988 A72-19864
- High energy inelastic interactions in cosmic ray showers, using Wilson chamber
07 p1060 A72-19866
- Methane pyrolysis in glow discharges /cold plasmas/, discussing chemical reactions initiated by high energy electrons inelastic collisions with gas molecules
07 p0937 A72-20286
- Forced vibrations of two-mass system with damping through inelastic collisions, determining periodic motions stability regions with allowance for elastic coupling and friction
09 p1352 A72-23179
- Dynamic equations for superconductors with electron-phonon and electron-electron inelastic collisions, investigating nonequilibrium stationary states
13 p2022 A72-29438
- Strong LF electromagnetic wave propagation in semiconductors with inelastic scattering of current carriers by optical phonons, calculating harmonics reflection coefficients
14 p2142 A72-30361
- Eikonal distorted wave analysis of inelastic electron-atom collisions at intermediate energies application to electron impact induced atomic hydrogen 2s and 2p states excitation
15 p2282 A72-32646
- Vibrational energy transfer probabilities for inelastic collisions between diatomic molecules, considering system represented by harmonic oscillators coupled by time dependent interaction potential
16 p2431 A72-33582
- Redistribution of resonance radiation. I - The effect of collisions.
17 p2605 A72-34534
- Perturbation method in inelastic interaction model for transport processes in reacting gases described by Boltzmann kinetic equation
18 p2713 A72-36807
- Influence of inelastic electron-energy losses on the development of ionization instability in a plasma
22 p3209 A72-41877
- Molecular gas presence effect on electron energy balance in atomic gases, noting inelastic collisions loss factor in heated Ar plasma containing nitrogen molecules
22 p3213 A72-43110
- Multiplicity of particles generated in inelastic interactions of nucleons with LiH nuclei at energies from 150 to 550 GeV
23 p3329 A72-44405
- High energy inelastic interactions in cosmic ray showers from Wilson chamber and ionization calorimeter observations, noting secondary particles occurrence dependence on primary energy
23 p3330 A72-44406

- Particle production in inelastic high energy interactions, noting correlation between particle pairs and groups
23 p3330 A72-44407
- Effective cross section of the inelastic interaction of hadrons with lead-atom nuclei at energies from 3 to 30 TeV
23 p3330 A72-44410
- Multifireball theory of particle production in inelastic high energy interactions, using elastic scattering amplitude for inelastic processes model
23 p3316 A72-44412
- Multiple collisions and an optical model of the inelastic interaction between cosmic particles and nuclei
23 p3330 A72-44413
- Approximation for Monte Carlo method modeling of pion-nucleon and nucleon-nucleon inelastic collisions at high energies
23 p3317 A72-44414
- High energy inelastic collisions of pions and protons with nuclear emulsion nucleons, noting pion pulse spectra
23 p3317 A72-44417
- Certain characteristics of the muon and electron components of extensive air showers at mountain level
23 p3331 A72-44425
- Energy dependence of muon-nucleon inelastic interaction, calculating photonuclear cross section for high energy interactions in iron
23 p3331 A72-44429
- Coherent cross section effects on primary particle energy in inelastic proton interaction with carbon nuclei at 20-600 GeV
23 p3332 A72-44439
- Study of the angular distribution of charged and neutral pions during inelastic interactions in the energy region above 1 TeV
23 p3291 A72-44443
- High energy nucleon inelastic collision characteristics dependence on secondary particle energy and meson velocity, using Wilson chamber measurement
23 p3291 A72-44445
- INELASTIC SCATTERING**
Vibrationally inelastic scattering of CO cations by Ar collision, measuring ion energy, mass and angular distribution with high resolution ion beam apparatus
05 p0693 A72-17169
- Inelastic nuclear interactions between 200-GeV cosmic ray particles and polyethylene targets, correlating similarity property, angular momentum spectra and secondary particle pairs
06 p0868 A72-17258
- Particle multiplicity and momentum spectra for high energy inelastic nuclear interactions in Wilson chamber with polyethylene target
06 p0868 A72-17261
- Cosmic ray hadrons inelastic collision cross sections and partial K-neutral pion inelasticity factor in ionization calorimeter
06 p0868 A72-17262
- Inelasticity factor dependence on particle energy spectra to explain nucleon flux calculations and Proton satellite data, considering scattering cross sections
06 p0869 A72-17264
- K-neutral pion inelasticity factor measurement for nucleon interactions in carbon corresponding to primary neutron energy transferred to pions
06 p0869 A72-17269
- Va crystal lattice interatomic bonds and elastic and inelastic X ray scattering intensity calculation
09 p1329 A72-23042
- Elastic, inelastic and reactive scattering experiments with low, high and intermediate energy molecular beams
11 p1691 A72-25675
- Particle-proton total cross section from cosmic ray data on proton-air inelastic cross sections
11 p1712 A72-25884
- Gas temperature from Raman rotational line intensities generated by lidar techniques applied to inelastic Raman scattering
15 p2232 A72-31373
- Out-of-plane density distribution and in-plane velocity distribution measurements for low energy helium scattering inelastically from 550 K silver
15 p2276 A72-31861
- Elastic and one-phonon inelastic scattering of monoenergetic He atoms from cleaved LiF crystal surface
15 p2281 A72-31862
- A dynamical theory for the contrast of perfect and imperfect crystals in the scanning electron microscope using backscattered electrons.
18 p2692 A72-36749
- An integral test of the inelastic cross sections of Pb and Mo using measured neutron spectra.
19 p2837 A72-37634
- Nonelastic interactions of nucleons and pi mesons with complex nuclei at energies below 3 GeV.
19 p2837 A72-38027
- Application of the Harris-Nesbet method to a dipole coupling potential.
21 p3083 A72-40103

Inelasticity of cosmic neutron interactions in carbon 21 p3102 A72-41840

Characteristics of pion and nucleon interaction with carbon and aluminum nuclei over the energy range from 30 to 300 GeV 23 p3331 A72-44435

NELASTICITY

U ELASTIC PROPERTIES

NEQUALITIES

NT SCHWARTZ INEQUALITY

Nth order linear differential inequalities reduction to first order, permitting Chaplygin theorem infinite applicability limit and solution by quadratures 03 p0382 A72-14313

Cauchy problem for nonlinear biharmonic equation in Euclidean n-space, deriving a priori inequality estimate by logarithmic convexity of functional F 04 p0539 A72-15044

N-port resistive network synthesis involving use of vectors, cones, bilinear inequalities and matrices 05 p0639 A72-15801

Feasible solutions to automatic control problems satisfying multiple state and control variable inequality constraints, discussing algorithmic numerical implementation 07 p0959 A72-19281

Difference equation inequalities in sampled data system stability analysis, discussing solution asymptotic behavior 09 p1342 A72-23252

Rectilinear motions in three body problem with null live forces constant, using inequality deduced from virial theorem 09 p1392 A72-23542

Liapunov functions and integral inequalities for study of finite time stability of motion, noting small parameter system subjected to continuous disturbances 13 p2004 A72-29496

Single closed loop discontinuous control system, determining discrete correcting element parameters from linear inequalities 15 p2212 A72-32175

Differential inequalities for semilinear hyperbolic operators with two independent variables 18 p2705 A72-36618

Thermoelasticity and magnetohydrodynamics equations and inequalities, covering Fourier law, stress relations, Bingham fluids, Ohms law, variational formulations and functional analysis 20 p2952 A72-39183

Linear estimation stochastic filtering and deterministic linear optimal regulation duality concept extension to problems with inequality constraints 21 p3074 A72-40228

A priori estimates and Harnack's inequality for general solutions of second-order degenerate quasi-linear parabolic equations 22 p3198 A72-42159

On the ergodic coefficients concerning generalized random systems with complete bonds 22 p3199 A72-42637

Closed loop pulsed automatic control system, determining discrete correcting element parameters from linear equalities 22 p3163 A72-43009

Navier-Stokes evolution inequality bounded solution existence and uniqueness theorems for two dimensional space 22 p3200 A72-43201

Boundary value problems for a mixed-composite type of equation in an unbounded domain 23 p3308 A72-43628

Linear inequalities and P matrices, with applications to stability of nonlinear systems 23 p3309 A72-43859

Cauchy problem for abstract Love equations 23 p3309 A72-44042

A 'length and area principle' type inequality for images in which certain integral functionals remain bounded in an n-dimensional space 24 p3419 A72-45261

Finite Boolean function computation on sequential machine models, developing exchange inequalities between storage, time, et cetera, for relation of combinational and time complexities 24 p3383 A72-45650

NERT ATMOSPHERE

Inert gas-oxygen mixtures fire retardant properties under atmospheric and hypobaric pressures, measuring effectiveness by standard fabric burning rate 12 p1890 A72-28309

High temperature forging apparatus for refractory metals under vacuum or inert atmosphere 15 p2241 A72-32443

Influence of the protective medium during sintering on the properties of iron-base cermets 23 p3299 A72-43289

NERT GASES

U RARE GASES

NERTIA

NT INERTIA PRINCIPLE

NT MACH INERTIA PRINCIPLE

Inertia effects in fully developed axisymmetric laminar flow between two parallel rotating walls, solving Navier-Stokes equation in nonlinear form [ASME PAPER 71-LUB-J] 02 p0234 A72-11529

Thermoelasticity theory coupled linear equations for thin orthotropic shells, taking into account rotatory inertia and lateral shear 04 p0588 A72-15060

Kinematic impact theory for inertial motion of rigid bodies of revolution and energy flow through wire grid 10 p1512 A72-24520

Time-space nonholonomic characteristics of curvature tensor for three dimensional physical space in gravitational and inertial fields 12 p1843 A72-27049

Dynamic deflection of elastic rectangular plate hinged to rigid base moving under sinusoidal pressure impulse action, noting base inertia effect 12 p1879 A72-27091

Natural frequencies of beams with stepwise variable cross sections, approximating deflection shape by sectionwise representation of inertia load 15 p2323 A72-31454

Kinetic forming of conical Al component from solid cylindrical billet, analyzing forming and inertia stresses, impact velocity and displacement-time history 15 p2244 A72-31708

Timoshenko finite element beam theory application to flexural vibration problems, considering shear deformation and rotary inertia effects 18 p2740 A72-37206

Measurement of unsteady hydrometeorological processes on inertial devices 19 p2830 A72-38774

Hysteresis curve equation for calculation of elastoplastic deformations caused by forced vibrations, taking into account medium compressibility and inertial forces 21 p3123 A72-41359

Eigenvalue spectrum translation and frequency shifting by inertia and stiffness matrix modifications in iteration techniques 22 p3207 A72-42850

Inertial effects in motion driven by hydrodynamic fluctuations 24 p3430 A72-45560

Time-space nonholonomic characteristics of curvature tensor for three dimensional physical space in gravitational and inertial fields 24 p3425 A72-45702

INERTIA MOMENTS

U MOMENTS OF INERTIA

INERTIA PRINCIPLE

NT MACH INERTIA PRINCIPLE

Whirling elastic shaft-disk system, investigating interaction effects of external and linear/nonlinear material damping, elastic restoring forces and inertia forces 01 p0101 A72-10036

Inertial and gravitational mass equivalence principle verified for aluminum and platinum, using torsional pendulum with large relaxation time 03 p0388 A72-13076

Gravitational and inertial masses equivalence principle verification by pendulum torsional oscillation experiment with laser beam 04 p0519 A72-15070

Concentrated inertias effects on cantilever beams and shafts free vibrations by Laplace transform technique 04 p0591 A72-15276

Satellite attitude control in circular orbit by actively varying inertia via angular rate sensing and use of fluid transfer logic 05 p0725 A72-16440

Turbopump rotating assembly bearing parameters and inertia products estimation and identification by extended Kalman filtering 08 p1173 A72-20844

Spacecraft orientation angle measurement by inertial sensors, analyzing equipment kinematic efficiency and limitations 11 p1684 A72-26913

Inertial and gravitational mass equivalence principle verified for Al and Pt, using torsional pendulum with large relaxation time 13 p2004 A72-29426

Statistical self-similarity and inertial subrange turbulence 18 p2678 A72-36021

INERTIA WHEELS

U REACTION WHEELS

INERTIAL ACCELEROMETERS

U ACCELEROMETERS

INERTIAL FORCES

U INERTIA

INERTIAL GUIDANCE

NT STRAPDOWN INERTIAL GUIDANCE

Scientific satellite with simple inertial system, deriving discrete feedback reentry guidance algorithms based on closed-form equations solvable by onboard computer 01 p0098 A72-10944

Soviet book on gyroscopic systems and inertial guidance instruments, emphasizing system motion under various dynamic conditions and systematic errors 03 p0362 A72-14167

Dynamic test facility and methods for Europa 2 launch vehicle inertial guidance system 05 p0643 A72-16433

Optimization algorithms for jet transport aircraft inertially based flight trajectory control in turbulent atmosphere, comparing with ILS 05 p0685 A72-16472

Cellular electronic logic circuit planar array representing objects inertial motion, applying to traffic control, image processing and artificial intelligence 06 p0779 A72-17496

Statistical analysis of system component error propagation by digital simulation using Continuous System Modeling program, considering strapped down inertial guidance computer 07 p1033 A72-20347

Inertial sensing principles interrelationship, stressing electric and magnetic procedures 12 p1809 A72-27788

Fighter bomber Loran-inertial data processing with digital computer to combine navigation, guidance and weapon delivery into fully integrated system 16 p2420 A72-33246

Mathematical model of seismic isolation block and pneumatic suspension for inertial guidance component tests to describe design factors effects on vibration behavior 20 p2950 A72-39085

Three dimensional seismic monitoring system developed from inertial guidance gyroscopes and accelerometers, noting pole shift observation, tilting under earth tides and earthquakes forecasting [AIAA PAPER 72-844] 20 p2923 A72-39088

Development and optimization of the SRAM guidance and control software 20 p2951 A72-39102

Black Arrow satellite launch vehicle attitude control as part of inertial guidance system, describing four-gimbal gyroscopically stabilized platform and associated electronics 21 p3115 A72-40121

Three solid stage Minuteman ICBM, discussing all-inertial guidance system, ablative reentry vehicle and management arrangements 23 p3358 A72-44357

The application of error control techniques in the design of an advanced augmented inertial surveying system 24 p3421 A72-44641

Examination of rocket control system by means of analog computer 24 p3450 A72-45175

INERTIAL MEASURING UNITS

U INERTIAL PLATFORMS

INERTIAL NAVIGATION

Passenger aircraft onboard automated inertial navigation devices, emphasizing accelerometer and gyroscope design and construction 01 p0096 A72-10070

Inertial navigation role in automatic ATC systems, discussing path control accuracies, environmental conditions, noise and air pollution, etc 01 p0098 A72-11118

Second order Markov process statistical model for gravity anomalies in local region, applying to error analysis in inertial navigation system computerized simulation 02 p0207 A72-11596

Optimal smoothing application to testing of inertial navigation systems, gyros and component failure detection during mission 02 p0258 A72-12810

Military aircraft inertial navigation system design, discussing gyroscope, gyro compassing alignment, accuracy and performance 04 p0545 A72-15666

Equations of motion for stable member of three axis gyro stabilized platform for inertial navigation, including friction, inertia and torque motor effects 05 p0662 A72-16557

Sensitivity algorithms for finite memory batch processing smoother [Kalman filter], applying to ship inertial velocity error estimation 05 p0686 A72-16572

Flight control systems development, discussing onboard computers use in subsystems functional integration, stabilization and landing systems, inertial navigation and flight simulation 05 p0687 A72-16736

Flight navigation technology current state and development trends, discussing transition from Doppler to inertial systems, use of computers and satellites, collision avoidance, etc 05 p0687 A72-16737

All-weather landing aids for civil VTOI aircraft and helicopters, discussing Doppler and inertial navigations, instrument landing systems and ground visibility improvement 05 p0688 A72-16780

Inertial navigation system accelerometer error autocompensation, using reversal by accelerometer forced rotation in stabilized platform plane

05 p0664 A72-17148

Book on mechanization and error analysis of inertial navigation systems, stressing terrestrial applications

06 p0845 A72-17944

Combined inertial/radio navigation systems for cost reduction, noting superior accuracy of VOR and DME

06 p0846 A72-18286

Switching sequence analysis of gas bearing gyros for low cost inertial sensors in short risetime navigation devices

07 p0989 A72-20281

Strapdown inertial guidance and navigation systems state of art, discussing recent developments in computers, sensors and systems technology

08 p1204 A72-21089

Local level and space stable inertial navigation systems, comparing position error propagation

08 p1204 A72-21410

Algorithm to compute inertial navigation system altitude and vertical velocity by closed feedback loop with accelerometer output mixed with pressure altitude reference

08 p1204 A72-21411

Area navigation systems, discussing VOR/DME, Doppler and inertial systems, CRT displays, data links, etc

08 p1204 A72-21523

Moving and inertial trihedron orientation determination from absolute angular velocity vector, solving Poisson equations system

08 p1205 A72-21802

Vertical deflections estimation with inertial navigation system, geodetic position and velocity reference and optimal data smoother, noting applicability to surveys from moving vehicles

12 p1843 A72-27634

Russian book on flight navigation cybernetics covering Doppler, astro and radio inertial schemes and satellite systems

12 p1843 A72-28344

OMEGA effect on oceanic airway safety, noting improvement over inertial navigation systems

13 p1998 A72-29197

Kalman filter application to inertial navigation systems optimal alignment, discussing linear systems representation in state space and filter algorithm recursive equations

14 p2129 A72-30330

Aircraft inertial navigation system, discussing mode selection unit, digital computer and control display for operator communication with system

15 p2267 A72-31596

Great circle intermediate waypoint computation method for inertial navigation equipped aircraft

15 p2271 A72-32205

Inertial navigation system platform alignment and calibration by state space technique similar to Kalman filtering

16 p2420 A72-33697

Coordinate and speed error dependence on instrumental errors of inertial navigation system using gyrohorizoncompass

16 p2420 A72-33960

Integrated inertial-VOR-DME or inertial-TACAN navigation system, presenting slant range and bearing adjustment procedure via least squares method

16 p2421 A72-34136

Helicopter testing of inertial navigation systems.

[AHS PREPRINT 634] 17 p2578 A72-34478
Configuration and flight test of the only operational Air Force area navigation system.

17 p2578 A72-35557

USAF development of electrostatic gyros for inertial air navigation, noting flight tests and associated airborne digital computer

17 p2578 A72-35558

A suboptimal error reduction scheme for a long-term self-contained inertial navigation system.

17 p2578 A72-35560

Motion stability of inertial navigation gyroscopic system with gyro horizon compass, noting constant and time dependent coefficients of motion equations

19 p2830 A72-37320

Inertial platform pursuant to ARINC-571 specifications, noting capability for integration into surface navigation system or autonomous operation

19 p2831 A72-37799

The impact of gradiometer techniques on the performance of inertial navigation systems.

[AIAA PAPER 72-850] 20 p2949 A72-39079

Design of a reduced-state suboptimal filter for self-calibration of a terrestrial inertial navigation system.

[AIAA PAPER 72-849] 20 p2949 A72-39080

Error analysis of hybrid aircraft inertial navigation systems.

[AIAA PAPER 72-848] 20 p2950 A72-39081

Optimum aiding of inertial navigation systems using air data.

[AIAA PAPER 72-847] 20 p2950 A72-39082

Updating inertial navigation systems with VOR/DME information.

[AIAA PAPER 72-846] 20 p2950 A72-39083

Space shuttle terminal navigation with conventional navigation aids.

[AIAA PAPER 72-832] 20 p2950 A72-39095

A simplified analysis of the computational requirements for strapdown attitude reference.

[AIAA PAPER 72-827] 20 p2951 A72-39098

Maximum likelihood failure detection for redundant inertial instruments.

[AIAA PAPER 72-864] 20 p2923 A72-39133

Star scanner attitude determination for the OSO-7 spacecraft.

[AIAA PAPER 72-922] 21 p3082 A72-41566

The INAS device of Ferranti as integrated weapon system for the HS Harrier

21 p3083 A72-41846

Great circle navigation for inertial equipped aircraft, describing procedure for determining waypoint coordinates with reference to VORTAC stations

22 p3203 A72-42949

Ballistic deviations of a gyroscopic navigation system

23 p3311 A72-43417

Space Shuttle landing navigation using precision distance measuring equipment.

24 p3421 A72-44637

Development and testing of a precise marine electrostatic gyroscope.

24 p3401 A72-44638

Kalman filter design considerations for space-stable inertial navigation systems.

24 p3421 A72-44640

Integrated navigation systems and Kalman filtering - A perspective.

24 p3386 A72-44642

Application of external information about the linear velocity of an object for correcting inertial navigation systems

24 p3423 A72-45319

INERTIAL PLATFORMS

Optimal control algorithm synthesized from linear sampling theory for inertial platform alignment, requiring systematic error free optimal digital computer

02 p0258 A72-12899

Linear scheme to calculate errors of inconvertible inertial systems

03 p0387 A72-13911

Time optimal self alignment of inertial platforms using gyros and accelerometers with Kalman-Bucy filter

07 p0989 A72-20279

German monograph on inertial platform stabilization by optical sensors for space vehicle guidance covering aircraft position determination

09 p1394 A72-22334

Soft gyro and accelerometer failure detection for redundant gimbaled inertial measurement units by skew sensors

15 p2270 A72-32187

Failure detection techniques for Space Shuttle redundant multiple gimbaled inertial measurement units, using simulated boost and entry trajectories

15 p2270 A72-32189

Gyro drift detection and isolation for redundant inertial measuring unit configuration of Carousel V system

15 p2270 A72-32190

Inertial navigation system platform alignment and calibration by state space technique similar to Kalman filtering

16 p2420 A72-33697

Inertial platform pursuant to ARINC-571 specifications, noting capability for integration into surface navigation system or autonomous operation

19 p2831 A72-37799

Pneumatically isolated test platform local gravity vector active control to investigate seismic level disturbance effects on precision inertial components evaluation

[AIAA PAPER 72-843] 20 p2923 A72-39086

Stable microprecision test platforms construction and microseismic effects on motion sensing instrument calibration including gyroscopes and inertial navigation and guidance systems

[AIAA PAPER 72-893] 20 p2911 A72-39110

Autonomous navigation systems, discussing Doppler navigation, inertial platforms and onboard computers

21 p3079 A72-40283

In-flight alignment and calibration of inertial measurement units. I - General formulation. II - Experimental results.

21 p3081 A72-41079

The application of error control techniques in the design of an advanced augmented inertial surveying system.

24 p3421 A72-44641

INERTIAL REFERENCE SYSTEMS

Gravitational biology theory problems, discussing possibility of applying relativistic phenomena to living organisms in inertial or inertialess systems

02 p0160 A72-12016

Lorentz transformation between fixed and inertial reference frame in uniform gravitational field, discussing application to clock paradox problem

03 p0388 A72-13228

High accuracy north-seeking course-attitude inertial reference system for air navigation, using platform unit and automatic alignment for Schuler tuned operation

07 p0990 A72-20282

Attitude reference platforms in ASTRID and DACHS control systems for high altitude research rockets

07 p0990 A72-20283

System methodology application to filter design for inertial reference unit calibration in digital test station for FB-111 aircraft navigation system

10 p1456 A72-23820

Earth pointing rotating satellites attitude control system based on two-degree of freedom gyroscope, determining conditions for rotor spin axis fixation in inertial space

10 p1509 A72-24646

Linear and rotational quartz fiber accelerometers suitable for geophysical and inertial use.

[AIAA PAPER 72-822] 20 p2923 A72-39103

Lorentz contraction and transformation of equilibrium forces and moments in inertial reference systems transition, discussing special relativity theory

21 p3084 A72-40938

INFARCTION

Incidence rates of myocardial infarction and sudden death from coronary heart disease for adult black and white populations in Nashville

02 p0156 A72-11425

Hemodynamic response to hypoxia in dogs with experimental myocardial infarction, discussing changes in cardiac output, stroke volume, left ventricular pressure and systemic vascular resistance

05 p0617 A72-16152

Myokinase activity determination as diagnostic test for human myocardial infarction, comparing to creatine phosphokinase activity test

05 p0618 A72-16388

Sudden death in myocardial infarction, discussing heart electrical stability, neural control, arrhythmias and cardiac conduction disturbances

06 p0761 A72-17381

Coronary artery disease and vessel involvement severity predictions from electrocardiographic and vectorcardiographic patterns of anterior wall myocardial infarction

07 p0931 A72-19994

ECG and VCG in diagnosis of myocardial infarction and QRS changes

07 p0920 A72-20174

Glucose and fatty acid metabolic response during impending myocardial infarction in animals

07 p0921 A72-20175

Hyperbaric chamber tests for hemodynamic response to oxygen inhalation at 1 and 2 atm pressure for myocardial infarction treatment assessment

08 p1114 A72-20891

Myocardial infarction effects on drug tolerance and hemodynamic changes due to digitalis doses, discussing toxic arrhythmias

08 p1115 A72-21082

Intraventricular conduction defects incidence and mortality in acute myocardial infarction, noting left anterior hemiblock dominance

09 p1266 A72-23273

Serum petidase activity determination as enzymatic diagnostic test for myocardial infarction

11 p1579 A72-25851

Myocardial infarction stress effect on serum cortisol, plasma free fatty acid and urinary catecholamine levels

11 p1582 A72-26787

Serial ECG change detection and description in myocardial infarction survivors, using computer analysis to find best diagnostic discriminants from multiple criteria

16 p2357 A72-34008

Induction of ventricular arrhythmias by elevation of arterial free fatty acids in experimental myocardial infarction.

17 p2502 A72-34997

Prognostic value of an electrocardiographic sign in acute myocardial infarction.

19 p2756 A72-37871

Systematic detection of myocardial infarction in the course of medical screening of flight personnel

19 p2757 A72-37881

An indirect method for evaluation of left ventricular function in acute myocardial infarction.

20 p2892 A72-39462

Vectorcardiographic and electrocardiographic differentiation between cor pulmonale and anterior wall myocardial infarction.

21 p3001 A72-40769

Clinical and anatomic implications of intraventricular conduction blocks in acute myocardial infarction.

24 p3374 A72-45691

INFECTIONS

U INFECTIOUS DISEASES

INFECTIOUS DISEASES

NT TUBERCULOSIS

ECG P-wave-like deflections caused by strong diaphragmatic action potentials in obese woman with fever and erysipelas

13 p1908 A72-28569

The magnetic field, infection and immunity
17 p2503 A72-35009

INFERENCE
Inferential structure of variational statements for equations of motion and constitutive relations, noting function space choice
11 p1690 A72-26554

INFLATABLE DEVICES
U INFLATABLE STRUCTURES
INFLATABLE SPACECRAFT
NT BEACON SATELLITES
INFLATABLE STRUCTURES
NT BALLOONS
NT BEACON SATELLITES
NT GAS BAGS
NT HIGH ALTITUDE BALLOONS
NT METEOROLOGICAL BALLOONS
NT TETHERED BALLOONS
Finite inflation of toroidal shell with edges bonded to rigid rim, using Runge-Kutta method to solve differential equations based on Mooney strain energy function
[ASME PAPER 71-WA/APM-20]
05 p0733 A72-15960
Rocket-borne inflatable sphere for radar signal backscatter calibrations at reentry altitudes and for simultaneous atmospheric density determination
13 p1918 A72-28819
Deceleration attenuation effectiveness of airbag restraint systems compared with seat belt-shoulder harness for aircraft occupants crash protection
15 p2191 A72-32605
Inflation pressure caused deformations of thin toroidal shells, discussing wrinkle development due to pressure reduction
[ASME PAPER 72-APM-32]
17 p2628 A72-34787
Development of an inflatable fabric structure for the early stabilization of the B-1 crew escape capsule.
[AIAA PAPER 72-801]
20 p2888 A72-40053
On the asymptotically spherical deformations of arbitrary membranes of revolution fixed along an edge and inflated by large pressures - A nonlinear boundary layer phenomenon.
21 p3118 A72-40840
Investigation of the parachute inflation aid utilizing liquid vapor pressure.
22 p3139 A72-43141

INFLATING
Parachute opening shock and filling time calculation based on aerodynamic drag, air mass and effective porosity time functions, using momentum and continuity equations
01 p0004 A72-10310
Parachute inflation loads and times, presenting calculation method based on unsteady pressure distribution on decelerating inflating parabolic shell of revolution with unsteady starting vortex
01 p0004 A72-10311

INFLUENCE COEFFICIENT
NT STRUCTURAL INFLUENCE COEFFICIENTS
Multistage axial flow compressor adjustment by flow geometrical dimension changes obtaining influence coefficient from linearized mathematical model
05 p0708 A72-17064
Multistage gas turbine flow area dimension change influence coefficient calculation from discrete nonlinear mathematical model through equation linearization
05 p0708 A72-17065
Influence coefficients method accuracy for design and adjustment of gas turbines, engines and parts
07 p1054 A72-18998
Influence coefficients for circumferential stress resultants in long conical shell elements without edges interaction
10 p1555 A72-24192
Supersonic aerodynamic influence coefficients matrices calculation for wings of arbitrary planform, constructing computer program
12 p1752 A72-28142
Computer program for gas turbine characteristics and influence coefficients calculation, allowing for cascade loss distribution during flow choking
12 p1862 A72-28151
Stability of compressed elastic rod with continuously varying stiffness, deriving solution via influence function
14 p2166 A72-30691
Feedback influence coefficient on amplifier gain, using recurrent difference concept
19 p2777 A72-37314
Evaluation of the coefficients of influence of initial information and model errors on optimization results
19 p2779 A72-37996
Statistical analysis of influence coefficients and unbalance forces measurement errors in balancing of rotors
21 p2996 A72-41229

INFORMATION DISSEMINATION
Automated system pathfinder application to systems design and analysis for engineering information exchange
03 p0326 A72-14198

Educational and social applications of communication and meteorological satellite data dissemination, discussing learning and teaching model development
06 p0777 A72-18624
Book on NASA technology transfer program covering regional university-based dissemination center evaluation and comparison with other transfer mechanisms
07 p1102 A72-19182
Space communication application for information, education and cultural exchange, noting need for international cooperation
07 p1104 A72-19473
Meteor trail radar data processing for upper atmosphere research, proposing dissemination for dynamical synoptic exploration
10 p1438 A72-24716
Fixed and broadcast communication satellites for educational information dissemination in U.S., discussing commercial, multipurpose domestic and hybrid systems
[AIAA PAPER 72-523]
12 p1779 A72-27352
Cost effectiveness model for evaluating general aviation weather dissemination techniques, stressing design variables and time periods
13 p1994 A72-28871
Time data dissemination techniques, discussing astronomical and atomic time scales, frequency standards, broadcasting and TV, navigation and satellite systems
14 p2085 A72-30364
Structural mechanics computer programs compendium covering subject oriented information according to structure type, load environment and analytical models
15 p2328 A72-31771
Reliability, safety, maintainability and system effectiveness disciplines acquisition, processing, dissemination and exchange via Government-Industry Data Exchange Program and Failure Rate Data Program
24 p3467 A72-44660
Cross section parameters for electron impact excitation, noting mathematical models for aeronautical users
24 p3400 A72-45591

INFORMATION FLOW
Information feedback application to AM laser communication system, predicting multiplicative error, background shot noise and photon arrival fluctuation effects on continuous parameter transmission
[AD-736731]
01 p0025 A72-10326
Aircraft optimal control for case of continuous data flow on time variable flight conditions
07 p1032 A72-18979
Technology transfer model in terms of donor-recipient activities for information implementation, forecasting and long range planning in developing countries and regional economics
07 p1106 A72-20271
Cortical synthesis and information handling properties of evoked potential in human normal and pathological behavior
08 p1119 A72-21840
NASA technology transfer from information dissemination and service to product development, noting firemen breathing system
17 p2639 A72-35506
Systematic approach to study energy and information flow through measuring system in experimental mechanics, using transducer model
18 p2690 A72-36356
The Gander automated air traffic system.
19 p2830 A72-37748
Control center relation to process control computers in production engineering, discussing information flow and communication in man machine systems
19 p2761 A72-38310
Man machine system functions and display and control role descriptions by flow diagrams, giving examples of keying and task in guided weapon system
21 p3011 A72-41415

INFORMATION MANAGEMENT
Project management mathematical models for task scheduling, resource allocation, information planning and decision making
06 p0905 A72-18067
Soviet papers on industrial plants automatic control systems organization, design and technological arrangement, covering information handling requirements and man machine interfaces
08 p1256 A72-22144
Selection, arrangement and use of computers and peripheral equipment in automated administrative control management system within industrial enterprise
08 p1256 A72-22147
Data transmission system design in computerized administrative control system for industrial enterprise management
08 p1257 A72-22148
Industrial enterprises preparation for computerized administrative control systems introduction
08 p1257 A72-22149

INFORMATION RETRIEVAL
Information content in simulated ERTS space photographs as function of various levels of image resolution
02 p0212 A72-11834
United Air Lines computerized information retrieval system for message switching, flight planning and monitoring and aircraft parts inventory control
[IEEE PAPER 23,3]
04 p0598 A72-15713
Retrieval model based on probability distribution defined on set of all admissible arrays of elements in loci set
10 p1446 A72-25191
Language description of remotely sensed image data, noting application to artificial intelligence, linguistic analysis and retrieval
13 p1924 A72-28525
Random retrieval algorithms in finite set of preset movement directions, considering quadratic function minimization
13 p1924 A72-28610
Parameter identification method using combined acceleration search /Partan/ and continuous parameter tracking techniques
13 p1935 A72-29102
Data file optimal arrangement for retrieval by programmed procedures formulated as combinatorial problem, using branch-and-bound method for solution
19 p2770 A72-38619
Reading of holograms by a semiconductor injection laser.
20 p2933 A72-39518

INFORMATION SYSTEMS
NT MANAGEMENT INFORMATION SYSTEMS
Earth resources information systems using satellite and aerial IR terrain photography and ground teams for international cooperation, emphasizing timber inventory
01 p0063 A72-10950
United Air Lines computerized information retrieval system for message switching, flight planning and monitoring and aircraft parts inventory control
[IEEE PAPER 23,3]
04 p0598 A72-15713
System properties of information patterns in complex hierarchical automatic control systems
07 p0949 A72-18927
Instructor station design for automated flight training systems, considering human factors and informational requirements
07 p0928 A72-19277
Optoelectronic elements for information system applications, discussing photomultipliers, photodiodes, photoresistors, avalanche and photoparametric diodes response and bandwidth characteristics
08 p1169 A72-21844
Reliability of recoverable information systems with temporal redundancy
08 p1180 A72-22058
Ground based ATC information processing systems analysis, considering controllers work load
09 p1348 A72-22778
System reliability improvement technique for identification and prevention of failures, using Experience Storage Program for design problem documentation collecting, storage and retrieval
10 p1486 A72-24021
Informational reliability of automatic control system comparators, considering tolerance field contraction effect
10 p1456 A72-24081
Avionics systems electrical interface connection design information document creation and dissemination, using EMPRENT computer program
10 p1453 A72-24864
Measuring information systems optimization, considering first order system with time lag
11 p1611 A72-26436
Effectiveness and reliability criteria for information and monitoring systems performance evaluation, suggesting use of revenue ratio
11 p1611 A72-26437
Individuals with high information potential in informal communications networks of government R and D organizations, discussing personal characteristics
12 p1891 A72-27654
Man machine system to repack weather information for easy assimilation, considering computer driven keyboard CRT displays
13 p1924 A72-28872
Ground station with control, communication and information processing centers, discussing automation, data transfer, system control and emergencies
[DGLR PAPER 72-007]
13 p1939 A72-28965
Human operator decision making role in information presentation system determined by experiments using laboratory performance and test measures, field observation, electrical and biochemical measures
21 p3010 A72-41408
Computerized weight data storage, recording and information system to aid in aerospace vehicle design
[SAWE PAPER 933]
23 p3266 A72-43473

INFORMATION THEORY
EEG parameters estimation and statistical uncertainty calculation by computer program
01 p0016 A72-10073

Two element matrix patterns generation with different degrees of internal constraint, developing objective complexity measures based on information theory or symmetry and grouping considerations
01 p0013 A72-10715

Methodological problems in unidimensional information transmission involving circular light identification tasks
01 p0013 A72-10715

Report on U.S. telecommunications telemetry information theory in period 1966-1969, discussing ionospheric and tropospheric data transmission
02 p0171 A72-11687

Information theory in metrology, comparing measurement techniques and calculating quantity of measurement information
06 p0817 A72-18164

Optimal design of dynamic system with universality for series of maneuvers with various degrees of informativeness, considering flight mechanics of limited power engine system
06 p0848 A72-18299

Conformal electron interactions in biopolymer and hypermolecular biological systems, discussing calcium ions effects, enzyme activity, muscle contractions and information theory
07 p0915 A72-18803

Estimation-correlation principle and optimal detector for incomplete a priori information signal reception on random and white noise background
08 p1131 A72-20790

ATC operator stress factor evaluation from information theory analysis of radio telecommunication information content
09 p1271 A72-23134

Internal and integral aerial photointerpretation, discussing enhancement of information quality, quantity and reliability through participation of experts in various specialized fields
09 p1303 A72-23300

Information theory and ambiguity concept generalization for signal distinction by phase displacement in time and frequency
09 p1281 A72-23470

Mathematical model as basis for equipment design-sensitive maintainability prediction technique, using information theory concepts of design interpretation
10 p1503 A72-23979

Book on telemetry and remote control covering information theory, analog/digital techniques, signal transmission, data processing and coding, etc
10 p1436 A72-24550

Linear least mean square estimate of additive white noise-corrupted signal considered as purely nondeterministic process of multiplicity one
11 p1591 A72-25352

Book on information theory of atmospheric visibility covering vision threshold conditions, eye as radiation detector and short waves field near ground
11 p1691 A72-26697

Information theory approaches to air navigation, discussing ATC, collision avoidance and computer applications
13 p1996 A72-29013

Optimal design of dynamic system with universality for series of maneuvers with various degrees of informativeness, considering flight mechanics of limited power engine system
13 p2052 A72-29439

Probabilistic information model of adaptive predictor filters /APF/ with latent memory simulated on digital and analog computers
15 p2211 A72-31896

Information propagation time direction of cosmological models in terms of conventional electrodynamical theory, contrasting with Wheeler-Feynman theory
16 p2424 A72-33286

Magnetic recording head designs, covering information density, head-tape subsystems and head materials electrical and mechanical suitability
16 p2394 A72-33643

A method for generalized statistical studies of discrete information transmission systems
19 p2764 A72-37301

Evaluation of the coefficients of influence of initial information and model errors on optimization results
19 p2779 A72-37996

A statistical information theory for extremum search of a function
19 p2827 A72-38576

Operator to minimize information loss, deleterious truncation and aliasing effects introduced by linear interpolation
21 p3077 A72-40104

Investigation of the redundancy of telemetry information from the automatic lunar stations Luna 9 and Luna 13
21 p3014 A72-40312

Statistical analysis of information from remote space vehicles
21 p3015 A72-40327

Data link design for planetary video data transmission back to earth based on rate distortion theory generalization of information theory
21 p3019 A72-40891

Kullback-Leibler information function and the sequential selection of experiments to discriminate among several linear models.
21 p3075 A72-41187

Information theory application for structural complexity measure of microelectronic logic circuits for digital computers, noting elements standardization for design quality criteria
23 p3269 A72-43441

Information aspects in visual perimetry, obtaining memory requirement for control computer in automated perimetry
23 p3261 A72-44378

Information theory and statistical mechanics applications to thermodynamics, discussing entropy and superiority of Georgian to Kelvin temperature scale
24 p3465 A72-45372

Man in a control circuit during an information game synthesis
24 p3377 A72-45520

INFORMATION TRANSMISSION

U DATA TRANSMISSION

INFRARED ASTRONOMY

Galactic IR astronomy, discussing findings on emission from H II regions of Orion Nebula and late and early type stars
02 p0276 A72-11643

Galactic nucleus IR measurements in terms of forbidden NE II emission line at 12.8 microns
07 p1081 A72-20229

Planetary nebula IR continuum and line radiation from spectrophotometric observation relation to visual and radio wave data
08 p1235 A72-21387

IR emission sources in NGC 2264, IC 2087 and M1-82 H II regions
08 p1236 A72-21397

Ground based IR astronomical telescope detectors, relating F number and optical requirements to near, far, and intermediate IR observation
10 p1481 A72-24249

IR observation and theoretical considerations for Jupiter atmosphere inhomogeneous model with two cloud layers
[AD-742156] 11 p1721 A72-26119

IR and optical observations of cluster surrounding Herbig Be type star BD plus 40.4124, noting extreme youth of group
11 p1721 A72-26122

Lunar occultations of IRC plus 10216 for IR radiation distribution, deducing model of late type carbon star surrounded by thermally reemitting dust shell
11 p1721 A72-26123

Lunar surface roughness mapping by combined IR and radar measurements
12 p1869 A72-27328

Lunar surface roughness thermal characteristics, comparing IR data with three realistic models
12 p1870 A72-27335

IR photometry of IR-OH sources, showing IR colors correlation with velocity separation of OH emission peaks
15 p2315 A72-32711

Planetary nebula M2-9 spectrum analysis, discussing IR excess, internal motions and Fe II emission lines
16 p2455 A72-33459

Compact extragalactic nonthermal sources.
17 p2604 A72-34519

Direct infrared measurements of thermal radiation from the nucleus of comet Bennett.
17 p2604 A72-34525

The measurement of polarized 10-micron radiation from cool stars with circumstellar shells.
19 p2854 A72-37232

Variable radio objects BL Lac, OJ 287, A P Lib, B2 1212+30 and ON 231 observed in IR spectral range, noting variations in flux
21 p3107 A72-41270

Interstellar nitrogen-15 and U169.3 - Possibly a new methanol line.
21 p3107 A72-41272

Extragalactic object categorization according to IR luminosities, considering radiation mechanism models and IR spectra relation to radio spectrum
22 p3228 A72-42571

UV and IR observations of galactic and intergalactic matter from space stations, noting spatial resolution increase
24 p3446 A72-45532

OAO IR instruments development to observe IR stars, diffuse galactic objects, galactic center and extragalactic objects
24 p3446 A72-45534

INFRARED DETECTORS

Absorption cell heterodyne method for nondispersive IR detection of trace gases with molecular vibrational-rotational spectrum
01 p0023 A72-10532

Gaseous pollutants remote detection by IR heterodyne radiometer with tunable lasers
[AIAA PAPER 71-1079] 01 p0080 A72-10538

Carbon dioxide laser IR heterodyne radiometer for remote sensing of atmospheric pollution
[AIAA PAPER 71-1083] 01 p0067 A72-10540

Thermovisors /recording IR detectors/ development, discussing application to biomedical investigations and disease diagnostics
01 p0022 A72-11293

Thermal IR remote sensing of surface geothermal heat flow, presenting nighttime heat budget equation based on solar and geothermal energy
02 p0208 A72-11786

Calibration technique for low energy IR radiometers, calculating detector field of view energy content or photons number from mirror reflectivity and temperature
[AD-740035] 03 p0359 A72-13441

Miniature refrigerators design for electronic devices, noting application to IR detectors cooling
03 p0313 A72-14366

Airborne CAT detection by passive IR radiometry, reducing false alarms due to temperature anomalies
04 p0543 A72-14828

Gallium-doped Ge bolometers and triglycine sulfate pyroelectric far IR detector, testing performance as functions of frequency and temperature
04 p0525 A72-15601

Pyroelectric IR detectors hf performance in direct and heterodyne modes, including thermal expansion effects
04 p0563 A72-15603

Photoconductive detection and generation of far IR radiation in high purity epitaxial GaAs
04 p0563 A72-15605

Low temperature Ga doped Ge bolometer for IR detection, improving sensitivity by load resistance noise elimination
05 p0662 A72-16195

HF tracer gas detection in inert and combustions flows, using IR absorption technique for gaseous flow visualization
[AIAA PAPER 72-70] 05 p0651 A72-16904

Image enhancement techniques for sea-ice mapping from satellite IR data, discussing gray scale contrast augmentation scheme for visual quantitative information
06 p0807 A72-17825

Meteorological satellites TV, visual and IR cloud imaging and atmospheric sounding techniques for short and long range weather forecasting
06 p0892 A72-18066

Nimbus 4 satellite selective chopper IR radiometer atmospheric temperature measurements from earth surface to 50 km altitude, describing instrument design, operation and performance
07 p1029 A72-19097

Wideband IR heterodyne receiver in spatially coherent array, discussing signal conversion efficiency, beam crossover control, mixer characteristics and microwave antenna comparison
07 p0940 A72-19237

IR radiation detection by microwave biased photoconductor, lead-tin telluride photovoltaic detector and thermal imaging pyroelectric detector and array system
07 p1034 A72-19425

Nonideal black body temperature measurement with IR radiometer, discussing error dependence on object temperature and emissivity and background temperature
07 p0993 A72-20692

IR image tube with electronic scanning and pyroelectric target for uncooled operation at ambient temperature, noting wideband spectral sensitivity
08 p1171 A72-21966

Ground based IR astronomical telescope detectors, relating F number and optical requirements to near, far, and intermediate IR observation
10 p1481 A72-24249

Russian book on satellite-borne electro-optical IR radiometers design for celestial bodies spectral radiance and energy distribution measurement
11 p1634 A72-26376

IR pupillography for screening narcoleptics and fatigue prone individuals from driver and pilot training applicants
12 p1777 A72-28323

Satellite IR telescopes in oceanography for data acquisition on ocean state, circulation, surface temperature, salinity, pollution, etc
15 p2221 A72-31238

Aircraft or helicopter-borne IR radiometer for surface temperature of snow covers and glaciers and air-snow energy balance measurements
15 p2232 A72-31244

Aerial IR line scanner systems for forest fire detection, considering escalation from aircraft to space platform
15 p2221 A72-31250

Sea surface temperature determination on Nimbus 2 satellite, using three channels in medium resolution IR radiometer
15 p2224 A72-31674

Liquid crystal detector design for IR holography and interferometry with applications to NDT of semiconductors, plasma diagnostics and material research
15 p2237 A72-32055

Coherent IR heterodyne receivers with quantum noise threshold sensitivity for laser communications and radar transmission

15 p2198 A72-32063

High temperature lattice and radiative thermal conductivity measurements utilizing carbon dioxide laser and IR detector for diffusivity and mean extinction coefficient phase data

15 p2250 A72-32507

Pyroelectric radiation detector with ferroelectric crystals, discussing operation mode, construction, sensitivity and IR applications

17 p2530 A72-35445

Procedure for the calibration of photoelectronic components in the IR spectral range

18 p2693 A72-37005

Reliability of HgTe-CdTe photovoltaic detectors

18 p2670 A72-37139

Clinical IR thermography with Thermovision camera for body temperature discontinuity detection, discussing image resolution

18 p2655 A72-37196

Remote sensing of urban 'heat islands' from an environmental satellite

20 p2919 A72-39717

Thermal imaging with pyroelectric IR detector arrays, discussing signal processing by digital technique to eliminate voltage offset variations effects in preamplifiers

20 p2928 A72-39968

Generation of infrared radiation in a metal-to-metal point-contact diode at synthesized frequencies of incident fields - A high-speed broad-band light modulator

22 p3157 A72-41971

Rocket radiometers measurement of oxygen IR atmospheric system altitude profile at night, noting auroral enhancement possibility

22 p3170 A72-42365

Mercury-cadmium telluride photodiode detectors for near IR laser receivers, discussing time response and I-V characteristics as function of temperature

23 p3296 A72-43881

Nimbus limb radiometer, Apollo fine sun sensor, and Skylab multispectral scanner

23 p3288 A72-43882

Sunspots and solar granulation recording and imaging with 64-element array of PbS IR detector for obtaining high SNR and resolution

23 p3288 A72-43883

Circular and linear dichrometer for the near infrared

23 p3289 A72-43899

Heterodyne, microwave bias and pyroelectric photon infrared detectors, noting mixed crystal photoconductive and photovoltaic detectors

23 p3291 A72-44392

IR detector specifications, construction and applications to industry science and military

23 p3291 A72-44393

INFRARED FILTERS

Transmission and passband properties of polyethylene echelette gratings and combined filters for long wave IR spectrum

08 p1210 A72-22038

Far IR filters for rocket-borne radiometer, discussing Ulrich theory and characteristic impedance determination

11 p1629 A72-25310

Low temperature interference filter design for atmospheric windows far IR photometers based on selective reststrahlen reflection of crystals

19 p2796 A72-37586

An Irtran-I reflection filter for the 20-micron atmospheric window

20 p2928 A72-39897

Signal voltage density, pulse shape and noise power spectrum analysis of matched filter configurations in IR scanning system model

21 p3033 A72-41078

INFRARED HORIZON SCANNERS

U HORIZON SCANNERS

U INFRARED SCANNERS

INFRARED IMAGERY

Direct readout ground system/DRGS/ for receiving, recording and displaying visible and IR imagery collected by ITOS and synchronous meteorological satellite radiometers

01 p0047 A72-10452

EROS program thematic mapping system for binary graphic overlays of open water, snow and ice, reflective IR vegetation and human works

01 p0066 A72-10460

Cloud temperature determination from satellite IR images, presenting error corrections for various U.S.S.R. locations

01 p0095 A72-10956

Quantitative cloud information from satellite IR thermal imagery and vertical temperature profile data

02 p0211 A72-11808

Synoptic sea surface temperature mapping off Eastern United States using NASA ITOS satellite IR imagery data

02 p0211 A72-11813

Earth surface feature recognition with IR imagery, evaluating Meteor satellite data

02 p0213 A72-11836

Multichannel multispectral airborne IR imaging system and video data processing for U.S. geological survey

02 p0227 A72-11851

Passive microwave remote sensing, discussing thermal imaging, radiometer tracking and image deterioration due to antenna imperfections

02 p0214 A72-11865

Spectral texture effects on remotely sensed high altitude automatic IR image interpretation, using Bayesian probability techniques

[AD-734261] 02 p0228 A72-11873

Thermal modeling for IR images geologic interpretation, discussing physical parameters role in materials natural environmental diurnal temperature behavior

02 p0214 A72-11877

Automatic geologic mapping with calibrated narrow band visible and near IR rock reflectivity data and computer processing

02 p0215 A72-11878

Airborne remote CAT detection equipment, examining pulsed Doppler laser and IR radiometry

04 p0521 A72-14831

Thermal IR imaging remote sensing device for aerial earth resource surveys, noting hydrogeology, volcanology, forest fire and geothermal region detection and ice sheet study applications

06 p0807 A72-17789

Environmental applications of airborne IR imagery, discussing detection, mapping and monitoring of water bodies thermal patterns and anomalous heat manifestations on land

09 p1312 A72-23301

Color enhanced black and white IR satellite images for oceanographic applications

11 p1620 A72-25346

Image conversion from 10.6 to 0.65 micron wavelength by nonlinear optical method in proustite crystal

12 p1821 A72-27604

Cloud top temperature measurement by satellite through comparison of visible and IR cloud images with concurrent airborne radar and lidar measurements

13 p1944 A72-28444

Infrared and radar maps of the lunar equatorial region

18 p2725 A72-36289

Sunspots and solar granulation recording and imaging with 64-element array of PbS IR detector for obtaining high SNR and resolution

23 p3288 A72-43883

INFRARED INSPECTION

IR ray thermography, discussing application to tires testing and rubber manufacture

07 p0991 A72-20422

INFRARED INSTRUMENTS

NT INFRARED DETECTORS

NT INFRARED SCANNERS

NT INFRARED SPECTROMETERS

NT INFRARED SPECTROPHOTOMETERS

Two dimensional time resolved and real time IR interferograms obtained with pulsed Nd doped glass laser illuminated Michelson interferometer

03 p0362 A72-14200

IR measurement of hot jets turbulence intensity axial and transverse profiles, noting application to sound sources detection

10 p1563 A72-24656

IR night vision instruments range calculation, taking into account atmospheric optics and electro-optical image converter characteristics

21 p3059 A72-41816

Spacecraft local vertical estimation and error limits in meridional and equatorial planes based on terrestrial IR radiation measuring instruments

22 p3223 A72-42205

OAO IR instruments development to observe IR stars, diffuse galactic objects, galactic center and extragalactic objects

24 p3446 A72-45534

INFRARED LASERS

Molecular Stark effect modulation of IR carbon dioxide laser radiation, using density matrix technique

01 p0079 A72-10515

Carbon dioxide IR laser construction, laboratory implementation and experimental results

02 p0239 A72-12693

Electrically excited tunable IR molecular gas lasers with rotational lines overlapping due to high pressure broadening

03 p0366 A72-12965

HCN laser amplifier gain measurement at IR wavelengths in gas mixtures by recording with pyroelectric receiver

03 p0368 A72-13667

Tunable optical and IR radiation source by rotating lithium niobate crystal in front of Q switched ruby laser

04 p0550 A72-15599

Far IR molecular laser variable interference filter for optimization of output coupling conditions and maximum power output

04 p0532 A72-15616

Tunable semiconductor and spin-flip Raman lasers for IR applications

[AD-738713] 05 p0667 A72-15788

Three frequency IR laser signal heterodyne detection with 40-MHz if narrow-band reception, measuring SNR

05 p0669 A72-16607

High power tunable IR gas lasers based on anharmonic molecules vibrational-rotational transitions excitation at gas pressures of 10 atm

06 p0825 A72-17786

Carbon dioxide laser IR radiation modulation by application of Stark effect in various molecular absorbers, showing absence of saturation

07 p1000 A72-19035

Time behavior and spectra of relaxation oscillations in high gain IR xenon laser

07 p1001 A72-19199

High repetition rate pulsed IR xenon laser using transversely excited discharge

07 p1003 A72-19221

Lamp pumped IR solid state laser obtaining 20 W output and 4 percent efficiency from transition of Ho ion in sensitized YAG

07 p1004 A72-19234

High sensitivity wideband heterodyne receiver system for spaceborne and ground-based IR laser communications

07 p0940 A72-19238

Atmospheric heating and kinetic cooling nonlinear effects on IR carbon dioxide laser beam propagation, comparing digital simulation results with geometrical optics

[CLEA PAPER 2.6] 07 p0942 A72-19381

Pulsed IR carbon dioxide TEA laser for two dimensional interferometry of theta pinch plasma during discharge

07 p1005 A72-19416

CW gas laser operating in far IR, discussing water vapor excitation by dc discharges

07 p0946 A72-19961

Defocused confocal Fabry-Perot spherical interferometer for analysis of Q switched visible and near IR lasers longitudinal mode outputs

10 p1481 A72-24564

IR carbon dioxide laser amplifier with fundamental mode output power in excess of 500 W, describing multistage mirror section design and test results

10 p1492 A72-24581

Extremal feedback control system for IR and sub-millimeter range laser emission frequency stabilization

11 p1650 A72-26358

Mathematical model for thermal lensing of IR laser window, discussing aberrations effect on diffraction-limited far field focus time

12 p1819 A72-27284

Carbon dioxide-helium-nitrogen mixture laser, comparing GaAs, CdSe, CdS and CdTe electro-optical crystals suitability for radiation modulation at 20.6 microns

12 p1822 A72-27610

Microwave source four hundredth order harmonic mixing with laser radiation, using Josephson junction and maser

12 p1827 A72-28221

Tunable monochromatic IR laser based on magneto-Raman scattering from conduction electrons in n-type InSb, discussing physical processes and experimental techniques

15 p2250 A72-32393

Sealed room temperature gas laser output oscillating on 5-micron carbon monoxide or 10-micron carbon dioxide lines

15 p2251 A72-32533

Holograms on bismuth and paraffin thin films with pulsed high power TEA carbon dioxide IR laser, discussing photosensitivity and capability for interferometric measurement

16 p2392 A72-33390

Magnetic field effect on polarization plane rotation and emission frequency shift of He-Ne ring laser at 3.39 micron wavelength

16 p2402 A72-33485

Extremal feedback control system for IR and sub-millimeter range laser emission frequency stabilization

16 p2403 A72-33711

Variable output coupling device for far infrared laser

17 p2562 A72-34643

Competition effects on spatial coherence in a CO2 laser

17 p2562 A72-34725

IR carbon dioxide laser radar with heterodyne detection, measuring SNR and atmospheric scattering coefficients for various weather conditions

17 p2516 A72-35192

Atmospheric pressure carbon dioxide pulsed IR laser to obtain 80 W peak power by optical pumping with TEA HBr laser and filter

17 p2565 A72-35816

Continuous arc generation in Ar via focused CW carbon dioxide TEA laser, inducing gas breakdown by focal volume preionization with single pulse
18 p2697 A72-36082

Certain results of a study of the emission-frequency stability of gas lasers at 0.63, 1.5, 3.39, and 9.6 micron wavelengths
19 p2814 A72-38786

Pulsed IR laser for heating supersonic plasma to high temperature, featuring inertial confinement by use of short duration energy and strong magnetic field
19 p2843 A72-38823

Pump laser design for an infrared upconverter.
20 p2934 A72-39873

Thermal decay of an infrared-laser-heated arc plasma.
21 p3090 A72-40341

Resonance absorption of laser emission by methane behind the shock front
21 p3063 A72-40986

IR CW laser emission from arc generated flowing CO active medium, describing thermal dissociation of oxygen followed by carbon disulfide injection
22 p3185 A72-42611

Spontaneous self mode locking in transversely excited nitrogen laser operation in first positive system
22 p3186 A72-42618

Pulsed room temperature laser action of Si-doped double heterostructure GaAs p type diodes within 9100-9500 A wavelengths, discussing threshold current densities and power efficiency
22 p3186 A72-42621

Laser magnetic resonance of the O₂ molecule using the 337-micron HCN laser.
22 p3209 A72-42896

INFRARED MASERS

U INFRARED LASERS

INFRARED PHOTOGRAPHY

Airborne remote sensing of earth surface physical properties, using panchromatic and IR black and white, true color and IR false color photography
02 p0208 A72-11782

Silicate rocks mapping from aerial IR data, discussing method for discriminating emission from background radiation
02 p0208 A72-11787

Photogeological remote sensing of high voltage dc power transmission system induced ground current paths, discussing X-15 near IR photographic recordings
02 p0212 A72-11826

Digital computer mapping of terrain by clustering techniques, using color IR film emulsion layers as three band spectrometer
02 p0215 A72-11879

Southeast Florida 13 year urban and agricultural development recorded by high altitude color and color-IR photographs, demonstrating capability for detail and macroscale patterns
02 p0230 A72-12199

Infrared telescopes /light collectors/, discussing diameter, photography, photometry and spectroscopy
06 p0818 A72-18298

Terrain evaluation by aerial imagery, discussing various film types for conventional visible and IR black and white and color photography, thermal IR and/or radar
09 p1303 A72-23303

Multispectral remote sensing techniques, equipment and applications, discussing color and IR camera, line scanning and radar systems and automated interpretation devices
09 p1312 A72-23304

Dynamic particle field in-line holographic recordings using IR film and p-n junction GaAs lasers
15 p2237 A72-32056

Two dimensional images from remote sensors, discussing geometrical properties and imaging equations for aerial, IR and radar photographs
17 p2555 A72-35335

Lunar color boundaries and their relationship to topographic features - A preliminary survey.
18 p2724 A72-36281

Landscape site and vegetation /timber/ predictions from color and IR aerial imagery compared with ground data
18 p2686 A72-36318

Multispectral photography in soil moisture determination and soil series differentiation.
18 p2686 A72-36320

Near-infrared photometry of Mira variables.
18 p2729 A72-37018

Use of an infrared-imaging camera to obtain convective heating distributions.
20 p2926 A72-39640

Optical quenching of the Gudden-Pohl effect in zinc sulfide luminophors and IR photography
21 p3057 A72-41680

Waterways outfall detection from color and IR color aerial photography, describing photointerpretation technique
22 p3181 A72-43197

INFRARED RADIATION

NT FAR INFRARED RADIATION

NT NEAR INFRARED RADIATION

Planetary atmosphere IR radiative transfer model using matched asymptotic expansions method
01 p0125 A72-10099

Centaurus A NGC 5128 nucleus IR radiation measurement, suggesting small nonstellar core superposed on extended reddened stellar component
01 p0132 A72-11091

IR radiation variability from circumstellar grains around carbon-rich supergiant R Coronae Borealis, noting spectrum similarity to black bodies
01 p0121 A72-11093

Automated operational procedure for sea surface temperature determination from ITOS IR data, discussing error analysis
02 p0211 A72-11810

Computer program for atmospheric effects on IR radiation, calculating transmission and radiance spectra for various remotely sensed atmospheric, path and target conditions
02 p0187 A72-11862

Thermal IR radiation attenuation by atmospheric particulates, comparing computer simulated brightness temperatures with airborne radiometer and Nimbus 3 observed data
02 p0213 A72-11863

Earth surface remote sensing with thermal IR radiation, investigating uncovered soils with heat balance equations under various weather conditions and times of day
02 p0172 A72-12017

Excited IR fluorescence in gas compounds with negligible absorption, using CW carbon dioxide laser
03 p0367 A72-13554

Statistical processing of phase dependence of Martian integral brightness at 0.3-1.1 microns, noting abrupt reflectivity decrease
03 p0436 A72-13816

Temperature reduction produced by partial cloud cover effect on radiation received by Nimbus 3 IR radiometer
03 p0385 A72-14226

Cloud interference-free sea surface temperatures, using techniques to reduce noise effect in Nimbus IR radiometer data
03 p0385 A72-14227

Nonisothermal gas layer IR radiation in multiaxial molecular vibrational-rotational band range, determining lowest level energy for wide line spectrum
04 p0547 A72-14657

Solar energy exchange by thermal radiation, investigating monochromatic emission factors at 0.3-15 micron
04 p0596 A72-14702

Tunable coherent IR signal generation and propagation by mixing carbon dioxide laser and millimeter wave klystron output in GaAs loaded waveguide
04 p0532 A72-15614

Curved-wall annular exhaust diffusers for hot engine parts IR shielding, evaluating performance tests for swirl flow and ejector secondary flow effects on pressure recovery
05 p0646 A72-15922

Hydrogen plasma absorption coefficients at laser frequencies over 0.3371-10.6 microns
05 p0694 A72-15997

Brightness temperatures and directionality of IR emission from rough lunar surface of crater field
05 p0714 A72-16104

Venus, M17 and M82 observation on ground through 345 micron atmospheric window, discussing IR fluxes
05 p0710 A72-16709

Young cluster NGC 2264 stellar radiation flux measurements, suggesting surrounding circumstellar shells producing observable IR excesses
05 p0720 A72-16716

Normal diathermancy coefficient determination from quartz and distilled water spectral transmittance data, applying to diathermic cooling system design
05 p0751 A72-17071

IR chemiluminescence study of chlorine reaction with hydrogen iodide at enhanced collision energies, investigating energy conversion efficiency and forward scattering
06 p0770 A72-17300

Piezoresonance modulation of IR amplitude in GaAs crystal by electric field at single, doubled and quadrupled frequencies
06 p0866 A72-17843

Galactic nuclei and quasars as IR source, noting critical accretion of gas at neutron stars
06 p0883 A72-18015

Azimuthal IR radiation distribution of atmospheric brightness cross sections at various zenith angles from balloon programmed-control radiometer data
06 p0808 A72-18042

Brightness temperatures over Mars south polar cap from Mariner 9 IR radiometry, comparing to Mariner 6 and 7
06 p0890 A72-18343

MHz IR/OH sources, discussing M type Mira variables or M supergiants photospheric temperature and dust shell structure
07 p1069 A72-19075

Comparative IR schlieren and interferometry techniques for measuring electron density profiles from refractive index effects of rotationally symmetric plasmas
07 p0986 A72-19613

Ruby laser telemetry station operated at 0.7 microns, describing telescope pointing system
07 p0947 A72-20257

IR radiation radiative transfer calculation for selected spectral intervals due to various model cloud droplet size distribution
07 p0980 A72-20456

Temperature and physical state effects on rubidium optical constants at 0.3-2.4 microns
07 p1050 A72-20522

Band averaged optical constants and IR characteristics of thin plastic films with/without metal substrate, using transmittance measurements [ASME PAPER 70-WA/HT-15]
08 p1205 A72-20874

IR luminescence and photoconductivity in p-type GaSe single crystals alloyed with Sn and Ge impurities
08 p1216 A72-21069

Martian height gradients from 1.6 micron carbon dioxide band intensity, using telescopes with prismatic quartz spectrometer
08 p1231 A72-21125

Vertical ozone distribution observed by Umkehr and IR methods
08 p1159 A72-21226

Quasi-elastic scattering differential cross section for nonpolarized IR radiation in electron plasma of semiconductors in strong elastic fields
09 p1366 A72-22210

Atmospheric refraction effects on IR far field irradiance distribution based on model of nonlinear interaction including absorption, transverse flow and vibrational relaxation effects
09 p1350 A72-22607

Nongray treatment of nonisothermal IR radiative transfer problem in terms of mean absorption coefficient
09 p1354 A72-22668

Coherent and incoherent structures of aerodynamic noise, analyzing compressor near field and hot jet IR emission source [ONERA, TP NO. 983]
09 p1294 A72-22816

IR emission at 2.7 microns from carbon dioxide-molecular nitrogen mixture flow, noting energy redistribution
09 p1357 A72-22854

Optical properties of Gd polycrystals in IR, explaining frequency dependence of complex permittivity
09 p1372 A72-23040

Mitogenic and IR radiation and plant bioelectricity in photogrammetry, using metabolic energy-photoemulsion relation
09 p1312 A72-23283

Intense IR radiation from galaxies central regions, comparing power levels with galactic nuclei optical and radio emission
10 p1534 A72-23899

He-Ne laser output dependence on transverse magnetic field, ascribing magneto-optical effects to IR radiation decrease
10 p1490 A72-24046

IR emission of oxygen reaction with carbon oxysulfide, investigating molecular vibrational transitions
10 p1510 A72-24133

IR absorption spectrum of gaseous ozone, obtaining mechanical anharmonicity coefficients and zero order wave numbers
10 p1511 A72-24226

IR measurement of hot jets turbulence intensity axial and transverse profiles, noting application to sound sources detection
10 p1563 A72-24656

Cygnus X-1 model with hard X rays from inverse Compton scattering of B star UV photons and IR synchrotron radiation from other component
10 p1530 A72-24944

IR radiative energy transfer to laminar flow of nongray absorbing emitting gases through circular tube
10 p1563 A72-25038

Multiple reflection absorption cell for gaseous air pollutants IR radiation measurements over wide temperature, pressure and distance ranges [AIAA PAPER 72-276]
11 p1619 A72-25216

IR refractivity measurement for atmospheric aerosol substances and sea salts [AD-744397]
11 p1620 A72-25306

Heat conduction and radiative transfer equations of IR cooling by atomic O in thermosphere
11 p1622 A72-25848

Galactic nuclei and quasars as IR sources, noting critical accretion of gas at neutron stars
11 p1718 A72-25951

IR radiation generation by Raman scattering and difference frequency mixing with Q switched Nd-YAG laser, noting peak power and photon conversion efficiency
11 p1647 A72-26149

Atmospheric ozone inference from satellite IR horizon radiance measurements
12 p1799 A72-27030

- Grain heating model of H II region to explain 100 micron emission predominance in IR sources
12 p1871 A72-27693
- Low photon IR photovoltaic response of CdS-metal junction, noting energy conversion efficiency
12 p1855 A72-28009
- IR absorption coefficients in air at 6000-8500 K and 40-95 atm, interpreting absorption due to free-free electron transitions in neutral particle fields
13 p2006 A72-29676
- IR radiation amplification due to high pressure colliding reacting molecular gas phototransitions
13 p1971 A72-29917
- Sulfur alloyed CdTe single crystals IR absorption spectrum, noting temperature effects
13 p2023 A72-29918
- Averaged atmospheric IR counter radiation values in cumulus clouds, using statistical characteristics
14 p2099 A72-30249
- Light intensity and linear polarization for single scattering by ice clouds in visible and IR, approximating crystals with long circular cylinders
14 p2128 A72-30349
- OH and IR emission from NML Cygnus, discussing gas cloud model with flattening and gas expansion
14 p2157 A72-30681
- Radiation measurements and thermal IR and photographic imaging techniques in meteorology and earth resources survey applications
15 p2221 A72-31241
- IR absorption coefficients of oxygen atom and molecule fields due to free-free electron transfers at specific elastic scattering cross sections
15 p2274 A72-31409
- Human vision sensitivity to covert IR illuminators for image intensification during night observation
15 p2189 A72-32046
- IR and visible parametric laser image upconversion experiments, demonstrating wavelength dependence on view field by black body radiometric measurements
15 p2249 A72-32152
- IR radiant energy emission from conical jet exhaust of turbojet aircraft
15 p2298 A72-32399
- Two beam optical recording instrument for atmospheric IR transmissivity, discussing spectrophotometers with changeable NaCl, KBr and LiF prisms
16 p2392 A72-33294
- Theory of photon-induced hopping on acceptors in p-type germanium.
17 p2595 A72-34750
- IR heterodyne radiometer SNR and spectral resolution, noting application to solar physics and air pollution detection
17 p2555 A72-35196
- Laser IR radiation attenuation in natural and artificial fogs, noting dependence on particle size distribution
18 p2697 A72-36102
- Laser optical and IR radiation attenuation in atmospheric precipitation, considering snow, rain and drizzle
18 p2697 A72-36103
- Meteorological applications of the Nimbus 4 temperature-humidity infrared radiometer, 6.7 micron channel data.
18 p2707 A72-36718
- Infrared dispersion of second-order electric susceptibilities in semiconducting compounds.
19 p2844 A72-37944
- IR emission of nitrogen layer heated by reflected shock wave, noting absorption cross sections under free-free electron transitions in neutral particle fields
19 p2835 A72-38776
- The use of infrared absorption to determine density of liquid hydrogen.
19 p2805 A72-38836
- OH airglow IR observation from high altitude sites with bandpass filter, noting average spatial and diurnal fluctuations
19 p2794 A72-38861
- Frequency-tunable stimulated IR parametric fluorescence produced by barium sodium niobate crystal pumped with picosecond pulses from frequency-doubled mode locked Nd-glass laser
20 p2933 A72-39560
- Calculation of solar CO vibration-rotation line profiles and equivalent widths.
20 p2973 A72-39889
- Mechanism and controlling factors of infrared-to-visible conversion process in Er³⁺/ and Yb³⁺/doped phosphors.
21 p3096 A72-40186
- Description and use of a method for characterizing noise sources in jets
21 p3046 A72-41160
- [ICAS PAPER 72-35]
- Optical quenching of the Gudden-Pohl effect in zinc sulfide lumiphosphors and IR photography
21 p3057 A72-41680
- Measurement of the vertical atmosphere transmittance in the IR spectral region with the aid of an artificial source
21 p3079 A72-41800
- Generation of infrared radiation in a metal-to-metal point-contact diode at synthesized frequencies of incident fields - A high-speed broad-band light modulator.
22 p3157 A72-41971
- Rocket measurement after sunset for altitude distribution of 1.27 micron band nightglow emission from diatomic oxygen molecules
22 p3172 A72-42435
- Mathematical models from UV, IR and radio observations of chromosphere and transition region to corona, noting temperature effects of shock wave dissipation
22 p3229 A72-42903
- Atmospheric thermal IR radiation transmission function dependence on carbon dioxide concentration, calculating spectral and vertical distributions for standard, summer and winter model atmospheres
22 p3174 A72-43005
- Cloud structure and cover determination from actinometric short wave solar radiation and IR cloud radiation measurements
23 p3311 A72-43627
- 3.39 micron resonance line absorption in shocked methane.
24 p3410 A72-45044
- Wideband parametric up-conversion of infrared waves into visible region using tunable dye laser pumping.
24 p3410 A72-45286
- INFRARED REFLECTION**
- Automatic geologic mapping with calibrated narrow band visible and near IR rock reflectivity data and computer processing
02 p0215 A72-11878
- Vacuum deposited films on CsI, AgCl, TiBr and TiCl for IR antireflection coatings on silicon [AD-736289]
03 p0380 A72-13431
- Uranus IR spectral albedo, discussing methane absorption
04 p0580 A72-15365
- Water and ice clouds spectral brightness coefficients in IR region of spectra from aircraft measurements
06 p0842 A72-18049
- Multilayer heat reflective coating optical thickness effect on temperature distributions, taking into account interlayer contact resistance and thermal radiation volume absorption
06 p0904 A72-18511
- Cloud tops height determination, considering IR radiation reflection by plane layer
12 p1841 A72-27990
- Silicon solar cells IR reflectance improvement by reflecting back electrode, obtaining 10 percent efficiency increase
12 p1758 A72-28032
- Cloud tops height determination, considering IR radiation reflection from plane layer
22 p3174 A72-43004
- INFRARED SCANNERS**
- IR scanner for Indian land areas and oceans thermal mapping, using satellite-borne multispectral photography
02 p0225 A72-11777
- IR remote detection of natural resources, discussing thermal to optical image conversion on photographic film
02 p0208 A72-11781
- Northern Alps geology, hydrology, lithology and tectonic survey, using aircraft-borne thermal IR scanner remote sensor
02 p0209 A72-11795
- Clear air turbulence radiometric detection by IR vertical scan technique, associating atmospheric lapse rate anomalies with CAT related temperature inversions
02 p0225 A72-11820
- Oil spills remote detection by multispectral photography, IR scanner imagery and microwave radiometry
02 p0226 A72-11830
- Moving window displays for IR scanner signals, producing images on magnetic video tape
02 p0228 A72-11852
- Improved Tiroso operational satellite visual and IR scanning radiometer data processing for polar and mercator map projection
02 p0173 A72-12127
- Water vapor injection into stratosphere by thunderstorms from IR radiometric inference measurements on NASA jet laboratory
04 p0544 A72-15358
- Microwave and IR radiometer surveillance of oil spills, discussing sources tracking, sea surface oil volume and flow rate determination and terminal location prediction
05 p0658 A72-16600
- Buffalo photographic aircraft for oil slick remote sensing, using aerial cameras and thermal IR scanner
05 p0658 A72-16600
- IR image tube with electronic scanning and pyroelectric target for uncooled operation at ambient temperature, noting wideband spectral sensitivity
08 p1171 A72-21966
- Rock type discrimination from ratioed airborne thermal IR scanner images of Pisgah Crater /California/
08 p1162 A72-22018
- High resolution Hadamard transform IR spectrometer with single slit and multiplex scan operation modes determined by signal strength, noise characteristics and scanning time
09 p1313 A72-23327
- Viking Mars Orbiter IR thermal mapper /IRTM/ to study surface kinetic temperature, thermal balance, anomalous cooling regions, ground frosts and water vapor
10 p1539 A72-24379
- Electrothermal NDT of metal structures by IR scanning camera or thermal image transducer
12 p1813 A72-27200
- Statistical characteristics of IR receivers with parametric carrier frequency conversion, describing noise index minimization technique
12 p1846 A72-27889
- Broad scale remote mapping of spectral composition of silicate rocks from thermal IR scanner data
14 p2099 A72-30321
- Nighttime lunar surface thermal properties from differential IR flux scans with earth based Cassegrain telescope, noting difference in brightness temperature gradients between highlands and maria
14 p2153 A72-30503
- Aerial IR line scanner systems for forest fire detection, considering escalation from aircraft to space platform
15 p2221 A72-31250
- Airborne external instrumentation pod containing IR scanner and associated test equipment for land and water surveys
16 p2393 A72-33635
- Statistical characteristics of IR receivers with parametric carrier frequency conversion, describing noise index minimization technique
16 p2427 A72-33998
- Direct infrared measurements of thermal radiation from the nucleus of comet Bennett.
17 p2604 A72-34525
- The accuracy of the intermittent photographic film advance in the camera of an airborne thermal scanner.
18 p2692 A72-36697
- Infrared testing of solar cell arrays.
20 p2890 A72-39339
- The cost-effectiveness of advanced remote sensing systems.
21 p3131 A72-40864
- Signal voltage density, pulse shape and noise power spectrum analysis of matched filter configurations in IR scanning system model
21 p3033 A72-41078
- Signal voltage density, pulse shape and noise power spectrum analysis of running integrator output in IR scanner model
21 p3056 A72-41086
- INFRARED SPECTRA**
- Quantitative interpretation of correlation mask remote sensors UV, visible and IR spectral data, discussing beam transmittance attenuation by absorption, scattering and emission [AIAA PAPER 71-1061]
01 p0066 A72-10530
- Empirical model with near IR spectra from expanding circumstellar envelope, normal pulsating atmosphere, shock front and relaxation layers and expanding radiative cooling layer
01 p0128 A72-10791
- IR radiation variability from circumstellar grains around carbon-rich supergiant R Coronae Borealis, noting spectrum similarity to black bodies
01 p0121 A72-11093
- Eta Carinae model with IR spectrum details described by compact H II region photoionized by hot massive star radiation
02 p0277 A72-11668
- Grating spectra of Jupiter North Equatorial Belt, noting absorption feature at 4.73 microns
02 p0280 A72-12206
- IR spectra of rock forming terrestrial and meteoritic silicates important in cosmic silicate dust
02 p0284 A72-12635
- Temperature fluctuations and fine structures in solar atmosphere from Ca II IR lines
03 p0414 A72-12926
- Solar magnetic field measurement with 10,830 Å He I line photoelectric spectroheliograms, observing filamentary fine structure in active regions
03 p0429 A72-13310
- Venus cloudy atmosphere IR absorption line spectra interpretation, suggesting HCl and HF formations dependence on condensation phases
03 p0439 A72-14149
- Vibrational IR and Raman spectra of dimethylaminodichlorophosphine, determining molecular structure symmetry in liquid and solid phases
04 p0481 A72-14444
- Planetary nebula IC 418 reddening constant from Paschen line intensities of IR spectrum
04 p0570 A72-14554

Atmospheric directional scattering coefficients from vertical measurements of IR spectral sky brightness near solar almucantar and direct radiation
06 p0842 A72-18048

Time behavior and spectra of relaxation oscillations in high gain IR xenon laser
07 p1001 A72-19199

Carbon dioxide IR absorption lines broadening at 298 and 207 K by evacuated high-resolution Czerny-Turner spectrograph, comparing with values based on fixed collision cross section
07 p1038 A72-19834

Room temperature IR absorption spectra of B alloyed powdered synthetic diamonds
07 p1050 A72-20253

Low temperature Si photoconverters transparent in IR solar spectrum tested on Cosmos satellites
07 p0915 A72-20616

Monograph on solar IR limb profiles covering intensity observations, apparatus, instrumental distortions and data reduction and analysis
08 p1236 A72-21489

IR spectral emittance measurement with airborne spectrometer for geological mapping over Pisgah Crater/California/
08 p1162 A72-22017

Mesospheric ozone measurement for altitude profiles, comparing rocket and ground based observations of 1.27 micron emission band at twilight
09 p1296 A72-22355

Electron phonon coupling and IR optical constants relationship to superconductivity in transition metals
09 p1369 A72-22566

Transition metals IR spectral absorptivity evaluation at room and liquid He temperatures from reflectivity measurement relative to vapor deposited Au mirror
09 p1309 A72-22604

Carbon monoxide in carbon dioxide atmosphere, determining IR absorption lines broadening at reduced temperatures
09 p1351 A72-22612

Chlorine, bromine and iodine first spectral lines observation in IR region with liquid nitrogen cooled lead sulfide detector
09 p1276 A72-22614

Airglow IR spectrum between 3 and 4 microns during morning and evening twilight, showing OH intensity drop
09 p1299 A72-22903

Seyfert galaxies emission, absorption, IR and optical spectral characteristics, suggesting model with sharp forbidden and Balmer line outer region and broad wing core
10 p1532 A72-23885

Saturated absorption spectroscopy of ammonia, considering Stark effect on IR transition
10 p1491 A72-24122

IR spectra and intermolecular potentials of nitrogen matrix-isolated protonated and deuterated nitromethane
10 p1434 A72-24339

Airborne IR radiometric measurements of upward vertical radiance from tropical sea surface at 10-12 microns, noting absorption coefficient dependence on water vapor
10 p1474 A72-24747

R Coronae Borealis type variable stars spectral, IR and polarimetric studies, outlining common features and hypotheses for phenomenon explanation
10 p1549 A72-25055

Fine structure and IR transmission functions of carbon dioxide absorption bands at high pressure and temperature, calculating transition lines strength and position
11 p1620 A72-25275

Paschen beta emission line equivalent width variation in IR spectra of omicron Ceti
11 p1716 A72-25679

Laser stimulated Raman scattering and IR absorption on crystal defects leading to atomic migration in solids
11 p1647 A72-26144

Radial temperature and water vapor concentration profiles of radiating combustion source from optical method, using IR band model
12 p1811 A72-27945

IR absorption bands in mechanically and chemically polished GaAs single crystals irradiated with varying neutron and electron doses
12 p1859 A72-28069

Venus atmosphere IR synthetic spectra of carbon dioxide band and water line formation for isotropic scattering, comparing with terrestrial clouds
13 p2040 A72-29410

Solar corona IR Fe XIII lines during 12 November 1966 solar eclipse, discussing proton collisions as line-producing excitation mechanism
13 p2042 A72-29537

Carbon dioxide power laser effects on IR spectra of HCl-ethylene and sulfur dioxide-ethylene mixtures, focusing with Ge lens
13 p1971 A72-29870

Sky spectral brightness, transmittance and indicatrix measurements at near IR wavelengths
15 p2222 A72-31398

Radiation effects measurement on neutron, proton and electron irradiated Li-drifted Si detectors by IR response technique, comparing characteristics with photovoltage effect
15 p2234 A72-31538

High resolution atmospheric millimeter wave spectrum of attenuated solar radiation from sea level observations, using Fourier type IR techniques
15 p2224 A72-31671

Chemical and spectroscopic activity of germanium tetrahydride in Jovian atmosphere in 4.7 micron window
15 p2312 A72-32094

Jupiter cloud models, observational characteristics and temperature error at 5 micron wavelength
15 p2312 A72-32095

Intermolecular hydrogen bond study of hydroxyl group in caranol and caranol-ol compounds, listing IR absorption bands for valence oscillations
15 p2192 A72-32100

Molecular nitrogen pulsed laser wavelength measurements, observing IR bands, stimulated emission lines and population inversion mechanisms
15 p2249 A72-32151

Air pressure effects on absorption dependence at IR wavelengths, using water vapor transmittance windows
15 p2202 A72-32657

Solar Fe XIII IR lines intensity ratio at 10747 and 10798 Å, deriving electron density as function of dilution factor with allowance for proton impact effect
15 p2318 A72-32784

Azomethane and azomethane-d6 IR and Raman spectra, discussing fundamental modes vibrational assignment based on band contours, isotopic shift ratios and group frequency correlations
16 p2360 A72-32923

Computerized analysis of overlapping Raman and IR spectral lines, describing routine for resolving complex spectrum into component lines via operator intervention
16 p2366 A72-33027

IR mass spectrometric study of OBF in Ne and Ar matrices, discussing molecular structure
16 p2360 A72-33223

Atmospheric transmittance calculation from 0.76-micron oxygen band fine structure parameters
16 p2417 A72-33289

Band model and scaling approximation validity for computation of transmission profile in V4 band of methane in Jovian atmosphere
16 p2461 A72-34099

The spectrum of Mars between 8 and 13 microns.
17 p2606 A72-34575

Minimum-light spectra of nine M-type variable stars.
17 p2610 A72-35118

The identification of the 1-0 and 2-1 bands of HCl in the infrared sunspot spectrum.
17 p2611 A72-35299

Limb darkening for B-type main sequence stars in the infrared.
17 p2612 A72-35383

Radiation absorption and emission in atmosphere IR spectrum influenced by water droplets around atmosphere contamination particles
17 p2552 A72-35942

Infrared and Raman spectra of lunar samples from Apollo 11, 12 and 14.
18 p2724 A72-36279

Facility and procedure for measuring the spectral transmittance of the atmosphere in the range from 0.48 to 12 microns with moderate resolution
18 p2692 A72-36965

Titan and its atmosphere.
18 p2729 A72-36989

Temperature effects on water refractive index from normal incidence IR spectral reflectance measurements
21 p3012 A72-40150

Turbulent plasma 'caldrons' in galactic nuclei
21 p3114 A72-41772

Polarimeter for recording of magnetooptical rotation dispersion and Kerr equatorial effect in visible, near UV and near IR spectral ranges
22 p3176 A72-42108

Fundamental infrared lattice vibration spectrum and the laser-excited Raman spectrum of MoSe₂.
22 p3185 A72-42321

Infrared observations of the moon and their interpretation.
22 p3225 A72-42527

Extragalactic object categorization according to IR luminosities, considering radiation mechanism models and IR spectra relation to radio spectrum
22 p3228 A72-42571

Indirect transitions and absorption in the mid-IR region of the spectrum in SbSBr crystals
23 p3323 A72-43337

Infrared photometry of Northern Wolf-Rayet stars.
23 p3337 A72-43827

A meteor spectrum in the infrared region.

23 p3341 A72-44473

The spectral albedo of water clouds in the 1- to 6-micron range
24 p3395 A72-44636

INFRARED SPECTROMETERS

Spaceborne Fourier interference spectrometer for environmental pollutant sensor, discussing IR detection systems, instrument servo, data reduction and handling systems and optical tolerance
01 p0067 A72-10552

Atmospheric water vapor vertical distribution from satellite IR spectrometer measurements, noting effects, absorption coefficients and temperature profiles errors
01 p0095 A72-10831

Orbiting multispectral scanner with independent land and oceanographic spectrometers for ground controlled dual mode operation
02 p0226 A72-11823

Far IR Fourier spectrometer with built-in real time digital computer for routine physical and chemical spectroscopy
04 p0520 A72-14523

Visual display IR spectrometer for pulsed transversely excited carbon dioxide laser, tabulating observed wavelengths
04 p0524 A72-15540

Ruling defects of echelette diffraction gratings for far IR high luminosity spectrometers
05 p0689 A72-16192

Carbon dioxide IR absorption lines broadening at 298 and 207 K by evacuated high-resolution Czerny-Turner spectrograph, comparing with values based on fixed collision cross section
07 p1038 A72-19834

Mariner Mars 1969 IR spectrometer for Mars atmosphere and surface spectra recording, describing design specifications and optimization for low light level sensitivity
09 p1313 A72-23326

High resolution Hadamard transform IR spectrometer with single slit and multiplex scan operation modes determined by signal strength, noise characteristics and scanning time
09 p1313 A72-23327

Ballistic density and wind determination from radiances observed by satellite IR spectrometer (SIRS) onboard Nimbus 3
13 p1991 A72-28825

Fourier transform spectrometer observation of IR coronal emission lines during 7 March 1970 solar eclipse from high altitude aircraft
13 p2042 A72-29538

Stepwise multiple regression techniques for Nimbus 3 IR interferometer-spectrometer (IRIS) data inversion, obtaining radiation predictors of meteorological parameters
16 p2418 A72-33666

Spectroscopy of pulsed HF chemical lasers using an infrared vidicon camera tube.
17 p2562 A72-34641

Evaluation of the possibilities of IR diffraction spectrometers
19 p2801 A72-37965

The composition of the Martian atmosphere - Minor constituents.
21 p3110 A72-41458

INFRARED SPECTROPHOTOMETERS

Aqueous solutions specular reflectance measurement, using organic dye laser spectrophotometer at 360-650 nm and reflectometer equipped spectrophotometer at 0.2-20 micron wavelengths
02 p0226 A72-11831

IR spectrophotometric data for Jupiter, determining limb darkening nature and ammonia and methane absorption variations over belts, zones and Red spot
10 p1548 A72-24971

Grid polarisers for use in the near infrared.
20 p2922 A72-39046

INFRARED SPECTROSCOPY

Venusian polar tropopause and cloud layer from IR spectral recording in carbon dioxide band near inferior conjunction for crescent regions
03 p0436 A72-13814

IR spectroscopy analysis of oxidation treatment, chemical and structural changes during carbon fiber formation from acrylic precursors
05 p0680 A72-16076

Emission spectra of exploding copper wires in air and vacuum in IR, UV, visible and vacuum UV regions
05 p0691 A72-16991

Infrared telescopes/light collectors/, discussing diameter, photography, photometry and spectroscopy
06 p0818 A72-18298

Mariner 9 experiments, discussing IR interferometric spectroscopy observations of Mars dust composition and pole flattening
06 p0889 A72-18340

Mariner 9 IR spectroscopy observations of Mars surface, indicating dust with silicon oxide content and atmospheric warming and water vapor over south polar cap
06 p0890 A72-18342

- Astronomical IR spectroscopy of Alpha Ori, discussing OH line formation, LTE, rms turbulence velocity and abundance
07 p1072 A72-19345
Press for air sensitive materials preparation for IR spectroscopic examination
07 p0965 A72-20577
Spectroscopic moments of molecular collision induced far IR and Raman spectra, stressing gas dimers contribution
09 p1276 A72-22859
Michelson interferometer application for continuous gas analysis in far IR
10 p1480 A72-24174
Satellite IR spectrometer sounding measurements reduction for atmospheric temperature profiles, obtaining coefficients by statistical regression and minimum information solutions
10 p1508 A72-25081
Spherical specularly reflecting nonresonant cavities for use as absorption cells in far IR spectroscopy, predicting performance
11 p1629 A72-25301
Autumnal stratospheric temperature variations in northern and southern hemispheres from Nimbus 3 IR spectrometer
11 p1680 A72-25761
Emission spectra of exploding copper wires in air and vacuum in IR, UV, visible and vacuum UV regions
12 p1843 A72-27134
Ion bombardment and partial discharges effects on polyethylene sheet, observing structural changes by IR spectroscopy
13 p1984 A72-29788
Calibrated thermal emission spectra under extreme temperature, surface reststrahlen and cloud conditions from Nimbus 4 IR spectroscopy
15 p2223 A72-31510
Internal reflection IR spectroscopy application to composite and double base propellants study, discussing merits as quality control technique
15 p2296 A72-32312
IR internal reflection spectroscopy application to dynamic chemical changes study on ammonium perchlorate surface during thermal decomposition, observing crystal lattice transformation
15 p2296 A72-32313
Oxygen molecule parameters from frequency data in microwave, submillimeter and IR spectroscopy
15 p2283 A72-32654
Hydrogen to helium mixing ratio in giant planets from far IR spectroscopy for atmospheric thermal models and greenhouse effect calculations
15 p2315 A72-32727
IR spectroscopy of Luna 16 regolith samples, noting differences in reflection, emission and transmission spectra of related terrestrial rocks
17 p2610 A72-35212
Comparison of infrared and activation analysis results in determining the oxygen and carbon content in silicon.
17 p2511 A72-35330
IR-spectroscopic investigation of the effectiveness of oxidation inhibitors in lubricants
19 p2823 A72-38092
IR chemiluminescence technique /method of arrested relaxation/ to measure spectral energy distribution among Cl and H1 and DI reaction products
19 p2763 A72-38802
Quantitative spectroscopy of the aurora. I - The spectrum of bright aurora between 7000 and 9000 Å at 7.5 Å resolution.
21 p3049 A72-41724
Spectroscopic study of the interaction of oxides with metallic surfaces. II - SiO₂-Fe /Cu, Al, Ni, Co, Ti, W/ systems
22 p3189 A72-42197
Absolute measurement of the solar brightness in the spectral region between 100 and 500 microns.
22 p3225 A72-42389
IR reflectance [or emittance] remote spectroscopy of mineral particulate surfaces, discussing particle size, surface roughness, porosity and mixing ratios effects
22 p3178 A72-42526
Coriolis constants for prolate symmetric top molecules from gas phase Raman band contours observation, noting comparison with IR spectroscopy
22 p3209 A72-42719
Measurement of the temperature of flames containing scattering particles on the basis of IR radiation
23 p3356 A72-43678
IR spectroscopy techniques based on Pfund triple-pass absorption cell, image slicer and achromatic doublet lenses, presenting graphs for prism dispersion design parameters
23 p3289 A72-43895
Infrared spectroscopy for chemical composition of inorganic and organic products formed on friction surfaces of gas turbine parts immersed in hydrocarbon fuels
23 p3325 A72-43974
Quartz and feldspar glasses produced by natural and experimental shock.
23 p3285 A72-44136
- Some infrared diagnostic techniques in high temperature gasdynamics.
24 p3402 A72-45043
- INFRARED STARS**
IR point source Becklin star spectrum consistent with highly reddened early-type supergiant with weak absorption masked by low resolution
01 p0133 A72-11094
Galactic plane 100 micron survey, detecting continuum radio sources, bright and dark nebula and IR stars
04 p0570 A72-14524
IR emission sources in NGC 2264, IC 2087 and M1-82 H II regions
08 p1236 A72-21397
OH emission characteristics of IR stars from model with asymmetrical expansion outward of circumstellar OH clouds
10 p1542 A72-24613
Photometric observations of Haro-Chavira IR stars, noting variable nature predominance
17 p2604 A72-34443
- INFRASONIC FREQUENCIES**
NT MICROSONICS
Portable detector-recorder for automobile, blast furnace, railroad car, engine room and helicopter infrasonic noise measurements, discussing peak frequencies and subjective effects
01 p0101 A72-10157
Microbaroms produced by ocean waves radiated infrasonic, noting dependence on upper atmosphere temperature and winds
09 p1348 A72-23656
Infrasonic pressure disturbance generation during 31 October 1968 polar substorms growth and decay from North American stations observations
10 p1475 A72-24953
Supersonic auroral motions relationship to infrasonic waves generation, showing acoustic pulse within electrojet arcs due to collisions with neutral gas of positive ions
11 p1624 A72-26403
Infrasonic research - Conference, Pullman, Washington and Moscow, Idaho, November 1970
11 p1627 A72-26508
Atmospheric infrasound measurement techniques and instrumentation for long distance propagation, considering wind and temperature effects
11 p1635 A72-26509
Atmospheric turbulent coherent noise in pipe arrays design for infrasonic wave detection
11 p1689 A72-26511
Acoustic ray tracing of long range infrasonic signals from launch and reentry of Saturn 5 rockets
11 p1690 A72-26512
Infrasound observations of natural background and signals from Apollo 14 and aircraft, using thermistor flowmeter microphone array
11 p1690 A72-26515
Negative auroral arc infrasonic wave observations during substorm poleward expansions at Inuvik, Canada
11 p1627 A72-26516
Infrasonic observations of acoustic auroras, using microbarographs and resonant detector recordings
11 p1627 A72-26517
Bibliography on infrasonic sound wave generation, propagation and detection at ground level and ionospheric heights
11 p1690 A72-26520
Infrasound excitation of red oxygen emission at 6300 Å during geomagnetic storms at middle latitudes
14 p2098 A72-30146
- INGESTION (BIOLOGY)**
NT DRINKING
NT EATING
INGESTION (ENGINES)
Simulated testing of turbojet engine ingestion of missile exhaust, determining design criteria for aircraft engine inlets from altitude chamber test data
07 p1052 A72-18758
Gas turbine engine icing, discussing atmospheric conditions, damage due to ice ingestion and anticice systems
[ASME PAPER 72-GT-6]
11 p1703 A72-25609
Ion thruster performance calibration investigating double ion content, back ingestion, beam spreading and propellant flow rate
[AIAA PAPER 72-475]
11 p1709 A72-26206
Erosion effects on gas turbine engine compressor blades due to dust ingestion, discussing means for alleviating performance and service life losses
[ICAS PAPER 72-02]
21 p3099 A72-41127
- INGOTS**
Carbon impurity effects on molybdenum ingot formation, detailing crystal growth, size reduction and length
04 p0533 A72-14987
Ti alloys evaluation technique of arc melting, processing and testing of miniature ingots, discussing alloying and microstructural effects and correlation with plate properties
05 p0674 A72-16390
- INHABITANTS**
NT MOUNTAIN INHABITANTS
- INHALATION**
U RESPIRATION
INHIBITION
The role of inhibition in the fatigue phenomenon
17 p2503 A72-35015
- INHIBITION (PSYCHOLOGY)**
Lateral spatial interactions of sensory receptors, discussing mathematical theory for monocular visual inputs described by real valued functions on continuum
01 p0021 A72-11196
Lateral inhibition effect on disappearance mode of visual perceptual units /lines and angles/
02 p0164 A72-12489
Neurophysiological mechanisms responsible for conditioned reflexes, considering cells, reaction relationship to animal behavior, neuronal stimuli interactions, internal inhibitions and trace process reproduction
08 p1118 A72-21835
Conditioned stimuli presentation role in successive differentiation and inhibition limits in monkeys
13 p1902 A72-28644
Lateral inhibition in auditory perception proved by psychophysical study of nervous activity stimuli patterns, noting erroneous measurement of pure tone masked threshold
16 p2357 A72-33970
Evoked potentials of the primary auditory cortical zone produced by positive and inhibitive conditioned stimuli
21 p3001 A72-40806
Electrophysiological investigation of the excitation and inhibition processes in the auditory cortex
22 p3148 A72-43165
Synaptic events during specific and nonspecific inhibition of visual cortex neurons
23 p3257 A72-44088
- INHIBITORS**
NT WEAR INHIBITORS
Beta-adrenergic inhibitors effects on coronary blood flow and myocardial oxygen consumption of normal and coronary artery disease patients
08 p1118 A72-21549
Burning velocity inhibitors effect on hydrocarbon-oxygen-nitrogen mixtures ignition by hot wires
[AD-744624]
08 p1129 A72-22039
Double base propellant nitroglycerin interactions with inhibition materials cellulose acetate and ethyl cellulose, noting time and temperature effects
14 p2145 A72-30767
Refractory materials fabrication characteristics for aerospace technology, presenting listing of synergic agents for use with halogenous inhibitors
17 p2571 A72-35277
Austenitic steel stress corrosion prevention at high temperatures and pressures, investigating inhibitor adsorption properties from capacitance measurements and polarization curves
17 p2568 A72-35474
Aromatic hydrocarbons - Methane ignition inhibitors
19 p2879 A72-37364
Chain interaction during the inhibited burning of hydrogen
19 p2880 A72-37741
IR-spectroscopic investigation of the effectiveness of oxidation inhibitors in lubricants
19 p2823 A72-38092
- INHOMOGENEITY**
Nonhomogeneous media electrodynamics with varying permittivity and permeability, solving nonstationary equations by differential operators
03 p0389 A72-13654
Hf wave scattering in inhomogeneous medium, examining asymptotic methods
03 p0390 A72-13973
Soviet book on nonlinear problems of inhomogeneous shallow shell theory covering bending, stability, bearing capacity, plasticity criteria, compressibility, etc
03 p0454 A72-14225
Structural inhomogeneities effect on fatigue phenomenon in rolling motion, discussing stress cycles preceding active surface degradation
04 p0526 A72-14473
Complex transmission coefficient of waveguide with two arbitrarily spaced infinitely thin plane parallel inhomogeneities, using Galerkin method for single-parameter approximation of electrodynamic problem
07 p0938 A72-19002
Holographic interferometry application to weak inhomogeneities visualization in gas flows, using photographic emulsion nonlinear properties
09 p1311 A72-22965
One dimensional shock wave propagation in inhomogeneous elastic materials, showing wave amplitude behavior dependence on critical jump in strain gradient
09 p1405 A72-22990
Inverse boundary value problem of optically inhomogeneous layer nonuniform profile construction from optical field distribution
10 p1510 A72-24050

Electromagnetic wave scattering on inhomogeneities by Born approximation, estimating maximum error for small correlation radius

10 p1436 A72-24503

Two dimensional approximation for viscoelastic inhomogeneous material with hereditary properties varying in radial direction, deriving integrodifferential equations

12 p1878 A72-27088

General analysis and synthesis of alloys and materials with inhomogeneous physical properties, noting thermal physicochemical methods for laminates and metal powders

16 p2405 A72-33095

The perturbation of alternating geomagnetic fields by three-dimensional conductivity inhomogeneities.

17 p2545 A72-34350

Holographic interferometry application to weak inhomogeneities visualization in gas flows, using photographic emulsion nonlinear properties

17 p2558 A72-35893

Microinhomogeneous elastic media with moduli tensor as coordinate random function, investigating stress and strain tensors

18 p2735 A72-36668

Influence of an optically nonhomogeneous medium on the coherence of laser radiation and the possibility of obtaining a holographic image

19 p2812 A72-38536

Reflection coefficient method of remote probing for inhomogeneous media, using plane wave incidence angle dependence

20 p2927 A72-39719

Book on nonhomogeneous boundary value problems covering Hilbert theory for trace and interpolation spaces, elliptic operators and variational equations

21 p3076 A72-41526

Reissner-Sagoci problem for semiinfinite elastic solid stress and displacement determination, discussing generalization to nonhomogeneous media with circular part under axisymmetric twisting

23 p3314 A72-44266

INITIAL VALUE PROBLEMS

U BOUNDARY VALUE PROBLEMS

INITIATION

Liquid and solid explosives detonation, initiation and shock interaction with inert materials for precision work

16 p2476 A72-33352

INITIATORS (EXPLOSIVES)

NT BOOSTERS (EXPLOSIVES)

NT DETONATORS

NT PRIMERS (EXPLOSIVES)

Firing characteristics of insensitive electroexplosive devices under impulsive waveforms, discussing theory, design and application of waveform generators

08 p1220 A72-20763

Nondestructive testing of electroexplosive devices, considering bridgewire-explosive interface and faults-abnormalities interrelationship

08 p1220 A72-20764

Aluminum plated pyrotechnics physical properties and performance for electroexplosive device applications, describing particle size distribution and loading pressure dependence of density

08 p1221 A72-20772

Fully redundant hermetically sealed cable cutter for application to electroexplosive devices in space

08 p1221 A72-20775

System reliability demonstration test cost minimization for one-shot electroexplosive device

13 p2024 A72-28367

Electroexplosive devices firing energy parameters determination by capacitor discharge system providing exponential pulses terminated at adjustable width

14 p2143 A72-30200

Aerospace vehicle explosive components initiation, separation and destruct systems

16 p2443 A72-33361

Sensor selection for electromagnetic instrumentation system with sufficient sensitivity and bandwidth to demonstrate electroexplosive device compliance with MIL-E-6051D specified safety margin

20 p2962 A72-38979

INJECTION

NT CARRIER INJECTION

NT FLUID INJECTION

NT FUEL INJECTION

NT GAS INJECTION

NT ION INJECTION

NT LIQUID INJECTION

NT SECONDARY INJECTION

NT WATER INJECTION

INJECTION CARBURETORS

U CARBURETORS

U FUEL INJECTION

INJECTION GUIDANCE

Optimum instantaneous impulsive orbital injection for specified asymptotic velocity vector, noting results of radius and asymptotic vector angular separations

03 p0437 A72-13837

Satellite launch vehicles guidance and control systems, discussing control parameters for minimum injection error

07 p1033 A72-20604

Mars Viking 1975 mission objectives and navigation activities from trans-Mars injection through post-landing stationkeeping phase, considering trajectory dispersions

15 p2269 A72-32180

INJECTION LASERS

Emitted light power of CW injection laser related to threshold current, electrical and thermal resistances and external quantum efficiency

01 p0079 A72-10325

Current dependent intensity of spontaneous emission of GaAs injection laser operated at 300 K

02 p0238 A72-12204

Minimum threshold current density of double heterojunction injection lasers

03 p0367 A72-13412

Magneto-optic storage density and read-write rate, discussing transducer cost, solid state injection lasers, holographic techniques and high activity data base applications

[IEEE PAPER 19,1] 03 p0361 A72-13774

Pulsed injection laser current pulse height, width and rise time controls, comparing use of tube, transistor and SCR discharge circuits

04 p0528 A72-14420

Radiative noise effect on threshold current, output power and quantum yield of injection laser, evaluating noise loss factor

04 p0531 A72-15077

Lasing onset moments distribution over emitting surface of injection lasers at room temperature

04 p0531 A72-15082

Injection laser threshold current density, radiation pattern and electric field distribution relation to layer thickness and dielectric constants, using waveguide theory

06 p0825 A72-17772

Handbook on lasers and optical technology covering gas, dye, liquid, injection and insulating crystal lasers, materials, sources, transmission, hazards and holographic recording

06 p0826 A72-17945

GaAs, injection lasers with homojunctions and single and double heterostructures, observing energy dependence of internal optical losses due to band-to-band absorption

07 p1006 A72-19823

Uncooled GaAs injection laser with high pulse repetition rate, discussing structural features and current-power characteristics

08 p1181 A72-20748

Pulse rate and pumping power effects on emission spectra and I-V characteristics of multielement GaAs injection lasers

08 p1181 A72-20796

Physical and operating principles of CW heterojunction injection lasers at room temperature

08 p1181 A72-21056

Pulsed GaAs injection laser active region anisotropy and radiation polarization under spontaneous and coherent emission conditions

08 p1183 A72-21772

GaAs semiconductor injection lasers, discussing time characteristics of current carriers, population inversion and resonator Q factor modulation

08 p1184 A72-22032

Gold-Weisberg phonon kick and extended Longini field-inhibited diffusion degradation mechanisms for GaAs double heterostructure injection lasers, discussing experimental tests

09 p1325 A72-23088

GaAs injection laser optical link assembly with silicon photodiode and optical transistor, noting applicability to optical data processing

11 p1648 A72-26328

Semiconductor injection laser with distributed radiative loss, calculating radiation line shape and width and quantum efficiency

11 p1648 A72-26329

Frequency modulation of CW GaAs laser emission by injection current, noting temperature effects

11 p1648 A72-26337

Optimal active layer thickness in heterogeneous injection lasers, estimating minimal threshold currents

11 p1649 A72-26346

Injection laser pulsed emission mode effect on spectral characteristics

11 p1650 A72-26359

Light power coupling efficiency from GaAs injection laser into single- and multimode fibers

12 p1820 A72-27507

Injection semiconductor laser mode selection and output enhancement by introducing external spectrally selective elements into resonator

12 p1821 A72-27589

Optical interaction of inhomogeneously excited semiconductor injection laser diodes, noting power efficiency increase with inhomogeneity

12 p1822 A72-27606

Te-doped GaAs injection laser, investigating crystal growth dislocations effects on output radiation-injection current characteristics

12 p1822 A72-27617

Low threshold current mesa-stripe-geometry double heterostructure injection lasers, eliminating current spreading by etching method

12 p1823 A72-27838

Instantaneous and averaged emission spectra of injection laser under spontaneous pulsation as function of operation mode and photon distribution

12 p1824 A72-27875

Pumping current pulse duration effect on lasing threshold of injection lasers with diffusion junctions and heterojunctions in GaAs-AlAs system

12 p1824 A72-27877

Internal parameters of injection lasers based on diffusion and epitaxial p-n junctions and heterojunctions in GaAs-AlAs system at 300 K

12 p1825 A72-27878

Radiation coherence enhancement in pulsed semiconductor injection laser by voltage controlled barium zirconite piezoceramic element

15 p2245 A72-31416

Moderate power GaAs single heterojunction injection laser diodes fabrication and operation characteristics in pulsed mode at 250-400 K

15 p2247 A72-32033

Avalanche photodiodes for Nd and injection lasers radiation detection, reducing noise equivalent power

15 p2247 A72-32035

Double heterostructure injection lasers with narrow active regions, discussing threshold current densities, emission polar diagrams and optical field penetration into boundary regions

15 p2249 A72-32237

Injection laser pulsed emission mode effect on spectral characteristics

16 p2403 A72-33712

Instantaneous and averaged spiking emission spectra of injection laser under spontaneous pulsation as function of oscillation mode and photon distribution

16 p2404 A72-33984

Pumping current pulse duration effect on lasing threshold of injection lasers with diffusion junctions and heterojunctions in GaAs-AlAs system

16 p2404 A72-33986

Internal parameters of injection lasers based on diffusion and epitaxial p-n junctions and heterojunctions in GaAs-AlAs system at 300 K

16 p2404 A72-33987

Book - Semiconductor diode lasers

17 p2563 A72-35300

High-radiance room-temperature GaAs laser with controlled radiation in a single transverse mode.

17 p2563 A72-35342

Wave-guiding properties of stripe-geometry double heterostructure injection lasers.

18 p2698 A72-36981

Radiation coherence in a monopulse single-mode semiconductor injection laser

19 p2811 A72-37736

Reduction in the rate of increase of spontaneous emission from double-heterostructure injection lasers at threshold.

19 p2811 A72-37866

Transverse mode selection in injection lasers with widely spaced heterojunctions.

19 p2812 A72-38595

Injection laser under self-Q-switching conditions.

20 p2933 A72-39515

Time characteristics of heterojunction injection lasers.

20 p2933 A72-39516

Reading of holograms by a semiconductor injection laser.

20 p2933 A72-39518

Effect of uniaxial pressure on the threshold current of double-heterostructure GaAs lasers.

20 p2933 A72-39559

Self-induced pulsations in the light output from double-heterostructure injection lasers.

20 p2934 A72-39710

Injection laser and light emitting diode techniques to transmit digital data in local distribution

21 p3018 A72-40869

An arrangement for studying the time characteristics of injection lasers

21 p3064 A72-41738

Pulsed GaAs injection laser heating application to thermal conductivity coefficient measurement in thin films, discussing lasing spectra kinetics

21 p3064 A72-41740

Absorption coefficient and gain of a GaAs injection laser

22 p3184 A72-42104

Experimental studies of injection lasers - Spontaneous spectrum at room temperature.

24 p3409 A72-44713

Commutation switch based on an injection semiconductor laser.

24 p3412 A72-45620

INJECTORS

NT VORTEX INJECTORS

Acceleration equations for plasma injectors with capacitive and inductive energy storage elements
05 p0697 A72-16985

Acceleration equations for plasma injectors with capacitive and inductive energy storage elements
12 p1850 A72-27129

High pressure injector optimum design and performance for gas jet boosters, using one dimensional theory with friction allowance
12 p1861 A72-27535

INJURIES

NT BACK INJURIES

NT BAROTRAUMA

NT BRAIN DAMAGE

NT BURNS (INJURIES)

NT CRASH INJURIES

NT EJECTION INJURIES

NT LESIONS

NT NOISE INJURIES

NT PARACHUTING INJURY

NT PULMONARY LESIONS

NT RADIATION INJURIES

Blood coagulation behavior in rats under fall induced intense trauma, attributing phenomenon to increase in extrinsic thromboplastin from damaged tissue
21 p3002 A72-41194

New mechanical device for producing traumatic shock in dogs - Circulatory and respiratory responses.
22 p3142 A72-42490

INLET FLOW

Velocity and temperature effects on momentum and temperature equalization in coaxial turbulent jet mixing in pipe inlet section
[DFVLR-SONDDR-183] 01 p0051 A72-11257

Injection geometry and inlet flow conditions application to open cycle gas nuclear reactor engine, evaluating fuel containment from cylindrical and spherical chambers experiments
01 p0100 A72-11350

Two dimensional diffusers flow patterns with laminar boundary layer entry, investigating wall shape and vanes effects with water table test facility
02 p0204 A72-12231

Optically thin radiation effects on local heat transfer in gas flow narrow duct thermal entrance region, presenting Nusselt number variations terms for uniform and parabolic velocity profiles
02 p0303 A72-12321

Start-up flow of viscous incompressible fluid under constant head in entrance region of circular tube
03 p0344 A72-14343

Rectangular and triangular duct entrance region laminar flow pressure losses from velocity profiles and integral energy equation
04 p0512 A72-15194

Mach 2.65 axisymmetric mixed-compression inlet system diffuser and boundary layer bleed system performance estimates confirmed by tests
[AIAA PAPER 72-45] 05 p0609 A72-16959

Rectangular channel mixed boundary layer flow patterns dependence on inlet edge configurations, channel geometry and hydrodynamic flow core parameters
08 p1150 A72-21317

Conical diffuser response to velocity distribution and turbulence intensity at inlet
10 p1416 A72-23858

Wind tunnel inlet effect on pulsed flow, relating velocity and pressure pulses
10 p1417 A72-24216

Three component flow calculation at inlet of axial flow compressor stage, linearizing hydrodynamic equations of ideal incompressible fluid with velocity perturbations
10 p1420 A72-25132

Viscous incompressible gas turbulent flow in axisymmetric channel under preliminary twist conditions at inlet, using computer numerical solution
12 p1752 A72-28126

Turbulent intensity induced by wakes near secondary air jet inlet to gas turbine engine flame tube
12 p1861 A72-28131

Nonuniform inlet velocity profile effect on laminar flow development between parallel plates, solving equations by finite difference method
13 p1941 A72-28706

Time dependent and stationary two dimensional calculation of current and potential distributions in MHD generator preionizer and entrance region flow
13 p2013 A72-29358

Axisymmetric convergent cone profile synthesis to transform parallel flow at inlet to uniform sonic flow at outlet, examining solution convergence
15 p2177 A72-31206

Flow distribution, vibration, wear and rupturing of rods in vertical pipe for various inlet flows investigated with high speed cameras, photography and transducers
16 p2376 A72-32996

German monograph on pressure loss and heat transfer in heat exchangers, taking into account hydrodynamic and thermal inflow velocity and temperature distribution
16 p2478 A72-33504

Influence of contraction section shape and inlet flow direction on supersonic nozzle flow and performance.
17 p2483 A72-34204

Heat and mass transfer in initial section of circular pipe under stabilized laminar flow, using modified Leveque method
17 p2637 A72-35131

MHD inlet flow into channel, obtaining velocity profile numerical solution in Prandtl approximation with modified boundary conditions
18 p2714 A72-36121

Investigation of the critical heat flux density in heat transfer with and without turbulization of the flow at the inlet of an annular channel
21 p3129 A72-41057

Investigation of the influence of nonuniform conditions at the inlet and of secondary flows on the flow parameters in arbitrarily twisted channels
21 p3045 A72-41067

The development of inlet flow distortions in multistage axial compressors of high hub-tip ratio.
[ICAS PAPER 72-20] 21 p3099 A72-41145

Installation caused flow distortion and its effect on noise from a fan designed for turbofan engines.
[AIAA PAPER 72-1006] 21 p2993 A72-41590

Researches on the two-dimensional retarded cascade. I, II.
22 p3133 A72-41944

Variational formulation and computer solution for thermal boundary layer flow over flat plate in entrance region, assuming temperature dependent thermal conductivity and viscosity
22 p3156 A72-41959

High response two-transducer pressure measurement for evaluating nonuniform and unsteady inlet airflow distortion effects on supersonic jet engine stability and performance
22 p3216 A72-42683

Unsteady convective heat transfer in the initial section of a pipe with a smooth inlet
23 p3356 A72-43670

Experiment of supersonic air intake buzz.
23 p3249 A72-44496

Linearized analysis of magnetohydrodynamic channel entrance flow.
24 p3430 A72-45573

INLET NOZZLES

Thermal shock fatigue tests on aircraft gas turbine engine inlet nozzles, showing cracks as function of material
01 p0143 A72-11373

F-111A inlet nozzle dynamic distortion diagnostics for airframe-propulsion integration based on flight and transonic wind tunnel tests
[ICAS PAPER 72-18] 21 p2991 A72-41143

INLET PRESSURE

Circumferential inlet pressure distortion index derivation for high hub-tip ratio multistage axial flow compressor from one dimensional isentropic flow expressions
07 p1053 A72-18762

Steady state radial inlet pressure distortion index for axial flow compressor, examining radial velocity, continuity equation and mathematical model
[ASME PAPER 72-GT-109] 11 p1571 A72-25673

Low inlet pressure performance of gerotor lube and scavenge pumps.
18 p2694 A72-36047

INLETS (DEVICES)

U INTAKE SYSTEMS

INNER RADIATION BELT

Longitudinal variations of inner radiation belt particle flux density at low altitudes from Proton 2 satellite data
01 p0119 A72-10604

Inner and outer belt electron differential energy spectra from Cosmos 228 satellite data, discussing fluxes of precipitating and quasi-captured particles
02 p0272 A72-11916

Inner radiation belt proton source and loss processes, obtaining flux intensities, energy spectrums and radial distributions
03 p0412 A72-13513

Azur satellite for investigating polar regions, inner radiation belt and solar particle emission
05 p0715 A72-16135

Long time variations of proton energy spectra in inner radiation belt during solar cycle
05 p0710 A72-16767

Integral and differential electron energy spectra in inner radiation belt from Cosmos 219 satellite observation
05 p0711 A72-16768

Fast charged particles measurement in inner radiation belt by Cerenkov counter mounted on Cosmos 137 satellite indicating presence of high energy electrons
05 p0711 A72-17035

Geomagnetically trapped protons, electrons and alpha particles verification and measurements in inner and outer radiation belts
07 p1062 A72-20227

Earth albedo neutrons energy and angular distributions, suggesting neutron source of inner radiation belt trapped protons
11 p1712 A72-25880

Fast charged particle flux measurement in inner radiation belt by Cosmos 137 satellite in January-February 1967
11 p1713 A72-25947

Inner and outer belt electron differential energy spectra from Cosmos 228 satellite data, discussing fluxes of precipitating and quasi-captured particles
13 p2030 A72-29228

Inner Van Allen zone proton energy spectrum at 30-300 MeV from ESRO 2 satellite measurements
13 p2031 A72-29383

Long term variations of proton flux and energy spectra in inner radiation belt during solar cycle
17 p2600 A72-35270

Integral and differential electron energy spectra in inner radiation belt from Cosmos 219 satellite observation
17 p2600 A72-35271

Energetic electron intrusion into inner radiation zone during and after 2 September 1966 geomagnetic storm, noting radial diffusion role
17 p2601 A72-35596

INOCULATION

Normal and germ free rat antibody response to sheep erythrocyte inoculation in He-O atmosphere, analyzing microagglutinin and hemolysin titres
[AD-736324] 04 p0471 A72-14861

INORGANIC COATINGS

NT ANODIC COATINGS

NT CERAMIC COATINGS

Vacuum deposited films on CsI, AgCl, TlBr and TiCl for IR antireflection coatings on silicon
[AD-736289] 03 p0380 A72-13431

INORGANIC COMPOUNDS

NT AMMONIA

NT LIQUID AMMONIA

Anion sorption mechanisms and product composition in anodic aluminum oxide filled with phosphate, chromate and sulfate solutions, discussing chemisorptive compound formation and oxide dehydration
05 p0624 A72-17053

Soviet monograph on solid inorganic compounds as high temperature lubricants covering powder lubricants mechanism under different friction conditions, gas media, temperature effects, etc
08 p1191 A72-20913

Self-propagating high-temperature synthesis of refractory inorganic compounds
22 p3188 A72-42165

INORGANIC MATERIALS

Inorganic photochromic and cathodochromic recording materials in single crystal and powder forms, considering color change properties during light or electron beam exposures
06 p0866 A72-17950

Inorganic single crystal titanate whisker fibers with high modulus strength for plastic reinforcement, noting mechanical, thermal and physical properties
08 p1193 A72-21685

Neutron diffraction study of inorganic materials atomic structure, examining symmetry properties and group arrangements of hydrogen compounds
09 p1358 A72-23478

Laser induced degradation as rapid reproducible method for characterization of inorganic materials exhibiting low vapor pressures at usual temperatures
10 p1433 A72-23953

Physicochemical principles of inorganic materials production, considering heat resistant alloys, oxygen free and oxide cermets, glasses, glass ceramics and protective coatings
10 p1501 A72-24408

Book - Solid lubricants and self-lubricating solids.
21 p3073 A72-41529

INORGANIC NITRATES

NT AMMONIUM NITRATES

INORGANIC PEROXIDES

NT HYDROGEN PEROXIDE

INORGANIC SULFIDES

NT CADMIUM SULFIDES

NT COPPER SULFIDES

NT HYDROGEN SULFIDE

NT LEAD SULFIDES

NT MOLYBDENUM DISULFIDES

NT POLYSULFIDES

NT WURTZITE

NT ZINC SULFIDES

NT ZINCLENDE

INPUT

Saturating nonlinear feedback systems stability under bounded input excitation, discussing error signals magnitude and duration
15 p2212 A72-32246

INPUT/OUTPUT ROUTINES

Model for I/O channel traffic in computer systems, obtaining closed solution for stationary probabilities of state
10 p1446 A72-25148

Simultaneous operation of digital computer units to reduce input times and prolong useful computer operation time

13 p1925 A72-29944

Texture synthesis by image processing equipment consisting of digital computer and input/output unit, noting image signatures of constant parameter areas

17 p2555 A72-35338

Berner simulation method /BERSIM/ based on lumping recurring combinations of operations into component subsystems representing specified transformations of input into output variables

23 p3267 A72-44143

INSECTICIDES

NT CARBAMATES [TRADENAME]

NT URETHANES

Insecticide dichlorvos vapor toxicity in aircraft cabin atmosphere at 8000 ft, studying plasma cholinesterase activity, erythrocytes, dark adaptation and bronchial resistance

14 p2081 A72-31082

INSECTS

NT COLEOPTERA

NT DROSOPHILA

Coincidence model tests of photoperiodic time measurement relation to circadian system in moth *Pectinophora gossypiella*, using induction by skeleton photoperiods and light cycles

07 p0919 A72-19533

INSENSITIVITY

U SENSITIVITY

INSEQUENT STREAMS

U STREAMS

INSERTION LOSS

Reciprocal dual mode millimeter wavelength phase shifter design for use in phased array antennas, calculating phase shift and insertion loss vs frequency

04 p0498 A72-14719

Wideband microwave acoustic delay line design featuring superior bandwidth, phase linearity, spurious echo and insertion loss characteristics

04 p0521 A72-14720

Dissipative magnetic parameters measurement in ferrite and insertion loss measurement in waveguide Y-circulators below microwave resonance

06 p0786 A72-18367

Top wall and multiple branch hybrid junction waveguide couplers for millimeter wavelengths, measuring insertion loss performance

06 p0787 A72-18378

Optoacoustic processing of large time-bandwidth signals, calculating insertion loss vs delay time

12 p1810 A72-27935

Epitaxial YIG film separated from conductive plane by thin dielectric layer, considering magnetostatic propagation dispersion and insertion loss

15 p2294 A72-32502

Technique for varying the conversion loss against frequency of a surface-wave transducer without apodization.

18 p2667 A72-36692

Slotted-line measurement of insertion loss in three-port ferrite junction circulator.

19 p2775 A72-38636

An improved design and measurement of attenuation characteristics of RF suppressors.

20 p2902 A72-38997

INSERTS

NT NOZZLE INSERTS

Scale factor and surface imbedded inserts effect on bending cyclic fatigue strength of nonhardened and roll hardened Al-Ti alloy

03 p0372 A72-13596

INSOMNIA

EEG diurnal rhythms during 72 hour insomnia, considering adaptation to altered work-rest cycle in subjects with stable and unstable brain activity rhythms

13 p1904 A72-29319

INSPECTION

NT INFRARED INSPECTION

NT X RAY INSPECTION

Metal fatigue damage nondestructive detection, discussing inspection methods, equipment, advantages, limitations and test results [AD-741977]

02 p0296 A72-12498

Reliability estimates for continuously inspected recoverable systems, determining readiness factor for periodic checkout

08 p1180 A72-22054

Functional readiness of periodically inspected recoverable systems with different failure causes

08 p1180 A72-22055

Automatic computer-controlled system with laser technology for quality inspection of mass produced automobile master brake cylinders

09 p1319 A72-22979

Tolerance intervals in multiple type acceptance sampling plans with attribute-based inspection

11 p1749 A72-26790

Price adjusted single sampling with linear indifference.

17 p2560 A72-34943

Single and double sample Dodge-Romig lot tolerance percent defective /LTPD/ rectifying inspection plans, using standard tables

21 p3059 A72-40827

Approaches to verification and solution of magnetic particle inspection problems.

24 p3407 A72-44903

INSTABILITY

U STABILITY

INSTALLATION

U INSTALLING

INSTALLING

Proposed gas turbine procurement standards for shipment and installation preparation

[ASME PAPER 71-WA/GT-4] 05 p0703 A72-15897

INSTRUCTIONS

U EDUCATION

INSTRUCTORS

ECG heart rate recording of helicopter instructor pilots during flight training tasks, administrative work, automobile driving and eating

14 p2082 A72-31097

INSTRUMENT APPROACH

Aircraft pilot performance during instrument approach in low visibility conditions

07 p0925 A72-18832

Civil aviation approach and landing guidance systems evolution, discussing ILS development, state of art and future requirements

13 p1996 A72-29014

A pilot's opinion - VTOL control design requirements for the instrument approach task. [AHS PREPRINT 644]

17 p2490 A72-34504

INSTRUMENT COMPENSATION

NT TEMPERATURE COMPENSATION

Transfer function compensation technique for processing sampled imagery data prior to recording on hard copy to remove degrading effect for quality improvement

01 p0046 A72-10873

Direct phase measuring and measured phase compensating microwave devices designed for plasma diagnostics applications

02 p0223 A72-11416

Laser station coordinate and Geos B satellite position compensation with simultaneous optical and laser observations

02 p0219 A72-12045

Gyro drift random error dispersion reduction in compensated closed loop multirator gyroscopic systems by cross couplings

02 p0231 A72-12566

Neuroelectric signal recognition system with computerized compensation for variations due to small random changes, slow trends and interference potentials

04 p0481 A72-15253

Light source fluctuations compensation in Raman spectroscopy, describing ratio recording system for photon counters

04 p0523 A72-15491

Inertial navigation system accelerometer error autocompensation, using reversal by accelerometer forced rotation in stabilized platform plane

05 p0664 A72-17148

Compensation of shock wave attenuation due to boundary layer by varying shock tube driver chamber area, using central body of suitable length and profile

06 p0797 A72-18546

Low pressure gauge with compensation of dry friction forces in servomechanism with respect to mean value

07 p0982 A72-18929

Gyroscopic device for compensating displacement of sextants or binoculars optical axis due to spontaneous hand movements

07 p0988 A72-19894

Wide gap spark chamber feeding technique for compensation of charged particle track drift due to avalanches

07 p0988 A72-19956

Aircraft altitude two-loop feedback control system designed by compensation parameter variation technique, determining correlation between system sensitivity computations and observations

07 p0963 A72-20592

Zero velocity lag servomechanism transient response sensitivity from intuitive approach to convolution problem, noting feedback compensation advantages in sensitivity reduction

07 p0964 A72-20593

Compensated Kalman filter as suboptimal state estimator to eliminate steady state bias errors in use with mismatched asymptotic time-invariant case

08 p1144 A72-20845

Temperature dependence and error compensation of Si strain sensors, using coupled dc generators

09 p1316 A72-23649

Holographic correction of reflecting refracting telescope objective mirror deformation aberrations, noting interferometric attachment

10 p1479 A72-24049

Compensation of nonlinear selectivity distortions in radio receivers with broadband preamplification

stages, noting circuit diagrams for preselector correctors

13 p1927 A72-28412

Measuring tape recorder, properties and utilization for signal recording and processing, discussing digital computer techniques and compensation for interference effects

14 p2104 A72-30287

Modulated laser beam record wideband signals on photographic film, discussing noise sources and compensation methods for SNR improvement

15 p2248 A72-32039

Ku band radio interferometer for discrete radio sources mapping, discussing construction and incorporated PDP-8 computer for pointing, tracking, delay compensation and data analysis

15 p2207 A72-32107

Integrated inertial-VOR-DME or inertial-TACAN navigation system, presenting slant range and bearing adjustment procedure via least squares method

16 p2421 A72-34136

Sampled imagery transfer function compensation by inverse function, noting truncation effects on processing array SNR performance

17 p2521 A72-34412

Feedback circuitry for dc amplifiers voltage drift compensation, discussing performance criteria in terms of residual offset voltage, system stability, correction and measurement time

18 p2671 A72-37150

Design of a system for automatic compensation of atmospheric dispersion

19 p2801 A72-37962

Enlarging the region of convergence of Kalman filters that encounter nonlinear elongation of measured range. [AIAA PAPER 72-879]

20 p2907 A72-39121

Fabry-Perot spectrometer adjustment for the compensation of Doppler shift from rapidly rotating and rapidly flowing sources.

21 p3053 A72-40607

Compensation of Fabry-Perot surface defects. II - Silicon oxide compensating layers.

21 p3053 A72-40608

ASW aircraft magnetic anomaly detection (MAD)/system range limitation due to residual maneuver noise, discussing real time compensation for geomagnetic gradient interference

22 p3177 A72-42322

Optimal control of the speed of a two-shaft helicopter turbine

23 p3326 A72-44278

Application of N equalizing and compensating signals in a single-cell reciprocal magnetoelectric transducer

24 p3386 A72-45315

INSTRUMENT DRIFT

U DRIFT [INSTRUMENTATION]

INSTRUMENT ERRORS

System distortion error characteristics for carrier gas type radiorespirometers, considering relation to system time constant

01 p0017 A72-10399

Linearization errors and calibration functions for hot-wire anemometry taking into account higher order velocity fluctuations

01 p0071 A72-11170

Optimal stochastic /Kalman/ filters application to integrated air and submarine navigation systems, discussing measurement errors modeling as bias and colored noise

02 p0256 A72-12050

Precision alignment device using He-Ne laser with small beam divergence

02 p0238 A72-12115

Phase error in 136 MHz interferometer due to galactic nucleus passage, obtaining lower bound

02 p0175 A72-12160

Oscillographically measured semiconductor element I-V characteristics plotting optimization by considering measuring instrument and sampling signal shape and frequency effects on hysteresis

03 p0330 A72-12968

Photoelectric and visual timings of occultations for lunar motions, comparing accuracy and systematic instrument errors

03 p0420 A72-13127

Systematic errors of Crimean vector magnetograph related to miscentering of spectral lines

03 p0357 A72-13285

Submillimeter wave stratospheric emission spectra measurement by aircraft- or balloon-borne phase modulated Fourier spectrometry, noting SNR and small errors

03 p0348 A72-13399

Meridian and local vertical gyro errors effects on geomagnetic field elements determination accuracy

03 p0359 A72-13559

Quadrupole mass spectrometer ultimate characteristics concerning resolution, range, recording speed, working pressure and sensitivity

03 p0360 A72-13665

- Temperature gradients measurements in transit-instrument pavilion and errors in time determination for two year period 03 p0361 A72-13822
- Soviet book on gyroscopic systems and inertial guidance instruments, emphasizing system motion under various dynamic conditions and systematic errors 03 p0362 A72-14167
- Aberration correction in collimator of Schmidt spectrograph camera by changing surface geometry and grating positioning 03 p0362 A72-14358
- Pressure broadened water vapor line shape resonance dispersion at 22 GHz, deriving expression for instrument induced deviation from Lorentzian behavior 04 p0552 A72-14891
- Error distribution computation for combined Rayleigh-Gaussian statistics data, applying to antenna radiation beam-pointing example 04 p0500 A72-15303
- Ground secondary radar interrogator system using monopulse technique for bearing measurement, accuracy and interference reduction 04 p0493 A72-15523
- High precision strain gage dynamometers design and testing at ONERA Modane test center, discussing accuracy limitation due to hysteresis and creep effects [ONERA, TP NO. 995] 05 p0642 A72-15859
- Microwave antenna efficiency measurement by integrated isotropic levels comparison, featuring elimination of error due to specular ground reflections 05 p0637 A72-16421
- Incorrect or unmodeled error sources effects on arbitrary linear navigation filters design and performance [AIAA PAPER 72-14] 05 p0688 A72-16911
- Inertial navigation system accelerometer error auto-compensation, using reversal by accelerator forced rotation in stabilized platform plane 05 p0664 A72-17148
- Airborne or satellite-mounted millimeter wave radiometer for atmospheric water vapor determination noting accuracy advantage over IR measurement 06 p0814 A72-17589
- Principle stress errors in biaxial stress fields expressed in terms of transverse sensitivity, stress and Poisson ratios of material during strain gage calibration 06 p0895 A72-17798
- Transit instrument system year-to-year stability in astronomical time determination, considering seasonal wave causes and star coordinate errors 06 p0885 A72-18037
- Square wave source gated detector bridge for square resistance measurement, discussing design and performance, and application in Pt resistance thermometry 06 p0785 A72-18244
- Gyroscopic error analysis, solving nonlinear equations by continuous Markov processes theory 06 p0819 A72-18724
- Angular and linear vibrations effect on dynamic errors of two stage gyrocompass, obtaining nonlinear equations of motion approximate solutions 07 p0981 A72-18928
- Numerically controlled machine tools accuracy, discussing feed spindle and displacement/angle measuring system errors determination through angular step transducers and laser interferometer 07 p0995 A72-19684
- Laser gyro operational principles, discussing passive Sagnac and active ring laser interferometers, readout, errors due to null shift, lock-in and mode pulling, etc 07 p1007 A72-20223
- Viscosity measurement error estimates for Newtonian incompressible fluid flow through deformed capillary tube 07 p0991 A72-20535
- Nonideal black body temperature measurement with IR radiometer, discussing error dependence on object temperature and emissivity and background temperature 07 p0993 A72-20692
- Quantization errors effect on recursive filter design for strapdown inertial navigation systems, developing suboptimal linear minimum variance 08 p1144 A72-20848
- French Geole satellite system for geodetic survey, discussing frequency selection, antenna problems, distance measuring equipment and instrument errors 08 p1158 A72-21206
- Sidewall reflection induced bore sight error in anechoic chamber used for missile test or simulation 08 p1141 A72-21421
- Systematic errors in scan-and-measure devices for tracking cameras photographs analysis, discussing correction during measurements 08 p1209 A72-21913
- Gaussian noise quasi-optimal filtering in optical communication system, evaluating signal timing accuracy in detector-amplifier circuits 08 p1136 A72-21914
- Component evaluation of linearity error of measuring instruments 09 p1284 A72-22241
- Skylab S-193 altimeter experimental mission objectives and spacecraft instrumentation, considering precision designs, oceanographic surface remote sensing and electromagnetic scattering measurement 09 p1306 A72-22317
- Static strain measurement errors due to nonstationary thermal conditions in semiconductor resistance gages 09 p1310 A72-22739
- Vibration string static strain gage for high temperature operation, proposing relations for measurement error calculation 09 p1310 A72-22741
- Radio receiver-transmitter system for synchronous heterodyne signal detection of 6 GHz band electromagnetic channel pulsed response, discussing operational principles and accuracy 09 p1280 A72-23353
- Air velocity calculation from hot-wire anemometer measurements in variable density flow, discussing correction factors checking method and application to internal combustion engine 09 p1315 A72-23390
- High pressure bulk modulus test rig for composite material specimen nondestructive test, discussing measurement method and errors 09 p1315 A72-23391
- Temperature dependence and error compensation of Si strain sensors, using coupled dc generators 09 p1316 A72-23649
- Measured quantity distribution effect on measurement errors, noting application in mass production process control 09 p1316 A72-23662
- Capacitance gap sensor with logarithmic output response and adjustment for minimum error 10 p1482 A72-24641
- Sensitivity loss from approximation to radar and sonar signal square law detectors in quadrature systems with postdetection integration 10 p1437 A72-24690
- Magnetometers for balloon-borne X ray astronomy payload azimuth determination, noting misorientation, earth and spurious magnetic fields effects on measurement effectiveness 10 p1530 A72-24954
- Semiautomatic measurement of human oxygen uptake, discussing apparatus and accuracy 10 p1432 A72-24991
- Hair hygrometer for FM radioisotope in-flight air humidity measurements, discussing design, operation and accuracy test in extreme weather conditions 10 p1483 A72-25005
- LiCl dew point hygrometer operation investigated by double ventilation psychrometers, noting measurement error dependence on relative humidity and temperature 10 p1483 A72-25015
- Sensors measurement accuracy for rainfall amount and duration determination by automatic remote transmitting meteorological station 10 p1483 A72-25017
- Two-laser optical distance measuring instrument with atmospheric refractivity correction, noting accuracy 11 p1646 A72-25305
- Cybernetic equipment reliability and precision analysis from algorithmic, conversion and instrumental errors, surveying digital, analog and hybrid computers and converters 11 p1608 A72-25427
- Solar chromosphere double limb effect attributed to instrument, discussing application to height measurement 11 p1717 A72-25905
- Transit instrument system year-to-year stability in astronomical time determination, considering seasonal wave causes and star coordinate errors 11 p1719 A72-25973
- Deterministic methods to calculate quantization error in digital control system 11 p1610 A72-25976
- Retarding potential analyzer errors and performance degradation due to grid plane potential depressions 11 p1634 A72-26411
- Double passed Michelson interferometer with polarizing beam splitter, quarter wave plates and cube corner reflectors to obtain immunity to mirror misalignment 11 p1635 A72-26500
- Latitude measurement at international stations during 1935-1947 period, discussing computation difficulties, instrument errors and correction 12 p1866 A72-27201
- Bonded strain gage type load cell design, construction and application, explaining methods to achieve high accuracy 12 p1806 A72-27315
- Spaceborne scatterometer measurement standard deviation derivation, noting integration time, signal bandwidth and SNR effects on accuracy 12 p1783 A72-27636
- Adcock direction finder errors due to diurnal and sporadic ionospheric variations and tilting layers effects on reflected signal 12 p1804 A72-27780
- Low noise receivers in radio astronomy, discussing accuracy requirements for line measurements and very long baseline interferometry 12 p1792 A72-27806
- Ultrasonic inspection effectiveness and equipment errors relationship to a priori acceptability of products 13 p1963 A72-28925
- Instrument errors of RF phase comparison altimeter for meteor height measurements, using radar tracked aircraft flights calibration 13 p1957 A72-29029
- Algorithm for optimal strategy in statistical plant control for machine parts production and assembly, discussing measuring equipment errors effects 13 p1965 A72-29168
- Systematic deviation of flat gyroscopic pendulum during irregular motions of ridden vehicle, comparing with physical pendulum 13 p1957 A72-29273
- Differential error of fused quartz Bourdon tube precision pressure gages as function of absolute pressure level tested for nitrogen 13 p1959 A72-29764
- Impurities effect on platinum resistance thermometers temperature reading accuracy, presenting empirical formula for approximate error estimate as function of operational conditions 13 p1960 A72-29906
- Combined hydrostatic suspension Hg cushion effects on gyrocompass response precision during irregular roll of platform 13 p1961 A72-30022
- Correcting electronic transducer for rapidly changing temperature measurement, discussing design peculiarities for superior metrological characteristics 13 p1961 A72-30024
- Adaptive radiometer dynamic properties and parameters optimization based on minimum mean square error criterion 14 p2088 A72-30373
- Lunar physical libration measurement from Apollo laser experiment with retroreflectors, assessing obtained data 14 p2154 A72-30516
- Turbulent friction values diminished by reading errors in pitot tube flow measurement of solid particles suspensions and polymer solutions caused by viscoelastic associations 14 p2106 A72-31007
- Instrumental errors estimation in photomultipliers and photodiodes during measurement of short time phase fluctuations in quasi-harmonic signals 15 p2246 A72-31424
- Radio phase interferometers for emitter position location, predicting polarization mismatch errors effects on accuracy 15 p2206 A72-31777
- Vehicle orientation degrees of freedom remote measurement with mounted passive devices and polarization-modulated light, discussing data reduction and system accuracy 15 p2267 A72-31780
- Background spallation source errors in satellite measurements of diffuse cosmic X ray spectrum with crystal scintillators 15 p2300 A72-31986
- Time-frequency dissemination system design, discussing radio propagation, time signals, noise effects, synchronous satellite transponders and TV use, accuracy, geographical coverage and costs 15 p2198 A72-32065
- Precise time and frequency dissemination via Loran C navigation system, discussing user techniques, economics and radio propagation mode and terrain effects on accuracy 15 p2268 A72-32067
- VLF signal role in long range time dissemination, communication and navigation, comparing conventional and modern techniques with emphasis on OMEGA system accuracy 15 p2199 A72-32068
- Lunar radar measurement for remotely located clock time synchronization, discussing applications to deep space tracking, computer technique for time delay correction and accuracy 15 p2199 A72-32069
- Timing requirements in geodetic measurements with optical and electronic equipment, considering lunar laser ranging technique for high accuracy 15 p2229 A72-32075
- NASA global tracking network clock time synchronization to microseconds accuracy via GEOS-11 satellite 15 p2199 A72-32079
- Circumsolar radiation measurement discrepancy explanation based on comparison with results obtained by international pyrheliometer scale 15 p2238 A72-32169
- Optically pumped magnetometer error, predicting atomic g-factor modification by nonresonant RF field 15 p2239 A72-32335

X band radar target cross section representation by discrete point reflector models, deriving boresight error mean and variance in presence of n-target sources

15 p2201 A72-32474

Angular measurement error for group and repetition techniques as function of observation time, deriving formulas for comparison in terms of economy and efficiency

16 p2389 A72-33030

Laser interferometric calibration for vibration measurement, discussing operation principle and detector error

16 p2391 A72-33248

Hot-wire anemometer output linearization by squaring and straight line sequence circuits combination, supplementing Bruun error estimates

16 p2392 A72-33606

Additive noise effect on accuracy of integrating digital voltmeters using pulse frequency and pulse time converters

16 p2370 A72-33955

Coordinate and speed error dependence on instrumental errors of inertial navigation system using gyrohorizoncompass

16 p2420 A72-33960

Instrument for Hall and Gauss effects measurement in semiconductors and metals, noting instrument error analysis

17 p2529 A72-34758

The effect of atmospheric turbulence on the error of an optoelectronic angle sensor.

17 p2554 A72-34941

Measurement of the error of temperature sensors in flowing gases.

17 p2555 A72-35247

Dynamic errors of a metering system with successive correction of the sensor's time constant for certain types of aperiodic input

17 p2557 A72-35787

Problem of improving the accuracy of differential meters with commutation of the compared harmonic signals

17 p2519 A72-35788

Around-the-world atomic clocks - Observed relativistic time gains.

17 p2584 A72-35839

Hybrid and pyrotechnic IR flare generated plasma effects on dual frequency Doppler range measurement system, discussing diagnostics and contamination concentration analysis

18 p2660 A72-36339

Bearing azimuth measurement accuracy improvement by ATC beacon system/secondary surveillance radar using monopulse technique

18 p2662 A72-37047

Elastically supported dry two degrees of freedom tuned gyroscopes, analyzing open-loop transfer function for characteristic errors

19 p2794 A72-37280

Errors due to gimbaling system asymmetries and rotor angular offsets effects in multigimbal elastically supported tuned gyroscope, deriving gyro translational transfer function

19 p2794 A72-37281

Comparison of several methods for determining the magnitude of turn for the screw of a positional contact micrometer in an astronomical universal instrument

19 p2795 A72-37347

Gage-length errors in the resolution of dispersive stress waves.

19 p2800 A72-37729

Analysis of the division-line errors of the Pulkovo meridian circle by observations of stars

19 p2801 A72-37912

Thermistor temperature observation and correction for errors due to refraction anomalies in latitude measurements

19 p2801 A72-37913

Lateral chromatic aberration of a double-meniscus telescope in Chile

19 p2801 A72-37919

Preliminary results of discussions of latitude observations by the prismatic astrolabe in Pulkovo /1963.2-1968.7/

19 p2861 A72-37977

Investigation of the Talcott levels of zenith telescopes and determination of their division value

19 p2802 A72-37980

Some effects of bias errors in redundant flight control systems.

19 p2779 A72-38237

Effect of plasma resistance on electron temperature measurement by means of an electrostatic probe.

19 p2804 A72-38593

Measurement of unsteady hydrometeorological processes on inertial devices

19 p2830 A72-38774

Cup anemometer response to fluctuating wind speeds.

20 p2920 A72-38966

Double-ended, folded-path and double-reflecting transmissometers operation principles, and measure-

ment error sources consideration for relative merits and disadvantages

20 p2923 A72-39054

The impact of gradiometer techniques on the performance of inertial navigation systems

[AIAA PAPER 72-850] 20 p2949 A72-39079

Error analysis of hybrid aircraft inertial navigation systems.

[AIAA PAPER 72-848] 20 p2950 A72-39081

A new approach to a cruise navigator evaluation using sparse reference data.

[AIAA PAPER 72-835] 20 p2950 A72-39092

Maximum likelihood failure detection for redundant inertial instruments.

[AIAA PAPER 72-864] 20 p2923 A72-39133

Astronomical telescope hybrid pointing control system with double gimbal control moment gyros and orthogonally mounted reaction wheels to achieve extreme accuracy and stability

[AIAA PAPER 72-854] 20 p2924 A72-39138

Some results of calibrating CG-2 gravimeters /Sharpe/ by the tilt method.

21 p3053 A72-40499

In-flight alignment and calibration of inertial measurement units. I - General formulation. II - Experimental results.

21 p3081 A72-41079

Statistical analysis of influence coefficients and unbalanced forces measurement errors in balancing of rotors

21 p2996 A72-41229

Optical pyrometers with dual spectral ratios to eliminate instrument error due to selective radiation

22 p3175 A72-41887

Radiogoniometer error analysis for receiver internal noise and external interference sources, noting sources angular distribution effect on instrument error

22 p3158 A72-42233

Evaluation of flight instrumentation for the identification of stability and control derivatives.

[AIAA PAPER 72-963] 22 p3136 A72-42346

Engine compressor face rake for flight test instrumentation F-14A/TF-30.

22 p3216 A72-42686

A new stagnation pressure probe having a high pressure recovery in supersonic flow.

22 p3179 A72-42687

Low frequency measurement of mechanical impedance and frequency response.

22 p3164 A72-42700

Air temperature measurement errors due to instrument inertia under various meteorological conditions and atmospheric stratification

23 p3310 A72-43536

Spectrophotometer linearity testing using the double-aperture method.

23 p3289 A72-43894

Spectrometer for absolute stellar spectrometry

23 p3290 A72-44039

Electric field orientation, magnetic field strength and high voltage pulse delay effects on spark chamber track displacement from true particle trajectory

23 p3291 A72-44441

Radiation influences on a white-coated thermistor temperature sensor in a radiosonde.

24 p3401 A72-44620

Errors caused by hot-wire filament vibration.

24 p3402 A72-44949

Integrating digital voltmeter - Operating principles and accuracy.

24 p3403 A72-45275

High accuracy contactless torque-measuring shaft with strain gage as sensor, describing circuit wiring

24 p3403 A72-45296

Optimal linear inertia-free processing of meter readouts with allowance for control-equipment signals

24 p3403 A72-45316

Application of external information about the linear velocity of an object for correcting inertial navigation systems

24 p3423 A72-45319

Pulse transient response function for gyroscopic course indicator with gyrocompass error filtered out and nondistorted directional gyroscope error

24 p3403 A72-45320

The wedge probe - A review.

24 p3404 A72-45355

INSTRUMENT FLIGHT RULES

Instrument flying skills retention, discussing initial training, discrete procedural and tracking responses

01 p0018 A72-10564

UFO sighting case history and analysis, discussing bright light approaching on collision course during night instrument flight rules

09 p1269 A72-22646

Aircraft collision near misses under IFR and VFR conditions, discussing ATC coordination, equipment failure and personal and planning problems

09 p1349 A72-22972

General aviation aircraft structural safety studied with 1547 accident histories, noting IFR and turbulent weather conditions predominance

[SAE PAPER 720308] 11 p1575 A72-25572

Low cost flight simulator for general aviation pilot training, containing IFB instrumentation and turbulence injection device

15 p2214 A72-32211

Magnetic compass use in instrument flight conditions, suggesting emergency procedures during aircraft system failures

15 p2238 A72-32212

Prototype interurban IFR STOL transportation system demonstration project, considering area navigation, scanning beam microwave landing systems and STOL-port planning

[ICAS PAPER 72-41] 21 p3040 A72-41166

INSTRUMENT LANDING SYSTEMS

NT AUTOMATIC LANDING CONTROL

Aircraft ILS, covering history, adverse weather operations and replacement systems

02 p0257 A72-12645

Operational requirements of instrument landing systems, interferometers, correlation protected instruments, landing guidance systems and navigation aids

03 p0386 A72-13421

R and D requirements for international standard vhf instrument landing system for Category I, II and III operations in next decade

04 p0545 A72-14827

Low cost vertical crossed beam radar systems for nonprecision approach in small airports, reducing track error

04 p0545 A72-14829

Computed performance of ILS glide slope transmitting arrays sited over flat ground planes of one dimensional perfectly conducting strips in free space

05 p0686 A72-16559

All-weather landing aids for civil VTOL aircraft and helicopters, discussing Doppler and inertial navigations, instrument landing systems and ground visibility improvement

05 p0688 A72-16780

Proposed microwave ILS, discussing continuous step and Doppler scanned radar scanning beams

06 p0846 A72-18396

Step-scan landing system technique, using microwave fixed linear array for area coverage with pattern of narrow overlapping individually coded sequentially switched beams

06 p0846 A72-18397

Microwave instrument landing systems based on continuous radar scanning technique, using pulse format for data transmission

06 p0846 A72-18399

ILS development, discussing four course radar ranges, autoland and radar systems

09 p1349 A72-23449

Microwave equipment and technology application for instrument landing, terminal ATC, millimeter wave CAT detection and satellite communications

10 p1509 A72-24036

Static and dynamic analysis of legged planetary instrument landers, taking into account structural flexibility, elastic-plastic gear load characteristics and soil properties

[AIAA PAPER 72-371] 11 p1725 A72-25396

Aircraft miniaturized ILS with transmitter and localizer antenna to provide pilot with bearing and glide slope information for alignment with runway

12 p1842 A72-27106

Instrument landing systems specifications for civil and military aviation, suggesting replacement type development based on existing configurations

12 p1842 A72-27110

Pilot glide slope and localizer tracking performance during successive in-flight simulated ILS approaches

12 p1773 A72-28260

Civil aviation approach and landing guidance systems evolution, discussing ILS development, state of art and future requirements

13 p1996 A72-29014

Microwave scale model of ILS glide path, considering interference and aircraft taxiing effects

14 p2129 A72-30944

Tactical approach landing radar tests for low lift drag ratio aircraft in unpowered flight, using F-104D as test aircraft

15 p2267 A72-31694

Hybrid area navigation and microwave instrument landing system, discussing approach control and terminal guidance

15 p2271 A72-32206

Low cost microwave scanning beam landing systems for interim instrument landing system replacement in civil aviation

15 p2272 A72-32217

STRADA landing trajectory recording system for real time flight path restitution during approach and landing, using computer and lidar techniques

16 p2420 A72-32895

Autoland system flight testing in Trident 3B and British Civil Aviation Authority approval for ICAO Cat 3a weather

16 p2420 A72-33539

Log periodic dipole antenna systems for ILS localizers, noting reduced sensitivity to snow and ice

19 p2830 A72-37279

All weather landing for a STOL system.
[AIAA PAPER 72-788] 19 p2831 A72-38105
Microwave landing system effect on the flight guidance and control system.
[AIAA PAPER 72-755] 20 p2952 A72-40057
ILS replacement by microwave landing system, considering landing phase range from acquisition to touchdown, terminal approach handling by airborne navigation system and economic advantages
21 p3081 A72-40294
Automatic landing and microwave guidance system potential.
21 p3040 A72-41072
Future trends in air traffic control and landing.
[ICAS PAPER 72-04] 21 p3082 A72-41129
Prototype interurban IFR STOL transportation system demonstration project, considering area navigation, scanning beam microwave landing systems and STOL port planning
[ICAS PAPER 72-41] 21 p3040 A72-41166
Dala /Sweden/ regional airport, describing planning and financing, approach lighting, ILS system and facilities for tourist traffic and industrial development
23 p3278 A72-43248
Possible impact of area navigation upon MLS requirements for azimuth angular coverage and range.
24 p3422 A72-44643

INSTRUMENT ORIENTATION
Magnetometers for balloon-borne X ray astronomy payload azimuth determination, noting misorientation, earth and spurious magnetic fields effects on measurement effectiveness
10 p1530 A72-24954
Kalman filter application to inertial navigation systems optimal alignment, discussing linear systems representation in state space and filter algorithm recursive equations
14 p2129 A72-30330
Orion spaceborne astronomical observatory automatic control system for instrument orientation and star tracking, discussing servomechanism and pulse duration modulation
15 p2242 A72-32743
Inertial navigation system platform alignment and calibration by state space technique similar to Kalman filtering
16 p2420 A72-33697
Orientation of astrographs in observations and measurements
19 p2802 A72-37972
Process control of the 100-m telescope - Digital control
19 p2803 A72-38486
Process control of the 100-m telescope - Communication of the observer with the computer-controlled telescope
19 p2804 A72-38487
A multislot shadow sensor of direction to a luminous object
21 p3052 A72-40308

INSTRUMENT PACKAGES
NT APOLLO LUNAR SURFACE EXPERIMENTS PACKAGE
NT EASEP
Airborne external instrumentation pod containing IR scanner and associated test equipment for land and water surveys
16 p2393 A72-33635
TCE-71A area navigation system based on modular design with provision for 20 waypoints parameter storage, describing computer, control display and automatic data entry units
21 p3079 A72-40278
Aircraft instrument panel redesign to alleviate crew task, proposing integral displays and controls for flight information
21 p3080 A72-40291

INSTRUMENT TRANSFORMERS
Choice of optimal geometrical relationships in a transformer-type angle converter
21 p3058 A72-41805

INSTRUMENT TRANSMITTERS
Prototype compact ruggedized crystal-controlled L-band artillery telemetry transmitter design and performance
02 p0192 A72-12156
Navy uhf telemetry transmitter production system, discussing test program contribution to quality control
02 p0177 A72-12322
Pressure transmitter for flow parameter measurements of aerodynamic nozzles and static pressure taps rotating on turbine rotor blades
22 p3176 A72-42250

INSTRUMENTAL ANALYSIS
U AUTOMATION
INSULATED STRUCTURES
One dimensional heat insulated structure under dynamic loads, showing thermoviscoelastic effects on spontaneous heating and stress-strain state
03 p0444 A72-13460
Electric model of bridging losses and optimal insulation layer thickness for small size resistance strain gages
21 p3056 A72-41367

One dimensional heat insulated structure under dynamic loads, showing thermoviscoelastic effects on spontaneous heating and stress-strain state
24 p3458 A72-44935

INSULATING MATERIALS
U INSULATION
INSULATION
NT ELECTRICAL INSULATION
NT MULTILAYER INSULATION
NT THERMAL INSULATION
Refractory material development for space shuttle hydrogen tank reusable internal gas layer insulation
01 p0139 A72-10777
Temperature and compressive loading cycles effects on high performance multilayer insulation materials and composites, discussing application to space shuttle orbiter
01 p0092 A72-10779
Low conductivity insulating coating /graded thermal barrier/ to cool gas turbine engine with high pressure ratio and inlet temperature
[AIAA PAPER 72-361] 11 p1669 A72-25389
Insulation and bonding materials effects on double base solid propellants stability, using vacuum reactivity testing technique
14 p2145 A72-30766

INSULATORS
Metals, insulators, semiconductors and ceramics thermophysical parameters measurement during monotonic heating or cooling at 123-3273 K
06 p0904 A72-18514
Hubbard mathematical model for metal-insulator transition due to electrons correlations, noting schematic phase diagram and transition metal oxides
10 p1527 A72-24939
Transition series oxides metal-insulator phase transition based on electron phonon interaction model
11 p1701 A72-26024
Design and performance characteristics of ion thruster feed system components including high voltage isolator, liquid Hg flowmeter and W vaporiser
[AIAA PAPER 72-487] 11 p1710 A72-26213
Thermal noise in double injection diodes operating in the insulator regime.
18 p2667 A72-36979
Experimentally observed admittance properties of the semiconductor-insulator-semiconductor /SIS/ diode.
19 p2772 A72-37568
Metal-insulator-semiconductor-insulator-metal structure light pulse amplification investigating power gain and photocurrent dependences on applied voltage and applicability as radiation detector
20 p2960 A72-39517
Boundary conditions in the exciton absorption region.
21 p3096 A72-40139

INSULIN
Short term response of insulin, glucose, growth hormone and corticosterone to acute vibration stress in rats
01 p0015 A72-11289
Insulin injection or carbohydrate consumption effects on serotonin and tryptophan concentrations in rat brains
02 p0165 A72-12845
Prediction of vegetative reactions in the case of stress and extreme effects upon the organism
22 p3149 A72-42069
Prediction of vegetative reactions to extremal actions on the organism
22 p3141 A72-42168
Water-soluble insulin receptors from human lymphocytes.
24 p3373 A72-45375

INTAKE SYSTEMS
NT AIR INTAKES
NT ENGINE INLETS
NT HYPERSONIC INLETS
NT SUPERSONIC INLETS
Gas generator performance shifts involving military trim level variations by TF-30 engines in high relative humidity environment caused by condensation in inlet duct
07 p1052 A72-18759
Electrical analog simulation of internal combustion engines intake and exhaust systems nonstationary gas flow, considering cylinder, turbine and supercharger operation
13 p2027 A72-29136
Mathematical model for gas turbine engine inlet noise caused by shock wave impingement, noting dynamic wave system with overpressure and distortion
13 p2028 A72-29576
Three dimensional boundary layer separation on slender bodies, delta wings and propulsion intake systems, reviewing computing techniques for interfering inviscid flow fields
16 p2341 A72-32826

INTEGERS
Computational solutions of matrix problems over an integral domain.
21 p3076 A72-41315

INTEGRAL CALCULUS
Integrals for atomic wave functions of Slater orbitals, obviating numerical snags by Euler transformation
02 p0262 A72-11980
Nonlinear transformation for improper integral calculation, noting faster convergence than linear methods
10 p1506 A72-24997
McShane belated stochastic integral existence theorem with quasi-martingale process for sample continuity assumption
11 p1678 A72-26156
Nonsymmetrical stellar motion in galaxies, finding number of isolating integrals in systems with three degrees of freedom from four dimensional mapping
12 p1874 A72-27911
Periodic two-parameter solution families of dynamic systems having first integral, showing stability and bifurcation existence criteria relationships to dimensionality and Hamiltonian systems
15 p2261 A72-31309
Table of indefinite and definite integrals of products of error functions with transcendental and special functions
15 p2262 A72-31589
Infinite integral evaluation with integrand formed by product of H function and double contour integral, with application to boundary value problems solution
15 p2265 A72-32600
Calculation of steady modes of operation of RC circuits with jumpwise varying parameters
17 p2533 A72-34761
Integration of equations of motion for nonconservative holonomic systems with pulsed coupling factors
19 p2825 A72-38192
Relation between the first integrals of a non-holonomic mechanical system and a corresponding system freed of constraints
22 p3204 A72-41902
Dynamic equations integration with constraint factors, discussing Hamilton-Jacobi method applicability conditions
22 p3205 A72-42100
Conditions for complete continuity of integral operators with stationary features in a space of continuous functions
23 p3307 A72-43224
Path independent integrals to predict onset of crack instability in an elastic plastic material.
23 p3346 A72-43711

INTEGRAL EQUATIONS
NT FREDHOLM EQUATIONS
NT SINGULAR INTEGRAL EQUATIONS
NT VOLTERRA EQUATIONS
NT WIENER HOPF EQUATIONS
Numerical-integral equation approach to plane wave scattering from nonplanar conducting surface with sinusoidal height profile for magnetic field parallel to surface ridges
[AD-735574] 01 p0032 A72-11237
Alternative derivation of Mei integral equation for numerical determination of current distribution along thin wire antennas
01 p0043 A72-11246
MHD boundary layer calculation for conducting fluid along semiinfinite flat plate with transverse magnetic field, deriving momentum and kinetic energy integral equations
01 p0113 A72-11383
Direct method for dual and triple integral equations involving inverse Mellin transforms in potential mixed boundary value problems
01 p0094 A72-11390
Contact problem of rigid sphere intrusion into viscoelastic half space, obtaining solution by Green function construction and integral-operator equation formulation
02 p0289 A72-11615
Aerodynamic behavior of thin jet-flapped airfoil, investigating integrodifferential equation solution
02 p0149 A72-11669
Reactive and nonreactive channels full particle scattering amplitudes using coupled integral equations
02 p0262 A72-11910
Turbulent flow development in concentric annuli from modified Reichart integral equation model for eddy diffusivity of momentum
02 p0203 A72-12103
Nonlinear development of instability wave in turbulent wake behind thin body based on integrals of mean flow momentum and kinetic energy equations
02 p0152 A72-12351
Convolution type integral equations over arbitrary finite segment number with kernels, showing solvability in spaces, applications and correctness
02 p0294 A72-12430
Contact stress between half plane and elastic cover plate, reducing problem to Prandtl type integrodifferential equation with Hilbert kernel
02 p0294 A72-12433
Anisotropic and compressible work hardening materials three dimensional elastoplastic flow quasi-linear theory, deriving boundary integral equations
02 p0296 A72-12530

Electric and magnetic field scattering on ellipsoidal inhomogeneities in circular waveguides from integrodifferential equation derived expressions
03 p0322 A72-13735

Two dimensional elasticity theory, discussing first, second and mixed boundary value problems solution in contour integral form
03 p0451 A72-14116

Dual integral equations method application to elastic bodies with plane circular cracks in torsion
03 p0452 A72-14135

Numerical solutions of integral equation for transition and turbulent flows through pipes and channels, discussing computer simulations
04 p0510 A72-14469

Boltzmann equation collision integral statistical models, solving shock structure in monatomic gas
04 p0513 A72-15339

Synthesis of currents along linear antennas, reducing to solution of integral equation
04 p0500 A72-15406

Spacecraft antenna radiation pattern numerical analysis using combined electric and magnetic integral equations
04 p0500 A72-15407

Feld modification for integrodifferential equation solution for voltage on exponentially narrow waveguide slit, discussing further changes in method
04 p0501 A72-15409

Open resonators stability analysis, describing integral equations eigenfunctions and eigenvalues short wave asymptotic expansions
04 p0502 A72-15435

Integral equation for lowest natural frequency of vibrating beams, using eigenfunction theory
04 p0593 A72-15565

Integral equations derived for single and composite radio signals with maximum energy concentration in given time interval or frequency band
05 p0625 A72-15824

Integral methods application to turbulent corner flow problem, obtaining mean velocity profile first approximation for turbulent boundary layer with streamwise pressure gradient
[ASME PAPER 71-WA/FE-36] 05 p0646 A72-15921

Integral computation for nonequilibrium compressible turbulent boundary layers using moment, momentum and skin friction equations
[ASME PAPER 71-WA/APM-12] 05 p0647 A72-15968

Nonlinear transient coupled thermoviscoelasticity problems solution by finite element method and iterative solution for integrodifferential equation
05 p0736 A72-16085

Periodic integral convolution equations in elasticity theory and mathematical physics, demonstrating solution existence
05 p0739 A72-16589

Thermal stresses in thin symmetrically heated disk with time and temperature dependent mechanical properties, deriving integrodifferential equation defining stress function
05 p0740 A72-16624

Thin wing harmonic oscillation in subsonic flow, developing analytical form of kernel function in generalized Possio integral equation
05 p0603 A72-16707

Integro-differential initial value problem solution, differentiating for time variable and integrating for space variable
06 p0838 A72-17383

Dual integral equations solutions to electromagnetic wave diffraction at plane conducting slotted screen
06 p0773 A72-17689

Two body problem trajectory equation method simplification, reducing entire solution to two integral evaluations
06 p0881 A72-17931

Numerical integration of N-body problem in integrodifferential equations, using integrals as constraints and for correction application in least squares procedure
06 p0885 A72-18074

Hollow waveguide performance numerical solution review covering finite difference and element methods, polynomial approximation, point matching, integral equations and conformal transformation
06 p0784 A72-18237

Waveguide integral equation numerical solution by moment method, suggesting algorithm for detecting and alleviating relative convergence behavior
[AD-745595] 06 p0775 A72-18368

Computer simulated data analysis procedure for improved resolution of optical instrument by integral equation numerical solution
06 p0840 A72-18738

Classical elasticity displacement problem solution by integral equation method based on Betti tensor counterpart of Green procedure in potential theory
07 p1026 A72-18815

Second order differential equations system solution in convergent integrals, describing solution limit in vector form as special case of linear system solution property
07 p1026 A72-18815

Averaging techniques for nonlinear integral and integrodifferential equations, considering standard equations with and without rapid and slow variables, asymptotic series application to unsolved problems
07 p1027 A72-19609

Toeplitz matrix in numerical solution of integral equation for cylindrical antenna and array, presenting rapid inversion algorithm by exploiting symmetry properties
[AD-743577] 07 p0957 A72-19795

Thin antenna hf time response from thin wire approximation and source gap model for integral equation solution
07 p0957 A72-19798

Multiple point boundary value problem with linear integrodifferential equation simplification
07 p1028 A72-19983

Transformation of integrodifferential equation of motion of heavy solid body about fixed point
08 p1207 A72-21341

Polynomial solutions to integrodifferential equation of motion of solid body with fixed point for Lagrange conditions
08 p1207 A72-21342

Algebraic invariant relation of integrodifferential equation of motion of solid body about fixed point for Hess conditions, proving uniqueness
08 p1207 A72-21344

Solutions existence for algebraic invariant relation to integrodifferential equation of motion of solid body about fixed point in trigonometric and exponential polynomials class
08 p1207 A72-21346

Solutions existence for nonlinear invariant relation to integrodifferential equations of motion of solid body about fixed point
08 p1207 A72-21347

Solutions existence conditions for integrodifferential equation of motion of solid body about fixed point
08 p1207 A72-21349

Integrodifferential equation exponential solutions for body motion about fixed point
08 p1208 A72-21353

Fourth algebraic integral in Kovalevskaya solution of rotating body motion about fixed point regarding angular momentum components
08 p1208 A72-21357

Variational solutions to linear integral equations and extremal functions in physical gas dynamics problems, using stepwise constant trial functions
08 p1150 A72-21620

Ideal gas many particle distribution functions in microspace from solution of chain of integrodifferential equations
09 p1354 A72-22220

Thirteen moment closed system of approximate integral equations for rarefied gases density, velocity, temperature, stress tensor and thermal flux vector
09 p1259 A72-22425

Numerical solution of integral equations for dislocation densities and stress singularities associated with cracks and pile ups in bimetallic media
09 p1398 A72-22622

Molodenski integral equation for gravitational field calculation at point M on earth surface as function of neighboring region astronomical geodetic measurements
09 p1299 A72-22675

Equivalence of integral equation form and infinite system of linear equations with eigenvalue localization, applying to linear ordinary differential equations
09 p1342 A72-23367

Plane and antiplane elasticity boundary value problems reduced to integral equations by dislocation layers, noting closed form solutions for half and whole space
10 p1557 A72-24561

Integrodifferential equation for rigid tunnel walls effect on supercavitating flow past thin jet flapped airfoil, noting lift coefficient derivatives
10 p1469 A72-24562

Minimum time thrust start-up of nuclear rocket as optimal control problem with integrodifferential constraints, using Pontryagin maximum principle and calculus of variations
11 p1685 A72-25870

Inhomogeneous strings oscillations determination in nonstationary inverse boundary value problems with integral equations
11 p1689 A72-26381

Nonlinear integral equations solution for heavily loaded actuator disk induced flow field, taking into account blade tip vortices and thrust coefficient effects
11 p1573 A72-26577

Integral equation numerical solution applications to rectangular solid capacitance calculation and mixed boundary value problems
11 p1679 A72-26954

Two dimensional approximation for viscoelastic inhomogeneous material with hereditary properties varying in radial direction, deriving integrodifferential equations
12 p1878 A72-27088

Laplace-Carson transform solution for integrodifferential equation of motion for droplet suspended in viscous gas slipstream
12 p1796 A72-27093

Microstrip transmission lines analysis by integral equations approach, assuming TEM mode
12 p1782 A72-27492

Russian papers on functional analysis covering approximate solution of linear integral equations, averaging principle for partial differential equations and boundary value problems
12 p1837 A72-27994

Orthogonalization method application to problems of diffraction on several bodies through reduction to integral equations
13 p1920 A72-29278

Direct and inverse problems of scattering theory for hyperbolic system of equations on plane, emphasizing unsteady approach and integral equation class with kernels
13 p2004 A72-29468

Harmonic functions skew derivative problem reduction to study of integrodifferential equation by constraints imposition on boundary condition coefficients
13 p1987 A72-29469

Integral equation for calculation of unsteady aerodynamic forces on helicopter lifting rotor blades, taking into account air compressibility
[ONERA, TP NO. 1081] 13 p1895 A72-29671

Electromagnetic processes computation in circuits with SHF currents by reduction to integral equation, using dipoles system representation
13 p1937 A72-29945

Wire antenna half-space problem analysis by Sommerfeld integral approach and plane wave reflection coefficient approximation
14 p2085 A72-30338

Initial value method for Ambarzumian integral equation by transformation to Cauchy system
14 p2126 A72-30889

Arbitrary cascade profiles aerodynamic characteristics calculation via integral equation numerical solution for attached potential incompressible fluid problem
14 p2070 A72-31014

Axisymmetric celestial bodies equilibrium shapes in post-Newtonian approximation of general relativity using integrodifferential equation
14 p2161 A72-31077

Electromagnetic boundary value problem of two rectangular waveguides coupled by aperture radiating into free space, solving integral equation by moments method
15 p2205 A72-31357

Elastic body stress concentration problem formulation for singular integral operator eigenvalue problem for half space
15 p2323 A72-31478

Numerical solution of singular integral equations system for stress concentration in elastic plane with curvilinear crack
15 p2327 A72-31735

Optimal controller design for parabolic type second-order linear stationary systems, discussing integrodifferential equation solution possibility
15 p2211 A72-32170

Reduced density matrix dependence on nonzero boundary conditions, considering Salzburg-Kirkwood integral equations
15 p2282 A72-32448

Narrow strongly radiating slot voltage distribution, investigating cavity coupling with integral equation
15 p2209 A72-32659

Direct integral method to calculate subsonic and supersonic regions in planar and axisymmetric hyper-sonic flow, using stream function for velocity and density
[DFVLR-SONDDR-202] 16 p2343 A72-33421

Triple and quadruple integral equations solution in analogy to Fourier-Bessel series with mixed boundary values, using Erdelyi, Kober, Sneddon and Srivastava operators
16 p2416 A72-33663

Differential equations system solution satisfying dual integral equations, noting biomechanics applications
16 p2417 A72-33828

Compressible boundary layer with normal pressure gradients, investigating quasi-similar, nonlinear integro-differential equations properties at wall and sharp and blunt leading edges
[AIAA PAPER 72-696] 16 p2345 A72-34048

Integral equation for electromagnetic wave scattering by thin dielectric ring
17 p2526 A72-34379

Mathematical model for nonequilibrium gas composed of hard spherical nonattracting molecules, deriving gas dynamics theory in terms of multiple integrals
17 p2538 A72-34424

Distribution of current in centre-fed cylindrical dipole antennas with arbitrarily displaced feed points.
17 p2526 A72-34517

Use of fast Fourier transforms for solving partial differential equations in physics. 17 p2575 A72-34645

Relationship between finite differences and quadratures of a Green's function for a second-order ordinary differential operator 17 p2577 A72-35803

General theory of spherically symmetric boundary-value problems of the linear transport theory. 17 p2583 A72-35825

Three point distribution function related to lower order functions for closure of hierarchy of equations for turbulent probability distribution functions 18 p2677 A72-36005

Motion integrals conservation under Hamiltonian function variations, examining gyroscope equations of motion with parameter disturbances 18 p2711 A72-36666

Two body problem trajectory equation method simplification, reducing entire solution to two integral evaluations 18 p2730 A72-37156

Integral equation method for solution of boundary value problems of structural mechanics. I - Ordinary differential equations. II - Elliptic partial differential equations. 18 p2739 A72-37169

An initial value method for dual integral equations. 19 p2824 A72-37413

Formal extension of the possibilities of the method of integral transforms in the study of linear distributed systems with constant parameters 19 p2834 A72-37432

Periodic integral convolution equations in elasticity theory and mathematical physics, demonstrating solution existence 19 p2872 A72-37561

Application of the Bubnov-Galerkin method to the approximate integration of a Timoshenko-type equation 19 p2877 A72-38188

The Dirichlet problem of the Poisson integrodifferential equation 19 p2825 A72-38208

Waveguides of arbitrary cross section by solution of a nonlinear integral eigenvalue equation. 19 p2773 A72-38292

Application of dual integral equations to the problem of electromagnetic wave diffraction by a thin conducting ribbon 19 p2766 A72-38526

Complex resonant frequencies calculation in external diffraction problems for arbitrary shaped bodies, noting Green function poles correspondence to eigenvalue zeros of integral equation 19 p2767 A72-38652

Certain algorithms for obtaining an approximate solution of incorrect problems on a set of monotonic functions 19 p2828 A72-38846

Maxwell electromagnetic field theory review, emphasizing relationship between integral forms of Faraday and Ampere laws in conventional space and time concepts 20 p2904 A72-39778

An integro-differential equation approach to acoustic scattering from fluid-immersed elastic bodies. 21 p3083 A72-40102

Integral equations of a multiport network with a digital control automaton 21 p3036 A72-40154

Russian book - Mechanics of deformable one-dimensional bodies of variable length. 21 p3116 A72-40387

Integral equation and optics methods for far field radiation characteristics calculation of plane antennas with arbitrary reflector-source configurations 21 p3029 A72-40522

Integral equation method for boundary value problem of logarithmic spiral antenna, noting suitability for digital computers 21 p3031 A72-40535

Bubnov-Galerkin solutions to wire-antenna problems. 21 p3032 A72-40631

Synthesis of Tolubinskii's integral method and the perturbation method in nonstationary transport problems with nonlinear boundary conditions 21 p3129 A72-41053

Laplace transformation for unsteady convective heat transfer with nonlinear and time dependent heat transfer coefficients, obtaining nonlinear integral equation solution 21 p3130 A72-41066

Integral equation for pressure distribution by rigid punch contact with elastic half space, solving by Mathieu function expansion in Fourier series 21 p3126 A72-41541

Solution for shallow shells of revolution with allowance for large deflections by the method of integral relations 22 p3232 A72-41869

Optimal controller design for parabolic type second-order linear stationary systems, discussing integro-differential equation solution possibility 22 p3162 A72-42079

A simple quadrature method for computing laminar boundary layers. 22 p3165 A72-42110

Approximate solution, in generalized functions, to integral and integrodifferential equations with difference kernels 22 p3198 A72-42145

Numerical solution of integral equations of the first kind, using a priori information about the function to be restored 22 p3198 A72-42276

Integral equations and transformations in application to problems of elasticity theory 22 p3236 A72-42625

Numerical integration of integral equation for phased array radiation modeled by impedance filaments in conductive plane, noting excitation by magnetic flux 22 p3159 A72-42663

Effects of non-homogeneity on the stresses in a rotating cylinder. 22 p3240 A72-42877

Light scattering in a sphere in the presence of an arbitrary source distribution 22 p3207 A72-42965

Integral equations derived for single and composite radio signals with maximum energy concentration band in given time interval or frequency 23 p3263 A72-43432

Influence of a nonlinearity in a coherent accumulator of pulse signals on the gain in the signal-to-noise ratio 23 p3264 A72-43762

Numerical evaluation of elastic stress intensity factors by the boundary-integral equation method. 23 p3353 A72-44233

Generalized integral equations of radiative heat exchange. 23 p3357 A72-44536

Axisymmetric and two-dimensional flow with attached shock waves. 24 p3361 A72-45161

Integrodifferential equations for curved walls effect on laminar boundary layer characteristics, noting wall friction, layer thickness and transverse pressure 24 p3394 A72-45447

A priori estimates at the boundary for solving second-order elliptic integrodifferential equations 24 p3420 A72-45648

INTEGRAL FUNCTIONS

U ENTIRE FUNCTIONS

INTEGRAL TRANSFORMATIONS

NT CONVOLUTION INTEGRALS

NT FOURIER TRANSFORMATION

NT HILBERT TRANSFORMATION

NT LAPLACE TRANSFORMATION

Stokes and Love integral representations for elastodynamic displacement fields in elastic solid deduced by potential theory method 01 p0138 A72-10513

Book on integral transforms for solving ordinary and partial differential equations in applied mathematics covering Laplace, Fourier and Hankel transforms 01 p0094 A72-11274

Sampling theorem application to time varying systems, considering Hankel transform as example 11 p1675 A72-25293

Point source wave field diffraction on nontransparent circular cone, using steepest descent method and integral transformations 11 p1597 A72-26385

Digital dynamics simulation of continuous controlled processes based on repeated integral transformation of differential equations 13 p1934 A72-28607

Unsteady spherical shock wave effect on thin infinite elastic plate covering acoustic semispace, using integral transformation method 13 p1943 A72-29946

Discrete frequencies search in time series via anharmonic frequency analysis, using integral transform 17 p2574 A72-34450

Power law behavior of autocorrelation and memory functions of statistical mechanics as t approaches infinity 23 p3309 A72-43870

Dispersion relations of scalar hereditary theory of nonlinear viscoelasticity, representing integral operators as orthonormalized function series in Fourier space 24 p3459 A72-45264

INTEGRATED CIRCUITS

NT LARGE SCALE INTEGRATION

Large-signal IC equivalent circuit model for DC, linear and nonlinear transient time circuit analysis of lateral p-n-p transistors, including isolation junction interactions 01 p0044 A72-10126

X band power, bandwidth, efficiency and temperature performance of one watt CW microwave integrated avalanche diode oscillator 01 p0038 A72-10650

Computer program for design optimization of three-stage wideband low-noise integrated microwave amplifier 01 p0041 A72-10690

Hybrid microwave integrated circuits, discussing distributed circuits with strip transmission lines and lumped element circuits with inductors and capacitors 01 p0045 A72-10698

Hybrid IC at 30 GHz, considering IMPATT oscillators, circulators, frequency multipliers and filters configuration and performance 01 p0046 A72-10699

GaAs, Si and alumina performance as substrates in integrated microwave circuits 01 p0046 A72-10700

Directional couplers design for broadband microwave integrated circuits 01 p0046 A72-10702

MHD boundary waves properties, noting application to traveling wave nonreciprocal devices and planar structures based on microwave integrated circuits 01 p0029 A72-10703

Generation-recombination model of large signal silicon transistor operating in IC microwatt range 02 p0188 A72-11521

Failure modes of IC containing MOS devices, considering threshold voltage variations, oxide and silicon defects and leakage 02 p0194 A72-12443

Book on microelectronics covering integrated circuits, semiconductors, p-n junctions, transistors, Schottky and MOS structures, epitaxy, ion implantation, photomechanical operation, fabrication techniques, etc 02 p0194 A72-12574

Computer programs and program systems for IC synthesis, emphasizing models, analysis methods, optimized design and monolithic and hybrid IC configurations 02 p0197 A72-12668

Digital IC of ECL series without temperature compensation, discussing emitter coupled logic circuits interconnection methods 02 p0197 A72-12669

Wireless electronic time distributing system, investigating integrable digital receiver circuit and frequency bandwidths 02 p0197 A72-12696

Plaquette program for logic network wiring on IC box cards 03 p0327 A72-13167

Reliable Permalloy integrated magnetic memories with realizable low switching coefficients and square-loop properties, discussing design and fabrication [IEEE PAPER 21.4] 03 p0328 A72-13779

Book on microwave semiconductor devices, considering point contact crystal, varactor, Schottky-barrier, tunnel, backward and p-i-n diodes, transistors, Gunn effect devices and integrated circuits 03 p0333 A72-13845

Book on field effect electronics covering junction and insulated gate transistors and allied devices, monolithic and film IC and design techniques 03 p0333 A72-13846

GaAs Schottky barrier and germanium backward diodes in microwave integrated circuit applications, describing design and performance as frequency changers and low level detectors 03 p0334 A72-14073

Dc, ac and transient models of IC operational amplifier for computer aided circuit design and analysis applications 03 p0329 A72-14180

Random access memory based on multichip array with MOS-bipolar device combinations by hybrid techniques, bypassing handling and cost limitations 03 p0329 A72-14185

Laminate materials, sockets and connectors for cost-effective high temperature accelerated life testing of IC 03 p0336 A72-14283

Defective IC device glass surface passivation effects on scanning electron microscope analysis 03 p0365 A72-14287

Thermal control methods for high density packaging, discussing cooling techniques for hybrid circuit consisting of semiconductor chips and/or thin film components 03 p0337 A72-14293

Semiconductor-thermoplastic-dielectric hybrid ICs reliability, discussing interelement adhesive bonding properties and thermally induced strains effects 03 p0337 A72-14294

Circuit application consideration in selecting design, materials, processes and packaging for IC component reliability 03 p0337 A72-14295

Low temperature liquid bath tests for IC environmental reliability, monitoring wire bonding, metallization, surface contamination, sealing and die bonding
03 p0337 A72-14296

All digital IC FM discriminator design, computing output SNR above threshold
04 p0486 A72-14489

RC network synthesis technique using grounded gyrator and summing amplifier, applying to thin film RC networks and IC operational amplifiers
04 p0504 A72-14570

Microwave IC power amplifiers for radio relay, telemetry, phased array radar and TWT replacement
05 p0634 A72-15784

Plastic encapsulated transistors and IC moisture resistance tests for reliability under laboratory and field conditions
06 p0782 A72-17363

Interactive computer graphics design aids to IC mask layouts, discussing hardware and software techniques including IMP program
06 p0778 A72-17473

IC microcircuit for time-pulse voltage converter for conversion of dc voltage into electric pulses of length proportional to input signal
06 p0784 A72-17836

Computer aided design in electronics, discussing interactive computing with time sharing teletype keyboards or CRT graphics and applications in IC, network analysis and optimization
06 p0780 A72-18236

DC 9 aircraft integrated data system simulator to facilitate interacting systems checking, input circuit integrity, performance degradation and calibration
06 p0796 A72-18284

High power L-band microminiaturized hybrid type integrated transistor amplifier design and realization by computer
06 p0785 A72-18314

Microwave IC oscillators design for broadband high performance receivers, exemplifying thin film Gunn effect, step- and varactor-tuned transistor oscillators
06 p0786 A72-18373

Microwave thin film microstrip IC tunnel diode amplifiers for broadband high performance receivers, discussing design, construction and performance
06 p0786 A72-18374

FM/CW varactor Gunn diode oscillator powered subminiature IC radar altimeter design on homodyne principle for ultrahigh reliable minimum chance detection
06 p0819 A72-18473

Papers on thin film and semiconductor IC and contact and connection technology
06 p0790 A72-18570

Thin film conductors, distributed film resistors and capacitors design and associated IC layout to form functional arrays
06 p0790 A72-18574

Monolithic Si IC design and fabrication including resistors, capacitors, diodes, p-n-p, p-n-p, p-n-p and field effect transistors and inductors
06 p0791 A72-18576

Semiconductor device IC encapsulation, thermal design, stress analysis, testing and applications
06 p0791 A72-18577

Nd-YAG laser system generating gold conductor patterns on ceramic substrates, using numerical control system for Si production
07 p1002 A72-19213

Integrated miniature guided wave optical transmission systems using crystals adapted to thin film nonlinear interaction and photolithographic technique
07 p1004 A72-19228

Microwave IC front end receiver synthesis for radio relay system, considering low noise figure achievement by Si Schottky barrier diodes
07 p0955 A72-19356

YIG tuning of X band Gunn effect stripline oscillator circuit, noting application to microwave ICs
07 p0955 A72-19357

Optimization algorithm for minimum margin efficiency of electronic circuits, applying to IC TTL gate and transistorized bistable multivibrator (flip-flop)
07 p0944 A72-19568

Miniature modular wideband parametric amplifier for centimeter range, using IC optimal coupled circuit with passband dependent on diode time constant
07 p0956 A72-19570

Adhesives use for assembly of mechanical, optical, nucleonic and electronic instruments including printed and integrated circuits
07 p0992 A72-20576

Battery powered dc integrated circuit for temperature regulation in small experimental animals, using thermistor probes and heating pads
08 p1114 A72-20895

Schottky barrier semiconductor devices characteristics, fabrication and application to pulse microwave diodes and IC elements
08 p1139 A72-21053

MOS IC reliability based on p-channel enhancement mode transistors, discussing failure modes and mechanisms
08 p1142 A72-21588

IC technology review, considering computer applications and microelectronics prospects
08 p1142 A72-21843

Linear IC amplifier analysis by admittance parameters of equivalent two terminal pair network as function of frequency, temperature and supply voltage
09 p1285 A72-22342

Fast IC signal delay time reduction by high packing density, discussing yield, power dissipation and cost problems
09 p1290 A72-22820

Book on digital and analog monolithic IC systems, covering manufacturing methods, component design, MOS logic, arithmetic, error correction, codes, applications, etc
09 p1286 A72-23044

Automatic assembly machines for IC batch production, involving terminal cutting and bending and RC element insertion
09 p1292 A72-23255

Thin organosilicon films for integrated optical circuits and devices, discussing transparency and loss characteristics and refractive index control
09 p1314 A72-23339

Six channel integrated MOS switch, discussing MOS transistor operation and circuits structure
09 p1288 A72-23363

Mass storage systems technologies covering magnetic recording, surface wave acoustics, magneto-optic beam addressing, magnetic bubbles, switchable resistances and IC memories
09 p1283 A72-23413

Numerical linear interpolator design with ICs, noting application to digital filters and sampled data systems
09 p1289 A72-23677

Ion implantation doping of MOSFET and IC for wafer production, using automatic vacuum pumpdown and cycle control
10 p1447 A72-23950

Reliability prediction for MOS/LSI devices based on chip circuit configurations evaluation, extrapolating bipolar IC failure rate model
10 p1447 A72-24009

Failure mode control in plastic packaged IC for screening and quality assurance
10 p1447 A72-24010

Large scale integrated circuits for digital differential analyzers, giving operational specifications for shift registers, adders and integrators
10 p1448 A72-24276

Homogeneous computing media, examining microelectronic fabrication, interconnection and control problems for MOSFET, bipolar transistors and IC structures
10 p1448 A72-24277

Microelectronic IC functional logic systems design with S-type semiconductor devices, describing procedures for logic functions, shift register and directional transmission line
10 p1448 A72-24278

Magnetic integrated circuits design and fabrication problems involving branched and logic circuits and solid state structures controlled domains
10 p1448 A72-24279

Thermal and electric fields interaction in LF integrated circuits design, applying thermal feedback loops to bandpass filter, delay circuit and Schmidt-trigger oscillator
10 p1448 A72-24280

Semiconductor IC transducers for electrical readout of optical radiation, mechanical stress and magnetic field strength
10 p1448 A72-24282

Integrated circuits fabrication and design, describing internal physical processes, input and output signal values, functional operations and topological features
10 p1448 A72-24283

Response time and noise stability measurements of integrated circuit TTL /transistor-transistor logic/ and DTL /diode-transistor logic/ elements performing invert functions
10 p1449 A72-24286

Monolithic IC semiconductor components layout density evaluation for isolation, active and edge regions utilization efficiency
10 p1449 A72-24287

Statistical analysis of MOS integrated circuits from initial data of electrophysical and geometric distribution laws and covariance matrix
10 p1449 A72-24289

Monolithic, thin film and LSI technology development trends in microelectronics, noting heteroepitaxy, ion implantation and laser beam techniques
10 p1454 A72-25175

Radio electronic equipment IC and microelectronics development trends, considering bipolar and MOS transistors applications in digital and analog computers and telemetry
10 p1454 A72-25176

Bipolar insulated gate FET IC buffer driver, discussing input and output interface capacitance and impedance characteristics and application to transistor-transistor logic
11 p1603 A72-25269

IC plastic encapsulation reliability problems related to die stability, wire bond and package moisture integrity
11 p1606 A72-26546

Binary multiplication algorithms adaptable to IC functional elements for ultrahigh speed operations
11 p1602 A72-26547

Complex bipolar IC logic circuits realization by economical high speed techniques using metal bonding or cells available in library
11 p1606 A72-26548

Common collector micropower monolithic transmitter for single or multichannel biomedical telemetry
11 p1586 A72-26563

Micropower IC approach based on complementary transistor-transistor logic
11 p1606 A72-26566

Complementary monolithic IC n-p-n and p-n-p transistor circuit structure with high sheet and low saturation resistance
11 p1606 A72-26567

Aluminum-silicon Schottky diode clamped transistor-transistor logic circuits parameters optimization for high switching speed and IC applications
11 p1606 A72-26568

Path connection algorithms for optimal IC layout on circuit board, using digital computer
11 p1607 A72-26784

IC lateral p-n-p multijunction transistor frequency characteristics analysis, noting parasitic effects, cutoff frequencies and power gain
12 p1788 A72-27311

Nonlinear mathematical dc models of planar transistors for computerized IC design and analysis obtained by continuity equation approximate solution
12 p1789 A72-27313

Programming system for automatic plotting of mask patterns for ICs
12 p1791 A72-27551

Circuitry and operational characteristics of variable output voltage regulator with low temperature coefficient, noting suitability for monolithic integration
12 p1792 A72-27740

Integrated inductorless quadratic bandpass filters for constant bandwidth wide frequency range, using IC analog multipliers network
13 p1927 A72-28403

Automatic electrostatic contour welding of IC microcircuit metallic casings, using contact and electrode voltage feedback signals
13 p1963 A72-28921

Digital precision frequency synthesizers constructed on IC logic modules without using LCI filters, analyzing restrictive factors
13 p1930 A72-29050

IC reliability assessment based on defects and failure mechanisms analysis instead of MTBF estimations
14 p2091 A72-31166

Low power TTL IC in plastic and hermetic packages tested for reliability via critical dc parameters measurement in initial and post-stress states
14 p2091 A72-31168

Lumped approximation to distributed RC notch networks for linear IC, deriving open circuit voltage transfer functions and root locus graphs
14 p2092 A72-31170

Linear ICs application to RF probe for ionospheric electron density measurements from rockets or satellites
15 p2240 A72-32389

Electric measurement and defect localization in monolithic IC elements by incorporating test structures
15 p2212 A72-32755

Physical phenomena limitations on MOS IC miniaturization, considering gate oxide breakdown, drain source punch through, doping fluctuations, power dissipation and metal migration
16 p2370 A72-34102

A simulation method permitting the direct construction of an integrated fluidic circuit with predetermined frequency response curve
17 p2494 A72-34197

Microwave integrated circuits
17 p2527 A72-34570

A study of the heat flow and thermal instabilities in high power hybrid integrated circuits
17 p2527 A72-34678

Techniques for control of long-term reliability of complex integrated circuits. I - Reliability assurance by test vehicle qualification
17 p2528 A72-34686

Failure analysis of plastic and ceramic packaged IC, describing plastic encapsulants chemical removal and radiographic failure detection procedures
17 p2528 A72-34707

Laser computer technology - Today and tomorrow
III p2523 A72-35186

Ceramic waveguide microwave integrated circuits
17 p2534 A72-35570

X- and Ku-band microelectronic phase shifters
17 p2531 A72-35767

- Numerical control component insertion for missile IC electronic module, tabulating producer-user survey data for designs usage and machine tools
17 p2532 A72-35923
- A thermal oscillator using the thermo-electric /Seebeck/ effect in silicon.
18 p2667 A72-36978
- Limitations in microelectronics. II - Bipolar technology.
18 p2667 A72-36980
- ATC IC transponder used with secondary surveillance radar, discussing design features
18 p2662 A72-37048
- Analysis of sensitization mechanisms of low consumption integrated circuits
18 p2668 A72-37107
- Reliability of integrated circuits with plastic encapsulation
18 p2669 A72-37114
- Microwave and optoelectronic devices performance and component reliability, considering varactors, p-i-n, avalanche and Gunn diodes, ICs, FETs, light emitters and liquid crystals
18 p2720 A72-37137
- Quality and reliability evaluation method for integrated circuits using MOS transistors - Option: Circuits on request
18 p2671 A72-37141
- Test structures - Powerful technique for quality evaluation and reliability assessment of MSI and LSI /medium and large scale integrated circuits/.
18 p2671 A72-37143
- Low noise high power bipolar and field effect transistors monolithic integration potentials for microwave applications
19 p2771 A72-37261
- An all solid-state MIC transmit-receive module.
19 p2771 A72-37268
- Single and dual gate GaAs FET integrated amplifiers in C band.
19 p2771 A72-37270
- P-i-n variable attenuator with low phase shift.
19 p2773 A72-38294
- Electrical properties and fabrication details of integral diode matrices with controllable avalanche breakdown produced from zone melted silicon under temperature gradient
19 p2774 A72-38416
- Eigenfrequencies of monolithic filters.
19 p2774 A72-38608
- Microelectronic component system temperature distribution measurement by IR microscope and electrical technique to determine beam-lead IC thermal performance
20 p2908 A72-39498
- Burn-in technique cost effectiveness in semiconductor and IC reliability enhancement, noting failure rate relationship to operating time
20 p2909 A72-39770
- Probability model and causal approach to failure mechanisms and reliability of control systems applied to IC
21 p3024 A72-40711
- Low noise compact down converter for 12 GHz to UHF based on waveguide mounting microwave ICs, measuring conversion loss for GaAs Schottky diode
21 p3033 A72-40885
- Microelectronics developments and limitations, considering bipolar IC, metal-dielectric-semiconductor structures and optoelectronic communication links
21 p3033 A72-40940
- Miniaturized IC semiconductor device fabrication and failure under electrical load, using scanning electron microscope
21 p3035 A72-41492
- Optimization algorithm for minimum margin efficiency of electronic circuits, applying to IC TTL gate and transistorized bistable multivibrator /flip-flop/.
22 p3158 A72-42086
- Miniature modular wideband parametric amplifier for centimeter range, using Q optimal coupled circuit with passband dependent on diode time constant
22 p3158 A72-42088
- Masking techniques for thin film and semiconductor devices and ICs fabrication, discussing conventional and computerized optical and electron beam systems
22 p3159 A72-42634
- Semiconductor/IC Processing and Production Conference, Anaheim, Calif., February 8-10, 1972 and New York, N.Y., June 13-15, 1972, Proceedings of the Technical Program.
22 p3160 A72-42822
- Niobium superconductive tunnel diode integrated circuit arrays.
22 p3161 A72-43090
- Microstrip matching networks synthesis for microwave integrated circuits, calculating passband of configurations with lumped and distributed elements
23 p3269 A72-43445
- Design optimization of an integrated-circuit direct access memory unit
23 p3267 A72-43841
- Monolithic quartz and ceramic bandpass filters for narrow band analog data transmission systems
23 p3273 A72-44347
- Book - Electronic integrated systems design.
23 p3274 A72-44475
- Shielded silicon gate complementary MOS integrated circuit.
24 p3385 A72-44972
- INTEGRATION (REAL VARIABLES)**
U MEASURE AND INTEGRATION
INTEGRATORS
NT DIGITAL INTEGRATORS
Self oscillations and drift motion of gyroscopic integrator of linear accelerations under hf vibrations, assuming ideal relay gimbal compensation
02 p0231 A72-12567
- Computer designed optical integrating devices for semiconductor laser arrays, considering diode, collection, projection and zoom parameters
15 p2248 A72-32048
- Reversible integrodifferentiator with automatic data input
21 p3024 A72-40162
- Dynamic error of storing voltages at capacitors in the storage channel of an integrator of variable structure
21 p3024 A72-40165
- Decomposition of multidimensional nonlinear equations of heat-conduction type and construction of nonlinear electrical integrators
21 p3128 A72-40181
- Signal voltage density, pulse shape and noise power spectrum analysis of running integrator output in IR scanner model
21 p3056 A72-41086
- INTEGRODIFFERENTIAL EQUATIONS**
U DIFFERENTIAL EQUATIONS
U INTEGRAL EQUATIONS
INTELLIGENCE
NT ARTIFICIAL INTELLIGENCE
Hologram data treatment comparison to human brain function, discussing recognition signals, Pavlovian qualities and intelligence function
06 p0768 A72-17997
- Frontal cerebrum region and elementary mental activity
18 p2649 A72-36400
- INTELLIGIBILITY**
NT SPEECH RECOGNITION
Message circuit noise evaluation in commercial telephone system, discussing noise measurements and weighting curves
15 p2202 A72-32575
- Visual information electronic display systems from human factors engineering viewpoint, discussing intelligibility optimization in terms of human vision physiological characteristics
19 p2803 A72-38309
- INTELSAT SATELLITES**
Design and performance of Intelsat III dual TWT power supply, noting space, weight and cost savings
01 p0007 A72-11056
- Ionospheric turbulence induced scintillations of Intelsat geostationary satellite signals at 4 and 6 GHz [AIAA PAPER 72-179]
05 p0631 A72-16966
- Legal structure of governmental and operational agreement by international organizations for Intelsat satellite communications system
06 p0905 A72-18169
- Communication satellite technology progress survey, discussing Early Bird and Intelsat satellites and Comsat program
06 p0777 A72-18620
- International space communication systems legal and operational aspects, discussing Intelsat and Intersputnik systems
07 p1104 A72-19470
- Intelsat functions, discussing international cooperation, United Nations resolutions and financial arrangements
07 p1104 A72-19471
- Rotor components vibration destabilizing effects on dual spin spacecraft dynamics, considering turbulent liquid sloshing in Intelsat 4 propellant tank
07 p0973 A72-20488
- Intelsat 4 satellite communication transponder design for broadband multicarrier operation, using frequency and pulse modulation techniques [AIAA PAPER 72-535]
12 p1780 A72-27358
- Intelsat V satellite system with large telephone channels capacity and full earth station network connectivity, discussing system concepts and technology [AIAA PAPER 72-536]
12 p1780 A72-27359
- Intelsat 4 nutation dynamics and gyrostat stabilization technique for precision pointing in international telecommunication, discussing damper and fuel sloshing [AIAA PAPER 72-537]
12 p1780 A72-27360
- TDMA system for Intelsat 4 and subsequent satellites, discussing automatic synchronization acquisition, terrestrial network-satellite transmission channel modular interface, etc [AIAA PAPER 72-538]
12 p1780 A72-27361
- Intelsat satellite time division multiple access system /TDMA/ using semiconductor technology with burst synchronization [AIAA PAPER 72-546]
12 p1781 A72-27369
- Intelsat 3 global multichannel wideband multiple access communication system, describing technological advancements in communication performance, attitude control and testing procedures [AIAA PAPER 72-534]
13 p1918 A72-28982
- Geostationary Intelsat satellite networks for retransmission of data received by earth resources satellites
15 p2221 A72-31243
- Intelsat satellite SPADE demand-assignment multiple access system design for increased communication flexibility and efficiency
17 p2512 A72-34269
- Intelsat 4 multichannel communication network earth station equipment components and characteristics experimental system /SPADE/ study to realize demand assignment
18 p2659 A72-36272
- Earth station receivers for global and domestic FM systems.
18 p2662 A72-36848
- INTENSIFICATION**
U AMPLIFICATION
INTENSIFIER TUBES
U IMAGE INTENSIFIERS
INTENSIFIERS
NT IMAGE INTENSIFIERS
NT IMAGE ORTHICONS
INTERACTIONS
NT AIR WATER INTERACTIONS
Longitudinal wave interaction and excitation by plasma instability in equatorial electrojet, considering energy transfer mechanism
05 p0656 A72-16242
- INTERATOMIC FORCES**
Interatomic force model for elastic properties of alpha quartz and alkali halides generalized for specified structure under arbitrary pressure
07 p0980 A72-20519
- Va crystal lattice interatomic bonds and elastic and inelastic X ray scattering intensity calculation
09 p1329 A72-23042
- Al inhibitive of Ti oxidation at 800-1000 C due to interatomic bonds, lower oxygen solubility and diffusion rates
14 p2113 A72-30166
- Iron carbide single crystal growth texture due to anisotropy of interatomic interactions associated with oriented covalent Fe-C bonds
14 p2121 A72-30774
- Some data on interatomic interaction in solid high-melting compounds of titanium, vanadium, and chromium with light metals
17 p2569 A72-35520
- Molecular and atomic interaction forces as interfacial free energy sources, discussing molecular attachment kinetics and surface configuration models
18 p2718 A72-36393
- An atomistic study of cracks in diamond-structure crystals.
18 p2718 A72-36509
- Ion-atom scattering and interatomic potentials for ions of noble metals and period II elements incident on neon and argon with energies in the range 8-25 keV.
19 p2837 A72-37883
- Direct fitting of spin wave energies to interatomic exchange parameters in the ferromagnetic rare earth metals.
21 p3097 A72-40625
- Hydrogen cold work peak measurements in Nb, showing hydrogen atoms-dislocations binding energy extent and temperature effects on internal friction
22 p3189 A72-42440
- INTERCEPTION**
Optimal allocation and guidance for linear time varying interception and rendezvous problems of dynamic deterministic or stochastic systems
05 p0686 A72-16558
- Minimum time duration rocket interception, calculating trajectory parameters and target orbits in Earth gravitational field
09 p1393 A72-23573
- Aircraft interception avoidance problem solved by differential game theory, discussing human operator decision making for random pursuit tracking
24 p3377 A72-45523
- INTERCEPTOR AIRCRAFT**
U FIGHTER AIRCRAFT
INTERCEPTORS
Real time homing guidance geometry and interceptor/sensor tradeoff studies based on reachable sets of target states analysis [AIAA PAPER 72-825]
20 p2951 A72-39101
- INTERCONTINENTAL BALLISTIC MISSILES**
NT MINUTEMAN ICBM
NASA ICBM/IRBM space program major management decisions and highlights concerning Atlas, Titan and Thor
23 p3358 A72-44356
- INTERCOSMOS SATELLITES**
Investigation of energetic charged particles and VLF emissions on the 'Intercosmos-3' satellite
17 p2600 A72-35209

INTERCRANIAL CIRCULATION

Russian book - Algorithms for calculation of navigation data on spacecraft position. 21 p3103 A72-40460

INTERCRANIAL CIRCULATION

Adrenergic innervation of internal carotid arteries in extra- and intracranial regions in dogs, using luminescence method 08 p1121 A72-22184

INTERFACE STABILITY

Dynamic stabilization of Rayleigh-Taylor instability at interface between two heavy fluids by viscosity and interfacial tension 01 p0108 A72-10231

Interface stability of floating liquid zones of water/ethanol solutions in simulated zero gravity 07 p1036 A72-20561

Chopped fiber glass reinforced high density thermoplastic polyethylene composite, determining critical fiber length, interfacial adhesion and fracture toughness 08 p1193 A72-21684

Adverse environmental effects on epoxy composites resin-glass interface properties, investigating epoxy-compatible silanes contribution to composite performance 08 p1194 A72-21696

Shock wave passage through curved interface from low to high density medium, showing interaction dependence on density ratio 10 p1469 A72-24541

Model for large signal losses prediction in charge coupled devices due to fast interface state trapping 10 p1526 A72-24625

Two dimensional Lagrangian hydrodynamic code for stability of shock acceleration perturbed interface between two gases of different density 13 p1942 A72-29114

Theoretical investigation of the interfacial stability of inviscid fluids in motion, considering surface tension. 18 p2681 A72-36482

Interface morphology development during stress corrosion cracking. I - Via surface diffusion. 18 p2700 A72-36583

Interfacial characteristics of silicon carbide-coated boron-reinforced aluminium matrix composites. 20 p2941 A72-39791

Precipitation thermodynamics of unstable and metastable solid solutions, discussing interfaces, vacancies, spinodal decomposition, nucleation, reversion and macroscopic diffusion 20 p2943 A72-40000

Baroclinic long wave dynamic instability in Kochin two layer frontal model, noting beta effect on wave disturbances 22 p3202 A72-43001

INTERFACES

NT FLUID BOUNDARIES

NT GAS-SOLID INTERFACES

NT JET BOUNDARIES

NT LIQUID-LIQUID INTERFACES

NT LIQUID-SOLID INTERFACES

NT LIQUID-VAPOR INTERFACES

NT SOLID-SOLID INTERFACES

Coaxial connector standard interfaces for optimum microwave performance, discussing single connector reflection coefficient measurement equipment and procedures 01 p0041 A72-10693

Data transmission and distribution systems interface, using semiconductor technology in multiplexing, asynchronous data transfer, A-D and D-A data conversion and sensor signal conditioning 02 p0194 A72-12404

Fock reflecting formulae expansion to moving interfaces from Fresnel laws, interpret ing solution in terms of geometrical optics 04 p0491 A72-15422

Digital computer equipped facility for training simulators environmental simulation capability testing, describing electronics interface, control and display equipment 22 p3164 A72-42928

Nuclear and dipole relaxation at polymer-polymer interfaces 23 p3307 A72-43931

INTERFACIAL ENERGY

Surface and interfacial energies measurement by multiphase equilibrium method for refractory metal monocarbides with liquid cobalt 07 p1010 A72-19136

Molecular and atomic interaction forces as interfacial free energy sources, discussing molecular attachment kinetics and surface configuration models 18 p2718 A72-36393

Acceleration stress tolerance dependence on electron or ion transport across cell surface activation energy barrier, studying rat survival times 18 p2650 A72-36448

INTERFACIAL STRAIN

U INTERFACIAL TENSION

INTERFACIAL TENSION

Dynamic stabilization of Rayleigh-Taylor instability at interface between two heavy fluids by viscosity and interfacial tension 01 p0108 A72-10231

Physical processes of fluids atomization in electric field, discussing droplet surface instability and boundary values of surface tension coefficient 05 p0667 A72-17185

Glass fiber reinforced polymer composite model for tensile stress distribution in matrix and fibers and at bond interface 08 p1194 A72-21753

Fluid sealing theory based on surface tension effects at roughness asperities within seal film 08 p1177 A72-21928

Surface tension determination at immiscible liquids or liquid-gas phase interfaces by capillary rise measurement of droplet 09 p1294 A72-22678

Embedded strain gage technique for subsurface tensile testing of boron-epoxy composites 11 p1671 A72-25467

Modified geometrical model for sintering Ni-doped W, including surface tension effect at Ni-vapor interface 14 p2121 A72-30770

Lunar dumbbell shaped glass globules formation due to rotation and surface tension effects of ejecta from meteoric impacts 15 p2306 A72-31628

Theoretical investigation of the interfacial stability of inviscid fluids in motion, considering surface tension. 18 p2681 A72-36482

Mathematical model for surface tension induced thermocapillary fluid flow influence on conductive heat transfer through condensate film broken by non-wetting strips [ASME PAPER 72-HT-H] 20 p2985 A72-39654

Concentration dependence of surface tension in solutions of surface-inactive polymers 21 p3072 A72-40079

INTERFERENCE

Noise reduction by acoustic interference, using sound generators operating in antiphase mode to noise input 02 p0262 A72-12897

Multifrequency ultrasonic pulse echo interference effect applying to flaw detection in metals 11 p1687 A72-26051

The interference function of molten metals 17 p2568 A72-35175

Aerodynamic interference between aircraft components - Illustration of the possibility for prediction. [ICAS PAPER 72-49] 21 p2992 A72-41174

Wall interference effects on cone-cylinder pressure distribution in variable porosity trisonic wind tunnel as function of model blockage and Mach number [AIAA PAPER 72-1010] 21 p3041 A72-41592

Analysis of a lateral-directional airframe/propulsion system interaction of a Mach 3 cruise aircraft. [AIAA PAPER 72-961] 22 p3137 A72-42348

Problems of interference between oscillating surfaces in subsonic flow 23 p3248 A72-43809

INTERFERENCE DRAG

Aerodynamic interference between parallel bodies for estimating aerodynamic characteristics of rocket engine with auxiliary boosters, obtaining flow field by slender body theory 05 p0600 A72-16005

Wind tunnel data correction for interference due to flow boundary constraints /wall effects/, acoustic and model support effects 21 p3043 A72-41640

An experimental investigation of a jet issuing from a wing in crossflow. 24 p3362 A72-45332

Transonic wall interference effects on bodies of revolution. [AIAA PAPER 72-1008] 24 p3389 A72-45404

INTERFERENCE GRATING

Far IR molecular laser variable interference filter for optimization of output coupling conditions and maximum power output 04 p0532 A72-15616

Characteristic impedance formulas for rectangular waveguides with dielectric slab, discussing interference filter design application 05 p0627 A72-16343

Lattice source interference method for detection of X ray diffraction in Al-Zn solid solutions, taking into account precipitation effects 10 p1499 A72-24981

Retina visual acuity testing by zero and first order moire fringes, using square-wave amplitude gratings 12 p1772 A72-27953

Three dimensional model images information content increasing in coherent light interference shadow marking, noting automatic systems for distant objects recognition 17 p2529 A72-34844

Surface evaluation of airfoils via contouring. 19 p2806 A72-37605

Surface distortion and strain fields visualization by grating produced diffraction patterns, discussing different detection techniques 22 p3234 A72-42391

Moire screens coded with pseudo-random sequences. 23 p3289 A72-43892

INTERFERENCE LIFT

Low subsonic region unsteady interference effects on harmonically oscillating wing-tailplane model with variable sweep wing [DGLR PAPER 71-081] 02 p0152 A72-12709

Wind tunnel wall blockage and lift interference reduction by streamwise porosity distribution 11 p1613 A72-26001

Wind tunnel data correction for interference due to flow boundary constraints /wall effects/, acoustic and model support effects 21 p3043 A72-41640

A new method for the evaluation of slotted wind tunnel interference parameters applicable to subsonic oscillatory tests. 21 p3043 A72-41642

An experimental investigation of a jet issuing from a wing in crossflow. 24 p3362 A72-45332

Computation of wall effects in ventilated transonic wind tunnels. [AIAA PAPER 72-1007] 24 p3388 A72-45403

INTERFERENCE MONOCHROMATIZATION

U DIFFRACTION

U MONOCHROMATIZATION

INTERFEROGRAMS

U INTERFEROMETRY

INTERFEROMETERS

NT FABRY-PEROT INTERFEROMETERS

NT MACH-ZEHNDER INTERFEROMETERS

NT MICHELSON INTERFEROMETERS

NT MICROWAVE INTERFEROMETERS

NT RADIO INTERFEROMETERS

Multifrequency interferometer for inhomogeneous plasma density soundings, determining time dependence, spatial distribution and plasma layer size. 02 p0263 A72-11413

Absolute gravity acceleration determination using free-falling laser interferometer apparatus with rotation-insensitive mirror at different sites. 02 p0207 A72-11597

Focused image holographic interferometer for reduced blur in deep object image reconstruction with white light source 02 p0224 A72-11747

Jones matrix representation of optical instruments applied to Fourier interferometers /spectrometers and spectropolarimeters/ 03 p0358 A72-13434

Plasma diagnostic technique using three-mirror He-Ne laser interferometer for electron concentration measurement 04 p0555 A72-14654

Laser interferometer for quality control of optical parts and instruments 05 p0668 A72-16191

Blunt bodies-shock wave interaction in shock tubes, using interferometer with laser light source and high speed streak camera 05 p0601 A72-16225

Accelerometer sensitivity calibration by laser interferometer for vibration measurement, discussing frequency range, accuracy and advantage over spectral lamp 07 p0984 A72-19350

Laser interferometers for displacement, length, gas refractivity, laser wavelength and relative object position measurements [CLEA PAPER 15,1] 07 p1005 A72-19396

Absolute gravity measurement methods and instruments, noting portable laser interferometer and formula derived from satellite observations 07 p1034 A72-19595

Displacement measuring instrument based on holographic interferometry using He-Ne laser with split beam for interference fringes on photographic plate 07 p0987 A72-19848

Laser gyro operational principles, discussing passive Sagnac and active ring laser interferometers, readout, errors due to null shift, lock-in and mode pulling, etc 07 p1007 A72-20223

Fast responding mark/space ratio decoder for use with slug Josephson interferometers, presenting circuit waveforms 07 p0992 A72-20580

FM/CW interferometric ionosonde used for interferometric direction finding, computing incident azimuth and elevation from baseline array phase differences 09 p1281 A72-23514

Holographic interferometer and fringe analyzer with laser sources, discussing design and application to supersonic flow imaging in wind tunnel 12 p1809 A72-27760

He-Cd laser emission wavelength determination at Lamb dip center for development of interferometer operation in violet spectral region 13 p1970 A72-29688

- Random variations in interferometer complex visibility function magnitude and phase, refractive index and source angular size 14 p2156 A72-30561
- German monograph on optical transmission measurement interferometer with plane-parallel birefringent crystal plates covering plate combination selection based on interference pattern mathematics 15 p2233 A72-31525
- Three Josephson junction asymmetric feed quantum interferometer, discussing magnetic field sensitivity and amplitude variation increase 15 p2241 A72-32536
- Construction, tuning and characteristics of high resolution spectrometers with scanning interferometers for He-Ne laser radiation analysis 16 p2400 A72-33080
- Electron interferometer based on second order interference effects from laser modulated electron beam, applying quantum mechanical analysis 16 p2402 A72-33398
- Holographic interferometer employing spherical mirrors. 18 p2692 A72-36699
- Twyman-Green interferometer to test large aperture optical systems. 19 p2811 A72-37590
- Application of video techniques and speckle pattern interferometry to engineering measurement. 19 p2799 A72-37628
- Experimental investigation of optical aberrations, due to temperature deformation and convective fluxes, by using a nonequal-arm interferometer with a coherent light source 19 p2801 A72-37920
- Critical current periodicity of Josephson junction interferometers. 19 p2846 A72-38601
- Optical measurement of wave front lens or mirror surface contours by laser unequal path interferometer combined with computer data reduction 20 p2922 A72-39034
- Heat transfer measurements with a Wollaston prism schlieren interferometer. [ASME PAPER 72-HT-9] 20 p2927 A72-39680
- An immersion interferometer for monitoring the quality of second-order aspherical surfaces 21 p3058 A72-41808
- German monograph - A hologram interferometer for the determination of amplitude and phase of optical excitation in diffraction patterns. 22 p3181 A72-43056
- A neoteric interferometer for use in holographic photoelasticity. 23 p3290 A72-43985
- ### INTERFEROMETRY
- #### NT DIFFERENTIAL INTERFEROMETRY
- Remote sensing of atmospheric pollutants and trace contaminants, presenting high speed high resolution, Fourier interferometer broadband model [AIAA PAPER 71-1109] 01 p0068 A72-10553
- Air holography interferometry for acrylic model materials inspection and selection for optical flatness, comparing with photoelasticity [SESA PAPER 1941] 02 p0224 A72-11516
- Interferometric observations of pulsars at 2.7 and 8.1 GHz, determining radiant flux densities 02 p0278 A72-11906
- Projected interference fringes in holographic interferometry for large surface movements measurements 02 p0231 A72-12544
- Nonperiodically moving object holographic interferometry by time-averaging method, considering single exposure technique advantage over multiple exposure in thermal deformation observation 03 p0357 A72-13373
- TV time lapse interferometry and contouring for photoelastic nondestructive testing, comparing with photographic techniques 03 p0358 A72-13436
- High resolution Galactic center interferometric observations at 5 GHz, showing compact components in Sagittarius A 04 p0580 A72-15511
- Holographic interferometer for heat transfer measurement, studying free convection thermal boundary layer on heated isothermal vertical flat plate 04 p0524 A72-15531
- Brownian particle sedimentation rate and diffusion coefficient determination by holographic double exposure interferometry 06 p0816 A72-17982
- Radio sources and quasar structure angular resolution determination with distant radio telescope interferometry and microwave relay links 06 p0886 A72-18177
- German monograph on vibration amplitudes interferometric measurement, discussing methods for resolution improvement and phase measurements, distortion and sonic field effects, etc 07 p0983 A72-19264
- Optical coupling effects in frequency stabilized He-Ne lasers, finding instabilities for interferometric length measurement 07 p1005 A72-19414
- Pulsed IR carbon dioxide TEA laser for two dimensional interferometry of theta pinch plasma during discharge 07 p1005 A72-19416
- Wave front division interferometry for small scale solar features study at visible wavelengths 07 p1076 A72-19598
- Comparative IR schlieren and interferometry techniques for measuring electron density profiles from refractive index effects of rotationally symmetric plasmas 07 p0986 A72-19613
- Hologram interference fringe relationship to nonlinearity of simple oscillations 07 p0987 A72-19836
- Holography applications and processes, discussing holographic microscopy, particle analysis, high speed photography, data storage and retrieval, interferometry, nondestructive testing, etc 07 p0989 A72-20221
- Laser applications in metrology and geodesy, discussing use of beam directionality for alignment purposes, interference patterns and interferometry, modulated light methods, optical Doppler methods, etc 07 p1007 A72-20222
- Transient plasma diagnostics using carbon dioxide laser interferometry and absorption for electron density and temperature determination 07 p1008 A72-20557
- Plasma diagnostics using carbon dioxide laser absorption and interferometry, comparing electron densities with shock data 07 p1008 A72-20565
- Placeholder for on site wet processing of holograms in real time holographic interferometry, obtaining undistorted reconstructed image by liquid gate immersion 07 p0992 A72-20581
- Strain measurements by holographic interferometry, considering data input to computer by digitization of video signals 08 p1163 A72-20917
- Holographic interferometry for nondestructive testing, discussing applicability to laminate structures 08 p1164 A72-20924
- Physical analysis of photoelastic interferometry and holography, considering retardation, isochromic and isopachic fringe systems and model materials 08 p1166 A72-21330
- Holographic interferometry application to weak inhomogeneities visualization in gas flows, using photographic emulsion nonlinear properties 09 p1311 A72-22965
- Interferometry in volume holograms with recording of wave fronts by double exposure technique and reconstruction by diffraction 09 p1315 A72-23350
- Atmospheric refractive index inhomogeneity statistics from interferometer measurements of distance-dependent phase fluctuations in near-ground horizontal optical propagation paths under turbulence conditions 09 p1354 A72-23696
- Interferometric measurements of time dependent electron density in Xe pinched plasma laser, showing laser lines due to transitions in triply ionized species 09 p1366 A72-23700
- Interferometric testing of optical systems, discussing test plates, Fizeau, Lloyd moire, transmission, Twyman-Green, shearing, Ronchi, scatter fringe, grazing and holographic methods 10 p1482 A72-24567
- Material testing by holographic interferometry, discussing application to early detection of delayed cracking, fatigue damage and bond imperfections 10 p1482 A72-24575
- Interferometric photoelectric scans of interstellar Ca K lines in stellar spectra, noting interstellar Na lines presence 10 p1544 A72-24663
- Reflecting surface roughness measurement by holographic interferometry, applying to lapped steel specimens 11 p1629 A72-25309
- Real time hologram-moire interferometry for visualization of turbulence phenomena in liquid flow through cylindrical pipe 11 p1629 A72-25317
- Satellite orbit tracking data accuracy estimation by partial differentiation, using Doppler and interferometric methods 11 p1593 A72-26097
- Continuous He-Ne laser radiation power interferometry using Michelson interferometer with frequency doubler 12 p1819 A72-27051
- Laser-interferometer instrumentation for shock stress wave measurements in solids, using velocity and displacement techniques 12 p1808 A72-27638
- Three station interferometer observations of Jovian decametric burst at 18 MHz, discussing possible solar wind interference 12 p1871 A72-27743
- Holographic interferometry for impact loaded object transient impulse response recording with double-pulse Q switched laser 12 p1809 A72-27761
- Electronic fringe counter with CdS cell photosensors, dc bridge and strip recorder for interferometric applications 12 p1792 A72-27762
- Spark interferometry of plasma filaments in gases from self focused single mode ruby laser beam 12 p1852 A72-27869
- Analog computer for practical evaluation of hologram interference fringes, analyzing errors 12 p1811 A72-27940
- Off center sampled interferograms correction by change of origin in Fourier transform, noting overlapping aliases effect 12 p1811 A72-27941
- Transparent materials study by interferometric methods, emphasizing holographic bench advantages for stress analysis and aerodynamic flows observation [ONERA, TP NO. 1037] 12 p1812 A72-28048
- Composite materials evaluation methods, discussing high quality photographs, radiography, laser holographic interferometry, thermographic fluorescent phosphors, liquid crystals and acoustic techniques 12 p1815 A72-28101
- Space center tractography and telemetry systems, including radar stations, interferometric equipment, optical methods and interlinked computers [DGLR PAPER 72-014] 13 p1938 A72-28961
- Spatial coherence measurement of ruby laser light by interference method, calculating diffraction pattern contrast curves 13 p1968 A72-29510
- Sensitivity limits in moire picture application to holographic interferometry 13 p1958 A72-29514
- Opaque scatterers disadvantages in interferometric images recording of transparent objects obtained by double exposure holography, noting phase type diffraction gratings 13 p1958 A72-29616
- Interferometric investigation of temperature fields and heat transfer in air layers between vertical, inclined and horizontal parallel walls 14 p2170 A72-30251
- Holographic interferometry for strain measurements in bodies, obtaining frozen interference fringes for stressed plane mechanical component via double exposure 14 p2105 A72-30840
- Three dimensional medium recording of multicolor holographic interferometry, comparing scale factor, spatial frequency and optical distortions with two dimensional medium 15 p2233 A72-31412
- Real time focused image holographic interferometry for deformation recording in diffusively reflecting plate under compression 15 p2233 A72-31415
- Liquid crystal detector design for IR holography and interferometry with applications to NDT of semiconductors, plasma diagnostics and material research 15 p2237 A72-32055
- Dynamic in situ thin film thickness monitoring during vacuum deposition by holographic interferometry, noting independence from high quality optical components 15 p2240 A72-32381
- Interference measurement techniques for small phase difference changes, noting diffraction and noise effects as limiting factors 15 p2243 A72-32769
- Holographic interferometric measurement of materials time dependent deformation responses to various environmental influences, discussing CW and pulsed laser techniques and holographic microscopy 16 p2388 A72-32820
- Quasars 3C273 and 3C279 superlight velocity and distances from interferometer pattern changes in 1970-1971 16 p2450 A72-32865
- Compact radio sources observation by long coherence intercontinental interferometry in trans-Pacific experiments 16 p2452 A72-33047
- Laser interferometric calibration for vibration measurement, discussing operation principle and detector error 16 p2391 A72-33248
- Holograms on bismuth and paraffin thin films with pulsed high power TEA carbon dioxide IR laser, discussing photosensitivity and capability for interferometric measurement 16 p2392 A72-33390
- Spark interferometry of plasma filaments in gases from self focused single mode-locked ruby laser pulses 16 p2439 A72-33978
- The spectrum of Mars between 8 and 13 microns. 17 p2606 A72-34575
- An improved method for obtaining the general-displacement field from a holographic interferogram. 17 p2553 A72-34721

Holographic interferometry application to weak inhomogeneities visualization in gas flows, using photographic emulsion nonlinear properties

17 p2558 A72-35893

Signal generator designed for calibration and control of interferometric radar station to observe and study radio echoes induced by meteor trails

17 p2519 A72-35959

Holographic interferometry analyzed from the point of view of moiré patterns.

18 p2690 A72-36362

Mechanical component acceleration-induced stress and transient phenomena analysis by dynamic photoelasticity and interferometry, applying to elastic birefringent and other materials

18 p2734 A72-36373

Method of stationary phase for analysis of fringe functions in hologram interferometry.

19 p2796 A72-37582

Optical holography and holographic interferometry applications in solid mechanics, considering surface physics, bomb breakup, transverse wave propagation, nondestructive testing and vibration analysis

19 p2797 A72-37603

Real time holographic contouring and coherent light interferometry of gear tooth surfaces.

19 p2797 A72-37606

Interferometric holography for bond inspection in aerospace composite materials and honeycomb structures

19 p2806 A72-37607

Holographic strain analysis using spline functions.

19 p2797 A72-37611

Quantitative data reduction with the use of fringe control techniques in conjunction with holographic interferometry.

19 p2797 A72-37612

Displacement field analysis via holographic interferogram, measuring fringe pattern shift due to change of observation direction through double exposure hologram

19 p2797 A72-37613

Determination of influence coefficients for composite structures by holographic interferometry.

19 p2873 A72-37614

Holographic strain measurement on a tensile specimen.

19 p2798 A72-37615

Holometric deformation measurement on carbon carbon biaxial test specimens.

19 p2822 A72-37616

Applications of holography to vibrations of segmented shells.

19 p2873 A72-37617

The non-stroboscopic visualisation of vibrational patterns by real-time/time averaged hologram interferometry.

19 p2873 A72-37618

Three dimensional flow field visualization, data acquisition and reduction via holography, noting applications in schlieren and interferometric techniques

19 p2798 A72-37620

Measurement of three-dimensional refractive-index fields by holographic interferometry.

19 p2798 A72-37621

Single pulse holographic flow visualization.

19 p2798 A72-37622

Interferometric holography of laser-produced gas breakdown.

19 p2798 A72-37623

A general theory of polarization holography and its application to photoelastic analysis.

19 p2799 A72-37627

Three dimensional holographic interferometry program for study of fringes due to displacement or deformation

19 p2799 A72-37630

Holography for aerodynamics.

19 p2799 A72-37682

Historical review of holographic interferometry development, giving attention to contouring technique and image reconstruction

19 p2800 A72-37775

The non-stroboscopic visualisation of vibration patterns by the real time-time averaged hologram interferometry.

20 p2921 A72-39028

Double-beam interferometry method for investigating axisymmetric configurations of dense plasma.

20 p2958 A72-39505

Interferometric study of a TEA-CO₂ laser produced plasma.

20 p2958 A72-39816

The study of vibration patterns using real-time hologram interferometry.

20 p2927 A72-39848

Recording holographic interferograms in a lanthanum-doped fluorite crystal

21 p3053 A72-40476

Transparent film thickness, refractivity and birefringence measurements by white light interferometric gage, noting performance insensitivity to chemical composition, film temperature and haze level

21 p3053 A72-40601

Opaque scatterers disadvantages in interferometric images recording of transparent objects obtained by double exposure holography, noting phase type diffraction gratings

21 p3054 A72-40669

Holographic interferometry with variable sensitivity

21 p3058 A72-41745

Double exposure holographic interferometry for distinguishing surface deformations by changing illuminating beam inclination in successive exposures

22 p3175 A72-41992

Interferometric investigation of natural convection in rectangular air cavities of different orientation

22 p3244 A72-42262

Absolute measurement of the solar brightness in the spectral region between 100 and 500 microns.

22 p3255 A72-42389

Measurements of the local velocity of shock and detonation waves by schlieren interferometry of Doppler-shifted laser light.

22 p3178 A72-42455

Laser interferometer for studying boundary layers in liquids

22 p3178 A72-42473

Interferometric observations of lunar occultations of radio sources, showing positions, brightness distributions, spectral index variations and quasar coincidence

23 p3334 A72-43260

Determination of the refractive index by the X-ray interferometry method

23 p3287 A72-43414

Holographic techniques in high intensity acoustic fields analysis, applying to chemistry, medicine and engineering

23 p3287 A72-43549

Upper limit on the gravitational flux reaching the earth from the Crab pulsar.

23 p3337 A72-43874

Interferometric spectropolarimetry - Alternate experimental methods.

23 p3289 A72-43890

Full-field surface-strain and displacement analysis of three-dimensional objects by speckle interferometry.

23 p3349 A72-43984

Interferometric measurement of the elongation of a pulsed diode laser.

23 p3297 A72-44185

Phase correlation between two sources formed on a diffusing surface - Application to the human retina

23 p3261 A72-44379

Closed-path interferometric experiments on the speed of light from moving sources.

24 p3425 A72-44788

INTERFERON

Blood self purification enteral mechanism in dogs, determining leukocyte population changes before and after feeding and intravenous interferon injections

07 p0915 A72-18867

INTERGALACTIC MEDIA

Interacting radio galaxies, considering dynamics of streaming through intergalactic medium and secondary radio structures origin

01 p0126 A72-10288

Extragalactic cosmic ray hypothesis plausibility from viewpoints of energy supply, acceleration process efficiency, galactic nucleus activity and intergalactic space

01 p0122 A72-11268

Fast particle interaction with intergalactic matter, discussing relaxation of power law cosmic ray spectra

04 p0570 A72-14553

Cosmic gamma radiation theoretical and experimental investigations, discussing sources, interactions with interstellar and intergalactic media, atmospheric backgrounds, balloon and satellite measurements, etc

05 p0709 A72-16328

Intergalactic matter and radiation relation to origin and evolution of universe

05 p0717 A72-16385

Intergalactic matter infall in galaxies, discussing quasar absorption spectra, hydrogen clouds, accretion rate and relations to spiral structure

09 p1386 A72-22660

Extragalactic clouds supersonic collisions with galactic gases, discussing high velocity neutral hydrogen gas result of recombination following post-shock surplus energy radiation

10 p1538 A72-24248

Coma galaxy cluster X ray and radio source region magnetic field origin as primordial metagalactic flux or strong radio source remnant

10 p1542 A72-24617

Intergalactic medium presence in clusters of galaxies from investigation of separation and size-separation ratio of double radio sources located inside and outside clusters

10 p1544 A72-24670

Fluid dynamics stability of double radio sources intergalactic medium, discussing evolution, ram pressure mechanism and Rayleigh-Taylor and Kelvin-Helmholtz effects

10 p1550 A72-25196

Intergalactic extinction relationship to large galactic clusters from statistical analysis of fourth and fifth Zwicky catalogs

12 p1872 A72-27759

Electromagnetic emission in universe, discussing background radiation spectrum, extragalactic source brightness, intergalactic gas and energy density

14 p2152 A72-30479

Double radio extensions in galactic cluster members, rejecting interacting galaxy hypothesis in favor of independent nonoptical radio galaxies in cluster intergalactic media

16 p2451 A72-32989

Sounding rocket observations of quasar 3C 273 X ray spectrum for upper limits to absolute abundance of He in intergalactic medium

16 p2446 A72-33451

Negligible intergalactic matter model, deriving distance-red shift relation and comparing to acceleration parameter of homogeneous model

16 p2455 A72-33470

Intergalactic ionized gas and member galaxies mass relationship in local group and nearby galactic clusters, considering gravitational potential

17 p2604 A72-34475

Heavy element enrichment of protogalactic primordial gas by quasars matter ejection into intergalactic medium

17 p2604 A72-34526

Interpretation of rotation measures of radio sources.

17 p2606 A72-34573

Faraday rotation in connection with Hoyle theory of intergalactic magnetic field existence in steady state cosmology, considering cosmological model with cosmic magnetic field

17 p2614 A72-35504

Observational evidence for strength and structure of intergalactic magnetic fields, discussing primordial fields effects on galaxy formations and early universe evolution

18 p2726 A72-36728

Soft X-ray emission from intergalactic gas in the neighbourhood of the Galaxy.

19 p2855 A72-37345

Extragalactic origin of the transient X-ray sources.

19 p2856 A72-37502

X-ray emission from intergalactic gas in the neighbourhood of galaxies.

20 p2964 A72-39240

Formation of clusters of galaxies - Photocluster fragmentation and intergalactic gas heating.

22 p3324 A72-42377

UV and IR observations of galactic and intergalactic matter from space stations, noting spatial resolution increase

24 p3446 A72-45532

INTERGRANULAR CORROSION

Al-Zn-Mg alloy intergranular corrosion in unstressed condition, detecting anodic paths at grain boundaries by potentiostatic technique

04 p0535 A72-15731

Preferential concentration of impurities and alloying elements at grain boundaries, noting role of equilibrium type interfacial segregation in intergranular corrosion

04 p0535 A72-15734

Pitting potential and intergranular corrosion of anodically polarized Al and Al alloys in electrolytes

04 p0536 A72-15736

High Cr ferritic steels intergranular and stress corrosion properties and resistance to sea water, organic and inorganic acids and acid mixtures

07 p0995 A72-19572

Accelerated intergranular corrosion and grain boundary precipitation mechanisms in stainless steel Fe-Ni-Cr alloy, using Huey, acid and Strauss tests

14 p2118 A72-30548

Critical species in the transgranular stress corrosion cracking of titanium alloys in aqueous solutions.

17 p2567 A72-34733

Active corrosion in aqueous solutions, discussing reactions, adsorption, intergranular attack, pitting, crevice corrosion and stress corrosion cracking

19 p2815 A72-37446

Electrochemical protection potential of metals and alloys in pitting, intergranular corrosion and stress corrosion cracking in presence of chlorides

21 p3065 A72-40087

Chemistry of grain boundaries and its relation to intergranular corrosion of austenitic stainless steel.

22 p3195 A72-43126

Surface layer grain boundary corrosion damage of Ti alloys during vacuum annealing, reducing rupture strength, vibration resistance and bending fatigue limit

23 p3293 A72-43589

INTERIOR BALLISTICS

Metallized solid propellants burning rate augmentation by internal ballistics effect of spinning rocket motor, deriving relationship between burning rate, pressure level and acceleration

13 p2025 A72-29302

Nonlinear equations solutions for interior ballistics parameters of solid rocket propellants combustion during rocket engine nozzle opening

19 p2878 A72-37352

INTERLAYERS

NT MULTILAYER INSULATION
Interlaminar shear testing of composite materials, discussing short beam, scissor and torsional methods [PI PAPER 7] 09 p1337 A72-22542
Shielding metallic interlayer technique to protect MIS device against degradation due to ionizing radiation effects 13 p2023 A72-29836

INTERMEDIATE FREQUENCIES

Phase measurements at if in microwave plasma diagnostics, examining phase stabilization processes 02 p0223 A72-11417
Telemetry receiver signal data quality in terms of RF, if AGC, AFC and AM rejection circuitry requirements 02 p0192 A72-12149
Sky wave propagation curves from MF observations for 7500 km distances 12 p1784 A72-27784
Linear detectors for broadband and high intermediate frequency measurements in radio astronomy 12 p1793 A72-27810

INTERMEDIATE FREQUENCY AMPLIFIERS

FM mf equipment for 2700-channel Hertzian beam, considering thermal noise, intermodulation and equivalent distortion of amplifiers, discriminator, limiter, etc 07 p0954 A72-19190
Microwave amplifier with internal negative feedback, using IF output for frequency modulation of mixer oscillator signal 13 p1930 A72-29057

Equivalent-damping and generalized-stagger distributions in single-circuit stagger-stage IF amplifiers at critical staggering 20 p2906 A72-38894

Allowance for transistor parameter dispersion in transistor IF amplifier designs with staggered-cascade pairs 20 p2906 A72-38895

Transient response of threshold lowering circuit with frequency converter for single contour IF amplifier with resonant frequency equal to carrier frequency 22 p3153 A72-42121

INTERMEDIATE RANGE BALLISTIC MISSILES

NT POLARIS MISSILES
NASA ICBM/IRBM space program major management decisions and highlights concerning Atlas, Titan and Thor 23 p3358 A72-44356

INTERMETALLICS

High transition temperature alloys, layered intermetallic and organic superconductors development and properties 01 p0113 A72-10163

Diffusion aluminide protective coating formation mechanisms on Ni-base superalloys observed from microstructures and compositions in Ni-Al intermetallics 01 p0089 A72-11165

Al-Mo alloys under high temperature, determining phase equilibria and intermetallic phases 03 p0370 A72-12961

Sigma phase formation in chromous ferrite, investigating vacuum diffusion, hot and cold working, welding and additives effects 03 p0375 A72-13940

Phase composition and structure of Be alloys containing Ru, Os, Rh or Ir, noting isomorphous beryllides existence 03 p0375 A72-13942

Nb-Co-Sn and Nb-Ni-Sn ternary systems, investigating intermetallic compounds existence by X ray analysis 03 p0375 A72-13944

Dilatometric investigation of martensitic transformation in TiNi compound, observing plastic memory effect 03 p0377 A72-14021

Au-Al wire bond, discussing intermetallic phase formation under elevated temperature treatments and reliability design limitations 03 p0364 A72-14284

NMR behavior and magnetic susceptibility of intermetallic compound CeAl, noting exchange polarization of RKKY type between 4f electrons and conduction electrons 05 p0702 A72-16784

Al-AlCu intermetallic unidirectionally solidified eutectic composite structure and heat treatment effects on room temperature tensile properties 05 p0676 A72-17104

Directionally solidified Al-AlNi intermetallic eutectic composites creep tests, identifying time dependent fracture mechanism 05 p0678 A72-17114

Gas turbine superalloys high temperature oxidation resistance by fiber strengthening, rare earth alloying, precipitation hardening and intermetallic compounds 06 p0828 A72-17611

Anomalous temperature-strain rate dependence of Ni-Al intermetallic compound mechanical properties from plastic deformation mechanism 06 p0832 A72-18417

Hardening mechanisms of interaction between superlattice dislocations and point defects in Ni-Al intermetallic compound mechanical properties strain rate and temperature dependence 06 p0832 A72-18420

Heat resistant weldable precipitation hardened Ni base alloy, discussing intermetallic phase hardening 07 p1014 A72-19842

Ni-Cr-Ti alloy hardening during intermetallic phases precipitation, discussing atom segregations, Guinier-Preston zones and fcc and hcp lattices 07 p1019 A72-20152

Critical temperature dependence of Nb-Al-Ge superconducting alloys on composition and heat treatment, discussing phase boundaries and electron state densities 07 p1049 A72-20154

Precipitation hardening of quenched superconducting Nb-Al alloys, examining polycrystalline and single crystal samples and intermetallic phases 07 p1050 A72-20155

Ni-Cr-Nb alloys structure and phase composition changes from W-Mo additions and hardening by intermetallic Ni-Nb precipitated from supersaturated solid solution 08 p1187 A72-21782

Ti-Co intermediate phase transformations discussing lattice formation, intermetallics melting points and stoichiometric composition 08 p1187 A72-21783

Intermetallics and carbide forming additions of Cr, Ti, Ce, V and Nb for hardening of cold worked Mn rich steel from crystal dislocations growth 09 p1327 A72-22230

Transition metal superconductors transition temperatures survey, considering d-band solid solution alloys and intermetallics and ferromagnetic element compounds 09 p1367 A72-22552

Parabolic oxidation kinetics of Ni-Ti alloy compound at elevated temperatures 09 p1330 A72-23358

Atomic radius ratios and lattice constants in intermetallic compounds Laves phases, presenting semistatistically calculated values for niobium diferride based on rigid sphere model 10 p1527 A72-24978

X ray analysis of internal friction strains in nickel molybdenide during ordering process at 650-700 C, using torsional pendulum method for friction measurements 11 p1662 A72-26654

Slip and mechanical twinning in nickel-nickel niobide directionally solidified eutectic alloy, showing variation with temperature of stress-strain curves 11 p1667 A72-26935

Electron microscope study of commercial Ni superalloys, discussing intermetallic compound and carbide precipitation hardening 12 p1827 A72-27137

Mo addition effect on Al and Ti diffusion from intermetallic compounds into Ni matrix, noting increased high temperature stress rupture life 13 p1975 A72-28670

Ti-Ni alloy strengthening by titanium nickelide intermetallic epsilon phase formation control via heat treatment 13 p1981 A72-29829

Chemical bond in Cu-Ti intermetallic phases, from X ray K absorption edges studies 13 p1981 A72-29914

Equiatomic ordered, bcc TiFe and TiNi electron density in outer energy band from X ray K emission spectra 13 p1981 A72-30006

Metallurgical and superconducting properties of beta-tungsten structure niobium aluminide with high critical temperature 14 p2119 A72-30607

Slip band blocking effect of disperse particles on crack suppression and creep rupture strength of intermetallic Al-Fe-Ni alloy 14 p2124 A72-31033

Primary crystallization of intermetallic compounds in Al alloy as function of high melting metal concentration and casting temperature 14 p2124 A72-31034

Binary Al alloys intermetallic phases effects on microcracks nucleation and propagation at 300 C in uniaxial tension, considering alloying elements influence on mechanical properties 14 p2124 A72-31036

Russian papers on intermetallic compounds covering structure, properties and applications of carbides, nitrides, oxides, phosphides, aluminides, antimonides, arsenides and chalcogenides 15 p2252 A72-31192

Composition diagrams and properties of intermetallic compounds of magnesium in binary and ternary systems 15 p2252 A72-31196

Pd-Al intermetallic compound contact materials. 18 p2698 A72-35985

Complexonometrical analysis of molybdenum aluminides and Cu-Mo alloys without preliminary separation of components 18 p2655 A72-36097

Composition dependence of density in NiTi and CoTi. 18 p2701 A72-36592

Formation of voids and dislocation loops in near-stoichiometric NiAl by aging at 700 to 900 C, and some effects on alloy properties. 20 p2937 A72-39288

The effect of elastic anisotropy on dislocations in Ni3Fe. 20 p2937 A72-39293

Phase diagram study of Cr-Ga alloys, investigating intermetallic compounds presence and polymorphic transformation and temperature effects 20 p2942 A72-39987

Fabrication studies of Nb3Al superconductors. 21 p0397 A72-41182

Hydrogen in intermetallic phases, taking into account as an example the system titanium-nickel-hydrogen 21 p3070 A72-41647

Nickel-titanium intermetallic phase effect on recrystallization of dispersion hardening high melting point steel during furnace and induction heating 21 p3071 A72-41789

Equiatomic ordered bcc TiFe and TiNi electron density in outer energy band from X ray K emission spectra 22 p3190 A72-42733

INTERMITTENCY

Turbulent flow internal intermittency and fine structure distribution as function of Reynolds number, using hot-wire anemometer for velocity field measurements 03 p0340 A72-13156

Intermittency factor of diffuser flow boundary layer with positive pressure gradient, using hot wire anemometers and multichannel analyzer 04 p0461 A72-14411

Clear air intermittent turbulence energy budget from aircraft data, obtaining turbulence parameters along aircraft path through application of electronic filters 09 p1344 A72-22437

Asymmetry and intermittency factors of temperature and velocity fluctuations in viscous substrate of hot plate turbulent boundary layer 10 p1464 A72-24064

Turbulent free shear flow intermittency factor determination by electronic circuit, discussing calibration and errors 11 p1617 A72-25997

Electromagnetic waves scattering by underdense plasmas, examining intermittency phenomenon due to mixing between turbulent inner and outer inviscid wake 13 p1922 A72-29473

Two fluid model for qualitative interpretation of turbulent intermittency, noting governing equations analogy to Landau equations for superfluidity 19 p2787 A72-38428

INTERMODULATION

Analog FM multiplex signal intermodulation formula based on time-variable electromagnetic waves tropospheric scatter propagation 01 p0027 A72-10411

Multichannel space station communications using PCM-PSK-PM interplex modulation for reducing cross modulation loss 02 p0174 A72-12131

Intermodulation noise in multichannel frequency division multiplex telemetry systems due to nonlinearities in transmitter-receiver links and tape recorder 02 p0175 A72-12145

Graphical and tubular methods for frequency assignment to avoid intermodulation interference in channelized bands 03 p0325 A72-14046

Intermodulation noise distortion due to multipath transmission over FM/FDM microwave links, deriving distortion probability distribution for Nakagami-Rice randomly distributed signal reception 04 p0493 A72-15517

AM/PM distortion intermodulation in FM/FDM radio systems during two-path propagation, using Fourier series method for noise power spectra calculation 06 p0775 A72-18239

FM mf equipment for 2700-channel Hertzian beam, considering thermal noise, intermodulation and equivalent distortion of amplifiers, discriminator, limiter, etc 07 p0954 A72-19190

Cross modulation relationship to intermodulation product based on third order distortions in nonlinear system 07 p0941 A72-19255

Harmonics, intermodulation noise and small signal effects in discrete image points holographic recording on photopolymer material characterized by linear phase shift vs exposure 15 p2238 A72-32158

- Baseband distortion caused by intermodulation in multicarrier FM systems. 17 p2512 A72-34266
- Intermodulation characteristics of X-band IMPATT amplifiers. 19 p2771 A72-37265
- A numerical evaluation and experimental study of the intermodulation noise spectra of traveling wave tubes. 21 p3033 A72-40880
- Intermodulation distortion of FDM-FM in injection locked oscillator. 21 p3020 A72-40899
- Cross-modulation in tuning circuits with nonlinear capacitances. 21 p3039 A72-41830

INTERMOLECULAR FORCES

- Intermolecular potentials determination by inverting phase shifts obtained from high resolution measurements of protons differential elastic scattering by rare gas atoms 04 p0552 A72-14577
- Model intermolecular interaction potentials constants determination for extrapolating thermodynamic properties of gases at high temperatures and pressures 05 p0692 A72-15842
- Intermolecular interaction potential parameters determination from gas compressibility data based on equation of state in kinetic theory 05 p0692 A72-17068
- Small distance range anisotropic intermolecular interaction potentials for carbon dioxide and nitrogen oxide from beams elastic scattering data 06 p0852 A72-17983
- Nonspherical and nonadditive interactions contribution to third virial coefficient of polyatomic gas, discussing anisotropy, shape factor, and intermolecular forces 08 p1211 A72-21292
- Electronic factors role in intermolecular interactions and biochemical evolution, applying quantum biochemistry 08 p1128 A72-22006
- IR spectra and intermolecular potentials of nitrogen matrix-isolated protonated and deuterated nitromethane 10 p1434 A72-24339
- Model intermolecular interaction potentials constants determination for extrapolating thermodynamic properties of gases at high temperatures and pressures 15 p2280 A72-31261
- Intermolecular hydrogen bond study of hydroxyl group in caranol and caranol-ol compounds, listing IR absorption bands for valence oscillations 15 p2192 A72-32100
- Energetic and topological effects in surface chemical reactions, considering intermolecular dispersion and dipole forces and chemisorption 18 p2657 A72-36828
- Adhesive joints strength and polymeric film breakdown dependence on substrate molecular forces at base interface 19 p2806 A72-37533
- Intramolecular interactions and vibronic spectra of polyatomic molecules. IV - Electronic relaxations: Configurational and relaxational spectra - The four-level arrangement 19 p2838 A72-38778
- On the application of perturbation theory for the calculation of molecular constants due to small mass changes and on the determination of force constants from very heavy isotope substitution. 19 p2763 A72-38806
- Computer-graphics studies of dipole-dipole collisions - Evidence for neutral collision complexes. 21 p3087 A72-40559

INTERMONTANE FLOORS

U VALLEYS

INTERNAL COMBUSTION ENGINES

- NT DIESEL ENGINES
- NT GAS TURBINE ENGINES
- NT HELICOPTER ENGINES
- NT JET ENGINES
- NT PULSEJET ENGINES
- NT RAMJET ENGINES
- NT SUPERSONIC COMBUSTION RAMJET ENGINES
- NT TURBOFAN ENGINES
- NT TURBOJET ENGINES
- NT TURBOPROP ENGINES
- Rate controlled partial thermodynamic equilibrium method for treating reacting gas mixtures, applying to freezing reactions in internal combustion engine 07 p1099 A72-19371
- Electrical analog simulation of internal combustion engines intake and exhaust systems nonstationary gas flow, considering cylinder, turbine and supercharger operation 13 p2027 A72-29136

INTERNAL ENERGY

- Temperature dependent gas internal diatomic laminar heat transfer, investigating continuity, energy, momentum for two dimensional flow between heated parallel plates [ASME PAPER 71-HT-N] 02 p0302 A72-12317

Monatomic He-Ar binary gas mixtures heat transfer to cylinders in low Reynolds number flow, considering internal energy effects 02 p0303 A72-12358

Plastic strain and fracture of metals by specific internal energy change method, investigating mechanical work and heat release 06 p0900 A72-18691

GaAs, injection lasers with homojunctions and single and double heterostructures, observing energy dependence of internal optical losses due to band-to-band absorption 07 p1006 A72-19823

Elastic rod system stationary vibrations under combinational parametric resonance due to internal energy dissipation, using matrix method 12 p1885 A72-27969

Reversible instantaneous deformations and internal energy in viscoelastic incompressible fluids, using Oldroyd and De Witt hydrodynamic models 16 p2376 A72-32937

Energetic boundedness conditions for internal work of deformation in elastic isotropic body 16 p2470 A72-33527

Fe-Ni-C alloys internal damping, martensitic structure and mechanical properties after quenching and tempering, discussing Mo and Cr additions 19 p2806 A72-37418

Estimation of the cleavage strength of polycrystalline metals from the internal energy 19 p2818 A72-38010

Internal energy and conductive and frictional dissipation, mass, momentum and energy production as functions of density, entropy and geometric state variables 21 p3130 A72-41228

Influence of the intermodal exchange on the wall heat flow in a gas possessing internal energy 22 p3244 A72-42641

Internal to total energy relation dependence on deformation time in impulsive loading of homogeneous free rod, noting energy conversion efficiency 23 p3344 A72-43338

Photothermoelastic study of stress concentrations in a plate with internal heating. 23 p3349 A72-43986

INTERNAL FRICTION

Macroscopic metal crystal plastic deformation applications to aircraft and spacecraft materials production, considering internal friction and energy conversion into strain energy and heat 01 p0071 A72-11020

Alloy steels temper brittleness analysis, using internal friction characteristics as functions of time and temperature 02 p0247 A72-12816

Stress induced oxygen diffusion in alpha Zr, attributing temperature dependent internal friction peak to oxygen-titanium interactions 02 p0247 A72-12818

Q values contradiction between lunar and earth rocks, discussing internal friction 04 p0580 A72-15450

Internal friction changes in aluminum single crystal after uniaxial plastic deformation and irradiation 05 p0673 A72-16148

Neutron irradiation effect on grain boundary relaxation in Al and Al-Li alloy by internal friction investigation 06 p0830 A72-18292

Internal friction spectrum peaks in Fe-Ni alloy at 20-1100 C upon heating and cooling, explaining by grain boundary relaxation and martensitic transformations 06 p0830 A72-18293

Internal friction and plastic microstrains in martensitic transformation of Fe-Ni, Co-Ni, and Fe-Cr-Ni alloys 06 p0830 A72-18294

Internal friction in annealed and deformed tungsten at room temperature to 950 C, examining carbon contents, dislocations and temperature effects on carbon Snoek peak 06 p0830 A72-18295

Bcc Mo and Nb after cold working observing internal friction relaxation peaks as function of stress, strain, temperature and strain rate 06 p0831 A72-18296

Small elastoplastic cyclic strain effects on internal friction and energy dissipation in metals during vibrations 06 p0834 A72-18679

Internal friction measurements of tempered martensitic Cr steel quenched from 1100 C, connecting friction peaks with precipitation phenomena 07 p1021 A72-20486

Mo single crystal internal dislocational friction and ultrasound damping dependence on oscillation amplitude, exposure time and annealing temperature 08 p1185 A72-21073

Earth Love waves and toroidal oscillations attenuation, presenting frequency dependent model of internal friction 09 p1299 A72-22801

Maximum internal friction onset temperature and magnitude in Co as function of thermomechanical treatment and crystal lattice defects 09 p1329 A72-23035

Carbon effects on internal friction of low temperature Fe-Ni alloy during martensitic transformation 10 p1495 A72-24083

Internal friction peak in fresh tempered martensite from Fe-Ni-C alloy cooled to 77 K, suggesting hypothetical carbon atoms interactions with mobile dislocations 10 p1496 A72-24232

Ohmic and internal friction loss minimization in stationary rotating incompressible plasmas, assuming magnetic and velocity fields as Trkal fields 10 p1524 A72-24928

Dislocation damping by point defects entrapment, calculating internal friction force rate dependence based on weak interactions continuum model 10 p1527 A72-24979

X ray analysis of internal friction strains in nickel molybdenide during ordering process at 650-700 C, using torsional pendulum method for friction measurements 11 p1662 A72-26654

Simultaneous nonhomogeneous internal and external friction effects on nonconservative force systems motion stability, considering cantilever beam compression 12 p1845 A72-27321

Electronic system for continuous automatic recording of internal friction and modulus of elasticity at high temperatures 12 p1807 A72-27462

Stress relaxation in anelastic materials, calculating spectra, complex modulus of elasticity and internal friction 12 p1883 A72-27541

Cu-Al-Ni alloys single crystals internal friction temperature dependence during martensitic transformations 13 p1977 A72-28912

Energy losses due to hysteresis friction during oscillations of dislocations in elastic field of point defect in solids, discussing temperature and amplitude effects 14 p2121 A72-30955

Dislocation substructures effect on relaxation and internal friction peak in cold rolled Mo single crystals after annealing 14 p2122 A72-30956

Relaxation and internal friction characteristics of beta-rhombohedral B at 80-1000 K, using LF vacuum oscillator with inverted torsion pendulum 14 p2122 A72-30958

Internal friction and relaxation mechanisms in substructure hardened fcc alloys and bcc metals, presenting dislocation parameters for annealed and cold worked Fe alloys 14 p2122 A72-30960

Dislocation motions as internal friction mechanism in solids due to medium frequency acoustic waves, considering motional energy transfer to thermal phonons and lattice vibrations 15 p2292 A72-31833

Grain-size dependence of Snoek peaks in niobium. 17 p2566 A72-34671

V-Ti alloys interstitial scavenging action dependence on titanium concentration via internal friction study 17 p2567 A72-34732

Nitrogen interactions in Nb-Zr alloys, investigating interior friction spectra peaks 18 p2702 A72-36707

Determination of flexural-vibration deflections of structural elements with allowance for internal friction damping 20 p2981 A72-39921

Thermal unpinning of dislocations - Hasiguti peaks of internal friction. 20 p2962 A72-39993

On the destabilizing effect in a non-conservative system with slight internal and external damping. 21 p3124 A72-41483

Inelastic effects during metal fatigue 22 p3195 A72-43156

Measurement of small strain amplitudes in internal friction experiments by means of a laser interferometer. 24 p3402 A72-44947

INTERNAL PRESSURE

Two-layered plane strain elastic cylinder with cracked inner bore under internal pressure loading, obtaining stress intensity factors by finite element method 01 p0141 A72-10994

Thin walled sandwich cylindrical shells under internal pressure, calculating elastic-plastic zone propagation 01 p0141 A72-11001

Truncated conical shell buckling under combined torsion and internal pressure load, discussing prebuckling stress conditions 02 p0298 A72-12666

Bending stresses in composite shell at conical interface between metal and fiberglass reinforced plastic portions under internal pressure

02 p0298 A72-12683

Rupture induced perturbation loads in pressurized orthotropic circular cylindrical shells

02 p0299 A72-12704

Elastoplastic stress distribution in thin spherical metallic shells with cylindrical branch pipe under internal pressure

03 p0448 A72-13905

Stress concentration at hypotrochoid hole in cylindrical shell under internal pressure and axial tensile stresses

03 p0453 A72-14138

Small parameter method solutions to linear viscoelasticity problems with nonhomogeneous temperature field applied to reinforced tube under internal pressure

03 p0454 A72-14217

Soft uniaxial crosswise reinforced shell stability under internal pressure, determining equilibrium state

04 p0587 A72-15015

Linearized equilibrium equations for thin spherical shell with internal pressure, obtaining free vibration modes

04 p0587 A72-15018

Cylindrical shell stability and load capacity at large plastic deformations under internal pressure

04 p0587 A72-15019

Mathematical analysis of Vuilleumier refrigerator, calculating internal pressures, temperatures and gas flow rates via computer program

[ASME PAPER 71-WA/HT-33] 05 p0745 A72-15886
Plasticity of Al alloy thin walled tubular specimens under axial tension and internal pressure at 293, 173 and 93 K

06 p0833 A72-18561

Cylindrical shell under internal pressure, detailing axial thermal stresses relaxation

06 p0900 A72-18669

Stress and deflection distribution for circular and elliptical toroidal shells under internal pressure from first order differential equations solutions

07 p1088 A72-19118

Axisymmetric deformation of infinite cylindrical shell under stress-strain data arising from internal pressure in statistically inhomogeneous Winklerian medium

07 p1088 A72-19258

Fatigue strength and life estimation method for thick walled cylinders under pulsating internal pressure, using fracture mechanics crack propagation law

[ASME PAPER 71-PVP-15] 08 p1244 A72-21482
Thermal stress analysis of laminated alternate ply cylindrical shells under internal pressure, using Donnell equations

10 p1556 A72-24257

Thin walled tubular carbon steel specimen deformation pattern under biaxial tension and internal pressure at normal and low temperatures

12 p1830 A72-28227

Isotropy postulate corollary verification for strain vectors measurement of annealed steel tubular specimens under combined tension and internal pressure

12 p1887 A72-28232

Internal pressure induced stresses, displacements and time-variable plasticity radii for thick walled fiber reinforced cylinder with hereditary elastic binder interlayers

13 p2055 A72-28557

Tubular materials plane stress-strain test facility for combined axial load and internal pressure effects, describing principal components

14 p2092 A72-30442

Surface stress solution for elastic half space weakened by spherical cut under internal pressure

15 p2333 A72-32681

Composite cylinders of helically wound fiber laminates, predicting burst fracture strength under internal pressure for comparison with experiment on epoxy-glass cylinders

16 p2472 A72-33950

Stress criterion for creep rupture in tubes under combined axial load and internal pressure, deriving stress concentration from high temperature tests

19 p2874 A72-37715

The unit stress state in a cylindrical tank with a flat bottom and a partly cantilevered shell

20 p2979 A72-39594

Nonlinear equilibrium equations for hinged flat circular and spherical membranes under large axisymmetric elastic deformations due to internal pressure

21 p3125 A72-41516

Calculation of the stress concentration at the joint between a cylindrical casing and a branch pipe for internal pressure

21 p3127 A72-41710

Equilibrium equation for unsteady creep of thin truncated conical shell under internal pressure, solving in successive time steps with Taylor series expansion

22 p3233 A72-42062

Theory of thin elastic shells applied to pipe bends subjected to bending and internal pressure.

24 p3456 A72-44795

INTERNAL STRESS U RESIDUAL STRESS

INTERNATIONAL COOPERATION

Planetary quarantine cost and mission success constraints, formulating mathematical models for international goals and implementation systems

01 p0019 A72-10819

Organization, management, contract placement and financing of CECLES/ELDO European multinational program for launcher development

01 p0146 A72-10947

Earth resources information systems using satellite and aerial IR terrain photography and ground teams for international cooperation, emphasizing timber inventory

01 p0063 A72-10950

Soviet-French Project Omega for near space disturbance studies, using ground and balloon measurements at conjugate points

01 p0063 A72-11075

Space law existence, contents and legal sources, discussing international decisions on outer space and celestial bodies use

01 p0147 A72-11108

Joint venture and international collaboration in guided weapon systems design, development and production, discussing cost sharing coordination between governments and contractors

01 p0147 A72-11156

Geomagnetic survey by Cosmos-49 satellite as international program, discussing data analysis and observation accuracy

02 p0219 A72-12082

Uhf aeronautical satellite system, presenting ATC trends, international aspects, available flight levels, weather conditions and long haul conflicts

02 p0257 A72-12383

International frequency allocation table revision by World Administrative Radio Conference for Space Telecommunications

02 p0177 A72-12385

Helios solar probe mission, describing project management, data reception system, trajectory monitoring and international cooperation

[DGLR PAPER 71-052] 02 p0284 A72-12720

German-American interplanetary solar probes Helios A and B mission characteristics and ground operations system, discussing planning phase

[DGLR PAPER 71-122] 02 p0285 A72-12741

R and D requirements for international standard vhf instrument landing system for Category I, II and III operations in next decade

04 p0545 A72-14827

International Satellite Geodesy Experiment based on laser telemetry technique, discussing ground stations network and tracking cameras

04 p0520 A72-15726

Aircraft hijacking control, examining international cooperation, extradition and treaties

05 p0752 A72-15834

Committee organization and international law concepts on outer-space peaceful uses, detailing Ukrainian delegation position

05 p0752 A72-16203

Europa 3 booster rocket development for future European space programs, discussing performance characteristics, project management and international cooperation aspects

05 p0724 A72-16310

Flight safety and ATC planning in German Federal Republic and on international level, discussing regional control stations, radio frequencies, navigation systems, automation, etc

05 p0687 A72-16738

Skylink project as prospective joint American-Soviet space mission, combining Skylab and Soyuz spacecraft

05 p0731 A72-17092

Civil and military aircraft forced diversion, discussing legal counters and aircraft restoration

05 p0753 A72-17166

Legal structure of governmental and operational agreement by international organizations for Intelsat satellite communications system

06 p0905 A72-18169

International Satellite Geodetic Experiment /ISAGEX/, using laser telemetry techniques for accurate measurement of earth gravitational field

06 p0888 A72-18261

United Nations role as center of international cooperation in space law norms elaboration

07 p1102 A72-19454

International space agency necessity, discussing registry of space objects, claims settlement, cooperation and space rescue

07 p1103 A72-19456

Space treaties, discussing factors of UN contribution success

07 p1103 A72-19457

INTERNATIONAL COOPERATION

Liability for space activities, considering international organizations status before international tribunals

07 p1103 A72-19459

Legal aspects of international manned orbiting laboratories, discussing space objects registry and liability for damage

07 p1103 A72-19461

Manned orbital laboratories within framework of space treaty

07 p1103 A72-19462

UN registry of space vehicles, reviewing historical development of registration procedures in U.S. and U.S.S.R.

07 p1103 A72-19463

UN agencies role in communication satellites technology exploitation, discussing international cooperation in outer space peaceful use and exploration and development of space law

07 p1074 A72-19468

International space communication systems legal and operational aspects, discussing Intelsat and Inter-sputnik systems

07 p1104 A72-19470

Intelsat functions, discussing international cooperation, United Nations resolutions and financial arrangements

07 p1104 A72-19471

Space communication application for information, education and cultural exchange, noting need for international cooperation

07 p1104 A72-19473

International cooperation in space law problems, considering space communication systems, geostationary orbits use, frequency band allocation, world weather watch and earth resources survey programs

07 p1105 A72-19475

International and national satellite TV systems, discussing technical and operational characteristics, artificial emission dispersion and costs

07 p0944 A72-19656

Collaboration of World Health Organization and various international astronomical organizations for space technology applications to man-environment relationships and medical and communication sciences

07 p0933 A72-20300

Conventions on international responsibility for damage caused by space objects, studying UN juridical subcommittee resolution

08 p1255 A72-21076

Satellite communication activities on French national level, European multinational level /Symphonie/ and worldwide level /Intelsat/

08 p1132 A72-21202

Aerosat program for ATC and communications via four geostationary satellites over Atlantic and Pacific Oceans, discussing technical and financial international provisions

08 p1256 A72-21203

Meteosat geostationary satellite international program for earth cloud cover observation and meteorological data relays between ground stations as part of Global Atmospheric Research Program

08 p1241 A72-21204

International TV broadcasting satellite system, discussing technical problems and cost effectiveness in competition with conventional TV systems

08 p1132 A72-21205

International standardization of manned spacecraft components for rescue efforts and joint multinational space missions

09 p1395 A72-23154

German-French DIAL aeronomy satellite project, describing geocoronal radiation, electron density and equatorial electrojet measurements

10 p1535 A72-24029

Legal aspects of international cooperation on aircraft design and production, discussing work distribution, project management and liabilities sharing

10 p1565 A72-24881

Collaborating parties cooperation with outsiders, examining relationship with government organizations, airworthiness authorities, financial institutions and marketing agencies

10 p1565 A72-24882

Noctilucent cloud kinematics as indicators of mesospheric circulation and turbulence characteristics, discussing need for international scientific cooperation

10 p1476 A72-25006

Book on world airlines economic regulation, analyzing multilateral international agreements, national aviation interests and competitive situation

11 p1748 A72-25923

Latitude measurement at international stations during 1935-1947 period, discussing computation difficulties, instrument errors and correction

12 p1866 A72-27201

Upper atmosphere observatory, noting application to long distance radio communication, long range weather prediction and international cooperation in research and education

13 p1947 A72-28613

European Airbus program, noting international cooperation juridical sources, content and organization, aircraft performance, financing, project chronology and Franco-German agreement

13 p2067 A72-28795

West German-United States Barium Ion Cloud Project meteorological support at Wallops Station, discussing magnetospheric magnetic and electric fields

13 p1947 A72-28802

Upper atmosphere research rockets missions, payloads and measurements, describing various international aeronomy research projects

13 p2052 A72-30081

Warsaw Air Transport Convention second revision by Guatemala Protocol of 8 March 1971, discussing provisions for air carrier liability

14 p2174 A72-30821

International cooperation in space operations and exploration - AAS Conference, Washington, D.C., March 1971

14 p2175 A72-31135

European programs on space stations, tugs, shuttles, propulsion and avionics and consideration for participation in NASA programs for 1970s and 1980s

14 p2175 A72-31137

European space project priority in terms of technological competition, budget limitation and participation in NASA post-Apollo program

14 p2175 A72-31138

Earth resources survey systems, discussing benefits, ground truth problem, data analysis, experimental satellites, operational system, and developing countries needs and activities

14 p2175 A72-31142

Space applications benefits through international cooperation, emphasizing environmental problems

14 p2175 A72-31143

U.S.-Canadian Alouette/ISIS satellites case history, considering hardware, lunar sample analysis and satellite transmitted radio beacon signal reception and analysis

14 p2175 A72-31144

U.S.-U.S.S.R. space cooperation, considering Eisenhower and Kennedy initiatives, NASA-Soviet Academy negotiations and current situation

14 p2176 A72-31145

International telephone hierarchical earth network organization for satellite communication extension, considering guidelines and constitution

15 p2193 A72-31179

United Nations activity in international space program for earth resources and environmental pollution surveillance by satellites

15 p2220 A72-31227

International programs for simultaneous ecological study via remote sensing techniques, discussing European and Italian space programs

15 p2220 A72-31230

NASA ATS F/G satellites for educational TV broadcasting in foreign countries, discussing technologies and case histories

15 p2196 A72-31829

Report to COSPAR on Indian space program covering organizations, ground station facilities, atmosphere and astronomy studies and international collaborations

15 p2338 A72-32012

Report to COSPAR on Argentina space program covering sounding rockets and balloons and Experimental Inter-American Meteorological Network meteorological rocket launchings

15 p2338 A72-32015

European unity as prerequisite for technological and scientific progress with respect to U.S. and Soviet superiority

16 p2480 A72-32893

ICAO assistance to member states in various transport airports and navigation facilities economics including accounting and financial statistics

16 p2481 A72-33334

The role of the International Civil Aviation Organization (ICAO) in organizing Search and Rescue Services (SAR)

17 p2638 A72-34430

International UV Explorer synchronous satellite program objectives and technology, describing spacecraft design, instrumentation, ground system, telescope control and data handling

17 p2621 A72-34900

Space tracking stations in Spain. I - The Madrid space station and its activities

17 p2536 A72-34945

Extension of lunar nomenclature to the far side of the moon

17 p2610 A72-35213

International Space Rescue Symposium, 2nd, Mar del Plata, Argentina, October 9, 1969, Proceedings

17 p2622 A72-35549

Satellite communications and the Pleumeur-Bodou centre

18 p2659 A72-36273

Canadian industrial participation in domestic, U.S. and overseas space projects, emphasizing technology advancement as national objective

18 p2742 A72-36544

Global network of ground based facilities /infrastructure/ including spacecraft launching, tracking, communication and readout sites for international space operations

18 p2742 A72-36545

Orbiting space laboratories for earth resources program, discussing satellites and Skylab missions and international cooperation

18 p2742 A72-36547

Canadian program for global environmental and world resources monitoring system, discussing management, technology and user interface

18 p2742 A72-36548

International space cooperation, emphasizing arrangements and prospects between U.S. and U.S.S.R.

18 p2743 A72-36549

The use of satellites to meet future press requirements

18 p2743 A72-37012

Standardization and reliability assurance on the national and European levels

18 p2743 A72-37128

European co-ordination activities with particular reference to the Space Components Co-ordination Committee

18 p2743 A72-37130

Book - Eleventh report by the International Telecommunication Union on telecommunication and the peaceful uses of outer space

20 p2988 A72-39025

ESOC-Darmstadt - ESRO's European center of operations for space exploration

20 p2988 A72-39415

European participation in space shuttle and space tug programs, discussing funding and technical aspects

21 p3103 A72-40456

Planning of a broadcast-satellite service

21 p3016 A72-40771

Space shuttle technological evolution prospects, discussing cooperative development phases toward space transportation system with globally dispersed launch and landing bases

21 p3132 A72-40966

Implementation status of the Omega Navigation System

22 p3203 A72-42945

Satellite relay and Omega navigation system for distress signal transmission and reception in global rescue alarm network serving ships, aircraft and spacecraft

24 p3467 A72-45134

Flight mechanics aspects in space transportation system for international rescue, analyzing potential crises situations requiring emergency action

24 p3451 A72-45217

Mission objectives, hardware development and international cooperation aspects in U.S. future space flight programs, discussing space shuttle, space tug, Apollo 17 and Skylab

24 p3441 A72-45219

INTERNATIONAL GEOPHYSICAL YEAR

Ionospheric disturbance in American zone during IGY-IGC, showing latitudinal, annual and diurnal solar variations effects and regional geomagnetic anomaly

06 p0806 A72-17641

The occurrence of radio aurora at high latitudes - The IGY period, 1957-1959

20 p2904 A72-39982

INTERNATIONAL LAW

Papers on air piracy and international law based on McGill University Conference (October 1970), covering legal problem solving, hijacking, etc

01 p0146 A72-10321

Air law concept as totality of legal regulations related to atmosphere use by flying devices, discussing relation to international environmental protection

01 p0147 A72-11107

Book on global communication law covering maritime transport, civil aviation, radio, space communication postal services, international cooperation, etc

02 p0305 A72-12575

Legal problems of aircraft hijacking, discussing jurisdiction, duty to prosecute, penalties, extradition, sanctions and international criminal tribunal

05 p0752 A72-15833

International and domestic governmental interests in aircraft hijacking, discussing deterrents, enforcement and accepted action

05 p0752 A72-15835

Hague convention on aircraft hijacking, discussing international extradition, prosecution and punishment

05 p0752 A72-15836

International criminal court for aircraft hijacking, examining political and jurisdictional aspects

05 p0752 A72-15837

Hague convention of 16 December 1970 for repression of skyjacking, discussing definition, punishment, jurisdictional competence, arrest and preliminary inquiry, pursuit, extradition and prevention

05 p0753 A72-17165

Legal structure of governmental and operational agreement by international organizations for Intelsat satellite communications system

06 p0905 A72-18169

International space agency necessity, discussing registry of space objects, claims settlement, cooperation and space rescue

07 p1103 A72-19456

International legal aspects of earth resources survey from space

07 p1104 A72-19467

International space communication systems legal and operational aspects, discussing Intelsat and Intersputnik systems

07 p1104 A72-19470

Satellite broadcasting for direct individual and community reception as mass communication means, discussing UN role and international juridical problems

07 p1104 A72-19472

Earth satellite legal aspects under space treaty discussing orbiting military remote sensing devices national obligations and security issues

07 p1105 A72-19476

Discrimination preference and effect on insurance of limit liability of international air carrier according to modified Montreal Interim Agreement

07 p1106 A72-20674

Legal aspects in prevention of aircraft unlawful seizure in view of international cooperation, noting German Democratic Republic agreements

12 p1890 A72-27272

The onboard authority of the aircraft commanding officer as provided by the 1963 Tokyo Convention

17 p2639 A72-35763

Book - Eleventh report by the International Telecommunication Union on telecommunication and the peaceful uses of outer space

20 p2988 A72-39025

International space telecommunication law and UN resolution concerning geostationary satellite orbit use for radio transmission

21 p3132 A72-41319

Government, military safety, police permission and insurance regulations for European rocket activities

24 p3467 A72-45124

The role of the United Nations in earth resources satellites

24 p3468 A72-45185

INTERNATIONAL PRACTICAL TEMPERATURE

U TEMPERATURE SCALES

INTERNATIONAL QUIET SUN YEAR

Precipitated electron energy latitude and time variations from auroral-height measurement during IQSY, using meridian scanning photometers

01 p0120 A72-10896

Diurnal and seasonal variations of F region irregularities drift and anisotropy parameters during IQSY from aerial fading records, noting magnetic activity effect

04 p0517 A72-14955

Arctic polar region geomagnetic perturbations during IQSY, noting diurnal variations

05 p0658 A72-16278

Soviet papers on ionospheric propagation and meteor trail drifts during IQSY, covering Doppler frequencies recording and mountains effect on radio transmission

08 p1238 A72-21881

Air masses circulation in atmospheric upper layers during IQSY from meteor trail drifts observation by radar tracking method

08 p1161 A72-21882

Geomagnetic activity index Ap correlation with daily magnetic variations during quiet sun year 1964

15 p2230 A72-32260

Comprehensive investigation of individual geomagnetic storms

18 p2686 A72-36226

Earth outer radiation belt and unstable radiation zone dynamics during IQSY magnetically quiet and disturbed period based on Elektron-series satellite data

22 p3218 A72-42211

INTERNATIONAL RELATIONS

NT INTERNATIONAL COOPERATION

INTERNATIONAL SATS FOR IONOSPHERIC STUDY

U ISIS SATELLITES

INTERNATIONAL TRADE

Book on IATA organization and functions, discussing international aviation history, conference machinery, enforcement of conference resolutions, air transportation economics, public corporations, etc

10 p1564 A72-23846

INTERNUCLEAR PROPERTIES

Evidence for protonated cyclopropane intermediates in crossed-beam ion molecule reactions

24 p3379 A72-45475

INTERPLANETARY DUST

NT METEOROID DUST CLOUDS

Interplanetary and terrestrial dust detection, discussing zodiacal light photometric measurements by Helios space probe and light pressure, solar wind and Poynting-Robertson effect

01 p0126 A72-10201

Interplanetary medium spherical solid component model from radio meteor orbit catalog, discussing density of interplanetary dust, meteor matter and cosmic fallout on sun

02 p0282 A72-12332

Astronomical interpretation of dust particle data recorded by Pioneer spacecraft, suggesting sensor surface orientation role for error correction

08 p1232 A72-21149

Heavy ions from interplanetary dust, estimating contribution to solar wind flux

11 p1713 A72-26393

Interplanetary medium spherical solid component model from radio meteor orbit catalog, discussing density of interplanetary dust, meteor matter and cosmic fallout on sun

13 p2039 A72-29216

Explorer 35 and OGO 3 data on picogram size dust particle distribution in cislunar and selenocentric space, showing fluctuations during meteor shower periods

15 p2309 A72-31937

Lunar surface microerosion relationship to interplanetary dust particle flux distributions, investigating sputter erosion and lunar rocks lifetimes

15 p2310 A72-31988

Astronomical interpretation of dust particle data recorded by Pioneer spacecraft, suggesting sensor surface orientation role for error correction

20 p2968 A72-39254

The structure and formation of comets.

24 p3445 A72-45464

INTERPLANETARY FLIGHT NT GRAND TOURS

Mars and Venus instrumented spacecraft flight results, describing planetary topographies, atmospheres and magnetic fields

12 p1877 A72-27650

U.S. industry views on NASA plans for 1970s, emphasizing interplanetary nuclear propulsion, space transportation, shuttle costs and economics

14 p2175 A72-31139

Nonchemical space propulsion systems for lunar and planetary flights, discussing fission, fusion and electric rockets

15 p2297 A72-31810

Outer planets masses and ephemerides, noting guidance system and fuel quantity for orbit corrections on interplanetary flight

15 p2312 A72-32181

Spacecraft and missions for Jupiter exploration, discussing launch vehicle requirements, solar electric propulsion for midcourse correction, Pioneer flyby and orbiter missions, TOPS mission, etc

21 p3103 A72-40457

Study of shuttle-based systems for high-energy planetary missions.

24 p3441 A72-45189

Electrostatic ion propulsion engines development for near-earth and interplanetary space missions, noting payload increase and flight time reduction capabilities

24 p3434 A72-45278

Maneuver strategies for multi-planetary missions.

[AIAA PAPER 72-914] 24 p3443 A72-45431

INTERPLANETARY GAS

Interplanetary high energy electron flux association with solar flares from HEOS-A1 data

15 p2302 A72-32792

Energy spectrum of interplanetary-plasma discontinuities

18 p2715 A72-36653

Interplanetary-gas motion induced by a solar flare

19 p2855 A72-37391

INTERPLANETARY MAGNETIC FIELDS

Tago-Sato-Kosaka and Bennett comets plasma tails interaction with interplanetary magnetic field, demonstrating cometary events correlatability with solar wind data

01 p0128 A72-10419

Interplanetary magnetic field angular gradient and sectorial effects on solar wind, discussing wind velocity

01 p0118 A72-10583

Open magnetosphere mathematical models application to dayside auroras, investigating interplanetary magnetic field topology

01 p0060 A72-10885

North-south asymmetry of cosmic ray intensity dependence on interplanetary sector magnetic field sign, based on spherical harmonic analysis during several sector structure passages

01 p0120 A72-10908

Magnetospheric diagnostics from ground stations data, considering dimensions, cusp, ring current, tail flux, electric fields, radiation zone, solar wind and interplanetary field

01 p0132 A72-11072

Solar wind plasma spherically symmetrical outflow allowing for equations of motion of velocity components, discussing interplanetary field and single fluid MHD

02 p0278 A72-11914

Galactic cosmic ray-solar wind nonlinear interaction effects on solar wind geometry near and far from sun

02 p0272 A72-11917

Broadband geomagnetic micropulsations relations to magnetospheric, interplanetary and solar phenomena

[AD-739038] 02 p0222 A72-12869

Low energy solar proton propagation and interplanetary magnetic field measurements, comparing with population in solar wind

03 p0407 A72-12943

Astronomical model for solar cosmic ray bursts propagation including anisotropic particle diffusion along interplanetary magnetic field

03 p0407 A72-12944

Solar coronal magnetic field large scale structure relation to photospheric and interplanetary sector patterns

[AD-734628] 03 p0422 A72-13207

Solar polar and general magnetic field fine structure and statistical nature, discussing time fluctuations and interplanetary field

03 p0432 A72-13353

Rotating dipole sector structure of interplanetary and solar photospheric magnetic fields from spacecraft observations

[AD-740309] 03 p0437 A72-13871

Geomagnetic micropulsation activity relationship to magnetospheric processes and interplanetary magnetic field, investigating time dependence of telluric current

04 p0515 A72-14927

Collisionless solar wind in spiral interplanetary magnetic field, using two fluid model with hydrodynamically treated electrons

06 p0872 A72-17441

Interplanetary magnetic field effect on flare-generated weak shock wave propagation speed and transit time

06 p0875 A72-17461

Interplanetary magnetic field fluctuations correlation with trapped particles redistribution, deriving magnetospheric electric field properties

06 p0875 A72-17468

Cosmic ray muon intensity in interplanetary magnetic field, revealing sidereal variation due to motion of solar system relative to local galactic rotation frame

06 p0873 A72-17648

Interplanetary magnetic sector structure at 1962-1969 solar maxima, noting Pioneer 9 magnetometer experiment observations

[AD-740308] 07 p1071 A72-19161

Solar wind radial velocity variations effects on interplanetary magnetic field spiral structure

07 p1079 A72-20019

Three dimensional structure of interplanetary magnetic field from observed line of sight field component in solar photosphere

07 p1082 A72-20379

Interplanetary origin of magnetospheric electric fields responsible for polar magnetic disturbances

07 p0979 A72-20382

Solar wind magnetic fields characteristics relative to 11 year cosmic ray modulation in interplanetary space

07 p1065 A72-20642

Solar active regions effects on galactic cosmic ray distribution and interplanetary magnetic field structure

07 p1065 A72-20646

Earth and interplanetary magnetic fields spectral power density characteristics at 0.0001-1 Hz

08 p1153 A72-20718

Atmospheric model for plasma motion along surface of geomagnetic tail under action of interplanetary, magnetic lines of forces

08 p1153 A72-20722

Outer radiation belt parameters dependence on interplanetary magnetic field sectorial structure and solar wind velocity

08 p1226 A72-20811

Interplanetary medium physical parameters from spacecraft measurements, noting solar wind properties, magnetic fields and MHD discontinuities

08 p1228 A72-20826

Solar modulation process for galactic cosmic ray particle time variation, discussing interplanetary magnetic fields and plasma, energy losses from solar wind deceleration, etc

08 p1227 A72-21188

Polar magnetic substorm generation through ionospheric current intensification in westward electrojet localized region, noting interplanetary magnetic field role

08 p1159 A72-21494

Solar energetic particle access characteristics to magnetosphere from PCA riometer and satellite measurements, determining relationship between earth dipole field and interplanetary field

08 p1228 A72-21497

Solar wind properties and discontinuity characteristics, describing particle densities, wind speed, magnetic field level and near earth electron and ion temperatures

09 p1377 A72-22756

Interplanetary magnetic field perturbations by solar wind and moon, noting lunar wake anomalies positive correlation with plasma beta value

09 p1387 A72-23003

Satellite, space probe and observatory data impact on space physics, considering solar wind, interplanetary

ry magnetic field, Van Allen belt and Chapman-Ferraro theory

10 p1538 A72-24268

Search coil magnetometer for measurement of weak alternating magnetic fields encountered by Helios solar probe in space

11 p1632 A72-25804

Interplanetary and magnetospheric magnetic force lines reconnection and effects on geomagnetic activity

11 p1718 A72-25933

Outer space and earth surface galactic cosmic ray intensity data correlation analysis for studying interplanetary magnetic field structure

11 p1713 A72-25936

Earth bow shock nonuniform structure observation correlation with interplanetary field orientation, using Explorer 33 and 35 data

11 p1722 A72-26395

Interplanetary magnetic field direction and high latitude ionospheric currents in dayside auroral regions, showing plasma drift induced magnetic disturbances

11 p1626 A72-26419

Magnetosheath pressure, magnetic field, temperature, particle density and stream velocity computed for earth bow shock in oblique interplanetary field with solar wind

11 p1723 A72-26526

Cosmic ray diffusion in radial divergent flow of magnetic discontinuities in interplanetary plasma, discussing isotropy in presence of regular magnetic field

13 p2029 A72-28591

Meteor-induced magnetic effect on cosmic ray intensity for meteor streams with orbits normal or parallel to interplanetary magnetic field lines of force

13 p2029 A72-28592

Solar wind plasma spherically symmetrical outflow allowing for equations of motion of velocity components, discussing interplanetary field and single fluid MHD

13 p2039 A72-29226

Galactic cosmic ray-solar wind nonlinear interaction effects on solar wind geometry near and far from sun

13 p2030 A72-29229

Interplanetary electrons quiet-time intensity increases, considering trans-earth-orbital modulating region due to solar wind transport of photospheric field lines

13 p2030 A72-29377

Large amplitude interplanetary solar wind discontinuities observed by OGO-5 plasma spectrometer and magnetometers, considering magnetic drift waves mechanism for plasma turbulence generation

13 p2031 A72-29378

Outer corona and interplanetary space magnetic fields calculated from photosphere magnetic fields measured during 7 March 1970 solar eclipse

13 p2041 A72-29528

Galactic cosmic ray anisotropy due to radial and diffusive streaming in direction of interplanetary magnetic field, using neutron monitor data

13 p1033 A72-29747

Solar magnetogram recorded mean photospheric magnetic field cross correlation with interplanetary magnetic field

13 p2049 A72-29935

Strong shock wave formation and propagation in interplanetary space after chromospheric flares calculated by gas dynamic approximation, determining magnetic field configuration

13 p2050 A72-29955

Gas dynamics of steady rotating azimuthally dependent solar wind under magnetic field influence, calculating azimuthal distribution of radial velocity near earth orbit

13 p2034 A72-29960

Cylindrical model of interplanetary magnetic field-moon interaction, taking into account solar wind flow boundary condition asymmetries

14 p2154 A72-30514

Cosmic ray density gradient perpendicular to ecliptic plane, noting component introduction into diurnal variation depending on sense and direction of interplanetary magnetic field

15 p2298 A72-31436

Low energy electron flux in magnetosphere, discussing relation to geophysical phenomena, solar wind, interplanetary magnetic field and charged particle longitudinal drift trajectories

15 p2225 A72-31903

F 2 layer electron concentration and maximum height variation with interplanetary magnetic field direction

15 p2226 A72-31920

Magnetospheric particles and interplanetary magnetic field measurements for solar proton event of March 1970, noting polar cap structures

16 p2444 A72-32956

Low energy outer zone electrons high latitude boundary variation with interplanetary magnetic field direction and with geomagnetic activity from Alouette and Explorer data

16 p2382 A72-32957

- Nighttime magnetosphere convection electric field from motions of whistler ducts within plasmasphere, considering interplanetary magnetic field theta component 16 p2382 A72-32960
- Interplanetary magnetic field variations and auroral zone substorm activity observation, noting time delay between IMF southward turning and negative magnetic bay 16 p2451 A72-32974
- Solar radio bursts time sequence and positions observation during 24 January 1971 proton event, noting relation to relativistic particles acceleration into interplanetary field 16 p2445 A72-33045
- Interplanetary magnetic field irregularities and shock effects associated with cosmic ray Forbush decreases 16 p2449 A72-33939
- Diurnal cosmic ray neutron variation dependence on interplanetary magnetic field based on neutron monitor data 16 p2449 A72-33940
- Spatial characteristics of magnetic field fluctuation in the magnetosheath. 17 p2545 A72-34474
- On neutral sheets in the solar wind. 17 p2599 A72-35096
- Heat conduction in a turbulent magnetic field, with application to solar-wind electrons. 17 p2601 A72-35584
- An analysis of Pioneer 9 low-frequency wave observations near interplanetary discontinuities. 17 p2614 A72-35585
- Critical component of the interplanetary magnetic field responsible for large geomagnetic effects in the polar cap. 17 p2548 A72-35590
- Satellite measurements of the moon's magnetic field - A preliminary report. 18 p2724 A72-36287
- The diurnal effect of the cosmic rays during the period 15 October 1965-30 June 1966. II - The equatorial cosmic-ray anisotropy and the interplanetary magnetic field. 18 p2722 A72-37160
- Heos 1 data on interplanetary magnetic field, solar wind and proton characteristics, noting barium cloud experiment 19 p2850 A72-37492
- Earth and interplanetary magnetic fields spectral power density characteristics at 0.0001-1 Hz, noting ambiguities due to variable investigation conditions 19 p2791 A72-38346
- Atmospherical model for plasma motion along surface of geomagnetic tail under action of interplanetary magnetic lines of force 19 p2791 A72-38350
- Numerical calculation of the lunar wake in a magnetohydrodynamic model. 19 p2864 A72-38435
- Rotation period variation in long term behavior of interplanetary magnetic sector structure during nearly four solar cycles 19 p2868 A72-38731
- Relationship of interplanetary magnetic field structure with development of substorm and storm main phase. 20 p2968 A72-39232
- Polar-cap electric field distributions related to the interplanetary magnetic field direction. 22 p3172 A72-42432
- Solar-wind parameter variation, magnetic activity, and electrons in the magnetospheric tail and outer radiation belt 23 p3283 A72-43367
- Families of geomagnetic storms, direction of the interplanetary magnetic field, and solar activity 23 p3283 A72-43371
- Annual and solar-magnetic-cycle variations in the interplanetary magnetic field, 1926-1971. 23 p3286 A72-44504
- Preconditions for the triggering of polar magnetic substorms by storm sudden commencements. 23 p3286 A72-44531
- Quiet, growth, expansive and recovery phases of auroral morphology, noting interplanetary magnetic field turning relation to substorm 24 p3396 A72-44848
- Cosmic ray diffusion in radial divergent flow of magnetic discontinuities in interplanetary plasma, discussing isotropy in presence of regular magnetic field 24 p3435 A72-45091
- Meteor-induced magnetic effect on cosmic ray intensity for meteor streams with orbits normal or parallel to interplanetary magnetic field lines of force 24 p3435 A72-45092
- Microscale MHD wave and stationary structure fluctuations in interplanetary medium solar wind, considering theoretical constraints 01 p0129 A72-10883
- Solar wind electron density variations, discussing radio source interplanetary scintillation and angular distribution measurements at various distances from sun 02 p0277 A72-11902
- Interplanetary medium spherical solid component model from radio meteor orbit catalog, discussing density of interplanetary dust, meteor matter and cosmic fallout on sun 02 p0282 A72-12332
- Large-scale solar coronal magnetic field from optical and radio observations for corpuscular propagation in corona and interplanetary medium 03 p0432 A72-13346
- Geomagnetic field and interplanetary plasma parameters daily variations correlation, taking into account corrections for storm time effects 03 p0348 A72-13511
- Nonuniform solar wind velocity effect on interplanetary medium and on cosmic radiation, observing diurnal variations 04 p0567 A72-14928
- Interplanetary media plasma density fluctuations and power law spectra effects on radio wave scintillation 05 p0695 A72-16068
- Geomagnetic tail natural oscillations, applying model of plasma cylinder with free boundary immersed in interplanetary medium 05 p0659 A72-17044
- Interplanetary plasma electron and proton density fluctuation measurements by space probes and from radio sources scintillation spectra, noting agreement with power-law irregularity spectrum 06 p0881 A72-17901
- Interplanetary shock wave inclination to ecliptic plane dependence on chromospheric flare and earth projection heliolatitude differences 06 p0884 A72-18027
- Interplanetary scintillation and angular dimensions of radio sources at 81.5 MHz, using diffraction theory 06 p0889 A72-18327
- Future deep space missions, discussing exploration of interplanetary conditions outside ecliptic plane and solar system Grand Tour with outer planets flyby 07 p1068 A72-19059
- Interplanetary scintillation of two pulsars, discussing scattering and amplitude modulation of incident radiation propagated through interstellar medium 07 p1069 A72-19073
- Scattering and scintillations of rf radiation from distant discrete astronomical sources as measure of interplanetary plasma irregularities 07 p1079 A72-20020
- Galactic cosmic ray modulation by interplanetary medium, including solar wind boundary problem 07 p1061 A72-20021
- Diffusion models of energetic solar particles in interplanetary medium, considering impulsive emission from solar flares 07 p1061 A72-20023
- Interplanetary medium physical parameters from spacecraft measurements, noting solar wind properties, magnetic fields and MHD discontinuities 08 p1228 A72-20826
- Solar cosmic ray diffusion in interplanetary medium, describing solar flare proton and heavy nuclei propagation in terms of time of arrival measurements 08 p1227 A72-21157
- Solar wind velocity determination from interplanetary scintillation, deriving equations by smooth perturbations method 09 p1375 A72-22285
- Interplanetary shock wave inclination to ecliptic plane dependence on chromospheric flare and earth projection heliolatitude differences 11 p1719 A72-25963
- Ionospheric disturbances relation to interplanetary positive ion and proton fluxes intensity and velocity from Mariner 2, Venus 3 and Vela 2 observations, discussing F 2 region 11 p1713 A72-26268
- Solar current flow penetration to 1 AU in interplanetary medium, discussing inhibition of field line reconnection across neutral sheet 11 p1714 A72-26528
- Interplanetary plasma microinstabilities within framework of underlying electron-proton solar exosphere, discussing solar wind high beta effects 11 p1714 A72-26529
- Radio wave propagation characteristics in Venusian atmosphere and interplanetary plasma from Venera 7 probe data 11 p1599 A72-26907
- Interplanetary medium spherical solid component model from radio meteor orbit catalog, discussing density of interplanetary dust, meteor matter and cosmic fallout on sun 13 p2039 A72-29216
- Interplanetary electrons quiet-time intensity increases, considering trans-earth-orbital modulating region due to solar wind transport of photospheric field lines 13 p2030 A72-29377
- Large amplitude interplanetary solar wind discontinuities observed byOGO-5 plasma spectrometer and magnetometers, considering magnetic drift waves mechanism for plasma turbulence generation 13 p2031 A72-29378
- Earth-solar wind bow shock structure fromOGO-5 observations during passage from interplanetary medium into magnetosheath 13 p1950 A72-29379
- Low energy proton flux increases associated with geomagnetic storms due to interplanetary shock waves occurring during solar cosmic ray flare event decay 13 p2032 A72-29724
- Interplanetary particles intensity relationship with solar activity based on Heos A1 observations during 1969-1971 15 p2300 A72-31992
- Geocorona and interplanetary He glow EUV emission altitude distribution measured by exospheric sounding rocket-borne thin film photon counters 15 p2231 A72-32327
- Monochromatic radio wave propagation in interplanetary plasma, deriving frequency spectrum and phase and amplitude fluctuations 15 p2202 A72-32656
- Probability density for interplanetary scintillation at 74 MHz, noting log normal distribution 16 p2450 A72-32953
- Interplanetary scintillation technique application to structure of flare induced shocks and corotating streams within interplanetary medium 16 p2451 A72-33033
- Radio source power spectra modulation dependence on distance and thickness of solar wind scattering region and on wind velocity component multiplicity 16 p2451 A72-33034
- Solar flare producing regions statistical correlation to SC/SI events accounting for geomagnetic storms and Forbush decreases in terms of interplanetary streams 16 p2445 A72-33376
- Alfven wave propagation in interplanetary medium for solar wind microscale fluctuations, using stationary spherically symmetrical model 16 p2449 A72-33912
- Cosmic ray anisotropy and conditions in the interplanetary medium during a solar cycle 17 p2603 A72-35871
- Study of the solar wind using the power spectrum of interplanetary scintillation of radio sources. 18 p2722 A72-36730
- Determination of shock wave velocity in the interplanetary medium 18 p2728 A72-36875
- Solar cosmic ray diffusion in interplanetary medium, describing solar flare proton and heavy nuclei propagation in terms of time of arrival measurements 20 p2964 A72-39262
- Pioneer 7 observations of the August 29, 1966, interplanetary shock-wave ensemble. 21 p3104 A72-40481
- Characteristics of interplanetary electron inhomogeneities according to observations in the period from 1967 to 1969 21 p3114 A72-41765
- Comet tail wave motion explanation via consideration as plasma cylinder with free boundary tangential discontinuity surface immersed in interplanetary plasma 22 p3221 A72-42011
- Error sensitivity of statistical models with pattern rearrangement for analysis of interplanetary scintillation in ecliptic plane 22 p3218 A72-42402
- Solar-wind and interplanetary electron measurements on the Apollo 15 subsatellite. 22 p3218 A72-42403
- Magnetohydrodynamic theory for the interaction of an interplanetary double-shock ensemble with the earth's bow shock. 22 p3170 A72-42404
- Association between interplanetary shock waves and delayed solar particle events. 23 p3332 A72-44503
- Annual variation of the interplanetary He⁺ velocity distribution at 1 AU. 23 p3332 A72-44505
- Detection of interplanetary electrons from 18 keV to 1.8 MeV during solar quiet times. 23 p3333 A72-44546
- Origin of 200-keV interplanetary electrons. 23 p3333 A72-44547
- Observations of the interplanetary medium and of the structure of radio sources using higher moments of interplanetary scintillations. 24 p3437 A72-44830
- Interplanetary scintillation of radio sources observed through solar corona, deriving higher central

INTERPLANETARY MEDIUM
 NT INTERPLANETARY DUST
 NT INTERPLANETARY GAS
 NT METEOROID DUST CLOUDS

- moments from skewness coefficient of probability density function 24 p3437 A72-44831
- INTERPLANETARY NAVIGATION
 - Cruise guidance, trajectory and navigation analysis for solar electric Mercury orbiter, considering engine performance, thrust and terminal errors [AIAA PAPER 72-427] 11 p1684 A72-26172
 - Navigational aspects of two impulse transfer initiated rendezvous with Deimos using modified Viking Monte Carlo error analysis program 15 p2269 A72-32177
 - Deep space navigation requirements for interplanetary missions (1978-1990) 15 p2269 A72-32178
 - Mars Viking 1975 mission objectives and navigation activities from trans-Mars injection through post-landing stationkeeping phase, considering trajectory dispersions 15 p2269 A72-32180
 - Fuzzy algorithms and artificial intelligence for deep space navigation of vehicles from earth to space /planet/ location 15 p2270 A72-32185
 - Image tube /TV/ and scanning photometer sensor comparison for outer planet mission onboard navigation 15 p2270 A72-32192
 - Multiple probe targeting from spacecraft for 1977 Venus mission, considering trajectory, spin, release, attack angle, location and navigation and control accuracy effects 15 p2312 A72-32193
 - A detailed analysis of Mariner nine TV navigation data. [AIAA PAPER 72-866] 20 p2977 A72-40061
 - Evaluation of optical data for Mars approach navigation. 24 p3422 A72-44646
 - Earth-based navigation capabilities for outer planet missions. [AIAA PAPER 72-925] 24 p3423 A72-45430
 - Spacecraft navigation systems for Mariner Jupiter-Saturn 1977 Project, considering maneuvers, orbit determination and data requirements [AIAA PAPER 72-926] 24 p3423 A72-45432
- INTERPLANETARY PROPULSION
 - U INTERPLANETARY SPACECRAFT
 - U ROCKET ENGINES
- INTERPLANETARY SPACE
 - Correlation coefficients for galactic cosmic rays relation to solar activity indices in interplanetary space 02 p0273 A72-11937
 - Areas index relationship to different phenomena in chromosphere, corona and interplanetary space, investigating coronal radio diameter during solar cycle and cosmic rays 03 p0423 A72-13214
 - Cosmic ray energy changes in interplanetary space by model for solar X-ray bursts 03 p0413 A72-13534
 - Optical observation program for upper atmosphere and interplanetary space investigations, discussing zodiacal light, earth atmosphere composition and stratification, interplanetary dust clouds, etc 06 p0881 A72-17927
 - Geomagnetic field intensity fluctuations due to events in atmosphere, ionosphere, magnetosphere and in interplanetary space connected with solar activity 06 p0809 A72-18276
 - Solar electrons and protons measurements in interplanetary space and in magnetotail, noting access to north polar cap [AD-744404] 07 p1058 A72-19156
 - Active region sources of solar proton streams, discussing 27-day recurrence, acceleration and confinement in interplanetary space 07 p1060 A72-20010
 - Solar magnetic fields configuration in corona ii: relation to energetic proton escape into interplanetary space 07 p1060 A72-20015
 - Low energy solar cosmic ray measurements in interplanetary space with Zond space probes, comparing to galactic cosmic rays 07 p1061 A72-20022
 - Comet characteristics as indicators of cosmic space conditions, including relation to solar activity 07 p1081 A72-20272
 - Three dimensional cosmic ray anisotropy and density distribution at earth orbit and in interplanetary space with allowance for primary particle and nucleon energy spectrum 07 p1065 A72-20645
 - Comet brightness variations correlation with geomagnetic field and solar corpuscular flux variations in interplanetary space 08 p1231 A72-21132
 - Interplanetary space three dimensional cosmic ray anisotropy from harmonic components of diurnal variations 09 p1377 A72-22926
 - Helios solar probe-borne zodiacal light photometer for diffuse light measurements in interplanetary space 11 p1632 A72-25805
 - Ferrite core memory for storage of Helios probe perisolar space data before transmission to telemetry system 11 p1601 A72-25806
 - Geomagnetic activity index response time to fluctuations in interplanetary electric field azimuthal component, relating to magnetosphere average energy content 11 p1627 A72-26670
 - Correlation coefficients for galactic cosmic rays relationship to solar activity indices in interplanetary space 13 p2030 A72-29249
 - Strong shock wave formation and propagation in interplanetary space after chromospheric flares calculated by gas dynamic approximation, determining magnetic field configuration 13 p2050 A72-29955
 - Micrometeorite and cosmic dust flux rates for near earth orbit and interplanetary space from satellite and ground based measurements 15 p2309 A72-31955
 - Unshocked solar wind detection by ATS 5 satellite during 8 March 1970 geomagnetic storm 15 p2299 A72-31960
 - Solar wind model dividing interplanetary space in one fluid and two fluid collisionless regions, discussing proton thermal anisotropy 15 p2300 A72-31996
 - Relativistic electron characteristics in interplanetary space from onboard satellite detector measurements beyond magnetospheric influence [IGPP-UCR-72-11] 15 p2300 A72-31998
 - Neutral hydrogen Lyman-alpha measurements in outer geocorona and in interplanetary space by two channel photometer onOGO 5 16 p2450 A72-32955
 - Solar wind thermal anisotropy effects on least squares estimates of interplanetary shock parameters and associated normals from Rankine-Hugoniot equations 16 p2444 A72-32973
 - Near earth interplanetary electron source detection related to coronal site type 3 bursts, using 80 MHz radioheliograph observations 16 p2445 A72-33044
 - Conservation equations for wave and/or turbulence momentum and energy flux in interplanetary space shock vicinity, developing modifications for electron temperature calculations 16 p2459 A72-33913
 - Fermi acceleration effects in low energy particle transport in interplanetary space, assuming kinetic energy contained in Alfvén and bidirectional traveling waves 16 p2460 A72-33938
 - Optical observation program for upper atmosphere and interplanetary space investigations, discussing zodiacal light, earth atmosphere composition and stratification, interplanetary dust clouds, etc 18 p2730 A72-37152
 - Shock wave propagation in the solar corona as the cause of type II radio bursts 19 p2851 A72-38064
 - Cosmic-ray diffusion coefficient in interplanetary space. 19 p2853 A72-38756
 - Three-dimensional cosmic ray anisotropy in interplanetary space. III, IV. 21 p3101 A72-41385
 - Electromagnetic instabilities produced by neutral-particle ionization in interplanetary space. 23 p3332 A72-44506
 - Interplanetary objects in review - Statistics of their masses and dynamics. 24 p3435 A72-44688
- INTERPLANETARY SPACECRAFT
 - NT JUPITER PROBES
 - NT MARINER SPACE PROBES
 - NT MARINER SPACECRAFT
 - NT MARS PROBES
 - NT PIONEER SPACE PROBES
 - NT TOPS (SPACECRAFT)
 - NT VENERA SATELLITES
 - NT VENUS PROBES
 - NT VIKING LANDER SPACECRAFT
 - NT VIKING ORBITER SPACECRAFT
 - NT ZOND SPACE PROBES
 - Reusable space tug mission profile for interplanetary spacecraft recovery, using branched trajectory, steepest descent optimization and propellant minimization [AIAA PAPER 72-113] 05 p0730 A72-16949
 - Soviet space program review from Sputnik 1 launch, discussing launch sites and vehicles, lunar, planetary and manned missions, civil and military programs and future goals 05 p0722 A72-17091
 - Atmospheric freestream pressure profiles determination from base pressure and flow phenomena of Mars, Venus or Jupiter entry probes [AIAA PAPER 72-202] 07 p0982 A72-18959
 - Interplanetary spacecraft midcourse guidance stochastic control, deriving algorithm for computing optimum velocity correction and execution time with allowance for correction-dependent errors 10 p1508 A72-23778
 - Anomalies detected in Mars 3 solar wind recordings interpreted as possibly caused by geomagnetic tail crossed by interplanetary probe 13 p2034 A72-30010
 - Interplanetary spacecraft transfer maneuver for hyperbolic trajectory change into eccentric orbit, using aerodynamic drag to obtain nearly circular orbit 14 p2151 A72-30471
 - Steering algorithm for fail-safe guidance of continuously thrusting interplanetary spacecraft to maintain ballistic intercept target objective 15 p2271 A72-32195
- INTERPLANETARY TRAJECTORIES
 - Outer planet low thrust orbiter missions, comparing three body numerical results with two methods of patching together two body solutions 01 p0128 A72-10379
 - Interplanetary spacecraft trajectory error analysis by closed form approximation to state transition matrix, enabling rapid estimation with computer program 05 p0718 A72-16443
 - Two point boundary value solution for N-body trajectories, comparing asymptotic with numerical integration solutions for several lunar and interplanetary trajectories [AIAA PAPER 72-49] 07 p1068 A72-18945
 - Interplanetary single impulse flight trajectories optimization and computation, determining geometrical and kinematic characteristics 11 p1718 A72-25927
 - Spacecraft interplanetary guidance trajectory correction, deriving algorithm for optimal accuracy and minimum fuel expenditure 11 p1718 A72-25931
 - Optimal deterministic guidance for bounded-thrust spacecrafts. 17 p2609 A72-35101
 - Optimum aim point biasing in case of a planetary quarantine constraint. 20 p2968 A72-39196
 - Guidance and navigation techniques for a solar electric Mercury orbiter. [AIAA PAPER 72-917] 21 p3082 A72-41562
 - Mission design and navigation for a 1977-1978 Venus Swingby/Mercury Orbiter. [AIAA PAPER 72-941] 21 p3113 A72-41577
 - Choice of parameters to be measured in determination of a spacecraft trajectory 22 p3223 A72-42201
 - Low thrust constant acceleration trajectories for a Mercury orbit. 24 p3441 A72-45208
 - Application of advanced filtering methods to the determination of the interplanetary orbit of Mariner '71. [AIAA PAPER 72-906] 24 p3443 A72-45427
- INTERPLANETARY TRANSFER ORBITS
 - Optimal transfer trajectories between Earth and Mars presented as functions of idealized Hohmann transfer approximation 07 p1077 A72-19824
 - Planetary swingby optimum transfer between hyperbolic asymptotes with less than maximum natural turn angle 10 p1552 A72-24487
 - Interplanetary single impulse flight trajectories optimization and computation, determining geometrical and kinematic characteristics 11 p1718 A72-25927
 - Electrostatic ion thruster ESKA 28 for interplanetary missions, calculating earth escape and optimal transfer orbits [AIAA PAPER 72-434] 11 p1707 A72-26177
 - Gradient method and Euler equations application to low thrust earth-to-Mars spacecraft orbital transfer trajectory optimization 13 p2034 A72-28438
 - Navigational aspects of two impulse transfer initiated rendezvous with Deimos using modified Viking Monte Carlo error analysis program 15 p2269 A72-32177
 - Orbital trim by velocity factoring for Viking Mars mission terminal rendezvous and intermediate timing constraints involving orbital operations 15 p2269 A72-32179
 - A method of solving the problem of choosing an optimal transfer orbit with the aid of an invariant nomographic scale 17 p2610 A72-35217
 - Thermonuclear fusion spacecraft propulsion systems operation principles, interplanetary orbit-to-orbit mission capabilities and environmental safeguard problems 17 p2598 A72-35953
 - Maneuver design and implementation for the Mariner 9 mission. [AIAA PAPER 72-913] 24 p3443 A72-45429
- INTERPOLATION
 - Linear interpolation for homogeneous isotropic random field observed on denumerable system of

spheres, deriving explicit formula analogous to Kotelnikov-Shannon

01 p0094 A72-11266

Stiffness matrix method application to finite deformation theory, noting convergence through use of iterative interpolation in numerical calculations

02 p0298 A72-12667

Sequential interpolating estimation algorithm derivation for distributed-parameter noisy dynamic systems described by nonlinear partial differential equations

04 p0538 A72-14669

Second and third degree harmonic interpolation formulas for given point in bounded simply connected n-dimensional region, indicating approximate solution of Dirichlet problem

04 p0538 A72-14727

Meteorological fields matching by Sasaki method combined with optimum interpolation, using weighting functions

05 p0683 A72-16724

Interpolation in numerical photogrammetry by least squares method

06 p0815 A72-17752

Computing techniques for finite Fourier transform, applying to Poisson equation, interpolation and quadrature and data smoothing

07 p1025 A72-18784

Interpolation of function of two variables by surface splines method, solving linear equations system by digital computer

07 p1026 A72-19095

Hybrid computation interpolation procedure, using table of function values represented by two dimensional array stored in digital computer core memory

10 p1445 A72-24092

Poised and nonpoised Hermite-Birkhoff interpolation problems application to quadratic formulas and expansions and completely convex functions

11 p1732 A72-25504

High order explicit Runge-Kutta method for linear autonomous systems of differential equations, using interpolation formulas integration

11 p1680 A72-26962

Computer algorithms and programs for complex surface geometrical parameters calculation and discrete curve coordinates determination by interpolation

13 p1924 A72-29141

Isoelectronic wavelength calculations for Ar line spectra, presenting table with identifications and interpolations

13 p2045 A72-29704

Lagrange interpolation formula to determine flow elements shape in pneumatic sensor head with extended measurement range

14 p2104 A72-30372

Shape functions for finite element analysis in n-dimensional space, examining completeness of polynomial interpolation and computational efficiency

15 p2326 A72-31713

Compact self adjoint differential operators in family of Hilbert interpolation spaces, applying perturbation theorem to boundary value problems

18 p2704 A72-36511

Interpolation theorems for nonlinear operators acting on locally convex spaces constituting projective and inductive limits of Banach spaces

18 p2704 A72-36513

Operator to minimize information loss, deleterious truncation and aliasing effects introduced by linear interpolation

21 p3077 A72-40104

Interpolation formulae for the electron impact excitation of ions in the H-, He-, Li-, and Ne-sequences.

22 p3224 A72-42379

Schauder bases in certain spaces of holomorphic functions

24 p3418 A72-44826

INTERPRETATION

Man-machine systems communication ambiguities due to information misinterpretation involving sense organs, previous experience and expectational bias

04 p0478 A72-14850

INTERROGATION

Ground secondary radar interrogator system using monopulse technique for bearing measurement, accuracy and interference reduction

04 p0493 A72-15523

Automatic meteorological station MME-1 data storage and interrogation device for transmission to central station

10 p1445 A72-25019

INTERRUPTION

Computer-controlled queuing system with service interruptions.

23 p3275 A72-43605

INTERSECTIONS

Nonlinear algebraic transformation to determine straight line and second order curve intersection point in aircraft lofting problem

13 p1986 A72-28742

INTERSTELLAR COMMUNICATION

Extraterrestrial life and civilization possibility in other planetary systems in universe, suggesting communication by hydrogen line frequency low harmonics

02 p0276 A72-11642

Engraved message on Au anodized Al plate aboard Pioneer 10 spacecraft for extraterrestrials after exiting solar system via momentum exchange with Jupiter

08 p1236 A72-21459

Life beyond solar system, discussing planetary formation and prebiological organic chemistry developments and interstellar communication

08 p1120 A72-22016

Extraterrestrial life search, noting radio contact with civilizations, bioastronautics, Martian conditions and physicochemical experiments

14 p2076 A72-30694

Extrasolar civilization search via possibly used electromagnetic signal types, discussing frequency and time domains

15 p2302 A72-31292

Soviet book on extraterrestrial civilizations and problems of interstellar communication

19 p2868 A72-38674

Biological aspects of communications with extraterrestrial intelligence, discussing life existence possibility on wandering planets

24 p3372 A72-45127

State of the art in the detection of intelligent extraterrestrial signals.

24 p3441 A72-45190

Linguistic message decoding algorithms for communication with extraterrestrial intelligences, considering unified procedure and key problems solutions

24 p3382 A72-45226

INTERSTELLAR EXTINCTION

Cosmic and X ray irradiated quartz particles as contributor to interstellar extinction, discussing grain radiation damage measurements and absorption spectra in wavelengths of approximately 1600 Å to 20 micrometers

01 p0134 A72-11163

Extinction curves for Mie scattering by interstellar grains, including refractive index differences in vacuum UV for methane, ammonia and water ice absorption

02 p0284 A72-12633

Circumstellar dust formation hypothesis based on O stars mean circumstellar extinction, explaining Ca and Na abundance in interstellar gas

02 p0284 A72-12636

Magellanic Clouds bright star intermediate band photometry, discussing interstellar extinction and luminous supergiants

03 p0425 A72-13257

Interstellar absorption in Perseus OB 2 association direction from UVBY-beta photometry of early type stars in four fields

03 p0438 A72-13875

Absorption effects on circular polarization in synchrotron radiation, discussing frequency and magnetic field dependence

04 p0570 A72-14550

Astrophysics of interstellar medium, discussing direct and indirect observations including 21 cm H lines and starlight extinction and polarization

04 p0581 A72-15622

Interstellar extinction curves for stellar far UV radiation, discussing required multicomponent interstellar dust model

05 p0720 A72-16717

Interstellar Ca II, H and K optical absorption lines of bright O and early B stars in Orion region

05 p0723 A72-17200

Spherical ice and graphite particles absorption, scattering and radiation pressure coefficients and albedo, noting application to interstellar extinction

06 p0875 A72-17296

Interstellar dust distribution, nature and physicochemical and dynamic evolution, discussing star and galaxy observation, light diffusion, star reddening and IR sources

06 p0882 A72-17995

M supergiants in Carina arm, discussing photometric studies at 4-18 microns, interstellar extinction uncertainties and spatial distribution

07 p1072 A72-19344

Quasar and galactic nuclei emission line spectral data corrected for interstellar extinction

10 p1534 A72-23898

Galactic plane distance effect on interstellar reddening in north galactic polar cap, discussing line blanketing and surface gravity role

10 p1546 A72-24834

Stellar statistics method for determining interstellar extinction to reddening ratio in dark cloud area

10 p1546 A72-24836

Perseus two armed spiral shock model based on O associations, young open clusters, H II regions, interstellar absorption lines and 21 cm hydrogen maps

11 p1720 A72-26110

Stellar population in Galactic nuclear bulge, considering interstellar reddening and variable stars

13 p2038 A72-29011

Stellar photometric observations in Magellanic Clouds, presenting photoelectric sequences in UVB system, interstellar reddening and extinction data

14 p2159 A72-30737

Planetary nebulae RF observations comparison with optically determined H-beta intensity for extinction coefficients

15 p2307 A72-31797

Interstellar absorption of Crab Nebula soft X ray from Aerobee rocket photographic scan, estimating average volume densities for H, O, Ne, Si and Mg

16 p2445 A72-33129

Molecular equilibrium abundances in interstellar H I gas clouds, noting formation dependence on gas density and degree of interstellar radiation extinction

19 p2854 A72-37230

Attenuation of X rays in interstellar space.

19 p2852 A72-38600

A study of the interstellar extinction in the Carina-Centaurus region.

20 p2973 A72-39881

Individual reddening laws of O-type stars. I - Computation method, first results

24 p3437 A72-44829

On the possible existence of different interstellar extinction laws in the spiral arms and in the field regions.

24 p3438 A72-44836

INTERSTELLAR GAS

High speed interstellar gas dynamic resonant hydromagnetic wave interaction with cosmic ray shocks

01 p0121 A72-11140

Interstellar OH formation through inverse predissociation from continuum to vibrational level of repulsive molecular state originating from asymptotic atomic ground state

01 p0133 A72-11141

Interstellar OH and water maser regions, deriving density, diameter and temperature

01 p0133 A72-11142

H I radio recombination line observation in H II region NGC 2024 microwave spectrum, detailing radiation frequency dependence

01 p0133 A72-11143

High precision rotational constants and transition frequencies in ground state interstellar molecule cyanoacetylene

01 p0023 A72-11147

Waterless amino acid synthesis in interstellar space, describing ammonia, methanol vapor, formic acid and formaldehyde reaction under UV radiation

01 p0023 A72-11157

High velocity interstellar Ca II near Vela pulsar 0833-45, discussing absorption line association with Vela X, Y, Z supernova remnant complex

02 p0279 A72-12191

Polycyclic hydrocarbon molecules formation in cool stars atmospheres and gases ejected by supernovae and Seyfert galaxies, discussing Platt particles origin

02 p0284 A72-12634

Circumstellar dust formation hypothesis based on O stars mean circumstellar extinction, explaining Ca and Na abundance in interstellar gas

02 p0284 A72-12636

Interstellar formaldehyde and ammonia molecules effects on prebiological amino acids evolution

02 p0165 A72-12846

He production from H to maintain Galactic luminosity, discussing interstellar gas enrichment

03 p0419 A72-13116

Interstellar molecular microwave observations, emphasizing theoretical production rates and modes

03 p0419 A72-13119

Interstellar molecules formation by radiative association and chemical reactions

03 p0320 A72-13121

Organic cosmochemistry evolution, discussing radio astronomical observations, lunar soil samples, meteorite analysis and interstellar gas cloud molecules

03 p0320 A72-13171

Gum Nebula size, emission features and expansion dynamics, discussing Zeta Puppis UV spectrum and Vela X radio emission

03 p0440 A72-14364

Interstellar formaldehyde, ammonia, water, methane and carbon dioxide photochemistry, discussing decomposition and lifetime

04 p0578 A72-15311

D-2A satellite antisolar mission, examining Lyman alpha emission from geocorona and interstellar hydrogen wind

04 p0582 A72-15688

Li, Be and B production rate in interstellar gas by galactic cosmic rays from diffusion model of fast particles, accounting for He component

05 p0708 A72-15760

Low velocity neutral hydrogen spur coincidence with radio continuum Loop IV, discussing average excess surface density and total mass

05 p0711 A72-15765

Distance estimation for supernova remnants and H II regions from H I absorption measurements

05 p0712 A72-15770

Weak D type ionization waves stability in optically thick plasma layer behind front of interstellar gas 05 p0715 A72-16210

Neutral hydrogen distribution in spiral and irregular galaxies, discussing H II regions 05 p0716 A72-16371

Be stars emission line profile broadening due to surrounding gaseous ring in circular motion according to Kepler law 06 p0880 A72-17892

Interstellar gas motion model of nebulae formation by Wolf-Rayet stars 06 p0883 A72-18016

Galactic evolution model, tracing stellar and supernova nucleosynthesis influence on interstellar gas composition 06 p0886 A72-18082

Neutral interstellar hydrogen atoms mean volume density from Lyman alpha absorption and radio measurements in solar region 06 p0886 A72-18098

Unsolved fluid dynamic problems, considering viscous fluids, epiphydrodynamics, magnetohydrodynamics, relativistic field dynamics and interstellar gas dynamics 06 p0800 A72-18112

High radial velocity neutral hydrogen outside galactic plane, noting inability to correlate with radio spurs, absorption and emission regions 07 p1069 A72-19082

Galactic nucleus explosive events and mass expulsion evidence from high velocity hydrogen survey with 20 ft horn reflector 07 p1070 A72-19086

Interstellar cloud properties based on electron concentration integral along line of sight from pulsar radiation measurements 07 p1080 A72-20053

Mathematical model for superheavy cosmic ray production by spallation on interstellar hydrogen, assuming single source for particle injection with given charge spectrum 07 p1062 A72-20197

Ionization loss effects on cosmic ray lifetime in galactic interstellar medium, noting dependence on particle energy 07 p1064 A72-20637

Interstellar gas role in cosmic ray yearly variations determined from solar short wave radiation induced gas ionization 07 p1065 A72-20640

Solar wind propagation limitations by galactic magnetic field and cosmic rays and solar system motion relative to interstellar gas 08 p1225 A72-20701

Cyclotron magnetoacoustic wave generation by planets and binary stars in circular orbits, deriving interstellar gas density variations 08 p1231 A72-21122

Formaldehyde concentration into cloud formation compared to atomic hydrogen from analysis of molecular lines near galactic center 08 p1235 A72-21386

Local interstellar hydrogen survey from OAO-2 observations of Lyman alpha absorption at 1216 A for B2 or earlier stars 08 p1235 A72-21392

IR emission sources in NGC 2264, IC 2087 and M1-82 H II regions 08 p1236 A72-21397

Astronomical models for gas kinematics near galactic center, discussing gas jets origin and kinetic energy 09 p1386 A72-22687

Future interstellar ramjet concepts, considering interstellar hydrogen fuel use for thermonuclear reactor and problems of fuel energy losses, plasma containment and structural limitations 09 p1374 A72-23250

Hydrogen cloud structure of interstellar medium, assuming UV star Stromgren sphere radiation effects 09 p1390 A72-23526

Interstellar gas streaming velocity due to galactic spiral density waves, deriving mathematical expressions for Oort constant and differential galactic rotation nodes from Lin theory 09 p1391 A72-23538

Solar wind termination distance as function of flux, velocity and interstellar hydrogen density, velocity and magnetic field strength 10 p1528 A72-23716

Extragalactic clouds supersonic collisions with galactic gases, discussing high velocity neutral hydrogen gas result of recombination following post-shock surplus energy radiation 10 p1538 A72-24248

Large Magellanic Cloud spiral structure and motion through interstellar gas, determining old and young stars spatial distribution near major spiral arm 10 p1544 A72-24662

Cosmic ray ionization rate for hydrogen calculated for ambipolar diffusion efficiency in decoupling magnetic flux from gas during cloud collapse with angular momentum 10 p1544 A72-24664

Stellar absorption spectral line fineness indication for cold interstellar molecular clouds between observer and star 10 p1546 A72-24848

High density models for ambient gas of eta Carinae star from X ray observations 10 p1530 A72-24947

Astronomical models of solar wind interaction with interstellar medium, determining magnetic field effects on shock wave 11 p1713 A72-25946

Interstellar gas motion model of nebulae formation by Wolf-Rayet stars 11 p1718 A72-25952

Antiproton energy spectrum in cosmic rays from primary proton-interstellar hydrogen collision in two fireball model 12 p1863 A72-27186

Galactic center region neutral hydrogen self absorbing cold cloud, discussing matter, spatial and radial velocity distributions and cloud temperature and density 12 p1867 A72-27208

Interstellar atomic hydrogen observations in radio nebula W 3 direction, noting 21-cm absorption line profile coincidence with Cn alpha recombination line in radial velocity 12 p1868 A72-27219

Hydromagnetic wave scattering of high energy cosmic rays in highly ionized interstellar gas to confine cosmic rays to Milky Way 12 p1864 A72-27745

Interstellar gas motions and density and temperature variations, discussing galactic structure, radiation fields and cosmic ray effects 13 p2038 A72-29009

Two phase flow model of cloud and star formation by galactic shocks in quasi-steady interstellar gas flow in spiral gravitational field 13 p2040 A72-29404

Model of solar wind expansion beyond heliosphere, taking into account effect of relative motion between cold interstellar atomic hydrogen and solar wind protons 13 p1033 A72-29801

Stellar radiation and gravitational effects on neutral atoms and dust grains at large distances for various spectral type stars in schematic evolutionary galaxy 14 p2158 A72-30735

Stellar UV radiation spectral energy distribution investigation of stellar composition and atmosphere and interstellar gas, discussing observation restriction by earth atmosphere absorption 15 p2302 A72-31284

Light elements production from primary cosmic rays spallation in interstellar gas, noting diffusion coefficient of relativistic particles in galaxy 15 p2301 A72-32754

Interstellar H I region strong polarization shock structure, obtaining charge separation field via beam continuum distribution and Mott-Smith approach 16 p2453 A72-33168

Li, Be and B nuclei production via nuclear spallation reactions generated by Galactic cosmic ray bombardment of interstellar gas 16 p2448 A72-33737

Be isotopic ratio in galactic cosmic rays, noting mean interstellar hydrogen density and rays age 16 p2448 A72-33738

Interstellar cosmic ray electron component and isotopic composition relations from positron observations 16 p2448 A72-33741

Solar wind expansion analysis with allowance for interaction with neutral interstellar matter, discussing kinetic energy loss due to EUV ionization of interstellar gas 16 p2449 A72-33910

Galactic magnetic field origin and large scale instability associated with Galactic field and cosmic rays, discussing thermal instability in interstellar gas 16 p2460 A72-33922

Interstellar molecular hydrogen formation on water, ice and solid CO, using laboratory adsorption energy measurements 16 p2461 A72-34160

Carbon 12/13 isotope ratio measurement for interstellar ionized CH molecules toward stars with strong interstellar lines 17 p2604 A72-34524

On the kinematic distribution of galactic neutral hydrogen. 17 p2606 A72-34572

Backscatter of solar resonance radiation. I. 17 p2598 A72-34626

Cosmic-ray heating of low-density interstellar H II regions. 17 p2600 A72-35296

The equilibrium configuration of the gaseous component of the Galaxy. 17 p2611 A72-35312

The stability of a self-gravitating, nonrotating gas layer with stellar, magnetic, and cosmic-ray components. I. 17 p2611 A72-35313

Slipping stream instability of a self-gravitating hydromagnetic gas cloud. 17 p2613 A72-35501

Molecular equilibrium abundances in interstellar H I gas clouds, noting formation dependence on gas density and degree of interstellar radiation extinction 19 p2854 A72-37230

Formation of clouds in a cooling interstellar medium. 19 p2854 A72-37231

Bright nebulae near concentrations of high-velocity gas. 19 p2856 A72-37504

Negative index polytropic sphere gravitational collapse structure, noting application to interstellar gas clouds thermal equilibrium 19 p2857 A72-37794

Gas ejections in NGC 4486 and activity problems of galactic nuclei 19 p2862 A72-38051

Solar wind propagation limitations by galactic magnetic field and cosmic ray pressure and solar system motion relative to interstellar gas 19 p2851 A72-38329

Hot rarefied neutral gas existence in interstellar space on basis of data collected in 21 cm hydrogen line 19 p2865 A72-38480

Low energy cosmic particle and soft X ray photon produced nonthermal electrons effect on interstellar gas ionization and thermal energy equilibrium 19 p2867 A72-38508

Ionisation equilibrium and line intensities for an X-ray heated H I gas. 19 p2852 A72-38509

Star cluster age relation to mass ratios of stars and interstellar hydrogen and dust 19 p2867 A72-38511

Intercloud atomic H gas density distribution from 21 cm line width variations with galactic longitude 19 p2867 A72-38512

Gas density as function of galactic radius according to Jeans unstable criterion for star formation from known galactic rotation curve and gas sound speed 20 p2966 A72-38917

Inviscid non-monatomic interstellar gas radial flow, considering gravitational and heat conducting effects in stellar winds 20 p2967 A72-39193

Interstellar molecules and dense clouds. 20 p2970 A72-39600

Interstellar gas electron temperature determination from recombination line spectra observations along galactic ridge 20 p2971 A72-39858

The interaction of Sco X-1 with its environment. 22 p3218 A72-42387

Angular distribution of interstellar atomic hydrogen. 23 p3315 A72-43834

Upper limits on the atomic hydrogen abundance in 12 globular clusters. 23 p3340 A72-44246

Annual variation of the interplanetary He+ velocity distribution at 1 AU. 23 p3332 A72-44505

Interaction of the solar wind with the neutral component of the interstellar gas. 23 p3332 A72-44507

Collapse of massless nonrotating gas particle nonuniform spheroidal shell contracting around gravitating massive point nucleus, interpreting galactic evolution 24 p3438 A72-44844

Microwave observations of a partially ionized interstellar cloud. 24 p3447 A72-45551

INTERSTELLAR MAGNETIC FIELDS

Radio Astronomy Explorer Satellite data on solar bursts, interstellar medium ionized component distribution, cosmic rays and galactic halo magnetic fields 03 p0330 A72-13067

Interstellar electron density and magnetic field fluctuations effects on Faraday rotation and signal dispersion measure in radio band 04 p0487 A72-14901

Repeated explosions mechanism in nuclei of galaxies and quasars due to instability in twisted magnetic fields, noting clouds and relativistic plasma ejection 05 p0717 A72-16379

Cyclonic turbulence generation of large scale magnetic field of Galaxy, using Steenbeck differential rotation mechanism 06 p0883 A72-18017

Pulsar rotation and dispersion from polarization and pulse arrival time observations, calculating magnetic field components in path to pulsars 07 p1072 A72-19343

Solar wind propagation limitations by galactic magnetic field and cosmic rays and solar system motion relative to interstellar gas 08 p1225 A72-20701

Rotating stellar system with stars and interstellar gas within magnetic field, discussing gravitational and magnetic effects on gas pressure 09 p1384 A72-22511

Solar wind termination distance as function of flux, velocity and interstellar hydrogen density, velocity and magnetic field strength

10 p1528 A72-23716

Radio continuum survey of spiral galaxies M51 and NGC 5195 for study of galactic magnetic field and cosmic rays origin and distribution

10 p1543 A72-24623

Cyclonic turbulence generation of large scale magnetic field of Galaxy, using Steenbeck differential rotation mechanism

11 p1718 A72-25953

Metagalactic magnetic field contributions to observed Faraday rotation measurements for distant extragalactic radio sources

13 p2039 A72-29088

Parker dynamo theory failure in explanation for galactic magnetic field origin and form, noting reasons

13 p2050 A72-29957

Turbulent plasma dynamo mechanisms of magnetic field origin in astrophysics, noting Steenbeck and Parker theories

14 p2162 A72-31150

Galactic magnetic field origin and large scale instability associated with Galactic field and cosmic rays, discussing thermal instability in interstellar gas

16 p2460 A72-33922

Interpretation of rotation measures of radio sources.

17 p2606 A72-34573

Generation of the large-scale magnetic field of the galaxy. II

19 p2864 A72-38079

Solar wind propagation limitations by galactic magnetic field and cosmic ray pressure and solar system motion relative to interstellar gas

19 p2851 A72-38329

The origin and form of the galactic magnetic field. II.

21 p3104 A72-40479

Interpretation of rotation measures of radio sources. II.

23 p3337 A72-43828

INTERSTELLAR MATTER

Molecular processes in interstellar space and life origin, discussing radio astronomy observations, catalytic action and hydroxyl radicals in galaxies

01 p0128 A72-10398

Interstellar medium physical properties and distribution, discussing ionization heating by starlight, cosmic X rays and subcosmic rays

01 p0128 A72-10413

Radiative, segregation and evaporation processes of ice particles surrounding early type stars of Orion association, justifying ice particle model for dust grains

01 p0129 A72-10794

Similarity models of interstellar loop structures, investigating magnetic field and energy losses effects and cosmic ray emission

01 p0131 A72-11011

IR radiation variability from circumstellar grains around carbon-rich supergiant R Coronae Borealis, noting spectrum similarity to black bodies

01 p0121 A72-11093

Pulsar distances and energy from assumed interstellar electron density, considering nonplausibility of associations with supernovae

02 p0278 A72-12047

Interstellar C12/C13 abundance ratio lower limit in direction of 20 Tau

02 p0280 A72-12192

Interstellar dust - IAU Conference, Jena, East Germany, August 1969

02 p0283 A72-12626

Dust grain orientation parameter from Fokker-Planck equation, considering magnetic relaxation time, nearly spherical grains and oblate spheroids

02 p0283 A72-12627

Dust grain existence at large distances from galactic plane by computing interstellar radiation field pressure effects on grains

02 p0283 A72-12629

Dust particle dynamical behavior during cloud collisions, discussing grain distribution in resultant cloud

02 p0284 A72-12638

Reflection nebulae genetic relationship to illuminating stars from catalogs based on Palomar Observatory Sky Survey

02 p0284 A72-12639

Supernovae remnants intrinsic luminosity-diameter correlations from soft X ray emission data, taking into account interstellar medium

03 p0408 A72-13008

Diffuse galactic light absolute intensity interpretation, showing interstellar dust discrete cloud structure effect on grain properties determination

03 p0416 A72-13015

Radio Astronomy Explorer Satellite data on solar bursts, interstellar medium ionized component distribution, cosmic rays and galactic halo magnetic fields

03 p0330 A72-13067

Space observation of stars and interstellar medium, considering stellar energy distributions and line spec-

tra, interstellar absorption lines, galactic nebulae and X ray sources

03 p0420 A72-13122

Linear polarization of pulsar PSR 22 18 plus 47 radio emission pulses, attributing periodic fine structure of spectrum to rotation of polarization plane in interstellar medium

03 p0436 A72-13824

Pulsar radiation scattering in interstellar medium, using Gaussian spatial autocorrelation function

04 p0577 A72-15281

Astrophysics of interstellar medium, discussing direct and indirect observations including 21 cm H lines and starlight extinction and polarization

04 p0581 A72-15622

UV astronomy techniques and devices, discussing hot stars, stellar chemical composition and interstellar medium

04 p0582 A72-15686

Galactic cluster lifetimes compared with star cluster model evaporation times, discussing general galactic and interstellar clouds tidal fields effects

05 p0713 A72-16051

Cosmic gamma radiation theoretical and experimental investigations, discussing sources, interactions with interstellar and intergalactic media, atmospheric backgrounds, balloon and satellite measurements, etc.

05 p0709 A72-16328

Young cluster NGC 2264 stellar radiation flux measurements, suggesting surrounding circumstellar shells producing observable IR excesses

05 p0720 A72-16716

Interstellar extinction curves for stellar far UV radiation, discussing required multicomponent interstellar dust model

05 p0720 A72-16717

Equilibrium temperatures of interstellar grains around early stars, discussing dependency on grain size and stellar distance

06 p0875 A72-17297

Interstellar heterocyclic carbon ring molecules furan and imidazole search from upper limits in galactic sources brightness temperature

06 p0891 A72-18502

Ejection behavior of relativistic particle magnetized clouds in radio galaxies central parts, noting interaction with interstellar medium

06 p0891 A72-18503

Large diatomic and polyatomic molecules formation from big radicals in interstellar medium, noting association reaction role

06 p0891 A72-18506

Spiral galaxies hypothesis for higher mass-luminosity ratio of outer parts from undetected cold neutral hydrogen, using model of NGC 300

07 p1068 A72-19071

Interstellar matter cooling and recombination after supernova ionization, comparing X ray and cosmic ray heating mechanisms

07 p1070 A72-19083

Papers on pulsar physics covering interstellar cloud properties, optical and X ray observations, rotating neutron stars, cosmic rays, etc

07 p1079 A72-20048

Plasma inhomogeneities effect on radio wave absorption in interstellar clouds of ionized hydrogen, analyzing cosmic radio emission spectrum

08 p1231 A72-21120

North Polar Spur soft X rays observed by Aerobee 150 rocket launched from Woomera for enhanced emission

08 p1227 A72-21398

Review of NASA Ames Research Center 1971 conference on interstellar molecules and origin of life

09 p1265 A72-22645

Pulsars CP 0328 and NP 0531 twinkling explained by interstellar electron density fluctuations due to Alfvén wave passage and coupling of cosmic rays to interstellar gas

09 p1377 A72-22753

Book on astronomy and cosmology covering big bang, steady state and oscillating universe theories, radio sources, galaxies, interstellar meteor relativity and extraterrestrial life

09 p1389 A72-23248

LF radiation effect on angular momentum distribution of interstellar grains with permanent dipole moments

10 p1541 A72-24473

Southern Hemisphere interstellar clouds radial velocities from optical and radio observations

10 p1542 A72-24612

High atomic energy levels population at low temperature, density and thermal radiation fields conditions in interstellar medium

11 p1720 A72-26111

Interstellar anomalous 6 centimeter formaldehyde absorption in diffuse dark nebulae, discussing quantum mechanics of collisional pumping process

11 p1720 A72-26112

Interstellar free radicals and molecules spectra, noting catalyzers, temperature and abundances role

11 p1722 A72-26434

Grain heating model of H II region to explain 100 micron emission predominance in IR sources

12 p1871 A72-27693

Ca and Na ionization equilibrium ratio in dust filled interstellar clouds, considering cosmic ray and charge transfer influence

13 p2040 A72-29405

RKR Franck-Condon factors for blue and UV transitions of metal oxides, hydrides and halides, discussing interstellar abundances

14 p2160 A72-30898

Extraterrestrial He I 584 Å background radiation suggested from rocket and satellite observations, noting interstellar medium temperature determination from isophotes

15 p2309 A72-31945

C-13 and C-12 formaldehyde absorption near Sgr A and Sgr B2, noting optical depths and abundance ratio

15 p2315 A72-32712

H I region molecular formation on interstellar dust grains, discussing nonequilibrium evaporation mechanism for adsorbed particles

16 p2452 A72-33128

Diffuse galactic light polarization characteristics from OSO-5 observations, discussing model of starlight scattering by interstellar dust

16 p2446 A72-33468

Interstellar OH maser size determination, discussing scattering by inhomogeneities in electron distribution

16 p2456 A72-33473

Pulsar pulse broadening due to multiple scattering by interstellar medium, finding exponential decay time constant relation to rms broadening of angular size

16 p2457 A72-33686

Complex organic molecules in interstellar space, discussing molecular identification reliability, prebiological organic synthesis, interstellar and planetary biology and UV natural selection

18 p2657 A72-36620

Central galactic plane, interstellar medium and spiral arm conditions for star formation in Milky Way

19 p2855 A72-37249

On circumstellar molecules in the Pleiades.

19 p2856 A72-37508

Decay of pregalactic vortex motions

19 p2862 A72-38057

Star cluster age relation to mass ratios of stars and interstellar hydrogen and dust

19 p2867 A72-38511

Attenuation of X rays in interstellar space.

19 p2852 A72-38600

The influence of local conditions in the interstellar medium upon star formation.

19 p2868 A72-38699

Interstellar medium hydroxyl radiation model, considering amplified spontaneous emission and hot spots

20 p2964 A72-38919

Interstellar molecules and dense clouds.

20 p2970 A72-39600

Physical properties of interstellar matter surrounding binary stars from astronomical spectroscopy, discussing eruptions and photometric changes

20 p2975 A72-40069

Emission and absorption RF recombination lines of interstellar neutral atomic H and He, discussing electron transition processes in nebula

20 p2975 A72-40070

Interstellar lines in the ultraviolet spectrum of zeta Ophiuchi.

21 p3105 A72-41035

Hydrogen sulfide detection in Galactic sources via observation of single line corresponding to rotational transition, comparing abundance to formaldehyde, CS, HCN and CO

21 p3107 A72-41271

Interstellar nitrogen-15 and U169.3 - Possibly a new methanol line.

21 p3107 A72-41272

Sodium to calcium ion abundances ratio variation model in interstellar clouds, comparing with pulsar dispersion and LF radio absorption measurements

22 p3224 A72-42383

The density of H₂ molecules in dark interstellar clouds.

22 p3224 A72-42385

Collisional excitation of carbon monoxide in interstellar clouds.

22 p3227 A72-42553

Interstellar circular polarization.

23 p3336 A72-43556

Discovery of interstellar circular polarization in the direction of the Crab Nebula.

23 p3336 A72-43557

Stellar implosion, gas cloud collapse into white dwarf or neutron star and atomic hydrogen cloud collapse, considering effects of cosmic bodies at high velocities

24 p3439 A72-45017

UV and IR observations of galactic and intergalactic matter from space stations, noting spatial resolution increase

24 p3446 A72-45532

INTERSTELLAR MICROWAVE SPECTRA U INTERSTELLAR RADIATION

U MICROWAVE SPECTRA

INTERSTELLAR RADIATION

- Interferometric photoelectric scans of interstellar Ca I 4226 line for stars with interstellar Ca II K-lines, discussing deduced electron densities 02 p0280 A72-12197
- Dust grain existence at large distances from galactic plane by computing interstellar radiation field pressure effects on grains 02 p0283 A72-12629
- Absorption spectrum of atomic Ca trapped in solid hydrocarbons, comparing with diffuse interstellar band at 4430 Å 02 p0284 A72-12632
- Stellar field structure in NGC 2129 cluster direction, discussing interstellar radiation absorption and star distribution 03 p0433 A72-13491
- Rf diagnostic technique for carbon and hydrogen /H I/ cloud recombination lines in cool interstellar medium 04 p0570 A72-14525
- Interstellar sodium lines intensities and widths as discriminants for two component models of galactic H I cloud regions 04 p0578 A72-15310
- Interplanetary scintillation of two pulsars, discussing scattering and amplitude modulation of incident radiation propagated through interstellar medium 07 p1069 A72-19073
- LF radiation effect on angular momentum distribution of interstellar grains with permanent dipole moments 10 p1541 A72-24473
- Time variable energy losses effects on cosmic ray nuclei composition, discussing fragmentation processes during heavy nuclei propagation through interstellar matter 12 p1864 A72-27692
- Interstellar gas motions and density and temperature variations, discussing galactic structure, radiation fields and cosmic ray effects 13 p2038 A72-29009
- Galactic structure, ionized gas distribution and radio source diameter studies from interstellar scattering at 81.5 MHz, comparing with pulsars 13 p2050 A72-29962
- Average interstellar electron and early star density in Galactic disk, examining hot stars ionizing photons and H II regions photoionization 14 p2161 A72-31044
- High gain laser amplifier spectral linewidth dependence on external signal or spontaneous emission source, noting saturation role and relevance to interstellar medium radiation 16 p2453 A72-33166
- Hydroxyl and water radio sources scale and geometry constraints placed by interstellar maser gain saturation relation to emission solid angle 21 p3062 A72-40565
- Recoil effect on inverted molecules changing pumping conditions and gain for interstellar, OH maser intensity and radial velocity variations 21 p3102 A72-41773
- A longitude survey of radio recombination lines from the diffuse interstellar medium. 22 p3227 A72-42552
- Interstellar circular polarization - Data for six stars and the wavelength dependence. 22 p3228 A72-42572
- Cross correlated interstellar scintillation patterns of circumpolar pulsar PSR 0329+54 at 408 MHz, interpreting transverse velocities in Galaxy 23 p3334 A72-43253
- INTERSTELLAR SPACE**
- Pulsar PSR 0833-45 linear polarization measurements at 300 and 1420 MHz, showing frequency invariance with interstellar scattering and Faraday rotation allowance 01 p0133 A72-11119
- Cosmic soft X ray and UV radiation sources, discussing transition radiation emission in interstellar space 01 p0121 A72-11121
- Dust particle formation in circumstellar space accompanying star formation, discussing necessary and sufficient condition for grain escape by fragmentation 02 p0284 A72-12637
- Antiproton flux energy spectrum in Galactic interstellar space, discussing flux peak 03 p0408 A72-13005
- Dust particle composition and effect on light transmission in interstellar medium, discussing gas, magnetic fields, cosmic rays and background radiation 07 p1074 A72-19557
- Cosmic sources of organic compounds from chemical evolution viewpoint, discussing comets, interstellar space, prestellar nebulae and cool stellar atmospheres 08 p1120 A72-22014
- Ionized gas effect on interstellar space synchrotron emission, noting magnetic field orientation-dependent low frequency cut-off 14 p2156 A72-30559

- Interstellar medium physical conditions from 21 cm hydrogen emission line observations in direction of pulsars, using 25 meter Dwingeloo radiotelescope 14 p2159 A72-30744
- Reaction rate coefficient evaluation for charge transfer from doubly positive carbon ion to helium at 100-100,000 K, discussing effect on interstellar medium 16 p2360 A72-33455
- Be 7 destruction via nuclear decay instigated by atomic electron capture in interstellar medium, considering Ar 37, Ca 41, Ti 44, V 49, Cr 51, Mn 53 and Fe 54 16 p2447 A72-33736
- Influence of interstellar discontinuities on the shape of radio pulses from pulsars 18 p2726 A72-36652
- A photon rest mass and the dispersion of longitudinal electric waves in interstellar space. 18 p2728 A72-36923
- Longitudinal electric waves absorption in interstellar space due to electron-heavy particle collisions, considering photon rest mass 20 p2969 A72-39348
- Emission and absorption spectral behavior observation by millimeter radio telescopes for molecules in interstellar space of Milky Way galaxy spiral arms 24 p3439 A72-44905
- Early stage condensation in planetary formation, discussing atomic and molecular reactions in interstellar space and earth outer atmosphere properties 24 p3444 A72-45452
- INTERSTELLAR TRAVEL**
- Interstellar flight conditions in photon vehicle 05 p0713 A72-15979
- Structural limitations of interstellar ramjet, investigating operation during travel in high matter number density space 07 p1054 A72-20249
- Future interstellar ramjet concepts, considering interstellar hydrogen fuel use for thermonuclear reactor and problems of fuel energy losses, plasma containment and structural limitations 09 p1374 A72-23250
- Requirements and techniques of interstellar navigation, discussing astronomical maps and observational phenomena at relativistic travel velocities 15 p2267 A72-31291
- INTERSTITIALS**
- Interstitial impurities and grain size effects on cold brittleness in W melts in deformed and recrystallized states 01 p0088 A72-11082
- Statistical mechanical calculation of thermodynamic properties of interstitial solid solutions involving second nearest neighbor solute atom mutual interactions based on Kirkwood expansions 03 p0459 A72-14252
- Oxygen and/or nitrogen interstitial solute pick-up effects on yield stress during Nb annealing, discussing Hall-Petch plot parameter values 05 p0676 A72-16730
- Prolonged jet flight effect on passenger interstitial and intracellular fluid volumes from plasma, extracellular and total body water measurements, noting dehydration and foot swelling 06 p0767 A72-17866
- Steady state creep model for high activation energy role in interstitial formation and migration in particle strengthened alloys 08 p1185 A72-20992
- Coupling of interstitial liquid and porous elastic medium deformation, calculating solidification by numerical integration of partial differential equations system of Lamé type 10 p1465 A72-24116
- Dimensionless thermal contact conductance parameter for determination of interstitial thermal contact materials effectiveness for metallic junctions [AIAA PAPER 72-284] 11 p1741 A72-25224
- Gas side, coolant side and interstitial heat transfer in gas turbines transpiration air cooling 11 p1860 A72-27350
- Mechanical strength of interstitial solid tantalum-oxygen solutions obtained by electron beam fusion, thermal cycling and saturation as function of temperature and oxygen contents 14 p2112 A72-30163
- Interstitial phases, crystal structure and chemical bonds of titanium, vanadium and niobium carbides, comparing with transition metal carbides 15 p2252 A72-31195
- Boltzmann-Matano analysis of substitutional interstitial diffusion profiles of Zn in GaAs by radio tracer techniques 16 p2441 A72-33209
- Grain-size dependence of Snoek peaks in niobium. 17 p2566 A72-34671
- V-Ti alloys interstitial scavenging action dependence on titanium concentration via internal friction study 12 p1267 A72-34732
- Properties of high-purity chromium 17 p2569 A72-35525

- Electron work function change of interstitial compounds of the 4a and 5a metals in dependence on the nonmetal content. 18 p2656 A72-36129
- Impurity controlled deformation mechanism for softening control of interstitial bcc alloys, discussing low temperature and composition effects 18 p2699 A72-36341
- Substitutional-interstitial interactions in bcc alloys. 18 p2699 A72-36396
- The influence of interstitial nitrogen on the asymmetry of the yield stress of tantalum. 20 p2935 A72-39006
- Hydrogen in intermetallic phases, taking into account as an example the system titanium-nickel-hydrogen 21 p3070 A72-41647
- Recombination and annihilation rates of interstitial atoms and vacancies in crystal lattices, taking account of diffusion 21 p3088 A72-41690
- Field-ion microscopic study of the interstitial plasticity of tungsten single crystals 23 p3304 A72-44484
- INTERVALS**
- German monograph - Internal-analytic methods in systems of linear equations with interval coefficients and relations to error analysis. 22 p3200 A72-43061
- INTESTINES**
- Hypoxia, hypercapnia and hyperoxia effects on active glucose transport in rat small intestines 05 p0618 A72-16633
- Intestinal disбактерiosis and autoinfection occurrence in guinea pigs and rats under magnetic field effect, noting Escherichia population changes 05 p0622 A72-16647
- Dog mesentery terminal venous microvessel distensibility characteristics from response to arterial and venous pressure changes 06 p0765 A72-18196
- Hermetic chamber medico-engineering experiment for long term isolation effects on human intestinal microflora, showing reduction and disappearance of certain microbe populations 13 p1904 A72-29323
- INTOXICATION**
- Effect of neurohomologous phospholipids associated with other substances on experimental intoxication by asymmetrical dimethylhydrazine. II - Biochemical aspects of the pyridoxine-phospholipid association 21 p3009 A72-41195
- Intoxicating liquor and the general aviation pilot in 1971. 24 p3377 A72-45662
- INTRACRANIAL CAVITY**
- Sudden pilot incapacitation and death due to subarachnoid hemorrhage secondary to ruptured intracranial aneurysm 10 p1429 A72-23742
- INTRACRANIAL PRESSURE**
- Cerebro-spinal fluid pressure remote monitoring by intracranially implanted radio pressure transducers, describing receiver-detector-recorder system 07 p0930 A72-19911
- Russian book - Intracranial blood circulation under conditions of accelerations and weightlessness 17 p2509 A72-35460
- INTRAOCULAR PRESSURE**
- Isotopic labeled microspheres for cat uveal and retinal blood flow and oxygen consumption determination, studying increased intraocular pressure and carbon dioxide tension effects 12 p1763 A72-27841
- Contact pressure between an elastic spherical shell and a rigid plate. [ASME PAPER 72-APM-31] 17 p2628 A72-34788
- INTRAVASCULAR SYSTEM**
- Dog mesentery terminal venous microvessel distensibility characteristics from response to arterial and venous pressure changes 06 p0765 A72-18196
- Microcirculation study of intravascular erythrocyte aggregation/blood sludge/ in rats 07 p0920 A72-19686
- Intravascular pressure and extravascular structure effects on radial and longitudinal distensibility of arterial microvessels in dog mesentery 07 p0922 A72-20426
- Wien intravascular effect on plasma carbon dioxide gradients near pulmonary capillary wall, discussing free energy requirements 08 p1114 A72-20890
- Interactions between gas bubbles and components of the blood - Implications in decompression sickness. 24 p3374 A72-45652
- INTRAVENOUS PROCEDURES**
- Blood self purification external mechanism in dogs, determining leukocyte population changes before and after feeding and intravenous interferon injections 07 p0915 A72-18867

INTROVERSION

Noise effects on human attention and work efficiency in extroverted and introverted individuals

08 p1128 A72-22137

Circadian rhythm effects on introverts and extroverts biochemistry, physiology and performance, suggesting arousal mechanism differences

11 p1581 A72-26693

INVARIANCE

NT GAUGE INVARIANCE

Pattern recognition, invariance, redundancy and information reduction in computer aided image processing

01 p0034 A72-10475

Stability theory invariance principle extension to generalized dynamical systems, considering problems in thermoelasticity, viscoelasticity and distributed nonlinear networks

02 p0251 A72-11497

Structure, controllability and synthesis of n-dimensional invariant systems under perturbation vector, using governing equations

05 p0641 A72-16352

Liapunov functions generation, using auxiliary functional differential equations table for invariance determination

06 p0838 A72-17378

Invariant characteristics of hydrodynamic systems with stationary boundaries, 3 degrees of freedom and second order nonlinear motion of Liouville type

06 p0801 A72-18136

Linear multivariable systems feedback invariant structure of controllable matrix pair under rich transformation group including regular linear coordinate and state-feedback transformations

07 p0960 A72-19700

Linear invariant solution to gyrostat motion under nonholonomic constraint

08 p1208 A72-21361

Learning systems mathematical scheme to identify classes invariant with respect to transformation groups, realizing functionals with coherent and incoherent optics

09 p1282 A72-22218

Riemann invariants method for plasticity theory application to first order quasi-linear systems, considering plastic flow in arbitrary die

09 p1403 A72-22760

Linear theories of gravitational fields, discussing Lorentz invariant approximation use to obtain Einstein equations approximation

09 p1352 A72-23386

Third order nonlinear differential equation invariants use to obtain integrable forms

10 p1504 A72-24053

Phenomenological symmetry for spatial, mechanical and relativistic physical laws, providing invariance to subsets of described objects

10 p1512 A72-24781

Structure, controllability and synthesis of n-dimensional invariant systems under perturbation vector, using governing equations

11 p1608 A72-25328

Boundary value problems to initial value problems transformation method extended by physical parameters invariant properties, noting fluid mechanics nonlinear equations

11 p1616 A72-25878

Relativistic statistical mechanics invariant formula for coherence degree of plane blackbody radiation beam in arbitrary Lorentz frame, noting transformation law of temperature

12 p1846 A72-27741

Iterative method for continuous one dimensional linear systems with space-time invariant properties, applying to dynamic mixed problem of linear viscoelasticity

13 p2006 A72-29783

Scaling invariance hypothesis for local structure of turbulence, using quantum field theory methods

13 p1943 A72-29994

Local Lorentz transformation in chronometric invariants, demonstrating appropriate operation for general covariant tensors from tetrad formalism

14 p2130 A72-30218

Time invariance violation in charge asymmetry experiment, showing K-meson decay rate difference reversal from world to antiworld with particle unchanged

14 p2130 A72-30265

Green operator first invariant upper bound for free oscillations eigenvalue upper limit, exemplifying for quadratic plate with two free and two clamped edges

15 p2274 A72-31459

Poincare noninvariance of Stigma equation as alternative to Dirac equation for spin one-half finite mass particles

15 p2280 A72-31519

Computer graphics for invariant torus behavior in four dimensional phase space, varying equation parameter over large intervals

15 p2263 A72-31758

German book on principles and applications of similarity theory in physical-technical research cover-

ing coherent dimensional units and invariance principle, physical dimensions, etc

15 p2218 A72-31900

Invariant solutions of the Navier-Stokes equations describing motions with a free boundary.

18 p2679 A72-36234

Universe expansion induced electromagnetic wave backscattering absence in Robertson-Walker space-time as consequence of motion equations conformal invariance

18 p2711 A72-36711

On the adiabatic invariants of a quantified system perturbed by a coherent wave

19 p2834 A72-37789

Variational method in the control system invariance problem

19 p2778 A72-37990

Invariant poles feedback control of flexible, highly variable spacecraft.

19 p2869 A72-38240

Investigation of the stability of solutions of second-order differential equations with periodic coefficients by the differential invariant method

19 p2827 A72-38467

Harmonic frames of reference in Einstein's theory of gravitation

20 p2953 A72-39406

Invariance problems in terms of Lagrangian domain of definition and Euler-Lagrange mapping intrinsic geometric characterization, reviewing theory of fiber bundles

20 p2954 A72-40006

Group properties and invariant solutions of electric-field equations in the case of nonlinear Ohm's laws

21 p3086 A72-41654

Invariant solutions of the differential equations of the uniform motion of a Hooke medium

22 p3233 A72-42058

Accuracy of the conservation of the third adiabatic invariant of charged-particle motion in axisymmetric fields. II

22 p3217 A72-42209

Variational method for invariance problem solution for optimal finite state of nonlinear dynamic systems under external disturbances

22 p3162 A72-42240

The construction of invariant transformations in plane rotational gasdynamics.

22 p3199 A72-42399

Conditions for space invariance in optical data processors used with coherent or noncoherent light.

23 p3288 A72-43887

Controllability properties of right invariant nonlinear systems described by evolution differential equation in Lie group

23 p3309 A72-43981

Mean square invariant forecasts for the Weibull distribution.

24 p3418 A72-44664

Differential games problem of pursuit tracking solved by invariants theory, noting explicit laws of pursuer activity control

24 p3387 A72-45518

Mathematical consequences of physical laws invariance hypothesis under space-time-dependent changes in unit length, discussing conformally covariant and cosmological theories interrelationship

24 p3447 A72-45626

INVARIANT IMBEDDINGS

Invariant imbedding theory of aerosols multiple scattering induced telephotometric errors, determining scattering coefficients relative to optical thickness by Monte Carlo method

[AIAA PAPER 71-1062] 01 p0066 A72-10531

Invariant imbedding technique application to linear partial differential equations boundary value problems conversion to Cauchy problem via generalized Riccati transformations

01 p0093 A72-11116

Dirichlet problem reduction to boundary value problem via invariant imbedding techniques and Fredholm integral equation method

04 p0540 A72-15632

Hybrid computer solution of partial differential equations by invariant imbedding application to serial method

06 p0839 A72-17631

Differential geometry extremal problem of holomorphic embedding of complex curves in Kaehler manifold with constant holomorphic curvature, using Riemann surface moduli theory

10 p1506 A72-24862

Neuronal network numerical and analytic studies, using invariant imbedding and matrix Fredholm integral equation

13 p1986 A72-29400

Poisson ratio changes effect on equilibrium problems solutions in thin plate theory via invariant imbedding technique, using Cauchy system formulation

15 p2330 A72-32444

Riemann invariants method for nonelliptic first order systems with two independent variables,

presenting application to perfectly plastic material flow in die without friction

16 p2467 A72-33140

Optimal filtering estimate of noisy nonlinear partial differential distributed parameter system, using least squares and invariant imbedding techniques

16 p2416 A72-33575

Stress concentration in elastic layer with circular slot analyzed by reducing mixed boundary value problem to initial condition problem via invariant imbedding

16 p2471 A72-33827

Invariant imbedding in time-varying homogeneous nondispersive media.

17 p2513 A72-34366

Invariant imbedding and optimum beam design with displacement constraints.

17 p2634 A72-35406

Dynamic programming and the optimum design of rotating disks.

23 p3356 A72-44550

INVENTORIES

NT TIMBER INVENTORY

INVENTORY CONTROLS

Interflug national economic control system, discussing objectives, costs, labor, science and technology, material and price management plans

05 p0753 A72-16778

INVENTORY MANAGEMENT

NT INVENTORY CONTROLS

Decision making models application to systems configuration, reliability, repair level and spares optimization and availability analysis

10 p1486 A72-24006

Electronic data processing in airline materiel supplies operations, discussing procedural efficiency improvement through reduction of stochastic effects inherent in aircraft maintenance operations

14 p2174 A72-30823

INVERSIONS

NT CENTRIFUGING STRESS

NT POPULATION INVERSION

NT TEMPERATURE INVERSIONS

Reinforcement method algorithm for inversion of matrix with rational function terms

21 p3075 A72-41313

INVERTEBRATES

NT AMOEBA

NT COLEOPTERA

NT DROSOPHILA

NT FLAGELLATA

NT INSECTS

NT MOLLUSKS

NT PROTOZOA

NT PUPA

NT SPORES

NT WORMS

INVERTERS

NT STATIC INVERTERS

Pulse width modulated transistor series inverter with inductor transformer in low power applications, noting short circuit and no-load protection

01 p0007 A72-11060

Output voltage characteristics of single phase thyristor inverter based on pulse duration modulation with direct shaping of control pulses, considering harmonic coefficients

11 p1603 A72-25277

Condenser charging by dc-dc converter consisting of SCR series inverter, transformer and rectifier-filter circuit, considering power consumption

11 p1577 A72-25278

Binary logic circuits with interconnected repeaters and inverters, discussing signal level selection to ensure maximum noise stability

12 p1786 A72-28120

Binary logic circuits with interconnected repeaters and inverters, discussing signal level selection to ensure maximum noise stability

19 p2767 A72-38621

MOS logic circuit design simplification by replacing series and parallel transistor networks by equivalent single transistor inverter circuit

23 p3271 A72-43843

INVESTIGATION

NT ACCIDENT INVESTIGATION

NT AIRCRAFT ACCIDENT INVESTIGATION

INVESTMENT CASTING

Materials research for investment cast turbine wheel, investigating Fe base specimens

05 p0666 A72-16496

INVESTMENTS

Management alternatives evaluation methodology for capital expenditures on large facilities in terms of competitive capability enhancement for aerospace contracts

15 p2340 A72-32615

INVISCID FLOW

NT STAGNATION FLOW

Two dimensional MHD channel flow of inviscid fluid in circular nonuniform magnetic field

02 p0267 A72-12771

Method of characteristics calculations of inviscid free jet flow with low specific heat ratios for perfect gas at 1.10 Mach number

Boundary value problem for steady parallel axisymmetric irrotational flow of inviscid incompressible fluid past cylinder having common axis with tube

Inviscid incompressible conducting fluid motion under line sink in uniform strong magnetic field

Hydroelastic vibrations of incompressible inviscid liquid with free surface in uniformly rotating infinitely long circular cylindrical container, investigating response to cylinder walls forced excitations

Inviscid variable density core flow in thin compressible boundary layer near stagnation point of smooth blunt body

Finite difference calculations for two dimensional unsteady inviscid expanding flow of perfect gas through nozzle, obtaining flow field patterns

Steady inviscid diabatic complex lamellar gas flow geometric properties, correlating stream and vortex lines via Beltrami surfaces in Euclidean space

Internal axisymmetric steady inviscid rotational flow velocity profiles simulation by means of shaped wire gauze screens

Numerical analysis of three dimensional inviscid supersonic flow field about complex vehicle geometry, using finite difference technique and Rankine-Hugoniot relations

Turbulent boundary layer development for airfoil at high transonic speeds, discussing viscous-inviscid flow interaction

Nonlinear effects of inviscid supersonic flow field surrounding bodies in coning motion, using shock capturing finite difference technique

Combined viscous-inviscid analytical procedure for predicting boundary layer effects on supersonic inlet flow field

Viscoelastic effect on cylindrical liquid jets capillary breakup after ejection into inviscid atmosphere

Circular vortex rings with nonsimilar vorticity distributions submerged in inviscid stream, considering motion and decay by inner and outer asymptotic expansions matching

Inviscid solar wind equations supersonic solutions existence domain from critical point boundary conditions

Lax finite difference scheme application to transonic two dimensional Laval nozzle and supersonic blunt body flow with detached shock wave, considering inviscid thermally nonconducting

Inviscid relaxing gas flow through tube with variable cross sectional area, deriving governing equation for weak discontinuity amplitude evolution

High altitude rocket plume rarefaction effects, predicting inviscid, merged, transition, first collision and free molecular flow regimes

Inviscid conducting gas steady one-dimensional MHD flow, using three-dimensional phase diagram for differential equations analysis

Electric eddy currents formation during thermal acceleration of inviscid quasi-linear plasma in profiled channel

Numerical integration of viscous and inviscid fluid flow equations, comparing various methods with exact solution

Taylor series truncation method for steady supersonic inviscid gas flow past nonaxisymmetric conical bodies

German monograph on flow calculation in axial thermal turbomachines covering boundary conditions and field computation for steady state inviscid flow

Steady inviscid irrotational transonic flow in two dimensional symmetric and axially symmetric nozzle throats

Pseudoviscous method application to computation of supersonic flow of inviscid ideal gas through two dimensional or annular axisymmetric ducts

Reduction of governing equation for thin nonstretching vortex filament in incompressible inviscid

fluid to nonlinear Schroedinger equation describing helical motion propagation

Inviscid parallel stratified shear flow stability to two dimensional disturbances, solving Taylor-Goldstein stability equation for eigenvalues by computerized numerical integration

Small cross section steady vortex rings existence in inviscid uniformly dense ideal fluid, deriving asymptotic formulas for rings shape and properties

Internal Alfvén gravity waves propagation in rotating Boussinesq inviscid adiabatic conducting fluid shear flow within transverse magnetic field, considering electromagnetic and Coriolis forces effects

Small gap approximation for axial magnetic field effects on stability of nonrotationally symmetric disturbances in inviscid flow between concentric rotating cylinders

Forced heat convection from sphere immersed in inviscid fluid stream at small Peclet number, using matched asymptotic expansions

Inviscid incompressible flow past longitudinally curved small aspect ratio slender wing, investigating aerodynamic characteristics

Axisymmetric hypersonic motion around thin solid of revolution, taking into account boundary layer interaction with inviscid external flow

Hypersonic flow of nonequilibrium ionized monatomic inviscid radiating gas past axisymmetric blunt body with allowance for electron and ion temperatures difference

Nonequilibrium dissociating inviscid nitrogen flow pattern over spheres and circular cylinders, obtaining temperature, pressure and density fields

Inviscid plane Couette flow infinitesimal instability as initial value problem, using distribution-theoretic approach

Numerical analysis of inviscid hypersonic flow characteristics in shock layer between bow shock and cone at angles of attack, taking into account laminar separated flow

Aerodynamic properties prediction procedure for thin jet-flapped airfoil in incompressible inviscid flow bounded by different types of boundaries

Time dependent finite difference (fluid-in-cell) method for supersonic aerodynamic problems concerning inviscid compressible flow with contact surface and shock discontinuities

Asymptotic solution for inviscid conducting fluid flow past arbitrary wing profile in magnetic field

Plane vortex sheet in incompressible inviscid and finitely conducting fluids, investigating discontinuity in density and conductivity on hydromagnetic stability

Inviscid surface streamlines and laminar, transitional and turbulent heating of blunt nose shuttle configurations in hypersonic flow

Closed form solution to conical inviscid hypersonic flow over circular cone at zero angle of attack

Kinetic and kinematic equations for inviscid unsteady gas flow, noting pseudostationary vortex geometry

The inviscid flowfield of an unsteady airfoil

Inviscid perfect gas supersonic steady irrotational flow past wedge, investigating analytical solution validity in downstream region behind shock

Finite amplitude disturbances in the flow 8019 of inviscid rotating and stratified fluids over obstacles

Theoretical investigation of the interfacial stability of inviscid fluids in motion, considering surface tension

Boundary layer and inviscid main stream interaction in asymmetric supersonic steady gas flow incident on circular cone at high Reynolds numbers

The influence of geostrophic force on the stability of an heterogeneous conducting fluid with a radial gravitational force

Multiplicity theorem for aligned steady MHD flows of inviscid perfectly conducting gas, assuming constant density along streamline

On a method of computing the plane steady flow around a profile situated between straight parallel lines

Inviscid non-monatomic interstellar gas radial flow, considering gravitational and heat conducting effects in stellar winds

Asymptotic theory of an optically thick radiating gas flow past a smooth boundary at moderate radiation strength

Free and forced trapped oscillation properties in inviscid rotating fluid, considering modifications for viscosity

Axial velocity distribution and streamline boundary selection to derive two dimensional infinite duct shapes for inviscid irrotational compressible flows

A steady vortex ring close to Hill's spherical vortex

Polish book - Fluid mechanics. Volume 2 - Gasdynamics.

INVISIBILITY

U VISIBILITY

INVOLUNTARINESS

U INVOLUNTARY ACTIONS

INVOLUNTARY ACTIONS

Involuntary eye movements effects on visual images, emphasizing drift and tremor effects on spatial frequency distortion

Involuntary head movement and helmet motion displacements during human centrifuge runs to 6 Gz from photographic recordings

IO

Photometric radii of Io and Europa

The determination of the diameter of Io from its occultation of beta Scorpii C on May 14, 1971

Io apparent equatorial radius, taking into account distortion due to Jupiter effects on rotation and tides

Upper limits for an atmosphere on Io

Thin ice crust, chondritic composition and ionosphere considerations for Io electrical conductivity and decametric radio emission modulation in unipolar inductor model

IODATES

Properties of a pulsed LiIO₃ doubly resonant parametric oscillator

IODIDES

NT CESIUM IODIDES

NT SODIUM IODIDES

Hydrogen iodide flash photolysis in presence of nitrous oxide, carbon dioxide and water investigated by kinetic spectroscopy, observing iodoigen as intermediate reaction product

Kinetic model and analysis of elementary characteristics of carbon trifluoriodide photodissociation laser

IR chemiluminescence study of chlorine reaction with hydrogen iodide at enhanced collision energies, investigating energy conversion efficiency and forward scattering

Kinetic model and analysis of time characteristics of trifluoriodomethane photodissociation laser

The photochemical iodine laser - A high-power laser

IODINE

NT IODINE ISOTOPES

Chlorine, bromine and iodine first spectral lines observation in IR region with liquid nitrogen cooled lead sulfide detector

Vapor pressure and composition in As-I system, investigating entropy and enthalpy changes and temperature dependence of equilibrium constant

Fast iodine ions charge exchange in dense carbon dioxide supersonic jet, determining electron capture cross sections by least squares method

Zeeman effects in hyperfine structure of atomic iodine photodissociation laser emission, noting magnetic fields effect on time behavior

Time estimate criterion of lasing breakdown in photodissociative iodine-alkyl lasers with iodine molecule buildup

Molecular iodine photolysis in photodissociative laser due to selective pumping, noting recombination-like storage mechanism

14 p2110 A72-30354

Stimulated emission in molecular iodine vapor phase laser optically pumped by Q switched Nd-YAG laser second harmonics

15 p2251 A72-32538

Molecular and atomic mechanisms for hydrogen-iodine exchange reaction dynamics, using classical trajectory analysis

16 p2360 A72-33581

Gaseous and particulate iodine in the marine atmosphere.

22 p3173 A72-42469

Generation spectrum kinetics of a photodissociative iodine laser

23 p3297 A72-44480

Analytic criteria for laser quenching moment, generation power and stimulated emission energy for photodissociative iodine-alkyl lasers with iodine molecule buildup

24 p3412 A72-45706

IODINE COMPOUNDS

NT CESIUM IODIDES

NT IODATES

NT IODIDES

NT SODIUM IODIDES

Dielectric dispersion in SrSI filamentary single crystals as function of Curie temperature in If and shf range

09 p1367 A72-22422

Semiconductor properties of iodine and bromine molecular complexes of /1-phenyl-3-isoindolyl-/ /1-phenyl-3-pseudoisodolylidene-/ phenylmethane and /1-p-tolyl-3-isoindolyl-/ /1-p-tolyl-3-pseudoisodolylidene-/ phenylmethane.

19 p2847 A72-38641

IODINE ISOTOPES

Thermal release Xe analysis of neutron irradiated white inclusion samples from Allende carbonaceous meteorite, noting iodine and plutonium isotopes abundance

18 p2728 A72-36971

ION ACCELERATORS

Ion accelerating system for minimum angular ion beam divergence with plasma ions ejection from source through slits in electrodes

05 p0701 A72-17236

Electromagnetic plasma accelerator with electron drift and diffusion towards anodes, neutral gas ionization and extended ion acceleration zone

09 p1361 A72-22955

Multiply charged heavy ion sources and accelerating systems - Conference, Gatlinburg, Tennessee, October 1971

10 p1516 A72-25026

Multiply charged ion plasmas production in heavy ion accelerator by laser beam interaction with vaporized target material

10 p1516 A72-25033

Heavy ion acceleration from strong electron beam in metallic plasma obtained with ruby laser and positive voltage pulses

10 p1524 A72-25034

Hydrogen, deuterium, helium, nitrogen and argon ion production and acceleration by intense pulsed relativistic electron beam

10 p1517 A72-25037

Grid translation accelerator system for Kaufman ion thrusters beam deflection, noting response time and accelerated life tests

[AIAA PAPER 72-485]

11 p1710 A72-26211

Microscopic processes within high energy ion acceleration in laser-produced plasmas, discussing transient electric field role

14 p2136 A72-30178

Electromagnetic plasma accelerator with electron drift and diffusion towards anodes, neutral gas ionization and extended ion acceleration zone

17 p2593 A72-35884

A theoretical analysis of the acceleration of ions in axially symmetric crossed fields with an external source and sectioned electrodes

17 p2593 A72-35902

Mercury Hall ion engine principles and design, discussing plasma ion acceleration, mercury evaporation and ionization and acceleration channel electrical and thermal insulation

20 p2963 A72-39937

ION ATOM INTERACTIONS

Intermolecular potentials determination by inverting phase shifts obtained from high resolution measurements of protons differential elastic scattering by rare gas atoms

04 p0552 A72-14577

Vanadium carbide diffraction spectrum reflection intensity under Mo and CuK-alpha irradiation, showing crystalline structure and interatomic ionic interaction

04 p0533 A72-14618

Nonuniform sinusoidal electric field anomalous influence on ion motion in gas with allowance for ion-atom collisions

04 p0547 A72-14622

Ground state He long range interaction with triplet metastable He, discussing gerade and ungerade states

07 p1037 A72-19495

Energy and angular distributions of electrons released during ion atom collisions from energy spectra studies, discussing autoionization transitions

08 p1210 A72-20836

Exothermic capture processes with ionization during nonelastic ion atom collisions, discussing cross sections of He ion collisions with Ar, Kr and Xe atoms

08 p1210 A72-20837

D and E region ion chemistry reaction rate measurements, noting hydration, charge exchange and ion-atom interchanges

09 p1275 A72-22366

Resonance theory of three body ion-atom association reactions in rare gases, estimating quasi-bound electron state population and deactivation cross section

09 p1356 A72-22792

Ionospheric oxygen ions loss rate in charge exchange reactions with hydrogen, molecular nitrogen and oxygen and atomic oxygen photoionization rate

13 p1953 A72-29811

Charge states and charge-changing cross sections of fast heavy ions penetrating through gaseous and solid media.

19 p2837 A72-37849

Ion-atom scattering and interatomic potentials for ions of noble metals and period II elements incident on neon and argon with energies in the range 8-25 keV.

19 p2837 A72-37883

Evidence for radiative electron capture by fast, highly stripped heavy ions.

23 p3316 A72-44073

Mass spectra stimulated by O+ and Ar+ interacting with a surface.

24 p3378 A72-45312

ION BEAMS

Energy levels and mean life measurements of Cl ions at 500-2800 A using beam-foil spectra technique

02 p0170 A72-12547

Moving plasma beam capture by transverse magnetic field due to polarization space charges electrostatic separation

03 p0396 A72-13657

Depth ionization properties and biological effects of bevatron produced heavy ion beams, discussing utilization in tumor therapy, space biology and radiobiology

03 p0316 A72-13693

Quasi-linear relaxation of fast ion beam in cold plasma moving transverse to magnetic field

04 p0554 A72-14403

Hanle effect mean-life measurements on aligned Ar fast ion beam particles, comparing results with beam-foil measurement

04 p0552 A72-15151

Single collision beam experiments, swarms, Townsend current and capture processes in negative ions

05 p0693 A72-17219

Collisionless relaxation of interpenetrating ion beams in Ar plasma, showing velocity spectrum broadening during Langmuir frequency periods

06 p0853 A72-17394

Nonlinear oscillation amplitude of ion beam due to phase bunching in interaction with plasma electrons

06 p0853 A72-17395

Two body ion-ion neutralization rates measurement by merged beam technique, considering D region reactions

06 p0805 A72-17465

Computerized simulation of high intensity beam charged particle trajectories in electromagnetic fields with rotational symmetry, applying to ion extraction

06 p0852 A72-17491

Thermal noise and ion-acoustic waves excitation in Q machine two beam plasma with high temperature ratio in presence of inhomogeneous B-field, observing instability

06 p0856 A72-17517

Cross-field current driven ion acoustic instability in two plasma devices, causing neutral sheet phenomena, anomalous dispersion and ion heating

[AD-740261]

06 p0858 A72-17541

Numerical model for ion beam instability in nonisothermal plasma with electron temperature much greater than ion temperature

06 p0861 A72-17915

Magnetic and electric field intensities measurement with charged particle beams in coaxial high temperature plasma sources

06 p0863 A72-18415

Electron bombardment ion engines scaling laws, considering electron energy, current density, propellant properties and magnetic flux density

07 p1054 A72-19602

Ion heating in high Mach number oblique collisionless shock waves, noting role of two-ion beam instability from digital simulation

07 p1043 A72-19665

Collisionless ion beam plasma simulation of ionospheric plasma with Langmuir interpretation of density and frequency agreement

07 p1044 A72-20367

Langmuir electron oscillation excitation by ion beam at velocity exceeding average electron thermal velocity in plasma formed by residual gas ionization

07 p1046 A72-20505

Plasma beam cutting of Al sheets, discussing heat effect on surface oxides and microstructure and plasmagentic gas influence

08 p1176 A72-21047

Steady state charged cylindrical electron-ion beam with high current in kinetics model framework, discussing densities proportionality and relativistic factor

09 p1360 A72-22951

Electron, ion and laser beam technology - IEEE Conference, Boulder, Colorado, May 1971

10 p1517 A72-23926

Ion trajectories equations of motion solution for E x B type mass separator, presenting curves for mass species dispersion inside separator channel

10 p1509 A72-23942

Nuclear reaction-produced high energy ion beams for gas laser pumping and output enhancement

10 p1489 A72-23948

Duoplasmatron as negative hydrogen ion source to study geometrical and electrical parameters effects on beam and analyze composition, energy spectrum and emittance

10 p1518 A72-23963

Collisionless thermalization of ion beam by interaction with plasma, noting acoustic instability growth

10 p1524 A72-24921

Radial density profiles and emittance for nitrogen ion beams from Penning-type cyclotron ion source with hot filament

10 p1516 A72-25028

Penning ion source for multiply charged ions high intensity beams generation, describing axial type design with electron focusing magnetic coil

10 p1516 A72-25030

Electron bombardment ion thruster ESKA 18-P thrust measurements by critically loaded columns suspension instrument and simultaneous beam diagnostics by electrostatic probes

11 p1707 A72-26176

Grid translation accelerator system for Kaufman ion thrusters beam deflection, noting response time and accelerated life tests

11 p1710 A72-26211

Nonlinear interactions between synthesized plasma positive and negative ion beams, discussing effect on individual velocity distribution functions

12 p1849 A72-27058

Plasma-ion beam system drift beam instability in longitudinal magnetic field, noting oscillations frequencies dependence

12 p1849 A72-27060

Design and tests of dual deflectable beam strip ion thruster, noting application to two axes satellite attitude control and stationkeeping

[AIAA PAPER 72-494]

13 p2027 A72-28951

Low energy Cs ion beam energy loss during traverse through near-thermal equilibrium Cs plasma as function of plasma density, comparing measurements with theoretical predictions

13 p2011 A72-29000

Dynamic behavior of long-period oscillations of surface wave type in system of inhomogeneous ion beams moving in dense plasma along magnetic field

14 p2136 A72-30307

Solid bodies microanalysis by mass spectrum microscopy based on secondary ion-ion emission, discussing ion source and focusing systems

14 p2104 A72-30449

Neutral atom concentration measurement in Cs ion beam, using high sensitivity detection gate to obtain emission indicatrices

[ONERA, TP NO. 1112]

16 p2434 A72-32862

Plasma-ion beam nonlinear interaction for beam velocity exceeding electrons thermal velocity, noting plasma heating and beam energy dissipation

16 p2440 A72-34154

Magnetic and electric field intensities measurement with charged particle beams in coaxial high temperature plasma sources

17 p2588 A72-34864

Steady state charged cylindrical electron-ion beam with high current in kinetic model framework, discussing densities proportionality and relativistic factor

17 p2593 A72-35880

Production of intense ion beams by high-frequency electric fields.

19 p2839 A72-37331

Solitary waves properties and propagation at right angles to magnetic field in two ion beam magnetized plasma

19 p2841 A72-38441

External high-frequency modulation of an ion beam and the absorption of beam-plasma instability oscillations in a plasma situated in a magnetic field of mirror configuration

21 p3095 A72-41683

An ion-cyclotron instability of a plasma produced by a fast-ion beam

22 p3213 A72-43113

Dynamic behavior of long-period oscillations of surface wave type in system of inhomogeneous ion beams moving in dense plasma along magnetic field
23 p3317 A72-43209

Collisionless heating of plasma ions by an ion beam
23 p3318 A72-43321

Visual perception of accelerated nitrogen nuclei interacting with the human retina.
23 p3256 A72-43940

Nonlinear interactions between synthesized plasma positive and negative ion beams, discussing effect on individual velocity distribution functions
24 p3431 A72-45711

Plasma-ion beam system drift beam instability in longitudinal magnetic field, noting oscillations frequencies dependence
24 p3431 A72-45713

ION CHAMBERS
U IONIZATION CHAMBERS
ION CHARGE

Ionic focusing of electron beam in transverse gas flow, using air, argon and helium
02 p0261 A72-12764

Ion charge composition in plasma-electron beam system in strong longitudinal magnetic field, noting multiply charged ions production under high temperature conditions
05 p0701 A72-17235

Multiple charge Al and C ions X-UV spectra use for studying laser produced plasmas build up and expansion regions
09 p1359 A72-22830

Nickel ion charge sign and magnitude estimation in Ni-Cr alloy by electron transfer method
14 p2116 A72-30415

Charge states and charge-changing cross sections of fast heavy ions penetrating through gaseous and solid media.
19 p2837 A72-37849

ION CONCENTRATION

Ionospheric composition of ions and neutral gases during magnetic storm, using coupled differential equations
01 p0054 A72-10425

Hydrogen ions concentration in dayside region of plasmasphere from OGO 5 satellite mass spectrometry, noting plasmopause position as function of magnetic activity
01 p0061 A72-10892

Sounding rocket spectral measurements of low energy auroral ion composition during premidnight breakup
09 p1300 A72-23020

Chloride ion concentration effect on polarization behavior of Fe-Ni alloy, noting cathodic curve parallel shift in noble potential direction
11 p1652 A72-25290

Electroretinographic illumination potentials dependence on extracellular chloride ion concentration in isolated frog retina
15 p2186 A72-32491

Positive and negative ions relative intensity measurement during nitrous oxide target molecules injection into sonic Ar plasma reaction channel, using quadrupole mass spectrometer
[AIAA PAPER 72-675] 16 p2440 A72-34064

Structure of ion acoustic solitons and shock waves in a two-component plasma.
19 p2841 A72-38440

An investigation of a possible correlation between the laser output of a ruby rod and the chromous ion concentration.
20 p2934 A72-39643

Experimental determination of ion density trapped by electron beam.
21 p3034 A72-41463

Oxygen ion anticorrelation to molecular ion concentrations from OGO 6 observations in F 2 region
22 p3169 A72-42016

The density dependent ionization balance of carbon, oxygen and neon in the solar atmosphere.
23 p3334 A72-43252

Diffusive spreading of weak plasma discontinuities in the presence of two kinds of positive ion
23 p3283 A72-43363

Intracellular potassium in cells of the distal tubule.
24 p3373 A72-45231

ION CURRENTS

Ion-wave current instabilities theory, showing inhomogeneities generated by field aligned currents in collisionless plasma
04 p0559 A72-15350

Balloon measurements of lower stratosphere ion conductivity, noting deviation from predicted values based on Thompson ion-ion recombination theory
06 p0808 A72-18094

High temperature and ZrO₂ ceramic electrolyte effects on ionic partial conductivity and fuel cells longevity
06 p0760 A72-18337

Plasma turbulent heating effectiveness by longitudinal ion current in mirror machine, determining hot ion lifetime and energy distribution function
07 p1039 A72-18913

Continuum plasma turbulent boundary layer structure in shear flow, showing electron to ion saturation currents ratio decrease from laminar case
[AIAA PAPER 72-107] 07 p1040 A72-18953

Diffused electron and ion currents through grid anode of cesium thermionic diode, determining electron temperature and potential distribution in electrode gap
08 p1113 A72-21747

Cs diode discharge current oscillations in Knudsen plasma containing electron and positive ion fluxes from thermionic emission and surface Cs ionization
09 p1361 A72-22960

Plasma ion temperature determination by measuring transient current to cylindrical Langmuir probe under collision free conditions
12 p1851 A72-27399

Qualitative microscopic model for biologic postsynaptic membrane with tunneling chemical bonds, noting selective ionic conductivity as function of electric field
13 p1909 A72-28769

Destabilization and aging mechanisms for ionic conductivity decrease in stabilized zirconia type electrolytes, discussing yttria stabilization
16 p2361 A72-33895

Ion temperature diagnostic using a high power alternating current probe.
17 p2557 A72-35617

Cs diode discharge current oscillations in collisionless Knudsen plasma containing electron and positive ion fluxes from thermionic emission and surface Cs ionization
17 p2593 A72-35889

Solid-body-surface and thin-layer analyses by the static method of secondary-ion mass spectroscopy
18 p2719 A72-36830

Relation between the plasma ion current and the surface defects produced by ruby and neodymium laser emission
19 p2812 A72-38210

Plasma turbulent heating effectiveness by longitudinal ion current in mirror machine, determining hot ion lifetime and energy distribution function
20 p2957 A72-39379

Magnetospheric interactions with topside ionosphere in terms of polar wind ion flows and density related to plasma temperature, F 2 region and cusp observations
20 p2918 A72-39537

ION CYCLOTRON RADIATION

Ion electromagnetic cyclotron modes growth rates in multicompound magnetospheric plasmas, discussing instabilities enhancement
01 p0062 A72-10906

Traveling wave antenna for exciting ion cyclotron waves in cylindrical anisotropic magnetoplasma
02 p0188 A72-11468

Ion transit time in ion cyclotron resonance spectrometer, using combination of pulsed ion formation and time dependent trapping conditions
04 p0523 A72-15484

Anisotropic plasma stability to magnetosonic wave near ion cyclotron frequency propagating almost perpendicular to magnetic field
05 p0698 A72-17017

Weakly damped Alfvén ion-cyclotron waves and fast magnetoacoustic waves in infinite plasma cylinder inserted into current bearing finite coil
07 p1046 A72-20516

Magnetized large volume plasma heating by hf ring field at ion cyclotron frequency
08 p1215 A72-21727

Strong pitch angle scattering of energetic electrons in presence of electrostatic waves due to ion cyclotron instability above midlatitude ionospheric trough region
11 p1714 A72-26398

Dispersion equations for electron and ion cyclotron waves propagating perpendicularly to magnetic field in plasma
13 p2016 A72-29602

Relative cross sections for gas phase photodetachment of electrons from amide and arsenide ions using ion cyclotron resonance spectrometer
13 p1914 A72-30064

Ion-molecule collision frequencies in gases by phase coherent pulsed ion cyclotron resonance spectrometry [ONERA, TP NO. 1071] 14 p2133 A72-30524

Dispersion equations solved for electron and ion cyclotron waves propagating perpendicularly to magnetic field in plasma
21 p3091 A72-40656

Ionospheric refractivity and attenuation surface deformation relationship to ion cyclotron whistlers near cross-over level between zero and critical coupling angles
22 p3168 A72-42006

An ion-cyclotron instability of a plasma produced by a fast-ion beam
22 p3213 A72-43113

Parasitic pitch angle diffusion of radiation belt particles by ion cyclotron waves.
23 p3333 A72-44527

ION DENSITY [CONCENTRATION]
NT IONOSPHERIC ION DENSITY

NT MAGNETOSPHERIC ION DENSITY
NT MAGNETOSPHERIC PROTON DENSITY
NT PROTON DENSITY [CONCENTRATION]

Line radiation from theta pinch with oscillatory ion and electron density applied to solar spectral studies
01 p0106 A72-10098

Flowing plasma ionization density measurement by stagnation probe, comparing measured with calculated plasma sheath convection current values
[AD-738692] 01 p0110 A72-11189

Plasma sheet positive ions flux enhancement detection at lunar distance during lunar eclipse and geomagnetic storm
02 p0283 A72-12452

Single-ended Q machine grid-excited density perturbation and ion wave propagation properties from linearized Vlasov equations
06 p0855 A72-17514

Ion density perturbations propagation through plasma with double-humped Maxwellian ion velocity distribution in single-ended Q machine
06 p0855 A72-17515

Spectrographic measurement of electron temperature and ion density profiles in cesium plasma thermionic converter
06 p0862 A72-18309

Thermal positive ion densities measurement in outer ionosphere and magnetosphere by OGO 1 satellite, relating plasmopause distribution and magnetic activity level
[AD-742186] 09 p1300 A72-23011

Multipole magnetic field configuration effectiveness in electromagnet plasma trap, discussing electron losses critical angle and captured ions maximum density
09 p1363 A72-23221

Atmospheric electricity problems, considering air pollution effects on ion concentration and air conductivity and solar activity effects on ionosphere-earth potential difference
10 p1473 A72-24528

Quasi-steady operation establishment in pulsed MPD arc jet, investigating ion density radial distribution and initial tank pressure and magnetic field effects on plasma front arrival
[AIAA PAPER 72-496] 11 p1696 A72-26219

Ionospheric disturbances relation to interplanetary positive ion and proton fluxes intensity and velocity from Mariner 2, Venus 3 and Vela 2 observations, discussing F 2 region
11 p1713 A72-26268

Artificial barium ion cloud spatial-temporal growth in ionosphere, solving ion diffusion equation by numerical methods
13 p1950 A72-29387

Solar X-ray spectral lines at 1-60 Å from coronal ion relative abundances obtained from Jordan ionization equilibrium calculations
13 p2034 A72-29940

Hydrogen plasma ion density determination from atomic beam attenuation by resonant charge exchange with protons
15 p2284 A72-31582

Annual variations of singly charged positive He ion density distribution in solar wind from Vela 3 observations
15 p2299 A72-31944

Ion density and electron acceleration region location from satellite-borne solar flare X-ray measurements
15 p2302 A72-32790

Mathematical model for atmospheric ions density fluctuation with time, noting absence of oscillating solutions
16 p2386 A72-33652

Plasma velocity, ion density and electrical conductivity from electron density and temperature and electromagnetic field profile measurements in Ar plasma inverse pinch
19 p2841 A72-38437

Measurement of ion parameters of a cesium plasma with the help of a grid probe with a cooled collector
22 p3211 A72-42645

ION DISTRIBUTION

Potential and ion charge distribution in proximity to conducting sphere moving in low density collisionless ion-electron plasma
01 p0109 A72-10371

Three body ionic recombination as Markov process, deriving ion pairs quasi-equilibrium distribution equation identical to Bates-Flannery statistical theory
01 p0104 A72-10860

F 1 region ion structure during ionospheric magnetic disturbances by numerical simulation of quiet and disturbed conditions based on electron concentration profiles
05 p0656 A72-16247

Oxygen ions vertical flux altitude distribution in F layer from incoherent scatter radar measurements, noting existence in protonosphere during daytime [AD-737929] 05 p0629 A72-16616

Ion distribution function oscillations in first order ionic waves of single ended Q device, noting plasma confinement in static magnetic field
06 p0855 A72-17507

Non-Maxwellian plasma response to acoustic wave propagation in single ended Q device, investigating ion distribution function

06 p0855 A72-17509

Pseudowaves and ion acoustic waves simulation, calculating time evolution of ion distribution for oscillating negative plasma potentials applied at grid

06 p0855 A72-17512

Wake behind obstacle immersed in plasma flow of single ended Q-machine, using experiment as diagnostic of ion distribution function

06 p0856 A72-17526

Hf instability on whistler branch of finite pressure plasma with nonmonotonic ion distribution function under Landau damping effect

07 p1042 A72-19615

Lower F 2 region positive oxygen ion distribution with allowance for vertical motions, production and recombination processes, using atmospheric models

08 p1152 A72-20705

Multiple charge Al and C ions X-UV spectra use for studying laser produced plasmas build up and expansion regions

09 p1359 A72-22830

Ferries electrical conductivity variations with time caused by cations distribution modification after cooling

10 p1525 A72-24121

Magnetospheric electrons precipitation into ionosphere due to conjugate conductivity asymmetry caused by wind induced ions vertical redistribution, using atmospheric model

10 p1530 A72-24791

Linear antenna in anisotropic plasma with ion depletion, calculating reactance change due to surrounding dielectric layer thickness

11 p1593 A72-25949

Apollo 14 basaltic rocks cooling deduced from divalent Mg and Fe ionic distribution in pyroxene, noting process interruption below 840 C

11 p1724 A72-26574

Vertical distribution of atomic nitrogen ions in F region produced by dissociative photoionization and charge transfer, suggesting undiscovered source at 300 km altitude

13 p1954 A72-29815

Kinetic equation of repeatedly ionized plasma from hyperbolic diffusion method, calculating direct transitions between excited ion states

13 p2008 A72-29895

Potassium, sodium and calcium ion distribution in skeletal muscle subcellular organelles, discussing lipid, protein and nucleic acid binding

14 p2076 A72-30670

Atmospheric stratification, wind profiles and vertical density distribution of ions and neutral particles determined by rocket sounding

15 p2228 A72-31968

Excess white noise source in photomultiplier as function of temperature from voltage, intensity and ion pulse measurements, noting effect on photon counting statistics

15 p2207 A72-32238

Experimental evidences for a transient ion layer formation in connection with sudden ionospheric disturbances in the height range 20-50 km

17 p2545 A72-34630

Lower F 2 region positive oxygen ion distribution with allowance for vertical motions, production and recombination processes, using atmospheric models

19 p2790 A72-38333

Dissociation of molecular ions formed by charge exchange in an in-line tandem mass spectrometer

19 p2763 A72-38801

Metal ions effect on sporadic E layer formation, noting magnesium ions profile redistribution by vertical gradient in neutral particles wind

23 p3284 A72-43376

Circularly polarized waves in magnetoplasmas containing negative ions

23 p3323 A72-44533

O/plus/ H/plus/ and He/plus/ ion distributions in a new polar wind model

24 p3400 A72-45587

Plasma produced by laser irradiation of solid targets as a source of highly stripped ions

24 p3430 A72-45603

ION EMISSION

Intermittent ion emission enhancement from tungsten surface in He-W field-ion microscope upon Ne addition to imaging gas

04 p0552 A72-14547

Energy spectra of positive ion bursts on lunar night side from Apollo 12 and 14 Alsep suprathermal ion detectors data

06 p0872 A72-17462

Emission characteristics of relativistic charge in rectilinear motion within gravitational wave field

08 p1206 A72-21072

Secondary molecular ion emission of Li as function of atoms number

11 p1701 A72-26506

Local emission coefficients fields for ionized gas in arbitrary and rectangular cross section streams

13 p2008 A72-29894

Solid bodies microanalysis by mass spectrum microscopy based on secondary ion-ion emission, discussing ion source and focusing systems

14 p2104 A72-30449

Energy level population and emission spectrum of C IV ion in planetary nebula with radiative excitation

16 p2458 A72-33688

Investigation by the method of secondary ion-ion emission of the initial phase of the formation process of a silver vacuum condensate on a nickel substrate

21 p3068 A72-40960

ION ENGINES

One millipound colloid thruster power conditioning and control system design, presenting circuit diagrams, fault protection efficiency and high voltage transformer

01 p0009 A72-11070

Maximum propellant utilization in electron bombardment ion thruster for space applications

04 p0564 A72-14432

Kaufman thruster ion sources, discussing refractory metal, oxide coated, liquid mercury and hollow cathodes design, performance and durability

04 p0564 A72-14433

Mercury electron bombardment ion thrusters research program, discussing mission requirements, size, propulsion type and beam current range

04 p0565 A72-14434

Electrostatic surface and bulk ionization ion thrusters current densities for propulsive and working fluid utilization efficiency

05 p0705 A72-16772

Optical radiation from plasma discharge of electron bombardment mercury ion thruster, discussing electron temperature and primary electron fraction

[AIAA PAPER 72-205]

05 p0706 A72-16851

Ion engine performance optimization by power sharing with secondary batteries on synchronous equatorial satellites

05 p0706 A72-16852

Hollow cathode neutralizer for electron bombardment ion thruster, discussing performance from SERT II flight

05 p0706 A72-16853

Electrostatic rf ion thruster development, including power conditioning and control units

07 p1054 A72-19600

Electron bombardment ion engines scaling laws, considering electron energy, current density, propellant properties and magnetic flux density

07 p1054 A72-19602

Critical magnetic flux indications of microanomalous plasma diffusion in electron bombardment ion engines

07 p1054 A72-19614

Ar plasma in ion engine discharge chamber with primary and Maxwell electron bombardment, discussing ion production probabilities in perturbed and unperturbed cases

08 p1223 A72-21209

Electron bombardment SERT II ion thruster operation using Xe, Kr, Ar, Ne, He, nitrogen and carbon dioxide

10 p1528 A72-23964

Current flow across double layer plasma in SERT 2 type hollow cathode ion thruster, using Langmuir probes

[AIAA PAPER 72-418]

11 p1706 A72-26168

Hollow cathode discharge effects on throttled electron bombardment ion thruster performance, considering discharge region diameter and length and baffle aperture area

[AIAA PAPER 72-421]

11 p1706 A72-26169

Space simulation facility for one year SERT 2 mercury ion thruster testing, discussing cryogenic operation and electrical and thermal insulation

[AIAA PAPER 72-430]

11 p1613 A72-26174

Electron bombardment ion thruster ESKA 18-P thrust measurements by critically loaded columns suspension instrument and simultaneous beam diagnostics by electrostatic probes

[AIAA PAPER 72-433]

11 p1707 A72-26176

ATS F ion thruster system for north-south station-keeping, discussing specific impulse, thrust vectoring, propellant system and power conditioning circuitry

[AIAA PAPER 72-439]

11 p1707 A72-26180

Optical radiation from Hg bombardment ion thrusters downstream regions due to excited atoms radiative decay, examining exhaust interference with star tracker

[AIAA PAPER 72-441]

11 p1707 A72-26182

Electric propulsion spacecraft design for ion thruster systems testing with circular solar cells array as gyroscopic stable platform

[AIAA PAPER 72-466]

11 p1578 A72-26200

RF ion thruster flight prototype development, describing test facilities, design and performance

[AIAA PAPER 72-471]

11 p1709 A72-26202

Plasma diagnostics of inductively coupled RF Hg discharge in RIT-10 ion thruster

[AIAA PAPER 72-472]

11 p1709 A72-26203

RF ion microthruster discharge vessel and plasma holder material investigation, considering quartz, boron nitride and aluminum oxide

[AIAA PAPER 72-473]

11 p1709 A72-26204

RF ion thruster for spacecraft propulsion, discussing tests and digital computer calculations to optimize design parameter

[AIAA PAPER 72-474]

11 p1709 A72-26205

Ion thruster performance calibration investigating double ion content, back ingestion, beam spreading and propellant flow rate

[AIAA PAPER 72-475]

11 p1709 A72-26206

Grid translation accelerator system for Kaufman ion thrusters beam deflection, noting response time and accelerated life tests

[AIAA PAPER 72-485]

11 p1710 A72-26211

Dished accelerator grids design, fabrication and operation in electron bombardment ion thruster, studying ion extraction capability and discharge chamber performance

[AIAA PAPER 72-486]

11 p1710 A72-26212

Design and performance characteristics of ion thruster feed system components including high voltage isolator, liquid Hg flowmeter and W vaporiser

[AIAA PAPER 72-487]

11 p1710 A72-26213

Electron bombardment ion thruster performance characteristics with variable magnetic baffle and hollow cathode

[AIAA PAPER 72-489]

11 p1710 A72-26214

Ion thruster development for Communications Technology Satellite, discussing synchronous orbit stationkeeping requirements, thrust vector control and mounting positions

[AIAA PAPER 72-491]

11 p1711 A72-26216

Electric propulsion systems assessment for military spacecraft, discussing ion, colloid, pulsed and quasi-steady plasma thrusters

[AIAA PAPER 72-493]

11 p1711 A72-26217

Cs contact ion microthrusters, neutral fraction measurements, analytical methods and testing procedures

[AIAA PAPER 72-495]

11 p1711 A72-26218

Communication satellites design and technology for future launchings, discussing ion engine development, antenna beams and thermal control

[AIAA PAPER 72-540]

12 p1780 A72-27363

Canada-NASA communications technology satellite /CTS/ for 12 and 14 GHz TV transmission, considering mission profile, spacecraft design, attitude control system and ion thruster

[AIAA PAPER 72-580]

12 p1877 A72-27382

Computer aided thermomechanical design of mercury bombardment ion thrusters, involving heat transfer, vibration and stress analysis

[AIAA PAPER 72-431]

12 p1860 A72-27420

Lifetime limitations of ion extraction systems for electron bombardment ion thrusters due to sputter erosion of electrode by ion beam

[AIAA PAPER 72-477]

12 p1860 A72-27421

Ion thruster module design for primary electric propulsion systems, discussing optical configurations, discharge chamber, control and performance tests

[AIAA PAPER 72-508]

12 p1860 A72-27423

Prime 30 cm ion thruster power conditioning and control system development, integration and testing

[AIAA PAPER 72-509]

12 p1860 A72-27424

Argon and mercury ion engines operation, performance and control, evaluating safety and ease of handling from laboratory test data

13 p2026 A72-28931

Model for mercury vapor electron bombardment ion thruster hollow cathodes operation and effects on thrust subsystem performance predictability

[AIAA PAPER 72-420]

13 p2026 A72-28936

Hg flow and hollow cathode temperature effects on ion thruster neutralizer stability and lifetime capability, using bell jar tests

[AIAA PAPER 72-422]

13 p2026 A72-28937

Hg fed hollow cathode ion thruster thermal and plasma heating characteristics, using Wiener-Kalman filtered temperature measurements

[AIAA PAPER 72-476]

13 p2027 A72-28947

Radial magnetic field geometry for total ion utilization in Kaufman thrusters, noting uniform current density and plasma generation and high electrical efficiency

[AIAA PAPER 72-481]

13 p2027 A72-28948

Variable magnetic baffle as control device for Kaufman electron bombardment ion thrusters with hollow cathode

[AIAA PAPER 72-488]

13 p2027 A72-28949

Structurally integrated ion thruster /SIT-5/ for synchronous satellites attitude control and station-keeping, presenting design and performance data

[AIAA PAPER 72-492]

13 p2027 A72-28950

Design and tests of dual deflectable beam strip ion thruster, noting application to two axes satellite attitude control and stationkeeping

[AIAA PAPER 72-494]

13 p2027 A72-28951

Characteristics of nonredundant auxiliary and prime propulsion power processors for electron bombardment ion thruster in communication satellites, discussing modular transistorized and SCR systems

[AIAA PAPER 72-518]

13 p2027 A72-28980

Mission operations for unmanned nuclear electric propulsion outer planet exploration with a thermionic reactor spacecraft

17 p2606 A72-34578

Thermionic reactor system for auxiliary power and electric propulsion.

17 p2494 A72-34579

Thermionic reactors design based on flashlight and external fuel concepts for nuclear electric propulsion

17 p2494 A72-34580

Constant voltage and constant emitter-temperature control schemes dynamics in thermionic reactor, showing closed loop responses to load changes, converter failures and reactivity perturbations

17 p2494 A72-34581

Thermionic reactor power conditioner design for nuclear electric propulsion.

17 p2495 A72-34582

Design features, fabrication technology and in-pile testing of thermionic reactor fuel elements

17 p2495 A72-34584

Sizing an external-fueled in-core thermionic reactor.

17 p2495 A72-34588

Development of the insulating multilayer collector system for ITR/Status report/.

17 p2559 A72-34594

Electrostatic surface ionization and electron bombardment ion thrusters current densities for propulsive and working fluid utilization efficiency

17 p2597 A72-35275

Ion-thruster propellant utilization.

17 p2597 A72-35490

Effect of neutron spectra on the swelling of ceramic insulators and implications for thermionic reactor design.

18 p2703 A72-36146

Investigations concerning metal-hydride technology and hydrogen transport in the incore thermionic reactor /ITR/-core.

18 p2699 A72-36157

Thermionic reactor electric propulsion system requirements.

18 p2720 A72-36167

Auxiliary power and electric propulsion applications of the thermionic reactor power systems in manned and unmanned space missions

18 p2644 A72-36168

Controlled dc to dc converter for a space-qualified thermionic-reactor.

18 p2644 A72-36170

High-voltage thermionic reactor using double-sheath fuel elements.

18 p2644 A72-36171

Electronic temperature-flattening of thermionic reactors.

18 p2644 A72-36172

Closed loop dynamics of in-core thermionic reactor systems.

18 p2644 A72-36173

Dynamics and control of an incore-thermionic-reactor in the power region.

18 p2644 A72-36174

Aspects on the modular lay-out of incore thermionic reactors.

18 p2645 A72-36175

Completely modular thermionic reactor ion propulsion system /trips/.

18 p2721 A72-36177

Significance of the results of the ITR critical experiments for the calculation of an incore-thermionic reactor.

18 p2645 A72-36180

A comparison of thermionic reactor designs employing a common thermionic fuel element.

18 p2645 A72-36183

Feedback synthesis of an incore thermionic reactor control system for space.

18 p2645 A72-36186

Control of the incore thermionic reactor /ITR/ by movable reflector elements.

18 p2645 A72-36189

Developmental status of thermionic materials. [GULF-GA-A12128]

19 p2833 A72-38575

Mercury Hall ion engine principles and design, discussing plasma ion acceleration, mercury evaporation and ionization and acceleration channel electrical and thermal insulation

20 p2963 A72-39937

Thermionic reactor systems for space applications.

24 p3423 A72-45177

Low thrust constant acceleration trajectories for a Mercury orbit.

24 p3441 A72-45208

Electrostatic ion propulsion engines development for near-earth and interplanetary space missions, noting payload increase and flight time reduction capabilities

24 p3434 A72-45278

ION EXCHANGE MEMBRANE ELECTROLYTES

Solute rejection in hyperfiltration of sodium chloride and urea with porous glass ion exchange membrane as function of pressure, temperature and concentration

07 p0937 A72-20601

Exchange diffusion process contribution to human red blood cell transmembrane cation movement from sodium tracer influx studies

15 p2187 A72-32746

Biomembrane hydration mechanism of Na-K ion pump of living cell based on fractionation at air-sea interface

18 p2649 A72-36441

ION EXCHANGE RESINS

Water disinfection by Ag coated filters obtained by silver nitrate reduction with ascorbic acid, hydroquinone, formaldehyde and sodium tartrate activated carbon and ion exchange resin surfaces

05 p0622 A72-16637

ION EXCHANGING

Newton cooling law applicability to unsteady heat and mass transfer approximate calculation for ion exchange process

09 p1412 A72-23685

ION EXTRACTION

High resolution RF linear mass spectrometer for separation of ions formed by electron impact on organic molecules

01 p0064 A72-10043

Primitive earth model of ion selective enzymatic asymmetric synthetic membrane for accelerated nutrients and metabolites transfer studies

04 p0469 A72-14787

Lifetime limitations of ion extraction systems for electron bombardment ion thrusters due to sputter erosion of electrode by ion beam [AIAA PAPER 72-477]

12 p1860 A72-27421

ION GAGES

U IONIZATION GAGES

ION IMPACT

High stability and power IMPATT oscillator design for line-of-sight communication links, avoiding spurious resonances and mode jumping

01 p0037 A72-10645

Voltage and current waveforms monitoring on sampling oscilloscope for TRAPATT microwave oscillator performance optimization

01 p0038 A72-10653

Hybrid IC at 30 GHz, considering IMPATT oscillators, circulators, frequency multipliers and filters configuration and performance

01 p0046 A72-10699

Gunn and IMPATT diodes applications for microwave power oscillators and amplifiers in radio link equipment

01 p0042 A72-10711

IMPATT driven pumps replacement of klystron for parametric amplifiers producing over 100 mW at 38-40 GHz with good stability and noise performance

06 p0788 A72-18470

GaAs IMPATT diodes performance improvement, describing fabrication methods to achieve 6.7 watts output at 15 percent efficiency

06 p0789 A72-18474

Differential sputtering yield of Ni-Cu alloy solid solution bombarded by Ar ions

10 p1495 A72-24057

Cesium contact ion thruster, investigating carburized thoriated tungsten filaments electron emission under ion bombardment [AIAA PAPER 72-440]

11 p1707 A72-26181

Ion bombardment and partial discharges effects on polyethylene sheet, observing structural changes by IR spectroscopy

13 p1984 A72-29788

EHF double-drift IMPATT oscillator small and large signal behavior analysis with computer program, noting second harmonic tuning and single frequency operation possibilities

15 p2204 A72-31314

Surface damage induced by ion bombardment of monocrystalline W and Mo, determining degradation rate dependence on collisional energy transfer

15 p2276 A72-31853

Novel and accurate methods for measuring small-signal and large-signal impedances of IMPATT diodes.

18 p2664 A72-35997

ION INJECTION

Pseudowave front spreading at leading edge of plasma slab during injection at high velocity into denser background plasma

02 p0265 A72-12364

Plasma beams injection into toroidal magnetic field along gradient or radius, using polarizational interaction

03 p0396 A72-13658

Trapped He, Ne and Ar isotopic variations presence in meteorites due to rare gas ions implantation by solar wind and flares

09 p1385 A72-22599

Ion implantation doping of MOSFET and IC for wafer production, using automatic vacuum pumpdown and cycle control

10 p1447 A72-23950

Toroidal plasmas heating by neutral injection, discussing ion acceleration, charge exchange and fast ion trajectories

11 p1697 A72-26582

Irradiation produced defects and electrical properties of n and p-type Si, discussing radiation damage due to neutron and ion implantation

12 p1857 A72-28058

A field-ion microscope study of ion-implantation in iridium. I, II.

18 p2719 A72-36747

Characteristics of P-channel MOS field effect transistors with ion-implanted channels.

24 p3385 A72-44981

ION IRRADIATION

NT DEUTERON IRRADIATION

NT PROTON IRRADIATION

Excited state and electron densities in noble and atmospheric gas plasmas created by alpha particle induced ion irradiation, discussing plasma kinetic processes and superimposed electric field effects

01 p0112 A72-11335

High purity W ion irradiated in situ under ultrahigh vacuum at high temperature, examining depleted zone defect structure by field ion microscope

02 p0242 A72-11909

Single crystal Si defect accumulation and transition to amorphous state under Xe, Ar, Ne, O and P ion irradiation, using EPR

02 p0269 A72-12884

Low energy He ion bombardment effects on Ni alloy single crystal surface, observing defect structure with stacking faults, tangled dislocations and carbide precipitation

04 p0533 A72-15159

Dislocation loops in thin W foil due to ion irradiation, using electron microscopic analysis

09 p1331 A72-23505

Radiation damage in bcc metal Mo and W foils under energetic Au ion irradiation, noting vacancy dislocation loops

09 p1331 A72-23506

Lunar surface darkening caused by solar wind effect, noting Fe valence state changes evaluation from photoelectron spectroscopy of foil samples exposed to ion bombardment

09 p1394 A72-23665

Ion implantation for varicaps and p-n-p bipolar transistors fabrication, examining implanted impurities profiles

10 p1449 A72-24285

Spacecraft thermal control coating damage by energetic Hg ion bombardment, using absorbance measurements [AIAA PAPER 72-445]

11 p1746 A72-26183

Lattice disorder effects in ion implanted Si and compound semiconductors, using IR and EPR measurements

12 p1859 A72-28074

Lattice damage measurement of Cd ion implanted GaAs semiconductors by optical reflection and scanning electron microscope

12 p1859 A72-28075

Surface damage equations for heavy ion irradiated Si and GaAs single crystals in terms of incident fluence

13 p2020 A72-28430

Low energy electron diffraction structures due to CO and oxygen adsorption on clean Re surfaces produced by Ar ion bombardment at 20 to 920°C

13 p2020 A72-28522

Energetic Hg ion bombardment erosive and chemical effects on spacecraft surfaces downstream of electrostatic rockets

13 p1983 A72-28944

The vapor deposition of high work function materials in a gas discharge.

18 p2656 A72-36149

Thin films deposited by evaporation and sputtering - A comparative study

18 p2696 A72-36834

Visual perception of accelerated nitrogen nuclei interacting with the human retina.

23 p3256 A72-43940

ION MICROSCOPES

Intermittent ion emission enhancement from tungsten surface in He-W field-ion microscope upon Ne addition to imaging gas

04 p0552 A72-14547

Ordered Cu-Au alloy atomic order parameters, using field ion microscopy

04 p0560 A72-14548

Two mechanism model for anomalous field ion microscope images in W, noting end form difference in high and low evaporation rates

09 p1370 A72-22803

Ti crystallographic and topographical features determination by hydrogen-ion microscopy, noting temperature effects on surface films and low index facets production

09 p1327 A72-22805

Field-ion microscopy as experimental metallurgical technique for metal surface atomic structure studies, discussing image formation, ionization and field evaporation

16 p2392 A72-33444

A field-ion microscope study of ion-implantation in iridium. I, II.

18 p2719 A72-36747

Image point formation in field ion microscopy of metal surfaces, using atom probe detection of noble gas apex adsorption

21 p3050 A72-40086

- Field-ion microscopic study of the interstitial plasticity of tungsten single crystals
23 p3304 A72-44484
- ION MOTION**
Electron and ion drift rate effect on floating double probe characteristics in Maxwellian plasmas
02 p0266 A72-12768
Ion transit time effects on plasma sheath RF admittance, using equivalent circuits for representation in low and high frequency ranges
03 p0394 A72-13150
Ions acceleration during current passage through plasma, discussing maximum energies, threshold current and electron beam flux density
03 p0396 A72-13661
Nonuniform sinusoidal electric field anomalous influence on ion motion in gas with allowance for ion-atom collisions
04 p0547 A72-14622
Wave exciting grid-plasma interaction in single ended Q device, determining ion velocity distribution function
06 p0855 A72-17510
Spontaneous collisionless drift waves due to pressure gradient in hydrogen plasma column, studying magnetic field and reflecting conditions effects
06 p0857 A72-17534
Collisionless drift waves in thermally ionized Li plasma column under variable shear magnetic field
06 p0857 A72-17535
Electrostatic energy analyzer for local ion velocity distribution function measurement in double ended Q machine plasma column
06 p0814 A72-17551
Metallic ion convergent flow role in sporadic E layer formation in auroral and equatorial ionosphere
06 p0810 A72-18730
Ion-electron collisions effect on ion cloud motion in magnetoactive plasma immersed in uniform external electric field
07 p1055 A72-18894
Ionic winds with restricted entrainment and gauze electrode, considering diffusion flame aeration in combustion systems
07 p1037 A72-19372
Plasma rotation during theta pinch collapse, determining ion azimuthal velocity from fields and pressure gradient measurements via Ohms law
08 p1213 A72-21255
Aspiration condenser spectrometry of small ion mobility as function of height and atmospheric conditions
09 p1346 A72-23267
Ion acceleration by relativistic electron-beam-formed plasma, explaining ion energy dependence on neutral gas pressure by potential well model
10 p1518 A72-23961
Momentum transfer theory for ion drift velocity in multicomponent gas mixture at arbitrary electric field strengths
10 p1519 A72-24096
Electron density maxima position relationship to wind profiles in sporadic E layer with electric fields and vertical ion motion
10 p1530 A72-25165
I.F. oscillations due to drift-diffusion of current free weakly ionized inhomogeneous plasma in magnetic field
12 p1850 A72-27128
Weak ion-acoustic quasi-shock wave propagation in collisionless plasma, determining long time behavior of precursor ion stream reflected by electrostatic potential
13 p2012 A72-29125
He ions motion normal to magnetic field under induced electric field, analyzing resonance mechanism
13 p2016 A72-29606
Burgers binary and Shkarofsky multiple collision theory numerical application to electrical conductivity in partially ionized solar magnetoplasma
13 p2018 A72-29714
Multiply charged ions motion velocity measurement for pulsed discharge plasma in nitrogen, krypton and xenon
14 p2139 A72-30777
Ionospheric ion temperatures and velocities and electron and neutral densities from incoherent scatter observations during 11 February 1969 magnetic storm
15 p2229 A72-32254
Finite beta plasma drift cone instability relationship to mirror ratio and plasma temperature changes
15 p2288 A72-32422
Geomagnetic field line tracing by plasma clouds produced by Ba vapor release, noting different ion drift rates and directions
16 p2384 A72-32977
Motion of ion-cloud in the ionosphere, field-aligned cloud with Gaussian distribution of ionization density.
17 p2546 A72-35060
Electron beam focusing by ions in transverse gas flows, considering air, argon and helium residuals
20 p2952 A72-39070
He ions motion normal to magnetic field under induced electric field, analyzing resonance mechanism
21 p3091 A72-40660
- Height structure of tidal winds as inferred from incoherent scatter observations.
22 p3169 A72-42014
Instability of a magnetically active plasma in the presence of a specified transverse velocity of the ions
24 p3429 A72-45488
- ION OSCILLATION**
U PLASMA OSCILLATIONS
ION PROBES
Supersonic and subsonic measurements of mesospheric ionization at night, using Arcas rocket parachute borne nose-tip and blunt probes
09 p1296 A72-22362
Ion and laser microprobes for concentration measurements of hot salt stress corrosion produced hydrogen on Ti alloy on microscopic scale
09 p1276 A72-23477
Determination of the velocity field of the wake of a hypersonic sphere with the aid of ion probe arrays
21 p3057 A72-41725
- ION PRODUCTION RATES**
Ion production rates during electron-flux-atmosphere interactions based on atmospheric models with different energy and angular distributions
01 p0059 A72-10597
Ionospheric ion formation and neutralization reaction rate coefficients determination by fitting measured electron concentration profiles with computer generated profiles
01 p0059 A72-10616
Nonequilibrium effects on ionization growth in molecular hydrogen, tabulating experimental data for comparison with Monte Carlo computation
02 p0267 A72-12793
Associative attachment and gas-to-particle conversion mechanisms in positive and negative ion formation up to 50 km
03 p0347 A72-13390
Ionospheric ion-molecule and ion-electron reaction rate constants determination from nighttime flight of rocket-borne ion mass spectrometer data least square fitting
03 p0347 A72-13396
D region ion and electron density rocket measurement during sunrise, discussing negative ion electron affinity and ion production functions
03 p0347 A72-13397
Compressible turbulent boundary layer equations for flow on B wall of MHD accelerator, including electron thermal nonequilibrium and finite rate ionization
03 p0397 A72-13923
Effective cross sections for charged and excited particles formation from He, Ne and Ar ion collisions with CO molecules, using mass spectrometry
03 p0393 A72-14065
Excitation and ionization cross sections and rate coefficients of hydrogen-like ions by electron and proton impact in Bethe-Born approximation
06 p0852 A72-18052
Recombination coefficient, ionization rates and average lifetime of ions in rarefied carbon-air flames, investigating pressure and additives effects
06 p0904 A72-18213
Negative hydrogen ion production during charge exchange between protons in thick Li, Na, K and Mg vapor jets
06 p0863 A72-18410
Methanol and formaldehyde photoionization by UV irradiation, determining ion yields as function of wavelength by mass spectrometric analysis
07 p1038 A72-20498
F 2 region magnetic disturbances conjugacy mechanisms, considering vertical ionization profiles
08 p1155 A72-20801
Auroral charged particle fluxes electrodynamic interaction with atmosphere, determining ion formation rate and electron concentration and conductivity
08 p1155 A72-20804
Ar plasma in ion engine discharge chamber with primary and Maxwell electron bombardment, discussing ion production probabilities in perturbed and unperturbed cases
08 p1223 A72-21209
Diatomic oxygen and carbon dioxide density profiles effects on photoionization rates in D region [AD-741091]
09 p1274 A72-22356
Nighttime D region ionization production by cosmic X rays from various celestial sources and galactic background
09 p1375 A72-22359
D and F regions positive ion chemistry based on E and F regions ion-molecule reaction rate constants comparison with laboratory measurement
09 p1275 A72-22360
Oxygen, nitric oxide and water cluster positive ion composition from mass spectrometer experiments in lower ionosphere, noting ion production and low temperature effects
09 p1375 A72-22363
Room temperature reactions involving ionospheric cluster ions, discussing rate constants measurement by stationary afterglow and drift tube facilities
09 p1275 A72-22367
- Laboratory ionization chamber measurement of ion chemistry and production rates from partial simulation of disturbed nighttime ionosphere at 300 K
09 p1275 A72-22368
Plasma emitter shape determination in accelerating electric field for charged particle flux production
09 p1358 A72-22490
NO ion production rate in D region in relation to electron densities
09 p1300 A72-23027
Cosmic ray ionization rate for hydrogen calculated for ambipolar diffusion efficiency in decoupling magnetic flux from gas during cloud collapse with angular momentum
10 p1544 A72-24664
Lower ionospheric structure, discussing electron production, loss and transport effects and diurnal variations
10 p1473 A72-24703
Magnetic mirrors for highly stripped heavy ions production in hot electron plasmas by low voltage high current electron beam
10 p1524 A72-25035
Hydrogen, deuterium, helium, nitrogen and argon ion production and acceleration by intense pulsed relativistic electron beam
10 p1517 A72-25037
Wind shear and midlatitude sporadic E layer theories, discussing metal ions production and loss
10 p1477 A72-25158
Electrostatic ion thruster theoretical model, deriving ionization rate density as function of discharge current
[AIAA PAPER 72-432]
11 p1707 A72-26175
Electron temperature determination from rate of ionization due to collisions between electrons and neutral particles in plasma
11 p1697 A72-26586
Energy spectra of multiply charged ions formed in laser beam interaction with plasma, noting recombination process role
12 p1849 A72-27065
Solar cosmic rays spectrum and geomagnetic cut-off rigidity determination from ion production rates in lower ionosphere
14 p2147 A72-30627
Ion pair production rate and electron number density in ionospheric D region from ground based and rocket measurements, discussing two ion model
15 p2229 A72-32252
Ion chemistry and heating of daytime ionosphere E and lower F regions, calculating neutral atmosphere densities, ion production rates and solar EUV radiation absorption
15 p2192 A72-32253
Solar activity effects on integrated ion production rates at sunrise using atmospheric model
15 p2301 A72-32266
Plasma emitter shape determination in accelerating electric field for charged particle flux production
17 p2588 A72-34653
Collisional excitation and impact ionization coefficients of hydrogen
19 p2837 A72-37807
Nature of ion generation during the action of laser emission on a solid body
19 p2811 A72-38193
Electron attachment and compound formation in flames. V - Negative ion formation in flames containing chromium and potassium.
22 p3244 A72-42717
The ionization of caesium vapour by the method of space charge amplification.
23 p3316 A72-44344
Formation and loss of O₂⁺ and O₄⁺ ions in krypton-oxygen afterglow plasmas.
23 p3316 A72-44345
A theoretical model of the ionosphere dynamics with interhemispheric coupling.
24 p3400 A72-45588
Energy spectra of multiply charged ions formed in laser beam interaction with plasma, noting recombination process role
24 p3431 A72-45718
- ION PROPULSION**
Vaporizer temperature effect on ion propulsion system thrust vector, presenting temperature control loop circuit diagram
10 p1528 A72-24652
Langmuir probe techniques for plasma measurement in ion thruster hollow cathode discharge configurations
[AIAA PAPER 72-416]
11 p1706 A72-26166
Electrostatic ion thruster ESKA 28 for interplanetary missions, calculating earth escape and optimal transfer orbits
[AIAA PAPER 72-434]
11 p1707 A72-26177
French R and D work on ion propulsion systems for communication satellite stabilization, discussing principal characteristics, mathematical modeling, design and economic problems
[AIAA PAPER 72-437]
11 p1727 A72-26179
Propulsion system based on ion tunneling through preferentially oriented metal crystal lattice
[AIAA PAPER 72-480]
11 p1710 A72-26208

Ion-thruster propellant utilization.
17 p2597 A72-35490
Completely modular thermionic reactor ion propulsion system /trips/.
18 p2721 A72-36177

ION PUMPS
IMPATT driven pumps replacement of klystron for parametric amplifiers producing over 100 mW at 38-40 GHz with good stability and noise performance
06 p0788 A72-18470
Prepumped systems with ion sorption and titanium sublimation vacuum pumps for ultrahigh vacuum production
07 p0914 A72-19906
Quadrupole ion pump performance characteristics, presenting pumping speed as function of pressure at different peak voltages
12 p1805 A72-27040

ION RECOMBINATION
Three body ionic recombination as Markov process, deriving ion pairs quasi-equilibrium distribution equation identical to Bates-Flannery statistical theory
01 p0104 A72-10860
Interstellar matter cooling and recombination after supernova ionization, comparing X ray and cosmic ray heating mechanisms
07 p1070 A72-19083
Lower F 2 region positive oxygen ion distribution with allowance for vertical motions, production and recombination processes, using atmospheric models
08 p1152 A72-20705
D region negative ion reaction schemes, discussing reaction rates of nitrogen dioxide with hydrogen
09 p1275 A72-22592
Radiative transition probabilities and recombination coefficients of ion C IV
09 p1354 A72-22664
Mathematical model of ion capture and annihilation by aerosol particles from ground level to 60 km
09 p1346 A72-23266
Absorbing sphere model for ion-ion recombination upper limit thermal energy reaction rate and total cross section energy dependence
10 p1515 A72-24342
F region plasma one dimensional nonisothermal diffusion for positive ions with allowance for ionization and recombinations and gravitational forces
15 p2232 A72-32731
Acceleration and recombination effects on ion energy spectra, discussing energy distributions of hydrogen, zirconium, lithium, and deuterium ions in laser plasmas
16 p2428 A72-32910
Lifetime and quenching of metastable CO produced by dissociative recombination of positive carbon dioxide ions in He afterglow
16 p2432 A72-33771
Short cesium plasma discharge diode as physical model for thermionic converter, studying ionization, recombination and microwave radiation
18 p2714 A72-36212
Recombination of protons and negative hydrogen ions in slow collisions.
18 p2713 A72-36953
Lower F 2 region positive oxygen ion distribution with allowance for vertical motions, production and recombination processes, using atmospheric models
19 p2790 A72-38333
D region ion compositions model during quiet and intense PCA conditions associated with dissociative recombination and ion-ion neutralization
20 p2917 A72-39530
Special features of photoresonance perturbation relaxation in a low-temperature discharge plasma
23 p3319 A72-43409
Formation and loss of O₂+/ and O₄+/ ions in krypton-oxygen afterglow plasmas.
23 p3316 A72-44345

ION SCATTERING
Alkali ion scattering by NbTi alloy and SiC and components, comparing scattering coefficients
03 p0401 A72-13424
Elastic scattering without dissociation of nitrogen molecular ions by noble gas targets in 0.3-3 keV range, analyzing energy loss
03 p0393 A72-14357
Electrons and ionized impurities interaction in thin quantizing layers, discussing donor activation energy and kinetic characteristics
07 p1048 A72-19640
Dense isothermal plasma heating due to electron and ion scattering on turbulent pulsations of electric field oscillations
13 p2019 A72-29916
Negative ions and collision frequency effects on circularly polarized E1F and V1F wave propagation in ionosphere
14 p2084 A72-30128
Helicon /whistler/ turbulence spectra in collisionless plasma due to ion scattering, considering self trapping and stability along magnetic field with Landau absorption decay
14 p2137 A72-30357
Influence of reflected ions on the magnetic structure of a collisionless shock front.
17 p2592 A72-35819

Energy spectra of Cs+ ions scattered by the surface of a tungsten single crystal
24 p3429 A72-45501

ION SELECTIVE ELECTRODES
Intracellular potassium in cells of the distal tubule.
24 p3373 A72-45231

ION SHEATHS
Space charge layer /ion sheath/ effects on impedance of lf transmitting electric dipole in ionospheric plasma
04 p0490 A72-15399
Metal ion sheaths in midlatitude sporadic E layer caused by vertical redistribution of neutral ionization, discussing wind shear discontinuities
10 p1477 A72-25159

ION SOURCES
NT DUOPLASMATRONS
NT PLASMATRONS
Low energy and strong current density ion source using mesh grid extraction
02 p0266 A72-12491
Kaufman thruster ion sources, discussing refractory metal, oxide coated, liquid mercury and hollow cathodes design, performance and durability
04 p0564 A72-14433
Rocket-borne mass spectrometer with helium cooled electron bombardment ion source to reduce gas-wall interactions effects
04 p0524 A72-15538
Ion accelerating system for minimum angular ion beam divergence with plasma ions ejection from source through slits in electrodes
05 p0701 A72-17236
Tungsten and rhenium oxides negative ions source, presenting mass analysis table
07 p1037 A72-19323
PIG discharge system with plasma feed from duoplasmatron ion source for steady state operation with ion energies 1.5-5 keV
08 p1214 A72-21435
German monograph on electron beam focusing in partial pressure analyzer with two compartment ion source, eliminating residual gas-filament interaction
09 p1306 A72-22318
Duoplasmatron as negative hydrogen ion source to study geometrical and electrical parameters effects on beam and analyze composition, energy spectrum and emittance
10 p1518 A72-23963
Electron bombardment type simplified ion source with magnetic field induction by filament heating current, discussing design and characteristics
10 p1518 A72-23965
Incompressible fluid jet propagation beyond charged particle source exit section, investigating electrohydrodynamic interaction parameter
10 p1522 A72-24549
Multiply charged heavy ion sources and accelerating systems - Conference, Gatlinburg, Tennessee, October 1971
10 p1516 A72-25026
Performance characteristics of various types of PIG sources for multiply charged heavy ions production
10 p1516 A72-25027
Electron cyclotron resonance in Penning ion source, measuring electron temperature from X ray emission spectra
10 p1516 A72-25029
Penning ion source for multiply charged ions high intensity beams generation, describing axial type design with electron focusing magnetic coil
10 p1516 A72-25030
Ion sources for high temperature operation based on electron bombardment and beam-plasma interactions
10 p1516 A72-25031
Solid bodies microanalysis by mass spectrum microscopy based on secondary ion-ion emission, discussing ion source and focusing systems
14 p2104 A72-30449
Minimum ion source temperatures for glow discharge ion flux deposition of films and coatings on metallic and nonmetallic substrates
15 p2244 A72-31573
Production of intense ion beams by high-frequency electric fields.
19 p2839 A72-37331
Low-frequency oscillations in a Penning-discharge plasma under conditions of a cyclotron ion source
21 p3095 A72-41682
Source and identification of heavy ions in the equatorial F layer.
23 p3286 A72-44516
Longitudinal magnetic field effect on the characteristics of a high frequency ion source
24 p3428 A72-45015
Plasma produced by laser irradiation of solid targets as a source of highly stripped ions.
24 p3430 A72-45603

ION TEMPERATURE
Similarity theory for electrostatic and magnetic collisionless shocks at zero ion temperature, using numerical simulation results
01 p0106 A72-10029

Ion and electron temperature increases by friction heating between neutral gas winds and plasma in ionosphere
01 p0054 A72-10424
Plasma ion temperature and neutral collision frequency determination by Langmuir probes [AD-739452]
02 p0264 A72-12262
Low energy and strong current density ion source using mesh grid extraction
02 p0266 A72-12491
Ion and electron temperatures difference relaxation rate in uniform plasma, noting relationship to Debye length
02 p0267 A72-12769
Plasma sheath drift origin of hot ions in modified Penning discharge
04 p0551 A72-14439
Magnetospheric heat flux effect on height variation of electron and ion temperatures and ion composition in topside ionosphere
04 p0515 A72-14929
Equilibrium diffusion of rotating plasma in toroidal systems, deriving two fluid hydrodynamic equations with allowance for ion temperature perturbation
05 p0701 A72-17242
Nighttime plasmopause and thermal ion plasma structures relationship to micropulsations, considering excitation in post storm recovery and diurnal plasma bulge regions
06 p0804 A72-17453
Energy absorption measurements of ion heating by ion-acoustic waves in ion streaming plasma
06 p0856 A72-17518
Ion acoustic waves instability from electron-ion temperature difference in homogeneous collisional ionized plasma, using fluid equations perturbation analysis
06 p0856 A72-17524
Linear dispersion relation for pressure gradient driven drift waves instabilities from ion and electron thermal conductivity effects in collisional plasma
06 p0857 A72-17529
Cross-field current driven ion acoustic instability in two plasma devices, causing neutral sheet phenomena, anomalous dispersion and ion heating [AD-740261]
06 p0858 A72-17541
Single ended Q machine Ba plasma probe measurements of ion temperatures perpendicular to magnetic field, electron temperatures and plasma densities and potentials
06 p0859 A72-17550
Resonance charge exchange cross section measurements for Cs at 2 eV within Q machine, discussing ion energy resolution improvement
06 p0859 A72-17552
Plasma turbulent heating effectiveness by longitudinal ion current in mirror machine, determining hot ion lifetime and energy distribution function
07 p1039 A72-18913
Interstellar matter cooling and recombination after supernova ionization, comparing X ray and cosmic ray heating mechanisms
07 p1070 A72-19083
Solar wind properties and discontinuity characteristics, describing particle densities, wind speed, magnetic field level and near earth electron and ion temperatures
09 p1377 A72-22756
Ionic and atomic temperature measurement in low pressure Ar plasma by X ray absorption spectroscopy
09 p1360 A72-22832
Low energy ions and negative particle fluxes simultaneous enhancements due to Apollo 14 lunar module impact, suggesting solar wind and gas cloud interaction as acceleration mechanism
09 p1388 A72-23018
Ar/He plasma acoustic wave properties, expressing phase velocity and damping as function of ion-electron temperature ratio and relative species densities
10 p1520 A72-24300
Deionization mechanism of expanding plasma cloud produced by arc burning in vacuum, discussing charged particle concentration and ion thermal velocity
10 p1521 A72-24356
Ion and electron temperature ratios in hot plasma, discussing energy relaxation, heating and cooling effects and electrostatic confinement by ambipolar diffusion
10 p1524 A72-25032
Thomson scattering of electromagnetic wave in plasma and ionosphere for studying electron and ion temperatures
11 p1621 A72-25838
Pulsed plasma thruster arc electron density measurement by Mach-Zehnder interferometer and He-Ne laser, determining exhaust ion temperature and total charge [AIAA PAPER 72-463]
11 p1709 A72-26198
Solar wind ion temperature association with influx of neutral hydrogen from heliosphere boundary
11 p1714 A72-26527

Energy spectra of multiply charged ions formed in laser beam interaction with plasma, noting recombination process role

12 p1849 A72-27065

Averaged equations for laser heating of two temperature plasma with allowance for nuclear fusion energy, noting inequality of ion and electron temperature

12 p1851 A72-27395

Plasma ion temperature determination by measuring transient current to cylindrical Langmuir probe under collision free conditions

[AD-739815] 12 p1851 A72-27399

Satellite and ground station observed ionospheric plasma parameters comparison, considering electron density and temperature and ion temperature and composition

12 p1804 A72-27785

Magnetic field effect on ruby laser generated plasma in solid target, measuring thermal ion energy increase

12 p1852 A72-27879

Self stabilization, measurement of two-ion beam instability generated by microturbulent ion heating in plasma with variable temperature ratio

13 p2007 A72-28428

Maximum ion energy dependence on radiation density in laser plasma

14 p2137 A72-30315

Magnetized nonuniform plasmas, discussing description to all orders in electron and ion temperatures of waves by operator method

14 p2139 A72-30879

Minimum ion source temperatures for glow discharge ion flux deposition of films and coatings on metallic and nonmetallic substrates

15 p2244 A72-31573

Apollo lunar surface experiments package suprathreshold ion detector measurements in lunar environment

15 p2309 A72-31957

Suprathreshold ion detector measurements on lunar surface by Apollo 12 and 14 astronauts to provide search for lunar exosphere phenomena

15 p2301 A72-32092

Ionospheric ion temperatures and velocities and electron and neutral densities from incoherent scatter observations during 11 February 1969 magnetic storm

15 p2229 A72-32254

Solitons propagation in two ion streams plasma for cold and finite temperature ions, noting periodic waves condition

15 p2286 A72-32276

End effect in current response of highly negative cylindrical Langmuir probe in collisionless plasma flow, discussing use for ion temperature determination

15 p2288 A72-32418

Acceleration and recombination effects on ion energy spectra, discussing energy distributions of hydrogen, zirconium, lithium, and deuterium ions in laser plasmas

16 p2428 A72-32910

H-He ions solar wind expansion absence for case of equal gas temperature, noting mass flux relationship to He ion temperature

16 p2449 A72-33911

Electron-ion heating in high beta perpendicular collisionless shock waves by plasma cylinder magnetic compression using theta pinch

16 p2439 A72-33936

Magnetic field effect on ruby laser generated plasma in solid target, measuring thermal ion energy increase

16 p2439 A72-33988

Ion heating via turbulent ion acoustic waves

17 p2588 A72-34873

Deionization mechanism of expanding plasma cloud produced by arc burning in vacuum, discussing charged particle concentration and ion thermal velocity

17 p2589 A72-34956

Ion temperature diagnostic using a high power alternating current probe

17 p2557 A72-35617

Turbulent heating of electrons and ions in a collisionless shock wave

18 p2715 A72-36599

Laser-beam-scattering measurement of ion temperature in a theta-pinch plasma and evidence for thermonuclear reactions

19 p2840 A72-37548

Mathematical model for perfectly absorbing spherical Langmuir probe in collisionless plasma, obtaining plasma density and ion temperature

19 p2842 A72-38524

Comparison between observed and numerically calculated atmospheric gravity waves in the F-region

19 p2794 A72-38864

Plasma turbulent heating effectiveness by longitudinal ion current in mirror machine, determining hot ion lifetime and energy distribution function

20 p2957 A72-39379

Transit time heating in stochastic electromagnetic fields

21 p3092 A72-41222

Measurement of ionic parameters of a cesium plasma with the help of a grid probe with a cooled collector

22 p3211 A72-42645

Maximum ion energy dependence on radiation density in laser plasma

23 p3318 A72-43218

Investigation of the heating of the plasma ion component by a collisionless shock wave

23 p3318 A72-43310

Particle distribution function evolution effect on turbulent plasma heating by wave interaction, considering stochastic heating of ions

23 p3318 A72-43314

The development of a theoretical model of the atmosphere and the ionosphere

24 p3399 A72-45585

Energy spectra of multiply charged ions formed in laser beam interaction with plasma, noting recombination process role

24 p3431 A72-45718

ION TRAPS [INSTRUMENTATION]

Ion transit time in ion cyclotron resonance spectrometer, using combination of pulsed ion formation and time dependent trapping conditions

04 p0523 A72-15484

Operational optimization of ion traps with dc amplifiers mounted on nonoriented earth satellite, proposing control circuit

07 p0993 A72-20664

Reflector-analyzers for studies of rarefied low-energy plasmas

21 p3058 A72-41731

ION-GAS INTERACTIONS

U GAS-ION INTERACTIONS

IONIC COLLISIONS

Characteristic scale lengths of stationary ionic collisional shocks in Q device perpendicular to magnetic field, presenting shock thickness variation with Mach number and density

01 p0105 A72-10028

Helium shock wave two step collisional ionization model comparison to observed profile data from laser Fabry-Perot interferometer

02 p0266 A72-12368

Effective cross sections of ion collisions with gaseous target and argon atoms collision with argon target by molecular beam intensity attenuation method

03 p0392 A72-14060

Effective cross sections for charged and excited particles formation from He, Ne and Ar ion collisions with CO molecules, using mass spectrometry

03 p0393 A72-14065

Surface potential effects on splitting of p- and d-orbitals of atoms and ions approaching bcc and fcc substrates

03 p0393 A72-14340

Plasma ion collision transport analogy with turbulent velocity space momentum transfer, explaining confined plasma runaway electron absence in strong electric fields

04 p0560 A72-15469

Colliding ion streams thermalization beyond plasmapause via unstable ion waves excitation or Coulomb collisions

06 p0805 A72-17464

Ion-electron collisions effect on ion cloud motion in magnetoactive plasma immersed in uniform external electric field

07 p1055 A72-18894

Colliding plasmas transverse instabilities, investigating ion dynamic and electron beam induced return currents effects

07 p1041 A72-19508

Exothermic capture processes with ionization during nonelastic ion atom collisions, discussing cross sections of He ion collisions with Ar, Kr and Xe atoms

08 p1210 A72-20837

Ion quadrupole effects in ion-molecule collisions, calculating capture cross sections and ion trajectories

09 p1354 A72-22658

Polyatomic ions interaction with neutral molecules in gases, calculating ion mobility as function of temperature from core model representation

09 p1355 A72-22788

Relative intensity of solar XUV emission lines of Li isoelectronic sequence ions, taking into account transitional collision strengths

09 p1391 A72-23532

Ion dipole capture cross sections at low ion and rotational energies compared with reaction cross sections for ammonia and water parent-ion collisions

11 p1692 A72-26014

Electron-ion collision frequency and conductivity of non-Debye plasma formed in high pressure discharge from Ar, Kr and Xe tubes

13 p2018 A72-29891

Density and electric field oscillations of plasma in stellarator, considering magnetic field strength effect, stabilization by ionic collisions and energy pumping mechanism

13 p2019 A72-29985

Dissipative instability produced by colliding ions and atoms in weakly ionized plasma

14 p2136 A72-30303

Ion-molecule collision frequencies in gases by phase coherent pulsed ion cyclotron resonance spectrometry [ONERA, TP NO. 1071]

14 p2133 A72-30524

Ionized plasma line widths and intensities due to Landau and collisional damping, observing effects by light scattering techniques

14 p2140 A72-30901

Lateral diffusion measurement for mass identified positive ions in oxygen, noting spiralling, charge exchange and collisions effects on ion-molecule system

15 p2281 A72-32224

Plasma containment in toroidal systems investigated on basis of fluid model containing inertia, momentum transfer, ionic collisions and thermal conductivity effects

15 p2285 A72-32273

Ionic collision effects on spatial ion wave echoes in single-ended Q machine plasma, noting echo peak amplitude damping

15 p2288 A72-32423

Booker theorem generalization to cover wide range of ionospheric refractivity profiles containing variable electron density and collision frequency

16 p2386 A72-33662

Diatomic molecules dissociation investigation from effective cross section measurement of slow atomic negative ions formation by molecules collisions with fast ions and atoms

16 p2432 A72-34152

Collisional losses in a very-low-frequency duct associated with the lower-hybrid-resonance frequency

17 p2517 A72-35608

Collisional-rate coefficients for sodiumlike Ar VIII ions

17 p2585 A72-35770

Recombination of protons and negative hydrogen ions in slow collisions

18 p2713 A72-36953

Effects of collisions on perpendicular longitudinal ion wave propagation in a magnetized plasma

19 p2841 A72-38438

Computer-graphics studies of dipole-dipole collisions - Evidence for neutral collision complexes

21 p3087 A72-40559

Cross sections for the excitation of Ar II laser lines in electron-ion collisions

21 p3063 A72-40725

Deuterium-tritium heating to thermonuclear temperatures by means of ion-ion collisions in the presence of intense laser radiation

21 p3094 A72-41632

Dissipative instability produced by colliding ions and atoms in weakly ionized plasma

23 p3317 A72-43205

Evidence for radiative electron capture by fast, highly stripped heavy ions

23 p3316 A72-44073

IONIC CONDUCTIVITY

U ION CURRENTS

IONIC CRYSTALS

Vertically oriented double crystal attachment to vacuum X ray spectrograph for enhanced resolution of ionic solids and solutions molecular spectra

07 p0983 A72-19317

Uranyl fluoride crystals luminescence spectrum study, calculating anion normal vibration frequencies

20 p2960 A72-39413

IONIC DIFFUSION

Diffusion equations of ion components of plane stratified plasma/ionosphere, taking into account wind effect and vertical temperature distribution

05 p0658 A72-16402

Artificial barium ion cloud spatial-temporal growth in ionosphere, solving ion diffusion equation by numerical methods

13 p1950 A72-29387

Lateral diffusion measurement for mass identified positive ions in oxygen, noting spiralling, charge exchange and collisions effects on ion-molecule system

15 p2281 A72-32224

Exchange diffusion process contribution to human red blood cell transmembrane cation movement from sodium tracer influx studies

15 p2187 A72-32746

Spectral dependence of diffusion in a magnetized plasma

17 p2592 A72-35623

Influence of a variable electric field on the diffusion of ions in a gas

21 p3086 A72-41676

Drift velocities, diffusion coefficients, and temperatures of photoions in argon, nitrogen, and oxygen

22 p3209 A72-42926

Diffusive spreading of weak plasma discontinuities in the presence of two kinds of positive ion

23 p3283 A72-43363

IONIC MOBILITY

Ionospheric ion mobilities and densities measurements over Sardinia, using parachute mesosphere probe

01 p0055 A72-10436

Plasma shock wave oscillation profile dependence on ion and electron friction and viscosity

04 p0555 A72-14620

Oxygen ionization and ion mobility measurements in air by open proportional counting chamber with electron counter and exoelectron emitter
09 p1305 A72-22203

Mesosphere region positively and negatively charged particles concentration and mobility measurements by sounding rocket experiments
09 p1375 A72-22361

Polyatomic ions interaction with neutral molecules in gases, calculating ion mobility as function of temperature from core model representation
09 p1355 A72-22788

Plasma diffusion coefficient in crossed electric and magnetic fields, discussing lifetime in magnetic trap and expression for ion mobility
13 p2019 A72-29942

Acceleration stress tolerance dependence on electron or ion transport across cell surface activation energy barrier, studying rat survival times
18 p2650 A72-36448

Ion mobilities and ion-molecule reaction rates in oxygen.
19 p2836 A72-37457

Field dependence of gaseous-ion mobility - Theoretical tests of approximate formulas.
23 p3316 A72-43871

IONIC PROPELLANTS
U ION ENGINES
IONIC REACTIONS

Photochemical ion-molecule reactions in ionosphere by air exhaust device and RF mass spectrometer observation in geophysical rocket experiment
01 p0068 A72-10591

D region positive and negative ion chemistry review, noting dominant roles of water ion clusters, NO cation and hydrates
02 p0219 A72-11979

Laboratory measurements of D region ion-molecule reactions using flowing afterglow system
03 p0347 A72-13388

Ionospheric ion-molecule and ion-electron reaction rate constants determination from nighttime flight of rocket-borne ion mass spectrometer data least square fitting
03 p0347 A72-13396

Mass spectroscopic rate constants for reactions of negative ions of rhenium and tungsten oxides with chlorine and nitrogen dioxide
04 p0484 A72-15639

Venus daytime ionosphere at 100-500 km, discussing ion clustering processes below 100 km forming UV haze layer and atmospheric composition
05 p0723 A72-17163

Additive and natural ionization in combustion reactions, discussing flame chemistry, ionic species and measurements
05 p0751 A72-17224

Two body ion-ion neutralization rates measurement by merged beam technique, considering D region reactions
06 p0805 A72-17465

D and E region ion chemistry - Conference, University of Illinois, Urbana, July 1971
09 p1274 A72-22352

D and E regions positive ion chemistry based on E and F regions ion-molecule reaction rate constants comparison with laboratory measurement
09 p1275 A72-22360

D and E region ion chemistry reaction rate measurements, noting hydration, charge exchange and ion-atom interchanges
09 p1275 A72-22366

Room temperature reactions involving ionospheric cluster ions, discussing rate constants measurement by stationary afterglow and drift tube facilities
09 p1275 A72-22367

Laboratory ionization chamber measurement of ion chemistry and production rates from partial simulation of disturbed nighttime ionosphere at 300 K
09 p1275 A72-22368

Resonance theory of three body ion-atom association reactions in rare gases, estimating quasi-bound electron state population and deactivation cross section
09 p1356 A72-22792

Low altitude electron-ion dissociative recombination and ion-ion neutralization coefficients during PCA event from ESRO rocket flights data
13 p2032 A72-29653

Solar flare flux effects on D region effective ion recombination coefficient decrease, discussing electron and negative ion densities
13 p1913 A72-29654

Hydrogen atom exchange in ion-molecule reactions of methane and ethylene determined from reaction products distribution, using ion cyclotron resonance techniques
14 p2084 A72-30522

Ionic and hydrophobic interactions effects on *Micrococcus lysodeikticus* membrane stabilization process
14 p2075 A72-30595

Disturbed ionospheric electron and ion kinetics, detailing dissociative recombination as regulating process for temporal evolution
14 p2102 A72-30654

Electric arc plasma, investigating reaction energy effects on radial temperature distribution
14 p2139 A72-30779

Positive and negative ions relative intensity measurement during nitrous oxide target molecules injection into sonic Ar plasma reaction channel, using quadrupole mass spectrometer
16 p2440 A72-34064

Particle excitation processes in solar corona, ionosphere and astrophysics, discussing electron affinities, ion-molecule reactions, forbidden atomic transitions and Fe II problem
16 p2432 A72-34150

High temperature turbulent jet facility for studying ionic species produced by high temperature air and ablation products interaction with cool ambient air [AIAA PAPER 72-676]
17 p2536 A72-35480

Ion mobilities and ion-molecule reaction rates in oxygen.
19 p2836 A72-37457

Observability of hyperfine structure and Lamb, nuclear-volume shifts in $1s_{n1}-1s_{n1}'$ transitions of helium-like ions.
19 p2837 A72-37544

Laboratory positive and negative ion composition measurements compared with D region ion-molecule reaction observations
20 p2917 A72-39527

Repulsive potential determination for alkali cations, halide anions and anisotropic molecules from scattering experiments and bond energy data
21 p3087 A72-40555

Bond energy electrostatic potential calculation and equilibrium and rate constants prediction for alkali and halide ions association with neutrals
21 p3087 A72-40556

Evidence for protonated cyclopropane intermediates in crossed-beam ion molecule reactions.
24 p3379 A72-45475

IONIC WAVES

LF large scale oblique Alfvén wave propagation in turbulent ion acoustic plasma, investigating dispersion relation, Landau damping and interactions
01 p0107 A72-10137

Ion oscillation theory for electrodynamic channel Poiseuille and Hagen-Poiseuille type flows, using transport and dispersion equations in various ionized media
01 p0111 A72-11214

Ionization waves linear theory for low pressure noble gas strong current column, showing self excitation limit and temperature dependence of energy loss rate
03 p0400 A72-14351

Hf electric field influence on electron drift instability and slow ion-acoustic waves for inhomogeneous magnetized plasma stabilization
04 p0555 A72-14617

Ion-wave current instabilities theory, showing inhomogeneities generated by field aligned currents in collisionless plasma
04 p0559 A72-15350

Weak D type ionization waves stability in optically thick plasma layer behind front of interstellar gas
05 p0715 A72-16210

Dispersion properties of drift waves in low-beta weakly collisional plasma in presence of ion acoustic or Langmuir waves parallel to magnetic lines
05 p0698 A72-17019

Perturbation theory, saturation and relaxation effects in electron and ion plasma wave echoes
05 p0699 A72-17220

Ion-acoustic waves and ionization waves instabilities in gas discharge plasmas
05 p0699 A72-17222

Ion distribution function oscillations in first order ion waves of single ended Q device, noting plasma confinement in static magnetic field
06 p0855 A72-17507

Perturbed density and ion velocity distribution functions of grid-excited ion acoustic waves in collisionless plasma in single ended Q device
06 p0855 A72-17511

Pseudowaves and ion acoustic waves simulation, calculating time evolution of ion distribution for oscillating negative plasma potentials applied at grid
06 p0855 A72-17512

Parametric excitation of ion-acoustic waves in Q machine plasma, controlling electron temperature by amplitude modulated rf heating
06 p0855 A72-17513

Single-ended Q machine grid-excited density perturbation and ion wave propagation properties from linearized Vlasov equations
06 p0855 A72-17514

Plasma microinstabilities due to ion acoustic waves propagation with double-humped ion velocity distribution function in Q machine
06 p0855 A72-17516

Energy absorption measurements of ion heating by ion-acoustic waves in ion streaming plasma
06 p0856 A72-17518

Ion acoustic wave excitation in plasma by modulated energetic electron beam, compared with grid excitation
06 p0856 A72-17519

Cylindrical plasma ion-acoustic resonance measurements from various excitation methods for noise component identification
06 p0856 A72-17523

Ion acoustic waves instability from electron-ion temperature difference in homogeneous collisional ionized plasma, using fluid equations perturbation analysis
06 p0856 A72-17524

Wake behind body moving in plasma parallel to magnetic field, observing coupling with parallel ion acoustic waves and with perpendicular Bernstein modes
06 p0875 A72-17525

Trapped ion instability in collisionless plasma ion acoustic waves, discussing sideband waves frequency spectrum and growth rate
06 p0859 A72-17545

Ion sound waves decay instability induced by large amplitude Bernstein mode in plasma
06 p0859 A72-17546

Ion heating caused by ion acoustic waves in ion streaming argon plasma
06 p0860 A72-17746

Ion acoustic and cyclotron harmonic plasma waves parametric excitation by hf electric field, measuring thresholds and growth rates agreeable with theory
06 p0861 A72-17827

Electric field induced ionizing potential waves in dense gas, describing avalanching electron gas breakdown into filaments by fluid dynamic and Maxwell field equations
06 p0864 A72-18534

Ionization wave propagation in inert gas due to microwave resonance quanta diffusion, explaining plasmaguide phenomena
07 p1040 A72-18916

Ion-acoustic solitary waves formation and interaction in collisionless warm plasma, using Vlasov equation for ions and Boltzmann distribution for electrons
07 p1041 A72-19507

High frequency heating of dense toroidal plasma by nonaxisymmetric ion cyclotron waves resonant excitation in closed magnetic trap
07 p1043 A72-19636

Ion-sound plasma turbulence theory, considering collisionless shock waves data and anomalous resistivity calculations
07 p1045 A72-20480

Stepwise ionization effects on ionic wave propagation and oscillation stability in inert gas dc discharges
07 p1046 A72-20503

Reactive mechanism of nonlinear mixing in resonant excitation of ion plasma waves by vlf and whistler waves
07 p1046 A72-20540

Nonlinear ion acoustic instability in plasma for subharmonic and harmonic forcing oscillations similar to Van der Pol effect
07 p1046 A72-20541

Growth rate estimation of negative energy Bernstein and ion acoustic waves explosive interaction, noting collisionless shock turbulence
08 p1212 A72-21248

Electrostatic ion wave Landau damping in magnetic field of Ar plasma QP machine
08 p1213 A72-21250

Electrostatic ion wave stability in magnetogasdynamic channel flow from approximate numerical solution of dispersion equations
08 p1211 A72-21305

Slow and fast longitudinal ion acoustic waves in plasma cylinder under axial magnetic field
08 p1215 A72-21873

Electron Larmor radius effect on hf hose and mirror instabilities of fast magnetoacoustic and ion acoustic waves in nonisothermal plasma
08 p1215 A72-21874

Large amplitude electrostatic ion acoustic shock production by superposing pulsed photoionized plasma slab on dc background
09 p1360 A72-22871

Self consistent collisionless theory of turbulent low Mach number ion-acoustic shocks, noting resistive heating
09 p1360 A72-22872

Stable large amplitude high Mach number ion acoustic shocks in collisionless plasma, obtaining electron density as function of time
09 p1364 A72-23445

Phase velocity and Landau damping of ion acoustic waves propagating through plasma boundary layer at conducting sphere or cylinder based on two fluid model
10 p1523 A72-24746

Fast and slow ion acoustic free streaming wave propagation in drifting plasma, showing phase velocity and damping in agreement with Maxwellian distribution
11 p1692 A72-25518

Perturbation technique application to nonlinear behavior of ion waves produced by two-beam instability in plasma
11 p1692 A72-25519

Grid produced LF electrostatic perturbations propagation and damping in near isothermal plasma, discussing ion ballistic contributions to ion acoustic waves

11 p1692 A72-25520

Plasma parametric instabilities excitation by radio waves in ionosphere, noting LF ionic and HF electrostatic wave growth

11 p1628 A72-26767

Plasma sheath from plane negatively biased electrode immersed in low pressure discharge investigated by ion acoustic waves and hot probe

12 p1850 A72-27279

Weak ion-acoustic quasi-shock wave propagation in collisionless plasma, determining long time behavior of precursor ion stream reflected by electrostatic potential

13 p2012 A72-29125

Alternating magnetic field effect on collisionless nonhomogeneous magnetoplasma ion acoustic oscillations stability, examining parametric excitation of Langmuir oscillations

13 p2016 A72-29604

Radio aurora ion-acoustic wave propagation direction divergence due to magnetic field distortion by large ionospheric horizontal sheet current [AD-746367]

13 p1923 A72-29662

Dispersion characteristics of ion-acoustic waves in positive gas discharge plasma column

13 p2019 A72-29912

Stationary nonlinear ion acoustic oscillations in dense weakly ionized current carrying plasma, considering wave propagation velocity and instability process

13 p2019 A72-29988

Ion-acoustic oscillations effect on turbulent plasma electric conductivity within weak external electric field

13 p2019 A72-29990

Ion sound turbulence in dense plasma within magnetic field, representing global equilibrium spectrum

14 p2137 A72-30356

Signal spectrum sidebands asymmetry of LF waves in plasma with electric current and ion stream, suggesting amplitude and frequency modulation

15 p2284 A72-31650

Ionic collision effects on spatial ion wave echoes in single-ended Q machine plasma, noting echo peak amplitude damping

15 p2288 A72-32423

Postfrontal ion acoustic shock turbulence as function of Mach number and electron/ion temperature ratio, using particle in cell technique

15 p2281 A72-32424

Ion acoustic and guided electron plasma waves excitation by grid antenna produced LF signals in cylindrical plasma column

15 p2289 A72-32650

Potential waves generation by transverse current in ionospheric electrojet region, discussing lower hybrid resonance domain

15 p2232 A72-32732

Random ionization waves convective instability in glow discharge positive column, calculating fluctuations spectrum as function of position along column for localized white noise source

16 p2437 A72-33747

Ion heating via turbulent ion acoustic waves.

17 p2588 A72-34873

A stability mechanism for the ion-acoustic waves.

17 p2592 A72-35625

Beam-generated collisionless ion-acoustic shocks.

17 p2592 A72-35626

Nonlinear saturation of 'type I' irregularities in the equatorial electrojet.

18 p2685 A72-35990

Effects of collisions on perpendicular longitudinal ion wave propagation in a magnetized plasma.

19 p2841 A72-38438

Radiation belt protons and ion-cyclotron wave interactions accounting for magnetospheric ring current instabilities during storm at plasmapause

20 p2919 A72-39545

Fresnel-like interference on an ion-wave decay in a plasma.

21 p3089 A72-40200

Microwave scattering from a radially propagating ion acoustic wave in a positive column.

21 p3089 A72-40201

Nonexistence of ion acoustic waves and Landau damping driven electrostatically in an ideal Q machine.

21 p3090 A72-40340

Nonlinear ion sound in a fully ionized current-carrying plasma

21 p3090 A72-40411

Alternating magnetic field effect on ionoacoustic oscillations stability of collisionless nonhomogeneous magnetoplasma, examining parametric excitation of Langmuir oscillations

21 p3091 A72-40658

Coulomb-collision corrected ion-acoustic line profiles.

21 p3092 A72-40819

Excitation of volume ion-acoustic oscillations in an inhomogeneous dense plasma by the field of an electromagnetic wave.

21 p3092 A72-40836

Linear and nonlinear aspects of ion-sound current instability for solar atmosphere conditions of full ionization, noting implications for flare mechanism

21 p3100 A72-41040

Sideband waves excitation by large amplitude ion-acoustic waves in collisionless plasma, noting frequency spectrum and growth rate agreement with trapped particles theory

21 p3094 A72-41629

Stationary solitary, snoidal and sinusoidal ion acoustic waves.

23 p3320 A72-43520

Role of nonlinear effects in the problem of the anomalous resistance of a plasma

23 p3322 A72-44481

Ion acceleration during expansion of a rarefied plasma

23 p3322 A72-44482

Magnetic pulsation spectra in a nonisothermal plasma

23 p3323 A72-44483

High frequency heating of dense toroidal plasma by nonaxisymmetric cyclotron waves resonant excitation in closed magnetic trap

24 p3427 A72-44568

Instability of a magnetically active plasma in the presence of a specified transverse velocity of the ions

24 p3429 A72-45488

High-frequency instabilities in a plasma with a nonlinear ion-acoustic wave

24 p3429 A72-45489

IONIZATION

NT ATMOSPHERIC IONIZATION

NT AURORAL IONIZATION

NT AUTOIONIZATION

NT FLAME IONIZATION

NT GAS IONIZATION

NT ION PRODUCTION RATES

NT NONEQUILIBRIUM IONIZATION

NT PHOTOIONIZATION

NT SURFACE IONIZATION

Solid state colloidal plasma physics, discussing statistical ionization mechanics, electron emission and recombination, rocket exhausts, MHD generation, metal vapors electrostatic precipitation, etc

02 p0267 A72-12842

Depth ionization properties and biological effects of bevatron produced heavy ion beams, discussing utilization in tumor therapy, space biology and radiobiology

03 p0316 A72-13693

High power Q switched ruby laser beam one dimensional penetration depth into metal as function of time, emphasizing ionization and plasma heating

04 p0528 A72-14536

Transverse electromagnetic field and electron velocity vectors during rectangular pulse incidence on ionization front moving at light speed, describing steady state encounter region

08 p1136 A72-21741

Chemionization in oxyhydrogen plasma detonation waves

08 p1129 A72-22045

Nonlinear initial boundary value problem for time dependent convection-diffusion equation with ionization and recombination reactions

09 p1341 A72-22472

Inner shell ionized atoms, discussing orbital electrons rearrangement processes based on shakeoff events and radiative Auger transition

09 p1356 A72-22834

Be and Mg ion generation and p-type layer electrical properties production by implantation in GaAs substrates

09 p1372 A72-23245

Microwave equipment for electron density profiles determination used in ionization relaxation start study of shock induced Ar plasma

10 p1519 A72-24067

F region plasma one dimensional nonisothermal diffusion for positive ions with allowance for ionization and recombinations and gravitational forces

15 p2232 A72-32731

Ionization structure and coarse and fine analyses in planetary nebulae spatial spectroscopic diagnostics based on line profile monochromatic intensity integral equation inversion

23 p3339 A72-44236

IONIZATION CHAMBERS

NT BUBBLE CHAMBERS

NT CLOUD CHAMBERS

NT PROPORTIONAL COUNTERS

NT SPARK CHAMBERS

Monte Carlo simulation on high energy cosmic ray propagation and multiplication in high altitude emulsion chamber observations, examining two-fire-ball and H-quantum models

01 p0121 A72-11123

Ionization chamber for direct measurement of radiation dose equivalent, describing high voltage switching circuit

[CERN-71-16]

02 p0168 A72-12072

Nuclear-electron cascades longitudinal evolution calculation in ionization calorimeter for primary nucleons and pions, using Monte Carlo method

06 p0811 A72-17260

Transient effect in electron-photon shower on readings of ionization chamber and scintillation counter

06 p0871 A72-17291

Transient effects due to electromagnetic cascades in Pb during Cu wall passage in ionization calorimeter

07 p0988 A72-19871

Ar plasma in ion engine discharge chamber with primary and Maxwell electron bombardment, discussing ion production probabilities in perturbed and unperturbed cases

08 p1223 A72-21209

Laboratory ionization chamber measurement of ion chemistry and production rates from partial simulation of disturbed nighttime ionosphere at 300 K

09 p1275 A72-22368

Picoampere charged particle beam symmetry and magnitude monitor consisting of four transmission ion chambers

09 p1315 A72-23405

Multiplicative factors for energy scale corrections of OSO-3 ion chamber for solar X-ray monitoring

13 p1035 A72-29748

Solar and geocoronal hydrogen Lyman alpha radiation detector, discussing ion chamber with magnesium difluoride window and nitric oxide gas

15 p2239 A72-32336

Experimental investigation of electromagnetic cascades at an energy greater than 20 GeV

23 p3291 A72-44444

IONIZATION COEFFICIENTS

Cosmic ray spectrum at nonrelativistic energy region, noting ionization loss effects

05 p0709 A72-16238

Interelectrode gas-filled gap electron avalanche formation effects in weak electric field, calculating ionization coefficient

06 p0863 A72-18411

Seasonal features of nocturnal 6300 A emission variation and decay coefficient in nightglow related to recombination coefficient for F layer ionization

14 p2097 A72-30132

Experimental technique for oxygen negative ions destruction by associative detachment reaction with hydrogen in oxygen-hydrogen mixtures, calculating transport and ionization coefficients

19 p2836 A72-37458

Secondary ionization coefficients in a low-pressure discharge in mercury vapour.

19 p2836 A72-37459

Collisional excitation and impact ionization coefficients of hydrogen

19 p2837 A72-37807

Singly and doubly ionized He plasma recombination and ionization coefficients due to electronic collisions and radiative absorption

19 p2841 A72-38083

Nickel single crystal target ionization by high voltage electron beam bombardment, using flight time mass spectroscopic analysis

19 p2835 A72-38666

The density dependent ionization balance of carbon, oxygen and neon in the solar atmosphere.

23 p3334 A72-43252

IONIZATION COUNTERS

U IONIZATION CHAMBERS

U RADIATION CHAMBERS

IONIZATION CROSS SECTIONS

Daytime bottomsides polar F layer latitudinal cross section construction from ionograms recorded in aircraft

[AD-738278]

01 p0061 A72-10900

Molecular continuity relationship relating discrete absorption oscillator strengths to photodissociation cross sections

01 p1004 A72-11115

Effective cross sections for charged and excited particles formation from He, Ne and Ar ion collisions with CO molecules, using mass spectrometry

03 p0393 A72-14065

Fe group transition metal impurities in semiconductors, calculating ground state wave functions and photoionization cross section dependence on wavelength

04 p0563 A72-15473

Velocity dependence of ionization cross section of Ar, Kr and Xe during thermal energy metastable neon atoms impact, obtaining secondary electron ejection efficiency

04 p0553 A72-15640

Ar core polarizability effect on photoionization cross section calculation for ground state configuration

05 p0693 A72-17173

Inelastic ionization cross section of cosmic ray hadrons with carbon nuclei at energies of 100 to 300 GeV
06 p0869 A72-17271

Excitation and ionization cross sections and rate coefficients of hydrogen-like ions by electron and proton impact in Bethe-Born approximation
06 p0852 A72-18052

Phosphorus hydride electron affinity determination by electron photodetachment cross section measurement, using ion cyclotron resonance spectrometer
07 p0935 A72-19432

Exothermic capture processes with ionization during nonelastic ion atom collisions, discussing cross sections of He ion collisions with Ar, Kr and Xe atoms
08 p1210 A72-20837

Auroral emission rates for various transitions from cross section data and secondary electron spectra measurements
08 p1227 A72-21114

Semiquantal theory application to cross section calculation for excitation and ionization produced by impact between two H atoms
09 p1355 A72-22791

Absorbing sphere model for ion-ion recombination upper limit thermal energy reaction rate and total cross section energy dependence
10 p1515 A72-24342

Differential and total ionization cross sections of multielectron atoms by electron and proton impact
10 p1515 A72-24602

Positive ions excitation cross sections calculated for proton impact induced transitions among fine structure states
10 p1543 A72-24619

Photoionization cross sections for atoms and ions of Al, Si and Ar on basis of Hartree-Fock bound-electron and close coupling approximation free-electron wave functions
10 p1516 A72-24669

Collisional ionization cross sections measurement for gaseous metal atoms in hydrogen-oxygen flames at 2000-2800 K
11 p1591 A72-26659

Fe light emission for simulated meteor conditions, measuring ionization and spectral emission cross sections for Fe reactions with nitrogen and oxygen for 350-2000 eV
14 p2156 A72-30562

Atomic hydrogen 3s state destruction by impact on nitrogen, argon and hydrogen molecules, considering collisional ionization and electron capture mechanisms
14 p2134 A72-30883

Electron production cross section during He atom ionization by proton impact, noting peak existence for electrons near incident proton velocities
15 p2281 A72-32220

Hydrogen direct photoionization and photoexcited autoionization cross sections calculation for radiation in 600-800 Å region
16 p2431 A72-33579

Oscillator strength and ground state photoionization cross sections computation for Na, K, Rb and Cs atoms, including core polarization correction to dipole moment
16 p2431 A72-33724

Brueckner-Goldstone many-body perturbation calculation of helium photoionization.
17 p2586 A72-35773

The measurement of partial pressure in vacuum technology and vacuum physics
18 p2692 A72-36836

On the influence of excited ions and crossed electric and magnetic fields on ionisation cross-sections.
18 p2714 A72-36956

Excited-state cesium photoionization cross sections.
19 p2837 A72-37838

Cross sections for the excitation of Ar II laser lines in electron-ion collisions.
21 p3063 A72-40725

Interpolation formulae for the electron impact excitation of ions in the H-, He-, Li-, and Ne-sequences.
22 p3224 A72-42379

Coulomb approximation method for photoionization cross sections of hydrogen molecule singly excited states
22 p3208 A72-42718

Electron impact ionization of ions trapped in a hollow electron beam.
23 p3316 A72-44343

Photoionization and photoabsorption cross sections of CO₂ at 584 Å.
23 p3317 A72-44519

A portable self-contained gas chromatograph.
23 p3292 A72-44544

Photoionization of N₂, O₂, NO, CO, and CO₂ by soft X rays.
24 p3426 A72-45302

Mathematical model for secondary electron production fall-off, calculating ionization cross section from electron distribution
24 p3400 A72-45592

IONIZATION FREQUENCIES

Ionization behind shock waves in nitrogen-oxygen mixtures.
20 p2958 A72-39601

Determination of the duration of the diffusional motion of charges in a plasma with allowance for bulk ionization
22 p3213 A72-43116

IONIZATION GAGES

NT BAYARD-ALPERT IONIZATION GAGES

NT PENNING GAGES

Bayard-Albert ionization vacuum meter use as primary standard, investigating ion orbiting and collecting processes
03 p0361 A72-13880

German monograph on experimental search for quarks in cosmic ultraradiation, describing hodoscope for particle ionization measurement
09 p1378 A72-23100

Reference transfer method for in situ calibration of ionization gages, determining pressure ratio of molecular gas flow through fixed orifices
10 p1480 A72-24147

Lunar surface neutral gas pressure measurement by Apollo 14 cold cathode ionization gage, determining day and night temperature effects on vacuum quality
12 p1805 A72-27041

Thermoemission ion gage stability and design aspects, discussing application as secondary standard for vacuum measurements
16 p2394 A72-33871

IONIZATION POTENTIALS

Fe I and Ti I excitation temperatures and ionization potentials of late G and K giant stellar atmospheres, comparing with model predictions
07 p1069 A72-19077

Saha equation for plasma ionization energy lowering, using three particle distribution function and BBGKY hierarchy
08 p1212 A72-20939

Ions classification by ionization potential to explain existence of empirically defined classes for visible solar corona lines
10 p1542 A72-24614

Structure of lower main sequence stars, considering ionization equilibrium in outer convection zone
10 p1546 A72-24835

Air composition and thermodynamic properties at 12,000-25,000 K and 0.1-100 atm with allowance for Coulomb interaction effect on pressure and for ionization potential decrease
13 p2018 A72-29878

HD absorption spectrum measurements in vacuum UV region for Rydberg states and ionization energy determination
16 p2431 A72-33583

Transverse magnetic field effects on cylindrical hollow cathode discharge voltage-current characteristics, noting sustaining potential and recombination probability changes
17 p2593 A72-35886

The ionization of caesium vapour by the method of space charge amplification.
23 p3316 A72-44344

IONIZED GASES

NT CATIONS

NT CESIUM PLASMA

NT CHARGED PARTICLES

NT COLD PLASMAS

NT COLLISIONLESS PLASMAS

NT COSMIC PLASMA

NT ELECTRON PLASMA

NT PLASMA CLOUDS

NT PLASMA JETS

NT PLASMA LAYERS

NT PLASMA SHEATHS

NT PLASMA SLABS

NT RELATIVISTIC PLASMAS

NT SOLAR WIND

NT STELLAR WINDS

NT THERMAL PLASMAS

NT TOROIDAL PLASMAS

Ionized argon recombination rate constant determination as function of temperature, using dual frequency laser interferometry measurement of corner expansion flow
01 p0050 A72-10851

Thermal conductivity, electrical conductivity, viscosity and diffusivity of ionized gas-solid suspension in electric field, using transport equations and particle interaction potentials
01 p0111 A72-11332

Electron temperature profile across nonequilibrium stagnation point boundary layer in partially ionized gas, investigating charged particles interaction with body in ionosphere
02 p0262 A72-12268

Electron impact Stark broadening of ionized chlorine lines in pulsed arc plasma using laser interferometric and spectroscopic measurements
03 p0396 A72-13748

Small sphere hydrodynamic drag in ionized gas at local thermodynamic equilibrium, taking into account

nonlinear transport properties variations with temperature
[ASME PAPER 71-APM-CC] 04 p0558 A72-15176

Nonequilibrium stagnation heat transfer mathematical models for injecting He, Ar or H into ionizing air laminar viscous layers at low Reynolds numbers
[ASME PAPER 71-WA/HT-18] 05 p0744 A72-15877

Energetic electrons absorption cross sections in weakly ionized atomic oxygen gas, showing energy losses through excitation
05 p0655 A72-16071

Electron density and diffusion measurements in ionized air in front of strong shock wave with resonant microwave probe and electromagnetic induction technique
05 p0648 A72-16211

Neutral atoms pressure distribution along capillary and pressure compensating channel during discharge in argon ion laser
05 p0670 A72-16990

Phenomena in ionized gases - Conference, Oxford, England, September 1971
05 p0699 A72-17216

Interelectrode gas-filled gap electron avalanche formation effects in weak electric field, calculating ionization coefficient
06 p0863 A72-18411

Contraststreaming electron beams instability in finite length one dimensional system with stationary neutralizing ion background, analyzing electrostatic waves space/time development by numerical simulation
06 p0865 A72-18540

Monatomic ionized radiating gas nonequilibrium flow in blunt body stagnation region behind shock wave during hypersonic atmospheric reentry
07 p0909 A72-20083

Galactic nucleus IR measurements in terms of forbidden NE II emission line at 12.8 microns
07 p1081 A72-20229

F region electron-ion gas dynamic model with stability dependence on periodic solutions convergence of continuity equations
08 p1153 A72-20725

Redshifted L alpha flux upper limit restricting hot ionized gas models for gravitational binding of Coma galactic cluster
09 p1383 A72-22292

Transition probabilities of ionized Ar spectral lines for excitation temperature measurements
09 p1355 A72-22672

Fast response pressure gage for short duration shock reflection measurements in shock tubes, using dual capacitive sensing elements with signal differencing for ionized gases
09 p1315 A72-23401

Radio telescope observation of galaxy NGC 5253 in 21 cm line, noting centrally condensed emission complex of ionized gas
10 p1543 A72-24620

Nonequilibrium partially ionized viscous shock layer on blunt body, determining electron temperature and electron-ion density profiles
11 p1744 A72-25560

Neutral atoms pressure distribution along capillary and pressure compensating channel during discharge in argon ion laser
12 p1819 A72-27133

Local emission coefficients fields for ionized gas in arbitrary and rectangular cross section streams
13 p2008 A72-29894

Galactic structure, ionized gas distribution and radio source diameter studies from interstellar scattering at 81.5 MHz, comparing with pulsars
13 p2050 A72-29962

Microwave interferometry as plasma diagnostic technique to measure electron densities in partially ionized dense gases
14 p2103 A72-30177

Ionized gas effect on interstellar space synchrotron emission, noting magnetic field orientation-dependent low frequency cut-off
14 p2156 A72-30559

Dc and RF sputter deposition in ionized inert gas of thin film coatings solid state microelectronics, solid lubricants and corrosion resistance applications
[ASME PAPER 72-DE-37] 14 p2108 A72-30871

Ionized and neutral species concentration in rarefied hypersonic wake flow behind cone, using electrostatic and electron density probes
15 p2177 A72-31209

Monatomic ionized gas thermodynamic properties direct computation by numerical method without iteration or numerical differentiation
15 p2335 A72-31714

Potential energy curves for exothermic reaction between oxygen cations and nitrogen molecules to form nitric oxide and atomic nitrogen
16 p2360 A72-32921

CW laser transitions in singly ionized Te vapor spectrum at 4843-9378 Å, indicating charge transfer as dominant excitation mechanism
16 p2401 A72-33394

- Ionized gas-solid suspension thermal physical properties verification by micro-sized MgO dispersion in Ar plasma
[AIAA PAPER 72-688] 16 p2439 A72-34054
- Statistical correlation of X-band microwave scattering by overdense intermittently turbulent ionized Ar jet with flux fluctuations from electrostatic probe observations
[AIAA PAPER 72-674] 16 p2440 A72-34065
- Intergalactic ionized gas and member galaxies mass relationship in local group and nearby galactic clusters, considering gravitational potential
17 p2604 A72-34475
- Simplified expressions for the calculation of the contribution of the heavy components to the transport coefficients of partially ionized gases.
17 p2589 A72-34896
- Study of the motion of ionized artificial clouds in the upper atmosphere
18 p2688 A72-36864
- Nonstationary electron-ion gas distribution in the ionosphere
18 p2689 A72-36878
- Yugoslav Symposium on Physics of Ionized Gases, 6th, Miljevac, Yugoslavia, July 16-21, 1972, Proceedings.
18 p2713 A72-36951
- Singly and doubly ionized He plasma recombination and ionization coefficients due to electronic collisions and radiative absorption
19 p2841 A72-38083
- F region electron-ion gas dynamic model with stability dependence on continuity equations periodic solutions convergence
19 p2791 A72-38353
- Shock tube boundary layers in ionized argon-helium mixtures.
20 p2914 A72-39639
- Sound propagation in ionized gases and electroacoustic effect.
21 p3085 A72-40993
- Multicomponent diffusion and heat transfer in flows of a chemically balanced ionized gas past bodies
21 p3047 A72-41658
- Gum nebula origin as ionized hydrogen cloud from prehistorical supernova explosion, discussing different ionization mechanisms
22 p3227 A72-42543
- New lines of neon ions in the range 50-200 Å.
23 p3315 A72-43802
- ### IONIZED PLASMAS
- #### U PLASMAS (PHYSICS)
- ### IONIZERS
- Time dependent and stationary two dimensional calculation of current and potential distributions in MHD generator preionizer and entrance region flow
13 p2013 A72-29358
- ### IONIZING RADIATION
- NT ALPHA PARTICLES
NT BETA PARTICLES
NT COSMIC RAY SHOWERS
NT COSMIC RAYS
NT FAR ULTRAVIOLET RADIATION
NT GAMMA RAY BEAMS
NT GAMMA RAYS
NT LYMAN ALPHA RADIATION
NT LYMAN BETA RADIATION
NT NEAR ULTRAVIOLET RADIATION
NT PRIMARY COSMIC RAYS
NT SECONDARY COSMIC RAYS
NT SOLAR COSMIC RAYS
NT SOLAR X-RAYS
NT ULTRAVIOLET RADIATION
NT X RAYS
- Inner and outer belt electron differential energy spectra from Cosmos 228 satellite data, discussing fluxes of precipitating and quasi-captured particles
02 p0272 A72-11916
- Penetration depth of hf electromagnetic waves in weakly ionized plasma, considering nonlinearity effect on ionization balance
03 p0394 A72-13085
- Vitreous silica and silicon-silicon dioxide interface defect structure and behavior during ionizing or particle irradiation
03 p0403 A72-14081
- Ionizing radiation effects in cavities of microwave Gunn oscillators, noting large dose rate effects on circuit performance
03 p0335 A72-14094
- Carbohydrate metabolism, glycolytic ferment activities and leukocyte size under ionizing radiation, showing compensatory bone marrow cell formation with leukopenia
04 p0467 A72-14609
- Ionizing radiation as effective energy in primordial organic synthesis, discussing small molecule formation and subsequent condensation into polypeptides and polynucleotides
05 p0617 A72-16127
- Pulsed and hf electric field effects on ionizing particle recording in nuclear and photographic emulsions
06 p0816 A72-17833
- Bacteriophage synergistic inactivation by heat and ionizing radiation from kinetic model describing dose rate and temperature dependences
06 p0768 A72-18185
- Circadian periodicity of resistance to ionizing radiation in pocket mouse at high and low metabolic rate
07 p0918 A72-19532
- High energy particle and ionizing radiation effects on glasses in aerospace environment
09 p1336 A72-22402
- Burn in technique in nonvolatile metal oxide semiconductor /MOS/ memory using ionizing radiation of reprogrammable electron beam
10 p1443 A72-23927
- Luminous filaments model of density condensations optically thick to ionizing radiation in planetary nebulae
10 p1550 A72-25197
- Inner and outer belt electron differential energy spectra from Cosmos 228 satellite data, discussing fluxes of precipitating and quasi-captured particles
13 p2030 A72-29228
- Penetration depth of HF electromagnetic waves in weakly ionized plasma, considering nonlinearity effect on ionization balance
13 p2015 A72-29435
- Shielding metallic interlayer technique to protect MIS device against degradation due to ionizing radiation effects
13 p2023 A72-29836
- P channel MOS transistors hardening against ionizing radiation based on positive space charge density and electrode injection efficiency
13 p2023 A72-29837
- Scintillation $\text{TiCl}_4/\text{I,Be}$ / crystal response to 8 GeV ionizing negative pions, noting pulse shape and resolution characteristics
15 p2291 A72-31535
- Hypothermia, asphyxia and ionizing radiation effects on rat immunological defense mechanisms against particulate antigens
16 p2355 A72-33555
- French monograph - Experimental characterization and analysis of the effect of ionizing radiation on the electrical properties of MOS transistors
17 p2531 A72-35650
- Theoretical investigation of nitric oxide and its role in D-region ionization.
20 p2918 A72-39531
- Ionizing radiation effects on mitosis and nucleic acid synthesis, noting protective chemical agents and hematological evaluation of radiation damage and marrow regeneration
22 p3141 A72-41986
- Influence of ionizing radiation on the tooth organ
22 p3141 A72-41987
- Variation of the output of radioluminescence of organic scintillators with energy loss and the number of charges of ionizing particles
22 p3180 A72-42938
- Electronic detection of ionizing-particle tracks in liquid argon
23 p3291 A72-44442
- ### IONOGRAMS
- Daytime bottomsides polar F layer latitudinal cross section construction from ionograms recorded in aircraft
[AD-738278] 01 p0061 A72-10900
- Daytime ionogram corrections for underlying ionization in absence of X-trace of sporadic E layer
05 p0657 A72-16265
- F 2 layer diffuse reflections and critical frequencies increase on ionogram recordings during Northern Hemisphere nighttime magnetic storm of 2 December 1967, noting cosmic radio emission decrease
08 p1154 A72-20738
- Ionogram electron density-height distributions for analysis of multiple cusp structure near E region critical frequency
08 p1156 A72-21101
- Lower ionosphere N/H/ profile calculation from ionograms with incomplete layer information
18 p2689 A72-36880
- F 2 layer spread reflections and critical frequencies increase on ionogram recordings during Northern Hemisphere nighttime magnetic storm of 2 December 1967, noting cosmic radio emission decrease
19 p2791 A72-38366
- ### IONOSONDES
- Directional ionosonde aerials and instrumentation for ionospheric reflection angle of arrival measurements
01 p0053 A72-10091
- Ionospheric heating effects of vlf radio wave transmitters, relating changes in electron density and collision frequencies, reflection coefficients and wave fields
08 p1132 A72-21104
- FM/CW interferometric ionosonde used for interferometric direction finding, computing incident azimuth and elevation from baseline array phase differences
09 p1281 A72-23514
- Sporadic E layer structure model from radiosonde observation, noting peak plasma frequency variation and total reflection by blobs
10 p1441 A72-25153
- Ionosonde observations and Faraday rotation measurements of E and F region total electron content during two solar eclipses
12 p1801 A72-27154
- Sporadic E layer structure and dynamics diurnal and seasonal variations from ionosondes frequency and drift measurements
12 p1804 A72-27781
- Ground recorded Pc 1 micropulsations occurrence frequency relationship to ionospheric spread F based on long term ionosonde recordings
18 p2685 A72-35987
- Ionosonde receiver with automatic noise suppression and digital-analogue recording of the first ionospheric reflection.
19 p2805 A72-38867
- ### IONOSPHERE
- NT D REGION
NT E REGION
NT F REGION
NT LOWER IONOSPHERE
NT SPORADIC E LAYER
NT UPPER IONOSPHERE
- Discrete ionospheric model of supersonic two dimensional low density plasma flow past large bodies, using quasi-neutrality condition
01 p0001 A72-10588
- Nighttime ionosphere dynamical behavior, discussing motions effect on OI emission intensity
01 p0063 A72-10919
- Annual movements of satellite signals scintillation boundary in subauroral ionosphere
01 p0031 A72-10920
- Antenna lf impedance measurements of lower terrestrial plasma wave characteristics, using equivalent impedance probe circuit
02 p0172 A72-11946
- Papers on plasma physics, covering ionospheric plasma resonances, fusion research, electrostatic precipitator, two stream instability, adiabatic motion and relativistic beam equilibria
02 p0267 A72-12837
- Altitude, photon wavelength and solar activity effects on photoionization yield of ionospheric monatomic and diatomic oxygen and nitrogen via Monte Carlo simulation
03 p0345 A72-12983
- Ionospheric hydromagnetic and acoustic gravity wave interactions, examining stratified nonisothermal atmospheric model
04 p0516 A72-14934
- Transverse electric field in ionosphere and magnetosphere during inhomogeneities consisting of fast electrons
05 p0656 A72-16246
- Diffusion equations of ion components of plane stratified plasma /ionosphere/, taking into account wind effect and vertical temperature distribution
05 p0658 A72-16402
- European Space Research and Technology Center /ESTEC/ results in cosmic rays, ionospheric physics and surface physics
05 p0644 A72-16754
- Ionospheric geocoronal L alpha emission intensity related to solar activity level from Cosmos 215 satellite data
05 p0659 A72-17038
- Venus daytime ionosphere at 100-500 km, discussing ion clustering processes below 100 km forming UV haze layer and atmospheric composition
05 p0723 A72-17163
- Plasma line enhancement variabilities in ionospheric modification experiments due to radar wave scattering, number density gradient and diagnostic beam temperature and orientation
06 p0805 A72-17470
- Geomagnetic field intensity fluctuations due to events in atmosphere, ionosphere, magnetosphere and in interplanetary space connected with solar activity
06 p0809 A72-18276
- Structural interactions between magnetosphere and ionosphere in terms of electrostatic field associated with plasma temperature difference
07 p0979 A72-20046
- Collisionless ion beam plasma simulation of ionospheric plasma with Langmuir interpretation of density and frequency agreement
07 p1044 A72-20367
- Thermal positive ion densities measurement in outer ionosphere and magnetosphere by OGO 1 satellite, relating plasmopause distribution and magnetic activity level
[AD-742186] 09 p1300 A72-23011
- Ionospheric and magnetospheric electric field measurements by rocket, satellite or balloon-borne electrostatic probes or by plasma drift methods
10 p1473 A72-24529
- Book on earth environment covering atmospheric structure, terrestrial magnetic field, solar radiation, micrometeorites, ionosphere and van Allen belts
10 p1478 A72-25173

Twilight and nighttime ionospheric temperatures from oxygen 6300 and 5577 Å spectral line profiles obtained with Fabry-Perot interferometers 11 p1625 A72-26406

Solar activity maximum annual variations effect on ionospheric parameters 12 p1868 A72-27306

Ionosphere - Conference, Kleinheubach, West Germany, September 1971 12 p1802 A72-27769

Upper atmosphere electric fields derived from ionosphere-earth electric potential measurements following solar flare activity 12 p1804 A72-27805

Solar activity effects in magnetosphere and ionosphere relation to geomagnetic activity and biospheric development, noting 11 year geomagnetic perturbation cycles 12 p1805 A72-28209

Antenna LF impedance measurements of lower terrestrial plasma wave characteristics, using equivalent impedance probe circuit 13 p1920 A72-29258

Artificial barium ion cloud spatial-temporal growth in ionosphere, solving ion diffusion equation by numerical methods 13 p1950 A72-29387

Positively and negatively charged plasma components thermodynamic density fluctuations effect on ionospheric and magnetospheric slowly varying electric fields measurement 13 p1953 A72-29810

Magnetospheric and ionospheric potential electric fields, using variational process based on transverse/longitudinal conductivity ratios in plasma 14 p2100 A72-30633

Ionospheric plasma resonance time duration variation with latitude, altitude and ratio of electron plasma frequency to electron cyclotron frequency 15 p2223 A72-31429

Report to COSPAR on West German space program covering meteorology, aeronomy, ionospheric physics, magnetosphere, solar wind and radiation, solar system and life sciences 15 p2338 A72-32014

Geomagnetic substorm magneto-ionospheric effect, discussing electric field transmission, magnetic field variations and currents flowing in dynamo region 15 p2230 A72-32259

Theory of magnetically conjugate transport of cold plasma in the outer low-latitude ionosphere 17 p2548 A72-35218

Russian book - Morphology and physics of the polar ionosphere 17 p2550 A72-35851

Determination of the quenching of O(1D) by molecular nitrogen using the ionospheric modification experiment. 18 p2685 A72-35991

Phase-plane solution for the electrostatic field of an ionospheric satellite. 18 p2728 A72-36950

Diurnal variation of the H⁺ flux between the ionosphere and the plasmasphere. 19 p2793 A72-38759

Magnetosphere-ionosphere interactions; Proceedings of the Advanced Study Institute, Dalseter, Norway, April 14-23, 1971. 20 p2917 A72-39526

Analytic expressions for electron energy transfer rates for nitrogen and oxygen vibrational excitation in ionosphere, applying to atmospheric and ionospheric computer modeling 22 p3168 A72-42001

A measurement of ionospheric electric fields at high latitude. 22 p3169 A72-42015

Conference on Theoretical Ionospheric Models, Pennsylvania State University, University Park, Pa., June 14-16, 1971, Proceedings. 24 p3399 A72-45579

A numerical integration method useful for studying ionospheric phenomena. 24 p3399 A72-45582

A theoretical model of the ionosphere dynamics with interhemispheric coupling. 24 p3400 A72-45588

Continuity equation for dynamic auroral ionospheric model relating electron density profiles to auroral arc brightness 24 p3400 A72-45589

Photoionization and photoabsorption cross sections for ionospheric calculations. 24 p3400 A72-45590

IONOSPHERIC ABSORPTION
U ELECTROMAGNETIC ABSORPTION
U IONOSPHERIC PROPAGATION
IONOSPHERIC BLACKOUT
U BLACKOUT [PROPAGATION]
IONOSPHERIC COMPOSITION
 Ionospheric composition of ions and neutral gases during magnetic storm, using coupled differential equations 01 p0054 A72-10425

Positive ion composition in equatorial D region, investigating reaction kinetics 03 p0412 A72-13522

Magnetospheric heat flux effect on height variation of electron and ion temperatures and ion composition in topside ionosphere 04 p0515 A72-14929

Upper atmosphere and ionosphere magnetic storm phenomena, showing atomic to molecular concentration ratio decrease 04 p0516 A72-14938

Ionospheric neutral composition variations as function of height, local time and solar activity 05 p0656 A72-16235

Nighttime polar atmospheric structure and temperature variations due to gas kinetic and electron energy changes 05 p0656 A72-16240

Oxygen, nitric oxide and water cluster positive ion composition from mass spectrometer experiments in lower ionosphere, noting ion production and low temperature effects 09 p1375 A72-22363

E region ion density and composition determination by incoherent scatter radar measurement [AD-742618] 09 p1375 A72-22365

Day, night and sunset mesospheric nitric oxide concentrations during polar cap absorption from rocket measurements of cation composition and charged particle densities [AD-741709] 09 p1300 A72-23026

Van Allen proton belt model, considering ionosphere particle acceleration by stochastic interaction with hydromagnetic waves due to solar wind at magnetosphere shock front 10 p1529 A72-24245

Ionosphere composition and ion concentration measurements for D and E region, including aerodynamic and plasma dynamic effects 11 p1621 A72-25836

Rocket-borne mass spectrometric studies of composition of lower thermosphere 11 p1622 A72-25847

Nitric oxide and oxygen molecular ion composition of lower ionosphere during solar eclipses from rocket measurements [AD-744403] 12 p1801 A72-27150

Thermospheric ion, electron and neutral particle concentration, composition and temperature changes during 7 March 1970 solar eclipse from rocket measurements 12 p1778 A72-27152

ATS F Environmental Measurements Experiment package for synchronous altitude space environment and electromagnetic-ionospheric interactions studies 12 p1795 A72-27525

Atomic/molecular oxygen concentration ratio semi-annual variation at 130 km altitude from mass spectroscopic data analysis 13 p1949 A72-29259

Photochemical model of N and NO distribution based on E region ion composition 15 p2226 A72-31916

Nighttime molecular nitrogen and oxygen number density profiles at 130-220 km over Sardinia from ESRO mass spectrometer measurements 15 p2226 A72-31938

An investigation of the ionospheric D region at sunrise. I - Time variations of ozone, metastable molecular oxygen, and atomic oxygen. II - Estimation of some photodetachment rates. III - Time variations of negative-ion and electron densities. 18 p2656 A72-36295

Laboratory positive and negative ion composition measurements compared with D region ion-molecule reaction observations 20 p2917 A72-39527

Recent positive and negative ion composition measurements in the lower ionosphere by means of mass spectrometers. 20 p2917 A72-39528

D region ion compositions model during quiet and intense PCA conditions associated with dissociative recombination and ion-ion neutralization 20 p2917 A72-39530

About the interaction between a satellite and its environmental ionospheric plasma. 21 p3090 A72-40454

Thermospheric atomic oxygen and molecular nitrogen densities from OGO 6 neutral atmospheric composition experiment, comparing with prediction by Jacchia models 22 p3172 A72-42431

Theoretical estimate of the effective recombination coefficient in the D region. 23 p3284 A72-43818

Theoretical models of the D-region. 24 p3399 A72-45580

The development of a theoretical model of the atmosphere and the ionosphere. 24 p3399 A72-45585

A theoretical model of the ionosphere dynamics with interhemispheric coupling. 24 p3400 A72-45588

IONOSPHERIC CONDUCTIVITY

Collision frequencies definition in kinetic theory of gases, expressing ionospheric electron conductivity 03 p0345 A72-12979

Electrical conduction in orthogonal coordinates from nondipole geomagnetic field effect on conductivity tensor of ionospheric dynamo region 05 p0657 A72-16260

D region positive ion and electron conductivities and densities measurement by parachute borne blunt probes during 1970-1971 winter anomaly 09 p1376 A72-22373

Height integrated ionospheric conductivity calculated using numerical model and approximate formulas 09 p1300 A72-23017

Topside ionosphere characteristics, discussing particle mean free path and geomagnetic field effects on conductivity, plasma anisotropies and latitudinal variations 10 p1473 A72-24704

Magnetospheric electrons precipitation into ionosphere due to conjugate conductivity asymmetry caused by wind induced ions vertical redistribution, using atmospheric model 10 p1530 A72-24791

Charged particle thermodynamics in ionosphere, considering energy exchange due to collisions or thermal conductivity 11 p1621 A72-25837

Characteristic functions of potential distribution on sphere with longitude dependent conductivity for application to ionosphere electrodynamics 14 p2101 A72-30644

Potential waves generation by transverse current in ionospheric electrojet region, discussing lower hybrid resonance domain 15 p2232 A72-32732

Dawn and dusk ionospheric conductivity gradients effects on equatorial electrojet, deriving vertical currents existence 16 p2385 A72-33377

Low latitude equatorial electrojet analysis based on three dimensional electric field equation for ionosphere and magnetosphere 18 p2687 A72-36854

IONOSPHERIC CROSS MODULATION
 Observations of D-region modifications at low and very low frequencies. 18 p2662 A72-37009

Monochromatic plasma waves linear and nonlinear coupling, discussing LF modulation partial transfer /Luxembourg effect/ and application to ionospheric diagnostics 23 p3319 A72-43517

IONOSPHERIC CURRENTS

NT AURORAL ELECTROJETS
NT ELECTROJETS
NT EQUATORIAL ELECTROJET
 Hall effect and magnetic field characteristics in lower ionosphere by vertical magnetospheric currents, using gyrotronic model 01 p0059 A72-10590

Auroral absorption and DR currents development during magnetic storms, discussing corpuscular fluxes arrival from magnetospheric tail into lower ionosphere 01 p0059 A72-10619

Rocket-borne measurement of Birkeland ionospheric current density associated with auroral arc and electrojet 01 p0061 A72-10898

Spectrum analysis of synchronous recordings of Pi 1 irregular pulsations and auroral brightness at Sogra for ionospheric electric fields 02 p0216 A72-11923

Magnetospheric substorm model for auroral activity sudden increase and ionospheric current development explanation by shock wave excitation in magnetospheric tail neutral layer 02 p0217 A72-11927

Incomplete ring current decay during magnetic storm development, discussing field asymmetry based on global network synchronous observations and generation mechanism by protons 02 p0218 A72-11949

Ionospheric effects related to production, maintenance and control of geomagnetically aligned Birkeland current system 02 p0219 A72-11978

Quiet auroral arcs formation by ionospheric instability and field aligned current triggering 02 p0220 A72-12451

Longitudinal wave interaction and excitation by plasma instability in equatorial electrojet, considering energy transfer mechanism 05 p0656 A72-16242

Noncircular ionospheric current conversion into longitudinal currents in magnetosphere along lines of force of geomagnetic field 05 p0657 A72-16259

Lower ionospheric currents fields, determining Hall conductivity and geomagnetic lines of force slope effects 05 p0657 A72-16266

Magnetic perturbations in near polar region and morning-night sectors of auroral oval as function of current sources and modulation by universal time

05 p0657 A72-16276

Magnetic baylike disturbances and multiple midlatitude 6300-A auroral arcs during geomagnetic storm recovery phase and concurrent ionospheric current system

05 p0630 A72-16620

Rocket-borne vector magnetometer measurements of midlatitude ionospheric currents near sporadic E, noting nearly uniform vertical distribution

06 p0804 A72-17459

Magnetoguided whistler propagation, observing longitudinal current in ionospheric plasma

06 p0808 A72-18064

Nighttime ionospheric dynamo current modulation due to galactic X ray ionization, observing diurnal sidereal time variation in geomagnetic field

07 p1056 A72-18898

Ionosphere electric field sources, magnitudes, relation to currents and effects on ionization distributions and electron density irregularities

07 p0978 A72-20043

Geomagnetic effect of solar wind rotational discontinuity observed by Explorer 34, noting high latitude nonstationary ionospheric current attenuation and magnetic disturbances

08 p1225 A72-20715

Polar magnetic substorm generation through ionospheric current intensification in westward electrojet localized region, noting interplanetary magnetic field role

08 p1159 A72-21494

Interplanetary magnetic field direction and high latitude ionospheric currents in dayside auroral regions, showing plasma drift induced magnetic disturbances

11 p1626 A72-26419

Electric field nature required for DP current system development in disturbed high latitude ionosphere, discussing F 2 region ionization drift

13 p1946 A72-28596

Spectrum analysis of synchronous recordings of Pi 1 irregular pulsations and auroral brightness at Sogra for ionospheric electric fields

13 p1948 A72-29235

Magnetospheric substorm model for auroral activity sudden increase and ionospheric current development explanation by shock wave excitation in magnetospheric tail neutral layer

13 p1948 A72-29239

Incomplete ring current decay during magnetic storm development, discussing field asymmetry based on global network synchronous observations and generation mechanism by protons

13 p1949 A72-29261

Radio aurora ion-acoustic wave propagation direction divergence due to magnetic field distortion by large ionospheric horizontal sheet current [AD-746367]

13 p1923 A72-29662

E region electron density distortion at magnetic equator by Sq current system, noting dependence on alpha coefficient profiles

13 p1952 A72-29663

Three layer atmospheric model for neutral gas motion-produced ionosphere and magnetosphere currents, electromagnetic field and charged particle concentration perturbations

14 p2100 A72-30632

Dawn and dusk ionospheric conductivity gradients effects on equatorial electrojet, deriving vertical currents existence

16 p2385 A72-33377

Dispersive motions in the ionosphere.

17 p2546 A72-34696

Book on ionosphere and magnetosphere covering solar radiation effects, ionospheric layers, currents and storms, charged particle movement and various wave propagations

17 p2550 A72-35850

Auroral zone splitting into various radiation intensity regions, discussing DR currents influence on particle motion in magnetosphere and structural relationship

17 p2550 A72-35856

Influence of ionospheric currents on the geometry of auroral radio echoes

17 p2519 A72-35875

Models for F region and topside ionospheric storms morphology, discussing electric current disturbance at polar region

18 p2685 A72-35994

Geomagnetic effect of solar wind rotational discontinuity observed by Explorer 34, noting magnetic storm initial phase relation to high latitude nonstationary ionospheric current attenuation

19 p2852 A72-38343

Elliptically polarized ionospheric source generation of short period geomagnetic disturbances at earth surface

19 p2791 A72-38347

Radial penetration of a hot plasma associated with a large-scale electric field in the magnetosphere, and some related problems.

20 p2916 A72-39228

Polar upper ionosphere morphology above E layer, discussing effects of winds, field aligned currents and electron precipitation

20 p2918 A72-39534

Ionospheric and magnetospheric electric field strength measurements in auroral and polar cap regions by Ba ion cloud and double floating probe techniques

20 p2918 A72-39543

The Harang discontinuity in auroral belt ionospheric currents.

20 p2920 A72-39980

Geomagnetic DP-2 variation base level from E region electron drift velocity measurements in equatorial electrojets

22 p3169 A72-42013

Different conductivities effect in ionospheric E layer of polar cap regions, noting electric current along high latitude magnetic field force lines

23 p3283 A72-43370

Ionospheric current relation to magnetospheric field-aligned and ring currents, noting effect of magnetospheric tail electric field on polar magnetic substorms

24 p3396 A72-44852

Polar cap magnetic field induced by currents along magnetospheric lines of force during polar substorm

24 p3397 A72-45087

Electric field nature for DP current system development in disturbed high latitude ionosphere, discussing F 2 region ionization drift

24 p3398 A72-45096

IONOSPHERIC DISTURBANCES

NT IONOSPHERIC STORMS

NT SUDDEN IONOSPHERIC DISTURBANCES

NT TRAVELING IONOSPHERIC

DISTURBANCES

Lower ionosphere ionization response to auroral particle fallout during 1968 substorms, using geomagnetic, VLF and balloon measurements

01 p0053 A72-10366

Ionogram observations of F layer electron rarefaction wake disturbance during small rocket ascent

01 p0054 A72-10423

Wind profile determinations at 90-100 km from meteor trail drift and ionosphere inhomogeneity radar data, noting semidiurnal harmonics in wind components

01 p0058 A72-10563

VLF noise spectra in earth-ionosphere cavity due to thunderstorm discharges, noting resonance level splitting by geomagnetic field

01 p0028 A72-10598

Log normal random fluctuations of ionospheric electron concentration in F region from vertical sounding and incoherent scatter data

01 p0059 A72-10609

Sizes, shapes and temporal characteristics of small scale inhomogeneities in F region, using vertical sounding, space diversity reception and radio astronomy

01 p0059 A72-10610

Midlatitude vhf phase detection of magnetic field aligned ionospheric irregularities

01 p0031 A72-10916

Night sky upper ionospheric electron concentration perturbations during magnetic storm, noting latitudinal distribution

02 p0217 A72-11940

Quiet auroral arcs formation by ionospheric instability and field aligned current triggering

02 p0220 A72-12451

Nighttime radio satellite scintillation from ionospheric irregularities heights associated with magnetic activity at subauroral latitudes

02 p0221 A72-12468

Three frequency radar spectral measurements of two stream and gradient plasma instabilities in equatorial electrojet as function of wavelength

03 p0349 A72-13521

Quiet day diurnal variability of equatorial geomagnetic field H component related to ionospheric dynamics

04 p0515 A72-14878

F 2 layer anomalies association with equatorial electrojet, investigating midday critical frequencies of sporadic E layer

04 p0515 A72-14932

High latitude scintillation effects on vhf and S band polar orbiting satellite transmissions, examining ionospheric irregularities

04 p0487 A72-14952

Small scale F region irregularities at Varanasi, plotting horizontal drift velocities and directions, axial ratios and orientations and rms random velocity values histograms

04 p0517 A72-14954

F 1 region ion structure during ionospheric magnetic disturbances by numerical simulation of quiet and

disturbed conditions based on electron concentration profiles

05 p0656 A72-16247

Magnetic storm disturbing effect on integral electron density in F 2 layer and in topside ionosphere

05 p0657 A72-16262

F 2 layer critical frequency deviations and negative disturbance zones during solar eclipse of 22 September 1968

05 p0657 A72-16264

Geomagnetic pulsations correlation with h type ionospheric sporadic echoes, considering effects on electromagnetic disturbances transmission

05 p0659 A72-16725

Ionospheric scintillation fading observations by NASA satellite tracking and data acquisition networks, noting frequency dependence in auroral regions

[AIAA PAPER 72-220]

05 p0631 A72-16858

Structure and movements of E region inhomogeneities, describing ionospheric drift velocities and directions for different seasons

05 p0660 A72-17178

Cosmic plasma phenomena in astrophysics, discussing distribution, ionospheric disturbances, magnetospheric waves, solar wind, etc.

05 p0723 A72-17217

Ionospheric disturbance in American zone during IGY-IGC, showing latitudinal, annual and diurnal solar variations effects and regional geomagnetic anomaly

06 p0806 A72-17641

Sunspot cycles effect on F region drifts and irregularities from observations at Ibadan during 1966/67, noting seasonal and diurnal variations

06 p0806 A72-17643

Electrodynamics of ionosphere and magnetosphere, discussing irregularities, red arc and auroral thermosphere density and temperature changes

06 p0809 A72-18279

Midlatitude F region wavelike disturbances detection by hf radio echo techniques, discussing correlation with jet stream associated tropopause wind patterns

07 p0974 A72-18885

Ionospheric scintillations relationship to airglow emission spectrum at 6300 A

07 p0974 A72-18895

F region electron density variation above North America during geomagnetic disturbance on 28 May 1970

[AD-739792]

07 p0976 A72-19162

Radio wave alternating electric field heating of ionospheric plasma electrons with density increase below 200 km and decrease at F layer maximum

08 p1152 A72-20703

Wave-like ionospheric disturbance effect on phase polarization fading of vertical sounding signal, using numerical integration by computer

08 p1130 A72-20709

F 2 region magnetic disturbances conjugacy mechanisms, considering vertical ionization profiles

08 p1155 A72-20801

Vertical distribution of electron density seasonal anomaly and storm effects in daytime midlatitudes topside ionosphere from Alouette 1 data

08 p1155 A72-20814

Perturbation effects on F 2 layer and outer ionosphere electron density profiles during successive magnetic storms from Alouette 1 satellite data

08 p1157 A72-21145

Propagation by direct backscatter on aligned irregularities in auroral F layer, noting horizontal ionization gradients role

08 p1158 A72-21220

F region disturbances, explaining critical frequency changes on basis of neutral winds, electrodynamic drift and temperature and chemical composition variation

08 p1158 A72-21222

Laboratory ionization chamber measurement of ion chemistry and production rates from partial simulation of disturbed nighttime ionosphere at 300 K

09 p1275 A72-22368

HF radio waves induced incoherent scatter spectrum enhancement, noting parametric instabilities in ionosphere

09 p1279 A72-23014

Wave propagation effects on irregularities observation in equatorial electrojet, presenting velocity profile and typical ray path

09 p1300 A72-23024

Turbulent LF electric field fluctuations relationship with disturbed F region, spread F and scintillations of radio stars and satellites

09 p1300 A72-23025

Ionospheric disturbances due to shock front from Apollo 15 launching, using split signal observation in ion acoustic and normal mode

09 p1397 A72-23569

Ionospheric inhomogeneity studies from angle of arrival recordings of satellite beacon transmissions, using phase radiometer interferometry

09 p1305 A72-23576

Three dimensional linear analysis of ionosphere cross field instability, noting potential as E region irregularities source
10 p1478 A72-25166

Ionospheric physics, attributing anomalies to plasma motions
11 p1621 A72-25835

Russian papers on ionospheric perturbations and effects on radio communication covering vertical ionization profiles, F 2 critical frequencies, short wave propagation, etc
11 p1593 A72-26266

Ionospheric disturbances relation to interplanetary positive ion and proton fluxes intensity and velocity from Mariner 2, Venus 3 and Vela 2 observations, discussing F 2 region
11 p1713 A72-26268

F 2 region critical radio frequencies forecasts from solar cycles, ionospheric disturbances data, latitude and annual and diurnal variations
11 p1594 A72-26272

Geometric parameters variations of ionospheric N/h/ profiles and characteristics during magnetic storm, discussing prognosis procedures from solar activity, latitude and season
11 p1594 A72-26273

Diurnal variations of F 2 region critical frequencies and quiet and perturbed ionosphere N/h/ profiles during solar cycle, estimating signal reflection altitudes
11 p1594 A72-26274

Angles of arrival and skip distances prediction of radio waves near MUF, using monthly forecasts of quiet and perturbed ionospheric parameters and N/h/ profiles
11 p1594 A72-26276

Ionospheric and magnetic disturbances effects on short wave radio links, using directional antennas and 1.5-24 MHz frequencies
11 p1594 A72-26279

Magnetic field line connection between F region irregularities causing scintillation and ionospheric conditions inducing spread E
11 p1625 A72-26405

Ionospheric weather index in terms of ionization irregularities at given time and place derived from continuous steep incidence HF Doppler soundings
11 p1627 A72-26518

Ionospheric irregularities-magnetospheric parameters relationship from satellite scintillation measurement, noting use as indirect electron precipitation indicator
12 p1803 A72-27772

Disturbed D layer electron density profiles at high energy particle incidence, using partial reflection method
12 p1864 A72-27783

Coincidence effects of subionospheric extraterrestrial radiation focusing on ionospheric changes and stratospheric warmings
12 p1804 A72-27804

Subauroral zone F region disturbances latitudinal variations catalogs from vertical sounding data, taking into account ionospheric states
13 p1946 A72-28598

Night sky upper ionospheric electron concentration perturbations during magnetic storm, noting latitudinal distribution
13 p1949 A72-29252

Transequatorial off-path propagation outside of great circle at decametric waves associated with forward scattering by field aligned irregularities in equatorial ionosphere
14 p2084 A72-30129

Disturbed ionospheric electron and ion kinetics, detailing dissociative recombination as regulating process for temporal evolution
14 p2102 A72-30654

Monitoring system for ionospheric disturbances prediction from satellite observation, discussing optimum locations for space stations
15 p2220 A72-31233

Atmospheric gravity waves effects in ionosphere, discussing F region traveling ionospheric disturbances, sporadic E layer and D region radar scattering
15 p2222 A72-31285

Solar event-related ionospheric horizontal electric fields derived from balloon measurement of mid-European and equatorial ionosphere potentials
15 p2223 A72-31556

Calculations of electron-profile disturbances in the F region during the passage of a neutral wave
17 p2551 A72-35861

Solution to a nonstationary continuity equation for disturbed ionospheric conditions
17 p2551 A72-35862

Certain characteristics of ionospheric disturbances in the F region during type A red colored polar auroras
17 p2551 A72-35866

Equatorial anomaly changes caused by ionospheric disturbances, noting diurnal variations of magnetic storm effect
17 p2551 A72-35868

Ground recorded Pc 1 micropulsations occurrence frequency relationship to ionospheric spread F based on long term ionosonde recordings
18 p2685 A72-35987

Nonlinear saturation of 'type I' irregularities in the equatorial electrojet.
18 p2685 A72-35990

Study of unsteady processes in the ionosphere and outer space by using quantum frequency stabilizers
18 p2687 A72-36853

Ionospheric magnetic disturbances during March 1970 related to solar flare corpuscular and proton fluxes, generating ring current and PCA absorption
18 p2688 A72-36857

Magnetospheric and ionospheric conjugate point phenomena as solar events manifestations via solar wind shock wave interaction with geomagnetic field
19 p2790 A72-37858

Radio wave alternating electric field heating of ionospheric plasma electrons with density increase below 200 km and decrease at F layer maximum
19 p2790 A72-38331

Ring current growth effects on midlatitude F region electron density change during large magnetic disturbances
19 p2790 A72-38334

Wave-like ionospheric disturbance effect on phase polarization fading of vertical sounding signal, using numerical integration by computer
19 p2765 A72-38337

A satellite survey of vector electric fields in the ionosphere at frequencies of 10 to 500 hertz. III - Low-frequency equatorial emissions and their relationship to ionospheric turbulence.
19 p2768 A72-38744

Determination of the orientation of ionospheric irregularities causing scintillation of signals from earth satellites.
19 p2794 A72-38866

Quiet day daily geomagnetic field variability associated with equatorial ionospheric upheavals, noting longitudinal extent
19 p2794 A72-38869

Seasonal, diurnal and magnetic dependence of ionospheric scintillation at 64 deg invariant latitude.
20 p2916 A72-39226

Observations of scintillations of two satellite beacons near the boundary of the irregularity region.
20 p2916 A72-39227

The interpretation of surface equatorial magnetic daily variations on disturbed days.
20 p2916 A72-39238

Formation of auroral patches in the midday sector during a substorm.
20 p2916 A72-39239

Perturbation effects on F 2 layer and outer ionosphere electron density profiles during successive magnetic storms from Alouette 1 satellite data
20 p2916 A72-39250

Characteristics of the abrupt scintillation boundary.
22 p3170 A72-42363

Aspect-sensitive reflections from ionization irregularities in the F-region.
22 p3154 A72-42364

Equatorial ionosphere irregularities vertical drift velocity calculation, showing agreement with incoherent scatter results
22 p3170 A72-42370

Radar auroral echo VHF power spectrum analysis of ionospheric irregularities, using range-time-intensity film strips
22 p3171 A72-42415

Power-law wavenumber spectrum deduced from ionospheric scintillation observations.
22 p3171 A72-42416

A possible connection between a barium cloud and electron intensity fluctuations observed on a rocket flight at Kiruna.
22 p3172 A72-42433

Geomagnetic storm and seasonal effects on spread of monthly distribution and average behavior of midlatitude F region electron peak density and slab thickness
22 p3172 A72-42434

Geometrical dimensions and effective number of large scale ionospheric inhomogeneities by F 2 critical frequency variability analysis
23 p3283 A72-43360

Radar observations of equatorial spread F in a region of electrostatic turbulence.
23 p3286 A72-44528

Subauroral zone F region disturbances latitudinal variations catalogs from vertical sounding data, taking into account ionospheric states
24 p3398 A72-45098

IONOSPHERIC DRIFT

Drift shells and pitch angle evolution of energetic particle motion in magnetospheric model including convection electric field
01 p0117 A72-10077

Ionospheric horizontal drifts during large vertical convection of mid dip-latitude postmidnight F region, using spaced antenna measurements
01 p0052 A72-10087

Substorm electron drift relationship to cosmic noise absorption on auroral zone morning side, calculating electron energy loss
01 p0063 A72-10918

Sporadic E layer motion and spreading under constant horizontal wind action, estimating lifetime
02 p0218 A72-11942

Equatorial ionospheric drift measurements and relation to electrojet from H component geomagnetic field variations
02 p0221 A72-12459

Small scale F region irregularities at Varanasi, plotting horizontal drift velocities and directions, axial ratios and orientations and rms random velocity values histograms
04 p0517 A72-14954

Diurnal and seasonal variations of F region irregularities drift and anisotropy parameters during IQSY from aerial fading records, noting magnetic activity effect
04 p0517 A72-14955

Ionospheric plasma drift instability, showing electric and magnetic fields, electron density and temperature effects
04 p0517 A72-14956

Magnetic latitude effect on wave dispersion in drifts and random movements of ionization irregularities in E region, suggesting charged particle precipitation role
04 p0518 A72-14964

Ion-acoustic instability in ionosphere in presence of fast particles inhomogeneity, estimating ions and electrons drift velocities
05 p0656 A72-16245

F 2 region electron density spatial and temporal distribution, investigating plasma vertical drift effects
05 p0657 A72-16263

Altitude dependent vertical drift velocity of small scale ionospheric inhomogeneities, using correlation of signal time lag scanning in frequency domain
05 p0657 A72-16270

Seasonal variations of semidiurnal tidal winds at 90-110 km from harmonic analysis of ionospheric inhomogeneity drift data
05 p0658 A72-16290

Structure and movements of E region inhomogeneities, describing ionospheric drift velocities and directions for different seasons
05 p0660 A72-17178

Sunspot cycles effect on F region drifts and irregularities from observations at Ibadan during 1966/67, noting seasonal and diurnal variations
06 p0806 A72-17643

Ionospheric movements measured by frequency spectra of signals incoherently scattered by ionospheric electrons [AD-738717]
06 p0808 A72-18085

PE sub s harmonic components diurnal and seasonal variations and latitudinal dependence, investigating relationship to drift velocity in E region
06 p0811 A72-18749

Electric field measurements in ionosphere and magnetosphere by double probe and electron and ion drift techniques
07 p0978 A72-20042

Ionospheric drifts measurement by small base diversity reception method, investigating dependence on receiving antennas orientation
08 p1154 A72-20731

Ionospheric drift characteristics from vertical and oblique radio soundings, discussing instrumental effects
08 p1156 A72-20818

Horizontal neutral winds meridional component from incoherent scatter measurements of F region ionization drifts, noting diurnal variations
08 p1156 A72-21098

Seasonal variation in ionospheric horizontal drift velocities under normal E and sporadic E conditions for middle latitudes
08 p1157 A72-21115

Tidal and seasonal wind variations from ionospheric drift If range measurements, comparing with radar-meteor data
08 p1160 A72-21528

Harmonic analysis of E layer drift measurements by closely spaced receiver method combined with on-line analog computer
08 p1160 A72-21529

Ionospheric drift patterns diurnal, seasonal and solar cycle variations from synoptic measurements over east Siberia by closely spaced receivers, using Briggs similar fades method
08 p1160 A72-21530

Fading method measurement of normal and sporadic E region drift, reviewing height gradient data
08 p1161 A72-21539

Radio meteor measurements of ionospheric drifts by two separated stations, obtaining wind velocities mean hourly values correlation coefficient
08 p1238 A72-21883

North-south ionospheric movements at low latitude station, investigating diurnal and seasonal velocity variations from cross correlation and similar fades time delays measurements
08 p1136 A72-21981

Nocturnal F region electrodynamic drift at conjugate point sunrise time, discussing dynamo electrostatic field normal component change as cause of ionosphere vertical movement

09 p1297 A72-22576

Atmospheric wind velocity time variations at 80-100 km altitudes from ionospheric drift data, finding planetary oscillation periodicities relationship to solar activity cycle

11 p1620 A72-25273

E and F region apparent and true drifts over magnetic equator correlated to solar activity, comparing electron density sensitivity to geomagnetic range

11 p1623 A72-26104

Lunar variations of Peruvian electrojet, analyzing E region electron drift and geomagnetic field H component data

11 p1626 A72-26415

Interplanetary magnetic field direction and high latitude ionospheric currents in dayside auroral regions, showing plasma drift induced magnetic disturbances

11 p1626 A72-26419

Semiannual variation in ionospheric drifts, zonal winds and vertical shear at thermosphere base

11 p1626 A72-26475

Sporadic E layer structure and dynamics diurnal and seasonal variations from ionosondes frequency and drift measurements

12 p1804 A72-27781

Drift measurement of lower ionosphere ionizational inhomogeneities by space-diversity LF band broadcast reception

13 p1948 A72-29037

Virtual height dependence of ionospheric F region parameters including angular divergence of reflected radio waves, heterogeneity coefficient and random and drift motions velocity

13 p1948 A72-29038

Sporadic E layer motion and spreading under constant horizontal wind action, estimating lifetime

13 p1949 A72-29254

Daily variations in E region horizontal drift at Thumba/India/, showing daytime westward and nighttime eastward drifts

13 p1949 A72-29275

Equatorial F region photoionization and chemical loss rates for electrons from simultaneous observations of vertical drift velocity and electron concentration, deriving plasma transport

13 p1949 A72-29336

E and F regions plasma horizontal drift measurements by oblique incidence incoherent scatter radar system, suggesting solar semidiurnal tidal oscillation dynamo action

13 p2031 A72-29386

B type discrete radio aurora theoretical prediction based on drift gradient instability, comparing with observations

13 p1951 A72-29651

E region drift velocity estimates from amplitude and phase measurements of pulsed radio waves reflected from lower ionosphere

13 p1923 A72-29664

Spread F association with ionospheric tilts due to total electron content drift, using incoherent scatter radar

15 p2230 A72-32261

Tropical sporadic E reflections and vertical plasma instabilities as function of equatorial electrojet and electron drift ratio based on ionogram observations

16 p2382 A72-32867

Real height variations of the ionospheric F2-layer above some pairs of geomagnetically conjugate stations.

17 p2545 A72-34689

The magnetic control of the lower ionospheric absorption at lower latitudes.

17 p2546 A72-34697

The interpretation of ionospheric radio drift measurements. IV - The effects of signal coupling among spaced sensor channels.

17 p2515 A72-34699

Ion concentration inhomogeneities in the ionosphere at an altitude of 600 km

17 p2547 A72-35207

Dispersion and random changes in the ground pattern of radio waves reflected from the ionosphere.

18 p2660 A72-36459

Structure of ionospheric inhomogeneities according to simultaneous observations of two magnetoionic components

18 p2688 A72-36856

Ionospheric drifts measurement by small base diversity reception method, investigating dependence on receiving antennas orientation

19 p2791 A72-38359

Similarity method to compute ionosphere drift velocity and direction from radio sounding data

19 p2792 A72-38640

Direct measurements of plasma drift velocities at high magnetic latitudes.

19 p2793 A72-38757

The interpretation of ionospheric radio drift measurements. V - Demonstration of the point effect in time-averaged correlations and drift calculations.

19 p2794 A72-38862

Recent work on ionospheric irregularities and drifts.

20 p2920 A72-39981

Horizontal and vertical electron drifts in the F-region at Thumba.

21 p3049 A72-41324

Height structure of tidal winds as inferred from incoherent scatter observations.

22 p3169 A72-42014

Results of a comparison between radar meteor wind measurements and simultaneous lower ionosphere drift measurements in the same area.

22 p3154 A72-42361

Equatorial ionosphere irregularities vertical drift velocity calculation, showing agreement with incoherent scatter results

22 p3170 A72-42370

Synchronous observations of lower-ionospheric wind conditions in Dushanbe and at the equator

23 p3285 A72-44166

Electric field nature for DP current system development in disturbed high latitude ionosphere, discussing F2 region ionization drift

24 p3398 A72-45096

IONOSPHERIC ELECTRON DENSITY

Topside electron density profile from empirical relation between ionospheric slab thickness and mean gradient temperature in F region, using Saint Santin scatter data

01 p0052 A72-10085

Lunar tidal variations of ionospheric electron density at fixed heights for different solar hours over Huan-cayo and Puerto Rico

01 p0053 A72-10089

Lindauer electron density profile for maximum F layer over sunspot cycle using frequency dependent radio ground echo in satellite ionograms

01 p0054 A72-10421

Statistical analysis of ionospheric electron content observations over European stations with nonstationary satellites, taking into account solar radiation and magnetic activity

01 p0054 A72-10422

Ionogram observations of F layer electron refraction wake disturbance during small rocket ascent

01 p0054 A72-10423

Lower ionosphere continuous electron density measurements with ground vlf transmitter, determining limiting altitude ceiling for diurnal and seasonal data

01 p0027 A72-10442

Electron density profile determination in D region based on frequency dependence of radio waves absorption, discussing lower ionosphere anomalous ionization

01 p0059 A72-10595

Log normal random fluctuations of ionospheric electron concentration in F region from vertical sounding and incoherent scatter data

01 p0059 A72-10609

Electron concentration profiles in D region from radio wave partial reflection coefficients

01 p0028 A72-10614

Ionospheric ion formation and neutralization reaction rate coefficients determination by fitting measured electron concentration profiles with computer generated profiles

01 p0059 A72-10616

Differential phase shift and absorption measurements of partially reflected radio waves, providing electron density and collision frequency data from 70-90 km

01 p0030 A72-10836

Ionospheric total electron content measurement with geostationary ATS 3 satellite during solar eclipse of 7 March 1970, plotting Faraday rotation as function of time

01 p0059 A72-10838

Stable red arc 6300 A emission calculation from satellite electron temperature and density data during geomagnetic storms

01 p0061 A72-10893

Phase difference measurement between magnetoionic components returned from lower ionosphere due to pulsed radio signal, obtaining electron density profiles

01 p0063 A72-10914

Midlatitude ionospheric trough characteristics from computer analysis of Ariel 3 electron density data, correlating with geomagnetic phenomena

01 p0120 A72-10921

Electron density measurements for traveling ionospheric disturbances by Thomson scatter technique using Faraday rotation

01 p0031 A72-10922

ATS Faraday rotation measurement data on total electron content during geomagnetic storms, giving first midlatitude ionosphere average storm patterns and seasonal influence analysis

02 p0216 A72-11900

Ionospheric spread-F mechanism as electromagnetic wave scattering on electron density in-

homogeneities, calculating characteristic dependence of height interval on operational frequency

02 p0216 A72-11920

Night sky upper ionospheric electron concentration perturbations during magnetic storm, noting latitudinal distribution

02 p0217 A72-11940

F2 region maximum electron density level height and molecular temperature diurnal variations at equatorial latitudes from Ibadan station data

02 p0218 A72-11941

Nighttime lower ionosphere electron density distribution models for vertically polarized radio wave propagation parameters

02 p0173 A72-12112

Beacon satellite transmission determination of ionosphere total electron content, describing equivalent slab thickness and diurnal, seasonal and solar cycle behavior

02 p0221 A72-12460

Manual reduction of Faraday rotation observations of ionospheric electron density at low latitudes, comparing with computer ray trace analysis

02 p0221 A72-12462

Ionospheric D region electron concentration, deriving correlation coefficient expression with allowance for scattering layer electrons/molecules collisions

02 p0222 A72-12593

Global morphology of integrated product with respect to D and E regions electron concentration height and collision frequency

03 p0345 A72-12981

Ionospheric small scale electron density irregularity structure from power spectral analysis of radio source scintillation observations

03 p0345 A72-12985

Dissociative recombination coefficients of water vapor and nitric oxide in determining D region electron densities

03 p0347 A72-13389

D region ion and electron density rocket measure-ment during sunrise, discussing negative ion electron affinity and ion production functions

03 p0347 A72-13397

Ionospheric photoelectron fluxes and motions simulated by Monte Carlo technique, including transport effects, elastic and inelastic collisions and energy losses

03 p0412 A72-13517

Starlight intensity modulation at discrete radio frequencies due to enhanced ionospheric electron density fluctuations

03 p0438 A72-14096

Long range satellite signal Faraday fading rate revealing electron density profile near F layer peak

04 p0486 A72-14883

Ionospheric electron content over New Delhi, observing seasonal and solar cycle variations of diurnal changes

04 p0515 A72-14930

Geomagnetic control over latitude variation of total electron content in equatorial ionosphere

04 p0515 A72-14931

Ionospheric electron content changes during 25-26 May 1967 magnetic storm event from geostationary satellite monitoring

04 p0516 A72-14940

Ionospheric plasma drift instability, showing electric and magnetic fields, electron density and temperature effects

04 p0517 A72-14956

Thumba night time equatorial E region electron density profiles from rocket-borne Langmuir probe experiments

04 p0517 A72-14957

F2 layer 6300 A night airglow emission photometric data on 31 January 1968, showing large electron content and movements

04 p0517 A72-14958

Power spectra of ionospheric electron content fluctuations from 6 year continuous records, noting gravity wave and seasonal daily variations

05 p0655 A72-16066

Electron concentration and collisions number fluctuations effect on D region profiles based on radio waves partial reflection data

05 p0656 A72-16244

Magnetic storm disturbing effect on integral electron density in F2 layer and in topside ionosphere

05 p0657 A72-16262

F2 region electron density spatial and temporal distribution, investigating plasma vertical drift effects

05 p0657 A72-16263

N/h electron concentration profile in ionospheric D layer by exponent of frequency dependence of radio wave absorption

05 p0627 A72-16401

Latitudinal, diurnal, seasonal and solar cycle variations in vhf-uhf scintillation producing irregularities in F layer electron density

05 p0630 A72-16617

Ionospheric electron content from Faraday rotation observed on satellite radio signals at various frequencies

05 p0659 A72-17095

F 1 layer diurnal and seasonal model for medium to high latitudes, comparing calculated and observed electron density diurnal variations

06 p0804 A72-17458

Ionospheric electron content diurnal and latitudinal variations from differential Faraday effect, discussing solar elevation and geophysical mechanisms

06 p0805 A72-17640

Ionospheric movements measured by frequency spectra of signals incoherently scattered by ionospheric electrons

[AD-738717]

06 p0808 A72-18085

Ionospheric effects of solar flares, considering flare spectrum below 10 Å, flare X-rays relationship to sudden ionospheric disturbances and electron density profiles

06 p0874 A72-18087

Ionospheric electron density profiles and time variation of electron production rate for X-ray flare of 30 January 1968, observing decrease in effective recombination coefficient

06 p0874 A72-18088

Thermal behavior of electron and ion gases in ionosphere, analyzing heat gain, transfer, loss and conductivity terms of energy equation

06 p0809 A72-18278

Quantum efficiency at 6300 and 6364 Å of recombination mechanism in nighttime F layer, obtaining ionospheric electron density profiles

07 p0974 A72-18893

F region electron density variation above North America during geomagnetic disturbance on 28 May 1970

[AD-739792]

07 p0976 A72-19162

Ionosphere electric field sources, magnitudes, relation to currents and effects on ionization distributions and electron density irregularities

07 p0978 A72-20043

Ionospheric F region storms model accounting for global electron density changes due to abundance ratio of atomic oxygen to molecular oxygen or nitrogen

07 p0979 A72-20047

Radio wave alternating electric field heating of ionospheric plasma electrons with density increase below 200 km and decrease at F layer maximum

08 p1152 A72-20703

Ring current growth effects on midlatitude F region electron density change during large magnetic disturbances

08 p1152 A72-20706

Sudden ionospheric perturbation effect on D region vertical distribution profiles, finding sixfold electron concentration increase at 75-80 km

08 p1154 A72-20729

Lower ionospheric electron density profile determination at high latitudes from riometric observations, discussing cosmic radio emission absorption representation

08 p1225 A72-20730

Ionospheric electron concentration and temperature as function of solar zenith angle from rocket sounding

08 p1154 A72-20734

Internal atmospheric gravity wave effects on ionospheric parameters obtained by vertical sounding, considering electron concentration isoline pattern

08 p1154 A72-20735

Ionospheric integral electron concentration data from measurements of Elektron 1 and 3 satellites coherent radio wave emission

08 p1155 A72-20800

Auroral charged particle fluxes electrodynamic interaction with atmosphere, determining ion formation rate and electron concentration and conductivity

08 p1155 A72-20804

Multicomponent meteoritic composition effects on meteor trails radio wave reflections, obtaining ionospheric electron concentration distribution

08 p1131 A72-20805

Vertical distribution of electron density seasonal anomaly and storm effects in daytime midlatitudes topside ionosphere from Alouette 1 data

08 p1155 A72-20814

Quasi-periodic ionospheric electron density fluctuations effects on electromagnetic waves propagation, noting effect on surface recordings as geomagnetic variations

08 p1156 A72-20824

Polar orbiting satellite ESRO-1A 1-13 keV electron measurements compared to bottomside ionosonde measurements for auroral particle precipitation and F region electron density

08 p1226 A72-21099

Ionogram electron density-height distributions for analysis of multiple cusp structure near E region critical frequency

08 p1156 A72-21101

Nighttime and sunrise period ionospheric electron density profiles with respect to time after sunset and solar zenith angle

08 p1226 A72-21102

Ionospheric heating effects of vlf radio wave transmitters, relating changes in electron density and collision frequencies, reflection coefficients and wave fields

08 p1132 A72-21104

Auroral F region electron density enhancement relation to sporadic F2 and red oxygen emission

08 p1226 A72-21111

Neutral wind influence on lower ionosphere nighttime electron and NO ion density profiles

08 p1157 A72-21112

Ionospheric electron density nighttime changes as function of local time, height and latitude during geomagnetic storms

08 p1157 A72-21113

Local and integral ionospheric electron concentrations and horizontal gradients effects on reduced Doppler frequency shift difference along satellite orbit

08 p1232 A72-21144

Perturbation effects on F 2 layer and outer ionosphere electron density profiles during successive magnetic storms from Alouette 1 satellite data

08 p1157 A72-21145

Radio absorption and scattering cross sections of thin cylinder with arbitrary electron density distribution in ionosphere, observing resonance effects

08 p1239 A72-21890

Model calculation for electron production rates due to photoionization and particle precipitation below 100 km at midlatitude during solar minimum and maximum years

09 p1375 A72-22357

Nightglow evidence of precipitating energetic electrons in midlatitude nighttime D region based on intensity determination from satellite and rocket data

09 p1375 A72-22358

D and E region electron density profile, investigating geographical, diurnal, seasonal and sunspot cycle variations

09 p1376 A72-22370

D and E regions electron densities measurement by incoherent scattering technique, noting sporadic E layer and echoes

[AD-742616]

09 p1376 A72-22371

Synoptic measurement of midlatitude D region electron density diurnal and seasonal variations under quiet conditions, using differential absorption partial reflection experiment

09 p1376 A72-22372

D region positive ion and electron conductivities and densities measurement by parachute borne blunt probes during 1970-1971 winter anomaly

09 p1376 A72-22373

Meteorological synoptic analysis of stratospheric planetary wave interaction with lower ionosphere in terms of wind, temperature and ionospheric electron density profiles

09 p1297 A72-22375

NO ion production rate in D region in relation to electron densities

09 p1300 A72-23027

Ionospheric potential and thunderstorm activity annual variations during 1959-70 solar cycle from radiosonde measurements in free atmosphere

09 p1301 A72-23265

Ionospheric electron concentrations and temperatures determined by time dependent continuity equations model during 11 September 1969 solar eclipse

09 p1390 A72-23518

VLF waves propagation dependence on ionospheric horizontal electron density gradients associated with midlatitude depression from FR-1 satellite observation

10 p1472 A72-24060

Reflected short wave signal frequency shift due to reflecting ionospheric layer movement and electron concentration changes, considering oblique incidence on isotropic and anisotropic layers

10 p1436 A72-24576

Lower ionospheric structure, discussing electron production, loss and transport effects and diurnal variations

10 p1473 A72-24703

Neutral atmosphere effects on lower ionosphere, considering D region atomic oxygen, nitric oxide and water vapor and electron density distributions

10 p1474 A72-24712

Ionospheric electron content determination at different latitudes from geostationary satellite signal Faraday rotation

10 p1475 A72-24955

Equatorial Faraday rotation measurements for night ionospheric electron density peak structures during equinoctial months, using ATS-C geostationary satellite radiation

10 p1476 A72-24958

Simultaneous rocket observation of wind shear and electron density profile in lower ionosphere, noting sporadic E layer formation

10 p1477 A72-25154

Midlatitude sporadic E layer observed by rocket and radio sounding, deriving plasma frequency from peak electron density

10 p1477 A72-25156

Temporal variations of sporadic E layer blanketing frequency, virtual height and occurrence rate, calculating electron density profiles and tidal wind influence

10 p1441 A72-25162

IONOSPHERIC ELECTRON DENSITY

Electron density maxima position relationship to wind profiles in sporadic E layer with electric fields and vertical ion motion

10 p1530 A72-25165

Ionospheric total electron content measurement by satellite radio emissions

11 p1632 A72-25840

Nighttime E region electron density variation effects on MF and HF radio wave propagation, discussing ionospheric absorption detection experiments

11 p1593 A72-26070

Daytime electron density profile in E and D regions from rocket lower ionosphere sounding, noting winter electromagnetic absorption anomaly

11 p1622 A72-26101

Ground based synoptic measurement of mesospheric electron densities, noting variations relationship to solar radiation changes

11 p1626 A72-26424

E layer effective recombination coefficient determination from solar flare enhanced electron density and solar X-ray flux measurements and ionospheric relaxation time constant evaluation

11 p1627 A72-26766

Ionospheric and neutral atmospheric temperature profile, composition and electron density and energy measurements by MR-12 rocket

11 p1628 A72-26905

Vertical electron concentration and temperature profiles at 80-170 km measured by rocket launched on 10 July 1969 at Volgograd

11 p1628 A72-26917

Simultaneous measurements of ionospheric electrons number vertical distribution by incoherent ground radar wave scattering and coherent signals from Intercoms 2 and Cosmos 321 satellites

11 p1628 A72-26918

Electron density and ionization changes in lower ionosphere during 7 March 1970 solar eclipse from 2.66 MHz absorption and Langmuir probe rocket measurements

12 p1800 A72-27148

Electron recombination loss coefficients and concentration profiles for D region during solar eclipses from rocket measurements

12 p1800 A72-27149

Ionospheric electron and ion densities during 12 November 1966 solar eclipse from rocket probe measurements

[AD-744390]

12 p1863 A72-27151

Conjugate point photoelectron flux measurements in ionosphere during 7 March 1970 solar eclipse, using retarding potential analyzer onboard Nike-Tomahawk rocket

12 p1801 A72-27153

Ionosonde observations and Faraday rotation measurements of E and F region total electron content during two solar eclipses

12 p1801 A72-27154

ATS observed ionospheric columnar electron content variation during March 1970 solar eclipse, discussing neutral winds effects

12 p1801 A72-27155

Traveling ionospheric disturbances observations during March 1970 solar eclipse from ATS 3 total electron content measurements

12 p1801 A72-27156

Electron density profiles calculation from ionograms, obtaining equivalent delay caused by ionization below minimum plasma frequency

12 p1802 A72-27307

F region parameters relationship to night sky optical emission, considering electron distribution produced by dissociative recombination

12 p1802 A72-27308

ATS F/G radio beacon experiments for study of exosphere and ionosphere integrated electron content, spatial structure and time dependent behavior

12 p1782 A72-27526

Ionosphere electron content annual mean difference from semiannual amplitude as seasonal fluctuation indication for tropospheric circulation

12 p1803 A72-27774

F region mean electron density profile seasonal and solar cycle dependence, using Chapman function for nighttime F layer description

12 p1803 A72-27775

Disturbed D layer electron density profiles at high energy particle incidence, using partial reflection method

12 p1864 A72-27783

Satellite and ground station observed ionospheric plasma parameters comparison, considering electron density and temperature and ion temperature and composition

12 p1804 A72-27785

Peak electron energy spectra during auroral substorm from high energy resolution balloon X ray measurements

12 p1804 A72-27787

D region electron density profiles calculated as function of solar zenith angles, noting LF radio wave propagation

13 p1945 A72-28582

Latitudinal and diurnal development of seasonal anomaly in upper ionosphere from Alouette 1 data, discussing vertical electron density profiles

13 p1946 A72-28594

Ionospheric spread-F mechanism as electromagnetic wave scattering on electron density inhomogeneities, calculating characteristic dependence of height interval on operational frequency

13 p1948 A72-29232

Night sky upper ionospheric electron concentration perturbations during magnetic storm, noting latitudinal distribution

13 p1949 A72-29252

F 2 region maximum electron density level height and molecular temperature diurnal variations at equatorial latitudes from Ibadan station data

13 p1949 A72-29253

Equatorial F region photoionization and chemical loss rates for electrons from simultaneous observations of vertical drift velocity and electron concentration, deriving plasma transport

13 p1949 A72-29336

E region electron density distortion at magnetic equator by Sq current system, noting dependence on alpha coefficient profiles

13 p1952 A72-29663

Global ionospheric electron density variations and associated thermospheric winds during 15-21 June 1965 geomagnetic storm from ground based and satellite data

13 p1953 A72-29805

Daytime F region inverse relationship between electron density and temperature, determining energy input profile and thermal flux

14 p2097 A72-30127

Incoherent scatter and filter photometer search for 6300 A predawn enhancement by magnetically conjugate photoelectron impact excitation, comparing with ionospheric electron density

14 p2098 A72-30148

E region electron collision frequency vertical distribution by ground measurement of radio wave absorption, using electron concentration data obtained by rocket-borne interferometer

14 p2100 A72-30462

Global electron concentration disturbances in low and middle latitude F 2 during magnetic storm

14 p2100 A72-30635

Ionospheric electrons and neutral particles temperature and concentration profiles explained by electron gas cooling due to atomic hydrogen excitation, calculating heat flow

14 p2101 A72-30641

Lower ionospheric seasonal anomaly in electron density levels, noting diurnal and latitudinal characteristics at various heights

14 p2102 A72-30653

Ionospheric electron density changes caused by strong radio waves induced plasma heating

14 p2102 A72-30657

Partial reflection method to obtain D region electron density profiles and collision number

14 p2086 A72-30791

Ionospheric electron density measurement by radio propagation method, recording traveling ionospheric disturbance effect and sporadic E strata thicknesses

15 p2223 A72-31438

F 2 layer electron concentration and maximum height variation with interplanetary magnetic field direction

15 p2226 A72-31920

Equatorial ionospheric vertical electron density profiles measurement by rocket-borne phase measuring swept RF probe with dc biased sensor, comparing data with ionograms

15 p2226 A72-31940

Anisotropic electron pitch angle distributions at synchronous altitude due to wave-particle scattering and ionospheric acceleration along field lines

15 p2299 A72-31961

Ion pair production rate and electron number density in ionospheric D region from ground based and rocket measurements, discussing two ion model

15 p2229 A72-32252

Ionospheric ion temperatures and velocities and electron and neutral densities from incoherent scatter observations during 11 February 1969 magnetic storm

15 p2229 A72-32254

Ionized and neutral atmospheres coupled ionospheric continuity and motion equations, discussing nonlinear force effects on F 2 height and electron density

15 p2230 A72-32257

Spread F association with ionospheric tilts due to total electron content drift, using incoherent scatter radar

15 p2230 A72-32261

Ionospheric models with constant electron density contours axially symmetrical to earth centered dipole magnetic field, discussing radio ray paths

15 p2230 A72-32263

Nighttime F region vertical velocity estimation, using electron density profiles vs true height

15 p2231 A72-32267

Linear ICs application to RF probe for ionospheric electron density measurements from rockets or satellites

15 p2240 A72-32389

Ionospheric gravity waves spectral frequency distribution from ATS 3 electron concentration measurements, using numerical filters for statistical frequency analysis

16 p2382 A72-32891

Ionospheric electron content semiannual and seasonal variations as function of solar and geomagnetic activity from low and mid-northern latitude observations

16 p2385 A72-33378

D region electron concentration and collision frequency with neutral molecules from radio waves backscattered by inhomogeneities in propagation medium

16 p2385 A72-33484

Booker theorem generalization to cover wide range of ionospheric refractivity profiles containing variable electron density and collision frequency

16 p2386 A72-33662

Electrostatic flush disk and cylindrical probe construction and electron density data during atmospheric reentry from beryllium sphere experiments [AIAA PAPER 72-691]

16 p2346 A72-34051

On the winter anomaly of ionospheric absorption.

17 p2546 A72-34695

Correlation of solar radio bursts and sudden increases of the total electron content (SITEC) of the ionosphere.

17 p2598 A72-34698

Satellite beacons observations from 1964 to 1970.

17 p2547 A72-35125

Atomic oxygen green line emission in nightglow from OGO-F photometer observations, calculating tropical F region electron density spatial distribution

17 p2549 A72-35604

Electron profiles during negative magnetic bays in the auroral zone

17 p2551 A72-35860

Calculations of electron-profile disturbances in the F region during the passage of a neutral wave

17 p2551 A72-35861

Determination of electron concentration profiles in the lower ionosphere from the absorption at several frequencies

17 p2551 A72-35863

UHF radio signals refraction angles and group delay times for biexponential model of ionospheric electron density profile

18 p2657 A72-36101

An investigation of the ionospheric D region at sunrise. I - Time variations of ozone, metastable molecular oxygen, and atomic oxygen. II - Estimation of some photodetachment rates. III - Time variations of negative-ion and electron densities.

18 p2656 A72-36295

Atmospheric model synthesis of observed electron temperatures and concentrations in tropical ionosphere during 8 March 1970 magnetic storm, noting F 2 region features

18 p2686 A72-36296

Photodetachment of electrons from major negative ions in the lower D region.

18 p2686 A72-36622

Properties of plane asymmetric plasma waveguides in applications to the propagation of short radio waves along inhomogeneities in the outer ionosphere

18 p2662 A72-36855

Nonstationary electron-ion gas distribution in the ionosphere

18 p2689 A72-36878

D region electron density profile determination based on LF link operating on one-hop ionospheric propagation of ordinary and quasi-transverse wave

18 p2689 A72-37163

Model ionosphere for D region at summer noon during sunspot maximum.

18 p2689 A72-37207

Radio wave alternating electric field heating of ionospheric plasma electrons with density increase below 200 km and decrease at F layer maximum

19 p2790 A72-38331

Ring current growth effects on midlatitude F region electron density change during large magnetic disturbances

19 p2790 A72-38334

Sudden ionospheric disturbance effect on D region vertical distribution profiles, finding sixfold electron concentration increase at 75-80 km

19 p2791 A72-38357

Lower ionospheric electron density profile determination at high latitudes from riometric observations, proposing cosmic radio emission absorption representation

19 p2791 A72-38358

Ionospheric electron concentration and temperature as function of solar zenith angle from rocket sounding

19 p2791 A72-38362

Internal atmospheric gravity wave effects on ionospheric parameters obtained by vertical sounding, considering electron concentration solin pattern

19 p2791 A72-38363

D-region electron densities and collision frequencies from Faraday rotation and differential absorption measurements.

19 p2793 A72-38858

Comparison between observed and numerically calculated atmospheric gravity waves in the F-region.

19 p2794 A72-38864

Electron temperature and density determination from RF impedance probe measurements in the lower ionosphere.

20 p2916 A72-39229

Local and integral ionospheric electron concentrations and horizontal gradients effects on reduced Doppler frequency shift difference along satellite orbit

20 p2903 A72-39249

Perturbation effects on F 2 layer and outer ionosphere electron density profiles during successive magnetic storms from Alouette 1 satellite data

20 p2916 A72-39250

Mid-latitude D-region ionization associated with the 'slot' in radiation belt electrons.

20 p2964 A72-39533

High latitude variations of F-region electron temperature.

20 p2918 A72-39535

Ionospheric heating and electron density modification by high powered radio waves, describing research facility

20 p2919 A72-39724

Electron-density increase in the E layer below an artificial barium cloud.

20 p2920 A72-39983

Some topside electron density measurements from Ariel III satellite during the geomagnetic storm of 25-27 May 1967.

22 p3169 A72-42017

Electron and positive ion density altitude distributions in the equatorial D-region.

22 p3170 A72-42366

D-region measurements with the differential-absorption, differential-phase partial-reflection experiments.

22 p3172 A72-42423

A possible connection between a barium cloud and electron intensity fluctuations observed on a rocket flight at Kiruna.

22 p3172 A72-42433

Geomagnetic storm and seasonal effects on spread of monthly distribution and average behavior of midlatitude F region electron peak density and slab thickness

22 p3172 A72-42434

A method of estimating the excess electron density in random irregularities embedded in the ionosphere.

22 p3173 A72-42883

A method for determining the electron density distribution about the F2 peak of the ionosphere.

22 p3174 A72-42992

Relative movements of mid-latitude trough and scintillation boundary.

23 p3282 A72-43267

Geometrical dimensions and effective number of large scale ionospheric inhomogeneities by F 2 critical frequency variability analysis

23 p3283 A72-43360

Variations of the planetary values of the F2 layer thickness and the parameters of the neutral atmosphere

23 p3284 A72-43375

A study of the dependence of the maximum usable frequency on the electron content.

23 p3266 A72-44333

D region electron density profiles calculated as function of solar zenith angles, noting LF radio wave propagation

24 p3397 A72-45082

Latitudinal and diurnal development of seasonal anomaly in upper ionosphere from Alouette 1 data, discussing vertical electron density profiles

24 p3398 A72-45094

Sunrise effects on the latitudinal variations of topside ionospheric densities and scale heights.

24 p3399 A72-45552

IONOSPHERIC F-SCATTER PROPAGATION

Supermode F range spreading and evening type transequatorial propagation, considering single scattering in east-west plane

03 p0321 A72-12994

Propagation by direct backscatter on aligned irregularities in auroral F layer, noting horizontal ionization gradients role

08 p1158 A72-21220

Equatorial spread F spatial and temporal distribution from short wave side reflection observations along Lindau-Tsumeb transequatorial HF radio transmission path

12 p1803 A72-27778

IONOSPHERIC HEATING

Ion and electron temperature increases by friction heating between neutral gas winds and plasma in ionosphere

01 p0054 A72-10424

Ionospheric F region heating by hf transmitter, obtaining electron temperature maps and heating/cooling time constants

01 p0062 A72-10910

- Vertical distribution of ionospheric and magneto-
spheric electric fields, estimating Joule heating
02 p0220 A72-12324
- Ionospheric heating effects of vlf radio wave trans-
mitters, relating changes in electron density and col-
lision frequencies, reflection coefficients and wave
fields
08 p1132 A72-21104
- Artificial heating of lower ionosphere in controlled
experiment, measuring electron temperature increase
by radar backscatter system
11 p1625 A72-26412
- Arecibo observatory research, discussing pulsars,
radio source scintillation and ionospheric heating
12 p1795 A72-27427
- Ionosphere heating effects produced by transverse
electric field, discussing strong nighttime source
14 p2100 A72-30631
- Ionospheric electron density changes caused by
strong radio waves induced plasma heating
14 p2102 A72-30657
- Ion chemistry and heating of daytime ionosphere E
and lower F regions, calculating neutral atmosphere
densities, ion production rates and solar EUV radia-
tion absorption
15 p2192 A72-32253
- Simultaneous F-region conjugate point dawn effects
at two mid-latitude stations.
20 p2916 A72-39234
- Ionospheric heating and electron density modifica-
tion by high powered radio waves, describing research
facility
20 p2919 A72-39724
- IONOSPHERIC ION DENSITY**
- Ionospheric ion mobilities and densities measure-
ments over Sardinia, using parachute mesosphere
probe
01 p0055 A72-10436
- Positive Fe ion concentration relationship to equa-
torial spread F fromOGO 6 satellite observation near
magnetic equator
01 p0062 A72-10902
- Equilibrium concentrations of negative ions in
nighttime D region, comparing computations to mass
spectrometric measurements
01 p0063 A72-10917
- D region ion and electron density rocket measure-
ment during sunrise, discussing negative ion electron
affinity and ion production functions
03 p0347 A72-13397
- Lower D region ion density measurement with
parachuted blunt probe consisting of disk-shaped col-
lector with guard ring at bottom
03 p0347 A72-13398
- Positive ion composition in equatorial D region, in-
vestigating reaction kinetics
03 p0412 A72-13522
- Venusian ionosphere thermal proton destruction,
discussing helium and oxygen replacement candidates
for principal ion components
03 p0434 A72-13537
- Lagrange method extended to method of charac-
teristics for solving first order hyperbolic partial dif-
ferential equations, applying to ionospheric ion den-
sity distribution
04 p0539 A72-14885
- Atmospheric composition and temperature effects
on F1 region ion concentration structure from 140 to
220 km for low solar activity conditions
05 p0657 A72-16261
- Ionospheric ion density distribution at 600 km height
and medium and low latitudes from Cosmos 184 satel-
lite data analysis
05 p0659 A72-16766
- Thermal behavior of electron and ion gases in iono-
sphere, analyzing heat gain, transfer, loss and conduc-
tivity terms of energy equation
06 p0809 A72-18278
- Ionosphere electric field sources, magnitudes, rela-
tion to currents and effects on ionization distributions
and electron density irregularities
07 p0978 A72-20043
- Neutral wind influence on lower ionosphere
nighttime electron and NO ion density profiles
08 p1157 A72-21112
- Diatomic oxygen and carbon dioxide density
profiles effects on photoionization rates in D region
[AD-741091]
09 p1274 A72-22356
- Nighttime D region ionization production by cosmic
X rays from various celestial sources and galactic
background
09 p1375 A72-22359
- Mesosphere region positively and negatively
charged particles concentration and mobility measure-
ments by sounding rocket experiments
09 p1375 A72-22361
- Supersonic and subsonic measurements of meso-
spheric ionization at night, using Arcas rocket
parachute borne nose-tip and blunt probes
09 p1296 A72-22362
- Oxygen, nitric oxide and water cluster positive ion
composition from mass spectrometer experiments in
lower ionosphere, noting ion production and low tem-
perature effects
09 p1375 A72-22363
- Midlatitude auroral zone positive ion mass spec-
trometer observations in E region, noting diurnal
variation and sporadic E events
09 p1375 A72-22364
- E region ion density and composition determination
by incoherent scatter radar measurement
[AD-742618]
09 p1375 A72-22365
- Room temperature reactions involving ionospheric
cluster ions, discussing rate constants measurement
by stationary afterglow and drift tube facilities
09 p1275 A72-22367
- D region positive ion and electron conductivities
and densities measurement by parachute borne blunt
probes during 1970-1971 winter anomaly
09 p1376 A72-22373
- Day, night and sunset mesospheric nitric oxide con-
centrations during polar cap absorption from rocket
measurements of cation composition and charged par-
ticle densities
[AD-741709]
09 p1300 A72-23026
- Ionosphere composition and ion concentration mea-
surements for D and E region, including aerodynamic
and plasma dynamic effects
11 p1621 A72-25836
- D region ionization by solar corpuscular streams,
considering formation of charged particle concentra-
tion profiles
11 p1622 A72-25948
- Ionospheric weather index in terms of ionization ir-
regularities at given time and place derived from con-
tinuous steep incidence HF Doppler soundings
11 p1627 A72-26518
- Mass spectrometer measurements of hydrogen,
helium, nitrogen, oxygen and nitrogen oxide ion con-
centrations vertical profiles in ionosphere at
midlatitudes
11 p1628 A72-26906
- Nitric oxide and oxygen molecular ion composition
of lower ionosphere during solar eclipses from rocket
measurements
[AD-744403]
12 p1801 A72-27150
- Ionospheric electron and ion densities during 12
November 1966 solar eclipse from rocket probe mea-
surements
[AD-744390]
12 p1863 A72-27151
- Satellite and ground station observed ionospheric
plasma parameters comparison, considering electron
density and temperature and ion temperature and com-
position
12 p1804 A72-27785
- Ionospheric oxygen ions loss rate in charge
exchange reactions with hydrogen, molecular nitrogen
and oxygen and atomic oxygen photoionization rate
13 p1953 A72-29811
- Aladdin experiment atmospheric composition, total
neutral density, temperature and ion density vertical
profiles
15 p2228 A72-31969
- Motion of ion-cloud in the ionosphere, field-aligned
cloud with Gaussian distribution of ionization density.
17 p2546 A72-35060
- Ion concentration inhomogeneities in the iono-
sphere at an altitude of 600 km
17 p2547 A72-35207
- Ionospheric ion density distribution at 600 km height
and medium and low latitudes from Cosmos 184 satel-
lite data analysis
17 p2548 A72-35269
- Photodetachment of electrons from major negative
ions in the lower D region.
18 p2686 A72-36622
- Nonstationary electron-ion gas distribution in the
ionosphere
18 p2689 A72-36878
- Lower ionosphere N/H₁ profile calculation from
ionograms with incomplete layer information
18 p2689 A72-36880
- Magnetospheric interactions with topside iono-
sphere in terms of polar wind ion flows and density re-
lated to plasma temperature, F2 region and cusp ob-
servations
20 p2918 A72-39537
- Electron and positive ion density altitude distribu-
tions in the equatorial D-region.
22 p3170 A72-42366
- Dayglow nitrogen ion 3914 A emission profiles for
average solar activity at 110-240 km heights from
Cosmos 224 observations
23 p3282 A72-43357
- Source and identification of heavy ions in the equa-
torial F layer.
23 p3286 A72-44516
- Sunrise effects on the latitudinal variations of top-
side ionospheric densities and scale heights.
24 p3399 A72-45552
- IONOSPHERIC NOISE**
- NT WHISTLERS**
- Tweaks contribution to atmospheric radio noise
background, discussing nighttime ionospheric source
information
01 p0056 A72-10444
- Hypotheses for excess background radiation at 200-
500 km, suggesting single high energy electrons or
electron clusters
07 p1064 A72-20638
- Characteristic features of ELF-noise spectra during
the excitation of the earth-ionosphere resonator by
cosmic sources
18 p2662 A72-36861
- Auroral ionosphere radio self emission at supercriti-
cal frequencies from accelerated protons charge
exchange effects, comprising radio noise bursts,
storms and amplifications
19 p2790 A72-38341
- Ionosonde receiver with automatic noise suppres-
sion and digital-analogue recording of the first iono-
spheric reflection.
19 p2805 A72-38867
- Polar ionosphere ELF/VLF noise distribution from
Alouette 2 electric dipole observations
20 p2903 A72-39538
- IONOSPHERIC PROPAGATION**
- NT IONOSPHERIC F-SCATTER PROPAGA-
TION**
- Directional ionosonde aeriels and instrumentation
for ionospheric reflection angle of arrival measure-
ments
01 p0053 A72-10091
- Ionospheric propagation - Conference, Kleinhe-
bach, West Germany, October 1970
01 p0054 A72-10401
- Magnetic declination effect on elevation control of
F2 layer maximum, considering east component of
geomagnetic field from Capetown and Canberra ob-
servations
01 p0054 A72-10427
- Sporadic E layer reflection behavior measurements
from two closely located stations, deriving drift
direction and critical frequencies daily variation
01 p0055 A72-10431
- Daily, annual and long term ionoscat and
sporadic E variations above Europe, using hf propaga-
tion measurements
01 p0055 A72-10432
- Spanish winter anomalous ionospheric short wave
absorption observed by high precision ground based
measurements
01 p0055 A72-10434
- Ionospheric neutral gas wind and altitude effects on
Spanish short wave absorption winter anomaly
01 p0055 A72-10435
- Equatorial E region short wave oblique incidence
propagation experiment showing transmitted impulse
delay increase with frequency decrease
01 p0056 A72-10437
- Spread F effects on transequatorial ionospheric
short wave oblique incidence path great circle devia-
tions
01 p0056 A72-10438
- Auroral backscatter echoes observations in iono-
spheric short wave propagation, using satellite oblique
propagation ionograms and magnetograms
01 p0056 A72-10439
- Magnetoinic component with fluctuating elliptical
polarization during wave reflection from F2 layer,
discussing suppression mechanism
01 p0028 A72-10593
- Radio communication accuracy characteristics in
calculation of maximum frequency, skip distance and
emission angle by transmission curves for midlatitude
ionosphere
01 p0028 A72-10600
- Short wave skip distance calculation as function of
path inclination to ionospheric layer for linear and
parabolic ionization distributions
01 p0028 A72-10612
- Transient electromagnetic plane wave ionospheric
transmission and reflection, considering impulsive and
step modulated sine wave excitations
01 p0031 A72-11102
- Spatial correlation coefficients measurements on
one-hop hf radio waves obliquely reflected from iono-
sphere for various antenna spacings
01 p0032 A72-11252
- Report on U.S. telecommunications telemetry infor-
mation theory in period 1966-1969, discussing iono-
spheric and tropospheric data transmission
02 p0171 A72-11687
- Lower ionospheric nighttime absorption as ioniza-
tion processes indicator, discussing relationship to
geomagnetic activity
02 p0216 A72-11921
- Spectral characteristics of ionospheric signal by
phase lags introduced in multichannel field recorder
02 p0172 A72-11926
- Ionospheric reflection height calculation according to
oblique electromagnetic backscatter sounding data
at two frequencies
02 p0172 A72-11943
- Nighttime ionospheric radio wave propagation,
determining geomagnetic latitude variations effects on
absorption and reflection
02 p0218 A72-11944
- Midlatitude ionospheric radio wave absorption mea-
surements, using radio astronomical polarization
method
02 p0172 A72-11945
- Nighttime lower ionosphere electron density dis-
tribution models for vertically polarized radio wave
propagation parameters
02 p0173 A72-12112

One-way error correcting system with 1/3 rate interleaved block code, testing code performance over 1300 km vhf ionosscatter path and 1500 km hf path
02 p0175 A72-12153

Ionospheric propagation, reflection and absorption of vlf hiss in aurora from rocket observation during quiet and substorm conditions
02 p0221 A72-12458

Cosmic noise ionospheric absorption measurements with riometers, showing mid and low latitudinal variation
02 p0221 A72-12464

Sporadic E layer shielding frequency correlation to limiting reflection frequency calculated by diurnal data from nine ground stations
02 p0221 A72-12522

Shielding and semitransparent sporadic E layer fine structure characteristics from summer observations data analysis
02 p0222 A72-12523

Ray path and absorption calculation for mf and hf radio wave oblique propagation through model ionosphere in nighttime, noting E region ionization role
02 p0184 A72-12875

Sunspot cycle 1958/70 effects on D region ionospheric absorption and stratospheric temperature measured by radiosonde
03 p0345 A72-12978

Radio wave scattering observation in turbulent lower ionosphere, determining vertical propagation velocity dispersion by statistical analysis
03 p0322 A72-13476

D region echo amplitude distribution, observing coherent scattering contribution
03 p0349 A72-13523

Italian monograph on ionospheric radio propagation, covering weather forecasts and radio communications
03 p0323 A72-13844

Rf interference measurements on guided hf ionospheric propagation in OV-41 dual satellite experiment
03 p0324 A72-14042

Vlf phase regressions at sunrise related to variations of reflection coefficient in D region, using IENGf data
04 p0485 A72-14465

Long range satellite signal Faraday fading rate revealing electron density profile near F layer peak
04 p0486 A72-14883

Hf radio wave reflection at vertical incidence from ionosphere, calculating distance attenuation by ray-tracing techniques
04 p0487 A72-14886

Geomagnetic effects on lower ionosphere at lower midlatitude station, discussing long wave propagation
04 p0516 A72-14939

Radio stars wave amplitude scintillation during passage through ionosphere observed by interferometer, noting association with geomagnetic field fluctuation
04 p0567 A72-14953

Ionospheric absorption measurements at 2.2 MHz by vertical incidence pulse sounding method, observing diurnal and seasonal variations
04 p0518 A72-14965

Ionospheric radio absorption, observing diurnal and seasonal variations and sunspot numbers and solar flares effects
04 p0518 A72-14966

Anomalous changes in ionospheric radio absorption during winter at midlatitudes, investigating diurnal and seasonal variations and stratospheric warming
04 p0518 A72-14967

Book on radio wave propagation covering ground, tropospheric and ionospheric waves, atmospheric and cosmic noise, reflection, attenuation, signal distortion, space communication, etc
04 p0487 A72-15269

Radio propagation from transmitter moving through irregular stationary ionospheric plasma, obtaining fluctuation dispersions for Faraday rotation angle and rate, phase, Doppler shift and refractions
04 p0489 A72-15395

Space charge layer /ion sheath/ effects on impedance of lf transmitting electric dipole in ionospheric plasma
04 p0490 A72-15399

Ricocheting mechanism in short radio wave propagation in ionosphere, using ray trajectories and field intensities equations
04 p0492 A72-15439

Long range ionospheric guided hf signal propagation from low orbiting San Marco 1 and 2 satellites
04 p0492 A72-15440

Complex eigenvalues computation for vlf wave propagation in spherical earth-ionosphere waveguide
04 p0492 A72-15442

Elliptical polarization and depolarization coefficients for monochromatic radio waves reflected from F2 ionosphere using Stokes parameters
05 p0656 A72-16241

D region ionization by electron fluxes as explanation for latitudinal radio wave absorption
05 p0656 A72-16249

Radio signal group trajectory in ionosphere expressed as series expansion in terms of increasing power of beam reflection height
05 p0626 A72-16250

Radio wave absorption during oblique propagation through ionosphere from vertical measurements, using rhombic antenna at 25 MHz
05 p0657 A72-16267

Vlf propagation and D region aeronomy model for vlf phase behavior predictions and observations during two solar eclipses
05 p0630 A72-16618

Geomagnetic field-hf sky wave orthogonality conditions, discussing ray tracing for signals reflected in ionosphere
05 p0630 A72-16619

Vhf waves transhorizontal propagation and day types correlation with sporadic E ionospheric layers in temperate zone, discussing wind shear theories
05 p0659 A72-16782

Ionospheric turbulence induced scintillations of Intelsat geostationary satellite signals at 4 and 6 GHz [AIAA PAPER 72-179]
05 p0631 A72-16966

Plasma models of topside ionosphere, investigating electrostatic wave propagation
05 p0698 A72-17022

Diurnal variation of lower ionosphere, analyzing nature and behavior of absorption long range variations over solar activity cycle
05 p0660 A72-17182

Pulsed FM radio pulse signal reflection from inhomogeneous plasma or ionosphere calculating electron collision loss effects on distortion
06 p0854 A72-17487

Interference above ionosphere of lf radio waves emitted by multiple lightning discharges concluded from spectrographic observation of whistler received onboard Injun 5 satellite
06 p0773 A72-17567

Phase velocity of first order mode of vlf waves propagating in earth ionosphere
06 p0773 A72-17598

Ionospheric absorption and atmospheric planetary scale waves fluctuations correlation
06 p0808 A72-18090

Geophysical aspects of ionospheric scintillation problems, considering correlation with spread F and sporadic E
06 p0889 A72-18282

Pulse reflection of polarized plane electromagnetic wave from cold plasma ionosphere model with vertical magnetic field
06 p0777 A72-18729

Forbush decreases in galactic cosmic ray flux and associated vlf nighttime ionospheric propagation phenomena
07 p1056 A72-18900

Ogo 6 ionospheric measurement of proton whistlers wave-normal vector, investigating propagation modes
07 p1057 A72-19148

Round-the-world short wave signals propagation and waveguides effective volume and attenuation characteristics, relating ionospheric effects and nonlinear beam defocusing
08 p1130 A72-20704

Slip effect in diurnal phase and amplitude cycles of vlf signals in lower ionosphere due to wave interference at transmitting point
08 p1130 A72-20710

Geomagnetic variations propagation theory for lf electromagnetic and Alfvén waves diffraction at stratified earth in thin gyrotopical ionosphere
08 p1130 A72-20711

Auroral ionosphere radio self emission at supercritical frequencies from accelerated protons charge exchange effects, comprising radio bursts, storms and amplifications
08 p1153 A72-20713

Unified coordinate system for earth planetary distribution of F2 and sporadic E layer transmission parameters, suggesting geomagnetic longitude and modified magnetic inclination
08 p1153 A72-20726

Critical frequencies and geometrical parameters of parabolic model in oblique backscatter ionospheric sounding, using distance-frequency characteristics
08 p1154 A72-20732

Altitude dependence of vlf field of vertical electric dipole in spherical waveguide of radially inhomogeneous ionosphere and earth, using Sommerfeld integral representations
08 p1130 A72-20736

Long radio waves slant incidence on isotropic inhomogeneous ionospheric plasma
08 p1131 A72-20737

Long distance atmospheric propagation in earth-ionosphere waveguide, obtaining phase velocities and damping factors
08 p1131 A72-20802

Radio absorption in lower ionosphere obtained from vertical distribution of electron density and production rates from solar protons energy spectrum
08 p1226 A72-20816

Errors in ionospheric sounding of sporadic E layers with auroral presence, discussing continuous reflections duration distribution
08 p1155 A72-20817

Diurnal fluctuations in radio echo producing ionospheric region horizontal scale and height, discussing dependence on solar position
08 p1131 A72-20819

Quasi-periodic ionospheric electron density fluctuations effects on electromagnetic waves propagation, noting effect on surface recordings as geomagnetic variations
08 p1156 A72-20824

Median true height atmospheric profile model synthesis from propagation parameters, using polynomial representations and alpha-Chapman layers
08 p1157 A72-21106

Soviet papers on ionospheric propagation and meteor trail drifts during IQSY, covering Doppler frequencies recording and mountains effect on radio transmission
08 p1238 A72-21881

Horizontally polarized impulsive plane electromagnetic wave reflection from perturbed linear ionosphere model, obtaining transient response as inverse Fourier transform
08 p1136 A72-21979

Acoustic approximation of pressure step discontinuity sound propagation in attenuating and dispersive ionosphere
08 p1162 A72-22139

Diurnal, seasonal and solar cycle variations in cosmic noise absorption during 1957-1966, showing various ionospheric layers contribution
09 p1385 A72-22586

Polarization characteristics measurement for PC I geomagnetic micropulsations propagated through ionospheric ducts, noting hydromagnetic emissions and whistlers relation to high latitude source region
09 p1299 A72-22989

Vlf hiss with lower hybrid resonance cut-off recorded by Alouette 1, emphasizing midlatitude events and electromagnetic energy transportation by multion duct in topside ionosphere
09 p1279 A72-23007

Laboratory simulation of VLF/ELF radio waves transpolar ionospheric propagation, taking into account polar cap absorption
09 p1279 A72-23016

Whistler damping factor dependence on magnetic field strength in geometrical optics approximation, emphasizing nonlinear effects at low frequencies in ionospheric propagation
09 p1282 A72-23516

Orthogonality conditions for VLF height gains in vertically inhomogeneous anisotropic earth ionosphere waveguide
09 p1282 A72-23517

Background medium anisotropy effect on electromagnetic waves scattering from ionospheric irregularities, calculating scattered power by Green function
09 p1282 A72-23519

Mode theory of long distance VLF propagation, deriving equation for flat earth-ionosphere waveguides
09 p1282 A72-23570

X ray effect from Scorpio XR-1 on lower ionosphere long wave transmissions, considering transit times and field intensity variations
09 p1305 A72-23572

French monograph on riometer measurement of abnormal ionospheric absorption, noting nighttime events association with F region lacunae
10 p1472 A72-23848

Sporadic E layer critical frequency relationship to ionospheric wind direction for midlatitudes in summer period
10 p1472 A72-24079

Reflected short wave signal frequency shift due to reflecting ionospheric layer movement and electron concentration changes, considering oblique incidence on isotropic and anisotropic layers
10 p1436 A72-24576

Optical path calculation in ionosphere and troposphere, determining term due to astronomical refraction with respect to frequency
10 p1475 A72-24859

Nonlinear HF ionospheric instabilities classification on unified basis by coupled mode theory
10 p1440 A72-24936

Wave particle interaction around lower hybrid resonance frequency, deriving whistler mode wave growth rate during propagation in magnetoactive plasma penetrated by nonthermal particles
10 p1476 A72-24959

Sporadic E layer structure model from radiosonde observation, noting peak plasma frequency variation and total reflection by blobs
10 p1441 A72-25153

Nighttime E region electron density variation effects on MF and HF radio wave propagation, discussing ionospheric absorption detection experiments
11 p1593 A72-26070

Radio wave scattering observation in turbulent lower ionosphere, determining vertical propagation velocity dispersion by statistical analysis

11 p1593 A72-26246

Ionospheric radio wave absorption and intensity calculation, using vertical sounding data and riometric measurements

11 p1594 A72-26278

Ionospheric detection of cosmic X rays by VLF links using nova sources

11 p1714 A72-26417

Ionospheric scattered wave propagation mode and weak echo delay explained by analysis-derived model

11 p1597 A72-26570

Transmission and reflection coefficients of ULF waves incident on lower ionosphere layer with exponential electron density profile

11 p1597 A72-26707

Analytic ray path solutions for HF radio wave transmission through plane stratified isotropic ionospheric model

11 p1599 A72-26763

Mode coupling effects on radio wave partial reflection from lower ionosphere at vertical incidence, using matrix perturbation analysis

11 p1599 A72-26764

VLF phase changes due to particle precipitation into geomagnetic anomaly during solar proton events explained by exponential ionospheric models with effective reflecting height

11 p1599 A72-26765

Plasma parametric instabilities excitation by radio waves in ionosphere, noting LF ionic and HF electrostatic wave growth

11 p1628 A72-26767

Ionospheric HF Doppler dispersion during 7 March 1970 solar eclipse, noting traveling ionospheric disturbance

12 p1801 A72-27157

Multiplicative noise envelope distribution for ionospheric scatter channel from single and diversity radio reception, noting meteor trails effects on electromagnetic wave propagation

12 p1782 A72-27627

Adcock direction finder errors due to diurnal and sporadic ionospheric variations and tilting layers effects on reflected signal

12 p1804 A72-27780

Ionospheric absorption measurements during sunspot cycle at fixed frequencies, noting monthly and seasonal variations

12 p1804 A72-27782

Sky wave propagation curves from MF observations for 7500 km distances

12 p1784 A72-27784

ELF wave propagation velocities in earth-ionosphere waveguide, studying fast and slow modes

12 p1784 A72-27789

Statistical model for short wave radio signal fading at oblique signal reflection from ionosphere, determining pulse amplitude and duration distribution laws

13 p1915 A72-28468

Beamed radio waves interaction in E and F1 regions propagation, noting beam width and field amplitude changes caused by defocusing

13 p1945 A72-28579

D region electron density profiles calculated as function of solar zenith angles, noting LF radio wave propagation

13 p1945 A72-28582

Multilayer plasma model for MHD pulse propagation in ionospheric waveguide, noting approximation of Alfvén velocity distribution by plasma layers

13 p1946 A72-28585

Worldwide thunderstorm activity model selection from Schumann resonance observations, using ELF noise measurements in lowest earth-ionosphere cavity modes

13 p1988 A72-28600

Arrival angles of radio wave reflected from ionosphere for remote short wave transmitter direction finding

13 p1917 A72-28601

Ionospheric radio adsorption measuring device with readout data convenient for visual and computer processing, discussing block and circuit diagrams

13 p1955 A72-28602

Lower ionospheric nighttime absorption as ionization processes indicator, discussing relationship to geomagnetic activity

13 p1948 A72-29233

Spectral characteristics of ionospheric signal by phase lags introduced in multichannel field recorder

13 p1920 A72-29238

Ionospheric reflection height calculation according to oblique electromagnetic backscatter sounding data at two frequencies

13 p1920 A72-29255

Nighttime ionospheric radio wave propagation, determining geomagnetic latitude variations effects on absorption and reflection

13 p1949 A72-29256

Midlatitude ionospheric radio wave absorption measurements, using radio astronomical polarization method

13 p1920 A72-29257

Error analysis of ionospheric parameter measurement by satellite transmitted or reflected multiple frequency pulsed radiation signal, using perturbation method

13 p1920 A72-29276

ELF and VLF waves propagation, deriving ionospheric field stable solutions by modified matrix multiplication technique for vertical geomagnetic field and large local refractivity

13 p1921 A72-29337

Amplitude probability distribution of radio waves reflected from traveling ionospheric disturbances superimposed on small scale irregularities

13 p1921 A72-29338

Daytime 30 MHz PCA from satellite and riometer measurements, noting linear relationship to square root of integral and differential solar proton fluxes

13 p2030 A72-29339

High latitude ionospheric transmission and reflection properties for oblique hydromagnetic plane waves at micropulsation frequencies for daytime and nighttime conditions

13 p1951 A72-29390

Diurnal and seasonal variations of ionospheric absorption in D and E regions, discussing blanketing sporadic E presence effect

13 p1922 A72-29392

Martian ionosphere electromagnetic wave propagation characteristics for E, F1 and F2 models, calculating refractive index for zero and nonzero collision frequencies

13 p1922 A72-29474

VLF long distance radio propagation in earth-ionosphere waveguide, considering earth magnetic field effects in mode conversion and refraction error calculation

13 p1922 A72-29655

Oblique radio wave propagation through horizontally stratified ionosphere, considering electron collisions effects, reflection behavior and coupling levels

13 p1923 A72-29657

Ionospheric absorption measurement by 1F mode field strength recording with A3 circuit at 6 MHz, noting diurnal and seasonal variations

13 p1952 A72-29660

VLF and LF electromagnetic waves amplitude and phase velocity in spherical earth-ionosphere waveguide, discussing wave hop method

13 p1923 A72-29661

Radio aurora ion-acoustic wave propagation direction divergence due to magnetic field distortion by large ionospheric horizontal sheet current [AD-746367]

13 p1923 A72-29662

E region drift velocity estimates from amplitude and phase measurements of pulsed radio waves reflected from lower ionosphere

13 p1923 A72-29664

Regular cyclic fading of HF and VHF radio signals due to ionospheric scintillation, noting consistency with two ray interference formula

13 p1952 A72-29665

Ionospheric multifrequency absorption measurement description by empirical expressions in terms of E layer critical frequency, solar activity and seasonal effects

13 p1952 A72-29667

Gravity wave observation in nighttime F region by measuring phase path length changes of stable CW signal reflected obliquely from ionosphere

13 p1953 A72-29814

Negative ions and collision frequency effects on circularly polarized ELF and VLF wave propagation in ionosphere

14 p2084 A72-30128

Cosmic ray anomalous absorption height dependence on zenith distance in midlatitude ionosphere during solar flare emission from polarization study

14 p2146 A72-30461

E region electron collision frequency vertical distribution by ground measurement of radio wave absorption, using electron concentration data obtained by rocket-borne interferometer

14 p2100 A72-30462

Ionospheric radio signal reflection fields verified via quantitative statistical reliability criterion

14 p2100 A72-30634

Radio wave reflection from ionosphere, determining polarization and fluctuation characteristics via Stokes parameters

14 p2100 A72-30636

HF radio signal reception behavior near maximum usable frequency during evening and at midnight, noting SNR

14 p2085 A72-30656

Ionospheric attenuation of 3-100 MHz radio waves, interpreting scatter mode propagation mechanism as total reflection from lower ionizational irregularities

14 p2086 A72-30658

Ionosphere radio wave propagation from fluid plasma wave and magnetically nonpermeable medium electrodynamic studies

15 p2193 A72-31281

Ionospheric electron density measurement by radio propagation method, recording traveling ionospheric disturbance effect and sporadic E strata thicknesses

15 p2223 A72-31438

Ionospheric radio waves absorption and stratosphere temperature variations with respect to season and sunspot cycles, examining 1963-5 winter anomaly

15 p2195 A72-31555

Pulse and monochromatic short wave signals phase/amplitude autocorrelation functions and probability distributions during oblique incidence reflection from ionosphere

15 p2197 A72-31876

Antarctic D region reflection heights from relative phase measurements on VLF transmissions at several phase locked frequencies, interpreting results by waveguide mode theory

15 p2200 A72-32105

VLF wave normal direction measurement during propagation through ionosphere by Doppler technique, using rocket-borne receivers

15 p2201 A72-32332

Rayleigh distribution of radio signals partially reflected from D region, noting amplitude fluctuations dependence on antenna radiation pattern

15 p2202 A72-32733

Tropical sporadic E reflections and vertical plasma instabilities as function of equatorial electrojet and electron drift ratio based on ionogram observations

16 p2382 A72-32867

Booker theorem generalization to cover wide range of ionospheric refractivity profiles containing variable electron density and collision frequency

16 p2386 A72-33662

Russian monograph on ionospheric measurements covering plasma parameters, wave propagation, absorption sounding methods and radio communication applications

16 p2387 A72-33875

Time delay measurements in the Athens/Greece/Roma/Lesotho/ VHF trans-equatorial propagation circuit

17 p2515 A72-34693

On the winter anomaly of ionospheric absorption

17 p2546 A72-34695

The magnetic control of the lower ionospheric absorption at lower latitudes

17 p2546 A72-34697

Wave interference effect in whistler mode reflection coefficients for model lower ionospheres

17 p2548 A72-35465

Book on ionosphere and magnetosphere covering solar radiation effects, ionospheric layers, currents and storms, charged particle movement and various wave propagations

17 p2550 A72-35850

Height of the region of principal auroral radio-wave absorption in the presence of a sporadic E layer

17 p2519 A72-35869

Investigation of the characteristics of short wave propagation along the auroral radio path

17 p2519 A72-35877

Influence of horizontal electron-concentration gradients on the magnitude of the maximum usable frequency and the trajectory of radio wave propagation in the ionosphere

17 p2519 A72-35878

Investigation of radio-wave propagation by the oblique sounding method/Survey/

17 p2519 A72-35879

Local characteristics of ray propagation in an inhomogeneous anisotropic ionosphere

18 p2686 A72-36229

Sunspot control of ionospheric absorption

18 p2686 A72-36231

On an anomaly in long-range short-wave propagation from the equatorial region to central Europe

18 p2657 A72-36232

On the reflection of whistler mode waves from model lower ionospheres

18 p2660 A72-36430

Dispersion and random changes in the ground pattern of radio waves reflected from the ionosphere

18 p2660 A72-36459

Properties of plane asymmetric plasma waveguides in applications to the propagation of short radio waves along inhomogeneities in the outer ionosphere

18 p2662 A72-36855

Measurement of integral parameters of the nighttime ionosphere by observations of signals from the 'Intercosmos 2' artificial earth satellite

18 p2689 A72-36877

Fluctuation frequency correlation for radio waves reflected from the ionosphere

18 p2662 A72-36879

Signal reflection height seasonal variations effect on radio waves absorption estimation from vertical ionospheric sounding

18 p2662 A72-36881

Reflection of microwave through laboratory plasma

18 p2716 A72-36947

Reflectionless ionospheric propagation of non-guided VLF descending wave near low hybrid resonance maximum frequency, investigating energy trajectory

19 p2790 A72-37793

Circumterrestrial short wave signals propagation and waveguides effective volume and attenuation characteristics, relating ionospheric effects and non-linear beam defocusing

19 p2765 A72-38332

Slip effect in diurnal phase and amplitude cycles of VLF signals in lower ionosphere due to wave interference at transmitting point

19 p2765 A72-38338

Geomagnetic variations propagation theory for LF electromagnetic and Alfvén waves diffraction at stratified earth in thin gyrotopical ionosphere

19 p2765 A72-38339

Unified coordinate system for global distribution of F 2 and sporadic E layer transmission parameters, suggesting geomagnetic longitude and modified magnetic inclination

19 p2791 A72-38354

Critical frequencies and geometric parameters of parabolic ionosphere layer model in oblique backscatter sounding, using distance-frequency characteristics

19 p2791 A72-38360

Altitude dependence of VLF field of vertical electric dipole in spherical waveguide of radially inhomogeneous ionosphere and earth, using Sommerfeld integral representations

19 p2766 A72-38364

Long radio waves oblique incidence on isotropic inhomogeneous ionospheric plasma

19 p2766 A72-38365

On the source of sunrise effects in the low ionosphere.

19 p2792 A72-38627

Numerical solution to the problem of propagation of ELF electromagnetic waves in the lower ionosphere

19 p2767 A72-38651

The interpretation of ionospheric radio drift measurements. V - Demonstration of the point effect in time-averaged correlations and drift calculations.

19 p2794 A72-38862

Determination of the orientation of ionospheric irregularities causing scintillation of signals from earth satellites.

19 p2794 A72-38866

Ionosonde receiver with automatic noise suppression and digital-analogue recording of the first ionospheric reflection.

19 p2805 A72-38867

The propagation of very low-frequency waves in ducts in the magnetosphere. II.

20 p2916 A72-39192

On the diurnal and seasonal variations of the D- and E-regions above Kjeller.

20 p2917 A72-39529

Recent work on ionospheric irregularities and drifts.

20 p2920 A72-39981

The generation and propagation of VLF emissions.

20 p2904 A72-39984

A high-frequency dynamic phase metering instrument for ionospheric research.

21 p3051 A72-40214

Propagation of HM-waves with periods corresponding to periods of Pcl micropulsations through the lower ionosphere.

21 p3015 A72-40497

Whistler propagation through magnetosphere.

21 p3049 A72-40975

Linear HF radar antenna array aperture synthesis for ionospherically propagated signal reception in airplane for achievement of ideal directivity without ionospheric compensation

21 p3022 A72-41080

Lateral deviation of radio waves reflected from ionosphere.

21 p3022 A72-41321

Ionospheric refractivity and attenuation surface deformation relationship to ion cyclotron whistlers near cross-over level between zero and critical coupling angles

22 p3168 A72-42006

Admittance measurements of a 36-m dipole antenna in the topside ionosphere.

22 p3153 A72-42007

Pc 1 hydromagnetic whistlers and emissions polarization characteristics measured in plane of earth surface

22 p3169 A72-42019

Reflection and refraction of radio waves from the ionosphere in presence of time-varying irregularities.

22 p3154 A72-42302

An investigation of the ground diffraction pattern of radio waves reflected by the ionosphere.

22 p3154 A72-42362

Very-high-frequency wave propagation by the temperate-latitude sporadic-E layer.

22 p3154 A72-42367

Partial reflections from a thin parabolic layer in the lower D-region.

22 p3170 A72-42374

D-region measurements with the differential-absorption, differential-phase partial-reflection experiments.

22 p3172 A72-42423

A method of estimating the excess electron density in random irregularities embedded in the ionosphere.

22 p3173 A72-42883

Propagation of electromagnetic waves in a weakly ionized warm magnetoplasma.

22 p3155 A72-42991

The effective recombination coefficient in the ionospheric D region

23 p3283 A72-43364

Analytic ray trajectory model of radio wave lateral incidence on traveling large scale ionospheric inhomogeneities as function of location and azimuthal angle departure

23 p3263 A72-43377

Ray tracing in ionosphere and magnetoionic theory application to coupling in cold plasma waves, considering linear waves, electrodes, particles and echoes as exciters

23 p3319 A72-43516

Relation between satellite radio signal scintillations and magnetic activity

23 p3264 A72-43850

Polarization of the central field of a wave reflected from the ionosphere

23 p3265 A72-44173

A study of the dependence of the maximum usable frequency on the electron content.

23 p3266 A72-44333

Rocket observation of topside resonances.

23 p3286 A72-44517

Quadruple conjugate pair observations of the sudden commencement absorption event on June 17, 1965.

23 p3286 A72-44526

Beamed radio waves interaction in E and F 1 regions propagation, noting beam width and field amplitude changes caused by defocusing

24 p3397 A72-45079

D region electron density profiles calculated as function of solar zenith angles, noting LF radio wave propagation

24 p3397 A72-45082

Multilayer plasma model for MHD pulse propagation in ionospheric waveguide, noting approximation of Alfvén velocity distribution by plasma layers

24 p3397 A72-45085

Worldwide thunderstorm activity model selection from Schumann resonance observations, using ELF noise measurements in lowest earth-ionosphere cavity modes

24 p3380 A72-45100

Arrival angles of radio wave reflected from ionosphere for remote short wave transmitter direction finding

24 p3380 A72-45101

Ionospheric radio absorption measuring device with readout data convenient for visual and computer processing, discussing block and circuit diagrams

24 p3402 A72-45102

Potential of the navy navigation satellite system in predicting ionospheric characteristics.

24 p3447 A72-45555

Phenomena associated with very high power, high frequency F-region modification below the critical frequency.

24 p3400 A72-45596

Measurement of best time-delay resolution obtainable along east-west and north-south ionospheric paths.

24 p3381 A72-45637

IONOSPHERIC REFLECTION

U IONOSPHERIC PROPAGATION

IONOSPHERIC SOUNDING

Skylark rocket observations of sporadic E layer magnetic fields, winds and ionization indicating ion divergence region

01 p0052 A72-10086

Ionospheric ion mobilities and densities measurements over Sardinia, using parachute mesosphere probe

01 p0055 A72-10436

Lower ionosphere continuous electron density measurements with ground vlf transmitter, determining limiting altitude ceiling for diurnal and seasonal data

01 p0027 A72-10442

Photochemical ion-molecule reactions in ionosphere by air exhaust device and RF mass spectrometer observation in geophysical rocket experiment

01 p0068 A72-10591

Sporadic E layer occurrence frequency distribution during 1958-1960, investigating characteristics over equatorial, temperate and auroral zones

01 p0059 A72-10596

Sizes, shapes and temporal characteristics of small scale inhomogeneities in F region, using vertical sounding, space diversity reception and radio astronomy

01 p0059 A72-10610

Daytime and nighttime sporadic F layer regularities correlation with other ionospheric phenomena based on vertical sounding data

01 p0059 A72-10611

Design, construction and testing of wideband circularly polarized dipole antenna suitable for ionospheric research

01 p0043 A72-11235

Ionospheric reflection height calculation according to oblique electromagnetic backscatter sounding data at two frequencies

02 p0172 A72-11943

Plasma resonances due to satellite antenna from ionospheric topside sounder observations

02 p0222 A72-12838

Ionospheric ion-molecule and ion-electron reaction rate constants determination from nighttime flight of rocket-borne ion mass spectrometer data least square fitting

03 p0347 A72-13396

Lower D region ion density measurement with parachuted blunt probe consisting of disk-shaped collector with guard ring at bottom

03 p0347 A72-13398

Electron temperature measurements in ionospheric isotropic nonequilibrium plasma by electrostatic probes and radar backscatter

03 p0349 A72-13520

Collision resonance effects on transverse wave propagation direction in collisionless plasma for upper ionospheric sounding

04 p0490 A72-15403

Traveling ionospheric perturbations investigation by vertical sounding with interference method, presenting group path difference measurements as function of frequency and time

05 p0657 A72-16269

Automatic interplanetary station adapter to obtain reflected signals amplitude-altitude-frequency characteristics during ionospheric probes

05 p0657 A72-16271

Ionospheric ion density distribution at 600 km height and medium and low latitudes from Cosmos 184 satellite data analysis

05 p0659 A72-16766

Dipolar rf probe admittance measurements in simulated ionosphere for satellite plasma experiments

06 p0811 A72-18733

Electric field measurements in ionosphere and magnetosphere by double probe and electron and ion drift techniques

07 p0978 A72-20042

Plasmasphere structure as outermost ionospheric region from direct measurements by particle traps, ion mass spectrometers and Langmuir probes on satellites

07 p0978 A72-20044

Large scale structure of plasmopause in equatorial plane based on whistler and upper ionosphere sounding data

07 p0978 A72-20045

Wave-like ionospheric disturbance effect on phase polarization fading of vertical sounding signal, using numerical integration by computer

08 p1130 A72-20709

Critical frequencies and geometrical parameters of parabolic model in oblique backscatter ionospheric sounding, using distance-frequency characteristics

08 p1154 A72-20732

Scattered signal power approximation during ionospheric oblique backscatter sounding, using geometrical optics method

08 p1130 A72-20733

Internal atmospheric gravity wave effects on ionospheric parameters obtained by vertical sounding, considering electron concentration isoline pattern

08 p1154 A72-20735

Errors in ionospheric sounding of sporadic E layers with auroral presence, discussing continuous reflections duration distribution

08 p1155 A72-20817

Ionospheric drift characteristics from vertical and oblique radio soundings, discussing instrumental effects

08 p1156 A72-20818

Optimum pulse duration for ionospheric oblique backscatter sounding, determining receiver signal power input dependence on pulse duration

08 p1131 A72-20820

Polar orbiting satellite ESRO-1A 1-13 keV electron measurements compared to bottomside ionosonde measurements for auroral particle precipitation and F region electron density

08 p1226 A72-21099

Wind and density measurements by small sounding rockets, comparing results with ground observed radio wave absorption diurnal variations

08 p1160 A72-21531

Mesospheric ozone measurement for altitude profiles, comparing rocket and ground based observations of 1.27 micron emission band at twilight

09 p1296 A72-22355

Mesosphere region positively and negatively charged particles concentration and mobility measurements by sounding rocket experiments

09 p1375 A72-22361

Rocket sounding of auroral zone F region low energy electron precipitation and excitation and ionization processes

09 p1298 A72-22585

- Ionospheric electron content determination at different latitudes from geostationary satellite signal Faraday rotation
10 p1475 A72-24955
- Equatorial Faraday rotation measurements for night ionospheric electron density peak structures during equinoctial months, using ATS-C geostationary satellite radiation
10 p1476 A72-24958
- Wind shear theory expectations tested by wind profiles and sporadic E layer observations, stressing time variations significance
10 p1477 A72-25155
- Frequency distribution of ionospheric horizontal winds vertical shear, noting altitude independence, turbulence and viscous energy dissipation
10 p1477 A72-25157
- Electrostatic and electron temperature probes compared during ionospheric rocket soundings, noting lower ionosphere discrepancies due to surface contamination
11 p1633 A72-26102
- Ground based synoptic measurement of mesospheric electron densities, noting variations relationship to solar radiation changes
11 p1626 A72-26424
- Ionospheric weather index in terms of ionization irregularities at given time and place derived from continuous steep incidence HF Doppler soundings
11 p1627 A72-26518
- Traveling ionospheric disturbances radio sounding during 7 March 1970 solar eclipse time, noting wave front orientation
12 p1801 A72-27158
- Ion velocity height profiles, ion temperature and electron density measurement with Thomson scatter facility during F region traveling ionospheric disturbance/gravity waves/
12 p1803 A72-27777
- Variations of F 1 layer thickness and maximum ionization height for high and low solar activity periods obtained from vertical ionospheric sounding
13 p1946 A72-28595
- Sporadic E layer frequency variations from space-diversity sounding data from three ionospheric stations
13 p1946 A72-28599
- Ionospheric reflection height calculation according to oblique electromagnetic backscatter sounding data at two frequencies
13 p1920 A72-29255
- Pulse-sounding position finding device for light parachute probes conducting ionospheric studies, discussing design features
13 p1922 A72-29350
- Cosmos 381 onboard ionospheric station signals received from magnetically conjugate region by ground wideband antennas
14 p2085 A72-30476
- Signal level fluctuations line spectra energy characteristics comparison for oblique and oblique-backscatter sounding, noting changes in harmonics intensity and period
14 p2085 A72-30638
- Monitoring system for ionospheric disturbances prediction from satellite observation, discussing optimum locations for space stations
15 p2220 A72-31233
- Atmospheric ion composition analysis by RF mass spectrometer during rocket ionosphere sounding, discussing meteor ionization layers
15 p2225 A72-31915
- Nitric oxide gas release by rocket in auroral glow to determine atomic oxygen densities in ionosphere via observation of auroral light emission
15 p2226 A72-31936
- Ionospheric molecular oxygen density measurements during solar grazing ray absorption experiment on Ariel 3 satellite
15 p2226 A72-31950
- Ionospheric neutral density profile measurement by ultrasensitive triaxial electrostatic force rebalance accelerometer onboard Cannon Ball 2
15 p2227 A72-31962
- Antarctic D region reflection heights from relative phase measurements on VLF transmissions at several phase locked frequencies, interpreting results by waveguide mode theory
15 p2200 A72-32105
- Monostatic radar measurement for incoherent scatter correlation function in lower ionosphere, using spaced short pulses transmission to obtain adequate height resolution
15 p2200 A72-32106
- Sounding rocket experiment on nonlinear interaction between two electron plasma waves and ion acoustic wave in ionosphere to investigate artificial realization feasibility
15 p2231 A72-32333
- Direct display plasma density and temperature meter with Langmuir probe for ionospheric observation
15 p2231 A72-32338
- Rayleigh distribution of radio signals partially reflected from D region, noting amplitude fluctuations dependence on antenna radiation pattern
15 p2202 A72-32733
- Lower thermosphere neutral composition from February 1969 rocket-borne mass spectrometer measurements over Fort Churchill, Canada
16 p2383 A72-32965
- Russian monograph on ionospheric measurements covering plasma parameters, wave propagation, absorption sounding methods and radio communication applications
16 p2387 A72-33875
- Barium cloud striations deformation in ionosphere explained by equations of motion for plasma cloud thin bar model, discussing pinch effect
16 p2387 A72-33907
- On the possibility of a simultaneous measurement of wind speed, wind direction, air density and air temperatures at heights which correspond to the upper D-region /max. 95 km/ with chaff cloud sensors.
17 p2545 A72-34631
- Experimental evidence of an electron temperature enhancement in the wake of an ionospheric satellite.
17 p2545 A72-34633
- Alouette 2 plasma resonances observation near ionospheric electron cyclotron frequency harmonics, interpreting frequency shift as wave dispersion effects
17 p2546 A72-34692
- Ionospheric ion density distribution at 600 km height and medium and low latitudes from Cosmos 184 satellite data analysis
17 p2548 A72-35269
- Geomagnetic effect on the neutral temperature of the F region during the magnetic storm of September 1969.
17 p2549 A72-35603
- Auroral proton energy time behavior estimation based on magnetic and ionospheric data from ground observations
17 p2550 A72-35855
- Investigation of radio-wave propagation by the oblique sounding method /Survey/
17 p2519 A72-35879
- Midlatitude red arc observations by satellite and ground station, suggesting thermal conduction theory of formation from ionospheric electron and ion temperatures and densities
18 p2685 A72-35989
- Chatanika, Alaska, auroral-zone incoherent-scatter facility.
18 p2674 A72-36297
- Incoherent scatter observations at Arecibo using compressed pulses.
18 p2659 A72-36299
- Structure of ionospheric inhomogeneities according to simultaneous observations of two magnetoionic components
18 p2688 A72-36856
- Fluctuation frequency correlation for radio waves reflected from the ionosphere
18 p2662 A72-36879
- Signal reflection height seasonal variations effect on radio waves absorption estimation from vertical ionospheric sounding
18 p2662 A72-36881
- Wave-like ionospheric disturbance effect on phase polarization fading of vertical sounding signal, using numerical integration by computer
19 p2765 A72-38337
- Critical frequencies and geometric parameters of parabolic ionosphere layer model in oblique backscatter sounding, using distance-frequency characteristics
19 p2791 A72-38360
- Scattered signal power approximation during ionospheric oblique backscatter sounding, using geometrical optics method
19 p2766 A72-38361
- Internal atmospheric gravity wave effects on ionospheric parameters obtained by vertical sounding, considering electron concentration soline pattern
19 p2791 A72-38363
- Quasi-periodic variation in F 2 layer reflected signal field strength, noting predominance during periods with type 4 bursts, auroras and geomagnetic disturbances
19 p2792 A72-38639
- Similarity method to compute ionosphere drift velocity and direction from radio sounding data
19 p2792 A72-38640
- A satellite survey of vector electric fields in the ionosphere at frequencies of 10 to 500 hertz. I - Isotropic, high-latitude electrostatic emissions.
19 p2768 A72-38742
- A satellite survey of vector electric fields in the ionosphere at frequencies of 10 to 500 hertz. II - The electric component of ELF hiss.
19 p2768 A72-38743
- A new method for in situ electron temperature determinations from plasma wave phenomena.
19 p2793 A72-38758
- Regression-line studies of E-region seasonal anomaly.
19 p2794 A72-38863
- Altitudinal dependence of upper atmosphere winds according to radar and ionosphere data
20 p2920 A72-40074
- Horizontal and vertical electron drifts in the F-region at Thumba.
21 p3049 A72-41324
- Some topside electron density measurements from Ariel III satellite during the geomagnetic storm of 25-27 May 1967.
22 p3169 A72-42017
- Geometrical dimensions and effective number of large scale ionospheric inhomogeneities by F 2 critical frequency variability analysis
23 p3283 A72-43360
- Group delay times of magnetoionic components for horizontal electron density profiles in magnetic meridian plane, noting comparison with ionospheric sounding data
23 p3283 A72-43361
- High power radio transmitter for structural investigation of ionospheric D and E regions by signal reflection and electron concentration profiles
23 p3263 A72-43378
- Plasma frequency, hybrid frequency and harmonic gyrofrequency electron resonances due to electrostatic waves in ionosphere observed with topside sounders aboard rockets and satellites
23 p3263 A72-43513
- Rocket observation of topside resonances.
23 p3286 A72-44517
- Equatorial spread F - Recent observations and a new interpretation.
23 p3286 A72-44530
- Solar control over the evolution of F2-layer after sunrise.
24 p3395 A72-44822
- Variations of F 1 layer thickness and maximum ionization height for high and low solar activity periods obtained from vertical ionospheric sounding
24 p3398 A72-45095
- Sporadic E layer frequency variations from space-diversity sounding data from three ionospheric stations
24 p3398 A72-45099
- Measurement of best time-delay resolution obtainable along east-west and north-south ionospheric paths.
24 p3381 A72-45637
- Evaluation of the performance of an ionospheric sounder with incoherent scatter
24 p3381 A72-45768
- IONOSPHERIC STORMS
NT SUDDEN IONOSPHERIC DISTURBANCES
Upper atmosphere and ionosphere magnetic storm phenomena, showing atomic to molecular concentration ratio decrease
04 p0516 A72-14938
- Ionospheric storms features based on F2 critical frequency data, investigating magnetosphere during geomagnetic storms
06 p0810 A72-18280
- Ionospheric F region storms model accounting for global electron density changes due to abundance ratio of atomic oxygen to molecular oxygen or nitrogen
07 p0979 A72-20047
- F region N/h/ profiles and parameters deviations during ionospheric and magnetic storms, discussing perturbation index
11 p1594 A72-26275
- Book on ionosphere and magnetosphere covering solar radiation effects, ionospheric layers, currents and storms, charged particle movement and various wave propagations
17 p2550 A72-35850
- Models for F region and topside ionospheric storms morphology, discussing electric current disturbance at polar region
18 p2685 A72-35994
- Measurements of MeV-electrons during the recovery-phase of a polar magnetic substorm on March 6, 1970.
19 p2789 A72-37409
- Anomalous ionization in lower ionosphere recorded by riometers, considering ionospheric substorms caused by auroral absorption
24 p3396 A72-44849
- IONOSPHERIC TEMPERATURE
Topside electron density profile from empirical relation between ionospheric slab thickness and mean gradient temperature in F region, using Saint Santin scatter data
01 p0052 A72-10085
- Lower thermosphere temperature, air density and pressure models, using auroral zone midlatitude neutral thermal and molecular diffusion coefficient measurements
01 p0053 A72-10187
- F region neutral thermosphere temperature perturbation and circulation pattern due to global wind with anomalies of ionization calculated from two dimensional dynamic model
01 p0096 A72-11283

F 2 region maximum electron density level height and molecular temperature diurnal variations at equatorial latitudes from Ibadan station data
02 p0218 A72-11941

Thomson scattering of electromagnetic wave in plasma and ionosphere for studying electron and ion temperatures
11 p1621 A72-25838

Thermospheric ion, electron and neutral particle concentration, composition and temperature changes during 7 March 1970 solar eclipse from rocket measurements
12 p1778 A72-27152

Neutral upper ionosphere temperature measurement with manometer device onboard Cosmos 320 satellite, noting equatorial fluctuations at 250 km
13 p1955 A72-28586

F 2 region maximum electron density level height and molecular temperature diurnal variations at equatorial latitudes from Ibadan station data
13 p1949 A72-29253

Ionospheric rotational temperature and density measurement, using fluorescence produced by rocket-borne electron beam gun
14 p2106 A72-30974

Geomagnetic effect on the neutral temperature of the F region during the magnetic storm of September 1969.
17 p2549 A72-35603

Design considerations in the measurement of electron temperature in the ionosphere.
19 p2801 A72-37926

Variations of the planetary values of the F2 layer thickness and the parameters of the neutral atmosphere
23 p3284 A72-43375

Neutral upper ionosphere temperature measurement with manometer device onboard Cosmos 320 satellite, noting equatorial fluctuations at 250 km
24 p3402 A72-45086

IONOSPHERICS

NT DAWN CHORUS

NT HISS

Collisional losses in a very-low-frequency duct associated with the lower-hybrid-resonance frequency.
17 p2517 A72-35608

IONS

NT ANIONS

NT ANTIPROTONS

NT CATIONS

NT CESIUM ION

NT DEUTERONS

NT FERRIC IONS

NT HEAVY IONS

NT HELIUM IONS

NT HYDROGEN IONS

NT MANGANESE IONS

NT METAL IONS

NT MOLECULAR IONS

NT NITROGEN IONS

NT PROTONS

NT SOLAR PROTONS

Ions classification by ionization potential to explain existence of empirically defined classes for visible solar corona lines
10 p1542 A72-24614

Ground state and metastable atoms and ions optical pumping, presenting critical survey on pumping and relaxation mechanisms, light propagation and spin exchange
14 p2109 A72-30325

IP [IMPACT PREDICTION]

U COMPUTERIZED SIMULATION

IQSY [INTERNATIONAL YEAR]

U INTERNATIONAL QUIET SUN YEAR

IRASERS

U INFRARED LASERS

IRBM [MISSILES]

U INTERMEDIATE RANGE BALLISTIC MISSILES

IRIDIUM

Iridium and tantalum foils for spaceflight neutron dosimetry.
17 p2558 A72-35901

A field-ion microscope study of ion-implantation in iridium. I, II.
18 p2719 A72-36747

Phase diagrams, solubility and alloying of Pt, Pd, Ru, Ir and Rh with noble, alkali earth, rare earth and transition metals
22 p3191 A72-42810

IRISES [MECHANICAL APERTURES]

Phased antenna array blind spot detection and elimination, describing aperture match with inductive irises
04 p0486 A72-14493

Equivalent network for symmetric inductive irises, investigating simultaneous effect of finite thickness and higher order mode interaction by variational approach
11 p1607 A72-26993

Open terminations of cylindrical waveguide periodically loaded by metallic irises, investigating cavity

resonator size effects on resonant frequency, mode and quality factor
15 p2194 A72-31547

IRON

NT FERRIC IONS

Single domain grain distribution deduction method obtained from Neel theory, applying to Apollo 11 lunar dust iron grains
01 p0125 A72-10071

Cation distribution observation over nonequivalent lattice sites in shocked orthopyroxene, noting Mg and Fe order-disorder
01 p0053 A72-10293

Mossbauer spectra measurement of metallic iron, sodium nitroprusside, sodium ferrocyanide and ferrocyanide absorbers at 78-293 K, fitting temperature dependences and resonant velocity to models
01 p0114 A72-10324

Positive Fe ion concentration relationship to equatorial spread F from OGO 6 satellite observation near magnetic equator
01 p0062 A72-10902

Presintering effects on dimensional change of iron powder compacts, using dilatometric, thermogravimetric, differential thermal analyses and resistivity measurements
02 p0233 A72-11461

Siderophilic element content relation to oxidation state of ordinary chondrites, using Ir/Ni concentrations from neutron activation analysis
02 p0277 A72-11896

Solar corona transition probabilities in intermediate coupling between Fe XVII configurations, including full configuration mixing
03 p0416 A72-13006

Terrestrial planets internal constitution and thermal history model, emphasizing iron fractionation in structure
03 p0418 A72-13110

Solar magnetic field observations with birefringent filter for 5324 A Fe I line, showing H alpha fine structure
03 p0430 A72-13316

Fe XI to XV emission lines from transitions and isoelectronic spectra in manganese, chromium and vanadium
03 p0391 A72-13750

Hydrogen diffusivity in Fe with cavities at room temperature calculated by mathematical model and numerical methods
03 p0378 A72-14256

Fe-S segregation role in early chemical and physical history, giving model of early lunar differentiation
03 p0439 A72-14274

Fe line emission during solar X-ray flares recorded by Bragg crystal spectrometers on OSO-6, resolving fine structure components of hydrogenic Ar
04 p0566 A72-14560

Carburization of various irons in methane-hydrogen atmosphere at 750 C, comparing activity coefficients and solubility limits
04 p0533 A72-14978

Magneto-optical effects on circular polarization in sunspots within Fe I 6302.5 A line
05 p0719 A72-16514

Electron density profiles as function of position in enhanced coronal region from Ni XV and Fe XIII emission lines observation
05 p0719 A72-16517

Alloying elements effects upon iron mechanical properties, investigating lattice parameters, temperature dependence of yielding and plastic flow, solid solution strengthening and softening, etc
05 p0676 A72-17101

Fe effect on dispersion hardened Ni alloys with various quantities of Nb and Ti during cryogenic operation
05 p0679 A72-17202

Muon generated cascade showers in iron, using ionization calorimeter and hodoscopic detectors
06 p0871 A72-17290

Solar Fe I oscillator strengths determination by hook method on shock heated gases
07 p1037 A72-19349

Alpha iron lattice dilation by titanium, measuring densities and lattice parameters
07 p1016 A72-19942

Coronal condensation of 10 September 1970, observing iron and calcium emission lines
07 p1082 A72-20297

Hyperfine interactions of Fe cations in ilmenite determined by Mossbauer spectroscopy, noting internal magnetic field and quadrupole coupling constant
09 p1367 A72-22457

Lunar surface darkening caused by solar wind effect, noting Fe valence state changes evaluation from photoelectron spectroscopy of foil samples exposed to ion bombardment
09 p1394 A72-23665

Statistical equilibrium analysis of fluorescent Fe I emission in long period variables
10 p1542 A72-24610

Fe powder preform hot rolling, investigating mechanical properties, microstructure and internal oxidation resistance as function of final density
10 p1488 A72-24695

Iron rotational hysteresis effect in cold magnetic balance wind tunnel system for spinning aircraft configurations and subsonic flow regimes
10 p1462 A72-24776

Metal adhesive forces to clean Fe surface measured with LEED and Auger emission spectroscopy, noting binding energy correlation to oxygen
10 p1497 A72-24821

Mercury porosimetry for iron powders void and internal particle porosity change as function of compacting pressure, noting compressibility improvement by precompacting and annealing
11 p1639 A72-25828

Bloch walls and Landau domain configurations in iron whiskers from DC to 200 kHz by direct magnetization measurements
11 p1659 A72-25912

Fe effect on plasticity and ductility of dispersion hardened Ni alloys with various quantities of Nb and Ti at cryogenic temperature
11 p1660 A72-26137

Iron base powders material requirements and forging processes, discussing powder composition, inclusions effect and preform densification
11 p1639 A72-26241

Solar curve of iron growth, noting damping dependence on excitation potentials
12 p1867 A72-27204

Magnetically unaffected Fe I line profiles in sunspots from high resolution photographic spectra observation
12 p1867 A72-27205

Secondary autoionization reduction of recombination coefficient during dielectronic recombination process, considering importance in Fe ions
12 p1864 A72-27747

Machine oil wear degree and Fe content determination by placing sample into induction coil and measuring coil Q at RF
13 p1957 A72-29142

Solar corona IR Fe XIII lines during 12 November 1966 solar eclipse, discussing proton collisions as line-producing excitation mechanism
13 p2042 A72-29537

Solar corona intensification analysis based on ionized Fe monochromatic emission spectra, investigating spectral lines behavior as function of temperature and electron density
13 p2047 A72-29736

Iron powder specific surface and particle size effect on shrinkage during sintering
13 p1966 A72-29800

Iron content and stress level effect on flaking corrosion of Al alloy sheets, describing experimental technique
13 p1980 A72-29826

Solar magnetic fields filamentary structure from Mount Wilson magnetograph recordings in Fe I 5250 A and Fe I 5233 A spectral lines
13 p2049 A72-29934

Fe light emission for simulated meteor conditions, measuring ionization and spectral emission cross sections for Fe reactions with nitrogen and oxygen for 350-2000 eV
14 p2156 A72-30562

Temperature dependent Mg and Fe hyperfine doublets in lunar olivine, indicating slow cooling crystallization
15 p2303 A72-31302

Solar Fe XIII IR lines intensity ratio at 10747 and 10798 A, deriving electron density as function of dilution factor with allowance for proton impact effect
15 p2318 A72-32784

Al-Zn-Mg-Cu forgings fracture toughness increase with Fe content reduction, discussing overload fracture following grain and stringers
16 p2405 A72-33000

X ray photoelectron spectroscopic measurements of Fe and Cu valence states produced by ion sputtering reduction, applying to multiplet splitting and isoelectronic shifts
16 p2389 A72-33026

Transition metal-modified matrix resins for composite materials.
17 p2570 A72-34672

Study by Mossbauer spectrometry of the iron distribution in mineralogical fractions separated from lunar rocks brought back by Apollo 12
17 p2607 A72-34917

Study of the diffusion of iron and cobalt along the grain boundaries of tungsten
17 p2569 A72-35522

The classification of transitions between levels of principal quantum numbers 3 and 4 in Fe IX to XVI and Mn VIII to XV.
17 p2586 A72-35834

Standard iron wavelengths for determining the radial velocities of stars
19 p2859 A72-37910

Regularities in the deformation and failure of commercial iron in a complex stress state under low-temperature conditions

19 p2818 A72-38005

Radiative lifetimes for some resonance transitions of Fe I and Fe II in the region between 2300 Å and 3050 Å, and the application to iron abundance determinations in the sun and in the QSO PHL 938.

20 p2966 A72-38915

Fabrication and properties of carbon-containing iron fibers and fiber sinter bodies

20 p2939 A72-39439

Iron transport in chondrites - Evidence from the Warrenton meteorite.

21 p3104 A72-40491

Cosmic abundance of iron and nature of primitive material in meteorites.

22 p3220 A72-41963

Low abundance of solar photosphere iron from Fe I excitation and ionization computations, showing LTE departure effects on spectral lines

22 p3228 A72-42569

Rate of molybdenum solution in carbon-saturated liquid iron.

22 p3193 A72-43027

German monograph - Contribution to the investigation of the fatigue strength of sintered iron.

22 p3194 A72-43066

Giant stars iron abundance from narrow band spectrophotometric analysis and model atmospheres, isolating super metal rich stars below H-R diagram subgiant branch

23 p3334 A72-43256

Thermophysical properties of highly porous thermochemically treated metal-ceramic iron

23 p3299 A72-43295

Simultaneous neutron-activation analyses of scandium, cobalt, iron, and zinc in biological objects with the aid of a total-absorption gamma spectrometer

23 p3259 A72-43347

The difference in the plastic deformation of the surface and bulk layers of polycrystalline iron under fatigue loading

23 p3304 A72-44490

A further high-resolution search for Fe XXV line emission from Scorpius X-1.

24 p3438 A72-44838

IRON ALLOYS

NT AUSTENITIC STAINLESS STEELS

NT BAINITIC STEEL

NT CARBON STEELS

NT CHROMIUM STEELS

NT FERRITIC STAINLESS STEELS

NT HIGH STRENGTH STEELS

NT MARAGING STEELS

NT MARTENSITIC STAINLESS STEELS

NT NICKEL STEELS

NT STAINLESS STEELS

NT STEELS

Carbon atoms thermodynamic properties in bcc and fcc Fe-Si-C solid solutions from equilibrium measurements with hydrogen-methane gas mixtures as function of temperature and carburizing gas composition

01 p0083 A72-10207

Ni, Fe and Ti alloys creep rupture characteristics in high temperature, high pressure gaseous hydrogen and helium

01 p0086 A72-10979

Critique of theoretical and experimental findings on slip geometry in bcc metals, especially Fe-Si alloy single crystals

01 p0089 A72-11300

Alumina dispersions structural stability in Fe and Ni based alloys metal matrices

02 p0241 A72-11445

Carbon content effect on phase relationships and mechanical properties of sintered Fe-WC alloys, noting high strength

02 p0241 A72-11452

Atomic structural mechanism of solid solution decomposition by nucleation and equilibrium phase particles in Fe-Co-Ti alloy, using X ray analysis and transmission microscopy

02 p0242 A72-12008

Anodic polarization curves of Ni-Fe alloys relating reaction to attack at controlled voltage of gamma joints and Ni content, using electron microprobe

02 p0243 A72-12168

Microstructure and mechanical properties of iron base superalloys, examining precipitation hardening by gamma prime and secondary intermetallic compounds formation

02 p0245 A72-12505

Titanium and aluminum variations effects on eta and gamma prime solvus temperatures and on mechanical properties of iron-nickel superalloy

02 p0245 A72-12508

Yield stress of solid solution iron and Fe-Ge alloys with bcc structure, obtaining interaction energy between solute atoms and screw dislocation

03 p0402 A72-13974

Alloying elements effects on aging response of austenitic-ferritic alloys in Fe-Cr-Mn-Ni base, deter-

mining mechanical properties dependence on processing and heat treatment

03 p0377 A72-14170

Substitutional dynamic strain aging effects on Fe-Nb alloys mechanical properties, attributing ductility reduction to work hardening and strain rate effects

04 p0534 A72-15576

Hardening of Fe-Mn-Ti ferritic and martensitic alloys, investigating microstructure and mechanical properties

05 p0672 A72-16144

Materials research for investment cast turbine wheel, investigating Fe base specimens

05 p0666 A72-16496

Laser pulse heating inability to quench in disorder in Fe-Al alloy

05 p0669 A72-16796

Binary and ternary alloys of Cr and Fe with Ni, determining interaction coefficient and molar enthalpy for Cr at 1600 C by mass spectrometry

05 p0676 A72-17103

Dynamic yielding of annealed and cold worked Fe-Ti alloy determined in shock compression tests

05 p0679 A72-17121

Fe-Co alloy athermal transformation to bcc martensite at industrial cooling rates, investigating effects on mechanical properties

06 p0829 A72-17830

Internal friction spectrum peaks in Fe-Ni alloy at 20-1100 C upon heating and cooling, explaining by grain boundary relaxation and martensitic transformations

06 p0830 A72-18293

Y-Fe-Al alloys ternary system X ray structural analysis after arc furnace preparation, annealing and quench hardening

07 p1048 A72-19681

Aluminized layer phase and chemical composition on heat resistant iron and nickel alloys

07 p1013 A72-19748

Phase and microstructure changes during nitriding process of Fe-Ti alloys, stressing Ti concentration effect

07 p1013 A72-19749

Formation kinetics, phase composition and structure of oxide films in binary and ternary iron-base chromium aluminum alloys, studying hydrogen penetration characteristics

07 p1013 A72-19771

Martensitic transformations induced by plastic deformation in Fe-Ni-Cr system, noting stacking fault energy dependence on temperature

07 p1015 A72-19928

Tensile strength enhancement of dislocated martensites in Fe alloys by precipitate dispersion in austenite prior to transformation

07 p1016 A72-19936

Microstructure and high temperature mechanical properties of unidirectionally solidified pseudobinary Fe-Cr-Nb eutectic alloy

07 p1016 A72-19938

Aging effect on brittleness and hardening of Fe-Ni-Mn alloy at various temperatures

07 p1016 A72-19939

Gas quenching technique for vacuum brazing of Al, Ti and ferrous alloys, evaluating mechanical properties, surface contamination and He leak tightness

07 p0997 A72-19997

Al, Ti and ferrous alloys suitability for vacuum brazing-gas quenching processing for He leak-tight joints, using photomicrography

07 p0997 A72-19999

Fe addition effects on structural and mechanical properties of heat resistant Ni-Cr alloys

07 p1020 A72-20416

X ray study of martensite fine structure produced by plastic deformation in Fe-Ni alloy

08 p1188 A72-21788

Plastic deformation characteristics of Fe-Cr-Ni alloy single crystals at low temperatures

08 p1188 A72-21790

X ray K absorption edges in binary solid solutions of Co, Fe and Ni with localized hole increases

09 p1371 A72-22846

Order-disorder transition in metastable splat cooled Ti rich Ti-Fe alloys from phase formation, constitution and crystal chemistry viewpoint

09 p1330 A72-23378

Graphite morphology in metallic materials from scanning electron micrographs, discussing sulfur contents effect in tempered cast iron

10 p1500 A72-23825

Carbon effects on internal friction of low temperature Fe-Ni alloy during martensitic transformation

10 p1495 A72-24083

Internal friction peak in fresh tempered martensite from Fe-Ni-C alloy cooled to 77 K, suggesting hypothetical carbon atoms interactions with mobile dislocations

10 p1496 A72-24232

Chloride ion concentration effect on polarization behavior of Fe-Ni alloy, noting cathodic curve parallel shift in noble potential direction

11 p1652 A72-25290

Fe-Cr-Mn alloys structural changes during high temperature oxidation, noting subscale layer thickening and alpha phase detection after heat treatment

11 p1655 A72-25498

Fe-Mo solid solutions transient creep behavior as function of applied stress, noting temperature effect

11 p1662 A72-26656

Grain boundary network of allotropic phase change for ductility enhancement in Fe-Ta alloys

11 p1668 A72-26941

Relative valence effect of transition metal additions on alpha-gamma phase equilibrium in Fe-Cr-Mn system

12 p1827 A72-27099

Hydrostatic pressure effect on itinerant antiferromagnetic ordering in Cr-Fe alloys with Ru and Mn additions

12 p1828 A72-27432

Nitride phase microstructure in ferrochromium nitrided in liquid state, comparing electrolytic etching and film coloration methods

12 p1829 A72-27454

Annealed and quenched Fe-Mo-Co system, defining phase relationships in Fe-rich corner at 2200, 2000 and 1800 F

13 p1973 A72-28650

Electron diffraction study of transformation twin rotations in Fe-Ni martensites, showing foil plane uncertainty effect with respect to image plane

13 p1975 A72-28666

Fcc lattice ferronickel alloys para-process susceptibility anomalous increase explanation by phase transition thermodynamic theory

13 p1977 A72-28911

Sintering of binary systems Co-Ni Co-Fe and Fe-Ni with infinite mutual solubility at different temperatures

13 p1966 A72-29954

Microstructure and mechanical properties of heat resistant Fe-Mn-Al alloys at 650-1150 C

13 p1981 A72-30093

Antifriction phase structure of friction formed thin surface layer of sulfurized iron-graphite metal-ceramic materials, using transmission microscopy

13 p1967 A72-30108

Phase precipitated helicoidal dislocations and vacancy-type stacking faults in aged austenite Fe-Ni-Ti alloy, using electron microscope diffraction contrast analysis

14 p2112 A72-30162

Maraging Fe-Ni-Co-Mo alloy ordered metastable omega phase formation during martensite aging from electron microscopic investigation, noting Co addition effects and precipitation

14 p2115 A72-30404

Martensitic transformation athermal kinetics and accompanied martensite morphology change in Fe-Ni and Fe-Ni-Cr alloys

14 p2115 A72-30407

Ni additions effect on Fe-Cr alloys oxidation behavior at high temperatures during varied exposure time periods, noting dichromium trioxide scale formation

14 p2118 A72-30545

Cr-containing Fe-alloy and Ni steels, investigating thermal cycling effects on thermal resistance by factorial program

14 p2118 A72-30546

Accelerated intergranular corrosion and grain boundary precipitation mechanisms in stainless steel Fe-Ni-Cr alloy, using Huey, acid and Strauss tests

14 p2118 A72-30548

Surface phase transformation during cavitation erosion in Co and Fe alloys, suggesting stacking fault energy effect on erosion resistance

14 p2119 A72-30603

Molybdenum carbide needle formation, growth in kinetics and morphology Fe-C-Mo alloy from lattice parameters measurements

14 p2120 A72-30618

Internal friction and relaxation mechanisms in substructure hardened fcc alloys and bcc metals, presenting dislocation parameters for annealed and cold worked Fe alloys

14 p2122 A72-30960

High temperature oxidation resistance and mechanical properties of Fe-Al-Cr alloys with Ti and Mo additions

15 p2253 A72-31520

Hyperfine magnetic field reduction produced in Fe-Cr alloy single crystal by Cr atoms observed by Mossbauer method, proposing spin disturbance mechanism

15 p2293 A72-32230

Mobile dislocation density and strain rate sensitivity of bcc Fe-Ni alloys from deformation onset to high temperature plateau

15 p2258 A72-32639

Si stabilization of laves and intermediate phases in Nb-Fe-Si and Nb-Co-Si systems

16 p2409 A72-33805

High temperature oxide scale adherence on Fe-Cr-Al alloys with Y or Sc additions as promoting agents

16 p2410 A72-33817

Ti comparison with Al for effects on Fe alloy deformation and fracture, discussing intergranular failure suppression

16 p2411 A72-33823

Separation of iron and annealing-out of lattice defects in rapidly-solidified aluminum-iron alloys. I - Microstructure and properties of quenched samples. II - Tempering behavior

17 p2567 A72-35174

Study of certain features of the electronic structure of the ternary alloys Ni₃/Mn, Fe/ and Ni₃/Mn, Co/

17 p2568 A72-35518

Charge carriers interaction with metal ions studied from electrical transport of Fe and Co in Fe-Cr alloy

17 p2569 A72-35521

Interstitial and substitutional dynamic strain aging of Fe-Nb alloy and Al-Nb bearing steel at 295-950 K

18 p2699 A72-36342

Grain-boundary relaxations in an Fe-Ni-Cr alloy.

18 p2700 A72-36588

Behavior of Fe-21.6 Ni, Fe-18.4 Ni-15.0 Co, Fe-16.8 Ni-5.0 Mo subjected to cumulative thermal cycling at 300 C/hr

18 p2701 A72-36701

Self-diffusion of cobalt in the ternary system Co-Ni-Fe

19 p2814 A72-37416

Some problems concerning microplastic deformation and isothermal transformation of Fe-Ni-C alloy. III - Effect of aging in the temperature range from 203 to 304 K on microplastic deformation at 77 K

19 p2814 A72-37419

Some problems concerning microplastic deformation and isothermal transformation of Fe-Ni-C alloy. IV - Effect of transformation plasticity on microplastic deformation at 77 K

19 p2815 A72-37420

X-ray analysis of iron-chrome solid solutions

19 p2821 A72-38572

Young and shear moduli of binary Fe base alloys as functions of composition and temperature by ultrasonic pulse echo technique

20 p2937 A72-39287

Effect of residual elements on radiation strengthening in iron alloys, pressure vessel steels, and welds.

20 p2937 A72-39289

The effect of elastic anisotropy on dislocations in Ni₃Fe.

20 p2937 A72-39293

Alloying element effects on C free energy interaction coefficients in liquid Fe alloys at 1550 C by equilibrium distribution method

20 p2937 A72-39295

The effect of plastic deformation on the martensite-to-austenite transition in an iron-nickel alloy.

20 p2938 A72-39298

Investigation of solid solution decay in cobalt-titanium, iron-cobalt-titanium-aluminum and iron-nickel-titanium-aluminum alloys

20 p2939 A72-39314

Fe-Ni sheet with austenitic cube texture by rolling and annealing, investigating plastic deformation during martensitic transformation

21 p3065 A72-40090

Interaction of nonmetallic refractory compounds with transition metals and ferroalloys

21 p3066 A72-40394

Contribution of the invar anomaly and the elinvar effect to the formation of the thermal stability of the modulus of elasticity of iron-nickel invars

21 p3068 A72-40952

On the growth kinetics of Laves phase precipitates in Fe-Ti alloys at elevated temperatures.

21 p3069 A72-41011

Martensite formation temperature decrease and grain size reduction caused by martensite crystals interaction with barriers in Fe alloy containing austenite beta phase particles

21 p3070 A72-41679

Crystallization and structure of hypereutectic iron-carbon-chromium alloys

21 p3071 A72-41788

Investigation of the influence of cobalt on the redistribution of the atoms of the alloying elements in iron-base alloys by the NGR method

22 p3188 A72-42162

Kinetic aspects of plastic strain induced martensite in polycrystalline Fe-Ni-C alloy from tensile tests on austenitic specimens

22 p3189 A72-42437

Magnetic properties and texture of a thin strip of nickel-iron-molybdenum alloys

22 p3192 A72-43012

Fe-Ni-C martensite reverse transformation to austenite during large and rapid applied shear, evaluating shear zone neighboring partially pierced hole

22 p3193 A72-43031

Enhanced strengthening of a spinodal Fe-Ni-Cu alloy by martensitic transformation.

22 p3194 A72-43040

German monograph - Determination of the diffusion coefficient of hydrogen in the binary iron-nickel system at 25 and 58 C.

22 p3194 A72-43057

Thermal stability of sulphides of some metals in iron-base cermets

23 p3298 A72-43285

Magnetic properties of the powders of highly dispersed iron-cobalt-nickel alloys

23 p3299 A72-43288

A study of the hardening of the subspinoidal alloy Fe-Ni-Al

24 p3415 A72-45395

IRON CHLORIDES

Spectrophotometric observations of Venus, showing unreliability of evidence for dihydrated ferrous chloride in upper cloud layers

10 p1532 A72-23715

IRON COMPOUNDS

NT CHROMITES

NT FAYALITE

NT FERRITES

NT FERROCENES

NT HEMATITE

NT ILMENITE

NT IRON CHLORIDES

NT IRON OXIDES

NT MAGNETITE

NT TROILITE

Iron aluminides and borides diffusion layers morphology on alpha iron surface by metal surface/gas phase interaction, observing preferential orientation

03 p0376 A72-13971

Crystal structure of iron-zincium disulfide and cobalt-zincium disulfide systems

10 p1496 A72-24089

Hydrated iron silicon fluoride internal motion pressure dependence examined by wideline and NMR techniques, noting corrections of second moments for bulk paramagnetic effects

13 p1914 A72-30061

Iron carbide single crystal growth texture due to anisotropy of interatomic interactions associated with oriented covalent Fe-C bonds

14 p2121 A72-30774

Iron-containing catalysts action mechanism during ammonium perchlorate-poly(methyl methacrylate) mixture burning in nitrogen atmosphere

19 p2847 A72-38456

Ground and low-lying excited electronic states of FeH.

21 p3096 A72-40563

Iron-nickel-molybdenum carbonyl powders

23 p3298 A72-43276

Influence of the protective medium during sintering on the properties of iron-base cermets

23 p3299 A72-43289

IRON METEORITES

NT SIKHOTE-ALIN METEORITE

Iron meteorite formation model based on metal carbonyls low temperature thermal decomposition in comets

01 p0124 A72-10061

Structure and characteristics of craters and pits in Sikhote-Alin iron meteorite shower, searching for meteor and meteorite dusts and micrometeorites

01 p0125 A72-10101

Logarithmic equation for iron meteorite cooling rate determination from kamacite bandwidths and Ni concentrations

01 p0126 A72-10102

Iron River meteorite, discussing history, physical characteristics, element distribution and Widmanstatten structure

01 p0126 A72-10105

Chemical analysis of iron meteorites, tabulating Ni, Co, P and C content

01 p0126 A72-10108

Chondrules occurrence in iron meteorite, investigating bulk chemical composition and mineral properties

01 p0127 A72-10294

Oxygen isotope ratios in iron meteorites magnetite crust and cosmic spherules as indicators for atmospheric oxygen development

02 p0279 A72-12117

Xe and Kr abundance and isotopic composition in silicate inclusions of iron meteorites

03 p0435 A72-13690

Theoretical model for radiating metallic gas produced around iron meteor entering earth atmosphere, presenting temperature, pressure and density distributions

[AIAA PAPER 72-204] Phosphorus effect on Widmanstatten pattern in iron meteorites, using Fe-Ni-P phase diagram and cooling experiments

05 p0721 A72-16884

Thermal release patterns and activation energies of spallogenic He, Ne and Ar from Carbo iron meteorite

12 p1866 A72-27116

Neutron activation data for Ru, Os, Ir, Pt and Au in iron meteorites, noting correlation

14 p2157 A72-30582

Natural remanent magnetism creation in meteorites via shock passage in collisional fragments

16 p2451 A72-32990

Parent-body models for the formation of iron meteorites.

17 p2615 A72-35687

The isotopic composition and elemental abundance of gallium in meteorites and in terrestrial samples.

18 p2723 A72-36061

Nuclear particle fluxes and radioactive isotopes production rate distribution from cosmic rays data along orbits, calculating iron meteorite dimensions prior to atmosphere entry

22 p3220 A72-41919

Falls of meteorites in Germany: Temporal distribution of the falls and deductions with regard to their origin - Hypotheses concerning the origin of the meteorites as well as further falls and findings in Germany

22 p3227 A72-42542

Determination of Ni, Ga, and Ge in iron meteorites by X-ray fluorescence analysis.

23 p3262 A72-44128

The chemical classification of iron meteorites. VI - A reinvestigation of irons with Ge concentrations lower than 1 ppm.

24 p3436 A72-44697

IRON ORES

NT HEMATITE

IRON OXIDES

NT CHROMITES

NT HEMATITE

NT ILMENITE

NT MAGNETITE

Lunar basalts 10044 and 12021 Fe oxidation state in plagioclase and distribution in crystal structure, using Mossbauer spectroscopy

01 p0124 A72-10064

Logic functions for magnetic bubble devices based on interaction of circular magnetic domains in rare earth iron oxides, considering gates for dynamic memory [IEEE PAPER 2,3]

03 p0327 A72-13753

Fine oxide particle inclusions in mild steel weld metal deposited by carbon dioxide shielded metal arc process, using electron microscopy and diffraction pattern photography

06 p0820 A72-17706

V, Nb and Ta deoxidizing capability in liquid Fe from oxide phase formation identification by electronographic and X ray analyses

07 p0101 A72-19545

Artificial meteor ablation on iron oxides by arc heated air plasma stream for product and environment identification studies

14 p2150 A72-30319

IRON 57

Gamma ray scattering asymmetries of Fe 57 nucleus, discussing hyperfine structure and conjugate spin transition

22 p3209 A72-42924

IRRADIANCE

NT ILLUMINANCE

NT SOLAR CONSTANT

Radiative transfer equation for solar irradiance penetration of turbid atmosphere and plant canopy, using four point quadrature method

09 p1297 A72-22442

Sunlight resonance scattering by spherically symmetric optically thick artificial Sr clouds, comparing photometric data with computed theoretical isophotes, line profiles and irradiances

09 p1297 A72-22579

Fresnel diffraction integrals for irradiance and power distribution calculations of Gaussian beams focused through annular apertures

09 p1352 A72-23334

Fourier transform plane irradiance distribution for random phase data masks in holographic data recording, discussing phase quantization level change effects

09 p1314 A72-23335

IRRADIATION

NT AURORAL IRRADIATION

NT DEUTERON IRRADIATION

NT ELECTRON IRRADIATION

NT ION IRRADIATION

NT NEUTRON IRRADIATION

NT PROTON IRRADIATION

NT X RAY IRRADIATION

Linear polyethylene irradiation, investigating chain scission processes importance, critical conditions for gelation and sol/gel partitioning

04 p0484 A72-15258

Laser irradiations inhibitory effect on cornea vascularization after treatment with supranatural total extract

13 p1906 A72-29867

Interaction energy and force between screw dislocation and spherical inhomogeneity, discussing voids growth in irradiated materials

18 p2718 A72-36510

Irradiation history of grain aggregates in ordinary chondrites - Possible clues to the advanced stages of accretion.

24 p3444 A72-45455

IRREVERSIBLE PROCESSES

- Irreversible thermodynamics applications to physicochemical and biological stability, including allosteric activation model 04 p0482 A72-14754
- General relativistic kinetic theory of gases, discussing microscopic model, space-time, self-consistent Einstein-Maxwell-Liouville equations and irreversible processes 06 p0847 A72-17255
- Basic thermodynamic efficiency relationships for irreversible processes under all system circumstances, introducing high grade energy concept 07 p1101 A72-20543
- Shock wave profile equation derivation based on minimal entropy rate variational principle for stationary irreversible processes, using local potential for Boltzmann type equation 09 p1295 A72-23473
- Generalized thermodynamic potentials and universal criteria for direction of evolution of irreversible processes from Gibbs function stability analysis 10 p1562 A72-24250
- Local and cosmological irreversibility and time anisotropy theories from thermodynamics, statistical mechanics, astrophysics and quantum-relativity viewpoints 11 p1716 A72-25775
- Irreversibility mechanism in postpartum ductus arteriosus closure in guinea pigs, studying vessel cellular changes and smooth muscle response to oxygen pressure 12 p1762 A72-27826
- Hard superconductors cylindrical samples irreversible magnetization and size effect calculation, comparing results with experiment on Nb-Ti alloy specimens 16 p2441 A72-33523
- Onsager irreversibility theory extension to nonlinear constitutive relations and with allowance for inclusion of all thermodynamic variables 16 p2479 A72-33826
- A study of the liquid-vapor phase change of mercury based on irreversible thermodynamics. [ASME PAPER 72-HT-A] 20 p2983 A72-39481
- Flux vortices and transport currents in type II superconductors. 20 p2961 A72-39809
- Some reflections on the nature of entropy, irreversibility and the second law of thermodynamics. 24 p3465 A72-45628
- IRRITATION**
- NT TOXICITY AND SAFETY HAZARD**
- IRROTATIONAL FLOW**
- U POTENTIAL FLOW**
- ISCHEMIA**
- Myocardial blood flow measurement value in ischemic heart disease assessment, discussing Xenon 133 injection into coronary arteries 03 p0315 A72-13179
- Clinical assessment of degree of obstruction from coronary arteriograms of ischemic and rheumatic heart patients 03 p0316 A72-13847
- Regional myocardial contraction mechanics during transient ischemia and reoxygenation in anesthetized dogs 04 p0476 A72-15719
- ECG evidence of myocardial ischemia in patients without arteriographic evidence of coronary artery disease, studying myocardial oxygen supply 07 p0920 A72-19995
- Atypical ECG of sportsmen, considering repolarization disorders due to ischemia, lesion, excitability and conduction signs 07 p0924 A72-20575
- Hypertension and blood sugar and lipid level increase as ischemic heart disease risk factors 08 p1117 A72-21542
- Triglyceridemia relation to age, relative weight and ischemic cardiopathy probability from ECG, anthropometry and lipid and glucid metabolism studies 12 p1759 A72-27238
- Heart enzyme activity under experimental myocardial ischemia in rabbits determined for blood, left and right ventricles and atrium 13 p1901 A72-28463
- Quantitative angiocardiology of abnormal left ventricular function and contractile spectrum in ischemic heart disease patients 14 p2077 A72-30968
- Metabolism of the hypoxic and ischaemic heart; Proceedings of the Symposium, Geneva, Switzerland, June 14-17, 1971. Part I. 17 p2501 A72-34976
- Myocardial protein synthesis in acute myocardial hypoxia and ischemia. 17 p2501 A72-34980
- Extracellular acid-base changes in the dog myocardium during hypoxia and local ischemia, measured by means of glass micro-electrodes. 17 p2501 A72-34983
- Ion alterations during myocardial ischemia. 17 p2502 A72-34994
- Morphological alterations in the ischaemic heart. 17 p2502 A72-34995

- Effects of hypoxia and ischemia on myocardial contraction - Alterations in the time course of force and ischemia-dependent inhomogeneity of contractility. 17 p2502 A72-34996
- The incidence of hypertension and associated factors - The Israel ischemic heart disease study. 19 p2756 A72-37870
- Influence of inotropic alteration on the severity of myocardial ischemia after experimental coronary occlusion. 19 p2758 A72-38552
- Yield of ischaemic exercise electrocardiograms in relation to exercise intensity in a normal population. 22 p3151 A72-42900
- Excitation contraction correlates in true ischemia. 23 p3255 A72-43814

ISENTROPIC PROCESSES

- Seigel state equation validity limit application to isentropic hydrogen and nitrogen steady and unsteady flow expansions at high pressure 02 p0206 A72-12597
- Rocket acceleration effect on internal isentropic nozzle flow, giving formulas for thermodynamic variables 03 p0441 A72-13627
- Characteristic schemes comparison for three dimensional steady isentropic supersonic flow [AIAA PAPER 72-190] 05 p0605 A72-16846
- Relativistic hydrodynamics, considering Cauchy problem in fluid evolution, ideal isentropic fluids, electromagnetic field effect and viscous/heat conducting thermodynamic flow models 06 p0846 A72-17252
- Mixed subsonic-supersonic flows solution for choked isentropic flow in convergent-divergent nozzle, comparing results with series solution 10 p1561 A72-23721
- Shock wave and isentropic compression/expansion in plasma with anomalous thermodynamic properties due to strong particle interactions, discussing phase transitions types 13 p2019 A72-29904
- Steady flow of compressible heat conducting fluid, discussing effect of small transfer coefficient on isentropic sonic singularity in Laval nozzle 14 p2171 A72-30713
- Ideal fluids isentropic flow equations solution via Riemann invariants method, describing nonlinear waves linear interactions 16 p2376 A72-33110
- Calculation of two-dimensional cascades in isentropic flow 17 p2484 A72-34893
- Entropy and simple waves in multidimensional gas flow. 22 p3166 A72-42314
- On the instability of a three-layer atmosphere with an isentropic stratosphere. 24 p3399 A72-45484
- ISING MODEL**
- U FERROMAGNETISM**
- U MATHEMATICAL MODELS**
- ISIS SATELLITES**
- U.S.-Canadian Alouette/ISIS satellites case history, considering hardware, lunar sample analysis and satellite transmitted radio beacon signal reception and analysis 14 p2175 A72-31144
- ISLANDS**
- NT JAPAN**
- Ecogenesis of volcanic island of Surtsey after 1967 lava eruption, discussing terrestrial and marine littoral and sublittoral biomes 04 p0473 A72-14916

ISOBARS

- Aerodynamic structure analysis of steady flame of homogeneous gas mixtures, noting streamlines, isotherms, isobars and flame front curves 21 p3129 A72-40979

ISOBARS (PRESSURE)

- Isobaric correlation coefficient functions for wind and geopotential, describing relationship by two differential equations derived from geostrophic wind equations 09 p1344 A72-22432

ISOBUTANE

U BUTANES

ISOBUTYLENE

U BUTENES

ISOCHORIC PROCESSES

- Isochoric heat capacity peaks of water and argon near boundary in two phase region at critical state 11 p1747 A72-26964
- Benzene isochoric specific heat curves along saturation line in biphasic and single phase states, noting variations near critical point 15 p2334 A72-31393
- Simplified theory for optimizing the design of a heat shield in an isochorically operated toroidal dewar. 19 p2805 A72-38843

ISOCHROMATICS

- Physical analysis of photoelastic interferometry and holography, considering retardation, isochromac and isopachic fringe systems and model materials 08 p1166 A72-21330

- Ti, Zr and Hf hcp-bcc phase transformation isochromat spectroscopic investigation, noting fine structures to confirm electron state density 09 p1371 A72-22849

- Aplanatic mirror-lens telescope systems with spherical optics, discussing isochromatic corrective lens specifications 14 p2104 A72-30497

- Differential stress-holo-interferometry. [SESA PAPER 1989A] 17 p2554 A72-34816

- Polarization offset angle effect on isochromatic fringe visibility of holographic photoelasticity recordings, noting reference beam ellipticity adjustment 18 p2733 A72-36360

- Aplanatic mirror-lens telescope systems with spherical optics, discussing isochromatic corrective lens specifications 19 p2803 A72-38326

- Determination of stresses along the symmetry axis in the isometric problem on the basis of an elastooptical image of isochromes 21 p3122 A72-41347

ISOENERGETIC PROCESSES

- Isoenergetic and irrotational planar supersonic cascade ideal gas flow computation by analytic method of characteristics 15 p2178 A72-31466

ISOLATION

NT SOCIAL ISOLATION

- Human electrophysiological changes during perceptual isolation from EEG, EMG, vertical eye movements and electrodermal measurements 12 p1771 A72-27484

ISOLATORS

NT VIBRATION ISOLATORS

- Anisotropic effects use in passive semiconductor magnetoplasma for submillimeter isolators and circulators development, describing transmission devices based on Faraday rotation 04 p0563 A72-15600

ISOMERS

- Mass spectral analysis of aliphatic amino acid derivatives, obtaining diagnostic criteria for distinction of alpha, beta, gamma and N-methyl isomers 07 p0935 A72-18905
- Artificial intelligence application to mass spectra interpretation, discussing heuristic Dendritic Algorithm based computer program to generate structural isomers 07 p0950 A72-19608
- Diastereomeric S-prolyl dipeptide derivatives adaptation to gas chromatographic quantitative estimation of R- and S-leucine enantiomers 11 p1590 A72-26366
- Cooperative direction changing isomer movement on polymer chain lattice describing equations derivation procedure 14 p2125 A72-30962
- Geochemistry of amino acid enantiomers - Gas chromatography of their diastereomeric derivatives. 19 p2762 A72-38224

ISOMORPHISM

- System theory on group manifolds and coset spaces. 17 p2575 A72-34949
- Phase diagram, isomorphism and temperature dependence of hexagonal, monoclinic and triclinic modifications of Sr-Ba polycrystalline aluminosilicates 21 p3072 A72-40382
- Mechanical properties of titanium alloys with isomorphous beta-stabilizing elements 23 p3300 A72-43590

ISOPERIMETRIC PROBLEM

- Classical isoperimetric problem approximation via multipliers method, generating minimizing convergent sequence of arcs 12 p1836 A72-27510

ISOPHOTES

- Solar corona observations during total eclipse of 22 September 1968, presenting photographs, polarization measurements, photometric data, structure and isophotes 03 p0434 A72-13492
- Mercury isophotometric measurements in white and H alpha light during transit across sun on 9 May 1970 04 p0573 A72-14904
- Large aperture ratio wide field VCN-UV camera exploration of night sky, presenting isophotes of zodiacal light and Milky Way 04 p0525 A72-15685
- Planetary nebulae NGC 2392, 6210, 6826, 6720 and 6853 observations, presenting monochromatic photographs and isophotic contours 05 p0713 A72-16021
- Isophote equidensity role in astronomical photometric investigation of solar corona, galactic nebulas, comets and extragalactic stellar systems 07 p1082 A72-20301
- Tago-Sato-Kosaka comet isophote picture of 5 February 1970, noting tail composition, photographic magnitude and emission spectrum 08 p1229 A72-20831

- Sunlight resonance scattering by spherically symmetric optically thick artificial Sr clouds, comparing photometric data with computed theoretical isophotes, line profiles and irradiances
09 p1297 A72-22579
- Lunar eclipse of 25 September 1965, observing penumbra densities and isophotes in B and V spectral regions by photoelectric photometry
14 p2161 A72-30915
- Photographic technique to obtain isophotic contours of solar corona polarized light during total eclipse
16 p2393 A72-33624
- Monte Carlo calculation of radial and time dependence of isophote diagrams for Cerenkov light in 0.1 to 1 TeV extensive air shower
17 p2599 A72-35142

ISOPLETHS

U NOMOGRAPHS

ISOPROPYL COMPOUNDS

- Catalytic action of metal oxides on isopropylbenzene hydroperoxide decomposition in liquid phase
08 p1129 A72-22094

ISOSTASY

- Two-layer lunar model from variable viscosity media-isostatic processes selenological investigation, suggesting hard top crust and deeper asthenosphere
04 p0569 A72-14505
- Geoid isostasy, protrusions and hollows, discussing attenuations and intensifications of gravity
17 p2548 A72-35425

ISOSTATIC PRESSURE

- Hot isostatic pressing techniques for thin wall Be tubes manufacture
11 p1643 A72-26831

ISOTENSOID STRUCTURES

- Filament wound pressure vessel isotensoid theory, considering composite material as macroscopically homogeneous anisotropic continuum
22 p3238 A72-42838

ISOTHERMAL FLOW

- Power law sealant effects on high aspect ratio viscoseal performance under laminar isothermal conditions
02 p0237 A72-12851
- Turbulent mixing of three plane isothermal jets with various velocity ratios, showing jet initial length shortening due to initial turbulence increase
23 p3279 A72-43657

ISOTHERMAL LAYERS

- Ta-Ra-B ternary alloy, investigating phase equilibria and isothermal cross sections with X ray analysis
03 p0374 A72-13739
- Loitsiankii parametric method application to universalize isothermal laminar boundary layer partial differential equations in Crocco variables
05 p0649 A72-16221
- Shape factors of heat conduction for fin arrangements with isothermal boundaries, using conformal mapping
09 p1412 A72-23688
- Sound waves radiative damping in isothermal atmosphere, discussing relaxation influence on model response to body force and chromosphere dissipation effect on oscillation
10 p1543 A72-24622

- Hydromagnetic stability of isothermal stratified plasma atmosphere uniform flow over conducting liquid along magnetic field, discussing dispersion relation for static configuration
11 p1695 A72-26115

- Three dimensional free convection boundary layer equations solution at two dimensional isothermal stagnation point with various Prandtl numbers
11 p1747 A72-26662

- Isothermal vertical plate turbulent thermal boundary layer during free convection, noting temperature pulsations dispersion
13 p2066 A72-29899

- Shear stresses distribution in isothermal incompressible turbulent boundary layer with positive pressure gradient by diffusers in open jet wind tunnel
17 p2544 A72-35931

- Surface reactions in similar boundary layers.
20 p2915 A72-40014
- Calculation of the radiation of two plane isothermal layers of carbon dioxide and/or water vapor
22 p3242 A72-41884

- Radiative transfer in a gray isothermal spherical layer.
24 p3461 A72-44805

ISOTHERMAL PROCESSES

- Isothermally contracting turbulent gas sphere for stellar formation from extension of Chandrasekhar work on Jeans criterion for static turbulent medium
01 p0129 A72-10799

- Low strength polymeric materials specimen geometry and lateral constraints effects on isothermal compressibility by compression tests
[SESA PAPER 1935] 02 p0248 A72-11518

- Isothermal uniaxial stress analysis of material consistent with linear law of heredity theory, determining viscoelastic relaxation function
02 p0290 A72-11621

- Isothermal analogy for thermal stress in cylindrical shells, presenting orthogonal coordinate boundary condition equations
[ASME PAPER 71-PVP-18] 02 p0294 A72-12471

- Thermodynamic and dissipative restrictions on isothermal stress relaxation functions in linear viscoelasticity
04 p0583 A72-14462

- Transformations of Ti alloy in isothermal conditions, observing hardening and loss of ductility
05 p0673 A72-16149

- Solar five minute oscillations in isothermal atmosphere by base pressure fluctuations
09 p1382 A72-22287

- Mo powder sintering kinetics and disperse mechanism in isothermal and nonisothermal conditions
11 p1643 A72-26836

- Statistical mechanics of one dimensional model for many body self gravitating system with canonical and microcanonical ensembles, noting isothermal solution of Vlasov equation
12 p1846 A72-27907

- Crystallization discontinuity and layer thickness in welded joints as function of overcooling and isotherm shape
13 p1963 A72-28922

- Hydrogen and hydrogen-helium isothermal radiative intensity at various temperatures, density ratios and path lengths, accounting for reabsorption due to overlapping lines
13 p2008 A72-30056

- U-Zr-Nb and U-Nb-Mo alloys gamma solid solution phase isothermal transformation kinetics at 500-600 C from dilatometric, microstructural and X ray analyses, noting decomposition
14 p2114 A72-30403

- Reflectivity-emissivity relationship for isothermal atmosphere with coherent scattering and continuous absorption, generalizing for noncoherent case with line opacity
14 p2131 A72-30890

- Radiation effect on isothermal discontinuity amplitude for stationary shock wave structure with heat transfer and dissipation
15 p2335 A72-32099

- Heteroplastic materials creep characteristics from constant strain rate isothermal traction tests, deriving deformation functions for material behavior beyond elastic range
16 p2412 A72-34120

- Some problems concerning microplastic deformation and isothermal transformation of Fe-Ni-C alloy. IV - Effect of transformation plasticity on microplastic deformation at 77 K
19 p2815 A72-37420

- Compressor exergetic efficiency calculation from gas exergy losses caused by pressure drop and cooling, noting relations to isothermal, adiabatic and polytropic efficiencies
19 p2746 A72-37668

- Influence of isothermic reaction levels on the diffusion growth of compounds with a binary equilibrium diagram
19 p2817 A72-37792

- Rotationally symmetric temperature distribution in region between two coaxial circular cones for isothermal and adiabatic conditions, solving heat conduction equation
20 p2983 A72-39329

- Radiation effects on isothermal discontinuity amplitude for stationary shock wave structure with heat transfer and dissipation
21 p3128 A72-40266

- Deformation-induced martensitic transformation in isothermal and athermal Fe-Ni-C alloys.
21 p3066 A72-40272

- Isothermal ionization of the lower ionosphere under the action of radio waves
23 p3283 A72-43362

- Molecular mechanical aspects of the isothermal rupture of elastomers.
23 p3305 A72-43507

- High temperature interaction between W and ZrC constructing isothermal structure
23 p3303 A72-44151

- Isothermal atmosphere inhomogeneities effects on electromagnetic cascade electrons integral energy spatial distribution
23 p3331 A72-44433

- Kinetic equations solution approximation for two species isothermal reactions in homogeneous turbulent mixing
24 p3392 A72-45059

ISOTHERMS

- Isothermal profiles for Nb-Zr-C and Nb-Ti-C alloys from microstructural and X ray analyses, noting Widmanstatten structure, and second phase formation
12 p1829 A72-27643

- Yttrium alloys isoperiodic lines, solidus isotherms, equal hardness lines and resistivity presented diagrammatically
15 p2289 A72-31185

- Aerodynamic structure analysis of steady flame of homogeneous gas mixtures, noting streamlines, isotherms, isobars and flame front curves
21 p3129 A72-40979

ISOTONICITY

- Force-velocity relations in cat papillary muscles isotonic relaxation, discussing effects of preloads and afterloads, temperature and stimulation frequency
09 p1265 A72-22864

ISOTOPE EFFECT

- Interstellar C12/C13 abundance ratio lower limit in direction of 20 Tau
02 p0280 A72-12192

- Single isotope He-Ne laser gyro comparison with multiisotope system, noting strong mode competition in ring laser
07 p1005 A72-19402

- Radiation damage in carbon doped silicon irradiated at low temperatures by 2 MeV electrons, noting isotope shifts
12 p1857 A72-28059

- Light polarization modes in gas ring laser with optically active isotopic cell, showing dependence on circular field coupling coefficient
13 p1968 A72-29512

- Isotopic composition of primary cosmic radiation - Conference, Lyngby, Denmark, March 1971
16 p2446 A72-33726

- Cosmic ray nuclei charge and isotope composition measurement, discussing data for Li, Be, B and 15-30Z nuclei
16 p2447 A72-33727

- Cosmic ray isotopic data extraction via geomagnetic field, discussing magnetic effects on particle flux and finite resolution limitations of counters
16 p2447 A72-33728

- Balloon flight observation of charge composition fine details and gross features of isotopic abundance in near relativistic cosmic rays
16 p2447 A72-33729

- HEAO experiment proposal for Be to Fe isotopic composition of galactic primary cosmic rays
16 p2447 A72-33733

- Isotopic effect in photodissociation processes of triplet excited molecules
19 p2838 A72-38779

- On the application of perturbation theory for the calculation of molecular constants due to small mass changes and on the determination of force constants from very heavy isotope substitution.
19 p2763 A72-38806

- Formation of hydrogen from amine oxidation and pyrolysis.
19 p2883 A72-38874

- The mechanisms of diffusion in metals and alloys.
20 p2962 A72-39999

- Isotope effect measurements application to determination of sodium diffusion mechanism and rate in sodium silicate glass
22 p3196 A72-42794

ISOTOPE SEPARATION

- Density and flux measurements by Langmuir probes in uranium plasma produced in single ended Q device, noting application to isotope separation
06 p0855 A72-17506

- Cosmic ray nuclei isotope identification with cryogenic magnet plus plastic scintillators to measure charge composition and rigidity
16 p2447 A72-33732

ISOTOPE SHIFT

U ISOTOPE EFFECT

ISOTOPES

- NT ALUMINUM ISOTOPES
NT ANTIMONY ISOTOPES
NT ARGON ISOTOPES
NT BARIUM ISOTOPES
NT BERYLLIUM ISOTOPES
NT BORON ISOTOPES
NT CALCIUM ISOTOPES
NT CARBON ISOTOPES
NT CESIUM VAPOR
NT DEUTERIUM
NT GALLIUM ISOTOPES
NT HELIUM ISOTOPES
NT HYDROGEN ISOTOPES
NT IODINE ISOTOPES
NT KRYPTON ISOTOPES
NT LEAD ISOTOPES
NT LITHIUM ISOTOPES
NT LUTETIUM
NT MAGNESIUM ISOTOPES
NT MANGANESE ISOTOPES
NT METALLIC HYDROGEN
NT NEON ISOTOPES
NT NITROGEN ISOTOPES
NT OXYGEN ISOTOPES
NT PLUTONIUM ISOTOPES
NT POTASSIUM ISOTOPES
NT RADIOACTIVE ISOTOPES
NT RADON ISOTOPES
NT RUBIDIUM ISOTOPES
NT SAMARIUM ISOTOPES
NT STANTONIUM ISOTOPES
NT SULFUR ISOTOPES

NT TELLURIUM
NT THORIUM ISOTOPES
NT TIN ISOTOPES
NT TITANIUM ISOTOPES
NT TRANSURANIUM ELEMENTS
NT TRITIUM
NT URANIUM ISOTOPES
NT XENON ISOTOPES

Nuclear astrophysics review, discussing chemical elements and isotopes abundance and cosmic nucleosynthesis

Trapped He, Ne and Ar isotopic variations presence in meteorites due to rare gas ions implantation by solar wind and flares

Neutron capture effects on Gd isotopic composition and irradiation histories of lunar rocks from Apollo sites, using mass spectroscopic measurements

Rare gases concentrations and isotope ratios in Haverø ureilite meteorite, including He, Ar, Ne, Kr and Xe

Inclusive isotope spectra of secondary nuclear produced by Bevatron heavy ion fragmentation in carbon and polyethylene targets, noting partial differential cross sections

Satellite-borne semiconductor particle detector telescope for C and Mn isotopes identification in heavy primary cosmic rays, considering scintillation counter and mass resolutions

Enstatite chondrite Abee isotopic ratios of Gd, Sm and Eu comparison with terrestrial samples

Isotopic abundance analysis of primary cosmic radiation with nuclear emulsion technique, discussing mass measurements in Be, C, O, Ne, Mg and Fe tracks

Interstellar cosmic ray electron component and isotopic composition relations from positron observations

Stratospheric balloons role in galactic cosmic radiation research with detection techniques for study of rate and heavy elements abundances and isotopic composition analysis

Isotopic compositions of rare gases in the carbonaceous chondrites Mokoia and Allende.

ISOTOPIC LABELING

Human left ventricular volume determined by peripheral venous scintillation angiocardigraph isotope method, comparing with X ray method

Myocardial blood flow measurement value in ischemic heart disease assessment, discussing Xenon 133 injection into coronary arteries

Xenon 133 method for coronary blood flow measurement during exercise, noting unsuitability for patients with coronary disease

Xenon 133 myocardial clearance method accuracy and reliability in determining high and low left coronary artery blood flow under different hemodynamic conditions

Myocardial blood flow measurement by Xe 133 clearance method after direct application of isotope into subendocardial and subepicardial layers of left ventricle

C 14 diffusion coefficients in W and W-Re alloys single crystals at 1500-1800 C, discussing tracer activation energy and frequency factor

Muscle blood flow relation to oxygen consumption from measurements during bicycle ergometer exercises, using Xe 133 clearance method

Autoradiographic study of stress intensity factor influence on hydrogen distribution at crack tips in Ti-Al-V alloy, using tritium doped salt water as corrosive medium

Isotopic labeled microspheres for cat uveal and retinal blood flow and oxygen consumption determination, studying increased intraocular pressure and carbon dioxide tension effects

Radiocardiography method for ventricular volume measurements, recording subclavian vein-injected radioisotope passage through cardiac cavities

Exchange diffusion process contribution to human red blood cell transmembrane cation movement from sodium tracer influx studies

Cell proliferation in lungs of mice exposed to elevated concentrations of oxygen.

The uptake, metabolism and release of C/14-laurine by rat retina in vitro.

Rat pulmonary lipid metabolism during feeding and fasting from studies of lung lecithin half life after C-14/1/palmitate and H-3/U/glucose injection

Needle type solid state detectors for in vivo measurement of tracer activity.

Some aspects of the use of small needle-shaped semiconductor detectors in the determination of regional distribution and transport of labelled compounds.

Coronary flow determination in experimental conditions with the use of radioactive xenon.

Regional lung function during early acclimatization to 3,100 m altitude.

New cancer therapy treatment techniques using space dosimetric concepts.

ISOTOPIC SPIN

Extension of the Curie principle and constitutive relations for fluids with antisymmetric stress.

ISOTROPIC MEDIA

Perturbed vibrational motion in isotropic elastic solid, using nonlinear Truesdell equations

Elastic incompressible isotropic transparent media, deriving photoelastic effect relationship to stress function

Hydroxyapatite isotropic and anisotropic elastic properties compared with experimentally observed anisotropic behavior of bone

Three dimensional problems in stability, elasticity and plasticity theory for isotropic, anisotropic and inhomogeneous bodies, noting applications to machine construction, civil engineering, geophysics, etc

Wave propagation in nonlocal isotropic elastic medium of ordinary kinematic structure with energy density as functional of displacement gradient field

Nonlinear boundary value problem of creep for isotropic bodies with random mechanical properties under random loads, calculating structural component reliability and service life

Nonlinear viscoelasticity theory, considering simplified stress-strain functional relationships with respect to time based on isotropy postulate

Frequency variations from uniformly moving source in homogeneous and inhomogeneous isotropic plasmas, calculating source-to-transmitted-wave group velocity ratio from Doppler curves slopes

Finite stretching of isotropic incompressible annular plate with inner edge rigid inclusion, noting edge zone thickness variation due to transverse normal strain

Static isotropic elastic body first and second boundary value problems solutions for inside and outside m dimensional sphere

Homogeneous isotropic elastic medium free vibration in unbounded space, obtaining relativistic relations in wave field from mathematical model

Electron temperature measurements in ionospheric isotropic nonequilibrium plasma by electrostatic probes and radar backscatter

Homogeneous isotropic thin elastic shells under forces along edge and with faces free of tractions, deriving refined interior equilibrium equations

Elasticity tensor formulas for wave propagation, vibration and stability of deformed isotropic solids

Polarization and stress tensor characteristics as function of interaction between mechanical, thermal and electromagnetic processes in elastic isotropic dielectrics

Infinite elastic isotropic multiply connected plate, determining stress-strain state by asymmetric stress tensors and moment stresses

Transversely isotropic plates with elastic circular insert, calculating stress concentration at holes under bending

Tangential stress pulse effects on transversally isotropic half space surface wave motion under torsion

Variable-modulus isotropic material finite elastic deformation, deriving two dimensional stress concentration by dual series expansion

Stress concentration at circular, elliptical, square, rectangular and triangular holes in isotropic plates stiffened by discontinuous elements under uniaxial tension

Stress-strain state of transverse isotropic plate with hole under bending and torsional moments

Stress channelling in transversely isotropic elastic composites, comparing classical theory with ideal fiber reinforced composite plane deformation theory

Current source generated electromagnetic and electroacoustic wave propagation through homogeneous, isotropic compressible electron-ion plasma, using two fluid continuum theory

Torsion of hollow beam consisting of two homogeneous isotropic rods with different elastic properties and simply connected cross sections, solving by conformal mapping

Stress-strain tensor component relations for isotropic elastic bodies with different tension and compression resistance

Fiber reinforced composites with transversely isotropic constituents, discussing various mathematical models for elastic constants calculation

Wave harmonics method application to problems of free oscillations in longitudinally regular screened waveguides partially filled with homogeneous isotropic media

Self focusing of electromagnetic waves in isotropic plasma, investigating nonlinear relaxation processes

Electromagnetic wave reflection from region with variable drift velocity and polarization of waves propagating in nonuniformly moving medium, applying to isotropic plasma

Linear two-temperature theory of thermoelasticity for investigating transient stresses arising from solid isotropic sphere aerodynamic heating [ASME PAPER 71-WA/APM-14]

Bimetallic rectangular plate with two interconnected layers of anisotropic and isotropic materials and large deflections in nonuniform pressure and temperature field

Tensor calculus theorem application to elastic isotropic materials finite deformation, considering acceleration waves propagation and moduli of elasticity

Refraction theory applied to isotropic absorbing media, noting spatial distribution of incoherent components according to polarization states

Scattering of arbitrarily impinging monochromatic electromagnetic waves by thin infinitely long isotropic, dielectric and metal rods of elliptic cross section

Equilibrium equations solution for displacements of inhomogeneous isotropic elastic media

Inverse periodic plane deformation of isotropic elastoplastic surface with infinite series of curvilinear holes

Two dimensional network class port behavior equivalence to three layer structures of linear passive isotropic materials based on depth and surface properties analysis

Radio wave beam trajectories in laminar isotropic plasma layer, using dynamic systems theory

Resonant frequency, phase velocities and dispersion curves for wave propagation in isotropic elastic cylinders

Large deformations of incompressible isotropic materials with parabolic stress-strain relations, deriving constitutive equation from strain energy function

Isotropic and anisotropic materials strength criteria and boundary surfaces in invariant stress tensor spaces

Thin walled elastic isotropic shallow shell with thermal boundary conditions, obtaining thermoelastic solution in series form

Thermal equilibrium fluctuations and Rayleigh light scattering in isotropic gyrotropic continuous medium with internal rotational degrees of freedom

- Stress-strain state of homogeneous isotropic medium bounded by noncanonical surfaces of revolution, using perturbation method
07 p1091 A72-19755
- Moving isotropic plasma half space effect on magnetic or electric line source radiation patterns
07 p1044 A72-20192
- Stressed state of isotropic nonlinear plate with doubly periodic system of curvilinear holes
07 p1094 A72-20208
- Stressed state approximate determination for isotropic slab with randomly positioned circular holes
07 p1094 A72-20210
- Stressed state of infinite isotropic plate weakened by curvilinear hole with elastic plug, using asymptotic integration method
07 p1094 A72-20212
- Stressed state of isotropic plate with curvilinear holes under tension, using computer techniques
07 p1094 A72-20215
- Three dimensional stressed state of isotropic plate with elliptical holes under tension, solving boundary value problems
07 p1095 A72-20216
- Long radio waves slant incidence on isotropic inhomogeneous ionospheric plasma
08 p1131 A72-20737
- Markov type isotropic random Gaussian field analysis in n -dimensional Euclidean space
08 p1198 A72-20999
- Laser holographic imagery of plane and three dimensional objects for supersonic field representation of standing wave in isotropic liquid
08 p1165 A72-21078
- Steady phase direction at time of electromagnetic wave transmission from one isotropic absorbing medium to another
08 p1132 A72-21221
- Local deviation limits of universe from homogeneous isotropic model, considering velocity field perturbations and galaxy counts
08 p1234 A72-21381
- Axisymmetric thermoelastic state of isotropic infinitely long circular cylinder with external annular cut, determining cut plane normal thermal stresses
08 p1245 A72-21668
- Plane stability of isotropic plate with straight line series of holes reinforced by complex elements or multicomponent rings, determining stress concentrations
08 p1246 A72-21710
- Thermoelasticity theory for transversely isotropic shells, obtaining variational formulation of noncoupled quasi-static problem
08 p1247 A72-21811
- Stress analysis of isotropic linearly elastic square plate of constant thickness loaded by concentrated forces at edges
09 p1399 A72-22698
- Variable rigidity circular isotropic plate vibration and bending, determining flexure surface and natural frequencies in terms of Fourier-Bessel series
09 p1399 A72-22699
- Bending theory of homogeneous isotropic micropolar cantilever beam loaded by moments at edges
09 p1399 A72-22700
- Crack propagation in two dimensional geometry with isotropic homogeneous and linearly elastic properties under in-plane tension loading
09 p1405 A72-22921
- Homogeneous isotropic elastic medium thermoelasticity equations based on variational principles noting definite integrals solutions by means of delayed potentials
09 p1406 A72-23070
- Linear theory of elasticity application to wave propagation in homogeneous isotropic material with deformable microstructure, presenting approximate solution method
09 p1353 A72-23552
- Stress distribution determination for long isotropic elastic cylinder with strip crack on diametral plane by complex variable technique and Fredholm equation solution
09 p1409 A72-23574
- Radial vibrations of isotropic homogeneous sphere and cylinder bonded to thin nonhomogeneous casting outside
10 p1557 A72-24406
- Dyadic Green functions for cylindrical circular or rectangular waveguides with moving isotropic homogeneous media
10 p1440 A72-25046
- Field and geodetic line equations for light rays in open and closed isotropic radiative universe model
10 p1549 A72-25059
- Radio wave beam trajectories in laminar isotropic plasma layer, using dynamic systems theory
11 p1591 A72-25335
- Direct numerical integration scheme for viscoelastoplastic response of isotropic axisymmetric shells under impulsive loads
[AIAA PAPER 72-400]
11 p1731 A72-25421
- Thermoelastic waves propagation in homogeneous isotropic medium under external generic forces and with distributed heat sources
11 p1734 A72-25676
- Finite element method for buckling coefficients of isotropic rectangular plate subject to linearly varying axial compression, using general linear geometric matrix
11 p1736 A72-25999
- Thermoelastic stresses in solid transparent isotropic homogeneous dielectric under self-focused laser beam
11 p1648 A72-26334
- Elasticity theory dynamic equations solutions concentrated near longitudinal or transverse wave beams propagating in inhomogeneous isotropic space
11 p1689 A72-26383
- Thermal stresses in homogeneous isotropic and composite curved beams for temperature distribution in polynomial form with coefficients representing functions of two remaining coordinates
11 p1737 A72-26665
- Axisymmetric stress field in infinite homogeneous isotropic elastic solid with crack surrounding cylindrical cavity, solving elastic equilibrium equations
11 p1738 A72-26720
- Shallow isotropic and orthotropic shells vibration, investigating dynamic rigidity for concentrated mass
12 p1878 A72-27079
- Stress-strain state and temperature distribution in transversely isotropic layer under mixed heat transfer conditions
12 p1878 A72-27085
- Variable shear modulus circular isotropic plate torsion by rigid circular stamp, obtaining stresses and displacements by Fourier analysis
12 p1881 A72-27319
- Ultimate safe load estimates for stability of isotropic elastic materials
12 p1883 A72-27563
- Elastic fields of dislocation loop in two phase material consisting of isotropic elastic half spaces
12 p1884 A72-27567
- Relations between normal mode radio propagation parameters and properties of earth-lower ionosphere isotropic waveguide, allowing for geomagnetic field
13 p1945 A72-28583
- Thermal stress distribution determination in isotropic plate with rigid circular insert, using small parameter technique
13 p2056 A72-28913
- Axisymmetric geometry and load finite element structural analysis of isotropic elastic materials for parametric and optimization studies
13 p2062 A72-29875
- Kinetic model for electromagnetic field fluctuations in bounded isotropic plasma half space with specular reflection of electrons at boundary
14 p2135 A72-30170
- Harmonic waves propagation in infinite transversely isotropic cylinder with elliptic cross section, obtaining solution in terms of Mathieu functions
14 p2163 A72-30190
- Refraction theory applied to isotropic absorbing media, noting spatial distribution of incoherent components according to polarization states
14 p2130 A72-30242
- Constitutive equations for incremental stress-strain relations in elastoplastic media, noting plane stress and strain in isotropic materials
14 p2131 A72-30715
- Noncoherent isotropic scattering in plane parallel finite layer, considering Doppler line broadening
15 p2273 A72-31331
- Stress analysis of boron fiber-reinforced and isotropic Al panels under identical loading conditions
15 p2323 A72-31479
- Exact nonlinear equation derived approximation for second order effects in thermoelasticity theory for isotropic and transversely isotropic heat conducting elastic materials
15 p2329 A72-32282
- Nonlinear elastic material approximation by piecewise linear material with linear boundary value problems, discussing isotropic case based on singular surfaces theory
15 p2330 A72-32295
- Antiplane shear wave diffraction by two coplanar Griffith cracks in infinite isotropic homogeneous elastic medium
16 p2464 A72-32919
- Static boundary value problem of axisymmetric elasticity for elastic isotropic media with small energy contribution to potential due to moment effects
16 p2464 A72-32934
- Optical measurement for simultaneous determination of transparent isotropic medium thermal diffusivity and conductivity
16 p2389 A72-32947
- Singular integral representations of displacement and rotation vectors for homogeneous isotropic centrosymmetric body, using Nowacki couple stress theory of thermoelasticity
16 p2465 A72-32984
- Strain energy method for finite deformation of solid and tubular cylinders of incompressible isotropic elastic material, noting torsional and tensile tests on natural rubber
16 p2468 A72-33198
- Upper and lower bounds for complex elastic moduli of composite materials with isotropic linear viscoelastic phases behaving as homogeneous isotropic materials
16 p2468 A72-33199
- Energetic boundedness conditions for internal work of deformation in elastic isotropic body
16 p2470 A72-33527
- Growth of an acceleration wave in an elastoplastic isotropic medium undergoing finite deformation
17 p2580 A72-34277
- Geometric instabilities in isotropic plastic solids under increasing uniaxial compression.
[ASME PAPER 72-APM-28]
17 p2624 A72-34310
- A first initial boundary value problem for a semilinear heat equation.
17 p2573 A72-34339
- Strain history effect on isotropic and anisotropic plastic behavior.
[SESA PAPER 1940]
17 p2631 A72-34820
- Free vibrations of a spherically isotropic hollow sphere.
18 p2736 A72-37004
- Electromagnetic and space charge disturbance transmission and reflection at plasma boundary and oblique incidence, discussing isotropic Vlasov plasma.
19 p2839 A72-37336
- Wave propagation in generalized thermoelasticity.
19 p2870 A72-37412
- A note on the low frequency diffraction of elastic waves by a Griffith crack.
19 p2870 A72-37414
- The thermal conductivity of a statistically isotropic heterogeneous medium.
19 p2880 A72-37462
- Equilibrium equations solution for displacements of inhomogeneous isotropic elastic media
19 p2872 A72-37560
- Shells of revolution free of bending under uniform axial loading.
19 p2876 A72-37886
- Long radio waves oblique incidence on isotropic inhomogeneous ionospheric plasma
19 p2766 A72-38365
- Forced motion of isotropic and transversely isotropic viscoelastic Timoshenko beams using measured material.
21 p3116 A72-40331
- Time dependent deformation of isotropic viscoelastic materials, discussing rectilinear shear, circular cylinder torsion, spiral shear of layer and conical layer torsion
21 p3119 A72-41075
- A hyperboloidal notch in a transversely isotropic material under pure shear.
21 p3119 A72-41105
- Elastic isotropic material mechanical and thermal constitutive equations restrictions investigation to ensure local stability under perturbations of deformation gradient and temperature field
21 p3120 A72-41203
- Optimal compression of constant-thickness media in a plane stress state
21 p3123 A72-41391
- Radiation of an oscillator moving parallel with the interface of two media
21 p3036 A72-41843
- Structural stability of anisotropic plates and structures, developing method based on data for corresponding isotropic problem
22 p3239 A72-42847
- The method of Muskhelishvili applied to coupled isotropic elastic plates
22 p3242 A72-43202
- Strictional nonlinearity effect on uniform non-relativistic monoenergetic beam interaction with isotropic bounded plasma, investigating plasma oscillations and stability
23 p3320 A72-43576
- Edge and screw dislocations induced stress fields in isotropic medium, using Kauderer nonlinear elasticity theory
23 p3345 A72-43622
- Isotropic materials nonlinear rheonomic behavior at small strains, deriving model structure deformation laws
23 p3345 A72-43623
- Parabolic approximation of spatially bounded square and Lorentz two dimensional light pulse propagation in homogeneous isotropic linear medium without dispersion
23 p3313 A72-43682
- A note on the twisting deformation of a non-homogeneous shaft containing a circular crack.
23 p3346 A72-43708
- Acceleration waves in orthotropic elastic materials.
23 p3354 A72-44342
- Electromagnetic-wave propagation in a random nonlinear dispersive medium.
24 p3379 A72-44784

- Pure antiplane stress and equilibrium of isotropic elastic beams, considering suspended cylinders 24 p3459 A72-44989
- Relations between normal mode radio propagation parameters and properties of earth-lower ionosphere isotropic waveguides, taking into account geomagnetic field 24 p3397 A72-45083
- Thermoelastic waves propagation in homogeneous isotropic medium, considering potential functions 24 p3460 A72-45598
- Reflection and transmission of electromagnetic waves by a moving inhomogeneous medium. 24 p3381 A72-45644

ISOTROPIC TURBULENCE

- Isotropic incompressible turbulence numerical simulation, presenting algorithm for convolution sums calculation 02 p0205 A72-12367
- Isotropic turbulence energy transport approximation by local differential equation analogous to Fokker-Planck equation, noting Kolmogoroff distribution for infinite Reynolds number 02 p0205 A72-12449
- Closure problem in statistical theory of isotropic turbulent velocity field 03 p0342 A72-13900
- Ray statistics of electromagnetic wave scattering in homogeneous isotropic turbulent medium with ellipsoidal inhomogeneities of refractive index, using Fokker-Planck equation 05 p0626 A72-16243
- German book on turbulent flow theory and applications covering isotropic and homogeneous nonisotropic fields, shear flows, pipe flows, free turbulence, boundary layers, etc 05 p0649 A72-16286
- Numerical simulations of three dimensional homogeneous isotropic turbulence at wind tunnel Reynolds numbers, solving Navier-Stokes equations for incompressible flow 05 p0649 A72-16685
- Closure approximation for energy transfer mechanism of stationary locally isotropic turbulence in inertial and dissipation ranges 06 p0802 A72-18545
- Selective summation techniques for coherent Green function in random isotropic turbulent media, comparing Dyson, Keller and renormalization methods 06 p0777 A72-18735
- Isotropic turbulence spectrum based on Heisenberg theory of viscosity limiting effect on fluid motion degrees of freedom, taking into account nonlinear inertial transfer term 07 p0968 A72-19671
- Atmospheric isotropic turbulence kinetic energy dissipation and wind spectra estimation from Doppler spectra of precipitation particle velocities 10 p1507 A72-25001
- Transverse particle diffusion across external homogeneous magnetic field under random isotropic large scale hydromagnetic turbulence 14 p2102 A72-30650
- The Reynolds tensor in a homogeneous turbulence associated with a pure deformation 17 p2539 A72-34909
- Numerical simulations of three dimensional isotropic turbulence in incompressible fluid at low wind tunnel Reynolds numbers 18 p2677 A72-36007
- Approximations yielding closed equations for isotropic turbulence compared to laboratory and computer experiments, emphasizing Langevin type model equation for velocity 18 p2677 A72-36008
- Computer aided study of nondiffusive plane convection mixing of scalar field by isotropic turbulence of single velocity modes 18 p2678 A72-36017
- Decay of isotropic turbulence generated by a mechanically agitated grid. 19 p2787 A72-38426
- Statistical continuous random process theory of homogeneous and isotropic turbulence in terms of energy transfer in wave number space based on Kolmogoroff hypothesis 21 p3045 A72-41025
- On a resolution of the equations governing the second order correlation functions for an isotropic hydromagnetic turbulence. 22 p3212 A72-43100
- Drag spectra of simple structures in turbulence. 23 p3281 A72-44102
- Experimental determination of the turbulent exchange coefficient in the case of homogeneous isotropic turbulence 23 p3282 A72-44489
- A theory of homogeneous, isotropic turbulence of incompressible fluids. 24 p3392 A72-45245

ISOTROPISM

- Einstein equations reduction to friction systems in homogeneous cosmological models, investigating Bianchi models isotropization and statistical analysis 23 p3335 A72-43301

ISOTROPY

- NT ISOTROPIC MEDIA
- Roller metals and alloys with various lattice types and packing defect energies, showing elastic properties isotropy and Young modulus anisotropy 03 p0371 A72-13188
- Isotropy postulate corollary verification for strain vectors measurement of annealed steel tubular specimens under combined tension and internal pressure 12 p1887 A72-28232
- Anisotropic and isotropic descriptions of physical process speeds in special relativity theory space-time metric 15 p2279 A72-32768
- Linearly elastic, transversely isotropic multilayer system, presenting stress and stability problem for two dimensional strain states 16 p2466 A72-33022
- Exponential representation of isotropy groups of simple solids, noting conditions for conjugation of unimodular to orthogonal group subgroups 16 p2423 A72-33111
- Transverse isotropy effects on beams static behavior, considering Green functions, deflection under distributed loads and beam-column deflection 20 p2980 A72-39613

ITERATION

- NT ITERATIVE SOLUTION
- Simultaneous iteration for eigenvalue problem numerical solution by mutually orthogonal trial vectors close to required eigenvectors, applying to flutter analysis and Markov chains 11 p1679 A72-26959
- Computation method for rotating and nonrotating viscous flows boundary vorticity iteration parameters for use with time centered or alternating direction implicit time differencing approximation 14 p2093 A72-30228

ITERATIVE NETWORKS

- An iterative array which can represent the rotation and translation of objects. 20 p2905 A72-39422
- A variation-iteration technique for the design of wall-impedance waveguides. 20 p2903 A72-39429

ITERATIVE SOLUTION

- Network synthesis of cascaded threshold logic elements to separate binary patterns into two classes by iterative computation of parameters 01 p0034 A72-10474
- Reachable sets calculation for linear dynamical system control, suggesting iterative procedures for numerical approximations 01 p0034 A72-11124
- Flutter equation approximate true damping or rate-of-decay solution by determinant iteration 01 p0142 A72-11133
- Iterative solutions for three dimensional turbulent boundary layers on rotating nose-body, using streamwise and cross flow momentum equations 01 p0002 A72-11397
- Iterative truncation error estimates in solution for plane wave diffraction by grating 02 p0171 A72-11738
- Network sensitivity analysis emphasizing first, higher and mixed higher derivatives computation and iterative synthesis techniques 02 p0197 A72-12114
- Axisymmetric circular membranes large deflections, solving nonlinear partial differential equations by iterative method in conjunction with finite difference approximations 02 p0296 A72-12526
- Elasticity theory Lamé difference equations system solved by two-step iteration procedure based on Samarskii regularization 03 p0447 A72-13727
- Nonlinear programming iteration scheme for fuel-time optimization of satellite orbital rendezvous terminal phase 03 p0437 A72-13838
- Biharmonic problem of displacements in plane theory of elasticity, analyzing stress-strain state by iterative solution in series form 03 p0454 A72-14312
- Hsu-Howe iterative hybrid method for partial differential equations solution by time sharing analog components, using dynamic scaling and incremental formulations for reduced sensitivity 04 p0495 A72-14418
- Natural vibration frequencies calculation of straight bars with stepwise variable cross sections by iterative technique based on method of three unknowns 04 p0584 A72-14522
- Freezing of hot fluid flowing onto flat cold wall, solving nonlinear integrodifferential equation for temperature distribution by iteration method 04 p0595 A72-14650
- Iterative procedure for computing optimal controls in distributed parameter systems described by linear parabolic differential equations, applying to metal slab temperature profile problem 04 p0504 A72-14664

Optical angle of refraction through earth mean atmosphere determination by three models of refractivity and iterative methods 04 p0515 A72-14884

Extended iterative weighted least squares estimation of coefficients for linearly independent component signals in linear model 04 p0539 A72-14913

Convergence of iterative schemes for calculating stress state of thin shells with allowance for nonlinear terms in differential equilibrium equations 04 p0587 A72-15048

Iterative synthesis of dipole antenna array for maximum directivity radiation pattern, considering amplitude-phase distributions 04 p0499 A72-15142

Matrix representation of nonlinear equation iterations based on polynomial methods, considering convergence and application to parallel computation 04 p0540 A72-15373

Diffraction anomaly from infinitely extended strip grating solution by successive approximation technique combination with singular integral equation 04 p0491 A72-15418

Iterative method to solve planetary boundary layer differential equations, overcoming difficulties of previous approaches 04 p0519 A72-15460

Minimal-time control of linear systems with energy constraints on input components, obtaining functional analysis solution by iterative method for nonlinear problem 05 p0639 A72-15802

Flow separation of turbulent boundary layer ahead of inward-projecting normal step predicted by rotational flow analysis via iterative solution [ASME PAPER 71-WA/FE-32] 05 p0599 A72-15924

Computational algorithm for optimal control problem with variable terminal point constrained on state space surface, using iteration technique for satisfying transversality condition [ASME PAPER 71-WA/AUT-6] 05 p0640 A72-15957

Nonlinear transient coupled thermoviscoelasticity problems solution by finite element method and iterative solution for integrodifferential equation 05 p0736 A72-16085

Laplace equation under Robin boundary conditions over unit square, discussing numerical solution by difference approximation and iterative procedure 05 p0682 A72-16100

Iterative method for approximate determination of local minima in fuel optimal finite thrust orbit transfer 05 p0719 A72-16541

Bayes theorem based iterative method for image restoration by treating degraded images as probability-frequency functions, noting adaptability to computer processing 05 p0690 A72-16671

Iterative process convergence in least squares and maximum likelihood methods of processing measurements in spacecraft trajectory control, space navigation and geodesy systems 05 p0633 A72-16761

Transient compressible heat and mass transfer in porous media, solving coupled nonlinear partial differential equations in finite difference form by iterative technique [AIAA PAPER 72-23] 05 p0749 A72-16914

Second variational algorithm for iterative solution of unconstrained optimal control problems, examining linearized feedback control 06 p0839 A72-17592

Triangular points linear stability in elliptic restricted three body problem, determining exponents by convergent iteration method 06 p0878 A72-17664

Conjugate gradient iterative method for optimal control problems with state variable constraint, noting optimal trajectory cases 06 p0793 A72-17953

Iterative solution for non-Levy rectangular plates with corner supports, assuming small deflection theory 06 p0896 A72-17966

Rotational flow computation, using iteration methods for irrotational and solenoidal vector field components 07 p0966 A72-18811

Tangent methods for nonlinear equations iterative solution using alternate tangent and derivative values 07 p1026 A72-19039

Dynamic programming for optimal stochastic control problem with Gaussian shot noise involving parabolic or elliptic differential equation in unbounded domain, discussing iterative solution and quasi-linearization 07 p1027 A72-19292

Iterative and direct modification procedures for structural analysis matrix displacement method, discussing computer program implementation 07 p1089 A72-19329

Algorithm for iterative computation of time and fuel optimal control functions for linear systems, presenting flow chart 07 p0962 A72-19714

Iterative solution of differential equations for steady plane flow with heat and mass transfer at high Reynolds numbers

07 p0971 A72-20098

Iteration procedure for approximate integration of nonlinear system of partial differential equations with time lag, presenting upper and lower estimates

07 p1028 A72-20209

Iterative solution of Cauchy problem of partial differential equations nonlinear system with time lag, formulating uniqueness theorem

08 p1198 A72-20904

Iterative solution to gas dynamics equations for hypersonic flow past slender three dimensional body, applying to Cauchy problem

08 p1107 A72-20971

Conjugate gradient method for computerized antenna radiation pattern synthesis using error functional minimization and iterative procedure

08 p1143 A72-21988

Gradient iterative techniques application to finite element vibration and stability analysis of skew plates

10 p1558 A72-24878

Partial orderings applications to convergence of iterative methods for solution of linear equation systems involving positive definiteness or monotonicity

11 p1677 A72-25862

Iterative formula for constructing Liapunov functions in convergent series form

12 p1836 A72-27073

Iterative solution for linear and nonlinear dc networks with independent voltage sources, noting convergence conditions

12 p1794 A72-27398

Iterative solution existence for elastic equilibrium problem of thin plates and shells near boundary layer

12 p1886 A72-27997

Laplace equation iterative solution for boundary value problems in structural hardening and heat resistance formulation, noting convergence

12 p1887 A72-28226

Iterative method for synthesis of reflector antenna array of dipole elements to provide given radiation pattern, obtaining impedance matching values

13 p1926 A72-28372

Predictor-corrector multiple iteration technique for three dimensional viscous flow problems applied to hypersonic leading edges and Burger equation [PIBAL-72-19]

13 p1893 A72-28422

Iterative solution of coupled nonlinear differential equations under boundary conditions for flow and heat transfer of Rivlin-Ericksen fluid between rotating parallel disks

13 p1986 A72-28881

Computer algorithm to calculate surfaces formed by equidistant conic sections, using successive approximation method

13 p1966 A72-29461

Iterative-zonal method for radiative heat transfer calculations with capability to numerically determine radiation characteristics of optically and energetically homogeneous zones

13 p2065 A72-29643

Iterative method for continuous one dimensional linear systems with space-time invariant properties, applying to dynamic mixed problem of linear viscoelasticity

13 p2006 A72-29783

Sandwich beams structural optimization for given deflection by iterative finite element procedure

14 p2168 A72-30927

German monograph on superconductors transition temperature calculation by iteration method using phonon spectrum approximation

14 p2143 A72-30947

Iterative numerical solution of linear differential equations system for wind vertical velocity and local pressure variation along vertical line

15 p2265 A72-31344

Elastic plates and shallow shells in finite deflection, obtaining iterative solution with good convergence for thermal stresses

15 p2324 A72-31488

Iteration methods to compute inverse for nonsingular linear operator on Banach space

15 p2261 A72-31495

Baird Method extension with restored convergence for multiple quadratic factors using interval arithmetic

15 p2262 A72-31631

Iterative solution of boundary value problem in multiple burn rocket trajectory optimization

15 p2308 A72-31820

Gravity anomalies interpretation by iterative data processing, discussing convergence improvement

15 p2231 A72-32347

Nonlinear equations systems iterative solution methods convergence, generalizing Varga matrix splitting technique to nonlinear mappings in Banach space

15 p2264 A72-32465

Structural design optimization procedure based on sequence of linearizations with iterative convergence

through series of least critical intermediate solutions in hyperspace

15 p2331 A72-32551

Iterative computational procedure for system parameter identification and optimization, using multilevel technique

16 p2371 A72-33192

Joint maximum likelihood estimation of three parameters of Weibull distribution, obtaining modified quasi-linearization algorithm for nonlinear equations iterative solution

16 p2416 A72-33348

Iterative procedure for Maxwell equations exact solution for anisotropic birefringent medium, applying result to limiting polarization problem

16 p2425 A72-33490

Nonlinear generalizations of matrix diagonal dominance with application to Gauss-Seidel iterations.

17 p2573 A72-34220

Chebyshev acceleration application to Jacobi, Gauss-Seidel and related iterative methods for solution of coupled harmonic equations, comparing to block SOR method

17 p2574 A72-34447

Norms of the successive overrelaxation method.

17 p2574 A72-34448

Study of circular arc airfoils with asymptotic critical Mach number. II

17 p2484 A72-34745

Iterative method for the calculation of two-impulse spacecraft rendezvous maneuvers

17 p2622 A72-35216

Minimum norm and gradient projection constrained optimization techniques for iterative solution of trajectory optimization problems, presenting mathematical relations to prove equivalence

17 p2576 A72-35232

Iterative process convergence in least squares and maximum likelihood methods of processing measurements in spacecraft trajectory control, space navigation and geodesy systems

17 p2523 A72-35264

Iterative calculation of a three-dimensional boundary layer and comparison with experiment

17 p2543 A72-35748

A rapidly convergent iterative method for the solution of the generalised nonlinear least squares problem.

17 p2577 A72-35849

Higher vibration modes by matrix iteration.

18 p2736 A72-36772

Note on the 'alpha'-constant stiffness method for the analysis of non-linear problems.

18 p2739 A72-37172

Some properties of iterative square-rooting methods using high-speed multiplication.

19 p2769 A72-37577

Strong convergence in the whole of an iteration process for ordinary differential equations

19 p2825 A72-37733

Convergence of a simple iteration scheme in equilibrium problems of flexible plates

19 p2877 A72-38201

Convergence of a multipoint iteration method for solving nonlinear equations

19 p2826 A72-38215

Existence of a unique solution for a class of nonlinear systems of equations and its calculation by iterative methods

19 p2827 A72-38546

Some results of a numerical experiment in the reconstruction of a temperature profile by a 'regularized' iteration method

19 p2829 A72-38769

Compressible boundary-layer equations solved by the method of parametric differentiation.

20 p2914 A72-39614

Iterative solution of nonlinear structural problems, using convergence criteria based on displacement quantities

20 p2946 A72-39625

Solution of the equations of consumption in gasdynamic problems

20 p2914 A72-39927

Gravitational field of arbitrarily thick steadily rotating shell in general relativity, using successive approximation method

20 p2955 A72-40010

Numerical solution of quasi-conservative hyperbolic systems - The cylindrical shock problem.

21 p3043 A72-40101

Modified Hestenes method of Lagrange multipliers for numerical iterative solution of mathematical programming problems in function minimizing noting improved convergence

21 p3074 A72-40226

Perturbation theory for field moments in inhomogeneous media

21 p3016 A72-40780

An iterative procedure to obtain exact buckling criteria for columns under combined action of variable continuous load and concentrated forces.

21 p3118 A72-40927

Iterative solution to aerodynamic design of axial flow compressors used in turbojet engines, calculating meridional velocity distribution

21 p3099 A72-40930

Computer simulation of retargeting procedure with closed form iterative solution and parameter optimization for nonlinear low thrust spacecraft guidance scheme

[AIAA PAPER 72-916] 21 p3082 A72-41561

Polak-Ribiere conjugate gradient algorithm modifications to eliminate minimization at each iteration for efficient implementation with convergence

22 p3198 A72-41931

On the solution of non-linear simultaneous equations with particular reference to fluid-dynamics.

22 p3199 A72-42325

Iteration process convergence improvement based on stiffness change expression as linear combination of two matrices in structural reanalysis

22 p3235 A72-42602

Eigenvalue spectrum translation and frequency shifting by inertia and stiffness matrix modifications in iteration techniques

22 p3207 A72-42850

Iterative method for calculating the deformations of an induced flow

22 p3136 A72-42919

German monograph - Iterative algorithms for ordinary differential equations and their suitability for parallel processing by means of symbol manipulation.

22 p3200 A72-43063

Extension of the range of convergence of precise iterative methods

22 p3200 A72-43133

An iterative technique for determining the minimal number of variables for a totally symmetric function with repeated variables.

23 p3308 A72-43421

Iterative method of computing the limiting solution of the matrix Riccati differential equation.

23 p3275 A72-43610

Calculation of transport coefficients of a non-Lorentzian plasma

23 p3321 A72-43821

Optimal design of a class of nonlinear networks.

23 p3276 A72-43865

The elastic analysis of the part-circular surface flow problem by the alternating method.

23 p3353 A72-44232

Iterative solution for adiabatic radial pulsation in massive main sequence star, noting transition to non-linearity via Eddington stability integral extension

24 p3438 A72-44833

Iterative methods for the aerodynamic calculation of thin wings in a subsonic flow

24 p3363 A72-45378

Satellite orbital motion numerical integration method, using Picard iteration relative to reference orbit to calculate short-term anomalous period intervals [AIAA PAPER 72-909]

24 p3443 A72-45428

ITOS 1

Direct readout ground system /DRGS/ for receiving, recording and displaying visible and IR imagery collected by Itos and synchronous meteorological satellite radiometers

01 p0047 A72-10452

ITOS-1 /Tiroso M/ satellite design, describing structure, thermal and attitude control, primary and secondary sensor subsystems, power supply and operational goals

09 p1396 A72-23373

Global sea surface temperature distribution determination with ITOS 1 radiation measurements and composite histogram, discussing RMS errors

11 p1620 A72-25763

IZSAK ELLIPSOID

U ELLIPSOIDS

U GEODESY

J

J-52 ENGINE

Sound pressure levels and acoustic fatigue tests for 11,200 and 9,300 pound thrust J-52 engines comparison in A-6A aircraft

07 p0910 A72-18757

JACKS [ELECTRICAL]

U ELECTRIC CONNECTORS

JACOBI INTEGRAL

Zero relative velocity surfaces in bounded circular three body problem in presence of magnetic dipole, deriving Jacobi integral

01 p0127 A72-10358

Mass changes in restricted quasi-circular variable mass three body problem with particle equations of motion having Jacobi integral

03 p0436 A72-13828

Jacobi integrals in restricted three body problem of small bodies with massive sun and Jupiter in solar system

09 p1389 A72-23394

JACOBI MATRIX METHOD

Jacobian matrix partial derivatives for orbital motion representation by time step power series
06 p0877 A72-17651
Quasi-classical mechanical approximation in molecular scattering, using Monte Carlo methods for Jacobian determinant evaluation
14 p2134 A72-30836

Chebyshev acceleration application to Jacobi, Gauss-Seidel and related iterative methods for solution of coupled harmonic equations, comparing to block SOR method
17 p2574 A72-34447

JACOBI POLYNOMIALS

U HYPERGEOMETRIC FUNCTIONS

JAGUAR AIRCRAFT

Jaguar powered flight controls, discussing wing spoilers, slab tailplane, rudder, autostabilization system and integrated packaging of actuators
16 p2353 A72-34144

JAMMING

Radar measurement accuracy in log-normal clutter of fluctuating targets in random noise or intentional interference
02 p0178 A72-12401

JAPAN

Japanese lava geochemical analysis, determining K, Rb, Sr, Ba and rare earth concentrations with mass spectrometric stable isotope dilution
01 p0051 A72-10059

JARRING

U MECHANICAL SHOCK

JEANS THEORY

Jeans escape rate prediction validity for hydrogen atoms in upper atmosphere and error sources in physical models
08 p1159 A72-21401

Orbital elements evolution for two body problem with decreasing mass according to Jeans model
08 p1236 A72-21638

Numerical experimentation in collisionless systems for Jeans instability, static self consistent models and spiral patterns
12 p1874 A72-27908

Gas density as function of galactic radius according to Jeans unstable criterion for star formation from known galaxy rotation curve and gas sound speed
20 p2966 A72-38917

JEEPS

U AUTOMOBILES

JET AIRCRAFT

NT BUCCANEER AIRCRAFT
NT CONCORDE AIRCRAFT
NT ELECTRA AIRCRAFT
NT TURBOFAN AIRCRAFT
NT TURBOPROP AIRCRAFT

Augmentor wing jet STOL research aircraft development progress report covering design, engine tests, performance prediction, control simulation and stability augmentation
[SAE PAPER 710757] 01 p0003 A72-10254
Handling qualities simulation program for augmentor wing jet STOL research aircraft considering control devices design
02 p0154 A72-11654

Carrier system for controlled approach of Naval aircraft to provide pilot window to deck for tactical jet guidance for poor visibility landing
02 p0256 A72-12323

Externally blown flaps for STOL characteristics in medium and heavy jet transport aircraft, demonstrating aerodynamic and flight mechanical feasibility
02 p0155 A72-12502

Jet aircraft brake parachute loads under engine wake, evaluating velocity and drag coefficient influences
02 p0155 A72-12504

U.S.S.R. high-subsonic freight transport jet aircraft II-76 for arctic areas, Siberia and Far East, noting independence of large airports availability
03 p0310 A72-13471

Trainer-combat turbojet or turbofan aircraft characteristics, comparing flight, weight, size, maintenance and development costs
05 p0611 A72-16178

Dynamic stability, control and structural response of transonic jet transport to atmospheric turbulence
05 p0611 A72-16348

Prolonged jet flight effect on passenger interstitial and intracellular fluid volumes from plasma, extracellular and total body water measurements, noting dehydration and foot swelling
06 p0767 A72-17866

Cockpit instrumentation for jet transport aircraft flight path management, emphasizing dependability, safety and economy
08 p1168 A72-21524

Physiological evaluation of modified jet transport passenger oxygen mask from altitude chamber experiments
08 p1126 A72-21571

Jet-STOL augmentor wing consisting of moderately thick airfoil with full span leading edge slat and double surface trailing edge flap
08 p1110 A72-21899

Mystere business jet aircraft flight instruments, acceleration, control and stall characteristics
08 p1110 A72-21900

Corrosion resistant fabrication methods in jumbo jetliners components to reduce maintenance and repair downtime, discussing clad wing and fuselage skins
10 p1487 A72-24025

Combat jet helicopter maneuverability, considering aircraft flying characteristics, pilot capability, flight configuration, altitude and load factor
10 p1421 A72-24923

Mitsubishi XT-2 jet trainer aircraft, presenting design, structural and performance data
10 p1421 A72-25107

NASA aerodynamic technology program, emphasizing airframe and engine development for next generation subsonic CTOL jet transport requirements
[SAE PAPER 720319] 11 p1575 A72-25582

Factor analysis of grades for successful performance skill identification during undergraduate and graduate jet pilot training
12 p1769 A72-27472

Pilots seating active and passive isolation from LF vibrations in helicopters and jet aircrafts, discussing human factors and dynamic environment
13 p1910 A72-29558

VFW 614 twin jet transport aircraft flight test program, detailing general task plan, test equipment installations and test schedule
14 p2072 A72-30679

Dynamic input to cargo in turbojet aircraft studied during C141 and C5A flights, discussing instrumentation, test procedures, data reduction processes and results
15 p2181 A72-32625

Jet aircraft gas turbine engine technology impact on safety, reliability, airline profitability and international trade
16 p2443 A72-33315

Statistical correlation techniques applied to jet aircraft autoland system dynamic ground tests with simulated engine and aerodynamic characteristics
16 p2420 A72-33641

Numerical study of the characteristic magnitudes of turbulence on the far sound field radiated by a subsonic jet
[ONERA, TP NO. 1058] 19 p2786 A72-37761

Flyover noise testing of commercial jet airplanes.
[AIAA PAPER 72-786] 19 p2749 A72-38103

High performance jet aircraft variable feel flight control systems for simulation of aerodynamic reaction forces proportional to dynamic pressure
21 p3039 A72-41069

Description and use of a method for characterizing noise sources in jets
[ICAS PAPER 72-35] 21 p3046 A72-41160

Empty weight and cruise performance of very large subsonic jet transports.
[SAE PAPER 7191] 23 p3251 A72-43466

JET AIRCRAFT NOISE

Liquid-base foam sound absorbing properties for jet aircraft noise reduction
01 p0115 A72-10160

Acoustic power radiated by jet aircraft fuselage structure exposed to turbulent boundary layer pressure field, evaluating noise reduction treatments
01 p0002 A72-10216

Jet aircraft turbofan engine fan compressor noise reduction by acoustic linings, giving R and D results
[BAS PAPER 71 SA6] 01 p0115 A72-10223

Jet noise reduction technology, hardware and tests for NASA Quiet Engine Program to develop low noise subsonic civil transport aircraft propulsion system
[SAE PAPER 710774] 01 p0116 A72-10266

High speed jet noise source physical properties interpretation by theory and scale-model experiments for supersonic transport aircraft noise suppression problem
02 p0154 A72-11973

Q/STOL jet aircraft engines design for low noise levels, describing takeoff thrust, bypass ratio and turbine stages
02 p0271 A72-12501

Aladin 2 noiseless STOL jet aircraft project, describing exhaust nozzle configuration, design and economics
02 p0155 A72-12503

Jet noise suppression near airports, discussing noise physical description, source relation to engine technology and ICAO certification standards
03 p3039 A72-13097

Air breathing propulsion systems for reducing engine noise level, discussing stoichiometric gas turbine engines, V/STOL, propfans and variable-geometry supersonic inlet and exhaust nozzles
03 p0406 A72-13486

NASA Quiet Engine experimental program for jet aircraft noise reduction, discussing aerodynamic and acoustic evaluation and tests of three fans
03 p0406 A72-13679

French jet aircraft noise reduction research facilities, discussing in-flight and overfly noise measure-

ments, various silencer configurations and Concorde engine tests
03 p0406 A72-13680

Turbojet engine noise causes and reduction techniques, noting U.S. antinoise standards
04 p0465 A72-14925

Jet aircraft noise reduction, discussing engine design modifications
04 p0465 A72-15167

Noise generation from turbulent supersonic shear layers, including low supersonic and transonic ranges for jet noise applications
04 p0463 A72-15566

Turbofan multiple pure tone noise analysis, discussing rotor geometry, relative Mach number and incidence angle effect on sound emission
[AIAA PAPER 72-127] 05 p0706 A72-16824

Jet engine silencing plug nozzle suppressor configurations acoustic and thrust performance measurements
[AIAA PAPER 72-160] 05 p0706 A72-16826

Directionality and far field structure of combustion generated noise, using premixed turbulent flame models
[AIAA PAPER 72-198] 05 p0748 A72-16875

Jet noise simple-source theory experimental verification, determining relation of measured sound power and jet pressure levels of turbojet engine
06 p0867 A72-17856

Hybrid computer method of nonstationary spectrum analysis of aircraft noise, applying to flyover and jet aircraft noise abatement under operational conditions
07 p0911 A72-18778

Spectral measurements of jet turbulence noise in core and annular mixing region, using subsonic test experiments
[AIAA PAPER 72-158] 07 p0966 A72-18957

Ground focus line location of sonic bang propagating in stratified atmosphere with wind for transonically accelerating aircraft
07 p0912 A72-19645

Jet noise intensity reduction by screen across nozzle exit, using acoustic and hot wire measurements
07 p0968 A72-19873

Circular jets sound generation analysis, using Lighthill equation and Michalke spectral method
[DFVLR-SONDDR-179] 07 p0910 A72-20100

Turbojet and turbofan engines noise signatures and sonic boom effects, discussing frequency spectra, atmospheric attenuation and noise suppression systems
07 p0912 A72-20163

Acoustic tests of jet aircraft noise and sonic boom effects on sleep pattern and human performance, using EEG analysis
[ASA PAPER W 11] 08 p1125 A72-21487

Olympus engine flight testing for relighting and anticipating, engine control and noise and vibration assessments in support of Concorde aircraft development
08 p1224 A72-21898

Subsonic jet noise directivity prediction from acoustic pressure measurements
11 p1706 A72-26041

Jet aircraft noise effect on sleeping EEG and subsequent waking performance, showing presence of carry-over effects
12 p1770 A72-27474

Supersonic jet noise and sonic boom sources, propagation and reduction, considering airport community disturbances, aircraft cabin noise and fatigue problems
13 p1898 A72-29578

Stress levels and fatigue in aircraft structures subjected to jet noise, noting stress calculation for skin panels and control surfaces
13 p1898 A72-29579

Supersonic jet exhaust noise radiation from turbulent shear layer instability waves, noting acoustic energy flux dependence on streamwise distance
13 p2028 A72-29581

Maximum overpressures of supersonic aircraft maneuvering-produced sonic booms occurring at geometrical acoustic ray focus points/caustic cusps/
13 p1898 A72-29586

Tu-104 turboprop aircraft flight noise measurements and spectral changes at different distances from landing strip, evaluating public nuisance and resident reactions
14 p2072 A72-30446

Hyperersonic commercial aircraft operational problems, considering passenger physiology limits flight profile, sonic pollution, traffic demands, route structure, etc
14 p2073 A72-30830

Noise measurements during shock free and underexpanded operation modes of supersonic cold model jet at moderate exit Mach number
15 p2179 A72-32017

Aerodynamic noise and structural fatigue failure research and test facility, concerning supersonic jet and V/STOL aircraft
16 p2342 A72-32900

Rotating flow introduction effects on jet noise levels, combustion and turbulent mixing processes and flame stability
[AIAA PAPER 72-645] 16 p2480 A72-34087

- Jet noise reduction by screen placed across jet flow, investigating acoustic properties, velocity and pressure in mixing zone
[AIAA PAPER 72-644] 16 p2381 A72-34088
- Data correlation of jet noise total sound power and peak sideline overall sound pressure level for subsonic and supersonic convergent exhaust nozzles
[AIAA PAPER 72-643] 16 p2381 A72-34089
- Acoustic attenuation and thrust loss incurred by shrouded multibute supersonic jet noise suppressor
[AIAA PAPER 72-642] 16 p2381 A72-34090
- Supersonic jet noise mechanisms and scaling laws, studying acoustic fields for rectangular and axisymmetric nozzle configurations
[AIAA PAPER 72-641] 16 p2381 A72-34091
- Sonic jet noise pressure source model for radiated sound power and jet pressure frequency spectra ratio derivation with application to noise suppression
18 p2680 A72-36414
- Noise generated by STOL core-jet thrust reversers.
[AIAA PAPER 72-791] 19 p2849 A72-38108
- Forward flight effects on mixer nozzle design and noise considerations for STOL externally blown flap systems.
[AIAA PAPER 72-792] 19 p2746 A72-38109
- Flight evaluation of three-dimensional area navigation for jet transport noise abatement.
[AIAA PAPER 72-814] 19 p2750 A72-38116
- Jet aircraft noise sources in subsonic and supersonic exhaust mixing process, suppressing noise via turbobfan exhaust speed reduction
19 p2849 A72-38380
- Advanced technology applications to present and future transport aircraft.
[AIAA PAPER 72-759] 20 p2888 A72-40051
- Tu-104 turboprop aircraft flight noise measurements and spectral changes at different distances from landing strip, evaluating annoyance factors and resident reactions
21 p3009 A72-41110
- Hypersonic transports commercial applications, examining economic and noise and air pollution aspects
[ICAS PAPER 72-32] 21 p2995 A72-41157
- NASA Quiet Engine program R and D on conventional takeoff and landing subsonic cruise aircraft engine noise
[ICAS PAPER 72-48] 21 p3100 A72-41173
- Noise control technology for jet-powered STOL vehicles.
[ICAS PAPER 72-50] 21 p2995 A72-41175
- Jet noise generation theory /Lighthill-Ffowcs Williams/ verification by model tests, discussing means of reducing or eliminating shock cells
[ICAS PAPER 72-55] 21 p3047 A72-41852
- Vibration measurements of an airplane fuselage structure. I - Turbulent boundary layer excitation. II - Jet noise excitation.
22 p3139 A72-42912
- German monograph - Studies of the ground effect on the noise levels and their frequency distribution in the near field of an engine jet directed vertically against the ground.
22 p3217 A72-43060
- NASA's quiet engine programs.
22 p3217 A72-43152
- Community noise levels of the L-1011 Tristar Jet Transport.
24 p3365 A72-44677
- JET AIRSTREAMS**
U JET STREAMS [METEOROLOGY]
- JET AMPLIFIERS**
Contacting-both-wall switching transients of bistable fluidic amplifiers with low setbacks, including unsteady effects in jet and attachment zone
[ASME PAPER 71-WA/FLCS-6] 05 p0615 A72-15917
- Permanent state operation optimization for fluid amplifier with jet interaction
10 p1422 A72-24125
- Pneumatic amplifiers with controlled pressure during subcritical and supercritical flow, considering jet-resonant choke, conical and membrane systems
11 p1578 A72-26783
- Jet turbulence interaction and velocity effects on noise level of proportional fluid amplifiers
16 p2350 A72-33177
- Pressure recovery and control characteristics of turbulence amplifiers with jet of rectangular section, using large scale water model
16 p2350 A72-33178
- JET AUGMENTED WING FLAPS**
U JET FLAPS
U WING FLAPS
- JET BLAST EFFECTS**
Scale model tests of high thrust engine blast deflection fence combinations for protection of adjacent roadway traffic
16 p2374 A72-33698
- Direct correlation measurement of turbulent jet noise and flow by cross correlating narrow filtered input turbulence and output acoustic signals
[AIAA PAPER 72-640] 16 p2381 A72-34092
- German monograph - Studies of the ground effect on the noise levels and their frequency distribution in

the near field of an engine jet directed vertically against the ground.
22 p3217 A72-43060

JET BOUNDARIES

Boundary configuration of supersonic under-expanded jet discharging into stationary medium
09 p1259 A72-22410

JET DAMPING

U DAMPING
U SPIN REDUCTION

JET DRIVE

U JET PROPULSION

JET ENGINE FUELS

Viscosity and additive effects on jet engine fuel antiwear properties improvement
02 p0270 A72-11968

Jet fuels hydrocarbon composition effect on thermal stability, considering nonaromatic components influence on aromatic hydrocarbons oxidation products coagulation
02 p0271 A72-12800

Surface active agent detection by device using ultrasonic vibrating mechanism to emulsify water with fuel, determining water retention or turbidity by photoelectric cell
04 p0564 A72-14419

Fuels and lubricants development trends for subsonic and supersonic aircraft, discussing thermostable hydrocarbons, ramjet fuels, esters, oxidation inhibitors, metal deactivators, high pressure lubricant additives, etc
05 p0681 A72-16739

JP-5 fuel sulfur content effect on aircraft engine turbine blades hot corrosion under marine environmental conditions
07 p1010 A72-18752

Jet engine fuel fire hazard evaluation by controlled laboratory tests, analyzing ignition characteristics under simulated survivable aircraft crash accidents
[SAE PAPER 72-0324] 11 p1702 A72-25587

Jet engine fuel modification to decrease fire hazard in survivable aircraft crashes
[ASME PAPER 72-GT-25] 11 p1702 A72-25621

Jet fuel hydrocarbon group chemical composition effects on antiwear characteristics in sliding friction and rolling simulation experiments
13 p2024 A72-29073

Continuous NDT of coalescers /jet fuel filters/ by liquid crystals, detecting split seams, cap leaks, cracks, material imperfections and epoxy filled voids
[ASME PAPER 72-DE-25] 14 p2108 A72-30867

Properties of pyrolytic oil hydrogenated aromatic fraction, noting suitability for jet fuels applications
14 p2145 A72-31075

Review of jet engine emissions.
19 p2848 A72-37645

Effect of fuel on gas corrosion in jet engine combustion chambers
19 p2849 A72-38091

Static electricity in fueling of superjets.
21 p3040 A72-41375

Supersonic jet engine fuels production by gasoline vapor pyrolysis, discussing physico-chemical characteristics and combustion properties
24 p3432 A72-44625

JET ENGINES

NT PULSEJET ENGINES

NT RAMJET ENGINES

NT SUPERSONIC COMBUSTION RAMJET ENGINES

NT TURBOFAN ENGINES

NT TURBOJET ENGINES

NT TURBOPROP ENGINES

Electrodischarge and electrochemical machining applications in continuous repetitive production of aircraft jet engine components
01 p0078 A72-11150

Jet engine component overhaul procedures for fatigue damage repair, detailing distressed metal removal, replacement and welding techniques
02 p0271 A72-12499

Automated jet engine development facility, discussing assembly and test area and computer controlled operation
[ASME PAPER 71-WA/GT-6] 05 p0642 A72-15899

Jet engine test facilities for JT9D experimental and production models
[ASME PAPER 71-WA/GT-12] 05 p0642 A72-15904

High intensity combustion chamber design for gas turbine of jet engine, considering primary, secondary and dilution zones
05 p0705 A72-16491

Papers on critical and exploratory flight testing covering rotary wings, lifting bodies and jet engine airstart
06 p0758 A72-18487

Airstart flight testing for single engine fighter/attack aircraft, including flight conditions, windmilling, fuel flows, gas temperature, ignition and acceleration
06 p0868 A72-18496

Statistical evaluation for forged jet engine parts tensile tests cost reduction, using regression analysis
07 p0995 A72-19484

Friction coefficient, standard wear and surface layer temperature of seal for dry friction pairs in jet engines, investigating crystal lattice parameters
07 p0996 A72-19768

Deterministic model for new product innovation adoption rate in commercial aircraft jet engine market
07 p1105 A72-20269

Twin spool jet engine system, predicting shaft speed effects on whirling frequencies due to gyroscopic action with computer model
08 p1224 A72-22130

Pod-mounted jet engine follower force instability, analyzing two degrees of freedom system dynamics
09 p1374 A72-22938

Two spool geared fan jet engine design and development for general aviation, discussing performance, reliability and ecological aspects
[SAE PAPER 72-0351] 11 p1703 A72-25602

Jet turbine engine front fans with and without snubbers, estimating flow field by streamline curvature technique
[ASME PAPER 72-GT-4] 11 p1568 A72-25607

Mixing parameter design of high loading spray type combustor for lift jet engine, using primary zone
[ASME PAPER 72-GT-99] 11 p1705 A72-25668

Propulsion system/airframe matching in hybrid V/STOL airplanes, stressing thrust vector management, lift engine bypass ratio and power plant packaging design
[ASME PAPER 72-GT-106] 11 p1576 A72-25671

Open-air jet engine test stand for flame stabilization, jet and compressor noise studies, noting provisions for rapid installation changes
12 p1795 A72-27416

Surface integrity machining practices application to jet engines production, noting cost reduction and process selection and quality control improvement
[ASM PAPER W 72-27.2] 12 p1862 A72-28163

Russian book on combustion and turbulent mixing processes in jet engines covering temperature and velocity profiles, combustion chamber design and fuel injection characteristics
12 p1862 A72-28340

Lifetime nomogram for evaporating drop at vapor combustion, applying thermomechanical and aerodynamic decay to jet engine combustion chamber
[DFVLR-SONDDR-203] 16 p2477 A72-33422

Effect on supersonic jet noise of nozzle plenum pressure fluctuations.
17 p2597 A72-35243

Inlet throttle centrifugal fuel pumps for jet engine augmentation, discussing design features, performance, noise, life and reliability characteristics
18 p2694 A72-36044

Proportional control of space vehicles with the aid of auxiliary jet engines
20 p2977 A72-39593

Optimization of controlled plants sequence with stochastic process described by partial differential equations, noting hydropneumatic system of liquid fuel jet engine
20 p2947 A72-39903

In-flight and flight-line monitor system to detect foreign object damage in jet engines.
22 p3179 A72-42690

Aircraft jet-engine control; Conference, Velešín, Czechoslovakia, June 12-16, 1972, Proceedings
23 p3326 A72-44276

Fluidic heat sensors for measuring fuel temperature in jet engines
23 p3326 A72-44280

Reliability analysis of a jet engine fuel system with the aid of an analog computer using operational data
23 p3326 A72-44282

Optimal synthesis of a two-parameter continuous controller for a jet engine with an afterburner
23 p3326 A72-44284

Planning and management requirements for aircraft jet engine control system research and development
23 p3294 A72-44285

Dynamic and static characteristics of jet engine simulators
23 p3327 A72-44286

Use of fluidic elements for jet engine controllers
23 p3327 A72-44290

A digital model of jet engine hydraulic fuel controller
23 p3327 A72-44291

JET EXHAUST

Aircraft engine exhaust geometry effects on smoke plume visibility, describing carbon particles light absorption characteristics by Beer-Lambert law
[ASME PAPER 71-WA/GT-10] 05 p0704 A72-15903

Jet flap type exhaust flows acoustic and fluid dynamic characteristics, measuring sound power output and noise spectra for various configurations
[AIAA PAPER 72-130] 05 p0608 A72-16920

JT8D engine exhaust noise field, considering internal noise sources contribution from exhaust duct sound pressure measurements
07 p1054 A72-19331

Combustion research for reducing jet aircraft pollutant emissions, discussing fuel atomization improve-

ment, smoke reduction and combustor design techniques

11 p1705 A72-26037
Russian monograph on self oscillatory noise generation during gas jet ejection covering single, parallel, supersonic, flat and cylindrical jets stability

11 p1617 A72-26066
Quasi-steady Ar MPD arc exhaust plume structure from spectroscopic and photographic investigation, noting dependence on arc current and mass flow rate [AIAA PAPER 72-499]

11 p1696 A72-26222
Near field megawatt single shot exhaust flow and propulsion characteristics of pulsed MPD arc thruster [AIAA PAPER 72-500]

11 p1711 A72-26223
Estimated peak regional concentration of SST exhaust in stratosphere from expected flight operation levels

13 p1991 A72-28837
SST water vapor and nitrogen oxides exhausts effect on stratospheric composition, developing nonequilibrium photochemical model

13 p1994 A72-28878
Supersonic jet exhaust noise radiation from turbulent shear layer instability waves, noting acoustic energy flux dependence on streamwise distance

13 p2028 A72-29581
IR radiant energy emission from conical jet exhaust of turbojet aircraft

15 p2298 A72-32399
Review of jet engine emissions.

19 p2848 A72-37645
Jet aircraft noise sources in subsonic and supersonic exhaust mixing process, suppressing noise via turbofan exhaust speed reduction

19 p2849 A72-38380
The study of gaseous jet exhausting into vacuum. [ICAS PAPER 72-36]

21 p3046 A72-41161
Detection of crystals in CO₂ jet plumes.

21 p3046 A72-41306

JET FLAMES

U FLAMES

U JET FLOW

JET FLAPS

STOL aircraft roll moment control possibility for externally-blown jet flap due to engine failure

02 p0154 A72-11700
Closed loop fluidic bidirectional jet flap airfoil lift control system, considering application to helicopter rotor blades

05 p0603 A72-16659
Jet flap type exhaust flows acoustic and fluid dynamic characteristics, measuring sound power output and noise spectra for various configurations

05 p0608 A72-16920
Integrodifferential equation for rigid tunnel walls effect on supercavitating flow past thin jet flapped airfoil, noting lift coefficient derivatives

10 p1469 A72-24562
Dynamic pressure distribution and propulsive contours of trailing vortex wake downwind of external flow jet flap, using five-hole probe measurements

10 p1420 A72-25070
Jet flaps for high turning compressor cascades in incompressible axial flow, calculating blade pressure and jet slope distributions

11 p1569 A72-25615
[ASME PAPER 72-GT-16]
Aerodynamic properties prediction procedure for thin jet-flapped airfoil in incompressible inviscid flow bounded by different types of boundaries

15 p2179 A72-32147
Lift and induced drag characteristics of jet flapped finite span wings in close proximity to ground, using method of matched asymptotic expansions

16 p2341 A72-32827
Oscillating flapped vane system for large amplitude uniform sinusoidal lateral gust generation in semiopen jet wind tunnel

16 p2374 A72-33699
Hydrodynamic characteristics of a cambered hydrofoil with a jet flap.

17 p2537 A72-34303
[ASME PAPER 71-APMW-17]
Forward flight effects on mixer nozzle design and noise considerations for STOL. externally blown flap systems.

19 p2746 A72-38109
[AIAA PAPER 72-792]
STOL transport stability and control derivative prediction methods and accuracy requirements.

19 p2752 A72-38139
[AIAA PAPER 72-780]
Lift and control augmentation by spanwise blowing over trailing edge flaps and control surfaces.

19 p2746 A72-38140
[AIAA PAPER 72-781]
The lift coefficient of a supercavitating jet-flapped foil in a free jet.

21 p2992 A72-41236
An improved solution of the two-dimensional jet-flapped airfoil problem.

23 p3247 A72-43329

JET FLIGHT

U JET AIRCRAFT

JET FLOW

NT AIR JETS

NT SUPERSONIC JET FLOW

Momentum jet and electric discharge from same hole in plane wall bounding viscous incompressible

conducting fluid, investigating flow field with similari-ty solutions

01 p0107 A72-10139
Harmonium reed self excited oscillation mechanism, describing flow visualization, jet instability potential flow and aerodynamic forces

01 p0002 A72-11232
Nozzle boundary layers effect on reattachment position of two dimensional jet to adjacent flat plate, noting Reynolds number influence

02 p0150 A72-11729
Laminar free jets characteristics, investigating transition to turbulence

02 p0150 A72-11730
Differential equations solution for turbulent two dimensional jet flows bounded by parallel planes

02 p0156 A72-12000
Incompressible two dimensional plane jet spatial stability analysis, presenting disturbance vorticity, Reynolds stress and energetics distribution in cross stream direction

02 p0152 A72-12352
[AD-741988]
Incompressible two dimensional laminar/turbulent wall jet characteristics, obtaining Prandtl mixing theory from apparent kinematic viscosity

02 p0206 A72-12619
Acoustical oscillations effect on free jet flow stability and boundary layer structure, using inviscid Orr-Sommerfeld equation for flow disturbances frequency, wavelength and velocity

03 p0340 A72-12913
Wall jet flow displacement on curved surface, deriving two dimensional solution for second-order boundary layer equations

03 p0307 A72-13159
German monograph on gas type and nozzle flow conditions effect on condensed molecular jets properties

03 p0391 A72-13275
Base pressure determination for subsonic isothermal central and peripheral jets of incompressible fluid discharging into subsonic slipstream

03 p0342 A72-13912
Axisymmetric deflected turbulent jet flow, analyzing physical features and trajectories

04 p0462 A72-15177
[ASME PAPER 71-APM-SS]
Underexpanded nitrogen jet from sonic orifice, investigating axial rotational temperature distribution

04 p0597 A72-15335
Theoretical and experimental heat transfer at plate in longitudinal jet flow with strong transverse inhomogeneity

05 p0649 A72-16228
Composite three-dimensional axisymmetric turbulent jet system, discussing jet interaction relation to boundary layer contact and resulting turbulent mixing

05 p0649 A72-16229
Turbulent jets interaction with cross flow, presenting longitudinal and transverse velocity, temperature and turbulence distributions

05 p0651 A72-16870
[AIAA PAPER 72-149]
Recirculating cells in laminar coaxial jets investigated by smoke introduction into flow field and hot-wire techniques

05 p0651 A72-16880
[AIAA PAPER 72-150]
Axial sound sources number, strengths and phases in jets, using experimental measurements of audio pressure in near field

05 p0652 A72-16910
[AIAA PAPER 72-159]
Jet flap type exhaust flows acoustic and fluid dynamic characteristics, measuring sound power output and noise spectra for various configurations

05 p0608 A72-16920
[AIAA PAPER 72-130]
Jet peak velocity decay in single and multielement nozzles for STOL aircraft externally blown flaps, noting noise reduction due to flow mixing

05 p0608 A72-16927
[AIAA PAPER 72-48]
Cumulative jet formation in elliptical cavity, investigating effect on liquid explosives ignition

06 p0799 A72-17909
Two dimensional flow of gas jet around dihedral obstacle, investigating screen proximity and fluid compressibility effects

06 p0799 A72-17912
Compressible axisymmetric coaxial jets turbulent mixing in constant area duct, considering axial and radial pressure distributions

07 p0967 A72-19094
Cross correlation analysis of turbulent jet flow noise with pressure fluctuation as acoustic source

08 p1150 A72-21488
[ASA PAPER H 12]
Durando model overprediction of deflected jet vortex strength in subsonic cross flow

08 p1151 A72-21631
Ray trace of sound refraction by point source on jet flow axis, numerically calculating directivity pattern

08 p1152 A72-21893
Sound refraction by sinusoidal point source in subsonic jet flow, obtaining solution by finite difference method for comparison with ray tracing results

08 p1152 A72-21894
Capacitive electret pressure sensors calibration for interior measurements in turbine engines, jets and exhaust nozzles

09 p1310 A72-22815
[ONERA, TP NO. 982]

Coherent and incoherent structures of aerodynamic noise, analyzing compressor near field and hot jet IR emission source

09 p1294 A72-22816
[ONERA, TP NO. 983]
Recirculation criteria for confined jet flames in cylindrical combustion chamber, using Thring-Newby number

09 p1411 A72-23144
Monodirectional jet mass ejection from black holes, developing hypothetical model based on squeezed toothpaste analogy

10 p1535 A72-23910
Aerodynamic noise produced by gas jet flow around airfoil, discussing sound reduction

10 p1471 A72-24107
Initial disturbance level effects on laminar viscous jet stability from calculation of maximum amplification rate as function of physical parameters

10 p1465 A72-24149
Incompressible fluid jet propagation beyond charged particle source exit section, investigating electrohydrodynamic interaction parameter

10 p1522 A72-24549
Aerodynamic throttling effect due to air jet flow interaction in throat region of mainstream two dimensional nozzle flow

10 p1419 A72-24845
Plane laminar semibounded incompressible fluid jet propagation into slipstream along moving plate, solving boundary layer equations

10 p1471 A72-25136
Two dimensional transverse subsonic hot-air jet interaction with freestream flow at various jet/freestream velocity ratios, measuring jet velocity and temperature distributions

11 p1567 A72-15230
[AIAA PAPER 72-292]
Laminar and turbulent compressible wall jet characteristics, obtaining density variation as function of velocity and Mach number at exit

11 p1618 A72-26593
Frictionless, Helmholtz and flat jet incompressible flows from slot in thick plane wall, comparing characteristics with free jet vicinity

15 p2216 A72-31464
Flow induction by cylinder performing transverse periodic vibrations in viscous fluid, noting jet flow with large streaming Reynolds number

15 p2217 A72-31617
Nonfriction vortices generation by jet flow in stationary fluid, using conservation of momentum principle

15 p2219 A72-32554
Spherical source jet flow expansion of single monatomic gas into vacuum on basis of BGK kinetic equation

16 p2375 A72-32887
Axisymmetric jet impact on ground board for different nozzle configurations and heights in VTOI. aircraft aerodynamic studies

16 p2377 A72-33404
Numerical finite difference prediction of inert turbulent boundary layer swirling jet flow, using nonisotropic energy-length model

16 p2380 A72-34044
[AIAA PAPER 72-699]
Jet noise reduction by screen placed across jet flow, investigating acoustic properties, velocity and pressure in mixing zone

16 p2381 A72-34088
[AIAA PAPER 72-644]
Direct correlation measurement of turbulent jet noise and flow by cross correlating narrow filtered input turbulence and output acoustic signals

16 p2381 A72-34092
[AIAA PAPER 72-640]
Vortex growth in two-dimensional coalescing jets.

17 p2539 A72-34970
Acoustic power spectrum of a subsonic jet

17 p2541 A72-35544
The turbulence diffusion in free jets and flames

18 p2740 A72-36245
Free hot jet turbulence space-time correlation function measurement based on IR detection

18 p2680 A72-36468
Thrust recovery factor and base drag losses in annular jets as function of jet thickness to base diameter ratio, determining recirculation mass flow

18 p2641 A72-36769
Circular-elliptical transformation of jet propagating in homogeneous slipstream within unperturbed uniform transverse magnetic field, using linearized three dimensional boundary layer equations

18 p2716 A72-36815
Nonlinear development of capillary waves in a fluid jet

18 p2682 A72-36885
An expansion scheme for the noise from circular jets.

18 p2683 A72-36941
[DFVLR-SONDDR-217]
Study by phase detection of the velocity of a molecular jet

18 p2714 A72-37200
Output impedance of a jet element

19 p2754 A72-37994
Analysis of the interaction of jets and airfoils in two dimensions.

19 p2746 A72-38136
[AIAA PAPER 72-777]

JET FUELS

- Burke-Shumann-Zeldovich model for aerodynamic characteristics of straight jet laminar diffusion flames, considering free, semibounded and slipstream types
19 p2882 A72-38460
- Axisymmetric jet stretcher diffuser performance for ramjet engine inlet configurations, testing at angles of attack and supersonic flow velocities
[AIAA PAPER 72-1024] 21 p2993 A72-41602
- Conformal mapping for interaction of two dimensional flow of ideal fluid and injected counterflow with jet formation, calculating cavitation void dimensions
22 p3165 A72-42065
- Characteristics of the propagation of swirling jets of variable density
22 p3166 A72-42255
- Equations of plane potential electrohydrodynamic flow, noting jet and quasi-one dimensional flows of charged particles in curvilinear electrostatic field
22 p3210 A72-42269
- Laminar to turbulent transition in axisymmetrical submerged jets and slipstream flows of air and He, discussing Reynolds number effect
22 p3166 A72-42270
- Steady two-dimensional viscous flow in a jet.
23 p3282 A72-44303
- Waves generated in the configuration of a magnetically confined and field-permeated axisymmetric jet.
23 p3322 A72-44307
- Stability of coaxial rotating jet and vortex of different densities.
24 p3394 A72-45562

JET FUELS

U JET ENGINE FUELS

JET IMPINGEMENT

- Sonic line neighborhood of uniform axisymmetric supersonic air jet impinging on perpendicular flat plate, measuring shock shapes and surface pressures
01 p0002 A72-11398
- Circular jet discharging perpendicular to solid surface into transverse flow, discussing effects on infinitely thin circular wing aerodynamic characteristics
03 p0309 A72-13915
- Interaction forces of gas jet injected into supersonic stream, examining data from thrust vector control gas injection tests
03 p0342 A72-13958
- Jet interaction induced supersonic turbulent boundary layer separation, obtaining flat plate pressure measurements and jet plume shadowgraphs
05 p0602 A72-16537
- Interaction produced by diametrically opposed plane turbulent wall jet collision in still air, discussing resultant free jet
[AIAA PAPER 72-211] 05 p0606 A72-16854
- Heat transfer rates of impingement cooling in gas turbine airfoils, noting leading edge sharpness effects for slot and circular jet configurations
[ASME PAPER 72-GT-7] 11 p1703 A72-25610
- Nonstationary interaction flow field between subsonic and composite jet on flat plate with vortex formation and reverse currents, using finite difference technique
12 p1799 A72-28168
- Vorticity and energy transfer equations for subsonic jet impingement on flat plate, noting turbulent jet effect on friction factor
12 p1799 A72-28171
- Holographic determination of local convective mass transfer coefficients over flat plate normally impinged with laminar air jet, using swollen polymer transparent coating
15 p2239 A72-32349
- Interaction between free oil jets and plates of various profiles
17 p2539 A72-34915
- Flow pattern of two impinging circular jets.
17 p2540 A72-35233
- Externally blown flap impingement noise.
[AIAA PAPER 72-664] 17 p2487 A72-35961
- Experimental study of heat transfer in a subsonic jet impinging normally on a plane baffle.
21 p3128 A72-40949
- Plume impingement force during tandem stage separation at high altitudes.
22 p3231 A72-42872
- German monograph - Studies of the ground effect on the noise levels and their frequency distribution in the near field of an engine jet directed vertically against the ground.
22 p3217 A72-43060
- Transverse oscillations of a jet in a jet-splitter system.
[ASME PAPER 72-FLCS-1] 23 p3281 A72-44065
- Jet impingement under VTOL aircraft.
24 p3364 A72-45779

JET LIFT

- Mixing parameter design of high loading spray type combustor for lift jet engine, using primary zone
[ASME PAPER 72-GT-99] 11 p1705 A72-25668
- Lift jet VTOL flight path optimization for minimum landing transition distance, evaluating deceleration as function of incidence and thrust vector angles
15 p2272 A72-32323

- Calculation of the recirculation flow of VTOL lift engines.
[ICAS PAPER 72-42] 21 p3099 A72-41167
- An experimental investigation of a jet issuing from a wing in crossflow.
24 p3362 A72-45332

JET MIXING FLOW

- Velocity and temperature effects on momentum and temperature equalization in coaxial turbulent jet mixing in pipe inlet section
[DFVLR-SONDDR-183] 01 p0051 A72-11257
- Plane mixing boundary layer flow of high temperature turbulent gas jet in longitudinal magnetic field
03 p0397 A72-13998
- Finite difference scheme for collision of two axially symmetric liquid jets with free boundary in cylindrical coordinate system
03 p0344 A72-14370
- Theoretical model for turbulent mixing of confined jet, including wall boundary layer
[ASME PAPER 71-WA/FE-31] 05 p0646 A72-15925
- Confined laminar jet mixing of two uniform streams flowing in parallel plate channel, obtaining velocity field from linearized governing equation
[ASME PAPER 71-WA/APM-2] 05 p0647 A72-15973
- Jet mixing flow from slotted source into longitudinal cross flow shown analogous to heat expansion in plane jets
05 p0648 A72-16220
- Air stream from air entry holes of aeronautical gas turbine combustor, investigating jets maximum penetration, flow path, and mixing
05 p0705 A72-16493
- Turbulent shear stress, intensity and velocity field in coflowing axisymmetric jets, using eddy viscosity model
[AIAA PAPER 72-47] 05 p0652 A72-16926
- Ejector nozzle design criteria, analyzing primary-secondary flow interactions and diameter, spacing and temperature ratio effects
[AIAA PAPER 72-46] 05 p0609 A72-16963
- Approximation method for gas ejection calculation, assuming zero mixer flow velocity and ejection coefficient and suction side optimum operation for uniform pressure distribution
08 p1107 A72-21320
- Turbulent mixing of high temperature Ar jet injected into ring slipstream of air in dc plasmatron with coaxial nozzle and fixed arc
09 p1410 A72-22677
- Flow phenomena, mixing and stability of high speed enclosed multijet turbulent diffusion flames fed by propane and air
10 p1563 A72-25139
- Ammonia-air opposed reacting jet /ORJ/ for flame stabilization, solving partial differential equations for flow field
10 p1564 A72-25141
- Mixing parameter design of high loading spray type combustor for lift jet engine, using primary zone
[ASME PAPER 72-GT-99] 11 p1705 A72-25668
- Jet compression role in high temperature mechanical energy conversion heat exchanger based on ejector principle
12 p1755 A72-27724
- Round air jet turbulent mixing with incompressible transverse flow, examining interaction behavior as function of relative momentum
13 p1943 A72-29641
- French monograph on turbulent free flow boundaries covering two dimensional plane jet mixing zone characteristics from thermal signal measurements
14 p2095 A72-30948
- Thermal molecular jets mixing produced by Knudsen effusion from porous wall, obtaining Boltzmann equation approximate solution by moment method via assumed distribution function
16 p2429 A72-33055
- Water vapor condensation in jet turbulent mixing zone of confluent high velocity high temperature gas streams for finite axisymmetric nozzle
16 p2377 A72-33260
- Free jet reenergization efficiency, mixing distance and similarity analysis for boundary layer control at sharp trailing edges and cusps
[AIAA PAPER 72-700] 16 p2345 A72-34043
- Jet noise reduction by screen placed across jet flow, investigating acoustic properties, velocity and pressure in mixing zone
[AIAA PAPER 72-644] 16 p2381 A72-34088
- Combustion process in mixing gas jets of different density, using argon and nitrogen for internal flow and air for external jet
16 p2381 A72-34169
- Circulating toroidal vortex pattern in initial region of turbulent coaxial jet stream mixing obtained with hot-wire anemometer, static pressure probes and shadowgraphy
[ASME PAPER 72-APM-30] 17 p2538 A72-34789
- A new theoretical model for representing jet penetration into a subsonic stream
17 p2538 A72-34888
- Binary diffusion of a jet embedded in a boundary layer.
17 p2541 A72-35238

- Determination of the stream function of a perturbation associated with a plane jet
18 p2680 A72-36470
- Structure of turbulent underexpanded jets expelled into a submerged space and into a slipstream
18 p2642 A72-36884
- The linearized solutions as applied to the half-jet mixing.
18 p2683 A72-36928
- The intrinsic structure of turbulent jets
18 p2684 A72-37201
- Jet aircraft noise sources in subsonic and supersonic exhaust mixing process, suppressing noise via turbofan exhaust speed reduction
19 p2849 A72-38380
- Free gas jets turbulent mixing flow, considering development of submerged air jet with action of mechanical turbulence generator ahead of nozzle
20 p2913 A72-39367
- Turbulent diffusion in Laval nozzle, studying mixing of weakly heated jet coaxial with main flow in subsonic flow region
20 p2913 A72-39368
- Mixing in initial portion of coflowing jets of incompressible gases of different densities, defining mixing zone widths relationship to velocity and density ratios
20 p2913 A72-39369
- Heat and mass transfer in the initial mixing region of confined coaxial laminar jets.
[ASME PAPER 72-HT-22] 20 p2986 A72-39674
- German monograph - Turbulence behavior and degree of nonmixing of jets and jet flames.
22 p3245 A72-43077
- Turbulent mixing of three plane isothermal jets with various velocity ratios, showing jet initial length shortening due to initial turbulence increase
23 p3279 A72-43657
- Flow parameters and geometric factors effect on wake structure behind nozzle cascades with cooling air ejection through blade trailing edges, evaluating energy losses due to flow mixing process
23 p3248 A72-43665
- An experimental study of turbulent diffusion of helium jets issued upwards into the air at rest.
23 p3281 A72-44273
- Laminar high speed mixing of nonequilibrium dissociating gases.
24 p3392 A72-45056
- High speed mixing of nitrogen vibrationally excited with carbon dioxide
24 p3464 A72-45065

JET NOISE

U JET AIRCRAFT NOISE

JET NOZZLES

- Jet peak velocity decay in single and multielement nozzles for STOL aircraft externally blown flaps, noting noise reduction due to flow mixing
[AIAA PAPER 72-48] 05 p0608 A72-16927

JET PILOTS

U AIRCRAFT PILOTS

JET PLUMES

U PLUMES

JET PROPULSION

- Rotating dumbbell shaped satellites orientation optimization by system of jets, calculating energy losses
05 p0731 A72-17043
- Air jet propelled flight vehicles optimal design parameters for constant altitude flight at given speed
07 p0911 A72-18991

JET PUMPS

- Soviet book on hydraulics, hydraulic machines and hydraulic drives covering fluid dynamics, pipe flows, jet pumps, turbines, bladed transmissions, etc
04 p0466 A72-15247
- Jet pumps for compressible fluids at supersonic velocities.
24 p3393 A72-45362

JET STREAMS [METEOROLOGY]

- Wind velocity and direction vertical changes for weather dynamics, emphasizing jet streams
02 p0255 A72-12785
- Wind altitude and maximal velocity computation for jet stream structure and turbulence
02 p0255 A72-12786
- Atmospheric deviations of ageostrophic wind in jet stream domain, using dimensionless vector characteristics
02 p0255 A72-12787
- Midlatitude F region wavelike disturbances detection by hf radio echo techniques, discussing correlation with jet stream associated tropopause wind patterns
07 p0974 A72-18885
- Polar night jet idealized model with zero tropospheric and constant vertical stratospheric shear, considering instability due to small wave disturbances
07 p1030 A72-19103
- Horizontal ozone distribution in middle stratospheric macro-synoptic situations, considering anticyclonic side and jet stream delta region
09 p1301 A72-23194
- Jet stream types derived from vector conditions for surface with maximum geostrophic wind velocity
10 p1507 A72-25002

GMD-1 tracking system for mesoscale wind data, minimizing elevation angle errors in jet stream CAT program by upwind release of rawinsonde 10 p1508 A72-25080

Jet streams development in rotating gaseous disk at discrete orbital distances in solar system 20 p2972 A72-39859

Internal wave instability in stratified jet streams 20 p2949 A72-39944

JET THRUST

Spacecraft precision off-on attitude control by pure jet torquing, using electronics based on control system idealized model 05 p0726 A72-16459

Sound pressure levels and acoustic fatigue tests for 11, 200 and 9,300 pound thrust J-52 engines comparison in A-6A aircraft 07 p0910 A72-18757

Propulsion system flexibility in V/STOL aircraft with one lift-cruise engine, discussing takeoff thrust requirements and cruise fuel consumption efficiency [ASME PAPER 72-GT-105] 11 p1576 A72-25670

Time optimal transfer trajectory in central Newtonian force field between two arbitrary points under jet acceleration 11 p1718 A72-25942

Digital autopilot for SKYLAB orbital assembly attitude control during docking, discussing jet selection logic, inter-axis dependence and onboard computer 15 p2269 A72-32183

STOL aircraft minimum noise takeoff trajectories determination, taking into account engine thrust and listeners distance from noise source [AIAA PAPER 72-665] 16 p2349 A72-34072

Thrust recovery factor and base drag losses in annular jets as function of jet thickness to base diameter ratio, determining recirculation mass flow 18 p2641 A72-36769

JET VANES

Oscillating flapped vane system for large amplitude uniform sinusoidal lateral gust generation in semiopen jet wind tunnel 16 p2374 A72-33699

JETAVATORS

U GUIDE VANES

JETS

Collision kinetics of jet streams of inelastic grains in neighboring orbits around central gravitating body 02 p0281 A72-12304

JETTISON SYSTEMS

Emergency escape from high performance military aircraft in flight and on ground, using explosive cord for transparent canopy material breakup 12 p1753 A72-27017

JETTISONING

Magnetic simulation of gravity for wind tunnel investigations of aircraft jettison processes, considering Froude number and relationships between model and full scale aircraft 10 p1462 A72-24775

JITTER

U VIBRATION

JOINING

Webbing joints stitching strain, considering nylon and flax yarns stretching properties and various stitching patterns strengths 01 p0005 A72-10315

JOINTS [ANATOMY]

Wear resistance and friction coefficients in physiologic solution of thermoplastic materials for prosthetic application in hip joints 08 p1194 A72-21760

JOINTS [JUNCTIONS]

NT BUTT JOINTS

NT LAP JOINTS

NT METAL JOINTS

NT RIVETED JOINTS

NT SEAMS [JOINTS]

NT SOLDERED JOINTS

NT SPOT WELDS

NT WELDED JOINTS

Strength analysis of hyperboloidal electric wire joint designs, expressing stress as function of contact loads 05 p0616 A72-17059

Rectangular and orthogonal circular waveguides hybrid junction with magnetized ferrite resonators along axes, discussing design and applications 07 p0952 A72-18844

Modal matching method evaluating planar surface waveguide junction transmission and reflection coefficients, comparing to integral equation method 07 p0955 A72-19253

Slip contact joint frictional damping of vibration of beam on elastic support 09 p1408 A72-23464

Rough surfaces thermal contact resistance in vacuum for normal height distribution, discussing bolted joint nonuniform stress distribution effect [AIAA PAPER 72-281] 11 p1741 A72-25221

Metallic foils effects on thermal joint resistance of interface between lathe turned and optically flat surfaces, noting optimal thickness [AIAA PAPER 72-283] 11 p1685 A72-25223

Solid state joining in gas turbine engines, discussing diffusion bonding, friction welding and coextrusion metal bonding [ASME PAPER 72-GT-74] 11 p1639 A72-25656

Ferrite loaded X band waveguide Y junctions eigenvalue frequency dependence measurement to identify modal resonance and arrange displacement for circulator operation 12 p1790 A72-27508

Tensile strength of fiber glass reinforced plastic elements joined by cover plates and nonlinearly elastic adhesives 13 p1962 A72-28737

Disks with inclined face, investigating effects of joint between hub and disk face on stress-strain state 14 p2164 A72-30430

Free and forced vibrations of two dimensional grids with simple and bridge-type boundary conditions, presenting closed form solutions for nodal deflections and moments 15 p2332 A72-32561

Automatic control for selective precision joint assembly of fuel pump equipment, reducing unfinished product volume 16 p2397 A72-33261

Fracture mechanics approach to adhesive joints. 17 p2633 A72-35282

Scattering characteristics of a cross-junction of oversized waveguides. 18 p2660 A72-36486

A multi-channel rotary joint for spacecraft applications. 19 p2770 A72-37260

Adhesive joints strength and polymeric film breakdown dependence on substrate molecular forces at base interface 19 p2806 A72-37533

Calculation of the stress concentration at the joint between a cylindrical casing and a branch pipe for internal pressure 21 p3127 A72-41710

Russian book - Design principles in aircraft construction. 22 p3136 A72-42074

Fatigue strength and fail-safe aspects of lug joint in aircraft structures, considering tension-compression load, fretting corrosion, prestress and residual stress 22 p3329 A72-42851

Junction circulator shunt conductance and susceptance-slope parameter calculation by constituent resonator input admittance formation, describing quarter wave mode operation 23 p3270 A72-43604

Limiting equilibrium of orthogonally coupled cylindrical shells 23 p3346 A72-43656

Optimum design of joints - The stress severity factor concept. 24 p3455 A72-44728

JORDAN FORM

Solution stability of linear differential equations systems with harmonic coefficients, using Jordan canonical forms and perturbation method 03 p0382 A72-13918

Algorithm for transformation of generalized companion forms for multivariable linear systems into Jordan canonical form 09 p1341 A72-23071

JOSEPHSON JUNCTIONS

Dc and ac Josephson effects in bulk granular superconductor, presenting junction I-V characteristics 02 p0268 A72-11472

Point contact Josephson junctions arrangement for millimeter and submillimeter region, showing mechanical stability 04 p0561 A72-14919

Josephson junction as 100 GHz oscillator-mixer for heterodyne frequency conversion in millimeter and submillimeter regions, observing I-V characteristics 04 p0503 A72-15604

Microwave parametric amplification and conversion in circuits with Josephson junctions, describing stable oscillation measurements 06 p0866 A72-18477

Nb-Nb point-contact Josephson junctions response to submillimeter radiation from HCN and DCN lasers 07 p0992 A72-20551

Fast responding mark/space ratio decoder for use with slug Josephson interferometers, presenting circuit waveforms 07 p0992 A72-20580

Josephson effect /superconducting weak link/ devices for low frequency magnetic field sensing, noting applications in magnetocardiography and absolute noise thermometry 08 p1218 A72-21919

Microwave induced dc voltages across unbiased Josephson tunnel junctions, showing power spectra dependence on magnetic field 09 p1367 A72-22458

Alternating Josephson effect and junctions applications to radiation generators and detectors, electromotive force regulators, oscillators, mixers and noise thermometers 09 p1370 A72-22799

Josephson dc and ac effects in plane junctions with thin semiconductor film barrier of evaporated material between two superconductors 09 p1370 A72-22800

Cryogenic Josephson junction tunneling in magnetocardiography, discussing high ambient noise levels in unshielded environment 12 p1769 A72-27288

Microwave source four hundredth order harmonic mixing with laser radiation, using Josephson junction and maser 12 p1827 A72-28221

Analog simulation of Josephson superconducting junctions dc characteristics for two mixed microwave frequencies, discussing signal detection sensitivity improvement 13 p2021 A72-28648

Parametric regeneration in Josephson superconducting point contacts for combination frequency signal amplification and conversion in microwave application 13 p1932 A72-29298

One electron and Josephson tunneling in superconductors in terms of energy level concepts 15 p2293 A72-32326

Three Josephson junction asymmetric feed quantum interferometer, discussing magnetic field sensitivity and amplitude variation increase 15 p2241 A72-32536

Superconductivity. 17 p2594 A72-34565

The temperature dependence of the critical current of a double Josephson junction. 19 p2846 A72-38556

Critical current periodicity of Josephson junction interferometers. 19 p2846 A72-38601

Effect of an alternating current on the steady characteristics of Josephson point contacts 22 p3208 A72-43109

Influence of fluctuations on the electromagnetic properties of Josephson tunneling contacts 22 p3208 A72-43124

Comparison of microwave-induced constant-voltage tests in Pb and Sn Josephson junctions. 23 p3323 A72-43272

Properties of a superconducting point contact contained in a resonator 23 p3324 A72-44221

JOULE HEATING

U OHMIC DISSIPATION

U RESISTANCE HEATING

JOURNAL BEARINGS

Load capacity, attitude angle and power loss of herringbone grooved gas lubricated journal bearings operating in air at 60,000 rpm 02 p0234 A72-11530

Unbalance response of rotor supported in hydrodynamic gas lubricated journal bearings [ASME PAPER 71-LUB-10] 02 p0235 A72-11534

Hydrodynamic journal gas bearing with herringbone grooved portion for self generating air supply pump hydrostatic starting and stopping [ASME PAPER 71-WA/DE-7] 05 p0664 A72-15944

Mathematical model for derivation of asperity or metal-metal contact load sharing of lubricated machine components in journal and roller bearings 09 p1317 A72-22248

Radial bearing placed on journal of Cardan suspension, investigating ball dimension errors effect on gyro drift rate 13 p1962 A72-28385

Stability considerations for a gas-lubricated tilting pad bearing. II - Analytical refinements and stability data. 19 p2807 A72-37697

Stability characteristics of floating bush bearings [ASME PAPER 71-LUB-9] 19 p2807 A72-37698

Flow between eccentric rotating cylinders. 19 p2786 A72-37699

High Reynolds number turbulence and vortices in journal bearings, discussing validity of flow field models based on mixing length and pipe flow theory 20 p2930 A72-39972

Shaft support improvement by combining rolling and hydrodynamic journal bearings, noting wear and friction torque reduction 21 p3060 A72-40928

Non-linear rotor bearing behavior. 21 p3061 A72-41518

JOURNALS [SHAFTS]

U SHAFTS [MACHINE ELEMENTS]

JUDGMENTS

Visual guidance of locomotion, discussing expansion information and target drift theories 03 p0319 A72-13879

Loudness and noisiness judgment contours, considering experimental subjective and objective conditions, subject age and sex and sound field characteristics 07 p0932 A72-20171

JUNCTION DIODES

Transferred electron microwave oscillator diodes with n-n-n structure by liquid phase epitaxy, reducing high resistance layer in interfaces and crystal defects 01 p0036 A72-10629

P-I-N diodes power handling characteristics in high power solid state TR switches

01 p0042 A72-10708

Mode guiding improvement in p-n junction of symmetrical AlGaAs-GaAs heterojunction laser diode with narrow active region, obtaining low room temperature threshold current

01 p0080 A72-10788

High peak power LSA epitaxial GaAs diode relaxation oscillator breakdown under neutron irradiation

01 p0044 A72-11309

Metal-semiconductor-metal Schottky barrier microwave diode impedance and shot noise calculation

02 p0191 A72-11894

Millimeter wave pulse signal transmission path length modulator with P-I-N diode switch, discussing system design and experimental results

02 p0196 A72-12798

GaAs Schottky barrier and germanium backward diodes in microwave integrated circuit applications, describing design and performance as frequency changers and low level detectors

03 p0334 A72-14073

Transient radiation effects on silicon diodes in avalanche breakdown, considering voltage regulating diode response and temperature compensating junction effects

03 p0334 A72-14090

Gaussian envelope microwave pulse generation using absorption p-i-n diode modulator, predicting performance by digital simulation

04 p0498 A72-14718

Space charge recombination in forward biased diffused p-n junction silicon diodes

04 p0562 A72-15127

Power Schottky diode design and advantages, comparing with junction diode

04 p0498 A72-15130

Heat flow resistance measurement in avalanche diodes, noting junction temperature effect

04 p0498 A72-15133

Si p-n-p and Cr-n-p junction transit time diode oscillators microwave and dc characteristics comparison, noting similarity

04 p0499 A72-15206

GaAs Schottky barrier diodes design, manufacture and characteristics, discussing radar receiver and communication equipment applications

05 p0638 A72-16595

Analytical model of Gunn diode oscillating in resonant mode with domain quenching, determining current harmonics

06 p0783 A72-17573

S band module with Gunn diode oscillators in series connection used as phased array radar 250 W power sources with efficient heat sink

06 p0789 A72-18476

GaAs and Si millimeter wave Schottky barrier mixer diodes fabrication, noting low noise broadband mixer/preamp

06 p0790 A72-18486

Neutron damage effects on red and green output of GaP light emitting diodes at 300 K

07 p1047 A72-19043

Schottky barrier and n-n heterojunction diodes hf noise, considering ideality factor effect

07 p0955 A72-19358

Physical and operational characteristics of Si and Ge photoelectric semiconductor devices with p-n junctions, discussing photodiodes, phototransistors, mosaic arrays and coordinate sensitive structures

08 p1139 A72-21055

Noise in optical output of small area electroluminescent GaAs diffused junction diodes, comparing with theoretical shot noise limit

09 p1286 A72-23087

Au-Si n and Al-Si p diodes noise operating in avalanche with charges injected by radiation

09 p1287 A72-23113

1/f excess flicker noise in metal semiconductor Schottky barrier diodes due to barrier height fluctuation

09 p1287 A72-23114

Metal probe potentials during mechanical displacement along surface of n-region of forward biased Si diode

09 p1288 A72-23362

Diode junction parameters and inverse saturation current measurements as function of current density and temperature

09 p1289 A72-23418

Validity range of applied voltage relationship to majority carrier current in Schottky diodes, assessing minority carrier current importance

10 p1448 A72-24108

Response time and noise stability measurements of integrated circuit TTI, (transistor-transistor logic/ and DTL, /diode-transistor logic/ elements performing invert functions

10 p1449 A72-24286

Lead tin telluride photovoltaic p-n junction diode and lasers, discussing n-type layer fabrication by proton bombardment

10 p1450 A72-24552

Schottky barrier crystal microwave video diodes design and fabrication to maximize burnout resistance and dynamic range for given detection sensitivity

10 p1450 A72-24553

GaAs abrupt junction IMPATT diode large signal operation analysis, noting oscillation efficiency HF fall-off characteristics

10 p1450 A72-24557

Electrical properties of Te/p-Si/N/ heterodiodes at room and liquid air temperatures

10 p1527 A72-24937

Si Pd-n-p/plus/ transit time diode microwave oscillator, discussing fabrication, FM noise spectrum and bias current fluctuation

11 p1604 A72-25748

Aluminum-silicon Schottky diode clamped transistor-transistor logic circuits parameters optimization for high switching speed and IC applications

11 p1606 A72-26568

Heterojunction p-GaAs-n-ZnSe diodes electrical and photovoltaic properties, showing space charge limited current effects

11 p1606 A72-26624

Fall time calculation and junction capacitance effect in diodes with nonuniform base doping switched off by voltage and current generators

11 p1607 A72-26963

P-n junction diodes fabricated by ion implantation doping, calculating I-V characteristics for comparison with measured breakdown voltages

12 p1789 A72-27312

Boron doped n-type Si planar diode and n-p-n epitaxial planar Si transistor junctions investigating hydrostatic pressure effects on static characteristics and breakdown voltage

12 p1789 A72-27314

Postdip heat treatment effects on thin film copper sulfide-cadmium sulfide junction solar cells spectral response, diode parameters and resistance

12 p1855 A72-28010

Laser light induced high-low impedance switch in Cd doped n-type Si diodes with p-p-n junctions and negative resistance

13 p1928 A72-28676

Forward voltage vs temperature characteristics for Si planar p-n junction diodes, determining zero temperature energy gaps for silicon, germanium and GaAs

13 p1933 A72-29824

Conversion efficiency and polarization behavior of Gunn diodes in resonant cavities, using I-V characteristics

13 p1937 A72-29866

N region capture centers effects on small signal impedance in p-n-n diode structure during passage of strong dc current

13 p1933 A72-29977

Schottky diode microwave down-converter conversion loss calculation as function of image terminal with consideration of barrier capacitance, series resistance and voltage drop

14 p2088 A72-30586

Nonlinear processes in oscillatory systems with semiconductor diodes, calculating amplitude and phase characteristics in steady state and transient conditions

14 p2090 A72-31133

Gallium aluminum arsenide light emitting diode thin structures grown on GaP substrates by liquid phase epitaxial method

15 p2290 A72-31381

IMPATT diode junction temperature effects on operation explained by small signal analysis

15 p2206 A72-31545

Microwave waveguide semiconductor modulator with p-n-n diode as control element, taking into account semiconductor control element conductivity change along waveguide wall

15 p2206 A72-31662

Room temperature GaAlAs single-heterojunction diode lasers structure, fabrication, threshold current density and quantum efficiency dependence on wavelength and temperature

15 p2247 A72-32032

Moderate power GaAs single heterojunction injection laser diodes fabrication and operation characteristics in pulsed mode at 250-400 K

15 p2247 A72-32033

GaAs laser properties determination by gallium arsenide-aluminum gallium arsenide double heterostructure junction diode laser, noting gain and loss at room temperature

15 p2250 A72-32519

Trapped charge effect on photovoltaic properties of copper sulfide-cadmium sulfide single crystal heterojunction in terms of tunneling by photocapacitance technique

15 p2294 A72-32520

Near junction doping characteristics of p-n GaP red emitting diodes by scanning electron microscope correlated with electrical and electroluminescent measurements

15 p2208 A72-32521

Coherent orange emission and bright electroluminescence from indium gallium phosphides vapor grown p-n junction laser diodes

15 p2251 A72-32532

Advances in LSI technology.

17 p2527 A72-34569

Application of the moving-slit X-ray automonochromatization method in structural studies of planar diodes and an attempt to correlate electrical properties with lattice defects.

17 p2595 A72-34749

Millimeter-wavelength frequency multipliers employing gallium arsenide diodes

17 p2529 A72-34851

Book - Semiconductor diode lasers

17 p2563 A72-35300

Frequency-modulation sensitivity and frequency-pushing factor of a Pd-n-p/+ punchthrough microwave diode.

18 p2667 A72-36686

Installation of a production line for high-reliability silicon diodes - Results obtained: Application of the underlying principles to more complex components

18 p2670 A72-37121

The use of semiconductor diodes to protect a radar receiver

18 p2663 A72-37217

High burnout gallium arsenide Schottky barrier diodes.

19 p2770 A72-37259

Experimentally observed admittance properties of the semiconductor-insulator-semiconductor /SIS/ diode.

19 p2772 A72-37568

Schottky diode frequency converter characteristics, considering series resistance, housing reactance, barrier layer capacitance, noise sources and noise temperature

19 p2773 A72-37937

Average energy to form electron-hole pairs in GaP diodes with alpha particles.

20 p2908 A72-39564

Digital p-i-n diode microwave drive amplifier design guidelines, discussing sharp switching pulses and short circuit protection features

20 p2904 A72-39734

High speed logic circuit interconnecting transmission line matching by nonlinear resistance, recommending use of Schottky diodes

20 p2909 A72-39737

Effects of impurities on gamma-irradiated silicon crystal examined by photovoltaic effect of p-n junction diode.

21 p3097 A72-40693

GaAsSb-AlGaAsSb double heterojunction lasers.

21 p3063 A72-40696

Observation on phenomena associated with a slowly varying surface barrier at niobium oxide and aluminum interface.

21 p3097 A72-40702

Influence of a magnetic field on the operation of an oscillator employing a two-base diode

21 p3032 A72-40791

Semiconductor diodes for microwave power control

21 p3033 A72-40939

Electrical fluctuations in ideal straight-staggered nondegenerate diodes

21 p3033 A72-40945

Thermal resistance of Gunn diodes - Analysis and measurement.

21 p3035 A72-41491

Design and frequency characteristics of cylindrical waveguide diode for microwave range, noting semiconductor junction effect on device efficiency

21 p3036 A72-41837

GaP /Zn-O/ diodes light emission efficiency increase by forward bias, relating to precipitation in n and p layers

22 p3159 A72-42613

Pulsed room temperature laser action of Si-doped double heterostructure GaAs p type diodes within 9100-9500 A wavelengths, discussing threshold current densities and power efficiency

22 p3186 A72-42621

Recent advances in diode and ferrite phaser technology for phased-array radars. I.

23 p3270 A72-43572

Interferometric measurement of the elongation of a pulsed diode laser.

23 p3297 A72-44185

JUNCTION TRANSISTORS

Large-signal IC equivalent circuit model for DC, linear and nonlinear transient time circuit analysis of lateral p-n-p transistors, including isolation junction interactions

01 p0044 A72-10126

Lateral photoelectric effect in junction FET under homogeneous illumination, detailing current-voltage characteristics

01 p0114 A72-10859

Static I-V characteristics and gain properties of lateral p-n-p transistors, using multijunction analysis

02 p0189 A72-11522

- Book on field effect electronics covering junction and insulated gate transistors and allied devices, monolithic and film IC and design techniques
03 p0333 A72-13846
- Matched Si junction FET under neutron burst and pulsed gamma radiation, investigating device parameters degradation
03 p0335 A72-14093
- Avalanche injected current relationship to emitter-base junction breakdown damage in planar n-p-n gated transistors
03 p0336 A72-14279
- Two section model of junction-gate field effect transistor with short channel length
04 p0498 A72-15134
- Si planar unijunction transistor fabrication, operation principles, parameter measurements and applications
05 p0635 A72-16196
- One dimensional bipolar junction transistor, comparing charge control and regional mathematical models for suitability in device and circuit computerized analysis and design
05 p0636 A72-16359
- One dimensional analysis computer program for junction device modeling, exemplifying hf bipolar transistor Fermi statistics effect and velocity limitation in high current density
06 p0779 A72-17478
- High temperature GaAs bipolar transistor n-p-n junction fabrication by vapor phase growth technique, considering I-V characteristics dependence on procedure
06 p0783 A72-17607
- Wide range bias dependence of planar bipolar transistor dc and small signal current gain, comparing analytical findings with Si junction experiment
06 p0783 A72-17608
- Semiconductor device physical behavior, discussing energy levels, impurity conduction, p-n junction capacitance and bipolar and unipolar transistor I-V characteristics
06 p0790 A72-18575
- Monolithic Si IC design and fabrication including resistors, capacitors, diodes, n-p-n, p-n-p, p-n-p-n and field effect transistors and inductors
06 p0791 A72-18576
- I-V characteristics of junction transistors with avalanche breakdown mechanism
07 p0958 A72-19895
- Junction and MOS FETs noise sources interaction with small signal model parameters and signal source admittance parameters, investigating amplifier If performance
08 p1141 A72-21428
- Multichannel junction gate FET /Gridstor/ for microwave power amplifier, discussing design, fabrication and performance
08 p1141 A72-21429
- Junction FET drain source capacitance theory based on two-region physical model, taking into account carrier drift velocity saturation effect
08 p1142 A72-21745
- Two dimensional dynamic model for background noise generation in bipolar transistors, using equivalent circuit
09 p1286 A72-23105
- Burst noise relationship to Si crystal dislocations and defects near emitter-base junction and surface zone in bipolar transistors
09 p1286 A72-23106
- Background noise in FETs with junction gate, formulating hypothesis of warm carriers for transistor channel
09 p1287 A72-23110
- Excess, shot and channel thermal noises performance-limiting effects on junction FETs in high input impedance applications, considering minimization method
09 p1287 A72-23111
- Ion implantation for varicaps and p-n-p bipolar transistors fabrication, examining implanted impurities profiles
10 p1449 A72-24285
- Junction transistor equivalent circuit small signal parameters determination at VHF and UHF
10 p1450 A72-24324
- Alloy p-n-p junction transistor diffusion capacity variation with emitter current as function of temperature at 80-320 K
10 p1451 A72-24558
- Width of space charge layer of reverse-biased p-n junction in p-n-p-n structure effect on current density, mobile charge carriers and constituent transistors gain coefficients
10 p1526 A72-24584
- Design analysis of emitter- and collector-base gain stabilized junction transistor amplifier at elevated temperatures using passive elements
11 p1606 A72-26569
- Schottky barrier gate FET design, device packaging and low noise characteristics
12 p1788 A72-27294
- IC lateral p-n-p multijunction transistor frequency characteristics analysis, noting parasitic effects, cutoff frequencies and power gain
12 p1788 A72-27311
- Nonlinear mathematical dc models of planar transistors for computerized IC design and analysis obtained by continuity equation approximate solution
12 p1789 A72-27313
- Boron doped n-type Si planar diode and n-p-n epitaxial planar Si transistor junctions investigating hydrostatic pressure effects on static characteristics and breakdown voltage
12 p1789 A72-27314
- Solid state array camera based on diffused junction phototransistors, discussing sensor technology and fabrication
12 p1810 A72-27931
- Nonequilibrium carrier distribution in drift junction transistor, considering base region hindering field effect on transit time, current gain cut-off and frequency response
13 p1926 A72-28371
- Relaxation oscillator synchronized by quartz crystal between emitter and base of unijunction transistor, obtaining sinusoidal output by series-connected RC load
13 p1926 A72-28377
- Quasi-linear approximation of input impedance of epitaxial n-type Si unijunction transistors for predominant drift conditions
13 p1927 A72-28406
- Fetron high voltage hybrid junction field effect (J-FET) devices for direct replacement of vacuum tubes in unchanged circuits
13 p1928 A72-28431
- Temperature dependent small signal operation of junction transistors at low supply voltage
13 p1930 A72-29058
- Distributed base resistance effect on stripline geometry transistor input characteristic, using equivalent circuit with pseudo-junction having high saturation current
13 p1930 A72-29059
- Metal-dielectric-semiconductor junction transistor HF response analysis by digital computer, deriving switching time as function of impurity concentration and electrode voltage
13 p1932 A72-29294
- P channel MOS transistors hardening against ionizing radiation based on positive space charge density and electrode injection efficiency
13 p2023 A72-29837
- Two dimensional numerical solution of semiconductor steady state transport equations, applying to MOS and bipolar transistors
14 p2142 A72-30847
- MOS junction transistor turn-off behavior calculation based on model with carrier source and drain for channel formation
15 p2207 A72-31891
- Three-dimensional small-signal analysis of bipolar transistors.
17 p2530 A72-35099
- Junction field-effect transistor circuits for prescribed output functions.
18 p2665 A72-36307
- The effects of electron bombardment on the noise properties of field effect transistors.
18 p2666 A72-36322
- Noise in bipolar junction transistors at low temperatures.
18 p2666 A72-36323
- Thermal effects in JFET and MOSFET devices at cryogenic temperatures.
18 p2666 A72-36453
- Temperature dependence of low-frequency excess noise in junction-gate FET's.
18 p2666 A72-36454
- Microwave power junction transistor design factors effects on long and short term reliability and MTBF
18 p2666 A72-36552
- Microwave junction transistor geometric design factors effect on reliability and performance, comparing overlay, interdigitated, mesh and inverse overlay structures
18 p2666 A72-36553
- Au alloys metallization system as alternative to aluminumizing for junction transistor reliability improvement, considering metal migration, microcracking and current leakage
18 p2666 A72-36554
- Mixing process at the emitter-base junction of a high-frequency transistor.
18 p2667 A72-36948
- Limitations in microelectronics. II - Bipolar technology.
18 p2667 A72-36980
- Behavior of epitaxial bipolar transistors in the strong injection regime
18 p2668 A72-37103
- Low noise high power bipolar and field effect transistors monolithic integration potentials for microwave applications
19 p2771 A72-37261
- Effect of temperature on the base resistance and the noise factor of a bipolar junction transistor.
19 p2773 A72-37848
- Boron p-type region impurity concentration calculation technique to establish anomalous base profile in n-p-n bipolar transistors
20 p2908 A72-39567
- Voltage controlled miniaturized n-type negative resistance circuit based on junction transistor and FET without internal bias
21 p3038 A72-40998
- Parameters and properties of special avalanche transistors
21 p3035 A72-41809
- Final stages of transistorized sweep generators
22 p3158 A72-42114
- The relative merits of thyristors and power transistors for fast power-switching applications.
22 p3159 A72-42306
- Influence of polycrystallinity on transconductance of thin-film transistor.
22 p3159 A72-42309
- P-n-p and p-n-p-n transistors and thyristors with lateral structure geometry, discussing operational characteristics and effects of structural modification on semiconductor parameters
23 p3271 A72-43835
- Excitation of oscillations in transistor oscillators
23 p3271 A72-43840
- Digital parallel correlator with LSI single-chip bipolar transistor construction, discussing triple diffusion process for n-p-n and p-n-p junctions
23 p3273 A72-44453
- The field-effect modified transistor - A high-responsivity photosensor.
23 p3273 A72-44455
- JUNCTIONS**
Waveguide model for calculating microstrip discontinuities and T-junctions wave impedances, using orthogonal series procedure
15 p2201 A72-32470
- Nonequilibrium phenomena in electron tunneling in normal metal-insulator-metal junctions.
21 p3096 A72-40343
- JUPITER [PLANET]**
Io modulation of Jupiter decametric emissions, using cyclotron magnetosphere model and coupling by whistler mode electromagnetic waves
01 p0125 A72-10084
- Review of papers on planetology given at Brighton symposium, covering moon, Venus, Mars and Jupiter.
01 p0132 A72-11071
- Jupiter outer satellite origin, considering capture orbit dimensions based on three body elliptical problem
02 p0275 A72-11594
- Jupiter decameter radio burst possibility as indicator of high velocity fluxes and shock waves in solar wind
02 p0273 A72-11935
- Grating spectra of Jupiter North Equatorial Belt, noting absorption feature at 4.73 microns
02 p0280 A72-12206
- Jovian disk brightness distribution at zero phase angle by expanding scattering indicatrix in Legendre polynomial series
02 p0282 A72-12329
- Rotation production in giant planets by gaseous impact, discussing Jupiter and Saturn formation
02 p0282 A72-12331
- Jupiter mass from motion of /76/ Freia, plotting residuals in right ascension and declination
02 p0286 A72-12893
- Giant planets internal constitution models, discussing Jupiter visual magnitude variability, Saturn ring system, cold matter equations of state and He abundances
03 p0418 A72-13111
- Jupiter decametric radio emission relation to solar wind, geomagnetic activity and shock waves causing Forbush decreases
03 p0436 A72-13820
- Orbit distributions of hypothetical comets from Jovian surface eruptions, calculating orbital elements with computer
03 p0439 A72-14240
- Comet orbits with perihelion distances and inclinations from Jupiter, calculating osculating orbital elements and distributions
03 p0439 A72-14241
- Jupiter outer satellite group formation theory, suggesting asteroid-larger satellite collision
04 p0569 A72-14496
- Jupiter equatorial radius and oblateness at atmospheric level from timings of 13-14 May 1971 occultations of beta Scorpi
04 p0571 A72-14615
- Jupiter-induced perturbations in orbital elements of Calisto artificial satellite, noting correction requirement due to Jupiter polar flattening
04 p0572 A72-14634
- Jupiter mass correction from minor planets /153/ Hilda, /279/ Thule and /334/ Chicago observations
04 p0576 A72-15036

Jovian decametric radiation observations, showing satellite Io relative position correlated to highest frequency

04 p0581 A72-15515

X ray detection on Jupiter with actively collimated balloonborne scintillation counter, noting decametric emission due to electron precipitation

06 p0872 A72-17445

Jupiter mass from discrete time observations of J1X satellite positions and velocities, using sequential Kalman-Bucy filter

06 p0876 A72-17580

Near resonance due to commensurability between Jupiter-Saturn mean motions, discussing effect on planetary system secular disturbing function

06 p0877 A72-17659

Radiation polarization from Jovian disk center as function of phase angle from polarimetric observations

06 p0884 A72-18033

Astronomical model for Jovian decametric radio emission control by Io satellite based on two surface sources on planet and particle interaction with plasma

06 p0891 A72-18504

Maximum cut-off frequency of Io controlled Jovian decametric radiation as function of lambda coordinates

07 p1059 A72-19599

Jupiter investigation by Pioneer F and G after asteroid belt traversal, discussing Jovian physical characteristics, spacecraft systems and experiments

08 p1230 A72-20979

UV absorption levels in different areas of Jupiter disk from spectrophotometric studies at 3300-4800 Å, noting temporal variations in reflectance

08 p1237 A72-21828

Photoelectric measurements of brightness of Galilean satellites of Jupiter as function of solar phase angle

08 p1238 A72-21831

Jupiter evolution from summer 1969 to autumn 1970, noting north equatorial and south temperate bands and Red Spot intensity and surroundings

08 p1239 A72-21925

Venus, Mars, Jupiter and Saturn UV spectra from OAO-2 objective grating spectrophotometry, obtaining planetary albedos from G-type stars observations

09 p1382 A72-22288

Book on perturbation theory in celestial mechanics, covering absolute perturbation, Hill lunar theory and application to Jupiter satellites

09 p1389 A72-23247

Jacobi integrals in restricted three body problem of small bodies with massive sun and Jupiter in solar system

09 p1389 A72-23394

Narrow band frequency drifts of polarized Jovian L bursts from simultaneous radio observations

10 p1532 A72-23713

Negative search for post eclipse brightening of Io and Europa satellites in 1970 based on single beam photometric observation

10 p1532 A72-23714

Short period comets origin and orbital evolution, discussing Jupiter perturbations and statistical study

10 p1536 A72-24143

Jupiter polar caps, Red Spot and equatorial belts visual observations during 1970 opposition

10 p1542 A72-24570

Photoelectric observation of beta Scorpii occultation by Jovian satellite Io, noting Fresnel diffraction effects

10 p1548 A72-24969

Occultation of beta Scorpii by Jupiter and Io to determine Jovian equatorial radius and oblateness

10 p1548 A72-24970

Radiation polarization from Jovian disk center as function of phase angle from polarimetric observations

11 p1719 A72-25969

Flash symmetry observed during fading and brightening of beta Scorpii A in occultation by Jupiter

12 p1868 A72-27297

Jupiter, Saturn, Uranus, Neptune and Pluto state of knowledge, noting angular momentum fraction, red spot, albedos, densities, atmospheric compositions, natural satellites, etc

12 p1870 A72-27345

Three station interferometer observations of Jovian decametric burst at 18 MHz, discussing possible solar wind interference

12 p1871 A72-27743

Jupiter and Saturn gravitational moments from available models, taking into account rotation, density and radius

12 p1871 A72-27744

Jupiter occultations of multiple star beta Scorpii and Io close approach to beta sub 2 Sco

12 p1871 A72-27757

Jovian disk brightness distribution at zero phase angle by expanding scattering indicatrix in Legendre polynomial series

13 p2039 A72-29213

Rotation production in giant planets by gaseous impact, discussing Jupiter and Saturn formation

13 p2039 A72-29215

Jupiter decimeter radio bursts as indicator of high velocity fluxes and shock waves in solar wind

13 p2030 A72-29247

Titan and Galilean satellites effective temperatures from broadband observations, suggesting low surface emissivity or high opacity for Titan

13 p2041 A72-29417

Jupiter electropolarimetric observations, showing polar regions polarization dependence on phase angle

13 p2050 A72-30069

Trajectory analysis for swingby technique using Jovian gravitational field for leaving ecliptic plane along heliocentric orbit and for solar flyby at specified distance

14 p2150 A72-30452

Monochromatic brightness coefficient measurements for Jupiter and Saturn disk centers and Uranus geometric albedo

14 p2152 A72-30491

Jupiter decametric radiation modulation by photoelectron emission by satellite Io, describing future probe experimental test

14 p2156 A72-30558

Comets formation from Jupiter satellite Io surface eruption using particle trajectory analysis and comet orbital elements calculation

15 p2305 A72-31391

Jovian synchrotron emission measurements by radioheliograph at 80 MHz, passing square law detector outputs through RC integrators

15 p2307 A72-31799

Callisto radio emission analysis by ice body model, noting brightness temperature calculation of ice surface

15 p2308 A72-31904

Solar activity long term effects on Jupiter cloud structure rotational periods, using Chree superposition analysis

15 p2308 A72-31930

Secular and long term periodic perturbation effects of third body upon particle motion in three body problem, discussing mass motion in Jovian gravitational field

15 p2312 A72-32120

Planetary atmospheres and interiors in terms of dynamics, rotation, magnetic fields, Jupiter features, geomagnetism, earth baroclinic waves, global circulation and gravitation, etc

16 p2384 A72-33339

Io effects on Jupiter decametric radio bursts, discussing ionosphere vs solid surface for required conductivity

16 p2455 A72-33465

The plasma physics of the Jovian decameter radiation.

17 p2605 A72-34539

Occultations of stars by Jupiter

17 p2607 A72-34751

A revision of Jupiter brightness temperatures in the frequency interval 18.5-24.0 GHz/1968/.

17 p2610 A72-35119

Strong beaming of Jupiter's non-Io-related radio emission.

17 p2610 A72-35224

Sheath effects and related charged-particle acceleration by Jupiter's satellite Io.

17 p2611 A72-35320

Influence of the Galilean Jovian satellites on the motion of an artificial satellite of Callisto

17 p2618 A72-35811

Secular variations of the first order of elements for the four major planets - Comparison with Le Verrier and Gaillot

18 p2727 A72-36734

Gravitational fields of Jupiter and Saturn

19 p2857 A72-37734

Occultation of beta Scorpii by Jupiter on May 13, 1971.

19 p2859 A72-37890

Determination of major planet coordinates by an expeditionary astrograph

19 p2861 A72-37986

Gas-liquid hydrogen mixture and helium adiabatic model of Jupiter temperature and pressure distribution, estimating planet center temperature

19 p2863 A72-38074

Measurement of Jovian radio emission at a wavelength of 2.94 m

19 p2864 A72-38080

Monochromatic brightness coefficient measurements for Jupiter and Saturn disk centers and Uranus geometric albedo

19 p2864 A72-38320

Electrodynamic effects of Jupiter's satellite Io.

21 p3104 A72-40483

Statistical mechanics of light elements at high pressure. II - Hydrogen and helium alloys.

21 p3106 A72-41044

Jupiter - New evidence of long-term variations of its decimeter flux density.

21 p3107 A72-41274

Cometary parent bodies transfer to short period orbits by Jupiter caused gravitational disturbances, noting qualitative analysis of orbits evolution

22 p3219 A72-41913

Photometric characteristics of Jupiter and Saturn at wavelengths between 0.48 to 0.33 micron

22 p3219 A72-41915

Jupiter surface maps for 1965-70 from drawings obtained with astrograph, noting high activity and eruptive changes after 1961-63 outburst

22 p3220 A72-41920

Jupiter surface maps from synoptic observations with refracting telescope, considering white cloud formations and atmosphere motions

22 p3220 A72-41921

The role of eruptive centers of the atmosphere of Jupiter in the determination of the rotation velocity of the core

23 p3336 A72-43548

Structure of Jupiter's decametric radio sources - Two-dimensional probability and flux studies, 1957-1970.

24 p3436 A72-44691

The determination of the diameter of Io from its occultation of beta Scorpii C on May 14, 1971.

24 p3436 A72-44700

Observation of the occultation of beta Sco C by Io.

24 p3436 A72-44702

Upper limits for an atmosphere on Io.

24 p3436 A72-44703

Mariner spacecraft Jupiter-Saturn 1977 gravity assisted flyby, discussing mission objectives and trajectory options

24 p3444 A72-45438

JUPITER ATMOSPHERE

Jupiter atmospheric hydrogen-helium mixing ratio from binary star beta Sco occultation by planet in May 1971

03 p0416 A72-13009

Jupiter and Venus cloudy atmosphere reflected sunlight circular polarization measurement, noting sense variations with phase angle and location on disk

03 p0439 A72-14150

Laboratory simulation of Jovian atmospheric reactions, observing amino nitriles formation

04 p0572 A72-14764

Polymer fractionation in simulated Jovian atmosphere according to molecular weight, suggesting substance responsible for red color

04 p0572 A72-14773

Extraterrestrial life on Mars and Venus and Jupiter atmospheres, discussing abiogenesis failures on life-supportable planets

04 p0471 A72-14805

Jovian atmosphere and clouds explained by physico-chemical and meteorological data, discussing cloud motions, colors and Great Red Spot

04 p0580 A72-15363

Jupiter atmosphere chemical and photochemical analysis, using solar-composition adiabatic equilibrium model for coloration, electric discharge and UV irradiation studies

05 p0714 A72-16132

Photoelectric spectrophotometric measurements of Jupiter atmosphere optical properties and structure, showing methane absorption band intensity latitudinal variations

06 p0881 A72-17928

Jovian atmosphere effect on photometric observations of beta Sco C occultation by Jupiter on 13 May 1971

06 p0886 A72-18153

Jovian belts, zones, great red spot, white ovals and atmospheric rotation and circulation from methane photographs analysis, comparing to earth atmosphere

06 p0889 A72-18331

Jovian atmospheric absorption coefficient at 6-14 microns as function of frequency from hydrogen, methane and ammonia contributions

07 p1069 A72-19078

Mars, Venus and Jupiter atmosphere composition and structure from spectral analysis, discussing equilibrium temperature, radiative heat transfer, integrated density and adiabatic temperature gradient

07 p1073 A72-19353

Circulation mechanics of gaseous atmospheres with zonal symmetry in motions and other properties, applying to Jupiter atmosphere

07 p1083 A72-20453

Hydrogen and helium thermal dissociation and ionization at Jupiter and Saturn adiabatic atmospheric models conditions

08 p1211 A72-21127

Thermodynamic properties of atomic hydrogen-helium plasma for postulated conditions present in stagnation shock layer of spacecraft entering Jupiter atmosphere

08 p1254 A72-21598

Planetary atmospheres composition diversity, discussing evolution of Mars, Venus, earth and Jupiter from primitive solar nebula

08 p1119 A72-22012

Jupiter atmosphere thermospheric temperature profile from heat conduction equation, noting radiative and convective transfer

09 p1393 A72-23658

- Atmospheric vertical shear at visible cloud level in Jupiter equatorial zone from blue and red wavelength photographs 10 p1531 A72-23712
- Jupiter spectral observations, discussing presence of deuterated methane in atmosphere and comparison with solar spectra for telluric features identification 10 p1539 A72-24347
- Beta Scorpil occultation by Jupiter, obtaining light curves, atmospheric scale height and stratification 10 p1548 A72-24968
- IR spectrophotometric data for Jupiter, determining limb darkening nature and ammonia and methane absorption variations over belts, zones and Red spot 10 p1548 A72-24971
- IR observation and theoretical considerations for Jupiter atmosphere inhomogeneous model with two cloud layers [AD-742156] 11 p1721 A72-26119
- Jupiter, Saturn and earth atmospheric circulation seasonal variation data analogies, noting factors governing planetary atmospheric circulation 13 p2048 A72-29813
- Jupiter and Saturn atmosphere composition, structure and radiative properties, presenting two zone stratosphere-troposphere model 14 p2161 A72-31072
- Environmental chamber simulation to show terrestrial microorganisms survival under Jovian atmospheric conditions 15 p2183 A72-31293
- Spacecraft bacteria population resistance to simulated Jovian trapped radiation belt electrons and solar wind protons, noting dependence on isolate, dose and electron energy 15 p2186 A72-31993
- Chemical and spectroscopic activity of germanium tetrahydride in Jovian atmosphere in 4.7 micron window 15 p2312 A72-32094
- Jupiter cloud models, observational characteristics and temperature error at 5 micron wavelength 15 p2312 A72-32095
- Jupiter atmospheric greenhouse effect modeled by two layer emission, deriving temperatures from non-gray step function approximation of IR absorption 15 p2312 A72-32096
- Solar wind velocity near Jupiter correlated to Io geocentric phase during radio bursts, noting plasma-sphere models 16 p2459 A72-33904
- Band model and scaling approximation validity for computation of transmission profile in V4 band of methane in Jovian atmosphere 16 p2461 A72-34099
- Temperature sounding experiments for the Jovian planets. 18 p2726 A72-36641
- Photoelectric spectrophotometric measurements of Jupiter atmosphere optical properties and structure, showing methane absorption band intensity latitudinal variations 18 p2730 A72-37153
- Survival of common terrestrial microorganisms under simulated Jovian conditions. 19 p2755 A72-37721
- Extensive air showers and the sporadic decimeter radio emission of Jupiter 19 p2863 A72-38073
- Scientific problem resolution during Jupiter missions, discussing Pioneer probes, trapped particle belts, Red Spot, atmosphere, biological activity, internal heat sources and radio emission 19 p2864 A72-38381
- Jupiter atmosphere methane deuterium/hydrogen ratio estimate from exchange reaction and temperature studies 20 p2968 A72-39242
- Shapes and widths of ammonia lines collision-broadened by hydrogen. 21 p3013 A72-40817
- Jupiter atmospheric C12/C13 ratio for methane from equivalent width measurements in R[2] multiplet 21 p3107 A72-41273
- Optical properties and structure of the Jovian atmosphere. V - Probable structure of the ammonium aerosol layer 22 p3219 A72-41914
- Jupiter surface maps from synoptic observations with refracting telescope, considering white cloud formations and atmospheric motions 22 p3220 A72-41921
- Limits to energetic proton fluxes trapped in Jupiter's magnetosphere. 22 p3221 A72-42021
- Taylor instability in the shock layer on a Jovian atmosphere entry probe. 22 p3136 A72-42873
- The role of eruptive centers of the atmosphere of Jupiter in the determination of the rotation velocity of the core 23 p3336 A72-43548
- The physical properties of the Jovian atmosphere inferred from eclipses of the Galilean satellites. II - 1971 apparition. 24 p3435 A72-44689
- The occultation of beta Sco by Jupiter. 24 p3436 A72-44699
- JUPITER PROBES**
- Environmental analysis of gas particle/probe aeroshell interaction in rarefied flow of high altitude Jupiter entry [AIAA PAPER 72-203] 05 p0721 A72-16844
- Jupiter investigation by Pioneer F and G after asteroid belt traversal, discussing Jovian physical characteristics, spacecraft systems and experiments 08 p1230 A72-20979
- Pioneer 10 probe survival hazards during passage through asteroids belt and intense Jupiter radiation fields 10 p1551 A72-24272
- Scientific problem resolution during Jupiter missions, discussing Pioneer probes, trapped particle belts, Red Spot, atmosphere, biological activity, internal heat sources and radio emission 19 p2864 A72-38381
- Spacecraft and missions for Jupiter exploration, discussing launch vehicle requirements, solar electric propulsion for midcourse correction, Pioneer flyby and orbiter missions, TOPS mission, etc 21 p3103 A72-40457
- Attitude perturbations of a spinning Jupiter Orbiter spacecraft. [AIAA PAPER 72-920] 21 p3115 A72-41565
- Spacecraft navigation systems for Mariner Jupiter-Saturn 1977 Project, considering maneuvers, orbit determination and data requirements [AIAA PAPER 72-926] 24 p3423 A72-45432
- JUPITER RED SPOT**
- Polymer fractionation in simulated Jovian atmosphere according to molecular weight, suggesting substance responsible for red color 04 p0572 A72-14773
- Jovian atmosphere and clouds explained by physico-chemical and meteorological data, discussing cloud motions, colors and Great Red Spot 04 p0580 A72-15363
- Jupiter Red Spot 1968-1970 isodensity maps, deriving east-west and north-south photometric profiles for asymmetries 05 p0712 A72-15766
- Jovian belts, zones, great red spot, white ovals and atmospheric rotation and circulation from methane photographs analysis, comparing to earth atmosphere 06 p0889 A72-18331
- Jupiter evolution from summer 1969 to autumn 1970, noting north equatorial and south temperate bands and Red Spot intensity and surroundings 08 p1239 A72-21925
- Jupiter polar caps, Red Spot and equatorial belts visual observations during 1970 opposition 10 p1542 A72-24570
- IR spectrophotometric data for Jupiter, determining limb darkening nature and ammonia and methane absorption variations over belts, zones and Red spot 10 p1548 A72-24971
- Jupiter Red Spot position determinations by East German observers tabulated 16 p2456 A72-33496
- Jupiter - Its Red Spot and disturbances in 1970-1971. 24 p3435 A72-44690
- K**
- K BAND**
- U EXTREMELY HIGH FREQUENCIES**
- K LINES**
- Photoelectric measurements of Ca K line of southern/equatorial A stars, discussing abundance variation 05 p0712 A72-15796
- Photoelectric photometry of Ca K-line for A stars of population I clusters 05 p0712 A72-15797
- Intensity variations of CN photospheric and K line chromospheric network with time 05 p0718 A72-16505
- High dispersion spectroscopic study of H alpha and K lines profile and velocity structure in quiescent prominences 05 p0719 A72-16516
- Red shift determination for two galaxies near PSK 2251 plus 11 quasar from Ca II H and K absorption line measurements 06 p0881 A72-17898
- Chemical bond effect on K emission spectrum of oxygen and fluorine 09 p1275 A72-22522
- Multiconfigurational interactions in atoms with incomplete electron shells, identifying K-alpha satellite emission lines 09 p1357 A72-22837
- Fluorescent X ray spectroscopy for K and L emission band structures of Mg, Al and V and metal compounds 09 p1370 A72-22839
- X ray emission bands related to K line intensity for iron group transition metals, using orthogonalized plane wave method 09 p1370 A72-22840
- Ca II K line profiles in front of distant OB stars, using pressure scanned Fabry-Perot interferometer and coude spectrograph 10 p1542 A72-24616
- Interferometric photoelectric scans of interstellar Ca K lines in stellar spectra, noting interstellar Na lines presence 10 p1544 A72-24663
- X ray spectral analysis of Ti-Mo system alloys, investigating K and L lines and electronic structure 13 p1972 A72-28491
- K line of X ray absorption spectra for pure Ti and compounds, discussing effects of valence, microstructure and electron configuration 15 p2259 A72-32700
- K and L lines of X ray emission spectra of Ti in alloys with Nb, noting atomic structure change during alloy formation 15 p2259 A72-32701
- Temporal properties of Ca II K line profile in solar disk nonmagnetic regions, noting time sequences of spectrograms and spectroheliograms 15 p2317 A72-32773
- Quiescent solar prominences internal motions from fine structure wavelength shift observations in Ca II K line spectra 15 p2318 A72-32780
- H and K emission intensity and line width dependence on stars age and luminosity, discussing dwarf stars and giants 19 p2866 A72-38503
- Characteristics of the Ca II K-line profiles in the quiet sun. 21 p3108 A72-41280
- Nonvelocity origin of excess red shift in companion galaxies from observation of H and K absorption lines of Ca II 22 p3220 A72-41962
- High resolution spectroscopy of the disk chromosphere. II - Time sequence observations of Ca II H and K emissions. 22 p3221 A72-42032
- KA BAND**
- U EXTREMELY HIGH FREQUENCIES**
- KALMAN FILTERS**
- On discrete-time Kalman filter in singular case and a kind of pseudo-inverse of a matrix. 18 p2672 A72-36059
- Extended Kalman filter application to delayed systems for state and time delay estimation, discussing two nonlinear estimators 21 p3039 A72-41553
- A design procedure for intermediate-order observer-estimators for linear discrete-time dynamical systems. 22 p3161 A72-41994
- Measurement system decomposition for aerodynamic coefficient estimation. [AIAA PAPER 72-964] 22 p3177 A72-42345
- Development and performance analysis of a trajectory estimator for an entry through the Martian atmosphere. [AIAA PAPER 72-953] 22 p3224 A72-42352
- On application of Kalman filtering technique to on-line orbit estimation of a launching vehicle. 22 p3203 A72-43142
- The application of Monte Carlo methods to the nonlinear filtering problem. 23 p3274 A72-43541
- Adaptive filtering algorithms for Kalman filter optimal gain estimation, discussing Bayesian, maximum likelihood, correlation and covariance matching methods relationship 23 p3274 A72-43542
- Kalman filter design considerations for space-stable inertial navigation systems. 24 p3421 A72-44640
- The application of error control techniques in the design of an advanced augmented inertial surveying system. 24 p3421 A72-44641
- Integrated navigation systems and Kalman filtering - A perspective. 24 p3386 A72-44642
- Application of advanced filtering methods to the determination of the interplanetary orbit of Mariner '71. [AIAA PAPER 72-906] 24 p3443 A72-45427
- KALMAN-SCHMIDT FILTERING**
- Kalman and linear numerical filtering, discussing data processing from wind tunnel and rocket flight tests 06 p0774 A72-17847

KAOLINITE

Preferential polymerization and adsorption of L-optical isomers of amino acids on kaolinite, indicating role in prebiotic protein origin

03 p0321 A72-13743

KAPTON [TRADEMARK]

Photoemission from polyethylene, Kapton, Teflon and polyvinyl chloride under photon irradiation

03 p0403 A72-14084

KARHUNEN-LOEVE EXPANSION

Performance criteria for transform data coding schemes evaluation under computational constraints, presenting numerical examples for Fourier, Walsh, Haar and Karhunen-Loeve transforms

16 p2366 A72-33214

KARL FISCHER REAGENT

Free and dissolved water contents determination in light petroleum products by modified Karl Fischer method using ethylene glycol solvent mixture

05 p0702 A72-16669

KARMAN VORTEX STREET

Turbulent flow field velocity fluctuations errors by hot-wire anemometer filaments vibrations from fluctuating aerodynamic loads in Karman vortex street

05 p0664 A72-17013

Reynolds number and cylindrical spacing effect on Karman vortex street formation from smoke visualizations of single and tandem cylinder wakes

09 p1261 A72-22939

A wind-tunnel experiment concerning atmospheric vortex streets.

20 p2948 A72-39796

Karman vortex street in a uniform shear flow.

21 p2992 A72-41247

The vortex street in the wake of a vibrating cylinder.

23 p3281 A72-44302

KELVIN TEMPERATURE SCALE

U TEMPERATURE SCALES

KEPLER LAWS

Satellite in eccentric Keplerian orbit transgressing Roche limit about rigid sphere, considering time dependent evolution problem with various centrifugal and tidal forces

01 p0134 A72-11145

General perturbations theory for canonical systems extended to noncanonical systems, applying to perturbed Kepler motion

04 p0573 A72-14875

Soviet book on geometrical space geodesy covering satellite observation, Keplerian laws, two body problem and orbit element determination

06 p0879 A72-17817

Secular perturbations of artificial earth satellites Keplerian orbital elements from arbitrary-order zonal harmonics in geopotential series expansion

07 p1078 A72-19982

Post-Newtonian approximation for calculation of energy and angular momentum radiated in form of gravitational waves by two point particles system, noting masses in hyperbolic Kepler orbit

10 p1547 A72-24933

Electromagnetic radiation frequency spectrum and mean power from accelerated magnetic dipoles in circular and Keplerian orbits, noting implications for pulsars

16 p2453 A72-33285

Interaction between attitude libration and orbital motion of a rigid body in a near Keplerian orbit of low eccentricity.

20 p2968 A72-39197

Numerical stabilization of the differential equations of Keplerian motion.

21 p3106 A72-41050

Interactions between stars and local dust formations

21 p3113 A72-41758

Transcendental equations solution for satellite Kepler orbit determination from coordinates, velocity and time components, using Lambert-Euler relation

22 p3223 A72-42204

Kepler second law based moment of gyration concept application to spacecraft and missiles mechanics and kinematics, proposing Skylab weightless environment experiment for validation

23 p3342 A72-43471

Spinor differential equation of generalized unperturbed Kepler motion, using motor method and Lie algebra

24 p3442 A72-45238

KERNEL FUNCTIONS

High temperature nongray kernel functions application to radiative heat transfer for bounded hydrogen plasma

01 p0145 A72-10100

Convolution type integral equations over arbitrary finite segment number with kernels, showing solvability in spaces, applications and correctness

02 p0294 A72-12430

Airfoil theory singular integrodifferential equation reduction to integral equations with quasi-regular and regular kernels, applying to jet flapped wing problem

03 p0381 A72-12987

Gaussian periodic data optimal smoothing, describing convolution kernel and computer program

03 p0381 A72-13200

Thin wing harmonic oscillation in subsonic flow, developing analytical form of kernel function in generalized Possio integral equation

05 p0603 A72-16707

Numerical solution of integral equations with singular and weakly singular kernels by weighted residuals method

07 p1025 A72-18781

Hyperstability conditions generalization for model reference adaptive systems, using positive definite kernels properties

09 p1290 A72-23098

Finite range Fredholm integral equations with band limited displacement kernels in terms of prolate spheroidal wave functions

10 p1506 A72-24460

Antisymmetric pseudorandom signal performance in measurement of second order kernels in Volterra series representation of nonlinear system by cross correlation

10 p1439 A72-24805

Direct and inverse problems of scattering theory for hyperbolic system of equations on plane, emphasizing unsteady approach and integral equation class with kernels

13 p2004 A72-29468

Gas surface interactions models, computing scattering kernels by reduction to boundary value problem

14 p2134 A72-30880

Heat equation kernel functions existence proof based on Harnack selection principle and inequality

16 p2476 A72-33187

Solar radiation anisotropic nonconservative scattering in seminfinitesimal atmosphere, calculating plane and spherical albedo by exponential kernel approximation

16 p2446 A72-33463

Quantum Boltzmann equation for a laser.

17 p2563 A72-35160

Structure, analysis and synthesis of time series models, discussing kernel Hilbert space, spectral estimation, moving averages, identification, etc

18 p2678 A72-36023

The numerical solution of Fredholm integral equations of the second kind with singular kernels.

18 p2705 A72-36603

Approximate solution, in generalized functions, to integral and integrodifferential equations with difference kernels

22 p3198 A72-42145

Approximate optimal control solution to boundary value problem for one dimensional heat conduction equation, using Fredholm linear integral and degenerate kernels

23 p3274 A72-43526

Power law behavior of autocorrelation and memory functions of statistical mechanics as t approaches infinity

23 p3309 A72-43870

A power-law model for the multiple-integral theory of non-linear viscoelasticity.

24 p3460 A72-45696

KEROSENE

Antismoking kerosene fuels for aircraft crash fires reduction

07 p1050 A72-18837

Nitrogen oxide emission characteristics of experimental compact combustors with kerosene type fuel, showing dependence on primary zone temperature and air-fuel ratio

[ASME PAPER 72-GT-108]

11 p1705 A72-25672

Multicomponent system combustion of Al suspensions in kerosene, determining ignition temperature as function of metal particle size and concentration

16 p2476 A72-33256

KERR CELLS

Ultrahigh speed electro-optical cameras with exposure times of several picoseconds, using biplanar image converter, electron multiplier and Kerr cell

06 p0812 A72-17415

High speed photography in high temperature short duration plasmas, using Kerr cell, image converter, framing and streak cameras

06 p0813 A72-17435

KERR EFFECTS

Q switched high power laser pulse compression based on optical polarization change on passing through Kerr-active medium

07 p1000 A72-19038

Microwaves interaction with ultrashort laser pulse generated traveling refractive index changes in liquids with orientational Kerr effect

15 p2252 A72-32652

Orientational Kerr effect direct observation via birefringence relaxation time measurement in self focusing region of mode locked Q switched laser picosecond pulses

17 p2561 A72-34190

Magnetic materials.

17 p2595 A72-34571

High energy particle and photon orbital and vortical motions in Kerr metric outside equatorial plane in gravitational field

20 p2953 A72-39341

KERR ELECTROOPTICAL EFFECT

Light beam time stationary multifocal structure in medium with Kerr type nonlinearity, relating maximum energy density and absorption coefficients

07 p0944 A72-19635

Optical Kerr constant measurement in liquid phosphoryl chloride and toluene and glasses, noting nonlinear refractivity

12 p1823 A72-27756

Transient high voltage and electric field measurement with electro-optical fringe pattern method employing pulsed laser Kerr system polarimeter

15 p2240 A72-32434

Passive mode-locking and Q-switching of high power lasers by means of the optical Kerr effect.

19 p2811 A72-37844

Influence of steric effects and compressibility on nonlinear response to laser pulses and the diameters of self-trapped filaments.

23 p3296 A72-43873

Light beam time stationary multifocal structure in medium with Kerr type nonlinearity, relating maximum energy density and absorption coefficients

24 p3408 A72-44567

KERR MAGNETOOPTICAL EFFECT

Polarimeter for recording of magnetooptical rotation dispersion and Kerr equatorial effect in visible, near UV and near IR spectral ranges

22 p3176 A72-42108

KETONES

NT ACETONE

NT ACETYLACETONE

NT NEMBUTAL [TRADEMARK]

Cation polymerization of beta-propiolactone without initial kinetics dependence on monomers concentration, relating acyl ion bonding and electron donor groups

09 p1275 A72-22496

Ti-Al-V foil stress corrosion methanol cracking resistance improved by treatment with pentanedione, suggesting metal ions removal from protective film

15 p2253 A72-31297

KEYING

NT FREQUENCY SHIFT KEYING

NT PHASE SHIFT KEYING

Optimum performance typewriter keyboard design, discussing biomechanical improvements in finger positioning facilitation, operator postural muscular strain reduction, etc

[AD-740259]

10 p1433 A72-25114

KIDNEY DISEASES

Renin in differential diagnosis of hypertension.

19 p2757 A72-38144

KIDNEYS

Hypoxia effect on kidney blood flow erythropoietic properties in rabbits, noting inhibiting effect on erythroblast cells mitotic activity in bone marrow culture

06 p0765 A72-18061

Aortic constriction and release effects on kidney glomerulotubular balance in saline- and water-loaded dogs, studying sodium reabsorption changes

08 p1115 A72-21084

Morphological changes in the lungs and kidneys during prolonged intoxication of the organism by carbon tetrachloride

19 p2760 A72-38035

The effect of space flight conditions and prolonged hypokinesia on the kidney function in man

22 p3149 A72-42068

Hypoxic acclimation effects on rats heart, liver and kidney mitochondria, measuring cytochrome oxidase and succinic dehydrogenase activities

22 p3144 A72-42673

Intracellular potassium in cells of the distal tubule.

24 p3373 A72-45231

KIMBERLITE

U BIOTITE

U PERIDOTITE

KINEMATIC EQUATIONS

Kharlamov kinematic equations application to gyrostat motion problem, deriving angular velocity hodograph

08 p1207 A72-21350

Dynamic and kinematic equations of attitude and translational motions of symmetric rigid body under body fixed force

09 p1351 A72-22991

Dynamic equations integration with constraint factors, discussing Hamilton-Jacobi method applicability conditions

13 p2003 A72-28724

Kinematic equations derivation for traveling displacements field in Cosserat continuum by Lagrange formalism, noting analogy with Maxwell equations

15 p2274 A72-31474

Kinematic equations of motion for elastic shaft with circular plane under external forces and moments, noting transverse and torsional vibrations

16 p2469 A72-33250

On the state of the geomagnetic field and its reversals.

17 p2548 A72-35323

- Kinetic and kinematic equations for inviscid unsteady gas flow, noting pseudostationary vortex geometry 17 p2541 A72-35436
- On the intrinsic representation of flows with Lamb surfaces. 18 p2684 A72-37085
- A kinematic theory of large magnetic Reynolds number dynamos. 19 p2833 A72-37248
- Lagrangian approach to kinematic-dynamo equations for astrophysical bodies, obtaining variational principle for eigenvalue computation 20 p2966 A72-38911
- The Nyquist criterion for kinematic-dynamo action. 20 p2956 A72-38912

KINEMATICS

NT BODY KINEMATICS

- Small amplitude velocity waves turbulent distribution in infinite medium, demonstrating kinematic dynamo regeneration 04 p0573 A72-14906
- Geomagnetic dipole field kinematic reversals due to cyclonic convective cell distribution fluctuations in earth core 06 p0807 A72-17895
- Kinematics of five-link hinged mechanisms containing two driving links, applying to spherical and flat links 07 p0987 A72-19858
- Aeromechanical analysis of flight conditions for conventional aircraft, including kinematics of curvilinear motions with constant speed 07 p0913 A72-20372
- AS type solar prominence kinematics of 10 September 1956, noting hyperbolic spiral knot motion from recorded data analysis 09 p1390 A72-23398
- Oscillatory relaxation combustion in annular chamber, applying kinematic theory to combustion frequencies and regions calculation 11 p1745 A72-25752
- Kinematic estimate of large scale atmospheric vertical motion field patterns, using polynomial approximation of wind profiles 12 p1840 A72-27707
- Axiomatic development of mechanics from geometrically formulated kinematics to statics of rigid bodies and systems, using virtual rate of work and reaction principles 13 p2000 A72-28477
- Asymmetrical mechanics theory of nematic liquid crystals, noting relation for local moment of inertia and tensor analysis of kinematic characteristics 13 p2022 A72-29497
- Impulse excited spatial systems of rigid bodies linked by pivot joints with arbitrary kinematics, applying Maxwell-Betti theorem 15 p2323 A72-31461
- Nonlinear Cosserat continuum theory of elasticity, discussing kinematics and stressed state as functions of angular velocity, acceleration, volume forces and moments 15 p2274 A72-31476
- Anisotropic and isotropic descriptions of physical process speeds in special relativity theory space-time metric 15 p2279 A72-32768
- On the kinematic distribution of galactic neutral hydrogen. 17 p2606 A72-34572
- Motion concept formulation by linear algebra of n dimensional spaces, emphasizing tensor character of velocity and acceleration 21 p3084 A72-40816
- Kepler second law based moment of gyration concept application to spacecraft and missiles mechanics and kinematics, proposing Skylab weightless environment experiment for validation [SAWE PAPER 931] 23 p3342 A72-43471
- Method of equivalent turns in the kinematics of inertial systems 23 p3311 A72-43583
- Streamline and fieldline geometry with applications to MHD flow kinematic properties, discussing field and momentum relations decomposition in terms of sound velocity 23 p3322 A72-44270
- KINESCOPIES**
- U PICTURE TUBES**
- KINESTHESIA**
- Supplementary cues and delayed-alternation performance of frontal monkeys. 20 p2892 A72-39372
- KINESTHESIS**
- U PROPRIOCEPTION**
- KINETIC ENERGY**
- MHD boundary layer calculation for conducting fluid along semiinfinite flat plate with transverse magnetic field, deriving momentum and kinetic energy integral equations 01 p0113 A72-11383

- Kinetic energy velocity and acceleration formulas of penny shaped crack propagation in brittle body under triaxial tensile stress 01 p0144 A72-11391
- Kinetic energy correction in capillary viscometry, observing pressure drops and mass flow rates 02 p0202 A72-11724
- Nonlinear development of instability wave in turbulent wake behind thin body based on integrals of mean flow momentum and kinetic energy equations 02 p0152 A72-12351
- Kinetic energy losses due to liquid-to-solid phase transformation in heated two-component flow ascending in tube 03 p0342 A72-14161
- Closure schemes and retention of third moments in stochastic dynamic equations for numerical weather prediction, discussing imperfect forcing effects and kinetic energy relations 03 p0385 A72-14230
- Short period height and longer period kinetic energy oscillations in 10-level primitive equation model for circulation prediction in tropical region 03 p0385 A72-14232
- Northern Hemisphere mean zonal flow across arbitrary horizontal surfaces, evaluating vertical transports of kinetic energy 04 p0541 A72-14454
- Gliding flight atmospheric energy utilization through aerology, discussing value of weather forecasts to glider pilots 04 p0542 A72-14684
- Interstellar propagation of 2-8 Z galactic cosmic ray nuclei at 10-1000 MeV/nucleon, analyzing differential kinetic energy spectra 04 p0567 A72-15323
- Turbine blade row coolant flow velocity, injection location and temperature effects on kinetic energy output [AIAA PAPER 72-12] 05 p0707 A72-16866
- Ultrahigh enthalpy gas generation by steady multicomponent flow process with kinetic energy transfer from low molecular weight gas to higher weight working medium [AIAA PAPER 72-167] 05 p0750 A72-16979
- Incompressible fluid unsteady kinetic energy equation periodic solution for harmonic oscillation viscous dissipation influence on temperature field, considering Couette steady flow solution 05 p0750 A72-17007
- Quasi-biennial modulation of kinetic energy transfer in stratosphere, comparing with hemispheric energy, eddy transports and tropical zonal wind and temperature 06 p0841 A72-17632
- Incompressible microstretch fluid flow in rigidly bounded domain, deriving kinetic energy decay rate via linear model subject to entropy principle and boundary adherence condition 06 p0799 A72-17918
- Multiparticle time regularization technique based on kinetic energy potential, noting application to two body encounters 06 p0885 A72-18073
- Turbulence model for near-wall boundary layer flows, solving differential equations for kinetic energy and length scale 06 p0802 A72-18527
- Atmospheric kinetic and temperature energy spectral balances in thermally stratified turbulent flow without shear 07 p0980 A72-20454
- Synoptic velocity fluctuations from empirical structural functions of wind fields, proposing spectral kinetic energy distribution model for atmospheric turbulence 07 p1031 A72-20694
- Turbulent flow model based on two equations for kinetic energy distribution and vorticity fluctuations, comparing flow and heat transfer prediction with experimental data 08 p1152 A72-22169
- Solar wind kinetic energy from flare associated solar wind disturbances relation to types 2 and 4 radio bursts, using satellite observations 09 p1378 A72-23399
- Asymmetric flow in plane channel characterized by diffusional transport of turbulent shear stress and kinetic energy from rough to smooth wall regions 10 p1467 A72-24368
- Quasars energy source and structure in terms of kinetic energy conversion to radiation in shock fronts of colliding gas clouds 10 p1544 A72-24671
- Atmospheric isotropic turbulence kinetic energy dissipation and wind spectra estimation from Doppler spectra of precipitation particle velocities 10 p1507 A72-25001
- Galactic tidal field and multiple encounters role in stellar escape from star clusters, noting escape rates and kinetic energy involved 12 p1873 A72-27898
- Na atoms D line radiation excited in collisions with molecular gases, noting transfer cross section dependence on kinetic energy for given quantum number change 13 p2009 A72-30063
- Kinetic forming of conical Al component from solid cylindrical billet, analyzing forming and inertia stresses, impact velocity and displacement-time history 15 p2244 A72-31708
- Kinetic energy and momentum of longitudinal waves in plasmas, deriving Landau dispersion equation from conservation laws 15 p2285 A72-32272
- Stellar winds and breezes classification using energy flux and particles kinetic and thermal energies for criteria, noting coronal temperature effects 15 p2313 A72-32298
- Water bag model in cylindrical rotating two dimensional rod stellar system, showing kinetic energy minimum correspondence to collisionless Boltzmann equation 15 p2315 A72-32717
- Solar wind expansion analysis with allowance for interaction with neutral interstellar matter, discussing kinetic energy loss due to EUV ionization of interstellar gas 16 p2449 A72-33910
- Fermi acceleration effects in low energy particle transport in interplanetary space, assuming kinetic energy contained in Alfvén and bidirectional traveling waves 16 p2460 A72-33938
- Aircraft measurements of dissipation of turbulent kinetic energy. 19 p2829 A72-38561
- Discussion of the thermal state of an open air premixed methane-oxygen flame. 19 p2883 A72-38871
- Synoptic velocity fluctuations from empirical structural functions of wind fields, proposing spectral kinetic energy distribution model for atmospheric turbulence 20 p2948 A72-39009
- An assessment of energy absorbing devices for prospective use in aircraft impact situations. 22 p3237 A72-42764
- Calculation of the parameters of a plasma accelerated in a high-frequency electric field and a static magnetic field 23 p3320 A72-43660
- Chemical explosion energy distribution between gases and propelled mass, discussing momentum and kinetic energy transfer 24 p3463 A72-45040
- On the power law for the kinetic energy spectrum of large scale atmospheric flow. 24 p3398 A72-45483

KINETIC EQUATIONS

NT HYDRODYNAMIC EQUATIONS

NT KINEMATIC EQUATIONS

- Brownian motion kinetic equation from Boltzmann equation for two component neutral gas by simultaneous expansion in density and mass ratios 01 p0050 A72-10233
- Kinetic equation for gases with rotational degrees of freedom under equality of probabilities of direct and inverse transitions and stereoisomerism of molecules 01 p0050 A72-10350
- Collision kinetics of jet streams of inelastic grains in neighboring orbits around central gravitating body 02 p0281 A72-12304
- Self consistent kinetic equations for evolution of particle distribution functions and wave intensity spectra of relativistic spatially homogeneous multippecies plasma in ambient magnetic field 04 p0553 A72-14401
- Macroscopic integrodifferential transport equations for gas mixture with internal degrees of freedom and chemical reactions from model kinetic equation 04 p0552 A72-14633
- Supersaturated semiconductor solid solutions decay kinetic equations and time constants, noting free current carriers effect 04 p0561 A72-15081
- Self consistent theory of waves in fluctuating plasma, discussing Klimontovich-Maxwell electromagnetic field equations uniqueness solution and kinetic equation 04 p0493 A72-15449
- Resonant transport properties of polyatomic gases in collinear static and oscillating magnetic fields, using microscopic kinetic equation 04 p0553 A72-15633
- Kinetic equations for laser active medium disturbances and electromagnetic field modes in cavities with losses 07 p1006 A72-20117
- Machine metals fatigue life, creep theory and stress and strain kinetics in severe environments, formulating physical equations 08 p1246 A72-21805
- Kinetic equations derivation for rarefied chemically reacting monatomic or stable molecular gases 10 p1514 A72-23845

Kinetic equations solution for homogeneous multiatomic gas relaxation, proving solution existence and uniqueness

10 p1516 A72-24629

Impulse and kinetic momentum equations for dynamics of variable mass solid using mechanical model

12 p1846 A72-27543

Nd-fiberglass laser intensity fluctuations due to fibers absorption centers, deriving population inversion threshold, pumping power and center formation rate from kinetic equations

12 p1825 A72-27884

Time constant limited stability of numerical integration procedures for systems of kinetic equations, examining causes and effects of stiffness

13 p1985 A72-28419

Kinetic approximation for bounded electron beam stability in plasma situated in magnetic field, deriving instability increments and dispersion relations

13 p2010 A72-28578

Source gas expansion flow into vacuum, solving spherical coordinates representation of BGK kinetic equation by numerical method

13 p1942 A72-29116

Kinetic equations derived for electromagnetic field inside cavity with resonance medium and external source, determining sensitivity thresholds, gain factors and spectral compositions

13 p1969 A72-29677

Kinetic equation of repeatedly ionized plasma from hyperbolic diffusion method, calculating direct transitions between excited ion states

13 p2008 A72-29895

Quantum kinetic equation for monatomic and molecular gases optical characteristics calculation, considering spontaneous emission spectrum of atoms

14 p2110 A72-30358

Failure phenomena relationship to kinetic equation for defect buildup from brittle fracture analysis of composite glass plastic in uniaxial eccentric tension

14 p2164 A72-30426

Kinetic equations for turbulent magnetized plasma, considering wave-wave interactions and wave energy in terms of second order Markov differential equation

14 p2141 A72-30940

Binary gas mixture slipping rate determination from joined solution of Hamel kinetic model linearized equations, and Navier-Stokes and Boltzmann equations

14 p2096 A72-31013

Weak homogeneous turbulence analysis by Bogoliubov statistical mechanics theory, deriving kinetic equations for nonlinear wave interaction

15 p2278 A72-32383

Multispecies magnetoplasma ac electrical conductivity tensor collision factor from quantum mechanical convergent kinetic equation

15 p2287 A72-32411

Spherical source jet flow expansion of single monatomic gas into vacuum on basis of BGK kinetic equation

16 p2375 A72-32887

Internal aerodynamic problem solution by kinetic equation for Couette and Poiseuille flows and heat transfer between plane plates

16 p2343 A72-33153

Papers on kinetic equations covering axiomatics, quantum and relativistics, plasma kinetic theory role in spectral line width, etc

17 p2590 A72-35151

Self-consistent kinetic equations.

17 p2581 A72-35152

An application of the generalized Langevin equation to the study of correlations in simple, classical fluids.

17 p2581 A72-35154

Kinetic equations with radiation effects.

17 p2590 A72-35155

A review of the unified theory of relaxations in plasmas.

17 p2590 A72-35159

Kinetic theory of waves in hot, low density plasma.

17 p2591 A72-35161

Wave-wave interactions due to scattering by electrons.

17 p2591 A72-35162

Kinetic and kinematic equations for inviscid unsteady gas flow, noting pseudostationary vortex geometry

17 p2541 A72-35436

Kinetic theory of surface waves in a cylindrical plasma waveguide

19 p2842 A72-38531

Collisionless solar wind protons - A comparison of kinetic and hydrodynamic descriptions.

19 p2853 A72-38732

Balescu-Guernsey-Lenard kinetic equation for homogeneous dilute electron gas extended to higher densities, specifying conditions for BBGKY hierarchy correlation functions solution

20 p2958 A72-39815

Kinetic equations for ultradense matter neutronization, noting stellar configuration of given mass with variable volume

21 p3086 A72-40096

Boltzmann kinetic equation for nonideal plasma with allowance for polarization effects, noting collision integral convergence

21 p3090 A72-40412

Influence of a variable electric field on the diffusion of ions in a gas

21 p3086 A72-41676

Kinetic equations of chemically reacting gas mixtures

22 p3152 A72-42267

Multiple scattering of bending waves by random inhomogeneities.

22 p3235 A72-42460

Application of multiple-scattering theory to the derivation of kinetic equations for waves in a weakly turbulent plasma

22 p3212 A72-42665

Kinetic equation for electron distribution in high temperature laser plasma, calculating nonequilibrium conditions for strong field and plasma parameters

23 p3318 A72-43323

Method of equivalent turns in the kinematics of inertial systems

23 p3311 A72-43583

Pulsed carbon dioxide laser medium composition, pressure and electrical parameters effects on output power, energy and efficiency from mathematical model solution of kinetic equation:

24 p3409 A72-44966

Characteristics and constants of motion method for collisional kinetic equations.

24 p3426 A72-44984

Kinetic equations solution approximation for two species isothermal reactions in homogeneous turbulent mixing

24 p3392 A72-45059

Kinetic approximation for confined electron beam stability in plasma situated in magnetic field, deriving instability increments and dispersion relations

24 p3428 A72-45078

Kinetic equations for a chemically reacting plasma.

24 p3430 A72-45566

KINETIC FRICTION

NT SLIDING FRICTION

Solar magnetic fields forced latitudinal drift rate due to differential rotation, taking into account turbulent friction and pressure forces

09 p1382 A72-22286

Friction and molecular structure - The behaviour of some thermoplastics.

20 p2945 A72-39974

KINETIC HEATING

NT AERODYNAMIC HEATING

NT SHOCK HEATING

Electronic energy transfer phenomena in rare gases.

24 p3429 A72-45310

KINETIC THEORY

NT CHAPMAN-ENSKOG THEORY

NT MIXING LENGTH FLOW THEORY

NT TRANSPORT THEORY

Quiet solar wind kinetic model, comparing with exospheric, semikinetic and hydrodynamic models

01 p0119 A72-10878

Approximate solution in gas kinetic theory, considering temperature jump, velocity and viscous slip problems

02 p0205 A72-12356

Collision frequencies definition in kinetic theory of gases, expressing ionospheric electron conductivity

03 p0345 A72-12979

Kinetic theory application to initially nonuniform gas relaxation to equilibrium, obtaining macroscopic velocity, density and temperature solutions by multitime scale perturbation methods

03 p0340 A72-13155

Gaseous general relativistic kinetic theory, detailing matter model, thermodynamics, cosmology and Einstein field equation completion with Liouville or Boltzmann equation

03 p0388 A72-13266

Shocks structure and kinetic theory of gases, discussing density profiles, velocity and temperature measurement techniques

03 p0341 A72-13686

Maxwell boundary conditions method application in kinetic theory of gases, investigating linearized plane Couette flow

04 p0510 A72-14594

Initial viscous heat conducting gas dynamic state one dimensional decay problem solution, using kinetic theory with Boltzmann equation

04 p0512 A72-14982

Kinetic rate theory extended to time dependent flow behavior of viscoelastic materials /polymers/ under constant stress and shear

04 p0512 A72-15263

Monograph on nonequilibrium relativistic kinetic theory covering heuristic approach, Boltzmann equation, H theorem, equilibrium distributions, relativistic thermodynamics, phenomenological transport theory, heat conduction coefficients, etc

05 p0689 A72-16289

General relativistic kinetic theory of gases, discussing microscopic model, space-time, self con-

sistent Einstein-Maxwell-Liouville equations and irreversible processes

06 p0847 A72-17255

Electromagnetic wave propagation and thermal spread in uniform magnetoplasma at electron-cyclotron resonance frequencies, discussing kinetic and multifluid theory

06 p0854 A72-17489

Kinetic model for propane pyrolysis based on most important free radical reaction steps

06 p0770 A72-17777

Kinetic theory of wall temperature jump and near-wall temperature distribution in polyatomic gases, solving simultaneous singular linear integral equations by numerical methods

06 p0904 A72-18528

Kinetic theory and nonequilibrium distribution functions of reacting gases with simultaneous reactions

07 p1035 A72-20114

Averaged Bogoliubov-derived chains of kinetic theory gas dynamics equations with strong statistical correlation for macroprocess description

08 p1149 A72-21175

Steady state charged cylindrical electron-ion beam with high current in kinetics model framework, discussing densities proportionality and relativistic factor

09 p1360 A72-22951

Kinetic model for polyatomic gas heat transfer between parallel plates, considering boundary value problem with arbitrary accommodation coefficients

11 p1744 A72-25559

Russian monograph on laser kinetic theory covering quanta dissipative systems, lasing equations, steady state, semiconductor emission, giant pulses, magnetic quantization, etc

12 p1827 A72-28338

Kinetics of monopulse development in cavity with nonlinear element converting generated radiation into second harmonic, considering energy and time characteristics

13 p1970 A72-29683

Kinetic model for electromagnetic field fluctuations in bounded isotropic plasma half space with specular reflection of electrons at boundary

14 p2135 A72-30170

First positive and first negative nitrogen emission excitation kinetic mechanisms, investigating shock tube measurements of nonequilibrium radiation

14 p2134 A72-30837

Azimuthal electric fields role in toroidal plasma transport properties based on kinetic theory for collision dominated regime

16 p2432 A72-32806

Papers on kinetic equations covering axiomatics, quantum and relativistics, plasma kinetic theory role in spectral line width, etc

17 p2590 A72-35151

The self-consistent test particle approach to relativistic kinetic theory.

17 p2590 A72-35156

Kinetic theory of waves in hot, low density plasma.

17 p2591 A72-35161

Superposition principle in test particle method for reducing plasma cloud kinetic theory to determination of conditional probability function involving Vlasov equation

17 p2591 A72-35163

The two-particle correlation function in nonequilibrium statistical mechanics.

17 p2581 A72-35164

Relativistic kinetic theory combined with surface layer theory in curved space-time to study counter-rotating disks with fine central red shift

17 p2582 A72-35389

Book - Introduction to the kinetic theory of gas flows

17 p2541 A72-35450

Closed rotating cosmologies containing matter described by the kinetic theory - Entropy production in the collision time approximation.

17 p2618 A72-35823

Steady state charged cylindrical electron-ion beam with high current in kinetic model framework, discussing densities proportionality and relativistic factor

17 p2593 A72-35880

Gas discharge plasma detection characteristics, examining electron and ion densities and collision rates dependence on electromagnetic field frequency and amplitude

17 p2593 A72-35885

Combined finite element-weighted residuals method for linearized BGK Boltzmann kinetic theory equation, considering cylindrical Couette flow

18 p2684 A72-37168

Structure of ion acoustic solitons and shock waves in a two-component plasma.

19 p2841 A72-38440

Kinetic theory of density fluctuations in a magnetized collision-dominated plasma in an electric field.

19 p2792 A72-38745

The self-consistent test-particle approach to relativistic kinetic theory.

20 p2955 A72-40013

Higher harmonics and transport coefficients of plasmas in circular polarized magnetic fields and additional electromagnetic fields.

21 p3091 A72-40489

Kinetic theory of the lasing bandwidth in a spectrally inhomogeneous medium

21 p3064 A72-41695

Kinetic theory of a modified Knudsen's absolute manometer.

22 p3175 A72-41941

Transient oscillator analysis of a high-pressure electrically excited CO laser.

22 p3184 A72-41970

The molecular-kinetic theory of polymer adhesion

23 p3307 A72-43930

Elements of a theory of CW gasdynamic quantum generators.

23 p3297 A72-44225

A kinetic-theory description of a chemically reacting gas.

23 p3357 A72-44272

The concepts of mean force, mean velocity, and ensemble velocity for a particle ensemble

24 p3425 A72-45070

KINETICS

NT ELECTROKINETICS

NT KINETIC ENERGY

NT NEWTON SECOND LAW

NT NEWTON THEORY

NT REACTION KINETICS

NT VARIABLE MASS SYSTEMS

Martensite first stage decomposition mechanism and kinetics during tempering of quenched Re steels with varying carbon concentration

08 p1187 A72-21779

Ionization kinetics influence on light absorption zone behind plane stationary shock wave in hydrogen

10 p1467 A72-24358

Mo powder sintering kinetics and disperse mechanism in isothermal and nonisothermal conditions

11 p1643 A72-26836

Ionization kinetics influence on light absorption zone behind plane stationary shock wave in hydrogen

17 p2539 A72-34957

Molecular and atomic interaction forces as interfacial free energy sources, discussing molecular attachment kinetics and surface configuration models

18 p2718 A72-36393

Kinetics and annealing and mechanical properties of W chemical vapor deposition, discussing high temperature tests

18 p2656 A72-36398

Excess metal buildup kinetics and work function of oxide thermionic cathode activated by emission current, noting effect of metal and oxygen concentrations

21 p2997 A72-40789

Kinetics, spectrum, and specific loss properties of radiation emitted by rhodamine 6G in the case of pumping by a self-constricting discharge

24 p3410 A72-45417

KIRCHHOFF LAW

Triangular (KLI) and quadrilateral (KQT) thin shallow shell elements with 20 degrees of freedom, basing bending behavior on discrete Kirchhoff formulation

05 p0739 A72-16549

KIRCHHOFF LAW OF RADIATION

Electromagnetic wave scattering from rough surfaces by Kirchhoff approach and small perturbation method, discussing validity near grazing angle

01 p0032 A72-11249

Radiative heat transfer damping rates of turbulent temperature pulsations in upper planetary atmospheres, assuming Kirchhoff radiation law validity

06 p0882 A72-17935

Kirchhoff method application to asymptotic solution of plane wave diffraction on dielectric conical shells, calculating electromagnetic field vector

08 p1131 A72-20931

Radiative heat transfer damping rates of turbulent temperature pulsations in upper planetary atmospheres, assuming Kirchhoff radiation law validity

16 p2459 A72-33776

On the validity of a generalized Kirchhoff's Law for a nonisothermal scattering and absorptive medium.

24 p3424 A72-44698

KIRCHHOFF-HELMHOLTZ FLOW

U PIPE FLOW

KIRCHHOFF-HUYGENS PRINCIPLE

U DIFFRACTION

U WAVE PROPAGATION

KITE BALLOONS

U TETHERED BALLOONS

KLEIN-GORDON EQUATION

Hulthen and Schwarzschild potentials in the Klein-Gordon equation.

18 p2711 A72-36515

KLYSTRONS

FM homodyne phase meter with klystron oscillator for measuring plasma electron concentration, presenting block diagrams of meter, detector and oscillator

02 p0223 A72-11414

Nonlinear nonlaminar 3D electron motion calculation through output cavity of klystron amplifier by Green function

04 p0497 A72-14697

Tunable coherent IR signal generation and propagation by mixing carbon dioxide laser and millimeter wave klystron output in GaAs loaded waveguide

04 p0532 A72-15614

Ten-stage electrostatic depressed collector designed with analog computer for improving klystron power conversion efficiency

05 p0637 A72-16365

Transistorized automatic feedback power level control for centimeter band reflex klystron oscillator for electron paramagnetic resonance studies

06 p0784 A72-18166

IMPATT driven pumps replacement of klystron for parametric amplifiers producing over 100 mW at 38-40 GHz with good stability and noise performance

06 p0788 A72-18470

Low noise Ku band klystron oscillators for Doppler radar, discussing FM noise induced frequency deviation, spurious modulation and countermeasures

07 p0954 A72-19049

Ultrasensitive measurement technique for low microwave susceptibility on ferrite samples featuring feedback scheme for signal klystron locking

07 p0955 A72-19320

Microwave signals detection with virtual cathode in klystron repeller by electrons screening at velocity modulated electron beam

08 p1136 A72-21766

Broadband electrostatically focused klystron for airborne radar application, discussing focusing cell design, amplification and efficiency

10 p1446 A72-23821

Short and long term frequency stability improvement in X band klystron oscillator stabilized by high Q superconducting cavity

10 p1449 A72-24303

Short term frequency instability in mm wave reflex klystrons, obtaining rms frequency drift

11 p1605 A72-26319

Vacuum tube developments for radar, TV and communication applications, discussing microwave, traveling wave, cathode ray, memory and vidicon tubes, magnetrons, klystrons and tetrodes

11 p1606 A72-26544

Nonlinear harmonic analysis of reflex klystrons with high electron conductance, using average method in second approximation

13 p1931 A72-29290

Russian book on microwave electronics covering linear-beam and cross-field backward and traveling wave amplifiers and oscillators, klystrons, masers, plasma devices, etc

17 p2532 A72-34650

Electron bunching and output gap interaction in broad-band klystrons.

19 p2772 A72-37566

Dispersion signal recording for klystron AFC radio spectrometer by low frequency magnetic field modulation

22 p3175 A72-41900

KNOWLEDGE

NT PARADOXES

NT PHILOSOPHY

Earth Resources Survey (ERS) program personnel training and education, discussing trainee selection, knowledge categories and training methods for remote sensing

02 p0304 A72-11855

Physical and biological sciences approaches to attainment of knowledge, noting indeterminateness in organic realm

07 p0934 A72-20394

KNUDSEN CELLS

U KNUDSEN GAGES

KNUDSEN FLOW

Multimoment solutions to convective heat transfer from sphere, discussing maximum drag coefficient and validity at all Knudsen numbers

[ASME PAPER 71-WA/HT-1] 05 p0743 A72-15863

Knudsen boundary layer role in physicochemical hydrodynamics of heterogeneous reactions and flows with surface reactions, using Boltzmann equation

05 p0746 A72-16209

Thermomolecular pressure gradients and temperatures in flow between parallel planes for statistical gas models at arbitrary Knudsen numbers

07 p1101 A72-20513

Body drag measurement in low density supersonic gas stream in various Knudsen number ranges

08 p1166 A72-21409

Stationary heat conduction between stagnant binary gas mixture and two constant temperature plane parallel walls for arbitrary Knudsen numbers

15 p2334 A72-31462

Computer simulation by Monte Carlo technique of particulate fluxes in divergent conical Knudsen cell orifices, considering specular reflection and surface diffusion effects

15 p2218 A72-32380

Molecular flux distribution in cylindrical vacuum chambers with various inlet and pumping configurations under assumption of Knudsen law validity, describing computer program

15 p2183 A72-32382

Thermal molecular jets mixing produced by Knudsen effusion from porous wall, obtaining Boltzmann equation approximate solution by moment method via assumed distribution function

16 p2429 A72-33055

Strong shock propagation through decreasing density.

19 p2789 A72-38796

A semiempirical method for the evaluation of aerothermodynamic properties in the intermediate hypersonic flow regimes.

21 p2990 A72-41128

Pressure effect at arbitrary Knudsen numbers.

23 p3279 A72-43216

KNUDSEN GAGES

Computer simulation by Monte Carlo technique of particulate fluxes in divergent conical Knudsen cell orifices, considering specular reflection and surface diffusion effects

15 p2218 A72-32380

Kinetic theory of a modified Knudsen's absolute manometer.

22 p3175 A72-41941

KNUDSEN NUMBER

U KNUDSEN FLOW

KNURLING

Study of the process of powder knurling to articles

23 p3292 A72-43279

KOLMOGOROFF THEORY

Ocean winds velocity, temperature and humidity fluctuations second and third order structure functions, deriving Kolmogoroff constants

03 p0383 A72-13154

Turbulence velocity field analysis by repeated cascade theory via partial Fourier transform, predicting Kolmogoroff law in line with experimental results

07 p0972 A72-20112

Motion of body similar to Lagrange gyroscope, using Kolmogoroff theorem

08 p1207 A72-21343

Servo systems operational reliability analysis for variable intensity of fluctuating interference, discussing Markov process probability determination and Kolmogoroff equations solution

11 p1609 A72-25441

Flow velocity fluctuation intensity relationship to turbulent energy dissipation based on Kolmogoroff similarity hypothesis

12 p1799 A72-28133

Statistical continuous random process theory of homogeneous and isotropic turbulence in terms of energy transfer in wave number space based on Kolmogoroff hypothesis

21 p3045 A72-41025

The intermittent small-scale structure of turbulence - Data-processing hazards.

23 p3282 A72-44305

Experimental determination of the turbulent exchange coefficient in the case of homogeneous isotropic turbulence

23 p3282 A72-44489

KOLMOGOROFF-SMIRNOFF TEST

System diagnosis based on ordered statistical samples, discussing Kolmogoroff-Smirnoff detector use for on-line computers in testing noisy systems

10 p1482 A72-24597

KOVAR (TRADEMARK)

Nonmetallized aluminum oxide ceramics brazing with metals under pressure using copper solder, noting optimum conditions for Kovar

15 p2243 A72-31225

KP INDEX

Auroral sporadic E layer diurnal distribution correlation to charged particle integral flux diurnal variations observed by satellite in winter, noting Kp index effect

14 p2102 A72-30655

Diurnal variation of the correlation of Pc 3 and Pc 4 micropulsation characteristics with magnetic activity.

23 p3286 A72-44524

KRONECKER PRODUCT

U ORTHOGONALITY

KROOK EQUATION

Source gas expansion flow into vacuum, solving spherical coordinates representation of BGK kinetic equation by numerical method

13 p1942 A72-29116

Kinetic equations for a chemically reacting plasma.

24 p3430 A72-45566

KRYPTON

NT KRYPTON ISOTOPES

Dimer formation effect on thermal diffusion factor at low temperatures for krypton-argon system

03 p0391 A72-13749

Ar, Kr, methane and nitrogen physiosorption isotherms on stainless steel in low pressure cryogenic baths calculating mean adsorption energies

05 p0624 A72-16395

Output power dependence on pressure and magnetic field strength in Kr ion laser for green, yellow and red lines

06 p0826 A72-18010

CW Kr arc lamps for high power Nd-YAG laser pumping, testing operating life and electrical and spectral characteristics as function of design

09 p1324 A72-23080

High power CW Nd-YAG laser efficiency improvement by optical pump wavelength, power coupling and balance factors, noting krypton arc lamp contribution

15 p2247 A72-32029

Kr I and II lines strength and relative transition probabilities, using thermal plasma behind reflected shock wave as spectroscopic light source

21 p3089 A72-40137

The mass spectrographic measurement of gas separation with the aid of ambipolar effusion in neon-krypton mixtures

21 p3053 A72-40486

Energy and angular distributions of secondary electrons resulting from ionizing collisions of electrons with helium and krypton.

21 p3088 A72-41493

Formation and loss of O₂⁺/+ and O₄⁺/+ ions in krypton-oxygen afterglow plasmas

23 p3316 A72-44345

Dissociative recombination at elevated temperatures. I - Experimental measurements in krypton afterglows.

23 p3316 A72-44346

KRYPTON ISOTOPES

Apollo 12 lunar igneous rocks 12004, 12040, 12051 and 12053, obtaining Kr 78/Kr 83 and Xe 131/Xe 126 spallation component ratios correlation line

01 p0124 A72-10065

Xe and Kr abundance and isotopic composition in silicate inclusions of iron meteorites

03 p0435 A72-13690

Xe and Kr mass fractionation and isotopic anomalies in ordinary chondrites, analyzing meteorite samples by mass spectrometry

07 p1084 A72-20497

KRYPTON 85

Kr 85 clouds released by instantaneous point sources, measuring speed, height, short period concentrations, crosswind and downwind concentration integrations and dimensions

01 p0095 A72-10828

Test method and apparatus to pressurize hermetically sealed components with Kr 85, comparing obtained leak rates with He mass spectrometric values

12 p1854 A72-27550

KU BAND

U SUPERHIGH FREQUENCIES

KUTTA-JOUKOWSKI CONDITION

Aerodynamic noise generation in turbulent fluid at low Mach number due to source near half plane by applying Kutta-Joukowski condition

10 p1415 A72-23724

L

L BAND

U ULTRAHIGH FREQUENCIES

L-1011 AIRCRAFT

Tristar commercial jet transport aircraft development, discussing design and flight tests for operating efficiency, reliability and safety

[SAE PAPER 710755] 01 p0003 A72-10252

Automated navigation management in cockpit, considering modular navigation /MONA/ dual channel system of L-1011 Tristar

09 p1349 A72-23450

Flight testing of automated modular area navigation system for L-1011, describing computer, data storage and control-display units and electronic automatic chart system

10 p1509 A72-24271

Dynamic model of high bypass ratio turbofan engines for L-1011 wind tunnel flutter test program

[AIAA PAPER 72-376] 11 p1703 A72-25400

L-1011 flight test program, discussing aircraft design, flight station, controls, flying qualities, etc

12 p1754 A72-27519

Fiberglass replacement by organic fiber for L-1011 interior sandwich panels and laminates, considering Nomex fiber in woven fabric

12 p1835 A72-28099

L-1011 Tristar cartridge valves and manifolds, reservoirs and hydraulic service center design for speedy maintenance and servicing

14 p2073 A72-31050

L-1011 propulsion, fuel, flight control, navigation, avionics, communication, electrical, environmental control and auxiliary power systems, discussing structure and high lift devices

15 p2181 A72-32427

Adhesive bonding of L-1011 body shell panels for improved fatigue strength and corrosion resistance

15 p2245 A72-32429

Flight test report on L-1011 aerodynamic characteristics, discussing high and low speed performance, stability and control, stall behavior, etc

19 p2748 A72-38030

Application of advanced methods to the determination of design loads of the Lockheed L-1011 Tristar. [AIAA PAPER 72-775] 19 p2752 A72-38134

Structural development of the L-1011 Tri-Star.

[AIAA PAPER 72-776] 19 p2876 A72-38135

L-1011 computerized weight reporting system present and future capabilities.

[SAE PAPER 932] 23 p3251 A72-43472

Community noise levels of the L-1011 Tristar Jet Transport.

24 p3365 A72-44677

LABELING [MARKING]

U MARKING

LABORATORIES

NT ENGINE TESTING LABORATORIES

NT ENVIRONMENTAL LABORATORIES

NT HUMAN FACTORS LABORATORIES

NT MANNED ORBITAL LABORATORIES

NT MANNED ORBITAL RESEARCH LABORATORIES

NT SPACE LABORATORIES

In-house R and D laboratory organization cost effectiveness evaluation methods, discussing supervisory, program and special appraisals, visiting committees and natural competition

07 p1105 A72-19551

LABORATORY EQUIPMENT

Integrated medical and behavioral laboratory for detection and measurement of space flight stresses, specific etiologies and human tolerances and adaptivity

12 p1796 A72-28279

Modular microbiology laboratory design considerations and zero gravity experiments to investigate microbial culture systems behavior

12 p1765 A72-28280

Digital control and data processing system to replace analog instrumentation in vibration test laboratories, discussing signal generation, data acquisition, storage and analysis

15 p2215 A72-32618

Components analysis laboratory with curve tracers, third harmonic index equipment, noise meters, TV X ray system and metallographic microscopes

18 p2676 A72-37132

LABYRINTH

NT COCHLEA

NT VESTIBULES

Histological examination of transverse acceleration stress effect on inner ear development of gestating rat embryos

07 p0923 A72-20446

Vestibular labyrinth reactions and nystagmus thresholds in dogs during negative angular accelerations and simulated chronic galactic radiation from Co 60 gamma source

21 p2998 A72-40439

Vestibular system functional relationship to postural reflex mechanism involving labyrinth and gravireceptors responses

22 p3147 A72-42788

LACQUERS

Brittle lacquer of air-drying type, investigating coating ingredients and plasticizers effect on strain sensitivity for various temperature and humidity levels

20 p2920 A72-38890

LACTATES

Acute and chronic hypercapnia effect on lactate, pyruvate, alpha-ketoglutarate, glutamate and phosphocreatine contents of rat brain

03 p0316 A72-13677

In vitro measurements of oxygen tension effect on teleost and amphibian retinal lactate dehydrogenase activity, discussing acetazolamide produced hypoxia effects

10 p1424 A72-23729

Muscle cell ATP, creatine phosphate and lactate concentration changes relation to oxygen uptake during and after exercise

14 p2080 A72-30705

Muscle metabolism of ATP, CP, glycogen and lactates at rest and during submaximal and maximal exercise

21 p3005 A72-40421

Lactate dehydrogenase from an extremely thermophilic bacillus.

23 p3259 A72-44450

LACTIC ACID

Human oxygen intake and blood lactic acid removal kinetics during recovery from mild steady work on bicycle ergometer

10 p1426 A72-24989

Human plasma free fatty acids relation to lactic acid concentration and maximum aerobic power, noting carbohydrate availability as exercise capacity limiter

21 p3003 A72-41520

LADDERS

Two-variable resonant ladder network synthesis for prescribed amplitude response with closed-form solution, illustrating with waveguide bandstop filter

14 p2091 A72-30945

LAGRANGE COORDINATES

Two dimensional Lagrangian hydrodynamic code for stability of shock acceleration perturbed interface between two gases of different density

13 p1942 A72-29114

LAGRANGE EQUATIONS OF MOTION

U EULER-LAGRANGE EQUATION

LAGRANGE MULTIPLIERS

Static deflections determination of thin rectangular plates with point clamped restraints, using Ritz method with Lagrange multipliers

10 p1555 A72-24193

Nonlocal variational mechanics problems approach by Balakrishnan epsilon technique, deriving methods for Lagrange function construction and Lagrange multipliers introduction

11 p1691 A72-26722

Lagrange multiplier method derivation of variational functional for finite element method and applications to plate and shell problems

13 p2055 A72-28623

Method of Lagrange multipliers for exploitation of the entropy principle.

19 p2825 A72-37842

Modified Hestenes method of Lagrange multipliers for numerical iterative solution of mathematical programming problems in function minimizing noting improved convergence

21 p3074 A72-40226

LAGRANGIAN EQUILIBRIUM POINTS

Trojan deep space communications systems, maintaining powerful relay satellites in equilibrium at Lagrangian points of earth, Mars and Venus orbits

10 p1548 A72-24975

Celestial mechanics principles application to geostationary satellites in equatorial plane and in earth-moon system libration points, considering Jupiter and Saturn stationary satellites

22 p3222 A72-42141

LAGUERRE FUNCTIONS

Incoherent optical system model with photodetectors governed by Laguerre counting statistics obtaining error probabilities for comparison with Poisson counting

06 p0776 A72-18394

Laguerre filters parameters choice for correlator input networks application, noting output SNR improvement

16 p2368 A72-33089

The possible use of Laguerre polynomials for representing the vertical structure of numerical models of the atmosphere.

19 p2829 A72-38562

Correlator with orthogonal filters for acoustic diagnostics, noting Laguerre functions variations in signal pairs autocorrelation

22 p3176 A72-42133

Approximation of a continuous function of two variables by particular sums of a Fourier-Laguerre series

24 p3419 A72-45647

LAKES

Lake effect cloud examination by TIROS and ESSA photography, noting parallel bands with larger dimensions than cloud streaks

01 p0095 A72-11280

LALLEMAND CAMERAS

Interference fringes production from binary stars focal images obtained with Lallemand electronic camera

03 p0435 A72-13798

Electronography in space astronomy, discussing use of Lallemand electronic camera as photon receptor onboard balloons or rockets

08 p1170 A72-21963

LAMB WAVES

Piezoelectric interaction between Lamb waves and charge carriers in piezoelectric plate inserted into semiconductor

06 p0865 A72-17388

Lamb waves interaction with conduction electrons in piezosemiconductor, deriving dispersion equation for CdS wafers

06 p0865 A72-17393

Temperature distribution and dissipation effects on compressible isothermal atmosphere Lamb waves vertical structure

12 p1839 A72-27504

Lamb dip for 119 micron line of CW gas laser, noting decay constants due to pressure

14 p2110 A72-30424

Lamb acoustic surface wave method for rapid non-destructive evaluation of rolling texture in arbitrarily thick metal sheets and plates

14 p2107 A72-30615

Lamb wave technique for bond strength testing of laminated or clad metal sheets, calculating displacement and stress dispersion and amplitude distribution for different modes

16 p2391 A72-33230

Guided elastic wave propagation near curved surfaces and in nonconstant thickness layers, discussing asymptotic solution and applications to Love, Rayleigh and Lamb waves

[ASME PAPER 72-APM-00] 17 p2580 A72-34306

LAME FUNCTIONS

Computer generated Lame functions of first kind definable by polynomial coefficients and eigenvalues

01 p0093 A72-10005

Elasticity theory Lame difference equations system solved by two-step iteration procedure based on Samarskii regularization

03 p0447 A72-13727

- Homogeneous first order solutions to Lame equations in statistical elasticity theory, yielding harmonic surface displacement for elastic body
03 p0454 A72-14371
- Stress and displacement solution to Lame problem for multilayer spherical vessels and cylindrical tubes in nonlinear elasticity theory
15 p2333 A72-32679
- LAME WAVE EQUATIONS**
- Coupling of interstitial liquid and porous elastic medium deformation, calculating solidification by numerical integration of partial differential equations system of Lame type
10 p1465 A72-24116
- Cylindrical elastic wave diffraction on semiinfinite screen, describing motion with displacement vector consistent with Lame equation
11 p1688 A72-26380
- Almansi strain tensor comparison with Lame elastostatics equations, noting distinction between strained and unstrained state
15 p2330 A72-32291
- Finite difference theory for Lame equations of elastic waves propagation in two dimensional body under mixed boundary conditions
22 p3234 A72-42144
- LAMINAR BOUNDARY LAYER**
- Wall conduction effect on heat transfer to laminar boundary layer, obtaining temperature distributions at plate surface by energy transport equation
02 p0202 A72-11670
- Self similar solutions for three dimensional laminar boundary layer equations under arbitrary surface conditions by quasi-linearization method
02 p0203 A72-11739
- Temperature profiles calculation for laminar boundary layer outside vibratory equilibrium
02 p0203 A72-11969
- Circular cone in supersonic flow, obtaining self similar solution for effect of angle of attack on laminar boundary layer by finite difference method
02 p0150 A72-12095
- Two dimensional diffusers flow patterns with laminar boundary layer entry, investigating wall shape and vanes effects with water table test facility
02 p0204 A72-12231
- Critique of self similar solutions for physical property models of laminar boundary layer separation due to adverse pressure gradients, noting viscosity-enthalpy relation
02 p0204 A72-12265
- Three dimensional laminar boundary layer about finite body nonuniformly moving along rectilinear trajectory
02 p0206 A72-12618
- Unsteady flow in laminar boundary layers along infinite porous flat plate with time dependent suction
02 p0206 A72-12620
- Elastico-viscous incompressible fluid laminar boundary layer flow past infinite plane porous wall, deriving velocity and temperature distributions by two-sided Laplace transform technique
03 p0340 A72-13024
- Two dimensional elasto-viscous incompressible fluid flow past porous wall with variable suction, analyzing temperature field of laminar thermal boundary layers
03 p0341 A72-13500
- Rigid and compliant walls longitudinal curvature and compliance effects on incompressible laminar boundary layer hydrodynamic stability
03 p0342 A72-13854
- Generalized equation for incompressible unsteady laminar boundary layer in external flow with arbitrary time dependent velocity distribution, discussing expanding cylindrical body
03 p0343 A72-14315
- Laminar boundary layers on heated plane wall behind shock wave in dissociating oxygen for thermodynamic and frozen flow
03 p0344 A72-14342
- Velocity and shear stress in laminar boundary layer flow on flat plate with narrow suction slot
04 p0461 A72-14461
- Gas flow fluctuations near stagnation point on hot wall, taking into account laminar boundary layer compressibility effects
04 p0462 A72-15178
- Thermal laminar boundary layer equations solution for power-law velocity distribution in external flow and arbitrary surface temperature distribution
05 p0742 A72-15844
- Longitudinal curvature effects on laminar and turbulent boundary layer flows predicted from Navier-Stokes equations, noting mixing length assumption validity
05 p0645 A72-15920
- Loitsianskii parametric method application to universalize isothermal laminar boundary layer partial differential equations in Crocco variables
05 p0649 A72-16221
- Heat flux calculation in laminar turbulent boundary layer transition zone using Schlichting model of turbulent spot formation
05 p0649 A72-16222
- Finite element algorithm derived for partial differential equation system governing laminar three dimensional boundary layer flow of multicomponent compressible fluid
05 p0604 A72-16817
- Laser schlieren measurement of density gradients in laminar hypersonic boundary layer interacting with corner expansion wave in shock tunnel
05 p0606 A72-16879
- Numerical solution method for laminar, time dependent and three dimensional boundary layer equations, applying to rotating flat plate in forward flight
05 p0652 A72-16944
- Truncated series use in laminar boundary layer calculation, noting computer time saving
06 p0756 A72-18115
- Wall curvature and flexibility effect on incompressible laminar boundary layer hydrodynamic stability, considering Tollmein-Schlichting transverse wave disturbances
06 p0801 A72-18134
- Steady two dimensional laminar compressible boundary layer of reacting gas mixture with surface vaporization and fuel injection, using integral method
07 p0967 A72-19129
- Thermal laminar three dimensional boundary layer on finite uniformly accelerated body in nonstationary regime, taking into account buoyancy effect
07 p1100 A72-19624
- Hydrodynamic flow parameters in laminar incompressible water boundary layer on heated plate, noting plate surface heating effect on velocity profile
07 p0968 A72-19766
- Two phase boundary layer flow for laminar two dimensional steady forced film condensation with pressure gradients for fluids of small Prandtl numbers
08 p1251 A72-20878
- Laminar and turbulent wall boundary layer and shock attenuation effects on flow uniformity in shock tubes
08 p1149 A72-21018
- Laminar thermal boundary layer analysis, comparing heat transfer characteristics of continuous surface and semiinfinite plate
08 p1254 A72-21613
- Plane potential flow problem for laminar boundary layer on rotating infinite cylindrical blade, using conformal coordinate transformation
08 p1108 A72-21614
- Accuracy tests of Wang method for calculating three dimensional laminar compressible boundary layer flow equations
08 p1150 A72-21625
- Laminar MHD boundary layer lateral velocity component profile for conducting fluid injection at oblique incidence, considering drag force and pressure gradient effects
08 p1214 A72-21647
- Heat and mass exchange in laminar boundary layer in air-carbon dioxide binary mixture under free convection on porous heated vertical surface
08 p1255 A72-21664
- Unsteady incompressible laminar boundary layer theory on two dimensional body motion through fluid at rest at infinity, considering skin friction
08 p1151 A72-21794
- Book on ideal and real compressible fluid dynamics covering supersonic flow past airfoils and shock wave interaction with laminar boundary layer
09 p1295 A72-23045
- Similarity method solution of differential equations of motion for supersonic laminar boundary near symmetry plane of cone at angle of incidence
10 p1418 A72-24326
- Unsteady laminar boundary layer on semiinfinite flat plate induced by small free stream velocity fluctuations, showing far downstream double layer structure via asymptotic and numerical solutions
10 p1467 A72-24334
- Laminar and turbulent boundary layer flow stability with forward separation areas
10 p1418 A72-24535
- Laminar boundary layer instability to longitudinal vortices onset due to homogeneous suction from slightly concave permeable wall, determining Goertler parameter and wavenumber critical values
10 p1470 A72-25064
- Laminar boundary layer velocity profiles in convergent nozzle incompressible swirling flow, considering boundary layer growth effects on free stream axial and tangential velocities
10 p1471 A72-25068
- Free convection-radiative heat transfer interaction of real gases in laminar boundary layer on vertical plate, using exponential wideband model for total band absorptance
11 p1740 A72-25218
- Boundary layer model for laminar transient forced convection film boiling on isothermal flat plate, noting one dimensional conduction, intermediate and steady state regions
11 p1741 A72-25227
- Double slot laminar film cooling, considering tangential gas injection velocities into laminar boundary layer and heat transfer to wall
11 p1741 A72-25228
- Heat transfer and laminarization prediction by two equation turbulence model for accelerated boundary layer flows at low Reynolds number
11 p1743 A72-25260
- Three dimensional laminar boundary layer on slender circular cone at angle of attack in supersonic flow, determining separated flow region via finite difference method
11 p1572 A72-25818
- Unsteady laminar wall boundary layers formation within finite expansion or compression waves in tube with gas at rest
11 p1616 A72-25981
- Mass transfer effect on adiabatic wall enthalpy and recovery factors in laminar boundary layer flow at high injection rates, using self similar solutions
11 p1746 A72-26535
- Dynamic and thermal laminar compressible boundary layers on flat plate, noting interaction of two quasi-steady flows
12 p1797 A72-27167
- Asymptotic behavior of velocity profiles in laminar boundary layers of steady incompressible fluid two dimensional flow past rigid wall
12 p1798 A72-27713
- Steady laminar boundary layer generated by vortex over fixed coaxial disk, solving governing equations by numerical integration
12 p1798 A72-27833
- Parametric approximation of unsteady laminar boundary layer in incompressible fluid in terms of flow velocity and friction characteristics
12 p1799 A72-28177
- Natural instabilities development in laminar boundary layer of incompressible flow, considering AM spectrum and abscissa-ordinate development compared to Orr-Sommerfeld equation solution
13 p1943 A72-29784
- Laminar Ekman boundary layer instability for incompressible fluid over rigid boundary with fixed vertical temperature gradient, investigating internal gravity waves generation
14 p2100 A72-30347
- French monograph on velocity profile in laminar boundary layer on semiinfinite flat plate in harmonic oscillation of uniform incompressible flow
14 p2095 A72-30949
- Hypersonic limit for equilibrium laminar constant pressure boundary layer equations of planetary entry, obtaining skin friction and heat transfer parameters
14 p2071 A72-31052
- Steady asymptotic suction profiles in free convection laminar boundary layer flows on heated vertical circular cylinder
14 p2096 A72-31070
- Shear stress distribution and local heat flux at surface of axisymmetric bodies for laminar and turbulent boundary layer flows
14 p2071 A72-31163
- Thermal laminar boundary layer equations solution for power-law velocity distribution in external flow and arbitrary surface temperature distribution
15 p2334 A72-31263
- Unsteady laminar boundary layer on body of revolution with axial and torsional oscillations, calculating velocity distribution and shear stress variation
15 p2178 A72-31402
- Energy supply calculation for two dimensional steady laminar compressible boundary layer flows with hypersonic hydrogen-air combustion
15 p2334 A72-31465
- Approximate model of weak shock wave interaction with laminar MHD boundary layers for perfectly conducting supersonic streams
15 p2284 A72-31633
- Velocity gradient induced by local wall deformation, investigating effect on unstable natural frequency amplification in laminar boundary layer
15 p2217 A72-31683
- Energy equation for solution compressible laminar boundary layer generalized with orthogonal curvilinear coordinates
15 p2218 A72-32146
- Laminar boundary layer separation point in steady two dimensional constant density flow past solid surface, deriving pressure-vorticity gradient relationship
15 p2218 A72-32467
- Unsteady Falkner-Skan flow solution by finite difference method for pressure gradient effect on transient response of laminar boundary layer
16 p2376 A72-33015
- Small disturbance behavior in laminar boundary layer on elastic surface experiencing deformation under perturbing pressure, noting surface resilience effect
16 p2377 A72-33164
- Heat transfer through laminar boundary layer with allowance for streamwise pressure gradient effect on velocity field, using I.lichtill method
16 p2477 A72-33427

Pohlhausen type integral method for dissociative binary mixture nonequilibrium laminar boundary layer on flat plate, using Crocco relationship between enthalpy and velocity profile

16 p2378 A72-33436

Mass flow rate and mean density measurements in separated laminar boundary layers with large transverse density gradients, analyzing density difference effects on instability

16 p2379 A72-33571

Incompressible flow drag caused by slot suction provided in bodies of revolution for preventing laminar boundary layer transition into turbulent state

16 p2344 A72-33678

Three dimensional small perturbation effects on laminar and turbulent low and high speed boundary layer flows

[AIAA PAPER 72-713]

16 p2344 A72-34034

Lateral pressure gradient and suction effects on laminar incompressible boundary layer separation on curved surfaces predicted by generalized tow-layer flow model

[AIAA PAPER 72-698]

16 p2380 A72-34045

Downstream effects of discontinuous injection of foreign gases in inert laminar boundary layer flows

17 p2542 A72-35632

Incident thermal flux parameters and wall temperature effects on flow characteristics in pre-separation zone of laminar boundary layer and separation point location

17 p2487 A72-35927

Self-similar separation flows in a laminar magnetohydrodynamic boundary layer during injection and suction

18 p2716 A72-36886

Rotational theory of laminar boundary layer separation of incompressible fluid from smooth surface under pressure gradients

18 p2682 A72-36887

A study of the asymptotic behaviour of the external fringes of compressible, laminar boundary layers of a dissociating gas.

18 p2683 A72-36937

Recent results on the effect of longitudinal curvature on a laminar layer

18 p2685 A72-37213

Solution of the equations of the compressible boundary layer / laminar, transition, turbulent / by an implicit finite difference technique.

19 p2785 A72-37521

Inversion of a laminar boundary layer during the injection of CO₂ through a vertical porous surface under natural convection conditions

19 p2881 A72-38191

Numerical analysis of three dimensional steady laminar free convection boundary layer due to heated ellipsoid, solving flow equations

19 p2881 A72-38394

Hypersonic unsteady compressible boundary layer dependence on Prandtl number.

19 p2787 A72-38429

Heat transfer during uniform injection on a vertical surface under conditions of combined free and forced convection

20 p2982 A72-39225

MHD instability of two dimensional laminar boundary layer in incompressible electrically conducting fluid along concave wall with periodic three dimensional disturbances

20 p2957 A72-39328

An analytical solution of wall-temperature distribution for transpiration and local mass injection over a flat plate.

[ASME PAPER 72-HT-57]

20 p2985 A72-39659

Film cooling effect on surface heat transfer in laminarizing mainstream turbulent boundary layer for injection through flush angled two dimensional slots

[ASME PAPER 72-HT-11]

20 p2986 A72-39682

A thermal boundary layer on a nonisothermal plate

20 p2987 A72-39917

Surface reactions in similar boundary layers.

20 p2915 A72-40014

Stability of laminar boundary layers on concave walls in presence of magnetic field.

20 p2958 A72-40066

An application of the shooting method to the stability problem for a stratified, rotating boundary layer.

21 p3043 A72-40106

A method for determining the motion in a laminar boundary layer.

21 p3045 A72-40813

Theory of laminar film condensation of flowing vapor.

21 p3128 A72-40950

Laminar and turbulent boundary-layer studies at hypersonic speeds.

[ICAS PAPER 72-09]

21 p2990 A72-41134

Behavior of a laminar boundary layer in the presence of a positive pressure gradient

[ICAS PAPER 72-17]

21 p3045 A72-41142

A method of computing skin friction and adiabatic wall temperature in a laminar boundary-layer without pressure gradient.

21 p3046 A72-41202

Calculation of heat shield with local mass injection in hypersonic flow.

21 p3131 A72-41235

The cooling problem in the case of laminar boundary layers of real gases

[DFVLR-SONDDR-223]

21 p3131 A72-41619

Transverse magnetic field effect on unsteady incompressible laminar MHD boundary layer flow, noting cylindrical body oscillations in fluid

21 p3095 A72-41786

Symmetrical plane-parallel boundary layer at a sudden onset of motion

22 p3164 A72-41909

Anode heat transfer for a flowing argon plasma at elevated electron temperature.

22 p3210 A72-41952

A simple quadrature method for computing laminar boundary layers.

22 p3165 A72-42110

Laminar boundary layer at critical point of blunt body in molecular oxygen flow, noting wall influence on condensation

22 p3243 A72-42257

Calculation of laminar boundary layers by means of a differential-difference method.

22 p3167 A72-42578

Evaluation of windward streamline effective cone boundary-layer analyses.

22 p3136 A72-42874

German monograph - Solution of the boundary layer equations for chemically reacting gases by a collocation method.

22 p3167 A72-43071

Calculation of separation points in incompressible turbulent flows.

23 p3279 A72-43328

Second order boundary layer solutions on a curved surface.

[ASME PAPER 72-FE-21]

23 p3280 A72-44063

Falkner-Skan flows with slip.

23 p3281 A72-44068

A note on the laminar mixing of two uniform parallel semi-infinite streams.

23 p3281 A72-44301

Measurement of the velocity distribution in the boundary layer over a flat plate with a diffusion flame.

24 p3464 A72-45062

Intermittent character of the viscous sublayer and interpretation of probability density measurements

24 p3392 A72-45072

Longitudinal curvature and displacement speed effects on incompressible laminar boundary layers.

24 p3393 A72-45249

Hydrodynamic weak-turbulence facility, equipment, and procedure for studying the stability of laminar boundary layers

24 p3388 A72-45258

Integrodifferential equations for curved walls effect on laminar boundary layer characteristics, noting wall friction, layer thickness and transverse pressure

24 p3394 A72-45447

Nonsimilar solution for laminar and turbulent boundary-layer flows over ablating surfaces.

24 p3364 A72-45782

LAMINAR BOUNDARY LAYER SEPARATION

U BOUNDARY LAYER SEPARATION

U LAMINAR BOUNDARY LAYER

LAMINAR FLAMES

U FLAMES

U LAMINAR FLOW

LAMINAR FLOW

NT BLASIUS FLOW

NT HARTMANN FLOW

NT STRATIFIED FLOW

Ion oscillation theory for electrogasdynamic channel Poiseuille and Hagen-Poiseuille type flows, using transport and dispersion equations in various ionized media

01 p0111 A72-11214

Inertia effects in fully developed axisymmetric laminar flow between two parallel rotating walls, solving Navier-Stokes equation in nonlinear form

[ASME PAPER 71-LUB-J]

02 p0234 A72-11529

Conical hydrostatic bearing optimization for minimum friction in laminar and turbulent flows, developing flow rate, load capacity and friction torque equations

[ASME PAPER 71-LUB-19]

02 p0235 A72-11539

Laminar liquid flow stability in vertical slots under natural convection, showing critical layer level for nonstationary perturbations

02 p0202 A72-11591

Laminar free jets characteristics, investigating transition to turbulence

02 p0150 A72-11730

Pure solid and composite propellants combustion theory based on laminarized solutions to energy and flow conservation equations

02 p0270 A72-11766

Laminar flow between stationary and rotating disk with mass flow through concentric circular opening by finite difference method

02 p0203 A72-12098

Slit element flow in shear flow turbopump rotors, presenting solutions for laminar and turbulent flow between two parallel disks rotating with same angular velocity

02 p0204 A72-12227

Laminar free convection from vertical nonisothermal right circular cone with boundary layer control by injection or suction, investigating heat transfer by perturbation method

02 p0204 A72-12232

Incompressible two dimensional laminar/turbulent wall jet characteristics, obtaining Prandtl mixing theory from apparent kinematic viscosity

02 p0206 A72-12619

Power law sealant effects on high aspect ratio viscoelastic performance under laminar isothermal conditions

02 p0237 A72-12851

Solar streamline flow patterns analysis test on terrestrial wind data

03 p0414 A72-12928

Velocity and temperature distributions for unsteady plane Poiseuille flow of viscous incompressible fluid between two parallel plates

03 p0340 A72-13000

Laminar flame front surface area determination, presenting graphical constructions from generatrix of arbitrary segment number

03 p0455 A72-13099

Residence time of foreign gas introduced within wake recirculation region behind slender body in axisymmetric supersonic laminar/turbulent flow

[AD-733525]

03 p0308 A72-13633

Annular MHD channel laminar flow generation at supercritical Reynolds numbers by strong magnetic fields

03 p0398 A72-14005

Steady laminar viscous conducting fluid flow in infinite rectangular channel in crossed electric and magnetic fields, deriving flow rate and potential distribution

03 p0398 A72-14008

Premixed combustible system in laminar axisymmetric stagnation flow, considering steady state and transient response of state variables, blow off extinction, ignition and heat flux

[AD-743387]

03 p0458 A72-14222

Thermal boundary layer of incompressible fluid unsteady laminar flow, obtaining temperature field from energy equation for various wall temperature conditions

03 p0343 A72-14314

Ekman boundary layer shear stress due to laminar and turbulent flow over hills

03 p0386 A72-14336

Forced convective heat transfer of laminar flow in curved channel with square cross section at constant wall heat flux

04 p0510 A72-14595

Laminar viscous flow past finite flat plate at high Reynolds numbers, solving Navier-Stokes equations

04 p0511 A72-14859

Hydrodynamic field around sphere moving along Poiseuille flow axis determined by least squares method, formulating flow resistance

04 p0511 A72-14968

Laminar shear flow over impulsively started wedges, describing flow field by Goldstein-Rosenhead method of approximate series expansion

04 p0590 A72-15190

Rectangular and triangular duct entrance region laminar flow pressure losses from velocity profiles and integral energy equation

04 p0512 A72-15194

Conducting incompressible fluid in laminar pipe flow under traveling magnetic field, investigating friction coefficient and energy balance

04 p0558 A72-15341

Bearing operating characteristics within transition range between laminar and fully developed turbulent flow, accounting for film thickness variation and pressure gradients

04 p0528 A72-15701

Radial pressure distribution in laminar flow of compressible fluid between two coaxial disks from analog computer study

04 p0514 A72-15702

Navier-Stokes equations solution by finite difference methods for steady incompressible laminar vapor flow in symmetrical and unsymmetrical heat pipes, calculating pressure losses

[ASME PAPER 71-WA/HT-15]

05 p0744 A72-15874

Incompressible laminar flow in conduit with arbitrary cross section, time varying pressure gradient and initial velocity, constructing finite series solution by orthonormalizing procedure

[ASME PAPER 71-WA/FE-22]

05 p0646 A72-15927

Confined laminar jet mixing of two uniform streams flowing in parallel plate channel, obtaining velocity field from linearized governing equation

[ASME PAPER 71-WA/APM-2]

05 p0647 A72-15973

Nonlinear disturbances of viscous flow in pipes and between rotating cylinders, considering Couette and Poiseuille flows

05 p0648 A72-16027

Cascade nozzle gas particle flow properties, discussing flow pressure experiments and theory at different streamlines

05 p0602 A72-16490

Steady inviscid diabatic complex lamellar gas flow geometric properties, correlating stream and vortex lines via Beltrami surfaces in Euclidian space

05 p0747 A72-16667

High speed boundary layer flow three dimensional disturbances interaction with thermal and ablative response in adjacent surface material, considering laminar and turbulent compressible flows

[AIAA PAPER 72-93] 05 p0748 A72-16811

Navier-Stokes equations numerical solution for laminar incompressible flow past paraboloid of revolution at zero angle of attack

[AIAA PAPER 72-110] 05 p0604 A72-16818

Laminar incompressible flow over yawed spinning bodies of revolution by Navier-Stokes solutions, discussing flow fields and corresponding force coefficients

[AIAA PAPER 72-112] 05 p0605 A72-16820

Recirculating cells in laminar coaxial jets investigated by smoke introduction into flow field and hot-wire techniques

[AIAA PAPER 72-150] 05 p0651 A72-16880

Wall thermal radiation influence on solid propellants burning rate in electrically heated tube furnace, noting correlation with laminar flame theory

[AIAA PAPER 72-35] 05 p0703 A72-16938

Vector analysis of three dimensional nonequilibrium dissociative gas flow quantity variations along stream lines

05 p0652 A72-17001

Plane Poiseuille flow stability from Orr-Sommerfeld equation solution by Chebyshev polynomials expansion and QR matrix eigenvalue algorithm

05 p0653 A72-17009

Compressibility and total enthalpy difference effects on laminar free shear layer from numerical integration of equations of motion

05 p0653 A72-17011

Polarographic method for simultaneous measurement of wall gradients of velocity and of concentration in unsteady laminar or steady turbulent flow

06 p0797 A72-17558

Navier-Stokes equation solution for laminar incompressible flow past parabolic cylinder, investigating skin friction and pressure drag

06 p0798 A72-17782

Acoustic waves refraction, reflection and transmission from moving medium layer with space-dependent velocity, considering Poiseuille flow three sublayer approximation

06 p0848 A72-17852

Perturbation methods for laminar flows near leading edge, discussing approximations of Navier-Stokes equations and domain connection

06 p0756 A72-18108

Laminar to turbulent flow transition spectral evolution and catastrophic transition, discussing visual experiments and analytical methods

06 p0800 A72-18121

Nonlinear motion stability of finite amplitude wave solution in thin viscous incompressible liquid film

06 p0801 A72-18142

Heat transfer and drag during air laminar flow in circular pipe with constant heat flux density at wall

07 p0966 A72-18938

Droplets coalescence in clouds, considering microturbulence effects due to laminar shear flow

07 p1030 A72-19102

Forced convective heat transfer for laminar flow of Newtonian fluid inside noncircular duct, taking into account viscous dissipation and work compression

07 p1100 A72-19628

Correlation for Prandtl number effect on laminar forced convective heat transfer with secondary flow

07 p1100 A72-19629

Transpiration cooling of laminar tangential Newtonian flow in annuli, obtaining temperature distribution

07 p1100 A72-19631

Heat and mass transfer in initial section of circular pipe under stabilized laminar flow, using modified Leveque method

07 p0968 A72-19883

Homogeneous laminar combustion in semiclosed cylindrical tube, relating stability to hydrodynamic and thermodynamic flow parameters longitudinal high frequency disturbances

07 p1101 A72-19988

Nonlinear stability theory for laminar flow of viscous incompressible liquids, noting application to Couette-Taylor flow between two concentric rotating cylinders

07 p0971 A72-20091

Unsteady laminar viscous incompressible electrically conducting flow between nonconducting parallel flat plates with applied constant magnetic field

07 p1044 A72-20245

Temperature fields and mass and heat transfer at surface of solid spherical particle in laminar viscous fluid flow

07 p0973 A72-20318

Heat transfer in laminar and turbulent Newtonian fluid flow in narrow channels with allowance for temperature dependence of viscosity and energy dissipation

08 p1148 A72-20955

Heat transfer effect on Poiseuille flow in channel, using modified Orr-Sommerfeld equation with additional viscosity gradient terms

08 p1252 A72-21253

Parameter calculation for laminar incompressible fluid jet expanding in gradient slipstream along moving surface, determining velocity distribution in jet axis

08 p1149 A72-21309

Surface friction coefficient dependence on Mach number and velocity gradients in adiabatic compressible laminar gas flow

08 p1107 A72-21311

Conjugate solution for Poisson equation of heat transfer in laminar flow with developed velocity profile in flat channel with internal constant heat sources

08 p1252 A72-21314

Free convection and hydrodynamics of inclined liquid layers in laminar flow and in stepwise change of heat exchange surfaces temperature

08 p1151 A72-21663

Laminar free convective flow of viscoelastic fluid past infinite porous plate

08 p1151 A72-21748

Concentric double and single screw seals in laminar Newtonian fluid flow operation, using mathematical methods for optimum thread geometry and maximum sealing coefficients

08 p1178 A72-21930

Sealing pressure and optimal groove form for concentric running screw viscosity seals in laminar flow

08 p1178 A72-21931

Test apparatus and measurement of sealing pressure and temperature in threads of concentric running screw viscosity seals in laminar flow

08 p1178 A72-21932

Boundary value solutions and computer programs for one dimensional laminar flame propagation equations

08 p1129 A72-22040

Bromine additions effect on normal laminar flame propagation velocity of methane-air mixture at high pressures

09 p1411 A72-22889

Resonant frequencies of viscous liquid in rectangular tank calculated from stream functions, assuming two dimensional oscillations and laminar flow

09 p1295 A72-23074

Flame structure studies of stabilizing region of near stoichiometric laminar burner methane-air flame

09 p1411 A72-23147

Adiabatic velocity profiles and pressure variations of developing laminar flow in circular tube, using finite difference computation in FORTRAN IV

10 p1463 A72-23863

Fully developed laminar flows in ducts with secondary motions, considering annuli with rotating core, pipe with swirl generator and straight rectangular duct

10 p1463 A72-23865

Electromagnetic coupling between one dimensional laminar flows of viscous conducting fluid in presence of magnetic field, noting static and dynamic efficiencies dependence on Hartmann number

10 p1519 A72-24065

Initial disturbance level effects on laminar viscous jet stability from calculation of maximum amplification rate as function of physical parameters

10 p1465 A72-24149

Navier-Stokes equations numerical solution for symmetric laminar incompressible flow past parabolic cylinder, presenting surface pressure, friction and pressure drag results

10 p1465 A72-24291

Laminar flow dispersion coefficient for curved tubes and channels determined by mathematical model, permitting concentration distribution computation

10 p1468 A72-24371

Antisymmetric turbulences linear stability in incompressible plane Poiseuille flow between flexible walls solved by variational boundary value problem formulation

10 p1468 A72-24372

Finite amplitude disturbances effect on plane Poiseuille flow hydrodynamic stability, presenting numerical method for solving parabolic partial differential equations derived from Navier-Stokes equation

10 p1468 A72-24422

Infinitesimal centered disturbance effect on plane Poiseuille flow at supercritical Reynolds number, determining modulated wave as function of position and time

10 p1562 A72-24423

Conducting fluid laminar free convective flow over heated rotating horizontal plate in presence of strong magnetic field aligned with rotation vector

10 p1522 A72-24465

Diffuser performance and idling characteristics in shock tube at Mach 8, discussing pressure recovery factor laminar and transition flows in boundary layer

10 p1419 A72-24545

Perturbation analysis for forced flow past semi-infinite flat plate parallel to uniform mainstream, calculating two dimensional laminar film condensation by boundary layer theory

10 p1469 A72-24563

Spheres drag coefficient measurements in laminar flow as function of Reynolds number, using wind tunnel model magnetic suspension system

10 p1419 A72-24772

Energy transfer in thermally developing laminar gas flows with radiative interaction, using total band absorptance model

[AD-745475] 10 p1563 A72-25043

Second order fluids plane Poiseuille flow instability to finite amplitude disturbances, noting implications to Toms friction pressure reduction phenomenon in pipe flow

10 p1470 A72-25065

Friction drag coefficient determination for cylindrical bodies in laminar and turbulent incompressible fluid flow

10 p1420 A72-25135

Plane laminar semibounded incompressible fluid jet propagation into slipstream along moving plate, solving boundary layer equations

10 p1471 A72-25136

Axial pressure variations in incompressible laminar tube flow with uniform suction, noting application to heat pipes

[AIAA PAPER 72-257] 11 p1614 A72-25202

Noncondensable gas and forced convection effects on laminar film condensation for two phase flows

11 p1743 A72-25261

Laminar viscous flow past semiinfinite flat plate at zero incidence, using Oseen approximation in matching leading edge and potential flow regions

11 p1615 A72-25522

Flow fields and inviscid core of two dimensional diffuser with fluid extraction on diverging walls, describing streamline patterns, stagnation region and stall conditions

[ASME PAPER 72-GT-2] 11 p1568 A72-25605

Thermodynamic coupling effects on temperature distribution, Nusselt number and cooling requirements in laminar nonisothermal pipe flow with coolant injection

11 p1745 A72-25734

Stationary MHD aligned flows of ideal incompressible fluids with same streamline patterns in plane, axisymmetric and spatial flows

11 p1695 A72-25910

Fluid compressibility effect on nonstationary laminar flow within infinite cylindrical pipe

11 p1618 A72-26502

Laminar transition and turbulent natural convection mass transfer measurements on inclined and vertical surfaces by electromechanical method

11 p1635 A72-26536

Laminar and turbulent compressible wall jet characteristics, obtaining density variation as function of velocity and Mach number at exit

11 p1618 A72-26593

Turbulent pipe flow laminarization by fluid injection, measuring axial turbulence intensity field and streamwise velocity distribution by hot-film anemometer

11 p1619 A72-26636

Incompressible laminar subcritical flow with separated wake past symmetric two dimensional bluff body, calculating upstream pressure distribution and separation point

12 p1751 A72-27172

Plane Poiseuille flow Orr-Sommerfeld problem numerical solutions comparison and computer program implementation

12 p1797 A72-27192

Galerkin boundary method as variational approach to low Peclet number heat transfer in laminar flow

13 p2063 A72-28418

Theoretical and computer simulation of laminar interactions of plasmas with different mass and density, discussing piston-ion dynamics solutions

13 p2009 A72-28427

Nonuniform inlet velocity profile effect on laminar flow development between parallel plates, solving equations by finite difference method

13 p1941 A72-28706

Laminar channel flow stability loss dependence on Reynolds number and wave number, discussing conditions for separated flow self oscillations

13 p1941 A72-28765

Orr-Sommerfeld equation solution by variable mesh finite difference method, applying to plane Poiseuille flow

13 p1986 A72-29112

Two dimensional laminar compressible flow of electrically conducting gas at thermodynamic equilibrium and perpendicular to magnetic field lines

13 p2013 A72-29362

Nonstationary laminar zero-discharge MHD Couette flow produced by sudden movement of highly conductive plate in closed volume filled with conducting liquid

13 p2016 A72-29607

Unsteady laminar natural and forced convection at transparent medium boundary layer radiating surface, noting turbulence effects on heat exchange

13 p2066 A72-29902

Large scale motion of turbulent boundary layer during relaminarization under strong pressure gradient, obtaining fluctuating velocity components and tangential Reynolds stress

13 p1944 A72-30028

Localized point centered initial disturbances effects on marginally unstable plane parallel flow, presenting differential equations solution for nonlinear response

14 p2094 A72-30366

Magnetic and electric field effects on steady state laminar MHD Couette flow of non-Newtonian fluids governed by Prandtl rheological law or Ostwald-de Waele power law

14 p2139 A72-30717

Velocity perturbation functions in linear theory for bounded stream flow past slender profile

14 p2070 A72-31018

Velocity and temperature profiles of plane Poiseuille flow with finite amplitude convection and longitudinal vortices, investigating uniform axial temperature gradient effect

14 p2173 A72-31063

German monograph on mass transport in thin fluid layers covering diffusion, convection, laminar flow rate distribution, flame ionization and gas chromatography measurements, etc

15 p2216 A72-31350

Heat conductivity equation solution for laminar gas flow in tubes, calculating temperature field and heat removal for molecular lasers with gas pumping

15 p2245 A72-31421

Wind tunnel measurement of intermittency in turbulent boundary layer on porous plate for alternating laminar and turbulent air flow

15 p2217 A72-31610

Flow induction by cylinder performing transverse periodic vibrations in viscous fluid, noting jet flow with large streaming Reynolds number

15 p2217 A72-31617

Contracting or diverging stream flow mean velocity change effects on airfoil pressure distribution, circulation and lift, deriving vortex distribution expression

15 p2179 A72-32023

Steady laminar MHD flow of viscous incompressible electrically conducting fluid between long concentric rotating porous cylinders under radial magnetic field

15 p2287 A72-32397

Nonlinear stability theory for plane Poiseuille flow under finite amplitude perturbations, solving Orr-Sommerfeld boundary value problem via finite difference method

15 p2218 A72-32469

Heat transfer to two dimensional laminar flow, calculating axial conduction and fluid preheating effects on adiabatic forced convection at low Peclet number

15 p2336 A72-32478

Flow theory improvement for laminar radial flow between parallel plates, considering inertial effects

15 p2219 A72-32479

Converging plane-walled channels, calculating laminar flow development and heat transfer by finite difference method

15 p2336 A72-32481

Space charge electron flow between parallel conducting walls, developing relativistic method for potential and field distribution time variation

15 p2279 A72-32510

Incompressible elastico-viscous liquid steady state laminar source flow between stationary infinite porous disks, noting Reynolds number effects

15 p2219 A72-32512

Heated thin film gages calibration for skin friction measurements in laminar and turbulent flows, discussing wall temperature distribution and turbulence effects

15 p2241 A72-32577

Internal aerodynamic problem solution by kinetic equation for Couette and Poiseuille flows and heat transfer between plane plates

16 p2343 A72-33153

Thermal protection by liquid-gas laminar flow near critical point with coolant film liquid oxygen injection incident on blunt body

16 p2343 A72-33156

Linearization and perturbation procedures to calculate nonlinear effects in fluid stability problems with application to nonlinear critical layer

16 p2377 A72-33338

Time behavior of two dimensional laminar free convection flow between heated vertical parallel plates, calculating temperature and velocity distributions as function of Grashof number

16 p2477 A72-33426

Energy and momentum losses of high temperature gas flow through externally cooled tube, solving laminar flow differential equations numerically on digital computer

16 p2378 A72-33430

Curved surface laminar flow turbulence front expansion rates measurement at high Reynolds number on experimental setup, considering centrifugal forces

16 p2379 A72-33792

Plane Poiseuille flow stability of incompressible second order fluids, noting destabilizing influence of viscoelasticity

16 p2379 A72-33829

Flat flame deflagration tube measurements of laminar flame velocities for propane-ammonia-air mixtures in fuel rich region

16 p2480 A72-34006

Reattachment heat transfer for laminar or turbulent separated shear layers, comparing predictions with measurements for cavities, ramps, spiked-nose bodies and forward facing step

[AIAA PAPER 72-717] 16 p2344 A72-34031

Flat plate leading edge blunting and wall cooling effects on supersonic laminar flow ramp-induced separation

[AIAA PAPER 72-716] 16 p2344 A72-34032

Theoretical study of electromagnetic coupling in the forced oscillatory regime of two one-dimensional laminar flows of a viscous and electroconducting liquid in the presence of a transverse uniform magnetic field

17 p2587 A72-34281

Flows between stationary surfaces of revolution, having similarity solutions.

[ASME PAPER 72-APM-4] 17 p2537 A72-34304

An asymptotic solution for the laminar flow of a thin film on a rotating disk.

[ASME PAPER 72-APM-38] 17 p2538 A72-34783

Determination of the excess air coefficient with the aid of electrical properties in the case of laminar flames of gaseous fuels

17 p2636 A72-34931

Effect of rotation on laminar compressible fluid flow in a vertical cylinder.

17 p2539 A72-34972

Heat and mass transfer in initial section of circular pipe under stabilized laminar flow, using modified Leveque method

17 p2637 A72-35131

Unsteady temperature distribution for laminar flow in a porous straight channel.

17 p2541 A72-35434

Laminar gas flow in narrow channels of constant and variable cross sections in the presence of heat transfer

17 p2543 A72-35807

Flow problems solutions estimation by variational principles application, exemplifying by plane Couette and Poiseuille and axisymmetric pipe flow

18 p2679 A72-36391

The stability of Poiseuille flow in a pipe of circular cross-section.

18 p2681 A72-36480

Poiseuille flow linear spatial stability in rigid pipe under infinitesimal disturbances, obtaining propagation modes eigenvalues

18 p2681 A72-36481

Moving periodic thermal wave induction of nonlinear motions in Boussinesq fluid layer, solving nonlinear two dimensional momentum and temperature equations

18 p2681 A72-36485

A new method of analysis in laminar flow theory.

18 p2681 A72-36551

Solution of some mixed boundary value problems of conducting medium thermodynamics by the method of variable separation

18 p2715 A72-36802

Flow phenomena in turbomolecular pumps

18 p2696 A72-36837

Instability of a moving plane-parallel layer

18 p2682 A72-36883

Propagation of an impurity in a laminar flow in a circular tube

18 p2682 A72-36892

Laminar flow in an annulus with porous outer wall.

18 p2683 A72-37054

Time dependent solution to motion and energy equations for unsteady laminar spherical Couette flow of incompressible constant viscosity fluid

18 p2684 A72-37055

Calculation of thermal fluxes and temperatures on the surfaces of a plate in the presence of heat exchange between fluids incident on the surfaces

18 p2742 A72-37183

Topler schlieren study of diffusion flame structure of plane laminar hydrogen-air jets in rectangular channel with vortex generators

19 p2879 A72-37365

General solutions of the heat equation in finite regions.

19 p2880 A72-37411

Perturbations development in laminar flow and transition to turbulent flow based on nonlinear theory of hydrodynamic stability

19 p2785 A72-37468

Heat transfer and resistance in a laminar gas flow with variable properties in an annular channel

19 p2786 A72-38040

Burke-Shumann-Zeldovich model for aerodynamic characteristics of straight jet laminar diffusion flames, considering free, semibounded and slipstream types

19 p2882 A72-38460

Heat transfer by laminar natural convection in low aspect ratio cavities.

[ASME PAPER 72-HT-52] 20 p2985 A72-39661

Viscous non-adiabatic laminar flow through a supersonic nozzle - Experimental results and numerical calculations.

[ASME PAPER 72-HT-49] 20 p2985 A72-39662

Laminar free convection from a rotating radial plate.

[ASME PAPER 72-HT-46] 20 p2985 A72-39664

Non-isothermal laminar flow of gases through cooled tubes.

[ASME PAPER 72-HT-45] 20 p2985 A72-39665

Heat and mass transfer in the initial mixing region of confined coaxial laminar jets.

[ASME PAPER 72-HT-22] 20 p2986 A72-39674

Optical measurements in a pulsating flame.

[ASME PAPER 72-HT-8] 20 p2926 A72-39679

Sting-free measurements of sphere drag in laminar flow.

21 p2989 A72-40110

Stability loss in Poiseuille flow within two dimensional channel during Reynolds number passage through critical value

21 p3044 A72-40265

Periodic wave of oscillating and stationary two dimensional bodies immersed in uniform incompressible stream, investigating semiinfinite vortex trails relationship to oscillating airfoils

21 p2989 A72-40651

Nonstationary laminar zero-discharge MHD Couette flow produced by sudden movement of highly conductive plate in closed volume filled with conducting liquid

21 p3091 A72-40661

Axial velocity distribution and streamline boundary selection to derive two dimensional infinite duct shapes for inviscid irrotational compressible flows

[ICAS PAPER 72-08] 21 p2990 A72-41133

Influence of blowing on the resistance of a sphere in laminar viscous fluid flow

21 p3047 A72-41665

Propagation of viscous fluid jets in a medium with a density discontinuity

21 p3047 A72-41666

Trajectory equations of laminar electron flow in exponential magnetic field, calculating electrode shapes of magnetron injection electron gun

21 p3088 A72-41835

Heat transfer, adiabatic enthalpy /temperature/ of the wall, and hydrodynamic resistance in the presence of turbulent and laminar flow of a compressible fluid in a round tube

22 p3164 A72-41883

Experimental investigation of the effect of an electric field on a laminar flame

22 p3243 A72-41889

Unsteady laminar flow in a tube with arbitrary variation of the flow rate in time

22 p3164 A72-41892

Studies on the convective heat transfer from a rotating disk. VI - Experiment on the laminar mass transfer from a stepwise discontinuous naphthalene disk rotating in a uniform forced stream.

22 p3243 A72-41946

Laminar to turbulent transition in axisymmetrical submerged jets and slipstream flows of air and He, discussing Reynolds number effect

22 p3166 A72-42270

Approximate calculation of a laminar arc discharge in a cylindrical channel

22 p3210 A72-42285

Extremal bounds for mass flow rate of laminar MHD flow in circular and thin walled conducting pipes at high Hartmann number

22 p3210 A72-42315

Singular points in conical flow streamline patterns, considering rotational and irrotational flows

22 p3135 A72-42580

Behavior of the lines of flow in the proximity of the stagnation points of blunt bodies

22 p3136 A72-42905

Fluid dynamic forces exerted by Newtonian fluid axisymmetric creeping flow on accelerating body of arbitrary shape, calculating pressure gradient via Navier-Stokes equation

23 p3347 A72-43726

Approximation for boundary value problem of homogeneous stationary combustion in laminar gas flow through cylindrical tube

23 p3356 A72-43798

Noncoaxial rotations of a disk and a fluid at infinity

23 p3248 A72-43824

A numerical experiment on two-dimensional turbulent separation. 24 p3389 A72-44687

Developing laminar and turbulent duct flow with chemical reaction. 24 p3378 A72-45061

Stability of the laminar flow of a 'power-law' non-Newtonian fluid in the boundary layer on a flat plate. 24 p3393 A72-45255

Diffusion flame in homologous turbulent shear flows. 24 p3395 A72-45564

LAMINAR FLOW AIRFOILS

Laminar flow airfoils for gliders, optimizing profiles for favorable velocity and pressure distribution. 05 p0610 A72-17194

LAMINAR FLOW CONTROL

U BOUNDARY LAYER CONTROL

U LAMINAR BOUNDARY LAYER

LAMINAR HEAT TRANSFER

Finite difference technique for heat transfer rate in laminar flow in tube with step change in cross section, discussing velocity profiles. 02 p0301 A72-11723

Temperature dependent gas internal diatomic laminar heat transfer, investigating continuity, energy, momentum for two dimensional flow between heated parallel plates. 02 p0302 A72-12317

[ASME PAPER 71-HT-N] Newtonian fluid laminar free convection over curved wall with arbitrary temperature variation, investigating similarity solutions existence by method of free parameters. 04 p0596 A72-15193

Laminar natural convection heat transfer from leading edge of isothermal plate under nonuniform gravity. 08 p1250 A72-20875

[ASME PAPER 71-HT-CC] German monograph on heat transfer in chemically reacting gases covering laminar and turbulent tube flows for dissociated dinitrogen tetroxide. 09 p1274 A72-22339

IR radiative energy transfer to laminar flow of non-gray absorbing emitting gases through circular tube. 10 p1563 A72-25038

Laminar and turbulent convective heating distributions on delta wing space shuttle boosters with interference effects. 11 p1567 A72-25249

[AIAA PAPER 72-315] Laminar free convection about isothermal horizontal cylinders with constant heat flux, calculating velocity and temperature profiles. 11 p1743 A72-25263

Converging plane-walled channels, calculating laminar flow development and heat transfer by finite difference method. 15 p2336 A72-32481

Effects of vorticity, displacement speed and curvature on heat transfer with dissipation. 17 p2638 A72-35747

Iterative calculation of a three-dimensional boundary layer and comparison with experiment. 17 p2543 A72-35748

Transient laminar free convection in closed spherical containers. 20 p2986 A72-39669

[ASME PAPER 72-HT-37] Buoyancy effects on laminar heat transfer in the thermal entrance region of horizontal rectangular channels with uniform wall heat flux for large Prandtl number fluid. 22 p3243 A72-41956

LAMINAR JETS

U JET FLOW

U LAMINAR FLOW

LAMINAR MIXING

Velocity distribution in mixing layer between fluid at rest and in uniform stream by solving Blasius equation with boundary points. 05 p0653 A72-17078

Nonequilibrium dissociating gases high speed laminar mixing layers, comparing approximate closed form solution with numerical solution. 05 p0653 A72-17150

[VPI-E-71-22] Laminar mixing zone calculated for two homogeneous compressible gas flows with pressure gradient, noting coincidence of velocity distribution for identical gas dynamic parameters. 14 p2070 A72-31009

A note on the laminar mixing of two uniform parallel semi-infinite streams. 23 p3281 A72-44301

Laminar high speed mixing of nonequilibrium dissociating gases. 24 p3392 A72-45056

LAMINAR WAKES

Laminar near wake solutions for slender ablating cone under supersonic atmospheric entry conditions including boundary layer reactions. 07 p0907 A72-18954

[AIAA PAPER 72-116] Book on steady laminar supersonic and hypersonic wakes covering near and far region solutions, boundary layer separation, etc. 09 p1261 A72-23029

Solution of the two-dimensional, unsteady, compressible Navier-Stokes equations using a second-order accurate numerical scheme. 17 p2538 A72-34666

Compressible laminar wake behind a thin flat plate. 19 p2747 A72-38798

LAMINATED MATERIALS

U LAMINATES

LAMINATES

Yield-fracture criterion for angle ply laminate cylinders wound with filament in biaxial tension. 01 p0090 A72-10521

Temperature and compressive loading cycles effects on high performance multilayer insulation materials and composites, discussing application to space shuttle orbiter. 01 p0092 A72-10779

Laminated orthotropic plates and shallow shells structural analysis using finite element program. 01 p0140 A72-10984

Two-layered plane strain elastic cylinder with cracked inner bore under internal pressure loading, obtaining stress intensity factors by finite element method. 01 p0141 A72-10994

Mechanical strength and performance of combined multicomponent bonded materials, including laminar, fiber, flake filled and metal matrix composites. 01 p0093 A72-11086

Three dimensional heat conduction behavior in laminated composites calculated from continuum model using asymptotic developments. 02 p0300 A72-11547

Stress-strain characteristics of stochastically reinforced materials of high rigidity orthotropic elastic layers alternating with isotropic elastic or viscoelastic layers. 02 p0248 A72-11623

Macroscopic fracture mechanics of composite laminates, discussing flawed specimen static strength prediction. 02 p0249 A72-11983

Thick orthotropic off-axis laminated plates vibration equations solution, presenting natural frequencies spectra and modal functions. 02 p0249 A72-11988

Unidirectional and bidirectional composite laminates subjected to cylindrical bending under uniformly distributed and concentrated loads. 02 p0292 A72-11989

Ultrasonic measurement of orthotropic laminated composites elastic moduli, describing stress-strain response. 02 p0249 A72-11994

[AD-736007] Postshear buckling, diagonal tension behavior of rectangular laminated boron-epoxy plates clamped on each side, observing stacking sequence effect. 02 p0249 A72-11995

Orthotropic glass fabric laminate creep under combined torsion and tension, describing test facility. 02 p0250 A72-12677

Three layer plates elastoplastic stability, describing breakdown conditions by five differential equations with five unknown variables. 02 p0299 A72-12690

Microwave propagation through laminated metallic media with gyromagnetic effects, applying dc magnetizing field normal to film plane. 03 p0323 A72-13784

[IEEE PAPER 31.6] Axisymmetric contact problem for circular flat stamp on laminated half space, using matrix calculus and Hankel transforms. 03 p0448 A72-13903

Laminate materials, sockets and connectors for cost-effective high temperature accelerated life testing of IC. 03 p0336 A72-14283

Carbon fiber-resin laminates ballistic impact resistance, discussing damage and interlaminar shear strength. 04 p0537 A72-15089

Maraging steel laminates stress corrosion cracking behavior, showing composite base plate and weld structure influence on crack propagation reduction. 04 p0534 A72-15569

Discrete variable approach for stress wave propagation in axisymmetric layered elastic-plastic solids. 04 p0593 A72-15626

Mechanical behavior of uniaxially loaded multilayered oriented fiber cylindrical composites, observing tensile transverse stresses. 05 p0732 A72-15792

[ASME PAPER 71-MET-O] Composite multilayer fibrous shell structural design optimization, using nonlinear mathematical programming methods. 05 p0733 A72-15943

[ASME PAPER 71-WA/DE-12] Bimetallic rectangular plate with two interconnected layers of anisotropic and isotropic materials and large deflections in nonuniform pressure and temperature field. 05 p0735 A72-16016

Laminated anisotropic imperfect circular cylindrical shells under axial compression, obtaining upper bound buckling load solution. 05 p0740 A72-16893

Carbon fiber laminates for helicopter components weight reduction. 05 p0681 A72-16999

Flexure analysis of isotropic Reissner flat plates bonded by adhesive layer, deriving stress distribution equations in general tensor form. 07 p1089 A72-19688

[AIAA PAPER 71-148] Elastic stability of laminated circular plate with rectangular anisotropy under in-plane compression forces along edge. 07 p1090 A72-19693

Buckling under uniaxial compressive load of structural sections and stiffened flat plates reinforced with laminated composites. 07 p1090 A72-19732

Strength and plasticity characteristics of hardened multilayer structural steels, investigating layer thickness effect. 07 p1013 A72-19746

Elastic properties of bonded orthotropic layer plates, finding good agreement with fiberglass reinforced plastic laminates. 07 p1097 A72-20596

Freely supported three layer cylindrical panel stability and critical loads under combined uniform axial compression and transverse pressure. 08 p1242 A72-20907

Holographic interferometry for nondestructive testing, discussing applicability to laminate structures. 08 p1164 A72-20924

Elastic unbounded homogeneous layer separation from half plane under normal load pressures, determining contact area with base for elastic moduli relationships. 08 p1243 A72-21233

Rational parameters and reinforcement of stiffened laminar plates with instability tendencies under compression loads. 08 p1243 A72-21236

Chlorogenic acid based Hetrion 92C fire retardant chemical resistant polyester for fiberglass reinforced structure applications. 08 p1192 A72-21677

Betatron electron beam evaluation for flaw detection in laminated materials by radiographic and radiometric methods. 08 p1177 A72-21774

Plane wave propagation in laminated reinforced elastic plates with difference-differential equations analysis. 08 p1247 A72-21809

Heat absorption and liberation by glass fabric laminates under uniaxial tension, determining thermal effects dependence on strain rate and test temperature by calorimetric measurements. 08 p1195 A72-21853

Bending under concentrated load of laminated cantilever plate with low interlaminar rigidity, taking into account low shear resistance effects. 08 p1248 A72-21860

Creep test for microfailures of glass reinforced epoxy and polyester laminates immersed in water at ultimate flexural stress. 09 p1336 A72-22537

Interlaminar shear testing of composite materials, discussing short beam, scissor and torsional methods. 09 p1337 A72-22542

[PI PAPER 7] Unidirectional and orthogonally cross-ply carbon fiber reinforced plastics laminates, determining interlaminar shear strength and fatigue life. 09 p1337 A72-22543

[PI PAPER 8] Stress-strain state of circular three layer laminar plates freely supported at circumference and loaded at edge. 09 p1399 A72-22694

Thermoelastic problem of open orthotropic multilayer shell of revolution, obtaining one dimensional boundary value problem solutions by numerical orthogonalization method. 09 p1400 A72-22712

Thermal insulations in form of thin shells of revolution with rigid external and elastic internal layers resting on rigid core. 09 p1400 A72-22713

Elastoplastic stressed state of multilayer cylinder during loading, unloading and cyclic loading processes. 09 p1401 A72-22721

Axisymmetrically heated orthotropic multilayer cylindrical shell with shear sensitive couplings and elastic stiffener, investigating stability and critical force under compression. 09 p1402 A72-22735

Continuum model for cylindrical and spherical elastic laminated composites deformation, using balance and constitutive equations. 09 p1405 A72-22992

Microelastic stress mechanics of thinly laminated orthotropic multilayered plates, taking into account skin effect. 09 p1405 A72-22994

[AD-739807] Three dimensional dynamic analysis of multilayered orthotropic viscoelastic plates, taking into account skin effect. 09 p1405 A72-22995

[AD-739806]

Loading process behind reflected and refracted shock waves in plastic layered media with linear elastic unloading

09 p1353 A72-23555

Electrical resistivity restoration in Van Arke type Zr deformed by lamination at 78 K attributed to point defects elimination

10 p1495 A72-24085

Macroscopic elastic constants of three dimensional multilaminar composites with anisotropic layers, assuming stress and displacement continuity

10 p1555 A72-24256

Thermal stress analysis of laminated alternate ply cylindrical shells under internal pressure, using Donnell equations

10 p1556 A72-24257

Crack toughness tests of fiber composite laminates, using linear elastic fracture mechanics

10 p1500 A72-24258

Cross-ply laminates effective elastic moduli relations based on generalized Hooke's law

10 p1556 A72-24264

Interaction diagram for mixed crack extension modes in unidirectional graphite-epoxy laminates from critical load test data

10 p1501 A72-24265

Glass content and temperature effects on fabric reinforced plastic laminates static behavior, analyzing tensile and bending strength and elastic moduli

10 p1501 A72-24660

Colaminated boron-polyimide film effect on strength of graphite fiber-epoxy resin composite double lap bolted joints

[AIAA PAPER 72-382]

11 p1730 A72-25405

Linear elastic fracture mechanics extension to fiber reinforced plastic composite laminates, noting dependence on homogeneous model validity

[AIAA PAPER 72-384]

11 p1730 A72-25406

Heterogeneous shear deformation effect on dynamic response of laminated plates for various local elastic deformation and interface conditions

[AIAA PAPER 72-398]

11 p1731 A72-25419

Two stress level cumulative fatigue damage prediction for glass fiber-epoxy laminates

11 p1670 A72-25462

Interlaminar shear properties of polymer matrix composites from dual element beam moment test

11 p1671 A72-25465

Stress concentrations around circular openings and failure criteria for orthotropic and anisotropic composite laminated plates subjected to uniaxial, biaxial and shear loading

11 p1732 A72-25474

Anisotropic graphite composite laminates cutouts stress analysis by finite element method, predicting structural reinforcement behavior

11 p1672 A72-25475

Moment stress-strain state of two layer circular cylindrical shells under creep conditions

11 p1733 A72-25542

Bending deflection calculation for laminated beams with layers of different rigidity

11 p1733 A72-25546

Multilevel structural analysis for multilayered fiber-epoxy and metal matrix composites, using FORTRAN IV

11 p1601 A72-26033

Laminated reinforced plastics structural design criteria obtained by statistical and deterministic approach

11 p1737 A72-26235

Multilayer dielectric reflective coatings performance in solid state laser pumping systems

11 p1649 A72-26345

Bending problem for circular three layer plate with rigid circular insert, studying deflection under bending moment

12 p1879 A72-27090

Plane unstable deformation and stability loss of incompressible laminated composites under highly elastic strains

12 p1880 A72-27229

Algebraic equations for displacement and stress vectors at faces and interfaces of elastic multilayered cylinders and infinite wedges, using matrix method

12 p1884 A72-27565

Crowded photographic emulsions, predicting granularity of multilayer sandwich as function of layers number

12 p1808 A72-27676

Fiberglass replacement by organic fiber for L-1011 interior sandwich panels and laminates, considering Nomex fiber in woven fabric

12 p1835 A72-28099

Thin surface film lamination in antifurcation carbon-graphite materials under critical specific pressure, discussing crystalline phase in wear products

12 p1818 A72-28192

Stress calculation in inflexible overlapping cemented joint of orthotropic layers, taking into account joining geometry and elastic properties anisotropy

13 p1962 A72-28396

Vibrations and plane wave propagation in laminated elastic plates and cylinders, noting finite element method for conical shells

[AIAA PAPER 72-406]

13 p2056 A72-28959

Transient stress pulses propagation in obliquely laminated composites, comparing analytically predicted waveforms with experimental results

13 p2060 A72-29693

Static deformation of laminar orthotropic shells of revolution with variable rigidity, using integral correlation method

13 p2061 A72-29795

System of equations derived for unsteady temperature field of arbitrary multilayer shell, using polynomial expression as temperature approximation for shell thickness

13 p2066 A72-29949

Coating materials for metal surface wear inhibition by adhesive and abrasive interactions minimization, discussing laminar solids, plastics, ceramics and soft metals

[ASME PAPER 72-DE-48]

14 p2108 A72-30874

Bending deflections of rectangular plates with laminated orthotropic layers analysis by finite element displacement, comparing with carbon fiber reinforced plastic structures

14 p2167 A72-30905

Laminated plate continuum theory with microstructure, studying one dimensional harmonic wave propagation in infinite laminate

14 p2169 A72-31147

Heat flux nondestructive inspection methods for laminate and sandwich structures and electronic components

15 p2232 A72-31322

Stress analysis and deflection equation for uniformly loaded and heated two layer clamped rectangular plate

15 p2322 A72-31362

Debonded laminar composite torsional stress intensification analysis near circular shaped imperfection based on Hankel transform and dual integral equations solution

15 p2261 A72-32247

Stress and displacement solution to Lamé problem for multilayer spherical vessels and cylindrical tubes in nonlinear elasticity theory

15 p2333 A72-32679

Transverse shear deformations in laminated anisotropic plates from generalized treatment for isotropic and sandwich plates with homogeneous cores

[AD-745613]

16 p2375 A72-32846

Linearly elastic, transversely isotropic multilayer system, presenting stress and stability problem for two dimensional strain states

16 p2466 A72-33022

General analysis and synthesis of alloys and materials with inhomogeneous physical properties, noting thermal physicochemical methods for laminates and metal powders

16 p2405 A72-33095

Optimal composite structures of multilayer spherical vessels in terms of elastic deformation under critical loads in thermal field

16 p2467 A72-33158

Lamb wave technique for bond strength testing of laminated or clad metal sheets, calculating displacement and stress dispersion and amplitude distribution for different modes

16 p2391 A72-33230

Fillers effect on polytetrafluoroethylene friction properties, electroconductivity and thermal conductivity, noting friction coefficient reduction by laminar filler structures

16 p2413 A72-33269

Elastic buckling of simply supported sandwich panels with fiber reinforced laminated face plates and honeycomb cores subjected to uniform end loading

16 p2469 A72-33405

Composite cylinder of helically wound fiber laminates, calculating torsional fracture strength with allowance for plastic deformation due to matrix distortion

16 p2472 A72-33949

Composite cylinders of helically wound fiber laminates, predicting burst fracture strength under internal pressure for comparison with experiment on epoxy-glass cylinders

16 p2472 A72-33950

Anisotropic laminated plates theories reliability comparison, noting applications to thin and sandwich plates

17 p2625 A72-34326

On the analysis of unsymmetrical cross-ply rectangular plates.

17 p2626 A72-34328

On natural vibrations and waves in laminated orthotropic plates.

[ASME PAPER 72-APM-14]

17 p2581 A72-34803

On a laminated orthotropic shell theory including transverse shear deformation.

[ASME PAPER 72-APM-7]

17 p2629 A72-34807

Calculation of sum-frequency electromagnetic waves emitted by a multilayer nonlinear plate

17 p2516 A72-35168

Elastic behavior of multilayered bidirectional composites.

17 p2632 A72-35234

Stress pulse attenuation in cloth-laminate quartz phenolic.

17 p2571 A72-35284

Static and tension fatigue and free edge delamination damage induced by uniaxial tensile loads in flat graphite/epoxy laminate coupons

17 p2571 A72-35291

Finite element solutions for laminated thick plates.

17 p2633 A72-35292

Shear deformation in heterogeneous anisotropic plates.

17 p2633 A72-35294

A sandwiched layer of dissimilar material weakened by crack-like imperfections.

18 p2737 A72-37058

Internal buckling of a laminated medium.

18 p2737 A72-37059

Thermal expansion at elevated temperatures. III - A hemispherical laminar composite of pyrolytic graphite, silicon carbide and its constituents between 300 and 800 K.

19 p2822 A72-37463

Heat-conduction equations for multilayer shells

19 p2881 A72-38158

Elastic impact on a three-layer plate in the presence of concentrated masses and nonlinear restraints

19 p2877 A72-38159

Dispersion hardening fabrication of hollow cooled blades of thin cermet layer and embedded plastic metal core, using aluminum oxynitrate in water-alcohol solution

19 p2809 A72-38282

Features of deformation and stress distribution in a laminated plastic

20 p2944 A72-38948

Laminar composite materials with special physical properties

20 p2940 A72-39451

Aluminum/plastic semifinished material - A new material for multiple applications

20 p2944 A72-39452

Dynamic characteristics of composite laminates.

20 p2979 A72-39558

Plane strain bending of laminated fibre-reinforced plates.

20 p2982 A72-40021

Boron polyimide composite development.

21 p3072 A72-40553

Multilayer shell theories with allowance for transverse shear and transverse normal deformation of layers, noting viscoelastic material and anisotropic shallow shells

21 p3125 A72-41537

Numerical analysis of wave processes in a three-layer strip with rigid filler

22 p3232 A72-41872

Simple thickness modes for laminated composite materials.

22 p3235 A72-42465

Multilayer shells structural analysis via equilibrium equations transformation into system of equivalent equations

22 p3238 A72-42836

German monograph - Contribution to the reinforcement of plastics with special allowance for the reinforcement and matrix materials.

22 p3197 A72-43078

Finite element method optimization of orthotropic layered shells of revolution under mechanical and thermal loadings, considering stress-strain relationships

[SAWE PAPER 939]

23 p3344 A72-43479

A crack stopper concept for filamentary composite laminates.

23 p3305 A72-43498

Modified Hellinger-Reissner variational method applicable to harmonic waves moving normal to fiber reinforced layered elastic composite, tabulating eigenfrequencies

23 p3351 A72-44061

Transfer matrix approach for determining stresses and displacements in elastostatics of laminated composites

[ASCE PREPRINT 1674]

23 p3351 A72-44105

Triangular element for multilayer sandwich plates.

23 p3351 A72-44108

Temperature calculation in a multilayered wall acted on by a thermal pulse.

23 p3357 A72-44537

Laminated thick plate and shell analysis by the assumed stress hybrid model.

24 p3453 A72-44601

Free vibration frequencies and critical buckling loads for thin walled shells of revolution constructed out of layered or heterogeneous anisotropic materials.

24 p3455 A72-44676

Determination of the radial heat conductivity of multilayer tubes for thermionic converters

24 p3461 A72-44875

Free vibrations of thick, layered cylinders having finite length with various boundary conditions. 24 p3425 A72-44884

Technique for measuring damping properties of thin viscoelastic layers. 24 p3402 A72-44885

Supersonic flutter of plane, rectangular, anisotropic, heterogeneous structures 24 p3459 A72-45440

Energy dissipation associated with transverse vibrations of sandwich metallic samples with damping coatings 24 p3461 A72-45760

LAMINATIONS

U LAMINATES

LAMPS

U LUMINAIRES

LAND USE

Agricultural land use analysis by remote sensing, discussing side-looking airborne radar systems and image interpretation for local needs 01 p0056 A72-10456

STOL aircraft for solving noise reduction and land use problems in future transportation systems, discussing airport location and layout for growing air traffic 01 p0005 A72-11153

Remote sensing for land use soil limitations recognition and mapping, using color encoded density slicing analysis 02 p0209 A72-11793

Environments susceptibility to low resolution imaging for land-use mapping, relating landscapes spatial frequency distributions to expected ERTS resolutions 02 p0210 A72-11796

Multistage resource inventory and analysis program combining remote sensing techniques and ecological principles in California Desert pilot area, discussing photointerpretation and ground truthing 02 p0210 A72-11802

Remote sensing with sounding rockets and balloons, discussing cost, mineralogical surveys, land use and hydrological assessments 05 p0654 A72-15756

Newark airport program, discussing land preparation, public facilities, terminal area, building design, support systems, organization and scheduling 05 p0644 A72-16696

Aerial photography for rural soil mapping, considering geographic, ecologic and agricultural production interpretation 09 p1301 A72-23279

Aerial photointerpretation for landscape analysis with respect to agricultural land use, considering geomorphologic, hydrographic, soil and microclimatic conditions 09 p1301 A72-23280

Black and white aerial photographs quantitative evaluation for differentiation and identification of land use patterns by microdensitometry, using statistical methods 09 p1313 A72-23306

Building soundproofing codes for airport zoning ordinances, emphasizing wider latitude in land use options 13 p2067 A72-29561

LANDAU DAMPING

Large amplitude linearly or elliptically polarized Alfvén wave propagation parallel to magnetic field, calculating nonlinear Landau damping rate 01 p0111 A72-11227

Coulomb collisions nonlinear effects on Landau damping of weakly damped plasma electron wave 04 p0559 A72-15347

Longitudinal instability of electron beams interacting with passive resonator, considering Landau damping influence by linear differential equations of motion solution 05 p0701 A72-17243

Electrostatic wave propagation and damping in thermally ionized collisionless alkali plasma, determining electron and ion densities, electron temperature and ion distribution function 06 p0856 A72-17521

Plasma density inhomogeneity effects on beam-plasma instability and Landau damping from digital simulation using charge sheet model 06 p0865 A72-18541

Nonlinear Landau damping of longitudinal plasma waves in dc magnetic field, obtaining wave-particle interactions from Vlasov equation by perturbation theory and method of characteristics 07 p1041 A72-19505

Nonlinear Landau damping and growth of finite amplitude cyclotron harmonic plasma waves in magnetic field, measuring coupling coefficients by calibrated interferometer 07 p1041 A72-19506

Hf instability on whistler branch of finite pressure plasma with nonmonotonic ion distribution function under Landau damping effect 07 p1042 A72-19615

Magnetospheric instabilities theory based on Vlasov equation and Landau damping 07 p0978 A72-20033

Electrostatic ion wave Landau damping in magnetic field of Ar plasma QP machine 08 p1213 A72-21250

Landau instability effect on density waves propagation in self gravitating disk of differentially rotating and nonrotating stars populations, noting radial flow of matter 09 p1384 A72-22518

Electrostatic longitudinal waves propagation and detection in isotropic collisionless hot electron plasma, calculating Landau dispersion curve and damping 09 p1359 A72-22794

Phase velocity and Landau damping of ion acoustic waves propagating through plasma boundary layer at conducting sphere or cylinder based on two fluid model 10 p1523 A72-24746

Vlasov perturbation theory of nonlinear plasma wave with Landau damping based on Korteweg-de Vries equation 11 p1692 A72-25517

Fast and slow ion acoustic free streaming wave propagation in drifting plasma, showing phase velocity and damping in agreement with Maxwellian distribution 11 p1692 A72-25518

Plasma beam cyclotron instability theory based on computer simulation, noting stabilizing effect due to Landau damping 11 p1693 A72-25562

Ionized plasma line widths and intensities due to Landau and collisional damping, observing effects by light scattering techniques 14 p2140 A72-30901

Lagrangian complex amplitude derivation for monochromatic electrostatic wave in unmagnetized collisionless plasma, investigating nonlinear Landau damping effects on instability 14 p2140 A72-30939

One dimensional Maxwellian electron plasma simulation by electron bunches, describing Landau damping of wave initially excited in medium and nonlinear effects of trapping 15 p2284 A72-31678

Kinetic energy and momentum of longitudinal waves in plasmas, deriving Landau dispersion equation from conservation laws 15 p2285 A72-32272

Optical measurements of electric fields turbulence level in gun plasma, noting compatibility with spatial Landau damping 15 p2287 A72-32409

HF electrostatic instabilities driven by electron-ion relative drift velocity across external magnetic field for inhomogeneous plasma, noting Landau damping role 16 p2433 A72-32809

A stability mechanism for the ion-acoustic waves. 17 p2592 A72-35625

Nonlinear equations for explosive instabilities of three plasma waves interaction with mutually different linear damping 19 p2838 A72-37326

Sideband growth in nonlinear Landau wave-particle interaction. 19 p2838 A72-37327

Effects of Landau damping on nonlinear wave modulation in plasma. 21 p3089 A72-40189

An asymptotic method for the Vlasov equation. III - Transition from amplitude oscillation to linear Landau damping. 21 p3089 A72-40190

Nonexistence of ion acoustic waves and Landau damping driven electrostatically in an ideal Q machine. 21 p3090 A72-40340

Electromagnetic disturbances within a degenerate electron plasma in a quantizing magnetic field 22 p3212 A72-43010

Landau dispersion equations for oscillations damping of bounded electron plasma, noting application to plasma cylinder in conducting tube 23 p3319 A72-43410

Damping of finite-amplitude electron plasma waves in a collisionless plasma. 23 p3321 A72-44075

Wave growth in a strongly turbulent plasma. 24 p3430 A72-45568

LANDAU FACTOR

Marginally unstable plane parallel flow nonlinear response to two dimensional disturbance, noting localized burst relationship to Landau constant 06 p0801 A72-18163

Landau orbital ferromagnetism appearance likelihood in white dwarf stars, noting temperature requirements of noninteracting electron gas 19 p2859 A72-37891

LANDAU-GINZBURG EQUATIONS

Abrikosov and Mendelsohn models of nonideal superconductors of second kind in transverse magnetic field, discussing Landau-Ginzburg parameters and critical current density 07 p1049 A72-20153

Critical supercurrents in heat treated and cold worked Nb-Ti wires, proposing pinning model based on enhancement of Ginzburg-Landau parameter in cell walls 08 p1186 A72-21594

LANDFORMS

NT CALDERAS

NT ISLANDS

NT MOUNTAINS

NT RIDGES

LANDING

NT AIRCRAFT LANDING

NT BLIND LANDING

NT CRASH LANDING

NT GLIDE LANDINGS

NT LUNAR LANDING

NT MARS LANDING

NT PLANETARY LANDING

NT SOFT LANDING

NT SPACECRAFT LANDING

NT TOUCHDOWN

NT WATER LANDING

LANDING AIDS

NT AIRPORT BEACONS

NT AIRPORT LIGHTS

NT APPROACH INDICATORS

NT AUTOMATIC LANDING CONTROL

NT INSTRUMENT LANDING SYSTEMS

NT LANDING INSTRUMENTS

NT LANDING RADAR

NT RUNWAY LIGHTS

Carrier system for controlled approach of Naval aircraft to provide pilot window to deck for tactical jet guidance for poor visibility landing 02 p0256 A72-12323

Microwave aircraft landing system development, discussing contract definition, feasibility, prototype development, management planning and program costs 02 p0304 A72-12377

Airline schedule keeping by Sud Lear all-weather landing system, discussing crew training 04 p0544 A72-14688

All-weather landing aids for civil VTOL aircraft and helicopters, discussing Doppler and inertial navigations, instrument landing systems and ground visibility improvement 05 p0688 A72-16780

V/STOL development for short haul air transportation, discussing requirements for quiet pollution-free operation, ATC systems, navigation and landing aids 08 p1108 A72-21010

Aircraft and airports weather instrumentation for all-weather landing and takeoff, discussing application of laser technology and digital presentation 08 p1168 A72-21522

Minimum safety flight altitudes for aircraft landing systems and lateral deviations for correction maneuver 12 p1842 A72-27269

Airport lights system design for optical landing aids, discussing runway illumination conditions 12 p1795 A72-27402

Civil aviation approach and landing guidance systems evolution, discussing ILS development, state of art and future requirements 13 p1996 A72-29014

Airport lighting for pilot guidance during approach and landing under category I-III visibility conditions, discussing runway layouts and power requirements 14 p2092 A72-30621

Air cushion landing system application for civil air transportation, discussing operation, braking and parking 16 p2348 A72-33184

Runway marking requirements for visibility under day and night conditions, considering night reflection value, color stability, durability, noninterference with flight operations, etc 17 p2535 A72-34243

Helicopter/ship dynamic interface testing for launch and recovery capabilities under sea environment conditions, discussing visual landing aids, wind, visibility and ship motions 17 p2491 A72-34505

[AHS PREPRINT 650] Computer control of aircraft landing. 17 p2578 A72-35950

Microwave holographic imaging techniques for aircraft landing aids and airport security applications, discussing real time operation 19 p2798 A72-37625

Aircraft accidents during nonprecision approaches under adverse weather conditions, discussing landing aids use for corporate jet aircraft 20 p2952 A72-39745

Meteorological and takeoff and landing information transmission by proposed automated meteorological and information service, discussing air-ground data link 21 p3080 A72-40287

Characteristics and prospects for a new landing guidance system. 21 p3080 A72-40293

LANDING GEAR

European A300B airbus flying control hydraulic system and landing gear design for safety and reliability, fatigue life, weight and maintenance

01 p0005 A72-10724

B-1 strategic supersonic bomber design, emphasizing variable sweep wing, landing gear, control and instrumentation

02 p0154 A72-12226

Pressure determination in kinematic pairs of spatial landing gear mechanism, describing rotatory and spherical pairs reactions to various combinations of momenta

05 p0614 A72-17057

Carrier suitability testing for aircraft landing, considering landing gear and supporting structure under simulated shipboard conditions

06 p0759 A72-18497

F-111 aircraft landing gear and speedbrake hydraulic system control by single dual-function valve, describing design features and performance characteristics

08 p1111 A72-21024

Aircraft landing gear wheel damage and antiskid mechanisms under operational conditions

08 p1109 A72-21485

Carbon/epoxy composite reinforced plastic materials feasibility for application to aircraft landing gear wheel fabrication

08 p1193 A72-21686

Higher order forces effect on shock absorbing systems of masses interconnected by elastic and damping members of aircraft landing gears

09 p1318 A72-22861

Runway unevenness and landing gear characteristics effects on SST vibration during taxiing, taking off and landing

09 p1263 A72-23459

Aircraft wheel mechanics, discussing freely turning and braked wheels, tire drift and antiskid braking systems for landing gear

11 p1574 A72-25287

Cessna 210 aircraft electrically driven hydraulic power pack for landing gear system, noting engine and flight tests

[SAE PAPER 720327]

11 p1577 A72-25589

Runway motion stability of aircraft with three wheel landing gear, assuming elastic response to moment induced drift

12 p1753 A72-27235

Air cushion aircraft landing systems advantages and suitability for arctic transportation applications

13 p1897 A72-28793

Aircraft landing gears structural systems design, taking into account different design criteria imposed by various national impact load norms

13 p1898 A72-30025

Aluminum aircraft wheels ultrasonic inspection, noting reliability, simplicity and time economy as compared to eddy current or fluorescent penetrant methods

13 p1966 A72-30037

Welded steel airframe residual fatigue life tests by nonstationary random loading, applying to jet trainer aircraft landing gear

14 p2107 A72-30277

Aircraft landing gear stress spectrum and design data during ground loading on airport runways, using linearized theory for model investigation

14 p2071 A72-30283

Undercarriage loadings of three aircraft - Porter PC-6, Venom DH-112 and Mirage IIIS.

24 p3367 A72-44738

LANDING INSTRUMENTS

NT APPROACH INDICATORS

Operational requirements of instrument landing systems, interferometers, correlation protected instruments, landing guidance systems and navigation aids

03 p0386 A72-13421

Soviet book on aircraft radio equipment covering transmission and reception, velocity and coordinates measurements, siting and navigation, flying target interception, reconnaissance, landing systems, etc

05 p0637 A72-16530

Microwave Doppler scanning landing guidance system with radar beam comparison and signal format simplification suggestion

06 p0846 A72-18398

Computerized aircraft landing measurement system for civil airport, using optical, seismic and IR sensors

16 p2374 A72-33627

Possible impact of area navigation upon MLS requirements for azimuth angular coverage and range.

24 p3422 A72-44643

LANDING LOADS

Dutch monograph - Analysis of dynamic aircraft landing loads, and a proposal for rational design landing load requirements.

21 p2994 A72-40925

Modern landing impact load calculations and old-fashioned requirements.

[ICAS PAPER 72-31]

21 p2995 A72-41156

Undercarriage loadings of three aircraft - Porter PC-6, Venom DH-112 and Mirage IIIS.

24 p3367 A72-44738

LANDING MODULES

NT LSSM

NT LUNAR MODULE

LANDING RADAR

Aircraft radar for weather data, ground mapping, avoidance modes and independent landing monitor function, presenting straight and slant approach simulation data

21 p3080 A72-40290

LANDING SIMULATION

Feedback gains for STOL aircraft display pilot interactive flight director design, using computerized approach-touchdown simulation and optimal control theory

[ASME PAPER 71-WA/AUT-9]

05 p0684 A72-15956

Unpowered shuttle orbiter piloted control during approach and landing, discussing energy management technique based on fixed base six degree of freedom simulation

[AIAA PAPER 72-227]

10 p1551 A72-24438

Simulator for physical forces experienced by carrier aircraft during catapult launches and arrested landings, considering external stores safe suspension

15 p2215 A72-32620

Statistical correlation techniques applied to jet aircraft autoland system dynamic ground tests with simulated engine and aerodynamic characteristics

16 p2420 A72-33641

Direct lift control feasibility for integration into F-14A automatic carrier landing system /ACLS/, using moving-base six-degree-of-freedom simulation

[AIAA PAPER 72-873]

20 p2951 A72-39127

LANDING SITES

NT LUNAR LANDING SITES

Viking Mars Orbiter imaging experiment with high resolution contiguous coverage by vidicon cameras for landing sites selection and surface study

10 p1539 A72-24377

Booster launch vehicle guidance scheme for critical aborts from staging through burnout, minimizing aerodynamic phases for different landing sites

15 p2269 A72-32182

Experimental and simulation study results on the development of a planetary landing site selection system.

[AIAA PAPER 72-868]

20 p2951 A72-39131

Landing-site and orientation determination for a spacecraft on Mars

21 p3103 A72-40302

LANDING SYSTEMS

U LANDING AIDS

LANDMARKS

Computer programs for global disk and landmarks registration of cloud motions from satellite data for ocean weather monitoring applications

01 p0070 A72-10871

Landmark navigation with angle measurements for roving vehicle guidance on lunar and planetary surfaces

15 p2268 A72-31790

Computer program algorithm for processing local landmark and cloud motion data recorded by satellite observation

17 p2520 A72-34410

Landmark navigation rule, a new navigation device.

19 p2830 A72-37296

LANDSCAPE

U TERRAIN

U TOPOGRAPHY

LANGEVIN FORMULA

Weakly interacting waves Langevin equation in fluid, using characteristic functionals and time asymptotic methods

04 p0549 A72-15289

Bcc lattice sum calculation method in Langevin function terms, noting validity at low temperatures

16 p2442 A72-34175

An application of the generalized Langevin equation to the study of correlations in simple, classical fluids.

17 p2581 A72-35154

LANGMUIR PROBES

U ELECTROSTATIC PROBES

LANGUAGE PROGRAMMING

Partial differential equation language /PDEL/ for batch and interactive digital simulation of PDE models

07 p0951 A72-20327

Terminal context in context-sensitive grammars.

17 p2524 A72-35924

LANGUAGES

NT ALGOL

NT CONTEXT FREE LANGUAGES

NT FORTRAN

NT MACHINE ORIENTED LANGUAGES

NT PROGRAMMING LANGUAGES

NT SYLLABLES

NT WORDS [LANGUAGE]

LANTHANIDE SERIES METALS

U RARE EARTH ELEMENTS

LANTHANUM

Cobalt and lanthanum with face and body centered lattices, studying plastic deformation during allotropic transformations under sliding friction and gripping

01 p0074 A72-10579

Ta, Nb and La superconductivity, investigating surface contamination effects on electron tunneling characteristics

09 p1367 A72-22554

La superconductivity pressure dependence based on valency considerations, noting actinides metals and alloys localized magnetism explanation by simple model

09 p1368 A72-22557

Isolation and sintering techniques and thermoelectric properties of lanthanum, yttrium and gadolinium borides

11 p1645 A72-26858

Y and La action on oxidation rates of Cr and Mo at high temperature in air

15 p2252 A72-31191

Exploratory investigation of Y, La, and Hf coatings for nitridation protection of chromium alloys.

20 p2944 A72-39290

Eu, La and Sm in sunspot spectra.

20 p2973 A72-39884

Recording holographic interferograms in a lanthanum-doped fluorite crystal

21 p3053 A72-40476

LANTHANUM ALLOYS

Rare earth metals effects on chromium brittle transition temperature, showing maximum plasticity with lanthanum addition

07 p1019 A72-20151

LANTHANUM COMPOUNDS

NT LANTHANUM FLUORIDES

Scandium substitution for lanthanum in lanthanum hexaboride crystal lattice, investigating effect on thermionic characteristics

12 p1854 A72-27309

LANTHANUM FLUORIDES

Phononless lines shift and broadening and electron phonon interaction in lanthanum trifluoride-Nd crystal, obtaining temperature dependence of non-radiative transition probability

14 p2142 A72-30359

LAP JOINTS

Colaminated boron-polyimide film effect on strength of graphite fiber-epoxy resin composite double lap bolted joints

[AIAA PAPER 72-382]

11 p1730 A72-25405

Stress calculation in inflexible overlapping cemented joint of orthotropic layers, taking into account joining geometry and elastic properties anisotropy

13 p1962 A72-28396

A fracture mechanics analysis of adhesive failure in a single lap shear joint.

[SESA PAPER 1990A]

17 p2630 A72-34815

Stress distribution and displacements in adhesive bonded lap-jointed aerospace structures, presenting approximate solution

18 p2740 A72-37214

LAPLACE EQUATION

Mixed boundary value problem of Laplace equation solution by dual trigonometric series equations approach, applying to microstrip transmission line capacitance determination

01 p0093 A72-10508

Three dimensional elasticity mixed boundary value problems associated with Laplace equation in half space, including slotted regions and stamp contact solutions

02 p0289 A72-11610

Howe gyroscope mounted on fixed base, deriving equations of motion with Laplace method

03 p0359 A72-13558

Spreading currents in parabolic rotating coordinates, determining magnetic field components consistent with Laplace equation series expansion

03 p0311 A72-13565

Laplace equation under Robin boundary conditions over unit square, discussing numerical solution by difference approximation and iterative procedure

05 p0682 A72-16100

Hybrid computer aided design of thick electrostatic electron lenses by Laplace equation solution in terms of cylindrical harmonics, applying to CRT

06 p0779 A72-17481

Planetary disturbing function expansion, using classical binomial or Laplace series methods on large scale digital computer with Poisson program

06 p0878 A72-17665

Laplace equation internal Dirichlet and Neumann boundary value problems solution procedure for thermal potential of steady temperature field

07 p1098 A72-18988

R function and variational methods solution for mixed boundary value problem of Laplace equation applied to stationary heat conduction and electrodynamic problems

08 p1209 A72-21704

Algorithm for automatic construction of finite element approximation to Laplace equation, noting convergence

10 p1502 A72-23719

Hybrid computer aided synthesis of thick electrostatic electron lenses by Laplace equation solution in terms of cylindrical harmonics with gradient used in trajectory integration

10 p1509 A72-23940

- Converging or diverging high intensity charged particle beams arbitrary profile shaping, obtaining solution via Laplace equation through reduction to Cauchy problem
10 p1521 A72-24362
- Spreading currents in parabolic rotating coordinates, determining magnetic field components consistency with Laplace equation series expansion
11 p1607 A72-26752
- Laplace equation iterative solution for boundary value problems in structural hardening and heat resistance formulation, noting convergence
12 p1887 A72-28226
- Complex eigenvalues of frequency for Laplace tidal equation with negative equivalent depth, noting unstable modes role in solar differential rotation
14 p2100 A72-30344
- Poisson equations solution in orthogonal curvilinear coordinate systems to allow Laplace and Helmholtz equations separability, applying to hydrodynamic, electrostatic, electromagnetic and MHD problems
15 p2278 A72-32249
- Variables separability conditions within Riemann space for Schroedinger and Laplace equations
15 p2264 A72-32278
- Laplace equation to generate stationary electromagnetic vacuum fields, generalizing from Papapetrou-Majumdar class of static fields
17 p2580 A72-34425
- Converging or diverging high intensity charged particle beams arbitrary profile shaping, obtaining solution via Laplace equation through reduction to Cauchy problem
17 p2589 A72-34961
- Modified Ritz method to find optimum boundaries to elliptic systems governed by Laplace or Poisson equation
19 p2826 A72-38246
- Book - The method of fractional steps: The solution of problems of mathematical physics in several variables
22 p3208 A72-43200
- Laplace equation for homogeneous magnetic field perturbation by superconducting elliptical cylinder and by two parallel circular cylinders
23 p3313 A72-43779
- LAPLACE OPERATORS**
U LAPLACE TRANSFORMATION
LAPLACE TRANSFORMATION
Positive additive functionals of homogeneous processes with independent increments in phase space, considering continuity condition for process distribution Laplace transform
01 p0094 A72-11264
- Concentrated inertias effects on cantilever beams and shafts free vibrations by Laplace transform technique
04 p0591 A72-15276
- Multiple-input multiple-output linear time invariant feedback systems stability, investigating continuous-time case
04 p0507 A72-15694
- Laplace operator eigenvalue computation for simply connected region with homogeneous Dirichlet and Neumann boundary conditions and finite difference problem
09 p1340 A72-22296
- Two independent damping systems impact vibration analysis from solution of equations of motion by Laplace transformation
09 p1399 A72-22695
- German book on unsteady heat conduction and temperature field equalization covering mathematical treatment with Laplace transformations
09 p1412 A72-23175
- Huffman sequence synthesis by z transform zero pattern selection to obtain high energy for given peak amplitude, noting signal ambiguity functions
10 p1437 A72-24679
- Laplace-Carson transform solution for integrodifferential equation of motion for droplet suspended in viscous gas slipstream
12 p1796 A72-27093
- Analytical expression for digital element transfer function derived with Laplace transforms
13 p1927 A72-28413
- Laplace transform method in unsteady radiation field theory, discussing generalization from steady luminescence to inhomogeneous media and forbidden band frequency radiative transport
13 p2001 A72-28506
- Laplace transformation for mechanical response of piezoelectric composite transducer under action of thermal field and electric potential, noting time dependent modulus of elasticity
13 p1955 A72-28621
- Difference scheme application to Laplace operator eigenvalues determination for regions composed of rectangles, using summary representation formulas
13 p1986 A72-29082
- Integral Laplace-Fourier transform stability during transient response functions reconstruction from frequency characteristics in linear circuits
15 p2264 A72-31879
- Standard and bilinear z transformation techniques for digital sampling filters block diagrams derivation
16 p2369 A72-33671
- Exponential signal reconstruction sampling rate restriction derivation based on pole-zero cancellations in Z transform
16 p2365 A72-33756
- Solution of heat transfer problems with the aid of Laplace transforms. I - Development of analytical solutions for two specific boundary value problems
18 p2740 A72-36422
- Fourier-Bessel superposition and Laplace transformation methods for surface displacement produced by time dependent dipole in elastic half space, noting buried dipole case
19 p2876 A72-37887
- Real time flight flutter testing via Z-transform analysis technique.
[AIAA PAPER 72-784]
19 p2749 A72-38101
- An approximate method for inverse Laplace transformation
19 p2828 A72-38853
- Use of the multidimensional Laplace transform for the analysis of nonlinear systems with variable parameters
21 p3036 A72-40185
- Laplace transformation for unsteady convective heat transfer with nonlinear and time dependent heat transfer coefficients, obtaining nonlinear integral equation solution
21 p3130 A72-41066
- Free vibrations of a system with a generalized piecewise-continuous characteristic
21 p3122 A72-41349
- Stability conditions and effective bandwidths of first and second degree pulsed phase locked AFC systems with proportionately integrating filter, using Z transform method
23 p3263 A72-43433
- Recent results in convolution feedback systems
23 p3276 A72-43861
- LAPSE RATE**
Clear air turbulence radiometric detection by IR vertical scan technique, associating atmospheric lapse rate anomalies with CAT related temperature inversions
02 p0225 A72-11820
- LARGE APERTURE SEISMIC ARRAY**
Long range air coupled seismic wave recording from Apollo launchings, using microphones and seismographs arrays
11 p1690 A72-26514
- LARGE SCALE INTEGRATION**
LSI/MOS logic circuits radiation effects prediction from modeling studies of individual devices on test chip
03 p0334 A72-14087
- Thermal deformation effects on metal bond fatigue failure modes in small signal transistors, micro and LSI circuits
03 p0365 A72-14291
- Digital simulation for steady state and transient thermal responses of LSI with metal within substrate, considering computer time cost
07 p0954 A72-19176
- Reliability prediction for MOS/LSI devices based on chip circuit configurations evaluation, extrapolating bipolar IC failure rate model
10 p1447 A72-24009
- Large scale integrated circuits for digital differential analyzers, giving operational specifications for shift registers, adders and integrators
10 p1448 A72-24276
- Monolithic, thin film and LSI technology development trends in microelectronics, noting heteroepitaxy, ion implantation and laser beam techniques
10 p1454 A72-25175
- Signal transmission through LSI logic circuit chains, discussing time delay measurement by step function testing
15 p2211 A72-31846
- Computer aided thermal design of LSI module packs for forced convection air cooling, using modal conductance matrix method
16 p2368 A72-33195
- Univac 1616 computer design featuring uses of 16-bit word technology, medium and large scale integration, and transistor-transistor logic
16 p2366 A72-33243
- Advances in LSI technology.
17 p2527 A72-34569
- Computer-aided thermal design of LSI packages.
17 p2527 A72-34681
- Hybrid LSI logic modules for aerospace.
17 p2527 A72-34683
- Techniques for control of long-term reliability of complex integrated circuits. I - Reliability assurance by test vehicle qualification.
17 p2528 A72-34686
- Techniques for control of long-term reliability of complex integrated circuits. II - A technique for the prediction of failure rates for MSI and LSI devices.
17 p2528 A72-34687
- Modularized digital controller for closed loop systems using MOS, MSI and LSI components
17 p2521 A72-34703
- Microelectronic module application to LSI set for implementation of digital filters, division and square root operations, polynomials, matrix computations, etc
17 p2522 A72-34704
- Stress and parametric change analysis for failure mode identification and reliability screen tests of LSI circuits, noting MOS inverter operation and RAM mechanization
17 p2528 A72-34706
- Advantages of MOS/LSI computers in avionics systems.
17 p2523 A72-35579
- Zero overhead testing relationship to software requirements, testing dynamic accuracies, LSI product types and function and parametric speeds related to product lines
18 p2664 A72-37109
- Technology and performance of n-channel MOS-LSIs using depletion-type load elements.
20 p2961 A72-39712
- Electronic packaging and LSI techniques cost efficient use in meeting weight, volume, reliability, circuit speed and thermal protection requirements
20 p2909 A72-39769
- Semiconductor/IC Processing and Production Conference, Anaheim, Calif., February 8-10, 1972 and New York, N.Y., June 13-15, 1972, Proceedings of the Technical Program.
22 p3160 A72-42822
- Cascade computer controlled system for LSI devices testing, considering interim buffer storage and programmable pattern generator
22 p3160 A72-42823
- Performance prediction of large-scale integrated logic circuits.
22 p3160 A72-42824
- Digital parallel correlator with LSI single-chip bipolar transistor construction, discussing triple diffusion process for p-n-p and p-n-p junctions
23 p3273 A72-44453
- A means of reducing custom LSI interconnection requirements.
23 p3273 A72-44454
- LARMOR PRECESSION**
Finite Larmor radius effect on Rayleigh-Taylor plasma instability in vertical magnetic field, characterizing solution by variational principle
04 p0557 A72-15022
- Electron Larmor radius effect on hf hose and mirror instabilities of fast magnetoacoustic and ion acoustic waves in nonisothermal plasma
08 p1215 A72-21874
- Larmor frequency influence on Rayleigh-Taylor instability of viscous Hall plasma with magnetic field
11 p1698 A72-26604
- Boundary conditions in the presence of Hall current or finite ion Larmor radius effects.
19 p2839 A72-37338
- Larmor radius and collisional effects on the dynamic stability of a composite medium.
22 p3212 A72-42990
- LARYNX**
Laryngeal motoneuron activity during Hering-Breuer reflexes, noting inspiratory fibers firing inhibition and activation during lung inflation
09 p1266 A72-22975
- LASER ALTIMETERS**
Flight laser altimeter for Apollo vehicle height measurements above lunar surface, using telescope relay and quartz crystal oscillator
05 p0660 A72-15786
- International Satellite Geodetic Experiment (ISAGEX), using laser telemetry techniques for accurate measurement of earth gravitational field
06 p0888 A72-18261
- Apollo mapping camera system synchronized laser altimetry utilization in astro-photogrammetric triangulation
12 p1872 A72-27816
- Cartographic and environmental surveys by Skylab orbiting stations and ERTS satellite using panoramic and mapping cameras and laser altimeter
15 p2322 A72-31247
- Comments on the figure of the moon based on preliminary results from laser altimetry.
18 p2724 A72-36280
- LASER BEAM DEFOCUSING**
U THERMAL BLOOMING
LASER COMMUNICATION
U OPTICAL COMMUNICATION
LASER HEATING
Internal electrostatic field effect on ion separation in expanding pulsed laser produced plasmas
01 p0105 A72-10021
- Mass spectrometric investigation of high power laser beam plasma on solid target, determining multicharged ion yield, energy, angular distribution and recombination effect
01 p0079 A72-10349

Magnetic field effects on ruby laser radiation kinetics and spectral composition, studying crystal heating and light emission

01 p0080 A72-10577

Flame propagation and overdense heating in laser beam created plasma, calculating density and temperature profiles by one dimensional continuum hydrodynamic theory

02 p0238 A72-12363

Confined small diameter PETN, RDX and tetryl columns longitudinal detonations, using focused Q switched ruby laser

03 p0367 A72-13604

Focused laser beam interaction with liquid metal particles, discussing fluid phase light screening effect, droplet evaporation and mass expulsion characteristics

03 p0368 A72-13668

Pulsed Nd laser drilling and welding of metal, metal-semiconductor and semiconductor elements, discussing bond penetration and character, mechanical strength and I-V characteristics

03 p0363 A72-13860

High temperature dense plasma formation by laser heating of gas target, noting fusion reaction in deuterium-tritium mixture

03 p0399 A72-14066

Amorphous polymer dielectric luminescence and destruction under Q switched laser radiation with subthreshold power and picosecond pulses

03 p0369 A72-14071

Nuclear fusion by laser radiation, discussing plasma heating mechanisms and limitations in DD reaction production

04 p0557 A72-15172

Hydrogen plasma absorption coefficients at laser frequencies over 0.3371-10.6 microns

05 p0694 A72-15997

Cumulation-laser heating of D-T plasma for cylindrical wave, investigating pulse energy increase for critical temperature attainment from average value mathematical model

05 p0695 A72-16279

Nuclear microfusion energy recovery threshold increase during laser pulse heating process of D-T plasma

05 p0695 A72-16280

Laser pulse heating inability to quench in disorder in Fe-Al alloy

05 p0669 A72-16796

Boron ignition and combustion mechanisms based on high speed photographs of laser ignited boron particles [AIAA PAPER 72-72]

05 p0703 A72-16801

Molecular Cs role in multiphoton ionization process during interaction with low intensity Q switched Nd-glass laser radiation

05 p0670 A72-17082

Heating dynamics of transparent dielectrics exposed to pulsed laser beam operating in free laser mode

06 p0825 A72-17697

Shielding of solid surface vaporizing under laser radiation effect in presence of thermal and ionizational nonequilibrium, investigating absorption flare onset mechanism

06 p0825 A72-17905

Laser beam welding by solid state pulsed lasers, discussing heat conduction relation to power density utilization

06 p0822 A72-18254

Gas breakdown in front of metal targets laser flare from UV radiation ionizing action, using pulsed holographic technique

06 p0818 A72-18412

Fast ionization fronts ahead of laser produced plasma expansion into low density gas, noting Langmuir probe and microwave diagnostics indication of photoionization density augmentation

06 p0864 A72-18532

Bulk vapor formation processes during laser beam heating of metals, considering effect on mass transfer

07 p1000 A72-18939

High intensity laser beams for solid surface material removal by vaporization and explosion, noting surface and subsurface temperature relations

07 p1002 A72-19210

Moving heat source model of temperature profile and thermal stress propagation for laser drilled holes in alumina ceramic material

07 p0994 A72-19211

High intensity pulsed laser beam heating of solid transparent materials

07 p1002 A72-19212

Nd-YAG laser system generating gold conductor patterns on ceramic substrates, using numerical control system for Si production

07 p1002 A72-19213

High power carbon dioxide laser beam applications to deep penetration metal welding, including cutting tests

07 p0994 A72-19214

Schlieren cinematographic and holographic diagnostic of giant pulse ruby laser produced plasma in Xe [CLEA PAPER 12,2]

07 p1040 A72-19393

X ray spectrum and D-D neutrons emission from high temperature plasma produced by two pulsed Nd-glass laser systems

[CLEA PAPER 12,3] 07 p1041 A72-19394

Thermal blooming of laser beams in liquids and gases, investigating short and long time behavior under thermal conduction and viscosity effects

07 p1005 A72-19408

Far UV Al line spectra from laser produced plasma in 35-50 A range

07 p1038 A72-19835

Laser flare luminosity front displacements and atom density at surfaces of transparent dielectrics as function of pulse intensities

07 p1007 A72-20123

Photometric monitoring of film thickness of stacked structures for high strength and laser flux resistance

07 p1049 A72-20126

Laser microdrilling of synthetic ruby, sapphire, silicon and ferrite materials, showing hole parameters dependent on focal length, beam power and pulse rate

07 p0997 A72-20200

Faraday rotators acting as optical isolators for high power giant pulse lasers used for plasma production

07 p1008 A72-20368

Laser beam welding operational and economic aspects, discussing comparative merits vs conventional welding techniques in terms of quality, speed, depth and power limitations

07 p0998 A72-20397

Plastics cutting and drilling with carbon dioxide IR laser beam, discussing economics and commercially available equipment

07 p0999 A72-20554

Phase composition changes, crater formation and metal ejection during erosion by pulsed laser beam

07 p1009 A72-20610

Direct detonation of insensitive PETN, RDX and tetryl explosives with Q switched ruby laser radiation

08 p1220 A72-20771

Pulsed carbon dioxide laser welding of miniature explosive detonators

08 p1221 A72-20778

Spatial-temporal temperature distribution on CW laser irradiated materials, noting application to water film

08 p1252 A72-21289

Laser heating of plasma based on thermal conductivity mechanism, considering nuclear microfusion energy recovery

08 p1213 A72-21303

Laser plasma density and velocity distributions and mass flow from surface and plasma pressure in target heating process based on interferometric measurements

08 p1215 A72-21719

Absorption by Nd laser generated ionized Al plasma of extreme UV radiation due to inverse bremsstrahlung and photoionization

09 p1360 A72-22831

Carbon dioxide laser radiation interaction with solids, applying to fused quartz drilling

09 p1323 A72-22904

Early phase time development of far UV line radiation from plasma production by focusing Q switched ruby laser onto solid Mg target

09 p1325 A72-23232

Pulsed carbon dioxide laser heating of theta pinch plasma by inverse bremsstrahlung and induced Compton processes

09 p1364 A72-23233

Plasma production from hydrogen solid targets by pulsed carbon dioxide TEA laser, noting diagnostic methods

09 p1325 A72-23237

Short laser pulses for plasma heating, considering turbulent heating mechanisms, neutron yield and electromagnetic radiation

09 p1364 A72-23444

Turbulent gas flow induced by laser heating, emphasizing Rayleigh number as stability criterion

09 p1295 A72-23492

Laser heating of plasma based on heat conduction mechanism of spherical thermal wave, taking into account nuclear fusion heat generation

09 p1365 A72-23551

Laser heating and fusion energy recovery of D-T plasma by mechanical-magnetic cumulation, considering cylindrical wave system

09 p1365 A72-23553

Gas jet combination with laser for cutting operations, discussing laser characteristics, beam guiding mirror, lens, nozzle, nozzle gas and workpiece materials

09 p1320 A72-23629

Oxygen jet-carbon dioxide laser beam cutting in mild and stainless steels, noting speed and material thickness limitations

09 p1321 A72-23639

Laser induced chemical decomposition of copper malate and fumarate and fragment reaction with low hydrocarbons, comparing with thermal heating

10 p1433 A72-23951

Laser induced degradation as rapid reproducible method for characterization of inorganic materials exhibiting low vapor pressures at usual temperatures

10 p1433 A72-23953

High intensity laser radiation absorption in plasma produced from thick metal targets and thin Au foil

10 p1490 A72-23967

Laser welding theory and applications to microelectronics, nuclear and aerospace fields

10 p1485 A72-23968

Materials processing with carbon dioxide lasers, noting cutting, welding and hole drilling applications

10 p1485 A72-23969

Absorption spectra and plasma of laser spark in hydrogen, studying electron and atoms temperature and concentrations time variations

10 p1491 A72-24359

Closed form solution for spherical and cylindrical wave propagation in laser conductively heated plasma, considering account of nuclear fusion energy recovery

10 p1522 A72-24721

Laser conductive heating of plasma with accounted nuclear fusion energy, assuming plane thermal wave

10 p1522 A72-24722

Ignition and incandescence of laser irradiated single micron size Mg particles suspended in stoichiometric methane air mixture

10 p1564 A72-25140

Anomalous heating due to nonlinear parametric interaction between plasma and laser radiation, calculating laser power thresholds for nonlinear instability effects

11 p1695 A72-25857

Anomalous plasma heating by laser irradiation with superimposed electric field oscillating near plasma frequency

11 p1696 A72-26326

Laser light intensity relationship to temperature distribution in completely ionized plasma, defining optimal heating conditions

11 p1696 A72-26342

Laser pulse form effect on confined plasma heating, taking into account inverse electron-ion bremsstrahlung and stimulated Compton scattering

11 p1651 A72-26672

Commercially available laser systems applications to welding, drilling, scribing and other machining operations

11 p1652 A72-26984

High temperature deuterium plasma production by laser heating of gas filled cylindrical tube, optimizing pulse duration and configuration

12 p1849 A72-27059

High power Nd glass laser with stepwise pulse amplification for intensive heating of solid target plasmas

12 p1849 A72-27061

Temperature dependence of destruction threshold of lithium niobate surface under laser irradiation, noting ferroelectric properties effects

12 p1853 A72-27069

Rapid laser heating induced stress generation in carbon fiber-polymethyl methacrylate composite

12 p1833 A72-27286

Averaged equations for laser heating of two temperature plasma with allowance for nuclear fusion energy, noting inequality of ion and electron temperature

12 p1851 A72-27395

High temperature heating of plasma by ultrashort laser pulses focused onto lithium deuteride, noting various diagnostic methods

12 p1851 A72-27581

Laser pulse heating of plasma, predicting efficiency enhancement by addition of heavy element impurities or deuterides to solid target surface

12 p1852 A72-27621

Heat conduction heating of plasma by high power ultrashort laser pulse incident on solid target, noting focusing and energy absorption role

12 p1852 A72-27622

High brightness picosecond light pulses generation by laser with multiple internal reflection amplifier for plasma heating

12 p1824 A72-27872

Theta pinch plasma heating by carbon dioxide laser transverse pulses, substantiating theoretical considerations by experimental observations

12 p1852 A72-27880

Deep penetration welding and cutting with high power CW carbon dioxide lasers, describing experimental setup

13 p1965 A72-29422

Nd laser irradiation of LiH particles in magnetic trap, investigating resultant plasma expansion and diffusion

13 p2015 A72-29431

Steels structural and microhardness changes by pulsed laser beam induced local heat treatment, noting needleshaped grain refinement

13 p1979 A72-29482

Material removal nature during focused laser radiation action on substances with different thermal diffusivity coefficients

13 p1968 A72-29508

- Thermal diffusivity measurements by laser flash technique for liquid metals at high temperatures
13 p1971 A72-29756
- Laser irradiations inhibitory effect on cornea vascularization after treatment with suprarenal total extract
13 p1906 A72-29867
- Pulsed laser plasma temperature determination by radiation measurements in X ray and visible spectral regions using foil method
13 p2018 A72-29887
- Mass spectroscopic determination of vapor composition during GaAs and GaP single crystals exposure to ruby laser radiation
14 p2109 A72-30316
- Spectral changes of light reflected back from plasma during heating by mode locked Nd laser, noting equidistant lines presence
14 p2138 A72-30447
- Pavel stony meteorite microspectral analysis to obtain metallic elements weight percentages in chondrules, matrix and core, using laser source for local vaporization and excitation
14 p2159 A72-30785
- High power carbon dioxide laser construction, specifications and operation for applications to laboratory and industrial processing of glass, ceramics and metals
14 p2111 A72-30857
- Chondrule like spherules from supercooled molten oxide and silicate droplets by carbon dioxide laser heating compared with meteoritic chondrules
15 p2303 A72-31306
- Nd glass laser drilling and welding applications and tests on materials to evaluate feasibility and operational advantages, identifying optimal pulse energies and durations
15 p2244 A72-32028
- High power carbon dioxide laser produced dense He plasma, comparing experimental and theoretical Stark profile of forbidden and allowed transitions
15 p2285 A72-32223
- Bremsstrahlung photon emission rate from Maxwellian plasma, determining soft X ray diagnostic techniques applicability for laser produced plasmas
15 p2285 A72-32271
- Dense helium theta pinch plasma heating by TEA carbon dioxide laser, studying temperature and density with high speed photography and spectrography
15 p2251 A72-32530
- Plasma corona electron temperature decoupling from core of solid deuterium pellet heated in vacuum by convergent laser beams
16 p2433 A72-32810
- Chondrite Pawel microspectral analysis with laser beam vaporization of sample from microzone
16 p2450 A72-32850
- Laser heating of two temperature plasma based on conductive heat transfer, taking into account nuclear fusion energy
16 p2434 A72-32876
- Conditions defined for recombination induced inversion of populations of resonance and fundamental levels in laser beam produced plasma
16 p2438 A72-33835
- High brightness picosecond light pulses generation by laser with multiple internal reflection amplifier for plasma heating
16 p2403 A72-33981
- Temperature distribution and heat dissipation calculations for CW and pulsed laser optical elements
16 p2403 A72-33982
- Theta pinch plasma heating by carbon dioxide laser transverse pulses, substantiating theoretical considerations by experimental observations
16 p2439 A72-33989
- Laser pulse produced high temperature plasma engine propulsion system, noting thrust/power ratio and requirements for orbital applications [AIAA PAPER 72-719]
16 p2443 A72-34029
- Laser systems.
17 p2562 A72-34567
- Possible mechanism for CO₂-discharge current variation under the influence of laser radiation
17 p2562 A72-34840
- Gas breakdown in front of metal targets laser flare from UV radiation ionizing action, using pulsed holographic technique
17 p2554 A72-34860
- Absorption spectra and plasma of laser spark in hydrogen, studying electron and atoms temperature and concentrations time variations
17 p2562 A72-34958
- Welding with a CW YAG laser beam
17 p2563 A72-35181
- The potential of a laser-induced fusion device as a thermal-neutron source.
17 p2591 A72-35353
- Temperature distribution in solids under laser irradiation.
17 p2564 A72-35355
- Breakdown in argon and nitrogen under the influence of a 0.35-micron picosecond laser pulse.
17 p2564 A72-35508
- Electrothermal cutting processes using a CO₂ laser. [IEEE PAPER TOD-71-118]
17 p2560 A72-35644
- Transient behaviour of laser generated carrier mobility in n-Ge.
18 p2697 A72-36351
- Laser machining of thin films. I - Irradiation characteristics of a focused Q-switched YAG laser beam.
18 p2695 A72-36518
- Experimental indications of plasma instabilities induced by laser heating.
19 p2840 A72-37549
- Averaged equations of the combined process of hydrodynamic expansion and conduction heating of plasma, the recovered energy of nuclear fusion being taken into consideration. I - The plane problem.
19 p2841 A72-38095
- Alternative description of the conduction-type laser heating process of two-temperature plasma in the spherically symmetric case, the nuclear fusion energy being taken into consideration.
19 p2841 A72-38096
- Nature of ion generation during the action of laser emission on a solid body
19 p2811 A72-38193
- Plasma formation on Al target surface by ruby laser beam irradiation, discussing electron and ion velocities as functions of beam power density
19 p2811 A72-38197
- Determination of the time of hole formation in a metallic film under the action of single-pulse laser radiation
19 p2812 A72-38540
- Successive graphitization of amorphous carbon
19 p2823 A72-38676
- Pulsed IR laser for heating superdense plasma to high temperature, featuring inertial confinement by use of short duration energy and strong magnetic field
19 p2843 A72-38823
- Laser power and pulse duration requirements for hot plasma production by flame propagation in solid DT targets for controlled thermonuclear fusion
20 p2931 A72-39354
- Inverse bremsstrahlung caused fast cascade of electrons with Boltzmann energy distribution to explain laser induced gas breakdown via plasma heating
20 p2934 A72-39645
- Interferometric study of a TEA-CO₂ laser produced plasma.
20 p2958 A72-39816
- Laser-induced damage in transparent dielectrics - The relationship between surface damage and surface plasmas.
21 p3062 A72-40241
- Anatomy and thermal history of laser self-focusing damage tracks in glass.
21 p3062 A72-40245
- Collisionless momentum transfer interactions in laser produced plasma on solid target, refuting Wright model
21 p3090 A72-40339
- Thermal decay of an infrared-laser-heated arc plasma.
21 p3090 A72-40341
- Plasma heating by nonlinear damping of resonantly excited longitudinal oscillations produced by two parallel laser beams with difference frequency equal to plasma frequency
21 p3090 A72-40342
- Far UV radiating hot dense microplasma production by laser heating for measuring by resonant absorption small quantities of gaseous element
21 p3093 A72-41341
- The problem of conductivity-type laser heating of two-temperature plasma, the nuclear fusion energy being taken into consideration, in the spherically symmetric case.
21 p3093 A72-41480
- Averaged equations of laser heating of Z-pinch plasma the nuclear fusion energy being taken into consideration.
21 p3093 A72-41481
- Deuterium-tritium heating to thermonuclear temperatures by means of ion-ion collisions in the presence of intense laser radiation.
21 p3094 A72-41632
- Pulsed GaAs injection laser heating application to thermal conductivity coefficient measurement in thin films, discussing lasing spectra kinetics
21 p3064 A72-41740
- Possible mechanisms of turbulent heating of a plasma by ultrashort laser emission pulses
21 p3095 A72-41823
- Magnetic-field-enhanced heating of plasmas with CO₂ lasers.
22 p3210 A72-41969
- Influence of single-pulse emission from a ruby laser on the plasma of a mercury vapor lamp
22 p3184 A72-42105
- Usability of a graphite dish for atom absorption analyses of laser collected samples
22 p3176 A72-42175
- Nature of radiation defects formed by ruby laser emission on the surface of solids
22 p3185 A72-42273
- Fundamental infrared lattice vibration spectrum and the laser-excited Raman spectrum of MoSe₂.
22 p3185 A72-42321
- Bubble and strip magnetic domains creation, annihilation and manipulation in epitaxial magnetic garnet films by laser beam thermal absorption induced local heating
22 p3185 A72-42612
- Alternative description of laser plasma heating for spherical thermal wave, the fusion energy being taken into account.
22 p3211 A72-42629
- Averaged equations for joint treatment of hydrodynamic expansion and conduction-type heating of plasma, the energy of nuclear fusion being taken into consideration. II - Spherical problem.
22 p3211 A72-42630
- Self-ignited impulsive optical discharge in a laser erosion plasma
23 p3295 A72-43308
- Electron and plasma particle acceleration by moving pulsed laser, noting appearance of fast particles, hard radiation and neutrons
23 p3295 A72-43312
- Kinetic equation for electron distribution in high temperature laser plasma, calculating nonequilibrium conditions for strong field and plasma parameters
23 p3318 A72-43323
- Pulsed laser produced high temperature plasma for electric power generation by controlled nuclear fusion, discussing gas dynamic model
23 p3321 A72-43723
- Averaged equations of laser heating of plasma in a focus-type system taking into account the heat of nuclear fusion.
23 p3322 A72-44223
- Averaged equations of laser heating of two-temperature plasma in a focus-type system taking into account the heat of nuclear fusion.
23 p3322 A72-44224
- Stimulated emission in vacuum far ultraviolet during rapid heating of the plasma electrons by ultrashort light pulses
23 p3322 A72-44466
- Evaporation of metallic targets by intense optical radiation
23 p3297 A72-44485
- Nanosecond and picosecond laser-produced CD₂ plasmas.
24 p3427 A72-44709
- Focusing characteristics of CO₂ laser beam.
24 p3409 A72-44776
- Electron-ion recombination in a helium plasma produced by laser.
24 p3428 A72-44799
- Initiation of a detonation by a laser beam focused in a gaseous medium
24 p3410 A72-45026
- Laser spin melting experiments for glass production in space from high melting metal and rare earth oxide ceramics
24 p3417 A72-45156
- High temperature deuterium plasma production by laser heating of gas filled cylindrical tube, optimizing pulse duration and tube configuration
24 p3431 A72-45712
- High power Nd glass laser with stepwise pulse amplification for intensive heating of solid target plasmas
24 p3431 A72-45714
- Temperature dependence of destruction threshold of lithium niobate surface under laser irradiation, noting ferroelectric properties effects
24 p3432 A72-45722

LASER MATERIALS

- Active and passive parameters correlations of solid state laser ruby crystals and Nd glass, using mechanical, thermal, chemical, optical, spectroscopic and electrical measurements
01 p0081 A72-11183
- Spectral heterogeneous lasing media with asymmetric luminescence bands, considering neodymium phosphate and germanate glass
06 p0824 A72-17392
- Handbook on lasers and optical technology covering gas, dye, liquid, injection and insulating crystal lasers, materials, sources, transmission, hazards and holographic recording
06 p0826 A72-17945
- Performance characteristics of electro-optical material cadmium telluride for intracavity modulator of carbon dioxide lasers
07 p1003 A72-19223
- Stimulated emission cross section, loss coefficient and terminal level lifetime of high power Nd-phosphorus oxychloride liquid lasers
07 p1004 A72-19226
- Energy transfer rates and spectral line inhomogeneity of narrow band oscillation phosphate glass and inorganic liquid lasers with Nd
07 p1004 A72-19227
- Optically pumped semiconductor lasers, discussing two photon absorption, emission from compounds and mixed crystals and smooth frequency variation
07 p1006 A72-20118
- Spectroluminescent and lasing properties of Nd ions in anisotropic scheelite crystal structures
07 p1007 A72-20121

- Nd glass absorption of flash pump emission energies with varying discharge parameters, Xe pressure and glass thickness 08 p1184 A72-22030
- Ceramic laser materials failure due to optically induced damage, estimating stresses and changes in refractive indices under thermal effects 09 p1336 A72-22403
- Longitudinal electro-optical effect in oblique cut lithium niobate crystal with minimum half wave voltage between incident beam and optical axis angle 12 p1855 A72-27603
- Low threshold current mesa-stripe-geometry double heterostructure injection lasers, eliminating current spreading by etching method 12 p1823 A72-27838
- Single crystal scheelite material for Nd doped intermediate gain laser host substance, considering optimum growth conditions, lasing parameter and Nd concentration 15 p2292 A72-32030
- Viscous boundary layer generated weak shock wave effects on gas dynamic laser medium density homogeneity [AIAA PAPER 72-709] 16 p2380 A72-34037
- Single-mode laser with a continuously variable pulse duration. 20 p2933 A72-39511
- Flash lamp optimal operating parameters determination by impedance matching to driving circuit and spectral matching to material of optically pumped solid state pulsed lasers 21 p3061 A72-40204
- Lasing properties of yttrium orthoaluminate doped with rare-earth metals 22 p3187 A72-42943
- Change in the sign of the thermal lens of glass laser rods during variation of the thermo-optical constant of glass 23 p3296 A72-43926
- Theory of pulsed internal optical parametric oscillators. 24 p3409 A72-44714
- Cadmium sulfide single crystals suitable for electron-beam-pumped lasers. 24 p3432 A72-45607
- ### LASER MODE LOCKING
- Radiation spectral properties in mode locking region of He-Ne 20 laser at 0.63 microns, generating three axial modes 01 p0078 A72-10154
- Unlocked multimode He-Ne lasers If noise, discussing different modes intensity fluctuations mutual correlations 01 p0080 A72-10850
- Mode locked He-Ne laser for optical communication, investigating steady state pulse behavior from injection locking theory 02 p0237 A72-11559
- Mode locked oscillation in ring cavity Nd glass laser, showing satellite pulse and spectral broadening due to self phase modulation 02 p0238 A72-12203
- Pulsed ruby laser with complex mirror resonator including optical delay line, observing mode locking effects in emission dynamics 02 p0238 A72-12290
- Picosecond pulse production and measurement from mode locked Nd glass laser 02 p0238 A72-12492
- Sequential dielectric breakdown of air by focused radiation from mode locked pulsed carbon dioxide TEA laser 03 p0366 A72-12966
- Gas laser longitudinal mode locking during single sideband modulation with nonuniform broadening in mode intensity distribution 03 p0366 A72-13365
- Traveling wave Ar laser with only fundamental TEM modes, examining mode self locking and composition and intensity as functions of frequency misalignment 03 p0366 A72-13366
- Passively mode locked Rhodamine 6G dye laser, obtaining frequency tuning with intracavity Fabry-Perot filter and transform limited duration picosecond pulses 03 p0368 A72-13605
- Mode-locked transversely excited atmospheric pressure carbon dioxide laser pulse duration dependence on cavity modulation frequency and loss 04 p0529 A72-14588
- Self mode locked dual polarization carbon dioxide laser, obtaining simultaneous active stabilization and frequency modulation 04 p0529 A72-14604
- Short duration high peak power laser pulses generation and measurement, examining active and passive mode locking, chirping, pulse compression and optical pumping 04 p0530 A72-14735
- Gas lasers mode locking, describing use of amplitude and frequency modulation and moving mirrors 04 p0530 A72-14738
- Ultrashort light pulse emission during mode locking in ruby lasers in free emission operation, examining first spike radiation 05 p0668 A72-16413
- Passive nonlinear output coupler for mode-locked high power picosecond pulse laser, using optical Kerr effect 05 p0670 A72-17190
- Coupled mode locking equations solved for homogeneously broadened lasers modulated near axial mode separation frequency 07 p1001 A72-19192
- GaAs junction laser, determining second order dispersion in mode locking and self pulsing from output field amplitude correlation measurement 07 p1001 A72-19198
- Second order mode locked GaAs junction laser, observing mode frequencies and phases configurations during self pulsing 07 p1001 A72-19200
- Millimeter wave techniques for laser stabilization to frequency standards, using phase locked HCN laser and high resolution IR spectrometer [CLEA PAPER 6,7] 07 p1004 A72-19383
- Laser gyro operational principles, discussing passive Sagnac and active ring laser interferometers, readout, errors due to null shift, lock-in and mode pulling, etc 07 p1007 A72-20223
- Laser triggered spark gaps characteristics initiated by switched out picosecond pulse from mode locked Nd-glass laser, investigating breakdown formation time delay 07 p1008 A72-20547
- Signal injection through laser transmitting window, showing effects on resonant frequency and locking mode [AD-738988] 07 p1009 A72-20680
- Self mode locking operation of transversely excited atmospheric pressure carbon dioxide pulsed laser with helical pumping 08 p1184 A72-22075
- Flashlamp and laser pumped cresyl violet laser emission characteristics between 620 and 710 nm, noting self mode locking in 3 component solution 09 p1324 A72-23048
- Single picosecond light pulses from mode locked Nd-glass laser, discussing temporal structure, spectral energy distribution and pulse shape measurements 09 p1324 A72-23082
- Multimode ring laser gyro with intracavity phase modulation, discussing experimental results concerned with lock-in at low rotation rates 09 p1324 A72-23085
- FM mode locked Nd-YAG pulsed laser controlled bistable phase position operation, using modulator cut as Brewster angle prism [AD-741511] 09 p1325 A72-23089
- Pulsed ruby laser with complex mirror resonator with optical delay line, observing mode locking effects in emission dynamics 10 p1488 A72-23764
- Solid state laser with slow relaxation bleachable filter, calculating modes self synchronization probability statistics relationship to relaxation time 10 p1492 A72-24512
- Mode locked ruby laser having triangular ring cavity with four prisms to obtain reliable single-transverse-mode Q switched and normal operation 11 p1647 A72-26150
- Transparent dielectrics destruction by mode-locked laser ultrashort pulses, discussing filamentary defect presence indication of radiation self focusing 12 p1853 A72-27068
- Picosecond pulse efficient second harmonic generation by crystals inside high power dye mode locked Nd-glass laser folded cavity 12 p1826 A72-28220
- Pulse energy and temporal width produced in self locking operation of laser with homogeneous gain line 13 p1968 A72-28686
- Energy conversion efficiency of xanthene dye laser pumped by mode-locked Nd-glass laser second harmonic, discussing effect of excited molecules transition to triplet state 13 p1970 A72-29686
- Steady state laser mode locking with saturable absorber, describing pulse shape and amplitude as function of quantity of absorbing medium 14 p2111 A72-30793
- Optical field emission effects on photoelectron emission nonlinearity from metal cathode using ultrashort mode locked laser pulses 15 p2250 A72-32303
- Dye-induced saturated frequency sweeping effects on mode-locked laser pulse broadening and substructures 15 p2250 A72-32523
- High speed photography ultrafast shutter based on polymethylene cyanide dyes saturability for measuring mode locked ruby laser pulse duration 15 p2241 A72-32535
- Russian papers on physical processes in lasers covering mode locking regime, pinch discharge, electronic transitions in diatomic molecules and laser control 16 p2400 A72-33295
- Q switched and free emission mode locking of neodymium glass and ruby lasers via liquid bleachable dye filter 16 p2400 A72-33296
- Mode locked lasers, investigating effect of grating-induced phase and spatial modulations by multiple transverse modes on pulse compression across beam cross section 16 p2403 A72-33840
- Spark interferometry of plasma filaments in gases from self focused single mode-locked ruby laser pulses 16 p2439 A72-33978
- Orientational Kerr effect direct observation via birefringence relaxation time measurement in self focusing region of mode locked Q switched laser picosecond pulses 17 p2561 A72-34190
- Pulse length evaluation from frequency domain phase function, applying to mode locked laser theory 17 p2562 A72-34292
- Off-axis hologram recording on thin bismuth film with picosecond pulse train from mode-locked Nd-glass laser 17 p2558 A72-35817
- Effects of thermal lensing in glass lasers. 19 p2810 A72-37512
- Double exposure holographic recording of rapidly changing object via mode locked ruby laser generated interference pattern 19 p2796 A72-37580
- Behavior of spontaneous emission across threshold in GaAs junction lasers. 19 p2811 A72-37865
- Nonlinear optics with picosecond laser pulses. 19 p2812 A72-38379
- Harmonic mode locking of the Nd:YAG laser. 19 p2813 A72-38688
- Theory of spontaneous mode locking in lasers using a circuit model. 19 p2813 A72-38690
- A simple self-mode-locked atmospheric pressure CO2 laser. 19 p2813 A72-38695
- Amplification of mode-locked trains with a liquid laser amplifier, Nd/3+/:POCl3:ZrCl4. 20 p2934 A72-39642
- Mode locked carbon dioxide with transverse pulse pumping, using Ge ultrasonic diffraction cell as active loss modulator 20 p2934 A72-39965
- Transition metal complex organic dye solution for Nd-glass laser Q-switching and mode locking, noting high photochemical stability 21 p3062 A72-40244
- Stimulated thermal scattering of picosecond laser pulses. 21 p3063 A72-40779
- Observation of transient behavior of picosecond laser pulses. 21 p3064 A72-41380
- Wavelength tuning of an intracavity pumped CW mode-locked dye laser. 22 p3184 A72-41989
- Spontaneous self mode locking in transversely excited nitrogen laser operation in first positive system 22 p3186 A72-42618
- Investigation of the shape of the radiation pulse of a self-mode-locked laser 23 p3294 A72-43303
- Molecular-beam-stabilized argon laser. 23 p3296 A72-43817
- Fluctuation mechanism of ultrashort pulse generation by laser with saturable absorber. 23 p3297 A72-44184
- Alkali metal vapor Q switches for synchronizing mode-locked laser pulse trains with external events. 23 p3297 A72-44189
- Time dependence of laser characteristics on external HF modulation of parameters by mirror oscillation and electrooptical and acoustooptical effects, noting laser mode locking 24 p3410 A72-45416
- Transparent dielectrics destruction by mode-locked laser ultrashort pulses, discussing filamentary defect presence indication of radiation self focusing 24 p3432 A72-45721
- ### LASER MODES
- Axial mode locking and equidistant frequency generation in solid state lasers due to active medium saturation, using self consistent equations with broadened amplification line 01 p0079 A72-10347
- Molecular Stark effect modulation of IR carbon dioxide laser radiation, using density matrix technique 01 p0079 A72-10515
- Airborne and spaceborne remote measurement and mapping of atmospheric nitric oxide, describing system configuration with mono or bistatic and pulsed or CW laser [AIAA PAPER 71-1112] 01 p0068 A72-10556

Single mode carbon dioxide laser action from quasi-optical mirror emission channels

01 p0080 A72-10578

Mode guiding improvement in p-n junction of symmetrical AlGaAs-GaAs heterojunction laser diode with narrow active region, obtaining low room temperature threshold current

01 p0080 A72-10788

Multimode Q switched ruby laser temporal coherence, comparing theoretical with experimental results from Michelson two-beam interferometer measurements

01 p0080 A72-10849

Unlocked multimode He-Ne lasers. If noise, discussing different modes intensity fluctuations mutual correlations

01 p0080 A72-10850

Laser optical anemometry system, describing fringe, Doppler and reference beam operation modes

01 p0081 A72-11168

Instabilities in dye switched ruby lasers emission distribution, investigating filament modes

01 p0081 A72-11314

Hypersonic projectiles wake visualization with holography, using single mode ruby laser and reflected diffuse light techniques

02 p0224 A72-11742

Laser flow anemometer technology, discussing velocity and spatial resolution, chromatic and temporal coherence, signal processing, frequency discrimination, spectrum analyzer and tracking filter

02 p0224 A72-11743

He-Ne traversing laser velocimeter for instantaneous axial fluid velocity measurement, describing signal analyzing system, construction and calibration

02 p0224 A72-11744

He-Ne laser velocimeter for roller bearing elements rotational speed measurements, discussing instrument construction and spatial resolution

02 p0224 A72-11745

Large steerable radio reflectors profile measurement with laser system, describing instrument design, accuracy and modifications

02 p0238 A72-12113

He-Ne laser active medium excitation and resonator geometry effects on TEM wave field

02 p0239 A72-12520

Laser with convex-plane resonator and cross sectional variable mirror transmission, showing effective transverse mode selection and diffraction divergence

02 p0239 A72-12767

Ruby ring laser single mode operation with Fabry-Perot etalons for selective feedback, discussing laser emission spectrograms

03 p0366 A72-13194

Focused image holography in multimode He-Ne laser radiation, using diffusely scattered reference wave and lens for high quality reconstruction

03 p0357 A72-13370

Single mode solid state laser periodic Q switching effects on spike pulse shape and synchronization by harmonic analysis with convergent series

03 p0366 A72-13371

Instrument and technique for Gaussian mode laser beam parameters measurement

03 p0367 A72-13444

Fluctuation theory for single mode laser detuning effect on photon intensity and spectral line width

03 p0368 A72-13671

Two photon method of measuring ultrashort pulses and nonlinear optical effectiveness of lasers in synchronized mode

03 p0369 A72-14063

Self focusing effect of Q switched single mode ruby laser emission in CdS crystal, noting 60 kw minimum threshold power

03 p0369 A72-14064

Electron energy distribution in carbon dioxide laser mixtures under lasing and nonlasing conditions

04 p0528 A72-14540

High power CW gas dynamic laser mode-control experiment with unstable resonator at high Fresnel number, obtaining near and far field intensity distribution

04 p0529 A72-14605

Multimode Ne-He laser in strong magnetic field, discussing plasma-optical effects, emission cut-off magnetic field strength for various discharge levels and single-mode construction

04 p0530 A72-14656

Airborne remote CAT detection equipment, examining pulsed Doppler laser and IR radiometry

04 p0521 A72-14831

Weakly ionized turbulent gas flow in pipe, comparing neutral and plasma fluctuations with laser beam scintillations

04 p0558 A72-15331

Output coupling apertures effect on carbon dioxide laser spatial coherence, considering resonator mode structure

05 p0667 A72-16001

Two mode lasers with photon intensity coupling near threshold treated by fluctuation theory detailing intensity, correlations and line widths

05 p0667 A72-16017

Monograph on semiclassical gas laser theory covering electromagnetic fields, atomic polarization, multimode theory, traveling- and standing-wave laser principles, collision effects, etc

05 p0668 A72-16398

Algebraic prediction formalism for ring laser mode coupling by phase modulation

05 p0668 A72-16566

Ultrasonic diffraction grating for noninterference sampling of high power carbon dioxide laser beam, discussing diffraction profiles obtained from lasers operating in Gaussian and donut modes

05 p0669 A72-16608

Carbon dioxide laser single mode operation dynamics measured by scanning Fabry-Perot interferometer and conventional reference oscillator

[AD-739101] 05 p0670 A72-17191

Heating dynamics of transparent dielectrics exposed to pulsed laser beam operating in free laser mode

06 p0825 A72-17697

Semiconductor lasers at room temperature, discussing hetero structures and diffused and epitaxial homostructures from basic operation modes and GaAs laser CW operation

06 p0825 A72-17771

Spectral characteristics of Ar ion laser emission for determination of stability region, mode sequence and beat signal levels

06 p0826 A72-18009

Junction lasers operating principles and device capabilities, considering reliability and mode properties

06 p0827 A72-18462

Laser quantum theory for single mode steady state emission fluctuations and instability region with high density of excited atoms

07 p0999 A72-18910

Optical sweep generator using single frequency He-Ne lasers with Michelson interferometer for mode selection to provide smooth tuning throughout Doppler width

07 p1000 A72-19010

Continuously pumped repetitively Q switched Nd-yttrium-aluminum trioxide laser, discussing mode selection technique based on gain excess over hold-off loss

07 p1000 A72-19045

Coupled mode locking equations solved for homogeneously broadened lasers modulated near axial mode separation frequency

07 p1001 A72-19192

Pulsed ruby laser mode structure effects on quartz damage, noting dependence on propagation and polarization directions with crystal

07 p1001 A72-19196

GaAs junction laser, determining second order dispersion in mode locking and self pulsing from output field amplitude correlation measurement

07 p1001 A72-19198

Second order mode locked GaAs junction laser, observing mode frequencies and phases configurations during self pulsing

07 p1001 A72-19200

Single mode high power pulsed nitrogen/carbon dioxide laser with unstable resonator coupling and diffraction limited focusing

07 p1002 A72-19215

Continuous TEM power from single longitudinal mode Nd-YAG laser pumped with tungsten-iodine lamp

07 p1004 A72-19235

Thermal distortion insensitive TEM mode beam of hf YAG laser for high precision drilling machine

07 p1004 A72-19236

Optical resonators using lossy anisotropic metal film linear polarizer for oscillation mode selection

[CLEA PAPER 6.3] 07 p1004 A72-19382

Single isotope He-Ne laser gyro comparison with multiisotope system, noting strong mode competition in ring laser

[CLEA PAPER 18.9] 07 p1005 A72-19402

Transverse mode effects on gain and dispersion focusing in high gain Xe laser

07 p1005 A72-19409

Density matrix equation solution in Liouville space, using variational procedure for laser mode equation and separable interaction method

07 p1006 A72-19670

Kinetic equations for laser active medium disturbances and electromagnetic field modes in cavities with losses

07 p1006 A72-20117

Spectral distributions of laser emission as dynamic variables of electromagnetic field modes and active medium excitations, using perturbation theory

07 p1007 A72-20120

Ruby laser emission losses for free lasing modes and threshold and above threshold pumping

07 p1007 A72-20122

Single mode laser line width calculation by reduction to non-Hermitian eigenvalue problem using Fokker-Planck equation

07 p1008 A72-20440

He-Ne laser discharge gap oscillation modes observation, noting applied magnetic field, gas parameters and cathode type effects on stimulated emission

07 p1008 A72-20510

Nonlinear mode relationship of gas ring laser due to light scattering at inhomogeneities in active medium

07 p1009 A72-20612

Internal asynchronous modulation of multifrequency He-Ne laser with Doppler broadened transition line

08 p1181 A72-20793

Nonlinear vibrational relaxation equations for expanding carbon dioxide-helium-nitrogen laser gas mixture, obtaining mode temperatures and gain coefficients by Runge-Kutta technique

08 p1149 A72-21261

Diffraction losses and corrections for lower order transverse modes and resonance conditions in optical resonators with cylindrical mirrors

08 p1133 A72-21371

Continuous chemical laser optimum optic axis position for maximum multimode power operation and intensity distribution

08 p1182 A72-21557

Two mode coupling and frequency pulling in He-Ne laser without absorbing medium in resonator

08 p1183 A72-21728

Holographic image reconstruction for individual transverse laser modes radiation intensity distribution

08 p1169 A72-21915

High resolution Raman spectroscopy of low pressure gases, using single mode Ar laser

09 p1323 A72-22613

Modal behavior and temperature tuning of pulsed room temperature GaAs laser, using hyperfine energy level separation

09 p1323 A72-22768

Laser pulse description by Fourier analysis, showing broadened spectral line widths relationship to cavity modes

09 p1324 A72-23078

Single mode He-Ne laser output, predicting intensity correlation function form and decay time near threshold

09 p1324 A72-23081

Multimode ring laser gyro phase modulation theory based on oppositely directed traveling waves

09 p1324 A72-23084

Smooth variation of He-Ne laser spectral line width in single to multifrequency mode transition, passing laser beam through coated quartz plate

10 p1490 A72-24051

Traveling wave mode ring laser operation, obtaining active medium polarization changes through longitudinal magnetic field excitation by capacitor discharge through spiral pump lamps

10 p1492 A72-24363

Polarization characteristics and losses of anisotropic laser resonators composed of arbitrary number of mirrors

10 p1492 A72-24364

Coherent and noncoherent modes of optical beating in laser Doppler velocity measurement using light scattered from single and multiple particles

10 p1481 A72-24412

IR carbon dioxide laser amplifier with fundamental mode output power in excess of 500 W, describing multistage mirror section design and test results

10 p1492 A72-24581

Frequency stabilization of He-Ne two mode laser with internal mirror plasma tube

11 p1646 A72-25303

Mode properties and energy losses for unstable laser resonator with curved and sharp edged mirrors

11 p1648 A72-26336

Two axial modes competition in He-Ne laser with uniform line broadening, noting application for high stability frequency standards

11 p1649 A72-26349

Injection laser pulsed emission mode effect on spectral characteristics

11 p1650 A72-26359

Near and far field energy and power density distributions of multi-transverse mode double discharge TEA laser beam

11 p1651 A72-26671

Two dimensional characteristic and distribution functions of monomode laser radiation random processes with nonlinear optics application

11 p1651 A72-26716

Ultrashort pulse lasing techniques, covering mode formation, secondary effects and two photon recording of emission structures

11 p1652 A72-26792

Thin Se film for recording mode structure of 10.6 micron carbon dioxide laser emission, describing optical equipment

11 p1652 A72-26795

Angular spectra and frequency characteristics of quasi-continuous monomode and two mode Nd-YAG lasers with spherical resonator

12 p1819 A72-27054

Single mode gas laser with internal absorption cell, emphasizing frequency standard application

12 p1819 A72-27285

Light power coupling efficiency from GaAs injection laser into single- and multimode fibers
12 p1820 A72-27507

Injection semiconductor laser mode selection and output enhancement by introducing external spectrally selective elements into resonator
12 p1821 A72-27589

Q switched ruby laser radiation spatial coherence, considering modes relationship to permittivity inhomogeneities and changes due to holes burning in population inversion
12 p1821 A72-27591

High order optical harmonic generation and many-quantum processes efficiency in multimode laser radiation field
12 p1821 A72-27593

Emission characteristics of single mode ring ruby laser under free oscillation conditions, discussing mode selection difficulties
12 p1821 A72-27598

Gas laser oscillation frequency stabilization by comparing mode separation with RF standard
12 p1822 A72-27608

Mode selection in high coherence ruby laser using KDP Q switch
12 p1823 A72-27618

Polarization modes of anisotropic optical traveling wave resonator using half wave plate and Faraday rotation cell
12 p1824 A72-27870

Active elements for high power Nd-glass laser facility to generate short and ultrashort pulses
12 p1825 A72-27881

Second harmonic conversion of CW YAG-Nd laser radiation on lithium metaniobate crystals, discussing conversion coefficient optimization
12 p1825 A72-27886

Laser resonator transverse and longitudinal mode selection techniques, considering single frequency stabilization, gain saturation theory and applications
12 p1826 A72-27964

Fabry-Perot interferometer for line structure of helical TEA-carbon dioxide laser, noting variable frequency single mode emission
13 p1968 A72-28687

Gas dynamic lasers and combustion driven devices design, operation, performance and industrial applications
13 p1965 A72-29420

Standing wave and colliding wave lasing and synchronization region in ring laser using active gas isotope mixture
13 p1968 A72-29511

Light polarization modes in gas ring laser with optically active isotopic cell, showing dependence on circular field coupling coefficient
13 p1968 A72-29512

Periodic motions of weakly interacting modes in solid state lasers, using active matter pellet-resonator model
13 p1969 A72-29517

Approximate analytical method for diffraction losses and corrections to lower transverse modes and resonance condition in symmetrical stable cavities with round spherical mirrors
13 p1970 A72-29679

Stable single frequency operation of molecular laser using carbon dioxide-helium mixture, ensuring vibrational-rotational transition by special selection of active element parameters
13 p1970 A72-29682

High power monopulse Nd laser, obtaining single longitudinal frequency stabilized mode with anisotropic spar or quartz plates
13 p1971 A72-29922

TEA carbon dioxide laser time dependent gain and cavity losses analysis, using lasing onset delay with current pulse
14 p2109 A72-30184

Visual observation of continuous hydrocyanic acid laser modes and beam energy distribution, using cholesteric liquid crystal image converter
14 p2111 A72-30851

Beam divergence prediction for multiple transverse laser modes, proposing tables and graphs to determine angular spread in far field
15 p2247 A72-32031

Wave packet theory application to multimode laser cavity electromagnetic/optical/field analysis
15 p2251 A72-32649

Q switched laser operation with electro-optic switch mechanism, measuring initial photon number per mode of Nd-glass and Nd-YAG lasers
16 p2399 A72-33014

Carbon dioxide waveguide gas laser performance characteristics, noting mode pattern stability and insensitivity to resonator disturbances
16 p2402 A72-33396

Single frequency and mode carbon dioxide laser frequency and power stabilization by phase control with electronic servosystem
16 p2402 A72-33621

Two axial modes competition in He-Ne laser with uniform line broadening, noting application for high stability frequency standards
16 p2402 A72-33702

Injection laser pulsed emission mode effect on spectral characteristics
16 p2403 A72-33712

Transverse modes competition in high power homogeneously broadened gas laser with confocal geometry, noting corresponding longitudinal mode in atomic excitation
16 p2403 A72-33841

Polarization modes and phase shifts of normal oscillation modes in anisotropic optical traveling wave resonator with Brewster winders half wave plate and Faraday rotation cell
16 p2403 A72-33979

Instantaneous and averaged spiking emission spectra of injection laser under spontaneous pulsation as function of oscillation mode and photon distribution
16 p2404 A72-33984

Active elements for high power Nd-glass laser facility to generate short and ultrashort pulses
16 p2404 A72-33990

Second harmonic conversion of CW YAG-Nd laser radiation on lithium metaniobate crystals, discussing conversion coefficient optimization
16 p2404 A72-33995

Competition effects on spatial coherence in a CO₂ laser.
17 p2562 A72-34725

Traveling wave mode ring laser operation, obtaining active medium polarization changes through longitudinal magnetic field excitation by capacitor discharge through spiral pump lamps
17 p2563 A72-34962

Polarization characteristics and losses of anisotropic laser resonators composed of arbitrary number of mirrors
17 p2563 A72-34963

Mode stability in a gas laser with nonlinear selection losses
17 p2563 A72-35304

High-radiance room-temperature GaAs laser with controlled radiation in a single transverse mode.
17 p2563 A72-35342

Hollow dielectric waveguide for distributed feedback lasers.
17 p2564 A72-35346

CW optically pumped tunable dye laser wavelength ranges, linewidth, mode purity, polarization and power output characteristics
17 p2565 A72-35947

Excitation modes and operating characteristics of electric discharge convection lasers
[AIAA PAPER 72-722] 17 p2565 A72-35962

Laser mode suppression arrangements consisting of Michelson interferometers with polarization prism as beam splitting element
18 p2697 A72-36112

Excitation of a confocal spherical laser resonator.
19 p2810 A72-37403

Gain and visualization of the modes of a thermally stabilized HCN laser.
19 p2810 A72-37455

Breakdown of some transparent dielectrics under the action of neodymium and ruby lasers in free light emission modes
19 p2810 A72-37542

Radiation coherence in a monopulse single-mode semiconductor injection laser
19 p2811 A72-37736

Passive mode-locking and Q-switching of high power lasers by means of the optical Kerr effect.
19 p2811 A72-37844

Active Q switching technique for producing high laser power in a single longitudinal mode.
19 p2811 A72-37845

Optimum generation conditions for a neon-helium laser operating in the axial TEM/sub 00/ mode
19 p2814 A72-38784

Frequency stabilization of a gas laser using mode-interaction effects.
19 p2814 A72-38822

Laser with convex-plane resonator and cross sectional variable mirror transmission, showing effective transverse mode selection and diffraction divergence
20 p2931 A72-39073

Laser action with coupled types of oscillations
20 p2931 A72-39319

Laser quantum theory for single mode emission fluctuations and instability region with high density of excited atoms, noting self consistent field effects
20 p2931 A72-39376

Rectangular aperture diaphragm dimension determination for ring laser resonator principal transverse mode selection and higher modes suppression
20 p2933 A72-39510

Single-mode laser with a continuously variable pulse duration.
20 p2933 A72-39511

High-resolution spectroscopy using magnetic-field-tuned semiconductor lasers.
20 p2933 A72-39561

Investigations on spectroscopy by nonlinear Zeeman-resonances of a multimode laser.
20 p2934 A72-39845

Measurements of a mode-competition discriminator in a single-frequency argon ion ring laser.
21 p3062 A72-40240

Single longitudinal mode operation of a transversely excited CO₂ laser.
21 p3062 A72-40243

Active gas mixture pressure relationship to excitation during single to multifrequency operation transition in He-Ne laser
21 p3063 A72-40667

Investigation by the photon count method of the statistical properties of the emission of a laser operating in the mode of several axial oscillations
21 p3063 A72-40784

Light pulse structure and bandwidth bounds in ruby laser with delay line inside variable effective length resonator
21 p3066 A72-40799

Single transverse mode operation of a pulsed volume excited atmospheric pressure CO₂ laser using an unstable resonator.
21 p3064 A72-41197

Mode-coupling effects in thin platelet semiconductor lasers.
21 p3064 A72-41381

Investigation of laser light spatial correlation by the photon coincidence method
21 p3064 A72-41691

The phase difference between coupled laser oscillations
22 p3184 A72-42109

Electromagnetic field, polarization and population inversion equations for spiked emission operation analysis in single mode laser
22 p3184 A72-42153

Hysteresis in a gas laser when passing from a single-frequency emission mode to a two-frequency mode
23 p3295 A72-43680

Effects of radiation trapping on mode competition and dispersion in the ring laser.
23 p3296 A72-43878

High gain He-Ne laser with forbidden cavity configuration, discussing elimination of unwanted lasing mode by temperature detuning with mirrors
23 p3296 A72-43903

Ultrasensitive response of a CW dye laser to selective extinction.
23 p3297 A72-44186

Time variations in the far-field diffraction patterns of spatial modes from electron-beam-pumped semiconductor lasers.
24 p3409 A72-44712

Investigation of the uniformity of neodymium-glass laser emission
24 p3410 A72-45419

Threshold characteristics of receivers with optical quantum amplifiers.
24 p3412 A72-45617

Angular spectra and frequency characteristics of quasi-continuous monomode and two mode Nd-YAG lasers with spherical resonator
24 p3412 A72-45707

LASER OUTPUTS

Goos-Hanchen nonpolarized light effect for laser beam separation into rectilinearly polarized beams during reflection
01 p0101 A72-10042

Channel clearing through clouds by laser beam, considering cross section expansion dynamics, channel growth rate, cloud motion and blurring
01 p0078 A72-10155

Emitted light power of CW injection laser related to threshold current, electrical and thermal resistances and external quantum efficiency
01 p0079 A72-10325

Laser light scattering by fuel droplets in flame combustion zone, measuring intensity distribution with contactless optical probe
01 p0066 A72-10495

Pin electrode transversely excited atmospheric pressure carbon dioxide laser construction and pulse power outputs up to 60 kW
[AD-738684] 01 p0079 A72-10516

Two dimensional scanning electron beam pumped laser, describing production of coherent emission
01 p0079 A72-10522

Gaseous pollutants remote detection by IR heterodyne radiometer with tunable lasers
[AIAA PAPER 71-1079] 01 p0080 A72-10538

Water quality monitoring by radiative transport equation for reflectance measurements of laser light scattered from turbid water polluted with absorber and scatterer particles
[AIAA PAPER 71-1098] 01 p0058 A72-10547

Completely sealed off room temperature CO laser system, discussing performance and continuous wave power
01 p0080 A72-10852

Laser power transmission, examining heat transformation into coherent radiation by closed cycle gas dynamic laser system
01 p0080 A72-10925

Solid state laser emission angular divergence, considering active medium optical inhomogeneity and cavity parameters effects

01 p0081 A72-10976

Instabilities in dye switched ruby lasers emission distribution, investigating filament modes

01 p0081 A72-11314

Nuclear radiation enhancement of carbon dioxide laser performance, discussing low pressure CW and high pressure pulsed discharges

01 p0082 A72-11330

Carbon dioxide laser pumping with nuclear reactions, indicating improved laser performance due to additional ionization by energetic charged particles

01 p0082 A72-11331

Pulsed hf discharge in hydrogen based on laser light scattering on plasma electrons, noting position of satellites in spectra

02 p0237 A72-11406

Optical distortion induced by heated windows in high power laser systems, deriving figures of merit for window materials

02 p0237 A72-11470

Pulsed laser emission in carbon monoxide, calculating molecular excited state populations

02 p0237 A72-11471

Plasma state variables diagnosis using laser light scattering

02 p0263 A72-11697

Calorimeter for measuring energy pulses and wavelengths from frequency doubled neodymium to carbon dioxide lasers

02 p0224 A72-11748

Contactless optical strain measurement based on speckle pattern change of diffusely reflected laser light

02 p0225 A72-11755

Spectral broadening in laser Doppler velocimeter, showing identity of wave vectors spread for incident and detected fields and scattering center finite volumetric stay

02 p0229 A72-12094

Solid state Q switched laser emission frequency drift from Fabry-Perot rings interferograms

02 p0237 A72-12108

Digital telemetry/communication laser link system design for operation at 1 gigabit/sec

02 p0174 A72-12143

Rabbit and monkey corneal damage following CW carbon dioxide laser irradiation, discussing hazard level derivation

02 p0163 A72-12413

Phototropic substance effect on spatial structure of passive Q switched ruby laser emission, considering gallium phthalocyanine solution

02 p0239 A72-12568

Fm of gas laser emission during sinusoidal modulation of relative excitation, evaluating collision parameters determination method

02 p0180 A72-12581

Dispersion characteristics and frequency stabilization of 0.63 micron laser in magnetic field

02 p0180 A72-12583

Mechanical breakdown characteristics of polymethyl methacrylate and polystyrene samples exposed to picosecond pulses emitted by Q switched laser

02 p0250 A72-12680

Impurities effects on crack initiation and propagation in polymethyl methacrylate under laser pulsed radiation

02 p0250 A72-12689

Carbon dioxide IR laser construction, laboratory implementation and experimental results

02 p0239 A72-12693

Directly heated cathode effect on He-Ne laser power output and relaxation oscillations in discharge gap

02 p0239 A72-12763

Cross-excited carbon-dioxide-nitrogen laser with pulse sharpening effect due to self-Q-switching, finding optimal nitrogen mixing ratio for peak power

02 p0239 A72-12827

Ruby and Nd lasers fundamental emission effects on excitation of stimulated Raman scattering in liquid and crystalline media by second harmonics

03 p0366 A72-13364

Traveling wave Ar laser with only fundamental TEM modes, examining mode self locking and composition and intensity as functions of frequency misalignment

03 p0366 A72-13366

Laser pumping pulse shape effects on second harmonic emission waveform during nonlinear crystal excitation by ultrashort light pulse

03 p0366 A72-13368

Atmospheric turbulence induced laser beam spread estimation from spherical wave modulation transfer function

03 p0367 A72-13442

Tunable multiple wavelength organic dye laser using optical feedback through partially transparent mirrors

03 p0367 A72-13443

Spectral and energetic characteristics of ruby laser radiation with two types of three-level radiation centers

03 p0367 A72-13582

Liquid breakdown and subsequent propagation by focused high power laser irradiation, presenting short term photography of event sequence

[AD-736005] 03 p0368 A72-13606

HCN laser amplifier gain measurement at IR wavelengths in gas mixtures by recording with pyroelectric receiver

03 p0368 A72-13667

Fluctuation theory for single mode laser detuning effect on photon intensity and spectral line width

03 p0368 A72-13671

Small signal gain and radiant power of carbon dioxide gas dynamic laser, presenting temperature distribution and population inversion

03 p0368 A72-13920

Two dimensional time resolved and real time IR interferograms obtained with pulsed Nd doped glass laser illuminated Michelson interferometer

03 p0362 A72-14200

Superradiative properties of high gain flashlamp-pumped dye laser amplifier, determining small signal amplification as function of pumping power and frequency

03 p0369 A72-14393

Uniform discharges in flowing carbon dioxide laser mixtures at atmospheric pressure, observing fluorescence intensity variation with discharge power density

03 p0369 A72-14400

High power Q switched ruby laser beam one dimensional penetration depth into metal as function of time, emphasizing ionization and plasma heating

04 p0528 A72-14536

Wavelength tuning effect on lasing threshold in electron beam pumped GaAs lasers as function of current density and voltage

04 p0528 A72-14545

Internal Q switching in CdS laser activated by exciton recombination, observing lag in emission onset after input pulses delivery

04 p0528 A72-14575

Statistical properties of random-phase modulated laser beams, calculating coherence functions of optical fields

04 p0528 A72-14580

Atmospheric pressure pulsed carbon dioxide laser using preionization by injected high energy electrons from surrounding glow discharge, obtaining highest output from gas mixture

04 p0529 A72-14586

Enhanced He-Ne laser frequency and output power stabilities obtained by constructing mirror and gas discharge tube as integral unit

04 p0529 A72-14603

High power CW gas dynamic laser mode-control experiment with unstable resonator at high Fresnel number, obtaining near and far field intensity distribution

04 p0529 A72-14605

Book on optics covering gas lasers, power output vs frequency, picosecond laser pulses, Q switching principles, mode locking, optical propagation through turbulent atmosphere, etc

04 p0548 A72-14733

Air pollutant detection by multiple slit correlation spectrometry and laser absorption technique, noting sensitivity enhancement by laser output increase

04 p0530 A72-14894

Digital measurement of pulsed laser energy, using planar vacuum photodiode detector with photocurrent capacitance integration and voltmeter display

04 p0530 A72-14921

Pulsed chemical laser started by transverse electrical discharge, observing output energy dependence on fluorine compound used

04 p0530 A72-14974

Laser light beam attenuation, considering turbulent pulsation effects in closed channel fluid flow axial region

04 p0530 A72-14989

Radiative noise effect on threshold current, output power and quantum yield of injection laser, evaluating noise loss factor

04 p0531 A72-15077

Lasing onset moments distribution over emitting surface of injection lasers at room temperature

04 p0531 A72-15082

Laser beam deflection as temperature sensor in optically inhomogeneous medium discussing gas density and temperature gradient relations

04 p0531 A72-15136

Laser coherent monochromatic light for cybernetics research in pattern classification, discussing fingerprints and letters

04 p0531 A72-15137

Neon lower laser level spontaneous emission double resonance phenomena, discussing depopulation rates and resonance line profile changes

04 p0531 A72-15138

Ultrahigh speed holographic camera for three-dimensional photographs and interferograms, using ruby laser output

04 p0522 A72-15139

Amplitude characteristics of Q switched He-Xe laser at 3.5 microns, using rotating reflection prism and velocity equations

04 p0531 A72-15149

Electron-ion-plasmon-photon interactions and energy exchange mechanism in plasma-field /laser pulse/ systems

04 p0557 A72-15155

Carbon dioxide gas dynamic laser mixture at high pressure, investigating gain and vibrational kinetics

04 p0531 A72-15336

He plasma generation by transversely excited carbon dioxide laser, determining density and temperature profiles of luminous fireball

04 p0558 A72-15345

Laser produced spark plasma, calculating threshold conditions for onset of stimulated scattering process and self focusing

04 p0559 A72-15346

Flow distribution behind shock wave with intense laser radiation absorption and laser-triggered thermomolecular reactions

04 p0559 A72-15351

Amplitude fluctuations of laser beam with Gaussian amplitude distribution on short line-of-sight path propagation through artificial turbulent atmosphere

04 p0488 A72-15383

Single and double channel laser triggered 1-3 MV switches design in high pressure gas, noting low jitter and built-in voltage isolation

04 p0532 A72-15532

Organic dye lasers radiation nonlinear interaction with alkali metals spark discharge plasma, showing angular and spectral broadening

04 p0532 A72-15573

Submillimeter wavelength HCN laser stabilization, describing AFC and phase locking

04 p0532 A72-15596

Far IR molecular laser variable interference filter for optimization of output coupling conditions and maximum power output

04 p0532 A72-15616

Nonlinear ponderomotive forces in intense laser light interaction with plasma

04 p0560 A72-15618

High accuracy laser reflector telemetric measurement for earth-moon distance variation in time by correlation method

04 p0495 A72-15727

Output coupling apertures effect on carbon dioxide laser spatial coherence, considering resonator mode structure

05 p0667 A72-16001

Giant pulse ruby laser operated at 6 Hz, describing shutter, shutter control unit, cooling system and electrical power supply and control circuits

05 p0667 A72-16035

Microwave-range optical heterodyne system with magnetically tuned /Zeeman effect/ laser emissions mixing and AFC

05 p0668 A72-16345

Pyroelectric laser power meter with built-in calibration based on reference heating by If current, describing operation, design and testing

05 p0662 A72-16347

Laser radiation amplification, investigating opposing laser pulses interaction in plasma

05 p0668 A72-16414

Laser induced gas breakdown in chemical reactions and explosions during plasma creation, using time resolved spectroscopy and titanium oxide probes

05 p0624 A72-16666

Unmodulated He-Ne laser output frequency stabilization, using quartz Fabry-Perot etalon

05 p0669 A72-16670

Continuously burning optical discharge in Ar and Xe at atmospheric pressures, evaluating laser beam energy absorption, electron density and plasma temperature

05 p0669 A72-16679

Two-photon time distribution in mixture of light from He-Ne laser and Gaussian source of same central frequency

05 p0669 A72-16691

Gas dynamic laser analysis based on phase cancellation model, showing flow induced phase nonuniformity minimization for far field intensity improvement

05 p0669 A72-16857

Gas dynamic laser technology advances, discussing water content, temperature and Na effects and nozzle design

05 p0669 A72-16895

HF and/or HF-carbon dioxide transfer laser potential power output and design criteria, considering deuterium and fluorine combustion, reaction product expansion and mixing rate

05 p0670 A72-16970

Hot plasma transverse and longitudinal wave parametric excitation by intense laser light near

plasma frequency, noting instability role in resonant coupling mechanism

05 p0699 A72-17172

Passive nonlinear output coupler for mode-locked high power picosecond pulse laser, using optical Kerr effect

05 p0670 A72-17190

Laser radiation intensity modulation by time varying magnetic field

06 p0825 A72-17685

Automatic frequency adjustment of pair of He-Ne lasers with different oscillation frequency fluctuations under various heating conditions

06 p0825 A72-17840

Polarizer circuit for reduction of output power fluctuations in He-Ne laser

06 p0825 A72-17842

Output power dependence on pressure and magnetic field strength in Kr ion laser for green, yellow and red lines

06 p0826 A72-18010

Laser radiation pressure applications to isotope and particle separation, optical levitation, high velocity acceleration and atomic beam analysis

06 p0826 A72-18176

Accurately stabilized lasers application to frequency standards, reporting inverted Lamb dip experiments data

06 p0827 A72-18461

Atmospheric pressure pulsed chemical laser based on reaction between fluorine and hydrogen or deuterium

07 p0999 A72-18877

Laser action in pulsed transverse discharge initiated chemical reactions forming hydrogen and deuterium halides, noting production of previously unobserved transitions

07 p0999 A72-18879

Laser triggered avalanche transistor voltage generator for picosecond streak camera used in laser pulse diagnostics

07 p0999 A72-18881

Spectral analysis of light reflected from Nd laser produced deuterium plasma, observing Doppler shift

07 p1039 A72-18888

Electro-optical multiple transit laser beam deflection system using KDP crystals and quadrupolar electrode arrangements

07 p1000 A72-19011

Tunable lasers using improved Littrow-mounted diffraction grating technique with mirror for spectral characteristics control

07 p1000 A72-19037

Q switched high power laser pulse compression based on optical polarization change on passing through Kerr-active medium

07 p1000 A72-19038

Kinetic model for gas dynamic laser energy extraction from carbon dioxide-nitrogen-helium mixture, predicting gain, saturation and pulse length

07 p1001 A72-19195

High voltage axially pulsed carbon dioxide laser performance test, determining output energy dependence on tube parameters

07 p1001 A72-19197

High gain xenon laser spectral narrowing dependence on line-broadening mechanism including saturation and distributed loss effects

07 p1001 A72-19201

High power UV light pulse generation using Nd-YAG laser with frequency doubling

07 p1002 A72-19202

Flashlamp pumped dye-doped polymethyl methacrylate laser thermal and photochemical effects decrease and peak power output increase by light converter

07 p1002 A72-19206

Dye laser system with narrow linewidth oscillator, transverse mode selector, power amplifier and nitrogen pumping, noting 50 kw and 5 nsec pulse generation capability

07 p1002 A72-19209

High power nitrogen-carbon dioxide cross beam electric discharge convection laser amplifier with rectangular channel

07 p1003 A72-19216

Atmospheric pressure carbon dioxide-nitrogen-helium lasers with high output energy densities, using auxiliary discharge for volumetric excitation

07 p1003 A72-19217

Spectral characteristics and small signal gains of carbon monoxide laser, using optimum gas compositions

07 p1003 A72-19218

Lamp pumped IR solid state laser obtaining 20 W output and 4 percent efficiency from transition of Ho ion in sensitized YAG

07 p1004 A72-19234

Self focusing of laser amplifier beam with Gaussian transverse intensity profile, discussing sample length and beam diameter, convergence and divergence

[AD-741092] 07 p0941 A72-19240

Accelerometer sensitivity calibration by laser interferometer for vibration measurement, discussing

frequency range, accuracy and advantage over spectral lamp

07 p0984 A72-19350

Pulsed and CW laser beam propagation through atmosphere

[CLEA PAPER 2,5] 07 p0942 A72-19380

Closed line magnetic confinement device filled with laser produced hydrogen plasma, discussing laser beam high speed numerical control for injected pellet interception

[CLEA PAPER 12,1] 07 p1040 A72-19392

Atomic selective two step photoionization and molecular photodissociation by tunable laser radiation, experimenting on Rb vapor and HCl respectively

[CLEA PAPER 12,4] 07 p1005 A72-19395

Neodymium-glass laser emission spectral and temporal correlations during Q switching by rotating prisms and passive shutter

07 p1006 A72-19633

Pulsed laser beam effect on residual stresses behavior in transverse weld on cylindrical shell

07 p0996 A72-19776

Laser telemetry performance, considering means of noise reduction

07 p0947 A72-20256

Ruby laser telemetry station operated at 0.7 microns, describing telescope pointing system

07 p0947 A72-20257

Aberration introduced by high satellite velocities, investigating application to laser telemetry

07 p0947 A72-20258

Tracking efficiency of laser telemetry on reflector carrying satellites

07 p0947 A72-20259

Tracking efficiency calculation for laser telemetry with laser reflector on nonstabilized satellite

07 p0947 A72-20260

Laser probes for acoustic surface wave amplitude and phase measurements

07 p1008 A72-20385

High speed rotating mirror camera adapted to solid state laser radiation, noting continuous recording and simultaneous imaging

07 p0990 A72-20401

He-Ne laser discharge gap oscillation modes observation, noting applied magnetic field, gas parameters and cathode type effects on stimulated emission

07 p1008 A72-20510

Liquid pulsed laser active element lens parameters effects on output radiation divergence

07 p1008 A72-20511

Output characteristics of Q switched liquid laser as function of pumping pulse, cavity mirror reflectivity and cavity length

07 p1008 A72-20544

Laser triggered spark gaps characteristics initiated by switched out picosecond pulse from mode locked Nd-glass laser, investigating breakdown formation time delay

07 p1008 A72-20547

Frequency stability of free running methane stabilized He-Ne lasers with dc excitation, comparing to rf excitation

07 p1008 A72-20562

Na deactivation effect on carbon dioxide-nitrogen gas dynamic laser gain

07 p1008 A72-20564

Repetitive dye laser with monochromatic beam of tunable wavelength, noting spectroscopic applications

07 p1009 A72-20588

Optimum lasing conditions and spectral characteristics of organic dye lasers at 3,100-11,000 Å

07 p1009 A72-20613

Magneto-optical effect on CW radiation intensity of Ar laser with cell in magnetic field for various gain conditions

07 p1009 A72-20615

Signal injection through laser transmitting window, showing effects on resonant frequency and locking mode

[AD-738988] 07 p1009 A72-20680

Two coupled lasers theory, obtaining fields equations of motion

[AD-739802] 07 p1009 A72-20681

Laser induced line narrowing effects in coupled Doppler broadened transitions within standing wave field

07 p1039 A72-20682

Constant period discrete holograms features, investigating laser visualization, recording, reconstruction and image focusing

08 p1163 A72-20747

Sensitivity threshold of optical heterodyne receiver as function of laser radiation amplitude spectrum, using photodetector output noise

08 p1181 A72-20794

Emission dynamics of pulsed laser with optical delay line in resonator

08 p1181 A72-20797

He-Ne laser resonator misalignment effect on output power, determining mirror arrangement precision tolerance for set fluctuation levels

08 p1181 A72-21163

High power visible output gas dynamic lasers, discussing supersonic flow generation

08 p1182 A72-21337

Single band optical mixer heterodyne spectrum analyzer for laser radiation image spectrum suppression

08 p1182 A72-21375

Spectral density curves for intensity fluctuations of stimulated emission from low and ultralow frequency gas lasers as function of thermal oscillation, mode interference and beat effects

08 p1182 A72-21379

Sealed-off He-Se laser construction and performance, comparing with He-Cd, He-Zn and He-Ne lasers

08 p1182 A72-21437

Laser radiation effects on optical glass volume and surface, discussing failure characteristics

08 p1182 A72-21655

TEA atmospheric pressure carbon dioxide laser driven by 200 kV Marx generator pulse

08 p1183 A72-21800

Ruby laser power output losses at 80 K with spectral line suppression dependence on surface reflection coefficient of plane parallel plate in resonator

08 p1183 A72-22026

Organic dyes molecular photodecay effect on output and power losses of laser activated by flash pump white light

08 p1184 A72-22029

Output power calculation of gas lasers with active elements of varying lengths, using extreme emission fluxes equations

08 p1184 A72-22031

Reduced air pressure effect on He-Ne laser output power via self heating

08 p1184 A72-22033

Magnetic field effect on gain saturation in CW Ar laser associated with Zeeman splitting

08 p1184 A72-22036

Resonator dielectric waveguide structure in electron beam pumped semiconductor laser, noting reduction of diffraction losses and of laser action threshold

08 p1184 A72-22089

Transparent and opaque materials fracture mechanism analogies under laser beam action, determining dislocation structure

08 p1185 A72-22093

Two photon absorption of ruby laser emission in mixed zinc cadmium sulfide crystals, plotting laser light damping vs beam power density

09 p1322 A72-22212

Electron and hole recombination at deep impurity centers during nonequilibrium current carriers excitation by Nd-glass laser light in p- and n-type germanium

09 p1322 A72-22214

Quartz crystals ultrasonic vibrations produced by laser beam, noting light modulation depth dependence on effective cross section and amplitude

09 p1322 A72-22415

High power electron beam pumped nitrogen super-radiant laser with 60 kW output

09 p1323 A72-22624

Hollow sphere calorimeter for high power pulsed laser energy measurements in broad spectral range, comparing with liquid calorimeter

09 p1323 A72-22656

Automatic computer-controlled system with laser technology for quality inspection of mass produced automobile master brake cylinders

09 p1319 A72-22979

Pulsed carbon dioxide laser operation, measuring pulse energy variation with gas pressure, expansion nozzle shape and output mirror transmission

09 p1323 A72-22980

Laser pulse description by Fourier analysis, showing broadened spectral line widths relationship to cavity modes

09 p1324 A72-23078

Uniform plane wave theory of internal upconversion and frequency doubling in optical parametric oscillators

09 p1324 A72-23079

CW Kr arc lamps for high power Nd-YAG laser pumping, testing operating life and electrical and spectral characteristics as function of design

09 p1324 A72-23080

Single mode He-Ne laser output, predicting intensity correlation function form and decay time near threshold

[AD-742154] 09 p1324 A72-23081

Laser induced surface damage probability as function of power density, suggesting electron avalanche breakdown as cause

09 p1324 A72-23083

Lasing length, power and efficiency of cw HF chemical laser with nitrogen or He diluent

[AD-742962] 09 p1325 A72-23241

Laser beam induced thermal blooming in absorbing gases from combined fluid dynamics and eikonal geometric optics theory, considering wind effects

09 p1352 A72-23333

Thin GaP film composition and structure determination by laser Raman scattering

09 p1314 A72-23345

- Neutral density glass collimating absorption lens for ideally uniform laser beams production
09 p1315 A72-23347
- Laser damage resistance properties of thin film multilayer antireflection coatings for quartz optics
09 p1326 A72-23348
- Ruby laser radiation modulation by mirror ultrasonic vibrations, discussing mechanism
09 p1326 A72-23681
- Interferometric measurements of time dependent electron density in Xe pinched plasma laser, showing laser lines due to transitions in triply ionized species
09 p1366 A72-23700
- Vesicular films in electron and laser beam recording suitable for computer output microfilm duplication and graphic arts
10 p1488 A72-23930
- Electric discharge carbon dioxide laser performance in terms of optical beam quality, electrical efficiency and gas utilization
10 p1489 A72-23943
- High power Ar ion laser with plasma tube using current conducting graphite bore for stable long life operation
10 p1489 A72-23944
- High power Nd-glass laser systems, discussing oscillator and amplifier operating parameters optimization
10 p1489 A72-23945
- Nuclear reaction-produced high energy ion beams for gas laser pumping and output enhancement
10 p1489 A72-23948
- Laser beams cross-sectional power distribution measurement by spinning disk scanner, using dual beam oscilloscope for laser beam profile display
10 p1489 A72-23949
- He-Ne laser output dependence on transverse magnetic field, describing magneto-optical effects to IR radiation decrease
10 p1490 A72-24046
- Smooth variation of He-Ne laser spectral line width in single to multifrequency mode transition, passing laser beam through coated quartz plate
10 p1490 A72-24051
- Nonlinear effects in optical pumping of Ne transition by laser line
10 p1491 A72-24109
- 50 MW laser amplifier at 3371 Å in molecular nitrogen via transverse electron pumping
10 p1491 A72-24225
- Laser source spectroscopic determination of pure and nitrogen perturbed carbon dioxide transition lines half-widths
10 p1491 A72-24227
- Superradiant laser stationary behavior and photon statistics, solving Fokker-Planck equation for quantum mechanical distribution function in Hilbert space of atomic system
10 p1514 A72-24247
- Inversion spatial nonuniformity effects on spectrum and kinetics of ruby laser, using spherical mirrors
10 p1491 A72-24361
- Defocused confocal Fabry-Perot spherical interferometer for analysis of Q switched visible and near IR lasers longitudinal mode outputs
10 p1481 A72-24564
- Modular carbon dioxide laser design and operational features, reporting measured data on plasma tube current, pressure and gas mixture flow rate effects on power output
10 p1492 A72-24565
- Semiconductor laser continuous emission conditions at room temperature, assuming output power drop with increasing current due to p-n junction heating
10 p1492 A72-24582
- Optical hyperfine structure of Ne 21 excited states and quadrupole moment obtained by laser induced line narrowing techniques
10 p1515 A72-24601
- Pressure dependence of gas laser intensity, taking into account velocity changing collisions with foreign gas atoms
[AD-740403] 10 p1492 A72-24604
- Induced Compton scattering and nonlinear electromagnetic wave propagation in laser beam focused plasma
10 p1522 A72-24605
- Intensity dependent propagation characteristics of circularly polarized high power laser radiation in dense electron plasma, calculating energy losses
10 p1522 A72-24607
- Maximum likelihood receiver performance for optical detection of multimode laser or scattered radiation, considering photocounting distribution, decision threshold and error probability
10 p1452 A72-24681
- Stochastic optimization of airborne laser seeker system design parameters to maximize target acquisition probability through regression analysis of data from computerized model
10 p1437 A72-24682
- Carbon dioxide laser output power enhancement methods, discussing gas transport, atmospheric pressure and gas dynamic lasers
10 p1492 A72-24849
- Rb87 vapor laser with optical pumping, measuring nitrogen or nitrogen argon mixture buffer gas partial pressure effect on power output
10 p1493 A72-24911
- Multiply charged ion plasmas production in heavy ion accelerator by laser beam interaction with vaporized target material
10 p1516 A72-25033
- Low voltage transversely excited gas transport CW carbon dioxide laser, discussing construction and power output, gain and efficiency
11 p1646 A72-25304
- Two-laser optical distance measuring instrument with atmospheric refractivity correction, noting accuracy
11 p1646 A72-25305
- Coordinate transformation equations derivation to determine third orthogonal velocity component from measurements at common point by two rotationally displaced laser Doppler velocimeter systems
11 p1629 A72-25308
- Rhesus monkey retinal image diameter estimation during exposure to Ar and He-Ne laser irradiation, using microphotometer scans
11 p1582 A72-25314
- Carbon dioxide-helium-nitrogen laser with nonlinearly absorbing cell, presenting emission pulse duration and rate
11 p1646 A72-25712
- Dielectrics breakdown under ultrashort neodymium laser pulses at fundamental and second harmonic frequencies
11 p1647 A72-25719
- Ruby laser light scattering method for measuring magnetic field direction in Tokamak plasma, testing validity by numerical calculation of scattered spectrum
11 p1694 A72-25793
- Anomalous heating due to nonlinear parametric interaction between plasma and laser radiation, calculating laser power thresholds for nonlinear instability effects
11 p1695 A72-25857
- IR radiation generation by Raman scattering and difference frequency mixing with Q switched Nd-YAG laser, noting peak power and photon conversion efficiency
11 p1647 A72-26149
- Laser induced transparent dielectrics surface fracture mechanism determination based on electron microscopic photograph analysis and disturbed specular reflection under predischARGE conditions study
11 p1648 A72-26333
- Thermoelastic stresses in solid transparent isotropic homogeneous dielectric under self-focused laser beam
11 p1648 A72-26334
- Frequency modulation of CW GaAs laser emission by injection current, noting temperature effects
11 p1648 A72-26337
- He-Ne laser with absorption cell, investigating high contrast power resonances due to Lamb dip at nonuniformly broadened absorption line center
11 p1649 A72-26340
- Laser emission spectrum broadening due to saturable dye filter bleaching, discussing amplitude and phase modulation contributions
11 p1649 A72-26341
- Q switched laser system emitting light pulses for high speed cinematography synchronized illumination
11 p1649 A72-26343
- Pumping conditions relationship to tube filling in Nd-YAG pulsed laser
11 p1649 A72-26344
- Populations modulation and spatial harmonics influence on gas and solid state laser radiation characteristics, discussing uniform and nonuniform line broadening
11 p1650 A72-26353
- Polyhedral radiation energy guides for laser sources and amplifiers, presenting solid state resonator design computation methods
11 p1650 A72-26354
- Stable single frequency Ar laser radiation with coupled transitions emission
11 p1650 A72-26356
- Solenoid-produced local axial magnetic field influence on beat signal frequency characteristics in ring laser with nearly linearly polarized emission
11 p1650 A72-26357
- Extremal feedback control system for IR and submillimeter range laser emission frequency stabilization
11 p1650 A72-26358
- Lithium niobate crystal refractive index inhomogeneity influence on second harmonic generation from He-Ne laser
11 p1650 A72-26360
- Total emitted power calculated for transversely pumped pulsed molecular nitrogen laser at 3371 Å
11 p1651 A72-26504
- Laser emission in near IR by flash lamp pumped fluorescent dyes, presenting oscillograms
11 p1651 A72-26505
- Alpha particles effect on carbon dioxide laser output power and emission spectra, using uranium acetate as radioactive source
11 p1651 A72-26552
- Zeeman effects in hyperfine structure of atomic iodine photodissociation laser emission, noting magnetic fields effect on time behavior
11 p1692 A72-26558
- Rare gas ion laser excited by electrodeless microwave discharges, noting external magnetic field effects on output
11 p1651 A72-26571
- Magnetic field direction measurement in Tokamak toroidal plasma by laser light scattering, using Fabry-Perot interferometer
11 p1697 A72-26583
- Near and far field energy and power density distributions of multi-transverse mode double discharge TEA laser beam
[AD-743823] 11 p1651 A72-26671
- Calorimeter calibration for laser energy and power measurements in terms of electrical energy based on voltage, resistance and frequency standards
11 p1652 A72-26781
- Ultrashort pulse lasing techniques, covering mode formation, secondary effects and two photon recording of emission structures
11 p1652 A72-26792
- Thin Se film for recording mode structure of 10.6 micron carbon dioxide laser emission, describing optical equipment
11 p1652 A72-26795
- Glass sample mechanical strength testing, considering abrasion process, concentric ring stress calculation and laser light scattering techniques
12 p1832 A72-27007
- Continuous He-Ne laser radiation power interferometry using Michelson interferometer with frequency doubler
12 p1819 A72-27051
- Time estimate criterion of lasing breakdown in photodissociative iodine-alkyl lasers with iodine molecule buildup
12 p1819 A72-27053
- Energy spectra of multiply charged ions formed in laser beam interaction with plasma, noting recombination process role
12 p1849 A72-27065
- Be foil electrical resistance change during and after pulsed laser irradiation and annealing
12 p1853 A72-27067
- Double discharge transversely excited atmospheric pressure /TEA/ carbon dioxide laser construction, operation and output energy
12 p1819 A72-27266
- Mathematical model for thermal lensing of IR laser window, discussing aberrations effect on diffraction-limited far field focus time
12 p1819 A72-27284
- Kinetics and cavity intensity models for output characteristics of pulsed electric discharge carbon dioxide lasers
12 p1820 A72-27287
- Cascade ionization of air by RF electric fields and intense laser pulses, solving Boltzmann equation for electron distribution
12 p1848 A72-27390
- Angular variation and spot dancing of laser beam in atmospheric propagation, obtaining standard deviation
12 p1782 A72-27493
- Russian book on spectral, spatial and time characteristics of lasers covering luminescence and resonator theories, electromagnetic field structure and radiation dispersion
12 p1820 A72-27500
- Phase matched nonlinear frequency conversion of laser light in tetragonal mercury thiocyanate complex crystals
12 p1854 A72-27549
- Stimulated laser emission in vacuum UV by liquid Xe excitation with electron beam, determining threshold current density, radiation divergence and line half width
12 p1820 A72-27582
- High power light pulse generation with steep leading edges in Nd-glass laser, noting duration change based on transparency increase under light transmission
12 p1820 A72-27583
- Gas laser with strong absorption saturation to obtain high peak power and frequency self stabilization by generation of quasi-traveling wave in resonator
12 p1820 A72-27585
- Laser emission intensity enhancement based on stimulated Brillouin scattering effect by raising pumping level, energy density and pulse duration
12 p1821 A72-27587
- Injection semiconductor laser mode selection and output enhancement by introducing external spectrally selective elements into resonator
12 p1821 A72-27589
- Laser with unstable telescopic resonator and large radiation loss, calculating energy characteristics and power efficiency
12 p1821 A72-27590
- High order optical harmonic generation and many-quantum processes efficiency in multimode laser radiation field
12 p1821 A72-27593

Second, third and fourth optical harmonics generation of Nd-doped YAG laser radiation under Q switching fast repetition pulse conditions

12 p1821 A72-27594

Discrete ten stage system for laser beam deflection based on electro-optical effect in lithium niobate crystals

12 p1808 A72-27595

High power pulse generation by ruby laser under free oscillation, using resonator with dielectric mirrors

12 p1821 A72-27597

Emission characteristics of single mode ring ruby laser under free oscillation conditions, discussing mode selection difficulties

12 p1821 A72-27598

Radiation distribution and power output characteristics of Nd in phosphorus oxychloride solution circulating liquid pulsed laser for various flow velocities

12 p1821 A72-27599

Solid state laser resonator inhomogeneous dielectric and mirror elements matching effects on Q factor and output power

12 p1822 A72-27609

Ruby laser electro-optical modulator with low modulation voltage, discussing layout, operating principle and laser energy characteristics

12 p1822 A72-27611

Thin polymer film bleachable dye switches for Q switched laser to achieve high power single pulse radiation

12 p1822 A72-27612

Transparent dielectric surface photoelectric emission current under laser pulse illumination, noting correlation to surface treatment and damage threshold

12 p1822 A72-27613

Industrial safety rules recommendations for lasers based on radiation biological effects and eye optical and physiological properties

12 p1771 A72-27615

Many element GaAs and CdS semiconductor laser achieving high power output by electron beam pumping

12 p1822 A72-27616

Te-doped GaAs injection laser, investigating crystal growth dislocations effects on output radiation-injection current characteristics

12 p1822 A72-27617

Transmitter aperture size and focus effects on scintillations of laser beam propagating through turbulent atmosphere

12 p1791 A72-27678

Laser irradiance modulation effect on high error fringes brightness in time average hologram reconstruction, noting exposure time increase

12 p1809 A72-27682

Time delayed amplification effects in TEA carbon dioxide lasers, measuring gain decay times for various gas mixtures

12 p1823 A72-27753

Carbon monoxide laser output power variation as function of oxygen tension

12 p1823 A72-27755

Holographic interferometer and fringe analyzer with laser sources, discussing design and application to supersonic flow imaging in wind tunnel

12 p1809 A72-27760

Intracavity gas cell for carbon monoxide laser oscillations restriction to lines coincident with atmosphere transmission bands, noting absorption by atmospheric water vapor

12 p1823 A72-27837

Spectral output of pulsed discharge initiated hydrogen fluoride chemical laser as function of pressure and gas composition

12 p1823 A72-27839

Crystal characteristics of optical detectors for direct measurement of high power laser radiation

12 p1824 A72-27874

Effect of pumping radiation absorption by electron-excited molecules on organic compounds lasing efficiency

12 p1825 A72-27883

Nd-fiberglass laser intensity fluctuations due to fibers absorption centers, deriving population inversion threshold, pumping power and center formation rate from kinetic equations

12 p1825 A72-27884

Frequency tuning and intracavity high efficiency extraction of second harmonic radiation from prism type Nd laser

12 p1825 A72-27885

Pressure effects on resonance fluorescence lifetimes in sulfur hexafluoride-air mixtures exposed to carbon dioxide laser radiation

12 p1826 A72-27929

Multiple laser light scattering from turbid medium, relating reflectance to polluted water parameters for aerial photographic surveillance

12 p1826 A72-27948

Organic dye desensitization of bleached AgBr phase holograms against printout darkening by Ar ion laser light

12 p1811 A72-27949

Gas and solid state lasers amplitude and phase fluctuations calculated from Langevin equations, noting spectral line width and collision waves

12 p1826 A72-28050

GaAs laser array Fabry-Perot structure to produce uniform TE polarization in emitted light

12 p1827 A72-28223

TEA pulsed carbon dioxide laser with continuous shaped electrodes, investigating hydrogen addition effects on power output and gain

12 p1827 A72-28224

Spacecraft propulsion into orbit by ground based high-power lasers via thrust generation by material evaporation, emphasizing advantages in launching small payloads

13 p2025 A72-28454

Free convection excitation and maintenance method, discussing occurrence around high power laser beam

13 p2063 A72-28628

Laser light induced high-low impedance switch in Cd doped n-type Si diodes with p-p-n junctions and negative resistance

13 p1928 A72-28676

Pulse energy and temporal width produced in self locking operation of laser with homogeneous gain line

13 p1968 A72-28686

Fabry-Perot interferometer for line structure of helical TEA-carbon dioxide laser, noting variable frequency single mode emission

13 p1968 A72-28687

Diffraction antenna use in visual range to study troposphere modulated laser radiation propagation in turbulent atmosphere, presenting light intensity distribution

13 p1917 A72-28690

Laser Doppler-type remote sensor for wind velocity and atmospheric turbulence measurements

13 p1956 A72-28859

Heating mechanisms in laser pulse produced plasma from electron temperature and reflectivity measurements

13 p2011 A72-28999

MHD laser discharge characteristics under generator conditions, emphasizing interaction of gas ionization instabilities and lasing radiation field

13 p2014 A72-29367

Statistical method of Pearson moments applied to temperature regimes effects on ruby laser output energy distribution

13 p1968 A72-29506

Helium-neon laser with Hg cathode in gas discharge tube, providing 250 mW output at 6328 Å

13 p1969 A72-29518

Energy and time characteristics of Raman scattering by benzene in laser cavity as function of medium thickness and cavity length

13 p1969 A72-29523

Electron density and temperature measurement from scattering of laser radiation in plasma within axisymmetric toroidal magnetic mirror machine

13 p2017 A72-29609

Optimal energy response conditions for single pulse emission by noninstantaneous switching of ruby and Nd glass lasers

13 p1969 A72-29612

Cosmological geodetic survey network construction via spacecraft tracking and laser beams, calculating power required for balloon satellite photography

13 p1922 A72-29631

He-Ne laser light modulation with lithium niobate crystals, noting lower light power and modulator volume requirements, better mechanical properties and lower thermal sensitivity

13 p1969 A72-29632

Interference method for gas laser phase front measurements based on comparison with radiation shifted in mirror plane

13 p1970 A72-29681

He-Cd laser emission wavelength determination at Lamb dip center for development of interferometer operation in violet spectral region

13 p1970 A72-29688

Pulsed chemical high pressure laser efficiency and output energy increase due to carbon dioxide introduction into deuterium-fluorine mixture

13 p1970 A72-29698

Helium use to minimize deflection of modulated laser beam in measurement of free surface motion of expanding annular cylinder loaded by exploding wire

13 p1960 A72-29765

Superradiant laser emission from organic dyes rhodamine 6G and B with coaxial flashlamp pumping source, relating input threshold energy to dye concentration

13 p1971 A72-29864

High power monopulse Nd laser, obtaining single longitudinal frequency stabilized mode with anisotropic spar or quartz plates

13 p1971 A72-29922

Visible light flash emission due to strong shock wave of laser spark, investigating strong external magnetic field effect and time variation of luminous intensity

13 p1972 A72-29983

Stimulated Compton scattering of laser radiation by electron plasma, determining electrons diffusion coefficient and velocity distribution function

13 p1972 A72-29987

Co 60 gamma radiation effect on stimulated ruby laser emission delay time, pulse duration, energy curve and intensity

13 p1972 A72-30005

Microscopic processes within high energy ion acceleration in laser-produced plasmas, discussing transient electric field role

14 p2136 A72-30178

Lightly doped InP and vapor epitaxial GaAs laser, observing long wavelength shift in photoemission spectra peak

14 p2108 A72-30182

Absorption effects on 10.6 micron laser beam in fluidized particulate crosswind, discussing calcium hydroxide performance

14 p2109 A72-30186

Proton beam effect on carbon dioxide laser discharge I-V characteristics and emission power

14 p2109 A72-30352

Lamb dip for 119 micron line of CW gas laser, noting decay constants due to pressure

14 p2110 A72-30424

Spectral changes of light reflected back from plasma during heating by mode locked Nd laser, noting equidistant lines presence

14 p2138 A72-30447

Lunar physical libration measurement from Apollo laser experiment with retroreflectors, assessing obtained data

14 p2154 A72-30516

Holographic diffraction grating production by impressing interference fringes with photographic procedure, using two laser beams

14 p2105 A72-30579

Small spectral width emission from dye laser with interference filter and quartz plate Fabry-Perot interferometer for spectroscopic investigations

14 p2110 A72-30674

Flashlamp pumped tunable narrowband traveling wave dye ring laser, stabilizing emission frequency by intracavity Fabry-Perot etalon

14 p2110 A72-30675

Free electron waves interaction with coherent laser light in crystalline medium, discussing quantum mechanical treatment and path integral approach

14 p2110 A72-30725

Laser radiation time characteristics measurement based on multiphoton processes in opposite light beams, estimating accuracy necessary for registration of ultrashort pulses

14 p2111 A72-30794

Soft X ray emission for plasma temperature determination in laser induced gas breakdown for air and He

14 p2139 A72-30805

Photon correlation spectrometer for laboratory wind tunnel measurement of laser Doppler signals backscattered from dust particles

14 p2111 A72-30854

High power carbon dioxide laser construction, specifications and operation for applications to laboratory and industrial processing of glass, ceramics and metals

14 p2111 A72-30857

CW oscillator model for laser amplifier, including nonlinear effect of gain saturation

14 p2111 A72-30896

Atmospheric air pollution study by space techniques via thermal radiation spectral measurements and laser sounding, considering spaceborne photography

15 p2220 A72-31237

Joint photon-count probability distribution measurement of electric field amplitude correlation function for random-Gaussian light fields produced by laser beam scattering

15 p2280 A72-31378

Human eye relative luminous efficiency for near IR and UV coherent light, using ruby laser pumped tunable dye laser primary and second harmonic outputs

15 p2184 A72-31380

Laser emission from pulsed transverse electric discharge in supersonic nozzle downstream region gas dynamic cooled mixture

15 p2245 A72-31385

Hollow dielectric waveguide used for carbon dioxide laser gas discharge, noting increased gain, volumetric output and saturation parameters

15 p2245 A72-31386

Properties of natural waves excited in Fabry-Perot resonator by external laser beams, noting stability dependence on wave type

15 p2245 A72-31420

Green luminescence intensity dependence on lasing power during two-photon excitation of Er and Ho ions in calcium difluoride by neodymium laser

15 p2246 A72-31422

Carbon dioxide TEA high output pulsed laser, testing wide range of carbon dioxide-nitrogen-helium mixtures at various pressures

15 p2246 A72-31638

Gas laser asynchronous coupling modulation, examining dependence on lasing threshold, optical spectrum and transition line shape

15 p2246 A72-31660

Laser effect in solution of neodymium oxide in mixture of phosphorus oxychloride and heavy water, presenting preparation procedure

15 p2246 A72-31680

Transient phase object high sensitivity measurement by He-Ne laser beam transmission through differential interferometer and signal detection with p-i-n photodiode

15 p2235 A72-31784

Frequency modulated laser radiation detection, studying photomultiplier current harmonics, phase/amplitude detector nonlinearities and noise-resonator coupling effects

15 p2246 A72-31882

Laser coupling through nonlinear gas filled absorber cell, discussing molecules mean free path

15 p2246 A72-31883

High power CW Nd-YAG laser efficiency improvement by optical pump wavelength, power coupling and balance factors, noting krypton arc lamp contribution

15 p2247 A72-32029

Beam divergence prediction for multiple transverse laser modes, proposing tables and graphs to determine angular spread in far field

15 p2247 A72-32031

Two dimensional acousto-optical light beam deflection system for laser recorder error correction

15 p2248 A72-32038

Modulated laser beam record wideband signals on photographic film, discussing noise sources and compensation methods for SNR improvement

15 p2248 A72-32039

High speed facsimile transmission system based on LR70 laser scanner, presenting typical system output image

15 p2248 A72-32041

Optical, mechanical and electrical arrangements of laser Doppler velocimeter, presenting Doppler signals displays and three dimensional gas velocity profiles in vortex region

15 p2236 A72-32044

Laser Doppler velocimetry system design for optical measurement of intrablade flow velocity in turbomachinery

15 p2237 A72-32045

IR and visible parametric laser image upconversion experiments, demonstrating wavelength dependence on view field by black body radiometric measurements

15 p2249 A72-32152

Turbulence and nonlinear thermal blooming effects as cause of refractive attenuation of laser beam intensities

15 p2249 A72-32160

Transverse wind self-induced thermal lens effects on target image quality in laser beam tracking systems

15 p2249 A72-32164

Laser interference fringe jitter due to wavelength instability, suggesting pulse shape blurring intensity variation control by flat or large-angle wedge beam splitter

15 p2249 A72-32166

Double heterostructure injection lasers with narrow active regions, discussing threshold current densities, emission polar diagrams and optical field penetration into boundary regions

15 p2249 A72-32237

High gain CW He-Xe laser transitions due to Xe 5d level long-lived decaying emission

15 p2250 A72-32301

Photodiode assembly for fast laser pulses and optical signal detection, utilizing Hewlett-Packard 5082-4220 diode in impedance matched holder

15 p2208 A72-32432

GaAs laser properties determination by gallium arsenide-aluminum gallium arsenide double heterostructure junction diode laser, noting gain and loss at room temperature

15 p2250 A72-32519

Dye-induced saturated frequency sweeping effects on mode-locked laser pulse broadening and substructures

15 p2250 A72-32523

Spiking response of luminescent diode pumped CW Nd-YAG laser to sinusoidal modulation, showing agreement with relaxation oscillation resonance prediction

15 p2250 A72-32526

Coherent orange emission and bright electroluminescence from indium gallium phosphides vapor grown p-n junction laser diodes

15 p2251 A72-32532

Sealed room temperature gas laser output oscillating on 5-micron carbon monoxide or 10-micron carbon dioxide lines

15 p2251 A72-32533

Stimulated emission in molecular iodine vapor phase laser optically pumped by Q switched Nd-YAG laser second harmonics

15 p2251 A72-32538

Oil spills remote sensing in marine environment, using laser excited fluorescence for detection, identification and quantification

15 p2251 A72-32623

Speckle pattern method of laser holography for structural vibration and surface strain study, noting real time operation

16 p2388 A72-32821

High power carbon dioxide lasers review covering CW, Q switched and pulsed atmospheric pressure lasers and various excitation techniques

16 p2399 A72-32848

Liquid optoacoustical modulator for laser radiation control operating on pulse amplitude modulated ultrasonic traveling waves with membrane partitions

16 p2400 A72-33081

Electro-optical Q switch synchronized by laser radiation for nanosecond light pulse shaping with energy dependent triggering

16 p2400 A72-33082

High voltage nanosecond pulse generator triggered by laser radiation from transmission stripline discharger for multichannel synchronous operation

16 p2400 A72-33083

High gain laser amplifier spectral linewidth dependence on external signal or spontaneous emission source, noting saturation role and relevance to interstellar medium radiation

16 p2453 A72-33166

Passive shutter power absorption effect on periodically triggered pulsed ruby laser output instability, showing optical inhomogeneity interferograms

16 p2400 A72-33189

Pulsed discharge development mechanism relationship to carbon dioxide laser lasing process, considering positive space charge ion role

16 p2401 A72-33369

CW dye laser output tuning by mirror-grating combination with interspersed output coupling element, noting orders of magnitude reduction of fluorescence background intensity

16 p2401 A72-33388

Intense emission from high pressure pulsed carbon dioxide chemical transfer laser by flash photolysis initiated deuterium-fluorine exothermic chain reactions

16 p2401 A72-33392

Coherent CW radiation by tunable GaAs injection laser in external dispersive cavity at 77 K, discussing monochromatic output spectral analysis by Fabry-Perot interferometer

16 p2401 A72-33393

CW laser transitions in singly ionized Te vapor spectrum at 4843-9378 A, indicating charge transfer as dominant excitation mechanism

16 p2401 A72-33394

Photodiode-operational amplifier circuit for pulsed laser systems energy variations monitoring, noting insensitivity to ambient light conditions

16 p2402 A72-33607

Single frequency and mode carbon dioxide laser frequency and power stabilization by phase control with electronic servosystem

16 p2402 A72-33621

Digital recording techniques for airborne data acquisition, emphasizing laser beam holographic recorders

16 p2394 A72-33642

Continuously burning optical discharge in Ar and Xe at atmospheric pressures, evaluating laser beam energy absorption, electron density and plasma temperature

16 p2402 A72-33691

Populations modulation and spatial harmonics influence on gas and solid state laser radiation characteristics, discussing uniform and nonuniform line broadening

16 p2402 A72-33706

Polyhedral radiation energy guides for laser sources and amplifiers, presenting solid state resonator design computation methods

16 p2402 A72-33707

Stable single frequency Ar laser radiation with coupled transitions emission

16 p2403 A72-33709

Solenoid-produced local axial magnetic field influence on beat signal frequency characteristics in ring laser with nearly linearly polarized emission

16 p2403 A72-33710

Extremal feedback control system for IR and sub-millimeter range laser emission frequency stabilization

16 p2403 A72-33711

Lithium niobate crystal refractive index inhomogeneity influence on second harmonic generation from He-Ne laser

16 p2403 A72-33713

Proton bombarded stripe geometry heterojunction lasers for 300 K CW operation compared with oxide insulated lasers

16 p2403 A72-33757

Transverse modes competition in high power homogeneously broadened gas laser with confocal geometry, noting corresponding longitudinal mode in atomic excitation

16 p2403 A72-33841

Transversely excited high pressure carbon dioxide laser cavity dumping with reproducible time delay between current excitation and gain-switched laser pulses

16 p2403 A72-33844

Spark interferometry of plasma filaments in gases from self focused single mode-locked ruby laser pulses

16 p2399 A72-33978

Crystal characteristics of optical detectors for direct measurement of high power laser radiation

16 p2403 A72-33983

Multielectron electron beam pumped semiconductor laser using emitting GaAs disks with vapor deposited dielectric mirror coatings

16 p2404 A72-33985

Effect of pumping radiation absorption by electron-excited molecules on organic compounds lasing efficiency

16 p2404 A72-33992

Nd-fiberglass laser intensity fluctuations due to fibers absorption centers, deriving population inversion threshold, pumping power and center formation rate

16 p2404 A72-33993

Frequency tuning and intracavity high efficiency extraction of second harmonic radiation from prism type Nd laser

16 p2404 A72-33994

Discharge stabilization in closed cycle carbon dioxide electric discharge convection lasers by aerodynamic, RF power and tandem techniques

16 p2404 A72-34026

Mathematical model for deuterium slab solid and plasma under laser pulses irradiation, noting shock wave propagation and slab acceleration

16 p2439 A72-34027

Q switched laser produced hemispherical shock waves in Ar and He plasmas, determining primary and secondary wave trajectories

16 p2439 A72-34028

CW argon ion laser characteristics at high steady discharge currents, discussing output limitation by low inversion utilization efficiency due to cavity mirrors optical degradation

16 p2404 A72-34035

Supersonic flow aerodynamic window for high power laser beam extraction through nonabsorbing gas medium while supporting pressure difference between cavity and ambient atmosphere

16 p2404 A72-34036

Atomic, molecular and ionic species detection in upper atmosphere by measurement of resonance fluorescence radiation excited by tunable laser radiation

16 p2388 A72-34073

He-Ne laser resonator misalignment effect on output power, determining mirror arrangement precision tolerance for set fluctuation levels

17 p2562 A72-34454

Variable output coupling device for far infrared laser.

17 p2562 A72-34463

Resonator dielectric waveguide structure in electron beam pumped semiconductor laser, noting reduction of diffraction losses and of laser action threshold

17 p2562 A72-34460

Transparent and opaque crystal surface fracture mechanism analogies under laser beam action, determining dislocation structure

17 p2562 A72-34664

Laser beam welding of small components

17 p2559 A72-34925

Inversion spatial nonuniformity effects on spectrum and kinetics of ruby laser with spherical mirrors

17 p2563 A72-34960

Simple technique for sequential Q-switching of molecular lasers.

17 p2563 A72-35193

Nonpeaked emission from a ruby laser obtained with the aid of bleachable solutions

17 p2563 A72-35306

A gas laser with external mirrors generating non-polarized radiation

17 p2563 A72-35308

High-radiance room-temperature GaAs laser with controlled radiation in a single transverse mode.

17 p2563 A72-35342

Hybrid injection locking of higher power CO2 lasers.

17 p2564 A72-35343

Output fluctuations of CW-pumped Nd:YAG lasers.

17 p2564 A72-35345

Passive Q switching extension of carbon dioxide laser output frequency range using dichloro-difluoro methane as saturable absorber

17 p2564 A72-35347

Tunable output dye and semiconductor lasers application to absorption spectroscopy and air pollution monitoring

17 p2564 A72-35381

Monochromatic carbon dioxide TFA laser

17 p2564 A72-35424

LASER OUTPUTS

Multicomponent structure of Nd-glass laser radiation, observing active medium gain band portions interrelationships in free running and stimulated emission operation modes

17 p2564 A72-35507

Displacement measurement from double-exposure laser photographs.

17 p2564 A72-35751

Laser and mercury lamp outputs spatial coherence measurement by speckle patterns produced with ground glass as random inhomogeneous medium

17 p2565 A72-35752

Atmospheric pressure carbon dioxide pulsed IR laser to obtain 80 w peak power by optical pumping with TEA HBr laser and filter

17 p2565 A72-35816

RF augmentation in CO₂ closed-cycle dc electric-discharge convection lasers.

17 p2565 A72-35818

CW optically pumped tunable dye laser wavelength ranges, linewidth, mode purity, polarization and power output characteristics

17 p2565 A72-35947

A relative performance analysis of atmospheric laser Doppler velocimeter methods.

17 p2558 A72-35949

Laser IR radiation attenuation in natural and artificial fogs, noting dependence on particle size distribution

18 p2697 A72-36102

Laser optical and IR radiation attenuation in atmospheric precipitation, considering snow, rain and drizzle

18 p2697 A72-36103

He-Ne laser radiation modulator at 1.5 GHz using X and Z cut lithium niobate crystals in toroidal microwave cavity

18 p2697 A72-36113

The influence of a nonuniform transversal magnetic field on the power output of a gas laser.

18 p2715 A72-36338

Quantum noise in semiconductor lasers.

18 p2697 A72-36345

Experimental analysis of the vibrational-rotational line content of a Q-switched CO₂ laser.

18 p2697 A72-36501

Field fluctuations of a laser beam propagating in a turbulent atmosphere

18 p2661 A72-36656

Resolution of optical-memory matrices prepared from photochromatic materials when using a focused beam to record information

18 p2692 A72-36658

Single-crystal, electro-optic shutter for Q-switching lasers emitting unpolarized radiation.

18 p2698 A72-36698

Propagation of laser beams through the atmosphere.

II

18 p2661 A72-36793

Investigation of the atmospheric boundary layer and clouds by the laser tracking method

18 p2698 A72-36969

Variation of the longitudinal electric field by the internally modulated beam in a He-Ne laser.

19 p2810 A72-37408

Gain and visualization of the modes of a thermally stabilized HCN laser.

19 p2810 A72-37455

Effects of thermal lensing in glass lasers.

19 p2810 A72-37512

High power pulsed HCN laser.

19 p2811 A72-37583

Interferometric holography of laser-produced gas breakdown.

19 p2798 A72-37623

Use of generalized theory of optical diffraction for the study of second harmonic generation.

19 p2811 A72-37673

A holographic method for optical adjustment of pulsed laser beams

19 p2811 A72-37674

Active Q switching technique for producing high laser power in a single longitudinal mode.

19 p2811 A72-37845

Momentum transfer and plasma formation above a surface with a high-power CO₂ laser.

19 p2811 A72-37864

Importance of nozzle geometry to high-pressure gas-dynamic lasers.

19 p2811 A72-37867

Fluid mechanics anemometry based on laser light frequency modulation /Doppler effect/, describing measurement of extensions of vortices and oscillations in flow boundary layers

19 p2801 A72-37934

Measurements of the laser linewidth due to quantum phase and quantum amplitude noise above and below threshold. I.

19 p2811 A72-38084

CW gasdynamic thermally excited and selectively pumped CO₂-N₂ mixing laser.

19 p2811 A72-38097

Quantum yield variations of Nd ion activated glass as function of electron beam energy and intensity, noting nuclear particles effect on laser radiation

19 p2823 A72-38205

Relation between the plasma ion current and the surface defects produced by ruby and neodymium laser emission

19 p2812 A72-38210

Effect of optical constants on the energy distribution in homogeneous particles illuminated by a parallel beam of light

19 p2812 A72-38216

Nonlinear optics with picosecond laser pulses.

19 p2812 A72-38379

Influence of an optically nonhomogeneous medium on the coherence of laser radiation and the possibility of obtaining a holographic image

19 p2812 A72-38536

Fracture of nonlinear KDP and LiNbO₃ crystals by ruby laser radiation

19 p2812 A72-38537

Analogy in the evolution of surface and bulk damage features produced by laser radiation in transparent glasses

19 p2812 A72-38541

Electric discharge concept to uncouple electron density from temperature for production of stable uniform electric laser discharges

19 p2812 A72-38596

Optical communications in Japan.

19 p2766 A72-38602

Possibility for buildup of laser radiation scattered by an electron beam

19 p2812 A72-38662

Multipulsing behavior of electrooptically Q-switched lasers.

19 p2813 A72-38692

Calculations of gain and power output for a gas-dynamic laser.

19 p2813 A72-38693

Radio-frequency preionization in a supersonic transverse electrical discharge laser.

19 p2813 A72-38694

A simple self-mode-locked atmospheric pressure CO₂ laser.

19 p2813 A72-38695

Pulse nitrogen laser at high repetition rate.

19 p2813 A72-38696

A helium-neon laser active element with a metallic inner wall surface

19 p2814 A72-38785

Certain results of a study of the emission-frequency stability of gas lasers at 0.63, 1.5, 3.39, and 9.6 micron wavelengths

19 p2814 A72-38786

Experimental achievement of optical pumping of a carbon dioxide molecular laser

19 p2814 A72-38790

Surface tilt and vibration measurements by laser speckle pattern photography, comparing with moire fringes in strain analysis

20 p2930 A72-39032

Electro-optical TV technique with laser source illumination to provide engineering metrology and NDT procedure resembling real time holographic interferometry

20 p2930 A72-39038

Laser beam scanning and recording in two dimensional pattern on silver halide, evaluating systems performance based on signal response, granularity and noise characteristics

20 p2930 A72-39040

Directly heated cathode effect on He-Ne laser power output and relaxation oscillations in discharge gap

20 p2931 A72-39069

Light attenuation coefficient measurement in water of various turbidity with AR and Kr lasers, interpreting results by Mie scattering theory

20 p2931 A72-39270

Investigation of radiation field distribution in a ruby laser with a SFR high speed camera

20 p2931 A72-39318

Isotropically and anisotropically polarized He-Ne lasers output dependence on longitudinal magnetic fields, noting electron density radial redistribution in gas discharge plasma

20 p2932 A72-39411

Polarization effect of attenuation of opposed-wave competition in ring lasers

20 p2932 A72-39412

Experimental effects of finite transmitter-apertures on scintillations.

20 p2932 A72-39500

Unstable resonator theory with geometrical optics and diffraction approximation, applying to laser mode selection and beam divergence reduction

20 p2932 A72-39501

Influence of the refractive index nonlinearity on the dynamics of emission from semiconductor lasers.

20 p2932 A72-39504

Air cooled CW 30 W carbon dioxide laser construction for technological applications, using radiation energy extraction through GeAs or GaAs plate

20 p2932 A72-39507

Utilization of photorecombination of radicals and atoms in continuous-wave lasers.

20 p2932 A72-39508

Spectral characteristics of a single-frequency argon laser with an absorbing film.

20 p2932 A72-39509

Energy characteristics of the laser action in rhodamine 6G pumped by a pinched discharge.

20 p2933 A72-39512

Generation of controllable light pulses in an electron-beam-pumped laser.

20 p2933 A72-39514

Time characteristics of heterojunction injection lasers.

20 p2933 A72-39516

Diffraction of a laser beam by domains in yttrium iron garnet.

20 p2933 A72-39521

Shock waves resulting from interaction of laser radiation with transparent solids.

20 p2933 A72-39522

Q switched Nd-YAG laser with lithium niobate crystal cut at Brewster angle for reproducible and controllable giant pulse generation

20 p2933 A72-39562

Continuously tunable dye laser to obtain output wavelength variation by changing pump laser beam incidence angle on prism lateral face

20 p2933 A72-39563

Gas breakdown in the laser as the limitation of pulsed high-pressure CO₂ lasers.

20 p2934 A72-39565

An investigation of a possible correlation between the laser output of a ruby rod and the chromium ion concentration.

20 p2934 A72-39643

Amorphous semiconductors for optical memory and other devices.

20 p2961 A72-39707

Self-induced pulsations in the light output from double-heterostructure injection lasers.

20 p2934 A72-39710

Single-cycle electron acceleration in focused laser fields.

20 p2934 A72-39720

Observation of quantum-phase and quantum-amplitude noise for a laser below and above threshold.

20 p2934 A72-39813

Effect of spatio-temporal laser light structure on multiphoton ionization.

20 p2934 A72-39814

Shock front radius of subsonic radiation front driven by plasma fireball during final stages of decaying laser spark

20 p2934 A72-39844

Investigations on spectroscopy by nonlinear Zeeman-resonances of a multimode laser.

20 p2934 A72-39845

Active spectroscopy of Raman scattering of light with the aid of a quasicontinuously tunable parametric generator.

20 p2934 A72-39852

Laser output power increase with plasma dynamic carbon dioxide laser configuration, noting steady population inversion in pure hydrogen atoms

20 p2934 A72-39932

HCN laser mechanical, pressure, temperature and voltage environmental factors effects on output power stability

20 p2934 A72-39967

Anisotropy of Raman scattering by optical phonons in cubic zinc blende crystals, describing experimental arrangements

21 p3061 A72-40141

Fabry-Perot interferometer measurements of Brillouin scattering from He-Ne laser excited low temperature condensed gases

21 p3051 A72-40151

Optical diffractometer with laser beam having approximately uniform transverse intensity distribution

21 p3051 A72-40210

Laser action on unclassified xenon transitions in a highly ionized plasma.

21 p3089 A72-40242

Explanation of limiting diameters of the self-focusing of light.

21 p3062 A72-40337

Multiple mirror astronomical telescope using laser source light collimated with central Cassegrain system, presenting expected diffraction patterns

21 p3052 A72-40378

Output power saturation with increasing discharge current in powerful argon CW lasers

21 p3062 A72-40404

Influence of polarization of laser fields on nonlinear interference effects

21 p3062 A72-40405

A new method of exciting uniform discharges for high pressure lasers.

21 p3062 A72-40568

Transverse CO₂ laser action at several atmospheres.

21 p3062 A72-40572

High resolution Michelson interferometer for spectral investigations of lasers.

21 p3062 A72-40610

HF chemical lasers pumped by atomic fluorine with molecular hydrogen, calculating intensity and efficiency by reaction kinetics analysis for comparison with computer solutions

21 p3062 A72-40617

One-to-one telescope with pressurized Ar gas for nanosecond and picosecond laser output pulse sensitive detection via gas breakdown and energy absorption

21 p3062 A72-40618

Electron density and temperature measurement from laser radiation scattering in plasma within axisymmetric toroidal magnetic mirror machine

21 p3091 A72-40663

Optimal energy response conditions for single pulse emission by noninstantaneous switching of ruby and Nd glass lasers

21 p3063 A72-40665

GaAsSb-AlGaAsSb double heterojunction lasers.

21 p3063 A72-40696

Two-step photodissociation of ammonia molecules excited by laser radiation.

21 p3013 A72-40724

Populating excited states of incoherent atoms using coherent light.

21 p3088 A72-40778

Frequency deviation equations for FM gas laser with modulation achieved by resonator optical length variations

21 p3063 A72-40798

Experimental CW chemical laser studies.

[AIAA PAPER 72-712] 21 p3063 A72-40920

Resonance absorption of laser emission by methane behind the shock front

21 p3063 A72-40986

Local necrosis, parenchyma incisions and vascularization of rabbit liver tissue under pulsed and continuous laser beams

21 p3002 A72-40991

Q-switched CO₂ lasers with variable pulse delay.

21 p3064 A72-41006

Single transverse mode operation of a pulsed volume excited atmospheric pressure CO₂ laser using an unstable resonator.

21 p3064 A72-41197

A new test of the second postulate of special relativity sensitive to first-order effects.

21 p3085 A72-41214

Observation of transient behavior of picosecond laser pulses.

21 p3064 A72-41380

Investigation of laser light spatial correlation by the photon coincidence method

21 p3064 A72-41691

Kinetic theory of the lasing bandwidth in a spectrally inhomogeneous medium

21 p3064 A72-41695

Pulsed monochromatic laser with toluene, xylene, ethanol, isoamyl alcohol and dimethylformamide solutions of organic dyes, discussing wavelength variations and power outputs

21 p3064 A72-41736

Emission synchronization in pulsed lasers

21 p3064 A72-41741

Investigation of amplification spectra and triplet-triplet absorption in a laser with a rhodamine 6G solution

21 p3064 A72-41743

Forced-convective-flow carbon monoxide laser.

22 p3184 A72-41968

High-intensity X-ray spectra and stimulated emission from laser plasmas.

22 p3210 A72-41990

Energy exchange processes in a low temperature N₂-CO transfer laser.

22 p3184 A72-41993

Nonlinear molecular absorption cell for frequency stabilization of carbon dioxide laser radiation, discussing stability limit dependence on amplification, absorptivity and Q value

22 p3184 A72-42102

Nonpeaked emission of a ruby laser with frequency tuning and selection

22 p3184 A72-42103

Absorption coefficient and gain of a GaAs injection laser

22 p3184 A72-42104

Electromagnetic field, polarization and population inversion equations for polarized emission operation analysis in single mode laser

22 p3184 A72-42153

Spectrum of stimulated emission in a resonator with plane mirrors

22 p3184 A72-42154

Effects of thermo-optical distortion on the radiation loss magnitude and spatial-angular radiation characteristics for a lamp-pumped rhodamine-6G laser

22 p3185 A72-42173

The effect of an interferometer selector on the spectrum of the characteristic frequencies of a dispersion resonator

22 p3176 A72-42245

Simultaneous recording of laser radiation and signal related to secondary processes, using ruby luminescence for oscillograph triggering

22 p3185 A72-42274

Self-aligning comparison beam methods for one-, two- and three-dimensional optical velocity measurements.

22 p3177 A72-42395

Measurement of the electron density distribution in plasmas from the bending of a gas laser beam.

22 p3211 A72-42396

IR CW laser emission from arc generated flowing CO active medium, describing thermal dissociation of oxygen followed by carbon disulfide injection

22 p3185 A72-42611

Unidirectional single frequency traveling wave CW pumped Nd-YAG ring laser, noting spatial hole burning elimination

22 p3185 A72-42614

Superradiant laser excitation at 3371 Å in molecular nitrogen second positive band system by high energy electron beam, noting 6 nsec pulse outputs to 24 MW

22 p3186 A72-42623

Approximate theory of the CW gasdynamic laser with an unstable resonator.

22 p3186 A72-42631

Multisectional CW gas dynamic laser output radiation density distribution control via transmitting mirror with variable reflection coefficient

22 p3186 A72-42632

Interferometric investigation of the phase fluctuations of coherent optical emission in the atmosphere

22 p3186 A72-42661

Pulse modulation of a laser during the tuning of an auxiliary passive resonator with the aid of ultrasound

22 p3186 A72-42666

Fluid velocity measurement of oscillatory flow generated from vortex shedding by laser Doppler system, discussing frequency tracker design, continuous detection problem and application

22 p3178 A72-42677

Laser Doppler velocimeter operating in forward- and back-scatter modes for supplementing wind tunnel flow field measurements in subsonic, transonic and supersonic regimes

22 p3179 A72-42678

A large viewfield laser photographic system for in-flight model contour measurements in an aeroballistic range.

22 p3179 A72-42679

Co 60 gamma radiation effect on stimulated ruby laser emission delay time, pulse duration, energy curve and intensity

22 p3186 A72-42731

The photochemical iodine laser - A high-power laser

22 p3186 A72-42940

Application of gasdynamic flows in laser technology

22 p3187 A72-43176

A laser beam divider with continuous adjustment of the intensity ratio

23 p3294 A72-43225

Laser compression of matter to super-high densities - Thermonuclear /CTR/ applications.

23 p3294 A72-43262

Investigation of the shape of the radiation pulse of a self-mode-locked laser

23 p3294 A72-43303

Self-ignited impulsive optical discharge in a laser erosion plasma

23 p3295 A72-43308

Investigation of the fast recombination channel in InSe during excitation by neodymium laser light

23 p3295 A72-43339

Use of light transformers in organic dye lasers

23 p3295 A72-43413

Book - Introduction to optical electronics.

23 p3295 A72-43650

Dynamic thermo-optical distortions compensation in lamp pumped rhodamine 6G liquid laser by introducing auxiliary dish with dye into cavity

23 p3295 A72-43679

Steady-state lasing spectrum of a CO₂ laser at reduced working-mixture pressures

23 p3295 A72-43681

Geometrical interpretation of Gaussian beam optics.

23 p3288 A72-43877

Laser beam periodic coupler design based on radiation property reciprocity theorem, suggesting use of reflecting layers and long wavelength gratings

23 p3288 A72-43888

Master oscillator/power amplifier laser systems output beam divergence and far field brightness, comparing to Gaussian plane waves

23 p3296 A72-43901

Laser radiation geometric divergence and variation of transmitted intensity with mirror transmissivity at centerline for unstable cavity viewed as oscillator-amplifier

23 p3296 A72-43902

High gain He-Ne laser with forbidden cavity configuration, discussing elimination of unwanted lasing mode by temperature detuning with mirrors

23 p3296 A72-43903

Gain measurements of matrix-type TEA CO₂ laser.

23 p3296 A72-44072

Fluorescent organic dyes solutions for Nd:YAG laser output performance improvement

23 p3297 A72-44191

Utilization of a composite resonator for improving the monochromaticity of a semiconductor laser with electron-beam excitation

23 p3297 A72-44468

Optical signal envelopes recording and reproduction with parametric superregenerative frequency converters, noting optical pumping by continuous wave YAG laser emission

23 p3292 A72-44471

Generation spectrum kinetics of a photodissociative iodine laser

23 p3297 A72-44480

Neodymium-glass laser emission spectral and temporal correlations during Q switching by rotating prisms and passive shutter

24 p3408 A72-44565

Experimental studies of injection lasers - Spontaneous spectrum at room temperature.

24 p3409 A72-44713

The efficient generation of coherent radiation continuously tunable from 2500 Å to 3250 Å.

24 p3409 A72-44803

Measurement of small strain amplitudes in internal friction experiments by means of a laser interferometer.

24 p3402 A72-44947

Pulsed carbon dioxide laser medium composition, pressure and electrical parameters effects on output power, energy and efficiency from mathematical model solution of kinetic equations

24 p3409 A72-44966

Noise characteristics of a digital system of light-beam deflection

24 p3410 A72-45323

Kinetics, spectrum, and specific loss properties of radiation emitted by rhodamine 6G in the case of pumping by a self-constricting discharge

24 p3410 A72-45417

Rhodamine laser emission spectral band control by plane parallel plates and polarizing prisms, noting band widening by resonator loss modulation with Fabry-Perot interferometer

24 p3410 A72-45418

Investigation of the uniformity of neodymium-glass laser emission

24 p3410 A72-45419

High power monopulse laser with a stabilized spectrum and radiation directivity close to that of diffraction

24 p3410 A72-45422

Attenuation of ruby laser radiation in the boundary layer of the atmosphere during the temperature-dependent variations of the wavelength

24 p3411 A72-45424

Laser frequency measurement by comparison with stable molecular oscillator Doppler shift produced by reflection of UHF modulated coherent optical signal

24 p3411 A72-45425

Analysis of the polarization properties of TW laser emission

24 p3411 A72-45497

Pulsed laser employing a rhodamine 6G solution in ethyl alcohol with an output energy of 110 J

24 p3411 A72-45498

Electrical characteristics of a CO laser discharge plasma

24 p3411 A72-45500

Plasma produced by laser irradiation of solid targets as a source of highly stripped ions.

24 p3430 A72-45603

Linear corrector for laser beam intensity distribution transformation into random distribution with rectangular envelope, noting uniform energy distribution result of spatial fluctuations averaging

24 p3411 A72-45608

Pulsating conditions in the evaporation of optical materials under the influence of CO₂ laser radiation.

24 p3411 A72-45610

Measurement of the angular divergence and of the refraction of a laser beam in the ground layer of the atmosphere.

24 p3380 A72-45611

Time dependence of the divergence of the radiation emitted by a rhodamine laser pumped by a pinched discharge.

24 p3411 A72-45612

Increase in the ratio of the energy of ultrashort laser pulses to the energy of the background radiation.

24 p3411 A72-45613

Temperature and angular widths of the phase-matching curve of a lithium niobate crystal.

24 p3432 A72-45615

Gain and line width in stimulated Brillouin scattering in gases.

24 p3412 A72-45616

Periodic control of the emission from a ruby laser achieved by a Q switch utilizing the transverse electro-optical effect.

24 p3412 A72-45618

Continuous He-He laser radiation intensity correlation function measurement, using Michelson interferometer and frequency doubler

24 p3412 A72-45704

Analytic criteria for laser quenching moment, generation power and stimulated emission energy for photodissociative iodine-alkyl lasers with iodine molecule buildup 24 p3412 A72-45706

Energy spectra of multiply charged ions formed in laser beam interaction with plasma, noting recombination process role 24 p3431 A72-45718

Be foil electrical resistance change during and after pulsed laser irradiation and annealing 24 p3432 A72-45720

LASER RADAR

U OPTICAL RADAR

LASER RANGE FINDERS

Precision phase indicating pulsed optical range finder, using uncooled semiconductor laser 01 p0080 A72-10621

Geos B satellite laser range experiment, discussing ruby oscillator and amplifier as transmitter and optical Schmidt system as receiver 03 p0365 A72-12950

Laser satellite range measurement at Ondrejov astronomical observatory, describing radar system and experiment design 03 p0326 A72-14332

Laser ranging retroreflector deployed by Apollo missions, discussing array design, structural support and thermal control 04 p0509 A72-15099

Military pulsed range finder design involving modularity, cooling, optical system and solid state receiver [CLEA PAPER 9.2] 07 p0942 A72-19384

Transportable lunar ranging with neodymium glass laser and Coude optical system, noting geophysical applications [CLEA PAPER 9.6] 07 p0943 A72-19388

Satellite angular coordinates determination by laser ranging from single station, using echo recording by Schmidt telescope 07 p0947 A72-20255

Laser systems for lunar ranging and high temperature plasma generation 08 p1182 A72-21336

Cloud height measurements and instrumentation, discussing rotating and fixed beam triangulation and French lidar and ruby laser ranging ceilometers 10 p1484 A72-25094

Earth-moon distance measurement by laser ranging methods, discussing retroreflectors, light collectors, time interval measuring devices and moon ranging stations 13 p2037 A72-28993

Earth chord length determinations, using synchronous photographic satellite observations with simultaneous topocentric distance data from laser measurement 14 p2103 A72-31076

Lunar laser ranging experiment single photon detection and nanosecond timing precision 15 p2233 A72-31530

Mathematical adjustment model for lunar laser ranging, noting accuracy improvement of points coordinates and orientation parameters 15 p2310 A72-31971

LASER RANGER/TRACKER

Optical radar target range estimation, determining suboptimum post detection signal processing algorithms in photon counting mode 01 p0024 A72-10047

Lunar laser ranging for orbital and rotational motion, continental drift and pole studies, discussing Lunokhod I roving vehicle mounted laser reflector 01 p0031 A72-11152

Geodetic applications of earth-moon laser ranging, discussing methods, accuracy, equipment, experiments and station characteristics 02 p0207 A72-11698

Lunar laser tracking determination of geodetic coordinates relative to earth gravity center 05 p0659 A72-16726

Nighttime laser ranging of French reflector for Soviet Lunokhod, discussing universal-ephemeris time difference determination 05 p0721 A72-16771

Automatic laser tracking and ranging system for cooperative retroreflective aircraft targets, discussing design, performance, eyesafe distance and atmospheric attenuation [CLEA PAPER 9.3] 07 p0942 A72-19385

Laser ranging techniques application to ground baseline measurements, discussing maximum range of satellites tracking laser system 07 p0947 A72-20264

Atmospheric turbulence induced wave front distortion effects on fast-tracking laser antenna performance, considering infinite plane wave random complex phase modulation 14 p2110 A72-30550

Dust influx into upper atmosphere above 30 km determined from laser radar measurement 16 p2386 A72-33610

Nighttime laser ranging of French reflector for Soviet Lunokhod, discussing universal-ephemeris time difference determination 17 p2611 A72-35274

Gravitational constant time variations measurement by high flying laser tracked satellite, considering non-conservative forces effects on orbital perturbations 22 p3174 A72-42925

Determination of the mutual position of points on the earth's surface from synchronous laser observations of artificial earth satellites 24 p3397 A72-44860

LASERS

NT ARGON LASERS

NT CARBON DIOXIDE LASERS

NT CARBON MONOXIDE LASERS

NT CHEMICAL LASERS

NT GALLIUM ARSENIDE LASERS

NT GAS LASERS

NT HCN LASERS

NT HELIUM-NEON LASERS

NT INFRARED LASERS

NT INJECTION LASERS

NT LIQUID LASERS

NT ORGANIC LASERS

NT PULSED LASERS

NT Q SWITCHED LASERS

NT RAMAN LASERS

NT RING LASERS

NT RUBY LASERS

NT SEMICONDUCTOR LASERS

NT SOLID STATE LASERS

NT YAG LASERS

FM/CW laser radar technique for smoke plume opacity remote measurement, discussing eye safety [ALAA PAPER 71-1081] 01 p0080 A72-10539

Environmental pollution sensing by vibrational Raman scattering probe measuring species constituency and temperature, discussing fluorescence, scattering cross sections and band shape [ALAA PAPER 71-1084] 01 p0067 A72-10541

Laser fluorensor for remote environmental probing, considering applications to oil slick mapping, locating lignin sulphonate pollution sources and hydrologic monitoring of tracer dye dispersal [ALAA PAPER 71-1121] 01 p0080 A72-10559

Plasma generation and continuous sustainment by laser beam and optical plasmatron 01 p0109 A72-11073

Laser anemometer system for instantaneous velocity measurement in turbulent pipe flow, determining two point velocity correlation coefficients 01 p0071 A72-11169

Microwaves and optical generation and amplification - Conference, Amsterdam, September 1970, covering microwave tubes, solid state devices and quantum electronics 01 p0044 A72-11278

Laser spark plasma initial development phase showing high electron temperature and concentration, continuous spectrum emission, line broadening and shock wave formation 02 p0237 A72-11405

Air pollution measurements by laser radar, using coherence properties to discriminate between backscatter due to molecular atmospheric constituents and pollutant particulates 02 p0212 A72-11816

Materials remote active sensing from ground, air and space by UV and visible laser induced luminescence, using excitation and emission spectral specificity for species identification 02 p0225 A72-11822

Laser station coordinate determination by geometrical method and satellite observations 02 p0219 A72-12046

Tensor description of laser beam second harmonic generation in dc magnetic field, using group theory derivation of nonzero element relations for all crystallographical classes 03 p0365 A72-12963

Bulk data storage and retrieval with scanning laser and electron beams, discussing spot formation focal sensitivity, noise, beam deflection, speed and media environment [IEEE PAPER 19.2] 03 p0368 A72-13775

Biological effects of unfocused laser radiation on DNA and RNA synthesis and cell activities in thymine dependent E. coli strain 04 p0477 A72-14610

Computer laser devices for logical operations, discussing analog-digital converter, gate circuits, bistable elements, flip-flop and shift register 04 p0496 A72-15141

Book on holographic technology covering fundamentals of holography and classical optics, diffraction theory, Huygens principle, lasers, illumination sources, holographic interferometry, etc 04 p0522 A72-15271

Atomic clocks application to spacecraft position determination, discussing ground stations synchronization and accuracy improvement by lasers [ONERA, TP NO. 1020] 05 p0660 A72-15858

Laser interferometer for quality control of optical parts and instruments 05 p0668 A72-16191

Blunt bodies-shock wave interaction in shock tubes, using interferometer with laser light source and high speed streak camera 05 p0601 A72-16225

Book on lasers and applications covering theories of light, polarization, coherence, resonators, mirrors, modes, electro-optical effect, communication, holography, etc 06 p0827 A72-18524

Random bias holographic technique for imaging three dimensional objects, using laser, one mirror, one diffuser and photographic plate [AD-743777] 07 p0982 A72-19036

Laser engineering and applications - Conference, Washington, D.C., June 1971 07 p1002 A72-19207

Scintillation measurement of transverse component of wind blowing across laser beam, using correlation method [CLEA PAPER 2.3] 07 p0942 A72-19378

Laser technology applications, considering economic factors in terms of market oriented products 07 p1105 A72-19554

Absolute gravity measurement methods and instruments, noting portable laser interferometer and formula derived from satellite observations 07 p1034 A72-19595

Papers on laser applications covering holography, metrology, geodesy, etc 07 p1007 A72-20220

Laser applications in metrology and geodesy, discussing use of beam directionality for alignment purposes, interference patterns and interferometry, modulated light methods, optical Doppler methods, etc 07 p1007 A72-20222

Lunar laser reflectors specifications and fabrication procedures, discussing lunar environment simulator and optical test equipment, techniques and results 07 p0947 A72-20261

Optical high precision surfaces correction method for laser based reflectors on vacuum vapor differential deposition 07 p1007 A72-20262

Laser Doppler velocimeter signals statistical properties, examining bandwidth, counting time and input SNR effects on zero crossing counter output fluctuations rms value 07 p0990 A72-20370

Industrial applications of lasers, considering programmable machining, distance measurement, computer memories, communication, night clubs, machine shops, aircraft manufacture and tunnel boring machine alignment 08 p1182 A72-21207

Design and operation of scanning laser based on exciting electron beam directional variation, discussing laser characteristics for various operating modes 08 p1182 A72-21268

Two dimensional laser Doppler forward and backscatter velocimetry in turbulent flows, applying to four inch pipe 09 p1305 A72-22303

Air pollution monitoring with tunable lasers employing Raman scattering, resonantly excited or hot gases emission and resonant absorption 09 p1322 A72-22313

Simulated superposed coherent and chaotic /thermal/ radiation of arbitrary spectral shape, using laser beam modulation and photocount statistics 09 p1352 A72-23240

Biological cell sorting by differential fluorescence generated electric signals via laser beam illuminated liquid stream 09 p1273 A72-23403

Laser reflection studies of surface morphology of growing or evaporating crystals 09 p1326 A72-23409

Ion and laser microprobes for concentration measurements of hot salt stress corrosion produced hydrogen on Ti alloy on microscopic scale 09 p1276 A72-23477

Electron, ion and laser beam technology - IEEE Conference, Boulder, Colorado, May 1971 10 p1517 A72-23926

Laser recording real time imagery for use in tactical reconnaissance aircraft 10 p1488 A72-23928

Broadband 100 MHz multichannel laser recorder and automatic data readout system using digital signal processing 10 p1488 A72-23932

Air pollution monitoring by remote optical sensing techniques based on light scattering measurements, noting suitability of high power laser probes 10 p1480 A72-24100

Classical laser theory, investigating anharmonic oscillators interaction with electromagnetic field in resonant cavity [AD-740404] 10 p1492 A72-24603

Confocal spherical laser resonator deformation analysis based on perturbation method, investigating forced oscillation 10 p1493 A72-25150

Non-Newtonian pipe flow turbulence measurements by laser anemometer, describing optical system and signal processing instrumentation [AD-742872] 11 p1646 A72-25554

Jones matrix method for polarization natural states, frequencies and mode losses calculation in anisotropic optical resonators

11 p1688 A72-26347

Laser apparatus for resonant frequencies and oscillation amplitudes measurement of semiconductor devices structural elements

11 p1649 A72-26348

Correlation function of depolarized finite collimated Gaussian laser beam in atmospheric turbulent medium

11 p1599 A72-26748

Commercially available laser systems applications to welding, drilling, scribing and other machining operations

11 p1652 A72-26984

Laser-interferometer instrumentation for shock stress wave measurements in solids, using velocity and displacement techniques

12 p1808 A72-27638

Frequency modulation demodulation technique for turbulence velocity measurements by laser Doppler velocimeter

[AD-744534]

12 p1809 A72-27836

Microwave and optical quantum electronic sources for frequency standards, noting primary Cs reference and multimode laser-RF oscillator beat technique

12 p1824 A72-27867

Book on density matrix theory application to lasers and masers, covering quantum mechanics, perturbation theory, magnetism and magnetic resonance, statistical ensembles, etc

12 p1826 A72-28203

Russian monograph on laser kinetic theory covering quanta dissipative systems, lasing equations, steady state, semiconductor emission, giant pulses, magnetic quantization, etc

12 p1827 A72-28338

Single frequency generation stability of one dimensional model of traveling wave laser using inhomogeneously broadened active material

13 p1967 A72-28470

Coherent laser light propagation in resonance media with level splitting, determining Lorentz and broadened resonance lines

13 p1969 A72-29515

Laser beam propagation in vacuum, imperfectly transparent medium and turbulent atmosphere

13 p1971 A72-29865

Doppler laser velocimeter and hot-wire anemometer readings in cylinder wake compared, describing instrument caused spectrum broadening effects neutralization method

13 p1960 A72-29889

Laser amplifier nonlinear properties by simplification of partial differential equations of amplitude and phase behavior, considering signal pulse deformation

14 p2111 A72-31113

Fine wire thermocouple probe use for measurement of total temperature in shock tube lasers

15 p2241 A72-32524

Lasing kinetics in coupled lasers pair, noting generation of steady state oscillations without relaxation

15 p2252 A72-32696

Russian papers on physical processes in lasers covering mode locking regime, pinch discharge, electronic transitions in diatomic molecules and laser control

16 p2400 A72-33295

Laser irradiation induced refractive index change in evaporated chalcogenide glass films of As-S-Ge system

16 p2401 A72-33395

Laser apparatus for natural resonant frequencies and oscillation amplitudes measurement of semiconductor devices structural elements

16 p2402 A72-33701

Microwave and optical quantum electronic sources for frequency standards, noting primary Cs reference and multimode laser-RF oscillator beat technique

16 p2403 A72-33976

The laser - A source of light in high speed photography

17 p2563 A72-35182

Precision laser system for micromachining applications, describing optical system

17 p2563 A72-35183

A laser velocimeter for Reynolds stress and other turbulence measurements.

17 p2555 A72-35235

Laser velocimeter measurement of Reynolds stress and turbulence in dilute polymer solutions.

17 p2541 A72-35252

Laser beam power transmission to lunar bases or spacecraft from nuclear fueled satellite power station, discussing achievable ranges and efficiencies

17 p2611 A72-35328

Density distribution in a high-pressure gas jet measured by laser-induced gas breakdown.

17 p2486 A72-35630

Simple two-dimensional laser velocimeter optics.

17 p2558 A72-35845

An automatic data processing system for laser anemometers.

19 p2795 A72-37287

German monograph - Development and testing of a laser autocollimator

19 p2810 A72-37480

Twyman-Green interferometer to test large aperture optical systems.

19 p2811 A72-37590

New proposition of the mechanism of self-focusing of laser beams in semiconductors.

19 p2811 A72-37945

Optical measurement of wave front lens or mirror surface contours by laser unequal path interferometer combined with computer data reduction

20 p2922 A72-39034

Theoretical considerations of significance to the design of optical anemometers.

[ASME PAPER 72-HT-7]

20 p2926 A72-39678

A unified analysis on laser Doppler velocimeters.

21 p3061 A72-40211

Ground, satellite, terrestrial glass fiber channel and waveguide radiation systems for laser communications

21 p3023 A72-41398

A high-frequency transmitted power meter using a laser signal

21 p3064 A72-41730

An arrangement for the holographic study of electrical explosions of wires

21 p3058 A72-41742

Noise-cancelling signal difference method for optical velocity measurements.

22 p3177 A72-42394

Laser interferometer for studying boundary layers in liquids

22 p3178 A72-42473

Nonlinearity and inhomogeneity effects on plasma wave excitation by beating two laser beams, taking into account Lorentz force modulation by large amplitude plasma wave

22 p3185 A72-42475

Mercury-cadmium telluride photodiode detectors for near IR laser receivers, discussing time response and I-V characteristics as function of temperature

23 p3296 A72-43881

Automatic acquisition and tracking system for laser communication.

23 p3265 A72-44176

Broad-band information transfer with the aid of laser-beam coupling fields

23 p3266 A72-44359

LATENCY

U REACTION TIME

LATERAL CONTROL

Three dimensional roll-controlled missile trajectory model for simple time-sharing digital or analog simulation, using wind-to-inertial axis transformation

01 p0130 A72-10964

STOL aircraft roll moment control possibility for externally-blown jet flap due to engine failure

02 p0154 A72-11700

Combat aircraft lateral aiming performance optimization and evaluation based on criterion of bullet stream response to pilot roll commands

05 p0611 A72-16657

Spacecraft roll stabilization during parabolic earth atmosphere reentry, developing single parameter multistep algorithm

11 p1684 A72-26897

Minimum safety flight altitudes for aircraft landing systems and lateral deviations for correction maneuver

12 p1842 A72-27269

Flight test of direct side force control by rudder deflection and asymmetrical drag on T-33 airplane, noting use in dive bombing

12 p1754 A72-27520

Limit-cycle bounds of a satellite attitude-control system.

17 p2622 A72-35529

An analysis of aircraft lateral-directional handling qualities using pilot models.

[AIAA PAPER 72-962]

22 p3137 A72-42347

Lateral flight path control during aircraft landing in gusty cross-winds by lateral thrust deflection, discussing design optimization

24 p3368 A72-45330

Flight test evaluation of a fluidically actuated monopropellant hydrazine roll control system.

[AIAA PAPER 72-975]

24 p3452 A72-45410

LATERAL OSCILLATION

Lateral vibration of thin conical bar with clamped base and free tip, calculating characteristic modes and frequencies

01 p0138 A72-10509

Damping of lateral oscillatory processes by end terminal displacement compensation, noting spring energy

05 p0691 A72-17132

Rotating machines self excited lateral vibration and instability avoidance and identification

[ASME PAPER 72-DE-21]

14 p2167 A72-30865

Effect on entry vehicle dynamic stability of aerodynamic and mass asymmetry coupling.

[AIAA PAPER 72-973]

22 p3231 A72-42338

LATERAL STABILITY

Hypersonic vehicles lateral dynamics during great circle flight, using linearized equations of motion and Newtonian theory for stability derivatives estimation

08 p1110 A72-21603

Hovercraft internal and external aerodynamic forces, discussing control, suspension, yawing moments, directional and roll stability and random surfaces performances

09 p1260 A72-22824

State sensitivity functions in aircraft parameter identification for lateral dynamics under aileron deflection from model response and in-flight test data

10 p1421 A72-23807

Analysis of a lateral-directional airframe/propulsion system interaction of a Mach 3 cruise aircraft.

[AIAA PAPER 72-961]

22 p3137 A72-42348

LATERALITY

U LATERAL STABILITY

LATERALIZATION

U LATERAL CONTROL

LATITUDE

NT GEOMAGNETIC LATITUDE

Latitude dependence of upper atmosphere corpuscular radiation intensity, analyzing sounding data from Indian Ocean area

01 p0118 A72-10369

Geomagnetic control over latitude variation of total electron content in equatorial ionosphere

04 p0515 A72-14931

PE sub s harmonic components diurnal and seasonal variations and latitudinal dependence, investigating relationship to drift velocity in E region

06 p0811 A72-18749

Saturn rotation period latitudinal difference, presenting graphic plots derived from various visual observations

17 p2619 A72-35958

LATITUDE MEASUREMENT

Astrolabe design and operation for reconnaissance and simultaneous determination of latitude and longitude

08 p1165 A72-21022

Optimal method selection for astronomical measurements on lunar surface, discussing instrumental and technical difficulties with selenographic longitudes and latitudes determination

08 p1231 A72-21130

Earth free diurnal nutation parameters comparison based on determinations from latitude observations at various observations

09 p1388 A72-23059

Poltava latitude changes derived from Boss catalog stars observations with Bamberg zenith telescope, deducing declination system from 12 year observation cycle

09 p1300 A72-23069

Latitude measurement at international stations during 1935-1947 period, discussing computation difficulties, instrument errors and correction

12 p1866 A72-27201

Paris Observatory Danjon astrolabe observation of latitude variations, obtaining periodograms by Fourier analysis

12 p1868 A72-27217

Circumzenithal instrument for latitude and longitude determination and star transits observation through almcantar

15 p2238 A72-32122

The Chandlerian wobble from 1900 to 1970.

18 p2727 A72-36731

Preliminary results of discussions of latitude observations by the prismatic astrolabe in Pulkovo /1963.2-1968.7/

19 p2861 A72-37977

Comparison of the declinations of Talcott pair centers, obtained from latitude observations by ZTF-135 in Pulkovo, with certain catalogs

19 p2861 A72-37978

Whittaker method for astronomical observational data smoothing, noting correlation function for latitude weighting functions determination

24 p3447 A72-45677

LATTICE IMPERFECTIONS

U CRYSTAL DEFECTS

LATTICE PARAMETERS

Order-disorder transition cooling effects on V carbide superlattice domain structure, using electron and optical microscopy

03 p0370 A72-12997

X ray diffraction analysis of dilute Nb-C alloys epsilon phase, discussing Bravais lattice and unit cell dimensions

03 p0375 A72-13932

Substructure variations and crystal lattice periods dependence on compression stress in beryllium single crystals during plastic deformation due to base slip

03 p0376 A72-14018

Alloying elements effects upon iron mechanical properties, investigating lattice parameters, temperature dependence of yielding and plastic flow, solid solution strengthening and softening, etc

05 p0676 A72-17101

Face-centered orthorhombic martensite in Ti-V alloy, determining axial ratios and lattice parameters by transmission electron microscopy and X ray diffraction

05 p0676 A72-17102

Thermal conductivity of aluminum, beryllium and magnesium oxides lattices at high temperatures

06 p0828 A72-17615

Structural changes, mechanical properties, electrical resistance and lattice constant during aging of Al alloys containing Mg, Li and Mn

06 p0834 A72-18743

Lattice and photon components of thermal conductivity of cerium dioxide at high temperatures

07 p1044 A72-19881

Alpha iron lattice dilation by titanium, measuring densities and lattice parameters

07 p1016 A72-19942

Lattice expansion of metal chalcogenide superconducting organometallic structures with aromatic or aliphatic Lewis bases sandwiched into van der Waal gap

08 p1216 A72-21214

UV radiation effects on pyrolytic boron nitride lattice imperfections, using space environment simulator

09 p1336 A72-22404

Atomic radius ratios and lattice constants in intermetallic compounds Laves phases, presenting semistatistically calculated values for niobium diferride based on rigid sphere model

10 p1527 A72-24978

Lattice damage measurement of Cd ion implanted GaAs semiconductors by optical reflection and scanning electron microscope

12 p1859 A72-28075

Mo influence on gamma prime phase precipitate in wrought Ni-base superalloys, considering solvus temperature, weight fraction and lattice parameters

13 p1975 A72-28669

Diamond powder lattice parameter changes during fast electron irradiation at various temperatures, discussing crystal defect stability and neutron irradiation comparison

13 p1983 A72-28760

Tin lead telluride rock salt structure solid solutions phase stability at 356-500 C, using room temperature lattice parameter measurements

13 p1913 A72-29750

Molybdenum carbide needle formation, growth in kinetics and morphology Fe-C-Mo alloy from lattice parameters measurements

14 p2120 A72-30618

Cooperative direction changing isomer movement on polymer chain lattice describing equations derivation procedure

14 p2125 A72-30962

Superlattice structure and electron correlation of Co-Sn system, using X ray and metallographic analyses

15 p2257 A72-32115

High temperature lattice and radiative thermal conductivity measurements utilizing carbon dioxide laser and IR detector for diffusivity and mean extinction coefficient phase data

15 p2250 A72-32507

Alpha to beta transformation of rhombohedral B, investigating lattice structure on heating stage in electron microscope

16 p2405 A72-33204

Geometric/chemical model of lattice dimensions of Laves phases of binary alloy bcc and fcc structures

16 p2409 A72-33801

A lattice model for stress wave propagation in composite materials.

[ASME PAPER 72-APM-52] Dilatometric studies of volume compression effect during aging of nimonic alloy showing linear dependence of matrix lattice constant on gamma prime phase

21 p3068 A72-40957

A study of cold-worked titanium-aluminum alloys by X-ray diffraction.

24 p3413 A72-44720

LATTICE VIBRATIONS

Jahn-Teller Hamiltonian for triplet electron state coupling to phonon vibrations in cubic symmetry

03 p0404 A72-14264

Damping effect in discrete one dimensional non-linear lattice model leading to weakly dissipative Korteweg-de Vries equation

06 p0838 A72-17301

Phonon dispersion curves of bcc transition metals for normal lattice vibration modes

09 p1369 A72-22680

Raman spectra of azoanisole and anizaldazin in liquid crystal states excited by Ar laser, revealing lattice vibrations attenuation near transition point

10 p1490 A72-24042

Thermodynamic perturbation and scaling theory for multidimensional spherical models of lattice structure in terms of field of critical phenomena

15 p2293 A72-32219

Angular force models with electron-ion interaction applied to bcc and fcc metals, calculating phonon dispersion curves for V, Nb and Ta

15 p2258 A72-32226

Premartensitic beta phase instability, lattice vibration and shape memory effect in noble metal base and Ti alloys

15 p2259 A72-32641

Lattice dynamical model for Cs vibration frequency distribution, specific heat and electrical and thermal resistivity calculations

16 p2441 A72-33584

Infrared dispersion of second-order electric susceptibilities in semiconducting compounds.

19 p2844 A72-37944

Fundamental infrared lattice vibration spectrum and the laser-excited Raman spectrum of MoSe₂.

22 p3185 A72-42321

Phonon dispersion relations and Debye characteristic temperature for Ti, Hf and Y hcp lattices

24 p3415 A72-45629

LATTICES

Plane electromagnetic wave diffraction by periodic lattice of long finite conductivity cylinders with arbitrary electric radius

04 p0491 A72-15414

Electromagnetic wave scattering and diffraction on lattice of dipole vibrators

04 p0491 A72-15415

Numerical solution for diffraction on conducting finite and infinite lattice of cylinders with circumferential cross section

04 p0491 A72-15416

Electromagnetic wave diffraction on infinite lattice of perfectly conducting arbitrary flat elements from numerical method, determining secondary field and strips current distribution

04 p0491 A72-15417

Lattice type structures as discrete elasticity problem, determining potential of thin rods connecting rigid nodes pairs from equations of motion and constitutive equations

08 p1244 A72-21302

Optimization of load-carrying elastic lattice structures designed on prescribed surface

09 p1402 A72-22746

Determination of the limits of applicability of a continuous model when calculating a discrete polar lattice disk

21 p3122 A72-41346

Drag spectra of simple structures in turbulence.

23 p3281 A72-44102

LATTICES [MATHEMATICS]

NT BOOLEAN ALGEBRA

NT BOOLEAN FUNCTIONS

Monatomic gas atoms scattering by solid surfaces, using classical three dimensional lattice model

07 p0969 A72-20064

Local limit theorems for sequence of nonidentically distributed independent integral-valued lattice random variables

11 p1676 A72-25356

Centered difference approximation for atmospheric model advection equation by two step Lax-Wendroff method, discussing computational instability due to lattice separation

11 p1680 A72-25768

Lower and upper bounds for number of lattice points in simplex, using linear programming algorithm for generating feasible cutting patterns for paper reels

11 p1678 A72-26157

Heisenberg antiferromagnet with noncollinear sublattices and linear dislocation, considering coupled spin wave states and density

13 p2023 A72-29910

Cluster variation method for boundary free energy solution in lattice model applied to Ising phase and gas-liquid interface and longer range interaction

18 p2711 A72-36565

Mathematical model for lattice-type error distribution of parallel channels communication system, noting metric for algebraic signal coding method

22 p3154 A72-42234

LAUNCH COMPLEXES

U LAUNCHING BASES

LAUNCH TIME

U LAUNCH WINDOWS

LAUNCH VEHICLES

NT ATLAS CENTAUR LAUNCH VEHICLE

NT DELTA LAUNCH VEHICLE

NT DIAMANT LAUNCH VEHICLE

NT ELDO LAUNCH VEHICLE

NT EUROPA LAUNCH VEHICLES

NT RECOVERABLE LAUNCH VEHICLES

NT REUSABLE LAUNCH VEHICLES

NT SATURN LAUNCH VEHICLES

NT SCOUT LAUNCH VEHICLE

NT THOR AGENA LAUNCH VEHICLE

Large launch vehicle attitude control system absolute stability mathematical model, using quadratic Liapunov function for exponential property description

05 p0728 A72-16475

Soviet space program review from Sputnik I launch, discussing launch sites and vehicles, lunar, planetary and manned missions, civil and military programs and future goals

05 p0722 A72-17091

Satellite launch vehicles guidance and control systems, discussing control parameters for minimum injection error

07 p1033 A72-20604

Digital computers application as filters in launch vehicles and high performance aircraft attitude control systems, estimating number of computer operations

10 p1444 A72-24031

Second generation European multi-mission launcher system for scientific and application satellites, using high energy propulsion modular design

15 p2320 A72-31804

Flexible launch vehicle optimal and constrained-optimal control for performance index minimization, using sensors and constant feedback gains

15 p2321 A72-32585

Expendable space transportation - A 1972 assessment.

[AIAA PAPER 72-732] 18 p2730 A72-36542

Hydraulic duct transfer function determination for prediction of liquid-fuel engine space launcher LF vibrations, investigating incompressible flow rate modulation by deformable walls

24 p3392 A72-45117

LAUNCH WINDOWS

Minimum engine trajectory and propellant consumption considerations for launch windows to Mars and Venus planets with Grand Tour mission possibilities

23 p3336 A72-43553

LAUNCHERS

NT AIRCRAFT LAUNCHING DEVICES

NT CATAPULTS

NT HYPERVELOCITY LAUNCHERS

NT MISSILE LAUNCHERS

NT ROCKET LAUNCHERS

LAUNCHING

NT ORBITAL LAUNCHING

NT ROCKET LAUNCHING

NT SEA LAUNCHING

NT SPACECRAFT LAUNCHING

LAUNCHING BASES

NT CAPE KENNEDY LAUNCH COMPLEX

Guiana Space Center launch complexes for Diamant B and Europa satellite launchers and rocket probes, discussing trajectory, telemetry and safety measures

03 p0339 A72-12912

Automatic optical tracking instrumentation at rocket launching station Tanegashima, describing automatic cinetheodolite

06 p0795 A72-17432

Launch center for solid-liquid propellant rocket probes, Diamant and Europa 2, describing payload preparation hall

[DGLR PAPER 72-0137] 13 p1939 A72-28962

The El Arenosillo launch base, a rocket test center in Huelva province

17 p2536 A72-34944

LAUNCHING SITES

Soviet space program review from Sputnik I launch, discussing launch sites and vehicles, lunar, planetary and manned missions, civil and military programs and future goals

05 p0722 A72-17091

Global network of ground based facilities/infrastructure/ including spacecraft launching, tracking, communication and readout sites for international space operations

[AIAA PAPER 72-739] 18 p2742 A72-36545

LAVA

Japanese lava geochemical analysis, determining K, Rb, Sr, Ba and rare earth concentrations with mass spectrometric stable isotope dilution

01 p0051 A72-10059

Ecogenesis of volcanic island of Surtsey after 1967 lava eruption, discussing terrestrial and marine littoral and sublittoral biomes

04 p0473 A72-14916

Lunar sea surface model derivation from morphology data analysis, suggesting four-layer bottom relief of basaltoid lava, rocks, breccia and surface regolith

04 p0576 A72-15069

Papers on moon geology and physics covering lunar volcanic lava flow, water and crater origin

06 p0886 A72-18216

Lunar Mare Ibrum lava flow geology and nature, mascon origins and explosive, collapse and impact mechanisms for small crater origin

06 p0887 A72-18218

Tycho, Aristarchas and neighboring small craters volcanic origin, discussing inner and outer rim lava flows and impact crater resemblance

06 p0887 A72-18221

Geomorphic evidence for basalt lava tubes and channels in Lunar Marius Hills, comparing with terrestrial analogs

07 p1067 A72-18870

Lava tube formation in pahoehoe basalt and flow activity in vent near Alae Crater, Hawaii

07 p0980 A72-20462

Sr isotope data indication of Glass Mountain rhyolite lava as part of parent silicic magma

11 p1623 A72-26240

Terrestrial volcanic lava conduits origin and development association with lunar maria channels and sinuous rills

13 p2037 A72-28992

Eruptive center location and flow direction measurements for andesite and quartz latite lava flows in Mogollon Mountains

15 p2223 A72-31579

Two phase heating of lunar crust for formation of lava filled Mare Smythii and Tsiolkovsky craters

15 p2313 A72-32198

Lava tubes of the Cave Basalt, Mount St. Helens, Washington.

19 p2790 A72-38296

Rates of solidification of Apollo 11 basalt and Hawaiian tholeiite.

20 p2967 A72-39181

LAW [JURISPRUDENCE]

NT INTERNATIONAL LAW

NT LEGAL LIABILITY

NT PENALTIES

NT SPACE LAW

Air law concept as totality of legal regulations related to atmosphere use by flying devices, discussing relation to international environmental protection

01 p0147 A72-11107

German book on air traffic law covering norms relative to vehicles and air space, international air law, organizations, etc

02 p0305 A72-12622

Satellite broadcasting juridical aspects, discussing control over frequency spectrum, geostationary orbits appropriation, copyrights, broadcast contents and advertising

04 p0494 A72-15679

Aircraft hijacking control, examining international cooperation, extradition and treaties

05 p0752 A72-15834

Civil and military aircraft forced diversion, discussing legal counters and aircraft restoration

05 p0753 A72-17166

Control concepts for future ATC system relative to airspace structure, management and geographic and jurisdictional boundaries

06 p0844 A72-17333

Airfield law in Schleswig-Holstein Appeals Court decision concerning property owner suit against operator for unnecessary noise

06 p0906 A72-18170

Charter air traffic regulations under German air law, discussing legal safeguards relative to economic, personnel, technical and organizational aspects

11 p1748 A72-26559

National and international legal aspects relative to levying user fees for flight safety services in Germany

11 p1748 A72-26560

Aircraft and spacecraft conceptual definitions in national and international law

11 p1749 A72-26561

Private and governmental regulatory aspects of environmental noise abatement and control, discussing legal efforts and trends at local, state and federal levels

15 p2340 A72-32614

Jurisdictional problems in the autopsy of aircraft accident victims.

17 p2639 A72-34558

The legal position of civil air personnel

17 p2639 A72-35762

Federal legislation impact on airport and airway system planning, considering budget and schedule requirements

18 p2743 A72-36777

FAA implemented airport certification legislation covering minimum safety standards, operation manual, emergency plan, fire and rescue service and pavement requirements

18 p2675 A72-36785

LAWS

NT CLOSURE LAW

NT CONSERVATION LAWS

NT FOURIER LAW

NT HOOKES LAW

NT KEPLER LAWS

NT KIRCHHOFF LAW OF RADIATION

NT NEWTON SECOND LAW

NT NEWTON-BUSEMANN LAW

NT OHMS LAW

NT SCALING LAWS

NT SIMILITUDE LAW

NT STEFAN-BOLTZMANN LAW

LAYOUTS

Monolithic IC semiconductor components layout density evaluation for isolation, active and edge regions utilization efficiency

10 p1449 A72-24287

Display device layout based on human operator manual control information requirements considera-

tion, discussing functional categories, motion compatibility, indicators relation and integration

21 p3009 A72-41404

LC CIRCUITS

German monograph on optimal design of HF band-pass filters with lumped elements, covering LC coupled two- and four-circuit systems

09 p1284 A72-22328

Transfer function sensitivity characteristics comparison of doubly terminated LC filters with active cascade and inductance simulation schemes

10 p1452 A72-24801

Variable saturation of series LC circuit, discussing current response, ferromagnetic jump, symmetry and subharmonic oscillations

14 p2090 A72-31116

Theoretical model for computer calculation of transients in oscillator consisting of nonlinear amplifier with feedback through sequence of matched LC circuits

16 p2371 A72-33280

Transient characteristics of lumped-parameter delay lines

18 p2674 A72-37216

A new circuit for the contactless thickness measurement with the aid of pulse-excited LC measuring circuits

20 p2927 A72-39696

Multiloop LC oscillators with negative resistance and nonlinear capacitances

23 p3271 A72-43838

LEAD [METAL]

NT LEAD ISOTOPES

Sphene U-Pb age resistance to thermal metamorphism, discussing zircon U-Pb and biotite and hornblende K-Ar ages within thermal aureole

01 p0052 A72-10069

Energy transfer to electron-photon component during hadron interaction in lead, using ionization calorimeter

06 p0869 A72-17268

Epitaxial and textured Pb films on mica and glass, using reflection electron diffraction, etching and optical microscopy for structure study

12 p1854 A72-27289

Steady state creep measurements of lead-phosphor bronze discontinuous fiber composites under nonuniform deformation, comparing to fiber and matrix alone

15 p2261 A72-32299

Electron showers of high primary energy in lead.

17 p2585 A72-35472

An integral test of the inelastic cross sections of Pb and Mo using measured neutron spectra.

19 p2763 A72-37634

Influence of the properties of the materials on junction tunnelling characteristics.

22 p3214 A72-42454

Comparison of microwave-induced constant-voltage steps in Pb and Sn Josephson junctions.

23 p3323 A72-43272

Effective cross section of the inelastic interaction of hadrons with lead-atom nuclei at energies from 3 to 30 TeV

23 p3330 A72-44410

Experimental investigation of electromagnetic cascades at an energy greater than 20 GeV

23 p3291 A72-44444

LEAD ALLOYS

Wear mechanism of lead-bronze dry sliding in air on hardened steel ring

11 p1638 A72-25510

LEAD COMPOUNDS

NT LEAD SULFIDES

NT LEAD TELLURIDES

LEAD ISOTOPES

Pb and Sr isotopic composition measurements on eclogites from South Africa

05 p0658 A72-16551

Lunar soil radiogenic U-Th-Pb analyses of Lunik 16 samples from Sea of Fertility

09 p1381 A72-22278

LEAD POISONING

Experimental studies on the alkali-acid equilibrium in the blood gases under the chronic action of low concentrations of lead.

24 p3374 A72-44824

LEAD SULFIDES

Hysteresis loops during breakdown in reverse bias segment of p-PbS point contact diodes I-V curves

05 p0638 A72-17177

LEAD TELLURIDES

Quantizing magnetic field effect on electromagnetic wave propagation in multivalley n-type Si and Ge and PbTe semiconductors

08 p1218 A72-21878

Lead tin telluride photovoltaic p-n junction diode and lasers, discussing n-type layer fabrication by proton bombardment

10 p1450 A72-24552

Tin lead telluride rock salt structure solid solutions phase stability at 356-500 C, using room temperature lattice parameter measurements

13 p1913 A72-29750

Low capacitance high speed lead tin telluride photodiodes via liquid phase epitaxial growth, discussing frequency response to Nd-YAG and carbon dioxide lasers

22 p3159 A72-42620

LEADING EDGE SLATS

European A300B airbus flap and slat systems and tailplane actuator for longitudinal pitch trim control

01 p0006 A72-10725

Slat-airfoil combinations aerodynamics modeled by single point vortex to represent leading edge slat, discussing on-line computer graphics program

05 p0603 A72-16798

Jet-STOL augmentor wing consisting of moderately thick airfoil with full span leading edge slat and double surface trailing edge flap

08 p1110 A72-21899

Three dimensional wind tunnel investigation of vortex augmented unswept wing with leading edge cusp flap and split upper and lower trailing edge flaps

11 p1568 A72-25584

LEADING EDGE SWEEP

Three-dimensional structure and equivalence rule of transonic flows.

20 p2886 A72-39631

LEADING EDGES

NT SHARP LEADING EDGES

Zirconium diboride-silicon carbon-graphite composition for lifting entry vehicle hot leading edges, investigating mechanical behavior by tension and flexural tests

01 p0091 A72-10767

Pseudowave front spreading at leading edge of plasma slab during injection at high velocity into denser background plasma

02 p0265 A72-12364

Symmetrically deformed delta wing in supersonic flow, considering leading edge flow separation induced vortices effects on downwash, pressure distribution and aerodynamic characteristics

04 p0463 A72-15741

Laminar leading edge of collisionless plasma perpendicular shock structure and distribution functions, considering instability calculations

05 p0654 A72-17227

Perturbation methods for laminar flows near leading edge, discussing approximations of Navier-Stokes equations and domain connection

06 p0756 A72-18108

Hypersonic gas flow around asymmetric triangular metal plate with blunt leading edges, using two layer model

07 p0909 A72-19985

Laminar natural convection heat transfer from leading edge of isothermal plate under nonuniform gravity

08 p1250 A72-20875

Steady heat conduction solution for intensified cooling of turbine rotor blade leading edge with holes and air channel

08 p1223 A72-20951

Laminar/turbulent boundary layer transition on parabolic wing profile in supersonic wind tunnel, noting critical Reynolds number increase with leading edge thickness

09 p1259 A72-22407

Optimal configuration of lifting bodies for hypersonic speeds, noting negligible effect of blunt leading edges

10 p1418 A72-24536

Vorticity effect on shock wave-boundary layer interactions on blunt edged compression surfaces of hypersonic inlets

10 p1419 A72-24649

Supersonic flow around thin cruciform wing with antisymmetrical angle of attack distribution and horizontal plane with leading edge, considering flow separation at edges

10 p1420 A72-25118

Viscous liquid impulsive flow past semiinfinite plate, showing leading edge effects and boundary layer singularity existence

11 p1614 A72-25351

Linearized method of characteristics application to supersonic flow past oscillating flat plate cascades with supersonic leading edge locus

11 p1730 A72-25401

Liquid film transpiration cooling concept application to space shuttle leading edge heating and shock heating

11 p1744 A72-25410

Numerical calculation of sonic flow around wing section with rounded leading edges, obtaining Mach number distribution, boundary characteristic shape and velocity field

12 p1751 A72-27181

High power light pulse generation with steep leading edges in Nd-glass laser, noting duration change based on transparency increase under light transmission

12 p1820 A72-27583

Predictor-corrector multiple iteration technique for three dimensional viscous flow problems applied to hypersonic leading edges and Burger equation

13 p1893 A72-28422

Initial dihedral wing-body interaction for supersonic leading edges, determining expansion of velocity potential on root chord 14 p2069 A72-30365

Pressure distribution over delta wing with blunted edges at small angles of attack in hypersonic wind tunnel tests 14 p2071 A72-31022

Leading edge boundary layer flow separation and reattachment processes in airfoil dynamic stall, considering effect of angle of attack rate of change 15 p2179 A72-32024

Thermal radiation effects on semiinfinite planar blunt leading edged body hypersonic flow field, using Lax and Rusanov artificial viscosity methods 15 p2337 A72-32593

Flat plate leading edge blunting and wall cooling effects on supersonic laminar flow ramp-induced separation [AIAA PAPER 72-716] 16 p2344 A72-34032

Compressible boundary layer with normal pressure gradients, investigating quasi-similar, nonlinear integro-differential equations properties at wall and sharp and blunt leading edges [AIAA PAPER 72-696] 16 p2345 A72-34048

Leading edge serrations effect on rotor noise and aerodynamic characteristics, noting vortex and rotational noise reduction and overall efficiency decrease [AIAA PAPER 72-655] 16 p2349 A72-34079

Quasi-homogeneous approximation for wing with curved subsonic leading edges at supersonic speeds. [ICAS PAPER 72-54] 21 p2992 A72-41176

Hypersonic leading edge problem - Wedges and cones. 24 p3364 A72-45778

LEAKAGE

Test method and apparatus to pressurize hermetically sealed components with Kr 85, comparing obtained leak rates with He mass spectrometric values 12 p1854 A72-27550

Probe gas flow modulation in leak search device tested in vacuum system 13 p2007 A72-29921

Leak detection in pressurized installations via NDT, discussing uses of fluid tracers, thermal and acoustic sensors, halogen detectors, He mass spectrometers and radioactive tracers 14 p2104 A72-30374

LEARNING

NT ASYMPTOTIC METHODS

NT CONDITIONING [LEARNING]

NT ITERATIVE SOLUTION

NT PROBLEM SOLVING

NT THEOREM PROVING

NT TRANSFER OF TRAINING

Nonsupervised learning algorithm steady state behavior for multicategory pattern classification by analysis and digital computer simulations 06 p0780 A72-18256

Mental rehearsal and physical practice relation to learning rate for rotary pursuit tracking skill acquisition 07 p0925 A72-18801

Stochastic time varying patterns classification by Kalman filter, discussing optimum dichotomizer with supervised learning 12 p1790 A72-27498

Relationship of visibility fluctuations in set of luminous circles to verbal response learned for each circle, showing word association influence on stimuli perception 13 p1911 A72-29851

Response-dependent electric shock punishment schedule preference during response sequence in food-deprived pigeons 16 p2357 A72-33773

Some data on the interrelations of conscious and unconscious reactions 23 p3257 A72-44076

LEARNING MACHINES

Sequential behavior and inherent tolerance to memory faults in terms of minimum redundancy 07 p0950 A72-19300

Learning systems mathematical scheme to identify classes invariant with respect to transformation groups, realizing functionals with coherent and incoherent optics 09 p1282 A72-22218

Multiple function stochastic automata performance in environment with random control processes, showing improved learning rate 12 p1787 A72-27922

Optimal random search noise recognition systems with Bayes teaching technique 13 p1924 A72-29162

Dynamic programming for optimal statistical control of self adaptive systems with fixed learning experiments, noting structural constraints for suboptimality 13 p1965 A72-29178

Learning strategy-based pattern recognition system for automatic classification of terrain type from aerial photography 18 p2691 A72-36494

Stochastic analogs of finite-converging learning algorithms for recognition systems 19 p2769 A72-37421

Optimal recurrent and nonrecurrent algorithms for polynomial dividing functions of learning and recognition in form of adaptive threshold elements 19 p2769 A72-38465

A learning approach to the parameter-adaptive self-organizing control problem. 23 p3277 A72-44198

LEARNING THEORY

Learning-identification of unknown nonlinear discrete systems, using local estimation results for global function learning 01 p0046 A72-11199

Discrete-time adaptive Kalman filter based on learning process and parameter estimate updating in operational cycle, comparing with simple Kalman and Wiener filters 05 p0639 A72-15758

Smoothed randomized functionals and algorithms in adaptation and learning theory, accounting for constraints by generalized penalty function method 07 p0960 A72-19653

Self learning estimator for tracking, using heuristic technique for time-varying estimates sequence determination 10 p1457 A72-24500

Heuristic recognition algorithms with learning for homogeneous irreducible stationary Markov chain sequence of recognized objects 12 p1837 A72-27824

Russian papers on adaptive control systems covering automata and game theory, learning models, Markov processes and probability theory 12 p1787 A72-27921

Ergodic theorems for operators generated by Markov transients, examining asymptotic properties of stochastic learning model 12 p1787 A72-27924

Optimal cross section selection of rectangular beams in oblique bending by nonlinear programming and learning algorithm 13 p2056 A72-28914

Application of a learning recognition system for classification of game situations 19 p2769 A72-37422

Learning and solving complex problems of reasoning - A test-theoretical investigation of the complexity of compound problems of predictive logic 24 p3373 A72-45244

LEAST SQUARES METHOD

Redundancy reduction method for multichannel spectrometer solar radio data processing, using least squares technique 01 p0128 A72-10418

Field and test data analysis with time share computer, using Weibull probability plotting, hazard rates and least squares regression 02 p0185 A72-11555

Least squares and point matching techniques compared for solution of two dimensional steady state heat conduction problems with irregularly shaped boundaries [ASME PAPER 71-HT-P] 02 p0302 A72-12318

Lunar occultation light curve model for photoelectric data analysis, using least squares method 03 p0421 A72-13133

Extended iterative weighted least squares estimation of coefficients for linearly independent component signals in linear model 04 p0539 A72-14913

Interpolation in numerical photogrammetry by least squares method 06 p0815 A72-17752

Deschamps graphical method application to multipoint waveguide junction scattering coefficient measurement with averaging and least square fitting for error reduction 06 p0787 A72-18379

Collocation least square solutions of boundary value problems, applying to prismatic bar torsion and plate bending 07 p1025 A72-18790

Image noise reduction by least squares polynomial filtering method, comparing with Wiener filtering 07 p0987 A72-19829

Couette flow between eccentric cylinders with inner cylinder rotating, using least squares numerical method for partial differential equations solution 07 p0970 A72-20070

Geomagnetic field optimal model with expansion of spherical harmonic series by least squares method 07 p0980 A72-20657

Near earth satellite orbit parameters correction, discussing least squares approach 09 p1387 A72-22770

Weighted least squares stationary approximations to time varying linear systems, noting criterion for matrix choice 09 p1341 A72-23094

Linear least squares estimation of Stratonovich-Kalman-Bucy formulas by innovations method 10 p1503 A72-23801

Observation errors effects on satellite attitude best least squares estimate based on direction measurements, using Monte Carlo method computer simulation 10 p1438 A72-24692

Linear least mean square estimate of additive white noise-corrupted signal considered as purely nondeterministic process of multiplicity one 11 p1591 A72-25352

Control surface dynamic hinge moment coefficients estimation based on system state measurements from flight tests, using least squares criterion [AIAA PAPER 72-379] 11 p1730 A72-25403

Least squares method algorithm for estimating unsteady harmonic signal parameter in presence of normally distributed additive noise 13 p1915 A72-28435

OMEGA short term range precision for broad ocean area navigation, using four range least squares position solution 13 p1997 A72-29181

Nonlinear regression method for nonlinear least squares problem compared to other solution techniques, discussing convergence theorems and computational results 15 p2262 A72-31632

Measurement data processing in celestial navigation based on least squares method, calculating errors correlation matrix 15 p2267 A72-31731

Helmert solution for least squares method application to mean scale factor, orientation and positioning of free geodetic net 16 p2384 A72-33028

Optimization of noise impeding observation of dynamic system subjected to random perturbations, discussing optimal control based on least square estimate 16 p2371 A72-33090

Weibull distribution parameters estimation for general device class from limited failure data through regression models, using least squares method 16 p2398 A72-33349

Optimal filtering estimate of noisy nonlinear partial differential distributed parameter system, using least squares and invariant imbedding techniques 16 p2416 A72-33575

The approximate solution of parabolic initial boundary value problems by weighted least-squares methods. 17 p2573 A72-34217

Finite element method matrices in least squares approximation and elliptic partial differential equations, discussing numerical stability properties 17 p2573 A72-34219

A gradient method for estimating the covariational matrix of unknown parameters 17 p2523 A72-35039

A rapidly convergent iterative method for the solution of the generalised nonlinear least squares problem. 17 p2577 A72-35849

Least squares method for Y Cyg spectroscopic elements improvement based on radial velocity measurements, noting nonexistence of gamma velocity variability 19 p2858 A72-37809

Necessary and sufficient conditions for differentiable non-scalar-valued functions to attain extrema. 19 p2826 A72-38244

Square root least squares and filtering solutions for fixed point and interval smoothing problems, comparing computational stability and precision and computer requirements [AIAA PAPER 72-877] 20 p2910 A72-39122

Comparison of two methods of astrogeodetic geoid determination based on least squares prediction and collocation. 21 p3048 A72-40469

A recursive least-squares approach to the on-line adaptive control problem. 21 p3037 A72-40640

Gaussian elimination with floating point arithmetic, discussing algorithm for least squares scaling of matrices with less error than row and column norms equilibration 21 p3076 A72-41317

Least squares estimation of cosmological model parameters, comparing confidence limits with Solheim trial method 21 p3109 A72-41440

Eclipsed binary brightness curve determination by least squares method, using weighted gravity center point observations 21 p3113 A72-41760

Least squares method for satellite motion parameters determination in orbital plane, using altimeter distance to planet surface measurements 22 p3223 A72-42202

Statistical synthesis of navigation aids systems with unsteady random interferences, obtaining optimization criterion by least squares method 22 p3202 A72-42232

The efficiency of the method of the least squares for adjusting observations with non-normal distributions
22 p3199 A72-42998

LEATHER

Chamois leather mechanical response, comparing stress relaxation and frequency response characteristics to human skin for applications in anthropometric dummy construction
15 p2191 A72-32606

LEAVES

Southern corn leaf blight detectability by remote sensing based on pattern recognition technique application to multispectral color and IR photographic and scanner data
02 p0212 A72-11814

Plant leaves light reflectance, transmittance and absorbance characteristics relationship to leaf mesophyll arrangement, considering interpretation of aircraft/spacecraft remotely sensed data
02 p0213 A72-11856

Plant leaves biochemical activities study by light scattering techniques, discussing photometric, spectroscopic and bionics methods
13 p1955 A72-28518

LEBESGUE THEOREM

Intermediate space concept extension to Sobolev-Orlicz spaces defined over subset with Lebesgue measure, generalizing trace theorems
18 p2704 A72-36460

LEE WAVES

Lee waves characteristics relationship to air flow and temperature layers in troposphere based on satellite pictures
02 p0255 A72-12791

Atmospheric lee waves three dimensional structures through high sensitivity Doppler radar measurements based on backscatter from refractive index inhomogeneities
07 p1029 A72-19100

Energy and momentum removal from troposphere and lower atmosphere by mountain lee wave breaking, discussing effects on atmospheric circulation evolution and maintenance
08 p1203 A72-22167

Winds aloft forecast use to predict southwestern mountain lee wave behavior for general aviation cross country flights
13 p1993 A72-28863

LEG [ANATOMY]

Leg cooling effect improving tolerance to positive headward acceleration in sitting position
04 p0479 A72-15210

Peripheral thermoregulation in arctic canines, showing subzero bath-immersed foot temperature maintenance above tissue freezing point
08 p1120 A72-22019

Anatomy, pathology, etiology, diagnosis and therapy of posterior tibial nerve compression lesion, discussing tarsal tunnel syndrome
21 p3005 A72-40396

The foot as input device for control operation
21 p3012 A72-41428

LEGAL LIABILITY

United Nations international space law development, discussing concepts of state jurisdiction, territorial sovereignty, damage liability, etc
06 p0905 A72-17814

Liability for space activities, considering international organizations status before international tribunals
07 p1103 A72-19459

Liability for damage caused by space objects, noting UN resolution
07 p1103 A72-19460

Legal aspects of international manned orbiting laboratories, discussing space objects registry and liability for damage
07 p1103 A72-19461

Common law liability of aviation manufacturers, discussing safety, airworthiness, maintenance, reporting, modifications and inspection requirements and evidence of negligence
07 p1106 A72-20671

Forum choice in aircraft disaster litigation, discussing res ipsa loquitur, guest statute and vicarious liability
07 p1106 A72-20672

Aviation insurance and claim servicing risks in aircraft accidents, discussing coverage, claims investigation, litigation and settlement
07 p1106 A72-20673

Discrimination preference and effect on insurance of limit liability of international air carrier according to modified Montreal Interim Agreement
07 p1106 A72-20674

Conventions on international responsibility for damage caused by space objects, studying UN juridical subcommittee resolution
08 p1255 A72-21076

Legal aspects of international cooperation on aircraft design and production, discussing work distribution, project management and liabilities sharing
10 p1565 A72-24881

Swiss franc revaluation effect on Warsaw Treaty liability limits, discussing legal problems
11 p1749 A72-26562

Legal aspects in prevention of aircraft unlawful seizure in view of international cooperation, noting German Democratic Republic agreements
12 p1890 A72-27272

Warsaw Air Transport Convention second revision by Guatemala Protocol of 8 March 1971, discussing provisions for air carrier liability
14 p2174 A72-30821

LEGENDRE CODE

U COMPUTER PROGRAMMING

U NEUTRON SCATTERING

LEGENDRE FUNCTIONS

Jovian disk brightness distribution at zero phase angle by expanding scattering indicatrix in Legendre polynomial series
02 p0282 A72-12329

Linear antenna input admittance calculation, computing excitation integral by field expansion in Legendre functions
04 p0501 A72-15431

Particular solutions to inhomogeneous Bessel and Legendre equations in resonance case
08 p1198 A72-20973

Aerodynamic field around singular stagnation point of blunt body tip with detached shock, using Legendre functions
09 p1261 A72-22932

Series representations of p-analytic functions in Legendre functions of first and second kind, applying to axisymmetric problems solution in elasticity theory
13 p0257 A72-29079

Jovian disk brightness distribution at zero phase angle by expanding scattering indicatrix in Legendre polynomial series
13 p0309 A72-29213

Radiative transfer equations solution for stellar spherical atmosphere by Grant-Hunt method, approximating intensity derivative over angular variable with Legendre polynomials
21 p3109 A72-41433

LEGENDRE POLYNOMIALS

U LEGENDRE FUNCTIONS

LEGENDRE TRANSFORMATION

U LEGENDRE FUNCTIONS

LEGIBILITY

Legibility of cold cathode, side illumination and straight projection electronic digital displays under varying ambient light and viewing positions
01 p0016 A72-10118

Legibility criterion of records from X-Y recorders, applying to Lissajous figures of stationary signals and phase trajectories
06 p0817 A72-18165

Criterion for signals records legibility obtained by analog recorders, deriving relationship between normalized root-mean-square error and apparent frequency
09 p1316 A72-23663

Alphanumeric characters for small TV type raster displays, describing legibility experiment for character height optimization
13 p1911 A72-29821

LEIDENFROST PHENOMENON

Unconstrained liquid mass /Leidenfrost phenomenon/ pool and forced convective film boiling at cryogenic temperature
19 p2883 A72-38841

LEM [LUNAR MODULE]

U LUNAR MODULE

LEMMAS

U THEOREMS

LENS ANTENNAS

Horn lens antennas for millimeter wave radiometric applications, discussing medium gain polystyrene lens design to obtain low peak sidelobes
04 p0503 A72-15608

Lens antennas for amplitude and phase transformations, examining existence of solutions and bounds in terms of parameters
07 p0985 A72-19404

Communication and data relay satellites multibeam antennas characteristics, discussing multiple feed reflectors, bootlace lens configuration and phased arrays
12 p1789 A72-27355

[AIAA PAPER 72-530] Microwave horn and lens antennas radiation spatial coherence characteristics, noting effect on picture contrast
13 p1928 A72-28475

An electromagnetic analysis of a cylindrical homogeneous lens
17 p2525 A72-34362

Focusing properties and efficiency of EHF waveguide lens with Al honeycomb as guiding medium, noting design considerations and performance test results
17 p2525 A72-34368

An artificial dielectric lens suitable for high power applications
18 p2671 A72-37148

Luneburg lens spherical antenna microwave radiation pattern, computing Maxwell equations via Tai method
21 p3030 A72-40529

LENS DESIGN

Cascaded annular lens systems for focusing electromagnetic waves, noting advantages of axicon
03 p0388 A72-12967

Solar prominence telescope design parameters and structural dimensions calculation using lens equation
03 p0356 A72-13197

Fourier transform lens design in coherent optical filtering systems
03 p0358 A72-13439

Isoplanatic instrument wave aberration determination, using longitudinal defocusing
03 p0360 A72-13563

Lens type beam waveguide for optical trunk communication, discussing transmission medium, terrain layout, bandwidth, terminal equipment, misalignment and multibeam application
04 p0497 A72-14483

Conical logarithmic foil type spiral antenna, presenting model of wavelength lenses used in dielectric rod antennas
04 p0500 A72-15408

Pinhole, fly-eye and holographic stereogram methods, examining resolution relationships, horizontal and vertical parallax and aberrations
05 p0663 A72-16673

Gathering power, geometrical factor and directional response of single and multielement particle telescopes
06 p0811 A72-17317

Hybrid computer aided design of thick electrostatic electron lenses by Laplace equation solution in terms of cylindrical harmonics, applying to CRT
06 p0779 A72-17481

Lens antennas for amplitude and phase transformations, examining existence of solutions and bounds in terms of parameters
07 p0985 A72-19404

Liquid pulsed laser active element lens parameters effects on output radiation divergence
07 p1008 A72-20511

Three element einzel and asymmetric voltage lenses for electron optics, calculating focal lengths and spherical aberrations based on potential distribution inside equidiameter coaxial cylinders
07 p0992 A72-20585

Zeiss aerial photographic lens systems imaging quality characteristics in visible and near IR spectral ranges
09 p1313 A72-23311

Neutral density glass collimating absorption lens for ideally uniform laser beams production
09 p1315 A72-23347

Hybrid computer aided synthesis of thick electrostatic electron lenses by Laplace equation solution in terms of cylindrical harmonics with gradient used in trajectory integration
10 p1509 A72-23940

Third order aberration coefficients of electron trajectories for two tube electrostatic lenses
10 p1510 A72-23941

Dark field electron microscopy with small annular zone of objective lens to reduce chromatic aberration effects on resolution
11 p1633 A72-26322

Critical values for two surface optical systems of refracting imaginary case modules in coupling and lens design
11 p1691 A72-26746

Lens parameters selection and prisms position optimization in light beam to avoid premature damage
12 p1808 A72-27623

Aplanatic mirror-lens telescope systems with spherical optics, discussing isochromatic corrective lens specifications
14 p2104 A72-30497

Book on coherent optical computers covering lens design, power sources, computation mathematics, modulation, detection, digital techniques and applications
15 p2203 A72-31499

Apollo-borne modified Hasselblad 500 EL Data moon camera and lenses, discussing design features and photographic applications
16 p2388 A72-32825

Glass choice for two lens uncemented objectives, calculating surface and aberration coefficients
16 p2395 A72-33965

An artificial dielectric lens suitable for high power applications
18 p2671 A72-37148

Lateral chromatic aberration of a double-meniscus telescope in Chile
19 p2801 A72-37919

Aplanatic mirror-lens telescope systems with spherical optics, discussing isochromatic corrective lens specifications
19 p2803 A72-38326

Low light level optics for image forming photoemissive sensors, discussing refractive and catadioptric lenses and reflective systems with magnetic focusing
20 p2921 A72-39029

Significance of OTF methods in assessing lenses to be used with partially coherent illumination.
20 p2931 A72-39049

Scattering from inhomogeneous cylindrically symmetric lenses with a line infinity in the index of refraction.
21 p3050 A72-40148

The use of high refractive index glasses of low dispersion for the correction of medium and high ametropia.
21 p3084 A72-40731

IR spectroscopy techniques based on Pfund triple-pass absorption cell, image slicer and achromatic doublet lenses, presenting graphs for prism dispersion design parameters
23 p3289 A72-43895

LENSES

NT CONTACT LENSES

NT MAGNETIC LENSES

NT WIDE ANGLE LENSES

NT WIRE GRID LENSES

Gravitational lens effect in black holes detection, computing light curves
03 p0416 A72-13011

Lens waveguides characteristics, analyzing Gaussian beams propagation through periodic system of thin plane-parallel nonlinear dielectric plates
04 p0489 A72-15389

Holographic measurement for optical transfer function of lenses, considering negative black and white photographic indicator emulsion effect
05 p0663 A72-16728

Fabry lens application in stellar photometry, describing technique of image construction on photomultiplier tube cathode
07 p0985 A72-19419

Transparency and polarization characteristics of three four-component Industrar-52 lenses with 1.5 aperture ratio and 50 cm focal length
09 p1309 A72-22516

Mathematical model for thermal lensing of IR laser window, discussing aberrations effect on diffraction-limited far field focus time
12 p1819 A72-27284

In situ measurement of objective lens data for high resolution electron microscope, using Bragg reflex images of crystallites with known orientation
12 p1807 A72-27528

Lens evaluation procedure based on optical transfer function data, discussing computer displays and merit parameters
12 p1810 A72-27936

Lens MTF calculation in presence of diffraction patterns via image mathematical model construction yielding Fourier transform
12 p1810 A72-27937

Experimental method to directly determine frequency-contrast and phase-frequency characteristics of optical objectives from boundary curve.
13 p2003 A72-28798

Experiments on the phase contrast transfer functions of a superconducting lens
17 p2594 A72-34284

Analysis of an optical beam waveguide consisting of a tapered lens-like medium and its applications.
17 p2580 A72-34382

Superposition method for potential distribution in plane tetraed field with unipotential and bipotential grids, noting electro-optical effect in cylindrical lenses
19 p2776 A72-38667

Numerical analysis of microwave heat generation in disc-shaped Luneberg lenses.
21 p3032 A72-40627

Crystalline lens optical structure in human eye, representing on and off axis imaging characteristics by mathematical model
21 p3007 A72-40737

Effect of spherical spectacle lenses on the monochromatic aberration of the eye
21 p3007 A72-40746

Gravitational deflection of light by radially and cylindrically symmetric masses, considering effect on apparent luminosity of distant object
22 p3204 A72-42000

Self focusing effect on wave beam propagation in optical lens waveguides, discussing system nonlinearity
22 p3186 A72-42656

LEONID METEORIDS

Leonid meteor trail drift measurements in upper atmosphere, comparing radar system with precise goniometric capabilities to photographic methods
09 p1383 A72-22509

Photometric parameters of Leonid meteor ionized trail and turbulent diffusion in M zone, determining electron attachment rate
09 p1384 A72-22510

LEPTONS

NT ELECTRONS

NT MUONS

NT NEUTRINOS

NT POSITRONS

Neutrino interactions in lepton era of universe and hot big bang cosmology according to proton-neutrino coupling theory
07 p1084 A72-20538

Direct particle theory of weak interactions, considering two component spinors and leptonic decay
13 p2007 A72-28500

LESIONS

NT PULMONARY LESIONS

Acute hypoxia of the myocardium - Ultrastructural changes.
17 p2501 A72-34982

Local necrosis, parenchyma incisions and vascularization of rabbit liver tissue under pulsed and continuous laser beams
21 p3002 A72-40991

LETHALITY

Sudden death in myocardial infarction, discussing heart electrical stability, neural control, arrhythmias and cardiac conduction disturbances
06 p0761 A72-17381

Remotely manned vehicles (RMV) application in aerial warfare, considering antiaircraft defenses lethality increase, equipment costs and role of man during combat mission
13 p1896 A72-28451

Effects of long periods of clinical death from drowning or lethal blood loss on higher nervous activity in reanimated dogs
13 p1902 A72-28642

Hypothermia and resistance of mice to lethal exposures to high gravitational forces.
22 p3142 A72-42494

LETTERS (SYMBOLS)

U SYMBOLS

LEUCINE

Diastereometric S-prolyl dipeptide derivatives adaptation to gas chromatographic quantitative estimation of R- and S-leucine enantiomers
11 p1590 A72-26366

LEUKEMIAS

Increased tolerance of leukemic mice to arabinosyl cytosine with schedule adjusted to circadian system.
17 p2505 A72-35397

LEUKOCYTES

NT LYMPHOCYTES

Carbohydrate metabolism, glycolytic ferment activities and leukocyte size under ionizing radiation, showing compensatory bone marrow cell formation with leukopenia
04 p0467 A72-14609

Blood self purification enteral mechanism in dogs, determining leukocyte population changes before and after feeding and intravenous interferon injections
07 p0915 A72-18867

Crowding phenomenon effect on blood cell oxygen consumption, using Cartesian diver technique for polymorphonuclear leukocyte, lymphocyte and platelet measurements
12 p1763 A72-27842

EEG investigation of circadian variations in qualitative and quantitative RNA content in human leukocytes, noting changes during sleep
18 p2651 A72-36624

Effect of prolonged gamma irradiation on the functional capacity of leukocytes
21 p3103 A72-40438

Pyrogenal injection test for hematopoietic tissue function in dogs, describing response as transient leukopenia followed by pronounced leukocytosis due to bone marrow granulocyte ejection
23 p3255 A72-43911

LEUKOPENIA

Pyrogenal injection test for hematopoietic tissue function in dogs, describing response as transient leukopenia followed by pronounced leukocytosis due to bone marrow granulocyte ejection
23 p3255 A72-43911

LEVEL (HORIZONTAL)

Heat conduction in vacuum insulated capillaries to prevent failure of level indicators and controllers based on condensation in evaporating cryogenic liquid
03 p0456 A72-13883

Contact-type level gauge with a transistorized decimal code converter
17 p2529 A72-34764

LEVEL (QUANTITY)

NT ATOMIC ENERGY LEVELS

NT ELECTRON STATES

NT ENERGY LEVELS

NT GROUND STATE

NT INTERMOLECULAR FORCES

NT MOLECULAR ENERGY LEVELS

LEVERS

Bent lever equilibrium and relativistic mass for point body in motion, introducing von Laue energy flow inertia into d'Alembert principle
10 p1505 A72-24074

LEVITATION

Superconducting levitron machine for trapped hot plasma stability and confinement studies in vacuum, discussing construction and coil performance
10 p1460 A72-24758

Critical levitation loci for spheres on cryogenic fluids.
19 p2836 A72-38844

LEWIS BASE

Intercalation complexes of Lewis bases and layered tantalum and niobium disulfide superconductors, noting critical temperatures
01 p0113 A72-10018

Lattice expansion of metal chalcogenide superconducting organometallic structures with aromatic or aliphatic Lewis bases sandwiched into van der Waal gap
08 p1216 A72-21214

LEWIS NUMBERS

Hydrodynamic convective stability in catalytic chemical reaction with thermal and concentration coupling dependent on Lewis number
02 p0301 A72-12092

Binary gas mixtures calculation for Schmidt, Prandtl and Lewis number dependence on pressure, temperature and chemical composition
07 p1101 A72-20600

LIABILITIES

NT LEGAL LIABILITY

LIAPUNOV FUNCTIONS

Sixth order nonlinear differential equation isolated equilibrium point stability determination, constructing Liapunov function
01 p0094 A72-11125

Energy-phase time transformations of damped Liapunov system applied to nonlinear spring pendulum and betatron transient oscillations
01 p1013 A72-11387

Linear systems partial stability via Liapunov second method, examining relation between uniformly and exponentially asymptotic partial stability
02 p0251 A72-11493

Stability theorems reformulation with one-parameter families of Liapunov functions, discussing applications to Matrosov and Rouche asymptotic stability theorems
02 p0251 A72-11495

Nonautonomous systems periodic solutions through Liapunov functions construction, considering application to nth-order dynamic systems forced oscillations
02 p0251 A72-11498

Uniformly and asymptotically stable solutions to linear Volterra integrodifferential equation system, discussing Liapunov stability
02 p0252 A72-11997

Stability properties of functional differential system solutions, discussing Liapunov functions construction
02 p0252 A72-12173

Unperturbed motion asymptotic stability and instability theorems, considering Liapunov function method
02 p0260 A72-12432

Liapunov functionals synthesis for continuous system stability study, discussing linear combinations of moments of governing partial differential operators
04 p0538 A72-14671

Control system synthesis from transient process estimates with Liapunov functions, proposing optimality criteria based on Gaussian minimum constraint principle extension
04 p0505 A72-14997

Linear feedback control systems with time lag, calculating integrated squared error by Liapunov function
04 p0506 A72-15110

Steady state angular motion stability of passive magnetically stabilized satellites, using Liapunov method
05 p0726 A72-16464

Large launch vehicle attitude control system absolute stability mathematical model, using quadratic Liapunov function for exponential property description
05 p0728 A72-16475

Liapunov direct method based approaches to hybrid dynamical systems stability, applying to attitude stability of flexible earth pointing satellite
05 p0729 A72-16867

[AIAA PAPER 72-18]
Liapunov functions generation, using auxiliary functional differential equations table for invariance determination
06 p0838 A72-17378

Spinning satellite with rigid central body and flexible appendages, deriving equations of motion and Liapunov stability
06 p0892 A72-17652

Generalized restricted three body problem with one point not exerting influence on others, discussing variational equations and Liapunov stability
06 p0877 A72-17662

Sufficient conditions for asymptotic stability and instability for elastic systems with dissipation, using Liapunov direct method
07 p1026 A72-18809

Book on asymptotic behavior and stability in ordinary differential equations covering linear and nonlinear systems, Liapunov and analytical-topological methods
07 p1026 A72-19184

Liapunov theorem for polynomial solution existence for first order inhomogeneous system of linear partial differential equations

08 p1205 A72-20958

Nonlinear differential equations system stability conditions for arbitrary initial perturbations of zero solution, using Liapunov functions

08 p1199 A72-21461

Liapunov stability of circular equatorial motions of light bodies in Kerr gravitational field of massive rotating body, using geodesic lines equations

08 p1210 A72-22071

Hamiltonian used as Liapunov function in stability evaluation of one dimensional continuous system loaded with polygenic forces

09 p1406 A72-23077

Stability analysis of composite systems, applying scalar and vector Liapunov function approach to specific examples

09 p1290 A72-23091

Liapunov theory solutions stability for oscillations along galactic axis of symmetry

09 p1390 A72-23396

Liapunov direct method in synthesis of frequency-pulse system for automatic stabilization of spacecraft position

09 p1397 A72-23427

Liapunov functional stability analysis in structural dynamics problems including wave equations with nonlinear damping

09 p1407 A72-23457

Stability criteria for continuous dynamic system under parametric excitation derived by Liapunov direct method, using time dependent functionals and Rayleigh operators quotients

[ASME PAPER 71-APM-EEE] 10 p1510 A72-24187

Asymptotic stability of astatic pulse frequency modulated feedback control systems with discrete correction, obtaining sufficient conditions in closed form with Liapunov method

11 p1610 A72-25450

Linearization and Liapunov stability analysis of nongyroscopic holonomic conservative dynamic differential equations system

11 p1677 A72-25979

Iterative formula for constructing Liapunov functions in convergent series form

12 p1836 A72-27073

Liapunov direct stability method extension to partial differential equations, using functional analysis and wave equation example

13 p1985 A72-28483

Convective hydromagnetic stability of hot conducting fluid layer in magnetic field by Liapunov method

13 p2011 A72-28891

Dynamic control stability on given time interval, using Liapunov-like functions and integral manifolds in quadratic forms

13 p2004 A72-29471

Liapunov functions and integral inequalities for study of finite time stability of motion, noting small parameter system subjected to continuous disturbances

13 p2004 A72-29496

Dynamic system motion stability estimation with Liapunov function in quadratic form, applying to circular satellite orbit stability in axisymmetric gravitational field

14 p2161 A72-31079

Automatic control theory trends /1950-1970/, discussing nonlinear, discontinuous and adaptive systems, optimization problems, Liapunov stability theory, etc

15 p2212 A72-32576

Numerical methods for Liapunov linear matrix equations solution in control systems analysis and design

15 p2265 A72-32798

Liapunov functions for nonlinear autonomous difference equations stability analysis, defining difference gradient, principal sum and definite sum

15 p2265 A72-32802

Damping perturbation of high order nonlinear autonomous Liapunov system, reducing system equations integration to quadratures via transformation to lower order quasi-linear nonautonomous system

16 p2422 A72-32938

Liapunov function application to stability of unperturbed motion of differential equations with respect to part of variables

16 p2422 A72-32940

Coefficient criterion of stability for Liapunov indices in a two dimensional linear system

17 p2575 A72-34774

Comparison principle and finite time stability of control systems.

17 p2581 A72-35052

Stability and transient behavior of composite nonlinear systems.

17 p2534 A72-35530

Equivalent predictions of the circle criterion and an optimum quadratic form for a second-order system.

17 p2577 A72-35534

Lyapunov functionals for a class of delay-differential systems.

18 p2709 A72-36052

Russian book - Introduction to the theory of stability of motion

18 p2711 A72-36523

A stability theory for perturbed difference equations.

19 p2826 A72-38249

Liapunov theory application to stability analysis of large scale dynamic systems, developing methods for vector Liapunov functions construction

19 p2781 A72-38262

Effects of incomplete adaptation and disturbance in adaptive control.

19 p2781 A72-38263

Lyapunov functions for quadratic differential equations with applications to adaptive control.

19 p2826 A72-38264

Investigation of the stability of solutions of second-order differential equations with periodic coefficients by the differential invariant method

19 p2827 A72-38467

One realization of Liapunov's method for integrating linear equations

19 p2827 A72-38469

A theorem of the Liapunov theorem type for the stability of a multidimensional system

20 p2954 A72-39866

Liapunov stability analysis of hybrid dynamical systems with multi-elastic domains.

21 p3086 A72-41519

Instability of the equilibrium position of a multidimensional system consisting of 'neutrally' unstable subsystems

21 p3126 A72-41546

Asymptotic motion stability analysis with respect to part of variables, using Liapunov functions for solution boundedness conditions

22 p3204 A72-41901

Construction of Liapunov functions for time-dependent systems containing inertialess nonlinearities

22 p3205 A72-42176

Liapunov function method in control problems of distributed parameter systems /Survey/

22 p3205 A72-42180

A constructive method of solving the Liapunov equation for complex matrices.

22 p3199 A72-42775

Nonlinear mechanics perturbation method for Liapunov functions construction, noting application to nonlinear differential equations

23 p3308 A72-43582

Regions of absolute ultimate boundedness for discrete-time systems.

23 p3309 A72-43857

Liapunov method extension to dynamically loaded elastically end-restrained columns stability and frames forced vibration boundedness problems

[ASCE PREPRINT 1639] 23 p3352 A72-44110

Analytical designing of regulators for second-order nonlinear systems

24 p3387 A72-45519

LIBRATION

Liapunov stability of rigorous particular solutions /corresponding to libration points/ of three body problem, determining motions of satellite influenced by two spherical bodies

03 p0436 A72-13823

Terrestrial dust belt particles origin, character and trapped time from observations of earth-moon system libration points

08 p1229 A72-20839

Lunar topography measurement by libration method based on stereoscopy and by photographic method

08 p1230 A72-21020

Second order libration solution of ideal resonance problem, using Lie series perturbation technique

08 p1236 A72-21637

Quasi-periodic orbits about the translunar libration point.

[AIAA PAPER 72-935] 21 p3112 A72-41573

A catalog of selenographic coordinates of points of the libration zones and the reverse side of the moon

21 p3114 A72-41767

Celestial mechanics principles application to geostationary satellites in equatorial plane and in earth-moon system libration points, considering Jupiter and Saturn stationary satellites

22 p3222 A72-42141

Stability of motion at collinear libration centers in the restricted problem of three bodies with allowance for light pressure

24 p3437 A72-44762

LIBRATIONAL MOTION

Triangular points stability in restricted three body problem by computer program

01 p0122 A72-10004

Stability of and motion about L4 in restricted three body problem with 3 to 1 commensurability between long and short periods of motion

01 p0122 A72-10010

Attitude motion at equilibrium libration points of axisymmetric smallest body in restricted three body problem

01 p0123 A72-10011

Periodic orbit families emanating from Lagrange triangular point L4 in restricted three body problem with mass ratio parameter equal to Routh critical mass ratio

01 p0123 A72-10013

Satellite attitude and libration control by solar radiation pressure

01 p0135 A72-10928

Solar radiation effects on planar libration motion and attitude of gravity oriented satellites at high altitudes

03 p0434 A72-13613

Magnetic damper for gravity gradient stabilized satellite rotational and librational motions, deriving formula for calculating damping coefficients

05 p0726 A72-16463

Solar radiation pressure effects on gravity oriented satellites librational dynamics, using digital computer aided numerical analysis and analog simulation

07 p1067 A72-18789

Librational transverse oscillations boundary value problems of heavy thread on orbiting satellite, determining equilibrium and eigenfunctions

08 p1240 A72-21142

Coupled librational motion of gravity oriented satellite in circular orbit under aerodynamic forces, discussing limiting stability and periodic solutions

11 p1726 A72-25914

Lunar crust mass distribution relation to moments of inertia derivation from librations, inferring non-validity of lunar evolution fluid phase hypothesis

14 p2153 A72-30504

Lunar physical libration measurement from Apollo laser experiment with retroreflectors, assessing obtained data

14 p2154 A72-30516

Aerodynamic effects on circular-orbiting cylindrical satellites coupled librational motion, analyzing equilibrium configurations stability by linearized and Liapunov direct method

15 p2320 A72-31818

Small amplitude libration stability and damping system for gravitationally stabilized tethered orbiting radio interferometer satellite system

16 p2462 A72-34020

Periodic libration solutions in attitude control stability study of slowly spinning satellites under gravity gradient torques, using Floquet theory

20 p2968 A72-39195

Interaction between attitude libration and orbital motion of a rigid body in a near Keplerian orbit of low eccentricity.

20 p2968 A72-39197

Librational transverse oscillations boundary value problems of heavy thread on orbiting satellite, determining equilibrium and eigenfunctions

20 p2977 A72-39247

Solar pressure control of a spinning satellite with a stabilized platform.

[AIAA PAPER 72-918] 21 p3115 A72-41563

Explicit series solutions for the frequencies of motion around the Lagrangean points in the restricted problem of three bodies.

24 p3440 A72-45136

Celestial mechanics ideal resonance problem global solution via Bohlin-von Zeipel perturbation technique, modifying Hamiltonian expansion point and separatrix and libration region singularities suppression method

24 p3440 A72-45138

LIDAR

U OPTICAL RADAR

LIE GROUPS

NT SPINOR GROUPS

Hamiltonian algorithms based on Lie transforms and von Zeipel method, discussing application to non-Hamiltonian system perturbation solution

06 p0839 A72-17660

Second order libration solution of ideal resonance problem, using Lie series perturbation technique

08 p1236 A72-21637

Dimensional analysis pi-theorem local generalization by Lie transformation group investigation, constructing local canonical coordinate systems to obtain factoring properties of certain functions

10 p1503 A72-23921

Differential equations similarity analysis, using Lie infinitesimal contact transformation group as search method for other possible transformation groups

10 p1503 A72-23922

Lie group theory application to linear differential equations of motion with variable parameters, considering flight vehicle example

12 p1847 A72-28127

Linear differential equations solution symmetry properties, using Lie algebraic methods and finite dimensional linear systems theory

15 p2264 A72-31761

System theory on group manifolds and coset spaces.

17 p2575 A72-34949

On the algebraic structure of a class of solvable quantum problems.

18 p2711 A72-36514

LIFE [BIOLOGY]

- Satellite vibration-rotation motions studied via canonical transformations.
[AIAA PAPER 72-919] 21 p3115 A72-41564
- An application of the theory of Lie groups in the optimal control problem for linear dynamic systems with time-variable coefficients
22 p3162 A72-42181
- Decision surface estimate of nonlinear system stability domain by Lie series method.
23 p3274 A72-43540
- Controllability properties of right invariant nonlinear systems described by evolution differential equation in Lie group
23 p3309 A72-43981

LIFE [BIOLOGY]

U LIFE SCIENCES

LIFE [DURABILITY]

- NT FATIGUE LIFE
NT PLASMA LIFETIME
NT SATELLITE LIFETIME
NT SERVICE LIFE
NT STORAGE STABILITY
- Test equipment for glass and polymer fibers strength and lifetime in vacuum and inert bases under static loads
01 p0093 A72-11382
- Energy levels and mean life measurements of Cl ions at 500-2800 A using beam-foil spectra technique
02 p0170 A72-12547
- Hanle effect mean-life measurements on aligned Ar fast ion beam particles, comparing results with beam-foil measurement
04 p0552 A72-15151

- Ionization loss effects on cosmic ray lifetime in galactic interstellar medium, noting dependence on particle energy
07 p1064 A72-20637
- Stress rupture data from S glass composite matrix effectiveness tests, noting skewed lifetime distribution in statistical patterns
08 p1192 A72-21683

- Galactic cluster lifetimes from observed age distribution comparison to evaporation times by numerical experiments with star cluster models
12 p1873 A72-27897

- Heat treatment and grain size effects on stress corrosion resistance and life duration of maraging steels, investigating crack initiation and propagation
14 p2117 A72-30539

- Random temperature variations effect on life of Euler column with sandwich cross section under constant axial compressive load, using Norton nonlinear creep law
15 p2324 A72-31494

- Components creep-rupture life prediction for multiaxial stress from uniaxial test data, discussing crack initiation and propagation phases stress states
16 p2412 A72-34114

- Microstructural damage effect on high temperature materials creep life, considering Robinson and Odqvist correlation laws
16 p2474 A72-34127

- Measurement of carrier lifetime in the base of silicon diodes - Application to the control of manufacturing techniques.
18 p2669 A72-37108

- The field strength conditions for measuring the carrier lifetime in semiconductor crystals by the light flash method
21 p3098 A72-41487

- On the determination of minority carrier lifetime and surface recombination velocity from the transient response of MOS capacitors.
23 p3324 A72-44071

LIFE DETECTORS

- Ti leaching from granitic rocks by Penicillium, sim-plicissimum, discussing extraterrestrial life detection
05 p0616 A72-15809

- Life detection on earth from satellite 100 meter resolution photographs, discussing potential false positives and implications for Mars probes
10 p1471 A72-23718

- Viking Mars 1975 mission with spacecraft orbiters and landers, describing experiments with emphasis on life detection
10 p1539 A72-24376

- Viking I lander carbon 14 assimilation experiment for life detection in Martian soils
10 p1540 A72-24385

- Viking I lander detection of metabolically produced radioactive labeled gas in Mars surface samples
10 p1540 A72-24386

- Viking I lander light scattering experiment to detect microbial growth from aqueous turbidity changes in contact with Martian soil
10 p1430 A72-24387

- Mars 1975 Viking mission profile, describing soft landing/orbiter probes and life detection experiments
12 p1877 A72-27687

- Viking mission gas exchange experiment for life detection in Martian soil, covering design of experiment
14 p2084 A72-30876

LIFE RAFTS

- Aircrews tolerance to cold water and life raft exposure, discussing prediction model based on thermal insulation effectiveness, assumed metabolism and body surface area and mass
[AD-740276] 10 p1428 A72-23734

- Thermally protective life rafts and clothing evaluation for cold sea survival potential assessment and tolerance limit determination
14 p2081 A72-31088

- Survival equipment for life raft in conjunction with Mercury, Gemini, Apollo, Skylab and space shuttle NASA programs
17 p2620 A72-34433

LIFE SCIENCES

NT MOLECULAR BIOLOGY

- Physical and biological sciences approaches to attainment of knowledge, noting indeterminateness in organic realm
07 p0934 A72-20394

- Living organisms defense and preservation via refrigeration and vacuum combined use in lyophilization technique
12 p1769 A72-27293

- Life sciences and space research X; Proceedings of the Fourteenth Plenary Meeting, Seattle, Wash., June 21-July 2, 1971.
23 p3253 A72-43381

LIFE SPAN

- Reliability theory distribution function construction for failure analysis in physical processes, considering mechanical system service life and living organisms life span
08 p1180 A72-22062

- Erythrocyte life span in mice under normal atmospheric pressure and various degrees of hypoxia acclimatization, using radioactive labeled diisopropyl phosphorofluoridate
11 p1579 A72-26608

- Assessment of life span age difference relations in visual perceptual tasks, taking into account maturational and generational differences
18 p2653 A72-36910

- Natural aging and radiation-induced life shortening in Drosophila melanogaster.
24 p3373 A72-45279

- Longevity and cardiovascular mortality among former college athletes.
24 p3374 A72-45689

LIFE SUPPORT SYSTEMS

NT CLOSED ECOLOGICAL SYSTEMS

NT EMERGENCY LIFE SUSTAINING SYSTEMS

- Electrochemical carbon dioxide concentrator materials compatibility to space shuttle life support environment, comparing with LiOH method
01 p0018 A72-10768

- Custom fit oxygen mask for life support of crew members
08 p1126 A72-21567

- Extravehicular life support systems for shuttle, space station, lunar base and Mars missions, considering thermal control, carbon dioxide control and oxygen supply subsystems
[AIAA PAPER 72-231] 10 p1430 A72-24441

- Malfunction detection for space station environmental/thermal control and life support system, using onboard computer
10 p1423 A72-24447

- Life support equipment and pressure suit operational requirements from viewpoint of flight crews and test pilots
12 p1771 A72-27516

- USAF custom fit oxygen mask program.
17 p2508 A72-34559

- Lunar horticulture possible role as life support system of earth independent lunar colony
17 p2505 A72-35938

- Continuous flow general aviation oxygen masks.
[SAE AS 1224] 18 p2653 A72-36536

- Space station prototype environmental/thermal control and life system - A current overview.
[ASME PAPER 72-ENAV-35] 20 p2894 A72-39143

- Design criteria for the modular space station environmental control and life support system selection.
[ASME PAPER 72-ENAV-25] 20 p2894 A72-39152

- Space station atmospheric revitalization system design, covering temperature, humidity, carbon dioxide, contaminant and oxygen generation and composition control and vehicle configuration
[ASME PAPER 72-ENAV-24] 20 p2894 A72-39153

- Potential applications of NASA-developed technology to problems of the environment.
[ASME PAPER 72-ENAV-23] 20 p2895 A72-39154

- Environmental control and life support subsystem conceptual design studies for shuttle launched 6-12 man crew modular space station
[ASME PAPER 72-ENAV-22] 20 p2895 A72-39155

- Significant factors in environmental and thermal control/life support system design for space shuttle orbiter
[ASME PAPER 72-ENAV-21] 20 p2895 A72-39156

- Optimal shuttle research applications module /RAM/ environmental control and life support system for sortie missions
[ASME PAPER 72-ENAV-20] 20 p2895 A72-39157

- Comparative evaluation of environmental control and life support systems for the space shuttle orbiter.
[ASME PAPER 72-ENAV-19] 20 p2895 A72-39158

- Space shuttle environmental temperature control/life support system program changes, discussing air cooled electronic equipment, cryogenic stores, crew size and mission duration
[ASME PAPER 72-ENAV-18] 20 p2895 A72-39159

- Modular environmental control/life support system design for low cost shuttle launched space station, evaluating humidity, carbon dioxide, water and waste management
[ASME PAPER 72-ENAV-17] 20 p2895 A72-39160

- Bosch CO2 reduction unit research and development.
[ASME PAPER 72-ENAV-10] 20 p2896 A72-39167

- Bosch carbon dioxide reduction process for manned spacecraft oxygen recovery, analyzing carbon and water forming reactions with iron as catalyst
[ASME PAPER 72-ENAV-9] 20 p2896 A72-39168

- Integrated water vapor electrolysis oxygen generator and hydrogen depolarized carbon dioxide concentrator development.
[ASME PAPER 72-ENAV-7] 20 p2896 A72-39170

- Integration of an automated onboard data management system with a manned spacecraft environmental thermal control and life support system.
[ASME PAPER 72-ENAV-6] 20 p2896 A72-39171

- Six-month test program of two water electrolysis systems for spacecraft cabin oxygen generation.
[ASME PAPER 72-ENAV-5] 20 p2896 A72-39172

- Functional reliability of the biological component of a life support system
21 p2998 A72-40448

- Design features of Soyuz life support and launch escape systems and Vostok rocket booster stage
23 p3343 A72-44335

- Biochemical and physiological evaluation of nourishment of subjects feeding on dehydrated products in test chamber with regenerative life support system, discussing metabolic data and hormone function
24 p3375 A72-45128

- Mathematical model for life support system optimization in terms of reduced mass minimization as quality criteria for energy conversion and metabolic processes
24 p3375 A72-45133

- R and D on environmental and thermal control/life support system application to lunar base mission, discussing reliability and food regeneration
24 p3375 A72-45164

- System design of a near-self-supporting lunar colony.
24 p3388 A72-45192

- The Space Station Prototype Program - The development of a regenerative life support system for extended-duration missions.
24 p3375 A72-45193

- Spacecraft food synthesis, using carbon dioxide and water from chemically regenerated human metabolic and waste products
24 p3376 A72-45277

LIFEBOATS

- Aircraft emergency evacuation systems, discussing door designs, inflatable escape slide and slide/lifeboat combination
22 p3138 A72-42520

LIFETIME [DURABILITY]

U LIFE [DURABILITY]

LIFT

NT INTERFERENCE LIFT

NT JET LIFT

NT ROTOR LIFT

NT ZERO LIFT

- Sound radiation from axial flow fans running in turbulent flow, evaluating fluctuating lift on rotor blades due to incident gusts
01 p0002 A72-10220

- Steady sonic flow around three dimensional obstacles by pseudo-axisymmetrical flow approach, revealing singular perturbation of lift downstream at infinity
02 p0150 A72-12096

- Area rule for change in lift/drag ratio of hypersonic delta wing due to conical body addition on compression side
02 p0151 A72-12270

- Power law bodies lift and drag coefficients interrelationship under Newtonian nonaffine similarity laws, presenting rules for equivalent transformations identification
02 p0151 A72-12273

- Drag and lift experimental determination for low aspect ratio rectangular wings with blunt trailing edges at Mach numbers 0.5-2.2
[DGLR PAPER 71-114] 02 p0152 A72-12712

- Gas-metal surface interactions effect on aerodynamic lift and drag coefficients in free molecular flow
03 p0342 A72-14059

- Heat transfer, drag and lift coefficients for free molecular flow over concave surfaces, describing Monte Carlo simulation technique
[ASME PAPER 71-WA/HT-17] 05 p0744 A72-15876

Inverse integral Fourier transforms to solve steady periodic motions of wing close to solid surface, deriving equations of lift and principal moment

08 p1108 A72-21701

Two dimensional MHD conducting fluid flow past insulating cylinder in presence of arbitrarily oriented magnetic field, determining lift and drag coefficients for small Hartmann numbers

09 p1359 A72-22533

Transfer matrix method application to rocket vehicles structural dynamics, incorporating axial and aerodynamic lift forces in vibrational analysis

09 p1397 A72-23499

Perfectly conducting incompressible fluid motion past thin body in oblique field, discussing magnetic field influence on lift

09 p1365 A72-23559

Oblique magnetic fields effect on compressible conductive fluids motion in presence of thin foil, noting lift values in hyperlipitic and double hyperbolic cases

09 p1365 A72-23560

Unsteady lift on airfoils in moving cascades with inlet axial flow disturbances, estimating lift on reference blade between blade channels

11 p1568 A72-25608

Lift and pressure fluctuations of cambered airfoil under periodic longitudinal and transverse gusts, applying to axial flow turbomachines

11 p1569 A72-25626

High intensity free stream turbulence effects on flow past circular cylinder at subcritical Reynolds numbers, measuring unsteady lift and drag

11 p1573 A72-26640

Rotating airfoil experimental test program for verification of Himmelskamp and Dwyer-McCroskey theoretical analysis, presenting graphs of lift coefficient vs angle of attack

12 p1752 A72-28124

Aerodynamic profiles lift coefficient determination by empirical formula based on potential flow lines obtained by conformal mapping

13 p1894 A72-29132

Roughened and smooth spherical wind sensors lift and drag, calculating aerodynamic coefficient spectra from velocity

13 p1894 A72-29620

Shock wave interaction with supersonic moving plate, calculating plate lift as function of time

14 p2071 A72-31024

Two dimensional viscous flow past semiinfinite flat plate and smooth obstacle, using Navier-Stokes equations for lift force relationship investigation

15 p2216 A72-31312

Contracting or diverging stream flow mean velocity change effects on airfoil pressure distribution, circulation and lift, deriving vortex distribution expression

15 p2179 A72-32023

Lift and induced drag characteristics of jet flapped finite span wings in close proximity to ground, using method of matched asymptotic expansions

16 p2341 A72-32827

Free molecular flow over rotating sphere satellite, deriving aerodynamic forces on differential surface to determine drag and lift coefficients

16 p2341 A72-32844

Three dimensional potential flow with lift about solid body calculated by distribution of sink, source and vortex type singularities satisfying Laplace equation

16 p2342 A72-32896

Lift and drag on conical, cylindrical and spherical artificial satellites from spatial impulsive interaction model depending on gas temperature and surface conditions

16 p2347 A72-34167

Rotary wings lift and efficiency increase by circulation control via tangential blowing about bluff trailing edge airfoils

17 p2489 A72-34492

Angle of attack increase of an airfoil in decelerating flow

18 p2641 A72-36773

A vortex model for the study of the flow at the rotor blade of a helicopter

18 p2642 A72-36975

Prediction of the stalling of a wing section in incompressible flow

19 p2746 A72-37760

Three-dimensional structure and equivalence rule of transonic flows

20 p2886 A72-39631

The lift coefficient of a supercavitating jet-flapped foil in a free jet

21 p2992 A72-41236

Lift on airfoils with separated boundary layers

21 p2992 A72-41264

LIFT AUGMENTATION

Disk shaped lift engine providing additional thrust during takeoff and transition phases of V/STOL aircraft, returning to ground by jet after task accomplishment

02 p0272 A72-12900

TU-154 lift and drag augmenting devices for takeoff and landing characteristics improvement

03 p0310 A72-13472

Closed loop fluidic bidirectional jet flap airfoil lift control system, considering application to helicopter rotor blades

05 p0603 A72-16659

Three dimensional wind tunnel investigation of vortex augmented unswept wing with leading edge cusp flap and split upper and lower trailing edge flaps

[SAE PAPER 720321] 11 p1568 A72-25584

The flight mechanics of STOL aircraft

17 p2488 A72-34241

Methodology for estimating STOL aircraft high lift systems characteristics

[AIAA PAPER 72-779] 19 p2752 A72-38138

Lift and control augmentation by spanwise blowing over trailing edge flaps and control surfaces

[AIAA PAPER 72-781] 19 p2746 A72-38140

Augmentor wing design for Buffalo STOL aircraft, discussing operational principle and wind tunnel test results

21 p2994 A72-40684

An improved solution of the two-dimensional jet-flapped airfoil problem

23 p3247 A72-43329

LIFT COEFFICIENTS

U AERODYNAMIC COEFFICIENTS

U LIFT

LIFT DEVICES

Lifting surface linearized potential theory for unsteady aerodynamic forces on wing and horizontal tail surfaces, using computer program

03 p0308 A72-13541

Steady and oscillatory subsonic aerodynamic loads prediction based on Doublet-Lattice method and method of images, determining chord and spanwise loading on lifting surfaces

[AIAA PAPER 72-26] 05 p0607 A72-16917

Two dimensional lift characteristics of multielement airfoils, using potential flow method based on surface source distribution and finite difference boundary layer method

[AIAA PAPER 72-3] 05 p0608 A72-16935

Wind tunnel investigation of Reynolds number effects on boundary layer separation incidence and maximum lift coefficient of high-lift device equipped aircraft model

10 p1419 A72-24657

Propulsion system/airframe matching in hybrid V/STOL airplanes, stressing thrust vector management, lift engine bypass ratio and power plant packaging design

[ASME PAPER 72-GT-106] 11 p1576 A72-25671

L-1011 propulsion, fuel, flight control, navigation, avionics, communication, electrical, environmental control and auxiliary power systems, discussing structure and high lift devices

15 p2181 A72-32427

Analysis of the interaction of j's and airfoils in two dimensions

[AIAA PAPER 72-777] 19 p2746 A72-38136

Methodology for estimating STOL aircraft high lift systems characteristics

[AIAA PAPER 72-779] 19 p2752 A72-38138

Potential flow calculations to support two-dimensional wind tunnel tests on high-lift devices

[ICAS PAPER 72-13] 21 p2991 A72-41138

The sweepback effect in the subsonic region in the lower atmosphere and in the hypersonic region at high altitudes

24 p3359 A72-44983

LIFT DISTRIBUTION

U FORCE DISTRIBUTION

U LIFT

LIFT DRAG RATIO

Newtonian theory for maximum lift drag ratio of blunt-cone cylinder bodies, optimizing rocket reentry nose shape

05 p0602 A72-16535

Tactical approach landing radar tests for low lift drag ratio aircraft in unpowered flight, using F-104D as test aircraft

15 p2267 A72-31694

Book on airfoil section designs for light aircraft covering wind tunnel studies of lift drag ratio as function of angle of attack

15 p2179 A72-32250

Triangular and conical wings in hypersonic flow with Mach reflection of shock waves from leading edge with optimal L/D ratio

18 p2642 A72-36893

LIFT FANS

Leaning vanes for fan noise reduction, discussing rotor-stator plane fluctuating pressure amplitude decrease and radial distribution modification

[AIAA PAPER 72-126] 05 p0706 A72-16823

Cross flow effect on lifting fan noise at subsonic blade tip speeds, analyzing radiation pattern change due to inlet flow distortion

[AIAA PAPER 72-128] 05 p0608 A72-16921

STOL and V/STOL transport aircraft design requirements consideration based on common propulsion and lift engine types use, noting fan lift solution superiority

10 p1421 A72-24865

Integral and remote powered lift fan engines design for large civilian VTOL transports

[ASME PAPER 72-GT-65] 11 p1704 A72-25654

Turbotip lift fan design developed for XV-5 VTOL research aircraft, reviewing changes for future commercial and research transport systems

[ASME PAPER 72-GT-111] 11 p1576 A72-25674

Aircraft fan and compressor noise generation mechanism, considering mass flow and lift forces fluctuations from rotor and stator airfoils

13 p2028 A72-29569

Lift fan blade interaction discrete frequency noise, discussing potential and viscous interactions relation to rotor-stator spacing

15 p2297 A72-32019

Blade characteristics of axial flow fan with orifice fan guide investigation by theoretical model with flat plate parallel to wing tip surface

15 p2179 A72-32142

LIFT FORCES

U LIFT

LIFTING BODIES

NT LIFTING REENTRY VEHICLES

Hydroelastic behavior of heavily loaded lifting surfaces, investigating flutter and divergence

04 p0592 A72-15562

Subsonic doublet-lattice lifting surface method non-planar aspects refinement, using wing-tail configurations

05 p0600 A72-16109

Steady and oscillatory subsonic aerodynamic loads prediction based on Doublet-Lattice method and method of images, determining chord and spanwise loading on lifting surfaces

[AIAA PAPER 72-26] 05 p0607 A72-16917

Papers on critical and exploratory flight testing covering rotary wings, lifting bodies and jet engine airstart

06 p0758 A72-18487

Rocket powered air launched lifting body reentry vehicles testing, stressing performance, handling qualities and crew preparation

06 p0892 A72-18494

Subsonic three dimensional potential flow computational method lifting aerodynamic configurations analysis and design

[AIAA PAPER 72-188] 07 p0907 A72-18958

Downwash behind lifting surface related to loading in ideal incompressible gas by equations of motion linearization

07 p0908 A72-19110

Aircraft performance parameters in terms of effect on lifting system service and fatigue life and on design

07 p0912 A72-19111

Book on matrix structural analysis covering matrix algebra concepts, direct stiffness matrix methods, lifting surface, nonlinear truss and structural partitioning analysis, etc

07 p1092 A72-19908

Optimal configuration of lifting bodies for hypersonic speeds, noting negligible effect of blunt leading edges

10 p1418 A72-24536

Lift variation effect on rolling reentry vehicle trajectory, calculating deviation from zero-lift impact point

10 p1552 A72-24651

Parachute based recovery system for experimental lifting body LB-21 developed and flight tested

12 p1877 A72-27411

LB 21 and space shuttle orbiter aerodynamic testing, discussing computer program supplanting reentry vehicle free flight aerodynamic testing

13 p1894 A72-28934

Sonic boom magnitude and location in stratified atmosphere calculated from gas dynamical equations for lifting body of revolution

13 p1898 A72-29585

Vortex-lattice method for subsonic aircraft aerodynamic coefficients calculation, verifying results with airbus lifting surface wind tunnel test data

15 p2178 A72-31401

Bumerang lifting body design for reentry vehicles, discussing optimal configurations and experimental flight testing

16 p2462 A72-33050

Transonic viscous flow around lifting two-dimensional airfoils

[AIAA PAPER 72-678] 17 p2486 A72-35479

Supercritical aerodynamics technology, noting lifting surface cross sectional profile and structural weight reduction

19 p2746 A72-37678

The application of non-planar lifting surface theory to the calculation of external-store loads

[AIAA PAPER 72-971] 22 p3135 A72-42340

Flutter analysis and unsteady pressure fields induced by pitching motions of wall mounted sweepback wing, verifying experimentally lifting surface theory in high subsonic range

22 p3241 A72-43094

LIFTING REENTRY VEHICLES

Reentry glider approximate optimal atmospheric entry trajectories, maximizing function of terminal velocity, altitude, flight path and heading angles subject to three terminal nonlinear constraints

01 p0128 A72-10377

Zirconium diboride-silicon carbon-graphite composition for lifting entry vehicle hot leading edges, investigating mechanical behavior by tension and flexural tests

01 p0091 A72-10767

Thin shock layer theory of lifting properties of reentry caret and flat delta wings and waveriders at high incidence angles and Mach number

02 p0152 A72-12345

Lifting reentry vehicle Bumerang design and development, discussing experimental verification of theoretical design concepts by aircraft launched unmanned flying model

05 p0724 A72-16312

Delta wing configuration design with anhedral heat shield for high lift reentry in 6-20 Mach number range [AIAA PAPER 72-132]

09 p1259 A72-22501

Real time estimation of trajectory for lifting reentry vehicle of shuttle orbiter type, discussing iterated nonlinear filter and adaptive filter [AIAA PAPER 72-874]

20 p2966 A72-39126

Theoretical and experimental investigations on the problem of aerodynamic heating of re-entry vehicles. [ICAS PAPER 72-39]

21 p3130 A72-41164

Lifting entry optimization equations for fixed angle of attack with path control for roll modulation of lift, considering space shuttle orbiter configuration [AIAA PAPER 72-933]

24 p3443 A72-45435

Aerodynamic characteristics of two-dimensional waverider configurations.

24 p3365 A72-45793

LIFTING ROTORS

Helicopter rotor tip drag relief estimate based on two dimensional drag divergence with Mach number, airfoil parameters and flight conditions

02 p0154 A72-12882

General solution for thin airfoil rectilinear motion in ideal incompressible gas, applying to rotor blade lift calculation

09 p1260 A72-22860

Bell lifting rotor systems, examining company contributions in electronics and avionics

10 p1421 A72-24877

Random vibration statistics of lifting rotors with feedback controls, solving response variance matrix by random inputs shaping filters

13 p2057 A72-29096

Integral equation for calculation of unsteady aerodynamic forces on helicopter lifting rotor blades, taking into account air compressibility [ONERA, TP NO. 1081]

13 p1895 A72-29671

Russian book - Experimental studies of helicopter aerodynamics.

20 p2887 A72-39598

V/STOL aircraft configurations with lifting counter-rotating disks, presenting aerodynamic coefficients from rotating water tank experiments

21 p2990 A72-41070

LIFTING SURFACES

U LIFT DEVICES

U LIFTING BODIES

U SURFACES

LIGHT [VISIBLE RADIATION]

NT AIRGLOW

NT COHERENT LIGHT

NT DAYGLOW

NT GEGENSCHIEIN

NT GEOCORONAL EMISSIONS

NT LIGHT BEAMS

NT NIGHTGLOW

NT POLARIZED LIGHT

NT SKY RADIATION

NT SUNLIGHT

NT TWILIGHT GLOW

NT ZODIACAL LIGHT

Gravitational lens effect in black holes detection, computing light curves

03 p0416 A72-13011

DT Cyg and T Vul cepheid variables light curves and periodic variations from photoelectric observations

03 p0416 A72-13018

Light distribution photometry in Japan, discussing photometers, luminous flux integration and source distribution and positioning errors

03 p0358 A72-13426

Critique of quasar model of independent random pulse emitting sources conglomeration, noting brightness fluctuations incompatibility

03 p0435 A72-13802

Telescopic meteors light curves, showing maximum point brightness distribution in visible trajectory with respect to stellar magnitudes

03 p0438 A72-13985

Quasar radio and optical luminosity evolution, criticizing Arakelian method

03 p0439 A72-14297

Light wave electric field Franz-Keldysh effect on GaAs absorption edge, using electroabsorption, electrophotorefractive and photoconductivity spectrum and internal photoeffect analysis

04 p0561 A72-14621

Structural lipids role in accumulating light energy during prebiological evolution, using conductance studies in lipid-chlorophyll-water system

04 p0468 A72-14779

Blue green algae *Anacystis nidulans* photorecovery after Co 60 gamma radiation exposures, using white and red light

04 p0475 A72-15516

Optical spectra of compact objects, reviewing emission line spectra of quasars

05 p0716 A72-16372

Optical radiation from plasma discharge of electron bombardment mercury ion thruster, discussing electron temperature and primary electron fraction [AIAA PAPER 72-205]

05 p0706 A72-16851

Eclipsing variable binary AI Draconis BV photoelectric observations, using wideband filters

06 p0882 A72-18007

Observed light curve amplitude phase relations in Ap magnetic star UVB system, using oblique rotator model

06 p0882 A72-18008

Photon counting system for low level radiation measurement in UV visible region, discussing simplifications

07 p0983 A72-19133

Wave front division interferometry for small scale solar features study at visible wavelengths

07 p1076 A72-19598

Light curve of TW Delphini from visual observations, noting relationship to RV Tauri-type stars

10 p1546 A72-24830

Field and geodetic line equations for light rays in open and closed isotropic radiative universe model

10 p1549 A72-25059

Optical radiation from Hg bombardment ion thrusters downstream regions due to excited atoms radiative decay, examining exhaust interference with star tracker

11 p1707 A72-26182

Be foil electrical resistance change during and after pulsed laser irradiation and annealing

12 p1853 A72-27067

High angular resolution optical system to measure light reflection from rough surfaces

13 p2002 A72-28513

D region chemistry based on earth albedo effects from airborne radio sounding experiments, suggesting visible light energy flux role

13 p1950 A72-29342

Carbon dioxide arc plasma emissivity in visible range at atmospheric pressure and 6500-9500 K, discussing diatomic carbon concentration

13 p2016 A72-29520

Single layer overcast clouds visible light angular transmittance profiles, noting correlation with hemispheric and narrow-angle pyrheliometric transmittances

13 p1995 A72-29621

Pulsed laser plasma temperature determination by radiation measurements in X ray and visible spectral regions using foil method

13 p2018 A72-29887

Variable circular polarization of X ray star SCO X-1 optical radiation due to Thomson scattering in magnetoactive plasma shell

15 p2304 A72-31328

Electro-optical media for initial light radiation frequency shift maximum, analyzing circular light/modulating wave interactions

15 p2197 A72-31880

IR and visible parametric laser image upconversion experiments, demonstrating wavelength dependence on view field by black body radiometric measurements

15 p2249 A72-32152

Visible and UV stimulated emission in plasma of direct pinch discharge on Ar II and III ions, discussing application possibility to plasma diagnostics

16 p2400 A72-33297

Visible and invisible nonionizing radiation produced human injuries, considering visual and retinal effects and induced thermal stresses

17 p2499 A72-34300

Compact extragalactic nonthermal sources.

17 p2604 A72-34519

Laser optical and IR radiation attenuation in atmospheric precipitation, considering snow, rain and drizzle

18 p2697 A72-36103

On depolarization of visible light from water clouds for a monostatic lidar.

18 p2706 A72-36646

Long range holography theory based on reference beam technique for removing distorting effects of atmosphere on imaging, discussing visible light use

19 p2796 A72-37579

Venus observation experiment with the aid of a television system

19 p2858 A72-37820

Evaluating the light from the sun.

19 p2790 A72-37933

Emission lines and optical continuum of Seyfert radio galaxy 3C 120 from spectrophotometric scans

20 p2965 A72-38905

Mechanism and controlling factors of infrared-to-visible conversion process in Er³⁺/ and Yb³⁺/doped phosphors.

21 p3096 A72-40186

Search for high frequency optical variability in X-ray sources.

21 p3100 A72-40685

Gravitational deflection of light by radially and cylindrically symmetric masses, considering effect on apparent luminosity of distant object

22 p3204 A72-42000

Use of light transformers in organic dye lasers

23 p3295 A72-43413

Be foil electrical resistance change during and after pulsed laser irradiation and annealing

24 p3432 A72-45720

LIGHT ABSORPTION

U ELECTROMAGNETIC ABSORPTION

LIGHT ADAPTATION

Sensitization by annular surrounds, tracing early light and dark adaptation curves

03 p0317 A72-13936

Visual adaptation to light and dark in humans and animals, discussing cellular mechanisms

06 p0762 A72-17720

Human vision light adaptation effects on dichromatic color matches for bipartite centrally fixated circular matching field

07 p0927 A72-19033

Computerized simulation from model of human pupillary motor behavioral response to light, accommodation and fusional inputs

07 p0928 A72-19310

Stereoscopic acuity for photometrically matched background wavelengths at scotopic and photopic levels, plotting variable depth error as function of retinal illuminance

10 p1425 A72-24269

Average evoked potentials correlates of two flash perceptual discrimination in cats, discussing parallel changes as function of interflash intervals and peripheral level

10 p1427 A72-25178

Foveal luminosity magnitude estimations validity, measuring relative effects of preadaptation and contrast

10 p1427 A72-25179

Flicker adaptation, discussing intermittent lights effect on apparent brightness

10 p1427 A72-25181

Gain control of cat retina rapid light adaptation process to attenuate signals reaching retinal ganglion cells from photoreceptors

12 p1760 A72-27299

Physiological effects of intense anticollision flash light backscatter pulses on instrument rated pilots

12 p1775 A72-28303

Illumination intensity effects on circadian periodicity and behavioral thresholds in Rhesus monkey, demonstrating exception to Aschoff rule

13 p1906 A72-29844

Opponent color responses of monkey optic tract fibers to monochromatic lights, using chromatic adaptation and microelectrode recording

15 p2184 A72-31369

Colorimetric photometric matching tests, showing subject differences in parafoveal spectral sensitivity indicated by photopic curve peaks

17 p2508 A72-34882

Linear-nonlinear-linear transition as a function of frequency in the retinal response to light.

17 p2508 A72-34885

Psychophysical procedures to investigate selective visual adaptation to light of different wavelengths from test gratings with various orientations and spatial frequencies

19 p2756 A72-37829

Spatial interaction with different-diameter stimuli matched on the basis of threshold, luminance, or total luminous flux.

21 p3004 A72-40152

The detectability of a brief gap in a pulse of light as a function of its temporal location within the pulse.

21 p3002 A72-41023

Localization and dynamic changes of glycogen in frog retina adapted to darkness or light, I, II.

23 p3258 A72-44377

Photopic and scotopic contributions to the human visually evoked cortical potential.

23 p3261 A72-44380

Component analysis of electroretinogram in dark and light adapted sheep eye, noting rod and cone receptor potentials and transient and dc responses

23 p3261 A72-44382

Line length detectors in the human visual system - Evidence from selective adaptation.

23 p3258 A72-44384

The suppression-recovery effect in relation to stimulus repetition and rapid light adaptation.

24 p3372 A72-44909

LIGHT AIRCRAFT

NT PIPER AIRCRAFT

General aviation type light airplanes pilot workload during steep landing approach, comparing flight tested

control response parameters with handling qualities criteria
[AIAA PAPER 72-125] 05 p0613 A72-16941
Energy absorbing seat design for light aircraft, describing development and static and dynamic testing [SAE PAPER 720322] 11 p1583 A72-25585
Commercial applications of quiet light aircraft technology, discussing cost and noise reduction [SAE PAPER 720339] 11 p1576 A72-25596
Flight tests of stability augmentation system for light airplane improving pilot control during IFR encounter 12 p1754 A72-27513

Small aircraft navigation over 10-400 mile course segments by raw OMEGA phase information dc presentation on conventional ID-249 course deviation indicator 13 p1999 A72-29201

Low altitude gust load spectra above Czechoslovak territory interpreted in terms of equivalent velocity cumulative frequencies for light aircraft 14 p2071 A72-30282

German Bo 105 five/six seat light utility helicopter with rigid glass-fiber reinforced plastic rotor blades, presenting design and performance 14 p2072 A72-30678

Book on airfoil section designs for light aircraft covering wind tunnel studies of lift drag ratio as function of angle of attack 15 p2179 A72-32250

The integration of composite structures into aircraft design. 17 p2492 A72-35281

The New Zealand light aircraft fatigue meter program. 24 p3401 A72-44735

Effects of variations in lift and drag response to longitudinal control on the ease and quality of landing. 24 p3368 A72-45333

LIGHT ALLOYS

NT ALUMINUM ALLOYS
NT BERYLLIUM ALLOYS
NT MAGNESIUM ALLOYS
Aircraft light alloy integral construction for stress concentration and fatigue failure avoidance, describing continuous casting process, stress relieving and ultrasonic flaw testing procedures 07 p0995 A72-19725
Russian papers on light and nonferrous alloys structure and properties covering phase diagrams, alloying effects, reduction, crystallization and recrystallization, solid solutions decomposition, etc 14 p2123 A72-31027
Heat treated light alloy bar deformation, temperature and time factor effects macrostructure and mechanical properties 14 p2124 A72-31038

Composition, strength and plasticity of ultralight Mn-Li alloys with two-phase alpha-beta base 14 p2125 A72-31040

LIGHT AMPLIFIERS

Axial mode locking and equidistant frequency generation in solid state lasers due to active medium saturation, using self consistent equations with broadened amplification line 01 p0079 A72-10347

Microwaves and optical generation and amplification - Conference, Amsterdam, September 1970, covering microwave tubes, solid state devices and quantum electronics 01 p0044 A72-11278

Saturation effect on power gain-bandwidth product of carbon dioxide regenerative ring laser amplifiers operating below threshold 03 p0366 A72-12964

HCN laser amplifier gain measurement at IR wavelengths in gas mixtures by recording with pyroelectric receiver 03 p0368 A72-13667

Superradiative properties of high gain flashlamp-pumped dye laser amplifier, determining small signal amplification as function of pumping power and frequency 03 p0369 A72-14393

Superregenerative linear mode amplification in Q switched He-Xe laser as function of resonator phase, length and signal angle 04 p0531 A72-15147

Amplitude characteristics of Q switched He-Xe laser at 3.5 microns, using rotating reflection prism and velocity equations 04 p0531 A72-15149

Laser radiation amplification, investigating opposing laser pulses interaction in plasma 05 p0668 A72-16414

Stimulated Raman emission in glass fiber optical waveguides with low threshold broadband gain, permitting construction of wideband amplifiers and oscillators 07 p0953 A72-18876

Light amplifier steady state pi pulse local instability against amplitude perturbations in absence of relaxation or inhomogeneous broadening 07 p1002 A72-19204

High power nitrogen-carbon dioxide cross beam electric discharge convection laser amplifier with rectangular channel 07 p1003 A72-19216

Self focusing of laser amplifier beam with Gaussian transverse intensity profile, discussing sample length and beam diameter, convergence and divergence [AD-741092] 07 p0941 A72-19240
Gain saturation measurements in carbon dioxide TEA pulsed amplifiers at 330 torr 07 p1009 A72-20569

German monograph on luminous intensity amplification by means of solid state lasers covering experiments with GaAs and ruby lasers and traveling wave amplifiers 09 p1322 A72-22331

Giant pulse amplification with neodymium-phosphorus oxychloride liquid laser amplifier 09 p1323 A72-22655

High power Nd-glass laser systems, discussing oscillator and amplifier operating parameters optimization 10 p1489 A72-23945

50 MW laser amplifier at 3371 A in molecular nitrogen via transverse electron pumping 10 p1491 A72-24225

IR carbon dioxide laser amplifier with fundamental mode output power in excess of 500 W, describing multistage mirror section design and test results 10 p1492 A72-24581

Time resolved gain in water and water-gas mixtures as function of composition and excitation current, considering relaxation rate in pulsed water vapor laser 11 p1691 A72-25302

Transversely excited pulsed carbon dioxide laser, measuring spatial resolution of gain 11 p1647 A72-26323

Polyhedral radiation energy guides for laser sources and amplifiers, presenting solid state resonator design computation methods 11 p1650 A72-26354

Nd-glass amplifier gain saturation by 1.06 micron light pulses determined by two laser states lifetimes and degeneracies and thermalization rates 12 p1792 A72-27752

Time delayed amplification effects in TEA carbon dioxide lasers, measuring gain decay times for various gas mixtures 12 p1823 A72-27753

High brightness picosecond light pulses generation by laser with multiple internal reflection amplifier for plasma heating 12 p1824 A72-27872

Spatially resolved gain measurements in carbon dioxide laser amplifier, considering gas mixture, flow rate, temperature, pressure and current effects 13 p1967 A72-28448

Nonlinear light amplification in molecular nitrogen amplifier as function of input pulse delay relative to excitation start 13 p1969 A72-29522

IR radiation amplification due to high pressure colliding reacting molecular gas phototransitions 13 p1971 A72-29917

CW oscillator model for laser amplifier, including nonlinear effect of gain saturation 14 p2111 A72-30896

Laser amplifier nonlinear properties by simplification of partial differential equations of amplitude and phase behavior, considering signal pulse deformation 14 p2111 A72-31113

High gain laser amplifier spectral linewidth dependence on external signal or spontaneous emission source, noting saturation role and relevance to interstellar medium radiation 16 p2453 A72-33166

Polyhedral radiation energy guides for laser sources and amplifiers, presenting solid state resonator design computation methods 16 p2402 A72-33707

Frequency dependent loss in self-pulsing ring laser. 18 p2697 A72-36337

Coherent optical signal superregenerative amplification in Q switched gas laser, calculating sensitivity of He-Ne laser light amplifier 19 p2813 A72-38663

Metal-insulator-semiconductor-insulator-metal structure light pulse amplification investigating power gain and photocurrent dependences on applied voltage and applicability as radiation detector 20 p2960 A72-39517

Amplification of mode-locked trains with a liquid laser amplifier, Nd³⁺/POCl₃:ZrCl₄. 20 p2934 A72-39642

The effect of pump coherence on frequency conversion and parametric amplification. 21 p3014 A72-40238

Optical communication channel optimization with binary signals preamplified in optical parametric amplifier, noting amplifier gain and SNR 21 p3016 A72-40783

Regenerative optical link assembly for weak image amplification and spectral conversion, using photosensor as light receiver 22 p3159 A72-42272

The photochemical iodine laser - A high-power laser 22 p3186 A72-42940

German monograph - Amplification measurements and investigation of 'super radiation' characteristics in the case of optically pumped rubies. 22 p3187 A72-43065

Master oscillator/power amplifier laser systems output beam divergence and far field brightness, comparing to Gaussian plane waves 23 p3296 A72-43901

Wave and polarization equations for short coherent light pulses transmission in linear amplifying and absorbing media, noting single pulse formation in lasers 24 p3410 A72-45420

Threshold characteristics of receivers with optical quantum amplifiers. 24 p3412 A72-45617

GaAs semiconductor injection laser and amplifier-absorber emission and light pulse transmission characteristics determination, noting nonlinear absorptivity, bleaching threshold and pulse compression factor 24 p3412 A72-45619

LIGHT BEAMS

Mass spectrometric investigation of high power laser beam plasma on solid target, determining multicharged ion yield, energy, angular distribution and recombination effect 01 p0079 A72-10349

Plasma generation and continuous sustainment by laser beam and optical plasmatron 01 p0109 A72-11073

Double reference beam holograms, evaluating interference effects of misalignment on image reconstruction 02 p0225 A72-11749

Angular straying of gravity center over cross section of diverging light beam in turbulent atmosphere 02 p0181 A72-12594

Instrument and technique for Gaussian mode laser beam parameters measurement 03 p0367 A72-13444

Coherence of excitations produced in crystal by Raman effect via two beam method 03 p0368 A72-13796

Multiphotonic ionization of atomic cesium jet by Q switched ruby laser beam 03 p0392 A72-14061

Self focusing effect of Q switched single mode ruby laser emission in CdS crystal, noting 60 kw minimum threshold power 03 p0369 A72-14064

Laser light beam attenuation, considering turbulent pulsation effects in closed channel fluid flow axial region 04 p0530 A72-14989

Laser induced gas breakdown in chemical reactions and explosions during plasma creation, using time resolved spectroscopy and titanium oxide probes 05 p0624 A72-16666

Heating dynamics of transparent dielectrics exposed to pulsed laser beam operating in free laser mode 06 p0825 A72-17697

Light field in cloud and fog plane layers from stationary collimated point source propagation 06 p0848 A72-17937

Holographic recording of focused images using reference laser beam reflected from object in direction of diffraction maxima 06 p0817 A72-18012

Complex filter properties of Fresnel hologram with converging beam for optical filtration of three dimensional objects in Fourier or image planes 06 p0817 A72-18013

Complete measurement in holography using complex coefficients of conversion matrix of interaction between coherent beam and recorded object 06 p0817 A72-18014

Laser radiation pressure applications to isotope and particle separation, optical levitation, high velocity acceleration and atomic beam analysis 06 p0826 A72-18176

Electro-optical multiple transit laser beam deflection system using KDP crystals and quadrupolar electrode arrangements 07 p1000 A72-19011

High intensity pulsed laser beam heating of solid transparent materials 07 p1002 A72-19212

High power carbon dioxide laser beam applications to deep penetration metal welding, including cutting tests 07 p0994 A72-19214

In-line eight stage digital light deflector with prisms and polarization switch, using Pockels effect with transverse field 07 p1003 A72-19222

Mode conversion effects on Gaussian laser beam in acousto-optical modulation for optical communications 07 p1004 A72-19225

Thermal distortion insensitive TFM mode beam of hf YAG laser for high precision drilling machine 07 p1004 A72-19236

Self focusing of laser amplifier beam with Gaussian transverse intensity profile, discussing sample length and beam diameter, convergence and divergence [AD-741092] 07 p0941 A72-19240

Scintillation measurement of transverse component of wind blowing across laser beam, using correlation method [CLEA PAPER 2,3] 07 p0942 A72-19378

Laser beam diffraction effects on self induced thermal distortion in crosswind, noting dependence on Fresnel number [CLEA PAPER 2,4] 07 p0942 A72-19379

Light beam time stationary multifocal structure in medium with Kerr type nonlinearity, relating maximum energy density and absorption coefficients 07 p0944 A72-19635

Nonlinear wave propagation of laser beams in absorbing fluid media, comparing computer model calculation results with experiment on liquid carbon disulfide cell 07 p1006 A72-19837

Dynamics of flare formation by pulsed laser beam at surface of alkali halide crystals 07 p1007 A72-20124

Phase composition changes, crater formation and metal ejection during erosion by pulsed laser beam 07 p1009 A72-20610

Photogrammetric light beam refraction during aerial surveys, considering air pressure, temperature and humidity gradients in and out of camera carrier 08 p1165 A72-21161

Amplitude-phase distortions of optical beam during nonlinear amplification in carbon dioxide laser with periodic correction 08 p1182 A72-21264

Correlation radius of intensity fluctuations of light beam focused in turbulent atmosphere 08 p1135 A72-21733

Displacement measurement of weight center of light beam transmitted through turbulent atmosphere 08 p1135 A72-21734

Spatial structure of sinusoidally modulated light beam propagating in medium with forward extended scattering characteristics 08 p1136 A72-21742

Fresnel diffraction integrals for irradiance and power distribution calculations of Gaussian beams focused through annular apertures 09 p1352 A72-23334

Speckle reference beam holography for object motion compensation with reduced vibration isolation requirements, discussing CW and pulsed laser use 09 p1314 A72-23338

Neutral density glass collimating absorption lens for ideally uniform laser beams production 09 p1315 A72-23347

Gas jet combination with laser for cutting operations, discussing laser characteristics, beam guiding mirror, lens, nozzle, nozzle gas and workpiece materials 09 p1320 A72-23629

Holographic method for investigating piston type vibrations with phase modulated reference light beam 09 p1317 A72-23682

Vesicular films in electron and laser beam recording suitable for computer output microfilm duplication and graphic arts 10 p1488 A72-23930

Laser beams cross-sectional power distribution measurement by spinning disk scanner, using dual beam oscilloscope for laser beam profile display 10 p1489 A72-23949

Light beams diffraction patterns of thin plexiglass plate for load induced thickness variations, noting crack opening and edge sliding modes stress intensity factors [ASME PAPER 71-APM-QQ] 10 p1553 A72-24178

Reflected light beam transverse shift calculated by energy flux conservation argument, noting circular polarization and quasi-limit total reflection 10 p1513 A72-24932

Cloud height measurements and instrumentation, discussing rotating and fixed beam triangulation and French lidar and ruby laser ranging ceilometers 10 p1484 A72-25094

Far field diffraction of Gaussian light beam passing through ultrasonic cylindrical standing waves 11 p1687 A72-26052

Near and far field energy and power density distributions of multi-transverse mode double discharge TEA laser beam [AD-743823] 11 p1651 A72-26671

Nonlinear thermal effects of atmospheric absorption for high power carbon dioxide laser beams 11 p1651 A72-26747

Correlation function of depolarized finite collimated Gaussian laser beam in atmospheric turbulent medium 11 p1599 A72-26748

Discrete ten stage system for laser beam deflection based on electro-optical effect in lithium niobate crystals 12 p1808 A72-27595

Multiple exposure hologram recording on photosensitive plate for extended reference-beam source 12 p1808 A72-27601

Lens parameters selection and prisms position optimization in light beam to avoid premature damage 12 p1808 A72-27623

Free convection excitation and maintenance method, discussing occurrence around high power laser beam 13 p2063 A72-28628

Destructive changes in rabbit brain and eyes under pulsed laser beam irradiation 13 p1910 A72-29333

Meteorological formations investigation with lidar, discussing laser beam interaction with clouds, fog and precipitation with allowance for multiple scattering 13 p1995 A72-29595

Cosmological geodetic survey network construction via spacecraft tracking and laser beams, calculating power required for balloon satellite photography 13 p1922 A72-29631

Helium use to minimize deflection of modulated laser beam in measurement of free surface motion of expanding annular cylinder loaded by exploding wire 13 p1960 A72-29765

Laser beam propagation in vacuum, imperfectly transparent medium and turbulent atmosphere 13 p1971 A72-29865

Laser radiation time characteristics measurement based on multiphoton processes in opposite light beams, estimating accuracy necessary for registration of ultrashort pulses 14 p2111 A72-30794

Random parameters effect on divergence of focused light beams in turbulent atmosphere, noting light patch dependence on illumination source diameter 14 p2131 A72-30810

Properties of natural waves excited in Fabry-Perot resonator by external laser beams, noting stability dependence on wave type 15 p2245 A72-31420

Light rays total, astronomical and photogrammetric refraction in planetary atmospheres with arbitrary composition 15 p2224 A72-31602

Beam trajectory distortions due to turbulent air refractive index fluctuations in optical transmission line 15 p2197 A72-31885

Two dimensional acousto-optical light beam deflection system for laser recorder error correction 15 p2248 A72-32038

Turbulence and nonlinear thermal blooming effects as cause of refractive attenuation of laser beam intensities 15 p2249 A72-32160

Extended Huygens-Fresnel principle for mutual coherence [cross correlation/ function of finite optical beam propagation in turbulent medium] 15 p2249 A72-32161

Statistical analysis of photocounts of arbitrary spectral profile Gaussian light, discussing two incoherent beams superposition 15 p2277 A72-32231

Interfering beams amplitude modulation, applying optical heterodyne techniques 15 p2202 A72-32676

Correlation function measurements of optical gravity center roaming of spatially limited light beams in turbulent atmosphere 16 p2364 A72-33486

Atmospheric turbulence from illuminance and intensity fluctuation measurements at focused light beam 16 p2364 A72-33488

Turbulent divergence of laser beams along oblique atmospheric path for vertical refractive index distribution, using Markov coherence model 16 p2364 A72-33489

Focused light beam intensity fluctuations measurement during passage through turbulent atmosphere, discussing random walks effects on dispersion 16 p2364 A72-33494

Light field in cloud and fog plane layers from stationary collimated point source propagation 16 p2426 A72-33778

Mathematical model for deuterium slab solid and plasma under laser pulses irradiation, noting shock wave propagation and slab acceleration [AIAA PAPER 72-721] 16 p2439 A72-34027

Analysis of an optical beam waveguide consisting of a tapered lens-like medium and its applications. 17 p2580 A72-34382

Photogrammetric light beam refraction during aerial surveys, considering air pressure, temperature and humidity gradients in an out of camera carrier 17 p2552 A72-34452

Resolution of optical-memory matrices prepared from photochromatic materials when using a focused beam to record information 18 p2692 A72-36658

Propagation of laser beams through the atmosphere. II 18 p2661 A72-36793

Russian book - Refraction of light rays in the atmosphere 19 p2834 A72-37448

Use of generalized theory of optical diffraction for the study of second harmonic generation. 19 p2811 A72-37673

A holographic method for optical adjustment of pulsed laser beams 19 p2811 A72-37674

New proposition of the mechanism of self-focusing of laser beams in semiconductors. 19 p2811 A72-37945

Effect of optical constants on the energy distribution in homogeneous particles illuminated by a parallel beam of light 19 p2812 A72-38216

Distribution of illumination in a point image in the presence of birefringence in the optical system /case of axial symmetry/ 19 p2836 A72-38789

Filaments formation behind nonlinear focus and frequency shift in transient self focusing of light beam in medium with given time dependent permittivity 20 p2953 A72-39502

Optical diffractometer with laser beam having approximately uniform transverse intensity distribution 21 p3051 A72-40210

Light pulse structure and bandwidth bounds in ruby laser with delay line inside variable effective length resonator 21 p3066 A72-40799

Self-aligning comparison beam methods for one-, two- and three-dimensional optical velocity measurements. 22 p3177 A72-42395

Measurement of the electron density distribution in plasmas from the bending of a gas laser beam. 22 p3211 A72-42396

The diffraction of light by progressive supersonic waves: Oblique incidence of light. I - Approximate solution of the Raman-Nath equations. 22 p3207 A72-42852

Geometrical interpretation of Gaussian beam optics. 23 p3288 A72-43877

Interferometric spectropolarimetry - Alternate experimental methods. 23 p3289 A72-43890

Light beam modulated by uniformly spaced circular apertures, calculating Fourier power spectrum for homogeneous and bivariate normal intensity distributions 23 p3289 A72-43900

Evaporation of metallic targets by intense optical radiation 23 p3297 A72-44485

Light beam time stationary multifocal structure in medium with Kerr type nonlinearity, relating maximum energy density and absorption coefficients 24 p3408 A72-44567

Focusing characteristics of CO₂ laser beam. 24 p3409 A72-44776

Initiation of a detonation by a laser beam focused in a gaseous medium 24 p3410 A72-45026

Noise characteristics of a digital system of light-beam deflection 24 p3410 A72-45323

Influence of the heating of a turbulent atmosphere by a light beam on the fluctuations of the beam intensity. 24 p3425 A72-45601

Focusing properties of converging-beam holograms. 24 p3405 A72-45602

Use of oblique-cut lithium niobate in optical-beam control systems. 24 p3411 A72-45606

Some features of the behavior of an intense light beam in a nonideal gas. 24 p3411 A72-45609

Measurement of the angular divergence and of the refraction of a laser beam in the ground layer of the atmosphere. 24 p3380 A72-45611

LIGHT BULBS

U LUMINAIRES

LIGHT COMMUNICATION

U OPTICAL COMMUNICATION

LIGHT DURATION

U FLASH

U PULSE DURATION

LIGHT ELEMENTS

Book on nuclear reactions in stellar surfaces and relations with stellar evolution covering high energy L elements formation, Li-Be observations and thermonuclear and spallative theories 01 p0122 A72-10002

Pulsar produced cosmic rays energy spectrum, investigating light elements origin 06 p0874 A72-18161

Spectrographic analysis of K-type supergiant epsilon Pegasi for effective temperature, surface gravity and heavy and light element abundances 10 p1543 A72-24621

Light elements production from primary cosmic rays spallation in interstellar gas, noting diffusion coefficient of relativistic particles in galaxy 15 p2301 A72-32754

Production of light elements in the solar system. 23 p3335 A72-43487

LIGHT EMISSION

NT BIOLUMINESCENCE

NT CHEMILUMINESCENCE

NT ELECTROLUMINESCENCE
NT FLUORESCENCE
NT INCANDESCENCE
NT LUMINESCENCE
NT LUNAR LUMINESCENCE
NT OPTICAL RESONANCE
NT PHOSPHORESCENCE
NT PHOTOLUMINESCENCE
NT SHOCK WAVE LUMINESCENCE
NT THERMOLUMINESCENCE
NT X RAY FLUORESCENCE

High resolution apparatus to record time dependent light flux variations at 380-700 nm, discussing He plasma decay investigation

01 p0064 A72-10375

Magnetic field effects on ruby laser radiation kinetics and spectral composition, studying crystal heating and light emission

01 p0080 A72-10577

Single mode carbon dioxide laser action from quasi-optical mirror emission channels

01 p0080 A72-10578

Stable red arc 6300 A emission calculation from satellite electron temperature and density data during geomagnetic storms

01 p0061 A72-10893

Optical emission spectrum of Ba and CuO combustion products during nozzle expansion into vacuum

01 p0146 A72-11312

Light emission intensity correlation functions associated with lf oscillations in beam plasma discharge

02 p0263 A72-11421

Crab Nebula pulsar NP 0532 model for interaction and polarization of radio radiation with surrounding media

02 p0277 A72-11772

Neon lower laser level spontaneous emission double resonance phenomena, discussing depopulation rates and resonance line profile changes

04 p0531 A72-15138

Airglow considered as faint light emission during atomic and molecular dissociations in atmosphere, yielding clues to physical and chemical processes from spectrum

04 p0520 A72-15642

Ultrashort light pulse emission during mode locking in ruby lasers in free emission operation, examining first spike radiation

05 p0668 A72-16413

Variable circular polarization in optical emission of X ray source Sco X-1, noting oscillations amplitude

06 p0878 A72-17785

Scintillation crystal light yield dependence on emission energy in particle flux measurements with semiconductor spectrometer

06 p0816 A72-17835

VV Pup binary light variations correlation with primary component variable disk dimensions, considering nova-like processes

06 p0882 A72-18003

Beta Cephei type variable stars, determining KP Persei times of maximum light, mean UBV magnitudes and light ranges

06 p0882 A72-18006

Neutron damage effects on red and green output of GaP light emitting diodes at 300 K

07 p1047 A72-19043

Simultaneous auroral X ray, bremsstrahlung and visible bursts observations from balloons.

07 p1058 A72-19166

Induction period, light emission, pressure change and cool flame explosion limits in butane oxidation, studying reaction products in negative temperature coefficient region

07 p1099 A72-19368

Quasar 3C 273 light variation periodicities search, noting confidence level concerning resonance periods

07 p1073 A72-19424

Magnetic bremsstrahlung energy straggling and radiation reaction, calculating particle and emitted photon distribution

07 p1037 A72-19668

Earth horizons nighttime, twilight and daytime visual observations from manned Soyuz spacecraft, discussing upper atmosphere emission layer structure and aureole development

08 p1158 A72-21148

Spectrophotographic recording of UV auroral emissions during rocket probe flight, noting excitation by electron impact on molecular nitrogen

08 p1159 A72-21225

Light emitting diodes for efficient conversion of electrical energy into electromagnetic radiation, discussing photometry, electrical injection, electroluminescence, design and applications

08 p1141 A72-21430

Rhodium solution laser emission pulse characteristics relation to pumping energy distribution over container end surface

08 p1184 A72-22048

Spectroscopic measurements of light emission from carbon dioxide positive ions and carbon monoxide in metastable He interaction with carbon dioxide

09 p1354 A72-22667

Optical and inner shell X ray transitions in highly ionized Cu, Fe and Ti observed from point plasma source generated in linear vacuum discharge

09 p1360 A72-22833

Visual aurora and Explorer 40 satellite simultaneous observations of VLF radio noise, noting hiss associated with light emissions and associated charged particle flux

[AD-740047] 09 p1299 A72-23006

Spectroscopic techniques for high temperature materials research program, studying light emission from plasmas generated by intense electron beam

10 p1518 A72-23937

Nuclear reaction-produced high energy ion beams for gas laser pumping and output enhancement

10 p1489 A72-23948

Ultramicromanometer based on photomultiplier for low pressure Penning discharge light flux emission measurement

10 p1480 A72-24208

Astronomical identification of optical objects near 5C2 radio sources position, noting probability parameters and measurement error

10 p1546 A72-24837

Sco X-1 simultaneous hard X ray and optical observations from balloon and ground correlating thermal X rays and optical emissions

10 p1530 A72-24949

Time dependent light emission from mesoplasmas in Si p-n junctions in pulse mode, showing carrier heating effect

11 p1700 A72-25780

Auroral spectrum analysis in 1200-4000 A band, obtaining photon emission rates

11 p1624 A72-26402

Luminous emissions of upper atmosphere, discussing relation to airglow and auroral phenomena

11 p1626 A72-26431

Evanescent photons absorption and emission in light excited molecules fluorescence

11 p1691 A72-26745

Combined photon and particle diffusion of two level system with ground and excited atomic states and photon emission-formed radiation field

13 p2001 A72-28509

GaAs doped Si light emitting diode as light source for optical timing system calibration, studying fast luminescent decay characteristics

13 p2000 A72-29763

Visible light flash emission due to strong shock wave of laser spark, investigating strong external magnetic field effect and time variation of luminous intensity

13 p1972 A72-29983

Nocturnal low intensity auroral red arcs observations by meridian scanning photometer, comparing with green emission

14 p2097 A72-30137

Auroral emission spectrum intensity ratios for IBC 2 system observed via aircraft flown digital multichannel photometer

14 p2097 A72-30137

Airglow and auroral OI and NI allowed and spin forbidden transitions for above 9 eV excitation potential lines

14 p2098 A72-30145

Fe light emission for simulated meteor conditions, measuring ionization and spectral emission cross sections for Fe reactions with nitrogen and oxygen for 350-2000 eV

14 p2156 A72-30562

Color photoelectric light pulsations curve of RU Cam variable star during October 1969-August 1970, noting constant mean luminosity and color

14 p2158 A72-30729

Gallium aluminum arsenide light emitting diode thin structures grown on GaP substrates by liquid phase epitaxial method

15 p2290 A72-31381

Laser effect in solution of neodymium oxide in mixture of phosphorus oxychloride and heavy water, presenting preparation procedure

15 p2246 A72-31680

Nitric oxide gas release by rocket in auroral glow to determine atomic oxygen densities in ionosphere via observation of auroral light emission

15 p2226 A72-31936

Light emitting diodes, photodiodes and photon coupled pair temperature compensation schemes, including uses of n-p-n transistors, operational amplifier and thermistor-resistor network

15 p2247 A72-32034

Bremsstrahlung photon emission rate from Maxwellian plasma, determining soft X ray diagnostic techniques applicability for laser produced plasmas

15 p2285 A72-32271

Optical field emission effects on photoelectron emission nonlinearity from metal cathode using ultrashort mode locked laser pulses

15 p2250 A72-32303

Photometric all sky observations of stable auroral red arcs on 8-9 March 1970, determining altitudes of 6300 A, 5577 A and 4278 A emissions

16 p2384 A72-32978

Radio source Oj 287 photometric and polarimetric observations, noting optical intensity and plane polarization variability

16 p2452 A72-33134

Pulsar radio and optical observations, discussing periods, pulse shapes at various frequencies and marching subpulses

16 p2460 A72-33925

Semiconductor optoelectronic devices, discussing light emitting indicator diodes, data display systems, photosensitive arrays and optical data transmission links

17 p2594 A72-34332

Nd-glass laser interaction with singly stimulated two-photon emission and anti-Stokes Raman scattering from metastable state He, calculating cross sections

17 p2565 A72-35831

On the radiation of discontinuous gold films by electric current transmission.

18 p2718 A72-36349

Reliability of semiconductor optoelectronic components - Analysis of the long-term behavior

18 p2670 A72-37138

Electronic and optical phenomena in semiconductors.

19 p2844 A72-37445

Coherent radiation emission by indium antimonide in a transverse magnetic field

19 p2845 A72-38176

Earth horizons nighttime, twilight and daytime visual observations from manned Soyuz spacecraft, discussing upper atmosphere emission layer structure and aureole development

20 p2916 A72-39253

Investigation by the photon count method of the statistical properties of the emission of a laser operating in the mode of several axial oscillations

21 p3063 A72-40784

Injection laser and light emitting diode techniques to transmit digital data in local distribution

21 p3018 A72-40869

Light emitting diodes (LED) materials characteristics, heterojunction band structures and optical spectral ranges, considering application to information processing

21 p3035 A72-41649

Auroral EUV flux observation by Javelin sounding rocket photometers, comparing with visible and X ray emissions

22 p3171 A72-42417

Double star components light aberration dependence on relative velocity of source and observer, considering two reference systems

22 p3225 A72-42458

GaP /Zn-O/ diodes light emission efficiency increase by forward bias, relating to precipitation in n and p layers

22 p3159 A72-42613

German monograph - Amplification measurements and investigation of 'super radiation' characteristics in the case of optically pumped rubies.

22 p3187 A72-43065

A cathode-ray tube with a semiconductor laser screen

23 p3272 A72-43925

GaAs light emitting diodes intensity fluctuations measurements at .025-20 kHz

23 p3297 A72-44190

LIGHT GAS GUNS

Dc X ray timing pulse generator for light gas gun triggering based on projectile interruption technique

15 p2241 A72-32441

LIGHT INTENSITY

U LUMINOUS INTENSITY

LIGHT MODULATION

NT ULTRASONIC LIGHT MODULATION

Parametric amplification of laser waves with amplitude and phase modulation under exponential signal growth applied to Raman scattering picosecond pulse field

01 p0079 A72-10346

Molecular Stark effect modulation of IR carbon dioxide laser radiation, using density matrix technique

01 p0079 A72-10515

Intracavity modulation of high-gain gas laser with traveling light waves nonuniform amplitude distribution, presenting results for lithium niobate crystal resonator equipped He-Ne laser

02 p0183 A72-12762

Gas laser longitudinal mode locking during single sideband modulation with nonuniform broadening in mode intensity distribution

03 p0366 A72-13365

Starlight intensity modulation at discrete radio frequencies due to enhanced ionospheric electron density fluctuations

03 p0438 A72-14096

Statistical properties of random-phase modulated laser beams, calculating coherence functions of optical fields

04 p0528 A72-14580

Carbon dioxide laser modulation by molecular Stark effect in deuterated ammonia, observing pressure broadening coefficient

04 p0528 A72-14585

Carbon dioxide laser Q switching by molecular gases intracavity Stark modulation with sine or square wave electric field, using methyl chloride and difluoroethane

05 p0669 A72-16609

Wideband electro-optic FM of laser light for optical communication, discussing modulator design, construction and testing

[AIAA PAPER 72-177]

05 p0631 A72-16961

Laser radiation intensity modulation by time varying magnetic field

06 p0825 A72-17685

Piezoresonance modulation of IR amplitude in GaAs crystal by electric field at single, doubled and quadrupled frequencies

06 p0866 A72-17843

Harmonically modulated reflected light signals phase shift and demodulation, assuming single scattering

06 p0848 A72-18047

Optical image transfer functions characteristics and modulation in isolated retinas and retinal receptors, noting similarity to optical fiber bundles

07 p0916 A72-19027

Carbon dioxide laser IR radiation modulation by application of Stark effect in various molecular absorbers, showing absence of saturation

07 p1000 A72-19035

Gases for carbon dioxide laser lines modulation by molecular Stark effect, presenting data for fluoroethane, monomethylamine, methyl mercaptan, vapors methanol and trichloroethylene

07 p1001 A72-19193

Performance characteristics of electro-optical material cadmium telluride for intracavity modulator of carbon dioxide lasers

07 p1003 A72-19223

Mode conversion effects on Gaussian laser beam in acousto-optical modulation for optical communications

07 p1004 A72-19225

Carbon dioxide lasers and GaAs electro-optical crystals 110-MHz bandwidth with coupling modulation technique

07 p1005 A72-19413

Holographic information storage with reference wave modulation by Fabry-Perot interferometer, using two coherent sources

07 p0985 A72-19417

Optical bidirectional modulator for two beam spectrophotometer, using tuning fork as oscillatory system

07 p0988 A72-19962

Laser applications in metrology and geodesy, discussing use of beam directionality for alignment purposes, interference patterns and interferometry, modulated light methods, optical Doppler methods, etc

07 p1007 A72-20222

Internal asynchronous modulation of multifrequency He-Ne laser with Doppler broadened transition line

08 p1181 A72-20793

Optimal continuous recording of amplitude-phase distributions on spatial carrier frequency for light wave modulation and optical antenna simulation

08 p1132 A72-21263

Spatial structure of sinusoidally modulated light beam propagating in medium with forward extended scattering characteristics

08 p1136 A72-21742

Light modulation by exciton electric absorption in thin high impedance recrystallized CdTe films within strong electric fields, showing spectral distribution curves

09 p1366 A72-22419

Multimode ring laser gyro phase modulation theory based on oppositely directed traveling waves

09 p1324 A72-23084

Multimode ring laser gyro with intracavity phase modulation, discussing experimental results concerned with lock-in at low rotation rates

09 p1324 A72-23085

Simulated superposed coherent and chaotic /thermal/ radiation of arbitrary spectral shape, using laser beam modulation and photocount statistics

09 p1352 A72-23240

Geodetic optical distance measuring instruments with electro-optical polarization modulators, comparing characteristics of four possible configurations

09 p1314 A72-23336

Electro-optical Fabry-Perot modulator with KDP and ADP crystals as optical resonators, determining modulation and frequency response characteristics

10 p1492 A72-24583

Nonlinear interaction between circular coherent light and modulating electromagnetic waves in presence of quadratic electrooptical effect, noting frequency shift

10 p1493 A72-24912

Muller matrix derivation for microwave light modulation studies in quasi-homogeneous magneto-optical

and electrooptical media, taking into account finite light speed

10 p1493 A72-24914

Carbon dioxide-helium-nitrogen mixture laser, comparing GaAs, CdSe, CdS and CdTe electro-optical crystals suitability for radiation modulation at 20.6 microns

12 p1822 A72-27610

Ruby laser electro-optical modulator with low modulation voltage, discussing layout, operating principle and laser energy characteristics

12 p1822 A72-27611

Laser irradiance modulation effect on high error fringes brightness in time average hologram reconstruction, noting exposure time increase

12 p1809 A72-27682

He-Ne laser light modulation with lithium niobate crystals, noting lower light power and modulator volume requirements, better mechanical properties and lower thermal sensitivity

13 p1969 A72-29632

Helium use to minimize deflection of modulated laser beam in measurement of free surface motion of expanding annular cylinder loaded by exploding wire

13 p1960 A72-29765

Modulation transfer functions of optical system producing image of distant object in turbulent boundary layer of atmosphere, determining refractive index fluctuation intensities

14 p2130 A72-30241

Book on coherent optical computers covering lens design, power sources, computation mathematics, modulation, detection, digital techniques and applications

15 p2203 A72-31499

Sine, square and triangular wave targets for optical transfer function measurements, comparing modulations in partial coherent light under different illumination conditions

15 p2246 A72-31613

Optical communications photodetector sensitivity assessed from input power ratio of ideal and actual detector, noting amplitude modulated systems

15 p2235 A72-31621

Gas laser asynchronous coupling modulation, examining dependence on lasing threshold, optical spectrum and transition line shape

15 p2246 A72-31660

Design data of guided wave structures for electro-optical modulation, evaluating propagation wave numbers, attenuation rate, phase modulation rate and dispersion characteristic

15 p2246 A72-31667

Light signal modulation by traveling wave in circular waveguide with coaxial KDP crystal

15 p2207 A72-31881

Modulated laser beam record wideband signals on photographic film, discussing noise sources and compensation methods for SNR improvement

15 p2248 A72-32039

Two dimensional optical phased array beam steering based on membrane light modulation and high speed digital techniques

15 p2248 A72-32053

Variable area modulation dual signal recording onto single input device for coherent optical correlators

15 p2249 A72-32165

Microwave modulated incoherent light for large volume scenes holography, noting object image reconstruction by coherent light transillumination of hologram

15 p2242 A72-32675

Interfering beams amplitude modulation, applying optical heterodyne techniques

15 p2202 A72-32676

Optical system production acceptance test based on modulation transfer function, discussing instrument design and test philosophy

16 p2389 A72-32847

Feedback averaging procedure application to M-ary polarization modulated laser communication system, obtaining error rate improvement over systems without feedback

16 p2362 A72-33215

Modulation measurement applied to the focusing of aerial cameras

17 p2558 A72-35948

He-Ne laser radiation modulator at 1.5 GHz using X and Z cut lithium niobate crystals in toroidal microwave cavity

18 p2697 A72-36113

Generalized multi-dimensional sampling theory and applications in optical systems

18 p2672 A72-36333

Hue shifts accompany phase induced modulation enhancement of sinusoidally flickering lights

18 p2651 A72-36613

Variation of the longitudinal electric field by the internally modulated beam in a He-Ne laser

19 p2810 A72-37408

Passive mode-locking and Q-switching of high power lasers by means of the optical Kerr effect

19 p2811 A72-37844

Fluid mechanics anemometry based on laser light frequency modulation /Doppler effect/, describing measurement of extensions of vortices and oscillations in flow boundary layers

19 p2801 A72-37934

Intracavity modulation of high-gain gas laser with traveling light waves nonuniform amplitude distribution, considering lithium niobate crystal resonator equipped He-Ne laser

20 p2931 A72-39068

Pulse generator for modulation of a low-voltage Pockels cell

20 p2933 A72-39525

Optical propagation in space-time-modulated media using many-space-scale perturbation theory

21 p3014 A72-40142

Frequency deviation equations for FM gas laser with modulation achieved by resonator optical length variations

21 p3063 A72-40798

Generation of infrared radiation in a metal-to-metal point-contact diode at synthesized frequencies of incident fields - A high-speed broad-band light modulator

22 p3157 A72-41971

Light beam modulated by uniformly spaced circular apertures, calculating Fourier power spectrum for homogeneous and bivariate normal intensity distributions

23 p3289 A72-43900

Approximate formulae for mixed modulated coherent and partially polarized chaotic light

24 p3425 A72-44769

Measurement of the modulation transfer functions of focusing screens

24 p3425 A72-44770

Time dependence of laser characteristics on external HF modulation of parameters by mirror oscillation and electrooptical and acoustooptical effects, noting laser mode locking

24 p3410 A72-45416

Laser frequency measurement by comparison with stable molecular oscillator Doppler shift produced by reflection of UHF modulated coherent optical signal

24 p3411 A72-45425

Effect of plasma mirror in the breakdown of air in a CO2 laser cavity

24 p3412 A72-45775

LIGHT PRESSURE

U ILLUMINANCE

LIGHT PROBES

U LIGHT BEAMS

LIGHT SCATTERING

NT HALOS

Laser light scattering by fuel droplets in flame combustion zone, measuring intensity distribution with contactless optical probe

01 p0066 A72-10495

Water quality monitoring by radiative transport equation for reflectance measurements of laser light scattered from turbid water polluted with absorber and scatterer particles

[AIAA PAPER 71-1098]

01 p0058 A72-10547

Atmospheric aerosol chemical composition analysis by nephelometer light scattering measurement of suspended particle mass concentration, visibility and size distribution and scattering-humidity relationship

[AIAA PAPER 71-1101]

01 p0058 A72-10549

Multiple scattering of incident coherent light wave propagating in turbulent medium, considering irradiance intensity fluctuations and spectral and correlation characteristics

01 p0103 A72-11167

Pulsed hf discharge in hydrogen based on laser light scattering on plasma electrons, noting position of satellites in spectra

02 p0237 A72-11406

Plasma state variables diagnosis using laser light scattering

02 p0263 A72-11697

Topmost soil layer moisture content measurement by reflected visible light polarization enhancement

02 p0209 A72-11794

Low temperature plasma electron density measurements using ruby laser light scattering method

02 p0264 A72-12210

Jovian disk brightness distribution at zero phase angle by expanding scattering indicatrix in Legendre polynomial series

02 p0282 A72-12329

Scattering media visibility improvement analysis, using theoretical evaluations and experimental electro-optical measurement techniques in fog and underwater

02 p0253 A72-12644

Ruby and Nd lasers fundamental emission effects on excitation of stimulated Raman scattering in liquid and crystalline media by second harmonics

03 p0366 A72-13364

Focused image holography in multimode He-Ne laser radiation, using diffusely scattered reference wave and lens for high quality reconstruction

03 p0357 A72-13370

Electrostrictively induced stimulated Brillouin light scattering effect on atmospheric depolarization, ob-

- taining solutions for steady state and transient conditions
[AD-736316] 03 p0367 A72-13429
- Plasma conductivity frequencies, including electromagnetic wave propagation in alternating field and scattered light intensities
03 p0396 A72-13653
- Plasma satellite linewidth broadening due to density inhomogeneity, considering evidence based on light scattering from Ar plasma jet
04 p0559 A72-15355
- Boundary effects on light incoherent scattering by dispersing molecules, using quantum statistics
04 p0490 A72-15398
- Inverse scattering by ray optics for conducting wedge, considering TE and TM edge diffracted fields
04 p0551 A72-15671
- Light scattering time dependence, erythrocyte aggregation rates and hydrodynamic characteristics in ox, pig and horse blood stream
05 p0621 A72-16230
- Short narrow light pulse reflection from thick turbid medium with strong anisotropic scattering, obtaining backscattering signal power from unsteady transport equation solution
05 p0690 A72-16292
- Atmospheric optics and geophysics problems modeling arrangement reproducing radiation field within light scattering medium
05 p0658 A72-16293
- Laser pulse induced stimulated Raman scattering (SRS) in linearly dispersionless medium measuring delay between laser and Stokes pulse maxima by photon absorption fluorescence technique
05 p0693 A72-17170
- Data transmitting dielectric light waveguide production problems, noting light scattering and absorption losses due to glass material imperfections
06 p0825 A72-17774
- Narrow light beam attenuation and scattering characteristics in turbid medium as function of distance from source from transport equation solution
06 p0774 A72-17938
- Twilight atmospheric sounding in oxygen absorption bands to reduce noise level in secondary light scattering
06 p0807 A72-17943
- Harmonically modulated reflected light signals phase shift and demodulation, assuming single scattering
06 p0848 A72-18047
- Lunar photometric studies, discussing surface light scattering properties, data reduction and relative and systematic errors in brightness
06 p0817 A72-18224
- Thermal equilibrium fluctuations and Rayleigh light scattering in isotropic gyrotropic continuous medium with internal rotational degrees of freedom
07 p1034 A72-18909
- Angular transmittance model of visible light scattering through overcast cloud layer
07 p1030 A72-19411
- Spherical scatterers extinction efficiency effect on photometer optical systems transmittances, using Mie equation and numerical methods
07 p0987 A72-19831
- Stokes Q branch fundamental vibrational Raman light scattering cross sections and depolarization ratio measurement for molecular gases
07 p1038 A72-20292
- Nonlinear mode relationship of gas ring laser due to light scattering at inhomogeneities in active medium
07 p1009 A72-20612
- Atmospheric light scattering matrices from nighttime air flows, showing climatic variability and similarity between Crimean and Moscow measurements
07 p1031 A72-20700
- Scattered light coherence in optically thin vapors and ideal gases in energy level crossing experiment formulated in terms of autocorrelation function
08 p1206 A72-21294
- Velocity measurement by Doppler light scattering due to particle finite residence time, estimating ambiguity and noise effects on turbulent spectra of frequency fluctuation
09 p1305 A72-22302
- Light scattering by spherical particles, noting cost effectiveness of logarithmic derivatives calculation method
09 p1350 A72-22412
- Atmospheric temperature vertical profiles by laser Raman backscatter measurements
09 p1307 A72-22439
- Nonuniform non-Lambertian diffusely scattering surface optical transfer characteristics and initial irradiance distribution inside sphere, discussing spherical harmonic moment measurement
09 p1309 A72-22610
- Thin GaP film composition and structure determination by laser Raman scattering
09 p1314 A72-23345
- CW carbon dioxide laser Doppler radar for remote measurement of atmospheric wind velocity and turbulence, obtaining Doppler signal via homodyned radiation scattered by airborne particles
09 p1315 A72-23407
- Raman spectra of azoanisole and anizaldazine in liquid crystal states excited by Ar laser, revealing lattice vibrations attenuation near transition point
10 p1490 A72-24042
- Air pollution monitoring by remote optical sensing techniques based on light scattering measurements, noting suitability of high power laser probes
10 p1480 A72-24100
- Viking Lander light scattering experiment to detect microbial growth from aqueous turbidity changes in contact with Martian soil
10 p1430 A72-24387
- Coherent and noncoherent modes of optical beating in laser Doppler velocity measurement using light scattered from single and multiple particles
10 p1481 A72-24412
- Induced Compton scattering and nonlinear electromagnetic wave propagation in laser beam focused plasma
10 p1522 A72-24605
- Maximum likelihood receiver performance for optical detection of multimode laser or scattered radiation, considering photocounting distribution, decision threshold and error probability
10 p1452 A72-24681
- Low temperature plasma electron density measurements using ruby laser light scattering method
11 p1693 A72-25706
- Ruby laser light scattering method for measuring magnetic field direction in Tokamak plasma, testing validity by numerical calculation of scattered spectrum
11 p1694 A72-25793
- Atmospheric constituents dimension, composition and dynamics from optical radar echo observation of laser light scattering
11 p1592 A72-25849
- Magnetic field direction measurement in Tokamak toroidal plasma by laser light scattering, using Fabry-Perot interferometer
11 p1697 A72-26583
- Light absorption and scattering factors in whole blood related to hemoglobin concentration, discussing oxygen saturation, cardiac output and pathological conditions
11 p1588 A72-26630
- Glass sample mechanical strength testing, considering abrasion process, concentric ring stress calculation and laser light scattering techniques
12 p1832 A72-27007
- Daytime sky polarimetry of scattered light in atmosphere during solar eclipses
12 p1800 A72-27141
- Ruby laser coherent light scattering by cylindrical electron beam under longitudinal magnetic field
12 p1820 A72-27586
- Laser emission intensity enhancement based on stimulated Brillouin scattering effect by raising pumping level, energy density and pulse duration
12 p1821 A72-27587
- Spatial noise in holographic images of diffusely scattering objects with allowance for recording apparatus resolving capacity
12 p1810 A72-27871
- Multiple laser light scattering from turbid medium, relating reflectance to polluted water parameters for aerial photographic surveillance
12 p1826 A72-27948
- Physiological effects of intense anticollision flash light backscatter pulses on instrument rated pilots
12 p1775 A72-28303
- Russian papers on light scattering covering electromagnetic propagation in turbid media, transport equation solution methods, unsteady scattering, spectral line radiation and nonlinear phenomena
13 p2001 A72-28501
- Anisotropic light scattering layer radiation intensity dependence on optical coordinate, obtaining integral equations for seminfinit and finitely thick layers
13 p2001 A72-28502
- Asymptotic and exact methods for light scattering problems in radiative transport theory, discussing finitely thick plane layer luminescence
13 p2001 A72-28503
- Numerical methods to solve boundary value problems of monochromatic transport equations in light scattering media optics
13 p2001 A72-28504
- Monte Carlo method for radiative transport theory problems, considering mathematical models of light scattering media and photon trajectory random elements
13 p2001 A72-28505
- Light propagation from unsteady source through homogeneous turbid light scattering media, using analytic and numerical methods for unsteady radiative transport equation solution
13 p2001 A72-28507
- Light propagation patterns in absorbing and scattering medium with radiation density dependent optical properties
13 p2002 A72-28510
- Light scattering media optical characteristics measurement techniques and equipment
13 p1955 A72-28515
- Daytime sky brightness and scattered light polarization, emphasizing atmospheric radiation field characteristics
13 p1945 A72-28516
- Plant leaves biochemical activities study by light scattering techniques, discussing photometric, spectroscopic and bionics methods
13 p1955 A72-28518
- Human and instrumental observations of aviation visibility, discussing measurements of extinction coefficient and light scatter and sensors testing
13 p1992 A72-28845
- Jovian disk brightness distribution at zero phase angle by expanding scattering indicatrix in Legendre polynomial series
13 p2039 A72-29213
- Meteorological formations investigation with lidar, discussing laser beam interaction with clouds, fog and precipitation with allowance for multiple scattering
13 p1995 A72-29595
- Electron density and temperature measurement from scattering of laser radiation in plasma within axisymmetric toroidal magnetic mirror machine
13 p2017 A72-29609
- Opaque scatterers disadvantages in interferometric images recording of transparent objects obtained by double exposure holography, noting phase type diffraction gratings
13 p1958 A72-29616
- Carbon dioxide laser light scattering measurements of turbulence in high beta collisionless plasma shock wave
13 p2018 A72-29853
- Angular distribution of first Stokes component for stimulated combinational scattering investigated under various excitation conditions
13 p1972 A72-29982
- Stimulated Compton scattering of laser radiation by electron plasma, determining electrons diffusion coefficient and velocity distribution function
13 p1972 A72-29987
- Secondary scattered light component of tropospheric twilight from electrophotometric observations, comparing with upper atmospheric scattering
13 p1954 A72-30070
- Light intensity and linear polarization for single scattering by ice clouds in visible and IR, approximating crystals with long circular cylinders
14 p2128 A72-30349
- Gas temperature from Raman rotational line intensities generated by lidar techniques applied to inelastic Raman scattering
15 p2232 A72-31373
- Joint photon-count probability distribution measurement of electric field amplitude correlation function for random-Gaussian light fields produced by laser beam scattering
15 p2280 A72-31378
- Planetary cloudy atmosphere synthetic spectral line profile computation, using analytic scattering diagrams
15 p2192 A72-31649
- Coherence narrowing during multiple scattering of resonance radiation in atomic vapor, treating polarization transfer in terms of classical tensors
15 p2281 A72-32221
- Photoelasticity with stress induced optical activity analysis using Stokes parameters, discussing rotational effects in scattered light problems
15 p2277 A72-32235
- Rocket-borne laser radar for aerosol observation in upper atmosphere, noting light scattering layer relation to noctilucent cloud appearance
15 p2231 A72-32331
- Cooperative enhanced scattering cross section of far IR laser radiation from nonthermal theta pinch plasmas in weak magnetic field
15 p2288 A72-32417
- Light scattering by fluids - Conference, France, July 1971
16 p2428 A72-32941
- Rayleigh-Brillouin light scattering in He-Xe gas mixtures, noting thermal fluctuations effect
16 p2422 A72-32943
- Light scattering by monatomic and polyatomic gases, superimposing effects due to rotational and translational molecular relaxation
16 p2428 A72-32944
- Angular distribution and intensity of light scattered by carbon dioxide near critical point, noting temperature dependence of isothermal compressibility and long range correlation length
16 p2422 A72-32945
- Hypersonic sound attenuation and velocity dispersion in sulfur fluoride near critical point determined by light scattering measurement
16 p2422 A72-32946
- Power spectrum of light scattered from surface waves thermally excited on carbon dioxide liquid-vapor interface near critical point
16 p2423 A72-32948

Depolarized light scattering spectra splitting in nonassociated liquids, noting viscoelastic theory with allowance for antisymmetric part of microscopic stress tensor

16 p2428 A72-32950

I.F. spectrum of depolarized light scattered from liquids composed of molecules with anisotropic polarizabilities, noting sharp line spectra with VH shear doublets

16 p2429 A72-32951

Mathematical models for depolarized light scattering by particle pair in gas, noting molecular collisions effect

16 p2423 A72-32952

Room temperature vibrational relaxation measurements in gases subsequent to laser pumping by picosecond pulse generated transient stimulated Raman scattering

16 p2401 A72-33389

Diffuse galactic light polarization characteristics from OSO-5 observations, discussing model of starlight scattering by interstellar dust

16 p2446 A72-33468

Interstellar OH maser size determination, discussing scattering by inhomogeneities in electron distribution

16 p2456 A72-33473

Monochromatic light beam propagation and scattering in optically nonhomogeneous medium containing matter in near critical state, determining exciting wave electric field strength

16 p2426 A72-33694

Narrow light beam attenuation and scattering characteristics in turbid medium as function of distance from source from transport equation solution

16 p2426 A72-33779

Twilight atmospheric sounding in oxygen absorption bands to reduce noise level in secondary light scattering

16 p2386 A72-33784

Bidirectional optical scattering from dielectric materials of various pigmentation and surface roughnesses, obtaining cross section data to determine angular, spectral and polarization behavior

16 p2427 A72-33839

Spatial noise in holographic images of diffusely scattering objects with allowance for recording apparatus resolving capacity

16 p2395 A72-33980

Carbon dioxide laser light scattering from cyclotron-harmonic waves in steady state rarefied collisionless plasma, noting associated electron density fluctuations

17 p2591 A72-35378

Poincare sphere application to polarimetry and two- and three-dimensional photoelasticity by scatter light photoelasticity

18 p2691 A72-36381

German monograph - A method for the determination of the differential albedo for photons in the range from 1-17 MeV

19 p2836 A72-37484

Laser-beam-scattering measurement of ion temperature in a theta-pinch plasma and evidence for thermonuclear reactions.

19 p2840 A72-37548

Experimental indications of plasma instabilities induced by laser heating.

19 p2840 A72-37549

Mie scattering models of zodiacal light based on spherical particles, commenting on inadequacy for nonspherical particles at elongations above 120 deg

19 p2792 A72-38506

Microwave-analogy tests regarding light scattering at cosmic dust particles

19 p2804 A72-38507

Possibility for buildup of laser radiation scattered by an electron beam

19 p2812 A72-38662

Brightness matrix of a flat powdered layer with opaque particles in the single-scattering approximation

19 p2836 A72-38783

Atmospheric surface layer light scattering matrices from nighttime air flows, showing climatic variability and similarity between Crimean and Moscow measurements

20 p2948 A72-39014

An application of atmospheric light scattering for contrast analysis in electro-optical detection systems.

20 p2923 A72-39056

Antiferromagnetic dispersion, absorption and light scattering in NiO and other face centred cubic crystals.

20 p2960 A72-39458

Stimulated thermal and Mandelstam-Brillouin scattering of light in liquid nitrogen and oxygen.

20 p2933 A72-39520

The redistribution function of polarized light in the presence of collisions and of small magnetic fields - Discussion of the polarization of the solar line Ca I 4227 A.

20 p2971 A72-39756

Thermalization lengths and mean numbers of scatterings for line photons.

20 p2956 A72-39759

Active spectroscopy of Raman scattering of light with the aid of a quasicontinuously tunable parametric generator.

20 p2934 A72-39852

Fabry-Perot interferometer measurements of Brillouin scattering from He-Ne laser excited low temperature condensed gases

21 p3051 A72-40151

An application of the concepts and methods of linear systems analysis to the scattering of resonance radiation by an atomic vapour.

21 p3084 A72-40470

Electron density and temperature measurement from laser radiation scattering in plasma within axisymmetric toroidal magnetic mirror machine

21 p3091 A72-40663

Opaque scatterers disadvantages in interferometric images recording of transparent objects obtained by double exposure holography, noting phase type diffraction gratings

21 p3054 A72-40669

Gravitational wave detector design based on fine components of scattered light spectrum

21 p3086 A72-41696

Determination of the characteristics of scattering particles in the Venusian atmosphere on the basis of photometric measurements

22 p3223 A72-42215

Light scattering by the medium created by a spacecraft. I - Luminescence of the gas jets of the spacecraft microthrusters

22 p3230 A72-42216

Internal dust effects on nebulae structure and spectrum, solving radiation transfer equation for spherical models with nonisotropic scattering

22 p3227 A72-42558

Laser Doppler velocimeter operating in forward- and back-scatter modes for supplementing wind tunnel flow field measurements in subsonic, transonic and supersonic regimes

22 p3179 A72-42678

Electro-optical design and performance parameters of polluted air liquid droplet size distribution measurement by pulsed junction diode laser light external scattering

22 p3179 A72-42680

Light scattering studies in amorphous media.

22 p3206 A72-42798

Light scattering in a sphere in the presence of an arbitrary source distribution

22 p3207 A72-42965

Sunlight scattering by double reflection on rough and absorbing surfaces, deriving fractional circular polarization from models for comparison with observation

23 p3334 A72-43254

Polarization characteristics and wave vector direction effect on cross section of incident and diffuse light scattered in liquid, determining frequency shift functions

23 p3312 A72-43318

Forward scattering of laser coherent light by acoustic or turbulent wave pressure variations, noting phase fluctuation spectrum

23 p3313 A72-44113

Spectral composition and phase function of plane monochromatic light wave scattering by electrons in high temperature plasma

23 p3322 A72-44465

Stimulated entropy /temperature/ scattering and its influence on stimulated Mandelstam-Brillouin scattering

23 p3297 A72-44478

Light spectral width and constant frequency shift during spontaneous diffusion in ideal gas for fixed photon wave

23 p3315 A72-44479

An experimental investigation of radiative properties of aluminum oxide particles.

24 p3461 A72-44809

Gain and line width in stimulated Brillouin scattering in gases.

24 p3412 A72-45616

LIGHT SOURCES

NT ILLUMINATORS

Stabilized hydrogen plasma arc spectral radiation as light source for vacuum UV radiometry, comparing output with W strip and carbon sources

01 p0073 A72-11400

Fabry-Perot interferometer for studying spatial distribution of plasma electron concentration, discussing resolution using solid state gas laser light source

02 p0223 A72-11403

Light source fluctuations compensation in Raman spectroscopy, describing ratio recording system for photon counters

04 p0523 A72-15491

White light shadowgram production during holographically recorded distorted wavefront reconstruction, discussing illuminating slit performance, image producing diaphragm, lenses and collimator

06 p0815 A72-17790

Neutral B I vacuum UV spectra from hollow cathode light source, remeasuring electron transitions to higher accuracy

06 p0852 A72-17896

Resolution dependence on coherent properties of light source for aberration free annular aperture operating in partially coherent light, presenting composite intensity curves

07 p1008 A72-20545

Multipole network characteristics of optical link assemblies /optons/ using photosensitive element and light source

08 p1139 A72-21057

Biological hazards of high intensity light sources, considering physiological factors involved in threshold eye damage values determination

08 p1125 A72-21333

Mathematical description of frequency difference hologram obtained by superposition of two holograms of same object produced with light of different frequencies

10 p1483 A72-24915

Diffuse galactic light observation, suggesting emanation from discrete sources

11 p1720 A72-26113

Spectropyrrometric device for pulsed light or plasma source temperature measurement, noting operation in 2000-40000 C range

11 p1635 A72-26465

Light propagation from unsteady source through homogeneous turbid light scattering media, using analytic and numerical methods for unsteady radiative transport equation solution

13 p2001 A72-28507

GaAs doped Si light emitting diode as light source for optical timing system calibration, studying fast luminescent decay characteristics

13 p2000 A72-29763

Random parameters effect on divergence of focused light beams in turbulent atmosphere, noting light path dependence on illumination source diameter

14 p2131 A72-30810

Spark discharge light source for shock wave multiple exposure schlieren photography, describing pulse separator and spark trigger circuits

15 p2240 A72-32437

Holographic image reconstruction using He-Ne laser as coherent light source and black-white and color photographic emulsions

17 p2554 A72-34930

The laser - A source of light in high speed photography

17 p2563 A72-35182

Relativistic beaming from periodically orbiting light point source in terms of photon fluxes, relating to pulsar radiation theory

19 p2835 A72-38697

Kr I and II lines strength and relative transition probabilities, using thermal plasma behind reflected shock wave as spectroscopic light source

21 p3089 A72-40137

Optical communication with distant spacecraft, discussing electro-optical transducers, light sources and receivers

21 p3014 A72-40321

Fabry-Perot spectrometer adjustment for the compensation of Doppler shift from rapidly rotating and rapidly flowing sources.

21 p3053 A72-40607

Pulsed photoexcitation /flash photolysis/ spectrophotometers in terms of light sources, recording sensitivity enhancement, data processing, laser use and performance requirements

21 p3058 A72-41726

Automatic coaxial alignment system with photoelectric positioning sensors, discussing alignment errors as function of light source distance and components spacing

21 p3059 A72-41817

Martian light sources generated by suspended crystals producing parhelic halo in atmosphere, noting randomly oriented and gravitationally arranged suspensions

22 p3223 A72-42142

Comparative studies of various spectral lamp designs for atom-absorption analyses and use of double-discharge multielement lamps to account for non-selective interference

22 p3176 A72-42170

Light scattering in a sphere in the presence of an arbitrary source distribution

22 p3207 A72-42965

Vacuum ultraviolet absorption measurements on ionized species.

23 p3316 A72-44330

Closed-path interferometric experiments on the speed of light from moving sources.

24 p3425 A72-44788

LIGHT SPEED

Velocity ratio /1.468/ of light received from quasar PKS 2134 plus 004 to light propagation velocity in vacuum

07 p1073 A72-19412

Disturbing parameters effect on spacecraft trajectory X coordinate values estimation, including planetary masses and coordinates, astronomical unit and light speed

08 p1232 A72-21151

Transverse electromagnetic field and electron velocity vectors during rectangular pulse incidence on ionization front moving at light speed, describing steady state encounter region 08 p1136 A72-21741

Red shift-absolute magnitude relation for uniform time-dependent universe expansion rate suggesting large scale clustering modifications based on light propagation model 10 p1545 A72-24810

Muller matrix derivation for microwave light modulation studies in quasi-homogeneous magneto-optical and electro-optical media, taking into account finite light speed 10 p1493 A72-24914

Electromagnetic and gravitational waves emission by superlight sources in vacuum, considering multi-particle and form factor cut-off effect 14 p2130 A72-30625

Radiation source motion at superluminal speed in vacuum, defining conditions for Vavilov-Cerenkov and Doppler effects 15 p2279 A72-32767

Quasars 3C273 and 3C279 superlight velocity and distances from interferometer pattern changes in 1970-1971 16 p2450 A72-32865

Time constancy of physical constants in expanding universe, discussing light speed, Planck constant and electron and proton mass in context of Dirac hypothesis 16 p2425 A72-33517

Combustion fronts velocity comparison with light speed in relativistic hydrodynamics and MHD 17 p2589 A72-34911

Disturbing parameters effect on spacecraft trajectory X coordinate values estimation, including planetary masses and coordinates, astronomical unit and light speed 20 p2969 A72-39256

A new test of the second postulate of special relativity sensitive to first-order effects. 21 p3085 A72-41214

Closed-path interferometric experiments on the speed of light from moving sources. 24 p3425 A72-44788

LIGHT TRANSMISSION

NT LIGHT SCATTERING

Asymptotic intensity fluctuations of plane light wave propagating in turbulent medium, using parabolic equation and Markov model 01 p0050 A72-10348

Far field diffraction due to annular apertures of plane wave light rendered partially coherent by atmospheric turbulence 01 p0103 A72-11166

Multiple scattering of incident coherent light wave propagating in turbulent medium, considering irradiance intensity fluctuations and spectral and correlation characteristics 01 p0103 A72-11167

Fused silica optical transmittance at elevated temperatures during high energy electron bombardment, noting optical absorption at short wavelengths 01 p0103 A72-11357

Distribution moments mathematical method for partially coherent light beam propagation through random phase screens in linear and nonlinear media 02 p0181 A72-12589

Laser with convex-plane resonator and cross sectional variable mirror transmission, showing effective transverse mode selection and diffraction divergence 02 p0239 A72-12767

Birefringent filter theory and optical properties, discussing transmission profile and error sources 03 p0352 A72-12947

Scanning Fabry-Perot interferometer for He-Ne laser spectral composition, discussing transmission coefficient, resolution, resonator dissipative losses, active medium saturation and light field spatial nonuniformity 03 p0356 A72-13190

Au thin film effective optical constant calculation from measured reflection and transmission coefficients and thickness by approximate formulas 03 p0401 A72-13363

Lens type beam waveguide for optical trunk communication, discussing transmission medium, terrain layout, bandwidth, terminal equipment, misalignment and multibeam application 04 p0497 A72-14483

Turbulent tropospheric temperature fluctuations effects on optical waves propagation with random scattering, considering amplitude, phase, angle-of-arrival and polarization 04 p0548 A72-14736

Optical angle of refraction through earth mean atmosphere determination by three models of refractivity and iterative methods 04 p0515 A72-14884

Light phase curve model for nonatmospheric bodies covered with porous or dust-like surface layer 04 p0574 A72-14910

Light transmission in medium with random inhomogeneities in Markov random process approximation, obtaining short wave field statistical characteristics 04 p0488 A72-15380

Amplitude fluctuations of laser beam with Gaussian amplitude distribution on short line-of-sight path propagation through artificial turbulent atmosphere 04 p0488 A72-15383

Optical image recording, transformation, readout, transmission and data processing techniques and instruments, discussing transfer function, cut-off frequency and information quantity concepts and holography 04 p0525 A72-15700

Optical wave front transmission through turbulent atmosphere, predicting saturation phenomenon accompanying sea level turbulence 05 p0690 A72-16675

Monochromatic light beam propagation in optically nonhomogeneous medium containing matter in near critical state, determining exciting wave electric field strength 05 p0691 A72-16683

Self induced transparency effect in ruby laser, investigating light transmission and pulse delay and broadening as function of input energy 05 p0670 A72-17171

SNR expressions for image transmission through turbid medium, showing quality dependence on energy transfer, contrast frequency and sensor phonon illumination level 06 p0774 A72-17936

Light diffuse transmission and reflection by semi-infinite atmosphere with four term scattering indicatrix 06 p0884 A72-18029

Quantum optics analysis of light propagation and photon flux fluctuations in medium with random dielectric constant inhomogeneities 07 p0938 A72-18912

Integrated miniature guided wave optical transmission systems using crystals adapted to thin film nonlinear interaction and photolithographic technique 07 p1004 A72-19228

Pulsed and CW laser beam propagation through atmosphere [CLEA PAPER 2,5] 07 p0942 A72-19380

Atmospheric heating and kinetic cooling nonlinear effects on IR carbon dioxide laser beam propagation, comparing digital simulation results with geometrical optics [CLEA PAPER 2,6] 07 p0942 A72-19381

Dust particle composition and effect on light transmission in interstellar medium, discussing gas, magnetic fields, cosmic rays and background radiation 07 p1074 A72-19557

Spherical scatterers extinction efficiency effect on photometer optical systems transmittances, using Mie equation and numerical methods 07 p0987 A72-19831

Nonlinear wave propagation of laser beams in absorbing fluid media, comparing computer model calculation results with experiment on liquid carbon disulfide cell 07 p1006 A72-19837

Signal injection through laser transmitting window, showing effects on resonant frequency and locking mode [AD-738988] 07 p1009 A72-20680

Remote ignition with noncoherent light from pyrotechnic, electric and explosive sources through fiber optics 08 p1219 A72-20757

Displacement measurement of weight center of light beam transmitted through turbulent atmosphere 08 p1135 A72-21734

Spatial structure of sinusoidally modulated light beam propagating in medium with forward extended scattering characteristics 08 p1136 A72-21742

Light absorptivity measurement in low loss liquid with interferometer based on refractivity dependence on temperature change due to absorption 09 p1309 A72-22602

Incoherently light radiating object and background light focusing on photosensitive mosaic, observing linear restoration by comparison of mean square error with Wiener filter theory 09 p1350 A72-22611

Pulsed carbon dioxide laser operation, measuring pulse energy variation with gas pressure, expansion nozzle shape and output mirror transmission 09 p1323 A72-22980

Atmospheric turbulence inner scale measuring configuration consisting of light transmitter and two scintillation counter detectors 09 p1314 A72-23343

Fourier transform and angular distribution of light diffusion by plasma with strong correlations 10 p1519 A72-24129

Radiative transfer theory for passage wall surface roughness effects on light transmission and reflection [AIAA PAPER 72-303] 11 p1742 A72-25237

Light diffuse transmission and reflection by semi-infinite atmosphere with four term scattering indicatrix 11 p1719 A72-25965

Pulse width relationship to frequency broadening during self phase modulation of propagating short laser pulse 11 p1647 A72-26151

Telescope performance reciprocity in laser transmitter or optical heterodyne receiver functionalities, considering atmospheric turbulence effects 11 p1636 A72-26750

Power transfer in optical fiber with nonuniform refractivity in mode propagation direction, using coupled mode theory 12 p1779 A72-27164

Angular variation and spot dancing of laser beam in atmospheric propagation, obtaining standard deviation 12 p1782 A72-27493

Phase matched nonlinear frequency conversion of laser light in tetragonal mercury thiocyanate complex crystals 12 p1854 A72-27549

Transmitter aperture size and focus effects on scintillations of laser beam propagating through turbulent atmosphere 12 p1791 A72-27678

Light pulse propagation in ring laser model employing homogeneously broadened gain line and discrete loss 12 p1823 A72-27754

Frequency modulation and transient effects in resonant propagation of coherent light pulses 12 p1826 A72-27939

Light propagation from unsteady source through homogeneous turbid light scattering media, using analytic and numerical methods for unsteady radiative transport equation solution 13 p2001 A72-28507

Light propagation patterns in absorbing and scattering medium with radiation density dependent optical properties 13 p2002 A72-28510

Propagation theory and quantum electrodynamics for light transmission in scattering media 13 p2002 A72-28511

Light beams propagation in clouds and fog, discussing scattering and attenuation coefficients 13 p1988 A72-28517

Diffraction antenna use in visual range to study troposphere modulated laser radiation propagation in turbulent atmosphere, presenting light intensity distribution 13 p1917 A72-28690

Coherent laser light propagation in resonance media with level splitting, determining Lorentz and broadened resonance lines 13 p1969 A72-29515

High power Q switched ruby laser radiation transmission through optically dense plasma, noting bleaching and increased absorptivity 13 p2016 A72-29521

Enhanced indirect optical absorption measurement in AlAs and GaP with energy denominator variation for direct band gap evaluation 13 p2022 A72-29627

Optical weak absorption measurements in amorphous semiconductors AsS, GeAs and GeSbSe, showing dependence on band gap localized states 13 p2022 A72-29629

Laser beam propagation in vacuum, imperfectly transparent medium and turbulent atmosphere 13 p1971 A72-29865

High light transmission electrically conducting Hyviz and gold film laminates for aircraft windshields and window heating applications 13 p1898 A72-30038

Random parameters effect on divergence of focused light beams in turbulent atmosphere, noting light patch dependence on illumination source diameter 14 p2131 A72-30810

Spectral transmittance enhancement in Fabry-Perot narrow band light filter by wavelength shifted dielectric mirror technique 15 p2233 A72-31414

Whole blood flow dependence on optical density from light transmission measurement, showing photometric effects of red cell aggregation, deformation and orientation 15 p2185 A72-31639

Light transmission measurements of blood flow to quantify red cell aggregation and dispersion 15 p2185 A72-31640

Transient phase object high sensitivity measurement by He-Ne laser beam transmission through differential interferometer and signal detection with p-i-n photodiode 15 p2235 A72-31784

Optical pulse wave field longitudinal and transverse statistical correlations during propagation in turbulent atmosphere 15 p2198 A72-32061

Time transfer measurement between two locations using nearly simultaneous reception times from optical pulsar signal transmission 15 p2199 A72-32076

Extended Huygens-Fresnel principle for mutual coherence /cross correlation/ function of finite optical beam propagation in turbulent medium

15 p2249 A72-32161

Quasi-optical transmission line stability improvement, investigating pulsating light beam concept

15 p2202 A72-32663

Electromagnetic single scattering near critical point in inhomogeneous optical medium with variable refractivity, discussing reflected light effect and Poynting vector reduction to Bragg conditions

15 p2279 A72-32693

Turbulent divergence of laser beams along oblique atmospheric path for vertical refractive index distribution, using Markov coherence model

16 p2364 A72-33489

Monochromatic light beam propagation and scattering in optically nonhomogeneous medium containing matter in near critical state, determining exciting wave electric field strength

16 p2426 A72-33694

SNR expressions for image transmission through turbid medium, showing quality dependence on energy transfer, contrast frequency and sensor photon illumination level

16 p2426 A72-33777

Band model and scaling approximation validity for computation of transmission profile in V4 band of methane in Jovian atmosphere

16 p2461 A72-34099

First and second moment of an optical wave propagating in a random medium - Equivalence of the solution of the Dyson and Bethe-Salpeter equation to that obtained by the Huygens-Fresnel principle.

17 p2580 A72-34290

German monograph - Wave propagation in glass-fiber light waveguides

18 p2697 A72-36249

Field fluctuations of a laser beam propagating in a turbulent atmosphere

18 p2661 A72-36656

Propagation of laser beams through the atmosphere.

18 p2661 A72-36793

Fourth moment of a wave propagating in a random medium.

18 p2712 A72-37025

Laser with convex-plane resonator and cross sectional variable mirror transmission, showing effective transverse mode selection and diffraction divergence.

20 p2931 A72-39073

Vector wave solution of light beam propagating along lenslike medium.

20 p2903 A72-39266

Reduction of temperature difference in shielding pipes for light-beam transmission.

20 p2903 A72-39267

Quantum optics analysis of light propagation and photon flux fluctuations in medium with random dielectric constant inhomogeneities

20 p2932 A72-39378

Optical devices to produce transmitted image rotation about axis, comparing derotation systems and roll and high-speed prisms

20 p2927 A72-39849

The geometry of free fall and light propagation.

20 p2954 A72-40005

Measurement of the thermal diffusivity of semiconductors by the light pulse technique

21 p3095 A72-40133

Optical propagation in space-time-modulated media using many-space-scale perturbation theory.

21 p3014 A72-40142

Simplified equation for amplitude scintillations in a turbulent atmosphere.

21 p3083 A72-40143

Energy absorption mechanisms of thin film optical waveguide surface in contact with low index dyes

21 p3050 A72-40147

Photogrammetric method for determining the deflection of light beams by spacecraft windows during flight

21 p3052 A72-40305

Light pulse propagation through clouds - Models and experiments.

21 p3063 A72-40857

Light transmission, reflection and environment problems of hydrophilic coatings for fog and frost protection in aviation instrument window design

22 p3196 A72-42519

Fundamental transverse electric field /TE-sub 0/ mode selection for thin-film asymmetric light guides.

22 p3186 A72-42622

Self focusing effect on wave beam propagation in optical lens waveguides, discussing system nonlinearity

22 p3186 A72-42656

Interferometric investigation of the phase fluctuations of coherent optical emission in the atmosphere

22 p3186 A72-42661

Gas absorption lines detection based on multiple light passage through absorbing medium during generation process, noting radiation spectra of neodymium glass laser

23 p3295 A72-43305

Subharmonic generation in plane-parallel plate for light wave propagation perpendicularly to plate, noting frequency division near multiplicative resonance

23 p3295 A72-43408

Parabolic approximation of spatially bounded square and Lorentz two dimensional light pulse propagation in homogeneous isotropic linear medium without dispersion

23 p3313 A72-43682

Laser radiation geometric divergence and variation of transmitted intensity with mirror transmissivity at centerline for unstable cavity viewed as oscillator-amplifier

23 p3296 A72-43902

Automatic acquisition and tracking system for laser communication.

23 p3265 A72-44176

Semigray approximation to nongray radiative transfer, taking into account mean absorption coefficient variation with spatial position and photon propagation direction

23 p3314 A72-44328

Propagation of the mutual coherence of optical waves in a random medium.

24 p3424 A72-44711

Fiber optics development and physical foundations, discussing reflection, optical waveguides, vibrational modes during light transmission and fabrication from inhomogeneous glass and mixed monomers

24 p3425 A72-44782

Transmission losses in glass and plastic single mode and liquid core optic fibers for long distance data links and image transmission

24 p3380 A72-45252

Wave and polarization equations for short coherent light pulses transmission in linear amplifying and absorbing media, noting single pulse formation in lasers

24 p3410 A72-45420

Attenuation of ruby laser radiation in the boundary layer of the atmosphere during the temperature-dependent variations of the wavelength

24 p3411 A72-45424

GaAs semiconductor injection laser and amplifier-absorber emission and light pulse transmission characteristics determination, noting nonlinear absorptivity, bleaching threshold and pulse compression factor

24 p3412 A72-45619

LIGHTHILL METHOD

Circular jets sound generation analysis, using Lighthill equation and Michalke spectral method [DFVLR-SONDDR-179]

07 p0910 A72-20100

Lighthill method for ohmic dissipation pulsation effect on sound field generated by turbulent flow of conducting fluid

14 p2141 A72-31001

Heat transfer through laminar boundary layer with allowance for streamwise pressure gradient effect on velocity field, using Lighthill method

16 p2477 A72-33427

The Poincare Lighthill perturbation technique and its generalizations.

19 p2827 A72-38383

LIGHTING

U ILLUMINATING

LIGHTING EQUIPMENT

NT AIRCRAFT LIGHTS

NT AIRPORT LIGHTS

NT ARC LAMPS

NT FLASH LAMPS

NT ILLUMINATORS

NT LUMINAIRES

NT MERCURY LAMPS

NT QUARTZ LAMPS

NT RUNWAY LIGHTS

NT XENON LAMPS

Airport runway lighting systems development, noting lamp for night flights and control console

13 p1940 A72-30119

The laser - A source of light in high speed photography

17 p2563 A72-35182

LIGHTNING

Lightning protective coatings for boron/epoxy composite materials, discussing high current damage mechanisms, simulation facility and test results on aluminum foils, meshes, etc

01 p0092 A72-10783

Air shower cores or relativistic monopoles as sources of straight lightning, considering thundercloud conditions over ocean and land areas

03 p0350 A72-14100

Electrostatic field changes in vertical intracloud discharges, discussing positive streamers and return strokes

04 p0543 A72-14881

Low latitude low dispersion whistlers, discussing origin as vlf waves radiated from return stroke of lightning discharge

04 p0517 A72-14949

Interference above ionosphere of lf radio waves emitted by multiple lightning discharges concluded from spectrographic observation of whistler received onboard Injun 5 satellite

06 p0773 A72-17567

Electric field rise times of first and subsequent lightning return strokes, discussing waveform oscillograms

06 p0841 A72-17822

Thunderstorm flight testing for evaluation of rain, ice, lightning and turbulence effects on aircraft, engine and systems operating characteristics

06 p0760 A72-18500

Aircraft hydrocarbon fuel tank lightning protection in airframes, using adhesive bonding, high strength materials and high modulus fiber structures

07 p1086 A72-18767

Multiple swept stroke flash technique to test lightning effects on aircraft

07 p0964 A72-18768

Lightning simulation laboratory for aircraft strike testing, using high energy generators

07 p0964 A72-18774

Ball lightning theory based on thin conducting ladder networks and three dimensional fine particle structures formation in electric fields

09 p1346 A72-22963

Digital lightning goniometry for flash locations at great distances by atmospheric and whistlers analysis

09 p1304 A72-23471

Tropical thunderstorm precipitation current variations due to lightning produced atmospheric electric field changes, considering charged raindrops turbulent diffusion

12 p1839 A72-27502

Thunderstorms physical mechanisms of charge generation and separation, considering correlation between lightning and precipitation

13 p1995 A72-29873

Lightning current tests of aircraft glass/carbon fiber reinforced plastics materials

13 p1898 A72-30040

Gas dynamics and chemistry of lightning-produced shock waves /thunder/ in postulated primordial reducing atmosphere, noting amino acid production

18 p2650 A72-36443

Bremsstrahlung as a possible source of UHF emissions from lightning.

19 p2828 A72-37894

The lightning arrestor-connector - A new concept in system electrical protection.

20 p2889 A72-38989

Radar as a diagnostic tool for lightning.

20 p2948 A72-39350

Electrostatic charge on an aircraft and lightning striking the aircraft

21 p2994 A72-40171

Zodiacal light, airflow and lightning monitoring by wide field broad bandpass OSO-5 experiment, obtaining height profile, cell size and intensity variations of nightglow

21 p3054 A72-40619

Computer-aided numerical solution for electric field structure of rod and plate, calculating field distortion by rod antennas and near lightning rod

21 p3086 A72-41671

Triggered lightning and some unsolved lightning hazards.

22 p3170 A72-42375

LIGHTS

U LUMINAIRES

LIMB DARKENING

The limb darkening problem in eclipsing binaries.

17 p2612 A72-35382

Limb darkening for B-type main sequence stars in the infrared.

17 p2612 A72-35383

A first order analysis of variations of the limb darkening and the shapes for solar Fraunhofer lines.

17 p2616 A72-35694

LIMBS [ANATOMY]

NT ARM [ANATOMY]

NT FOREARM

NT HAND [ANATOMY]

NT LEG [ANATOMY]

Human body dynamics, discussing configuration, modeling techniques, kinematics, equations of motions and various limb motions examples

01 p0016 A72-10110

Steady state heat transfer problem solutions in living tissue modeled as cylindrical shells, discussing blood flow and temperature distributions in extremities

[ASME PAPER 71-WA/HT-34] 05 p0745 A72-15885

Pure biocarbons for skeletal fixation of limb prosthetic devices, noting load bearing applications dependence on brittle characteristics

12 p1773 A72-28095

Techniques and procedure for differential ballistooculography of extremities.

20 p2897 A72-39325

LIME

U CALCIUM OXIDES

LIMITATIONS

U CONSTRAINTS

LIMITER CIRCUITS

Transistorized microwave amplifier/limiter for upper part of decimeter wave range, suggesting limitation in automatic gain control transistors

10 p1451 A72-24588

Ferrite microwave limiter-filters and circulators using resonant rotation of polarization plane
13 p1927 A72-28409

Book on phase locked and frequency feedback systems covering FM and multiple loop principles, limiter-discriminator operation, phase detection techniques, etc
15 p2210 A72-31500

Filtering and hard-limiting effects on digital FM signals power spectra, using Postl direct method
15 p2194 A72-31543

Search radar constant false alarm rate receiver circuit for background noise and clutter compensation, using matched dispersive delay lines flanking hard limiter
16 p2365 A72-33762

RF discharge gap in cascaded plasma limiters, using tritium igniter as reliable electron priming source
18 p2715 A72-36451

Transmission of two partially time coincident linearly frequency modulated signals through limiter-filter system, noting distortion and satellite signals generation
19 p2766 A72-38419

Frequency conversion and limiter action for an angle-modulated wave with amplitude fluctuation in a half-wave linear mixer.
23 p3265 A72-44179

On the performance of digital communication systems with bandpass limiters. I - One-link system. II - Two-link system.
23 p3265 A72-44181

Determination of the energy spectrum of the initial process in an amplitude gate subjected to the action of a random signal
24 p3380 A72-44897

LIMITS [MATHEMATICS]
Second order differential equations system solution in convergent integrals, describing solution limit in vector form as special case of linear system solution property
07 p1026 A72-18815

Markovian characteristics of time dependent excursions and independent incursions processes provided with limits to left and continuous to right, noting Poisson punctual process and Borel sets
10 p1505 A72-24114

Local limit theorems for sequence of nonidentically distributed independent integral-valued lattice random variables
11 p1676 A72-25356

Limit set configuration of optimal nonlinear feedback control scheme in n-dimensional state space
15 p2213 A72-32797

Application of a limit theorem to solutions of a stochastic differential equation.
17 p2575 A72-34866

Limit distributions for sums of random values specified in a denumerable Markov chain with absorption
19 p2827 A72-38470

Riccati equation asymptotic theory, deriving a priori bound dependence on information and control energy rates and state dimensions
20 p2945 A72-39347

Probability theory central limit theorem application to dynamic system generated by billiard scattering motion
20 p2945 A72-39403

LINE SHAPE
Pressure broadened water vapor line shape resonance dispersion at 22 GHz, deriving expression for instrument induced deviation from Lorentzian behavior
04 p0552 A72-14891

Hough transformation for detection of lines and curves in pictures, using angle radius instead of slope intercept parameters for efficient computation
05 p0664 A72-17164

Solar Fraunhofer line profiles determination by digital data recording double-pass spectrophotometer, presenting observed atomic Ni and Fe lines intensity distributions
06 p0884 A72-18028

Oxygen telluric lines contours shape analysis, allowing for atmospheric nonisothermicity and inhomogeneity
06 p0852 A72-18050

Coupled coherent and incoherent excitons motion effect on optical absorption line shape, deriving diffusion equation from density matrix equation of motion
07 p1035 A72-19672

Pressure broadened atomic line shapes calculation for Cs resonance line pressurized by Ar, using Lennard-Jones potentials
09 p1354 A72-22663

Photoelectric Fabry-Perot measurements of M8 and M42 nebulae H alpha and forbidden N II emission lines profiles, determining temperatures and turbulent motions
09 p1390 A72-23528

Transition probabilities and line shapes and widths of unimolecular problem computed using numerical methods for scattering processes
10 p1514 A72-24337

Solar Fraunhofer line profiles determination by digital data recording double-pass spectrophotometer, presenting observed atomic Ni and Fe lines intensity distributions
11 p1719 A72-25964

HCl and HF in carbon dioxide atmosphere, determining line intensities, halfwidths and shapes at room temperature
14 p2135 A72-30894

Photoelectric observation of H alpha, sodium deuteride and He solar umbral line profiles, using pressure scanning spectrometer
17 p2608 A72-35082

The influence of line shape and band structure on temperatures in planetary atmospheres.
18 p2726 A72-36640

Absorption line profile and equivalent line width derivation for planetary atmosphere with low and high optical thicknesses, assuming arbitrary scattering coefficients
19 p2863 A72-38071

A line-profile Stokesmeter - Preliminary results on non-sunspot fields.
20 p2971 A72-39761

Observation of quantum-phase and quantum-amplitude noise for a laser below and above threshold.
20 p2934 A72-39813

Speed-dependent collisional width and shift parameters in spectral profiles.
21 p3088 A72-40820

Characteristics of the Ca II K-line profiles in the quiet sun.
21 p3108 A72-41280

LINE SPECTRA
NT BALMER SERIES
NT D LINES
NT ELECTRONIC SPECTRA
NT FRAUNHOFER LINES
NT H ALPHA LINE
NT H BETA LINE
NT H GAMMA LINE
NT H LINES
NT K LINES
NT LYMAN SPECTRA
NT PASCHEN SERIES
NT RYDBERG SERIES
NT TELLURIC LINES
Redistribution function of line radiation during scattering without atom velocity restriction
01 p0104 A72-10093

Atomic models of velocity noncorrelated radiation line scattering with frequency redistribution at large distance from atmosphere
01 p0104 A72-10094

Self broadened rotational half widths for Lorentzian line shape and slit function in CO fundamental, using line center transmission measurements
01 p0104 A72-10095

Line radiation from theta pinch with oscillatory ion and electron density applied to solar spectral studies
01 p0106 A72-10098

He emission line star G61-29, discussing spectral features and proper motion limits on maximum distance
01 p0133 A72-11095

Phosphorus absolute transition probabilities determination from P I and P II lines strength measurement, using gas-driven shock tube
01 p0104 A72-11111

H I radio recombination line observation in H II region NGC 2024 microwave spectrum, detailing radiation frequency dependence
01 p0133 A72-11143

Line splitting in emission near plasma frequency in drift pair solar radio bursts, considering causes by model involving electrons bunching through solar corona
02 p0276 A72-11646

Interferometric photoelectric scans of interstellar Ca I 4226 line for stars with interstellar Ca II K-lines, discussing deduced electron densities
02 p0280 A72-12197

Absorption spectrum of atomic Ca trapped in solid hydrocarbons, comparing with diffuse interstellar band at 4430 A
02 p0284 A72-12632

Line spectrum of Of star zeta Puppis at 3150-8600 A, comparing absorption spectrum to 9 Sgr
03 p0416 A72-13014

Electron impact broadening of ionized Be and Ba lines in electric shock tube plasma, measuring electron density and temperatures
03 p0393 A72-13020

Absorption profiles of neutral helium lines lambda 4471 and lambda 4026 for BoV star tau Sco, observing flux near peak of forbidden component
03 p0417 A72-13022

High spectral resolution balloon-borne spectrograph for near UV solar Mg II resonance lines
03 p0354 A72-13053

Space observation of stars and interstellar medium, considering stellar energy distributions and line spectra, interstellar absorption lines, galactic nebulae and X ray sources
03 p0420 A72-13122

Solar UV line spectrum identification and intensity analysis, emphasizing electron spectra in soft X ray region and forbidden transitions
03 p0420 A72-13124

Active and quiet solar atmosphere models from OSO satellite data, presenting emission lines and continua from abundant elements
03 p0423 A72-13215

Solar flare 1.9 A line feature identification from X ray observation by OSO-4 proportional counter spectrometer
03 p0424 A72-13218

Systematic errors of Crimean vector magnetograph related to miscentering of spectral lines
03 p0357 A72-13285

Absorption line formation in magnetic field for magnetograph interpretation of solar atmosphere
03 p0427 A72-13291

Collisional relaxation rate effects of atomic level polarization on spectral line formation in solar magnetic regions
03 p0427 A72-13294

Magnetic field strengths from umbral spectral lines in sunspots
03 p0428 A72-13301

Spectroheliogram movies of magnetic, velocity and intensity field in solar atmosphere, showing time resolution of line spectra
03 p0429 A72-13314

Zeeman spectroheliograms of photospheric magnetic fields in Ca I 6102.7 A line
03 p0430 A72-13317

Magnetic fields orientation in solar corona from polarization measurements in green line
03 p0431 A72-13343

Midday oval, cusp region and polar cap auroral electron precipitation at low magnetic activity, presenting intensity vs altitude profiles for nitrogen ion line emissions
03 p0350 A72-13531

Fe XI to XV emission lines from transitions and isoelectronic spectra in manganese, chromium and vanadium
03 p0391 A72-13750

Differential line shifts in spectrum of supergiant beta Ori attributed to radial spreading of stellar atmosphere
03 p0436 A72-13810

Mars short wave line spectra from measurement with reflector, estimating nitrogen dioxide content in atmosphere
03 p0436 A72-13815

Venus cloudy atmosphere IR absorption line spectra interpretation, suggesting HCl and HF formations dependence on condensation phases
03 p0439 A72-14149

Wolf-Rayet type stars emission line variations from outer convective zone opening and matter ejection
03 p0439 A72-14243

Forbidden O I and molecular nitrogen ions emission lines ratio variation with height in aurora
03 p0352 A72-14382

Mars atmospheric water vapor observations, examining spectroscopic plates water line strengths at 8200 A
04 p0569 A72-14497

RF diagnostic technique for carbon and hydrogen /H I/ cloud recombination lines in cool interstellar medium
04 p0570 A72-14525

Fe line emission during solar X-ray flares recorded by Bragg crystal spectrometers on OSO-6, resolving fine structure components of hydrogenic Ar
04 p0566 A72-14560

Nonisothermal gas layer IR radiation in multiatomic molecular vibrational-rotational band range, determining lowest level energy for wide line spectrum
04 p0547 A72-14657

Blanketing effect of strong line spectra collisionally broadened wings, evaluating stellar atmospheric model computation
04 p0573 A72-14907

Spectral line data on terminal flare and wake of double-station meteor 38421
04 p0574 A72-14922

Markarian galaxies photometric observations, presenting emission line intensities and UVB magnitudes
04 p0578 A72-15309

Solar radio recombination lines observation at hydrogen and helium frequencies
04 p0568 A72-15328

Submillimeter wave sulfur dioxide molecular laser, investigating lasing lines, plasma decay and relaxation, line interactions and signal temporal behavior
04 p0532 A72-15595

Optical spectra of compact objects, reviewing emission line spectra of quasars
05 p0716 A72-16372

High dispersion spectroscopic study of H alpha and K lines profile and velocity structure in quiescent prominences
05 p0719 A72-16516

Electron density profiles as function of position in enhanced coronal region from Ni XV and Fe XIII emission lines observation

05 p0719 A72-16517

Solar wind velocity correlation with 5303 Å coronal intensity

05 p0710 A72-16523

Quasar photoionization and emission line spectra, determining radiation/gas density

05 p0720 A72-16713

Radio quiet quasar PHL 957 absorption line spectra obtained at telescope with Cassegrain image tube and multichannel spectrometer and integrating TV camera

05 p0720 A72-16714

Plasma line enhancement variabilities in ionospheric modification experiments due to radar wave scattering, number density gradient and diagnostic beam temperature and orientation

06 p0805 A72-17470

Emission line of neutral carbon in solar spectrum at 1993.6 Å from balloon-borne spectrography

06 p0876 A72-17566

Temperature and density fluctuations in photosphere from Fe and Mg line intensities, noting variations due to granulation in solar atmosphere model

06 p0876 A72-17579

Atomic hydrogen 6300 Å forbidden line emission altitude and intensity during predawn enhancement, using rotating photometer

06 p0806 A72-17644

Be stars emission line profile broadening due to surrounding gaseous ring in circular motion according to Kepler law

06 p0880 A72-17892

UV spectrophotometry of late-type giant star *Arc-turus*/ from Aerobee rocket, identifying Mg II doublet resonance line for stellar chromospheric

06 p0881 A72-17893

Temperature scale for classifying spectra of peculiar and metallic line stars

06 p0883 A72-18021

Early type stars photoelectric spectra obtained with Mariner 9 UV spectrometer, obtaining resonant line features and spectral energy distribution

06 p0890 A72-18347

Photoelectron flux measurement of intensities of plasma lines in radar incoherent scatter spectrum by uhf radar

06 p0874 A72-18732

Far UV Al line spectra from laser produced plasma in 35-50 Å range

07 p1038 A72-19835

Coronal condensation of 10 September 1970, observing iron and calcium emission lines

07 p1082 A72-20297

Zeta Puppis visual line spectrum discrepancy from non-LTE stellar atmospheres models, necessitating hydrostatic equilibrium deviations consideration for temperature derivation

08 p1232 A72-21178

Planetary nebula IR continuum and line radiation from spectrophotometric observation relation to visual and radio wave data

08 p1235 A72-21387

Coalescence /collapse/ of overlapping spectral lines due to nonadiabatic broadening for Stark structure of hydrogen and helium lines in discharge plasma

08 p1211 A72-21717

Stellar atmosphere UV spectral line broadening by electron collision, radiative and classical damping

08 p1237 A72-21750

Ruby laser power output losses at 80 K with spectral line suppression dependence on surface reflection coefficient of plane parallel plate in resonator

08 p1183 A72-22026

Quasi-stellar objects hydrogen L-alpha lines computation via cloud collapse and ionizing radiation flux model, comparing computed distribution with PHL 957 and 4C 05.34 observations

09 p1382 A72-22280

Chlorine, bromine and iodine first spectral lines observation in IR region with liquid nitrogen cooled lead sulfide detector

09 p1276 A72-22614

Tabulation of calculated rotational line intensities relative to integrated vibration-rotation band intensity for various electron transitions of nitrous oxide

09 p1276 A72-22665

Spectral line formation in cloudy planetary atmospheres, applying to Venus

09 p1386 A72-22669

Spectroscopic evidence for spectral line structure of visible Venus cloud layers

09 p1386 A72-22670

Transition probabilities of ionized Ar spectral lines for excitation temperature measurements

09 p1355 A72-22672

Excitation accompanying photoionization in atoms and molecules and relationship to electron correlation observed from rare gases inner and valence shell satellite lines measurements

09 p1356 A72-22835

Line intensity variation simulation in Raman spectrum of oxygen with allowance for spin splitting of rotational levels

09 p1358 A72-23049

Pulsating polar auroral line emission spectra observation at 3914 and 5577 Å by rocket-borne photometers

09 p1301 A72-23262

Standard deviation in ghost lines size due to random sampling position errors of monochromatic spectral line in Fourier transform spectroscopy

09 p1314 A72-23344

Rapid rotation effect on weak and intermediate strength early type stellar radiation spectral absorption lines

09 p1390 A72-23527

Gravity darkening effects on rapidly rotating B stars He I and Mg II spectral lines

09 p1391 A72-23530

Relative intensity of solar XUV emission lines of Li isoelectronic sequence ions, taking into account transitional collision strengths

09 p1391 A72-23532

Galaxy NGC 253 mass and distance from neutral hydrogen spectral line observations with radio telescope

09 p1391 A72-23533

Book on stellar atmospheric physics covering gray and nongray atmospheres, radiation emission and absorption, transfer equation, Eddington approximation, spectral lines formation, etc

10 p1532 A72-23725

Seyfert, N-type, compact and radio galaxies spectroscopic properties, noting two dwarf emission line galaxies as possible young galactic nuclei

10 p1534 A72-23896

Radio-emitting and radio-quiet quasar optical emission and absorption line spectra

10 p1534 A72-23897

Quasar and galactic nuclei emission line spectral data corrected for interstellar extinction

10 p1534 A72-23898

Rb 87 line shift produced by rare buffer gases and molecular nitrogen measured from applied magnetic field magnitude and hyperfine structure of D lines

10 p1490 A72-24040

Spectral line formation in atmosphere with plane parallel layers and frequency independent source function, using matrix approach for transfer equation solution

10 p1535 A72-24058

Auroral spectrophotometric measurements in *J*-S-1 region and of O I line /5577/, discussing digital recording and computer averaging techniques

10 p1474 A72-24745

Spectral measurements of temperature in low temperature plasma, describing line reversal method

10 p1485 A72-25110

Optical method based on spectral line center intensity recording to measure plasma temperature in MHD generators channels and combustion chambers

10 p1525 A72-25111

Close binary stars system model for totally eclipsing AW UMa light curves and line profiles, noting very low mass ratio

10 p1550 A72-25195

Fine structure and IR transmission functions of carbon dioxide absorption bands at high pressure and temperature, calculating transition lines strength and position

11 p1620 A72-25275

Temperature scale for classifying spectra of peculiar and metallic line stars

11 p1718 A72-25957

Twilight and nighttime ionospheric temperatures from oxygen 6300 and 5577 Å spectral line profiles obtained with Fabry-Perot interferometers

11 p1625 A72-26406

Cosmological origin of red shift in spectral lines of astronomic bodies, suggesting interpretation based on inelastic interactions between photons of essentially nonzero mass

11 p1723 A72-26507

He-like lines in solar X-ray spectrum observed by Bragg crystal spectrometer, noting absolute wavelengths determination with shaft encoder for angle readout

11 p1714 A72-26572

Magnetically unaffected Fe I line profiles in sunspots from high resolution photographic spectra observation

12 p1867 A72-27205

Magnetic field gradient in sunspot umbrae from magnetically split line profiles

12 p1867 A72-27206

Planetary nebula classification based on forbidden line ratios and morphology, discussing galactic plane distribution, radial velocities and evolution

12 p1867 A72-27209

Heavily obscured galaxy IC 10 21-cm line observation with radio telescope and neutral hydrogen diameter measurement for distance estimation

12 p1868 A72-27215

Interstellar atomic hydrogen observations in radio nebula W 3 direction, noting 21-cm absorption line profile coincidence with Cn alpha recombination line in radial velocity

12 p1868 A72-27219

Russian papers on light scattering covering electromagnetic propagation in turbid media, transport equation solution methods, unsteady scattering, spectral line radiation and nonlinear phenomena

13 p2001 A72-28501

Approximate solution to spectral line frequency resonance radiation transport equation, assuming total radiation redistribution with respect to frequencies

13 p2001 A72-28508

Fabry-Perot interferometer for line structure of helical TEA-carbon dioxide laser, noting variable frequency single mode emission

13 p1968 A72-28687

Velocity field measurements from M82 /NGC 3034/ galaxy H alpha, forbidden N II and S II emission lines, suggesting expanding ejecta cloud rotating about axis normal to galactic plane

13 p2040 A72-29401

Spectrographic observation of flash spectrum during 7 March 1970 solar eclipse, showing significant coronal line emission origin in chromosphere interspectral regions

13 p2042 A72-29534

Inner corona spectral data of 7 March 1970 solar eclipse, noting line half widths and emission line origin area relationship

13 p2042 A72-29535

Fourier transform spectrometer observation of IR coronal emission lines during 7 March 1970 solar eclipse from high altitude aircraft

13 p2042 A72-29538

Wavelength, intensity and spatial distribution identification of far UV solar coronal forbidden lines observed during 7 March 1970 solar eclipse

13 p2043 A72-29540

Photographic polarimeter measurement of linear polarization of coronal emission lines during 7 March 1970 solar eclipse

13 p2043 A72-29547

Transverse magnetic field effect on electron temperature and energy distribution and spectral lines of gas discharge plasma

13 p2017 A72-29635

Interaction between generating lines in coupled channels with arbitrary line broadening, studying radiation generation regimes in cascade circuit

13 p1970 A72-29680

Isoelectronic wavelength calculations for Ar line spectra, presenting table with identifications and interpolations

13 p2045 A72-29704

Flare related impulsive EUV solar emission lines enhancement in chromosphere-corona transition region

13 p2032 A72-29720

Semiempirical line blanketing in solar model atmospheres, including limb darkening predictions

13 p2047 A72-29735

Solar corona intensification analysis based on ionized Fe monochromatic emission spectra, investigating spectral lines behavior as function of temperature and electron density

13 p2047 A72-29736

Solar plasmas intensity ratios of He-like ion line emission, showing dependence on atomic number and electron temperature

13 p2018 A72-29737

Crossover and magneto-optical effects of line splitting in sunspot spectra, considering instrumental circular polarization

13 p2047 A72-29738

Electron beam excited P-15 phosphor 3900 Å spectral component fast decay time measurement by delayed coincidence technique

13 p2000 A72-29762

Total line intensities interpretation from optically thin gases, considering matter partitioning bivariate distribution function and chemical composition

13 p2008 A72-29930

Solar magnetic fields filamentary structure from Mount Wilson magnetograph recordings in Fe I 5250 Å and Fe I 5233 Å spectral lines

13 p2049 A72-29934

Solar transition zone and corona EUV lines formation heights measurement from OSO-4 spectroheliograms

13 p2050 A72-29939

Solar X-ray spectral lines at 1-60 Å from coronal ion relative abundances obtained from Jordan ionization equilibrium calculations

13 p2034 A72-29940

Spectral line identifications and classifications of Li like spectra of elements K through Mn in extreme UV region, detailing extrapolation procedures

14 p2133 A72-30563

Signal level fluctuations line spectra energy characteristics comparison for oblique and oblique-backscatter sounding, noting changes in harmonics intensity and period

14 p2085 A72-30638

Solar spectrum Mg I multiplet lines hyperfine structures, examining emission lines with Fabry-Perot and Fourier transform spectrometers

14 p2158 A72-30730

Spectral line profile of optical transition spontaneous radiation during resonance with strong field on adjacent transition

14 p2110 A72-30781

Ar plasma spectral lines, calculating temperature functions of excitation to fourth ionization multiple at atmospheric pressure

14 p2139 A72-30782

Dc arc plasma, investigating applied magnetic field, trace elements and gap spacing effects on spectral line intensity spatial distribution

14 p2139 A72-30783

Spectrochemical trace analyses in electric arc plasma, examining external magnetic field effects on spectral line intensity variation

14 p2139 A72-30784

Pressure effects of Ar and He mixtures on Cs atomic line shapes calculated assuming additivity of perturber interactions

14 p2134 A72-30838

Electronic density measurement in ionized Cs vapor by observation of fundamental series lines mixture, comparing to Stark widening theory based profiles

14 p2134 A72-30852

Hg vapor absorptivity dependence on wave number, atomic density and temperature in 2537 A resonance line region, discussing measurement by magnetic scanning or monochromator

14 p2131 A72-30853

Methane collision broadened rotational fundamental line, calculating line width dependence on temperature

14 p2135 A72-30893

Noncoherent isotropic scattering in plane parallel finite layer, considering Doppler line broadening

15 p2273 A72-31331

CW tunable semiconductor laser measurement of CO laser amplifier gain line shape for several vibration-rotation lines

15 p2245 A72-31382

Planetary cloudy atmosphere synthetic spectral line profile computation, using analytic scattering diagrams

15 p2192 A72-31649

Rocket-borne spectrometric measurement of small solar flare O VII and Ne IX resonance lines and 5 keV X-ray continuum emission, analyzing data via nonisothermal model

15 p2300 A72-31990

Ar plasma radiation dispersion by plane grating, measuring ionic spectral lines and continuous spectrum intensity time variation

15 p2286 A72-32340

Hydroxyl emission sources classification from observed main line polarization and satellite lines

15 p2315 A72-32710

Tabulation of diatomic molecular lines observed in sunspot spectra with rotation branch, quantum number and vibration band

15 p2316 A72-32750

Solar photosphere and low chromosphere spectral lines non-LTE empirical analysis, relating coefficients of departure from LTE to elemental state temperatures

15 p2317 A72-32771

Large sunspot umbra high resolution spectrogram obtained by beam splitter with monochromatic polarization optics, noting blends near Zeeman lines

15 p2317 A72-32775

Solar O VI, Ne VIII and Mg X spectral lines intensity ratios from XUV rocket measurements, comparing data with Jordan-Allen-Dupree ionization equilibrium calculations [AD-745811]

15 p2318 A72-32783

Solar Fe XIII IR lines intensity ratio at 10747 and 10798 A, deriving electron density as function of dilution factor with allowance for proton impact effect

15 p2318 A72-32784

Astronomical objects spectral lines red shift interpretation in terms of noncosmological origin and photon-photon interactions

16 p2450 A72-32863

LF spectrum of depolarized light scattered from liquids composed of molecules with anisotropic polarizabilities, noting sharp line spectra with VH shear doublets

16 p2429 A72-32951

Computerized analysis of overlapping Raman and IR spectral lines, describing routine for resolving complex spectrum into component lines via operator intervention

16 p2366 A72-33027

Quasars spectroscopic observations, noting red shift and line spectra errors and corrections

16 p2452 A72-33133

K2 III star Arcturus far UV chromospheric emission line spectrum observation with rocket-borne spectrometer, identifying hydrogen I, alpha and O I

16 p2453 A72-33136

OSO I observation of 300 second oscillation in solar transition region and coronal extreme UV emission line intensity

16 p2453 A72-33137

Coherent emission lines in visible spectrum from triply ionized Er in barium yttrium fluoride, discussing energy level transitions associated with various lines

16 p2401 A72-33387

Heavily doped ruby optical properties review, discussing N-lines, absorption and fluorescence spectra, interactions with phonon and photon fields and ionic reactions

16 p2441 A72-33522

Flowing air glow discharge near IR emission spectrum as function of pressure, noting atomic lines

16 p2427 A72-34097

Spectral characteristics of hot stars with emission lines, discussing Ba, Of, P Cygni, Wolf-Rayet and B type supergiant stars

16 p2462 A72-34183

Titan spectrum absorption features, estimating hydrogen abundances

17 p2606 A72-34540

On the dependence of the linear velocity of solar rotation on latitude and optical depth.

17 p2607 A72-35076

The solar abundance of gold.

17 p2607 A72-35077

Measurements of the limb darkening in the forbidden MgI line at 4571.1 A.

17 p2608 A72-35078

A compact grating spectroheliograph for the MgII resonance lines.

17 p2554 A72-35079

Spectral analyses of solar photospheric fluctuations. II.

17 p2608 A72-35081

Solar corona emission line polarization numerical computation based on magnetic dipole transition scattering function for interpretation in terms of magnetic field direction

17 p2608 A72-35084

Solar flares and prominences rotational motions from spectrographic observations of atomic Al absorption line periodic asymmetry

17 p2608 A72-35086

The identification of the 1-0 and 2-1 bands of HCl in the infrared sunspot spectrum.

17 p2611 A72-35299

Metallic abundances in the solar chromosphere.

17 p2613 A72-35498

Theoretical He-triplet line strengths compared with astronomical observations of planetary nebulae and H II regions

17 p2614 A72-35646

Some new Dy II identifications in the solar spectrum.

17 p2616 A72-35696

Doppler shift of solar photospheric spectral lines related to downward motions over plages

17 p2617 A72-35705

Improved Stark-profile calculations for the He II lines at 256, 304, 1085, 1216, 3203, and 4686 A.

17 p2585 A72-35768

The classification of transitions between levels of principal quantum numbers 3 and 4 in Fe IX to XVI and Mn VIII to XV.

17 p2586 A72-35834

Galactic nebulae electron temperature and density from forbidden line emissions interpreted in terms of transition probabilities and collision strengths

18 p2723 A72-36090

Experimental analysis of the vibrational-rotational line content of a Q-switched CO₂ laser.

18 p2697 A72-36501

Changes in the spectrum of the star Be HD 217050

18 p2727 A72-36733

Pm existence evidence for HR 465 from analysis of Pm II spectral line data

18 p2727 A72-36738

The use of known helium line cross sections for investigation of unknown transition in neon.

18 p2713 A72-36954

Time-dependent ionization equilibrium and line radiation under flarelike conditions.

19 p2849 A72-37241

On circumstellar molecules in the Pleiades.

19 p2856 A72-37508

Photon count circuit conjugation with photomultiplier for spectrometric measurement of lines emitted by atomic barium jet excited by slow electron beam

19 p2799 A72-37671

Coma, astigmatism and spectral line curvature derivation for spherical mirror-concave grating assembly, calculating mounting resolution in terms of wavelength

19 p2799 A72-37672

Continuous emission localization in solar flare nuclei

19 p2850 A72-37814

Pressure shift of the magnetic resonance line of neon in a He-Ne laser.

19 p2811 A72-37930

Spectral line profiles of the solar chromosphere. III - Relationship between the line profiles and their intensity gradients

19 p2860 A72-37950

Study of the spectrally variable silicon Ap star 56 Ari

19 p2862 A72-38055

L-S coupling interpretation of high-resolution LMM Auger spectra of Cu and Zn.

19 p2846 A72-38597

Nightglow observations and ionospheric soundings for red oxygen line intensity relation to F region parameters

19 p2792 A72-38638

Investigation of the 0.63-micron line shift in an He-Ne/20/laser with an absorbing cell

19 p2814 A72-38787

Emission lines and optical continuum of Seyfert radio galaxy 3C 120 from spectrophotometric scans

20 p2965 A72-38905

Interstellar molecules and dense clouds.

20 p2970 A72-39600

Line formation in the presence of magnetic fields: Proceedings of the Conference, Boulder, Colo., August 30-September 2, 1971.

20 p2970 A72-39752

The treatment of the Stokes parameters and measurement of magnetic field.

20 p2970 A72-39755

The redistribution function of polarized light in the presence of collisions and of small magnetic fields - Discussion of the polarization of the solar line Ca I 4227 A.

20 p2971 A72-39756

Computer program for solar corona emission line polarization computation to interpret measurements in terms of coronal magnetic field direction

20 p2971 A72-39757

Stellar multilevel spectral line formation solution by preconditioning procedure based on core frequency transfer determination by local saturation approximation

20 p2954 A72-39758

Thermalization lengths and mean numbers of scatterings for line photons.

20 p2956 A72-39759

Line spectra and continuum polarization in magnetic white dwarfs.

20 p2971 A72-39760

On the filamentary nature of solar magnetic fields.

20 p2971 A72-39762

On the filamentary nature of active-region magnetic fields.

20 p2971 A72-39764

Interstellar gas electron temperature determination from recombination line spectra observations along galactic ridge

20 p2971 A72-39858

Emission and absorption line spectra of type I supernovae after luminosity maximum interpreted by heating and ionization mechanisms in shell and intensity computation

20 p2973 A72-39886

Calculation of solar CO vibration-rotation line profiles and equivalent widths.

20 p2973 A72-39889

Temperature and emission measure deduced by coronal visible lines.

20 p2974 A72-39896

Emission and absorption RF recombination lines of interstellar neutral atomic H and He, discussing electron transition processes in nebula

20 p2975 A72-40070

Kr I and II lines strength and relative transition probabilities, using thermal plasma behind reflected shock wave as spectroscopic light source

21 p3089 A72-40137

Cross sections for the excitation of Ar II laser lines in electron-ion collisions.

21 p3063 A72-40725

Shapes and widths of ammonia lines collision-broadened by hydrogen.

21 p3013 A72-40817

Coulomb-collision corrected ion-acoustic line profiles.

21 p3092 A72-40819

Numerical model of NGC 7662 consistent with line strengths and ratios, considering double shell structure and central star flux deviation from black body

21 p3105 A72-41033

Interstellar lines in the ultraviolet spectrum of zeta Ophiuchi.

21 p3105 A72-41035

Transfer of resonance-line radiation in differentially expanding atmospheres. I - General considerations and Monte Carlo calculations.

21 p3106 A72-41037

New observations on the Kuiper bands of Uranus.

21 p3106 A72-41043

Temperature range estimation method for planetary atmospheric component generating spectral lines, applying to Venus observations at 7820 A carbon dioxide band

21 p3106 A72-41045

Hydrogen sulfide detection in Galactic sources via observation of single line corresponding to rotational transition, comparing abundance to formaldehyde, CS, HCN and CO

21 p3107 A72-41271

Probability interpretation of radiative transfer to calculate magnetic field-originating spectral line for-

mation dependence on solar atmosphere mean optical depth 21 p3107 A72-41276

He II line emission in cold regions of solar prominences and chromosphere, noting hydrogen, metal and He I emissions 21 p3108 A72-41281

Coexisting weak and strong opposite-polarity magnetic field regions as cause of sunspot umbra Zeeman spectra pi-component splitting 21 p3108 A72-41283

Photoelectrically observed diatomic carbon absorption lines in sunspot spectra for two energy bands 21 p3108 A72-41284

Diatomic carbon lines search in sunspot umbras spectrum from solar telescope observations 21 p3108 A72-41285

Various ground configuration level intervals from gaseous nebulae and solar coronal forbidden transitions observations and laboratory investigations of resonance lines 21 p3108 A72-41286

Coronagraphic observations of an enhanced coronal region. II - Temperature and density structure through the enhanced region. 21 p3108 A72-41288

Spectrum of P Cygni in 1968-1969. 21 p3110 A72-41445

Stratification of the emission in the envelope of a Wolf-Rayet type eclipsing binary V444 Cyg 21 p3113 A72-41759

Effect of a random magnetic field on the absorption line characteristics of stars 21 p3113 A72-41761

Solar silver abundance from spectral scans for Ag 3280.7 and 3382.9 A resonance lines, using spectral synthesis method, model atmosphere and limb darkening observations 22 p3221 A72-42028

Transuranium elements in HD 25354. 22 p3224 A72-42381

Molecular vibration levels inversion ratios increase by vibrationally cold CO addition to CW CO chemical laser, observing R-branch emission lines 22 p3185 A72-42615

Observations of the airglow continuum. 22 p3174 A72-42888

Spectrophotometric study of the cometary nebula NGC 2261 22 p3229 A72-42961

21 cm observations of NGC45. 22 p3229 A72-42995

The emission-line spectrum of Cygnus A. 22 p3334 A72-43251

Type II supernova spectral intensity minima due to blueshifted absorption lines of hydrogen and Fe II based on observed and synthetic spectra wavelength comparison 23 p3334 A72-43257

Gas absorption lines detection based on multiple light passage through absorbing medium during generation process, noting radiation spectra of neodymium glass laser 23 p3295 A72-43305

New lines of neon ions in the range 50-200 A. 23 p3315 A72-43802

Ultraviolet absorption lines in the spectrum of Vega. 23 p3337 A72-43826

Digitally pressure-scanned Fabry-Perot interferometer for studying weak spectral lines. 23 p3289 A72-43891

Spectral line identification computer program determining wavelength and equivalent line width from photometric measurements 23 p3267 A72-44029

Structural characteristics of high resolution NMR spectra, noting interrelationships between line positions and intensities 23 p3290 A72-44171

Ionization structure and coarse and fine analyses in planetary nebulae spatial spectroscopic diagnostics based on line profile monochromatic intensity integral equation inversion 23 p3339 A72-44236

Coronal lines photometry systematic error dependence on aureola spectral intensity, line half width, gradation curve slope, and neutral filter transmission coefficient 23 p3340 A72-44240

A meteor spectrum in the infrared region. 23 p3341 A72-44473

The influence of ultraviolet line blanketing on the neutral helium triplet lines in B-type stars. 24 p3438 A72-44834

A further high-resolution search for Fe XXV line emission from Scorpius X-1. 24 p3438 A72-44838

Fast Fourier transform algorithm for astronomical line spectra resolution enhancement, estimating central line intensity, line width parameter and line shape. 24 p3438 A72-44841

Profile of a parametric luminescence line emitted by lithium niobate crystals. 24 p3432 A72-45614

LINEAR ACCELERATORS

Nb superconducting resonant cavities application to linear accelerator and RF particle separator structures in GHz region for wall energy loss reduction 13 p1922 A72-29348

Radiographic measurement of gas turbine components during response to thrust changes, using linear accelerator for X ray generation 14 p2092 A72-30620

LINEAR AMPLIFIERS

Hf and shf power transistor gain, efficiency and electrical characteristics for wideband linear amplifiers 08 p1139 A72-21051

Linear IC amplifier analysis by admittance parameters of equivalent two terminal pair network as function of frequency, temperature and supply voltage 09 p1285 A72-22342

LINEAR ARRAYS

NT ENDFIRE ARRAYS

NT YAGI ANTENNAS

X-band linear phased array tracking antenna with digital phase shifters and beam steering, evaluating beamwidth, gain and direction error 01 p0028 A72-10663

Linear antenna array optimal power pattern synthesis by best approximation, using weighting function in man-machine iteration 01 p0029 A72-10665

Optimal synthesis for radiator coordinates and complex amplitudes of linear antenna array for given radiation pattern 02 p0196 A72-12756

Waveguide radiators linear phased array impedance matching during E-plane wide angle scanning improved by reflection coefficient variation compensation 04 p0499 A72-15239

Synthesis of currents along linear antennas, reducing to solution of integral equation 04 p0500 A72-15406

Linear antenna input admittance calculation, computing excitation integral by field expansion in Legendre functions 04 p0501 A72-15431

Rectangular planar antenna array directivity from constituent linear arrays of dipoles or isotropic elements, using Forman method 06 p0782 A72-17358

Antenna pattern sidelobe control for line sources and uniformly spaced linear arrays, using iterative sampling method 06 p0782 A72-17359

Single slotted waveguide linear arrays, discussing microwave antenna design and feeding and cross polarization suppression 06 p0784 A72-17740

Bearing estimation performance of monopulse tracking with passive linear arrays, using computer simulation for various integration times and input S/N ratios 06 p0774 A72-17809

Ground based Doppler navigation system for wide range elevation and azimuth aircraft approach guidance, using linear directive antenna array for conical surface definition 06 p0845 A72-18183

Hansen-Woodyard condition applicability in continuous linear array design for increased directivity with optimal excitation 06 p0775 A72-18238

Microwave attenuation due to ohmic losses in periodic linear arrays of metallic cylinders, ribbons and slots in metallic ground plane 06 p0786 A72-18372

Step-scan landing system technique, using microwave fixed linear array for area coverage with pattern of narrow overlapping individually coded sequentially switched beams 06 p0846 A72-18397

Linear array antenna radiation pattern synthesis for minimum sidelobe level outside of given intervals, calculating current distribution 07 p0953 A72-19005

Linear antenna synthesis for minimum sidelobe level, eliminating superdirectivity effect 07 p0956 A72-19567

Improved circuit theory for linear antenna array design, obtaining maximum directivity and corresponding current distributions and driving-point voltages and currents 07 p0958 A72-20193

Synthesis of linear antenna with integrated currents for specified ratio of antenna radiation to elementary radiator patterns 10 p1436 A72-24504

Parasitic sidelobe suppression in radiation patterns of phase switching linear antenna array without gain loss 11 p1598 A72-26717

Local FM radio pulse scattering by cylinder and linear cylinder array in Kirchhoff approximation 13 p1914 A72-28407

Radiation patterns of linear equidistant fishbone-type dipole antenna array fed by long symmetrical transmission line 13 p1930 A72-29056

Mathematical analysis of feed point displacement effects on linear dipole antennas, investigating radiation properties 16 p2362 A72-32852

Computer calculations of horizontal linear antenna impedance for multilayer plane stratified medium, using induced emf method 16 p2368 A72-33492

Shaped-beam synthesis of nonuniformly spaced linear arrays. 17 p2525 A72-34370

A portable coaxial collinear antenna. 17 p2526 A72-34377

Pattern synthesis of linear arrays using Fourier coefficient matching. 18 p2659 A72-36298

Analysis of the correlation functions of space-time wideband signals received by linear antennas 19 p2775 A72-38657

Antenna pattern analysis for compatibility prediction. 20 p2902 A72-39000

Optimal synthesis for radiator coordinates and complex amplitudes of linear antenna array for given radiation pattern 20 p2907 A72-39062

The optimum design of small nonuniformly spaced arrays. 21 p3027 A72-40362

On the relationship between classical and matrix design methods for arrays of wire antennas. 21 p3027 A72-40373

Linear HF radar antenna array aperture synthesis for ionospherically propagated signal reception in air-plane for achievement of ideal directivity without ionospheric compensation 21 p3022 A72-41080

Linear antenna synthesis for minimum sidelobe level, eliminating superdirectivity effect 22 p3158 A72-42085

Multimoded components wavefront arrival angle from measurements of signal induced in linear array, discussing numerical calculation from linear equation solution and polynomial roots 23 p3264 A72-43601

Butler-matrix fed arrays, discussing phase differences, scan steps and sectors, sidelobe structure and attenuation 23 p3273 A72-44363

Acoustical holography with a scanned linear array. 24 p3401 A72-44705

LINEAR CIRCUITS

Linear active two-port networks, considering concept of noise figures F less than 1 in signal and noise transmission 07 p0944 A72-19659

Numerical linear interpolator design with ICs, noting application to digital filters and sampled data systems 09 p1289 A72-23677

Modulated filter theory for AM signal analysis in linear resonant circuits, noting use for superheterodyne amplifier and phase discriminator design 13 p1930 A72-29046

Hysteretic motor in steady synchronous operation with nonsinusoidal supply voltage, computing stator winding current based on superposition with two linear equivalent circuits 13 p1900 A72-29975

Integral Laplace-Fourier transform stability during transient response functions reconstruction from frequency characteristics in linear circuits 15 p2264 A72-31879

Linear ICs application to RF probe for ionospheric electron density measurements from rockets or satellites 15 p2240 A72-32389

Development of a continuous linear model of a d-c to d-c flyback converter. 18 p2643 A72-36073

Linear electric circuits optimal synthesis as non-linear programming of network parameters, discussing approximation algorithms 19 p2776 A72-37306

Programming method for computer analysis of linear passive circuits powered by voltage sources 19 p2777 A72-37311

Determination of linear circuit sensitivity to circuit parameter changes in the equations of state variables 19 p2777 A72-37312

Differential equations for digital model of linear quadrupole, discussing digital simulation of analog radio equipment circuits 19 p2775 A72-38659

New active all-pass network with linear group delay. 20 p2910 A72-39431

Possibility of developing combination method for calculating, with a controlled quantization step, the response of a nonlinear network 21 p3074 A72-40184

- Digraphs application to electronic linear networks analysis, developing computer program
21 p3024 A72-40992
 - Low cost design of linear pulse stretcher circuit for short duration pulse time measurement in nuclear instrumentation and computing counters
21 p3033 A72-40997
 - Inductive frequency converter with a characteristic having enhanced linearity
21 p3058 A72-41802
 - Computation of optimal parameter domains of components in the design of electronic circuits
23 p3268 A72-43440
 - Generalized numbers method for analysis and synthesis of linear circuits described by signal flow graph, noting algorithms for computer programming
23 p3269 A72-43443
 - Linear theory of a microwave distributed amplifier based on an avalanche transit-time diode
23 p3271 A72-43776
 - Linear electronic networks analysis and synthesis via equations of variable states, noting structural features of circuits without component related degeneration
23 p3271 A72-43844
 - Frequency conversion and limiter action for an angle-modulated wave with amplitude fluctuation in a half-wave linear mixer.
23 p3265 A72-44179
- LINEAR EQUATIONS**
- Uniformly and asymptotically stable solutions to linear Volterra integrodifferential equation system, discussing Liapunov stability
02 p0252 A72-11997
 - Stability of plane rotating galaxies in magnetic field parallel to axis of rotation, showing linearized MHD equations self conjugate for radial disturbance case
03 p0435 A72-13806
 - Rotationally symmetric force free magnetic field boundary value problem, using linear elliptic differential equation
03 p0400 A72-14352
 - Quasi-linear parabolic equations, investigating conditions for Cauchy-Dirichlet problem solution
03 p0383 A72-14380
 - Second order differential equations system solution in convergent integrals, describing solution limit in vector form as special case of linear system solution property
07 p1026 A72-18815
 - Algorithm for constructing linear and nonlinear differential and algebraic equations of state variables of nonlinear electronic circuits
07 p0958 A72-18846
 - Interpolation of function of two variables by surface splines method, solving linear equations system by digital computer
07 p1026 A72-19095
 - Multiple point boundary value problem with linear integrodifferential equation simplification
07 p1028 A72-19983
 - Wave diffusion related to phenomena governed by linear hyperbolic partial differential equations of second order, presenting Cauchy problem solution
07 p1035 A72-20090
 - Linear equations with periodic coefficients in mathematical models for systems with rotating components, discussing methods for obtaining closed form solutions
07 p0913 A72-20204
 - Theorems for averaging of first order linear hyperbolic system with time lag, proving existence and uniqueness of solution to Cauchy problem
07 p1028 A72-20214
 - Linear first order differential equation transient response computer simulation using transition matrix method
07 p1028 A72-20340
 - Liapunov theorem for polynomial solution existence for first order inhomogeneous system of linear partial differential equations
08 p1205 A72-20958
 - Autonomous linear second order equations system reduction to Poincare normal form in oscillations theory
08 p1206 A72-21169
 - Uniqueness theorems for linearized Boltzmann equation with Maxwell boundary conditions, using Gauss theorem and Schwartz inequality
08 p1149 A72-21252
 - Convergence and stability criteria of monotonic difference schemes for linear parabolic differential equations with interface boundary conditions
08 p1199 A72-21286
 - Bergman operators construction for second order linear partial differential equations
08 p1199 A72-21288
 - Ordinary linear differential equation boundary value problem solution in form of asymptotic series in powers of small parameter
08 p1199 A72-21462
 - Optimal controllers analytic design for linear steady controlled differential equations system
08 p1145 A72-21467
 - Variational solutions to linear integral equations and extremal functions in physical gas dynamics problems, using stepwise constant trial functions
08 p1150 A72-21620
 - Functional analysis techniques for existence of holonomic solutions to linear differential equation systems with singular points
09 p1342 A72-23254
 - Equivalence of integral equation form and infinite system of linear equations with eigenvalue localization, applying to linear ordinary differential equations.
09 p1342 A72-23367
 - Numerical solutions of linear and nonlinear hydrostatic primitive equations for frontogenesis forced by nondivergent horizontal wind, noting discontinuities prediction
09 p1347 A72-23651
 - Collision operator behavior in linear Boltzmann equation model of molecular gas in Hilbert space
10 p1510 A72-24102
 - Predictor-corrector method for stiff linear differential equations, considering truncation error estimation and system stability
11 p1675 A72-25272
 - Lower bound estimates of error distributions for analog computer solutions of linear algebraic equations
11 p1600 A72-25433
 - Numerical stability in linear algebraic equations, considering mapping from input data to desired output information
11 p1677 A72-25861
 - Partial orderings applications to convergence of iterative methods for solution of linear equation systems involving positive definiteness or monotonicity
11 p1677 A72-25862
 - Dynamical torsion theory of rods deduced from linear elasticity equations, using averaging technique
11 p1736 A72-25987
 - Regular matrices inversion for linear equations solution, using modified method of completing
11 p1678 A72-26495
 - Linear difference equations solved by indefinite Z transformations technique using Cramer rule for simultaneous algebraic equations
11 p1678 A72-26664
 - Russian papers on functional analysis covering approximate solution of linear integral equations, averaging principle for partial differential equations and boundary value problems
12 p1837 A72-27994
 - Lie group theory application to linear differential equations of motion with variable parameters, considering flight vehicle example
12 p1847 A72-28127
 - Flight vehicle motion described by linear differential equations with variable parameters, discussing programmed optimal control solution by functional analysis
12 p1755 A72-28128
 - Russian monograph on three dimensional deformable bodies stability covering linearized equations for subcritical deformations and strength analysis of low shear rigidity structures
12 p1888 A72-28337
 - Asymptotic approximation methods for boundary layers in singular perturbation theory for linear elliptic partial differential equations in two independent variables
13 p1940 A72-28425
 - Bending of rectangular plates clamped at three edges, establishing sufficient conditions for application of simple iterations to linear algebraic equations solution
13 p2057 A72-29077
 - Generalized solution regularity of arbitrary order quasi-linear elliptic equations, indicating continuity conditions of variational problems
13 p1987 A72-30001
 - Linear functional equations with constant coefficients for generalized partial derivative operators introduced in certain spaces of functions of many complex variables
13 p1987 A72-30083
 - Delayed argument linear partial differential equations system integration, constructing asymptotic solution in nonresonant case
13 p1988 A72-30084
 - Linear stiff differential equations subdominant solutions, developing numerical integration algorithm
14 p2126 A72-30525
 - Iterative numerical solution of linear differential equations system for wind vertical velocity and local pressure variation along vertical line
15 p2265 A72-31344
 - Iteration methods to compute inverse for nonsingular linear operator on Banach space
15 p2261 A72-31495
 - Linear differential equations solution symmetry properties, using Lie algebraic methods and finite dimensional linear systems theory
15 p2264 A72-31761
 - Linear autonomous differential equations finite time stability theory, extending to systems driven by white noise
15 p2264 A72-31764
 - Microscopic theory of weakly ionized plasma conductivity, showing particle diffusion function or transition probability description by linear Boltzmann equation
15 p2287 A72-32412
 - Plane wave dispersion and nonlocal elasticity equations linearization, demonstrating continuum treatment of lattice dynamics
15 p2330 A72-32445
 - Numerical methods for Liapunov linear matrix equations solution in control systems analysis and design
15 p2265 A72-32798
 - Completeness proof for linear elasticity theory set of three harmonic functions based on theory of linear differential equations with constant coefficients
16 p2466 A72-33018
 - First eigenvalue and first eigenfunction properties of linear elliptic partial differential equation in variational form with discontinuous coefficients, considering Dirichlet problem
16 p2416 A72-33502
 - Turbulent solutions of certain linear and nonlinear partial differential equations
17 p2537 A72-34194
 - Coefficient criterion of stability for Liapunov indices in a two dimensional linear system
17 p2575 A72-34774
 - Feedback controller synthesis from nonlinear system modeling by linear equations, proving theorem relating stability properties
18 p2672 A72-36060
 - Necessary and sufficient conditions for space linear operator factorization, noting summation operators theory
18 p2704 A72-36462
 - A basic theorem in the computation of ellipsoidal error bounds.
18 p2705 A72-36602
 - Variational principle of linear differential equations.
18 p2705 A72-36717
 - A posteriori error bounds for approximate solutions of linear second-order ordinary differential equations.
19 p2824 A72-37372
 - The problem of encounter avoidance in linear differential games
19 p2824 A72-37377
 - Asymptotic solution of a second-order linear differential system
19 p2824 A72-37382
 - Linear partial differential equations with random forcing.
19 p2825 A72-37573
 - Method of Lagrange multipliers for exploitation of the entropy principle.
19 p2825 A72-37842
 - Solution of certain systems of partial differential equations in linear commutative differential operators
19 p2825 A72-38183
 - Distributed parameter linear and nonlinear systems analysis, deriving theorem for solution stability of linear partial differential equations
19 p2826 A72-38247
 - The Galerkin method for the numerical solution of Fredholm integral equations of the second kind.
19 p2827 A72-38384
 - One realization of Liapunov's method for integrating linear equations
19 p2827 A72-38469
 - Limit distributions for sums of random values specified in a denumerable Markov chain with absorption
19 p2827 A72-38470
 - Asymptotic behavior of solutions of boundary value problems for systems of linear ordinary differential equations with a small parameter by the derivative
20 p2945 A72-39464
 - Group properties of ordinary linear second-order differential equations
20 p2946 A72-39471
 - Variability of solutions to higher-order time-lag linear differential equations
20 p2947 A72-39864
 - Solution to the encounter avoidance problem in a linear differential game
20 p2947 A72-39865
 - Accuracy of alpha-analog simulation of linear algebraic equations in the case of a nonzero discrepancy vector
21 p3074 A72-40170
 - Classes of uniqueness of solutions to a boundary value problem in an infinite layer for systems of linear difference-differential equations
21 p3074 A72-40257
 - Initial-value methods in the theory of Fredholm integral equations. II.
21 p3075 A72-40550
 - Motion concept formulation by linear algebra of n dimensional spaces, emphasizing tensor character of velocity and acceleration
21 p3084 A72-40816

Characteristic equation coefficients of monodromy matrix for linear system of second order homogeneous differential equations with periodic coefficients

21 p3075 A72-41092

On the calculation of variances of solutions to linear simultaneous equation.

21 p3075 A72-41233

Regularized linear problem with perturbed equation as solution, presenting error overestimate

21 p3076 A72-41336

A system of linear equations with partial derivatives

21 p3077 A72-41822

Instability of the characteristic indices of systems of linear differential equations with almost periodic coefficients

22 p3197 A72-41853

Discontinuities propagation in quasi-linear hyperbolic partial differential equation systems, noting MHD flow and crystal optics equations

22 p3204 A72-41905

A regularity theorem for linear second order elliptic divergence equations.

22 p3198 A72-41947

Analogies between linearized and linear problems in elasticity theory in the case of uniform initial states

22 p3233 A72-42061

Necessary and sufficient conditions for the absolute asymptotic stability of linear systems of differential equations with constant delay

22 p3198 A72-42143

Certain necessary conditions for the local solvability of first-order differential equations with infinitely differentiable coefficients

22 p3198 A72-42158

Algorithm for identification of unsteady dynamic objects described by linear differential equation, noting quasi-optimal system operation

22 p3205 A72-42290

Second order differential equations with general boundary conditions.

22 p3199 A72-42915

German monograph - Internal-analytic methods in systems of linear equations with interval coefficients and relations to error analysis.

22 p3200 A72-43061

A method for partitioning the phase space into regions with constant-sign increments of phase coordinates

23 p3275 A72-43780

Estimates of derivative solutions of linear non-homogeneous elliptic-type equations of arbitrary order near the domain boundary in the L_2 metric

23 p3309 A72-44041

Poorly founded systems of equations in astronomical practice and methods for their solution

24 p3437 A72-44760

On zeros of solutions of the second-order linear differential equation with retardation.

24 p3419 A72-45577

Comparison of linear and Riccati equations used to solve optimal control problems.

24 p3420 A72-45775

LINEAR FILTERS

NT KALMAN FILTERS

Kalman filtering process digital simulation by numerical integration of matrix differential equations describing linear system random process model and optimal filter

01 p0024 A72-10225

RF interference in angle-modulated system with predetection linear bandpass filter, calculating output power spectral density in baseband

01 p0045 A72-10332

Dynamic model for estimating Bayesian recursive images by linear Kalman filtering

01 p0046 A72-10866

Optimal stochastic /Kalman/ filters application to integrated air and submarine navigation systems, discussing measurement errors modeling as bias and colored noise

02 p0256 A72-12050

Discrete time square root Kalman filtering techniques, discussing computational requirements and covariance and information implementations

02 p0198 A72-12804

Kalman filter divergence due to errors, applying to orbital navigation

02 p0198 A72-12805

Computational time and computer storage requirements for discrete Kalman filter, comparing simultaneous and sequential types of measurement processing

02 p0198 A72-12806

Satellite tracking by combined optimal estimation and control techniques with Kalman filter, considering radio antenna and optical tracking systems

02 p0285 A72-12812

Fading medium transfer function estimation via homomorphic and Kalman filtering, considering multiplicative noise

03 p0326 A72-14195

Kalman type optimal filter for linear distributed-parameter systems under white Gaussian and boundary noise, obtaining Wiener-Hopf equation by calculus of variations

04 p0505 A72-14668

Discrete-time adaptive Kalman filter based on learning process and parameter estimate updating in operational cycle, comparing with simple Kalman and Wiener filters

05 p0639 A72-15758

Optimal digital Kalman filtering for systems with continuous input noise by autocorrelation function matching

[ASME PAPER 71-WA/AUT-21]

05 p0640 A72-15952

Kalman linear filtering technique for spinning satellite attitude restitution, evaluating reliability by model for simulation of measurements by sensors

[ONERA, TP NO. 953]

05 p0724 A72-16436

Satellite attitude estimation on elliptic orbits by Kalman filters with periodic coefficients, demonstrating efficiency by earth pointing satellite using different instrumentation noise models

05 p0685 A72-16442

Optimal linear filtering for unmodeled time correlated driving disturbances of forcing function, applying to space navigation

05 p0685 A72-16461

Sensitivity algorithms for finite memory batch processing smoother /Kalman filter/, applying to ship inertial velocity error estimation

05 p0686 A72-16572

Incorrect or unmodeled error sources effects on arbitrary linear navigation filters design and performance

[AIAA PAPER 72-14]

05 p0688 A72-16911

Generalized matrix inverse application to dynamic system state vector estimation, determining covariance matrix for comparison with optimal Kalman type procedure

05 p0641 A72-17089

Jupiter mass from discrete time observations of J1X satellite positions and velocities, using sequential Kalman-Bucy filter

06 p0876 A72-17580

Kalman and linear numerical filtering, discussing data processing from wind tunnel and rocket flight tests

06 p0774 A72-17847

Kalman-Bucy colored noise filtering discrete time results and continuous time linear minimum variance estimation by calculus of variations

06 p0793 A72-17955

Suboptimal Kalman filter design for system state estimation in presence of plant dynamics uncertainties and measurements noise, optimizing tradeoff between sensitivity and estimation error

07 p0959 A72-19302

Time optimal self alignment of inertial platforms using gyros and accelerometers with Kalman-Bucy filter

07 p0989 A72-20279

Turbopump rotating assembly bearing parameters and inertia products estimation and identification by extended Kalman filtering

08 p1173 A72-20844

Compensated Kalman filter as suboptimal state estimator to eliminate steady state bias errors in use with mismatched asymptotic time-invariant case

08 p1144 A72-20845

Dynamic system time varying parameters on-line estimation using adaptive extended Kalman filter based on predicted error covariance matrix alteration

08 p1144 A72-20847

Quantization errors effect on recursive filter design for strapdown inertial navigation systems, developing suboptimal linear minimum variance

08 p1144 A72-20848

On-line equalization of digital communication channels, discussing extended discrete Kalman filter use as adaptive equalizer

08 p1131 A72-20855

Onboard orbital navigation system analysis on space shuttle radio range and range rate measurement data relative to ground beacon, using Kalman filter

08 p1203 A72-20856

Sequential testing of actual and calculated error covariances consistency in recursive nonlinear estimators, noting method application to linear filters

08 p1197 A72-20857

Omega radio navigation system laning problem, discussing ambiguity resolution by multiple state vector Kalman filter

08 p1144 A72-20860

Kalman filter estimator for nonlinear human pilot model parameters including time delay

08 p1145 A72-20861

Orbit determination using Kalman-Bucy filter to estimate state and unmodeled acceleration approximated as first order stationary Gauss-Markov process

08 p1145 A72-20867

Input binary sequence transformation in chain of series connected on-off neuron models, applying to n-stage linear filter analysis

08 p1138 A72-20870

Pontryagin maximum principle application to optimal linear filtration for multivariable systems with signal processing

08 p1133 A72-21374

Stationary Kalman-Bucy filter synthesis from filter coefficients and correlation matrix of filtration errors, discussing random process estimation application

09 p1289 A72-23434

Optimum bounding filter design based on error covariance for Kalman-Bucy and Wiener filters with inexact known parameters, obtaining performance figure of merit

10 p1454 A72-23785

Recursive minimum variance linear filter and controller for systems with white state-dependent noise

10 p1455 A72-23800

Linear least squares estimation of Stratonovich-Kalman-Bucy formulas by innovations method

10 p1503 A72-23801

Fixed point smoothing of sequentially correlated processes by extending filtering technique to simultaneous estimation of state and process noise contribution

11 p1610 A72-25871

Linear multiple section binary filters analysis and synthesis, discussing mesh functions spectra for signal measurement in automatic control systems

11 p1612 A72-26452

Stochastic time varying patterns classification by Kalman filter, discussing optimum dichotomizer with supervised learning

12 p1790 A72-27498

Narrow band linear filter output SNR relationship to orthogonal radiating elements system directional gain and radiation patterns

13 p1931 A72-29281

Kalman filter stability analysis by mathematical modeling, using floating point computer algorithm

13 p1934 A72-30000

Kalman filter application to inertial navigation systems optimal alignment, discussing linear systems representation in state space and filter algorithm recursive equations

14 p2129 A72-30330

Fourth order linear filter function suggested for pulse signal detection from gravitational antennas, noting parameters optimization

14 p2086 A72-30800

Optimal filter synthesis for linear time varying parameter control systems, using computer-aided solution of multidimensional Riccati equations

14 p2090 A72-31120

Signal with bounded spectrum, obtaining higher derivatives by reduction to stationary random process filtering problem solvable with Kolmogorov-Wiener and Kalman-Bucy techniques

15 p2207 A72-32171

Optimal filtering estimate of noisy nonlinear partial differential distributed parameter system, using least squares and invariant imbedding techniques

16 p2416 A72-33575

Inertial navigation system platform alignment and calibration by state space technique similar to Kalman filtering

16 p2420 A72-33697

Recursive filtering techniques in space navigation, describing initialization procedure to account for state vector errors correlation

17 p2532 A72-34214

Bayesian recursive linear Kalman filtering technique for image estimation with noise background elimination, proposing time invariant dynamic model to provide stationary statistics

17 p2520 A72-34403

Helicopter stability derivative extraction and data processing using Kalman filtering techniques.

[AHS PREPRINT 641]

17 p2490 A72-34501

The identification of parameters in nonlinear thermal networks with the aid of a Kalman filter

17 p2533 A72-34827

Filtering with perfectly correlated measurement noise.

17 p2533 A72-35240

Spectral factorization in periodically time-varying systems and application to navigation problems.

17 p2578 A72-35492

Bayesian recursive estimation by Kalman filtering for enhancement of image corrupted by additive random noise

17 p2557 A72-35539

Optimal filtering in linear distributed-parameter systems.

18 p2673 A72-36823

Optimal minimal-order observers for discrete-time systems - A unified theory.

18 p2674 A72-37099

Linear stochastic system optimal measurement strategy and matched Kalman type filter computation via transformation into deterministic control problem

18 p2674 A72-37100

Target tracking based on the Kalman-Bucy filter

19 p2778 A72-37750

Extended Kalman filter with fictitious noise input for adaptive tracking of time varying parameters applied to VTOL aircraft

19 p2781 A72-38265

A biased filter for linear discrete dynamic systems.

19 p2781 A72-38273

Recursive updating of smoothing and filtering algorithms for discretely observed continuous dynamic linear systems

19 p2826 A72-38274

Stationary Kalman-Bucy filter synthesis from filter coefficients and correlation matrix of filtration errors, discussing random process estimation application

19 p2782 A72-38517

Filtration and extrapolation of multidimensional random processes described by linear differential equations system, examining adaptive filter synthesis

19 p2770 A72-38519

Calculation of pulsed signal amplitudes at linear filter output in optical communication systems

19 p2768 A72-38671

Design of a reduced-state suboptimal filter for self-calibration of a terrestrial inertial navigation system. [AIAA PAPER 72-849]

20 p2949 A72-39080

Optimum aiding of inertial navigation systems using air data.

20 p2950 A72-39082

Space shuttle terminal navigation with conventional navigation aids.

20 p2950 A72-39095

Minimax technique for direct synthesis of Kalman-like filter under large uncertainties in a priority statistics of plant and measurement noises

20 p2907 A72-39120

Enlarging the region of convergence of Kalman filters that encounter nonlinear elongation of measured range.

20 p2907 A72-39121

The observability of unforced physical systems by linear non-sequential estimators in the validation of linear error analysis.

20 p2910 A72-39123

Linear estimation stochastic filtering and deterministic linear optimal regulation duality concept extension to problems with inequality constraints

21 p3074 A72-40228

In-flight alignment and calibration of inertial measurement units. I - General formulation. II - Experimental results.

21 p3081 A72-41079

Investigations on the use of a Kalman filtering method in tracking systems for air traffic control.

21 p3082 A72-41168

Optimal, on-line linear filtering with noisy, time-delayed observations.

23 p3276 A72-43855

Conditions for space invariance in optical data processors used with coherent or noncoherent light.

23 p3288 A72-43887

Linear filtration of random signals based on the criterion of maximum signal-to-noise ratio

23 p3273 A72-44215

LINEAR PREDICTION

Learning-identification of unknown nonlinear discrete systems, using local estimation results for global function learning

01 p0046 A72-11199

Discrete-time adaptive Kalman filter based on learning process and parameter estimate updating in operational cycle, comparing with simple Kalman and Wiener filters

05 p0639 A72-15758

Satellite attitude estimation on elliptic orbits by Kalman filters with periodic coefficients, demonstrating efficiency by earth pointing satellite using different instrumentation noise models

05 p0685 A72-16442

Biased estimator as alternative to linear unbiased estimator for dynamic system model states and parameters optimization and regulation, noting squared errors sum

08 p1144 A72-20852

Standard linear estimation and control problem with quadratic loss, optimizing information rate by minimizing total measurements number through Riccati equation singular solution

08 p1144 A72-20859

Linear statistical forecasting with noncorrelated predictors by multiple regression equations, showing degradation dependence on sampled cross covariances

13 p1995 A72-29591

Target tracking based on the Kalman-Bucy filter

19 p2778 A72-37750

Best linear invariant estimation of Weibull parameters - Samples censored by time and truncated distributions.

22 p3199 A72-42969

LINEAR PROGRAMMING

Optimal frequency domain design of two dimensional low pass finite impulse response digital filters by linear programming

01 p0046 A72-10868

Thin shell creep and plasticity analyses reduced to linear programming problem by functionals and finite difference equations

02 p0290 A72-11622

Linear and quadratic programming procedures in optimal control problems of stochastic and deterministic system design

02 p0198 A72-12807

Sandwich beam design, deriving linear programming formulation suitable for computer treatment

04 p0590 A72-15191

Optimization algorithm for simultaneous solutions to bivalent 0-1 Knapsack problems with linear target function and linear restrictions, using ALGOL.

05 p0632 A72-15817

Automatic plastic minimum weight design of structural frames comparing with linear programming techniques

05 p0737 A72-16117

Optimum directional arrays design with linear programming simplex method generation of point elements excitation

06 p0774 A72-17855

Structural design primal and dual linear programming problem decomposition into sum and difference problems with form of original equation

07 p1026 A72-18810

Optimal multivariable control systems theory, considering linear programming, maximum principle and differential games

07 p0963 A72-19724

Linear programming procedure for efficiency and cost optimization in aerial survey mission

08 p1165 A72-21164

Optimality conditions for nonconvex optimization problems from linear programming solution

08 p1199 A72-21285

Linear programming application to aircraft selection for tactical airlift fleet contingency planning [AD-736074]

08 p1256 A72-21468

Man machine decision making procedures for multicriterial aggregate estimates, using pairwise comparisons and linear programming

09 p1273 A72-23430

Lower and upper bounds for number of lattice points in simplex, using linear programming algorithm for generating feasible cutting patterns for paper reels

11 p1678 A72-26157

Trajectory correction problem optimal measurement set, showing solution by linear programming simplex algorithm method

11 p1684 A72-26901

Linear programming simplex method for static load limit of circular arch

11 p1739 A72-26921

Computer calculation of minimum weight ribbed plates under axial compression by random search method and linear programming

12 p1878 A72-27083

Optimal design of thin walled minimum weight aircraft shell structures, using linear programming

13 p2058 A72-29143

Economic interpretation of dual variables in linear fractional programming, noting coherence of marginal pricing

14 p2087 A72-30714

Frequency domain design of two-dimensional finite impulse response digital filters.

17 p2532 A72-34406

Linear programming procedure for efficiency and cost optimization in aerial survey mission

17 p2521 A72-34455

An operations research approach to solve complex and unstructured problems illustrated for the case of cost-plus-award fee contracts.

17 p2639 A72-35341

The use of linear programming to design digital filters from impulse-response specifications.

18 p2663 A72-36304

Linear programming application to the solution of some optimum problems of reliability theory

19 p2825 A72-37995

Solution of the general linear programming problem by electronic simulation using the regularization method

21 p3023 A72-40155

Frequency-sampling and transversal digital filter equalizers optimal design from specified unit impulse time response, using linear programming algorithm

21 p3033 A72-40900

Characterization and algorithm for optimal solution of stochastic linear programming to minimize cost

21 p3075 A72-41234

Irreducible sparse matrix transformation to upper triangular form by row-column permutation formulated as linear integer programming problem

21 p3075 A72-41312

Mathematical formulation of linear programming problem, reducing vector value optimal management plan determination to quadratic programming problem

22 p3198 A72-42179

Plotting of composition vs property curves for superconducting systems with a digital computer by the method of simplex arrays

22 p3191 A72-42813

Design of a military air cargo transportation system by use of a large scale mathematical programming model.

24 p3466 A72-44577

LINEAR RECEIVERS

Linear detectors for broadband and high intermediate frequency measurements in radio astronomy

12 p1793 A72-27810

LINEAR SYSTEMS

Linear stochastic-parameter output channel, examining signal quadrature components statistical characteristics

01 p0024 A72-10199

Closed linear systems optimal stabilization determining transfer function from Wiener Hopf equation

01 p0045 A72-10572

Reachable sets calculation for linear dynamical system control, suggesting iterative procedures for numerical approximations

01 p0034 A72-11124

Linear systems partial stability via Liapunov second method, examining relation between uniformly and exponentially asymptotic partial stability

02 p0251 A72-11493

Feedback control dynamic system described by linear differential equation with random coefficients, calculating parameters distribution effect on behavior precision

02 p0197 A72-12339

Anelastic solid energy dissipation linear memory models based on viscoelasticity theory, applied to earth and metals experimental data and dynamic loading problems

02 p0294 A72-12447

Nomogram determination of frequency characteristics of closed loop linear automatic control systems

02 p0197 A72-12563

Linear aperture antennas approximate synthesis method, determining radiation pattern characteristics by solution of extremal problems in theory of linear integral operators

02 p0195 A72-12592

Noninteracting decoupling control theory for linear constant multivariable systems, using dynamic feedback matrix compensators

02 p0198 A72-12802

Linear regulator and servomechanism theories modification to account for fluctuation disturbances, obtaining deterministic controller design to maintain set point regulation or servotracking

02 p0198 A72-12803

Discrete-time linear quadratic stochastic control system with perfect measurements of state, obtaining optimal solution by dynamic programming

02 p0198 A72-12808

Optimal limited state variable feedback controllers design for static and dynamic linear systems [AD-738770]

02 p0198 A72-12809

Linear multivariable interacting feedback control system optimal design by heuristic approach to determine input-output pairing and controller settings for satisfactory disturbance attenuation

03 p0337 A72-12905

Linear time optimal control system with retardations in controls, discussing controllability, existence and uniqueness, synthesis techniques and dynamic programming [AD-737927]

03 p0338 A72-13406

Symmetrical three component pancratic system with intermediate constant image plane and linear displacement of components

03 p0360 A72-13562

Small parameter linear differential systems approximate solution, noting Liapunov reduction as particular case

03 p0389 A72-13785

Linear radio receiver circuit synthesis for output signal structure and rotational choice, using reduction algorithm

03 p0323 A72-13894

Limiting approximation theorems for synthesis of linear circuits and signals in time-frequency domains

03 p0338 A72-13896

Solution stability of linear differential equations systems with harmonic coefficients, using Jordan canonical forms and perturbation method

03 p0382 A72-13918

Soviet book on linear automatic control systems with variable parameters covering pulse transfer function determination algorithms, signal transmission characteristics and systems stability

03 p0339 A72-14245

Linear nongyroscopic conservative system stability from modified Lagrange equations of motion, using pseudo degree of freedom concepts and vibration method

03 p0362 A72-14394

Computer analysis of linear electric circuits without restrictions on network topology and component composition, using system matrix

04 p0495 A72-14464

Optimization programs for linear control systems with nonconvex constraints on phase coordinates applied to material point transfer

04 p0504 A72-14624

Kalman type optimal filter for linear distributed-parameter systems under white Gaussian and boundary noise, obtaining Wiener-Hopf equation by calculus of variations

04 p0505 A72-14668

Linear distributed parameter system optimal boundary control by direct method using linear combination of finite number of orthonormal functions

04 p0505 A72-14670

Linear dynamic system sensitivity models simplification conditions application to adaptive nonsearching system synthesis algorithms

04 p0505 A72-14999

Minimal order precompensator with state feedback for decoupling linear time-invariant multivariable control system, discussing design parameters determination from linear equations

04 p0506 A72-15109

Linear feedback control systems with time lag, calculating integrated squared error by Liapunov function

04 p0506 A72-15110

Large linear time invariant dynamic control system optimum simplified model based on performance index connecting feedback errors

04 p0506 A72-15113

Electric network scattering matrix and associated incident and reflected wave variables concepts applications in linear optimal control problem

04 p0507 A72-15528

Modal theory of state observers for control of multivariable time-invariant linear systems with plant matrices possessing distinct eigenvalues

04 p0507 A72-15529

Optimal control of linear systems (continuous and discrete), using quadratic performance criterion

04 p0507 A72-15667

Multiple-input multiple-output linear time invariant feedback systems stability, investigating continuous-time case

04 p0507 A72-15694

Continuous linear elastic systems characteristic vibrations differential operator eigenvalues lower bounds calculation, obtaining Green integral operator first invariant upper bound via stress function

04 p0540 A72-15706

Bang-bang automatic control of linear plant with periodic characteristics element, investigating periodic function oscillation

05 p0639 A72-15757

Minimal-time control of linear systems with energy constraints on input components, obtaining functional analysis solution by iterative method for nonlinear problem

05 p0639 A72-15802

Analytical inversion of quasi-orthogonal matrix for Simpson method of state feedback gains calculation in multiloop linear mode control systems

05 p0639 A72-15807

Stability-instability criterion of time varying linear systems, using canonical form of differential equations

[ASME PAPER 71-WA/AUT-20]

05 p0682 A72-15953

Linear single and multiloop control system synthesis for sensitivity reduction by introducing signals proportional to sensitivity functions with analyzer

05 p0640 A72-16207

Optimal control synthesis for linear systems with quadratic functional under random white noise

05 p0641 A72-16314

Parameter adjustment algorithm for simplified sensitivity model in adaptive nonsearching control system of linear plant with polynomial transfer function

05 p0641 A72-16318

Linear dynamic control system identification by local impulse response approximation, comparing with Goodman-Reswick model

05 p0641 A72-16319

Minimax solution of linear regulator problem, presenting algorithm for numerical computation

05 p0682 A72-16451

Nonlinear multivariable and linear systems optimal control in aerospace field, discussing use of performance indexes for fuel consumption, process evolution time or combination

05 p0725 A72-16453

Optimal control problem formulation as nonlinear two point boundary value problems, comparing linear systems and Riccati equations for solution

05 p0726 A72-16455

Controllability regions of linear steady system with two and three control constraints, presenting initial states set determination procedure

05 p0690 A72-16585

Helicopter rotor blade response to random loads treated by theory of linear dynamic systems with time-varying coefficients

[AIAA PAPER 72-169]

05 p0613 A72-16940

Linear time-varying control systems with one feedback nonlinearity, determining combined time-frequency condition for stability

05 p0642 A72-17090

Optimal control synthesis for linear stochastic systems with random piecewise-continuous coefficients as function of time

05 p0683 A72-17139

Adaptive control for linear discrete time stochastic systems with unknown gain parameters, considering

open loop feedback optimal control using quadratic performance index

[AD-739126] 06 p0791 A72-17305

Parameter adaptive self organizing control of linear discrete time systems, presenting stochastic approximation algorithms for feedback systems identification

06 p0791 A72-17306

Time domain infinite matrices analysis methods for linear stationary and nonstationary multivariable systems, presenting recursion formulae

06 p0792 A72-17310

Linear time-varying control system synthesis for specific input and maximum admissible error, considering various weighting functions and constraints

06 p0792 A72-17311

Optimal linear multivariable control systems design with prescribed eigenvalues, presenting method for corresponding weighting matrix elements

06 p0792 A72-17315

Linear time-varying system under modulated signal excitation, obtaining quasi-stationary response by separable system approximation with parameter optimization

06 p0771 A72-17379

Linear network sensitivity and group delay evaluation without topology or component restraints, using computer technique

06 p0793 A72-17594

Linear system digital simulation by matrix exponentiation with generalized hold order algorithm for accuracy improvement at less computer time

06 p0839 A72-17630

Linear airspeed and runway rate field displays, measuring initial response latencies, control reversals and root mean square tracking errors

06 p0845 A72-17717

Linear plants time optimal control, deriving auxiliary equations system solution in accordance with Pontryagin maximum principle

07 p0959 A72-19127

Book on asymptotic behavior and stability in ordinary differential equations covering linear and nonlinear systems, Liapunov and analytical-topological methods

07 p1026 A72-19184

Minimax terminal state estimator existence and structure for linear discrete system, applying to stochastic pursuit evasion games of LQG variety

07 p1027 A72-19283

Multinput and multioutput linear and nonlinear dynamic system maximum likelihood identification based on state vector formulation and optimal filter use

07 p0959 A72-19286

Minimal order controller for decoupling of linear multivariable systems with low order control devices and reduced control effort

07 p0960 A72-19697

Linear dynamic control systems controllability and observability quality analysis and optimization, considering determinant, trace and maximal eigenvalue

07 p0960 A72-19699

Linear multivariable systems feedback invariant structure of controllable matrix pair under rich transformation group including regular linear coordinate and state-feedback transformations

07 p0960 A72-19700

Algorithm for low order linear state variable models construction from measured data

07 p0950 A72-19701

Algebraic algorithm for reducing to state form multivariable control systems defined by linear constant differential operators

07 p0950 A72-19702

Statistical analysis of linear systems with additive environmental inputs and behavioral uncertainties, obtaining transfer function matrix, cross covariance matrix and power spectrum

07 p0960 A72-19703

Linear time-invariant controllable plant, determining semiclosed loop nominally equivalent control realization for reduced sensitivity to plant parameter perturbations

07 p0961 A72-19705

Linear multivariable discrete time cyclic system sensitivity model yielding sensitivity functions with respect to any system parameters and initial conditions

07 p0961 A72-19706

Linear multivariable control system state observation by sampling with arbitrary but fixed distribution of sampling instants, emphasizing dual control by step functions

07 p0961 A72-19707

Linear multivariable system design based on relationship between performance index parameters and optimal response in frequency domain, exemplifying gas turbine feedback controller design

07 p0961 A72-19710

Multivariable linear systems control structure via optimal control theory with quadratic criterion, permitting compensation for nonzero mean value and slowly varying perturbations

07 p0961 A72-19711

Weighting matrices effect on optimal regulator for linear time invariant multivariable systems

07 p0961 A72-19713

Algorithm for iterative computation of time and fuel optimal control functions for linear systems, presenting flow chart

07 p0962 A72-19714

Optimal control of linear multivariable plants with one or more quality criteria, considering control channels and game theory

07 p0962 A72-19720

Linear multivariable feedback control system design techniques

07 p0963 A72-19723

Microdensitometer system analysis by partial coherence theory, determining optical transfer function for linear operation

07 p0987 A72-19830

Minimum dimensionality determination for control process stabilizing linear mechanical system equilibrium position, obtaining necessary and sufficient conditions

07 p1036 A72-20320

Cross correlation identification of linear time varying processes based on pseudorandom sequences, presenting digital simulation results

07 p0948 A72-20390

Interactive graphics technique for design of single input linear feedback systems described by state equations or cascaded transfer functions

07 p0963 A72-20391

Maximum likelihood estimates of covariance parameters of time discrete nonstationary linear systems from residuals measurement of suboptimal sequential filter

08 p1145 A72-20865

Orthogonal functions representation of received signals in ideal signal sequences transmission in linear systems with matched filters and frequency band limitation

08 p1132 A72-21326

Feedback control dynamic system described by linear differential equation with random coefficients, calculating parameters distribution effect on behavior precision

08 p1146 A72-21554

Linear system oscillations and stability under random disturbances, using Laplace transform and Sh-tokalo method

08 p1146 A72-21730

Deviation accumulation conditions and maximum dynamic error of linear automatic control system under perturbation, including theorem for Bellman equation

08 p1146 A72-22177

German monograph on multielement linear mechanical oscillator analysis covering behavior of harmonically excited bar chains of arbitrary structure

09 p1350 A72-22337

Linear analysis and synthesis of three dimensional interference system stationary in space and time domains

09 p1278 A72-22573

Algorithm for transformation of generalized companion forms for multivariable linear systems into Jordan canonical form

09 p1341 A72-23071

Weighted least squares stationary approximations to time varying linear systems, noting criterion for matrix choice

09 p1341 A72-23094

Linear multivariable system stabilization by output feedback technique based on gradient approach

09 p1290 A72-23097

Linear time invariant multirate sampled data control systems characteristic equation simplification

09 p1290 A72-23099

Stability degree analysis of linear feedback control systems with dead time, presenting proportional and integral compensation diagrams produced with digital computer program

09 p1291 A72-23370

Digital computer prepared optimal controls setting diagrams for single loop, linear and concentrated parameter control circuit design

09 p1291 A72-23372

Motion stability of linear discrete deterministic and random systems over finite time interval

09 p1291 A72-23428

Optimal control synthesis for linear passive stationary plants with symmetrical coefficient matrices of minimized functional

09 p1291 A72-23431

Quadratic performance index generation for optimal design of completely controllable, scalar linear system with state feedback

10 p1454 A72-23783

Differential geometric methods to extend linear system theory to nonlinear classes, considering differential equations, controllability, optimal control, stochastic processes and bilinear system problems

10 p1503 A72-23788

Computer aided design of linear time-invariant multivariable feedback control systems, given specifications in frequency domain in stability margin form 10 p1455 A72-23789

Quadratic cost, nonlinear optimal adaptive stochastic control of linear plant and measurement models excited by white Gaussian noise and with unknown parameters 10 p1455 A72-23792

Linear mechanical elastic systems divergence with infinitely large frequency onset, noting discrete cantilever beam under nonconservative forces [ASME PAPER 71-APM-DDD] 10 p1555 A72-24189

Closed and open loop transfer function coefficients relationship for steady state linear system with proportional elements in feedback and parallel paths 10 p1457 A72-24724

Approximate model to reduce differential equation order for linear system of series connected elementary aperiodic components with different time constants 10 p1457 A72-24753

Time optimal control system for linear plant with transfer functions containing zeros 10 p1458 A72-24999

Parameter adjustment algorithm for simplified sensitivity model in adaptive nonsearching control system of linear plant with polynomial transfer function 10 p1458 A72-25072

Linear dynamic control system identification by local impulse response approximation, comparing with Goodman-Reswick model 10 p1458 A72-25073

Linear constant systems synthesis with structural constraints in state space form, applying to RC filter circuit 10 p1453 A72-25101

Optimal control of linear stochastic feedback systems described by functional differential equations 10 p1458 A72-25145

Linear continuous time systems optimal dual control problem solution by reduction to partial differential equation in finite domain with suitable boundary conditions 10 p1458 A72-25170

Power spectral density function parameters with random vibration applications, considering response spectra of multidegree of freedom linear systems [ASCE PREPRINT 1375] 10 p1560 A72-25189

Stationary weighting pattern synthesis by linear time varying dynamic system, noting feedback system input-output mapping properly 11 p1608 A72-25321

Global controllability of nonlinear differential systems during linear system perturbation, discussing controllable and uncontrollable parts splitting and null domain nature 11 p1608 A72-25323

Input-output stability of linear time invariant multivariable closed loop control systems 11 p1608 A72-25327

Optimal control synthesis for linear systems with quadratic functional under random white noise 11 p1610 A72-25797

Optimal control systems with time delays described by linear Volterra integral equations 11 p1677 A72-26090

Weighting patterns application to linear finite dimensional systems analysis and synthesis, presenting discrete time realizability condition 11 p1677 A72-26154

Absolute and convective plasma instabilities distinction in one dimensional linear infinite system, discussing saddle points method 11 p1697 A72-26585

High order explicit Runge-Kutta method for linear autonomous systems of differential equations, using interpolation formulas integration 11 p1680 A72-26962

Linear oscillatory system, investigating effects of pulsed dynamic damper with mass vibrations bounded by limiters 12 p1887 A72-28235

Stability and oscillation in linear and nonlinear systems, examining existence of T-periodic solutions /harmonic forced vibrations/ 13 p2000 A72-28484

Suboptimal controls of linear multidimensional plants with variable parameters, considering asymptotic stability 13 p1935 A72-28609

Fourier transforms for linear systems transient time and frequency characteristics, using discrete functional values for initial information 13 p1985 A72-28675

Linear product demodulator for quadrature double sideband signal, evaluating channel noise and phase jitter effect on carrier 13 p1920 A72-29105

Two step adaptive control of multidimensional linear static system, using first and second step ratio and optimization equations 13 p1936 A72-29159

Transfer function of polynomial discrete linear pulse systems for differential equation solution 13 p1936 A72-29269

Iterative method for continuous one dimensional linear systems with space-time invariant properties, applying to dynamic mixed problem of linear viscoelasticity 13 p2006 A72-29783

Linear automatic control systems diagnostics and synthesis 13 p1937 A72-29998

Linear systems theory for mathematical model of retinal image and ganglion cell excitation, calculating receptor layer luminance distributions for several stimulus patterns 15 p2184 A72-31367

Parameter-dependent linear and nonlinear equation systems solution by approximation polynomials, developing numerical algorithms 15 p2261 A72-31496

German monograph on theory of simple waves and application in continuum mechanics covering phase curves for quasi-linear autonomous system 15 p2275 A72-31505

Linear stochastic-parameter output channel, examining signal quadrature components statistical characteristics 15 p2195 A72-31623

Linear control systems optimal synthesis using ALGOL program for digital computers minimizing error square integral 15 p2210 A72-31687

Generalized differential system for Hamiltonian, Hermitian and corresponding symmetric nonreal linear matrix differential equations systems 15 p2263 A72-31756

Globally controllable nonlinear differential systems arising from linear system under perturbation 15 p2264 A72-31762

Equivalent baseband and passband delay line and transversal equalizers derivation for linear modulation systems, obtaining relationship between tap coefficients 15 p2211 A72-31844

SIDERAL program organization and computational method application to calculation of malfunction by drift of linear analog equipment 15 p2207 A72-31872

Optimal controller design for parabolic type second-order linear stationary systems, discussing integro-differential equation solution possibility 15 p2211 A72-32170

Multidegree of freedom linear systems mean-square response to nonstationary random vibratory excitation, using staircase approximation to continuous intensity functions 15 p2331 A72-32552

Linear radio receiver circuit synthesis for output signal structure and rational selection, using reduction algorithm 15 p2202 A72-32705

Limiting approximation theorems for synthesis of linear circuits and signals in time-frequency domains 15 p2212 A72-32707

Optimal state space synthesis of discrete linear computer controlled systems with quadratic cost function, using Liapunov, Pontryagin, and Bellman techniques 15 p2212 A72-32765

High speed deterministic adaptive controller for linear and nonlinear plants, identifying control law from state and input data by linear regression procedure 15 p2212 A72-32794

Sensitivity design of multiple input controller for dynamic optimization applied to linear systems with quadratic performance index 15 p2212 A72-32795

Noninteractive compensation of linear multivariable control systems based on matrix block diagram technique 15 p2213 A72-32799

State space approach to linear multivariable servomechanism problem, deriving controllability conditions and design procedure 15 p2213 A72-32801

Linearly elastic, transversely isotropic multilayer system, presenting stress and stability problem for two dimensional strain states 16 p2466 A72-33022

Observability conditions for nonlinear and unsteady linear systems, noting control systems design 16 p2371 A72-33092

State space technique application to discrete linear control systems synthesis, discussing time-optimal and quadratic-cost problems, and pole assignment method 17 p2532 A72-34246

Calculation of correlation matrices for linear systems subjected to nonwhite excitation. [ASME PAPER 71-APMW-10] 17 p2625 A72-34316

The elastic stability of two-parameter nonconservative systems. [ASME PAPER 72-APM-43] 17 p2627 A72-34782

Smooth empirical Bayes estimation of observation error variances in linear systems. 17 p2576 A72-35248

Finite group homomorphic sequential systems generalization from linear system theory, developing

controllability, observability, minimality and realizability concepts 17 p2523 A72-35526

Controllability of linear continuous systems with a time-variable delay. 17 p2534 A72-35532

Stability of linear time-invariant distributed parameter single-loop feedback systems. 17 p2534 A72-35535

Counting theorems for random processes discretization in linear systems described by finite spectrum functions 17 p2534 A72-35776

State feedback control law for linear multiinput multioutput time-invariant dynamic system under disturbance to obtain output with zero steady state error 18 p2672 A72-36054

Recursive bootstrap maximum likelihood estimators algorithms for identification of process modeled by stable linear difference equation under additive output measurement noise 18 p2672 A72-36056

Effective dimensional reduction in the computation of linear, discrete, time-delay problems. 18 p2672 A72-36302

Digital simulation of stiff linear dynamic systems. 18 p2663 A72-36315

Linear homogeneous system of differential equations as model for perturbation problems including functions with retarded and/or advanced arguments 18 p2705 A72-36614

Optimal minimal-order observers for discrete-time systems - A unified theory. 18 p2674 A72-37099

Linear stochastic system optimal measurement strategy and matched Kalman filter computation via transformation into deterministic control problem 18 p2674 A72-37100

Choice of parameters for measuring devices in a closed-loop linear control system 19 p2777 A72-37319

French monograph - Linear estimation of the parameters of multidimensional dynamic systems and statistical validation of the model - Applications to process identification 19 p2778 A72-37486

Stability of linear systems with constraint damping and integrals of the motion. 19 p2856 A72-37519

Controllability regions of linear steady system with two and three control constraints, presenting initial states set determination procedure 19 p2825 A72-37556

Uniqueness of the solution for identification of linear systems by the modulating function method 19 p2779 A72-38086

Investigation of the structure of processes in discrete automatic control systems by the application of graph theory 19 p2779 A72-38180

The output control of linear time-invariant multivariable systems with unmeasurable arbitrary disturbances. 19 p2779 A72-38231

Algorithm for linear multivariable systems synthesis via combined dynamic feedforward compensation and linear state variable feedback 19 p2779 A72-38232

Pontryagin Minimum Principle application to stochastic optimal control problems formulated around linear systems with Gaussian noise and general cost criteria 19 p2779 A72-38234

Optimal decentralized control of two coupled linear stochastic systems, introducing fake plant white noise for weak coupling effects compensation 19 p2779 A72-38236

Transfer-characterization and the unique realization of linear time-invariant multivariable systems. 19 p2780 A72-38238

Linear control system design with parameter uncertainties, using stochastic control approach based on minimization of state vector-dependent quadratic performance index expected value 19 p2780 A72-38239

Transfer function concept extension to analytical representation of linear time-invariant plants and controllers with multiple inputs and outputs 19 p2780 A72-38242

Suboptimal stochastic control of a class of linear distributed parameter regulators. 19 p2780 A72-38243

Hyperstability concepts and their application to discrete control systems. 19 p2780 A72-38248

Recent results concerning a graphical test for checking the stability of a linear time-invariant system. 19 p2826 A72-38251

Discrete optimal terminal control, with application to missile guidance. 19 p2780 A72-38257

Parameter identification of a class of multiple input/multiple output linear discrete-time systems. 19 p2826 A72-38269

Linear dynamic systems parameter identification via optimal input design, noting eigenfunction dependence on positive self adjoint operator
19 p2781 A72-38271

A biased filter for linear discrete dynamic systems.
19 p2781 A72-38273

Recursive updating of smoothing and filtering algorithms for discretely observed continuous dynamic linear systems
19 p2826 A72-38274

Optimal control synthesis for linear passive stationary plants with symmetrical coefficient matrices of minimized functional
19 p2782 A72-38514

Decoupling of linear discrete time systems by state variable feedback.
19 p2827 A72-38563

Response of discrete linear systems to forcing functions with inequality constraints.
20 p2910 A72-39604

Response of linear periodically time varying systems to random excitation.
20 p2946 A72-39636

Book - Some aspects of the optimal control of distributed parameter systems.
20 p2946 A72-39731

An application of the concepts and methods of linear systems analysis to the scattering of resonance radiation by an atomic vapour.
21 p3084 A72-40470

Optimal single stage control law applicable to linear multivariable systems based on discrete-time analysis, discussing real time simulation on hybrid computer
21 p3037 A72-40637

Isochronic corner generated difficulties avoidance in linear multivariable system minimum time controller, noting association with switchings
21 p3037 A72-40638

Synthesis of feedback systems with large plant ignorance for prescribed time-domain tolerances.
21 p3037 A72-40643

Linear distributed parameter systems modal analysis and design for low sensitivity optimal feedback control, using linear differential operators
21 p3037 A72-40646

General solution of a system of differential equations with an irregular singular point
21 p3075 A72-41095

Six dimensional vector space of stresses in elastic piecewise linear material divided into separate regions having different linear stress-strain relation
21 p3122 A72-41345

Constitutive equations and boundary value problems in discrete theory of elasticity, noting linear systems of prismatic rods and lattice type shells
21 p3123 A72-41390

A comparison of the effects of small nonlinearities on several estimation schemes.
[AIAA PAPER 72-905] 21 p3076 A72-41555

Entropy criterion in the estimation of the dynamic quality of automatic control systems
21 p3039 A72-41803

Compatible controllers for time-varying linear plants.
22 p3161 A72-41939

A design procedure for intermediate-order observer-estimators for linear discrete-time dynamical systems.
22 p3161 A72-41994

Optimal controller design for parabolic type second-order linear stationary systems, discussing integro-differential equation solution possibility
22 p3162 A72-42079

Construction of Liapunov functions for time-dependent systems containing inertialess nonlinearities
22 p3205 A72-42176

Linear dynamic control system synthesis methods based on aggregation and suboptimal control by decomposition, considering quadratic performance criterion
22 p3162 A72-42177

An application of the theory of Lie groups in the optimal control problem for linear dynamic systems with time-variable coefficients
22 p3162 A72-42181

Frequency stability criterion for variable-structure automatic control systems
22 p3162 A72-42185

Optimal control of complex time lag systems with series connected lumped and distributed parameters described by linear differential equations
22 p3162 A72-42241

Synthesis of linear stationary systems with the aid of proportional elements
22 p3162 A72-42738

Linear system proper frequencies and vibration dampings obtained by mathematical smoothing of mechanical admittance measurements
22 p3241 A72-43093

On discrete linear time-invariant systems with singular transition matrix.
23 p3275 A72-43545

Control of jump parameter systems with discontinuous state trajectories.
23 p3275 A72-43547

Optimisation of contraction-mapping algorithm for calculating optimal controls.
23 p3275 A72-43607

Iterative method of computing the limiting solution of the matrix Riccati differential equation.
23 p3275 A72-43610

A direct method for computing optimal feedback control for linear systems.
23 p3275 A72-43613

The rotating noncircular shaft as stability problem of a linear periodic system
23 p3347 A72-43718

Optimal control of stochastic systems with continuous and discontinuous random disturbances, obtaining problem solution conditions for linear system via dynamic programming
23 p3276 A72-43782

Reduced order observers design for optimal control of linear discrete time stochastic systems, considering velocity-aided tracking filter
23 p3276 A72-43856

A method for calculating canonic realizations for linear, unsteady, discrete systems
23 p3277 A72-43989

The inverse problem of optimal process theory and the synthesis of linear optimal systems in the case of restricted phase coordinates
23 p3277 A72-44008

Cumulants of multidimensional response of linear and nonlinear systems to Poisson distributed impulses, estimating joint probability distribution and evaluating threshold statistics
23 p3314 A72-44368

Equivalence conditions for classes of linear and non-linear distributed parameter systems.
23 p3277 A72-44369

Determination and quality estimation of stability in discrete linear systems
24 p3386 A72-44722

Linear analysis and synthesis of three dimensional interference system stationary in space and time domains
24 p3379 A72-44752

Modelled time optimal control process investigation for system with relay components, noting Hausdorff maximum principle application for optimal linear control
24 p3386 A72-45389

LINEAR TRANSFORMATIONS

Quasi-linear tensor operator derived in form of series converging inside circle, proving theorem concerning reciprocity conditions and existence of potential
03 p0445 A72-13579

Multivalued logical function synthesis with multistage logical network through hypercomplex representation and linear transformation
12 p1794 A72-27497

Linear transformation and absorption of electromagnetic waves in plasma
17 p2591 A72-35165

Symmetries of the boundary-layer equations under groups of linear transformations.
17 p2541 A72-35241

Picture coding via linear transformation and quantization on subpictures with applications to monochromatic image processing
18 p2658 A72-36254

Linear vector formulation of pursuit problems with pursuer discrimination, using Mischchenko-Pontryagin curvature conditions
23 p3307 A72-43220

LINEAR VIBRATION

Algorithm for selective computation of large structural modifications effect on eigenmodes of linear structure
06 p0895 A72-17848

Angular and linear vibrations effect on dynamic errors of two stage gyrocompass, obtaining nonlinear equations of motion approximate solutions
07 p0981 A72-18928

Random vibrational stress and displacement spectra for linear complex mechanical dissipative systems with strong resistance and finite degrees of freedom
07 p1091 A72-19763

Linear system oscillations and stability under random disturbances, using Laplace transform and Sh-tokalo method
08 p1146 A72-21730

New methods of measuring the parameters of multidimensional vibrations of linear mechanical systems
22 p3176 A72-42130

Linear system proper frequencies and vibration dampings obtained by mathematical smoothing of mechanical admittance measurements
22 p3241 A72-43093

LINEARITY

NT COLLINEARITY

Hologram interference fringe relationship to non-linearity of simple oscillations
07 p0987 A72-19836

Carbon dioxide concentration effect on calibration of linearized hot-wire anemometer in operation at constant temperature
10 p1480 A72-24217

Analog measuring data transmission systems optimization by computers, noting improvement of dynamic response and linearity in digital systems
12 p1786 A72-27580

LINEARIZATION

Statistical linearization approach to determine approximate instantaneous correlation matrices of nonlinear structure response to nonwhite excitation
02 p0298 A72-12663

Remes algorithm modification for linear approximation problem solution, discussing geometric interpretation and convergence
03 p0381 A72-13619

One dimensional Boltzmann equation with linearized small perturbation, determining secondary conditions
03 p0399 A72-14347

Elastoplastic body random vibration analysis by statistical linearization, obtaining free elastic vibration mode shapes and damping constants
04 p0586 A72-15005

Modified quasi-linearization algorithm for solving nonlinear two-point boundary value problems based on performance index and cumulative error in differential equations
04 p0539 A72-15045

Numerical integration solution of nonlinear equations and two point boundary value problems, using quasi-linearization and imbedding methods
06 p0839 A72-17957

Stability analysis of steady control systems acted upon by random signal in single valued one dimensional nonlinearity form, using statistical linearization
07 p0959 A72-18989

Spectrometers for phase audible frequencies, discussing linearization theory and application to spectrum analyzer calculation
07 p0983 A72-19186

Hydrodynamic stability problems with reference to Navier-Stokes equation solutions, discussing linearization principle application
07 p0969 A72-20066

Applied nonlinear mechanics problems solutions by variable scale method, choosing transformations for linearization of differential equations
09 p1343 A72-23602

Dynamic systems stability problems, differential equations linearization and random processes
09 p1343 A72-23603

Nonlinear vibrations under random excitation, discussing equivalent linearization and small parameter perturbation methods and Fokker-Planck equation
09 p1353 A72-23604

Zaidenberg correlation method for nonlinear systems dynamic properties under random excitation, determining statistically equivalent linearized terms for equations of motion
09 p1353 A72-23607

Statistical linearization of stochastic differential equations for optimal terms in mean square distance
10 p1506 A72-24993

Approximate statistical analysis of PFM and combined modulation systems, proposing linearization method
11 p1609 A72-25447

Linearization and Liapunov stability analysis of nongyroscopic holonomic conservative dynamic differential equations system
11 p1677 A72-25979

Linear multistep methods with variable matrix coefficients for asymptotic numerical integration of ordinary differential equations system
11 p1679 A72-26960

Linearized steady motion of gas with mass sources and sinks, determining resonance onset conditions
13 p1893 A72-28731

Variational principles for linearized dynamic and static problems of elastic incompressible bodies for highly elastic initial deformations
13 p2059 A72-29499

Linearization method to determine changes in principal harmonic resulting from nonlinear device characteristic deformation due to HF components
13 p1937 A72-30019

Earth-moon system periodic orbits calculation by modified quasi-linearization combined with particular solutions method, using restricted three body model
14 p2149 A72-30232

Nonlinear autooscillatory systems forced vibration under random perturbations, calculating dynamic processes by statistical linearization
14 p2132 A72-31114

Nonlinear elastic material approximation by piecewise linear material with linear boundary value problems, discussing isotropic case based on singular surfaces theory
15 p2330 A72-32295

Structural design optimization procedure based on sequence of linearizations with iterative convergence through series of least critical intermediate solutions in hyperspace
15 p2331 A72-32551

Linearization and perturbation procedures to calculate nonlinear effects in fluid stability problems with application to nonlinear critical layer
16 p2377 A72-33338

Joint maximum likelihood estimation of three parameters of Weibull distribution, obtaining modified quasi-linearization algorithm for nonlinear equations iterative solution 16 p2416 A72-33348

Hot-wire anemometer output linearization by squaring and straight line sequence circuits combination, supplementing Bruun error estimates 16 p2392 A72-33606

Application of statistical linearization techniques to nonlinear multidegree-of-freedom systems. [ASME PAPER 71-WA/APM-5] 17 p2624 A72-34315

Computation of optimal controls by a method combining quasi-linearization and quadratic programming. 18 p2673 A72-36824

Heat production effects in general linearized thermoviscoelasticity theory, deriving equations of motion, state and energy and boundary conditions for intensely strained objects 19 p2871 A72-37526

Linearized problem of one-dimensional periodic gas flow in a pipe 19 p2786 A72-37666

Dynamic nonlinear system direct statistical analysis by Covariance Analysis Describing Function Technique with linearization, giving illustrative examples [AIAA PAPER 72-875] 20 p2905 A72-39124

Electronic circuit for linearizing the transfer function of a photographic plate used in mass-spectrometry. 20 p2925 A72-39428

Qualitative analysis of the linearization of quasi-linear problems of nonstationary heat conduction 21 p3129 A72-41055

Analogies between linearized and linear problems in elasticity theory in the case of uniform initial states 22 p3233 A72-42061

Linearization of relaxation-time control in a transistorized multivibrator 23 p3270 A72-43765

Linearizing compensation for nonlinear control system transformation into linear system without approximation, discussing differential operator matrix definition and random noise effects 23 p3277 A72-43945

Multicomponent plasmas with static magnetic field, deriving dielectric tensor and dispersion relation for wave propagation by linearization technique 24 p3428 A72-44967

Linear theory of a solid propellant rocket motor with modulated exhaust 24 p3433 A72-45116

LINERS

U LININGS

LINES [GEOMETRY]

NT CHORDS [GEOMETRY]

Phi-spatial filter method for straight or curved line geometric feature extraction of characters, using coherent optical system 12 p1820 A72-27494

Nonlinear algebraic transformation to determine straight line and second order curve intersection point in aircraft lofting problem 13 p1986 A72-28742

Complete assimilation of briefly presented lines. 23 p3261 A72-44150

LINES OF FORCE

Faraday rotation as perturbation for analytic solution of system of differential equations for line formation in inhomogeneous magnetic fields 03 p0427 A72-13295

Solar polar magnetic fields, discussing inversion line location, observations, data analysis, general field and computer reduction 03 p0432 A72-13356

Equilibrium state linear theta pinch plasma confinement dependence on nonuniform magnetic force lines curvature radius 03 p0396 A72-13655

Dielectrophoresis force measurements and wedge shaped capacitor separation properties in satellite zero gravity conditions 04 p0549 A72-14988

Noncircular ionospheric current conversion into longitudinal currents in magnetosphere along lines of force of geomagnetic field 05 p0657 A72-16259

Lower ionospheric currents fields, determining Hall conductivity and geomagnetic lines of force slope effects 05 p0657 A72-16266

Nonlinear propagation effects of monochromatic circularly polarized vlf waves /whistlers, heli cons/ along field lines in magnetosphere 05 p0658 A72-16603

Sounding rocket observations of magnetic field aligned electron pitch angle distributions coincident with auroral precipitation band northern boundary 06 p0804 A72-17457

Atmospherical model for plasma motion along surface of geomagnetic tail under action of interplanetary, magnetic lines of forces 08 p1153 A72-20722

Electromagnetic field around thin linear receiving antenna by superposition of incident wave with antenna scattered field, deriving differential equations solution for field lines 08 p1132 A72-21327

Solar particles latitudes dayside profiles as function of geomagnetic activity, suggesting closed field lines limit location 09 p1378 A72-23002

Single helix magnetic field with axial current, discussing field lines rotatory transformation and magnetic well and shear effect on plasma behavior 09 p1363 A72-23216

Double helix magnetic field in longitudinal and axial current fields of stellarators, noting rotatory transformation and shear of field lines 09 p1363 A72-23217

Interplanetary and magnetospheric magnetic force lines reconnection and effects on geomagnetic activity 11 p1718 A72-25933

Solar current flow penetration to 1 AU in interplanetary medium, discussing inhibition of field line reconnection across neutral sheet 11 p1714 A72-26528

Geomagnetic invariant coordinates and related field line parameters calculation via field model and fast numerical method 12 p1803 A72-27771

Polar cap magnetic field induced by currents along magnetospheric lines of force during polar substorm 13 p1946 A72-28587

Meteor-induced magnetic effect on cosmic ray intensity for meteor streams with orbits normal or parallel to interplanetary magnetic field lines of force 13 p2029 A72-28592

Interplanetary electrons quiet-time intensity increases, considering trans-earth-orbital modulating region due to solar wind transport of photospheric field lines 13 p2030 A72-29377

Geomagnetic field line tracing by plasma clouds produced by Ba vapor release, noting different ion drift rates and directions 16 p2384 A72-32977

Magnetic field rapid dissipation induced by stochastic topology of lines of force, discussing implications for hydromagnetic turbulence, solar activity and cosmic ray diffusion 16 p2378 A72-33454

Plasma motion relation to magnetic field line motion for imperfect electroconductivity, noting comparison with total particle drift distance 16 p2439 A72-33931

Transverse diffusion and conductivity coefficients for a three-dimensional magnetized equilibrium plasma. 17 p2592 A72-35379

Multiplicity theorem for aligned steady MHD flows of inviscid perfectly conducting gas, assuming constant density along streamline 19 p2840 A72-37405

Atmospherical model for plasma motion along surface of geomagnetic tail under action of interplanetary magnetic lines of force 19 p2791 A72-38350

Sweet's mechanism for the destruction of magnetic flux. 20 p2955 A72-40017

Height structure of tidal winds as inferred from incoherent scatter observations. 22 p3169 A72-42014

Different conductivities effect in ionospheric E layer of polar cap regions, noting electric current along high latitude magnetic field force lines 23 p3283 A72-43370

Electron polar cap and the boundary of open geomagnetic field lines. 23 p3286 A72-44522

Polar cap magnetic field induced by currents along magnetospheric lines of force during polar substorm 24 p3397 A72-45087

Meteor-induced magnetic effect on cosmic ray intensity for meteor streams with orbits normal or parallel to interplanetary magnetic field lines of force 24 p3435 A72-45092

LING-TEMCO-VOUGHT MILITARY AIRCRAFT

U MILITARY AIRCRAFT

LINGUISTICS

NT MACHINE TRANSLATION

NT PHONEMICS

NT SYLLABLES

NT WORDS [LANGUAGE]

Language description of remotely sensed image data, noting application to artificial intelligence, linguistic analysis and retrieval 13 p1924 A72-28525

Terminal context in context-sensitive grammars. 17 p2524 A72-35924

Linguistic message decoding algorithms for communication with extraterrestrial intelligences, considering unified procedure and key problems solutions 24 p3382 A72-45226

LININGS

NT ROCKET LININGS

Analytical model for acoustic impedance of perforated plate liner with multiple frequency excitation, discussing effects of fluid motion, grazing flow and spectral excitation 04 p0548 A72-14699

Engine fan-compressor maximum noise reduction for given aircraft configuration by acoustic linings on nacelle inlet and exhaust walls 07 p1054 A72-19268

Combined plasma and magnetic field cumulation due to heavy conducting liner implosion, noting compression parameters for plane and cylindrical bodies 10 p1523 A72-24723

Low thermal flux glass fiber composite over-wrapped tubing with metallic liners for leak free cryogenic propulsion plumbing systems [AIAA PAPER 72-328] 11 p1637 A72-25364

Fiberglass performance as duct liner in presence of spinning modes from free field measurements, noting ineffectiveness for plane wave attenuation 13 p2028 A72-29573

Sound attenuation in lined air ducts, describing experimental determination of lining materials acoustical properties for central air heating systems 13 p2005 A72-29577

Sound attenuation in acoustically lined circular ducts in the presence of uniform flow and shear flow. 17 p2582 A72-35411

Optimization of acoustic linings in presence of wall shear layers. 21 p3083 A72-40334

LINKAGES

Rigid body model for nonholonomic kinematic linkages of tangentially sliding nonrolling bearings, noting virtual displacements and mechanical work 12 p1845 A72-27539

LINKING

U JOINING

LINKS

Kinematics of five-link hinged mechanisms containing two driving links, applying to spherical and flat links 07 p0987 A72-19858

Impulse excited spatial systems of rigid bodies linked by pivot joints with arbitrary kinematics, applying Maxwell-Betti theorem 15 p2323 A72-31461

LIOUVILLE EQUATIONS

Two dimensional plasma under dc magnetic field, investigating thermal equilibrium with Liouville equation and BBGKY hierarchy 01 p0107 A72-10145

Invariant characteristics of hydrodynamic systems with stationary boundaries, 3 degrees of freedom and second order nonlinear motion of Liouville type 06 p0801 A72-18136

Density matrix equation solution in Liouville space, using variational procedure for laser mode equation and separable interaction method 07 p1006 A72-19670

Electrical conductivity of two dimensional strongly magnetized guiding center plasma, using Liouville equation 11 p1693 A72-25563

Statistical mechanics of magneto-active plasma. 17 p2590 A72-35144

Master equations for finite systems. 17 p2576 A72-35153

LIPID METABOLISM

Hypoxic hypothermia effects on endocrine organs phospholipid metabolism during chronic hypoxic hypoxia 02 p0165 A72-12516

Potassium cyanide effect on phospholipid exchange in rat brain and liver during histotoxic hypoxia as function of body temperature 05 p0618 A72-16357

Hypertension and blood sugar and lipid level increase as ischemic heart disease risk factors 08 p1117 A72-21542

Dietary lipid effect on platelet adhesion and aggregation, blood coagulation and fibrinolysis and relation to atherosclerosis and thrombosis 08 p1117 A72-21543

Lipid metabolism abnormality relation to hypothyroidism leading to atherosclerosis, noting thyroid parenchyma atrophy from autoimmune thyroiditis 08 p1117 A72-21544

Hyperlipidemia progressive increase among flying personnel, showing Clofibrate treatment effect on lowering rate 08 p1117 A72-21545

Blood lipid levels and dietary habits in atherosclerotic and healthy subjects, showing lipid and glucose metabolism disturbance increase in coronary cases 08 p1117 A72-21546

Dietary and pharmacological treatment of atherogenic hyperlipidemias from lipid-sugar balance and drug efficacy studies 08 p1117 A72-21547

Pure oxygen atmosphere effects at 450 and 600 mm Hg on rats in vitro liver and adipose tissue lipid

synthesis, measuring food intake and plasma components

10 p1424 A72-23739

Triglyceridemia relation to age, relative weight and ischemic cardiopathy probability from ECG, anthropometry and lipid and glucid metabolism studies

12 p1759 A72-27238

Serum cholesterol, phospholipid and lipoprotein levels relation to atherosclerotic heart disease occurrence in USAF personnel

12 p1766 A72-28292

Hydrogen peroxide formation relationship to lipid peroxidation and seizures in brain during high pressure oxygen exposure

12 p1766 A72-28300

Myocardial lipid and carbohydrate metabolism in fasting men during prolonged exercise.

17 p2499 A72-34347

Effects of in vivo inhalation of 100% oxygen at reduced pressure on serum and red cell lipids.

[AD-746090]

17 p2508 A72-34553

The effects of acute hypoxia on lipid synthesis in the rat heart.

17 p2501 A72-34979

Lipid composition of growing and starving cells of *Arthrobacter crystallopoietes*.

17 p2505 A72-35835

Effect of nicotinic acid on myocardial metabolism in man at rest and during exercise.

17 p2506 A72-35968

Rat pulmonary lipid metabolism during feeding and fasting from studies of lung lecithin half life after C-14/1/palmitate and H-3/U/glucose injection

18 p2651 A72-36573

LIPIDS

NT LIPOPROTEINS

NT OLEIC ACID

Human patients with chest pain and normal ECG, examining diagnostic value of graded exercise test, history and lipid levels with coronary arteriography data

01 p0010 A72-10146

Structural lipids role in accumulating light energy during prebiological evolution, using conductance studies in lipid-chlorophyll-water system

04 p0468 A72-14779

Pigments participation in lipid systems formation, considering chlorophyll photochemical activity in surface active agents

04 p0469 A72-14785

Molecular evolution of biological membrane from lipid film to lipoprotein particle assembly, using bacterial biocompatibility

04 p0469 A72-14786

Lipid peroxidation on the human skin surface following erythrogenic UV irradiation

19 p2757 A72-38087

Effect of neurohomologous phospholipids associated with other substances on experimental intoxication by asymmetrical dimethylhydrazine. II - Biochemical aspects of the pyridoxine-phospholipid association

21 p3009 A72-41195

LIPOPROTEINS

Serum cholesterol, phospholipid and lipoprotein levels relation to atherosclerotic heart disease occurrence in USAF personnel

12 p1766 A72-28292

LIPSCHITZ CONDITION

Nonlinear resistive network analysis by piecewise linear mappings, studying Lipschitz condition and global homomorphism

11 p1608 A72-25360

Classical flow problem solution by fixed point approach, using quasi-Lipschitz conditions for Newtonian potential gradients

15 p2216 A72-31468

LIQUEFACTION

Book - Advances in cryogenic engineering, Volume 17

19 p2883 A72-38826

LIQUEFIED GASES

NT LIQUID AMMONIA

NT LIQUID HELIUM

NT LIQUID HYDROGEN

NT LIQUID NITROGEN

NT LIQUID OXYGEN

Hard sphere liquid Bernal model with cell method extension, determining liquid argon behavior near melting

03 p0388 A72-13151

Fabry-Perot interferometer measurements of Brillouin scattering from He-Ne laser excited low temperature condensed gases

21 p3051 A72-40151

Electronic detection of ionizing-particle tracks in liquid argon

23 p3291 A72-44442

LIQUID AIR

German monograph on liquid air fractionation during flight of recoverable spacecraft carrier propelled by air breathing propulsion systems

09 p1374 A72-23160

LIQUID ALLOYS

Al alloy melts with Fe, Cr, Co and Ni, measuring kinematic viscosity by oscillatory-rotary method using logarithmic damping decrement

07 p1012 A72-19550

X ray diffraction study of molten Mg-U alloy atomic structure, demonstrating existence of Mg-Cd compounds

10 p1497 A72-24678

Study of the flow kinetics of metal melt spread over hard surfaces

23 p3293 A72-43284

LIQUID AMMONIA

Ti anodic behavior in anhydrous liquid ammonia, noting oxidation by halogen intermediary

04 p0484 A72-14976

High thermal power density ammonia heat pipe with porous grooved wick concept

[ASME PAPER 71-WA/HT-20]

05 p0744 A72-15879

LIQUID ATOMIZATION

Airport cold fog attenuation by propane atomization technique, discussing application at Orly

04 p0508 A72-14686

Electric field voltage effect on dispersion of electrostatically atomized liquids and hydrocarbon fuels with and without gamma irradiation

09 p1350 A72-22546

The behavior of two-phase systems during adiabatic expansion

20 p2953 A72-39595

LIQUID BEARINGS

Squeeze-film bearings nonlinear vibration performance in aircraft gas turbine engines, emphasizing lubricant viscosity importance

07 p0999 A72-20532

LIQUID BREATHING

Pulmonary atelectasis and arterial-venous shunting and heart displacement prevention during centrifuging of dogs breathing oxygenated liquid fluorocarbon in water immersion respirator

11 p1579 A72-26609

Oxygen consumption in liquid breathing mice.

22 p3142 A72-42488

LIQUID COOLED REACTORS

NT WATER COOLED REACTORS

LIQUID COOLING

NT FILM COOLING

Positive pressure cooling of cryogenic baths of liquid nitrogen by helium gas addition for frequency shift of ruby laser

09 p1326 A72-23411

Energy capacity margin of heat absorbing liquid /water/ in cooling system, considering specific heat and maximum critical heat flux

11 p1747 A72-26969

Water cooled suits efficiency and effectiveness for heat removal, noting importance of head area

14 p2081 A72-31085

Microelectronic devices liquid cooling by free and forced convection, investigating component size effects on heat transfer by boundary layer analysis and experiment

14 p2091 A72-31172

Heat transfer in water droplets and its role in the calculation of highly stressed injection coolers [DFVLR-SONDDR-196]

20 p2911 A72-39075

Investigation of heat transfer at high temperature heads in the case of cooling by a dispersed flow of liquid nitrogen

23 p3356 A72-43683

LIQUID CRYSTALS

Nematic liquid crystals application to real time optical data processing

06 p0847 A72-17565

Molecular ordering in smectic A liquid crystals, evaluating spectrum hyperfine splitting as function of orientation to spectrometer magnetic field

08 p1217 A72-21490

Optical properties of nematic and cholesteric liquid crystals, noting application for visualization and display systems

09 p1373 A72-23598

Raman spectra of azoanisole and anizaldazine in liquid crystal states excited by Ar laser, revealing lattice vibrations attenuation near transition point

10 p1490 A72-24042

Composite materials evaluation methods, discussing high quality photographs, radiography, laser holographic interferometry, thermographic fluorescent phosphors, liquid crystals and acoustic techniques

12 p1815 A72-28101

Asymmetrical mechanics theory of nematic liquid crystals, noting relation for local moment of inertia and tensor analysis of kinematic characteristics

13 p2022 A72-29497

Visual observation of continuous hydrocyanic acid laser modes and beam energy distribution, using cholesteric liquid crystal image converter

14 p2111 A72-30851

Continuous NDT of coalescers /jet fuel filters/ by liquid crystals, detecting split seams, cap leaks, cracks, material imperfections and epoxy filled voids [ASME PAPER 72-DE-25]

14 p2108 A72-30867

Liquid crystal structure, physical properties, discussing electronics applications and technical development trends

15 p2291 A72-31594

Liquid crystal detector design for IR holography and interferometry with applications to NDT of semiconductors, plasma diagnostics and material research

15 p2237 A72-32055

Liquid crystals synthesis, physical chemistry and material parameters effects on mesomorphic and electro-optical behavior

15 p2240 A72-32363

Study of transient phenomena by a TEA CO₂ laser associated with a liquid-crystal detector

17 p2562 A72-34285

Nematic liquid crystals application to monochromatic or multicolor display devices based on vertical phase elastoelectric deformation effect

18 p2719 A72-36679

Some optical properties of liquid crystals

20 p2961 A72-39850

Electron paramagnetic resonance spectrum of vanadyl acetylacetonate dissolved in liquid crystal or isotropic solvent

21 p3013 A72-41177

The use of cholesteric liquid crystals in the study of skin temperature and their applications in aviation medicine

21 p3009 A72-41192

LIQUID DROPS

U DROPS (LIQUIDS)

LIQUID DYNAMICS

U FLUID DYNAMICS

U LIQUID FLOW

LIQUID FILLED SHELLS

Liquid motion in circular cylinder with elastic bottom under longitudinal excitation, representing dynamic and kinematic free surface conditions as nonlinear equations

02 p0204 A72-12254

Vertical thin circular cylindrical shells partially or completely filled with stationary liquid, determining free vibration characteristics with finite element theory

02 p0293 A72-12371

Fluid filled fiber reinforced spherical shells extensional vibrations, evaluating equivalent elastic orthotropic compliance constants, natural frequencies and mode shapes

03 p0443 A72-13403

Thin walled elastic axisymmetric fluid filled tanks under longitudinal vibrations, determining dynamic characteristics

04 p0586 A72-15011

Free oscillations of liquid masses contained in tanks, analyzing variational and Ritz methods

04 p0513 A72-15557

Zhukovskii potentials for ideal fluid motion in spherical or cylindrical cavity with arbitrary radial partitions

05 p0648 A72-16218

Equations of motion for oscillating heavy symmetrical gyroscope with cylindrical cavity partially filled with inviscid incompressible liquid

05 p0664 A72-17145

Flutter of thin elastic circular cylindrical fluid filled shells, presenting potential flow theory for coupled hydrodynamic forces

06 p0894 A72-17763

Dynamics of two dimensional body with cavity containing viscous incompressible fluid, noting obstacle interaction and free surface motion problems

06 p0801 A72-18139

Nonlinear oscillations of liquids in complex geometrically shaped moving vessels, using approximation methods for boundary value problem solution in Cartesian coordinate system

06 p0802 A72-18712

Branching theory application to convection and axisymmetric flow formation in internally heated self gravitating liquid filled sphere

07 p0968 A72-19973

Nonlinear oscillations of liquid in movable conical containers, presenting approximate procedures for solving weight boundary value problem of eigenvalues

07 p0972 A72-20211

Ideal liquid small oscillations natural frequencies and mode shapes in shell of revolution under weak gravitational field

08 p1148 A72-20956

Dynamic characteristics and nonlinear oscillations of liquid in spherical shell of revolution, modifying Lukovskii approximation method

08 p1148 A72-20962

Liquid sloshing in circular cylindrical cavity with ribs mounted radially to walls, calculating oscillation frequencies and virtual masses

08 p1148 A72-20968

Axial impact of semiinfinite elastic cylindrical shell filled with inviscid compressible fluid, obtaining equations of motion

08 p1149 A72-21166

Ideal incompressible fluid sloshing under centrifugal force in partially filled conical cavity rotating at constant angular velocity

08 p1149 A72-21244

Descriptive geometric method for distribution of axes of uniform rotation of body containing ideal homogeneous incompressible fluid in uniform turbulent motion

08 p1209 A72-21364

Liquid filled spinning projectiles and satellites flight stability based on Stewartson gyroscopic analysis method

08 p1168 A72-21600

Variable wall thickness influence on axisymmetric vibrations frequencies and reduced masses of cylindrical elastic shell filled with ideal incompressible fluid

08 p1247 A72-21815

Normal axial impact of thin liquid filled elastic cylindrical shell with rigid bottom on compressible fluid half space surface

09 p1350 A72-22207

Perturbed motion of rotating solid body with viscous fluid filled cavity, linearizing motion and Navier-Stokes equations

09 p1295 A72-23487

Piston exerting pressure on liquid filled cylinder, determining deformation state based on thin elastic orthotropic plate theory

10 p1556 A72-24266

Hemispherical elastic nonexpandable weightless film fastened along equator to inner wall of closed cylindrical vessel under hydrostatic pressure, determining film axisymmetric equilibrium shapes

13 p1940 A72-28392

Harmonic functions system for resonant vibrations of liquid in elastic circular cylindrical tank, calculating shells surface pressure from equations of motion

13 p1940 A72-28394

Orbital and rotational motion stability of solid body containing elastic rods and fluid-filled cavity

13 p2002 A72-28715

Natural oscillation frequencies of cavity-contained liquid in weak gravitational field, using variational principles

13 p1943 A72-29791

Dynamic behavior of thin walled semiinfinite elastic cylindrical shell with liquid under axial impact loads

13 p1943 A72-30008

Gravitational wave diffraction by liquid on surface of rigid circular cylindrical shells, determining velocity potentials

14 p2093 A72-30192

Average stress and strain across thickness of liquid filled cylindrical elastic thin walled shell with rigid bottom under axial impact loads

14 p2166 A72-30698

Natural frequency of free beam-like vibration of coupled fluid/structural system of cylindrical rod submerged in ideal fluid enclosed by cylindrical shell

16 p2465 A72-32985

Elastic momentless shell completely filled with ideal incompressible liquid, detailing small steady free vibrations

18 p2681 A72-36667

Fluid oscillations in a partially filled cylindrical tank with a spring supported elastic floor

18 p2684 A72-37062

Forced axisymmetric response of fluid filled spherical shells

18 p2684 A72-37063

Rotatory motions of a body with a liquid-containing cavity

19 p2787 A72-38151

Branching theory application to convection and axisymmetric flow formation in internally heated self gravitating liquid filled sphere

20 p2915 A72-40030

Orbital and rotational motion stability of rigid body containing elastic rods and fluid-filled cavity

22 p3204 A72-42092

Convective interaction in a partially-liquid-filled vertical vessel with heat influxes in its lateral and free surfaces and bottom

22 p3244 A72-42261

Dynamic behavior of thin walled semiinfinite elastic cylindrical shell with compressible liquid under axial impact loads

22 p3167 A72-42736

Dynamic loading of a fluid-filled spherical shell

22 p3240 A72-42891

Hydrodynamic fluid pressure on a shell during hydraulic impact

23 p3280 A72-43788

Forced and free vibrations of shallow cylindrical shell in rectangular duct filled with ideal fluid

24 p3459 A72-45004

The calculation of elastic tanks partially filled with liquids for prediction of the Pogo effect

24 p3392 A72-45152

German book on liquids flow rate measurement techniques covering physical principles of flow measurement including pressure, magnetic or inductive and ultrasonic methods

02 p0230 A72-12299

Photomultiplier signal for water axial velocity in glass pipe, providing turbulent liquid flow information and laser Doppler velocimeter evaluation

04 p0520 A72-14438

Unsteady boundary layer on hemisphere embedded on infinite plane during normal liquid impingement, using inner and outer expansions method to study separation time

05 p0653 A72-17003

Nonlinear motion stability of finite amplitude wave solution in thin viscous incompressible liquid film

06 p0801 A72-18142

Invariant free boundary problems of Navier-Stokes equations with nonzero vector of volume forces, investigating liquid layer flow on vertical cylinder surface

07 p0972 A72-20105

Flow characteristics of liquid layers adjacent to vapor bubble, visualizing flow via particle motion

08 p1151 A72-21670

Liquid flow cavitation impact on rotating disk surfaces, showing pitting characteristics dependence on physicochemical properties of specimens

09 p1327 A72-22297

Damping measurements of hydrodynamic vibrations of cylinder excited by random pressure field of liquid flow

10 p1465 A72-24073

Pump and unloading valve hydraulic system model with waves processes allowance in connecting pipe, discussing liquid mass and leakage effects on stability

11 p1578 A72-25770

Reynolds analogy for twisted liquid flow in tube with swirl vane

11 p1619 A72-26968

Shock wave propagation and damping in system of constant density gas bubble suspension in liquid flow with uniform velocity

13 p1940 A72-28436

Convection instability in viscous incompressible liquid layer with free boundaries under modulated external force field

13 p2064 A72-28723

Turbulent friction relation to averaged velocity profile of liquid flow in pipes and channels

14 p2096 A72-31019

Plane unsteady convective motion of viscous incompressible liquid in infinite horizontal vessel of rectangular cross section due to wall temperature fluctuations

14 p2174 A72-31157

Optimization of heat pipe with wick and annulus liquid flow, investigating effect of pressure loss and recovery in vapor passage

[ASME PAPER 71-HT-V] 15 p2335 A72-31767

Stability analysis of ideal incompressible liquid steady flow for given distribution, discussing velocity distribution effect on longitudinal cylindrical flow instability

16 p2376 A72-33093

Turbulent flow of viscous incompressible liquid film falling down semiinfinite vertical plate under gravity influence

16 p2376 A72-33142

Theoretical study of electromagnetic coupling in the forced oscillatory regime of two one-dimensional laminar flows of a viscous and electroconducting liquid in the presence of a transverse uniform magnetic field

17 p2587 A72-34281

Initial value techniques in free-surface hydrodynamics

17 p2538 A72-34644

An asymptotic solution for the laminar flow of a thin film on a rotating disk

[ASME PAPER 72-APM-38] 17 p2538 A72-34783

Transient turbulent free convection in a closed container with heating at the sides only

17 p2638 A72-35642

Flat plate withdrawal at high speed from quiescent liquid baths, calculating velocity profile via boundary condition transformation and eigenfunction expansion method

18 p2678 A72-36122

An integral analysis of condensing annular-mist flow

18 p2682 A72-36720

Nonlinear development of capillary waves in a fluid jet

18 p2682 A72-36885

Dynamics of stratified liquids in the presence of space charge

19 p2788 A72-38432

Two phase flow types defined as flow problems of two-phase matter mixtures /solid, liquid, gas or plasma/ and interface interaction

20 p2915 A72-39971

Metallic corrosion testing in high velocity liquids

22 p3183 A72-42858

LIQUID HELIUM

High conductivity superfluid region in cryogenic liquid helium 4 bath with temperature gradient in equilibrium with saturating vapor

01 p0101 A72-10040

Superconducting magnetic suspension systems safety aspects, discussing relief valves for He boil-off, flowmeters, cryostat temperature monitors, power supply diodes and safety interlocks

10 p1462 A72-24774

Torsional crystal measurements of viscosity for He 4 and He 3-He 4 mixture at lambda points

12 p1888 A72-27388

Carbon resistance thermometers time response and thermal diffusivity measurements in liquid helium temperature range

15 p2234 A72-31581

Glass silvered Dewar for liquid helium without auxiliary shielding cryogen, using surrounding annular space for radiation shielding

15 p2214 A72-32431

Solute quenching technique to determine hydrogen solubility in Ta to liquid He temperature, comparing with equilibrium measurements

15 p2259 A72-32640

Heat transfer with the helium II superfluid film

19 p2883 A72-38839

Breakdown of superfluidity for cylinders in saturated liquid helium II

19 p2836 A72-38840

Thermohydrodynamic conditions at the peak flux of horizontal heaters in superfluid liquid helium II at zero net mass flow

20 p2984 A72-39647

Reflection and transformation of sound waves in a superfluid liquid at a solid boundary

22 p3207 A72-42956

LIQUID HELIUM 2 U HELIUM ISOTOPES LIQUID HYDROGEN

Discretely oriented thread reinforced polyurethane cryogenic foam insulation systems for liquid hydrogen fuel tanks

01 p0092 A72-10981

Design, development and operation of liquid hydrogen plant, using production for rocket thrust chamber tests and tank pressurization studies

06 p0867 A72-17593

Shock tube rotational relaxation time measurements in cryogenic hydrogen, using laser schlieren optical system

11 p1691 A72-26008

Liquid and two phase liquid-gaseous hydrogen density determination via dielectric constant measurement by open-ended microwave cavity

14 p2103 A72-30197

Temperature and pressure requirements for producing superfluid liquid molecular hydrogen, noting use of solid deuterium or Ne walls to prevent hydrogen solidification

16 p2422 A72-32911

Gas-liquid hydrogen mixture and helium adiabatic model of Jupiter temperature and pressure distribution, estimating planet center temperature

19 p2863 A72-38074

A 10,000-gpm liquid hydrogen transfer system for the Saturn/Apollo program

19 p2784 A72-38829

The use of infrared absorption to determine density of liquid hydrogen

19 p2805 A72-38836

Development of a rocket propulsion system with 500 kgf vacuum thrust for liquid hydrogen/liquid fluorine

23 p3325 A72-43620

LIQUID INJECTION

NT WATER INJECTION

Drill hole heat transfer upon hot liquid injection into productive layer, enhancing oil extraction process effectiveness

04 p0594 A72-14515

Heat losses in oil wells hot liquid injections, modifying Oroveanu approximation method for exact solution

04 p0597 A72-15743

Evaporation and combustion of liquids injected into high temperature supersonic flow, considering interrelation with pressure variations

08 p1253 A72-21454

Cold flow tests of mixing and atomization characteristics of gas/liquid circular coaxial injector elements in pressurized facilities

14 p2146 A72-30920

Thermal protection by liquid-gas laminar flow near critical point with coolant film liquid oxygen injection incident on blunt body

16 p2343 A72-33156

Impulse liquid jet pressure reduction in closed vessel under adiabatic conditions and evaporation intensity dependence on jet velocity

16 p2476 A72-33259

Prediction of electron concentration reductions in re-entry flow fields due to electrophilic liquid and water injection

18 p2730 A72-36537

LIQUID LASERS

Laser generator research, discussing metallic vapor, heterojunction semiconductor, liquid, neodymium and organic colorant types

02 p0237 A72-11696

Handbook on lasers and optical technology covering gas, dye, liquid, injection and insulating crystal lasers, materials, sources, transmission, hazards and holographic recording

06 p0826 A72-17945

Stimulated emission cross section, loss coefficient and terminal level lifetime of high power Nd-phosphorus oxychloride liquid lasers

07 p1004 A72-19226

Energy transfer rates and spectral line inhomogeneity of narrow band oscillation phosphate glass and inorganic liquid lasers with Nd

07 p1004 A72-19227

Liquid pulsed laser active element lens parameters effects on output radiation divergence

07 p1008 A72-20511

Output characteristics of Q switched liquid laser as function of pumping pulse, cavity mirror reflectivity and cavity length

07 p1008 A72-20544

Giant pulse amplification with neodymium-phosphorus oxychloride liquid laser amplifier

09 p1323 A72-22655

Fast coaxial flash lamp pumped liquid dye laser /I.D.L./ for photolysis and biophysical and biochemical applications

09 p1326 A72-23406

Radiation distribution and power output characteristics of Nd in phosphorus oxychloride solution circulating liquid pulsed laser for various flow velocities

12 p1821 A72-27599

Energy characteristics of the laser action in rhodamine 6G pumped by a pinched discharge

20 p2933 A72-39512

Amplification of mode-locked trains with a liquid laser amplifier, Nd³⁺/POCl₃:ZrCl₄

20 p2934 A72-39642

Dynamic thermo-optical distortions compensation in lamp pumped rhodamine 6G liquid laser by introducing auxiliary dish with dye into cavity

23 p3295 A72-43679

Pulsed laser employing a rhodamine 6G solution in ethyl alcohol with an output energy of 110 J

24 p3411 A72-45498

LIQUID LEVELS

Continuous volume-temperature dilatometer measurement of small liquid samples in biological application

13 p1959 A72-29752

Contact-type level gauge with a transistorized decimal code converter

17 p2529 A72-34764

LIQUID MERCURY

U MERCURY [METAL]

LIQUID METALS

NT LIQUID POTASSIUM

NT LIQUID SODIUM

NT MERCURY [METAL]

NT MERCURY VAPOR

Focused laser beam interaction with liquid metal particles, discussing fluid phase light screening effect, droplet evaporation and mass expulsion characteristics

03 p0368 A72-13668

Potentials, currents and velocity variation of rotating conducting disk system in liquid metal medium under uniform longitudinal magnetic field

03 p0397 A72-13996

Visual investigation of semibounded axisymmetric MHD flow of liquid eutectic K-Na alloy under strong magnetic field effect

03 p0399 A72-14014

High temperature thermal properties of solid and liquid metals and rocks and minerals, discussing earth heat balance and measurement methods for heat capacity and conductivity

04 p0596 A72-14653

Alkali liquid metal heat pipes, showing heat transport rate for boiling initiation

05 p0743 A72-15870

Book on electronic processes in noncrystalline materials covering liquid metals, semimetals and semiconductors, Hall effect, phonons and polarons, thermoelectricity, photoconductivity, etc

06 p0866 A72-18516

Surface and interfacial energies measurement by multiphase equilibrium method for refractory metal monocarbides with liquid cobalt

07 p1010 A72-19136

V, Nb and Ta deoxidizing capability in liquid Fe from oxide phase formation identification by electronographic and X ray analyses

07 p1011 A72-19545

Thermal conductivity measurements of liquid InSb and Ga at 250-550 C

07 p1036 A72-20566

Liquid metal regenerator design and test evaluation for gas turbine engine fuel consumption improvement

[ASME PAPER 72-GT-33] 11 p1704 A72-25629

Heat transfer characteristics of liquid metal filled closed thermophons for hot wall boundary conditions of constant temperature and uniform heat flux

[ASME PAPER 72-GT-36] 11 p1745 A72-25631

Liquid Rb and Cs density and thermal expansion measurements near fusion point, discussing temperature dependence and gamma ray irradiation method

11 p1746 A72-26237

Semiconductor layers alloying by directional crystallization of compressed metals doped by contact with Ag, Ge, Te, Al and Sb films

13 p2020 A72-28564

Thermal diffusivity measurements by laser flash technique for liquid metals at high temperatures

13 p1971 A72-29756

Graphite wetting with liquid V, Nb and Mo as function of metal melting point and sample temperature

15 p2243 A72-31223

Hexagonal and cubic boron nitride surface wetting by liquid metals as function of contact interaction and chemical affinity

15 p2253 A72-31224

Capillary heat convective diffusion model of liquid layer sandwiched between two planes for calculating slag and metal movement rates

16 p2476 A72-33157

Variable amplitude and phase velocity electromagnetic traveling wave field distribution in diverging MHD induction machine channel with liquid metal flow

16 p2435 A72-33282

Steady state temperature field and heat flux at wall for metallic coolant flow in thin walled axisymmetric pipe with nonhomogeneous Neumann boundary condition

16 p2477 A72-33413

C concentration and temperature dependence of graphite wetting by liquid Ni and Co and melts of Ni-C and Co-C alloys, noting nonequilibrium effect

16 p2415 A72-33537

Pure metal unidirectional solidification as function of liquid superheat, metal/mold heat transfer coefficient and mold material

16 p2399 A72-33804

Liquid metals thermodynamic properties tabulation, including high melting transition metals, based on levitation data and periodic table correlations

16 p2479 A72-34000

Thermodynamic properties of liquid Co and Pd metals by levitation calorimetry, including specific heat, heats of fusion and surface emissivities

16 p2480 A72-34025

The interference function of molten metals

17 p2568 A72-35175

Investigation of the viscosity and density of solution melts intended for growing yttrium-iron garnet /YIG/ single crystals

19 p2847 A72-38684

The grain-size-dependences of the failure mode and ductility transition temperatures of melted chromium and tungsten

20 p2935 A72-39139

Alloying element effects on C free energy interaction coefficients in liquid Fe alloys at 1550 C by equilibrium distribution method

20 p2937 A72-39295

Rate of molybdenum solution in carbon-saturated liquid iron

22 p3193 A72-43027

Some contributions to energetics by the Lewis Research Center and a review of their potential aerospace applications

[ASME PAPER 72-AERO-12] 22 p3245 A72-43148

Design of high-temperature liquid-metal systems

[ASME PAPER 72-AERO-13] 22 p3204 A72-43149

Contact interaction between high-melting compounds and liquid metals. I - Interaction between subgroup IVA metals and metals of the iron family

23 p3299 A72-43287

Diffusion coefficients measurement in solid and liquid Al, discussing experimental techniques and temperature dependence

23 p3304 A72-44300

Optical constants of cesium in the wavelength range from 0.3 to 2.5 microns and their dependence on temperature and state of matter

24 p3426 A72-44800

LIQUID NITROGEN

Arterial and grooved Wick cryogenic nitrogen heat pipe performance tests, comparing elevation sensitivity, priming and heat transfer characteristics

[ASME PAPER 71-WA/HT-42] 05 p0745 A72-15889

Positive pressure cooling of cryogenic baths of liquid nitrogen by helium gas addition for frequency shift of ruby laser

09 p1326 A72-23411

Investigation of heat exchange during film boiling of underheated liquid under conditions of forced flow in channels

19 p2881 A72-38036

Stimulated thermal and Mandelstam-Brillouin scattering of light in liquid nitrogen and oxygen

20 p2933 A72-39520

Method of investigating the wear of hard tungsten carbide cobalt alloys in a liquid nitrogen medium

20 p2941 A72-39715

Combined buoyancy and flow direction effects on saturated boiling critical heat flux in liquid nitrogen

21 p3130 A72-41184

Strain hardening of maraging steels in liquid nitrogen

22 p3187 A72-41867

Investigation of heat transfer at high temperature heads in the case of cooling by a dispersed flow of liquid nitrogen

23 p3356 A72-43683

Investigation of the process of D16-alloy quenching in liquid nitrogen

23 p3294 A72-44095

LIQUID OXYGEN

Impact sensitivity of space shuttle materials in liquid and gaseous oxygen at high pressures

01 p0102 A72-10772

Apollo 12 liquid oxygen cloud spectrum observations, describing spectrograph with off axis zone plate for transmission grating and sieve plate collimator

01 p0071 A72-11172

Finite element analysis of hydroelastic properties of Saturn 5 full scale S-2 LOX tank, comparing with water tests

[AIAA PAPER 72-173] 05 p0740 A72-16833

Cavitation erosion of Al in liquid oxygen as function of static pressure and ultrasound frequency

07 p1034 A72-18921

LOX supply systems installation for civil transport aircraft crew and/or passenger breathing oxygen

[SAE AIR 1223] 11 p1584 A72-26030

Dielectric constant measurements of compressed gaseous and liquid oxygen for computing Clausius-Mossotti function

11 p1691 A72-26782

Cavitation erosion of Al in liquid oxygen as function of static pressure and ultrasound frequency

13 p1942 A72-29207

Detonation and burning characteristics of liquid oxygen-liquid methane mixtures

19 p2848 A72-38834

Stimulated thermal and Mandelstam-Brillouin scattering of light in liquid nitrogen and oxygen

20 p2933 A72-39520

LIQUID PHASES

Transferred electron microwave oscillator diodes with n-n structure by liquid phase epitaxy, reducing high resistance layer in interfaces and crystal defects

01 p0036 A72-10629

Oxygen content and stoichiometry effects on metal carbides grain growth in liquid phase sintering, discussing carbide-metal interface solution reaction as rate controlling mechanism

02 p0240 A72-11434

Catalytic action of metal oxides on isopropylbenzene hydroperoxide decomposition in liquid phase

08 p1129 A72-22094

Binary system molar energy diagram plotting, covering superheated, saturation and liquid phase regions

08 p1255 A72-22170

High temperature radiographic techniques for measurements of molten ceramics density, melting point, phase transitions, surface tension and viscosity up to 3000 C

09 p1333 A72-22378

Growth rate of semiconductor epitaxial films obtained by forced cooling from liquid phase

09 p1372 A72-23360

Minority carrier diffusion length in liquid epitaxial GaP, noting dependence on dominant impurity and substrate growth orientation from Schottky diode photocurrent technique

10 p1526 A72-24551

Liquid phase epitaxy GaAs growth in rotary reactors from Ga solution, noting thickness, doping uniformity, reproducibility and surface morphology

10 p1526 A72-24556

Oxygen, carbon and boron effect on liquid phase sintering behavior and mechanical properties of Ni base superalloys

11 p1645 A72-26848

Gallium arsenide-aluminum gallium arsenide double heterostructure wafer fabrication, describing reproducible liquid phase epitaxial growth

15 p2250 A72-32518

Effect of the process of crystallization of the liquid phase under pressure on the properties of Silumin

22 p3192 A72-42959

LIQUID POTASSIUM

Compatibility of brazed joints with potassium and vacuum

17 p2567 A72-34938

LIQUID PROPELLANT ROCKET ENGINES

NT HYDRAZINE ENGINES

NT HYDROGEN OXYGEN ENGINES

Liquid propellant rocket abort fireball model, specifying heat flux as function of time

03 p0457 A72-13953

Soviet book on thermal and gas dynamic design of gas turbines in aircraft and liquid propellant rocket en-

gines, covering three dimensional flows, temperature distribution, component cooling, etc
04 p0565 A72-15246

Mirage 3E liquid propellant auxiliary rocket engine, discussing intercept performance enhancement
05 p0705 A72-16708

Dynamic stability of controlled spacecraft with liquid propellant rocket engines, considering acceleration and braking sections of trajectory
05 p0730 A72-17027

Onboard equipment layout effect on dynamic stability against liquid propellant sloshing in spacecraft
05 p0730 A72-17028

Specific impulse, mass and propellant efficiency characteristics of miniature motors using cryogenic fuels for auxiliary rocket thrusters
07 p0914 A72-18983

Liquid fuel elastic rocket motion stability in supersonic flight, using vibration and thrust vector control equations for dynamic properties description
08 p1241 A72-21633

Soviet book on longitudinal vibrations of rocket with liquid propellant engine covering rocket element dynamic characteristics and free vibration mode shape and frequency calculations
08 p1241 A72-22025

Flame autostabilization mechanism during gaseous oxygen-liquid ammonia mixture combustion in liquid fuel rocket engine chamber, measuring mean burnout time
08 p1224 A72-22091

Control system for stabilization of liquid propellant rockets Pogo oscillations, discussing structure, fuel tank and feed system, combustion chamber, control gain and accelerometer installations
10 p1551 A72-24027

Liquid rocket LF unsteady transient behavior calculation from droplet evaporation and combustion parameters
10 p1528 A72-24644

Liquid fuel rocket engines design for space applications, describing combustion chambers, thrust and vector control systems and propellant mixtures physicochemical properties
12 p1861 A72-27861

Launch center for solid-liquid propellant rocket probes, Diamant and Europa 2, describing payload preparation hall
[DGLR PAPER 72-0137] 13 p1939 A72-28962

Liquid propellant rocket performance, stability and compatibility prediction techniques, noting effect on design time and cost
14 p2146 A72-30919

Flame autostabilization mechanism during gaseous oxygen-liquid ammonia mixture combustion in liquid fuel rocket engine chamber, measuring mean burnout time
17 p2597 A72-34662

Transmission line with feedback, deriving Nyquist stability from Michailov criterion with application to liquid fuel rocket model
17 p2621 A72-35100

Digital controller for high pressure rocket engine
18 p2721 A72-36335

Development of a rocket propulsion system with 500 kgf vacuum thrust for liquid hydrogen/liquid fluorine
23 p3325 A72-43620

Jets breakup, liquid propellant evaporation and cross sectional area variation in rocket motor combustion chambers
24 p3433 A72-44998

Theoretical analysis of a rotating two-phase detonation in liquid rocket motors.
24 p3433 A72-45053

LIQUID ROCKET PROPELLANTS

NT AEROZINE
NT CRYOGENIC ROCKET PROPELLANTS
NT HYPERGOLIC ROCKET PROPELLANTS
NT MONOPROPELLANTS

Fluorine-ammonia as high energy liquid bipropellant for rocket engines, presenting ground test results regarding velocity and specific impulse characteristics as functions of mixture ratio
01 p0114 A72-11220

Bipropellant fuel droplets combustion in oxidizing atmospheres from spherico-symmetrical nonconvective quasi-steady state model, discussing supercritical pressures and forced convection probability
04 p0596 A72-15273

Solid charge design for hybrid rocket engine with constant liquid propellant component consumption, deriving differential equation for perforated grain burning rate
07 p1053 A72-18994

Liquid propellants coupling effects on parallel stage space shuttle configuration structural dynamics, using forty degree of freedom analytical model
[AIAA PAPER 72-347] 11 p1725 A72-25376

Combustion of liquid propellants under supercritical conditions
17 p2637 A72-34946

Book on liquid rocket propellants development, history and ignition problem covering nitrogen tetroxide,

hydrogen peroxide, fluorine compounds, boranes and monopropellants
19 p2884 A72-38675

Popping phenomena with the hydrazine nitrogen-tetroxide propellant system.
22 p3215 A72-42866

Apollo/Saturn 5 spacecraft liquid propellants safety procedures in event of fire on explosion in operations building at Kennedy Space Center
23 p3343 A72-43552

Ideal high energy liquid rocket propellants combinations for high propulsive efficiencies, considering hydrogen, hydrazine, diborane and ammonia and various oxidizers
23 p3358 A72-44355

Contribution to the discussion of mixed-mode propulsion and reusable one-stage-to-orbit vehicles.
24 p3450 A72-45191

LIQUID ROTATION

U ROTATING LIQUIDS

LIQUID SLOSHING

Liquid motion in circular cylinder with elastic bottom under longitudinal excitation, representing dynamic and kinematic free surface conditions as nonlinear equations
02 p0204 A72-12254

Onboard equipment layout effect on dynamic stability against liquid propellant sloshing in spacecraft
05 p0730 A72-17028

Nonlinear oscillations of liquids in complex geometrically shaped moving vessels, using approximation methods for boundary value problem solution in Cartesian coordinate system
06 p0802 A72-18712

Capillary forces effects on free surface liquid behavior in partial or total weightlessness, reviewing sloshing problem mathematical treatments
06 p0802 A72-18717

Rotor components vibration destabilizing effects on dual spin spacecraft dynamics, considering turbulent liquid sloshing in Intelsat 4 propellant tank
07 p0973 A72-20488

Ideal liquid small oscillations natural frequencies and mode shapes in shell of revolution under weak gravitational field
08 p1148 A72-20956

Dynamic characteristics and nonlinear oscillations of liquid in spherical shell of revolution, modifying Lukovskii approximation method
08 p1148 A72-20962

Liquid sloshing in circular cylindrical cavity with ribs mounted radially to walls, calculating oscillation frequencies and virtual masses
08 p1148 A72-20968

Ideal incompressible fluid sloshing under centrifugal force in partially filled conical cavity rotating at constant angular velocity
08 p1149 A72-21244

Intelsat 4 nutation dynamics and gyrostabilization technique for precision pointing in international telecommunication, discussing damper and fuel sloshing
[AIAA PAPER 72-537] 12 p1780 A72-27360

Free small steady oscillations of liquid in solid tanks, considering HF modes
16 p2375 A72-32931

LIQUID SODIUM

The effect of oxygen on tantalum-sodium compatibility
20 p2938 A72-39297

LIQUID SURFACES

NT MENISCI

Dynamics of two dimensional body with cavity containing viscous incompressible fluid, noting obstacle interaction and free surface motion problems
06 p0801 A72-18139

Pulsating flame spread on liquid alcohol surface over range of liquid temperatures, using shadow streak photography
07 p1099 A72-19375

Dissolved gases effect on liquid surface state during high pressure liquid monopropellant strand combustion
08 p1222 A72-22046

Gravity waves parametric generation on liquid surface, presenting threshold values for space distribution of amplitudes and phases
14 p2097 A72-31111

Coupled oscillations of inviscid homogeneous liquid with free surface under vacuum or gas filled space in elastic cylindrical container
15 p2217 A72-31472

Unsteady axisymmetric flows of a liquid draining from a circular tank.
20 p2913 A72-39605

Draining of a fluid from a rotating cylindrical tank.
21 p3046 A72-41307

Laser interferometer for studying boundary layers in liquids
22 p3178 A72-42473

LIQUID-GAS MIXTURES

NT AEROSOLS

NT FOG

Liquid containment in gas driven vortex with air-water mixture densities above 100 times gas flow, discussing applicability to colloidal core nuclear reactor performance estimation
01 p0100 A72-11360

Shock wave damping and droplet atomization function of relaxation zone in noncombustible two phase gas-liquid mixtures
02 p0202 A72-11592

Gas-liquid bipropellant rocket motor system instability boundaries under various operating and design conditions, interpreting experimental results via time lag model
[AD-733596] 03 p0406 A72-13632

Two phase flow model of water droplets velocity in air stream, using Fresnel biprism and laser differential scheme
07 p1000 A72-18940

Flame autostabilization mechanism during gaseous oxygen-liquid ammonia mixture combustion in liquid fuel rocket engine chamber, measuring mean burnout time
08 p1224 A72-22091

Hydrothermodynamic foundations of hydrofoil engines employing gas-water mixtures and gas turbine generators, analyzing thrust coefficient and power efficiency
10 p1528 A72-25128

Liquid and two phase liquid-gaseous hydrogen density determination via dielectric constant measurement by open-ended microwave cavity
14 p2103 A72-30197

Flame autostabilization mechanism during gaseous oxygen-liquid ammonia mixture combustion in liquid fuel rocket engine chamber, measuring mean burnout time
17 p2597 A72-34662

Atomization of liquid droplets in a convective gas stream.
17 p2540 A72-35044

Motion of a fluid and gas bubbles with allowance for their relative displacement
18 p2682 A72-36891

Temperature field of a gas turbine rotor blade externally cooled by an air-liquid mixture
19 p2849 A72-38043

Investigation of the formation of local concentrations near the critical liquid-gas point by the electron paramagnetic resonance
23 p3356 A72-43326

Low speed steady one dimensional flow models for monodisperse spray deflagration, considering homogeneous, heterogeneous and premixed combustion
24 p3464 A72-45054

Fraunhofer single beam holography application to gas/liquid mixture high velocity flow cross section determination, observing liquid component effects on droplet dispersion composition
24 p3405 A72-45624

LIQUID-LIQUID INTERFACES

Plane steady flow of two viscous fluids in contact, presenting normal and tangential pressure
04 p0510 A72-14513

Interface stability of floating liquid zones of water/ethanol solutions in simulated zero gravity
07 p1036 A72-20561

Free convection and hydrodynamics of inclined liquid layers in laminar flow and in stepwise change of heat exchange surfaces temperature
08 p1151 A72-21663

Surface tension determination at immiscible liquids or liquid-gas phase interfaces by capillary rise measurement of droplet
09 p1294 A72-22678

Interior and exterior hydrodynamics of spherical droplet submerged in unbounded arbitrary velocity field, including effects of surface active agents
10 p1470 A72-25042

The linearized solutions as applied to the half-jet mixing.
18 p2683 A72-36928

The Rayleigh-Taylor problem with a vertical magnetic field, including the effects of Hall current and resistivity.
19 p2839 A72-37339

Critical levitation loci for spheres on cryogenic fluids.
19 p2836 A72-38844

Propagation of viscous fluid jets in a medium with a density discontinuity
21 p3047 A72-41666

LIQUID-SOLID INTERFACES

Sound pressure in liquid layer bounded by oscillating plate under bending as function of boundary acoustic impedance
07 p1034 A72-18923

Binary alloys concentration distribution determination in migrating liquid-solid plane phase interfaces range during crystallization
07 p1022 A72-20571

Surface active medium effect on free surface energy and strength of pyrographite in ethyl alcohol solution, using crack kinetics experiment
08 p1197 A72-22182

- Temperature dependence of emf coefficient Hall constant and conductivity in solid and liquid phases of InSe semiconductor during melting
10 p1526 A72-24267
- Acoustic measurement of solid-liquid interface motion and solidification during freezing of Hg and paraffins
10 p1563 A72-25044
- Cylindrical shell vibrations in incompressible inviscid fluid near free interface, calculating natural frequencies with Fourier transforms
10 p1471 A72-25130
- Schlieren visualization of radiated wave fronts for Al plates illuminated with short acoustical pulses in water, comparing with Lamb theory
11 p1687 A72-26057
- Periodic liquid heating through infinite plate, taking into account temperature induced variation in heat capacity and conductivity
12 p1888 A72-27227
- Momentum and energy equations for pool film boiling heat transfer from horizontal cylinder to saturated liquids, using integral boundary layer analysis
14 p2173 A72-31067
- Thin liquid films on rotating horizontal disk, measuring flow, thickness and stability with asymptotic-expansion solution
15 p2334 A72-31616
- Motion of a fluid and gas bubbles with allowance for their relative displacement
18 p2682 A72-36891
- Damping characteristics of a liquid squeeze film.
18 p2683 A72-37053
- German monograph - A photometric method for measuring the concentration distribution in turbulent boundary layers
19 p2799 A72-37652
- Correctness of boundary conditions in the method of measuring the heat exchange coefficient by the rate of the thermal deformation of samples
19 p2881 A72-38038
- A technique for determining the transient heat flux at a solid interface using the measured transient interfacial temperature.
[ASME PAPER 72-HT-18] 20 p2987 A72-39687
- X-ray diffraction studies on liquids at very high pressures along the melting curve. I, II.
21 p3084 A72-40558
- Water film formation and breakdown during motion over solid surfaces, predicting flow rate difference due to contact angle hysteresis
21 p3085 A72-41178
- LIQUID-VAPOR EQUILIBRIUM**
- Vapor bubble growth on heated surface with random temperature distribution and liquid microfilm for water and boiling potassium
02 p0303 A72-12862
- Papers on high pressure-high temperature research techniques covering laboratory procedures for control, calibration and measurement of solid-vapor and liquid-vapor equilibria
12 p1778 A72-28103
- Vapor-liquid equilibrium analysis of water soluble volatile organic compounds in closed airtight systems by gas chromatography
13 p1910 A72-29326
- Method of characteristics application to supersonic jet and nozzle gas flow with allowance for equilibrium and nonequilibrium condensation
17 p2544 A72-35929
- A generalized virial equation of state and its application to vapor-liquid equilibria at low temperatures.
19 p2883 A72-38838
- Breakdown of superfluidity for cylinders in saturated liquid helium II.
19 p2836 A72-38840
- Evaporation of metallic targets by intense optical radiation
23 p3297 A72-44485
- LIQUID-VAPOR INTERFACES**
- Two dimensional molecular dynamics digital simulation of Ar liquid-vapor interface at triple point, yielding strongly oscillatory density profile
03 p0393 A72-14263
- Surface tension determination at immiscible liquids or liquid-gas phase interfaces by capillary rise measurement of droplet
09 p1294 A72-22678
- Temperature oscillations associated with surface gravity waves at two fluid model compressible vapor-incompressible superfluid interface
12 p1845 A72-27386
- Shock wave propagation and damping in system of constant density gas bubble suspension in liquid flow with uniform velocity
13 p1940 A72-28436
- Coupled oscillations of inviscid homogeneous liquid with free surface under vacuum or gas filled space in elastic cylindrical container
15 p2217 A72-31472
- Power spectrum of light scattered from surface waves thermally excited on carbon dioxide liquid-vapor interface near critical point
16 p2423 A72-32948
- An integral analysis of condensing annular-mist flow.
18 p2682 A72-36720
- Convective heat exchange of metastable liquid during suspension of boiling
19 p2881 A72-38037
- A study of the liquid-vapor phase change of mercury based on irreversible thermodynamics.
[ASME PAPER 72-HT-A] 20 p2983 A72-39481
- Saturated liquid film boiling on vertical surface, calculating local heat transfer rates as function of height and superheat from turbulent vapor flow model
[ASME PAPER 72-HT-38] 20 p2986 A72-39668
- Diffusive and radiative effects on vaporization times of drops in film boiling.
21 p3130 A72-41185
- Interactions between gas bubbles and components of the blood - Implications in decompression sickness.
24 p3374 A72-45652
- LIQUIDS**
- NT AEROZINE
NT CRYOGENIC FLUIDS
NT CRYOGENIC ROCKET PROPELLANTS
NT FLOX
NT HYDRAULIC FLUIDS
NT HYPERGOLIC ROCKET PROPELLANTS
NT LIQUEFIED GASES
NT LIQUID AMMONIA
NT LIQUID HELIUM
NT LIQUID HYDROGEN
NT LIQUID METALS
NT LIQUID NITROGEN
NT LIQUID OXYGEN
NT LIQUID POTASSIUM
NT LIQUID ROCKET PROPELLANTS
NT LIQUID SODIUM
NT MERCURY [METAL]
NT MERCURY VAPOR
NT MONOPROPELLANTS
NT ORGANIC LIQUIDS
NT ROTATING LIQUIDS
- Liquid n-octane, n-decane and n-undecane densities and adiabatic/isothermal compressibilities from sound velocity measurements at high pressures and 30-140 C
02 p0261 A72-12829
- Liquid breakdown and subsequent propagation by focused high power laser irradiation, presenting short term photography of event sequence
03 p0368 A72-13606
- Sphere unsteady motion in viscoelastic liquids, noting falling-ball technique use for elastic parameters determination
07 p0973 A72-20549
- Light absorptivity measurement in low loss liquid with interferometer based on refractivity dependence on temperature change due to absorption
09 p1309 A72-22602
- Acoustic waves generation in liquids by Q-switched ruby laser, noting transition from plane to spherical waves with dye concentration and focusing configuration variations
10 p1490 A72-23954
- Lunar anorthosites and parent liquids chemical composition from trace element analysis
10 p1537 A72-24158
- Quenched specimen anisotropic surface heating effect in liquid vaporization characteristics determination
10 p1561 A72-24207
- Liquid environments effect on mild steel fatigue strength, discussing effects of viscosity, compressibility and entry rate into cracks
11 p1656 A72-25738
- Volume and enthalpy changes at critical point of condensed state, noting Ar enthalpy dependence on temperature
19 p2881 A72-38045
- X-ray diffraction studies on liquids at very high pressures along the melting curve. I, II.
21 p3084 A72-40558
- Stimulated thermal scattering of picosecond laser pulses.
21 p3063 A72-40779
- Nonstationary method for measuring the heat conductivity of liquids and gases under high pressures
22 p3243 A72-41886
- Polarization characteristics and wave vector direction effect on cross section of incident and diffuse light scattered in liquid, determining frequency shift functions
23 p3312 A72-43318
- Influence of steric effects and compressibility on nonlinear response to laser pulses and the diameters of self-trapped filaments.
23 p3296 A72-43873
- LIQUIDS**
- Liquidus temperatures and isothermals in Al corner of Al-Ti-B alloy phase diagram, using differential thermal analysis
16 p2409 A72-33808
- LITERATURE**
NT DOCUMENTATION
LITHERGOLIC PROPELLANTS
U HYBRID PROPELLANTS
- LITHIUM**
NT LITHIUM ISOTOPES
- Thermal flux model of lithium plasma source at various temperatures and pressures, using arc channel model with conducting cross section
02 p0268 A72-12859
- Magnetic splitting of lines dependence on Paschen-Back effect for Li resonance doublet in sunspots
03 p0427 A72-13293
- Low energy phase shifts for elastic scattering of electrons by Li and Na
03 p0391 A72-13745
- Li-diffused Si compared to conventionally doped materials under neutron irradiation, considering carrier removal
03 p0403 A72-14078
- Li-containing solar cell damage and recovery characteristics measurement under 1-MeV electron irradiation, deriving diffusion-length damage coefficient
03 p0312 A72-14092
- Li, Be and B production rate in interstellar gas by galactic cosmic rays from diffusion model of fast particles, accounting for He component
05 p0708 A72-15760
- Angular momentum and Li diffusive transport induced by mild thermally driven turbulence associated with Goldreich-Schubert-Fricke instability, discussing solar rotation slowdown
[AD-735988] 05 p0720 A72-16718
- Collisionless drift waves in thermally ionized Li plasma column under variable shear magnetic field
06 p0857 A72-17535
- Positive electrode materials for high energy density batteries with Li negative electrode, calculating discharge emf for various salts
06 p0760 A72-17575
- Atmospheric Na, Li and K layers height, width, abundance and thickness from twilight glow measurements, using birefringent filter type photometers
08 p1159 A72-21224
- Radiation induced extrinsic photoconductivity in Li doped Si, examining localized energy levels in forbidden gap
09 p1372 A72-23238
- Cross sections of Li nonresonant capture of Na ion charge, interpreting quasi-oscillatory structure
10 p1517 A72-25047
- Electrothermal thruster supersonic convergent-divergent nozzle performance with lithium vapor propellant, predicting exhaust velocity by isentropic flow equations
[AIAA PAPER 72-453] 11 p1708 A72-26189
- Secondary molecular ion emission of Li as function of atoms number
11 p1701 A72-26506
- Electron irradiation effects on Li doped silicon solar cells, noting changes in donor concentration and defects formation
12 p1757 A72-28022
- Li dopant radiation damage inhibiting effect on electron irradiated n-type silicon, discussing EPR and photoconductivity experimental results
12 p1856 A72-28023
- Electron bombardment effects on transport properties and carrier lifetime degradation of Li doped Si solar cells
12 p1856 A72-28024
- Lithium diffusion into silicon by evaporation and homogenization technique, discussing dislocations and oxygen effects from aging in Ar at 150 C
12 p1757 A72-28025
- Li defect interactions in electron irradiated n-type single crystal Si from electron paramagnetic resonance measurements
12 p1858 A72-28063
- Acceptor level study of thermally diffused Be and Be-Li complexes in single crystal Si after quenching and annealing
13 p2022 A72-29628
- Umbral model effect on Li abundance determination from sunspot spectra
13 p2045 A72-29711
- Spectral line identifications and classifications of Li like spectra of elements K through Mn in extreme UV region, detailing extrapolation procedures
14 p2133 A72-30563
- Model for low energy galactic cosmic ray effects on young and F star Li abundance and H I region heating
16 p2448 A72-33740
- Properties of lithium greases as a function of the saturation level of commercial 12-oxysearic acid
19 p2823 A72-38093
- Investigation of the structure of a high-current discharge in a lithium plasma
22 p3209 A72-41878
- Recombination continuum in a lithium plasma spectrum
22 p3210 A72-42171
- Model potential calculations of lithium transitions.
24 p3426 A72-44808
- LITHIUM ALLOYS**
- Phase equilibrium of Mg base solid solutions of Mg-Li-Sn system at 200-500 C, analyzing microstructure, microhardness and electrical resistivity
14 p2124 A72-31029

Alloying effect on structural transformations and strain hardening during aging of two phase α -phase/Mg-Li-Zn alloys

14 p1214 A72-31031

Al-Mu-Li alloys phases mechanical and thermal properties under tensile and fatigue tests at room and elevated temperatures

14 p1214 A72-31037

Composition, strength and plasticity of ultrahigh Mn-Li alloys with two-phase α -phase base

14 p1215 A72-31040

Li addition effects on Mg mechanical properties temperature dependence and notch sensitivity of binary Mg-Li alloys

14 p1215 A72-31041

Peritectic solid phase transformations in cast homogenized Al-Cu-Li-Mn-Cd alloy, noting Li strengthening effect

23 p3303 A72-44093

LITHIUM BORATES

The role of Sm and Mn as activators in calcium sulphate and lithium tetraborate.

18 p2718 A72-36347

LITHIUM CHLORIDES

LiCl dew point hygrometer operation investigated by double ventilation psychrometers, noting measurement error dependence on relative humidity and temperature

10 p1483 A72-25015

Phase transition between solid hydrate and saturated solution of lithium chloride electrically detected on a lithium chloride heated hygrometer.

21 p3054 A72-40689

LITHIUM COMPOUNDS

NT LITHIUM BORATES

NT LITHIUM CHLORIDES

NT LITHIUM FLUORIDES

NT LITHIUM HYDRIDES

NT ORGANIC LITHIUM COMPOUNDS

Tunable optical, and IR radiation source by rotating lithium niobate crystal in front of Q switched ruby laser

04 p0550 A72-15599

Optical holographic storage in lithium niobate single crystals, noting erasability and rewritability

07 p0981 A72-18890

Ho doped YLF and YAG laser threshold and slope characteristics at room temperature, considering Q-switched operation lifetime

07 p1004 A72-19233

Lithium niobate crystal refractive index inhomogeneity influence on second harmonic generation from He-Ne laser

11 p1650 A72-26360

Temperature dependence of destruction threshold of lithium niobate surface under laser irradiation, noting ferroelectric properties effects

12 p1853 A72-27069

High temperature heating of plasma by ultrashort laser pulses focused onto lithium deuteride, noting various diagnostic methods

12 p1851 A72-27581

Discrete ten stage system for laser beam deflection based on electro-optical effect in lithium niobate crystals

12 p1808 A72-27595

Longitudinal electro-optical effect in oblique cut lithium niobate crystal with minimum half wave voltage between incident beam and optical axis angle

12 p1855 A72-27603

Second harmonic conversion of CW YAG-Nd laser radiation on lithium metaniobate crystals, discussing conversion coefficient optimization

12 p1825 A72-27886

He-Ne laser light modulation with lithium niobate crystals, noting lower light power and modulator volume requirements, better mechanical properties and lower thermal sensitivity

13 p1969 A72-29632

Undoped lithium niobate for holographic storage applications, reviewing physics and recording performance

15 p2239 A72-32353

Transition metal doped lithium niobate for holographic storage, measuring recording sensitivity, maximum diffraction efficiency and erase behavior

15 p2239 A72-32354

Lithium niobate crystal refractive index inhomogeneity influence on second harmonic generation from He-Ne laser

16 p2403 A72-33713

Second harmonic conversion of CW YAG-Nd laser radiation on lithium metaniobate crystals, discussing conversion coefficient optimization

16 p2404 A72-33995

He-Ne laser radiation modulator at 1.5 GHz using X and Z cut lithium niobate crystals in toroidal microwave cavity

18 p2697 A72-36113

Fracture of nonlinear KDP and LiNbO₃ crystals by ruby laser radiation

19 p2812 A72-38537

Synthesis of polymers with conjugate bonds on the basis of dilithium-derivative aromatic hydrocarbons

23 p3262 A72-43929

Properties of a pulsed LiO₃ doubly resonant parametric oscillator.

23 p3297 A72-44187

Use of oblique-cut lithium niobate in optical-beam control systems.

24 p3411 A72-45606

Profile of a parametric luminescence line emitted by lithium niobate crystals.

24 p3432 A72-45614

Temperature and angular widths of the phase-matching curve of a lithium niobate crystal.

24 p3432 A72-45615

Temperature dependence of destruction threshold of lithium niobate surface under laser irradiation, noting ferroelectric properties effects

24 p3432 A72-45722

LITHIUM FLUORIDES

Elastic and one-phonon inelastic scattering of monoenergetic He atoms from cleaved LiF crystal surface

15 p2281 A72-31862

LITHIUM HYDRIDES

Neodymium laser plasma dispersion and diffusion in magnetic field, using electrostatic injection of LiH particles

03 p0393 A72-13081

Multiple meson production in 250 GeV nucleon-nucleon collisions in LiH targets, noting 40 per cent formation of heavy meson cluster fireballs

06 p0868 A72-17259

Nd laser irradiation of LiH particles in magnetic trap, investigating resultant plasma expansion and diffusion

13 p2015 A72-29431

Multiplicity of particles generated in inelastic interactions of nucleons with LiH nuclei at energies from 150 to 550 GeV

23 p3329 A72-44405

LITHIUM ISOTOPES

Cosmic Li, Be and B nuclei charge and isotopic composition measured by particle telescopes, finding L/M ratio

01 p0121 A72-11120

Slowly rotating F, G and early K field stars data, computing Li abundance and isotope ratio

04 p0578 A72-15316

Pionic X ray fields and transitions in Li6, Be9, C12 and O16, obtaining 2p level absorption broadening

10 p1515 A72-24418

LITHIUM 4

U LITHIUM ISOTOPES

LITHIUM 6

U LITHIUM ISOTOPES

LITHOGRAPHY

Electron image projection system using converter tube technique for microcircuit lithography, discussing performance tests and design changes

10 p1447 A72-23957

Microwave integrated circuits.

17 p2527 A72-34570

LITHOLOGY

Northern Alps geology, hydrology, lithology and tectonic survey, using aircraft-borne thermal IR scanner remote sensor

02 p0209 A72-11795

Lithology of Apollo 14 lunar clastic rocks from Fra Mauro region, noting different makeups of glassy matrix and particles, plagioclase, pyroxene and lithic clasts

16 p2457 A72-33675

LITHOSPHERE

NT EARTH CORE

NT EARTH CRUST

NT EARTH MANTLE

NT EARTH PLANETARY STRUCTURE

NT EARTH SURFACE

Lithic and vitreous particles in Lunik 16 core tube samples from Mare Fecunditatis, discussing particle type proportions and petrological and mineralogical aspects

09 p1379 A72-22256

Physical structure of the moon.

17 p2615 A72-35680

LIVER

Starvation effects on male rats, mice and guinea pigs hepatic drug metabolism, discussing ethylmorphine, p-nitroanisole and aniline

01 p0015 A72-11262

Dipeptidyl aminopeptidase I preparation from beef spleen and rat liver, discussing contamination with catheptic carboxypeptidase C and Ser-Met dipeptidase

07 p0935 A72-18906

Pulsed and continuous rf irradiation effects on mitotic activity and chromosomal aberrations in regenerating rat liver tissue

07 p0917 A72-19443

Splanchnic vascular bed role in human blood pressure regulation from lower body negative pressure tests, measuring blood flow from hepatic dye removal rates

08 p1123 A72-20889

Liver and muscle type isozymes of DPN-linked glycerol-3-P dehydrogenase in chickens in terms of tissue distribution, ontogeny and avian evolution

12 p1759 A72-27161

Synthetic carbohydrates toxicity effects on rat liver lysosomes application to astronaut potential food sources

14 p2074 A72-30381

High gravity, cold and starvation space stress effects on oxidative metabolism of ethylmorphine, aniline and p-nitroanisole in male rat liver

15 p2185 A72-31700

Dietary regulation of fatty acid synthesis in rat liver and hepatic autotransplants.

19 p2757 A72-38147

Local necrosis, parenchyma incisions and vascularization of rabbit liver tissue under pulsed and continuous laser beams

21 p3002 A72-40991

Hypoxic acclimation effects on rats heart, liver and kidney mitochondria, measuring cytochrome oxidase and succinic dehydrogenase activities

22 p3144 A72-42673

LOAD DISTRIBUTION [FORCES]

Airport apron surface pavement strain measurements under field loading conditions, considering static and dynamic loads with finite element method

01 p0047 A72-10192

Structural sandwich panel design, establishing simple stress and deflection formulas under transverse loading based on tests evaluating balsa as laminate core

01 p0138 A72-10723

Finite plasticity incremental and total strain theories for nonproportionate loading of circular steel and Al alloy torsion-tension members assuming von Mises yield

[SESA PAPER 1901] 02 p0288 A72-11519

Misalignment effect on load distribution and fatigue life of tapered roller bearings

[ASME PAPER 71-LUB-6] 02 p0234 A72-11532

Asymmetrically loaded cylindrical roller bearings, describing hollow ended design for fatigue life improvement

[ASME PAPER 71-LUB-14] 02 p0235 A72-11536

Unidirectional and bidirectional composite laminates subjected to cylindrical bending under uniformly distributed and concentrated loads

02 p0292 A72-11989

Elastic stability of body under conservative loads, deriving energy criterion with thermodynamic laws

02 p0292 A72-12003

Surface subsidence in semiinfinite resilient elastic solid mass supporting annular load distributed over circular ring

02 p0297 A72-12616

Square orthotropic and isotropic plates stability with square hole under uniformly distributed load

02 p0299 A72-12685

Microinhomogeneous elastoplastic cyclically strain hardenable material under symmetric loading, calculating stress-strain relationship

03 p0443 A72-13453

Variable cross section elastic stringer end loaded longitudinal force transmission to stiffened elastic plate

03 p0444 A72-13465

Static load transfer to discontinuous elastic filament in fiber reinforced composite, determining fiber force longitudinal distribution by approximation to Fredholm integral equation

03 p0455 A72-14384

Displacements in nonhomogeneous elastic layer, investigating uniformly distributed load surface settling behavior dependence on layer depth relationship to loaded area width

03 p0455 A72-14387

Time delay effect on stability of viscoelastic cantilever column under retarded follower load

04 p0590 A72-15186

Statically indeterminate and determinate elastic beams optimal design for maximum-minimum deflection under distributed load

04 p0590 A72-15192

Circular conical orthotropic shells of linearly variable thickness loaded by distributed and concentrated forces and moments, analyzing stress-strain state by numerical methods

04 p0594 A72-15749

Fatigue crack propagation rates for aluminum alloy plates under mode I extensional loads and transverse mode II bending loads

[ASME PAPER 71-MET-J] 05 p0732 A72-15793

Variable thickness shallow spherical shells of revolution axisymmetric loads carrying capacity, determining limit equilibrium through application of Tresca yield point concept

05 p0734 A72-15983

Stressed state of radial bearings hollow rollers under loads concentrated along generatrix, evaluating test results by statistical analysis

05 p0665 A72-15984

Load or compression eccentricity effect on buckling and postbuckling behavior of flat plates, presenting stress distribution curves

05 p0737 A72-16116

Elastically supported cantilever stability with continuous lateral restraint under uniform distributed axial load, developing boundary conditions

05 p0737 A72-16118

Crackline loaded edge crack stress corrosion specimen, investigating crack initiation and propagation 05 p0673 A72-16324

Equilibrium conditions of closed elastic spherical shell under uniform nearly critical compression loads, determining shell deformation in Hilbert spaces 05 p0739 A72-16587

Fiber pull-out from elastic matrix, calculating shear stress and load distribution dependence on elastic properties and fiber length 06 p0897 A72-18152

Shear and direct stresses on fuselage model cross section due to concentrated radial loads on frame comparing measurement with prediction by matrix force analysis 06 p0898 A72-18322

Interferometric holography application to photoelastic stress analysis of opaque anisotropic composite plates under static and dynamic transverse and in-plane loads 06 p0898 A72-18349

Optimal rigid-plastic limit load analysis of spherical shells under nonsymmetrical loadings, using SUMT and Rosenbrock method 07 p1087 A72-18791

Zero moment theory application to cylindrical shells with elliptical geometries under constant transverse loads 07 p1087 A72-18992

Rupture strength of disk with surface crack under concentrated loads, applying integral equation to stressed state 07 p1092 A72-19777

Matrices of fundamental solutions constructed for loading singularities and Green method in unbounded micropolar elastic continuum 07 p1095 A72-20243

Stress-strain state of unclamped thin elastic zero curvature shell under three component surface load and tangential boundary forces 07 p1095 A72-20313

Symmetrically loaded uniform thin circular ring natural vibration frequencies in radial and axial flexural modes, comparing experimental data with values predicted by group theory 07 p1096 A72-20499

Wilga 3 aircraft structure service life from structural fatigue theory and tests, emphasizing operational load distribution measurement 08 p1110 A72-21634

Nonsymmetrical cylinders and valves under nonsymmetrical loading 08 p1113 A72-22157

Mathematical model for derivation of asperity or metal-metal contact load sharing of lubricated machine components in journal and roller bearings 09 p1317 A72-22248

Trapezoidal plate thermoelasticity problem for various thermal load distributions, solving Poisson equation for sectorial annular region 09 p1400 A72-22711

Elastoplastic stressed state of multilayer cylinder during loading, unloading and cyclic loading processes 09 p1401 A72-22721

Loading path effect on yield surfaces of pure Al at elevated temperatures under tension 09 p1328 A72-22993

Electric contact phenomena in ultraclean and specifically contaminated metallic systems, noting resistance relationship to load curves and surface conditions 10 p1448 A72-24172

Wing load distribution and induced drag control by warping, summarizing linear theory and wind tunnel test results 10 p1417 A72-24218

External load effects on natural frequencies of free end and centrally loaded cantilever beams and supported or clamped circular plates 10 p1558 A72-24814

Photoelastic investigation of star shaped models for loading direction influence on shear stress distribution at notch tip region in uniform tensile field 10 p1559 A72-24897

Freely supported rectangular plate flexure under arbitrarily distributed load, obtaining differential equations solution in trigonometric polynomials 10 p1559 A72-24996

Prestressed circular ring snap-through under continuously distributed or discrete torsional loads, determining critical torque by asymptotic solution 11 p1734 A72-25721

Curved cylindrical shell finite element with reduced stiffness matrix, noting convergence for symmetrical and unsymmetrical loading 11 p1735 A72-25896

Incremental growth of beams under combined direct load and cyclically varying curvature 11 p1735 A72-25897

Bending of simply supported thin square plate clamped around central circular hole and under uniformly distributed transverse load 11 p1736 A72-25985

Annular plate with supporting edge beams and concentrated load, showing deflection decrease with stiffness 11 p1736 A72-25990

Anisotropic cylindrical beam bent by transverse load in elastic plane, reducing to Almansi problem 11 p1736 A72-26091

Elastic-plastic analysis of large deflection of axisymmetrically loaded circular plates, using incremental theory 11 p1737 A72-26426

Large deflection of variable thickness square plate under uniform load, using strain energy method 11 p1737 A72-26588

Structural effects of meridian imperfections in symmetrically loaded elastic thin shell of revolution 12 p1881 A72-27255

Closed form solution for dynamic response of infinite plate with elastic foundation and damping under arbitrary initial conditions and load distribution 12 p1883 A72-27559

Circular cylindrical shell under distributed edge load along circular hole contour, calculating stress concentration by trigonometric series solution for shallow shell equation 12 p1886 A72-28130

Conjunction mechanism of two real contacting bodies with rough surfaces under normal load 12 p1819 A72-28202

Uniformly loaded parabolic arches lateral-torsional buckling, deriving governing linear differential equations from Clebsch-Kirchhoff equilibrium equations for thin curved bars 12 p1888 A72-28349

Axisymmetric stability of spherical cap rigidly clamped at contour of shells of revolution, using variational difference method for uniformly distributed external pressure 13 p2053 A72-28393

Structural approach to elastic stability in buckling problems, simplifying deformation concepts and loading condition definition 13 p2054 A72-28479

Cylindrical shell stability with variable thickness and moderate length under distributed ring load and uniform pressure, determining critical load 13 p2058 A72-29459

Collapse loads of symmetrically tapered cantilever beams under uniformly distributed end shear, considering optimum tapering angle for minimum weight 13 p2059 A72-29596

Thin wedge shaped shell bending under normal loads, discussing boundary value problems 13 p2062 A72-30066

Shallow rectangular shell vibrations induced by moving band load, deriving frequency equation and load critical speed 14 p2166 A72-30688

Finite element method with compliance equations determining energy release rates and stress intensity factors for complex crack configurations and loadings 14 p2168 A72-30908

Loading conditions effect on relaxation and creep in inhomogeneous hereditary elastoplastic polycrystalline materials 14 p2168 A72-30953

Stress analysis and deflection equation for uniformly loaded and heated two layer clamped rectangular plate 15 p2322 A72-31362

Filler influence on critical load and buckling zone size in circular elastic three layer ring under uniformly distributed vertical load in rigid cavity 15 p2328 A72-31745

Stress concentrations in cylindrical shells with cut-outs under uniformly distributed axial tensile load, presenting exact solution of differential equation 15 p2328 A72-32138

Buckling behavior of simply supported elastic folded plate structures without and with transverse stiffeners under symmetrical and asymmetrical uniform vertical loads 15 p2332 A72-32562

Bending of uniformly loaded circular plate with mixed boundary conditions, calculating deflection and bending moments 15 p2332 A72-32579

Stress analysis for brittle body with thermoinsulated crack under mechanical load and temperature field, noting limiting equilibrium equation 16 p2469 A72-33272

Stress analysis for circular disk with diametral crack under symmetric and antisymmetric loads, solving integral equations via factorization 16 p2469 A72-33273

Imperfect circular cylindrical shells creep and elastic buckling under nonuniform external loads, solving ordinary differential equations via finite difference technique 16 p2474 A72-34133

Optimal design of static laterally loaded fiber reinforced plates, determining optimum load-path directions at all plate points 16 p2475 A72-34174

The plane solution for anisotropic elastic wedges under normal and shear loading. [ASME PAPER 72-APM-13] 17 p2629 A72-34802

Continuous elastic systems flutter and divergence instability under nonconservative loading, determining slopes of loading-frequency curves 17 p2633 A72-35255

Shear buckling of an elastically supported fiber. 17 p2633 A72-35290

On the finite deflections of thin beams. 17 p2634 A72-35404

Photoelastic investigation of a Hertzian contact with shallow grooves in the contact area. 18 p2734 A72-36374

Steady flow of conducting fluid in MHD ball bearing clearance between two eccentric spheres, deriving load, friction moment and optimum operation mode 18 p2696 A72-36818

Vibration of a stiffened ring considered as a cyclic structure. 18 p2739 A72-37205

Computer method for plasticity theory boundary value problem for medium with unknown equations of state, using complex load simulating device 19 p2870 A72-37387

Determination of the parameters of motion of a container and its load with allowance for their interaction during internal vibrational finishing operations 19 p2824 A72-37426

Equilibrium conditions of closed elastic spherical shell under uniform nearly critical compression loads, determining shell deformation in Hilbert spaces 19 p2872 A72-37558

Limit analysis for plates - A simple loading problem involving a complex exact solution. 19 p2872 A72-37599

Free vibrations of multilayer sandwich plates in the presence of in-plane loads. 19 p2876 A72-38020

Method of sources for solving axisymmetrical problems in the theory of elasticity 19 p2877 A72-38202

Elastoplastic axisymmetric bending of a clamped circular plate under the action of a conically-distributed variable load 20 p2978 A72-39022

Uniformly loaded thin elastic isotropic circular plate with partly clamped and simply supported edges, determining deflection via solution of biharmonic differential equation 20 p2979 A72-39331

Deformation of the earth by surface loads. 20 p2916 A72-39335

Transverse isotropy effects on beams static behavior, considering Green functions, deflection under distributed loads and beam-column deflection 20 p2980 A72-39613

Thin elastic rings subjected to radial load sets. [ASME PAPER 71-WA/DE-2] 20 p2980 A72-39812

The carrying capacity of frames under the influence of concentrated forces 20 p2981 A72-39919

Stress intensity factors for transversely loaded elastic plates and their application to predictions of crack arrest. 20 p2981 A72-39956

Stresses in a perforated, continuously loaded cantilever beam. 21 p3117 A72-40453

An iterative procedure to obtain exact buckling criteria for columns under combined action of variable continuous load and concentrated forces. 21 p3118 A72-40927

Non-Hertzian contact stresses in a smoothly cradled heavy cylinder. 21 p3119 A72-41108

The vertical stress distribution due to parabolical strip load and uniform load over an ellipse in the interior of a semi-infinite solid. 21 p3121 A72-41243

A consistent approach for treating distributed loading in the matrix force method. 21 p3122 A72-41261

Stress distribution at crack tips in elastic plate loaded by two concentrated opposite forces perpendicular to crack 21 p3123 A72-41389

Perfectly plastic media under the action of multiparameter loads 21 p3123 A72-41393

Weight minimization for elastic circular plates of variable thickness under uniformly distributed load with given stress function conditions 22 p2332 A72-41896

Carrying capacity of thin-walled shells subjected to impulsive radial pressure loads 22 p2333 A72-42052

A practical method for determining Dugdale model solutions for cracked bodies of arbitrary shape. 23 p3466 A72-43701

Computer simulation of fracture spreading in a visco-elastic solid. 23 p3267 A72-43702

Load distribution in a single-edge-notch tensile specimen. 23 p3306 A72-43710

Large deflection of rectangular orthotropic plates. 23 p3352 A72-44111

Microinhomogeneous elastoplastic cyclically strain hardenable material under symmetric loading, calculating stress-strain relationship 24 p3458 A72-44928

Variable cross section elastic stringer end loaded longitudinal force transmission to stiffened elastic plate 24 p3458 A72-44940

Variable thickness shallow spherical shells of revolution axisymmetric loads carrying capacity, determining limit equilibrium through application of Tresca yield point concept 24 p3460 A72-45725

Stressed state of radial bearings hollow rollers under loads concentrated along generatrix, evaluating test results by statistical analysis 24 p3408 A72-45726

LOAD FACTORS

U LOADS [FORCES]

LOAD TESTING MACHINES

Automatic testing machine for mechanical properties of metals under static loading 06 p0796 A72-18365

Bonded strain gage type load cell design, construction and application, explaining methods to achieve high accuracy 12 p1806 A72-27315

Polymer testing machine for simultaneous structural and mechanical properties measurement of specimens subjected to uniaxial tensile loads for broad temperature range 12 p1795 A72-27465

Testing machine for synthetic plastic cylindrical specimens cyclic cophasal compression-torsion load tests, describing mechanical and hydraulic subsystems and testing techniques 13 p1938 A72-28559

A mechanical pulsator for testing plastics with the capacity for adjusting cyclic and mean load during test 18 p2676 A72-37097

A new creep rupture testing machine with loading by tubular springs and electronic temperature control 22 p3164 A72-42860

Automatic testing machine for mechanical properties of metals under static loading 24 p3389 A72-45751

LOAD TESTS

NDT program for detectability changes of tight defects in Al as function of applied load 01 p0085 A72-10756

Structural analysis of cable stayed bridge scale model with fractional and full loading, showing system linear behavior with small displacements and real nonlinearities, respectively [SESA PAPER 1896] 02 p0199 A72-11515

Load capacity, attitude angle and power loss of heringbone grooved gas lubricated journal bearings operating in air at 60,000 rpm [ASME PAPER 71-LUB-B] 02 p0234 A72-11530

Plastic strain and rupture characteristics of thin walled tubular Ni samples under complex loading and biaxial tension 04 p0588 A72-15058

Composite materials testing with four point loading method, studying environmental and creep effects in flexure 04 p0537 A72-15091

Ti-Al-Mo-V alloy sustained load stress corrosion crack growth in salt and distilled water environments 04 p0534 A72-15570

Titanium alloy microstructure effect on fatigue strength under symmetric bending load cycles in air and NaCl solution 04 p0535 A72-15663

Bend tests for minimum radius/thickness ratio of Ti and Be alloy sheets in pressurized fluid [ASME PAPER 71-WA/PT-8] 05 p0671 A72-15913

Fatigue testing machines for axial and torsional loadings at low temperatures in vacuum 06 p0797 A72-18667

Notch length effect on stress concentration in polymethyl methacrylate sample from tensile, impact and bending tests 08 p1196 A72-21867

Structural Acoustic Monitor system for airframe structural proof testing, providing multichannel recording and aural monitoring of acoustic data derived from aircraft mounted accelerometers 10 p1459 A72-24146

Crack arrest in transversely loaded elastic plates from fracture mechanics combined with stress intensity factor for tensile and compression loads 10 p1499 A72-24890

Tubular specimens for testing mechanical properties of fiber reinforced composites under axial loading, discussing design, fabrication and end attachment problems 11 p1670 A72-25456

Uniaxial, biaxial and shear loading tests on filament wound carbon-carbon composite tubes and rings 11 p1670 A72-25458

Vacuum mold preparation and flexural testing of miniature carbon fiber reinforced composite specimens 11 p1671 A72-25468

Creep characteristics of weakly strain-hardenable alloy under variable tensile load and temperature conditions 11 p1663 A72-26808

Added elastic load tests for thoracic elastance change effects on human response to carbon dioxide inhalation, using rebreathing technique 12 p1762 A72-27726

High modulus fiber composite circular tube specimens multiaxial load testing, noting gripping methods to reduce transitional strains 12 p1886 A72-28000

Temperature effects on nonelastic behavior of turbine rotor disk for steady and cyclic loading, noting creep solutions, transient stress and plastic strain 14 p2167 A72-30906

Low temperature environmental chamber for F-111 proof load testing, describing components of cold air forced convection recirculation system with liquid nitrogen injection 15 p2214 A72-32612

Ti alloy fracture strength determination by crack propagation observation in specimen center, noting load-displacement curve construction from cyclic loading test 15 p2259 A72-32804

Russian book on metal fatigue and inelasticity covering structural inhomogeneities, static and dynamic loading, failure mechanisms, deformation, temperature effects and test methods 17 p2566 A72-34649

The comparison of torsion and tension creep data for a 0.18 per cent carbon steel. 19 p2816 A72-37709

Effect of the loading frequency on the fatigue strength of metals 19 p2818 A72-38012

The octahedral shear strain theory and its relation to biaxial cumulative fatigue damage. 20 p2978 A72-39202

Load tests in air to evaluate maraging steels weldments for rocket motor case applications 20 p2942 A72-39955

Creep test diagrams plotted to estimate heat resistance for turbine blades design, predicting fatigue life with allowance for loading cycle form and duration 21 p3123 A72-41366

Machine with programmed load control for studying the fatigue and inelasticity of metals at room and elevated temperatures 23 p3278 A72-43969

Plane-stress fracture toughness testing using a crack-line-loaded specimen. 24 p3456 A72-44810

Crack growth resistance in plane-stress fracture testing. 24 p3456 A72-44811

Compliance calibrations of a contoured and face grooved double cantilever beam specimen. 24 p3413 A72-44817

LOADING FORCES
U LOADS [FORCES]

LOADING MOMENTS

Rheological relations of moment-stress plasticity for steady and cyclic loads, using small elastoplastic strains 03 p0453 A72-14212

Axisymmetric load influence on stability of eccentrically reinforced shells of revolution, determining critical loads and linear and nonlinear relations for moment-subcritical states 04 p0587 A72-15014

Interlaminar shear properties of polymer matrix composites from dual element beam moment test 11 p1671 A72-25465

Viscoelasticity analysis of bending displacements in thin walled closed cylindrical shell loaded by moving moment 11 p1739 A72-26920

Dead load static stability of elastic solids in terms of zero moment condition of Beatty theory 12 p1883 A72-27557

Equilibrium equations for boundary value problems in Vekua theory with moments allowance for plate with circular hole under bending and torsion 15 p2333 A72-32682

Zero-moment reinforced axisymmetric shells 19 p2876 A72-38155

Lorentz contraction and transformation of equilibrium forces and moments in inertial reference systems transition, discussing special relativity theory 21 p3084 A72-40938

LOADING OPERATIONS

Proposed gas turbine procurement standards for shipment and installation preparation [ASME PAPER 71-WA/GT-4] 05 p0703 A72-15897

Super Guppy four engine aircraft characteristics, performance and loading device for bulky cargo air transportation 11 p1577 A72-25812

LOADING RATE

High speed tensile impact test for polymers at large loading rate, describing equipment design and test technique 01 p0048 A72-10782

Rigid plastic circular plate dynamic model with yield time delay, discussing residual deflection as function of load duration 02 p0293 A72-12426

Deformation kinetics relationship to scale effect in notched samples during elastoplastic loading phase 03 p0443 A72-13455

German monograph on Zn and Zn-Cu-Ti-Al alloy creep resistance under high loads covering grain boundary precipitation, rotation-shear hole and annealing 04 p0535 A72-15697

Metal powder materials at high loading rates, obtaining stress state diagram from Cauchy problem solution with inertia components in equilibrium equations 05 p0672 A72-16088

Temperature and compression rate effects on metal powder packing density, obtaining activation energy from Boltzmann equation 05 p0665 A72-16089

Creep behavior during and immediately after loading of Nimonic 90 and H 46 Cr steel under various stresses, temperatures and rates 06 p0829 A72-17801

Plastic deformation fatigue theory extended to tests at stresses below elastic limit, explaining cyclic loading frequency effect on fatigue life 06 p0899 A72-18652

Thermostable and heat resistant steels and alloys vibration loading frequency effects on fatigue at high temperatures 06 p0834 A72-18688

High speed testing of materials mechanical behavior over range of loading rates 14 p2165 A72-30441

Structural rings impulsively loaded by magnetic pressure between two parallel current-carrying conductors 15 p2322 A72-31348

A mechanical pulsator for testing plastics with the capacity for adjusting cyclic and mean load during test 18 p2676 A72-37097

Dynamic photoelasticity application to periodic/vibrating and pulse/stress wave fields, considering loading rate effect on material fringe value 22 p3237 A72-42767

Technical cohesive strength of welded joints at various temperatures and loading rates 23 p3293 A72-43961

Deformation kinetics relationship to scale effect in notched samples during elastoplastic loading phase 24 p3458 A72-44930

LOADING WAVES

U ELASTIC WAVES

U LOADS [FORCES]

LOADS [FORCES]

NT AERODYNAMIC LOADS

NT AXIAL COMPRESSION LOADS

NT AXIAL LOADS

NT BLAST LOADS

NT COMPRESSION LOADS

NT CRITICAL LOADING

NT CYCLIC LOADS

NT DYNAMIC LOADS

NT EDGE LOADING

NT GUST LOADS

NT IMPACT LOADS

NT LANDING LOADS

NT RANDOM LOADS

NT ROLLING CONTACT LOADS

NT SHOCK LOADS

NT STATIC LOADS

NT THRUST LOADS

NT TRANSIENT LOADS

NT VIBRATORY LOADS

NT WING LOADING

Optimal design of elastic beams under alternative loads and constraints on generalized compliance and bending stiffness [AD-743419] 02 p0291 A72-11962

Lower bound deformation theorem for rigid plastic continua under impulsive loads, emphasizing kinematically admissible velocity field 02 p0259 A72-12237

Elastoplastic material crack propagation behavior under arbitrary loading, introducing plastic zone, intensity and retardation factor concepts [DGLR PAPER 71-111] 02 p0300 A72-12726

Temperature and loading conditions effects on structural element service life, showing partial healing process of microdefects 03 p0443 A72-13454

Subcritical crack extension in elastoplastic or viscoelastic-plastic matrix, showing similar mathe-

matematical representations for fatigue crack propagation and creep rupture under sustained loads

05 p0737 A72-16302

Soviet book on nonmetallic material strength during nonuniform heating covering, load endurance, bending phenomena and thermal stability of fiberglass, pyroceramics and reinforced plastics

06 p0796 A72-18521

Metals and alloys breakdown toughness and mechanical properties predictions under various loading conditions, discussing interatomic bonds and plastic deformation zone size

07 p1019 A72-20146

Snapping process dynamics of shallow elastic hinged cylindrical panel of rectangular planform under gaseous, liquid and solid loads

08 p1242 A72-21228

Elastic unbounded homogeneous layer separation from half plane under normal load pressures, determining contact area with base for elastic moduli relationships

08 p1243 A72-21233

Elasticity theory doubly periodic problem for unbounded anisotropic plate weakened by system of identical arbitrary holes with self balanced loads

08 p1246 A72-21807

Nonlinear dynamic response of deformable solids under time and space dependent thermal and mechanical loads determined by finite element method

08 p1248 A72-21822

Two dimensional thermoelasticity problem with nonstationary temperature field and external boundary forces, using algorithm to evaluate stress-strain state of welded plates

09 p1401 A72-22725

Hamiltonian used as Liapunov function in stability evaluation of one dimensional continuous system loaded with polygenic forces

09 p1406 A72-23077

Photoelastic studies of plane stress fields in plate induced by moving loads at subsonic, transonic and supersonic speeds

10 p1553 A72-23746

Upper bounds on lumped and continuous dynamic systems motion under loads and perturbations, discussing structure stability conditions

[ASME PAPER 71-APMW-3] 10 p1554 A72-24188

Literature review of structural safety, treating load, strength, dynamic structural and structural reliability analyses and design aspects

10 p1560 A72-25174

Dynamic deflections and bending moments of simply supported Bernoulli-Euler beam under traveling mass loads

[AIAA PAPER 72-338] 11 p1728 A72-25371

Ring assembly with hinged cross section and uniform radial and transverse loads, determining deflection dependence on bulkheads and rigidity of supports

[AIAA PAPER 72-355] 11 p1729 A72-25384

Infinite elastic thick plate with loads symmetrical to axis of revolution and middle plane, analyzing stress functions, Fourier-Bessel expansion and photoelastic experiment

11 p1626 A72-26427

Cantilever beam transverse vibrations induced by time varying linear displacements of clamped end under external loads, taking into account internal energy dissipation

11 p1738 A72-26797

Thin lubricant film angular inertia effect on externally pressurized MGD bearings load carrying capacity, solving nonlinear differential equation by Runge-Kutta method

13 p1963 A72-28747

Molybdenum disulfide-tantalum compact solid lubricant wear rate as function of load and sliding velocity, presenting test data statistical interpretation

[ASLE PREPRINT 72AM 15] 13 p1964 A72-28972

Natural frequencies of beams with stepwise variable cross sections, approximating deflection shape by sectionwise representation of inertia load

15 p2323 A72-31454

Stress function method for calculating stress-strain state in homogeneous shallow spherical shell under arbitrary load

15 p2324 A72-31485

Stability and control dynamics of helicopter hovering with heavy sling load, analyzing maneuvers for minimal excitation of pendulous motion

[AHS PREPRINT 630] 17 p2489 A72-34488

Bifurcation of circular rings under normal concentrated loads

[ASME PAPER 72-APM-55] 17 p2627 A72-34776

Optimization of self-acting step thrust bearings for load capacity and stiffness

19 p2807 A72-37895

Solution manifolds for dynamic elasticity equations corresponding to the action of a concentrated load

19 p2878 A72-38213

On the diffusion of a load from a semi-infinite stringer bonded to a sheet

22 p2328 A72-42833

The accuracy of Donnell's theory for very high harmonic loading on closed cylinders

23 p3350 A72-44059

The New Zealand light aircraft fatigue meter program

24 p3401 A72-44735

Temperature and loading conditions effects on structural element service life, showing partial healing process of microdefects

24 p3458 A72-44929

LOBES

Equiphase radiating apertures maximum directivity under nonaxial orientation conditions, discussing limitation dependence on illumination law for major and lateral lobes

02 p0194 A72-12570

Switching curves and lobesweeping in origin seeking time optimal control for Duffing oscillator, using Pontryagin maximum principle

19 p2777 A72-37373

LOCALIZATION

U POSITION [LOCATION]

LOCATES SYSTEM

Wind profiles determination by Locate System in connection with OMEGA navigation system as sensing device

13 p1997 A72-29183

LOCATION OF AIR TRAFFIC SATELLITES

U LOCATES SYSTEM

LOCI

Generalized root locus graphical plotting by method of normals, comparing to Rimsii method while applying to third order systems

06 p0840 A72-18664

The concept of reference loci applied to four-body dynamics

24 p3440 A72-45137

LOCKHEED AIRCRAFT

NT ELECTRA AIRCRAFT

LOCKHEED MILITARY AIRCRAFT

U MILITARY AIRCRAFT

LOCKING

NT LASER MODE LOCKING

Generalized locking equation for microwave oscillator bandwidth prediction for arbitrary cavity configurations and waveforms, considering strong harmonics presence

15 p2205 A72-31358

LOCOMOTION

NT ASTRONAUT LOCOMOTION

NT WALKING

Visual guidance of locomotion, discussing expansion information and target drift theories

03 p0319 A72-13879

Classification of neurons in the lumbosacral section of the spinal cord according to their discharge during evoked locomotion

23 p3257 A72-44092

LOFTING

Computer calculation of second order curve segment discriminant in geometrical problem associated with aircraft lofting, assessing method accuracy

13 p1986 A72-28739

Nonlinear algebraic transformation to determine straight line and second order curve intersection point in aircraft lofting problem

13 p1986 A72-28742

LOG PERIODIC ANTENNAS

Mutual microwave coupling effects on element VSWR in linear dipole log periodic antenna array

01 p0043 A72-11242

Vertically polarized logarithmically periodic monopole antenna for incoming wave front reception with low elevation angles in 1.5 to 30 MHz frequency range

02 p0195 A72-12697

Two center-fed feed-point displaced dipole antennas, calculating mutual impedance for various combinations of displacements and heights

04 p0501 A72-15433

Log periodic dipole antenna design with loop elements, discussing radiation patterns and resistance, efficiency, polarization and gain

04 p0503 A72-15673

Log periodic dipole antenna design parameters effects on bidirectional radiation pattern

09 p1282 A72-23571

Parabolic reflector fed by log-periodic dipole antenna array, predicting combined effects of feed phase center lateral and axial displacement on secondary performance

15 p2205 A72-31541

Bandwidth log-periodic dipole array radiation pattern and impedance characteristics as function of design parameters

15 p2208 A72-32390

Log periodic dipole antenna input impedance and gain characteristics derivation via periodically loaded line theory and Poynting vector method, discussing separation angle effect

15 p2208 A72-32473

Log periodic dipole antenna systems for ILS localizers, noting reduced sensitivity to snow and ice

19 p2830 A72-37279

New combination of logarithmic-periodic dipole antennas for the short wave range

21 p3031 A72-40537

LOG SPIRAL ANTENNAS

Conical logarithmic foil type spiral antenna, presenting model of wavelength lenses used in dielectric rod antennas

04 p0500 A72-15408

Dispersion and energy characteristics of azimuthally asymmetrical waves in microwave logarithmic or arithmetical spiral antenna deposited on isotropic magnetodielectric layer

05 p0636 A72-16338

Circular-polarization antennas with controlled radiation patterns

21 p3026 A72-40314

Controlling the directive gain of weakly directional antennas during space-vehicle flight

21 p3026 A72-40324

Integral equation method for boundary value problem of logarithmic spiral antenna, noting suitability for digital computers

21 p3031 A72-40535

LOGARITHMIC RECEIVERS

Pulsed dye lasers logarithmic detector circuit with two ultrafast photodiodes, eliminating intensity variations problem

07 p1005 A72-19415

Thermally stable six stage transistorized amplifier with logarithmic relationship between input and output voltage

10 p1450 A72-24494

Postdetection integration loss for logarithmic detectors

19 p2763 A72-37295

Characteristics of an optimal algorithm for detecting Gaussian signals against a pulse noise background for receivers with a logarithmic amplifier

22 p3154 A72-42238

LOGARITHMS

Book on logarithmic video amplifiers covering design, analysis, performance and applications

10 p1452 A72-24698

Comment on paper on Gaussian logarithms use in air navigation

13 p1996 A72-29016

Automatic computation of exponentials, logarithms, ratios and square roots

18 p2705 A72-37021

Application of logarithmic characteristics to calculate wideband load matching of an oscillator

23 p3271 A72-43836

The automatic computation of exponentials, logarithms, ratios, and square roots

24 p3383 A72-45668

LOGIC

Learning and solving complex problems of reasoning - A test-theoretical investigation of the complexity of compound problems of predictive logic

24 p3373 A72-45244

LOGIC CIRCUITS

NT THRESHOLD GATES

Optimal design of logic networks in homogeneous microelectronic structures, using shortest link search and graph continuity parameters

01 p0034 A72-10300

General purpose electronic modular units for human factors research instrumentation, considering digital and analog computers, logic modules and interface and auxiliary equipment

01 p0048 A72-10569

Irredundant multiple output combinational logic network fault detection and diagnosis theorems derivation from structural models in labeled direct graph form

02 p0184 A72-11478

Random and algorithmic procedures employing three-valued logic system for sequential circuits fault detection test sequence generation

02 p0185 A72-11486

Reliable combinational logic networks, deriving conditions for fault locatability from directed graph formal model

02 p0185 A72-11491

Digital IC of ECL series without temperature compensation, discussing emitter coupled logic circuits interconnection methods

02 p0197 A72-12669

Plaquette program for logic network wiring on IC box cards

03 p0327 A72-13167

Logic networks with hydraulic elements, considering dynamic qualities of hydraulic transmission system

03 p0312 A72-13965

LSI/MOS logic circuits radiation effects prediction from modeling studies of individual devices on test chip

03 p0334 A72-14087

Logically stable failures of discrete combination devices by practical behavior in response to given input vectors, using alpha state Boolean algebras

04 p0496 A72-14994

Programmable cellular cascades and arrays synthesis for realizing arbitrary Boolean functions or parallel arithmetic operations

04 p0498 A72-15107

Computer laser devices for logical operations, discussing analog-digital converter, gate circuits, bistable elements, flip-flop and shift register

04 p0496 A72-15141

Floating point cellular logic multiplier with variable dynamic range suitable for scientific satellites, missiles, desk calculators and cellular computers

04 p0499 A72-15208

Optimal nonlinear logical filters for noise protection of space vehicle servosystems

05 p0726 A72-16460

Logic circuit binary signal autocorrelation determination as function of 0 and 1 signals duration distribution considering AND and OR gates

05 p0632 A72-17094

Cellular electronic logic circuit planar array representing objects inertial motion, applying to traffic control, image processing and artificial intelligence

06 p0779 A72-17496

Book on digital and analog monolithic IC systems, covering manufacturing methods, component design, MOS logic, arithmetic, error correction, codes, applications, etc

09 p1286 A72-23044

N fail-safe logics for circuit fault restoration, comparing with failure probability of majority voting scheme and quadded logic

09 p1283 A72-23420

Response time and noise stability measurements of integrated circuit TTL (transistor-transistor logic) and DTL (diode-transistor logic) elements performing invert functions

10 p1449 A72-24286

MOS transistor logic circuits pulse noise stability dependence on transient response, emphasizing supply voltage effect

10 p1449 A72-24290

Dynamic processes of electric drive system with electromagnetic clutch modeled by analog computer element with logical input-output relation

10 p1423 A72-24755

Accuracy and reliability in engineering design of discrete automata without memory (logic circuits), using Boolean algebra for mathematical models

11 p1600 A72-25434

Logic character generator for CRT test display and DEC PDP 8/S graphics

11 p1601 A72-26290

Matrix and graphic test construction methods for optimal design of logic networks in automatic control systems

11 p1612 A72-26443

Digital indicators design and logic circuits employing gas discharge tubes and illuminated and synthesizing indicators

11 p1605 A72-26458

Complex bipolar IC logic circuits realization by economical high speed techniques using metal bonding or cells available in library

11 p1606 A72-26548

Automatic search for Huffman sequential logic circuit breakdown detection sequence, using VEGA program through matrices and graphs utilization

11 p1612 A72-26549

Aluminum-silicon Schottky diode clamped transistor-transistor logic circuits parameters optimization for high switching speed and IC applications

11 p1606 A72-26568

Polish monograph on minimal representations and identification of Boolean function symmetry in combinational logic network synthesis, using two dimensional topological model

12 p1793 A72-27224

Multivalued logical function synthesis with multistage logical network through hypercomplex representation and linear transformation

12 p1794 A72-27497

Binary logic circuits with interconnected repeaters and inverters, discussing signal level selection to ensure maximum noise stability

12 p1786 A72-28120

Software models to test operating conditions of logic nets, discussing application to network faults diagnostics

15 p2203 A72-31749

Signal transmission through LSI logic circuit chains, discussing time delay measurement by step function testing

15 p2211 A72-31846

Registers and digital circuits with FETs and integrated operational amplifiers to permit analog measurements storage for display on CRT oscilloscope

15 p2204 A72-32499

Hybrid LSI logic modules for aerospace

17 p2527 A72-34683

An algorithm for the automatic synthesis of nearly optimal 2-level and-or combinational circuits

17 p2533 A72-35058

NAND gate logic transistor circuit design, layout, fabrication and electrical parameters, noting base and resistors diffusion welding

17 p2530 A72-35069

Laser computer technology - Today and tomorrow.

III

17 p2523 A72-35186

Analysis of sensitization mechanisms of low consumption integrated circuits

18 p2668 A72-37107

Zero overhead testing relationship to software requirements, testing dynamic accuracies, LSI product types and function and parametric speeds related to product lines

18 p2664 A72-37109

Error correction in redundant logic circuits without application of majority elements

19 p2769 A72-37758

Binary logic circuits with interconnected repeaters and inverters, discussing signal level selection to ensure maximum noise stability

19 p2767 A72-38621

Multivariable static /combination/ switching characteristics of TRIMELOG pneumatic logic elements

19 p2754 A72-38644

Probability density - A new approach to system electromagnetic compatibility testing of digital circuits.

20 p2906 A72-38980

An iterative array which can represent the rotation and translation of objects.

20 p2905 A72-39422

Realization of static /combination/ logic switches with the aid of TRIMELOG pneumatic elements. II

20 p2890 A72-39423

Two dimensional microprogrammed cellular arrays logic organization and control structure for multifunctional digital subsystems

20 p2906 A72-39736

High speed logic circuit interconnecting transmission line matching by nonlinear resistance, recommending use of Schottky diodes

20 p2909 A72-39737

Unknown plant self organizing time optimal controller with variable switching surface and adaptation logic net, noting effectiveness by computer simulation

21 p3037 A72-40639

Phase locked feedback circuit for FM demodulation, discussing all digital circuit design and voltage controlled oscillator algorithm to avoid analog implementation problems

21 p3018 A72-40873

A procedure for the design of asynchronous time division multiplexers.

21 p3021 A72-40909

Parameters and properties of special avalanche transistors

21 p3035 A72-41809

The mathematical synthesis and analysis of fluid logic networks.

22 p3161 A72-42049

Performance prediction of large-scale integrated logic circuits.

22 p3160 A72-42824

Input delay influence on dynamic stability of potential finite automata in transition between two states, noting logic circuits synthesis based on Boolean algebra

23 p3274 A72-43350

Information theory application for structural complexity measure of microelectronic logic circuits for digital computers, noting elements standardization for design quality criteria

23 p3269 A72-43441

Flawless operation probability for information transmission reliability of electronic logic circuits with binary data inputs

23 p3271 A72-43784

MOS logic circuit design simplification by replacing series and parallel transistor networks by equivalent single transistor inverter circuit

23 p3271 A72-43843

Bistable trigger stages composed of digital multiplexer with IC logic modulus replacing NAND or NOR circuits

23 p3267 A72-43990

Asymptotic reliability estimates of monotonically structured complex logic systems with low and high component failure rates equivalent with exponential or Weibull distributions

23 p3267 A72-44004

An interactive approach for the generation and verification of test sequences in a logic system

24 p3382 A72-44662

LOGIC DESIGN

Soviet book on reliable logic units design covering adaptive redundant and nonredundant control systems, threshold functions, optimal adaptation algorithms, restoring circuits, etc

01 p0033 A72-10296

Optimal design of logic networks in homogeneous microelectronic structures, using shortest link search and graph continuity parameters

01 p0034 A72-10300

Fault-tolerant digital computer logic design for dynamic and interactive recovery with data integrity after error, discussing hardware and software functions requirements

02 p0184 A72-11480

Minimum length fault tests design for irredundant combinational logic circuits containing single faults based on Boolean difference function

02 p0185 A72-11485

Format logic design for airborne memory controlled PCM telemetry multiplex digital and analog data system

02 p0187 A72-12130

Digital computer memory system for real time processing of air and naval traffic data, discussing logic design, time comparisons and optimum use

02 p0188 A72-12647

Computer laser devices for logical operations, discussing analog-digital converter, gate circuits, bistable elements, flip-flop and shift register

04 p0496 A72-15141

Logical synthesis of hybrid off-on control systems with proportional and binary variables, presenting example of fluid power, electronic and fluidic implementation [ASME PAPER 71-WA/FLCS-1]

05 p0640 A72-15919

Satellite attitude control with gimballed reaction wheel digital system, discussing logic and computerized design, implementation, fabrication and performance tests

05 p0726 A72-16458

Interactive computerized design and programs for computer logic design block assignment to modules, comparing performance with manual solutions

06 p0778 A72-17472

Axiomatic determination of dynamic logic control systems based on Moore automaton elements and combined continuous and finite models

06 p0781 A72-18660

Microelectronic IC functional logic systems design with S-type semiconductor devices, describing procedures for logic functions, shift register and directional transmission line

10 p1448 A72-24278

Magnetic integrated circuits design and fabrication problems involving branched and logic circuits and solid state structures controlled domains

10 p1448 A72-24279

Pneumatic fluidic logic elements design based on Coanda effect to realize conjunction, equivalence, nonequivalence, alternative and implication functions

10 p1423 A72-25112

Matrix and graphic test construction methods for optimal design of logic networks in automatic control systems

11 p1612 A72-26443

Threshold logic network synthesis with specific threshold-gate sensitivities.

17 p2533 A72-35364

Future trends of airborne computers. [AIAA PAPER 72-895]

20 p2905 A72-39109

Synthesis of threshold-logic networks using Karnaugh-mapping techniques.

21 p3037 A72-40636

Development and evaluation of an energy-oriented guidance logic for air combat models.

22 p3137 A72-42354

Input delay influence on dynamic stability of potential finite automata in transition between two states, noting logic circuits synthesis based on Boolean algebra

23 p3274 A72-43350

Design optimization of an integrated-circuit direct access memory unit

23 p3267 A72-43841

LOGIC NETWORKS

U LOGIC CIRCUITS

LOGICAL ELEMENTS

Network synthesis of cascaded threshold logic elements to separate binary patterns into two classes by iterative computation of parameters

01 p0034 A72-10474

German book on fluidics covering pneumatic logic elements and systems with and without moving parts and applications in sensors, transducers, power amplifiers, analog-to-digital converters, decoders, etc

01 p0072 A72-11276

Pneumatic fluidic logic elements design based on Coanda effect to realize conjunction, equivalence, nonequivalence, alternative and implication functions

10 p1423 A72-25112

Binary multiplication algorithms adaptable to IC functional elements for ultrahigh speed operations

11 p1602 A72-26547

Complex bipolar IC logic circuits realization by economical high speed techniques using metal bonding or cells available in library

11 p1606 A72-26548

Digital precision frequency synthesizers constructed on IC logic modules without using LC filters, analyzing restrictive factors

13 p1930 A72-29050

Fluidic digital logic devices vs electromechanical-electronic equivalents, describing Coanda effect application to bistable jet amplifiers /flip-flops/ as switching or memory devices

15 p2182 A72-31218

Information theory application for structural complexity measure of microelectronic logic circuits for digital computers, noting elements standardization for design quality criteria

23 p3269 A72-43441

An iterative algorithm for solving the realization problem of a Boolean function by a single threshold element.

24 p3419 A72-45576

LOGISTICS

NT LUNAR LOGISTICS

Military aircraft operations and logistics computerized simulation for support and maintenance cost estimates

06 p0758 A72-17974

Task oriented maintainability engineering relationship to systems engineering and logistics support requirements

10 p1564 A72-23852

Book on man machine system experiments covering ATC, air defense, logistics organizations, space flight, battlefield operation, police dispatching, communications, etc

16 p2359 A72-33796

The heavy lift helicopter - An operations research/technology/performance blend.

24 p3466 A72-44581

LOGISTICS MANAGEMENT

NT INVENTORY MANAGEMENT

Concorde on-time operation as total management problem from design to airline operations, discussing techniques for in-flight failure diagnosis and onward reporting

15 p2181 A72-32460

LONG RANGE NAVIGATION

U LORAN

U LORAN D

LONG RANGE WEATHER FORECASTING

Thermal advection statistical relation to vertical motion, discussing conventional synoptic meteorological empirical facts utilization in numerical models for long term weather forecasting

02 p0254 A72-12779

Satellite measurements of tropospheric and earth surface state parameters for long term numerical weather forecasting, discussing data fluctuations

02 p0255 A72-12789

Pressure and temperature fields expansion in natural orthogonal components, considering application to long range forecasts construction

11 p1683 A72-26889

Upper atmosphere observatory, noting application to long distance radio communication, long range weather prediction and international cooperation in research and education

13 p1947 A72-28613

Geomagnetic pulsations long term statistical forecast, obtaining averaged yearly pearls activity

15 p2222 A72-31426

Spatial variations in atmospheric predictability

18 p2706 A72-36627

Computerized long term weather forecasting via mathematical modeling of atmospheric processes based on meteorological parameters worldwide observational data

20 p2948 A72-39939

Allowance for the ocean surface temperature in monthly weather forecasts for the Northern Atlantic Ocean

20 p2949 A72-39946

Russian book - Long-term variations of atmospheric circulation and long-range hydrometeorological forecasts.

22 p3200 A72-42078

LONG TERM EFFECTS

Geomagnetism, discussing world field distribution, secular variation, paleomagnetism, archaeomagnetism, origin, magnetic anomaly and earth electromagnetic induction

01 p0053 A72-10168

Daily, annual and long term ionosscatter and sporadic E variations above Europe, using hf propagation measurements

01 p0055 A72-10432

Long term bed rest effect on humans and primates, detailing cardiovascular metabolic and musculoskeletal physiological systems

[AD-737557]

01 p0014 A72-10932

Mice tolerance to long term accelerations or supergravities, detailing physiological consequences

01 p0014 A72-10934

Cosmic ray intensity long term modulation and 27 day recurrence relationship to solar activity

03 p0407 A72-12945

Stellar secular stability during complex roots onset in model evolution, discussing radiative heat transport coefficient effects

03 p0416 A72-13004

Excess secular change in ecliptic obliquity in relation to earth internal motion due to mantle-core coupling

04 p0575 A72-15028

Pulsar CP 0328 wideband rf spectrum long term periodicity, considering origin during propagation through interstellar medium

04 p0580 A72-15369

Solar wind structure from long lived inhomogeneities in corona, allowing for velocity, density and temperature perturbations

06 p0872 A72-17444

Near resonance due to commensurability between Jupiter-Saturn mean motions, discussing effect on planetary system secular disturbing function

06 p0877 A72-17659

Pulsar long term intensity variations due to intrinsic structure or propagation effects

06 p0878 A72-17670

Trapped particle motion response to collapsing dipole moment in secularly varying geomagnetic field

07 p1058 A72-19158

Secular geomagnetic dipole moment decrease effect on inner proton belt proton energy distribution, comparing with radial diffusion influences

07 p1058 A72-19159

Thermal blooming of laser beams in liquids and gases, investigating short and long time behavior under thermal conduction and viscosity effects

07 p1005 A72-19408

Secular perturbations of artificial earth satellites Keplerian orbital elements from arbitrary-order zonal harmonics in geopotential series expansion

07 p1078 A72-19982

Long term variations in height of solar activity maxima and sunspot numbers during 11 year cycle

07 p1079 A72-20016

S glass/epoxy composites strength retention properties under long duration tensile load, proposing use of stress rupture data for reliable safe structural design

10 p1501 A72-24263

Abridged version of 1970 Soviet conference on constant geomagnetic field and paleomagnetism, reviewing secular variation data

13 p1946 A72-28588

Human organism readaptation after prolonged hypokinesia and weightlessness, discussing coordination disturbances, vegetative and vascular system instabilities, reduced orthostatic stability and asthenia

14 p2076 A72-30745

Nitrate ester propellants self ignition hazard and ballistic stability, describing heat generation test at various temperatures for long term storage

14 p2144 A72-30754

Meteor streams secular perturbations computation by Gauss-Halphen-Goriachev method

14 p2161 A72-31078

Earth core hydromagnetic oscillations with respect to geomagnetic secular variation time scales and role in dynamo process-produced geomagnetic field

15 p2222 A72-31279

Solar activity long term effects on Jupiter cloud structure rotational periods, using Chree superposition analysis

15 p2308 A72-31930

Geopotential induced secular perturbations, using second approximation to achieve analytic accuracy

15 p2309 A72-31934

Secular and long term periodic perturbation effects of third body upon particle motion in three body problem, discussing mass motion in Jovian gravitational field

15 p2312 A72-32120

Technology R and D program to qualify man for long term weightlessness, assessing space flight stress effects on physiology and psychology

16 p2358 A72-33544

Prolonged weightlessness effects on cardiovascular, digestive, musculoskeletal and nervous systems, blood and metabolism, noting compensatory reactions

16 p2354 A72-33546

Physiological effects on prolonged weightlessness in dogs aboard Cosmos 110 biosatellite, emphasizing body weight loss and enzyme activity and bone tissue mineral concentration changes

16 p2354 A72-33547

Long term space flight weightlessness and hypodynamic effects on orthostatic and vestibular tolerances, infection susceptibility and drug reactivity

16 p2355 A72-33550

Influence of prolonged starvation on the frequency of occurrence of decompression-induced pulmonary hemorrhage.

17 p2508 A72-34545

Techniques for control of long-term reliability of complex integrated circuits. I - Reliability assurance by test vehicle qualification.

17 p2528 A72-34686

Techniques for control of long-term reliability of complex integrated circuits. II - A technique for the prediction of failure rates for MSI and LSI devices.

17 p2528 A72-34687

Exchangeable potassium in heart disease - Long-term effects of potassium supplements and amiloride.

17 p2500 A72-34932

Long-term prediction of artificial satellite motion along almost circular orbits allowing for a random number of zonal harmonics

17 p2607 A72-35033

In-core thermionic converter emitters irradiation tests to determine fuel, fission gas venting system and emission layer performances

18 p2708 A72-36158

Body weight decreases in some proton exposed primates.

18 p2650 A72-36447

Microwave power junction transistor design factors effects on long and short term reliability and MTBF

18 p2666 A72-36552

Secular variations of the first order of elements for the four major planets - Comparison with Le Verrier and Gaillot

18 p2727 A72-36734

Secular variation of the geomagnetic field in epoch 1965 to 1970 according to observatory and satellite data

18 p2689 A72-36871

Drift characteristics of the main eccentric geomagnetic dipole

18 p2689 A72-36872

Possibility of determining the secular variation of geomagnetic field components from the distribution of total-vector modulus variation

18 p2689 A72-36873

Spherical analyses of the principal geomagnetic field for the years 1550 through 1800

18 p2689 A72-36874

Reliability of semiconductor optoelectronic components - Analysis of the long-term behavior

18 p2670 A72-37138

Nature of the 80-90 year cycle of solar activity

19 p2860 A72-37952

Secular stability. I - A Population I star near the main sequence.

19 p2864 A72-38099

Rotation period variation in long term behavior of interplanetary magnetic sector structure during nearly four solar cycles

19 p2868 A72-38731

Effect of prolonged gamma irradiation on the functional capacity of leukocytes

21 p3103 A72-40438

Acceleration tolerance of man after a lasting exposure to conditions of simulated weightlessness

21 p3006 A72-40442

The properties and structures of a heat resistant 1Cr-Mo-V steel and alloy A-286 after long time exposures at elev. temps.

21 p3069 A72-41012

An integrated medical system for long-duration space missions.

21 p3009 A72-41305

Secular perturbations in the motion of artificial earth satellites

21 p3114 A72-41770

Activity of the secular behavior of the geomagnetic field

22 p3168 A72-41924

Psychic adaptation of man to a long-duration stay in space

22 p3149 A72-41988

Analysis of survival and cause of death statistics for mice under single and duration-of-life gamma irradiation.

23 p3254 A72-43394

Heat resistant ZrSi₂ alloy precision and ground cast specimens, determining short and long term strength and fatigue

23 p3301 A72-43761

Energy and mass content of high-speed solar-wind streams.

23 p3332 A72-44508

Nature of the long-term and short-term modulations of cosmic-ray intensity.

23 p3332 A72-44521

Abridged version of 1970 Soviet conference on constant geomagnetic field and paleomagnetism, reviewing secular variation data

24 p3397 A72-45088

Experimental development of a method for long-term implantation of plastic catheters in different sections of the cardiovascular system

24 p3375 A72-45118

The Space Station Prototype Program - The development of a regenerative life support system for extended-duration missions.

24 p3375 A72-45193

Longevity and cardiovascular mortality among former college athletes.

24 p3374 A72-45689

LONG WAVE RADIATION

Power flow approximation for long distance long wave propagation of ground source between earth and ionosphere, comparing mode theory to heuristic approach

01 p0033 A72-11310

Long wave radiation and surface friction effects on midlatitude cyclone development in eight-level primitive equation orographic model

03 p0385 A72-14229

Long wave propagation in curved ducts and pipes, considering plane wave transition and distortion 04 p0548 A72-14698

Diurnal phase and amplitude variations of long radio waves at great distances, explaining sunrise and sunset fading 04 p0492 A72-15443

APZ-2 daytime actinometric radiosonde measuring long wave radiation balance in presence of short wave solar radiation 06 p0814 A72-17626

Ionospheric absorption and atmospheric planetary scale waves fluctuations correlation 06 p0808 A72-18090

X ray effect from Scorpio XR-1 on lower ionosphere long wave transmissions, considering transit times and field intensity variations 09 p1305 A72-23572

Critique of Rees theory of primordial gravitational radiation concerning galaxy clusters interaction with very long wavelength universal gravitational waves 10 p1550 A72-25200

Long wave radio and acoustic holograms recording by complex scanning for transmission over communication channels 11 p1636 A72-26714

Negative ions and collision frequency effects on circularly polarized ELF and VLF wave propagation in ionosphere 14 p2084 A72-30128

Vertical propagation of large scale disturbances in long wave radiation field into upper atmosphere, using linearized hydrothermodynamic equations 14 p2127 A72-30262

Venus long wave radiation spectral composition, angular distribution and carbon dioxide transmission from thermal, structure and vertical radiation absorption profile 15 p2305 A72-31394

Long wave fluctuations in nonequilibrium gas with pair collisions, using Bogoliubov equations for simultaneous correlation functions 15 p2282 A72-32450

The distribution of the long wave photoreceptors in the compound eye of the honey bee as revealed by selective osmic staining. 17 p2500 A72-34877

Book - Terrestrial propagation of long electromagnetic waves. 21 p3023 A72-41532

Some results of measurements of short-wave and long-wave radiation fluxes from the Cosmos-320 satellite 22 p3168 A72-41875

Long wave oscillations attenuation by charged particle collisions in one- and two-component hot and cold Boltzmann plasma, using kinetic and polarization vector equations 23 p3318 A72-43325

LONGITUDE

NT SOLAR LONGITUDE

Longitudinal variations of inner radiation belt particle flux density at low altitudes from Proton 2 satellite data 01 p0119 A72-10604

Meridian direction determination with angular accelerometer, noting reduction in effects of component imperfections on accuracy 16 p2421 A72-33962

LONGITUDE MEASUREMENT

Grazing lunar occultation method application to geodetic measurement of geographical longitude differences, noting advantage over equal-limb-line method 03 p0420 A72-13128

Astrolabe design and operation for reconnaissance and simultaneous determination of latitude and longitude 08 p1165 A72-21022

Optimal method selection for astronomical measurements on lunar surface, discussing instrumental and technical difficulties with selenographic longitudes and latitudes determination 08 p1231 A72-21130

Circumzenithal instrument for latitude and longitude determination and star transits observation through almucentar 15 p2238 A72-32122

Observation error in time determination of solar limb contact with optical instrument hair, noting effect on accuracy of time and longitude measurement 24 p3438 A72-44859

LONGITUDINAL CONTROL

Time optimal control for pitch damping of gravity gradient stabilized satellite by mass distribution variation 05 p0727 A72-16465

Aft center of gravity travel effects on aircraft longitudinal control response characteristics [SAE PAPER 720318] 11 p1575 A72-25581

An experimental investigation of STOL longitudinal flying qualities in the landing approach using the variable stability X-22A aircraft. 17 p2490 A72-34502

Multiloop piloting aspects of longitudinal approach path control. [ICAS PAPER 72-46] 21 p2995 A72-41171

Control requirements for control configured vehicles. 24 p3368 A72-45349

LONGITUDINAL STABILITY

Wind tunnel study of space shuttle longitudinal dynamic stability at supersonic speeds, discussing damping-in-pitch [AIAA PAPER 72-135] 05 p0730 A72-16890

Longitudinal vibrations stability of launching rocket body, allowing for propellant sloshing, body dynamic deformation and motor dynamics 05 p0731 A72-17186

Longitudinal instability of electron beams interacting with passive resonator, considering Landau damping influence by linear differential equations of motion solution 05 p0701 A72-17243

Pitching moments effect on phugoid and height mode stability of aircraft in supersonic flight 09 p1263 A72-23622

Control system for stabilization of liquid propellant rockets Pogo oscillations, discussing structure, fuel tank and feed system, combustion chamber, control gain and accelerometer installations 10 p1551 A72-24027

Longitudinal bending stability of hard polymer rods under compression load and creep 11 p1675 A72-26824

Plasma stability in field of longitudinal monochromatic wave, examining satellites excitation by Langmuir wave 16 p2437 A72-33693

Longitudinal dynamic stability of hypersonic shuttle vehicle designed for operation to planetary atmosphere rim 16 p2462 A72-34019

Problems and solutions related to the design of a control augmentation system for a longitudinally unstable supersonic transport. [AIAA PAPER 72-871] 20 p2887 A72-39128

Aerodynamic characteristics of the slotted fin. 21 p2992 A72-41262

Aircraft longitudinal stability under conditions of varying atmospheric density, thrust force and velocity, determining critical altitude for vanishing oscillations [AIAA PAPER 72-951] 22 p3138 A72-42358

LONGITUDINAL WAVES

NT PLANE WAVES

Periodic inhomogeneous plasma electrostatic waves, considering dispersion relation and longitudinal oscillations 01 p0107 A72-10141

Oxygen effect on dynamic elastic modulus of titanium-oxygen alloys by density and longitudinal ultrasonic wave velocity measurements 01 p0083 A72-10393

Zinc oxide longitudinal acoustic microwave transducer, measuring untuned insertion loss and electroacoustic coupling constant 01 p0042 A72-10705

Longitudinal stress pulse amplification during propagation along tapered elastic bars in direction of decreasing cross section [SESA PAPER 1894] 02 p0287 A72-11504

Transient response of Al cylindrical shells to longitudinal impact, indicating wave front propagation at plate velocity [SESA PAPER 1885] 02 p0287 A72-11505

Rigid mass impact against viscoelastic beam of finite length, investigating longitudinal waves propagation and interaction 02 p0298 A72-12682

Perturbation induced long waves boundary effects in ideal incompressible fluid in uniformly rotating basin with stepwise depth difference, using Schwarz symmetry principle 03 p0340 A72-13094

Longitudinal and transverse wave diffraction on cavities, investigating field pattern by dynamic photoelasticity method with flat models 03 p0452 A72-14131

Longitudinal wave interaction and excitation by plasma instability in equatorial electrojet, considering energy transfer mechanism 05 p0656 A72-16242

Plasma stability in field of longitudinal monochromatic wave, examining satellites excitation by Langmuir wave 05 p0696 A72-16681

Longitudinal electrostatic waves in perpendicular collisionless plasma shock, investigating stability 05 p0698 A72-17021

Coupled longitudinal and transverse plasma waves propagating normal to applied magnetic field, using three fluid model 05 p0700 A72-17230

Longitudinal hf oscillations in homogeneous magnetoactive plasma by fast monoenergetic electron excitation 06 p0853 A72-17389

Longitudinal electron plasma waves interaction with electron distribution, investigating energy transfer 06 p0858 A72-17543

Stability of weakly ionized homogeneous plasma placed in weak microwave field and in constant magnetic field, expressing growth increments of longitudinal waves 06 p0861 A72-17902

Numerical approximation of Pochhammer-Chree longitudinal vibration modes in elastic cylinders by quadratic spline functions 07 p1087 A72-18797

Nonlinear Landau damping of longitudinal plasma waves in dc magnetic field, obtaining wave-particle interactions from Vlasov equation by perturbation theory and method of characteristics 07 p1041 A72-19505

Longitudinal plane harmonic elastic wave scattering and stress concentration at rough circular hole boundary in thin isotropic plate 08 p1243 A72-21230

Longitudinal elastic wave propagation along composite bar with conical sections and interface discontinuities in material properties, solving multiple reflection by finite difference method 08 p1245 A72-21606

Slow and fast longitudinal ion acoustic waves in plasma cylinder under axial magnetic field 08 p1215 A72-21873

Soviet book on longitudinal vibrations of rocket with liquid propellant engine covering rocket element dynamic characteristics and free vibration mode shape and frequency calculations 08 p1241 A72-22025

Electrostatic longitudinal waves propagation and detection in isotropic collisionless hot electron plasma, calculating Landau dispersion curve and damping 09 p1359 A72-22794

Wave propagation in bonded discretely inhomogeneous elastic cylindrical rods, including longitudinal and radial motions 09 p1409 A72-23563

Longitudinal plasma oscillations nonlinear instability due to energy transformation into harmonics and subharmonics 11 p1695 A72-25795

Stationary HF Rayleigh waves in surface waveguide, considering transverse and longitudinal wave velocities in half space with elastic medium 11 p1688 A72-26378

Elasticity theory dynamic equations solutions concentrated near longitudinal or transverse wave beams propagating in inhomogeneous isotropic space 11 p1689 A72-26383

Longitudinal propagation of elastic disturbance in conical rod, discussing Young modulus, material density and periodic and impulsive stress 11 p1737 A72-26589

Longitudinal electromagnetic wave excitation in restricted plasma by relativistic electron beam injection, determining increments, frequency distribution and width of spectra 12 p1849 A72-27064

Longitudinal elastic impact wave propagation along branched thin rods, using Timoshenko theory 12 p1881 A72-27256

Plane longitudinal displacement wave reflection from fixed surface in micropolar elastic half space, presenting reflection laws and amplitude ratios for specific cases 13 p2056 A72-29001

Partial differential equations for longitudinal, torsional and transverse vibrations of bars with variable composition 13 p2006 A72-29885

Variable cross section rod free longitudinal and torsional vibration frequencies and mode shapes determined by slowly varying parameters approximation method 15 p2327 A72-31740

Kinetic energy and momentum of longitudinal waves in plasmas, deriving Landau dispersion equation from conservation laws 15 p2285 A72-32272

Longitudinal, transverse and bending waves propagation in elastic shells, using Hadamard method within linear shell theory 16 p2465 A72-32982

Longitudinal and transverse waves propagation and decay in elastic membranes with allowance for coupling effects, using Hadamard method 16 p2465 A72-32983

Elastic longitudinal or shear wave scattering by movable rigid sphere embedded in elastic solid, showing inverse Rayleigh limit dependence 16 p2423 A72-32988

Growth of an acceleration wave in an elastoplastic isotropic medium undergoing finite deformation 17 p2580 A72-34277

Longitudinal pulses propagation in straight hollow circular elastic tubes, presenting strain-time records [ASME PAPER 72-APM-10] 17 p2629 A72-34806

A photon rest mass and the dispersion of longitudinal electric waves in interstellar space.

18 p2728 A72-36923

Longitudinal impact on a thin cylindrical shell

19 p2870 A72-37321

Buckling of an elastic cylindrical shell during longitudinal impact against an obstacle

19 p2870 A72-37322

Longitudinal waves in a perpendicular collisionless plasma shock. IV - Gradient B.

19 p2838 A72-37329

Effects of collisions on perpendicular longitudinal ion wave propagation in a magnetized plasma.

19 p2841 A72-38438

Electromagnetic self induced vibrations in homogeneous unbounded electron beam moving with time dependent velocity, noting longitudinal and transverse wave generation

19 p2842 A72-38527

Longitudinal electric waves absorption in interstellar space due to electron-heavy particle collisions, considering photon rest mass

20 p2969 A72-39348

Investigation by the photon count method of the statistical properties of the emission of a laser operating in the mode of several axial oscillations

21 p3063 A72-40784

Spontaneous emission of plasma waves in the presence of a finite amplitude wave.

21 p3093 A72-41494

Longitudinal-torsional vibrations of a screw beam under axial excitation

22 p3240 A72-42954

Plasma-electromagnetic interaction with surface wave propagation along boundary, obtaining boundary conditions for longitudinal and transverse wave amplitudes with allowance for particles interaction

22 p3213 A72-43117

Conditions for magnetoactive plasma longitudinal waves with phase velocity near light velocity existence, investigating increments during synchrotron instability due to relativistic particles

23 p3262 A72-43311

On the instability of nonlinear longitudinal oscillations of magnetoactive plasma.

23 p3320 A72-43524

Thermomechanical coupling effects in the longitudinal oscillations of a viscoelastic cylinder.

23 p3352 A72-44122

Probability distribution of vertical longitudinal shear fluctuations.

23 p3281 A72-44146

Unsteady longitudinal viscoelastic vibrations of a rod of variable thickness at small values of time

24 p3459 A72-45265

Longitudinal electromagnetic wave excitation in restricted plasma by relativistic electron beam injection, determining increments frequency distribution and width of spectra

24 p3431 A72-45717

LOOK ANGLES

U AZIMUTH

U ELEVATION ANGLE

LOOP ANTENNAS

Active loop-dipole antennas with height reduction properties at resonance, deriving input impedance power gain and radiation patterns

04 p0502 A72-15519

Double parasitic loop counterpoise antenna radiation properties comparison to VOR systems, noting sitting error reduction

06 p0782 A72-17357

Input resistance derivation for finite horizontal loops with uniform current distribution located above lossy half-space ground

06 p0777 A72-18737

Radiation patterns of circular loop antenna in isotropic compressible plasma, discussing far fields for electromagnetic and electron plasma waves

12 p1790 A72-27491

Active loop dipole aeriels with height reduction properties at resonance, investigating transistor configurations in loop monopole aerial

12 p1792 A72-27699

Cross loop antenna for apparent azimuthal direction of incidence of VLF transmitter, showing night time bearing direction changes

12 p1784 A72-27794

Quasi-static and full wave calculation of VLF/ELF input impedance of arbitrarily oriented loop antenna in cold collisionless multicomponent magnetoplasma

13 p2009 A72-28542

Thin circular loop antenna input admittance and current distribution calculation comparison

15 p2209 A72-32673

Signal-to-noise performance of cryogenic electrically small receiving antennas.

17 p2525 A72-34375

The loop antenna with director arrays of loops and rods.

17 p2526 A72-34378

Design of an array of circular-loop antennas with optimum directivity.

17 p2514 A72-34387

Fourier series analysis of multielement circular loop antenna with arbitrary circumference for current distribution and self and mutual admittances

19 p2775 A72-38615

Analysis and design of TEM-line antennas.

21 p3026 A72-40353

Radiation efficiency of electrically small multielement loop antennas.

21 p3027 A72-40370

Detection of whistler mode signals from VLF transmitter in Australia.

21 p3023 A72-41386

Frequency dependent antenna impedance characteristics in ionospheric plasma, discussing anisotropic and isotropic electron plasmas, loop antennas, resonance rectification and ion effects

23 p3319 A72-43512

Field expressions for a circular loop antenna in terms of a new set of functions.

24 p3379 A72-44707

LOOPS

Elastic fields of dislocation loop in two phase material consisting of isotropic elastic half spaces

12 p1884 A72-27567

Digital command system second-order subcarrier tracking loop performance.

21 p3038 A72-40870

Near optimum digital phase locked loops.

21 p3038 A72-40871

Decision directed phase locked loops acquisition properties improvement technique for PCM bit synchronizer of random nonreturn to zero data

21 p3038 A72-40872

LORAN

Toran O long range navigation system based on circular coordinates and rubidium vapor clocks for beat phase measurements, noting use of portable transmitters

06 p0846 A72-18287

Loran-Omega course and track equipment /LO-CATE/ of integrated upper air meteorological sounding systems, describing radiosonde navigational aids

10 p1484 A72-25086

Loran/OMEGA course and track equipment /LO-CATE/ for remote object tracking by retransmission technique, eliminating search from search and rescue missions

13 p1997 A72-29182

Fighter bomber Loran-inertial data processing with digital computer to combine navigation, guidance and weapon delivery into fully integrated system

16 p2420 A72-33246

An area navigation system for a long range airplane.

21 p3079 A72-40281

LORAN C

Loran C system time tick transmission delay during solar eclipse of 7 March 1970, discussing atmospheric electron density effects

03 p0322 A72-13533

Radiosonde balloon tracking errors in upper atmosphere wind measurement with Loran C, Omega and radar transmitters

10 p1441 A72-25092

Hardware and software integration of OMEGA and LORAN C and D receivers based on hyperbolic navigation systems compatibility

13 p1999 A72-29205

Precise time and frequency dissemination via Loran C navigation system, discussing user techniques, economics and radio propagation mode and terrain effects on accuracy

15 p2268 A72-32067

LORAN D

Hardware and software integration of OMEGA and LORAN C and D receivers based on hyperbolic navigation systems compatibility

13 p1999 A72-29205

LORENTZ CONTRACTION

Model with large Lorentz factor and relativistic relations violations to explain theoretical estimate disparity with experimental data for high energy primary cosmic rays

01 p0118 A72-10156

Poincare, Lorentz and Einstein contributions to relativity theory construction according to Whittaker, discussing influence on contemporary scientists

20 p2954 A72-40003

Lorentz contraction and transformation of equilibrium forces and moments in inertial reference systems transition, discussing special relativity theory

21 p3084 A72-40938

On the gauge groups of linear conservative gravitational theories.

24 p3447 A72-45630

LORENTZ FORCE

Lorentz polarization effects on complex refractive index and wave polarization of magnetoionic theory

04 p0548 A72-14944

Magnetodiode model of intrinsic semiconductor slab under Lorentz force and double injection inducing ambipolar drift and carrier redistribution

08 p1142 A72-21746

Nonlinearity and inhomogeneity effects on plasma wave excitation by beating two laser beams, taking

into account Lorentz force modulation by large amplitude plasma wave

22 p3185 A72-42475

Optimal gyroresonator control in electric oscillating field by HF magnetic Lorentz force in terms of relativistic electron trajectory drifts

23 p3290 A72-44200

LORENTZ GAS

Self absorption and temperature gradient effects on fluorine-hydrogen flame spectroscopic temperature determination, comparing calculated and theoretical Lorentz intensity profile

04 p0596 A72-14890

Boltzmann equation solution analysis for Maxwell-Lorentz gas in electric field, discussing conditions for electron velocity distribution isotropic part evolution towards Maxwellian distribution

06 p0861 A72-18162

Magnetic effects on Lorentz plasma collision processes, calculating electron distribution function in presence of strong arbitrarily oriented magnetic and weak electric fields

06 p0864 A72-18535

Magnetic mirror system to study Lorentz ionization of highly excited hydrogen atoms with quantum numbers 6-7 in strong magnetic fields

09 p1363 A72-23222

FM electromagnetic wave propagation in Lorentzian plasma, taking into account harmonic generations effect

10 p1520 A72-24209

Third harmonic current density excitation by HF electric field in Lorentz plasma, calculating electron distribution function with unnormalized spherical harmonics and Fourier series

11 p1697 A72-26553

High momentum transfer collisions importance for anisotropic part of distribution function in Lorentz and single component plasmas

14 p2134 A72-30802

LORENTZ TRANSFORMATIONS

Thomas precession description with Lorentz transformation

03 p0388 A72-12989

Lorentz transformation between fixed and inertial reference frame in uniform gravitational field, discussing application to clock paradox problem

03 p0388 A72-13228

Lorentz transformation role in special to general relativity theory transition, noting neglect by Einstein and general covariance physical meaning exaggeration

06 p0848 A72-17991

Linear theories of gravitational fields, discussing Lorentz invariant approximation use to obtain Einstein equations approximation

09 p1352 A72-23386

Relativistic statistical mechanics invariant formula for coherence degree of plane blackbody radiation beam in arbitrary Lorentz frame, noting transformation law of temperature

12 p1846 A72-27741

Local Lorentz transformation in chronometric invariants, demonstrating appropriate operation for general covariant tensors from tetrad formalism

14 p2130 A72-30218

Zeeman triplet with unsplit upper level formation in isothermic atmosphere under magnetic field, considering Doppler and Lorentz frequency profiles of transitions

15 p2304 A72-31332

Poincare, Lorentz and Einstein contributions to relativity theory construction according to Whittaker, discussing influence on contemporary scientists

20 p2954 A72-40003

Inhomogeneous cosmological models in terms of impulse energy tensor, discussing coupled Einstein equations, gauge invariance and Lorentz gauge

21 p3110 A72-41442

Lorentz-covariant reference-tetrad theories of gravitation

24 p3425 A72-44913

LOS ALAMOS TURRET REACTOR

U HIGH TEMPERATURE NUCLEAR REACTORS

LOSSLESS MATERIALS

Microwaves propagation through circular waveguide partially filled with lossless cold electron plasma dielectric, presenting computed dispersion curves for waveguide and plasmasguide modes

10 p1522 A72-24677

Optimal flexible ferrite keeper for ferromagnetic thin film memories performance improvement, noting requirements for high permeability, low loss factor and dielectric constant, etc

11 p1601 A72-25899

LOST WAX PROCESS

U INVESTMENT CASTING

LOUDNESS

Loudness scaling methods for transportation noises, discussing matching procedures, reference sources, etc

07 p0931 A72-20165

Loudness and noisiness judgment contours, considering experimental subjective and objective condi-

- tions, subject age and sex and sound field characteristics
07 p0932 A72-20171
- Loudness function correlations to illusory spiral aftereffect persistence, motion sickness susceptibility and auditory reaction time in individuals
08 p1128 A72-22138
- Auditory sensation overall loudness prediction for steady broad-band noise from summation of weighted intensities of power spectrum sub-bands
11 p1686 A72-25800
- Acoustic stimuli transients rise time and repetition rate effects on loudness, applying various steady state noise calculation methods to transients Fourier transforms
13 p2004 A72-29097
- Mathematical determination of decibel-loudness index, tables for various frequencies.
20 p2956 A72-40076
- 1971 Rayleigh Gold Medal Address - Calculating the perceived level of light and sound.
22 p3205 A72-42462
- LOUNGE**
Lounge planning model for airport terminal design simulation, taking into account scheduled arrivals and departures, aircraft types, passenger number, gate assignments, etc
06 p0780 A72-17979
- LOUVERS**
ATS specular thermal control louver system performance in simulated solar vacuum environment as function of sun and blade angle, noting white paint effect
[AIAA PAPER 72-268] 11 p1740 A72-25209
- LOVE WAVES**
Love surface wave excitation in thin film layer by line source as function of propagation direction, frequency and film thickness
07 p1089 A72-19683
- Earth Love waves and toroidal oscillations attenuation, presenting frequency dependent model of internal friction
09 p1299 A72-22801
- Love wave tapping in isotropic microacoustic surface waveguide by partial transduction into bulk wave at discontinuity
16 p2428 A72-34178
- Guided elastic wave propagation near curved surfaces and in nonconstant thickness layers, discussing asymptotic solution and applications to Love, Rayleigh and Lamb waves
[ASME PAPER 72-APM-00] 17 p2580 A72-34306
- Partial derivatives of dispersion curves for higher modes of Love waves in a single-layered medium.
21 p3084 A72-40496
- On the propagation of Love type waves in an infinite cylinder with rigidity and density varying linearly with the radial distance.
22 p3207 A72-42878
- LOW ALTITUDE**
Low altitude electron-ion dissociative recombination and ion-ion neutralization coefficients during PCA event from ESRO rocket flights data
13 p2032 A72-29653
- Low altitude gust load spectra above Czechoslovak territory interpreted in terms of equivalent velocity cumulative frequencies for light aircraft
14 p2071 A72-30282
- Low-altitude flight imposed psychophysiological stresses due to air turbulence discomfort, instrument dial vibration and ground-based navigational objects recognition difficulty
14 p2080 A72-30747
- Local-time survey of plasma at low altitudes over the auroral zones.
19 p2792 A72-38739
- Studies of outer belt and slot region protons at low altitudes.
19 p2853 A72-38740
- Low-altitude atmospheric turbulence around an airport.
24 p3421 A72-45334
- LOW ASPECT RATIO**
Viscous incompressible flow past longitudinally cambered small aspect ratio slender wing near solid interface
05 p0600 A72-16215
- Vibration analysis of shaft supported low aspect ratio control surfaces on guided rockets, using Rayleigh-Ritz method
07 p1097 A72-20602
- Slender body theory for flow calculation past low aspect ratio delta wing with straight trailing edge, noting lifting vortices distribution
10 p1420 A72-25131
- Heat transfer by laminar natural convection in low aspect ratio cavities.
[ASME PAPER 72-HT-52] 20 p2985 A72-39661
- An experimental study of flows in planar nozzles.
[ASME PAPER 72-FLCS-2] 23 p3249 A72-44066
- An investigation of confined vortex flow phenomena.
[ASME PAPER 72-FLCS-3] 23 p3281 A72-44067
- LOW ASPECT RATIO WINGS**
NT DELTA WINGS
- Force and pressure distribution measurements on delta wing-body combination in compressible flow, investigating Reynolds number effect
[DGLR PAPER 71-118] 02 p0152 A72-12707
- Drag and lift experimental determination for low aspect ratio rectangular wings with blunt trailing edges at Mach numbers 0.5-2.2
[DGLR PAPER 71-114] 02 p0152 A72-12712
- Tip clearance effect on compressor blade aerodynamic characteristics, applying Bolay analysis to low aspect ratio rectangular wing
02 p0153 A72-12825
- Aerodynamic center and center of pressure of slender small aspect ratio wing near solid or free surface, determining angle of attack effect
13 p1894 A72-29131
- Calculation of a thin-walled small-aspect-ratio wing beyond the limit of proportionality
23 p3346 A72-43654
- LOW CURRENTS**
Generation-recombination model of large signal silicon transistor operating in IC microwatt range
02 p0188 A72-11521
- LOW DENSITY FLOW**
Alternating directional implicit numerical solution for three dimensional steady low density hypersonic flow over finite width flat plate
[AD-736572] 01 p0049 A72-10230
- Temperature distribution in hot wires in high-enthalpy low-density flows
[DFVLR-SONDDR-216] 19 p2804 A72-38685
- LOW DENSITY GASES**
U RAREFIED GASES
- LOW DENSITY MATERIALS**
High strength, stiffness and low density properties of boron/aluminum matrix composites in flight structures
04 p0585 A72-14745
- Structural design characteristics of low density fiber ceramic materials coated with refractory ceramics for space shuttle reusable surface insulation thermal protection systems
[AIAA PAPER 72-372] 13 p2056 A72-28957
- LOW DENSITY RESEARCH**
High speed streak cameras applicability to low density theta pinch studies, describing image converters design, operation and block diagrams
02 p0263 A72-11410
- High vacuum technology applications in surface physics research, discussing atomic collisions and adsorption processes
18 p2712 A72-36827
- LOW DENSITY WIND TUNNELS**
Optical TV scanning for wind tunnel model position detection in magnetic suspension system for sphere low density drag measurements
[ONERA, TP NO. 988] 10 p1461 A72-24764
- Magnetic balance measurements of aerodynamic forces on spheres and slender cones in hypersonic low density wind tunnels, noting sting effect
10 p1462 A72-24771
- Electron beam visualization in hypersonic air flows.
[AIAA PAPER 72-1017] 21 p3042 A72-41596
- Simulation of the interaction of high altitude plumes and a high-speed free-stream flow.
[AIAA PAPER 72-1019] 21 p3042 A72-41598
- Nitrogen temperature determination in arc tunnel air flows.
[AIAA PAPER 72-1022] 21 p3042 A72-41600
- LOW FINENESS RATIO**
U FINENESS RATIO
- LOW FREQUENCIES**
NT VERY LOW FREQUENCIES
- Lf noise measurements of mercury telluride and Cd-Hg-Te semiconducting thin films using vacuum tube preamplifier and step-up transformer
02 p0268 A72-11523
- Antenna lf impedance measurements of lower terrestrial plasma wave characteristics, using equivalent impedance probe circuit
02 p0172 A72-11946
- Lf oscillations of magnetic field at ATS 1, presenting local time and frequency distributions
07 p0975 A72-19160
- LF radiation effect on angular momentum distribution of interstellar grains with permanent dipole moments
10 p1541 A72-24473
- Antenna LF impedance measurements of lower terrestrial plasma wave characteristics, using equivalent impedance probe circuit
13 p1920 A72-29258
- VLF and LF electromagnetic waves amplitude and phase velocity in spherical earth-ionosphere waveguide, discussing wave hop method
13 p1923 A72-29661
- Lf white noise voltage theory of avalanche diode extended to small multiplication M values and unequal hole and electron avalanche ionization coefficients
15 p2206 A72-31642
- VLF wave propagation and its interaction with the magnetoplasma.
17 p2516 A72-35357
- An analysis of Pioneer 9 low-frequency wave observations near interplanetary discontinuities.
17 p2614 A72-35585
- Observations of D-region modifications at low and very low frequencies.
18 p2662 A72-37009
- Analysis of a procedure for the transmission of low-frequency signals in time-compressed, analog form
21 p3023 A72-41399
- A comparison of field-strengths of 164 kHz radio waves transmitted from Tashkent and received at Ahmabad with flare-time solar X-ray emissions measured in satellites.
23 p3262 A72-43275
- LOW FREQUENCY BANDS**
NT VERY LOW FREQUENCIES
- Spectral density curves for intensity fluctuations of stimulated emission from low and ultralow frequency gas lasers as function of thermal oscillation, mode interference and beat effects
08 p1182 A72-21379
- Drift measurement of lower ionosphere ionizational inhomogeneities by space-diversity LF band broadcast reception
13 p1948 A72-29037
- LOW GRAVITY**
U REDUCED GRAVITY
- LOW GRAVITY MANUFACTURING**
NASA materials science and manufacturing in space program involving space shuttle reusable equipment and weightlessness applications experiments
06 p0797 A72-18621
- Immiscible materials processing experiments in near weightlessness environments during Apollo 14 mission and on NASA short duration low gravity test facilities
24 p3407 A72-45155
- LOW LATITUDES**
U TROPICAL REGIONS
- LOW LEVEL TURBULENCE**
Density function for lower troposphere vertical turbulence diffusion coefficient derived from atmosphere radiometric probe data
13 p2029 A72-28456
- Aircraft flight conditions effect on low altitude critical air turbulence in terms of gust velocity components for CAT prediction
13 p1993 A72-28861
- LOW MASS**
U MASS
- LOW NOISE**
Lf noise measurements of mercury telluride and Cd-Hg-Te semiconducting thin films using vacuum tube preamplifier and step-up transformer
02 p0268 A72-11523
- Satellite tracking radio interferometer with 1 deg sec directional accuracy, discussing low noise level and precise time allocation requirements
[DGLR PAPER 71-125] 02 p0182 A72-12738
- Low noise IMPATT diode design for arbitrary signal levels, using Read model
06 p0787 A72-18382
- Si p-n-p punchthrough X band oscillator, discussing wideband tuning and low noise properties and applications
07 p0955 A72-19252
- Microwave IC front end receiver synthesis for radio relay system, considering low noise figure achievement by Si Schottky barrier diodes
07 p0955 A72-19356
- Low noise power level measurement at microwave frequencies, noting Nyquist equation applicability and cooled-to-uncooled element connections effects in receivers
12 p1779 A72-27175
- Avalanche photodiode with n-p-pi double diffused reach-through structure for visible and near-IR regions, noting high efficiency, low noise and gain stability
15 p2248 A72-32036
- Quiescent large-volume collisionless HF discharge plasma generator with zero magnetic field, noting low noise level due to self-stabilizing feature
17 p2592 A72-35814
- Microwave low noise amplifiers for use in radar systems.
20 p2907 A72-39220
- Low-noise parametric amplifiers for radio astronomical observations at 18 to 21 cm wavelengths
21 p3025 A72-40303
- Low noise microwave parametric amplifier design for space communication receivers, using inverted diode balanced mixers
21 p3025 A72-40304
- Simplified, low-noise processing technique for photographic phase holograms.
24 p3401 A72-44804
- LOW PASS FILTERS**
Computer program for microwave circuit scattering matrix sensitivity, applying to stripline elliptic low pass filters and thin-film negative resistance transistor amplifier
01 p0034 A72-10688
- Optimal frequency domain design of two dimensional low pass finite impulse response digital filters by linear programming
01 p0046 A72-10868

Staged corrector, transformer and low pass filter two terminal pair matching network for resonant circuits using semiconductor elements

03 p0333 A72-13897

Unified design charts for communication systems filter networks with inverse Chebyshev and elliptic function responses

06 p0787 A72-18400

Low and high pass, bandpass and bandstop active filters, tabulating cut-off frequencies, thermal stability, impedance, power dissipation and voltage specifications

07 p0955 A72-19248

PCM systems low pass filter characteristics from PAM off-band signals noise attenuation calculations

07 p0943 A72-19435

Linear constant systems synthesis with structural constraints in state space form, applying to RC filter circuit

10 p1453 A72-25101

Phase shift methods for data transmission vestigial sideband signal generation, providing shaping functions by shift registers, weighting resistors, summing amplifiers and low pass filters

11 p1592 A72-25890

Ideal low pass filter with fastest monotonic step response to permit no signal transmission outside prescribed frequency band

11 p1605 A72-26469

Active transistorized low pass RC filter providing fourth-order transfer function and uniform frequency response

13 p1927 A72-28381

Lossless low pass ladder network synthesis in terms of reflection coefficient poles and zeros with application to bandpass matching problem

15 p2212 A72-32248

Frequency domain design of two-dimensional finite impulse response digital filters.

17 p2532 A72-34406

LOW PRESSURE

NT HIGH ALTITUDE PRESSURE

Temperature dependence of gas flow coefficients at low pressures, determining isothermal permeability and heats of transport of He, Ne and Ar capillary flow

10 p1469 A72-24600

Low pressure ratio Q-FAN propulsor noise reduction tests on wind tunnel model, discussing source components and design configurations

[ASME PAPER 72-GT-40]

11 p1569 A72-25634

Low carbon and nitrogen concentrations in chromium ferritic stainless steel obtained with gas rinsing at reduced pressure, noting weldability and corrosion resistance

14 p2119 A72-30606

Low pressure gas ejector operation with cylindrical mixing chamber, discussing design procedure with compression rate and ejection coefficient calculation

19 p2746 A72-37667

Experimental investigation of the combustion process of two-component heterogeneous condensed systems at low pressures

20 p2987 A72-40042

Throttle characteristics and mixing chamber geometry effects on low pressure gas ejector operation, noting air flow and pressure rates in air ejectors

22 p3133 A72-41859

LOW PRESSURE CHAMBERS

U VACUUM CHAMBERS

LOW SPEED HANDLING

U CONTROLLABILITY

LOW SPEED WIND TUNNELS

NT SUBSONIC WIND TUNNELS

Indian low speed wind tunnel, describing design, six component balance and calibration

04 p0509 A72-15277

Spatial boundary layer variations in low speed wind tunnel working section due to settling chamber screens, discussing mesh variations effects on Preston tube measured pressure coefficient distributions

07 p0966 A72-19061

Base pressure drag reduction on rectangular wings with blunt trailing edges from low speed wind tunnel measurements

[DFVLR-SONDDR-219]

10 p1419 A72-24842

Thermoanemometer measurements of turbulence degree in wake behind square mesh grids in water flow within low speed wind tunnel

20 p2912 A72-39364

Reynolds number and drive power variation with Mach number, pressure and temperature in cryogenic wind tunnel

[AIAA PAPER 72-995]

21 p3040 A72-41581

LOW TEMPERATURE

Heat resistant metals long time creep prediction at low stresses or temperatures

06 p0834 A72-18668

High atomic energy levels population at low temperature, density and thermal radiation fields conditions in interstellar medium

11 p1720 A72-26111

Chemical equilibrium models of low temperature condensation from solar nebula relating to planetary composition

15 p2311 A72-32083

Transport phenomena in an electron-phonon system in strong magnetic fields at low temperatures

20 p2953 A72-39310

Radiation heat transfer between closely spaced metal surfaces at low temperature - The impact of discrete modes of the radiation field.

[ASME PAPER 72-HT-0]

20 p2983 A72-39483

Model of degenerate semiconductor near semiconducting phase transformation, noting superconducting state at low temperatures with corresponding impurity concentrations

23 p3323 A72-43317

LOW TEMPERATURE ENVIRONMENTS

Fiber reinforced plastic composite seals for liquid hydrogen and nuclear radiation environments, stressing polyquinoxaline fitness

01 p0075 A72-10773

Ventilatory and metabolic responses of unanesthetized dogs exposed to various carbon dioxide concentrations at 2 and 18 C, discussing oxygen uptake relation to cold

02 p0159 A72-11954

Aging effect on duraluminum electrical resistivity alteration at low temperature plastic deformation

05 p0679 A72-17181

Fe effect on dispersion hardened Ni alloys with various quantities of Nb and Ti during cryogenic operation

05 p0679 A72-17202

Low temperature tensile strength and plasticity of Ti alloys containing zirconium

05 p0679 A72-17203

Electron transmission microscope study of quenched Mo-N alloys supersaturated solid solution low temperature aging behavior, investigating recovery processes

06 p0830 A72-18056

Temperature dependence of strain rate sensitivity in low temperature deformation processes, considering inherent lattice conditions and impurity atoms effects

07 p1022 A72-20573

Calibration technique for conductive thermal flux sensors operating at low temperatures

08 p1166 A72-21315

Transition metals IR spectral absorptivity evaluation at room and liquid He temperatures from reflectivity measurement relative to vapor deposited Au mirror

09 p1309 A72-22604

Low temperature resistant stainless steels mechanical properties, microstructure and weldability, discussing compositions and heat treatments

10 p1498 A72-24838

Fe effect on plasticity and ductility of dispersion hardened Ni alloys with various quantities of Nb and Ti at cryogenic temperature

11 p1660 A72-26137

Low temperature tensile strength and plasticity of Ti alloys with zirconium, investigating sensitivity to stress concentrations

11 p1660 A72-26138

Thermoregulation in deeply hibernating rodents during separate chilling and steady hibernation temperature maintenance of skin and brain

12 p1762 A72-27827

Silicon dislocation density relationship to solar cell current loss at low temperature, presenting temperature-diffusion length and I-V characteristics

15 p2183 A72-32132

Laser ignition and combustion of boron particles, developing oxide coating and droplet burning models for low and high temperature stages respectively

15 p2296 A72-32582

Noise in bipolar junction transistors at low temperatures.

18 p2666 A72-36323

Space environment simulation and testing techniques, considering vacuum systems, low temperature, solar radiation and motion simulation

18 p2676 A72-36833

Low-temperature measurements of the three-body electron-attachment coefficient in O₂

19 p2837 A72-37545

Low temperature interference filter design for atmospheric windows far IR photometers based on selective reststrahlen reflection of crystals

19 p2796 A72-37586

High-sensitivity resonant-quartz scales operating in high vacuum at very low temperature - Application to the study of gas-solid interactions

19 p2800 A72-37834

Low-temperature photoluminescence of GaAs under conditions of strong interaction of the non-equilibrium carriers.

19 p2847 A72-38821

Static and dynamic fatigue behavior of glass filament-wound pressure vessels at ambient and cryogenic temperatures.

19 p2823 A72-38832

Self-diffusion of cobalt in coarse grained polycrystalline Ni-Co alloys at low temperature.

20 p2935 A72-39016

Laser action with coupled types of oscillations

20 p2931 A72-39319

Anomalous line broadening in the low temperature X-ray diffraction pattern of niobium.

20 p2942 A72-39989

A novel specimen stage permitting high-resolution electron microscopy at low temperatures.

21 p3051 A72-40218

Thermal properties of polymers below 4 K.

22 p3197 A72-42800

Apparatus for measurement of specific heats between 0.3 and 3 K in the oscillating thermal region

22 p3180 A72-42936

LOW TEMPERATURE PHYSICS

Czech FET properties in low temperature region, measuring static characteristics, electrical parameters and noise levels at 4.2-296 K

02 p0195 A72-12670

Dimer formation effect on thermal diffusion factor at low temperatures for krypton-argon system

03 p0391 A72-13749

Quasi-static measurement and electron phonon interpretation of specific heat of metals at low temperature

03 p0456 A72-13843

Electron correlation effects on low temperature thermodynamics of amorphous semiconductors, predicting Curie law magnetic susceptibility and equilibrium electronic specific heat dependence on temperature

04 p0562 A72-15153

Low temperature Ga doped Ge bolometer for IR detection, improving sensitivity by load resistance noise elimination

05 p0662 A72-16195

Al and Al-Si alloy thermal expansion at low temperatures, noting near-eutectic crystalline composition

07 p1019 A72-20156

Spectral measurements of temperature in low temperature plasma, describing line reversal method

10 p1485 A72-25110

Electronic model for low temperature transition in magnetite with nonintegral average electron number on site

11 p1701 A72-26023

Thermal conduction anomalies and electron phonon interaction in thin metallic sheet at low temperatures

12 p1888 A72-27182

Low temperature homogeneous plasma electric conductivity in magnetic field, noting monotonic decrease

13 p2018 A72-29892

Electrical conductivity, reluctance and Hall effect of n-type semiconductors determined at extremely low temperatures

15 p2291 A72-31389

Bcc lattice sum calculation method in Langevin function terms, noting validity at low temperatures

16 p2442 A72-34175

Low-temperature properties of nitrogen-alloyed austenitic chromium-nickel/molybdenum steels and chromium-manganese-nickel steels and their applicability as low-temperature ductile steels

17 p2566 A72-34395

Quantum crystals in the single-particle picture.

19 p2844 A72-37943

Study of the solidification of cryogenic fluids by means of evacuation

19 p2881 A72-38039

A generalized virial equation of state and its application to vapor-liquid equilibria at low temperatures.

19 p2883 A72-38838

Electron-electron collision induced anomalous Hall effect in ferromagnetic d metals at low temperatures

20 p2959 A72-39309

Formation of deformation martensite in Fe-Ni-C alloys which do not undergo transformation on cooling.

21 p3066 A72-40270

LOW TEMPERATURE TESTS

Fatigue test machine for alternating cantilever bend and torsion testings at 50 He and 1.5-300 K

01 p0049 A72-11381

Uniform low temperature compression effect on accelerated aging of Duralumin specimens, noting Plateau due to Guinier-Preston zones

02 p0245 A72-12539

Resistive force on moving dislocations at low temperature in solids and crystal defect studies by ultrasonic methods, determining temperature dependence of mechanical properties

03 p0362 A72-13224

Temperature dependence of low temperature endurance of Cr-Ni steels in bending fatigue tests

03 p0371 A72-13463

Plane strain fracture toughness of notched high strength Al and Ti alloys at low temperatures

03 p0371 A72-13464

Low temperature heat capacity of chromium silicide, observing superconducting transition and magnetic susceptibility

03 p0377 A72-14024

Low temperature liquid bath tests for IC environmental reliability, monitoring wire bonding, metallization, surface contamination, sealing and die bonding

03 p0337 A72-14296

Low temperatures and deformation rates effect on martensitic phase formation in Cr-Ni austenitic stainless steel under compression and tension

03 p0379 A72-14378

Ar, Kr, methane and nitrogen physisorption isotherms on stainless steel in low pressure cryogenic baths calculating mean adsorption energies

05 p0624 A72-16395

Hydrogen environment effects on fatigue crack growth rates in Ti-Al-V weldments over low ambient temperature range

05 p0678 A72-17116

Thermostated integrating sphere for low temperature measurements of reflection and transmission coefficients of materials with arbitrary scattering functions

06 p0816 A72-17838

Low temperature slip discontinuity and strength of pure Al crystals as function of strain rate

06 p0831 A72-18355

Al and Ti alloy fatigue after temperature reduction to 253, 77 and 4 K as function of surface purity after machining

06 p0831 A72-18356

Plasticity of Al alloy thin walled tubular specimens under axial tension and internal pressure at 293, 173 and 93 K

06 p0833 A72-18561

Deformability and strength of soft fiber reinforced plastics under biaxial tension, determining low temperature critical tensile stresses and elongation ratios

06 p0836 A72-18562

Low temperature test facility for cryogenic and rocket materials under combined tension and torsion

06 p0797 A72-18648

Fatigue testing machines for axial and torsional loadings at low temperatures in vacuum

06 p0797 A72-18667

Product of net branching factor and induction period in hydrocarbon oxidation at low temperatures, tabulating results

07 p1051 A72-19374

Book on materials low temperature mechanical properties covering metals, polymers, ceramics and composites, temperature effects on deformation processes, fracture mechanics, test methods, etc

07 p1015 A72-19909

Mechanical properties and structural strength evaluation methods for metallic materials at low temperatures, describing hydraulic and pneumatic testing facilities

07 p1017 A72-20130

Stress-strain behavior of steel under elastic compression at 4.2 K, observing discontinuous twinning

07 p1020 A72-20413

Plastic deformation characteristics of Fe-Cr-Ni alloy single crystals at low temperatures

08 p1188 A72-21790

Plastic deformation effect on structure and properties of steel sheet under biaxial tension at liquid nitrogen temperature

09 p1330 A72-23187

Crystal grain size effect on fracture initiation in mild steel under triaxial stress, using notch tests at low temperatures

11 p1657 A72-25756

Low temperature mechanical properties of Ti-base alloys, examining notched samples impact strength as function of temperature and notch depth

11 p1663 A72-26806

Low temperature solid state phase transformations in 2H silicon carbide single crystals, noting time and temperature dependence

12 p1854 A72-27276

Low temperature irradiation and annealing effects in germanium, calculating charge states for donor and acceptor centers

12 p1857 A72-28054

Electron irradiation of Li doped Ge at low temperatures, measuring Hall effect and minority carriers diffusion length

12 p1857 A72-28055

Radiation damage in carbon doped silicon irradiated at low temperatures by 2 MeV electrons, noting isotope shifts

12 p1857 A72-28059

Tensile strength, plastic properties and notch sensitivity from low temperature tests of binary Ti alloys, noting effects of Sn content and temperature

12 p1831 A72-28239

Crack and notch induced stress concentrations effect on steel mechanical properties at 20-293 K, using static and dynamic test methods

12 p1831 A72-28240

Mechanical properties of nitrated austenitic steels at low temperatures, noting improved tensile strength

13 p1977 A72-29017

Ti-V and Ti-Nb alloys mechanical strength and stress concentration resistance at low temperatures

13 p1977 A72-29018

Uniaxial compressive stress apparatus for InSb investigation at low temperatures in large magnetic fields

13 p1959 A72-29753

Tensile strength and martensitic transformation effect on stainless steel plastic deformation at cryogenic temperatures

15 p2253 A72-31521

Microcalorimetric investigation of energy transfer from atomic and molecular hydrogen beams to various surfaces at liquid helium temperatures and ultrahigh vacuum conditions

15 p2281 A72-31863

Surface treatment effects on light and X ray irradiated surface photoconductivity of InSb semiconductor single crystals at liquid nitrogen temperature

15 p2292 A72-31866

Varian HR-60 NMR spectrometer probe with Dewared insert for low temperature operation

15 p2240 A72-32435

Rising temperature reactor technique to evaluate catalysts for initiating hydrogen-oxygen reaction in gas mixtures at 78 K

15 p2193 A72-32550

Low temperature environmental chamber for F-111 proof load testing, describing components of cold air forced convection recirculation system with liquid nitrogen injection

15 p2214 A72-32612

Impurity controlled deformation mechanism for softening control of interstitial bcc alloys, discussing low temperature and composition effects

18 p2699 A72-36341

Regularities in the deformation and failure of commercial iron in a complex stress state under low-temperature conditions

19 p2818 A72-38005

Investigation of the influence of surface treatment purity and procedure on the strength of the Kh18N10T and Kh16N6 steels and the AMG6 alloy at normal and low temperatures

19 p2819 A72-38016

Influence of temperature shocks on seed formation after irradiation of pollen from *Tradescantia paludosa*.

19 p2761 A72-38642

Mechanical properties of Ti-Mo alloys at low temperatures

20 p2942 A72-39824

Characteristics of the low temperature effect of an electric field on the sensitivity of photographic emulsions

21 p3053 A72-40391

Tempered hardness and tensile strength of ausforming Mn-Cr-B spring steels at low temperatures in austenite stable phase by electron microscopy

21 p3066 A72-40718

Pure and compensated Ge and Si far IR spectral properties at liquid He temperatures for bolometer detector application

21 p3013 A72-40822

On some aspects of low-temperature and anodic oxidation of metals and semiconductors.

21 p3067 A72-40914

Strength of welded joints of high-strength stainless steels at cryogenic temperatures

21 p3061 A72-41365

Yielding and fracture of D16T alloy at low temperatures under conditions of complex stress-strain state

21 p3071 A72-41706

Quadrisectional facility for studying creep and fatigue strength under deep freezing conditions

21 p3057 A72-41719

Fatigue properties of 18-8 stainless steel at cryogenic temperatures.

21 p3071 A72-41845

Low temperature characteristics of the Gunn diode.

22 p3159 A72-42307

Ultrasonic evidence against multiple energy gaps in superconducting niobium.

22 p3190 A72-42476

Relaxations in polymers at low temperatures.

22 p3196 A72-42793

Fatigue test equipment for 293-233 K and 50-100 ton static or 25-50 ton cyclic loads, using Freon 22 as coolant

23 p3278 A72-43759

Elastic stiffness of AT-2 and AT-3 titanium alloys and their welds at high and low temperatures

23 p3302 A72-43966

Stress-strain diagrams from high and low temperature tests of Y alloy rods, noting temperature effects on plastic deformation

24 p3413 A72-44724

Temperature dependence of low temperature endurance of Cr-Ni steels in bending fatigue tests

24 p3413 A72-44938

Plane strain fracture toughness of notched high strength Al and Ti alloys at low temperatures

24 p3413 A72-44939

Low temperature slip discontinuity and strength of pure Al crystals as function of strain rate

24 p3416 A72-45742

Al and Ti alloy fatigue after temperature reduction to 253, 77 and 4 K as function of surface purity after machining

24 p3416 A72-45743

Mechanical properties and structural strength evaluation methods for metallic materials at low tem-

peratures, describing hydraulic and pneumatic testing facilities

24 p3416 A72-45756

LOW THRUST

NT MICROTHRUST

Optimal flight of material point in central field of forces subject to controlled small thrust

01 p0127 A72-10356

Minimum fuel continuous low thrust orbit transfer problem of optimal control, solving boundary value problem with Multiple Substitution Polynomials and Marquardt method

10 p1552 A72-24486

Analytic partial derivatives for estimating low-thrust parameters.

22 p3231 A72-42865

LOW THRUST PROPULSION

NT ELECTROMAGNETIC PROPULSION

NT ELECTROSTATIC PROPULSION

NT ION PROPULSION

NT PHOTONIC PROPULSION

NT PLASMA PROPULSION

NT SOLAR PROPULSION

Outer planet low thrust orbiter missions, comparing three body numerical results with two methods of patching together two body solutions

01 p0128 A72-10379

Mini-cavity gas core reactor concept for low thrust high impulse probe propulsion, using U 233 or 235 fuel

04 p0546 A72-14422

Trajectory optimization for low thrust mission and system analysis, exemplifying by Jupiter flyby and comet rendezvous missions

[AIAA PAPER 72-426]

11 p1721 A72-26171

Gradient method and Euler equations application to low thrust earth-to-Mars spacecraft orbital transfer trajectory optimization

13 p2034 A72-28438

Low thrust propulsion system effects on communication satellites subsystems, discussing mercury, cesium and Teflon rocket placement and effects of exhaust

[AIAA PAPER 72-519]

13 p2027 A72-28981

Low thrust spacecraft navigation requirements for minimum propellant guidance, using neighboring extremal law

15 p2270 A72-32194

Computer simulation of retargeting procedure with closed form iterative solution and parameter optimization for nonlinear low thrust spacecraft guidance scheme

[AIAA PAPER 72-916]

21 p3082 A72-41561

Development and testing of a radioisotope-fueled thruster for spacecraft propulsion.

24 p3434 A72-45178

Low thrust constant acceleration trajectories for a Mercury orbit.

24 p3441 A72-45208

LOW TURBULENCE

Low turbulence wind tunnel with closed circuit design and pressure gradient adjustment capability for turbulent boundary layer studies

06 p0795 A72-17713

LOW VISIBILITY

Pilot perception tests on estimating flight path inclination, ground image and touchdown time under poor visibility

05 p0684 A72-16180

Aircraft pilot performance during instrument approach in low visibility conditions

07 p0925 A72-18832

Coastal and inland fog microphysical features, discussing visibility, liquid water content, drop size distributions and haze droplet concentrations

13 p1991 A72-28842

Autoland system flight testing in Trident 3B and British Civil Aviation Authority approval for ICAO Cat 3a weather

16 p2420 A72-33539

Investigation of data rate requirements for low visibility approach with a scanning beam landing guidance system.

17 p2578 A72-35562

Investigation of data rate requirements for low visibility approach with a scanning beam landing guidance system.

19 p2832 A72-38259

LOW VOLTAGE

Efficiency/reliability design requirements of driven transistor synchronous rectifiers in low output voltage applications

01 p0042 A72-11053

Low voltage arc discharge development in cesium vapor with glowing spherical plasma cluster formation in electrode gap

05 p0701 A72-17238

Temperature dependent small signal operation of junction transistors at low supply voltage

13 p1930 A72-29058

LOWER ATMOSPHERE

NT OZONOSPHERE

NT TROPOSPHERE

Venus subcloud layer, investigating radiant heat transfer in convective lower atmosphere

01 p0128 A72-10370

Terrestrial biosphere back contamination from outer space organisms, discussing microbiologic control and prevention requirements

01 p0020 A72-10825

Atmospheric refractive index structure parameter variation with height and measurement near ground [AD-739059]

02 p0253 A72-12546

Biochemical functions of organisms in evolution of biosphere, discussing redox reactions, elementary compositions and metal compounds role in photosynthesis

04 p0470 A72-14796

Combined radar-acoustic system for lower atmosphere temperature sounding, considering use in air pollution studies and short range weather forecasting [AD-739790]

05 p0663 A72-16690

Energy and momentum removal from troposphere and lower atmosphere by mountain lee wave breaking, discussing effects on atmospheric circulation evolution and maintenance

08 p1203 A72-22167

High energy UV solar radiation transfer by stratospheric aerosols to biosphere, considering radiation injury to human lung

09 p1298 A72-22662

Mathematical model of ion capture and annihilation by aerosol particles from ground level to 60 km

09 p1346 A72-23266

Mathematical model for compressed gas convection into lower atmosphere with substantial density changes

10 p1563 A72-24778

Atmospheric temperature measurement up to 2 km height, reviewing sounding equipment and techniques

10 p1508 A72-25091

Lower atmosphere vertical temperature profiles determination from clear air ground based measurements of microwave thermal emission by oxygen

11 p1591 A72-25764

Real time measurements of ground level and airborne particle concentrations and diffusion in 10-100 km range

11 p1681 A72-26081

Geomagnetic Sq current electric field mapping into lower atmosphere, calculating equipotential surfaces

11 p1626 A72-26416

Venus lower atmosphere enhanced microwave attenuation explained by water vapor and droplet layer, calculating mass density distributions

11 p1724 A72-26762

Analytic models of large scale electric fields in atmosphere, considering geomagnetic Sq current in lower atmosphere and inner magnetosphere

12 p1804 A72-27790

Russian papers on solar activity effects on earth atmosphere and biosphere covering climate, vegetation, animals and man

12 p1763 A72-28206

Solar activity effects in magnetosphere and ionosphere relation to geomagnetic activity and biospheric development, noting 11 year geomagnetic perturbation cycles

12 p1805 A72-28209

Solar activity effects on biospheric processes for biological and physicochemical systems in unsteady state, considering maximum effects on man at certain electromagnetic wave frequencies

12 p1773 A72-28211

Mathematical model for compressed gas thermal convection into lower atmosphere with substantial density changes

14 p2170 A72-30215

Microscale static pressure fluctuation measurements in lower atmospheric boundary layer turbulent flow using Eulerian measurements

15 p2265 A72-31618

Two layer model for diurnal temperature variations analysis for radiative heat transfer between lower atmosphere and underlying layer

16 p2417 A72-33293

Observations of Helmholtz waves in the lower atmosphere with an acoustic sounder

18 p2687 A72-36635

Relation between impurity shear dispersion in the atmospheric ground layer and the turbulence characteristics

19 p2829 A72-38772

Investigation of the mesoscale convective processes during the forthcoming GARP implementation.

20 p2948 A72-39800

Russian book - Calculated wind velocities at heights of the lower atmospheric layer.

22 p3200 A72-42077

Spatial distribution of excess-radiation intensity at low altitudes

22 p3218 A72-42212

Radiation, evaporation and the maintenance of turbulence under stable conditions in the lower atmosphere.

22 p3201 A72-42597

Thermal equilibrium calculations of the lower Venus atmosphere.

24 p3439 A72-44955

The sweepback effect in the subsonic region in the lower atmosphere and in the hypersonic region at high altitudes

24 p3359 A72-44983

LOWER IONOSPHERE NT D REGION

Lower ionosphere ionization response to auroral particle fallout during 1968 substorms, using geomagnetic, VLF and balloon measurements

01 p0053 A72-10366

Lower ionosphere continuous electron density measurements with ground vlf transmitter, determining limiting altitude ceiling for diurnal and seasonal data

01 p0027 A72-10442

Wind resonance in ionosphere under pressure fluctuations, noting turbulent friction factor above 110 km

01 p0058 A72-10589

Auroral absorption and DR currents development during magnetic storms, discussing corpuscular fluxes arrival from magnetospheric tail into lower ionosphere

01 p0059 A72-10619

Lower ionospheric nighttime absorption as ionization processes indicator, discussing relationship to geomagnetic activity

02 p0216 A72-11921

Radio wave scattering observation in turbulent lower ionosphere, determining vertical propagation velocity dispersion by statistical analysis

03 p0322 A72-13476

Geomagnetic effects on lower ionosphere at lower midlatitude station, discussing long wave propagation

04 p0516 A72-14939

Lower ionosphere 5577 and 5893 A and hydroxyl band emissions interrelationships, observing atomic O and vertical eddy transport effects

04 p0518 A72-14961

Diurnal variation of lower ionosphere, analyzing nature and behavior of absorption long range variations over solar activity cycle

05 p0660 A72-17182

Vlf wave excitation during sudden storm commencement, causing magnetosphere trapped energetic electrons to diffuse and precipitate into lower ionosphere

06 p0803 A72-17451

Solar cosmic ray flare of 11-18 April 1969, investigating effect on polar cap absorption in lower ionosphere

07 p1066 A72-20650

Slip effect in diurnal phase and amplitude cycles of vlf signals in lower ionosphere due to wave interference at transmitting point

08 p1130 A72-20710

Lower ionospheric electron density profile determination at high latitudes from riometric observations, discussing cosmic radio emission absorption representation

08 p1225 A72-20730

Oxygen, nitric oxide and water cluster positive ion composition from mass spectrometer experiments in lower ionosphere, noting ion production and low temperature effects

09 p1375 A72-22363

Meteorological synoptic analysis of stratospheric planetary wave interaction with lower ionosphere in terms of wind, temperature and ionospheric electron density profiles

09 p1297 A72-22375

Differential photoelectron flux in lower ionosphere during 7 March 1970 solar eclipse observed by Nike-Apache rockets

09 p1378 A72-23012

X ray effect from Scorpio XR-1 on lower ionosphere long wave transmissions, considering transit times and field intensity variations

09 p1305 A72-23572

Lower ionospheric structure, discussing electron production, loss and transport effects and diurnal variations

10 p1473 A72-24703

Simultaneous rocket observation of wind shear and electron density profile in lower ionosphere, noting sporadic E layer formation

10 p1477 A72-25154

Electrostatic and electron temperature probes compared during ionospheric rocket soundings, noting lower ionosphere discrepancies due to surface contamination

11 p1633 A72-26102

Radio wave scattering observation in turbulent lower ionosphere, determining vertical propagation velocity dispersion by statistical analysis

11 p1593 A72-26246

Atmospheric density annual and diurnal variations in lower ionosphere, from satellite radar tracking data, considering drag coefficient modeling and orbit determination techniques

11 p1625 A72-26410

Artificial heating of lower ionosphere in controlled experiment, measuring electron temperature increase by radar backscatter system

11 p1625 A72-26412

Transmission and reflection coefficients of ULF waves incident on lower ionosphere layer with exponential electron density profile

11 p1597 A72-26707

Mode coupling effects on radio wave partial reflection from lower ionosphere at vertical incidence, using matrix perturbation analysis

11 p1599 A72-26764

Electron density and ionization changes in lower ionosphere during 7 March 1970 solar eclipse from 2.66 MHz absorption and Langmuir probe rocket measurements

12 p1800 A72-27148

Nitric oxide and oxygen molecular ion composition of lower ionosphere during solar eclipses from rocket measurements

12 p1801 A72-27150

Upper atmosphere particle flux density determined from nocturnal electromagnetic absorption caused by geomagnetic storms, noting ionization process time lag in lower ionosphere

13 p1945 A72-28580

Relations between normal mode radio propagation parameters and properties of earth-lower ionosphere isotropic waveguide, allowing for geomagnetic field

13 p1945 A72-28583

Drift measurement of lower ionosphere ionizational inhomogeneities by space-diversity LF band broadcast reception

13 p1948 A72-29037

Lower ionospheric nighttime absorption as ionization processes indicator, discussing relationship to geomagnetic activity

13 p1948 A72-29233

Solar cosmic rays spectrum and geomagnetic cut-off rigidity determination from ion production rates in lower ionosphere

14 p2147 A72-30627

Lower ionospheric seasonal anomaly in electron density levels, noting diurnal and latitudinal characteristics at various heights

14 p2102 A72-30653

Surface contamination effect on electron temperature measurement using rocket-borne Langmuir probe in lower ionosphere

15 p2236 A72-31926

Monostatic radar measurement for incoherent scatter correlation function in lower ionosphere, using spaced short pulses transmission to obtain adequate height resolution

15 p2200 A72-32106

Sudden decreases of atmospherics due to solar flares effects on lower ionosphere, discussing noise propagation

15 p2230 A72-32256

Oxygen molecule electron affinity role in ion chemistry of lower ionosphere, noting binding energy of ground state

17 p2585 A72-34260

Wave interference effect in whistler mode reflection coefficients for model lower ionospheres.

17 p2548 A72-35465

Determination of electron concentration profiles in the lower ionosphere from the absorption at several frequencies

17 p2551 A72-35863

On the reflection of whistler mode waves from model lower ionospheres.

18 p2660 A72-36430

Lower ionosphere N/H/ profile calculation from ionograms with incomplete layer information

18 p2689 A72-36880

Slip effect in diurnal phase and amplitude cycles of VLF signals in lower ionosphere due to wave interference at transmitting point

19 p2765 A72-38338

Lower ionospheric electron density profile determination at high latitudes from riometric observations, proposing cosmic radio emission absorption representation

19 p2791 A72-38358

On the source of sunrise effects in the low ionosphere.

19 p2792 A72-38627

Numerical solution to the problem of propagation of ELF electromagnetic waves in the lower ionosphere

19 p2767 A72-38651

Electron temperature and density determination from RF impedance probe measurements in the lower ionosphere.

20 p2916 A72-39229

Recent positive and negative ion composition measurements in the lower ionosphere by means of mass spectrometers.

20 p2917 A72-39528

Propagation of HM-waves with periods corresponding to periods of Pc1 micropulsations through the lower ionosphere.

21 p3015 A72-40497

Isothermal ionization of the lower ionosphere under the action of radio waves

23 p3283 A72-43362

Variation with electron velocity powers of electron collision frequency and energy transport coefficients in weakly ionised plasmas - Earth's lower ionosphere. 23 p3285 A72-43994

Synchronous observations of lower-ionospheric wind conditions in Dushanbe and at the equator 23 p3285 A72-44166

Anomalous ionization in lower ionosphere recorded by riometers, considering ionospheric substorms caused by auroral absorption 24 p3396 A72-44849

Upper atmosphere particle flux density determined from nocturnal electromagnetic absorption caused by geomagnetic storms, noting ionization process time lag in lower ionosphere 24 p3397 A72-45080

Relations between normal mode radio propagation parameters and properties of earth-lower ionosphere isotropic waveguides, taking into account geomagnetic field 24 p3397 A72-45083

The relationship of theory and experiment in the D-region. 24 p3399 A72-45581

LOX [OXYGEN]

U LIQUID OXYGEN

LOX-HYDROGEN ENGINES

U HYDROGEN OXYGEN ENGINES

LR CIRCUITS

U RL CIRCUITS

LRC CIRCUITS

U RLC CIRCUITS

LRV [VEHICLE]

U LUNAR ROVING VEHICLES

LSI

U LARGE SCALE INTEGRATION

LSSM

Lunar ejecta and meteorites experiment, determining speed, direction, mass and flux density of cosmic dust particles 04 p0509 A72-15102

Lunar mass spectrometer experiment, determining global distributions and diurnal variations of lunar atmosphere 04 p0509 A72-15103

Lunar seismic profiling experiment, describing explosives package, electronics and SAFE/ARM assembly 04 p0509 A72-15104

Apollo 16 far-ultraviolet camera/spectrograph - Earth observations. 21 p3105 A72-40600

LUBRICANT TESTS

Hydrodynamic lubricating films with viscosity variations perpendicular to direction of motion, evaluating friction coefficient changes for constant film thickness and load carrying capacity [ASME PAPER 72-LUB-E] 06 p0821 A72-17806

Molybdenum disulfide and layer lattice materials lubricating mechanism and effectiveness from sulfur atoms strong polarization, using scanning electron microscope 06 p0822 A72-18157

Molybdenum disulfides with varying purity level evaluated as solid lubricants and as lubricant additives in standard lubricating testing devices 06 p0836 A72-18588

Methyl phenyl polysiloxane bonded solid film lubricants, discussing air curing at ambient temperatures and performance tests 06 p0836 A72-18592

Self lubricating polytetrafluoroethylene and polyimide composites transfer film formation tests, studying film thickness and uniformity 06 p0824 A72-18596

Aircraft gas turbine engines synthetic lubricants thermal stability characteristics, describing coke deposition test apparatus and results [ASLE PREPRINT 72AM 14] 13 p1983 A72-28971

Metallic, ceramic, polymeric, composite and solid film lubricant friction and wear properties and testing [ASME PAPER 72-DE-28] 14 p2108 A72-30869

The testing of contact materials for slip rings and brushes for space application. 18 p2698 A72-36117

Shear modulus of liquids at elastohydrodynamic lubrication pressures. 21 p3059 A72-40688

Testing of plastic lubricants in ball bearings with rocking motion on the TsKB 16-T test stand 23 p3307 A72-43975

LUBRICANTS

NT GAS LUBRICANTS

NT HIGH TEMPERATURE LUBRICANTS

NT LUBRICATING OILS

NT SOLID LUBRICANTS

Physical inconsistencies of mechanico-mathematical concepts of metal deformation, considering friction forces, lubricant action and plastic tensors and deviators 01 p0102 A72-11077

Organophosphorus antiwear additives in neopentyl polyol ester lubricants on 440C stainless steel surfaces, using four ball wear test machine [AD-740055] 02 p0250 A72-12849

Fuels and lubricants development trends for subsonic and supersonic aircraft, discussing thermostable hydrocarbons, ramjet fuels, esters, oxidation inhibitors, metal deactivators, high pressure lubricant additives, etc 05 p0681 A72-16739

Deep groove ball bearing endurance tests to determine running conditions and lubricant film thickness/surface roughness ratio effects on fatigue life 12 p1816 A72-28112

Solids deformation resistance increased by active lubricants effects on coupled friction surfaces, noting damage localization to thin surface layers 12 p1817 A72-28181

Contact potential difference effects on lubricant film thickness in electronic equipment joints, noting molecules orientation in electric field 13 p1930 A72-29052

Apiezone lubricants physicochemical properties comparison, noting aromatic hydrocarbons effect on thermo-oxidation stability and polyisoprene rubber type polymer additive effect on adhesiveness 16 p2413 A72-33171

Complex Ca lubricants strength, colloidal and mechanical stability and thermal hardening relationship to dispersion medium viscosity 16 p2413 A72-33172

Antioxidant additives effect on chemical stability and rheological properties of silica gel lubricants with SU type mineral oil dispersion medium 16 p2413 A72-33173

Plane-strain compression of rigid plastic material between flat platens, approximating frictional boundary conditions by entrapped viscous fluid lubricant 16 p2428 A72-34171

Influence of the polarity of the dispersive medium on the structure and properties of plastic lubricants 17 p2571 A72-35176

Damping characteristics of a liquid squeeze film. 18 p2683 A72-37053

IR-spectroscopic investigation of the effectiveness of oxidation inhibitors in lubricants 19 p2823 A72-38092

LUBRICATING OILS

Oil pumping ability of tapered roller bearing, using boundary layer theory [ASME PAPER 71-LUB-21] 02 p0236 A72-11541

Engine lubrication under cold weather conditions, discussing polymer thickened and synthetic oils, automotive and industrial gear oils, hydraulic oils and lubricating greases 03 p0363 A72-13450

Lubricating mixtures of mineral oil with inorganic phosphates, hydroxides and sulfides, discussing lubrication mechanism and physical properties 06 p0837 A72-18603

Laboratory evaluation of engine oils, transmission lubricants and hydraulic fluids utilization in hydraulic power transmission systems 08 p1192 A72-21635

Antiwear properties of mixed anhydrides of alkyl xanthogene and phosphorus containing acids for use as oil lubricant additives 09 p1336 A72-22499

Thickening properties of butoxyacrosil products of butyl alcohol vapor and silicon dioxide surface reactions for use as oil lubricant additives 09 p1336 A72-22500

Ball bearing rolling contact lubricating oil film thickness theoretical prediction compared with experiment 09 p1318 A72-22850

Ball bearings lubricated with oils and fire-resistant fluids, testing fatigue life relationship to steel quality, fluid film thickness and viscosity 12 p1816 A72-28108

Antioxidative and antiwear action of S-containing and S-free phosphoric acid ester additives in lubricating oils 12 p1835 A72-28201

Machine oil wear degree and Fe content determination by placing sample into induction coil and measuring coil Q at RF 13 p1957 A72-29142

Negative slip reversal effect formation mechanism during friction, discussing elimination via oleic acid as lubricant additive 17 p2559 A72-34663

Derivative graph method of thermal analysis for lubricating oils 17 p2571 A72-35180

Unbalanced shafts vibration and stability characteristics, considering elastic and damping properties of sliding bearings oil films 18 p2731 A72-36069

A method for the study of wear particles in lubricating oil. 19 p2803 A72-38376

Fuels, lubricating oils and hydraulic fluids for supersonic aircraft, discussing chemical properties, propellant combustion efficiency and production 20 p2945 A72-39930

Developing a synthetic turbine oil. 23 p3306 A72-43810

LUBRICATION

NT BOUNDARY LUBRICATION

NT SELF LUBRICATION

NT SPACECRAFT LUBRICATION

Graphite and molybdenum disulfide surface and lubricating properties, examining basal plane proportion relationship with edge sites 02 p0236 A72-12847

Sputtered molybdenum disulfide film lubrication, discussing adherence to metal surfaces, particle size, friction experiments and tensile tests 02 p0236 A72-12848

Engine lubrication under cold weather conditions, discussing polymer thickened and synthetic oils, automotive and industrial gear oils, hydraulic oils and lubricating greases 03 p0363 A72-13450

Lubrication and friction problems regrouping in thin viscous fluid films mechanics 03 p0364 A72-14271

Non-Newtonian real fluids flow characteristics, determining stress-deformation relationship by tensor analysis, with application to lubrication theory 04 p0528 A72-15742

MHD squeeze film lubrication between electrically conducting parallel plates, showing graphically approach time under magnetic field in free space 05 p0665 A72-16031

Lubricating action of sulfur-containing additives and chlorine compounds in lubricants and cermet materials, noting effects of iron compounds formation in contact region 07 p0996 A72-19967

Elastohydrodynamic lubrication of soft elastic-deformed contact surfaces, determining lubricant film thickness as function of inlet and outlet parameters 07 p0998 A72-20530

Fuel lubricity effects on aircraft engine fuel pump wear, discussing remedial use of corrosion inhibitors and change to noncorroding pump construction materials 08 p1222 A72-21450

Surface reaction mechanisms analysis in adhesion, friction, wear and lubrication, using electron diffraction, Auger spectroscopy and ellipsometry techniques 12 p1813 A72-27036

Molybdenum disulfide addition effect on compounded model greases lubricating performance, determining oxidation stability, rust preventive behavior and consistency 12 p1832 A72-27047

Resonant contact vibrations of sliding element in direction normal to friction surface, noting lubrication damping effect 12 p1818 A72-28188

Carbon fibers reinforced polymer wear rate decrease in organic fluids associated with films development on steel counterface, noting application in lubricated systems 16 p2397 A72-33124

Molybdenum disulfide lubricating effectiveness due to surface film properties, suggesting chemical reaction effect with sliding metal surface 16 p2397 A72-33125

Tribological properties of gold for electric contacts. 18 p2693 A72-35980

Low inlet pressure performance of gerotor lube and scavenge pumps. 18 p2694 A72-36047

Technological utilization of Weissenberg viscoelastic effect for sliding bearings centripetal pressure lubrication, noting analogy with human and animal skeletal joints lubrication 22 p3183 A72-42875

LUBRICATION SYSTEMS

Lightweight low pressure plastic hose assemblies in aircraft and missile petroleum base fuel and synthetic lubricating oil systems at 395-710 R and up to 200 psi [SAE ARP 1180] 01 p0006 A72-10388

Full lubrication characteristics, discussing pressure pump, viscosity, MHD, volume elasticity, centrifugal and rheodynamic techniques 03 p0365 A72-14299

Molybdenum disulfide lubricating film and wear-in study by scanning electron microscopy and testing machine 06 p0836 A72-18586

Lubrication system filtration effects on rolling element bearing life and extended mean time to failure of gas turbine engines 07 p1052 A72-18754

Hydrodynamically lubricated mechanical seal design, predicting duty variation effects on performance 08 p1179 A72-21942

Mathematical model for derivation of asperity or metal-metal contact load sharing of lubricated machine components in journal and roller bearings 09 p1317 A72-22248

Elastohydrodynamic lubrication - Conference, Leeds University, England, April 1972 12 p1816 A72-28107

- Combined centrifugal oil filter, pump and deaerator for gas turbine engine lubrication systems, noting heat transfer effectiveness increase 18 p2694 A72-36050
- Lubrication with solids. 19 p2807 A72-37771
- Non-linear rotor bearing behavior. 21 p3061 A72-41518

LUCITE [TRADEMARK]

U POLYMETHYL METHACRYLATE

LUDER BANDS

U PLASTIC DEFORMATION

U YIELD POINT

LUGS

- Fatigue strength and fail-safe aspects of lug joint in aircraft structures, considering tension-compression load, fretting corrosion, prestress and residual stress 22 p3239 A72-42851

LUMBAR REGION

- Synaptic mechanisms of vestibulospinal and reticulospinal effect on transmission to lumbar motoneurons in monkeys 02 p0158 A72-11760

LUMBERING AREAS

U FORESTS

LUMINAIRES

NT AIRCRAFT LIGHTS

NT AIRPORT LIGHTS

NT ARC LAMPS

NT FLASH LAMPS

NT MERCURY LAMPS

NT QUARTZ LAMPS

NT RUNWAY LIGHTS

NT XENON LAMPS

- Efficiency of pulsed tubular pumping lamps made of quartz glass investigated by active element luminescence measurement, noting dependence on current density 15 p2246 A72-31425

- Comparative studies of various spectral lamp designs for atom-absorption analyses and use of double-discharge multiple element lamps to account for non-selective interference 22 p3176 A72-42170

LUMINANCE

- Human visual system multiple channels sensitivity to patterns at low luminance or high drift rates, noting retinal ganglion cells selective sensitivity 06 p0761 A72-17602

- Dark adaptation with logarithmically time decreasing background luminance, noting threshold time lag variation with rate of background change 07 p0930 A72-19827

- Achromatic and chromatic thresholds during dark adaptation against varying background luminances, noting trend change at transition from cone to rod function 07 p0930 A72-19828

- Visual latencies measurement as function of stimulus luminance and adaptation state by stereoscopic null method, characterizing relationship by inverse power function 13 p1911 A72-29968

- Matched luminance chromatic stimuli wavelength effects on human visual latency 14 p2074 A72-30267

- Effect of target-background luminance contrast on binocular depth discrimination at photopic levels of illumination. 17 p2508 A72-34879

- Mach band measurement by psychological compensation technique, causing band disappearance by changes in stimulus pattern luminance and brightness distribution relations 19 p2760 A72-37827

- Spatial interaction with different-diameter stimuli matched on the basis of threshold, luminance, or total luminous flux. 21 p3004 A72-40152

- Perceptual latency as a function of stimulus onset and offset and retinal location. 23 p3258 A72-44386

LUMINESCENCE

NT BIOLUMINESCENCE

NT CHEMILUMINESCENCE

NT ELECTROLUMINESCENCE

NT FLUORESCENCE

NT LUNAR LUMINESCENCE

NT OPTICAL RESONANCE

NT PHOSPHORESCENCE

NT PHOTOLUMINESCENCE

NT SHOCK WAVE LUMINESCENCE

NT THERMOLUMINESCENCE

NT X RAY FLUORESCENCE

- Materials remote active sensing from ground, air and space by UV and visible laser induced luminescence, using excitation and emission spectral specificity for species identification 02 p0225 A72-11822

- Amorphous polymer dielectric luminescence and destruction under Q switched laser radiation with subthreshold power and picosecond pulses 03 p0369 A72-14071

- Isothermal annealing measurements of zero-phonon line luminescence at 0.97 eV in electron irradiated Si, obtaining activation energy 04 p0560 A72-14546

- Spectral heterogeneous lasing media with asymmetric luminescence bands, considering neodymium phosphate and germanate glass 06 p0824 A72-17392

- Ionization mechanisms of quiescent prominence of He II 4686 line luminescence under coronal UV radiation at high temperatures 07 p1077 A72-19812

- Spectroluminescent and lasing properties of Nd ions in anisotropic scheelite crystal structures 07 p1007 A72-20121

- Quantum yield of ruby crystals luminescence for excitation in UV region, noting Cr concentration effect 10 p1490 A72-24043

- Automated scanning spectroradiometer for color vision test stimuli and luminescence measurements, applying computer analysis of spectral data 12 p1811 A72-27944

- Recombination luminescence in irradiated Si, investigating uniaxial stress and temperature variations effects 12 p1858 A72-28061

- Recombination luminescence in irradiated Si, investigating thermal annealing and Li impurity effects 12 p1858 A72-28062

- Electron radiation damage and edge emission of cadmium telluride, presenting cathodoluminescence spectra 12 p1859 A72-28071

- Asymptotic and exact methods for light scattering problems in radiative transport theory, discussing finitely thick plane layer luminescence 13 p2001 A72-28503

- Laplace transform method in unsteady radiation field theory, discussing generalization from steady luminescence to inhomogeneous media and forbidden band frequency radiative transport 13 p2001 A72-28506

- Stimulated luminescence in activated Nd glass by pulsed laser radiation at 1060 nm wavelength 13 p1969 A72-29519

- GaAs doped Si light emitting diode as light source for optical timing system calibration, studying fast luminescent decay characteristics 13 p2000 A72-29763

- Semiconducting glass filter time dependent transition, absorption coefficient and luminescent spectral dependences, using monolayered ruby laser 13 p1971 A72-29909

- Green luminescence intensity dependence on lasing power during two-photon excitation of Er and Ho ions in calcium difluoride by neodymium laser 15 p2246 A72-31422

- Efficiency of pulsed tubular pumping lamps made of quartz glass investigated by active element luminescence measurement, noting dependence on current density 15 p2246 A72-31425

- Luminescence behavior of single-crystal semiconductor compounds under electron bombardment 17 p2596 A72-35721

- Photometric observations from sounding rockets - Selection of horizontal sightings 19 p2789 A72-37784

- Some results of studies of cathode luminescence in cerium-activated glass 19 p2845 A72-38190

- Uranyl fluoride crystals luminescence spectrum study, calculating anion normal vibration frequencies 20 p2960 A72-39413

- Influence of cerium additions on the luminescence of europium and samarium ions in NaF single crystals 20 p2932 A72-39414

- Mechanism and controlling factors of infrared-to-visible conversion process in Er³⁺ and Yb³⁺-doped phosphors. 21 p3096 A72-40186

- Light scattering by the medium created by a spacecraft. I - Luminescence of the gas jets of the spacecraft microthrusters 22 p3230 A72-42216

- Simultaneous recording of laser radiation and signal related to secondary processes, using ruby luminescence for oscillograph triggering 22 p3185 A72-42274

- Variation of the output of radioluminescence of organic scintillators with energy loss and the number of charges of ionizing particles 22 p3180 A72-42938

- Profile of a parametric luminescence line emitted by lithium niobate crystals. 24 p3432 A72-45614

LUMINESCENT INTENSITY

U LUMINOUS INTENSITY

LUMINOSITY

NT STELLAR LUMINOSITY

- N galaxies and quasars properties comparison, suggesting continuous distribution and luminosity function 04 p0578 A72-15285

- Meteor count by naked eye and binocular visual observation in Crimea, obtaining luminosity functions 06 p0881 A72-17932

- Radial velocity effects on diameter and luminosity functions of dwarf galaxies 06 p0883 A72-18019

- Laser flare luminosity front displacements and atom density at surfaces of transparent dielectrics as function of pulse intensities 07 p1007 A72-20123

- Quasars as cosmological and local objects, considering red shift origin and optical and radio luminosities comparison with galaxies 10 p1541 A72-24522

- Zero-pressure universe model parameters from red shift and apparent magnitude data for clusters of galaxies 10 p1545 A72-24809

- Radial velocity effects on diameter and luminosity functions of dwarf galaxies 11 p1718 A72-25955

- Luminosity distribution in plane of image produced by radiation from plane parallel plate, taking into account rays real path 13 p1955 A72-28498

- Luminous molecular absorption cross sections in aeronomy, considering photodissociation, actinic solar radiation attenuation and UV to IR analysis 14 p2097 A72-30135

- Spectral index-luminosity relation for radio galaxies and quasi-stellar sources with power law spectra 15 p2315 A72-32714

- Meteor count by naked eye and binocular visual observation in Crimea, obtaining luminosity functions 18 p2730 A72-37157

- Finite sized optically thin radiating plasma stability analysis, deriving luminosity function for metastable state existence from mathematical model 20 p2958 A72-39456

- Gross properties of five Scd galaxies as determined from 21-centimeter observations. 21 p3105 A72-41027

- A photoelectric study of Messier 81. 22 p3229 A72-42975

LUMINOUS FLUX DENSITY

U LUMINOUS INTENSITY

LUMINOUS INTENSITY

NT ILLUMINANCE

NT LUMINANCE

- Asymptotic intensity fluctuations of plane light wave propagating in turbulent medium, using parabolic equation and Markov model 01 p0050 A72-10348

- Luminosity function at 400 and 2700 MHz of radio galaxies in Parkes Catalog, discussing optical and radio flux densities 01 p0131 A72-11004

- Critique on luminosity volume test for quasars, considering space distribution and luminous function 01 p0133 A72-11126

- Quasar model proposal as giant pulsar rejected discussing mass, radius, magnetic field strength, luminosity and gamma radiation 01 p0134 A72-11144

- Light emission intensity correlation functions associated with If oscillations in beam plasma discharge 02 p0263 A72-11421

- Martian equatorial zone brightness distribution formula, noting agreement with observations near zero phase and 6-45 deg phase angles 02 p0282 A72-12328

- Jovian disk brightness distribution at zero phase angle by expanding scattering indicatrix in Legendre polynomial series 02 p0282 A72-12329

- Diffuse galactic light absolute intensity interpretation, showing interstellar dust discrete cloud structure effect on grain properties determination 03 p0416 A72-13015

- He production from H to maintain Galactic luminosity, discussing interstellar gas enrichment 03 p0419 A72-13116

- Seeing effects on light curve of stellar occultation by moon, calculating limitation on angular resolution 03 p0420 A72-13131

- Magnetic and velocity fields and brightness in solar atmosphere, using double magnetograph 03 p0429 A72-13309

- Photopic spectral curves of relative luminous efficiency for congenital deficiencies of color vision, using optical bench, interference filters and Bachstein flicker photometer 03 p0316 A72-13935

- Ishihara charts readings in artificial daylight at low color temperatures, low light intensity and limited exposure time by normal and color defective subjects 03 p0317 A72-13939

- Telescopic meteors light curves, showing maximum point brightness distribution in visible trajectory with respect to stellar magnitudes 03 p0438 A72-13985

- Starlight intensity modulation at discrete radio frequencies due to enhanced ionospheric electron density fluctuations 03 p0438 A72-14096

Optical search for Ryle-Neville radio sources, discussing cosmological model constraints and quasar and radio galaxies optical and radio luminosity functions

04 p0570 A72-14549

High stability electrodeless discharge lamps with less than 0.1 percent intensity variation, discussing construction and quality control procedures

04 p0509 A72-15485

Two mode lasers with photon intensity coupling near threshold treated by fluctuation theory detailing intensity, correlations and line widths

05 p0667 A72-16017

Charged particles injection effects on magnetic perturbations relation to integral auroral luminance intensity from whole sky photometry measurements

05 p0658 A72-16277

Light fluctuations of quasars in Harvard historical plate collection

05 p0716 A72-16375

Hubble parameter derivation for regions beyond local anisotropy, discussing cluster galaxies magnitude-red shift diagram

05 p0717 A72-16380

Virgo cluster galaxies evolutionary sequence in radial velocity-nuclear magnitude diagram in terms of morphology, radial color variations, nuclear size and radio emission

05 p0717 A72-16382

Intensity variations of CN photospheric and K line chromospheric network with time

05 p0718 A72-16505

Solar wind velocity correlation with 5303 A coronal intensity

05 p0710 A72-16523

Illumination effect on proton and gamma irradiated cabbage plant growth, height and foliage, indicating radiation protective effect for certain light intensities

05 p0622 A72-16649

Plasma line enhancement variabilities in ionospheric modification experiments due to radar wave scattering, number density gradient and diagnostic beam temperature and orientation

06 p0805 A72-17470

Asteroid diameters and absolute magnitude distributions, noting characteristics, methods of calculation and hypotheses

06 p0875 A72-17494

Quasar luminosity due to unique big bang in specific space-time region, considering Minkowski geometry

06 p0878 A72-17669

Pulsar long term intensity variations due to intrinsic structure or propagation effects

06 p0878 A72-17670

Light intensity distribution from ultrasonic surface waves reflection to probe surface acoustic propagation characteristics

06 p0848 A72-17851

Powder combustion rate dependence on light irradiation intensity

06 p0902 A72-17908

Southern globular clusters /NGC 6362 and NGC 6752/ photometric standards, stellar photographic and color-magnitude diagrams

07 p1069 A72-19076

Self focusing of laser amplifier beam with Gaussian transverse intensity profile, discussing sample length and beam diameter, convergence and divergence

07 p0941 A72-19240

Seyfert galaxy hypothesis with galactic center containing hot gas region with density decreasing toward boundary, discussing nucleus brightness variability

07 p1075 A72-19560

Supraluminous wave instability in weakly turbulent plasmas, using Vlasov equations

07 p1043 A72-19619

Resolution dependence on coherent properties of light source for aberration free annular aperture operating in partially coherent light, presenting composite intensity curves

07 p1008 A72-20545

Tago-Sato-Kosaka comet isophote picture of 5 February 1970, noting tail composition, photographic magnitude and emission spectrum

08 p1229 A72-20831

N Her 1963 distance, absolute magnitude, stellar mass and explosion-ejected shell mass, using maximum and relative intensity calculation methods

08 p1229 A72-20840

Intense discrete extragalactic radio source counts at 1400 MHz, noting number-flux density relation and separation dependence of surface brightness

08 p1233 A72-21213

Quasars and optical quasi-stellar galaxies comparisons for red shifts and luminosities distributions

08 p1234 A72-21283

Biological hazards of high intensity light sources, considering physiological factors involved in threshold eye damage values determination

08 p1125 A72-21333

Continuous chemical laser optimum optic axis position for maximum multimode power operation and intensity distribution

08 p1182 A72-21557

Correlation radius of intensity fluctuations of light beam focused in turbulent atmosphere

08 p1135 A72-21733

Quasi-stellar radio sources spectroscopic and photometric observations, determining spatial distribution and bivariate radio and optical luminosity function

09 p1382 A72-22279

German monograph on luminous intensity amplification by means of solid state lasers covering experiments with GaAs and ruby lasers and traveling wave amplifiers

09 p1322 A72-22331

Quasar redshift distribution and optical and radio luminosity functions analysis

10 p1534 A72-23904

Red shift-absolute magnitude relation for uniform time-dependent universe expansion rate suggesting large scale clustering modifications based on light propagation model

10 p1545 A72-24810

Brightness estimates of Markarian galaxies on photographic plates, measuring light variation amplitude

10 p1546 A72-24831

Foveal luminosity magnitude estimations validity, measuring relative effects of preadaptation and contrast

10 p1427 A72-25179

Flicker adaptation, discussing intermittent lights effect on apparent brightness

10 p1427 A72-25181

Compact galaxies morphology and related properties from blue and red prints of Palomar Sky Survey, correlating to color and apparent magnitude

11 p1717 A72-25902

Laser light intensity relationship to temperature distribution in completely ionized plasma, defining optimal heating conditions

11 p1696 A72-26342

Inclination and absorption effects on galaxies apparent diameters, optical luminosities and neutral atomic hydrogen radiation

11 p1724 A72-26725

Airport lights systems control with thyristors, discussing light intensity regulation, command board design and insulation test equipment

12 p1794 A72-27401

Laser irradiance modulation effect on high error fringes brightness in time average hologram reconstruction, noting exposure time increase

12 p1809 A72-27682

High brightness picosecond light pulses generation by laser with multiple internal reflection amplifier for plasma heating

12 p1824 A72-27872

Diffraction antenna use in visual range to study troposphere modulated laser radiation propagation in turbulent atmosphere, presenting light intensity distribution

13 p1917 A72-28690

Martian equatorial zone brightness distribution formula, noting agreement with observations near zero phase and 6-45 deg phase angles

13 p2039 A72-29212

Jovian disk brightness distribution at zero phase angle by expanding scattering indicatrix in Legendre polynomial series

13 p2039 A72-29213

Visibility function change of low red shift radio galaxy 3C 120 from interferometer observations, noting high speed expansion

13 p2041 A72-29418

Illumination intensity effects on circadian periodicity and behavioral thresholds in Rhesus monkey, demonstrating exception to Aschoff rule

13 p1906 A72-29844

Total line intensities interpretation from optically thin gases, considering matter partitioning bivariate distribution function and chemical composition

13 p2008 A72-29930

Visible light flash emission due to strong shock wave of laser spark, investigating strong external magnetic field effect and time variation of luminous intensity

13 p1972 A72-29983

Free carrier mobility dependence on excitation light intensity in CdSe single crystals with negative photoconductivity

14 p2141 A72-30169

Light intensity and linear polarization for single scattering by ice clouds in visible and IR, approximating crystals with long circular cylinders

14 p2128 A72-30349

Green luminescence intensity dependence on lasing power during two-photon excitation of Er and Ho ions in calcium difluoride by neodymium laser

15 p2246 A72-31422

Foveal light pulse duration effects on reaction time, showing stimulus intensity-time reciprocity

15 p2188 A72-31509

Daytime zodiacal light intensity and polarization measurement at elongation angles between 15-30 degrees from Skylark rocket photometric observations

15 p2227 A72-31951

V/Vm insensitivity to red shift random shuffling based on luminosity function in Einstein-de Sitter cosmological model

15 p2314 A72-32375

Photometric, photographic and spectroscopic observations of Seyfert galaxies NGC 1068 and 1566, noting nuclear luminosity and surface brightness

15 p2315 A72-32713

Radio source Oj 287 photometric and polarimetric observations, noting optical intensity and plane polarization variability

16 p2452 A72-33134

Focused light beam intensity fluctuations measurement during passage through turbulent atmosphere, discussing random walks effects on dispersion

16 p2364 A72-33494

High brightness picosecond light pulses generation by laser with multiple internal reflection amplifier for plasma heating

16 p2403 A72-33981

Light induced alterations in growth pattern of the avian eye.

17 p2500 A72-34880

Clustering properties of the luminosity function in galactic globular clusters.

18 p2723 A72-36091

Luminous intensity, visibility duration, condensation nuclei and mass balance of noctilucent clouds

18 p2686 A72-36504

Radio galaxies monochromatic luminosity-spectral index relationship from 3CR spectra studied at 10 MHz to 10,700 MHz

18 p2726 A72-36621

Earth magnetosphere pinch effect related to geomagnetic field pulsations and polar aurora luminosity fluctuations

18 p2688 A72-36867

The determination of diffusion coefficient for Na in dc arc plasma by measurements of intensity distribution of emitted light.

18 p2716 A72-36959

On the ability of the luminosity-volume test to reveal the statistical evolution of the luminosity of quasi-stellar sources.

19 p2854 A72-37226

The correlation of redshift with magnitude and morphology in the coma cluster.

19 p2854 A72-37228

Luminance profiles photometry for axisymmetrical propagation in propane-air turbulent flow combustion with turbulence level control in jet core

19 p2879 A72-37366

Absolute magnitudes of E and S0 galaxies in the Virgo and Coma clusters as a function of U-B color.

20 p2965 A72-38902

Atmospheric turbulence induced optical effects due to refractive index fluctuations, solving Maxwell equations for instantaneous intensity distribution function

20 p2948 A72-39055

Discrimination sensitivity and black light density in the mesopic range

21 p3007 A72-40735

Spectral sensitivity after prolonged intense spectral light exposure of rhesus monkey corneas, demonstrating long term loss of cone photopigment response

21 p3000 A72-40739

Corrugated image screens advantages over flat screens, determining light intensity per corrugation, maximum viewing angle and reflection factor

21 p3055 A72-40743

Statistical studies of the evolution of extra-galactic radio sources. I, II, & III.

21 p3105 A72-41026

Gravitational deflection of light by radially and cylindrically symmetric masses, considering effect on apparent luminosity of distant object

22 p3204 A72-42000

Skylight intensity, polarization and airglow measurements during the total solar eclipse of 30 May 1965.

22 p3170 A72-42371

Brightness and polarization structure of four supernova remnants 3C58, IC443, W28, and W44 at 2.8 centimeter wavelength.

22 p3224 A72-42382

Extragalactic object categorization according to IR luminosities, considering radiation mechanism models and IR spectra relation to radio spectrum

22 p3228 A72-42571

Observations of the airglow continuum.

22 p3174 A72-42888

German monograph - A hologram interferometer for the determination of amplitude and phase of optical excitation in diffraction patterns.

22 p3181 A72-43056

Determination of the optimum concentration level of solar radiation in solar batteries with different types of cooling

22 p3140 A72-43189

Nature of polar-aurora light intensity pulsations associated with Pi2-type geomagnetic pulsations

23 p3282 A72-43359

Characteristics and measurements of an aperture-limited in-line hologram image.

23 p3288 A72-43886

- GaAs light emitting diodes intensity fluctuations measurements at 0.25-20 kHz 23 p3297 A72-44190
- Fluorescent organic dyes solutions for Nd:YAG laser output performance improvement 23 p3297 A72-44191
- Coronal lines photometry systematic error dependence on aureola spectral intensity, line half width, gradation curve slope, and neutral filter transmission coefficient 23 p3340 A72-44240
- Influence of the heating of a turbulent atmosphere by a light beam on the fluctuations of the beam intensity. 24 p3425 A72-45601
- Linear corrector for laser beam intensity distribution transformation into random distribution with rectangular envelope, noting uniform energy distribution result of spatial fluctuations averaging 24 p3411 A72-45608
- Statistical analysis of comet observations, calculating relationships between comet head angular diameter and heliocentric and geocentric distances and apparent brightness 24 p3448 A72-45687
- LUMPING**
- Lumped approximation to distributed RC notch networks for linear IC, deriving open circuit voltage transfer functions and root locus graphs 14 p2092 A72-31170
- Nodal equations derivation for lumped circuit representation of Gunn diode with steadily propagating domain under steady state and transient conditions 15 p2205 A72-31317
- LUNAR ATMOSPHERES**
- Lunar mass spectrometer experiment, determining global distributions and diurnal variations of lunar atmosphere 04 p0509 A72-15103
- Neutral gases density and flux distribution in lunar atmosphere, using kinetic theory of gases 11 p1722 A72-26394
- Lunar surface neutral gas pressure measurement by Apollo 14 cold cathode ionization gage, determining day and night temperature effects on vacuum quality 12 p1805 A72-27041
- Suprathermal ion detector measurements on lunar surface by Apollo 12 and 14 astronauts to provide search for lunar exosphere phenomena 15 p2301 A72-32092
- Lunar volcanic gas release rate estimation from orbiting Apollo spacecraft-borne mass spectrometer detection, noting atmospheric perturbation 19 p2868 A72-38736
- Equilibrium lunar atmospheric content of radon-222, noting earth based diffusion constants inapplicability in moon vacuum conditions 20 p2972 A72-39861
- LUNAR BASES**
- Permanent manned lunar stations electrical power systems, discussing nuclear energy, solar cells and electrochemical power cells 15 p2214 A72-31814
- Lunar horticulture possible role as life support system of earth independent lunar colony 17 p2505 A72-35938
- R and D on environmental and thermal control/life support system application to lunar base mission, discussing reliability and food regeneration 24 p3375 A72-45164
- System design of a near-self-supporting lunar colony. 24 p3388 A72-45192
- Implications of new transport vehicles and cost analysis of supplying and maintaining a manned lunar laboratory. 24 p3441 A72-45209
- LUNAR CINEMATOGRAPHY**
- LUNAR PHOTOGRAPHY**
- LUNAR COMMUNICATION**
- Lunar crust exploration by vlf electromagnetic surface waves, discussing frequency dependent depth penetration, conducting layers detection and communication or navigation use 03 p0436 A72-13821
- Electromagnetic-thermal properties of lunar surface layers for radio communication around moon 04 p0577 A72-15121
- Investigation of the redundancy of telemetry information from the automatic lunar stations Luna 9 and Luna 13 21 p3014 A72-40312
- LUNAR COMPOSITION**
- NT LUNAR CORE**
- Glass compositions in Apollo 14 soil, discussing correspondence to Fra Mauro basalts, mare basalts and soils, and gabbroic anorthosite and potash granite 01 p0123 A72-10054
- Apollo 11 and 12 lunar soil samples, calculating mixing models by least squares and end member groups by Q mode factor analysis 01 p0124 A72-10057
- Apollo 14 lunar soil sample 14163 orthopyroxene composition, determining K, P and rare earth elements 01 p0125 A72-10066

- Apollo flight lunar spinels compositional variations, formulating modified Johnstone prism projections 01 p0134 A72-11162
- Critique of paper by Ringwood on petrogenesis of Apollo 11 lunar basalts composition and implications for lunar origin 02 p0275 A72-11600
- Apollo 11 and 12 rock samples depth profiles for Al, Na, Mn, S, V, Ca, P, Co, Fe, Cu and Sc isotopic contents, estimating solar proton flux 02 p0282 A72-12327
- Apollo 12 lunar soil samples solar wind noble gas analysis of KREEP fragments, estimating Surveyor Crater age 03 p0414 A72-12902
- Lunar structure and evolution from mineral composition, density, gravity, magnetic and heat measurements and seismic events 03 p0440 A72-14303
- Carbon chemistry of moon based on lunar samples analysis 04 p0573 A72-14807
- Lunar ejecta and meteorites experiment, determining speed, direction, mass and flux density of cosmic dust particles 04 p0509 A72-15102
- Lunar mineral resources from analyses of moon samples, discussing solar cell and vacuum process manufacturing 05 p0722 A72-17099
- Lunar surface rocks, soil and breccia chemical composition, discussing element concentration, radiation effects on surface chemistry and volcanism 06 p0887 A72-18226
- Earth and moon chemical composition differences based on model of lunar formation from circumterrestrial swarm of particles and larger objects 07 p1077 A72-19820
- Carbon compound distribution on moon from Apollo 11 samples, comparing with earth data 08 p1120 A72-22013
- Lunik 16 microbasalt sample containing skeletal olivine, plagioclase, ilmenite and interstitial pyroxene, comparing to ferromagnesian rich Apollo 11 and 12 basalts 09 p1379 A72-22258
- Electron microprobe analyses of Lunik 16 mare basalt fragment G37 with high Al and low Mg content, discussing fragments G46 and G51 09 p1380 A72-22260
- Mass spectroscopic measurement of inert gases in Lunik 16 fragments and dust samples 09 p1380 A72-22267
- Neutron capture effect on isotopic composition variations of Sm in Apollo lunar samples, comparing with terrestrial abundance 10 p1537 A72-24156
- Lunar basalt Eu abundance anomaly in Apollo 11 and 12 samples, considering partial melting with or without plagioclase 10 p1537 A72-24162
- Gas rich meteorites and lunar materials solar rare gases component observed and predicted relative abundance agreement indicating absence of fractionation in solar nebula formation 11 p1721 A72-26118
- Apollo 12 and 14 lunar soils K, Rb and Sr isotopic composition evaluation, noting microbreccia as major nonbasaltic constituent 11 p1723 A72-26497
- U, Th, Pb and rare earth elements abundances and Pb 207/Pb 206 ages of Apollo lunar minerals by ion microprobe mass analysis 12 p1866 A72-27114
- Apollo 15 lunar heat flow experiment, discussing temperature data from probes and long lived radioisotopes decay effects 12 p1869 A72-27332
- Apollo 11 and 12 rock samples depth profiles for cosmogenic Al, Na, Mn, S, V, Ca, P, Co, Fe, Cu and Sc isotopic contents, estimating solar proton flux 13 p2039 A72-29211
- Lunar interior temperature profile estimation from electrical conductivity distribution based on forsteritic olivine composition 14 p2153 A72-30505
- Thermal history, heterogeneity, refraction and transition phenomena of lunar glassy fragments and spherules, using electron microprobe analysis 15 p2306 A72-31586
- Lunar interior structure and crust composition from artificial impact data recorded by Apollo seismometers 15 p2314 A72-32377
- Electron spectroscopy for chemical analysis /ESCA/ technique for nondestructive elemental analysis of lunar and terrestrial minerals 16 p2454 A72-33447
- Diopside and Cr-Zr-armalcolite occurrence on moon from Apollo 14166.6 fines, using petrographic and electron microprobe examination 16 p2461 A72-34163
- Lunar composition as a clue to the early history of the solar system. 17 p2614 A72-35678

- Earth and moon chemical composition differences based on model of lunar formation, from circumterrestrial swarm of particles and larger objects 17 p2618 A72-35745
- A new, earth-based radar technique for the measurement of lunar topography. 18 p2659 A72-36277
- Evidence for objects of lunar mass in the early solar system. 18 p2724 A72-36284
- Lunar surface mapping for Mg, Al and Si along ground tracks swept out by orbiting Apollo 16 spacecraft, noting geochemical X ray fluorescent analysis 18 p2726 A72-36556
- Apollo and terrestrial geochemical samples examination for indigenous amino acids distribution and optical configuration, stressing close monitoring of contamination sources 19 p2762 A72-37648
- In-situ geochemical analysis of Martian and lunar composition via alpha particle activation technique, discussing Surveyor instrument performance 20 p2899 A72-39828
- Neutron activation and mass spectrometry methods for geochemical analysis of rare earth elements in meteoritic, lunar and terrestrial materials 20 p2899 A72-39835
- Highly aluminous glasses in lunar soils and the nature of the lunar highlands. 21 p3104 A72-40490
- Lunar thermal history model, considering nonuniform initial composition, radioactive element partitioning and melt cutoff value 22 p3225 A72-42529
- Lunar interior composition constraints from chemical composition of igneous rocks on surface 22 p3226 A72-42533
- Lunar ultramafic glasses, chondrules and rocks. 23 p3340 A72-44340
- Lunar composition in terms of evolutionary mode based on inhomogeneous planetary accretion and high temperature condensation 24 p3439 A72-44977
- Chemical composition of Luna 16 and Luna 20 rock samples from Sea of Fertility and Apollonius Crater 24 p3440 A72-45109
- LUNAR CORE**
- Mars and moon cores elastic properties inferred from hydrostatic equilibrium based on observed data for total mass, radius and moment of inertia 13 p2048 A72-29809
- Lunar core-crust conductivity models compatibility with lunar surface field/interplanetary magnetic field transfer function from Apollo 12 magnetometer data 14 p2153 A72-30502
- Lunar interior temperature profile estimation from electrical conductivity distribution based on forsteritic olivine composition 14 p2153 A72-30505
- Lunar interior electrical conductivity from surface magnetic field measurements by Apollo magnetometers, calculating temperature profile for olivine moon model 14 p2154 A72-30508
- Internal structure dynamics of earth, moon and planets, showing density variation and bulk modulus as function of pressure with correction of Bullen hypothesis 16 p2461 A72-34176
- Physical structure of the moon. 17 p2615 A72-35680
- Thermoluminescence lunar samples - Measurement of temperature gradients in core material. 18 p2724 A72-36278
- Lunar electrical conductivity. 18 p2729 A72-37000
- Moon model - An offset core. 20 p2969 A72-39374
- Dynamo theory for lunar magnetic field based on hypothetical thermal convection in rotating moon core analogous to earth 23 p3341 A72-44448
- LUNAR CRATERS**
- NT TYCHO CRATER**
- Lunar crater population and distribution time development under meteoroid and solar wind bombardment, developing model for absolute formation ages 01 p0124 A72-10056
- Height-depth ratios of lunar craters and terrestrial calderas from topographic measurements 02 p0278 A72-11908
- Apollo 12 lunar soil samples solar wind noble gas analysis of KREEP fragments, estimating Surveyor Crater age 03 p0414 A72-12902
- Apollo mission profiles, discussing lunar landings, craters, evolution, samples and spacecraft instruments and hardware improvements 03 p0418 A72-13106
- Lunar craters and maria origin from rock and sample chemical composition and magnetic differentiation 03 p0439 A72-14302

Rille Rima Goclenius II formation, describing fractures mechanisms

04 p0571 A72-14563

Lunar seas small craters morphology from Soviet Lunar Rover panoramic picture data, suggesting impact-explosion formation mechanism

04 p0576 A72-15064

Lunar surface small crater statistical analysis and age prediction based on density and diameter correlation from Soviet Lunar Rover panoramic pictures

04 p0576 A72-15065

Brightness temperatures and directionality of IR emission from rough lunar surface of crater field

05 p0714 A72-16104

Small lunar maria craters morphological maturity as function of age and dimensions

05 p0722 A72-17041

Papers on moon geology and physics covering lunar volcanic lava flow, water and crater origin

06 p0886 A72-18216

Recent moon exploration, discussing Ranger and Lunar Orbiter photographs for crater and volcano studies and landing site mapping and Apollo program rock studies

06 p0887 A72-18217

Lunar Mare Ibrum lava flow geology and nature, mascon origins and explosive, collapse and impact mechanisms for small crater origin

06 p0887 A72-18218

Tycho, Aristarchas and neighboring small craters volcanic origin, discussing inner and outer rim lava flows and impact crater resemblance

06 p0887 A72-18221

Lunar far side crater Tsiolkovsky geology, indicating formation by meteoroid, asteroid or comet impact explosion

06 p0887 A72-18222

Lunar crater origin mechanisms, considering single and multiple meteor impact and volcanic explosions, low velocity excavation, collapse and material emission

06 p0887 A72-18223

Selenographic coordinate system development, using lunar craters as reference point selection criteria

07 p1067 A72-18869

Copernicus rays and ejecta blanket V-features form and distribution, suggesting association with satellite craters of secondary impact origin

07 p1067 A72-18872

Lunar crater tectonic and endogenic origin in maria from Orbiter photographs analysis

07 p1076 A72-19610

Catalog of lunar craters central peaks and floor objects on visible hemisphere based on Kuiper photographic atlas

08 p1236 A72-21476

Reference grid construction for lunar craters in system with scale and orientation independent of other systems, discussing preliminary catalog compilation from lunar photographs

09 p1388 A72-23055

Gosses Bluff impact structure in Central Australia, discussing geologic, seismic, gravity, and magnetic surveys and lunar crater analog

09 p1304 A72-23494

Meteorite flux at lunar surface as function of position and earth-moon distance, applying to crater counting

10 p1531 A72-23703

Lunar and Mars crater genetic similarities, discussing scale dependent effects and post-impact geologic development

10 p1531 A72-23704

Apollo 16 planned mission to moon surface near crater Descartes, describing objectives

10 p1547 A72-24942

Lunar crater region ray systems origin and brightness variation mechanism from surface vitreous spherules examination

11 p1715 A72-25300

Orbiter 4 photographs to update System of Lunar Craters /1966/, cataloging positions, diameters and morphological data

13 p2037 A72-28991

July 1952 polarization change in lunar crater Posidonius from polarimeter observations

14 p2152 A72-30488

Glazed rock fragments and glassy splatter origin in bottom of small lunar craters from Apollo 15 observation

15 p2306 A72-31577

Two phase heating of lunar crust for formation of lava filled Mare Smythii and Tsiolkovsky craters

15 p2313 A72-32198

Lunar surface breccias origin, using exploration data to reappraise ballistic theory of giant craters and maria formation in favor of volcanic concepts

16 p2461 A72-34180

Geometric similitude of lunar and terrestrial craters.

17 p2615 A72-35681

July 1952 polarization change in lunar crater Posidonius from polarimeter observations

19 p2864 A72-38317

Craters formed in mineral dust by hypervelocity microparticles.

20 p2970 A72-39474

Structure of Sierra Madera, Texas, as a guide to central peaks of lunar craters.

21 p3049 A72-41114

Comments on the figure of the moon from Apollo landmark tracking.

22 p3226 A72-42534

Lunar crater origins due to external impact of particles moving within earth-moon gravitational dipole during earliest history stage

22 p3226 A72-42538

Trace element geochemistry of Apollo 16 soil 68501.

23 p3337 A72-43939

Chemical composition of Luna 16 and Luna 20 rock samples from Sea of Fertility and Apollonius C crater

24 p3440 A72-45109

The distribution of craters on the surfaces of the moon and Mars in relation to their origin

24 p3441 A72-45222

LUNAR CRUST

NT LUNAR CORE

Lunar igneous activity and differentiation, discussing volcanic flows near Tycho, flow patterns in maria, sinuous rilles and crust lineaments

03 p0418 A72-13107

Lunar crust exploration by vlf electromagnetic surface waves, discussing frequency dependent depth penetration, conducting layers detection and communication or navigation use

03 p0436 A72-13821

Earth mantle and core density using Monte Carlo models compared with lunar structure from crust and seismology data, noting planetological contrast

04 p0571 A72-14616

Electromagnetic-thermal properties of lunar surface layers for radio communication around moon

04 p0577 A72-15121

Apollo 15 geochemical X ray fluorescence experiment, noting differential lunar highland crust existence

06 p0889 A72-18273

Lunar crust and mantle evolution from Rb-Sr ages of Apollo 15 mare basalt samples

10 p1537 A72-24161

Random walk atomic migration model for radon diffusion through lunar regolith into atmosphere

13 p2038 A72-28995

Lunar core-crust conductivity models compatibility with lunar surface field/interplanetary magnetic field transfer function from Apollo 12 magnetometer data

14 p2153 A72-30502

Lunar crust mass distribution relation to moments of inertia derivation from librations, inferring non-validity of lunar evolution fluid phase hypothesis

14 p2153 A72-30504

Lunar interior electrical conductivity from surface magnetic field measurements by Apollo magnetometers, calculating temperature profile for olivine moon model

14 p2154 A72-30508

Two phase heating of lunar crust for formation of lava filled Mare Smythii and Tsiolkovsky craters

15 p2313 A72-32198

Lunar rock nature and properties from Apollo samples, discussing crust, Fra Mauro, interior, chronology, surface processes and earth-moon environment

15 p2314 A72-32376

Lunar interior structure and crust composition from artificial impact data recorded by Apollo seismometers

15 p2314 A72-32377

Rock size, mineralogy and fines size distribution in lunar regolith

17 p2615 A72-35683

Seismic data from lunar geophysical stations network, noting moonquakes and meteoroid impacts

18 p2724 A72-36283

Velocity structure and properties of the lunar crust.

18 p2725 A72-36292

Lunar electrical conductivity.

18 p2729 A72-37000

Xenon isotope fission component due to extinct Pu-244 in lunar breccia, noting storage details in terms of crustal material dating

20 p2967 A72-39182

LUNAR DUST

Single domain grain distribution deduction method obtained from Neel theory, applying to Apollo 11 lunar dust iron grains

01 p0125 A72-10071

Apollo 12 lunar crystalline rock and fines magnetic properties measurement, noting magnetic minerals composition

02 p0278 A72-12026

Heat conduction model of surface thermal history of moon as function of dust, anorthosite, basalt and dunite layers

04 p0571 A72-14598

Transient lunar phenomena as changes in albedo due to dust movement or fluidization from lunar sample tests

06 p0877 A72-17650

Lunar dust grain fossil coatings of ultrathin metamictized amorphous layers resulting from solar wind ion implantation

08 p1230 A72-20982

Rare gas concentrations in Luna 16 fines, using stepwise heating technique

09 p1380 A72-22266

Mass spectroscopic measurement of inert gases in Lunik 16 fragments and dust samples

09 p1380 A72-22267

Alpha corundum grains from Apollo 11 lunar dust sample, using X ray diffraction and electron microprobe analyses

10 p1536 A72-24152

Lunar seismogram characteristics interpretation in terms of Gold-Soter powder layer theory, taking into account elastic wave scattering by surface undulations

14 p2154 A72-30506

Thermal history, heterogeneity, refraction and transition phenomena of lunar glassy fragments and spherules, using electron microprobe analysis

15 p2306 A72-31586

Ferromagnetic and paramagnetic resonance spectra of lunar material - Apollo 12.

18 p2724 A72-36276

Infrared and Raman spectra of lunar samples from Apollo 11, 12 and 14.

18 p2724 A72-36279

Effect of fluidization on the polarization of reflected light from lunar dust layers.

18 p2729 A72-36987

Ejected lunar particles in meteoric sporadic background, noting brightness relation to yearly particle concentration

19 p2864 A72-38324

Craters formed in mineral dust by hypervelocity microparticles.

20 p2970 A72-39474

LUNAR ECHOES

NT LUNAR RADAR ECHOES

Lunar laser ranging for orbital and rotational motion, continental drift and pole studies, discussing Lunokhod I roving vehicle mounted laser reflector

01 p0031 A72-11152

Lunar laser tracking determination of geodetic coordinates relative to earth gravity center

05 p0659 A72-16726

Quasi-specular and Lambert reflection of short radio waves from lunar surface dependent on central portion of near side

05 p0631 A72-17039

Transportable lunar ranging with neodymium glass laser and Coude optical system, noting geophysical applications

07 p0943 A72-19388

Laser systems for lunar ranging and high temperature plasma generation

08 p1182 A72-21336

Earth-moon distance measurement by laser ranging methods, discussing retroreflectors, light collectors, time interval measuring devices and moon ranging stations

13 p2037 A72-28993

Lunar radar backscattering measurement of 0.86 cm circularly polarized radiation, noting echo polarization ratio and depolarization variations with incidence angle

19 p2868 A72-38735

LUNAR ECLIPSES

Plasma sheet positive ions flux enhancement detection at lunar distance during lunar eclipse and geomagnetic storm

02 p0283 A72-12452

Lunar eclipse of 25 September 1965, observing penumbra densities and isophotes in B and V spectral regions by photoelectric photometry

14 p2161 A72-30915

Lunar eclipse observations at millimeter wavelengths on 10 February 1971, determining surface cooling for Copernicus, Mare Serenitatis and highland region

15 p2311 A72-32087

Infrared observations of the moon and their interpretation.

22 p3225 A72-42527

LUNAR EFFECTS

NT LUNAR GRAVITATIONAL EFFECTS

NT LUNAR TIDES

Critique of Brown lunar theory, discussing planetary orbits, earth and moon figure effects and second order terms

01 p0122 A72-10009

Unisolar precession and equinox motion from Cepheids proper motion, using recently determined distance values

04 p0576 A72-15038

Higher harmonics in lunar transfer functions for surface magnetic field tangential components, discussing lunar electrical conductivity models

06 p0875 A72-17448

Semidiurnal lunar variation, solar and sidereal effects on cosmic radiation intensity, using zenith pointed particle telescopes

06 p0873 A72-17490

Transient lunar phenomena as changes in albedo due to dust movement or fluidization from lunar sample tests

06 p0877 A72-17650

Sporadic E layer altitude and density variations caused by lunar influences, using model for electrostatic field and wind shear effects

10 p1478 A72-25163

Lunar variations of Peruvian electrojet, analyzing E region electron drift and geomagnetic field H component data

11 p1626 A72-26415

Lunar transient phenomena during 1540-1970, tabulating observation reports

15 p2312 A72-32093

Geomagnetic and meteorological elements lunar daily variation calculation by modified Chapman-Miller method, estimating confidence limits for parameters reliability

16 p2384 A72-32972

Lunar semidiurnal variations of the geomagnetic field determined from the 2.5-min data scalings.

17 p2545 A72-34691

Numerical calculation of the lunar wake in a magnetohydrodynamic model.

19 p2864 A72-38435

Lunar magnetic variations at Trelew/Argentina/.

19 p2794 A72-38860

LUNAR ENVIRONMENT

NT LUNAR ATMOSPHERES

Apollo 14 charged particle lunar environment experiment, describing ALSEP particle spectrometer

04 p0508 A72-15097

Lunar laser reflectors specifications and fabrication procedures, discussing lunar environment simulator and optical test equipment, techniques and results

07 p0947 A72-20261

Apollo 14 charged particle lunar environment experiment data analysis, noting earth plasma sheet absence at lunar distance during geomagnetically quiet times

10 p1476 A72-24961

VLF and LF electromagnetic ground wave propagation between points on smooth curved lunar surface surrounded by free space or cold isotropic plasma

12 p1783 A72-27635

Apollo lunar surface experiments package suprathermal ion detector measurements in lunar environment

15 p2309 A72-31957

Detection of earthward flow of keV protons in the geomagnetic tail at lunar distances.

23 p3333 A72-44532

The lunar conductivity profile and the nonuniqueness of electromagnetic data inversion.

24 p3436 A72-44693

LUNAR EVOLUTION

Lunar crater population and distribution time development under meteoroid and solar wind bombardment, developing model for absolute formation ages

01 p0124 A72-10056

Apollo 12 lunar samples exoelectrons of thermally stimulated emission, noting concentration of traps for radiation history measurement

01 p0124 A72-10063

Critique of paper by Ringwood on petrogenesis of Apollo 11 lunar basalts composition and implications for lunar origin

02 p0275 A72-11600

Apollo mission profiles, discussing lunar landings, craters, evolution, samples and spacecraft instruments and hardware improvements

03 p0418 A72-13106

Lunar igneous activity and differentiation, discussing volcanic flows near Tycho, flow patterns in maria, sinuous rilles and crust lineaments

03 p0418 A72-13107

Mascon free lunar gravitational potential calculations, showing hydrostatic equilibrium in early evolution

03 p0434 A72-13552

Apollo 14 basaltic evidence for selective volatilization on lunar surface, using electron probe analysis

03 p0439 A72-14273

Fe-S segregation role in early chemical and physical history, giving model of early lunar differentiation

03 p0439 A72-14274

Lunar craters and maria origin from rock and sample chemical composition and magnetic differentiation

03 p0439 A72-14302

Lunar structure and evolution from mineral composition, density, gravity, magnetic and heat measurements and seismic events

03 p0440 A72-14303

Two-layer lunar model from variable viscosity media isostatic processes selenological investigation, suggesting hard top crust and deeper asthenosphere

04 p0569 A72-14505

Rille Rima Goclenius II formation, describing fractures mechanisms

04 p0571 A72-14563

Heat conduction model of surface thermal history of moon as function of dust, anorthosite, basalt and dunite layers

04 p0571 A72-14598

Lunar surface small crater statistical analysis and age prediction based on density and diameter correlation from Soviet Lunar Rover panoramic pictures

04 p0576 A72-15065

Lunar stone and rock morphological characteristics from Soviet Lunar Rover, Luna and Surveyor orbiters and Apollo mission pictures, noting evolution

04 p0576 A72-15066

Lunar stone distribution statistical analysis according to size on Soviet Lunar Rover panoramic pictures, estimating rock ages

04 p0576 A72-15067

Lunar thermal history and radioactivity upper limits determination consistent with proposed temperature distribution and Apollo chondrite data, implying low uranium content

04 p0581 A72-15579

Lunar volcanology, discussing domes, crater chains, halos, sinuous rills, mare wrinkle ridges, dark smooth level material and ring dike-like structures

04 p0581 A72-15619

Lunar Imbrian Basin formation, discussing micrometeorite component composition of Apollo 14 soil samples

05 p0715 A72-16160

Relative age determination of lunar surface regions using orbital photography and model of small impact erosion

06 p0878 A72-17759

Lunar crater origin mechanisms, considering single and multiple meteor impact and volcanic explosions, low velocity excavation, collapse and material emission

06 p0887 A72-18223

Texture, mineralogy and metamorphic history of lunar anorthosite 15415

06 p0889 A72-18272

Copernicus rays and ejecta blanket V-features form and distribution, suggesting association with satellite craters of secondary impact origin

07 p1067 A72-18872

Lunar crater tectonic and endogenic origin in maria from Orbiter photographs analysis

07 p1076 A72-19610

Earth and moon chemical composition differences based on model of lunar formation from circumterrestrial swarm of particles and larger objects

07 p1077 A72-19820

Lunar evolution theory, discussing terrestrial cluster dynamics during earth accumulation

08 p1231 A72-21129

Chondrite normalized rare earth abundances in lunar solidified liquid-type materials from Mare Tranquillitatis and Oceanus Procellarum associated with evolution

08 p1233 A72-21218

Lunar near side visual appearance reconstruction at two geologically significant points of evolution of Imbrian period

10 p1530 A72-23702

Lunar and Mars crater genetic similarities, discussing scale dependent effects and post-impact geologic development

10 p1531 A72-23704

Stable remanent magnetization components of lunar rock samples from Apollo 11 and 12 missions, indicating liquid core origin

10 p1536 A72-24155

Lunar crust and mantle evolution from Rb-Sr ages of Apollo 15 mare basalt samples

10 p1537 A72-24161

Lunar crater region ray systems origin and brightness variation mechanism from surface vitreous spherules examination

11 p1715 A72-25300

Radiogenic Ar 40/Ar 39 age and cosmic ray irradiation history of Apollo 15 anorthosite sample 15415, indicating Imbrian impact heating

12 p1862 A72-27111

Lunar interior thermal history discussing mathematical models for radioactive heat source, initial conditions, temperature distribution and time dependent fractionation

12 p1870 A72-27336

Significance of Apollo 11 and 12 lunar rock fragments of noritic rich in K, rare earth elements and P/KREEP/ for lunar evolution assessment

13 p2037 A72-28990

Lunar crust mass distribution relation to moments of inertia derivation from librations, inferring nonvalidity of lunar evolution fluid phase hypothesis

14 p2153 A72-30504

Lunar interior thermal history and current state from theoretical temperature models, taking into account initial conditions, heat sources, differentiation and simulated convection

14 p2155 A72-30519

Lunar origin and evolution, considering gravitational energy, radioactive isotopes and tidal deformations as heat sources

14 p2161 A72-30997

Apollo 15 orbital science payload instruments for exploring lunar origin and evolution to relate to earth history

15 p2310 A72-31984

Thermal history and early magmatism for lunar models, considering high near-surface temperatures and radionuclides upward transport during melting

15 p2311 A72-32082

Two phase heating of lunar crust for formation of lava filled Mare Smythii and Tsolkovsky craters

15 p2313 A72-32198

Lunar rock nature and properties from Apollo samples, discussing crust, Fra Mauro, interior, chronology, surface processes and earth-moon environment

15 p2314 A72-32376

Apollo 14 Rb-Sr isotope rock sample data, relating isochron age to igneous crystallization time

17 p2607 A72-35073

Earth and moon chemical composition differences based on model of lunar formation, from circumterrestrial swarm of particles and larger objects

17 p2618 A72-35745

Evidence for objects of lunar mass in the early solar system.

18 p2724 A72-36284

Geochemically and geophysically consistent model of lunar accretion process to explain initial temperature distribution

18 p2725 A72-36291

Chronology of first phases of formation of solar system solid objects, meteorites and primitive lunar rocks, describing models

19 p2867 A72-38548

Xenon isotope fission component due to extinct Pu-244 in lunar breccia, noting storage details in terms of crustal material dating

20 p2967 A72-39182

Chemical and structural classification of Apollo 11 lunar rocks, showing lunar surface material temperature history and meteoritic component presence

20 p2900 A72-39842

Fragments of terra rock in the Apollo 12 soil samples and a structural model of the moon.

21 p3110 A72-41452

Role of the swarm of satellite-particles on the origin of the earth's rotation

22 p3220 A72-41916

Lunar thermal history model, considering nonuniform initial composition, radioactive element partitioning and melt cutoff value

22 p3225 A72-42529

Lunar crater origins due to external impact of particles moving within earth-moon gravitational dipole during earliest history stage

22 p3226 A72-42538

Earth geophysical effects due to tidal capture of moon from direct orbit, discussing volcanism, atmosphere and hydrosphere origins and biological evolution

22 p3226 A72-42539

Origin and evolution of the earth-moon system.

22 p3227 A72-42540

Lunar composition in terms of evolutionary mode based on inhomogeneous planetary accretion and high temperature condensation

24 p3439 A72-44977

The distribution of craters on the surfaces of the moon and Mars in relation to their origin

24 p3441 A72-45222

LUNAR EXPLORATION

Lunar crust exploration by vlf electromagnetic surface waves, discussing frequency dependent depth penetration, conducting layers detection and communication or navigation use

03 p0436 A72-13821

Luna 16 and 17 and Lunokhod 1 flight, landing, operations and lunar surface activities

03 p0440 A72-14307

Recent moon exploration, discussing Ranger and Lunar Orbiter photographs for crater and volcano studies and landing site mapping and Apollo program rock studies

06 p0887 A72-18217

Apollo 15 mission report, discussing lunar module powered descent, surface exploration with LRV, scientific instrument module, extravehicular activity, etc

08 p1230 A72-21007

Apollo, Luna and Zond lunar exploration contribution to solar system formation knowledge, discussing post-Apollo lunar and planetary exploration programs

11 p1715 A72-25252

Manned-Unmanned Lunar Explorer (MULE) for NASA integrated program plan after 1980, discussing weight, locomotion system and mission capabilities [AIAA PAPER 72-369]

11 p1612 A72-25394

Lunar physical libration measurement from Apollo laser experiment with retroreflectors, assessing obtained data

14 p2154 A72-30516

Lunar research bibliography covering earth-moon system, moon motion, gravitational field, structure, thermal history, composition, photometry, spacecraft exploration, etc

14 p2155 A72-30521

Apollo lunar exploration program survey, reviewing information on lunar crust composition and thickness, lunar evolutionary processes and chronology and extraterrestrial particle fluxes

15 p2309 A72-31970

Report to COSPAR on U.S. space program covering stellar astronomy, lunar and planetary research under atmospheric physics, earth and life sciences, etc

15 p2337 A72-32006

Lunar exploration integrated program for 1980s, discussing halo orbit lunar far side data relay satellite advantages vs lunar orbit space station

15 p2321 A72-32318

Lunar volcanic gas release rate estimation from orbiting Apollo spacecraft-borne mass spectrometer detection, noting atmospheric perturbation

19 p2868 A72-38736

Remote control and navigation tests for application to long-range lunar surface exploration.

22 p2303 A72-43131

Investigation of solar system evolution by automatic vehicles on the moon.

24 p3445 A72-45466

LUNAR FAR SIDE

Lunar configuration, limb relief and coordinates of western hemisphere and far side from Zond 6 photograph reduction

05 p0721 A72-17040

Lunar far side crater Tsiolkovsky geology, indicating formation by meteoroid, asteroid or comet impact explosion

06 p0887 A72-18222

Lunar exploration integrated program for 1980s, discussing halo orbit lunar far side data relay satellite advantages vs lunar orbit space station

15 p2321 A72-32318

Extension of lunar nomenclature to the far side of the moon

17 p2610 A72-35213

Comments on the figure of the moon based on preliminary results from laser altimetry.

18 p2724 A72-36280

A catalog of selenographic coordinates of points of the libration zones and the reverse side of the moon

21 p3114 A72-41767

A new unified system for designating objects on the lunar surface

21 p3114 A72-41780

LUNAR GEOLOGY

NT LUNAR CORE

Lunar remanent magnetism origin theory from Apollo and Explorer data, suggesting solar wind, earth magnetosphere and lunar dynamo sources

01 p0134 A72-11269

Lunar passive seismic experiment deducing internal structure constitution and tectonic processes

03 p0418 A72-13108

Lunar structure and evolution from mineral composition, density, gravity, magnetic and heat measurements and seismic events

03 p0440 A72-14303

Two-layer lunar model from variable viscosity media isostatic processes selenological investigation, suggesting hard top crust and deeper asthenosphere

04 p0569 A72-14505

ALSEP active seismic experiment design, investigating lunar subsurface geologic structure

04 p0508 A72-15096

Papers on moon geology and physics covering lunar volcanic lava flow, water and crater origin

06 p0886 A72-18216

Tycho, Aristarchas and neighboring small craters volcanic origin, discussing inner and outer rim lava flows and impact crater resemblance

06 p0887 A72-18221

Lunar far side crater Tsiolkovsky geology, indicating formation by meteoroid, asteroid or comet impact explosion

06 p0887 A72-18222

Geologic setting of Apollo 15 breccias and basalts

06 p0888 A72-18263

Lunik 16 landing site geologic similarity to Apollo 11 and 12 sites on basaltic mare fill, noting impact bombardment developed regolith presence

09 p1379 A72-22251

Lunik 16 soil sample chemical composition indicating similarity of Sea of Fertility to Sea of Tranquility sites geochemical characteristics

09 p1381 A72-22273

Model for volcanic origin of Descartes Formation high albedo region, suggesting young age and endogenic nature of bright surface deposit

09 p1394 A72-23666

Geological provinces of lunar near side, showing nature and distribution patterns of five surface shaping periods

10 p1530 A72-23701

Lunar near side visual appearance reconstruction at two geologically significant points of evolution of Imbrian period

10 p1530 A72-23702

Geological setting, petrography and history of Apollo 15 anorthosite sample, tracing fragmentation and thermal metamorphic events

11 p1722 A72-26239

Lunar regolith glassy particles formation processes modeling with molten soil samples, emphasizing liquid particles spattering with subsequent cooling during meteoritic impact

13 p2036 A72-28767

Lunar geophysics - Conference, Houston, October 1971

14 p2153 A72-30501

Apollo 15 manned lunar landing, discussing geological data and surface experiment package and instruments

15 p2310 A72-31983

Lunar Science Institute, Conference on Lunar Geophysics, Houston, Tex., October 18-21, 1971, Proceedings.

18 p2724 A72-36275

Laboratory studies on seismic and electrical properties of the moon.

18 p2724 A72-36282

Seismic data from lunar geophysical stations network, noting moonquakes and meteoroid impacts

18 p2724 A72-36283

Q values from lunar seismic record measurements indicating separation of scattering and real loss parameters effects on energy propagation, discussing geophysical models

18 p2724 A72-36288

Gd and Sm isotope composition in Apollo 15 soils and drill stem samples, discussing lunar sedimentary processes dating from neutron capture dependence on depth

18 p2729 A72-36974

Relation between tectonic processes on the earth and moon

19 p2860 A72-37958

Craters formed in mineral dust by hypervelocity microparticles.

20 p2970 A72-39474

Lunar regolith glassy particles formation processes modeling with molten soil samples, emphasizing liquid particles spattering with subsequent cooling during meteoritic impact

21 p3102 A72-40268

Trace element geochemistry of Apollo 16 soil 68501.

23 p3337 A72-43939

LUNAR GRAVITATION

Apollo 14 landing site gravity determination from accelerometer data

02 p0285 A72-12844

Mascon free lunar gravitational potential calculations, showing hydrostatic equilibrium in early evolution

03 p0434 A72-13552

Lunar gravitational potential determination from Stokes and selenocentric constant

03 p0440 A72-14326

Lunar surface gravimeter experiment to search for gravitational radiation from cosmic sources exciting moon if free oscillations

04 p0509 A72-15105

Lunar gravity measurements via Apollo 14 Doppler radio tracking over 100 kilometer band during low periaapsis altitude orbits, relating to surface features

05 p0722 A72-17126

Lunar gravitational field, relief and internal structure, suggesting two layer model and crust thickness change relation to field characteristics

06 p0881 A72-17926

Mass distribution gravitationally equivalent to L1 lunar potential model for finite torus shaped shell region sampled by Apollo spacecraft

07 p1067 A72-18871

Lunar gravitational anomalies and plumb deviations mapping, reflecting global structure of Llorell JPL-3 model

07 p0976 A72-19818

Semiautomatic self leveling transverse gravimeter for gravity measurement along Lunar Rover Vehicle route on lunar surface

09 p1306 A72-22316

Lunar mass, gravitational field and moments of inertia from Lunar Orbiter spacecraft Doppler tracking data

13 p2037 A72-28989

Lunar gravitational field expansion coefficients C20 and C22 calculation, using Cassini equator inclination and radial bulk density distribution

14 p2149 A72-30213

Lunar orbiting dumbbell gravity gradiometer for measurement and mapping of lunar gravity field anomalies

14 p2104 A72-30511

Best fitting triaxial ellipsoid representation of seleno-equipotential surface at Apollo 12 landing site based on observed local gravity and moon angular velocity

15 p2308 A72-31922

Gravitational absorption investigation from lunisolar attraction observed by tracking high flying satellite in eccentric polar orbit

16 p2382 A72-32892

Physical structure of the moon.

17 p2615 A72-35680

Lunar gravitational anomalies and plumb deviations mapping, reflecting global structure of Llorell JPL-3 model

17 p2618 A72-35743

Apollo 15 gravity analysis from the S-band transponder experiment.

18 p2724 A72-36286

On the effects of gravitational absorption on orbits of artificial earth satellites.

18 p2728 A72-36761

Lunar gravitational field, relief and internal structure, suggesting two layer model and crust thickness change relation to field characteristics

18 p2730 A72-37151

Generalization of the sphere of interaction for the restricted four-body problem

20 p2975 A72-40073

Lunar gravitational field expansion coefficients C20 and C22 calculation, using Cassini equator inclination and radial bulk density distribution

23 p3334 A72-43243

Lunar and solar gravitational effects on earth atmosphere, describing latitudinal distribution of cyclone centers by momentum distribution of horizontal tide-generating forces

23 p3310 A72-43249

Russian book - Space research 1970: Investigation of the gravitational fields and shapes of the earth, other planets, and the moon on the basis of spacecraft observations.

24 p3443 A72-45399

LUNAR GRAVITATIONAL EFFECTS

Lunar gravitational field for placing spacecraft into static earth satellite orbit with standing position with respect to rotating earth

01 p0127 A72-10351

Moonquakes as recorded by seismic stations installed during Apollo 12 and 14 missions, observing periodic occurrence correlation with lunar gravity variations

01 p0134 A72-11225

Luni-solar perturbations of the geostationary vehicle at arbitrary latitude.

24 p3448 A72-44990

Dynamic model compensation algorithm accuracy for sequential estimation of time history of lunar satellite acceleration due to modeled surface mascons effects

24 p3440 A72-45139

LUNAR IONOSPHERE

U LUNAR ATMOSPHERES

LUNAR LANDING

Apollo spacecraft guidance and control systems, reviewing navigation objectives, concepts and performances during cislunar, rendezvous and landing maneuver phases

01 p0097 A72-10943

Apollo 14 mission report covering crew training, launch, docking, lunar landing and surface activities

08 p1230 A72-21006

Lunar landing mission escape and rescue concepts, considering emergencies during earth orbit, translunar, lunar orbit, surface and rendezvous, transearth and earth reentry phases

09 p1396 A72-21357

Soviet unmanned Luna 20 mission, describing launch, lunar trajectory injection, midcourse correction, lunar orbit and landing, surface soil sampling and return to earth

14 p2163 A72-30680

Lunar topsoil-solid bodies interaction in terms of hardness and friction, discussing simulation equipment

14 p2161 A72-31074

Apollo 15 manned lunar landing, discussing geological data and surface experiment package and instruments

15 p2310 A72-31983

Unique charts for space missions.

24 p3422 A72-44644

LUNAR LANDING MODULES

NT LSSM

LUNAR LANDING SITES

Apollo 14 Fra Mauro site basaltic rocks and breccia clast internal Rb-Sr isochrons, comparing to Tranquility Sea basalts

01 p0123 A72-10053

Radiometric upper limit to Fra Mauro Formation pebble age by Rb-Sr isotopic dating method

01 p0124 A72-10055

Lunar surface soil mechanical properties from computer simulation of Surveyor spacecraft observation data for each landing site, estimating cohesion

02 p0275 A72-11595

Photogrammetric techniques for Tranquility base experiment locations map based on surface and spacecraft photographs

02 p0280 A72-12198

Apollo 14 landing site gravity determination from accelerometer data

02 p0285 A72-12844

Apollo mission profiles, discussing lunar landings, craters, evolution, samples and spacecraft instruments and hardware improvements

03 p0418 A72-13106

- Lunik 16 landing site geologic similarity to Apollo 11 and 12 sites on basaltic mare fill, noting impact bombardment developed regolith presence
09 p1379 A72-22251
- Radiation damage by heavy solar particles in soil grains from Lunik 16 and landing Apollo sites
09 p1381 A72-22269
- Tranquility Base rocks irradiation depths and cosmic rays exposure ages from rare gases in samples, noting correlated variations in He 3/Ne 21 and Ar 38/Ne 21 due to shielding differences
09 p1377 A72-22596
- Apollo 16 planned mission to moon surface near crater Descartes, describing objectives
10 p1547 A72-24942
- Photogeologic evidence of differentiation and deposition of lunar highland volcanic rocks at Apollo 16 landing site
12 p1866 A72-27115
- Best fitting triaxial ellipsoid representation of seleno-equipotential surface at Apollo 12 landing site based on observed local gravity and moon angular velocity
15 p2308 A72-31922
- Anomalistic lunar tide vs latitudinal or declinational tidal wave for moonquakes recorded at Apollo 12 landing site
16 p2457 A72-33565
- Lunar landing sites selection approach for Apollo missions, examining mission design requirements, launch vehicle considerations and lunar composition
19 p2857 A72-37700
- Apollo 11 and 12 mare basalts and gabbros - Classification, compositional variations, and possible petrogenetic relations.
19 p2864 A72-38295
- Spectrophotometry /0.3 to 1.1 micron/ of visited and proposed Apollo lunar landing sites.
22 p3225 A72-42530
- Soil mechanical properties at the Apollo 14 site.
24 p3447 A72-45556

LUNAR LIMB

- Stellar intensity effect on angular navigation sighting accuracy attainable between star and lunar limb using Apollo T2 sextant
01 p0097 A72-10566
- Lunar limb structure from occultation traces from point source stars, constructing model with levels and slopes
03 p0420 A72-13129
- Lunar configuration, limb relief and coordinates of western hemisphere and far side from Zond 6 photograph reduction
05 p0721 A72-17040
- Lunar limb slope from photoelectric measurements of occultations, noting relation to double star astronomy
06 p0879 A72-17861
- Lunar limb charts comparison, computing corrections to orbital elements and systematic and random errors
09 p1388 A72-23056
- Algorithm and formulas for lunar limb absolute heights determination in selenodetic reference points system from lunar photographs
09 p1388 A72-23057
- Model solar atmosphere from mm and cm wavelength high resolution observations of chromosphere by lunar limb antenna tracking during 7 March 1970 eclipse
13 p2042 A72-29532

LUNAR LOGISTICS

- System design of a near-self-supporting lunar colony.
24 p3388 A72-45192

LUNAR LUMINESCENCE

- Transient lunar phenomena theories, investigating surface features obscuration, lunar material melting, ejected gas glow discharge luminescence processes
08 p1233 A72-21212
- Thermoluminescent and luminescent properties of Apollo 12 lunar fines, core tube samples and rock chips
10 p1537 A72-24163

LUNAR MAGNETIC FIELDS

- Lunar remanent magnetism origin theory from Apollo and Explorer data, suggesting solar wind, earth magnetosphere and lunar dynamo sources
01 p0134 A72-11269
- Lunar surface magnetic field variations, considering solar wind effect
02 p0285 A72-12871
- Lunar induced and permanent magnetism, discussing solar wind dynamic pressure effects and Apollo data
03 p0418 A72-13109
- Lunar electrical conductivity model, determining vacuum transient response to time varying spatially uniform magnetic field
03 p0434 A72-13508
- Magnetic monopole search in lunar samples by electromagnetic measurement, determining flux limits for cosmic radiation and pair production in proton-nucleon collisions
06 p0880 A72-17884

Solar wind perturbations downstream of moon outside of diamagnetic cavity, considering lunar surface magnetized areas as possible sources
07 p1057 A72-19144

Interplanetary magnetic field perturbations by solar wind and moon, noting lunar wake anomalies positive correlation with plasma beta value
09 p1387 A72-23003

Stable remanent magnetization components of lunar rock samples from Apollo 11 and 12 missions, indicating liquid core origin
10 p1536 A72-24155

Remanent lunar magnetic field compression by solar wind from magnetic measurements at Apollo landing sites
12 p1871 A72-27691

Lunar core-crust conductivity models compatibility with lunar surface field/interplanetary magnetic field transfer function from Apollo 12 magnetometer data
14 p2153 A72-30502

Lunar interior electrical conductivity from surface magnetic field measurements by Apollo magnetometers, calculating temperature profile for olivine moon model
14 p2154 A72-30508

Lunar local surface magnetic fields production mechanism, considering convection currents due to ionization of volcanic-ash-particle flow by electrodynamic model
17 p2614 A72-35586

Satellite measurements of the moon's magnetic field - A preliminary report.
18 p2724 A72-36287

Lunar shadowing of charged particles with arbitrary gyroradii and steady drift transverse to magnetic field applied to detector in low lunar orbit
21 p3104 A72-40482

On the applicability of lunar breccias for paleomagnetic interpretations.
22 p3226 A72-42532

The sunspot cycle and solar and lunar daily variations in H.
22 p3228 A72-42882

Dynamo theory for lunar magnetic field based on hypothetical thermal convection in rotating moon core analogous to earth
23 p3341 A72-44448

LUNAR MAPS

- Photogrammetric techniques for Tranquility base experiment locations map based on surface and spacecraft photographs
02 p0280 A72-12198
- Soviet lunar rover-carrying Luna 17 lander, obtaining topography and map in Sea of Rains
04 p0576 A72-15063
- Lunar surface details absolute and relative heights, estimating accuracy by comparison of data from different catalogs
06 p0884 A72-18034
- Selenographic coordinate system development, using lunar craters as reference point selection criteria
07 p1067 A72-18869
- Lunar gravitational anomalies and plumb deviations mapping, reflecting global structure of Lorell JPL-3 model
07 p0976 A72-19818
- Catalog of lunar craters central peaks and floor objects on visible hemisphere based on Kuiper photographic atlas
08 p1236 A72-21476
- Geological provinces of lunar near side, showing nature and distribution patterns of five surface shaping periods
10 p1530 A72-23701
- Lunar surface features absolute and relative heights, estimating accuracy by comparison of data from different catalogs
11 p1719 A72-25970
- Selenodetic catalog centers mutual positions determination from lunar near side hypsometric charts
11 p1724 A72-26911
- Lunar surface roughness mapping by combined IR and radar measurements
12 p1869 A72-27328
- Position information in lunar cartographic products evaluated by Apollo data, obtaining reliability factors
12 p1871 A72-27530
- Isogram map of Mare Imbrium reddening coefficients, noting correlation between chromaticity and relief details
14 p2148 A72-30208
- Stellar oriented Apollo metric mapping camera system for photo geodesy, discussing planned coverage triangulation methods, control network and gravity model improvements
16 p2396 A72-34105
- Lunar gravitational anomalies and plumb deviations mapping, reflecting global structure of Lorell JPL-3 model
17 p2618 A72-35743
- A new, earth-based radar technique for the measurement of lunar topography.
18 p2659 A72-36277

Infrared and radar maps of the lunar equatorial region.
18 p2725 A72-36289

A catalog of selenographic coordinates of points of the libration zones and the reverse side of the moon
21 p3114 A72-41767

Elevations and depressions frequencies determined for visible lunar continents and maria
21 p3114 A72-41768

A new unified system for designating objects on the lunar surface
21 p3114 A72-41780

Isogram map of Mare Imbrium reddening coefficients, noting correlation between chromaticity and relief details
23 p3333 A72-43238

LUNAR MARIA

Lunar craters and maria origin from rock and sample chemical composition and magnetic differentiation
03 p0439 A72-14302

Lunar mare soil deformation and cracking from Surveyor and Apollo photographs
04 p0574 A72-14918

Lunar seas small craters morphology from Soviet Lunar Rover panoramic picture data, suggesting impact-explosion formation mechanism
04 p0576 A72-15064

Luna 16 sampled lunar rock size distribution near craters in Sea of Rains from Lunokhod panoramic pictures
04 p0576 A72-15068

Lunar sea surface model derivation from morphology data analysis, suggesting four-layer bottom relief of basaltoidal lava, rocks, breccia and surface regolith
04 p0576 A72-15069

Small lunar maria craters morphological maturity as function of age and dimensions
05 p0722 A72-17041

Lunar Mare Imbrium lava flow geology and nature, mascon origins and explosive, collapse and impact mechanisms for small crater origin
06 p0887 A72-18218

Lunar sinuous rills location and origin, discussing Orbiter photographic maps, predominance in maria and similarity to terrestrial lava tubes
06 p0887 A72-18219

Lunar maria material igneous origin, relating surface features to various volcanic eruption types
06 p0887 A72-18220

Geomorphic evidence for basalt lava tubes and channels in Lunar Marius Hills, comparing with terrestrial analogs
07 p1067 A72-18870

Lunar crater tectonic and endogenic origin in maria from Orbiter photographs analysis
07 p1076 A72-19610

Petrological analysis of Mare Fecunditatis regolith returned from Luna 16 mission
09 p1379 A72-22254

Electron microprobe analyses of Lunik 16 mare basalt fragment G37 with high Al and low Mg content, discussing fragments G46 and G51
09 p1380 A72-22260

Rb-Sr internal isochron determination of Luna 16 maria basalt age, discussing major lunar magmatic activity time interval
09 p1380 A72-22263

Particle track densities in Lunik 16 soil column grains from Sea of Plenty, noting surface irradiation and regolith age
09 p1380 A72-22268

Lunik 16 soil sample chemical composition indicating similarity of Sea of Fertility to Sea of Tranquility sites geochemical characteristics
09 p1381 A72-22273

Spectral reflectance properties of lunar surface areas, discussing materials identification and maria depth determination
09 p1393 A72-23664

Terrestrial volcanic lava conduits origin and development association with lunar maria channels and sinuous rills
13 p2037 A72-28992

Isogram map of Mare Imbrium reddening coefficients, noting correlation between chromaticity and relief details
14 p2148 A72-30208

Lunar surface breccias origin, using exploration data to reappraise ballistic theory of giant craters and maria formation in favor of volcanic concepts
16 p2461 A72-34180

Comments on the figure of the moon based on preliminary results from laser altimetry.
18 p2724 A72-36280

Lunar color boundaries and their relationship to topographic features - A preliminary survey.
18 p2724 A72-36281

Apollo 11 and 12 mare basalts and gabbros - Classification, compositional variations, and possible petrogenetic relations.
19 p2864 A72-38295

Elevations and depressions frequencies determined for visible lunar continents and maria
21 p3114 A72-41768

Isogram map of Mare Imbrium reddening coefficients, noting correlation between chromaticity and relief details

23 p3333 A72-43238

LUNAR MODULE

NT LSSM

Toxicological control and chemical analysis of outgassing products from nonmetals in high temperature oxygen atmosphere, investigating use within LM crew compartment

01 p0019 A72-10771

Astronaut training obtained visually in lunar module simulator via film, spacecraft models and landing site relief models as sources for complex TV system

08 p1147 A72-21335

Low energy ions and negative particle fluxes simultaneous enhancements due to Apollo 14 lunar module impact, suggesting solar wind and gas cloud interaction as acceleration mechanism

09 p1388 A72-23018

Apollo 15 gravity analysis from the S-band transponder experiment.

18 p2724 A72-36286

LUNAR OBSERVATORIES

Cer-Vit glass mirror replacement for AFCRL lunar laser observatory inverted Dall-Kirkham Cassegrain telescope, noting one arc sec resolution from wire and null optics tests

07 p0985 A72-19410

Small lunar based reflecting telescopes with Cassegrainian and catadioptric optical systems, discussing design and operation

08 p1164 A72-20976

Optimal method selection for astronomical measurements on lunar surface, discussing instrumental and technical difficulties with selenographic longitudes and latitudes determination

08 p1231 A72-21130

Operational tests of the AFCRL 152-cm telescope.

17 p2555 A72-35198

LUNAR OCCULTATION

NT SOLAR ECLIPSES

Orbiting lunar spacecraft Endeavor radio transmission postoccultation reception, considering surface wave propagation and maintain formation prismatic refraction

02 p0171 A72-11753

Lunar occultation observations of radio source PKS 1514-24, presenting brightness distributions

02 p0277 A72-11905

Photoelectric and visual timings of occultations for lunar motions, comparing accuracy and systematic instrument errors

03 p0420 A72-13127

Grazing lunar occultation method application to geodetic measurement of geographical longitude differences, noting advantage over equal-limb-line method

03 p0420 A72-13128

Lunar limb structure from occultation traces from point source stars, constructing model with levels and slopes

03 p0420 A72-13129

Occultation curves for optical and radio lunar occultation analysis of radio sources, considering detection and measurement of binary systems

03 p0420 A72-13130

Seeing effects on light curve of stellar occultation by moon, calculating limitation on angular resolution

03 p0420 A72-13131

Filters and color effects on lunar occultation of stars and appropriate deconvolution procedures

03 p0420 A72-13132

Lunar occultation light curve model for photoelectric data analysis, using least squares method

03 p0421 A72-13133

Lunar limb slope from photoelectric measurements of occultations, noting relation to double star astronomy

06 p0879 A72-17861

Photoelectric lunar occultation measurements of multiple star systems, determining separate colors from simultaneous multichannel observations

06 p0880 A72-17862

GX3 plus 1 identification by sounding rocket during lunar occultations, discussing magnitude

07 p1070 A72-19123

Lunar occultations of IRC plus 10216 for IR radiation distribution, deducing model of late type carbon star surrounded by thermally reemitting dust shell

11 p1721 A72-26123

Solar flare X-ray emission occultation observed during 7 March 1970 eclipse by NRL instrument on OSO-5 satellite

13 p2031 A72-29549

Radio sources position determination by lunar occultation, noting observation technique and data analysis method

16 p2453 A72-33287

Radio position accuracy of pulsar PSR 1749-28 from lunar occultations compared to time of arrival measurements

20 p2969 A72-39388

Interferometric observations of lunar occultations of radio sources, showing positions, brightness distributions, spectral index variations and quasar coincidence

23 p3334 A72-43260

LUNAR ORBITER

Lunar sinuous rills location and origin, discussing Orbiter photographic maps, predominance in maria and similarity to terrestrial lava tubes

06 p0887 A72-18219

Lunar center of mass position with respect to visible hemisphere physical surface calculated from photogrammetric analysis and Lunar Orbiter 1 data

08 p1232 A72-21158

Lunar orbiting rescue vehicle design for Apollo missions, discussing guidance, navigation and communications

09 p1396 A72-23156

Lunar mass, gravitational field and moments of inertia from Lunar Orbiter spacecraft Doppler tracking data

13 p2037 A72-28989

Orbiter 4 photographs to update System of Lunar Craters /1966/, cataloging positions, diameters and morphological data

13 p2037 A72-28991

Lunar orbiting dumbbell gravity gradiometer for measurement and mapping of lunar gravity field anomalies

14 p2104 A72-30511

Lunar exploration integrated program for 1980s, discussing halo orbit lunar far side data relay satellite advantages vs lunar orbit space station

15 p2321 A72-32318

Moon radius from Lunar Orbiter 1 angular velocity data obtained from camera image motion compensator sensor /V/H sensor/

17 p2603 A72-34207

Lunar center of mass position with respect to visible hemisphere physical surface calculated from photogrammetric analysis and Lunar Orbiter 1 data

20 p2969 A72-39263

Long term stability of earth and lunar orbiters - Theory and analysis.

[AIAA PAPER 72-936]

21 p3112 A72-41574

High resolution lunar surface stereophotographs from pairing overlapping Lunar Orbiter photographs

22 p3230 A72-43195

LUNAR ORBITS

Flight laser altimeter for Apollo vehicle height measurements above lunar surface, using telescope relay and quartz crystal oscillator

05 p0660 A72-15786

Average plasma sheet configuration in geomagnetic tail at lunar orbit, presenting seasonal dependence and variations with geomagnetic activity

11 p1624 A72-26396

Explorer 35 and OGO 3 data on picogram size dust particle distribution in cislunar and selenocentric space, showing fluctuations during meteor shower periods

15 p2309 A72-31937

Apollo 15 orbital science payload instruments for exploring lunar origin and evolution to relate to earth history

15 p2310 A72-31984

Terrestrial and lunar orbital and rotational motion behavior, discussing kinematic theory and ground and space vehicle based observation techniques

19 p2865 A72-38479

Quasi-periodic orbits about the translunar libration point.

[AIAA PAPER 72-935]

21 p3112 A72-41573

Unique charts for space missions.

24 p3422 A72-44644

Analysis of the Radio Astronomy Explorer lunar orbit mission.

[AIAA PAPER 72-940]

24 p3444 A72-45437

LUNAR PERTURBATION

U LUNAR EFFECTS

LUNAR PHOTOGRAPHS

Photogrammetric techniques for Tranquility base experiment locations map based on surface and spacecraft photographs

02 p0280 A72-12198

Lunar stone and rock morphological characteristics from Soviet Lunar Rover, Luna and Surveyor orbiters and Apollo mission pictures, noting evolution

04 p0576 A72-15066

Lunar stone distribution statistical analysis according to size on Soviet Lunar Rover panoramic pictures, estimating rock ages

04 p0576 A72-15067

Luna 16 sampled lunar rock size distribution near craters in Sea of Rains from Lunokhod panoramic pictures

04 p0576 A72-15068

Reference grid construction for lunar craters in system with scale and orientation independent of other systems, discussing preliminary catalog compilation from lunar photographs

09 p1388 A72-23055

Algorithm and formulas for lunar limb absolute heights determination in selenodetic reference points system from lunar photographs

09 p1388 A72-23057

Orbiter 4 photographs to update System of Lunar Craters /1966/, cataloging positions, diameters and morphological data

13 p2037 A72-28991

A catalog of selenographic coordinates of points of the libration zones and the reverse side of the moon

21 p3114 A72-41767

LUNAR PHOTOGRAPHY

Book on earth, moon and planet space photography, discussing synoptic meteorological data, mapping, surface detail inspection and planetary exploration

03 p0438 A72-14099

Relative age determination of lunar surface regions using orbital photography and model of small impact erosion

06 p0878 A72-17759

Recent moon exploration, discussing Ranger and Lunar Orbiter photographs for crater and volcano studies and landing site mapping and Apollo program rock studies

06 p0887 A72-18217

Lunar sinuous rills location and origin, discussing Orbiter photographic maps, predominance in maria and similarity to terrestrial lava tubes

06 p0887 A72-18219

Photographic telescope Gautier used for photographs of moon together with stellar background, noting reduction method for lunar positions deduction

11 p1716 A72-25771

Apollo-borne modified Hasselblad 500 EL Data moon camera and lenses, discussing design features and photographic applications

16 p2388 A72-32825

Stellar oriented Apollo metric mapping camera system for photo geodesy, discussing planned coverage triangulation methods, control network and gravity model improvements

16 p2396 A72-34105

Moon radius from Lunar Orbiter 1 angular velocity data obtained from camera image motion compensator sensor /V/H sensor/

17 p2603 A72-34207

Lunar color boundaries and their relationship to topographic features - A preliminary survey.

18 p2724 A72-36281

Infrared and radar maps of the lunar equatorial region.

18 p2725 A72-36289

High resolution lunar surface stereophotographs from pairing overlapping Lunar Orbiter photographs

22 p3230 A72-43195

LUNAR PROBES

NT LUNIK LUNAR PROBES

NT RANGER LUNAR PROBES

NT SURVEYOR LUNAR PROBES

Luna 16 and 17 and Lunokhod 1 flight, landing, operations and lunar surface activities

03 p0440 A72-14307

LUNAR PROGRAMS

NT APOLLO PROJECT

Apollo spacecraft guidance and control systems, reviewing navigation objectives, concepts and performances during cislunar, rendezvous and landing maneuver phases

01 p0097 A72-10943

Soviet space program review from Sputnik I launch, discussing launch sites and vehicles, lunar, planetary and manned missions, civil and military programs and future goals

05 p0722 A72-17091

Lunar laser ranging experiment single photon detection and nanosecond timing precision

15 p2233 A72-31530

Apollo lunar exploration program survey, reviewing information on lunar crust composition and thickness, lunar evolutionary processes and chronology and extraterrestrial particle fluxes

15 p2309 A72-31970

LUNAR RADAR ECHOES

Moon and Venus relief from backscattering diagrams based on radar echoes, calculating root-mean-square angles of surface inclination

14 p2151 A72-30468

Lunar radar measurement for remotely located clock time synchronization, discussing applications to deep space tracking, computer technique for time delay correction and accuracy

15 p2199 A72-32069

A multiple-scattering model of the diffuse component of lunar radar echoes.

20 p2903 A72-39473

Methods of radar studies of the moon and planets from spacecraft

21 p3103 A72-40307

Specific effective scattering area of the lunar, Martian, and Venusian surfaces in the radio range

22 p3223 A72-42214

LUNAR RADIATION

Monte Carlo calculations of lunar photon albedo from galactic and solar proton bombardment for lunar soil composition information

07 p1070 A72-19139

Mesosphere ozone number densities from rocket photometric measurement of lunar UV radiation absorption

09 p1385 A72-22583

Lunar microwave emission, constructing thermophysical models for radio observations and brightness temperature variations

12 p1869 A72-27327

July 1952 polarization change in lunar crater Posidonius from polarimeter observations

14 p2152 A72-30488

July 1952 polarization change in lunar crater Posidonius from polarimeter observations

19 p2864 A72-38317

Infrared observations of the moon and their interpretation.

22 p3225 A72-42527

Directional far IR emission from sunlit lunar surface, determining brightness temperature as function of observer and sun elevation angles and surface parameters

22 p3226 A72-42537

On the validity of a generalized Kirchhoff's Law for a nonisothermal scattering and absorptive medium.

24 p3424 A72-44698

LUNAR RAYS

Copernicus rays and ejecta blanket V-features form and distribution, suggesting association with satellite craters of secondary impact origin

07 p1067 A72-18872

Lunar crater region ray systems origin and brightness variation mechanism from surface vitreous spherules examination

11 p1715 A72-25300

LUNAR ROCKS

Book on Apollo 11 lunar rocks and minerals covering mineralogy, petrology, chemical and isotope analyses, bioscience, organic geochemistry, physical properties and measurements

01 p0122 A72-10001

Apollo 14 crystalline rocks and fragments Rb/Sr, Ar 40/Ar 39 or cosmic ray exposure ages from electron microprobe and petrographic microscope examination

01 p0123 A72-10051

Apollo 14 rocks, breccia fragments and soil samples ages from Ar 40/Ar 39 and cosmic ray dating, discussing basalt Ar release patterns

01 p0117 A72-10052

Apollo 14 Rb-Mauro site basaltic rocks and breccia clast internal Rb-Sr isochrons, comparing to Tranquility Sea basalts

01 p0123 A72-10053

Radiometric upper limit to Fra Mauro Formation pebble age by Rb-Sr isotopic dating method

01 p0124 A72-10055

Apollo 12 lunar rock 12013, examining uranium distribution in apatite, whitlockite, zircon and beta phases

01 p0124 A72-10062

Apollo 12 lunar samples exoelectrons of thermally stimulated emission, noting concentration of traps for radiation history measurement

01 p0124 A72-10063

Lunar basalts 10044 and 12021 Fe oxidation state in plagioclase and distribution in crystal structure, using Mossbauer spectroscopy

01 p0124 A72-10064

Apollo 12 lunar igneous rocks 12004, 12040, 12051 and 12053, obtaining Kr 78/Kr 83 and Xe 131/Xe 126 spallation component ratios correlation line

01 p0124 A72-10065

Apollo flight lunar spinels compositional variations, formulating modified Johnstone prism projections

01 p0134 A72-11162

Critique of paper by Ringwood on petrogenesis of Apollo 11 lunar basalts composition and implications for lunar origin

02 p0275 A72-11600

Apollo 12 lunar crystalline rock and fines magnetic properties measurement, noting magnetic minerals composition

02 p0278 A72-12026

Chemical composition and morphology of silicate spherules, comparing to lunar rocks, meteorites and tektites

02 p0280 A72-12283

Lunar regolith powder weight density, compressibility and torsional strength determination at atmospheric pressure and He atmosphere

02 p0281 A72-12288

Apollo 11 and 12 rock samples depth profiles for Al, Na, Mn, S, V, Ca, P, Co, Fe, Cu and Sc isotopic contents, estimating solar proton flux

02 p0282 A72-12327

Electron microprobe analysis of plagioclase points and pyroxene grains of Apollo 15415 anorthositic genesis rock

02 p0282 A72-12411

Excess Xe 131 in lunar Ba feldspar rocks, discussing results of reactor irradiation experiments with fast and epithermal neutrons

03 p0414 A72-12901

Lunar igneous activity and differentiation, discussing volcanic flows near Tycho, flow patterns in maria, sinuous rilles and crust lineaments

03 p0418 A72-13107

Nonequilibrium subsolidus reduction of lunar spinels at low oxygen fugacities based on Cr-Al ulspinel and olivine decomposition

03 p0439 A72-14298

Lunar craters and maria origin from rock and sample chemical composition and magnetic differentiation

03 p0439 A72-14302

Lunar structure and evolution from mineral composition, density, gravity, magnetic and heat measurements and seismic events

03 p0440 A72-14303

Lunar stone and rock morphological characteristics from Soviet Lunar Rover, Luna and Surveyor orbiters and Apollo mission pictures, noting evolution

04 p0576 A72-15066

Lunar stone distribution statistical analysis according to size on Soviet Lunar Rover panoramic pictures, estimating rock ages

04 p0576 A72-15067

Luna 16 sampled lunar rock size distribution near craters in Sea of Rains from Lunokhod panoramic pictures

04 p0576 A72-15068

Lunar sea surface model derivation from morphology data analysis, suggesting four-layer bottom relief of basaltoid lava, rocks, breccia and surface regolith

04 p0576 A72-15069

High energy cosmic ray track angular azimuthal distribution in lunar silicate rocks

04 p0577 A72-15154

Q values contradiction between lunar and earth rocks, discussing internal friction

04 p0580 A72-15450

Lunar thermal history and radioactivity upper limits determination consistent with proposed temperature distribution and Apollo chondrite data, implying low uranium content

04 p0581 A72-15579

Lunar rock 12013 sawdust and fragment composition from neutron activation analysis, comparing to Java tektite J2

05 p0722 A72-17127

Chromian pleonaste and aluminous picotite in Apollo 14 fine grained microbreccias comparing with spinel composition in lunar basalts

06 p0878 A72-17672

Magnetic monopole search in lunar samples by electromagnetism measurement, determining flux limits for cosmic radiation and pair production in proton-nucleon collisions

06 p0880 A72-17884

Lunar maria material igneous origin, relating surface features to various volcanic eruption types

06 p0887 A72-18220

Lunar regolith top surface polarimetric properties of sunlight-exposed rocks and fines compared to terrestrial rocks and meteorites

06 p0887 A72-18225

Lunar surface rocks, soil and breccia chemical composition, discussing element concentration, radiation effects on surface chemistry and volcanism

06 p0887 A72-18226

Apollo 15 mare basalts and breccias and premare igneous rocks, analyzing chemical composition and microstructure

06 p0888 A72-18262

Chemical, geochronological and petrogenetic analyses of Apollo 15 lunar mare basalt rock from Hadley Rille, comparing with Apollo 12 and 14 basalts

06 p0888 A72-18264

Apollo 15 rock 15555 age by argon-40-argon-39 dating

06 p0888 A72-18265

Lunar mare basalt 15555 age by Rb-Sr and K-Ar techniques

06 p0888 A72-18266

Largest Apollo 15 lunar rock mass spectrometry analyses of noble gases with gas retention age estimation and spallation Kr data

06 p0888 A72-18267

Gas retention and cosmic ray exposure ages of lunar rock from Hadley Rille, using isotopic dilution method

06 p0888 A72-18268

Crystallization age of Apollo 15 anorthositic rock 15415.9

06 p0888 A72-18270

Mineralogic and petrologic study of lunar anorthositic slide 15415.18

06 p0888 A72-18271

Texture, mineralogy and metamorphic history of lunar anorthositic 15415

06 p0889 A72-18272

Critique of paper on heat capacity and thermal conductivity of Apollo 11 lunar rocks at liquid helium temperatures, noting constraints imposed by Mossbauer data

07 p1084 A72-20521

Electron microprobe analysis of Lunik 16 basalt fragments, noting similarity to Apollo 11 and 12 igneous rocks

09 p1379 A72-22252

Shock metamorphism in Luna 16 soil sample, indicating regolith formation by meteorite impact

09 p1380 A72-22259

Electron microprobe analyses of Lunik 16 mare basalt fragment G37 with high Al and low Mg content, discussing fragments G46 and G51

09 p1380 A72-22260

Luna 16 rock sample B-1 petrology, mineralogy and chemistry, noting fine grained ophitic basalt nature

09 p1380 A72-22262

Gas retention and cosmic ray exposure ages of Luna 16 basalt fragment from Mare Feconditatis

09 p1380 A72-22264

Mass spectroscopic measurement of inert gases in Lunik 16 fragments and dust samples

09 p1380 A72-22267

Fossil track densities and thermoluminescence measurements of Luna 16 feldspar crystal samples compared to Apollo 12 samples

09 p1381 A72-22270

Tranquility Base rocks irradiation depths and cosmic rays exposure ages from rare gases in samples, noting correlated variations in He 3/Ne 21 and Ar 38/Ne 21 due to shielding differences

09 p1377 A72-22596

Apollo 14 explosion seismic refraction data, showing lunar near surface regolith thickness and compressional wave velocity

09 p1390 A72-23495

Lunar regolith powder weight density, compressibility and torsional strength determination at atmospheric pressure and He atmosphere

10 p1532 A72-23757

Neutron capture effects on Gd isotopic composition and irradiation histories of lunar rocks from Apollo sites, using mass spectroscopic measurements

10 p1536 A72-24154

Stable remanent magnetization components of lunar rock samples from Apollo 11 and 12 missions, indicating liquid core origin

10 p1536 A72-24155

Differentiated igneous textures of Apollo 11 lunar ferrobasalt samples, indicating fractional crystallization followed by crystal-liquid separation

10 p1537 A72-24157

Lunar anorthosites and parent liquids chemical composition from trace element analysis

10 p1537 A72-24158

Crystallization sequence, petrology and mineralogy of Apollo 12 basalt sample 12009

10 p1537 A72-24160

Lunar basalt Eu abundance anomaly in Apollo 11 and 12 samples, considering partial melting with or without plagioclase

10 p1537 A72-24162

Thermoluminescent and luminescent properties of Apollo 12 lunar fines, core tube samples and rock chips

10 p1537 A72-24163

Geochemistry of lunar opaque minerals in Apollo 14 crystalline rocks, including FeNi metal, ilmenite, spinels, schreibersite, baddeleyite, fayalite and tranquillityite

10 p1538 A72-24164

Apollo 12 lunar rocks and fines sulfur concentrations and isotope ratios measurement

10 p1538 A72-24168

Zirconium rich metal oxides mineral group in Apollo 14 and 15 lunar rocks from feldspar-phryic basalt and pyroxene ferrobasalt, noting optical and chemical properties

11 p1717 A72-25868

Luna 16 automatic probe drilling experiment, obtaining lunar rocks physicochemical properties for comparison with terrestrial rocks

11 p1613 A72-25938

Surface orientation reconstruction of Apollo 14 lunar rocks from microstereoscopic studies of microcraters, soil covers and glass coatings, determining micrometeoroid erosion

11 p1719 A72-25975

Geological setting, petrography and history of Apollo 15 anorthositic sample, tracing fragmentation and thermal metamorphic events

11 p1722 A72-26239

Vaporization and condensation effects on Apollo 11 glass spherules from microbreccia samples, suggesting concentration gradients as result of impact event

11 p1723 A72-26522

Crystallization experiments on Apollo 11 magmas of K and Rb-rich basalt, discussing plagioclase characteristics

11 p1723 A72-26523

Apollo 14 basaltic rocks cooling deduced from divalent Mg and Fe ionic distribution in pyroxene, noting process interruption below 840 C

11 p1724 A72-26574

Luna 16 Sea of Abundance rock volume weight, destruction pattern, compressibility, shear strength and carrying ability, comparing to terrestrial rock

11 p1724 A72-26910

Shock deformation microstructures in Apollo 14 breccia and comparative terrestrial minerals, using transmission electron microscopy

11 p1724 A72-26951

Lunar and terrestrial pyroxenes phase structure electron microscopic investigation, using ion-thinned samples

11 p1725 A72-26952

Apollo 14 breccia sample inverted pigeonites/pyroxenes/ as evidence of lunar plutonic rocks, using optical, electron probe and X ray diffraction techniques

12 p1865 A72-27112

Electron microprobe analysis of chromian spinels from Apollo 14 rocks indicating crystallization from high aluminum low iron magma

12 p1865 A72-27113

Photogeologic evidence of differentiation and deposition of lunar highland volcanic rocks at Apollo 16 landing site

12 p1866 A72-27115

Apollo 11 and 12 lunar samples thermal properties, presenting diffusivity, conductivity and specific heat

12 p1869 A72-27334

Lunar glass particle micrometeorite crater morphology, showing radial fracture and spallation zone relationships

13 p2036 A72-28755

Significance of Apollo 11 and 12 lunar rock fragments of norite rich in K, rare earth elements and P /KREEP/ for lunar evolution assessment

13 p2037 A72-28990

Apollo 11 and 12 rock samples depth profiles for cosmogenic Al, Na, Mn, S, V, Ca, P, Co, Fe, Cu and Sc isotopic contents, estimating solar proton flux

13 p2039 A72-29211

Low temperature shock effects on lunar glass spherules from two beam interferometry, discussing mechanical and thermal causes of fragmentation

14 p2149 A72-30266

Ejected lunar particles in meteoric sporadic background, noting brightness relation to yearly particle concentration

14 p2153 A72-30495

Lunar breccia and crystalline rocks thermomagnetic magnetization characteristics, presenting alternating field and thermal demagnetization curves

14 p2154 A72-30507

Fe and Ti ion bands in lunar pyroxenes and olivines single crystals polarized absorption spectra

14 p2154 A72-30510

Ferric ion traces evidenced in lunar and meteoritic titanates by charge transfer bands observations during heating, interpreting origin as caused by cosmic radiation

14 p2154 A72-30515

Magnetization and temperature interrelationship in high constant magnetic field for Apollo 11, 12 and 14 rocks, obtaining magnetic hysteresis curves

14 p2155 A72-30517

Apollo 11 and 12 lunar surface rocks electrical conductivity at 300-1200 K in vacuum, Ar, He and H₂ hydrogen atmospheres, noting large hysteresis above 500 C

14 p2155 A72-30518

Lunar rock and mineral shock melting and vaporization from hypervelocity meteoroid impacts, calculating entropy, phase changes and thermal equilibrium

14 p2155 A72-30520

Thermal expansion measurements of simulated volcanic and nonvolcanic lunar rocks as function of temperature

15 p2222 A72-31258

U-Th-Pb ages in Apollo 14 basalts and initial radiogenic Pb in lunar rocks, comparing with Rb-Sr and K-Ar isotopic method

15 p2303 A72-31301

Temperature dependent Mg and Fe hyperfine doublets in lunar olivine, indicating slow cooling crystallization

15 p2303 A72-31302

U bearing phase zirkelite in Apollo 12 and 14 lunar rocks, using electron microprobe

15 p2303 A72-31303

Low radioactivity of surface exposed lunar rock from alpha spectrometry, indicating absence of radon outgassing

15 p2303 A72-31304

Glazed rock fragments and glassy splatter origin in bottom of small lunar craters from Apollo 15 observation

15 p2306 A72-31577

Pu 244/U 238 fission track retention age of whitlockite crystal in lunar breccia 14321 from Fra Mauro formation

15 p2307 A72-31722

Lunar rock abrasion and catastrophic rupture lifetimes for near earth micrometeoroid flux determination, using hypervelocity impact tests

15 p2309 A72-31956

Lunar surface microerosion relationship to interplanetary dust particle flux distributions, investigating sputter erosion and lunar rocks lifetimes

15 p2310 A72-31988

Lunar rock nature and properties from Apollo samples, discussing crust, Fra Mauro, interior, chronology, surface processes and earth-moon environment

15 p2314 A72-32376

Lunar rock 14310 whitlockite richness in rare earth elements relative to associated apatite

16 p2454 A72-33446

Lunar rock 12052 euhedral clinopyroxenes composed of honey yellow pigeonite cores overgrown by dark brown augite

16 p2454 A72-33448

Lithology of Apollo 14 lunar clastic rocks from Fra Mauro region, noting different makeups of glassy matrix and particles, plagioclase, pyroxene and lithic clasts

16 p2457 A72-33675

Study by Mossbauer spectrometry of the iron distribution in mineralogical fractions separated from lunar rocks brought back by Apollo 12

17 p2607 A72-34917

Apollo 14 Rb-Sr isotope rock sample data, relating isochron age to igneous crystallization time

17 p2607 A72-35073

Electron paramagnetic resonance of radiation damage in a lunar rock.

17 p2609 A72-35098

IR spectroscopy of Luna 16 regolith samples, noting differences in reflection, emission and transmission spectra of related terrestrial rocks

17 p2610 A72-35212

Effect of lunar ground on radiation damage in mice

17 p2504 A72-35214

Glass lined microcraters on lunar rocks attributed to hypervelocity impact of extralunar particles

17 p2615 A72-35682

Rock size, mineralogy and fines size distribution in lunar regolith

17 p2615 A72-35683

Petrologic comparisons of lunar terra materials.

17 p2615 A72-35684

The distribution of carbon in lunar samples from Apollo 11, 12 and 14.

17 p2615 A72-35685

Transition element distribution in stony meteorites and in terrestrial and lunar rocks.

17 p2619 A72-35936

Compositional characteristics of olivines from Apollo 12 samples.

18 p2723 A72-36063

Ferromagnetic and paramagnetic resonance spectra of lunar material - Apollo 12.

18 p2724 A72-36276

Infrared and Raman spectra of lunar samples from Apollo 11, 12 and 14.

18 p2724 A72-36279

Laboratory studies on seismic and electrical properties of the moon.

18 p2724 A72-36282

Thermophysical properties of lunar material returned by Apollo missions.

18 p2725 A72-36290

Lunar pentlandite and sulfidization reactions in microbreccia 14315.9.

18 p2729 A72-36973

Gd and Sm isotope composition in Apollo 15 soils and drill stem samples, discussing lunar sedimentary processes dating from neutron capture dependence on depth

18 p2729 A72-36974

Apollo 11 and 12 mare basalts and gabbros - Classification, compositional variations, and possible petrogenetic relations.

19 p2864 A72-38295

Ejected lunar particles in meteoric sporadic background, noting brightness relation to yearly particle concentration

19 p2864 A72-38324

Chronology of first phases of formation of solar system solid objects, meteorites and primitive lunar rocks, describing models

19 p2867 A72-38548

Anomalous high concentration of lunar rock Xe-131 relation to Ba-130 nonthermal neutron-capture cross section in resonance energy region

20 p2967 A72-39180

Rates of solidification of Apollo 11 basalt and Hawaiian tholeiite.

20 p2967 A72-39181

Brief review of thermoluminescence studies in lunar samples.

20 p2970 A72-39402

Aluminum 26 and manganese 53 produced by solar-flare particles in lunar rock and cosmic dust.

20 p2970 A72-39472

Phase transformations and exsolution in lunar and terrestrial calcic plagioclases.

20 p2970 A72-39480

Rocks and meteorites analysis techniques evaluation, using Apollo 11 fines results to evaluate activation analysis for geochemistry and cosmochemistry applications

20 p2899 A72-39827

Instrumental neutron activation analysis of igneous rock abundances in petrogenic and stratigraphic

problems, applying to Colombia River basalts and Apollo 11 rock samples

20 p2899 A72-39829

Multielement neutron activation analysis of geological and lunar material using chemical group separations and high resolution gamma spectrometry.

20 p2899 A72-39830

Neutron activation techniques for nondestructive analysis of meteorites and lunar rocks, noting types of nuclear reactions for geochemical application

20 p2899 A72-39832

Chemical and structural classification of Apollo 11 lunar rocks, showing lunar surface material temperature history and meteoritic component presence

20 p2900 A72-39842

Experimental evidence against the role of selective volatilization on the lunar surface.

21 p3013 A72-40452

Phenocryst fabric in lunar basalt sample 12052 from the Ocean of Storms.

21 p3106 A72-41115

On the applicability of lunar breccias for paleomagnetic interpretations.

22 p3226 A72-42532

Lunar interior composition constraints from chemical composition of igneous rocks on surface

22 p3226 A72-42533

Thermal stability of lunar rock remanence, indicating magnetization components acquired after initial cooling

22 p3226 A72-42535

Occurrence of chromian, hercynitic spinel /-pleonaste/ in Apollo-14 samples and its petrologic implications.

22 p3153 A72-42862

Uranium distribution in basalt fragments of five lunar samples.

23 p3261 A72-43399

Mineralogy, petrology and chemistry of lunar rock 12039.

23 p3339 A72-44127

Metastable growth patterns in some terrestrial and lunar rocks.

23 p3339 A72-44133

Major element composition of glasses in three Apollo 15 soils.

23 p3339 A72-44137

Lunar ultramafic glasses, chondrules and rocks.

23 p3340 A72-44340

A study of the vestigial records of cosmic rays in lunar rocks using a thick section technique.

23 p3341 A72-44459

Chemical composition of Luna 16 and Luna 20 rock samples from Sea of Fertility and Apollonius C crater

24 p3440 A72-45109

LUNAR ROVING VEHICLES

NT LUNOKHOD LUNAR ROVING VEHICLES

NT MANNED LUNAR SURFACE VEHICLES

Lunar Roving Vehicle navigation subsystem power converter design, discussing circuits, performance and voltage regulators and preregulators

01 p0009 A72-11069

Soviet lunar rover-carrying Luna 17 lander, obtaining topography and map in Sea of Rains

04 p0576 A72-15063

Lunar seas small craters morphology from Soviet Lunar Rover panoramic picture data, suggesting impact-explosion formation mechanism

04 p0576 A72-15064

Apollo lunar roving vehicle design requirements based on environmental conditions, emphasizing wheel drive control and steering systems optimization and navigational instrumentation

05 p0643 A72-16428

Apollo 15 mission report, discussing lunar module powered descent, surface exploration with LRV, scientific instrument module, extravehicular activity, etc

08 p1230 A72-21007

Semiautomatic self leveling transverse gravimeter for gravity measurement along Lunar Rover Vehicle route on lunar surface

09 p1306 A72-22316

Lunar roving vehicle reliability program and design features of mobility, electrical power and navigation subsystems

10 p1460 A72-24443

[AIAA PAPER 72-233] Landmark navigation with angle measurements for roving vehicle guidance on lunar and planetary surfaces

15 p2268 A72-31790

Lunar roving vehicle qualification program to meet performance specifications under lunar conditions, describing testing procedures and project management techniques

15 p2214 A72-32613

Thermal control system incorporation into lunar roving vehicle /LRV/ for electronic component protection during translunar transportation and lunar surface operation

20 p2894 A72-39150

Investigation of solar system evolution by automatic vehicles on the moon.

24 p3445 A72-45466

LUNAR SATELLITES

NT LUNAR ORBITER

Apollo 15 lunar subsatellite particle experiment subsystem design for studying magnetosphere dynamics, plasmas-moon interaction and solar flare physics
08 p1168 A72-21519

Dynamic model compensation algorithm accuracy for sequential estimation of time history of lunar satellite acceleration due to modeled surface mascons effects
24 p3440 A72-45139

LUNAR SCATTERING

U DIFFUSE RADIATION

U LUNAR RADAR ECHOES

LUNAR SEISMOGRAPHS

Moonquakes as recorded by seismic stations installed during Apollo 12 and 14 missions, observing periodic occurrence correlation with lunar gravity variations
01 p0134 A72-11225

Lunar passive seismic experiment deducing internal structure constitution and tectonic processes
03 p0418 A72-13108

Earth mantle and core density using Monte Carlo models compared with lunar structure from crust and seismology data, noting planetological contrast
04 p0571 A72-14616

ALSEP passive seismic experiment design, discussing instrument operation and performance parameters
04 p0508 A72-15095

ALSEP active seismic experiment design, investigating lunar subsurface geologic structure
04 p0508 A72-15096

Lunar seismic profiling experiment, describing explosives package, electronics and SAFE/ARM assembly
04 p0509 A72-15104

Apollo 14 explosion seismic refraction data, showing lunar near surface regolith thickness and compressional wave velocity
09 p1390 A72-23495

Lunar seismograms for LM and S-4B impacts in Apollo 12 experiment, indicating modulation mirage effect on signal distortion
10 p1536 A72-24153

ALSEP seismic records from Apollo 12 lunar module and Apollo 13 rocket stage impact, showing ringing phenomenon due to sphere curvature-caused energy dissipation
13 p2035 A72-28618

Ultrasonic signal propagation with distance along steel sphere surface compared with lunar seismic signal, discussing surface dent and lunar crater effects
13 p2035 A72-28619

Moonquakes and meteorite and manmade impacts as sources of seismic signals detected by Apollo lunar seismic stations
13 p2037 A72-28988

Lunar seismogram characteristics interpretation in terms of Gold-Soter powder layer theory, taking into account elastic wave scattering by surface undulations
14 p2154 A72-30506

Lunar interior structure and crust composition from artificial impact data recorded by Apollo seismometers
15 p2314 A72-32377

Seismic data from lunar geophysical stations network, noting moonquakes and meteoroid impacts
18 p2724 A72-36283

Q values from lunar seismic record measurements indicating separation of scattering and real loss parameters effects on energy propagation, discussing geophysical models
18 p2724 A72-36288

Velocity structure and properties of the lunar crust.
18 p2725 A72-36292

LUNAR SHADOW

Lunar shadowing of charged particles with arbitrary gyroradii and steady drift transverse to magnetic field applied to detector in low lunar orbit
21 p3104 A72-40482

LUNAR SOIL

NT LUNAR DUST

Apollo 14 rocks, breccia fragments and soil samples ages from Ar 40/Ar 39 and cosmic ray dating, discussing basalt Ar release patterns
01 p0117 A72-10052

Glass compositions in Apollo 14 soil, discussing correspondence to Fra Mauro basalts, mare basalts and soils, and gabbroic anorthositic and potash granite
01 p0123 A72-10054

Apollo 11 and 12 lunar soil samples, calculating mixing models by least squares and end member groups by Q mode factor analysis
01 p0124 A72-10057

Apollo 14 lunar soil sample 14163 orthopyroxene composition, determining K, P and rare earth elements
01 p0125 A72-10066

Dunite-norite olivine-rich microbreccia in Apollo 14 lunar fines sample 14002.8, discussing origin and chemical composition
01 p0126 A72-10106

Lunik 16 core-tube soil sample petrology and chemical composition
01 p0126 A72-10107

Martian surface nature from Surveyor and Apollo missions data on lunar particle size distribution
01 p0132 A72-11037

Lunar surface soil mechanical properties from computer simulation of Surveyor spacecraft observation data for each landing site, estimating cohesion
02 p0275 A72-11595

Luna 16 lunar soil sample tests, comparing friction coefficients and microhardness with terrestrial analogs
02 p0280 A72-12286

Lunar soil dielectric constant and loss-tangent and electrical resistivity measurement by Q meter method, noting resemblance to dense terrestrial rock powders
02 p0281 A72-12287

Apollo 12 lunar soil samples solar wind noble gas analysis of KREEP fragments, estimating Surveyor Crater age
03 p0414 A72-12902

Li, Be and B abundances in Apollo 11, 12 and 14 and Lunik 16 missions fine and core samples
03 p0414 A72-12903

Organic cosmochemistry evolution, discussing radio astronomical observations, lunar soil samples, meteorite analysis and interstellar gas cloud molecules
03 p0320 A72-13171

Sedimentology of Apollo 11 and 12 soils, investigating grain size distribution
03 p0440 A72-14325

Apollo 11 lunar fines behavior and gas evolution characteristics from high vacuum differential thermal analysis and mass spectroscopy
04 p0569 A72-14504

Lunar mare soil deformation and cracking from Surveyor and Apollo photographs
04 p0574 A72-14918

Vacuum handling system for lunar materials thermal-mophysical properties measurements under contamination preventive conditions
04 p0509 A72-15496

Apollo 11 lunar samples carbon compound geochemical analysis, using sequential scheme with minimum handling of solids and extracts
05 p0714 A72-16131

Lunar Imbrian Basin formation, discussing micrometeorite component composition of Apollo 14 soil samples
05 p0715 A72-16160

Apollo 14 lunar breccia samples, observing chondrules from meteoritic impact event
05 p0715 A72-16161

Lunar surface rocks, soil and breccia chemical composition, discussing element concentration, radiation effects on surface chemistry and volcanism
06 p0887 A72-18226

Apollo 15 mare basalts and breccias and premare igneous rocks, analyzing chemical composition and microstructure
06 p0888 A72-18262

Trace element concentrations of Apollo 15 basalt and soil samples by atomic spectrophotometry, colorimetry and isotope dilution
06 p0888 A72-18269

Primordial radioelements and cosmogenic radionuclides in Apollo 15 basalt, breccia and soil samples
06 p0889 A72-18274

Lunar surface bearing strength vs penetration curves from Surveyor 3 soil sample, comparing with in-situ remote measurements
07 p1067 A72-18873

Radionuclides formation rate as function of depth in moon for bombardments by galactic cosmic ray particles and by solar protons
07 p1057 A72-19140

Lunar soil electric properties, density, microhardness, abrasive properties and frictional and shear resistance determinations by Tor I operating in high vacuum
07 p1075 A72-19562

Tobacco tissue cultures with Apollo 12 lunar material, determining endogenous sterols and fatty acids concentrations by gas chromatography and mass spectrometry
07 p0920 A72-19850

Carbon chemistry of Apollo 14 size-fractionated fines, noting solar wind activity effect
07 p1082 A72-20290

Simulation study of lunar carbon chemistry, noting hydrocarbon production by solar wind interaction with fines
07 p1082 A72-20291

Lunar and terrestrial soil thermal and electrical properties measurement in vacuum and He atmospheres
08 p1232 A72-21150

Transient lunar phenomena theories, investigating surface features obscuration, lunar material melting, ejected gas glow discharge luminescence processes
08 p1233 A72-21212

Low power X ray diffractometer with multiwire proportional counter detector array for remote

mineralogical analysis of lunar, planetary or asteroid soils detector array
08 p1167 A72-21507

Lunar rheolite cosmogenic Al 26 and Na 22 distribution in Lunik 16 sample interpreted by lunar surface soil impact induced mixing
08 p1240 A72-22190

Igneous and microbreccia lithic fragments, glasses and chondrules from Luna 16 fines, confirming lunar surface melting and igneous differentiation
09 p1379 A72-22253

Petrological analysis of Mare Fecunditatis regolith returned from Luna 16 mission
09 p1379 A72-22254

Microscopic and electron microprobe analyses of silicate melt inclusions and glasses in lunar soil fragments from Lunik 16 core sample
09 p1379 A72-22255

Lithic and vitreous particles in Lunik 16 core tube samples from Mare Fecunditatis, discussing particle type proportions and petrological and mineralogical aspects
09 p1379 A72-22256

Optical petrographic, electron microprobe and single crystal X ray diffraction analysis of basaltic and monomineralic soil fragments of Lunik 16 core sample from Sea of Fertility
09 p1379 A72-22257

Lunik 16 microbasalt sample containing skeletal olivine, plagioclase, ilmenite and interstitial pyroxene, comparing to ferromagnesian rich Apollo 11 and 12 basalts
09 p1379 A72-22258

Shock metamorphism in Luna 16 soil sample, indicating regolith formation by meteorite impact
09 p1380 A72-22259

Opaque mineralogy of Luna 16 soil sample, emphasizing compositional variations of Fe-Ti-Cr-Al-Mg spinels
09 p1380 A72-22261

Rb-Sr internal isochron determination of Luna 16 maria basalt age, discussing major lunar magmatic activity time interval
09 p1380 A72-22263

Gd and Sm isotopic composition measurement in Luna 16 soil with largest low energy neutron fluence
09 p1380 A72-22265

Particle track densities in Lunik 16 soil column grains from Sea of Plenty, noting surface irradiation and regolith age
09 p1380 A72-22268

Radiation damage by heavy solar particles in soil grains from Lunik 16 and landing Apollo sites
09 p1381 A72-22269

Lunik 16 lunar soil samples petrogenesis and chemical composition, comparing to Apollo regoliths
09 p1381 A72-22271

Lunik 16 samples trace element concentration, suggesting feldspar excess and local regolith derivation
09 p1381 A72-22272

Lunik 16 soil sample chemical composition indicating similarity of Sea of Fertility to Sea of Tranquility sites geochemical characteristics
09 p1381 A72-22273

Rare earth and trace elements in Lunik 16 soil, comparing abundances with chondrites and Apollo samples
09 p1381 A72-22274

Bulk and rare earth abundances in Luna 16 soil levels A and D by sequential instrumental neutron activation analysis
09 p1381 A72-22275

Lunik 16 soil samples trace elements composition suggesting meteoritic component presence and similarity to Apollo soils
09 p1381 A72-22276

Oxygen 18/16 composition of Lunik 16 soil, comparing with Apollo soils
09 p1381 A72-22277

Lunar soil radiogenic U-Th-Pb analyses of Lunik 16 samples from Sea of Fertility
09 p1381 A72-22278

Apollo lunar fine samples total emittance as function of temperature, using spectral emittance measurement technique
09 p1388 A72-23028

Lunar surface darkening caused by solar wind effect, noting Fe valence state changes evaluation from photoelectronic spectroscopy of foil samples exposed to ion bombardment
09 p1394 A72-23665

Thermal conductivity, diffusivity and specific heat of lunar soil and basalt analogs, using Luna 16 samples
10 p1532 A72-23753

Vacuum and inert gas TOR-I device for studying physical properties of lunar soil and terrestrial analogs
10 p1478 A72-23754

Luna 16 lunar soil sample tests, comparing friction coefficients and microhardness with terrestrial analogs
10 p1532 A72-23755

Lunar soil dielectric constant and loss-tangent and electrical resistivity measurement by Q meter method, noting resemblance to dense terrestrial rock powders
10 p1532 A72-23756

Rb-Sr isotopic age determination on density and size fractions of Apollo 11 fine soil and basaltic materials
10 p1538 A72-24165

Apollo 12 and 14 lunar soils K, Rb and Sr isotopic composition evaluation, noting microbreccia as major nonbasaltic constituent
11 p1723 A72-26497

Lunar topsoil density variations from Lunik and Surveyor radio wave, alpha and gamma scattering data, discussing Lunik 13 and Surveyor 7 landing sites
11 p1724 A72-26909

Lunar granular materials thermophysical properties, emphasizing thermal conductivity data and heat transfer mechanisms
12 p1869 A72-27333

Lunar regolith glassy particles formation processes modeling with molten soil samples, emphasizing liquid particles spattering with subsequent cooling during meteoritic impact
13 p2036 A72-28767

Disturbance-induced lunar surface darkening due to soil photometric function changes resulting from particle rearrangement
13 p2037 A72-28994

X ray milliprobe apparatus adaptation for examining single crystals from lunar samples
13 p1960 A72-29839

Luna 16 fine lunar soil fraction biological effect on mice
14 p2079 A72-30469

Apollo 12 fines thermal conductivity in vacuum at 200-400 K, using least squares technique for curve fit
14 p2154 A72-30509

Apollo 12 lunar fines spectral and thermal radiation properties as function of bulk density, presenting emittance as function of temperature and solar reflectance
14 p2154 A72-30513

Soviet unmanned Luna 20 mission, describing launch, lunar trajectory injection, midcourse correction, lunar orbit and landing, surface soil sampling and return to earth
14 p2163 A72-30680

Lunar topsoil-solid bodies interaction in terms of hardness and friction, discussing simulation equipment
14 p2161 A72-31074

Cosmic ray irradiations study of gas rich meteoroid aubrites by track method, comparing with lunar soils
15 p2303 A72-31308

Lunar dumbbell shaped glass globules formation due to rotation and surface tension effects of ejecta from meteoric impacts
15 p2306 A72-31628

Lunar surface diurnal temperature variations calculation based on Apollo 12 lunar fines thermophysical properties and surface layer core-tube sample density
16 p2454 A72-33432

Lunar surface breccias origin, using exploration data to reappraise ballistic theory of giant craters and maria formation in favor of volcanic concepts
16 p2461 A72-34180

Petrologic comparisons of lunar terra materials.
17 p2615 A72-35684

The distribution of carbon in lunar samples from Apollo 11, 12 and 14.
17 p2615 A72-35685

Analysis of vegetable seedlings grown in contact with Apollo 14 lunar surface fines.
17 p2505 A72-35925

Lunar ash flows - Isothermal approximation.
18 p2723 A72-36026

Thermoluminescence lunar samples - Measurement of temperature gradients in core material.
18 p2724 A72-36278

Laboratory studies on seismic and electrical properties of the moon.
18 p2724 A72-36282

Thermophysical properties of lunar material returned by Apollo missions.
18 p2725 A72-36290

Measurements of radon emanation from Apollo 11, 12, and 14 fines.
18 p2728 A72-36970

Gd and Sm isotope composition in Apollo 15 soils and drill stem samples, discussing lunar sedimentary processes dating from neutron capture dependence on depth
18 p2729 A72-36974

Lunar and terrestrial soil thermal and electrical properties measurement in vacuum and He atmospheres
20 p2968 A72-39255

Brief review of thermoluminescence studies in lunar samples.
20 p2970 A72-39402

Spectral emittance of Apollo-12 lunar fines.
20 p2970 A72-39486

Spectral reflectance and emittance of Apollo 11 and 12 lunar material.
20 p2970 A72-39609

Improved techniques for separation and determination of rare-earth elements in extraterrestrial material.
20 p2900 A72-39836

Lunar regolith glassy particles formation processes modeling with molten soil samples, emphasizing liquid

particles spattering with subsequent cooling during meteoritic impact
21 p3102 A72-40268

Highly aluminous glasses in lunar soils and the nature of the lunar highlands.
21 p3104 A72-40490

Fragments of terra rock in the Apollo 12 soil samples and a structural model of the moon.
21 p3110 A72-41452

Uranium distribution in basalt fragments of five lunar samples.
23 p3261 A72-43399

Trace element geochemistry of Apollo 16 soil 68501.
23 p3337 A72-43939

Solid solution, subsolidus reduction and compositional characteristics of spinels in some Apollo 15 basalts.
23 p3262 A72-44135

Major element composition of glasses in three Apollo 15 soils.
23 p3339 A72-44137

The carbon chemistry of the moon.
23 p3339 A72-44149

Thermal cycling tests for natural remanent magnetism of lunar soil samples, proposing magnetization mechanism of material buried in regolith
24 p3443 A72-45373

Soil mechanical properties at the Apollo 14 site.
24 p3447 A72-45556

LUNAR SPACECRAFT
NT APOLLO SPACECRAFT
NT LUNAR MODULE
NT LUNAR ORBITER
NT LUNAR PROBES
NT LUNAR SATELLITES
NT LUNIK LUNAR PROBES
NT RANGER LUNAR PROBES
NT SURVEYOR LUNAR PROBES

LUNAR SURFACE
U LUNAR TOPOGRAPHY

LUNAR SURFACE SCIENTIFIC MODULES
U LSSM

LUNAR SURFACE VEHICLES
NT LUNAR ROVING VEHICLES
NT LUNOKHOD LUNAR ROVING VEHICLES
NT MANNED LUNAR SURFACE VEHICLES

Remote control and navigation tests for application to long-range lunar surface exploration.
22 p3203 A72-43131

LUNAR TEMPERATURE
Heat conduction model of surface thermal history of moon as function of dust, anorthosite, basalt and dunite layers
04 p0571 A72-14598

Lunar thermal history and radioactivity upper limits determination consistent with proposed temperature distribution and Apollo chondrite data, implying low uranium content
04 p0581 A72-15579

Lunar surface temperature-independent and dependent plane homogeneous models for thermal properties study, discussing surface roughness and localized thermal anomalies
06 p0887 A72-18227

Diurnal temperature variations in lunar surface layer from Apollo 12 samples, comparing with Apollo 11 samples and IR measurements
07 p1068 A72-18874

Lunar surface roughness effect on temperature distribution, noting solar elevation and observation angle dependence
11 p1715 A72-25244

[AIAA PAPER 72-310]
Russian book on radar studies of moon covering lunar motion, dimensions, mass, density and surface layer thermal and optical properties
11 p1720 A72-26047

Papers on thermal characteristics of moon covering earth based and in situ surface temperature measurements, radar mapping, heat flow experiments, etc
12 p1869 A72-27326

Surveyor spacecraft lunar thermal data, comparing spatial resolution with earth based measurements
12 p1869 A72-27329

Apollo 11 EASEP nickel resistance thermometer lunar surface data, presenting unshadowed equivalent brightness temperature and thermal parameters and emission directional dependence
12 p1869 A72-27330

ALSEP heat flow experiment design and calibration, presenting independent vertical temperature gradient and thermal conductivity measurements in regolith
12 p1869 A72-27331

Apollo 15 lunar heat flow experiment, discussing temperature data from probes and long lived radioisotopes decay effects
12 p1869 A72-27332

Lunar granular materials thermophysical properties, emphasizing thermal conductivity data and heat transfer mechanisms
12 p1869 A72-27333

Lunar interior thermal history discussing mathematical models for radioactive heat source, initial con-

ditions, temperature distribution and time dependent fractionation
12 p1870 A72-27336

Nighttime lunar surface thermal properties from differential IR flux scans with earth based Cassegrain telescope, noting difference in brightness temperature gradients between highlands and maria
14 p2153 A72-30503

Lunar interior electrical conductivity from surface magnetic field measurements by Apollo magnetometers, calculating temperature profile for olivine moon model
14 p2154 A72-30508

Lunar interior thermal history and current state from theoretical temperature models, taking into account initial conditions, heat sources, differentiation and simulated convection
14 p2155 A72-30519

Thermal history, heterogeneity, refraction and transition phenomena of lunar glassy fragments and spherules, using electron microprobe analysis
15 p2306 A72-31586

Thermal history and early magmatism for lunar models, considering high near-surface temperatures and radionuclides upward transport during melting
15 p2311 A72-32082

Lunar eclipse observations at millimeter wavelengths on 10 February 1971, determining surface cooling for Copernicus, Mare Serenitatis and highland region
15 p2311 A72-32087

Lunar surface diurnal temperature variations calculation based on Apollo 12 lunar fines thermophysical properties and surface layer core-tube sample density
16 p2454 A72-33432

Physical structure of the moon.
17 p2615 A72-35680

Geochemically and geophysically consistent model of lunar accretion process to explain initial temperature distribution
18 p2725 A72-36291

Lunar temperature profiles from electrical conductivity profile of olivine single crystal as lunar interior material representative sample
20 p2967 A72-39179

Lunar thermal history model, considering nonuniform initial composition, radioactive element partitioning and melt cutoff value
22 p3225 A72-42529

The moon's thermal state and an interpretation of the lunar electrical conductivity distribution.
22 p3226 A72-42531

Lunar albedo and temperature distribution from simultaneous photoelectric and far IR brightness temperature measurements of sunlit lunar surface
22 p3226 A72-42536

LUNAR TIDES
Lunar tidal variations of ionospheric electron density at fixed heights for different solar hours over Huan-cayo and Puerto Rico
01 p0053 A72-10089

Declinational component of geomagnetic lunar tide diurnal variations, noting effects of electric currents induced in oceans
11 p1622 A72-26103

Observational bias source in lunar transient events correlation with perigee and tidal stresses, using statistical analysis for 1947-1967 period
14 p2150 A72-30324

Lunar origin and evolution, considering gravitational energy, radioactive isotopes and tidal deformations as heat sources
14 p2161 A72-30997

Semidiurnal variation in O I 5577 A nightglow due to lunar tidal dynamics effect in E and F regions
16 p3283 A72-32971

Anomalistic lunar tide vs latitudinal or declinational tidal wave for moonquakes recorded at Apollo 12 landing site
16 p2457 A72-33565

Information-prediction value of the tidal solar-lunar rhythmicity of certain meteorological processes
17 p2577 A72-35779

LUNAR TOPOGRAPHY
Lunar crater population and distribution time development under meteoroid and solar wind bombardment, developing model for absolute formation ages
01 p0124 A72-10056

Lunar surface soil mechanical properties from computer simulation of Surveyor spacecraft observation data for each landing site, estimating cohesion
02 p0275 A72-11595

Height-depth ratios of lunar craters and terrestrial calderas from topographic measurements
02 p0278 A72-11908

Photogrammetric techniques for Tranquility base experiment locations map based on surface and spacecraft photographs
02 p0280 A72-12198

Lunar limb structure from occultation traces from point source stars, constructing model with levels and slopes
03 p0420 A72-13129

Lunar surface altitude measurements, considering difficulty due to reference level absence and accuracy improvement by photometric procedure

03 p0421 A72-13195

Apollo 14 basaltic evidence for selective volatilization on lunar surface, using electron probe analysis

03 p0439 A72-14273

Soviet lunar rover-carrying Luna 17 lander, obtaining topography and map in Sea of Rains

04 p0576 A72-15063

Lunar surface small crater statistical analysis and age prediction based on density and diameter correlation from Soviet Lunar Rover panoramic pictures

04 p0576 A72-15065

Lunar sea surface model derivation from morphology data analysis, suggesting four-layer bottom relief of basaltoidal lava, rocks, breccia and surface regolith

04 p0576 A72-15069

Lunar volcanology, discussing domes, crater chains, halos, sinuous rills, mare wrinkle ridges, dark smooth level material and ring dike-like structures

04 p0581 A72-15619

Photogrammetric coordinate relation of points on lunar surface and stereo panoramas of scanning photographs by Luna 9 and 13 orbiters

05 p0660 A72-15832

Quasi-specular and Lambert reflection of short radio waves from lunar surface dependent on central portion of near side

05 p0631 A72-17039

Lunar configuration, limb relief and coordinates of western hemisphere and far side from Zond 6 photograph reduction

05 p0721 A72-17040

Lunar gravity measurements via Apollo 14 Doppler radio tracking over 100 kilometer band during low periaxis altitude orbits, relating to surface features

05 p0722 A72-17126

Relative age determination of lunar surface regions using orbital photography and model of small impact erosion

06 p0878 A72-17759

Lunar gravitational field, relief and internal structure, suggesting two layer model and crust thickness change relation to field characteristics

06 p0881 A72-17926

Lunar surface details absolute and relative heights, estimating accuracy by comparison of data from different catalogs

06 p0884 A72-18034

Lunar sinuous rills location and origin, discussing Orbiter photographic maps, predominance in maria and similarity to terrestrial lava tubes

06 p0887 A72-18219

Lunar maria material igneous origin, relating surface features to various volcanic eruption types

06 p0887 A72-18220

Lunar photometric studies, discussing surface light scattering properties, data reduction and relative and systematic errors in brightness

06 p0817 A72-18224

Lunar regolith top surface polarimetric properties of sunlight-exposed rocks and fines compared to terrestrial rocks and meteorites

06 p0887 A72-18225

Lunar surface temperature-independent and dependent plane homogeneous models for thermal properties study, discussing surface roughness and localized thermal anomalies

06 p0887 A72-18227

Copernicus rays and ejecta blanket V-features form and distribution, suggesting association with satellite craters of secondary impact origin

07 p1067 A72-18872

Diurnal temperature variations in lunar surface layer from Apollo 12 samples, comparing with Apollo 11 samples and IR measurements

07 p1068 A72-18874

Lunar topography measurement by libration method based on stereoscopy and by photographic method

08 p1230 A72-21020

Determination method for selenographic coordinates of points on lunar surface, discussing astronomical observations from moon

08 p1231 A72-21131

Lunar center of mass position with respect to visible hemisphere physical surface calculated from photogrammetric analysis and Lunar Orbiter 1 data

08 p1232 A72-21158

Catalog of lunar craters central peaks and floor objects on visible hemisphere based on Kuiper photographic atlas

08 p1236 A72-21476

Planetary and lunar surface relief reconstruction from photographic imagery, discussing statistical morphological characteristics determination from relief

08 p1238 A72-21833

Lunik 16 landing site geologic similarity to Apollo 11 and 12 sites on basaltic mare fill, noting impact bombardment developed regolith presence

09 p1379 A72-22251

Lunar objects position accuracy assessment based on pairwise comparison of current selenodetic reference catalogs

09 p1388 A72-23054

Algorithm and formulas for lunar limb absolute heights determination in selenodetic reference points system from lunar photographs

09 p1388 A72-23057

Spectral reflectance properties of lunar surface areas, discussing materials identification and maria depth determination

09 p1393 A72-23664

Geological provinces of lunar near side, showing nature and distribution patterns of five surface shaping periods

10 p1530 A72-23701

Lunar near side visual appearance reconstruction at two geologically significant points of evolution of Imbrian period

10 p1530 A72-23702

Lunar surface roughness effect on temperature distribution, noting solar elevation and observation angle dependence

[AIAA PAPER 72-310]

11 p1715 A72-25244

Lunar surface features absolute and relative heights, estimating accuracy by comparison of data from different catalogs

11 p1719 A72-25970

Russian book on radar studies of moon covering lunar motion, dimensions, mass, density and surface layer thermal and optical properties

11 p1720 A72-26047

Circularly polarized ultrashort radio wave reflection from lunar and planetary surfaces, determining angular scattering spectrum

11 p1599 A72-26908

Photogeologic evidence of differentiation and deposition of lunar highland volcanic rocks at Apollo 16 landing site

12 p1866 A72-27115

Lunar surface roughness mapping by combined IR and radar measurements

12 p1869 A72-27328

Lunar surface roughness thermal characteristics, comparing IR data with three realistic models

12 p1870 A72-27335

Terrestrial volcanic lava conduits origin and development association with lunar maria channels and sinuous rills

13 p2037 A72-28992

Disturbance-induced lunar surface darkening due to soil photometric function changes resulting from particle rearrangement

13 p2037 A72-28994

Isogram map of Mare Imbrium reddening coefficients, noting correlation between chromaticity and relief details

14 p1248 A72-30208

Moon and Venus relief from backscattering diagrams based on radar echoes, calculating root-mean-square angles of surface inclination

14 p1251 A72-30468

Nighttime lunar surface thermal properties from differential IR flux scans with earth based Cassegrain telescope, noting difference in brightness temperature gradients between highlands and maria

14 p1253 A72-30503

Lunar seismogram characteristics interpretation in terms of Gold-Soter power layer theory, taking into account elastic wave scattering by surface undulations

14 p1254 A72-30506

Lunar surface profile, subsurface features and electrical properties measurement for Apollo 17 coherent radar and optical recording system

14 p2085 A72-30512

Lunar surface microerosion relationship to interplanetary dust particle flux distributions, investigating sputter erosion and lunar rocks lifetimes

15 p2310 A72-31988

Lunar eclipse observations at millimeter wavelengths on 10 February 1971, determining surface cooling for Copernicus, Mare Serenitatis and highland region

15 p2311 A72-32087

Lunik 14 spacecraft radio signal reflection from lunar surface, showing energy spectrum dependence on surface roughness

15 p2202 A72-32655

Lunokhod 1 17 November 1970-30 September 1972 day by day activity, noting distance traveled, TV pictures, physicochemical analyses and still photographs transmitted

16 p2456 A72-33497

Theoretical analyses on Apollo lunar surface electrical properties experiment transmitter antenna

17 p2515 A72-34423

Extension of lunar nomenclature to the far side of the moon

17 p2610 A72-35213

A new, earth-based radar technique for the measurement of lunar topography

18 p2659 A72-36277

Comments on the figure of the moon based on preliminary results from laser altimetry

18 p2724 A72-36280

Lunar color boundaries and their relationship to topographic features - A preliminary survey

18 p2724 A72-36281

Lunar surface mapping for Mg, Al and Si along ground tracks swept out by orbiting Apollo 16 spacecraft, noting geochemical X ray fluorescent analysis

18 p2726 A72-36556

Lunar gravitational field, relief and internal structure, suggesting two layer model and crust thickness change relation to field characteristics

18 p2730 A72-37151

Determination of mutual orientation in Euler angles for nine selenodetic catalogs

19 p2863 A72-38076

Lunar center of mass position with respect to visible hemisphere physical surface calculated from photogrammetric analysis and Lunar Orbiter 1 data

20 p2969 A72-39263

Experimental evidence against the role of selective volatilization on the lunar surface

21 p3013 A72-40452

Highly aluminous glasses in lunar soils and the nature of the lunar highlands

21 p3104 A72-40490

Elevations and depressions frequencies determined for visible lunar continents and maria

21 p3114 A72-41768

A new unified system for designating objects on the lunar surface

21 p3114 A72-41780

Comments on the figure of the moon from Apollo landmark tracking

22 p3226 A72-42534

Lunar crater origins due to external impact of particles moving within earth-moon gravitational dipole during earliest history stage

22 p3226 A72-42538

High resolution lunar surface stereophotographs from pairing overlapping Lunar Orbiter photographs

22 p3230 A72-43195

Isogram map of Mare Imbrium reddening coefficients, noting correlation between chromaticity and relief details

23 p3333 A72-43238

LUNAR TRAJECTORIES

NT EARTH-MOON TRAJECTORIES

NT MOON-EARTH TRAJECTORIES

Two point boundary value solution for N-body trajectories, comparing asymptotic with numerical integration solutions for several lunar and interplanetary trajectories

07 p1068 A72-18945

LUNEBERG LENSES

U RADAR CORNER REFLECTORS

LUNG MORPHOLOGY

Electron microscope examination of freeze-etched air-filled lung alveoli extracellular lining layer, discussing sample preparation techniques

05 p0623 A72-16787

Ultrastructural and morphometric studies of beryllium oxide-contaminated environment effect on monkey and dog lung tissue

07 p0925 A72-20686

Electron microscope study of hyperoxia-induced pathogenetic ultrastructural changes in rat lung

12 p1761 A72-27531

Morphological changes in the lungs and kidneys during prolonged intoxication of the organism by carbon tetrachloride

19 p2760 A72-38035

Morphometric evaluation of changes in lung structure due to high altitude

22 p3143 A72-42585

LUNGS

Pulmonary functional inhomogeneities effects on steady state oxygen and CO diffusing capacity estimates in gas transfer resistances terms

01 p0014 A72-10847

Lung ventilation nonuniformity determination by single calm breath method, showing nitrogen concentration in alveolar phases

02 p0165 A72-12515

Single breath method for pulmonary diffusing capacity measurement with respect to total lung capacity and inspiration time

05 p0620 A72-17174

Compression cycles effects on alveolar volumes of sea lions and dogs excised lungs, noting decompression sickness prevention by airways cartilaginous reinforcement

08 p1116 A72-21186

Vasomotor efferent effects on rabbit lung posterior lobe blood content in response to electrical stimulation of vagus nerve peripheral ends

09 p1268 A72-23693

Quasi-steady creeping flow in small airways of spherical, oblate and prolate ellipsoid and circular cylinder lung models, obtaining Stokes equations solutions

10 p1431 A72-24469

Chest strapping-induced increased lung recoil pressure effects on maximal expiratory flow relation to lung surface compliance decrease

10 p1425 A72-24478

- Elastic lung shaped model for distribution analysis of weight induced stresses, strains and surface pressures in lung
10 p1425 A72-24479
- Pulmonary capillary bed filling as function of arterial pressure in perfused frozen dog lungs
10 p1425 A72-24480
- Blood flow stratification effect on alveolar gas exchange in liquid filled lungs in dogs from Xe 133 concentration measurements
10 p1425 A72-24481
- Artificial heart-lungs model with contractile polymer membrane as synthetic muscles to react with gases and liquids, discussing design features
10 p1431 A72-24640
- Lumped parameter nonlinear RC circuit lung model for positive pressure respirator design
11 p1588 A72-26631
- Pulmonary oxygen transport dynamic model representing lung gas-side airway and alveolar regions and blood-side capillary bed
13 p1909 A72-28996
- Four-parallel-compartment lung model for emptying pattern study, using expired nitrogen concentration data to calculate alveolar dilution ratio and emptying rate
14 p2079 A72-30703
- Nonlinear theory of pulmonary ventilation distribution in two compartment model of human lungs
16 p2358 A72-33025
- Effects of vagotomy and increased blood pressure on the incidence of decompression-induced pulmonary hemorrhage.
18 p2650 A72-36446
- Role of the autonomic nervous system in the hypoxic response of the pulmonary vascular bed.
18 p2650 A72-36572
- Rat pulmonary lipid metabolism during feeding and fasting from studies of lung lecithin half life after C-14/1/palmitate and H-3/U/glucose injection
18 p2651 A72-36573
- Regional lung function in man during immersion with the head above water.
19 p2758 A72-38701
- Pulmonary air-trapping induced by water immersion.
19 p2759 A72-38711
- Relation of the electrocardiogram to hemodynamic alterations in pulmonary embolism.
19 p2759 A72-38816
- Vectorcardiographic and electrocardiographic differentiation between cor pulmonale and anterior wall myocardial infarction.
21 p3001 A72-40769
- Control of the circulating blood mass in the case of a functional detachment of various amounts of pulmonary tissue
21 p3012 A72-41825
- Lung volume changes of people in antihypostatic position in hospital beds for control, exercising and muscle electric-stimulated groups
23 p3256 A72-43918
- Possibility of determining the lung ventilation volume by the mathematical modeling method
24 p3374 A72-44597
- Determination of the diffusional capability of lungs by the method of delayed respiration
24 p3374 A72-44598
- Gas exchange mechanism in lung alveoles and capillaries, discussing cell metabolism for oxygen uptake and carbon dioxide formation
24 p3371 A72-44599
- LUNIK LUNAR PROBES**
Lunik 16 core-tube soil sample petrology and chemical composition
01 p0126 A72-10107
- Li, Be and B abundances in Apollo 11, 12 and 14 and Lunik 16 missions fine and core samples
03 p0414 A72-12903
- Soviet lunar rover-carrying Luna 17 lander, obtaining topography and map in Sea of Rains
04 p0576 A72-15063
- Lunar rheolite cosmogenic Al 26 and Na 22 distribution in Lunik 16 sample interpreted by lunar surface soil impact induced mixing
08 p1240 A72-22190
- Lunik 16 landing site geologic similarity to Apollo 11 and 12 sites on basaltic mare fill, noting impact bombardment developed regolith presence
09 p1379 A72-22251
- Electron microprobe analysis of Lunik 16 basalt fragments, noting similarity to Apollo 11 and 12 igneous rocks
09 p1379 A72-22252
- Igneous and microbreccia lithic fragments, glasses and chondrules from Luna 16 fines, confirming lunar surface melting and igneous differentiation
09 p1379 A72-22253
- Petrological analysis of Mare Fecunditatis regolith returned from Luna 16 mission
09 p1379 A72-22254
- Microscopic and electron microprobe analyses of silicate melt inclusions and glasses in lunar soil fragments from Lunik 16 core sample
09 p1379 A72-22255
- Lithic and vitreous particles in Lunik 16 core tube samples from Mare Fecunditatis, discussing particle type proportions and petrological and mineralogical aspects
09 p1379 A72-22256
- Optical petrographic, electron microprobe and single crystal X ray diffraction analysis of basaltic and monomineralic soil fragments of Lunik 16 core sample from Sea of Fertility
09 p1379 A72-22257
- Lunik 16 microbasalt sample containing skeletal olivine, plagioclase, ilmenite and interstitial pyroxene, comparing to ferromagnesian rich Apollo 11 and 12 basalts
09 p1379 A72-22258
- Electron microprobe analyses of Lunik 16 mare basalt fragment G37 with high Al and low Mg content, discussing fragments G46 and G51
09 p1380 A72-22260
- Opaque mineralogy of Luna 16 soil sample, emphasizing compositional variations of Fe-Ti-Cr-Al-Mg spinels
09 p1380 A72-22261
- Luna 16 rock sample B-1 petrology, mineralogy and chemistry, noting fine grained ophitic basalt nature
09 p1380 A72-22262
- Rb-Sr internal isochron determination of Luna 16 maria basalt age, discussing major lunar magmatic activity time interval
09 p1380 A72-22263
- Gas retention and cosmic ray exposure ages of Luna 16 basalt fragment from Mare Fecunditatis
09 p1380 A72-22264
- Gd and Sm isotopic composition measurement in Luna 16 soil with largest low energy neutron fluence
09 p1380 A72-22265
- Rare gas concentrations in Luna 16 fines, using stepwise heating technique
09 p1380 A72-22266
- Mass spectroscopic measurement of inert gases in Lunik 16 fragments and dust samples
09 p1380 A72-22267
- Particle track densities in Lunik 16 soil column grains from Sea of Plenty, noting surface irradiation and regolith age
09 p1380 A72-22268
- Fossil track densities and thermoluminescence measurements of Luna 16 feldspar crystal samples compared to Apollo 12 samples
09 p1381 A72-22270
- Lunik 16 lunar soil samples petrogenesis and chemical composition, comparing to Apollo regoliths
09 p1381 A72-22271
- Lunik 16 samples trace element concentration, suggesting feldspar excess and local regolith derivation
09 p1381 A72-22272
- Lunik 16 soil sample chemical composition indicating similarity of Sea of Fertility to Sea of Tranquility sites geochemical characteristics
09 p1381 A72-22273
- Rare earth and trace elements in Lunik 16 soil, comparing abundances with chondrites and Apollo samples
09 p1381 A72-22274
- Bulk and rare earth abundances in Luna 16 soil levels A and D by sequential instrumental neutron activation analysis
09 p1381 A72-22275
- Lunik 16 soil samples trace elements composition suggesting meteoritic component presence and similarity to Apollo soils
09 p1381 A72-22276
- Oxygen 18/16 composition of Lunik 16 soil, comparing with Apollo soils
09 p1381 A72-22277
- Lunar soil radiogenic U-Th-Pb analyses of Lunik 16 samples from Sea of Fertility
09 p1381 A72-22278
- Luna 16 automatic probe drilling experiment, obtaining lunar rocks physicochemical properties for comparison with terrestrial rocks
11 p1613 A72-25938
- Luna 16 Sea of Abundance rock volume weight, destruction pattern, compressibility, shear strength and carrying ability, comparing to terrestrial rock
11 p1724 A72-26910
- Soviet unmanned Luna 20 mission, describing launch, lunar trajectory injection, midcourse correction, lunar orbit and landing, surface soil sampling and return to earth
14 p2163 A72-30680
- Chemical composition of Luna 16 and Luna 20 rock samples from Sea of Fertility and Apollonius C crater
24 p3440 A72-45109
- LUNIK 9 LUNAR PROBE**
Investigation of the redundancy of telemetry information from the automatic lunar stations Luna 9 and Luna 13
21 p3014 A72-40312
- LUNIK 13 LUNAR PROBE**
Investigation of the redundancy of telemetry information from the automatic lunar stations Luna 9 and Luna 13
21 p3014 A72-40312
- LUNIK 16 LUNAR PROBE**
Luna 16 fine lunar soil fraction biological effect on mice
14 p2079 A72-30469
- IR spectroscopy of Luna 16 regolith samples, noting differences in reflection, emission and transmission spectra of related terrestrial rocks
17 p2610 A72-35212
- LUNOKHOD LUNAR ROVING VEHICLES**
Lunar laser ranging for orbital and rotational motion, continental drift and pole studies, discussing Lunokhod I roving vehicle mounted laser reflector
01 p0031 A72-11152
- Luna 16 and 17 and Lunokhod I flight, landing, operations and lunar surface activities
03 p0440 A72-14307
- Nighttime laser ranging of French reflector for Soviet Lunokhod, discussing universal-ephemeris time difference determination
05 p0721 A72-16771
- Laser tracking measurements of distance to light reflector mounted on Lunokhod 1, describing equipment and procedure
12 p1825 A72-27888
- Lunokhod 1 17 November 1970-30 September 1972 day by day activity, noting distance traveled, TV pictures, physicochemical analyses and still photographs transmitted
16 p2456 A72-33497
- Laser tracking measurements of distance to light reflector mounted on Lunokhod 1, describing equipment and procedure
16 p2404 A72-33997
- Nighttime laser ranging of French reflector for Soviet Lunokhod, discussing universal-ephemeris time difference determination
17 p2611 A72-35274
- Galactic X rays investigation with X ray telescope on Lunokhod 1, noting observed singularities connection with statistical distribution of quasars and radio galaxies
19 p2802 A72-38090
- LUTETIUM**
Lutetium strength and plastic deformation characteristics under tension, presenting temperature and strain rate effects
23 p3301 A72-43754
- LUXEMBOURG EFFECT**
Monochromatic plasma waves linear and nonlinear coupling, discussing LF modulation partial transfer /Luxembourg effect/ and application to ionospheric diagnostics
23 p3319 A72-43517
- LYAPUNOV FUNCTIONS**
U LYAPUNOV FUNCTIONS
LYMAN ALPHA RADIATION
Lyman alpha, Lyman beta and Balmer alpha hydrogen airglow emission simultaneous measurements compared with solar radiation resonant scattering models
01 p0061 A72-10899
- Far UV astronomical studies with moderate spectral and spatial resolution instruments, discussing Lyman alpha line background
03 p0417 A72-13049
- French Lyman alpha photometer experiment onOGO 5 satellite, describing geocoronal observations, extraterrestrial emission and Bennett and Encke comets hydrogen envelopes
04 p0582 A72-15684
- D-2A satellite antisolar mission, examining Lyman alpha emission from geocorona and interstellar hydrogen wind
04 p0582 A72-15688
- Ionospheric geocoronal L alpha emission intensity related to solar activity level from Cosmos 215 satellite data
05 p0659 A72-17038
- Hydrogen 2p and 2s states formation during 1-25 keV atomic collisions with rare gases from Lyman alpha radiation cross section measurement
05 p0693 A72-17168
- Refractometer design based on air dielectric constant dependence on humidity, comparing performance with Ly-alpha humidimeter
06 p0841 A72-17668
- Argon ion spectra overlap with satellites to carbon and boron Lyman alpha lines, employing theta pinch
06 p0852 A72-17897
- Neutral interstellar hydrogen atoms mean volume density from Lyman alpha absorption and radio measurements in solar region
06 p0886 A72-18098
- Lyman alpha radiation emission cross sections due to H/2p/ and H/2s/ formation in protons and hydrogen atoms collisions with hydrogen molecules
07 p1038 A72-20678
- Local interstellar hydrogen survey from OAO-2 observations of Lyman alpha absorption at 1216 A for B2 or earlier stars
08 p1235 A72-21392
- Quasi-stellar objects hydrogen L-alpha lines computation via cloud collapse and ionizing radiation flux

model, comparing computed distribution with PHL 957 and 4C 05.34 observations

09 p1382 A72-22280

Redshifted L alpha flux upper limit restricting hot ionized gas models for gravitational binding of Coma galactic cluster

09 p1383 A72-22292

Geocoronal hydrogen Lyman alpha glow intensity and zenith angle dependence from observations by rocket-borne extreme UV photometers

09 p1298 A72-22593

Polarization fraction calculation for Lyman alpha radiation from excited H atom collisions, using Glauber, Born and Vainshtein approximations

09 p1355 A72-22790

Solar UV radiation and Lyman alpha flux observation during 7 March 1970 solar eclipse with Nike-Apache rocket photometer soundings

12 p1862 A72-27145

Solar Lyman alpha radiation flux over disk during solar eclipse from rocket measurements

12 p1863 A72-27147

Rocket-borne photographic measurement of Lyman alpha corona brightness during 7 March 1970 eclipse, comparing limb white light variations

13 p2043 A72-29541

Carbon origin in comets associated with propyne photodissociation by solar 1216 A Lyman alpha radiation

13 p2050 A72-29995

Solar UV Lyman alpha radiation intensity measurements, using Vertikal-1 rocket-borne photometer and photoelectron analyzer

14 p2128 A72-30465

Molecular oxygen concentrations from solar Lyman alpha radiation absorption profile in mesosphere, using rocket-borne nitric oxide filled ion chamber

15 p2230 A72-32264

Solar and geocoronal hydrogen Lyman alpha radiation detector, discussing ion chamber with magnesium difluoride window and nitric oxide gas

15 p2239 A72-32336

Neutral hydrogen Lyman-alpha measurements in outer geocorona and in interplanetary space by two channel photometer onOGO 5

16 p2450 A72-32955

Monte Carlo treatment of Lyman-alpha radiation in a plane-parallel atmosphere.

17 p2598 A72-34538

Backscatter of solar resonance radiation. I.

17 p2598 A72-34626

Atmospheric pressure, density and scale height calculated from H Lyman-alpha absorption allowing for the variation in cross-section with wavelength.

19 p2793 A72-38859

Lyman alpha resonance line asymmetry calculation in dense hydrogen plasma, noting disagreement between theory and experiment

22 p3212 A72-42917

Equatorial UV airglow azimuthal variations from spinning rocket measurements, attributing origin to electron collision excited atomic hydrogen Lyman alpha emission

23 p3282 A72-43263

LYMAN BETA RADIATION

Lyman alpha, Lyman beta and Balmer alpha hydrogen airglow emission simultaneous measurements compared with solar radiation resonant scattering models

01 p0061 A72-10899

LYMAN SPECTRA

Electric quadrupole to magnetic dipole f-values for CO fourth positive and nitrogen Lyman-Birge-Hopfield systems, using curve of growth method

01 p0103 A72-10092

Exosphere geocoronal hydrogen density, vertical structure and diurnal variability from Lyman spectra observational data, discussing polar wind origins

07 p0978 A72-20041

Time evolution of chromosphere layer heated by energetic particle stream during solar flare, noting cooling by Lyman continuum radiation transfer

13 p2032 A72-29721

Solar chromosphere model based on Lyman spectra observations, calculating temperature, gas and electron pressure and particle densities as function of height

13 p2049 A72-29932

UV laser parameters calculation for operation on Lyman transition between H atom resonant excited state and ground state

17 p2562 A72-34349

LYMPH

NT LYMPHOCYTES

Histologic analysis of hypoxia exposure effects on mouse skin homograft reaction due to lymphatic organ function changes

22 p3144 A72-42675

LYMPHOCYTES

Inhaled ozone effect on chromosome aberrations break frequencies in circulating blood lymphocytes of irradiated Chinese hamsters

01 p0015 A72-11149

Chronic microwave irradiation effects on experimental animal blood forming systems, examining peripheral blood count changes and nuclei and mitosis abnormalities in erythroblastic and lymphoid cells

02 p0158 A72-11708

Crowding phenomenon effect on blood cell oxygen consumption, using Cartesian diver technique for polymorphonuclear leukocyte, lymphocyte and platelet measurements

12 p1763 A72-27842

Stress and adaptation responses to repeated acute acceleration.

17 p2500 A72-34729

Water-soluble insulin receptors from human lymphocytes.

24 p3373 A72-45375

LYOPHILIZATION

U COLLOIDING

LYOPHILS

U COLLOIDS

LYSOGENESIS

Rat tissue autolysis rate during hypokinesia, discussing relation to free amino acid background changes

05 p0619 A72-16648

LYSOZYME

Lysosomal enzymes of eye tissues during the action of hydrocortisone

22 p3141 A72-42279



AIAA TECHNICAL INFORMATION SERVICE

750 THIRD AVENUE

NEW YORK, N. Y. 10017